PHYSICS LETTERS B

VOLUME 592, 2004

REVIEW OF PARTICLE PHYSICS

ELSEVIER

Amsterdam – Boston – Jena – London – New York – Oxford
Paris – Philadelphia – San Diego – St. Louis

PHYSICS LETTERS B

Aims and scope
Physics Letters B ensures the rapid publication of letter-type communications in the fields of Nuclear Physics, Particle Physics and Astrophysics. Articles should influence the physics community significantly.

Abstracted/indexed in:
Current Contents: Physical, Chemical & Earth Sciences; INSPEC.

Publication information
PHYSICS LETTERS A (ISSN 0375-9601) and PHYSICS LETTERS B (ISSN 0370-2693) will each be published weekly. For 2004, volumes 320–333 of Physics Letters A are scheduled for publication. For 2004, volumes 578–604 of Physics Letters B are scheduled for publication. Subscription prices are available upon request from the Publisher or from the Regional Sales Office nearest you or from these journals websites (http://www.elsevier.com/locate/physleta) (http://www.elsevier.com/locate/physletb). Further information is available on these journals and other Elsevier products through Elsevier's website: (http://www.elsevier.com). PHYSICS REPORTS (ISSN 0370-1573) will be published approximately weekly. For 2004, volumes 388–404 of Physics Reports are scheduled for publication. Subscription prices are available upon request from the Publisher or from the Regional Sales Office nearest you or from this journal's website (http://www.elsevier.com/locate/physrep). Further information is available on this journal and other Elsevier products through Elsevier's website: (http://www.elsevier.com).
A combined subscription to the 2004 issues of Physics Letters A, Physics Letters B and Physics Reports is available at a reduced rate.
Subscriptions are accepted on a prepaid basis only and are entered on a calendar year basis. Issues are sent by standard mail (surface within Europe, air delivery outside Europe). Priority rates are available upon request. Claims for missing issues should be made within six months of the date of dispatch.

Orders, claims and journal enquiries: please contact the Customer Support Department at the Regional Sales Office nearest to you:
Orlando, Elsevier, Customer Service Department, 6277 Sea Harbor Drive, Orlando, FL 32887-4800, USA; phone: (+1) (877) 8397126 [toll free number for US customers], or (+1) (407) 3454020 [customers outside US]; fax: (+1) (407) 3631354; e-mail: usjcs@elsevier.com
Amsterdam, Elsevier, Customer Service Department, P.O. Box 211, 1000 AE Amsterdam, The Netherlands; phone: (+31) (20) 485 3757; fax: (+31) (20) 485 3432; e-mail: nlinfo-f@elsevier.com
Tokyo, Elsevier, Customer Service Department, 4F Higashi Azabu, 1 Chome Bldg, 1-9-15 Higashi-Azabu, Minato-ku, Tokyo 106-0044, Japan; phone: (+81) (3) 5561 5037; fax: (+81) (3) 5561 5047; e-mail: jp.info@elsevier.com
Singapore, Elsevier, Customer Service Department, 3 Killiney Road, #08-01 Winsland House I, Singapore 239519; phone: (+65) 6349 0222; fax: (+65) 6733 1510; e-mail: asiainfo@elsevier.com

Advertising information
Advertising orders and enquiries can be sent to:
South America: Mr Tino DeCarlo, The Advertising Department, Elsevier Inc., 360 Park Avenue South, New York, NY 10010-1710, USA; phone: (+1) (212) 633 3815; fax: (+1) (212) 633 3820; e-mail: t.decarlo@elsevier.com
Europe, USA, Canada and ROW: Miss Katrina Barton, Commercial Sales, Elsevier, 84 Theobald's Road, London, WC1X 8RR, UK; phone: (+44) (0) 20 7611 4117; fax: (+44) (0) 20 7611 4463; e-mail: commercialsales@elsevier.com

USA mailing notice: Physics Letters B (ISSN 0370-2693) is published weekly by Elsevier B.V. (P.O. Box 211, 1000 AE Amsterdam, The Netherlands). Annual subscription price in the USA US$ 9884.00 (valid in North, Central and South America), including air speed delivery. Periodicals postage rate paid at Jamaica, NY 11431.
USA POSTMASTER: Send address changes to Physics Letters B, Publications Expediting, Inc., 200 Meacham Avenue, Elmont, NY 11003.
AIRFREIGHT AND MAILING in the USA by Publications Expediting, Inc., 200 Meacham Avenue, Elmont, NY 11003.

♾ The paper used in this publication meets the requirements of ANSI/NISO Z39.48-1992 (Permanence of Paper).

Printed in The Netherlands

Available online at www.sciencedirect.com
SCIENCE DIRECT®
Physics Letters B 592 (2004) 1–1109
PHYSICS LETTERS B
www.elsevier.com/locate/physletb

REVIEW OF PARTICLE PHYSICS*

Particle Data Group

Abstract

This biennial *Review* summarizes much of Particle Physics. Using data from previous editions, plus 1726 new measurements from 512 papers, we list, evaluate, and average measured properties of gauge bosons, leptons, quarks, mesons, and baryons. We also summarize searches for hypothetical particles such as Higgs bosons, heavy neutrinos, and supersymmetric particles. All the particle properties and search limits are listed in Summary Tables. We also give numerous tables, figures, formulae, and reviews of topics such as the Standard Model, particle detectors, probability, and statistics. Among the 119 reviews are many that are new or heavily revised including those on neutrino mixing, CP violation in K, D, and B mesons, V_{cb}, the new exotic $\Theta(1540)$ particle, extra-dimensions, grand unified theories, cosmic background radiation, dark matter, cosmological parameters, and big bang cosmology. A booklet is available containing the Summary Tables and abbreviated versions of some of the other sections of this full *Review*. All tables, listings, and reviews (and errata) are also available on the Particle Data Group website: `http://pdg.lbl.gov`.

*The publication of the *Review of Particle Physics* is supported by the Director, Office of Science, Office of High Energy and Nuclear Physics, the Division of High Energy Physics of the U.S. Department of Energy under Contract No. DE–AC03–76SF00098; by the U.S. National Science Foundation under Agreement No. PHY-0070972; by the European Laboratory for Particle Physics (CERN); by an implementing arrangement between the governments of Japan (MEXT: Ministry of Education, Culture, Sports, Science and Technology) and the United States (DOE) on cooperative research and development; and by the Italian National Institute of Nuclear Physics (INFN).

0370-2693/$ – see front matter © 2004 Elsevier B.V. All rights reserved.
doi:10.1016/j.physletb.2004.06.001

PARTICLE DATA GROUP AUTHORS:
S. Eidelman,[1] K.G. Hayes,[2] K.A. Olive,[3] M. Aguilar-Benitez,[4] C. Amsler,[5] D. Asner,[6] K.S. Babu,[7] R.M. Barnett,[8] J. Beringer,[8] P.R. Burchat,[9] C.D. Carone,[10] C. Caso,[11] G. Conforto,[12,13] O. Dahl,[8] G. D'Ambrosio,[14] M. Doser,[15] J.L. Feng,[16] T. Gherghetta,[3] L. Gibbons,[17] M. Goodman,[18] C. Grab,[19] D.E. Groom,[8] A. Gurtu,[20,15] K. Hagiwara,[21] J.J. Hernández-Rey,[22†] K. Hikasa,[23] K. Honscheid,[24] H. Jawahery,[25] C. Kolda,[26] Y. Kwon,[27] M.L. Mangano,[15] A.V. Manohar,[28] J. March-Russell,[15] A. Masoni,[29] R. Miquel,[8] K. Mönig,[30] H. Murayama,[8,31] K. Nakamura,[21] S. Navas,[32†] L. Pape,[15] C. Patrignani,[11] A. Piepke,[33] G. Raffelt,[34] M. Roos,[35] M. Tanabashi,[23] J. Terning,[36] N.A. Törnqvist,[35] T.G. Trippe,[8] P. Vogel,[37] C.G. Wohl,[8] R.L. Workman,[38] W.-M. Yao,[8] P.A. Zyla[8]

Technical Associates: B. Armstrong,[8] P.S. Gee,[8] G. Harper,[8] K.S. Lugovsky,[39] S.B. Lugovsky,[39] V.S. Lugovsky,[39] A. Rom[8]

OTHER AUTHORS WHO HAVE MADE SUBSTANTIAL CONTRIBUTIONS TO REVIEWS:
M. Artuso,[40] E. Barberio,[41] M. Battaglia,[31] H. Bichsel,[42] O. Biebel,[34] P. Bloch,[15] R.N. Cahn,[8] D. Casper,[16] A. Cattai,[15] R.S. Chivukula,[43] G. Cowan,[44] T. Damour,[45] K. Desler,[46] M.A. Dobbs,[8] M. Drees,[47] A. Edwards,[9] D.A. Edwards,[46] V.D. Elvira,[48] J. Erler,[49] V.V. Ezhela,[39] W. Fetscher,[19] B.D. Fields,[50] B. Foster,[46,51] D. Froidevaux,[15] M. Fukugita,[52] T.K. Gaisser,[53] L. Garren,[48] H.-J. Gerber,[19] G. Gerbier,[54] F.J. Gilman,[55] H.E. Haber,[56] C. Hagmann,[57] J. Hewett,[58] I. Hinchliffe,[8] C.J. Hogan,[42] G. Höhler,[59] P. Igo-Kemenes,[60] J.D. Jackson,[8] K.F. Johnson,[61] D. Karlen,[62] B. Kayser,[48] D. Kirkby,[16] S.R. Klein,[63] K. Kleinknecht,[64] I.G. Knowles,[65] P. Kreitz,[58] Yu.V. Kuyanov,[39] O. Lahav,[66] P. Langacker,[67] A. Liddle,[68] L. Littenberg,[69] D.M. Manley,[70] A.D. Martin,[71] M. Narain,[72] P. Nason,[73] Y. Nir,[74] J.A. Peacock,[65] H.R. Quinn,[58] S. Raby,[24] B.N. Ratcliff,[58] E.A. Razuvaev,[39] B. Renk,[64] G. Rolandi,[15] M.T. Ronan,[8] L.J. Rosenberg,[75] C.T. Sachrajda,[76] Y. Sakai,[21] A.I. Sanda,[77] S. Sarkar,[78] M. Schmitt,[79] O. Schneider,[80] D. Scott,[81] W.G. Seligman,[82] M.H. Shaevitz,[83] T. Sjöstrand,[84] G.F. Smoot,[8] S. Spanier,[58] H. Spieler,[8] N.J.C. Spooner,[85] M. Srednicki,[86] A. Stahl,[30] T. Stanev,[53] M. Suzuki,[8] N.P. Tkachenko,[39] G.H. Trilling,[8] G. Valencia,[87] K. van Bibber,[57] M.G. Vincter,[88] D.R. Ward,[89] B.R. Webber,[89] M. Whalley,[71] L. Wolfenstein,[55] J. Womersley,[48] C.L. Woody,[69] O.V. Zenin,[39] R.-Y. Zhu[90]

1. *Budker Institute of Nuclear Physics, RU-630090, Novosibirsk, Russia*
2. *Department of Physics, Hillsdale College, Hillsdale, MI 49242, USA*
3. *School of Physics and Astronomy, University of Minnesota, Minneapolis, MN 55455, USA*
4. *C.I.E.M.A.T., E-28040, Madrid, Spain*
5. *Institute of Physics, University of Zürich, CH-8057 Zürich, Switzerland*
6. *University of Pittsburgh, Department of Physics and Astronomy, 3951 O'Hara St, Pittsburgh PA, 15260, USA*
7. *Department of Physics, Oklahoma State University, Stillwater, OK 74078, USA*
8. *Physics Division, Lawrence Berkeley National Laboratory, 1 Cyclotron Road, Berkeley, CA 94720, USA*
9. *Department of Physics, Stanford University, Stanford, CA 94305, USA*
10. *Nuclear and Particle Theory Group, Department of Physics, College of William and Mary, Williamsburg, VA 23187, USA*
11. *Dipartimento di Fisica e INFN, Università di Genova, I-16146 Genova, Italy*
12. *Università degli Studi, I-61029 Urbino, Italy*
13. *Istituto Nazionale di Fisica Nucleare, Sezione di Firenze, I-50125 Firenze, Italy*
14. *Dipartimento di Scienze Fisiche, Univ. di Napoli "Federico II," Complesso Universitario Monte S. Angelo, Via Cintia, I-80126 Napoli, Italy*
15. *CERN, European Organization for Nuclear Research, CH-1211 Genève 23, Switzerland*
16. *Department of Physics and Astronomy, University of California, Irvine, CA 92697-4576, USA*
17. *Newman Laboratory for Elementary Particle Physics, Cornell University, Ithaca, NY 14853-5001, USA*
18. *Argonne National Laboratory, 9700 S. Cass Ave., Argonne, IL 60439-4815, USA*
19. *Institute for Particle Physics, ETH Zürich, CH-8093 Zürich, Switzerland*
20. *Tata Institute of Fundamental Research, Mumbai (Bombay) 400 005, India*
21. *KEK, High Energy Accelerator Research Organization, Oho, Tsukuba-shi, Ibaraki-ken 305-0801, Japan*
22. *IFIC — Instituto de Física Corpuscular, Universitat de València — C.S.I.C., E-46071 Valencia, Spain*
23. *Department of Physics, Tohoku University, Aoba-ku, Sendai 980-8578, Japan*
24. *Department of Physics, The Ohio State University, 174 W. 28th Ave., Columbus, OH 43210 USA*
25. *University of Maryland, Department of Physics and Astronomy, College Park, MD 20742-4111, USA*
26. *Department of Physics, University of Notre Dame, 225 Niewland Hall, Notre Dame, IN 46556 USA*
27. *Yonsei University, Department of Physics, 134 Sinchon-dong, Sudaemoon-gu, Seoul 120-749, South Korea*
28. *Department of Physics, University of California at San Diego, La Jolla, CA 92093, USA*
29. *INFN Sezione di Cagliari, Cittadella Universitaria de Monserrato, Casella postale 170, I-09042 Monserrato (CA), Italy*
30. *DESY-Zeuthen, D-15735 Zeuthen, Germany*
31. *Department of Physics, University of California, Berkeley, CA 94720, USA*

† J.J. Hernández-Rey and S. Navas acknowledge support from MCYT, Spain (FPA2002-12065-E).

32. *Dpto. de Física Teórica y del Cosmos & C.A.F.P.E., Universidad de Granada, 18071 Granada, Spain*
33. *Department of Physics and Astronomy University of Alabama, 206 Gallalee Hall, Box 870324, Tuscaloosa, AL 35487-0324, USA*
34. *Max-Planck-Institut für Physik (Werner-Heisenberg-Institut), Föhringer Ring 6, D-80805 München, Germany*
35. *Department of Physical Sciences, POB 64 FIN-00014 University of Helsinki, Finland*
36. *Los Alamos National Laboratory, Los Alamos, NM 87545, USA*
37. *California Institute of Technology, Kellogg Radiation Laboratory 106-38, Pasadena, CA 91125, USA*
38. *Department of Physics, George Washington University Virginia Campus, Ashburn, VA 20147-2604, USA*
39. *COMPAS Group, Institute for High Energy Physics, RU-142284, Protvino, Russia*
40. *Department of Physics, Syracuse University, Syracuse, NY, 13244-1130, USA*
41. *University of Melbourne, School of Physics, Parkville, Victoria 3052, Australia*
42. *Department of Astronomy, University of Washington, Physics/Astronomy Bldg., Stevens Way, POB 351580, Seattle, WA 98195-1580, USA*
43. *Michigan State University, Dept. of Physics and Astronomy, East Lansing, MI 48824-2320, USA*
44. *Department of Physics, Royal Holloway, University of London, Egham, Surrey TW20 0EX, UK*
45. *Institut des Hautes Etudes Scientifiques, F-91440 Bures-sur-Yvette, France*
46. *Deutsches Elektronen-Synchrotron DESY, 85 Notkestraße, D-22603 Hamburg, Germany*
47. *Technische Universität München, Fakultät Für Physik Department, James Franck Str., D-85748 Garching, Germany*
48. *Fermilab, P.O. Box 500, Batavia, IL 60510, USA*
49. *Instituto de Física, Universidad Nacional Autónoma de México, Apartado Postal 20-364, 01000 México D.F., México*
50. *Department of Astronomy, University of Illinois, 1002 W. Green St., Urbana, IL 61801, USA*
51. *H.H. Wills Physics Lab., University of Bristol, Royal Fort, Tyndall Ave., Bristol BS8 1TL, UK*
52. *University of Tokyo, Institute for Cosmic Ray Research, Kashiwa 2778582, Japan*
53. *Bartol Research Institute, University of Delaware, Newark, DE 19716, USA*
54. *CEA/Saclay, B.P.2, Orme des Merisiers, F-91191 Gif-sur-Yvette Cedex, France*
55. *Department of Physics, Carnegie Mellon University, Pittsburgh, PA 15213, USA*
56. *Santa Cruz Institute for Particle Physics, University of California, Santa Cruz, CA 95064, USA*
57. *Lawrence Livermore National Laboratory, 7000 East Ave., Livermore, CA 94550, USA*
58. *Stanford Linear Accelerator Center, P.O. box 4349, Stanford, CA 94309, USA*
59. *Institut für Theoretische Teilchenphysik, University of Karlsruhe, Postfach 6980, D-76128 Karlsruhe, Germany*
60. *Physikalisches Institut, Universität Heidelberg, Philosophenweg 12, D-69120 Heidelberg, Germany*
61. *Department of Physics, Florida State University, Tallahassee, FL 32306, USA*
62. *Department of Physics, Carleton University, 1125 Colonel By Drive, Ottawa, ON K1S 5B6, Canada*
63. *Nuclear Science Division, Lawrence Berkeley National Laboratory, 1 Cyclotron Road, Berkeley, CA 94720, USA*
64. *Institut für Physik, Johannes-Gutenberg Universität Mainz, D-55099 Mainz, Germany*
65. *Institute for Astronomy, University of Edinburgh, Royal Observatory, Blackford Hill, Edinburgh, EH9 3JZ, Scotland, UK*
66. *University of Cambridge, Institute of Astronomy, Madingley Road, Cambridge, CB3 0HA, UK*
67. *Department of Physics and Astronomy, University of Pennsylvania, Philadelphia, PA 19104, USA*
68. *University of Sussex, Astronomy Centre, Falmer Brighton BN1 9RH, UK*
69. *Physics Department, Brookhaven National Laboratory, Upton, NY 11973, USA*
70. *Department of Physics, Kent State University, Kent, OH 44242, USA*
71. *Institute for Particle Physics Phenomenology, Department of Physics, University of Durham, Durham DH1 3LE, UK*
72. *Boston University, Department of Physics, 590 Commonwealth Ave., Boston, MA 02215, USA*
73. *INFN Sezione di Milano, via Celoria 16, I-20133 Milano, Italy*
74. *Weizmann Institue of Science, Department of Particle Physics, P.O. Box 26 Rehovot 76100, Israel*
75. *Department of Physics and Laboratory for Nuclear Science, Massachusetts Institute of Technology, 77 Massachusetts Avenue, Cambridge, MA 02139, USA*
76. *Department of Physics and Astronomy, University of Southampton, Highfield, Southampton S017 1BJ, UK*
77. *Nagoya University, Department of Physics, Chikusa-ku, Nagoya, 464-8602, Japan*
78. *Theoretical Physics, University of Oxford, 1 Keble Road, Oxford OX1 3NP, UK*
79. *Department of Physics and Astronomy, Northwestern University, Evanston, IL 60208, USA*
80. *Laboratoire de Physique des Hautes Energies, Swiss Federal Institute of Technology, Lausanne, CH-1015 Lausanne, Switzerland*
81. *Department of Physics and Astronomy, University of British Columbia, Vancouver, BC V6T 1Z1 Canada*
82. *Columbia University, Nevis Labs, PO Box 137, Irvington, NY 10533, USA*
83. *Department of Physics, Columbia University, 538 West 120th St., New York, NY 10027, USA*
84. *Department of Theoretical Physics, Lund University, S-223 62 Lund, Sweden*
85. *Department of Physics and Astronomy, University of Sheffield, Sheffield S3 7RH, UK*
86. *Department of Physics, University of California, Santa Barbara, CA 93106, USA*
87. *Department of Physics, Iowa State University, Ames, IA 50011, USA*
88. *Department of Physics, University of Alberta, Edmonton, Alberta, T6G 2J1, Canada*
89. *Cavendish Laboratory, Madingley Road, Cambridge CB3 0HE, UK*
90. *California Institute of Technology, Physics Department, 161-33, Pasadena, CA 91125, USA*

We dedicate this edition of the Review of Particle Physics to the memory of two long-time members of the Particle Data Group, Lucien Montanet and Giovanni Conforto, both of whom died in 2003.

†Lucien Montanet (1930–2003)

Lucien Montanet died on Thursday June 19, 2003. Lucien was a pioneer of high energy physics, becoming in 1957 one of the first physicists at CERN. For his PhD thesis, he analyzed interactions of cosmic rays in a Wilson cloud chamber run at the top of Switzerland's Jungfraujoch mountain. Later he joined Charles Peyrou and Raphael Armenteros to analyze photographs of proton-antiproton annihilations in an 81-cm bubble chamber, one of the earliest such analysis at CERN. He co-signed the discovery of the first meson resonance found at CERN and in Europe, the E meson, now call the $\eta(1440)$. Thus began a long career devoted to meson and baryon spectroscopy, a field in which he became one of the leading experts. He organized and lead numerous workshops and conferences on hadron spectroscopy, and was a frequent rapporteur for review talks on these topics. He was a key member of the Particle Data Group from 1977 through 1996.

Lucien initiated and coordinated several important experiments, including the European Hybrid Spectrometer at the CERN SPS, designed to study complex hadronic final states, strong-interaction dynamics, and features of the associated weak decays.

In 1985, Lucien was appointed coordinator of the CERN-USSR (now CERN-Russia) Committee, where he fostered excellent relations between CERN and Russia. In 1990, he became a member of the Scientific Council of the Joint Institute for Nuclear Research (JINR) at Dubna, and played a key role in defining JINR's scientific policy. In 1973, he became editor of "Physics Letters" and continued in this role even after his retirement in 1995. Many publications of CERN and other European laboratories underwent the expert and critical scrutiny of Lucien and his partner Klaus Winter.

In Lucien Montanet, we have lost one of the pioneers of modern high-energy physics, an inspired, generous, and friendly member of our community and a true lover of science.

†Giovanni Conforto (1938–2003)

Gianni Conforto died in May 2003. He was born in Rome on August 30, 1938 and received his Ph.D. from the University of Rome in 1961. He pursued a rich physics career at CERN, Enrico Fermi Institute of the University of Chicago, Rutherford Laboratory, INFN Roma, INFN Firenze, University of Michigan at Ann Arbor, University of Hamburg, and University of Urbino, working on many experiments, including NOMAD, L3, Crystal Ball, and Gargamelle. His wide-ranging research interests included weak decays of leptons and baryons, properties of mesons and baryons including states with strangeness, charm, and beauty, the Upsilon meson, the Z boson, neutrino physics, astrophysics, and cosmology.

From 1988 to 2003, he made significant contributions to the Review of Particle Physics in the W boson and K meson sections.

In Gianni Conforto, we have lost a charming person, a real gentleman, and an accomplished physicist.

TABLE OF CONTENTS

(Continued on next page.)

PARTICLE LISTINGS*

MAJOR REVIEWS IN THE PARTICLE LISTINGS

*The divider sheets give more detailed indices for each main section of the Particle Listings.

HIGHLIGHTS OF THE 2004 EDITION OF THE REVIEW OF PARTICLE PHYSICS

- 512 new papers with 1726 new measurements.
- 119 reviews (most are revised or new).
- Major update to Neutrino Mixing review. Also the three Neutrino Mixing summary plots are combined into one, with the latest results.
- Latest from B-meson physics: 106 papers with 466 measurements: CP violation, $\sin 2\beta$, mixing, V_{cb}, and V_{ud} *etc.*
- New combined review of CP Violation in K, D, and B mesons.
- Major updates of V_{ub}, V_{cb}, Mixing, and b decay reviews.
- Coverage of the new exotic $\Theta(1540)$, with a special review.
- Major update of CKM review.
- New fits for CP violation parameters in K meson decay.
- Reviews of extra-dimensions and grand unified theories.
- New Cosmic Background Radiation review with emphasis on WMAP and other new anisotropy results.
- New reviews on dark matter and cosmological parameters.
- Post-WMAP review on big bang cosmology.
- New and revised sections in Particle Detectors review, especially organic scintillators, Cherenkov detectors, and electromagnetic calorimeters.
- New, improved plots of $R_{e^+e^-}$, including detailed plots covering the low mass region and the regions around the $c\bar{c}$ and $b\bar{b}$ thresholds. Updated Z lineshape plot with the final results from LEP1.

INTRODUCTION

ONLINE PARTICLE PHYSICS INFORMATION

INTRODUCTION

1. Overview

The *Review of Particle Physics* and the abbreviated version, the *Particle Physics Booklet,* are reviews of the field of Particle Physics. This complete *Review* includes a compilation/evaluation of data on particle properties, called the "Particle Listings." These Listings include 1726 new measurements from 512 papers, in addition to the 20,200 measurements from 5903 papers that first appeared in previous editions.

Both books include Summary Tables with our best values and limits for particle properties such as masses, widths or lifetimes, and branching fractions, as well as an extensive summary of searches for hypothetical particles. In addition, we give a long section of "Reviews, Tables, and Plots" on a wide variety of theoretical and experimental topics, a quick reference for the practicing particle physicist.

The *Review* and the *Booklet* are published in even-numbered years. This edition is an updating through December 2003 (and, in some areas, well into 2004). As described in the section "Using Particle Physics Databases" following this introduction, the content of this *Review* is available on the World-Wide Web, and is updated between printed editions (`http://pdg.lbl.gov/`).

The Summary Tables give our best values of the properties of the particles we consider to be well established, a summary of search limits for hypothetical particles, and a summary of experimental tests of conservation laws.

The Particle Listings contain all the data used to get the values given in the Summary Tables. Other measurements considered recent enough or important enough to mention, but which for one reason or another are not used to get the best values, appear separately just beneath the data we do use for the Summary Tables. The Particle Listings also give information on unconfirmed particles and on particle searches, as well as short "reviews" on subjects of particular interest or controversy.

The Particle Listings were once an archive of all published data on particle properties. This is no longer possible because of the large quantity of data. We refer interested readers to earlier editions for data now considered to be obsolete.

We organize the particles into six categories:

Gauge and Higgs bosons
Leptons
Quarks
Mesons
Baryons
Searches for monopoles, supersymmetry, compositeness, extra dimensions, *etc.*

The last category only includes searches for particles that do not belong to the previous groups; searches for heavy charged leptons and massive neutrinos, by contrast, are with the leptons.

In Sec. 2 of this Introduction, we list the main areas of responsibility of the authors, and also list our large number of consultants, without whom we would not have been able to produce this *Review.* In Sec. 3, we mention briefly the naming scheme for hadrons. In Sec. 4, we discuss our procedures for choosing among measurements of particle properties and for obtaining best values of the properties from the measurements.

The accuracy and usefulness of this *Review* depend in large part on interaction between its users and the authors. We appreciate comments, criticisms, and suggestions for improvements of any kind. Please send them to the appropriate author, according to the list of responsibilities in Sec. 2 below, or to the LBNL addresses below.

To order a copy of the *Review* or the *Particle Physics Booklet* from North and South America, Australia, and the Far East, send email to `PDG@LBL.GOV`

or via the web at:
(`http://pdg.lbl.gov/pdgmail`)
or write to:
Particle Data Group, MS 50R6008
Lawrence Berkeley National Laboratory
Berkeley, CA 94720-8166, USA

From all other areas, see
(`http://weblib.cern.ch/publreq.php`)
or write to
CERN Scientific Information Service
CH-1211 Geneva 23
Switzerland

2. Authors and consultants

The authors' main areas of responsibility are shown below:
* Asterisk indicates the person to contact with questions or comments

Gauge and Higgs bosons	
γ	C. Grab, D.E. Groom*
Gluons	R.M. Barnett,* A.V. Manohar
Graviton	D.E. Groom*
W, Z	C. Caso,* A. Gurtu*
Higgs bosons	K. Hikasa, M.L. Mangano*
Heavy bosons	K.S. Babu, R. Miquel,* M. Tanabashi
Axions	J. March-Russell, H. Murayama, G. Raffelt*
Leptons	
Neutrinos	M. Goodman, R. Miquel,* K. Nakamura, K.A. Olive, A. Piepke, P. Vogel
e, μ	C. Grab, D.E. Groom*
ν_τ, τ	D.E. Groom, K.G. Hayes, K. Mönig*
Quarks	
Quarks	R.M. Barnett,* A.V. Manohar
Top quark	J.L. Feng,* K. Hagiwara
b'	J.L. Feng,* K. Hagiwara
Free quark	D.E. Groom*
Mesons	
π	C. Grab, D.E. Groom*
η	C. Grab, C.G. Wohl*
Unstable mesons	M. Aguilar-Benitez, C. Amsler, M. Doser,* S. Eidelman, J.J. Hernández-Rey, A. Masoni, S. Navas, C. Patrignani, M. Roos, N.A. Törnqvist
K (stable)	G. D'Ambrosio, T.G. Trippe*
D (stable)	P.R. Burchat, C.G. Wohl*
B (stable)	H. Jawahery, Y. Kwon, W.-M. Yao*

Baryons

Stable baryons	C. Grab, C.G. Wohl*
Unstable baryons	D.M. Manley, C.G. Wohl,* R.L. Workman
Charmed baryons	D. Asner, P.R. Burchat, C.G. Wohl*
Bottom baryons	H. Jawahery, Y. Kwon, W.-M. Yao*

Miscellaneous searches

Monopole	D.E. Groom*
Supersymmetry	M.L. Mangano,* H. Murayama, K.A. Olive, L. Pape
Technicolor	M. Tanabashi, J. Terning*
Compositeness	M. Tanabashi, J. Terning*
Extra Dimensions	J.L. Feng, T. Gherghetta*, C. Kolda, J. March-Russell
WIMPs and Other	J.L. Feng,* K. Hikasa

Reviews, tables, figures, and formulae

R.M. Barnett, D.E. Groom, R. Miquel, T.G. Trippe, C.G. Wohl, W.-M. Yao

Technical support

B. Armstrong, P.S. Gee, G. Harper, K.S. Lugovsky, S.B. Lugovsky, V.S. Lugovsky, A. Rom, P.A. Zyla*

The Particle Data Group benefits greatly from the assistance of some 700 physicists who are asked to verify every piece of data entered into this *Review*. Of special value is the advice of the PDG Advisory Committee which meets annually and thoroughly reviews all aspects of our operation. The members of the 2004 committee are:

H. Aihara (Tokyo)
P. Drell (SLAC)
R. Voss (CERN), Chair
M. Whalley (Durham)
P. Zerwas (DESY)

We have especially relied on the expertise of the following people for advice on particular topics:

- M.N. Achasov (BINP, Novosibirsk)
- S.I. Alekhin (COMPAS Group, IHEP, Protvino)
- A. Ali (DESY)
- J.A. Appel (Fermilab)
- G. Azuelos (University of Montreal)
- E. Barberis (LBNL, Northeastern University)
- A.R. Barker (University of Colorado)
- T. Barnes (University of Tennessee)
- J.-L. Basdevant (University of Paris)
- L. Baudis (Stanford University)
- T. Beers (Michigan State University)
- E. Berger (Argonne National Lab)
- S. Bethke (MPI, Munich)
- I.I. Bigi (Notre Dame University)
- S. Bilenky (Joint Inst. for Nuclear Research, Dubna)
- M. Billing (Cornell University)
- E. Blucher (University of Chicago)
- A.E. Bondar (BINP, Novosibirsk)
- R.A. Briere (Harvard University)
- T. Browder (University of Hawaii)
- O. Bruening (CERN)
- D. Bryman (TRIUMF)
- G. Buchalla (CERN)
- A. Buras (Tech. University of Munich)
- R.N. Cahn (LBNL)
- M. Cavalli (IFAE, Barcelona)
- A. Ceccucci (CERN)
- D. Chakraborty (Northern Illinois University)
- D.A. Cinabro (Wayne State University)
- F. Close (Oxford University)
- E.D. Commins (University of California, Berkeley)
- S. Derenzo (LBNL)
- L. Di Ciaccio (LAPP, Annecy)
- R. Dixon (Fermilab)
- J. Donoghue (University of Massachusetts, Amherst)
- M.S. Dubrovin (Cornell University)
- S.A. Dytman (University of Pittsburgh)
- G. Eigen (Bergen University)
- J. Engelfried (San Luis Potosi University)
- G.V. Fedotovich (BINP, Novosibirsk)
- T. Ferbel (Rochester University)
- M. Fidecaro (CERN)
- W. Fischer (Brookhaven National Lab)
- S.J. Freedman (University of California, Berkeley)
- H. Fritzsch (Ludwig-Maximilians University, Munich)
- M.A. Furman (LBNL)
- F. Gabbiani (Duke University)
- P. Gambino (INFN, Turin)
- A. Glazov (University of Chicago)
- M.C. Gonzalez-Garcia (SUNY Stony Brook and IFIC Valencia)
- H. Greenlee (Fermilab)
- E.M. Gullikson (LBNL)
- R. Hagstrom (Argonne National Lab)
- S. Heinemeyer (CERN)
- M. Hobson (MRAO, Cambridge)
- A. Hoecker (LAL-Orsay)
- J. Imazato (KEK)
- G. Isidori (INFN, Frascati)
- Yu.M. Ivanov (Petersburg Nuclear Physics Inst.)
- P. Janot (CERN)
- R.W. Kenney (LBNL)
- B.I. Khazin (BINP, Novosibirsk)
- B. Klima (Fermilab)
- I.A. Koop (BINP, Novosibirsk)
- A.A. Korol (BINP, Novosibirsk)
- P. Krizan (Stefan Inst., Ljubljana)
- P.P. Krokovny (BINP, Novosibirsk)
- S.-I. Kurokawa (KEK)
- A.S. Kuzmin (BINP, Novosibirsk)
- G. Landsberg (Brown University)
- U. Langenegger (Heidelberg University)
- L. Lellouch (Marseille, CPT)
- K. Lesko (LBNL)
- E.B. Levichev (BINP, Novosibirsk)
- W. Lewis (Los Alamos National Lab)
- Z. Ligeti (LBNL)
- E. Lisi (INFN Bari)
- I.B. Logashenko (BINP, Novosibirsk)
- O. Long (University of California, Santa Barbara)
- V. Luth (SLAC)
- G.R. Lynch (LBNL)
- W. MacKay (Brookhaven National Lab)
- W. Marciano (Brookhaven National Lab)

- P. Meyers (Princeton University)
- P.J. Mohr (NIST)
- D. Morgan (Rutherford Appleton Lab)
- B.M.K. Nefkens (University of California, Los Angeles)
- M. Neubert (Cornell University)
- H.N. Nelson (University of California, Santa Barbara)
- K. Oide (KEK)
- S. Olsen (University of Hawaii)
- F. Paige (Brookhaven National Lab)
- S. Pakvasa (University of Hawaii)
- F. Parodi (University of Genova)
- R. Partridge (Brown University)
- M. Paulini (Carnegie Mellon University)
- R. Peccei (University of California, Los Angeles)
- M.R. Pennington (University of Durham)
- K. Pitts (University of Illinois, Urbana)
- C. Pryke (University of Chicago)
- P. Raimondi (INFN, Frascati)
- J. Richman (University of California, Santa Barbara)
- B.L. Roberts (Boston University)
- S. Robertson (SLAC)
- R. Roser (Fermilab)
- T. Roser (Brookhaven National Lab)
- J.L. Rosner (University of Chicago)
- P. Roudeau (LAL, Orsay)
- G. Rudolph (University of Innsbruck)
- G. Schierholz (DESY)
- J.T. Seeman (SLAC)
- Yu.M. Shatunov (BINP, Novosibirsk)
- M. Shochet (University of Chicago)
- B.A. Shwartz (BINP, Novosibirsk)
- J. Smith (University of Colorado)
- M.D. Sokoloff (University of Cincinnati)
- T. Stelzer (University of Illinois, Urbana)
- S.L. Stone (Syracuse University)
- S.I. Striganov (COMPAS Group, IHEP, Protvino)
- M. Strovink (LBNL)
- B.N. Taylor (NIST)
- G. Unal (LAL, Orsay)
- N. Uraltsev (St. Petersburg, INP)
- J.E. Urheim (University of Minnesota)
- E. Vangioni-Flam (Paris, Inst. Astrophysics)
- R. Voss (CERN)
- Y. Wah (University of Chicago)
- H. Wahl (CERN)
- S. Wasserbaech (Utah Valley State College)
- A.J. Weinstein (California Institute of Technology)
- C. Weiser (CERN)
- F. Willeke (DESY)
- D.A. Williams (University of California, Santa Cruz)
- S. Willocq (University of Massachusetts, Amherst)
- B. Winstein (University of Chicago)
- J.E. Wiss (University of Illinois)
- B. Yabsley (Virginia Tech)
- O.P. Yushchenko (IHEP, Protvino)
- A.M. Zaitsev (IHEP, Protvino)
- M. Zeller (Yale University)
- P. Zerwas (DESY)
- C. Zhang (IHEP, Beijing)
- K. Zuber (Oxford University)

3. Naming scheme for hadrons

We introduced in the 1986 edition [2] a new naming scheme for the hadrons. Changes from older terminology affected mainly the heavier mesons made of u, d, and s quarks. Otherwise, the only important change to known hadrons was that the $F^{\pm}$ became the $D_s^{\pm}$. None of the lightest pseudoscalar or vector mesons changed names, nor did the $c\overline{c}$ or $b\overline{b}$ mesons (we do, however, now use χ_c for the $c\overline{c}$ χ states), nor did any of the established baryons. The Summary Tables give both the new and old names whenever a change has occurred.

The scheme is described in "Naming Scheme for Hadrons" (p. 102) of this *Review*.

We give here our conventions on type-setting style. Particle symbols are italic (or slanted) characters: e^-, p, Λ, π^0, K_L, D_s^+, b. Charge is indicated by a superscript: B^-, Δ^{++}. Charge is not normally indicated for p, n, or the quarks, and is optional for neutral isosinglets: η or η^0. Antiparticles and particles are distinguished by charge for charged leptons and mesons: τ^+, K^-. Otherwise, distinct antiparticles are indicated by a bar (overline): $\overline{\nu}_\mu$, $\overline{t}$, $\overline{p}$, $\overline{K}^0$, and $\overline{\Sigma}^+$ (the antiparticle of the Σ^-).

4. Procedures

4.1. ***Selection and treatment of data***: The Particle Listings contain all relevant data known to us that are published in journals. With very few exceptions, we do not include results from preprints or conference reports. Nor do we include data that are of historical importance only (the Listings are not an archival record). We search every volume of 20 journals through our cutoff date for relevant data. We also include later published papers that are sent to us by the authors (or others).

In the Particle Listings, we clearly separate measurements that are used to calculate or estimate values given in the Summary Tables from measurements that are not used. We give explanatory comments in many such cases. Among the reasons a measurement might be excluded are the following:

- It is superseded by or included in later results.
- No error is given.
- It involves assumptions we question.
- It has a poor signal-to-noise ratio, low statistical significance, or is otherwise of poorer quality than other data available.
- It is clearly inconsistent with other results that appear to be more reliable. Usually we then state the criterion, which sometimes is quite subjective, for selecting "more reliable" data for averaging. See Sec. 4.4.
- It is not independent of other results.
- It is not the best limit (see below).
- It is quoted from a preprint or a conference report.

In some cases, *none* of the measurements is entirely reliable and no average is calculated. For example, the masses of many of the baryon resonances, obtained from partial-wave analyses, are quoted as estimated ranges thought to probably include the true values, rather than as averages with errors. This is discussed in the Baryon Particle Listings.

For upper limits, we normally quote in the Summary Tables the strongest limit. We do not average or combine

upper limits except in a very few cases where they may be re-expressed as measured numbers with Gaussian errors.

As is customary, we assume that particle and antiparticle share the same spin, mass, and mean life. The Tests of Conservation Laws table, following the Summary Tables, lists tests of CPT as well as other conservation laws.

We use the following indicators in the Particle Listings to tell how we get values from the tabulated measurements:

- OUR AVERAGE—From a weighted average of selected data.
- OUR FIT—From a constrained or overdetermined multi-parameter fit of selected data.
- OUR EVALUATION—Not from a direct measurement, but evaluated from measurements of related quantities.
- OUR ESTIMATE—Based on the observed range of the data. Not from a formal statistical procedure.
- OUR LIMIT—For special cases where the limit is evaluated by us from measured ratios or other data. Not from a direct measurement.

An experimentalist who sees indications of a particle will of course want to know what has been seen in that region in the past. Hence we include in the Particle Listings all reported states that, in our opinion, have sufficient statistical merit and that have not been disproved by more reliable data. However, we promote to the Summary Tables only those states that we feel are well established. This judgment is, of course, somewhat subjective and no precise criteria can be given. For more detailed discussions, see the minireviews in the Particle Listings.

4.2. ***Averages and fits***: We divide this discussion on obtaining averages and errors into three sections: (1) treatment of errors; (2) unconstrained averaging; (3) constrained fits.

4.2.1. *Treatment of errors:* In what follows, the "error" δx means that the range $x \pm \delta x$ is intended to be a 68.3% confidence interval about the central value x. We treat this error as if it were Gaussian. Thus when the error *is* Gaussian, δx is the usual one standard deviation (1σ). Many experimenters now give statistical and systematic errors separately, in which case we usually quote both errors, with the statistical error first. For averages and fits, we then add the the two errors in quadrature and use this combined error for δx.

When experimenters quote asymmetric errors $(\delta x)^+$ and $(\delta x)^-$ for a measurement x, the error that we use for that measurement in making an average or a fit with other measurements is a continuous function of these three quantities. When the resultant average or fit $\overline{x}$ is less than $x-(\delta x)^-$, we use $(\delta x)^-$; when it is greater than $x+(\delta x)^+$, we use $(\delta x)^+$. In between, the error we use is a linear function of x. Since the errors we use are functions of the result, we iterate to get the final result. Asymmetric output errors are determined from the input errors assuming a linear relation between the input and output quantities.

In fitting or averaging, we usually do not include correlations between different measurements, but we try to select data in such a way as to reduce correlations. Correlated errors are, however, treated explicitly when there are a number of results of the form $A_i \pm \sigma_i \pm \Delta$ that have identical systematic errors Δ. In this case, one can first average the $A_i \pm \sigma_i$ and then combine the resulting statistical error with Δ. One obtains, however, the same result by averaging $A_i \pm (\sigma_i^2 + \Delta_i^2)^{1/2}$, where $\Delta_i = \sigma_i \Delta [\sum (1/\sigma_j^2)]^{1/2}$. This procedure has the advantage that, with the modified systematic errors Δ_i, each measurement may be treated as independent and averaged in the usual way with other data. Therefore, when appropriate, we adopt this procedure. We tabulate Δ and invoke an automated procedure that computes Δ_i before averaging and we include a note saying that there are common systematic errors.

Another common case of correlated errors occurs when experimenters measure two quantities and then quote the two and their difference, *e.g.*, m_1, m_2, and $\Delta = m_2 - m_1$. We cannot enter all of m_1, m_2 and Δ into a constrained fit because they are not independent. In some cases, it is a good approximation to ignore the quantity with the largest error and put the other two into the fit. However, in some cases correlations are such that the errors on m_1, m_2 and Δ are comparable and none of the three values can be ignored. In this case, we put all three values into the fit and invoke an automated procedure to increase the errors prior to fitting such that the three quantities can be treated as independent measurements in the constrained fit. We include a note saying that this has been done.

4.2.2. *Unconstrained averaging:* To average data, we use a standard weighted least-squares procedure and in some cases, discussed below, increase the errors with a "scale factor." We begin by assuming that measurements of a given quantity are uncorrelated, and calculate a weighted average and error as

$$\overline{x} \pm \delta\overline{x} = \frac{\sum_i w_i\, x_i}{\sum_i w_i} \pm \left(\sum_i w_i\right)^{-1/2} , \qquad (1)$$

where

$$w_i = 1/(\delta x_i)^2 .$$

Here x_i and δx_i are the value and error reported by the ith experiment, and the sums run over the N experiments. We then calculate $\chi^2 = \sum w_i(\overline{x} - x_i)^2$ and compare it with $N-1$, which is the expectation value of χ^2 if the measurements are from a Gaussian distribution.

If $\chi^2/(N-1)$ is less than or equal to 1, and there are no known problems with the data, we accept the results.

If $\chi^2/(N-1)$ is very large, we may choose not to use the average at all. Alternatively, we may quote the calculated average, but then make an educated guess of the error, a conservative estimate designed to take into account known problems with the data.

Finally, if $\chi^2/(N-1)$ is greater than 1, but not greatly so, we still average the data, but then also do the following:

(a) We increase our quoted error, $\delta\overline{x}$ in Eq. (1), by a scale factor S defined as

$$S = \left[\chi^2/(N-1)\right]^{1/2} . \qquad (2)$$

Our reasoning is as follows. The large value of the χ^2 is likely to be due to underestimation of errors in at least one of the experiments. Not knowing which of the errors are underestimated, we assume they are all underestimated by the same factor S. If we scale up all the input errors by this factor, the χ^2 becomes $N-1$, and of course the output error $\delta\overline{x}$ scales up by the same factor. See Ref. 3.

When combining data with widely varying errors, we modify this procedure slightly. We evaluate S using only the

experiments with smaller errors. Our cutoff or ceiling on δx_i is arbitrarily chosen to be

$$\delta_0 = 3N^{1/2}\,\delta\overline{x}\,,$$

where $\delta\overline{x}$ is the unscaled error of the mean of all the experiments. Our reasoning is that although the low-precision experiments have little influence on the values $\overline{x}$ and $\delta\overline{x}$, they can make significant contributions to the χ^2, and the contribution of the high-precision experiments thus tends to be obscured. Note that if each experiment has the same error δx_i, then $\delta\overline{x}$ is $\delta x_i/N^{1/2}$, so each δx_i is well below the cutoff. (More often, however, we simply exclude measurements with relatively large errors from averages and fits: new, precise data chase out old, imprecise data.)

Our scaling procedure has the property that if there are two values with comparable errors separated by much more than their stated errors (with or without a number of other values of lower accuracy), the scaled-up error $\delta\,\overline{x}$ is approximately half the interval between the two discrepant values.

We emphasize that our scaling procedure for *errors* in no way affects central values. And if you wish to recover the unscaled error $\delta\overline{x}$, simply divide the quoted error by S.

(b) If the number M of experiments with an error smaller than δ_0 is at least three, and if $\chi^2/(M-1)$ is greater than 1.25, we show in the Particle Listings an ideogram of the data. Figure 1 is an example. Sometimes one or two data points lie apart from the main body; other times the data split into two or more groups. We extract no numbers from these ideograms; they are simply visual aids, which the reader may use as he or she sees fit.

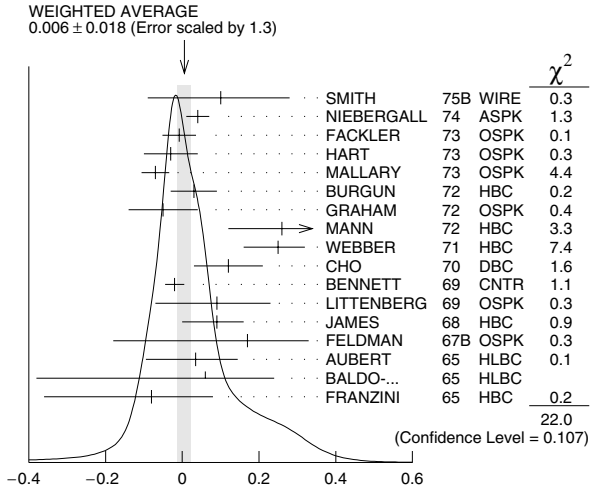

Figure 1: A typical ideogram. The arrow at the top shows the position of the weighted average, while the width of the shaded pattern shows the error in the average after scaling by the factor S. The column on the right gives the χ^2 contribution of each of the experiments. Note that the next-to-last experiment, denoted by the incomplete error flag ($\perp$), is not used in the calculation of S (see the text).

Each measurement in an ideogram is represented by a Gaussian with a central value x_i, error δx_i, and area proportional to $1/\delta x_i$. The choice of $1/\delta x_i$ for the area is somewhat arbitrary. With this choice, the center of gravity of the ideogram corresponds to an average that uses weights $1/\delta x_i$ rather than the $(1/\delta x_i)^2$ actually used in the averages. This may be appropriate when some of the experiments have seriously underestimated systematic errors. However, since for this choice of area the height of the Gaussian for each measurement is proportional to $(1/\delta\, x_i)^2$, the peak position of the ideogram will often favor the high-precision measurements at least as much as does the least-squares average. See our 1986 edition [2] for a detailed discussion of the use of ideograms.

4.2.3. *Constrained fits:* In some cases, such as branching ratios or masses and mass differences, a constrained fit may be needed to obtain the best values of a set of parameters. For example, most branching ratios and rate measurements are analyzed by making a simultaneous least-squares fit to all the data and extracting the partial decay fractions P_i, the partial widths Γ_i, the full width Γ (or mean life), and the associated error matrix.

Assume, for example, that a state has m partial decay fractions P_i, where $\sum P_i = 1$. These have been measured in N_r different ratios R_r, where, e.g., $R_1 = P_1/P_2$, $R_2 = P_1/P_3$, *etc.* [We can handle any ratio R of the form $\sum \alpha_i\, P_i/\sum \beta_i\, P_i$, where α_i and β_i are constants, usually 1 or 0. The forms $R = P_iP_j$ and $R = (P_iP_j)^{1/2}$ are also allowed.] Further assume that *each* ratio R has been measured by N_k experiments (we designate each experiment with a subscript k, e.g., R_{1k}). We then find the best values of the fractions P_i by minimizing the χ^2 as a function of the $m-1$ independent parameters:

$$\chi^2 = \sum_{r=1}^{N_r}\sum_{k=1}^{N_k}\left(\frac{R_{rk}-R_r}{\delta R_{rk}}\right)^2\,, \qquad (3)$$

where the R_{rk} are the measured values and R_r are the fitted values of the branching ratios.

In addition to the fitted values $\overline{P}_i$, we calculate an error matrix $\langle\delta\overline{P}_i\ \delta\overline{P}_j\rangle$. We tabulate the diagonal elements of $\delta\,\overline{P}_i = \langle\delta\,\overline{P}_i\ \delta\,\overline{P}_i\rangle^{1/2}$ (except that some errors are scaled as discussed below). In the Particle Listings, we give the complete correlation matrix; we also calculate the fitted value of each ratio, for comparison with the input data, and list it above the relevant input, along with a simple unconstrained average of the same input.

Three comments on the example above:

(1) There was no connection assumed between measurements of the full width and the branching ratios. But often we also have information on partial widths Γ_i as well as the total width Γ. In this case we must introduce Γ as a parameter in the fit, along with the P_i, and we give correlation matrices for the widths in the Particle Listings.

(2) We try to pick those ratios and widths that are as independent and as close to the original data as possible. When one experiment measures all the branching fractions and constrains their sum to be one, we leave one of them (usually the least well-determined one) out of the fit to make the set of input data more nearly independent. We now do allow for correlations between input data.

(3) We calculate scale factors for both the R_r and P_i when the measurements for any R give a larger-than-expected contribution to the χ^2. According to Eq. (3), the

double sum for χ^2 is first summed over experiments $k = 1$ to N_k, leaving a single sum over ratios $\chi^2 = \sum \chi_r^2$. One is tempted to define a scale factor for the ratio r as $S_r^2 = \chi_r^2/\langle\chi_r^2\rangle$. However, since $\langle\chi_r^2\rangle$ is not a fixed quantity (it is somewhere between N_k and N_{k-1}), we do not know how to evaluate this expression. Instead we define

$$S_r^2 = \frac{1}{N_k}\sum_{k=1}^{N_k}\frac{\left(R_{rk}-\overline{R}_r\right)^2}{\langle(R_{rk}-\overline{R}_r)^2\rangle}. \qquad (4)$$

With this definition the expected value of S_r^2 is one. We can show that

$$\langle(R_{rk}-\overline{R}_r)^2\rangle = (\delta R_{rk})^2 - (\delta\overline{R}_r)^2\ , \qquad (5)$$

where $\delta\overline{R}_r$ is the fitted error for ratio r.

The fit is redone using errors for the branching ratios that are scaled by the larger of S_r and unity, from which new and often larger errors $\delta\overline{P}_i'$ are obtained. The scale factors we finally list in such cases are defined by $S_i = \delta\overline{P}_i'/\delta\overline{P}_i$. However, in line with our policy of not letting S affect the central values, we give the values of $\overline{P}_i$ obtained from the original (unscaled) fit.

There is one special case in which the errors that are obtained by the preceding procedure may be changed. When a fitted branching ratio (or rate) $\overline{P}_i$ turns out to be less than three standard deviations ($\delta\overline{P}_i'$) from zero, a new smaller error $(\delta\overline{P}_i'')^-$ is calculated on the low side by requiring the area under the Gaussian between $\overline{P}_i - (\delta\overline{P}_i'')^-$ and $\overline{P}_i$ to be 68.3% of the area between zero and $\overline{P}_i$. A similar correction is made for branching fractions that are within three standard deviations of one. This keeps the quoted errors from overlapping the boundary of the physical region.

4.3. ***Rounding***: While the results shown in the Particle Listings are usually exactly those published by the experiments, the numbers that appear in the Summary Tables (means, averages and limits) are subject to a set of rounding rules.

The basic rule states that if the three highest order digits of the error lie between 100 and 354, we round to two significant digits. If they lie between 355 and 949, we round to one significant digit. Finally, if they lie between 950 and 999, we round up to 1000 and keep two significant digits. In all cases, the central value is given with a precision that matches that of the error. So, for example, the result (coming from an average) 0.827 ± 0.119 would appear as 0.83 ± 0.12, while 0.827 ± 0.367 would turn into 0.8 ± 0.4.

Rounding is not performed if a result in a Summary Table comes from a single measurement, without any averaging. In that case, the number of digits published in the original paper is kept, unless we feel it inappropriate. Note that, even for a single measurement, when we combine statistical and systematic errors in quadrature, rounding rules apply to the result of the combination. It should be noted also that most of the limits in the Summary Tables come from a single source (the best limit) and, therefore, are not subject to rounding.

Finally, we should point out that in several instances, when a group of results come from a single fit to a set of data, we have chosen to keep two significant digits for all the results. This happens, for instance, for several properties of the W and Z bosons and the τ lepton.

4.4. ***Discussion***: The problem of averaging data containing discrepant values is nicely discussed by Taylor in Ref. 4. He considers a number of algorithms that attempt to incorporate inconsistent data into a meaningful average. However, it is difficult to develop a procedure that handles simultaneously in a reasonable way two basic types of situations: (a) data that lie apart from the main body of the data are incorrect (contain unreported errors); and (b) the opposite—it is the main body of data that is incorrect. Unfortunately, as Taylor shows, case (b) is not infrequent. He concludes that the choice of procedure is less significant than the initial choice of data to include or exclude.

We place much emphasis on this choice of data. Often we solicit the help of outside experts (consultants). Sometimes, however, it is simply impossible to determine which of a set of discrepant measurements are correct. Our scale-factor technique is an attempt to address this ignorance by increasing the error. In effect, we are saying that present experiments do not allow a precise determination of this quantity because of unresolvable discrepancies, and one must await further measurements. The reader is warned of this situation by the size of the scale factor, and if he or she desires can go back to the literature (via the Particle Listings) and redo the average with a different choice of data.

Our situation is less severe than most of the cases Taylor considers, such as estimates of the fundamental constants like $\hbar$, *etc.* Most of the errors in his case are dominated by systematic effects. For our data, statistical errors are often at least as large as systematic errors, and statistical errors are usually easier to estimate. A notable exception occurs in partial-wave analyses, where different techniques applied to the same data yield different results. In this case, as stated earlier, we often do not make an average but just quote a range of values.

A brief history of early Particle Data Group averages is given in Ref. 3. Figure 2 shows some histories of our values of a few particle properties. Sometimes large changes occur. These usually reflect the introduction of significant new data or the discarding of older data. Older data are discarded in favor of newer data when it is felt that the newer data have smaller systematic errors, or have more checks on systematic errors, or have made corrections unknown at the time of the older experiments, or simply have much smaller errors. Sometimes, the scale factor becomes large near the time at which a large jump takes place, reflecting the uncertainty introduced by the new and inconsistent data. By and large, however, a full scan of our history plots shows a dull progression toward greater precision at central values quite consistent with the first data points shown.

We conclude that the reliability of the combination of experimental data and our averaging procedures is usually good, but it is important to be aware that fluctuations outside of the quoted errors can and do occur.

ACKNOWLEDGMENTS

The publication of the *Review of Particle Physics* is supported by the Director, Office of Science, Office of High Energy and Nuclear Physics, the Division of High Energy Physics of the U.S. Department of Energy under Contract No. DE–AC03–76SF00098; by the U.S. National Science Foundation under Agreement No. PHY-0070972; by the European Laboratory for Particle Physics (CERN); by an implementing arrangement between the governments of Japan (Monbusho) and the United States (DOE) on cooperative research and development; and by the Italian National Institute of Nuclear Physics (INFN).

We thank all those who have assisted in the many phases of preparing this *Review*. We particularly thank the many who have responded to our requests for verification of data entered in the Listings, and those who have made suggestions or pointed out errors.

REFERENCES

1. The previous edition was Particle Data Group: D.E. Groom *et al.*, Eur. Phys. J. **C15**, 1 (2000).
2. Particle Data Group: M. Aguilar-Benitez *et al.*, Phys. Lett. **170B** (1986).
3. A.H. Rosenfeld, Ann. Rev. Nucl. Sci. **25**, 555 (1975).
4. B.N. Taylor, "Numerical Comparisons of Several Algorithms for Treating Inconsistent Data in a Least-Squares Adjustment of the Fundamental Constants," U.S. National Bureau of Standards NBSIR 81-2426 (1982).

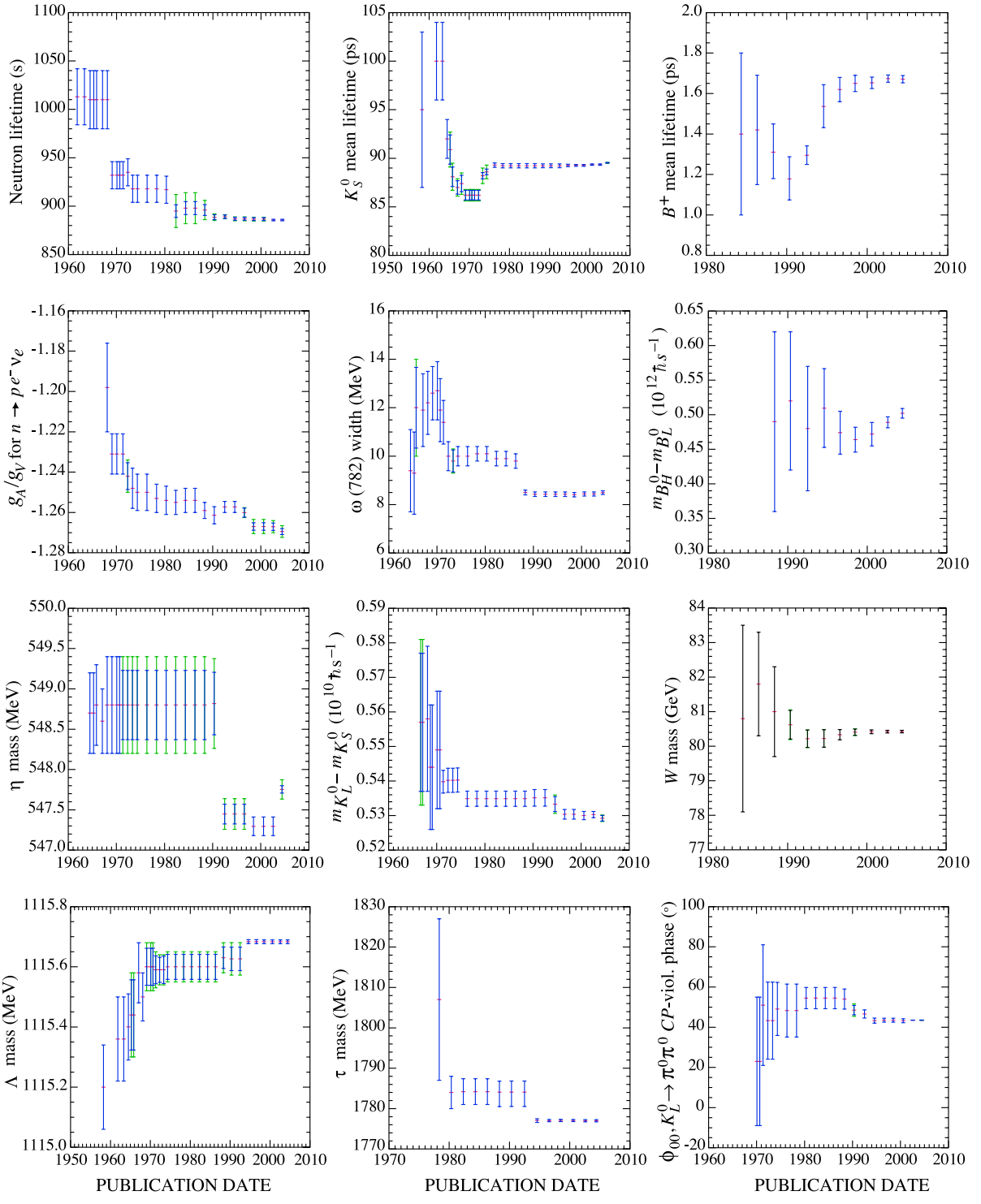

Figure 2: An historical perspective of values of a few particle properties tabulated in this *Review* as a function of date of publication of the *Review*. A full error bar indicates the quoted error; a thick-lined portion indicates the same but without the "scale factor."

ONLINE PARTICLE PHYSICS INFORMATION

Revised December 2003 by P. Kreitz (SLAC) with the substantial assistance in the Physics Education Section from L. Wolf (SLAC).

This annotated list provides a highly selective set of online resources that are useful to the particle physics community. It describes the scope, size, and organization of the resources so that efficient choices can be made amongst many sites which may appear similar. A resource is excluded if it provides information primarily of interest to only one institution. Because this list must be fixed in print, it is important to consult the updated version of this compilation which includes newly added resources and hypertext links to more complete information at:

`http://www.slac.stanford.edu/library/pdg/`

Accelerator physics resources have been excluded because they are covered well by the World Wide Web Virtual Library of Beam Physics and Accelerator Technology:

`http://home.earthlink.net/ whittum/vl/`

My thanks to Betty Armstrong and Piotr Zyla, Particle Data Group, Travis Brooks and Kim Sutton, SLAC Library, and the many particle physics Web site and database maintainers who have all given me their generous assistance. Please send comments and corrections by e-mail to `pkreitz@slac.stanford.edu`.

1. Particles & Properties Data:

- REVIEW OF PARTICLE PHYSICS (RPP): A biennial comprehensive review summarizing much of the known data about the field of particle physics produced by the international Particle Data Group (PDG). Includes a compilation/evaluation of data on particle properties, summary tables with best values and limits for particle properties, extensive summaries of searches for hypothetical particles, and a long section of reviews, tables, and plots on a wide variety of theoretical and experimental topics of interest to particle and astrophysicists. The linked table of contents provides access to particle listings, reviews, summary tables, errata, indices, *etc.* The current printed version is this edition: S. Eidelman, *et al.*, *Physics Letters* **B592** 1. Maintained at:
  `http://pdg.lbl.gov/`
- PARTICLE PHYSICS BOOKLET: A pocket-sized 300-page booklet containing the Summary Tables and abbreviated versions of some of the other sections of the full *Review of Particle Physics*. This is extracted from the most recent edition of the full *Review of Particle Physics*. Contains images in an easy-to-read print useful for classroom studies. The next edition will be in Spring 2004. Until the new edition is published and available via the Web, students, teachers, and researchers should use the full *Review of Particle Physics*:
  `http://pdg.lbl.gov/`
- COMPUTER-READABLE FILES: Currently available from the PDG: Tables of masses, widths, and PDG Monte Carlo particle numbers and cross-section data, including hadronic total and elastic cross sections vs laboratory momenta, and total center-of mass energy. The PDG Monte Carlo particle numbering scheme has been updated for the recent edition of the RPP and are also available as a MobileDB database. Palm Pilot products include physical constants, astrophysical constants and particle properties. These files are is updated in even-numbered years coinciding with the production of the *Review of Particle Properties*:
  `http://pdg.lbl.gov/computer_read.html`
- PARTICLE PHYSICS DATA SYSTEM: This site contains an indexed bibliography of particle physics (1895–1995), a database of computerized numerical data extracted from experimental publications, and an index of papers (1895–present) that contain experimental data or data analyses. The Web interface permits simple searching for for compilations of integrated cross-section data. The search interface for numerical data on observables in reactions (ReacData or RD), is under construction. Maintained by the COMPAS group at IHEP:
  `http://wwwppds.ihep.su:8001/ppds.html`
- HEPDATA: REACTION DATA DATABASE: A part of the HEPDATA databases at University of Durham/RAL, this database is compiled by the Durham Database Group (UK) with help from the COMPAS Group (Russia) for the PDG. Contains numerical values of HEP reaction data such as total and differential cross sections, fragmentation functions, structure functions, and polarization measurements from a wide range of experiments. Updated at regular intervals. Provides data reviews which contain precompiled reviewed data such as 'Structure Functions in DIS', 'Single Photon Production in Hadronic Interactions', and 'Drell-Yan Cross Sections':
  `http://durpdg.dur.ac.uk/HEPDATA/REAC`
- NIST PHYSICS LABORATORY: This unit of the National Institute of Standards and Technology provides measurement services and research for electronic, optical, and radiation technologies. Three sub-pages, on Physical Reference Data, on Constants, Units & Uncertainty, and on Measurements & Calibrations, are extremely useful. Additional links to other physical properties and data of tangential interest to particle physics are also available from this page:
  `http://physics.nist.gov/`

2. Collaborations & Experiments:

- EXPERIMENTS Database: Contains more than 2,200 past, present, and future experiments in elementary particle physics. Lists both accelerator and non-accelerator experiments. Includes official experiment name and number, location, spokespersons and collaboration lists. Simple searches by: participant, title, experiment number, institution, date approved, accelerator, or detector, return a result that fully describes the experiment, including a complete list of authors, title, description of the experiment's goals and methods, and a link to the experiment's Web page if available. Publication lists distinguish articles in refereed journals, theses, technical or instrumentation papers, and those which make the Topcite at 50+ subsequent citations or more:
  `http://www.slac.stanford.edu/spires/experiments/`
- HIGH ENERGY PHYSICS EXPERIMENTS: A HEPiC page of links to experimental collaboration Web pages. Experiments are arranged alphabetically by name or number under 18 major laboratories or in a miscellaneous group of 'Others':
  `http://www.hep.net/experiments/`
  `all_sites.html_sites.html`
- COSMIC RAY/GAMMA RAY/NEUTRINO AND SIMILAR EXPERIMENTS: This is an extensive collection of experimental Web sites organized by focus of study and also by location. Additional sections link to educational materials, organizations and related Web sites, *etc.* Maintained at the Max Planck Institute for Nuclear Physics by Konrad Bernlöhr:
  `www.mpi-hd.mpg.de/hfm/CosmicRay/CosmicRaySites.html`

3. Conferences:

- CONFERENCES: Database of more than 12,300 past, present and future conferences, schools, and meetings of interest to high-energy physics and related fields. Covers 1973 to the future. The current year covers more than 600 events. Search or browse by title, acronym, date, location. Includes information about published proceedings, links to submitted papers from the SPIRES-HEP database, and links to the conference Web site when available. Links to a form with which one can submit a new conference or edit an existing one:
  `http://www.slac.stanford.edu/spires/conferences/`
  `add_conference.shtml` to submit a new conference. Can also search for any conferences occurring by day, month, quarter, or year:
  `http://www.slac.stanford.edu/spires/conferences/`

- CONFERENCES AND CONFERENCES: Lists 150+ current meetings in many fields of physics. Provides post-conference information such as proceedings, *etc.*, in a second list at the end of the subject categories of conferences. Browse through an ASCII list of all conferences or specialized lists arranged by topic: particles/nuclei, quantum, condensed matter, mathematical, interdisciplinary physics, and related fields. Includes links to the conference Web page and the contact. Provides a useful set of links to universities, laboratories and institutions which host major conferences and/or schools:
  `http://www.physics.umd.edu/robot/confer/confmenu.html`
- CERN EVENTS: A list of current and upcoming conferences, schools, workshops, *etc.*, of interest to high-energy physicists. Organized by year and then by date. Covers from 1993 to one year beyond the current year. Includes about a hundred events. To post an event to this list use the Web form at:
  `http://wpedb.cern.ch/databases/requests/`
- EUROPHYSICS MEETINGS LIST: Maintained by the European Physical Society, this lists in chronological order all the current and future meetings, workshops, schools, *etc.*, organized or sponsored by EPS or organized in conjunction with an EPS-sponsored group. Provides a PDF form to electronically submit a notice of a new conference or to print and mail to EPS:
  `http://www.eps.org/ephconf.html`
- PHYSICSWEB EVENTS: Part of the Institute of Physics (IOP) Web site, this site contains approximately a hundred entries for meetings, workshops, exhibitions and schools occurring in the current year and the following year. Fills a gap by covering the smaller conferences and workshops around the world. Searchable by type of event, e.g., school, workshop, or by date or free text words. Provides a Web form and email address for adding a conference and for signing up to receive email notices of new events added:
  `http://physicsweb.org/events/`

4. Current Notices & Announcement Services:

- See also the conference and event sites above for links to email notification services or event submission forms.
- CURRENT SCIENCE NEWS: Lists news sites from around the world. A few sites are by subscription and so are labelled as available to Stanford only but most are free and publically accessible. Commercial sites often provide headlines and a brief abstract as a free service and require subscription or payment for a complete article.
  `http://www.slac.stanford.edu/library/eresources/news.html`
- E-PRINT ARCHIVES LISTSERV NOTICES: The Cornell-based E-Print Archives provides daily notices of preprints in the fields of physics, mathematics, nonlinear sciences, and computer sciences and quantitative biology which have been submitted to the archives as full text electronic documents. Use the Web-accessible listings:
  `http://arXiv.org/`
  or subscribe:
  `http://arXiv.org/help/subscribe`
- HEPJOBS DATABASE: Maintained by Fermilab and SLAC libraries, this database lists jobs in the fields of core interest to the particle physics and astroparticle physics communities. Use this page to post a job or to receive email notices of new job listings:
  `http://www.slac.stanford.edu/spires/jobs/`
- INTERACTIONS.ORG: Provides particle physics news and resources from the world's particle physics laboratories. Subscribe to Interactions.org Newswire:
  `http://www.interactions.org/cms/?pid=1000502`
- NASA ASTROPHYSICS DATA SYSTEM: This table of contents query page provides tables of contents for 24 core titles in the field:
  `http://adsabs.harvard.edu/custom_toc.html`
- PREPRINTS IN PARTICLES AND FIELDS (PPF): A weekly listing averaging 250 new preprints in particle physics and related fields. Contains bibliographic listings for and, in the Web version, full text links to, the new preprints received by and cataloged into the SPIRES High-Energy Physics (HEP) database. Includes that week's titles from the e-print archives as well as preprints and articles received from other sources. Directions for subscribing to an email version can be found on the page listing the most recent week's preprints:
  `http://www.slac.stanford.edu/library/documents/newppf.html`
- PSIGATE PHYSICS GATEWAY: IoP News and Jobs: Newsfeeds containing the latest jobs and news from the Institute of Physics' (IoP) PhysicsWeb with news headlines from Optics.org, Fibers.org and Nanotechweb.org:
  `http://www.psigate.ac.uk/newsite/awareness_iop.html`

Note: Use the library pages in Section 5.3 below to find additional announcement lists for recently received preprints, books, and proceedings. Use the online journal links in Section 7 below for journal table of contents.

5. Directories:

5.1. *Directories—Research Institutions:*

- HEP and Astrophysics INSTITUTIONS: SPIRES database of over 6,500 high-energy physics and astropartcle physics institutes, laboratories, and university departments in which research on particle physics is performed. Covers six continents and over a hundred countries. Provides an alphabetical list by country or an interface that is searchable by name, acronym, location, *etc.* Includes address, phone and fax numbers, e-mail address, and Web links where available. Has links to the recent HEP papers from each institution. Maintained by SLAC, DESY and Fermilab libraries:
  `http://www.slac.stanford.edu/spires/institution/`
- HEP INSTITUTES: Contains almost a thousand institutional addresses used in the CERN Library catalog. Includes, where available, the following: phone and fax numbers; e-mail addresses; and Web links. Provides free text searching and result sorting by organization, country, or town:
  `http://cdsweb.cern.ch/?c=HEP%20Institutes`
- HIGH ENERGY PHYSICS WEB SITES: An alphabetical listing of approximately 200 particle physics Web sites with links to the institutions' Web pages. Maintained by the CERN Web group for the WWW Virtual Library. Somewhat difficult to use because entries are listed by institutional acronym or by short name:
  `http://physics.web.cern.ch/physics/HEPWebSites.html`
- TOP 500 INSTITUTIONS IN HIGH-ENERGY PHYSICS: Lists the 500 HEP-related organizations and universities that have published the most papers in the past five years, as identified from the SPIRES HEP Database. Provides active links to the home pages and full INSTITUTIONS database records. Listed by country, and then alphabetically by institution:
  `http://www.slac.stanford.edu/spires/institution/major.shtml`

5.2. *Directories—People:*

- HEPNAMES: Searchable worldwide database of over 40,000 people associated with particle physics, synchrotron radiation, and related fields. Provides e-mail addresses, country in which the person is currently working, and a SPIRES HEP database search for their papers. If the person has supplied the following information, it lists the countries in which they did their undergraduate and graduate work, their url, and their graduate students. It also provides listings of Nobel Laureates, country statistics, Lab Directors, *etc.*:
  `http://www.slac.stanford.edu/spires/hepnames/`
- HEP VIRTUAL PHONEBOOK: A list of links to phonebooks and directories of high-energy physics sites and collaborations around the world organized by site. Often provides links to more specialized phone or e-mail listings, such as a department within a university, visiting scientists, or postdocs. Some phonebooks may require passwords or other authentication to access. Maintained by HEPiC:
  `http://www.hep.net/sites/directories.html`
- US-HEPFOLK DIRECTORY: A searchable directory and census of U.S. particle physicists updated annually. Contains more than 4,000 U.S. physicists. Searchable by first or last name, by affiliation, and/or by email address. Also provides demographic plots of the survey data for the past three years:
  `http://pdg.lbl.gov/us-hepfolk/index.html`

5.3. *Directories—Libraries:*

- Argonne National Laboratory (ANL) Library:
  `http://www.library.anl.gov/library/index.html`
- Brookhaven National Laboratory (BNL) Library:
  `http://inform.bnl.gov/RESLIB/reslib.html`
- (CERN) European Organization for Nuclear Research Library:
  `http://library.cern.ch/`
- Deutsches Elektronen-Synchrotron (DESY) Library:
  `http://www.desy.de/html/infodienste/bibliothek.html`
- Fermi National Accelerator Laboratory (Fermilab) Library:
  `http://fnalpubs.fnal.gov/`
- Idaho National Engineering and Environmental Laboratory (INEEL) Library:
  `http://www.inel.gov/library/`
- (KEK) National Laboratory for High Energy Physics Library:
  `http://www-lib.kek.jp/top-e.html`
- Lawrence Berkeley National Laboratory (LBNL) Library:
  `http://www-library.lbl.gov/teid/tmLib/aboutus/LibDefault.htm`
- Lawrence Livermore National Laboratory (LLNL) Library:
  `http://www.llnl.gov/library/`
- Los Alamos National Laboratory (LANL) Library:
  `http://lib-www.lanl.gov/`
- Oak Ridge National Laboratory (ORNL) Library:
  `http://www.ornl.gov/Library/library-home.html`
- Pacific Northwest National Laboratory (PNL) Library:
  `http://www.pnl.gov/tech_lib/home.html`
- Sandia National Laboratory Library:
  `http://www.sandia.gov/news-center/resources/tech-library/index.html`
- Stanford Linear Accelerator Center (SLAC) Library:
  `http://www.slac.stanford.edu/library`
- Thomas Jefferson National Accelerator Facility (JLab) Library:
  `http://www.jlab.org/IR/library/index.html`

5.4. *Directories—Publishers:*

- DIRECTORY OF PUBLISHERS AND VENDORS: Outstanding and comprehensive directory of publishers and vendors used by libraries. Organized by publisher name, by subject (e.g. Science, Mathematics, and Technology), and by location. Also provides an email directory.
  `http://acqweb.library.vanderbilt.edu/acqweb/pubr.html`

5.5. *Directories—Scholarly Societies:*

- American Association for the Advancement of Science:
  `http://www.aaas.org/`
- American Association of Physics Teachers:
  `http://www.aapt.org/`
- American Astronomical Society:
  `http://www.aas.org`
- American Institute of Physics:
  `http://www.aip.org/`
- American Mathematical Society:
  `http://www.ams.org/`
- American Physical Society:
  `http://www.aps.org`
- American Physical Society: Scholarly Societies: Use this list to find national and international scientific and professional societies:
  `http://www.aps.org/resources/society.html`
- European Physical Society:
  `http://epswww.epfl.ch/`
- IEEE Nuclear and Plasma Sciences Society:
  `http://ewh.ieee.org/soc/nps/aboutnpss.htm`
- Institute of Physics:
  `http://www.iop.org/`
- International Union of Pure and Applied Physics:
  `http://www.iupap.org/`
- Japan Society of Applied Physics:
  `http://www.jsap.or.jp/english/`
- Physical Society of Japan:
  `http://wwwsoc.nii.ac.jp/jps/`
- Physical Society of the Republic of China:
  `http://psroc.phys.ntu.edu.tw/english/index.html`
- SCHOLARLY SOCIETIES PROJECT: Directory of more than 3,700 scholarly and technical societies with links to their Web sites. Permits searching by subject, country, language, founding dates, and more. Includes acronyms and indicates when a Web site contains both its native language and an English-language version and when it has a permanent URL. Provides direct links to society meeting and conference announcement lists, standards, and full text journals. Maintained by the University of Waterloo:
  `http://www.scholarly-societies.org/`

6. E-Prints/Pre-Prints, Papers, & Reports:

- CERN ARTICLES & PREPRINTS: The CERN document server contains records of more than 500,000 CERN and non-CERN articles, preprints, theses. Includes records for CERN Yellow Reports, internal and technical notes, and official CERN committee documents. Provides access to full text of the documents for about 50 percent of the entries and to the references when available:

  `http://cdsweb.cern.ch/?`
  `c=Articles+%26+Preprints&as=0`

- ECONF: Electronic Conference Proceedings Archive: This site offers a fully electronic, Web-accessible archive for the proceedings of scientific conferences in High-Energy Physics and related fields. Conference editors can use the site tools to prepare and post an electronic version of their proceedings. Librarians and other indexers can download metadata from each proceedings. Researchers can browse an entire proceedings via a table of contents or search for papers through a link to the SPIRES HEP Database which indexes the EConf contents.

  `http://www.slac.stanford.edu/econf/`

- HEP DATABASE (SPIRES): Contains over 570,000 bibliographic records for particle physics articles, including journal papers, preprints, e-prints, technical reports, conference papers and theses. Comprehensively indexed with multiple links to full text as well as links to author and institutional information. Covers 1974 to the present with substantial older materials added. Updated daily with links to electronic texts, Durham Reaction Data, *Review of Particle Properties*, *etc.* Searchable by citation, by all authors and authors' affiliations, title, topic, report number, citation (footnotes), e-print archive number, date, journal, *etc.* A joint project of the SLAC and DESY libraries with the collaboration of Fermilab, Durham University (UK), KEK, Kyoto University, and many other research institutions and scholarly societies:

  `http://www.slac.stanford.edu/spires/hep/`

- JACoW: This Joint Accelerator Conference Website is organized by the editorial boards of the Asian, European and American Particle Accelerator Conferences and the CYCLOTRONS, DIPAC, ICALEPCS and LINAC conferences. It contains the full text of all the papers of these accelerator conferences. Search by conference name, author, title, keyword or full text of the paper:

  `http://www.JACoW.org/`

- KISS (KEK INFORMATION SERVICE SYSTEM) FOR PREPRINTS: KEK Library preprint and technical report database. Contains bibliographic records of preprints and technical reports held in the KEK library with links to the full text images of more than 100,000 papers scanned from their worldwide collection of preprints. Particularly userful for older scanned preprints:

  `http://www-lib.kek.jp/KISS/kiss_prepri.html`

- E-PRINT ARCHIVE: The arXiv.org's automated electronic repository of full text papers in physics, mathematics, computer, and nonlinear sciences and cosmology and quantitative biology. Papers, called pre-prints or e(electronic)-prints, are usually sent by their authors to arXiv in advance of submission to a journal for publication. Primarily covers 1991 to the present but authors are encouraged to post older papers retroactively. Permits searching by author, title, and keyword in abstract. Allows limiting by subfield archive or by date.

  `http://arXiv.org`

- NASA ASTROPHYSICS DATA SYSTEM: The ADS Abstract Service provides a search interface for four bibliographic databases covering: Astronomy and Astrophysics, Instrumentation, Physics and Geophysics, and arXiv Preprints. Contains abstracts from articles and monographs as well as conference proceedings:

  `http://adsabs.harvard.edu/ads_abstracts.html`

- PARTICLE PHYSICS DATA SYSTEM—PPDS: A search interface to the bibliography of the print publication *A Guide to Experimental Elementary Particle Physics Literature* (LBL-90). This bibliography covers the published literature of theoretical and experimental particle physics from 1895 to 1995. The url is sometimes difficult to reach:

  `http://wwwppds.ihep.su:8001/ppds.html`

- DIRECTORY OF MATHEMATICS PREPRINT AND E-PRINT SERVERS: Provides the current home page and email contacts for mathematical preprint and e-print servers throughout the world:

  `http://www.ams.org/global-preprints/`

7. Particle Physics Journals & Reviews:

7.1. *Online Journals and Tables of Contents:*

Please note, some of these journals, publishers, and reviews may limit access to subscribers. If you encounter access problems, check with your institution's library.

- ADVANCES IN THEORETICAL AND MATHEMATICAL PHYSICS (ATMP): Bimonthly electronic and hard copy publication. Table of contents has links to arXiv.org since this is the first e-journal to be an overlay to arXiv.org, where papers for this journal are submitted:

  `http://www.intlpress.com/journals/ATMP/archive/`

- AMERICAN JOURNAL OF PHYSICS: A monthly publication of the American Association of Physics Teachers on instructional and cultural aspects of physical science:

  `http://ojps.aip.org/ajp`

- APPLIED PHYSICS LETTERS: Weekly publication of short (3 pages maximum) articles:

  `http://ojps.aip.org/aplo/`

- ASTROPHYSICAL JOURNAL: Published three times a month by the American Astronomical Society (AAS). See also AAS entry under Journal Publishers (below):

  `http://www.journals.uchicago.edu/ApJ/`

- CLASSICAL AND QUANTUM GRAVITY: Published 24 times a year by the Institute of Physics (IOP) covering the fields of gravitation and spacetime theory:

  `http://www.iop.org/Journals/cq`

- EUROPEAN PHYSICAL JOURNAL A: HADRONS AND NUCLEI: This monthly journal merges *Il Nuovo Cimento A* and *Zeitschrift fur Physik A* and covers physics and astronomy:

  `http://www.springerlink.com/app/home/journal.asp`
  `?wasp=hb5c1gugrj2rwcvkybrl&referrer=parent`
  `&backto=linkingpublicationresults,id:101158,1`

- EUROPEAN PHYSICAL JOURNAL C: PARTICLES AND FIELDS: This twice monthly journal is the successor to *Zeitschrift fur Physik C*, covering physics and astronomy:

  `http://www.springerlink.com/app/home/journal.asp`
  `?wasp=4nc6tkmvqh3qgyjvudu7&referrer=parent`
  `&backto=linkingpublicationresults,id:101160,1`

- INTERNATIONAL JOURNAL OF MODERN PHYSICS C: PHYSICS AND COMPUTERS: Includes both revew and research articles. Published ten times per year:

  `http://ejournals.wspc.com.sg/ijmpc/ijmpc.shtml`

- INTERNATIONAL JOURNAL OF MODERN PHYSICS D: GRAVITATION, ASTROPHYSICS AND COSMOLOGY: Includes both revew and research articles. Published ten times per year:

  `http://ejournals.wspc.com.sg/ijmpd/ijmpd.shtml`

- INTERNATIONAL JOURNAL OF MODERN PHYSICS E: NULCEAR PHYSICS: Includes both revew and research articles. Bi-monthly:
  `http://ejournals.wspc.com.sg/ijmpe/ijmpe.shtml`
- JAPANESE JOURNAL OF APPLIED PHYSICS: Part 1 is monthly and covers papers, short notes, and review papers. Part 2 is semimonthly and publishes letters including a special *Express Letters* section:
  `http://www.jsap.or.jp/english/publication/journal.html`
- JOURNAL OF COSMOLOGY AND ASTROPARTICLE PHYSICS: An electronic peer-reviewed journal created by the International School for Advanced Studies (SSISA) and the Institute of Physics. Authors are encouraged to submit media files to enhance the online versions of articles:
  `http://jcap.sissa.it/`
- JOURNAL OF HIGH ENERGY PHYSICS: Electronic and print available. Like *ATMP*, this is a refereed journal written, run, and distributed by electronic means. It accepts email submission notices and 'fetches' the submitted paper from the arXiv.org E-print archives:
  `http://jhep.sissa.it/`
- JOURNAL OF PHYSICS G: NUCLEAR AND PARTICLE PHYSICS: Monthly, published by IOP:
  `http://www.iop.org/EJ/journal/0954-3899`
- JOURNAL OF THE PHYSICAL SOCIETY OF JAPAN: JPSJ ONLINE: Monthly, online since 1996:
  `http://jpsj.ipap.jp/`
- MODERN PHYSICS LETTERS A: Published 40 times a year, this contains research papers in gravitation, cosmology, nuclear physics, and particles and fields. *Brief Review* section for short reports on new findings and developments:
  `http://www.wspc.com.sg/journals/mpla/mpla.html`
- NEW JOURNAL OF PHYSICS: Co-owned by the Institute of Physics and the Deutsche Physikalische Gesellschaft, this journal is funded by article charges from authors of published papers and by scholarly societies, *NJP* is available in a free, electronic form:
  `http://www.iop.org/EJ/journal/1367-2630/1`
- NUCLEAR INSTRUMENTS AND METHODS IN PHYSICS RESEARCH A: ACCELERATORS, SPECTROMETERS, DETECTORS, AND ASSOCIATED EQUIPMENT: This journal was formerly part of *Nuclear Instruments and Methods in Physics Research*. Published approximately 36 times per year, this journal covers instrumentation and large scale facilities:
  `http://www.elsevier.nl/locate/nima`
- NUCLEAR PHYSICS A: NUCLEAR AND HADRONIC PHYSICS:
  `http://www.elsevier.nl/inca/publications/store/5/0/5/7/1/5/`
- NUCLEAR PHYSICS B: PARTICLE PHYSICS, FIELD THEORY, STATISTICAL SYSTEMS, AND MATHEMATICAL PHYSICS:
  `http://www.elsevier.nl/inca/publications/store/5/0/5/7/1/6/`
- NUCLEAR PHYSICS B: PROCEEDINGS SUPPLEMENTS: Publishes proceedings of international conferences and topical meetings in high-energy physics and related areas:
  `http://www.elsevier.nl/inca/publications/store/5/0/5/7/1/7/`
- PHYSICAL REVIEW D: PARTICLES, FIELDS, GRAVITATION, AND COSMOLOGY: Published 24 times a year:
  `http://prd.aps.org/`
- PHYSICAL REVIEW SPECIAL TOPICS – ACCELERATORS AND BEAMS: A peer-reviewed electronic journal freely available from the American Physical Society:
  `http://prst-ab.aps.org/`
- PHYSICS LETTERS B: Nuclear and Particle Physics: Published weekly:
  `http://www.elsevier.nl/locate/plb`
- PHYSICS—USPEKHI: English edition of *Uspekhi Fizicheskikh Nauk*:
  `http://ufn.ioc.ac.ru/`
- PROGRESS IN PARTICLE AND NUCLEAR PHYSICS: Published four times a year. Many, but not all, articles are at a level suitable for the general nuclear and particle physicist:
  `http://www.elsevier.nl/locate/inca/419`
- PROGRESS OF THEORETICAL PHYSICS: Published monthly covering all fields of theoretical physics. A supplement is published roughly quarterly containing either long original or review papers or collections of papers on specific topics:
  `http://www2.yukawa.kyoto-u.ac.jp/ptpwww/`

7.2. *Journals – Directories:*

- DESY Library Electronic Journals: Use this Web page for up-to-date links to electronic journals of interest to particle physics. Provides a further link to tables of contents services. Provides a broader list than is included in this compilation:
  `http://www-library.desy.de/eljnl.html`

7.3. *Journals – Publishers & Repositories:*

- NASA ASTROPHYSICS DATA SYSTEM: Provides free electronic access to back issues of the *Astrophysical Journal*, *Astrophysical Journal Letters*, and the *Astrophysical Journal Supplement Series* and to many other titles. Often a journal allows the ADS to provide free, full text access after a delay of some number of years. :
  `http://adswww.harvard.edu/`
- AIP JOURNAL CENTER: The American Institute of Physics' top-level page for their electronic journals may be found at:
  `http://www.aip.org/ojs/service.html`
- AMERICAN PHYSICAL SOCIETY: The top-level page for the APS research journals. From this page one can access their *Physical Review* Online Archive (PROLA) search engine which is free to users:
  `http://publish.aps.org/`
- ELSEVIER SCIENCE: This Web site enables browsing Elsevier-published journals by subject field. First select Physics and Astronomy and then on the next page you must select either physics or astronomy (no longer both) and then subsequently select a sub-field of physics or astronomy. This page permits one to also select publication type Journal. Then, one reaches an alphabetical listing of journal titles with links to the journal's home page:
  `http://www.elsevier.nl/homepage/`
- EUROPEAN PHYSICAL SOCIETY: This is the top-level page listing all the society's journals:
  `http://www.eps.org/publications.html`
- INSTITUTE OF PHYSICS (IOP): Journals: Information: A list of the IOP journals organized by subject. A page organized by title is also available linked to this page:
  `http://www.iop.org/EJ/S/3/418/main/-list=subject`

- SPRINGER PUBLISHING: Physics: From this link, one can reach a subject list of Springer journals in physics with two more clicks. Unfortunately, the URL to that page is prohibitively long and so this is the most practical route:
  `http://www.springer-ny.com/discipline.tpl?discipline=Physics&cart=10715351791679624`

7.4. *Review Publications:*

- LIVING REVIEWS IN RELATIVITY: A peer-refereed, solely online physics j ournal publishing invited reviews covering all areas of relativity. Provided as a free service to the scientific community. Published in yearly volumes, although articles appear throughout the year. Hyperlinks are kept checked and active and reviews are updated frequently:
  `http://relativity.livingreviews.org/`
- NET ADVANCE OF PHYSICS: A free electronic service providing review articles and tutorials in an encyclopedic format. Covers all areas of physics. Includes e-prints, book announcements, full text of electronic books, and other resources with hypertext links when available. Welcomes contributions of original review articles:
  `http://web.mit.edu/redingtn/www/netadv/welcome.html`
- PHYSICS REPORTS: A review section for *Physics Letters A* and *Physics Letters B*. Each report deals with one subject. The reviews are specialized in nature, more extensive than a literature survey but normally less than book length:
  `http://www.elsevier.nl/locate/physrep`
- REPORTS ON PROGRESS IN PHYSICS: Covers all areas of physics and is published monthly. All papers are free for 30 days from the date of online publication:
  `http://www.iop.org/EJ/journal/0034-4885/1`
- REVIEWS OF MODERN PHYSICS: Published quarterly, it includes traditional scholarly reviews and shorter colloquium papers intended to describe recent research of interest to a broad audience of physicists:
  `http://rmp.aps.org/`

8. Particle Physics Education Sites:

Please note, each site in this section containing student activities now lists the (U.S. educational system) school grade level(s) that best fit that site. Also listed are the National Science Education Content Standards for teaching science which are relevant to the classroom activities provided at that site. Further explanation of the National Science Educational Content Standards can be found at:

For Grades 5 - 8:
`http://www.nap.edu/readingroom/books/nses/html/6d.html`

For Grades 9 - 12:
`http://www.nap.edu/readingroom/books//nses/html/6e.html`

8.1. *Particle Physics Education: Background Knowledge:*

- ANTIMATTER: MIRROR OF THE UNIVERSE: Find out what antimatter is, where it is made, the history behind its discovery, and how it is a part of our lives. This award-winning site, sponsored by the European Organisation for Nuclear Research, (CERN), explains to big kids and little kids alike the truth (and fiction) about antimatter. Features colorful photos and illustrations, a Kids Corner, and CERN physicists answering your questions on antimatter.
  Grades 8-12+; National Science Education Content Standards: A, B, D, G
  `http://livefromcern.web.cern.ch/livefromcern/antimatter/index.html`
- BIG-BANG SCIENCE–EXPLORING THE ORIGINS OF MATTER: In clear, concise, yet elegant language, this Web site, produced by the Particle Physics and Astronomy Research Council of the UK (PPARC), explains what physicists are looking for with their giant instruments called accelerators and particle detectors. Includes a brief history on how scientists came to define what is fundamental in the universe. Big Bang Science focuses on CERN particle detectors and on United Kingdom scientists' contribution to the search for the fundamental building blocks of matter. In addition to information on the how and why of particle physics, this site also shows particle physics as an international collaborative endeavor.
  Grades 9-12; National Science Education Content Standards B, D, E, G
  `http://hepwww.rl.ac.uk/pub/bigbang/part1.html`
- LIFE, THE UNIVERSE, AND THE ELECTRON: Sponsored by the Institute of Physics (IOP) and the Science Museum, London, this interactive online exhibit celebrates the centenary of the discovery of the electron. Sections explain many aspects of the nature, history, and usefulness of electrons. Clear explanations and beautiful photography.
  Grades 9-12; National Science Education Content Standards: A, B, D
  `http://www.sciencemuseum.org.uk/on-line/electron/index.asp`
- THE WORLD OF BEAMS: A site to visit if you wish to know a little or a lot about laser beams, particle beams, and other kinds of beams. Includes interactive tutorials, such as: What are Beams?, Working with Beams, and Beam Research and Technology. A good resource for physical science units involving energy, structure and properties of matter, and motion and forces for Grades 8-12. The information here is also helpful if you plan to tour any of the national laboratories listed in the "Libraries" section of this guide.
  Grades 8-12; National Science Education Content Standards: A, B, E
  `http://cbp-1.lbl.gov/`

8.2. *Particle Physics Education: Particle Physics Lessons and Activities:*

- BNL/BSA ONLINE CLASSROOM: The objective of this site, developed by Brookhaven National Laboratory, is to use technology to bring the scientific research of BNL to students and teachers. BNL has created a series of nine units comprising an online, interactive classroom and provided a Multi User Object-Oriented (MOO) virtual classroom that enables group interactivity. Students can test their knowledge of physics by playing the delightfully interactive RHIC Adventure (Secrets of the Nucleus) that focuses on the science of the Relativistic Heavy Ion Collider. Games can be modified to match student knowledge levels from grades 8-12. Lesson plans are available on nuclear physics for high school and on solar neutrinos for K-8. Try The Mystery of the Sun for grades K-8 or Dippin' Dots Neutrinos for grades 9-12. Each lesson includes National Science Education Content Standards.
  Grades K-12 (mostly 9-12); National Science Education Content Standards 5-8 and 9-12: A, B, D, E, G
  `http://onlineclassroom.bnl.org/`
- CONTEMPORARY PHYSICS EDUCATION PROJECT (CPEP): This site is especially designed to help teachers bring four areas of physics to their students in an accessible and engaging format. Provides charts, brochures, Web links, and classroom activities. Online interactive courses include: Fundamental Particles and Interactions (includes lesson plans), Plasma Physics and Fusion, and Nuclear Science (includes lesson plans and simple experiments).
  Grade Level: 9-12; Some of the experiments may be of interest to grades 5-8; National Science Education Content Standards 9-12: A, B, D, E
  `http://www.cpepweb.org/`

- CENTER FOR PARTICLE ASTROPHYSICS ON-LINE DEMOS: A good source for do-it-yourself demos aimed at middle school students (modifiable for other levels). Demonstrations include: Air-Powered Rockets, Desktop Stars, Lunar Topography, Ping Pong Ball Launcher, Potato Power, and Solar System. Each includes an introduction, teacher and student worksheets, and a list of materials needed. Site has not been updated with new materials, but existing lesson plans are nevertheless well-written and relevant. Parents might be interested in doing some of these projects with their children.

  Grades 7-8+; National Science Education Content Standards: A, B, D, E

  `http://cfpa.berkeley.edu/Education/DEMOS/DEMOS.html`

- DOE ONLINE K-12 INSTRUCTIONAL RESOURCES: The U.S. Department of Energy (DOE) brings together a collection of online resources and lesson plans from the education sites of DOE-funded national laboratories such as Stanford Linear Accelerator Center, Lawrence Berkeley, Jefferson Lab, and Brookhaven. In the area of atomic and particle physics, see Jefferson Lab's All About Atoms slide show and clickable interactive table of elements which enables you to find out an element's properties, history, and uses.

  Grades: K-12; A variety of lesson plans are available in all scientific disciplines, conforming to National Science Education Content Standards.

  `http://www-ed.fnal.gov/doe/`

- FERMILAB EDUCATION OFFICE: Outstanding collection of resources from the "grandmother" of all physics lab educational programs. Thoughtful unit and lesson plans in both physics and the environment (Fermilab is located on a rare, protected prairie in Illinois). Sections are organized by grade level. Note in particular pedagogical resources for teachers, LInC Online, and the Lederman Science Center. Offers online guided tours and and science adventures.

  Grades K-12; National Science Education Content Standards: A, B, C, D, E, F. Many lesson plans designed to meet Illinois State Standards

  `http://www-ed.fnal.gov/`

- GLAST CLASSROOM MATERIALS: The Gamma Ray Large Area Space Telescope (GLAST) project and the National Aeronautics and Space Administration (NASA)'s Education and Public Outreach Office have developed this colorful, in depth, and engaging Web site teaching about the origin and structure of the universe and the fundamental relationship between energy and matter. Includes lesson plans and a teacher resource booklet which are available in PDF format, HTML, or can be ordered in print. Lesson plans are hands-on, student-group oriented and require common household objects. Activities such as: Three Mysteries, Alien Bandstand, Live! From 2-Alpha, and Starmarket build critical thinking and analytical skills as well as address at least one of the physical science standards. Full color posters and other educational materials also available. Provides links to other educational Web sites with classroom resources.

  Grades 9-12; National Science Education Content Standards A, B, D, E

  `http://glast.sonoma.edu/teachers/teachers.html`

- IMAGINE THE UNIVERSE: Created by the Laboratory for High-Energy Astrophysics at NASA/Goddard Space Flight Center, this site features astronomy and astrophysics lesson plans for age 14 and up, teacher's guides, classroom posters, and links to other classroom resources. Activities are linked to National Standards for Science and Math. Lessons include: What is Your Cosmic Connection to the Elements?, Life Cycle of Stars, and Gamma-Ray Bursts. Also included in the Teacher's Corner are links to math-science lesson plans for grades 6-12. The Multimedia Theatre Archive provides more than a dozen movies with free downloadable viewing software.

  Grades 9-12; National Science Education Content Standards: A, B, D, G

  `http://imagine.gsfc.nasa.gov`

- *Also note:* STARCHILD: Interlinked with Imagine the Universe, above, this site is a lively, age appropriate site for grade school level astronomy lessons.

  `http://starchild.gsfc.nasa.gov/docs/StarChild/StarChild.html`

- JEFFERSON LAB SCIENCE EDUCATION: This well-organized, visually attractive Web site from the Thomas Jefferson National Accelerator Facility, supports science and math education in K-12 classrooms. Features hands-on physics activities, math games, and puzzles. Check out the All About Atoms slide show and the interactive Table of Elements. Includes a question-and-answer page on Atoms, Elements and Molecules and one on Electricity and Magnetism. Science videos are available on loan.

  Grades K-12; Lessons follow Virginia State and National Science Education Content Standards

  `http://education.jlab.org/`

- PHYSICAL SCIENCE HOTLIST: Created by the Franklin Institute Science Museum, these hotlists contain a prescreened grouping of resources for science educators, students, and enthusiasts. Teacher resources include *The Physical Science Activity Manual* which contains 34 hands-on activities for the classroom. Included are Newtonian Physics for grades 9-12 and activities such as Floating Objects which may be appropriate for grades 5-8. The Project Labs offer student-centered experiments in the areas of general science, physical science, and the natural, biological and environmental sciences.

  Grades K-12; National Science Education Content Standards: Varies according to site visited from the listing.

  `http://sln.fi.edu/tfi/hotlists/physical.html`

- THE PARTICLE ADVENTURE: One of the most popular Web sites for learning the fundamentals of matter and force. Created by the Particle Data Group of Lawrence Berkeley National Laboratory. An award winning, interactive tour of the atom, with visits to quarks, neutrinos, antimatter, extra dimensions, dark matter, accelerators and particle detectors. Simple elegant graphics and translations into eleven languages. May be used by teachers or by students alone or in groups.

  Grades 9-12; National Science Education Content Standards A, B, D

  `http://ParticleAdventure.org`

- PARTICLE PHYSICAL EDUCATION SITES: This rich site maintained by the Particle Data Group provides links to many other educational sites. Organizes the links by subject, level, and type of educational experience.

  Grades 9-12; National Science Education Content Standards: Varies according to site

  `http://pdg.lbl.gov/outreach.html`

- QUARKNET: QuarkNet brings the excitement of particle physics research to high school teachers and their students. Teachers join research groups at sixty universities and labs across the country. These research groups are part of particle physics experiments at CERN, Fermilab, or SLAC. Students learn fundamental physics as they participate in inquiry-oriented investigations and analyze live, online data. QuarkNet is supported in part by the National Science Foundation and the U.S. Department of Energy.

  Grades 9-12; National Science Education Content Standards: A, B, E

  `http://QuarkNet.fnal.gov`

- VIRTUAL VISITOR'S CENTER: This Stanford Linear Accelerator Center Web site explains basic particle physics, linear and synchrotron accelerators, electron gamma showers, cosmic rays, and the experiments conducted at SLAC, including real-world applications. Intended for the general public as well as teachers and students.

  Grades 9-12; National Science Education Content Standards: A, B, D, E, G

  `http://www2.slac.stanford.edu/vvc/Default.htm`

8.3. *Particle Physics Education: Astronomy Lessons and Experiments:*

- HANDS-ON UNIVERSE: Enables students in middle and high schools to investigate the night sky without having to stay out late. Created by a collaboration of teachers and students including the Lawrence Hall of Science at the U.C., Berkeley, it uses high quality astronomical images to explore central concepts in math, science, and technology. Students analyze real images with image processing software similar to that used by professional astronomers. Lesson plans and activities are specifically tied to National Science Education Content Standards A and D, Science as Inquiry, and Earth and Space Science. Schools or districts much purchase the software, teacher and student booklets and materials. PDF color versions of the booklets are available from the Web, as well as a number of lesson plans and materials that do not require the purchased software.
  Grades 5-8 and 9-12; National Science Education Content Standards A, D
  `http://www.handsonuniverse.org`

- WINDOWS TO THE UNIVERSE: Provides a rich array of material for exploring earth and space, physics, geology, and chemistry in K-12 classrooms. Includes numerous, thorough lesson plans on topics ranging from the solar system to atmosphere and weather to physics and chemistry. Student-centered activities such as Building a Magnetometer or Create Your Own Cloud are simple, yet highly engaging. Content standards are detailed for most lesson plans. The People section of this vast but well-organized site traces the history of human scientific inquiry from Archimedes to Stephen Hawking. Three reading levels.
  Grades K-12; National Science Education Content Standards A, B, D, E, G
  `http://www.windows.ucar.edu/`

8.4. *Particle Physics Education: Ask-a-Scientist Sites:*

- ASK THE EXPERTS: Submit questions via a form to scientists at PhysLink.com. Questions are answered free. Beware that they won't answer questions from homework assignments or help design something for a science fair or competition.
  `http://www.physlink.com/Education/AskExperts/Index.cfm`

- HOW THINGS WORK: The author of the popular book, *How Things Work: the Physics of Everyday Life*, has created a site that functions as a virtual 'radio call-in program'. Submit questions about how something works or consult the sixty plus pages of most recent questions which are searchable by date, topic, or keyword.
  `http://howthingswork.virginia.edu/`

- MAD SCIENTIST'S NETWORK: ASK A QUESTION: Scientists at this Web site respond to hundreds of questions a week. Be sure to check out their extensive archive of answered questions and use their Science Fair Links for ideas for projects. Also note questions they decline to answer.
  `http://www.madsci.org/submit.html`

8.5. *Particle Physics Education: Experiments, Demos,* & *Fun*

- ALL ABOUT LIGHT: From Fermilab, this offers a delightful collection of pages giving classical, relativistic and quantum explanations of light. Advanced placement high school level or above.
  Grades 11-12+
  `http://www.fnal.gov/pub/inquiring/more/light/index.html`

- CANTEACH: PHYSICAL SCIENCE: Canadian elementary teachers have put together a list of investigations and hands-on physics experiments for elementary level. These well-written physical science lesson plans feature such activities as Making a Pinhole Camera, Air Takes Space, Acid and Basic Test, Growing Crystals, Potential and Kinetic Energy, and Evaporation Painting.
  Grades K-4; National Science Education Standards A, B, E
  `http://www.canteach.ca/elementary/physical.html`

- THE EDIBLE/INEDIBLE EXPERIMENTS ARCHIVE: Part of the Mad Scientist's Network, this Web site covers astronomy, mathematics, and physics. Each experiment uses common materials and identifies whether the experiment is edible, inedible, partially drinkable, or not all that edible (!).
  Grades K-8
  `http://www.madsci.org/experiments/`

- HELPING YOUR CHILD LEARN SCIENCE: A wonderful introduction and set of tools for parents of elementary-age children compiled by the U.S. Department of Education. Provides ideas, home experiments, community-based science activities, and more.
  Grades K-4
  `http://www.ed.gov/pubs/parents/Science/index.html`

- INSULTINGLY STUPID MOVIE PHYSICS: An entertaining and educational site to learn how many movie special effects violate the laws of physics. Includes a rating system for movie reviews. Heavy on text, with few graphics. Equations are included. A good way to emphasize, at the high school level, the immutability of the laws of physics in the real world. Provides instructions on how to use movie physics in the classroom and a bibliography.
  Grades 9-12;
  `http://www.intuitor.com/moviephysics`

- PHYSICS-SCIENCE PHYS/SCI DEMOS: This Web site provides over fifty physics demonstrations on the topics of density, motion, force, angular measurement, waves and sound, electricity and magnetism, optics and nuclear physics. Some of the demos feature photographs. Most of the demos are original, although a few were taken from the T.V. program, *Newton's Apple*. The high school teacher who created this site has won both a Presidential Award for Excellence in Mathematics and Science Teaching and the 2003 Classroom Connect Internet Educator of the Year Award.
  Grades to 5-8 and 9-12; National Science Education Content Standards 5-8 and 9-12: A, B, E
  `http://www.darylscience.com/DemoPhys.html`

8.6. *Particle Physics Education: Physics History and Diversity Sites:*

- AIP CENTER FOR HISTORY OF PHYSICS: This site, produced by the American Institute of Physics, aims to preserve and make known the history of modern physics and allied fields including astronomy, geophysics, and optics. Of interest to teachers and students is the Exhibit Hall, with award-winning exhibits including photos and facts about Marie Curie, Einstein, the discovery of the electron, and the invention of the transistor.
  Grades 7-12; National Science Education Content Standard: G
  `http://www.aip.org/history`

- A CENTURY OF PHYSICS: A timeline from the American Physical Society providing a comprehensive history of major physical science developments with a selection of other events from society, art, politics and literature. Provides a physical timeline, an index, a search sytem and reproductions of the posters and images.
  Grades 7-12; National Science Education Content Standard: G
  `http://timeline.aps.org/APS/home_HighRes.html`

- CONTRIBUTIONS OF 20TH CENTURY WOMEN TO PHYSICS: A great resource for that history of science paper, this archive features descriptions of important contributions to science made by 83 women in the 20th century. Provides historical essays and links to additional documentation such as primary source materials.
  Grades 7-12+; National Science Education Content Standard G
  `http://www.physics.ucla.edu/ cwp/`

- EDUCATION AND OUTREACH COMMITTEE ON THE STATUS OF WOMEN IN PHYSICS: Interested in inspiring a young woman to pursue physics? This American Physical Society site features *Physics in Your Future*, which conveys the exciting possibilities of a career in physics to middle and high school girls. Copies of this four-color booklet are available at no charge to students and their parents, educators, guidance counselors, and groups who work with young women. Also available in PDF. The popular, full color, *Celebrate Women in Physics* poster, is also available at no charge.
  Grades 7-12; National Science Education Content Standard G
  `http://www.aps.org/educ/cswp/`

- PHYSLINK.COM HISTORY OF PHYSICS AND ASTRONOMY: This site, which is a compendium of other history of physics, astronomy and science sites, organizes that historical world into: general guides, histories of physics, of astronomy and space exploration, and of mathematics, online archives, museums and exhibits, and famous scientists. Serves as a guide to some of the most well known people and events in the physical sciences.
  Grades 7-12; National Science Education Content Standard: G
  `http://www.physlink.com/Education/History.cfm`

- NOBEL LAUREATES IN PHYSICS 1901-PRESENT: Maintained by SLAC, this site provides very comprehensive information on physics laureates. Links to the Nobel Foundation's pages on each laureate. Also lists the location(s) of the laureate's prize-winning work, where, if appropriate, the laureate is currently working, and where she or he was working when the work was done. Links to books, related Web sites, and to the HEP Database for in-depth bibliography. An interesting Quick Facts section provides great trivia about some of the prize winners.
  Grades 7-12; National Science Education Content Standard: G
  `http://www.slac.stanford.edu/library/nobel/index.html`

8.7. *Particle Physics Education: Art in Physics:*

Note: This modest collection of physics art links is provided for high school art, photography and literature teachers who may be interested in the intersections between science and technology and art and literature, or who wish to take an interdisciplinary approach to the curriculum in collaborating with their science department colleagues.

- DESY IN A SPECIAL LIGHT: Six luminescent pages of particle physics technology photographed at the Deutsches Electronen Synchrotronen Laboratory (DESY) by Peter Ginter, German photographer, in 1997.
  `http://www.peterginter.de/01technology/desy_01.html`

- HIDDEN CATHEDRALS–SCIENCE OR ART?: Part of a secton of the Web site explaining how physicst study particles, this page provides fifteen brilliantly detailed color photographs of the inner workings of particle detectors at the European Organisation for Nuclear Research (CERN) which is the world's largest particle physics center.
  `http://public.web.cern.ch/public/about/how/art/art.html`

- PHYSICS ICONS: Particle physics as delicate, experiential art. The site description says that this is a meditation on the shifting nature of physics iconography. This video clip was featured in the New York P.S.1 exhibit, *Signatures of the Invisible.*
  `http://www-project.slac.stanford.edu/streaming-media/Sub-Movies.html`

- PRESS PHOTO PRIZE FOR CERN: This article describes the photos done by Peter Ginter for CERN. The photos won a third prize from the World Press Photo of the Year competition in 1998.
  `http://bulletin.cern.ch/9911/art4/Text_E.html`

- ESSAYS AND BOOKS ON ART IN PHYSICS AND SCIENCE:
  "Art and Physics–a Beautiful Friendship"
  `http://bulletin.cern.ch/9949/art1/Text_E.html`
  "Art and Physics" by Leonard Shlain
  `http://www.artandphysics.com/h_main.html`
  "Physics Meets Art and Literature"
  `http://physicsweb.org/article/world/15/11/7`
  "Signatures of the Invisible"
  `http://www.ps1.org/cut/press/signatures.html`

9. Software Directories:

- CERNLIB: CERN PROGRAM LIBRARY: A large collection of general purpose libraries and modules offered in both source code and object code forms from the CERN central computing division. Provides programs applicable to a wide range of physics research problems such as general mathematics, data analysis, detectors simulation, data-handling, *etc.* Also includes links to commercial, free, and other software:
  `http://wwwasd.web.cern.ch/wwwasd/index.html`

- FREEHEP: A collection of software and information about software useful in high-energy physics. Searching can be done by title, subject, date acquired, date updated, or by browsing an alphabetical list of all packages:
  `http://www.slac.stanford.edu/find/fhmain.html`

- FERMITOOLS: Fermilab's software tools program provides a repository of Fermilab-developed software packages of value to the HEP community. Permits searching for packages by title or subject category:
  `http://fermitools.fnal.gov/`

- HEPIC: SOFTWARE & TOOLS USED IN HEP RESEARCH: A meta-level site with links to other sites of HEP-related software and computing tools:
  `http://www.hep.net/resources/software.html`

- GRID PHYSICS NETWORK: The GriPhyN Project is developing grid technologies for scientific and engineering projects that collect and analyze distributed, petabyte-scale datasets. Proivdes links to project information such as documents, education, workspace, virtual data toolkits, Chimera and Sphinx, as well as people, activities and news and related projects:
  `http://www.griphyn.org/index.php`

- PARTICLE PHYSICS DATA GRID: The Web site for the U.S. collaboration of federal laboratories and universities to build a worldwide distributed computing model for current and future particle and nuclear physics experiments:
  `http://www.ppdg.net/`

10. Specialized Subject Pages:

10.1. *Subject Pages*

- CAMBRIDGE RELATIVITY: PUBLIC HOME PAGE: These pages focus on the non-technical learner and explain aspects of relativity such as: cosmology, black holes, cosmic strings, inflation, and quantum gravity. Provides links to movies, research-level home pages and to Stephen Hawking's Web site:
  `http://www.damtp.cam.ac.uk/user/gr/public/`

- NEUTRINO WEBSITE: John Bahcall has compiled links to: technical and popular articles, books, the Hubble Space Telescope and other images, models, viewgraphs, cross-section data, software, and more. The place to begin researching neutrinos at a graduate student level and beyond:
  `http://www.sns.ias.edu/~jnb/`

- THE OFFICIAL STRING THEORY WEB SITE: Outstanding compilation of information about string theory includes: basics, mathematics, experiments, cosmology, black holes, people (including interviews with string theorists), history, theater, links to other Web sites and a discussion forum:
  `http://superstringtheory.com/`
- RELATIVITY: BOOKMARKS: Presents over 100 links collected into subject or other logical divisions. Unfortunately, the site owner explains in a note that he has not been able to verify the links for awhile. However, it still represents one of the best initial collections on the subject.:
  `http://physics.syr.edu/research/relativity/RELATIVITY.html`
- RELATIVITY ON THE WORLD WIDE WEB: An excellent set of pages offering links and written information about relativity. Organized into: popular science sites; visualization sites; Web tutorials; observational and experimental evidence and rebuttals; course work (divided into undergraduate and graduate levels); software; research frontiers; and further reading:
  `http://www.math.washington.edu/~hillman/relativity.html`
- SUPERSTRINGS: An online introduction to superstring theory for the advanced student. Includes further links:
  `http://www.sukidog.com/jpierre/strings/`
- THE ULTIMATE NEUTRINO PAGE: This page provides a gateway to an extremely useful compilation of experimental data and results:
  `http://cupp.oulu.fi/neutrino/`

SUMMARY TABLES OF PARTICLE PHYSICS

* There are also search limits in the Summary Tables for the Gauge and Higgs Bosons, the Leptons, the Quarks, and the Mesons.

SUMMARY TABLES OF PARTICLE PROPERTIES

Extracted from the Particle Listings of the
Review of Particle Physics
S. Eidelman *et al.*, Phys. Lett. B **592**, 1 (2004)
Available at `http://pdg.lbl.gov`

Particle Data Group Authors:

S. Eidelman, K.G. Hayes, K.A. Olive, M. Aguilar-Benitez, C. Amsler, D. Asner, K.S. Babu, R.M. Barnett, J. Beringer, P.R. Burchat, C.D. Carone, C. Caso, G. Conforto, O. Dahl, G. D'Ambrosio, M. Doser, J.L. Feng, T. Gherghetta, L. Gibbons, M. Goodman, C. Grab, D.E. Groom, A. Gurtu, K. Hagiwara, J.J. Hernández-Rey, K. Hikasa, K. Honscheid, H. Jawahery, C. Kolda, Y. Kwon, M.L. Mangano, A.V. Manohar, J. March-Russell, A. Masoni, R. Miquel, K. Mönig, H. Murayama, K. Nakamura, S. Navas, L. Pape, C. Patrignani, A. Piepke, G. Raffelt, M. Roos, M. Tanabashi, J. Terning, N.A. Törnqvist, T.G. Trippe, P. Vogel, C.G. Wohl, R.L. Workman, W.-M. Yao, P.A. Zyla

Technical Associates:

B. Armstrong, P.S. Gee, G. Harper, K.S. Lugovsky, S.B. Lugovsky, V.S. Lugovsky, A. Rom

Other authors who have made substantial contributions to the reviews:

M. Artuso, E. Barberio, M. Battaglia, H. Bichsel, O. Biebel, P. Bloch, R.N. Cahn, D. Casper, A. Cattai, R.S. Chivukula, G. Cowan, T. Damour, K. Desler, M.A. Dobbs, M. Drees, A. Edwards, D.A. Edwards, V.D. Elvira, J. Erler, V.V. Ezhela, W. Fetscher, B.D. Fields, B. Foster, D. Froidevaux, M. Fukugita, T.K. Gaisser, L. Garren, H.-J. Gerber, G. Gerbier, F.J. Gilman, H.E. Haber, C. Hagmann, J. Hewett, I. Hinchliffe, C.J. Hogan, G. Höhler, P. Igo-Kemenes, J.D. Jackson, K.F. Johnson, D. Karlen, B. Kayser, D. Kirkby, S.R. Klein, K. Kleinknecht, I.G. Knowles, P. Kreitz, Yu.V. Kuyanov, O. Lahav, P. Langacker, A. Liddle, L. Littenberg, D.M. Manley, A.D. Martin, M. Narain, P. Nason, Y. Nir, J.A. Peacock, H.R. Quinn, S. Raby, B.N. Ratcliff, E.A. Razuvaev, B. Renk, G. Rolandi, M.T. Ronan, L.J. Rosenberg, C.T. Sachrajda, Y. Sakai, A.I. Sanda, S. Sarkar, M. Schmitt, O. Schneider, D. Scott, W.G. Seligman, M.H. Shaevitz, T. Sjöstrand, G.F. Smoot, S. Spanier, H. Spieler, N.J.C. Spooner, M. Srednicki, A. Stahl, T. Stanev, M. Suzuki, N.P. Tkachenko, G.H. Trilling, G. Valencia, K. van Bibber, M.G. Vincter, D.R. Ward, B.R. Webber, M. Whalley, L. Wolfenstein, J. Womersley, C.L. Woody, O.V. Zenin, R.-Y. Zhu

(Approximate closing date for data: January 1, 2004)

GAUGE AND HIGGS BOSONS

γ

$I(J^{PC}) = 0,1(1^{--})$

Mass $m < 6 \times 10^{-17}$ eV
Charge $q < 5 \times 10^{-30}$ e
Mean life τ = Stable

g or gluon

$I(J^{P}) = 0(1^{-})$

Mass $m = 0$ [a]
SU(3) color octet

W

$J = 1$

Charge $= \pm 1$ e
Mass $m = 80.425 \pm 0.038$ GeV
$m_Z - m_W = 10.763 \pm 0.038$ GeV
$m_{W^+} - m_{W^-} = -0.2 \pm 0.6$ GeV
Full width $\Gamma = 2.124 \pm 0.041$ GeV
$\langle N_{\pi^\pm} \rangle = 15.70 \pm 0.35$
$\langle N_{K^\pm} \rangle = 2.20 \pm 0.19$
$\langle N_p \rangle = 0.92 \pm 0.14$
$\langle N_{\text{charged}} \rangle = 19.41 \pm 0.15$

W^- modes are charge conjugates of the modes below.

W^+ DECAY MODES		Fraction (Γ_i/Γ)		Confidence level	p (MeV/c)
$\ell^+\nu$	[b]	(10.68 ± 0.12)	%		–
$e^+\nu$		(10.72 ± 0.16)	%		40212
$\mu^+\nu$		(10.57 ± 0.22)	%		40212
$\tau^+\nu$		(10.74 ± 0.27)	%		40193
hadrons		(67.96 ± 0.35)	%		–
$\pi^+\gamma$		< 8	$\times 10^{-5}$	95%	40212
$D_s^+\gamma$		< 1.3	$\times 10^{-3}$	95%	40188
cX		(33.6 ± 2.7)	%		–
$c\overline{s}$		(31 $^{+13}_{-11}$)	%		–
invisible	[c]	(1.4 ± 2.8)	%		–

Z

$J = 1$

Charge $= 0$
Mass $m = 91.1876 \pm 0.0021$ GeV [d]
Full width $\Gamma = 2.4952 \pm 0.0023$ GeV
$\Gamma(\ell^+\ell^-) = 83.984 \pm 0.086$ MeV [b]
$\Gamma(\text{invisible}) = 499.0 \pm 1.5$ MeV [e]
$\Gamma(\text{hadrons}) = 1744.4 \pm 2.0$ MeV
$\Gamma(\mu^+\mu^-)/\Gamma(e^+e^-) = 1.0009 \pm 0.0028$
$\Gamma(\tau^+\tau^-)/\Gamma(e^+e^-) = 1.0019 \pm 0.0032$ [f]

Average charged multiplicity

$\langle N_{charged} \rangle = 21.07 \pm 0.11$

Couplings to leptons

$g_V^\ell = -0.03783 \pm 0.00041$
$g_A^\ell = -0.50123 \pm 0.00026$
$g^{\nu_e} = 0.53 \pm 0.09$
$g^{\nu_\mu} = 0.502 \pm 0.017$

Asymmetry parameters [g]

$A_e = 0.1515 \pm 0.0019$
$A_\mu = 0.142 \pm 0.015$
$A_\tau = 0.143 \pm 0.004$
$A_s = 0.90 \pm 0.09$
$A_c = 0.666 \pm 0.036$
$A_b = 0.926 \pm 0.024$

Charge asymmetry (%) at Z pole

$A_{FB}^{(0\ell)} = 1.71 \pm 0.10$
$A_{FB}^{(0u)} = 4 \pm 7$
$A_{FB}^{(0s)} = 9.8 \pm 1.1$
$A_{FB}^{(0c)} = 7.04 \pm 0.36$
$A_{FB}^{(0b)} = 10.01 \pm 0.17$

Z DECAY MODES		Fraction (Γ_i/Γ)		Scale factor/ Confidence level	p (MeV/c)
e^+e^-		(3.363 ± 0.004)	%		45594
$\mu^+\mu^-$		(3.366 ± 0.007)	%		45594
$\tau^+\tau^-$		(3.370 ± 0.008)	%		45559
$\ell^+\ell^-$	[b]	(3.3658 ± 0.0023)	%		–
invisible		(20.00 ± 0.06)	%		–
hadrons		(69.91 ± 0.06)	%		–
$(u\overline{u}+c\overline{c})/2$		(10.1 ± 1.1)	%		–
$(d\overline{d}+s\overline{s}+b\overline{b})/3$		(16.6 ± 0.6)	%		–
$c\overline{c}$		(11.81 ± 0.33)	%		–
$b\overline{b}$		(15.13 ± 0.05)	%		–
$b\overline{b}b\overline{b}$		(3.6 ± 1.3)	$\times 10^{-4}$		–
ggg		< 1.1	%	CL=95%	–
$\pi^0\gamma$		< 5.2	$\times 10^{-5}$	CL=95%	45594
$\eta\gamma$		< 5.1	$\times 10^{-5}$	CL=95%	45592
$\omega\gamma$		< 6.5	$\times 10^{-4}$	CL=95%	45590
$\eta'(958)\gamma$		< 4.2	$\times 10^{-5}$	CL=95%	45589
$\gamma\gamma$		< 5.2	$\times 10^{-5}$	CL=95%	45594
$\gamma\gamma\gamma$		< 1.0	$\times 10^{-5}$	CL=95%	45594
$\pi^\pm W^\mp$	[h]	< 7	$\times 10^{-5}$	CL=95%	10127
$\rho^\pm W^\mp$	[h]	< 8.3	$\times 10^{-5}$	CL=95%	10101
$J/\psi(1S)$X		(3.51 $^{+0.23}_{-0.25}$)	$\times 10^{-3}$	S=1.1	–
$\psi(2S)$X		(1.60 ± 0.29)	$\times 10^{-3}$		–
$\chi_{c1}(1P)$X		(2.9 ± 0.7)	$\times 10^{-3}$		–

Gauge & Higgs Boson Summary Table

$\chi_{c2}(1P)$ X		< 3.2		$\times 10^{-3}$	CL=90%	–
$\Upsilon(1S)$ X + $\Upsilon(2S)$ X + $\Upsilon(3S)$ X		(1.0	±0.5)	$\times 10^{-4}$		–
$\Upsilon(1S)$X		< 4.4		$\times 10^{-5}$	CL=95%	–
$\Upsilon(2S)$X		< 1.39		$\times 10^{-4}$	CL=95%	–
$\Upsilon(3S)$X		< 9.4		$\times 10^{-5}$	CL=95%	–
(D^0 / $\overline{D}^0$) X		(20.7	±2.0) %			–
$D^{\pm}$X		(12.2	±1.7) %			–
$D^*(2010)^{\pm}$X	[h]	(11.4	±1.3) %			–
$D_{s1}(2536)^{\pm}$X		(3.6	±0.8)	$\times 10^{-3}$		–
$D_{sJ}(2573)^{\pm}$X		(5.8	±2.2)	$\times 10^{-3}$		–
$D^{*\prime}(2629)^{\pm}$X		searched for				–
B_s^0X		seen				–
$B_c^{\pm}$X		searched for				–
anomalous γ + hadrons	[i]	< 3.2		$\times 10^{-3}$	CL=95%	–
$e^+e^-\gamma$	[i]	< 5.2		$\times 10^{-4}$	CL=95%	45594
$\mu^+\mu^-\gamma$	[i]	< 5.6		$\times 10^{-4}$	CL=95%	45594
$\tau^+\tau^-\gamma$	[i]	< 7.3		$\times 10^{-4}$	CL=95%	45559
$\ell^+\ell^-\gamma\gamma$	[j]	< 6.8		$\times 10^{-6}$	CL=95%	–
$q\overline{q}\gamma\gamma$	[j]	< 5.5		$\times 10^{-6}$	CL=95%	–
$\nu\overline{\nu}\gamma\gamma$	[j]	< 3.1		$\times 10^{-6}$	CL=95%	45594
$e^{\pm}\mu^{\mp}$	LF [h]	< 1.7		$\times 10^{-6}$	CL=95%	45594
$e^{\pm}\tau^{\mp}$	LF [h]	< 9.8		$\times 10^{-6}$	CL=95%	45576
$\mu^{\pm}\tau^{\mp}$	LF [h]	< 1.2		$\times 10^{-5}$	CL=95%	45576
pe	L,B	< 1.8		$\times 10^{-6}$	CL=95%	45589
$p\mu$	L,B	< 1.8		$\times 10^{-6}$	CL=95%	45589

Higgs Bosons — H^0 and $H^{\pm}$, Searches for

H^0 Mass $m >$ 114.4 GeV, CL = 95%

H_1^0 in Supersymmetric Models ($m_{H_1^0} < m_{H_2^0}$)

Mass $m >$ 89.8 GeV, CL = 95%

A^0 Pseudoscalar Higgs Boson in Supersymmetric Models [k]

Mass $m >$ 90.4 GeV, CL = 95% $\tan\beta > 1$

$H^{\pm}$ Mass $m >$ 79.3 GeV, CL = 95%

See the Particle Listings for a Note giving details of Higgs Bosons.

Heavy Bosons Other Than Higgs Bosons, Searches for

Additional W Bosons

W' with standard couplings decaying to $e\nu$, $\mu\nu$
Mass $m >$ 786 GeV, CL = 95%

W_R — right-handed W
Mass $m >$ 715 GeV, CL = 90% (electroweak fit)

Additional Z Bosons

Z'_{SM} with standard couplings
Mass $m >$ 690 GeV, CL = 95% ($p\overline{p}$ direct search)
Mass $m >$ 1500 GeV, CL = 95% (electroweak fit)

Z_{LR} of $SU(2)_L \times SU(2)_R \times U(1)$ (with $g_L = g_R$)
Mass $m >$ 630 GeV, CL = 95% ($p\overline{p}$ direct search)
Mass $m >$ 860 GeV, CL = 95% (electroweak fit)

Z_χ of $SO(10) \rightarrow SU(5) \times U(1)_\chi$ (with $g_\chi = e/\cos\theta_W$)
Mass $m >$ 595 GeV, CL = 95% ($p\overline{p}$ direct search)
Mass $m >$ 680 GeV, CL = 95% (electroweak fit)

Z_ψ of $E_6 \rightarrow SO(10) \times U(1)_\psi$ (with $g_\psi = e/\cos\theta_W$)
Mass $m >$ 590 GeV, CL = 95% ($p\overline{p}$ direct search)
Mass $m >$ 350 GeV, CL = 95% (electroweak fit)

Z_η of $E_6 \rightarrow SU(3) \times SU(2) \times U(1) \times U(1)_\eta$ (with $g_\eta = e/\cos\theta_W$)
Mass $m >$ 620 GeV, CL = 95% ($p\overline{p}$ direct search)
Mass $m >$ 619 GeV, CL = 95% (electroweak fit)

Scalar Leptoquarks

Mass $m >$ 242 GeV, CL = 95% (1st generation, pair prod.)
Mass $m >$ 298 GeV, CL = 95% (1st gener., single prod.)
Mass $m >$ 202 GeV, CL = 95% (2nd gener., pair prod.)
Mass $m >$ 73 GeV, CL = 95% (2nd gener., single prod.)
Mass $m >$ 148 GeV, CL = 95% (3rd gener., pair prod.)
(See the Particle Listings for assumptions on leptoquark quantum numbers and branching fractions.)

Axions (A^0) and Other Very Light Bosons, Searches for

The standard Peccei-Quinn axion is ruled out. Variants with reduced couplings or much smaller masses are constrained by various data. The Particle Listings in the full *Review* contain a Note discussing axion searches.

The best limit for the half-life of neutrinoless double beta decay with Majoron emission is $> 7.2 \times 10^{24}$ years (CL = 90%).

NOTES

In this Summary Table:

When a quantity has "(S = ...)" to its right, the error on the quantity has been enlarged by the "scale factor" S, defined as $S = \sqrt{\chi^2/(N-1)}$, where N is the number of measurements used in calculating the quantity. We do this when $S > 1$, which often indicates that the measurements are inconsistent. When $S > 1.25$, we also show in the Particle Listings an ideogram of the measurements. For more about S, see the Introduction.

A decay momentum p is given for each decay mode. For a 2-body decay, p is the momentum of each decay product in the rest frame of the decaying particle. For a 3-or-more-body decay, p is the largest momentum any of the products can have in this frame.

[a] Theoretical value. A mass as large as a few MeV may not be precluded.
[b] ℓ indicates each type of lepton (e, μ, and τ), not sum over them.
[c] This represents the width for the decay of the W boson into a charged particle with momentum below detectability, p< 200 MeV.
[d] The Z-boson mass listed here corresponds to a Breit-Wigner resonance parameter. It lies approximately 34 MeV above the real part of the position of the pole (in the energy-squared plane) in the Z-boson propagator.
[e] This partial width takes into account Z decays into $\nu\overline{\nu}$ and any other possible undetected modes.
[f] This ratio has not been corrected for the τ mass.
[g] Here $A \equiv 2g_V g_A/(g_V^2+g_A^2)$.
[h] The value is for the sum of the charge states or particle/antiparticle states indicated.
[i] See the Z Particle Listings for the γ energy range used in this measurement.
[j] For $m_{\gamma\gamma} = (60 \pm 5)$ GeV.
[k] The limits assume no invisible decays.

LEPTONS

e

$J = \frac{1}{2}$

Mass $m = (548.57990945 \pm 0.00000024) \times 10^{-6}$ u
Mass $m = 0.51099892 \pm 0.00000004$ MeV
$|m_{e^+} - m_{e^-}|/m < 8 \times 10^{-9}$, CL = 90%
$|q_{e^+} + q_{e^-}|/e < 4 \times 10^{-8}$
Magnetic moment $\mu = 1.001159652187 \pm 0.000000000004\ \mu_B$
$(g_{e^+} - g_{e^-}) / g_{\rm average} = (-0.5 \pm 2.1) \times 10^{-12}$
Electric dipole moment $d = (0.07 \pm 0.07) \times 10^{-26}\ e$ cm
Mean life $\tau > 4.6 \times 10^{26}$ yr, CL = 90% [a]

μ

$J = \frac{1}{2}$

Mass $m = 0.1134289264 \pm 0.0000000030$ u
Mass $m = 105.658369 \pm 0.000009$ MeV
Mean life $\tau = (2.19703 \pm 0.00004) \times 10^{-6}$ s
$\tau_{\mu^+}/\tau_{\mu^-} = 1.00002 \pm 0.00008$
$c\tau = 658.654$ m
Magnetic moment $\mu = 1.0011659160 \pm 0.0000000006\ e\hbar/2m_\mu$
$(g_{\mu^+} - g_{\mu^-}) / g_{\rm average} = (-2.6 \pm 1.6) \times 10^{-8}$
Electric dipole moment $d = (3.7 \pm 3.4) \times 10^{-19}\ e$ cm

Decay parameters [b]

$\rho = 0.7518 \pm 0.0026$
$\eta = -0.007 \pm 0.013$
$\delta = 0.749 \pm 0.004$
$\xi P_\mu = 1.003 \pm 0.008$ [c]
$\xi P_\mu \delta/\rho > 0.99682$, CL = 90% [c]
$\xi' = 1.00 \pm 0.04$
$\xi'' = 0.7 \pm 0.4$
$\alpha/A = (0 \pm 4) \times 10^{-3}$
$\alpha'/A = (0 \pm 4) \times 10^{-3}$
$\beta/A = (4 \pm 6) \times 10^{-3}$
$\beta'/A = (2 \pm 6) \times 10^{-3}$
$\overline{\eta} = 0.02 \pm 0.08$

μ^+ modes are charge conjugates of the modes below.

μ^- DECAY MODES		Fraction (Γ_j/Γ)	Confidence level	p (MeV/c)
$e^- \overline{\nu}_e \nu_\mu$		$\approx 100\%$		53
$e^- \overline{\nu}_e \nu_\mu \gamma$	[d]	$(1.4 \pm 0.4)\%$		53
$e^- \overline{\nu}_e \nu_\mu e^+ e^-$	[e]	$(3.4 \pm 0.4) \times 10^{-5}$		53
Lepton Family number (LF) violating modes				
$e^- \nu_e \overline{\nu}_\mu$	LF	[f] < 1.2 %	90%	53
$e^- \gamma$	LF	$< 1.2 \times 10^{-11}$	90%	53
$e^- e^+ e^-$	LF	$< 1.0 \times 10^{-12}$	90%	53
$e^- 2\gamma$	LF	$< 7.2 \times 10^{-11}$	90%	53

τ

$J = \frac{1}{2}$

Mass $m = 1776.99^{+0.29}_{-0.26}$ MeV
$(m_{\tau^+} - m_{\tau^-})/m_{\rm average} < 3.0 \times 10^{-3}$, CL = 90%
Mean life $\tau = (290.6 \pm 1.1) \times 10^{-15}$ s
$c\tau = 87.11\ \mu$m
Magnetic moment anomaly > -0.052 and < 0.058, CL = 95%
$\mathrm{Re}(d_\tau) = -0.22$ to $0.45 \times 10^{-16}\ e$ cm, CL = 95%
$\mathrm{Im}(d_\tau) = -0.25$ to $0.008 \times 10^{-16}\ e$ cm, CL = 95%

Weak dipole moment

$\mathrm{Re}(d_\tau^w) < 0.50 \times 10^{-17}\ e$ cm, CL = 95%
$\mathrm{Im}(d_\tau^w) < 1.1 \times 10^{-17}\ e$ cm, CL = 95%

Weak anomalous magnetic dipole moment

$\mathrm{Re}(\alpha_\tau^w) < 1.1 \times 10^{-3}$, CL = 95%
$\mathrm{Im}(\alpha_\tau^w) < 2.7 \times 10^{-3}$, CL = 95%

Decay parameters

See the τ Particle Listings for a note concerning τ-decay parameters.

$\rho^\tau(e \text{ or } \mu) = 0.745 \pm 0.008$
$\rho^\tau(e) = 0.747 \pm 0.010$
$\rho^\tau(\mu) = 0.763 \pm 0.020$
$\xi^\tau(e \text{ or } \mu) = 0.985 \pm 0.030$
$\xi^\tau(e) = 0.994 \pm 0.040$
$\xi^\tau(\mu) = 1.030 \pm 0.059$
$\eta^\tau(e \text{ or } \mu) = 0.013 \pm 0.020$
$\eta^\tau(\mu) = 0.094 \pm 0.073$
$(\delta\xi)^\tau(e \text{ or } \mu) = 0.746 \pm 0.021$
$(\delta\xi)^\tau(e) = 0.734 \pm 0.028$
$(\delta\xi)^\tau(\mu) = 0.778 \pm 0.037$
$\xi^\tau(\pi) = 0.993 \pm 0.022$
$\xi^\tau(\rho) = 0.994 \pm 0.008$
$\xi^\tau(a_1) = 1.001 \pm 0.027$
$\xi^\tau(\text{all hadronic modes}) = 0.995 \pm 0.007$

τ^+ modes are charge conjugates of the modes below. "$h^\pm$" stands for $\pi^\pm$ or $K^\pm$. "ℓ" stands for e or μ. "Neutrals" stands for γ's and/or π^0's.

τ^- DECAY MODES		Fraction (Γ_j/Γ)	Scale factor/ Confidence level	p (MeV/c)
Modes with one charged particle				
particle$^- \geq 0$ neutrals $\geq 0 K^0 \nu_\tau$ ("1-prong")		$(85.35 \pm 0.07)\%$	S=1.1	–
particle$^- \geq 0$ neutrals $\geq 0 K_L^0 \nu_\tau$		$(84.72 \pm 0.07)\%$	S=1.1	–
$\mu^- \overline{\nu}_\mu \nu_\tau$	[g]	$(17.36 \pm 0.06)\%$		885
$\mu^- \overline{\nu}_\mu \nu_\tau \gamma$	[e]	$(3.6 \pm 0.4) \times 10^{-3}$		885
$e^- \overline{\nu}_e \nu_\tau$	[g]	$(17.84 \pm 0.06)\%$		888
$e^- \overline{\nu}_e \nu_\tau \gamma$	[e]	$(1.75 \pm 0.18)\%$		888
$h^- \geq 0 K_L^0 \nu_\tau$		$(12.30 \pm 0.11)\%$	S=1.4	883
$h^- \nu_\tau$		$(11.75 \pm 0.11)\%$	S=1.4	883
$\pi^- \nu_\tau$	[g]	$(11.06 \pm 0.11)\%$	S=1.4	883
$K^- \nu_\tau$	[g]	$(6.86 \pm 0.23) \times 10^{-3}$		820
$h^- \geq 1$ neutrals ν_τ		$(36.92 \pm 0.14)\%$	S=1.1	–
$h^- \pi^0 \nu_\tau$		$(25.87 \pm 0.13)\%$	S=1.1	878
$\pi^- \pi^0 \nu_\tau$	[g]	$(25.42 \pm 0.14)\%$	S=1.1	878
$\pi^- \pi^0$ non-$\rho(770) \nu_\tau$		$(3.0 \pm 3.2) \times 10^{-3}$		878
$K^- \pi^0 \nu_\tau$	[g]	$(4.50 \pm 0.30) \times 10^{-3}$		814
$h^- \geq 2\pi^0 \nu_\tau$		$(10.77 \pm 0.15)\%$	S=1.1	–
$h^- 2\pi^0 \nu_\tau$		$(9.39 \pm 0.14)\%$	S=1.1	862
$h^- 2\pi^0 \nu_\tau$ (ex. K^0)		$(9.23 \pm 0.14)\%$	S=1.1	862
$\pi^- 2\pi^0 \nu_\tau$ (ex. K^0)	[g]	$(9.17 \pm 0.14)\%$	S=1.1	862
$\pi^- 2\pi^0 \nu_\tau$ (ex. K^0), scalar		$< 9 \times 10^{-3}$	CL=95%	862
$\pi^- 2\pi^0 \nu_\tau$ (ex. K^0), vector		$< 7 \times 10^{-3}$	CL=95%	862
$K^- 2\pi^0 \nu_\tau$ (ex. K^0)	[g]	$(5.8 \pm 2.3) \times 10^{-4}$		796
$h^- \geq 3\pi^0 \nu_\tau$		$(1.37 \pm 0.11)\%$	S=1.1	–
$h^- 3\pi^0 \nu_\tau$		$(1.21 \pm 0.10)\%$		836
$\pi^- 3\pi^0 \nu_\tau$ (ex. K^0)	[g]	$(1.08 \pm 0.10)\%$		836
$K^- 3\pi^0 \nu_\tau$ (ex. K^0, η)	[g]	$(3.8^{+2.2}_{-2.0}) \times 10^{-4}$		766
$h^- 4\pi^0 \nu_\tau$ (ex. K^0)		$(1.6 \pm 0.6) \times 10^{-3}$		800
$h^- 4\pi^0 \nu_\tau$ (ex. K^0, η)	[g]	$(1.0^{+0.6}_{-0.5}) \times 10^{-3}$		800
$K^- \geq 0\pi^0 \geq 0 K^0 \geq 0\gamma\ \nu_\tau$		$(1.56 \pm 0.04)\%$		820
$K^- \geq 1$ (π^0 or K^0 or γ) ν_τ		$(8.74 \pm 0.35) \times 10^{-3}$		–

Lepton Summary Table

Modes with K^0's

K^0_S(particles)$^-\,\nu_\tau$		$(\ 9.2\ \pm0.4\ )\times10^{-3}$	S=1.1	–
$h^-\overline{K}^0\nu_\tau$		$(\ 1.05\pm0.04)$ %	S=1.1	812
$\pi^-\overline{K}^0\nu_\tau$	[g]	$(\ 8.9\ \pm0.4\ )\times10^{-3}$	S=1.1	812
$\pi^-\overline{K}^0$ (non-$K^*(892)^-$)$\,\nu_\tau$		$<\ 1.7\ \times10^{-3}$	CL=95%	812
$K^-K^0\nu_\tau$	[g]	$(\ 1.54\pm0.16)\times10^{-3}$		737
$K^-K^0\geq0\pi^0\,\nu_\tau$		$(\ 3.09\pm0.24)\times10^{-3}$		737
$h^-\overline{K}^0\pi^0\nu_\tau$		$(\ 5.2\ \pm0.4\ )\times10^{-3}$		794
$\pi^-\overline{K}^0\pi^0\nu_\tau$	[g]	$(\ 3.7\ \pm0.4\ )\times10^{-3}$		794
$\overline{K}^0\rho^-\nu_\tau$		$(\ 2.2\ \pm0.5\ )\times10^{-3}$		612
$K^-K^0\pi^0\nu_\tau$	[g]	$(\ 1.55\pm0.20)\times10^{-3}$		685
$\pi^-\overline{K}^0\geq1\pi^0\,\nu_\tau$		$(\ 3.2\ \pm1.0\ )\times10^{-3}$		–
$\pi^-\overline{K}^0\pi^0\pi^0\nu_\tau$		$(\ 2.6\ \pm2.4\ )\times10^{-4}$		763
$K^-K^0\pi^0\pi^0\nu_\tau$		$<\ 1.6\ \times10^{-4}$	CL=95%	619
$\pi^-K^0\overline{K}^0\nu_\tau$		$(\ 1.59\pm0.29)\times10^{-3}$	S=1.1	682
$\pi^-K^0_SK^0_S\nu_\tau$	[g]	$(\ 2.4\ \pm0.5\ )\times10^{-4}$		682
$\pi^-K^0_SK^0_L\nu_\tau$	[g]	$(\ 1.10\pm0.28)\times10^{-3}$	S=1.1	682
$\pi^-K^0\overline{K}^0\pi^0\nu_\tau$		$(\ 3.1\ \pm2.3\ )\times10^{-4}$		614
$\pi^-K^0_SK^0_S\pi^0\nu_\tau$		$<\ 2.0\ \times10^{-4}$	CL=95%	614
$\pi^-K^0_SK^0_L\pi^0\nu_\tau$		$(\ 3.1\ \pm1.2\ )\times10^{-4}$		614
$K^0h^+h^-h^-\geq0$ neutrals ν_τ		$<\ 1.7\ \times10^{-3}$	CL=95%	760
$K^0h^+h^-h^-\nu_\tau$		$(\ 2.3\ \pm2.0\ )\times10^{-4}$		760

Modes with three charged particles

$h^-h^-h^+\geq0K^0_L\nu_\tau$		(15.19 ± 0.07) %	S=1.1	861
$h^-h^-h^+\geq0$ neutrals ν_τ (ex. $K^0_S\to\pi^+\pi^-$) ("3-prong")		(14.57 ± 0.07) %	S=1.1	861
$h^-h^-h^+\nu_\tau$		(10.01 ± 0.09) %	S=1.2	861
$h^-h^-h^+\nu_\tau$(ex.K^0)		$(\ 9.65\pm0.09)$ %	S=1.2	861
$h^-h^-h^+\nu_\tau$(ex.K^0,ω)		$(\ 9.60\pm0.09)$ %	S=1.2	861
$\pi^-\pi^+\pi^-\nu_\tau$		$(\ 9.47\pm0.10)$ %	S=1.2	861
$\pi^-\pi^+\pi^-\nu_\tau$(ex.K^0)		$(\ 9.16\pm0.10)$ %	S=1.2	861
$\pi^-\pi^+\pi^-\nu_\tau$(ex.K^0), non-axial vector		$<\ 2.4\ $ %	CL=95%	861
$\pi^-\pi^+\pi^-\nu_\tau$(ex.K^0,ω)	[g]	$(\ 9.12\pm0.10)$ %	S=1.2	861
$h^-h^-h^+\geq1$ neutrals ν_τ		$(\ 5.19\pm0.10)$ %	S=1.3	–
$h^-h^-h^+\geq1$ neutrals ν_τ (ex. $K^0_S\to\pi^+\pi^-$)		$(\ 4.92\pm0.09)$ %	S=1.3	–
$h^-h^-h^+\pi^0\nu_\tau$		$(\ 4.53\pm0.09)$ %	S=1.3	834
$h^-h^-h^+\pi^0\nu_\tau$(ex.K^0)		$(\ 4.35\pm0.09)$ %	S=1.3	834
$h^-h^-h^+\pi^0\nu_\tau$(ex. K^0, ω)		$(\ 2.62\pm0.09)$ %	S=1.2	834
$\pi^-\pi^+\pi^-\pi^0\nu_\tau$		$(\ 4.37\pm0.09)$ %	S=1.3	834
$\pi^-\pi^+\pi^-\pi^0\nu_\tau$(ex.$K^0$)		$(\ 4.25\pm0.09)$ %	S=1.3	834
$\pi^-\pi^+\pi^-\pi^0\nu_\tau$(ex.$K^0$,$\omega$)	[g]	$(\ 2.51\pm0.09)$ %	S=1.2	834
$h^-h^-h^+2\pi^0\nu_\tau$		$(\ 5.5\ \pm0.4\ )\times10^{-3}$		797
$h^-h^-h^+2\pi^0\nu_\tau$(ex.K^0)		$(\ 5.4\ \pm0.4\ )\times10^{-3}$		797
$h^-h^-h^+2\pi^0\nu_\tau$(ex.K^0,ω,η)	[g]	$(\ 1.1\ \pm0.4\ )\times10^{-3}$		797
$h^-h^-h^+3\pi^0\nu_\tau$	[g]	$(\ 2.3\ \pm0.8\ )\times10^{-4}$	S=1.5	749
$K^-h^+h^-\geq0$ neutrals ν_τ		$(\ 6.9\ \pm0.4\ )\times10^{-3}$	S=1.3	794
$K^-h^+\pi^-\nu_\tau$(ex.K^0)		$(\ 4.8\ \pm0.4\ )\times10^{-3}$	S=1.5	794
$K^-h^+\pi^-\pi^0\nu_\tau$(ex.K^0)		$(\ 1.07\pm0.22)\times10^{-3}$		763
$K^-\pi^+\pi^-\geq0$ neutrals ν_τ		$(\ 5.0\ \pm0.4\ )\times10^{-3}$	S=1.3	794
$K^-\pi^+\pi^-\geq0\pi^0\nu_\tau$(ex.$K^0$)		$(\ 3.9\ \pm0.4\ )\times10^{-3}$	S=1.3	794
$K^-\pi^+\pi^-\nu_\tau$		$(\ 3.8\ \pm0.4\ )\times10^{-3}$	S=1.6	794
$K^-\pi^+\pi^-\nu_\tau$(ex.K^0)	[g]	$(\ 3.3\ \pm0.4\ )\times10^{-3}$	S=1.6	794
$K^-\rho^0\nu_\tau\to K^-\pi^+\pi^-\nu_\tau$		$(\ 1.6\ \pm0.6\ )\times10^{-3}$		–
$K^-\pi^+\pi^-\pi^0\nu_\tau$		$(\ 1.18\pm0.25)\times10^{-3}$		763
$K^-\pi^+\pi^-\pi^0\nu_\tau$(ex.$K^0$)		$(\ 6.5\ \pm2.4\ )\times10^{-4}$		763
$K^-\pi^+\pi^-\pi^0\nu_\tau$(ex.$K^0$,$\eta$)	[g]	$(\ 5.9\ \pm2.4\ )\times10^{-4}$		763
$K^-\pi^+K^-\geq0$ neut. ν_τ		$<\ 9\ \times10^{-4}$	CL=95%	685
$K^-K^+\pi^-\geq0$ neut. ν_τ		$(\ 1.97\pm0.18)\times10^{-3}$	S=1.1	685
$K^-K^+\pi^-\nu_\tau$	[g]	$(\ 1.55\pm0.07)\times10^{-3}$		685
$K^-K^+\pi^-\pi^0\nu_\tau$	[g]	$(\ 4.2\ \pm1.6\ )\times10^{-4}$	S=1.1	618
$K^-K^+K^-\geq0$ neut. ν_τ		$<\ 2.1\ \times10^{-3}$	CL=95%	472
$K^-K^+K^-\nu_\tau$		$<\ 3.7\ \times10^{-5}$	CL=90%	472
$\pi^-K^+\pi^-\geq0$ neut. ν_τ		$<\ 2.5\ \times10^{-3}$	CL=95%	794
$e^-e^-e^+\overline{\nu}_e\nu_\tau$		$(\ 2.8\ \pm1.5\ )\times10^{-5}$		888
$\mu^-e^-e^+\overline{\nu}_\mu\nu_\tau$		$<\ 3.6\ \times10^{-5}$	CL=90%	885

Modes with five charged particles

$3h^-2h^+\geq0$ neutrals ν_τ (ex. $K^0_S\to\pi^-\pi^+$) ("5-prong")		$(\ 1.00\pm0.06)\times10^{-3}$		794
$3h^-2h^+\nu_\tau$(ex.K^0)	[g]	$(\ 8.2\ \pm0.6\ )\times10^{-4}$		794
$3h^-2h^+\pi^0\nu_\tau$(ex.K^0)	[g]	$(\ 1.81\pm0.27)\times10^{-4}$		746
$3h^-2h^+2\pi^0\nu_\tau$		$<\ 1.1\ \times10^{-4}$	CL=90%	687

Miscellaneous other allowed modes

$(5\pi)^-\nu_\tau$		$(\ 8.0\ \pm0.7\ )\times10^{-3}$		800
$4h^-3h^+\geq0$ neutrals ν_τ ("7-prong")		$<\ 2.4\ \times10^{-6}$	CL=90%	683
$X^-(S{=}-1)\nu_\tau$		$(\ 2.91\pm0.08)$ %	S=1.1	–
$K^*(892)^-\geq0$ neutrals $\geq0K^0_L\nu_\tau$		$(\ 1.42\pm0.18)$ %	S=1.4	665
$K^*(892)^-\nu_\tau$		$(\ 1.29\pm0.05)$ %		665
$K^*(892)^0K^-\geq0$ neutrals ν_τ		$(\ 3.2\ \pm1.4\ )\times10^{-3}$		542
$K^*(892)^0K^-\nu_\tau$		$(\ 2.1\ \pm0.4\ )\times10^{-3}$		542
$\overline{K}^*(892)^0\pi^-\geq0$ neutrals ν_τ		$(\ 3.8\ \pm1.7\ )\times10^{-3}$		656
$\overline{K}^*(892)^0\pi^-\nu_\tau$		$(\ 2.2\ \pm0.5\ )\times10^{-3}$		656
$(\overline{K}^*(892)\pi)^-\nu_\tau\to\pi^-\overline{K}^0\pi^0\nu_\tau$		$(\ 1.0\ \pm0.4\ )\times10^{-3}$		–
$K_1(1270)^-\nu_\tau$		$(\ 4.7\ \pm1.1\ )\times10^{-3}$		433
$K_1(1400)^-\nu_\tau$		$(\ 1.7\ \pm2.6\ )\times10^{-3}$	S=1.7	335
$K^*(1410)^-\nu_\tau$		$(\ 1.5\ ^{+1.4}_{-1.0}\ )\times10^{-3}$		326
$K^*_0(1430)^-\nu_\tau$		$<\ 5\ \times10^{-4}$	CL=95%	328
$K^*_2(1430)^-\nu_\tau$		$<\ 3\ \times10^{-3}$	CL=95%	317
$\eta\pi^-\nu_\tau$		$<\ 1.4\ \times10^{-4}$	CL=95%	797
$\eta\pi^-\pi^0\nu_\tau$	[g]	$(\ 1.74\pm0.24)\times10^{-3}$		778
$\eta\pi^-\pi^0\pi^0\nu_\tau$		$(\ 1.5\ \pm0.5\ )\times10^{-4}$		746
$\eta K^-\nu_\tau$	[g]	$(\ 2.7\ \pm0.6\ )\times10^{-4}$		720
$\eta K^*(892)^-\nu_\tau$		$(\ 2.9\ \pm0.9\ )\times10^{-4}$		511
$\eta K^-\pi^0\nu_\tau$		$(\ 1.8\ \pm0.9\ )\times10^{-4}$		665
$\eta\overline{K}^0\pi^-\nu_\tau$		$(\ 2.2\ \pm0.7\ )\times10^{-4}$		661
$\eta\pi^+\pi^-\pi^-\geq0$ neutrals ν_τ		$<\ 3\ \times10^{-3}$	CL=90%	744
$\eta\pi^-\pi^+\pi^-\nu_\tau$		$(\ 2.3\ \pm0.5\ )\times10^{-4}$		744
$\eta a_1(1260)^-\nu_\tau\to\eta\pi^-\rho^0\nu_\tau$		$<\ 3.9\ \times10^{-4}$	CL=90%	–
$\eta\eta\pi^-\nu_\tau$		$<\ 1.1\ \times10^{-4}$	CL=95%	637
$\eta\eta\pi^-\pi^0\nu_\tau$		$<\ 2.0\ \times10^{-4}$	CL=95%	559
$\eta'(958)\pi^-\nu_\tau$		$<\ 7.4\ \times10^{-5}$	CL=90%	620
$\eta'(958)\pi^-\pi^0\nu_\tau$		$<\ 8.0\ \times10^{-5}$	CL=90%	591
$\phi\pi^-\nu_\tau$		$<\ 2.0\ \times10^{-4}$	CL=90%	585
$\phi K^-\nu_\tau$		$<\ 6.7\ \times10^{-5}$	CL=90%	445
$f_1(1285)\pi^-\nu_\tau$		$(\ 5.8\ \pm2.3\ )\times10^{-4}$		408
$f_1(1285)\pi^-\nu_\tau\to\eta\pi^-\pi^+\pi^-\nu_\tau$		$(\ 1.3\ \pm0.4\ )\times10^{-4}$		–
$\pi(1300)^-\nu_\tau\to(\rho\pi)^-\nu_\tau\to(3\pi)^-\nu_\tau$		$<\ 1.0\ \times10^{-4}$	CL=90%	–
$\pi(1300)^-\nu_\tau\to((\pi\pi)_{S-\text{wave}}\,\pi)^-\nu_\tau\to(3\pi)^-\nu_\tau$		$<\ 1.9\ \times10^{-4}$	CL=90%	–
$h^-\omega\geq0$ neutrals ν_τ		$(\ 2.38\pm0.08)$ %		708
$h^-\omega\nu_\tau$	[g]	$(\ 1.94\pm0.07)$ %		708
$h^-\omega\pi^0\nu_\tau$	[g]	$(\ 4.4\ \pm0.5\ )\times10^{-3}$		684
$h^-\omega2\pi^0\nu_\tau$		$(\ 1.4\ \pm0.5\ )\times10^{-4}$		644
$2h^-h^+\omega\nu_\tau$		$(\ 1.20\pm0.22)\times10^{-4}$		641

Lepton Family number (LF), Lepton number (L), or Baryon number (B) violating modes

L means lepton number violation (*e.g.* $\tau^- \to e^+\pi^-\pi^-$). Following common usage, LF means lepton family violation *and not* lepton number violation (*e.g.* $\tau^- \to e^-\pi^+\pi^-$). B means baryon number violation.

$e^-\gamma$	LF	$<$	2.7	$\times 10^{-6}$	CL=90%	888
$\mu^-\gamma$	LF	$<$	1.1	$\times 10^{-6}$	CL=90%	885
$e^-\pi^0$	LF	$<$	3.7	$\times 10^{-6}$	CL=90%	883
$\mu^-\pi^0$	LF	$<$	4.0	$\times 10^{-6}$	CL=90%	880
$e^-K^0_S$	LF	$<$	9.1	$\times 10^{-7}$	CL=90%	819
$\mu^-K^0_S$	LF	$<$	9.5	$\times 10^{-7}$	CL=90%	815
$e^-\eta$	LF	$<$	8.2	$\times 10^{-6}$	CL=90%	804
$\mu^-\eta$	LF	$<$	9.6	$\times 10^{-6}$	CL=90%	800
$e^-\rho^0$	LF	$<$	2.0	$\times 10^{-6}$	CL=90%	719
$\mu^-\rho^0$	LF	$<$	6.3	$\times 10^{-6}$	CL=90%	715
$e^-K^*(892)^0$	LF	$<$	5.1	$\times 10^{-6}$	CL=90%	665
$\mu^-K^*(892)^0$	LF	$<$	7.5	$\times 10^{-6}$	CL=90%	660
$e^-\overline{K}^*(892)^0$	LF	$<$	7.4	$\times 10^{-6}$	CL=90%	665
$\mu^-\overline{K}^*(892)^0$	LF	$<$	7.5	$\times 10^{-6}$	CL=90%	660
$e^-\phi$	LF	$<$	6.9	$\times 10^{-6}$	CL=90%	596
$\mu^-\phi$	LF	$<$	7.0	$\times 10^{-6}$	CL=90%	590
$e^-e^+e^-$	LF	$<$	2.9	$\times 10^{-6}$	CL=90%	888
$e^-\mu^+\mu^-$	LF	$<$	1.8	$\times 10^{-6}$	CL=90%	882
$e^+\mu^-\mu^-$	LF	$<$	1.5	$\times 10^{-6}$	CL=90%	882
$\mu^-e^+e^-$	LF	$<$	1.7	$\times 10^{-6}$	CL=90%	885
$\mu^+e^-e^-$	LF	$<$	1.5	$\times 10^{-6}$	CL=90%	885
$\mu^-\mu^+\mu^-$	LF	$<$	1.9	$\times 10^{-6}$	CL=90%	873
$e^-\pi^+\pi^-$	LF	$<$	2.2	$\times 10^{-6}$	CL=90%	877
$e^+\pi^-\pi^-$	L	$<$	1.9	$\times 10^{-6}$	CL=90%	877
$\mu^-\pi^+\pi^-$	LF	$<$	8.2	$\times 10^{-6}$	CL=90%	866
$\mu^+\pi^-\pi^-$	L	$<$	3.4	$\times 10^{-6}$	CL=90%	866
$e^-\pi^+K^-$	LF	$<$	6.4	$\times 10^{-6}$	CL=90%	813
$e^-\pi^-K^+$	LF	$<$	3.8	$\times 10^{-6}$	CL=90%	813
$e^+\pi^-K^-$	L	$<$	2.1	$\times 10^{-6}$	CL=90%	813
$e^-K^0_SK^0_S$	LF	$<$	2.2	$\times 10^{-6}$	CL=90%	736
$e^-K^+K^-$	LF	$<$	6.0	$\times 10^{-6}$	CL=90%	739
$e^+K^-K^-$	L	$<$	3.8	$\times 10^{-6}$	CL=90%	739
$\mu^-\pi^+K^-$	LF	$<$	7.5	$\times 10^{-6}$	CL=90%	800
$\mu^-\pi^-K^+$	LF	$<$	7.4	$\times 10^{-6}$	CL=90%	800
$\mu^+\pi^-K^-$	L	$<$	7.0	$\times 10^{-6}$	CL=90%	800
$\mu^-K^0_SK^0_S$	LF	$<$	3.4	$\times 10^{-6}$	CL=90%	696
$\mu^-K^+K^-$	LF	$<$	1.5	$\times 10^{-5}$	CL=90%	699
$\mu^+K^-K^-$	L	$<$	6.0	$\times 10^{-6}$	CL=90%	699
$e^-\pi^0\pi^0$	LF	$<$	6.5	$\times 10^{-6}$	CL=90%	878
$\mu^-\pi^0\pi^0$	LF	$<$	1.4	$\times 10^{-5}$	CL=90%	867
$e^-\eta\eta$	LF	$<$	3.5	$\times 10^{-5}$	CL=90%	699
$\mu^-\eta\eta$	LF	$<$	6.0	$\times 10^{-5}$	CL=90%	654
$e^-\pi^0\eta$	LF	$<$	2.4	$\times 10^{-5}$	CL=90%	798
$\mu^-\pi^0\eta$	LF	$<$	2.2	$\times 10^{-5}$	CL=90%	784
$\overline{p}\gamma$	L,B	$<$	3.5	$\times 10^{-6}$	CL=90%	641
$\overline{p}\pi^0$	L,B	$<$	1.5	$\times 10^{-5}$	CL=90%	632
$\overline{p}2\pi^0$	L,B	$<$	3.3	$\times 10^{-5}$	CL=90%	604
$\overline{p}\eta$	L,B	$<$	8.9	$\times 10^{-6}$	CL=90%	475
$\overline{p}\pi^0\eta$	L,B	$<$	2.7	$\times 10^{-5}$	CL=90%	360
e^- light boson	LF	$<$	2.7	$\times 10^{-3}$	CL=95%	–
μ^- light boson	LF	$<$	5	$\times 10^{-3}$	CL=95%	–

Heavy Charged Lepton Searches

$L^\pm$ – charged lepton

Mass $m >$ 100.8 GeV, CL = 95% [h] Decay to νW.

$L^\pm$ – stable charged heavy lepton

Mass $m >$ 102.6 GeV, CL = 95%

ν_e $J = \frac{1}{2}$

The following results are obtained using neutrinos associated with e^+ or e^-. See the Note on "Electron, muon, and tau neutrino listings" in the Particle Listings.

Mass $m <$ 3 eV Interpretation of tritium beta decay experiments is complicated by anomalies near the endpoint, and the limits are not without ambiguity.
Mean life/mass, $\tau/m_\nu > 7\times10^9$ s/eV [i] (solar)
Mean life/mass, $\tau/m_\nu >$ 300 s/eV, CL = 90% [i] (reactor)
Magnetic moment $\mu < 1.0\times10^{-10}\,\mu_B$, CL = 90%

ν_μ $J = \frac{1}{2}$

The following results are obtained using neutrinos associated with μ^+ or μ^-. See the Note on "Electron, muon, and tau neutrino listings" in the Particle Listings.

Mass $m <$ 0.19 MeV, CL = 90%
Mean life/mass, $\tau/m_\nu >$ 15.4 s/eV, CL = 90%
Magnetic moment $\mu < 6.8\times10^{-10}\,\mu_B$, CL = 90%

ν_τ $J = \frac{1}{2}$

The following results are obtained using neutrinos associated with τ^+ or τ^-. See the Note on "Electron, muon, and tau neutrino listings" in the Particle Listings.

Mass $m <$ 18.2 MeV, CL = 95%
Magnetic moment $\mu < 3.9\times10^{-7}\,\mu_B$, CL = 90%
Electric dipole moment $d < 5.2\times10^{-17}\,e$ cm, CL = 95%

Number of Neutrino Types and Sum of Neutrino Masses

Number $N = 2.994 \pm 0.012$ (Standard Model fits to LEP data)
Number $N = 2.92 \pm 0.07$ (Direct measurement of invisible Z width)

Lepton Summary Table

Neutrino Mixing

There is now compelling evidence that neutrinos have nonzero mass from the observation of neutrino flavor change, both from the study of atmospheric neutrino fluxes by SuperKamiokande, and from the study of solar neutrino cross sections by SNO (charged and neutral currents) and SuperKamiokande (elastic scattering). The flavor change observed in solar neutrinos has been confirmed by the KamLAND experiment using reactor antineutrinos.

Solar Neutrinos

Detectors using gallium ($E_\nu \gtrsim 0.2$ MeV), chlorine ($E_\nu \gtrsim 0.8$ MeV), and Cherenkov effect in water ($E_\nu \gtrsim 5$ MeV) measure significantly lower neutrino rates than are predicted from solar models. From the determination by SNO of the ^{8}B solar neutrino flux via elastic scattering, charged-current process interactions, and neutral-current interactions, one can determine the flux of non-ν_e active neutrinos to be $\phi(\nu_{\mu\,\tau}) = (3.41^{+0.66}_{-0.64}) \times 10^6\ \mathrm{cm}^{-2}\,\mathrm{s}^{-1}$, providing a $5.3\,\sigma$ evidence for neutrino flavor change. A global analysis of the solar neutrino data, including the KamLAND results that confirm the effect using reactor antineutrinos, favors large mixing angles and $\Delta(m^2) \simeq (6\text{–}9) \times 10^{-5}\ \mathrm{eV}^2$. See the Note "Solar Neutrinos" in the Listings and the review "Neutrino Mass, Mixing, and Flavor Change."

Atmospheric Neutrinos

Underground detectors observing neutrinos produced by cosmic rays in the atmosphere have measured a ν_μ/ν_e ratio much less than expected, and also a deficiency of upward going ν_μ compared to downward. This can be explained by oscillations leading to the disappearance of ν_μ with $\Delta m^2 \approx (1\text{–}3) \times 10^{-3}\ \mathrm{eV}^2$ and almost full mixing between ν_μ and ν_τ. The effect has been confirmed by the K2K experiment using accelerator neutrinos. See the review "Neutrino Mass, Mixing, and Flavor Change."

Heavy Neutral Leptons, Searches for

For excited leptons, see Compositeness Limits below.

Stable Neutral Heavy Lepton Mass Limits

Mass $m >$ 45.0 GeV, CL = 95% (Dirac)
Mass $m >$ 39.5 GeV, CL = 95% (Majorana)

Neutral Heavy Lepton Mass Limits

Mass $m >$ 90.3 GeV, CL = 95%
(Dirac ν_L coupling to e, μ, τ; conservative case(τ))
Mass $m >$ 80.5 GeV, CL = 95%
(Majorana ν_L coupling to e, μ, τ; conservative case(τ))

NOTES

In this Summary Table:

When a quantity has "(S = ...)" to its right, the error on the quantity has been enlarged by the "scale factor" S, defined as $S = \sqrt{\chi^2/(N-1)}$, where N is the number of measurements used in calculating the quantity. We do this when $S > 1$, which often indicates that the measurements are inconsistent. When $S > 1.25$, we also show in the Particle Listings an ideogram of the measurements. For more about S, see the Introduction.

A decay momentum p is given for each decay mode. For a 2-body decay, p is the momentum of each decay product in the rest frame of the decaying particle. For a 3-or-more-body decay, p is the largest momentum any of the products can have in this frame.

[a] This is the best limit for the mode $e^- \to \nu\gamma$. The best limit for "electron disappearance" is 6.4×10^{24} yr.

[b] See the "Note on Muon Decay Parameters" in the μ Particle Listings for definitions and details.

[c] P_μ is the longitudinal polarization of the muon from pion decay. In standard $V-A$ theory, $P_\mu = 1$ and $\rho = \delta = 3/4$.

[d] This only includes events with the γ energy > 10 MeV. Since the $e^-\overline{\nu}_e\nu_\mu$ and $e^-\overline{\nu}_e\nu_\mu\gamma$ modes cannot be clearly separated, we regard the latter mode as a subset of the former.

[e] See the relevant Particle Listings for the energy limits used in this measurement.

[f] A test of additive vs. multiplicative lepton family number conservation.

[g] Basis mode for the τ.

[h] $L^\pm$ mass limit depends on decay assumptions; see the Full Listings.

[i] Limit assumes radiative decay of neutrino.

QUARKS

The u-, d-, and s-quark masses are estimates of so-called "current-quark masses," in a mass-independent subtraction scheme such as $\overline{\text{MS}}$ at a scale $\mu \approx 2$ GeV. The c- and b-quark masses are the "running" masses in the $\overline{\text{MS}}$ scheme. For the b-quark we also quote the 1S mass. These can be different from the heavy quark masses obtained in potential models.

u

$I(J^P) = \frac{1}{2}(\frac{1}{2}^+)$

Mass $m = 1.5$ to 4 MeV [a] Charge $= \frac{2}{3}\,e$ $I_z = +\frac{1}{2}$
$m_u/m_d = 0.3$ to 0.7

d

$I(J^P) = \frac{1}{2}(\frac{1}{2}^+)$

Mass $m = 4$ to 8 MeV [a] Charge $= -\frac{1}{3}\,e$ $I_z = -\frac{1}{2}$
$m_s/m_d = 17$ to 22
$\overline{m} = (m_u + m_d)/2 = 3.0$ to 5.5 MeV

s

$I(J^P) = 0(\frac{1}{2}^+)$

Mass $m = 80$ to 130 MeV [a] Charge $= -\frac{1}{3}\,e$ Strangeness $= -1$
$(m_s - (m_u + m_d)/2)/(m_d - m_u) = 30$ to 50

c

$I(J^P) = 0(\frac{1}{2}^+)$

Mass $m = 1.15$ to 1.35 GeV Charge $= \frac{2}{3}\,e$ Charm $= +1$

b

$I(J^P) = 0(\frac{1}{2}^+)$

Charge $= -\frac{1}{3}\,e$ Bottom $= -1$

Mass $m = 4.1$ to 4.4 GeV ($\overline{\text{MS}}$ mass)
Mass $m = 4.6$ to 4.9 GeV (1S mass)

t

$I(J^P) = 0(\frac{1}{2}^+)$

Charge $= \frac{2}{3}\,e$ Top $= +1$

Mass $m = 174.3 \pm 5.1$ GeV (direct observation of top events)
Mass $m = 178.1^{+10.4}_{-8.3}$ GeV (Standard Model electroweak fit)

t DECAY MODES		Fraction (Γ_i/Γ)	Confidence level	p (MeV/c)
$W\,q\,(q = b,\ s,\ d)$				–
$W\,b$				–
$\ell\,\nu_\ell$ anything		[b,c] (9.4 ± 2.4) %		–
$\tau\,\nu_\tau\,b$				–
$\gamma\,q\,(q=u,c)$		[d] < 5.9 $\times 10^{-3}$	95%	–
$\Delta T = 1$ weak neutral current ($T1$) modes				
$Z\,q\,(q=u,c)$	$T1$	[e] < 13.7 %	95%	–

b′ (4th Generation) Quark, Searches for

Mass $m >$ 190 GeV, CL = 95% ($p\overline{p}$, quasi-stable b')
Mass $m >$ 199 GeV, CL = 95% ($p\overline{p}$, neutral-current decays)
Mass $m >$ 128 GeV, CL = 95% ($p\overline{p}$, charged-current decays)
Mass $m >$ 46.0 GeV, CL = 95% (e^+e^-, all decays)

Free Quark Searches

All searches since 1977 have had negative results.

NOTES

[a] The ratios m_u/m_d and m_s/m_d are extracted from pion and kaon masses using chiral symmetry. The estimates of u and d masses are not without controversy and remain under active investigation. Within the literature there are even suggestions that the u quark could be essentially massless. The s-quark mass is estimated from SU(3) splittings in hadron masses.

[b] ℓ means e or μ decay mode, not the sum over them.

[c] Assumes lepton universality and W-decay acceptance.

[d] This limit is for $\Gamma(t \to \gamma\,q)/\Gamma(t \to W\,b)$.

[e] This limit is for $\Gamma(t \to Z\,q)/\Gamma(t \to W\,b)$.

Meson Summary Table

LIGHT UNFLAVORED MESONS ($S = C = B = 0$)

For $I = 1$ (π, b, ρ, a): $u\overline{d}$, $(u\overline{u}-d\overline{d})/\sqrt{2}$, $d\overline{u}$;
for $I = 0$ (η, η', h, h', ω, ϕ, f, f'): $c_1(u\overline{u}+d\overline{d}) + c_2(s\overline{s})$

$\pi^\pm$

$I^G(J^P) = 1^-(0^-)$

Mass $m = 139.57018 \pm 0.00035$ MeV (S = 1.2)
Mean life $\tau = (2.6033 \pm 0.0005) \times 10^{-8}$ s (S = 1.2)
$c\tau = 7.8045$ m

$\pi^\pm \to \ell^\pm \nu\gamma$ form factors [a]

$F_V = 0.017 \pm 0.008$
$F_A = 0.0116 \pm 0.0016$ (S = 1.3)
$R = 0.059^{+0.009}_{-0.008}$

π^- modes are charge conjugates of the modes below.

For decay limits to particles which are not established, see the appropriate Search setions (Massive Neutrino Peak Search Test, A^0 (axion), and Other Light Boson (X^0) Searches, etc.).

π^+ DECAY MODES		Fraction (Γ_i/Γ)	Confidence level	p (MeV/c)
$\mu^+\nu_\mu$	[b]	(99.98770 ± 0.00004) %		30
$\mu^+\nu_\mu\gamma$	[c]	(2.00 ± 0.25) $\times 10^{-4}$		30
$e^+\nu_e$	[b]	(1.230 ± 0.004) $\times 10^{-4}$		70
$e^+\nu_e\gamma$	[c]	(1.61 ± 0.23) $\times 10^{-7}$		70
$e^+\nu_e\pi^0$		(1.025 ± 0.034) $\times 10^{-8}$		4
$e^+\nu_e e^+e^-$		(3.2 ± 0.5) $\times 10^{-9}$		70
$e^+\nu_e\nu\overline{\nu}$		< 5 $\times 10^{-6}$	90%	70
Lepton Family number (LF) or Lepton number (L) violating modes				
$\mu^+\overline{\nu}_e$	L	[d] < 1.5 $\times 10^{-3}$	90%	30
$\mu^+\nu_e$	LF	[d] < 8.0 $\times 10^{-3}$	90%	30
$\mu^- e^+e^+\nu$	LF	< 1.6 $\times 10^{-6}$	90%	30

π^0

$I^G(J^{PC}) = 1^-(0^{-+})$

Mass $m = 134.9766 \pm 0.0006$ MeV (S = 1.1)
$m_{\pi^\pm} - m_{\pi^0} = 4.5936 \pm 0.0005$ MeV
Mean life $\tau = (8.4 \pm 0.6) \times 10^{-17}$ s (S = 3.0)
$c\tau = 25.1$ nm

For decay limits to particles which are not established, see the appropriate Search setions (A^0 (axion), and Other Light Boson (X^0) Searches, etc.).

π^0 DECAY MODES		Fraction (Γ_i/Γ)	Scale factor/ Confidence level	p (MeV/c)
2γ		(98.798 ± 0.032) %	S=1.1	67
$e^+e^-\gamma$		(1.198 ± 0.032) %	S=1.1	67
γ positronium		(1.82 ± 0.29) $\times 10^{-9}$		67
$e^+e^+e^-e^-$		(3.14 ± 0.30) $\times 10^{-5}$		67
e^+e^-		(6.2 ± 0.5) $\times 10^{-8}$		67
4γ		< 2 $\times 10^{-8}$	CL=90%	67
$\nu\overline{\nu}$	[e]	< 8.3 $\times 10^{-7}$	CL=90%	67
$\nu_e\overline{\nu}_e$		< 1.7 $\times 10^{-6}$	CL=90%	67
$\nu_\mu\overline{\nu}_\mu$		< 3.1 $\times 10^{-6}$	CL=90%	67
$\nu_\tau\overline{\nu}_\tau$		< 2.1 $\times 10^{-6}$	CL=90%	67
$\gamma\nu\overline{\nu}$		< 6 $\times 10^{-4}$	CL=90%	67
Charge conjugation (C) or Lepton Family number (LF) violating modes				
3γ	C	< 3.1 $\times 10^{-8}$	CL=90%	67
μ^+e^-	LF	< 3.8 $\times 10^{-10}$	CL=90%	26
μ^-e^+	LF	< 3.4 $\times 10^{-9}$	CL=90%	26
$\mu^+e^- + \mu^-e^+$	LF	< 1.72 $\times 10^{-8}$	CL=90%	26

η

$I^G(J^{PC}) = 0^+(0^{-+})$

Mass $m = 547.75 \pm 0.12$ MeV [f] (S = 2.6)
Full width $\Gamma = 1.29 \pm 0.07$ keV [g]

C-nonconserving decay parameters

$\pi^+\pi^-\pi^0$ Left-right asymmetry = $(0.09 \pm 0.17) \times 10^{-2}$
$\pi^+\pi^-\pi^0$ Sextant asymmetry = $(0.18 \pm 0.16) \times 10^{-2}$
$\pi^+\pi^-\pi^0$ Quadrant asymmetry = $(-0.17 \pm 0.17) \times 10^{-2}$
$\pi^+\pi^-\gamma$ Left-right asymmetry = $(0.9 \pm 0.4) \times 10^{-2}$
$\pi^+\pi^-\gamma$ β (D-wave) = -0.02 ± 0.07 (S = 1.3)

Dalitz plot parameter

$\pi^0\pi^0\pi^0$ $\alpha = -0.031 \pm 0.004$ (S = 1.1)

η DECAY MODES		Fraction (Γ_i/Γ)	Scale factor/ Confidence level	p (MeV/c)
Neutral modes				
neutral modes		(72.0 ± 0.5) %	S=1.3	–
2γ	[g]	(39.43 ± 0.26) %	S=1.2	274
$3\pi^0$		(32.51 ± 0.29) %	S=1.2	179
$\pi^0 2\gamma$		(7.2 ± 1.4) $\times 10^{-4}$		257
other neutral modes		< 2.8 %	CL=90%	–
Charged modes				
charged modes		(28.0 ± 0.5) %	S=1.3	–
$\pi^+\pi^-\pi^0$		(22.6 ± 0.4) %	S=1.3	174
$\pi^+\pi^-\gamma$		(4.68 ± 0.11) %	S=1.2	236
$e^+e^-\gamma$		(6.0 ± 0.8) $\times 10^{-3}$	S=1.4	274
$\mu^+\mu^-\gamma$		(3.1 ± 0.4) $\times 10^{-4}$		253
e^+e^-		< 7.7 $\times 10^{-5}$	CL=90%	274
$\mu^+\mu^-$		(5.8 ± 0.8) $\times 10^{-6}$		253
$e^+e^-e^+e^-$		< 6.9 $\times 10^{-5}$	CL=90%	274
$\pi^+\pi^-e^+e^-$		(4.0 $^{+14.0}_{-2.7}$) $\times 10^{-4}$	S=5.8	235
$\pi^+\pi^-2\gamma$		< 2.0 $\times 10^{-3}$		236
$\pi^+\pi^-\pi^0\gamma$		< 5 $\times 10^{-4}$	CL=90%	174
$\pi^0\mu^+\mu^-\gamma$		< 3 $\times 10^{-6}$	CL=90%	210
Charge conjugation (C), Parity (P), Charge conjugation × Parity (CP), or Lepton Family number (LF) violating modes				
$\pi^+\pi^-$	P,CP	< 3.3 $\times 10^{-4}$	CL=90%	236
$\pi^0\pi^0$	P,CP	< 4.3 $\times 10^{-4}$	CL=90%	238
3γ	C	< 5 $\times 10^{-4}$	CL=95%	274
$4\pi^0$	P,CP	< 6.9 $\times 10^{-7}$	CL=90%	40
$\pi^0e^+e^-$	C	[h] < 4 $\times 10^{-5}$	CL=90%	257
$\pi^0\mu^+\mu^-$	C	[h] < 5 $\times 10^{-6}$	CL=90%	210
$\mu^+e^- + \mu^-e^+$	LF	< 6 $\times 10^{-6}$	CL=90%	264

$f_0(600)$ [i] or σ

$I^G(J^{PC}) = 0^+(0^{++})$

Mass $m = (400–1200)$ MeV
Full width $\Gamma = (600–1000)$ MeV

$f_0(600)$ DECAY MODES	Fraction (Γ_i/Γ)	p (MeV/c)
$\pi\pi$	dominant	–
$\gamma\gamma$	seen	–

$\rho(770)$ [j]

$I^G(J^{PC}) = 1^+(1^{--})$

Mass $m = 775.8 \pm 0.5$ MeV
Full width $\Gamma = 150.3 \pm 1.6$ MeV
$\Gamma_{ee} = 7.02 \pm 0.11$ keV

$\rho(770)$ DECAY MODES	Fraction (Γ_i/Γ)	Scale factor/ Confidence level	p (MeV/c)
$\pi\pi$	~ 100 %		364
$\rho(770)^\pm$ decays			
$\pi^\pm\gamma$	$(4.5 \pm 0.5) \times 10^{-4}$	S=2.2	375
$\pi^\pm\eta$	$< 6 \times 10^{-3}$	CL=84%	153
$\pi^\pm\pi^+\pi^-\pi^0$	$< 2.0 \times 10^{-3}$	CL=84%	254
$\rho(770)^0$ decays			
$\pi^+\pi^-\gamma$	$(9.9 \pm 1.6) \times 10^{-3}$		362
$\pi^0\gamma$	$(6.0 \pm 1.3) \times 10^{-4}$	S=1.1	376
$\eta\gamma$	$(3.0 \pm 0.4) \times 10^{-4}$	S=1.4	195
$\pi^0\pi^0\gamma$	$(4.5 \pm 0.8) \times 10^{-5}$		364
$\mu^+\mu^-$ [k]	$(4.55 \pm 0.28) \times 10^{-5}$		373
e^+e^- [k]	$(4.67 \pm 0.09) \times 10^{-5}$		388
$\pi^+\pi^-\pi^0$	$(1.01^{+0.54}_{-0.36} \pm 0.34) \times 10^{-4}$		323
$\pi^+\pi^-\pi^+\pi^-$	$(1.8 \pm 0.9) \times 10^{-5}$		251
$\pi^+\pi^-\pi^0\pi^0$	$< 4 \times 10^{-5}$	CL=90%	257

$\omega(782)$

$I^G(J^{PC}) = 0^-(1^{--})$

Mass $m = 782.59 \pm 0.11$ MeV (S = 1.7)
Full width $\Gamma = 8.49 \pm 0.08$ MeV
$\Gamma_{ee} = 0.60 \pm 0.02$ keV

$\omega(782)$ DECAY MODES	Fraction (Γ_i/Γ)	Scale factor/ Confidence level	p (MeV/c)
$\pi^+\pi^-\pi^0$	(89.1 ± 0.7) %	S=1.1	327
$\pi^0\gamma$	$(8.92^{+0.28}_{-0.24})$ %	S=1.1	380
$\pi^+\pi^-$	(1.70 ± 0.27) %	S=1.4	366
neutrals (excluding $\pi^0\gamma$)	$(1.4^{+7.0}_{-0.9}) \times 10^{-3}$		–
$\eta\gamma$	$(4.9 \pm 0.5) \times 10^{-4}$		200
$\pi^0 e^+e^-$	$(5.9 \pm 1.9) \times 10^{-4}$		380
$\pi^0\mu^+\mu^-$	$(9.6 \pm 2.3) \times 10^{-5}$		349
e^+e^-	$(7.14 \pm 0.13) \times 10^{-5}$	S=1.1	391
$\pi^+\pi^-\pi^0\pi^0$	< 2 %	CL=90%	262
$\pi^+\pi^-\gamma$	$< 3.6 \times 10^{-3}$	CL=95%	366
$\pi^+\pi^-\pi^+\pi^-$	$< 1 \times 10^{-3}$	CL=90%	256
$\pi^0\pi^0\gamma$	$(6.7 \pm 1.1) \times 10^{-5}$		367
$\eta\pi^0\gamma$	$< 3.3 \times 10^{-5}$	CL=90%	162
$\mu^+\mu^-$	$(9.0 \pm 3.1) \times 10^{-5}$		377
3γ	$< 1.9 \times 10^{-4}$	CL=95%	391
Charge conjugation (C) violating modes			
$\eta\pi^0$ C	$< 1 \times 10^{-3}$	CL=90%	162
$3\pi^0$ C	$< 3 \times 10^{-4}$	CL=90%	330

$\eta'(958)$

$I^G(J^{PC}) = 0^+(0^{-+})$

Mass $m = 957.78 \pm 0.14$ MeV
Full width $\Gamma = 0.202 \pm 0.016$ MeV (S = 1.3)

$\eta'(958)$ DECAY MODES	Fraction (Γ_i/Γ)	Scale factor/ Confidence level	p (MeV/c)
$\pi^+\pi^-\eta$	(44.3 ± 1.5) %	S=1.2	232
$\rho^0\gamma$ (including non-resonant $\pi^+\pi^-\gamma$)	(29.5 ± 1.0) %	S=1.2	165
$\pi^0\pi^0\eta$	(20.9 ± 1.2) %	S=1.2	239
$\omega\gamma$	(3.03 ± 0.31) %		159
$\gamma\gamma$	(2.12 ± 0.14) %	S=1.3	479
$3\pi^0$	$(1.56 \pm 0.26) \times 10^{-3}$		430
$\mu^+\mu^-\gamma$	$(1.04 \pm 0.26) \times 10^{-4}$		467
$\pi^+\pi^-\pi^0$	< 5 %	CL=90%	428
$\pi^0\rho^0$	< 4 %	CL=90%	110
$\pi^+\pi^+\pi^-\pi^-$	< 1 %	CL=90%	372
$\pi^+\pi^+\pi^-\pi^-$ neutrals	< 1 %	CL=95%	–
$\pi^+\pi^+\pi^-\pi^-\pi^0$	< 1 %	CL=90%	298
6π	< 1 %	CL=90%	211
$\pi^+\pi^- e^+e^-$	$< 6 \times 10^{-3}$	CL=90%	458
γe^+e^-	$< 9 \times 10^{-4}$	CL=90%	479
$\pi^0\gamma\gamma$	$< 8 \times 10^{-4}$	CL=90%	469
$4\pi^0$	$< 5 \times 10^{-4}$	CL=90%	380
e^+e^-	$< 2.1 \times 10^{-7}$	CL=90%	479
Charge conjugation (C), Parity (P), Lepton family number (LF) violating modes			
$\pi^+\pi^-$ P,CP	< 2 %	CL=90%	458
$\pi^0\pi^0$ P,CP	$< 9 \times 10^{-4}$	CL=90%	459
$\pi^0 e^+e^-$ C [h]	$< 1.4 \times 10^{-3}$	CL=90%	469
ηe^+e^- C [h]	$< 2.4 \times 10^{-3}$	CL=90%	322
3γ C	$< 1.0 \times 10^{-4}$	CL=90%	479
$\mu^+\mu^-\pi^0$ C [h]	$< 6.0 \times 10^{-5}$	CL=90%	445
$\mu^+\mu^-\eta$ C [h]	$< 1.5 \times 10^{-5}$	CL=90%	273
$e\mu$ LF	$< 4.7 \times 10^{-4}$	CL=90%	473

$f_0(980)$ [l]

$I^G(J^{PC}) = 0^+(0^{++})$

Mass $m = 980 \pm 10$ MeV
Full width $\Gamma = 40$ to 100 MeV

$f_0(980)$ DECAY MODES	Fraction (Γ_i/Γ)	p (MeV/c)
$\pi\pi$	dominant	471
$K\overline{K}$	seen	†
$\gamma\gamma$	seen	490

$a_0(980)$ [l]

$I^G(J^{PC}) = 1^-(0^{++})$

Mass $m = 984.7 \pm 1.2$ MeV (S = 1.5)
Full width $\Gamma = 50$ to 100 MeV

$a_0(980)$ DECAY MODES	Fraction (Γ_i/Γ)	p (MeV/c)
$\eta\pi$	dominant	322
$K\overline{K}$	seen	†
$\gamma\gamma$	seen	492

$\phi(1020)$

$I^G(J^{PC}) = 0^-(1^{--})$

Mass $m = 1019.456 \pm 0.020$ MeV (S = 1.1)
Full width $\Gamma = 4.26 \pm 0.05$ MeV (S = 1.7)

$\phi(1020)$ DECAY MODES	Fraction (Γ_i/Γ)	Scale factor/ Confidence level	p (MeV/c)
K^+K^-	(49.1 ± 0.6) %	S=1.2	127
$K^0_L K^0_S$	(34.0 ± 0.5) %	S=1.1	110
$\rho\pi + \pi^+\pi^-\pi^0$	(15.4 ± 0.5) %	S=1.3	–
$\eta\gamma$	(1.295 ± 0.025) %	S=1.1	363
$\pi^0\gamma$	$(1.23 \pm 0.10) \times 10^{-3}$		501
e^+e^-	$(2.98 \pm 0.04) \times 10^{-4}$	S=1.1	510
$\mu^+\mu^-$	$(2.85 \pm 0.19) \times 10^{-4}$		499
ηe^+e^-	$(1.15 \pm 0.10) \times 10^{-4}$		363
$\pi^+\pi^-$	$(7.3 \pm 1.3) \times 10^{-5}$		490
$\omega\pi^0$	$(5.2^{+1.3}_{-1.1}) \times 10^{-5}$		172
$\omega\gamma$	< 5 %	CL=84%	209
$\rho\gamma$	$< 1.2 \times 10^{-5}$	CL=90%	215
$\pi^+\pi^-\gamma$	$(4.1 \pm 1.3) \times 10^{-5}$		490
$f_0(980)\gamma$	$(4.40 \pm 0.21) \times 10^{-4}$		39
$\pi^0\pi^0\gamma$	$(1.09 \pm 0.06) \times 10^{-4}$		492
$\pi^+\pi^-\pi^+\pi^-$	$(3.9^{+2.8}_{-2.2}) \times 10^{-6}$		410
$\pi^+\pi^+\pi^-\pi^-\pi^0$	$< 4.6 \times 10^{-6}$	CL=90%	342
$\pi^0 e^+e^-$	$(1.12 \pm 0.28) \times 10^{-5}$		501
$\pi^0\eta\gamma$	$(8.3 \pm 0.5) \times 10^{-5}$		346
$a_0(980)\gamma$	$(7.6 \pm 0.6) \times 10^{-5}$		34
$\eta'(958)\gamma$	$(6.2 \pm 0.7) \times 10^{-5}$	S=1.1	60
$\eta\pi^0\pi^0\gamma$	$< 2 \times 10^{-5}$	CL=90%	293
$\mu^+\mu^-\gamma$	$(1.4 \pm 0.5) \times 10^{-5}$		499
$\rho\gamma\gamma$	$< 5 \times 10^{-4}$	CL=90%	215
$\eta\pi^+\pi^-$	$< 1.8 \times 10^{-5}$	CL=90%	288
$\eta\mu^+\mu^-$	$< 9.4 \times 10^{-6}$	CL=90%	321

Meson Summary Table

$h_1(1170)$ $I^G(J^{PC}) = 0^-(1^{+-})$

Mass $m = 1170 \pm 20$ MeV
Full width $\Gamma = 360 \pm 40$ MeV

$h_1(1170)$ DECAY MODES	Fraction (Γ_i/Γ)	p (MeV/c)
$\rho\pi$	seen	307

$b_1(1235)$ $I^G(J^{PC}) = 1^+(1^{+-})$

Mass $m = 1229.5 \pm 3.2$ MeV (S = 1.6)
Full width $\Gamma = 142 \pm 9$ MeV (S = 1.2)

$b_1(1235)$ DECAY MODES	Fraction (Γ_i/Γ)	Confidence level	p (MeV/c)
$\omega\pi$	dominant		348
[D/S amplitude ratio $= 0.277 \pm 0.027$]			
$\pi^\pm\gamma$	$(1.6 \pm 0.4) \times 10^{-3}$		607
$\eta\rho$	seen		†
$\pi^+\pi^+\pi^-\pi^0$	< 50 %	84%	535
$(K\overline{K})^\pm\pi^0$	< 8 %	90%	248
$K^0_S K^0_L \pi^\pm$	< 6 %	90%	235
$K^0_S K^0_S \pi^\pm$	< 2 %	90%	235
$\phi\pi$	< 1.5 %	84%	147

$a_1(1260)$ [m] $I^G(J^{PC}) = 1^-(1^{++})$

Mass $m = 1230 \pm 40$ MeV [n]
Full width $\Gamma = 250$ to 600 MeV

$a_1(1260)$ DECAY MODES	Fraction (Γ_i/Γ)	p (MeV/c)
$(\rho\pi)_{S-\text{wave}}$	seen	353
$(\rho\pi)_{D-\text{wave}}$	seen	353
$(\rho(1450)\pi)_{S-\text{wave}}$	seen	†
$(\rho(1450)\pi)_{D-\text{wave}}$	seen	†
$\sigma\pi$	seen	–
$f_0(980)\pi$	not seen	189
$f_0(1370)\pi$	seen	–
$f_2(1270)\pi$	seen	†
$K\overline{K}^*(892)+$ c.c.	seen	†
$\pi\gamma$	seen	608

$f_2(1270)$ $I^G(J^{PC}) = 0^+(2^{++})$

Mass $m = 1275.4 \pm 1.2$ MeV
Full width $\Gamma = 185.1^{+3.5}_{-2.6}$ MeV (S = 1.5)

$f_2(1270)$ DECAY MODES	Fraction (Γ_i/Γ)	Scale factor/ Confidence level	p (MeV/c)
$\pi\pi$	$(84.8\ ^{+2.5}_{-1.3})$ %	S=1.3	623
$\pi^+\pi^-2\pi^0$	$(7.1\ ^{+1.5}_{-2.7})$ %	S=1.3	563
$K\overline{K}$	(4.6 ± 0.4) %	S=2.7	404
$2\pi^+2\pi^-$	(2.8 ± 0.4) %	S=1.2	559
$\eta\eta$	$(4.5 \pm 1.0) \times 10^{-3}$	S=2.4	327
$4\pi^0$	$(3.0 \pm 1.0) \times 10^{-3}$		565
$\gamma\gamma$	$(1.41 \pm 0.13) \times 10^{-5}$		638
$\eta\pi\pi$	$< 8 \times 10^{-3}$	CL=95%	478
$K^0K^-\pi^+ +$ c.c.	$< 3.4 \times 10^{-3}$	CL=95%	293
e^+e^-	$< 6 \times 10^{-10}$	CL=90%	638

$f_1(1285)$ $I^G(J^{PC}) = 0^+(1^{++})$

Mass $m = 1281.8 \pm 0.6$ MeV (S = 1.6)
Full width $\Gamma = 24.1 \pm 1.1$ MeV (S = 1.3)

$f_1(1285)$ DECAY MODES	Fraction (Γ_i/Γ)	Scale factor/ Confidence level	p (MeV/c)
4π	$(33.1^{+\ 2.1}_{-\ 1.8})$ %	S=1.3	568
$\pi^0\pi^0\pi^+\pi^-$	$(22.0^{+\ 1.4}_{-\ 1.2})$ %	S=1.3	566
$2\pi^+2\pi^-$	$(11.0^{+\ 0.7}_{-\ 0.6})$ %	S=1.3	563
$\rho^0\pi^+\pi^-$	$(11.0^{+\ 0.7}_{-\ 0.6})$ %	S=1.3	336
$\rho^0\rho^0$	seen		†
$4\pi^0$	$< 7 \times 10^{-4}$	CL=90%	568
$\eta\pi\pi$	(5.2 ± 1.6) %		482
$a_0(980)\pi$ [ignoring $a_0(980) \to K\overline{K}$]	(3.6 ± 0.7) %		234
$\eta\pi\pi$ [excluding $a_0(980)\pi$]	(1.6 ± 0.7) %		482
$K\overline{K}\pi$	(9.0 ± 0.4) %	S=1.1	308
$K\overline{K}^*(892)$	not seen		†
$\gamma\rho^0$	(5.5 ± 1.3) %	S=2.8	406
$\phi\gamma$	$(7.4 \pm 2.6) \times 10^{-4}$		236

$\eta(1295)$ $I^G(J^{PC}) = 0^+(0^{-+})$

Mass $m = 1294 \pm 4$ MeV (S = 1.6)
Full width $\Gamma = 55 \pm 5$ MeV

$\eta(1295)$ DECAY MODES	Fraction (Γ_i/Γ)	p (MeV/c)
$\eta\pi^+\pi^-$	seen	487
$a_0(980)\pi$	seen	244
$\eta\pi^0\pi^0$	seen	490
$\eta(\pi\pi)_{S\text{-wave}}$	seen	–

$\pi(1300)$ $I^G(J^{PC}) = 1^-(0^{-+})$

Mass $m = 1300 \pm 100$ MeV [n]
Full width $\Gamma = 200$ to 600 MeV

$\pi(1300)$ DECAY MODES	Fraction (Γ_i/Γ)	p (MeV/c)
$\rho\pi$	seen	404
$\pi(\pi\pi)_{S\text{-wave}}$	seen	–

$a_2(1320)$ $I^G(J^{PC}) = 1^-(2^{++})$

Mass $m = 1318.3 \pm 0.6$ MeV (S = 1.2)
Full width $\Gamma = 107 \pm 5$ MeV [n]

$a_2(1320)$ DECAY MODES	Fraction (Γ_i/Γ)	Scale factor/ Confidence level	p (MeV/c)
$\rho\pi$	(70.1 ± 2.7) %	S=1.2	416
$\eta\pi$	(14.5 ± 1.2) %		535
$\omega\pi\pi$	(10.6 ± 3.2) %	S=1.3	366
$K\overline{K}$	(4.9 ± 0.8) %		437
$\eta'(958)\pi$	$(5.3 \pm 0.9) \times 10^{-3}$		288
$\pi^\pm\gamma$	$(2.68 \pm 0.31) \times 10^{-3}$		652
$\gamma\gamma$	$(9.4 \pm 0.7) \times 10^{-6}$		659
$\pi^+\pi^-\pi^-$	< 8 %	CL=90%	621
e^+e^-	$< 6 \times 10^{-9}$	CL=90%	659

$f_0(1370)$ [l] $I^G(J^{PC}) = 0^+(0^{++})$

Mass $m = 1200$ to 1500 MeV
Full width $\Gamma = 200$ to 500 MeV

$f_0(1370)$ DECAY MODES	Fraction (Γ_i/Γ)	p (MeV/c)
$\pi\pi$	seen	–
4π	seen	–
$4\pi^0$	seen	–
$2\pi^+2\pi^-$	seen	–
$\pi^+\pi^-2\pi^0$	seen	–
$\rho\rho$	dominant	–
$2(\pi\pi)_{S\text{-wave}}$	seen	–
$\pi(1300)\pi$	seen	–
$a_1(1260)\pi$	seen	–
$\eta\eta$	seen	–
$K\overline{K}$	seen	–
$\gamma\gamma$	seen	–
e^+e^-	not seen	–

$\pi_1(1400)$ [o]

$I^G(J^{PC}) = 1^-(1^{-+})$

Mass $m = 1376 \pm 17$ MeV
Full width $\Gamma = 300 \pm 40$ MeV

$\pi_1(1400)$ DECAY MODES	Fraction (Γ_i/Γ)	p (MeV/c)
$\eta\pi^0$	seen	570
$\eta\pi^-$	seen	569

$\eta(1405)$ [p] was $\eta(1440)$

$I^G(J^{PC}) = 0^+(0^{-+})$

Mass $m = 1410.3 \pm 2.6$ MeV [n] (S = 2.2)
Full width $\Gamma = 51 \pm 4$ MeV [n] (S = 2.2)

$\eta(1405)$ DECAY MODES	Fraction (Γ_i/Γ)	p (MeV/c)
$K\overline{K}\pi$	seen	425
$\eta\pi\pi$	seen	563
$a_0(980)\pi$	seen	342
$\eta(\pi\pi)_{S\text{-wave}}$	seen	–
$f_0(980)\eta$	seen	†
4π	seen	639
$K^*(892)K$	seen	127

$f_1(1420)$ [q]

$I^G(J^{PC}) = 0^+(1^{++})$

Mass $m = 1426.3 \pm 0.9$ MeV (S = 1.1)
Full width $\Gamma = 54.9 \pm 2.6$ MeV

$f_1(1420)$ DECAY MODES	Fraction (Γ_i/Γ)	p (MeV/c)
$K\overline{K}\pi$	dominant	438
$K\overline{K}^*(892)+$ c.c.	dominant	163
$\eta\pi\pi$	possibly seen	573
$\phi\gamma$	seen	349

$\omega(1420)$ [r]

$I^G(J^{PC}) = 0^-(1^{--})$

Mass m (1400–1450) MeV
Full width Γ (180–250) MeV

$\omega(1420)$ DECAY MODES	Fraction (Γ_i/Γ)	p (MeV/c)
$\rho\pi$	dominant	488
$\omega\pi\pi$	seen	–
$b_1(1235)\pi$	seen	–
e^+e^-	seen	–

$a_0(1450)$ [f]

$I^G(J^{PC}) = 1^-(0^{++})$

Mass $m = 1474 \pm 19$ MeV
Full width $\Gamma = 265 \pm 13$ MeV

$a_0(1450)$ DECAY MODES	Fraction (Γ_i/Γ)	p (MeV/c)
$\pi\eta$	seen	627
$\pi\eta'(958)$	seen	410
$K\overline{K}$	seen	547
$\omega\pi\pi$	seen	484

$\rho(1450)$ [s]

$I^G(J^{PC}) = 1^+(1^{--})$

Mass $m = 1465 \pm 25$ MeV [n]
Full width $\Gamma = 400 \pm 60$ MeV [n]

$\rho(1450)$ DECAY MODES	Fraction (Γ_i/Γ)	Confidence level	p (MeV/c)
$\pi\pi$	seen		720
4π	seen		669
$\omega\pi$	<2.0 %	95%	512
e^+e^-	seen		732
$\eta\rho$	<4 %		310
$a_2(1320)\pi$	not seen		55
$\phi\pi$	<1 %		360
$K\overline{K}$	$<1.6\times10^{-3}$	95%	541
$\eta\gamma$	possibly seen		630

$\eta(1475)$ [p] was $\eta(1440)$

$I^G(J^{PC}) = 0^+(0^{-+})$

Mass $m = 1476 \pm 4$ MeV (S = 1.4)
Full width $\Gamma = 87 \pm 9$ MeV (S = 1.6)

$\eta(1475)$ DECAY MODES	Fraction (Γ_i/Γ)	p (MeV/c)
$K\overline{K}\pi$	dominant	477
$K\overline{K}^*(892)+$ c.c.	seen	245
$a_0(980)\pi$	seen	393
$\gamma\gamma$	seen	738

$f_0(1500)$ [o]

$I^G(J^{PC}) = 0^+(0^{++})$

Mass $m = 1507 \pm 5$ MeV (S = 1.2)
Full width $\Gamma = 109 \pm 7$ MeV

$f_0(1500)$ DECAY MODES	Fraction (Γ_i/Γ)	Scale factor	p (MeV/c)
$\eta\eta'(958)$	(1.9±0.8) %	1.7	34
$\eta\eta$	(5.1±0.9) %	1.4	518
4π	(49.5±3.3) %	1.2	692
$4\pi^0$	seen		692
$2\pi^+2\pi^-$	seen		688
$\pi\pi$	(34.9±2.3) %	1.2	741
$\pi^+\pi^-$	seen		741
$2\pi^0$	seen		741
$K\overline{K}$	(8.6±1.0) %	1.1	569
$\gamma\gamma$	not seen		754

$f_2'(1525)$

$I^G(J^{PC}) = 0^+(2^{++})$

Mass $m = 1525 \pm 5$ MeV [n]
Full width $\Gamma = 73^{+6}_{-5}$ MeV [n]

$f_2'(1525)$ DECAY MODES	Fraction (Γ_i/Γ)	p (MeV/c)
$K\overline{K}$	(88.8 ±3.1) %	581
$\eta\eta$	(10.3 ±3.1) %	530
$\pi\pi$	(8.2 ±1.5) $\times10^{-3}$	750
$\gamma\gamma$	(1.11±0.14) $\times10^{-6}$	763

$\pi_1(1600)$ [o]

$I^G(J^{PC}) = 1^-(1^{-+})$

Mass $m = 1596^{+25}_{-14}$ MeV
Full width $\Gamma = 312^{+64}_{-24}$ MeV (S = 1.1)

$\pi_1(1600)$ DECAY MODES	Fraction (Γ_i/Γ)	p (MeV/c)
$\pi\pi\pi$	seen	769
$\rho^0\pi^-$	seen	600
$f_2(1270)\pi^-$	not seen	259
$\eta'(958)\pi^-$	seen	497

$\eta_2(1645)$

$I^G(J^{PC}) = 0^+(2^{-+})$

Mass $m = 1617 \pm 5$ MeV
Full width $\Gamma = 181 \pm 11$ MeV

$\eta_2(1645)$ DECAY MODES	Fraction (Γ_i/Γ)	p (MeV/c)
$a_2(1320)\pi$	seen	242
$K\overline{K}\pi$	seen	580
$K^*\overline{K}$	seen	404
$\eta\pi^+\pi^-$	seen	685
$a_0(980)\pi$	seen	496
$f_2(1270)\eta$	not seen	†

Meson Summary Table

$\omega(1650)$ [t] was $\omega(1600)$

$I^G(J^{PC}) = 0^-(1^{--})$

Mass $m = 1670 \pm 30$ MeV
Full width $\Gamma = 315 \pm 35$ MeV

$\omega(1650)$ DECAY MODES	Fraction (Γ_i/Γ)	p (MeV/c)
$\rho\pi$	seen	646
$\omega\pi\pi$	seen	617
$\omega\eta$	seen	500
e^+e^-	seen	835

$\omega_3(1670)$

$I^G(J^{PC}) = 0^-(3^{--})$

Mass $m = 1667 \pm 4$ MeV
Full width $\Gamma = 168 \pm 10$ MeV [n]

$\omega_3(1670)$ DECAY MODES	Fraction (Γ_i/Γ)	p (MeV/c)
$\rho\pi$	seen	645
$\omega\pi\pi$	seen	615
$b_1(1235)\pi$	possibly seen	361

$\pi_2(1670)$

$I^G(J^{PC}) = 1^-(2^{-+})$

Mass $m = 1672.4 \pm 3.2$ MeV [n] (S = 1.4)
Full width $\Gamma = 259 \pm 9$ MeV [n] (S = 1.3)

$\pi_2(1670)$ DECAY MODES	Fraction (Γ_i/Γ)	Confidence level	p (MeV/c)
3π	(95.8±1.4) %		809
$f_2(1270)\pi$	(56.2±3.2) %		329
$\rho\pi$	(31 ±4) %		648
$\sigma\pi$	(10.9±3.4) %		–
$(\pi\pi)_{S\text{-wave}}$	(8.7±3.4) %		–
$K\overline{K}^*(892)+$ c.c.	(4.2±1.4) %		455
$\omega\rho$	(2.7±1.1) %		303
$\rho(1450)\pi$	$< 3.6 \times 10^{-3}$	97.7%	148
$b_1(1235)\pi$	$< 1.9 \times 10^{-3}$	97.7%	366

$\phi(1680)$

$I^G(J^{PC}) = 0^-(1^{--})$

Mass $m = 1680 \pm 20$ MeV [n]
Full width $\Gamma = 150 \pm 50$ MeV [n]

$\phi(1680)$ DECAY MODES	Fraction (Γ_i/Γ)	p (MeV/c)
$K\overline{K}^*(892)+$ c.c.	dominant	462
$K^0_S K\pi$	seen	621
$K\overline{K}$	seen	680
e^+e^-	seen	840
$\omega\pi\pi$	not seen	623

$\rho_3(1690)$

$I^G(J^{PC}) = 1^+(3^{--})$

Mass $m = 1688.8 \pm 2.1$ MeV [n]
Full width $\Gamma = 161 \pm 10$ MeV [n] (S = 1.5)

$\rho_3(1690)$ DECAY MODES	Fraction (Γ_i/Γ)	Scale factor	p (MeV/c)
4π	(71.1 ± 1.9) %		790
$\pi^\pm\pi^+\pi^-\pi^0$	(67 ±22) %		787
$\omega\pi$	(16 ± 6) %		655
$\pi\pi$	(23.6 ± 1.3) %		834
$K\overline{K}\pi$	(3.8 ± 1.2) %		629
$K\overline{K}$	(1.58± 0.26) %	1.2	685
$\eta\pi^+\pi^-$	seen		727
$\rho(770)\eta$	seen		520
$\pi\pi\rho$	seen		633
Excluding 2ρ and $a_2(1320)\pi$.			
$a_2(1320)\pi$	seen		307
$\rho\rho$	seen		333

$\rho(1700)$ [s]

$I^G(J^{PC}) = 1^+(1^{--})$

Mass $m = 1720 \pm 20$ MeV [n] ($\eta\rho^0$ and $\pi^+\pi^-$ modes)
Full width $\Gamma = 250 \pm 100$ MeV [n] ($\eta\rho^0$ and $\pi^+\pi^-$ modes)

$\rho(1700)$ DECAY MODES	Fraction (Γ_i/Γ)	p (MeV/c)
$2(\pi^+\pi^-)$	large	803
$\rho\pi\pi$	dominant	653
$\rho^0\pi^+\pi^-$	large	650
$\rho^\pm\pi^\mp\pi^0$	large	651
$a_1(1260)\pi$	seen	404
$h_1(1170)\pi$	seen	447
$\pi(1300)\pi$	seen	349
$\rho\rho$	seen	371
$\pi^+\pi^-$	seen	849
$\pi\pi$	seen	849
$K\overline{K}^*(892)+$ c.c.	seen	496
$\eta\rho$	seen	544
$a_2(1320)\pi$	not seen	334
$K\overline{K}$	seen	704
e^+e^-	seen	860
$\pi^0\omega$	seen	674

$f_0(1710)$ [u]

$I^G(J^{PC}) = 0^+(0^{++})$

Mass $m = 1714 \pm 5$ MeV
Full width $\Gamma = 140 \pm 10$ MeV (S = 1.2)

$f_0(1710)$ DECAY MODES	Fraction (Γ_i/Γ)	p (MeV/c)
$K\overline{K}$	seen	701
$\eta\eta$	seen	659
$\pi\pi$	seen	846

$\pi(1800)$

$I^G(J^{PC}) = 1^-(0^{-+})$

Mass $m = 1812 \pm 14$ MeV (S = 2.3)
Full width $\Gamma = 207 \pm 13$ MeV

$\pi(1800)$ DECAY MODES	Fraction (Γ_i/Γ)	p (MeV/c)
$\pi^+\pi^-\pi^-$	seen	879
$f_0(600)\pi^-$	seen	–
$f_0(980)\pi^-$	seen	631
$f_0(1370)\pi^-$	seen	–
$f_0(1500)\pi^-$	not seen	248
$\rho\pi^-$	not seen	732
$\eta\eta\pi^-$	seen	661
$a_0(980)\eta$	seen	469
$f_0(1500)\pi^-$	seen	248
$\eta\eta'(958)\pi^-$	seen	376
$K^*_0(1430)K^-$	seen	†
$K^*(892)K^-$	not seen	570

$\phi_3(1850)$

$I^G(J^{PC}) = 0^-(3^{--})$

Mass $m = 1854 \pm 7$ MeV
Full width $\Gamma = 87^{+28}_{-23}$ MeV (S = 1.2)

$\phi_3(1850)$ DECAY MODES	Fraction (Γ_i/Γ)	p (MeV/c)
$K\overline{K}$	seen	785
$K\overline{K}^*(892)+$ c.c.	seen	602

$f_2(1950)$

$I^G(J^{PC}) = 0^+(2^{++})$

Mass $m = 1945 \pm 13$ MeV (S = 1.6)
Full width $\Gamma = 475 \pm 19$ MeV

$f_2(1950)$ DECAY MODES	Fraction (Γ_i/Γ)	p (MeV/c)
$K^*(892)\overline{K}^*(892)$	seen	389
$\pi^+\pi^-$	seen	963
4π	seen	925
$\eta\eta$	seen	804
$K\overline{K}$	seen	838
$\gamma\gamma$	seen	973

$f_2(2010)$

$I^G(J^{PC}) = 0^+(2^{++})$

Mass $m = 2011^{+60}_{-80}$ MeV
Full width $\Gamma = 202 \pm 60$ MeV

$f_2(2010)$ DECAY MODES	Fraction (Γ_i/Γ)	p (MeV/c)
$\phi\phi$	seen	†

$a_4(2040)$

$I^G(J^{PC}) = 1^-(4^{++})$

Mass $m = 2010 \pm 12$ MeV
Full width $\Gamma = 353 \pm 40$ MeV

$a_4(2040)$ DECAY MODES	Fraction (Γ_i/Γ)	p (MeV/c)
$K\overline{K}$	seen	875
$\pi^+\pi^-\pi^0$	seen	981
$\rho\pi$	seen	849
$f_2(1270)\pi$	seen	590
$\eta\pi^0$	seen	925
$\eta'(958)\pi$	seen	769

$f_4(2050)$

$I^G(J^{PC}) = 0^+(4^{++})$

Mass $m = 2034 \pm 11$ MeV (S = 1.6)
Full width $\Gamma = 222 \pm 19$ MeV (S = 1.8)

$f_4(2050)$ DECAY MODES	Fraction (Γ_i/Γ)	p (MeV/c)
$\omega\omega$	not seen	650
$\pi\pi$	(17.0 ± 1.5) %	1008
$K\overline{K}$	$(6.8^{+3.4}_{-1.8}) \times 10^{-3}$	889
$\eta\eta$	$(2.1 \pm 0.8) \times 10^{-3}$	857
$4\pi^0$	< 1.2 %	972
$a_2(1320)\pi$	seen	579

$f_2(2300)$

$I^G(J^{PC}) = 0^+(2^{++})$

Mass $m = 2297 \pm 28$ MeV
Full width $\Gamma = 149 \pm 40$ MeV

$f_2(2300)$ DECAY MODES	Fraction (Γ_i/Γ)	p (MeV/c)
$\phi\phi$	seen	529
$K\overline{K}$	seen	1037
$\gamma\gamma$	seen	1149

$f_2(2340)$

$I^G(J^{PC}) = 0^+(2^{++})$

Mass $m = 2339 \pm 60$ MeV
Full width $\Gamma = 319^{+80}_{-70}$ MeV

$f_2(2340)$ DECAY MODES	Fraction (Γ_i/Γ)	p (MeV/c)
$\phi\phi$	seen	573

STRANGE MESONS ($S = \pm 1$, $C = B = 0$)

$K^+ = u\overline{s}$, $K^0 = d\overline{s}$, $\overline{K}^0 = \overline{d}s$, $K^- = \overline{u}s$, similarly for K^*'s

$K^\pm$

$I(J^P) = \frac{1}{2}(0^-)$

Mass $m = 493.677 \pm 0.016$ MeV [v] (S = 2.8)
Mean life $\tau = (1.2384 \pm 0.0024) \times 10^{-8}$ s (S = 2.0)
$c\tau = 3.713$ m

Slope parameter g [w]

(See Particle Listings for quadratic coefficients)

$K^+ \to \pi^+\pi^+\pi^- = -0.2154 \pm 0.0035$ (S = 1.4)
$K^- \to \pi^-\pi^-\pi^+ = -0.217 \pm 0.007$ (S = 2.5)
$K^\pm \to \pi^\pm\pi^0\pi^0 = 0.638 \pm 0.020$ (S = 2.5)

$K^\pm$ decay form factors [a,x]

Assuming μ-e universality

$\lambda_+(K^+_{\mu 3}) = \lambda_+(K^+_{e3}) = (2.78 \pm 0.07) \times 10^{-2}$ (S = 1.5)
$\lambda_0(K^+_{\mu 3}) = (1.77 \pm 0.16) \times 10^{-2}$ (S = 1.5)

Not assuming μ-e universality

$\lambda_+(K^+_{e3}) = (2.77 \pm 0.05) \times 10^{-2}$
$\lambda_+(K^+_{\mu 3}) = (2.84 \pm 0.27) \times 10^{-2}$ (S = 1.8)
$\lambda_0(K^+_{\mu 3}) = (1.74 \pm 0.22) \times 10^{-2}$ (S = 1.8)

K^+_{e3} $|f_S/f_+| = (-0.3^{+0.8}_{-0.7}) \times 10^{-2}$
K^+_{e3} $|f_T/f_+| = (-1.2 \pm 2.3) \times 10^{-2}$
$K^+_{\mu 3}$ $|f_S/f_+| = (0.2 \pm 0.6) \times 10^{-2}$
$K^+_{\mu 3}$ $|f_T/f_+| = (-0.1 \pm 0.7) \times 10^{-2}$
$K^+ \to e^+\nu_e\gamma$ $|F_A + F_V| = 0.148 \pm 0.010$
$K^+ \to \mu^+\nu_\mu\gamma$ $|F_A + F_V| = 0.165 \pm 0.013$
$K^+ \to e^+\nu_e\gamma$ $|F_A - F_V| < 0.49$
$K^+ \to \mu^+\nu_\mu\gamma$ $|F_A - F_V| = -0.24$ to 0.04, CL = 90%

Charge Radius

$\langle r \rangle = 0.560 \pm 0.031$ fm

***CP* violation parameters**

$\Delta(K^\pm_{\pi\mu\mu}) = -0.02 \pm 0.12$

***T* violation parameters**

$K^+ \to \pi^0\mu^+\nu_\mu$ $P_T = (-4 \pm 5) \times 10^{-3}$
$K^+ \to \mu^+\nu_\mu\gamma$ $P_T = (-0.6 \pm 1.9) \times 10^{-2}$
$K^+ \to \pi^0\mu^+\nu_\mu$ $\mathrm{Im}(\xi) = -0.014 \pm 0.014$

K^- modes are charge conjugates of the modes below.

K^+ DECAY MODES	Fraction (Γ_i/Γ)	Scale factor/ Confidence level	p (MeV/c)
Leptonic and semileptonic modes			
$e^+\nu_e$	(1.55 ± 0.07) × 10^{-5}		247
$\mu^+\nu_\mu$	(63.43 ± 0.17) %	S=1.2	236
$\pi^0 e^+\nu_e$ Called K^+_{e3}.	(4.87 ± 0.06) %	S=1.2	228
$\pi^0\mu^+\nu_\mu$ Called $K^+_{\mu 3}$.	(3.27 ± 0.06) %	S=1.2	215
$\pi^0\pi^0 e^+\nu_e$	(2.1 ± 0.4) × 10^{-5}		206
$\pi^+\pi^- e^+\nu_e$	(4.08 ± 0.09) × 10^{-5}		203
$\pi^+\pi^-\mu^+\nu_\mu$	(1.4 ± 0.9) × 10^{-5}		151
$\pi^0\pi^0\pi^0 e^+\nu_e$	< 3.5 × 10^{-6}	CL=90%	135
Hadronic modes			
$\pi^+\pi^0$	(21.13 ± 0.14) %	S=1.1	205
$\pi^+\pi^0\pi^0$	(1.73 ± 0.04) %	S=1.2	133
$\pi^+\pi^+\pi^-$	(5.576 ± 0.031) %	S=1.1	125
Leptonic and semileptonic modes with photons			
$\mu^+\nu_\mu\gamma$	[y,z] (5.50 ± 0.28) × 10^{-3}		236
$\pi^0 e^+\nu_e\gamma$	[y,z] (2.65 ± 0.20) × 10^{-4}		228
$\pi^0 e^+\nu_e\gamma$(SD)	[aa] < 5.3 × 10^{-5}	CL=90%	228
$\pi^0\mu^+\nu_\mu\gamma$	[y,z] < 6.1 × 10^{-5}	CL=90%	215
$\pi^0\pi^0 e^+\nu_e\gamma$	< 5 × 10^{-6}	CL=90%	206

Meson Summary Table

Hadronic modes with photons

$\pi^+\pi^0\gamma$	[y,z]	$(2.75 \pm 0.15) \times 10^{-4}$	205
$\pi^+\pi^0\gamma$ (DE)	[z,bb]	$(4.4 \pm 0.8) \times 10^{-6}$	205
$\pi^+\pi^0\pi^0\gamma$	[y,z]	$(7.4 \ ^{+5.5}_{-2.9}) \times 10^{-6}$	133
$\pi^+\pi^+\pi^-\gamma$	[y,z]	$(1.04 \pm 0.31) \times 10^{-4}$	125
$\pi^+\gamma\gamma$	[z]	$(1.10 \pm 0.32) \times 10^{-6}$	227
$\pi^+ 3\gamma$	[z]	$< 1.0 \times 10^{-4}$ CL=90%	227

Leptonic modes with $\ell\overline{\ell}$ pairs

$e^+\nu_e\overline{\nu}$		$< 6 \times 10^{-5}$ CL=90%	247
$\mu^+\nu_\mu\overline{\nu}$		$< 6.0 \times 10^{-6}$ CL=90%	236
$e^+\nu_e e^+ e^-$		$(2.48 \pm 0.20) \times 10^{-8}$	247
$\mu^+\nu_\mu e^+ e^-$		$(7.06 \pm 0.31) \times 10^{-8}$	236
$e^+\nu_e\mu^+\mu^-$		$< 5 \times 10^{-7}$ CL=90%	223
$\mu^+\nu_\mu\mu^+\mu^-$		$< 4.1 \times 10^{-7}$ CL=90%	185

Lepton Family number (LF), Lepton number (L), $\Delta S = \Delta Q$ (SQ) violating modes, or $\Delta S = 1$ weak neutral current ($S1$) modes

$\pi^+\pi^+ e^-\overline{\nu}_e$	SQ	$< 1.2 \times 10^{-8}$ CL=90%	203
$\pi^+\pi^+\mu^-\overline{\nu}_\mu$	SQ	$< 3.0 \times 10^{-6}$ CL=95%	151
$\pi^+ e^+ e^-$	$S1$	$(2.88 \pm 0.13) \times 10^{-7}$	227
$\pi^+\mu^+\mu^-$	$S1$	$(8.1 \pm 1.4) \times 10^{-8}$ S=2.7	172
$\pi^+\nu\overline{\nu}$	$S1$	$(1.6 \ ^{+1.8}_{-0.8}) \times 10^{-10}$	227
$\pi^+\pi^0\nu\overline{\nu}$	$S1$	$< 4.3 \times 10^{-5}$ CL=90%	205
$\mu^-\nu e^+ e^+$	LF	$< 2.0 \times 10^{-8}$ CL=90%	236
$\mu^+\nu_e$	LF [d]	$< 4 \times 10^{-3}$ CL=90%	236
$\pi^+\mu^+ e^-$	LF	$< 2.8 \times 10^{-11}$ CL=90%	214
$\pi^+\mu^- e^+$	LF	$< 5.2 \times 10^{-10}$ CL=90%	214
$\pi^-\mu^+ e^+$	L	$< 5.0 \times 10^{-10}$ CL=90%	214
$\pi^- e^+ e^+$	L	$< 6.4 \times 10^{-10}$ CL=90%	227
$\pi^-\mu^+\mu^+$	L [d]	$< 3.0 \times 10^{-9}$ CL=90%	172
$\mu^+\overline{\nu}_e$	L [d]	$< 3.3 \times 10^{-3}$ CL=90%	236
$\pi^0 e^+\overline{\nu}_e$	L	$< 3 \times 10^{-3}$ CL=90%	228
$\pi^+\gamma$	[cc]	$< 3.6 \times 10^{-7}$ CL=90%	227

Modes with photons or $\ell\overline{\ell}$ pairs

$\pi^+\pi^-\gamma$	[y,ff]	$(1.79 \pm 0.05) \times 10^{-3}$	206
$\pi^+\pi^- e^+ e^-$		$(4.69 \pm 0.30) \times 10^{-5}$	206
$\pi^0\gamma\gamma$	[ff]	$(4.9 \pm 1.8) \times 10^{-8}$	231
$\gamma\gamma$		$(2.80 \pm 0.07) \times 10^{-6}$	249

Semileptonic modes

$\pi^\pm e^\mp\nu_e$	[gg]	$(6.9 \pm 0.4) \times 10^{-4}$	229

CP violating (CP) and $\Delta S = 1$ weak neutral current ($S1$) modes

$3\pi^0$	CP	$< 1.4 \times 10^{-5}$	CL=90%	139
$\mu^+\mu^-$	$S1$	$< 3.2 \times 10^{-7}$	CL=90%	225
$e^+ e^-$	$S1$	$< 1.4 \times 10^{-7}$	CL=90%	249
$\pi^0 e^+ e^-$	$S1$	[ff] $(3.0 \ ^{+1.5}_{-1.2}) \times 10^{-9}$		231

K^0

$I(J^P) = \frac{1}{2}(0^-)$

50% K_S, 50% K_L

Mass $m = 497.648 \pm 0.022$ MeV

$m_{K^0} - m_{K^\pm} = 3.972 \pm 0.027$ MeV (S = 1.2)

Mean Square Charge Radius

$\langle r^2 \rangle = -0.076 \pm 0.018$ fm^2 (S = 1.1)

***T*-violation parameters in K^0-$\overline{K}^0$ mixing** [x]

Asymmetry A_T in K^0-$\overline{K}^0$ mixing $= (6.6 \pm 1.6) \times 10^{-3}$

***CPT*-violation parameters** [x]

Re $\delta = (2.9 \pm 2.7) \times 10^{-4}$

Im $\delta = (0.02 \pm 0.05) \times 10^{-3}$

$\left|m_{K^0} - m_{\overline{K}^0}\right| / m_{\text{average}} < 10^{-18}$, CL = 90% [dd]

$(\Gamma_{K^0} - \Gamma_{\overline{K}^0})/m_{\text{average}} = (8 \pm 8) \times 10^{-18}$

K_S^0

$I(J^P) = \frac{1}{2}(0^-)$

Mean life $\tau = (0.8953 \pm 0.0006) \times 10^{-10}$ s (S = 1.4) Assuming CPT

Mean life $\tau = (0.8958 \pm 0.0006) \times 10^{-10}$ s (S = 1.2) Not assuming CPT

$c\tau = 2.6842$ cm Assuming CPT

***CP*-violation parameters** [ee]

Im$(\eta_{+-0}) = -0.002 \pm 0.009$

Im$(\eta_{000}) = -0.05 \pm 0.13$

CP asymmetry A in $\pi^+\pi^- e^+ e^- = (-1 \pm 4)\%$

K_S^0 DECAY MODES	Fraction (Γ_i/Γ)	Scale factor/ Confidence level	p (MeV/c)
Hadronic modes			
$\pi^0\pi^0$	(31.05 ±0.14) %	S=1.1	209
$\pi^+\pi^-$	(68.95 ±0.14) %	S=1.1	206
$\pi^+\pi^-\pi^0$	$(3.2 \ ^{+1.2}_{-1.0}) \times 10^{-7}$		133

K_L^0

$I(J^P) = \frac{1}{2}(0^-)$

$m_{K_L} - m_{K_S}$

$= (0.5292 \pm 0.0010) \times 10^{10}\ \hbar\ \text{s}^{-1}$ (S = 1.2) Assuming CPT

$= (3.483 \pm 0.006) \times 10^{-12}$ MeV Assuming CPT

$= (0.5290 \pm 0.0016) \times 10^{10}\ \hbar\ \text{s}^{-1}$ (S = 1.2) Not assuming CPT

Mean life $\tau = (5.18 \pm 0.04) \times 10^{-8}$ s (S = 1.1)

$c\tau = 15.51$ m

Slope parameter g [w]

(See Particle Listings for quadratic coefficients)

$K_L^0 \to \pi^+\pi^-\pi^0 = 0.678 \pm 0.008$ (S = 1.5)

***K_L* decay form factors** [x]

Assuming μ-e universality

$\lambda_+(K_{\mu 3}^0) = \lambda_+(K_{e3}^0) = 0.0300 \pm 0.0020$ (S = 2.0)

$\lambda_0(K_{\mu 3}^0) = 0.030 \pm 0.005$ (S = 2.0)

Not assuming μ-e universality

$\lambda_+(K_{e3}^0) = 0.0291 \pm 0.0018$ (S = 1.5)

$\lambda_+(K_{\mu 3}^0) = 0.033 \pm 0.005$ (S = 2.3)

$\lambda_0(K_{\mu 3}^0) = 0.027 \pm 0.006$ (S = 2.3)

$K_{e3}^0 \quad |f_S/f_+| < 0.04$, CL = 68%

$K_{e3}^0 \quad |f_T/f_+| < 0.23$, CL = 68%

$K_{\mu 3}^0 \quad |f_T/f_+| = 0.12 \pm 0.12$

$K_L \to e^+ e^-\gamma$: $\alpha_{K^*} = -0.33 \pm 0.05$

$K_L \to \mu^+\mu^-\gamma$: $\alpha_{K^*} = -0.158 \pm 0.027$

$K_L \to e^+ e^- e^+ e^-$: $\alpha_{K^*}^{\text{eff}} = -0.14 \pm 0.22$

$K_L \to \pi^+\pi^- e^+ e^-$: $a_1/a_2 = -0.734 \pm 0.022$ GeV^2

$K_L \to \pi^0 2\gamma$: $a_V = -0.54 \pm 0.12$ (S = 2.8)

***CP*-violation parameters** [ee]

$\delta_L = (0.327 \pm 0.012)\%$

$|\eta_{00}| = (2.276 \pm 0.014) \times 10^{-3}$

$|\eta_{+-}| = (2.288 \pm 0.014) \times 10^{-3}$

$|\epsilon| = (2.284 \pm 0.014) \times 10^{-3}$

$|\eta_{00}/\eta_{+-}| = 0.9950 \pm 0.0008$ [hh] (S = 1.6)

Re$(\epsilon'/\epsilon) = (1.67 \pm 0.26) \times 10^{-3}$ [hh] (S = 1.6)

Assuming CPT

$\phi_{+-} = (43.52 \pm 0.06)^\circ$ (S = 1.3)

$\phi_{00} = (43.50 \pm 0.06)^\circ$ (S = 1.3)

$\phi_\epsilon = \phi_{SW} = (43.51 \pm 0.05)^\circ$ (S = 1.2)

Not assuming CPT

$\phi_{+-} = (43.4 \pm 0.7)^\circ$ (S = 1.3)

$\phi_{00} = (43.7 \pm 0.8)^\circ$ (S = 1.2)

$\phi_\epsilon = (43.5 \pm 0.7)^\circ$ (S = 1.3)

CP asymmetry A in $K_L^0 \to \pi^+\pi^- e^+ e^- = (13.8 \pm 2.2)\%$

β_{CP} from $K_L^0 \to e^+e^-e^+e^- = -0.23 \pm 0.09$

γ_{CP} from $K_L^0 \to e^+e^-e^+e^- = -0.09 \pm 0.09$

j for $K_L^0 \to \pi^+\pi^-\pi^0 = 0.0012 \pm 0.0008$

f for $K_L^0 \to \pi^+\pi^-\pi^0 = 0.004 \pm 0.006$

$|\eta_{+-\gamma}| = (2.35 \pm 0.07) \times 10^{-3}$

$\phi_{+-\gamma} = (44 \pm 4)^\circ$

$|\epsilon'_{+-\gamma}|/\epsilon < 0.3$, CL = 90%

T-violation parameters

Im(ξ) in $K^0_{\mu 3} = -0.007 \pm 0.026$

CPT invariance tests

$\phi_{00} - \phi_{+-} = (0.2 \pm 0.4)^\circ$

Re$(\frac{2}{3}\eta_{+-} + \frac{1}{3}\eta_{00}) - \frac{\delta_L}{2} = (-3 \pm 35) \times 10^{-6}$

$\Delta S = -\Delta Q$ in $K^0_{\ell 3}$ decay

Re $x = -0.002 \pm 0.006$

Im $x = 0.0012 \pm 0.0021$

K_L^0 DECAY MODES		Fraction (Γ_i/Γ)	Scale factor/ Confidence level	p (MeV/c)
Semileptonic modes				
$\pi^\pm e^\mp \nu_e$ Called K^0_{e3}.	[gg]	(38.81 ±0.27) %	S=1.1	229
$\pi^\pm \mu^\mp \nu_\mu$ Called $K^0_{\mu 3}$.	[gg]	(27.19 ±0.25) %	S=1.1	216
$(\pi\mu$ atom$)\nu$		(1.06 ±0.11) $\times 10^{-7}$		188
$\pi^0\pi^\pm e^\mp \nu$	[gg]	(5.18 ±0.29) $\times 10^{-5}$		207
Hadronic modes, including Charge conjugation × Parity Violating (CPV) modes				
$3\pi^0$		(21.05 ±0.23) %	S=1.1	139
$\pi^+\pi^-\pi^0$		(12.59 ±0.19) %	S=1.6	133
$\pi^+\pi^-$	CPV	(2.090±0.025) $\times 10^{-3}$	S=1.1	206
$\pi^0\pi^0$	CPV	(9.32 ±0.12) $\times 10^{-4}$	S=1.1	209
Semileptonic modes with photons				
$\pi^\pm e^\mp \nu_e \gamma$	[y,gg,ii]	(3.53 ±0.06) $\times 10^{-3}$		229
$\pi^\pm \mu^\mp \nu_\mu \gamma$		(5.7 $^{+0.6}_{-0.7}$) $\times 10^{-4}$		216
Hadronic modes with photons or $\ell\overline{\ell}$ pairs				
$\pi^0\pi^0\gamma$		< 5.6 $\times 10^{-6}$		209
$\pi^+\pi^-\gamma$	[y,ii]	(4.39 ±0.12) $\times 10^{-5}$	S=1.8	206
$\pi^0 2\gamma$	[ii]	(1.41 ±0.12) $\times 10^{-6}$	S=2.8	231
$\pi^0\gamma e^+e^-$		(2.3 ±0.4) $\times 10^{-8}$		231
Other modes with photons or $\ell\overline{\ell}$ pairs				
2γ		(5.90 ±0.07) $\times 10^{-4}$	S=1.1	249
3γ		< 2.4 $\times 10^{-7}$	CL=90%	249
$e^+e^-\gamma$		(10.0 ±0.5) $\times 10^{-6}$	S=1.5	249
$\mu^+\mu^-\gamma$		(3.59 ±0.11) $\times 10^{-7}$	S=1.3	225
$e^+e^-\gamma\gamma$	[ii]	(5.95 ±0.33) $\times 10^{-7}$		249
$\mu^+\mu^-\gamma\gamma$	[ii]	(1.0 $^{+0.8}_{-0.6}$) $\times 10^{-8}$		225
Charge conjugation × Parity (CP) or Lepton Family number (LF) violating modes, or $\Delta S = 1$ weak neutral current ($S1$) modes				
$\mu^+\mu^-$	$S1$	(7.27 ±0.14) $\times 10^{-9}$		225
e^+e^-	$S1$	(9 $^{+6}_{-4}$) $\times 10^{-12}$		249
$\pi^+\pi^-e^+e^-$	$S1$ [ii]	(3.11 ±0.19) $\times 10^{-7}$		206
$\pi^0\pi^0e^+e^-$	$S1$	< 6.6 $\times 10^{-9}$	CL=90%	209
$\mu^+\mu^-e^+e^-$	$S1$	(2.69 ±0.27) $\times 10^{-9}$		225
$e^+e^-e^+e^-$	$S1$	(3.75 ±0.27) $\times 10^{-8}$		249
$\pi^0\mu^+\mu^-$	$CP,S1$ [jj]	< 3.8 $\times 10^{-10}$	CL=90%	177
$\pi^0 e^+e^-$	$CP,S1$ [jj]	< 5.1 $\times 10^{-10}$	CL=90%	231
$\pi^0\nu\overline{\nu}$	$CP,S1$ [kk]	< 5.9 $\times 10^{-7}$	CL=90%	231
$e^\pm\mu^\mp$	LF [gg]	< 4.7 $\times 10^{-12}$	CL=90%	238
$e^\pm e^\pm \mu^\mp \mu^\mp$	LF [gg]	< 4.12 $\times 10^{-11}$	CL=90%	225
$\pi^0\mu^\pm e^\mp$	LF [gg]	< 6.2 $\times 10^{-9}$	CL=90%	217

$K^*(892)$

$I(J^P) = \frac{1}{2}(1^-)$

$K^*(892)^\pm$ mass $m = 891.66 \pm 0.26$ MeV

$K^*(892)^0$ mass $m = 896.10 \pm 0.27$ MeV (S = 1.4)

$K^*(892)^\pm$ full width $\Gamma = 50.8 \pm 0.9$ MeV

$K^*(892)^0$ full width $\Gamma = 50.7 \pm 0.6$ MeV (S = 1.1)

$K^*(892)$ DECAY MODES	Fraction (Γ_i/Γ)	Confidence level	p (MeV/c)
$K\pi$	~ 100 %		289
$K^0\gamma$	(2.30±0.20) $\times 10^{-3}$		307
$K^\pm\gamma$	(9.9 ±0.9) $\times 10^{-4}$		309
$K\pi\pi$	< 7 $\times 10^{-4}$	95%	223

$K_1(1270)$

$I(J^P) = \frac{1}{2}(1^+)$

Mass $m = 1273 \pm 7$ MeV [n]

Full width $\Gamma = 90 \pm 20$ MeV [n]

$K_1(1270)$ DECAY MODES	Fraction (Γ_i/Γ)	p (MeV/c)
$K\rho$	(42 ±6) %	43
$K_0^*(1430)\pi$	(28 ±4) %	†
$K^*(892)\pi$	(16 ±5) %	302
$K\omega$	(11.0±2.0) %	†
$K f_0(1370)$	(3.0±2.0) %	–
γK^0	seen	539

$K_1(1400)$

$I(J^P) = \frac{1}{2}(1^+)$

Mass $m = 1402 \pm 7$ MeV

Full width $\Gamma = 174 \pm 13$ MeV (S = 1.6)

$K_1(1400)$ DECAY MODES	Fraction (Γ_i/Γ)	p (MeV/c)
$K^*(892)\pi$	(94 ±6) %	402
$K\rho$	(3.0±3.0) %	292
$K f_0(1370)$	(2.0±2.0) %	–
$K\omega$	(1.0±1.0) %	284
$K_0^*(1430)\pi$	not seen	†
γK^0	seen	613

$K^*(1410)$

$I(J^P) = \frac{1}{2}(1^-)$

Mass $m = 1414 \pm 15$ MeV (S = 1.3)

Full width $\Gamma = 232 \pm 21$ MeV (S = 1.1)

$K^*(1410)$ DECAY MODES	Fraction (Γ_i/Γ)	Confidence level	p (MeV/c)
$K^*(892)\pi$	> 40 %	95%	410
$K\pi$	(6.6±1.3) %		612
$K\rho$	< 7 %	95%	305
γK^0	seen		619

$K_0^*(1430)$ [l]

$I(J^P) = \frac{1}{2}(0^+)$

Mass $m = 1412 \pm 6$ MeV

Full width $\Gamma = 294 \pm 23$ MeV

$K_0^*(1430)$ DECAY MODES	Fraction (Γ_i/Γ)	p (MeV/c)
$K\pi$	(93±10) %	611

$K_2^*(1430)$

$I(J^P) = \frac{1}{2}(2^+)$

$K_2^*(1430)^\pm$ mass $m = 1425.6 \pm 1.5$ MeV (S = 1.1)

$K_2^*(1430)^0$ mass $m = 1432.4 \pm 1.3$ MeV

$K_2^*(1430)^\pm$ full width $\Gamma = 98.5 \pm 2.7$ MeV (S = 1.1)

$K_2^*(1430)^0$ full width $\Gamma = 109 \pm 5$ MeV (S = 1.9)

$K_2^*(1430)$ DECAY MODES	Fraction (Γ_i/Γ)	Scale factor/ Confidence level	p (MeV/c)
$K\pi$	(49.9±1.2) %		619
$K^*(892)\pi$	(24.7±1.5) %		419
$K^*(892)\pi\pi$	(13.4±2.2) %		372
$K\rho$	(8.7±0.8) %	S=1.2	318

$K\omega$	$(\ 2.9\pm0.8\ )$ %		311
$K^+\gamma$	$(\ 2.4\pm0.5\ )\times10^{-3}$	S=1.1	627
$K\eta$	$(\ 1.5^{+3.4}_{-1.0}\ )\times10^{-3}$	S=1.3	486
$K\omega\pi$	$<\ 7.2\ \times10^{-4}$	CL=95%	100
$K^0\gamma$	$<\ 9\ \times10^{-4}$	CL=90%	626

$K^*(1680)$

$I(J^P) = \frac{1}{2}(1^-)$

Mass $m = 1717 \pm 27$ MeV (S = 1.4)
Full width $\Gamma = 322 \pm 110$ MeV (S = 4.2)

$K^*(1680)$ DECAY MODES	Fraction (Γ_i/Γ)	p (MeV/c)
$K\pi$	(38.7 ± 2.5) %	781
$K\rho$	$(31.4^{+4.7}_{-2.1})$ %	570
$K^*(892)\pi$	$(29.9^{+2.2}_{-4.7})$ %	618

$K_2(1770)$ [mm]

$I(J^P) = \frac{1}{2}(2^-)$

Mass $m = 1773 \pm 8$ MeV
Full width $\Gamma = 186 \pm 14$ MeV

$K_2(1770)$ DECAY MODES	Fraction (Γ_i/Γ)	p (MeV/c)
$K\pi\pi$		794
$K_2^*(1430)\pi$	dominant	288
$K^*(892)\pi$	seen	654
$K f_2(1270)$	seen	53
$K\phi$	seen	441
$K\omega$	seen	607

$K_3^*(1780)$

$I(J^P) = \frac{1}{2}(3^-)$

Mass $m = 1776 \pm 7$ MeV (S = 1.1)
Full width $\Gamma = 159 \pm 21$ MeV (S = 1.3)

$K_3^*(1780)$ DECAY MODES	Fraction (Γ_i/Γ)	Confidence level	p (MeV/c)
$K\rho$	$(31\ \pm\ 9\ )$ %		613
$K^*(892)\pi$	$(20\ \pm\ 5\ )$ %		656
$K\pi$	$(18.8\pm\ 1.0)$ %		813
$K\eta$	$(30\ \pm13\ )$ %		719
$K_2^*(1430)\pi$	$<\ 16$ %	95%	291

$K_2(1820)$ [nn]

$I(J^P) = \frac{1}{2}(2^-)$

Mass $m = 1816 \pm 13$ MeV
Full width $\Gamma = 276 \pm 35$ MeV

$K_2(1820)$ DECAY MODES	Fraction (Γ_i/Γ)	p (MeV/c)
$K_2^*(1430)\pi$	seen	327
$K^*(892)\pi$	seen	681
$K f_2(1270)$	seen	185
$K\omega$	seen	638

$K_4^*(2045)$

$I(J^P) = \frac{1}{2}(4^+)$

Mass $m = 2045 \pm 9$ MeV (S = 1.1)
Full width $\Gamma = 198 \pm 30$ MeV

$K_4^*(2045)$ DECAY MODES	Fraction (Γ_i/Γ)	p (MeV/c)
$K\pi$	(9.9 ± 1.2) %	958
$K^*(892)\pi\pi$	$(9\ \pm5\ )$ %	802
$K^*(892)\pi\pi\pi$	$(7\ \pm5\ )$ %	768
$\rho K\pi$	(5.7 ± 3.2) %	741
$\omega K\pi$	(5.0 ± 3.0) %	738
$\phi K\pi$	(2.8 ± 1.4) %	594
$\phi K^*(892)$	(1.4 ± 0.7) %	363

CHARMED MESONS ($C = \pm1$)

$D^+ = c\overline{d}$, $D^0 = c\overline{u}$, $\overline{D}^0 = \overline{c}u$, $D^- = \overline{c}d$, similarly for D^*'s

$D^\pm$

$I(J^P) = \frac{1}{2}(0^-)$

Mass $m = 1869.4 \pm 0.5$ MeV (S = 1.1)
Mean life $\tau = (1040 \pm 7)\times10^{-15}$ s
$c\tau = 311.8\ \mu$m

c-quark decays

$\Gamma(c \to\ \ell^+$ anything$)/\Gamma(c \to\$ anything$) = 0.096 \pm 0.004$ [oo]
$\Gamma(c \to\ D^*(2010)^+$ anything$)/\Gamma(c \to\$ anything$) = 0.255 \pm 0.017$

CP-violation decay-rate asymmetries

$A_{CP}(K^0_S\pi^\pm) = -0.016 \pm 0.017$
$A_{CP}(K^0_S K^\pm) = 0.07 \pm 0.06$
$A_{CP}(K^+K^-\pi^\pm) = 0.002 \pm 0.011$
$A_{CP}(K^\pm K^{*0}) = -0.02 \pm 0.05$
$A_{CP}(\phi\pi^\pm) = -0.014 \pm 0.033$
$A_{CP}(\pi^+\pi^-\pi^\pm) = -0.02 \pm 0.04$

$D^+ \to\ \overline{K}^*(892)^0\ell^+\nu_\ell$ form factors

$r_V = 1.62 \pm 0.08$ (S = 1.5)
$r_2 = 0.83 \pm 0.05$
$r_3 = 0.0 \pm 0.4$
$\Gamma_L/\Gamma_T = 1.13 \pm 0.08$
$\Gamma_+/\Gamma_- = 0.22 \pm 0.06$ (S = 1.6)

D^- modes are charge conjugates of the modes below.

D^+ DECAY MODES		Fraction (Γ_i/Γ)	Scale factor/ Confidence level	p (MeV/c)
Inclusive modes				
e^+ anything		$(17.2\ \pm\ 1.9\ )$ %		–
K^- anything		$(27.5\ \pm\ 2.4\ )$ %		–
$\overline{K}^0$ anything + K^0 anything		$(61\ \pm\ 8\ )$ %		–
K^+ anything		$(\ 5.5\ \pm\ 1.6\ )$ %		–
η anything	[pp]	<13 %	CL=90%	–
ϕ anything		$<\ 1.8$ %	CL=90%	–
ϕe^+ anything		$<\ 1.6$ %	CL=90%	–
Leptonic and semileptonic modes				
$\mu^+\nu_\mu$		$(\ 8\ ^{+17}_{-\ 5}\ )\times10^{-4}$		932
$\overline{K}^0\ell^+\nu_\ell$	[qq]	$(\ 6.8\ \pm\ 0.8\ )$ %		868
$\overline{K}^0 e^+\nu_e$		$(\ 6.7\ \pm\ 0.9\ )$ %		868
$\overline{K}^0\mu^+\nu_\mu$		$(\ 7.0\ ^{+\ 3.0}_{-\ 2.0}\ )$ %		865
$K^-\pi^+e^+\nu_e$		$(\ 4.5\ ^{+\ 1.0}_{-\ 0.8}\ )$ %	S=1.1	863
$\overline{K}^*(892)^0e^+\nu_e$ × B($\overline{K}^*(892)^0 \to\ K^-\pi^+$)		$(\ 3.7\ \pm\ 0.5\ )$ %		722
$K^-\pi^+e^+\nu_e$ nonresonant		$<\ 7\ \times10^{-3}$	CL=90%	863
$K^-\pi^+\mu^+\nu_\mu$		$(\ 4.00\pm\ 0.32)$ %		851
$\overline{K}^*(892)^0\mu^+\nu_\mu$ × B($\overline{K}^*(892)^0 \to\ K^-\pi^+$)		$(\ 3.7\ \pm\ 0.3\ )$ %		717
$K^-\pi^+\mu^+\nu_\mu$ nonresonant		$(\ 3.3\ \pm\ 1.3\ )\times10^{-3}$		851
$(\overline{K}^*(892)\pi)^0e^+\nu_e$		$<\ 1.2$ %	CL=90%	712
$(\overline{K}\pi\pi)^0e^+\nu_e$ non-$\overline{K}^*(892)$		$<\ 9\ \times10^{-3}$	CL=90%	846
$K^-\pi^+\pi^0\mu^+\nu_\mu$		$<\ 1.7\ \times10^{-3}$	CL=90%	825
$\pi^0\ell^+\nu_\ell$	[rr]	$(\ 3.1\ \pm\ 1.5\ )\times10^{-3}$		930

Fractions of some of the following modes with resonances have already appeared above as submodes of particular charged-particle modes.

$\overline{K}^*(892)^0\ell^+\nu_\ell$	[qq]	$(\ 5.73\pm\ 0.35)$ %		722
$\overline{K}^*(892)^0e^+\nu_e$		$(\ 5.5\ \pm\ 0.7\ )$ %	S=1.4	722
$\overline{K}^*(892)^0\mu^+\nu_\mu$		$(\ 5.5\ \pm\ 0.4\ )$ %		717
$\overline{K}_1(1270)^0\mu^+\nu_\mu$		$<\ 4$ %	CL=95%	493
$\overline{K}_2^*(1430)^0\mu^+\nu_\mu$		$<\ 1.0$ %	CL=95%	380
$\rho^0e^+\nu_e$		$(\ 2.5\ \pm\ 1.0\ )\times10^{-3}$		774
$\rho^0\mu^+\nu_\mu$		$(\ 3.4\ \pm\ 0.8\ )\times10^{-3}$		769
$\phi e^+\nu_e$		$<\ 2.09$ %	CL=90%	657
$\phi\mu^+\nu_\mu$		$<\ 3.72$ %	CL=90%	651
$\eta\ell^+\nu_\ell$		$<\ 5\ \times10^{-3}$	CL=90%	854
$\eta'(958)\mu^+\nu_\mu$		$<\ 1.1$ %	CL=90%	684

Hadronic modes with a $\overline{K}$ or $\overline{K}K\overline{K}$

$\overline{K}^0\pi^+$		(2.82 ± 0.19) %		862
$K^-\pi^+\pi^+$	[ss]	(9.2 ± 0.6) %		845
$\overline{K}^*(892)^0\pi^+$		(1.30 ± 0.13) %		714
× B($\overline{K}^*(892)^0 \to K^-\pi^+$)				
$\overline{K}_0^*(1430)^0\pi^+$		(2.3 ± 0.3) %		382
× B($\overline{K}_0^*(1430)^0 \to K^-\pi^+$)				
$\overline{K}^*(1680)^0\pi^+$		(3.8 ± 0.8) × 10^{-3}		58
× B($\overline{K}^*(1680)^0 \to K^-\pi^+$)				
$K^-\pi^+\pi^+$ nonresonant		(8.8 ± 0.9) %		845
$\overline{K}^0\pi^+\pi^0$	[ss]	(9.7 ± 3.0) %	S=1.1	845
$\overline{K}^0\rho^+$		(6.6 ± 2.5) %		677
$\overline{K}^*(892)^0\pi^+$		(6.5 ± 0.6) × 10^{-3}		714
× B($\overline{K}^*(892)^0 \to \overline{K}^0\pi^0$)				
$\overline{K}^0\pi^+\pi^0$ nonresonant		(1.3 ± 1.1) %		845
$K^-\pi^+\pi^+\pi^0$	[ss]	(6.5 ± 1.1) %		816
$\overline{K}^*(892)^0\rho^+$ total		(1.4 ± 0.9) %		422
× B($\overline{K}^*(892)^0 \to K^-\pi^+$)				
$\overline{K}_1(1400)^0\pi^+$		(2.2 ± 0.6) %		390
× B($\overline{K}_1(1400)^0 \to K^-\pi^+\pi^0$)				
$K^-\rho^+\pi^+$ total		(3.1 ± 1.1) %		612
$K^-\rho^+\pi^+$ 3-body		(1.1 ± 0.4) %		612
$\overline{K}^*(892)^0\pi^+\pi^0$ total		(4.5 ± 0.9) %		690
× B($\overline{K}^*(892)^0 \to K^-\pi^+$)				
$\overline{K}^*(892)^0\pi^+\pi^0$ 3-body		(2.9 ± 0.9) %		690
× B($\overline{K}^*(892)^0 \to K^-\pi^+$)				
$K^*(892)^-\pi^+\pi^+$ 3-body		(7 ± 3) × 10^{-3}		688
× B($K^*(892)^- \to K^-\pi^0$)				
$K^-\pi^+\pi^+\pi^0$ nonresonant	[tt]	(1.2 ± 0.6) %		816
$\overline{K}^0\pi^+\pi^+\pi^-$	[ss]	(7.1 ± 1.0) %		814
$\overline{K}^0 a_1(1260)^+$		(4.0 ± 0.9) %		328
× B($a_1(1260)^+ \to \pi^+\pi^+\pi^-$)				
$\overline{K}_1(1400)^0\pi^+$		(2.2 ± 0.6) %		390
× B($\overline{K}_1(1400)^0 \to \overline{K}^0\pi^+\pi^-$)				
$K^*(892)^-\pi^+\pi^+$ 3-body		(1.4 ± 0.6) %		688
× B($K^*(892)^- \to \overline{K}^0\pi^-$)				
$\overline{K}^0\rho^0\pi^+$ total		(4.3 ± 0.9) %		610
$\overline{K}^0\rho^0\pi^+$ 3-body		(5 ± 5) × 10^{-3}		610
$\overline{K}^0\pi^+\pi^+\pi^-$ nonresonant		(9 ± 4) × 10^{-3}		814
$K^-3\pi^+\pi^-$	[ss]	(6.2 ± 0.8) × 10^{-3}	S=1.3	772
$\overline{K}^*(892)^0\pi^+\pi^+\pi^-$		(2.1 ± 0.8) × 10^{-3}		645
× B($\overline{K}^*(892)^0 \to K^-\pi^+$)				
$\overline{K}^*(892)^0\rho^0\pi^+$		(2.0 ± 0.5) × 10^{-3}		239
× B($\overline{K}^*(892)^0 \to K^-\pi^+$)				
$\overline{K}^*(892)^0\pi^+\pi^+\pi^-$ no-ρ		(2.9 ± 1.1) × 10^{-3}		645
× B($\overline{K}^*(892)^0 \to K^-\pi^+$)				
$K^-\rho^0\pi^+\pi^+$		(1.94 ± 0.35) × 10^{-3}	S=1.1	524
$K^-3\pi^+\pi^-$ nonresonant		(4.3 ± 3.2) × 10^{-4}		772
$\overline{K}^0\overline{K}^0K^+$		(1.8 ± 0.8) %		545
$K^+K^-\overline{K}^0\pi^+$		(5.5 ± 1.4) × 10^{-4}		435

Fractions of some of the following modes with resonances have already appeared above as submodes of particular charged-particle modes.

$\overline{K}^0\rho^+$		(6.6 ± 2.5) %		677
$\overline{K}^0 a_1(1260)^+$		(8.2 ± 1.7) %		328
$\overline{K}^0 a_2(1320)^+$		< 3 × 10^{-3}	CL=90%	199
$\overline{K}^*(892)^0\pi^+$		(1.95 ± 0.19) %		714
$\overline{K}^*(892)^0\rho^+$ total	[tt]	(2.1 ± 1.4) %		422
$\overline{K}^*(892)^0\rho^+$ S-wave	[tt]	(1.7 ± 1.6) %		422
$\overline{K}^*(892)^0\rho^+$ P-wave		< 1 × 10^{-3}	CL=90%	422
$\overline{K}^*(892)^0\rho^+$ D-wave		(10 ± 7) × 10^{-3}		422
$\overline{K}^*(892)^0\rho^+$ D-wave longitudinal		< 7 × 10^{-3}	CL=90%	422
$\overline{K}_1(1270)^0\pi^+$		< 7 × 10^{-3}	CL=90%	487
$\overline{K}_1(1400)^0\pi^+$		(5.0 ± 1.3) %		390
$\overline{K}_0^*(1430)^0\pi^+$		(3.8 ± 0.4) %		382
$\overline{K}^*(1680)^0\pi^+$		(1.47 ± 0.31) %		58
$\overline{K}^*(892)^0\pi^+\pi^0$ total		(6.8 ± 1.4) %		690
$\overline{K}^*(892)^0\pi^+\pi^0$ 3-body	[tt]	(4.3 ± 1.4) %		690
$K^*(892)^-\pi^+\pi^+$ total		—		688
$K^*(892)^-\pi^+\pi^+$ 3-body		(2.1 ± 0.9) %		688
$K^-\rho^+\pi^+$ total		(3.1 ± 1.1) %		612
$K^-\rho^+\pi^+$ 3-body		(1.1 ± 0.4) %		612
$\overline{K}^0\rho^0\pi^+$ total		(4.3 ± 0.9) %	CL=90%	610
$\overline{K}^0\rho^0\pi^+$ 3-body		(5 ± 5) × 10^{-3}		610
$\overline{K}^*(892)^0\pi^+\pi^+\pi^-$		(3.2 ± 1.2) × 10^{-3}	S=2.0	645
$\overline{K}^*(892)^0\rho^0\pi^+$		(3.0 ± 0.7) × 10^{-3}	S=1.3	239
$\overline{K}^*(892)^0\pi^+\pi^+\pi^-$ no-ρ		(4.4 ± 1.7) × 10^{-3}		645
$K^-\rho^0\pi^+\pi^+$		(1.94 ± 0.35) × 10^{-3}		524
$\overline{K}^*(892)^0 a_1(1260)^+$		(9.1 ± 1.9) × 10^{-3}		†

Pionic modes

$\pi^+\pi^0$		(2.6 ± 0.7) × 10^{-3}		925
$\pi^+\pi^+\pi^-$		(3.1 ± 0.4) × 10^{-3}		908
$\sigma\pi^+$		(2.2 ± 0.5) × 10^{-3}		–
$\rho^0\pi^+$		(1.05 ± 0.18) × 10^{-3}		766
$f_0(980)\pi^+$	[uu]	(1.9 ± 0.5) × 10^{-4}		669
× B($f_0 \to \pi^+\pi^-$)				
$f_2(1270)\pi^+$		(6.1 ± 1.1) × 10^{-4}		485
× B($f_2 \to \pi^+\pi^-$)				
$\pi^+\pi^+\pi^-$ nonresonant		(2.4 ± 2.1) × 10^{-4}		908
$\pi^+\pi^+\pi^-\pi^0$		—		883
$\eta\pi^+$ × B($\eta \to \pi^+\pi^-\pi^0$)		(6.8 ± 1.4) × 10^{-4}		848
$\omega\pi^+$ × B($\omega \to \pi^+\pi^-\pi^0$)		< 6 × 10^{-3}	CL=90%	763
$3\pi^+2\pi^-$		(1.82 ± 0.25) × 10^{-3}	S=1.2	845

Fractions of some of the following modes with resonances have already appeared above as submodes of particular charged-particle modes.

$\eta\pi^+$		(3.0 ± 0.6) × 10^{-3}		848
$\rho^0\pi^+$		(1.05 ± 0.18) × 10^{-3}		766
$\omega\pi^+$		< 7 × 10^{-3}	CL=90%	763
$\eta\rho^+$		< 7 × 10^{-3}	CL=90%	655
$\eta'(958)\pi^+$		(5.1 ± 1.0) × 10^{-3}		680
$\eta'(958)\rho^+$		< 5 × 10^{-3}	CL=90%	348
$f_2(1270)\pi^+$		(1.08 ± 0.20) × 10^{-3}		485

Hadronic modes with a $K\overline{K}$ pair

$K^+\overline{K}^0$		(5.9 ± 0.6) × 10^{-3}	S=1.2	792
$K^+K^-\pi^+$	[ss]	(8.9 ± 0.8) × 10^{-3}		744
$\phi\pi^+$ × B($\phi \to K^+K^-$)		(3.1 ± 0.3) × 10^{-3}		647
$K^+\overline{K}^*(892)^0$		(2.9 ± 0.4) × 10^{-3}		613
× B($\overline{K}^{*0} \to K^-\pi^+$)				
$K^+K^-\pi^+$ nonresonant		(4.6 ± 0.9) × 10^{-3}		744
$K^0\overline{K}^0\pi^+$		—		741
$K^*(892)^+\overline{K}^0$		(2.1 ± 0.9) %		611
× B($K^{*+} \to K^0\pi^+$)				
$K^+K^-\pi^+\pi^0$		—		682
$\phi\pi^+\pi^0$ × B($\phi \to K^+K^-$)		(1.1 ± 0.5) %		619
$\phi\rho^+$ × B($\phi \to K^+K^-$)		< 7 × 10^{-3}	CL=90%	258
$K^+K^-\pi^+\pi^0$ non-ϕ		(1.5 $^{+0.7}_{-0.6}$) %		682
$K^+\overline{K}^0\pi^+\pi^-$		(4.0 ± 0.7) × 10^{-3}		678
$K^0K^-\pi^+\pi^+$		(5.5 ± 0.8) × 10^{-3}		678
$K^*(892)^+\overline{K}^*(892)^0$		(1.2 ± 0.5) %		280
× B^2($K^*(892)^+ \to K^0\pi^+$)				
$K^0K^-\pi^+\pi^+$(non-$K^{*+}\overline{K}^{*0}$)		< 7.9 × 10^{-3}	CL=90%	678
$K^+K^-\pi^+\pi^+\pi^-$		(2.5 ± 1.3) × 10^{-4}		600

Fractions of some of the following modes with resonances have already appeared above as submodes of particular charged-particle modes.

$\phi\pi^+$		(6.2 ± 0.6) × 10^{-3}		647
$\phi\pi^+\pi^0$		(2.3 ± 1.0) %		619
$\phi\rho^+$		< 1.5 %	CL=90%	258
$K^+\overline{K}^*(892)^0$		(4.3 ± 0.6) × 10^{-3}		613
$K^*(892)^+\overline{K}^0$		(3.1 ± 1.4) %		611
$K^*(892)^+\overline{K}^*(892)^0$		(2.6 ± 1.1) %		280

Doubly Cabibbo suppressed (DC) modes, $\Delta C = 1$ weak neutral current ($C1$) modes, or Lepton Family number (LF) or Lepton number (L) violating modes

$K^+\pi^+\pi^-$	DC		(7.0 ± 1.5) × 10^{-4}		845
$K^+\rho^0$	DC		(2.6 ± 1.2) × 10^{-4}		678
$K^*(892)^0\pi^+$	DC	[vv]	(3.7 ± 1.7) × 10^{-4}		714
$K^+\pi^+\pi^-$ nonresonant	DC		(2.5 ± 1.2) × 10^{-4}		845
$K^+K^+K^-$	DC		(8.7 ± 2.1) × 10^{-5}		550
ϕK^+	DC	[vv]	< 1.3 × 10^{-4}	CL=90%	527
$\pi^+e^+e^-$	$C1$		< 5.2 × 10^{-5}	CL=90%	929
$\pi^+\mu^+\mu^-$	$C1$		< 8.8 × 10^{-6}	CL=90%	917
$\rho^+\mu^+\mu^-$	$C1$		< 5.6 × 10^{-4}	CL=90%	757
$K^+e^+e^-$		[ww]	< 2.0 × 10^{-4}	CL=90%	870
$K^+\mu^+\mu^-$		[ww]	< 9.2 × 10^{-6}	CL=90%	856
$\pi^+e^\pm\mu^\mp$	LF	[gg]	< 3.4 × 10^{-5}	CL=90%	926
$K^+e^\pm\mu^\mp$	LF	[gg]	< 6.8 × 10^{-5}	CL=90%	866
$\pi^-e^+e^+$	L		< 9.6 × 10^{-5}	CL=90%	929
$\pi^-\mu^+\mu^+$	L		< 4.8 × 10^{-6}	CL=90%	917

$\pi^- e^+ \mu^+$	L	$<$ 5.0	$\times 10^{-5}$	CL=90%	926
$\rho^- \mu^+ \mu^+$	L	$<$ 5.6	$\times 10^{-4}$	CL=90%	757
$K^- e^+ e^+$	L	$<$ 1.2	$\times 10^{-4}$	CL=90%	870
$K^- \mu^+ \mu^+$	L	$<$ 1.3	$\times 10^{-5}$	CL=90%	856
$K^- e^+ \mu^+$	L	$<$ 1.3	$\times 10^{-4}$	CL=90%	866
$K^*(892)^- \mu^+ \mu^+$	L	$<$ 8.5	$\times 10^{-4}$	CL=90%	703

D^0

$I(J^P) = \frac{1}{2}(0^-)$

Mass $m = 1864.6 \pm 0.5$ MeV (S = 1.1)
$m_{D^\pm} - m_{D^0} = 4.78 \pm 0.10$ MeV (S = 1.1)
Mean life $\tau = (410.3 \pm 1.5) \times 10^{-15}$ s
$c\tau = 123.0\ \mu$m
$\left|m_{D_1^0} - m_{D_2^0}\right| < 7 \times 10^{10}\ \hbar\ \mathrm{s}^{-1}$, CL = 95% [xx]
$(\Gamma_{D_1^0} - \Gamma_{D_2^0})/\Gamma = 2y = 0.016 \pm 0.010$
$\Gamma(K^+ \ell^- \overline{\nu}_\ell \text{ (via } \overline{D}^0))/\Gamma(K^- \ell^+ \nu_\ell) < 0.005$, CL = 90%
$\Gamma\left(K^+\pi^- \text{ (via } \overline{D}^0)\right)/\Gamma\left(K^-\pi^+\right) < 4.1 \times 10^{-4}$, CL = 95%

CP-violation decay-rate asymmetries

$A_{CP}(K^+K^-) = 0.005 \pm 0.016$
$A_{CP}(K^0_S K^0_S) = -0.23 \pm 0.19$
$A_{CP}(\pi^+\pi^-) = 0.021 \pm 0.026$
$A_{CP}(\pi^0\pi^0) = 0.00 \pm 0.05$
$A_{CP}(K^0_S \phi) = -0.03 \pm 0.09$
$A_{CP}(K^0_S \pi^0) = 0.001 \pm 0.013$
$A_{CP}(K^\pm\pi^\mp) = 0.08 \pm 0.09$
$A_{CP}(K^\mp\pi^\pm\pi^0) = -0.03 \pm 0.09$
$A_{CP}(K^\pm\pi^\mp\pi^0) = 0.09^{+0.25}_{-0.22}$

CPT-violation decay-rate asymmetry

$A_{CPT}(K^\mp\pi^\pm) = 0.008 \pm 0.008$

$\overline{D}^0$ modes are charge conjugates of the modes below.

D^0 DECAY MODES	Fraction (Γ_j/Γ)	Scale factor/ Confidence level	p (MeV/c)
Inclusive modes			
e^+ anything	[yy] (6.87 ± 0.28) %		–
μ^+ anything	(6.5 ± 0.8) %		–
K^- anything	(53 ± 4) %	S=1.3	–
$\overline{K}^0$ anything + K^0 anything	(42 ± 5) %		–
K^+ anything	(3.4 $^{+\ 0.6}_{-\ 0.4}$) %		–
η anything	[pp] < 13 %	CL=90%	–
ϕ anything	(1.7 ± 0.8) %		–
Semileptonic modes			
$K^- \ell^+ \nu_\ell$	[qq] (3.43 ± 0.14) %	S=1.2	867
$K^- e^+ \nu_e$	(3.58 ± 0.18) %	S=1.1	867
$K^- \mu^+ \nu_\mu$	(3.19 ± 0.17) %		864
$K^- \pi^0 e^+ \nu_e$	(1.1 $^{+\ 0.8}_{-\ 0.6}$) %	S=1.6	861
$\overline{K}^0 \pi^- e^+ \nu_e$	(1.8 ± 0.8) %	S=1.6	860
$\overline{K}^*(892)^- e^+ \nu_e$	(1.43 ± 0.23) %		719
× B($K^*(892)^- \to \overline{K}^0\pi^-$)			
$K^- \pi^+ \pi^- \mu^+ \nu_\mu$	< 1.2 $\times 10^{-3}$	CL=90%	821
$(\overline{K}^*(892)\pi)^- \mu^+ \nu_\mu$	< 1.4 $\times 10^{-3}$	CL=90%	692
$\pi^- e^+ \nu_e$	(3.6 ± 0.6) $\times 10^{-3}$		927
A fraction of the following resonance mode has already appeared above as a submode of a charged-particle mode.			
$K^*(892)^- e^+ \nu_e$	(2.15 ± 0.35) %		719
Hadronic modes with a $\overline{K}$ or $\overline{K}K\overline{K}$			
$K^- \pi^+$	(3.80 ± 0.09) %		861
$\overline{K}^0 \pi^0$	(2.30 ± 0.22) %		860
$\overline{K}^0 \pi^+ \pi^-$	[ss] (5.97 ± 0.35) %	S=1.1	842
$\overline{K}^0 \rho^0$	(1.55 $^{+\ 0.12}_{-\ 0.16}$) %		673
$\overline{K}^0 \omega$	(3.9 ± 0.9) $\times 10^{-4}$		670
× B($\omega \to \pi^+\pi^-$)			
$\overline{K}^0 f_0(980)$	(2.8 $^{+\ 0.6}_{-\ 0.4}$) $\times 10^{-3}$		549
× B($f_0(980) \to \pi^+\pi^-$)			
$\overline{K}^0 f_2(1270)$	(2.6 $^{+\ 2.3}_{-\ 1.4}$) $\times 10^{-4}$		262
× B($f_2(1270) \to \pi^+\pi^-$)			
$\overline{K}^0 f_0(1370)$	(5.1 $^{+\ 1.2}_{-\ 1.3}$) $\times 10^{-3}$		–
× B($f_0(1370) \to \pi^+\pi^-$)			
$K^*(892)^- \pi^+$	(3.9 ± 0.3) %		711
× B($K^*(892)^- \to \overline{K}^0\pi^-$)			
$K^*_0(1430)^- \pi^+$	(6.1 $^{+\ 1.2}_{-\ 0.8}$) $\times 10^{-3}$		378
× B($K^*_0(1430)^- \to \overline{K}^0\pi^-$)			
$K^*_2(1430)^- \pi^+$	(1.0 $^{+\ 0.7}_{-\ 0.4}$) $\times 10^{-3}$		367
× B($K^*_2(1430)^- \to \overline{K}^0\pi^-$)			
$K^*(1680)^- \pi^+$	(2.1 $^{+\ 1.0}_{-\ 0.9}$) $\times 10^{-3}$		46
× B($K^*(1680)^- \to \overline{K}^0\pi^-$)			
$K^*(892)^+ \pi^-$	(2.0 $^{+\ 2.6}_{-\ 0.9}$) $\times 10^{-4}$		711
× B($K^*(892)^+ \to K^0\pi^+$)			
$\overline{K}^0 \pi^+ \pi^-$ nonresonant	(5.4 $^{+12.0}_{-\ 3.4}$) $\times 10^{-4}$		842
$K^- \pi^+ \pi^0$	[ss] (13.0 ± 0.8) %	S=1.3	844
$K^- \rho^+$	(10.1 ± 0.8) %		675
$K^- \rho(1700)^+$	(7.4 ± 1.6) $\times 10^{-3}$		†
× B($\rho(1700)^+ \to \pi^+\pi^0$)			
$K^*(892)^- \pi^+$	(1.97 ± 0.13) %		711
× B($K^*(892)^- \to K^-\pi^0$)			
$\overline{K}^*(892)^0 \pi^0$	(1.87 ± 0.27) %		711
× B($\overline{K}^*(892)^0 \to K^-\pi^+$)			
$K^*_0(1430)^- \pi^+$	(3.0 $^{+\ 0.6}_{-\ 0.4}$) $\times 10^{-3}$		378
× B($K^*_0(1430)^- \to K^-\pi^0$)			
$\overline{K}^*_0(1430)^0 \pi^0$	(5.3 $^{+\ 4.2}_{-\ 1.4}$) $\times 10^{-3}$		379
× B($\overline{K}^*_0(1430)^0 \to K^-\pi^+$)			
$K^*(1680)^- \pi^+$	(1.1 ± 0.5) $\times 10^{-3}$		46
× B($K^*(1680)^- \to K^-\pi^0$)			
$K^- \pi^+ \pi^0$ nonresonant	(1.04 $^{+\ 0.50}_{-\ 0.19}$) %		844
$\overline{K}^0 \pi^0 \pi^0$	—		843
$\overline{K}^*(892)^0 \pi^0$	(9.3 ± 1.3) $\times 10^{-3}$		711
× B($\overline{K}^*(892)^0 \to \overline{K}^0\pi^0$)			
$\overline{K}^0 \pi^0 \pi^0$ nonresonant	(8.5 ± 2.2) $\times 10^{-3}$		843
$K^- \pi^+ \pi^+ \pi^-$	[ss] (7.46 ± 0.31) %		812
$K^- \pi^+ \rho^0$ total	(6.2 ± 0.4) %		609
$K^- \pi^+ \rho^0$ 3-body	(4.7 ± 2.1) $\times 10^{-3}$		609
$\overline{K}^*(892)^0 \rho^0$	(9.7 ± 2.1) $\times 10^{-3}$		416
× B($\overline{K}^*(892)^0 \to K^-\pi^+$)			
$K^- a_1(1260)^+$	(3.6 ± 0.6) %		327
× B($a_1(1260)^+ \to \pi^+\pi^+\pi^-$)			
$\overline{K}^*(892)^0 \pi^+\pi^-$ total	(1.5 ± 0.4) %		685
$\overline{K}^*(892)^0 \pi^+\pi^-$ 3-body	(9.5 ± 2.1) $\times 10^{-3}$		685
× B($\overline{K}^*(892)^0 \to K^-\pi^+$)			
$K_1(1270)^- \pi^+$	[tt] (2.9 ± 0.3) $\times 10^{-3}$		484
× B($K_1(1270)^- \to K^-\pi^+\pi^-$)			
$K^- \pi^+ \pi^+ \pi^-$ nonresonant	(1.74 ± 0.25) %		812
$\overline{K}^0 \pi^+ \pi^- \pi^0$	[ss] (10.9 ± 1.3) %		812
$\overline{K}^0 \eta \times$ B($\eta \to \pi^+\pi^-\pi^0$)	(1.74 ± 0.25) $\times 10^{-3}$		772
$\overline{K}^0 \omega \times$ B($\omega \to \pi^+\pi^-\pi^0$)	(2.1 ± 0.4) %		670
$K^*(892)^- \rho^+$	(4.4 ± 1.7) %		416
× B($K^*(892)^- \to \overline{K}^0\pi^-$)			
$\overline{K}^*(892)^0 \rho^0$	(4.8 ± 1.1) $\times 10^{-3}$		416
× B($\overline{K}^*(892)^0 \to \overline{K}^0\pi^0$)			
$K_1(1270)^- \pi^+$	[tt] (4.5 ± 1.2) $\times 10^{-3}$		484
× B($K_1(1270)^- \to \overline{K}^0\pi^-\pi^0$)			
$\overline{K}^*(892)^0 \pi^+\pi^-$ 3-body	(4.7 ± 1.0) $\times 10^{-3}$		685
× B($\overline{K}^*(892)^0 \to \overline{K}^0\pi^0$)			
$\overline{K}^0 \pi^+\pi^-\pi^0$ nonresonant	(2.3 ± 2.3) %		812
$K^- \pi^+ \pi^+ \pi^- \pi^0$	(4.0 ± 0.4) %		771
$\overline{K}^*(892)^0 \pi^+\pi^-\pi^0$	(1.2 ± 0.6) %		643
× B($\overline{K}^*(892)^0 \to K^-\pi^+$)			
$\overline{K}^*(892)^0 \eta$	(2.7 ± 0.6) $\times 10^{-3}$		582
× B($\overline{K}^*(892)^0 \to K^-\pi^+$)			
× B($\eta \to \pi^+\pi^-\pi^0$)			
$K^-\pi^+\omega \times$ B($\omega \to \pi^+\pi^-\pi^0$)	(2.7 ± 0.5) %		605
$\overline{K}^*(892)^0 \omega$	(6.5 ± 2.4) $\times 10^{-3}$		410
× B($\overline{K}^*(892)^0 \to K^-\pi^+$)			
× B($\omega \to \pi^+\pi^-\pi^0$)			
$\overline{K}^0 \pi^+\pi^+\pi^-\pi^-$	(6.4 ± 1.8) $\times 10^{-3}$		768
$\overline{K}^0 K^+ K^-$	(1.03 ± 0.10) %		544
$\overline{K}^0 \phi \times$ B($\phi \to K^+K^-$)	(4.7 ± 0.6) $\times 10^{-3}$		520
$\overline{K}^0 K^+ K^-$ non-ϕ	(5.6 ± 0.9) $\times 10^{-3}$		544
$K^0_S K^0_S K^0_S$	(9.2 ± 1.6) $\times 10^{-4}$		538
$K^+ K^- K^- \pi^+$	(2.04 ± 0.30) $\times 10^{-4}$		434
$K^+ K^- \overline{K}^*(892)^0$	(4.1 ± 1.7) $\times 10^{-5}$		†
× B($\overline{K}^*(892)^0 \to K^-\pi^+$)			

$K^-\pi^+\phi\times$ B($\phi\to K^+K^-$)		(3.8 ± 1.6) × 10^{-5}		422
$\phi\overline{K}^*(892)^0$ × B($\phi\to K^+K^-$) × B($\overline{K}^*(892)^0\to K^-\pi^+$)		(1.0 ± 0.2) × 10^{-4}		†
$K^+K^-K^-\pi^+$ nonresonant		(3.1 ± 1.4) × 10^{-5}		434

Fractions of many of the following modes with resonances have already appeared above as submodes of particular charged-particle modes. (Modes for which there are only upper limits and $\overline{K}^*(892)\rho$ submodes only appear below.)

$\overline{K}^0\eta$		(7.7 ± 1.1) × 10^{-3}		772
$\overline{K}^0\rho^0$		(1.55 $^{+0.12}_{-0.16}$) %		673
$K^-\rho^+$		(10.1 ± 0.8) %	S=1.2	675
$\overline{K}^0\omega$		(2.3 ± 0.4) %		670
$\overline{K}^0\eta'(958)$		(1.88± 0.28) %		565
$\overline{K}^0\phi$		(9.4 ± 1.1) × 10^{-3}		520
$K^-a_1(1260)^+$		(7.2 ± 1.1) %		327
$\overline{K}^0a_1(1260)^0$	<	1.9 %	CL=90%	323
$\overline{K}^0f_2(1270)$		(4.7 $^{+4.1}_{-2.4}$) × 10^{-4}		262
$K^-a_2(1320)^+$	<	2 × 10^{-3}	CL=90%	197
$K^*(892)^-\pi^+$		(5.9 ± 0.4) %	S=1.1	711
$\overline{K}^*(892)^0\pi^0$		(2.8 ± 0.4) %	S=1.1	711
$\overline{K}^*(892)^0\pi^+\pi^-$ total		(2.2 ± 0.5) %		685
$\overline{K}^*(892)^0\pi^+\pi^-$ 3-body		(1.42± 0.31) %		685
$K^-\pi^+\rho^0$ total		(6.2 ± 0.4) %		609
$K^-\pi^+\rho^0$ 3-body		(4.7 ± 2.1) × 10^{-3}		609
$\overline{K}^*(892)^0\rho^0$		(1.45± 0.32) %		416
$\overline{K}^*(892)^0\rho^0$ transverse		(1.5 ± 0.5) %		416
$\overline{K}^*(892)^0\rho^0$ S-wave		(2.8 ± 0.6) %		416
$\overline{K}^*(892)^0\rho^0$ S-wave long.	<	3 × 10^{-3}	CL=90%	416
$\overline{K}^*(892)^0\rho^0$ P-wave	<	3 × 10^{-3}	CL=90%	416
$\overline{K}^*(892)^0\rho^0$ D-wave		(1.9 ± 0.6) %		416
$K^*(892)^-\rho^+$		(6.6 ± 2.6) %		416
$K^*(892)^-\rho^+$ longitudinal		(3.2 ± 1.3) %		416
$K^*(892)^-\rho^+$ transverse		(3.4 ± 2.0) %		416
$K^*(892)^-\rho^+$ P-wave	<	1.5 %	CL=90%	416
$K_1(1270)^-\pi^+$	[tt]	(1.14± 0.31) %		484
$K_1(1400)^-\pi^+$	<	1.2 %	CL=90%	386
$\overline{K}_1(1400)^0\pi^0$	<	3.7 %	CL=90%	387
$K_0^*(1430)^-\pi^+$		(9.8 $^{+2.0}_{-1.3}$) × 10^{-3}		378
$\overline{K}_0^*(1430)^0\pi^0$		(8.6 $^{+6.8}_{-2.3}$) × 10^{-3}		379
$K_2^*(1430)^-\pi^+$		(2.0 $^{+1.3}_{-0.7}$) × 10^{-3}		367
$\overline{K}_2^*(1430)^0\pi^0$	<	3.3 × 10^{-3}	CL=90%	368
$K^*(1680)^-\pi^+$		(8.2 $^{+3.9}_{-3.5}$) × 10^{-3}	S=1.2	46
$\overline{K}^*(892)^0\pi^+\pi^-\pi^0$		(1.8 ± 0.9) %		643
$\overline{K}^*(892)^0\eta$		(1.8 ± 0.4) %		582
$K^-\pi^+\omega$		(3.0 ± 0.6) %		605
$\overline{K}^*(892)^0\omega$		(1.1 ± 0.4) %		410
$K^-\pi^+\eta'(958)$		(6.9 ± 1.8) × 10^{-3}		479
$\overline{K}^*(892)^0\eta'(958)$	<	1.0 × 10^{-3}	CL=90%	119
$K^-\pi^+\phi$		(7.6 ± 3.1) × 10^{-5}		422
$K^+K^-\overline{K}^*(892)^0$		(6.1 ± 2.5) × 10^{-5}		†
$\phi\overline{K}^*(892)^0$		(3.0 ± 0.6) × 10^{-4}		†

Pionic modes

$\pi^+\pi^-$		(1.38± 0.05) × 10^{-3}		922
$\pi^0\pi^0$		(8.4 ± 2.2) × 10^{-4}		922
$\pi^+\pi^-\pi^0$		(1.1 ± 0.4) %		907
$\pi^+\pi^+\pi^-\pi^-$		(7.3 ± 0.5) × 10^{-3}		880

Hadronic modes with a $K\overline{K}$ pair

K^+K^-		(3.89 $^{+0.12}_{-0.15}$) × 10^{-3}	S=1.2	791
$K^0\overline{K}^0$		(7.1 ± 1.9) × 10^{-4}	S=1.2	788
$K^0K^-\pi^+$		(6.9 ± 1.0) × 10^{-3}		739
$\overline{K}^*(892)^0K^0$ × B($\overline{K}^{*0}\to K^-\pi^+$)	<	1.1 × 10^{-3}	CL=90%	608
$K^*(892)^+K^-$ × B($K^{*+}\to K^0\pi^+$)		(2.5 ± 0.5) × 10^{-3}		610
$K^0K^-\pi^+$ nonresonant		(2.3 ± 2.3) × 10^{-3}		739
$\overline{K}^0K^+\pi^-$		(5.3 ± 1.0) × 10^{-3}		739
$K^*(892)^0\overline{K}^0$ × B($K^{*0}\to K^+\pi^-$)	<	6 × 10^{-4}	CL=90%	608
$K^*(892)^-K^+$ × B($K^{*-}\to\overline{K}^0\pi^-$)		(1.3 ± 0.7) × 10^{-3}		610
$\overline{K}^0K^+\pi^-$ nonresonant		(3.8 $^{+2.3}_{-1.9}$) × 10^{-3}		739
$K^+K^-\pi^0$		(1.24± 0.35) × 10^{-3}		743
$K_S^0K_S^0\pi^0$	<	5.9 × 10^{-4}		740
$K^+K^-\pi^+\pi^-$	[zz]	(2.49± 0.23) × 10^{-3}		677
$\phi\pi^+\pi^-\times$ B($\phi\to K^+K^-$)		(5.3 ± 1.4) × 10^{-4}		614
$\phi\rho^0\times$ B($\phi\to K^+K^-$)		(2.9 ± 1.5) × 10^{-4}		250
$K^+K^-\rho^0$ 3-body		(9.0 ± 2.3) × 10^{-4}		301
$K^*(892)^0K^-\pi^+$ + c.c. × B($K^{*0}\to K^+\pi^-$)	[aaa]	< 5 × 10^{-4}		531
$K^*(892)^0\overline{K}^*(892)^0$ × $B^2(K^{*0}\to K^+\pi^-)$		(6 ± 2) × 10^{-4}		272
$K^+K^-\pi^+\pi^-$ nonresonant	<	8 × 10^{-4}	CL=90%	677
$K^0\overline{K}^0\pi^+\pi^-$		(7.5 ± 2.9) × 10^{-3}		673
$K^+K^-\pi^+\pi^-\pi^0$		(3.1 ± 2.0) × 10^{-3}		600

Fractions of most of the following modes with resonances have already appeared above as submodes of particular charged-particle modes.

$\overline{K}^*(892)^0K^0$	<	1.7 × 10^{-3}	CL=90%	608
$K^*(892)^+K^-$		(3.8 ± 0.8) × 10^{-3}		610
$K^*(892)^0\overline{K}^0$	<	9 × 10^{-4}	CL=90%	608
$K^*(892)^-K^+$		(2.0 ± 1.1) × 10^{-3}		610
$\phi\pi^0$		(7.5 ± 0.5) × 10^{-4}		645
$\phi\eta$		(1.4 ± 0.5) × 10^{-4}		489
$\phi\omega$	<	2.1 × 10^{-3}	CL=90%	238
$\phi\pi^+\pi^-$		(1.06± 0.28) × 10^{-3}		614
$\phi\rho^0$		(5.7 ± 3.0) × 10^{-4}		250
$\phi\pi^+\pi^-$ 3-body		(7 ± 5) × 10^{-4}		614
$K^*(892)^0K^-\pi^+$ + c.c.	[aaa]	< 7 × 10^{-4}	CL=90%	531
$K^*(892)^0\overline{K}^*(892)^0$		(1.4 ± 0.5) × 10^{-3}		272

Radiative modes

$\rho^0\gamma$	<	2.4 × 10^{-4}	CL=90%	771
$\omega\gamma$	<	2.4 × 10^{-4}	CL=90%	768
$\phi\gamma$		(2.5 $^{+0.7}_{-0.6}$) × 10^{-5}		654
$\overline{K}^*(892)^0\gamma$	<	7.6 × 10^{-4}	CL=90%	719

Doubly Cabibbo suppressed (DC) modes, $\Delta C=2$ forbidden via mixing ($C2M$) modes, $\Delta C=1$ weak neutral current ($C1$) modes, Lepton Family number (LF) violating modes, or Lepton number (L) violating modes

$K^+\ell^-\overline{\nu}_\ell$ (via $\overline{D}^0$)	$C2M$	<	1.7 × 10^{-4}	CL=90%	–
$K^+\pi^-$	DC	(1.38± 0.11) × 10^{-4}			861
$K^+\pi^-$ (via $\overline{D}^0$)	$C2M$	<	1.6 × 10^{-5}	CL=95%	861
$K^*(892)^+\pi^-$		(3.0 $^{+3.8}_{-1.3}$) × 10^{-4}			711
$K^+\pi^-\pi^0$		(5.6 ± 1.7) × 10^{-4}			844
$K^+\pi^-\pi^+\pi^-$	DC	(3.1 ± 1.0) × 10^{-4}			812
$K^+\pi^-\pi^+\pi^-$ (via $\overline{D}^0$)	$C2M$	<	4 × 10^{-4}	CL=90%	812
$K^+\pi^-$ or $K^+\pi^-\pi^+\pi^-$ (via $\overline{D}^0$)		<	1.0 × 10^{-3}	CL=90%	–
μ^- anything (via $\overline{D}^0$)	$C2M$	<	4 × 10^{-4}	CL=90%	–
$\gamma\gamma$	$C1$	<	2.8 × 10^{-5}	CL=90%	932
e^+e^-	$C1$	<	6.2 × 10^{-6}	CL=90%	932
$\mu^+\mu^-$	$C1$	<	4.1 × 10^{-6}	CL=90%	926
$\pi^0e^+e^-$	$C1$	<	4.5 × 10^{-5}	CL=90%	927
$\pi^0\mu^+\mu^-$	$C1$	<	1.8 × 10^{-4}	CL=90%	915
ηe^+e^-	$C1$	<	1.1 × 10^{-4}	CL=90%	852
$\eta\mu^+\mu^-$	$C1$	<	5.3 × 10^{-4}	CL=90%	838
$\pi^+\pi^-e^+e^-$	$C1$	<	3.73 × 10^{-4}	CL=90%	922
$\rho^0e^+e^-$	$C1$	<	1.0 × 10^{-4}	CL=90%	771
$\pi^+\pi^-\mu^+\mu^-$	$C1$	<	3.0 × 10^{-5}	CL=90%	894
$\rho^0\mu^+\mu^-$	$C1$	<	2.2 × 10^{-5}	CL=90%	754
ωe^+e^-	$C1$	<	1.8 × 10^{-4}	CL=90%	768
$\omega\mu^+\mu^-$	$C1$	<	8.3 × 10^{-4}	CL=90%	751
$K^-K^+e^+e^-$	$C1$	<	3.15 × 10^{-4}	CL=90%	791
ϕe^+e^-	$C1$	<	5.2 × 10^{-5}	CL=90%	654
$K^-K^+\mu^+\mu^-$	$C1$	<	3.3 × 10^{-5}	CL=90%	710
$\phi\mu^+\mu^-$	$C1$	<	3.1 × 10^{-5}	CL=90%	631
$\overline{K}^0e^+e^-$	[ww]	<	1.1 × 10^{-4}	CL=90%	866
$\overline{K}^0\mu^+\mu^-$	[ww]	<	2.6 × 10^{-4}	CL=90%	852
$K^-\pi^+e^+e^-$	$C1$	<	3.85 × 10^{-4}	CL=90%	861
$\overline{K}^*(892)^0e^+e^-$	[ww]	<	4.7 × 10^{-5}	CL=90%	719
$K^-\pi^+\mu^+\mu^-$	$C1$	<	3.59 × 10^{-4}	CL=90%	829
$\overline{K}^*(892)^0\mu^+\mu^-$	[ww]	<	2.4 × 10^{-5}	CL=90%	700
$\pi^+\pi^-\pi^0\mu^+\mu^-$	$C1$	<	8.1 × 10^{-4}	CL=90%	863
$\mu^\pm e^\mp$	LF	[gg] <	8.1 × 10^{-6}	CL=90%	929

Meson Summary Table

$\pi^0 e^\pm \mu^\mp$	LF	[gg]	< 8.6	$\times 10^{-5}$	CL=90%	924
$\eta e^\pm \mu^\mp$	LF	[gg]	< 1.0	$\times 10^{-4}$	CL=90%	848
$\pi^+ \pi^- e^\pm \mu^\mp$	LF	[gg]	< 1.5	$\times 10^{-5}$	CL=90%	911
$\rho^0 e^\pm \mu^\mp$	LF	[gg]	< 4.9	$\times 10^{-5}$	CL=90%	767
$\omega e^\pm \mu^\mp$	LF	[gg]	< 1.2	$\times 10^{-4}$	CL=90%	764
$K^- K^+ e^\pm \mu^\mp$	LF	[gg]	< 1.8	$\times 10^{-4}$	CL=90%	754
$\phi e^\pm \mu^\mp$	LF	[gg]	< 3.4	$\times 10^{-5}$	CL=90%	648
$\overline{K}^0 e^\pm \mu^\mp$	LF	[gg]	< 1.0	$\times 10^{-4}$	CL=90%	862
$K^- \pi^+ e^\pm \mu^\mp$	LF	[gg]	< 5.53	$\times 10^{-4}$	CL=90%	848
$\overline{K}^*(892)^0 e^\pm \mu^\mp$	LF	[gg]	< 8.3	$\times 10^{-5}$	CL=90%	714
$\pi^- \pi^- e^+ e^+ +$ c.c.	L		< 1.12	$\times 10^{-4}$	CL=90%	922
$\pi^- \pi^- \mu^+ \mu^+ +$ c.c.	L		< 2.9	$\times 10^{-5}$	CL=90%	894
$K^- \pi^- e^+ e^+ +$ c.c.	L		< 2.06	$\times 10^{-4}$	CL=90%	861
$K^- \pi^- \mu^+ \mu^+ +$ c.c.	L		< 3.9	$\times 10^{-4}$	CL=90%	829
$K^- K^- e^+ e^+ +$ c.c.	L		< 1.52	$\times 10^{-4}$	CL=90%	791
$K^- K^- \mu^+ \mu^+ +$ c.c.	L		< 9.4	$\times 10^{-5}$	CL=90%	710
$\pi^- \pi^- e^+ \mu^+ +$ c.c.	L		< 7.9	$\times 10^{-5}$	CL=90%	911
$K^- \pi^- e^+ \mu^+ +$ c.c.	L		< 2.18	$\times 10^{-4}$	CL=90%	848
$K^- K^- e^+ \mu^+ +$ c.c.	L		< 5.7	$\times 10^{-5}$	CL=90%	754

$D^*(2007)^0$

$I(J^P) = \frac{1}{2}(1^-)$
I, J, P need confirmation.

Mass $m = 2006.7 \pm 0.5$ MeV (S = 1.1)
$m_{D^{*0}} - m_{D^0} = 142.12 \pm 0.07$ MeV
Full width $\Gamma < 2.1$ MeV, CL = 90%

$\overline{D}^*(2007)^0$ modes are charge conjugates of modes below.

$D^*(2007)^0$ DECAY MODES	Fraction (Γ_i/Γ)	p (MeV/c)
$D^0 \pi^0$	(61.9 ± 2.9) %	43
$D^0 \gamma$	(38.1 ± 2.9) %	137

$D^*(2010)^\pm$

$I(J^P) = \frac{1}{2}(1^-)$
I, J, P need confirmation.

Mass $m = 2010.0 \pm 0.5$ MeV (S = 1.1)
$m_{D^*(2010)^+} - m_{D^+} = 140.64 \pm 0.10$ MeV (S = 1.1)
$m_{D^*(2010)^+} - m_{D^0} = 145.421 \pm 0.010$ MeV (S = 1.1)
Full width $\Gamma = 96 \pm 22$ keV

$D^*(2010)^-$ modes are charge conjugates of the modes below.

$D^*(2010)^\pm$ DECAY MODES	Fraction (Γ_i/Γ)	p (MeV/c)
$D^0 \pi^+$	(67.7 ± 0.5) %	39
$D^+ \pi^0$	(30.7 ± 0.5) %	38
$D^+ \gamma$	(1.6 ± 0.4) %	136

$D_1(2420)^0$

$I(J^P) = \frac{1}{2}(1^+)$
I, J, P need confirmation.

Mass $m = 2422.2 \pm 1.8$ MeV (S = 1.2)
Full width $\Gamma = 18.9^{+4.6}_{-3.5}$ MeV

$\overline{D}_1(2420)^0$ modes are charge conjugates of modes below.

$D_1(2420)^0$ DECAY MODES	Fraction (Γ_i/Γ)	p (MeV/c)
$D^*(2010)^+ \pi^-$	seen	355
$D^+ \pi^-$	not seen	474

$D_2^*(2460)^0$

$I(J^P) = \frac{1}{2}(2^+)$

$J^P = 2^+$ assignment strongly favored.

Mass $m = 2458.9 \pm 2.0$ MeV (S = 1.2)
Full width $\Gamma = 23 \pm 5$ MeV

$\overline{D}_2^*(2460)^0$ modes are charge conjugates of modes below.

$D_2^*(2460)^0$ DECAY MODES	Fraction (Γ_i/Γ)	p (MeV/c)
$D^+ \pi^-$	seen	504
$D^*(2010)^+ \pi^-$	seen	387

$D_2^*(2460)^\pm$

$I(J^P) = \frac{1}{2}(2^+)$

$J^P = 2^+$ assignment strongly favored.

Mass $m = 2459 \pm 4$ MeV (S = 1.7)
$m_{D_2^*(2460)^\pm} - m_{D_2^*(2460)^0} = 0.9 \pm 3.3$ MeV (S = 1.1)
Full width $\Gamma = 25^{+8}_{-7}$ MeV

$D_2^*(2460)^-$ modes are charge conjugates of modes below.

$D_2^*(2460)^\pm$ DECAY MODES	Fraction (Γ_i/Γ)	p (MeV/c)
$D^0 \pi^+$	seen	507
$D^{*0} \pi^+$	seen	390

CHARMED, STRANGE MESONS ($C = S = \pm 1$)

$D_s^+ = c\overline{s}$, $D_s^- = \overline{c}s$, similarly for D_s^*'s

$D_s^\pm$ was $F^\pm$

$I(J^P) = 0(0^-)$

Mass $m = 1968.3 \pm 0.5$ MeV (S = 1.2)
$m_{D_s^\pm} - m_{D^\pm} = 98.87 \pm 0.31$ MeV (S = 1.4)
Mean life $\tau = (490 \pm 9) \times 10^{-15}$ s (S = 1.1)
$c\tau = 147.0\ \mu$m

D_s^+ form factors

$r_2 = 1.60 \pm 0.24$
$r_V = 1.92 \pm 0.32$
$\Gamma_L/\Gamma_T = 0.72 \pm 0.18$

Unless otherwise noted, the branching fractions for modes with a resonance in the final state include all the decay modes of the resonance. D_s^- modes are charge conjugates of the modes below.

D_s^+ DECAY MODES		Fraction (Γ_i/Γ)	Scale factor/ Confidence level	p (MeV/c)
Inclusive modes				
K^- anything		(13 $^{+14}_{-12}$) %		–
$\overline{K}^0$ anything + K^0 anything		(39 ±28) %		–
K^+ anything		(20 $^{+18}_{-14}$) %		–
(non-$K\overline{K}$) anything		(64 ±17) %		–
e^+ anything		(8 $^{+6}_{-5}$) %		–
ϕ anything		(18 $^{+15}_{-10}$) %		–
Leptonic and semileptonic modes				
$\mu^+ \nu_\mu$		(5.0 ± 1.9) $\times 10^{-3}$	S=1.3	981
$\tau^+ \nu_\tau$		(6.4 ± 1.5) %		182
$\phi \ell^+ \nu_\ell$	[bbb]	(2.0 ± 0.5) %		720
$\eta \ell^+ \nu_\ell + \eta'(958) \ell^+ \nu_\ell$	[bbb]	(3.4 ± 1.0) %		–
$\eta \ell^+ \nu_\ell$	[bbb]	(2.5 ± 0.7) %		908
$\eta'(958) \ell^+ \nu_\ell$	[bbb]	(8.9 ± 3.3) $\times 10^{-3}$		751
Hadronic modes with a $K\overline{K}$ pair (including from a ϕ)				
$K^+ \overline{K}^0$		(3.6 ± 1.1) %		850
$K^+ K^- \pi^+$	[ss]	(4.4 ± 1.2) %		805
$\phi \pi^+$	[ccc]	(3.6 ± 0.9) %		712
$K^+ \overline{K}^*(892)^0$	[ccc]	(3.3 ± 0.9) %		685
$f_0(980) \pi^+$	[ddd]	(4.9 ± 2.3) $\times 10^{-3}$		732
$\times$ B($f_0 \to K^+ K^-$)				
$K^+ \overline{K}_0^*(1430)^0$	[ccc]	(7 ± 4) $\times 10^{-3}$		218
$K^+ K^- \pi^+$ nonresonant		(9 ± 4) $\times 10^{-3}$		805
$K^0 \overline{K}^0 \pi^+$		—		802
$K^*(892)^+ \overline{K}^0$	[ccc]	(4.3 ± 1.4) %		683
$K^+ K^- \pi^+ \pi^0$		—		748
$\phi \pi^+ \pi^0$	[ccc]	(9 ± 5) %		686
$\phi \rho^+$	[ccc]	(6.7 ± 2.3) %		400
$\phi \pi^+ \pi^0$ 3-body	[ccc]	< 2.6 %	CL=90%	686
$K^+ K^- \pi^+ \pi^0$ non-ϕ		< 9 %	CL=90%	748

$K^+\overline{K}^0\pi^+\pi^-$		(2.5 ± 0.9) %		744
$K^0K^-\pi^+\pi^+$		(4.3 ± 1.5) %		744
$K^*(892)^+\overline{K}^*(892)^0$	[ccc]	(5.8 ± 2.5) %		416
$K^0K^-\pi^+\pi^+$(non-$K^{*+}\overline{K}^{*0}$)		< 2.9 %	CL=90%	744
$K^+K^-\pi^+\pi^+\pi^-$		(7.1 ± 2.2) × 10^{-3}		673
$\phi\pi^+\pi^+\pi^-$	[ccc]	(9.7 ± 2.6) × 10^{-3}		640
$K^+K^-\rho^0\pi^+$non-ϕ		< 2.1 × 10^{-4}	CL=90%	248
$\phi\rho^0\pi^+$	[ccc]	(1.06± 0.35) %		180
$\phi a_1(1260)^+$	[ccc]	(2.5 ± 0.8) %		†
$K^+K^-\pi^+\pi^+\pi^-$ nonresonant		(7 ± 6) × 10^{-4}		673
Hadronic modes without K's				
$\pi^+\pi^+\pi^-$		(1.01± 0.28) %	S=1.1	959
$\rho^0\pi^+$		< 7 × 10^{-4}	CL=90%	824
$f_0(980)\pi^+$ × B($f_0\to\pi^+\pi^-$)	[uu]	(5.7 ± 1.7) × 10^{-3}		732
$f_2(1270)\pi^+$	[ccc]	(3.5 ± 1.2) × 10^{-3}		559
$f_0(1370)\pi^+$ × B($f_0\to\pi^+\pi^-$)	[uu]	(3.3 ± 1.2) × 10^{-3}		493
$\rho(1450)^0\pi^+$ × B($\rho^0\to\pi^+\pi^-$)	[uu]	(4.4 ± 2.5) × 10^{-4}		421
$\pi^+\pi^+\pi^-$ nonresonant		(5 $^{+22}_{-5}$) × 10^{-5}		959
$\pi^+\pi^+\pi^-\pi^0$		< 12 %	CL=90%	935
$\eta\pi^+$	[ccc]	(1.7 ± 0.5) %		902
$\omega\pi^+$	[ccc]	(2.8 ± 1.1) × 10^{-3}		822
$3\pi^+2\pi^-$		(6.5 ± 1.8) × 10^{-3}		899
$\pi^+\pi^+\pi^-\pi^0\pi^0$		—		902
$\eta\rho^+$	[ccc]	(10.8 ± 3.1) %		723
$\eta\pi^+\pi^0$ 3-body	[ccc]	< 4 %	CL=90%	885
$3\pi^+2\pi^-\pi^0$		(4.9 ± 3.2) %		856
$\eta'(958)\pi^+$	[ccc]	(3.9 ± 1.0) %		743
$3\pi^+2\pi^-2\pi^0$		—		803
$\eta'(958)\rho^+$	[ccc]	(10.1 ± 2.8) %		464
$\eta'(958)\pi^+\pi^0$ 3-body	[ccc]	< 1.4 %	CL=90%	720
Modes with one or three K's				
$K^0\pi^+$		< 8 × 10^{-3}	CL=90%	916
$K^+\pi^+\pi^-$		(1.0 ± 0.4) %		900
$K^+\rho^0$		< 2.9 × 10^{-3}	CL=90%	744
$K^*(892)^0\pi^+$	[ccc]	(6.5 ± 2.8) × 10^{-3}		775
$K^+K^+K^-$		(4.0 ± 1.7) × 10^{-4}		627
ϕK^+	[ccc]	< 5 × 10^{-4}	CL=90%	607
$\Delta C=1$ weak neutral current ($C1$) modes, Lepton family number (LF), or Lepton number (L) violating modes				
$\pi^+e^+e^-$	[ww]	< 2.7 × 10^{-4}	CL=90%	979
$\pi^+\mu^+\mu^-$	[ww]	< 2.6 × 10^{-5}	CL=90%	968
$K^+e^+e^-$	$C1$	< 1.6 × 10^{-3}	CL=90%	922
$K^+\mu^+\mu^-$	$C1$	< 3.6 × 10^{-5}	CL=90%	909
$K^*(892)^+\mu^+\mu^-$	$C1$	< 1.4 × 10^{-3}	CL=90%	765
$\pi^+e^\pm\mu^\mp$	LF [gg]	< 6.1 × 10^{-4}	CL=90%	976
$K^+e^\pm\mu^\mp$	LF [gg]	< 6.3 × 10^{-4}	CL=90%	919
$\pi^-e^+e^+$	L	< 6.9 × 10^{-4}	CL=90%	979
$\pi^-\mu^+\mu^+$	L	< 2.9 × 10^{-5}	CL=90%	968
$\pi^-e^+\mu^+$	L	< 7.3 × 10^{-4}	CL=90%	976
$K^-e^+e^+$	L	< 6.3 × 10^{-4}	CL=90%	922
$K^-\mu^+\mu^+$	L	< 1.3 × 10^{-5}	CL=90%	909
$K^-e^+\mu^+$	L	< 6.8 × 10^{-4}	CL=90%	919
$K^*(892)^-\mu^+\mu^+$	L	< 1.4 × 10^{-3}	CL=90%	765

$D_s^{*\pm}$

$I(J^P) = 0(?^?)$

J^P is natural, width and decay modes consistent with 1^-.

Mass $m = 2112.1 \pm 0.7$ MeV (S = 1.1)

$m_{D_s^{*\pm}} - m_{D_s^\pm} = 143.8 \pm 0.4$ MeV

Full width $\Gamma < 1.9$ MeV, CL = 90%

D_s^{*-} modes are charge conjugates of the modes below.

D_s^{*+} DECAY MODES	Fraction (Γ_i/Γ)	p (MeV/c)
$D_s^+\gamma$	(94.2±2.5) %	139
$D_s^+\pi^0$	(5.8±2.5) %	48

$D_{sJ}^*(2317)^\pm$

$I(J^P) = 0(0^+)$

J, P need confirmation.

J^P is natural, low mass consistent with 0^+.

Mass $m = 2317.4 \pm 0.9$ MeV (S = 1.1)

$m_{D_{sJ}^*(2317)^\pm} - m_{D_s^\pm} = 349.2 \pm 0.7$ MeV

Full width $\Gamma < 4.6$ MeV, CL = 90%

$D_{sJ}(2460)^\pm$

$I(J^P) = 0(1^+)$

Mass $m = 2459.3 \pm 1.3$ MeV (S = 1.3)

$m_{D_{sJ}^*(2460)^\pm} - m_{D_s^{*\pm}} = 347.2 \pm 1.2$ MeV (S = 1.3)

$m_{D_{sJ}^*(2460)^\pm} - m_{D_s^\pm} = 491.0 \pm 1.2$ MeV (S = 1.3)

Full width $\Gamma < 5.5$ MeV, CL = 90%

$D_{s1}(2536)^\pm$

$I(J^P) = 0(1^+)$

J, P need confirmation.

Mass $m = 2535.35 \pm 0.34 \pm 0.5$ MeV

Full width $\Gamma < 2.3$ MeV, CL = 90%

$D_{s1}(2536)^-$ modes are charge conjugates of the modes below.

$D_{s1}(2536)^+$ DECAY MODES	Fraction (Γ_i/Γ)	p (MeV/c)
$D^*(2010)^+K^0$	seen	150
$D^*(2007)^0K^+$	seen	168
D^+K^0	not seen	382
D^0K^+	not seen	392
$D_s^{*+}\gamma$	possibly seen	388

$D_{s2}(2573)^\pm$

$I(J^P) = 0(?^?)$

J^P is natural, width and decay modes consistent with 2^+.

Mass $m = 2572.4 \pm 1.5$ MeV

Full width $\Gamma = 15^{+5}_{-4}$ MeV

$D_{s2}(2573)^-$ modes are charge conjugates of the modes below.

$D_{s2}(2573)^+$ DECAY MODES	Fraction (Γ_i/Γ)	p (MeV/c)
D^0K^+	seen	435
$D^*(2007)^0K^+$	not seen	244

Meson Summary Table

BOTTOM MESONS ($B = \pm 1$)

$B^+ = u\overline{b}$, $B^0 = d\overline{b}$, $\overline{B}^0 = \overline{d}b$, $B^- = \overline{u}b$, similarly for B^*'s

B-particle organization

Many measurements of B decays involve admixtures of B hadrons. Previously we arbitrarily included such admixtures in the $B^\pm$ section, but because of their importance we have created two new sections: "$B^\pm/B^0$ Admixture" for $\Upsilon(4S)$ results and "$B^\pm/B^0/B_s^0$/b-baryon Admixture" for results at higher energies. Most inclusive decay branching fractions and χ_b at high energy are found in the Admixture sections. B^0-$\overline{B}^0$ mixing data are found in the B^0 section, while B_s^0-$\overline{B}_s^0$ mixing data and B-$\overline{B}$ mixing data for a B^0/B_s^0 admixture are found in the B_s^0 section. CP-violation data are found in the $B^\pm$, B^0, and $B^\pm$ B^0 Admixture sections. b-baryons are found near the end of the Baryon section.

The organization of the B sections is now as follows, where bullets indicate particle sections and brackets indicate reviews.

- $B^\pm$
  - mass, mean life, branching fractions CP violation
- B^0
  - mass, mean life, branching fractions
  - polarization in B^0 decay, B^0-$\overline{B}^0$ mixing, CP violation
- $B^\pm$ B^0 Admixtures
  - branching fractions, CP violation
- $B^\pm/B^0/B_s^0$/b-baryon Admixtures
  - mean life, production fractions, branching fractions
  - χ_b at high energy, V_{cb} measurements
- B^*
  - mass
- B_s^0
  - mass, mean life, branching fractions
  - polarization in B_s^0 decay, B_s^0-$\overline{B}_s^0$ mixing
- $B_c^\pm$
  - mass, mean life, branching fractions

At end of Baryon Listings:

- Λ_b
  - mass, mean life, branching fractions
- b-baryon Admixture
  - mean life, branching fractions

$B^\pm$

$I(J^P) = \frac{1}{2}(0^-)$

I, J, P need confirmation. Quantum numbers shown are quark-model predictions.

Mass $m_{B^\pm} = 5279.0 \pm 0.5$ MeV
Mean life $\tau_{B^\pm} = (1.671 \pm 0.018) \times 10^{-12}$ s
$c\tau = 501$ μm

CP violation

$A_{CP}(B^+ \to J/\psi(1S)K^+) = -0.007 \pm 0.019$
$A_{CP}(B^+ \to J/\psi(1S)\pi^+) = -0.01 \pm 0.13$
$A_{CP}(B^+ \to \psi(2S)K^+) = -0.037 \pm 0.025$
$A_{CP}(B^+ \to \overline{D}^0 K^+) = 0.04 \pm 0.07$
$A_{CP}(B^+ \to D_{CP(+1)} K^+) = 0.06 \pm 0.19$
$A_{CP}(B^+ \to D_{CP(-1)} K^+) = -0.19 \pm 0.18$
$A_{CP}(B^+ \to \pi^+\pi^0) = 0.05 \pm 0.15$
$A_{CP}(B^+ \to K^+\pi^0) = -0.10 \pm 0.08$
$A_{CP}(B^+ \to K_S^0\pi^+) = 0.03 \pm 0.08$ (S = 1.1)
$A_{CP}(B^+ \to \pi^+\pi^-\pi^+) = -0.39 \pm 0.35$
$A_{CP}(B^+ \to \rho^+\rho^0) = -0.09 \pm 0.16$
$A_{CP}(B^+ \to K^+\pi^-\pi^+) = 0.01 \pm 0.08$
$A_{CP}(B^+ \to K^+K^-K^+) = 0.02 \pm 0.08$
$A_{CP}(B^+ \to K^+\eta') = 0.009 \pm 0.035$
$A_{CP}(B^+ \to \omega\pi^+) = -0.21 \pm 0.19$
$A_{CP}(B^+ \to \omega K^+) = -0.21 \pm 0.28$
$A_{CP}(B^+ \to \phi K^+) = 0.03 \pm 0.07$
$A_{CP}(B^+ \to \phi K^*(892)^+) = 0.09 \pm 0.15$
$A_{CP}(B^+ \to \rho^0 K^*(892)^+) = 0.20 \pm 0.31$

B^- modes are charge conjugates of the modes below. Modes which do not identify the charge state of the B are listed in the $B^\pm/B^0$ ADMIXTURE section.

The branching fractions listed below assume 50% $B^0\overline{B}^0$ and 50% B^+B^- production at the $\Upsilon(4S)$. We have attempted to bring older measurements up to date by rescaling their assumed $\Upsilon(4S)$ production ratio to 50:50 and their assumed D, D_s, D^*, and ψ branching ratios to current values whenever this would affect our averages and best limits significantly.

Indentation is used to indicate a subchannel of a previous reaction. All resonant subchannels have been corrected for resonance branching fractions to the final state so the sum of the subchannel branching fractions can exceed that of the final state.

For inclusive branching fractions, *e.g.*, $B \to D^\pm$ anything, the values usually are multiplicities, not branching fractions. They can be greater than one.

B^+ DECAY MODES	Fraction (Γ_j/Γ)	Scale factor/ Confidence level	p (MeV/c)
Semileptonic and leptonic modes			
$\ell^+\nu_\ell$ anything	[rr] (10.2 ±0.9) %		–
$\overline{D}^0\ell^+\nu_\ell$	[rr] (2.15±0.22) %		2310
$\overline{D}^*(2007)^0\ell^+\nu_\ell$	[rr] (6.5 ±0.5) %		2258
$\overline{D}_1(2420)^0\ell^+\nu_\ell$	(5.6 ±1.6) × 10^{-3}		2084
$\overline{D}_2^*(2460)^0\ell^+\nu_\ell$	< 8 × 10^{-3}	CL=90%	2067
$\pi^0 e^+\nu_e$	(9.0 ±2.8) × 10^{-5}		2638
$\eta\ell^+\nu_\ell$	(8 ±4) × 10^{-5}		2611
$\omega\ell^+\nu_\ell$	[rr] < 2.1 × 10^{-4}	CL=90%	2582
$\rho^0\ell^+\nu_\ell$	[rr] ($1.34^{+0.32}_{-0.35}$) × 10^{-4}		2583
$p\overline{p}e^+\nu_e$	< 5.2 × 10^{-3}	CL=90%	2467
$e^+\nu_e$	< 1.5 × 10^{-5}	CL=90%	2640
$\mu^+\nu_\mu$	< 2.1 × 10^{-5}	CL=90%	2638
$\tau^+\nu_\tau$	< 5.7 × 10^{-4}	CL=90%	2340
$e^+\nu_e\gamma$	< 2.0 × 10^{-4}	CL=90%	2640
$\mu^+\nu_\mu\gamma$	< 5.2 × 10^{-5}	CL=90%	2638
D, D^*, or D_s modes			
$\overline{D}^0\pi^+$	(4.98±0.29) × 10^{-3}		2308
$\overline{D}^0\rho^+$	(1.34±0.18) %		2236
$\overline{D}^0K^+$	(3.7 ±0.6) × 10^{-4}	S=1.1	2280
$\overline{D}^0K^*(892)^+$	(6.1 ±2.3) × 10^{-4}		2213
$\overline{D}^0K^+\overline{K}^0$	(5.5 ±1.6) × 10^{-4}		2189
$\overline{D}^0K^+\overline{K}^*(892)^0$	(7.5 ±1.7) × 10^{-4}		2071
$\overline{D}^0\pi^+\pi^+\pi^-$	(1.1 ±0.4) %		2289
$\overline{D}^0\pi^+\pi^+\pi^-$ nonresonant	(5 ±4) × 10^{-3}		2289
$\overline{D}^0\pi^+\rho^0$	(4.2 ±3.0) × 10^{-3}		2207
$\overline{D}^0a_1(1260)^+$	(5 ±4) × 10^{-3}		2123
$\overline{D}^0\omega\pi^+$	(4.1 ±0.9) × 10^{-3}		2206
$D^*(2010)^-\pi^+\pi^+$	(2.1 ±0.6) × 10^{-3}		2247
$D^-\pi^+\pi^+$	< 1.4 × 10^{-3}	CL=90%	2299
$\overline{D}^*(2007)^0\pi^+$	(4.6 ±0.4) × 10^{-3}		2256
$\overline{D}^*(2007)^0\omega\pi^+$	(4.5 ±1.2) × 10^{-3}		2149
$\overline{D}^*(2007)^0\rho^+$	(9.8 ±1.7) × 10^{-3}		2181
$\overline{D}^*(2007)^0K^+$	(3.6 ±1.0) × 10^{-4}		2227
$\overline{D}^*(2007)^0K^*(892)^+$	(7.2 ±3.4) × 10^{-4}		2156

$\overline{D}^*(2007)^0 K^+ \overline{K}^0$	< 1.06	$\times 10^{-3}$	CL=90%	2132
$\overline{D}^*(2007)^0 K^+ K^*(892)^0$	$(1.5 \pm 0.4) \times 10^{-3}$			2008
$\overline{D}^*(2007)^0 \pi^+ \pi^+ \pi^-$	$(9.4 \pm 2.6) \times 10^{-3}$			2236
$\overline{D}^*(2007)^0 a_1(1260)^+$	(1.9 ± 0.5) %			2062
$\overline{D}^*(2007)^0 \pi^- \pi^+ \pi^+ \pi^0$	(1.8 ± 0.4) %			2219
$D^*(2010)^+ \pi^0$	< 1.7	$\times 10^{-4}$	CL=90%	2255
$\overline{D}^*(2010)^+ K^0$	< 9.5	$\times 10^{-5}$	CL=90%	2225
$D^*(2010)^- \pi^+ \pi^+ \pi^0$	(1.5 ± 0.7) %			2235
$D^*(2010)^- \pi^+ \pi^+ \pi^+ \pi^-$	< 1	%	CL=90%	2217
$\overline{D}_1^*(2420)^0 \pi^+$	$(1.5 \pm 0.6) \times 10^{-3}$		S=1.3	2081
$\overline{D}_1^*(2420)^0 \rho^+$	< 1.4	$\times 10^{-3}$	CL=90%	1995
$\overline{D}_2^*(2460)^0 \pi^+$	< 1.3	$\times 10^{-3}$	CL=90%	2064
$\overline{D}_2^*(2460)^0 \rho^+$	< 4.7	$\times 10^{-3}$	CL=90%	1977
$\overline{D}^0 D_s^+$	(1.3 ± 0.4) %			1815
$\overline{D}^0 D_{sJ}(2317)^+$	seen			1605
$\overline{D}^0 D_{sJ}(2457)^+$	seen			–
$\overline{D}^0 D_{sJ}(2536)^+$	not seen			1447
$\overline{D}^*(2007)^0 D_{sJ}(2536)^+$	not seen			1338
$\overline{D}^0 D_{sJ}(2573)^+$	not seen			1417
$\overline{D}^*(2007)^0 D_{sJ}(2573)^+$	not seen			1306
$\overline{D}^0 D_s^{*+}$	$(9 \pm 4) \times 10^{-3}$			1734
$\overline{D}^*(2007)^0 D_s^+$	(1.2 ± 0.5) %			1737
$\overline{D}^*(2007)^0 D_s^{*+}$	(2.7 ± 1.0) %			1651
$D_s^{(*)+} \overline{D}^{**0}$	(2.7 ± 1.2) %			–
$\overline{D}^*(2007)^0 D^*(2010)^+$	< 1.1	%	CL=90%	1713
$\overline{D}^0 D^*(2010)^+ + \overline{D}^*(2007)^0 D^+$	< 1.3	%	CL=90%	1792
$\overline{D}^0 D^+$	< 6.7	$\times 10^{-3}$	CL=90%	1866
$\overline{D}^0 D^+ K^0$	< 2.8	$\times 10^{-3}$	CL=90%	1571
$\overline{D}^*(2007)^0 D^+ K^0$	< 6.1	$\times 10^{-3}$	CL=90%	1475
$\overline{D}^0 \overline{D}^*(2010)^+ K^0$	$(5.2 \pm 1.2) \times 10^{-3}$			1476
$\overline{D}^*(2007)^0 D^*(2010)^+ K^0$	$(7.8 \pm 2.6) \times 10^{-3}$			1362
$\overline{D}^0 D^0 K^+$	$(1.9 \pm 0.4) \times 10^{-3}$			1577
$\overline{D}^*(2010)^0 D^0 K^+$	< 3.8	$\times 10^{-3}$	CL=90%	–
$\overline{D}^0 D^*(2007)^0 K^+$	$(4.7 \pm 1.0) \times 10^{-3}$			1481
$\overline{D}^*(2007)^0 D^*(2007)^0 K^+$	$(5.3 \pm 1.6) \times 10^{-3}$			1368
$D^- D^+ K^+$	< 4	$\times 10^{-4}$	CL=90%	1571
$D^- D^*(2010)^+ K^+$	< 7	$\times 10^{-4}$	CL=90%	1475
$D^*(2010)^- D^+ K^+$	$(1.5 \pm 0.4) \times 10^{-3}$			1475
$D^*(2010)^- D^*(2010)^+ K^+$	< 1.8	$\times 10^{-3}$	CL=90%	1363
$(\overline{D} + \overline{D}^*)(D + D^*) K$	(3.5 ± 0.6) %			–
$D_s^+ \pi^0$	< 2.0	$\times 10^{-4}$	CL=90%	2270
$D_s^{*+} \pi^0$	< 3.3	$\times 10^{-4}$	CL=90%	2215
$D_s^+ \eta$	< 5	$\times 10^{-4}$	CL=90%	2235
$D_s^{*+} \eta$	< 8	$\times 10^{-4}$	CL=90%	2178
$D_s^+ \rho^0$	< 4	$\times 10^{-4}$	CL=90%	2197
$D_s^{*+} \rho^0$	< 5	$\times 10^{-4}$	CL=90%	2138
$D_s^+ \omega$	< 5	$\times 10^{-4}$	CL=90%	2195
$D_s^{*+} \omega$	< 7	$\times 10^{-4}$	CL=90%	2136
$D_s^+ a_1(1260)^0$	< 2.2	$\times 10^{-3}$	CL=90%	2079
$D_s^{*+} a_1(1260)^0$	< 1.6	$\times 10^{-3}$	CL=90%	2014
$D_s^+ \phi$	< 3.2	$\times 10^{-4}$	CL=90%	2141
$D_s^{*+} \phi$	< 4	$\times 10^{-4}$	CL=90%	2079
$D_s^+ \overline{K}^0$	< 1.1	$\times 10^{-3}$	CL=90%	2241
$D_s^{*+} \overline{K}^0$	< 1.1	$\times 10^{-3}$	CL=90%	2184
$D_s^+ \overline{K}^*(892)^0$	< 5	$\times 10^{-4}$	CL=90%	2172
$D_s^{*+} \overline{K}^*(892)^0$	< 4	$\times 10^{-4}$	CL=90%	2112
$D_s^- \pi^+ K^+$	< 8	$\times 10^{-4}$	CL=90%	2222
$D_s^{*-} \pi^+ K^+$	< 1.2	$\times 10^{-3}$	CL=90%	2164
$D_s^- \pi^+ K^*(892)^+$	< 6	$\times 10^{-3}$	CL=90%	2138
$D_s^{*-} \pi^+ K^*(892)^+$	< 8	$\times 10^{-3}$	CL=90%	2076

Charmonium modes

$\eta_c K^+$	$(9.0 \pm 2.7) \times 10^{-4}$			1754
$J/\psi(1S) K^+$	$(1.00 \pm 0.04) \times 10^{-3}$			1683
$J/\psi(1S) K^+ \pi^+ \pi^-$	$(7.7 \pm 2.0) \times 10^{-4}$			1612
$X(3872) K^+$	seen			–
$J/\psi(1S) K^*(892)^+$	$(1.35 \pm 0.10) \times 10^{-3}$			1571
$J/\psi(1S) K(1270)^+$	$(1.8 \pm 0.5) \times 10^{-3}$			1390
$J/\psi(1S) K(1400)^+$	< 5	$\times 10^{-4}$	CL=90%	1308
$J/\psi(1S) \phi K^+$	$(5.2 \pm 1.7) \times 10^{-5}$		S=1.2	1227
$J/\psi(1S) \pi^+$	$(4.0 \pm 0.5) \times 10^{-5}$			1727
$J/\psi(1S) \rho^+$	< 7.7	$\times 10^{-4}$	CL=90%	1611
$J/\psi(1S) a_1(1260)^+$	< 1.2	$\times 10^{-3}$	CL=90%	1414
$J/\psi(1S) p \overline{\Lambda}$	$(1.2 \, ^{+0.9}_{-0.6}) \times 10^{-5}$			567
$\psi(2S) K^+$	$(6.8 \pm 0.4) \times 10^{-4}$			1284
$\psi(2S) K^*(892)^+$	$(9.2 \pm 2.2) \times 10^{-4}$			1115
$\psi(2S) K^+ \pi^+ \pi^-$	$(1.9 \pm 1.2) \times 10^{-3}$			1178
$\chi_{c0}(1P) K^+$	$(6.0 \, ^{+2.4}_{-2.1}) \times 10^{-4}$			1478
$\chi_{c1}(1P) K^+$	$(6.8 \pm 1.2) \times 10^{-4}$			1411
$\chi_{c1}(1P) K^*(892)^+$	< 2.1	$\times 10^{-3}$	CL=90%	1265

K or K^* modes

$K^0 \pi^+$	$(1.88 \pm 0.21) \times 10^{-5}$			2614
$K^+ \pi^0$	$(1.29 \pm 0.12) \times 10^{-5}$			2615
$\eta' K^+$	$(7.8 \pm 0.5) \times 10^{-5}$			2528
$\eta' K^*(892)^+$	< 3.5	$\times 10^{-5}$	CL=90%	2472
ηK^+	< 6.9	$\times 10^{-6}$	CL=90%	2588
$\eta K^*(892)^+$	$(2.6 \, ^{+1.0}_{-0.9}) \times 10^{-5}$			2534
ωK^+	$(9.2 \, ^{+2.8}_{-2.5}) \times 10^{-6}$			2557
$\omega K^*(892)^+$	< 8.7	$\times 10^{-5}$	CL=90%	2503
$K^*(892)^0 \pi^+$	$(1.9 \, ^{+0.6}_{-0.8}) \times 10^{-5}$			2562
$K^*(892)^+ \pi^0$	< 3.1	$\times 10^{-5}$	CL=90%	2562
$K^+ \pi^- \pi^+$	$(5.7 \pm 0.4) \times 10^{-5}$			2609
$K^+ \pi^- \pi^+$ nonresonant	< 2.8	$\times 10^{-5}$	CL=90%	2609
$K^+ \rho^0$	< 1.2	$\times 10^{-5}$	CL=90%	2558
$K_2^*(1430)^0 \pi^+$	< 6.8	$\times 10^{-4}$	CL=90%	2445
$K^- \pi^+ \pi^+$	< 1.8	$\times 10^{-6}$	CL=90%	2609
$K^- \pi^+ \pi^+$ nonresonant	< 5.6	$\times 10^{-5}$	CL=90%	2609
$K_1(1400)^0 \pi^+$	< 2.6	$\times 10^{-3}$	CL=90%	2451
$K^0 \pi^+ \pi^0$	< 6.6	$\times 10^{-5}$	CL=90%	2609
$K^0 \rho^+$	< 4.8	$\times 10^{-5}$	CL=90%	2558
$K^*(892)^+ \pi^+ \pi^-$	< 1.1	$\times 10^{-3}$	CL=90%	2556
$K^*(892)^+ \rho^0$	$(1.1 \pm 0.4) \times 10^{-5}$			2504
$K^*(892)^+ K^*(892)^0$	< 7.1	$\times 10^{-5}$	CL=90%	2484
$K_1(1400)^+ \rho^0$	< 7.8	$\times 10^{-4}$	CL=90%	2387
$K_2^*(1430)^+ \rho^0$	< 1.5	$\times 10^{-3}$	CL=90%	2381
$K^+ \overline{K}^0$	< 2.0	$\times 10^{-6}$	CL=90%	2593
$\overline{K}^0 K^+ \pi^0$	< 2.4	$\times 10^{-5}$	CL=90%	2578
$K^+ K_S^0 K_S^0$	$(1.34 \pm 0.24) \times 10^{-5}$			2521
$K_S^0 K_S^0 \pi^+$	< 3.2	$\times 10^{-6}$	CL=90%	2577
$K^+ K^- \pi^+$	< 6.3	$\times 10^{-6}$	CL=90%	2578
$K^+ K^- \pi^+$ nonresonant	< 7.5	$\times 10^{-5}$	CL=90%	2578
$K^+ K^+ \pi^-$	< 1.3	$\times 10^{-6}$	CL=90%	2578
$K^+ K^+ \pi^-$ nonresonant	< 8.79	$\times 10^{-5}$	CL=90%	2578
$K^+ K^*(892)^0$	< 5.3	$\times 10^{-6}$	CL=90%	2540
$K^+ K^- K^+$	$(3.08 \pm 0.21) \times 10^{-5}$			2522
$K^+ \phi$	$(9.3 \pm 1.0) \times 10^{-6}$		S=1.3	2516
$K^+ K^- K^+$ nonresonant	< 3.8	$\times 10^{-5}$	CL=90%	2522
$K^*(892)^+ K^+ K^-$	< 1.6	$\times 10^{-3}$	CL=90%	2466
$K^*(892)^+ \phi$	$(9.6 \pm 3.0) \times 10^{-6}$		S=1.9	2460
$K_1(1400)^+ \phi$	< 1.1	$\times 10^{-3}$	CL=90%	2339
$K_2^*(1430)^+ \phi$	< 3.4	$\times 10^{-3}$	CL=90%	2332
$K^+ \phi \phi$	$(2.6 \, ^{+1.1}_{-0.9}) \times 10^{-6}$			2306
$K^*(892)^+ \gamma$	$(3.8 \pm 0.5) \times 10^{-5}$			2564
$K_1(1270)^+ \gamma$	< 9.9	$\times 10^{-5}$	CL=90%	2486
$\phi K^+ \gamma$	$(3.4 \pm 1.0) \times 10^{-6}$			2516
$K^+ \pi^- \pi^+ \gamma$	$(2.4 \, ^{+0.6}_{-0.5}) \times 10^{-5}$			2609
$K^*(892)^0 \pi^+ \gamma$	$(2.0 \, ^{+0.7}_{-0.6}) \times 10^{-5}$			2562
$K^+ \rho^0 \gamma$	< 2.0	$\times 10^{-5}$	CL=90%	2558
$K^+ \pi^- \pi^+ \gamma$ nonresonant	< 9.2	$\times 10^{-6}$	CL=90%	2609
$K_1(1400)^+ \gamma$	< 5.0	$\times 10^{-5}$	CL=90%	2453
$K_2^*(1430)^+ \gamma$	< 1.4	$\times 10^{-3}$	CL=90%	2447
$K^*(1680)^+ \gamma$	< 1.9	$\times 10^{-3}$	CL=90%	2360
$K_3^*(1780)^+ \gamma$	< 5.5	$\times 10^{-3}$	CL=90%	2341
$K_4^*(2045)^+ \gamma$	< 9.9	$\times 10^{-3}$	CL=90%	2243

Light unflavored meson modes

$\rho^+ \gamma$	< 2.1	$\times 10^{-6}$	CL=90%	2583
$\pi^+ \pi^0$	$(5.6 \, ^{+0.9}_{-1.1}) \times 10^{-6}$			2636
$\pi^+ \pi^+ \pi^-$	$(1.1 \pm 0.4) \times 10^{-5}$			2630
$\rho^0 \pi^+$	$(8.6 \pm 2.0) \times 10^{-6}$			2581
$\pi^+ f_0(980)$	< 1.4	$\times 10^{-4}$	CL=90%	2547
$\pi^+ f_2(1270)$	< 2.4	$\times 10^{-4}$	CL=90%	2483
$\pi^+ \pi^- \pi^+$ nonresonant	< 4.1	$\times 10^{-5}$	CL=90%	2630

Meson Summary Table

$\pi^+\pi^0\pi^0$	< 8.9	$\times 10^{-4}$	CL=90%	2631
$\rho^+\pi^0$	< 4.3	$\times 10^{-5}$	CL=90%	2581
$\pi^+\pi^-\pi^+\pi^0$	< 4.0	$\times 10^{-3}$	CL=90%	2621
$\rho^+\rho^0$	(2.6 ± 0.6)	$\times 10^{-5}$		2523
$a_1(1260)^+\pi^0$	< 1.7	$\times 10^{-3}$	CL=90%	2494
$a_1(1260)^0\pi^+$	< 9.0	$\times 10^{-4}$	CL=90%	2494
$\omega\pi^+$	(6.4 $^{+1.8}_{-1.6}$)	$\times 10^{-6}$	S=1.3	2580
$\omega\rho^+$	< 6.1	$\times 10^{-5}$	CL=90%	2522
$\eta\pi^+$	< 5.7	$\times 10^{-6}$	CL=90%	2609
$\eta'\pi^+$	< 7.0	$\times 10^{-6}$	CL=90%	2551
$\eta'\rho^+$	< 3.3	$\times 10^{-5}$	CL=90%	2492
$\eta\rho^+$	< 1.5	$\times 10^{-5}$	CL=90%	2553
$\phi\pi^+$	< 4.1	$\times 10^{-7}$	CL=90%	2539
$\phi\rho^+$	< 1.6	$\times 10^{-5}$		2480
$\pi^+\pi^+\pi^+\pi^-\pi^-$	< 8.6	$\times 10^{-4}$	CL=90%	2608
$\rho^0 a_1(1260)^+$	< 6.2	$\times 10^{-4}$	CL=90%	2433
$\rho^0 a_2(1320)^+$	< 7.2	$\times 10^{-4}$	CL=90%	2410
$\pi^+\pi^+\pi^+\pi^-\pi^-\pi^0$	< 6.3	$\times 10^{-3}$	CL=90%	2592
$a_1(1260)^+ a_1(1260)^0$	< 1.3	%	CL=90%	2335

Charged particle ($h^\pm$) modes

$h^\pm = K^\pm$ or $\pi^\pm$

$h^+\pi^0$	(1.6 $^{+0.7}_{-0.6}$)	$\times 10^{-5}$		2636
ωh^+	(1.38 $^{+0.27}_{-0.24}$)	$\times 10^{-5}$		2580
$h^+ X^0$ (Familon)	< 4.9	$\times 10^{-5}$	CL=90%	–

Baryon modes

$p\overline{p}\pi^+$	< 3.7	$\times 10^{-6}$	CL=90%	2439
$p\overline{p}\pi^+$ nonresonant	< 5.3	$\times 10^{-5}$	CL=90%	2439
$p\overline{p}\pi^+\pi^+\pi^-$	< 5.2	$\times 10^{-4}$	CL=90%	2369
$p\overline{p}K^+$	(4.3 $^{+1.2}_{-1.0}$)	$\times 10^{-6}$		2348
$p\overline{p}K^+$ nonresonant	< 8.9	$\times 10^{-5}$	CL=90%	2348
$p\overline{\Lambda}$	< 1.5	$\times 10^{-6}$	CL=90%	2430
$p\overline{\Lambda}\pi^+\pi^-$	< 2.0	$\times 10^{-4}$	CL=90%	2367
$\overline{\Delta}^0 p$	< 3.8	$\times 10^{-4}$	CL=90%	2402
$\Delta^{++}\overline{p}$	< 1.5	$\times 10^{-4}$	CL=90%	2402
$D^+ p\overline{p}$	< 1.5	$\times 10^{-5}$	CL=90%	1860
$D^*(2010)^+ p\overline{p}$	< 1.5	$\times 10^{-5}$	CL=90%	1786
$\overline{\Lambda}_c^- p\pi^+$	(2.1 ± 0.7)	$\times 10^{-4}$		1981
$\overline{\Lambda}_c^- p\pi^+\pi^0$	(1.8 ± 0.6)	$\times 10^{-3}$		1936
$\overline{\Lambda}_c^- p\pi^+\pi^+\pi^-$	(2.3 ± 0.7)	$\times 10^{-3}$		1881
$\overline{\Lambda}_c^- p\pi^+\pi^+\pi^-\pi^0$	< 1.34	%	CL=90%	1823
$\overline{\Sigma}_c(2455)^0 p$	< 8	$\times 10^{-5}$	CL=90%	1939
$\overline{\Sigma}_c(2520)^0 p$	< 4.6	$\times 10^{-5}$	CL=90%	1905
$\overline{\Sigma}_c(2455)^0 p\pi^0$	(4.4 ± 1.8)	$\times 10^{-4}$		1897
$\overline{\Sigma}_c(2455)^0 p\pi^-\pi^+$	(4.4 ± 1.7)	$\times 10^{-4}$		1845
$\overline{\Sigma}_c(2455)^{--} p\pi^+\pi^+$	(2.8 ± 1.2)	$\times 10^{-4}$		1845
$\overline{\Lambda}_c(2593)^- / \overline{\Lambda}_c(2625)^- p\pi^+$	< 1.9	$\times 10^{-4}$	CL=90%	–

Lepton Family number (LF) or Lepton number (L) violating modes, or $\Delta B = 1$ weak neutral current ($B1$) modes

$\pi^+ e^+ e^-$	$B1$	< 3.9	$\times 10^{-3}$	CL=90%	2638
$\pi^+\mu^+\mu^-$	$B1$	< 9.1	$\times 10^{-3}$	CL=90%	2633
$K^+ e^+ e^-$	$B1$	(6.3 $^{+1.9}_{-1.7}$)	$\times 10^{-7}$		2616
$K^+\mu^+\mu^-$	$B1$	(4.5 $^{+1.4}_{-1.2}$)	$\times 10^{-7}$		2612
$K^+\ell^+\ell^-$	$B1$	[rr] (5.3 ± 1.1)	$\times 10^{-7}$		2616
$K^+\overline{\nu}\nu$	$B1$	< 2.4	$\times 10^{-4}$	CL=90%	2616
$K^*(892)^+ e^+ e^-$	$B1$	< 4.6	$\times 10^{-6}$	CL=90%	2564
$K^*(892)^+\mu^+\mu^-$	$B1$	< 2.2	$\times 10^{-6}$	CL=90%	2560
$K^*(892)^+\ell^+\ell$	$B1$	[rr] < 2.2	$\times 10^{-6}$	CL=90%	2564
$\pi^+ e^+\mu^-$	LF	< 6.4	$\times 10^{-3}$	CL=90%	2637
$\pi^+ e^-\mu^+$	LF	< 6.4	$\times 10^{-3}$	CL=90%	2637
$K^+ e^+\mu^-$	LF	< 8	$\times 10^{-7}$	CL=90%	2615
$K^+ e^-\mu^+$	LF	< 6.4	$\times 10^{-3}$	CL=90%	2615
$K^*(892)^+ e^\pm\mu^\mp$	LF	< 7.9	$\times 10^{-6}$	CL=90%	2563
$\pi^- e^+ e^+$	L	< 1.6	$\times 10^{-6}$	CL=90%	2638
$\pi^-\mu^+\mu^+$	L	< 1.4	$\times 10^{-6}$	CL=90%	2633
$\pi^- e^+\mu^+$	L	< 1.3	$\times 10^{-6}$	CL=90%	2637
$\rho^- e^+ e^+$	L	< 2.6	$\times 10^{-6}$	CL=90%	2583
$\rho^-\mu^+\mu^+$	L	< 5.0	$\times 10^{-6}$	CL=90%	2578
$\rho^- e^+\mu^+$	LF	< 3.3	$\times 10^{-6}$	CL=90%	2581
$K^- e^+ e^+$	L	< 1.0	$\times 10^{-6}$	CL=90%	2616
$K^-\mu^+\mu^+$	L	< 1.8	$\times 10^{-6}$	CL=90%	2612
$K^- e^+\mu^+$	L	< 2.0	$\times 10^{-6}$	CL=90%	2615
$K^*(892)^- e^+ e^+$	L	< 2.8	$\times 10^{-6}$	CL=90%	2564
$K^*(892)^-\mu^+\mu^+$	L	< 8.3	$\times 10^{-6}$	CL=90%	2560
$K^*(892)^- e^+\mu^+$	LF	< 4.4	$\times 10^{-6}$	CL=90%	2563

B^0

$I(J^P) = \frac{1}{2}(0^-)$

I, J, P need confirmation. Quantum numbers shown are quark-model predictions.

Mass $m_{B^0} = 5279.4 \pm 0.5$ MeV
$m_{B^0} - m_{B^\pm} = 0.33 \pm 0.28$ MeV (S = 1.1)
Mean life $\tau_{B^0} = (1.536 \pm 0.014) \times 10^{-12}$ s
$c\tau = 460\ \mu$m
$\tau_{B^+}/\tau_{B^0} = 1.086 \pm 0.017$ (direct measurements)

B^0-$\overline{B}^0$ mixing parameters

$\chi_d = 0.186 \pm 0.004$
$\Delta m_{B^0} = m_{B^0_H} - m_{B^0_L} = (0.502 \pm 0.007) \times 10^{12}\ \hbar\ \mathrm{s}^{-1}$
$= (3.304 \pm 0.046) \times 10^{-10}$ MeV
$x_d = \Delta m_{B^0}/\Gamma_{B^0} = 0.771 \pm 0.012$

CP violation parameters

$\mathrm{Re}(\epsilon_{B^0})/(1+|\epsilon_{B^0}|^2) = (0.5 \pm 3.1) \times 10^{-3}$
$A_{T/CP} = 0.005 \pm 0.018$
$A_{CP}(B^0 \to K^+\pi^-) = -0.09 \pm 0.04$
$A_{CP}(B^0 \to \rho^+\pi^-) = -0.18 \pm 0.09$
$A_{CP}(B^0 \to \rho^+ K^-) = 0.28 \pm 0.19$
$A_{CP}(B^0 \to K^*(892)^+\pi^-) = 0.26 \pm 0.35$
$A_{CP}(B^0 \to K^*(892)^0\phi) = 0.05 \pm 0.10$
$A_{CP}(B^0 \to D^*(2010)^+ D^-) = -0.03 \pm 0.12$
$C_{\pi\pi}(B^0 \to \pi^+\pi^-) = -0.51 \pm 0.23$ (S = 1.2)
$S_{\pi\pi}(B^0 \to \pi^+\pi^-) = -0.5 \pm 0.6$ (S = 2.3)
$C_{\rho\pi}(B^0 \to \rho^+\pi^-) = 0.36 \pm 0.18$
$S_{\rho\pi}(B^0 \to \rho^+\pi^-) = 0.19 \pm 0.24$
$C_{\eta'(958)K}(B^0 \to \eta'(958)K^0_S) = 0.04 \pm 0.13$
$S_{\eta'(958)K}(B^0 \to \eta'(958)K^0_S) = 0.27 \pm 0.21$
$C_{\phi K^0_S}(B^0 \to \phi K^0_S) = 0.15 \pm 0.30$
$S_{\phi K^0_S}(B^0 \to \phi K^0_S) = -1.0 \pm 0.5$
$C_{K^+K^-K^0_S}(B^0 \to K^+K^-K^0_S) = 0.17 \pm 0.16$
$S_{K^+K^-K^0_S}(B^0 \to K^+K^-K^0_S) = -0.51 \pm 0.26$
$C_{D^*(2010)^- D^+}(B^0 \to D^*(2010)^- D^+) = -0.2 \pm 0.4$
$S_{D^*(2010)^- D^+}(B^0 \to D^*(2010)^- D^+) = -0.2 \pm 0.7$
$C_{D^*(2010)^+ D^-}(B^0 \to D^*(2010)^+ D^-) = -0.5 \pm 0.4$
$S_{D^*(2010)^+ D^-}(B^0 \to D^*(2010)^+ D^-) = -0.8 \pm 0.8$
$C_{J/\psi(1S)\pi^0}(B^0 \to J/\psi(1S)\pi^0) = 0.4 \pm 0.4$
$S_{J/\psi(1S)\pi^0}(B^0 \to J/\psi(1S)\pi^0) = 0.1 \pm 0.5$
$\Delta C_{\rho\pi}(B^0 \to \rho^+\pi^-) = 0.28 \pm 0.19$
$\Delta S_{\rho\pi}(B^0 \to \rho^+\pi^-) = 0.15 \pm 0.25$
$|\lambda|(B^0 \to c\overline{c}K^0) = 0.949 \pm 0.045$
$|\lambda|(B^0 \to D^{*+}D^{*-}) = 0.75 \pm 0.19$
$\mathrm{Im}(\lambda)(B^0 \to D^{*+}D^{*-}) = 0.05 \pm 0.31$
$\sin(2\beta) = 0.731 \pm 0.056$

$\overline{B}^0$ modes are charge conjugates of the modes below. Reactions indicate the weak decay vertex and do not include mixing. Modes which do not identify the charge state of the B are listed in the $B^\pm/B^0$ ADMIXTURE section.

The branching fractions listed below assume 50% $B^0\overline{B}^0$ and 50% B^+B^- production at the $\Upsilon(4S)$. We have attempted to bring older measurements up to date by rescaling their assumed $\Upsilon(4S)$ production ratio to 50:50 and their assumed D, D_S, D^*, and ψ branching ratios to current values whenever this would affect our averages and best limits significantly.

Indentation is used to indicate a subchannel of a previous reaction. All resonant subchannels have been corrected for resonance branching fractions to the final state so the sum of the subchannel branching fractions can exceed that of the final state.

For inclusive branching fractions, *e.g.*, $B \to D^\pm$ anything, the values usually are multiplicities, not branching fractions. They can be greater than one.

B^0 DECAY MODES		Fraction (Γ_i/Γ)	Scale factor/ Confidence level	p (MeV/c)
$\ell^+ \nu_\ell$ anything	[rr]	(10.5 ±0.8) %		–
$D^- \ell^+ \nu_\ell$	[rr]	(2.14±0.20) %		2309
$D^*(2010)^- \ell^+ \nu_\ell$	[rr]	(5.44±0.23) %		2257
$\rho^- \ell^+ \nu_\ell$	[rr]	(2.6 ±0.7) × 10^{-4}		2583
$\pi^- \ell^+ \nu_\ell$	[rr]	(1.33±0.22) × 10^{-4}		2638
Inclusive modes				
K^+ anything		(78 ±8) %		–
D, D^*, or D_s modes				
$D^- \pi^+$		(2.76±0.25) × 10^{-3}		2306
$D^- \rho^+$		(7.7 ±1.3) × 10^{-3}		2235
$D^- K^*(892)^+$		(3.7 ±1.8) × 10^{-4}		2211
$D^- \omega \pi^+$		(2.8 ±0.6) × 10^{-3}		2204
$D^- K^+$		(2.0 ±0.6) × 10^{-4}		2279
$D^- K^+ \overline{K}^0$		< 3.1 × 10^{-4}	CL=90%	2188
$D^- K^+ \overline{K}^*(892)^0$		(8.8 ±1.9) × 10^{-4}		2070
$\overline{D}^0 \pi^0$		(2.7 ±0.8) × 10^{-4}		2308
$\overline{D}^0 \pi^+ \pi^-$		(8.0 ±1.6) × 10^{-4}		2301
$D^*(2010)^- \pi^+$		(2.76±0.21) × 10^{-3}		2255
$D^- \pi^+ \pi^+ \pi^-$		(8.0 ±2.5) × 10^{-3}		2287
($D^- \pi^+ \pi^+ \pi^-$) nonresonant		(3.9 ±1.9) × 10^{-3}		2287
$D^- \pi^+ \rho^0$		(1.1 ±1.0) × 10^{-3}		2206
$D^- a_1(1260)^+$		(6.0 ±3.3) × 10^{-3}		2121
$D^*(2010)^- \pi^+ \pi^0$		(1.5 ±0.5) %		2247
$D^*(2010)^- \rho^+$		(6.8 ±0.9) × 10^{-3}		2180
$D^*(2010)^- K^+$		(2.0 ±0.5) × 10^{-4}		2226
$D^*(2010)^- K^*(892)^+$		(3.8 ±1.5) × 10^{-4}		2155
$D^*(2010)^- K^+ \overline{K}^0$		< 4.7 × 10^{-4}	CL=90%	2131
$D^*(2010)^- K^+ \overline{K}^*(892)^0$		(1.29±0.33) × 10^{-3}		2007
$D^*(2010)^- \pi^+ \pi^+ \pi^-$		(7.6 ±1.8) × 10^{-3}	S=1.4	2235
($D^*(2010)^- \pi^+ \pi^+ \pi^-$) non-resonant		(0.0 ±2.5) × 10^{-3}		2235
$D^*(2010)^- \pi^+ \rho^0$		(5.7 ±3.2) × 10^{-3}		2150
$D^*(2010)^- a_1(1260)^+$		(1.30±0.27) %		2061
$D^*(2010)^- \pi^+ \pi^+ \pi^- \pi^0$		(1.76±0.27) %		2218
$D^*(2010)^+ \pi^+ \pi^- \pi^- \pi^0$		(1.8 ±0.7) %		2218
$D^*(2010)^- p \overline{p} \pi^+$		(6.5 ±1.6) × 10^{-4}		1707
$D^*(2010)^- p \overline{n}$		(1.5 ±0.4) × 10^{-3}		1785
$\overline{D}^*(2010)^- \omega \pi^+$		(2.9 ±0.5) × 10^{-3}		2148
$\overline{D}_2^*(2460)^- \pi^+$		< 2.2 × 10^{-3}	CL=90%	2064
$\overline{D}_2^*(2460)^- \rho^+$		< 4.9 × 10^{-3}	CL=90%	1977
$D^- D^+$		< 9.4 × 10^{-4}	CL=90%	1864
$D^- D_s^+$		(8.0 ±3.0) × 10^{-3}		1812
$D^*(2010)^- D_s^+$		(1.07±0.29) %		1735
$D^- D_s^{*+}$		(1.0 ±0.5) %		1732
$D^*(2010)^- D_s^{*+}$		(1.9 ±0.5) %		1649
$D^- D_{sJ}(2317)^+$		seen		1602
$D^- D_{sJ}(2457)^+$		seen		–
$D^- D_{sJ}(2536)^+$		not seen		1444
$D^*(2010)^- D_{sJ}(2536)^+$		not seen		1336
$D^- D_{sJ}(2573)^+$		not seen		1414
$D^*(2010)^- D_{sJ}(2573)^+$		not seen		1303
$D_s^+ \pi^-$		(2.7 ±1.0) × 10^{-5}		2270
$D_s^{*+} \pi^-$		< 4.1 × 10^{-5}	CL=90%	2215
$D_s^+ \rho^-$		< 7 × 10^{-4}	CL=90%	2197
$D_s^{*+} \rho^-$		< 8 × 10^{-4}	CL=90%	2138
$D_s^+ a_1(1260)^-$		< 2.6 × 10^{-3}	CL=90%	2080
$D_s^{*+} a_1(1260)^-$		< 2.2 × 10^{-3}	CL=90%	2015
$D_s^- K^+$		(3.8 ±1.3) × 10^{-5}		2242
$D_s^{*-} K^+$		< 2.5 × 10^{-5}	CL=90%	2185
$D_s^- K^*(892)^+$		< 9.9 × 10^{-4}	CL=90%	2172
$D_s^{*-} K^*(892)^+$		< 1.1 × 10^{-3}	CL=90%	2112
$D_s^- \pi^+ K^0$		< 5 × 10^{-3}	CL=90%	2222
$D_s^{*-} \pi^+ K^0$		< 3.1 × 10^{-3}	CL=90%	2164
$D_s^- \pi^+ K^*(892)^0$		< 4 × 10^{-3}	CL=90%	2138
$D_s^{*-} \pi^+ K^*(892)^0$		< 2.0 × 10^{-3}	CL=90%	2076
$\overline{D}^0 K^0$		(5.0 ±1.4) × 10^{-5}		2280
$\overline{D}^0 K^*(892)^0$		(4.8 ±1.2) × 10^{-5}		2213
$\overline{D}^0 \pi^0$		(2.91±0.28) × 10^{-4}		2308
$\overline{D}^0 \rho^0$		(2.9 ±1.1) × 10^{-4}		2237
$\overline{D}^0 \eta$		(2.2 ±0.5) × 10^{-4}	S=1.6	2274
$\overline{D}^0 \eta'$		(1.7 ±0.4) × 10^{-4}		2198
$\overline{D}^0 \omega$		(2.5 ±0.6) × 10^{-4}	S=1.5	2235
$D^0 K^*(892)^0$		< 1.8 × 10^{-5}	CL=90%	2213
$\overline{D}^{*0} \gamma$		< 5.0 × 10^{-5}	CL=90%	2258
$\overline{D}^*(2007)^0 \pi^0$		(2.7 ±0.5) × 10^{-4}		2256
$\overline{D}^*(2007)^0 \rho^0$		< 5.1 × 10^{-4}	CL=90%	2181
$\overline{D}^*(2007)^0 \eta$		(2.6 ±0.6) × 10^{-4}		2220
$\overline{D}^*(2007)^0 \eta'$		< 2.6 × 10^{-4}	CL=90%	2141
$\overline{D}^*(2007)^0 \pi^+ \pi^-$		(6.2 ±2.2) × 10^{-4}		2248
$\overline{D}^*(2007)^0 K^0$		< 6.6 × 10^{-5}	CL=90%	2227
$\overline{D}^*(2007)^0 K^*(892)^0$		< 6.9 × 10^{-5}	CL=90%	2157
$D^*(2007)^0 K^*(892)^0$		< 4.0 × 10^{-5}	CL=90%	2157
$D^*(2007)^0 \pi^+ \pi^+ \pi^- \pi^-$		(3.0 ±0.9) × 10^{-3}		2219
$D^*(2010)^+ D^*(2010)^-$		(8.7 ±1.8) × 10^{-4}		1711
$\overline{D}^*(2007)^0 \omega$		(4.2 ±1.1) × 10^{-4}		2180
$D^*(2010)^+ D^-$		< 6.3 × 10^{-4}	CL=90%	1790
$D^*(2010)^- D^+$ + $D^*(2010)^+ D^-$		(9.3 ±1.5) × 10^{-4}		1790
$D^*(2007)^0 \overline{D}^*(2007)^0$		< 2.7 %	CL=90%	1715
$D^- D^0 K^+$		(1.7 ±0.4) × 10^{-3}		1574
$D^- D^*(2007)^0 K^+$		(4.6 ±1.0) × 10^{-3}		1478
$D^*(2010)^- D^0 K^+$		(3.1 $^{+0.6}_{-0.5}$) × 10^{-3}		1479
$D^*(2010)^- D^*(2007)^0 K^+$		(1.18±0.20) %		1366
$D^- D^+ K^0$		< 1.7 × 10^{-3}	CL=90%	1568
$D^*(2010)^- D^+ K^0$ + $D^- D^*(2010)^+ K^0$		(6.5 ±1.6) × 10^{-3}		1473
$D^*(2010)^- D^*(2010)^+ K^0$		(8.8 ±1.9) × 10^{-3}		1360
$\overline{D}^0 D^0 K^0$		< 1.4 × 10^{-3}	CL=90%	1575
$\overline{D}^0 D^*(2007)^0 K^0$ + $\overline{D}^*(2007)^0 D^0 K^0$		< 3.7 × 10^{-3}	CL=90%	1478
$\overline{D}^*(2007)^0 D^*(2007)^0 K^0$		< 6.6 × 10^{-3}	CL=90%	1365
$(\overline{D}+\overline{D}^*)(D+D^*) K$		(4.3 ±0.7) %		–
Charmonium modes				
$\eta_c K^0$		(1.2 ±0.4) × 10^{-3}		1753
$\eta_c K^*(892)^0$		(1.6 ±0.7) × 10^{-3}		1648
$J/\psi(1S) K^0$		(8.5 ±0.5) × 10^{-4}		1683
$J/\psi(1S) K^+ \pi^-$		(1.2 ±0.6) × 10^{-3}		1652
$J/\psi(1S) K^*(892)^0$		(1.31±0.07) × 10^{-3}		1571
$J/\psi(1S) \phi K^0$		(9.4 ±2.6) × 10^{-5}		1224
$J/\psi(1S) K(1270)^0$		(1.3 ±0.5) × 10^{-3}		1390
$J/\psi(1S) \pi^0$		(2.2 ±0.4) × 10^{-5}		1728
$J/\psi(1S) \eta$		< 2.7 × 10^{-5}	CL=90%	1672
$J/\psi(1S) \pi^+ \pi^-$		(4.6 ±0.9) × 10^{-5}		1716
$J/\psi(1S) \rho^0$		(1.6 ±0.7) × 10^{-5}		1611
$J/\psi(1S) \omega$		< 2.7 × 10^{-4}	CL=90%	1609
$J/\psi(1S) \phi$		< 9.2 × 10^{-6}	CL=90%	1519
$J/\psi(1S) \eta'(958)$		< 6.3 × 10^{-5}	CL=90%	1546
$J/\psi(1S) K^0 \pi^+ \pi^-$		(1.0 ±0.4) × 10^{-3}		1611
$J/\psi(1S) K^0 \rho^0$		(5.4 ±3.0) × 10^{-4}		1390
$J/\psi(1S) K^*(892)^+ \pi^-$		(8 ±4) × 10^{-4}		1514
$J/\psi(1S) K^*(892)^0 \pi^+ \pi^-$		(6.6 ±2.2) × 10^{-4}		1447
$J/\psi(1S) p \overline{p}$		< 1.9 × 10^{-6}	CL=90%	862
$\psi(2S) K^0$		(6.2 ±0.7) × 10^{-4}		1283
$\psi(2S) K^+ \pi^-$		< 1 × 10^{-3}	CL=90%	1238
$\psi(2S) K^*(892)^0$		(8.0 ±1.3) × 10^{-4}		1116
$\chi_{c0}(1P) K^0$		< 5.0 × 10^{-4}	CL=90%	1477
$\chi_{c1}(1P) K^0$		(4.0 $^{+1.2}_{-1.0}$) × 10^{-4}		1411
$\chi_{c1}(1P) K^*(892)^0$		(4.1 ±1.5) × 10^{-4}		1265
K or K^* modes				
$K^+ \pi^-$		(1.85±0.11) × 10^{-5}	S=1.2	2615
$K^0 \pi^0$		(9.5 $^{+2.1}_{-1.9}$) × 10^{-6}		2614
$\eta' K^0$		(6.3 ±0.7) × 10^{-5}	S=1.1	2528
$\eta' K^*(892)^0$		< 2.4 × 10^{-5}	CL=90%	2472
$\eta K^*(892)^0$		(1.4 $^{+0.6}_{-0.5}$) × 10^{-5}		2534
ηK^0		< 9.3 × 10^{-6}	CL=90%	2587
ωK^0		< 1.3 × 10^{-5}	CL=90%	2557
$K^0_S X^0$ (Familon)		< 5.3 × 10^{-5}	CL=90%	–
$\omega K^*(892)^0$		< 2.3 × 10^{-5}	CL=90%	2503
$K^0 \overline{K}^0$		< 3.3 × 10^{-6}	CL=90%	2592
$K^0_S K^0_S K^0_S$		(4.2 $^{+1.8}_{-1.5}$) × 10^{-6}		2521
$K^+ \pi^- \pi^0$		< 4.0 × 10^{-5}	CL=90%	2609
$K^+ \rho^-$		(7.3 ±1.8) × 10^{-6}		2559
$K^0 \pi^+ \pi^-$		(4.7 ±0.7) × 10^{-5}		2609

Meson Summary Table

$K^0\rho^0$	<	3.9	$\times 10^{-5}$	CL=90%	2558
$K^0 f_0(980)$	<	3.6	$\times 10^{-4}$	CL=90%	2524
$K^*(892)^+\pi^-$		$(1.6\ ^{+0.6}_{-0.5})$	$\times 10^{-5}$		2562
$K^*(892)^0\pi^0$	<	3.6	$\times 10^{-6}$	CL=90%	2563
$K_2^*(1430)^+\pi^-$	<	1.8	$\times 10^{-5}$	CL=90%	2445
$K^0 K^-\pi^+$	<	2.1	$\times 10^{-5}$	CL=90%	2578
$K^+ K^-\pi^0$	<	1.9	$\times 10^{-5}$	CL=90%	2579
$K^0 K^+ K^-$		(2.8 ± 0.5)	$\times 10^{-5}$		2522
$K^0\phi$		$(8.6\ ^{+1.3}_{-1.1})$	$\times 10^{-6}$		2516
$K^-\pi^+\pi^+\pi^-$	[eee] <	2.3	$\times 10^{-4}$	CL=90%	2600
$K^*(892)^0\pi^+\pi^-$	<	1.4	$\times 10^{-3}$	CL=90%	2557
$K^*(892)^0\rho^0$	<	3.4	$\times 10^{-5}$	CL=90%	2504
$K^*(892)^0 f_0(980)$	<	1.7	$\times 10^{-4}$	CL=90%	2468
$K_1(1400)^+\pi^-$	<	1.1	$\times 10^{-3}$	CL=90%	2451
$K^- a_1(1260)^+$	[eee] <	2.3	$\times 10^{-4}$	CL=90%	2471
$K^*(892)^0 K^+ K^-$	<	6.1	$\times 10^{-4}$	CL=90%	2466
$K^*(892)^0\phi$		(1.07 ± 0.11)	$\times 10^{-5}$		2460
$\overline{K}^*(892)^0 K^*(892)^0$	<	2.2	$\times 10^{-5}$	CL=90%	2485
$K^*(892)^0 K^*(892)^0$	<	3.7	$\times 10^{-5}$	CL=90%	2485
$K^*(892)^+ K^*(892)^-$	<	1.41	$\times 10^{-4}$	CL=90%	2485
$K_1(1400)^0\rho^0$	<	3.0	$\times 10^{-3}$	CL=90%	2388
$K_1(1400)^0\phi$	<	5.0	$\times 10^{-3}$	CL=90%	2339
$K_2^*(1430)^0\rho^0$	<	1.1	$\times 10^{-3}$	CL=90%	2381
$K_2^*(1430)^0\phi$	<	1.4	$\times 10^{-3}$	CL=90%	2333
$K^*(892)^0\gamma$		(4.3 ± 0.4)	$\times 10^{-5}$		2564
$K^0\phi\gamma$	<	8.3	$\times 10^{-6}$	CL=90%	2516
$K^+\pi^-\gamma$		(4.6 ± 1.4)	$\times 10^{-6}$		2615
$K^*(1410)\gamma$	<	1.3	$\times 10^{-4}$	CL=90%	2450
$K^+\pi^-\gamma$ nonresonant	<	2.6	$\times 10^{-6}$	CL=90%	2615
$K_1(1270)^0\gamma$	<	7.0	$\times 10^{-3}$	CL=90%	2486
$K_1(1400)^0\gamma$	<	4.3	$\times 10^{-3}$	CL=90%	2453
$K_2^*(1430)^0\gamma$		(1.3 ± 0.5)	$\times 10^{-5}$		2447
$K^*(1680)^0\gamma$	<	2.0	$\times 10^{-3}$	CL=90%	2360
$K_3^*(1780)^0\gamma$	<	1.0	%	CL=90%	2341
$K_4^*(2045)^0\gamma$	<	4.3	$\times 10^{-3}$	CL=90%	2244

Light unflavored meson modes

$\rho^0\gamma$	<	1.2	$\times 10^{-6}$	CL=90%	2583
$\omega\gamma$	<	1.0	$\times 10^{-6}$	CL=90%	2582
$\phi\gamma$	<	3.3	$\times 10^{-6}$	CL=90%	2541
$\pi^+\pi^-$		(4.8 ± 0.5)	$\times 10^{-6}$		2636
$\pi^0\pi^0$		(1.9 ± 0.5)	$\times 10^{-6}$		2636
$\eta\pi^0$	<	2.9	$\times 10^{-6}$	CL=90%	2610
$\eta\eta$	<	1.8	$\times 10^{-5}$	CL=90%	2582
$\eta'\pi^0$	<	5.7	$\times 10^{-6}$	CL=90%	2551
$\eta'\eta'$	<	4.7	$\times 10^{-5}$	CL=90%	2460
$\eta'\eta$	<	2.7	$\times 10^{-5}$	CL=90%	2522
$\eta'\rho^0$	<	1.2	$\times 10^{-5}$	CL=90%	2492
$\eta\rho^0$	<	1.0	$\times 10^{-5}$	CL=90%	2553
$\omega\eta$	<	1.2	$\times 10^{-5}$	CL=90%	2552
$\omega\eta'$	<	6.0	$\times 10^{-5}$	CL=90%	2491
$\omega\rho^0$	<	1.1	$\times 10^{-5}$	CL=90%	2522
$\omega\omega$	<	1.9	$\times 10^{-5}$	CL=90%	2521
$\phi\pi^0$	<	5	$\times 10^{-6}$	CL=90%	2539
$\phi\eta$	<	9	$\times 10^{-6}$	CL=90%	2511
$\phi\eta'$	<	3.1	$\times 10^{-5}$	CL=90%	2447
$\phi\rho^0$	<	1.3	$\times 10^{-5}$	CL=90%	2480
$\phi\omega$	<	2.1	$\times 10^{-5}$	CL=90%	2479
$\phi\phi$	<	1.2	$\times 10^{-5}$	CL=90%	2435
$\pi^+\pi^-\pi^0$	<	7.2	$\times 10^{-4}$	CL=90%	2631
$\rho^0\pi^0$	<	5.3	$\times 10^{-6}$	CL=90%	2581
$\rho^\mp\pi^\pm$	[gg]	(2.28 ± 0.25)	$\times 10^{-5}$		2581
$\pi^+\pi^-\pi^+\pi^-$	<	2.3	$\times 10^{-4}$	CL=90%	2621
$\rho^0\rho^0$	<	2.1	$\times 10^{-6}$	CL=90%	2523
$a_1(1260)^\mp\pi^\pm$	[gg] <	4.9	$\times 10^{-4}$	CL=90%	2494
$a_2(1320)^\mp\pi^\pm$	[gg] <	3.0	$\times 10^{-4}$	CL=90%	2473
$\pi^+\pi^-\pi^0\pi^0$	<	3.1	$\times 10^{-3}$	CL=90%	2622
$\rho^+\rho^-$	<	2.2	$\times 10^{-3}$	CL=90%	2523
$a_1(1260)^0\pi^0$	<	1.1	$\times 10^{-3}$	CL=90%	2494
$\omega\pi^0$	<	3	$\times 10^{-6}$	CL=90%	2580
$\pi^+\pi^+\pi^-\pi^-\pi^0$	<	9.0	$\times 10^{-3}$	CL=90%	2609
$a_1(1260)^+\rho^-$	<	3.4	$\times 10^{-3}$	CL=90%	2433
$a_1(1260)^0\rho^0$	<	2.4	$\times 10^{-3}$	CL=90%	2433
$\pi^+\pi^+\pi^+\pi^-\pi^-\pi^-$	<	3.0	$\times 10^{-3}$	CL=90%	2592
$a_1(1260)^+ a_1(1260)^-$	<	2.8	$\times 10^{-3}$	CL=90%	2336
$\pi^+\pi^+\pi^+\pi^-\pi^-\pi^-\pi^0$	<	1.1	%	CL=90%	2572

Baryon modes

$p\overline{p}$	<	1.2	$\times 10^{-6}$	CL=90%	2467
$p\overline{p}\pi^+\pi^-$	<	2.5	$\times 10^{-4}$	CL=90%	2406
$p\overline{p}K^0$	<	7.2	$\times 10^{-6}$	CL=90%	2347
$p\overline{\Lambda}\pi^-$		$(4.0\ ^{+1.1}_{-1.0})$	$\times 10^{-6}$		2401
$p\overline{\Lambda}K^-$	<	8.2	$\times 10^{-7}$	CL=90%	2308
$p\overline{\Sigma}^0\pi^-$	<	3.8	$\times 10^{-6}$	CL=90%	2383
$\overline{\Lambda}\Lambda$	<	1.0	$\times 10^{-6}$	CL=90%	2392
$\Delta^0\overline{\Delta}^0$	<	1.5	$\times 10^{-3}$	CL=90%	2335
$\Delta^{++}\overline{\Delta}^{--}$	<	1.1	$\times 10^{-4}$	CL=90%	2335
$\overline{D}^0 p\overline{p}$		(1.18 ± 0.22)	$\times 10^{-4}$		1862
$\overline{D}^*(2007)^0 p\overline{p}$		(1.2 ± 0.4)	$\times 10^{-4}$		1788
$\overline{\Sigma}_c^{--}\Delta^{++}$	<	1.0	$\times 10^{-3}$	CL=90%	1840
$\overline{\Lambda}_c^-\, p\pi^+\pi^-$		(1.3 ± 0.4)	$\times 10^{-3}$		1934
$\overline{\Lambda}_c^- p$		(2.2 ± 0.8)	$\times 10^{-5}$		2021
$\overline{\Lambda}_c^- p\pi^0$	<	5.9	$\times 10^{-4}$	CL=90%	1982
$\overline{\Lambda}_c^- p\pi^+\pi^-\pi^0$	<	5.07	$\times 10^{-3}$	CL=90%	1883
$\overline{\Lambda}_c^- p\pi^+\pi^-\pi^+\pi^-$	<	2.74	$\times 10^{-3}$	CL=90%	1821
$\overline{\Sigma}_c(2520)^{--} p\pi^+$		(1.6 ± 0.7)	$\times 10^{-4}$		1861
$\overline{\Sigma}_c(2520)^0 p\pi^-$	<	1.21	$\times 10^{-4}$	CL=90%	1861
$\overline{\Sigma}_c(2455)^0 p\pi^-$		$(10\ \pm8)$	$\times 10^{-5}$	S=1.7	1896
$\overline{\Sigma}_c(2455)^{--} p\pi^+$		(2.8 ± 0.9)	$\times 10^{-4}$		1896
$\overline{\Lambda}_c(2593)^-\ /\ \overline{\Lambda}_c(2625)^- p$	<	1.1	$\times 10^{-4}$	CL=90%	–

Lepton Family number (*LF*) violating modes, or $\Delta B = 1$ weak neutral current (*B1*) modes

$\gamma\gamma$	*B1*	<	1.7	$\times 10^{-6}$	CL=90%	2640
e^+e^-	*B1*	<	1.9	$\times 10^{-7}$	CL=90%	2640
$\mu^+\mu^-$	*B1*	<	1.6	$\times 10^{-7}$	CL=90%	2638
$K^0 e^+e^-$	*B1*	<	5.4	$\times 10^{-7}$	CL=90%	2616
$K^0\mu^+\mu^-$	*B1*		$(5.6\ ^{+2.9}_{-2.4})$	$\times 10^{-7}$		2612
$K^0\ell^+\ell^-$	*B1*	[rr] <	6.8	$\times 10^{-7}$	CL=90%	2616
$K^*(892)^0 e^+e^-$	*B1*	<	2.4	$\times 10^{-6}$	CL=90%	2564
$K^*(892)^0\mu^+\mu^-$	*B1*		(1.3 ± 0.4)	$\times 10^{-6}$		2560
$K^*(892)^0\nu\overline{\nu}$	*B1*	<	1.0	$\times 10^{-3}$	CL=90%	2564
$K^*(892)^0\ell^+\ell^-$	*B1*	[rr]	(1.17 ± 0.30)	$\times 10^{-6}$		2564
$e^\pm\mu^\mp$	*LF*	[gg] <	1.7	$\times 10^{-7}$	CL=90%	2639
$K^0 e^\pm\mu^\mp$	*LF*	<	4.0	$\times 10^{-6}$	CL=90%	2615
$K^*(892)^0 e^\pm\mu^\mp$	*LF*	<	3.4	$\times 10^{-6}$	CL=90%	2563
$e^\pm\tau^\mp$	*LF*	[gg] <	5.3	$\times 10^{-4}$	CL=90%	2341
$\mu^\pm\tau^\mp$	*LF*	[gg] <	8.3	$\times 10^{-4}$	CL=90%	2339

$B^\pm/B^0$ ADMIXTURE

CP violation

$A_{CP}(B \to K^*(892)\gamma) = -0.01 \pm 0.07$

$A_{CP}(B \to s\gamma) = -0.08 \pm 0.11$

The branching fraction measurements are for an admixture of B mesons at the $\Upsilon(4S)$. The values quoted assume that $B(\Upsilon(4S) \to B\overline{B}) = 100\%$.

For inclusive branching fractions, *e.g.*, $B \to D^\pm$ anything, the values usually are multiplicities, not branching fractions. They can be greater than one.

$\overline{B}$ modes are charge conjugates of the modes below. Reactions indicate the weak decay vertex and do not include mixing.

***B* DECAY MODES**	Fraction (Γ_i/Γ)		Scale factor/ Confidence level	p (MeV/c)
Semileptonic and leptonic modes				
$B \to e^+\nu_e$ anything	[fff]	$(10.73\ \pm\ 0.28)$ %		–
$B \to \overline{p}e^+\nu_e$ anything	<	5.9×10^{-4}	CL=90%	–
$B \to \ell^+\nu_\ell$ anything	[rr,fff]	$(10.73\ \pm\ 0.28)$ %		–
$B \to D^-\ell^+\nu_\ell$ anything	[rr]	$(2.8\ \pm\ 0.9)$ %		–
$B \to \overline{D}^0\ell^+\nu_\ell$ anything	[rr]	$(7.2\ \pm\ 1.5)$ %		–
$B \to \overline{D}^{**}\ell^+\nu_\ell$	[rr,ggg]	$(2.7\ \pm\ 0.7)$ %		–
$B \to \overline{D}_1(2420)\ell^+\nu_\ell$ anything		$(7.4\ \pm\ 1.6) \times 10^{-3}$		–
$B \to D\pi\ell^+\nu_\ell$ anything + $D^*\pi\ell^+\nu_\ell$ anything		$(2.6\ \pm\ 0.5)$ %	S=1.5	–
$B \to D\pi\ell^+\nu_\ell$ anything		$(1.5\ \pm\ 0.6)$ %		–
$B \to D^*\pi\ell^+\nu_\ell$ anything		$(1.9\ \pm\ 0.4)$ %		–
$B \to \overline{D}_2^*(2460)\ell^+\nu_\ell$ anything	<	6.5×10^{-3}	CL=95%	–

$B \to D^{*-}\pi^+\ell^+\nu_\ell$ anything		(1.00 ± 0.34) %			–
$B \to D_s^-\ell^+\nu_\ell$ anything	[rr]	< 9	$\times 10^{-3}$	CL=90%	–
$B \to D_s^-\ell^+\nu_\ell K^+$ anything	[rr]	< 6	$\times 10^{-3}$	CL=90%	–
$B \to D_s^-\ell^+\nu_\ell K^0$ anything	[rr]	< 9	$\times 10^{-3}$	CL=90%	–
$B \to K^+\ell^+\nu_\ell$ anything	[rr]	(6.2 ± 0.6) %			–
$B \to K^-\ell^+\nu_\ell$ anything	[rr]	(10 ± 4) $\times 10^{-3}$			–
$B \to K^0/\overline{K}^0\ell^+\nu_\ell$ anything	[rr]	(4.5 ± 0.5) %			–

D, D^*, or D_s modes

$B \to D^\pm$ anything		(23.5 ± 1.9) %			–
$B \to D^0/\overline{D}^0$ anything		(64.0 ± 3.0) %		S=1.1	–
$B \to D^*(2010)^\pm$ anything		(22.5 ± 1.5) %			–
$B \to D^*(2007)^0$ anything		(26.0 ± 2.7) %			–
$B \to D_s^\pm$ anything	[gg]	(10.5 ± 2.6) %			–
$B \to D_s^{*\pm}\overline{D}^{(*)}$		(7.9 ± 2.2) %			–
$B \to \overline{D}^{(*)}D_{sJ}(2317)$		(4.2 ± 1.2) %			–
$B \to \overline{D}D_{sJ}(2317)$		seen			1605
$B \to \overline{D}D_{sJ}(2457)$		seen			–
$B \to D^{(*)}\overline{D}^{(*)}K^0 + D^{(*)}\overline{D}^{(*)}K^\pm$	[gg,hhh]	(7.1 $^{+\ 2.7}_{-\ 1.7}$) %			–
$b \to c\overline{c}s$		(22 ± 4) %			–
$B \to D_s^{(*)}\overline{D}^{(*)}$	[gg,hhh]	(4.9 ± 1.2) %			–
$B \to D^*D^*(2010)^\pm$	[gg]	< 5.9	$\times 10^{-3}$	CL=90%	1711
$B \to D\,D^*(2010)^\pm + D^*D^\pm$	[gg]	< 5.5	$\times 10^{-3}$	CL=90%	–
$B \to D\,D^\pm$	[gg]	< 3.1	$\times 10^{-3}$	CL=90%	1866
$B \to D_s^{(*)\pm}\overline{D}^{(*)}X(n\pi^\pm)$	[gg,hhh]	(9 $^{+\ 5}_{-\ 4}$) %			–
$B \to D^*(2010)\gamma$		< 1.1	$\times 10^{-3}$	CL=90%	2257
$B \to D_s^+\pi^-$, $D_s^{*+}\pi^-$, $D_s^+\rho^-$, $D_s^{*+}\rho^-$, $D_s^+\pi^0$, $D_s^{*+}\pi^0$, $D_s^+\eta$, $D_s^{*+}\eta$, $D_s^+\rho^0$, $D_s^{*+}\rho^0$, $D_s^+\omega$, $D_s^{*+}\omega$	[gg]	< 5	$\times 10^{-4}$	CL=90%	–
$B \to D_{s1}(2536)^+$ anything		< 9.5	$\times 10^{-3}$	CL=90%	–

Charmonium modes

$B \to J/\psi(1S)$ anything		(1.094 ± 0.032) %		S=1.1	–
$B \to J/\psi(1S)$(direct) anything		(7.8 ± 0.4) $\times 10^{-3}$		S=1.1	–
$B \to \psi(2S)$ anything		(3.07 ± 0.21) $\times 10^{-3}$			–
$B \to \chi_{c1}(1P)$ anything		(3.86 ± 0.27) $\times 10^{-3}$			–
$B \to \chi_{c1}(1P)$(direct) anything		(3.34 ± 0.28) $\times 10^{-3}$			–
$B \to \chi_{c2}(1P)$ anything		(1.3 ± 0.4) $\times 10^{-3}$		S=1.9	–
$B \to \chi_{c2}(1P)$(direct) anything		(1.65 ± 0.31) $\times 10^{-3}$			–
$B \to \eta_c(1S)$ anything		< 9	$\times 10^{-3}$	CL=90%	–

K or K^* modes

$B \to K^\pm$ anything	[gg]	(78.9 ± 2.5) %			–
$B \to K^+$ anything		(66 ± 5) %			–
$B \to K^-$ anything		(13 ± 4) %			–
$B \to K^0/\overline{K}^0$ anything	[gg]	(64 ± 4) %			–
$B \to K^*(892)^\pm$ anything		(18 ± 6) %			–
$B \to K^*(892)^0/\overline{K}^*(892)^0$ anything	[gg]	(14.6 ± 2.6) %			–
$B \to K^*(892)\gamma$		(4.2 ± 0.6) $\times 10^{-5}$			2564
$B \to K_1(1400)\gamma$		< 1.27	$\times 10^{-4}$	CL=90%	2453
$B \to K_2^*(1430)\gamma$		(1.7 $^{+\ 0.6}_{-\ 0.5}$) $\times 10^{-5}$			2447
$B \to K_2(1770)\gamma$		< 1.2	$\times 10^{-3}$	CL=90%	2342
$B \to K_3^*(1780)\gamma$		< 3.0	$\times 10^{-3}$	CL=90%	2341
$B \to K_4^*(2045)\gamma$		< 1.0	$\times 10^{-3}$	CL=90%	2244
$B \to K\eta'(958)$		(8.3 ± 1.1) $\times 10^{-5}$			2528
$B \to K^*(892)\eta'(958)$		< 2.2	$\times 10^{-5}$	CL=90%	2472
$B \to K\eta$		< 5.2	$\times 10^{-6}$	CL=90%	2588
$B \to K^*(892)\eta$		(1.8 ± 0.5) $\times 10^{-5}$			2534
$B \to K\phi\phi$		(2.3 ± 0.9) $\times 10^{-6}$			2306
$B \to \overline{b} \to \overline{s}\gamma$		(3.3 ± 0.4) $\times 10^{-4}$			–
$B \to \overline{b} \to \overline{s}$gluon		< 6.8	%	CL=90%	–
$B \to \eta$ anything		< 4.4	$\times 10^{-4}$	CL=90%	–
$B \to \eta'$ anything		(4.6 ± 1.3) $\times 10^{-4}$			–

Light unflavored meson modes

$B \to \rho\gamma$		< 1.9	$\times 10^{-6}$	CL=90%	2583
$B \to \pi^\pm$ anything	[gg,iii]	(358 ± 7) %			–
$B \to \pi^0$ anything		(235 ± 11) %			–
$B \to \eta$ anything		(17.6 ± 1.6) %			–
$B \to \rho^0$ anything		(21 ± 5) %			–
$B \to \omega$ anything		< 81	%	CL=90%	–
$B \to \phi$ anything		(3.5 ± 0.7) %		S=1.8	–
$B \to \phi K^*(892)$		< 2.2	$\times 10^{-5}$	CL=90%	2460

Baryon modes

$B \to \Lambda_c^+ / \overline{\Lambda}_c^-$ anything		(6.4 ± 1.1) %			–
$B \to \overline{\Lambda}_c^- e^+$ anything		< 3.2	$\times 10^{-3}$	CL=90%	–
$B \to \overline{\Lambda}_c^- p$ anything		(3.6 ± 0.7) %			–
$B \to \overline{\Lambda}_c^- p e^+ \nu_e$		< 1.5	$\times 10^{-3}$	CL=90%	2021
$B \to \overline{\Sigma}_c^{--}$ anything		(4.2 ± 2.4) $\times 10^{-3}$			–
$B \to \overline{\Sigma}_c^-$ anything		< 9.6	$\times 10^{-3}$	CL=90%	–
$B \to \overline{\Sigma}_c^0$ anything		(4.6 ± 2.4) $\times 10^{-3}$			–
$B \to \overline{\Sigma}_c^0 N(N = p \text{ or } n)$		< 1.5	$\times 10^{-3}$	CL=90%	1939
$B \to \Xi_c^0$ anything $\times$ B($\Xi_c^0 \to \Xi^-\pi^+$)		(1.4 ± 0.5) $\times 10^{-4}$			–
$B \to \Xi_c^+$ anything $\times$ B($\Xi_c^+ \to \Xi^-\pi^+\pi^+$)		(4.5 $^{+\ 1.3}_{-\ 1.2}$) $\times 10^{-4}$			–
$B \to p/\overline{p}$ anything	[gg]	(8.0 ± 0.4) %			–
$B \to p/\overline{p}$(direct) anything	[gg]	(5.5 ± 0.5) %			–
$B \to \Lambda/\overline{\Lambda}$ anything	[gg]	(4.0 ± 0.5) %			–
$B \to \Xi^-/\overline{\Xi}^+$ anything	[gg]	(2.7 ± 0.6) $\times 10^{-3}$			–
$B \to$ baryons anything		(6.8 ± 0.6) %			–
$B \to p\overline{p}$ anything		(2.47 ± 0.23) %			–
$B \to \Lambda\overline{p}/\overline{\Lambda}p$ anything	[gg]	(2.5 ± 0.4) %			–
$B \to \Lambda\overline{\Lambda}$ anything		< 5	$\times 10^{-3}$	CL=90%	–

Lepton Family number (LF) violating modes or $\Delta B = 1$ weak neutral current ($B1$) modes

$B \to s e^+ e^-$	$B1$		(5.0 ± 2.6) $\times 10^{-6}$			–
$B \to s\mu^+\mu^-$	$B1$		(7.9 $^{+\ 3.0}_{-\ 2.6}$) $\times 10^{-6}$			–
$B \to s\ell^+\ell^-$	$B1$	[rr]	(6.1 $^{+\ 2.0}_{-\ 1.8}$) $\times 10^{-6}$			–
$B \to K e^+ e^-$	$B1$		(4.8 $^{+\ 1.5}_{-\ 1.3}$) $\times 10^{-7}$			2617
$B \to K^*(892) e^+ e^-$	$B1$		(1.5 ± 0.5) $\times 10^{-6}$			2564
$B \to K\mu^+\mu^-$	$B1$		(4.8 ± 1.2) $\times 10^{-7}$			2612
$B \to K^*(892)\mu^+\mu^-$	$B1$		(1.17 $^{+\ 0.37}_{-\ 0.33}$) $\times 10^{-6}$			2560
$B \to K\ell^+\ell^-$	$B1$		(5.4 ± 0.8) $\times 10^{-7}$			2617
$B \to K^*(892)\ell^+\ell^-$	$B1$		(1.05 ± 0.20) $\times 10^{-6}$			2564
$B \to e^\pm\mu^\mp s$	LF	[gg]	< 2.2	$\times 10^{-5}$	CL=90%	–
$B \to \pi e^\pm\mu^\mp$	LF		< 1.6	$\times 10^{-6}$	CL=90%	2637
$B \to \rho e^\pm\mu^\mp$	LF		< 3.2	$\times 10^{-6}$	CL=90%	2582
$B \to K e^\pm\mu^\mp$	LF		< 1.6	$\times 10^{-6}$	CL=90%	2616
$B \to K^*(892) e^\pm\mu^\mp$	LF		< 6.2	$\times 10^{-6}$	CL=90%	2563

$B^\pm/B^0/B_s^0/b$-baryon ADMIXTURE

These measurements are for an admixture of bottom particles at high energy (LEP, Tevatron, S$p\overline{p}$S).

Mean life $\tau = (1.564 \pm 0.014) \times 10^{-12}$ s

Mean life $\tau = (1.72 \pm 0.10) \times 10^{-12}$ s Charged b-hadron admixture

Mean life $\tau = (1.58 \pm 0.14) \times 10^{-12}$ s Neutral b-hadron admixture

$\tau_{\text{charged } b\text{-hadron}}/\tau_{\text{neutral } b\text{-hadron}} = 1.09 \pm 0.13$

$|\Delta\tau_b|/\tau_{b,\overline{b}} = -0.001 \pm 0.014$

The branching fraction measurements are for an admixture of B mesons and baryons at energies above the $\Upsilon(4S)$. Only the highest energy results (LEP, Tevatron, S$p\overline{p}$S) are used in the branching fraction averages. In the following, we assume that the production fractions are the same at the LEP and at the Tevatron.

For inclusive branching fractions, *e.g.*, $B \to D^\pm$ anything, the values usually are multiplicities, not branching fractions. They can be greater than one.

The modes below are listed for a $\overline{b}$ initial state. b modes are their charge conjugates. Reactions indicate the weak decay vertex and do not include mixing.

$\overline{b}$ DECAY MODES	Fraction (Γ_j/Γ)	Scale factor/ Confidence level	p (MeV/c)

Meson Summary Table

PRODUCTION FRACTIONS

The production fractions for weakly decaying b-hadrons at high energy have been calculated from the best values of mean lives, mixing parameters, and branching fractions in this edition by the Heavy Flavor Averaging Group (HFAG) as described in the note "B^0-$\overline{B}^0$ Mixing" in the B^0 Particle Listings. Values assume

$$B(\overline{b} \to B^+) = B(\overline{b} \to B^0)$$
$$B(\overline{b} \to B^+) + B(\overline{b} \to B^0) + B(\overline{b} \to B_s^0) + B(b \to b\text{-baryon}) = 100\ \%.$$

The notation for production fractions varies in the literature (f_d, d_{B^0}, $f(b \to \overline{B}^0)$, $\mathrm{Br}(b \to \overline{B}^0)$). We use our own branching fraction notation here, $B(\overline{b} \to B^0)$.

B^+	(39.7 ± 1.0) %		–
B^0	(39.7 ± 1.0) %		–
B_s^0	(10.7 ± 1.1) %		–
b-baryon	(9.9 ± 1.7) %		–
B_c	—		–

DECAY MODES

Semileptonic and leptonic modes

ν anything		(23.1 ± 1.5) %		–
$\ell^+ \nu_\ell$ anything	[rr]	(10.68 ± 0.22) %		–
$e^+ \nu_e$ anything		(10.86 ± 0.35) %		–
$\mu^+ \nu_\mu$ anything		(10.95 $^{+}_{-}$ 0.29 0.25) %		–
$D^- \ell^+ \nu_\ell$ anything	[rr]	(2.3 ± 0.4) %	S=1.7	–
$D^- \pi^+ \ell^+ \nu_\ell$ anything		(4.9 ± 1.9) × 10^{-3}		–
$D^- \pi^- \ell^+ \nu_\ell$ anything		(2.6 ± 1.6) × 10^{-3}		–
$\overline{D}^0 \ell^+ \nu_\ell$ anything	[rr]	(6.90 ± 0.35) %		–
$\overline{D}^0 \pi^- \ell^+ \nu_\ell$ anything		(1.07 ± 0.27) %		–
$\overline{D}^0 \pi^+ \ell^+ \nu_\ell$ anything		(2.3 ± 1.6) × 10^{-3}		–
$D^{*-} \ell^+ \nu_\ell$ anything	[rr]	(2.75 ± 0.19) %		–
$D^{*-} \pi^+ \ell^+ \nu_\ell$ anything		(4.8 ± 1.0) × 10^{-3}		–
$D^{*-} \pi^- \ell^+ \nu_\ell$ anything		(6 ± 7) × 10^{-4}		–
$D_j^- \ell^+ \nu_\ell$ anything	[rr,jjj]	seen		–
$D_2^*(2460)^- \ell^+ \nu_\ell$ anything		seen		–
charmless $\ell \overline{\nu}_\ell$	[rr]	(1.7 ± 0.5) × 10^{-3}		–
$\tau^+ \nu_\tau$ anything		(2.48 ± 0.26) %		–
$D^{*-} \tau \nu_\tau$ anything		(9 ± 4) × 10^{-3}		–
$\overline{c} \to \ell^- \overline{\nu}_\ell$ anything	[rr]	(8.0 ± 0.4) %		–
$c \to \ell^+ \nu$ anything		(1.6 $^{+}_{-}$ 0.4 0.5) %		–

Charmed meson and baryon modes

$\overline{D}^0$ anything		(61.0 ± 3.2) %		–
$D^0 D_s^\pm$ anything	[gg]	(9.1 $^{+}_{-}$ 3.9 2.8) %		–
$D^\mp D_s^\pm$ anything	[gg]	(4.0 $^{+}_{-}$ 2.3 1.8) %		–
$\overline{D}^0 D^0$ anything	[gg]	(5.1 $^{+}_{-}$ 2.0 1.8) %		–
$D^0 D^\pm$ anything	[gg]	(2.7 $^{+}_{-}$ 1.8 1.6) %		–
$D^\pm D^\mp$ anything	[gg]	< 9 × 10^{-3}	CL=90%	–
D^- anything		(23.1 ± 2.2) %		–
$D^*(2010)^+$ anything		(17.3 ± 2.0) %		–
$D_1(2420)^0$ anything		(5.0 ± 1.5) %		–
$D^*(2010)^\mp D_s^\pm$ anything	[gg]	(3.3 $^{+}_{-}$ 1.6 1.3) %		–
$D^0 D^*(2010)^\pm$ anything	[gg]	(3.0 $^{+}_{-}$ 1.1 0.9) %		–
$D^*(2010)^\pm D^\mp$ anything	[gg]	(2.5 $^{+}_{-}$ 1.2 1.0) %		–
$D^*(2010)^\pm D^*(2010)^\mp$ anything	[gg]	(1.2 ± 0.4) %		–
$D_2^*(2460)^0$ anything		(4.7 ± 2.7) %		–
D_s^- anything		(18 ± 5) %		–
D_s^+ anything		(10.1 ± 3.1) %		–
Λ_c^+ anything		(9.7 ± 2.9) %		–
$\overline{c}/c$ anything	[iii]	(116.6 ± 3.3) %		–

Charmonium modes

$J/\psi(1S)$ anything		(1.16 ± 0.10) %		–
$\psi(2S)$ anything		(4.8 ± 2.4) × 10^{-3}		–
$\chi_{c1}(1P)$ anything		(1.5 ± 0.5) %		–

K or K^* modes

$\overline{s}\gamma$		(3.1 ± 1.1) × 10^{-4}		–
$\overline{s}\nu\overline{\nu}$		< 6.4 × 10^{-4}	CL=90%	–
$K^\pm$ anything		(74 ± 6) %		–
K_S^0 anything		(29.0 ± 2.9) %		–

Pion modes

$\pi^\pm$ anything		(397 ± 21) %		–
π^0 anything	[iii]	(278 ± 60) %		–
ϕ anything		(2.82 ± 0.23) %		–

Baryon modes

$p/\overline{p}$ anything		(13.1 ± 1.1) %		–

Other modes

charged anything	[iii]	(497 ± 7) %		–
hadron$^+$ hadron$^-$		(1.7 $^{+}_{-}$ 1.0 0.7) × 10^{-5}		–
charmless		(7 ± 21) × 10^{-3}		–

Baryon modes

$\Lambda/\overline{\Lambda}$ anything		(5.9 ± 0.6) %		–
b-baryon anything		(10.2 ± 2.8) %		–

$\Delta B = 1$ weak neutral current ($B1$) modes

$\mu^+ \mu^-$ anything	$B1$	< 3.2 × 10^{-4}	CL=90%	–

B^*

$I(J^P) = \frac{1}{2}(1^-)$

I, J, P need confirmation. Quantum numbers shown are quark-model predictions.

Mass $m_{B^*} = 5325.0 \pm 0.6$ MeV

$m_{B^*} - m_B = 45.78 \pm 0.35$ MeV

B^* DECAY MODES	Fraction (Γ_i/Γ)	p (MeV/c)
$B\gamma$	dominant	45

BOTTOM, STRANGE MESONS ($B = \pm 1, S = \mp 1$)

$B_s^0 = s\overline{b}$, $\overline{B}_s^0 = \overline{s}b$, similarly for B_s^*'s

B_s^0

$I(J^P) = 0(0^-)$

I, J, P need confirmation. Quantum numbers shown are quark-model predictions.

Mass $m_{B_s^0} = 5369.6 \pm 2.4$ MeV

Mean life $\tau = (1.461 \pm 0.057) \times 10^{-12}$ s

$c\tau = 438\ \mu$m

B_s^0-$\overline{B}_s^0$ mixing parameters

$\Delta m_{B_s^0} = m_{B_{sH}^0} - m_{B_{sL}^0} > 14.4 \times 10^{12}\ \hbar\ \mathrm{s}^{-1}$, CL = 95%

$> 94.8 \times 10^{-10}$ MeV, CL = 95%

$x_s = \Delta m_{B_s^0}/\Gamma_{B_s^0} > 20.6$, CL = 95%

$\chi_s > 0.49883$, CL = 95%

These branching fractions all scale with $B(\overline{b} \to B_s^0)$, the LEP B_s^0 production fraction. The first four were evaluated using $B(\overline{b} \to B_s^0) = (10.7 \pm 1.4)\%$ and the rest assume $B(\overline{b} \to B_s^0) = 12\%$.

The branching fraction $B(B_s^0 \to D_s^- \ell^+ \nu_\ell \text{ anything})$ is not a pure measurement since the measured product branching fraction $B(\overline{b} \to B_s^0) \times B(B_s^0 \to D_s^- \ell^+ \nu_\ell \text{ anything})$ was used to determine $B(\overline{b} \to B_s^0)$, as described in the note on "Production and Decay of b-Flavored Hadrons."

For inclusive branching fractions, *e.g.*, $B \to D^\pm$ anything, the values usually are multiplicities, not branching fractions. They can be greater than one.

B_s^0 DECAY MODES		Fraction (Γ_i/Γ)	Confidence level	p (MeV/c)
D_s^- anything		(94 ± 30) %		–
$D_s^- \ell^+ \nu_\ell$ anything	[kkk]	(7.9 ± 2.4) %		–
$D_s^- \pi^+$		< 13 %		2322
$D_s(*)^+ D_s(*)^-$		(23 $^{+21}_{-13}$) %		–
$J/\psi(1S)\phi$		(9.3 ± 3.3) × 10^{-4}		1590
$J/\psi(1S)\pi^0$		< 1.2 × 10^{-3}	90%	1788
$J/\psi(1S)\eta$		< 3.8 × 10^{-3}	90%	1735
$\psi(2S)\phi$		seen		1123
$\pi^+\pi^-$		< 1.7 × 10^{-4}	90%	2681

$\pi^0\pi^0$	< 2.1	$\times 10^{-4}$	90%	2681
$\eta\pi^0$	< 1.0	$\times 10^{-3}$	90%	2655
$\eta\eta$	< 1.5	$\times 10^{-3}$	90%	2628
$\rho^0\rho^0$	< 3.20	$\times 10^{-4}$	90%	2570
$\phi\rho^0$	< 6.17	$\times 10^{-4}$	90%	2528
$\phi\phi$	< 1.183	$\times 10^{-3}$	90%	2484
π^+K^-	< 2.1	$\times 10^{-4}$	90%	2660
K^+K^-	< 5.9	$\times 10^{-5}$	90%	2639
$\overline{K}^*(892)^0\rho^0$	< 7.67	$\times 10^{-4}$	90%	2551
$\overline{K}^*(892)^0K^*(892)^0$	< 1.681	$\times 10^{-3}$	90%	2532
$\phi K^*(892)^0$	< 1.013	$\times 10^{-3}$	90%	2508
$p\overline{p}$	< 5.9	$\times 10^{-5}$	90%	2516
$\gamma\gamma$	< 1.48	$\times 10^{-4}$	90%	2685
$\phi\gamma$	< 1.2	$\times 10^{-4}$	90%	2588

Lepton Family number (LF) violating modes or $\Delta B = 1$ weak neutral current ($B1$) modes

$\mu^+\mu^-$	$B1$	< 2.0	$\times 10^{-6}$	90%	2683
e^+e^-	$B1$	< 5.4	$\times 10^{-5}$	90%	2685
$e^\pm\mu^\mp$	LF	[gg] < 6.1	$\times 10^{-6}$	90%	2684
$\phi(1020)\mu^+\mu^-$	$B1$	< 4.7	$\times 10^{-5}$	90%	2584
$\phi\nu\overline{\nu}$	$B1$	< 5.4	$\times 10^{-3}$	90%	2588

BOTTOM, CHARMED MESONS ($B = C = \pm 1$)

$B_c^+ = c\overline{b}$, $B_c^- = \overline{c}b$, similarly for B_c^*'s

$B_c^\pm$

$I(J^P) = 0(0^-)$
I, J, P need confirmation.

Quantum numbers shown are quark-model predicitions.

Mass $m = 6.4 \pm 0.4$ GeV
Mean life $\tau = (0.46^{+0.18}_{-0.16}) \times 10^{-12}$ s

B_c^- modes are charge conjugates of the modes below.

B_c^+ DECAY MODES × B($\overline{b} \to B_c$)	Fraction (Γ_i/Γ)	Confidence level	p (MeV/c)
The following quantities are not pure branching ratios; rather the fraction $\Gamma_i/\Gamma \times$ B($\overline{b} \to B_c$).			
$J/\psi(1S)\ell^+\nu_\ell$ anything	$(5.2^{+2.4}_{-2.1}) \times 10^{-5}$		–
$J/\psi(1S)\pi^+$	< 8.2 $\times 10^{-5}$	90%	2448
$J/\psi(1S)\pi^+\pi^+\pi^-$	< 5.7 $\times 10^{-4}$	90%	2429
$J/\psi(1S)a_1(1260)$	< 1.2 $\times 10^{-3}$	90%	2255
$D^*(2010)^+\overline{D}^0$	< 6.2 $\times 10^{-3}$	90%	2546

$c\overline{c}$ MESONS

$\eta_c(1S)$

$I^G(J^{PC}) = 0^+(0^{-+})$

Mass $m = 2979.6 \pm 1.2$ MeV (S = 1.7)
Full width $\Gamma = 17.3^{+2.7}_{-2.5}$ MeV (S = 1.1)

$\eta_c(1S)$ DECAY MODES	Fraction (Γ_i/Γ)	Confidence level	p (MeV/c)
Decays involving hadronic resonances			
$\eta'(958)\pi\pi$	(4.1 ±1.7) %		1321
$\rho\rho$	(2.6 ±0.9) %		1272
$K^*(892)^0K^-\pi^+$ + c.c.	(2.0 ±0.7) %		1275
$K^*(892)\overline{K}^*(892)$	(8.5 ±3.1) $\times 10^{-3}$		1194
ϕK^+K^-	(2.9 ±1.4) $\times 10^{-3}$		1101
$\phi\phi$	(2.6 ±0.9) $\times 10^{-3}$		1086
$a_0(980)\pi$	< 2 %	90%	1323
$a_2(1320)\pi$	< 2 %	90%	1194
$K^*(892)\overline{K}$ + c.c.	< 1.28 %	90%	1307
$f_2(1270)\eta$	< 1.1 %	90%	1143
$\omega\omega$	< 3.1 $\times 10^{-3}$	90%	1268
Decays into stable hadrons			
$K\overline{K}\pi$	(5.7 ±1.6) %		1379
$\eta\pi\pi$	(4.9 ±1.8) %		1426
$\pi^+\pi^-K^+K^-$	(1.5 ±0.6) %		1343
$2(K^+K^-)$	(1.5 ±0.7) $\times 10^{-3}$		1053
$2(\pi^+\pi^-)$	(1.20±0.30) %		1457
$p\overline{p}$	(1.3 ±0.4) $\times 10^{-3}$		1157
$K\overline{K}\eta$	< 3.1 %	90%	1263
$\pi^+\pi^-p\overline{p}$	< 1.2 %	90%	1024
$\Lambda\overline{\Lambda}$	< 2 $\times 10^{-3}$	90%	987
Radiative decays			
$\gamma\gamma$	(4.3 ±1.5) $\times 10^{-4}$		1490

$J/\psi(1S)$

$I^G(J^{PC}) = 0^-(1^{--})$

Mass $m = 3096.916 \pm 0.011$ MeV
Full width $\Gamma = 91.0 \pm 3.2$ keV
$\Gamma_{ee} = 5.40 \pm 0.15 \pm 0.07$ keV

$J/\psi(1S)$ DECAY MODES	Fraction (Γ_i/Γ)	Scale factor/ Confidence level	p (MeV/c)
hadrons	(87.7 ±0.5) %		–
virtual $\gamma \to$ hadrons	(17.0 ±2.0) %		–
e^+e^-	(5.93±0.10) %		1548
$\mu^+\mu^-$	(5.88±0.10) %		1545
Decays involving hadronic resonances			
$\rho\pi$	(1.27±0.09) %		1448
$\rho^0\pi^0$	(4.2 ±0.5) $\times 10^{-3}$		1448
$a_2(1320)\rho$	(1.09±0.22) %		1123
$\omega\pi^+\pi^+\pi^-\pi^-$	(8.5 ±3.4) $\times 10^{-3}$		1392
$\omega\pi^+\pi^-$	(7.2 ±1.0) $\times 10^{-3}$		1435
$\omega f_2(1270)$	(4.3 ±0.6) $\times 10^{-3}$		1142
$K^*(892)^0\overline{K}_2^*(1430)^0$ + c.c.	(6.7 ±2.6) $\times 10^{-3}$		1012
$\omega K^*(892)\overline{K}$ + c.c.	(5.3 ±2.0) $\times 10^{-3}$		1097
$K^+\overline{K}^*(892)^-$ + c.c.	(5.0 ±0.4) $\times 10^{-3}$		1373
$K^0\overline{K}^*(892)^0$ + c.c.	(4.2 ±0.4) $\times 10^{-3}$		1373
$K_1(1400)^\pm K^\mp$	(3.8 ±1.4) $\times 10^{-3}$		1171
$\omega\pi^0\pi^0$	(3.4 ±0.8) $\times 10^{-3}$		1436
$b_1(1235)^\pm\pi^\mp$	[gg] (3.0 ±0.5) $\times 10^{-3}$		1300
$\omega K^\pm K_S^0\pi^\mp$	[gg] (2.9 ±0.7) $\times 10^{-3}$		1210
$b_1(1235)^0\pi^0$	(2.3 ±0.6) $\times 10^{-3}$		1300
$\phi K^*(892)\overline{K}$ + c.c.	(2.04±0.28) $\times 10^{-3}$		969
$\omega K\overline{K}$	(1.9 ±0.4) $\times 10^{-3}$		1268
$\omega f_0(1710) \to \omega K\overline{K}$	(4.8 ±1.1) $\times 10^{-4}$		878
$\phi 2(\pi^+\pi^-)$	(1.60±0.32) $\times 10^{-3}$		1318
$\Delta(1232)^{++}\overline{p}\pi^-$	(1.6 ±0.5) $\times 10^{-3}$		1030
$\omega\eta$	(1.58±0.16) $\times 10^{-3}$		1394
$\phi K\overline{K}$	(1.54±0.21) $\times 10^{-3}$		1179
$\phi f_0(1710) \to \phi K\overline{K}$	(3.6 ±0.6) $\times 10^{-4}$		875
$p\overline{p}\omega$	(1.30±0.25) $\times 10^{-3}$	S=1.3	768
$\Delta(1232)^{++}\overline{\Delta}(1232)^{--}$	(1.10±0.29) $\times 10^{-3}$		938
$\Sigma(1385)^-\overline{\Sigma}(1385)^+$ (or c.c.)	[gg] (1.03±0.13) $\times 10^{-3}$		697
$p\overline{p}\eta'(958)$	(9 ±4) $\times 10^{-4}$	S=1.7	596
$\phi f_2'(1525)$	(8 ±4) $\times 10^{-4}$	S=2.7	871
$\phi\pi^+\pi^-$	(8.0 ±1.2) $\times 10^{-4}$		1365
$\phi K^\pm K_S^0\pi^\mp$	[gg] (7.2 ±0.9) $\times 10^{-4}$		1114
$\omega f_1(1420)$	(6.8 ±2.4) $\times 10^{-4}$		1062
$\phi\eta$	(6.5 ±0.7) $\times 10^{-4}$		1320
$\Xi(1530)^-\overline{\Xi}^+$	(5.9 ±1.5) $\times 10^{-4}$		601
$pK^-\overline{\Sigma}(1385)^0$	(5.1 ±3.2) $\times 10^{-4}$		646
$\omega\pi^0$	(4.2 ±0.6) $\times 10^{-4}$	S=1.4	1446
$\phi\eta'(958)$	(3.3 ±0.4) $\times 10^{-4}$		1192
$\phi f_0(980)$	(3.2 ±0.9) $\times 10^{-4}$	S=1.9	1182
$\Xi(1530)^0\overline{\Xi}^0$	(3.2 ±1.4) $\times 10^{-4}$		608
$\Sigma(1385)^-\overline{\Sigma}^+$ (or c.c.)	[gg] (3.1 ±0.5) $\times 10^{-4}$		855
$\phi f_1(1285)$	(2.6 ±0.5) $\times 10^{-4}$	S=1.1	1032
$\rho\eta$	(1.93±0.23) $\times 10^{-4}$		1396
$\omega\eta'(958)$	(1.67±0.25) $\times 10^{-4}$		1279
$\omega f_0(980)$	(1.4 ±0.5) $\times 10^{-4}$		1271
$\rho\eta'(958)$	(1.05±0.18) $\times 10^{-4}$		1281
$p\overline{p}\phi$	(4.5 ±1.5) $\times 10^{-5}$		527
$a_2(1320)^\pm\pi^\mp$	[gg] < 4.3 $\times 10^{-3}$	CL=90%	1263
$K\overline{K}_2^*(1430)$ + c.c.	< 4.0 $\times 10^{-3}$	CL=90%	1159
$K_1(1270)^\pm K^\mp$	< 3.0 $\times 10^{-3}$	CL=90%	1231
$K_2^*(1430)^0\overline{K}_2^*(1430)^0$	< 2.9 $\times 10^{-3}$	CL=90%	604

$K^*(892)^0\overline{K}^*(892)^0$	<	5	$\times 10^{-4}$	CL=90%	1266
$\phi f_2(1270)$	<	3.7	$\times 10^{-4}$	CL=90%	1036
$p\overline{p}\rho$	<	3.1	$\times 10^{-4}$	CL=90%	774
$\phi\eta(1405) \to \phi\eta\pi\pi$	<	2.5	$\times 10^{-4}$	CL=90%	946
$\omega f_2'(1525)$	<	2.2	$\times 10^{-4}$	CL=90%	1003
$\Sigma(1385)^0\overline{\Lambda}$	<	2	$\times 10^{-4}$	CL=90%	912
$\Delta(1232)^+\overline{p}$	<	1	$\times 10^{-4}$	CL=90%	1100
$\Sigma^0\overline{\Lambda}$	<	9	$\times 10^{-5}$	CL=90%	1032
$\phi\pi^0$	<	6.8	$\times 10^{-6}$	CL=90%	1377

Decays into stable hadrons

$2(\pi^+\pi^-)\pi^0$		(3.37 ± 0.26) %			1496
$3(\pi^+\pi^-)\pi^0$		(2.9 ± 0.6) %			1433
$\pi^+\pi^-\pi^0$		(1.50 ± 0.20) %			1533
$\pi^+\pi^-\pi^0 K^+K^-$		(1.20 ± 0.30) %			1368
$4(\pi^+\pi^-)\pi^0$		(9.0 ± 3.0)	$\times 10^{-3}$		1345
$\pi^+\pi^- K^+K^-$		(7.2 ± 2.3)	$\times 10^{-3}$		1407
$K\overline{K}\pi$		(6.1 ± 1.0)	$\times 10^{-3}$		1442
$p\overline{p}\pi^+\pi^-$		(6.0 ± 0.5)	$\times 10^{-3}$	S=1.3	1107
$2(\pi^+\pi^-)$		(4.0 ± 1.0)	$\times 10^{-3}$		1517
$3(\pi^+\pi^-)$		(4.0 ± 2.0)	$\times 10^{-3}$		1466
$n\overline{n}\pi^+\pi^-$		(4 ± 4)	$\times 10^{-3}$		1106
$\Sigma^0\overline{\Sigma}^0$		(1.27 ± 0.17)	$\times 10^{-3}$		988
$2(\pi^+\pi^-)K^+K^-$		(3.1 ± 1.3)	$\times 10^{-3}$		1320
$p\overline{p}\pi^+\pi^-\pi^0$	[*lll*]	(2.3 ± 0.9)	$\times 10^{-3}$	S=1.9	1033
$p\overline{p}$		(2.12 ± 0.10)	$\times 10^{-3}$		1232
$p\overline{p}\eta$		(2.09 ± 0.18)	$\times 10^{-3}$		948
$p\overline{n}\pi^-$		(2.00 ± 0.10)	$\times 10^{-3}$		1174
$n\overline{n}$		(2.2 ± 0.4)	$\times 10^{-3}$		1231
$\Xi\overline{\Xi}$		(1.8 ± 0.4)	$\times 10^{-3}$	S=1.8	818
$\Lambda\overline{\Lambda}$		(1.30 ± 0.12)	$\times 10^{-3}$	S=1.1	1074
$p\overline{p}\pi^0$		(1.09 ± 0.09)	$\times 10^{-3}$		1176
$\Lambda\overline{\Sigma}^-\pi^+$ (or c.c.)	[*gg*]	(1.06 ± 0.12)	$\times 10^{-3}$		950
$pK^-\overline{\Lambda}$		(8.9 ± 1.6)	$\times 10^{-4}$		876
$2(K^+K^-)$		(9.2 ± 3.3)	$\times 10^{-4}$	S=1.3	1131
$pK^-\overline{\Sigma}^0$		(2.9 ± 0.8)	$\times 10^{-4}$		819
K^+K^-		(2.37 ± 0.31)	$\times 10^{-4}$		1468
$K_S^0 K_L^0$		(1.46 ± 0.26)	$\times 10^{-4}$	S=2.7	1466
$\Lambda\overline{\Lambda}\pi^0$		(2.2 ± 0.6)	$\times 10^{-4}$		998
$\pi^+\pi^-$		(1.47 ± 0.23)	$\times 10^{-4}$		1542
$\Lambda\overline{\Sigma}+$ c.c.	<	1.5	$\times 10^{-4}$	CL=90%	1034
$K_S^0 K_S^0$	<	5.2	$\times 10^{-6}$	CL=90%	1466

Radiative decays

$\gamma\eta_c(1S)$		(1.3 ± 0.4) %			115
$\gamma\pi^+\pi^-2\pi^0$		(8.3 ± 3.1)	$\times 10^{-3}$		1518
$\gamma\eta\pi\pi$		(6.1 ± 1.0)	$\times 10^{-3}$		1487
$\gamma\eta(1405/1475) \to \gamma K\overline{K}\pi$	[*p*]	(2.8 ± 0.6)	$\times 10^{-3}$	S=1.6	1223
$\gamma\eta(1405/1475) \to \gamma\gamma\rho^0$		(6.4 ± 1.4)	$\times 10^{-5}$		1223
$\gamma\eta(1405/1475) \to \gamma\eta\pi^+\pi^-$		(3.0 ± 0.5)	$\times 10^{-4}$		–
$\gamma\rho\rho$		(4.5 ± 0.8)	$\times 10^{-3}$		1340
$\gamma\eta_2(1870) \to \gamma\pi^+\pi^-$		(6.2 ± 2.4)	$\times 10^{-4}$		–
$\gamma\eta'(958)$		(4.31 ± 0.30)	$\times 10^{-3}$		1400
$\gamma 2\pi^+2\pi^-$		(2.8 ± 0.5)	$\times 10^{-3}$	S=1.9	1517
$\gamma K^+K^-\pi^+\pi^-$		(2.1 ± 0.6)	$\times 10^{-3}$		1407
$\gamma f_4(2050)$		(2.7 ± 0.7)	$\times 10^{-3}$		880
$\gamma\omega\omega$		(1.59 ± 0.33)	$\times 10^{-3}$		1336
$\gamma\eta(1405/1475) \to \gamma\rho^0\rho^0$		(1.7 ± 0.4)	$\times 10^{-3}$	S=1.3	1223
$\gamma f_2(1270)$		(1.38 ± 0.14)	$\times 10^{-3}$		1286
$\gamma f_0(1710) \to \gamma K\overline{K}$		(8.5 $^{+1.2}_{-0.9}$)	$\times 10^{-4}$	S=1.2	1075
$\gamma\eta$		(8.6 ± 0.8)	$\times 10^{-4}$		1500
$\gamma f_1(1420) \to \gamma K\overline{K}\pi$		(7.9 ± 1.3)	$\times 10^{-4}$		1220
$\gamma f_1(1285)$		(6.1 ± 0.8)	$\times 10^{-4}$		1283
$\gamma f_1(1510) \to \gamma\eta\pi^+\pi^-$		(4.5 ± 1.2)	$\times 10^{-4}$		–
$\gamma f_2'(1525)$		(4.5 $^{+0.7}_{-0.4}$)	$\times 10^{-4}$		1173
$\gamma f_2(1950) \to \gamma K^*(892)\overline{K}^*(892)$		(7.0 ± 2.2)	$\times 10^{-4}$		–
$\gamma K^*(892)\overline{K}^*(892)$		(4.0 ± 1.3)	$\times 10^{-3}$		1266
$\gamma\phi\phi$		(4.0 ± 1.2)	$\times 10^{-4}$	S=2.1	1166
$\gamma p\overline{p}$		(3.8 ± 1.0)	$\times 10^{-4}$		1232
$\gamma\eta(2225)$		(2.9 ± 0.6)	$\times 10^{-4}$		752
$\gamma\eta(1760) \to \gamma\rho^0\rho^0$		(1.3 ± 0.9)	$\times 10^{-4}$		1048
$\gamma(K\overline{K}\pi)_{J^{PC}=0^{-+}}$		(7 ± 4)	$\times 10^{-4}$	S=2.1	1442
$\gamma\pi^0$		(3.9 ± 1.3)	$\times 10^{-5}$		1546
$\gamma p\overline{p}\pi^+\pi^-$	<	7.9	$\times 10^{-4}$	CL=90%	1107
$\gamma\gamma$	<	5	$\times 10^{-4}$	CL=90%	1548
$\gamma\Lambda\overline{\Lambda}$	<	1.3	$\times 10^{-4}$	CL=90%	1074
3γ	<	5.5	$\times 10^{-5}$	CL=90%	1548
$\gamma f_J(2220)$	>	2.50	$\times 10^{-3}$	CL=99.9%	745
$\gamma f_J(2220) \to \gamma\pi\pi$		(8 ± 4)	$\times 10^{-5}$		–
$\gamma f_J(2220) \to \gamma K\overline{K}$		(8.1 ± 3.0)	$\times 10^{-5}$		–
$\gamma f_J(2220) \to \gamma p\overline{p}$		(1.5 ± 0.8)	$\times 10^{-5}$		–
$\gamma f_0(1500)$	>	(5.7 ± 0.8)	$\times 10^{-4}$		1182
γe^+e^-		(8.8 ± 1.4)	$\times 10^{-3}$		1548

Lepton Family number (*LF*) violating modes

$e^\pm\mu^\mp$ *LF*	<	1.1	$\times 10^{-6}$	CL=90%	1547

$\chi_{c0}(1P)$ $I^G(J^{PC}) = 0^+(0^{++})$

Mass $m = 3415.19 \pm 0.34$ MeV
Full width $\Gamma = 10.1 \pm 0.8$ MeV

$\chi_{c0}(1P)$ DECAY MODES	Fraction (Γ_i/Γ)	Confidence level	p (MeV/c)
Hadronic decays			
$2(\pi^+\pi^-)$	(2.58 ± 0.31) %		1679
$\pi^+\pi^- K^+K^-$	(2.1 ± 0.5) %		1581
$\rho^0\pi^+\pi^-$	(1.6 ± 0.5) %		1607
$3(\pi^+\pi^-)$	(1.27 ± 0.22) %		1633
$K^+\overline{K}^*(892)^0\pi^-$ + c.c.	(1.2 ± 0.4) %		1524
K^+K^-	(6.0 ± 0.9)	$\times 10^{-3}$	1635
$\pi\pi$	(7.4 ± 0.8)	$\times 10^{-3}$	1702
$\eta\eta$	(2.1 ± 1.1)	$\times 10^{-3}$	1617
$K^+K^-K^+K^-$	(2.3 ± 0.5)	$\times 10^{-3}$	1334
$K_S^0 K_S^0$	(2.1 ± 0.6)	$\times 10^{-3}$	1633
$\pi^+\pi^- p\overline{p}$	(2.2 ± 0.8)	$\times 10^{-3}$	1320
$\phi\phi$	(1.0 ± 0.6)	$\times 10^{-3}$	1370
$p\overline{p}$	(2.24 ± 0.27)	$\times 10^{-4}$	1427
$\Lambda\overline{\Lambda}$	(4.7 ± 1.6)	$\times 10^{-4}$	1293
$K_S^0 K^+\pi^-$ + c.c.	< 8	$\times 10^{-4}$ 90%	1610
Radiative decays			
$\gamma J/\psi(1S)$	(1.18 ± 0.14) %		303
$\gamma\gamma$	(2.6 ± 0.5)	$\times 10^{-4}$	1708

$\chi_{c1}(1P)$ $I^G(J^{PC}) = 0^+(1^{++})$

Mass $m = 3510.59 \pm 0.10$ MeV (S = 1.1)
Full width $\Gamma = 0.91 \pm 0.13$ MeV

$\chi_{c1}(1P)$ DECAY MODES	Fraction (Γ_i/Γ)	p (MeV/c)
Hadronic decays		
$3(\pi^+\pi^-)$	(6.2 ± 1.6) $\times 10^{-3}$	1683
$2(\pi^+\pi^-)$	(8.2 ± 2.9) $\times 10^{-3}$	1727
$\pi^+\pi^- K^+K^-$	(4.9 ± 1.1) $\times 10^{-3}$	1632
$\rho^0\pi^+\pi^-$	(3.9 ± 3.5) $\times 10^{-3}$	1657
$K^+\overline{K}^*(892)^0\pi^-$ + c.c.	(3.2 ± 2.1) $\times 10^{-3}$	1577
$K_S^0 K^+\pi^-$ + c.c.	(2.5 ± 0.7) $\times 10^{-3}$	1660
$\pi^+\pi^- p\overline{p}$	(5.3 ± 2.1) $\times 10^{-4}$	1381
$K^+K^-K^+K^-$	(4.2 ± 1.9) $\times 10^{-4}$	1393
$p\overline{p}$	(7.2 ± 1.3) $\times 10^{-5}$	1483
$\Lambda\overline{\Lambda}$	(2.6 ± 1.2) $\times 10^{-4}$	1355
$\pi^+\pi^- + K^+K^-$	< 2.1 $\times 10^{-3}$	–
Radiative decays		
$\gamma J/\psi(1S)$	(31.6 ± 3.3) %	389

$\chi_{c2}(1P)$ $I^G(J^{PC}) = 0^+(2^{++})$

Mass $m = 3556.26 \pm 0.11$ MeV
Full width $\Gamma = 2.11 \pm 0.16$ MeV

$\chi_{c2}(1P)$ DECAY MODES	Fraction (Γ_i/Γ)	Confidence level	p (MeV/c)
Hadronic decays			
$2(\pi^+\pi^-)$	(1.48 ± 0.21) %		1751
$\pi^+\pi^- K^+K^-$	(1.24 ± 0.33) %		1656
$3(\pi^+\pi^-)$	(1.07 ± 0.24) %		1707
$\rho^0\pi^+\pi^-$	(7 ± 4)	$\times 10^{-3}$	1681
$K^+\overline{K}^*(892)^0\pi^-$ + c.c.	(4.8 ± 2.8)	$\times 10^{-3}$	1602
$\phi\phi$	(2.4 ± 0.9)	$\times 10^{-3}$	1457
$\pi^+\pi^-$	(1.77 ± 0.27)	$\times 10^{-3}$	1773

$\pi^0\pi^0$	(1.1 ±0.7) × 10^{-3}			1773
$\eta\eta$	< 1.5	× 10^{-3}	90%	1692
$K^+K^-K^+K^-$	(1.8 ±0.5) × 10^{-3}			1421
$\pi^+\pi^-p\overline{p}$	(1.7 ±0.4) × 10^{-3}			1410
K^+K^-	(9.4 ±2.1) × 10^{-4}			1708
$K^0_S K^0_S$	(7.2 ±2.7) × 10^{-4}			1707
$p\overline{p}$	(6.8 ±0.7) × 10^{-5}			1510
$\Lambda\overline{\Lambda}$	(3.4 ±1.7) × 10^{-4}			1385
$J/\psi(1S)\pi^+\pi^-\pi^0$	< 1.5	%	90%	186
$K^0_S K^+\pi^-$ + c.c.	< 1.3	× 10^{-3}	90%	1685
Radiative decays				
$\gamma J/\psi(1S)$	(20.2 ±1.7) %			430
$\gamma\gamma$	(2.46±0.23) × 10^{-4}			1778

$\psi(2S)$

$I^G(J^{PC}) = 0^-(1^{--})$

Mass m = 3686.093 ± 0.034 MeV (S = 1.4)
Full width Γ = 281 ± 17 keV
Γ_{ee} = 2.12 ± 0.12 keV

$\psi(2S)$ DECAY MODES	Fraction (Γ_i/Γ)	Scale factor/ Confidence level	p (MeV/c)
hadrons	(97.85 ±0.13) %		–
virtual γ → hadrons	(2.16±0.35) %	S=2.1	–
e^+e^-	(7.55±0.31) × 10^{-3}		1843
$\mu^+\mu^-$	(7.3 ±0.8) × 10^{-3}		1840
$\tau^+\tau^-$	(2.8 ±0.7) × 10^{-3}		489
Decays into $J/\psi(1S)$ and anything			
$J/\psi(1S)$ anything	(57.6 ±2.0) %		–
$J/\psi(1S)$ neutrals	(24.6 ±1.2) %		–
$J/\psi(1S)\pi^+\pi^-$	(31.7 ±1.1) %		477
$J/\psi(1S)\pi^0\pi^0$	(18.8 ±1.2) %		481
$J/\psi(1S)\eta$	(3.16±0.22) %		199
$J/\psi(1S)\pi^0$	(9.6 ±2.1) × 10^{-4}		528
Hadronic decays			
$3(\pi^+\pi^-)\pi^0$	(3.5 ±1.6) × 10^{-3}		1746
$2(\pi^+\pi^-)\pi^0$	(3.0 ±0.8) × 10^{-3}		1799
$\rho a_2(1320)$	< 2.3	× 10^{-4}	CL=90%	1500
$\omega\pi^+\pi^-$	(4.8 ±0.9) × 10^{-4}			1748
$b_1^\pm\pi^\mp$	(3.2 ±0.8) × 10^{-4}			1635
$\omega f_2(1270)$	< 1.5	× 10^{-4}	CL=90%	1515
$\pi^+\pi^-K^+K^-$	(1.6 ±0.4) × 10^{-3}			1726
$K^*(892)\overline{K}^*_2(1430)^0$	< 1.2	× 10^{-4}	CL=90%	1418
$K_1(1270)^\pm K^\mp$	(1.00±0.28) × 10^{-3}			1581
$\pi^+\pi^-p\overline{p}$	(8.0 ±2.0) × 10^{-4}			1491
$K^+\overline{K}^*(892)^0\pi^-$ + c.c.	(6.7 ±2.5) × 10^{-4}			1674
$2(\pi^+\pi^-)$	(4.5 ±1.0) × 10^{-4}			1817
$\rho^0\pi^+\pi^-$	(4.2 ±1.5) × 10^{-4}			1750
ωK^+K^-	(1.5 ±0.4) × 10^{-4}			1614
$\omega p\overline{p}$	(8.0 ±3.2) × 10^{-5}			1247
$\overline{p}p$	(2.07±0.31) × 10^{-4}			1586
$\Lambda\overline{\Lambda}$	(1.81±0.34) × 10^{-4}			1467
$3(\pi^+\pi^-)$	(1.5 ±1.0) × 10^{-4}			1774
$\overline{p}p\pi^0$	(1.4 ±0.5) × 10^{-4}			1543
$\Delta^{++}\overline{\Delta}^{--}$	(1.28±0.35) × 10^{-4}			1371
$\Sigma^0\overline{\Sigma}^0$	(1.2 ±0.6) × 10^{-4}			1405
$\Sigma^{*+}\overline{\Sigma}^{*-}$	(1.1 ±0.4) × 10^{-4}			1218
K^+K^-	(1.0 ±0.7) × 10^{-4}			1776
$K^0_S K^0_L$	(5.2 ±0.7) × 10^{-5}			1775
$\pi^+\pi^-\pi^0$	(8 ±5) × 10^{-5}			1830
$\rho\pi$	< 8.3	× 10^{-5}	CL=90%	1759
$\pi^+\pi^-$	(8 ±5) × 10^{-5}			1838
$\Xi^-\overline{\Xi}^+$	(9.4 ±3.1) × 10^{-5}			1285
$K_1(1400)^\pm K^\mp$	< 3.1	× 10^{-4}	CL=90%	1532
$\Xi^{*0}\overline{\Xi}^{*0}$	< 8.1	× 10^{-5}	CL=90%	1025
$\Omega^-\overline{\Omega}^+$	< 7.3	× 10^{-5}	CL=90%	774
$K^+K^-\pi^0$	< 2.96	× 10^{-5}	CL=90%	1754
$K^+\overline{K}^*(892)^-$ + c.c.	< 5.4	× 10^{-5}	CL=90%	1698
$\phi\pi^+\pi^-$	(1.50±0.28) × 10^{-4}			1690
$\phi f_0(980)$ → $\pi^+\pi^-$	(6.0 ±2.2) × 10^{-5}			–
ϕK^+K^-	(6.0 ±2.2) × 10^{-5}			1546
$\phi p\overline{p}$	< 2.6	× 10^{-5}	CL=90%	1109
$\phi f_2'(1525)$	< 4.5	× 10^{-5}	CL=90%	1321
Radiative decays				
$\gamma\chi_{c0}(1P)$	(8.6 ±0.7) %			261
$\gamma\chi_{c1}(1P)$	(8.4 ±0.8) %			171
$\gamma\chi_{c2}(1P)$	(6.4 ±0.6) %			128
$\gamma\eta_c(1S)$	(2.8 ±0.6) × 10^{-3}			639
$\gamma\eta'(958)$	(1.5 ±0.4) × 10^{-4}			1719
$\gamma f_2(1270)$	(2.1 ±0.4) × 10^{-4}			1622
$\gamma f_0(1710)$ → $\gamma\pi\pi$	(3.0 ±1.3) × 10^{-5}			–
$\gamma f_0(1710)$ → $\gamma K\overline{K}$	(6.0 ±1.6) × 10^{-5}			–
$\gamma\gamma$	< 1.5	× 10^{-4}	CL=90%	1843
$\gamma\eta$	< 9	× 10^{-5}	CL=90%	1802
$\gamma\eta(1405)$ → $\gamma K\overline{K}\pi$	< 1.2	× 10^{-4}	CL=90%	1569

$\psi(3770)$

$I^G(J^{PC}) = 0^-(1^{--})$

Mass m = 3770.0 ± 2.4 MeV (S = 1.8)
Full width Γ = 23.6 ± 2.7 MeV (S = 1.1)
Γ_{ee} = 0.26 ± 0.04 keV (S = 1.2)

$\psi(3770)$ DECAY MODES	Fraction (Γ_i/Γ)	Scale factor	p (MeV/c)
$D\overline{D}$	dominant		276
e^+e^-	(1.12±0.17) × 10^{-5}	1.2	1885

$\psi(4040)$ [mmm]

$I^G(J^{PC}) = 0^-(1^{--})$

Mass m = 4040 ± 10 MeV
Full width Γ = 52 ± 10 MeV
Γ_{ee} = 0.75 ± 0.15 keV

$\psi(4040)$ DECAY MODES	Fraction (Γ_i/Γ)	p (MeV/c)
e^+e^-	(1.4±0.4) × 10^{-5}	2020
$D^0\overline{D}^0$	seen	777
$D^*(2007)^0\overline{D}^0$ + c.c.	seen	577
$D^*(2007)^0\overline{D}^*(2007)^0$	seen	231

$\psi(4160)$ [mmm]

$I^G(J^{PC}) = 0^-(1^{--})$

Mass m = 4159 ± 20 MeV
Full width Γ = 78 ± 20 MeV
Γ_{ee} = 0.77 ± 0.23 keV

$\psi(4160)$ DECAY MODES	Fraction (Γ_i/Γ)	p (MeV/c)
e^+e^-	(10±4) × 10^{-6}	2080

$\psi(4415)$ [mmm]

$I^G(J^{PC}) = 0^-(1^{--})$

Mass m = 4415 ± 6 MeV
Full width Γ = 43 ± 15 MeV (S = 1.8)
Γ_{ee} = 0.47 ± 0.10 keV

$\psi(4415)$ DECAY MODES	Fraction (Γ_i/Γ)	p (MeV/c)
hadrons	dominant	–
e^+e^-	(1.1±0.4) × 10^{-5}	2207

$b\overline{b}$ MESONS

$\Upsilon(1S)$

$I^G(J^{PC}) = 0^-(1^{--})$

Mass m = 9460.30 ± 0.26 MeV (S = 3.3)
Full width Γ = 53.0 ± 1.5 keV
Γ_{ee} = 1.314 ± 0.029 keV

$\Upsilon(1S)$ DECAY MODES	Fraction (Γ_i/Γ)	Confidence level	p (MeV/c)
$\tau^+\tau^-$	$(2.67^{+0.14}_{-0.16})$ %		4384
e^+e^-	(2.38±0.11) %		4730
$\mu^+\mu^-$	(2.48±0.06) %		4729

Meson Summary Table

Hadronic decays				
$\eta'(958)$ anything	(2.8 ± 0.4) %			–
$J/\psi(1S)$ anything	$(1.1 \pm 0.4) \times 10^{-3}$			4223
$\rho\pi$	< 2	$\times 10^{-4}$	90%	4697
$\pi^+\pi^-$	< 5	$\times 10^{-4}$	90%	4728
K^+K^-	< 5	$\times 10^{-4}$	90%	4704
$p\overline{p}$	< 5	$\times 10^{-4}$	90%	4636
$\pi^0\pi^+\pi^-$	< 1.84	$\times 10^{-5}$	90%	4725
Radiative decays				
$\gamma\pi^+\pi^-$	$(6.3 \pm 1.8) \times 10^{-5}$			4728
$\gamma\pi^0\pi^0$	$(1.7 \pm 0.7) \times 10^{-5}$			4728
$\gamma 2h^+2h^-$	$(7.0 \pm 1.5) \times 10^{-4}$			4720
$\gamma 3h^+3h^-$	$(5.4 \pm 2.0) \times 10^{-4}$			4703
$\gamma 4h^+4h^-$	$(7.4 \pm 3.5) \times 10^{-4}$			4679
$\gamma\pi^+\pi^- K^+K^-$	$(2.9 \pm 0.9) \times 10^{-4}$			4686
$\gamma 2\pi^+2\pi^-$	$(2.5 \pm 0.9) \times 10^{-4}$			4720
$\gamma 3\pi^+3\pi^-$	$(2.5 \pm 1.2) \times 10^{-4}$			4703
$\gamma 2\pi^+2\pi^- K^+K^-$	$(2.4 \pm 1.2) \times 10^{-4}$			4658
$\gamma\pi^+\pi^- p\overline{p}$	$(1.5 \pm 0.6) \times 10^{-4}$			4604
$\gamma 2\pi^+2\pi^- p\overline{p}$	$(4 \pm 6) \times 10^{-5}$			4563
$\gamma 2K^+2K^-$	$(2.0 \pm 2.0) \times 10^{-5}$			4601
$\gamma\eta'(958)$	< 1.6	$\times 10^{-5}$	90%	4682
$\gamma\eta$	< 2.1	$\times 10^{-5}$	90%	4714
$\gamma f_2'(1525)$	< 1.4	$\times 10^{-4}$	90%	4607
$\gamma f_2(1270)$	$(8 \pm 4) \times 10^{-5}$			4644
$\gamma\eta(1405)$	< 8.2	$\times 10^{-5}$	90%	4625
$\gamma f_0(1710) \to \gamma K\overline{K}$	< 2.6	$\times 10^{-4}$	90%	4576
$\gamma f_0(2200) \to \gamma K^+K^-$	< 2	$\times 10^{-4}$	90%	4475
$\gamma f_J(2220) \to \gamma K^+K^-$	< 1.5	$\times 10^{-5}$	90%	4469
$\gamma f_J(2220) \to \gamma\pi^+\pi^-$	< 1.2	$\times 10^{-5}$	90%	–
$\gamma f_J(2220) \to \gamma p\overline{p}$	< 1.6	$\times 10^{-5}$	90%	–
$\gamma\eta(2225) \to \gamma\phi\phi$	< 3	$\times 10^{-3}$	90%	4469
γX (X = pseudoscalar with $m < 7.2$ GeV)	< 3	$\times 10^{-5}$	90%	–
$\gamma X\overline{X}$ ($X\overline{X}$ = vectors with $m < 3.1$ GeV)	< 1	$\times 10^{-3}$	90%	–

$\chi_{b0}(1P)$ [nnn]

$I^G(J^{PC}) = 0^+(0^{++})$
J needs confirmation.

Mass $m = 9859.9 \pm 1.0$ MeV

$\chi_{b0}(1P)$ DECAY MODES	Fraction (Γ_i/Γ)	Confidence level	p (MeV/c)
$\gamma\Upsilon(1S)$	<6 %	90%	391

$\chi_{b1}(1P)$ [nnn]

$I^G(J^{PC}) = 0^+(1^{++})$
J needs confirmation.

Mass $m = 9892.7 \pm 0.6$ MeV (S = 1.1)

$\chi_{b1}(1P)$ DECAY MODES	Fraction (Γ_i/Γ)	p (MeV/c)
$\gamma\Upsilon(1S)$	(35 ± 8) %	423

$\chi_{b2}(1P)$ [nnn]

$I^G(J^{PC}) = 0^+(2^{++})$
J needs confirmation.

Mass $m = 9912.6 \pm 0.5$ MeV (S = 1.1)

$\chi_{b2}(1P)$ DECAY MODES	Fraction (Γ_i/Γ)	p (MeV/c)
$\gamma\Upsilon(1S)$	(22±4) %	442

$\Upsilon(2S)$

$I^G(J^{PC}) = 0^-(1^{--})$

Mass $m = 10.02326 \pm 0.00031$ GeV
Full width $\Gamma = 43 \pm 6$ keV
$\Gamma_{ee} = 0.576 \pm 0.024$ keV

$\Upsilon(2S)$ DECAY MODES	Fraction (Γ_i/Γ)	Confidence level	p (MeV/c)
$\Upsilon(1S)\pi^+\pi^-$	(18.8 ± 0.6) %		475
$\Upsilon(1S)\pi^0\pi^0$	(9.0 ± 0.8) %		480
$\tau^+\tau^-$	(1.7 ± 1.6) %		4686
$\mu^+\mu^-$	(1.31 ± 0.21) %		5011
e^+e^-	(1.34 ± 0.20) %		5012
$\Upsilon(1S)\pi^0$	$< 1.1 \times 10^{-3}$	90%	531
$\Upsilon(1S)\eta$	$< 2 \times 10^{-3}$	90%	126
$J/\psi(1S)$ anything	$< 6 \times 10^{-3}$	90%	4533
Radiative decays			
$\gamma\chi_{b1}(1P)$	(6.8 ± 0.7) %		130
$\gamma\chi_{b2}(1P)$	(7.0 ± 0.6) %		110
$\gamma\chi_{b0}(1P)$	(3.8 ± 0.6) %		162
$\gamma f_0(1710)$	$< 5.9 \times 10^{-4}$	90%	4865
$\gamma f_2'(1525)$	$< 5.3 \times 10^{-4}$	90%	4896
$\gamma f_2(1270)$	$< 2.41 \times 10^{-4}$	90%	4930

$\chi_{b0}(2P)$ [nnn]

$I^G(J^{PC}) = 0^+(0^{++})$
J needs confirmation.

Mass $m = 10.2321 \pm 0.0006$ GeV

$\chi_{b0}(2P)$ DECAY MODES	Fraction (Γ_i/Γ)	p (MeV/c)
$\gamma\Upsilon(2S)$	(4.6 ± 2.1) %	207
$\gamma\Upsilon(1S)$	$(9 \pm 6) \times 10^{-3}$	743

$\chi_{b1}(2P)$ [nnn]

$I^G(J^{PC}) = 0^+(1^{++})$
J needs confirmation.

Mass $m = 10.2552 \pm 0.0005$ GeV
$m_{\chi_{b1}(2P)} - m_{\chi_{b0}(2P)} = 23.5 \pm 1.0$ MeV

$\chi_{b1}(2P)$ DECAY MODES	Fraction (Γ_i/Γ)	Scale factor	p (MeV/c)
$\gamma\Upsilon(2S)$	(21 ± 4) %	1.5	229
$\gamma\Upsilon(1S)$	(8.5 ± 1.3) %	1.3	764

$\chi_{b2}(2P)$ [nnn]

$I^G(J^{PC}) = 0^+(2^{++})$
J needs confirmation.

Mass $m = 10.2685 \pm 0.0004$ GeV
$m_{\chi_{b2}(2P)} - m_{\chi_{b1}(2P)} = 13.5 \pm 0.6$ MeV

$\chi_{b2}(2P)$ DECAY MODES	Fraction (Γ_i/Γ)	p (MeV/c)
$\gamma\Upsilon(2S)$	(16.2 ± 2.4) %	242
$\gamma\Upsilon(1S)$	(7.1 ± 1.0) %	776

$\Upsilon(3S)$

$I^G(J^{PC}) = 0^-(1^{--})$

Mass $m = 10.3552 \pm 0.0005$ GeV
Full width $\Gamma = 26.3 \pm 3.4$ keV

$\Upsilon(3S)$ DECAY MODES	Fraction (Γ_i/Γ)	Scale factor/ Confidence level	p (MeV/c)
$\Upsilon(2S)$ anything	(10.6 ± 0.8) %		296
$\Upsilon(2S)\pi^+\pi^-$	(2.8 ± 0.6) %	S=2.2	177
$\Upsilon(2S)\pi^0\pi^0$	(2.00 ± 0.32) %		190
$\Upsilon(2S)\gamma\gamma$	(5.0 ± 0.7) %		327
$\Upsilon(1S)\pi^+\pi^-$	(4.48 ± 0.21) %		813
$\Upsilon(1S)\pi^0\pi^0$	(2.06 ± 0.28) %		816
$\Upsilon(1S)\eta$	$< 2.2 \times 10^{-3}$	CL=90%	677
$\mu^+\mu^-$	(1.81 ± 0.17) %		5177
e^+e^-	seen		5178
Radiative decays			
$\gamma\chi_{b2}(2P)$	(11.4 ± 0.8) %	S=1.3	86
$\gamma\chi_{b1}(2P)$	(11.3 ± 0.6) %		100
$\gamma\chi_{b0}(2P)$	(5.4 ± 0.6) %	S=1.1	122

$\Upsilon(4S)$ or $\Upsilon(10580)$

$I^G(J^{PC}) = 0^-(1^{--})$

Mass $m = 10.5800 \pm 0.0035$ GeV
Full width $\Gamma = 20 \pm 4$ MeV
$\Gamma_{ee} = 0.248 \pm 0.031$ keV (S = 1.3)

$\Upsilon(4S)$ DECAY MODES	Fraction (Γ_i/Γ)	Confidence level	p (MeV/c)
$B\overline{B}$	> 96 %	95%	335
non-$B\overline{B}$	< 4 %	95%	–
e^+e^-	$(2.8 \pm 0.7) \times 10^{-5}$		5290
$J/\psi(1S)$ anything	$< 1.9 \times 10^{-4}$	95%	–

D^{*+} anything + c.c.	<	7.4	%	90%	5099
ϕ anything	<	2.3	$\times 10^{-3}$	90%	5240
$\Upsilon(1S)$ anything	<	4	$\times 10^{-3}$	90%	1053
$\Upsilon(1S)\pi^+\pi^-$	<	1.2	$\times 10^{-4}$	90%	1027
$\Upsilon(2S)\pi^+\pi^-$	<	3.9	$\times 10^{-4}$	90%	469

$\Upsilon(10860)$ $I^G(J^{PC}) = 0^-(1^{--})$

Mass $m = 10.865 \pm 0.008$ GeV (S = 1.1)
Full width $\Gamma = 110 \pm 13$ MeV
$\Gamma_{ee} = 0.31 \pm 0.07$ keV (S = 1.3)

$\Upsilon(10860)$ DECAY MODES	Fraction (Γ_i/Γ)	p (MeV/c)
e^+e^-	$(2.8 \pm 0.7) \times 10^{-6}$	5432

$\Upsilon(11020)$ $I^G(J^{PC}) = 0^-(1^{--})$

Mass $m = 11.019 \pm 0.008$ GeV
Full width $\Gamma = 79 \pm 16$ MeV
$\Gamma_{ee} = 0.130 \pm 0.030$ keV

$\Upsilon(11020)$ DECAY MODES	Fraction (Γ_i/Γ)	p (MeV/c)
e^+e^-	$(1.6 \pm 0.5) \times 10^{-6}$	5510

NOTES

In this Summary Table:

When a quantity has "(S = ...)" to its right, the error on the quantity has been enlarged by the "scale factor" S, defined as $S = \sqrt{\chi^2/(N-1)}$, where N is the number of measurements used in calculating the quantity. We do this when $S > 1$, which often indicates that the measurements are inconsistent. When $S > 1.25$, we also show in the Particle Listings an ideogram of the measurements. For more about S, see the Introduction.

A decay momentum p is given for each decay mode. For a 2-body decay, p is the momentum of each decay product in the rest frame of the decaying particle. For a 3-or-more-body decay, p is the largest momentum any of the products can have in this frame.

[a] See the "Note on $\pi^\pm \to \ell^\pm\nu\gamma$ and $K^\pm \to \ell^\pm\nu\gamma$ Form Factors" in the $\pi^\pm$ Particle Listings for definitions and details.

[b] Measurements of $\Gamma(e^+\nu_e)/\Gamma(\mu^+\nu_\mu)$ always include decays with γ's, and measurements of $\Gamma(e^+\nu_e\gamma)$ and $\Gamma(\mu^+\nu_\mu\gamma)$ never include low-energy γ's. Therefore, since no clean separation is possible, we consider the modes with γ's to be subreactions of the modes without them, and let $[\Gamma(e^+\nu_e) + \Gamma(\mu^+\nu_\mu)]/\Gamma_{\rm total} = 100\%$.

[c] See the $\pi^\pm$ Particle Listings for the energy limits used in this measurement; low-energy γ's are not included.

[d] Derived from an analysis of neutrino-oscillation experiments.

[e] Astrophysical and cosmological arguments give limits of order 10^{-13}; see the π^0 Particle Listings.

[f] Due to a new measurement in the average, this is 0.45 MeV larger than the mass we gave in our 2002 edition, 547.30 ± 0.12 MeV.

[g] Due to removing an old measurement from the average, this is 0.11 keV larger than the width we gave in our 2002 edition, 1.18 ± 0.11 keV. See the $\Gamma(2\gamma)$ data block in the Data Listings.

[h] C parity forbids this to occur as a single-photon process.

[i] See the "Note on scalar mesons" in the $f_0(1370)$ Particle Listings . The interpretation of this entry as a particle is controversial.

[j] See the "Note on $\rho(770)$" in the $\rho(770)$ Particle Listings .

[k] The $\omega\rho$ interference is then due to $\omega\rho$ mixing only, and is expected to be small. If $e\mu$ universality holds, $\Gamma(\rho^0 \to \mu^+\mu^-) = \Gamma(\rho^0 \to e^+e^-) \times 0.99785$.

[l] See the "Note on scalar mesons" in the $f_0(1370)$ Particle Listings .

[m] See the "Note on $a_1(1260)$" in the $a_1(1260)$ Particle Listings .

[n] This is only an educated guess; the error given is larger than the error on the average of the published values. See the Particle Listings for details.

[o] See the "Note on non-$q\overline{q}$ mesons" in the Particle Listings (see the index for the page number).

[p] See the "Note on the $\eta(1405)$" in the $\eta(1405)$ Particle Listings.

[q] See the "Note on the $f_1(1420)$" in the $\eta(1405)$ Particle Listings.

[r] See also the $\omega(1650)$ Particle Listings.

[s] See the "Note on the $\rho(1450)$ and the $\rho(1700)$" in the $\rho(1700)$ Particle Listings.

[t] See also the $\omega(1420)$ Particle Listings.

[u] See the "Note on $f_0(1710)$" in the $f_0(1710)$ Particle Listings .

[v] See the note in the $K^\pm$ Particle Listings.

[w] The definition of the slope parameter g of the $K \to 3\pi$ Dalitz plot is as follows (see also "Note on Dalitz Plot Parameters for $K \to 3\pi$ Decays" in the $K^\pm$ Particle Listings):

$$|M|^2 = 1 + g(s_3 - s_0)/m^2_{\pi^+} + \cdots .$$

[x] For more details and definitions of parameters see the Particle Listings.

[y] Most of this radiative mode, the low-momentum γ part, is also included in the parent mode listed without γ's.

[z] See the $K^\pm$ Particle Listings for the energy limits used in this measurement.

[aa] Structure-dependent part.

[bb] Direct-emission branching fraction.

[cc] Violates angular-momentum conservation.

[dd] Derived from measured values of ϕ_{+-}, ϕ_{00}, $|\eta|$, $|m_{K^0_L} - m_{K^0_S}|$, and $\tau_{K^0_S}$, as described in the introduction to "Tests of Conservation Laws."

[ee] The CP-violation parameters are defined as follows (see also "Note on CP Violation in $K_S \to 3\pi$" and "Note on CP Violation in K^0_L Decay" in the Particle Listings):

$$\eta_{+-} = |\eta_{+-}|e^{i\phi_{+-}} = \frac{A(K^0_L \to \pi^+\pi^-)}{A(K^0_S \to \pi^+\pi^-)} = \epsilon + \epsilon'$$

$$\eta_{00} = |\eta_{00}|e^{i\phi_{00}} = \frac{A(K^0_L \to \pi^0\pi^0)}{A(K^0_S \to \pi^0\pi^0)} = \epsilon - 2\epsilon'$$

$$\delta = \frac{\Gamma(K^0_L \to \pi^-\ell^+\nu) - \Gamma(K^0_L \to \pi^+\ell^-\nu)}{\Gamma(K^0_L \to \pi^-\ell^+\nu) + \Gamma(K^0_L \to \pi^+\ell^-\nu)} ,$$

$$|{\rm Im}(\eta_{+-0})|^2 = \frac{\Gamma(K^0_S \to \pi^+\pi^-\pi^0)^{CP\ \rm viol.}}{\Gamma(K^0_L \to \pi^+\pi^-\pi^0)} ,$$

$$|{\rm Im}(\eta_{000})|^2 = \frac{\Gamma(K^0_S \to \pi^0\pi^0\pi^0)}{\Gamma(K^0_L \to \pi^0\pi^0\pi^0)} .$$

where for the last two relations CPT is assumed valid, *i.e.*, ${\rm Re}(\eta_{+-0}) \simeq 0$ and ${\rm Re}(\eta_{000}) \simeq 0$.

[ff] See the K^0_S Particle Listings for the energy limits used in this measurement.

[gg] The value is for the sum of the charge states or particle/antiparticle states indicated.

[hh] ${\rm Re}(\epsilon'/\epsilon) = \epsilon'/\epsilon$ to a very good approximation provided the phases satisfy CPT invariance.

[ii] See the K^0_L Particle Listings for the energy limits used in this measurement.

[jj] Allowed by higher-order electroweak interactions.

[kk] Violates CP in leading order. Test of direct CP violation since the indirect CP-violating and CP-conserving contributions are expected to be suppressed.

[ll] See the "Note on $f_0(1370)$" in the $f_0(1370)$ Particle Listings and in the 1994 edition.

[mm] See the note in the $L(1770)$ Particle Listings in Reviews of Modern Physics **56** No. 2 Pt. II (1984), p. S200. See also the "Note on $K_2(1770)$ and the $K_2(1820)$" in the $K_2(1770)$ Particle Listings .

[nn] See the "Note on $K_2(1770)$ and the $K_2(1820)$" in the $K_2(1770)$ Particle Listings .

[oo] This result applies to $Z^0 \to c\overline{c}$ decays only. Here ℓ^+ is an average (not a sum) of e^+ and μ^+ decays.

[pp] This is a weighted average of $D^\pm$ (44%) and D^0 (56%) branching fractions. See "D^+ and $D^0 \to$ (η anything) / (total D^+ and D^0)" under "D^+ Branching Ratios" in the Particle Listings.

[qq] This value averages the e^+ and μ^+ branching fractions, after making a small phase-space adjustment to the μ^+ fraction to be able to use it as an e^+ fraction; hence our ℓ^+ here is really an e^+.

[rr] An ℓ indicates an e or a μ mode, not a sum over these modes.

Meson Summary Table

[ss] The branching fraction for this mode may differ from the sum of the submodes that contribute to it, due to interference effects. See the relevant papers in the Particle Listings.

[tt] The two experiments measuring this fraction are in serious disagreement. See the Particle Listings.

[uu] This value includes only $\pi^+\pi^-$ decays of the intermediate resonance, because branching fractions of this resonance are not known.

[vv] Unseen decay modes of the resonance are included.

[ww] This mode is not a useful test for a $\Delta C=1$ weak neutral current because both quarks must change flavor in this decay.

[xx] This $D_1^0 - D_2^0$ limit is inferred from the D^0-$\overline{D}^0$ mixing ratio $\Gamma(K^+\pi^-$ (via $\overline{D}^0$)) / $\Gamma(K^-\pi^+)$ near the end of the D^0 Listings.

[yy] The exclusive e^+ modes $K^-e^+\nu_e$, $K^-\pi^0e^+\nu_e$, $\overline{K}^0\pi^-e^+\nu_e$ and $\pi^-e^+\nu_e$ are constrained to equal this (well-measured) inclusive fraction.

[zz] The experiments on the division of this charge mode amongst its submodes disagree, and the submode branching fractions here add up to considerably more than the charged-mode fraction.

[aaa] However, these upper limits are in serious disagreement with values obtained in another experiment.

[bbb] For now, we average together measurements of the $Xe^+\nu_e$ and $X\mu^+\nu_\mu$ branching fractions. This is the *average*, not the *sum*.

[ccc] This branching fraction includes all the decay modes of the final-state resonance.

[ddd] This value includes only K^+K^- decays of the intermediate resonance, because branching fractions of this resonance are not known.

[eee] B^0 and B_s^0 contributions not separated. Limit is on weighted average of the two decay rates.

[fff] These values are model dependent. See 'Note on Semileptonic Decays' in the B^+ Particle Listings.

[ggg] D^{**} stands for the sum of the $D(1\,^1P_1)$, $D(1\,^3P_0)$, $D(1\,^3P_1)$, $D(1\,^3P_2)$, $D(2\,^1S_0)$, and $D(2\,^1S_1)$ resonances.

[hhh] $D^{(*)}\overline{D}^{(*)}$ stands for the sum of $D^*\overline{D}^*$, $D^*\overline{D}$, $D\overline{D}^*$, and $D\overline{D}$.

[iii] Inclusive branching fractions have a multiplicity definition and can be greater than 100%.

[jjj] D_j represents an unresolved mixture of pseudoscalar and tensor D^{**} (P-wave) states.

[kkk] Not a pure measurement. See note at head of B_s^0 Decay Modes.

[lll] Includes $p\overline{p}\pi^+\pi^-\gamma$ and excludes $p\overline{p}\eta$, $p\overline{p}\omega$, $p\overline{p}\eta'$.

[mmm] J^{PC} known by production in e^+e^- via single photon annihilation. I^G is not known; interpretation of this state as a single resonance is unclear because of the expectation of substantial threshold effects in this energy region.

[nnn] Spectroscopic labeling for these states is theoretical, pending experimental information.

Meson Summary Table

See also the table of suggested $q\overline{q}$ quark-model assignments in the Quark Model section.

• Indicates particles that appear in the preceding Meson Summary Table. We do not regard the other entries as being established.

† Indicates that the value of J given is preferred, but needs confirmation.

LIGHT UNFLAVORED ($S = C = B = 0$)

	$I^G(J^{PC})$
• $\pi^{\pm}$	$1^-(0^{-+})$
• π^0	$1^-(0^{-+})$
• η	$0^+(0^{-+})$
• $f_0(600)$	$0^+(0^{++})$
• $\rho(770)$	$1^+(1^{--})$
• $\omega(782)$	$0^-(1^{--})$
• $\eta'(958)$	$0^+(0^{-+})$
• $f_0(980)$	$0^+(0^{++})$
• $a_0(980)$	$1^-(0^{++})$
• $\phi(1020)$	$0^-(1^{--})$
• $h_1(1170)$	$0^-(1^{+-})$
• $b_1(1235)$	$1^+(1^{+-})$
• $a_1(1260)$	$1^-(1^{++})$
• $f_2(1270)$	$0^+(2^{++})$
• $f_1(1285)$	$0^+(1^{++})$
• $\eta(1295)$	$0^+(0^{-+})$
• $\pi(1300)$	$1^-(0^{-+})$
• $a_2(1320)$	$1^-(2^{++})$
• $f_0(1370)$	$0^+(0^{++})$
$h_1(1380)$	$?^-(1^{+-})$
• $\pi_1(1400)$	$1^-(1^{-+})$
• $\eta(1405)$	$0^+(0^{-+})$
• $f_1(1420)$	$0^+(1^{++})$
• $\omega(1420)$	$0^-(1^{--})$
$f_2(1430)$	$0^+(2^{++})$
• $a_0(1450)$	$1^-(0^{++})$
• $\rho(1450)$	$1^+(1^{--})$
• $\eta(1450)$	$0^+(0^{-+})$
• $f_0(1500)$	$0^+(0^{++})$
$f_1(1510)$	$0^+(1^{++})$
• $f_2'(1525)$	$0^+(2^{++})$
$f_2(1565)$	$0^+(2^{++})$
$h_1(1595)$	$0^-(1^{+-})$
• $\pi_1(1600)$	$1^-(1^{-+})$
$a_1(1640)$	$1^-(1^{++})$
$f_2(1640)$	$0^+(2^{++})$
• $\eta_2(1645)$	$0^+(2^{-+})$
• $\omega(1650)$	$0^-(1^{--})$
• $\omega_3(1670)$	$0^-(3^{--})$
• $\pi_2(1670)$	$1^-(2^{-+})$
• $\phi(1680)$	$0^-(1^{--})$
• $\rho_3(1690)$	$1^+(3^{--})$
• $\rho(1700)$	$1^+(1^{--})$
$a_2(1700)$	$1^-(2^{++})$
• $f_0(1710)$	$0^+(0^{++})$
$\eta(1760)$	$0^+(0^{-+})$
• $\pi(1800)$	$1^-(0^{-+})$
$f_2(1810)$	$0^+(2^{++})$
• $\phi_3(1850)$	$0^-(3^{--})$
$\eta_2(1870)$	$0^+(2^{-+})$
$\rho(1900)$	$1^+(1^{--})$
$f_2(1910)$	$0^+(2^{++})$
• $f_2(1950)$	$0^+(2^{++})$
$\rho_3(1990)$	$1^+(3^{--})$
• $f_2(2010)$	$0^+(2^{++})$
$f_0(2020)$	$0^+(0^{++})$
• $a_4(2040)$	$1^-(4^{++})$
• $f_4(2050)$	$0^+(4^{++})$
$\pi_2(2100)$	$1^-(2^{-+})$
$f_0(2100)$	$0^+(0^{++})$
$f_2(2150)$	$0^+(2^{++})$
$\rho(2150)$	$1^+(1^{--})$
$f_0(2200)$	$0^+(0^{++})$
$f_J(2220)$	$0^+(2^{++}$ or $4^{++})$
$\eta(2225)$	$0^+(0^{-+})$
$\rho_3(2250)$	$1^+(3^{--})$
• $f_2(2300)$	$0^+(2^{++})$
$f_4(2300)$	$0^+(4^{++})$
• $f_2(2340)$	$0^+(2^{++})$
$\rho_5(2350)$	$1^+(5^{--})$
$a_6(2450)$	$1^-(6^{++})$
$f_6(2510)$	$0^+(6^{++})$

OTHER LIGHT

Further States

STRANGE ($S = \pm 1$, $C = B = 0$)

	$I(J^P)$
• $K^{\pm}$	$1/2(0^-)$
• K^0	$1/2(0^-)$
• K_S^0	$1/2(0^-)$
• K_L^0	$1/2(0^-)$
$K_0^*(800)$	$1/2(0^+)$
• $K^*(892)$	$1/2(1^-)$
• $K_1(1270)$	$1/2(1^+)$
• $K_1(1400)$	$1/2(1^+)$
• $K^*(1410)$	$1/2(1^-)$
• $K_0^*(1430)$	$1/2(0^+)$
• $K_2^*(1430)$	$1/2(2^+)$
$K(1460)$	$1/2(0^-)$
$K_2(1580)$	$1/2(2^-)$
$K(1630)$	$1/2(?^?)$
$K_1(1650)$	$1/2(1^+)$
• $K^*(1680)$	$1/2(1^-)$
• $K_2(1770)$	$1/2(2^-)$
• $K_3^*(1780)$	$1/2(3^-)$
• $K_2(1820)$	$1/2(2^-)$
$K(1830)$	$1/2(0^-)$
$K_0^*(1950)$	$1/2(0^+)$
$K_2^*(1980)$	$1/2(2^+)$
• $K_4^*(2045)$	$1/2(4^+)$
$K_2(2250)$	$1/2(2^-)$
$K_3(2320)$	$1/2(3^+)$
$K_5^*(2380)$	$1/2(5^-)$
$K_4(2500)$	$1/2(4^-)$
$K(3100)$	$?^?(?^{??})$

CHARMED ($C = \pm 1$)

• $D^{\pm}$	$1/2(0^-)$
• D^0	$1/2(0^-)$
• $D^*(2007)^0$	$1/2(1^-)$
• $D^*(2010)^{\pm}$	$1/2(1^-)$
• $D_1(2420)^0$	$1/2(1^+)$
$D_1(2420)^{\pm}$	$1/2(?^?)$
• $D_2^*(2460)^0$	$1/2(2^+)$
• $D_2^*(2460)^{\pm}$	$1/2(2^+)$
$D^*(2640)^{\pm}$	$1/2(?^?)$

CHARMED, STRANGE ($C = S = \pm 1$)

• $D_s^{\pm}$	$0(0^-)$
• $D_s^{*\pm}$	$0(?^?)$
• $D_{sJ}^*(2317)^{\pm}$	$0(0^+)$
• $D_{sJ}(2460)^{\pm}$	$0(1^+)$
• $D_{s1}(2536)^{\pm}$	$0(1^+)$
• $D_{s2}(2573)^{\pm}$	$0(?^?)$

BOTTOM ($B = \pm 1$)

	$I^G(J^{PC})$
• $B^{\pm}$	$1/2(0^-)$
• B^0	$1/2(0^-)$
• $B^{\pm}/B^0$ ADMIXTURE	
• $B^{\pm}/B^0/B_s^0/b$-baryon ADMIXTURE V_{cb} and V_{ub} CKM Matrix Elements	
• B^*	$1/2(1^-)$
$B_J^*(5732)$	$?(?^?)$

BOTTOM, STRANGE ($B = \pm 1$, $S = \mp 1$)

• B_s^0	$0(0^-)$
B_s^*	$0(1^-)$
$B_{sJ}^*(5850)$	$?(?^?)$

BOTTOM, CHARMED ($B = C = \pm 1$)

• $B_c^{\pm}$	$0(0^-)$

$c\overline{c}$

• $\eta_c(1S)$	$0^+(0^{-+})$
• $J/\psi(1S)$	$0^-(1^{--})$
• $\chi_{c0}(1P)$	$0^+(0^{++})$
• $\chi_{c1}(1P)$	$0^+(1^{++})$
$h_c(1P)$	$?^?(?^{??})$
• $\chi_{c2}(1P)$	$0^+(2^{++})$
$\eta_c(2S)$	$0^+(0^{-+})$
• $\psi(2S)$	$0^-(1^{--})$
• $\psi(3770)$	$0^-(1^{--})$
$\psi(3836)$	$0^-(2^{--})$
$X(3872)$	$?^?(?^?)$
• $\psi(4040)$	$0^-(1^{--})$
• $\psi(4160)$	$0^-(1^{--})$
• $\psi(4415)$	$0^-(1^{--})$

$b\overline{b}$

$\eta_b(1S)$	$0^+(0^{-+})$
• $\Upsilon(1S)$	$0^-(1^{--})$
• $\chi_{b0}(1P)$	$0^+(0^{++})$
• $\chi_{b1}(1P)$	$0^+(1^{++})$
• $\chi_{b2}(1P)$	$0^+(2^{++})$
• $\Upsilon(2S)$	$0^-(1^{--})$
• $\chi_{b0}(2P)$	$0^+(0^{++})$
• $\chi_{b1}(2P)$	$0^+(1^{++})$
• $\chi_{b2}(2P)$	$0^+(2^{++})$
• $\Upsilon(3S)$	$0^-(1^{--})$
• $\Upsilon(4S)$	$0^-(1^{--})$
• $\Upsilon(10860)$	$0^-(1^{--})$
• $\Upsilon(11020)$	$0^-(1^{--})$

NON-$q\overline{q}$ CANDIDATES

NON-$q\overline{q}$ CANDIDATES

Baryon Summary Table

This short table gives the name, the quantum numbers (where known), and the status of baryons in the Review. Only the baryons with 3- or 4-star status are included in the main Baryon Summary Table. Due to insufficient data or uncertain interpretation, the other entries in the short table are not established as baryons. The names with masses are of baryons that decay strongly. For N, Δ, and Ξ resonances, the partial wave is indicated by the symbol $L_{2I,2J}$, where L is the orbital angular momuntum (S, P, D, ...), I is the isospin, and J is the total angular momentum. For Λ and Σ resonances, the symbol is $L_{I,2J}$.

p	P_{11}	****	$\Delta(1232)$	P_{33}	****	Λ	P_{01}	****	Σ^+	P_{11}	****	Ξ^0	P_{11}	****
n	P_{11}	****	$\Delta(1600)$	P_{33}	***	$\Lambda(1405)$	S_{01}	****	Σ^0	P_{11}	****	Ξ^-	P_{11}	****
$N(1440)$	P_{11}	****	$\Delta(1620)$	S_{31}	****	$\Lambda(1520)$	D_{03}	****	Σ^-	P_{11}	****	$\Xi(1530)$	P_{13}	****
$N(1520)$	D_{13}	****	$\Delta(1700)$	D_{33}	****	$\Lambda(1600)$	P_{01}	***	$\Sigma(1385)$	P_{13}	****	$\Xi(1620)$		*
$N(1535)$	S_{11}	****	$\Delta(1750)$	P_{31}	*	$\Lambda(1670)$	S_{01}	****	$\Sigma(1480)$		*	$\Xi(1690)$		***
$N(1650)$	S_{11}	****	$\Delta(1900)$	S_{31}	**	$\Lambda(1690)$	D_{03}	****	$\Sigma(1560)$		**	$\Xi(1820)$	D_{13}	***
$N(1675)$	D_{15}	****	$\Delta(1905)$	F_{35}	****	$\Lambda(1800)$	S_{01}	***	$\Sigma(1580)$	D_{13}	**	$\Xi(1950)$		***
$N(1680)$	F_{15}	****	$\Delta(1910)$	P_{31}	****	$\Lambda(1810)$	P_{01}	***	$\Sigma(1620)$	S_{11}	**	$\Xi(2030)$		***
$N(1700)$	D_{13}	***	$\Delta(1920)$	P_{33}	***	$\Lambda(1820)$	F_{05}	****	$\Sigma(1660)$	P_{11}	***	$\Xi(2120)$		*
$N(1710)$	P_{11}	***	$\Delta(1930)$	D_{35}	***	$\Lambda(1830)$	D_{05}	****	$\Sigma(1670)$	D_{13}	****	$\Xi(2250)$		**
$N(1720)$	P_{13}	****	$\Delta(1940)$	D_{33}	*	$\Lambda(1890)$	P_{03}	****	$\Sigma(1690)$		**	$\Xi(2370)$		**
$N(1900)$	P_{13}	**	$\Delta(1950)$	F_{37}	****	$\Lambda(2000)$		*	$\Sigma(1750)$	S_{11}	***	$\Xi(2500)$		*
$N(1990)$	F_{17}	**	$\Delta(2000)$	F_{35}	**	$\Lambda(2020)$	F_{07}	*	$\Sigma(1770)$	P_{11}	*			
$N(2000)$	F_{15}	**	$\Delta(2150)$	S_{31}	*	$\Lambda(2100)$	G_{07}	****	$\Sigma(1775)$	D_{15}	****	Ω^-		****
$N(2080)$	D_{13}	**	$\Delta(2200)$	G_{37}	*	$\Lambda(2110)$	F_{05}	***	$\Sigma(1840)$	P_{13}	*	$\Omega(2250)^-$		***
$N(2090)$	S_{11}	*	$\Delta(2300)$	H_{39}	**	$\Lambda(2325)$	D_{03}	*	$\Sigma(1880)$	P_{11}	**	$\Omega(2380)^-$		**
$N(2100)$	P_{11}	*	$\Delta(2350)$	D_{35}	*	$\Lambda(2350)$	H_{09}	***	$\Sigma(1915)$	F_{15}	****	$\Omega(2470)^-$		**
$N(2190)$	G_{17}	****	$\Delta(2390)$	F_{37}	*	$\Lambda(2585)$		**	$\Sigma(1940)$	D_{13}	***			
$N(2200)$	D_{15}	**	$\Delta(2400)$	G_{39}	**				$\Sigma(2000)$	S_{11}	*	Λ_c^+		****
$N(2220)$	H_{19}	****	$\Delta(2420)$	$H_{3,11}$	****				$\Sigma(2030)$	F_{17}	****	$\Lambda_c(2593)^+$		***
$N(2250)$	G_{19}	****	$\Delta(2750)$	$I_{3,13}$	**				$\Sigma(2070)$	F_{15}	*	$\Lambda_c(2625)^+$		***
$N(2600)$	$I_{1,11}$	***	$\Delta(2950)$	$K_{3,15}$	**				$\Sigma(2080)$	P_{13}	**	$\Lambda_c(2765)^+$		*
$N(2700)$	$K_{1,13}$	**							$\Sigma(2100)$	G_{17}	*	$\Lambda_c(2880)^+$		**
			$\Theta(1540)^+$		***				$\Sigma(2250)$		***	$\Sigma_c(2455)$		****
			$\Phi(1860)$		*				$\Sigma(2455)$		**	$\Sigma_c(2520)$		***
									$\Sigma(2620)$		**	Ξ_c^+		***
									$\Sigma(3000)$		*	Ξ_c^0		***
									$\Sigma(3170)$		*	$\Xi_c^{\prime+}$		***
												$\Xi_c^{\prime0}$		***
												$\Xi_c(2645)$		***
												$\Xi_c(2790)$		***
												$\Xi_c(2815)$		***
												Ω_c^0		***
												Ξ_{cc}^+		*
												Λ_b^0		***
												Ξ_b^0, Ξ_b^-		*

**** Existence is certain, and properties are at least fairly well explored.

*** Existence ranges from very likely to certain, but further confirmation is desirable and/or quantum numbers, branching fractions, etc. are not well determined.

** Evidence of existence is only fair.

* Evidence of existence is poor.

N BARYONS
$(S = 0, I = 1/2)$

p, $N^+ = uud$; n, $N^0 = udd$

p

$I(J^P) = \frac{1}{2}(\frac{1}{2}^+)$

Mass $m = 1.00727646688 \pm 0.00000000013$ u
Mass $m = 938.27203 \pm 0.00008$ MeV [a]
$\left|m_p - m_{\overline{p}}\right|/m_p < 1.0 \times 10^{-8}$, CL = 90% [b]
$\left|\frac{q_{\overline{p}}}{m_{\overline{p}}}\right|/(\frac{q_p}{m_p}) = 0.99999999991 \pm 0.00000000009$
$\left|q_p + q_{\overline{p}}\right|/e < 1.0 \times 10^{-8}$, CL = 90% [b]
$\left|q_p + q_e\right|/e < 1.0 \times 10^{-21}$ [c]
Magnetic moment $\mu = 2.792847351 \pm 0.000000028\ \mu_N$
$(\mu_p + \mu_{\overline{p}}) / \mu_p = (-2.6 \pm 2.9) \times 10^{-3}$
Electric dipole moment $d < 0.54 \times 10^{-23}\ e$ cm
Electric polarizability $\alpha = (12.0 \pm 0.6) \times 10^{-4}$ fm^3
Magnetic polarizability $\beta = (1.9 \pm 0.5) \times 10^{-4}$ fm^3
Charge radius = 0.870 ± 0.008 fm
Mean life $\tau > 2.1 \times 10^{29}$ years, CL = 90% ($p \to$ invisible mode)
Mean life $\tau > 10^{31}$ to 10^{33} years [d] (mode dependent)

See the "Note on Nucleon Decay" in our 1994 edition (Phys. Rev. **D50**, 1673) for a short review.

The "partial mean life" limits tabulated here are the limits on τ/B_i, where τ is the total mean life and B_i is the branching fraction for the mode in question. For N decays, p and n indicate proton and neutron partial lifetimes.

p DECAY MODES	Partial mean life (10^{30} years)	Confidence level	p (MeV/c)
Antilepton + meson			
$N \to e^+\pi$	$> 158\ (n)$, $> 1600\ (p)$	90%	459
$N \to \mu^+\pi$	$> 100\ (n)$, $> 473\ (p)$	90%	453
$N \to \nu\pi$	$> 112\ (n)$, $> 25\ (p)$	90%	459
$p \to e^+\eta$	> 313	90%	309
$p \to \mu^+\eta$	> 126	90%	297
$n \to \nu\eta$	> 158	90%	310
$N \to e^+\rho$	$> 217\ (n)$, $> 75\ (p)$	90%	148
$N \to \mu^+\rho$	$> 228\ (n)$, $> 110\ (p)$	90%	113
$N \to \nu\rho$	$> 19\ (n)$, $> 162\ (p)$	90%	148
$p \to e^+\omega$	> 107	90%	143
$p \to \mu^+\omega$	> 117	90%	105
$n \to \nu\omega$	> 108	90%	144
$N \to e^+K$	$> 17\ (n)$, $> 150\ (p)$	90%	339
$p \to e^+K^0_S$	> 120	90%	337
$p \to e^+K^0_L$	> 51	90%	337
$N \to \mu^+K$	$> 26\ (n)$, $> 120\ (p)$	90%	329
$p \to \mu^+K^0_S$	> 150	90%	326
$p \to \mu^+K^0_L$	> 83	90%	326
$N \to \nu K$	$> 86\ (n)$, $> 670\ (p)$	90%	339
$n \to \nu K^0_S$	> 51	90%	338
$p \to e^+K^*(892)^0$	> 84	90%	45
$N \to \nu K^*(892)$	$> 78\ (n)$, $> 51\ (p)$	90%	45
Antilepton + mesons			
$p \to e^+\pi^+\pi^-$	> 82	90%	448
$p \to e^+\pi^0\pi^0$	> 147	90%	449
$n \to e^+\pi^-\pi^0$	> 52	90%	449
$p \to \mu^+\pi^+\pi^-$	> 133	90%	425
$p \to \mu^+\pi^0\pi^0$	> 101	90%	427
$n \to \mu^+\pi^-\pi^0$	> 74	90%	427
$n \to e^+K^0\pi^-$	> 18	90%	319
Lepton + meson			
$n \to e^-\pi^+$	> 65	90%	459
$n \to \mu^-\pi^+$	> 49	90%	453
$n \to e^-\rho^+$	> 62	90%	149
$n \to \mu^-\rho^+$	> 7	90%	114
$n \to e^-K^+$	> 32	90%	340
$n \to \mu^-K^+$	> 57	90%	330
Lepton + mesons			
$p \to e^-\pi^+\pi^+$	> 30	90%	448
$n \to e^-\pi^+\pi^0$	> 29	90%	449
$p \to \mu^-\pi^+\pi^+$	> 17	90%	425
$n \to \mu^-\pi^+\pi^0$	> 34	90%	427
$p \to e^-\pi^+K^+$	> 75	90%	320
$p \to \mu^-\pi^+K^+$	> 245	90%	279
Antilepton + photon(s)			
$p \to e^+\gamma$	> 670	90%	469
$p \to \mu^+\gamma$	> 478	90%	463
$n \to \nu\gamma$	> 28	90%	470
$p \to e^+\gamma\gamma$	> 100	90%	469
$n \to \nu\gamma\gamma$	> 219	90%	470
Three (or more) leptons			
$p \to e^+e^+e^-$	> 793	90%	469
$p \to e^+\mu^+\mu^-$	> 359	90%	457
$p \to e^+\nu\nu$	> 17	90%	469
$n \to e^+e^-\nu$	> 257	90%	470
$n \to \mu^+e^-\nu$	> 83	90%	464
$n \to \mu^+\mu^-\nu$	> 79	90%	458
$p \to \mu^+e^+e^-$	> 529	90%	463
$p \to \mu^+\mu^+\mu^-$	> 675	90%	439
$p \to \mu^+\nu\nu$	> 21	90%	463
$p \to e^-\mu^+\mu^+$	> 6	90%	457
$n \to 3\nu$	> 0.0005	90%	470
Inclusive modes			
$N \to e^+$ anything	$> 0.6\ (n,\ p)$	90%	–
$N \to \mu^+$ anything	$> 12\ (n,\ p)$	90%	–
$N \to e^+\pi^0$ anything	$> 0.6\ (n,\ p)$	90%	–
$\Delta B = 2$ dinucleon modes			
The following are lifetime limits per iron nucleus.			
$pp \to \pi^+\pi^+$	> 0.7	90%	–
$pn \to \pi^+\pi^0$	> 2	90%	–
$nn \to \pi^+\pi^-$	> 0.7	90%	–
$nn \to \pi^0\pi^0$	> 3.4	90%	–
$pp \to e^+e^+$	> 5.8	90%	–
$pp \to e^+\mu^+$	> 3.6	90%	–
$pp \to \mu^+\mu^+$	> 1.7	90%	–
$pn \to e^+\overline{\nu}$	> 2.8	90%	–
$pn \to \mu^+\overline{\nu}$	> 1.6	90%	–
$nn \to \nu_e\overline{\nu}_e$	> 0.000049	90%	–
$pp \to$ neutrinos	> 0.00005	90%	–

$\overline{p}$ DECAY MODES

$\overline{p}$ DECAY MODES	Partial mean life (years)	Confidence level	p (MeV/c)
$\overline{p} \to e^-\gamma$	$> 7 \times 10^5$	90%	469
$\overline{p} \to \mu^-\gamma$	$> 5 \times 10^4$	90%	463
$\overline{p} \to e^-\pi^0$	$> 4 \times 10^5$	90%	459
$\overline{p} \to \mu^-\pi^0$	$> 5 \times 10^4$	90%	453
$\overline{p} \to e^-\eta$	$> 2 \times 10^4$	90%	309
$\overline{p} \to \mu^-\eta$	$> 8 \times 10^3$	90%	297
$\overline{p} \to e^-K^0_S$	> 900	90%	337
$\overline{p} \to \mu^-K^0_S$	$> 4 \times 10^3$	90%	326
$\overline{p} \to e^-K^0_L$	$> 9 \times 10^3$	90%	337
$\overline{p} \to \mu^-K^0_L$	$> 7 \times 10^3$	90%	326
$\overline{p} \to e^-\gamma\gamma$	$> 2 \times 10^4$	90%	469
$\overline{p} \to \mu^-\gamma\gamma$	$> 2 \times 10^4$	90%	463
$\overline{p} \to e^-\omega$	> 200	90%	143

Baryon Summary Table

n

$I(J^P) = \frac{1}{2}(\frac{1}{2}^+)$

Mass $m = 1.0086649156 \pm 0.0000000006$ u
Mass $m = 939.56536 \pm 0.00008$ MeV [a]
$m_n - m_p = 1.2933317 \pm 0.0000005$ MeV
$= 0.0013884487 \pm 0.0000000006$ u
Mean life $\tau = 885.7 \pm 0.8$ s
$c\tau = 2.655 \times 10^8$ km
Magnetic moment $\mu = -1.91304027 \pm 0.0000005\ \mu_N$
Electric dipole moment $d < 0.63 \times 10^{-25}$ e cm, CL = 90%
Mean-square charge radius $\langle r_n^2 \rangle = -0.1161 \pm 0.0022$ fm^2 (S = 1.3)
Electric polarizability $\alpha = (11.6 \pm 1.5) \times 10^{-4}$ fm^3
Magnetic polarizability $\beta = (3.7 \pm 2.0) \times 10^{-4}$ fm^3
Charge $q = (-0.4 \pm 1.1) \times 10^{-21}$ e
Mean $n\overline{n}$-oscillation time $> 8.6 \times 10^7$ s, CL = 90% (free n)
Mean $n\overline{n}$-oscillation time $> 1.3 \times 10^8$ s, CL = 90% [e] (bound n)

Decay parameters [f]

$pe^-\overline{\nu}_e$ $\lambda \equiv g_A / g_V = -1.2695 \pm 0.0029$ (S = 2.0)
" $A = -0.1173 \pm 0.0013$ (S = 2.3)
" $B = 0.983 \pm 0.004$
" $a = -0.103 \pm 0.004$
" $\phi_{AV} = (180.08 \pm 0.10)^\circ$ [g]
" $D = (-0.6 \pm 1.0) \times 10^{-3}$

n DECAY MODES	Fraction (Γ_i/Γ)	Confidence level	p (MeV/c)
$pe^-\overline{\nu}_e$	100 %		1
$pe^-\overline{\nu}_e\gamma$	[h] $< 6.9 \times 10^{-3}$	90%	1
Charge conservation (Q) violating mode			
$p\nu_e\overline{\nu}_e$	Q $< 8 \times 10^{-27}$	68%	1

$N(1440)$ P_{11}

$I(J^P) = \frac{1}{2}(\frac{1}{2}^+)$

Breit-Wigner mass = 1430 to 1470 (≈ 1440) MeV
Breit-Wigner full width = 250 to 450 (≈ 350) MeV
$p_{\text{beam}} = 0.61$ GeV/c $4\pi\lambda\!\!\!^{-2} = 31.0$ mb
Re(pole position) = 1345 to 1385 (≈ 1365) MeV
-2Im(pole position) = 160 to 260 (≈ 210) MeV

$N(1440)$ DECAY MODES	Fraction (Γ_i/Γ)	p (MeV/c)
$N\pi$	60–70 %	398
$N\pi\pi$	30–40 %	347
$\Delta\pi$	20–30 %	147
$N\rho$	<8 %	†
$N(\pi\pi)^{I=0}_{S\text{-wave}}$	5–10 %	–
$p\gamma$	0.035–0.048 %	414
$p\gamma$, helicity=1/2	0.035–0.048 %	414
$n\gamma$	0.009–0.032 %	413
$n\gamma$, helicity=1/2	0.009–0.032 %	413

$N(1520)$ D_{13}

$I(J^P) = \frac{1}{2}(\frac{3}{2}^-)$

Breit-Wigner mass = 1515 to 1530 (≈ 1520) MeV
Breit-Wigner full width = 110 to 135 (≈ 120) MeV
$p_{\text{beam}} = 0.74$ GeV/c $4\pi\lambda\!\!\!^{-2} = 23.5$ mb
Re(pole position) = 1505 to 1515 (≈ 1510) MeV
-2Im(pole position) = 110 to 120 (≈ 115) MeV

$N(1520)$ DECAY MODES	Fraction (Γ_i/Γ)	p (MeV/c)
$N\pi$	50–60 %	457
$N\eta$	$(2.3 \pm 0.4) \times 10^{-3}$	154
$N\pi\pi$	40–50 %	414
$\Delta\pi$	15–25 %	230
$N\rho$	15–25 %	†
$N(\pi\pi)^{I=0}_{S\text{-wave}}$	<8 %	–
$p\gamma$	0.46–0.56 %	470
$p\gamma$, helicity=1/2	0.001–0.034 %	470
$p\gamma$, helicity=3/2	0.44–0.53 %	470
$n\gamma$	0.30–0.53 %	470
$n\gamma$, helicity=1/2	0.04–0.10 %	470
$n\gamma$, helicity=3/2	0.25–0.45 %	470

$N(1535)$ S_{11}

$I(J^P) = \frac{1}{2}(\frac{1}{2}^-)$

Breit-Wigner mass = 1520 to 1555 (≈ 1535) MeV
Breit-Wigner full width = 100 to 200 (≈ 150) MeV
$p_{\text{beam}} = 0.76$ GeV/c $4\pi\lambda\!\!\!^{-2} = 22.5$ mb
Re(pole position) = 1495 to 1515 (≈ 1505) MeV
-2Im(pole position) = 90 to 250 (≈ 170) MeV

$N(1535)$ DECAY MODES	Fraction (Γ_i/Γ)	p (MeV/c)
$N\pi$	35–55 %	468
$N\eta$	30–55 %	186
$N\pi\pi$	1–10 %	426
$\Delta\pi$	<1 %	244
$N\rho$	<4 %	†
$N(\pi\pi)^{I=0}_{S\text{-wave}}$	<3 %	–
$N(1440)\pi$	<7 %	†
$p\gamma$	0.15–0.35 %	481
$p\gamma$, helicity=1/2	0.15–0.35 %	481
$n\gamma$	0.004–0.29 %	480
$n\gamma$, helicity=1/2	0.004–0.29 %	480

$N(1650)$ S_{11}

$I(J^P) = \frac{1}{2}(\frac{1}{2}^-)$

Breit-Wigner mass = 1640 to 1680 (≈ 1650) MeV
Breit-Wigner full width = 145 to 190 (≈ 150) MeV
$p_{\text{beam}} = 0.96$ GeV/c $4\pi\lambda\!\!\!^{-2} = 16.4$ mb
Re(pole position) = 1640 to 1680 (≈ 1660) MeV
-2Im(pole position) = 150 to 170 (≈ 160) MeV

$N(1650)$ DECAY MODES	Fraction (Γ_i/Γ)	p (MeV/c)
$N\pi$	55–90 %	547
$N\eta$	3–10 %	348
ΛK	3–11 %	169
$N\pi\pi$	10–20 %	514
$\Delta\pi$	1–7 %	345
$N\rho$	4–12 %	†
$N(\pi\pi)^{I=0}_{S\text{-wave}}$	<4 %	–
$N(1440)\pi$	<5 %	150
$p\gamma$	0.04–0.18 %	558
$p\gamma$, helicity=1/2	0.04–0.18 %	558
$n\gamma$	0.003–0.17 %	557
$n\gamma$, helicity=1/2	0.003–0.17 %	557

$N(1675)$ D_{15}

$I(J^P) = \frac{1}{2}(\frac{5}{2}^-)$

Breit-Wigner mass = 1670 to 1685 (≈ 1675) MeV
Breit-Wigner full width = 140 to 180 (≈ 150) MeV
$p_{\text{beam}} = 1.01$ GeV/c $4\pi\lambda\!\!\!^{-2} = 15.4$ mb
Re(pole position) = 1655 to 1665 (≈ 1660) MeV
-2Im(pole position) = 125 to 155 (≈ 140) MeV

$N(1675)$ DECAY MODES	Fraction (Γ_i/Γ)	p (MeV/c)
$N\pi$	40–50 %	564
$N\eta$	(0.0 ± 1.0) %	376
ΛK	<1 %	216
$N\pi\pi$	50–60 %	532
$\Delta\pi$	50–60 %	366
$N\rho$	< 1–3 %	†
$p\gamma$	0.004–0.023 %	575
$p\gamma$, helicity=1/2	0.0–0.015 %	575
$p\gamma$, helicity=3/2	0.0–0.011 %	575
$n\gamma$	0.02–0.12 %	574
$n\gamma$, helicity=1/2	0.006–0.046 %	574
$n\gamma$, helicity=3/2	0.01–0.08 %	574

$N(1680)$ F_{15} $I(J^P) = \frac{1}{2}(\frac{5}{2}^+)$

Breit-Wigner mass = 1675 to 1690 (≈ 1680) MeV
Breit-Wigner full width = 120 to 140 (≈ 130) MeV
p_{beam} = 1.01 GeV/c $4\pi\lambda^2$ = 15.2 mb
Re(pole position) = 1665 to 1675 (≈ 1670) MeV
−2Im(pole position) = 105 to 135 (≈ 120) MeV

$N(1680)$ DECAY MODES	Fraction (Γ_i/Γ)	p (MeV/c)
$N\pi$	60–70 %	568
$N\eta$	(0.0 ± 1.0) %	381
$N\pi\pi$	30–40 %	535
$\Delta\pi$	5–15 %	370
$N\rho$	3–15 %	†
$N(\pi\pi)^{I=0}_{S\text{-wave}}$	5–20 %	–
$p\gamma$	0.21–0.32 %	578
$p\gamma$, helicity=1/2	0.001–0.011 %	578
$p\gamma$, helicity=3/2	0.20–0.32 %	578
$n\gamma$	0.021–0.046 %	577
$n\gamma$, helicity=1/2	0.004–0.029 %	577
$n\gamma$, helicity=3/2	0.01–0.024 %	577

$N(1700)$ D_{13} $I(J^P) = \frac{1}{2}(\frac{3}{2}^-)$

Breit-Wigner mass = 1650 to 1750 (≈ 1700) MeV
Breit-Wigner full width = 50 to 150 (≈ 100) MeV
p_{beam} = 1.05 GeV/c $4\pi\lambda^2$ = 14.5 mb
Re(pole position) = 1630 to 1730 (≈ 1680) MeV
−2Im(pole position) = 50 to 150 (≈ 100) MeV

$N(1700)$ DECAY MODES	Fraction (Γ_i/Γ)	p (MeV/c)
$N\pi$	5–15 %	581
$N\eta$	(0.0 ± 1.0) %	402
ΛK	<3 %	255
$N\pi\pi$	85–95 %	550
$N\rho$	<35 %	†
$p\gamma$	0.01–0.05 %	591
$p\gamma$, helicity=1/2	0.0–0.024 %	591
$p\gamma$, helicity=3/2	0.002–0.026 %	591
$n\gamma$	0.01–0.13 %	590
$n\gamma$, helicity=1/2	0.0–0.09 %	590
$n\gamma$, helicity=3/2	0.01–0.05 %	590

$N(1710)$ P_{11} $I(J^P) = \frac{1}{2}(\frac{1}{2}^+)$

Breit-Wigner mass = 1680 to 1740 (≈ 1710) MeV
Breit-Wigner full width = 50 to 250 (≈ 100) MeV
p_{beam} = 1.07 GeV/c $4\pi\lambda^2$ = 14.2 mb
Re(pole position) = 1670 to 1770 (≈ 1720) MeV
−2Im(pole position) = 80 to 380 (≈ 230) MeV

$N(1710)$ DECAY MODES	Fraction (Γ_i/Γ)	p (MeV/c)
$N\pi$	10–20 %	588
$N\eta$	(6.2 ± 1.0) %	412
$N\omega$	(13.0 ± 2.0) %	†
ΛK	5–25 %	269
$N\pi\pi$	40–90 %	557
$\Delta\pi$	15–40 %	394
$N\rho$	5–25 %	†
$N(\pi\pi)^{I=0}_{S\text{-wave}}$	10–40 %	–
$p\gamma$	0.002–0.05%	598
$p\gamma$, helicity=1/2	0.002–0.05%	598
$n\gamma$	0.0–0.02%	597
$n\gamma$, helicity=1/2	0.0–0.02%	597

$N(1720)$ P_{13} $I(J^P) = \frac{1}{2}(\frac{3}{2}^+)$

Breit-Wigner mass = 1650 to 1750 (≈ 1720) MeV
Breit-Wigner full width = 100 to 200 (≈ 150) MeV
p_{beam} = 1.09 GeV/c $4\pi\lambda^2$ = 13.9 mb
Re(pole position) = 1650 to 1750 (≈ 1700) MeV
−2Im(pole position) = 110 to 390 (≈ 250) MeV

$N(1720)$ DECAY MODES	Fraction (Γ_i/Γ)	p (MeV/c)
$N\pi$	10–20 %	594
$N\eta$	(4.0 ± 1.0) %	422
ΛK	1–15 %	283
$N\pi\pi$	>70 %	564
$N\rho$	70–85 %	71
$p\gamma$	0.003–0.10 %	604
$p\gamma$, helicity=1/2	0.003–0.08 %	604
$p\gamma$, helicity=3/2	0.001–0.03 %	604
$n\gamma$	0.002–0.39 %	603
$n\gamma$, helicity=1/2	0.0–0.002 %	603
$n\gamma$, helicity=3/2	0.001–0.39 %	603

$N(2190)$ G_{17} $I(J^P) = \frac{1}{2}(\frac{7}{2}^-)$

Breit-Wigner mass = 2100 to 2200 (≈ 2190) MeV
Breit-Wigner full width = 350 to 550 (≈ 450) MeV
p_{beam} = 2.07 GeV/c $4\pi\lambda^2$ = 6.21 mb
Re(pole position) = 1950 to 2150 (≈ 2050) MeV
−2Im(pole position) = 350 to 550 (≈ 450) MeV

$N(2190)$ DECAY MODES	Fraction (Γ_i/Γ)	p (MeV/c)
$N\pi$	10–20 %	888
$N\eta$	(0.0 ± 1.0) %	791

$N(2220)$ H_{19} $I(J^P) = \frac{1}{2}(\frac{9}{2}^+)$

Breit-Wigner mass = 2180 to 2310 (≈ 2220) MeV
Breit-Wigner full width = 320 to 550 (≈ 400) MeV
p_{beam} = 2.14 GeV/c $4\pi\lambda^2$ = 5.97 mb
Re(pole position) = 2100 to 2240 (≈ 2170) MeV
−2Im(pole position) = 370 to 570 (≈ 470) MeV

$N(2220)$ DECAY MODES	Fraction (Γ_i/Γ)	p (MeV/c)
$N\pi$	10–20 %	906

$N(2250)$ G_{19} $I(J^P) = \frac{1}{2}(\frac{9}{2}^-)$

Breit-Wigner mass = 2170 to 2310 (≈ 2250) MeV
Breit-Wigner full width = 290 to 470 (≈ 400) MeV
p_{beam} = 2.21 GeV/c $4\pi\lambda^2$ = 5.74 mb
Re(pole position) = 2080 to 2200 (≈ 2140) MeV
−2Im(pole position) = 280 to 680 (≈ 480) MeV

$N(2250)$ DECAY MODES	Fraction (Γ_i/Γ)	p (MeV/c)
$N\pi$	5–15 %	924

$N(2600)$ $I_{1,11}$ $I(J^P) = \frac{1}{2}(\frac{11}{2}^-)$

Breit-Wigner mass = 2550 to 2750 (≈ 2600) MeV
Breit-Wigner full width = 500 to 800 (≈ 650) MeV
p_{beam} = 3.12 GeV/c $4\pi\lambda^2$ = 3.86 mb

$N(2600)$ DECAY MODES	Fraction (Γ_i/Γ)	p (MeV/c)
$N\pi$	5–10 %	1126

Δ BARYONS ($S = 0$, $I = 3/2$)

$\Delta^{++} = uuu$, $\Delta^{+} = uud$, $\Delta^{0} = udd$, $\Delta^{-} = ddd$

Δ(1232) P_{33}

$I(J^P) = \frac{3}{2}(\frac{3}{2}^+)$

Breit-Wigner mass (mixed charges) = 1230 to 1234 (≈ 1232) MeV
Breit-Wigner full width (mixed charges) = 115 to 125 (≈ 120) MeV
p_{beam} = 0.30 GeV/c $4\pi\lambda^2$ = 94.8 mb
Re(pole position) = 1209 to 1211 (≈ 1210) MeV
−2Im(pole position) = 98 to 102 (≈ 100) MeV

Δ(1232) DECAY MODES	Fraction (Γ_i/Γ)	p (MeV/c)
$N\pi$	>99 %	229
$N\gamma$	0.52–0.60 %	259
$N\gamma$, helicity=1/2	0.11–0.13 %	259
$N\gamma$, helicity=3/2	0.41–0.47 %	259

Δ(1600) P_{33}

$I(J^P) = \frac{3}{2}(\frac{3}{2}^+)$

Breit-Wigner mass = 1550 to 1700 (≈ 1600) MeV
Breit-Wigner full width = 250 to 450 (≈ 350) MeV
p_{beam} = 0.87 GeV/c $4\pi\lambda^2$ = 18.6 mb
Re(pole position) = 1500 to 1700 (≈ 1600) MeV
−2Im(pole position) = 200 to 400 (≈ 300) MeV

Δ(1600) DECAY MODES	Fraction (Γ_i/Γ)	p (MeV/c)
$N\pi$	10–25 %	513
$N\pi\pi$	75–90 %	477
$\Delta\pi$	40–70 %	303
$N\rho$	<25 %	†
$N(1440)\pi$	10–35 %	82
$N\gamma$	0.001–0.02 %	525
$N\gamma$, helicity=1/2	0.0–0.02 %	525
$N\gamma$, helicity=3/2	0.001–0.005 %	525

Δ(1620) S_{31}

$I(J^P) = \frac{3}{2}(\frac{1}{2}^-)$

Breit-Wigner mass = 1615 to 1675 (≈ 1620) MeV
Breit-Wigner full width = 120 to 180 (≈ 150) MeV
p_{beam} = 0.91 GeV/c $4\pi\lambda^2$ = 17.7 mb
Re(pole position) = 1580 to 1620 (≈ 1600) MeV
−2Im(pole position) = 100 to 130 (≈ 115) MeV

Δ(1620) DECAY MODES	Fraction (Γ_i/Γ)	p (MeV/c)
$N\pi$	20–30 %	527
$N\pi\pi$	70–80 %	492
$\Delta\pi$	30–60 %	320
$N\rho$	7–25 %	†
$N\gamma$	0.004–0.044 %	538
$N\gamma$, helicity=1/2	0.004–0.044 %	538

Δ(1700) D_{33}

$I(J^P) = \frac{3}{2}(\frac{3}{2}^-)$

Breit-Wigner mass = 1670 to 1770 (≈ 1700) MeV
Breit-Wigner full width = 200 to 400 (≈ 300) MeV
p_{beam} = 1.05 GeV/c $4\pi\lambda^2$ = 14.5 mb
Re(pole position) = 1620 to 1700 (≈ 1660) MeV
−2Im(pole position) = 150 to 250 (≈ 200) MeV

Δ(1700) DECAY MODES	Fraction (Γ_i/Γ)	p (MeV/c)
$N\pi$	10–20 %	581
$N\pi\pi$	80–90 %	550
$\Delta\pi$	30–60 %	386
$N\rho$	30–55 %	†
$N\gamma$	0.12–0.26 %	591
$N\gamma$, helicity=1/2	0.08–0.16 %	591
$N\gamma$, helicity=3/2	0.025–0.12 %	591

Δ(1905) F_{35}

$I(J^P) = \frac{3}{2}(\frac{5}{2}^+)$

Breit-Wigner mass = 1870 to 1920 (≈ 1905) MeV
Breit-Wigner full width = 280 to 440 (≈ 350) MeV
p_{beam} = 1.45 GeV/c $4\pi\lambda^2$ = 9.62 mb
Re(pole position) = 1800 to 1860 (≈ 1830) MeV
−2Im(pole position) = 230 to 330 (≈ 280) MeV

Δ(1905) DECAY MODES	Fraction (Γ_i/Γ)	p (MeV/c)
$N\pi$	5–15 %	714
$N\pi\pi$	85–95 %	690
$\Delta\pi$	<25 %	542
$N\rho$	>60 %	414
$N\gamma$	0.01–0.03 %	721
$N\gamma$, helicity=1/2	0.0–0.1 %	721
$N\gamma$, helicity=3/2	0.004–0.03 %	721

Δ(1910) P_{31}

$I(J^P) = \frac{3}{2}(\frac{1}{2}^+)$

Breit-Wigner mass = 1870 to 1920 (≈ 1910) MeV
Breit-Wigner full width = 190 to 270 (≈ 250) MeV
p_{beam} = 1.46 GeV/c $4\pi\lambda^2$ = 9.54 mb
Re(pole position) = 1830 to 1880 (≈ 1855) MeV
−2Im(pole position) = 200 to 500 (≈ 350) MeV

Δ(1910) DECAY MODES	Fraction (Γ_i/Γ)	p (MeV/c)
$N\pi$	15–30 %	717
$N\gamma$	0.0–0.2 %	725
$N\gamma$, helicity=1/2	0.0–0.2 %	725

Δ(1920) P_{33}

$I(J^P) = \frac{3}{2}(\frac{3}{2}^+)$

Breit-Wigner mass = 1900 to 1970 (≈ 1920) MeV
Breit-Wigner full width = 150 to 300 (≈ 200) MeV
p_{beam} = 1.48 GeV/c $4\pi\lambda^2$ = 9.37 mb
Re(pole position) = 1850 to 1950 (≈ 1900) MeV
−2Im(pole position) = 200 to 400 (≈ 300) MeV

Δ(1920) DECAY MODES	Fraction (Γ_i/Γ)	p (MeV/c)
$N\pi$	5–20 %	723
ΣK	(2.10 ± 0.30) %	431

Δ(1930) D_{35}

$I(J^P) = \frac{3}{2}(\frac{5}{2}^-)$

Breit-Wigner mass = 1920 to 1970 (≈ 1930) MeV
Breit-Wigner full width = 250 to 450 (≈ 350) MeV
p_{beam} = 1.50 GeV/c $4\pi\lambda^2$ = 9.21 mb
Re(pole position) = 1840 to 1940 (≈ 1890) MeV
−2Im(pole position) = 200 to 300 (≈ 250) MeV

Δ(1930) DECAY MODES	Fraction (Γ_i/Γ)	p (MeV/c)
$N\pi$	10–20 %	729
$N\gamma$	0.0–0.02 %	737
$N\gamma$, helicity=1/2	0.0–0.01 %	737
$N\gamma$, helicity=3/2	0.0–0.01 %	737

Δ(1950) F_{37}

$I(J^P) = \frac{3}{2}(\frac{7}{2}^+)$

Breit-Wigner mass = 1940 to 1960 (≈ 1950) MeV
Breit-Wigner full width = 290 to 350 (≈ 300) MeV
p_{beam} = 1.54 GeV/c $4\pi\lambda^2$ = 8.91 mb
Re(pole position) = 1880 to 1890 (≈ 1885) MeV
−2Im(pole position) = 210 to 270 (≈ 240) MeV

Δ(1950) DECAY MODES	Fraction (Γ_i/Γ)	p (MeV/c)
$N\pi$	35–40 %	742
$N\pi\pi$		719
$\Delta\pi$	20–30 %	575
$N\rho$	<10 %	463
$N\gamma$	0.08–0.13 %	749
$N\gamma$, helicity=1/2	0.03–0.055 %	749
$N\gamma$, helicity=3/2	0.05–0.075 %	749

Δ(2420) $H_{3,11}$ $I(J^P) = \frac{3}{2}(\frac{11}{2}^+)$

Breit-Wigner mass = 2300 to 2500 (≈ 2420) MeV
Breit-Wigner full width = 300 to 500 (≈ 400) MeV
p_{beam} = 2.64 GeV/c $4\pi\lambda\!\!\!^{-2}$ = 4.68 mb
Re(pole position) = 2260 to 2400 (≈ 2330) MeV
−2Im(pole position) = 350 to 750 (≈ 550) MeV

Δ(2420) DECAY MODES	Fraction (Γ_i/Γ)	p (MeV/c)
$N\pi$	5–15 %	1023

EXOTIC BARYONS

Minimum quark content: $\Theta^+ = uudd\overline{s}$, $\Phi^{--} = ssdd\overline{u}$, $\Phi^+ = ssuu\overline{d}$.

Θ(1540)$^+$ $I(J^P) = 0(?^?)$

It is difficult to deny a place in the Summary Tables for a state that six experiments claim to have seen. Nevertheless, we believe it reasonable to have some reservations about the existence of this state on the basis of the present evidence.

Mass m = 1539.2 ± 1.6 MeV
Full width Γ = 0.90 ± 0.30 MeV

NK is the only strong decay mode allowed for a strangeness S=+1 resonance of this mass.

Θ(1540)$^+$ DECAY MODES	Fraction (Γ_i/Γ)	p (MeV/c)
KN	100%	270

Λ BARYONS ($S = -1, I = 0$)

$\Lambda^0 = uds$

Λ $I(J^P) = 0(\frac{1}{2}^+)$

Mass m = 1115.683 ± 0.006 MeV
$(m_\Lambda - m_{\overline{\Lambda}}) / m_\Lambda = (-0.1 \pm 1.1) \times 10^{-5}$ (S = 1.6)
Mean life $\tau = (2.632 \pm 0.020) \times 10^{-10}$ s (S = 1.6)
$c\tau$ = 7.89 cm
Magnetic moment $\mu = -0.613 \pm 0.004\ \mu_N$
Electric dipole moment $d < 1.5 \times 10^{-16}$ e cm, CL = 95%

Decay parameters

$p\pi^-$	α_-	= 0.642 ± 0.013
"	ϕ_-	= (−6.5 ± 3.5)°
"	γ_-	= 0.76 [i]
"	Δ_-	= (8 ± 4)° [i]
$n\pi^0$	α_0	= +0.65 ± 0.05
$pe^-\overline{\nu}_e$	g_A/g_V	= −0.718 ± 0.015 [f]

Λ DECAY MODES	Fraction (Γ_i/Γ)	p (MeV/c)
$p\pi^-$	(63.9 ±0.5) %	101
$n\pi^0$	(35.8 ±0.5) %	104
$n\gamma$	(1.75±0.15) × 10^{-3}	162
$p\pi^-\gamma$	[j] (8.4 ±1.4) × 10^{-4}	101
$pe^-\overline{\nu}_e$	(8.32±0.14) × 10^{-4}	163
$p\mu^-\overline{\nu}_\mu$	(1.57±0.35) × 10^{-4}	131

Λ(1405) S_{01} $I(J^P) = 0(\frac{1}{2}^-)$

Mass m = 1406 ± 4 MeV
Full width Γ = 50.0 ± 2.0 MeV
Below $\overline{K}N$ threshold

Λ(1405) DECAY MODES	Fraction (Γ_i/Γ)	p (MeV/c)
$\Sigma\pi$	100 %	157

Λ(1520) D_{03} $I(J^P) = 0(\frac{3}{2}^-)$

Mass m = 1519.5 ± 1.0 MeV [k]
Full width Γ = 15.6 ± 1.0 MeV [k]
p_{beam} = 0.39 GeV/c $4\pi\lambda\!\!\!^{-2}$ = 82.8 mb

Λ(1520) DECAY MODES	Fraction (Γ_i/Γ)	p (MeV/c)
$N\overline{K}$	45 ± 1%	243
$\Sigma\pi$	42 ± 1%	268
$\Lambda\pi\pi$	10 ± 1%	259
$\Sigma\pi\pi$	0.9 ± 0.1%	169
$\Lambda\gamma$	0.8 ± 0.2%	350

Λ(1600) P_{01} $I(J^P) = 0(\frac{1}{2}^+)$

Mass m = 1560 to 1700 (≈ 1600) MeV
Full width Γ = 50 to 250 (≈ 150) MeV
p_{beam} = 0.58 GeV/c $4\pi\lambda\!\!\!^{-2}$ = 41.6 mb

Λ(1600) DECAY MODES	Fraction (Γ_i/Γ)	p (MeV/c)
$N\overline{K}$	15–30 %	343
$\Sigma\pi$	10–60 %	338

Λ(1670) S_{01} $I(J^P) = 0(\frac{1}{2}^-)$

Mass m = 1660 to 1680 (≈ 1670) MeV
Full width Γ = 25 to 50 (≈ 35) MeV
p_{beam} = 0.74 GeV/c $4\pi\lambda\!\!\!^{-2}$ = 28.5 mb

Λ(1670) DECAY MODES	Fraction (Γ_i/Γ)	p (MeV/c)
$N\overline{K}$	20–30 %	414
$\Sigma\pi$	25–55 %	394
$\Lambda\eta$	10–25 %	70

Λ(1690) D_{03} $I(J^P) = 0(\frac{3}{2}^-)$

Mass m = 1685 to 1695 (≈ 1690) MeV
Full width Γ = 50 to 70 (≈ 60) MeV
p_{beam} = 0.78 GeV/c $4\pi\lambda\!\!\!^{-2}$ = 26.1 mb

Λ(1690) DECAY MODES	Fraction (Γ_i/Γ)	p (MeV/c)
$N\overline{K}$	20–30 %	433
$\Sigma\pi$	20–40 %	410
$\Lambda\pi\pi$	~ 25 %	419
$\Sigma\pi\pi$	~ 20 %	358

Λ(1800) S_{01} $I(J^P) = 0(\frac{1}{2}^-)$

Mass m = 1720 to 1850 (≈ 1800) MeV
Full width Γ = 200 to 400 (≈ 300) MeV
p_{beam} = 1.01 GeV/c $4\pi\lambda\!\!\!^{-2}$ = 17.5 mb

Λ(1800) DECAY MODES	Fraction (Γ_i/Γ)	p (MeV/c)
$N\overline{K}$	25–40 %	528
$\Sigma\pi$	seen	494
$\Sigma(1385)\pi$	seen	349
$N\overline{K}^*(892)$	seen	†

Λ(1810) P_{01} $I(J^P) = 0(\frac{1}{2}^+)$

Mass m = 1750 to 1850 (≈ 1810) MeV
Full width Γ = 50 to 250 (≈ 150) MeV
p_{beam} = 1.04 GeV/c $4\pi\lambda\!\!\!^{-2}$ = 17.0 mb

Λ(1810) DECAY MODES	Fraction (Γ_i/Γ)	p (MeV/c)
$N\overline{K}$	20–50 %	537
$\Sigma\pi$	10–40 %	501
$\Sigma(1385)\pi$	seen	357
$N\overline{K}^*(892)$	30–60 %	†

Baryon Summary Table

$\Lambda(1820)$ F_{05} $I(J^P) = 0(\frac{5}{2}^+)$

Mass $m = 1815$ to 1825 (≈ 1820) MeV
Full width $\Gamma = 70$ to 90 (≈ 80) MeV
$p_{\text{beam}} = 1.06$ GeV/c $4\pi\lambda\!\!\!^{-2} = 16.5$ mb

$\Lambda(1820)$ DECAY MODES	Fraction (Γ_i/Γ)	p (MeV/c)
$N\overline{K}$	55–65 %	545
$\Sigma\pi$	8–14 %	509
$\Sigma(1385)\pi$	5–10 %	366

$\Lambda(1830)$ D_{05} $I(J^P) = 0(\frac{5}{2}^-)$

Mass $m = 1810$ to 1830 (≈ 1830) MeV
Full width $\Gamma = 60$ to 110 (≈ 95) MeV
$p_{\text{beam}} = 1.08$ GeV/c $4\pi\lambda\!\!\!^{-2} = 16.0$ mb

$\Lambda(1830)$ DECAY MODES	Fraction (Γ_i/Γ)	p (MeV/c)
$N\overline{K}$	3–10 %	553
$\Sigma\pi$	35–75 %	516
$\Sigma(1385)\pi$	>15 %	374

$\Lambda(1890)$ P_{03} $I(J^P) = 0(\frac{3}{2}^+)$

Mass $m = 1850$ to 1910 (≈ 1890) MeV
Full width $\Gamma = 60$ to 200 (≈ 100) MeV
$p_{\text{beam}} = 1.21$ GeV/c $4\pi\lambda\!\!\!^{-2} = 13.6$ mb

$\Lambda(1890)$ DECAY MODES	Fraction (Γ_i/Γ)	p (MeV/c)
$N\overline{K}$	20–35 %	599
$\Sigma\pi$	3–10 %	560
$\Sigma(1385)\pi$	seen	423
$N\overline{K}^*(892)$	seen	236

$\Lambda(2100)$ G_{07} $I(J^P) = 0(\frac{7}{2}^-)$

Mass $m = 2090$ to 2110 (≈ 2100) MeV
Full width $\Gamma = 100$ to 250 (≈ 200) MeV
$p_{\text{beam}} = 1.68$ GeV/c $4\pi\lambda\!\!\!^{-2} = 8.68$ mb

$\Lambda(2100)$ DECAY MODES	Fraction (Γ_i/Γ)	p (MeV/c)
$N\overline{K}$	25–35 %	751
$\Sigma\pi$	~ 5 %	705
$\Lambda\eta$	< 3 %	617
ΞK	< 3 %	491
$\Lambda\omega$	< 8 %	443
$N\overline{K}^*(892)$	10–20 %	515

$\Lambda(2110)$ F_{05} $I(J^P) = 0(\frac{5}{2}^+)$

Mass $m = 2090$ to 2140 (≈ 2110) MeV
Full width $\Gamma = 150$ to 250 (≈ 200) MeV
$p_{\text{beam}} = 1.70$ GeV/c $4\pi\lambda\!\!\!^{-2} = 8.53$ mb

$\Lambda(2110)$ DECAY MODES	Fraction (Γ_i/Γ)	p (MeV/c)
$N\overline{K}$	5–25 %	757
$\Sigma\pi$	10–40 %	711
$\Lambda\omega$	seen	455
$\Sigma(1385)\pi$	seen	591
$N\overline{K}^*(892)$	10–60 %	525

$\Lambda(2350)$ H_{09} $I(J^P) = 0(\frac{9}{2}^+)$

Mass $m = 2340$ to 2370 (≈ 2350) MeV
Full width $\Gamma = 100$ to 250 (≈ 150) MeV
$p_{\text{beam}} = 2.29$ GeV/c $4\pi\lambda\!\!\!^{-2} = 5.85$ mb

$\Lambda(2350)$ DECAY MODES	Fraction (Γ_i/Γ)	p (MeV/c)
$N\overline{K}$	~ 12 %	915
$\Sigma\pi$	~ 10 %	867

Σ BARYONS ($S = -1$, $I = 1$)

$\Sigma^+ = uus$, $\Sigma^0 = uds$, $\Sigma^- = dds$

Σ^+ $I(J^P) = 1(\frac{1}{2}^+)$

Mass $m = 1189.37 \pm 0.07$ MeV (S = 2.2)
Mean life $\tau = (0.8018 \pm 0.0026) \times 10^{-10}$ s
$c\tau = 2.404$ cm
$(\tau_{\Sigma^+} - \tau_{\overline{\Sigma}^-}) / \tau_{\Sigma^+} = (-0.6 \pm 1.2) \times 10^{-3}$
Magnetic moment $\mu = 2.458 \pm 0.010\ \mu_N$ (S = 2.1)
$\Gamma(\Sigma^+ \to n\ell^+\nu)/\Gamma(\Sigma^- \to n\ell^-\overline{\nu}) < 0.043$

Decay parameters

$p\pi^0$	$\alpha_0 = -0.980^{+0.017}_{-0.015}$
"	$\phi_0 = (36 \pm 34)^\circ$
"	$\gamma_0 = 0.16$ [i]
"	$\Delta_0 = (187 \pm 6)^\circ$ [i]
$n\pi^+$	$\alpha_+ = 0.068 \pm 0.013$
"	$\phi_+ = (167 \pm 20)^\circ$ (S = 1.1)
"	$\gamma_+ = -0.97$ [i]
"	$\Delta_+ = (-73^{+133}_{-10})^\circ$ [i]
$p\gamma$	$\alpha_\gamma = -0.76 \pm 0.08$

Σ^+ DECAY MODES		Fraction (Γ_i/Γ)	Confidence level	p (MeV/c)
$p\pi^0$		(51.57 ± 0.30) %		189
$n\pi^+$		(48.31 ± 0.30) %		185
$p\gamma$		(1.23 ± 0.05) × 10^{-3}		225
$n\pi^+\gamma$	[j]	(4.5 ± 0.5) × 10^{-4}		185
$\Lambda e^+\nu_e$		(2.0 ± 0.5) × 10^{-5}		71
$\Delta S = \Delta Q$ (SQ) violating modes or $\Delta S = 1$ weak neutral current ($S1$) modes				
$ne^+\nu_e$	SQ	< 5 × 10^{-6}	90%	224
$n\mu^+\nu_\mu$	SQ	< 3.0 × 10^{-5}	90%	202
pe^+e^-	$S1$	< 7 × 10^{-6}		225

Σ^0 $I(J^P) = 1(\frac{1}{2}^+)$

Mass $m = 1192.642 \pm 0.024$ MeV
$m_{\Sigma^-} - m_{\Sigma^0} = 4.807 \pm 0.035$ MeV (S = 1.1)
$m_{\Sigma^0} - m_\Lambda = 76.959 \pm 0.023$ MeV
Mean life $\tau = (7.4 \pm 0.7) \times 10^{-20}$ s
$c\tau = 2.22 \times 10^{-11}$ m
Transition magnetic moment $|\mu_{\Sigma\Lambda}| = 1.61 \pm 0.08\ \mu_N$

Σ^0 DECAY MODES		Fraction (Γ_i/Γ)	Confidence level	p (MeV/c)
$\Lambda\gamma$		100 %		74
$\Lambda\gamma\gamma$		< 3 %	90%	74
Λe^+e^-	[l]	5×10^{-3}		74

Σ^- $I(J^P) = 1(\frac{1}{2}^+)$

Mass $m = 1197.449 \pm 0.030$ MeV (S = 1.2)
$m_{\Sigma^-} - m_{\Sigma^+} = 8.08 \pm 0.08$ MeV (S = 1.9)
$m_{\Sigma^-} - m_\Lambda = 81.766 \pm 0.030$ MeV (S = 1.2)
Mean life $\tau = (1.479 \pm 0.011) \times 10^{-10}$ s (S = 1.3)
$c\tau = 4.434$ cm
Magnetic moment $\mu = -1.160 \pm 0.025\ \mu_N$ (S = 1.7)
Σ^- charge radius = 0.78 ± 0.10 fm

Decay parameters

$n\pi^-$	$\alpha_- = -0.068 \pm 0.008$
"	$\phi_- = (10 \pm 15)^\circ$
"	$\gamma_- = 0.98$ [i]
"	$\Delta_- = (249^{+12}_{-120})^\circ$ [i]
$ne^-\overline{\nu}_e$	$g_A/g_V = 0.340 \pm 0.017$ [f]
"	$f_2(0)/f_1(0) = 0.97 \pm 0.14$
"	$D = 0.11 \pm 0.10$
$\Lambda e^-\overline{\nu}_e$	$g_V/g_A = 0.01 \pm 0.10$ [f] (S = 1.5)
"	$g_{WM}/g_A = 2.4 \pm 1.7$ [f]

Σ^- DECAY MODES	Fraction (Γ_i/Γ)	p (MeV/c)
$n\pi^-$	(99.848 ± 0.005) %	193
$n\pi^-\gamma$	[j] (4.6 ± 0.6) × 10^{-4}	193
$ne^-\overline{\nu}_e$	(1.017 ± 0.034) × 10^{-3}	230
$n\mu^-\overline{\nu}_\mu$	(4.5 ± 0.4) × 10^{-4}	210
$\Lambda e^-\overline{\nu}_e$	(5.73 ± 0.27) × 10^{-5}	79

$\Sigma(1385)\ P_{13}$

$I(J^P) = 1(\frac{3}{2}^+)$

$\Sigma(1385)^+$ mass $m = 1382.8 \pm 0.4$ MeV (S = 2.0)
$\Sigma(1385)^0$ mass $m = 1383.7 \pm 1.0$ MeV (S = 1.4)
$\Sigma(1385)^-$ mass $m = 1387.2 \pm 0.5$ MeV (S = 2.2)
$\Sigma(1385)^+$ full width $\Gamma = 35.8 \pm 0.8$ MeV
$\Sigma(1385)^0$ full width $\Gamma = 36 \pm 5$ MeV
$\Sigma(1385)^-$ full width $\Gamma = 39.4 \pm 2.1$ MeV (S = 1.7)
Below $\overline{K}N$ threshold

$\Sigma(1385)$ DECAY MODES	Fraction (Γ_i/Γ)	p (MeV/c)
$\Lambda\pi$	88±2 %	208
$\Sigma\pi$	12±2 %	129

$\Sigma(1660)\ P_{11}$

$I(J^P) = 1(\frac{1}{2}^+)$

Mass $m = 1630$ to 1690 (≈ 1660) MeV
Full width $\Gamma = 40$ to 200 (≈ 100) MeV
$p_{\text{beam}} = 0.72$ GeV/c $\quad 4\pi\lambda\!\!\!^{-2} = 29.9$ mb

$\Sigma(1660)$ DECAY MODES	Fraction (Γ_i/Γ)	p (MeV/c)
$N\overline{K}$	10–30 %	405
$\Lambda\pi$	seen	440
$\Sigma\pi$	seen	387

$\Sigma(1670)\ D_{13}$

$I(J^P) = 1(\frac{3}{2}^-)$

Mass $m = 1665$ to 1685 (≈ 1670) MeV
Full width $\Gamma = 40$ to 80 (≈ 60) MeV
$p_{\text{beam}} = 0.74$ GeV/c $\quad 4\pi\lambda\!\!\!^{-2} = 28.5$ mb

$\Sigma(1670)$ DECAY MODES	Fraction (Γ_i/Γ)	p (MeV/c)
$N\overline{K}$	7–13 %	414
$\Lambda\pi$	5–15 %	448
$\Sigma\pi$	30–60 %	394

$\Sigma(1750)\ S_{11}$

$I(J^P) = 1(\frac{1}{2}^-)$

Mass $m = 1730$ to 1800 (≈ 1750) MeV
Full width $\Gamma = 60$ to 160 (≈ 90) MeV
$p_{\text{beam}} = 0.91$ GeV/c $\quad 4\pi\lambda\!\!\!^{-2} = 20.7$ mb

$\Sigma(1750)$ DECAY MODES	Fraction (Γ_i/Γ)	p (MeV/c)
$N\overline{K}$	10–40 %	486
$\Lambda\pi$	seen	507
$\Sigma\pi$	<8 %	456
$\Sigma\eta$	15–55 %	99

$\Sigma(1775)\ D_{15}$

$I(J^P) = 1(\frac{5}{2}^-)$

Mass $m = 1770$ to 1780 (≈ 1775) MeV
Full width $\Gamma = 105$ to 135 (≈ 120) MeV
$p_{\text{beam}} = 0.96$ GeV/c $\quad 4\pi\lambda\!\!\!^{-2} = 19.0$ mb

$\Sigma(1775)$ DECAY MODES	Fraction (Γ_i/Γ)	p (MeV/c)
$N\overline{K}$	37–43%	508
$\Lambda\pi$	14–20%	525
$\Sigma\pi$	2–5%	475
$\Sigma(1385)\pi$	8–12%	327
$\Lambda(1520)\pi$	17–23%	201

$\Sigma(1915)\ F_{15}$

$I(J^P) = 1(\frac{5}{2}^+)$

Mass $m = 1900$ to 1935 (≈ 1915) MeV
Full width $\Gamma = 80$ to 160 (≈ 120) MeV
$p_{\text{beam}} = 1.26$ GeV/c $\quad 4\pi\lambda\!\!\!^{-2} = 12.8$ mb

$\Sigma(1915)$ DECAY MODES	Fraction (Γ_i/Γ)	p (MeV/c)
$N\overline{K}$	5–15 %	618
$\Lambda\pi$	seen	623
$\Sigma\pi$	seen	577
$\Sigma(1385)\pi$	<5 %	443

$\Sigma(1940)\ D_{13}$

$I(J^P) = 1(\frac{3}{2}^-)$

Mass $m = 1900$ to 1950 (≈ 1940) MeV
Full width $\Gamma = 150$ to 300 (≈ 220) MeV
$p_{\text{beam}} = 1.32$ GeV/c $\quad 4\pi\lambda\!\!\!^{-2} = 12.1$ mb

$\Sigma(1940)$ DECAY MODES	Fraction (Γ_i/Γ)	p (MeV/c)
$N\overline{K}$	<20 %	637
$\Lambda\pi$	seen	640
$\Sigma\pi$	seen	595
$\Sigma(1385)\pi$	seen	463
$\Lambda(1520)\pi$	seen	355
$\Delta(1232)\overline{K}$	seen	410
$N\overline{K}^*(892)$	seen	322

$\Sigma(2030)\ F_{17}$

$I(J^P) = 1(\frac{7}{2}^+)$

Mass $m = 2025$ to 2040 (≈ 2030) MeV
Full width $\Gamma = 150$ to 200 (≈ 180) MeV
$p_{\text{beam}} = 1.52$ GeV/c $\quad 4\pi\lambda\!\!\!^{-2} = 9.93$ mb

$\Sigma(2030)$ DECAY MODES	Fraction (Γ_i/Γ)	p (MeV/c)
$N\overline{K}$	17–23 %	702
$\Lambda\pi$	17–23 %	700
$\Sigma\pi$	5–10 %	657
ΞK	<2 %	422
$\Sigma(1385)\pi$	5–15 %	532
$\Lambda(1520)\pi$	10–20 %	430
$\Delta(1232)\overline{K}$	10–20 %	498
$N\overline{K}^*(892)$	<5 %	439

$\Sigma(2250)$

$I(J^P) = 1(?^?)$

Mass $m = 2210$ to 2280 (≈ 2250) MeV
Full width $\Gamma = 60$ to 150 (≈ 100) MeV
$p_{\text{beam}} = 2.04$ GeV/c $\quad 4\pi\lambda\!\!\!^{-2} = 6.76$ mb

$\Sigma(2250)$ DECAY MODES	Fraction (Γ_i/Γ)	p (MeV/c)
$N\overline{K}$	<10 %	851
$\Lambda\pi$	seen	842
$\Sigma\pi$	seen	803

Ξ BARYONS ($S = -2$, $I = 1/2$)

$\Xi^0 = uss$, $\Xi^- = dss$

Ξ^0 $I(J^P) = \frac{1}{2}(\frac{1}{2}^+)$

P is not yet measured; + is the quark model prediction.

Mass $m = 1314.83 \pm 0.20$ MeV
$m_{\Xi^-} - m_{\Xi^0} = 6.48 \pm 0.24$ MeV
Mean life $\tau = (2.90 \pm 0.09) \times 10^{-10}$ s
$c\tau = 8.71$ cm
Magnetic moment $\mu = -1.250 \pm 0.014\ \mu_N$

Decay parameters

$\Lambda\pi^0$	$\alpha = -0.411 \pm 0.022$	(S = 2.1)
"	$\phi = (21 \pm 12)^\circ$	
"	$\gamma = 0.85$ [i]	
"	$\Delta = (218^{+12}_{-19})^\circ$ [i]	
$\Lambda\gamma$	$\alpha = -0.4 \pm 0.4$	
$\Sigma^0\gamma$	$\alpha = -0.63 \pm 0.09$	
$\Sigma^+ e^- \overline{\nu}_e$	$g_1(0)/f_1(0) = 1.32^{+0.22}_{-0.18}$	
$\Sigma^+ e^- \overline{\nu}_e$	$f_2(0)/f_1(0) = 2.0 \pm 1.3$	

Ξ^0 DECAY MODES	Fraction (Γ_i/Γ)	Scale factor/ Confidence level	p (MeV/c)
$\Lambda\pi^0$	(99.522 ± 0.032) %	S=1.7	135
$\Lambda\gamma$	$(1.18 \pm 0.30) \times 10^{-3}$	S=2.0	184
$\Sigma^0\gamma$	$(3.33 \pm 0.10) \times 10^{-3}$		117
$\Sigma^+ e^- \overline{\nu}_e$	$(2.7 \pm 0.4) \times 10^{-4}$		119
$\Sigma^+ \mu^- \overline{\nu}_\mu$	$< 1.1 \times 10^{-3}$	CL=90%	64
$\Delta S = \Delta Q$ (SQ) violating modes or $\Delta S = 2$ forbidden ($S2$) modes			
$\Sigma^- e^+ \nu_e$	SQ $< 9 \times 10^{-4}$	CL=90%	112
$\Sigma^- \mu^+ \nu_\mu$	SQ $< 9 \times 10^{-4}$	CL=90%	49
$p\pi^-$	$S2$ $< 4 \times 10^{-5}$	CL=90%	299
$p e^- \overline{\nu}_e$	$S2$ $< 1.3 \times 10^{-3}$		323
$p\mu^- \overline{\nu}_\mu$	$S2$ $< 1.3 \times 10^{-3}$		309

Ξ^- $I(J^P) = \frac{1}{2}(\frac{1}{2}^+)$

P is not yet measured; + is the quark model prediction.

Mass $m = 1321.31 \pm 0.13$ MeV
Mean life $\tau = (1.639 \pm 0.015) \times 10^{-10}$ s
$c\tau = 4.91$ cm
Magnetic moment $\mu = -0.6507 \pm 0.0025\ \mu_N$

Decay parameters

$\Lambda\pi^-$	$\alpha = -0.458 \pm 0.012$	(S = 1.8)
$[\alpha(\Xi^-)\alpha_-(\Lambda) - \alpha(\overline{\Xi}^+)\alpha_+(\overline{\Lambda})]/[\alpha(\Xi^-)\alpha_-(\Lambda) + \alpha(\overline{\Xi}^+)\alpha_+(\overline{\Lambda})]$	$= 0.012 \pm 0.014$	
"	$\phi = (-0.4 \pm 2.3)^\circ$	
"	$\gamma = 0.89$ [i]	
"	$\Delta = (179 \pm 4)^\circ$ [i]	
$\Lambda e^- \overline{\nu}_e$	$g_A/g_V = -0.25 \pm 0.05$ [f]	

Ξ^- DECAY MODES	Fraction (Γ_i/Γ)	Confidence level	p (MeV/c)
$\Lambda\pi^-$	(99.887 ± 0.035) %		139
$\Sigma^-\gamma$	$(1.27 \pm 0.23) \times 10^{-4}$		118
$\Lambda e^- \overline{\nu}_e$	$(5.63 \pm 0.31) \times 10^{-4}$		190
$\Lambda\mu^- \overline{\nu}_\mu$	$(3.5 \ ^{+3.5}_{-2.2}) \times 10^{-4}$		163
$\Sigma^0 e^- \overline{\nu}_e$	$(8.7 \pm 1.7) \times 10^{-5}$		122
$\Sigma^0 \mu^- \overline{\nu}_\mu$	$< 8 \times 10^{-4}$	90%	70
$\Xi^0 e^- \overline{\nu}_e$	$< 2.3 \times 10^{-3}$	90%	6
$\Delta S = 2$ forbidden ($S2$) modes			
$n\pi^-$	$S2$ $< 1.9 \times 10^{-5}$	90%	303
$n e^- \overline{\nu}_e$	$S2$ $< 3.2 \times 10^{-3}$	90%	327
$n\mu^- \overline{\nu}_\mu$	$S2$ < 1.5 %	90%	313
$p\pi^-\pi^-$	$S2$ $< 4 \times 10^{-4}$	90%	223
$p\pi^- e^- \overline{\nu}_e$	$S2$ $< 4 \times 10^{-4}$	90%	304
$p\pi^- \mu^- \overline{\nu}_\mu$	$S2$ $< 4 \times 10^{-4}$	90%	250
$p\mu^-\mu^-$	L $< 4 \times 10^{-4}$	90%	272

$\Xi(1530)$ P_{13} $I(J^P) = \frac{1}{2}(\frac{3}{2}^+)$

$\Xi(1530)^0$ mass $m = 1531.80 \pm 0.32$ MeV (S = 1.3)
$\Xi(1530)^-$ mass $m = 1535.0 \pm 0.6$ MeV
$\Xi(1530)^0$ full width $\Gamma = 9.1 \pm 0.5$ MeV
$\Xi(1530)^-$ full width $\Gamma = 9.9^{+1.7}_{-1.9}$ MeV

$\Xi(1530)$ DECAY MODES	Fraction (Γ_i/Γ)	Confidence level	p (MeV/c)
$\Xi\pi$	100 %		158
$\Xi\gamma$	<4 %	90%	202

$\Xi(1690)$ $I(J^P) = \frac{1}{2}(?^?)$

Mass $m = 1690 \pm 10$ MeV [k]
Full width $\Gamma < 30$ MeV

$\Xi(1690)$ DECAY MODES	Fraction (Γ_i/Γ)	p (MeV/c)
$\Lambda\overline{K}$	seen	240
$\Sigma\overline{K}$	seen	70
$\Xi\pi$	seen	311
$\Xi^-\pi^+\pi^-$	possibly seen	214

$\Xi(1820)$ D_{13} $I(J^P) = \frac{1}{2}(\frac{3}{2}^-)$

Mass $m = 1823 \pm 5$ MeV [k]
Full width $\Gamma = 24^{+15}_{-10}$ MeV [k]

$\Xi(1820)$ DECAY MODES	Fraction (Γ_i/Γ)	p (MeV/c)
$\Lambda\overline{K}$	large	402
$\Sigma\overline{K}$	small	324
$\Xi\pi$	small	421
$\Xi(1530)\pi$	small	237

$\Xi(1950)$ $I(J^P) = \frac{1}{2}(?^?)$

Mass $m = 1950 \pm 15$ MeV [k]
Full width $\Gamma = 60 \pm 20$ MeV [k]

$\Xi(1950)$ DECAY MODES	Fraction (Γ_i/Γ)	p (MeV/c)
$\Lambda\overline{K}$	seen	522
$\Sigma\overline{K}$	possibly seen	460
$\Xi\pi$	seen	519

$\Xi(2030)$ $I(J^P) = \frac{1}{2}(\geq \frac{5}{2}^?)$

Mass $m = 2025 \pm 5$ MeV [k]
Full width $\Gamma = 20^{+15}_{-5}$ MeV [k]

$\Xi(2030)$ DECAY MODES	Fraction (Γ_i/Γ)	p (MeV/c)
$\Lambda\overline{K}$	~ 20 %	585
$\Sigma\overline{K}$	~ 80 %	529
$\Xi\pi$	small	574
$\Xi(1530)\pi$	small	416
$\Lambda\overline{K}\pi$	small	499
$\Sigma\overline{K}\pi$	small	428

Ω BARYONS ($S=-3, I=0$)

$\Omega^- = sss$

Ω^-

$I(J^P) = 0(\frac{3}{2}^+)$

J^P is not yet measured; $\frac{3}{2}^+$ is the quark model prediction.

Mass $m = 1672.45 \pm 0.29$ MeV
$(m_{\Omega^-} - m_{\overline{\Omega}^+}) / m_{\Omega^-} = (-1 \pm 8) \times 10^{-5}$
Mean life $\tau = (0.821 \pm 0.011) \times 10^{-10}$ s
$c\tau = 2.461$ cm
$(\tau_{\Omega^-} - \tau_{\overline{\Omega}^+}) / \tau_{\Omega^-} = -0.002 \pm 0.040$
Magnetic moment $\mu = -2.02 \pm 0.05\ \mu_N$

Decay parameters

ΛK^- $\alpha = -0.026 \pm 0.023$
$\frac{1}{2}[\alpha(\Lambda K^-) + \alpha(\overline{\Lambda} K^+)] = -0.004 \pm 0.040$
$\Xi^0 \pi^-$ $\alpha = 0.09 \pm 0.14$
$\Xi^- \pi^0$ $\alpha = 0.05 \pm 0.21$

Ω^- DECAY MODES	Fraction (Γ_i/Γ)	Confidence level	p (MeV/c)
ΛK^-	(67.8 ± 0.7) %		211
$\Xi^0 \pi^-$	(23.6 ± 0.7) %		294
$\Xi^- \pi^0$	(8.6 ± 0.4) %		290
$\Xi^- \pi^+ \pi^-$	$(4.3^{+3.4}_{-1.3}) \times 10^{-4}$		190
$\Xi(1530)^0 \pi^-$	$(6.4^{+5.1}_{-2.0}) \times 10^{-4}$		17
$\Xi^0 e^- \overline{\nu}_e$	(5.6 ± 2.8) $\times 10^{-3}$		319
$\Xi^- \gamma$	< 4.6 $\times 10^{-4}$	90%	314
$\Delta S = 2$ forbidden ($S2$) modes			
$\Lambda \pi^-$	$S2$ < 1.9 $\times 10^{-4}$	90%	449

$\Omega(2250)^-$

$I(J^P) = 0(?^?)$

Mass $m = 2252 \pm 9$ MeV
Full width $\Gamma = 55 \pm 18$ MeV

$\Omega(2250)^-$ DECAY MODES	Fraction (Γ_i/Γ)	p (MeV/c)
$\Xi^- \pi^+ K^-$	seen	532
$\Xi(1530)^0 K^-$	seen	437

CHARMED BARYONS ($C=+1$)

$\Lambda_c^+ = udc$, $\Sigma_c^{++} = uuc$, $\Sigma_c^+ = udc$, $\Sigma_c^0 = ddc$,
$\Xi_c^+ = usc$, $\Xi_c^0 = dsc$, $\Omega_c^0 = ssc$

Λ_c^+

$I(J^P) = 0(\frac{1}{2}^+)$

J is not well measured; $\frac{1}{2}$ is the quark-model prediction.

Mass $m = 2284.9 \pm 0.6$ MeV
Mean life $\tau = (200 \pm 6) \times 10^{-15}$ s (S = 1.6)
$c\tau = 59.9\ \mu$m

Decay asymmetry parameters

$\Lambda \pi^+$ $\alpha = -0.98 \pm 0.19$
$\Sigma^+ \pi^0$ $\alpha = -0.45 \pm 0.32$
$\Lambda \ell^+ \nu_\ell$ $\alpha = -0.82^{+0.11}_{-0.07}$

Nearly all branching fractions of the Λ_c^+ are measured relative to the $pK^-\pi^+$ mode, but there are no model-independent measurements of this branching fraction. We explain how we arrive at our value of B($\Lambda_c^+ \to pK^-\pi^+$) in a Note at the beginning of the branching-ratio measurements in the Listings. When this branching fraction is eventually well determined, all the other branching fractions will slide up or down proportionally as the true value differs from the value we use here.

Λ_c^+ DECAY MODES	Fraction (Γ_i/Γ)	Scale factor/ Confidence level	p (MeV/c)
Hadronic modes with a p: $S=-1$ final states			
$p\overline{K}^0$	(2.3 ± 0.6) %		872
$pK^-\pi^+$ [m]	(5.0 ± 1.3) %		822
$p\overline{K}^*(892)^0$ [n]	(1.6 ± 0.5) %		684
$\Delta(1232)^{++} K^-$	(8.6 ± 3.0) $\times 10^{-3}$		709
$\Lambda(1520)\pi^+$ [n]	(5.9 ± 2.1) $\times 10^{-3}$		626
$pK^-\pi^+$ nonresonant	(2.8 ± 0.8) %		822
$p\overline{K}^0\pi^0$	(3.3 ± 1.0) %		822
$p\overline{K}^0\eta$	(1.2 ± 0.4) %		566
$p\overline{K}^0\pi^+\pi^-$	(2.6 ± 0.7) %		753
$pK^-\pi^+\pi^0$	(3.4 ± 1.0) %		758
$pK^*(892)^-\pi^+$ [n]	(1.1 ± 0.5) %		579
$p(K^-\pi^+)_{\text{nonresonant}}\pi^0$	(3.6 ± 1.2) %		758
$\Delta(1232)\overline{K}^*(892)$	seen		417
$pK^-\pi^+\pi^+\pi^-$	(1.1 ± 0.8) $\times 10^{-3}$		670
$pK^-\pi^+\pi^0\pi^0$	(8 ± 4) $\times 10^{-3}$		676
Hadronic modes with a p: $S=0$ final states			
$p\pi^+\pi^-$	(3.5 ± 2.0) $\times 10^{-3}$		926
$pf_0(980)$ [n]	(2.8 ± 1.9) $\times 10^{-3}$		621
$p\pi^+\pi^+\pi^-\pi^-$	(1.8 ± 1.2) $\times 10^{-3}$		851
pK^+K^-	(7.7 ± 3.5) $\times 10^{-4}$		615
$p\phi$ [n]	(8.2 ± 2.7) $\times 10^{-4}$		589
pK^+K^- non-ϕ	(3.5 ± 1.7) $\times 10^{-4}$		615
Hadronic modes with a hyperon: $S=-1$ final states			
$\Lambda\pi^+$	(9.0 ± 2.8) $\times 10^{-3}$		863
$\Lambda\pi^+\pi^0$	(3.6 ± 1.3) %		843
$\Lambda\rho^+$	< 5 %	CL=95%	634
$\Lambda\pi^+\pi^+\pi^-$	(3.3 ± 1.0) %		806
$\Lambda\pi^+\pi^+\pi^-\pi^0$ total	(1.8 ± 0.8) %		756
$\Lambda\pi^+\eta$	(1.8 ± 0.6) %		689
$\Sigma(1385)^+\eta$ [n]	(8.5 ± 3.3) $\times 10^{-3}$		569
$\Lambda\pi^+\omega$ [n]	(1.2 ± 0.5) %		515
$\Lambda\pi^+\pi^+\pi^-\pi^0$, no η or ω	< 7 $\times 10^{-3}$	CL=90%	756
$\Lambda K^+\overline{K}^0$	(6.0 ± 2.1) $\times 10^{-3}$		441
$\Xi(1690)^0 K^+$, $\Xi(1690)^0 \to \Lambda\overline{K}^0$	(1.6 ± 0.8) $\times 10^{-3}$		286
$\Sigma^0\pi^+$	(9.9 ± 3.2) $\times 10^{-3}$		824
$\Sigma^+\pi^0$	(1.00 ± 0.34) %		826
$\Sigma^+\eta$	(5.5 ± 2.3) $\times 10^{-3}$		712
$\Sigma^+\pi^+\pi^-$	(3.6 ± 1.0) %		803
$\Sigma^+\rho^0$	< 1.4 %	CL=95%	573
$\Sigma^-\pi^+\pi^+$	(1.9 ± 0.8) %		798
$\Sigma^0\pi^+\pi^0$	(1.8 ± 0.8) %		802
$\Sigma^0\pi^+\pi^+\pi^-$	(1.1 ± 0.4) %		762
$\Sigma^+\pi^+\pi^-\pi^0$	—		766
$\Sigma^+\omega$ [n]	(2.7 ± 1.0) %		568
$\Sigma^+K^+K^-$	(2.8 ± 0.8) $\times 10^{-3}$		346
$\Sigma^+\phi$ [n]	(3.2 ± 1.0) $\times 10^{-3}$		292
$\Xi(1690)^0 K^+$, $\Xi(1690)^0 \to \Sigma^+K^-$	(8.2 ± 3.1) $\times 10^{-4}$		286
$\Sigma^+K^+K^-$ nonresonant	< 7 $\times 10^{-4}$	CL=90%	346
$\Xi^0 K^+$	(3.9 ± 1.4) $\times 10^{-3}$		652
$\Xi^- K^+\pi^+$	(4.9 ± 1.7) $\times 10^{-3}$		564
$\Xi(1530)^0 K^+$ [n]	(2.6 ± 1.0) $\times 10^{-3}$		471
Hadronic modes with a hyperon: $S=0$ final states			
ΛK^+	(6.7 ± 2.5) $\times 10^{-4}$		780
$\Sigma^0 K^+$	(5.6 ± 2.4) $\times 10^{-4}$		734
$\Sigma^+K^+\pi^-$	(1.7 ± 0.7) $\times 10^{-3}$		668
$\Sigma^+K^*(892)^0$ [n]	(2.8 ± 1.1) $\times 10^{-3}$		468
$\Sigma^-K^+\pi^+$	< 1.0 $\times 10^{-3}$	CL=90%	662
Semileptonic modes			
$\Lambda\ell^+\nu_\ell$ [o]	(2.0 ± 0.6) %		870
$\Lambda e^+\nu_e$	(2.1 ± 0.6) %		870
$\Lambda\mu^+\nu_\mu$	(2.0 ± 0.7) %		866
Inclusive modes			
e^+ anything	(4.5 ± 1.7) %		–
pe^+ anything	(1.8 ± 0.9) %		–
p anything	(50 ±16) %		–
p anything (no Λ)	(12 ±19) %		–
n anything	(50 ±16) %		–
n anything (no Λ)	(29 ±17) %		–
Λ anything	(35 ±11) %	S=1.4	–
$\Sigma^\pm$ anything [p]	(10 ± 5) %		–
3prongs	(24 ± 8) %		–

Baryon Summary Table

$\Delta C = 1$ weak neutral current ($C1$) modes, or Lepton number (L) violating modes

$p\mu^+\mu^-$	$C1$	$<$	3.4	$\times 10^{-4}$	CL=90%	936
$\Sigma^-\mu^+\mu^+$	L	$<$	7.0	$\times 10^{-4}$	CL=90%	811

$\Lambda_c(2593)^+$

$I(J^P) = 0(\frac{1}{2}^-)$

The spin-parity follows from the fact that $\Sigma_c(2455)\pi$ decays, with little available phase space, are dominant. This assumes that $J^P = 1/2^+$ for the $\Sigma_c(2455)$.

Mass $m = 2593.9 \pm 0.8$ MeV
$m - m_{\Lambda_c^+} = 308.9 \pm 0.6$ MeV (S = 1.1)
Full width $\Gamma = 3.6^{+2.0}_{-1.3}$ MeV

$\Lambda_c^+\pi\pi$ and its submode $\Sigma_c(2455)\pi$ — the latter just barely — are the only strong decays allowed to an excited Λ_c^+ having this mass; and the submode seems to dominate.

$\Lambda_c(2593)^+$ DECAY MODES	Fraction (Γ_i/Γ)	p (MeV/c)
$\Lambda_c^+\pi^+\pi^-$	[q] ≈ 67 %	124
$\Sigma_c(2455)^{++}\pi^-$	24 ± 7 %	28
$\Sigma_c(2455)^0\pi^+$	24 ± 7 %	28
$\Lambda_c^+\pi^+\pi^-$ 3-body	18 ± 10 %	124
$\Lambda_c^+\pi^0$	[r] not seen	261
$\Lambda_c^+\gamma$	not seen	291

$\Lambda_c(2625)^+$

$I(J^P) = 0(\frac{3}{2}^-)$

J^P has not been measured; $\frac{3}{2}^-$ is the quark-model prediction.

Mass $m = 2626.6 \pm 0.8$ MeV (S = 1.2)
$m - m_{\Lambda_c^+} = 341.7 \pm 0.6$ MeV (S = 1.6)
Full width $\Gamma < 1.9$ MeV, CL = 90%

$\Lambda_c^+\pi\pi$ and its submode $\Sigma(2455)\pi$ are the only strong decays allowed to an excited Λ_c^+ having this mass.

$\Lambda_c(2625)^+$ DECAY MODES	Fraction (Γ_i/Γ)	Confidence level	p (MeV/c)
$\Lambda_c^+\pi^+\pi^-$	[q] $\approx 67\%$		184
$\Sigma_c(2455)^{++}\pi^-$	<5	90%	102
$\Sigma_c(2455)^0\pi^+$	<5	90%	102
$\Lambda_c^+\pi^+\pi^-$ 3-body	large		184
$\Lambda_c^+\pi^0$	[r] not seen		293
$\Lambda_c^+\gamma$	not seen		319

$\Sigma_c(2455)$

$I(J^P) = 1(\frac{1}{2}^+)$

J^P has not been measured; $\frac{1}{2}^+$ is the quark-model prediction.

$\Sigma_c(2455)^{++}$ mass $m = 2452.5 \pm 0.6$ MeV
$\Sigma_c(2455)^+$ mass $m = 2451.3 \pm 0.7$ MeV
$\Sigma_c(2455)^0$ mass $m = 2452.2 \pm 0.6$ MeV
$m_{\Sigma_c^{++}} - m_{\Lambda_c^+} = 167.58 \pm 0.12$ MeV
$m_{\Sigma_c^+} - m_{\Lambda_c^+} = 166.4 \pm 0.4$ MeV
$m_{\Sigma_c^0} - m_{\Lambda_c^+} = 167.32 \pm 0.12$ MeV
$m_{\Sigma_c^{++}} - m_{\Sigma_c^0} = 0.26 \pm 0.11$ MeV
$m_{\Sigma_c^+} - m_{\Sigma_c^0} = -0.9 \pm 0.4$ MeV
$\Sigma_c(2455)^{++}$ full width $\Gamma = 2.23 \pm 0.30$ MeV
$\Sigma_c(2455)^+$ full width $\Gamma < 4.6$ MeV, CL = 90%
$\Sigma_c(2455)^0$ full width $\Gamma = 2.2 \pm 0.4$ MeV (S = 1.4)

$\Lambda_c^+\pi$ is the only strong decay allowed to a Σ_c having this mass.

$\Sigma_c(2455)$ DECAY MODES	Fraction (Γ_i/Γ)	p (MeV/c)
$\Lambda_c^+\pi$	≈ 100 %	94

$\Sigma_c(2520)$

$I(J^P) = 1(\frac{3}{2}^+)$

J^P has not been measured; $\frac{3}{2}^+$ is the quark-model prediction.

$\Sigma_c(2520)^{++}$ mass $m = 2519.4 \pm 1.5$ MeV
$\Sigma_c(2520)^+$ mass $m = 2515.9 \pm 2.4$ MeV
$\Sigma_c(2520)^0$ mass $m = 2517.5 \pm 1.4$ MeV
$m_{\Sigma_c(2520)^{++}} - m_{\Lambda_c^+} = 234.5 \pm 1.4$ MeV
$m_{\Sigma_c(2520)^+} - m_{\Lambda_c^+} = 231.0 \pm 2.3$ MeV
$m_{\Sigma_c(2520)^0} - m_{\Lambda_c^+} = 232.6 \pm 1.3$ MeV
$m_{\Sigma_c(2520)^{++}} - m_{\Sigma_c(2520)^0} = 1.9 \pm 1.7$ MeV
$\Sigma_c(2520)^{++}$ full width $\Gamma = 18 \pm 5$ MeV
$\Sigma_c(2520)^+$ full width $\Gamma < 17$ MeV, CL = 90%
$\Sigma_c(2520)^0$ full width $\Gamma = 13 \pm 5$ MeV

$\Lambda_c^+\pi$ is the only strong decay allowed to a Σ_c having this mass.

$\Sigma_c(2520)$ DECAY MODES	Fraction (Γ_i/Γ)	p (MeV/c)
$\Lambda_c^+\pi$	≈ 100 %	180

Ξ_c^+

$I(J^P) = \frac{1}{2}(\frac{1}{2}^+)$

J^P has not been measured; $\frac{1}{2}^+$ is the quark-model prediction.

Mass $m = 2466.3 \pm 1.4$ MeV
Mean life $\tau = (442 \pm 26) \times 10^{-15}$ s (S = 1.3)
$c\tau = 132$ μm

Ξ_c^+ DECAY MODES	Fraction (Γ_i/Γ)	Confidence level	p (MeV/c)
No absolute branching fractions have been measured. The following are branching *ratios* relative to $\Xi^-\pi^+\pi^+$.			
Cabibbo-favored ($S = -2$) decays			
$\Lambda\overline{K}^0\pi^+$	—		851
$\Sigma(1385)^+\overline{K}^0$	[n,s] 1.0 ±0.5		745
$\Lambda K^-\pi^+\pi^+$	[s] 0.34 ± 0.12		785
$\Lambda\overline{K}^*(892)^0\pi^+$	[n,s] <0.2	90%	607
$\Sigma(1385)^+K^-\pi^+$	[n,s] <0.3	90%	677
$\Sigma^+K^-\pi^+$	[s] 0.94 ± 0.11		809
$\Sigma^+\overline{K}^*(892)^0$	[n,s] 0.81 ± 0.15		657
$\Sigma^0K^-\pi^+\pi^+$	[s] 0.29 ± 0.16		734
$\Xi^0\pi^+$	[s] 0.55 ± 0.16		876
$\Xi^-\pi^+\pi^+$	[s] DEFINED AS 1		850
$\Xi(1530)^0\pi^+$	[n,s] <0.1	90%	748
$\Xi^0\pi^+\pi^0$	[s] 2.34 ± 0.68		855
$\Xi^0\pi^+\pi^+\pi^-$	[s] 1.74 ± 0.50		817
$\Xi^0e^+\nu_e$	[s] $2.3\ ^{+0.7}_{-0.9}$		883
$\Omega^-K^+\pi^+$	[s] 0.07 ± 0.04		397
Cabibbo-suppressed decays			
$pK^-\pi^+$	[s] 0.21 ± 0.03		943
$p\overline{K}^*(892)^0$	[n,s] 0.12 ± 0.02		827
$\Sigma^+K^+K^-$	[s] 0.15 ± 0.07		578
$\Sigma^+\phi$	[n,s] <0.11	90%	547
$\Xi(1690)^0K^+$ $\times$ B($\Xi(1690)^0 \rightarrow \Sigma^+K^-$)	[s] <0.05	90%	501

Ξ_c^0

$I(J^P) = \frac{1}{2}(\frac{1}{2}^+)$

J^P has not been measured; $\frac{1}{2}^+$ is the quark-model prediction.

Mass $m = 2471.8 \pm 1.4$ MeV
$m_{\Xi_c^0} - m_{\Xi_c^+} = 5.5 \pm 1.8$ MeV
Mean life $\tau = (112^{+13}_{-10}) \times 10^{-15}$ s
$c\tau = 33.6\ \mu$m

Decay asymmetry parameters

$\Xi^-\pi^+$ $\alpha = -0.6 \pm 0.4$

Ξ_c^0 DECAY MODES	Fraction (Γ_i/Γ)	p (MeV/c)
$\Lambda\overline{K}^0$	seen	907
$\Lambda\overline{K}^0\pi^+\pi^-$	seen	788
$\Lambda K^-\pi^+\pi^+\pi^-$	seen	704
$\Xi^-\pi^+$	seen	876
$\Xi^-\pi^+\pi^+\pi^-$	seen	817
$pK^-\overline{K}^*(892)^0$	seen	414
$\Omega^- K^+$	seen	523
$\Xi^- e^+\nu_e$	seen	883
$\Xi^-\ell^+$ anything	seen	–

$\Xi_c'^+$

$I(J^P) = \frac{1}{2}(\frac{1}{2}^+)$

J^P has not been measured; $\frac{1}{2}^+$ is the quark-model prediction.

Mass $m = 2574.1 \pm 3.3$ MeV
$m_{\Xi_c'^+} - m_{\Xi_c^+} = 107.8 \pm 3.0$ MeV

The $\Xi_c'^+ - \Xi_c^+$ mass difference is too small for any strong decay to occur.

$\Xi_c'^+$ DECAY MODES	Fraction (Γ_i/Γ)	p (MeV/c)
$\Xi_c^+\gamma$	seen	106

$\Xi_c'^0$

$I(J^P) = \frac{1}{2}(\frac{1}{2}^+)$

J^P has not been measured; $\frac{1}{2}^+$ is the quark-model prediction.

Mass $m = 2578.8 \pm 3.2$ MeV
$m_{\Xi_c'^0} - m_{\Xi_c^0} = 107.0 \pm 2.9$ MeV

The $\Xi_c'^0 - \Xi_c^0$ mass difference is too small for any strong decay to occur.

$\Xi_c'^0$ DECAY MODES	Fraction (Γ_i/Γ)	p (MeV/c)
$\Xi_c^0\gamma$	seen	105

$\Xi_c(2645)$

$I(J^P) = \frac{1}{2}(\frac{3}{2}^+)$

J^P has not been measured; $\frac{3}{2}^+$ is the quark-model prediction.

$\Xi_c(2645)^+$ mass $m = 2647.4 \pm 2.0$ MeV (S = 1.2)
$\Xi_c(2645)^0$ mass $m = 2644.5 \pm 1.8$ MeV
$m_{\Xi_c(2645)^+} - m_{\Xi_c^0} = 175.6 \pm 1.4$ MeV (S = 1.7)
$m_{\Xi_c(2645)^0} - m_{\Xi_c^+} = 178.2 \pm 1.1$ MeV
$\Xi_c(2645)^+$ full width $\Gamma < 3.1$ MeV, CL = 90%
$\Xi_c(2645)^0$ full width $\Gamma < 5.5$ MeV, CL = 90%

$\Xi_c\pi$ is the only strong decay allowed to a Ξ_c resonance having this mass.

$\Xi_c(2645)$ DECAY MODES	Fraction (Γ_i/Γ)	p (MeV/c)
$\Xi_c^0\pi^+$	seen	98
$\Xi_c^+\pi^-$	seen	107

$\Xi_c(2790)$

$I(J^P) = \frac{1}{2}(\frac{1}{2}^-)$

J^P has not been measured; $\frac{1}{2}^-$ is the quark-model prediction.

$\Xi_c(2790)^+$ mass = 2790.0 ± 3.5 MeV
$\Xi_c(2790)^0$ mass = 2790 ± 4 MeV
$m_{\Xi_c(2790)^+} - m_{\Xi_c^0} = 318.2 \pm 3.2$ MeV
$m_{\Xi_c(2790)^0} - m_{\Xi_c^+} = 324.0 \pm 3.3$ MeV
$\Xi_c(2790)^+$ width < 15 MeV, CL = 90%
$\Xi_c(2790)^0$ width < 12 MeV, CL = 90%

$\Xi_c(2790)$ DECAY MODES	Fraction (Γ_i/Γ)	p (MeV/c)
$\Xi_c'\pi$	seen	162

$\Xi_c(2815)$

$I(J^P) = \frac{1}{2}(\frac{3}{2}^-)$

J^P has not been measured; $\frac{3}{2}^-$ is the quark-model prediction.

$\Xi_c(2815)^+$ mass $m = 2814.9 \pm 1.8$ MeV
$\Xi_c(2815)^0$ mass $m = 2819.0 \pm 2.5$ MeV
$m_{\Xi_c(2815)^+} - m_{\Xi_c^+} = 348.6 \pm 1.2$ MeV
$m_{\Xi_c(2815)^0} - m_{\Xi_c^0} = 347.2 \pm 2.1$ MeV
$\Xi_c(2815)^+$ full width $\Gamma < 3.5$ MeV, CL = 90%
$\Xi_c(2815)^0$ full width $\Gamma < 6.5$ MeV, CL = 90%

The $\Xi_c\pi\pi$ modes are consistent with being entirely via $\Xi_c(2645)\pi$.

$\Xi_c(2815)$ DECAY MODES	Fraction (Γ_i/Γ)	p (MeV/c)
$\Xi_c^+\pi^+\pi^-$	seen	196
$\Xi_c^0\pi^+\pi^-$	seen	187

Ω_c^0

$I(J^P) = 0(\frac{1}{2}^+)$

J^P has not been measured; $\frac{1}{2}^+$ is the quark-model prediction.

Mass $m = 2697.5 \pm 2.6$ MeV (S = 1.2)
Mean life $\tau = (69 \pm 12) \times 10^{-15}$ s
$c\tau = 21\ \mu$m

No absolute branching fractions have been measured.

Ω_c^0 DECAY MODES	Fraction (Γ_i/Γ)	p (MeV/c)
$\Sigma^+ K^- K^-\pi^+$	seen	691
$\Xi^0 K^-\pi^+$	seen	903
$\Xi^- K^-\pi^+\pi^+$	seen	832
$\Omega^- e^+\nu_e$	seen	830
$\Omega^-\pi^+$	seen	822
$\Omega^-\pi^+\pi^0$	seen	798
$\Omega^-\pi^-\pi^+\pi^+$	seen	754

Baryon Summary Table

BOTTOM BARYONS ($B = -1$)

$\Lambda_b^0 = udb$, $\Xi_b^0 = usb$, $\Xi_b^- = dsb$

Λ_b^0 $I(J^P) = 0(\frac{1}{2}^+)$

$I(J^P)$ not yet measured; $0(\frac{1}{2}^+)$ is the quark model prediction.

Mass $m = 5624 \pm 9$ MeV (S = 1.8)

Mean life $\tau = (1.229 \pm 0.080) \times 10^{-12}$ s

$c\tau = 368\ \mu$m

These branching fractions are actually an average over weakly decaying b-baryons weighted by their production rates in Z decay (or high-energy $p\overline{p}$), branching ratios, and detection efficiencies. They scale with the LEP b-baryon production fraction B($b \rightarrow$ b-baryon) and are evaluated for our value B($b \rightarrow$ b-baryon) = (9.9 ± 1.7)%.

The branching fractions B(b-baryon $\rightarrow$ $\Lambda \ell^- \overline{\nu}_\ell$ anything) and B($\Lambda_b^0 \rightarrow$ $\Lambda_c^+ \ell^- \overline{\nu}_\ell$ anything) are not pure measurements because the underlying measured products of these with B($b \rightarrow$ b-baryon) were used to determine B($b \rightarrow$ b-baryon), as described in the note "Production and Decay of b-Flavored Hadrons."

Λ_b^0 DECAY MODES	Fraction (Γ_i/Γ)	Confidence level	p (MeV/c)
$J/\psi(1S)\Lambda$	$(4.7 \pm 2.8) \times 10^{-4}$		1744
$\Lambda_c^+ \pi^-$	seen		2345
$\Lambda_c^+ a_1(1260)^-$	seen		2156
$\Lambda_c^+ \ell^- \overline{\nu}_\ell$ anything	[t] (9.2 ± 2.1) %		–
$p\pi^-$	$< 5.0 \times 10^{-5}$	90%	2732
pK^-	$< 5.0 \times 10^{-5}$	90%	2711
$\Lambda\gamma$	$< 1.3 \times 10^{-3}$	90%	2701

b-baryon ADMIXTURE (Λ_b, Ξ_b, Σ_b, Ω_b)

Mean life $\tau = (1.208 \pm 0.051) \times 10^{-12}$ s

These branching fractions are actually an average over weakly decaying b-baryons weighted by their production rates in Z decay (or high-energy $p\overline{p}$), branching ratios, and detection efficiencies. They scale with the LEP b-baryon production fraction B($b \rightarrow$ b-baryon) and are evaluated for our value B($b \rightarrow$ b-baryon) = (9.9 ± 1.7)%.

The branching fractions B(b-baryon $\rightarrow$ $\Lambda \ell^- \overline{\nu}_\ell$ anything) and B($\Lambda_b^0 \rightarrow$ $\Lambda_c^+ \ell^- \overline{\nu}_\ell$ anything) are not pure measurements because the underlying measured products of these with B($b \rightarrow$ b-baryon) were used to determine B($b \rightarrow$ b-baryon), as described in the note "Production and Decay of b-Flavored Hadrons."

b-baryon ADMIXTURE DECAY MODES (Λ_b,Ξ_b,Σ_b,Ω_b)	Fraction (Γ_i/Γ)	p (MeV/c)
$p\mu^- \overline{\nu}$ anything	$(4.9^{+2.1}_{-1.8})$ %	–
$p\ell\overline{\nu}_\ell$ anything	(4.8 ± 1.1) %	–
p anything	(60 ± 20) %	–
$\Lambda\ell^-\overline{\nu}_\ell$ anything	(3.2 ± 0.6) %	–
$\Lambda/\overline{\Lambda}$ anything	(33 ± 7) %	–
$\Xi^-\ell^-\overline{\nu}_\ell$ anything	$(5.6 \pm 1.5) \times 10^{-3}$	–

NOTES

This Summary Table only includes established baryons. The Particle Listings include evidence for other baryons. The masses, widths, and branching fractions for the resonances in this Table are Breit-Wigner parameters, but pole positions are also given for most of the N and Δ resonances.

For most of the resonances, the parameters come from various partial-wave analyses of more or less the same sets of data, and it is not appropriate to treat the results of the analyses as independent or to average them together. Furthermore, the systematic errors on the results are not well understood. Thus, we usually only give ranges for the parameters. We then also give a best guess for the mass (as part of the name of the resonance) and for the width. The *Note on N and Δ Resonances* and the *Note on Λ and Σ Resonances* in the Particle Listings review the partial-wave analyses.

When a quantity has "(S = ...)" to its right, the error on the quantity has been enlarged by the "scale factor" S, defined as $S = \sqrt{\chi^2/(N-1)}$, where N is the number of measurements used in calculating the quantity. We do this when S > 1, which often indicates that the measurements are inconsistent. When S > 1.25, we also show in the Particle Listings an ideogram of the measurements. For more about S, see the Introduction.

A decay momentum p is given for each decay mode. For a 2-body decay, p is the momentum of each decay product in the rest frame of the decaying particle. For a 3-or-more-body decay, p is the largest momentum any of the products can have in this frame. For any resonance, the *nominal* mass is used in calculating p. A dagger ("†") in this column indicates that the mode is forbidden when the nominal masses of resonances are used, but is in fact allowed due to the nonzero widths of the resonances.

[a] The masses of the p and n are most precisely known in u (unified atomic mass units). The conversion factor to MeV, 1 u = 931.494043 ± 0.000080 MeV, is less well known than are the masses in u.

[b] These two results are not independent, and both use the more precise measurement of $|q_{\overline{p}}/m_{\overline{p}}|/(q_p/m_p)$.

[c] The limit is from neutrality-of-matter experiments; it assumes $q_n = q_p + q_e$. See also the charge of the neutron.

[d] The first limit is for $p \rightarrow$ anything or "disappearance" modes of a bound proton. The second entry, a rough range of limits, assumes the dominant decay modes are among those investigated. For antiprotons the best limit, inferred from the observation of cosmic ray $\overline{p}$s is $\tau_{\overline{p}} > 10^7$ yr, the cosmic-ray storage time, but this limit depends on a number of assumptions. The best direct observation of stored antiprotons gives $\tau_{\overline{p}}/\mathrm{B}(\overline{p} \rightarrow e^-\gamma) > 7 \times 10^5$ yr.

[e] There is some controversy about whether nuclear physics and model dependence complicate the analysis for bound neutrons (from which the best limit comes). The first limit here is from reactor experiments with free neutrons.

[f] The parameters g_A, g_V, and g_{WM} for semileptonic modes are defined by $\overline{B}_f[\gamma_\lambda(g_V + g_A\gamma_5) + i(g_{WM}/m_{B_i})\ \sigma_{\lambda\nu}\ q^\nu]B_i$, and ϕ_{AV} is defined by $g_A/g_V = |g_A/g_V|e^{i\phi_{AV}}$. See the "Note on Baryon Decay Parameters" in the neutron Particle Listings.

[g] Time-reversal invariance requires this to be 0° or 180°.

[h] This limit is for γ energies between 35 and 100 keV.

[i] The decay parameters γ and Δ are calculated from α and ϕ using

$$\gamma = \sqrt{1-\alpha^2}\cos\phi, \qquad \tan\Delta = -\frac{1}{\alpha}\sqrt{1-\alpha^2}\sin\phi.$$

See the "Note on Baryon Decay Parameters" in the neutron Particle Listings.

[j] See the Listings for the pion momentum range used in this measurement.

[k] The error given here is only an educated guess. It is larger than the error on the weighted average of the published values.

[l] A theoretical value using QED.

[m] See the note on "Λ_c^+ Branching Fractions" in the Λ_c^+ Particle Listings.

[n] This branching fraction includes all the decay modes of the final-state resonance.

[o] An ℓ indicates an e or a μ mode, not a sum over these modes.

[p] The value is for the sum of the charge states or particle/antiparticle states indicated.

[q] Assuming isospin conservation, so that the other third is $\Lambda_c^+\pi^0\pi^0$.

[r] A test that the isospin is indeed 0, so that the particle is indeed a Λ_c^+.

[s] No absolute branching fractions have been measured. The following are branching *ratios* relative to $\Xi^-\pi^+\pi^+$.

[t] Not a pure measurement. See note at head of Λ_b^0 Decay Modes.

SEARCHES FOR MONOPOLES, SUPERSYMMETRY, TECHNICOLOR, COMPOSITENESS, EXTRA DIMENSIONS, etc.

Magnetic Monopole Searches

Isolated supermassive monopole candidate events have not been confirmed. The most sensitive experiments obtain negative results.

Best cosmic-ray supermassive monopole flux limit:

$< 1.0 \times 10^{-15}$ cm^{-2}sr^{-1}s^{-1} for $1.1 \times 10^{-4} < \beta < 0.1$

Supersymmetric Particle Searches

Limits are based on the Minimal Supersymmetric Standard Model.

Assumptions include: 1) $\widetilde{\chi}_1^0$ (or $\widetilde{\gamma}$) is lightest supersymmetric particle; 2) R-parity is conserved; 3) With the exception of $\widetilde{t}$ and $\widetilde{b}$, all scalar quarks are assumed to be degenerate in mass and $m_{\widetilde{q}_R} = m_{\widetilde{q}_L}$. 4) Limits for sleptons refer to the $\widetilde{\ell}_R$ states.

See the Particle Listings for a Note giving details of supersymmetry.

$\widetilde{\chi}_i^0$ — neutralinos (mixtures of $\widetilde{\gamma}$, $\widetilde{Z}^0$, and $\widetilde{H}_i^0$)

Mass $m_{\widetilde{\chi}_1^0} > 46$ GeV, CL = 95% [all tanβ, all Δm_0, all m_0]

Mass $m_{\widetilde{\chi}_2^0} > 62.4$ GeV, CL = 95%
[1<tanβ<40, all m_0, all $m_{\widetilde{\chi}_2^0} - m_{\widetilde{\chi}_1^0}$]

Mass $m_{\widetilde{\chi}_3^0} > 99.9$ GeV, CL = 95%
[1<tanβ<40, all m_0, all $m_{\widetilde{\chi}_2^0} - m_{\widetilde{\chi}_1^0}$]

$\widetilde{\chi}_i^\pm$ — charginos (mixtures of $\widetilde{W}^\pm$ and $\widetilde{H}_i^\pm$)

Mass $m_{\widetilde{\chi}_1^\pm} > 94$ GeV, CL = 95%
[tan$\beta < 40$, $m_{\widetilde{\chi}_1^\pm} - m_{\widetilde{\chi}_1^0} > 3$ GeV, all m_0]

$\widetilde{e}$ — scalar electron (selectron)

Mass $m > 73$ GeV, CL = 95% [all $m_{\widetilde{e}_R} - m_{\widetilde{\chi}_1^0}$]

$\widetilde{\mu}$ — scalar muon (smuon)

Mass $m > 94$ GeV, CL = 95%
[$1 \leq$ tan$\beta \leq 40$, $m_{\widetilde{\mu}_R} - m_{\widetilde{\chi}_1^0} > 10$ GeV]

$\widetilde{\tau}$ — scalar tau (stau)

Mass $m > 81.9$ GeV, CL = 95%
[$m_{\widetilde{\tau}_R} - m_{\widetilde{\chi}_1^0} > 15$ GeV, all θ_τ]

$\widetilde{q}$ — scalar quark (squark)

These limits include the effects of cascade decays, evaluated assuming a fixed value of the parameters μ and tanβ. The limits are weakly sensitive to these parameters over much of parameter space. Limits assume GUT relations between gaugino masses and the gauge coupling.

Mass $m > 250$ GeV, CL = 95% [tan$\beta = 2$, $\mu < 0$, $A = 0$]

$\widetilde{b}$ — scalar bottom (sbottom)

Mass $m > 89$ GeV, CL = 95% [$m_{\widetilde{b}_1} - m_{\widetilde{\chi}_1^0} > 8$ GeV, all θ_b]

$\widetilde{t}$ — scalar top (stop)

Mass $m > 95.7$ GeV, CL = 95%
[$\widetilde{t} \rightarrow c\widetilde{\chi}_1^0$, all θ_t, $m_{\widetilde{t}} - m_{\widetilde{\chi}_1^0} > 10$ GeV]

$\widetilde{g}$ — gluino

The limits summarised here refer to the high-mass region ($m_{\widetilde{g}} \gtrsim 5$ GeV), and include the effects of cascade decays, evaluated assuming a fixed value of the parameters μ and tanβ. The limits are weakly sensitive to these parameters over much of parameter space. Limits assume GUT relations between gaugino masses and the gauge coupling,

Mass $m > 195$ GeV, CL = 95% [any $m_{\widetilde{q}}$]

Mass $m > 300$ GeV, CL = 95% [$m_{\widetilde{q}} = m_{\widetilde{g}}$]

Technicolor

Searches for a color-octet techni-ρ constrain its mass to be greater than 260 to 480 GeV, depending on allowed decay channels. Similar bounds exist on the color-octet techni-ω.

Quark and Lepton Compositeness, Searches for

Scale Limits Λ for Contact Interactions
(the lowest dimensional interactions with four fermions)

If the Lagrangian has the form

$$\pm \frac{g^2}{2\Lambda^2} \overline{\psi}_L \gamma_\mu \psi_L \overline{\psi}_L \gamma^\mu \psi_L$$

(with $g^2/4\pi$ set equal to 1), then we define $\Lambda \equiv \Lambda_{LL}^\pm$. For the full definitions and for other forms, see the Note in the Listings on Searches for Quark and Lepton Compositeness in the full *Review* and the original literature.

$\Lambda_{LL}^+(eeee)$	>	8.3 TeV, CL = 95%
$\Lambda_{LL}^-(eeee)$	>	10.3 TeV, CL = 95%
$\Lambda_{LL}^+(ee\mu\mu)$	>	8.5 TeV, CL = 95%
$\Lambda_{LL}^-(ee\mu\mu)$	>	6.3 TeV, CL = 95%
$\Lambda_{LL}^+(ee\tau\tau)$	>	5.4 TeV, CL = 95%
$\Lambda_{LL}^-(ee\tau\tau)$	>	6.5 TeV, CL = 95%
$\Lambda_{LL}^+(\ell\ell\ell\ell)$	>	9.0 TeV, CL = 95%
$\Lambda_{LL}^-(\ell\ell\ell\ell)$	>	7.8 TeV, CL = 95%
$\Lambda_{LL}^+(eeuu)$	>	23.3 TeV, CL = 95%
$\Lambda_{LL}^-(eeuu)$	>	12.5 TeV, CL = 95%
$\Lambda_{LL}^+(eedd)$	>	11.1 TeV, CL = 95%
$\Lambda_{LL}^-(eedd)$	>	26.4 TeV, CL = 95%
$\Lambda_{LL}^+(eecc)$	>	1.0 TeV, CL = 95%
$\Lambda_{LL}^-(eecc)$	>	2.1 TeV, CL = 95%
$\Lambda_{LL}^+(eebb)$	>	5.6 TeV, CL = 95%
$\Lambda_{LL}^-(eebb)$	>	4.9 TeV, CL = 95%
$\Lambda_{LL}^+(\mu\mu qq)$	>	2.9 TeV, CL = 95%
$\Lambda_{LL}^-(\mu\mu qq)$	>	4.2 TeV, CL = 95%
$\Lambda(\ell\nu\ell\nu)$	>	3.10 TeV, CL = 90%
$\Lambda(e\nu qq)$	>	2.81 TeV, CL = 95%
$\Lambda_{LL}^+(qqqq)$	>	2.7 TeV, CL = 95%
$\Lambda_{LL}^-(qqqq)$	>	2.4 TeV, CL = 95%
$\Lambda_{LL}^+(\nu\nu qq)$	>	5.0 TeV, CL = 95%
$\Lambda_{LL}^-(\nu\nu qq)$	>	5.4 TeV, CL = 95%

Searches Summary Table

Excited Leptons

The limits from $\ell^{*+}\ell^{*-}$ do not depend on λ (where λ is the $\ell\ell^*$ transition coupling). The λ-dependent limits assume chiral coupling.

$e^{*\pm}$ — excited electron

Mass $m >$ 103.2 GeV, CL = 95% (from e^*e^*)
Mass $m >$ 255 GeV, CL = 95% (from ee^*)
Mass $m >$ 310 GeV, CL = 95% (if $\lambda_\gamma = 1$)

$\mu^{*\pm}$ — excited muon

Mass $m >$ 103.2 GeV, CL = 95% (from $\mu^*\mu^*$)
Mass $m >$ 190 GeV, CL = 95% (from $\mu\mu^*$)

$\tau^{*\pm}$ — excited tau

Mass $m >$ 103.2 GeV, CL = 95% (from $\tau^*\tau^*$)
Mass $m >$ 185 GeV, CL = 95% (from $\tau\tau^*$)

ν^* — excited neutrino

Mass $m >$ 102.6 GeV, CL = 95% (from $\nu^*\nu^*$)
Mass $m >$ 190 GeV, CL = 95% (from $\nu\nu^*$)

q^* — excited quark

Mass $m >$ 45.6 GeV, CL = 95% (from q^*q^*)
Mass $m >$ 570, none 580–760 GeV, CL = 95% (from q^*X)

Color Sextet and Octet Particles

Color Sextet Quarks (q_6)

Mass $m >$ 84 GeV, CL = 95% (Stable q_6)

Color Octet Charged Leptons (ℓ_8)

Mass $m >$ 86 GeV, CL = 95% (Stable ℓ_8)

Color Octet Neutrinos (ν_8)

Mass $m >$ 110 GeV, CL = 90% ($\nu_8 \rightarrow \nu g$)

Extra Dimensions

Please refer to the Extra Dimensions section of the full *Review* for a discussion of the model-dependence of these bounds, and further constraints.

Constraints on the fundamental gravity scale

$M_H >$ 1.1 TeV, CL = 95% (dim-8 operators; $p\overline{p} \rightarrow e^+e^-, \gamma\gamma$)
$M_D >$ 1.1 TeV, CL = 95% ($e^+e^- \rightarrow G\gamma$; 2-flat dimensions)
$M_D >$ 3–1000 TeV (astrophys. and cosmology; 2-flat dimensions; limits depend on technique and assumptions)

Constraints on the radius of the extra dimensions, for the case of two-flat dimensions of equal radii

$r <$ 90–660 nm (astrophysics; limits depend on technique and assumptions)
$r <$ 0.22 mm, CL = 95% (direct tests of Newton's law; cited in Extra Dimensions review)

TESTS OF CONSERVATION LAWS

Updated February 2004 by L. Wolfenstein and T.G. Trippe.

In keeping with the current interest in tests of conservation laws, we collect together a Table of experimental limits on all weak and electromagnetic decays, mass differences, and moments, and on a few reactions, whose observation would violate conservation laws. The Table is given only in the full *Review of Particle Physics*, not in the Particle Physics Booklet. For the benefit of Booklet readers, we include the best limits from the Table in the following text. Limits in this text are for CL=90% unless otherwise specified. The Table is in two parts: "Discrete Space-Time Symmetries," *i.e.*, C, P, T, CP, and CPT; and "Number Conservation Laws," *i.e.*, lepton, baryon, hadronic flavor, and charge conservation. The references for these data can be found in the the Particle Listings in the *Review*. A discussion of these tests follows.

CPT INVARIANCE

General principles of relativistic field theory require invariance under the combined transformation CPT. The simplest tests of CPT invariance are the equality of the masses and lifetimes of a particle and its antiparticle. The best test comes from the limit on the mass difference between K^0 and $\overline{K}^0$. Any such difference contributes to the CP-violating parameter ϵ. Assuming CPT invariance, ϕ_ϵ, the phase of ϵ should be very close to 44°. (See the review "CP Violation in K_L decay" in this edition.) In contrast, if the entire source of CP violation in K^0 decays were a $K^0 - \overline{K}^0$ mass difference, ϕ_ϵ would be $44° + 90°$.

Assuming that there is no other source of CPT violation than this mass difference, it is possible to deduce that[1]

$$m_{\overline{K}^0} - m_{K^0} \approx \frac{2(m_{K_L^0} - m_{K_S^0})\,|\eta|\,(\frac{2}{3}\phi_{+-} + \frac{1}{3}\phi_{00} - \phi_{\rm SW})}{\sin\phi_{\rm SW}}\ ,$$

where $\phi_{\rm SW} = (43.51 \pm 0.05)°$, the superweak angle. Using our best values of the CP-violation parameters, we get $|(m_{\overline{K}^0} - m_{K^0})/m_{K^0}| \leq 10^{-18}$ at CL=95%. Limits can also be placed on specific CPT-violating decay amplitudes. Given the small value of $(1 - |\eta_{00}/\eta_{+-}|)$, the value of $\phi_{00} - \phi_{+-}$ provides a measure of CPT violation in $K_L^0 \to 2\pi$ decay. Results from CERN[1] and Fermilab[2] indicate no CPT-violating effect.

CP AND T INVARIANCE

Given CPT invariance, CP violation and T violation are equivalent. The original evidence for CP violation came from the measurement of $|\eta_{+-}| = |A(K_L^0 \to \pi^+\pi^-)/A(K_S^0 \to \pi^+\pi^-)| = (2.288 \pm 0.014) \times 10^{-3}$. This could be explained in terms of K^0–$\overline{K}^0$ mixing, which also leads to the asymmetry $[\Gamma(K_L^0 \to \pi^- e^+ \nu) - \Gamma(K_L^0 \to \pi^+ e^- \overline{\nu})]/[\text{sum}] = (0.333 \pm 0.014)\%$. Evidence for CP violation in the kaon decay amplitide comes from the measurement of $(1 - |\eta_{00}/\eta_{+-}|)/3 = Re(\epsilon'/\epsilon) = (1.67 \pm 0.26) \times 10^{-3}$. In the Standard Model much larger CP-violating effects are expected. The first of these, which is associated with B–$\overline{B}$ mixing, is the parameter $sin(2\beta)$ now measured quite accurately to be 0.731 ± 0.056. A number of other CP-violating observables are being measured in B decays and preliminary results are available. Direct tests of T violation are much more difficult; a measurement by CPLEAR of the difference between the oscillation probabilities of K^0 to $\overline{K^0}$ and $\overline{K^0}$ to K^0 is related to T violation [3]. Other searches for CP or T violation involve effects that are expected to be unobservable in the Standard Model. The most sensitive are probably the searches for an electric dipole moment of the neutron, measured to be $< 6 \times 10^{-26}$ e cm, and the electron $(0.07 \pm 0.07) \times 10^{-26}$ e cm. A nonzero value requires both P and T violation.

CONSERVATION OF LEPTON NUMBERS

Present experimental evidence and the standard electroweak theory are consistent with the absolute conservation of three separate lepton numbers: electron number L_e, muon number L_μ, and tau number L_τ, except for the effect of neutrino mixing associated with neutrino masses. Searches for violations are of the following types:

a) $\Delta L = 2$ for one type of charged lepton. The best limit comes from the search for neutrinoless double beta decay $(Z, A) \to (Z + 2, A) + e^- + e^-$. The best laboratory limit is $t_{1/2} > 1.9 \times 10^{25}$ yr (CL=90%) for ^{76}Ge.

b) Conversion of one charged-lepton type to another. For purely leptonic processes, the best limits are on $\mu \to e\gamma$ and $\mu \to 3e$, measured as $\Gamma(\mu \to e\gamma)/\Gamma(\mu \to \text{all}) < 1.2 \times 10^{-11}$ and $\Gamma(\mu \to 3e)/\Gamma(\mu \to \text{all}) < 1.0 \times 10^{-12}$. For semileptonic processes, the best limit comes from the coherent conversion process in a muonic atom, $\mu^- + (Z, A) \to e^- + (Z, A)$, measured as $\Gamma(\mu^-\text{Ti} \to e^-\text{Ti})/\Gamma(\mu^-\text{Ti} \to \text{all}) < 4 \times 10^{-12}$. Of special interest is the case in which the hadronic flavor also changes, as in $K_L \to e\mu$ and $K^+ \to \pi^+ e^- \mu^+$, measured as $\Gamma(K_L \to e\mu)/\Gamma(K_L \to \text{all}) < 4.7 \times 10^{-12}$ and $\Gamma(K^+ \to \pi^+ e^- \mu^+)/\Gamma(K^+ \to \text{all}) < 2.8 \times 10^{-11}$. Limits on the conversion of τ into e or μ are found in τ decay and are much less stringent than those for $\mu \to e$ conversion, *e.g.*, $\Gamma(\tau \to \mu\gamma)/\Gamma(\tau \to \text{all}) < 1.1 \times 10^{-6}$ and $\Gamma(\tau \to e\gamma)/\Gamma(\tau \to \text{all}) < 2.7 \times 10^{-6}$.

c) Conversion of one type of charged lepton into another type of charged antilepton. The case most studied is $\mu^- + (Z, A) \to e^+ + (Z - 2, A)$, the strongest limit being $\Gamma(\mu^-\text{Ti} \to e^+\text{Ca})/\Gamma(\mu^-\text{Ti} \to \text{all}) < 3.6 \times 10^{-11}$.

d) Neutrino oscillations. If neutrinos have mass, then it is expected even in the standard electroweak theory that the lepton numbers are not separately conserved, as a consequence of lepton mixing analogous to Cabibbo quark mixing. However, if the only source of lepton-number violation is the mixing of low-mass neutrinos then processes such as $\mu \to e\gamma$ are expected to have extremely small unobservable probabilities. For small neutrino masses, the lepton-number violation would be observed first in neutrino oscillations, which have been the subject of extensive experimental searches. Strong evidence for neutrino mixing has come from atmospheric and solar neutrinos. The SNO experiment has detected the total flux of neutrinos from the sun measured via neutral current interactions and found it

greater than the flux of ν_e. This confirms previous indications of a deficit of ν_e and can be explained by oscillations with $\Delta(m^2) = (7.1^{+1.2}_{-0.6}) \times 10^{-5}$ eV^2. Evidence for such oscillations for reactor $\overline{\nu}$ has been found by the KAMLAND detector. In addition, underground detectors observing neutrinos produced by cosmic rays in the atmosphere have found a factor of 2 deficiency of upward going ν_μ compared to downward. This provides compelling evidence for ν_μ disappearance, for which the most probable explanation is $\nu_\mu \to \nu_\tau$ oscillations with nearly maximal mixing and $\Delta(m^2)$ of the order 0.0013–0.0030 eV^2.

CONSERVATION OF HADRONIC FLAVORS

In strong and electromagnetic interactions, hadronic flavor is conserved, *i.e.* the conversion of a quark of one flavor (d, u, s, c, b, t) into a quark of another flavor is forbidden. In the Standard Model, the weak interactions violate these conservation laws in a manner described by the Cabibbo-Kobayashi-Maskawa mixing (see the section "Cabibbo-Kobayashi-Maskawa Mixing Matrix"). The way in which these conservation laws are violated is tested as follows:

(a) $\Delta S = \Delta Q$ rule. In the strangeness-changing semileptonic decay of strange particles, the strangeness change equals the change in charge of the hadrons. Tests come from limits on decay rates such as $\Gamma(\Sigma^+ \to n e^+ \nu)/\Gamma(\Sigma^+ \to \text{all}) < 5 \times 10^{-6}$, and from a detailed analysis of $K_L \to \pi e \nu$, which yields the parameter x, measured to be $(\mathrm{Re}\, x, \mathrm{Im}\, x) = (-0.002 \pm 0.006, 0.0012 \pm 0.0021)$. Corresponding rules are $\Delta C = \Delta Q$ and $\Delta B = \Delta Q$.

(b) Change of flavor by two units. In the Standard Model this occurs only in second-order weak interactions. The classic example is $\Delta S = 2$ via $K^0 - \overline{K}^0$ mixing, which is directly measured by $m(K_L) - m(K_S) = (3.483 \pm 0.006) \times 10^{-12}$ MeV. There is now evidence for $B^0 - \overline{B}^0$ mixing ($\Delta B = 2$), with the corresponding mass difference between the eigenstates $(m_{B^0_{\rm H}} - m_{B^0_{\rm L}}) = (0.751 \pm 0.012)\Gamma_{B^0} = (3.304 \pm 0.045) \times 10^{-10}$ MeV, and for B^0_s–$\overline{B}^0_s$ mixing, with $(m_{B^0_{sH}} - m_{B^0_{sL}}) > 20.6\,\Gamma_{B^0_s}$ or $> 9 \times 10^{-9}$ MeV (CL=95%). For D^0–$\overline{D}^0$ mixing $m_{D^0_H} - m_{D^0_L} < 5 \times 10^{-11}$ MeV. All results are consistent with the second-order calculations in the Standard Model.

(c) Flavor-changing neutral currents. In the Standard Model the neutral-current interactions do not change flavor. The low rate $\Gamma(K_L \to \mu^+\mu^-)/\Gamma(K_L \to \text{all}) = (7.23 \pm 0.14) \times 10^{-9}$ puts limits on such interactions; the nonzero value for this rate is attributed to a combination of the weak and electromagnetic interactions. The best test should come from $K^+ \to \pi^+ \nu \overline{\nu}$, which occurs in the Standard Model only as a second-order weak process with a branching fraction of (0.4 to 1.2)$\times 10^{-10}$. Recent results, including observation of two events, yields $\Gamma(K^+ \to \pi^+ \nu \overline{\nu})/\Gamma(K^+ \to \text{all}) = (1.6^{+1.8}_{-0.8}) \times 10^{-10}$[4]. Limits for charm-changing or bottom-changing neutral currents are much less stringent: $\Gamma(D^0 \to \mu^+\mu^-)/\Gamma(D^0 \to \text{all}) < 4 \times 10^{-6}$ and $\Gamma(B^0 \to \mu^+\mu^-)/\Gamma(B^0 \to \text{all}) < 1.6 \times 10^{-7}$. One cannot isolate flavor-changing neutral current (FCNC) effects in non leptonic decays. For example, the FCNC transition $s \to d + (\overline{u} + u)$ is equivalent to the charged-current transition $s \to u + (\overline{u} + d)$. Tests for FCNC are therefore limited to hadron decays into lepton pairs. Such decays are expected only in second-order in the electroweak coupling in the Standard Model.

References

1. R. Carosi *et al.*, Phys. Lett. **B237**, 303 (1990).
2. B. Schwingenheuer *et al.*, Phys. Rev. Lett. **74**, 4376 (1995).
3. A. Angelopoulos *et al.*, Phys. Lett. **B444**, 43 (1998); L. Wolfenstein, Phys. Rev. Lett. **83**, 911 (1999).
4. S. Adler *et al.*, Phys. Rev. Lett. **88**, 041803 (2002).

Unless otherwise stated, limits are given at the 90% confidence level, while errors are given as ±1 standard deviation.

TESTS OF DISCRETE SPACE-TIME SYMMETRIES

CHARGE CONJUGATION (C) INVARIANCE

$\Gamma(\pi^0 \to 3\gamma)/\Gamma_{\rm total}$		$<3.1 \times 10^{-8}$, CL = 90%
η C-nonconserving decay parameters		
$\pi^+\pi^-\pi^0$ left-right asymmetry parameter		$(0.09 \pm 0.17) \times 10^{-2}$
$\pi^+\pi^-\pi^0$ sextant asymmetry parameter		$(0.18 \pm 0.16) \times 10^{-2}$
$\pi^+\pi^-\pi^0$ quadrant asymmetry parameter		$(-0.17 \pm 0.17) \times 10^{-2}$
$\pi^+\pi^-\gamma$ left-right asymmetry parameter		$(0.9 \pm 0.4) \times 10^{-2}$
$\pi^+\pi^-\gamma$ parameter β (D-wave)		-0.02 ± 0.07 (S = 1.3)
$\Gamma(\eta \to 3\gamma)/\Gamma_{\rm total}$		$<5 \times 10^{-4}$, CL = 95%
$\Gamma(\eta \to \pi^0 e^+ e^-)/\Gamma_{\rm total}$	[a]	$<4 \times 10^{-5}$, CL = 90%
$\Gamma(\eta \to \pi^0 \mu^+ \mu^-)/\Gamma_{\rm total}$	[a]	$<5 \times 10^{-6}$, CL = 90%
$\Gamma(\omega(782) \to \eta\pi^0)/\Gamma_{\rm total}$		$<1 \times 10^{-3}$, CL = 90%
$\Gamma(\omega(782) \to 3\pi^0)/\Gamma_{\rm total}$		$<3 \times 10^{-4}$, CL = 90%
$\Gamma(\eta'(958) \to \pi^0 e^+ e^-)/\Gamma_{\rm total}$	[a]	$<1.4 \times 10^{-3}$, CL = 90%
$\Gamma(\eta'(958) \to \eta e^+ e^-)/\Gamma_{\rm total}$	[a]	$<2.4 \times 10^{-3}$, CL = 90%
$\Gamma(\eta'(958) \to 3\gamma)/\Gamma_{\rm total}$		$<1.0 \times 10^{-4}$, CL = 90%
$\Gamma(\eta'(958) \to \mu^+\mu^-\pi^0)/\Gamma_{\rm total}$	[a]	$<6.0 \times 10^{-5}$, CL = 90%
$\Gamma(\eta'(958) \to \mu^+\mu^-\eta)/\Gamma_{\rm total}$	[a]	$<1.5 \times 10^{-5}$, CL = 90%

PARITY (P) INVARIANCE

e electric dipole moment		$(0.07 \pm 0.07) \times 10^{-26}$ e cm
μ electric dipole moment		$(3.7 \pm 3.4) \times 10^{-19}$ e cm
Re(d_τ)		-0.22 to 0.45×10^{-16} e cm, CL = 95%
$\Gamma(\eta \to \pi^+\pi^-)/\Gamma_{\rm total}$		$<3.3 \times 10^{-4}$, CL = 90%
$\Gamma(\eta \to \pi^0\pi^0)/\Gamma_{\rm total}$		$<4.3 \times 10^{-4}$, CL = 90%
$\Gamma(\eta \to 4\pi^0)/\Gamma_{\rm total}$		$<6.9 \times 10^{-7}$, CL = 90%
$\Gamma(\eta'(958) \to \pi^+\pi^-)/\Gamma_{\rm total}$		$<2 \times 10^{-2}$, CL = 90%
$\Gamma(\eta'(958) \to \pi^0\pi^0)/\Gamma_{\rm total}$		$<9 \times 10^{-4}$, CL = 90%
p electric dipole moment		$<0.54 \times 10^{-23}$ e cm
n electric dipole moment		$<0.63 \times 10^{-25}$ e cm, CL = 90%
Λ electric dipole moment		$<1.5 \times 10^{-16}$ e cm, CL = 95%

TIME REVERSAL (T) INVARIANCE

Limits on e, μ, τ, p, n, and Λ electric dipole moments under Parity Invariance above are also tests of Time Reversal Invariance.

μ decay parameters		
transverse e^+ polarization normal to plane of μ spin, e^+ momentum		0.007 ± 0.023
α'/A		$(0 \pm 4) \times 10^{-3}$
β'/A		$(2 \pm 6) \times 10^{-3}$
P_T in $K^+ \to \pi^0 \mu^+ \nu_\mu$		$(-4 \pm 5) \times 10^{-3}$
P_T in $K^+ \to \mu^+ \nu_\mu \gamma$		$(-0.6 \pm 1.9) \times 10^{-2}$
Im(ξ) in $K^+ \to \pi^0 \mu^+ \nu_\mu$ decay (from transverse μ pol.)		-0.014 ± 0.014
asymmetry A_T in K^0-$\overline{K}^0$ mixing		$(6.6 \pm 1.6) \times 10^{-3}$
Im(ξ) in $K^0_{\mu 3}$ decay (from transverse μ pol.)		-0.007 ± 0.026
$n \to p e^- \overline{\nu}_e$ decay parameters		
ϕ_{AV}, phase of g_A relative to g_V	[b]	$(180.08 \pm 0.10)^\circ$
triple correlation coefficient D		$(-0.6 \pm 1.0) \times 10^{-3}$
triple correlation coefficient D for $\Sigma^- \to n e^- \overline{\nu}_e$		0.11 ± 0.10

CP INVARIANCE

$\mathrm{Re}(d_\tau^W)$		$<0.50\times10^{-17}$ e cm, CL = 95%
$\mathrm{Im}(d_\tau^W)$		$<1.1\times10^{-17}$ e cm, CL = 95%
$\Gamma(\eta\to\pi^+\pi^-)/\Gamma_{\rm total}$		$<3.3\times10^{-4}$, CL = 90%
$\Gamma(\eta\to\pi^0\pi^0)/\Gamma_{\rm total}$		$<4.3\times10^{-4}$, CL = 90%
$\Gamma(\eta\to4\pi^0)/\Gamma_{\rm total}$		$<6.9\times10^{-7}$, CL = 90%
$\Gamma(\eta'(958)\to\pi^+\pi^-)/\Gamma_{\rm total}$		$<2\times10^{-2}$, CL = 90%
$\Gamma(\eta'(958)\to\pi^0\pi^0)/\Gamma_{\rm total}$		$<9\times10^{-4}$, CL = 90%
$K^\pm\to\pi^\pm\pi^+\pi^-$ rate difference/average		(0.07 ± 0.12)%
$K^\pm\to\pi^\pm\pi^0\pi^0$ rate difference/average		(0.0 ± 0.6)%
$K^\pm\to\pi^\pm\pi^0\gamma$ rate difference/average		(0.9 ± 3.3)%
$(g_{\tau^+}-g_{\tau^-})\,/\,(g_{\tau^+}+g_{\tau^-})$ for $K^\pm\to\pi^\pm\pi^+\pi^-$		(-0.7 ± 0.5)%
$\Delta(K^\pm_{\pi\mu\mu})=\frac{\Gamma(K^+_{\pi\mu\mu})-\Gamma(K^-_{\pi\mu\mu})}{\Gamma(K^+_{\pi\mu\mu})+\Gamma(K^-_{\pi\mu\mu})}$		-0.02 ± 0.12
$\mathrm{Im}(\eta_{+-0})=\mathrm{Im}(A(K^0_S\to\pi^+\pi^-\pi^0,$ *CP*-violating$)\,/\,A(K^0_L\to\pi^+\pi^-\pi^0))$		-0.002 ± 0.009
$\mathrm{Im}(\eta_{000})=\mathrm{Im}(A(K^0_S\to\pi^0\pi^0\pi^0)/A(K^0_L\to\pi^0\pi^0\pi^0))$		-0.05 ± 0.13
CP asymmetry A in $K^0_S\to\pi^+\pi^-e^+e^-$		(-1 ± 4)%
$\Gamma(K^0_S\to3\pi^0)/\Gamma_{\rm total}$		$<1.4\times10^{-5}$, CL = 90%
linear coefficient j for $K^0_L\to\pi^+\pi^-\pi^0$		0.0012 ± 0.0008
quadratic coefficient f for $K^0_L\to\pi^+\pi^-\pi^0$		0.004 ± 0.006
$\lvert\epsilon'_{+-\gamma}\rvert/\epsilon$ for $K^0_L\to\pi^+\pi^-\gamma$		<0.3, CL = 90%
$\Gamma(K^0_L\to\pi^0\mu^+\mu^-)/\Gamma_{\rm total}$	[c]	$<3.8\times10^{-10}$, CL = 90%
$\Gamma(K^0_L\to\pi^0e^+e^-)/\Gamma_{\rm total}$	[c]	$<5.1\times10^{-10}$, CL = 90%
$\Gamma(K^0_L\to\pi^0\nu\overline{\nu})/\Gamma_{\rm total}$	[d]	$<5.9\times10^{-7}$, CL = 90%
$A_{CP}(K^0_S\pi^\pm)$ in $D^\pm\to K^0_S\pi^\pm$		-0.016 ± 0.017
$A_{CP}(K^0_SK^\pm)$ in $D^\pm\to K^0_SK^\pm$		0.07 ± 0.06
$A_{CP}(K^+K^-\pi^\pm)$ in $D^\pm\to K^+K^-\pi^\pm$		0.002 ± 0.011
$A_{CP}(K^\pm K^{*0})$ in $D^+\to K^+\overline{K}^{*0}$, $D^-\to K^-K^{*0}$		-0.02 ± 0.05
$A_{CP}(\phi\pi^\pm)$ in $D^\pm\to\phi\pi^\pm$		-0.014 ± 0.033
$A_{CP}(\pi^+\pi^-\pi^\pm)$ in $D^\pm\to\pi^+\pi^-\pi^\pm$		-0.02 ± 0.04
$A_{CP}(K^+K^-)$ in D^0, $\overline{D}^0\to K^+K^-$		0.005 ± 0.016
$A_{CP}(K^0_SK^0_S)$ in D^0, $\overline{D}^0\to K^0_SK^0_S$		-0.23 ± 0.19
$A_{CP}(\pi^+\pi^-)$ in D^0, $\overline{D}^0\to\pi^+\pi^-$		0.021 ± 0.026
$A_{CP}(\pi^0\pi^0)$ in D^0, $\overline{D}^0\to\pi^0\pi^0$		0.00 ± 0.05
$A_{CP}(K^0_S\phi)$ in D^0, $\overline{D}^0\to K^0_S\phi$		-0.03 ± 0.09
$A_{CP}(K^0_S\pi^0)$ in D^0, $\overline{D}^0\to K^0_S\pi^0$		0.001 ± 0.013
$A_{CP}(K^\pm\pi^\mp)$ in $D^0\to K^+\pi^-$, $\overline{D}^0\to K^-\pi^+$		0.08 ± 0.09
$A_{CP}(K^\mp\pi^\pm\pi^0)$ in $D^0\to K^-\pi^+\pi^0$, $\overline{D}^0\to K^+\pi^-\pi^0$		-0.03 ± 0.09
$A_{CP}(K^\pm\pi^\mp\pi^0)$ in $D^0\to K^+\pi^-\pi^0$, $\overline{D}^0\to K^-\pi^+\pi^0$		$0.09^{+0.25}_{-0.22}$
$A_{CP}(B^+\to J/\psi(1S)K^+)$		-0.007 ± 0.019
$A_{CP}(B^+\to J/\psi(1S)\pi^+)$		-0.01 ± 0.13
$A_{CP}(B^+\to\psi(2S)K^+)$		-0.037 ± 0.025
$A_{CP}(B^+\to\overline{D}^0K^+)$		0.04 ± 0.07
$A_{CP}(B^+\to D_{CP(+1)}K^+)$		0.06 ± 0.19
$A_{CP}(B^+\to D_{CP(-1)}K^+)$		-0.19 ± 0.18
$A_{CP}(B^+\to\pi^+\pi^0)$		0.05 ± 0.15
$A_{CP}(B^+\to K^+\pi^0)$		-0.10 ± 0.08
$A_{CP}(B^+\to K^0_S\pi^+)$		0.03 ± 0.08 (S = 1.1)
$A_{CP}(B^+\to\pi^+\pi^-\pi^+)$		-0.39 ± 0.35
$A_{CP}(B^+\to\rho^+\rho^0)$		-0.09 ± 0.16
$A_{CP}(B^+\to K^+\pi^-\pi^+)$		0.01 ± 0.08
$A_{CP}(B^+\to K^+K^-K^+)$		0.02 ± 0.08
$A_{CP}(B^+\to K^+\eta')$		0.009 ± 0.035
$A_{CP}(B^+\to\omega\pi^+)$		-0.21 ± 0.19
$A_{CP}(B^+\to\omega K^+)$		-0.21 ± 0.28
$A_{CP}(B^+\to\phi K^+)$		0.03 ± 0.07
$A_{CP}(B^+\to\phi K^*(892)^+)$		0.09 ± 0.15
$A_{CP}(B^+\to\rho^0K^*(892)^+)$		0.20 ± 0.31
$\mathrm{Re}(\epsilon_{B^0})/(1+\lvert\epsilon_{B^0}\rvert^2)$		$(0.5\pm3.1)\times10^{-3}$
$A_{T/CP}$		0.005 ± 0.018
$A_{CP}(B^0\to K^+\pi^-)$		-0.09 ± 0.04
$A_{CP}(B^0\to\rho^+\pi^-)$		-0.18 ± 0.09
$A_{CP}(B^0\to\rho^+K^-)$		0.28 ± 0.19
$A_{CP}(B^0\to K^*(892)^+\pi^-)$		0.26 ± 0.35
$A_{CP}(B^0\to K^*(892)^0\phi)$		0.05 ± 0.10
$A_{CP}(B^0\to D^*(2010)^+D^-)$		-0.03 ± 0.12
$C_{\pi\pi}$ $(B^0\to\pi^+\pi^-)$		-0.51 ± 0.23 (S = 1.2)
$S_{\pi\pi}$ $(B^0\to\pi^+\pi^-)$		-0.5 ± 0.6 (S = 2.3)
$C_{\rho\pi}$ $(B^0\to\rho^+\pi^-)$		0.36 ± 0.18
$S_{\rho\pi}$ $(B^0\to\rho^+\pi^-)$		0.19 ± 0.24
$C_{\eta'(958)K}$ $(B^0\to\eta'(958)K^0_S)$		0.04 ± 0.13
$S_{\eta'(958)K}$ $(B^0\to\eta'(958)K^0_S)$		0.27 ± 0.21
$C_{\phi K^0_S}$ $(B^0\to\phi K^0_S)$		0.15 ± 0.30
$S_{\phi K^0_S}$ $(B^0\to\phi K^0_S)$		-1.0 ± 0.5
$C_{K^+K^-K^0_S}$ $(B^0\to K^+K^-K^0_S)$		0.17 ± 0.16
$S_{K^+K^-K^0_S}$ $(B^0\to K^+K^-K^0_S)$		-0.51 ± 0.26
$C_{D^*(2010)^-D^+}$ $(B^0\to D^*(2010)^-D^+)$		-0.2 ± 0.4
$S_{D^*(2010)^-D^+}$ $(B^0\to D^*(2010)^-D^+)$		-0.2 ± 0.7
$C_{D^*(2010)^+D^-}$ $(B^0\to D^*(2010)^+D^-)$		-0.5 ± 0.4
$S_{D^*(2010)^+D^-}$ $(B^0\to D^*(2010)^+D^-)$		-0.8 ± 0.8
$C_{J/\psi(1S)\pi^0}$ $(B^0\to J/\psi(1S)\pi^0)$		0.4 ± 0.4
$S_{J/\psi(1S)\pi^0}$ $(B^0\to J/\psi(1S)\pi^0)$		0.1 ± 0.5
$\Delta C_{\rho\pi}$ $(B^0\to\rho^+\pi^-)$		0.28 ± 0.19
$\Delta S_{\rho\pi}$ $(B^0\to\rho^+\pi^-)$		0.15 ± 0.25
$\lvert\lambda\rvert$ $(B^0\to c\overline{c}K^0)$		0.949 ± 0.045
$\lvert\lambda\rvert$ $(B^0\to D^{*+}D^{*-})$		0.75 ± 0.19
$\mathrm{Im}(\lambda)$ $(B^0\to D^{*+}D^{*-})$		0.05 ± 0.31
$A_{CP}(B\to K^*(892)\gamma)$		-0.01 ± 0.07
$A_{CP}(B\to s\gamma)$		-0.08 ± 0.11
$[\alpha_-(\Lambda)+\alpha_+(\overline{\Lambda})]\;/\;[\alpha_-(\Lambda)-\alpha_+(\overline{\Lambda})]$		0.012 ± 0.021
$\frac{[\alpha(\Xi^-)\alpha_-(\Lambda)-\alpha(\overline{\Xi}^+)\alpha_+(\overline{\Lambda})]}{[\alpha(\Xi^-)\alpha_-(\Lambda)+\alpha(\overline{\Xi}^+)\alpha_+(\overline{\Lambda})]}$		0.012 ± 0.014
$[\alpha(\Omega^-\to\Lambda K^-)+\alpha(\overline{\Omega}^+\to\overline{\Lambda}K^+)]/2$		-0.004 ± 0.040

CP VIOLATION OBSERVED

charge asymmetry in $K^0_{\ell3}$ decays		
$\delta_L=$ weighted average of $\delta_L(\mu)$ and $\delta_L(e)$		(0.327 ± 0.012)%
$\delta_L(\mu)=[\Gamma(\pi^-\mu^+\nu_\mu)-\Gamma(\pi^+\mu^-\overline{\nu}_\mu)]/$sum		(0.304 ± 0.025)%
$\delta_L(e)=[\Gamma(\pi^-e^+\nu_e)-\Gamma(\pi^+e^-\overline{\nu}_e)]/$sum		(0.333 ± 0.014)%
parameters for $K^0_L\to2\pi$ decay		
$\lvert\eta_{00}\rvert=\lvert A(K^0_L\to2\pi^0)\,/\,A(K^0_S\to2\pi^0)\rvert$		$(2.276\pm0.014)\times10^{-3}$
$\lvert\eta_{+-}\rvert=\lvert A(K^0_L\to\pi^+\pi^-)\,/\,A(K^0_S\to\pi^+\pi^-)\rvert$		$(2.288\pm0.014)\times10^{-3}$
$\lvert\epsilon\rvert=(2\lvert\eta_{+-}\rvert+\lvert\eta_{00}\rvert)/3$		$(2.284\pm0.014)\times10^{-3}$
$\lvert\eta_{00}/\eta_{+-}\rvert$	[e]	0.9950 ± 0.0008 (S = 1.6)
$\mathrm{Re}(\epsilon'/\epsilon)=(1-\lvert\eta_{00}/\eta_{+-}\rvert)/3$	[e]	$(1.67\pm0.26)\times10^{-3}$ (S = 1.6)
Assuming *CPT*		
ϕ_{+-}, phase of η_{+-}		$(43.52\pm0.06)^\circ$ (S = 1.3)
ϕ_{00}, phase of η_{00}		$(43.50\pm0.06)^\circ$ (S = 1.3)
$\phi_\epsilon=(2\phi_{+-}+\phi_{00})/3$		$(43.51\pm0.05)^\circ$ (S = 1.2)
Not assuming *CPT*		
ϕ_{+-}, phase of η_{+-}		$(43.4\pm0.7)^\circ$ (S = 1.3)
ϕ_{00}, phase of η_{00}		$(43.7\pm0.8)^\circ$ (S = 1.2)
$\phi_\epsilon=(2\phi_{+-}+\phi_{00})/3$		$(43.5\pm0.7)^\circ$ (S = 1.3)
CP asymmetry A in $K^0_L\to\pi^+\pi^-e^+e^-$		(13.8 ± 2.2)%
β_{CP} from $K^0_L\to e^+e^-e^+e^-$		-0.23 ± 0.09
γ_{CP} from $K^0_L\to e^+e^-e^+e^-$		-0.09 ± 0.09
parameters for $K^0_L\to\pi^+\pi^-\gamma$ decay		
$\lvert\eta_{+-\gamma}\rvert=\lvert A(K^0_L\to\pi^+\pi^-\gamma,$ *CP* violating$)/A(K^0_S\to\pi^+\pi^-\gamma)\rvert$		$(2.35\pm0.07)\times10^{-3}$
$\phi_{+-\gamma}=$ phase of $\eta_{+-\gamma}$		$(44\pm4)^\circ$
$\Gamma(K^0_L\to\pi^+\pi^-)/\Gamma_{\rm total}$		$(2.090\pm0.025)\times10^{-3}$ (S = 1.1)

Unless otherwise stated, limits are given at the 90% confidence level, while errors are given as ±1 standard deviation.

Tests of Conservation Laws

$\Gamma(K_L^0 \to \pi^0\pi^0)/\Gamma_{total}$		$(9.32 \pm 0.12) \times 10^{-4}$ (S = 1.1)
Parameters for $B^0 \to J/\psi K_S^0$		
$\sin(2\beta)$		0.731 ± 0.056

CPT INVARIANCE

$(m_{W^+} - m_{W^-}) / m_{average}$		-0.002 ± 0.007
$(m_{e^+} - m_{e^-}) / m_{average}$		$<8 \times 10^{-9}$, CL = 90%
$\lvert q_{e^+} + q_{e^-}\rvert/e$		$<4 \times 10^{-8}$
$(g_{e^+} - g_{e^-}) / g_{average}$		$(-0.5 \pm 2.1) \times 10^{-12}$
$(\tau_{\mu^+} - \tau_{\mu^-}) / \tau_{average}$		$(2 \pm 8) \times 10^{-5}$
$(g_{\mu^+} - g_{\mu^-}) / g_{average}$		$(-2.6 \pm 1.6) \times 10^{-8}$
$(m_{\pi^+} - m_{\pi^-}) / m_{average}$		$(2 \pm 5) \times 10^{-4}$
$(\tau_{\pi^+} - \tau_{\pi^-}) / \tau_{average}$		$(6 \pm 7) \times 10^{-4}$
$(m_{K^+} - m_{K^-}) / m_{average}$		$(-0.6 \pm 1.8) \times 10^{-4}$
$(\tau_{K^+} - \tau_{K^-}) / \tau_{average}$		$(0.11 \pm 0.09)\%$ (S = 1.2)
$K^\pm \to \mu^\pm\nu_\mu$ rate difference/average		$(-0.5 \pm 0.4)\%$
$K^\pm \to \pi^\pm\pi^0$ rate difference/average	[f]	$(0.8 \pm 1.2)\%$
δ in $K^0 - \overline{K}^0$ mixing		
real part of δ		$(2.9 \pm 2.7) \times 10^{-4}$
imaginary part of δ		$(0.02 \pm 0.05) \times 10^{-3}$
$\lvert m_{K^0} - m_{\overline{K}^0}\rvert / m_{average}$	[g]	$<10^{-18}$, CL = 90%
$(\Gamma_{K^0} - \Gamma_{\overline{K}^0})/m_{average}$		$(8 \pm 8) \times 10^{-18}$
phase difference $\phi_{00} - \phi_{+-}$		$(0.2 \pm 0.4)^\circ$
$\mathrm{Re}(\frac{2}{3}\eta_{+-} + \frac{1}{3}\eta_{00}) - \frac{\delta_L}{2}$		$(-3 \pm 35) \times 10^{-6}$
$A_{CPT}(K^\mp\pi^\pm)$ in $D^0 \to K^-\pi^+$, $\overline{D}^0 \to K^+\pi^-$		0.008 ± 0.008
$\lvert m_p - m_{\overline{p}}\rvert/m_p$	[h]	$<1.0 \times 10^{-8}$, CL = 90%
$(\lvert\frac{q_p}{m_p}\rvert - \lvert\frac{q_{\overline{p}}}{m_{\overline{p}}}\rvert)/\lvert\frac{q_p}{m_p}\rvert$		$(-9 \pm 9) \times 10^{-11}$
$\lvert q_p + q_{\overline{p}}\rvert/e$	[h]	$<1.0 \times 10^{-8}$, CL = 90%
$(\mu_p + \mu_{\overline{p}}) / \mu_p$		$(-2.6 \pm 2.9) \times 10^{-3}$
$(m_n - m_{\overline{n}}) / m_n$		$(9 \pm 5) \times 10^{-5}$
$(m_\Lambda - m_{\overline{\Lambda}}) / m_\Lambda$		$(-0.1 \pm 1.1) \times 10^{-5}$ (S = 1.6)
$(\tau_\Lambda - \tau_{\overline{\Lambda}}) / \tau_\Lambda$		-0.001 ± 0.009
$(\tau_{\Sigma^+} - \tau_{\overline{\Sigma}^-}) / \tau_{\Sigma^+}$		$(-0.6 \pm 1.2) \times 10^{-3}$
$(\mu_{\Sigma^+} + \mu_{\overline{\Sigma}^-}) / \mu_{\Sigma^+}$		0.014 ± 0.015
$(m_{\Xi^-} - m_{\overline{\Xi}^+}) / m_{\Xi^-}$		$(1.1 \pm 2.7) \times 10^{-4}$
$(\tau_{\Xi^-} - \tau_{\overline{\Xi}^+}) / \tau_{\Xi^-}$		0.02 ± 0.18
$(\mu_{\Xi^-} + \mu_{\overline{\Xi}^+}) / \lvert\mu_{\Xi^-}\rvert$		$+0.01 \pm 0.05$
$(m_{\Omega^-} - m_{\overline{\Omega}^+}) / m_{\Omega^-}$		$(-1 \pm 8) \times 10^{-5}$
$(\tau_{\Omega^-} - \tau_{\overline{\Omega}^+}) / \tau_{\Omega^-}$		-0.002 ± 0.040

TESTS OF NUMBER CONSERVATION LAWS

LEPTON FAMILY NUMBER

Lepton family number conservation means separate conservation of each of L_e, L_μ, L_τ.

$\Gamma(Z \to e^\pm\mu^\mp)/\Gamma_{total}$	[i]	$<1.7 \times 10^{-6}$, CL = 95%
$\Gamma(Z \to e^\pm\tau^\mp)/\Gamma_{total}$	[i]	$<9.8 \times 10^{-6}$, CL = 95%
$\Gamma(Z \to \mu^\pm\tau^\mp)/\Gamma_{total}$	[i]	$<1.2 \times 10^{-5}$, CL = 95%
limit on $\mu^- \to e^-$ conversion		
$\sigma(\mu^- {}^{32}\mathrm{S} \to e^- {}^{32}\mathrm{S}) / \sigma(\mu^- {}^{32}\mathrm{S} \to \nu_\mu {}^{32}\mathrm{P}^*)$		$<7 \times 10^{-11}$, CL = 90%
$\sigma(\mu^- \mathrm{Ti} \to e^- \mathrm{Ti}) / \sigma(\mu^- \mathrm{Ti} \to \text{capture})$		$<4.3 \times 10^{-12}$, CL = 90%
$\sigma(\mu^- \mathrm{Pb} \to e^- \mathrm{Pb}) / \sigma(\mu^- \mathrm{Pb} \to \text{capture})$		$<4.6 \times 10^{-11}$, CL = 90%
limit on muonium $\to$ antimuonium conversion $R_g = G_C / G_F$		<0.0030, CL = 90%
$\Gamma(\mu^- \to e^-\nu_e\overline{\nu}_\mu)/\Gamma_{total}$	[j]	$<1.2 \times 10^{-2}$, CL = 90%
$\Gamma(\mu^- \to e^-\gamma)/\Gamma_{total}$		$<1.2 \times 10^{-11}$, CL = 90%
$\Gamma(\mu^- \to e^- e^+ e^-)/\Gamma_{total}$		$<1.0 \times 10^{-12}$, CL = 90%
$\Gamma(\mu^- \to e^- 2\gamma)/\Gamma_{total}$		$<7.2 \times 10^{-11}$, CL = 90%
$\Gamma(\tau^- \to e^-\gamma)/\Gamma_{total}$		$<2.7 \times 10^{-6}$, CL = 90%
$\Gamma(\tau^- \to \mu^-\gamma)/\Gamma_{total}$		$<1.1 \times 10^{-6}$, CL = 90%
$\Gamma(\tau^- \to e^-\pi^0)/\Gamma_{total}$		$<3.7 \times 10^{-6}$, CL = 90%
$\Gamma(\tau^- \to \mu^-\pi^0)/\Gamma_{total}$		$<4.0 \times 10^{-6}$, CL = 90%
$\Gamma(\tau^- \to e^- K_S^0)/\Gamma_{total}$		$<9.1 \times 10^{-7}$, CL = 90%
$\Gamma(\tau^- \to \mu^- K_S^0)/\Gamma_{total}$		$<9.5 \times 10^{-7}$, CL = 90%
$\Gamma(\tau^- \to e^-\eta)/\Gamma_{total}$		$<8.2 \times 10^{-6}$, CL = 90%
$\Gamma(\tau^- \to \mu^-\eta)/\Gamma_{total}$		$<9.6 \times 10^{-6}$, CL = 90%
$\Gamma(\tau^- \to e^-\rho^0)/\Gamma_{total}$		$<2.0 \times 10^{-6}$, CL = 90%
$\Gamma(\tau^- \to \mu^-\rho^0)/\Gamma_{total}$		$<6.3 \times 10^{-6}$, CL = 90%
$\Gamma(\tau^- \to e^- K^*(892)^0)/\Gamma_{total}$		$<5.1 \times 10^{-6}$, CL = 90%
$\Gamma(\tau^- \to \mu^- K^*(892)^0)/\Gamma_{total}$		$<7.5 \times 10^{-6}$, CL = 90%
$\Gamma(\tau^- \to e^- \overline{K}^*(892)^0)/\Gamma_{total}$		$<7.4 \times 10^{-6}$, CL = 90%
$\Gamma(\tau^- \to \mu^- \overline{K}^*(892)^0)/\Gamma_{total}$		$<7.5 \times 10^{-6}$, CL = 90%
$\Gamma(\tau^- \to e^-\phi)/\Gamma_{total}$		$<6.9 \times 10^{-6}$, CL = 90%
$\Gamma(\tau^- \to \mu^-\phi)/\Gamma_{total}$		$<7.0 \times 10^{-6}$, CL = 90%
$\Gamma(\tau^- \to e^- e^+ e^-)/\Gamma_{total}$		$<2.9 \times 10^{-6}$, CL = 90%
$\Gamma(\tau^- \to e^-\mu^+\mu^-)/\Gamma_{total}$		$<1.8 \times 10^{-6}$, CL = 90%
$\Gamma(\tau^- \to e^+\mu^-\mu^-)/\Gamma_{total}$		$<1.5 \times 10^{-6}$, CL = 90%
$\Gamma(\tau^- \to \mu^- e^+ e^-)/\Gamma_{total}$		$<1.7 \times 10^{-6}$, CL = 90%
$\Gamma(\tau^- \to \mu^+ e^- e^-)/\Gamma_{total}$		$<1.5 \times 10^{-6}$, CL = 90%
$\Gamma(\tau^- \to \mu^-\mu^+\mu^-)/\Gamma_{total}$		$<1.9 \times 10^{-6}$, CL = 90%
$\Gamma(\tau^- \to e^-\pi^+\pi^-)/\Gamma_{total}$		$<2.2 \times 10^{-6}$, CL = 90%
$\Gamma(\tau^- \to \mu^-\pi^+\pi^-)/\Gamma_{total}$		$<8.2 \times 10^{-6}$, CL = 90%
$\Gamma(\tau^- \to e^-\pi^+ K^-)/\Gamma_{total}$		$<6.4 \times 10^{-6}$, CL = 90%
$\Gamma(\tau^- \to e^-\pi^- K^+)/\Gamma_{total}$		$<3.8 \times 10^{-6}$, CL = 90%
$\Gamma(\tau^- \to e^- K_S^0 K_S^0)/\Gamma_{total}$		$<2.2 \times 10^{-6}$, CL = 90%
$\Gamma(\tau^- \to e^- K^+ K^-)/\Gamma_{total}$		$<6.0 \times 10^{-6}$, CL = 90%
$\Gamma(\tau^- \to \mu^-\pi^+ K^-)/\Gamma_{total}$		$<7.5 \times 10^{-6}$, CL = 90%
$\Gamma(\tau^- \to \mu^-\pi^- K^+)/\Gamma_{total}$		$<7.4 \times 10^{-6}$, CL = 90%
$\Gamma(\tau^- \to \mu^- K_S^0 K_S^0)/\Gamma_{total}$		$<3.4 \times 10^{-6}$, CL = 90%
$\Gamma(\tau^- \to \mu^- K^+ K^-)/\Gamma_{total}$		$<1.5 \times 10^{-5}$, CL = 90%
$\Gamma(\tau^- \to e^-\pi^0\pi^0)/\Gamma_{total}$		$<6.5 \times 10^{-6}$, CL = 90%
$\Gamma(\tau^- \to \mu^-\pi^0\pi^0)/\Gamma_{total}$		$<1.4 \times 10^{-5}$, CL = 90%
$\Gamma(\tau^- \to e^-\eta\eta)/\Gamma_{total}$		$<3.5 \times 10^{-5}$, CL = 90%
$\Gamma(\tau^- \to \mu^-\eta\eta)/\Gamma_{total}$		$<6.0 \times 10^{-5}$, CL = 90%
$\Gamma(\tau^- \to e^-\pi^0\eta)/\Gamma_{total}$		$<2.4 \times 10^{-5}$, CL = 90%
$\Gamma(\tau^- \to \mu^-\pi^0\eta)/\Gamma_{total}$		$<2.2 \times 10^{-5}$, CL = 90%
$\Gamma(\tau^- \to e^-$ light boson$)/\Gamma_{total}$		$<2.7 \times 10^{-3}$, CL = 95%
$\Gamma(\tau^- \to \mu^-$ light boson$)/\Gamma_{total}$		$<5 \times 10^{-3}$, CL = 95%

LEPTON FAMILY NUMBER VIOLATION IN NEUTRINOS

Solar Neutrinos

$\theta_\odot = 32.5^\circ {}^{+2.4^\circ}_{-2.3^\circ}$

$\Delta m^2_\odot = \left(7.1^{+1.2}_{-0.6}\right) \times 10^{-5}\ \mathrm{eV}^2$

Atmospheric Neutrinos

$36^\circ < \theta_{atm} < 54^\circ$, CL = 90%

$1.3 \times 10^{-3}\,\mathrm{eV}^2 < \Delta m^2_{atm} < 3.0 \times 10^{-3}\,\mathrm{eV}^2$, CL = 90%

$\Gamma(\pi^+ \to \mu^+\nu_e)/\Gamma_{total}$	[k]	$<8.0 \times 10^{-3}$, CL = 90%
$\Gamma(\pi^+ \to \mu^- e^+ e^+\nu)/\Gamma_{total}$		$<1.6 \times 10^{-6}$, CL = 90%
$\Gamma(\pi^0 \to \mu^+ e^-)/\Gamma_{total}$		$<3.8 \times 10^{-10}$, CL = 90%
$\Gamma(\pi^0 \to \mu^- e^+)/\Gamma_{total}$		$<3.4 \times 10^{-9}$, CL = 90%
$\Gamma(\pi^0 \to \mu^+ e^- + \mu^- e^+)/\Gamma_{total}$		$<1.72 \times 10^{-8}$, CL = 90%
$\Gamma(\eta \to \mu^+ e^- + \mu^- e^+)/\Gamma_{total}$		$<6 \times 10^{-6}$, CL = 90%
$\Gamma(\eta'(958) \to e\mu)/\Gamma_{total}$		$<4.7 \times 10^{-4}$, CL = 90%
$\Gamma(K^+ \to \mu^-\nu e^+ e^+)/\Gamma_{total}$		$<2.0 \times 10^{-8}$, CL = 90%
$\Gamma(K^+ \to \mu^+\nu_e)/\Gamma_{total}$	[k]	$<4 \times 10^{-3}$, CL = 90%
$\Gamma(K^+ \to \pi^+\mu^+ e^-)/\Gamma_{total}$		$<2.8 \times 10^{-11}$, CL = 90%
$\Gamma(K^+ \to \pi^+\mu^- e^+)/\Gamma_{total}$		$<5.2 \times 10^{-10}$, CL = 90%
$\Gamma(K_L^0 \to e^\pm\mu^\mp)/\Gamma_{total}$	[i]	$<4.7 \times 10^{-12}$, CL = 90%
$\Gamma(K_L^0 \to e^\pm e^\pm\mu^\mp\mu^\mp)/\Gamma_{total}$	[i]	$<4.12 \times 10^{-11}$, CL = 90%
$\Gamma(K_L^0 \to \pi^0\mu^\pm e^\mp)/\Gamma_{total}$	[i]	$<6.2 \times 10^{-9}$, CL = 90%
$\Gamma(D^+ \to \pi^+ e^\pm\mu^\mp)/\Gamma_{total}$	[i]	$<3.4 \times 10^{-5}$, CL = 90%
$\Gamma(D^+ \to K^+ e^\pm\mu^\mp)/\Gamma_{total}$	[i]	$<6.8 \times 10^{-5}$, CL = 90%
$\Gamma(D^0 \to \mu^\pm e^\mp)/\Gamma_{total}$	[i]	$<8.1 \times 10^{-6}$, CL = 90%
$\Gamma(D^0 \to \pi^0 e^\pm\mu^\mp)/\Gamma_{total}$	[i]	$<8.6 \times 10^{-5}$, CL = 90%
$\Gamma(D^0 \to \eta e^\pm\mu^\mp)/\Gamma_{total}$	[i]	$<1.0 \times 10^{-4}$, CL = 90%
$\Gamma(D^0 \to \pi^+\pi^- e^\pm\mu^\mp)/\Gamma_{total}$	[i]	$<1.5 \times 10^{-5}$, CL = 90%
$\Gamma(D^0 \to \rho^0 e^\pm\mu^\mp)/\Gamma_{total}$	[i]	$<4.9 \times 10^{-5}$, CL = 90%
$\Gamma(D^0 \to \omega e^\pm\mu^\mp)/\Gamma_{total}$	[i]	$<1.2 \times 10^{-4}$, CL = 90%
$\Gamma(D^0 \to K^- K^+ e^\pm\mu^\mp)/\Gamma_{total}$	[i]	$<1.8 \times 10^{-4}$, CL = 90%
$\Gamma(D^0 \to \phi e^\pm\mu^\mp)/\Gamma_{total}$	[i]	$<3.4 \times 10^{-5}$, CL = 90%

Unless otherwise stated, limits are given at the 90% confidence level, while errors are given as ± 1 standard deviation.

$\Gamma(D^0 \to \overline{K}^0 e^\pm \mu^\mp)/\Gamma_{\text{total}}$	[i]	$<1.0\times10^{-4}$, CL = 90%
$\Gamma(D^0 \to K^-\pi^+ e^\pm \mu^\mp)/\Gamma_{\text{total}}$	[i]	$<5.53\times10^{-4}$, CL = 90%
$\Gamma(D^0 \to \overline{K}^*(892)^0 e^\pm \mu^\mp)/\Gamma_{\text{total}}$	[i]	$<8.3\times10^{-5}$, CL = 90%
$\Gamma(D_s^+ \to \pi^+ e^\pm \mu^\mp)/\Gamma_{\text{total}}$	[i]	$<6.1\times10^{-4}$, CL = 90%
$\Gamma(D_s^+ \to K^+ e^\pm \mu^\mp)/\Gamma_{\text{total}}$	[i]	$<6.3\times10^{-4}$, CL = 90%
$\Gamma(B^+ \to \pi^+ e^+ \mu^-)/\Gamma_{\text{total}}$		$<6.4\times10^{-3}$, CL = 90%
$\Gamma(B^+ \to \pi^+ e^- \mu^+)/\Gamma_{\text{total}}$		$<6.4\times10^{-3}$, CL = 90%
$\Gamma(B^+ \to K^+ e^+ \mu^-)/\Gamma_{\text{total}}$		$<8\times10^{-7}$, CL = 90%
$\Gamma(B^+ \to K^+ e^- \mu^+)/\Gamma_{\text{total}}$		$<6.4\times10^{-3}$, CL = 90%
$\Gamma(B^+ \to K^*(892)^+ e^\pm \mu^\mp)/\Gamma_{\text{total}}$		$<7.9\times10^{-6}$, CL = 90%
$\Gamma(B^+ \to \rho^- e^+ \mu^+)/\Gamma_{\text{total}}$		$<3.3\times10^{-6}$, CL = 90%
$\Gamma(B^+ \to K^*(892)^- e^+ \mu^+)/\Gamma_{\text{total}}$		$<4.4\times10^{-6}$, CL = 90%
$\Gamma(B^0 \to e^\pm \mu^\mp)/\Gamma_{\text{total}}$	[i]	$<1.7\times10^{-7}$, CL = 90%
$\Gamma(B^0 \to K^0 e^\pm \mu^\mp)/\Gamma_{\text{total}}$		$<4.0\times10^{-6}$, CL = 90%
$\Gamma(B^0 \to K^*(892)^0 e^\pm \mu^\mp)/\Gamma_{\text{total}}$		$<3.4\times10^{-6}$, CL = 90%
$\Gamma(B^0 \to e^\pm \tau^\mp)/\Gamma_{\text{total}}$	[i]	$<5.3\times10^{-4}$, CL = 90%
$\Gamma(B^0 \to \mu^\pm \tau^\mp)/\Gamma_{\text{total}}$	[i]	$<8.3\times10^{-4}$, CL = 90%
$\Gamma(B \to e^\pm \mu^\mp s)/\Gamma_{\text{total}}$	[i]	$<2.2\times10^{-5}$, CL = 90%
$\Gamma(B \to \pi e^\pm \mu^\mp)/\Gamma_{\text{total}}$		$<1.6\times10^{-6}$, CL = 90%
$\Gamma(B \to \rho e^\pm \mu^\mp)/\Gamma_{\text{total}}$		$<3.2\times10^{-6}$, CL = 90%
$\Gamma(B \to K e^\pm \mu^\mp)/\Gamma_{\text{total}}$		$<1.6\times10^{-6}$, CL = 90%
$\Gamma(B \to K^*(892) e^\pm \mu^\mp)/\Gamma_{\text{total}}$		$<6.2\times10^{-6}$, CL = 90%
$\Gamma(B_s^0 \to e^\pm \mu^\mp)/\Gamma_{\text{total}}$	[i]	$<6.1\times10^{-6}$, CL = 90%
$\Gamma(J/\psi(1S) \to e^\pm \mu^\mp)/\Gamma_{\text{total}}$		$<1.1\times10^{-6}$, CL = 90%

TOTAL LEPTON NUMBER

Violation of total lepton number conservation also implies violation of lepton family number conservation.

$\Gamma(Z \to pe)/\Gamma_{\text{total}}$		$<1.8\times10^{-6}$, CL = 95%
$\Gamma(Z \to p\mu)/\Gamma_{\text{total}}$		$<1.8\times10^{-6}$, CL = 95%
limit on $\mu^- \to e^+$ conversion		
$\sigma(\mu^- {}^{32}\text{S} \to e^+ {}^{32}\text{Si}^*)$ / $\sigma(\mu^- {}^{32}\text{S} \to \nu_\mu {}^{32}\text{P}^*)$		$<9\times10^{-10}$, CL = 90%
$\sigma(\mu^- {}^{127}\text{I} \to e^+ {}^{127}\text{Sb}^*)$ / $\sigma(\mu^- {}^{127}\text{I} \to \text{anything})$		$<3\times10^{-10}$, CL = 90%
$\sigma(\mu^- \text{Ti} \to e^+ \text{Ca})$ / $\sigma(\mu^- \text{Ti} \to \text{capture})$		$<3.6\times10^{-11}$, CL = 90%
$\Gamma(\tau^- \to e^+\pi^-\pi^-)/\Gamma_{\text{total}}$		$<1.9\times10^{-6}$, CL = 90%
$\Gamma(\tau^- \to \mu^+\pi^-\pi^-)/\Gamma_{\text{total}}$		$<3.4\times10^{-6}$, CL = 90%
$\Gamma(\tau^- \to e^+\pi^- K^-)/\Gamma_{\text{total}}$		$<2.1\times10^{-6}$, CL = 90%
$\Gamma(\tau^- \to e^+ K^- K^-)/\Gamma_{\text{total}}$		$<3.8\times10^{-6}$, CL = 90%
$\Gamma(\tau^- \to \mu^+\pi^- K^-)/\Gamma_{\text{total}}$		$<7.0\times10^{-6}$, CL = 90%
$\Gamma(\tau^- \to \mu^+ K^- K^-)/\Gamma_{\text{total}}$		$<6.0\times10^{-6}$, CL = 90%
$\Gamma(\tau^- \to \overline{p}\gamma)/\Gamma_{\text{total}}$		$<3.5\times10^{-6}$, CL = 90%
$\Gamma(\tau^- \to \overline{p}\pi^0)/\Gamma_{\text{total}}$		$<1.5\times10^{-5}$, CL = 90%
$\Gamma(\tau^- \to \overline{p}2\pi^0)/\Gamma_{\text{total}}$		$<3.3\times10^{-5}$, CL = 90%
$\Gamma(\tau^- \to \overline{p}\eta)/\Gamma_{\text{total}}$		$<8.9\times10^{-6}$, CL = 90%
$\Gamma(\tau^- \to \overline{p}\pi^0\eta)/\Gamma_{\text{total}}$		$<2.7\times10^{-5}$, CL = 90%
$t_{1/2}(\ {}^{76}\text{Ge} \to {}^{76}\text{Se} + 2e^-\ )$		$>1.9\times10^{25}$ yr, CL = 90%
$\Gamma(\pi^+ \to \mu^+\overline{\nu}_e)/\Gamma_{\text{total}}$	[k]	$<1.5\times10^{-3}$, CL = 90%
$\Gamma(K^+ \to \pi^-\mu^+e^+)/\Gamma_{\text{total}}$		$<5.0\times10^{-10}$, CL = 90%
$\Gamma(K^+ \to \pi^- e^+e^+)/\Gamma_{\text{total}}$		$<6.4\times10^{-10}$, CL = 90%
$\Gamma(K^+ \to \pi^-\mu^+\mu^+)/\Gamma_{\text{total}}$	[k]	$<3.0\times10^{-9}$, CL = 90%
$\Gamma(K^+ \to \mu^+\overline{\nu}_e)/\Gamma_{\text{total}}$	[k]	$<3.3\times10^{-3}$, CL = 90%
$\Gamma(K^+ \to \pi^0 e^+\overline{\nu}_e)/\Gamma_{\text{total}}$		$<3\times10^{-3}$, CL = 90%
$\Gamma(D^+ \to \pi^- e^+e^+)/\Gamma_{\text{total}}$		$<9.6\times10^{-5}$, CL = 90%
$\Gamma(D^+ \to \pi^-\mu^+\mu^+)/\Gamma_{\text{total}}$		$<4.8\times10^{-6}$, CL = 90%
$\Gamma(D^+ \to \pi^- e^+\mu^+)/\Gamma_{\text{total}}$		$<5.0\times10^{-5}$, CL = 90%
$\Gamma(D^+ \to \rho^-\mu^+\mu^+)/\Gamma_{\text{total}}$		$<5.6\times10^{-4}$, CL = 90%
$\Gamma(D^+ \to K^- e^+e^+)/\Gamma_{\text{total}}$		$<1.2\times10^{-4}$, CL = 90%
$\Gamma(D^+ \to K^-\mu^+\mu^+)/\Gamma_{\text{total}}$		$<1.3\times10^{-5}$, CL = 90%
$\Gamma(D^+ \to K^- e^+\mu^+)/\Gamma_{\text{total}}$		$<1.3\times10^{-4}$, CL = 90%
$\Gamma(D^+ \to K^*(892)^-\mu^+\mu^+)/\Gamma_{\text{total}}$		$<8.5\times10^{-4}$, CL = 90%
$\Gamma(D^0 \to \pi^-\pi^- e^+e^+ + \text{c.c.})/\Gamma_{\text{total}}$		$<1.12\times10^{-4}$, CL = 90%
$\Gamma(D^0 \to \pi^-\pi^-\mu^+\mu^+ + \text{c.c.})/\Gamma_{\text{total}}$		$<2.9\times10^{-5}$, CL = 90%
$\Gamma(D^0 \to K^-\pi^- e^+e^+ + \text{c.c.})/\Gamma_{\text{total}}$		$<2.06\times10^{-4}$, CL = 90%
$\Gamma(D^0 \to K^-\pi^-\mu^+\mu^+ + \text{c.c.})/\Gamma_{\text{total}}$		$<3.9\times10^{-4}$, CL = 90%
$\Gamma(D^0 \to K^- K^- e^+e^+ + \text{c.c.})/\Gamma_{\text{total}}$		$<1.52\times10^{-4}$, CL = 90%
$\Gamma(D^0 \to K^- K^-\mu^+\mu^+ + \text{c.c.})/\Gamma_{\text{total}}$		$<9.4\times10^{-5}$, CL = 90%
$\Gamma(D^0 \to \pi^-\pi^- e^+\mu^+ + \text{c.c.})/\Gamma_{\text{total}}$		$<7.9\times10^{-5}$, CL = 90%
$\Gamma(D^0 \to K^-\pi^- e^+\mu^+ + \text{c.c.})/\Gamma_{\text{total}}$		$<2.18\times10^{-4}$, CL = 90%
$\Gamma(D^0 \to K^- K^- e^+\mu^+ + \text{c.c.})/\Gamma_{\text{total}}$		$<5.7\times10^{-5}$, CL = 90%
$\Gamma(D_s^+ \to \pi^- e^+e^+)/\Gamma_{\text{total}}$		$<6.9\times10^{-4}$, CL = 90%
$\Gamma(D_s^+ \to \pi^-\mu^+\mu^+)/\Gamma_{\text{total}}$		$<2.9\times10^{-5}$, CL = 90%
$\Gamma(D_s^+ \to \pi^- e^+\mu^+)/\Gamma_{\text{total}}$		$<7.3\times10^{-4}$, CL = 90%
$\Gamma(D_s^+ \to K^- e^+e^+)/\Gamma_{\text{total}}$		$<6.3\times10^{-4}$, CL = 90%
$\Gamma(D_s^+ \to K^-\mu^+\mu^+)/\Gamma_{\text{total}}$		$<1.3\times10^{-5}$, CL = 90%
$\Gamma(D_s^+ \to K^- e^+\mu^+)/\Gamma_{\text{total}}$		$<6.8\times10^{-4}$, CL = 90%
$\Gamma(D_s^+ \to K^*(892)^-\mu^+\mu^+)/\Gamma_{\text{total}}$		$<1.4\times10^{-3}$, CL = 90%
$\Gamma(B^+ \to \pi^- e^+e^+)/\Gamma_{\text{total}}$		$<1.6\times10^{-6}$, CL = 90%
$\Gamma(B^+ \to \pi^-\mu^+\mu^+)/\Gamma_{\text{total}}$		$<1.4\times10^{-6}$, CL = 90%
$\Gamma(B^+ \to \pi^- e^+\mu^+)/\Gamma_{\text{total}}$		$<1.3\times10^{-6}$, CL = 90%
$\Gamma(B^+ \to \rho^- e^+e^+)/\Gamma_{\text{total}}$		$<2.6\times10^{-6}$, CL = 90%
$\Gamma(B^+ \to \rho^-\mu^+\mu^+)/\Gamma_{\text{total}}$		$<5.0\times10^{-6}$, CL = 90%
$\Gamma(B^+ \to K^- e^+e^+)/\Gamma_{\text{total}}$		$<1.0\times10^{-6}$, CL = 90%
$\Gamma(B^+ \to K^-\mu^+\mu^+)/\Gamma_{\text{total}}$		$<1.8\times10^{-6}$, CL = 90%
$\Gamma(B^+ \to K^- e^+\mu^+)/\Gamma_{\text{total}}$		$<2.0\times10^{-6}$, CL = 90%
$\Gamma(B^+ \to K^*(892)^- e^+e^+)/\Gamma_{\text{total}}$		$<2.8\times10^{-6}$, CL = 90%
$\Gamma(B^+ \to K^*(892)^-\mu^+\mu^+)/\Gamma_{\text{total}}$		$<8.3\times10^{-6}$, CL = 90%
$\Gamma(\Xi^- \to p\mu^-\mu^-)/\Gamma_{\text{total}}$		$<4\times10^{-4}$, CL = 90%
$\Gamma(\Lambda_c^+ \to \Sigma^-\mu^+\mu^+)/\Gamma_{\text{total}}$		$<7.0\times10^{-4}$, CL = 90%

BARYON NUMBER

$\Gamma(Z \to pe)/\Gamma_{\text{total}}$		$<1.8\times10^{-6}$, CL = 95%
$\Gamma(Z \to p\mu)/\Gamma_{\text{total}}$		$<1.8\times10^{-6}$, CL = 95%
$\Gamma(\tau^- \to \overline{p}\gamma)/\Gamma_{\text{total}}$		$<3.5\times10^{-6}$, CL = 90%
$\Gamma(\tau^- \to \overline{p}\pi^0)/\Gamma_{\text{total}}$		$<1.5\times10^{-5}$, CL = 90%
$\Gamma(\tau^- \to \overline{p}2\pi^0)/\Gamma_{\text{total}}$		$<3.3\times10^{-5}$, CL = 90%
$\Gamma(\tau^- \to \overline{p}\eta)/\Gamma_{\text{total}}$		$<8.9\times10^{-6}$, CL = 90%
$\Gamma(\tau^- \to \overline{p}\pi^0\eta)/\Gamma_{\text{total}}$		$<2.7\times10^{-5}$, CL = 90%
p mean life		$>2.1\times10^{29}$ years, CL = 90%
A few examples of proton or bound neutron decay follow. For limits on many other nucleon decay channels, see the Baryon Summary Table.		
$\tau(N \to e^+\pi)$		>158 (n), >1600 $(p)\times10^{30}$ years, CL = 90%
$\tau(N \to \mu^+\pi)$		>100 (n), >473 $(p)\times10^{30}$ years, CL = 90%
$\tau(N \to e^+K)$		>17 (n), >150 $(p)\times10^{30}$ years, CL = 90%
$\tau(N \to \mu^+K)$		>26 (n), >120 $(p)\times10^{30}$ years, CL = 90%
limit on $n\overline{n}$ oscillations (free n)		$>0.86\times10^8$ s, CL = 90%
limit on $n\overline{n}$ oscillations (bound n)	[l]	$>1.2\times10^8$ s, CL = 90%

ELECTRIC CHARGE (Q)

$e \to \nu_e\gamma$ and astrophysical limits	[m]	$>4.6\times10^{26}$ yr, CL = 90%
$\Gamma(n \to p\nu_e\overline{\nu}_e)/\Gamma_{\text{total}}$		$<8\times10^{-27}$, CL = 68%

$\Delta S = \Delta Q$ RULE

Violations allowed in second-order weak interactions.

$\Gamma(K^+ \to \pi^+\pi^+ e^-\overline{\nu}_e)/\Gamma_{\text{total}}$		$<1.2\times10^{-8}$, CL = 90%
$\Gamma(K^+ \to \pi^+\pi^+\mu^-\overline{\nu}_\mu)/\Gamma_{\text{total}}$		$<3.0\times10^{-6}$, CL = 95%
$x = A(\overline{K}^0 \to \pi^-\ell^+\nu)/A(K^0 \to \pi^-\ell^+\nu) = A(\Delta S{=}-\Delta Q)/A(\Delta S{=}\Delta Q)$		
real part of x		-0.002 ± 0.006
imaginary part of x		0.0012 ± 0.0021
$\Gamma(\Sigma^+ \to n\ell^+\nu)/\Gamma(\Sigma^- \to n\ell^-\overline{\nu})$		<0.043
$\Gamma(\Sigma^+ \to ne^+\nu_e)/\Gamma_{\text{total}}$		$<5\times10^{-6}$, CL = 90%
$\Gamma(\Sigma^+ \to n\mu^+\nu_\mu)/\Gamma_{\text{total}}$		$<3.0\times10^{-5}$, CL = 90%
$\Gamma(\Xi^0 \to \Sigma^- e^+\nu_e)/\Gamma_{\text{total}}$		$<9\times10^{-4}$, CL = 90%
$\Gamma(\Xi^0 \to \Sigma^-\mu^+\nu_\mu)/\Gamma_{\text{total}}$		$<9\times10^{-4}$, CL = 90%

Unless otherwise stated, limits are given at the 90% confidence level, while errors are given as ±1 standard deviation.

Tests of Conservation Laws

$\Delta S = 2$ FORBIDDEN

Allowed in second-order weak interactions.

$\Gamma(\Xi^0 \to p\pi^-)/\Gamma_{\text{total}}$	$<4 \times 10^{-5}$, CL = 90%
$\Gamma(\Xi^0 \to pe^-\overline{\nu}_e)/\Gamma_{\text{total}}$	$<1.3 \times 10^{-3}$
$\Gamma(\Xi^0 \to p\mu^-\overline{\nu}_\mu)/\Gamma_{\text{total}}$	$<1.3 \times 10^{-3}$
$\Gamma(\Xi^- \to n\pi^-)/\Gamma_{\text{total}}$	$<1.9 \times 10^{-5}$, CL = 90%
$\Gamma(\Xi^- \to ne^-\overline{\nu}_e)/\Gamma_{\text{total}}$	$<3.2 \times 10^{-3}$, CL = 90%
$\Gamma(\Xi^- \to n\mu^-\overline{\nu}_\mu)/\Gamma_{\text{total}}$	$<1.5 \times 10^{-2}$, CL = 90%
$\Gamma(\Xi^- \to p\pi^-\pi^-)/\Gamma_{\text{total}}$	$<4 \times 10^{-4}$, CL = 90%
$\Gamma(\Xi^- \to p\pi^-e^-\overline{\nu}_e)/\Gamma_{\text{total}}$	$<4 \times 10^{-4}$, CL = 90%
$\Gamma(\Xi^- \to p\pi^-\mu^-\overline{\nu}_\mu)/\Gamma_{\text{total}}$	$<4 \times 10^{-4}$, CL = 90%
$\Gamma(\Omega^- \to \Lambda\pi^-)/\Gamma_{\text{total}}$	$<1.9 \times 10^{-4}$, CL = 90%

$\Delta S = 2$ VIA MIXING

Allowed in second-order weak interactions, e.g. mixing.

$m_{K_L^0} - m_{K_S^0}$	$(0.5292 \pm 0.0010) \times 10^{10}\ \hbar\,\text{s}^{-1}$ (S = 1.2)
$m_{K_L^0} - m_{K_S^0}$	$(3.483 \pm 0.006) \times 10^{-12}$ MeV

$\Delta C = 2$ VIA MIXING

Allowed in second-order weak interactions, e.g. mixing.

$\lvert m_{D_1^0} - m_{D_2^0}\rvert$	[n]	$<7 \times 10^{10}\ \hbar\,\text{s}^{-1}$, CL = 95%
$(\Gamma_{D_1^0} - \Gamma_{D_2^0})/\Gamma = 2y$		0.016 ± 0.010
$\Gamma(D^0 \to K^+\ell^-\overline{\nu}_\ell(\text{via } \overline{D}^0))/\Gamma_{\text{total}}$		$<1.7 \times 10^{-4}$, CL = 90%
$\Gamma(D^0 \to K^+\pi^-(\text{via } \overline{D}^0))/\Gamma_{\text{total}}$		$<1.6 \times 10^{-5}$, CL = 95%
$\Gamma(D^0 \to K^+\pi^-\pi^+\pi^-(\text{via } \overline{D}^0))/\Gamma_{\text{total}}$		$<4 \times 10^{-4}$, CL = 90%
$\Gamma(D^0 \to \mu^-\text{ anything (via } \overline{D}^0))/\Gamma_{\text{total}}$		$<4 \times 10^{-4}$, CL = 90%

$\Delta B = 2$ VIA MIXING

Allowed in second-order weak interactions, e.g. mixing.

χ_d	0.186 ± 0.004
$\Delta m_{B^0} = m_{B_H^0} - m_{B_L^0}$	$(0.502 \pm 0.007) \times 10^{12}\ \hbar\,\text{s}^{-1}$
$x_d = \Delta m_{B^0}/\Gamma_{B^0}$	0.771 ± 0.012
$\Delta m_{B_s^0} = m_{B_{sH}^0} - m_{B_{sL}^0}$	$>14.4 \times 10^{12}\ \hbar\,\text{s}^{-1}$, CL = 95%
$x_s = \Delta m_{B_s^0}/\Gamma_{B_s^0}$	>20.6, CL = 95%
χ_s	>0.49883, CL = 95%

$\Delta S = 1$ WEAK NEUTRAL CURRENT FORBIDDEN

Allowed by higher-order electroweak interactions.

$\Gamma(K^+ \to \pi^+e^+e^-)/\Gamma_{\text{total}}$		$(2.88 \pm 0.13) \times 10^{-7}$
$\Gamma(K^+ \to \pi^+\mu^+\mu^-)/\Gamma_{\text{total}}$		$(8.1 \pm 1.4) \times 10^{-8}$ (S = 2.7)
$\Gamma(K^+ \to \pi^+\nu\overline{\nu})/\Gamma_{\text{total}}$		$(1.6^{+1.8}_{-0.8}) \times 10^{-10}$
$\Gamma(K^+ \to \pi^+\pi^0\nu\overline{\nu})/\Gamma_{\text{total}}$		$<4.3 \times 10^{-5}$, CL = 90%
$\Gamma(K_S^0 \to \mu^+\mu^-)/\Gamma_{\text{total}}$		$<3.2 \times 10^{-7}$, CL = 90%
$\Gamma(K_S^0 \to e^+e^-)/\Gamma_{\text{total}}$		$<1.4 \times 10^{-7}$, CL = 90%
$\Gamma(K_S^0 \to \pi^0e^+e^-)/\Gamma_{\text{total}}$	[o]	$(3.0^{+1.5}_{-1.2}) \times 10^{-9}$
$\Gamma(K_L^0 \to \mu^+\mu^-)/\Gamma_{\text{total}}$		$(7.27 \pm 0.14) \times 10^{-9}$
$\Gamma(K_L^0 \to e^+e^-)/\Gamma_{\text{total}}$		$(9^{+6}_{-4}) \times 10^{-12}$
$\Gamma(K_L^0 \to \pi^+\pi^-e^+e^-)/\Gamma_{\text{total}}$	[p]	$(3.11 \pm 0.19) \times 10^{-7}$
$\Gamma(K_L^0 \to \pi^0\pi^0e^+e^-)/\Gamma_{\text{total}}$		$<6.6 \times 10^{-9}$, CL = 90%
$\Gamma(K_L^0 \to \mu^+\mu^-e^+e^-)/\Gamma_{\text{total}}$		$(2.69 \pm 0.27) \times 10^{-9}$
$\Gamma(K_L^0 \to e^+e^-e^+e^-)/\Gamma_{\text{total}}$		$(3.75 \pm 0.27) \times 10^{-8}$
$\Gamma(K_L^0 \to \pi^0\mu^+\mu^-)/\Gamma_{\text{total}}$		$<3.8 \times 10^{-10}$, CL = 90%
$\Gamma(K_L^0 \to \pi^0e^+e^-)/\Gamma_{\text{total}}$		$<5.1 \times 10^{-10}$, CL = 90%
$\Gamma(K_L^0 \to \pi^0\nu\overline{\nu})/\Gamma_{\text{total}}$		$<5.9 \times 10^{-7}$, CL = 90%
$\Gamma(\Sigma^+ \to pe^+e^-)/\Gamma_{\text{total}}$		$<7 \times 10^{-6}$

Unless otherwise stated, limits are given at the 90% confidence level, while errors are given as ± 1 standard deviation.

$\Delta C = 1$ WEAK NEUTRAL CURRENT FORBIDDEN

Allowed by higher-order electroweak interactions.

$\Gamma(D^+ \to \pi^+e^+e^-)/\Gamma_{\text{total}}$	$<5.2 \times 10^{-5}$, CL = 90%
$\Gamma(D^+ \to \pi^+\mu^+\mu^-)/\Gamma_{\text{total}}$	$<8.8 \times 10^{-6}$, CL = 90%
$\Gamma(D^+ \to \rho^+\mu^+\mu^-)/\Gamma_{\text{total}}$	$<5.6 \times 10^{-4}$, CL = 90%
$\Gamma(D^0 \to \gamma\gamma)/\Gamma_{\text{total}}$	$<2.8 \times 10^{-5}$, CL = 90%
$\Gamma(D^0 \to e^+e^-)/\Gamma_{\text{total}}$	$<6.2 \times 10^{-6}$, CL = 90%
$\Gamma(D^0 \to \mu^+\mu^-)/\Gamma_{\text{total}}$	$<4.1 \times 10^{-6}$, CL = 90%
$\Gamma(D^0 \to \pi^0e^+e^-)/\Gamma_{\text{total}}$	$<4.5 \times 10^{-5}$, CL = 90%
$\Gamma(D^0 \to \pi^0\mu^+\mu^-)/\Gamma_{\text{total}}$	$<1.8 \times 10^{-4}$, CL = 90%
$\Gamma(D^0 \to \eta e^+e^-)/\Gamma_{\text{total}}$	$<1.1 \times 10^{-4}$, CL = 90%
$\Gamma(D^0 \to \eta\mu^+\mu^-)/\Gamma_{\text{total}}$	$<5.3 \times 10^{-4}$, CL = 90%
$\Gamma(D^0 \to \pi^+\pi^-e^+e^-)/\Gamma_{\text{total}}$	$<3.73 \times 10^{-4}$, CL = 90%
$\Gamma(D^0 \to \rho^0e^+e^-)/\Gamma_{\text{total}}$	$<1.0 \times 10^{-4}$, CL = 90%
$\Gamma(D^0 \to \pi^+\pi^-\mu^+\mu^-)/\Gamma_{\text{total}}$	$<3.0 \times 10^{-5}$, CL = 90%
$\Gamma(D^0 \to \rho^0\mu^+\mu^-)/\Gamma_{\text{total}}$	$<2.2 \times 10^{-5}$, CL = 90%
$\Gamma(D^0 \to \omega e^+e^-)/\Gamma_{\text{total}}$	$<1.8 \times 10^{-4}$, CL = 90%
$\Gamma(D^0 \to \omega\mu^+\mu^-)/\Gamma_{\text{total}}$	$<8.3 \times 10^{-4}$, CL = 90%
$\Gamma(D^0 \to K^-K^+e^+e^-)/\Gamma_{\text{total}}$	$<3.15 \times 10^{-4}$, CL = 90%
$\Gamma(D^0 \to \phi e^+e^-)/\Gamma_{\text{total}}$	$<5.2 \times 10^{-5}$, CL = 90%
$\Gamma(D^0 \to K^-K^+\mu^+\mu^-)/\Gamma_{\text{total}}$	$<3.3 \times 10^{-5}$, CL = 90%
$\Gamma(D^0 \to \phi\mu^+\mu^-)/\Gamma_{\text{total}}$	$<3.1 \times 10^{-5}$, CL = 90%
$\Gamma(D^0 \to K^-\pi^+e^+e^-)/\Gamma_{\text{total}}$	$<3.85 \times 10^{-4}$, CL = 90%
$\Gamma(D^0 \to K^-\pi^+\mu^+\mu^-)/\Gamma_{\text{total}}$	$<3.59 \times 10^{-4}$, CL = 90%
$\Gamma(D^0 \to \pi^+\pi^-\pi^0\mu^+\mu^-)/\Gamma_{\text{total}}$	$<8.1 \times 10^{-4}$, CL = 90%
$\Gamma(D_s^+ \to K^+e^+e^-)/\Gamma_{\text{total}}$	$<1.6 \times 10^{-3}$, CL = 90%
$\Gamma(D_s^+ \to K^+\mu^+\mu^-)/\Gamma_{\text{total}}$	$<3.6 \times 10^{-5}$, CL = 90%
$\Gamma(D_s^+ \to K^*(892)^+\mu^+\mu^-)/\Gamma_{\text{total}}$	$<1.4 \times 10^{-3}$, CL = 90%
$\Gamma(\Lambda_c^+ \to p\mu^+\mu^-)/\Gamma_{\text{total}}$	$<3.4 \times 10^{-4}$, CL = 90%

$\Delta B = 1$ WEAK NEUTRAL CURRENT FORBIDDEN

Allowed by higher-order electroweak interactions.

$\Gamma(B^+ \to \pi^+e^+e^-)/\Gamma_{\text{total}}$		$<3.9 \times 10^{-3}$, CL = 90%
$\Gamma(B^+ \to \pi^+\mu^+\mu^-)/\Gamma_{\text{total}}$		$<9.1 \times 10^{-3}$, CL = 90%
$\Gamma(B^+ \to K^+e^+e^-)/\Gamma_{\text{total}}$		$(6.3^{+1.9}_{-1.7}) \times 10^{-7}$
$\Gamma(B^+ \to K^+\mu^+\mu^-)/\Gamma_{\text{total}}$		$(4.5^{+1.4}_{-1.2}) \times 10^{-7}$
$\Gamma(B^+ \to K^+\ell^+\ell^-)/\Gamma_{\text{total}}$	[q]	$(5.3 \pm 1.1) \times 10^{-7}$
$\Gamma(B^+ \to K^+\overline{\nu}\nu)/\Gamma_{\text{total}}$		$<2.4 \times 10^{-4}$, CL = 90%
$\Gamma(B^+ \to K^*(892)^+e^+e^-)/\Gamma_{\text{total}}$		$<4.6 \times 10^{-6}$, CL = 90%
$\Gamma(B^+ \to K^*(892)^+\mu^+\mu^-)/\Gamma_{\text{total}}$		$<2.2 \times 10^{-6}$, CL = 90%
$\Gamma(B^+ \to K^*(892)^+\ell^+\ell)/\Gamma_{\text{total}}$	[q]	$<2.2 \times 10^{-6}$, CL = 90%
$\Gamma(B^0 \to \gamma\gamma)/\Gamma_{\text{total}}$		$<1.7 \times 10^{-6}$, CL = 90%
$\Gamma(B^0 \to e^+e^-)/\Gamma_{\text{total}}$		$<1.9 \times 10^{-7}$, CL = 90%
$\Gamma(B^0 \to \mu^+\mu^-)/\Gamma_{\text{total}}$		$<1.6 \times 10^{-7}$, CL = 90%
$\Gamma(B^0 \to K^0e^+e^-)/\Gamma_{\text{total}}$		$<5.4 \times 10^{-7}$, CL = 90%
$\Gamma(B^0 \to K^0\mu^+\mu^-)/\Gamma_{\text{total}}$		$(5.6^{+2.9}_{-2.4}) \times 10^{-7}$
$\Gamma(B^0 \to K^0\ell^+\ell^-)/\Gamma_{\text{total}}$	[q]	$<6.8 \times 10^{-7}$, CL = 90%
$\Gamma(B^0 \to K^*(892)^0e^+e^-)/\Gamma_{\text{total}}$		$<2.4 \times 10^{-6}$, CL = 90%
$\Gamma(B^0 \to K^*(892)^0\mu^+\mu^-)/\Gamma_{\text{total}}$		$(1.3 \pm 0.4) \times 10^{-6}$
$\Gamma(B^0 \to K^*(892)^0\nu\overline{\nu})/\Gamma_{\text{total}}$		$<1.0 \times 10^{-3}$, CL = 90%
$\Gamma(B^0 \to K^*(892)^0\ell^+\ell^-)/\Gamma_{\text{total}}$	[q]	$(1.17 \pm 0.30) \times 10^{-6}$
$\Gamma(B \to se^+e^-)/\Gamma_{\text{total}}$		$(5.0 \pm 2.6) \times 10^{-6}$
$\Gamma(B \to s\mu^+\mu^-)/\Gamma_{\text{total}}$		$(7.9^{+3.0}_{-2.6}) \times 10^{-6}$
$\Gamma(B \to s\ell^+\ell^-)/\Gamma_{\text{total}}$	[q]	$(6.1^{+2.0}_{-1.8}) \times 10^{-6}$
$\Gamma(B \to Ke^+e^-)/\Gamma_{\text{total}}$		$(4.8^{+1.5}_{-1.3}) \times 10^{-7}$
$\Gamma(B \to K^*(892)e^+e^-)/\Gamma_{\text{total}}$		$(1.5 \pm 0.5) \times 10^{-6}$
$\Gamma(B \to K\mu^+\mu^-)/\Gamma_{\text{total}}$		$(4.8 \pm 1.2) \times 10^{-7}$
$\Gamma(B \to K^*(892)\mu^+\mu^-)/\Gamma_{\text{total}}$		$(1.17^{+0.37}_{-0.33}) \times 10^{-6}$
$\Gamma(B \to K\ell^+\ell^-)/\Gamma_{\text{total}}$		$(5.4 \pm 0.8) \times 10^{-7}$
$\Gamma(B \to K^*(892)\ell^+\ell^-)/\Gamma_{\text{total}}$		$(1.05 \pm 0.20) \times 10^{-6}$
$\Gamma(\overline{b} \to \mu^+\mu^-\text{ anything})/\Gamma_{\text{total}}$		$<3.2 \times 10^{-4}$, CL = 90%
$\Gamma(B_s^0 \to \mu^+\mu^-)/\Gamma_{\text{total}}$		$<2.0 \times 10^{-6}$, CL = 90%
$\Gamma(B_s^0 \to e^+e^-)/\Gamma_{\text{total}}$		$<5.4 \times 10^{-5}$, CL = 90%
$\Gamma(B_s^0 \to \phi(1020)\mu^+\mu^-)/\Gamma_{\text{total}}$		$<4.7 \times 10^{-5}$, CL = 90%
$\Gamma(B_s^0 \to \phi\nu\overline{\nu})/\Gamma_{\text{total}}$		$<5.4 \times 10^{-3}$, CL = 90%

$\Delta T = 1$ WEAK NEUTRAL CURRENT FORBIDDEN

Allowed by higher-order electroweak interactions.

$\Gamma(t \to Zq(q{=}u,c))/\Gamma_{\text{total}}$	[r]	$<13.7 \times 10^{-2}$, CL = 95%

NOTES

In this Summary Table:

When a quantity has "(S = ...)" to its right, the error on the quantity has been enlarged by the "scale factor" S, defined as $S = \sqrt{\chi^2/(N-1)}$, where N is the number of measurements used in calculating the quantity. We do this when $S > 1$, which often indicates that the measurements are inconsistent. When $S > 1.25$, we also show in the Particle Listings an ideogram of the measurements. For more about S, see the Introduction.

[a] C parity forbids this to occur as a single-photon process.

[b] Time-reversal invariance requires this to be 0° or 180°.

[c] Allowed by higher-order electroweak interactions.

[d] Violates CP in leading order. Test of direct CP violation since the indirect CP-violating and CP-conserving contributions are expected to be suppressed.

[e] $\text{Re}(\epsilon'/\epsilon) = \epsilon'/\epsilon$ to a very good approximation provided the phases satisfy CPT invariance.

[f] Neglecting photon channels. See, *e.g.*, A. Pais and S.B. Treiman, Phys. Rev. **D12**, 2744 (1975).

[g] Derived from measured values of ϕ_{+-}, ϕ_{00}, $|\eta|$, $|m_{K_L^0} - m_{K_S^0}|$, and $\tau_{K_S^0}$, as described in the introduction to "Tests of Conservation Laws."

[h] These two results are not independent, and both use the more precise measurement of $|q_{\overline{p}}/m_{\overline{p}}|/(q_p/m_p)$.

[i] The value is for the sum of the charge states or particle/antiparticle states indicated.

[j] A test of additive vs. multiplicative lepton family number conservation.

[k] Derived from an analysis of neutrino-oscillation experiments.

[l] There is some controversy about whether nuclear physics and model dependence complicate the analysis for bound neutrons (from which the best limit comes). The first limit here is from reactor experiments with free neutrons.

[m] This is the best limit for the mode $e^- \to \nu\gamma$. The best limit for "electron disappearance" is 6.4×10^{24} yr.

[n] This $D_1^0 - D_2^0$ limit is inferred from the D^0-$\overline{D}^0$ mixing ratio $\Gamma(K^+\pi^-$ (via $\overline{D}^0$)) / $\Gamma(K^-\pi^+)$ near the end of the D^0 Listings.

[o] See the K_S^0 Particle Listings for the energy limits used in this measurement.

[p] See the K_L^0 Particle Listings for the energy limits used in this measurement.

[q] An ℓ indicates an e or a μ mode, not a sum over these modes.

[r] This limit is for $\Gamma(t \to Zq)/\Gamma(t \to Wb)$.

Unless otherwise stated, limits are given at the 90% confidence level, while errors are given as ± 1 standard deviation.

REVIEWS, TABLES, AND PLOTS

MAJOR REVIEWS IN THE PARTICLE LISTINGS

Additional Reviews and Notes related to specific particles are located in the Particle Listings.

1. PHYSICAL CONSTANTS

Table 1.1. Reviewed 2004 by P.J. Mohr and B.N. Taylor (NIST). Based mainly on the "CODATA Recommended Values of the Fundamental Physical Constants: 2002" by P.J. Mohr and B.N. Taylor, to be published in 2004. The last group of constants (beginning with the Fermi coupling constant) comes from the Particle Data Group. The figures in parentheses after the values give the 1-standard-deviation uncertainties in the last digits; the corresponding fractional uncertainties in parts per 10^9 (ppb) are given in the last column. This set of constants (aside from the last group) is recommended for international use by CODATA (the Committee on Data for Science and Technology). The full 2002 CODATA set of constants may be found at `http://physics.nist.gov/constants`

Quantity	Symbol, equation	Value	Uncertainty (ppb)
speed of light in vacuum	c	299 792 458 m s^{-1}	exact*
Planck constant	h	$6.626\ 0693(11)\times10^{-34}$ J s	170
Planck constant, reduced	$\hbar \equiv h/2\pi$	$1.054\ 571\ 68(18)\times10^{-34}$ J s	170
		$= 6.582\ 119\ 15(56)\times10^{-22}$ MeV s	85
electron charge magnitude	e	$1.602\ 176\ 53(14)\times10^{-19}$ C $= 4.803\ 204\ 41(41)\times10^{-10}$ esu	85, 85
conversion constant	$\hbar c$	197.326 968(17) MeV fm	85
conversion constant	$(\hbar c)^2$	0.389 379 323(67) GeV^2 mbarn	170
electron mass	m_e	0.510 998 918(44) MeV/c^2 $= 9.109\ 3826(16)\times10^{-31}$ kg	86, 170
proton mass	m_p	938.272 029(80) MeV/c^2 $= 1.672\ 621\ 71(29)\times10^{-27}$ kg	86, 170
		$= 1.007\ 276\ 466\ 88(13)$ u $= 1836.152\ 672\ 61(85)\ m_e$	0.13, 0.46
deuteron mass	m_d	1875.612 82(16) MeV/c^2	86
unified atomic mass unit (u)	(mass ^{12}C atom)/12 = (1 g)/(N_A mol)	931.494 043(80) MeV/c^2 $= 1.660\ 538\ 86(28)\times10^{-27}$ kg	86, 170
permittivity of free space	$\epsilon_0 = 1/\mu_0 c^2$	$8.854\ 187\ 817\ \ldots\times10^{-12}$ F m^{-1}	exact
permeability of free space	μ_0	$4\pi\times10^{-7}$ N A^{-2} $= 12.566\ 370\ 614\ \ldots\times10^{-7}$ N A^{-2}	exact
fine-structure constant	$\alpha = e^2/4\pi\epsilon_0\hbar c$	$7.297\ 352\ 568(24)\times10^{-3} = 1/137.035\ 999\ 11(46)^\dagger$	3.3, 3.3
classical electron radius	$r_e = e^2/4\pi\epsilon_0 m_e c^2$	$2.817\ 940\ 325(28)\times10^{-15}$ m	10
(e^- Compton wavelength)/2π	$\lambda\!\!\!^{-}_e = \hbar/m_e c = r_e\alpha^{-1}$	$3.861\ 592\ 678(26)\times10^{-13}$ m	6.7
Bohr radius ($m_{\rm nucleus} = \infty$)	$a_\infty = 4\pi\epsilon_0\hbar^2/m_e e^2 = r_e\alpha^{-2}$	$0.529\ 177\ 2108(18)\times10^{-10}$ m	3.3
wavelength of 1 eV/c particle	$hc/(1\ {\rm eV})$	$1.239\ 841\ 91(11)\times10^{-6}$ m	85
Rydberg energy	$hcR_\infty = m_e e^4/2(4\pi\epsilon_0)^2\hbar^2 = m_e c^2\alpha^2/2$	13.605 6923(12) eV	85
Thomson cross section	$\sigma_T = 8\pi r_e^2/3$	0.665 245 873(13) barn	20
Bohr magneton	$\mu_B = e\hbar/2m_e$	$5.788\ 381\ 804(39)\times10^{-11}$ MeV T^{-1}	6.7
nuclear magneton	$\mu_N = e\hbar/2m_p$	$3.152\ 451\ 259(21)\times10^{-14}$ MeV T^{-1}	6.7
electron cyclotron freq./field	$\omega^e_{\rm cycl}/B = e/m_e$	$1.758\ 820\ 12(15)\times10^{11}$ rad s^{-1} T^{-1}	86
proton cyclotron freq./field	$\omega^p_{\rm cycl}/B = e/m_p$	$9.578\ 833\ 76(82)\times10^{7}$ rad s^{-1} T^{-1}	86
gravitational constant‡	G_N	$6.6742(10)\times10^{-11}$ m^3 kg^{-1} s^{-2}	1.5×10^5
		$= 6.7087(10)\times10^{-39}\ \hbar c\ ({\rm GeV}/c^2)^{-2}$	1.5×10^5
standard gravitational accel.	g_n	9.806 65 m s^{-2}	exact
Avogadro constant	N_A	$6.022\ 1415(10)\times10^{23}$ mol^{-1}	170
Boltzmann constant	k	$1.380\ 6505(24)\times10^{-23}$ J K^{-1}	1800
		$= 8.617\ 343(15)\times10^{-5}$ eV K^{-1}	1800
molar volume, ideal gas at STP	$N_A k(273.15\ {\rm K})/(101\ 325\ {\rm Pa})$	22.413 996(39)$\times10^{-3}$ m^3 mol^{-1}	1700
Wien displacement law constant	$b = \lambda_{\rm max}T$	$2.897\ 7685(51)\times10^{-3}$ m K	1700
Stefan-Boltzmann constant	$\sigma = \pi^2 k^4/60\hbar^3 c^2$	$5.670\ 400(40)\times10^{-8}$ W m^{-2} K^{-4}	7000
Fermi coupling constant**	$G_F/(\hbar c)^3$	$1.166\ 37(1)\times10^{-5}$ GeV^{-2}	9000
weak-mixing angle	$\sin^2\widehat{\theta}(M_Z)$ ($\overline{\rm MS}$)	0.23120(15)††	6.5×10^5
$W^\pm$ boson mass	m_W	80.425(38) GeV/c^2	4.8×10^5
Z^0 boson mass	m_Z	91.1876(21) GeV/c^2	2.3×10^4
strong coupling constant	$\alpha_s(m_Z)$	0.1187(20)	1.7×10^7

$\pi = 3.141\ 592\ 653\ 589\ 793\ 238$	e $= 2.718\ 281\ 828\ 459\ 045\ 235$	$\gamma = 0.577\ 215\ 664\ 901\ 532\ 861$	
1 in $\equiv$ 0.0254 m	1 G $\equiv 10^{-4}$ T	1 eV $= 1.602\ 176\ 53(14)\times10^{-19}$ J	kT at 300 K $= [38.681\ 684(68)]^{-1}$ eV
1 Å $\equiv$ 0.1 nm	1 dyne $\equiv 10^{-5}$ N	1 eV/c^2 $= 1.782\ 661\ 81(15)\times10^{-36}$ kg	0 °C $\equiv$ 273.15 K
1 barn $\equiv 10^{-28}$ m^2	1 erg $\equiv 10^{-7}$ J	$2.997\ 924\ 58\times10^9$ esu $=$ 1 C	1 atmosphere $\equiv$ 760 Torr $\equiv$ 101 325 Pa

* The meter is the length of the path traveled by light in vacuum during a time interval of 1/299 792 458 of a second.
† At $Q^2 = 0$. At $Q^2 \approx m_W^2$ the value is $\sim 1/128$.
‡ Absolute lab measurements of G_N have been made only on scales of about 1 cm to 1 m.
** See the discussion in Sec. 10, "Electroweak model and constraints on new physics."
†† The corresponding $\sin^2\theta$ for the effective angle is 0.23149(15).

2. ASTROPHYSICAL CONSTANTS AND PARAMETERS

Table 2.1. Revised 2001 by D.E. Groom (LBNL), February 2004 by M.A. Dobbs (LBNL). The figures in parentheses after some values give the one-standard deviation uncertainties in the last digit(s). Physical constants are from Ref. 1. While every effort has been made to obtain the most accurate current values of the listed quantities, the table does not represent a critical review or adjustment of the constants, and is not intended as a primary reference. The values and uncertainties for the cosmological parameters depend on the exact datasets, priors, and basis parameters used in the fit. Many of the parameters reported in this table are derived parameters or have non-Gaussian likelihoods. Their error bars may be highly correlated with other parameters and care must be taken when extrapolating to higher significance levels. In most cases we report the best fit running spectral index model parameters from the WMAPext plus 2dFGRS and Lyman α forest dataset, as reported in Ref. 2. Refer to Ref. 3 and the original papers for more information.

Quantity	Symbol, equation	Value	Reference, footnote
speed of light	c	299 792 458 m s^{-1}	defined[4]
Newtonian gravitational constant	G_N	$6.6742(10) \times 10^{-11}$ $m^3 kg^{-1}$ s^{-2}	[1, 5]
astronomical unit (mean $\oplus$–$\odot$ distance)	au	149 597 870 660(20) m	[6, 7]
tropical year (equinox to equinox) (2005.0)	yr	31 556 925.2 s	[6]
sidereal year (fixed star to fixed star) (2005.0)		31 558 149.8 s	[6]
mean sidereal day (2005.0)		$23^h\ 56^m\ 04^s.090\,53$	[6]
Jansky	Jy	10^{-26} W m^{-2} Hz^{-1}	
Planck mass	$\sqrt{\hbar c/G_N}$	$1.22090(9) \times 10^{19}$ GeV/c^2 $= 2.17645(16) \times 10^{-8}$ kg	[1]
Planck length	$\sqrt{\hbar G_N/c^3}$	$1.61624(12) \times 10^{-35}$ m	[1]
Hubble length	c/H_0	$\sim 1.2 \times 10^{26}$ m	[8]
parsec (1 AU/1 arc sec)	pc	$3.085\,677\,580\,7(4) \times 10^{16}$ m $= 3.262\ldots$ ly	[9]
light year (deprecated unit)	ly	$0.306\,6\ldots$ pc $= 0.946\,1\ldots \times 10^{16}$ m	
Schwarzschild radius of the Sun	$2G_N M_\odot/c^2$	2.953 250 08 km	[10]
solar mass	$M_\odot$	$1.988\,44(30) \times 10^{30}$ kg	[11]
solar equatorial radius	$R_\odot$	6.961×10^8 m	[6]
solar luminosity	$L_\odot$	$(3.846 \pm 0.008) \times 10^{26}$ W	[12]
Schwarzschild radius of the Earth	$2G_N M_\oplus/c^2$	8.870 056 22 mm	[13]
Earth mass	$M_\oplus$	$5.972\,3(9) \times 10^{24}$ kg	[14]
Earth mean equatorial radius	$R_\oplus$	$6.378\,140 \times 10^6$ m	[6]
luminosity conversion	L	$3.02 \times 10^{28} \times 10^{-0.4\ M_{\rm bol}}$ W ($M_{\rm bol}$ = absolute bolometric magnitude = bolometric magnitude at 10 pc	[15]
flux conversion	$\mathscr{F}$	$2.52 \times 10^{-8} \times 10^{-0.4\ m_{\rm bol}}$ W m^{-2} ($m_{\rm bol}$ = apparent bolometric magnitude)	from above
$v_\odot$ around center of Galaxy	$\Theta_\circ$	220(20) km s^{-1}	[16]
solar distance from galactic center	$R_\circ$	8.0(5) kpc	[17]
local disk density	$\rho_{\rm disk}$	3–12 $\times 10^{-24}$ g cm^{-3} $\approx$ 2–7 GeV/c^2 cm^{-3}	[18]
local halo density	$\rho_{\rm halo}$	2–13 $\times 10^{-25}$ g cm^{-3} $\approx$ 0.1–0.7 GeV/$c^2$$cm^{-3}$	[19]
present day Hubble expansion rate	H_0	100 h km s^{-1} Mpc^{-1} $= h \times (9.778\,13$ Gyr$)^{-1}$	[20]
present day normalized Hubble expansion rate	h	$0.71^{+0.04}_{-0.03}$	[2]
critical density of the universe	$\rho_c = 3H_0^2/8\pi G_N$	$2.775\,366\,27 \times 10^{11}\ h^2\ M_\odot$Mpc^{-3} $= 1.878\,37(28) \times 10^{-29}\ h^2$ g cm^{-3} $= 1.053\,69(16) \times 10^{-5}\ h^2$ GeV cm^{-3}	derived
pressureless matter density of the universe	$\Omega_m \equiv \rho_m/\rho_c$	$0.135^{+0.008}_{0.009}/h^2 = 0.27 \pm 0.04$	[2]
baryon density of the universe	$\Omega_b \equiv \rho_b/\rho_c$	$0.0224 \pm 0.0009/h^2 = 0.044 \pm 0.004$	[2]
dark matter density of the universe	$\Omega_{dm} \equiv \Omega_m - \Omega_b$	$0.113^{+0.008}_{-0.009}/h^2 = 0.22 \pm 0.04$	[21]
radiation density of the universe	$\Omega_\gamma = \rho_\gamma/\rho_c$	$(2.471 \pm 0.004) \times 10^{-5}/h^2 = (4.9 \pm 0.5) \times 10^{-5}$	[22]
neutrino density of the universe	Ω_ν	$< (0.0076/h^2 = 0.015)$, 95% C.L.	[2]
dark energy density	Ω_Λ	0.73 ± 0.04	[2]
total energy density	$\Omega_{\rm tot} = \Omega_m + \ldots + \Omega_\Lambda$	1.02 ± 0.02	[2]
number density of baryons	n_b	$(2.5 \pm 0.1) \times 10^{-7}$/cm^3	[2]
number density of CMB photons	n_γ	(410.4 ± 0.5)/cm^{-3}	[23]
baryon-to-photon ratio	$\eta = n_b/n_\gamma$	$(6.1 \pm 0.2) \times 10^{-10}$	derived
scale factor for cosmological constant	$c^2/3H_0^2$	$2.853 \times 10^{51}\ h^{-2}$ m^2	
dark energy equation of state	w	< -0.78 at 95% C.L.	[2, 24]
fluctuation amplitude at $8h^{-1}$ Mpc scale	σ_8	0.84 ± 0.04	[2]
scalar spectral index at $k_0 = 0.05$ Mpc^{-1}	n_s	0.93 ± 0.03	[2]

Quantity	Symbol, equation	Value	Reference, footnote
running spectral index slope at $k_0 = 0.05$ Mpc^{-1}	$dn_s/d\,ln\,k$	$-0.031^{+0.016}_{-0.018}$	[2]
tensor to scalar field perturbations ratio at $k_0 = 0.002$ Mpc^{-1}	$r = T/S$	< 0.71 at 95% C.L.	[2, 25]
reionization optical depth	τ	0.17 ± 0.04	[2]
age of the universe	t_0	13.7 ± 0.2 Gyr	[2]
present day CBR temperature	T_0	2.725 ± 0.001 K	[26]
solar velocity with respect to CBR		368 ± 2 km/s towards $(\ell, b) = (263.85^\circ \pm 0.10^\circ, 48.25^\circ \pm 0.04^\circ)$	[27, 28]
Local group velocity with respect to CBR	$v_{\rm LG}$	627 ± 22 km s^{-1} towards $(\ell, b) = (276^\circ \pm 3^\circ, 30^\circ \pm 3^\circ)$	[27]
entropy density/Boltzmann constant	s/k	$2\,889.2\ (T/2.725)^3$ cm^{-3}	[15]

References:

1. P.J. Mohr and B.N. Taylor, CODATA 2002; `http://physics.nist.gov/cuu/Constants`.
2. D.N. Spergel *et al.*, Astrophys. J. Supp. **148**, 175 (2003).
3. O. Lahav, A.R. Liddle, "The Cosmological Parameters", this *Review*.
4. B.W. Petley, Nature **303**, 373 (1983).
5. In the context of the scale dependence of field theoretic quantities, it should be remarked that absolute lab measurements of G_N have been performed on scales of 0.01–1.0 m.
6. *The Astronomical Almanac for the year 2005*, U.S. Government Printing Office, Washington, and Her Majesty's Stationary Office, London (2003).
7. JPL Planetary Ephemerides, E. Myles Standish, Jr., private communication (1989).
8. Derived from H_0 [2].
9. 1 AU divided by $\pi/648\,000$; quoted error is from the JPL Planetary Ephemerides value of the AU [7].
10. Product of $2/c^2$ and the heliocentric gravitational constant [6]. The given 9-place accuracy seems consistent with uncertainties in defining the earth's orbital parameters.
11. Obtained from the heliocentric gravitational constant [6] and G_N [1]. The error is the 150 ppm standard deviation of G_N.
12. 1996 mean total solar irradiance (TSI) $= 1367.5 \pm 2.7$ [29]; the solar luminosity is $4\pi \times (1\,\mathrm{AU})^2$ times this quantity. This value increased by 0.036% between the minima of solar cycles 21 and 22. It was modulated with an amplitude of 0.039% during solar cycle 21 [30].

    Sackmann *et al.* [31] use TSI $= 1370 \pm 2$ W m^{-2}, but conclude that the solar luminosity ($L_\odot = 3.853 \times 10^{26}$ J s^{-1}) has an uncertainty of 1.5%. Their value comes from three 1977–83 papers, and they comment that the error is based on scatter among the reported values, which is substantially in excess of that expected from the individual quoted errors.

    The conclusion of the 1971 review by Thekaekara and Drummond [32] ($1353 \pm 1\%$ W m^{-2}) is often quoted [33]. The conversion to luminosity is not given in the Thekaekara and Drummond paper, and we cannot exactly reproduce the solar luminosity given in Ref. 33.

    Finally, a value based on the 1954 spectral curve due to Johnson [34] ($1395 \pm 1\%$ W m^{-2}, or $L_\odot = 3.92 \times 10^{26}$ J s^{-1}) has been used widely, and may be the basis for the higher value of the solar luminosity and the corresponding lower value of the solar absolute bolometric magnitude (4.72) still common in the literature [15].
13. Product of $2/c^2$, the heliocentric gravitational constant from Ref. 6, and the earth/sun mass ratio, also from Ref. 6. The given 9-place accuracy appears to be consistent with uncertainties in actually defining the earth's orbital parameters.
14. Obtained from the geocentric gravitational constant [6] and G_N [1]. The error is the 150 ppm standard deviation of G_N.
15. E.W. Kolb and M.S. Turner, *The Early Universe*, Addison-Wesley (1990).
16. F.J. Kerr and D. Lynden-Bell, Mon. Not. R. Astr. Soc. **221**, 1023–1038 (1985). "On the basis of this review these [$R_\circ = 8.5 \pm 1.1$ kpc and $\Theta_\circ = 220 \pm 20$ km s^{-1}] were adopted by resolution of IAU Commission 33 on 1985 November 21 at Delhi".
17. M.J. Reid, Annu. Rev. Astron. Astrophys. **31**, 345–372 (1993). Note that $\Theta_\circ$ from the 1985 IAU Commission 33 recommendations is adopted in this review, although the new value for $R_\circ$ is smaller.
18. G. Gilmore, R.F.G. Wyse, and K. Kuijken, Ann. Rev. Astron. Astrophys. **27**, 555 (1989).
19. E.I. Gates, G. Gyuk, and M.S. Turner (Astrophys. J. **449**, L133 (1995)) find the local halo density to be $9.2^{+3.8}_{-3.1} \times 10^{-25}$ g cm^{-3}, but also comment that previously published estimates are in the range $1\text{–}10 \times 10^{-25}$ g cm^{-3}.
    The value 0.3 GeV/c^2 has been taken as "standard" in several papers setting limits on WIMP mass limits, *e.g.* in M. Mori *et al.*, Phys. Lett. **B289**, 463 (1992).
20. Conversion using length of tropical year.
21. Derived from [2].
22. $\rho_\gamma = \dfrac{\pi^2}{15}\dfrac{(k_B T)^4}{(\hbar c)^3}$, using T_0 from Ref. 26.
23. $n_\gamma = \dfrac{2\zeta(3)}{\pi^2}\left(\dfrac{k_B T}{\hbar c}\right)^3$, using T_0 from Ref. 26.
24. Note that one of the priors assumed when deriving this parameter is $w \geq -1$.
25. There are several definitions of r used in the literature, here r corresponds to the definition used by Ref. 2.
26. J. Mather *et al.*, Astrophys. J. **512**, 511 (1999). This paper gives $T_0 = 2.725 \pm 0.002$K at 95%CL. We take 0.001 as the one-standard deviation uncertainty.
27. D. Scott and G.F. Smoot, "Cosmic Microwave Background", this *Review*.
28. C.L. Bennett *et al.*, Astrophys. J. Supp. **148**, 1 (2003).
29. R.C. Willson, Science **277**, 1963 (1997); the 0.2% error estimate is from R.C. Willson, private correspondence (1998).
30. R.C. Willson and H.S. Hudson, Nature **332**, 810 (1988).
31. I.-J. Sackmann, A.I. Boothroyd, and K.E. Kraemer, Astrophys. J. **418**, 457 (1993).
32. M.P. Thekaekara and A.J. Drummond, Nature Phys. Sci. **229**, 6 (1971).
33. K.R. Lang, *Astrophysical Formulae*, Springer-Verlag (1974); K.R. Lang, *Astrophysical Data: Planets and Stars*, Springer-Verlag (1992).
34. F.S. Johnson, J. Meterol. **11**, 431 (1954).

3. INTERNATIONAL SYSTEM OF UNITS (SI)

See "The International System of Units (SI)," NIST Special Publication **330**, B.N. Taylor, ed. (USGPO, Washington, DC, 1991); and "Guide for the Use of the International System of Units (SI)," NIST Special Publication **811**, 1995 edition, B.N. Taylor (USGPO, Washington, DC, 1995).

Physical quantity	Name of unit	Symbol
Base units		
length	meter	m
mass	kilogram	kg
time	second	s
electric current	ampere	A
thermodynamic temperature	kelvin	K
amount of substance	mole	mol
luminous intensity	candela	cd
Derived units with special names		
plane angle	radian	rad
solid angle	steradian	sr
frequency	hertz	Hz
energy	joule	J
force	newton	N
pressure	pascal	Pa
power	watt	W
electric charge	coulomb	C
electric potential	volt	V
electric resistance	ohm	Ω
electric conductance	siemens	S
electric capacitance	farad	F
magnetic flux	weber	Wb
inductance	henry	H
magnetic flux density	tesla	T
luminous flux	lumen	lm
illuminance	lux	lx
celsius temperature	degree celsius	°C
activity (of a radioactive source)*	becquerel	Bq
absorbed dose (of ionizing radiation)*	gray	Gy
dose equivalent*	sievert	Sv

*See our section 29, on "Radioactivity and radiation protection," p. 272.

SI prefixes

10^{24}	yotta	(Y)
10^{21}	zetta	(Z)
10^{18}	exa	(E)
10^{15}	peta	(P)
10^{12}	tera	(T)
10^{9}	giga	(G)
10^{6}	mega	(M)
10^{3}	kilo	(k)
10^{2}	hecto	(h)
10	deca	(da)
10^{-1}	deci	(d)
10^{-2}	centi	(c)
10^{-3}	milli	(m)
10^{-6}	micro	(μ)
10^{-9}	nano	(n)
10^{-12}	pico	(p)
10^{-15}	femto	(f)
10^{-18}	atto	(a)
10^{-21}	zepto	(z)
10^{-24}	yocto	(y)

Table 4.1. Revised 2004 by C.G. Wohl (LBNL). Adapted from the Commission of Atomic Weights and Isotopic Abundances, "Atomic Weights of the Elements 1995," Pure and Applied Chemistry **68**, 2339 (1996), and G. Audi and A.H. Wapstra, "The 1993 Mass Evaluation," Nucl. Phys. **A565**, 1 (1993). The atomic number (top left) is the number of protons in the nucleus. The atomic mass (bottom) is weighted by isotopic abundances in the Earth's surface. For a new determination of atomic masses, not weighted by abundances, see G. Audi, A.H. Wapstra, and C. Thibault, Nucl. Phys. **A729**, 337 (2003). Atomic masses are relative to the mass of the one isotope, isotope defined to be exactly 12 unified atomic mass units (u). Errors range from 1 to 9 in the last digit quoted. Relative isotopic abundances often vary considerably, both in natural and commercial samples. A number in the mass column is the mass of the longest-lived isotope of that element—no stable isotope exists. However, although Th, Pa, and U have no stable isotope they do have characteristic terrestrial compositions, and meaningful weighted masses can be given. For elements 110 and 111, the atomic number of confirmed isotopes are given.

PERIODIC TABLE OF THE ELEMENTS

1 IA												13 IIIA	14 IVA	15 VA	16 VIA	17 VIIA	18 VIIIA
1 H Hydrogen 1.00794	2 IIA																2 He Helium 4.002602
3 Li Lithium 6.941	4 Be Beryllium 9.012182											5 B Boron 10.811	6 C Carbon 12.0107	7 N Nitrogen 14.00674	8 O Oxygen 15.9994	9 F Fluorine 18.9984032	10 Ne Neon 20.1797
11 Na Sodium 22.989770	12 Mg Magnesium 24.3050	3 IIIB	4 IVB	5 VB	6 VIB	7 VIIB	8	9 VIII	10	11 IB	12 IIB	13 Al Aluminum 26.981538	14 Si Silicon 28.0855	15 P Phosph. 30.973761	16 S Sulfur 32.066	17 Cl Chlorine 35.4527	18 Ar Argon 39.948
19 K Potassium 39.0983	20 Ca Calcium 40.078	21 Sc Scandium 44.955910	22 Ti Titanium 47.867	23 V Vanadium 50.9415	24 Cr Chromium 51.9961	25 Mn Manganese 54.938049	26 Fe Iron 55.845	27 Co Cobalt 58.933200	28 Ni Nickel 58.6934	29 Cu Copper 63.546	30 Zn Zinc 65.39	31 Ga Gallium 69.723	32 Ge German. 72.61	33 As Arsenic 74.92160	34 Se Selenium 78.96	35 Br Bromine 79.904	36 Kr Krypton 83.80
37 Rb Rubidium 85.4678	38 Sr Strontium 87.62	39 Y Yttrium 88.90585	40 Zr Zirconium 91.224	41 Nb Niobium 92.90638	42 Mo Molyb. 95.94	43 Tc Technet. (97.907215)	44 Ru Ruthen. 101.07	45 Rh Rhodium 102.90550	46 Pd Palladium 106.42	47 Ag Silver 107.8682	48 Cd Cadmium 112.411	49 In Indium 114.818	50 Sn Tin 118.710	51 Sb Antimon. 121.760	52 Te Tellurium 127.60	53 I Iodine 126.90447	54 Xe Xenon 131.29
55 Cs Cesium 132.90545	56 Ba Barium 137.327	57–71 Lantha-nides	72 Hf Hafnium 178.49	73 Ta Tantalum 180.9479	74 W Tungsten 183.84	75 Re Rhenium 186.207	76 Os Osmium 190.23	77 Ir Iridium 192.217	78 Pt Platinum 195.078	79 Au Gold 196.96655	80 Hg Mercury 200.59	81 Tl Thallium 204.3833	82 Pb Lead 207.2	83 Bi Bismuth 208.98038	84 Po Polonium (208.982415)	85 At Astatine (209.987131)	86 Rn Radon (222.017570)
87 Fr Francium (223.019731)	88 Ra Radium (226.025402)	89–103 Actinides	104 Rf Rutherford. (261.1089)	105 Db Dubnium (262.1144)	106 Sg Seab. (263.1186)	107 Bh Bohrium (262.1231)	108 Hs Hassium (265.1306)	109 Mt Meitner. (266.1378)	110 Ds Darmstadt. [269,271]	111 [272]							

Lanthanide series	57 La Lanthan. 138.9055	58 Ce Cerium 140.116	59 Pr Praseo. 140.90765	60 Nd Neo. 144.24	61 Pm Prometh. (144.912745)	62 Sm Samarium 150.36	63 Eu Europium 151.964	64 Gd Gadolin. 157.25	65 Tb Terbium 158.92534	66 Dy Dyspros. 162.50	67 Ho Holmium 164.93032	68 Er Erbium 167.26	69 Tm Thulium 168.93421	70 Yb Ytterbium 173.04	71 Lu Lutetium 174.967

Actinide series	89 Ac Actinium (227.027747)	90 Th Thorium 232.0381	91 Pa Protactin. 231.03588	92 U Uranium 238.0289	93 Np Neptunium (237.048166)	94 Pu Plutonium (244.064197)	95 Am Americ. (243.061372)	96 Cm Curium (247.070346)	97 Bk Berkelium (247.070298)	98 Cf Californ. (251.079579)	99 Es Einstein. (252.08297)	100 Fm Fermium (257.095096)	101 Md Mendelev. (258.098427)	102 No Nobelium (259.1011)	103 Lr Lawrenc. (262.1098)

5. ELECTRONIC STRUCTURE OF THE ELEMENTS

Table 5.1. Reviewed 2002 by W.C. Martin (NIST). The electronic configurations and the ionization energies are from the NIST database *Ground Levels and Ionization Energies for the Neutral Atoms*, W.C. Martin and A. Musgrove (2002), `http://physics.nist.gov` (select "Physical Reference Data"). The electron configuration for, say, iron indicates an argon electronic core (see argon) plus six $3d$ electrons and two $4s$ electrons. The ionization energy is the least energy necessary to remove to infinity one electron from an atom of the element.

	Element		Electron configuration ($3d^5$ = five $3d$ electrons, *etc.*)		Ground state $^{2S+1}L_J$	Ionization energy (eV)
1	H	Hydrogen	$1s$		$^2S_{1/2}$	13.5984
2	He	Helium	$1s^2$		$^1S_0$	24.5874
3	Li	Lithium	(He) $2s$		$^2S_{1/2}$	5.3917
4	Be	Beryllium	(He) $2s^2$		$^1S_0$	9.3227
5	B	Boron	(He) $2s^2$ $2p$		$^2P_{1/2}$	8.2980
6	C	Carbon	(He) $2s^2$ $2p^2$		$^3P_0$	11.2603
7	N	Nitrogen	(He) $2s^2$ $2p^3$		$^4S_{3/2}$	14.5341
8	O	Oxygen	(He) $2s^2$ $2p^4$		$^3P_2$	13.6181
9	F	Fluorine	(He) $2s^2$ $2p^5$		$^2P_{3/2}$	17.4228
10	Ne	Neon	(He) $2s^2$ $2p^6$		$^1S_0$	21.5646
11	Na	Sodium	(Ne) $3s$		$^2S_{1/2}$	5.1391
12	Mg	Magnesium	(Ne) $3s^2$		$^1S_0$	7.6462
13	Al	Aluminum	(Ne) $3s^2$ $3p$		$^2P_{1/2}$	5.9858
14	Si	Silicon	(Ne) $3s^2$ $3p^2$		$^3P_0$	8.1517
15	P	Phosphorus	(Ne) $3s^2$ $3p^3$		$^4S_{3/2}$	10.4867
16	S	Sulfur	(Ne) $3s^2$ $3p^4$		$^3P_2$	10.3600
17	Cl	Chlorine	(Ne) $3s^2$ $3p^5$		$^2P_{3/2}$	12.9676
18	Ar	Argon	(Ne) $3s^2$ $3p^6$		$^1S_0$	15.7596
19	K	Potassium	(Ar) $4s$		$^2S_{1/2}$	4.3407
20	Ca	Calcium	(Ar) $4s^2$		$^1S_0$	6.1132
21	Sc	Scandium	(Ar) $3d$ $4s^2$	Transition elements	$^2D_{3/2}$	6.5615
22	Ti	Titanium	(Ar) $3d^2$ $4s^2$		$^3F_2$	6.8281
23	V	Vanadium	(Ar) $3d^3$ $4s^2$		$^4F_{3/2}$	6.7463
24	Cr	Chromium	(Ar) $3d^5$ $4s$		$^7S_3$	6.7665
25	Mn	Manganese	(Ar) $3d^5$ $4s^2$		$^6S_{5/2}$	7.4340
26	Fe	Iron	(Ar) $3d^6$ $4s^2$		$^5D_4$	7.9024
27	Co	Cobalt	(Ar) $3d^7$ $4s^2$		$^4F_{9/2}$	7.8810
28	Ni	Nickel	(Ar) $3d^8$ $4s^2$		$^3F_4$	7.6398
29	Cu	Copper	(Ar) $3d^{10}4s$		$^2S_{1/2}$	7.7264
30	Zn	Zinc	(Ar) $3d^{10}4s^2$		$^1S_0$	9.3942
31	Ga	Gallium	(Ar) $3d^{10}4s^2$ $4p$		$^2P_{1/2}$	5.9993
32	Ge	Germanium	(Ar) $3d^{10}4s^2$ $4p^2$		$^3P_0$	7.8994
33	As	Arsenic	(Ar) $3d^{10}4s^2$ $4p^3$		$^4S_{3/2}$	9.7886
34	Se	Selenium	(Ar) $3d^{10}4s^2$ $4p^4$		$^3P_2$	9.7524
35	Br	Bromine	(Ar) $3d^{10}4s^2$ $4p^5$		$^2P_{3/2}$	11.8138
36	Kr	Krypton	(Ar) $3d^{10}4s^2$ $4p^6$		$^1S_0$	13.9996
37	Rb	Rubidium	(Kr) $5s$		$^2S_{1/2}$	4.1771
38	Sr	Strontium	(Kr) $5s^2$		$^1S_0$	5.6949
39	Y	Yttrium	(Kr) $4d$ $5s^2$	Transition elements	$^2D_{3/2}$	6.2173
40	Zr	Zirconium	(Kr) $4d^2$ $5s^2$		$^3F_2$	6.6339
41	Nb	Niobium	(Kr) $4d^4$ $5s$		$^6D_{1/2}$	6.7589
42	Mo	Molybdenum	(Kr) $4d^5$ $5s$		$^7S_3$	7.0924
43	Tc	Technetium	(Kr) $4d^5$ $5s^2$		$^6S_{5/2}$	7.28
44	Ru	Ruthenium	(Kr) $4d^7$ $5s$		$^5F_5$	7.3605
45	Rh	Rhodium	(Kr) $4d^8$ $5s$		$^4F_{9/2}$	7.4589
46	Pd	Palladium	(Kr) $4d^{10}$		$^1S_0$	8.3369
47	Ag	Silver	(Kr) $4d^{10}5s$		$^2S_{1/2}$	7.5762
48	Cd	Cadmium	(Kr) $4d^{10}5s^2$		$^1S_0$	8.9938

49	In	Indium	(Kr) $4d^{10}5s^2$	$5p$				$^2P_{1/2}$	5.7864
50	Sn	Tin	(Kr) $4d^{10}5s^2$	$5p^2$				$^3P_0$	7.3439
51	Sb	Antimony	(Kr) $4d^{10}5s^2$	$5p^3$				$^4S_{3/2}$	8.6084
52	Te	Tellurium	(Kr) $4d^{10}5s^2$	$5p^4$				$^3P_2$	9.0096
53	I	Iodine	(Kr) $4d^{10}5s^2$	$5p^5$				$^2P_{3/2}$	10.4513
54	Xe	Xenon	(Kr) $4d^{10}5s^2$	$5p^6$				$^1S_0$	12.1298
55	Cs	Cesium	(Xe)	$6s$				$^2S_{1/2}$	3.8939
56	Ba	Barium	(Xe)	$6s^2$				$^1S_0$	5.2117
57	La	Lanthanum	(Xe) $5d$	$6s^2$				$^2D_{3/2}$	5.5770
58	Ce	Cerium	(Xe) $4f$ $5d$	$6s^2$				$^1G_4$	5.5387
59	Pr	Praseodymium	(Xe) $4f^3$	$6s^2$		L		$^4I_{9/2}$	5.464
60	Nd	Neodymium	(Xe) $4f^4$	$6s^2$		a		$^5I_4$	5.5250
61	Pm	Promethium	(Xe) $4f^5$	$6s^2$		n		$^6H_{5/2}$	5.58
62	Sm	Samarium	(Xe) $4f^6$	$6s^2$		t		$^7F_0$	5.6437
63	Eu	Europium	(Xe) $4f^7$	$6s^2$		h		$^8S_{7/2}$	5.6704
64	Gd	Gadolinium	(Xe) $4f^7$ $5d$	$6s^2$		a		$^9D_2$	6.1498
65	Tb	Terbium	(Xe) $4f^9$	$6s^2$		n		$^6H_{15/2}$	5.8638
66	Dy	Dysprosium	(Xe) $4f^{10}$	$6s^2$		i		$^5I_8$	5.9389
67	Ho	Holmium	(Xe) $4f^{11}$	$6s^2$		d		$^4I_{15/2}$	6.0215
68	Er	Erbium	(Xe) $4f^{12}$	$6s^2$		e		$^3H_6$	6.1077
69	Tm	Thulium	(Xe) $4f^{13}$	$6s^2$		s		$^2F_{7/2}$	6.1843
70	Yb	Ytterbium	(Xe) $4f^{14}$	$6s^2$				$^1S_0$	6.2542
71	Lu	Lutetium	(Xe) $4f^{14}5d$	$6s^2$				$^2D_{3/2}$	5.4259
72	Hf	Hafnium	(Xe) $4f^{14}5d^2$	$6s^2$		T		$^3F_2$	6.8251
73	Ta	Tantalum	(Xe) $4f^{14}5d^3$	$6s^2$		r	e	$^4F_{3/2}$	7.5496
74	W	Tungsten	(Xe) $4f^{14}5d^4$	$6s^2$		a	l	$^5D_0$	7.8640
75	Re	Rhenium	(Xe) $4f^{14}5d^5$	$6s^2$		n	e	$^6S_{5/2}$	7.8335
76	Os	Osmium	(Xe) $4f^{14}5d^6$	$6s^2$		s	m	$^5D_4$	8.4382
77	Ir	Iridium	(Xe) $4f^{14}5d^7$	$6s^2$		i	e	$^4F_{9/2}$	8.9670
78	Pt	Platinum	(Xe) $4f^{14}5d^9$	$6s$		t	n	$^3D_3$	8.9588
79	Au	Gold	(Xe) $4f^{14}5d^{10}$	$6s$		i	t	$2S_{1/2}$	9.2255
80	Hg	Mercury	(Xe) $4f^{14}5d^{10}$	$6s^2$		o	s	$^1S_0$	10.4375
81	Tl	Thallium	(Xe) $4f^{14}5d^{10}6s^2$	$6p$		n		$^2P_{1/2}$	6.1082
82	Pb	Lead	(Xe) $4f^{14}5d^{10}6s^2$	$6p^2$				$^3P_0$	7.4167
83	Bi	Bismuth	(Xe) $4f^{14}5d^{10}6s^2$	$6p^3$				$^4S_{3/2}$	7.2855
84	Po	Polonium	(Xe) $4f^{14}5d^{10}6s^2$	$6p^4$				$^3P_2$	8.4167
85	At	Astatine	(Xe) $4f^{14}5d^{10}6s^2$	$6p^5$				$^2P_{3/2}$	
86	Rn	Radon	(Xe) $4f^{14}5d^{10}6s^2$	$6p^6$				$^1S_0$	10.7485
87	Fr	Francium	(Rn)	$7s$				$^2S_{1/2}$	4.0727
88	Ra	Radium	(Rn)	$7s^2$				$^1S_0$	5.2784
89	Ac	Actinium	(Rn) $6d$	$7s^2$				$^2D_{3/2}$	5.17
90	Th	Thorium	(Rn) $6d^2$	$7s^2$				$^3F_2$	6.3067
91	Pa	Protactinium	(Rn) $5f^2$ $6d$	$7s^2$		A		$^4K_{11/2}$	5.89
92	U	Uranium	(Rn) $5f^3$ $6d$	$7s^2$		c		$^5L_6$	6.1941
93	Np	Neptunium	(Rn) $5f^4$ $6d$	$7s^2$		t		$^6L_{11/2}$	6.2657
94	Pu	Plutonium	(Rn) $5f^6$	$7s^2$		i		$^7F_0$	6.0262
95	Am	Americium	(Rn) $5f^7$	$7s^2$		n		$^8S_{7/2}$	5.9738
96	Cm	Curium	(Rn) $5f^7$ $6d$	$7s^2$		i		$^9D_2$	5.9915
97	Bk	Berkelium	(Rn) $5f^9$	$7s^2$		d		$^6H_{15/2}$	6.1979
98	Cf	Californium	(Rn) $5f^{10}$	$7s^2$		e		$^5I_8$	6.2817
99	Es	Einsteinium	(Rn) $5f^{11}$	$7s^2$		s		$^4I_{15/2}$	6.42
100	Fm	Fermium	(Rn) $5f^{12}$	$7s^2$				$^3H_6$	6.50
101	Md	Mendelevium	(Rn) $5f^{13}$	$7s^2$				$^2F_{7/2}$	6.58
102	No	Nobelium	(Rn) $5f^{14}$	$7s^2$				$^1S_0$	6.65
103	Lr	Lawrencium	(Rn) $5f^{14}$	$7s^2$ $7p$?				$^2P_{1/2}$?	
104	Rf	Rutherfordium	(Rn) $5f^{14}6d^2$	$7s^2$?				$^3F_2$?	6.0?

6. ATOMIC AND NUCLEAR PROPERTIES OF MATERIALS

Table 6.1. Revised May 2002 by D.E. Groom (LBNL). Gases are evaluated at 20°C and 1 atm (in parentheses) or at STP [square brackets]. Densities and refractive indices without parentheses or brackets are for solids or liquids, or are for cryogenic liquids at the indicated boiling point (BP) at 1 atm. Refractive indices are evaluated at the sodium D line. Data for compounds and mixtures are from Refs. 1 and 2. Futher materials and properties are given in Ref. 3 and at `http://pdg.lbl.gov/AtomicNuclearProperties`.

Material	Z	A	$\langle Z/A\rangle$	Nuclear [a] collision length λ_T {g/cm^2}	Nuclear [a] interaction length λ_I {g/cm^2}	$dE/dx\|_{\rm min}$ [b] $\left\{\frac{\rm MeV}{\rm g/cm^2}\right\}$	Radiation length [c] X_0 {g/cm^2}	{cm}	Density {g/cm^3} ({g/ℓ} for gas)	Liquid boiling point at 1 atm(K)	Refractive index n ($(n-1)\times10^6$ for gas)
H_2 gas	1	1.00794	0.99212	43.3	50.8	(4.103)	61.28 [d]	(731000)	(0.0838)[0.0899]		[139.2]
H_2 liquid	1	1.00794	0.99212	43.3	50.8	4.034	61.28 [d]	866	0.0708	20.39	1.112
D_2	1	2.0140	0.49652	45.7	54.7	(2.052)	122.4	724	0.169[0.179]	23.65	1.128 [138]
He	2	4.002602	0.49968	49.9	65.1	(1.937)	94.32	756	0.1249[0.1786]	4.224	1.024 [34.9]
Li	3	6.941	0.43221	54.6	73.4	1.639	82.76	155	0.534		—
Be	4	9.012182	0.44384	55.8	75.2	1.594	65.19	35.28	1.848		—
C	6	12.011	0.49954	60.2	86.3	1.745	42.70	18.8	2.265 [e]		—
N_2	7	14.00674	0.49976	61.4	87.8	(1.825)	37.99	47.1	0.8073[1.250]	77.36	1.205 [298]
O_2	8	15.9994	0.50002	63.2	91.0	(1.801)	34.24	30.0	1.141[1.428]	90.18	1.22 [296]
F_2	9	18.9984032	0.47372	65.5	95.3	(1.675)	32.93	21.85	1.507[1.696]	85.24	[195]
Ne	10	20.1797	0.49555	66.1	96.6	(1.724)	28.94	24.0	1.204[0.9005]	27.09	1.092 [67.1]
Al	13	26.981539	0.48181	70.6	106.4	1.615	24.01	8.9	2.70		—
Si	14	28.0855	0.49848	70.6	106.0	1.664	21.82	9.36	2.33		3.95
Ar	18	39.948	0.45059	76.4	117.2	(1.519)	19.55	14.0	1.396[1.782]	87.28	1.233 [283]
Ti	22	47.867	0.45948	79.9	124.9	1.476	16.17	3.56	4.54		—
Fe	26	55.845	0.46556	82.8	131.9	1.451	13.84	1.76	7.87		—
Cu	29	63.546	0.45636	85.6	134.9	1.403	12.86	1.43	8.96		—
Ge	32	72.61	0.44071	88.3	140.5	1.371	12.25	2.30	5.323		—
Sn	50	118.710	0.42120	100.2	163	1.264	8.82	1.21	7.31		—
Xe	54	131.29	0.41130	102.8	169	(1.255)	8.48	2.87	2.953[5.858]	165.1	[701]
W	74	183.84	0.40250	110.3	185	1.145	6.76	0.35	19.3		—
Pt	78	195.08	0.39984	113.3	189.7	1.129	6.54	0.305	21.45		—
Pb	82	207.2	0.39575	116.2	194	1.123	6.37	0.56	11.35		—
U	92	238.0289	0.38651	117.0	199	1.082	6.00	≈0.32	≈18.95		—
Air, (20°C, 1 atm.), [STP]			0.49919	62.0	90.0	(1.815)	36.66	[30420]	(1.205)[1.2931]	78.8	(273) [293]
H_2O			0.55509	60.1	83.6	1.991	36.08	36.1	1.00	373.15	1.33
CO_2 gas			0.49989	62.4	89.7	(1.819)	36.2	[18310]	[1.977]		[410]
CO_2 solid (dry ice)			0.49989	62.4	89.7	1.787	36.2	23.2	1.563	sublimes	—
Shielding concrete [f]			0.50274	67.4	99.9	1.711	26.7	10.7	2.5		—
SiO_2 (fused quartz)			0.49926	66.5	97.4	1.699	27.05	12.3	2.20 [g]		1.458
Dimethyl ether, $(CH_3)_2O$			0.54778	59.4	82.9	—	38.89	—	—	248.7	—
Methane, CH_4			0.62333	54.8	73.4	(2.417)	46.22	[64850]	0.4224[0.717]	111.7	[444]
Ethane, C_2H_6			0.59861	55.8	75.7	(2.304)	45.47	[34035]	0.509(1.356) [h]	184.5	(1.038) [h]
Propane, C_3H_8			0.58962	56.2	76.5	(2.262)	45.20	—	(1.879)	231.1	—
Isobutane, $(CH_3)_2CHCH_3$			0.58496	56.4	77.0	(2.239)	45.07	[16930]	[2.67]	261.42	[1900]
Octane, liquid, $CH_3(CH_2)_6CH_3$			0.57778	56.7	77.7	2.123	44.86	63.8	0.703	398.8	1.397
Paraffin wax, $CH_3(CH_2)_{n\approx23}CH_3$			0.57275	56.9	78.2	2.087	44.71	48.1	0.93		—
Nylon, type 6 [i]			0.54790	58.5	81.5	1.974	41.84	36.7	1.14		—
Polycarbonate (Lexan) [j]			0.52697	59.5	83.9	1.886	41.46	34.6	1.20		—
Polyethylene terephthlate (Mylar) [k]			0.52037	60.2	85.7	1.848	39.95	28.7	1.39		—
Polyethylene [l]			0.57034	57.0	78.4	2.076	44.64	≈47.9	0.92–0.95		—
Polyimide film (Kapton) [m]			0.51264	60.3	85.8	1.820	40.56	28.6	1.42		—
Lucite, Plexiglas [n]			0.53937	59.3	83.0	1.929	40.49	≈34.4	1.16–1.20		≈1.49
Polystyrene, scintillator [o]			0.53768	58.5	81.9	1.936	43.72	42.4	1.032		1.581
Polytetrafluoroethylene (Teflon) [p]			0.47992	64.2	93.0	1.671	34.84	15.8	2.20		—
Polyvinyltolulene, scintillator [q]			0.54155	58.3	81.5	1.956	43.83	42.5	1.032		—
Aluminum oxide (Al_2O_3)			0.49038	67.0	98.9	1.647	27.94	7.04	3.97		1.761
Barium fluoride (BaF_2)			0.42207	92.0	145	1.303	9.91	2.05	4.89		1.56
Bismuth germanate (BGO) [r]			0.42065	98.2	157	1.251	7.97	1.12	7.1		2.15
Cesium iodide (CsI)			0.41569	102	167	1.243	8.39	1.85	4.53		1.80
Lithium fluoride (LiF)			0.46262	62.2	88.2	1.614	39.25	14.91	2.632		1.392
Sodium fluoride (NaF)			0.47632	66.9	98.3	1.69	29.87	11.68	2.558		1.336
Sodium iodide (NaI)			0.42697	94.6	151	1.305	9.49	2.59	3.67		1.775
Silica Aerogel [s]			0.50093	66.3	96.9	1.740	27.25	136@ρ=0.2	0.04–0.6		1.0+0.21ρ
NEMA G10 plate [t]				62.6	90.2	1.87	33.0	19.4	1.7		—

Material	Dielectric constant ($\kappa = \epsilon/\epsilon_0$) () is $(\kappa-1)\times10^6$ for gas	Young's modulus [10^6 psi]	Coeff. of thermal expansion [10^{-6}cm/cm-°C]	Specific heat [cal/g-°C]	Electrical resistivity [$\mu\Omega$cm(@°C)]	Thermal conductivity [cal/cm-°C-sec]
H_2	(253.9)	—	—	—	—	—
He	(64)	—	—	—	—	—
Li	—	—	56	0.86	8.55(0°)	0.17
Be	—	37	12.4	0.436	5.885(0°)	0.38
C	—	0.7	0.6–4.3	0.165	1375(0°)	0.057
N_2	(548.5)	—	—	—	—	—
O_2	(495)	—	—	—	—	—
Ne	(127)	—	—	—	—	—
Al	—	10	23.9	0.215	2.65(20°)	0.53
Si	11.9	16	2.8–7.3	0.162	—	0.20
Ar	(517)	—	—	—	—	—
Ti	—	16.8	8.5	0.126	50(0°)	—
Fe	—	28.5	11.7	0.11	9.71(20°)	0.18
Cu	—	16	16.5	0.092	1.67(20°)	0.94
Ge	16.0	—	5.75	0.073	—	0.14
Sn	—	6	20	0.052	11.5(20°)	0.16
Xe	—	—	—	—	—	—
W	—	50	4.4	0.032	5.5(20°)	0.48
Pt	—	21	8.9	0.032	9.83(0°)	0.17
Pb	—	2.6	29.3	0.038	20.65(20°)	0.083
U	—	—	36.1	0.028	29(20°)	0.064

1. R.M. Sternheimer, M.J. Berger, and S.M. Seltzer, Atomic Data and Nuclear Data Tables **30**, 261–271 (1984).
2. S.M. Seltzer and M.J. Berger, Int. J. Appl. Radiat. **33**, 1189–1218 (1982).
3. D.E. Groom, N.V. Mokhov, and S.I. Striganov, "Muon stopping-power and range tables," Atomic Data and Nuclear Data Tables **78**, 183–356 (2001).
4. S.M. Seltzer and M.J. Berger, Int. J. Appl. Radiat. **35**, 665 (1984) & `http://physics.nist.gov/PhysRefData/Star/Text/contents.html`.

a. σ_T, λ_T and λ_I are energy dependent. Values quoted apply to high energy range, where energy dependence is weak. Mean free path between collisions (λ_T) or inelastic interactions (λ_I), calculated from $\lambda^{-1} = N_A \sum w_j \sigma_j / A_j$, where N is Avogadro's number and w_j is the weight fraction of the jth element in the element, compound, or mixture. $\sigma_{\rm total}$ at 80–240 GeV for neutrons ($\approx \sigma$ for protons) from Murthy *et al.*, Nucl. Phys. **B92**, 269 (1975). This scales approximately as $A^{0.77}$. $\sigma_{\rm inelastic} = \sigma_{\rm total} - \sigma_{\rm elastic} - \sigma_{\rm quasielastic}$; for neutrons at 60–375 GeV from Roberts *et al.*, Nucl. Phys. **B159**, 56 (1979). For protons and other particles, see Carroll *et al.*, Phys. Lett. **80B**, 319 (1979); note that $\sigma_I(p) \approx \sigma_I(n)$. σ_I scales approximately as $A^{0.71}$.

b. For minimum-ionizing muons (results are very slightly different for other particles). Minimum dE/dx from Ref. 3, using density effect correction coefficients from Ref. 1. For electrons and positrons see Ref. 4. Ionization energy loss is discussed in Sec. 27.

c. From Y.S. Tsai, Rev. Mod. Phys. **46**, 815 (1974); X_0 data for all elements up to uranium are given. Corrections for molecular binding applied for H_2 and D_2. For atomic H, $X_0 = 63.05$ g/cm^2.

d. For molecular hydrogen (deuterium). For atomic H, $X_0 = 63.047$ g cm^{-2}.

e. For pure graphite; industrial graphite density may vary 2.1–2.3 g/cm^3.

f. Standard shielding blocks, typical composition O_2 52%, Si 32.5%, Ca 6%, Na 1.5%, Fe 2%, Al 4%, plus reinforcing iron bars. The attenuation length, $\ell = 115 \pm 5$ g/cm^2, is also valid for earth (typical $\rho = 2.15$), from CERN–LRL–RHEL Shielding exp., UCRL–17841 (1968).

g. For typical fused quartz. The specific gravity of crystalline quartz is 2.64.

h. Solid ethane density at −60°C; gaseous refractive index at 0°C, 546 mm pressure.

i. Nylon, Type 6, $(NH(CH_2)_5CO)_n$

j. Polycarbonate (Lexan), $(C_{16}H_{14}O_3)_n$

k. Polyethylene terephthlate, monomer $C_5H_4O_2$

l. Polyethylene, monomer $CH_2 = CH_2$

m. Polymide film (Kapton), $(C_{22}H_{10}N_2O_5)_n$

n. Polymethylmethacralate, monomer $CH_2 = C(CH_3)CO_2CH_3$

o. Polystyrene, monomer $C_6H_5CH = CH_2$

p. Teflon, monomer $CF_2 = CF_2$

q. Polyvinyltolulene, monomer 2-$CH_3C_6H_4CH = CH_2$

r. Bismuth germanate (BGO), $(Bi_2O_3)_2(GeO_2)_3$

s. 97% SiO_2 + 3% H_2O by weight; see A. R. Buzykaev *et al.*, Nucl. Instrum. Methods **A433**, 396 (1999). Aerogel in the density range 0.04–0.06 g/cm^3 has been used in Čerenkov counters, but aerogel with higher and lower densities has been produced. ρ = density in g/cm^3.

t. G10-plate, typically 60% SiO_2 and 40% epoxy.

7. ELECTROMAGNETIC RELATIONS

Quantity	Gaussian CGS	SI
Conversion factors: Charge: Potential: Magnetic field:	 $2.997\ 924\ 58 \times 10^9$ esu $(1/299.792\ 458)$ statvolt (ergs/esu) 10^4 gauss $= 10^4$ dyne/esu	 $= 1$ C $= 1$ A s $= 1$ V $= 1$ J C^{-1} $= 1$ T $= 1$ N A^{-1}m^{-1}
Lorentz force:	$\mathbf{F} = q\left(\mathbf{E} + \frac{\mathbf{v}}{c} \times \mathbf{B}\right)$	$\mathbf{F} = q(\mathbf{E} + \mathbf{v} \times \mathbf{B})$
Maxwell equations:	$\boldsymbol{\nabla} \cdot \mathbf{D} = 4\pi\rho$ $\boldsymbol{\nabla} \times \mathbf{H} - \frac{1}{c}\frac{\partial \mathbf{D}}{\partial t} = \frac{4\pi}{c}\mathbf{J}$ $\boldsymbol{\nabla} \cdot \mathbf{B} = 0$ $\boldsymbol{\nabla} \times \mathbf{E} + \frac{1}{c}\frac{\partial \mathbf{B}}{\partial t} = 0$	$\boldsymbol{\nabla} \cdot \mathbf{D} = \rho$ $\boldsymbol{\nabla} \times \mathbf{H} - \frac{\partial \mathbf{D}}{\partial t} = \mathbf{J}$ $\boldsymbol{\nabla} \cdot \mathbf{B} = 0$ $\boldsymbol{\nabla} \times \mathbf{E} + \frac{\partial \mathbf{B}}{\partial t} = 0$
Constitutive relations:	$\mathbf{D} = \mathbf{E} + 4\pi\mathbf{P}, \quad \mathbf{H} = \mathbf{B} - 4\pi\mathbf{M}$	$\mathbf{D} = \epsilon_0\mathbf{E} + \mathbf{P}, \quad \mathbf{H} = \mathbf{B}/\mu_0 - \mathbf{M}$
Linear media: Permitivity of free space: Permeability of free space:	$\mathbf{D} = \epsilon\mathbf{E}, \quad \mathbf{H} = \mathbf{B}/\mu$ 1 1	$\mathbf{D} = \epsilon\mathbf{E}, \quad \mathbf{H} = \mathbf{B}/\mu$ $\epsilon_0 = 8.854\ 187 \ldots \times 10^{-12}$ F m^{-1} $\mu_0 = 4\pi \times 10^{-7}$ N A^{-2}
Fields from potentials:	$\mathbf{E} = -\boldsymbol{\nabla} V - \frac{1}{c}\frac{\partial \mathbf{A}}{\partial t}$ $\mathbf{B} = \boldsymbol{\nabla} \times \mathbf{A}$	$\mathbf{E} = -\boldsymbol{\nabla} V - \frac{\partial \mathbf{A}}{\partial t}$ $\mathbf{B} = \boldsymbol{\nabla} \times \mathbf{A}$
Static potentials: (coulomb gauge)	$V = \sum_{\text{charges}} \frac{q_i}{r_i} = \int \frac{\rho(\mathbf{r}')}{\lvert\mathbf{r} - \mathbf{r}'\rvert}\, d^3x'$ $\mathbf{A} = \frac{1}{c}\oint \frac{I\, d\boldsymbol{\ell}}{\lvert\mathbf{r} - \mathbf{r}'\rvert} = \frac{1}{c}\int \frac{\mathbf{J}(\mathbf{r}')}{\lvert\mathbf{r} - \mathbf{r}'\rvert}\, d^3x'$	$V = \frac{1}{4\pi\epsilon_0}\sum_{\text{charges}} \frac{q_i}{r_i} = \frac{1}{4\pi\epsilon_0}\int \frac{\rho(\mathbf{r}')}{\lvert\mathbf{r} - \mathbf{r}'\rvert}\, d^3x'$ $\mathbf{A} = \frac{\mu_0}{4\pi}\oint \frac{I\, d\boldsymbol{\ell}}{\lvert\mathbf{r} - \mathbf{r}'\rvert} = \frac{\mu_0}{4\pi}\int \frac{\mathbf{J}(\mathbf{r}')}{\lvert\mathbf{r} - \mathbf{r}'\rvert}\, d^3x'$
Relativistic transformations: ($\mathbf{v}$ is the velocity of the primed frame as seen in the unprimed frame)	$\mathbf{E}'_\parallel = \mathbf{E}_\parallel$ $\mathbf{E}'_\perp = \gamma(\mathbf{E}_\perp + \frac{1}{c}\mathbf{v} \times \mathbf{B})$ $\mathbf{B}'_\parallel = \mathbf{B}_\parallel$ $\mathbf{B}'_\perp = \gamma(\mathbf{B}_\perp - \frac{1}{c}\mathbf{v} \times \mathbf{E})$	$\mathbf{E}'_\parallel = \mathbf{E}_\parallel$ $\mathbf{E}'_\perp = \gamma(\mathbf{E}_\perp + \mathbf{v} \times \mathbf{B})$ $\mathbf{B}'_\parallel = \mathbf{B}_\parallel$ $\mathbf{B}'_\perp = \gamma(\mathbf{B}_\perp - \frac{1}{c^2}\mathbf{v} \times \mathbf{E})$
$\frac{1}{4\pi\epsilon_0} = c^2 \times 10^{-7}$ N A^{-2} $= 8.987\ 55 \ldots \times 10^9$ m F^{-1} ; $\quad \frac{\mu_0}{4\pi} = 10^{-7}$ N A^{-2} ; $\quad c = \frac{1}{\sqrt{\mu_0\epsilon_0}} = 2.997\ 924\ 58 \times 10^8$ m s^{-1}		

7.1. Impedances (SI units)

ρ = resistivity at room temperature in $10^{-8}\ \Omega$ m:
~ 1.7 for Cu ~ 5.5 for W
~ 2.4 for Au ~ 73 for SS 304
~ 2.8 for Al ~ 100 for Nichrome
(Al alloys may have double the Al value.)

For alternating currents, instantaneous current I, voltage V, angular frequency ω:

$$V = V_0\, e^{j\omega t} = ZI\ . \tag{7.1}$$

Impedance of self-inductance L: $Z = j\omega L$.

Impedance of capacitance C: $Z = 1/j\omega C$.

Impedance of free space: $Z = \sqrt{\mu_0/\epsilon_0} = 376.7\ \Omega$.

High-frequency surface impedance of a good conductor:

$$Z = \frac{(1+j)\,\rho}{\delta}\ , \quad \text{where } \delta = \text{skin depth}\ ; \tag{7.2}$$

$$\delta = \sqrt{\frac{\rho}{\pi\nu\mu}} \approx \frac{6.6\text{ cm}}{\sqrt{\nu\,(\text{Hz})}} \quad \text{for Cu}\ . \tag{7.3}$$

7.2. Capacitance $\widehat{C}$ and inductance $\widehat{L}$ per unit length (SI units) [negligible skin depth]

Flat rectangular plates of width w, separated by $d \ll w$ with linear medium (ϵ, μ) between:

$$\widehat{C} = \epsilon\,\frac{w}{d}\ ; \qquad \widehat{L} = \mu\,\frac{d}{w}\ ; \tag{7.4}$$

$$\epsilon/\epsilon_0 = 2 \text{ to } 6 \text{ for plastics; } 4 \text{ to } 8 \text{ for porcelain, glasses;} \tag{7.5}$$

$$\mu/\mu_0 \simeq 1\ . \tag{7.6}$$

Coaxial cable of inner radius r_1, outer radius r_2:

$$\widehat{C} = \frac{2\pi\,\epsilon}{\ln\,(r_2/r_1)}\ ; \qquad \widehat{L} = \frac{\mu}{2\pi}\,\ln\,(r_2/r_1)\ . \tag{7.7}$$

Transmission lines (no loss):

$$\text{Impedance: } Z = \sqrt{\widehat{L}/\widehat{C}}\ . \tag{7.8}$$

$$\text{Velocity: } v = 1/\sqrt{\widehat{L}\,\widehat{C}} = 1/\sqrt{\mu\,\epsilon}\ . \tag{7.9}$$

7.3. Synchrotron radiation (CGS units)

For a particle of charge e, velocity $v = \beta c$, and energy $E = \gamma mc^2$, traveling in a circular orbit of radius R, the classical energy loss per revolution δE is

$$\delta E = \frac{4\pi}{3}\,\frac{e^2}{R}\,\beta^3\,\gamma^4\ . \tag{7.10}$$

For high-energy electrons or positrons ($\beta \approx 1$), this becomes

$$\delta E\ (\text{in MeV}) \approx 0.0885\ [E(\text{in GeV})]^4/R(\text{in m})\ . \tag{7.11}$$

For $\gamma \gg 1$, the energy radiated per revolution into the photon energy interval $d(\hbar\omega)$ is

$$dI = \frac{8\pi}{9}\alpha\,\gamma\,F(\omega/\omega_c)\,d(\hbar\omega)\ , \tag{7.12}$$

where $\alpha = e^2/\hbar c$ is the fine-structure constant and

$$\omega_c = \frac{3\gamma^3 c}{2R} \tag{7.13}$$

is the critical frequency. The normalized function $F(y)$ is

$$F(y) = \frac{9}{8\pi}\sqrt{3}\,y\,\int_y^\infty K_{5/3}(x)\ dx\ , \tag{7.14}$$

where $K_{5/3}(x)$ is a modified Bessel function of the third kind. For electrons or positrons,

$$\hbar\omega_c\,(\text{in keV}) \approx 2.22\ [E(\text{in GeV})]^3/R(\text{in m})\ . \tag{7.15}$$

Fig. 7.1 shows $F(y)$ over the important range of y.

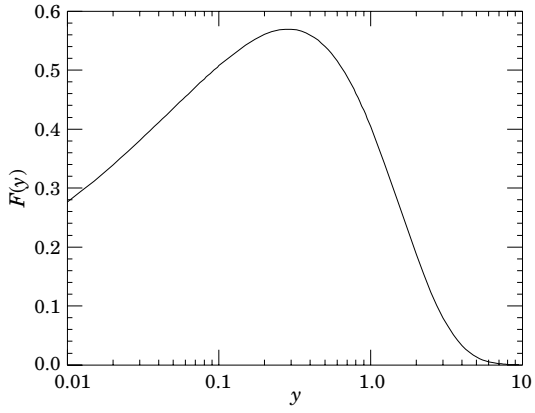

Figure 7.1: The normalized synchrotron radiation spectrum $F(y)$.

For $\gamma \gg 1$ and $\omega \ll \omega_c$,

$$\frac{dI}{d(\hbar\omega)} \approx 3.3\alpha\,(\omega R/c)^{1/3}\ , \tag{7.16}$$

whereas for

$$\gamma \gg 1 \text{ and } \omega \gtrsim 3\omega_c\ ,$$

$$\frac{dI}{d(\hbar\omega)} \approx \sqrt{\frac{3\pi}{2}}\,\alpha\,\gamma\,\left(\frac{\omega}{\omega_c}\right)^{1/2} e^{-\omega/\omega_c}\left[1 + \frac{55}{72}\frac{\omega_c}{\omega} + \ldots\right]\ . \tag{7.17}$$

The radiation is confined to angles $\lesssim 1/\gamma$ relative to the instantaneous direction of motion. For $\gamma \gg 1$, where Eq. (7.12) applies, the mean number of photons emitted per revolution is

$$N_\gamma = \frac{5\pi}{\sqrt{3}}\alpha\gamma\ , \tag{7.18}$$

and the mean energy per photon is

$$\langle\hbar\omega\rangle = \frac{8}{15\sqrt{3}}\hbar\omega_c\ . \tag{7.19}$$

When $\langle\hbar\omega\rangle \gtrsim \mathrm{O}(E)$, quantum corrections are important.

See J.D. Jackson, *Classical Electrodynamics*, 3rd edition (John Wiley & Sons, New York, 1998) for more formulae and details. (Note that ealier editions had ω_c twice as large as Eq. (7.13).

8. NAMING SCHEME FOR HADRONS

Revised 2004 by M. Roos (University of Finland) and C.G. Wohl (LBNL).

8.1. Introduction

We introduced in the 1986 edition [1] a new naming scheme for the hadrons. Changes from older terminology affected mainly the heavier mesons made of the light (u, d, and s) quarks. Old and new names were listed alongside until 1994. Names also change from edition to edition because some characteristic like mass or spin changes. The Summary Tables give both the new and old names whenever a change occurred.

8.2. "Neutral-flavor" mesons ($S = C = B = T = 0$)

Table 8.1 shows the names for mesons having the strangeness and all heavy-flavor quantum numbers equal to zero. The scheme is designed for all ordinary non-exotic mesons, but it will work for many exotic types too, if needed.

Table 8.1: Symbols for mesons with the strangeness and all heavy-flavor quantum numbers equal to zero.

	$J^{PC} =$	$\left\{\begin{array}{c} 0^{-+} \\ 2^{-+} \\ \vdots \end{array}\right.$	$\begin{array}{c} 1^{+-} \\ 3^{+-} \\ \vdots \end{array}$	$\begin{array}{c} 1^{--} \\ 2^{--} \\ \vdots \end{array}$	$\left.\begin{array}{c} 0^{++} \\ 1^{++} \\ \vdots \end{array}\right.$
$q\overline{q}$ content	$^{2S+1}L_J =$	$^1(L\,\text{even})_J$	$^1(L\,\text{odd})_J$	$^3(L\,\text{even})_J$	$^3(L\,\text{odd})_J$
$u\overline{d}, u\overline{u} - d\overline{d}, d\overline{u}$	$(I = 1)$	π	b	ρ	a
$d\overline{d} + u\overline{u}$ and/or $s\overline{s}$	$(I = 0)$	η, η'	h, h'	ω, ϕ	f, f'
$c\overline{c}$		η_c	h_c	$\psi^\dagger$	χ_c
$b\overline{b}$		η_b	h_b	Υ	χ_b
$t\overline{t}$		η_t	h_t	θ	χ_t

†The J/ψ remains the J/ψ.

First, we assign names to those states with quantum numbers compatible with being $q\overline{q}$ states. The rows of the Table give the possible $q\overline{q}$ content. The columns give the possible parity/charge-conjugation states,

$$PC = -+,\ +-,\ --, \text{ and } ++\ ;$$

these combinations correspond one-to-one with the angular-momentum state $^{2S+1}L_J$ of the $q\overline{q}$ system being

$$^1(L \text{ even})_J,\ ^1(L \text{ odd})_J,\ ^3(L \text{ even})_J, \text{ or } ^3(L \text{ odd})_J\ .$$

Here S, L, and J are the spin, orbital, and total angular momenta of the $q\overline{q}$ system. The quantum numbers are related by

$$P = (-1)^{L+1},\ C = (-1)^{L+S}, \text{ and } G \text{ parity } = (-1)^{L+S+I},$$

where of course the C quantum number is only relevant to neutral mesons.

The entries in the Table give the meson names. The spin J is added as a subscript except for pseudoscalar and vector mesons, and the mass is added in parentheses for mesons that decay strongly. However, for the lightest meson resonances, we omit the mass.

Measurements of the mass, quark content (where relevant), and quantum numbers I, J, P, and C (or G) of a meson thus fix its symbol. Conversely, these properties may be inferred unambiguously from the symbol.

If the main symbol cannot be assigned because the quantum numbers are unknown, X is used. Sometimes it is not known whether a meson is mainly the isospin-0 mix of $u\overline{u}$ and $d\overline{d}$ or is mainly $s\overline{s}$. A prime (or pair ω, ϕ) may be used to distinguish two such mixing states.

We follow custom and use spectroscopic names such as $\Upsilon(1S)$ as the primary name for most of those ψ, Υ, and χ states whose spectroscopic identity is known. We use the form $\Upsilon(9460)$ as an alternative, and as the primary name when the spectroscopic identity is not known.

Names are assigned for $t\overline{t}$ mesons, although the top quark is evidently so heavy that it is expected to decay too rapidly for bound states to form.

Gluonium states or other mesons that are not $q\overline{q}$ states are, if the quantum numbers are *not* exotic, to be named just as are the $q\overline{q}$ mesons. Such states will probably be difficult to distinguish from $q\overline{q}$ states and will likely mix with them, and we make no attempt to distinguish those "mostly gluonium" from those "mostly $q\overline{q}$."

An "exotic" meson with J^{PC} quantum numbers that a $q\overline{q}$ system cannot have, namely $J^{PC} = 0^{--}, 0^{+-}, 1^{-+}, 2^{+-}, 3^{-+}, \cdots$, would use the same symbol as does an ordinary meson with all the same quantum numbers as the exotic meson except for the C parity. But then the J subscript may still distinguish it; for example, an isospin-0 1^{-+} meson could be denoted ω_1.

8.3. Mesons with nonzero S, C, B, and/or T

Since the strangeness or a heavy flavor of these mesons is nonzero, none of them are eigenstates of charge conjugation, and in each of them one of the quarks is heavier than the other. The rules are:

1. The main symbol is an upper-case italic letter indicating the heavier quark as follows:
$$s \to \overline{K} \qquad c \to D \qquad b \to \overline{B} \qquad t \to T\ .$$
We use the convention that *the flavor and the charge of a quark have the same sign.* Thus the strangeness of the s quark is negative, the charm of the c quark is positive, and the bottom of the b quark is negative. In addition, I_3 of the u and d quarks are positive and negative, respectively. The effect of this convention is as follows: *Any flavor carried by a charged meson has the same sign as its charge.* Thus the K^+, D^+, and B^+ have positive strangeness, charm, and bottom, respectively, and all have positive I_3. The D_s^+ has positive charm *and* strangeness. Furthermore, the $\Delta(\text{flavor}) = \Delta Q$ rule, best known for the kaons, applies to every flavor.
2. If the lighter quark is not a u or a d quark, its identity is given by a subscript. The D_s^+ is an example.
3. If the spin-parity is in the "normal" series, $J^P = 0^+, 1^-, 2^+, \cdots$, a superscript "*" is added.
4. The spin is added as a subscript except for pseudoscalar or vector mesons.

8.4. Ordinary (3-quark) baryons

The symbols N, Δ, Λ, Σ, Ξ, and Ω used for more than 30 years for the baryons made of light quarks (u, d, and s quarks) tell the isospin and quark content, and the same information is conveyed by the symbols used for the baryons containing one or more heavy quarks (c and b quarks). The rules are:

1. Baryons with *three* u and/or d quarks are N's (isospin 1/2) or Δ's (isospin 3/2).
2. Baryons with *two* u and/or d quarks are Λ's (isospin 0) or Σ's (isospin 1). If the third quark is a c, b, or t quark, its identity is given by a subscript.
3. Baryons with *one* u or d quark are Ξ's (isospin 1/2). One or two subscripts are used if one or both of the remaining quarks are heavy: thus Ξ_c, Ξ_{cc}, Ξ_b, *etc.**
4. Baryons with *no* u or d quarks are Ω's (isospin 0), and subscripts indicate any heavy-quark content.
5. A baryon that decays strongly has its mass as part of its name. Thus p, Σ^-, Ω^-, Λ_c^+, *etc.*, but $\Delta(1232)^0$, $\Sigma(1385)^-$, $\Xi_c(2645)^+$, *etc.*

In short, the number of u plus d quarks together with the isospin determine the main symbol, and subscripts indicate any content of heavy quarks. A Σ always has isospin 1, an Ω always has isospin 0, *etc.*

8.5. Exotic baryons

In 2003, several experiments reported finding a strangeness $S = +1$, charge $Q = +1$ baryon, and one experiment reported finding an $S = -2$, $Q = -2$ baryon; see the "Exotic Baryons" section of the Data Listings. Baryons with such quantum numbers cannot be made from three quarks, and thus they are exotic. The $S = +1$ baryon, which once would have been called a Z, was quickly dubbed the $\Theta(1540)^+$, and we propose to name the $S = -2$ baryon the $\Phi(1860)$.

Footnote and Reference:

* Sometimes a prime is necessary to distinguish two Ξ_c's in the same SU(n) multiplet. See the "Note on Charmed Baryons" in the Charmed Baryon Listings.

1. Particle Data Group: M. Aguilar-Benitez *et al.,* Phys. Lett. **170B** (1986).

9. QUANTUM CHROMODYNAMICS

9.1. The QCD Lagrangian

Revised September 2003 by I. Hinchliffe (LBNL).

Quantum Chromodynamics (QCD), the gauge field theory which describes the strong interactions of colored quarks and gluons, is one of the components of the SU(3)×SU(2)×U(1) Standard Model. A quark of specific flavor (such as a charm quark) comes in 3 colors; gluons come in eight colors; hadrons are color-singlet combinations of quarks, anti-quarks, and gluons. The Lagrangian describing the interactions of quarks and gluons is (up to gauge-fixing terms)

$$L_{\rm QCD} = -\frac{1}{4}F^{(a)}_{\mu\nu}\ F^{(a)\mu\nu} + i\sum_q \overline{\psi}^i_q\ \gamma^\mu\ (D_\mu)_{ij}\ \psi^j_q - \sum_q m_q\ \overline{\psi}^i_q\ \psi_{qi}\ , \tag{9.1}$$

$$F^{(a)}_{\mu\nu} = \partial_\mu\ A^a_\nu - \partial_\nu\ A^a_\mu - g_s\ f_{abc}\ A^b_\mu\ A^c_\nu\ , \tag{9.2}$$

$$(D_\mu)_{ij} = \delta_{ij}\ \partial_\mu + ig_s\ \sum_a \frac{\lambda^a_{i,j}}{2} A^a_\mu\ , \tag{9.3}$$

where g_s is the QCD coupling constant, and the f_{abc} are the structure constants of the SU(3) algebra (the λ matrices and values for f_{abc} can be found in "SU(3) Isoscalar Factors and Representation Matrices," Sec. 36 of this *Review*). The $\psi^i_q(x)$ are the 4-component Dirac spinors associated with each quark field of (3) color i and flavor q, and the $A^a_\mu(x)$ are the (8) Yang-Mills (gluon) fields. A complete list of the Feynman rules which derive from this Lagrangian, together with some useful color-algebra identities, can be found in Ref. 1.

The principle of "asymptotic freedom" determines that the renormalized QCD coupling is small only at high energies, and it is only in this domain that high-precision tests—similar to those in QED—can be performed using perturbation theory. Nonetheless, there has been in recent years much progress in understanding and quantifying the predictions of QCD in the nonperturbative domain, for example, in soft hadronic processes and on the lattice [2]. This short review will concentrate on QCD at short distances (large momentum transfers), where perturbation theory is the standard tool. It will discuss the processes that are used to determine the coupling constant of QCD. Other recent reviews of the coupling constant measurements may be consulted for a different perspective [3–5].

9.2. The QCD coupling and renormalization scheme

The renormalization scale dependence of the effective QCD coupling $\alpha_s = g_s^2/4\pi$ is controlled by the β-function:

$$\mu\frac{\partial\alpha_s}{\partial\mu} = 2\beta(\alpha_s) = -\frac{\beta_0}{2\pi}\alpha_s^2 - \frac{\beta_1}{4\pi^2}\alpha_s^3 - \frac{\beta_2}{64\pi^3}\alpha_s^4 - \cdots\ , \tag{9.4a}$$

$$\beta_0 = 11 - \frac{2}{3}n_f\ , \tag{9.4b}$$

$$\beta_1 = 51 - \frac{19}{3}n_f\ , \tag{9.4c}$$

$$\beta_2 = 2857 - \frac{5033}{9}n_f + \frac{325}{27}n_f^2\ ; \tag{9.4d}$$

where n_f is the number of quarks with mass less than the energy scale μ. The expression for the next term in this series (β_3) can be found in Ref. 7. In solving this differential equation for α_s, a constant of integration is introduced. This constant is the one fundamental constant of QCD that must be determined from experiment. The most sensible choice for this constant is the value of α_s at a fixed-reference scale μ_0. It has become standard to choose $\mu_0 = M_Z$. The value at other values of μ can be obtained from $\log(\mu^2/\mu_0^2) = \int_{\alpha_s(\mu_0)}^{\alpha_s(\mu)} \frac{d\alpha}{\beta(\alpha)}$. It is also convenient to introduce the dimensional parameter Λ, since this provides a parameterization of the μ dependence of α_s. The definition of Λ is arbitrary. One way to define it (adopted here) is to write a solution of Eq. (9.4) as an expansion in inverse powers of $\ln(\mu^2)$:

$$\alpha_s(\mu) = \frac{4\pi}{\beta_0\ \ln(\mu^2/\Lambda^2)}\left[1 - \frac{2\beta_1}{\beta_0^2}\ \frac{\ln\left[\ln(\mu^2/\Lambda^2)\right]}{\ln(\mu^2/\Lambda^2)} + \frac{4\beta_1^2}{\beta_0^4\ln^2(\mu^2/\Lambda^2)} \times\left(\left(\ln\left[\ln(\mu^2/\Lambda^2)\right] - \frac{1}{2}\right)^2 + \frac{\beta_2\beta_0}{8\beta_1^2} - \frac{5}{4}\right)\right]\ . \tag{9.5}$$

This solution illustrates the *asymptotic freedom* property: $\alpha_s \to 0$ as $\mu \to \infty$ and shows that QCD becomes strongly coupled at $\mu \sim \Lambda$.

Consider a "typical" QCD cross section which, when calculated perturbatively [6], starts at $\mathcal{O}(\alpha_s)$:

$$\sigma = A_1\ \alpha_s + A_2\ \alpha_s^2 + \cdots\ . \tag{9.6}$$

The coefficients A_1, A_2 come from calculating the appropriate Feynman diagrams. In performing such calculations, various divergences arise, and these must be regulated in a consistent way. This requires a particular renormalization scheme (RS). The most commonly used one is the modified minimal subtraction ($\overline{\rm MS}$) scheme [8]. This involves continuing momentum integrals from 4 to 4–2ϵ dimensions, and then subtracting off the resulting $1/\epsilon$ poles and also ($\ln 4\pi - \gamma_E$), which is an artifact of continuing the dimension. (Here γ_E is the Euler-Mascheroni constant.) To preserve the dimensionless nature of the coupling, a mass scale μ must also be introduced: $g \to \mu^\epsilon g$. The finite coefficients A_i ($i \geq 2$) thus obtained depend implicitly on the renormalization convention used and explicitly on the scale μ.

The first two coefficients (β_0, β_1) in Eq. (9.4) are independent of the choice of RS's. In contrast, the coefficients of terms proportional to α_s^n for $n > 3$ *are* RS-dependent. The form given above for β_2 is in the $\overline{\rm MS}$ scheme.

The fundamental theorem of RS dependence is straightforward. Physical quantities, such as the cross section calculated to all orders in perturbation theory, do not depend on the RS. It follows that a truncated series *does* exhibit RS dependence. In practice, QCD cross sections are known to leading order (LO), or to next-to-leading order (NLO), or in some cases, to next-to-next-to-leading order (NNLO); and it is only the latter two cases, which have reduced RS dependence, that are useful for precision tests. At NLO the RS dependence is completely given by one condition which can be taken to be the value of the renormalization scale μ. At NNLO this is not sufficient, and μ is no longer equivalent to a choice of scheme; both must now be specified. One, therefore, has to address the question of what is the "best" choice for μ within a given scheme, usually $\overline{\rm MS}$. There is no definite answer to this question—higher-order corrections do not "fix" the scale, rather they render the theoretical predictions less sensitive to its variation.

One should expect that choosing a scale μ characteristic of the typical energy scale (E) in the process would be most appropriate. In general, a poor choice of scale generates terms of order $\ln(E/\mu)$ in the A_i's. Various methods have been proposed including choosing the scale for which the next-to-leading-order correction vanishes ("Fastest Apparent Convergence [9]"); the scale for which the next-to-leading-order prediction is stationary [10], (*i.e.*, the value of μ where $d\sigma/d\mu = 0$); or the scale dictated by the effective charge scheme [11] or by the BLM scheme [12]. By comparing the values of α_s that different reasonable schemes give, an estimate of theoretical errors can be obtained. It has also been suggested to replace the perturbation series by its Padé approximant [13]. Results obtained using this method have, in certain cases, a reduced scale dependence [14,15]. One can also attempt to determine the scale from data by allowing it to vary and using a fit to determine it. This method can allow a determination of the error due to the scale choice and can give more confidence in the end result [16]. In many of the cases discussed below this scale uncertainty is the dominant error.

An important corollary is that if the higher-order corrections are naturally small, then the additional uncertainties introduced by the μ dependence are likely to be small. There are some processes, however, for which the choice of scheme *can* influence the extracted value of $\alpha_s(M_Z)$. There is no resolution to this problem other than to try to calculate even more terms in the perturbation series. It is important to note that, since the perturbation series is an asymptotic expansion, there is a limit to the precision with which any theoretical quantity can be calculated. In some processes, the highest-order perturbative terms may be comparable in size to nonperturbative corrections (sometimes called higher-twist or renormalon effects, for a discussion see [17]); an estimate of these terms and their uncertainties is required if a value of α_s is to be extracted.

Cases occur where there is more than one large scale, say μ_1 and μ_2. In these cases, terms appear of the form $\log(\mu_1/\mu_2)$. If the ratio μ_1/μ_2 is large, these logarithms can render naive perturbation theory unreliable and a modified perturbation expansion that takes these terms into account must be used. A few examples are discussed below.

In the cases where the higher-order corrections to a process are known and are large, some caution should be exercised when quoting the value of α_s. In what follows, we will attempt to indicate the size of the theoretical uncertainties on the extracted value of α_s. There are two simple ways to determine this error. First, we can estimate it by comparing the value of $\alpha_s(\mu)$ obtained by fitting data using the QCD formula to highest known order in α_s, and then comparing it with the value obtained using the next-to-highest-order formula (μ is chosen as the typical energy scale in the process). The corresponding Λ's are then obtained by evolving $\alpha_s(\mu)$ to $\mu = M_Z$ using Eq. (9.4) to the same order in α_s as the fit. Alternatively, we can vary the value of μ over a reasonable range, extracting a value of Λ for each choice of μ. This method is by its nature imprecise, since "reasonable" involves a subjective judgment. In either case, if the perturbation series is well behaved, the resulting error on $\alpha_s(M_Z)$ will be small.

In the above discussion we have ignored quark-mass effects, *i.e.*, we have assumed an idealized situation where quarks of mass greater than μ are neglected completely. In this picture, the β-function coefficients change by discrete amounts as flavor thresholds (a quark of mass M) are crossed when integrating the differential equation for α_s. Now imagine an experiment at energy scale μ; for example, this could be $e^+e^- \to$ hadrons at center-of-mass energy μ. If $\mu \gg M$, the mass M is negligible and the process is well described by QCD with n_f massless flavors and its parameter $\alpha_{(n_f)}$ up to terms of order M^2/μ^2. Conversely if $\mu \ll M$, the heavy quark plays no role and the process is well described by QCD with $n_f - 1$ massless flavors and its parameter $\alpha_{(n_f-1)}$ up to terms of order μ^2/M^2. If $\mu \sim M$, the effects of the quark mass are process-dependent and cannot be absorbed into the running coupling. The values of $\alpha_{(n_f)}$ and $\alpha_{(n_f-1)}$ are related so that a physical quantity calculated in both "theories" gives the same result [18]. This implies, for $\mu = M$

$$\alpha_{(n_f)}(M) = \alpha_{(n_f-1)}(M) - \frac{11}{72\pi^2}\alpha^3_{(n_f-1)}(M) + \mathcal{O}\left(\alpha^4_{(n_f-1)}\right) \quad (9.7)$$

which is almost identical to the naive result $\alpha_{(n_f)}(M) = \alpha_{(n_f-1)}(M)$. Here M is the mass of the value of the running quark mass defined in the $\overline{\rm MS}$ scheme (see the note on "Quark Masses" in the Particle Listings for more details), *i.e.*, where $M_{\overline{\rm MS}}(M) = M$.

It also follows that, for a relationship such as Eq. (9.5) to remain valid for all values of μ, Λ must also change as flavor thresholds are crossed, the value corresponds to an effective number of massless quarks: $\Lambda \to \Lambda^{(n_f)}$ [18,19]. The formulae are given in the 1998 edition of this review.

Data from deep-inelastic scattering are in a range of energy where the bottom quark is not readily excited, and hence, these experiments quote $\Lambda^{(4)}_{\overline{\rm MS}}$. Most data from PEP, PETRA, TRISTAN, LEP, and SLC quote a value of $\Lambda^{(5)}_{\overline{\rm MS}}$ since these data are in an energy range where the bottom quark is light compared to the available energy. We have converted it to $\Lambda^{(4)}_{\overline{\rm MS}}$ as required. A few measurements, including the lattice gauge theory values from the J/ψ system, and from τ decay are at sufficiently low energy that $\Lambda^{(3)}_{\overline{\rm MS}}$ is appropriate.

In order to compare the values of α_s from various experiments, they must be evolved using the renormalization group to a common scale. For convenience, this is taken to be the mass of the Z boson. This evolution uses third-order perturbation theory and can introduce additional errors particularly if extrapolation from very small scales is used. The variation in the charm and bottom quark masses ($M_b = 4.3 \pm 0.2$ GeV and $M_c = 1.3 \pm 0.3$ GeV are used [20]) can also introduce errors. These result in a fixed value of $\alpha_s(2$ GeV) giving an uncertainty in $\alpha_s(M_Z) = \pm 0.001$ if only perturbative evolution is used. There could be additional errors from nonperturbative effects that enter at low energy.

9.3. QCD in deep-inelastic scattering

The original and still one of the most powerful quantitative tests of perturbative QCD is the breaking of Bjorken scaling in deep-inelastic lepton-hadron scattering. The review 'Structure Functions," (Sec. 16 of this *Review*) describes the basic formalism and reviews the data. α_s is obtained together with the structure functions. The global fit from MRST03 [30] of (Sec. 16) gives $\alpha_s(M_Z) = 0.1165 \pm 0.004$ from NLO and $\alpha_s(M_Z) = 0.1153 \pm 0.004$ from NNLO. Other fits are consistent with these values but cannot be averaged as they use overlapping data sets. The good agreement between the NLO and NNLO fits indicates that the theoretical uncertainties are under control. The NNLO result is used in the average below.

Nonsinglet structure function offers in principle the most precise test of the theory, since the Q^2 evolution is independent of the gluon distribution which is much more poorly constrained. The CCFR collaboration fit to the Gross-Llewellyn Smith sum rule [22] which is known to order α_s^3 [23,24](NNLO); estimates of the order α_s^4 term are available [25].

$$\int_0^1 dx \left(F_3^{\overline{\nu}p}(x,Q^2) + F_3^{\nu p}(x,Q^2)\right) = 3\left[1 - \frac{\alpha_s}{\pi}(1 + 3.58\frac{\alpha_s}{\pi} + 19.0\left(\frac{\alpha_s}{\pi}\right)^2\right) - \Delta HT\Big] \quad , \quad (9.8)$$

where the higher-twist contribution ΔHT is estimated to be $(0.09 \pm 0.045)/Q^2$ in Refs. 23,26 and to be somewhat smaller by Ref. 27. The CCFR collaboration [28], combines their data with that from other experiments [29] and gives α_s ($\sqrt{3}$ GeV) $= 0.28 \pm 0.035$ (expt.) ± 0.05 (sys)$^{+0.035}_{-0.03}$ (theory). The error from higher-twist terms (assumed to be $\Delta HT = 0.05 \pm 0.05$) dominates the theoretical error. If the higher twist result of Ref. 27 is used, the central value increases to 0.31 in agreement with the fit of [30]. This value corresponds to $\alpha_s(M_Z) = 0.118 \pm 0.011$. Fits of the Q^2 evolution [31] of xF_3 using the CCFR data using NNLO and estimates of NNNLO QCD and higher twist terms enables the effect of these terms to be studied.

The spin-dependent structure functions, measured in polarized lepton-nucleon scattering, can also be used to test QCD and to determine α_s. Note that these experiments measure asymmetries and rely on measurements of unpolarized data to extract the spin-dependent structure functions. Here the values of $Q^2 \sim 2.5$ GeV^2 are small, particularly for the E143 data [32], and higher-twist corrections are important. A fit [33] by an experimental group using the measured spin dependent structure functions for several experiments Refs. 32,34 as well as their own data has been made. When data from HERMES [35] and SMC are included [36] $\alpha_s(M_Z) = 0.120 \pm 0.009$ is obtained: this is used in the final average.

α_s can also be determined from the Bjorken spin sum rule [37]; a fit gives [38] $\alpha_s(M_Z) = 0.118^{+0.010}_{-0.024}$; consistent with an earlier determination [39], the larger error being due to the extrapolation into the (unmeasured) small x region. Theoretically, the sum rule is preferable as the perturbative QCD result is known to higher order and these terms are important at the low Q^2 involved. It has been shown that the theoretical errors associated with the choice of scale are considerably reduced by the use of Padé approximants [14] which results in $\alpha_s(1.7$ GeV) $= 0.328 \pm 0.03$(expt.) ± 0.025(theory) corresponding to $\alpha_s(M_Z) = 0.116^{+0.003}_{-0.005}$(expt.) ± 0.003(theory). No error is included from the extrapolation into the region of x that is unmeasured. Should data become available at smaller values of x so that this extrapolation could be more tightly constrained, the sum rule method could provide a better determination of α_s.

9.4. QCD in decays of the τ lepton

The semi-leptonic branching ratio of the tau ($\tau \to \nu_\tau +$ hadrons, R_τ) is an inclusive quantity. It is related to the contribution of hadrons to the imaginary part of the W self energy ($\Pi(s)$). It is sensitive to a range of energies since it involves an integral

$$R_\tau \sim \int_0^{m_\tau^2} \frac{ds}{m_\tau^2}(1 - \frac{s}{m_\tau^2})^2 \ {\rm Im}\,(\Pi(s)) \ . \quad (9.9)$$

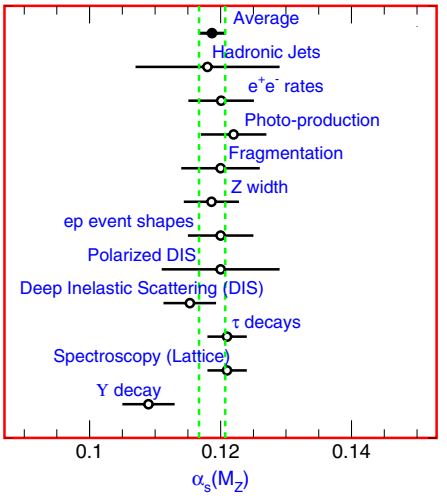

Figure 9.1: Summary of the value of $\alpha_s(M_Z)$ from various processes. The values shown indicate the process and the measured value of α_s extrapolated to $\mu = M_Z$. The error shown is the *total* error including theoretical uncertainties. The average quoted in this report which comes from these measurements is also shown. See text for discussion of errors.

Since the scale involved is low, one must take into account nonperturbative (higher-twist) contributions which are suppressed by powers of the τ mass.

$$R_\tau = 3.058\left[1 + \frac{\alpha_s(m_\tau)}{\pi} + 5.2\left(\frac{\alpha_s(m_\tau)}{\pi}\right)^2 + 26.4\left(\frac{\alpha_s(m_\tau)}{\pi}\right)^3 + a\frac{m^2}{m_\tau^2} + b\frac{m\bar{\psi}\psi}{m_\tau^4} + c\frac{\bar{\psi}\psi\bar{\psi}\psi}{m_\tau^6} + \cdots\right] . \quad (9.10)$$

Here a, b, and c are dimensionless constants and m is a light quark mass. The term of order $1/m_\tau^2$ is a kinematical effect due to the light quark masses and is consequently very small. The nonperturbative terms are estimated using sum rules [40]. In total, they are estimated to be -0.014 ± 0.005 [41,42]. This estimate relies on there being no term of order Λ^2/m_τ^2. Λ^2/m_τ^2 $\left(\text{note that } \frac{\alpha_s(m_\tau)}{\pi} \sim (\frac{0.5\ \text{GeV}}{m_\tau})^2\right)$. The a, b, and c can be determined from the data [43] by fitting to moments of the $\Pi(s)$ and separately to the final states accessed by the vector and axial parts of the W coupling. The values so extracted [44,45] are consistent with the theoretical estimates. If the nonperturbative terms are omitted from the fit, the extracted value of $\alpha_s(m_\tau)$ decreases by ~ 0.02.

For $\alpha_s(m_\tau) = 0.35$ the perturbative series for R_τ is $R_\tau \sim 3.058(1 + 0.112 + 0.064 + 0.036)$. The size (estimated error) of the nonperturbative term is 20% (7%) of the size of the order α_s^3 term. The perturbation series is not very well convergent; if the order α_s^3 term is omitted, the extracted value of $\alpha_s(m_\tau)$ increases by 0.05. The order α_s^4 term has been estimated [46] and attempts made to resum the entire series [47,48]. These estimates can be used to obtain an estimate of the errors due to these unknown terms [49,50]. We assign an uncertainty of ± 0.02 to $\alpha_s(m_\tau)$ from these sources.

R_τ can be extracted from the semi-leptonic branching ratio from the relation $R_\tau = 1/(\mathrm{B}(\tau \to e\nu\overline{\nu}) - 1.97256)$; where $\mathrm{B}(\tau \to e\nu\overline{\nu})$ is measured directly or extracted from the lifetime, the muon mass, and the muon lifetime assuming universality of lepton couplings. Using the average lifetime of 290.6 ± 1.1 fs and a τ mass of 1776.99 ± 0.29 MeV from the PDG fit gives $R_\tau = 3.645 \pm 0.020$. The direct measurement of $\mathrm{B}(\tau \to e\nu\overline{\nu})$ can be combined with $\mathrm{B}(\tau \to \mu\nu\overline{\nu})$ to give $\mathrm{B}(\tau \to e\nu\overline{\nu}) = 0.1785 \pm 0.0005$ which gives $R_\tau = 3.629 \pm 0.015$. Averaging these yields $\alpha_s(m_\tau) = 0.353 \pm 0.007$ using the experimental error alone. We assign a theoretical error equal to 40% of the contribution from the order α^3 term and all of the nonperturbative contributions. This then gives $\alpha_s(m_\tau) = 0.35 \pm 0.03$ for the final result. This corresponds to $\alpha_s(M_Z) = 0.121 \pm 0.003$. This result is consistent with that obtained by using the moments [51] and is used in the average below.

9.5. QCD in high-energy hadron collisions

There are many ways in which perturbative QCD can be tested in high-energy hadron colliders. The quantitative tests are only useful if the process in question has been calculated beyond leading order in QCD perturbation theory. The production of hadronic jets with large transverse momentum in hadron-hadron collisions provides a direct probe of the scattering of quarks and gluons: $qq \to qq$, $qg \to qg$, $gg \to gg$, *etc.* Higher–order QCD calculations of the jet rates [52] and shapes are in impressive agreement with data [53]. This agreement has led to the proposal that these data could be used to provide a determination of α_s [54]. A set of structure functions is assumed and jet data are fitted over a very large range of transverse momenta to the QCD prediction for the underlying scattering process that depends on α_s. The evolution of the coupling over this energy range (40 to 250 GeV) is therefore tested in the analysis. CDF obtains $\alpha_s(M_Z) = 0.1178 \pm 0.0001$ (stat.) ± 0.0085 (syst.) [55]. Estimation of the theoretical errors is not straightforward. The structure functions used depend implicitly on α_s and an iteration procedure must be used to obtain a consistent result; different sets of structure functions yield different correlations between the two values of α_s. CDF includes a scale error of 4% and a structure function error of 5% in the determination of α_s. Ref. 54 estimates the error from unknown higher order QCD corrections to be ± 0.005. Combining these then gives $\alpha_s(M_Z) = 0.118 \pm 0.011$ which is used in the final average. Data are also available on the angular distribution of jets; these are also in agreement with QCD expectations [56,57].

QCD corrections to Drell-Yan type cross sections (*i.e.*, the production in hadron collisions by quark-antiquark annihilation of lepton pairs of invariant mass Q from virtual photons, or of real W or Z bosons), are known [58]. These $\mathcal{O}(\alpha_s)$ QCD corrections are sizable at small values of Q. The correction to W and Z production, as measured in $p\overline{p}$ collisions at $\sqrt{s} = 0.63$ TeV and $\sqrt{s} = 1.8$ TeV, is of order 30%. The NNLO corrections to this process are known [59].

The production of W and Z bosons and photons at large transverse momentum can also be used to test QCD. The leading-order QCD subprocesses are $q\overline{q} \to Vg$ and $qg \to Vq$ ($V = W, Z, \gamma$). If the parton distributions are taken from other processes and a value of α_s assumed, then an absolute prediction is obtained. Conversely, the data can be used to extract information on quark and gluon distributions and on the value of α_s. The next-to-leading-order QCD corrections are known [60,61] (for photons), and for W/Z production [62], and so a precision test is possible. Data exist on photon production from the CDF and DØ collaborations [63,64] and from fixed target experiments [65]. Detailed comparisons with QCD predictions [66] may indicate an excess of the data over the theoretical prediction at low value of transverse momenta, although other authors [67] find smaller excesses.

The UA2 collaboration [68] extracted a value of $\alpha_s(M_W) = 0.123 \pm 0.018(\text{stat.}) \pm 0.017(\text{syst.})$ from the measured ratio $R_W = \frac{\sigma(W + 1\text{jet})}{\sigma(W + 0\text{jet})}$. The result depends on the algorithm used to define a jet, and the dominant systematic errors due to fragmentation and corrections for underlying events (the former causes jet energy to be lost, the latter causes it to be increased) are connected to the algorithm. There is also dependence on the parton distribution functions, and hence, α_s appears explicitly in the formula for R_W, and implicitly in the distribution functions. The UA2 result is not used in the final average. Data from CDF and DØ on the W p_t distribution [69] are in agreement with QCD but are not able to determine α_s with sufficient precision to have any weight in a global average.

In the region of low p_t, fixed order perturbation theory is not applicable; one must sum terms of order $\alpha_s^n \ln^n(p_t/M_W)$ [70]. Data from DØ [71] on the p_t distribution of Z bosons agree well with these predictions.

The production rates of b quarks in $p\overline{p}$ have been used to determine α_s [72]. The next-to-leading-order QCD production processes [73] have been used. By selecting events where the b quarks are back-to-back in azimuth, the next-to-leading-order calculation can be used to compare rates to the measured value and a value of α_s extracted. The errors are dominated by the measurement errors, the choice of μ and the scale at which the structure functions are evaluated, and uncertainties in the choice of structure functions. The last were estimated by varying the structure functions used. The result is $\alpha_s(M_Z) = 0.113^{+0.009}_{-0.013}$, which is not included in the final average, as the measured $b\overline{b}$ cross section is in poor agreement with perturbative QCD [74] and it is therefore difficult to interpret this result.

9.6. QCD in heavy-quarkonium decay

Under the assumption that the hadronic and leptonic decay widths of heavy $Q\overline{Q}$ resonances can be factorized into a nonperturbative part—dependent on the confining potential—and a calculable perturbative part, the ratios of partial decay widths allow measurements of α_s at the heavy-quark mass scale. The most precise data come from the decay widths of the 1^{--} $J/\psi(1S)$ and Υ resonances. The total decay width of the Υ is predicted by perturbative QCD [75,76]

$$R_\mu(\Upsilon) = \frac{\Gamma(\Upsilon \to \text{hadrons})}{\Gamma(\Upsilon \to \mu^+\mu^-)} = \frac{10(\pi^2-9)\alpha_s^3(M_b)}{9\pi\alpha_{\rm em}^2} \times \left[1 + \frac{\alpha_s}{\pi}\left(-19.36 + \frac{3\beta_0}{2}\left(1.161 + \ln\left(\frac{2M}{M_\Upsilon}\right)\right)\right)\right] . \quad (9.11)$$

Data are available for the Υ, Υ', Υ'', and J/ψ. The result is very sensitive to α_s and the data are sufficiently precise ($R_\mu(\Upsilon) = 39.11 \pm 0.4$) [77] that the theoretical errors will dominate. There are theoretical corrections to this formula due to the relativistic nature of the $Q\overline{Q}$ system which have been calculated [76] to order v^2/c^2. These corrections are more severe for the J/ψ. There are also nonperturbative corrections arising from annihilation from higher Fock states ("color octet" contribution) which can only be estimated [78]; again these are more severe for the J/ψ. The Υ gives $\alpha_s(M_b) = 0.177 \pm 0.01$, where the error includes that from the "color octet" term and the choice of scale which together dominate. The ratio of widths $\frac{\Upsilon \to \gamma gg}{\Upsilon \to ggg}$ has been measured by the CLEO collaboration and can be used to determine $\alpha_s(M_b) = 0.189 \pm 0.01 \pm 0.01$. The error is dominated by theoretical uncertainties associated with the scale choice; the uncertainty due to the "color octet" piece is not present in this case [79]. The theoretical uncertainties due to the production of photons in fragmentation [80] are small [81]. Higher order QCD calculations of the photon energy distribution are available [82]; this distribution could now be used to further test the theory. The width $\Gamma(\Upsilon \to e^+e^-)$ can also be used to determine α_s by using moments of the quantity $R_b(s) = \frac{\sigma(e^+e^- \to b\overline{b})}{\sigma(e^+e^- \to \mu^+\mu^-)}$ defined by $M_n = \int_0^\infty \frac{R_b(s)}{s^{n+1}}$ [83]. At large values of n, M_n is dominated by $\Gamma(\Upsilon \to e^+e^-)$. Higher order corrections are available and the method gives [84] $\alpha_s(M_b) = 0.220 \pm 0.027$. The dominant error is theoretical and is dominated by the choice of scale and by uncertainties in Coulomb corrections. These various Υ decay measurements can be combined and give $\alpha_s(M_b) = 0.185 \pm 0.01$ corresponding to $\alpha_s(M_Z) = 0.109 \pm 0.004$ which is used in the final average [79]

9.7. Perturbative QCD in e^+e^- collisions

The total cross section for $e^+e^- \to$ hadrons is obtained (at low values of $\sqrt{s}$) by multiplying the muon-pair cross section by the factor $R = 3\Sigma_q e_q^2$. The higher-order QCD corrections to this quantity have been calculated, and the results can be expressed in terms of the factor:

$$R = R^{(0)}\left[1 + \frac{\alpha_s}{\pi} + C_2\left(\frac{\alpha_s}{\pi}\right)^2 + C_3\left(\frac{\alpha_s}{\pi}\right)^3 + \cdots\right] , \quad (9.12)$$

where $C_2 = 1.411$ and $C_3 = -12.8$ [85].

$R^{(0)}$ can be obtained from the formula for $d\sigma/d\Omega$ for $e^+e^- \to f\overline{f}$ by integrating over Ω. The formula is given in Sec. 39.2 of this *Review*. This result is only correct in the zero-quark-mass limit. The $\mathcal{O}(\alpha_s)$ corrections are also known for massive quarks [86]. The principal advantage of determining α_s from R in e^+e^- annihilation is that there is no dependence on fragmentation models, jet algorithms, *etc.*

A measurement by CLEO [87] at $\sqrt{s} = 10.52$ GeV yields $\alpha_s(10.52\text{ GeV}) = 0.20 \pm 0.01 \pm 0.06$, which corresponds to $\alpha_s(M_Z) = 0.13 \pm 0.005 \pm 0.03$. A comparison of the theoretical prediction of Eq. (9.12) (corrected for the b-quark mass), with all the available data at values of $\sqrt{s}$ between 20 and 65 GeV, gives [88] $\alpha_s(35\text{ GeV}) = 0.146 \pm 0.030$. The size of the order α_s^3 term is of order 40% of that of the order α_s^2 and 3% of the order α_s. If the order α_s^3 term is not included, a fit to the data yields α_s (35 GeV) $= 0.142 \pm 0.03$, indicating that the theoretical uncertainty is smaller than the experimental error.

Measurements of the ratio of hadronic to leptonic width of the Z at LEP and SLC, Γ_h/Γ_μ probe the same quantity as R. Using the average of $\Gamma_h/\Gamma_\mu = 20.783 \pm 0.025$ gives $\alpha_s(M_Z) = 0.1224 \pm 0.0038$ [89]. There are theoretical errors arising from the values of top-quark and Higgs masses which enter due to electroweak corrections to the Z width and from the choice of scale. While this method has small theoretical uncertainties from QCD itself, it relies sensitively on the electroweak couplings of the Z to quarks [90]. The presence of new physics which changes these couplings via electroweak radiative corrections would invalidate the value of $\alpha_s(M_Z)$. An illustration of the sensitivity can be obtained by comparing this value with the one obtained from the global fits [89] of the various precision measurements at LEP/SLC and the W and top masses: $\alpha_s(M_Z) = 0.1186 \pm 0.0027$. The difference between these two values may be accounted for by systematic uncertainties as large as ± 0.003 [89], therefore $\alpha_s(M_Z) = 0.1186 \pm 0.0042$ will be used in the final average.

An alternative method of determining α_s in e^+e^- annihilation is from measuring quantities that are sensitive to the relative rates of two-, three-, and four-jet events. A review should be consulted for more details [91] of the issues mentioned briefly here. In addition to simply counting jets, there are many possible choices of such "shape variables": thrust [92], energy-energy correlations [93], average jet mass, *etc.* All of these are infrared safe, which means they can be reliably calculated in perturbation theory. The starting point for all these quantities is the multijet cross section. For example, at order α_s, for the process $e^+e^- \to q\overline{q}g$: [94]

$$\frac{1}{\sigma}\frac{d^2\sigma}{dx_1 dx_2} = \frac{2\alpha_s}{3\pi}\frac{x_1^2 + x_2^2}{(1-x_1)(1-x_2)} , \quad (9.13)$$

$$x_i = \frac{2E_i}{\sqrt{s}} \quad (9.14)$$

where x_i are the center-of-mass energy fractions of the final-state (massless) quarks. A distribution in a "three-jet" variable, such as those listed above, is obtained by integrating this differential cross section over an appropriate phase space region for a fixed value of the variable. The order α_s^2 corrections to this process have been computed, as well as the 4-jet final states such as $e^+e^- \to qqgg$ [95].

There are many methods used by the e^+e^- experimental groups to determine α_s from the event topology. The jet-counting algorithm, originally introduced by the JADE collaboration [96], has been used

by many other groups. Here, particles of momenta p_i and p_j are combined into a pseudo-particle of momentum $p_i + p_j$ if the invariant mass of the pair is less than $y_0\sqrt{s}$. The process is iterated until all pairs of particles or pseudoparticles have a mass-measure that exceeds $y_0\sqrt{s}$; the remaining number is then defined to be the jet multiplicity. The remaining number is then defined to be the number of jets in the event, and can be compared to the QCD prediction. The Durham algorithm is slightly different: in combining a pair of partons, it uses $M^2 = 2\min(E_i^2, E_j^2)(1 - \cos\theta_{ij})$ for partons of energies E_i and E_j separated by angle θ_{ij} [97].

There are theoretical ambiguities in the way this process is carried out. Quarks and gluons are massless, whereas the observed hadrons are not, so that the massive jets that result from this scheme cannot be compared directly to the massless jets of perturbative QCD. Different recombination schemes have been tried, for example combining 3-momenta and then rescaling the energy of the cluster so that it remains massless. These schemes result in the same data giving slightly different values [98,99] of α_s. These differences can be used to determine a systematic error. In addition, since what is observed are hadrons rather than quarks and gluons, a model is needed to describe the evolution of a partonic final state into one involving hadrons, so that detector corrections can be applied. The QCD matrix elements are combined with a parton-fragmentation model. This model can then be used to correct the data for a direct comparison with the parton calculation. The different hadronization models that are used [100–103] model the dynamics that are controlled by nonperturbative QCD effects which we cannot yet calculate. The fragmentation parameters of these Monte Carlos are tuned to get agreement with the observed data. The differences between these models contribute to the systematic errors. The systematic errors from recombination schemes and fragmentation effects dominate over the statistical and other errors of the LEP/SLD experiments.

The scale M at which $\alpha_s(M)$ is to be evaluated is not clear. The invariant mass of a typical jet (or $\sqrt{sy_0}$) is probably a more appropriate choice than the e^+e^- center-of-mass energy. While there is no justification for doing so, if the value is allowed to float in the fit to the data, the fit improves and the data tend to prefer values of order $\sqrt{s}/10$ GeV for some variables [99,104]; the exact value depends on the variable that is fitted.

The perturbative QCD formulae can break down in special kinematical configurations. For example, the thrust (T) distribution contains terms of the type $\alpha_s \ln^2(1-T)$. The higher orders in the perturbation expansion contain terms of order $\alpha_s^n \ln^m(1-T)$. For $T \sim 1$ (the region populated by 2-jet events), the perturbation expansion is unreliable. The terms with $n \leq m$ can be summed to all orders in α_s [105]. If the jet recombination methods are used higher-order terms involve $\alpha_s^n \ln^m(y_0)$, these too can be resummed [106]. The resummed results give better agreement with the data at large values of T. Some caution should be exercised in using these resummed results because of the possibility of overcounting; the showering Monte Carlos that are used for the fragmentation corrections also generate some of these leading-log corrections. Different schemes for combining the order α_s^2 and the resummations are available [107]. These different schemes result in shifts in α_s of order ± 0.002. The use of the resummed results improves the agreement between the data and the theory. An average of results at the Z resonance from SLD [99], OPAL [108], L3 [109], ALEPH [110], and DELPHI [111], using the combined α_s^2 and resummation fitting to a large set of shape variables, gives $\alpha_s(M_Z) = 0.122 \pm 0.007$. The errors in the values of $\alpha_s(M_Z)$ from these shape variables are totally dominated by the theoretical uncertainties associated with the choice of scale, and the effects of hadronization Monte Carlos on the different quantities fitted.

Estimates are available for the nonperturbative corrections to the mean value of $1-T$ [112]. These are of order $1/E$ and involve a single parameter to be determined from experiment. These corrections can then be used as an alternative to those modeled by the fragmentation Monte Carlos. The DELPHI collaboration has fitted its data using an additional parameter to take into account these $1/E$ effects [113] and quotes for the MSbar scheme $\alpha_s = 0.1217 \pm 0.0046$ and a significant $1/E$ term. This term vanishes in the RGI/ECH scheme and the data are well described by pure perturbation theory with consistent $\alpha_s = 0.1201 \pm 0.0020$.

Studies have been carried out at energies between $\sim$130 GeV [114] and $\sim$200 GeV [115]. These can be combined to give $\alpha_s(130\ \text{GeV}) = 0.114 \pm 0.008$ and $\alpha_s(189\ \text{GeV}) = 0.1104 \pm 0.005$. The dominant errors are theoretical and systematic and, most of these are in common at the two energies. These data and those at the Z resonance and below provide clear confirmation of the expected decrease in α_s as the energy is increased.

The LEP QCD working group [116] uses all LEP data Z mass and higher energies to perform a global fit using a large number of shape variables. It determines $\alpha_s(M_Z) = 0.1201 \pm 0.0003(stat) \pm 0.0048(syst)$, (result quoted in Ref. 5) the error being dominated by theoretical uncertainties which are the most difficult to quantify.

Similar studies on event shapes have been undertaken at lower energies at TRISTAN, PEP/PETRA, and CLEO. A combined result from various shape parameters by the TOPAZ collaboration gives $\alpha_s(58\ \text{GeV}) = 0.125 \pm 0.009$, using the fixed order QCD result, and $\alpha_s(58\ \text{GeV}) = 0.132 \pm 0.008$ (corresponding to $\alpha_s(M_Z) = 0.123 \pm 0.007$), using the same method as in the SLD and LEP average [117]. The measurements of event shapes at PEP/PETRA are summarized in earlier editions of this note. A recent reevaluation of the JADE data [118] obtained using resummed QCD results with modern models of jet fragmentation and by averaging over several shape variables gives $\alpha_s(22\ \text{GeV}) = 0.151 \pm 0.004(expt)^{+0.014}_{-0.012}(theory)$ which is used in the final average. These results also attempt to constrain the non-perurbative parameters and show a remarkable agreement with QCD even at low energies [119]. An analysis by the TPC group [120] gives $\alpha_s(29\ \text{GeV}) = 0.160 \pm 0.012$, using the same method as TOPAZ.

The CLEO collaboration fits to the order α_s^2 results for the two jet fraction at $\sqrt{s} = 10.53$ GeV, and obtains $\alpha_s(10.53\ \text{GeV}) = 0.164 \pm 0.004$ (expt.) ± 0.014 (theory) [121]. The dominant systematic error arises from the choice of scale (μ), and is determined from the range of α_s that results from fit with $\mu = 10.53$ GeV, and a fit where μ is allowed to vary to get the lowest χ^2. The latter results in $\mu = 1.2$ GeV. Since the quoted result corresponds to $\alpha_s(1.2\ \text{GeV}) = 0.35$, it is by no means clear that the perturbative QCD expression is reliable and the resulting error should, therefore, be treated with caution. A fit to many different variables as is done in the LEP/SLC analyses would give added confidence to the quoted error.

All these measurements are consistent with the LEP average quoted above which has the smallest statistical error; the systematic errors being mostly theoretical are likely to be strongly correlated between the measurements. The value of $\alpha_s(M_Z) = 0.1201 \pm 0.005$ is used in the final average.

9.8. Scaling violations in fragmentation functions

Measurements of the fragmentation function $d_i(z, E)$, (the probability that a hadron of type i be produced with energy zE in e^+e^- collisions at $\sqrt{s} = 2E$) can be used to determine α_s. (Detailed definitions and a discussion of the properties of fragmentation functions can be found in Sec. 17 of this *Review*). As in the case of scaling violations in structure functions, QCD predicts only the E dependence. Hence, measurements at different energies are needed to extract a value of α_s. Because the QCD evolution mixes the fragmentation functions for each quark flavor with the gluon fragmentation function, it is necessary to determine each of these before α_s can be extracted.

The ALEPH collaboration has used data from energies ranging from $\sqrt{s} = 22$ GeV to $\sqrt{s} = 91$ GeV. A flavor tag is used to discriminate between different quark species, and the longitudinal and transverse cross sections are used to extract the gluon fragmentation function [122]. The result obtained is $\alpha_s(M_Z) = 0.126 \pm 0.007$ (expt.) $\pm$ 0.006 (theory) [123]. The theory error is due mainly to the choice of scale. The OPAL collaboration [124] has also extracted the separate fragmentation functions. DELPHI [125] has also performed a similar analysis using data from other experiments at lower energy with the result $\alpha_s(M_Z) = 0.124 \pm 0.007 \pm 0.009$ (theory).

The larger theoretical error is due to the larger range of scales that were used in the fit. These results can be combined to give $\alpha_s(M_Z) = 0.125 \pm 0.005 \pm 0.008$ (theory).

A global analysis [126] uses data on the production of π, K, p, and $\overline{p}$ from SLC [127], DELPHI [128], OPAL [129], ALEPH [130], and lower-energy data from the TPC collaboration [131]. A flavor tag and a three-jet analysis is used to disentangle the quark and gluon fragmentation functions. The value $\alpha_s(M_Z) = 0.117^{+0.0055+0.0017}_{-0.0069-0.0025}$ is obtained. The second error is a theoretical one arising from the choice of scale. The fragmentation functions resulting from this fit are consistent with a recent fit of Ref. 132.

It is unclear how to combine the measurements discussed in the two previous paragraphs as much of the data used are common to both. If the theoretical errors dominate then a simple average is appropriate as the methods are different. For want of a better solution, the naive average of $\alpha_s(M_Z) = 0.1201 \pm 0.006$ is used for in the average value quoted below.

9.9. Photon structure functions

e^+e^- can also be used to study photon-photon interactions, which can be used to measure the structure function of a photon [133], by selecting events of the type $e^+e^- \to e^+e^- + hadrons$ which proceeds via two photon scattering. If events are selected where one of the photons is almost on mass shell and the other has a large invariant mass Q, then the latter probes the photon structure function at scale Q; the process is analogous to deep inelastic scattering where a highly virtual photon is used to probe the proton structure. This process was included in earlier versions of this *Review* which can be consulted for details on older measurements [134–137]. A review of the data can be found in Ref. 138. Data are available from LEP [139–143] and from TRISTAN [144,145] which extend the range of Q^2 to of order 300 GeV^2 and x as low as $2 \times 10^{-3}$and show Q^2 dependence of the structure function that is consistent with QCD expectations. There is evidence for a hadronic (non-perturbative) component to the photon structure function that complicates attempts to extract a value of α_s from the data.

Reference [146] uses data from PETRA, TRISTAN, and LEP to perform a combined fit. The higher data from LEP extend to higher Q^2 (< 780 GeV^2) and enable a measurement: $\alpha_s(m_Z) = 0.1198 \pm 0.0054$ which now is competitive with other results.

Experiments at HERA can also probe the photon structure function by looking at jet production in γp collisions; this is analogous to the jet production in hadron-hadron collisions which is sensitive to hadron structure functions. The data [147] are consistent with theoretical models [148].

9.10. Jet rates in ep collisions

At lowest order in α_s, the ep scattering process produces a final state of (1+1) jets, one from the proton fragment and the other from the quark knocked out by the process $e + quark \to e + quark$. At next order in α_s, a gluon can be radiated, and hence a (2+1) jet final state produced. By comparing the rates for these (1+1) and (2+1) jet processes, a value of α_s can be obtained. A NLO QCD calculation is available [149]. The basic methodology is similar to that used in the jet counting experiments in e^+e^- annihilation discussed above. Unlike those measurements, the ones in ep scattering are not at a fixed value of Q^2. In addition to the systematic errors associated with the jet definitions, there are additional ones since the structure functions enter into the rate calculations. Results from H1 [150] and ZEUS [152] can be combined to give [4] $\alpha_s(M_Z) = 0.120 \pm 0.002$ (expt.) ± 0.004 (theor.). which is used in the final average. The theoretical errors arise from scale choice, structure functions, and jet definitions.

Photoproduction of two or more jets via processes such as $\gamma + g \to q\overline{q}$ can also be observed at HERA. The process is similar to jet production in hadron-hadron collisions. Agreement with perturbative QCD is excellent and ZEUS [151] quotes $\alpha_s(M_Z) = 0.1224 \pm 0.0020$ (expt) ± 0.0050 (theory) which is used in the average below.

9.11. QCD in diffractive events

In approximately 10% of the deep-inelastic scattering events at HERA a rapidity gap is observed [153]; that is events are seen where there are almost no hadrons produced in the direction of the incident proton. This was unexpected; QCD based models of the final state predicted that the rapidity interval between the quark that is hit by the electron and the proton remnant should be populated approximately evenly by the hadrons. Similar phenomena have been observed at the Tevatron in W and jet production. For a review see Ref. 154.

9.12. Lattice QCD

Lattice gauge theory calculations can be used to calculate, using non-perturbative methods, a physical quantity that can be measured experimentally. The value of this quantity can then be used to determine the QCD coupling that enters in the calculation. For a review of the methodology see Ref. 155. For example, the energy levels of a $Q\overline{Q}$ system can be determined and then used to extract α_s. The masses of the $Q\overline{Q}$ states depend only on the quark mass and on α_s. A limitation until very recently is that calculations have not been performed for three light quark flavors. Results for zero ($n_f = 0$, quenched approximation) and two light flavors must be extrapolated to $n_f = 3$. The coupling constant so extracted is in a lattice renormalization scheme, and must be converted to the $\overline{\rm MS}$ scheme for comparison with other results. Using the mass differences of Υ and Υ' and Υ'' and χ_b, Davies *et al.* [156] extract a value of $\alpha_s(M_Z) = 0.121 \pm 0.003$. This result is the first to have three light flavors and allows the strange quark to have a different mass from the up and down. This result supersedes earlier estimates although it should be pointed out that in an earlier paper [157] a result with a smaller error was given. A similar result with larger errors is reported by [158], whose results are consistent with $\alpha_s(M_Z) = 0.111 \pm 0.006$. The SESAM collaboration [159] uses the Υ and Υ' and χ_b masses to obtain $\alpha_s(M_Z) = 0.1118 \pm 0.0017$ using Wilson fermions. While this result agrees with that of Ref. 160 which also uses Wilson fermions, and is consistent with Ref. 167 which uses a similar method and results from quenched and two massless flavors to get $\alpha_s(M_Z) = 0.1076 \pm 0.0038$, these authors point out that their result is more than 3σ from that of Davies *et al.* [157] which uses Kogut-Susskind fermions. Note that a combination of the older results from quenched [161] and ($n_f = 2$) [162] gives $\alpha_s(M_Z) = 0.116 \pm 0.003$ [163] which is remarkably consistent with the newer values. The ALPHA collaboration [164] who use the strength of the QCD potential from the Υ system inferred by Ref. 165 have begun to probe the systematic errors in detail for simulations involving two flavors of massless quarks.

There have also been investigations of the running of α_s [166]. These show remarkable agreement with the two loop perturbative result of Eq. (9.5).

There are several sources of error in these estimates of $\alpha_s(M_Z)$. The experimental error associated with the measurements of the particle masses is negligible. The conversion from the lattice coupling constant to the $\overline{\rm MS}$ constant is obtained using a perturbative expansion where one coupling expanded as a power series in the other. The series is known to third order [168]. The effect of the third-order term is a shift in the extracted value of $\alpha_s(M_Z)$ of $+0.002$. Other theoretical errors arising from the limited statistics of the Monte-Carlo calculation, extrapolation in n_f which is not needed in latest results [156], and corrections for light quark masses are smaller than this.

In this review, we will use only the new result [156] of $\alpha_s(M_Z) = 0.121 \pm 0.003$. It should be noted that this is 2σ away from the value $\alpha_s(M_Z) = 0.1134 \pm 0.003$ in the last version of this review that was obtained by averaging Refs. [157,159,160,161,167]

In addition to the strong coupling constant other quantities can be determined. Of particular interest are the decay constants of charmed and bottom mesons. These are required, for example, to facilitate the extraction of CKM elements from measurements of charm and bottom decay rates. See Ref. 169 for a recent review.

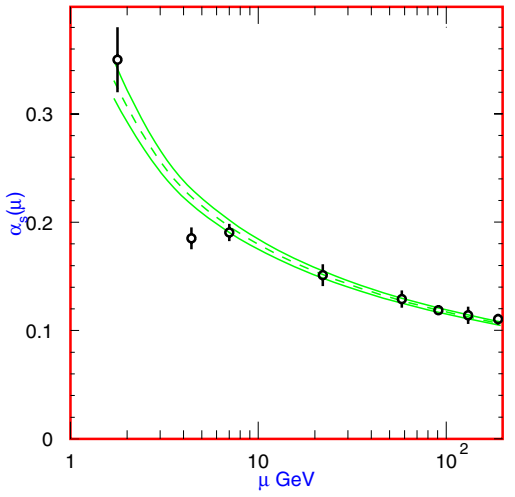

Figure 9.2: Summary of the values of $\alpha_s(\mu)$ at the values of μ where they are measured. The lines show the central values and the $\pm 1\sigma$ limits of our average. The figure clearly shows the decrease in $\alpha_s(\mu)$ with increasing μ. The data are, in increasing order of μ, τ width, Υ decays, deep inelastic scattering, e^+e^- event shapes at 22 GeV from the JADE data, shapes at TRISTAN at 58 GeV, Z width, and e^+e^- event shapes at 135 and 189 GeV.

9.13. Conclusions

The need for brevity has meant that many other important topics in QCD phenomenology have had to be omitted from this review. One should mention in particular the study of exclusive processes (form factors, elastic scattering, ...), the behavior of quarks and gluons in nuclei, the spin properties of the theory, and QCD effects in hadron spectroscopy.

We have focused on those high-energy processes which currently offer the most quantitative tests of perturbative QCD. Figure 9.1 shows the values of $\alpha_s(M_Z)$ deduced from the various experiments. Figure 9.2 shows the values and the values of Q where they are measured. This figure clearly shows the experimental evidence for the variation of $\alpha_s(Q)$ with Q.

An average of the values in Fig. 9.1 gives $\alpha_s(M_Z) = 0.1187$, with a total χ^2 of 9 for eleven fitted points, showing good consistency among the data. The error on this average, assuming that all of the errors in the contributing results are uncorrelated, is ± 0.0013, and may be an underestimate. Almost all of the values used in the average are dominated by systematic, usually theoretical, errors. Only some of these, notably from the choice of scale, are correlated. The average is not dominated by a single measurement; there are several results with comparable small errors: these are the ones from τ decay, lattice gauge theory, deep inelastic scattering, upsilon decay and the Z^0 width. We quote our average value as $\alpha_s(M_Z) = 0.1187 \pm 0.002$, which corresponds to $\Lambda^{(5)} = 217^{+25}_{-23}$ MeV using Eq. (9.5). Note that the average has moved by less than 1σ from the last version of this review. Future experiments can be expected to improve the measurements of α_s somewhat. Precision at the 1% level may be achievable if the systematic and theoretical errors can be reduced [170].

The value of α_s at any scale corresponding to our average can be obtained from `http://www-theory.lbl.gov/~ianh/alpha/alpha.html` which uses Eq. (9.5) to interpolate.

References:

1. R.K. Ellis, W.J. Stirling, and B.R. Webber, "QCD and Collider Physics" (Cambridge 1996).
2. For reviews see, for example, A.S. Kronfeld and P.B. Mackenzie, Ann. Rev. Nucl. and Part. Sci. **43**, 793 (1993);
   H. Wittig, Int. J. Mod. Phys. **A12**, 4477 (1997).
3. For example see, P Gambino , *International Conference on Lepton Photon Interactions*, Fermilab, USA, (2003).
4. S. Bethke, `hep-ex/0211012`;
   M. Davier, *33rd Rencontres de Moriond: Electroweak Interactions and Unified Theories*, Les Arcs, France (14–21 Mar. 1998);
   S. Bethke, J. Phys. **G26**, R27 (2000).
5. R. Hirosky, *International Conference on Lepton Photon Interactions*, Fermilab, USA, (2003).
6. See, for example, J. Collins "Renormalization: an introduction to renormalization, the renormalization group and the operator product expansion," (Cambridge University Press, Cambridge, 1984). "QCD and Collider Physics" (Cambridge 1996).
7. S.A. Larin, T. van Ritbergen, and J.A.M. Vermaseren, Phys. Lett. **B400**, 379 (1997).
8. W.A. Bardeen *et al.*, Phys. Rev. **D18**, 3998 (1978).
9. G. Grunberg, Phys. Lett. **95B**, 70 (1980); Phys. Rev. **D29**, 2315 (1984).
10. P.M. Stevenson, Phys. Rev. **D23**, 2916 (1981); and Nucl. Phys. **B203**, 472 (1982).
11. S. Brodsky and H.J. Lu, SLAC-PUB-6389 (Nov. 1993).
12. S. Brodsky, G.P. Lepage, and P.B. Mackenzie, Phys. Rev. **D28**, 228 (1983).
13. M.A. Samuel, G. Li, and E. Steinfelds, Phys. Lett. **B323**, 188 (1994);
    M.A. Samuel, J. Ellis, and M. Karliner, Phys. Rev. Lett. **74**, 4380 (1995).
14. J. Ellis *et al.*, Phys. Rev. **D54**, 6986 (1996).
15. P.N. Burrows *et al.*, Phys. Lett. **B382**, 157 (1996).
16. P. Abreu *et al.*, Z. Phys. **C54**, 55 (1992).
17. A.H. Mueller, Phys. Lett. **B308**, 355, (1993).
18. W. Bernreuther, Annals of Physics **151**, 127 (1983); Erratum Nucl. Phys. **B513**, 758 (1998);
    S.A. Larin, T. van Ritbergen, and J.A.M. Vermaseren, Nucl. Phys. **B438**, 278 (1995).
19. K.G. Chetyrkin, B.A. Kniehl, and M. Steinhauser, Phys. Rev. Lett. **79**, 2184 (1997);
    K.G. Chetyrkin, B.A. Kniehl, and M. Steinhauser, Nucl. Phys. **B510**, 61 (1998).
20. See the Review on the "Quark Mass" in the Particle Listings for *Review of Particle Physics*.
21. A.D. Martin *et al.*, `hep-ph/0307262`.
22. D. Gross and C.H. Llewellyn Smith, Nucl. Phys. **B14**, 337 (1969).
23. J. Chyla and A.L. Kataev, Phys. Lett. **B297**, 385 (1992).
24. S.A. Larin and J.A.M. Vermaseren, Phys. Lett. **B259**, 345 (1991).
25. A.L. Kataev and V.V. Starchenko, Mod. Phys. Lett. **A10**, 235 (1995).
26. V.M. Braun and A.V. Kolesnichenko, Nucl. Phys. **B283**, 723 (1987).
27. M. Dasgupta and B. Webber, Phys. Lett. **B382**, 273 (1993).
28. J. Kim *et al.*, Phys. Rev. Lett. **81**, 3595 (1998).
29. D. Allasia *et al.*, Z. Phys. **C28**, 321 (1985);
    K. Varvell *et al.*, Z. Phys. **C36**, 1 (1987);
    V.V. Ammosov *et al.*, Z. Phys. **C30**, 175 (1986);
    P.C. Bosetti *et al.*, Nucl. Phys. **B142**, 1 (1978).
30. A.L. Kataev *et al.*, Nucl. Phys. **A666 & 667**, 184 (2000); Nucl. Phys. **B573**, 405 (2000).
31. A.L. Kataev, G. Parente, and A.V. Sidorov, `hep-ph/0106221`;
    A.L. Kataev, G. Parente, and A.V. Sidorov, Nucl. Phys. Proc. Suppl. **116**, 105 (2003) `hep-ph/0211151`.

32. K. Abe *et al.*, Phys. Rev. Lett. **74**, 346 (1995); Phys. Lett. **B364**, 61 (1995); Phys. Rev. Lett. **75**, 25 (1995);
P.L. Anthony *et al.*, Phys. Rev. **D54**, 6620 (1996).
33. B. Adeva *et al.*, Phys. Rev. **D58**, 112002 (1998), Phys. Lett. **B420**, 180 (1998).
34. D. Adams *et al.*, Phys. Lett. **B329**, 399 (1995); Phys. Rev. **D56**, 5330 (1998); Phys. Rev. **D58**, 1112001 (1998);
K. Ackerstaff *et al.*, Phys. Lett. **B464**, 123 (1999).
35. P.L. Anthony *et al.*, Phys. Lett. **B463**, 339 (1999); Phys. Lett. **B493**, 19 (2000).
36. J. Blümlein and H. Böttcher, Nucl. Phys. **B636**, 225 (2002).
37. J.D. Bjorken, Phys. Rev. **148**, 1467 (1966).
38. G. Altarelli *et al.*, Nucl. Phys. **B496**, 337 (1997).
39. J. Ellis and M. Karliner, Phys. Lett. **B341**, 397 (1995).
40. M.A. Shifman, A.I Vainshtein, and V.I. Zakharov, Nucl. Phys. **B147**, 385 (1979).
41. S. Narison and A. Pich, Phys. Lett. **B211**, 183 (1988);
E. Braaten, S. Narison, and A. Pich, Nucl. Phys. **B373**, 581 (1992).
42. M. Neubert, Nucl. Phys. **B463**, 511 (1996).
43. F. Le Diberder and A. Pich, Phys. Lett. **B289**, 165 (1992).
44. R. Barate *et al.*, Z. Phys. **C76**, 1 (1997); Z. Phys. **C76**, 15 (1997);
K. Ackerstaff *et al.*, Eur. Phys. J. **C7**, 571 (1999).
45. T. Coan *et al.*, Phys. Lett. **B356**, 580 (1995).
46. A.L. Kataev and V.V. Starshenko, Mod. Phys. Lett. **A10**, 235 (1995).
47. F. Le Diberder and A. Pich, Phys. Lett. **B286**, 147 (1992).
48. C.J. Maxwell and D.J. Tong, Nucl. Phys. **B481**, 681 (1996).
49. G. Altarelli, Nucl. Phys. **B40**, 59 (1995);
G. Altarelli, P. Nason, and G. Ridolfi, Z. Phys. **C68**, 257 (1995).
50. S. Narison, Nucl. Phys. **B40**, 47 (1995).
51. S. Menke, `hep-ex/0106011`.
52. S.D. Ellis, Z. Kunszt, and D.E. Soper, Phys. Rev. Lett. **64**, 2121 (1990);
F. Aversa *et al.*, Phys. Rev. Lett. **65**, 401 (1990);
W.T. Giele, E.W.N. Glover, and D. Kosower, Phys. Rev. Lett. **73**, 2019 (1994);
S. Frixione, Z. Kunszt, and A. Signer, Nucl. Phys. **B467**, 399 (1996).
53. F. Abe *et al.*, Phys. Rev. Lett. **77**, 438 (1996);
B. Abbott *et al.*, Phys. Rev. Lett. **86**, 1707 (2001).
54. W.T. Giele, E.W.N. Glover, and J. Yu, Phys. Rev. **D53**, 120 (1996).
55. T. Affolder *et al.*, Phys. Rev. Lett. **88**, 042001 (2002).
56. UA1 Collaboration: G. Arnison *et al.*, Phys. Lett. **B177**, 244 (1986).
57. F. Abe *et al.*, Phys. Rev. Lett. **77**, 533 (1996);
ibid., erratum Phys. Rev. Lett. **78**, 4307 (1997);
B. Abbott, Phys. Rev. Lett. **80**, 666 (1998);
S. Abachi *et al.*, Phys. Rev. **D53**, 6000 (1996).
58. G. Altarelli, R.K. Ellis, and G. Martinelli, Nucl. Phys. **B143**, 521 (1978).
59. R. Hamberg, W.L. Van Neerven, and T. Matsuura, Nucl. Phys. **B359**, 343 (1991).
60. P. Aurenche, R. Baier, and M. Fontannaz, Phys. Rev. **D42**, 1440 (1990);
P. Aurenche *et al.*, Phys. Lett. **140B**, 87 (1984);
P. Aurenche *et al.*, Nucl. Phys. **B297**, 661 (1988).
61. H. Baer, J. Ohnemus, and J.F. Owens, Phys. Lett. **B234**, 127 (1990).
62. H. Baer and M.H. Reno, Phys. Rev. **D43**, 2892 (1991);
P.B. Arnold and M.H. Reno, Nucl. Phys. **B319**, 37 (1989).
63. F. Abe *et al.*, Phys. Rev. Lett. **73**, 2662 (1994).
64. B. Abbott *et al.*, Phys. Rev. Lett. **84**, 2786 (2001);
V.M. Abazov *et al.*, Phys. Rev. Lett. **87**, 251805 (2001).
65. G. Alverson *et al.*, Phys. Rev. **D48**, 5 (1993).
66. L. Apanasevich *et al.*, Phys. Rev. **D59**, 074007 (1999); Phys. Rev. Lett. **81**, 2642 (1998).
67. W. Vogelsang and A. Vogt, Nucl. Phys. **B453**, 334 (1995);
P. Aurenche *et al.*, Eur. Phys. J. **C9**, 107 (1999).
68. J. Alitti *et al.*, Phys. Lett. **B263**, 563 (1991).
69. S. Abachi *et al.*, Phys. Rev. Lett. **75**, 3226 (1995);
J. Womersley, private communication;
J. Huston, in the *Proceedings to the 29th International Conference on High-Energy Physics (ICHEP98)*, Vancouver, Canada (23–29 Jul 1998) `hep-ph/9901352`.
70. R.K. Ellis and S. Veseli, Nucl. Phys. **B511**, 649 (1998);
C.T. Davies, B.R. Webber, and W.J. Stirling, Nucl. Phys. **B256**, 413 (1985);
G. Parisi and R. Petronzio, Nucl. Phys. **B154**, 427 (1979);
J.C. Collins, D.E. Soper, G. Sterman, Nucl. Phys. **B250**, 199 (1985).
71. DØ Collaboration: B. Abbott *et al.*, Phys. Rev. **D61**, 032004 (2000);
T. Affolder *et al.*, FERMILAB-PUB-99/220.
72. C. Albajar *et al.*, Phys. Lett. **B369**, 46 (1996).
73. M.L. Mangano, P. Nason, and G. Ridolfi, Nucl. Phys. **B373**, 295 (1992).
74. D. Acosta *et al.*, Phys. Rev. **D65**, 052005 (2002).
75. R. Barbieri *et al.*, Phys. Lett. **95B**, 93 (1980);
P.B. Mackenzie and G.P. Lepage, Phys. Rev. Lett. **47**, 1244 (1981).
76. G.T. Bodwin, E. Braaten, and G.P. Lepage, Phys. Rev. **D51**, 1125 (1995).
77. *The Review of Particle Physics,* D.E. Groom *et al.*, Eur. Phys. J. **C15**, 1 (2000) and 2001 off-year partial update for the 2002 edition available on the PDG WWW pages (URL: `http://pdg.lbl.gov/`).
78. M. Gremm and A. Kapustin, Phys. Lett. **B407**, 323 (1997).
79. I. Hinchliffe and A.V. Manohar, Ann. Rev. Nucl. Part. Sci. **50**, 643 (2000).
80. S. Catani and F. Hautmann, Nucl. Phys. **B** (Proc. Supp.), vol. **39BC**, 359 (1995).
81. B. Nemati *et al.*, Phys. Rev. **D55**, 5273 (1997).
82. M. Kramer, Phys. Rev. **D60**, 111503 (1999).
83. M. Voloshin, Int. J. Mod. Phys. **A10**, 2865 (1995).
84. M. Jamin and A. Pich, Nucl. Phys. **B507**, 334 (1997).
85. S.G. Gorishny, A. Kataev, and S.A. Larin, Phys. Lett. **B259**, 144 (1991);
L.R. Surguladze and M.A. Samuel, Phys. Rev. Lett. **66**, 560 (1991).
86. K.G. Chetyrkin and J.H. Kuhn, Phys. Lett. **B308**, 127 (1993).
87. R. Ammar *et al.*, Phys. Rev. **D57**, 1350 (1998).
88. D. Haidt, in *Directions in High Energy Physics,* vol. 14, p. 201, ed. P. Langacker (World Scientific, 1995).
89. G. Quast, presented at the *International Europhysics Conference on High Energy Physics, EPS-HEP03*, Aachen Germany (July 2003);
D. Abbaneo, *et al.*, LEPEWWG/2003-01.

90. A. Blondel and C. Verzegrassi, Phys. Lett. **B311**, 346 (1993);
G. Altarelli *et al.*, Nucl. Phys. **B405**, 3 (1993).
91. G. Dissertori, I. Knowles, and M. Schmelling: "Quantum Chromodynamics: High Energy Experiments and Theory" (Oxford University Press, 2003).
92. E. Farhi, Phys. Rev. Lett. **39**, 1587 (1977).
93. C.L. Basham *et al.*, Phys. Rev. **D17**, 2298 (1978).
94. J. Ellis, M.K. Gaillard, and G. Ross, Nucl. Phys. **B111**, 253 (1976);
ibid., erratum Nucl. Phys. **B130**, 516 (1977);
P. Hoyer *et al.*, Nucl. Phys. **B161**, 349 (1979).
95. R.K. Ellis, D.A. Ross, A.E. Terrano, Phys. Rev. Lett. **45**, 1226 (1980);
Z. Kunszt and P. Nason, ETH-89-0836 (1989).
96. S. Bethke *et al.*, Phys. Lett. **B213**, 235 (1988).
97. S. Bethke *et al.*, Nucl. Phys. **B370**, 310 (1992).
98. M.Z. Akrawy *et al.*, Z. Phys. **C49**, 375 (1991).
99. K. Abe *et al.*, Phys. Rev. Lett. **71**, 2578 (1993); Phys. Rev. **D51**, 962 (1995).
100. B. Andersson *et al.*, Phys. Reports **97**, 33 (1983).
101. A. Ali *et al.*, Nucl. Phys. **B168**, 409 (1980);
A. Ali and R. Barreiro, Phys. Lett. **118B**, 155 (1982).
102. B.R. Webber, Nucl. Phys. **B238**, 492 (1984);
G. Marchesini *et al.*, Phys. Comm. **67**, 465 (1992).
103. T. Sjostrand and M. Bengtsson, Comp. Phys. Comm. **43**, 367 (1987);
T. Sjostrand, CERN-TH-7112/93 (1993).
104. O. Adriani *et al.*, Phys. Lett. **B284**, 471 (1992);
M. Akrawy *et al.*, Z. Phys. **C47**, 505 (1990);
B. Adeva *et al.*, Phys. Lett. **B248**, 473 (1990);
D. Decamp *et al.*, Phys. Lett. **B255**, 623 (1991).
105. S. Catani *et al.*, Phys. Lett. **B263**, 491 (1991).
106. S. Catani *et al.*, Phys. Lett. **B269**, 432 (1991);
S. Catani, B.R. Webber, and G. Turnock, Phys. Lett. **B272**, 368 (1991);
N. Brown and J. Stirling, Z. Phys. **C53**, 629 (1992).
107. S. Catani *et al.*, Phys. Lett. **B269**, 432 (1991); Phys. Lett. **B295**, 269 (1992); Nucl. Phys. **B607**, 3 (1993); Phys. Lett. **B269**, 432 (1991).
108. P.D. Acton *et al.*, Z. Phys. **C55**, 1 (1992); Z. Phys. **C58**, 386 (1993).
109. O. Adriani *et al.*, Phys. Lett. **B284**, 471 (1992).
110. D. Decamp *et al.*, Phys. Lett. **B255**, 623 (1992); Phys. Lett. **B257**, 479 (1992).
111. P. Abreu *et al.*, Z. Phys. **C59**, 21 (1993); Phys. Lett. **B456**, 322 (1999);
M. Acciarri *et al.*, Phys. Lett. **B404**, 390 (1997).
112. Y.L. Dokshitzer and B.R. Webber Phys. Lett. **B352**, 451 (1995);
Y.L. Dokshitzer *et al.*, Nucl. Phys. **B511**, 396 (1997);
Y.L. Dokshitzer *et al.*, JHEP **9801**, 011 (1998).
113. J. Abdallah *et al.*, [DELPHI Collaboration], Eur. Phys. J. **C29**, 285 (2003).
114. D. Buskulic *et al.*, Z. Phys. **C73**, 409 (1997); Z. Phys. **C73**, 229 (1997).
115. H. Stenzel *et al.* [ALEPH Collaboration], CERN-OPEN-99-303(1999);
DELPHI Collaboration: Eur. Phys. J. **C14**, 557 (2000);
M. Acciarri *et al.* [L3 Collaboration], Phys. Lett. **B489**, 65 (2000);
OPAL Collaboration, PN-403 (1999); all submitted to *International Conference on Lepton Photon Interactions*, Stanford, USA (Aug. 1999);
M. Acciarri *et al.* OPAL Collaboration], Phys. Lett. **B371**, 137 (1996); Z. Phys. **C72**, 191 (1996);
K. Ackerstaff *et al.*, Z. Phys. **C75**, 193 (1997);
ALEPH Collaboration: ALEPH 98-025 (1998).
116. `http://lepqcd.web.cern.ch/LEPQCD/annihilations/Welcome.html`.
117. Y. Ohnishi *et al.*, Phys. Lett. **B313**, 475 (1993).
118. P.A. Movilla Fernandez *et al.*, Eur. Phys. J. **C1**, 461 (1998);
O. Biebel *et al.*, Phys. Lett. **B459**, 326 (1999).
119. S. Kluth *et al.*, [JADE Collaboration], `hep-ex/0305023`.
120. D.A. Bauer *et al.*, SLAC-PUB-6518.
121. L. Gibbons *et al.*, CLNS 95-1323 (1995).
122. P. Nason and B.R. Webber, Nucl. Phys. **B421**, 473 (1994).
123. D. Buskulic *et al.*, Phys. Lett. **B357**, 487 (1995);
ibid., erratum Phys. Lett. **B364**, 247 (1995).
124. R. Akers *et al.*, Z. Phys. **C68**, 203 (1995).
125. P. Abreu *et al.*, Phys. Lett. **B398**, 194 (1997).
126. B.A. Kniehl, G. Kramer, and B. Potter, Phys. Rev. Lett. **85**, 5288 (2000).
127. K. Abe *et al.*, [SLD Collaboration], Phys. Rev. **D59**, 052001 (1999).
128. P. Abreu *et al.*, [DELPHI Collaboration], Eur. Phys. J. **C5**, 585 (1998).
129. G. Abbiendi *et al.*, [OPAL Collaboration], Eur. Phys. J. **C11**, 217 (1999).
130. D. Buskulic *et al.*, [ALEPH Collaboration], Z. Phys. **C66**, 355 (1995);
R. Barate *et al.*, Eur. Phys. J. **C17**, 1 (2000).
131. H. Aihara, *et al.*, LBL-23737 (1988) (Unpublished).
132. L. Bourhis, M. Fontannaz, J.P. Guillet, and M. Werlen, Eur. Phys. J. **C19**, 89 (2001).
133. E. Witten, Nucl. Phys. **B120**, 189 (1977).
134. C. Berger *et al.*, Nucl. Phys. **B281**, 365 (1987).
135. H. Aihara *et al.*, Z. Phys. **C34**, 1 (1987).
136. M. Althoff *et al.*, Z. Phys. **C31**, 527 (1986).
137. W. Bartel *et al.*, Z. Phys. **C24**, 231 (1984).
138. M. Erdmann, *International Conference on Lepton Photon Interactions*, Rome Italy (Aug. 2001).
139. K. Ackerstaff *et al.*, Phys. Lett. **B412**, 225 (1997); Phys. Lett. **B411**, 387 (1997).
140. G. Abbiendi *et al.*, [OPAL Collaboration], Eur. Phys. J. **C18**, 15 (2000).
141. R. Barate *et al.*, Phys. Lett. **B458**, 152 (1999).
142. M. Acciarri *et al.*, Phys. Lett. **B436**, 403 (1998); Phys. Lett. **B483**, 373 (2000).
143. P. Abreu *et al.*, Z. Phys. **C69**, 223 (1996).
144. K. Muramatsu *et al.*, Phys. Lett. **B332**, 477 (1994).
145. S.K. Sahu *et al.*, Phys. Lett. **B346**, 208 (1995).
146. S. Albino, M. Klasen and S. Soldner-Rembold, Phys. Rev. Lett. **89**, 122004 (2002).
147. C. Adloff *et al.*, Eur. Phys. J. **C13**, 397 (2000);
J. Breitweg *et al.*, Eur. Phys. J. **C11**, 35 (1999).
148. S. Frixione, Nucl. Phys. **B507**, 295 (1997);
B.W. Harris and J.F. Owens, Phys. Rev. **D56**, 4007 (1997);
M. Klasen and G. Kramer, Z. Phys. **C72**, 107 (1996).
149. D. Graudenz, Phys. Rev. **D49**, 3921 (1994);
J.G. Korner, E. Mirkes, and G.A. Schuler, Int. J. Mod. Phys. **A4**, 1781, (1989);
S. Catani and M. Seymour, Nucl. Phys. **B485**, 291 (1997);
M. Dasgupta and B.R. Webber, Eur. Phys. J. **C1**, 539 (1998);
E. Mirkes and D. Zeppenfeld, Phys. Lett. **B380**, 205 (1996).

150. C. Adloff *et al.*, Eur. Phys. J. **C19**, 289 (2001);
T. Ahmed *et al.*, Phys. Lett. **B346**, 415 (1995); Eur. Phys. J. **C5**, 575 (1998).
151. ZEUS Collaboration: Phys. Lett. **B560**, 7 (2003).
152. ZEUS Collaboration: S. Chekanov *et al.*, Phys. Lett. **B558**, 41 (2003);
E. Tassi at DIS2001 Conference, Bologna (April 2001).
153. M. Derrick *et al.*, Phys. Lett. **B**, 369 (1996);
T. Ahmed *et al.*, Nucl. Phys. **B435**, 3 (1995).
154. D.M. Janson, M. Albrow, and R. Brugnera, `hep-ex/9905537`.
155. P. Weisz, Nucl. Phys. **B** (Proc. Supp.) **47**, 71 (1996).
156. C.T.H. Davies *et al.*, `hep-lat/0304004`.
157. C.T.H. Davies *et al.*, Phys. Rev. **D56**, 2755 (1997).
158. S. Aoki *et al.*, Phys. Rev. Lett. **74**, 222 (1995).
159. A. Spitz *et al.*, Phys. Rev. **D60**, 074502 (1999).
160. P. Boucaud *et al.*, JHEP **0201**, 046 (2002).
161. A.X. El-Khadra *et al.*, Phys. Rev. Lett. **69**, 729 (1992);
A.X. El-Khadra *et al.*, FNAL 94-091/T (1994);
A.X. El-Khadra *et al.*, `hep-ph/9608220`.
162. S. Collins *et al.*, cited by Ref. 163.
163. J. Shigemitsu, Nucl. Phys. **B** (Proc. Supp.) **53**, 16 (1997).
164. A. Bode *et al.*, [ALPHA Collaboration], Phys. Lett. **B515**, 4 (2001).
165. R. Sommer, Nucl. Phys. **B411**, (1994).
166. G. de Divitiis *et al.*, Nucl. Phys. **B437**, 447 (1995);
M. Luscher *et al.*, Nucl. Phys. **B413**, 481 (1994).
167. S. Booth *et al.*, [QCDSF-UKQCD Collaboration], Phys. Lett. **B519**, 229 (2001).
168. M. Luscher and P. Weisz, Nucl. Phys. **B452**, 234 (1995);
C. Christou *et al.*, Nucl. Phys. **B525**, 387 (1998); and erratum Nucl. Phys. **B608**, 479 (2001).
169. C.T. Sachrajda, *International Conference on Lepton Photon Interactions*, Rome Italy (Aug. 2001);
P. Lepage *International Conference on Lepton Photon Interactions*, Fermilab (Aug. 2003).
170. P.N. Burrows *et al.*, in *Proceedings of 1996 DPF/DPB Snowmass Summer Study*, ed. D. Cassel *et al.*, (1997).

10. ELECTROWEAK MODEL AND CONSTRAINTS ON NEW PHYSICS

Revised December 2003 by J. Erler (U. Mexico) and P. Langacker (Univ. of Pennsylvania).

10.1. Introduction

The standard electroweak model (SM) is based on the gauge group [1] SU(2) × U(1), with gauge bosons W^i_μ, $i = 1, 2, 3$, and B_μ for the SU(2) and U(1) factors, respectively, and the corresponding gauge coupling constants g and g'. The left-handed fermion fields $\psi_i = \begin{pmatrix} \nu_i \\ \ell_i^- \end{pmatrix}$ and $\begin{pmatrix} u_i \\ d'_i \end{pmatrix}$ of the i^{th} fermion family transform as doublets under SU(2), where $d'_i \equiv \sum_j V_{ij}\, d_j$, and V is the Cabibbo-Kobayashi-Maskawa mixing matrix. (Constraints on V and tests of universality are discussed in Ref. 2 and in the Section on the Cabibbo-Kobayashi-Maskawa mixing matrix.) The right-handed fields are SU(2) singlets. In the minimal model there are three fermion families and a single complex Higgs doublet $\phi \equiv \begin{pmatrix} \phi^+ \\ \phi^0 \end{pmatrix}$.

After spontaneous symmetry breaking the Lagrangian for the fermion fields is

$$\begin{aligned}\mathscr{L}_F = &\sum_i \overline{\psi}_i \left(i\, \partial\!\!\!/ - m_i - \frac{g m_i H}{2M_W} \right) \psi_i \\ &- \frac{g}{2\sqrt{2}} \sum_i \overline{\psi}_i\, \gamma^\mu\, (1-\gamma^5)(T^+\, W^+_\mu + T^-\, W^-_\mu)\, \psi_i \\ &- e \sum_i q_i\, \overline{\psi}_i\, \gamma^\mu\, \psi_i\, A_\mu \\ &- \frac{g}{2\cos\theta_W} \sum_i \overline{\psi}_i\, \gamma^\mu (g^i_V - g^i_A \gamma^5)\, \psi_i\, Z_\mu\ . \end{aligned} \tag{10.1}$$

$\theta_W \equiv \tan^{-1}(g'/g)$ is the weak angle; $e = g \sin\theta_W$ is the positron electric charge; and $A \equiv B\cos\theta_W + W^3 \sin\theta_W$ is the (massless) photon field. $W^\pm \equiv (W^1 \mp i W^2)/\sqrt{2}$ and $Z \equiv -B \sin\theta_W + W^3 \cos\theta_W$ are the massive charged and neutral weak boson fields, respectively. T^+ and T^- are the weak isospin raising and lowering operators. The vector and axial-vector couplings are

$$g^i_V \equiv t_{3L}(i) - 2 q_i \sin^2\theta_W\ , \tag{10.2a}$$

$$g^i_A \equiv t_{3L}(i)\ , \tag{10.2b}$$

where $t_{3L}(i)$ is the weak isospin of fermion i ($+1/2$ for u_i and ν_i; $-1/2$ for d_i and e_i) and q_i is the charge of ψ_i in units of e.

The second term in $\mathscr{L}_F$ represents the charged-current weak interaction [3,4]. For example, the coupling of a W to an electron and a neutrino is

$$-\frac{e}{2\sqrt{2}\sin\theta_W} \left[W^-_\mu\ \overline{e}\, \gamma^\mu (1-\gamma^5)\nu + W^+_\mu\, \overline{\nu}\, \gamma^\mu\, (1-\gamma^5) e \right]\ . \tag{10.3}$$

For momenta small compared to M_W, this term gives rise to the effective four-fermion interaction with the Fermi constant given (at tree level, *i.e.*, lowest order in perturbation theory) by $G_F/\sqrt{2} = g^2/8M_W^2$. CP violation is incorporated in the SM by a single observable phase in V_{ij}. The third term in $\mathscr{L}_F$ describes electromagnetic interactions (QED), and the last is the weak neutral-current interaction.

In Eq. (10.1), m_i is the mass of the i^{th} fermion ψ_i. For the quarks these are the current masses. For the light quarks, as described in the Particle Listings, $\widehat{m}_u \approx$ 1.5–4.5 MeV, $\widehat{m}_d \approx$ 5–8.5 MeV, and $\widehat{m}_s \approx$ 80–155 MeV. These are running $\overline{\rm MS}$ masses evaluated at the scale $\mu = 2$ GeV. (In this Section we denote quantities defined in the $\overline{\rm MS}$ scheme by a caret; the exception is the strong coupling constant, α_s, which will always correspond to the $\overline{\rm MS}$ definition and where the caret will be dropped.) For the heavier quarks we use QCD sum rule constraints [5] and recalculate their masses in each call of our fits to account for their direct α_s dependence. We find, $\widehat{m}_c(\mu = \widehat{m}_c) = 1.290^{+0.040}_{-0.045}$ GeV and $\widehat{m}_b(\mu = \widehat{m}_b) = 4.206 \pm 0.031$ GeV, with a correlation of 29%. The top quark "pole" mass, $m_t = 177.9 \pm 4.4$ GeV, is an average of CDF results from run I [6] and run II [7], as well as the DØ dilepton [8] and lepton plus jets [9] channels. The latter has been recently reanalyzed, leading to a somewhat higher value. We computed the covariance matrix accounting for correlated systematic uncertainties between the different channels and experiments according to Refs. 6 and 10. Our covariance matrix also accounts for a common 0.6 GeV uncertainty (the size of the three-loop term [11]) due to the conversion from the pole mass to the $\overline{\rm MS}$ mass. We are using a BLM optimized [12] version of the two-loop perturbative QCD formula [13] which should correspond approximately to the kinematic mass extracted from the collider events. The three-loop formula [11] gives virtually identical results. We use $\overline{\rm MS}$ masses in all expressions to minimize theoretical uncertainties. We will use above value for m_t (together with $M_H = 117$ GeV) for the numerical values quoted in Sec. 10.2–Sec. 10.4. See "The Note on Quark Masses" in the Particle Listings for more information. In the presence of right-handed neutrinos, Eq. (10.1) gives rise also to Dirac neutrino masses. The possibility of Majorana masses is discussed in "Neutrino mass" in the Particle Listings.

H is the physical neutral Higgs scalar which is the only remaining part of ϕ after spontaneous symmetry breaking. The Yukawa coupling of H to ψ_i, which is flavor diagonal in the minimal model, is $g m_i/2M_W$. In non-minimal models there are additional charged and neutral scalar Higgs particles [14].

10.2. Renormalization and radiative corrections

The SM has three parameters (not counting the Higgs boson mass, M_H, and the fermion masses and mixings). A particularly useful set is:

(a) The fine structure constant $\alpha = 1/137.03599911(46)$, determined from the $e^\pm$ anomalous magnetic moment, the quantum Hall effect, and other measurements [15]. In most electroweak renormalization schemes, it is convenient to define a running α dependent on the energy scale of the process, with $\alpha^{-1} \sim 137$ appropriate at very low energy. (The running has also been observed directly [16].) For scales above a few hundred MeV this introduces an uncertainty due to the low-energy hadronic contribution to vacuum polarization. In the modified minimal subtraction ($\overline{\rm MS}$) scheme [17] (used for this *Review*), and with $\alpha_s(M_Z) = 0.120$ for the QCD coupling at M_Z, we have $\widehat{\alpha}(m_\tau)^{-1} = 133.498 \pm 0.017$ and $\widehat{\alpha}(M_Z)^{-1} = 127.918 \pm 0.018$. These values are updated from Ref. 18 and account for the latest results from τ decays and a reanalysis of the CMD 2 collaboration results after correcting a radiative correction [19]. See Ref. 20 for a discussion in the context of the anomalous magnetic moment of the muon. The correlation of the latter with $\widehat{\alpha}(M_Z)$, as well as the non-linear α_s dependence of $\widehat{\alpha}(M_Z)$ and the resulting correlation with the input variable α_s, are fully taken into account in the fits. The uncertainty is from e^+e^- annihilation data below 1.8 GeV and τ decay data, from isospin breaking effects (affecting the interpretation of the τ data), from uncalculated higher order perturbative and non-perturbative QCD corrections, and from the $\overline{\rm MS}$ quark masses. Such a short distance mass definition (unlike the pole mass) is free from non-perturbative and renormalon uncertainties. Various recent evaluations of the contributions of the five light quark flavors, $\Delta\alpha^{(5)}_{\rm had}$, to the conventional (on-shell) QED coupling, $\alpha(M_Z) = \dfrac{\alpha}{1 - \Delta\alpha}$, are summarized in Table 10.1. Most of the older results relied on $e^+e^- \to$ hadrons cross-section measurements up to energies of 40 GeV, which were somewhat higher than the QCD prediction, suggested stronger running, and were less precise. The most recent results typically assume the validity of perturbative QCD (PQCD) at scales of 1.8 GeV and above, and are in reasonable agreement with each other.

(Evaluations in the on-shell scheme utilize resonance data from BES [36] as further input.) There is, however, some discrepancy between analyzes based on $e^+e^- \to$ hadrons cross-section data

Table 10.1: Recent evaluations of the on-shell $\Delta\alpha^{(5)}_{\rm had}(M_Z)$. For better comparison we adjusted central values and errors to correspond to a common and fixed value of $\alpha_s(M_Z) = 0.120$. References quoting results without the top quark decoupled are converted to the five flavor definition. Ref. [31] uses $\Lambda_{\rm QCD} = 380 \pm 60$ MeV; for the conversion we assumed $\alpha_s(M_Z) = 0.118 \pm 0.003$.

Reference	Result	Comment
Martin & Zeppenfeld [21]	0.02744 ± 0.00036	PQCD for $\sqrt{s} > 3$ GeV
Eidelman & Jegerlehner [22]	0.02803 ± 0.00065	PQCD for $\sqrt{s} > 40$ GeV
Geshkenbein & Morgunov [23]	0.02780 ± 0.00006	$\mathcal{O}(\alpha_s)$ resonance model
Burkhardt & Pietrzyk [24]	0.0280 ± 0.0007	PQCD for $\sqrt{s} > 40$ GeV
Swartz [25]	0.02754 ± 0.00046	use of fitting function
Alemany, Davier, Höcker [26]	0.02816 ± 0.00062	includes τ decay data
Krasnikov & Rodenberg [27]	0.02737 ± 0.00039	PQCD for $\sqrt{s} > 2.3$ GeV
Davier & Höcker [28]	0.02784 ± 0.00022	PQCD for $\sqrt{s} > 1.8$ GeV
Kühn & Steinhauser [29]	0.02778 ± 0.00016	complete $\mathcal{O}(\alpha_s^2)$
Erler [18]	0.02779 ± 0.00020	converted from $\overline{\rm MS}$ scheme
Davier & Höcker [30]	0.02770 ± 0.00015	use of QCD sum rules
Groote *et al.* [31]	0.02787 ± 0.00032	use of QCD sum rules
Martin, Outhwaite, Ryskin [32]	0.02741 ± 0.00019	includes new BES data
Burkhardt & Pietrzyk [33]	0.02763 ± 0.00036	PQCD for $\sqrt{s} > 12$ GeV
de Troconiz & Yndurain [34]	0.02754 ± 0.00010	PQCD for $s > 2$ GeV^2
Jegerlehner [35]	0.02766 ± 0.00013	converted from MOM scheme

and those based on τ decay spectral functions [20]. The latter imply lower central values for the extracted M_H of $\mathcal{O}(10$ GeV). Further improvement of this dominant theoretical uncertainty in the interpretation of precision data will require better measurements of the cross-section for $e^+e^- \to$ hadrons below the charmonium resonances, as well as in the threshold region of the heavy quarks (to improve the precision in $\widehat{m}_c(\widehat{m}_c)$ and $\widehat{m}_b(\widehat{m}_b)$). As an alternative to cross-section scans, one can use the high statistics radiative return events [37] at e^+e^- accelerators operating at resonances such as the Φ or the $\Upsilon(4S)$. The method is systematics dominated. First preliminary results have been presented by the KLOE collaboration [38].

(b) The Fermi constant, $G_F = 1.16637(1) \times 10^{-5}$ GeV^{-2}, determined from the muon lifetime formula [39,40],

$$\tau_\mu^{-1} = \frac{G_F^2 m_\mu^5}{192\pi^3} F\left(\frac{m_e^2}{m_\mu^2}\right)\left(1 + \frac{3}{5}\frac{m_\mu^2}{M_W^2}\right) \times \left[1 + \left(\frac{25}{8} - \frac{\pi^2}{2}\right)\frac{\alpha(m_\mu)}{\pi} + C_2\frac{\alpha^2(m_\mu)}{\pi^2}\right] , \qquad (10.4a)$$

where

$$F(x) = 1 - 8x + 8x^3 - x^4 - 12x^2 \ln x , \qquad (10.4b)$$

$$C_2 = \frac{156815}{5184} - \frac{518}{81}\pi^2 - \frac{895}{36}\zeta(3) + \frac{67}{720}\pi^4 + \frac{53}{6}\pi^2 \ln(2) , \qquad (10.4c)$$

and

$$\alpha(m_\mu)^{-1} = \alpha^{-1} - \frac{2}{3\pi}\ln\left(\frac{m_\mu}{m_e}\right) + \frac{1}{6\pi} \approx 136 . \qquad (10.4d)$$

The $\mathcal{O}(\alpha^2)$ corrections to μ decay have been completed recently [40]. The remaining uncertainty in G_F is from the experimental input.

(c) The Z boson mass, $M_Z = 91.1876 \pm 0.0021$ GeV, determined from the Z-lineshape scan at LEP 1 [41].

With these inputs, $\sin^2\theta_W$ and the W boson mass, M_W, can be calculated when values for m_t and M_H are given; conversely (as is done at present), M_H can be constrained by $\sin^2\theta_W$ and M_W. The value of $\sin^2\theta_W$ is extracted from Z-pole observables and neutral-current processes [41,42], and depends on the renormalization prescription. There are a number of popular schemes [44–50] leading to values which differ by small factors depending on m_t and M_H. The notation for these schemes is shown in Table 10.2. Discussion of the schemes follows the table.

Table 10.2: Notations used to indicate the various schemes discussed in the text. Each definition of $\sin\theta_W$ leads to values that differ by small factors depending on m_t and M_H.

Scheme	Notation
On-shell	$s_W \equiv \sin\theta_W$
NOV	$s_{M_Z} \equiv \sin\theta_W$
$\overline{\rm MS}$	$\widehat{s}_Z \equiv \sin\theta_W$
$\overline{\rm MS}$ ND	$\widehat{s}_{\rm ND} \equiv \sin\theta_W$
Effective angle	$\overline{s}_f \equiv \sin\theta_W$

(i) The on-shell scheme [44] promotes the tree-level formula $\sin^2\theta_W = 1 - M_W^2/M_Z^2$ to a definition of the renormalized $\sin^2\theta_W$ to all orders in perturbation theory, *i.e.*, $\sin^2\theta_W \to s_W^2 \equiv 1 - M_W^2/M_Z^2$:

$$M_W = \frac{A_0}{s_W(1-\Delta r)^{1/2}} , \qquad (10.5a)$$

$$M_Z = \frac{M_W}{c_W} , \qquad (10.5b)$$

where $c_W \equiv \cos\theta_W$, $A_0 = (\pi\alpha/\sqrt{2}G_F)^{1/2} = 37.2805(2)$ GeV, and Δr includes the radiative corrections relating α, $\alpha(M_Z)$, G_F, M_W, and M_Z. One finds $\Delta r \sim \Delta r_0 - \rho_t/\tan^2\theta_W$, where $\Delta r_0 = 1 - \alpha/\widehat{\alpha}(M_Z) = 0.06654(14)$ is due to the running of α, and $\rho_t = 3G_F m_t^2/8\sqrt{2}\pi^2 = 0.00992(m_t/177.9\ {\rm GeV})^2$ represents the dominant (quadratic) m_t dependence. There are additional contributions to Δr from bosonic loops, including those which depend logarithmically on M_H. One has $\Delta r = 0.03434 \mp 0.0017 \pm 0.00014$, where the second uncertainty is from $\alpha(M_Z)$. Thus the value of s_W^2 extracted from M_Z includes an uncertainty (∓ 0.00054) from the currently allowed range of m_t. This scheme is simple conceptually. However, the relatively large ($\sim 3\%$) correction from ρ_t causes large spurious contributions in higher orders.

(ii) A more precisely determined quantity $s^2_{M_Z}$ can be obtained from M_Z by removing the (m_t, M_H) dependent term from Δr [45], *i.e.*,

$$s^2_{M_Z} c^2_{M_Z} \equiv \frac{\pi\alpha(M_Z)}{\sqrt{2}\, G_F\, M_Z^2} . \qquad (10.6)$$

Using $\alpha(M_Z)^{-1} = 128.91 \pm 0.02$ yields $s^2_{M_Z} = 0.23108 \mp 0.00005$. The small uncertainty in $s^2_{M_Z}$ compared to other schemes is because most of the m_t dependence has been removed by definition. However, the m_t uncertainty reemerges when other

quantities (*e.g.*, M_W or other Z-pole observables) are predicted in terms of M_Z.

Both s^2_W and $s^2_{M_Z}$ depend not only on the gauge couplings but also on the spontaneous-symmetry breaking, and both definitions are awkward in the presence of any extension of the SM which perturbs the value of M_Z (or M_W). Other definitions are motivated by the tree-level coupling constant definition $\theta_W = \tan^{-1}(g'/g)$.

(*iii*) In particular, the modified minimal subtraction ($\overline{\rm MS}$) scheme introduces the quantity $\sin^2\widehat{\theta}_W(\mu) \equiv \widehat{g}'^2(\mu)/[\widehat{g}^{\,2}(\mu) + \widehat{g}'^2(\mu)]$, where the couplings $\widehat{g}$ and $\widehat{g}'$ are defined by modified minimal subtraction and the scale μ is conveniently chosen to be M_Z for many electroweak processes. The value of $\widehat{s}^2_Z = \sin^2\widehat{\theta}_W(M_Z)$ extracted from M_Z is less sensitive than s^2_W to m_t (by a factor of $\tan^2\theta_W$), and is less sensitive to most types of new physics than s^2_W or $s^2_{M_Z}$. It is also very useful for comparing with the predictions of grand unification. There are actually several variant definitions of $\sin^2\widehat{\theta}_W(M_Z)$, differing according to whether or how finite $\alpha\ln(m_t/M_Z)$ terms are decoupled (subtracted from the couplings). One cannot entirely decouple the $\alpha\ln(m_t/M_Z)$ terms from all electroweak quantities because $m_t \gg m_b$ breaks SU(2) symmetry. The scheme that will be adopted here decouples the $\alpha\ln(m_t/M_Z)$ terms from the γ–Z mixing [17,46], essentially eliminating any $\ln(m_t/M_Z)$ dependence in the formulae for asymmetries at the Z-pole when written in terms of $\widehat{s}^2_Z$. (A similar definition is used for $\widehat{\alpha}$.) The various definitions are related by

$$\widehat{s}^2_Z = c(m_t, M_H)\, s^2_W = \overline{c}(m_t, M_H)\, s^2_{M_Z} \ , \qquad (10.7)$$

where $c = 1.0381 \pm 0.0019$ and $\overline{c} = 1.0003 \mp 0.0006$. The quadratic m_t dependence is given by $c \sim 1 + \rho_t/\tan^2\theta_W$ and $\overline{c} \sim 1 - \rho_t/(1-\tan^2\theta_W)$, respectively. The expressions for M_W and M_Z in the $\overline{\rm MS}$ scheme are

$$M_W = \frac{A_0}{\widehat{s}_Z(1-\Delta\widehat{r}_W)^{1/2}} \ , \qquad (10.8a)$$

$$M_Z = \frac{M_W}{\widehat{\rho}^{1/2}\widehat{c}_Z} \ , \qquad (10.8b)$$

and one predicts $\Delta\widehat{r}_W = 0.06976 \pm 0.00006 \pm 0.00014$. $\Delta\widehat{r}_W$ has no quadratic m_t dependence, because shifts in M_W are absorbed into the observed G_F, so that the error in $\Delta\widehat{r}_W$ is dominated by $\Delta r_0 = 1 - \alpha/\widehat{\alpha}(M_Z)$ which induces the second quoted uncertainty. The quadratic m_t dependence has been shifted into $\widehat{\rho} \sim 1 + \rho_t$, where including bosonic loops, $\widehat{\rho} = 1.0110 \pm 0.0005$.

(*iv*) A variant $\overline{\rm MS}$ quantity $\widehat{s}^2_{\rm ND}$ (used in the 1992 edition of this *Review*) does not decouple the $\alpha\ln(m_t/M_Z)$ terms [47]. It is related to $\widehat{s}^2_Z$ by

$$\widehat{s}^2_Z = \widehat{s}^2_{\rm ND}/\left(1 + \frac{\widehat{\alpha}}{\pi}d\right) \ , \qquad (10.9a)$$

$$d = \frac{1}{3}\left(\frac{1}{\widehat{s}^2} - \frac{8}{3}\right)\left[(1+\frac{\alpha_s}{\pi})\ln\frac{m_t}{M_Z} - \frac{15\alpha_s}{8\pi}\right], \qquad (10.9b)$$

Thus, $\widehat{s}^2_Z - \widehat{s}^2_{\rm ND} \sim -0.0002$ for $m_t = 177.9$ GeV.

(*v*) Yet another definition, the effective angle [48–50] $\overline{s}^2_f$ for the Z vector coupling to fermion f, is described in Sec. 10.3.

Experiments are at a level of precision that complete $\mathcal{O}(\alpha)$ radiative corrections must be applied. For neutral-current and Z-pole processes, these corrections are conveniently divided into two classes:

1. QED diagrams involving the emission of real photons or the exchange of virtual photons in loops, but not including vacuum polarization diagrams. These graphs often yield finite and gauge-invariant contributions to observable processes. However, they are dependent on energies, experimental cuts, *etc.*, and must be calculated individually for each experiment.
2. Electroweak corrections, including $\gamma\gamma$, γZ, ZZ, and WW vacuum polarization diagrams, as well as vertex corrections, box graphs, *etc.*, involving virtual W's and Z's. Many of these corrections are absorbed into the renormalized Fermi constant defined in Eq. (10.4). Others modify the tree-level expressions for Z-pole observables and neutral-current amplitudes in several ways [42]. One-loop corrections are included for all processes. In addition, certain two-loop corrections are also important. In particular, two-loop corrections involving the top quark modify ρ_t in $\widehat{\rho}$, Δr, and elsewhere by

$$\rho_t \to \rho_t[1 + R(M_H, m_t)\rho_t/3] \ . \qquad (10.10)$$

$R(M_H, m_t)$ is best described as an expansion in M^2_Z/m^2_t. The unsuppressed terms were first obtained in Ref. 51, and are known analytically [52]. Contributions suppressed by M^2_Z/m^2_t were first studied in Ref. 53 with the help of small and large Higgs mass expansions, which can be interpolated. These contributions are about as large as the leading ones in Refs. 51 and 52. In addition, the complete two-loop calculation of diagrams containing at least one fermion loop and contributing to Δr has been performed without further approximation in Ref. 54. The two-loop evaluation of Δr was completed with the purely bosonic contributions in Ref. 55. For M_H above its lower direct limit, $-17 < R \leq -13$. Mixed QCD-electroweak loops of order $\alpha\alpha_s m^2_t$ [56] and $\alpha\alpha^2_s m^2_t$ [57] increase the predicted value of m_t by 6%. This is, however, almost entirely an artifact of using the pole mass definition for m_t. The equivalent corrections when using the $\overline{\rm MS}$ definition $\widehat{m}_t(\widehat{m}_t)$ increase m_t by less than 0.5%. The leading electroweak [51,52] and mixed [58] two-loop terms are also known for the $Z \to b\bar{b}$ vertex, but not the respective subleading ones. $\mathcal{O}(\alpha\alpha_s)$-vertex corrections involving massless quarks have been obtained in Ref. [59]. Since they add coherently, the resulting effect is sizable, and shifts the extracted $\alpha_s(M_Z)$ by $\approx +0.0007$. Corrections of the same order to $Z \to b\bar{b}$ decays have also been completed [60].

Throughout this *Review* we utilize electroweak radiative corrections from the program GAPP [61], which works entirely in the $\overline{\rm MS}$ scheme, and which is independent of the package ZFITTER [50].

10.3. Cross-section and asymmetry formulas

It is convenient to write the four-fermion interactions relevant to ν-hadron, ν-e, and parity violating e-hadron neutral-current processes in a form that is valid in an arbitrary gauge theory (assuming massless left-handed neutrinos). One has

$$-\mathscr{L}^{\nu\rm Hadron} = \frac{G_F}{\sqrt{2}}\,\overline{\nu}\,\gamma^\mu\,(1-\gamma^5)\nu$$

$$\times\sum_i\left[\epsilon_L(i)\,\overline{q}_i\,\gamma_\mu(1-\gamma^5)q_i + \epsilon_R(i)\,\overline{q}_i\,\gamma_\mu(1+\gamma^5)q_i\right] \ , \qquad (10.11)$$

$$-\mathscr{L}^{\nu e} = \frac{G_F}{\sqrt{2}}\,\overline{\nu}_\mu\,\gamma^\mu(1-\gamma^5)\nu_\mu\,\overline{e}\,\gamma_\mu(g^{\nu e}_V - g^{\nu e}_A\gamma^5)e \qquad (10.12)$$

(for ν_e-e or $\overline{\nu}_e$-e, the charged-current contribution must be included), and

$$-\mathscr{L}^{e\rm Hadron} = -\frac{G_F}{\sqrt{2}}$$

$$\times\sum_i\left[C_{1i}\,\overline{e}\,\gamma_\mu\,\gamma^5\,e\,\overline{q}_i\,\gamma^\mu\,q_i + C_{2i}\,\overline{e}\,\gamma_\mu\,e\,\overline{q}_i\,\gamma^\mu\,\gamma^5\,q_i\right] \ . \qquad (10.13)$$

(One must add the parity-conserving QED contribution.)

The SM expressions for $\epsilon_{L,R}(i)$, $g^{\nu e}_{V,A}$, and C_{ij} are given in Table 10.3. Note, that $g^{\nu e}_{V,A}$ and the other quantities are coefficients of effective four-Fermi operators, which differ from the quantities defined in Eq. (10.2) in the radiative corrections and in the presence of possible physics beyond the SM.

A precise determination of the on-shell s^2_W, which depends only very weakly on m_t and M_H, is obtained from deep inelastic neutrino scattering from (approximately) isoscalar targets [62]. The ratio $R_\nu \equiv \sigma^{NC}_{\nu N}/\sigma^{CC}_{\nu N}$ of neutral- to charged-current cross-sections has been measured to 1% accuracy by the CDHS [63] and CHARM [64]

collaborations at CERN, and the CCFR [65] collaboration at Fermilab has obtained an even more precise result, so it is important to obtain theoretical expressions for R_ν and $R_{\overline{\nu}} \equiv \sigma^{NC}_{\overline{\nu}N}/\sigma^{CC}_{\overline{\nu}N}$ to comparable accuracy. Fortunately, most of the uncertainties from the strong interactions and neutrino spectra cancel in the ratio. The largest theoretical uncertainty is associated with the c-threshold, which mainly affects σ^{CC}. Using the slow rescaling prescription [66] the central value of $\sin^2\theta_W$ from CCFR varies as $0.0111(m_c\ [\mathrm{GeV}] - 1.31)$, where m_c is the effective mass which is numerically close to the $\overline{\rm MS}$ mass $\widehat{m}_c(\widehat{m}_c)$, but their exact relation is unknown at higher orders. For $m_c = 1.31 \pm 0.24$ GeV (determined from ν-induced dimuon production [67]) this contributes ± 0.003 to the total uncertainty $\Delta \sin^2\theta_W \sim \pm 0.004$. (The experimental uncertainty is also ± 0.003.) This uncertainty largely cancels, however, in the Paschos-Wolfenstein ratio [68],

$$R^- = \frac{\sigma^{NC}_{\nu N} - \sigma^{NC}_{\overline{\nu}N}}{\sigma^{CC}_{\nu N} - \sigma^{CC}_{\overline{\nu}N}} \,. \tag{10.14}$$

It was measured recently by the NuTeV collaboration [69] for the first time, and required a high-intensity and high-energy anti-neutrino beam.

Table 10.3: Standard Model expressions for the neutral-current parameters for ν-hadron, ν-e, and e-hadron processes. At tree level, $\rho = \kappa = 1$, $\lambda = 0$. If radiative corrections are included, $\rho^{NC}_{\nu N} = 1.0086$, $\widehat{\kappa}_{\nu N}(\langle Q^2\rangle = -12\ \mathrm{GeV}^2) = 0.9978$, $\widehat{\kappa}_{\nu N}(\langle Q^2\rangle = -35\ \mathrm{GeV}^2) = 0.9965$, $\lambda_{uL} = -0.0031$, $\lambda_{dL} = -0.0025$, and $\lambda_{dR} = 2\,\lambda_{uR} = 7.5 \times 10^{-5}$. For ν-e scattering, $\rho_{\nu e} = 1.0132$ and $\widehat{\kappa}_{\nu e} = 0.9967$ (at $\langle Q^2\rangle = 0$.). For atomic parity violation and the SLAC polarized electron experiment, $\rho'_{eq} = 0.9881$, $\rho_{eq} = 1.0011$, $\widehat{\kappa}'_{eq} = 1.0027$, $\widehat{\kappa}_{eq} = 1.0300$, $\lambda_{1d} = -2\,\lambda_{1u} = 3.7 \times 10^{-5}$, $\lambda_{2u} = -0.0121$ and $\lambda_{2d} = 0.0026$. The dominant m_t dependence is given by $\rho \sim 1 + \rho_t$, while $\widehat{\kappa} \sim 1$ ($\overline{\rm MS}$) or $\kappa \sim 1 + \rho_t/\tan^2\theta_W$ (on-shell).

Quantity	Standard Model Expression
$\epsilon_L(u)$	$\rho^{NC}_{\nu N}\left(\frac{1}{2} - \frac{2}{3}\widehat{\kappa}_{\nu N}\,\widehat{s}^2_Z\right) + \lambda_{uL}$
$\epsilon_L(d)$	$\rho^{NC}_{\nu N}\left(-\frac{1}{2} + \frac{1}{3}\widehat{\kappa}_{\nu N}\,\widehat{s}^2_Z\right) + \lambda_{dL}$
$\epsilon_R(u)$	$\rho^{NC}_{\nu N}\left(-\frac{2}{3}\widehat{\kappa}_{\nu N}\,\widehat{s}^2_Z\right) + \lambda_{u\,R}$
$\epsilon_R(d)$	$\rho^{NC}_{\nu N}\left(\frac{1}{3}\widehat{\kappa}_{\nu N}\,\widehat{s}^2_Z\right) + \lambda_{dR}$
$g^{\nu e}_V$	$\rho_{\nu e}\left(-\frac{1}{2} + 2\widehat{\kappa}_{\nu e}\,\widehat{s}^2_Z\right)$
$g^{\nu e}_A$	$\rho_{\nu e}\left(-\frac{1}{2}\right)$
C_{1u}	$\rho'_{eq}\left(-\frac{1}{2} + \frac{4}{3}\widehat{\kappa}'_{eq}\,\widehat{s}^2_Z\right) + \lambda_{1u}$
C_{1d}	$\rho'_{eq}\left(\frac{1}{2} - \frac{2}{3}\widehat{\kappa}'_{eq}\,\widehat{s}^2_Z\right) + \lambda_{1d}$
C_{2u}	$\rho_{eq}\left(-\frac{1}{2} + 2\widehat{\kappa}_{eq}\,\widehat{s}^2_Z\right) + \lambda_{2u}$
C_{2d}	$\rho_{eq}\left(\frac{1}{2} - 2\widehat{\kappa}_{eq}\,\widehat{s}^2_Z\right) + \lambda_{2d}$

A simple zeroth-order approximation is

$$R_\nu = g^2_L + g^2_R r \,, \tag{10.15a}$$

$$R_{\overline{\nu}} = g^2_L + \frac{g^2_R}{r} \,, \tag{10.15b}$$

$$R^- = g^2_L - g^2_R \,, \tag{10.15c}$$

where

$$g^2_L \equiv \epsilon_L(u)^2 + \epsilon_L(d)^2 \approx \frac{1}{2} - \sin^2\theta_W + \frac{5}{9}\sin^4\theta_W \,, \tag{10.16a}$$

$$g^2_R \equiv \epsilon_R(u)^2 + \epsilon_R(d)^2 \approx \frac{5}{9}\sin^4\theta_W \,, \tag{10.16b}$$

and $r \equiv \sigma^{CC}_{\overline{\nu}N}/\sigma^{CC}_{\nu N}$ is the ratio of $\overline{\nu}$ and ν charged-current cross-sections, which can be measured directly. (In the simple parton model, ignoring hadron energy cuts, $r \approx (\frac{1}{3} + \epsilon)/(1 + \frac{1}{3}\epsilon)$, where $\epsilon \sim 0.125$ is the ratio of the fraction of the nucleon's momentum carried by antiquarks to that carried by quarks.) In practice, Eq. (10.15) must be corrected for quark mixing, quark sea effects, c-quark threshold effects, non-isoscalarity, W–Z propagator differences, the finite muon mass, QED and electroweak radiative corrections. Details of the neutrino spectra, experimental cuts, x and Q^2 dependence of structure functions, and longitudinal structure functions enter only at the level of these corrections and therefore lead to very small uncertainties. The CCFR group quotes $s^2_W = 0.2236 \pm 0.0041$ for $(m_t, M_H) = (175, 150)$ GeV with very little sensitivity to (m_t, M_H). The NuTeV collaboration finds $s^2_W = 0.2277 \pm 0.0016$ (for the same reference values) which is 3.0 σ higher than the SM prediction. The discrepancy is in the left-handed coupling, $g^2_L = 0.3000 \pm 0.0014$, which is 2.9 σ low, while $g^2_R = 0.0308 \pm 0.0011$ is 0.6 σ high. It is conceivable that the effect is caused by an asymmetric strange sea [70]. A preliminary analysis of dimuon data [71] in the relevant kinematic regime, however, indicates an asymmetric strange sea with the wrong sign to explain the discrepancy [72]. Another possibility is that the parton distribution functions (PDFs) violate isospin symmetry at levels much stronger than generally expected. Isospin breaking, nuclear physics, and higher order QCD effects seem unlikely explanations of the NuTeV discrepancy but need further study. The extracted $g^2_{L,R}$ may also shift if analyzed using the most recent set of QED and electroweak radiative corrections [73].

The laboratory cross-section for $\nu_\mu e \to \nu_\mu e$ or $\overline{\nu}_\mu e \to \overline{\nu}_\mu e$ elastic scattering is

$$\frac{d\sigma_{\nu_\mu,\overline{\nu}_\mu}}{dy} = \frac{G^2_F m_e E_\nu}{2\pi} \times \left[(g^{\nu e}_V \pm g^{\nu e}_A)^2 + (g^{\nu e}_V \mp g^{\nu e}_A)^2(1-y)^2 - (g^{\nu e 2}_V - g^{\nu e 2}_A)\frac{y\,m_e}{E_\nu}\right] \,, \tag{10.17}$$

where the upper (lower) sign refers to $\nu_\mu(\overline{\nu}_\mu)$, and $y \equiv E_e/E_\nu$ (which runs from 0 to $(1 + m_e/2E_\nu)^{-1}$) is the ratio of the kinetic energy of the recoil electron to the incident ν or $\overline{\nu}$ energy. For $E_\nu \gg m_e$ this yields a total cross-section

$$\sigma = \frac{G^2_F\, m_e\, E_\nu}{2\pi}\left[(g^{\nu e}_V \pm g^{\nu e}_A)^2 + \frac{1}{3}(g^{\nu e}_V \mp g^{\nu e}_A)^2\right] \,. \tag{10.18}$$

The most accurate leptonic measurements [74–77] of $\sin^2\theta_W$ are from the ratio $R \equiv \sigma_{\nu_\mu e}/\sigma_{\overline{\nu}_\mu e}$ in which many of the systematic uncertainties cancel. Radiative corrections (other than m_t effects) are small compared to the precision of present experiments and have negligible effect on the extracted $\sin^2\theta_W$. The most precise experiment (CHARM II) [76] determined not only $\sin^2\theta_W$ but $g^{\nu e}_{V,A}$ as well. The cross-sections for ν_e-e and $\overline{\nu}_e$-e may be obtained from Eq. (10.17) by replacing $g^{\nu e}_{V,A}$ by $g^{\nu e}_{V,A} + 1$, where the 1 is due to the charged-current contribution [77,78].

The SLAC polarized-electron experiment [79] measured the parity-violating asymmetry

$$A = \frac{\sigma_R - \sigma_L}{\sigma_R + \sigma_L} \,, \tag{10.19}$$

where $\sigma_{R,L}$ is the cross-section for the deep-inelastic scattering of a right- or left-handed electron: $e_{R,L}N \to e\mathrm{X}$. In the quark parton model

$$\frac{A}{Q^2} = a_1 + a_2\,\frac{1-(1-y)^2}{1+(1-y)^2} \,, \tag{10.20}$$

where $Q^2 > 0$ is the momentum transfer and y is the fractional energy transfer from the electron to the hadrons. For the deuteron or other isoscalar targets, one has, neglecting the s-quark and antiquarks,

$$a_1 = \frac{3G_F}{5\sqrt{2}\pi\alpha}\left(C_{1u} - \frac{1}{2}C_{1d}\right) \approx \frac{3G_F}{5\sqrt{2}\pi\alpha}\left(-\frac{3}{4} + \frac{5}{3}\sin^2\theta_W\right) \,, \tag{10.21a}$$

$$a_2 = \frac{3G_F}{5\sqrt{2}\pi\alpha}\left(C_{2u} - \frac{1}{2}C_{2d}\right) \approx \frac{9G_F}{5\sqrt{2}\pi\alpha}\left(\sin^2\theta_W - \frac{1}{4}\right) . \quad (10.21b)$$

There are now precise experiments measuring atomic parity violation [80] in cesium (at the 0.4% level) [81], thallium [82], lead [83], and bismuth [84]. The uncertainties associated with atomic wave functions are quite small for cesium [85], and have been reduced recently to about 0.4% [86]. In the past, the semi-empirical value of the tensor polarizability added another source of theoretical uncertainty [87]. The ratio of the off-diagonal hyperfine amplitude to the polarizability has now been measured directly by the Boulder group [86]. Combined with the precisely known hyperfine amplitude [88] one finds excellent agreement with the earlier results, reducing the overall theory uncertainty to only 0.5% (while slightly increasing the experimental error). An earlier 2.3 σ deviation from the SM (see the year 2000 edition of this *Review*) is now seen at the 1 σ level, after the contributions from the Breit interaction have been reevaluated [89], and after the subsequent inclusion of other large and previously underestimated effects [90] (*e.g.*, from QED radiative corrections), and an update of the SM calculation [91] resulted in a vanishing net effect. The theoretical uncertainties are 3% for thallium [92] but larger for the other atoms. For heavy atoms one determines the "weak charge"

$$Q_W = -2\left[C_{1u}\,(2Z+N) + C_{1d}(Z+2N)\right]$$
$$\approx Z(1-4\sin^2\theta_W) - N . \quad (10.22)$$

The recent Boulder experiment in cesium also observed the parity-violating weak corrections to the nuclear electromagnetic vertex (the anapole moment [93]).

In the future it could be possible to reduce the theoretical wave function uncertainties by taking the ratios of parity violation in different isotopes [80,94]. There would still be some residual uncertainties from differences in the neutron charge radii, however [95].

The forward-backward asymmetry for $e^+e^- \to \ell^+\ell^-$, $\ell = \mu$ or τ, is defined as

$$A_{FB} \equiv \frac{\sigma_F - \sigma_B}{\sigma_F + \sigma_B} , \quad (10.23)$$

where $\sigma_F(\sigma_B)$ is the cross-section for ℓ^- to travel forward (backward) with respect to the e^- direction. A_{FB} and R, the total cross-section relative to pure QED, are given by

$$R = F_1 , \quad (10.24)$$

$$A_{FB} = 3F_2/4F_1 , \quad (10.25)$$

where

$$F_1 = 1 - 2\chi_0\, g_V^e\, g_V^\ell\, \cos\delta_R + \chi_0^2\left(g_V^{e2} + g_A^{e2}\right)\left(g_V^{\ell 2} + g_A^{\ell 2}\right), \quad (10.26a)$$

$$F_2 = -2\chi_0\, g_A^e\, g_A^\ell\, \cos\delta_R + 4\chi_0^2\, g_A^e\, g_A^\ell\, g_V^e\, g_V^\ell , \quad (10.26b)$$

$$\tan\delta_R = \frac{M_Z\Gamma_Z}{M_Z^2 - s} , \quad (10.27)$$

$$\chi_0 = \frac{G_F}{2\sqrt{2}\pi\alpha}\frac{sM_Z^2}{\left[(M_Z^2-s)^2 + M_Z^2\Gamma_Z^2\right]^{1/2}} , \quad (10.28)$$

and $\sqrt{s}$ is the CM energy. Eq. (10.26) is valid at tree level. If the data is radiatively corrected for QED effects (as described above), then the remaining electroweak corrections can be incorporated [96,97] (in an approximation adequate for existing PEP, PETRA, and TRISTAN data, which are well below the Z-pole) by replacing χ_0 by $\chi(s) \equiv (1+\rho_t)\chi_0(s)\alpha/\alpha(s)$, where $\alpha(s)$ is the running QED coupling, and evaluating g_V in the $\overline{\rm MS}$ scheme. Formulas for $e^+e^- \to$ hadrons may be found in Ref. 98.

At LEP and SLC, there were high-precision measurements of various Z-pole observables [41,99–105], as summarized in Table 10.4. These include the Z mass and total width, Γ_Z, and partial widths $\Gamma(f\overline{f})$ for $Z \to f\overline{f}$ where fermion $f = e$, μ, τ, hadrons, b, or c. It is convenient to use the variables M_Z, Γ_Z, $R_\ell \equiv \Gamma({\rm had})/\Gamma(\ell^+\ell^-)$, $\sigma_{\rm had} \equiv 12\pi\Gamma(e^+e^-)\Gamma({\rm had})/M_Z^2\Gamma_Z^2$, $R_b \equiv \Gamma(b\overline{b})/\Gamma({\rm had})$, and $R_c \equiv \Gamma(c\overline{c})/\Gamma({\rm had})$, most of which are weakly correlated experimentally. ($\Gamma({\rm had})$ is the partial width into hadrons.) $\mathcal{O}(\alpha^3)$ QED corrections introduce a large anticorrelation (-30%) between Γ_Z and $\sigma_{\rm had}$ [41], while the anticorrelation between R_b and R_c (-14%) is smaller than previously [100]. R_ℓ is insensitive to m_t except for the $Z \to b\overline{b}$ vertex and final state corrections and the implicit dependence through $\sin^2\theta_W$. Thus it is especially useful for constraining α_s. The width for invisible decays [41], $\Gamma({\rm inv}) = \Gamma_Z - 3\Gamma(\ell^+\ell^-) - \Gamma({\rm had}) = 499.0 \pm 1.5$ MeV, can be used to determine the number of neutrino flavors much lighter than $M_Z/2$, $N_\nu = \Gamma({\rm inv})/\Gamma^{\rm theory}(\nu\overline{\nu}) = 2.983 \pm 0.009$ for $(m_t, M_H) = (177.9, 117)$ GeV.

There were also measurements of various Z-pole asymmetries. These include the polarization or left-right asymmetry

$$A_{LR} \equiv \frac{\sigma_L - \sigma_R}{\sigma_L + \sigma_R} , \quad (10.29)$$

where $\sigma_L(\sigma_R)$ is the cross-section for a left-(right-)handed incident electron. A_{LR} has been measured precisely by the SLD collaboration at the SLC [101], and has the advantages of being extremely sensitive to $\sin^2\theta_W$ and that systematic uncertainties largely cancel. In addition, the SLD collaboration has extracted the final-state couplings A_b, A_c [41], A_s [102], A_τ, and A_μ [103] from left-right forward-backward asymmetries, using

$$A_{LR}^{FB}(f) = \frac{\sigma_{LF}^f - \sigma_{LB}^f - \sigma_{RF}^f + \sigma_{RB}^f}{\sigma_{LF}^f + \sigma_{LB}^f + \sigma_{RF}^f + \sigma_{RB}^f} = \frac{3}{4}A_f , \quad (10.30)$$

where, for example, σ_{LF} is the cross-section for a left-handed incident electron to produce a fermion f traveling in the forward hemisphere. Similarly, A_τ is measured at LEP [41] through the negative total τ polarization, $\mathcal{P}_\tau$, and A_e is extracted from the angular distribution of $\mathcal{P}_\tau$. An equation such as (10.30) assumes that initial state QED corrections, photon exchange, γ–Z interference, the tiny electroweak boxes, and corrections for $\sqrt{s} \neq M_Z$ are removed from the data, leaving the pure electroweak asymmetries. This allows the use of effective tree-level expressions,

$$A_{LR} = A_e P_e , \quad (10.31)$$

$$A_{FB} = \frac{3}{4}A_f\frac{A_e + P_e}{1 + P_e A_e} , \quad (10.32)$$

where

$$A_f \equiv \frac{2\overline{g}_V^f\,\overline{g}_A^f}{\overline{g}_V^{f2} + \overline{g}_A^{f2}} , \quad (10.33)$$

and

$$\overline{g}_V^f = \sqrt{\rho_f}\,(t_{3L}^{(f)} - 2q_f\kappa_f\sin^2\theta_W) , \quad (10.33b)$$
$$\overline{g}_A^f = \sqrt{\rho_f}\,t_{3L}^{(f)} . \quad (10.33c)$$

P_e is the initial e^- polarization, so that the second equality in Eq. (10.30) is reproduced for $P_e = 1$, and the Z-pole forward-backward asymmetries at LEP ($P_e = 0$) are given by $A_{FB}^{(0,f)} = \frac{3}{4}A_eA_f$ where $f = e$, μ, τ, b, c, s [104], and q, and where $A_{FB}^{(0,q)}$ refers to the hadronic charge asymmetry. Corrections for t-channel exchange and s/t-channel interference cause $A_{FB}^{(0,e)}$ to be strongly anticorrelated with R_e (-37%). The initial state coupling, A_e, is also determined through the left-right charge asymmetry [105] and in polarized Bhabba scattering at the SLC [103].

The electroweak radiative corrections have been absorbed into corrections $\rho_f - 1$ and $\kappa_f - 1$, which depend on the fermion f and on the renormalization scheme. In the on-shell scheme, the quadratic m_t dependence is given by $\rho_f \sim 1 + \rho_t$, $\kappa_f \sim 1 + \rho_t/\tan^2\theta_W$, while in $\overline{\rm MS}$, $\widehat{\rho}_f \sim \widehat{\kappa}_f \sim 1$, for $f \neq b$ ($\widehat{\rho}_b \sim 1 - \frac{4}{3}\rho_t$, $\widehat{\kappa}_b \sim 1 + \frac{2}{3}\rho_t$). In the $\overline{\rm MS}$ scheme the normalization is changed according to $G_FM_Z^2/2\sqrt{2}\pi \to \widehat{\alpha}/4\widehat{s}_Z^2\widehat{c}_Z^2$. (If one continues to normalize amplitudes by $G_FM_Z^2/2\sqrt{2}\pi$, as in the 1996 edition of this *Review*, then $\widehat{\rho}_f$ contains an additional factor of $\widehat{\rho}$.) In practice, additional bosonic and fermionic loops, vertex corrections, leading higher order contributions, *etc.*, must be included.

For example, in the $\overline{\rm MS}$ scheme one has $\widehat{\rho}_\ell = 0.9981$, $\widehat{\kappa}_\ell = 1.0013$, $\widehat{\rho}_b = 0.9861$, and $\widehat{\kappa}_b = 1.0071$. It is convenient to define an effective angle $\overline{s}^2_f \equiv \sin^2\overline{\theta}_{Wf} \equiv \widehat{\kappa}_f \widehat{s}^2_Z = \kappa_f s^2_W$, in terms of which $\overline{g}^f_V$ and $\overline{g}^f_A$ are given by $\sqrt{\rho_f}$ times their tree-level formulae. Because $\overline{g}^\ell_V$ is very small, not only $A^0_{LR} = A_e$, $A^{(0,\ell)}_{FB}$, and $\mathcal{P}_\tau$, but also $A^{(0,b)}_{FB}$, $A^{(0,c)}_{FB}$, $A^{(0,s)}_{FB}$, and the hadronic asymmetries are mainly sensitive to $\overline{s}^2_\ell$. One finds that $\widehat{\kappa}_f$ ($f \neq b$) is almost independent of (m_t, M_H), so that one can write

$$\overline{s}^2_\ell \sim \widehat{s}^{\,2}_Z + 0.00029\ . \tag{10.34}$$

Thus, the asymmetries determine values of $\overline{s}^2_\ell$ and $\widehat{s}^{\,2}_Z$ almost independent of m_t, while the κ's for the other schemes are m_t dependent.

LEP 2 [41] has run at several energies above the Z-pole up to ~ 209 GeV. Measurements have been made of a number of observables, including the cross-sections for $e^+e^- \to f\bar{f}$ for $f = q, \mu^-, \tau^-$; the differential cross-sections and A_{FB} for μ and τ; R and A_{FB} for b and c; W branching ratios; and WW, $WW\gamma$, ZZ, single W, and single Z cross-sections. They are in agreement with the SM predictions, with the exceptions of the total hadronic cross-section (1.7 σ high), R_b (2.1 σ low), and $A_{FB}(b)$ (1.6 σ low). Also, the SM Higgs has been excluded below 114.4 GeV [106].

The Z-boson properties are extracted assuming the SM expressions for the γ–Z interference terms. These have also been tested experimentally by performing more general fits [107] to the LEP 1 and LEP 2 data. Assuming family universality this approach introduces three additional parameters relative to the standard fit [41], describing the γ–Z interference contribution to the total hadronic and leptonic cross-sections, $j^{\rm tot}_{\rm had}$ and $j^{\rm tot}_\ell$, and to the leptonic forward-backward asymmetry, $j^{\rm fb}_\ell$. For example,

$$j^{\rm tot}_{\rm had} \sim g^\ell_V g^{\rm had}_V = 0.277 \pm 0.065\ , \tag{10.35}$$

which is in good agreement with the SM expectation [41] of $0.220^{+0.003}_{-0.014}$. Similarly, LEP data up to CM energies of 206 GeV were used to constrain the γ–Z interference terms for the heavy quarks. The results for $j^{\rm tot}_b$, $j^{\rm fb}_b$, $j^{\rm tot}_c$, and $j^{\rm fb}_c$ were found in perfect agreement with the SM. These are valuable tests of the SM; but it should be cautioned that new physics is not expected to be described by this set of parameters, since (i) they do not account for extra interactions beyond the standard weak neutral-current, and (ii) the photonic amplitude remains fixed to its SM value.

Strong constraints on anomalous triple and quartic gauge couplings have been obtained at LEP 2 and at the Tevatron, as are described in the Particle Listings.

The left-right asymmetry in polarized Møller scattering $e^+e^- \to e^+e^-$ is being measured in the SLAC E158 experiment. A precision of better than ± 0.001 in $\sin^2\theta_W$ at $Q^2 \sim 0.03$ GeV^2 is anticipated. The result of the first of three runs yields $\widehat{s}^{\,2}_Z = 0.2279 \pm 0.0032$ [108]. In a similar experiment and at about the same Q^2, Qweak at Jefferson Lab [109] will be able to measure $\sin^2\theta_W$ in polarized ep scattering with a relative precision of 0.3%. These experiments will provide the most precise determinations of the weak mixing angle off the Z peak and will be sensitive to various types of physics beyond the SM.

The Belle [110], CLEO [111], and BaBar [112] collaborations reported precise measurements of the flavor changing transition $b \to s\gamma$. The signal efficiencies (including the extrapolation to the full photon spectrum) depend on the bottom pole mass, m_b. We adjusted the Belle and BaBar results to agree with the m_b value used by CLEO. In the case of CLEO, a 3.8% component from the model error of the signal efficiency is moved from the systematic error to the model error. The results for the branching fractions are then given by,

$$\mathcal{B}[\text{Belle}] = 3.05 \times 10^{-4}[1 \pm 0.158 \pm 0.124 \pm 0.202 \pm 0]\ , \tag{10.36a}$$

$$\mathcal{B}[\text{CLEO}] = 3.21 \times 10^{-4}[1 \pm 0.134 \pm 0.076 \pm 0.059 \pm 0.016]\ , \tag{10.36b}$$

$$\mathcal{B}[\text{BaBar}] = 3.86 \times 10^{-4}[1 \pm 0.090 \pm 0.093 \pm 0.074 \pm 0.016]\ , \tag{10.36c}$$

where the first two errors are the statistical and systematic uncertainties (taken uncorrelated). The third error (taken 100% correlated) accounts for the extrapolation from the finite photon energy cutoff (2.25 GeV, 2.0 GeV, and 2.1 GeV, respectively) to the full theoretical branching ratio [113]. The last error is from the correction for the $b \to d\gamma$ component which is common to CLEO and BaBar. It is advantageous [114] to normalize the result with respect to the semi-leptonic branching fraction, $\mathcal{B}(b \to X e\nu) = 0.1064 \pm 0.0023$, yielding,

$$R = \frac{\mathcal{B}(b \to s\gamma)}{\mathcal{B}(b \to X e\nu)} = (3.39 \pm 0.43 \pm 0.37) \times 10^{-3}. \tag{10.37}$$

In the fits we use the variable $\ln R = -5.69 \pm 0.17$ to assure an approximately Gaussian error [115]. We added an 11% theory uncertainty (excluding parametric errors such as from α_s) in the SM prediction which is based on the next-to-leading order calculations of Refs. 114,116.

The present world average of the muon anomalous magnetic moment,

$$a^{\rm exp}_\mu = \frac{g_\mu - 2}{2} = (1165920.37 \pm 0.78) \times 10^{-9}\ , \tag{10.38}$$

is dominated by the 1999 and 2000 data runs of the E821 collaboration at BNL [117]. The final 2001 data run is currently being analyzed. The QED contribution has been calculated to four loops (fully analytically to three loops), and the leading logarithms are included to five loops [118]. The estimated SM electroweak contribution [119–121], $a^{\rm EW}_\mu = (1.52 \pm 0.03) \times 10^{-9}$, which includes leading two-loop [120] and three-loop [121] corrections, is at the level of the current uncertainty. The limiting factor in the interpretation of the result is the uncertainty from the two-loop hadronic contribution [20], $a^{\rm had}_\mu = (69.63 \pm 0.72) \times 10^{-9}$, which has been obtained using $e^+e^- \to$ hadrons cross-section data. The latter are dominated by the recently reanalyzed CMD 2 data [19]. This value suggests a 1.9 σ discrepancy between Eq. (10.38) and the SM prediction. In an alternative analysis, the authors of Ref. 20 use τ decay data and isospin symmetry (CVC) to obtain instead $a^{\rm had}_\mu = (71.10 \pm 0.58) \times 10^{-9}$. This result implies no conflict (0.7 σ) with Eq. (10.38). Thus, there is also a discrepancy between the 2π spectral functions obtained from the two methods. For example, if one uses the e^+e^- data and CVC to predict the branching ratio for $\tau^- \to \nu_\tau\pi^-\pi^0$ decays one obtains $24.52 \pm 0.32\%$ [20] while the average of the measured branching ratios by DELPHI [122], ALEPH, CLEO, L3, and OPAL [20] yields $25.43 \pm 0.09\%$, which is 2.8 σ higher. It is important to understand the origin of this difference and to obtain additional experimental information (*e.g.*, from the radiative return method [37]). Fortunately, this problem is less pronounced as far as $a^{\rm had}_\mu$ is concerned: due to the suppression at large s (from where the conflict originates) the difference is only 1.7 σ (or 1.9 σ if one adds the 4 π channel which by itself is consistent between the two methods). Note also that a part of this difference is due to the older e^+e^- data [20], and the direct conflict between τ decay data and CMD 2 is less significant. Isospin violating corrections have been estimated in Ref. 123 and found to be under control. The largest effect is due to higher-order electroweak corrections [39] but introduces a negligible uncertainty [124]. In the following we view the 1.7 σ difference as a fluctuation and average the results. An additional uncertainty is induced by the hadronic three-loop light-by-light scattering contribution [125], $a^{\rm LBLS}_\mu = (+0.83 \pm 0.19) \times 10^{-9}$, which was estimated within a form factor approach. The sign of this effect is opposite to the one quoted in the 2002 edition of this *Review*, and has subsequently been confirmed by two other groups [126]. Other hadronic effects at three-loop order contribute [127], $a^{\rm had}_\mu \left[\left(\frac{\alpha}{\pi}\right)^3\right] = (-1.00 \pm 0.06) \times 10^{-9}$. Correlations with the two-loop hadronic contribution and with $\Delta\alpha(M_Z)$ (see Sec. 10.2) were considered in Ref. 128, which also contains analytic results for the perturbative QCD contribution. The SM prediction is

$$a^{\rm theory}_\mu = (1165918.83 \pm 0.49) \times 10^{-9}\ , \tag{10.39}$$

where the error is from the hadronic uncertainties excluding parametric ones such as from α_s and the heavy quark masses. We estimate its correlation with $\Delta\alpha(M_Z)$ as 21%. The small overall discrepancy

between the experimental and theoretical values could be due to fluctuations or underestimates of the theoretical uncertainties. On the other hand, $g_\mu - 2$ is also affected by many types of new physics, such as supersymmetric models with large $\tan\beta$ and moderately light superparticle masses [129]. Thus, the deviation could also arise from physics beyond the SM.

Note added: After completion of this Section and the fits described here, the E821 collaboration announced its measurement on the anomalous magnetic moment of the negatively charged muon based on data taken in 2001 [130]. The result, $a_\mu^{\rm exp} = (1165921.4 \pm 0.8 \pm 0.3) \times 10^{-9}$, is consistent with the results on positive muons and appears to confirm the deviation. There also appeared two new evaluations [131,132] of $a_\mu^{\rm had}$. They are based on e^+e^- data only and are generally in good agreement with each other and other e^+e^- based analyzes. τ decay data are not used; it is argued [131] that CVC breaking effects (*e.g.*, through a relatively large mass difference between the $\rho^\pm$ and ρ^0 vector mesons) may be larger than expected. This may also be relevant in the context of the NuTeV discrepancy discussed above [131].

10.4. W and Z decays

The partial decay width for gauge bosons to decay into massless fermions $f_1\overline{f}_2$ is

$$\Gamma(W^+ \to e^+\nu_e) = \frac{G_F M_W^3}{6\sqrt{2}\pi} \approx 226.56 \pm 0.24 \text{ MeV} \quad , \tag{10.47a}$$

$$\Gamma(W^+ \to u_i\overline{d}_j) = \frac{C G_F M_W^3}{6\sqrt{2}\pi} |V_{ij}|^2 \approx (707.1 \pm 0.7)\,|V_{ij}|^2 \text{ MeV} \quad , \tag{10.47b}$$

$$\Gamma(Z \to \psi_i\overline{\psi}_i) = \frac{C G_F M_Z^3}{6\sqrt{2}\pi}\left[g_V^{i2} + g_A^{i2}\right] \tag{10.47c}$$

$$\approx \begin{cases} 300.4 \pm 0.2 \text{ MeV } (u\overline{u}), & 167.29 \pm 0.07 \text{ MeV } (\nu\overline{\nu}), \\ 383.2 \pm 0.2 \text{ MeV } (d\overline{d}), & 84.03 \pm 0.04 \text{ MeV } (e^+e^-), \\ 375.8 \mp 0.1 \text{ MeV } (b\overline{b}). \end{cases}$$

For leptons $C = 1$, while for quarks $C = 3\Big(1 + \alpha_s(M_V)/\pi + 1.409\alpha_s^2/\pi^2 - 12.77\alpha_s^3/\pi^3\Big)$, where the 3 is due to color and the factor in parentheses represents the universal part of the QCD corrections [133] for massless quarks [134]. The $Z \to f\overline{f}$ widths contain a number of additional corrections: universal (non-singlet) top quark mass contributions [135]; fermion mass effects and further QCD corrections proportional to $\widehat{m}_q^2(M_Z^2)$ [136] which are different for vector and axial-vector partial widths; and singlet contributions starting from two-loop order which are large, strongly top quark mass dependent, family universal, and flavor non-universal [137]. All QCD effects are known and included up to three-loop order. The QED factor $1 + 3\alpha q_f^2/4\pi$, as well as two-loop order $\alpha\alpha_s$ and α^2 self-energy corrections [138] are also included. Working in the on-shell scheme, *i.e.*, expressing the widths in terms of $G_F M_{W,Z}^3$, incorporates the largest radiative corrections from the running QED coupling [44,139]. Electroweak corrections to the Z widths are then incorporated by replacing $g_{V,A}^{i2}$ by $\overline{g}_{V,A}^{i2}$. Hence, in the on-shell scheme the Z widths are proportional to $\rho_i \sim 1 + \rho_t$. The $\overline{\rm MS}$ normalization accounts also for the leading electroweak corrections [48]. There is additional (negative) quadratic m_t dependence in the $Z \to b\overline{b}$ vertex corrections [140] which causes $\Gamma(b\overline{b})$ to decrease with m_t. The dominant effect is to multiply $\Gamma(b\overline{b})$ by the vertex correction $1 + \delta\rho_{b\overline{b}}$, where $\delta\rho_{b\overline{b}} \sim 10^{-2}(-\frac{1}{2}\frac{m_t^2}{M_Z^2} + \frac{1}{5})$. In practice, the corrections are included in ρ_b and κ_b, as discussed before.

For 3 fermion families the total widths are predicted to be

$$\Gamma_Z \approx 2.4968 \pm 0.0011 \text{ GeV} \quad , \tag{10.48}$$

$$\Gamma_W \approx 2.0936 \pm 0.0022 \text{ GeV} \quad . \tag{10.49}$$

We have assumed $\alpha_s(M_Z) = 0.1200$. An uncertainty in α_s of ± 0.0018 introduces an additional uncertainty of 0.05% in the hadronic widths, corresponding to ± 0.9 MeV in Γ_Z. These predictions are to be compared with the experimental results $\Gamma_Z = 2.4952 \pm 0.0023$ GeV [41] and $\Gamma_W = 2.124 \pm 0.041$ GeV (see the Particle Listings for more details).

Table 10.4: Principal Z-pole and other observables, compared with the SM predictions for the global best fit values $M_Z = 91.1874 \pm 0.0021$ GeV, $M_H = 113^{+56}_{-40}$ GeV, $m_t = 176.9 \pm 4.0$ GeV, $\alpha_s(M_Z) = 0.1213 \pm 0.0018$, and $\widehat{\alpha}(M_Z)^{-1} = 127.906 \pm 0.019$. The LEP averages of the ALEPH, DELPHI, L3, and OPAL results include common systematic errors and correlations [41]. The heavy flavor results of LEP and SLD are based on common inputs and correlated, as well [100]. $\overline{s}_\ell^2(A_{FB}^{(0,q)})$ is the effective angle extracted from the hadronic charge asymmetry, which has some correlation with $A_{FB}^{(0,b)}$ which is currently neglected. The values of $\Gamma(\ell^+\ell^-)$, Γ(had), and Γ(inv) are not independent of Γ_Z, the R_ℓ, and $\sigma_{\rm had}$. The m_t values are from the lepton plus jets channel of the CDF [6] and DØ [9] run I data, respectively. Results from the other channels and all correlations are also included. The first M_W value is from UA2, CDF, and DØ [141], while the second one is from LEP 2 [41]. The first M_W and M_Z are correlated, but the effect is negligible due to the tiny M_Z error. The three values of A_e are (i) from A_{LR} for hadronic final states [101]; (ii) from A_{LR} for leptonic final states and from polarized Bhabba scattering [103]; and (iii) from the angular distribution of the τ polarization. The two A_τ values are from SLD and the total τ polarization, respectively. g_L^2 and g_R^2 are from NuTeV [69] and have a very small (-1.7%) residual anticorrelation. The older deep-inelastic scattering (DIS) results from CDHS [63], CHARM [64], and CCFR [65] are included, as well, but not shown in the Table. The world averages for $g_{V,A}^{\nu e}$ are dominated by the CHARM II [76] results, $g_V^{\nu e} = -0.035 \pm 0.017$ and $g_A^{\nu e} = -0.503 \pm 0.017$. The errors in Q_W, DIS, $b \to s\gamma$, and $g_\mu - 2$ are the total (experimental plus theoretical) uncertainties. The τ_τ value is the τ lifetime world average computed by combining the direct measurements with values derived from the leptonic branching ratios [5]; the theory uncertainty is included in the SM prediction. In all other SM predictions, the uncertainty is from M_Z, M_H, m_t, m_b, m_c, $\widehat{\alpha}(M_Z)$, and α_s, and their correlations have been accounted for. The SM errors in Γ_Z, Γ(had), R_ℓ, and $\sigma_{\rm had}$ are largely dominated by the uncertainty in α_s.

Quantity	Value	Standard Model	Pull
m_t [GeV]	176.1 ± 7.4	176.9 ± 4.0	-0.1
	180.1 ± 5.4		0.6
M_W [GeV]	80.454 ± 0.059	80.390 ± 0.018	1.1
	80.412 ± 0.042		0.5
M_Z [GeV]	91.1876 ± 0.0021	91.1874 ± 0.0021	0.1
Γ_Z [GeV]	2.4952 ± 0.0023	2.4972 ± 0.0012	-0.9
Γ(had) [GeV]	1.7444 ± 0.0020	1.7435 ± 0.0011	—
Γ(inv) [MeV]	499.0 ± 1.5	501.81 ± 0.13	—
$\Gamma(\ell^+\ell^-)$ [MeV]	83.984 ± 0.086	84.024 ± 0.025	—
$\sigma_{\rm had}$ [nb]	41.541 ± 0.037	41.472 ± 0.009	1.9
R_e	20.804 ± 0.050	20.750 ± 0.012	1.1
R_μ	20.785 ± 0.033	20.751 ± 0.012	1.0
R_τ	20.764 ± 0.045	20.790 ± 0.018	-0.7
R_b	0.21638 ± 0.00066	0.21564 ± 0.00014	1.1
R_c	0.1720 ± 0.0030	0.17233 ± 0.00005	-0.1
$A_{FB}^{(0,e)}$	0.0145 ± 0.0025	0.01626 ± 0.00025	-0.7
$A_{FB}^{(0,\mu)}$	0.0169 ± 0.0013		0.5
$A_{FB}^{(0,\tau)}$	0.0188 ± 0.0017		1.5
$A_{FB}^{(0,b)}$	0.0997 ± 0.0016	0.1032 ± 0.0008	-2.2

Table 10.4: (continued)

Quantity	Value	Standard Model	Pull
$A_{FB}^{(0,c)}$	0.0706 ± 0.0035	0.0738 ± 0.0006	-0.9
$A_{FB}^{(0,s)}$	0.0976 ± 0.0114	0.1033 ± 0.0008	-0.5
$\bar{s}_\ell^2(A_{FB}^{(0,q)})$	0.2324 ± 0.0012	0.23149 ± 0.00015	0.8
A_e	0.15138 ± 0.00216	0.1472 ± 0.0011	1.9
	0.1544 ± 0.0060		1.2
	0.1498 ± 0.0049		0.5
A_μ	0.142 ± 0.015		-0.4
A_τ	0.136 ± 0.015		-0.8
	0.1439 ± 0.0043		-0.8
A_b	0.925 ± 0.020	0.9347 ± 0.0001	-0.5
A_c	0.670 ± 0.026	0.6678 ± 0.0005	0.1
A_s	0.895 ± 0.091	0.9357 ± 0.0001	-0.4
g_L^2	0.30005 ± 0.00137	0.30397 ± 0.00023	-2.9
g_R^2	0.03076 ± 0.00110	0.03007 ± 0.00003	0.6
$g_V^{\nu e}$	-0.040 ± 0.015	-0.0397 ± 0.0003	-0.1
$g_A^{\nu e}$	-0.507 ± 0.014	-0.5065 ± 0.0001	0.0
Q_W(Cs)	-72.69 ± 0.48	-73.19 ± 0.03	1.0
Q_W(Tl)	-116.6 ± 3.7	-116.81 ± 0.04	0.1
$\frac{\Gamma(b\to s\gamma)}{\Gamma(b\to Xe\nu)}$	$3.39^{+0.62}_{-0.54} \times 10^{-3}$	$(3.23 \pm 0.09) \times 10^{-3}$	0.3
$\frac{1}{2}(g_\mu - 2 - \frac{\alpha}{\pi})$	4510.64 ± 0.92	4509.13 ± 0.10	1.6
τ_τ [fs]	290.92 ± 0.55	291.83 ± 1.81	-0.4

10.5. Experimental results

The values of the principal Z-pole observables are listed in Table 10.4, along with the SM predictions for $M_Z = 91.1874 \pm 0.0021$ GeV, $M_H = 113^{+56}_{-40}$ GeV, $m_t = 176.9 \pm 4.0$ GeV, $\alpha_s(M_Z) = 0.1213 \pm 0.0018$, and $\widehat{\alpha}(M_Z)^{-1} = 127.906 \pm 0.019$ ($\Delta\alpha^{(5)}_{\rm had} \approx 0.02801 \pm 0.00015$). The values and predictions of M_W [41,141]; m_t [6,9]; the Q_W for cesium [81] and thallium [82]; deep inelastic [69] and ν_μ-e scattering [74–76]; the $b \to s\gamma$ observable [110–112]; the muon anomalous magnetic moment [117]; and the τ lifetime are also listed. The values of M_W and m_t differ from those in the Particle Listings because they include recent preliminary results. The agreement is excellent. Only g_L^2 from NuTeV is currently showing a large (2.9 σ) deviation. In addition, the hadronic peak cross-section, $\sigma_{\rm had}$, and the A_{LR}^0 from hadronic final states differ by 1.9 σ. On the other hand, $A_{FB}^{(0,b)}$ (2.2 σ) and $g_\mu - 2$ (1.6 σ, see Sec. 10.3) both moved closer to the SM predictions by about one standard deviation compared to the 2002 edition of this *Review*, while M_W (LEP 2) has moved closer by 0.8 σ. Observables like $R_b = \Gamma(b\bar{b})/\Gamma({\rm had})$, $R_c = \Gamma(c\bar{c})/\Gamma({\rm had})$, and the combined value for M_W which showed significant deviations in the past, are now in reasonable agreement. In particular, R_b whose measured value deviated as much as 3.7 σ from the SM prediction is now only 1.1 σ (0.34%) high.

A_b can be extracted from $A_{FB}^{(0,b)}$ when $A_e = 0.1501 \pm 0.0016$ is taken from a fit to leptonic asymmetries (using lepton universality). The result, $A_b = 0.886 \pm 0.017$, is 2.9 σ below the SM prediction†, and also 1.5 σ below $A_b = 0.925 \pm 0.020$ obtained from $A_{LR}^{FB}(b)$ at SLD. Thus, it appears that at least some of the problem in $A_{FB}^{(0,b)}$ is experimental. Note, however, that the uncertainty in $A_{FB}^{(0,b)}$ is strongly statistics dominated. The combined value, $A_b = 0.902 \pm 0.013$ deviates by 2.5 σ. It would be extremely difficult to account for this 3.5% deviation by new physics radiative corrections since an order of 20% correction to $\widehat{\kappa}_b$ would be necessary to account for the central value of A_b. If this deviation is due to new physics, it is most likely of tree-level type affecting preferentially the third generation. Examples include the decay of a scalar neutrino resonance [142], mixing of the b quark with heavy exotics [143], and a heavy Z' with family-nonuniversal couplings [144]. It is difficult, however, to simultaneously account for R_b, which has been measured on the Z peak and off-peak [145] at LEP 1. An average of R_b measurements at LEP 2 at energies between 133 and 207 GeV is 2.1 σ below the SM prediction, while $A_{FB}^{(b)}$(LEP 2) is 1.6 σ low.

The left-right asymmetry, $A_{LR}^0 = 0.15138 \pm 0.00216$ [101], based on all hadronic data from 1992–1998 differs 1.9 σ from the SM expectation of 0.1472 ± 0.0011. The combined value of $A_\ell = 0.1513 \pm 0.0021$ from SLD (using lepton-family universality and including correlations) is also 1.9 σ above the SM prediction; but there is now experimental agreement between this SLD value and the LEP value, $A_\ell = 0.1481 \pm 0.0027$, obtained from a fit to $A_{FB}^{(0,\ell)}$, $A_e(\mathcal{P}_\tau)$, and $A_\tau(\mathcal{P}_\tau)$, again assuming universality.

Despite these discrepancies the goodness of the fit to all data is excellent with a χ^2/d.o.f. = 45.5/45. The probability of a larger χ^2 is 45%. The observables in Table 10.4, as well as some other less precise observables, are used in the global fits described below. The correlations on the LEP lineshape and τ polarization, the LEP/SLD heavy flavor observables, the SLD lepton asymmetries, the deep inelastic and ν-e scattering observables, and the m_t measurements, are included. The theoretical correlations between $\Delta\alpha^{(5)}_{\rm had}$ and $g_\mu - 2$, and between the charm and bottom quark masses, are also accounted for.

Table 10.5: Values of $\widehat{s}^2_Z$, s^2_W, α_s, and M_H [in GeV] for various (combinations of) observables. Unless indicated otherwise, the top quark mass, $m_t = 177.9 \pm 4.4$ GeV, is used as an additional constraint in the fits. The (†) symbol indicates a fixed parameter.

Data	$\widehat{s}^2_Z$	s^2_W	$\alpha_s(M_Z)$	M_H
All data	0.23120(15)	0.2228(4)	0.1213(18)	113^{+56}_{-40}
All indirect (no m_t)	0.23116(17)	0.2229(4)	0.1213(18)	79^{+95}_{-38}
Z pole (no m_t)	0.23118(17)	0.2231(6)	0.1197(28)	79^{+94}_{-38}
LEP 1 (no m_t)	0.23148(20)	0.2237(7)	0.1210(29)	140^{+192}_{-74}
SLD + M_Z	0.23067(28)	0.2217(6)	0.1213 (†)	43^{+38}_{-23}
$A_{FB}^{(b,c)}$ + M_Z	0.23185(28)	0.2244(8)	0.1213 (†)	408^{+317}_{-179}
M_W + M_Z	0.23089(37)	0.2221(8)	0.1213 (†)	67^{+77}_{-45}
M_Z	0.23117(15)	0.2227(5)	0.1213 (†)	117 (†)
DIS (isoscalar)	0.2359(16)	0.2274(16)	0.1213 (†)	117 (†)
Q_W (APV)	0.2292(19)	0.2207(19)	0.1213 (†)	117 (†)
polarized Møller	0.2292(42)	0.2207(43)	0.1213 (†)	117 (†)
elastic $\nu_\mu(\overline{\nu_\mu})e$	0.2305(77)	0.2220(77)	0.1213 (†)	117 (†)
SLAC eD	0.222(18)	0.213(19)	0.1213 (†)	117 (†)
elastic $\nu_\mu(\overline{\nu_\mu})p$	0.211(33)	0.203(33)	0.1213 (†)	117 (†)

The data allow a simultaneous determination of M_H, m_t, $\sin^2\theta_W$, and the strong coupling $\alpha_s(M_Z)$. ($\widehat{m}_c$, $\widehat{m}_b$, and $\Delta\alpha^{(5)}_{\rm had}$ are also allowed to float in the fits, subject to the theoretical constraints [5,18] described in Sec. 10.1–Sec. 10.2. These are correlated with α_s.) α_s is determined mainly from R_ℓ, Γ_Z, $\sigma_{\rm had}$, and τ_τ and is only weakly correlated with the other variables (except for a 10% correlation with $\widehat{m}_c$). The global fit to all data, including the CDF/DØ average, $m_t = 177.9 \pm 4.4$ GeV, yields

$$\begin{aligned} M_H &= 113^{+56}_{-40}\ {\rm GeV}\ , \\ m_t &= 176.9 \pm 4.0\ {\rm GeV}\ , \\ \widehat{s}^2_Z &= 0.23120 \pm 0.00015\ , \\ \alpha_s(M_Z) &= 0.1213 \pm 0.0018\ . \end{aligned} \tag{10.50}$$

† Alternatively, one can use $A_\ell = 0.1481 \pm 0.0027$, which is from LEP alone and in excellent agreement with the SM, and obtain $A_b = 0.898 \pm 0.022$ which is 1.7 σ low. This illustrates that some of the discrepancy is related to the one in A_{LR}.

In the on-shell scheme one has $s^2_W = 0.22280 \pm 0.00035$, the larger error due to the stronger sensitivity to m_t, while the corresponding effective angle is related by Eq. (10.34), *i.e.*, $\overline{s}^2_\ell = 0.23149 \pm 0.00015$. The m_t pole mass corresponds to $\widehat{m}_t(\widehat{m}_t) = 166.8 \pm 3.8$ GeV. In all fits, the errors include full statistical, systematic, and theoretical uncertainties. The $\widehat{s}^2_Z$ ($\overline{s}^2_\ell$) error reflects the error on $\overline{s}^2_f = 0.23150 \pm 0.00016$ from a fit to the Z-pole asymmetries.

The weak mixing angle can be determined from Z-pole observables, M_W, and from a variety of neutral-current processes spanning a very wide Q^2 range. The results (for the older low-energy neutral-current data see [42,43]) shown in Table 10.5 are in reasonable agreement with each other, indicating the quantitative success of the SM. The largest discrepancy is the value $\widehat{s}^2_Z = 0.2358 \pm 0.0016$ from DIS which is 2.9 σ above the value 0.23120 ± 0.00015 from the global fit to all data. Similarly, $\widehat{s}^2_Z = 0.23185 \pm 0.00028$ from the forward-backward asymmetries into bottom and charm quarks, and $\widehat{s}^2_Z = 0.23067 \pm 0.00028$ from the SLD asymmetries (both when combined with M_Z) are 2.3 σ high and 1.9 σ low, respectively.

The extracted Z-pole value of $\alpha_s(M_Z)$ is based on a formula with negligible theoretical uncertainty (± 0.0005 in $\alpha_s(M_Z)$) if one assumes the exact validity of the SM. One should keep in mind, however, that this value, $\alpha_s = 0.1197 \pm 0.0028$, is very sensitive to such types of new physics as non-universal vertex corrections. In contrast, the value derived from τ decays, $\alpha_s(M_Z) = 0.1221^{+0.0026}_{-0.0023}$ [5], is theory dominated but less sensitive to new physics. The former is mainly due to the larger value of $\alpha_s(m_\tau)$, but just as the hadronic Z-width the τ lifetime is fully inclusive and can be computed reliably within the operator product expansion. The two values are in excellent agreement with each other. They are also in perfect agreement with other recent values, such as 0.1202 ± 0.0049 from jet-event shapes at LEP [146], and 0.121 ± 0.003 [147] from the most recent lattice calculation of the Υ spectrum. For more details and other determinations, see our Section 9 on "Quantum Chromodynamics" in this *Review*.

The data indicate a preference for a small Higgs mass. There is a strong correlation between the quadratic m_t and logarithmic M_H terms in $\widehat{\rho}$ in all of the indirect data except for the $Z \to b\overline{b}$ vertex. Therefore, observables (other than R_b) which favor m_t values higher than the Tevatron range favor lower values of M_H. This effect is enhanced by R_b, which has little direct M_H dependence but favors the lower end of the Tevatron m_t range. M_W has additional M_H dependence through $\Delta\widehat{r}_W$ which is not coupled to m^2_t effects. The strongest individual pulls toward smaller M_H are from M_W and A^0_{LR}, while $A^{(0b)}_{FB}$ and the NuTeV results favor high values. The difference in χ^2 for the global fit is $\Delta\chi^2 = \chi^2(M_H = 1000 \text{ GeV}) - \chi^2_{\rm min} = 34.6$. Hence, the data favor a small value of M_H, as in supersymmetric extensions of the SM. The central value of the global fit result, $M_H = 113^{+56}_{-40}$ GeV, is slightly below the direct lower bound, $M_H \geq 114.4$ GeV (95% CL) [106].

The 90% central confidence range from all precision data is

$$53 \text{ GeV} \leq M_H \leq 213 \text{ GeV} .$$

Including the results of the direct searches as an extra contribution to the likelihood function drives the 95% upper limit to $M_H \leq 241$ GeV. As two further refinements, we account for (i) theoretical uncertainties from uncalculated higher order contributions by allowing the T parameter (see next subsection) subject to the constraint $T = 0 \pm 0.02$, (ii) the M_H dependence of the correlation matrix which gives slightly more weight to lower Higgs masses [148]. The resulting limits at 95 (90, 99)% CL are

$$M_H \leq 246 \text{ (217, 311) GeV} ,$$

respectively. The extraction of M_H from the precision data depends strongly on the value used for $\alpha(M_Z)$. Upper limits, however, are more robust due to two compensating effects: the older results indicated more QED running and were less precise, yielding M_H distributions which were broader with centers shifted to smaller values. The hadronic contribution to $\alpha(M_Z)$ is correlated with $g_\mu - 2$ (see Sec. 10.3). The measurement of the latter is higher than the SM prediction, and its inclusion in the fit favors a larger $\alpha(M_Z)$ and a lower M_H (by 4 GeV).

One can also carry out a fit to the indirect data alone, *i.e.*, without including the constraint, $m_t = 177.9 \pm 4.4$ GeV, obtained by CDF and DØ. (The indirect prediction is for the $\overline{\rm MS}$ mass, $\widehat{m}_t(\widehat{m}_t) = 162.5^{+9.2}_{-6.9}$ GeV, which is in the end converted to the pole mass). One obtains $m_t = 172.4^{+9.8}_{-7.3}$ GeV, with little change in the $\sin^2\theta_W$ and α_s values, in remarkable agreement with the direct CDF/DØ average. The relations between M_H and m_t for various observables are shown in Fig. 10.1.

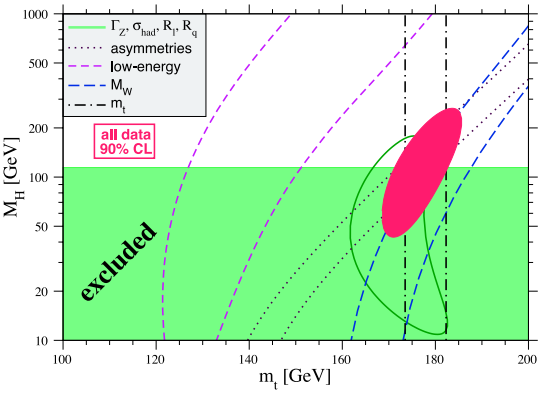

Figure 10.1: One-standard-deviation (39.35%) uncertainties in M_H as a function of m_t for various inputs, and the 90% CL region ($\Delta\chi^2 = 4.605$) allowed by all data. $\alpha_s(M_Z) = 0.120$ is assumed except for the fits including the Z-lineshape data. The 95% direct lower limit from LEP 2 is also shown See full-color version on color pages at end of book.

Using $\alpha(M_Z)$ and $\widehat{s}^2_Z$ as inputs, one can predict $\alpha_s(M_Z)$ assuming grand unification. One predicts [149] $\alpha_s(M_Z) = 0.130 \pm 0.001 \pm 0.01$ for the simplest theories based on the minimal supersymmetric extension of the SM, where the first (second) uncertainty is from the inputs (thresholds). This is slightly larger, but consistent with the experimental $\alpha_s(M_Z) = 0.1213 \pm 0.0018$ from the Z lineshape and the τ lifetime, as well as with other determinations. Non-supersymmetric unified theories predict the low value $\alpha_s(M_Z) = 0.073 \pm 0.001 \pm 0.001$. See also the note on "Low-Energy Supersymmetry" in the Particle Listings.

One can also determine the radiative correction parameters Δr: from the global fit one obtains $\Delta r = 0.0347 \pm 0.0011$ and $\Delta\widehat{r}_W = 0.06981 \pm 0.00032$. M_W measurements [41,141] (when combined with M_Z) are equivalent to measurements of $\Delta r = 0.0326 \pm 0.0021$, which is 1.2 σ below the result from all indirect data, $\Delta r = 0.0355 \pm 0.0013$. Fig. 10.2 shows the 1 σ contours in the $M_W - m_t$ plane from the direct and indirect determinations, as well as the combined 90% CL region. The indirect determination uses M_Z from LEP 1 as input, which is defined assuming an s-dependent decay width. M_W then corresponds to the s-dependent width definition, as well, and can be directly compared with the results from the Tevatron and LEP 2 which have been obtained using the same definition. The difference to a constant width definition is formally only of $\mathcal{O}(\alpha^2)$, but is strongly enhanced since the decay channels add up coherently. It is about 34 MeV for M_Z and 27 MeV for M_W. The residual difference between working consistently with one or the other definition is about 3 MeV, *i.e.*, of typical size for non-enhanced $\mathcal{O}(\alpha^2)$ corrections [54,55].

Most of the parameters relevant to ν-hadron, ν-e, e-hadron, and e^+e^- processes are determined uniquely and precisely from the data in "model-independent" fits (*i.e.*, fits which allow for an arbitrary electroweak gauge theory). The values for the parameters defined in Eqs. (10.11)–(10.13) are given in Table 10.6 along with the predictions of the SM. The agreement is reasonable, except for the values of g^2_L and $\epsilon_L(u,d)$, which reflect the discrepancy in the recent NuTeV results. (The ν-hadron results without the new NuTeV data can be found in

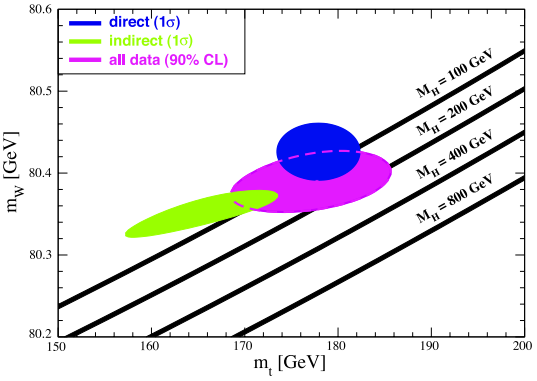

Figure 10.2: One-standard-deviation (39.35%) region in M_W as a function of m_t for the direct and indirect data, and the 90% CL region ($\Delta\chi^2 = 4.605$) allowed by all data. The SM prediction as a function of M_H is also indicated. The widths of the M_H bands reflect the theoretical uncertainty from $\alpha(M_Z)$. See full-color version on color pages at end of book.

Table 10.6: Values of the model-independent neutral-current parameters, compared with the SM predictions for the global best fit values $M_Z = 91.1874 \pm 0.0021$ GeV, $M_H = 113^{+56}_{-40}$ GeV, $m_t = 176.9 \pm 4.0$ GeV, $\alpha_s(M_Z) = 0.1213 \pm 0.0018$, and $\widehat{\alpha}(M_Z)^{-1} = 127.906 \pm 0.019$. There is a second $g^{\nu e}_{V,A}$ solution, given approximately by $g^{\nu e}_V \leftrightarrow g^{\nu e}_A$, which is eliminated by e^+e^- data under the assumption that the neutral current is dominated by the exchange of a single Z. The ϵ_L, as well as the ϵ_R, are strongly correlated and non-Gaussian, so that for implementations we recommend the parametrization using g_i and $\theta_i = \tan^{-1}[\epsilon_i(u)/\epsilon_i(d)]$, $i = L$ or R. θ_R is only weakly correlated with the g_i, while the correlation coefficient between θ_R and θ_L is 0.27.

Quantity	Experimental Value	SM	Correlation		
$\epsilon_L(u)$	0.326 ± 0.013	0.3460(2)			
$\epsilon_L(d)$	-0.441 ± 0.010	−0.4292(1)	non-		
$\epsilon_R(u)$	$-0.175\ ^{+0.013}_{-0.004}$	−0.1551(1)	Gaussian		
$\epsilon_R(d)$	$-0.022\ ^{+0.072}_{-0.047}$	0.0776			
g^2_L	0.3005±0.0012	0.3040(2)	−0.11	−0.21	−0.01
g^2_R	0.0311±0.0010	0.0301		−0.02	−0.03
θ_L	2.51 ± 0.033	2.4631(1)			0.26
θ_R	$4.59\ ^{+0.41}_{-0.28}$	5.1765			
$g^{\nu e}_V$	-0.040 ± 0.015	−0.0397(3)			−0.05
$g^{\nu e}_A$	-0.507 ± 0.014	−0.5065(1)			
$C_{1u} + C_{1d}$	0.148 ± 0.004	0.1529(1)	0.95	−0.55	−0.26
$C_{1u} - C_{1d}$	-0.597 ± 0.061	−0.5299(4)		−0.57	−0.27
$C_{2u} + C_{2d}$	0.62 ± 0.80	−0.0095			−0.38
$C_{2u} - C_{2d}$	-0.07 ± 0.12	−0.0623(6)			

the previous editions of this *Review*.). The off Z-pole e^+e^- results are difficult to present in a model-independent way because Z-propagator effects are non-negligible at TRISTAN, PETRA, PEP, and LEP 2 energies. However, assuming e-μ-τ universality, the low-energy lepton asymmetries imply [98] $4(g^e_A)^2 = 0.99 \pm 0.05$, in good agreement with the SM prediction $\simeq 1$.

The results presented here are generally in reasonable agreement with the ones obtained by the LEP Electroweak Working Group [41]. We obtain higher best fit values for α_s and a higher and slightly more precise M_H. We trace most of the differences to be due to (i) the inclusion of recent higher order radiative corrections, in particular, the leading $\mathcal{O}(\alpha^4_s)$ contribution to hadronic Z decays [150]; (ii) a different evaluation of $\alpha(M_Z)$ [18]; (iii) slightly different data sets (such as the recent DØ m_t value); and (iv) scheme dependences. Taking into account these differences, the agreement is excellent.

10.6. Constraints on new physics

The Z-pole, W mass, and neutral-current data can be used to search for and set limits on deviations from the SM. In particular, the combination of these indirect data with the direct CDF and DØ average for m_t allows one to set stringent limits on new physics. We will mainly discuss the effects of exotic particles (with heavy masses $M_{\rm new} \gg M_Z$ in an expansion in $M_Z/M_{\rm new}$) on the gauge boson self-energies. (Brief remarks are made on new physics which is not of this type.) Most of the effects on precision measurements can be described by three gauge self-energy parameters S, T, and U. We will define these, as well as related parameters, such as ρ_0, ϵ_i, and $\widehat{\epsilon}_i$, to arise from new physics only. *I.e.*, they are equal to zero ($\rho_0 = 1$) exactly in the SM, and do not include any contributions from m_t or M_H, which are treated separately. Our treatment differs from most of the original papers.

Many extensions of the SM are described by the ρ_0 parameter,

$$\rho_0 \equiv M^2_W/(M^2_Z\,\widehat{c}^2_Z\,\widehat{\rho})\ , \tag{10.51}$$

which describes new sources of SU(2) breaking that cannot be accounted for by the SM Higgs doublet or m_t effects. In the presence of $\rho_0 \neq 1$, Eq. (10.51) generalizes Eq. (10.8*b*) while Eq. (10.8*a*) remains unchanged. Provided that the new physics which yields $\rho_0 \neq 1$ is a small perturbation which does not significantly affect the radiative corrections, ρ_0 can be regarded as a phenomenological parameter which multiplies G_F in Eqs. (10.11)–(10.13), (10.28), and Γ_Z in Eq. (10.47). There is enough data to determine ρ_0, M_H, m_t, and α_s, simultaneously. From the global fit,

$$\rho_0 = 0.9998^{+0.0008}_{-0.0005}\ , \tag{10.52}$$

$$114.4\ \text{GeV} < M_H < 193\ \text{GeV}\ , \tag{10.53}$$

$$m_t = 178.0 \pm 4.1\ \text{GeV}\ , \tag{10.54}$$

$$\alpha_s(M_Z) = 0.1214 \pm 0.0018\ , \tag{10.55}$$

where the lower limit on M_H is the direct search bound. (If the direct limit is ignored one obtains $M_H = 66^{+86}_{-30}$ GeV and $\rho_0 = 0.9993^{+0.0010}_{-0.0008}$.) The error bar in Eq. (10.52) is highly asymmetric: at the 2 σ level one has $\rho_0 = 0.9998^{+0.0025}_{-0.0010}$ and $M_H < 664$ GeV. Clearly, in the presence of ρ_0 upper limits on M_H become much weaker. The result in Eq. (10.52) is in remarkable agreement with the SM expectation, $\rho_0 = 1$. It can be used to constrain higher-dimensional Higgs representations to have vacuum expectation values of less than a few percent of those of the doublets. Indeed, the relation between M_W and M_Z is modified if there are Higgs multiplets with weak isospin $> 1/2$ with significant vacuum expectation values. In order to calculate to higher orders in such theories one must define a set of four fundamental renormalized parameters which one may conveniently choose to be α, G_F, M_Z, and M_W, since M_W and M_Z are directly measurable. Then $\widehat{s}^2_Z$ and ρ_0 can be considered dependent parameters.

Eq. (10.52) can also be used to constrain other types of new physics. For example, non-degenerate multiplets of heavy fermions or scalars break the vector part of weak SU(2) and lead to a decrease in the value of M_Z/M_W. A non-degenerate SU(2) doublet $\binom{f_1}{f_2}$ yields a positive contribution to ρ_0 [151] of

$$\frac{CG_F}{8\sqrt{2}\pi^2}\Delta m^2\ , \tag{10.56}$$

where

$$\Delta m^2 \equiv m^2_1 + m^2_2 - \frac{4m^2_1 m^2_2}{m^2_1 - m^2_2}\ln\frac{m_1}{m_2} \geq (m_1 - m_2)^2\ , \tag{10.57}$$

and $C = 1$ (3) for color singlets (triplets). Thus, in the presence of such multiplets, one has

$$\frac{3G_F}{8\sqrt{2}\pi^2}\sum_i \frac{C_i}{3}\Delta m_i^2 = \rho_0 - 1\ , \tag{10.58}$$

where the sum includes fourth-family quark or lepton doublets, $\binom{t'}{b'}$ or $\binom{E^0}{E^-}$, and scalar doublets such as $\binom{\tilde{t}}{\tilde{b}}$ in Supersymmetry (in the absence of $L-R$ mixing). This implies

$$\sum_i \frac{C_i}{3}\Delta m_i^2 \le (85\ \text{GeV})^2 \tag{10.59}$$

at 95% CL. The corresponding constraints on non-degenerate squark and slepton doublets are even stronger, $\sum_i C_i \Delta m_i^2/3 \le (59\ \text{GeV})^2$. This is due to the MSSM Higgs mass bound, $m_{h^0} < 150$ GeV, and the very strong correlation between m_{h^0} and ρ_0 (79%).

Non-degenerate multiplets usually imply $\rho_0 > 1$. Similarly, heavy Z' bosons decrease the prediction for M_Z due to mixing and generally lead to $\rho_0 > 1$ [152]. On the other hand, additional Higgs doublets which participate in spontaneous symmetry breaking [153], heavy lepton doublets involving Majorana neutrinos [154], and the vacuum expectation values of Higgs triplets or higher-dimensional representations can contribute to ρ_0 with either sign. Allowing for the presence of heavy degenerate chiral multiplets (the S parameter, to be discussed below) affects the determination of ρ_0 from the data, at present leading to a smaller value (for fixed M_H).

A number of authors [155–160] have considered the general effects on neutral-current and Z and W boson observables of various types of heavy (*i.e.*, $M_{\text{new}} \gg M_Z$) physics which contribute to the W and Z self-energies but which do not have any direct coupling to the ordinary fermions. In addition to non-degenerate multiplets, which break the vector part of weak SU(2), these include heavy degenerate multiplets of chiral fermions which break the axial generators. The effects of one degenerate chiral doublet are small, but in Technicolor theories there may be many chiral doublets and therefore significant effects [155].

Such effects can be described by just three parameters, S, T, and U at the (electroweak) one-loop level. (Three additional parameters are needed if the new physics scale is comparable to M_Z [161].) T is proportional to the difference between the W and Z self-energies at $Q^2 = 0$ (*i.e.*, vector SU(2)-breaking), while S $(S+U)$ is associated with the difference between the Z (W) self-energy at $Q^2 = M_{Z,W}^2$ and $Q^2 = 0$ (axial SU(2)-breaking). Denoting the contributions of new physics to the various self-energies by Π_{ij}^{new}, we have

$$\widehat{\alpha}(M_Z)T \equiv \frac{\Pi_{WW}^{\text{new}}(0)}{M_W^2} - \frac{\Pi_{ZZ}^{\text{new}}(0)}{M_Z^2}\ , \tag{10.60a}$$

$$\frac{\widehat{\alpha}(M_Z)}{4\widehat{s}_Z^2\widehat{c}_Z^2}S \equiv \frac{\Pi_{ZZ}^{\text{new}}(M_Z^2) - \Pi_{ZZ}^{\text{new}}(0)}{M_Z^2} - \frac{\widehat{c}_Z^2 - \widehat{s}_Z^2}{\widehat{c}_Z\widehat{s}_Z}\frac{\Pi_{Z\gamma}^{\text{new}}(M_Z^2)}{M_Z^2} - \frac{\Pi_{\gamma\gamma}^{\text{new}}(M_Z^2)}{M_Z^2}\ , \tag{10.60b}$$

$$\frac{\widehat{\alpha}(M_Z)}{4\widehat{s}_Z^2}(S+U) \equiv \frac{\Pi_{WW}^{\text{new}}(M_W^2) - \Pi_{WW}^{\text{new}}(0)}{M_W^2} - \frac{\widehat{c}_Z}{\widehat{s}_Z}\frac{\Pi_{Z\gamma}^{\text{new}}(M_Z^2)}{M_Z^2} - \frac{\Pi_{\gamma\gamma}^{\text{new}}(M_Z^2)}{M_Z^2}\ . \tag{10.60c}$$

S, T, and U are defined with a factor proportional to $\widehat{\alpha}$ removed, so that they are expected to be of order unity in the presence of new physics. In the $\overline{\text{MS}}$ scheme as defined in Ref. 46, the last two terms in Eq. (10.60b) and Eq. (10.60c) can be omitted (as was done in some earlier editions of this *Review*). They are related to other parameters $(S_i,\ h_i,\ \widehat{\epsilon}_i)$ defined in [46,156,157] by

$$\begin{aligned} T &= h_V = \widehat{\epsilon}_1/\alpha\ , \\ S &= h_{AZ} = S_Z = 4\widehat{s}_Z^2\widehat{\epsilon}_3/\alpha\ , \\ U &= h_{AW} - h_{AZ} = S_W - S_Z = -4\widehat{s}_Z^2\widehat{\epsilon}_2/\alpha\ . \end{aligned} \tag{10.61}$$

A heavy non-degenerate multiplet of fermions or scalars contributes positively to T as

$$\rho_0 - 1 = \frac{1}{1-\alpha T} - 1 \simeq \alpha T\ , \tag{10.62}$$

where ρ_0 is given in Eq. (10.58). The effects of non-standard Higgs representations cannot be separated from heavy non-degenerate multiplets unless the new physics has other consequences, such as vertex corrections. Most of the original papers defined T to include the effects of loops only. However, we will redefine T to include all new sources of SU(2) breaking, including non-standard Higgs, so that T and ρ_0 are equivalent by Eq. (10.62).

A multiplet of heavy degenerate chiral fermions yields

$$S = C\sum_i \Big(t_{3L}(i) - t_{3R}(i)\Big)^2/3\pi\ , \tag{10.63}$$

where $t_{3L,R}(i)$ is the third component of weak isospin of the left-(right-)handed component of fermion i and C is the number of colors. For example, a heavy degenerate ordinary or mirror family would contribute $2/3\pi$ to S. In Technicolor models with QCD-like dynamics, one expects [155] $S \sim 0.45$ for an iso-doublet of techni-fermions, assuming $N_{TC} = 4$ techni-colors, while $S \sim 1.62$ for a full techni-generation with $N_{TC} = 4$; T is harder to estimate because it is model dependent. In these examples one has $S \ge 0$. However, the QCD-like models are excluded on other grounds (flavor changing neutral-currents, and too-light quarks and pseudo-Goldstone bosons [162]). In particular, these estimates do not apply to models of walking Technicolor [162], for which S can be smaller or even negative [163]. Other situations in which $S < 0$, such as loops involving scalars or Majorana particles, are also possible [164]. The simplest origin of $S < 0$ would probably be an additional heavy Z' boson [152], which could mimic $S < 0$. Supersymmetric extensions of the SM generally give very small effects. See Refs. 115,165 and the Section on Supersymmetry in this *Review* for a complete set of references.

[115,165]. Most simple types of new physics yield $U = 0$, although there are counter-examples, such as the effects of anomalous triple gauge vertices [157].

The SM expressions for observables are replaced by

$$\begin{aligned} M_Z^2 &= M_{Z0}^2\ \frac{1-\alpha T}{1 - G_F M_{Z0}^2 S/2\sqrt{2}\pi}\ , \\ M_W^2 &= M_{W0}^2\ \frac{1}{1 - G_F M_{W0}^2 (S+U)/2\sqrt{2}\pi}\ , \end{aligned} \tag{10.64}$$

where M_{Z0} and M_{W0} are the SM expressions (as functions of m_t and M_H) in the $\overline{\text{MS}}$ scheme. Furthermore,

$$\begin{aligned} \Gamma_Z &= \frac{1}{1-\alpha T} M_Z^3 \beta_Z\ , \\ \Gamma_W &= M_W^3 \beta_W\ , \\ A_i &= \frac{1}{1-\alpha T} A_{i0}\ , \end{aligned} \tag{10.65}$$

where β_Z and β_W are the SM expressions for the reduced widths Γ_{Z0}/M_{Z0}^3 and Γ_{W0}/M_{W0}^3, M_Z and M_W are the physical masses, and A_i (A_{i0}) is a neutral-current amplitude (in the SM).

The data allow a simultaneous determination of $\widehat{s}_Z^2$ (from the Z-pole asymmetries), S (from M_Z), U (from M_W), T (mainly from Γ_Z), α_s (from R_ℓ, σ_{had}, and τ_τ), and m_t (from CDF and DØ), with little correlation among the SM parameters:

$$\begin{aligned} S &= -0.13 \pm 0.10\ (-0.08)\ , \\ T &= -0.17 \pm 0.12\ (+0.09)\ , \\ U &= 0.22 \pm 0.13\ (+0.01)\ , \end{aligned} \tag{10.66}$$

and $\widehat{s}_Z^2 = 0.23119 \pm 0.00016$, $\alpha_s(M_Z) = 0.1222 \pm 0.0019$, $m_t = 177.2 \pm 4.2$ GeV, where the uncertainties are from the inputs. The central values assume $M_H = 117$ GeV, and in parentheses we show

the change for $M_H = 300$ GeV. As can be seen, the SM parameters (U) can be determined with no (little) M_H dependence. On the other hand, S, T, and M_H cannot be obtained simultaneously, because the Higgs boson loops themselves are resembled approximately by oblique effects. Eqs. (10.66) show that negative (positive) contributions to the S (T) parameter can weaken or entirely remove the strong constraints on M_H from the SM fits. Specific models in which a large M_H is compensated by new physics are reviewed in [166]. The parameters in Eqs. (10.66), which by definition are due to new physics only, all deviate by more than one standard deviation from the SM values of zero. However, these deviations are correlated. Fixing $U = 0$ (as is done in Fig. 10.3) will also move S and T to values compatible with zero within errors because the slightly high experimental value of M_W favors a positive value for $S + U$. Using Eq. (10.62) the value of ρ_0 corresponding to T is $0.9987 \pm 0.0009\,(+0.0007)$. The values of the $\widehat{\epsilon}$ parameters defined in Eq. (10.61) are

$$\begin{aligned}
\widehat{\epsilon}_3 &= -0.0011 \pm 0.0008\,(-0.0006)\,, \\
\widehat{\epsilon}_1 &= -0.0013 \pm 0.0009\,(+0.0007)\,, \\
\widehat{\epsilon}_2 &= -0.0019 \pm 0.0011\,(-0.0001)\,. \qquad (10.67)
\end{aligned}$$

Unlike the original definition, we defined the quantities in Eqs. (10.67) to vanish identically in the absence of new physics and to correspond directly to the parameters S, T, and U in Eqs. (10.66). There is a strong correlation (80%) between the S and T parameters. The allowed region in $S - T$ is shown in Fig. 10.3. From Eqs. (10.66) one obtains $S \leq 0.03\,(-0.05)$ and $T \leq 0.02\,(0.11)$ at 95% CL for $M_H = 117$ GeV (300 GeV). If one fixes $M_H = 600$ GeV and requires the constraint $S \geq 0$ (as is appropriate in QCD-like Technicolor models) then $S \leq 0.09$ (Bayesian) or $S \leq 0.06$ (frequentist). This rules out simple Technicolor models with many techni-doublets and QCD-like dynamics.

An extra generation of ordinary fermions is excluded at the 99.95% CL on the basis of the S parameter alone, corresponding to $N_F = 2.92 \pm 0.27$ for the number of families. This result assumes that there are no new contributions to T or U and therefore that any new families are degenerate. In principle this restriction can be relaxed by allowing T to vary as well, since $T > 0$ is expected from a non-degenerate extra family. However, the data currently favor $T < 0$, thus strengthening the exclusion limits. A more detailed analysis is required if the extra neutrino (or the extra down-type quark) is close to its direct mass limit [167]. This can drive S to small or even negative values but at the expense of too-large contributions to T. These results are in agreement with a fit to the number of light neutrinos, $N_\nu = 2.986 \pm 0.007$ (which favors a larger value for $\alpha_s(M_Z) = 0.1228 \pm 0.0021$ mainly from R_ℓ and τ_τ). However, the S parameter fits are valid even for a very heavy fourth family neutrino.

There is no simple parametrization that is powerful enough to describe the effects of every type of new physics on every possible observable. The S, T, and U formalism describes many types of heavy physics which affect only the gauge self-energies, and it can be applied to all precision observables. However, new physics which couples directly to ordinary fermions, such as heavy Z' bosons [152] or mixing with exotic fermions [168] cannot be fully parametrized in the S, T, and U framework. It is convenient to treat these types of new physics by parameterizations that are specialized to that particular class of theories (*e.g.*, extra Z' bosons), or to consider specific models (which might contain, *e.g.*, Z' bosons and exotic fermions with correlated parameters). Constraints on various types of new physics are reviewed in Refs. [43,91,169,170]. Fits to models with (extended) Technicolor and Supersymmetry are described, respectively, in Refs. [171], and [115,172]. The effects of compactified extra spatial dimensions at the TeV scale have been reviewed in [173], and constraints on Little Higgs models in [174].

An alternate formalism [175] defines parameters, ϵ_1, ϵ_2, ϵ_3, ϵ_b in terms of the specific observables M_W/M_Z, $\Gamma_{\ell\ell}$, $A_{FB}^{(0,\ell)}$, and R_b. The definitions coincide with those for $\widehat{\epsilon}_i$ in Eqs. (10.60) and (10.61) for physics which affects gauge self-energies only, but the ϵ's now parametrize arbitrary types of new physics. However, the ϵ's are not related to other observables unless additional model-dependent assumptions are made. Another approach [176–178] parametrizes new

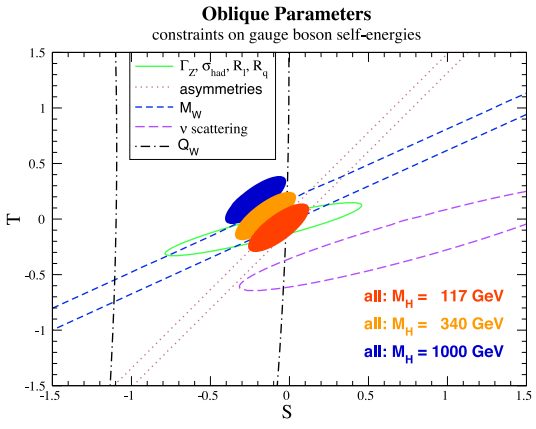

Figure 10.3: 1 σ constraints (39.35%) on S and T from various inputs. S and T represent the contributions of new physics only. (Uncertainties from m_t are included in the errors.) The contours assume $M_H = 117$ GeV except for the central and upper 90% CL contours allowed by all data, which are for $M_H = 340$ GeV and 1000 GeV, respectively. Data sets not involving M_W are insensitive to U. Due to higher order effects, however, $U = 0$ has to be assumed in all fits. α_s is constrained using the τ lifetime as additional input in all fits. See full-color version on color pages at end of book.

physics in terms of gauge-invariant sets of operators. It is especially powerful in studying the effects of new physics on non-Abelian gauge vertices. The most general approach introduces deviation vectors [169]. Each type of new physics defines a deviation vector, the components of which are the deviations of each observable from its SM prediction, normalized to the experimental uncertainty. The length (direction) of the vector represents the strength (type) of new physics.

Table 10.7: 95% CL lower mass limits (in GeV) from low energy and Z pole data on various extra Z' gauge bosons, appearing in models of unification and string theory. ρ_0 free indicates a completely arbitrary Higgs sector, while $\rho_0 = 1$ restricts to Higgs doublets and singlets with still unspecified charges. The CDF bounds from searches for $\bar{p}p \to e^+e^-, \mu^+\mu^-$ [183] and the LEP 2 $e^+e^- \to f\bar{f}$ [41,184] bounds are listed in the last two columns, respectively. (The CDF bounds would be weakend if there are open supersymmetric or exotic decay channels.)

Z'	ρ_0 free	$\rho_0 = 1$	CDF (direct)	LEP 2
Z_χ	551	545	595	673
Z_ψ	151	146	590	481
Z_η	379	365	620	434
Z_{LR}	570	564	630	804
Z_{SM}	822	809	690	1787
$Z_{\rm string}$	582	578	–	–

One of the best motivated kinds of physics beyond the SM besides Supersymmetry are extra Z' bosons. They do not spoil the observed approximate gauge coupling unification, and appear copiously in many Grand Unified Theories (GUTs), most Superstring models, as well as in dynamical symmetry breaking [171,179] and Little Higgs models [174]. For example, the SO(10) GUT contains an extra U(1) as can be seen from its maximal subgroup, $\mathrm{SU}(5) \times \mathrm{U}(1)_\chi$. Similarly, the E_6 GUT contains the subgroup $\mathrm{SO}(10) \times \mathrm{U}(1)_\psi$. The Z_ψ possesses only axial-vector couplings to the ordinary fermions, and its mass is generally less constrained. The Z_η boson is the linear combination $\sqrt{3/8}\,Z_\chi - \sqrt{5/8}\,Z_\psi$. The Z_{LR} boson occurs in left-right models with gauge group $\mathrm{SU}(3)_C \times \mathrm{SU}(2)_L \times \mathrm{SU}(2)_R \times \mathrm{U}(1)_{B-L} \subset \mathrm{SO}(10)$.

The sequential Z_{SM} boson is defined to have the same couplings to fermions as the SM Z boson. Such a boson is not expected in the context of gauge theories unless it has different couplings to exotic fermions than the ordinary Z. However, it serves as a useful reference case when comparing constraints from various sources. It could also play the role of an excited state of the ordinary Z in models with extra dimensions at the weak scale. Finally, we consider a Superstring motivated Z_{string} boson appearing in a specific model [180]. The potential Z' boson is in general a superposition of the SM Z and the new boson associated with the extra U(1). The mixing angle θ satisfies,

$$\tan^2\theta = \frac{M_{Z_1^0}^2 - M_Z^2}{M_{Z'}^2 - M_{Z_1^0}^2},$$

where $M_{Z_1^0}$ is the SM value for M_Z in the absence of mixing. Note, that $M_Z < M_{Z_1^0}$, and that the SM Z couplings are changed by the mixing. If the Higgs U(1)$'$ quantum numbers are known, there will be an extra constraint,

$$\theta = C\frac{g_2}{g_1}\frac{M_Z^2}{M_{Z'}^2}\ , \qquad (10.68)$$

where $g_{1,2}$ are the U(1) and U(1)$'$ gauge couplings with $g_2 = \sqrt{\frac{5}{3}}\sin\theta_W\sqrt{\lambda}\,g_1$. $\lambda \sim 1$ (which we assume) if the GUT group breaks directly to SU(3) $\times$ SU(2) $\times$ U(1) $\times$ U(1)$'$. C is a function of vacuum expectation values. For minimal Higgs sectors it can be found in reference [152]. Table 10.7 shows the 95% CL lower mass limits obtained from a somewhat earlier data set [181] for ρ_0 free and $\rho_0 = 1$, respectively. In cases of specific minimal Higgs sectors where C is known, the Z' mass limits are generally pushed into the TeV region. The limits on $|\theta|$ are typically $<$ few $\times 10^{-3}$. For more details see [181,182] and the Section on "The Z' Searches" in this *Review*. Also listed in Table 10.7 are the direct lower limits on Z' production from CDF [183] and LEP 2 bounds [41,184]. The final LEP 1 value for $\sigma_{\rm had}$, some previous values for Q_W(Cs), NuTeV, and $A_{FB}^{0,b}$ (for family-nonuniversal couplings [185]) modify the results and might even suggest the possible existence of a Z' [144,186].

References:

1. S. Weinberg, Phys. Rev. Lett. **19**, 1264 (1967);
   A. Salam, p. 367 of *Elementary Particle Theory*, ed. N. Svartholm (Almquist and Wiksells, Stockholm, 1969);
   S.L. Glashow, J. Iliopoulos, and L. Maiani, Phys. Rev. **D2**, 1285 (1970).
2. H. Abele *et al.*, `hep-ph/0312150`.
3. For reviews, see G. Barbiellini and C. Santoni, Riv. Nuovo Cimento **9(2)**, 1 (1986);
   E.D. Commins and P.H. Bucksbaum, *Weak Interactions of Leptons and Quarks*, (Cambridge Univ. Press, Cambridge, 1983);
   W. Fetscher and H.J. Gerber, p. 657 of Ref. 4;
   J. Deutsch and P. Quin, p. 706 of Ref. 4;
   J.M. Conrad, M.H. Shaevitz, and T. Bolton, Rev. Mod. Phys. **70**, 1341 (1998).
4. *Precision Tests of the Standard Electroweak Model*, ed. P. Langacker (World Scientific, Singapore, 1995).
5. J. Erler and M. Luo, Phys. Lett. **B558**, 125 (2003).
6. CDF: T. Affolder *et al.*, Phys. Rev. **D63**, 032003 (2001).
7. E. Thomson for the CDF Collaboration, presented at the *31st SLAC Summer Institute* (SSI 2003, Menlo Park).
8. DØ: B. Abbott *et al.*, Phys. Rev. **D58**, 052001 (1998).
9. F. Canelli for the DØ Collaboration, presented at the *8th Conference on the Intersections of Particle and Nuclear Physics* (CIPANP 2003, New York).
10. L. Demortier *et al.*, preprint FERMILAB-TM-2084.
11. K. Melnikov and T. v. Ritbergen, Phys. Lett. **B482**, 99 (2000).
12. S.J. Brodsky, G.P. Lepage, and P.B. Mackenzie, Phys. Rev. **D28**, 228 (1983).
13. N. Gray *et al.*, Z. Phys. **C48**, 673 (1990).
14. For reviews, see the article on "The Higgs boson" in this *Review*;
    J. Gunion, H.E. Haber, G.L. Kane, and S. Dawson, *The Higgs Hunter's Guide*, (Addison-Wesley, Redwood City, 1990);
    M. Sher, Phys. Reports **179**, 273 (1989);
    M. Carena and H.E. Haber, Prog. Part. Nucl. Phys. **50**, 63 (2003).
15. P.J. Mohr and B.N. Taylor, Rev. Mod. Phys. **72**, 351 (2000).
16. TOPAZ: I. Levine *et al.*, Phys. Rev. Lett. **78**, 424 (1997);
    VENUS: S. Okada *et al.*, Phys. Rev. Lett. **81**, 2428 (1998);
    OPAL: G. Abbiendi *et al.*, Eur. Phys. J. **C13**, 553 (2000);
    L3: M. Acciarri *et al.*, Phys. Lett. **B476**, 40 (2000).
17. S. Fanchiotti, B. Kniehl, and A. Sirlin, Phys. Rev. **D48**, 307 (1993) and references therein.
18. J. Erler, Phys. Rev. **D59**, 054008 (1999).
19. CMD 2: R.R. Akhmetshin *et al.*, `hep-ex/0308008`.
20. M. Davier, S. Eidelman, A. Höcker, and Z. Zhang, `hep-ph/0308213`.
21. A.D. Martin and D. Zeppenfeld, Phys. Lett. **B345**, 558 (1995).
22. S. Eidelman and F. Jegerlehner, Z. Phys. **C67**, 585 (1995).
23. B.V. Geshkenbein and V.L. Morgunov, Phys. Lett. **B340**, 185 (1995) and Phys. Lett. **B352**, 456 (1995).
24. H. Burkhardt and B. Pietrzyk, Phys. Lett. **B356**, 398 (1995).
25. M.L. Swartz, Phys. Rev. **D53**, 5268 (1996).
26. R. Alemany, M. Davier, and A. Höcker, Eur. Phys. J. **C2**, 123 (1998).
27. N.V. Krasnikov and R. Rodenberg, Nuovo Cimento **111A**, 217 (1998).
28. M. Davier and A. Höcker, Phys. Lett. **B419**, 419 (1998).
29. J.H. Kühn and M. Steinhauser, Phys. Lett. **B437**, 425 (1998).
30. M. Davier and A. Höcker, Phys. Lett. **B435**, 427 (1998).
31. S. Groote, J.G. Körner, K. Schilcher, N.F. Nasrallah, Phys. Lett. **B440**, 375 (1998).
32. A.D. Martin, J. Outhwaite, and M.G. Ryskin, Phys. Lett. **B492**, 69 (2000).
33. H. Burkhardt and B. Pietrzyk, Phys. Lett. **B513**, 46 (2001).
34. J.F. de Trocóniz and F.J. Yndurain, Phys. Rev. **D65**, 093002 (2002).
35. F. Jegerlehner, `hep-ph/0308117`.
36. BES: J.Z. Bai *et al.*, Phys. Rev. Lett. **88**, 101802 (2002);
    G.S. Huang, `hep-ex/0105074`.
37. S. Binner, J.H. Kühn, and K. Melnikov, Phys. Lett. **B459**, 279 (1999).
38. KLOE: A. Aloisio *et al.*, `hep-ex/0307051`.
39. W.J. Marciano and A. Sirlin, Phys. Rev. Lett. **61**, 1815 (1988).
40. T. van Ritbergen and R.G. Stuart, Phys. Rev. Lett. **82**, 488 (1999).
41. ALEPH, DELPHI, L3, OPAL, LEP Electroweak Working Group, and SLD Heavy Flavor Group, `hep-ex/0212036` and `http://www.cern.ch/LEPEWWG/`.
42. Earlier analyses include U. Amaldi *et al.*, Phys. Rev. **D36**, 1385 (1987);
    G. Costa *et al.*, Nucl. Phys. **B297**, 244 (1988);
    Deep inelastic scattering is considered by G.L. Fogli and D. Haidt, Z. Phys. **C40**, 379 (1988);
    P. Langacker and M. Luo, Phys. Rev. **D44**, 817 (1991);
    For more recent analyses, see Ref. 43.
43. P. Langacker, p. 883 of Ref. 4;
    J. Erler and P. Langacker, Phys. Rev. **D52**, 441 (1995);
    Neutrino scattering is reviewed by J.M. Conrad *et al.* in Ref. 3;
    Nonstandard neutrino interactions are surveyed in Z. Berezhiani and A. Rossi, Phys. Lett. **B535**, 207 (2002);
    S. Davidson, C. Pena-Garay, N. Rius, and A. Santamaria, JHEP **0303**, 011 (2003).

44. A. Sirlin, Phys. Rev. **D22**, 971 (1980) and *ibid.* **29**, 89 (1984);
D.C. Kennedy *et al.*, Nucl. Phys. **B321**, 83 (1989);
D.C. Kennedy and B.W. Lynn, Nucl. Phys. **B322**, 1 (1989);
D.Yu. Bardin *et al.*, Z. Phys. **C44**, 493 (1989);
W. Hollik, Fortsch. Phys. **38**, 165 (1990);
For reviews, see the articles by W. Hollik, pp. 37 and 117, and W. Marciano, p. 170 in Ref. 4. Extensive references to other papers are given in Ref. 42.
45. W. Hollik in Ref. 44 and references therein;
V.A. Novikov, L.B. Okun, and M.I. Vysotsky, Nucl. Phys. **B397**, 35 (1993).
46. W.J. Marciano and J.L. Rosner, Phys. Rev. Lett. **65**, 2963 (1990).
47. G. Degrassi, S. Fanchiotti, and A. Sirlin, Nucl. Phys. **B351**, 49 (1991).
48. G. Degrassi and A. Sirlin, Nucl. Phys. **B352**, 342 (1991).
49. P. Gambino and A. Sirlin, Phys. Rev. **D49**, 1160 (1994).
50. ZFITTER: D. Bardin *et al.*, Comput. Phys. Commun. **133**, 229 (2001) and references therein.
51. R. Barbieri *et al.*, Phys. Lett. **B288**, 95 (1992);
R. Barbieri *et al.*, Nucl. Phys. **B409**, 105 (1993).
52. J. Fleischer, O.V. Tarasov, and F. Jegerlehner, Phys. Lett. **B319**, 249 (1993).
53. G. Degrassi, P. Gambino, and A. Vicini, Phys. Lett. **B383**, 219 (1996);
G. Degrassi, P. Gambino, and A. Sirlin, Phys. Lett. **B394**, 188 (1997).
54. A. Freitas, W. Hollik, W. Walter, and G. Weiglein, Phys. Lett. **B495**, 338 (2000) and Nucl. Phys. **B632**, 189 (2002).
55. M. Awramik and M. Czakon, Phys. Rev. Lett. **89**, 241801 (2002);
A. Onishchenko and O. Veretin, Phys. Lett. **B551**, 111 (2003).
56. A. Djouadi and C. Verzegnassi, Phys. Lett. **B195**, 265 (1987);
A. Djouadi, Nuovo Cimento **100A**, 357 (1988);
B.A. Kniehl, Nucl. Phys. **B347**, 86 (1990);
A. Djouadi and P. Gambino, Phys. Rev. **D49**, 3499 (1994), **D49**, 4705 (1994), and **D53**, 4111(E) (1996).
57. K.G. Chetyrkin, J.H. Kühn, and M. Steinhauser, Phys. Lett. **B351**, 331 (1995);
L. Avdeev *et al.*, Phys. Lett. **B336**, 560 (1994) and **B349**, 597(E) (1995).
58. J. Fleischer *et al.*, Phys. Lett. **B293**, 437 (1992);
K.G. Chetyrkin, A. Kwiatkowski, and M. Steinhauser, Mod. Phys. Lett. **A8**, 2785 (1993).
59. A. Czarnecki and J.H. Kühn, Phys. Rev. Lett. **77**, 3955 (1996).
60. R. Harlander, T. Seidensticker, and M. Steinhauser, Phys. Lett. **B426**, 125 (1998);
J. Fleischer *et al.*, Phys. Lett. **B459**, 625 (1999).
61. J. Erler, `hep-ph/0005084`.
62. For reviews, see F. Perrier, p. 385 of Ref. 4;
J.M. Conrad *et al.* in Ref. 3.
63. CDHS: H. Abramowicz *et al.*, Phys. Rev. Lett. **57**, 298 (1986);
CDHS: A. Blondel *et al.*, Z. Phys. **C45**, 361 (1990).
64. CHARM: J.V. Allaby *et al.*, Phys. Lett. **B177**, 446 (1986);
CHARM: J.V. Allaby *et al.*, Z. Phys. **C36**, 611 (1987).
65. CCFR: C.G. Arroyo *et al.*, Phys. Rev. Lett. **72**, 3452 (1994);
CCFR: K.S. McFarland *et al.*, Eur. Phys. J. **C1**, 509 (1998).
66. R.M. Barnett, Phys. Rev. **D14**, 70 (1976);
H. Georgi and H.D. Politzer, Phys. Rev. **D14**, 1829 (1976).
67. LAB-E: S.A. Rabinowitz *et al.*, Phys. Rev. Lett. **70**, 134 (1993).
68. E.A. Paschos and L. Wolfenstein, Phys. Rev. **D7**, 91 (1973).
69. NuTeV: G. P. Zeller *et al.*, Phys. Rev. Lett. **88**, 091802 (2002).
70. S. Davidson *et al.*, JHEP **0202**, 037 (2002).
71. NuTeV: M. Goncharov *et al.*, Phys. Rev. **D64**, 112006 (2001).
72. NuTeV: G.P. Zeller *et al.*, Phys. Rev. **D65**, 111103 (2002);
NuTeV: R. H. Bernstein *et al.*, J. Phys. G **29**, 1919 (2003).
73. K.P.O. Diener, S. Dittmaier, and W. Hollik, `hep-ph/0310364`.
74. CHARM: J. Dorenbosch *et al.*, Z. Phys. **C41**, 567 (1989).
75. CALO: L.A. Ahrens *et al.*, Phys. Rev. **D41**, 3297 (1990).
76. CHARM II: P. Vilain *et al.*, Phys. Lett. **B335**, 246 (1994).
77. See also J. Panman, p. 504 of Ref. 4.
78. ILM: R.C. Allen *et al.*, Phys. Rev. **D47**, 11 (1993);
LSND: L.B. Auerbach *et al.*, Phys. Rev. **D63**, 112001 (2001).
79. SSF: C.Y. Prescott *et al.*, Phys. Lett. **B84**, 524 (1979);
For a review, see P. Souder, p. 599 of Ref. 4.
80. For reviews and references to earlier work, see M.A. Bouchiat and L. Pottier, Science **234**, 1203 (1986);
B.P. Masterson and C.E. Wieman, p. 545 of Ref. 4.
81. Cesium (Boulder): C.S. Wood *et al.*, Science **275**, 1759 (1997).
82. Thallium (Oxford): N.H. Edwards *et al.*, Phys. Rev. Lett. **74**, 2654 (1995);
Thallium (Seattle): P.A. Vetter *et al.*, Phys. Rev. Lett. **74**, 2658 (1995).
83. Lead (Seattle): D.M. Meekhof *et al.*, Phys. Rev. Lett. **71**, 3442 (1993).
84. Bismuth (Oxford): M.J.D. MacPherson *et al.*, Phys. Rev. Lett. **67**, 2784 (1991).
85. V.A. Dzuba, V.V. Flambaum, and O.P. Sushkov, Phys. Lett. **141A**, 147 (1989);
S.A. Blundell, J. Sapirstein, and W.R. Johnson, Phys. Rev. Lett. **65**, 1411 (1990) and Phys. Rev. **D45**, 1602 (1992);
For a review, see S.A. Blundell, W.R. Johnson, and J. Sapirstein, p. 577 of Ref. 4.
86. S.C. Bennett and C.E. Wieman, Phys. Rev. Lett. **82**, 2484 (1999).
87. V.A. Dzuba, V.V. Flambaum, and O.P. Sushkov, Phys. Rev. **A56**, R4357 (1997).
88. M.A. Bouchiat and J. Guéna, J. Phys. (France) **49**, 2037 (1988).
89. A. Derevianko, Phys. Rev. Lett. **85**, 1618 (2000);
V.A. Dzuba, C. Harabati, and W.R. Johnson, Phys. Rev. **A63**, 044103 (2001);
M.G. Kozlov, S.G. Porsev, and I.I. Tupitsyn, Phys. Rev. Lett. **86**, 3260 (2001).
90. A.I. Milstein and O.P. Sushkov, Phys. Rev. **A66**, 022108 (2002);
W.R. Johnson, I. Bednyakov, and G. Soff, Phys. Rev. Lett. **87**, 233001 (2001);
V.A. Dzuba, V.V. Flambaum, and J.S. Ginges, Phys. Rev. **D66**, 076013 (2002);
M.Y. Kuchiev and V.V. Flambaum, Phys. Rev. Lett. **89**, 283002 (2002);
A.I. Milstein, O.P. Sushkov, and I.S. Terekhov, Phys. Rev. Lett. **89**, 283003 (2002);
For a recent review, see J.S.M. Ginges and V.V. Flambaum, `physics/0309054`.
91. J. Erler, A. Kurylov, and M.J. Ramsey-Musolf, Phys. Rev. **D68**, 016006 (2003).
92. V.A. Dzuba *et al.*, J. Phys. **B20**, 3297 (1987).
93. Ya.B. Zel'dovich, Sov. Phys. JETP **6**, 1184 (1958);
For recent discussions, see V.V. Flambaum and D.W. Murray, Phys. Rev. **C56**, 1641 (1997);
W.C. Haxton and C.E. Wieman, Ann. Rev. Nucl. Part. Sci. **51**, 261 (2001).
94. J.L. Rosner, Phys. Rev. **D53**, 2724 (1996).
95. S.J. Pollock, E.N. Fortson, and L. Wilets, Phys. Rev. **C46**, 2587 (1992);
B.Q. Chen and P. Vogel, Phys. Rev. **C48**, 1392 (1993).
96. B.W. Lynn and R.G. Stuart, Nucl. Phys. **B253**, 216 (1985).

97. *Physics at LEP*, ed. J. Ellis and R. Peccei, CERN 86–02, Vol. 1.
98. C. Kiesling, *Tests of the Standard Theory of Electroweak Interactions*, (Springer-Verlag, New York, 1988);
R. Marshall, Z. Phys. **C43**, 607 (1989);
Y. Mori *et al.*, Phys. Lett. **B218**, 499 (1989);
D. Haidt, p. 203 of Ref. 4.
99. For reviews, see D. Schaile, p. 215, and A. Blondel, p. 277 of Ref. 4.
100. M. Elsing, presented at the *International Europhysics Conference on High Energy Physics* (EPS 2003, Aachen).
101. SLD: K. Abe *et al.*, Phys. Rev. Lett. **84**, 5945 (2000).
102. SLD: K. Abe *et al.*, Phys. Rev. Lett. **85**, 5059 (2000).
103. SLD: K. Abe *et al.*, Phys. Rev. Lett. **86**, 1162 (2001).
104. DELPHI: P. Abreu *et al.*, Z. Phys. **C67**, 1 (1995);
OPAL: K. Ackerstaff *et al.*, Z. Phys. **C76**, 387 (1997).
105. SLD: K. Abe *et al.*, Phys. Rev. Lett. **78**, 17 (1997).
106. ALEPH, DELPHI, L3, and OPAL Collaborations, and the LEP Working Group for Higgs Boson Searches: D. Abbaneo *et al.*, Phys. Lett. **B565**, 61 (2003).
107. A. Leike, T. Riemann, and J. Rose, Phys. Lett. **B273**, 513 (1991);
T. Riemann, Phys. Lett. **B293**, 451 (1992).
108. E158: P.L. Anthony *et al.*, `hep-ex/0312035`;
the implications are discussed in A. Czarnecki and W.J. Marciano, Int. J. Mod. Phys. A **15**, 2365 (2000).
109. G. S. Mitchell, `hep-ex/0308049`;
the implications are discussed in Ref. 91.
110. Belle: K. Abe *et al.*, Phys. Lett. **B511**, 151 (2001).
111. CLEO: S. Chen *et al.*, Phys. Rev. Lett. **87**, 251807 (2001).
112. BaBar: B. Aubert *et al.*, `hep-ex/0207076`.
113. A. Ali and C. Greub, Phys. Lett. **B259**, 182 (1991);
A.L. Kagan and M. Neubert, Eur. Phys. J. **C7**, 5 (1999).
114. A. Czarnecki and W.J. Marciano, Phys. Rev. Lett. **81**, 277 (1998).
115. J. Erler and D.M. Pierce, Nucl. Phys. **B526**, 53 (1998).
116. Y. Nir, Phys. Lett. **B221**, 184 (1989);
K. Adel and Y.P. Yao, Phys. Rev. **D49**, 4945 (1994);
C. Greub, T. Hurth, and D. Wyler, Phys. Rev. **D54**, 3350 (1996);
K.G. Chetyrkin, M. Misiak, and M. Münz, Phys. Lett. **B400**, 206 (1997);
C. Greub and T. Hurth, Phys. Rev. **D56**, 2934 (1997);
M. Ciuchini *et al.*, Nucl. Phys. **B527**, 21 (1998) and **B534**, 3 (1998);
F.M. Borzumati and C. Greub, Phys. Rev. **D58**, 074004 (1998) and **D59**, 057501 (1999);
A. Strumia, Nucl. Phys. **B532**, 28 (1998).
117. E821: H.N. Brown *et al.*, Phys. Rev. Lett. **86**, 2227 (2001);
E821: G.W. Bennett, *et al.*, Phys. Rev. Lett. **89**, 101804 (2002).
118. For reviews, see V.W. Hughes and T. Kinoshita, Rev. Mod. Phys. **71**, S133 (1999);
A. Czarnecki and W.J. Marciano, Phys. Rev. **D64**, 013014 (2001);
T. Kinoshita, J. Phys. **G29**, 9 (2003).
119. S.J. Brodsky and J.D. Sullivan, Phys. Rev. **D156**, 1644 (1967);
T. Burnett and M.J. Levine, Phys. Lett. **B24**, 467 (1967);
R. Jackiw and S. Weinberg, Phys. Rev. **D5**, 2473 (1972);
I. Bars and M. Yoshimura, Phys. Rev. **D6**, 374 (1972);
K. Fujikawa, B.W. Lee, and A.I. Sanda, Phys. Rev. **D6**, 2923 (1972);
G. Altarelli, N. Cabibbo, and L. Maiani, Phys. Lett. **B40**, 415 (1972);
W.A. Bardeen, R. Gastmans, and B.E. Laurup, Nucl. Phys. **B46**, 315 (1972).
120. T.V. Kukhto, E.A. Kuraev, A. Schiller, and Z.K. Silagadze, Nucl. Phys. **B371**, 567 (1992);
S. Peris, M. Perrottet, and E. de Rafael, Phys. Lett. **B355**, 523 (1995);
A. Czarnecki, B. Krause, and W.J. Marciano, Phys. Rev. **D52**, 2619 (1995) and Phys. Rev. Lett. **76**, 3267 (1996).
121. G. Degrassi and G. Giudice, Phys. Rev. **D58**, 053007 (1998).
122. F. Matorras (DELPHI), contributed paper to the *International Europhysics Conference on High Energy Physics* (EPS 2003, Aachen).
123. V. Cirigliano, G. Ecker and H. Neufeld, JHEP **0208**, 002 (2002).
124. J. Erler, `hep-ph/0211345`.
125. M. Knecht and A. Nyffeler, Phys. Rev. **D65**, 073034 (2002).
126. M. Hayakawa and T. Kinoshita, `hep-ph/0112102`;
J. Bijnens, E. Pallante and J. Prades, Nucl. Phys. **B626**, 410 (2002).
127. B. Krause, Phys. Lett. **B390**, 392 (1997).
128. J. Erler and M. Luo, Phys. Rev. Lett. **87**, 071804 (2001).
129. J.L. Lopez, D.V. Nanopoulos, and X. Wang, Phys. Rev. **D49**, 366 (1994);
for recent reviews, see Ref. 118.
130. E821: `http://www.g-2.bnl.gov/index.shtml/`.
131. S. Ghozzi and F. Jegerlehner, `hep-ph/0310181`.
132. K. Hagiwara, A.D. Martin, D. Nomura, and T. Teubner, `hep-ph/0312250`.
133. A comprehensive report and further references can be found in K.G. Chetyrkin, J.H. Kühn, and A. Kwiatkowski, Phys. Reports **277**, 189 (1996).
134. J. Schwinger, *Particles, Sources and Fields*, Vol. II, (Addison-Wesley, New York, 1973);
K.G. Chetyrkin, A.L. Kataev, and F.V. Tkachev, Phys. Lett. **B85**, 277 (1979);
M. Dine and J. Sapirstein, Phys. Rev. Lett. **43**, 668 (1979);
W. Celmaster, R.J. Gonsalves, Phys. Rev. Lett. **44**, 560 (1980);
S.G. Gorishnii, A.L. Kataev, and S.A. Larin, Phys. Lett. **B212**, 238 (1988) and **B259**, 144 (1991);
L.R. Surguladze and M.A. Samuel, Phys. Rev. Lett. **66**, 560 (1991) and 2416(E).
135. W. Bernreuther and W. Wetzel, Z. Phys. **11**, 113 (1981) and Phys. Rev. **D24**, 2724 (1982);
B.A. Kniehl, Phys. Lett. **B237**, 127 (1990);
K.G. Chetyrkin, Phys. Lett. **B307**, 169 (1993);
A.H. Hoang *et al.*, Phys. Lett. **B338**, 330 (1994);
S.A. Larin, T. van Ritbergen, and J.A.M. Vermaseren, Nucl. Phys. **B438**, 278 (1995).
136. T.H. Chang, K.J.F. Gaemers, and W.L. van Neerven, Nucl. Phys. **B202**, 407 (1980);
J. Jersak, E. Laermann, and P.M. Zerwas, Phys. Lett. **B98**, 363 (1981) and Phys. Rev. **D25**, 1218 (1982);
S.G. Gorishnii, A.L. Kataev, and S.A. Larin, Nuovo Cimento **92**, 117 (1986);
K.G. Chetyrkin and J.H. Kühn, Phys. Lett. **B248**, 359 (1990) and *ibid.* **406**, 102 (1997);
K.G. Chetyrkin, J.H. Kühn, and A. Kwiatkowski, Phys. Lett. **B282**, 221 (1992).
137. B.A. Kniehl and J.H. Kühn, Phys. Lett. **B224**, 229 (1990) and Nucl. Phys. **B329**, 547 (1990);
K.G. Chetyrkin and A. Kwiatkowski, Phys. Lett. **B305**, 285 (1993) and **B319**, 307 (1993);
S.A. Larin, T. van Ritbergen, and J.A.M. Vermaseren, Phys. Lett. **B320**, 159 (1994);
K.G. Chetyrkin and O.V. Tarasov, Phys. Lett. **B327**, 114 (1994).

138. A.L. Kataev, Phys. Lett. **B287**, 209 (1992).
139. D. Albert *et al.*, Nucl. Phys. **B166**, 460 (1980);
F. Jegerlehner, Z. Phys. **C32**, 425 (1986);
A. Djouadi, J.H. Kühn, and P.M. Zerwas, Z. Phys. **C46**, 411 (1990);
A. Borrelli *et al.*, Nucl. Phys. **B333**, 357 (1990).
140. A.A. Akhundov, D.Yu. Bardin, and T. Riemann, Nucl. Phys. **B276**, 1 (1986);
W. Beenakker and W. Hollik, Z. Phys. **C40**, 141 (1988);
B.W. Lynn and R.G. Stuart, Phys. Lett. **B352**, 676 (1990);
J. Bernabeu, A. Pich, and A. Santamaria, Nucl. Phys. **B363**, 326 (1991).
141. UA2: S. Alitti *et al.*, Phys. Lett. **B276**, 354 (1992);
CDF: T. Affolder *et al.*, Phys. Rev. **D64**, 052001 (2001);
DØ: V. M. Abazov *et al.*, Phys. Rev. **D66**, 012001 (2002);
CDF and DØ Collaborations: `hep-ex/0311039`.
142. J. Erler, J.L. Feng, and N. Polonsky, Phys. Rev. Lett. **78**, 3063 (1997).
143. D. Choudhury, T.M.P. Tait and C.E.M. Wagner, Phys. Rev. **D65**, 053002 (2002).
144. J. Erler and P. Langacker, Phys. Rev. Lett. **84**, 212 (2000).
145. DELPHI: P. Abreu *et al.*, Z. Phys. **C**, 70 (1996);
DELPHI: P. Abreu *et al.*, in the Proceedings of the *International Europhysics Conference on High Energy Physics* (Jerusalem, 1997).
146. P. Schleper, presented at the *International Europhysics Conference on High Energy Physics* (EPS 2003, Aachen).
147. HPQCD: C.T. Davies *et al.*, `hep-lat/0304004`.
148. J. Erler, Phys. Rev. **D63**, 071301 (2001).
149. P. Langacker and N. Polonsky, Phys. Rev. **D52**, 3081 (1995);
J. Bagger, K.T. Matchev, and D. Pierce, Phys. Lett. **B348**, 443 (1995).
150. A.L. Kataev and V.V. Starshenko, Mod. Phys. Lett. **A10**, 235 (1995).
151. M. Veltman, Nucl. Phys. **B123**, 89 (1977);
M. Chanowitz, M.A. Furman, and I. Hinchliffe, Phys. Lett. **B78**, 285 (1978).
152. P. Langacker and M. Luo, Phys. Rev. **D45**, 278 (1992) and references therein.
153. A. Denner, R.J. Guth, and J.H. Kühn, Phys. Lett. **B240**, 438 (1990).
154. S. Bertolini and A. Sirlin, Phys. Lett. **B257**, 179 (1991).
155. M. Peskin and T. Takeuchi, Phys. Rev. Lett. **65**, 964 (1990) and Phys. Rev. **D46**, 381 (1992);
M. Golden and L. Randall, Nucl. Phys. **B361**, 3 (1991).
156. D. Kennedy and P. Langacker, Phys. Rev. Lett. **65**, 2967 (1990) and Phys. Rev. **D44**, 1591 (1991).
157. G. Altarelli and R. Barbieri, Phys. Lett. **B253**, 161 (1990).
158. B. Holdom and J. Terning, Phys. Lett. **B247**, 88 (1990).
159. B.W. Lynn, M.E. Peskin, and R.G. Stuart, p. 90 of Ref. 97.
160. An alternative formulation is given by K. Hagiwara *et al.*, Z. Phys. **C64**, 559 (1994) and *ibid.* **C68**, 352(E) (1995);
K. Hagiwara, D. Haidt, and S. Matsumoto, Eur. Phys. J. **C2**, 95 (1998).
161. I. Maksymyk, C.P. Burgess, and D. London, Phys. Rev. **D50**, 529 (1994);
C.P. Burgess *et al.*, Phys. Lett. **B326**, 276 (1994).
162. K. Lane, in the Proceedings of the *27th International Conference on High Energy Physics* (Glasgow, 1994).
163. E. Gates and J. Terning, Phys. Rev. Lett. **67**, 1840 (1991);
R. Sundrum and S.D.H. Hsu, Nucl. Phys. **B391**, 127 (1993);
R. Sundrum, Nucl. Phys. **B395**, 60 (1993);
M. Luty and R. Sundrum, Phys. Rev. Lett. **70**, 529 (1993);
T. Appelquist and J. Terning, Phys. Lett. **B315**, 139 (1993).
164. H. Georgi, Nucl. Phys. **B363**, 301 (1991);
M.J. Dugan and L. Randall, Phys. Lett. **B264**, 154 (1991).
165. R. Barbieri *et al.*, Nucl. Phys. **B341**, 309 (1990).
166. M.E. Peskin and J.D. Wells, Phys. Rev. **D64**, 093003 (2001).
167. H.J. He, N. Polonsky, and S. Su, Phys. Rev. **D64**, 053004 (2001);
V.A. Novikov, L.B. Okun, A.N. Rozanov, and M.I. Vysotsky, Sov. Phys. JETP **76**, 127 (2002) and references therein.
168. For a review, see D. London, p. 951 of Ref. 4;
a recent analysis is M.B. Popovic and E.H. Simmons, Phys. Rev. **D58**, 095007 (1998);
for collider implications, see T.C. Andre and J.L. Rosner, `hep-ph/0309254`.
169. P. Langacker, M. Luo, and A.K. Mann, Rev. Mod. Phys. **64**, 87 (1992);
M. Luo, p. 977 of Ref. 4.
170. F.S. Merritt *et al.*, p. 19 of *Particle Physics: Perspectives and Opportunities: Report of the DPF Committee on Long Term Planning*, ed. R. Peccei *et al.* (World Scientific, Singapore, 1995).
171. C.T. Hill and E.H. Simmons, Phys. Reports **381**, 235 (2003).
172. G. Altarelli *et al.*, JHEP **0106**, 018 (2001);
A. Kurylov, M.J. Ramsey-Musolf, and S. Su, Nucl. Phys. **B667**, 321 (2003) and Phys. Rev. **D68**, 035008 (2003);
W. de Boer and C. Sander, `hep-ph/0307049`;
S. Heinemeyer and G. Weiglein, `hep-ph/0307177`;
J.R. Ellis, K.A. Olive, Y. Santoso, and V.C. Spanos, `hep-ph/0310356`.
173. K. Agashe, A. Delgado, M.J. May, and R. Sundrum, JHEP **0308**, 050 (2003);
M. Carena *et al.*, Phys. Rev. **D68**, 035010 (2003);
for reviews, see the articles on "Extra Dimensions" in this *Review* and I. Antoniadis, `hep-th/0102202`.
174. J.L. Hewett, F.J. Petriello, and T.G. Rizzo, JHEP **0310**, 062 (2003);
C. Csaki *et al.*, Phys. Rev. **D67**, 115002 (2003) and *ibid.* **68**, 035009 (2003);
T. Gregoire, D.R. Smith, and J.G. Wacker, `hep-ph/0305275`;
M. Perelstein, M.E. Peskin, and A. Pierce, `hep-ph/0310039`;
R. Casalbuoni, A. Deandrea, and M. Oertel, `hep-ph/0311038`;
W. Kilian and J. Reuter, `hep-ph/0311095`.
175. G. Altarelli, R. Barbieri, and S. Jadach, Nucl. Phys. **B369**, 3 (1992) and **B376**, 444(E) (1992).
176. A. De Rújula *et al.*, Nucl. Phys. **B384**, 3 (1992).
177. K. Hagiwara *et al.*, Phys. Rev. **D48**, 2182 (1993).
178. C.P. Burgess and D. London, Phys. Rev. **D48**, 4337 (1993).
179. R.S. Chivukula and E.H. Simmons, Phys. Rev. **D66**, 015006 (2002).
180. S. Chaudhuri *et al.*, Nucl. Phys. **B456**, 89 (1995);
G. Cleaver *et al.*, Phys. Rev. **D59**, 055005 (1999).
181. J. Erler and P. Langacker, Phys. Lett. **B456**, 68 (1999).
182. T. Appelquist, B.A. Dobrescu, and A.R. Hopper, Phys. Rev. **D68**, 035012 (2003);
R.S. Chivukula, H.J. He, J. Howard, and E.H. Simmons, `hep-ph/0307209`.
183. CDF: F. Abe *et al.*, Phys. Rev. Lett. **79**, 2192 (1997).
184. K.M. Cheung, Phys. Lett. **B517**, 167 (2001).
185. P. Langacker and M. Plümacher, Phys. Rev. **D62**, 013006 (2000).
186. R. Casalbuoni, S. De Curtis, D. Dominici, and R. Gatto, Phys. Lett. **B460**, 135 (1999);
J.L. Rosner, Phys. Rev. **D61**, 016006 (2000).

11. THE CABIBBO-KOBAYASHI-MASKAWA QUARK-MIXING MATRIX

Revised January 2004 by F.J. Gilman (Carnegie-Mellon University), K. Kleinknecht and B. Renk (Johannes-Gutenberg Universität Mainz).

In the Standard Model with SU(2)×U(1) as the gauge group of electroweak interactions, both the quarks and leptons are assigned to be left-handed doublets and right-handed singlets. The quark mass eigenstates are not the same as the weak eigenstates, and the matrix relating these bases was defined for six quarks and given an explicit parametrization by Kobayashi and Maskawa [1] in 1973. This generalizes the four-quark case, where the matrix is described by a single parameter, the Cabibbo angle [2].

By convention, the mixing is often expressed in terms of a 3×3 unitary matrix V operating on the charge $-e/3$ quark mass eigenstates (d, s, and b):

$$\begin{pmatrix} d' \\ s' \\ b' \end{pmatrix} = \begin{pmatrix} V_{ud} & V_{us} & V_{ub} \\ V_{cd} & V_{cs} & V_{cb} \\ V_{td} & V_{ts} & V_{tb} \end{pmatrix} \begin{pmatrix} d \\ s \\ b \end{pmatrix} \ . \tag{11.1}$$

The values of individual matrix elements can in principle all be determined from weak decays of the relevant quarks, or, in some cases, from deep inelastic neutrino scattering. Using the eight tree-level constraints discussed below together with unitarity, and assuming only three generations, the 90% confidence limits on the magnitude of the elements of the complete matrix are

$$\begin{pmatrix} 0.9739 \text{ to } 0.9751 & 0.221 \text{ to } 0.227 & 0.0029 \text{ to } 0.0045 \\ 0.221 \text{ to } 0.227 & 0.9730 \text{ to } 0.9744 & 0.039 \text{ to } 0.044 \\ 0.0048 \text{ to } 0.014 & 0.037 \text{ to } 0.043 & 0.9990 \text{ to } 0.9992 \end{pmatrix} \ . \tag{11.2}$$

The ranges shown are for the individual matrix elements. The constraints of unitarity connect different elements, so choosing a specific value for one element restricts the range of others.

There are several parametrizations of the Cabibbo-Kobayashi-Maskawa (CKM) matrix. We advocate a "standard" parametrization [3] of V that utilizes angles θ_{12}, θ_{23}, θ_{13}, and a phase, δ_{13}

$$V = \begin{pmatrix} c_{12}c_{13} & s_{12}c_{13} & s_{13}e^{-i\delta_{13}} \\ -s_{12}c_{23} - c_{12}s_{23}s_{13}e^{i\delta_{13}} & c_{12}c_{23} - s_{12}s_{23}s_{13}e^{i\delta_{13}} & s_{23}c_{13} \\ s_{12}s_{23} - c_{12}c_{23}s_{13}e^{i\delta_{13}} & -c_{12}s_{23} - s_{12}c_{23}s_{13}e^{i\delta_{13}} & c_{23}c_{13} \end{pmatrix} \ , \tag{11.3}$$

with $c_{ij} = \cos\theta_{ij}$ and $s_{ij} = \sin\theta_{ij}$ for the "generation" labels $i, j = 1, 2, 3$. This has distinct advantages of interpretation, for the rotation angles are defined and labeled in a way which relate to the mixing of two specific generations and if one of these angles vanishes, so does the mixing between those two generations; in the limit $\theta_{23} = \theta_{13} = 0$ the third generation decouples, and the situation reduces to the usual Cabibbo mixing of the first two generations with θ_{12} identified as the Cabibbo angle [2]. This parametrization is exact to all orders, and has four parameters; the real angles θ_{12}, θ_{23}, θ_{13} can all be made to lie in the first quadrant by an appropriate redefinition of quark field phases.

The matrix elements in the first row and third column, which have been directly measured in decay processes, are all of a simple form, and, as c_{13} is known to deviate from unity only in the sixth decimal place, $V_{ud} = c_{12}$, $V_{us} = s_{12}$, $V_{ub} = s_{13}\ e^{-i\delta_{13}}$, $V_{cb} = s_{23}$, and $V_{tb} = c_{23}$ to an excellent approximation. The phase δ_{13} lies in the range $0 \le \delta_{13} < 2\pi$, with non-zero values breaking CP invariance for the weak interactions. The generalization to the n generation case contains $n(n-1)/2$ angles and $(n-1)(n-2)/2$ phases. Using tree-level processes as constraints only, the matrix elements in Eq. (11.2) correspond to values of the sines of the angles of $s_{12} = 0.2243 \pm 0.0016$, $s_{23} = 0.0413 \pm 0.0015$, and $s_{13} = 0.0037 \pm 0.0005$.

If we use the loop-level processes discussed below as additional constraints, the central values of the sines of the angles do not change, and the CKM phase, sometimes referred to as the angle $\gamma = \phi_3$ of the unitarity triangle, is restricted to $\delta_{13} = (1.05 \pm 0.24)$ radians $= 60^o \pm 14^o$.

Kobayashi and Maskawa [1] originally chose a parametrization involving the four angles θ_1, θ_2, θ_3, and δ:

$$\begin{pmatrix} d' \\ s' \\ b' \end{pmatrix} = \begin{pmatrix} c_1 & -s_1c_3 & -s_1s_3 \\ s_1c_2 & c_1c_2c_3 - s_2s_3e^{i\delta} & c_1c_2s_3 + s_2c_3e^{i\delta} \\ s_1s_2 & c_1s_2c_3 + c_2s_3e^{i\delta} & c_1s_2s_3 - c_2c_3e^{i\delta} \end{pmatrix} \begin{pmatrix} d \\ s \\ b \end{pmatrix} \ , \tag{11.4}$$

where $c_i = \cos\theta_i$ and $s_i = \sin\theta_i$ for $i = 1, 2, 3$. In the limit $\theta_2 = \theta_3 = 0$, this reduces to the usual Cabibbo mixing with θ_1 identified (up to a sign) with the Cabibbo angle [2]. Note that in this case V_{ub} and V_{td} are real and V_{cb} complex, illustrating a different placement of the phase than in the standard parametrization.

An approximation to the standard parametrization proposed by Wolfenstein [4] emphasizes the hierarchy in the size of the angles, $s_{12} \gg s_{23} \gg s_{13}$. Setting $\lambda \equiv s_{12}$, the sine of the Cabibbo angle, one expresses the other elements in terms of powers of λ:

$$V = \begin{pmatrix} 1 - \lambda^2/2 & \lambda & A\lambda^3(\rho - i\eta) \\ -\lambda & 1 - \lambda^2/2 & A\lambda^2 \\ A\lambda^3(1 - \rho - i\eta) & -A\lambda^2 & 1 \end{pmatrix} + \mathcal{O}(\lambda^4) \ . \tag{11.5}$$

with A, ρ, and η real numbers that were intended to be of order unity. This approximate form is widely used, especially for B-physics, but care must be taken, especially for CP-violating effects in K-physics, since the phase enters V_{cd} and V_{cs} through terms that are higher order in λ. These higher order terms up to order (λ^5) are given in [5].

Another parametrization has been advocated [6] that arises naturally where one builds models of quark masses in which initially $m_u = m_d = 0$. With no phases in the third row or third column, the connection between measurements of CP-violating effects for B mesons and single CKM parameters is less direct than in the standard parametrization.

Different parametrizations shuffle the placement of phases between particular tree and loop (e.g., neutral meson mixing) amplitudes. No physics can depend on which of the above parametrizations (or any other) is used, as long as a single one is used consistently and care is taken to be sure that no other choice of phases is in conflict.

Our present knowledge of the matrix elements comes from the following sources:

(1) $|V_{ud}|$: Analyses have been performed comparing nuclear beta decays that proceed through a vector current to muon decay. Radiative corrections are essential to extracting the value of the matrix element. They already include effects [7] of order $Z\alpha^2$, and most of the theoretical argument centers on the nuclear mismatch and structure-dependent radiative corrections, [8], [9].

Taking the complete data set on superallowed $0^+ \to 0^+$ beta decays, [10], a value of $|V_{ud}| = 0.9740 \pm 0.0005$ has been obtained [11]. Calculations taking into account core polarization effects and charge symmetry breaking as well as charge independence breaking forces on the mean field potentials [12] get close results. This contradicts earlier results about changes in the charge-symmetry violation for quarks inside nucleons in nuclear matter. Therefore we do not apply further additional uncertainties.

The theoretical uncertainties in extracting a value of $|V_{ud}|$ from neutron decays are significantly smaller than for decays of mirror nuclei, but the value depends on both the value of g_A/g_V and the neutron lifetime. Experimental progress has been made on g_A/g_V using very highly polarized cold neutrons together with improved detectors. The recent experimental result [13], $g_A/g_V = -1.2739 \pm 0.0019$, by itself has a better precision than the former world average and results in $|V_{ud}| = 0.9713 \pm 0.0013$ if taken alone. Averaging over all recent experiments using polarizations of more than 90% [14] gives $g_A/g_V = -1.2720 \pm 0.0018$ and results in $|V_{ud}| = 0.9725 \pm 0.0013$ from neutron decay.

Since most of the contributions to the errors in these two determinations of $|V_{ud}|$ are independent, we average them to obtain

$$|V_{ud}| = 0.9738 \pm 0.0005 \ . \tag{11.6}$$

(2) $|V_{us}|$: The original analysis of K_{e3} decays yielded [15]

$$|V_{us}| = 0.2196 \pm 0.0023 \ . \tag{11.7}$$

With isospin violation taken into account in K^+ and K^0 decays, the extracted values of $|V_{us}|$ are in agreement at the 1% level. Radiative corrections have been recently calculated in chiral perturbation theory [16]. The combined effects of long-distance radiative corrections and nonlinear terms in the form factor can decrease the value of $|V_{us}|$ by up to 1% [17], and we take this into account by applying an additional correction of $(-0.5 \pm 0.5)\%$ which compensates the effect of radiative corrections in Ref. [16]. A new measurement of the K^+ semileptonic branching ratio [18] indicates a higher value of this quantity, in disagreement with the early measurements. It also would imply a contradiction to the value of $|V_{us}|$ derived from K^0 semileptonic decays. We average the new result with the older ones, leading mainly to an increase of the non-dominant experimental part of the uncertainty of $|V_{us}|$, and a slight increase of the derived value

$$|V_{us}| = 0.2200 \pm 0.0026 \ , \tag{11.8}$$

in very good agreement with the former analysis. New results on this will come from KLOE and NA48/2. The analysis [19] of hyperon decay data has larger theoretical uncertainties because of first order SU(3) symmetry breaking effects in the axial-vector couplings. This has been redone incorporating second order SU(3) symmetry breaking corrections in models [20] applied to the WA2 data [21] to give a value of $|V_{us}| = 0.2176 \pm 0.0026$, which is consistent with Eq. (11.8) using the "best-fit" model. A new analysis of the same hyperon decay data [22] yields $|V_{us}| = 0.2250 \pm 0.0027$, at variance with the earlier hyperon analysis. Since the values obtained in these models differ outside the errors and generally do not give good fits, we retain the value in Eq. (11.8) for $|V_{us}|$.

(3) $|V_{cd}|$: The magnitude of V_{cd} may be deduced from neutrino and antineutrino production of charm off valence d quarks. The dimuon production cross sections of the CDHS group [23] yield $\overline{B}_c\,|V_{cd}|^2 = (0.41 \pm 0.07) \times 10^{-2}$, where $\overline{B}_c$ is the semileptonic branching fraction of the charmed hadrons produced. The corresponding value from the more recent CCFR Tevatron experiment [24], where a next-to-leading-order QCD analysis has been carried out, is $0.534 \pm 0.046^{+0.025}_{-0.051} \times 10^{-2}$, where the last error is from the scale uncertainty. Assuming a similar scale error for the CDHS measurement and averaging these two values with the result from the Charm II experiment [25] $\overline{B}_c\,|V_{cd}|^2 = (0.442 \pm 0.049) \times 10^{-2}$, we obtain as an average $(0.463 \pm 0.034) \times 10^{-2}$. Supplementing this with data [26,27,28] on the mix of charmed particle species produced by neutrinos and values for their semileptonic branching fractions (to give $\overline{B}_c = 0.0923 \pm 0.0073$), this yields

$$|V_{cd}| = 0.224 \pm 0.012 \ . \tag{11.9}$$

(4) $|V_{cs}|$: Values for $|V_{cs}|$ obtained from neutrino production of charm and from semileptonic D decays have errors due to theoretical uncertainties that exceed 10%, as discussed in previous editions of this review. They have been superseded by direct measurements [29] of $|V_{cs}|$ in charm-tagged W decays that give $|V_{cs}| = 0.97 \pm 0.09$ (stat.) $\pm$ 0.07 (syst.). A tighter determination follows from the ratio of hadronic W decays to leptonic decays, which has been measured at LEP with the result [30] that $\sum_{i,j} |V_{ij}|^2 = 2.039 \pm 0.025 \pm 0.001$, where the sum extends over $i = u, c$ and $j = d, s, b$ and the last error is from knowledge of α_s. With a three-generation CKM matrix, unitarity requires that this sum has the value 2. Since five of the six CKM matrix elements in the sum are well measured or contribute negligibly to the measured sum of the squares, it can be converted into a greatly improved result [30]:

$$|V_{cs}| = 0.996 \pm 0.013 \ . \tag{11.10}$$

(5) $|V_{cb}|$: The heavy quark effective theory [31] (HQET) provides a nearly model-independent treatment of B semileptonic decays to charmed mesons, assuming that both the b and c quarks are heavy enough for the theory to apply. Measurements of the exclusive decay $B \to \overline{D}^* \ell^+ \nu_\ell$ have been used primarily to extract a value of $|V_{cb}|$ using corrections based on HQET. Exclusive $B \to \overline{D} \ell^+ \nu_\ell$ decays give a consistent, but less precise result. Analysis of inclusive decays, where the measured semileptonic bottom hadron partial width is assumed to be that of a b quark decaying through the usual $V-A$ interaction, depends on going from the quark to the hadron level and involves an assumption on the validity of quark-hadron duality. Improvements have been obtained in theoretical studies of the moments of inclusive semi leptonic and radiative decays and experimental measurements of such moments. The results for $|V_{cb}|$ from exclusive and inclusive decays generally are in good agreement. A more detailed discussion and references are found in a mini-review in the *Review of Particle Physics* [32]. We add an uncertainty due to the assumption of quark-hadron duality [32], [33] of 1% to the results from inclusive decays and average over the exclusive result $|V_{cb}| = (42.0 \pm 1.1 \pm 1.9) \times 10^{-3}$ and inclusive result $|V_{cb}| = (41.0 \pm 0.5 \pm 0.5 \pm 0.8) \times 10^{-3}$ with theoretical uncertainties combined linearly to obtain

$$|V_{cb}| = (41.3 \pm 1.5) \times 10^{-3} \ . \tag{11.11}$$

(6) $|V_{ub}|$: The decay $b \to u \ell \overline{\nu}$ and its charge conjugate can be observed in the semileptonic decay of B mesons produced on the $\Upsilon(4S)$ $(b\overline{b})$ resonance by measuring the lepton energy spectrum above the endpoint of the $b \to c \ell \overline{\nu}_\ell$ spectrum. There the $b \to u \ell \overline{\nu}_\ell$ decay rate can be obtained by subtracting the background from nonresonant e^+e^- reactions. This continuum background is determined from auxiliary measurements off the $\Upsilon(4S)$. The interpretation of this inclusive result in terms of $|V_{ub}|$ depends fairly strongly on the theoretical model used to generate the lepton energy spectrum, especially that for $b \to u$ transitions. At LEP, the separation between u-like and c-like decays is based on up to twenty different event parameters, and while the extraction of $|V_{ub}|$ is less sensitive to theoretical assumptions, it requires a detailed understanding of the decay $b \to c \ell \overline{\nu}_\ell$. The CLEO Collaboration [34] has recently employed an important technique that uses moments of measured distributions in $b \to s\gamma$ and $B \to D^* \ell \nu_\ell$ to fix the parameters in the inclusive distribution and thereby reduce the errors.

The huge data samples at the B factories, optimized cut variables which minimize theoretical uncertainties, measurements of spectral moments and event samples with fully reconstructed B decays contribute to an improved accuracy of $|V_{ub}|$.

The value of $|V_{ub}|$ can also be extracted from exclusive decays, such as $B \to \pi \ell \nu_\ell$ and $B \to \rho \ell \nu_\ell$, but there is an associated theoretical model dependence in the values of the matrix elements of the weak current between exclusive states. Detailed discussion and references on both the inclusive and exclusive analyses is found in the mini-review on $|V_{ub}|$ in the *Review of Particle Physics* [35]. They average the inclusive result $|V_{ub}| = (4.68 \pm 0.85) \times 10^{-3}$, with the exclusive result of $|V_{ub}| = (3.326 \pm 0.59) \times 10^{-3}$ to obtain a result dominated by the theoretical uncertainties,

$$|V_{ub}| = (3.67 \pm 0.47) \times 10^{-3} \ . \tag{11.12}$$

(7) V_{tb}: The discovery of the top quark by the CDF and D0 collaborations utilized in part the semileptonic decays of t to b. The CDF experiment has published a limit on the fraction of decays of the form $t \to b\ \ell^+\ \nu_\ell$, as opposed to semileptonic t decays that involve the light s or d quarks, of [36]

$$\frac{|V_{tb}|^2}{|V_{td}|^2 + |V_{ts}|^2 + |V_{tb}|^2} = 0.94^{+0.31}_{-0.24} \ . \tag{11.13}$$

For most of the CKM matrix elements the principal error is no longer experimental, but rather theoretical. This arises from explicit model dependence in interpreting inclusive data or in the direct use of specific hadronic matrix elements to relate decay rates for exclusive processes to weak transitions of quarks. This type of uncertainty often is even larger at present in extracting CKM matrix elements from loop diagrams, as discussed below. Such theoretical errors are not distributed in a Gaussian manner. We have judged what is a reasonable range in assigning the theoretical errors.

While we use the central values with the quoted errors in a consistent way [37] performing a random exploration of the full parameter space to make a best overall fit to the CKM matrix (interpreting a "1 σ" range in a theoretical error as corresponding to a 68% confidence level that the true value lies within a range of "± 1 σ" of the central value in making those fits), the result should be taken with appropriate care. The issue of how to use appropriate statistical methods to deal with these errors has been intensively discussed in the last few years by a number of authors [38]. The different fitting methods, if they use the same input parameters, give essentially the same result. Our limited knowledge of some of the theoretical uncertainties makes us cautious in extending this to results for multi-standard-deviation determinations of the allowed regions for CKM matrix elements.

We determine the best fit by searching for the minimum chi-squared by scanning the parameter spaces of the four angles. The results for three generations of quarks, from Eqs. (11.6), (11.8), (11.9), (11.10), (11.11), (11.12), and (11.13) plus unitarity, are summarized in the matrix in Eq. (11.2). The ranges given there are different from those given in Eqs. (11.6) – (11.13) because of the inclusion of unitarity, but are consistent with the one-standard-deviation errors on the input matrix elements. Note in particular that the unitarity constraint has pushed $|V_{ud}|$ about 1.4 standard deviations higher than given in Eq. (11.6). We observe a violation of unitarity in the first row of the CKM matrix by more than 2 standard deviations. While this bears watching and encourages another more accurate measurement of $|V_{us}|$ as well as more theoretical work, we do not see this as a major challenge to the validity of the three-generation Standard Model.

The data do not preclude there being more than three generations. Moreover, the entries deduced from unitarity might be altered when the CKM matrix is expanded to accommodate more generations. Conversely, the known entries restrict the possible values of additional elements if the matrix is expanded to account for additional generations. For example, unitarity and the known elements of the first row require that any additional element in the first row have a magnitude $|V_{ub'}| < 0.08$. When there are more than three generations the allowed ranges (at 90% CL) of the matrix elements connecting the first three generations are

$$\begin{pmatrix} 0.9730 \text{ to } 0.9746 & 0.2174 \text{ to } 0.2241 & 0.0030 \text{ to } 0.0044\ldots \\ 0.213 \text{ to } 0.226 & 0.968 \text{ to } 0.975 & 0.039 \text{ to } 0.044\ \ldots \\ 0 \text{ to } 0.08 & 0 \text{ to } 0.11 & 0.07 \text{ to } 0.9993\ldots \\ \vdots & \vdots & \vdots \end{pmatrix}, \tag{11.14}$$

where we have used unitarity (for the expanded matrix) and the measurements of the magnitudes of the CKM matrix elements (including the constraint from hadronic W decays), resulting in the weak bound $|V_{tb}| > 0.07$.

Direct and indirect information on the smallest matrix elements of the CKM matrix is neatly summarized in terms of the "unitarity triangle," one of six such triangles that correspond to the unitarity condition applied to two different rows or columns of the CKM matrix. Unitarity applied to the first and third columns yields

$$V_{ud}\ V_{ub}^* + V_{cd}\ V_{cb}^* + V_{td}\ V_{tb}^* = 0\ . \tag{11.15}$$

The unitarity triangle is just a geometrical presentation of this equation in the complex plane [39], as in Fig. 11.1(a). We can always choose to orient the triangle so that $V_{cd}\ V_{cb}^*$ lies along the horizontal; in the standard parametrization, V_{cb} is real and V_{cd} is real to a very good approximation in any case. Setting cosines of small angles to unity, Eq. (11.15) becomes

$$V_{ub}^* + V_{td} \approx s_{12}\ V_{cb}^*\ , \tag{11.16}$$

which is shown as the unitarity triangle. The sides of this triangle are of order 1% of the diagonal elements of the CKM matrix, which highlights the precision we are aiming to achieve of knowing each of these sides in turn to a precision of a few percent.

The angles α, β and γ of the triangle are also referred to as ϕ_2, ϕ_1, and ϕ_3, respectively, with β and $\gamma = \delta_{13}$ being the phases of the CKM elements V_{td} and V_{ub} as per

$$V_{td} = |V_{td}|e^{-i\beta}, V_{ub} = |V_{ub}|e^{-i\gamma}\ . \tag{11.17}$$

Rescaling the triangle so that the base is of unit length, the coordinates of the vertices A, B, and C become respectively:

$$\left(\mathrm{Re}(V_{ud}\ V_{ub}^*)/|V_{cd}\ V_{cb}^*|,\ \mathrm{Im}(V_{ud}\ V_{ub}^*)/|V_{cd}\ V_{cb}^*|\right),\ (1,0),\ \&\ (0,0)\ . \tag{11.18}$$

The coordinates of the apex of the rescaled unitarity triangle take the simple form $(\overline{\rho}, \overline{\eta})$, with $\overline{\rho} = \rho(1 - \lambda^2/2)$ and $\overline{\eta} = \eta(1 - \lambda^2/2)$ in the Wolfenstein approximation, [4] parametrization [4], as shown in Fig. 11.1(b).

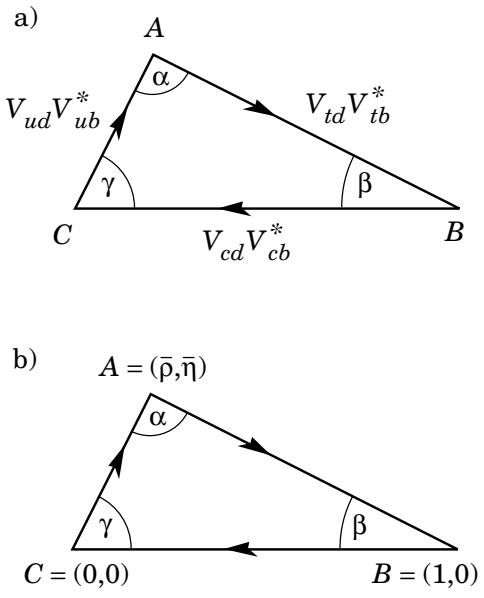

Figure 11.1: (a) Representation in the complex plane of the triangle formed by the CKM matrix elements $V_{ud}\ V_{ub}^*$, $V_{td}\ V_{tb}^*$, and $V_{cd}\ V_{cb}^*$. (b) Rescaled triangle with vertices A, B, and C at $(\overline{\rho}, \overline{\eta})$, $(1,0)$, and $(0,0)$, respectively.

CP-violating processes involve the phase in the CKM matrix, assuming that the observed CP violation is solely related to a nonzero value of this phase. More specifically, a necessary and sufficient condition for CP violation with three generations can be formulated in a parametrization-independent manner in terms of the non-vanishing of J, the determinant of the commutator of the mass matrices for the charge $2e/3$ and charge $-e/3$ quarks [40]. CP-violating amplitudes or differences of rates are all proportional to the product of CKM factors in this quantity, namely $s_{12}s_{13}s_{23}c_{12}c_{13}^2c_{23}\sin\delta_{13}$. This is just twice the area of the unitarity triangle.

Further information, particularly on CKM matrix elements involving the top quark, can be obtained from flavor-changing processes that occur at the one-loop level. We have not used this information up to this point since the derivation of values for V_{td} and V_{ts} in this manner from, for example, B mixing or $b \to s\gamma$, require an additional assumption that the top-quark loop, rather than new physics, gives the dominant contribution to the process in question. Conversely, when we find agreement between CKM matrix elements extracted from loop diagrams and the values above based on direct measurements plus the assumption of three generations, this can be used to place restrictions on new physics.

We first consider constraints from flavor-changing processes that are not CP-violating. The measured value [41] of $\Delta M_{B_d} = 0.502 \pm 0.007$ ps^{-1} from ${B_d}^0 - {\overline{B}_d}^0$ mixing can be turned into information on $|{V_{tb}}^* V_{td}|$, assuming that the dominant contribution to the mass difference arises from the matrix element between a B_d and a $\overline{B}_d$ of an operator that corresponds to a box diagram with W bosons and top quarks as sides. Using the characteristic hadronic matrix element that then occurs, $\hat{B}_{B_d} \cdot {f_{B_d}}^2 = (1.26 \pm 0.10) \cdot (196 \pm 32 \text{ MeV})^2$ from lattice QCD calculations [42], next-to-leading-order QCD corrections ($\eta_{\rm QCD} = 0.55$) [43], and the running top-quark mass, $\overline{m}_t(m_t) = (166 \pm 5)$ GeV as input, we obtain

$$|{V_{tb}}^* \cdot V_{td}| = 0.0083 \pm 0.0016 \ , \tag{11.19}$$

where the uncertainty comes primarily from that in the hadronic matrix elements, whose estimated errors are combined linearly.

In the ratio of B_s to B_d mass differences, many common factors (such as the QCD correction and dependence on the top-quark mass) cancel, and we have

$$\frac{\Delta M_{B_s}}{\Delta M_{B_d}} = \frac{M_{B_s}}{M_{B_d}} \frac{\widehat{B}_{B_s} {f_{B_s}}^2}{\widehat{B}_{B_d} {f_{B_d}}^2} \frac{|V_{tb}^* \cdot V_{ts}|^2}{|V_{tb}^* \cdot V_{td}|^2} \ . \tag{11.20}$$

With the experimentally measured masses, $\widehat{B}_{B_s} {f_{B_s}}^2 / (\widehat{B}_{B_d} {f_{B_d}}^2) = 1.56 \pm 0.26$ [42], and the experimental lower limit [41] at 95% CL of $\Delta M_{B_s} > 14.4$ ps^{-1} based on published data,

$$|V_{td}|/|V_{ts}| < 0.25 \ . \tag{11.21}$$

Since with three generations, $|V_{ts}| \approx |V_{cb}|$, this result converts to $|V_{td}| < 0.011$, which is a significant constraint by itself (see Figure 2).

The CLEO observation [44] of $b \to s\gamma$, confirmed by BELLE and BaBar [45], is in agreement with the Standard Model prediction. This observation can be restated, assuming the Standard Model, as a constraint [46]

$$V_{tb} {V_{td}}^* = (-47 \pm 8) \times 10^{-3} \ . \tag{11.22}$$

This is consistent in both sign and magnitude with the value that follows from the measured magnitudes of CKM matrix elements and the assumption of three generations, but has a much larger uncertainty.

In $K^+ \to \pi^+ \nu\overline{\nu}$ there are significant contributions from loop diagrams involving both charm and top quarks. Experiment is just beginning to probe the level predicted in the Standard Model [47].

All these additional indirect constraints are consistent with the CKM elements obtained from the direct measurements plus unitarity, assuming three generations. Adding the results on B mixing together with theoretical improvements in lattice calculations reduces the range allowed for $|V_{td}|$.

Now we turn to CP-violating processes. Just the added constraint from CP violation in the neutral kaon system, taken together with the restrictions above on the magnitudes of the CKM matrix elements, is tight enough to restrict considerably the range of angles and the phase of the CKM matrix. For example, the constraint obtained from the CP-violating parameter ϵ in the neutral K system corresponds to the vertex A of the unitarity triangle lying on a hyperbola for fixed values of the (imprecisely known) hadronic matrix elements [48], [49].

In addition, following the initial evidence [50], it is now established that direct CP violation in the weak transition from a neutral K to two pions exists, i.e., that the parameter ϵ' is non-zero [51]. While theoretical uncertainties in hadronic matrix elements of canceling amplitudes presently preclude this measurement from giving a significant constraint on the unitarity triangle, it supports the assumption that the observed CP violation is related to a non-zero value of the CKM phase.

Ultimately in the neutral K system, the CP-violating process $K_L \to \pi^0 \nu\overline{\nu}$ offers the possibility of a theoretically clean, high precision measurement of the imaginary part of $V_{td} \cdot {V_{ts}}^*$ and the area of the unitarity triangle. Given $|V_{ts}|$, this will yield the altitude of the unitarity triangle. However, the experimental upper limit is presently many orders of magnitude away from the required sensitivity.

Turning to the B-meson system, for CP-violating asymmetries of neutral B mesons decaying to CP eigenstates, the interference between mixing and a single weak decay amplitude for certain final states directly relates the asymmetry in a given decay to $\sin 2\phi$, where $\phi = \alpha$, β, γ is an appropriate angle of the unitarity triangle [39]. A new generation of experiments has established a non-vanishing asymmetry in the decays $B_d(\overline{B}_d) \to \psi K_S$ and in other B_d decay modes where the asymmetry is given by $\sin 2\beta$. The present experimental results from BaBar [52] and BELLE [53], when averaged yield

$$\sin 2\beta = 0.736 \pm 0.049 \ . \tag{11.23}$$

While the limits on the leptonic charge asymmetry for $B_d - \overline{B}_d$ mixing (measuring the analogue of 2Re ϵ in the neutral K system) have been reduced to the 1% level [41], this is still roughly an order of magnitude greater than the value expected without new physics. It provides no significant constraints on the CKM matrix for now [54].

The constraints on the apex of the unitarity triangle that follow from Eqs. (11.12), (11.19), (11.21), (11.23), and ϵ are shown in Fig. 11.2. Both the limit on ΔM_s and the value of ΔM_d indicate that the apex lies in the first rather than the second quadrant.

All constraints nicely overlap in one small area in the first quadrant with the sign of ϵ measured in the K system agreeing with the sign of $\sin 2\beta$ measured in the B system.

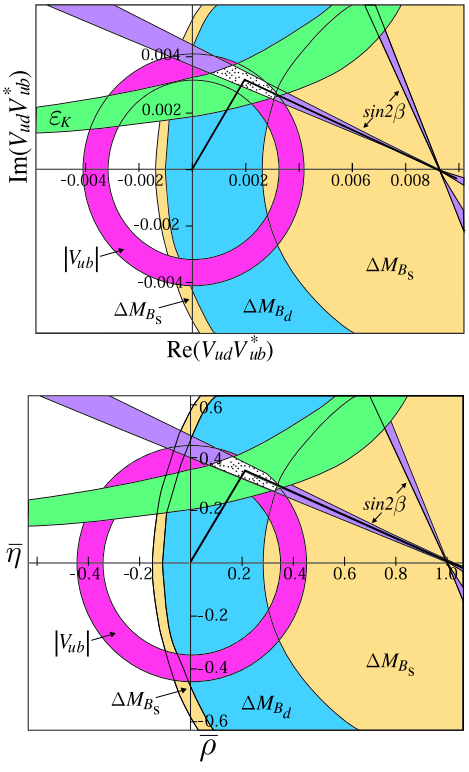

Figure 11.2: Constraints from the text on the position of the apex, A, of the unitarity triangle following from $|V_{ub}|$,B mixing, ϵ, and $\sin 2\beta$. A possible unitarity triangle is shown with A in the preferred region. See full-color version on color pages at end of book.

The situation with regard to the unitarity triangle has changed qualitatively in the past few years. Both the constraints from the lengths of the sides (from $|V_{ub}|$, $|V_{cb}|$, and $|V_{td}|$) and independently

those from CP-violating processes (ϵ from the K system and $\sin 2\beta$ from the B system) indicate the same region for the apex of the triangle. The first major test of the full CKM picture and CP violation has been passed successfully.

From a combined fit using the direct measurements, B mixing, ϵ, and $\sin 2\beta$, we obtain:

$$\text{Re } V_{td} = 0.0067 \pm 0.0008 \ , \tag{11.24}$$

$$\text{Im } V_{td} = -0.0031 \pm 0.0004 \ , \tag{11.25}$$

$$\overline{\rho} = 0.20 \pm 0.09 \ , \tag{11.26}$$

$$\overline{\eta} = 0.33 \pm 0.05 \ . \tag{11.27}$$

All processes can be quantitatively understood by one value of the CKM phase $\delta_{13} = \gamma = 60^\circ \pm 14^\circ$. The value of $\beta = 23.4^\circ \pm 2^\circ$ from the overall fit is consistent with the value from the CP-asymmetry measurements of $23.7^\circ \pm 2.1^\circ$. The invariant measure of CP violation is $J = (2.88 \pm 0.33) \times 10^{-5}$.

The limit in Eq. (11.21) is not far from the value we would expect from the other information on the unitarity triangle. This limit is more robust theoretically since it depends on ratios (rather than absolute values) of hadronic matrix elements and is independent of the top mass or QCD corrections (which cancel in the ratio). Thus, the significant increase in experimental sensitivity to B_s mixing that should become available in the CDF and D0 experiments in the next few years will lead either to an observation of mixing as predicted by our knowledge to date or to an indication of physics beyond the Standard Model.

Other experimental progress in the next few years includes: checking the unitarity of the first row of the CKM matrix by new precise measurements of $|V_{us}|$ in semileptonic decays of charged and neutral kaons; resolution of the apparent inconsistency between BELLE and BaBar in the measurement of the time-dependent particle-antiparticle asymmetry in the decay $B_d(\overline{B}_d) \to \phi K_S$; searches for direct CP violation in B decay modes; and measurement of the Dalitz plot asymmetry in $K^+(K^-) \to 3\pi$ at the 10^{-4} level by NA48/2.

Longer range, the frontiers are: extraction of the angle $\alpha = \phi_2$ from measurements of decays of B_d mesons; determination of the angle $\gamma = \phi_3$ from measurements of both B_d and B_s decays; and the pursuit of the CP-violating rare decay $K_L \to \pi^0 \nu\overline{\nu}$.

Acknowledgment:

This research work is supported in part by the Department of Energy under Grant No. DE-FG02-91ER40682 and by the Bundesministerium für Bildung und Forschung under Grant No. 05HE1UMA/3.

References:

1. M. Kobayashi and T. Maskawa, Prog. Theor. Phys. **49**, 652 (1973).
2. N. Cabibbo, Phys. Rev. Lett. **10**, 531 (1963).
3. L.-L. Chau and W.-Y. Keung, Phys. Rev. Lett. **53**, 1802 (1984);
   H. Harari and M Leurer, Phys. Lett. **B181**, 123 (1986);
   H. Fritzsch and J. Plankl, Phys. Rev. **D35**, 1732 (1987);
   F.J. Botella and L.-L. Chao, Phys. Lett. **B168**, 97 (1986).
4. L. Wolfenstein, Phys. Rev. Lett. **51**, 1945 (1983).
5. A. Buras *et al.*, Phys. Rev. **D50**, 3433 (1994);
   see also M. Schmidtler and K. Schubert, Z. Phys. **C53**, 347, (1992).
6. C.D. Frogatt and H.B. Nielsen, Nucl. Phys. **B147**, 277 (1979);
   H. Fritzsch, Nucl. Phys. **B155**, 189 (1979);
   S. Dimopoulos, L.J. Hall, and S. Rabi, Phys. Rev. Lett. **68**, 1984 (1992);
   H. Fritzsch and Z.-Z. Xing, Phys. Lett. **B413**, 396 (1997).
7. W.J. Marciano and A. Sirlin, Phys. Rev. Lett. **56**, 22 (1986);
   A. Sirlin and R. Zucchini, Phys. Rev. Lett. **57**, 1994 (1986);
   W. Jaus and G. Rasche, Phys. Rev. **D35**, 3420 (1987);
   A. Sirlin, Phys. Rev. **D35**, 3423 (1987).
8. B.A. Brown and W.E. Ormand, Phys. Rev. Lett. **62**, 866 (1989).
9. F.C. Barker *et al.*, Nucl. Phys. **A540**, 501 (1992);
   F.C. Barker *et al.*, Nucl. Phys. **A579**, 62 (1994).
10. G. Savard *et al.*, Phys. Rev. Lett. **74**, 1521 (1995).
11. J.C. Hardy and I.S. Towner, talk at WEIN98, Santa Fe, June 14-21, 1998 and `nucl-th/9809087`.
12. H. Sagawa, Proc. of the Workshop "Quark-Mixing, CKM Unitarity", 2002, Heidelberg, 162.
13. H. Abele *et al.*, Phys. Rev. Lett. **88**, 211801 (2002) as a final result of J. Reich *et al.*, Nucl. Instrum. Methods **A440**, 535 (2000), and H. Abele *et al.*, Nucl. Phys. **A612**, 53 (1997).
14. Yu. A. Mostovoi *et al.*, Phys. Atomic Nucl. **64**, 1955 (2001);
   P. Liaud, Nucl. Phys. **A612**, 53 (1997).
15. H. Leutwyler and M. Roos, Z. Phys. **C25**, 91 (1984);
   See also the work of R.E. Shrock and L.-L. Wang, Phys. Rev. Lett. **41**, 1692 (1978).
16. V. Cirigliano *et al.*, Eur. Phys. J. **C23**, 121 (2002).
17. G. Calderon and G. Lopez Castro , Phys. Rev. **D65**, 073032 (2002).
18. J. Thompson, talk given at CKM03 workshop, Durham, UK, April 5th to 9th, (2003), `hep-ex/0307053` .
19. J.F. Donoghue, B.R. Holstein, and S.W. Klimt, Phys. Rev. **D35**, 934 (1987).
20. R. Flores-Mendieta, A. Garcia, and G. Sanchez-Col'on, Phys. Rev. **D54**, 6855 (1996).
21. M. Bourquin *et al.*, Z. Phys. **C21**, 27 (1983).
22. N. Cabibbo *et al.*, `hep-ph/0307214` ; `hep-ph/0307298` , to be published in *Ann. Rev. Nucl. Part. Sci.*, Vol. 53 (2003).
23. H. Abramowicz *et al.*, Z. Phys. **C15**, 19 (1982).
24. S.A. Rabinowitz *et al.*, Phys. Rev. Lett. **70**, 134 (1993);
   A.O. Bazarko *et al.*, Z. Phys. **C65**, 189 (1995).
25. P. Vilain *et al.*, Eur. Phys. J. **C11**, 19 (1999).
26. N. Ushida *et al.*, Phys. Lett. **B206**, 375 (1988).
27. T. Bolton, `hep-ex/9708014` (1997).
28. A. Kayis-Topasku *et al.*, Phys. Lett. **B549**, 48 (2002).
29. P. Abreu *et al.*, Phys. Lett. **B439**, 209 (1998);
   R. Barate *et al.*, Phys. Lett. **B465**, 349 (1999).
30. The LEP Collaborations, the LEP Electroweak Working Group and the SLD Heavy Flavour and Electroweak Groups, `hep-ex/0112021v2` (2002).
31. N. Isgur and M.B. Wise, Phys. Lett. **B232**, 113 (1989), and Phys. Lett. **B237**, 527 (1990) E;
   E. Eichten and B. Hill, Phys. Lett. **B234**, 511 (1990);
   M.E. Luke, Phys. Lett. **B252**, 447 (1990).
32. See the review on "Determination of $|V_{cb}|$" by M. Artuso and E. Barberio in this *Review*.
33. A. Falk, presentation at the Fifth KEK Topical Conference, Tsukuba, Japan, November 20–22, 2001 and `hep-ph/0201094` .
34. A. Bornheim *et al.* (CLEO Collaboration), `hep-ex/0202019` , 2002.
35. See the review on "Determination of $|V_{ub}|$" by M. Battaglia and L. Gibbons in this *Review*.
36. T. Affolder *et al.*, Phys. Rev. Lett. **86**, 3233 (2001).
37. K. Kleinknecht and B. Renk, Phys. Lett. **86**, 130B (1983);
   Z. Phys. **C34**, 209 (1987).
38. A. Hocker *et al.*, Eur. Phys. J. **C21**, 225 (2001);
   C. Ciuchini *et al.*, JHEP **0107**, 013 (2001).
39. L.-L. Chau and W.Y. Keung, Ref. 3;

J.D. Bjorken, private communication and Phys. Rev. **D39**, 1396 (1989);

C. Jarlskog and R. Stora, Phys. Lett. **B208**, 268 (1988);

J.L. Rosner, A.I. Sanda, and M.P. Schmidt, in *Proceedings of the Workshop on High Sensitivity Beauty Physics at Fermilab*, Fermilab, November 11–14, 1987, edited by A.J. Slaughter, N. Lockyer, and M. Schmidt (Fermilab, Batavia, 1988), p. 165;

C. Hamzaoui, J.L. Rosner, and A.I. Sanda, *ibid.*, p. 215.

40. C. Jarlskog, Phys. Rev. Lett. **55**, 1039 (1985) and Z. Phys. **C29**, 491 (1985).
41. See the review on "B–$\overline{B}$ Mixing" by O. Schneider in this *Review*.
42. A. Kronfeld, `hep-lat/0310063v1`.
43. A.J. Buras *et al.*, Nucl. Phys. **B347**, 491 (1990).
44. M. S. Alam *et al.* (CLEO Collab.), Phys. Rev. Lett. **74**, 2885 (1995);

    S. Chen *et al.* (CLEO Collab.), Phys. Rev. Lett. **87**, 1807 (2001).
45. K. Abe *et al.* (BELLE Collab.), Phys. Lett. **B511**, 157 (2001);

    B. Aubert *et al.* (BaBar Collab.), `hep-ex/0207074` and `hep-ex/0207076` (2002).
46. A. Ali and M. Misiak, `hep-ph/0304132`, (2003).
47. S. Adler *et al.*, `hep-ex/0111091` (2001).
48. The relevant QCD corrections in leading order in F.J. Gilman and M.B. Wise Phys. Lett. **B93**, 129 (1980), and Phys. Rev. **D27**, 1128 (1983), have been extended to next-to-leading-order by A. Buras *et al.*, Ref. 43;

    S. Herrlich and U. Nierste Nucl. Phys. **B419**, 292 (1992) and Nucl. Phys. **B476**, 27 (1996).
49. The limiting curves in Fig. 11.2 arising from the value of $|\epsilon|$ correspond to values of the hadronic matrix element expressed in terms of the renormalization group invariant parameter $\widehat{B}_K$ from 0.68 to 1.06 . See, for example, D. Becirevic, plenary talk at Lattice 2003, Tsukuba, Japan, July 15 - 19, 2003.
50. H. Burkhardt *et al.*, Phys. Lett. **B206**, 169 (1988).
51. G.D. Barr *et al.*, Phys. Lett. **B317**, 233 (1993);

    L.K. Gibbons *et al.*, Phys. Rev. Lett. **70**, 1203 (1993);

    V. Fanti *et al.*, Phys. Lett. **B465**, 335 (1999);

    A. Alavi-Harati *et al.*, Phys. Rev. Lett. **83**, 22 (1999);

    A. Lai *et al.*, Eur. Phys. J. **C22**, 231 (2001);

    J.R. Batley *et al.*, Phys. Lett. **B544**, 97 (2002).
52. B. Aubert *et al.*, Phys. Rev. Lett. **89**, 201802 (2002).
53. K. Abe *et al.* Belle-CONF-0353, LP'03 (2003).
54. S. Laplace *et al.*, Phys. Rev. **D65**, 094040 (2002).

12. CP VIOLATION IN MESON DECAYS

Written December 2003 by D. Kirkby (UC, Irvine) and Y. Nir (Weizmann Inst.).

The CP transformation combines charge conjugation C with parity P. Under C, particles and antiparticles are interchanged, by conjugating all internal quantum numbers, *e.g.*, $Q \to -Q$ for electromagnetic charge. Under P, the handedness of space is reversed, $\vec{x} \to -\vec{x}$. Thus, for example, a left-handed electron e^-_L is transformed under CP into a right-handed positron, e^+_R.

If CP were an exact symmetry, the laws of Nature would be the same for matter and for antimatter. We observe that most phenomena are C- and P-symmetric, and therefore, also CP-symmetric. In particular, these symmetries are respected by the gravitational, electromagnetic, and strong interactions. The weak interactions, on the other hand, violate C and P in the strongest possible way. For example, the charged W bosons couple to left-handed electrons, e^-_L, and to their CP-conjugate right-handed positrons, e^+_R, but to neither their C-conjugate left-handed positrons, e^+_L, nor their P-conjugate right-handed electrons, e^-_R. While weak interactions violate C and P separately, CP is still preserved in most weak interaction processes. The CP symmetry is, however, violated in certain rare processes, as discovered in neutral K decays in 1964 [1], and recently observed in neutral B decays [2,3]. A K_L meson decays more often to $\pi^- e^+ \overline{\nu}_e$ than to $\pi^+ e^- \nu_e$, thus allowing electrons and positrons to be unambiguously distinguished, but the decay-rate asymmetry is only at the 0.003 level. The CP-violating effects observed in B decays are larger: the CP asymmetry in $B^0/\overline{B}^0$ meson decays to CP eigenstates like $J/\psi K_S$ is about 0.73. CP violation has not yet been observed in the decays of any charged mesons, or in neutral D or B_s mesons, or in the lepton sector.

In addition to parity and to continuous Lorentz transformations, there is one other spacetime operation that could be a symmetry of the interactions: time reversal T, $t \to -t$. Violations of T symmetry have been observed in neutral K decays [4], and are expected as a corollary of CP violation if the combined CPT transformation is a fundamental symmetry of Nature. All observations indicate that CPT is indeed a symmetry of Nature. Furthermore, one cannot build a Lorentz-invariant quantum field theory with a Hermitian Hamiltonian that violates CPT. (At several points in our discussion, we avoid assumptions about CPT, in order to identify cases where evidence for CP violation relies on assumptions about CPT.)

Within the Standard Model, CP symmetry is broken by complex phases in the Yukawa couplings (that is, the couplings of the Higgs scalar to quarks). When all manipulations to remove unphysical phases in this model are exhausted, one finds that there is a single CP-violating parameter [5]. In the basis of mass eigenstates, this single phase appears in the 3×3 unitary matrix that gives the W-boson couplings to an up-type antiquark and a down-type quark. (If the Standard Model is supplemented with Majorana mass terms for the neutrinos, the analogous mixing matrix for leptons has three CP-violating phases.) The beautifully consistent and economical Standard-Model description of CP violation in terms of Yukawa couplings, known as the Kobayashi-Maskawa (KM) mechanism [5], agrees with all measurements to date. In particular, one can account within this framework for the three measured CP-violating observables, ϵ and ϵ' in neutral K decays, and $S_{\psi K}$ in neutral B decays. This agreement implies that the matrix of three-generation quark mixing is, very likely, the dominant source of CP violation in meson decays.

The small number of observations, and the theoretical uncertainties involved in their interpretation, however, leave room for additional sources of CP violation from new physics. Indeed, almost all extensions of the Standard Model imply that there are such additional sources. Moreover, CP violation is a necessary condition for baryogenesis, the process of dynamically generating the matter-antimatter asymmetry of the Universe [6]. Despite the phenomenological success of the KM mechanism, it fails (by several orders of magnitude) to accommodate the observed asymmetry [7]. This discrepancy strongly suggests that Nature provides additional sources of CP violation beyond the KM mechanism. (Recent evidence for neutrino masses implies that CP can be violated also in the lepton sector. This situation makes leptogenesis [8], a scenario where such phases play a crucial role in the generation of the baryon asymmetry, a very attractive possibility.) The expectation of new sources motivates the large ongoing experimental effort to find deviations from the predictions of the KM mechanism.

CP violation can be experimentally searched for in a variety of processes, such as meson decays, electric dipole moments of neutrons, electrons and nuclei, and neutrino oscillations. Meson decays probe flavor-changing CP violation. The search for electric dipole moments may find (or constrain) sources of CP violation that, unlike the KM phase, are not related to flavor changing couplings. Future searches for CP violation in neutrino oscillations might provide further input on leptogenesis.

The present measurements of CP asymmetries provide some of the strongest constraints on the weak couplings of quarks. Future measurements of CP violation in K, D, B, and B_s meson decays will provide additional constraints on the flavor parameters of the Standard Model, and can probe new physics. In this review, we give the formalism and basic physics that are relevant to present and near future measurements of CP violation in meson decays.

12.1. Formalism

The phenomenology of CP violation is superficially different in K, D, B, and B_s decays. This is primarily because each of these systems is governed by a different balance between decay rates, oscillations, and lifetime splitting. However, the underlying mechanisms of CP violation are identical for all pseudoscalar mesons.

In this section we present a general formalism for, and classification of, CP violation in the decay of a pseudoscalar meson M that might be a charged or neutral K, D, B, or B_s meson. Subsequent sections describe the CP-violating phenomenology, approximations, and alternate formalisms that are specific to each system.

12.1.1. ***Charged- and neutral-meson decays***: We define decay amplitudes of M (which could be charged or neutral) and its CP conjugate $\overline{M}$ to a multi-particle final state f and its CP conjugate $\overline{f}$ as

$$A_f = \langle f\,|\mathcal{H}|\,M\rangle \quad , \quad \overline{A}_f = \langle f\,|\mathcal{H}|\,\overline{M}\rangle \quad ,$$
$$A_{\overline{f}} = \langle \overline{f}\,|\mathcal{H}|\,M\rangle \quad , \quad \overline{A}_{\overline{f}} = \langle \overline{f}\,|\mathcal{H}|\,\overline{M}\rangle \quad , \tag{12.1}$$

where $\mathcal{H}$ is the Hamiltonian governing weak interactions. The action of CP on these states introduces phases ξ_M and ξ_f that depend on their flavor content, according to

$$CP|M\rangle = e^{+i\xi_M}\,|\overline{M}\rangle \quad , \quad CP|f\rangle = e^{+i\xi_f}\,|\overline{f}\rangle\,, \tag{12.2}$$

with

$$CP|\overline{M}\rangle = e^{-i\xi_M}\,|M\rangle \quad , \quad CP|\overline{f}\rangle = e^{-i\xi_f}\,|f\rangle \tag{12.3}$$

so that $(CP)^2 = 1$. The phases ξ_M and ξ_f are arbitrary and unphysical because of the flavor symmetry of the strong interaction. If CP is conserved by the dynamics, $[CP, \mathcal{H}] = 0$, then A_f and $\overline{A}_{\overline{f}}$ have the same magnitude and an arbitrary unphysical relative phase

$$\overline{A}_{\overline{f}} = e^{i(\xi_f - \xi_M)}\,A_f\,. \tag{12.4}$$

12.1.2. ***Neutral-meson mixing***: A state that is initially a superposition of M^0 and $\overline{M}^0$, say

$$|\psi(0)\rangle = a(0)|M^0\rangle + b(0)|\overline{M}^0\rangle\,, \tag{12.5}$$

will evolve in time acquiring components that describe all possible decay final states $\{f_1, f_2, \ldots\}$, that is,

$$|\psi(t)\rangle = a(t)|M^0\rangle + b(t)|\overline{M}^0\rangle + c_1(t)|f_1\rangle + c_2(t)|f_2\rangle + \cdots\,. \tag{12.6}$$

If we are interested in computing only the values of $a(t)$ and $b(t)$ (and not the values of all $c_i(t)$), and if the times t in which we are interested are much larger than the typical strong interaction scale, then we can use a much simplified formalism [9]. The simplified time evolution is determined by a 2×2 effective Hamiltonian $\mathbf{H}$ that is not Hermitian, since otherwise the mesons would only oscillate and not decay. Any complex matrix, such as $\mathbf{H}$, can be written in terms of Hermitian matrices $\mathbf{M}$ and $\mathbf{\Gamma}$ as

$$\mathbf{H} = \mathbf{M} - \frac{i}{2}\mathbf{\Gamma}\,. \tag{12.7}$$

$\mathbf{M}$ and $\mathbf{\Gamma}$ are associated with $(M^0,\overline{M}^0)\leftrightarrow(M^0,\overline{M}^0)$ transitions via off-shell (dispersive), and on-shell (absorptive) intermediate states, respectively. Diagonal elements of $\mathbf{M}$ and $\mathbf{\Gamma}$ are associated with the flavor-conserving transitions $M^0\to M^0$ and $\overline{M}^0\to\overline{M}^0$, while off-diagonal elements are associated with flavor-changing transitions $M^0\leftrightarrow\overline{M}^0$.

The eigenvectors of $\mathbf{H}$ have well-defined masses and decay widths. To specify the components of the strong interaction eigenstates, M^0 and $\overline{M}^0$, in the light (M_L) and heavy (M_H) mass eigenstates, we introduce three complex parameters: p, q, and, for the case that both CP and CPT are violated in mixing, z:

$$\begin{aligned}|M_L\rangle &\propto p\sqrt{1-z}\,|M^0\rangle + q\sqrt{1+z}\,|\overline{M}^0\rangle\\ |M_H\rangle &\propto p\sqrt{1+z}\,|M^0\rangle - q\sqrt{1-z}\,|\overline{M}^0\rangle\,,\end{aligned} \tag{12.8}$$

with the normalization $|q|^2+|p|^2=1$ when $z=0$. (Another possible choice, which is in standard usage for K mesons, defines the mass eigenstates according to their lifetimes: K_S for the short-lived and K_L for the long-lived state. The K_L is the heavier state.)

The real and imaginary parts of the eigenvalues $\omega_{L,H}$ corresponding to $|M_{L,H}\rangle$ represent their masses and decay-widths, respectively. The mass and width splittings are

$$\begin{aligned}\Delta m &\equiv m_H - m_L = \mathcal{R}e(\omega_H-\omega_L)\quad,\\ \Delta\Gamma &\equiv \Gamma_H-\Gamma_L = -2\,\mathcal{I}m(\omega_H-\omega_L)\,.\end{aligned} \tag{12.9}$$

Note that here Δm is positive by definition, while the sign of $\Delta\Gamma$ is to be experimentally determined. (Alternatively, one can use the states defined by their lifetimes to have $\Delta\Gamma\equiv\Gamma_S-\Gamma_L$ positive by definition.) Solving the eigenvalue problem for $\mathbf{H}$ yields

$$\left(\frac{q}{p}\right)^2 = \frac{\mathbf{M}_{12}^* - (i/2)\mathbf{\Gamma}_{12}^*}{\mathbf{M}_{12}-(i/2)\mathbf{\Gamma}_{12}} \tag{12.10}$$

and

$$z \equiv \frac{\delta m - (i/2)\delta\Gamma}{\Delta m - (i/2)\Delta\Gamma}\,, \tag{12.11}$$

where

$$\delta m \equiv \mathbf{M}_{11}-\mathbf{M}_{22}\quad,\quad \delta\Gamma\equiv\mathbf{\Gamma}_{11}-\mathbf{\Gamma}_{22} \tag{12.12}$$

are the differences in effective mass and decay-rate expectation values for the strong interaction states M^0 and $\overline{M}^0$.

If either CP or CPT is a symmetry of $\mathbf{H}$ (independently of whether T is conserved or violated), then the values of δm and $\delta\Gamma$ are both zero, and hence $z=0$. We also find that

$$\omega_H-\omega_L = 2\sqrt{\left(\mathbf{M}_{12}-\frac{i}{2}\mathbf{\Gamma}_{12}\right)\left(\mathbf{M}_{12}^*-\frac{i}{2}\mathbf{\Gamma}_{12}^*\right)}\,. \tag{12.13}$$

If either CP or T is a symmetry of $\mathbf{H}$ (independently of whether CPT is conserved or violated), then $\mathbf{M}_{12}$ and $\mathbf{\Gamma}_{12}$ are relatively real, leading to

$$\left(\frac{q}{p}\right)^2 = e^{2i\xi_M} \quad\Rightarrow\quad \left|\frac{q}{p}\right| = 1\,, \tag{12.14}$$

where ξ_M is the arbitrary unphysical phase introduced in Eq. (12.3). If, and only if, CP is a symmetry of $\mathbf{H}$ (independently of CPT and T), then both of the above conditions hold, with the result that the mass eigenstates are orthogonal

$$\langle M_H|M_L\rangle = |p|^2-|q|^2 = 0\,. \tag{12.15}$$

12.1.3. ***CP-violating observables***: All CP-violating observables in M and $\overline{M}$ decays to final states f and $\overline{f}$ can be expressed in terms of phase-convention-independent combinations of A_f, $\overline{A}_f$, $A_{\overline{f}}$, and $\overline{A}_{\overline{f}}$, together with, for neutral-meson decays only, q/p. CP violation in charged-meson decays depends only on the combination $|\overline{A}_{\overline{f}}/A_f|$, while CP violation in neutral-meson decays is complicated by $M^0\leftrightarrow\overline{M}^0$ oscillations, and depends, additionally, on $|q/p|$ and on $\lambda_f\equiv(q/p)(\overline{A}_f/A_f)$.

The decay-rates of the two neutral K mass eigenstates, K_S and K_L, are different enough ($\Gamma_S/\Gamma_L\sim 500$) that one can, in most cases, actually study their decays independently. For neutral D, B, and B_s mesons, however, values of $\Delta\Gamma/\Gamma$ (where $\Gamma\equiv(\Gamma_H+\Gamma_L)/2$) are relatively small, and so both mass eigenstates must be considered in their evolution. We denote the state of an initially pure $|M^0\rangle$ or $|\overline{M}^0\rangle$ after an elapsed proper time t as $|M^0_{\rm phys}(t)\rangle$ or $|\overline{M}^0_{\rm phys}(t)\rangle$, respectively. Using the effective Hamiltonian approximation, but not assuming CPT is a good symmetry, we obtain

$$\begin{aligned}|M^0_{\rm phys}(t)\rangle &= \left(g_+(t)+z\,g_-(t)\right)|M^0\rangle - \sqrt{1-z^2}\,\frac{q}{p}\,g_-(t)|\overline{M}^0\rangle,\\ |\overline{M}^0_{\rm phys}(t)\rangle &= \left(g_+(t)-z\,g_-(t)\right)|\overline{M}^0\rangle - \sqrt{1-z^2}\,\frac{p}{q}\,g_-(t)|M^0\rangle\,,\end{aligned} \tag{12.16}$$

where

$$g_\pm(t) \equiv \frac{1}{2}\left(e^{-im_Ht-\frac{1}{2}\Gamma_Ht} \pm e^{-im_Lt-\frac{1}{2}\Gamma_Lt}\right) \tag{12.17}$$

and $z=0$ if either CPT or CP is conserved.

Defining $x\equiv\Delta m/\Gamma$ and $y\equiv\Delta\Gamma/(2\Gamma)$, and assuming $z=0$, one obtains the following time-dependent decay rates:

$$\begin{aligned}&\frac{d\Gamma\left[M^0_{\rm phys}(t)\to f\right]/dt}{e^{-\Gamma t}\mathcal{N}_f} =\\ &\left(|A_f|^2+|(q/p)\overline{A}_f|^2\right)\cosh(y\Gamma t) + \left(|A_f|^2-|(q/p)\overline{A}_f|^2\right)\cos(x\Gamma t)\\ &+2\,\mathcal{R}e((q/p)A_f^*\overline{A}_f)\sinh(y\Gamma t) - 2\,\mathcal{I}m((q/p)A_f^*\overline{A}_f)\sin(x\Gamma t)\,,\end{aligned} \tag{12.18}$$

$$\begin{aligned}&\frac{d\Gamma\left[\overline{M}^0_{\rm phys}(t)\to f\right]/dt}{e^{-\Gamma t}\mathcal{N}_f} =\\ &\left(|(p/q)A_f|^2+|\overline{A}_f|^2\right)\cosh(y\Gamma t) - \left(|(p/q)A_f|^2-|\overline{A}_f|^2\right)\cos(x\Gamma t)\\ &+2\,\mathcal{R}e((p/q)A_f\overline{A}_f^*)\sinh(y\Gamma t) - 2\,\mathcal{I}m((p/q)A_f\overline{A}_f^*)\sin(x\Gamma t)\,,\end{aligned} \tag{12.19}$$

where $\mathcal{N}_f$ is a common normalization factor. Decay rates to the CP-conjugate final state $\overline{f}$ are obtained analogously, with $\mathcal{N}_f=\mathcal{N}_{\overline{f}}$ and the substitutions $A_f\to A_{\overline{f}}$ and $\overline{A}_f\to\overline{A}_{\overline{f}}$ in Eqs. (12.18,12.19). Terms proportional to $|A_f|^2$ or $|\overline{A}_f|^2$ are associated with decays that occur without any net $M\leftrightarrow\overline{M}$ oscillation, while terms proportional to $|(q/p)\overline{A}_f|^2$ or $|(p/q)A_f|^2$ are associated with decays following a net oscillation. The $\sinh(y\Gamma t)$ and $\sin(x\Gamma t)$ terms of Eqs. (12.18,12.19) are associated with the interference between these two cases. Note that, in multi-body decays, amplitudes are functions of phase-space variables. Interference may be present in some regions but not others, and is strongly influenced by resonant substructure.

When neutral pseudoscalar mesons are produced coherently in pairs from the decay of a vector resonance, $V\to M^0\overline{M}^0$ (for example, $\Upsilon(4S)\to B^0\overline{B}^0$ or $\phi\to K^0\overline{K}^0$), the time-dependence of their subsequent decays to final states f_1 and f_2 has a similar form to Eqs. (12.18,12.19):

$$\begin{aligned}&\frac{d\Gamma\left[V_{\rm phys}(t_1,t_2)\to f_1f_2\right]/dt}{e^{-\Gamma|\Delta t|}\mathcal{N}_{f_1f_2}} =\\ &\left(|a_+|^2+|a_-|^2\right)\cosh(y\Gamma\Delta t) + \left(|a_+|^2-|a_-|^2\right)\cos(x\Gamma\Delta t)\\ &-2\,\mathcal{R}e(a_+^*a_-)\sinh(y\Gamma\Delta t) + 2\,\mathcal{I}m(a_+^*a_-)\sin(x\Gamma\Delta t)\,,\end{aligned} \tag{12.20}$$

where $\Delta t \equiv t_2 - t_1$ is the difference in the production times, t_1 and t_2, of f_1 and f_2, respectively, and the dependence on the average decay time and on decay angles has been integrated out. The coefficients in Eq. (12.20) are determined by the amplitudes for no net oscillation from $t_1 \to t_2$, $\overline{A}_{f_1} A_{f_2}$ and $A_{f_1}\overline{A}_{f_2}$, and for a net oscillation, $(q/p)\overline{A}_{f_1}\overline{A}_{f_2}$ and $(p/q)A_{f_1}A_{f_2}$, via

$$a_+ \equiv \overline{A}_{f_1}A_{f_2} - A_{f_1}\overline{A}_{f_2}\,, \tag{12.21}$$

$$a_- \equiv -\sqrt{1-z^2}\left(\frac{q}{p}\overline{A}_{f_1}\overline{A}_{f_2} - \frac{p}{q}A_{f_1}A_{f_2}\right) + z\left(\overline{A}_{f_1}A_{f_2} + A_{f_1}\overline{A}_{f_2}\right)\,.$$

Assuming CPT conservation, $z = 0$, and identifying $\Delta t \to t$ and $f_2 \to f$, we find that Eqs. (12.20) and (12.21) reduce to Eq. (12.18) with $A_{f_1} = 0$, $\overline{A}_{f_1} = 1$, or to Eq. (12.19) with $\overline{A}_{f_1} = 0$, $A_{f_1} = 1$. Indeed, such a situation plays an important role in experiments. Final states f_1 with $A_{f_1} = 0$ or $\overline{A}_{f_1} = 0$ are called tagging states, because they identify the decaying pseudoscalar meson as, respectively, $\overline{M}^0$ or M^0. Before one of M^0 or $\overline{M}^0$ decays, they evolve in phase, so that there is always one M^0 and one $\overline{M}^0$ present. A tagging decay of one meson sets the clock for the time evolution of the other: it starts at t_1 as purely M^0 or $\overline{M}^0$, with time evolution that depends only on $t_2 - t_1$.

When f_1 is a state that both M^0 and $\overline{M}^0$ can decay into, then Eq. (12.20) contains interference terms proportional to $A_{f_1}\overline{A}_{f_1} \neq 0$ that are not present in Eqs. (12.18,12.19). Even when f_1 is dominantly produced by M^0 decays rather than $\overline{M}^0$ decays, or vice versa, $A_{f_1}\overline{A}_{f_1}$ can be non-zero owing to doubly-CKM-suppressed decays, and these terms should be considered for precision studies of CP violation in coherent $V \to M^0\overline{M}^0$ decays [10].

12.1.4. ***Classification of CP-violating effects***: We distinguish three types of CP-violating effects in meson decays:

I. CP violation in decay is defined by

$$|\overline{A}_{\overline{f}}/A_f| \neq 1\,. \tag{12.22}$$

In charged meson decays, where mixing effects are absent, this is the only possible source of CP asymmetries:

$$\mathcal{A}_{f^\pm} \equiv \frac{\Gamma(M^- \to f^-) - \Gamma(M^+ \to f^+)}{\Gamma(M^- \to f^-) + \Gamma(M^+ \to f^+)} = \frac{|\overline{A}_{f^-}/A_{f^+}|^2 - 1}{|\overline{A}_{f^-}/A_{f^+}|^2 + 1}\,. \tag{12.23}$$

II. CP (and T) violation in mixing is defined by

$$|q/p| \neq 1\,. \tag{12.24}$$

In charged-current semileptonic neutral meson decays $M, \overline{M} \to \ell^\pm X$ (taking $|A_{\ell^+X}| = |\overline{A}_{\ell^-X}|$ and $A_{\ell^-X} = \overline{A}_{\ell^+X} = 0$, as is the case in the Standard Model, to lowest order, and in most of its reasonable extensions), this is the only source of CP violation, and can be measured via the asymmetry of "wrong-sign" decays induced by oscillations:

$$\mathcal{A}_{\rm SL}(t) \equiv \frac{d\Gamma/dt\left[\overline{M}^0_{\rm phys}(t) \to \ell^+X\right] - d\Gamma/dt\left[M^0_{\rm phys}(t) \to \ell^-X\right]}{d\Gamma/dt\left[\overline{M}^0_{\rm phys}(t) \to \ell^+X\right] + d\Gamma/dt\left[M^0_{\rm phys}(t) \to \ell^-X\right]} = \frac{1-|q/p|^4}{1+|q/p|^4}. \tag{12.25}$$

Note that this asymmetry of time-dependent decay rates is actually time-independent.

III. CP violation in interference between a decay without mixing, $M^0 \to f$, and a decay with mixing, $M^0 \to \overline{M}^0 \to f$ (such an effect occurs only in decays to final states that are common to M^0 and $\overline{M}^0$, including all CP eigenstates), is defined by

$$\mathcal{I}m(\lambda_f) \neq 0\,, \tag{12.26}$$

with

$$\lambda_f \equiv \frac{q}{p}\frac{\overline{A}_f}{A_f}\,. \tag{12.27}$$

This form of CP violation can be observed, for example, using the asymmetry of neutral meson decays into final CP eigenstates f_{CP}

$$\mathcal{A}_{f_{CP}}(t) \equiv \frac{d\Gamma/dt\left[\overline{M}^0_{\rm phys}(t) \to f_{CP}\right] - d\Gamma/dt\left[M^0_{\rm phys}(t) \to f_{CP}\right]}{d\Gamma/dt\left[\overline{M}^0_{\rm phys}(t) \to f_{CP}\right] + d\Gamma/dt\left[M^0_{\rm phys}(t) \to f_{CP}\right]}\,. \tag{12.28}$$

If $\Delta\Gamma = 0$ and $|q/p| = 1$, as expected to a good approximation for B mesons, but not for K mesons, then $\mathcal{A}_{f_{CP}}$ has a particularly simple form (see Eq. (12.60), below). If, in addition, the decay amplitudes fulfill $|\overline{A}_{f_{CP}}| = |A_{f_{CP}}|$, the interference between decays with and without mixing is the only source of the asymmetry and $\mathcal{A}_{f_{CP}}(t) = \mathcal{I}m(\lambda_{f_{CP}})\sin(x\Gamma t)$.

Examples of these three types of CP violation will be given in Sections 12.4, 12.5, and 12.6.

12.2. Theoretical Interpretation: General Considerations

Consider the $M \to f$ decay amplitude A_f, and the CP conjugate process, $\overline{M} \to \overline{f}$, with decay amplitude $\overline{A}_{\overline{f}}$. There are two types of phases that may appear in these decay amplitudes. Complex parameters in any Lagrangian term that contributes to the amplitude will appear in complex conjugate form in the CP-conjugate amplitude. Thus, their phases appear in A_f and $\overline{A}_{\overline{f}}$ with opposite signs. In the Standard Model, these phases occur only in the couplings of the $W^\pm$ bosons, and hence, are often called "weak phases". The weak phase of any single term is convention-dependent. However, the difference between the weak phases in two different terms in A_f is convention-independent. A second type of phase can appear in scattering or decay amplitudes, even when the Lagrangian is real. Their origin is the possible contribution from intermediate on-shell states in the decay process. Since these phases are generated by CP-invariant interactions, they are the same in A_f and $\overline{A}_{\overline{f}}$. Usually the dominant rescattering is due to strong interactions; hence the designation "strong phases" for the phase shifts so induced. Again, only the relative strong phases between different terms in the amplitude are physically meaningful.

The 'weak' and 'strong' phases discussed here appear in addition to the 'spurious' CP-transformation phases of Eq. (12.4). Those spurious phases are due to an arbitrary choice of phase convention, and do not originate from any dynamics or induce any CP violation. For simplicity, we set them to zero from here on.

It is useful to write each contribution a_i to A_f in three parts: its magnitude $|a_i|$, its weak phase ϕ_i, and its strong phase δ_i. If, for example, there are two such contributions, $A_f = a_1 + a_2$, we have

$$\begin{aligned} A_f &= |a_1|e^{i(\delta_1+\phi_1)} + |a_2|e^{i(\delta_2+\phi_2)}, \\ \overline{A}_{\overline{f}} &= |a_1|e^{i(\delta_1-\phi_1)} + |a_2|e^{i(\delta_2-\phi_2)}. \end{aligned} \tag{12.29}$$

Similarly, for neutral meson decays, it is useful to write

$$\mathbf{M}_{12} = |\mathbf{M}_{12}|e^{i\phi_M} \quad , \quad \mathbf{\Gamma}_{12} = |\mathbf{\Gamma}_{12}|e^{i\phi_\Gamma}\,. \tag{12.30}$$

Each of the phases appearing in Eqs. (12.29,12.30) is convention-dependent, but combinations such as $\delta_1 - \delta_2$, $\phi_1 - \phi_2$, $\phi_M - \phi_\Gamma$, and $\phi_M + \phi_1 - \overline{\phi}_1$ (where $\overline{\phi}_1$ is a weak phase contributing to $\overline{A}_f$) are physical.

It is now straightforward to evaluate the various asymmetries in terms of the theoretical parameters introduced here. We will do so with approximations that are often relevant to the most interesting measured asymmetries.

1. The CP asymmetry in charged meson decays [Eq. (12.23)] is given by

$$\mathcal{A}_{f^\pm} = -\frac{2|a_1a_2|\sin(\delta_2-\delta_1)\sin(\phi_2-\phi_1)}{|a_1|^2 + |a_2|^2 + 2|a_1a_2|\cos(\delta_2-\delta_1)\cos(\phi_2-\phi_1)}. \tag{12.31}$$

The quantity of most interest to theory is the weak phase difference $\phi_2 - \phi_1$. Its extraction from the asymmetry requires, however, that the amplitude ratio and the strong phase are known. Both quantities depend on non-perturbative hadronic parameters that are difficult to calculate.

2. In the approximation that $|\mathbf{\Gamma}_{12}/\mathbf{M}_{12}| \ll 1$ (valid for B and B_s mesons), the CP asymmetry in semileptonic neutral-meson decays [Eq. (12.25)] is given by

$$\mathcal{A}_{\rm SL} = -\left|\frac{\mathbf{\Gamma}_{12}}{\mathbf{M}_{12}}\right| \sin(\phi_M - \phi_\Gamma). \tag{12.32}$$

The quantity of most interest to theory is the weak phase $\phi_M - \phi_\Gamma$. Its extraction from the asymmetry requires, however, that $|\mathbf{\Gamma}_{12}/\mathbf{M}_{12}|$ is known. This quantity depends on long distance physics that is difficult to calculate.

3. In the approximations that only a single weak phase contributes to decay, $A_f = |a_f| e^{i(\delta_f + \phi_f)}$, and that $|\mathbf{\Gamma}_{12}/\mathbf{M}_{12}| = 0$, we obtain $|\lambda_f| = 1$, and the CP asymmetries in decays to a final CP eigenstate f [Eq. (12.28)] with eigenvalue $\eta_f = \pm 1$ are given by

$$\mathcal{A}_{f_{CP}}(t) = \mathcal{I}m(\lambda_f)\ \sin(\Delta m t)\ \ \text{with}\ \ \mathcal{I}m(\lambda_f) = \eta_f \sin(\phi_M + 2\phi_f). \tag{12.33}$$

Note that the phase so measured is purely a weak phase, and no hadronic parameters are involved in the extraction of its value from $\mathcal{I}m(\lambda_f)$.

The discussion above allows us to introduce another classification:

1. *Direct CP violation* is one that cannot be accounted for by just $\phi_M \neq 0$. CP violation in decay (type I) belongs to this class.
2. *Indirect CP violation* is consistent with taking $\phi_M \neq 0$ and setting all other CP violating phases to zero. CP violation in mixing (type II) belongs to this class.

As concerns type III CP violation, observing $\eta_{f_1}\mathcal{I}m(\lambda_{f_1}) \neq \eta_{f_2}\mathcal{I}m(\lambda_{f_2})$ (for the same decaying meson and two different final CP eigenstates f_1 and f_2) would establish direct CP violation. The significance of this classification is related to theory. In superweak models [11], CP violation appears only in diagrams that contribute to $\mathbf{M}_{12}$, hence they predict that there is no direct CP violation. In most models and, in particular, in the Standard Model, CP violation is both direct and indirect. The experimental observation of $\epsilon' \neq 0$ (see Section 12.4) excluded the superweak scenario.

12.3. Theoretical Interpretation: The KM Mechanism

Of all the Standard Model quark parameters, only the Kobayashi-Maskawa (KM) phase is CP violating. Having a single source of CP violation, the Standard Model is very predictive for CP asymmetries: some vanish, and those that do not are correlated.

To be precise, CP could be violated also by strong interactions. The experimental upper bound on the electric dipole moment of the neutron implies, however, that $\theta_{\rm QCD}$, the non-perturbative parameter that determines the strength of this type of CP violation, is tiny, if not zero. (The smallness of $\theta_{\rm QCD}$ constitutes a theoretical puzzle, known as 'the strong CP problem.') In particular, it is irrelevant to our discussion of meson decays.

The charged current interactions (that is, the $W^\pm$ interactions) for quarks are given by

$$-\mathcal{L}_{W^\pm} = \frac{g}{\sqrt{2}}\, \overline{u_{Li}}\, \gamma^\mu\, (V_{\rm CKM})_{ij}\, d_{Lj}\, W^+_\mu + \text{h.c.} \tag{12.34}$$

Here $i, j = 1, 2, 3$ are generation numbers. The Cabibbo-Kobayashi-Maskawa (CKM) mixing matrix for quarks is a 3×3 unitary matrix [12]. Ordering the quarks by their masses, *i.e.* $(u_1, u_2, u_3) \to (u, c, t)$ and $(d_1, d_2, d_3) \to (d, s, b)$, the elements of $V_{\rm CKM}$ are written as follows:

$$V_{\rm CKM} = \begin{pmatrix} V_{ud} & V_{us} & V_{ub} \\ V_{cd} & V_{cs} & V_{cb} \\ V_{td} & V_{ts} & V_{tb} \end{pmatrix} . \tag{12.35}$$

While a general 3×3 unitary matrix depends on three real angles and six phases, the freedom to redefine the phases of the quark mass eigenstates can be used to remove five of the phases, leaving a single physical phase, the Kobayashi-Maskawa phase, that is responsible for all CP violation in meson decays in the Standard Model.

The fact that one can parametrize $V_{\rm CKM}$ by three real and only one imaginary physical parameters can be made manifest by choosing an explicit parametrization. The Wolfenstein parametrization [13,14] is particularly useful:

$$V_{\rm CKM} = \begin{pmatrix} 1 - \frac{1}{2}\lambda^2 - \frac{1}{8}\lambda^4 & \lambda & A\lambda^3(\rho - i\eta) \\ -\lambda + \frac{1}{2}A^2\lambda^5[1 - 2(\rho + i\eta)] & 1 - \frac{1}{2}\lambda^2 - \frac{1}{8}\lambda^4(1 + 4A^2) & A\lambda^2 \\ A\lambda^3[1 - (1 - \frac{1}{2}\lambda^2)(\rho + i\eta)] & -A\lambda^2 + \frac{1}{2}A\lambda^4[1 - 2(\rho + i\eta)] & 1 - \frac{1}{2}A^2\lambda^4 \end{pmatrix} . \tag{12.36}$$

Here $\lambda = |V_{us}| = 0.22$ (not to be confused with λ_f) plays the role of an expansion parameter, and η represents the CP violating phase. Terms of $\mathcal{O}(\lambda^6)$ were neglected.

The unitarity of the CKM matrix leads to various relations among the matrix elements; *e.g.*,

$$V_{ud}V^*_{ub} + V_{cd}V^*_{cb} + V_{td}V^*_{tb} = 0\ . \tag{12.37}$$

This relation requires the sum of three complex quantities to vanish and so can be geometrically represented in the complex plane as a triangle (see Fig. 12.1). The angles of this triangle,

$$\begin{aligned} \alpha &\equiv \varphi_2 \equiv \arg\left(-\frac{V_{td}V^*_{tb}}{V_{ud}V^*_{ub}}\right), \\ \beta &\equiv \varphi_1 \equiv \arg\left(-\frac{V_{cd}V^*_{cb}}{V_{td}V^*_{tb}}\right), \\ \gamma &\equiv \varphi_3 \equiv \arg\left(-\frac{V_{ud}V^*_{ub}}{V_{cd}V^*_{cb}}\right), \end{aligned} \tag{12.38}$$

are physical quantities and can, in principle, be independently measured by CP asymmetries in B decays. The notations (α, β, γ) and $(\varphi_1, \varphi_2, \varphi_3)$ are both in common usage.

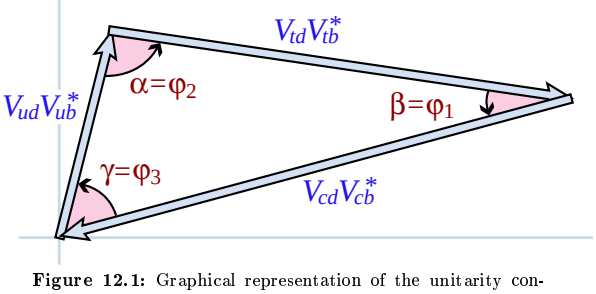

Figure 12.1: Graphical representation of the unitarity constraint $V_{ud}V^*_{ub} + V_{cd}V^*_{cb} + V_{td}V^*_{tb} = 0$ as a triangle in the complex plane.

All unitarity triangles that correspond to relations, such as Eq. (12.37) between two different columns or two different rows of the CKM matrix have the same area, commonly denoted by $J/2$ [15]. If CP is violated, J is different from zero and can be taken as the single CP-violating parameter. In the Wolfenstein parametrization of Eq. (12.36), $J \simeq \lambda^6 A^2 \eta$.

12.4. K Decays

CP violation was discovered in $K \to \pi\pi$ decays in 1964 [1]. The same mode provided the first evidence for direct CP violation [16–18].

The decay amplitudes actually measured in neutral K decays refer to the mass eigenstates K_L and K_S, rather than to the K and $\overline{K}$ states referred to in Eq. (12.1). We define CP-violating amplitude ratios for two-pion final states,

$$\eta_{00} \equiv \frac{\langle \pi^0\pi^0|\mathcal{H}|K_L\rangle}{\langle \pi^0\pi^0|\mathcal{H}|K_S\rangle} \quad , \quad \eta_{+-} \equiv \frac{\langle \pi^+\pi^-|\mathcal{H}|K_L\rangle}{\langle \pi^+\pi^-|\mathcal{H}|K_S\rangle} \, . \tag{12.39}$$

Another important observable is the asymmetry of time-integrated semileptonic decay rates:

$$\delta_L \equiv \frac{\Gamma(K_L \to \ell^+\nu_\ell\pi^-) - \Gamma(K_L \to \ell^-\overline{\nu}_\ell\pi^+)}{\Gamma(K_L \to \ell^+\nu_\ell\pi^-) + \Gamma(K_L \to \ell^-\overline{\nu}_\ell\pi^+)} \, . \tag{12.40}$$

CP violation has been observed as an appearance of K_L decays to two-pion final states [19],

$$\begin{aligned} |\eta_{00}| &= (2.276 \pm 0.014) \times 10^{-3} \qquad \phi_{00} &&= 43.7^\circ \pm 0.8^\circ \\ |\eta_{+-}| &= (2.286 \pm 0.014) \times 10^{-3} \qquad \phi_{+-} &&= 43.4^\circ \pm 0.7^\circ \\ |\eta_{00}/\eta_{+-}| &= 0.9950 \pm 0.0008 \qquad \phi_{00} - \phi_{+-} &&= 0.2^\circ \pm 0.4^\circ \, , \end{aligned} \tag{12.41}$$

where ϕ_{ij} is the phase of the amplitude ratio η_{ij} determined without assuming CPT invariance. (A fit that assumes CPT gives [19] $\phi_{00} = 43.49^\circ \pm 0.06^\circ$, $\phi_{+-} = 43.51^\circ \pm 0.05^\circ$ and $\phi_{00} - \phi_{+-} = -0.022^\circ \pm 0.020^\circ$.) CP violation has also been observed in semileptonic K_L decays [19]

$$\delta_L = (3.27 \pm 0.12) \times 10^{-3} \, , \tag{12.42}$$

where δ_L is a weighted average of muon and electron measurements, as well as in K_L decays to $\pi^+\pi^-\gamma$ and $\pi^+\pi^-e^+e^-$ [19]. CP violation in $K \to 3\pi$ decays has not yet been observed [19,20].

Historically, CP violation in neutral K decays has been described in terms of parameters ϵ and ϵ'. The observables η_{00}, η_{+-}, and δ_L are related to these parameters, and to those of Section 12.1, by

$$\begin{aligned} \eta_{00} &= \frac{1 - \lambda_{\pi^0\pi^0}}{1 + \lambda_{\pi^0\pi^0}} &&= \epsilon - 2\epsilon' \, , \\ \eta_{+-} &= \frac{1 - \lambda_{\pi^+\pi^-}}{1 + \lambda_{\pi^+\pi^-}} &&= \epsilon + \epsilon' \, , \\ \delta_L &= \frac{1 - |q/p|^2}{1 + |q/p|^2} &&= \frac{2\mathcal{R}e(\epsilon)}{1 + |\epsilon|^2} \, , \end{aligned} \tag{12.43}$$

where, in the last line, we have assumed that $\left|A_{\ell^+\nu_\ell\pi^-}\right| = \left|\overline{A}_{\ell^-\overline{\nu}_\ell\pi^+}\right|$ and $\left|A_{\ell^-\overline{\nu}_\ell\pi^+}\right| = \left|\overline{A}_{\ell^+\nu_\ell\pi^-}\right| = 0$. (The convention-dependent parameter $\bar{\epsilon} \equiv (1 - q/p)/(1 + q/p)$, sometimes used in the literature, is, in general, different from ϵ but yields a similar expression, $\delta_L = 2\mathcal{R}e(\bar{\epsilon})/(1 + |\bar{\epsilon}|^2)$.) A fit to the $K \to \pi\pi$ data yields [19]

$$\begin{aligned} |\epsilon| &= (2.284 \pm 0.014) \times 10^{-3} \, , \\ \mathcal{R}e(\epsilon'/\epsilon) &= (1.67 \pm 0.26) \times 10^{-3} \, . \end{aligned} \tag{12.44}$$

In discussing two-pion final states, it is useful to express the amplitudes $A_{\pi^0\pi^0}$ and $A_{\pi^+\pi^-}$ in terms of their isospin components via

$$\begin{aligned} A_{\pi^0\pi^0} &= \sqrt{\frac{1}{3}}\,|A_0|\,e^{i(\delta_0+\phi_0)} - \sqrt{\frac{2}{3}}\,|A_2|\,e^{i(\delta_2+\phi_2)}, \\ A_{\pi^+\pi^-} &= \sqrt{\frac{2}{3}}\,|A_0|\,e^{i(\delta_0+\phi_0)} + \sqrt{\frac{1}{3}}\,|A_2|\,e^{i(\delta_2+\phi_2)} \, , \end{aligned} \tag{12.45}$$

where we parameterize the amplitude $A_I(\overline{A}_I)$ for $K^0(\overline{K}^0)$ decay into two pions with total isospin $I = 0$ or 2 as

$$\begin{aligned} A_I &\equiv \langle(\pi\pi)_I\,|\mathcal{H}|\,K^0\rangle = |A_I|\,e^{i(\delta_I+\phi_I)} \, , \\ \overline{A}_I &\equiv \langle(\pi\pi)_I\,|\mathcal{H}|\,\overline{K}^0\rangle = |A_I|\,e^{i(\delta_I-\phi_I)} \, . \end{aligned} \tag{12.46}$$

The smallness of $|\eta_{00}|$ and $|\eta_{+-}|$ allows us to approximate

$$\epsilon \simeq \frac{1}{2}(1 - \lambda_{(\pi\pi)_{I=0}}), \qquad \epsilon' \simeq \frac{1}{6}\left(\lambda_{\pi^0\pi^0} - \lambda_{\pi^+\pi^-}\right) \, . \tag{12.47}$$

The parameter ϵ represents indirect CP violation, while ϵ' parameterizes direct CP violation: $\mathcal{R}e(\epsilon')$ measures CP violation in decay (type I), $\mathcal{R}e(\epsilon)$ measures CP violation in mixing (type II), and $\mathcal{I}m(\epsilon)$ and $\mathcal{I}m(\epsilon')$ measure the interference between decays with and without mixing (type III).

The following expressions for ϵ and ϵ' are useful for theoretical evaluations:

$$\epsilon \simeq \frac{e^{i\pi/4}}{\sqrt{2}} \frac{\mathcal{I}m(\mathbf{M}_{12})}{\Delta m}, \qquad \epsilon' = \frac{i}{\sqrt{2}} \left|\frac{A_2}{A_0}\right| e^{i(\delta_2-\delta_0)} \sin(\phi_2 - \phi_0). \tag{12.48}$$

The expression for ϵ is only valid in a phase convention where $\phi_2 = 0$, corresponding to a real $V_{ud}V_{us}^*$, and in the approximation that also $\phi_0 = 0$. The phase of ϵ, $\arg(\epsilon) \approx \arctan(-2\Delta m/\Delta\Gamma)$, is independent of the electroweak model and is experimentally determined to be about $\pi/4$. The calculation of ϵ benefits from the fact that $\mathcal{I}m(\mathbf{M}_{12})$ is dominated by short distance physics. Consequently, the main source of uncertainty in theoretical interpretations of ϵ are the values of matrix elements, such as $\langle K^0\,|(\overline{s}d)_{V-A}(\overline{s}d)_{V-A}|\,\overline{K}^0\rangle$. The expression for ϵ' is valid to first order in $|A_2/A_0| \sim 1/20$. The phase of ϵ' is experimentally determined, $\pi/2 + \delta_2 - \delta_0 \approx \pi/4$, and is independent of the electroweak model. Note that, accidentally, ϵ'/ϵ is real to a good approximation.

A future measurement of much interest is that of CP violation in the rare $K \to \pi\nu\overline{\nu}$ decays. The signal for CP violation is simply observing the $K_L \to \pi^0\nu\overline{\nu}$ decay. The effect here is that of interference between decays with and without mixing (type III) [21]:

$$\frac{\Gamma(K_L \to \pi^0\nu\overline{\nu})}{\Gamma(K^+ \to \pi^+\nu\overline{\nu})} = \frac{1}{2}\left[1 + |\lambda_{\pi\nu\overline{\nu}}|^2 - 2\,\mathcal{R}e(\lambda_{\pi\nu\overline{\nu}})\right] \simeq 1 - \mathcal{R}e(\lambda_{\pi\nu\overline{\nu}}), \tag{12.49}$$

where in the last equation we neglect CP violation in decay and in mixing (expected, model-independently, to be of order 10^{-5} and 10^{-3}, respectively). Such a measurement would be experimentally very challenging and theoretically very rewarding [22]. Similar to the CP asymmetry in $B \to J/\psi K_S$, the CP violation in $K \to \pi\nu\overline{\nu}$ decay is predicted to be large and can be very cleanly interpreted.

Within the Standard Model, the $K_L \to \pi^0\nu\overline{\nu}$ decay is dominated by an intermediate top quark contribution and, consequently, can be interpreted in terms of CKM parameters [23]. (For the charged mode, $K^+ \to \pi^+\nu\overline{\nu}$, the contribution from an intermediate charm quark is not negligible, and constitutes a source of hadronic uncertainty.) In particular, $\mathrm{B}(K_L \to \pi^0\nu\overline{\nu})$ provides a theoretically clean way to determine the Wolfenstein parameter η [24]:

$$\mathrm{B}(K_L \to \pi^0\nu\overline{\nu}) = \kappa_L X^2(m_t^2/m_W^2) A^4\eta^2, \tag{12.50}$$

where $\kappa_L = 1.80 \times 10^{-10}$ incorporates the value of the four-fermion matrix element which is deduced, using isospin relations, from $\mathrm{B}(K^+ \to \pi^0 e^+\nu)$, and $X(m_t^2/m_W^2)$ is a known function of the top mass.

12.5. D Decays

Unlike the case of neutral K, B, and B_s mixing, D^0–$\overline{D}^0$ mixing has not yet been observed [25]. Long-distance contributions make it difficult to calculate the Standard Model prediction for the D^0–$\overline{D}^0$ mixing parameters. Therefore, the goal of the search for D^0–$\overline{D}^0$ mixing is not to constrain the CKM parameters, but rather to probe new physics. Here CP violation plays an important role. Within the Standard Model, the CP-violating effects are predicted to be negligibly small, since the mixing and the relevant decays are described, to an excellent approximation, by physics of the first two generations. Observation of CP violation in D^0–$\overline{D}^0$ mixing (at a level much higher than $\mathcal{O}(10^{-3})$) will constitute an unambiguous signal of new physics. At present, the most sensitive searches involve the $D \to K^+K^-$ and $D \to K^\pm\pi^\mp$ modes.

The neutral D mesons decay via a singly-Cabibbo-suppressed transition to the CP eigenstate K^+K^-. Since the decay proceeds via a Standard-Model tree diagram, it is very likely unaffected by new physics and, furthermore, dominated by a single weak phase. It is safe then to assume that direct CP violation plays no role here. In addition, given the experimental bounds [26], $x \equiv \Delta m/\Gamma \lesssim 0.03$ and $y \equiv \Delta\Gamma/(2\Gamma) = 0.0045 \pm 0.0065$, we can expand the decay rates to first order in these parameters. Using Eq. (12.18) with these assumptions and approximations yields, for $xt, yt \lesssim \Gamma^{-1}$,

$$\begin{aligned}
&\Gamma[D^0_{\rm phys}(t) \to K^+K^-] \\
&\quad = e^{-\Gamma t}\,|A_{KK}|^2\,[1 - |q/p|\,(y\cos\phi_D - x\sin\phi_D)\Gamma t]\ , \\
&\Gamma[\overline{D}^0_{\rm phys}(t) \to K^+K^-] \\
&\quad = e^{-\Gamma t}\,|A_{KK}|^2\,[1 - |p/q|\,(y\cos\phi_D + x\sin\phi_D)\Gamma t]\ ,
\end{aligned} \tag{12.51}$$

where ϕ_D is defined via $\lambda_{K^+K^-} = -\,|q/p|\,e^{i\phi_D}$. (In the limit of CP conservation, choosing $\phi_D = 0$ is equivalent to defining the mass eigenstates by their CP eigenvalue: $|D_\mp\rangle = p|D^0\rangle \pm q|\overline{D}^0\rangle$, with $D_-(D_+)$ being the CP-odd (CP-even) state; that is, the state that does not (does) decay into K^+K^-.) Given the small values of x and y, the time dependences of the rates in Eq. (12.51) can be recast into purely exponential forms, but with modified decay-rate parameters [27]:

$$\begin{aligned}
\Gamma_{D^0\to K^+K^-} &= \Gamma \times [1 + |q/p|\,(y\cos\phi_D - x\sin\phi_D)]\ , \\
\Gamma_{\overline{D}^0\to K^+K^-} &= \Gamma \times [1 + |p/q|\,(y\cos\phi_D + x\sin\phi_D)]\ .
\end{aligned} \tag{12.52}$$

One can define CP-conserving and CP-violating combinations of these two observables (normalized to the true width Γ):

$$\begin{aligned}
Y &\equiv \frac{\Gamma_{\overline{D}^0\to K^+K^-} + \Gamma_{D^0\to K^+K^-}}{2\Gamma} - 1 \\
&= \frac{|q/p| + |p/q|}{2}\,y\cos\phi_D - \frac{|q/p| - |p/q|}{2}\,x\sin\phi_D\ , \\
\Delta Y &\equiv \frac{\Gamma_{\overline{D}^0\to K^+K^-} - \Gamma_{D^0\to K^+K^-}}{2\Gamma} \\
&= \frac{|q/p| + |p/q|}{2}\,x\sin\phi_D - \frac{|q/p| - |p/q|}{2}\,y\cos\phi_D\ .
\end{aligned} \tag{12.53}$$

In the limit of CP conservation (and, in particular, within the Standard Model), $Y = y$ and $\Delta Y = 0$.

The $K^\pm\pi^\mp$ states are not CP eigenstates, but they are still common final states for D^0 and $\overline{D}^0$ decays. Since $D^0(\overline{D}^0) \to K^-\pi^+$ is a Cabibbo-favored (doubly-Cabibbo-suppressed) process, these processes are particularly sensitive to x and/or $y = \mathcal{O}(\lambda^2)$. Taking into account that $\left|\lambda_{K^-\pi^+}\right|, \left|\lambda^{-1}_{K^+\pi^-}\right| \ll 1$ and $x, y \ll 1$, assuming that there is no direct CP violation (again, these are Standard Model tree level decays dominated by a single weak phase), and expanding the time-dependent rates for $xt, yt \lesssim \Gamma^{-1}$, one obtains

$$\begin{aligned}
&\frac{\Gamma[D^0_{\rm phys}(t) \to K^+\pi^-]}{\Gamma[\overline{D}^0_{\rm phys}(t) \to K^+\pi^-]} \\
&\quad = r_d^2 + r_d\left|\frac{q}{p}\right|(y'\cos\phi_D - x'\sin\phi_D)\Gamma t + \left|\frac{q}{p}\right|^2\frac{y^2+x^2}{4}(\Gamma t)^2\ , \\
&\frac{\Gamma[\overline{D}^0_{\rm phys}(t) \to K^-\pi^+]}{\Gamma[D^0_{\rm phys}(t) \to K^-\pi^+]} \\
&\quad = r_d^2 + r_d\left|\frac{p}{q}\right|(y'\cos\phi_D + x'\sin\phi_D)\Gamma t + \left|\frac{p}{q}\right|^2\frac{y^2+x^2}{4}(\Gamma t)^2\ ,
\end{aligned} \tag{12.54}$$

where

$$\begin{aligned}
y' &\equiv y\cos\delta - x\sin\delta\ , \\
x' &\equiv x\cos\delta + y\sin\delta\ .
\end{aligned} \tag{12.55}$$

The weak phase ϕ_D is the same as that of Eq. (12.51) (a consequence of the absence of direct CP violation), δ is a strong phase difference for these processes, and $r_d = \mathcal{O}(\tan^2\theta_c)$ is the amplitude ratio, $r_d = \left|\overline{A}_{K^-\pi^+}/A_{K^-\pi^+}\right| = \left|A_{K^+\pi^-}/\overline{A}_{K^+\pi^-}\right|$, that is, $\lambda_{K^-\pi^+} = r_d(q/p)e^{-i(\delta-\phi_D)}$ and $\lambda^{-1}_{K^+\pi^-} = r_d(p/q)e^{-i(\delta+\phi_D)}$. By fitting to the six coefficients of the various time-dependences, one can extract r_d, $|q/p|$, (x^2+y^2), $y'\cos\phi_D$, and $x'\sin\phi_D$. In particular, finding CP violation, that is, $|q/p| \neq 1$ and/or $\sin\phi_D \neq 0$, would constitute evidence for new physics.

More details on theoretical and experimental aspects of $D^0 - \overline{D}^0$ mixing can be found in [25]. Note that BABAR use $R_D \equiv r_d^2$ and $r_m \equiv |q/p|$. Belle use $R_m \equiv |q/p|$, $y_{CP} \equiv Y$, and $A_\Gamma \equiv -\Delta Y$.

12.6. B and B_s Decays

The upper bound on the CP asymmetry in semileptonic B decays [28] implies that CP violation in $B^0 - \overline{B}^0$ mixing is a small effect (we use $\mathcal{A}_{\rm SL}/2 \approx 1 - |q/p|$, see Eq. (12.25)):

$$\mathcal{A}_{\rm SL} = (0.3 \pm 1.3) \times 10^{-2} \implies |q/p| = 0.998 \pm 0.007. \tag{12.56}$$

The Standard Model prediction is

$$\mathcal{A}_{\rm SL} = \mathcal{O}\left(\frac{m_c^2}{m_t^2}\sin\beta\right) \lesssim 0.001. \tag{12.57}$$

In models where $\mathbf{\Gamma}_{12}/\mathbf{M}_{12}$ is approximately real, such as the Standard Model, an upper bound on $\Delta\Gamma/\Delta m \approx \mathcal{R}e(\mathbf{\Gamma}_{12}/\mathbf{M}_{12})$ provides yet another upper bound on the deviation of $|q/p|$ from one. This constraint does not hold if $\mathbf{\Gamma}_{12}/\mathbf{M}_{12}$ is approximately imaginary. (An alternative parameterization uses $q/p = (1-\bar{\epsilon}_B)/(1+\bar{\epsilon}_B)$, leading to $\mathcal{A}_{\rm SL} \simeq 4\mathcal{R}e(\bar{\epsilon}_B)$.)

The small deviation (less than one percent) of $|q/p|$ from 1 implies that, at the present level of experimental precision, CP violation in B mixing is a negligible effect. Thus, for the purpose of analyzing CP asymmetries in hadronic B decays, we can use

$$\lambda_f = e^{-i\phi_{M(B)}}(\overline{A}_f/A_f)\ , \tag{12.58}$$

where $\phi_{M(B)}$ refers to the phase of $\mathbf{M}_{12}$ appearing in Eq. (12.30) that is appropriate for $B^0 - \overline{B}^0$ oscillations. Within the Standard Model, the corresponding phase factor is given by

$$e^{-i\phi_{M(B)}} = (V_{tb}^*V_{td})/(V_{tb}V_{td}^*)\ . \tag{12.59}$$

Some of the most interesting decays involve final states that are common to B^0 and $\overline{B}^0$ [29,30]. It is convenient to rewrite Eq. (12.28) for B decays as [31,32,33]

$$\begin{aligned}
&\mathcal{A}_f(t) = S_f\sin(\Delta m t) - C_f\cos(\Delta m t), \\
&S_f \equiv \frac{2\mathcal{I}m(\lambda_f)}{1+|\lambda_f|^2}, \quad C_f \equiv \frac{1-|\lambda_f|^2}{1+|\lambda_f|^2}\ ,
\end{aligned} \tag{12.60}$$

where we assume that $\Delta\Gamma = 0$ and $|q/p| = 1$. An alternative notation in use is $A_f \equiv -C_f$, but this A_f should not be confused with the A_f of Eq. (12.1).

The processes of interest proceed via quark transitions of the form $\overline{b} \to \overline{q}q\overline{q}'$ with $q' = s$ or d. For $q = c$ or u, there are contributions from both tree (t) and penguin (p^{q_u}, where $q_u = u, c, t$ is the quark in the loop) diagrams (see Fig. 12.2) which carry different weak phases:

$$A_f = \left(V_{qb}^*V_{qq'}\right)t_f + \sum_{q_u=u,c,t}\left(V_{q_ub}^*V_{q_uq'}\right)p_f^{q_u}\ . \tag{12.61}$$

(The distinction between tree and penguin contributions is a heuristic one; the separation by the operator that enters is more precise. For a detailed discussion of the more complete operator product approach, which also includes higher order QCD corrections, see, for example, ref. [34].) Using CKM unitarity, these decay amplitudes can always

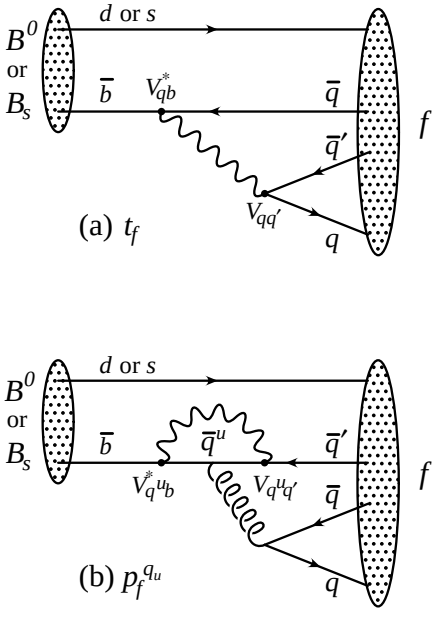

Figure 12.2: Feynman diagrams for (a) tree and (b) penguin amplitudes contributing to $B^0 \to f$ or $B_s \to f$ via a $\overline{b} \to \overline{q}q\overline{q}'$ quark-level process.

be written in terms of just two CKM combinations. For example, for $f = \pi\pi$, which proceeds via $\overline{b} \to \overline{u}u\overline{d}$ transition, we can write

$$A_{\pi\pi} = (V_{ub}^* V_{ud})\, T_{\pi\pi} + (V_{tb}^* V_{td})\, P_{\pi\pi}^t, \qquad (12.62)$$

where $T_{\pi\pi} = t_{\pi\pi} + p_{\pi\pi}^u - p_{\pi\pi}^c$ and $P_{\pi\pi}^t = p_{\pi\pi}^t - p_{\pi\pi}^c$. CP-violating phases in Eq. (12.62) appear only in the CKM elements, so that

$$\frac{\overline{A}_{\pi\pi}}{A_{\pi\pi}} = \frac{(V_{ub} V_{ud}^*)\, T_{\pi\pi} + (V_{tb} V_{td}^*)\, P_{\pi\pi}^t}{(V_{ub}^* V_{ud})\, T_{\pi\pi} + (V_{tb}^* V_{td})\, P_{\pi\pi}^t}. \qquad (12.63)$$

For $f = J/\psi K$, which proceeds via $\overline{b} \to \overline{c}c\overline{s}$ transition, we can write

$$A_{\psi K} = (V_{cb}^* V_{cs})\, T_{\psi K} + (V_{ub}^* V_{us})\, P_{\psi K}^u, \qquad (12.64)$$

where $T_{\psi K} = t_{\psi K} + p_{\psi K}^c - p_{\psi K}^t$ and $P_{\psi K}^u = p_{\psi K}^u - p_{\psi K}^t$. A subtlety arises in this decay that is related to the fact that $B^0 \to J/\psi K^0$ and $\overline{B}^0 \to J/\psi \overline{K}^0$. A common final state, *e.g.*, $J/\psi K_S$, is reached only via $K^0 - \overline{K}^0$ mixing. Consequently, the phase factor (defined in Eq. (12.30)) corresponding to neutral K mixing, $e^{-i\phi_{M(K)}} = (V_{cd}^* V_{cs})/(V_{cd} V_{cs}^*)$, plays a role:

$$\frac{\overline{A}_{\psi K_S}}{A_{\psi K_S}} = -\frac{(V_{cb} V_{cs}^*)\, T_{\psi K} + (V_{ub} V_{us}^*)\, P_{\psi K}^u}{(V_{cb}^* V_{cs})\, T_{\psi K} + (V_{ub}^* V_{us})\, P_{\psi K}^u} \times \frac{V_{cd}^* V_{cs}}{V_{cd} V_{cs}^*}. \qquad (12.65)$$

For $q = s$ or d, there are only penguin contributions to A_f, that is, $t_f = 0$ in Eq. (12.61). (The tree $\overline{b} \to \overline{u}u\overline{q}'$ transition followed by $\overline{u}u \to \overline{q}q$ rescattering is included below in the P^u terms.) Again, CKM unitarity allows us to write A_f in terms of two CKM combinations. For example, for $f = \phi K_S$, which proceeds via $\overline{b} \to \overline{s}s\overline{s}$ transition, we can write

$$\frac{\overline{A}_{\phi K_S}}{A_{\phi K_S}} = -\frac{(V_{cb} V_{cs}^*)\, P_{\phi K}^c + (V_{ub} V_{us}^*)\, P_{\phi K}^u}{(V_{cb}^* V_{cs})\, P_{\phi K}^c + (V_{ub}^* V_{us})\, P_{\phi K}^u} \times \frac{V_{cd}^* V_{cs}}{V_{cd} V_{cs}^*}, \qquad (12.66)$$

where $P_{\phi K}^c = p_{\phi K}^c - p_{\phi K}^t$ and $P_{\phi K}^u = p_{\phi K}^u - p_{\phi K}^t$.

Since the amplitude A_f involves two different weak phases, the corresponding decays can exhibit both CP violation in the interference of decays with and without mixing, $S_f \neq 0$, and CP violation in decays, $C_f \neq 0$. (At the present level of experimental precision, the contribution to C_f from CP violation in mixing is negligible, see Eq. (12.56).) If the contribution from a second weak phase is suppressed, then the interpretation of S_f in terms of Lagrangian CP-violating parameters is clean, while C_f is small. If such a second contribution is not suppressed, S_f depends on hadronic parameters and, if the relevant strong phase is large, C_f is large.

A summary of $\overline{b} \to \overline{q}q\overline{q}'$ modes with $q' = s$ or d is given in Table 12.1. The $\overline{b} \to \overline{d}d\overline{q}$ transitions lead to final states that are similar to the $\overline{b} \to \overline{u}u\overline{q}$ transitions and have similar phase dependence. Final states that consist of two vector-mesons ($\psi\phi$ and $\phi\phi$) are not CP eigenstates, and angular analysis will be needed to separate the CP-even from the CP-odd contributions.

Table 12.1: Summary of $\overline{b} \to \overline{q}q\overline{q}'$ modes with $q' = s$ or d. The second and third columns give examples of final hadronic states. The fourth column gives the CKM dependence of the amplitude A_f, using the notation of Eqs. (12.62,12.64,12.66), with the dominant term first and the sub-dominant second. The suppression factor of the second term compared to the first is given in the last column. "Loop" refers to a penguin versus tree suppression factor (it is mode-dependent and roughly $\mathcal{O}(0.2 - 0.3)$) and $\lambda = 0.22$ is the expansion parameter of Eq. (12.36).

$\overline{b} \to \overline{q}q\overline{q}'$	$B^0 \to f$	$B_s \to f$	CKM dependence of A_f	Suppression
$\overline{b} \to \overline{c}c\overline{s}$	ψK_S	$\psi\phi$	$(V_{cb}^* V_{cs})T + (V_{ub}^* V_{us})P^u$	loop $\times\, \lambda^2$
$\overline{b} \to \overline{s}s\overline{s}$	ϕK_S	$\phi\phi$	$(V_{cb}^* V_{cs})P^c + (V_{ub}^* V_{us})P^u$	λ^2
$\overline{b} \to \overline{u}u\overline{s}$	$\pi^0 K_S$	K^+K^-	$(V_{cb}^* V_{cs})P^c + (V_{ub}^* V_{us})T$	λ^2/loop
$\overline{b} \to \overline{c}c\overline{d}$	D^+D^-	ψK_S	$(V_{cb}^* V_{cd})T + (V_{tb}^* V_{td})P^t$	loop
$\overline{b} \to \overline{s}s\overline{d}$	$\phi\pi$	ϕK_S	$(V_{tb}^* V_{td})P^t + (V_{cb}^* V_{cd})P^c$	$\lesssim 1$
$\overline{b} \to \overline{u}u\overline{d}$	$\pi^+\pi^-$	$\pi^0 K_S$	$(V_{ub}^* V_{ud})T + (V_{tb}^* V_{td})P^t$	loop

The cleanliness of the theoretical interpretation of S_f can be assessed from the information in the last column of Table 12.1. In case of small uncertainties, the expression for S_f in terms of CKM phases can be deduced from the fourth column of Table 12.1 in combination with Eq. (12.59) (and, for $b \to q\overline{q}s$ decays, the example in Eq. (12.65)). Here we consider several interesting examples.

For $B \to J/\psi K_S$ and other $\overline{b} \to \overline{c}c\overline{s}$ processes, we can neglect the P^u contribution to A_f, in the Standard Model, to an approximation that is better than one percent:

$$\lambda_{\psi K_S} = -e^{-2i\beta} \;\Rightarrow\; S_{\psi K_S} = \sin 2\beta, \quad C_{\psi K_S} = 0\,. \qquad (12.67)$$

(Below the percent level, several effects have to be taken into account [35].) In the presence of new physics, A_f is still likely to be dominated by the T term, but the mixing amplitude might be modified. We learn that, model independently, $C_f \approx 0$ while S_f cleanly determines the mixing phase ($\phi_M - 2\arg(V_{cb}V_{cd}^*)$). The experimental measurement [28], $S_{\psi K} = 0.731 \pm 0.056$, gave the first precision test of the Kobayashi-Maskawa mechanism, and its consistency with the predictions for $\sin 2\beta$ makes it very likely that this mechanism is indeed the dominant source of CP violation in meson decays.

For $B \to \phi K_S$ and other $\overline{b} \to \overline{s}s\overline{s}$ processes, we can neglect the P^u contribution to A_f, in the Standard Model, to an approximation that is good to order of a few percent:

$$\lambda_{\phi K_S} = -e^{-2i\beta} \;\Rightarrow\; S_{\phi K_S} = \sin 2\beta, \quad C_{\phi K_S} = 0\,. \qquad (12.68)$$

In the presence of new physics, both A_f and $\mathbf{M}_{12}$ can get contributions that are comparable in size to those of the Standard Model and carry new weak phases. Such a situation gives several interesting consequences for $b \to \overline{s}s\overline{s}$ decays:

1. The value of S_f may be different from $S_{\psi K_S}$ by more than a few percent.
2. The values of S_f for different final states f may be different from each other by more than a few percent (for example, $S_{\phi K_S} \neq S_{\eta' K_S}$).
3. The value of C_f may be different from zero by more than a few percent.

While a clear interpretation of such signals in terms of Lagrangian parameters will be difficult because, under these circumstances, hadronic parameters do play a role, any of the above three options will clearly signal new physics. Present experimental results give [28] $S_{\eta' K} = 0.27 \pm 0.21$ and $S_{\phi K} = -1.0 \pm 0.5$. Thus, for this class of modes, neither $S_f \neq 0$ nor $S_f \neq S_{\psi K}$ is unambiguously established, but there is definitely still room for new physics.

For $B \to \pi\pi$ and other $\overline{b} \to \overline{u}u\overline{d}$ processes, the penguin-to-tree ratio can be estimated using SU(3) relations and experimental data on related $B \to K\pi$ decays. The result is that the suppression is of order $0.2 - 0.3$ and so cannot be neglected. The expressions for $S_{\pi\pi}$ and $C_{\pi\pi}$ to leading order in $R_{PT} \equiv (|V_{tb}V_{td}|\,P^t_{\pi\pi})/(|V_{ub}V_{ud}|\,T_{\pi\pi})$ are:

$$\lambda_{\pi\pi} = e^{2i\alpha}\left[(1 - R_{PT}e^{-i\alpha})/(1 - R_{PT}e^{+i\alpha})\right] \;\Rightarrow$$

$$S_{\pi\pi} \approx \sin 2\alpha + 2\,\mathcal{R}e(R_{PT})\cos 2\alpha \sin\alpha, \quad C_{\pi\pi} \approx 2\,\mathcal{I}m(R_{PT})\sin\alpha. \tag{12.69}$$

Note that R_{PT} is mode-dependent and, in particular, could be different for $\pi^+\pi^-$ and $\pi^0\pi^0$. If strong phases can be neglected then R_{PT} is real, resulting in $C_{\pi\pi} = 0$. The size of $C_{\pi\pi}$ is an indicator of how large the strong phase is. The present experimental range is [28] $C_{\pi\pi} = -0.51 \pm 0.23$. As concerns $S_{\pi\pi}$, it is clear from Eq. (12.69) that the relative size and strong phase of the penguin contribution must be known to extract α. This is the problem of penguin pollution.

The cleanest solution involves isospin relations among the $B \to \pi\pi$ amplitudes [36]:

$$\frac{1}{\sqrt{2}}A_{\pi^+\pi^-} + A_{\pi^0\pi^0} = A_{\pi^+\pi^0}. \tag{12.70}$$

The method exploits the fact that the penguin contribution to $P^t_{\pi\pi}$ is pure $\Delta I = \frac{1}{2}$ (this is not true for the electroweak penguins which, however, are expected to be small), while the tree contribution to $T_{\pi\pi}$ contains pieces which are both $\Delta I = \frac{1}{2}$ and $\Delta I = \frac{3}{2}$. A simple geometric construction then allows one to find R_{PT} and extract α cleanly from $S_{\pi^+\pi^-}$. The key experimental difficulty is that one must measure accurately the separate rates for $B^0, \overline{B}^0 \to \pi^0\pi^0$. It has been noted that an upper bound on the average rate allows one to put a useful upper bound on the deviation of $S_{\pi^+\pi^-}$ from $\sin 2\alpha$ [37,38,39]. Parametrizing the asymmetry by $S_{\pi^+\pi^-}/\sqrt{1-(C_{\pi^+\pi^-})^2} = \sin(2\alpha + 2\delta_{+-})$, the bound reads

$$\cos 2\delta_{+-} \geq \frac{1}{\sqrt{1-(C_{\pi^+\pi^-})^2}}\left[1 - \frac{2\mathcal{B}_{00}}{\mathcal{B}_{+0}} + \frac{(\mathcal{B}_{+-} - 2\mathcal{B}_{+0} + 2\mathcal{B}_{00})^2}{4\mathcal{B}_{+-}\mathcal{B}_{+0}}\right], \tag{12.71}$$

where $\mathcal{B}_{ij}$ are the averages over CP-conjugate branching ratios; *e.g.*, $\mathcal{B}_{00} = \frac{1}{2}[\mathcal{B}(B^0 \to \pi^0\pi^0) + \mathcal{B}(\overline{B}^0 \to \pi^0\pi^0)]$. CP asymmetries in $B \to \rho\pi$ and, in particular, in $B \to \rho\rho$ can also be used to determine α.

For B_s decays, one has to replace Eq. (12.59) with $e^{-i\phi_{M(B_s)}} = (V^*_{tb}V_{ts})/(V_{tb}V^*_{ts})$. Note that one expects $\Delta\Gamma/\Gamma = \mathcal{O}(0.1)$, and therefore, y should not be put to zero in Eqs. (12.18,12.19), but $|q/p| = 1$ is expected to hold to an even better approximation than for B mesons. The CP asymmetry in $B_s \to J/\psi\phi$ will determine (with angular analysis to disentangle the CP-even and CP-odd components of the final state) $\sin 2\beta_s$, where

$$\beta_s \equiv \arg\left(-\frac{V_{ts}V^*_{tb}}{V_{cs}V^*_{cb}}\right). \tag{12.72}$$

Another class of interesting decay modes is that of the tree level decays of B_s and $\overline{B}_s$ into $D_s^{\pm}K^{\mp}$. The quark sub-processes are $\overline{b} \to \overline{c}u\overline{s}$, $\overline{b} \to \overline{u}c\overline{s}$, and the two CP-conjugate processes. Measuring the four time dependent decay rates, one can cleanly extract the angle γ [40]. (Similarly, γ can be extracted from the time dependent rates of $B \to DK$ decays [41].)

12.7. Summary and Outlook

CP violation has been experimentally established in neutral K and B meson decays:

1. All three types of CP violation have been observed in $K \to \pi\pi$ decays:

$$\begin{aligned}
\mathcal{R}e(\epsilon') &= \frac{1}{6}\left(\left|\frac{\overline{A}_{\pi^0\pi^0}}{A_{\pi^0\pi^0}}\right| - \left|\frac{\overline{A}_{\pi^+\pi^-}}{A_{\pi^+\pi^-}}\right|\right) = (2.5 \pm 0.4) \times 10^{-6} \quad \text{(I)} \\
\mathcal{R}e(\epsilon) &= \frac{1}{2}\left(1 - \left|\frac{q}{p}\right|\right) = (1.657 \pm 0.021) \times 10^{-3} \quad \text{(II)} \\
\mathcal{I}m(\epsilon) &= -\frac{1}{2}\mathcal{I}m(\lambda_{(\pi\pi)_{I=0}}) = (1.572 \pm 0.022) \times 10^{-3} \quad \text{(III)}
\end{aligned} \tag{12.73}$$

2. CP violation in interference of decays with and without mixing has been observed in $B \to J/\psi K_S$ decays [28] (and related modes):

$$S_{\psi K} = \mathcal{I}m(\lambda_{\psi K}) = 0.731 \pm 0.056 \quad \text{(III)} \tag{12.74}$$

Searches for additional types of CP violation are ongoing in B, D, and K decays, and current limits are consistent with Standard Model expectations.

Based on Standard Model predictions, observation of direct CP violation in B decays seems promising for the near future, followed later by CP violation observed in B_s decays and in the process $K \to \pi\nu\overline{\nu}$. Observables that are subject to clean theoretical interpretation, such as $S_{\psi K_S}$ and $\mathcal{B}(K_L \to \pi^0\nu\overline{\nu})$, are of particular value for constraining the values of the CKM parameters and probing the flavor sector of extensions to the Standard Model. Other probes of CP violation now being pursued experimentally include the electric dipole moments of the neutron and electron, and the decays of tau leptons. Additional processes that are likely to play an important role in future CP studies include top-quark production and decay, and neutrino oscillations.

All measurements of CP violation to date are consistent with the predictions of the Kobayashi-Maskawa mechanism of the Standard Model. However, a dynamically-generated matter-antimatter asymmetry of the universe requires additional sources of CP violation, and such sources are naturally generated by extensions to the Standard Model. New sources might eventually reveal themselves as small deviations from the predictions of the KM mechanism in meson decay rates, or else might not be observable in meson decays at all, but observable with future probes such as neutrino oscillations or electric dipole moments. We cannot guarantee that new sources of CP violation will ever be found experimentally, but the fundamental nature of CP violation demands a vigorous effort.

A number of excellent reviews of CP violation are available [42–45], where the interested reader may find a detailed discussion of the various topics that are briefly reviewed here. Another book on CP violation that will shortly appear is Ref. 46.

References:

1. J.H. Christenson *et al.*, Phys. Rev. Lett. **13**, 138 (1964).
2. B. Aubert *et al.* [BABAR Collaboration], Phys. Rev. Lett. **87**, 091801 (2001).
3. K. Abe *et al.* [Belle Collaboration], Phys. Rev. Lett. **87**, 091802 (2001).
4. See results on the 'Time reversal invariance' within the review on 'Tests of conservation laws' in this report.

5. M. Kobayashi and T. Maskawa, Prog. Theor. Phys. **49**, 652 (1973).
6. A.D. Sakharov, Pisma Zh. Eksp. Teor. Fiz. **5**, 32 (1967) [Sov. Phys. JETP Lett. **5**, 24 (1967)].
7. For a review, see *e.g.* A. Riotto, "Theories of baryogenesis," `arXiv:hep-ph/9807454`.
8. M. Fukugita and T. Yanagida, Phys. Lett. **B174**, 45 (1986).
9. V. Weisskopf and E. P. Wigner, Z. Phys. **63**, 54 (1930); Z. Phys. **65**, 18 (1930). [See also Appendix A of P.K. Kabir, "The CP Puzzle: Strange Decays of the Neutral Kaon," Academic Press (1968)].
10. O. Long *et al.*, Phys. Rev. **D68**, 034010 (2003).
11. L. Wolfenstein, Phys. Rev. Lett. **13**, 562 (1964).
12. See the review on 'Cabibbo-Kobayashi-Maskawa mixing matrix' in this report.
13. L. Wolfenstein, Phys. Rev. Lett. **51**, 1945 (1983).
14. A.J. Buras, M.E. Lautenbacher, and G. Ostermaier, Phys. Rev. **D50**, 3433 (1994).
15. C. Jarlskog, Phys. Rev. Lett. **55**, 1039 (1985).
16. H. Burkhardt *et al.* [NA31 Collaboration], Phys. Lett. **B206**, 169 (1988).
17. V. Fanti *et al.* [NA48 Collaboration], Phys. Lett. **B465**, 335 (1999).
18. A. Alavi-Harati *et al.* [KTeV Collaboration], Phys. Rev. Lett. **83**, 22 (1999).
19. See the K-meson listings in this report.
20. See the review on 'CP violation in $K_S \to 3\pi$' in this report.
21. Y. Grossman and Y. Nir, Phys. Lett. **B398**, 163 (1997).
22. L.S. Littenberg, Phys. Rev. **D39**, 3322 (1989).
23. A.J. Buras, Phys. Lett. **B333**, 476 (1994).
24. G. Buchalla and A.J. Buras, Nucl. Phys. **B400**, 225 (1993).
25. See the review on '$D^0 - \overline{D}^0$ mixing' in this report.
26. See the D-meson listings in this report.
27. S. Bergmann *et al.*, Phys. Lett. **B486**, 418 (2000).
28. See the B-meson listings in this report.
29. A.B. Carter and A.I. Sanda, Phys. Rev. Lett. **45**, 952 (1980); Phys. Rev. **D23**, 1567 (1981).
30. I.I. Bigi and A.I. Sanda, Nucl. Phys. **B193**, 85 (1981).
31. I. Dunietz and J.L. Rosner, Phys. Rev. **D34**, 1404 (1986).
32. Ya.I. Azimov, N.G. Uraltsev, and V.A. Khoze, Sov. J. Nucl. Phys. **45**, 878 (1987) [Yad. Fiz. **45**, 1412 (1987)].
33. I.I. Bigi and A.I. Sanda, Nucl. Phys. **B281**, 41 (1987).
34. G. Buchalla, A.J. Buras, and M.E. Lautenbacher, Rev. Mod. Phys. **68**, 1125 (1996).
35. Y. Grossman, A.L. Kagan and Z. Ligeti, Phys. Lett. **B538**, 327 (2002).
36. M. Gronau and D. London, Phys. Rev. Lett. **65**, 3381 (1990).
37. Y. Grossman and H.R. Quinn, Phys. Rev. **D58**, 017504 (1998).
38. J. Charles, Phys. Rev. **D59**, 054007 (1999).
39. M. Gronau *et al.*, Phys. Lett. **B514**, 315 (2001).
40. R. Aleksan, I. Dunietz and B. Kayser, Z. Phys. **C54**, 653 (1992).
41. M. Gronau and D. Wyler, Phys. Lett. **B265**, 172 (1991).
42. G.C. Branco, L. Lavoura, and J.P. Silva, "CP violation," Oxford University Press, Oxford (1999).
43. I.I. Y. Bigi and A.I. Sanda, "CP Violation," Cambridge Monogr. Part. Phys. Nucl. Phys. Cosmol. **9**, 1 (2000).
44. P.F. Harrison and H.R. Quinn, editors [BABAR Collaboration], "The BABAR physics book: Physics at an asymmetric B factory," SLAC-R-0504.
45. K. Anikeev *et al.*, "B physics at the Tevatron: Run II and beyond," `arXiv:hep-ph/0201071`.
46. K. Kleinknecht, "Uncovering CP Violation," Springer tracts in modern physics **195** (2003).

13. NEUTRINO MASS, MIXING, AND FLAVOR CHANGE

Revised November 2003 by B. Kayser (Fermilab).

There is now convincing evidence that both atmospheric and solar neutrinos change from one flavor to another. There is also very strong evidence that reactor anti-neutrinos do this, and interesting evidence that accelerator neutrinos do it as well. Barring exotic possibilities, neutrino flavor change implies that neutrinos have masses and that leptons mix. In this review, we discuss the physics of flavor change and the evidence for it, summarize what has been learned so far about neutrino masses and leptonic mixing, consider the relation between neutrinos and their antiparticles, and discuss the open questions about neutrinos to be answered by future experiments.

I. The physics of flavor change: If neutrinos have masses, then there is a spectrum of three or more neutrino mass eigenstates, ν_1, ν_2, ν_3, ..., that are the analogues of the charged-lepton mass eigenstates, e, μ, and τ. If leptons mix, the weak interaction coupling the W boson to a charged lepton, and a neutrino can couple any charged-lepton mass eigenstate ℓ_α to any neutrino mass eigenstate ν_i. Here, $\alpha = e, \mu$, or τ, and ℓ_e is the electron, *etc.*. Leptonic W^+ decay can yield a particular ℓ_α^+ in association with any ν_i. The amplitude for this decay to produce the specific combination $\ell_\alpha^+ + \nu_i$ is $U_{\alpha i}^*$, where U is the unitary leptonic mixing matrix [1]. Thus, the neutrino state created in the decay $W^+ \to \ell_\alpha^+ + \nu$ is the state

$$|\nu_\alpha\rangle = \sum_i U_{\alpha i}^* |\nu_i\rangle \ . \tag{13.1}$$

This superposition of neutrino mass eigenstates, produced in association with the charged lepton of "flavor" α, is the state we refer to as the neutrino of flavor α.

While there are only three (known) charged lepton mass eigenstates, the experimental results suggest that perhaps there are more than three neutrino mass eigenstates. If, for example, there are four ν_i, then one linear combination of them,

$$|\nu_s\rangle = \sum_i U_{si}^* |\nu_i\rangle \ , \tag{13.2}$$

does not have a charged-lepton partner, and consequently does not couple to the Standard Model W boson. Indeed, since the decays $Z \to \nu_\alpha \overline{\nu}_\alpha$ of the Standard Model Z boson have been found to yield only three distinct neutrinos ν_α of definite flavor [2], ν_s does not couple to the Z boson either. Such a neutrino, which does not have any Standard Model weak couplings, is referred to as a "sterile" neutrino.

To understand neutrino flavor change, or "oscillation," in vacuum, let us consider how a neutrino born as the ν_α of Eq. (13.1) evolves in time. First, we apply Schrödinger's equation to the ν_i component of ν_α in the rest frame of that component. This tells us that

$$|\nu_i(\tau_i)\rangle = e^{-im_i\tau_i} |\nu_i(0)\rangle \ , \tag{13.3}$$

where m_i is the mass of ν_i, and τ_i is time in the ν_i frame. In terms of the time t and position L in the laboratory frame, the Lorentz-invariant phase factor in Eq. (13.3) may be written

$$e^{-im_i\tau_i} = e^{-i(E_i t - p_i L)} \ . \tag{13.4}$$

Here, E_i and p_i are respectively the energy and momentum of ν_i in the laboratory frame. In practice, our neutrino will be extremely relativistic, so we will be interested in evaluating the phase factor of Eq. (13.4) with $t \approx L$, where it becomes $\exp[-i(E_i - p_i)L]$.

Imagine now that our ν_α has been produced with a definite momentum p, so that all of its mass-eigenstate components have this common momentum. Then the ν_i component has $E_i = \sqrt{p^2 + m_i^2} \approx p + m_i^2/2p$, assuming that all neutrino masses m_i are small compared to the neutrino momentum. The phase factor of Eq. (13.4) is then approximately

$$e^{-i(m_i^2/2p)L} \ . \tag{13.5}$$

From this expression and Eq. (13.1), it follows that after a neutrino born as a ν_α has propagated a distance L, its state vector has become

$$|\nu_\alpha(L)\rangle \approx \sum_i U_{\alpha i}^* e^{-i(m_i^2/2E)L} |\nu_i\rangle \ . \tag{13.6}$$

Here, $E \simeq p$ is the average energy of the various mass eigenstate components of the neutrino. Using the unitarity of U to invert Eq. (13.1), and inserting the result in Eq. (13.6), we find that

$$|\nu_\alpha(L)\rangle \approx \sum_\beta \left[\sum_i U_{\alpha i}^* e^{-i(m_i^2/2E)L} U_{\beta i} \right] |\nu_\beta\rangle \ . \tag{13.7}$$

We see that our ν_α, in traveling the distance L, has turned into a superposition of all the flavors. The probability that it has flavor β, $P(\nu_\alpha \to \nu_\beta)$, is obviously $|\langle \nu_\beta | \nu_\alpha(L)\rangle|^2$. From Eq. (13.7) and the unitarity of U, we easily find that

$$\begin{aligned} P(\nu_\alpha \to \nu_\beta) = {} & \delta_{\alpha\beta} \\ & -4 \sum_{i>j} \Re(U_{\alpha i}^* U_{\beta i} U_{\alpha j} U_{\beta j}^*) \sin^2[1.27\, \Delta m_{ij}^2 (L/E)] \\ & +2 \sum_{i>j} \Im(U_{\alpha i}^* U_{\beta i} U_{\alpha j} U_{\beta j}^*) \sin[2.54\, \Delta m_{ij}^2 (L/E)] \ . \end{aligned} \tag{13.8}$$

Here, $\Delta m_{ij}^2 \equiv m_i^2 - m_j^2$ is in eV^2, L is in km, and E is in GeV. We have used the fact that when the previously omitted factors of $\hbar$ and c are included,

$$\Delta m_{ij}^2 (L/4E) \simeq 1.27\, \Delta m_{ij}^2 (\mathrm{eV}^2) \frac{L(\mathrm{km})}{E(\mathrm{GeV})} \ . \tag{13.9}$$

The quantum mechanics of neutrino oscillation leading to the result Eq. (13.8) is somewhat subtle. To do justice to the physics requires a more refined treatment [3] than the one we have given. Sophisticated treatments continue to yield new insights [4].

Assuming that CPT invariance holds,

$$P(\overline{\nu}_\alpha \to \overline{\nu}_\beta) = P(\nu_\beta \to \nu_\alpha) \ . \tag{13.10}$$

But, from Eq. (13.8) we see that

$$P(\nu_\beta \to \nu_\alpha; U) = P(\nu_\alpha \to \nu_\beta; U^*) \ . \tag{13.11}$$

Thus, when CPT holds,

$$P(\overline{\nu}_\alpha \to \overline{\nu}_\beta; U) = P(\nu_\alpha \to \nu_\beta; U^*) \ . \tag{13.12}$$

That is, the probability for oscillation of an anti-neutrino is the same as that for a neutrino, except that the mixing matrix U is replaced by its complex conjugate. Thus, if U is not real, the neutrino and anti-neutrino oscillation probabilities can differ by having opposite values of the last term in Eq. (13.8). When CPT holds, any difference between these probabilities indicates a violation of CP invariance.

As we shall see, the squared-mass splittings Δm_{ij}^2 called for by the various reported signals of oscillation are quite different from one another. It may be that one splitting, ΔM^2, is much bigger than all the others. If that is the case, then for an oscillation experiment with L/E such that $\Delta M^2 L/E = \mathcal{O}(1)$, Eq. (13.8) simplifies considerably, becoming

$$P(\overline{\nu}_\alpha \to (\overline{\nu}_\beta) \simeq S_{\alpha\beta} \sin^2[1.27\, \Delta M^2 (L/E)] \tag{13.13}$$

for $\beta \neq \alpha$, and

$$P(\overline{\nu}_\alpha \to (\overline{\nu}_\alpha) \simeq 1 - 4\, T_\alpha (1 - T_\alpha) \sin^2[1.27\, \Delta M^2 (L/E)] \ . \tag{13.14}$$

Here,

$$S_{\alpha\beta} \equiv 4 \left| \sum_{i \ \mathrm{Up}} U_{\alpha i}^* U_{\beta i} \right|^2 \tag{13.15}$$

and

$$T_\alpha \equiv \sum_{i\ \mathrm{Up}} |U_{\alpha i}|^2 \ , \tag{13.16}$$

where "i Up" denotes a sum over only those neutrino mass eigenstates that lie *above* ΔM^2 or, alternatively, only those that lie *below* it. The unitarity of U guarantees that summing over either of these two clusters will yield the same results for $S_{\alpha\beta}$ and for $T_\alpha(1-T_\alpha)$.

The situation described by Eqs. (13.13)–(13.16) may be called "quasi-two-neutrino oscillation." It has also been called "one mass scale dominance" [5]. It corresponds to an experiment whose L/E is such that the experiment can "see" only the big splitting ΔM^2. To this experiment, all the neutrinos above ΔM^2 appear to be a single neutrino, as do all those below ΔM^2.

The relations of Eqs. (13.13)–(13.16) also apply to the special case where, to a good approximation, only two mass eigenstates, and two corresponding flavor eigenstates (or two linear combinations of flavor eigenstates), are relevant. One encounters this case when, for example, only two mass eigenstates couple significantly to the charged lepton with which the neutrino being studied is produced. When only two mass eigenstates count, there is only a single splitting, Δm^2, and, omitting irrelevant phase factors, the unitary mixing matrix U takes the form

$$U = \begin{array}{c} \\ \nu_\alpha \\ \nu_\beta \end{array} \begin{array}{c} \begin{array}{cc} \nu_1 & \nu_2 \end{array} \\ \begin{bmatrix} \cos\theta & \sin\theta \\ -\sin\theta & \cos\theta \end{bmatrix} \end{array} \ . \tag{13.17}$$

Here, the symbols above and to the left of the matrix label the columns and rows, and θ is referred to as the mixing angle. From Eqs. (13.15) and (13.16), we now have $S_{\alpha\beta} = \sin^2 2\theta$ and $4\,T_\alpha(1-T_\alpha) = \sin^2 2\theta$, so that Eqs. (13.13) and (13.14) become, respectively,

$$P(\overset{(-)}{\nu}_\alpha \to \overset{(-)}{\nu}_\beta) = \sin^2 2\theta\ \sin^2[1.27\,\Delta m^2(L/E)] \tag{13.18}$$

with $\beta \neq \alpha$, and

$$P(\overset{(-)}{\nu}_\alpha \to \overset{(-)}{\nu}_\alpha) = 1 - \sin^2 2\theta\ \sin^2[1.27\,\Delta m^2(L/E)] \ . \tag{13.19}$$

Many experiments have been analyzed using these two expressions. Some of these experiments actually have been concerned with quasi-two-neutrino oscillation, rather than a genuinely two-neutrino situation. For these experiments, "$\sin^2 2\theta$" and "Δm^2" have the significance that follows from Eqs. (13.13)–(13.16).

When neutrinos travel through matter (*e.g.*in the Sun, Earth, or a supernova), their coherent forward scattering from particles they encounter along the way can significantly modify their propagation [6]. As a result, the probability for changing flavor can be rather different than it is in vacuum [7]. Flavor change that occurs in matter, and that grows out of the interplay between flavor-nonchanging neutrino-matter interactions and neutrino mass and mixing, is known as the Mikheyev-Smirnov-Wolfenstein (MSW) effect.

To a good approximation, one can describe neutrino propagation through matter via a Schrödinger-like equation. This equation governs the evolution of a neutrino state vector with several components, one for each flavor. The effective Hamiltonian in the equation, a matrix $\mathcal{H}$ in neutrino flavor space, differs from its vacuum counterpart by the addition of interaction energies arising from the coherent forward neutrino scattering. For example, the ν_e–ν_e element of $\mathcal{H}$ includes the interaction energy

$$V = \sqrt{2}\,G_F N_e \ , \tag{13.20}$$

arising from W-exchange-induced ν_e forward scattering from ambient electrons. Here, G_F is the Fermi constant, and N_e is the number of electrons per unit volume. In addition, the ν_e–ν_e, ν_μ–ν_μ, and ν_τ–ν_τ elements of $\mathcal{H}$ all contain a common interaction energy growing out of Z-exchange-induced forward scattering. However, when one is not considering the possibility of transitions to sterile neutrino flavors, this common interaction energy merely adds to $\mathcal{H}$ a multiple of the identity matrix, and such an addition has no effect on flavor transitions.

The effect of matter is illustrated by the propagation of solar neutrinos through solar matter. When combined with information on atmospheric neutrino oscillation, the experimental bounds on short-distance ($L \lesssim 1$ km) oscillation of reactor $\overline{\nu}_e$ [8] tell us that, if there are no sterile neutrinos, then only two neutrino mass eigenstates, ν_1 and ν_2, are significantly involved in the evolution of the solar neutrinos. Correspondingly, only two flavors are involved: the ν_e flavor with which every solar neutrino is born, and the effective flavor ν_x — some linear combination of ν_μ and ν_τ — which it may become. The Hamiltonian $\mathcal{H}$ is then a 2×2 matrix in ν_e–ν_x space. Apart from an irrelevant multiple of the identity, for a distance r from the center of the Sun, $\mathcal{H}$ is given by

$$\begin{aligned} \mathcal{H} &= \mathcal{H}_V + \mathcal{H}_M(r) \\ &= \frac{\Delta m^2_\odot}{4E} \begin{bmatrix} -\cos 2\theta_\odot & \sin 2\theta_\odot \\ \sin 2\theta_\odot & \cos 2\theta_\odot \end{bmatrix} + \begin{bmatrix} V(r) & 0 \\ 0 & 0 \end{bmatrix} \ . \end{aligned} \tag{13.21}$$

Here, the first matrix $\mathcal{H}_V$ is the Hamiltonian in vacuum, and the second matrix $\mathcal{H}_M(r)$ is the modification due to matter. In $\mathcal{H}_V$, $\theta_\odot$ is the solar mixing angle defined by the two-neutrino mixing matrix of Eq. (13.17) with $\theta = \theta_\odot$, $\nu_\alpha = \nu_e$, and $\nu_\beta = \nu_x$. The splitting $\Delta m^2_\odot$ is $m_2^2 - m_1^2$, and for the present purpose we *define* ν_2 to be the heavier of the two mass eigenstates, so that $\Delta m^2_\odot$ is positive. In $\mathcal{H}_M(r)$, $V(r)$ is the interaction energy of Eq. (13.20) with the electron density $N_e(r)$ evaluated at distance r from the Sun's center.

From Eqs. (13.18–13.19) (with $\theta = \theta_\odot$), we see that two-neutrino oscillation in vacuum cannot distinguish between a mixing angle $\theta_\odot$ and an angle $\theta'_\odot = \pi/2 - \theta_\odot$. But these two mixing angles represent physically different situations. Suppose, for example, that $\theta_\odot < \pi/4$. Then, from Eq. (13.17) we see that if the mixing angle is $\theta_\odot$, the lighter mass eigenstate (defined to be ν_1) is more ν_e than ν_x, while if it is $\theta'_\odot$, then this mass eigenstate is more ν_x than ν_e. While oscillation in vacuum cannot discriminate between these two possibilities, neutrino propagation through solar matter can do so. The neutrino interaction energy V of Eq. (13.20) is of definite, positive sign [9]. Thus, the ν_e–ν_e element of the solar $\mathcal{H}$, $-(\Delta m^2_\odot/4E)\cos 2\theta_\odot + V(r)$, has a different size when the mixing angle is $\theta'_\odot = \pi/2 - \theta_\odot$ than it does when this angle is $\theta_\odot$. As a result, the flavor content of the neutrinos coming from the Sun can be different in the two cases [10].

Solar and long-baseline reactor neutrino data establish that the behavior of solar neutrinos is governed by a Large-Mixing-Angle (LMA) MSW effect (see Sec. II). Let us estimate the probability $P(\nu_e \to \nu_e)$ that a solar neutrino which undergoes the LMA-MSW effect in the Sun still has its original ν_e flavor when it arrives at the Earth. We focus on the neutrinos produced by ^{8}B decay, which are at the high-energy end of the solar neutrino spectrum. At $r \simeq 0$, where the solar neutrinos are created, the electron density $N_e \simeq 6\times 10^{25}/\mathrm{cm}^3$ [11] yields for the interaction energy V of Eq. (13.20) the value 0.75×10^{-5} eV^2/MeV. Thus, for $\Delta m^2_\odot$ in the favored region, around 7×10^{-5} eV^2, and E a typical ^{8}B neutrino energy ($\sim$6-7 MeV), $\mathcal{H}_M$ dominates over $\mathcal{H}_V$. This means that, in first approximation, $\mathcal{H}(r \simeq 0)$ is diagonal. Thus, a ^{8}B neutrino is born not only in a ν_e flavor eigenstate, but also, again in first approximation, in an eigenstate of the Hamiltonian $\mathcal{H}(r \simeq 0)$. Since $V > 0$, the neutrino will be in the heavier of the two eigenstates. Now, under the conditions where the LMA-MSW effect occurs, the propagation of a neutrino from $r \simeq 0$ to the outer edge of the Sun is adiabatic. That is, $N_e(r)$ changes sufficiently slowly that we may solve Schrödinger's equation for one r at a time, and then patch together the solutions. This means that our neutrino propagates outward through the Sun as one of the r-dependent eigenstates of the r-dependent $\mathcal{H}(r)$. Since the eigenvalues of $\mathcal{H}(r)$ do not cross at any r, and our neutrino is born in the heavier of the two $r = 0$ eigenstates, it emerges from the Sun in the heavier of the two $\mathcal{H}_V$ eigenstates. The latter is the mass eigenstate we have called ν_2, given according to Eq. (13.17) by

$$\nu_2 = \nu_e \sin\theta_\odot + \nu_x \cos\theta_\odot \ . \tag{13.22}$$

Since this is an eigenstate of the vacuum Hamiltonian, the neutrino remains in it all the way to the surface of the Earth. The probability of observing the neutrino as a ν_e on Earth is then just the probability that ν_2 is a ν_e. That is [cf. Eq. (13.22)] [12],

$$P(\nu_e \to \nu_e) = \sin^2\theta_\odot \ . \tag{13.23}$$

We note that for $\theta_\odot < \pi/4$, this ν_e survival probability is less than 1/2. In constrast, when matter effects are negligible, the energy-averaged survival probability in two-neutrino oscillation cannot be less than 1/2 for any mixing angle [see Eq. (13.19)] [13].

II. The evidence for flavor metamorphosis: The persuasiveness of the evidence that neutrinos actually do change flavor in nature is summarized in Table 13.1. We discuss the different pieces of evidence.

Table 13.1: The persuasiveness of the evidence for neutrino flavor change. The symbol L denotes the distance travelled by the neutrinos. LSND is the Liquid Scintillator Neutrino Detector experiment.

Neutrinos	Evidence for Flavor Change
Atmospheric	Compelling
Accelerator ($L = 250\,\mathrm{km}$)	Interesting
Solar	Compelling
Reactor ($L \sim 180\,\mathrm{km}$)	Very Strong
From Stopped μ^+ Decay (LSND)	Unconfirmed

The atmospheric neutrinos are produced in the Earth's atmosphere by cosmic rays, and then detected in an underground detector. The flux of cosmic rays that lead to neutrinos with energies above a few GeV is isotropic, so that these neutrinos are produced at the same rate all around the Earth. This can easily be shown to imply that at any underground site, the downward- and upward-going fluxes of multi-GeV neutrinos of a given flavor must be equal. That is, unless some mechanism changes the flux of neutrinos of the given flavor as they propagate, the flux coming down from zenith angle θ_Z must equal that coming up from angle $\pi - \theta_Z$ [14].

The underground Super-Kamiokande (SK) detector finds that for multi-GeV atmospheric muon neutrinos [15],

$$\frac{\text{Flux Up}(-1.0 < \cos\theta_Z < -0.2)}{\text{Flux Down}(+0.2 < \cos\theta_Z < +1.0)} = 0.54 \pm 0.04 \ , \qquad (13.24)$$

in strong disagreement with equality of the upward and downward fluxes. Thus, some mechanism does change the ν_μ flux as the neutrinos travel to the detector. The most attractive candidate for this mechanism is the oscillation $\nu_\mu \to \nu_X$ of the muon neutrinos into neutrinos ν_X of another flavor. Since the upward-going muon neutrinos come from the atmosphere on the opposite side of the Earth from the detector, they travel much farther than the downward-going ones to reach the detector. Thus, they have more time to oscillate away into the other flavor, which explains why Flux Up < Flux Down. The null results of short-baseline reactor neutrino experiments [8] imply limits on $P(\overline{\nu}_e \to \overline{\nu}_\mu)$, which, assuming CPT invariance, are also limits on $P(\nu_\mu \to \nu_e)$. From the latter, we know that ν_X is not a ν_e, except possibly a small fraction of the time. Thus, ν_X is a ν_τ, a sterile neutrino ν_s, or sometimes one and sometimes the other. All of the voluminous, detailed SK atmospheric neutrino data are very well described by the hypothesis that the oscillation is purely $\nu_\mu \to \nu_\tau$, and that it is a quasi-two-neutrino oscillation with a splitting $\Delta m^2_{\mathrm{atm}}$ and a mixing angle θ_{atm} that, at 90% CL, are in the ranges [16]

$$1.3 \times 10^{-3}\,\mathrm{eV}^2 \lesssim \Delta m^2_{\mathrm{atm}} \lesssim 3.0 \times 10^{-3}\,\mathrm{eV}^2 \ , \qquad (13.25)$$

and

$$\sin^2 2\theta_{\mathrm{atm}} > 0.9 \ . \qquad (13.26)$$

Other experiments favor roughly similar regions of parameter space [17,18]. We note that the constraint (13.25) implies that at least one mass eigenstate ν_i has a mass exceeding 36 meV. From several pieces of evidence, the 90% CL upper limit on the fraction of ν_X that is sterile is 19% [19].

The oscillation interpretation of the atmospheric neutrino data has received support from the KEK to Kamioka (K2K) long-baseline experiment. This experiment produces a ν_μ beam using an accelerator, measures the beam intensity with a complex of near detectors, and then measures the ν_μ flux still in the beam 250 km away using the SK detector. The L/E of this experiment is such that one expects to see an oscillation dominated by the atmospheric squared-mass splitting $\Delta m^2_{\mathrm{atm}}$. K2K has reported on two data samples. In the first, 80 ν_μ events would be expected in SK if there were no oscillation, but only 56 events are seen [20]. These data are well described by the same oscillation hypothesis that describes the atmospheric neutrino data, with the same parameters [16]. In the second, newer data sample, 26 events would be expected in the absence of oscillation, but only 16 events are seen [16]. This degree of ν_μ disappearance is quite consistent with that observed in the earlier data.

The neutrinos created in the Sun have been detected on Earth by several experiments, as discussed by K. Nakamura in this *Review*. The nuclear processes that power the Sun make only ν_e, not ν_μ or ν_τ. For years, solar neutrino experiments had been finding that the solar ν_e flux arriving at the Earth is below the one expected from neutrino production calculations. Now, thanks especially to the Sudbury Neutrino Observatory (SNO), we have compelling evidence that the missing ν_e have simply changed into neutrinos of other flavors.

SNO has studied the flux of high-energy solar neutrinos from ^{8}B decay. This experiment detects these neutrinos via the reactions

$$\nu + d \to e^- + p + p \ , \qquad (13.27)$$

$$\nu + d \to \nu + p + n \ , \qquad (13.28)$$

and

$$\nu + e^- \to \nu + e^- \ . \qquad (13.29)$$

The first of these reactions, charged-current deuteron breakup, can be initiated only by a ν_e. Thus, it measures the flux $\phi(\nu_e)$ of ν_e from ^{8}B decay in the Sun. The second reaction, neutral-current deuteron breakup, can be initiated with equal cross sections by neutrinos of all active flavors. Thus, it measures $\phi(\nu_e) + \phi(\nu_{\mu,\tau})$, where $\phi(\nu_{\mu,\tau})$ is the flux of ν_μ and/or ν_τ from the Sun. Finally, the third reaction, neutrino electron elastic scattering, can be triggered by a neutrino of any active flavor, but $\sigma(\nu_{\mu,\tau}\, e \to \nu_{\mu,\tau}\, e) \simeq \sigma(\nu_e\, e \to \nu_e\, e)/6.5$. Thus, this reaction measures $\phi(\nu_e) + \phi(\nu_{\mu,\tau})/6.5$.

Recently, SNO has reported the results of measurements made with increased sensitivity to the neutral-current deuteron breakup [21]. From its observed rates for the two deuteron breakup reactions, SNO finds that [21]

$$\frac{\phi(\nu_e)}{\phi(\nu_e) + \phi(\nu_{\mu,\tau})} = 0.306 \pm 0.026\,(\mathrm{stat}) \pm 0.024\,(\mathrm{syst}) \ . \qquad (13.30)$$

Clearly, $\phi(\nu_{\mu,\tau})$ is not zero. This non-vanishing $\nu_{\mu,\tau}$ flux from the Sun is "smoking-gun" evidence that some of the ν_e produced in the solar core do indeed change flavor.

Corroborating information comes from the detection reaction $\nu e^- \to \nu e^-$, studied by both SNO and SK [22].

Change of neutrino flavor, whether in matter or vacuum, does not change the total neutrino flux. Thus, unless some of the solar ν_e are changing into sterile neutrinos, the total active high-energy flux measured by the neutral-current reaction (13.28) should agree with the predicted total ^{8}B solar neutrino flux based on calculations of neutrino production in the Sun. This predicted total is $(5.05\,^{+1.01}_{-0.81}) \times 10^6\ \mathrm{cm}^{-2}\mathrm{s}^{-1}$ [23]. By comparison, the total active flux measured by reaction (13.28) is $[5.21 \pm 0.27\,(\mathrm{stat}) \pm 0.38\,(\mathrm{syst})] \times 10^6\ \mathrm{cm}^{-2}\mathrm{s}^{-1}$, in good agreement. This agreement provides evidence that neutrino production in the Sun is correctly understood, further strengthens the evidence that neutrinos really do change flavor, and strengthens the evidence that the previously-reported deficits of solar ν_e flux are due to this change of flavor.

The strongly favored explanation of solar neutrino flavor change is the LMA-MSW effect. As pointed out after Eq. (13.23), a ν_e survival probability below 1/2, which is indicated by Eq. (13.30), requires that solar matter effects play a significant role [24]. The LMA-MSW interpretation of solar neutrino behavior implies that a substantial fraction of reactor $\overline{\nu}_e$ that travel more than a hundred kilometers should disappear into anti-neutrinos of other flavors. The KamLAND

experiment, which studies reactor $\overline{\nu}_e$ that typically travel ~ 180 km to reach the detector, finds that, indeed, the $\overline{\nu}_e$ flux at the detector is only $0.611 \pm 0.085\,(\mathrm{stat}) \pm 0.041\,(\mathrm{syst})$ of what it would be if no $\overline{\nu}_e$ were vanishing [25]. The KamLAND data establish that the "solar" mixing angle $\theta_\odot$ is indeed large. In addition, KamLAND helps to confirm the LMA-MSW explanation of solar neutrino behavior since both the KamLAND result and all the solar neutrino data [26] can be described by the same neutrino parameters, in the LMA-MSW region. A global fit to both the solar and KamLAND data constrains these parameters, the solar $\Delta m^2_\odot$ and $\theta_\odot$ defined after Eq. (13.21), to lie in the region shown in Fig. 13.1 [27]. That θ_{atm}, Eq. (13.26), and $\theta_\odot$, Fig. 13.1, are both large, in striking contrast to all quark mixing angles, is very interesting [28].

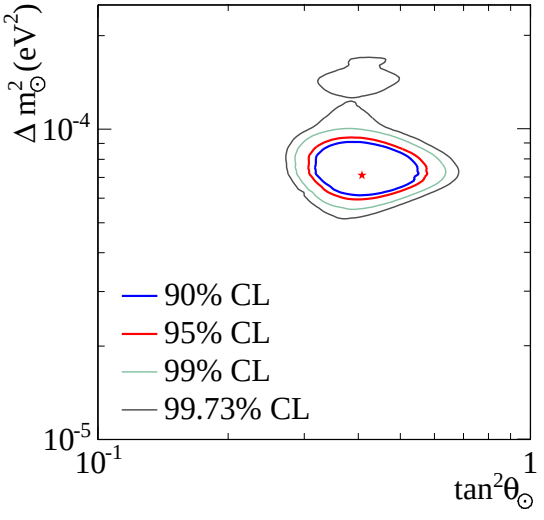

Figure 13.1: The region allowed for the neutrino parameters $\Delta m^2_\odot$ and $\theta_\odot$ by the solar and KamLAND data. The best-fit point, indicated by the star, is $\Delta m^2_\odot = 7.1 \times 10^{-5}\,\mathrm{eV}^2$ and $\theta_\odot = 32.5^\circ$. See full-color version on color pages at end of book.

While the total active solar neutrino flux measured by SNO via neutral-current deuteron breakup is compatible with the theoretically predicted total ^{8}B neutrino production by the Sun, we have seen that the uncertainties in these quantities are not negligible. It remains possible that some of the solar ν_e that change their flavor become sterile. Taking into account both the solar and KamLAND data, but not assuming the total ^{8}B solar neutrino flux to be known from theory, it has been found that, at 90% CL, the sterile fraction of the non-ν_e solar neutrino flux at Earth is less than 36% [29].

The neutrinos studied by the LSND experiment [30] come from the decay $\mu^+ \to e^+ \nu_e \overline{\nu}_\mu$ of muons at rest. While this decay does not produce $\overline{\nu}_e$, an excess of $\overline{\nu}_e$ over expected background is reported by the experiment. This excess is interpreted as due to oscillation of some of the $\overline{\nu}_\mu$ produced by μ^+ decay into $\overline{\nu}_e$. The related KArlsruhe Rutherford Medium Energy Neutrino (KARMEN) experiment [31] sees no indication for such an oscillation. However, the LSND and KARMEN experiments are not identical; at LSND the neutrino travels a distance $L \approx 30$ m before detection, while at KARMEN it travels $L \approx 18$ m. The KARMEN results exclude a portion of the neutrino parameter region favored by LSND, but not all of it. A joint analysis [32] of the results of both experiments finds that a splitting $0.2 \lesssim \Delta m^2_{\mathrm{LSND}} \lesssim 1\,\mathrm{eV}^2$ and mixing $0.003 \lesssim \sin^2 2\theta_{\mathrm{LSND}} \lesssim 0.03$, or a splitting $\Delta m^2_{\mathrm{LSND}} \simeq 7\,\mathrm{eV}^2$ and mixing $\sin^2 2\theta_{\mathrm{LSND}} \simeq 0.004$, might explain both experiments.

The regions of neutrino parameter space favored or excluded by various neutrino oscillation experiments are shown in Fig. 13.2.

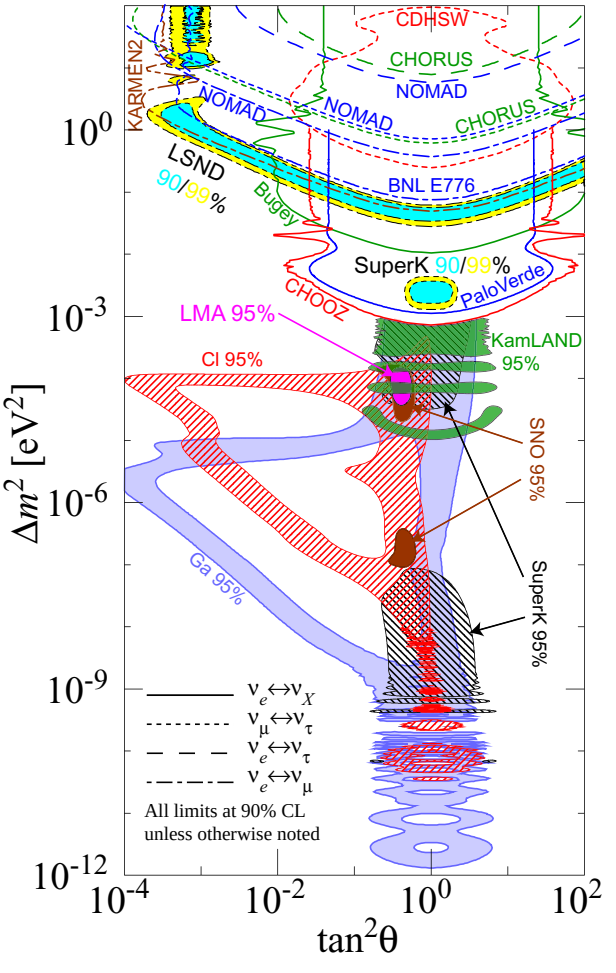

Figure 13.2: The regions of squared-mass splitting and mixing angle favored or excluded by various experiments. This figure was contributed by H. Murayama (University of California, Berkeley). References to the data used in the figure can be found at http://hitoshi.berkeley.edu/neutrino/ref.html. See full-color version on color pages at end of book.

III. Neutrino spectra and mixings: If there are only three neutrino mass eigenstates, ν_1, ν_2 and ν_3, then there are only three mass splittings Δm^2_{ij}, and they obviously satisfy

$$\Delta m^2_{32} + \Delta m^2_{21} + \Delta m^2_{13} = 0 \ . \qquad (13.31)$$

However, as we have seen, the Δm^2 values required to explain the flavor changes of the atmospheric, solar, and LSND neutrinos are of three different orders of magnitude. Thus, they cannot possibly obey the constraint of Eq. (13.31). If all of the reported changes of flavor are genuine, then nature must contain at least four neutrino mass eigenstates [33]. As explained in Sec. I, one linear combination of these mass eigenstates would have to be sterile.

If the LSND oscillation is not confirmed, then nature may well contain only three neutrino mass eigenstates. The neutrino spectrum then contains two mass eigenstates separated by the splitting $\Delta m^2_\odot$ needed to explain the solar and KamLAND data, and a third eigenstate separated from the first two by the larger splitting $\Delta m^2_{\rm atm}$ called for by the atmospheric and K2K data. Current experiments do not tell us whether the solar pair — the two eigenstates separated by $\Delta m^2_\odot$ — is at the bottom or the top of the spectrum. These two possibilities are usually referred to, respectively, as a normal and an inverted spectrum. The study of flavor changes of accelerator-generated neutrinos and anti-neutrinos that pass through matter can discriminate between these two spectra (see Sec. V). If the solar pair is at the bottom, then the spectrum is of the form shown in Fig. 13.3. There we include the approximate flavor content of each mass eigenstate, the flavor-α fraction of eigenstate ν_i being simply $|\langle\nu_\alpha|\nu_i\rangle|^2 = |U_{\alpha i}|^2$. The flavor content shown assumes that the atmospheric mixing angle of Eq. (13.26) is maximal (which gives the best fit to the atmospheric data [16]) and takes into account the now-established LMA-MSW explanation of solar neutrino behavior.

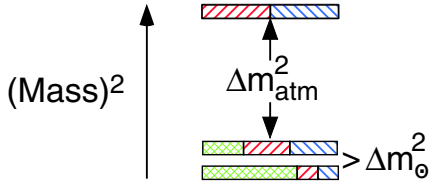

Figure 13.3: A three-neutrino squared-mass spectrum that accounts for the observed flavor changes of solar, reactor, atmospheric, and long-baseline accelerator neutrinos. The ν_e fraction of each mass eigenstate is crosshatched, the ν_μ fraction is indicated by right-leaning hatching, and the ν_τ fraction by left-leaning hatching.

When there are only three neutrino mass eigenstates, and the corresponding three familiar neutrinos of definite flavor, the leptonic mixing matrix U can be written as

$$U = \begin{array}{c} \\ \nu_e \\ \nu_\mu \\ \nu_\tau \end{array} \begin{array}{c} \begin{array}{ccc} \nu_1 & \nu_2 & \nu_3 \end{array} \\ \begin{bmatrix} c_{12}c_{13} & s_{12}c_{13} & s_{13}e^{-i\delta} \\ -s_{12}c_{23} - c_{12}s_{23}s_{13}e^{i\delta} & c_{12}c_{23} - s_{12}s_{23}s_{13}e^{i\delta} & s_{23}c_{13} \\ s_{12}s_{23} - c_{12}c_{23}s_{13}e^{i\delta} & -c_{12}s_{23} - s_{12}c_{23}s_{13}e^{i\delta} & c_{23}c_{13} \end{bmatrix} \end{array} \times \mathrm{diag}(e^{i\alpha_1/2},\ e^{i\,\alpha_2/2},\ 1)\ . \quad (13.32)$$

Here, ν_1 and ν_2 are the members of the solar pair, with $m_2 > m_1$, and ν_3 is the isolated neutrino, which may be heavier or lighter than the solar pair. Inside the matrix, $c_{ij} \equiv \cos\theta_{ij}$ and $s_{ij} \equiv \sin\theta_{ij}$, where the three θ_{ij}'s are mixing angles. The quantities δ, α_1, and α_2 are CP-violating phases. The phases α_1 and α_2, known as Majorana phases, have physical consequences only if neutrinos are Majorana particles, identical to their antiparticles. Then these phases influence neutrinoless double beta decay [see Sec. IV] and other processes [34]. However, as we see from Eq. (13.8), α_1 and α_2 do not affect neutrino oscillation, regardless of whether neutrinos are Majorana particles. Apart from the phases α_1, α_2, which have no quark analogues, the parametrization of the leptonic mixing matrix in Eq. (13.32) is identical to that [35] advocated for the quark mixing matrix by Gilman, Kleinknecht, and Renk in their article in this *Review*.

From bounds on the short-distance oscillation of reactor $\overline{\nu}_e$ [8] and other data, at $3\,\sigma$, $s^2_{13} < 0.067$ [36]. Taking this and the LMA-MSW explanation of solar neutrino behavior into account, and assuming that atmospheric neutrino mixing is maximal, the U of Eq. (13.32) simplifies to

$$U \simeq \begin{array}{c} \\ \nu_e \\ \nu_\mu \\ \nu_\tau \end{array} \begin{array}{c} \begin{array}{ccc} \nu_1 & \nu_2 & \nu_3 \end{array} \\ \begin{bmatrix} c\,e^{i\alpha_1/2} & s\,e^{i\alpha_2/2} & s_{13}\,e^{-i\delta} \\ -s\,e^{i\alpha_1/2}/\sqrt{2} & c\,e^{i\alpha_2/2}/\sqrt{2} & 1/\sqrt{2} \\ s\,e^{i\alpha_1/2}/\sqrt{2} & -c\,e^{i\alpha_2/2}/\sqrt{2} & 1/\sqrt{2} \end{bmatrix} \end{array} . \quad (13.33)$$

Here, $c \equiv \cos\theta_\odot$ and $s \equiv \sin\theta_\odot$, where $\theta_\odot$ is the solar mixing angle defined in Sec. I and constrained by Fig. 13.1. With θ_{13} small, $\theta_\odot \simeq \theta_{12}$. The illustrative flavor content shown in Fig. 13.3 is obtained from the U of Eq. (13.33) taking $s^2_{13} \simeq 0$, $s^2 \simeq 0.3$.

If the LSND oscillation is confirmed, then, as already noted, there must be at least four mass eigenstates. If there are exactly four, then the spectrum is either of the kind depicted in Fig. 13.4a, or of the kind shown in Fig. 13.4b.

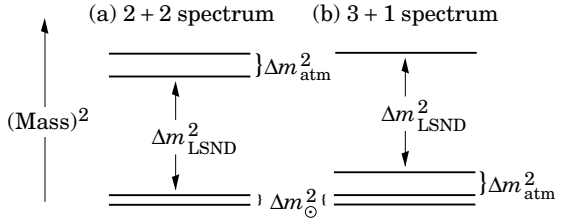

Figure 13.4: Possible four-neutrino squared-mass spectra.

In Fig. 13.4a, we have a "2+2" spectrum. This consists of a "solar pair" of eigenstates that are separated by the solar splitting $\Delta m^2_\odot$ and are the main contributors to the behavior of solar neutrinos, plus an "atmospheric pair" that are separated by the atmospheric splitting $\Delta m^2_{\rm atm}$ and are the main contributors to the atmospheric $\nu_\mu \to \nu_\tau$ oscillation. From the bounds on reactor $\overline{\nu}_e$ short-distance oscillation [8], we know that the ν_e fraction of the atmospheric pair is less than a few percent. From bounds on accelerator ν_μ short-distance oscillation [37], we know that the ν_μ fraction of the solar pair is similarly limited. Thus, the atmospheric (solar) pair of eigenstates plays only a small role in the behavior of the solar ν_e (atmospheric ν_μ). The solar and atmospheric pairs are separated from each other by the large LSND splitting $\Delta m^2_{\rm LSND}$, making possible the LSND oscillation. The solar pair may lie below the atmospheric pair, as shown in Fig. 13.4a, or above it.

In Fig. 13.4b, we have a "3+1" spectrum. This includes a trio, consisting of a solar pair separated by $\Delta m^2_\odot$, plus a third neutrino separated from the solar pair by $\Delta m^2_{\rm atm}$, and a fourth neutrino separated from the trio by $\Delta m^2_{\rm LSND}$. In the trio, the solar pair may lie below the third neutrino, as shown, or above it [38]. In addition, the fourth, isolated neutrino may lie above the other three, as shown, or below them. In the case of a 3+1 spectrum, the reactor $\overline{\nu}_e$ and accelerator ν_μ oscillation bounds mentioned previously imply that the isolated neutrino has very little ν_e or ν_μ flavor content. It is interesting to consider the possibility that it has very little ν_τ content as well, and consequently is largely sterile. Then, by unitarity, the other three neutrinos—the "3"—can have only very little sterile content. Those three neutrinos dominate the solar and atmospheric fluxes, so neither of these fluxes will contain sterile neutrinos to any significant degree. In contrast, it is characteristic of the 2+2 spectra that either the solar or atmospheric neutrino fluxes, or both, do include a substantial component of sterile neutrinos [39–40]. Thus, further information on the sterile neutrino content of these two fluxes can potentially discriminate between the 2+2 and 3+1 spectra.

Neither a 2+2 nor a 3+1 spectrum gives a statistically satisfactory fit to all the data. In particular, in the 3+1 spectra, there is tension between the bounds on short-baseline oscillation and the LSND signal for short-baseline oscillation [41]. However, if there are *at least* four neutrino mass eigenstates, there is no strong reason to believe that there are *exactly* four. The presence of more states may improve the quality of the fit. For example, it has been found that a "3+2"

spectrum fits all the short-baseline data significantly better than a 3+1 spectrum [42].

IV. The neutrino-anti-neutrino relation: Unlike quarks and charged leptons, neutrinos may be their own antiparticles. Whether they are depends on the nature of the physics that gives them mass.

In the Standard Model (SM), neutrinos are assumed to be massless. Now that we know they do have masses, it is straightforward to extend the SM to accommodate these masses in the same way that this model accommodates quark and charged lepton masses. When a neutrino ν is assumed to be massless, the SM does not contain the chirally right-handed neutrino field ν_R, but only the left-handed field ν_L that couples to the W and Z bosons. To accommodate the ν mass in the same manner as quark masses are acccommodated, we add ν_R to the Model. Then we may construct the "Dirac mass term"

$$\mathcal{L}_D = -m_D\,\overline{\nu}_L\,\nu_R + h.c. \quad , \tag{13.34}$$

in which m_D is a constant. This term, which mimics the mass terms of quarks and charged leptons, conserves the lepton number L that distinguishes neutrinos and negatively-charged leptons on the one hand from anti-neutrinos and positively-charged leptons on the other. Since everything else in the SM also conserves L, we then have an L-conserving world. In such a world, each neutrino mass eigenstate ν_i differs from its antiparticle $\overline{\nu}_i$, the difference being that $L(\overline{\nu}_i) = -L(\nu_i)$. When $\overline{\nu}_i \neq \nu_i$, we refer to the $\nu_i - \overline{\nu}_i$ complex as a "Dirac neutrino."

Once ν_R has been added to our description of neutrinos, a "Majorana mass term,"

$$\mathcal{L}_M = -m_R\,\overline{\nu_R^c}\,\nu_R + h.c. \quad , \tag{13.35}$$

can be constructed out of ν_R and its charge conjugate, ν_R^c. In this term, m_R is another constant. Since both ν_R and $\overline{\nu_R^c}$ absorb ν and create $\overline{\nu}$, $\mathcal{L}_M$ mixes ν and $\overline{\nu}$. Thus, a Majorana mass term does not conserve L. There is then no conserved lepton number to distinguish a neutrino mass eigenstate ν_i from its antiparticle. Hence, when Majorana mass terms are present, $\overline{\nu}_i = \nu_i$. That is, for a given helicity h, $\overline{\nu}_i(h) = \nu_i(h)$. We then refer to ν_i as a "Majorana neutrino."

Suppose the right-handed neutrinos required by Dirac mass terms have been added to the SM. If we insist that this extended SM conserve L, then, of course, Majorana mass terms are forbidden. However, if we do not impose L conservation, but require only the general principles of gauge invariance and renormalizability, then Majorana mass terms like that of Eq. (13.35) are expected to be present. As a result, L is violated, and neutrinos are Majorana particles [43].

In the see-saw mechanism [44], which is the most popular explanation of why neutrinos — although massive — are nevertheless so light, both Dirac and Majorana mass terms are present. Hence, the neutrinos are Majorana particles. However, while half of them are the familiar light neutrinos, the other half are extremely heavy Majorana particles referred to as the N_i, with masses possibly as large as the GUT scale. The N_i may have played a crucial role in baryogenesis in the early universe, as we shall discuss in Sec. V.

How can the theoretical expectation that L is violated and neutrinos are Majorana particles be confirmed experimentally? The interactions of neutrinos are well described by the SM, and the SM interactions conserve L. If we may neglect any non-SM L-violating interactions, then the only sources of L violation are the neutrino Majorana mass terms. This means that all L-violating effects disappear in the limit of vanishing neutrino masses. Thus, any experimental approach to confirming the violation of L, and the consequent Majorana character of neutrinos, must be able to see an L violation that is going to be very small because of the smallness of the neutrino masses that drive it. One approach that shows great promise is the search for neutrinoless double beta decay ($0\nu\beta\beta$). This is the process $(A,Z) \to (A,Z+2) + 2e^-$, in which a nucleus containing A nucleons, Z of which are protons, decays to a nucleus containing $Z+2$ protons by emitting two electrons. This process manifestly violates L conservation, so we expect it to be suppressed. However, if (A,Z) is a nucleus that is stable against single β (and α and γ) decay, then it can decay only via the process we are seeking, and the L-conserving two-neutrino process $(A,Z) \to (A,Z+2) + 2e^- + 2\overline{\nu}_e$. The latter decay mode is suppressed by the small phase space associated with the four light particles in the final state, so we have a chance to observe the neutrinoless mode, $(A,Z) \to (A,Z+2) + 2e^-$.

While $0\nu\beta\beta$ can in principle receive contributions from a variety of mechanisms (R-parity-violating supersymmetric couplings, for example), it is easy to show explicitly that the observation of $0\nu\beta\beta$ at any non-vanishing rate would imply that nature contains at least one Majorana neutrino mass term [45]. Now, quarks and charged leptons cannot have Majorana mass terms, because such terms mix fermion and antifermion, and $q \leftrightarrow \overline{q}$ or $\ell \leftrightarrow \overline{\ell}$ would not conserve electric charge. Thus, the discovery of $0\nu\beta\beta$ would demonstrate that the physics of neutrino masses is unlike that of the masses of all other fermions.

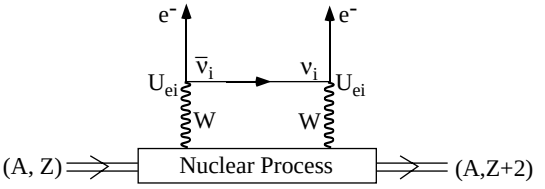

Figure 13.5: The dominant mechanism for $0\nu\beta\beta$. The diagram does not exist unless $\overline{\nu}_i = \nu_i$.

The dominant mechanism for $0\nu\beta\beta$ is expected to be the one depicted in Fig. 13.5. There, a pair of virtual W bosons are emitted by the parent nucleus, and then these W bosons exchange one or another of the light neutrino mass eigenstates ν_i to produce the outgoing electrons. The $0\nu\beta\beta$ amplitude is then a sum over the contributions of the different ν_i. It is assumed that the interactions at the two leptonic W vertices are those of the SM.

Since the exchanged ν_i is created together with an e^-, the left-handed SM current that creates it gives it the helicity we associate, in common parlance, with an "anti-neutrino." That is, the ν_i is almost totally right-handed, but has a small left-handed-helicity component, whose amplitude is of order m_i/E, where E is the ν_i energy. At the vertex where this ν_i is absorbed, the absorbing left-handed SM current can absorb only its small left-handed-helicity component without further suppression. Consequently, the ν_i-exchange contribution to the $0\nu\beta\beta$ amplitude is proportional to m_i. From Fig. 13.5, we see that this contribution is also proportional to U_{ei}^2. Thus, summing over the contributions of all the ν_i, we conclude that the amplitude for $0\nu\beta\beta$ is proportional to the quantity

$$\left| \sum_i m_i\,U_{ei}^2 \right| \equiv |<m_{\beta\beta}>| \quad , \tag{13.36}$$

commonly referred to as the "effective Majorana mass for neutrinoless double beta decay" [46].

That the $0\nu\beta\beta$ amplitude arising from the diagram in Fig. 13.5 is proportional to neutrino mass is no surprise, and illustrates our earlier general discussion. The diagram in Fig. 13.5 is manifestly L-nonconserving. But we are assuming that the interactions in this diagram are L-conserving. Thus, the L-nonconservation in the diagram as a whole must be coming from underlying Majorana neutrino mass terms. Hence, if all the neutrino masses vanish, the L-nonconservation will vanish as well.

To how small an $|<m_{\beta\beta}>|$ should a $0\nu\beta\beta$ search be sensitive? In answering this question, it makes sense to assume there are only three neutrino mass eigenstates — if there are more, $|<m_{\beta\beta}>|$ might be larger. Suppose that there are just three mass eigenstates, and that the solar pair, ν_1 and ν_2, is at the top of the spectrum, so that we

have an inverted spectrum. If the various ν_i are not much heavier than demanded by the observed splittings $\Delta m^2_{\rm atm}$ and $\Delta m^2_\odot$, then in $|<m_{\beta\beta}>|$, Eq. (13.36), the contribution of ν_3 may be neglected, because both m_3 and $|U^2_{e3}| = s^2_{13}$ are small. From Eqs. (13.36) and (13.33), we then have that

$$|<m_{\beta\beta}>| \simeq m_0\sqrt{1-\sin^2 2\theta_\odot \sin^2\left(\frac{\Delta\alpha}{2}\right)} \quad . \tag{13.37}$$

Here, m_0 is the average mass of the members of the solar pair, whose splitting will be invisible in a practical $0\nu\beta\beta$ experiment, and $\Delta\alpha \equiv \alpha_2 - \alpha_1$ is a CP-violating phase. Although $\Delta\alpha$ is completely unknown, we see from Eq. (13.37) that

$$|<m_{\beta\beta}>| \geq m_0 \cos 2\theta_\odot \quad . \tag{13.38}$$

Now, in an inverted spectrum, $m_0 \geq \sqrt{\Delta m^2_{\rm atm}}$. At 90% CL, $\sqrt{\Delta m^2_{\rm atm}} > 36$ meV [16], while $\cos 2\theta_\odot > 0.28$ [21]. Thus, if neutrinos are Majorana particles, and the spectrum is as we have assumed, a $0\nu\beta\beta$ experiment sensitive to $|<m_{\beta\beta}>| \gtrsim 10$ meV would have an excellent chance of observing a signal. If the spectrum is inverted, but the ν_i masses are larger than the $\Delta m^2_{\rm atm}$- and $\Delta m^2_\odot$-demanded minimum values we have assumed above, then once again $|<m_{\beta\beta}>|$ is larger than 10 meV [47], and an experiment sensitive to 10 meV still has an excellent chance of seeing a signal.

If the solar pair is at the bottom of the spectrum, rather than at the top, then $|<m_{\beta\beta}>|$ is not as tightly constrained, and can be anywhere from the present bound of 0.3–1.0 eV down to invisibly small [47,48]. For a discussion of the present bounds, see the article by Vogel and Piepke in this *Review* [49].

V. Questions to be answered: The strong evidence for neutrino flavor metamorphosis — hence neutrino mass — opens many questions about the neutrinos. These questions, which hopefully will be answered by future experiments, include the following:

i) Does neutrino flavor change truly oscillate?

Where matter effects are unimportant, flavor change probabilities are predicted to have an oscillatory $\sin^2[1.27\Delta m^2(L/E)]$ dependence on L/E. This so-far-unobserved characteristic signature of flavor change could in principle be seen in reactor experiments for $\Delta m^2 = \Delta m^2_\odot$, long base-line (LBL) accelerator experiments for $\Delta m^2 = \Delta m^2_{\rm atm}$, and short base-line (SBL) accelerator experiments for $\Delta m^2 = \Delta m^2_{\rm LSND}$.

ii) How many neutrino species are there? Do sterile neutrinos exist?

This question is being addressed by the MiniBooNE experiment [50],whose purpose is to confirm or refute LSND.

iii) What are the masses of the mass eigenstates ν_i?

The sizes of the squared-mass splittings $\Delta m^2_\odot$, $\Delta m^2_{\rm atm}$, and, if present, one or more large splittings $\Delta m^2_{\rm LSND}$, can be determined more precisely than they are currently known through future neutrino oscillation measurements. If there are only three ν_i, then one can find out whether the solar pair, $\nu_{1,2}$, is at the bottom of the spectrum or at its top by exploiting matter effects in LBL neutrino and anti-neutrino oscillations. These matter effects will determine the sign one wishes to learn — that of $\{m^2_3 - [(m^2_2 + m^2_1)/2]\}$ — relative to a sign that is already known — that of the interaction energy of Eq. (13.20).

While flavor-change experiments can determine a spectral pattern such as the one in Fig. 13.3, they cannot tell us the distance of the entire pattern from the zero of squared-mass. One might discover that distance via study of the β energy spectrum in tritium β decay, if the mass of some ν_i with appreciable coupling to an electron is large enough to be within reach of a feasible experiment. One might also gain some information on the distance from zero by measuring $|<m_{\beta\beta}>|$, the effective Majorana mass for neutrinoless double beta decay [47–49] (see Vogel and Piepke in this *Review*). Finally, one might obtain information on this distance from cosmology or astrophysics. Indeed, from relatively recent cosmological data and some cosmological assumptions, it is already concluded that, at 95% CL [51],

$$\sum_i m_i < 0.71\,{\rm eV} \quad . \tag{13.39}$$

Here, the sum runs over the masses of all the light neutrino mass eigenstates ν_i that may exist and that were in thermal equilibrium in the early universe.

If there are just three ν_i, and they are heavy enough to be constrained by the bound of Eq. (13.39), then, given that $\Delta m^2_\odot \ll \Delta m^2_{\rm atm} \ll 1\,{\rm eV}^2$, the ν_i are approximately degenerate. Then Eq. (13.39) requires that the mass of each of them be less than 0.71 eV / 3 = 0.23 eV. Now, the mass of the heaviest ν_i cannot be less than $\sqrt{\Delta m^2_{\rm atm}}$, which in turn is not less than 0.036 eV [see Eq. (13.25)]. Thus, if the cosmological assumptions behind Eq. (13.39) are correct, then

$$0.03\,{\rm eV} < {\rm Mass\,[Heaviest}\ \nu_i] < 0.23\,{\rm eV} \quad . \tag{13.40}$$

iv) Are the neutrino mass eigenstates Majorana particles?

The confirmed observation of neutrinoless double beta decay would establish that the answer is "yes." If there are only three ν_i, knowledge that the spectrum is inverted and a definitive upper bound on $|<m_{\beta\beta}>|$ that is well below 0.01 eV would establish that it is "no" [see discussion after Eq. (13.38)] [47], [48].

v) What are the mixing angles in the leptonic mixing matrix U?

The solar mixing angle $\theta_\odot$ can be determined more precisely through future solar and reactor neutrino measurements.

The atmospheric mixing angle $\theta_{\rm atm}$ is constrained at 90% CL to lie in the region where $\sin^2 2\theta_{\rm atm} > 0.9$ [see Eq. (13.26)], but this region is fairly large: 36° to 54° [52]. The value of $\theta_{\rm atm}$, and in particular, its deviation from maximal mixing, 45°, can be sought in precision LBL ν_μ disappearance experiments.

A knowledge of the small mixing angle θ_{13} is important not only to help complete our picture of leptonic mixing, but also because, as Eq. (13.32) makes clear, all CP-violating effects of the phase δ are proportional to $\sin\theta_{13}$. Thus, a knowledge of the order of magnitude of θ_{13} would help guide the design of experiments to probe CP violation. From Eq. (13.33), we see that $\sin^2\theta_{13}$ is the ν_e fraction of ν_3. The ν_3 is the isolated neutrino that lies at one end of the atmospheric squared-mass gap $\Delta m^2_{\rm atm}$, so an experiment seeking to measure θ_{13} should have an L/E that makes it sensitive to $\Delta m^2_{\rm atm}$, and should involve ν_e. Possibilities include a sensitive search for the disappearance of reactor $\overline{\nu}_e$ while they travel a distance $L \sim 1$ km, and an accelerator neutrino search for $\nu_\mu \to \nu_e$ or $\nu_e \to \nu_\mu$ with a beamline $L >$ several hundred km.

If LSND is confirmed, then the matrix U is at least 4×4, and contains many more than three angles. A rich program, including short baseline experiments with multiple detectors, will be needed to learn about both the squared-mass spectrum and the mixing matrix.

Given the large sizes of $\theta_{\rm atm}$ and $\theta_\odot$, we already know that leptonic mixing is very different from its quark counterpart, where all the mixing angles are small. This difference, and the striking contrast betwen the tiny neutrino masses and the very much larger quark masses, suggest that the physics underlying neutrino masses and mixing may be very different from the physics behind quark masses and mixing.

vi) Does the behavior of neutrinos violate CP?

From Eqs. (13.8), (13.12), and (13.33), we see that if the CP-violating phase δ and the small mixing angle θ_{13} are both non-vanishing, there will be CP-violating differences between neutrino and anti-neutrino oscillation probabilities. Observation of these differences would establish that CP violation is not a peculiarity of quarks.

The CP-violating difference $P(\nu_\alpha \to \nu_\beta) - P(\overline{\nu}_\alpha \to \overline{\nu}_\beta)$ between "neutrino" and " anti-neutrino" oscillation probabilities is independent of whether the mass eigenstates ν_i are Majorana or Dirac particles. To study $\nu_\mu \to \nu_e$ with a super-intense but conventionally-generated neutrino beam, for example, one would create the beam via the process $\pi^+ \to \mu^+\,\nu_i$, and detect it via ν_i + target $\to e^- + \ldots$. To study $\overline{\nu}_\mu \to \overline{\nu}_e$, one would create the beam via $\pi^- \to \mu^-\,\overline{\nu}_i$, and detect it

via $\overline{\nu}_i + \text{target} \to e^+ + \ldots$. Whether $\overline{\nu}_i = \nu_i$ or not, the amplitudes for the latter two processes are proportional to $U_{\mu i}$ and U_{ei}^*, respectively. In contrast, the amplitudes for their $\nu_\mu \to \nu_e$ counterparts are proportional to $U_{\mu i}^*$ and U_{ei}. As this illustrates, Eq. (13.12) relates "neutrino" and "anti-neutrino" oscillation probabilities even when the neutrino mass eigenstates are their own antiparticles.

The baryon asymmetry of the universe could not have developed without some violation of CP during the universe's early history. The one known source of CP violation — the complex phase in the quark mixing matrix — could not have produced sufficiently large effects. Thus, perhaps *leptonic* CP violation is responsible for the baryon asymmetry. The see-saw mechanism predicts very heavy Majorana neutral leptons N_i (see Sec. IV), which would have been produced in the Big Bang. Perhaps CP violation in the leptonic decays of an N_i led to the inequality

$$\Gamma(N_i \to \ell^+ + \ldots) \neq \Gamma(N_i \to \ell^- + \ldots) \ , \qquad (13.41)$$

which would have resulted in unequal numbers of ℓ^+ and ℓ^- in the early universe [53]. This leptogenesis could have been followed by nonperturbative SM processes that would have converted the lepton asymmetry, in part, into the observed baryon asymmetry [54].

While the connection between the CP violation that would have led to leptogenesis, and that which we hope to observe in neutrino oscillation, is model-dependent, it is not likely that we have either of these without the other [55]. This makes the search for CP violation in neutrino oscillation very interesting indeed. Depending on the rough size of θ_{13}, this CP violation may be observable with a very intense conventional neutrino beam, or may require a "neutrino factory," whose neutrinos come from the decay of stored muons. The detailed study of CP violation may require a neutrino factory in any case.

The questions we have discussed, and other questions about the world of neutrinos, will be the focus of a major experimental program in the years to come.

Acknowledgements

I am grateful to Susan Kayser for her crucial role in the production of this manuscript.

References:

1. This matrix is sometimes referred to as the Maki-Nakagawa-Sakata matrix, or as the Pontecorvo-Maki-Nakagawa-Sakata matrix, in recognition of the pioneering contributions of these scientists to the physics of mixing and oscillation. See Z. Maki, M. Nakagawa, and S. Sakata, Prog. Theor. Phys. **28**, 870 (1962);
   B. Pontecorvo, Zh. Eksp. Teor. Fiz. **53**, 1717 (1967) [Sov. Phys. JETP **26**, 984 (1968)].
2. D. Karlen in this *Review*.
3. B. Kayser, Phys. Rev. **D24**, 110 (1981);
   F. Boehm and P. Vogel, *Physics of Massive Neutrinos* (Cambridge University Press, Cambridge, 1987) p. 87;
   C. Giunti, C. Kim, and U. Lee, Phys. Rev. **D44**, 3635 (1991);
   J. Rich, Phys. Rev. **D48**, 4318 (1993);
   H. Lipkin, Phys. Lett. **B348**, 604 (1995);
   W. Grimus and P. Stockinger, Phys. Rev. **D54**, 3414 (1996);
   T. Goldman, `hep-ph/9604357`;
   Y. Grossman and H. Lipkin, Phys. Rev. **D55**, 2760 (1997);
   W. Grimus, S. Mohanty, and P. Stockinger, in *Proc. of the 17th Int. Workshop on Weak Interactions and Neutrinos*, eds. C. Dominguez and R. Viollier (World Scientific, Singapore, 2000) p. 355.
4. L. Stodolsky, Phys. Rev. **D58**, 036006 (1998);
   C. Giunti, Phys. Scripta **67**, 29 (2003);
   M. Beuthe, Phys. Rept. **375**, 105 (2003) and Phys. Rev. **D66**, 013003 (2002), and references therein;
   H. Lipkin, `hep-ph/0304187`.
5. G. Fogli, E. Lisi, and G. Scioscia, Phys. Rev. **D52**, 5334 (1995).
6. L. Wolfenstein, Phys. Rev. **D17**, 2369 (1978).
7. S. Mikheyev and A. Smirnov, Yad. Fiz. **42**, 1441 (1985) [Sov. J. Nucl. Phys. **42**, 913 (1986)]; Zh. Eksp. Teor. Fiz. **91**, 7, (1986) [Sov. Phys. JETP **64**, 4 (1986)]; Nuovo Cimento **9C**, 17 (1986).
8. The Bugey Collaboration (B. Achkar *et al.*), Nucl. Phys. **B434**, 503 (1995);
   The Palo Verde Collaboration (F. Boehm *et al.*), Phys. Rev. **D64**, 112001 (2001);
   The CHOOZ Collaboration (M. Apollonio *et al.*), Eur. Phys. J. **C27**, 331 (2003).
9. P. Langacker, J. Leveille, and J. Sheiman, Phys. Rev. **D27**, 1228 (1983);
   The corresponding energy for anti-neutrinos is negative.
10. G. L. Fogli, E. Lisi, and D. Montanino, Phys. Rev. **D54**, 2048 (1996);
    A. de Gouvêa, A. Friedland, and H. Murayama, Phys. Lett. **B490**, 125 (2000).
11. J. Bahcall, *Neutrino Astrophysics*, (Cambridge Univ. Press, Cambridge, UK 1989).
12. S. Parke, Phys. Rev. Lett. **57**, 1275 (1986).
13. We thank J. Beacom and A. Smirnov for invaluable conversations on how LMA-MSW works. For an early description, see S. Mikheyev and A. Smirnov, Ref. 7 (first paper).
14. D. Ayres *et al.*, in *Proc. of the 1982 DPF Summer Study on Elementary Particle Physics and Future Facilities*, p. 590;
    G. Dass and K. Sarma, Phys. Rev. **D30**, 80 (1984);
    J. Flanagan, J. Learned, and S. Pakvasa, Phys. Rev. **D57**, 2649 (1998);
    B. Kayser, in *Proc. of the 17th Int. Workshop on Weak Interactions and Neutrinos*, eds. C. Dominguez and R. Viollier (World Scientific, Singapore, 2000) p. 339.
15. E. Kearns, in *Proc. of the 30th Int. Conf. on High Energy Physics*, eds. C. Lim and T. Yamanaka (World Scientific, Singapore, 2001) p. 172.
16. K. Nishikawa, presented at the XXI Int. Symp. on Lepton and Photon Interactions at High Energies (Lepton Photon 2003), Fermilab, August, 2003.
17. The MACRO Collaboration (M. Ambrosio *et al.*), Phys. Lett. **B566**, 35 (2003);
    The Soudan 2 Collaboration (M. Sanchez *et al.*), `hep-ex/0307069`;
    For a review, see M. Goodman, *Proc. of the XXth Int. Conf. on Neutrino Physics and Astrophysics*, eds. F. von Feilitzsch and N. Schmitz, Nucl. Phys. B (Proc. Suppl.) **118**, 99 (2003).
18. For additional discussion of the atmospheric data, see T. Gaisser and T. Stanev in this *Review*.
19. M. Shiozawa, presented at the XXth Int. Conf. on Neutrino Physics and Astrophysics, Munich, May, 2002.
20. The K2K Collaboration (M. Ahn *et al.*), Phys. Rev. Lett. **90**, 041801 (2003).
21. The SNO Collaboration (S. Ahmed *et al.*), `nucl-ex/0309004`.
22. Y. Koshio, to appear in the Proceedings of 38th Rencontres de Moriond on Electroweak Interactions and Unified Theories, Les Arcs, France, March 15-22, 2003, `hep-ex/0306002`.
23. J. Bahcall, M. Pinsonneault, and S. Basu, Astrophys. J. **555**, 990 (2001).
24. G. Fogli, E. Lisi, A. Marrone, and A. Palazzo, `hep-ph/0309100`.
25. The KamLAND Collaboration (K. Eguchi *et al.*), Phys. Rev. Lett. **90**, 021802 (2003).
26. The latter include the data from the chlorine experiment: B. Cleveland *et al.*, Astrophys. J. **496**, 505 (1998);
    and from the gallium experiments: T. Kirsten (for the GNO Collaboration), *Proc. of the XXth Int. Conf. on Neutrino Physics*

and Astrophysics, eds. F. von Feilitzsch and N. Schmitz, Nucl. Phys. B (Proc. Suppl.) **118**, 33 (2003);

V. Gavrin (for the SAGE collaboration), presented at the 4th Int. Workshop on Low Energy and Solar Neutrinos, Paris, May, 2003.

27. The SNO Collaboration, Ref. [21]. We thank the collaboration for allowing us to use their figure.

28. Fits to the neutrino data incorporating the recent SNO results of Ref. [21] may be found in A.B. Balantekin and H. Yuksel, `hep-ph/0309079`;

A. Bandyopadhyay *et al.*, Phys. Rev. **D68**, 113002 (2003);

P. Holanda and Y, Smirnov, `hep-ph/0309299`;

M. Maltoni, T. Schwetz, M. Tortola, and J. Valle, Phys. Rev. **D68**, 113010 (2003).

29. J. Bahcall, M.C. Gonzalez-Garcia, and C. Peña-Garay, JHEP **0302**, 009 (2003);

See also P. Holanda and A. Smirnov, `hep-ph/0211264` and `hep-ph/0307266`.

30. The LSND Collaboration (A. Aguilar *et al.*), Phys. Rev. **D64**, 112007 (2001).

31. The KARMEN Collaboration (B. Armbruster *et al.*), Phys. Rev. **D65**, 112001 (2002).

32. E. Church *et al.*, Phys. Rev. **D66**, 013001 (2003).

33. For an alternative possibility entailing *CPT* violation, see H. Murayama and T. Yanagida, Phys. Lett. **B520**, 263 (2001);

G. Barenboim *et al.*, JHEP **0210**, 001 (2002);

However, after KamLAND, this alternative is disfavored. M. C. Gonzalez-Garcia, M. Maltoni, and T. Schwetz, Phys. Rev. **D68**, 053007 (2003);

G. Barenboim, L. Borissov, and J. Lykken, `hep-ph/0212116 v2`.

34. J. Schechter and J. Valle, Phys. Rev. **D23**, 1666 (1981);

J. Nieves and P. Pal, Phys. Rev. **D64**, 076005 (2001);

A. de Gouvêa, B. Kayser, and R. Mohapatra, Phys. Rev. **D67**, 053004 (2003).

35. L.-L. Chau and W.-Y. Keung, Phys. Rev. Lett. **53**, 1802 (1984);

H. Harari and M. Leurer, Phys. Lett. **B181**, 123 (1986);

F.J. Botella and L.-L. Chau, Phys. Lett. **B168**, 97 (1986);

H. Fritzsch and J. Plankl, Phys. Rev. **D35**, 1732 (1987).

36. G. Fogli *et al.*, `hep-ph/0308055`.

37. F. Dydak *et al.*, Phys. Lett. **B134**, 281 (1984).

38. A trio with its solar pair at the top is an interesting possibility that could reflect new physics that approximately conserves L_e–L_μ–L_τ, where L_α is the lepton number for flavor α. See K. Babu and R. Mohapatra, Phys. Lett. **B532**, 77 (2002).

39. O.L.G. Peres and A. Smirnov, Nucl. Phys. **B599**, 3 (2001);

M.C. Gonzalez-Garcia, M. Maltoni, and C. Peña-Garay, Phys. Rev. **D64**, 093001 (2001), and in *Budapest 2001, High Energy Physics (Proc. of the Int. Europhys. Conf. on High-Energy Physics)*.

40. See, however, H. Paes, L. Song, and T. Weiler, Phys. Rev. **D67**, 073019 (2003).

41. M. Maltoni, T. Schwetz, and J. Valle, Phys. Rev. **D65**, 093004 (2002);

G. Fogli, E. Lisi, and A. Marrone, Phys. Rev. **D63**, 053008 (2001);

References in these two papers.

42. M. Sorel, J. Conrad, and M. Shaevitz, `hep-ph/0305255`.

43. We thank Belen Gavela for introducing us to this argument.

44. M. Gell-Mann, P. Ramond, and R. Slansky, in: *Supergravity*, eds. D. Freedman and P. van Nieuwenhuizen (North Holland, Amsterdam, 1979) p. 315;

T. Yanagida, in: *Proceedings of the Workshop on Unified Theory and Baryon Number in the Universe*, eds. O. Sawada and A. Sugamoto (KEK, Tsukuba, Japan, 1979);

R. Mohapatra and G. Senjanovic: Phys. Rev. Lett. **44**, 912 (1980) and Phys. Rev. **D23**, 165 (1981).

45. J. Schechter and J. Valle, Phys. Rev. **D25**, 2951 (1982).

46. The physics of Majorana neutrinos and $0\nu\beta\beta$ are discussed in S. Bilenky and S. Petcov, Rev. Mod. Phys. **59**, 671 (1987) [Erratum–*ibid.* **61**, 169 (1987)];

B. Kayser, *The Physics of Massive Neutrinos* (World Scientific, Singapore, 1989).

47. S. Pascoli and S.T. Petcov, Phys. Lett. **B580**, 280 (2003).

48. Analyses of the possible values of $| < m_{\beta\beta} > |$ have been given by H. Murayama and C. Peña-Garay, `hep-ph/0309114`;

S. Pascoli and S. Petcov, Phys. Lett. **B544**, 239 (2002);

S. Bilenky, S. Pascoli, and S. Petcov, Phys. Rev. **D64**, 053010 (2001), and Phys. Rev. **D64**, 113003 (2001);

H. Klapdor-Kleingrothaus, H. Päs, and A. Smirnov, Phys. Rev. **D63**, 073005 (2001);

S. Bilenky *et al.*, Phys. Lett. **B465**, 193 (1999);

References in these papers.

49. See also S. Elliott and P Vogel, Ann. Rev. Nucl. Part. Sci. **52**, 115 (2002), and references therein.

50. The MiniBooNE Collaboration (E. Church *et al.*) FERMILAB-P-0898 (1997), available at http://library.fnal.gov/archive/test-proposal/0000/fermilab-proposal-0898.shtml.

51. D. Spergel *et al.*, Astrophys. J. Supp. **148**, 175 (2003).

52. This point has been stressed by S. Parke, private communication.

53. M. Fukugita and T. Yanagida, Phys. Lett. **B174**, 45 (1986).

54. G. 't Hooft, Phys. Rev. Lett. **37**, 8 (1976);

V. Kuzmin, V. Rubakov, and M. Shaposhnikov, Phys. Lett. **155B**, 36 (1985).

55. S. Pascoli, S. Petcov, and W. Rodejohann, Phys. Rev. **D68**, 093007 (2003);

S. Davidson, S. Pascoli, and S. Petcov, private communications.

14. QUARK MODEL

Revised January 2004 by C. Amsler (University of Zürich) and C.G. Wohl (LBNL).

14.1. Quantum numbers of the quarks

Quarks are strongly interacting fermions with spin 1/2 and, by convention, positive parity. Then antiquarks have negative parity. Quarks have the additive baryon number 1/3, antiquarks -1/3. Table 14.1 gives the other additive quantum numbers (flavors) for the three generations of quarks. They are related to the charge Q (in units of the elementary charge e) through the generalized Gell-Mann-Nishijima formula

$$\mathsf{Q} = \mathsf{I}_z + \frac{\mathcal{B} + \mathsf{S} + \mathsf{C} + \mathsf{B} + \mathsf{T}}{2} , \tag{14.1}$$

where $\mathcal{B}$ is the baryon number. The convention is that the *flavor* of a quark (I_z, S, C, B, or T) has the same sign as its *charge* Q. With this convention, any flavor carried by a charged meson has the same sign as its charge, e.g. the strangeness of the K^+ is +1, the bottomness of the B^+ is +1, and the charm and strangeness of the D_s^- are each −1. Antiquarks have the opposite flavor signs.

Table 14.1: Additive quantum numbers of the quarks.

Property \ Quark	d	u	s	c	b	t
Q – electric charge	$-\frac{1}{3}$	$+\frac{2}{3}$	$-\frac{1}{3}$	$+\frac{2}{3}$	$-\frac{1}{3}$	$+\frac{2}{3}$
I – isospin	$\frac{1}{2}$	$\frac{1}{2}$	0	0	0	0
I_z – isospin z-component	$-\frac{1}{2}$	$+\frac{1}{2}$	0	0	0	0
S – strangeness	0	0	−1	0	0	0
C – charm	0	0	0	+1	0	0
B – bottomness	0	0	0	0	−1	0
T – topness	0	0	0	0	0	+1

14.2. Mesons

Mesons have baryon number $\mathcal{B} = 0$. In the quark model they are $q\overline{q}'$ bound states of quarks q and antiquarks $\overline{q}'$ (the flavors of q and q' may be different). If the orbital angular momentum of the $q\overline{q}'$ state is ℓ, then the parity P is $(-1)^{\ell+1}$. The meson spin J is given by the usual relation $|\ell - s| < J < |\ell + s|$ where s is 0 (antiparallel quark spins) or 1 (parallel quark spins). The charge conjugation, or C-parity $C = (-1)^{\ell+s}$, is defined only for the $q\bar{q}$ states made of quarks and their own antiquarks. The C-parity can be generalized to the G-parity $G = (-1)^{I+\ell+s}$ for mesons made of quarks and their own antiquarks (isospin $\mathsf{I}_z = 0$) and for the charged $u\bar{d}$ and $d\bar{u}$ states (isospin I = 1).

The mesons are classified in J^{PC} multiplets. The $\ell = 0$ states are the pseudoscalars (0^{-+}) and the vectors (1^{--}). The orbital excitations $\ell = 1$ are the scalars (0^{++}), the axial vectors (1^{++}) and (1^{+-}), and the tensors (2^{++}). Assignments for many of the known mesons are given in Tables 14.2 and 14.3. Radial excitations are denoted by the principal quantum number n. The very short lifetime of the t quark makes it likely that bound state hadrons containing t quarks and/or antiquarks do not exist.

States in the natural spin-parity series $P = (-1)^J$ must, according to the above, have $s = 1$ and hence $CP = +1$. Thus mesons with natural spin-parity and $CP = -1$ (0^{+-}, 1^{-+}, 2^{+-}, 3^{-+}, etc) are forbidden in the $q\bar{q}'$ model. The $J^{PC} = 0^{--}$ state is forbidden as well. Mesons with such *exotic* quantum numbers may exist, but would lie outside the $q\bar{q}'$ model (see section below on exotic mesons).

Following SU(3) the nine possible $q\bar{q}'$ combinations containing the light u, d, and s quarks are grouped into an octet and a singlet of light quark mesons:

$$\mathbf{3} \otimes \overline{\mathbf{3}} = \mathbf{8} \oplus \mathbf{1} . \tag{14.2}$$

A fourth quark such as charm c can be included by extending SU(3) to SU(4). However, SU(4) is badly broken owing to the much heavier c quark. Nevertheless, in an SU(4) classification the sixteen mesons are grouped into a 15-plet and a singlet:

$$\mathbf{4} \otimes \overline{\mathbf{4}} = \mathbf{15} \oplus \mathbf{1} . \tag{14.3}$$

The *weight diagrams* for the ground-state pseudoscalar (0^{-+}) and vector (1^{--}) mesons are depicted in Fig. 14.1. The light quark mesons are members of nonets building the middle plane in Fig. 14.1(a) and (b).

Isoscalar states with the same J^{PC} will mix but mixing between the two light quark mesons and the much heavier charm or bottom states are generally assumed to be negligible. In the following we shall use the generic names a for the $I = 1$, K for the $I = 1/2$, f and f' for the $I = 0$ members of the light quark nonets. Thus the physical isoscalars are mixtures of the SU(3) wave function ψ_8 and ψ_1:

$$f' = \psi_8 \cos\theta - \psi_1 \sin\theta , \tag{14.4}$$

$$f = \psi_8 \sin\theta + \psi_1 \cos\theta , \tag{14.5}$$

where θ is the nonet mixing angle and

$$\psi_8 = \frac{1}{\sqrt{6}}(u\bar{u} + d\bar{d} - 2s\bar{s}) , \tag{14.6}$$

$$\psi_1 = \frac{1}{\sqrt{3}}(u\bar{u} + d\bar{d} + s\bar{s}) . \tag{14.7}$$

The mixing angle has to be determined experimentally.

These mixing relations are often rewritten to exhibit the $u\bar{u} + d\bar{d}$ and $s\bar{s}$ components which decouple for the "ideal" mixing angle θ_i such that $\tan\theta_i = 1/\sqrt{2}$ (or θ_i=35.3°). Defining $\alpha = \theta + 54.7°$, one obtains the physical isoscalar in the flavor basis

$$f' = \frac{1}{\sqrt{2}}(u\bar{u} + d\bar{d})\cos\alpha - s\bar{s}\ \sin\alpha , \tag{14.8}$$

and its orthogonal partner f (replace α by $\alpha - 90°$). Thus for ideal mixing ($\alpha_i = 90°$) the f' becomes pure $s\bar{s}$ and the f pure $u\bar{u} + d\bar{d}$. The mixing angle θ can be derived from the mass relation

$$\tan\theta = \frac{4m_K - m_a - 3m_{f'}}{2\sqrt{2}(m_a - m_K)} , \tag{14.9}$$

which also determines its sign or, alternatively, from

$$\tan^2\theta = \frac{4m_K - m_a - 3m_{f'}}{-4m_K + m_a + 3m_f} . \tag{14.10}$$

Eliminating θ from these equations leads to the sum rule [1]

$$(m_f + m_{f'})(4m_K - m_a) - 3m_f m_{f'} = 8m_K^2 - 8m_K m_a + 3m_a^2 . \tag{14.11}$$

This relation is verified for the ground-state vector mesons. We identify the $\phi(1020)$ with the f' and the $\omega(783)$ with the f. Thus

$$\phi(1020) = \psi_8 \cos\theta_V - \psi_1 \sin\theta_V , \tag{14.12}$$

$$\omega(782) = \psi_8 \sin\theta_V + \psi_1 \cos\theta_V , \tag{14.13}$$

with the vector mixing angle $\theta_V = 35°$ from Eq. (14.9), very close to ideal mixing. Thus $\phi(1020)$ is nearly pure $s\bar{s}$. For ideal mixing Eq. (14.9) and Eq. (14.10) lead to the relations

$$m_K = \frac{m_f + m_{f'}}{2} , \quad m_a = m_f , \tag{14.14}$$

Table 14.2: Suggested $q\overline{q}$ quark-model assignments for some of the observed light mesons. Mesons in bold face are included in the Meson Summary Table. The wave functions f and f' are given in the text. The singlet-octet mixing angles from the quadratic and linear mass formulae are also given for some of the nonets. The classification of the 0^{++} mesons is tentative and the mixing angle uncertain due to large uncertainties in some of the masses. The $f_0(1500)$ in the Meson Summary Table is not in this table as it is hard to accommodate in the scalar nonet. The light scalars $a_0(980)$, $f_0(980)$ and $f_0(600)$ are often considered as meson-meson resonances or four-quark states and are therefore not included in the table. See the "Note on Non-$q\overline{q}$ Mesons" at the end of the Meson Listings.

$n\,^{2s+1}\ell_J$	J^{PC}	$I=1$ $u\overline{d}$, $\overline{u}d$, $\frac{1}{\sqrt{2}}(d\overline{d}-u\overline{u})$	$I=\frac{1}{2}$ $u\overline{s}$, $d\overline{s}$; $\overline{d}s$, $-\overline{u}s$	$I=0$ f'	$I=0$ f	$\theta_{\rm quad}$ [°]	$\theta_{\rm lin}$ [°]
$1\,^1S_0$	0^{-+}	$\boldsymbol{\pi}$	$\boldsymbol{K}$	$\boldsymbol{\eta}$	$\boldsymbol{\eta'(958)}$	-11.5	-24.6
$1\,^3S_1$	1^{--}	$\boldsymbol{\rho(770)}$	$\boldsymbol{K^*(892)}$	$\boldsymbol{\phi(1020)}$	$\boldsymbol{\omega(782)}$	38.7	36.0
$1\,^1P_1$	1^{+-}	$\boldsymbol{b_1(1235)}$	$\boldsymbol{K_{1B}}^\dagger$	$h_1(1380)$	$\boldsymbol{h_1(1170)}$		
$1\,^3P_0$	0^{++}	$\boldsymbol{a_0(1450)}$	$\boldsymbol{K_0^*(1430)}$	$\boldsymbol{f_0(1710)}$	$\boldsymbol{f_0(1370)}$		
$1\,^3P_1$	1^{++}	$\boldsymbol{a_1(1260)}$	$\boldsymbol{K_{1A}}^\dagger$	$\boldsymbol{f_1(1420)}$	$\boldsymbol{f_1(1285)}$		
$1\,^3P_2$	2^{++}	$\boldsymbol{a_2(1320)}$	$\boldsymbol{K_2^*(1430)}$	$\boldsymbol{f_2'(1525)}$	$\boldsymbol{f_2(1270)}$	29.6	28.0
$1\,^1D_2$	2^{-+}	$\boldsymbol{\pi_2(1670)}$	$\boldsymbol{K_2(1770)}^\dagger$	$\eta_2(1870)$	$\boldsymbol{\eta_2(1645)}$		
$1\,^3D_1$	1^{--}	$\boldsymbol{\rho(1700)}$	$\boldsymbol{K^*(1680)}^\ddagger$		$\boldsymbol{\omega(1650)}$		
$1\,^3D_2$	2^{--}		$\boldsymbol{K_2(1820)}^\ddagger$				
$1\,^3D_3$	3^{--}	$\boldsymbol{\rho_3(1690)}$	$\boldsymbol{K_3^*(1780)}$	$\boldsymbol{\phi_3(1850)}$	$\boldsymbol{\omega_3(1670)}$	32.0	31.0
$1\,^3F_4$	4^{++}	$\boldsymbol{a_4(2040)}$	$\boldsymbol{K_4^*(2045)}$		$\boldsymbol{f_4(2050)}$		
$1\,^3G_5$	5^{--}	$\rho_5(2350)$					
$1\,^3H_6$	6^{++}	$a_6(2450)$			$f_6(2510)$		
$2\,^1S_0$	0^{-+}	$\boldsymbol{\pi(1300)}$	$K(1460)$	$\boldsymbol{\eta(1475)}$	$\boldsymbol{\eta(1295)}$	-22.4	-22.6
$2\,^3S_1$	1^{--}	$\boldsymbol{\rho(1450)}$	$\boldsymbol{K^*(1410)}^\ddagger$	$\boldsymbol{\phi(1680)}$	$\boldsymbol{\omega(1420)}$		

† The $1^{+\pm}$ and $2^{-\pm}$ isospin $\frac{1}{2}$ states mix. In particular, the K_{1A} and K_{1B} are nearly equal (45°) mixtures of the $K_1(1270)$ and $K_1(1400)$.

‡ The $K^*(1410)$ could be replaced by the $K^*(1680)$ as the $2\,^3S_1$ state.

Table 14.3: $q\overline{q}$ quark-model assignments for the observed heavy mesons. Mesons in bold face are included in the Meson Summary Table.

$n\,^{2s+1}\ell_J$	J^{PC}	$I=0$ $c\overline{c}$	$I=0$ $b\overline{b}$	$I=\frac{1}{2}$ $c\overline{u}$, $c\overline{d}$; $\overline{c}u$, $\overline{c}d$	$I=0$ $c\overline{s}$; $\overline{c}s$	$I=\frac{1}{2}$ $b\overline{u}$, $b\overline{d}$; $\overline{b}u$, $\overline{b}d$	$I=0$ $b\overline{s}$; $\overline{b}s$	$I=0$ $b\overline{c}$; $\overline{b}c$
$1\,^1S_0$	0^{-+}	$\boldsymbol{\eta_c(1S)}$	$\eta_b(1S)$	$\boldsymbol{D}$	$\boldsymbol{D_s^\pm}$	$\boldsymbol{B}$	$\boldsymbol{B_s}$	$\boldsymbol{B_c^\pm}$
$1\,^3S_1$	1^{--}	$\boldsymbol{J/\psi(1S)}$	$\boldsymbol{\Upsilon(1S)}$	$\boldsymbol{D^*}$	$\boldsymbol{D_s^{*\pm}}$	$\boldsymbol{B^*}$	$B_s^{*\pm}$	
$1\,^1P_1$	1^{+-}	$h_c(1P)$		$\boldsymbol{D_1(2420)}$	$\boldsymbol{D_{s1}(2536)^\pm}$			
$1\,^3P_0$	0^{++}	$\boldsymbol{\chi_{c0}(1P)}$	$\boldsymbol{\chi_{b0}(1P)}$		$\boldsymbol{D_{sJ}^*(2317)^{\pm\dagger}}$			
$1\,^3P_1$	1^{++}	$\boldsymbol{\chi_{c1}(1P)}$	$\boldsymbol{\chi_{b1}(1P)}$		$\boldsymbol{D_{sJ}^*(2460)^{\pm\dagger}}$			
$1\,^3P_2$	2^{++}	$\boldsymbol{\chi_{c2}(1P)}$	$\boldsymbol{\chi_{b2}(1P)}$	$\boldsymbol{D_2(2460)}$	$\boldsymbol{D_{s2}^*(2573)^\pm}$			
$1\,^3D_1$	1^{--}	$\boldsymbol{\psi(3770)}$						
$2\,^1S_0$	0^{-+}	$\boldsymbol{\eta_c(2S)}$						
$2\,^3S_1$	1^{--}	$\boldsymbol{\psi(2S)}$	$\boldsymbol{\Upsilon(2S)}$					
$2\,^3P_{0,1,2}$	$0^{++}, 1^{++}, 2^{++}$		$\boldsymbol{\chi_{b0,1,2}(2P)}$					

† The masses of these states are considerably smaller than most theoretical predictions. They have also been considered as four-quark states (See the "Note o No $\overline{\ }$ Meso s" at the e d of the Meso Listi gs)

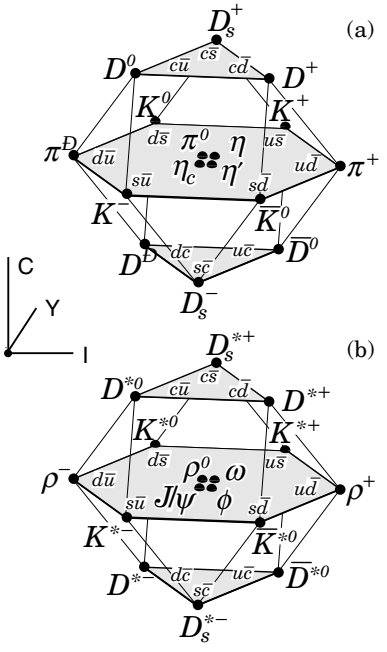

Figure 14.1: SU(4) weight diagram showing the 16-plets for the pseudoscalar (a) and vector mesons (b) made of the u, d, s and c quarks as a function of isospin I, charm C and hypercharge $Y = S + \mathcal{B} - \frac{C}{3}$. The nonets of light mesons occupy the central planes to which the $c\bar{c}$ states have been added.

which are satisfied for the vector mesons. However, for the pseudoscalar (and scalar mesons) Eq. (14.11) is satisfied only approximately. Then Eq. (14.9) and Eq. (14.10) lead to somewhat different values for the mixing angle. Identifying the η with the f' one gets

$$\eta = \psi_8 \cos\theta_P - \psi_1 \sin\theta_P \ , \qquad (14.15)$$

$$\eta' = \psi_8 \sin\theta_P + \psi_1 \cos\theta_P \ . \qquad (14.16)$$

Following chiral perturbation theory the meson masses in the mass formulae (Eq. (14.9)) and (Eq. (14.10)) should be replaced by their squares. Table 14.2 lists the mixing angle $\theta_{\rm lin}$ from Eq. (14.10) and the corresponding $\theta_{\rm quad}$ obtained by replacing the meson masses by their squares throughout.

The pseudoscalar mixing angle θ_P can also be measured by comparing the partial widths for radiative J/ψ decay into a vector and a pseudoscalar [2], radiative $\phi(1020)$ decay into η and η' [3], or $\bar{p}p$ annihilation at rest into a pair of vector and pseudoscalar or into two pseudoscalars [4,5]. One obtains a mixing angle between –10° and –20°.

The nonet mixing angles can be measured in $\gamma\gamma$ collisions, e.g. for the 0^{-+}, 0^{++} and 2^{++} nonets. In the quark model the coupling of neutral mesons to two photons is proportional to $\sum_i Q_i^2$, where Q_i is the charge of the i-th quark. The 2γ partial width of an isoscalar meson with mass m is then given in terms of the mixing angle α by

$$\Gamma_{2\gamma} = C(5\cos\alpha - \sqrt{2}\sin\alpha)^2 m^3 \ , \qquad (14.17)$$

for f' and f ($\alpha \to \alpha - 90°$). The coupling C may depend on the meson mass. It is often assumed to be a constant in the nonet. For the isovector a one then finds $\Gamma_{2\gamma} = 9\ C\ m^3$. Thus the members of an ideally mixed nonet couple to 2γ with partial widths in the ratios $f : f' : a = 25 : 2 : 9$. For tensor mesons one finds from the ratios of the measured 2γ partial widths for the $f_2(1270)$ and $f_2'(1525)$ mesons a mixing angle α_T of $(81 \pm 1)°$, or $\theta_T = (27 \pm 1)°$, in accord with the linear mass formula. For the pseudoscalars one finds from the ratios

Table 14.4: SU(3) couplings γ^2 for quarkonium decays as a function on nonet mixing angle α, up to a common multiplicative factor C ($\phi \equiv 54.7° + \theta_P$).

Isospin	Decay channel	γ^2
0	$\pi\pi$	$3\cos^2\alpha$
	$K\overline{K}$	$(\cos\alpha - \sqrt{2}\sin\alpha)^2$
	$\eta\eta$	$(\cos\alpha\cos^2\phi - \sqrt{2}\sin\alpha\sin^2\phi)^2$
	$\eta\eta'$	$\frac{1}{2}\sin^2 2\phi\ (\cos\alpha + \sqrt{2}\sin\alpha)^2$
1	$\eta\pi$	$2\cos^2\phi$
	$\eta'\pi$	$2\sin^2\phi$
	$K\overline{K}$	1
$\frac{1}{2}$	$K\pi$	$\frac{3}{2}$
	$K\eta$	$(\sin\phi - \frac{\cos\phi}{\sqrt{2}})^2$
	$K\eta'$	$(\cos\phi + \frac{\sin\phi}{\sqrt{2}})^2$

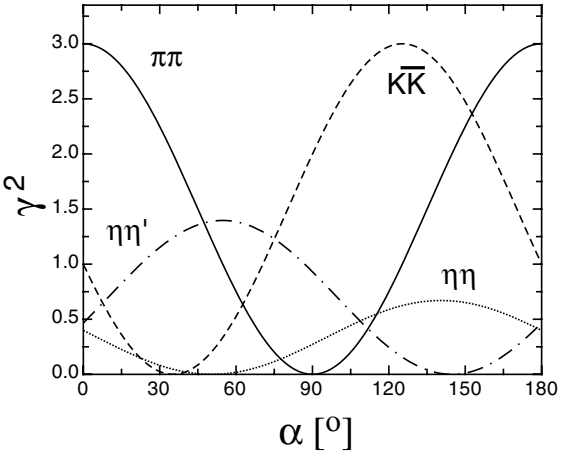

Figure 14.2: SU(3) couplings as a function of mixing angle α for isoscalar decays, up to a common multiplicative factor C and for $\theta_P = -17.3°$ (from Ref. 4).

of partial widths $\Gamma(\eta' \to 2\gamma)/\Gamma(\eta \to 2\gamma)$ a mixing angle $\theta_P = (-18 \pm 2)°$ while the ratio $\Gamma(\eta' \to 2\gamma)/\Gamma(\pi^0 \to 2\gamma)$ leads to $\sim$ –24 °. SU(3) breaking effects for pseudoscalars are discussed in Ref. 6.

The partial width for the decay of a scalar or a tensor meson into a pair of pseudoscalar mesons is model dependent. Following Ref. 7,

$$\Gamma = C \times \gamma^2 \times |F(q)|^2 \times q \ . \qquad (14.18)$$

C is a nonet constant, q the momentum of the decay products, $F(q)$ a form factor and γ^2 the SU(3) coupling. The model-dependent formfactor may be written as

$$|F(q)|^2 = q^{2\ell} \times \exp(-\frac{q^2}{8\beta^2}), \qquad (14.19)$$

where ℓ is the relative angular momentum between the decay products. The decay of a $q\bar{q}$ meson into a pair of mesons involves the creation of a $q\bar{q}$ pair from the vacuum and SU(3) symmetry assumes that the matrix elements for the creation of $s\bar{s}$, $u\bar{u}$ and $d\bar{d}$ pairs are equal. The couplings γ^2 are given in Table 14.4 and their dependence upon the mixing angle α is shown in Fig. 14.2 for isoscalar decays. The generalization to unequal $s\bar{s}$, $u\bar{u}$ and $d\bar{d}$ couplings is given in Ref. 7. An excellent fit to the tensor meson decay widths is obtained assuming SU(3) symmetry, with $\beta \simeq 0.5$ GeV/c, $\theta_V \simeq 26$ ° and $\theta_P \simeq$ -17 ° [7].

14.3. Exotic mesons

The existence of a light nonet composed of four quarks with masses below 1 GeV was suggested a long time ago [8]. Coupling two triplets of light quarks u, d and s one obtains nine states, of which the six symmetric (uu, dd, ss, $ud+du$, $us+su$, $ds+sd$) form the six dimensional representation **6**, while the three antisymmetric ($ud-du$, $us-su$, $ds-sd$) form the three dimensional representation $\bar{\mathbf{3}}$ of SU(3):

$$\mathbf{3} \otimes \mathbf{3} = \mathbf{6} \oplus \bar{\mathbf{3}} \ . \tag{14.20}$$

Combining with spin and color and requiring antisymmetry, one finds that the most deeply bound diquark (and hence the lightest) is the one in the $\bar{\mathbf{3}}$ and spin singlet state. The combinination of the diquark with an antidiquark in the **3** representation then gives a light nonet of four-quark scalar states. Letting the number of strange quarks determine the mass splitting one obtains a mass inverted spectrum with a light isosinglet ($ud\bar{u}\bar{d}$), a medium heavy isodublet (e.g. $ud\bar{s}\bar{d}$) and a heavy isotriplet (e.g. $ds\bar{u}\bar{s}$) + isosinglet (e.g. $us\bar{u}\bar{s}$). It is then tempting to identify the lightest state with the $f_0(600)$, and the heaviest states with the $a_0(980)$, and $f_0(980)$. Then the meson with strangeness $\kappa(800)$ would lie in between.

QCD predicts the existence of isoscalar mesons which contain only gluons, the glueballs. The ground state glueball is predicted by lattice gauge theories to be 0^{++}, the first excited state 2^{++}. Errors on the mass predictions are large. Ref. 9 predicts a mass of about 1600 MeV for the ground state with an uncertainty of 160 MeV. As an example for the glueball mass spectrum we show in Figure 14.3 a recent calculation from the lattice [10]. The first excited state has a mass of about 2.4 GeV and the lightest glueball with exotic quantum numbers (2^{+-}) has a mass of about 4 GeV.

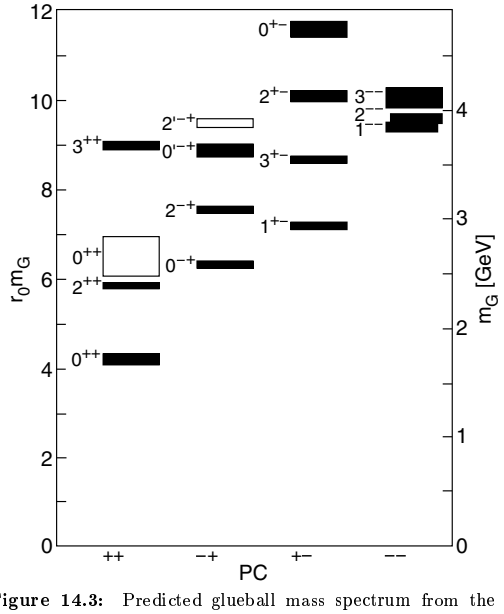

Figure 14.3: Predicted glueball mass spectrum from the lattice (from Ref. 10).

Lattice calculations assume that the quark masses are infinite and neglect $q\bar{q}$ loops. However, one expects that glueballs will mix with nearby $q\bar{q}$ states of the same quantum numbers [7,11]. For example, the two isoscalar 0^{++} mesons will mix with the pure ground state glueball to generate the observed physical states $f_0(1370)$, $f_0(1500)$, and $f_0(1710)$. Experimental evidence is mounting that the $f_0(1500)$ has considerable affinity for glue and that the $f_0(1370)$ and $f_0(1710)$ have large $u\bar{u}+d\bar{d}$ and $s\bar{s}$ components, respectively (See the "Note on Non-$q\bar{q}$ Mesons" at the end of the Meson Listings and Ref. 12).

Mesons made of $q\bar{q}$ pairs bound by excited gluons g, the hybrid states $q\bar{q}g$, are also predicted. They should lie in the 1.9 GeV mass region, according to gluon flux tube models [13]. Lattice QCD also predicts the lightest hybrid, an exotic 1^{-+}, at a mass of 1.9 GeV [14]. However, the bag model predicts four nonets, among them an exotic 1^{-+} around 1.4 GeV [15]. Most hybrids are rather broad but some can be as narrow as 100 MeV. There are so far two prominent candidates for exotic states with quantum numbers 1^{-+}, the $\pi_1(1400)$ and $\pi_1(1600)$, which could be hybrids or four-quark states (See the "Note on Non-$q\bar{q}$ Mesons" at the end of the Meson Listings and Ref. 12).

14.4. Baryons: qqq states

All the established baryons are apparently 3-quark (qqq) states, and each such state is an SU(3) color singlet, a completely antisymmetric state of the three possible colors. Since the quarks are fermions, the state function for any baryon must be antisymmetric under interchange of any two equal-mass quarks (up and down quarks in the limit of isospin symmetry). Thus the state function may be written as

$$|\, qqq \,\rangle_A = |\, \text{color} \,\rangle_A \times |\, \text{space, spin, flavor} \,\rangle_S \ , \tag{14.21}$$

where the subscripts S and A indicate symmetry or antisymmetry under interchange of any two of the equal-mass quarks. Note the contrast with the state function for the three nucleons in ^{3}H or ^{3}He:

$$|\, NNN \,\rangle_A = |\, \text{space, spin, isospin} \,\rangle_A \ . \tag{14.22}$$

This difference has major implications for internal structure, magnetic moments, *etc.* (For a nice discussion, see Ref. 16.)

The "ordinary" baryons are made up of u, d, and s quarks. The three flavors imply an approximate flavor SU(3), which requires that baryons made of these quarks belong to the multiplets on the right side of

$$\mathbf{3} \otimes \mathbf{3} \otimes \mathbf{3} = \mathbf{10}_S \oplus \mathbf{8}_M \oplus \mathbf{8}_M \oplus \mathbf{1}_A \tag{14.23}$$

(see Sec. 37, on "SU(n) Multiplets and Young Diagrams"). Here the subscripts indicate symmetric, mixed-symmetry, or antisymmetric states under interchange of any two quarks. The **1** is a uds state (Λ_1) and the octet contains a similar state (Λ_8). If these have the same spin and parity they can mix. An example is the mainly octet D_{03} $\Lambda(1690)$ and mainly singlet D_{03} $\Lambda(1520)$. In the ground state multiplet, the SU(3) flavor singlet Λ is forbidden by Fermi statistics. The mixing formalism is the same as for η-η' or ϕ-ω (see above), except that for baryons the mass M instead of M^2 is used. Section 36, on "SU(3) Isoscalar Factors and Representation Matrices", shows how relative decay rates in, say, $\mathbf{10} \to \mathbf{8} \otimes \mathbf{8}$ decays may be calculated. A summary of results of fits to the observed baryon masses and decay rates for the best-known SU(3) multiplets is given in Appendix II of our 1982 edition [17].

The addition of the c quark to the light quarks extends the flavor symmetry to SU(4). Figures 14.4(a) and 14.4(b) show the (badly broken) SU(4) baryon multiplets that have as their bottom levels an SU(3) octet, such as the octet that includes the nucleon, or an SU(3) decuplet, such as the decuplet that includes the $\Delta(1232)$. All the particles in a given SU(4) multiplet have the same spin and parity. The charmed baryons are discussed in more detail in the "Note on Charmed Baryons" in the Particle Listings. The addition of a b quark extends the flavor symmetry to SU(5); it would require four dimensions to draw the multiplets.

For the "ordinary" baryons (no c or b quark), flavor and spin may be combined in an approximate flavor-spin SU(6) in which the six basic states are $d\uparrow$, $d\downarrow$, $\cdots$, $s\downarrow$ ($\uparrow$, $\downarrow$ = spin up, down). Then the baryons belong to the multiplets on the right side of

$$\mathbf{6} \otimes \mathbf{6} \otimes \mathbf{6} = \mathbf{56}_S \oplus \mathbf{70}_M \oplus \mathbf{70}_M \oplus \mathbf{20}_A \ . \tag{14.24}$$

These SU(6) multiplets decompose into flavor SU(3) multiplets as follows:

$$\mathbf{56} = {}^4\mathbf{10} \oplus {}^2\mathbf{8} \tag{14.25a}$$

$$\mathbf{70} = {}^2\mathbf{10} \oplus {}^4\mathbf{8} \oplus {}^2\mathbf{8} \oplus {}^2\mathbf{1} \tag{14.25b}$$

$$\mathbf{20} = {}^2\mathbf{8} \oplus {}^4\mathbf{1} \ , \tag{14.25c}$$

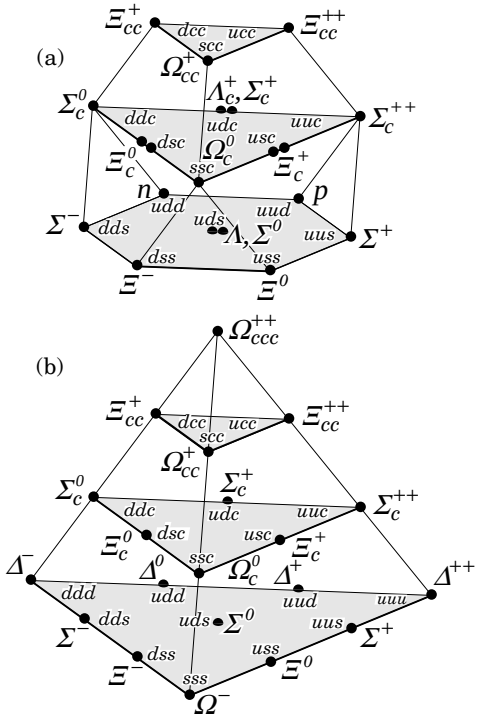

Figure 14.4: SU(4) multiplets of baryons made of u, d, s, and c quarks. (a) The 20-plet with an SU(3) octet. (b) The 20-plet with an SU(3) decuplet.

where the superscript $(2S+1)$ gives the net spin S of the quarks for each particle in the SU(3) multiplet. The $J^P = 1/2^+$ octet containing the nucleon and the $J^P = 3/2^+$ decuplet containing the $\Delta(1232)$ together make up the "ground-state" 56-plet in which the orbital angular momenta between the quark pairs are zero (so that the spatial part of the state function is trivially symmetric). The **70** and **20** require some excitation of the spatial part of the state function in order to make the overall state function symmetric. States with nonzero orbital angular momenta are classified in SU(6)⊗O(3) supermultiplets. Physical baryons with the same quantum numbers do not belong to a single supermultiplet, since SU(6) is broken by spin-dependent interactions, differences in quark masses, *etc.* Nevertheless, the SU(6)⊗O(3) basis provides a suitable framework for describing baryon state functions.

It is useful to classify the baryons into bands that have the same number N of quanta of excitation. Each band consists of a number of supermultiplets, specified by (D, L_N^P), where D is the dimensionality of the SU(6) representation, L is the total quark orbital angular momentum, and P is the total parity. Supermultiplets contained in bands up to $N = 12$ are given in Ref. 18. The $N = 0$ band, which contains the nucleon and $\Delta(1232)$, consists only of the $(56,0_0^+)$ supermultiplet. The $N = 1$ band consists only of the $(70,1_1^-)$ multiplet and contains the negative-parity baryons with masses below about 1.9 GeV. The $N = 2$ band contains five supermultiplets: $(56,0_2^+)$, $(70,0_2^+)$, $(56,2_2^+)$, $(70,2_2^+)$, and $(20,1_2^+)$. Baryons belonging to the $(20,1_2^+)$ supermultiplet are not ever likely to be observed, since a coupling from the ground-state baryons requires a two-quark excitation. Selection rules are similarly responsible for the fact that many other baryon resonances have not been observed [19].

In Table 14.5, quark-model assignments are given for many of the established baryons whose SU(6)⊗O(3) compositions are relatively unmixed. We note that the unestablished resonances $\Sigma(1480)$, $\Sigma(1560)$, $\Sigma(1580)$, $\Sigma(1770)$, and $\Xi(1620)$ in our Baryon Particle Listings are too low in mass to be accommodated in most quark models [19,20].

Table 14.5: Quark-model assignments for many of the known baryons in terms of a flavor-spin SU(6) basis. Only the dominant representation is listed. Assignments for some states, especially for the $\Lambda(1810)$, $\Lambda(2350)$, $\Xi(1820)$, and $\Xi(2030)$, are merely educated guesses. For assignments of the charmed baryons, see the "Note on Charmed Baryons" in the Particle Listings.

J^P	(D, L_N^P)	S	Octet members				Singlets
$1/2^+$	$(56,0_0^+)$	1/2	$N(939)$	$\Lambda(1116)$	$\Sigma(1193)$	$\Xi(1318)$	
$1/2^+$	$(56,0_2^+)$	1/2	$N(1440)$	$\Lambda(1600)$	$\Sigma(1660)$	$\Xi(?)$	
$1/2^-$	$(70,1_1^-)$	1/2	$N(1535)$	$\Lambda(1670)$	$\Sigma(1620)$	$\Xi(?)$	$\Lambda(1405)$
$3/2^-$	$(70,1_1^-)$	1/2	$N(1520)$	$\Lambda(1690)$	$\Sigma(1670)$	$\Xi(1820)$	$\Lambda(1520)$
$1/2^-$	$(70,1_1^-)$	3/2	$N(1650)$	$\Lambda(1800)$	$\Sigma(1750)$	$\Xi(?)$	
$3/2^-$	$(70,1_1^-)$	3/2	$N(1700)$	$\Lambda(?)$	$\Sigma(?)$	$\Xi(?)$	
$5/2^-$	$(70,1_1^-)$	3/2	$N(1675)$	$\Lambda(1830)$	$\Sigma(1775)$	$\Xi(?)$	
$1/2^+$	$(70,0_2^+)$	1/2	$N(1710)$	$\Lambda(1810)$	$\Sigma(1880)$	$\Xi(?)$	$\Lambda(?)$
$3/2^+$	$(56,2_2^+)$	1/2	$N(1720)$	$\Lambda(1890)$	$\Sigma(?)$	$\Xi(?)$	
$5/2^+$	$(56,2_2^+)$	1/2	$N(1680)$	$\Lambda(1820)$	$\Sigma(1915)$	$\Xi(2030)$	
$7/2^-$	$(70,3_3^-)$	1/2	$N(2190)$	$\Lambda(?)$	$\Sigma(?)$	$\Xi(?)$	$\Lambda(2100)$
$9/2^-$	$(70,3_3^-)$	3/2	$N(2250)$	$\Lambda(?)$	$\Sigma(?)$	$\Xi(?)$	
$9/2^+$	$(56,4_4^+)$	1/2	$N(2220)$	$\Lambda(2350)$	$\Sigma(?)$	$\Xi(?)$	
			Decuplet members				
$3/2^+$	$(56,0_0^+)$	3/2	$\Delta(1232)$	$\Sigma(1385)$	$\Xi(1530)$	$\Omega(1672)$	
$1/2^-$	$(70,1_1^-)$	1/2	$\Delta(1620)$	$\Sigma(?)$	$\Xi(?)$	$\Omega(?)$	
$3/2^-$	$(70,1_1^-)$	1/2	$\Delta(1700)$	$\Sigma(?)$	$\Xi(?)$	$\Omega(?)$	
$5/2^+$	$(56,2_2^+)$	3/2	$\Delta(1905)$	$\Sigma(?)$	$\Xi(?)$	$\Omega(?)$	
$7/2^+$	$(56,2_2^+)$	3/2	$\Delta(1950)$	$\Sigma(2030)$	$\Xi(?)$	$\Omega(?)$	
$11/2^+$	$(56,4_4^+)$	3/2	$\Delta(2420)$	$\Sigma(?)$	$\Xi(?)$	$\Omega(?)$	

The quark model for baryons is extensively reviewed in Ref. 21 and 22.

14.5. Dynamics

Many specific quark models exist, but most contain the same basic set of dynamical ingredients. These include:

i) A confining interaction, which is generally spin-independent.

ii) A spin-dependent interaction, modeled after the effects of gluon exchange in QCD. For example, in the S-wave states, there is a spin-spin hyperfine interaction of the form

$$H_{HF} = -\alpha_S M \sum_{i>j} (\vec{\sigma}\lambda_a)_i (\vec{\sigma}\lambda_a)_j \ , \qquad (14.26)$$

where M is a constant with units of energy, λ_a $(a = 1, \cdots, 8,)$ is the set of SU(3) unitary spin matrices, defined in Sec. 36, on "SU(3) Isoscalar Factors and Representation Matrices," and the sum runs over constituent quarks or antiquarks. Spin-orbit interactions, although allowed, seem to be small.

iii) A strange quark mass somewhat larger than the up and down quark masses, in order to split the SU(3) multiplets.

iv) In the case of isoscalar mesons, an interaction for mixing $q\overline{q}$ configurations of different flavors (*e.g.*, $u\overline{u} \leftrightarrow d\overline{d} \leftrightarrow s\overline{s}$), in a manner which is generally chosen to be flavor independent.

These four ingredients provide the basic mechanisms that determine the hadron spectrum.

References:

1. J. Schwinger, Phys. Rev. Lett. **12**, 237 (1964).
2. A. Bramon, R. Escribano, and M.D. Scadron, Phys. Lett. **B403**, 339 (1997).
3. A. Aloisio *et al.*, Phys. Lett. **B541**, 45 (2002).
4. C. Amsler *et al.*, Phys. Lett. **B294**, 451 (1992).
5. C. Amsler, Rev. Mod. Phys. **70**, 1293 (1998).
6. T. Feldmann, Int. J. Mod. Phys. **A915**, 159 (2000).
7. C. Amsler and F.E. Close, Phys. Rev. **D53**, 295 (1996).
8. R.L. Jaffe, Phys. Rev. **D 15** 267, 281 (1977).
9. C. Michael, AIP Conf. Proc. **432**, 657 (1998).
10. C. Morningstar and M. Peardon, Phys. Rev. **D60**, 034509 (1999).
11. F.E. Close and A. Kirk, Eur. Phys. J. **C21**, 531 (2001).
12. C. Amsler and N.A. Törnqvist, Phys. Rev. **389**, 61 (2004).
13. N. Isgur and J. Paton, Phys. Rev. **D31**, 2910 (1985).
14. P. Lacock *et al.*, Phys. Lett. **B401**, 308 (1997);
    C. Bernard *et al.*, Phys. Rev. **D56**, 7039 (1997).
15. T. Barnes, F.E. Close, F. de Viron Nucl. Phys. **B224**, 241 (1983).
16. F.E. Close, in *Quarks and Nuclear Forces* (Springer-Verlag, 1982), p. 56.
17. Particle Data Group, Phys. Lett. **111B** (1982).
18. R.H. Dalitz and L.J. Reinders, in *Hadron Structure as Known from Electromagnetic and Strong Interactions, Proceedings of the Hadron '77 Conference* (Veda, 1979), p. 11.
19. N. Isgur and G. Karl, Phys. Rev. **D18**, 4187 (1978); ibid. **D19**, 2653 (1979); ibid. **D20**, 1191 (1979);
    K.-T. Chao, N. Isgur, and G. Karl, Phys. Rev. **D23**, 155 (1981).
20. C.P. Forsyth and R.E. Cutkosky, Z. Phys. **C18**, 219 (1983).
21. A.J.G. Hey and R.L. Kelly, Phys. Reports **96**, 71 (1983). Also see S. Gasiorowicz and J.L. Rosner, Am. J. Phys. **49**, 954 (1981).
22. N. Isgur, Int. J. Mod. Phys. **E1**, 465 (1992);
    G. Karl, Int. J. Mod. Phys. **E1**, 491 (1992).

15. GRAND UNIFIED THEORIES

Written April 2002 by S. Raby (Ohio State University).

15.1. Grand Unification

15.1.1. *Standard Model: An Introduction*:

In spite of all the successes of the Standard Model [SM], it is unlikely to be the final theory. It leaves many unanswered questions. Why the local gauge interactions $SU(3)_C \times SU(2)_L \times U(1)_Y$, and why 3 families of quarks and leptons? Moreover, why does one family consist of the states $[Q, u^c, d^c; L, e^c]$ transforming as $[(3, 2, 1/3), (\bar{3}, 1, -4/3), (\bar{3}, 1, 2/3); (1, 2, -1), (1, 1, 2)]$, where $Q = (u, d)$, and $L = (\nu, e)$ are $SU(2)_L$ doublets, and u^c, d^c, e^c are charge conjugate $SU(2)_L$ singlet fields with the $U(1)_Y$ quantum numbers given? [We use the convention that electric charge $Q_{EM} = T_{3L} + Y/2$ and all fields are left-handed.] Note the SM gauge interactions of quarks and leptons are completely fixed by their gauge charges. Thus, if we understood the origin of this charge quantization, we would also understand why there are no fractionally charged hadrons. Finally, what is the origin of quark and lepton masses, or the apparent hierarchy of family masses and quark mixing angles? Perhaps if we understood this, we would also know the origin of CP violation, the solution to the strong CP problem, the origin of the cosmological matter-antimatter asymmetry, or the nature of dark matter.

The SM has 19 arbitrary parameters; their values are chosen to fit the data. Three arbitrary gauge couplings: g_3, g, g' (where g, g' are the $SU(2)_L$, $U(1)_Y$ couplings, respectively) or equivalently, $\alpha_s = (g_3^2/4\pi)$, $\alpha_{EM} = (e^2/4\pi)$ ($e = g \sin\theta_W$), and $\sin^2\theta_W = (g')^2/(g^2 + (g')^2)$. In addition, there are 13 parameters associated with the 9 charged fermion masses and the four mixing angles in the CKM matrix. The remaining 3 parameters are v, λ [the Higgs VEV (vacuum expectation value) and quartic coupling] (or equivalently, M_Z, m_h^0), and the QCD θ parameter. In addition, there are hints of new physics beyond the SM, such as neutrino masses. With 3 light Majorana neutrinos, there are at least 9 additional parameters in the neutrino sector; 3 masses and 6 mixing angles. In summary, the SM has too many arbitrary parameters, and leaves open too many unresolved questions to be considered complete. These are the problems which grand unified theories hope to address.

15.1.2. *Charge Quantization*:

In the Standard Model, quarks and leptons are on an equal footing; both fundamental particles without substructure. It is now clear that they may be two faces of the same coin; unified, for example, by extending QCD (or $SU(3)_C$) to include leptons as the fourth color, $SU(4)_C$ [1]. The complete Pati-Salam gauge group is $SU(4)_C \times SU(2)_L \times SU(2)_R$, with the states of one family $[(Q, L), (Q^c, L^c)]$ transforming as $[(4, 2, 1), (\bar{4}, 1, \bar{2})]$, where $Q^c = (d^c, u^c)$, $L^c = (e^c, \nu^c)$ are doublets under $SU(2)_R$. Electric charge is now given by the relation $Q_{EM} = T_{3L} + T_{3R} + 1/2(B-L)$, and $SU(4)_C$ contains the subgroup $SU(3)_C \times (B-L)$ where B (L) is baryon (lepton) number. Note ν^c has no SM quantum numbers and is thus completely "sterile." It is introduced to complete the $SU(2)_R$ lepton doublet. This additional state is desirable when considering neutrino masses.

Although quarks and leptons are unified with the states of one family forming two irreducible representations of the gauge group, there are still 3 independent gauge couplings (two if one also imposes parity, *i.e.*, $L \leftrightarrow R$ symmetry). As a result, the three low-energy gauge couplings are still independent arbitrary parameters. This difficulty is resolved by embedding the SM gauge group into the simple unified gauge group, Georgi-Glashow SU(5), with one universal gauge coupling α_G defined at the grand unification scale M_G [2]. Quarks and leptons still sit in two irreducible representations, as before, with a $\mathbf{10} = [Q, u^c, e^c]$ and $\bar{\mathbf{5}} = [d^c, L]$. Nevertheless, the three low energy gauge couplings are now determined in terms of two independent parameters : α_G and M_G. Hence, there is one prediction.

In order to break the electroweak symmetry at the weak scale and give mass to quarks and leptons, Higgs doublets are needed which can sit in either a $\mathbf{5_H}$ or $\bar{\mathbf{5}}_\mathbf{H}$. The additional 3 states are color triplet Higgs scalars. The couplings of these color triplets violate baryon and lepton number, and nucleons decay via the exchange of a single color triplet Higgs scalar. Hence, in order not to violently disagree with the non-observation of nucleon decay, their mass must be greater than $\sim 10^{10-11}$ GeV. Note, in supersymmetric GUTs, in order to cancel anomalies, as well as give mass to both up and down quarks, both Higgs multiplets $\mathbf{5_H}$, $\bar{\mathbf{5}}_\mathbf{H}$ are required. As we shall discuss later, nucleon decay now constrains the color triplet Higgs states in a SUSY GUT to have mass significantly greater than M_G.

Complete unification is possible with the symmetry group SO(10), with one universal gauge coupling α_G, and one family of quarks and leptons sitting in the 16-dimensional-spinor representation $\mathbf{16} = [\mathbf{10} + \bar{\mathbf{5}} + \mathbf{1}]$ [3]. The SU(5) singlet $\mathbf{1}$ is identified with ν^c. In Table 15.1 we present the states of one family of quarks and leptons, as they appear in the $\mathbf{16}$. It is an amazing and perhaps even profound fact that all the states of a single family of quarks and leptons can be represented digitally as a set of 5 zeros and/or ones or equivalently as the tensor product of 5 "spin" 1/2 states (see Table 15.1). The first three "spins" correspond to $SU(3)_C$ color quantum numbers, while the last two are $SU(2)_L$ weak quantum numbers. In fact, an $SU(3)_C$ rotation just raises one color index and lowers another, thereby changing colors $\{r, b, y\}$. Similarly an $SU(2)_L$ rotation raises one weak index and lowers another, thereby flipping the weak isospin from up to down or vice versa. In this representation, weak hypercharge Y is given by the simple relation $Y = 2/3(\sum \text{color spins}) - (\sum \text{weak spins})$ where the sum is over the spin values $\{\pm 1/2\}$. SU(5) rotations then raise (or lower) a color index, while at the same time lowering (or raising) a weak index. It is easy to see that such rotations can mix the states $\{Q, u^c, e^c\}$ and $\{d^c, L\}$ among themselves, and ν^c is a singlet. The new SO(10) rotations [not in SU(5)] are then given by either raising or lowering any two spins. For example, by lowering the two weak indices ν^c rotates into e^c, etc.

Table 15.1: The quantum numbers of the **16** dimensional representation of SO(10) are represented as a tensor product of 5 "spin" 1/2 states with the values $\pm$ denoting the spin states $|\pm\frac{1}{2}>$ and with the condition that we have an even number of $-$ spins.

State	Y	Color	Weak
$\boldsymbol{\nu^c}$	0	+ + +	+ +
$\boldsymbol{e^c}$	2	+ + +	− −
$\boldsymbol{u_r}$	1/3	− + +	+ −
$\boldsymbol{d_r}$	1/3	− + +	− +
$\boldsymbol{u_b}$	1/3	+ − +	+ −
$\boldsymbol{d_b}$	1/3	+ − +	− +
$\boldsymbol{u_y}$	1/3	+ + −	+ −
$\boldsymbol{d_y}$	1/3	+ + −	− +
$\boldsymbol{u_r^c}$	−4/3	+ − −	+ +
$\boldsymbol{u_b^c}$	−4/3	− + −	+ +
$\boldsymbol{u_y^c}$	−4/3	− − +	+ +
$\boldsymbol{d_r^c}$	2/3	+ − −	− −
$\boldsymbol{d_b^c}$	2/3	− + −	− −
$\boldsymbol{d_y^c}$	2/3	− − +	− −
$\boldsymbol{\nu}$	−1	− − −	+ −
$\boldsymbol{e}$	−1	− − −	− +

SO(10) has two inequivalent maximal breaking patterns: $SO(10) \to SU(5) \times U(1)_X$ and $SO(10) \to SU(4)_C \times SU(2)_L \times SU(2)_R$. In the first case, we obtain Georgi-Glashow SU(5) if Q_{EM} is given in terms of SU(5) generators alone, or so-called flipped SU(5) [4] if Q_{EM} is partly in $U(1)_X$. In the latter case, we have the Pati-Salam symmetry. If SO(10) breaks directly to the SM at M_G, then we

retain the prediction for gauge coupling unification. However, more possibilities for breaking (hence more breaking scales and more parameters) are available in SO(10). Nevertheless with one breaking pattern SO(10) → SU(5) → SM, where the last breaking scale is M_G, the predictions from gauge coupling unification are preserved. The Higgs multiplets in minimal SO(10) are contained in the fundamental $\mathbf{10_H} = [\mathbf{5_H}, \bar{\mathbf{5}}_\mathbf{H}]$ representation. Note only in SO(10) does the gauge symmetry distinguish quark and lepton multiplets from Higgs multiplets.

Finally, larger symmetry groups have been considered. For example, $E(6)$ has a fundamental representation **27**, which under SO(10) transforms as a $[\mathbf{16} + \mathbf{10} + \mathbf{1}]$. The breaking pattern $E(6) \to \mathrm{SU}(3)_C \times \mathrm{SU}(3)_L \times \mathrm{SU}(3)_R$ is also possible. With the additional permutation symmetry $Z(3)$ interchanging the three SU(3)s, we obtain so-called "trinification [5]," with a universal gauge coupling. The latter breaking pattern has been used in phenomenological analyses of the heterotic string [6]. Note, in larger symmetry groups, such as $E(6)$, SU(6), etc., there are now many more states which have not been observed and must be removed from the effective low-energy theory. In particular, three families of **27**s in $E(6)$ contain three Higgs type multiplets transforming as **10**s of SO(10). This makes these larger symmetry groups unattractive starting points for model building.

15.1.3. *Gauge coupling unification*:

The biggest paradox of grand unification is to understand how it is possible to have a universal gauge coupling g_G in a grand unified theory [GUT], and yet have three unequal gauge couplings at the weak scale with $g_3 > g > g'$. The solution is given in terms of the concept of an effective field theory [EFT] [7]. The GUT symmetry is spontaneously broken at the scale M_G, and all particles not in the SM obtain mass of order M_G. When calculating Green's functions with external energies $E \gg M_G$, we can neglect the mass of all particles in the loop and hence all particles contribute to the renormalization group running of the universal gauge coupling. However, for $E \ll M_G$, one can consider an effective field theory including only the states with mass $< E \ll M_G$. The gauge symmetry of the EFT is $\mathrm{SU}(3)_C \times \mathrm{SU}(2)_L \times \mathrm{U}(1)_Y$, and the three gauge couplings renormalize independently. The states of the EFT include only those of the SM; 12 gauge bosons, 3 families of quarks and leptons, and one or more Higgs doublets. At M_G, the two effective theories [the GUT itself is most likely the EFT of a more fundamental theory defined at a higher scale] must give identical results; hence we have the boundary conditions $g_3 = g_2 = g_1 \equiv g_G$, where at any scale $\mu < M_G$, we have $g_2 \equiv g$ and $g_1 = \sqrt{5/3}\, g'$. Then using two low-energy couplings, such as $\alpha_s(M_Z)$, $\alpha_{EM}(M_Z)$, the two independent parameters α_G, M_G can be fixed. The third gauge coupling, $\sin^2\theta_W$ in this case, is then predicted. This was the procedure up until about 1991 [8,9]. Subsequently, the uncertainties in $\sin^2\theta_W$ were reduced tenfold. Since then, $\alpha_{EM}(M_Z)$, $\sin^2\theta_W$ have been used as input to predict α_G, M_G, and $\alpha_s(M_Z)$ [10].

Note, the above boundary condition is only valid when using one-loop-renormalization group [RG] running. With precision electroweak data, however, it is necessary to use two-loop-RG running. Hence, one must include one-loop-threshold corrections to gauge coupling boundary conditions at both the weak and GUT scales. In this case, it is always possible to define the GUT scale as the point where $\alpha_1(M_G) = \alpha_2(M_G) \equiv \bar{\alpha}_G$ and $\alpha_3(M_G) = \bar{\alpha}_G\,(1 + \epsilon_3)$. The threshold correction ϵ_3 is a logarithmic function of all states with mass of order M_G and $\bar{\alpha}_G = \alpha_G + \Delta$, where α_G is the GUT coupling constant above M_G, and Δ is a one-loop-threshold correction. To the extent that gauge coupling unification is perturbative, the GUT threshold corrections are small and calculable. This presumes that the GUT scale is sufficiently below the Planck scale or any other strong coupling extension of the GUT, such as a strongly coupled string theory.

Supersymmetric grand unified theories [SUSY GUTs] are an extension of non-SUSY GUTs [11]. The key difference between SUSY GUTs and non-SUSY GUTs is the low-energy effective theory. The low-energy effective field theory in a SUSY GUT is assumed to satisfy $N = 1$ supersymmetry down to scales of order the weak scale, in addition to the SM gauge symmetry. Hence, the spectrum includes all the SM states, plus their supersymmetric partners. It also includes one pair (or more) of Higgs doublets; one to give mass to up-type quarks, and the other to down-type quarks and charged leptons. Two doublets with opposite hypercharge Y are also needed to cancel fermionic triangle anomalies. Note, a low-energy SUSY-breaking scale (the scale at which the SUSY partners of SM particles obtain mass) is necessary to solve the gauge hierarchy problem.

Simple non-SUSY SU(5) is ruled out, initially by the increased accuracy in the measurement of $\sin^2\theta_W$, and by early bounds on the proton lifetime (see below) [9]. However, by now LEP data [10] has conclusively shown that SUSY GUTs is the new Standard Model; by which we mean the theory used to guide the search for new physics beyond the present SM. SUSY extensions of the SM have the property that their effects decouple as the effective SUSY-breaking scale is increased. Any theory beyond the SM must have this property simply because the SM works so well. However, the SUSY-breaking scale cannot be increased with impunity, since this would reintroduce a gauge hierarchy problem. Unfortunately there is no clear-cut answer to the question, "When is the SUSY-breaking scale too high?" A conservative bound would suggest that the third generation squarks and sleptons must be lighter than about 1 TeV, in order that the one-loop corrections to the Higgs mass from Yukawa interactions remain of order the Higgs mass bound itself.

At present, gauge coupling unification within SUSY GUTs works extremely well. Exact unification at M_G, with two-loop-RG running from M_G to M_Z, and one-loop-threshold corrections at the weak scale, fits to within 3 σ of the present precise low-energy data. A small threshold correction at M_G ($\epsilon_3 \sim -4\%$) is sufficient to fit the low-energy data precisely.* This may be compared to non-SUSY GUTs, where the fit misses by $\sim 12\ \sigma$, and a precise fit requires new weak-scale states in incomplete GUT multiplets, or multiple GUT-breaking scales.**

15.1.4. *Nucleon Decay*:

Baryon number is necessarily violated in any GUT [15]. In SU(5), nucleons decay via the exchange of gauge bosons with GUT scale masses, resulting in dimension-6 baryon-number-violating operators suppressed by $(1/M_G^2)$. The nucleon lifetime is calculable and given by $\tau_N \propto M_G^4/(\alpha_G^2\, m_p^5)$. The dominant decay mode of the proton (and the baryon-violating decay mode of the neutron), via gauge exchange, is $p \to e^+\,\pi^0$ ($n \to e^+\,\pi^-$). In any simple gauge symmetry, with one universal GUT coupling and scale (α_G, M_G), the nucleon lifetime from gauge exchange is calculable. Hence, the GUT scale may be directly observed via the extremely rare decay of the nucleon. Experimental searches for nucleon decay began with the Kolar Gold Mine, Homestake, Soudan, NUSEX, Frejus, HPW, and IMB detectors [8]. The present experimental bounds come from Super-Kamiokande and Soudan II. We discuss these results shortly. Non-SUSY GUTs are also ruled out by the non-observation of nucleon decay [9]. In SUSY GUTs, the GUT scale is of order 3×10^{16} GeV, as compared to the GUT scale in non-SUSY GUTs, which is of order 10^{15} GeV. Hence, the dimension-6 baryon-violating operators are significantly suppressed in SUSY GUTs [11] with $\tau_p \sim 10^{34-38}$ yrs.

However, in SUSY GUTs, there are additional sources for baryon-number violation—dimension-4 and -5 operators [16]. Although the notation does not change, when discussing SUSY GUTs, all fields are implicitly bosonic superfields, and the operators

* This result implicitly assumes universal GUT boundary conditions for soft SUSY-breaking parameters at M_G. In the simplest case, we have a universal gaugino mass $M_{1/2}$, a universal mass for squarks and sleptons m_{16}, and a universal Higgs mass m_{10}, as motivated by SO(10). In some cases, threshold corrections to gauge coupling unification can be exchanged for threshold corrections to soft SUSY parameters. See for example, Ref. 12 and references therein.

** Non-SUSY GUTs with a more complicated breaking pattern can still fit the data. For example, non-SUSY SO(10) → $\mathrm{SU}(4)_C \times \mathrm{SU}(2)_L \times \mathrm{SU}(2)_R$ →SM, with the second breaking scale of order an intermediate scale, determined by light neutrino masses using the see-saw mechanism, can fit the low-energy data for gauge couplings [13], and at the same time survive nucleon decay bounds [14], discussed in the following section.

considered are the so-called F terms, which contain two fermionic components, and the rest scalars or products of scalars. Within the context of SU(5), the dimension-4 and -5 operators have the form $(\mathbf{10}\ \bar{\mathbf{5}}\ \bar{\mathbf{5}}) \supset (u^c\ d^c\ d^c) + (Q\ L\ d^c) + (e^c\ L\ L)$, and $(\mathbf{10}\ \mathbf{10}\ \mathbf{10}\ \bar{\mathbf{5}}) \supset (Q\ Q\ Q\ L) + (u^c\ u^c\ d^c\ e^c) + B$ and L conserving terms, respectively. The dimension-4 operators are renormalizable with dimensionless couplings; similar to Yukawa couplings. On the other hand, the dimension-5 operators have a dimensionful coupling of order $(1/M_G)$.

The dimension-4 operators violate baryon number or lepton number, respectively, but not both. The nucleon lifetime is extremely short if both types of dimension-4 operators are present in the low-energy theory. However, both types can be eliminated by requiring R parity. In SU(5), the Higgs doublets reside in a $\mathbf{5_H}$, $\bar{\mathbf{5}}_\mathbf{H}$, and R parity distinguishes the $\bar{\mathbf{5}}$ (quarks and leptons) from $\bar{\mathbf{5}}_\mathbf{H}$ (Higgs). R parity [17] (or more precisely, its cousin, family reflection symmetry (see Dimopoulos and Georgi [11] and DRW [18]) takes $F \to -F$, $H \to H$ with $F = \{\mathbf{10},\ \bar{\mathbf{5}}\}$, $H = \{\bar{\mathbf{5}}_\mathbf{H},\ \mathbf{5_H}\}$. This forbids the dimension-4 operator $(\mathbf{10}\ \bar{\mathbf{5}}\ \bar{\mathbf{5}})$, but allows the Yukawa couplings of the form $(\mathbf{10}\ \bar{\mathbf{5}}\ \bar{\mathbf{5}}_\mathbf{H})$ and $(\mathbf{10}\ \mathbf{10}\ \mathbf{5_H})$. It also forbids the dimension-3, lepton-number-violating operator $(\bar{\mathbf{5}}\ \mathbf{5_H}) \supset (L\ H_u)$, with a coefficient with dimensions of mass which, like the μ parameter, could be of order the weak scale and the dimension-5, baryon-number-violating operator $(\mathbf{10}\ \mathbf{10}\ \mathbf{10}\ \bar{\mathbf{5}}_\mathbf{H}) \supset (Q\ Q\ Q\ H_d) + \cdots$.

Note, in the MSSM, it is possible to retain R-parity-violating operators at low energy, as long as they violate either baryon number or lepton number only, but not both. Such schemes are natural if one assumes a low-energy symmetry, such as lepton number, baryon number, or a baryon parity [19]. However, these symmetries cannot be embedded in a GUT. Thus, in a SUSY GUT, only R parity can prevent unwanted dimension four operators. Hence, by naturalness arguments, R parity must be a symmetry in the effective low-energy theory of any SUSY GUT. This does not mean to say that R parity is guaranteed to be satisfied in any GUT.

Note also, R parity distinguishes Higgs multiplets from ordinary families. In SU(5), Higgs and quark/lepton multiplets have identical quantum numbers; while in $E(6)$, Higgs and families are unified within the fundamental **27** representation. Only in SO(10) are Higgs and ordinary families distinguished by their gauge quantum numbers. Moreover, the Z(4) center of SO(10) distinguishes **10**s from **16**s, and can be associated with R parity [20].

Dimension-5 baryon-number-violating operators may be forbidden at tree level by symmetries in SU(5), etc. These symmetries are typically broken, however, by the VEVs responsible for the color triplet Higgs masses. Consequently, these dimension-5 operators are generically generated via color triplet Higgsino exchange. Hence, the color triplet partners of Higgs doublets must necessarily obtain mass of order the GUT scale. The dominant decay modes from dimension-5 operators are $p \to K^+\ \overline{\nu}$ $(n \to K^0\ \overline{\nu})$. This is due to a simple symmetry argument; the operators $(Q_i\ Q_j\ Q_k\ L_l)$, $(u_i^c\ u_j^c\ d_k^c\ e_l^c)$ (where $i,\ j,\ k,\ l = 1, 2, 3$ are family indices, and color and weak indices are implicit) must be invariant under $SU(3)_C$ and $SU(2)_L$. As a result, their color and weak doublet indices must be anti-symmetrized. However, since these operators are given by bosonic superfields, they must be totally symmetric under interchange of all indices. Thus, the first operator vanishes for $i = j = k$, and the second vanishes for $i = j$. Hence, a second or third generation member must exist in the final state [18].

Recent Super-Kamiokande bounds on the proton lifetime severely constrain these dimension-6 operators with dimension-5 operators with $\tau_{(p\to e^+\pi^0)} > 5.0 \times 10^{33}$ yrs (79.3 ktyr exposure), $\tau_{(n\to e^+\pi^-)} > 5 \times 10^{33}$ yrs (61 ktyr), and $\tau_{(p\to K^+\overline{\nu})} > 1.6 \times 10^{33}$ yrs (79.3 ktyr), $\tau_{(n\to K^0\overline{\nu})} > 1.7 \times 10^{32}$ yrs (61 ktyr) at (90% CL) based on the listed exposures [21]. These constraints are now sufficient to rule out minimal SUSY SU(5) [22]. Non-minimal Higgs sectors in SU(5) or SO(10) theories still survive [24,25]. The upper bound on the proton lifetime from these theories is approximately a factor of 5 above the experimental bounds. They are also being pushed to their theoretical limits. Hence, if SUSY GUTs are correct, then nucleon decay must be seen soon.

Is there a way out of this conclusion? String theories, and recent field theoretic constructions [26,27], contain grand unified symmetries realized in higher dimensions. In most heterotic string models, when compactifying all but four of these extra dimensions, only the MSSM is recovered as a symmetry of the effective four dimensional field theory. [Of course, this is not required by string theory, and string theory models exist whose low-energy field theory is a SUSY GUT [28].] In the process of compactification and GUT symmetry breaking, color triplet Higgs states are removed (projected out of the massless sector of the theory). In addition, the same projections, in heterotic string models, typically rearrange the quark and lepton states so that the massless states which survive emanate from different GUT multiplets. In these models, proton decay due to dimension-5 operators can be severely suppressed, or eliminated completely. In addition, proton decay due to dimension-6 operators may be enhanced due to threshold corrections at the GUT scale which effectively lower the GUT scale [27], or eliminate it altogether, if the states of one family come from different irreducible representations. Hence, the observation of proton decay may distinguish extra-dimensional GUTs from four-dimensional ones.

Before concluding the topic of baryon-number violation, consider the status of $\Delta B = 2$ neutron- anti-neutron oscillations. Generically, the leading operator for this process is the dimension-9 six-quark operator $G_{(\Delta B=2)}$ $(u^c\ d^c\ d^c\ u^c\ d^c\ d^c)$, with dimensionful coefficient $G_{(\Delta B=2)} \sim 1/M^5$. The present experimental bound $\tau_{n-\overline{n}} \geq 0.86 \times 10^8$ sec. at 90% CL [30] probes only up to the scale $M \leq 10^6$ GeV. For $M \sim M_G$, $n-\overline{n}$ oscillations appear to be unobservable for any GUT (for a recent discussion see Ref. 29).

15.1.5. *Yukawa coupling unification:*

15.1.5.1. *3rd generation, b–τ or t–b–τ unification:*

If quarks and leptons are two sides of the same coin, related by a new grand unified gauge symmetry, then that same symmetry relates the Yukawa couplings (and hence the masses) of quarks and leptons. In SU(5), there are two independent renormalizable Yukawa interactions given by $\lambda_t\ (\mathbf{10}\ \mathbf{10}\ \mathbf{5_H}) + \lambda\ (\mathbf{10}\ \bar{\mathbf{5}}\ \bar{\mathbf{5}}_\mathbf{H})$. These contain the SM interactions $\lambda_t\ (\mathbf{Q}\ \mathbf{u^c}\ \mathbf{H_u}) + \lambda\ (\mathbf{Q}\ \mathbf{d^c}\ \mathbf{H_d} + \mathbf{e^c}\ \mathbf{L}\ \mathbf{H_d})$. Hence, at the GUT scale, we have the tree-level relation, $\lambda_b = \lambda_\tau \equiv \lambda$ [31]. In SO(10), there is only one independent renormalizable Yukawa interaction given by $\lambda\ (\mathbf{16}\ \mathbf{16}\ \mathbf{10_H})$, which gives the tree-level relation, $\lambda_t = \lambda_b = \lambda_\tau \equiv \lambda$ [32,33]. Note, in the discussion above, we assume the minimal Higgs content, with Higgs in $\mathbf{5}$, $\bar{\mathbf{5}}$ for SU(5) and $\mathbf{10}$ for SO(10). With Higgs in higher-dimensional representations, there are more possible Yukawa couplings.

In order to make contact with the data, one now renormalizes the top, bottom, and τ Yukawa couplings, using two-loop-RG equations, from M_G to M_Z. One then obtains the running quark masses $m_t(M_Z) = \lambda_t(M_Z)\ v_u$, $m_b(M_Z) = \lambda_b(M_Z)\ v_d$, and $m_\tau(M_Z) = \lambda_\tau(M_Z)\ v_d$, where $< H_u^0 > \equiv v_u = \sin\beta\ v/\sqrt{2}$, $< H_d^0 > \equiv v_d = \cos\beta\ v/\sqrt{2}$, $v_u/v_d \equiv \tan\beta$, and $v \sim 246$ GeV is fixed by the Fermi constant, G_μ.

Including one-loop-threshold corrections at M_Z, and additional RG running, one finds the top, bottom, and τ-pole masses. In SUSY, b–τ unification has two possible solutions, with $\tan\beta \sim 1$ or $40-50$. The small $\tan\beta$ solution is now disfavored by the LEP limit, $\tan\beta > 2.4$ [34]. The large $\tan\beta$ limit overlaps the SO(10) symmetry relation.

When $\tan\beta$ is large, there are significant weak-scale threshold corrections to down quark and charged lepton masses, from either gluino and/or chargino loops [35]. Yukawa unification (consistent with low energy data) is only possible in a restricted region of SUSY parameter space with important consequences for SUSY searches [36].

15.1.5.2. *Three families:*

Simple Yukawa unification is not possible for the first two generations, of quarks and leptons. Consider the SU(5) GUT scale relation $\lambda_b = \lambda_\tau$. If extended to the first two generations, one would have $\lambda_s = \lambda_\mu$, $\lambda_d = \lambda_e$, which gives $\lambda_s/\lambda_d = \lambda_\mu/\lambda_e$. The last relation is a renormalization group invariant, and is thus satisfied at any scale. In particular, at the weak scale, one obtains $m_s/m_d = m_\mu/m_e$, which is in serious disagreement with the data, namely $m_s/m_d \sim 20$ and

$m_\mu/m_e \sim 200$. An elegant solution to this problem was given by Georgi and Jarlskog [37]. Of course, a three-family model must also give the observed CKM mixing in the quark sector. Note, although there are typically many more parameters in the GUT theory above M_G, it is possible to obtain effective low-energy theories with many fewer parameters making strong predictions for quark and lepton masses. Three-family models exist which fit all the data, including neutrino masses and mixing [38].

15.1.6. ***Neutrino Masses***:

Atmospheric and solar neutrino oscillations require neutrino masses. Adding three "sterile" neutrinos ν^c with the Yukawa coupling λ_ν ($\nu^{\mathbf{c}}$ $\mathbf{L}$ $\mathbf{H_u}$), one easily obtains three massive Dirac neutrinos with mass $m_\nu = \lambda_\nu\, v_u$. However, in order to obtain a tau neutrino with mass of order 0.1 eV, one needs $\lambda_{\nu_\tau}/\lambda_\tau \leq 10^{-10}$. The see-saw mechanism, on the other hand, can naturally explain such small neutrino masses [15,39]. Since ν^c has no SM quantum numbers, there is no symmetry (other than global lepton number) which prevents the mass term $\frac{1}{2}\ \nu^c\ M\ \nu^c$. Moreover, one might expect $M \sim M_G$. Heavy "sterile" neutrinos can be integrated out of the theory, defining an effective low-energy theory with only light active Majorana neutrinos, with the effective dimension-5 operator $\frac{1}{2}$ ($\mathbf{L}$ $\mathbf{H_u}$) $\lambda_\nu^T\ M^{-1}\ \lambda_\nu$ ($\mathbf{L}$ $\mathbf{H_u}$). This then leads to a 3×3 Majorana neutrino mass matrix $\mathbf{m} = m_\nu^T\ M^{-1}\ m_\nu$.

Atmospheric neutrino oscillations require neutrino masses with $\Delta m_\nu^2 \sim 3\times 10^{-3}$ eV^2 with maximal mixing, in the simplest two-neutrino scenario. With hierarchical neutrino masses, $m_{\nu_\tau} = \sqrt{\Delta m_\nu^2} \sim 0.055$ eV. Moreover, via the "see-saw" mechanism, $m_{\nu_\tau} = m_t(m_t)^2/(3M)$. Hence, one finds $M \sim 2\times 10^{14}$ GeV—remarkably close to the GUT scale. Note we have related the neutrino-Yukawa coupling to the top-quark-Yukawa coupling $\lambda_{\nu_\tau} = \lambda_t$ at M_G, as given in SO(10) or $\mathrm{SU}(4)\times\mathrm{SU}(2)_L\times\mathrm{SU}(2)_R$. However, at low energies they are no longer equal, and we have estimated this RG effect by $\lambda_{\nu_\tau}(M_Z) \approx \lambda_t(M_Z)/\sqrt{3}$.

15.1.7. ***Selected Topics***:

15.1.7.1. *Magnetic Monopoles:*

In the broken phase of a GUT, there are typically localized classical solutions carrying magnetic charge under an unbroken U(1) symmetry [40]. These magnetic monopoles with mass of order M_G/α_G are produced during the GUT phase transition in the early universe. The flux of magnetic monopoles is experimentally found to be less than $\sim 10^{-16}$ cm^{-2} s^{-1} sr^{-1} [41]. Many more are predicted however, hence the GUT monopole problem. In fact, one of the original motivations for an inflationary universe is to solve the monopole problem by invoking an epoch of rapid inflation after the GUT phase transition [42]. This would have the effect of diluting the monopole density as long as the reheat temperature is sufficiently below M_G. Parenthetically, it was also shown that GUT monopoles can catalyze nucleon decay [43].

15.1.7.2. *Baryogenesis via Leptogenesis:*

Baryon-number-violating operators in SU(5) or SO(10) preserve the global symmetry $B-L$. Hence, the value of the cosmological $B-L$ density is an initial condition of the theory, and is typically assumed to be zero. On the other hand, anomalies of the electroweak symmetry violate $B+L$ while also preserving $B-L$. Hence, thermal fluctuations in the early universe, via so-called sphaleron processes, can drive $B+L$ to zero, washing out any net baryon number generated in the early universe at GUT temperatures.

One way out of this dilemma is to generate a net $B-L$ dynamically in the early universe. We have just seen that neutrino oscillations suggest a new scale of physics of order 10^{14} GeV. This scale is associated with heavy Majorana neutrinos with mass M. If in the early universe, the decay of the heavy neutrinos is out of equilibrium and violates both lepton number and CP, then a net lepton number may be generated. This lepton number will then be partially converted into baryon number via electroweak processes [44].

15.1.7.3. *GUT symmetry breaking:*

The grand unification symmetry is necessarily broken spontaneously. Scalar potentials (or superpotentials) exist whose vacua spontaneously break SU(5) and SO(10). These potentials are ad hoc (just like the Higgs potential in the SM), and, therefore it is hoped that they may be replaced with better motivated sectors. Gauge coupling unification now tests GUT-breaking sectors, since it is one of the two dominant corrections to the GUT threshold correction ϵ_3. The other dominant correction comes from the Higgs sector and doublet-triplet splitting. This latter contribution is always positive $\epsilon_3 \propto \ln(M_T/M_G)$ (where M_T is an effective color triplet Higgs mass), while the low-energy data requires $\epsilon_3 < 0$. Hence, the GUT-breaking sector must provide a significant (of order -8%) contribution to ϵ_3 to be consistent with the Super-K bound on the proton lifetime [23,24,25,38].

In string theory (and GUTs in extra-dimensions), GUT breaking may occur due to boundary conditions in the compactified dimensions [26,27]. This is still ad hoc. The major benefits are that it does not require complicated GUT-breaking sectors, and it can suppress dimension-5 baryon-violating operators.

15.1.7.4. *Doublet-triplet splitting:*

The Minimal Supersymmetric Standard Model has a μ problem: why is the coefficient of the bilinear Higgs term in the superpotential μ ($\mathbf{H_u}$ $\mathbf{H_d}$) of order the weak scale when, since it violates no low-energy symmetry, it could be as large as M_G? In a SUSY GUT, the μ problem is replaced by the problem of *doublet-triplet* splitting—giving mass of order M_G to the color triplet Higgs, and mass μ to the Higgs doublets. Several mechanisms for natural doublet-triplet splitting have been suggested, such as the sliding singlet, missing partner or missing VEV [45], and pseudo-Nambu-Goldstone boson mechanisms. Particular examples of the missing partner mechanism for SU(5) [25], the missing VEV mechanism for SO(10) [24,38], and the pseudo-Nambu-Goldstone boson mechanism for SU(6) [46], have been shown to be consistent with gauge coupling unification and proton decay. There are also several mechanisms for explaining why μ is of order the SUSY-breaking scale [47]. Finally, for a recent review of the μ problem and some suggested solutions in SUSY GUTs and string theory, see Ref. 48 and references therein.

15.2. Conclusion

Grand unification of the strong and electroweak interactions at a unique high energy scale $M_G \sim 3\times 10^{16}$ GeV requires

- gauge coupling unification,
- low-energy supersymmetry [with a large SUSY desert], and
- nucleon decay.

The first prediction has already been verified. Perhaps the next two will soon be seen. Whether or not Yukawa couplings unify is more model dependent. Nevertheless, the "digital" 16-dimensional representation of quarks and leptons in SO(10) is very compelling, and may yet lead to an understanding of fermion masses and mixing angles.

In any event, the experimental verification of the first three pillars of SUSY GUTs would forever change our view of Nature. Moreover, the concomitant evidence for a vast SUSY desert would expose a huge lever arm for discovery. For then it would become clear that experiments probing the TeV scale could reveal physics at the GUT scale and perhaps beyond.

References:

1. J. Pati and A. Salam, Phys. Rev. **D8**, 1240 (1973);
   For more discussion on the standard charge assignments in this formalism, see A. Davidson, Phys. Rev. **D20**, 776 (1979); and R.N. Mohapatra and R.E. Marshak, Phys. Lett. **B91**, 222 (1980).
2. H. Georgi and S.L. Glashow, Phys. Rev. Lett. **32**, 438 (1974).
3. H. Georgi, Particles and Fields, *Proceedings of the APS Div. of Particles and Fields*, ed. C. Carlson, p. 575 (1975);
   H. Fritzsch and P. Minkowski, Ann. Phys. **93**, 193 (1975).
4. S.M. Barr, Phys. Lett. **B112**, 219 (1982).

5. A. de Rujula, H. Georgi, and S.L. Glashow, p. 88, *5th Workshop on Grand Unification*, ed. K. Kang, H. Fried, and P. Frampton, World Scientific, Singapore (1984);
   See also earlier paper by Y. Achiman and B. Stech, p. 303, "New Phenomena in Lepton-Hadron Physics," ed. D.E.C. Fries and J. Wess, Plenum, NY (1979).
6. B.R. Greene *et al.*, Nucl. Phys. **B278**, 667 (1986), and Nucl. Phys. **B292**, 606 (1987);
   B.R. Greene, C.A. Lutken, and G.G. Ross, Nucl. Phys. **B325**, 101 (1989).
7. H. Georgi, H. Quinn, and S. Weinberg, Phys. Rev. Lett. **33**, 451 (1974);
   see also the definition of effective field theories by S. Weinberg, Phys. Lett. **91B**, 51 (1980).
8. See talks on proposed and running nucleon decay experiments, and theoretical talks by P. Langacker, p. 131, and W.J. Marciano and A. Sirlin, p. 151, in *The Second Workshop on Grand Unification*, eds. J.P. Leveille, L.R. Sulak, and D.G. Unger, Birkhäuser, Boston (1981).
9. W.J. Marciano, p. 190, *Eighth Workshop on Grand Unification*, ed. K. Wali, World Scientific Publishing Co., Singapore (1987).
10. U. Amaldi, W. de Boer, and H. Fürstenau, Phys. Lett. **B260**, 447 (1991);
    J. Ellis, S. Kelly and D.V. Nanopoulos, Phys. Lett. **B260**, 131 (1991);
    P. Langacker and M. Luo, Phys. Rev. **D44**, 817 (1991);
    P. Langacker and N. Polonsky, Phys. Rev. **D47**, 4028 (1993);
    M. Carena, S. Pokorski, and C.E.M. Wagner, Nucl. Phys. **B406**, 59 (1993);
    see also the review by S. Dimopoulos, S. Raby, and F. Wilczek, Physics Today, 25–33, October (1991).
11. S. Dimopoulos, S. Raby, and F. Wilczek, Phys. Rev. **D24**, 1681 (1981);
    S. Dimopoulos and H. Georgi, Nucl. Phys. **B193**, 150 (1981);
    L. Ibanez and G.G. Ross, Phys. Lett. **105B**, 439 (1981);
    N. Sakai, Z. Phys. **C11**, 153 (1981);
    M.B. Einhorn and D.R.T. Jones, Nucl. Phys. **B196**, 475 (1982);
    W.J. Marciano and G. Senjanovic, Phys. Rev. **D25**, 3092 (1982).
12. G. Anderson *et al.*, in *New directions for high-energy physics*, Snowmass 1996, eds. D.G. Cassel, L. Trindle Gennari, and R.H. Siemann, `hep-ph/9609457`.
13. R.N. Mohapatra and M.K. Parida, Phys. Rev. **D47**, 264 (1993).
14. D.G. Lee *et al.*, Phys. Rev. **D51**, 229 (1995).
15. M. Gell-Mann, P. Ramond, and R. Slansky, in *Supergravity*, eds. P. van Nieuwenhuizen and D.Z. Freedman, North-Holland, Amsterdam, 1979, p. 315.
16. S. Weinberg, Phys. Rev. **D26**, 287 (1982);
    N. Sakai and T Yanagida, Nucl. Phys. **B197**, 533 (1982).
17. G. Farrar and P. Fayet, Phys. Lett. **B76**, 575 (1978).
18. S. Dimopoulos, S. Raby, and F. Wilczek, Phys. Lett. **112B**, 133 (1982);
    J. Ellis, D.V. Nanopoulos, and S. Rudaz, Nucl. Phys. **B202**, 43 (1982).
19. L.E. Ibanez and G.G. Ross, Nucl. Phys. **B368**, 3 (1992).
20. For a recent discussion, see C.S. Aulakh *et al.*, Nucl. Phys. **B597**, 89 (2001).
21. See talks by Matthew Earl, *NNN workshop*, Irvine, February (2000);
    Y. Totsuka, *SUSY2K*, CERN, June (2000);
    Y. Suzuki, *International Workshop on Neutrino Oscillations and their Origins*, Tokyo, Japan, December (2000), and *Baksan School, Baksan Valley*, Russia, April (2001), `hep-ex/0110005`.
    For published results see : Y. Hayato *et al.* (Super-Kamiokande Collab.), Phys. Rev. Lett. **83**, 1529 (1999).
22. H. Murayama and A. Pierce, Phys. Rev. **D65**, 055009 (2002).
23. K.S. Babu and S.M. Barr, Phys. Rev. **D48**, 5354 (1993);
    V. Lucas and S. Raby, Phys. Rev. **D54**, 2261 (1996);
    S.M. Barr and S. Raby, Phys. Rev. Lett. **79**, 4748 (1997) and references therein.
24. R. Dermíšek, A. Mafi, and S. Raby, Phys. Rev. **D63**, 035001 (2001);
    K.S. Babu, J.C. Pati, and F. Wilczek, Nucl. Phys. **B566**, 33 (2000).
25. G. Altarelli, F. Feruglio, I. Masina, JHEP **0011**, 040 (2000);
    see also earlier papers by A. Masiero *et al.*, Phys. Lett. **B115**, 380 (1982);
    B. Grinstein, Nucl. Phys. **B206**, 387 (1982).
26. P. Candelas *et al.*, Nucl. Phys. **B258**, 46 (1985);
    L.J. Dixon *et al.*, Nucl. Phys. **B261**, 678 (1985), and Nucl. Phys. **B274**, 285 (1986).
27. Y. Kawamura, Prog. Theor. Phys. **105**, 999 (2001);
    L.J. Hall and Y. Nomura, Phys. Rev. **D64**, 055003 (2001);
    R. Barbieri, L.J. Hall, and Y. Nomura, `hep-ph/0106190 (2001)`.
28. Z. Kakushadze and S.H.H. Tye, Phys. Rev. **D54**, 7520 (1996);
    Z. Kakushadze *et al.*, Int. J. Mod. Phys. **A13**, 2551 (1998).
29. K.S. Babu and R.N. Mohapatra, Phys. Lett. **B518**, 269 (2001).
30. M. Baldoceolin *et al.*, Z. Phys. **C63**, 409 (1994).
31. M. Chanowitz, J. Ellis, and M.K. Gaillard, Nucl. Phys. **B135**, 66 (1978);
    For the corresponding SUSY analysis, see M. Einhorn and D.R.T. Jones, Nucl. Phys. **B196**, 475 (1982);
    K. Inoue *et al.*, Prog. Theor. Phys. **67**, 1889 (1982);
    L.E. Ibañez and C. Lopez, Nucl. Phys. **B233**, 511 (1984).
32. H. Georgi and D.V. Nanopoulos, Nucl. Phys. **B159**, 16 (1979);
    J. Harvey, P. Ramond, and D.B. Reiss, Phys. Lett. **92B**, 309 (1980);
    Nucl. Phys. **B199**, 223 (1982).
33. T. Banks, Nucl. Phys. **B303**, 172 (1988);
    M. Olechowski and S. Pokorski, Phys. Lett. **B214**, 393 (1988);
    S. Pokorski, Nucl. Phys. (Proc. Supp.) **B13**, 606 (1990);
    B. Ananthanarayan, G. Lazarides, and Q. Shafi, Phys. Rev. **D44**, 1613 (1991);
    Q. Shafi and B. Ananthanarayan, ICTP Summer School lectures (1991);
    S. Dimopoulos, L.J. Hall, and S. Raby, Phys. Rev. Lett. **68**, 1984 (1992), and Phys. Rev. **D45**, 4192 (1992);
    G. Anderson *et al.*, Phys. Rev. **D47**, 3702 (1993);
    B. Ananthanarayan, G. Lazarides, and Q. Shafi, Phys. Lett. **B300**, 245 (1993);
    G. Anderson *et al.*, Phys. Rev. **D49**, 3660 (1994);
    B. Ananthanarayan, Q. Shafi, and X.M. Wang, Phys. Rev. **D50**, 5980 (1994).
34. LEP Higgs Working Group and ALEPH Collab., DELPHI Collab., L3 Collab., and OPAL Collab., Preliminary results, `hep-ex/0107030 (2001)`.
35. L.J. Hall, R. Rattazzi, and U. Sarid, Phys. Rev. **D50**, 7048 (1994);
    M. Carena *et al.*, Nucl. Phys. **B419**, 213 (1994);
    R. Rattazzi and U. Sarid, Nucl. Phys. **B501**, 297 (1997).
36. T. Blažek, R. Dermíšek, and S. Raby, Phys. Rev. Lett. **88**, 111804 (2002) and `hep-ph/0201081`.
37. H. Georgi and C. Jarlskog, Phys. Lett. **86B**, 297 (1979).

38. K.S. Babu and R.N. Mohapatra, Phys. Rev. Lett. **74**, 2418 (1995);
V. Lucas and S. Raby, Phys. Rev. **D54**, 2261 (1996);
T. Blažek *et al.*, Phys. Rev. **D56**, 6919 (1997);
R. Barbieri *et al.*, Nucl. Phys. **B493**, 3 (1997);
T. Blazek, S. Raby, and K. Tobe, Phys. Rev. **D60**, 113001 (1999), and Phys. Rev. **D62**, 055001 (2000);
Q. Shafi and Z. Tavartkiladze, Phys. Lett. **B487**, 145 (2000);
C.H. Albright and S.M. Barr, Phys. Rev. Lett. **85**, 244 (2000);
K.S. Babu, J.C. Pati, and F. Wilczek, Nucl. Phys. **B566**, 33 (2000);
G. Altarelli, F. Feruglio, I. Masina, Ref. 25;
Z. Berezhiani and A. Rossi, Nucl. Phys. **B594**, 113 (2001).

39. T. Yanagida, in *Proceedings of the Workshop on the Unified Theory and the Baryon Number of the Universe*, eds. O. Sawada and A. Sugamoto, KEK report No. 79-18, Tsukuba, Japan, 1979;
R.N. Mohapatra and G. Senjanovic, Phys. Rev. Lett. **44**, 912 (1980).

40. G. 't Hooft, Nucl. Phys. **B79**, 276 (1974);
A.M. Polyakov, Pis'ma Zh. Eksp. Teor. Fiz. **20**, 430 (1974) [JETP Lett. **20**, 194 (1974)];
For a pedagogical introduction, see S. Coleman, in *Aspects of Symmetry*, Selected Erice Lectures, Cambridge University Press, Cambridge, (1985), and P. Goddard and D. Olive, Rep. Prog. Phys. **41**, 1357 (1978).

41. I. De Mitri, (MACRO Collab.), Nucl. Phys. (Proc. Suppl.) **B95**, 82 (2001).

42. For a review, see A.D. Linde, *Particle Physics and Inflationary Cosmology*, Harwood Academic, Switzerland (1990).

43. V. Rubakov, Nucl. Phys. **B203**, 311 (1982), Institute of Nuclear Research Report No. P-0211, Moscow (1981), unpublished;
C. Callan, Phys. Rev. **D26**, 2058 (1982);
F. Wilczek, Phys. Rev. Lett. **48**, 1146 (1982);
See also, S. Dawson and A.N. Schellekens, Phys. Rev. **D27**, 2119 (1983).

44. M. Fukugita and T. Yanagida, Phys. Lett. **B174**, 45 (1986);
see also the recent review by W. Buchmuller, `hep-ph/0107153 (2001)` and references therein.

45. S. Dimopoulos and F. Wilczek, *Proceedings Erice Summer School*, ed. A. Zichichi (1981);
K.S. Babu and S.M. Barr, Phys. Rev. **D50**, 3529 (1994).

46. R. Barbieri, G.R. Dvali, and A. Strumia, Nucl. Phys. **B391**, 487 (1993);
Z. Berezhiani, C. Csaki, and L. Randall, Nucl. Phys. **B444**, 61 (1995);
Q. Shafi and Z. Tavartkiladze, Phys. Lett. **B522**, 102 (2001).

47. G.F. Giudice and A. Masiero, Phys. Lett. **B206**, 480 (1988);
J.E. Kim and H.P. Nilles, Mod. Phys. Lett. **A9**, 3575 (1994).

48. L. Randall and C. Csaki, *Proceedings Pascos/Hopkins 1995*, `hep-ph/9508208`;
E. Witten, `hep-ph/0201018`.

16. STRUCTURE FUNCTIONS

Written Summer 2001 by B. Foster (University of Bristol), A.D. Martin (University of Durham), M.G. Vincter (University of Alberta). Updated Summer 2003.

16.1. Deep inelastic scattering

High energy lepton-nucleon scattering (deep inelastic scattering) plays a key role in determining the partonic structure of the proton. The process $\ell N \to \ell' X$ is illustrated in Fig. 16.1. The filled circle in this figure represents the internal structure of the proton which can be expressed in terms of structure functions.

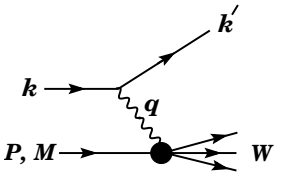

Figure 16.1: Kinematic quantities for the description of deep inelastic scattering. The quantities k and k' are the four-momenta of the incoming and outgoing leptons, P is the four-momentum of a nucleon with mass M, and W is the mass of the recoiling system X. The exchanged particle is a γ, $W^{\pm}$, or Z; it transfers four-momentum $q = k - k'$ to the nucleon.

Invariant quantities:

$\nu = \dfrac{q \cdot P}{M} = E - E'$ is the lepton's energy loss in the nucleon rest frame (in earlier literature sometimes $\nu = q \cdot P$). Here, E and E' are the initial and final lepton energies in the nucleon rest frame.

$Q^2 = -q^2 = 2(EE' - \vec{k} \cdot \vec{k}') - m_\ell^2 - m_{\ell'}^2$ where $m_\ell (m_{\ell'})$ is the initial (final) lepton mass. If $EE' \sin^2(\theta/2) \gg m_\ell^2,\, m_{\ell'}^2$, then

$\approx 4EE' \sin^2(\theta/2)$, where θ is the lepton's scattering angle in the nucleon rest frame with respect to the lepton beam direction.

$x = \dfrac{Q^2}{2M\nu}$ where, in the parton model, x is the fraction of the nucleon's momentum carried by the struck quark.

$y = \dfrac{q \cdot P}{k \cdot P} = \dfrac{\nu}{E}$ is the fraction of the lepton's energy lost in the nucleon rest frame.

$W^2 = (P+q)^2 = M^2 + 2M\nu - Q^2$ is the mass squared of the system X recoiling against the scattered lepton.

$s = (k+P)^2 = \dfrac{Q^2}{xy} + M^2 + m_\ell^2$ is the center-of-mass energy squared of the lepton-nucleon system.

The process in Fig. 16.1 is called deep ($Q^2 >> M^2$) inelastic ($W^2 >> M^2$) scattering (DIS). In what follows, the masses of the initial and scattered leptons, m_ℓ and m'_ℓ, are neglected.

16.1.1. *DIS cross sections*:

$$\frac{d^2\sigma}{dx\, dy} = x\,(s - M^2)\,\frac{d^2\sigma}{dx\, dQ^2} = \frac{2\pi\, M\nu}{E'}\,\frac{d^2\sigma}{d\Omega_{\rm Nrest}\, dE'}\,. \qquad (16.1)$$

In lowest-order perturbation theory, the cross section for the scattering of polarised leptons on polarised nucleons can be expressed in terms of the products of leptonic and hadronic tensors associated with the coupling of the exchanged bosons at the upper and lower vertices in Fig. 16.1 (see Refs. 1–4)

$$\frac{d^2\sigma}{dxdy} \;=\; \frac{2\pi y\alpha^2}{Q^4}\,\sum_j\, \eta_j\, L_j^{\mu\nu}\, W_{\mu\nu}^j\,. \qquad (16.2)$$

For neutral-current processes, the summation is over $j = \gamma, Z$ and γZ representing photon and Z exchange and the interference between them, whereas for charged-current interactions there is only W exchange, $j = W$. (For transverse nucleon polarization, there is a dependence on the azimuthal angle of the scattered lepton.) $L_{\mu\nu}$ is the lepton tensor associated with the coupling of the exchange boson to the leptons. For incoming leptons of charge $e = \pm 1$ and helicity $\lambda = \pm 1$,

$$\begin{aligned} L^{\gamma}_{\mu\nu} &= 2\left(k_\mu k'_\nu + k'_\mu k_\nu - k\cdot k' g_{\mu\nu} - i\lambda\varepsilon_{\mu\nu\alpha\beta}k^\alpha k'^\beta\right), \\ L^{\gamma Z}_{\mu\nu} &= (g_V^e + e\lambda g_A^e)\; L^{\gamma}_{\mu\nu},\; L^{Z}_{\mu\nu} = (g_V^e + e\lambda g_A^e)^2\; L^{\gamma}_{\mu\nu}, \\ L^{W}_{\mu\nu} &= (1+e\lambda)^2\; L^{\gamma}_{\mu\nu}, \end{aligned} \qquad (16.3)$$

where $g_V^e = -\frac{1}{2} - 2e\sin^2\theta_W, \qquad g_A^e = -\frac{1}{2}$.

Although here the helicity formalism is adopted, an alternative approach is to express the tensors in Eq. (16.3) in terms of the polarization of the lepton.

The factors η_j in Eq. (16.2) denote the ratios of the corresponding propagators and couplings to the photon propagator and coupling squared

$$\begin{aligned} \eta_\gamma &= 1 \;\;;\;\; \eta_{\gamma Z} = \left(\frac{G_F M_Z^2}{2\sqrt{2}\pi\alpha}\right)\left(\frac{Q^2}{Q^2+M_Z^2}\right); \\ \eta_Z &= \eta_{\gamma Z}^2 \;\;;\;\; \eta_W = \tfrac{1}{2}\left(\frac{G_F M_W^2}{4\pi\alpha}\,\frac{Q^2}{Q^2+M_W^2}\right)^2. \end{aligned} \qquad (16.4)$$

The hadronic tensor, which describes the interaction of the appropriate electroweak currents with the target nucleon, is given by

$$W_{\mu\nu} \;=\; \frac{1}{4\pi}\int d^4z\; e^{iq\cdot z}\,\left\langle P,S\left|\left[J_\mu^\dagger(z), J_\nu(0)\right]\right|P,S\right\rangle, \qquad (16.5)$$

where S denotes the nucleon-spin 4-vector, with $S^2 = -M^2$ and $S\cdot P = 0$.

16.2. Structure functions of the proton

The structure functions are defined in terms of the hadronic tensor (see Refs. 1–3)

$$\begin{aligned} W_{\mu\nu} = &\left(-g_{\mu\nu} + \frac{q_\mu q_\nu}{q^2}\right) F_1(x,Q^2) + \frac{\hat{P}_\mu \hat{P}_\nu}{P\cdot q}\, F_2(x,Q^2) \\ &- i\varepsilon_{\mu\nu\alpha\beta}\,\frac{q^\alpha P^\beta}{2P\cdot q}\, F_3(x,Q^2) \\ &+ i\varepsilon_{\mu\nu\alpha\beta}\,\frac{q^\alpha}{P\cdot q}\left[S^\beta g_1(x,Q^2) + \left(S^\beta - \frac{S\cdot q}{P\cdot q}\,P^\beta\right) g_2(x,Q^2)\right] \\ &+ \frac{1}{P\cdot q}\left[\tfrac{1}{2}\left(\hat{P}_\mu \hat{S}_\nu + \hat{S}_\mu \hat{P}_\nu\right) - \frac{S\cdot q}{P\cdot q}\,\hat{P}_\mu \hat{P}_\nu\right] g_3(x,Q^2) \\ &+ \frac{S\cdot q}{P\cdot q}\left[\frac{\hat{P}_\mu \hat{P}_\nu}{P\cdot q}\, g_4(x,Q^2) + \left(-g_{\mu\nu} + \frac{q_\mu q_\nu}{q^2}\right) g_5(x,Q^2)\right] \end{aligned} \qquad (16.6)$$

where

$$\hat{P}_\mu \;=\; P_\mu - \frac{P\cdot q}{q^2}\,q_\mu, \qquad \hat{S}_\mu \;=\; S_\mu - \frac{S\cdot q}{q^2}\,q_\mu\,. \qquad (16.7)$$

In Ref. 2, the definition of $W_{\mu\nu}$ with $\mu \leftrightarrow \nu$ is adopted, which changes the sign of the $\varepsilon_{\mu\nu\alpha\beta}$ terms in Eq. (16.6), although the formulae given here below are unchanged. Ref. 1 tabulates the relation between the structure functions defined in Eq. (16.6) and other choices available in the literature.

The cross sections for neutral and charged-current deep inelastic scattering on unpolarized nucleons can be written in terms of the structure functions in the generic form

$$\frac{d^2\sigma^i}{dxdy} = \frac{4\pi\alpha^2}{xyQ^2}\,\eta^i\left\{\left(1 - y - \frac{x^2y^2M^2}{Q^2}\right) F_2^i + y^2 x F_1^i \mp \left(y - \frac{y^2}{2}\right) x F_3^i\right\}, \tag{16.8}$$

where i = NC, CC corresponds to neutral-current ($eN \to eX$) or charged-current ($eN \to \nu X$ or $\nu N \to eX$) processes, respectively. In the last term, the $-$ sign is taken for an incoming e^+ or $\overline{\nu}$ and the $+$ sign for an incoming e^- or ν. The factor $\eta^{\rm NC} = 1$ for unpolarized $e^\pm$ beams, whereas*

$$\eta^{\rm CC} = (1 \pm \lambda)^2\eta_W \tag{16.9}$$

with $\pm$ for $\ell^\pm$ and where λ is the helicity of the incoming lepton. η_W is defined in Eq. (16.4). The CC structure functions, which derive exclusively from W exchange, are

$$F_1^{\rm CC} = F_1^W,\ F_2^{\rm CC} = F_2^W,\ xF_3^{\rm CC} = xF_3^W. \tag{16.10}$$

The NC structure functions F_2^γ, $F_2^{\gamma Z}$, F_2^Z are, for $e^\pm N \to e^\pm X$, given by Ref. 5,

$$F_2^{\rm NC} = F_2^\gamma - (g_V^e \pm \lambda g_A^e)\eta_{\gamma Z}F_2^{\gamma Z} + (g_V^{e\,2} + g_A^{e\,2} \pm 2\lambda g_V^e g_A^e)\,\eta_Z F_2^Z \tag{16.11}$$

and similarly for $F_1^{\rm NC}$, whereas

$$xF_3^{\rm NC} = -(g_A^e \pm \lambda g_V^e)\eta_{\gamma Z}xF_3^{\gamma Z} + [2g_V^e g_A^e \pm \lambda(g_V^{e\,2} + g_A^{e\,2})]\eta_{Z}xF_3^Z\ . \tag{16.12}$$

The polarized cross-section difference

$$\Delta\sigma = \sigma(\lambda_n = -1, \lambda_\ell) - \sigma(\lambda_n = 1, \lambda_\ell)\ , \tag{16.13}$$

where λ_ℓ, λ_n are the helicities (±1) of the incoming lepton and nucleon, respectively, may be expressed in terms of the five structure functions $g_{1,\ldots5}(x, Q^2)$ of Eq. (16.6). Thus,

$$\frac{d^2\Delta\sigma^i}{dxdy} = \frac{8\pi\alpha^2}{xyQ^2}\,\eta^i\left\{-\lambda_\ell y\left(2 - y - 2x^2y^2\frac{M^2}{Q^2}\right) xg_1^i + \lambda_\ell 4x^3y^2\,\frac{M^2}{Q^2}\,g_2^i + 2x^2y\frac{M^2}{Q^2}\left(1 - y - x^2y^2\frac{M^2}{Q^2}\right) g_3^i - \left(1 + 2x^2y\frac{M^2}{Q^2}\right)\left[\left(1 - y - x^2y^2\frac{M^2}{Q^2}\right) g_4^i + xy^2 g_5^i\right]\right\} \tag{16.14}$$

with i = NC or CC as before. The Eq. (16.13) corresponds to the difference of antiparallel minus parallel spins of the incoming particles for e^- or ν initiated reactions, but parallel minus antiparallel for e^+ or $\overline{\nu}$ initiated processes. For longitudinal nucleon polarization, the contributions of g_2 and g_3 are suppressed by powers of M^2/Q^2. These structure functions give an unsuppressed contribution to the cross section for transverse polarization [1], but in this case the cross-section difference vanishes as $M/Q \to 0$.

Because the same tensor structure occurs in the spin-dependent and spin-independent parts of the hadronic tensor of Eq. (16.6) in the $M^2/Q^2 \to 0$ limit, the differential cross-section difference of Eq. (16.14) may be obtained from the differential cross section Eq. (16.8) by replacing

$$F_1 \to -g_5\ ,\quad F_2 \to -g_4\ ,\quad F_3 \to 2g_1\ , \tag{16.15}$$

and multiplying by two, since the total cross section is the average over the initial-state polarizations. In this limit, Eq. (16.8) and Eq. (16.14) may be written in the form

$$\frac{d^2\sigma^i}{dxdy} = \frac{2\pi\alpha^2}{xyQ^2}\,\eta^i\left[Y_+F_2^i \mp Y_-xF_3^i - y^2F_L^i\right],$$
$$\frac{d^2\Delta\sigma^i}{dxdy} = \frac{4\pi\alpha^2}{xyQ^2}\,\eta^i\left[-Y_+g_4^i \mp Y_-2xg_1^i + y^2g_L^i\right], \tag{16.16}$$

with i = NC or CC, where $Y_\pm = 1 \pm (1-y)^2$ and

$$F_L^i = F_2^i - 2xF_1^i\ ,\qquad g_L^i = g_4^i - 2xg_5^i\ . \tag{16.17}$$

In the naive quark-parton model, the analogy with the Callan-Gross relations [6] $F_L^i = 0$, are the Dicus relations [7] $g_L^i = 0$. Therefore, there are only two independent polarized structure functions: g_1 (parity conserving) and g_5 (parity violating), in analogy with the unpolarized structure functions F_1 and F_3.

16.2.1. *Structure functions in the quark-parton model*:

In the quark-parton model [8,9], contributions to the structure functions F^i and g^i can be expressed in terms of the quark distribution functions $q(x, Q^2)$ of the proton, where $q = u, \overline{u}, d, \overline{d}$ etc. The quantity $q(x, Q^2)dx$ is the number of quarks (or antiquarks) of designated flavor that carry a momentum fraction between x and $x + dx$ of the proton's momentum in a frame in which the proton momentum is large.

For the neutral-current processes $ep \to eX$,

$$\left[F_2^\gamma,\ F_2^{\gamma Z},\ F_2^Z\right] = x\sum_q\left[e_q^2,\ 2e_qg_V^q,\ g_V^{q\,2} + g_A^{q\,2}\right]\ (q + \overline{q})\ ,$$
$$\left[F_3^\gamma,\ F_3^{\gamma Z},\ F_3^Z\right] = \sum_q\left[0,\ 2e_qg_A^q,\ 2g_V^qg_A^q\right]\ (q - \overline{q})\ ,$$
$$\left[g_1^\gamma,\ g_1^{\gamma Z},\ g_1^Z\right] = \tfrac{1}{2}\sum_q\left[e_q^2,\ 2e_qg_V^q,\ g_V^{q\,2} + g_A^{q\,2}\right]\ (\Delta q + \Delta\overline{q})\ ,$$
$$\left[g_5^\gamma,\ g_5^{\gamma Z},\ g_5^Z\right] = \sum_q\left[0,\ e_qg_A^q,\ g_V^qg_A^q\right]\ (\Delta q - \Delta\overline{q})\ , \tag{16.18}$$

where $g_V^q = \pm\frac{1}{2} - 2e_q\sin^2\theta_W$ and $g_A^q = \pm\frac{1}{2}$, with $\pm$ according to whether q is a $u-$ or $d-$type quark respectively. The quantity Δq is the difference $q\uparrow - q\downarrow$ of the distributions with the quark spin parallel and antiparallel to the proton spin.

For the charged-current processes $e^-p \to \nu X$ and $\overline{\nu}p \to e^+X$, the structure functions are:

$$F_2^{W^-} = 2x(u + \overline{d} + \overline{s} + c\ldots)\ ,$$
$$F_3^{W^-} = 2(u - \overline{d} - \overline{s} + c\ldots)\ ,$$
$$g_1^{W^-} = (\Delta u + \Delta\overline{d} + \Delta\overline{s} + \Delta c\ldots)\ ,$$
$$g_5^{W^-} = (-\Delta u + \Delta\overline{d} + \Delta\overline{s} - \Delta c\ldots)\ , \tag{16.19}$$

where only the active flavors are to be kept and where CKM mixing has been neglected. For $e^+p \to \overline{\nu}X$ and $\nu p \to e^-X$, the structure functions F^{W^+}, g^{W^+} are obtained by the flavor interchanges $d \leftrightarrow u, s \leftrightarrow c$ in the expressions for F^{W^-}, g^{W^-}. The structure functions for scattering on a neutron are obtained from those of the proton by the interchange $u \leftrightarrow d$. For both the neutral and charged-current processes, the quark-parton model predicts $2xF_1^i = F_2^i$ and $g_4^i = 2xg_5^i$.

Neglecting masses, the structure functions g_2 and g_3 contribute only to scattering from transversely polarized nucleons (for which $S \cdot q = 0$), and have no simple interpretation in terms of the quark-parton model. They arise from off-diagonal matrix elements $\langle P, \lambda'|[J_\mu^\dagger(z), J_\nu(0)]|P, \lambda\rangle$, where the proton helicities satisfy $\lambda' \neq \lambda$. In fact, the leading-twist contributions to both g_2 and g_3 are both twist-2 and twist-3, which contribute at the same order of Q^2. The Wandzura-Wilczek relation [10] expresses the twist-2 part of g_2 in terms of g_1 as

$$g_2^i(x) = -g_1^i(x) + \int_x^1 \frac{dy}{y}\,g_1^i(y)\ . \tag{16.20}$$

However, the twist-3 component of g_2 is unknown. Similarly, there is a relation expressing the twist-2 part of g_3 in terms of g_4. A complete set of relations, including M^2/Q^2 effects, can be found in Ref. 11.

16.2.2. *Structure functions and QCD*:

One of the most striking predictions of the quark-parton model is that the structure functions F^i, g^i *scale*, *i.e.*, $F^i(x,Q^2) \to F^i(x)$ in the Bjorken limit that Q^2 and $\nu \to \infty$ with x fixed [12]. This property is related to the assumption that the transverse momentum of the partons in the infinite-momentum frame of the proton is small. In QCD, however, the radiation of hard gluons from the quarks violates this assumption, leading to logarithmic scaling violations, which are particularly large at small x, see Fig. 16.2. The radiation of gluons produces the evolution of both the structure functions and the parton distribution functions. As Q^2 increases, more and more gluons are radiated, which in turn split into $q\overline{q}$ pairs. This process leads both to the softening of the initial quark momentum distributions and to the growth of the gluon density and the $q\overline{q}$ sea as x decreases.

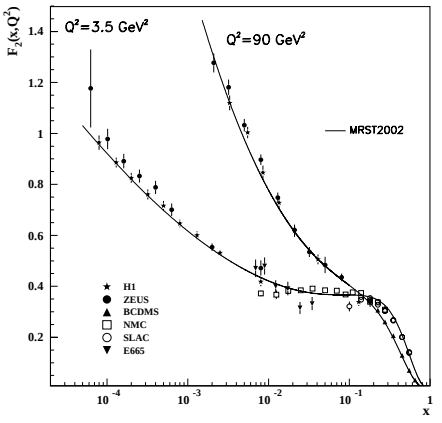

Figure 16.2: The proton structure function F_2^p given at two Q^2 values (3.5 GeV^2 and 90 GeV^2), which exhibit scaling at the 'pivot' point $x \sim 0.14$. See the caption in Fig. 16.6 for the references of the data. Also shown is the MRST2002 parameterization [13] given at the same scales.

In QCD, the above process is described in terms of scale-dependent parton distributions $f(x,\mu^2)$, where $f = g$ or q and, typically, μ is the scale of the probe Q. These distributions correspond, at a given x, to the density of partons in the proton integrated over transverse momentum k_t up to μ. Their evolution in μ is described in QCD by the DGLAP equations (see Refs. 14–17) which have the schematic form

$$\frac{\partial f}{\partial \ln \mu^2} \sim \frac{\alpha_s(\mu^2)}{2\pi}(P \otimes f) \ , \qquad (16.21)$$

where $\otimes$ denotes the convolution integral

$$P \otimes f \ = \ \int_x^1 \frac{dy}{y} \, P(y) \, f\left(\frac{x}{y}\right) \ . \qquad (16.22)$$

Although perturbative QCD can predict, via Eq. (16.21), the evolution of the parton distribution functions from a particular scale, μ_0, it cannot predict them *a priori* at any particular μ_0. Thus they must be measured at a starting point μ_0 before the predictions of QCD can be compared to the data at other scales, μ. In general, all observables involving a hard hadronic interaction (such as structure functions) can be expressed as a convolution of calculable, process-dependent coefficient functions and these universal parton distributions.

It is often convenient to write the evolution equations in terms of the gluon, non-singlet (q^{NS}) and singlet (q^S) quark distributions, such that

$$q^{NS} \ = \ q_i - \overline{q}_i, \qquad q^S \ = \ \sum_i (q_i + \overline{q}_i) \ . \qquad (16.23)$$

The non-singlet distributions have non-zero values of flavor quantum numbers, such as isospin and baryon number. The DGLAP evolution equations then take the form

$$\frac{\partial q^{NS}}{\partial \ln \mu^2} = \frac{\alpha_s(\mu^2)}{2\pi} \, P_{qq} \ \otimes \ q^{NS} \ ,$$

$$\frac{\partial}{\partial \ln \mu^2} \begin{pmatrix} q^S \\ g \end{pmatrix} = \frac{\alpha_s(\mu^2)}{2\pi} \begin{pmatrix} P_{qq} & 2n_f \, P_{qg} \\ P_{gq} & P_{gg} \end{pmatrix} \otimes \begin{pmatrix} q^S \\ g \end{pmatrix} \ , \qquad (16.24)$$

where P are splitting functions that describe the probability of a given parton splitting into two others, and n_f is the number of (active) quark flavors. The leading-order Altarelli-Parisi [16] splitting functions are

$$P_{qq} = \frac{4}{3}\left[\frac{1+x^2}{(1-x)}\right]_+ = \frac{4}{3}\left[\frac{1+x^2}{(1-x)_+}\right] + 2\delta(1-x) \ , \qquad (16.25)$$

$$P_{qg} = \frac{1}{2}\left[x^2 + (1-x)^2\right] \ , \qquad (16.26)$$

$$P_{gq} = \frac{4}{3}\left[\frac{1+(1-x)^2}{x}\right] \ , \qquad (16.27)$$

$$P_{gg} = 6\left[\frac{1-x}{x} + x(1-x) + \frac{x}{(1-x)_+}\right] + \left[\frac{11}{2} - \frac{n_f}{3}\right]\delta(1-x), \qquad (16.28)$$

where the notation $[F(x)]_+$ defines a distribution such that for any sufficiently regular test function, $f(x)$,

$$\int_0^1 dx f(x)[F(x)]_+ = \int_0^1 dx \ (f(x) - f(1))F(x) \ . \qquad (16.29)$$

In general, the structure functions can be expressed as a power series in α_s. The series contains both terms proportional to $\ln \mu^2$ and to $\ln 1/x$. The leading $\ln \mu^2$ terms come, in an axial gauge, from evolution along the parton chain that is strongly ordered in transverse momenta, that is $\mu^2 \gg k_{t,n}^2 \gg k_{t,n-1}^2 \gg \ldots$, where n denotes the n^{th} parton-branching process and k_t the parton transverse momentum. The leading-order DGLAP evolution sums up the $(\alpha_s \ln \mu^2)^n$ contributions. The next-to-leading order (NLO) sums up the $\alpha_s(\alpha_s \ln \mu^2)^{n-1}$ terms [18,19], which arise when two adjacent $k_{t,i}$'s are no longer strongly ordered but become comparable, thereby losing a factor of $\ln \mu^2$. The NNLO contributions are now almost all known (see Refs. 20–24).

In the small x kinematic region, it is essential to sum leading terms in $\ln 1/x$, independent of the value of $\ln \mu^2$. At leading order, this is done by the BFKL equation for the unintegrated distributions (see Refs. 25,26). The leading-order $(\alpha_s \ln(1/x))^n$ terms come from the configuration strongly ordered in x, *i.e.*, $x \ll x_n \ll x_{n-1} \ll \ldots$.

In general, however, QCD color coherence implies *angular* ordering along the chain, so that it is necessary to work in terms of $f_a(x, k_t^2, \mu^2)$, the parton distributions unintegrated over k_t. These distributions depend on two hard scales: k_t and the scale μ of the probe. Consequently they satisfy more complicated CCFM evolution equations [27,28]. The DGLAP and BFKL equations are two limits of angular-ordered evolution. In the DGLAP collinear approximation, the angle increases due to the growth of k_t, while, in the BFKL treatment, the angle ($\theta \simeq k_t/k_l$, where k_l is the longitudinal momentum) grows due to the decrease of the longitudinal-momentum fraction, x, along the chain of parton emissions from the proton.

As yet, there is no firm evidence in the data for $Q^2 \gtrsim 2$ GeV^2 for any deviation from standard DGLAP evolution, except that some DGLAP parton sets predict an unphysical behavior for F_L at low x [29], see however Ref. 30.

The precision of the contemporary experimental data demands that NLO (or even NNLO) DGLAP evolution be used in comparisons between QCD theory and experiment. At higher orders, it is necessary to specify, and to use consistently, both a renormalization and a factorization scheme. Whereas the renormalization scheme used is almost universally the modified minimal subtraction ($\overline{MS}$) scheme,

there are two popular choices for factorization scheme, in which the form of the correction for each structure function is different. The two most-used factorization schemes are: DIS [31], in which there are no higher-order corrections to the F_2 structure function, and $\overline{MS}$ (based on Refs. 32–34). They differ by how the higher-order gluon divergences are assimilated in the parton distribution functions.

Perturbative QCD predicts the Q^2 behavior of leading-twist (twist-2) contributions to the structure functions. Higher-twist terms, which involve their own non-perturbative input, can occur. These die off as powers of Q; specifically twist-n terms are damped by $1/Q^{n-2}$. The higher-twist terms appear to be numerically unimportant for Q^2 above a few GeV^2, except for x close to 1. At very large values of x, perturbative corrections proportional to $\log(1-x)$ can become important [35].

So far, it has been assumed that the quarks are massless. The effects of the c and b-quark masses on the evolution have been studied, for example, in Refs. 36–39. An approach using a variable flavor number is now generally adopted, in which evolution with $n_f = 3$ is matched to that with $n_f = 4$ at the charm threshold, with an analogous matching at the bottom threshold.

16.3. Determination of parton distributions

The parton distribution functions (PDFs) can be determined from data for deep inelastic lepton-nucleon scattering and for related hard-scattering processes initiated by nucleons. Table 16.1 given below (based on Ref. 40) highlights some processes and their primary sensitivity to PDFs.

Table 16.1: Lepton-nucleon and related hard-scattering processes and their primary sensitivity to the parton distributions that are probed.

Process	Main Subprocess	PDFs Probed
$\ell^\pm N \to \ell^\pm X$	$\gamma^* q \to q$	$g(x \lesssim 0.01), q, \overline{q}$
$\ell^+(\ell^-)N \to \overline{\nu}(\nu)X$	$W^* q \to q'$	
$\nu(\overline{\nu})N \to \ell^-(\ell^+)X$	$W^* q \to q'$	
$\nu\ N \to \mu^+\mu^- X$	$W^* s \to c \to \mu^+$	s
$pp \to \gamma X$	$qg \to \gamma q$	$g(x \sim 0.4)$
$pN \to \mu^+\mu^- X$	$q\overline{q} \to \gamma^*$	$\overline{q}$
$pp, pn \to \mu^+\mu^- X$	$u\overline{u}, d\overline{d} \to \gamma^*$	$\overline{u} - \overline{d}$
	$u\overline{d}, d\overline{u} \to \gamma^*$	
$ep, en \to e\pi X$	$\gamma^* q \to q$	
$p\overline{p} \to W \to \ell^\pm X$	$ud \to W$	$u, d, u/d$
$p\overline{p} \to$ jet $+X$	$gg, qg, qq \to 2j$	$q, g(0.01 \lesssim x \lesssim 0.5)$

The kinematic ranges of fixed-target and collider experiments are complementary (as is shown in Fig. 16.3) which enables the determination of PDFs over a wide range in x and Q^2. Recent determinations of the unpolarized PDF's from NLO global analyses are given in Refs. 29,13 and Ref. 41, and at NNLO in Refs. 42,30, see also Ref. 43. Recent studies of the uncertainties in the PDFs and observables can be found in Refs. 44,45 and Refs. 13,30, see also Ref. 46. The result of one analysis is shown in Fig. 16.4 at a scale $\mu^2 = 10$ GeV^2. The polarized PDFs are obtained through NLO global analyses of measurements of the g_1 structure function in inclusive polarized deep inelastic scattering (for recent examples see Refs. 47–49). The inclusive data do not provide enough observables to determine all polarized PDFs. These polarized PDFs may be fully accessed via flavor tagging in semi-inclusive deep inelastic scattering. Fig. 16.5 shows several global analyses at a scale of 2.5 GeV^2 along with the data from semi-inclusive DIS.

Comprehensive sets of PDFs available as program-callable functions can be obtained from several sources *e.g.*, Refs. 52,53. As a result of a Les Houches Accord, a PDF package (LHAPDF) exists [54] which facilitates the inclusion of recent PDFs in Monte Carlo/Matrix Element programs in a very compact and efficient format.

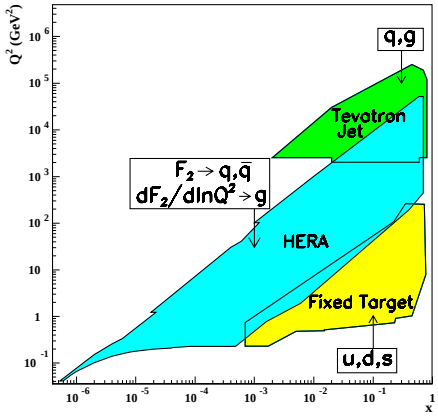

Figure 16.3: Kinematic domains in x and Q^2 probed by fixed-target and collider experiments, shown together with the important constraints they make on the various parton distributions.

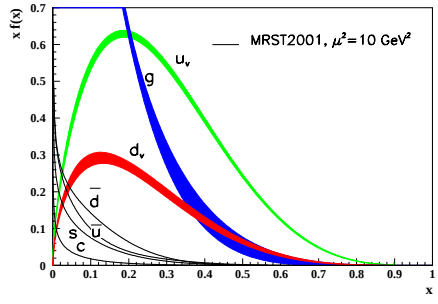

Figure 16.4: Distributions of x times the unpolarized parton distributions $f(x)$ (where $f = u_v, d_v, \overline{u}, \overline{d}, s, c, g$) using the MRST2001 parameterization [29,13](with uncertainties for u_v, d_v, and g) at a scale $\mu^2 = 10$ GeV^2.

16.4. DIS determinations of α_s

Table 16.2 shows the values of $\alpha_S(M_Z^2)$ found in recent fits to DIS and related data in which the coupling is left as a free parameter.

There have been several other studies of α_s at NNLO, and beyond, using subsets of DIS data (see, for example, Refs. 57–59). Moreover, there exist global NLO analyses of polarised DIS data which give $\alpha_s(M_Z^2) = 0.120 \pm 0.009$ [60] and 0.114 ± 0.009 [49].

16.5. The hadronic structure of the photon

Besides the *direct* interactions of the photon, it is possible for it to fluctuate into a hadronic state via the process $\gamma \to q\overline{q}$. While in this state, the partonic content of the photon may be *resolved*, for example, through the process $e^+e^- \to e^+e^-\gamma^*\gamma \to e^+e^-X$ where the virtual photon emitted by the deep inelastic scattering lepton probes the hadronic structure of the quasi-real photon emitted by the other lepton. The perturbative LO contributions, $\gamma \to q\overline{q}$ followed by $\gamma^* q \to q$, are subject to QCD corrections due to the coupling of quarks to gluons.

Often the equivalent-photon approximation is used to express the differential cross section for deep inelastic electron–photon scattering

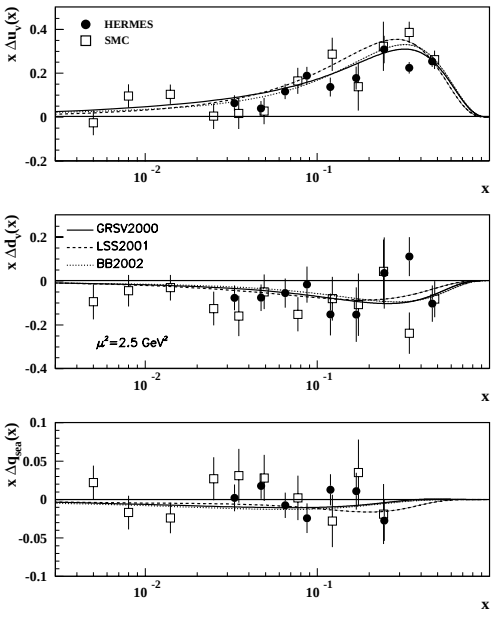

Figure 16.5: Distributions of x times the polarized parton distributions $\Delta q(x)$ (where $q = u_v, d_v, q_{sea}$) using the GRSV2000 [47], LSS2001 [48], and BB2002 [49] parameterizations at a scale $\mu^2 = 2.5$ GeV^2. Points represent data from semi-inclusive positron (HERMES [50]) and muon (SMC [51]) deep inelastic scattering given at $Q^2 = 2.5$ GeV^2.

Table 16.2: The values of $\alpha_S(M_Z^2)$ found in NLO and NNLO fits to DIS data. The experimental errors quoted correspond to an increase $\Delta\chi^2$ from the best fit value of χ^2. CTEQ6 [41] and MRST03 [30] are global fits. H1 [56] fit only a subset of the F_2^{ep} data, while Alekhin [43] also includes F_2^{ed} and ZEUS [55] in addition include xF_3^{ν} data.

	$\Delta\chi^2$	$\alpha_S(M_Z^2)$ $\pm$ expt $\pm$ theory $\pm$ model	
NLO			
CTEQ6	100	0.1165 ± 0.0065	
ZEUS	50	0.1166 ± 0.0049	± 0.0018
MRST03	5	$0.1165 \pm 0.002 \pm 0.003$	
H1	1	$0.115 \pm 0.0017 \pm 0.005^{+0.0009}_{-0.0005}$	
Alekhin	1	$0.1171 \pm 0.0015 \pm 0.0033$	
NNLO			
MRST03	5	$0.1153 \pm 0.002 \pm 0.003$	
Alekhin	1	$0.1143 \pm 0.0014 \pm 0.0009$	

in terms of the structure functions of the transverse quasi-real photon times a flux factor N for the incoming quasi-real photons of transverse polarisation

$$\frac{d^2\sigma}{dxdQ^2} = N\frac{2\pi\alpha^2}{xQ^4}\left[\left(1+(1-y)^2\right)F_2^{\gamma}(x,Q^2) - y^2 F_L^{\gamma}(x,Q^2)\right],$$

where we have used $F_2^{\gamma} = 2xF_T^{\gamma} + F_L^{\gamma}$. Complete formulae are given, for example, in the comprehensive review of Ref. 61.

The hadronic photon structure function F_2^{γ} evolves from the 'hadron-like' behavior, calculable via the vector-meson-dominance model, to the dominating 'point-like' behaviour, calculable in perturbative QCD, with increasing Q^2. Due to the point-like coupling, the logarithmic evolution of F_2^{γ} with Q^2 has a *positive* slope for all values of x, see Fig. 16.13. The 'loss' of quarks at large x due to gluon radiation is over-compensated by the 'creation' of quarks via the point-like $\gamma \to q\bar{q}$ coupling. The logarithmic evolution was first predicted in the quark–parton model ($\gamma^*\gamma \to q\bar{q}$) [62,63] and then in QCD in the limit of large Q^2 [64].

* The value of $\eta^{\rm CC}$ deduced from Ref. 1 is found to be a factor of two too small; $\eta^{\rm CC}$ of Eq. (16.9) agrees with Refs. 2,3.

References:

1. J. Blümlein and N. Kochelev, Nucl. Phys. **B498**, 285 (1997).
2. S. Forte, M.L. Mangano, and G. Ridolfi, Nucl. Phys. **B602**, 585 (2001).
3. M. Anselmino, P. Gambino, and J. Kalinowski, Z. Phys. **C64**, 267 (1994).
4. M. Anselmino, A. Efremov, and E. Leader, Phys. Rep. **261**, 1 (1995).
5. M. Klein and T. Riemann, Z. Phys. **C24**, 151 (1984).
6. C.G. Callan and D.J. Gross, Phys. Rev. Lett. **22**, 156 (1969).
7. D.A. Dicus, Phys. Rev. **D5**, 1367 (1972).
8. J.D. Bjorken and E.A. Paschos, Phys. Rev. **185**, 1975 (1969).
9. R.P. Feynman, Photon Hadron Interactions (Benjamin, New York, 1972).
10. S. Wandzura and F. Wilczek, Phys. Rev. **B72**, 195 (1977).
11. J. Blümlein and A. Tkabladze, Nucl. Phys. **B553**, 427 (1999).
12. J.D. Bjorken, Phys. Rev. **179**, 1547 (1969).
13. A.D. Martin, R.G. Roberts, W.J. Stirling, and R.S. Thorne, Eur. Phys. J. **C28**, 455 (2003).
14. V.N. Gribov and L.N. Lipatov, Sov. J. Nucl. Phys. **15**, 438 (1972).
15. L.N. Lipatov, Sov. J. Nucl. Phys. **20**, 95 (1975).
16. G. Altarelli and G. Parisi, Nucl. Phys. **B126**, 298 (1977).
17. Yu.L. Dokshitzer, Sov. Phys. JETP **46**, 641 (1977).
18. G. Curci, W. Furmanski, and R. Petronzio, Nucl. Phys. **B175**, 27 (1980).
19. R.K. Ellis, W.J. Stirling, and B.R. Webber, QCD and Collider Physics (Cambridge UP, 1996).
20. E.B. Zijlstra and W.L. van Neerven, Nucl. Phys. **B383**, 525 (1992).
21. S. Moch and J.A.M. Vermaseren, Nucl. Phys. **B573**, 853 (2000).
22. S.A. Larin, P. Nogueira, T. van Ritbergen and J.A.M. Vermaseren, Nucl. Phys. **B492**, 338 (1997).
23. A. Retey and J.A.M. Vermaseren, Nucl. Phys. **B604**, 281 (2001).
24. S. Moch, J.A.M. Vermaseren and A. Vogt, Nucl. Phys. **B646**, 181 (2002).
25. E.A. Kuraev, L.N. Lipatov, and V.S. Fadin, Phys. Lett. **B60**, 50 (1975); Sov. Phys. JETP **44**, 443 (1976); Sov. Phys. JETP **45**, 199 (1977).
26. Ya.Ya. Balitsky and L.N. Lipatov, Sov. J. Nucl. Phys. **28**, 822 (1978).
27. M. Ciafaloni, Nucl. Phys. **B296**, 49 (1988).
28. S. Catani, F. Fiorani, and G. Marchesini, Phys. Lett. **B234**, 339 (1990); Nucl. Phys. **B336**, 18 (1990).
29. A.D. Martin, R.G. Roberts, W.J. Stirling, and R.S. Thorne, Eur. Phys. J. **C23**, 73 (2002).
30. A.D. Martin, R.G. Roberts, W.J. Stirling and R.S. Thorne, (MRST2003) `hep-ph/0308087`.
31. G. Altarelli, R.K. Ellis, and G. Martinelli, Nucl. Phys. **B143**, 521 (1978) and erratum: Nucl. Phys. **B146**, 544 (1978).
32. G. 't Hooft and M. Veltman, Nucl. Phys. **B44**, 189 (1972).

33. G. 't Hooft, Nucl. Phys. **B61**, 455 (1973).
34. W.A. Bardeen *et al.*, Phys. Rev. **D18**, 3998 (1978).
35. G. Sterman, Nucl. Phys. **B281**, 310 (1987).
36. M.A.G. Aivazis *et al.*, Phys. Rev. **D50**, 3102 (1994).
37. J.C. Collins, Phys. Rev. **D58**, 094002 (1998).
38. R.S. Thorne and R.G. Roberts, Phys. Rev. **D57**, 1998 (1998); Phys. Lett. **B421**, 303 (1998); Eur. Phys. J. **C19**, 339 (2001).
39. W.-K. Tung, S. Kretzer and C. Schmidt, J. Phys. **G28**, 983 (2002).
40. A.D. Martin, R.G. Roberts, W.J. Stirling, and R.S. Thorne, Eur. Phys. J. **C4**, 463 (1998).
41. CTEQ, J. Pumplin *et al.*, JHEP **0207**, 012 (2002).
42. A.D. Martin, R.G. Roberts, W.J. Stirling, and R.S. Thorne, Phys. Lett. **B531**, 216 (2002).
43. S. Alekhin, JHEP **0302**, 015 (2003).
44. CTEQ, D. Stump *et al.*, Phys. Rev. **D65**, 014012 (2001).
45. CTEQ, J. Pumplin *et al.*, Phys. Rev. **D65**, 014013 (2001).
46. W.T. Giele, S. Keller and D.A. Kosower, `hep-ph/0104052`.
47. M. Glück, E. Reya, M. Stratmann, and W. Vogelsang, Phys. Rev. **D63**, 094005 (2001).
48. E. Leader, A.V. Sidorov and D.B. Stamenov, Eur. Phys. J. **C23**, 479 (2002).
49. J. Blümlein and H. Böttcher, Nucl. Phys. **B636**, 225 (2002).
50. HERMES, K. Ackerstaff *et al.*, Phys. Lett. **B464**, 123 (1999).
51. SMC, B. Adeva *et al.*, Phys. Lett. **B420**, 180 (1998).
52. H. Plothow-Besch, CERN PDFLIB, W5051 (2000).
53. `http://durpdg.dur.ac.uk/HEPDATA/PDF`.
54. `http://durpdg.dur.ac.uk/lhapdf/index.html`.
55. ZEUS, S. Chenakov *et al.*, Phys. Rev. **D67**, 012007 (2003).
56. H1, C. Adloff *et al.*, Eur. Phys. J. **C21**, 33 (2001).
57. W.L. van Neerven and A. Vogt, Nucl. Phys. **B603**, 42 (2001).
58. J. Santiago and F.J. Yndurain, Nucl. Phys. **B611**, 447 (2001).
59. A.L. Kataev, G. Parente, and A.V. Sidorov, Nucl. Phys. Proc. Supp. **116**, 105 (2003).
60. G. Altarelli, R.D. Ball, S. Forte, and G. Ridolfi, Nucl. Phys. **B496**, 337 (1997).
61. R. Nisius, Phys. Reports **332**, 165 (2000).
62. T.F. Walsh and P.M. Zerwas, Phys. Lett. **B44**, 195 (1973).
63. R.L. Kingsley, Nucl. Phys. **B60**, 45 (1973).
64. E. Witten, Nucl. Phys. **B120**, 189 (1977).

NOTE: THE FIGURES IN THIS SECTION ARE INTENDED TO SHOW THE REPRESENTATIVE DATA.
THEY ARE NOT MEANT TO BE COMPLETE COMPILATIONS OF ALL THE WORLD'S RELIABLE DATA.

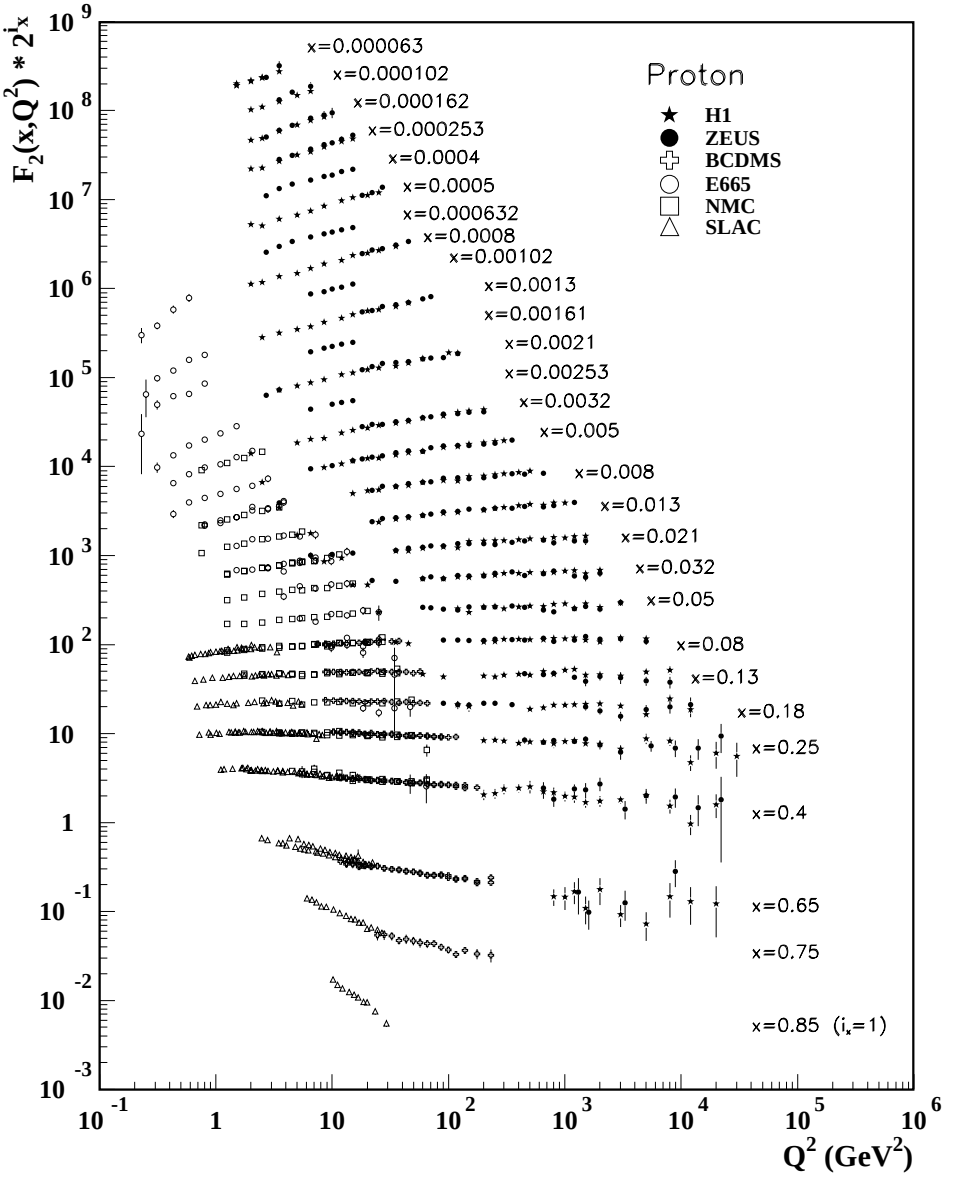

Figure 16.6: The proton structure function F_2^p measured in electromagnetic scattering of positrons on protons (collider experiments ZEUS and H1), in the kinematic domain of the HERA data, for $x > 0.00006$ (*cf.* Fig. 16.9 for data at smaller x and Q^2), and for electrons (SLAC) and muons (BCDMS, E665, NMC) on a fixed target. Statistical and systematic errors added in quadrature are shown. The data are plotted as a function of Q^2 in bins of fixed x. Some points have been slightly offset in Q^2 for clarity. The ZEUS binning in x is used in this plot; all other data are rebinned to the x values of the ZEUS data. For the purpose of plotting, F_2^p has been multiplied by 2^{i_x}, where i_x is the number of the x bin, ranging from $i_x = 1$ ($x = 0.85$) to $i_x = 28$ ($x = 0.000063$). References: **H1**—C. Adloff *et al.*, Eur. Phys. J. **C21**, 33 (2001); C. Adloff *et al.*, Eur. Phys. J. (accepted for publication) hep-ex/0304003; **ZEUS**—S. Chekanov *et al.*, Eur. Phys. J. **C21**, 443 (2001); **BCDMS**—A.C. Benvenuti *et al.*, Phys. Lett. **B223**, 485 (1989) (as given in [53]); **E665**—M.R. Adams *et al.*, Phys. Rev. **D54**, 3006 (1996); **NMC**—M. Arneodo *et al.*, Nucl. Phys. **B483**, 3 (97); **SLAC**—L.W. Whitlow *et al.*, Phys. Lett. **B282**, 475 (1992).

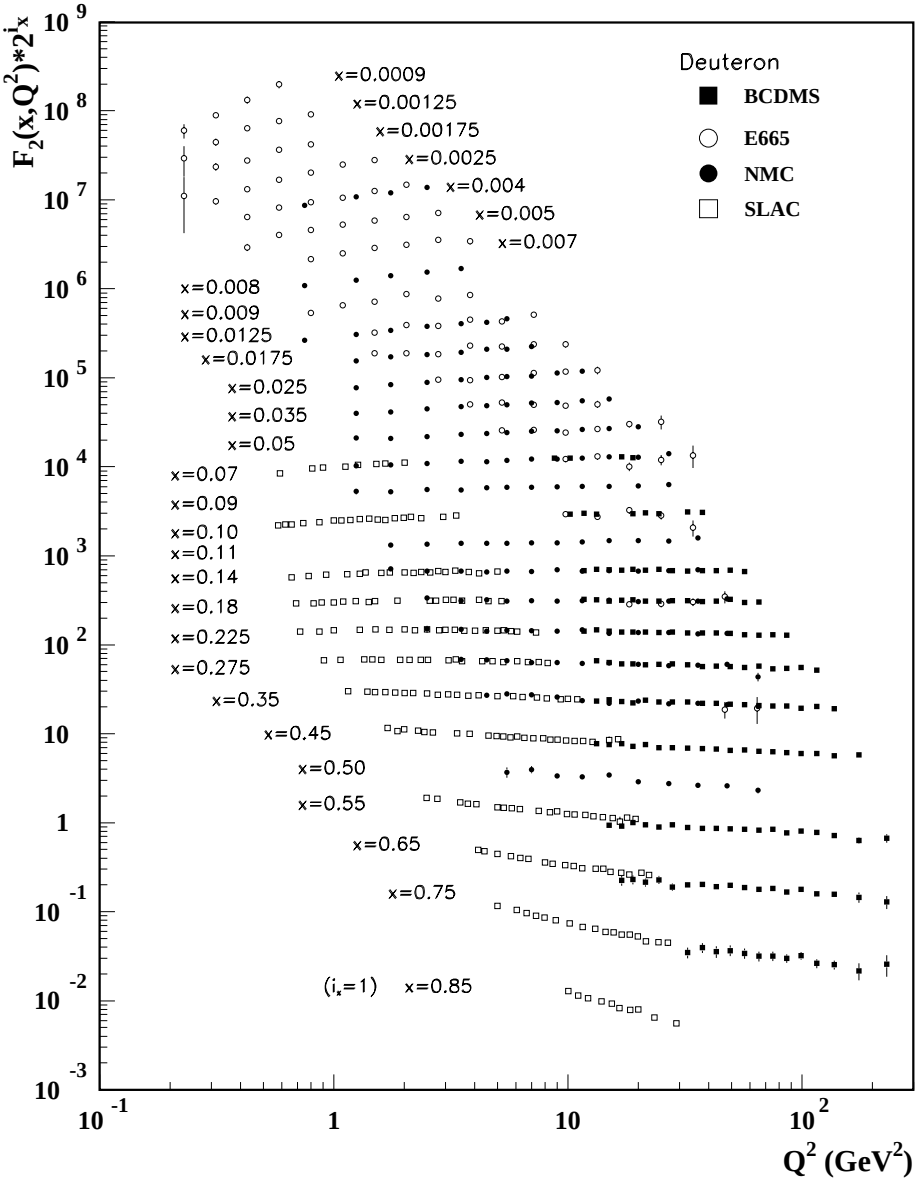

Figure 16.7: The deuteron structure function F_2^d measured in electromagnetic scattering of electrons (SLAC) and muons (BCDMS, E665, NMC) on a fixed target, shown as a function of Q^2 for bins of fixed x. Statistical and systematic errors added in quadrature are shown. For the purpose of plotting, F_2^p has been multiplied by 2^{ix}, where i_x is the number of the x bin, ranging from 1 ($x = 0.85$) to 29 ($x = 0.0009$). References: **BCDMS**—A.C. Benvenuti *et al.*, Phys. Lett. **B237**, 592 (1990). **E665, NMC, SLAC**—same references as Fig. 16.6.

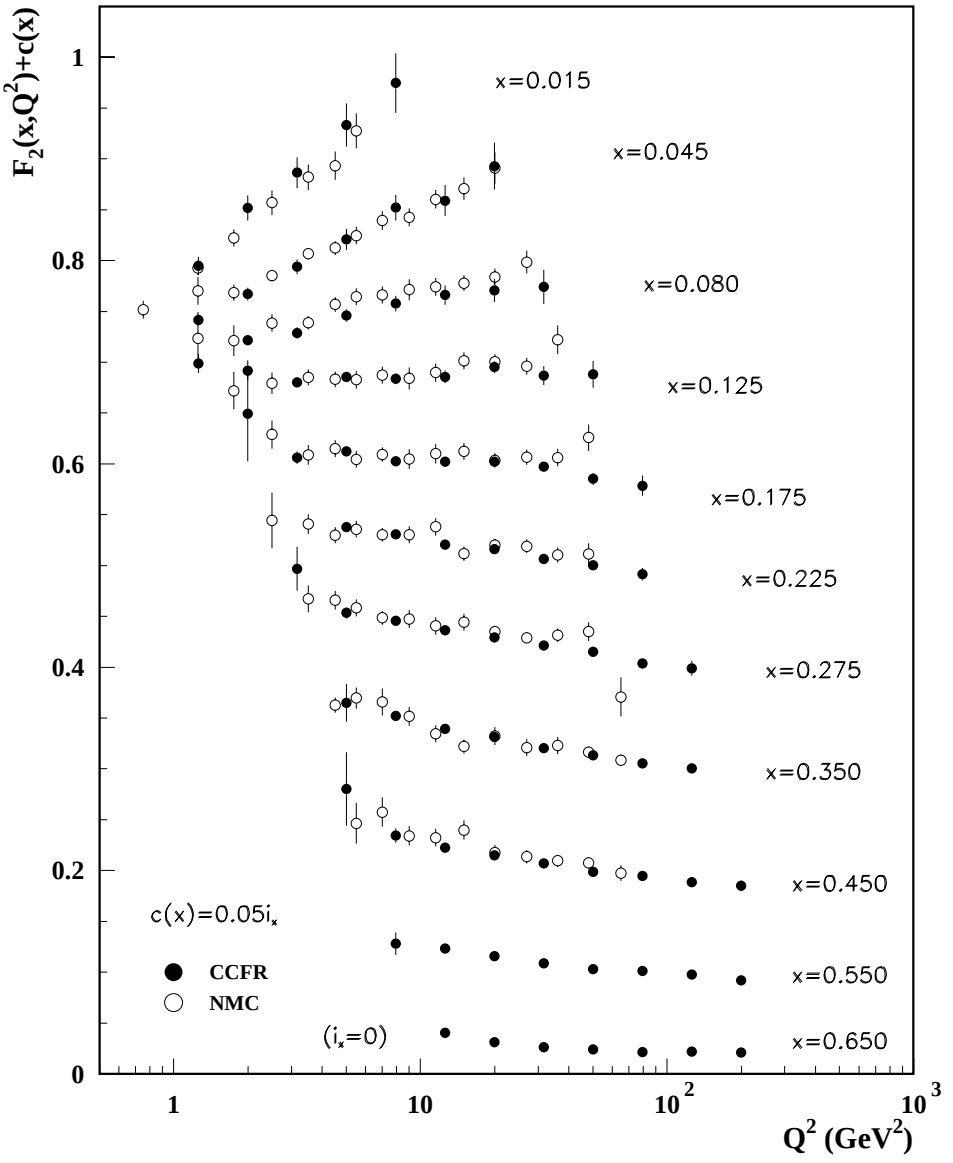

Figure 16.8: The deuteron structure function F_2 measured in deep inelastic scattering of muons on a fixed target (NMC) is compared to the structure function F_2 from neutrino-iron scattering (CCFR) using $F_2^\mu = (5/18)F_2^\nu - x(s+\bar{s})/6$, where heavy target effects have been taken into account. The data are shown versus Q^2, for bins of fixed x. The NMC data have been rebinned to CCFR x values. Statistical and systematic errors added in quadrature are shown. For the purpose of plotting, a constant $c(x) = 0.05 i_x$ is added to F_2 where i_x is the number of the x bin, ranging from 0 ($x = 0.65$) to 10 ($x = 0.015$). References: **NMC**—M. Arneodo *et al.*, Nucl. Phys. **B483**, 3 (97); **CCFR/NuTeV**—U.K. Yang *et al.*, Phys. Rev. Lett. **86**, 2741 (2001).

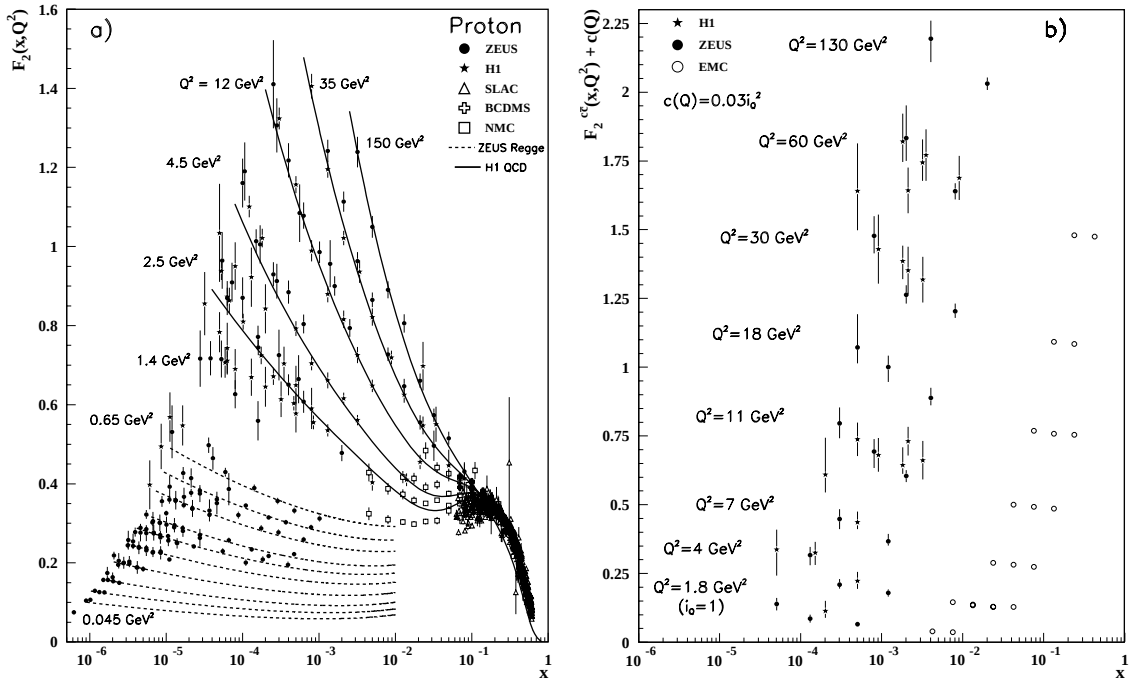

Figure 16.9: a) The proton structure function F_2^p mostly at small x and Q^2, measured in electromagnetic scattering of positrons (H1, ZEUS), electrons (SLAC), and muons (BCDMS, NMC) on protons. Lines are ZEUS and H1 parameterizations for lower (Regge) and higher (QCD) Q^2. Some points are only within 10% of the stated Q^2. Some points have been slightly offset in x for clarity. References: **ZEUS**—J. Breitweg *et al.*, Phys. Lett. **B407**, 432 (1997); J. Breitweg *et al.*, Eur. Phys. J. **C7**, 609 (1999); J. Breitweg *et al.*, Phys. Lett. **B487**, 53 (2000) (both data and ZEUS Regge parameterization); S. Chekanov *et al.*, Eur. Phys. J. **C21**, 443 (2001); **H1**—C. Adloff *et al.*, Nucl. Phys. **B497**, 3 (1997); C. Adloff *et al.*, Eur. Phys. J. **C21**, 33 (2001) (both data and H1 QCD parameterization) ; **BCDMS, NMC, SLAC**—same references as Fig. 16.6.

b) The charm structure function $F_2^{c\overline{c}}(x)$, i.e. that part of the inclusive structure function F_2^p arising from the production of charm quarks, measured in electromagnetic scattering of positrons on protons (H1, ZEUS) and muons on iron (EMC). The H1 points have been slightly offset in x for clarity. For the purpose of plotting, a constant $c(Q) = 0.03 i_Q^2$ is added to $F_2^{c\overline{c}}$ where i_Q is the number of the Q^2 bin, ranging from 1 ($Q^2 = 1.8$ GeV^2) to 8 ($Q^2 = 130$ GeV^2). References: **ZEUS**—J. Breitweg *et al.*, Eur. Phys. J. **C12**, 35 (2000); **H1**—C. Adloff *et al.*, Z. Phys. **C72**, 593 (1996); C. Adloff *et al.*, Phys. Lett. **B528**, 199 (2002); **EMC**—J.J. Aubert *et al.*, Nucl. Phys. **B213**, 31 (1983).

Statistical and systematic errors added in quadrature are shown for both plots. The data are given as a function of x in bins of Q^2.

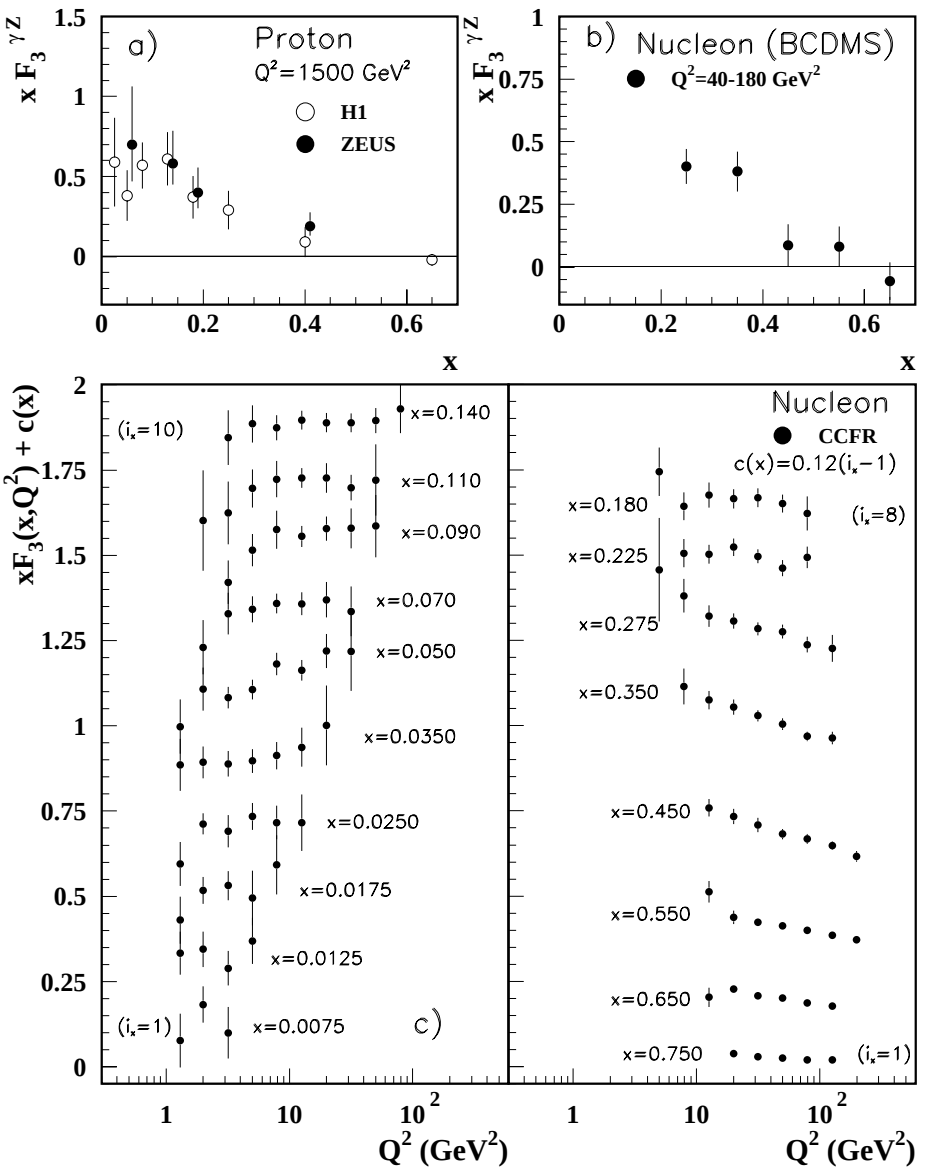

Figure 16.10: The structure function $xF_3^{\gamma Z}$ measured in electroweak scattering of **a)** electrons on protons (H1 and ZEUS) and **b)** muons on carbon (BCDMS). The ZEUS points have been slightly offset in x for clarity. References: **H1**—C. Adloff *et al.*, Eur. Phys. J. (accepted for publication) hep-ex/0304003; **ZEUS**–S. Chekanov *et al.*, Eur. Phys. J. **C28**, 175 (2003); **BCDMS**—A. Argento *et al.*, Phys. Lett. **B140**, 142 (1984).

c) The structure function xF_3 of the nucleon measured in ν-Fe scattering. The data are plotted as a function of Q^2 in bins of fixed x. For the purpose of plotting, a constant $c(x) = 0.12(i_x - 1)$ is added to xF_3, where i_x is the number of the x bin as shown in the plot. References: **CCFR**–W.G. Seligman *et al.*, Phys. Rev. Lett. **79**, 1213 (1997).

Statistical and systematic errors added in quadrature are shown for all plots.

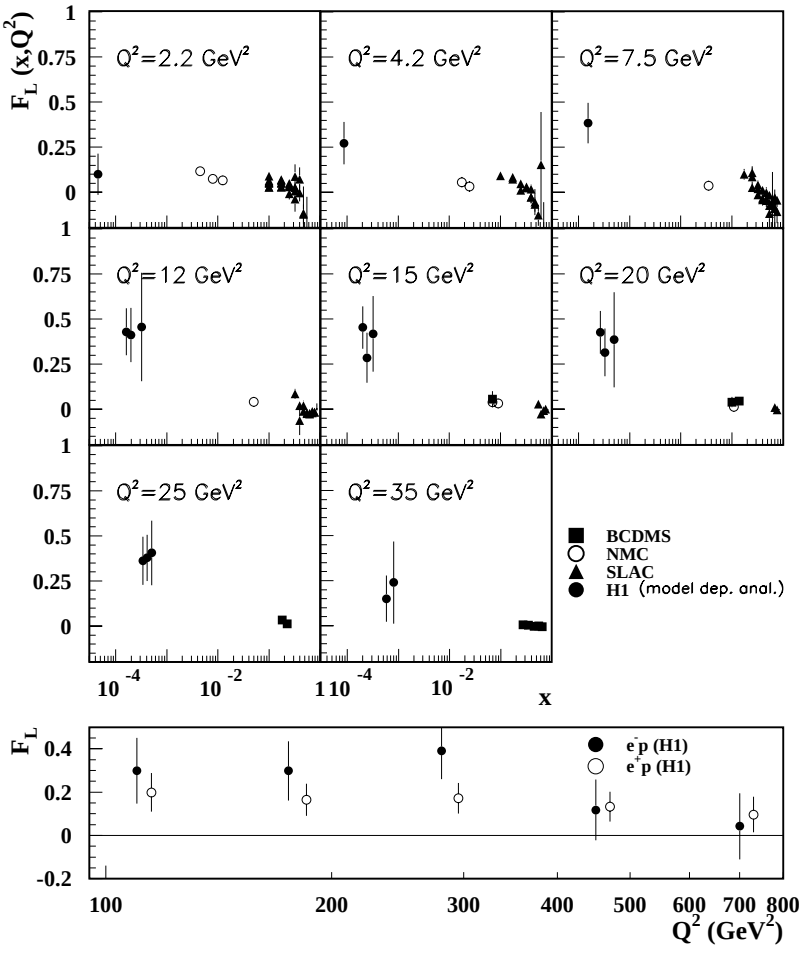

Figure 16.11: Top panel: The longitudinal structure function F_L as a function of x in bins of fixed Q^2 measured on the proton (except for the SLAC data which also contain deuterium data). BCDMS, NMC, and SLAC results are from measurements of R (the ratio of longitudinal to transverse photon absorption cross sections) which are converted to F_L by using the BDCMS parameterization of F_2 (A.C. Benvenuti *et al.*, Phys. Lett. **B223**, 485 (1989)). It is assumed that the Q^2 dependence of the fix-target data is small within a given Q^2 bin. References: **H1**—C. Adloff *et al.*, Eur. Phys. J. **C21**, 33 (2001); **BCDMS**—A. Benvenuti *et al.*, Phys. Lett. **B223**, 485 (1989); **NMC**—M. Arneodo *et al.*, Nucl. Phys. **B483**, 3 (1997); **SLAC**— L.W. Whitlow *et al.*, Phys. Lett. **B250**, 193 (1990) and numerical values from the thesis of L.W. Whitlow (SLAC-357).

Bottom panel: Higher Q^2 values of the longitudinal structure function F_L as a function of Q^2 given at the measured x for e^+/e^--proton scattering. Points have been slightly offset in Q^2 for clarity. References: **H1**—C. Adloff *et al.*, Eur. Phys. J. (accepted for publication) hep-ex/0304003.

The H1 results shown in both plots require the assumption of the validity of the QCD form for the F_2 structure function in order to extract F_L. Statistical and systematic errors added in quadrature are shown for both plots.

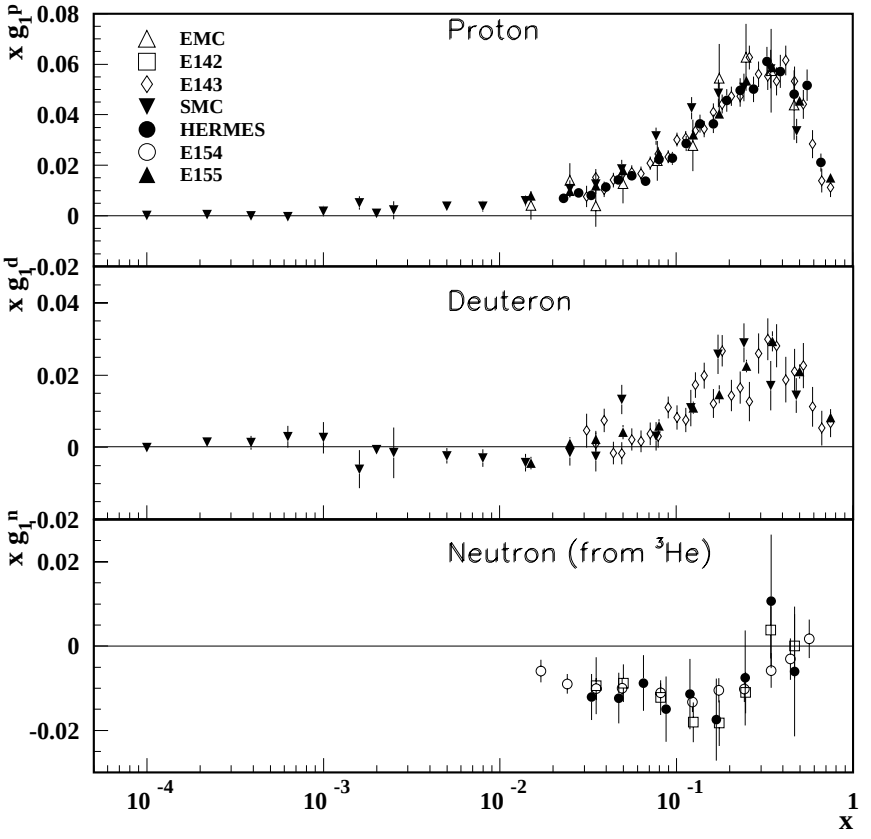

Figure 16.12: The spin-dependent structure function $xg_1(x)$ of the proton, deuteron, and neutron (from ^{3}He target) measured in deep inelastic scattering of polarized electrons/positrons: E142 ($Q^2 \sim 0.3 - 10$ GeV^2), E143 ($Q^2 \sim 0.3 - 10$ GeV^2), E154 ($Q^2 \sim 1 - 17$ GeV^2), E155 ($Q^2 \sim 1 - 40$ GeV^2), HERMES ($Q^2 \sim 0.8 - 20$ GeV^2) and muons: EMC ($Q^2 \sim 1.5 - 100$ GeV^2), SMC ($Q^2 \sim 0.01 - 100$ GeV^2), shown at the measured Q^2 (except for EMC data given $Q^2 = 10.7$ GeV^2 and E155 data given at $Q^2 = 5$ GeV^2). Note that $g_1^n(x)$ may also be extracted by taking the difference between $g_1^d(x)$ and $g_1^p(x)$, but these values have been omitted in the bottom plot for clarity. Statistical and systematic errors added in quadrature are shown. References: **EMC**—J. Ashman *et al.*, Nucl. Phys. **B328**, 1 (1989); **E142**—P.L. Anthony *et al.*, Phys. Rev. **D54**, 6620 (1996); **E143**—K. Abe *et al.*, Phys. Rev. **D58**, 112003 (1998); **SMC**—B. Adeva *et al.*, Phys. Rev. **D58**, 112001 (1998), B. Adeva *et al.*, Phys. Rev. **D60**, 072004 (1999) and Erratum-Phys. Rev. **D62**, 079902 (2000); **HERMES**—A. Airapetian *et al.*, Phys. Lett. **B442**, 484 (1998) and K. Ackerstaff *et al.*, Phys. Lett. **B404**, 383 (1997); **E154**—K. Abe *et al.*, Phys. Rev. Lett. **79**, 26 (1997); **E155**—P.L. Anthony *et al.*, Phys. Lett. **B463**, 339 (1999) and P.L. Anthony *et al.*, Phys. Lett. **B493**, 19 (2000).

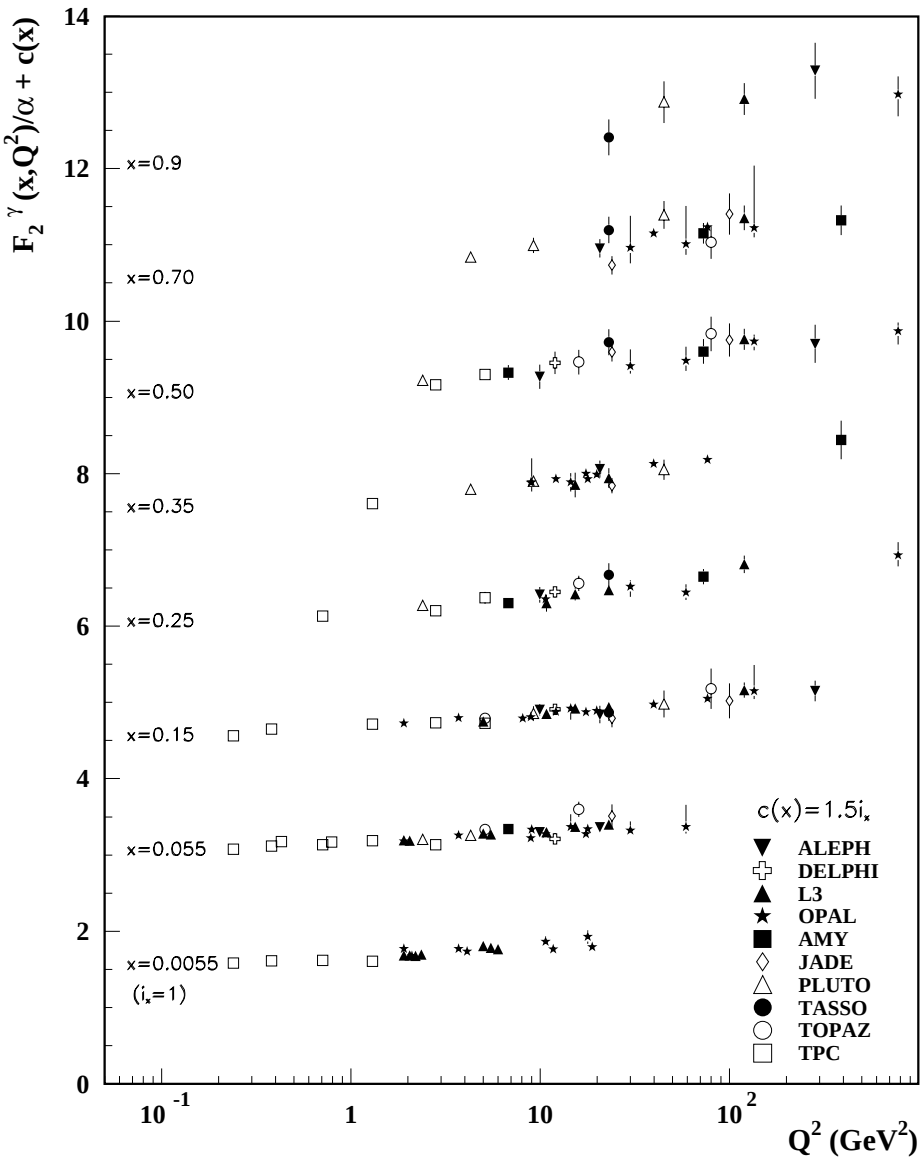

Figure 16.13: The hadronic structure function of the photon F_2^γ divided by the fine structure constant α measured in e^+e^- scattering, shown as a function of Q^2 for bins of x. Data points have been shifted to the nearest corresponding x bin as given in the plot. Some points have been offset in Q^2 for clarity. Statistical and systematic errors added in quadrature are shown. For the purpose of plotting, a constant $c(x) = 1.5i_x$ is added to F_2^γ/α where i_x is the number of the x bin, ranging from 1 ($x = 0.0055$) to 8 ($x = 0.9$). References: **ALEPH**–R. Barate *et al.*, Phys. Lett. **B458**, 152 (1999); **DELPHI**–P. Abreu *et al.*, Z. Phys. **C69**, 223 (1995); **L3**–M. Acciarri *et al.*, Phys. Lett. **B436**, 403 (1998); M. Acciarri *et al.*, Phys. Lett. **B447**, 147 (1999); M. Acciarri *et al.*, Phys. Lett. **B483**, 373 (2000); **OPAL**–A. Ackerstaff *et al.*, Phys. Lett. **B411**, 387 (1997); A. Ackerstaff *et al.*, Z. Phys. **C74**, 33 (1997); G. Abbiendi *et al.*, Eur. Phys. J. **C18**, 15 (2000); G. Abbiendi *et al.*, Phys. Lett. **B533**, 207 (2002) (note that there is some non-trivial statistical correlation between these last two papers); **AMY**–S.K. Sahu *et al.*, Phys. Lett. **B346**, 208 (1995); T. Kojima *et al.*, Phys. Lett. **B400**, 395 (1997); **JADE**–W. Bartel *et al.*, Z. Phys. **C24**, 231 (1984); **PLUTO**–C. Berger *et al.*, Phys. Lett. **142B**, 111 (1984); C. Berger *et al.*, Nucl. Phys. **B281**, 365 (1987); **TASSO**–M. Althoff *et al.*, Z. Phys. **C31**, 527 (1986); **TOPAZ**–K. Muramatsu *et al.*, Phys. Lett. **B332**, 477 (1994); **TPC/Two Gamma**–H. Aihara *et al.*, Z. Phys. **C34**, 1 (1987).

17. FRAGMENTATION FUNCTIONS IN e^+e^- ANNIHILATION

Revised September 2003 by O. Biebel (Max-Planck-Institut für Physik, Munich, Germany), P. Nason (INFN, Sez. di Milano, Milan, Italy), and B.R. Webber (Cavendish Laboratory, Cambridge, UK). An extended version of the 2001 version of this review can be found in Ref. 1

17.1. Introduction

Fragmentation functions are dimensionless functions that describe the final-state single-particle energy distributions in hard scattering processes. The total e^+e^- fragmentation function for hadrons of type h in annihilation at c.m. energy $\sqrt{s}$, via an intermediate vector boson $V = \gamma/Z^0$, is defined as

$$F^h(x,s) = \frac{1}{\sigma_{\rm tot}}\frac{d\sigma}{dx}(e^+e^- \to V \to hX) \qquad (17.1)$$

where $x = 2E_h/\sqrt{s} \le 1$ is the scaled hadron energy (in practice, the approximation $x = x_p = 2p_h/\sqrt{s}$ is often used). Its integral with respect to x gives the average multiplicity of those hadrons:

$$\langle n_h(s)\rangle = \int_0^1 dx\, F^h(x,s)\,. \qquad (17.2)$$

Neglecting contributions suppressed by inverse powers of s, the fragmentation function (17.1) can be represented as a sum of contributions from the different parton types $i = u, \overline{u}, d, \overline{d}, \ldots, g$:

$$F^h(x,s) = \sum_i \int_x^1 \frac{dz}{z} C_i(s;z,\alpha_{\rm S}) D_i^h(x/z,s)\,. \qquad (17.3)$$

where D_i^h are the parton fragmentation functions. At lowest order in $\alpha_{\rm S}$ the coefficient function C_g for gluons is zero, while for quarks $C_i = g_i(s)\delta(1-z)$ where $g_i(s)$ is the appropriate electroweak coupling. In particular, $g_i(s)$ is proportional to the charge-squared of parton i at $s \ll M_Z^2$, when weak effects can be neglected. In higher orders the coefficient functions and parton fragmentation functions are factorization-scheme dependent.

Parton fragmentation functions are analogous to the parton distributions in deep inelastic scattering (see sections on QCD and Stucture Functions (9 and 16 of this *Review*). In both cases, the simplest parton-model approach would predict a scale-independent x distribution. Furthermore we obtain similar violations of this scaling behaviour when QCD corrections are taken into account.

17.2. Scaling violation

The evolution of the parton fragmentation function $D_i(x,t)$ with increasing scale $t = s$, like that of the parton distribution function $f_i(x,t)$ with $t = s$ (see Sec. 39 of this *Review*), is governed by the DGLAP equation [2]

$$t\frac{\partial}{\partial t}D_i(x,t) = \sum_j \int_x^1 \frac{dz}{z}\frac{\alpha_{\rm S}}{2\pi}P_{ji}(z,\alpha_{\rm S})D_j(x/z,t)\,. \qquad (17.4)$$

In analogy to DIS, in some cases an evolution equation for the fragmentation function F itself (Eq. (17.3)) can be derived from Eq. (17.4) [3]. Notice that the splitting function is now P_{ji} rather than P_{ij} since here D_j represents the fragmentation of the final parton. The splitting functions again have perturbative expansions of the form

$$P_{ji}(z,\alpha_{\rm S}) = P_{ji}^{(0)}(z) + \frac{\alpha_{\rm S}}{2\pi}P_{ji}^{(1)}(z) + \cdots \qquad (17.5)$$

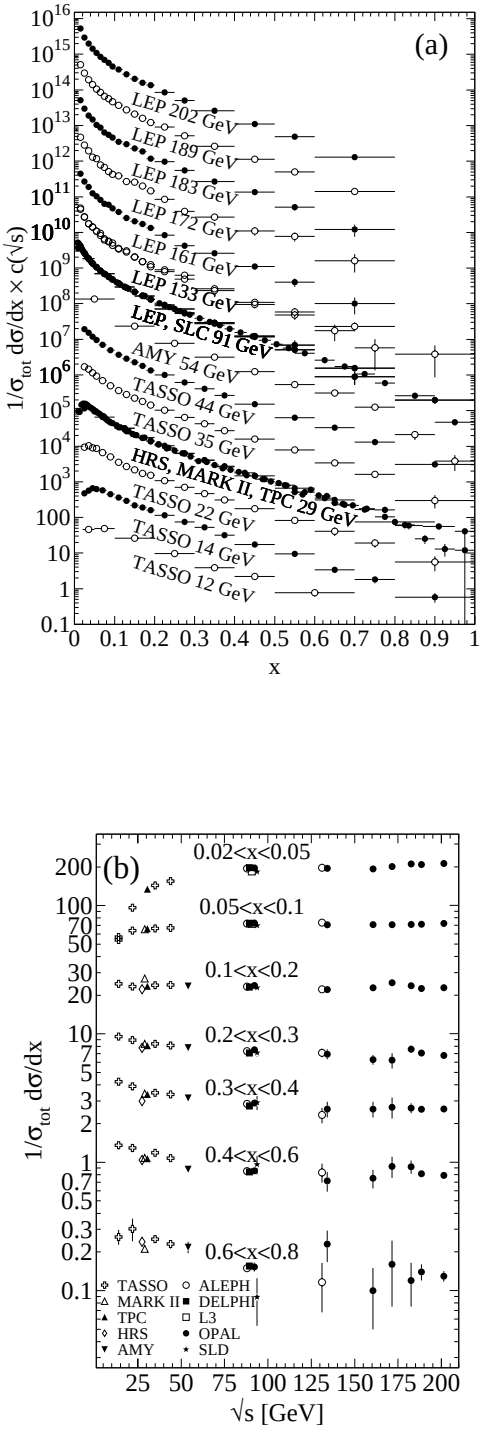

Figure 17.1: The e^+e^- fragmentation function for all charged particles is shown [6,7,8,9](a) for different c.m. energies, $\sqrt{s}$, versus x and (b) for various ranges of x versus $\sqrt{s}$. For the purpose of plotting (a), the distributions were scaled by $c(\sqrt{s}) = 10^i$ where i is ranging from $i = 0$ ($\sqrt{s} = 12$ GeV) to $i = 13$ ($\sqrt{s} = 202$ GeV).

where the lowest-order functions $P_{ji}^{(0)}(z)$ are the same as those in deep inelastic scattering but the higher-order terms [4] [1] are different. The effect of evolution is, however, the same in both cases: as the scale increases, one observes a scaling violation in which the x distribution is shifted towards lower values. This can be seen from Fig. 17.1.

The coefficient functions C_i in Eq. (17.3) and the splitting functions P_{ji} contain singularities at $z = 0$ and 1, which have important effects on fragmentation at small and large values of x, respectively. For details see *e.g.*, Ref. 1.

Quantitative results of studies of scaling violation in e^+e^- fragmentation are reported in Refs. 10,12. The values of α_S obtained are consistent with the world average (see section on QCD in Sec. 9 of this *Review*).

17.3. Longitudinal Fragmentation

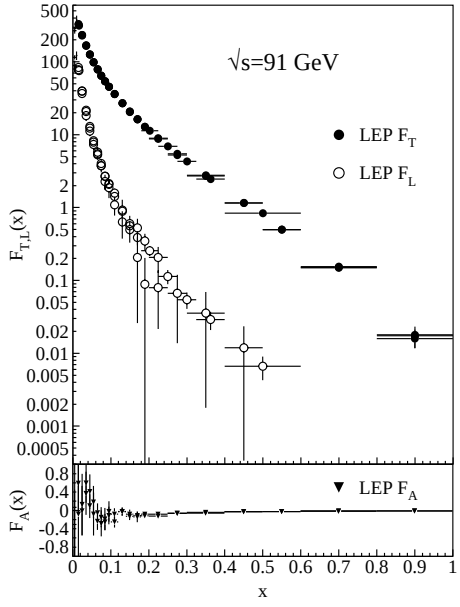

Figure 17.2: Transverse (F_T), longitudinal (F_L), and asymmetric (F_A) fragmentation functions are shown [8,11,13]. Data points with relative errors greater than 100% are omitted.

In the process $e^+e^- \to V \to hX$, the joint distribution in the energy fraction x and the angle θ between the observed hadron h and the incoming electron beam has the general form

$$\frac{1}{\sigma_{\rm tot}}\frac{d^2\sigma}{dx\,d\cos\theta} = \frac{3}{8}(1+\cos^2\theta)\,F_T(x) + \frac{3}{4}\sin^2\theta\,F_L(x) + \frac{3}{4}\cos\theta\,F_A(x)\,, \tag{17.6}$$

where F_T, F_L and F_A are respectively the transverse, longitudinal and asymmetric fragmentation functions. All these functions also depend on the c.m. energy $\sqrt{s}$. Eq. (17.6) is the most general form of the inclusive single particle production from the decay of a massive vector boson [3]. As their names imply, F_T and F_L represent the contributions from virtual bosons polarized transversely or longitudinally with respect to the direction of motion of the hadron h. F_A is a parity-violating contribution which comes from the interference between vector and axial vector contributions. Integrating over all angles, we obtain the total fragmentation function, $F = F_T + F_L$. Each of these functions can be represented as a convolution of the parton fragmentation functions D_i with appropriate coefficient functions $C_i^{\rm T,L,A}$ as in Eq. (17.3). This representation works in the high energy limit. As $x \cdot \sqrt{s}/2$ approaches hadronic scales $\simeq m_\rho$, power suppressed effects can no longer be neglected, and the fragmentation function formalism no longer accounts correctly for the separation of F_T, F_L, and F_A. In Fig. 17.2, F_T, F_L, and F_A measured at $\sqrt{s} = 91$ GeV are shown.

[1] There are misprints in the formulae in the published article. The correct expressions can be found in the preprint version or in Ref. 5.

17.4. Gluon fragmentation

The gluon fragmentation function $D_g(x)$ can be extracted from the longitudinal fragmentation function defined in Eq. (17.6). Since the coefficient functions $C_i^{\rm L}$ for quarks and gluons are comparable in $\mathcal{O}(\alpha_S)$, F_L can be expressed in terms of F_T and D_g which allows one to obtain D_g from the measured F_L and F_T. It can also be deduced from the fragmentation of three-jet events in which the gluon jet is identified, for example by tagging the other two jets with heavy quark decays. To leading order the measured distributions of $x = E_{\rm had}/E_{\rm jet}$ for particles in gluon jets can be identified directly with the gluon fragmentation functions $D_g(x)$. The experimentally measured gluon fragmentation functions are shown in Fig. 17.3.

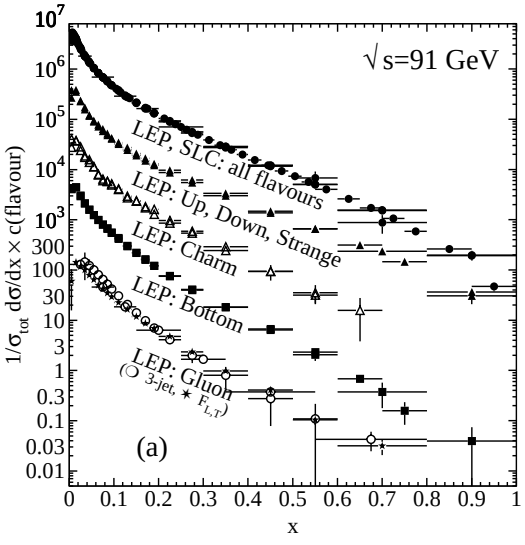

Figure 17.3: Comparison of the charged-particle and the flavour-dependent e^+e^- fragmentation functions obtained at $\sqrt{s} = 91$ GeV. The data [8,9,10,13,14] are shown for the inclusive, light (up, down, strange) quarks, charm quark, bottom quark, and the gluon versus x. For the purpose of plotting, the distributions were scaled by $c(\text{flavour}) = 10^i$ where i is ranging from $i = 0$ (Gluon) to $i = 4$ (all flavours).

17.5. Fragmentation models

Although the scaling violation can be calculated perturbatively, the actual form of the parton fragmentation functions is non-perturbative. Perturbative evolution gives rise to a shower of quarks and gluons (partons). Phenomenological schemes are then used to model the carry-over of parton momenta and flavour to the hadrons. Two of the very popular models are the *string fragmentation* [15,16], implemented in the JETSET [17] and UCLA [18] Monte Carlo event generation programs, and the *cluster fragmentation* of the HERWIG Monte Carlo event generator [19].

17.5.1. ***String fragmentation***: The string-fragmentation scheme considers the colour field between the partons, *i.e.*, quarks and gluons, to be the fragmenting entity rather than the partons themselves. The string can be viewed as a colour flux tube formed by gluon self-interaction as two coloured partons move apart. Energetic gluon emission is regarded as energy-momentum carrying "kinks" on the string. When the energy stored in the string is sufficient, a $q\overline{q}$ pair may be created from the vacuum. Thus the string breaks up repeatedly

into colour singlet systems as long as the invariant mass of the string pieces exceeds the on-shell mass of a hadron. The $q\bar{q}$ pairs are created according to the probability of a tunnelling process $\exp(-\pi m^2_{q,\perp}/\kappa)$ which depends on the transverse mass squared $m^2_{q,\perp} \equiv m^2_q + p^2_{q,\perp}$ and the string tension $\kappa \approx 1$ GeV/fm. The transverse momentum $p_{q,\perp}$ is locally compensated between quark and antiquark. Due to the dependence on the parton mass m_q and/or hadron mass, m_h, the production of strange and, in particular, heavy-quark hadrons is suppressed. The light-cone momentum fraction $z = (E+p_\parallel)_h/(E+p)_q$, where $p_\parallel$ is the momentum of the formed hadron h along the direction of the quark q, is given by the string-fragmentation function

$$f(z) \sim \frac{1}{z}(1-z)^a \exp\left(-\frac{bm^2_{h,\perp}}{z}\right) \qquad (17.7)$$

where a and b are free parameters. These parameters need to be adjusted to bring the fragmentation into accordance with measured data, *e.g.*, $a = 0.11$ and $b = 0.52$ GeV^{-2} as determined in Ref. 20 (for an overview on tuned parameters see Ref. 21).

17.5.2. ***Cluster fragmentation***: Assuming a local compensation of colour based on the *pre-confinement* property of perturbative QCD [22], the remaining gluons at the end of the parton shower evolution are split non-perturbatively into quark-antiquark pairs. Colour singlet clusters of typical mass of a couple of GeV are then formed from quark and antiquark of colour-connected splittings. These clusters decay directly into two hadrons unless they are either too heavy (relative to an adjustable parameter `CLMAX`, default value 3.35 GeV), when they decay into two clusters, or too light, in which case a cluster decays into a single hadron, requiring a small rearrangement of energy and momentum with neighbouring clusters. The decay of a cluster into two hadrons is assumed to be isotropic in the rest frame of the cluster except if a perturbative-formed quark is involved. A decay channel is chosen based on the phase-space probability, the density of states, and the spin degeneracy of the hadrons. Cluster fragmentation has a compact description with few parameters, due to the phase-space dominance in the hadron formation.

17.6. Experimental studies

A great wealth of measurements of e^+e^- fragmentation into identified particles exists. A collection of references to find data on the fragmentation into identified particles is given for Table 40.1. As representatives of all the data, Fig. 17.4 shows fragmentation functions as the scaled momentum spectra of charged particles at several c.m. energies. Heavy flavour particles are dealt with separately in Sec. 17.7.

The measured fragmentation functions are solutions to the DGLAP equation (17.4) but need to be parametrized at some initial scale t_0 (usually 2 GeV^2 for light quarks and gluons). A general parametrization is [24]

$$D_{p\to h}(x,t_0) = Nx^\alpha(1-x)^\beta\left(1+\frac{\gamma}{x}\right) \qquad (17.8)$$

where the normalization N, and the parameters α, β, and γ in general depend on the energy scale t_0 and also on the type of the parton, p, and the hadron, h. Frequently the term involving γ is left out [25]. The parameters of Eq. (17.8), listed in Ref. 25, were obtained by fitting data on various hadron types for different combinations of partons and hadrons in $p \to h$ in the range $\sqrt{s} \approx$ 5–200 GeV.

17.7. Heavy quark fragmentation

It was recognized very early [26] that a heavy flavoured meson should retain a large fraction of the momentum of the primordial heavy quark, and therefore its fragmentation function should be much harder than that of a light hadron. In the limit of a very heavy quark, one expects the fragmentation function for a heavy quark to go into any heavy hadron to be peaked near 1.

When the heavy quark is produced at a momentum much larger than its mass, one expects important perturbative effects, enhanced by powers of the logarithm of the transverse momentum over

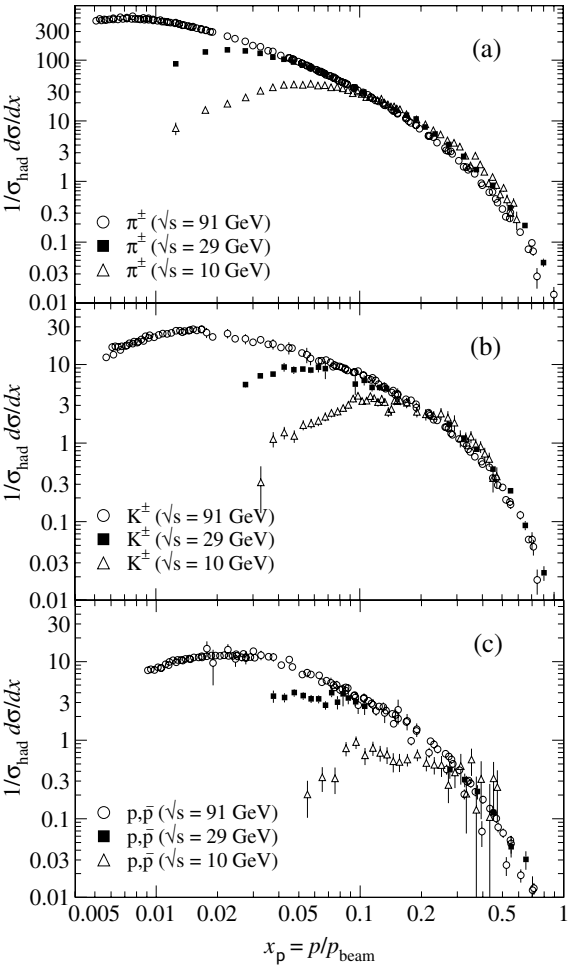

Figure 17.4: Scaled momentum spectra of (a) $\pi^\pm$, (b) $K^\pm$, and (c) $p/\overline{p}$ at $\sqrt{s} = 10$, 29, and 91 GeV are shown [7,23].

the heavy quark mass, to intervene and modify the shape of the fragmentation function. In leading logarithmic order (*i.e.*, including all powers of $\alpha_S \log m_Q/p_T$) the total (*i.e.*, summed over all hadron types) perturbative fragmentation function is simply obtained by solving the leading evolution equation for fragmentation functions, Eq. (17.4), with the initial condition at a scale $\mu^2 = m^2_Q$ given by $D_Q(z, m^2_Q) = \delta(1-z)$ and $D_i(z, m^2_Q) = 0$ for $i \neq Q$ (the notation $D_i(z)$ stands for the probability to produce a heavy quark Q from parton i with a fraction z of the parton momentum).

Several extensions of the leading logarithmic result have appeared in the literature. Next-to-leading-log (NLL) order results for the perturbative heavy quark fragmentation function have been obtained in Ref. 27. At large z, phase space for gluon radiation is suppressed. This exposes large perturbative corrections due to the incomplete cancellation of real gluon radiation and virtual gluon exchange (Sudakov effects), which should be resummed in order to get accurate results. A leading-log (LL) resummation formula has been obtained in Refs. 27,28. Next-to-leading-log resummation has been performed in Ref. 29. Fixed-order calculations of the fragmentation function at order α_S^2 in e^+e^- annihilation have appeared in Ref. 30. This result does not include terms of order $(\alpha_S \log s/m^2)^k$ and $\alpha_S(\alpha_S \log s/m^2)^k$, but it does include correctly all terms up to the order α_S^2, including terms without any logarithmic enhancements.

Inclusion of non-perturbative effects in the calculation of the heavy quark fragmentation function is done in practice by convolving the perturbative result with a phenomenological non-perturbative form. Among the most popular parametrizations we have the following:

$$\text{Peterson } \textit{et al.} \ [3]: \quad D_{\rm np}(z) \propto \frac{1}{z}\left(1-\frac{1}{z}-\frac{\epsilon}{1-z}\right)^{-2}, \tag{17.9}$$

$$\text{Kartvelishvili } \textit{et al.} \ [32]: \quad D_{\rm np}(z) \propto z^{\alpha}(1-z), \tag{17.10}$$

$$\text{Collins\&Spiller} \ [33]: \quad D_{\rm np}(z) \propto \left(\frac{1-z}{z}+\frac{(2-z)\epsilon_C}{1-z}\right)\times (1+z^2)\left(1-\frac{1}{z}-\frac{\epsilon_C}{1-z}\right)^{-2} \tag{17.11}$$

where ϵ, α, and ϵ_C are non-perturbative parameters, depending upon the heavy hadron considered. In general, the non-perturbative parameters do not have an absolute meaning. They are fitted together with some model of hard radiation, which can be either a shower Monte Carlo, a leading-log or NLL calculation (which may or may not include Sudakov resummation), or a fixed order calculation. In Ref. 30, for example, the ϵ parameter for charm and bottom production is fitted from the measured distributions of Refs. 34,35 for charm, and of Ref. 36 for bottom. If the leading-logarithmic approximation (LLA) is used for the perturbative part, one finds $\epsilon_c \approx 0.05$ and $\epsilon_b \approx 0.006$; if a second order calculation is used one finds $\epsilon_c \approx 0.035$ and $\epsilon_b \approx 0.0033$; if a NLLO calculation is used instead one finds $\epsilon_c \approx 0.022$ and $\epsilon_b \approx 0.0023$. The larger values found in the LL approximation are consistent with what is obtained in the context of parton shower models [37], as expected. The ϵ parameter for charm and bottom scales roughly with the inverse square of the heavy flavour mass. This behaviour can be justified by several arguments [26,38]. It can be used to relate the non-perturbative parts of the fragmentation functions of charm and bottom quarks [30,39].

The bulk of the available fragmentation function data on charmed mesons (excluding $J/\psi(1S)$) is from measurements in e^+e^- annihilation at $\sqrt{s} \approx 10$ GeV. Shown in Fig. 17.5(a) are the efficiency-corrected (but not branching ratio corrected) CLEO and ARGUS inclusive cross sections, $s \cdot \mathcal{B}\, d\sigma/dx_p$, for the production of D^0 and D^{*+}. The variable x_p approximates the light-cone momentum fraction z in Eq. (17.9), but is not identical to it.

For the D^0, $\mathcal{B}$ represents the product branching fraction: $D^{*+} \to D^0\pi^+$, $D^0 \to K^-\pi^+$. These inclusive spectra have not been corrected for cascades from higher states, nor for radiative effects. Since the momentum spectra are sensitive to QED and QCD radiative corrections, charm spectra at $\sqrt{s} = 10$ GeV cannot be compared directly with spectra at higher c.m. energies, and must be appropriately evolved. Tuning ϵ of (17.9) in the JETSET 7.4 Monte Carlo generator [17] using the parameter set of Ref. 20 and including radiative corrections to describe the combined CLEO and ARGUS D^0 and D^{*+} data gives $\epsilon_c = 0.043 \pm 0.004$; this is indicated in the solid curves.[2]

Experimental studies of the fragmentation function for b quarks, shown in Fig. 17.5(b), have been performed at LEP and SLD [36,41,42]. Commonly used methods identify the B meson through its semileptonic decay or based upon tracks emerging from the B secondary vertex. The most recent studies [42] fit the B spectrum using a Monte Carlo shower model supplemented with non-perturbative fragmentation functions yielding consistent results.

The experiments measure primarily the spectrum of B mesons. This defines a fragmentation function which includes the effect of the decay of higher mass excitations, like the B^* and B^{**}. In the literature there is sometimes ambiguity in what is defined to be the bottom fragmentation function. Instead of using what is directly measured (*i.e.*, the B meson spectrum) corrections are applied to account for B^* or B^{**} production in some cases. For a more detailed discussion see Ref. 1.

[2] This paragraph is adapted from D. Besson's contribution to C. Caso *et al.*, Eur. Phys. J. **C3**, 1 (1998).

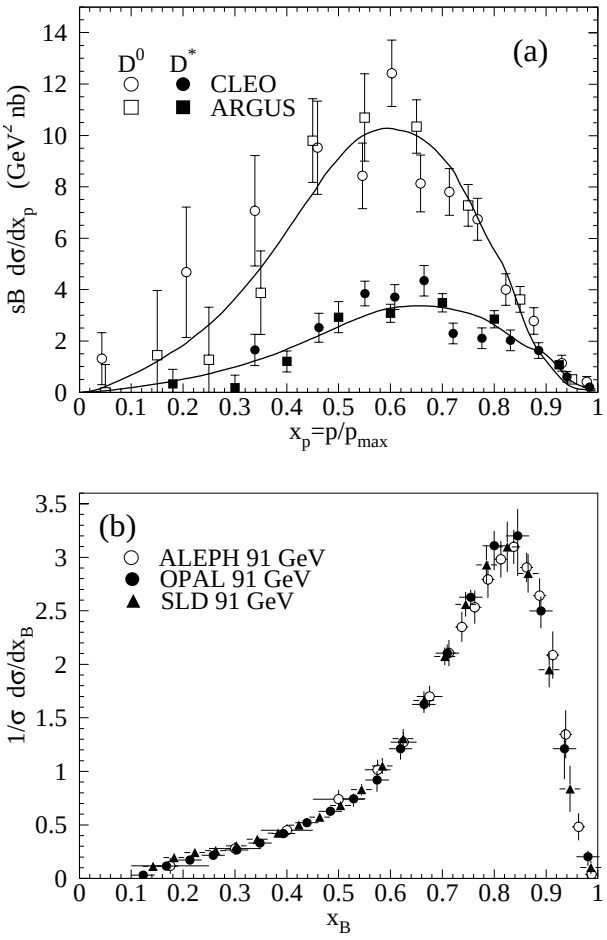

Figure 17.5: (a) Efficiency-corrected inclusive cross-section measurements for the production of D^0 and D^{*+} in e^+e^- measurements at $\sqrt{s} \approx 10$ GeV [35,40]. (b) Measured e^+e^- fragmentation function of b quarks into B hadrons at $\sqrt{s} \approx$ 91 GeV [41,42].

Besides degrading the fragmentation function by gluon radiation, QCD evolution can also generate soft heavy quarks, increasing in the small x region as s increases. Several theoretical studies are available on the issue of how often $b\overline{b}$ or $c\overline{c}$ pairs are produced indirectly, via a gluon splitting mechanism [43–45]. Experimental results from studies on charm production via gluon splitting [46,47], and measurements of $g \to b\overline{b}$ [48–50] are given in Table 17.1.

In Ref. 44 an explicit calculation of these quantities has been performed. Using these results, charm and bottom multiplicities as reported in Table 17.1 for different values of the masses and of $\Lambda^{(5)}_{\overline{\rm MS}}$ were computed in Ref. 51. The averaged experimental result for charm, $(3.23 \pm 0.42)\%$, is 1–2 standard deviations above the theoretical prediction, preferring lower values of the quark mass and/or a larger value of $\Lambda^{(5)}_{\overline{\rm MS}}$. However, higher-order corrections may well be substantial at the charm quark mass scale. Better agreement is achieved for bottom.

As reported in Ref. 44, Monte Carlo models are in qualitative agreement with these results, although the spread of the values they obtain is somewhat larger than the theoretical error estimated by the direct calculation. In particular, for charm one finds that while HERWIG [19] and JETSET [17] agree quite well with the theoretical calculation, ARIADNE [52] is higher by roughly a factor of 2, and

Table 17.1: Measured fraction of events containing $g \to c\bar{c}$ and $g \to b\bar{b}$ subprocesses in Z decays, compared with theoretical predictions. The central/lower/upper values for the theoretical predictions are obtained with $m_c = (1.5 \pm 0.3)$ and $m_b = (4.75 \pm 0.25)$ GeV.

	$\overline{n}_{g\to c\bar{c}}$ (%)	$\overline{n}_{g\to b\bar{b}}$ (%)
OPAL	[46] $3.20 \pm 0.21 \pm 0.38$	
ALEPH	[47] $3.26 \pm 0.23 \pm 0.42$	[49] $0.277 \pm 0.042 \pm 0.057$
DELPHI		[48] $0.21 \pm 0.11 \pm 0.09$
SLD		[50] $0.307 \pm 0.071 \pm 0.066$
Theory [44]		
$\Lambda^{(5)}_{\overline{\rm MS}} = 150$ MeV	$1.35^{+0.48}_{-0.30}$	0.20 ± 0.02
$\Lambda^{(5)}_{\overline{\rm MS}} = 300$ MeV	$1.85^{+0.69}_{-0.44}$	0.26 ± 0.03

thus is in better agreement with data. For bottom, agreement between theory, models and data is adequate. For a detailed discussion see Ref. 53.

The discrepancy with the charm prediction may be due to experimental cuts forcing the final state configuration to be more 3-jet like, which increases the charm multiplicity. Calculations that take this possibility into account are given in Ref. 45.

References:

1. O. Biebel, P. Nason, and B.R. Webber, Bicocca-FT-01-20, Cavendish-HEP-01/12, MPI-PhE/2001-14, hep-ph/0109282.
2. L.N. Lipatov, Sov. J. Nucl. Phys. **20**, 95 (1975);
   V.N. Gribov and L.N. Lipatov, Sov. J. Nucl. Phys. **15**, 438 (1972);
   G. Altarelli and G. Parisi, Nucl. Phys. **B126**, 298 (1977);
   Yu.L. Dokshitzer, Sov. Phys. JETP **46**, 641 (1977).
3. P. Nason and B.R. Webber, Nucl. Phys. **B421**, 473 (1994); erratum *ibid.*; **B480**, 755 (1996).
4. W. Furmanski and R. Petronzio, preprint TH.2933–CERN (1980), Phys. Lett. **97B**, 437 (1980).
5. R.K. Ellis, J. Stirling, and B.R. Webber: *QCD and Collider Physics*, Cambridge University Press, Cambridge (1996).
6. TASSO Collaboration: R. Brandelik *et al.*, Phys. Lett. **B114**, 65 (1982);
   W. Braunschweig *et al.*, Z. Phys. **C47**, 187 (1990);
   HRS Collaboration: D.Bender *et al.*, Phys. Rev. **D31**, 1 (1984);
   MARK II Collaboration: A. Petersen *et al.*, Phys. Rev. **D37**, 1 (1988);
   AMY Collaboration: Y.K. Li *et al.*, Phys. Rev. **D41**, 2675 (1990);
   ALEPH Collaboration: D. Buskulic *et al.*, Z. Phys. **C73**, 409 (1997);
   OPAL Collaboration: R. Akers *et al.*, Z. Phys. **C72**, 191 (1996);
   G. Abbiendi *et al.*, Eur. Phys. J. **C27**, 467 (2003);
   K. Ackerstaff *et al.*, Z. Phys. **C75**, 193 (1997);
   G. Abbiendi *et al.*, Eur. Phys. J. **C16**, 185 (2000).
7. TPC Collaboration: H. Aihara *et al.*, Phys. Rev. Lett. **61**, 1263 (1988).
8. DELPHI Collaboration: P. Abreu *et al.*, Eur. Phys. J. **C6**, 19 (1999).
9. ALEPH Collaboration: E. Barate *et al.*, Phys. Reports **294**, 1 (1998);
   L3 Collaboration: B. Adeva *et al.*, Phys. Lett. **B259**, 199 (1991);
   OPAL Collaboration: K. Ackerstaff *et al.*, Eur. Phys. J. **C7**, 369 (1998);
   MARK II Collaboration: G.S. Abrams *et al.*, Phys. Rev. Lett. **64**, 1334 (1990).
10. DELPHI Collaboration: P. Abreu *et al.*, Phys. Lett. **B398**, 194 (1997).
11. ALEPH Collaboration: D. Barate *et al.*, Phys. Lett. **B357**, 487 (1995); erratum *ibid.*; **B364**, 247 (1995).
12. DELPHI Collaboration: P. Abreu *et al.*, Eur. Phys. J. **C13**, 573 (2000); Phys. Lett. **B311**, 408 (1993);
    W. de Boer and T. Kußmaul, IEKP-KA/93-8, hep-ph/9309280;;
    B.A. Kniehl, G. Kramer, and B. Pötter, Phys. Rev. Lett. **85**, 5288 (2001).
13. OPAL Collaboration: R. Akers *et al.*, Z. Phys. **C86**, 203 (1995).
14. ALEPH Collaboration: R. Barate *et al.*, Eur. Phys. J. **C17**, 1 (2000);
    OPAL Collaboration: G. Abbiendi *et al.*, Eur. Phys. J. **C11**, 217 (1999);
    R. Akers *et al.*, Z. Phys. **C68**, 179 (1995).
15. X. Artru and G. Mennessier, Nucl. Phys. **B70**, 93 (1974).
16. B. Andersson, G. Gustafson, G. Ingelman, T. Sjöstrand, Phys. Reports **97**, 31 (1983).
17. T. Sjöstrand and M. Bengtsson, Comp. Phys. Comm. **43**, 367 (1987);
    T. Sjöstrand, Comp. Phys. Comm. **82**, 74 (1994).
18. S. Chun and C. Buchanan, Phys. Reports **292**, 239 (1998).
19. G. Marchesini *et al.*, Comp. Phys. Comm. **67**, 465 (1992);
    G. Corcella *et al.*, JHEP **0101**, 010 (2001).
20. OPAL Collaboration: G. Alexander *et al.*, Z. Phys. **C69**, 543 (1996).
21. M. Schmelling, Phys. Scripta **51**, 683 (1995).
22. D. Amati and G. Veneziano, Phys. Lett. **B83**, 87 (1979).
23. ALEPH Collaboration: D. Buskulic *et al.*, Z. Phys. **C66**, 355 (1995);
    ARGUS Collaboration: H. Albrecht *et al.*, Z. Phys. **C44**, 547 (1989);
    DELPHI Collaboration: P. Abreu *et al.*, Eur. Phys. J. **C5**, 585 (1998);
    OPAL Collaboration: R. Akers *et al.*, Z. Phys. **C63**, 181 (1994);
    SLD Collaboration: K. Abe *et al.*, Phys. Rev. **D59**, 052001 (1999).
24. B.A. Kniehl, G. Kramer and B. Pötter, Nucl. Phys. **B597**, 337 (2001).
25. L. Bourhis *et al.*, Eur. Phys. J. **C19**, 89 (2001);
    B.A. Kniehl, G. Kramer, and B. Pötter, Nucl. Phys. **B582**, 514 (2000);
    J. Binnewies, B.A. Kniehl, and G. Kramer, Phys. Rev. **D52**, 4947 (1995);
    Z. Phys. **C65**, 471 (1995);
    J. Binnewies, Hamburg University PhD Thesis, DESY 97-128, hep-ph/9707269.
26. V.A. Khoze, Ya.I. Azimov, and L.L. Frankfurt, Proceedings, Conference on High Energy Physics, Tbilisi 1976;
    J.D. Bjorken, Phys. Rev. **D17**, 171 (1978).
27. B. Mele and P. Nason, Phys. Lett. **B245**, 635 (1990); Nucl. Phys. **B361**, 626 (1991).
28. Y. Dokshitzer, V.A. Khoze, and S.I. Troyan, Phys. Rev. **D53**, 89 (1996).
29. M. Cacciari and S. Catani, Nucl. Phys. **B617**, 253 (2001).
30. P. Nason and C. Oleari, Phys. Lett. **B418**, 199 (1998) *ibid.*; **B447**, 327 (1999); Nucl. Phys. **B565**, 245 (2000).
31. C. Peterson *et al.*, Phys. Rev. **D27**, 105 (1983).
32. V.G. Kartvelishvili, A.K. Likehoded, and V.A. Petrov, Phys. Lett. **B78**, 615 (1978).
33. P. Collins and T. Spiller, J. Phys. **G11**, 1289 (1985).
34. OPAL Collaboration: R. Akers *et al.*, Z. Phys. **C67**, 27 (1995).
35. ARGUS Collaboration: H. Albrecht *et al.*, Z. Phys. **C52**, 353 (1991).

36. ALEPH Collaboration: D. Buskulic *et al.*, Phys. Lett. **B357**, 699 (1995).
37. J. Chrin, Z. Phys. **C36**, 163 (1987).
38. R.L. Jaffe and L. Randall, Nucl. Phys. **B412**, 79 (1994);
    P. Nason and B. Webber, Phys. Lett. **B395**, 355 (1997).
39. G. Colangelo and P. Nason, Phys. Lett. **B285**, 167 (1992);
    L. Randall and N. Rius, Nucl. Phys. **B441**, 167 (1995).
40. CLEO Collaborations: D. Bortoletto *et al.*, Phys. Rev. **D37**, 1719 (1988).
41. OPAL Collaboration: G. Alexander *et al.*, Phys. Lett. **B364**, 93 (1995);
    L3 Collaboration: B. Adeva *et al.*, Phys. Lett. **B261**, 177 (1991).
42. SLD Collaboration: K. Abe *et al.*, Phys. Rev. Lett. **84**, 4300 (2000);
    K. Abe *et al.*, Phys. Rev. **D65**, 092006 (2002); erratum **D66**, 079905 (2002);
    ALEPH Collaboration: A. Heister *et al.*, Phys. Lett. **B512**, 30 (2001);
    OPAL Collaboration: G. Abbiendi *et al.*, Eur. Phys. J. **C29**, 463 (2003).
43. A.H. Mueller and P. Nason, Nucl. Phys. **B266**, 265 (1986);
    M.L. Mangano and P. Nason, Phys. Lett. **B285**, 160 (1992).
44. M.H. Seymour, Nucl. Phys. **B436**, 163 (1995).
45. D.J. Miller and M.H. Seymour, Phys. Lett. **B435**, 213 (1998).
46. OPAL Collaboration: G. Abbiendi *et al.*, Eur. Phys. J. **C13**, 1 (2000).
47. ALEPH Collaboration: R. Barate *et al.*, Eur. Phys. J. **C16**, 597 (2000);
    ALEPH Collaboration: R. Barate *et al.*, Phys. Lett. **B561**, 213 (2003).
48. DELPHI Collaboration: P. Abreu *et al.*, Phys. Lett. **B405**, 202 (1997).
49. ALEPH Collaboration: R. Barate *et al.*, Phys. Lett. **B434**, 437 (1998).
50. SLD Collaboration: K. Abe *et al.*, SLAC-PUB-8157, `hep-ex/9908028`.
51. S. Frixione, M.L. Mangano, P. Nason, and G. Ridolfi: Heavy Quark Production, in A.J. Buras and M. Lindner (eds.), *Heavy Flavours II*, World Scientific, Singapore (1998), `hep-ph/9702287`.
52. L. Lönnblad, Comp. Phys. Comm. **71**, 15 (1992).
53. A. Ballestrero *et al.*, CERN-2000-09-B, `hep-ph/0006259`.

18. EXPERIMENTAL TESTS OF GRAVITATIONAL THEORY

Revised September 2003 by T. Damour (IHES, Bures-sur-Yvette, France).

Einstein's General Relativity, the current "standard" theory of gravitation, describes gravity as a universal deformation of the Minkowski metric:

$$g_{\mu\nu}(x^\lambda) = \eta_{\mu\nu} + h_{\mu\nu}(x^\lambda)\ , \text{ where } \eta_{\mu\nu} = \mathrm{diag}(-1,+1,+1,+1)\ . \quad (18.1)$$

Alternatively, it can be defined as the unique, consistent, local theory of a massless spin-2 field, $h_{\mu\nu}$, whose source must then be the total, conserved energy-momentum tensor [1]. General Relativity is classically defined by two postulates. One postulate states that the Lagrangian density describing the propagation and self-interaction of the gravitational field is

$$\mathcal{L}_{\rm Ein}[g_{\mu\nu}] = \frac{c^4}{16\pi G_N}\sqrt{g}g^{\mu\nu}R_{\mu\nu}(g)\ , \quad (18.2)$$

$$R_{\mu\nu}(g) = \partial_\alpha\Gamma^\alpha_{\mu\nu} - \partial_\nu\Gamma^\alpha_{\mu\alpha} + \Gamma^\beta_{\alpha\beta}\Gamma^\alpha_{\mu\nu} - \Gamma^\beta_{\alpha\nu}\Gamma^\alpha_{\mu\beta}\ , \quad (18.3)$$

$$\Gamma^\lambda_{\mu\nu} = \tfrac{1}{2}g^{\lambda\sigma}(\partial_\mu g_{\nu\sigma} + \partial_\nu g_{\mu\sigma} - \partial_\sigma g_{\mu\nu})\ , \quad (18.4)$$

where G_N is Newton's constant, $g = -\det(g_{\mu\nu})$, and $g^{\mu\nu}$ is the matrix inverse of $g_{\mu\nu}$. A second postulate states that $g_{\mu\nu}$ couples universally, and minimally, to all the fields of the Standard Model by replacing everywhere the Minkowski metric $\eta_{\mu\nu}$. Schematically (suppressing matrix indices and labels for the various gauge fields and fermions, and for the Higgs doublet),

$$\begin{aligned}\mathcal{L}_{\rm SM}[\psi, A_\mu, H, g_{\mu\nu}] = &-\tfrac{1}{4}\sum\sqrt{g}g^{\mu\alpha}g^{\nu\beta}F^a_{\mu\nu}F^a_{\alpha\beta}\\ &-\sum\sqrt{g}\,\overline{\psi}\,\gamma^\mu D_\mu\psi\\ &-\tfrac{1}{2}\sqrt{g}g^{\mu\nu}\overline{D_\mu H}D_\nu H - \sqrt{g}\,V(H)\\ &-\sum\lambda\sqrt{g}\,\overline{\psi}\,H\psi\ ,\end{aligned} \quad (18.5)$$

where $\gamma^\mu\gamma^\nu + \gamma^\nu\gamma^\mu = 2g^{\mu\nu}$, and where the covariant derivative D_μ contains, besides the usual gauge field terms, a (spin-dependent) gravitational contribution $\Gamma_\mu(x)$ [2]. From the total action $S_{\rm tot}[g_{\mu\nu},\psi,A_\mu,H] = c^{-1}\int d^4x(\mathcal{L}_{\rm Ein} + \mathcal{L}_{\rm SM})$ follows Einstein's field equations,

$$R_{\mu\nu} - \tfrac{1}{2}Rg_{\mu\nu} = \frac{8\pi G_N}{c^4}T_{\mu\nu}\ . \quad (18.6)$$

Here, $R = g^{\mu\nu}R_{\mu\nu}$, $T_{\mu\nu} = g_{\mu\alpha}g_{\nu\beta}T^{\alpha\beta}$, and $T^{\mu\nu} = (2/\sqrt{g})\delta\mathcal{L}_{\rm SM}/\delta g_{\mu\nu}$ is the (symmetric) energy-momentum tensor of the Standard Model matter. The theory is invariant under arbitrary coordinate transformations: $x'^\mu = f^\mu(x^\nu)$. To solve the field equations Eq. (18.6), one needs to fix this coordinate gauge freedom. *E.g.*, the "harmonic gauge" (which is the analogue of the Lorentz gauge, $\partial_\mu A^\mu = 0$, in electromagnetism) corresponds to imposing the condition $\partial_\nu(\sqrt{g}g^{\mu\nu}) = 0$.

In this *Review*, we only consider the classical limit of gravitation (*i.e.*, classical matter and classical gravity). Considering quantum matter in a classical gravitational background already poses interesting challenges, notably the possibility that the zero-point fluctuations of the matter fields generate a nonvanishing vacuum energy density $\rho_{\rm vac}$, corresponding to a term $-\sqrt{g}\ \rho_{\rm vac}$ in $\mathcal{L}_{\rm SM}$ [3]. This is equivalent to adding a "cosmological constant" term $+\Lambda g_{\mu\nu}$ on the left-hand side of Einstein's equations Eq. (18.6), with $\Lambda = 8\pi G_N\rho_{\rm vac}/c^4$. Recent cosmological observations (see the following Reviews) suggest a positive value of Λ corresponding to $\rho_{\rm vac} \approx (2.3\times10^{-3}\mathrm{eV})^4$. Such a small value has a negligible effect on the tests discussed below. Quantizing the gravitational field itself poses a very difficult challenge because of the perturbative non-renormalizability of Einstein's Lagrangian. Superstring theory offers a promising avenue toward solving this challenge.

18.1. Experimental tests of the coupling between matter and gravity

The universality of the coupling between $g_{\mu\nu}$ and the Standard Model matter postulated in Eq. (18.5) ("Equivalence Principle") has many observable consequences. First, it predicts that the outcome of a local non-gravitational experiment, referred to local standards, does not depend on where, when, and in which locally inertial frame the experiment is performed. This means, for instance, that local experiments should neither feel the cosmological evolution of the universe (constancy of the "constants"), nor exhibit preferred directions in spacetime (isotropy of space, local Lorentz invariance). These predictions are consistent with many experiments and observations. The best limit on a possible time variation of the basic coupling constants concerns the fine-structure constant $\alpha_{\rm em}$, and has been obtained by analyzing a natural fission reactor phenomenon which took place at Oklo, Gabon, two billion years ago [4]. A conservative estimate of the (95% C.L.) Oklo limit on the variability of $\alpha_{\rm em}$ is (see second reference in [4])

$$-0.9\times10^{-7} < \frac{\alpha_{\rm em}^{\rm Oklo} - \alpha_{\rm em}^{\rm now}}{\alpha_{\rm em}} < 1.2\times10^{-7}\ , \quad (18.7)$$

which corresponds to the following limit on the average time derivative of $\alpha_{\rm em}$

$$-6.7\times10^{-17}\mathrm{yr}^{-1} < \dot{\alpha}_{\rm em}/\alpha_{\rm em} < 5.0\times10^{-17}\mathrm{yr}^{-1}\ . \quad (18.8)$$

Direct laboratory limits on the time variation of $\alpha_{\rm em}$ [5] are less stringent than Eq. (18.8). Recently, Ref. 6 claimed to have measured a cosmological change of $\alpha_{\rm em}$ of magnitude $\Delta\alpha_{\rm em}/\alpha_{\rm em} = (-0.72\pm0.18)\times10^{-5}$ around redshifts $z\simeq0.5-3.5$. When analyzed within various dilaton-like theoretical models of $\alpha_{\rm em}$ variability [7–9], such a large cosmological variation of $\alpha_{\rm em}$ appears incompatible with the combined set of other experimental limits, notably the Oklo bound quoted above, a comparable "rhenium" geological bound [10], and the limits on possible violations of the universality of free fall quoted below. See Refs. 11,12 for discussions of systematic errors in astronomical measurements of $\alpha_{\rm em}$, and Ref. 13 for a general review of the issue of "variable constants".

The highest precision tests of the isotropy of space have been performed by looking for possible quadrupolar shifts of nuclear energy levels [14]. The (null) results can be interpreted as testing the fact that the various pieces in the matter Lagrangian Eq. (18.5) are indeed coupled to one and the same external metric $g_{\mu\nu}$ to the 10^{-27} level. For astrophysical constraints on possible Planck-scale violations of Lorentz invariance, see Refs. 15,16.

The universal coupling to $g_{\mu\nu}$ postulated in Eq. (18.5) implies that two (electrically neutral) test bodies dropped at the same location and with the same velocity in an external gravitational field fall in the same way, independently of their masses and compositions. The universality of the acceleration of free fall has been verified at the 10^{-12} level both for laboratory bodies [17],

$$(\Delta a/a)_{\rm BeCu} = (-1.9\pm2.5)\times10^{-12}\ , \quad (18.9)$$

and for the gravitational accelerations of the Moon and the Earth toward the Sun [18],

$$(\Delta a/a)_{\rm MoonEarth} = (-3.2\pm4.6)\times10^{-13}\ . \quad (18.10)$$

See also Ref. 19 for a $\pm0.94\times10^{-12}$ limit on the fractional difference in free-fall acceleration toward the Sun of earth-core-like and moon-mantle-like laboratory bodies, and Ref. 20 for *short-range* tests of the universality of free-fall.

Finally, Eq. (18.5) also implies that two identically constructed clocks located at two different positions in a static external Newtonian potential $U(\boldsymbol{x}) = \sum G_N m/r$ exhibit, when intercompared by means of electromagnetic signals, the (apparent) difference in clock rate,

$$\frac{\tau_1}{\tau_2} = \frac{\nu_2}{\nu_1} = 1 + \frac{1}{c^2}[U(\boldsymbol{x}_1) - U(\boldsymbol{x}_2)] + O\left(\frac{1}{c^4}\right)\ , \quad (18.11)$$

independently of their nature and constitution. This universal gravitational redshift of clock rates has been verified at the 10^{-4} level by comparing a hydrogen-maser clock, flying on a rocket up to an altitude $\sim 10,000$ km, to a similar clock on the ground [21]. For more details and references on experimental gravity see, *e.g.*, Refs. 22 and 23.

18.2. Tests of the dynamics of the gravitational field in the weak field regime

The effect on matter of one-graviton exchange, *i.e.*, the interaction Lagrangian obtained when solving Einstein's field equations Eq. (18.6) written in, say, the harmonic gauge at first order in $h_{\mu\nu}$,

$$\Box h_{\mu\nu} = -\frac{16\pi G_N}{c^4}(T_{\mu\nu} - \tfrac{1}{2}T\eta_{\mu\nu}) + O(h^2) + O(hT)\ , \qquad (18.12)$$

reads $-(8\pi G_N/c^4)T^{\mu\nu}\Box^{-1}(T_{\mu\nu} - \frac{1}{2}T\eta_{\mu\nu})$. For a system of N moving point masses, with free Lagrangian $L^{(1)} = \sum_{A=1}^{N} - m_A c^2\sqrt{1 - \boldsymbol{v}_A^2/c^2}$, this interaction, expanded to order v^2/c^2, reads (with $r_{AB} \equiv |\boldsymbol{x}_A - \boldsymbol{x}_B|$, $\boldsymbol{n}_{AB} \equiv (\boldsymbol{x}_A - \boldsymbol{x}_B)/r_{AB}$)

$$L^{(2)} = \tfrac{1}{2}\sum_{A\neq B}\frac{G_N m_A m_B}{r_{AB}}\left[1 + \frac{3}{2c^2}(\boldsymbol{v}_A^2 + \boldsymbol{v}_B^2) - \frac{7}{2c^2}(\boldsymbol{v}_A\cdot\boldsymbol{v}_B) - \frac{1}{2c^2}(\boldsymbol{n}_{AB}\cdot\boldsymbol{v}_A)(\boldsymbol{n}_{AB}\cdot\boldsymbol{v}_B) + O\left(\frac{1}{c^4}\right)\right]\ . \qquad (18.13)$$

The two-body interactions Eq. (18.13) exhibit v^2/c^2 corrections to Newton's $1/r$ potential induced by spin-2 exchange. Consistency at the "post-Newtonian" level $v^2/c^2 \sim G_N m/rc^2$ requires that one also consider the three-body interactions induced by some of the three-graviton vertices, and other nonlinearities (terms $O(h^2)$ and $O(hT)$ in Eq. (18.12)),

$$L^{(3)} = -\frac{1}{2}\sum_{B\neq A\neq C}\frac{G_N^2 m_A m_B m_C}{r_{AB}\, r_{AC}\, c^2} + O\left(\frac{1}{c^4}\right)\ . \qquad (18.14)$$

All currently performed gravitational experiments in the solar system, including perihelion advances of planetary orbits, the bending and delay of electromagnetic signals passing near the Sun, and very accurate ranging data to the Moon obtained by laser echoes, are compatible with the post-Newtonian results Eqs. (18.12)–(18.14).

Similarly to what is done in discussions of precision electroweak experiments (see Section 10 in this *Review*), it is useful to quantify the significance of precision gravitational experiments by parameterizing plausible deviations from General Relativity. The addition of a mass-term in Einstein's field equations leads to a score of theoretical difficulties [24], which have not yet received any consensual solution. We shall, therefore, not consider here the ill-defined "mass of the graviton" as a possible deviation parameter from General Relativity (see, however, the phenomenological limits quoted in the Section "Gauge and Higgs Bosons" of this *Review*). Deviations from Einstein's pure spin-2 theory are then defined by adding new bosonic light or massless macroscopically coupled fields. The possibility of new gravitational-strength couplings leading (on small, and possibly large, scales) to deviations from Einsteinian (and Newtonian) gravity is suggested by String Theory [25], and by Brane World ideas [26]. For compilations of experimental constraints on Yukawa-type additional interactions, see Refs. [17,27,28] and the Section "Extra Dimensions" in this *Review*. Recent experiments have set limits on non-Newtonian forces below 0.1 mm [29].

Here, we shall focus on the parametrization of long-range deviations from relativistic gravity obtained by adding a massless scalar field φ, coupled to the trace of the energy-momentum tensor $T = g_{\mu\nu}T^{\mu\nu}$ [30]. The most general such theory contains an arbitrary function $a(\varphi)$ of the scalar field, and can be defined by the Lagrangian

$$\mathcal{L}_{\rm tot}[g_{\mu\nu},\varphi,\psi,A_\mu,H] = \frac{c^4}{16\pi G}\sqrt{g}(R(g) - 2g^{\mu\nu}\partial_\mu\varphi\partial_\nu\varphi) + \mathcal{L}_{\rm SM}[\psi, A_\mu, H, \tilde{g}_{\mu\nu}]\ , \qquad (18.15)$$

where G is a "bare" Newton constant, and where the Standard Model matter is coupled not to the "Einstein" (pure spin-2) metric $g_{\mu\nu}$, but to the conformally related ("Jordan-Fierz") metric $\tilde{g}_{\mu\nu} = \exp(2a(\varphi))g_{\mu\nu}$. The scalar field equation $\Box_g\varphi = -(4\pi G/c^4)\alpha(\varphi)T$ displays $\alpha(\varphi) \equiv \partial a(\varphi)/\partial\varphi$ as the basic (field-dependent) coupling between φ and matter [31]. The one-parameter (ω) Jordan-Fierz-Brans-Dicke theory [30] is the special case $a(\varphi) = \alpha_0\varphi$, leading to a field-independent coupling $\alpha(\varphi) = \alpha_0$ (with ${\alpha_0}^2 = 1/(2\omega+3)$).

In the weak field, slow motion limit, appropriate to describing gravitational experiments in the solar system, the addition of φ modifies Einstein's predictions only through the appearance of two "post-Einstein" dimensionless parameters: $\overline{\gamma} = -2\alpha_0^2/(1+\alpha_0^2)$ and $\overline{\beta} = +\frac{1}{2}\beta_0\alpha_0^2/(1+\alpha_0^2)^2$, where $\alpha_0 \equiv \alpha(\varphi_0)$, $\beta_0 \equiv \partial\alpha(\varphi_0)/\partial\varphi_0$, φ_0 denoting the vacuum expectation value of φ. These parameters also show up naturally (in the form $\gamma_{\rm PPN} = 1 + \overline{\gamma}$, $\beta_{\rm PPN} = 1 + \overline{\beta}$) in phenomenological discussions of possible deviations from General Relativity [32,22]. The parameter $\overline{\gamma}$ measures the admixture of spin 0 to Einstein's graviton, and contributes an extra term $+\overline{\gamma}(\boldsymbol{v}_A - \boldsymbol{v}_B)^2/c^2$ in the square brackets of the two-body Lagrangian Eq. (18.13). The parameter $\overline{\beta}$ modifies the three-body interaction Eq. (18.14) by a factor $1 + 2\overline{\beta}$. Moreover, the combination $\eta \equiv 4\overline{\beta} - \overline{\gamma}$ parameterizes the lowest order effect of the self-gravity of orbiting masses by modifying the Newtonian interaction energy terms in Eq. (18.13) into $G_{AB}m_A m_B/r_{AB}$, with a body-dependent gravitational "constant" $G_{AB} = G_N[1 + \eta(E_A^{\rm grav}/m_A c^2 + E_B^{\rm grav}/m_B c^2) + O(1/c^4)]$, where $G_N = G\exp[2a(\varphi_0)](1+\alpha_0^2)$, and where $E_A^{\rm grav}$ denotes the gravitational binding energy of body A.

The best current limits on the post-Einstein parameters $\overline{\gamma}$ and $\overline{\beta}$ are (at the 68% confidence level): (i) $\overline{\gamma} = (2.1 \pm 2.3)\times 10^{-5}$, deduced from the additional Doppler shift experienced by radio-wave beams connecting the Earth to the Cassini spacecraft when they passed near the Sun [33], and (ii) $4\overline{\beta} - \overline{\gamma} = -0.0007 \pm 0.0010$ [18] from Lunar Laser Ranging measurements of a possible polarization of the Moon toward the Sun [34]. More stringent limits on $\overline{\gamma}$ are obtained in models (*e.g.*, string-inspired ones [35]) where scalar couplings violate the Equivalence Principle.

18.3. Tests of the dynamics of the gravitational field in the radiative and/or strong field regimes

The discovery of pulsars (*i.e.*, rotating neutron stars emitting a beam of radio noise) in gravitationally bound orbits [36,37] has opened up an entirely new testing ground for relativistic gravity, giving us an experimental handle on the regime of radiative and/or strong gravitational fields. In these systems, the finite velocity of propagation of the gravitational interaction between the pulsar and its companion generates damping-like terms at order $(v/c)^5$ in the equations of motion [38]. These damping forces are the local counterparts of the gravitational radiation emitted at infinity by the system ("gravitational radiation reaction"). They cause the binary orbit to shrink and its orbital period P_b to decrease. The remarkable stability of the pulsar clock has allowed Taylor and collaborators to measure the corresponding very small orbital period decay $\dot{P}_b \equiv dP_b/dt \sim -(v/c)^5 \sim -10^{-12}$ [37,39,40], thereby giving us a direct experimental confirmation of the propagation properties of the gravitational field, and, in particular, an experimental confirmation that the speed of propagation of gravity is equal to the velocity of light to better than a part in a thousand [41]. In addition, the surface gravitational potential of a neutron star $h_{00}(R) \simeq 2Gm/c^2R \simeq 0.4$ being a factor $\sim 10^8$ higher than the surface potential of the Earth, and a mere factor 2.5 below the black hole limit ($h_{00} = 1$), pulsar data are sensitive probes of the strong-gravitational-field regime.

Binary pulsar timing data record the times of arrival of successive electromagnetic pulses emitted by a pulsar orbiting around the center of mass of a binary system. After correcting for the Earth motion around the Sun, and for the dispersion due to propagation in the interstellar plasma, the time of arrival of the Nth pulse t_N can be described by a generic, parameterized "timing formula," [42] whose functional form is common to the whole class of tensor-scalar gravitation theories:

$$t_N - t_0 = F[T_N(\nu_p, \dot{\nu}_p, \ddot{\nu}_p)\,;\,\{p^K\}\,;\,\{p^{PK}\}]\ . \qquad (18.16)$$

Here, T_N is the pulsar proper time corresponding to the Nth turn given by $N/2\pi = \nu_p T_N + \frac{1}{2}\dot{\nu}_p T_N^2 + \frac{1}{6}\ddot{\nu}_p T_N^3$ (with $\nu_p \equiv 1/P_p$ the spin frequency of the pulsar, *etc.*), $\{p^K\} = \{P_b, T_0, e, \omega_0, x\}$ is the set of "Keplerian" parameters, (notably, orbital period P_b, eccentricity e and projected semi-major axis $x = a \sin i/c$), and $\{p^{PK}\} = \{k, \gamma_{\rm timing}, \dot{P}_b, r, s, \delta_\theta, \dot{e}, \dot{x}\}$ denotes the set of (separately measurable) "post-Keplerian" parameters. Most important among these are: the fractional periastron advance per orbit $k \equiv \dot{\omega} P_b/2\pi$, a dimensionful time-dilation parameter $\gamma_{\rm timing}$, the orbital period derivative $\dot{P}_b$, and the "range" and "shape" parameters of the gravitational time delay caused by the companion, r and s.

Without assuming any specific theory of gravity, one can phenomenologically analyze the data from any binary pulsar by least-squares fitting the observed sequence of pulse arrival times to the timing formula Eq. (18.16). This fit yields the "measured" values of the parameters $\{\nu_p, \dot{\nu}_p, \ddot{\nu}_p\}$, $\{p^K\}$, $\{p^{PK}\}$. Now, each specific relativistic theory of gravity predicts that, for instance, k, $\gamma_{\rm timing}$, $\dot{P}_b$, r, and s (to quote parameters that have been successfully measured from some binary pulsar data) are some theory-dependent functions of the Keplerian parameters and of the (unknown) masses m_1, m_2 of the pulsar and its companion. For instance, in General Relativity, one finds (with $M \equiv m_1 + m_2$, $n \equiv 2\pi/P_b$)

$$\begin{aligned} k^{\rm GR}(m_1,m_2) &= 3(1-e^2)^{-1}(G_N M n/c^3)^{2/3} \ , \\ \gamma^{\rm GR}_{\rm timing}(m_1,m_2) &= e n^{-1}(G_N M n/c^3)^{2/3} m_2(m_1+2m_2)/M^2 \ , \\ \dot{P}_b^{\rm GR}(m_1,m_2) &= -(192\pi/5)(1-e^2)^{-7/2}\left(1+\tfrac{73}{24}e^2+\tfrac{37}{96}e^4\right) \\ &\quad \times (G_N M n/c^3)^{5/3} m_1 m_2/M^2 \ , \\ r(m_1,m_2) &= G_N m_2/c^3 \ , \quad \text{and} \\ s(m_1,m_2) &= n x (G_N M n/c^3)^{-1/3} M/m_2 \ . \end{aligned} \tag{18.17}$$

In tensor-scalar theories, each of the functions $k^{\rm theory}(m_1,m_2)$, $\gamma^{\rm theory}_{\rm timing}(m_1,m_2)$, $\dot{P}_b^{\rm theory}(m_1,m_2)$, *etc.* is modified by quasi-static strong field effects (associated with the self-gravities of the pulsar and its companion), while the particular function $\dot{P}_b^{\rm theory}(m_1,m_2)$ is further modified by radiative effects (associated with the spin 0 propagator) [31,43].

Let us summarize the current experimental situation (see Ref. 44 for a more extensive review). In the first discovered binary pulsar PSR1913 + 16 [36,37], it has been possible to measure with accuracy the three post-Keplerian parameters k, $\gamma_{\rm timing}$ and $\dot{P}_b$. The three equations $k^{\rm measured} = k^{\rm theory}(m_1,m_2)$, $\gamma^{\rm measured}_{\rm timing} = \gamma^{\rm theory}_{\rm timing}(m_1,m_2)$, $\dot{P}_b^{\rm measured} = \dot{P}_b^{\rm theory}(m_1,m_2)$ determine, for each given theory, three curves in the two-dimensional mass plane. This yields *one* (combined radiative/strong-field) test of the specified theory, according to whether the three curves meet at one point, as they should. After subtracting a small ($\sim 10^{-14}$ level in $\dot{P}_b^{\rm obs} = (-2.4211 \pm 0.0014) \times 10^{-12}$), but significant Newtonian perturbing effect caused by the Galaxy [45], one finds that General Relativity passes this $(k - \gamma_{\rm timing} - \dot{P}_b)_{1913+16}$ test with complete success at the 10^{-3} level [37,39,40]

$$\begin{aligned} \left[\frac{\dot{P}_b^{\rm obs} - \dot{P}_b^{\rm galactic}}{\dot{P}_b^{\rm GR}[k^{\rm obs}, \gamma^{\rm obs}_{\rm timing}]}\right]_{1913+16} &= 1.0026 \pm 0.0006({\rm obs}) \pm 0.0021({\rm galactic}) \\ &= 1.0026 \pm 0.0022 \ . \end{aligned} \tag{18.18}$$

Here $\dot{P}_b^{\rm GR}[k^{\rm obs}, \gamma^{\rm obs}_{\rm timing}]$ is the result of inserting in $\dot{P}_b^{\rm GR}(m_1,m_2)$ the values of the masses predicted by the two equations $k^{\rm obs} = k^{\rm GR}(m_1,m_2)$, $\gamma^{\rm obs}_{\rm timing} = \gamma^{\rm GR}_{\rm timing}(m_1,m_2)$. This experimental evidence for the reality of gravitational radiation damping forces at the 0.3% level is illustrated in Fig. 18.1, which shows actual orbital phase data (after subtraction of a linear drift).

The discovery of the binary pulsar PSR1534 + 12 [46] has allowed one to measure the four post-Keplerian parameters k, $\gamma_{\rm timing}$, r and s, and thereby to obtain *two* (four observables minus two masses) tests of strong field gravity, without mixing of radiative effects [47]. General Relativity passes these tests within the measurement accuracy [37,47]. The most precise of these new, pure, strong-field tests is the one obtained by combining the measurements of k, γ, and s. Using the most recent data [48], one finds agreement at the 1% level:

$$\left[\frac{s^{\rm obs}}{s^{\rm GR}[k^{\rm obs}, \gamma^{\rm obs}_{\rm timing}]}\right]_{1534+12} = 1.000 \pm 0.007 \ . \tag{18.19}$$

It has also been possible to measure the orbital period change of PSR1534 + 12. General Relativity passes the corresponding $(k - \gamma_{\rm timing} - \dot{P}_b)_{1534+12}$ test with success at the 15% level [48].

The discovery of the binary pulsar PSR J1141 − 6545 [49] (whose companion is probably a white dwarf) has recently led to the measurement of the three post-Keplerian parameters k, $\gamma_{\rm timing}$ and $\dot{P}_b$ [50]. As in the PSR 1913 + 16 system, this yields *one* combined radiative/strong-field test of relativistic gravity. One finds that General Relativity passes this $(k - \gamma_{\rm timing} - \dot{P}_b)_{1141-6545}$ test with success at the 25% level [50]. Several other binary pulsar systems, of a nonsymmetric type (nearly circular systems made of a neutron star and a white dwarf), can also be used to test relativistic gravity [51–54]. The constraints on tensor-scalar theories provided by three binary-pulsar "experiments" have been analyzed in Ref. 43, and shown to exclude a large portion of the parameter space allowed by solar-system tests. Measurements of the pulse shape of PSR1913 + 16 [55] have detected a time variation of the pulse shape, compatible with the prediction [56] that the general relativistic spin-orbit coupling should cause a secular change in the orientation of the pulsar beam, with respect to the line of sight ("geodetic precession").

The tests considered above have examined the gravitational interaction on scales between a fraction of a millimeter and a few

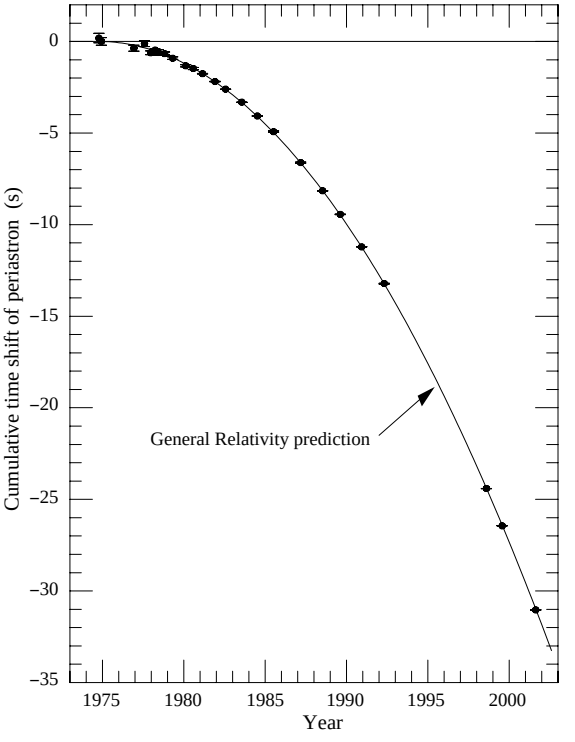

Figure 18.1: Accumulated shift of the times of periastron passage in the PSR 1913+16 system, relative to an assumed orbit with a constant period. The parabolic curve represents the general relativistic prediction, modified by Galactic effects, for orbital period decay from gravitational radiation damping forces. (Figure obtained with permission from Ref. 40.)

astronomical units. On the other hand, the general relativistic action on light and matter of an external gravitational field on a length scale ~ 100 kpc has been verified to $\sim 30\%$ in some gravitational lensing systems (see, *e.g.*, Ref. 57). Some tests on cosmological scales are also available. In particular, Big Bang Nucleosynthesis (see Section 20 of this *Review*) has been used to set significant constraints on the variability of the gravitational "constant" [58]. For other cosmological tests of the "constancy of constants," see the review [13].

18.4. Conclusions

All present experimental tests are compatible with the predictions of the current "standard" theory of gravitation: Einstein's General Relativity. The universality of the coupling between matter and gravity (Equivalence Principle) has been verified at the 10^{-12} level. Solar system experiments have tested all the weak-field predictions of Einstein's theory at better than the 10^{-3} level (and down to the 2×10^{-5} level for the post-Einstein parameter $\overline{\gamma}$). The propagation properties of relativistic gravity, as well as several of its strong-field aspects, have been verified at the 10^{-3} level in binary pulsar experiments. Recent laboratory experiments have set strong constraints on sub-millimeter modifications of Newtonian gravity.

Several important new developments in experimental gravitation are expected in the near future. The approved NASA Gravity Probe B mission [59] (a space gyroscope experiment; due for launch in December 2003) will directly measure the gravitational spin-orbit and spin-spin couplings, thereby measuring the parameter $\overline{\gamma}$ to better than the 10^{-5} level. The universality of free-fall acceleration should soon be tested to much better than the 10^{-12} level by some satellite experiments: the approved CNES MICROSCOPE [60] mission (10^{-15} level), and the planned (cryogenic) NASA-ESA STEP [61] mission (10^{-18} level). The recently constructed kilometer-size laser interferometers (notably LIGO [62] in the USA, and VIRGO [63] and GEO600 [64] in Europe), should soon directly detect gravitational waves arriving on Earth. As the sources of these waves are expected to be extremely relativistic objects with strong internal gravitational fields (*e.g.*, coalescing binary black holes), their detection will allow one to experimentally probe gravity in highly dynamical circumstances. Note finally that arrays of millisecond pulsars are sensitive detectors of (very low frequency) gravitational waves [65,66].

References:

1. S.N. Gupta, Phys. Rev. **96**, 1683 (1954);
   R.H. Kraichnan, Phys. Rev. **98**, 1118 (1955);
   R.P. Feynman, F.B. Morinigo, and W.G. Wagner, *Feynman Lectures on Gravitation*, edited by Brian Hatfield (Addison-Wesley, Reading, 1995);
   S. Weinberg, Phys. Rev. **138**, B988 (1965);
   V.I. Ogievetsky and I.V. Polubarinov, Ann. Phys. (NY) **35**, 167 (1965);
   W. Wyss, Helv. Phys. Acta **38**, 469 (1965);
   S. Deser, Gen. Rel. Grav. **1**, 9 (1970);
   D.G. Boulware and S. Deser, Ann. Phys. (NY) **89**, 193 (1975);
   J. Fang and C. Fronsdal, J. Math. Phys. **20**, 2264 (1979);
   R.M. Wald, Phys. Rev. **D33**, 3613 (1986);
   C. Cutler and R.M. Wald, Class. Quantum Grav. **4**, 1267 (1987);
   R.M. Wald, Class. Quantum Grav. **4**, 1279 (1987);
   N. Boulanger *et al.*, Nucl. Phys. **B597**, 127 (2001).
2. S. Weinberg, *Gravitation and Cosmology* (John Wiley, New York, 1972).
3. S. Weinberg, Rev. Mod. Phys. **61**, 1 (1989).
4. A.I. Shlyakhter, Nature **264**, 340 (1976);
   T. Damour and F. Dyson, Nucl. Phys. **B480**, 37 (1996);
   Y. Fujii *et al.*, Nucl. Phys. **B573**, 377 (2000).
5. J.D. Prestage, R.L. Tjoelker, and L. Maleki, Phys. Rev. Lett. **74**, 3511 (1995);
   Y. Sortais *et al.*, Physica Scripta **95**, 50 (2001).
6. J.K. Webb *et al.*, Phys. Rev. Lett. **87**, 091301 (2001);
   M.T. Murphy *et al.*, Mon. Not. Roy. Astron. Soc. **327**, 1208 (2001).
7. K.A. Olive and M. Pospelov, Phys. Rev. **D65**, 085044 (2002).
8. H.B. Sandvik, J.D. Barrow, and J. Magueijo, Phys. Rev. Lett. **88**, 031302 (2002).
9. T. Damour, F. Piazza, and G. Veneziano, Phys. Rev. Lett. **89**, 081601 (2002); and Phys. Rev. **D66**, 046007 (2002).
10. K.A. Olive *et al.*, Phys. Rev. **D66**, 045022 (2002).
11. M.T. Murphy *et al.*, Astrophys. Space Sci. **283**, 577 (2003).
12. J.N. Bahcall, C.L. Steinhardt, and D. Schlegel, `astro-ph/0301507`.
13. J.P. Uzan, Rev. Mod. Phys. **75**, 403 (2003).
14. J.D. Prestage *et al.*, Phys. Rev. Lett. **54**, 2387 (1985);
    S.K. Lamoreaux *et al.*, Phys. Rev. Lett. **57**, 3125 (1986);
    T.E. Chupp *et al.*, Phys. Rev. Lett. **63**, 1541 (1989).
15. T. Jacobson, S. Liberati, and D. Mattingly, Nature **424**, 1019 (2003).
16. R.C. Myers and M. Pospelov, Phys. Rev. Lett. **90**, 211601 (2003).
17. Y. Su *et al.*, Phys. Rev. **D50**, 3614 (1994).
18. J.O. Dickey *et al.*, Science **265**, 482 (1994);
    J.G. Williams, X.X. Newhall, and J.O. Dickey, Phys. Rev. **D53**, 6730 (1996).
19. S. Baessler *et al.*, Phys. Rev. Lett. **83**, 3585 (1999).
20. G.L. Smith *et al.*, Phys. Rev. **D61**, 022001 (1999).
21. R.F.C. Vessot and M.W. Levine, Gen. Rel. Grav. **10**, 181 (1978);
    R.F.C. Vessot *et al.*, Phys. Rev. Lett. **45**, 2081 (1980).
22. C.M. Will, *Theory and Experiment in Gravitational Physics* (Cambridge University Press, Cambridge, 1993); and Living Rev. Rel. **4**, 4 (2001).
23. T. Damour, in *Gravitation and Quantizations*, ed. B. Julia and J. Zinn-Justin, Les Houches, Session LVII (Elsevier, Amsterdam, 1995), pp. 1–61.
24. H. van Dam and M.J. Veltman, Nucl. Phys. **B22**, 397 (1970);
    V.I. Zakharov, Sov. Phys. JETP Lett. **12**, 312 (1970);
    D.G. Boulware and S. Deser, Phys. Rev. **D6**, 3368 (1972);
    C. Aragone and J. Chela-Flores, Nuovo Cim. **10A**, 818 (1972);
    A.I. Vainshtein, Phys. Lett. **B39**, 393 (1972);
    C. Deffayet *et al.*, Phys. Rev. **D65**, 044026 (2002);
    M. Porrati, Phys. Lett. **B534**, 209 (2002);
    N. Arkani-Hamed, H. Georgi, and M.D. Schwartz, Annals Phys. **305**, 96 (2003);
    T. Damour, I.I. Kogan, and A. Papazoglou, Phys. Rev. **D67**, 064009 (2003);
    G. Dvali, A. Gruzinov, and M. Zaldarriaga, Phys. Rev. **D68**, 024012 (2003).
25. T.R. Taylor and G. Veneziano, Phys. Lett. **B213**, 450 (1988);
    S. Dimopoulos and G. Giudice, Phys. Lett. **B379**, 105 (1996);
    I. Antoniadis, S. Dimopoulos, and G. Dvali, Nucl. Phys. **B516**, 70 (1998).
26. V.A. Rubakov, Phys. Usp **44**, 871 (2001);
    I.I. Kogan, in *Proceedings of the XXXVIth Rencontres de Moriond, Electro-Weak Interactions and Unified Theories* (March 2001); `astro-ph/0108220`.
27. E. Fischbach and C.L. Talmadge, *The search for non-Newtonian gravity* (Springer-Verlag, New York, 1999).
28. J.C. Long, H.W. Chan, and J.C. Price, Nucl. Phys. **B539**, 23 (1999).
29. C.D. Hoyle *et al.*, Phys. Rev. Lett. **86**, 1418 (2001);
    J. Chiaverini *et al.*, Phys. Rev. Lett. **90**, 151101 (2003);
    J.C. Long *et al.*, Nature **421**, 922 (2003).

30. P. Jordan, *Schwerkraft und Weltall* (Vieweg, Braunschweig, 1955); M. Fierz, Helv. Phys. Acta **29**, 128 (1956); C. Brans and R.H. Dicke, Phys. Rev. **124**, 925 (1961).
31. T. Damour and G. Esposito-Farèse, Class. Quantum Grav. **9**, 2093 (1992).
32. A.S. Eddington, *The Mathematical Theory of Relativity* (Cambridge University Press, Cambridge, 1923); K. Nordtvedt, Phys. Rev. **169**, 1017 (1968); C.M. Will, Astrophys. J. **163**, 611 (1971).
33. B. Bertotti, L. Iess and P. Tortora, Nature, **425**, 374 (2003).
34. K. Nordtvedt, Phys. Rev. **170**, 1186 (1968).
35. T.R. Taylor and G. Veneziano, Phys. Lett. **B213**, 450 (1988); T. Damour and A.M. Polyakov, Nucl. Phys. **B423**, 532 (1994).
36. R.A. Hulse, Rev. Mod. Phys. **66**, 699 (1994).
37. J.H. Taylor, Rev. Mod. Phys. **66**, 711 (1994).
38. T. Damour and N. Deruelle, Phys. Lett. **A87**, 81 (1981); T. Damour, C.R. Acad. Sci. Paris **294**, 1335 (1982).
39. J.H. Taylor, Class. Quantum Grav. **10**, S167 (Supplement 1993).
40. J. Weisberg and J.H. Taylor, in *Radio Pulsars, ASP Conference Series* **302**, 93 (2003); `astro-ph/0211217`.
41. By contrast to the binary pulsar case, which does involve the gauge-invariant, helicity-two propagating degrees of freedom of the gravitational field, the recent measurement of light deflection from Jupiter (E.B. Fomalont and S.M. Kopeikin, `astro-ph/0302294`) does not depend (in spite of contrary claims: S.M. Kopeikin, Astrophys. J. **556**, L1 (2001)), at the considered precision level, on the propagation speed of gravity (see C.M. Will, Astrophys. J. **590**, 683 (2003) and S. Samuel, Phys. Rev. Lett. **90**, 231101 (2003)).
42. T. Damour and J.H. Taylor, Phys. Rev. **D45**, 1840 (1992).
43. T. Damour and G. Esposito-Farèse, Phys. Rev. **D54**, 1474 (1996); and Phys. Rev. **D58**, 042001 (1998).
44. I.H. Stairs, Living Rev. Rel. **6** 5 (2003).
45. T. Damour and J.H. Taylor, Astrophys. J. **366**, 501 (1991).
46. A. Wolszczan, Nature **350**, 688 (1991).
47. J.H. Taylor *et al.*, Nature **355**, 132 (1992).
48. I.H. Stairs *et al.*, Astrophys. J. **505**, 352 (1998); I.H. Stairs *et al.*, Astrophys. J. **581**, 501 (2002).
49. V.M. Kaspi *et al.*, Astrophys. J. **528**, 445 (2000).
50. M. Bailes *et al.*, Astrophys. J. **595**, L49 (2003).
51. C.M. Will and H.W. Zaglauer, Astrophys. J. **346**, 366 (1989).
52. T. Damour and G. Schäfer, Phys. Rev. Lett. **66**, 2549 (1991).
53. Ch. Lange *et al.*, Mon. Not. Roy. Astron. Soc. **326**, 274 (2001).
54. Z. Arzoumanian, in *Radio Pulsars, ASP Conference Series* **302**, 69 (2003); `astro-ph/0212180`.
55. M. Kramer, Astrophys. J. **509**, 856 (1998); J.M. Weisberg and J.H. Taylor, Astrophys. J. **576**, 942 (2002).
56. T. Damour and R. Ruffini, C. R. Acad. Sc. Paris **279**, série A, 971 (1974); B.M. Barker and R.F. O'Connell, Phys. Rev. D 12, 329 (1975).
57. A. Dar, Nucl. Phys. (Proc. Supp.) **B28**, 321 (1992).
58. J. Yang *et al.*, Astrophys. J. **227**, 697 (1979); T. Rothman and R. Matzner, Astrophys. J. **257**, 450 (1982); F.S. Accetta, L.M. Krauss, and P. Romanelli, Phys. Lett. **B248**, 146 (1990).
59. `http://einstein.stanford.edu`.
60. P. Touboul *et al.*, C.R.Acad. Sci. Paris **2** (série IV) 1271 (2001).
61. P.W. Worden, in *Proc. 7th Marcel Grossmann Meeting on General Relativity*, edited by R.J. Jantzen and G. MacKeiser, (World Scientific, Singapore, 1995), pp. 1569-1573.
62. `http://www.ligo.caltech.edu` .
63. `http://www.virgo.infn.it` .
64. `http://www.geo600.uni-hannover.de` .
65. V.M. Kaspi, J.H. Taylor and M.F. Ryba, Astrophys. J. **428**, 713 (1994).
66. A.N. Lommen and D.C. Backer, Bulletin of the American Astronomical Society **33**, 1347 (2001); and Astrophys. J. **562**, 297 (2001).

19. BIG-BANG COSMOLOGY

Written July 2001 by K.A. Olive (University of Minnesota) and J.A. Peacock (University of Edinburgh). Revised November 2003.

19.1. Introduction to Standard Big-Bang Model

The observed expansion of the Universe [1,2,3] is a natural (almost inevitable) result of any homogeneous and isotropic cosmological model based on general relativity. However, by itself, the Hubble expansion does not provide sufficient evidence for what we generally refer to as the Big-Bang model of cosmology. While general relativity is in principle capable of describing the cosmology of any given distribution of matter, it is extremely fortunate that our Universe appears to be homogeneous and isotropic on large scales. Together, homogeneity and isotropy allow us to extend the Copernican Principle to the Cosmological Principle, stating that all spatial positions in the Universe are essentially equivalent.

The formulation of the Big-Bang model began in the 1940s with the work of George Gamow and his collaborators, Alpher and Herman. In order to account for the possibility that the abundances of the elements had a cosmological origin, they proposed that the early Universe which was once very hot and dense (enough so as to allow for the nucleosynthetic processing of hydrogen), and has expanded and cooled to its present state [4,5]. In 1948, Alpher and Herman predicted that a direct consequence of this model is the presence of a relic background radiation with a temperature of order a few K [6,7]. Of course this radiation was observed 16 years later as the microwave background radiation [8]. Indeed, it was the observation of the 3 K background radiation that singled out the Big-Bang model as the prime candidate to describe our Universe. Subsequent work on Big-Bang nucleosynthesis further confirmed the necessity of our hot and dense past. (See the review on BBN—Sec. 20 of this *Review* for a detailed discussion of BBN.) These relativistic cosmological models face severe problems with their initial conditions, to which the best modern solution is inflationary cosmology, discussed in Sec. 19.3.5. If correct, these ideas would strictly render the term 'Big Bang' redundant, since it was first coined by Hoyle to represent a criticism of the lack of understanding of the initial conditions.

19.1.1. *The Robertson-Walker Universe*:

The observed homogeneity and isotropy enable us to describe the overall geometry and evolution of the Universe in terms of two cosmological parameters accounting for the spatial curvature and the overall expansion (or contraction) of the Universe. These two quantities appear in the most general expression for a space-time metric which has a (3D) maximally symmetric subspace of a 4D space-time, known as the Robertson-Walker metric:

$$ds^2 = dt^2 - R^2(t)\left[\frac{dr^2}{1-kr^2} + r^2\left(d\theta^2 + \sin^2\theta\, d\phi^2\right)\right] . \qquad (19.1)$$

Note that we adopt $c = 1$ throughout. By rescaling the radial coordinate, we can choose the curvature constant k to take only the discrete values $+1$, -1, or 0 corresponding to closed, open, or spatially flat geometries. In this case, it is often more convenient to re-express the metric as

$$ds^2 = dt^2 - R^2(t)\left[d\chi^2 + S_k^2(\chi)\left(d\theta^2 + \sin^2\theta\, d\phi^2\right)\right] , \qquad (19.2)$$

where the function $S_k(\chi)$ is $(\sin\chi, \chi, \sinh\chi)$ for $k = (+1, 0, -1)$. The coordinate r (in Eq. (19.1)) and the 'angle' χ (in Eq. (19.2)) are both dimensionless; the dimensions are carried by $R(t)$, which is the cosmological scale factor which determines proper distances in terms of the comoving coordinates. A common alternative is to define a dimensionless scale factor, $a(t) = R(t)/R_0$, where $R_0 \equiv R(t_0)$ is R at the present epoch. It is also sometimes convenient to define a dimensionless or conformal time coordinate, η, by $d\eta = dt/R(t)$. Along constant spatial sections, the proper time is defined by the time coordinate, t. Similarly, for $dt = d\theta = d\phi = 0$, the proper distance is given by $R(t)\chi$. For standard texts on cosmological models see *e.g.*, Refs. [9–14].

19.1.2. *The redshift*:

The cosmological redshift is a direct consequence of the Hubble expansion, determined by $R(t)$. A local observer detecting light from a distant emitter sees a redshift in frequency. We can define the redshift as

$$z \equiv \frac{\nu_1 - \nu_2}{\nu_2} \simeq \frac{v_{12}}{c} , \qquad (19.3)$$

where ν_1 is the frequency of the emitted light, ν_2 is the observed frequency and v_{12} is the relative velocity between the emitter and the observer. While the definition, $z = (\nu_1 - \nu_2)/\nu_2$ is valid on all distance scales, relating the redshift to the relative velocity in this simple way is only true on small scales (*i.e.*, less than cosmological scales) such that the expansion velocity is non-relativistic. For light signals, we can use the metric given by Eq. (19.1) and $ds^2 = 0$ to write

$$\frac{v_{12}}{c} = \dot{R}\,\delta r = \frac{\dot{R}}{R}\,\delta t = \frac{\delta R}{R} = \frac{R_2 - R_1}{R_1} , \qquad (19.4)$$

where $\delta r(\delta t)$ is the radial coordinate (temporal) separation between the emitter and observer. Thus, we obtain the simple relation between the redshift and the scale factor

$$1 + z = \frac{\nu_1}{\nu_2} = \frac{R_2}{R_1} . \qquad (19.5)$$

This result does not depend on the non-relativistic approximation.

19.1.3. *The Friedmann-Lemaître equations of motion*:

The cosmological equations of motion are derived from Einstein's equations

$$\mathcal{R}_{\mu\nu} - \tfrac{1}{2} g_{\mu\nu}\mathcal{R} = 8\pi G_{\rm N} T_{\mu\nu} + \Lambda g_{\mu\nu} . \qquad (19.6)$$

Gliner [15] and Zeldovich [16] seem to have pioneered the modern view, in which the Λ term is taken to the rhs and interpreted as particle-physics processes yielding an effective energy–momentum tensor $T_{\mu\nu}$ for the vacuum of $\Lambda g_{\mu\nu}/8\pi G_{\rm N}$. It is common to assume that the matter content of the Universe is a perfect fluid, for which

$$T_{\mu\nu} = -p g_{\mu\nu} + (p + \rho)\, u_\mu u_\nu , \qquad (19.7)$$

where $g_{\mu\nu}$ is the space-time metric described by Eq. (19.1), p is the isotropic pressure, ρ is the energy density and $u = (1, 0, 0, 0)$ is the velocity vector for the isotropic fluid in co-moving coordinates. With the perfect fluid source, Einstein's equations lead to the Friedmann-Lemaître equations

$$H^2 \equiv \left(\frac{\dot{R}}{R}\right)^2 = \frac{8\pi\ G_{\rm N}\,\rho}{3} - \frac{k}{R^2} + \frac{\Lambda}{3} , \qquad (19.8)$$

and

$$\frac{\ddot{R}}{R} = \frac{\Lambda}{3} - \frac{4\pi G_{\rm N}}{3}\ (\rho + 3p) , \qquad (19.9)$$

where $H(t)$ is the Hubble parameter and Λ is the cosmological constant. The first of these is sometimes called the Friedmann equation. Energy conservation via $T^{\mu\nu}{}_{;\mu} = 0$, leads to a third useful equation [which can also be derived from Eq. (19.8) and Eq. (19.9)]

$$\dot{\rho} = -3H\,(\rho + p) . \qquad (19.10)$$

Eq. (19.10) can also be simply derived as a consequence of the first law of thermodynamics.

Eq. (19.8) has a simple classical mechanical analog if we neglect (for the moment) the cosmological term Λ. By interpreting $-k/R^2$ as a "total energy", then we see that the evolution of the Universe is governed by a competition between the potential energy, $8\pi G_{\rm N}\rho/3$ and the kinetic term $(\dot{R}/R)^2$. For $\Lambda = 0$, it is clear that the Universe must be expanding or contracting (except at the turning point prior to collapse in a closed Universe). The ultimate fate of the Universe is determined by the curvature constant k. For $k = +1$, the Universe will recollapse in a finite time, whereas for $k = 0, -1$, the Universe will expand indefinitely. These simple conclusions can be altered when $\Lambda \neq 0$ or more generally with some component with $(\rho + 3p) < 0$.

19.1.4. ***Definition of cosmological parameters*:**

In addition to the Hubble parameter, it is useful to define several other measurable cosmological parameters. The Friedmann equation can be used to define a critical density such that $k = 0$ when $\Lambda = 0$,

$$\rho_c \equiv \frac{3H^2}{8\pi G_N} = 1.88 \times 10^{-26}\, h^2 \text{ kg m}^{-3} = 1.05 \times 10^{-5}\, h^2 \text{ GeV cm}^{-3} , \quad (19.11)$$

where the scaled Hubble parameter, h, is defined by

$$H \equiv 100\, h \text{ km s}^{-1} \text{ Mpc}^{-1} \Rightarrow H^{-1} = 9.78\, h^{-1} \text{ Gyr} = 2998\, h^{-1} \text{ Mpc} . \quad (19.12)$$

The cosmological density parameter $\Omega_{\rm tot}$ is defined as the energy density relative to the critical density,

$$\Omega_{\rm tot} = \rho/\rho_c . \quad (19.13)$$

Note that one can now rewrite the Friedmann equation as

$$k/R^2 = H^2(\Omega_{\rm tot} - 1) , \quad (19.14)$$

From Eq. (19.14), one can see that when $\Omega_{\rm tot} > 1$, $k = +1$ and the Universe is closed, when $\Omega_{\rm tot} < 1$, $k = -1$ and the Universe is open, and when $\Omega_{\rm tot} = 1$, $k = 0$, and the Universe is spatially flat.

It is often necessary to distinguish different contributions to the density. It is therefore convenient to define present-day density parameters for pressureless matter (Ω_m) and relativistic particles (Ω_r), plus the quantity $\Omega_\Lambda = \Lambda/3H^2$. In more general models, we may wish to drop the assumption that the vacuum energy density is constant, and we therefore denote the present-day density parameter of the vacuum by Ω_v. The Friedmann equation then becomes

$$k/R_0^2 = H_0^2(\Omega_m + \Omega_r + \Omega_v - 1) , \quad (19.15)$$

where the subscript 0 indicates present-day values. Thus, it is the sum of the densities in matter, relativistic particles and vacuum that determines the overall sign of the curvature. Note that the quantity $-k/R_0^2H_0^2$ is sometimes referred to as Ω_k. This usage is unfortunate: it encourages one to think of curvature as a contribution to the energy density of the Universe, which is not correct.

19.1.5. ***Standard Model solutions*:**

Much of the history of the Universe in the standard Big-Bang model can be easily described by assuming that either matter or radiation dominates the total energy density. During inflation or perhaps even today if we are living in an accelerating Universe, domination by a cosmological constant or some other form of dark energy should be considered. In the following, we shall delineate the solutions to the Friedmann equation when a single component dominates the energy density. Each component is distinguished by an equation of state parameter $w = p/\rho$.

19.1.5.1. *Solutions for a general equation of state:*

Let us first assume a general equation of state parameter for a single component, w which is constant. In this case, Eq. (19.10) can be written as $\dot\rho = -3(1+w)\rho\dot R/R$ and is easily integrated to yield

$$\rho \propto R^{-3(1+w)} . \quad (19.16)$$

Note that at early times when R is small, the less singular curvature term k/R^2 in the Friedmann equation can be neglected so long as $w > -1/3$. Curvature domination occurs at rather late times (if a cosmological constant term does not dominate sooner). For $w \neq -1$, one can insert this result into the Friedmann equation Eq. (19.8) and if one neglects the curvature and cosmological constant terms, it is easy to integrate the equation to obtain,

$$R(t) \propto t^{2/[3(1+w)]} . \quad (19.17)$$

19.1.5.2. *A Radiation-dominated Universe:*

In the early hot and dense Universe, it is appropriate to assume an equation of state corresponding to a gas of radiation (or relativistic particles) for which $w = 1/3$. In this case, Eq. (19.16) becomes $\rho \propto R^{-4}$. The "extra" factor of $1/R$ is due to the cosmological redshift; not only is the number density of particles in the radiation background decreasing as R^{-3} since volumes scales as R^3, but in addition, each particle's energy is decreasing as $E \propto \nu \propto R^{-1}$. Similarly, one can substitute $w = 1/3$ into Eq. (19.17) to obtain

$$R(t) \propto t^{1/2} ; \qquad H = 1/2t . \quad (19.18)$$

19.1.5.3. *A Matter-dominated Universe:*

At relatively late times, non-relativistic matter eventually dominates the energy density over radiation (see Sec. 19.3.8). A pressureless gas ($w = 0$) leads to the expected dependence $\rho \propto R^{-3}$ from Eq. (19.16) and, if $k = 0$, we get

$$R(t) \propto t^{2/3} ; \qquad H = 2/3t . \quad (19.19)$$

19.1.5.4. *A Universe dominated by vacuum energy:*

If there is a dominant source of vacuum energy, V_0, it would act as a cosmological constant with $\Lambda = 8\pi G_N V_0$ and equation of state $w = -1$. In this case, the solution to the Friedmann equation is particularly simple and leads to an exponential expansion of the Universe

$$R(t) \propto e^{\sqrt{\Lambda/3}t} . \quad (19.20)$$

A key parameter is the equation of state of the vacuum, $w \equiv p/\rho$: this need not be the $w = -1$ of Λ, and may not even be constant [17,18,19]. It is now common to use w to stand for this vacuum equation of state, rather than of any other constituent of the Universe, and we use the symbol in this sense hereafter. We generally assume w to be independent of time, and where results relating to the vacuum are quoted without an explicit w dependence, we have adopted $w = -1$.

The presence of vacuum energy can dramatically alter the fate of the Universe. For example, if $\Lambda < 0$, the Universe will eventually recollapse independent of the sign of k. For large values of Λ (larger than the Einstein static value needed to halt any cosmological expansion or contraction), even a closed Universe will expand forever. One way to quantify this is the deceleration parameter, q_0, defined as

$$q_0 = -\left.\frac{R\ddot R}{\dot R^2}\right|_0 = \frac{1}{2}\Omega_m + \Omega_r + \frac{(1+3w)}{2}\Omega_v . \quad (19.21)$$

This equation shows us that $w < -1/3$ for the vacuum may lead to an accelerating expansion. Astonishingly, it appears that such an effect has been observed in the Supernova Hubble diagram [20–23] (see Fig. 19.1 below); current data indicate that vacuum energy is indeed the largest contributor to the cosmological density budget, with $\Omega_v = 0.72 \pm 0.05$ and $\Omega_m = 0.28 \pm 0.05$ if $k = 0$ is assumed [23].

The nature of this dominant term is presently uncertain, but much effort is being invested in dynamical models (*e.g.*, rolling scalar fields), under the catch-all heading of "quintessence."

19.2. Introduction to Observational Cosmology

19.2.1. ***Fluxes, luminosities, and distances*:**

The key quantities for observational cosmology can be deduced quite directly from the metric.

(1) The *proper* transverse size of an object seen by us to subtend an angle $d\psi$ is its comoving size $d\psi\, S_k(\chi)$ times the scale factor at the time of emission:

$$d\ell = d\psi\ R_0 S_k(\chi)/(1+z) . \quad (19.22)$$

(2) The apparent flux density of an object is deduced by allowing its photons to flow through a sphere of current radius $R_0 S_k(\chi)$; but photon energies and arrival rates are redshifted, and the bandwidth $d\nu$ is reduced. The observed photons at frequency ν_0 were emitted at frequency $\nu_0(1+z)$, so the flux density is the luminosity at this frequency, divided by the total area, divided by $1+z$:

$$S_\nu(\nu_0) = \frac{L_\nu([1+z]\nu_0)}{4\pi R_0^2 S_k^2(\chi)(1+z)} \ . \tag{19.23}$$

These relations lead to the following common definitions:

$$\begin{aligned} \text{angular-diameter distance:} \quad & D_{\rm A} = (1+z)^{-1} R_0 S_k(\chi) \\ \text{luminosity distance:} \quad & D_{\rm L} = (1+z)\ R_0 S_k(\chi) \end{aligned} \tag{19.24}$$

These distance-redshift relations are expressed in terms of observables by using the equation of a null radial geodesic ($R(t)d\chi = dt$) plus the Friedmann equation:

$$\begin{aligned} R_0 d\chi = & \frac{1}{H(z)}\,dz = \frac{1}{H_0}\,\Big[(1-\Omega_m-\Omega_v-\Omega_r)(1+z)^2 \\ & +\ \Omega_v(1+z)^{3+3w} \ + \ \Omega_m(1+z)^3 + \Omega_r(1+z)^4\Big]^{-1/2}\ dz \ . \end{aligned} \tag{19.25}$$

The main scale for the distance here is the Hubble length, $1/H_0$.

The flux density is the product of the specific intensity I_ν and the solid angle $d\Omega$ subtended by the source: $S_\nu = I_\nu\ d\Omega$. Combining the angular size and flux-density relations thus gives the relativistic version of surface-brightness conservation:

$$I_\nu(\nu_0) = \frac{B_\nu([1+z]\nu_0)}{(1+z)^3} \ , \tag{19.26}$$

where B_ν is surface brightness (luminosity emitted into unit solid angle per unit area of source). We can integrate over ν_0 to obtain the corresponding total or bolometric formula:

$$I_{\rm tot} = \frac{B_{\rm tot}}{(1+z)^4} \ . \tag{19.27}$$

This cosmology-independent form expresses Liouville's Theorem: photon phase-space density is conserved along rays.

19.2.2. *Distance data and geometrical tests of cosmology*:

In order to confront these theoretical predictions with data, we have to bridge the divide between two extremes. Nearby objects may have their distances measured quite easily, but their radial velocities are dominated by deviations from the ideal Hubble flow, which typically have a magnitude of several hundred km s^{-1}. On the other hand, objects at redshifts $z \gtrsim 0.01$ will have observed recessional velocities that differ from their ideal values by $\lesssim 10\%$, but absolute distances are much harder to supply in this case. The traditional solution to this problem is the construction of the distance ladder: an interlocking set of methods for obtaining relative distances between various classes of object, which begins with absolute distances at the 10 to 100 pc level and terminates with galaxies at significant redshifts. This is reviewed in the review on Global cosmological parameters—Sec. 21 of this *Review*.

By far the most exciting development in this area has been the use of type Ia Supernovae (SNe), which now allow measurement of relative distances with 5% precision. In combination with Cepheid data from the HST key project on the distance scale, SNe results are the dominant contributor to the best modern value for H_0: 72 km s^{-1}Mpc^{-1} $\pm$ 10% [24]. Better still, the analysis of high-z SNe has allowed the first meaningful test of cosmological geometry to be carried out: as shown in Fig. 19.1 and Fig. 19.2, a combination of supernova data and measurements of microwave-background anisotropies strongly favors a $k = 0$ model dominated by vacuum energy. (See the review on Global cosmological parameters—Sec. 21 of this *Review* for a more comprehensive review of Hubble parameter determinations.)

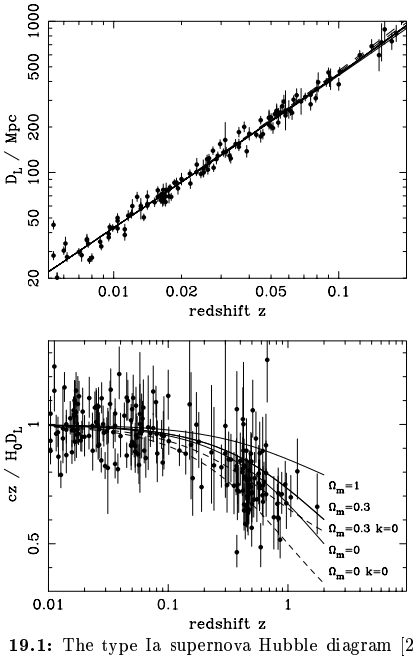

Figure 19.1: The type Ia supernova Hubble diagram [20–22]. The first panel shows that for $z \ll 1$ the large-scale Hubble flow is indeed linear and uniform; the second panel shows an expanded scale, with the linear trend divided out, and with the redshift range extended to show how the Hubble law becomes nonlinear. ($\Omega_r = 0$ is assumed.) Comparison with the prediction of Friedmann-Lemaître models appears to favor a vacuum-dominated Universe.

19.2.3. *Age of the Universe*:

The most striking conclusion of relativistic cosmology is that the Universe has not existed forever. The dynamical result for the age of the Universe may be written as

$$\begin{aligned} H_0 t_0 &= \int_0^\infty \frac{dz}{(1+z)H(z)} \\ &= \int_0^\infty \frac{dz}{(1+z)\,\left[(1+z)^2(1+\Omega_m z) - z(2+z)\Omega_v\right]^{1/2}} \ , \end{aligned} \tag{19.28}$$

where we have neglected Ω_r and chosen $w = -1$. Over the range of interest ($0.1 \lesssim \Omega_m \lesssim 1$, $|\Omega_v| \lesssim 1$), this exact answer may be approximated to a few % accuracy by

$$H_0 t_0 \simeq \tfrac{2}{3}\,(0.7\Omega_m + 0.3 - 0.3\Omega_v)^{-0.3} \ . \tag{19.29}$$

For the special case that $\Omega_m + \Omega_v = 1$, the integral in Eq. (19.28) can be expressed analytically as

$$H_0 t_0 = \frac{2}{3\sqrt{\Omega_v}}\,\ln\frac{1+\sqrt{\Omega_v}}{\sqrt{1-\Omega_v}} \quad (\Omega_m < 1) \ . \tag{19.30}$$

The most accurate means of obtaining ages for astronomical objects is based on the natural clocks provided by radioactive decay. The use of these clocks is complicated by a lack of knowledge of the initial conditions of the decay. In the Solar System, chemical fractionation of different elements helps pin down a precise age for the pre-Solar nebula of 4.6 Gyr, but for stars it is necessary to attempt an a priori calculation of the relative abundances of nuclei that result from supernova explosions. In this way, a lower limit for the age of stars in the local part of the Milky Way of about 11 Gyr is obtained [25].

The other major means of obtaining cosmological age estimates is based on the theory of stellar evolution. In principle, the main-sequence turnoff point in the color-magnitude diagram of a globular cluster should yield a reliable age. However, these have been controversial owing to theoretical uncertainties in the evolution model, as well as observational uncertainties in the distance, dust extinction and metallicity of clusters. The present consensus favors ages for the oldest clusters of about 12 Gyr [26,27].

These methods are all consistent with the age deduced from studies of structure formation, using the microwave background and large-scale structure: $t_0 = 13.7 \pm 0.2$ Gyr [28], where the extra accuracy comes at the price of assuming the Cold Dark Matter model to be true.

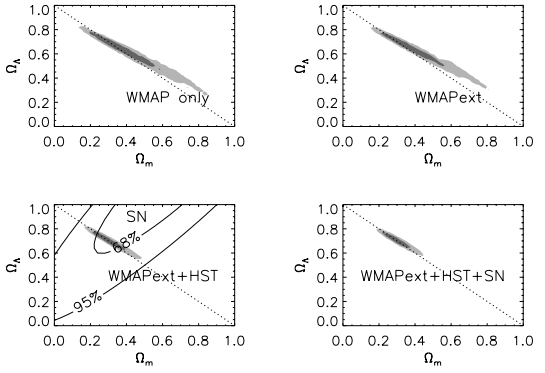

Figure 19.2: Likelihood-based confidence contours [28] over the plane Ω_Λ (*i.e.* Ω_v assuming $w = -1$) vs Ω_m. The SNe Ia results very nearly constrain $\Omega_v - \Omega_m$, whereas the results of CMB anisotropies (from the first-year WMAP data) favor a flat model with $\Omega_v + \Omega_m \simeq 1$. The intersection of these constraints is the most direct (but far from the only) piece of evidence favoring a flat model with $\Omega_m \simeq 0.3$.

19.2.4. *Horizon, isotropy, flatness problems*:

For photons, the radial equation of motion is just $c\,dt = R\,d\chi$. How far can a photon get in a given time? The answer is clearly

$$\Delta\chi = \int_{t_1}^{t_2} \frac{dt}{R(t)} \equiv \Delta\eta \ , \tag{19.31}$$

i.e., just the interval of conformal time. We can replace dt by $dR/\dot{R}$, which the Friedmann equation says is $\propto dR/\sqrt{\rho R^2}$ at early times. Thus, this integral converges if $\rho R^2 \to \infty$ as $t_1 \to 0$, otherwise it diverges. Provided the equation of state is such that ρ changes faster than R^{-2}, light signals can only propagate a finite distance between the Big Bang and the present; there is then said to be a particle horizon. Such a horizon therefore exists in conventional Big-Bang models, which are dominated by radiation ($\rho \propto R^{-4}$) at early times.

At late times, the integral for the horizon is largely determined by the matter-dominated phase, for which

$$D_{\rm H} = R_0\,\chi_{\rm H} \equiv R_0 \int_0^{t(z)} \frac{dt}{R(t)} \simeq \frac{6000}{\sqrt{\Omega z}}\,h^{-1}\,{\rm Mpc} \quad (z \gg 1) \ . \tag{19.32}$$

The horizon at the time of formation of the microwave background ('last scattering': $z \simeq 1100$) was thus of order 100 Mpc in size, subtending an angle of about 1°. Why then are the large number of causally disconnected regions we see on the microwave sky all at the same temperature? The Universe is very nearly isotropic and homogeneous, even though the initial conditions appear not to permit such a state to be constructed.

A related problem is that the $\Omega = 1$ Universe is unstable:

$$\Omega(a) - 1 = \frac{\Omega - 1}{1 - \Omega + \Omega_v a^2 + \Omega_m a^{-1} + \Omega_r a^{-2}} \ , \tag{19.33}$$

where Ω with no subscript is the total density parameter, and $a(t) = R(t)/R_0$. This requires $\Omega(t)$ to be unity to arbitrary precision as the initial time tends to zero; a universe of non-zero curvature today requires very finely tuned initial conditions.

19.3. The Hot Thermal Universe

19.3.1. *Thermodynamics of the early Universe*:

As alluded to above, we expect that much of the early Universe can be described by a radiation-dominated equation of state. In addition, through much of the radiation-dominated period, thermal equilibrium is established by the rapid rate of particle interactions relative to the expansion rate of the Universe (see Sec. 19.3.3 below). In equilibrium, it is straightforward to compute the thermodynamic quantities, ρ, p, and the entropy density, s. In general, the energy density for a given particle type i can be written as

$$\rho_i = \int E_i\,dn_{q_i} \ , \tag{19.34}$$

with the density of states given by

$$dn_{q_i} = \frac{g_i}{2\pi^2}\left(\exp[(E_{q_i} - \mu_i)/T_i] \pm 1\right)^{-1}\ q_i^2\,dq_i \ , \tag{19.35}$$

where g_i counts the number of degrees of freedom for particle type i, $E_{q_i}^2 = m_i^2 + q_i^2$, μ_i is the chemical potential, and the $\pm$ corresponds to either Fermi or Bose statistics. Similarly, we can define the pressure of a perfect gas as

$$p_i = \frac{1}{3}\int \frac{q_i^2}{E_i}\,dn_{q_i} \ . \tag{19.36}$$

The number density of species i is simply

$$n_i = \int dn_{q_i} \ , \tag{19.37}$$

and the entropy density is

$$s_i = \frac{\rho_i + p_i - \mu_i n_i}{T_i} \ , \tag{19.38}$$

In the Standard Model, a chemical potential is often associated with baryon number, and since the net baryon density relative to the photon density is known to be very small (of order 10^{-10}), we can neglect the chemical potential.

For photons, we can compute all of the thermodynamic quantities rather easily. Taking $g_i = 2$ for the 2 photon polarization states, we have

$$\rho_\gamma = \frac{\pi^2}{15}T^4 \ ; \quad p_\gamma = \frac{1}{3}\rho_\gamma \ ; \quad s_\gamma = \frac{4\rho_\gamma}{3T} \ ; \quad n_\gamma = \frac{2\zeta(3)}{\pi^2}T^3 \ , \tag{19.39}$$

with $2\zeta(3)/\pi^2 \simeq 0.2436$. Note that Eq. (19.10) can be converted into an equation for entropy conservation. Recognizing that $\dot{p} = s\dot{T}$, Eq. (19.10) becomes

$$d(sR^3)/dt = 0 \ . \tag{19.40}$$

For radiation, this corresponds to the relationship between expansion and cooling, $T \propto R^{-1}$ in an adiabatically expanding Universe. Note also that both s and n_γ scale as T^3.

19.3.2. *Radiation content of the Early Universe*:

At the very high temperatures associated with the early Universe, massive particles are pair produced, and are part of the thermal bath. If for a given particle species i we have $T \gg m_i$, then we can neglect the mass in Eq. (19.34) to Eq. (19.38), and the thermodynamic quantities are easily computed as in Eq. (19.39). In general, we can approximate the energy density (at high temperatures) by including only those particles with $m_i \ll T$. In this case, we have

$$\rho = \left(\sum_B g_B + \frac{7}{8}\sum_F g_F\right)\frac{\pi^2}{30}T^4 \equiv \frac{\pi^2}{30}\,N(T)\,T^4 \ , \tag{19.41}$$

Temperature	New Particles	$4N(T)$
$T < m_e$	γ's + ν's	29
$m_e < T < m_\mu$	$e^\pm$	43
$m_\mu < T < m_\pi$	$\mu^\pm$	57
$m_\pi < T < T_c$ †	π's	69
$T_c < T < m_{\rm strange}$	π's + u, $\bar{u}$, d, $\bar{d}$ + gluons	205
$m_s < T < m_{\rm charm}$	s, $\bar{s}$	247
$m_c < T < m_\tau$	c, $\bar{c}$	289
$m_\tau < T < m_{\rm bottom}$	$\tau^\pm$	303
$m_b < T < m_{\rm W,Z}$	b, $\bar{b}$	345
$m_{W,Z} < T < m_{\rm Higgs}$	$W^\pm$, Z	381
$m_H < T < m_{\rm top}$	H^0	385
$m_t < T$	t, $\bar{t}$	427

†T_c corresponds to the confinement-deconfinement transition between quarks and hadrons.

where $g_{B(F)}$ is the number of degrees of freedom of each boson (fermion) and the sum runs over all boson and fermion states with $m \ll T$. The factor of 7/8 is due to the difference between the Fermi and Bose integrals. Eq. (19.41) defines the effective number of degrees of freedom, $N(T)$, by taking into account new particle degrees of freedom as the temperature is raised. This quantity is plotted in Fig. 19.3 [29].

The value of $N(T)$ at any given temperature depends on the particle physics model. In the standard SU(3) × SU(2) × U(1) model, we can specify $N(T)$ up to temperatures of O(100) GeV. The change in N (ignoring mass effects) can be seen in the following table.

At higher temperatures, $N(T)$ will be model dependent. For example, in the minimal SU(5) model, one needs to add 24 states to $N(T)$ for the X and Y gauge bosons, another 24 from the adjoint Higgs, and another 6 (in addition to the 4 already counted in $W^\pm$, Z, and H) from the $\overline{5}$ of Higgs. Hence for $T > m_{\rm X}$ in minimal SU(5), $N(T) = 160.75$. In a supersymmetric model this would at least double, with some changes possibly necessary in the table if the lightest supersymmetric particle has a mass below m_t.

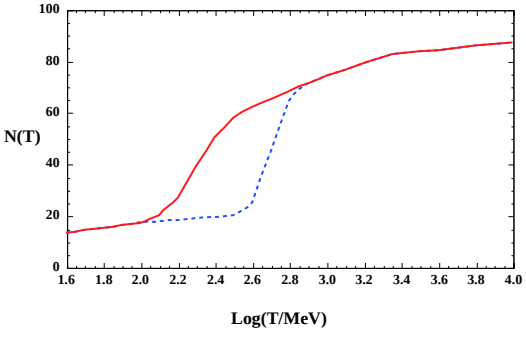

Figure 19.3: The effective numbers of relativistic degrees of freedom as a function of temperature. The sharp drop corresponds to the quark-hadron transition. The solid curve assume a QCD scale of 150 MeV, while the dashed curve assumes 450 MeV.

In the radiation-dominated epoch, Eq. (19.10) can be integrated (neglecting the T-dependence of N) giving us a relationship between the age of the Universe and its temperature

$$t = \left(\frac{90}{32\pi^3 G_{\rm N} N(T)}\right)^{1/2} T^{-2} \ , \tag{19.42}$$

Put into a more convenient form

$$t\, T_{\rm MeV}^2 = 2.4[N(T)]^{-1/2} \ , \tag{19.43}$$

where t is measured in seconds and $T_{\rm MeV}$ in units of MeV.

19.3.3. ***Neutrinos and equilibrium:***

Due to the expansion of the Universe, certain rates may be too slow to either establish or maintain equilibrium. Quantitatively, for each particle i, as a minimal condition for equilibrium, we will require that some rate Γ_i involving that type be larger than the expansion rate of the Universe or

$$\Gamma_i > H \ . \tag{19.44}$$

Recalling that the age of the Universe is determined by H^{-1}, this condition is equivalent to requiring that on average, at least one interaction has occurred over the lifetime of the Universe.

A good example for a process which goes in and out of equilibrium is the weak interactions of neutrinos. On dimensional grounds, one can estimate the thermally averaged scattering cross section

$$\langle \sigma v \rangle \sim O(10^{-2}) T^2 / m_{\rm W}^4 \tag{19.45}$$

for $T \lesssim m_{\rm W}$. Recalling that the number density of leptons is $n \propto T^3$, we can compare the weak interaction rate, $\Gamma \sim n \langle \sigma v \rangle$, with the expansion rate,

$$\begin{aligned} H = \left(\frac{8\pi G_{\rm N}\rho}{3}\right)^{1/2} &= \left(\frac{8\pi^3}{90} N(T)\right)^{1/2} T^2/M_{\rm P} \\ &\sim 1.66 N(T)^{1/2} T^2/M_{\rm P}. \end{aligned} \tag{19.46}$$

The Planck mass $M_{\rm P} = G_{\rm N}^{-1/2} = 1.22 \times 10^{19}$ GeV.

Neutrinos will be in equilibrium when $\Gamma_{\rm wk} > H$ or

$$T > (500\, m_{\rm W}^4/M_{\rm P})^{1/3} \sim 1 \text{ MeV} \ . \tag{19.47}$$

The temperature at which these rates are equal is commonly referred to as the neutrino decoupling or freeze-out temperature and is defined by $\Gamma(T_d) = H(T_d)$.

At very high temperatures, the Universe is too young for equilibrium to have been established. For $T \gg m_{\rm W}$, we should write $\langle \sigma v \rangle \sim O(10^{-2})/T^2$, so that $\Gamma \sim 10^{-2} T$. Thus at temperatures $T \gtrsim 10^{-2} M_{\rm P}/\sqrt{N}$, equilibrium will not have been established.

For $T < T_d$, neutrinos drop out of equilibrium. The Universe becomes transparent to neutrinos and their momenta simply redshift with the cosmic expansion. The effective neutrino temperature will simply fall with $T \sim 1/R$.

Soon after decoupling, $e^\pm$ pairs in the thermal background begin to annihilate (when $T \lesssim m_e$). Because the neutrinos are decoupled, the energy released due to annihilation heats up the photon background relative to the neutrinos. The change in the photon temperature can be easily computed from entropy conservation. The neutrino entropy must be conserved separately from the entropy of interacting particles. A straightforward computation yields

$$T_\nu = (4/11)^{1/3} T_\gamma \simeq 1.9 \text{ K} \ . \tag{19.48}$$

Today, the total entropy density is therefore given by

$$s = \frac{4}{3}\frac{\pi^2}{30}\left(2 + \frac{21}{4}(T_\nu/T_\gamma)^3\right) T_\gamma^3 = \frac{4}{3}\frac{\pi^2}{30}\left(2 + \frac{21}{11}\right) T_\gamma^3 = 7.04\, n_\gamma \ . \tag{19.49}$$

Similarly, the total relativistic energy density today is given by

$$\rho_r = \frac{\pi^2}{30}\left[2 + \frac{21}{4}(T_\nu/T_\gamma)^4\right] T_\gamma^4 \simeq 1.68 \rho_\gamma \ . \tag{19.50}$$

In practice, a small correction is needed to this, since neutrinos are not totally decoupled at $e^\pm$ annihilation: the effective number of massless neutrino species is 3.04, rather than 3 [30].

This expression ignores neutrino rest masses, but current oscillation data require at least one neutrino eigenstate to have a mass exceeding 0.05 eV. In this minimal case, $\Omega_\nu h^2 = 5 \times 10^{-4}$, so the neutrino contribution to the matter budget would be negligibly small (which is our normal assumption). However, a nearly degenerate pattern of mass eigenstates could allow larger densities, since oscillation experiments only measure differences in m^2 values. Note that a 0.05-eV neutrino becomes non-relativistic at redshift $z = 2.2$, so the above expression for the total present relativistic density is really only an extrapolation. However, neutrinos are almost certainly relativistic at all epochs where the radiation content of the universe is dynamically significant.

19.3.4. ***Field Theory and Phase transitions***:

It is very likely that the Universe has undergone one or more phase transitions during the course of its evolution [31–34]. Our current vacuum state is described by $SU(3)_c \times U(1)_{em}$ which in the Standard Model is a remnant of an unbroken $SU(3)_c \times SU(2)_L \times U(1)_Y$ gauge symmetry. Symmetry breaking occurs when a non-singlet gauge field (the Higgs field in the Standard Model) picks up a non-vanishing vacuum expectation value, determined by a scalar potential. For example, a simple (non-gauged) potential describing symmetry breaking is $V(\phi) = \frac{1}{4}\lambda\phi^4 - \frac{1}{2}\mu^2\phi^2 + V(0)$. The resulting expectation value is simply $\langle\phi\rangle = \mu/\sqrt{\lambda}$.

In the early Universe, finite temperature radiative corrections typically add terms to the potential of the form $\phi^2 T^2$. Thus, at very high temperatures, the symmetry is restored and $\langle\phi\rangle = 0$. As the Universe cools, depending on the details of the potential, symmetry breaking will occur via a first order phase transition in which the field tunnels through a potential barrier, or via a second order transition in which the field evolves smoothly from one state to another (as would be the case for the above example potential).

The evolution of scalar fields can have a profound impact on the early Universe. The equation of motion for a scalar field ϕ can be derived from the energy-momentum tensor

$$T_{\mu\nu} = \partial_\mu\phi\partial_\nu\phi - \frac{1}{2}g_{\mu\nu}\partial_\rho\phi\partial^\rho\phi - g_{\mu\nu}V(\phi)\ . \tag{19.51}$$

By associating $\rho = T_{00}$ and $p = R^{-2}(t)T_{ii}$ we have

$$\begin{aligned} \rho &= \frac{1}{2}\dot{\phi}^2 + \frac{1}{2}R^{-2}(t)(\nabla\phi)^2 + V(\phi) \\ p &= \frac{1}{2}\dot{\phi}^2 - \frac{1}{6}R^{-2}(t)(\nabla\phi)^2 - V(\phi) \end{aligned} \tag{19.52}$$

and from Eq. (19.10) we can write the equation of motion (by considering a homogeneous region, we can ignore the gradient terms)

$$\ddot{\phi} + 3H\dot{\phi} = -\partial V/\partial\phi\ . \tag{19.53}$$

19.3.5. ***Inflation***:

In Sec. 19.2.4, we discussed some of the problems associated with the standard Big-Bang model. However, during a phase transition, our assumptions of an adiabatically expanding universe are generally not valid. If, for example, a phase transition occurred in the early Universe such that the field evolved slowly from the symmetric state to the global minimum, the Universe may have been dominated by the vacuum energy density associated with the potential near $\phi \approx 0$. During this period of slow evolution, the energy density due to radiation will fall below the vacuum energy density, $\rho \ll V(0)$. When this happens, the expansion rate will be dominated by the constant V(0) and we obtain the exponentially expanding solution given in Eq. (19.20). When the field evolves towards the global minimum it will begin to oscillate about the minimum, energy will be released during its decay and a hot thermal universe will be restored. If released fast enough, it will produce radiation at a temperature $NT_R{}^4 \lesssim V(0)$. In this reheating process entropy has been created and the final value of RT is greater than the initial value of RT. Thus, we see that, during a phase transition, the relation $RT \sim$ constant need not hold true. This is the basis of the inflationary Universe scenario [35–37].

If during the phase transition the value of RT changed by a factor of $O(10^{29})$, the cosmological problems discussed above would be solved. The observed isotropy would be generated by the immense expansion; one small causal region could get blown up and hence our entire visible Universe would have been in thermal contact some time in the past. In addition, the density parameter Ω would have been driven to 1 (with exponential precision). Density perturbations will be stretched by the expansion, $\lambda \sim R(t)$. Thus it will appear that $\lambda \gg H^{-1}$ or that the perturbations have left the horizon, where in fact the size of the causally connected region is now no longer simply H^{-1}. However, not only does inflation offer an explanation for large scale perturbations, it also offers a source for the perturbations themselves through quantum fluctuations.

Early models of inflation were based on a first order phase transition of a Grand Unified theory [38]. Although these models led to sufficient exponential expansion, completion of the transition through bubble percolation did not occur. Later models of inflation [39,40], also based on Grand Unified symmetry breaking, through second order transitions were also doomed. While they successfully inflated and reheated, and in fact produced density perturbations due to quantum fluctuations during the evolution of the scalar field, they predicted density perturbations many orders of magnitude too large. Most models today are based on an unknown symmetry breaking involving a new scalar field, the inflaton, ϕ.

19.3.6. ***Baryogenesis***:

The Universe appears to be populated exclusively with matter rather than antimatter. Indeed antimatter is only detected in accelerators or in cosmic rays. However, the presence of antimatter in the latter is understood to be the result of collisions of primary particles in the interstellar medium. There is in fact strong evidence against primary forms of antimatter in the Universe. Furthermore, the density of baryons compared to the density of photons is extremely small, $\eta \sim 10^{-10}$.

The production of a net baryon asymmetry requires baryon number violating interactions, C and CP violation and a departure from thermal equilibrium [41]. The first two of these ingredients are expected to be contained in grand unified theories as well as in the non-perturbative sector of the standard model, the third can be realized in an expanding universe where as we have seen interactions come in and out of equilibrium.

There are several interesting and viable mechanisms for the production of the baryon asymmetry. While, we can not review any of them here in any detail, we mention some of the important scenarios. In all cases, all three ingredients listed above are incorporated. One of the first mechanisms was based on the out of equilibrium decay of a massive particle such as a superheavy GUT gauge of Higgs boson [42,43]. A novel mechanism involving the decay of flat directions in supersymmetric models is known as the Affleck-Dine scenario [44]. Recently, much attention has been focused on the possibility of generating the baryon asymmetry at the electro-weak scale using the non-perturbative interactions of sphalerons [45]. Because these interactions conserve the sum of baryon and lepton number, $B + L$, it is possible to first generate a lepton asymmetry (*e.g.*, by the out-of-equilibrium decay of a superheavy right-handed neutrino), which is converted to a baryon asymmetry at the electro-weak scale [46]. This mechanism is known as lepto-baryogenesis.

19.3.7. ***Nucleosynthesis***:

An essential element of the standard cosmological model is Big-Bang nucleosynthesis (BBN), the theory which predicts the abundances of the light element isotopes D, ^{3}He, ^{4}He, and ^{7}Li. Nucleosynthesis takes place at a temperature scale of order 1 MeV. The nuclear processes lead primarily to ^{4}He, with a primordial mass fraction of about 24%. Lesser amounts of the other light elements are produced: about 10^{-5} of D and ^{3}He and about 10^{-10} of ^{7}Li by number relative to H. The abundances of the light elements depend almost solely on one key parameter, the baryon-to-photon ratio, η. The nucleosynthesis predictions can be compared with observational determinations of the abundances of the light elements. Consistency between theory and observations leads to a conservative range of

$$3.4 \times 10^{-10} < \eta < 6.9 \times 10^{-10}\ . \tag{19.54}$$

η is related to the fraction of Ω contained in baryons, Ω_b

$$\Omega_b = 3.66 \times 10^7 \eta\, h^{-2}\ , \tag{19.55}$$

or $10^{10}\eta = 274\Omega_b h^2$. The WMAP result [28] for $\Omega_b h^2$ of 0.0224 ± 0.0009 translates into a value of $\eta = 6.15 \pm 0.25$. This result can be used to 'predict' the light element abundance which can in turn be compared with observation [47]. The resulting D/H abundance is in excellent agreement with that found in quasar absorption systems. It is in reasonable agreement with the helium abundance observed in extra-galactic HII regions (once systematic uncertainties are accounted

for) but is in poor agreement with the Li abundance observed in the atmospheres of halo dwarf stars. (See the review on BBN—Sec. 20 of this *Review* for a detailed discussion of BBN or references [48,49].)

19.3.8. ***The transition to a matter-dominated Universe***:

In the Standard Model, the temperature (or redshift) at which the Universe undergoes a transition from a radiation dominated to a matter dominated Universe is determined by the amount of dark matter. Assuming three nearly massless neutrinos, the energy density in radiation at temperatures $T \ll 1$ MeV, is given by

$$\rho_r = \frac{\pi^2}{30}\left[2 + \frac{21}{4}\left(\frac{4}{11}\right)^{4/3}\right] T^4 \ . \tag{19.56}$$

In the absence of non-baryonic dark matter, the matter density can be written as

$$\rho_m = m_{\rm N}\eta\, n_\gamma \ , \tag{19.57}$$

where $m_{\rm N}$ is the nucleon mass. Recalling that $n_\gamma \propto T^3$ [cf. Eq. (19.39)], we can solve for the temperature or redshift at the matter-radiation equality when $\rho_r = \rho_m$,

$$T_{eq} = 0.22\, m_{\rm N}\,\eta \qquad \text{or} \qquad (1+z_{\rm eq}) = 0.22\,\eta\frac{m_{\rm N}}{T_0} \ , \tag{19.58}$$

where T_0 is the present temperature of the microwave background. For $\eta = 5\times10^{-10}$, this corresponds to a temperature $T_{\rm eq} \simeq 0.1$ eV or $(1+z_{\rm eq}) \simeq 425$. A transition this late is very problematic for structure formation (see Sec. 19.4.5).

The redshift of matter domination can be pushed back significantly if non-baryonic dark matter is present. If instead of Eq. (19.57), we write

$$\rho_m = \Omega_m \rho_c \left(\frac{T}{T_0}\right)^3 \ , \tag{19.59}$$

we find that

$$T_{eq} = 0.9\frac{\Omega_m \rho_c}{T_0^3} \qquad \text{or} \qquad (1+z_{eq}) = 2.4\times10^4 \Omega_m h^2 \ . \tag{19.60}$$

19.4. The Universe at late times

19.4.1. ***The CMB***:

One form of the infamous Olbers' paradox says that, in Euclidean space, surface brightness is independent of distance. Every line of sight will terminate on matter that is hot enough to be ionized and so scatter photons: $T \gtrsim 10^3$ K; the sky should therefore shine as brightly as the surface of the Sun. The reason the night sky is dark is entirely due to the expansion, which cools the radiation temperature to 2.73 K. This gives a Planck function peaking at around 1 mm to produce the microwave background (CMB).

The CMB spectrum is a very accurate match to a Planck function [50]. (See the review on CBR–Sec. 23 of this *Review*.) The COBE estimate of the temperature is [51]

$$T = 2.725 \pm 0.002\,{\rm K} \ . \tag{19.61}$$

The lack of any distortion of the Planck spectrum is a strong physical constraint. It is very difficult to account for in any expanding universe other than one that passes through a hot stage. Alternative schemes for generating the radiation, such as thermalization of starlight by dust grains, inevitably generate a superposition of temperatures. What is required in addition to thermal equilibrium is that $T \propto 1/R$, so that radiation from different parts of space appears identical.

Although it is common to speak of the CMB as originating at "recombination," a more accurate terminology is the era of "last scattering," In practice, this takes place at $z \simeq 1100$, almost independently of the main cosmological parameters, at which time the fractional ionization is very small. This occurred when the age of the Universe was a few hundred thousand years. (See the review on CBR–Sec. 23 of this *Review* for a full discussion of the CMB.)

19.4.2. ***Matter in the Universe***:

One of the main tasks of cosmology is to measure the density of the Universe, and how this is divided between dark matter and baryons. The baryons consist partly of stars, with $0.002 \lesssim \Omega_* \lesssim 0.003$ [52] but mainly inhabit the IGM. One powerful way in which this can be studied is via the absorption of light from distant luminous objects such as quasars. Even very small amounts of neutral hydrogen can absorb rest-frame UV photons (the Gunn-Peterson effect), and should suppress the continuum by a factor $\exp(-\tau)$, where

$$\tau \simeq \left[\frac{n_{\rm HI}(z)}{(1+z)\sqrt{1+\Omega_m z}}\right] \Big/\ 10^{-4.62}\ h\,{\rm m}^{-3}, \tag{19.62}$$

and this expression applies while the Universe is matter dominated ($z \gtrsim 1$ in the $\Omega_m = 0.3$ $\Omega_v = 0.7$ model). It is possible that this general absorption has now been seen at $z = 6.2$ [53]. In any case, the dominant effect on the spectrum is a 'forest' of narrow absorption lines, which produce a mean $\tau = 1$ in the Lyα forest at about $z = 3$, and so we have $\Omega_{\rm HI} \simeq 10^{-5.5} h^{-1}$. This is such a small number that clearly the IGM is very highly ionized at these redshifts.

The Lyα forest is of great importance in pinning down the abundance of deuterium. Because electrons in deuterium differ in reduced mass by about 1 part in 4000 compared to Hydrogen, each absorption system in the Lyα forest is accompanied by an offset deuterium line. By careful selection of systems with an optimal HI column density, a measurement of the D/H ratio can be made. This has now been done in 5 quasars, with relatively consistent results [49]. Combining these determinations with the theory of primordial nucleosynthesis yields a baryon density of $\Omega_b h^2 = 0.021 \pm 0.004$ (95% confidence). (See also the review on BBN—Sec. 20 of this *Review*.)

Ionized IGM can also be detected in emission when it is densely clumped, via bremsstrahlung radiation. This generates the spectacular X-ray emission from rich clusters of galaxies. Studies of this phenomenon allow us to achieve an accounting of the total baryonic material in clusters. Within the central $\simeq 1$ Mpc, the masses in stars, X-ray emitting gas and total dark matter can be determined with reasonable accuracy (perhaps 20% rms), and this allows a minimum baryon fraction to be determined [54,55]:

$$\frac{M_{\rm baryons}}{M_{\rm total}} \gtrsim 0.009 + (0.066 \pm 0.003)\, h^{-3/2} \ . \tag{19.63}$$

Because clusters are the largest collapsed structures, it is reasonable to take this as applying to the Universe as a whole. This equation implies a minimum baryon fraction of perhaps 12% (for reasonable h), which is too high for $\Omega_m = 1$ if we take $\Omega_b h^2 \simeq 0.02$ from nucleosynthesis. This is therefore one of the more robust arguments in favor of $\Omega_m \simeq 0.3$. (See the review on Global cosmological parameters—Sec. 21 of this *Review*.) This argument is also consistent with the inference on Ω_m that can be made from Fig. 19.2.

This method is much more robust than the older classical technique for weighing the Universe: '$L \times M/L$'. The overall light density of the Universe is reasonably well determined from redshift surveys of galaxies, so that a good determination of mass M and luminosity L for a single object suffices to determine Ω_m *if* the mass-to-light ratio is universal.

Galaxy redshift surveys allow us to deduce the galaxy luminosity function, ϕ, which is the comoving number density of galaxies; this may be described by the Schechter function, which is a power law with an exponential cutoff:

$$\phi = \phi^* \left(\frac{L}{L^*}\right)^{-\alpha} e^{-L/L^*}\,\frac{dL}{L^*} \tag{19.64}$$

The total luminosity density produced by integrating over the distribution is

$$\rho_L = \phi^* L^* \Gamma(2-\alpha) \ , \tag{19.65}$$

and this tells us the average mass-to-light ratio needed to close the Universe. Answers vary (principally owing to uncertainties in ϕ^*). In blue light, the total luminosity density is

$\rho_{\rm L} = 2 \pm 0.2 \times 10^8\ h L_\odot {\rm Mpc}^{-3}$ [56,57]. The critical density is $2.78 \times 10^{11}\ \Omega h^2 M_\odot {\rm Mpc}^{-3}$, so the critical M/L for closure is

$$(M/L)_{\rm crit,\,B} = 1390\, h \pm 10\% \ . \tag{19.66}$$

Dynamical determinations of mass on the largest accessible scales consistently yield blue M/L values of at least $300\,h$, but normally fall short of the closure value [58]. This was a long-standing argument against the $\Omega_m = 1$ model, but it was never conclusive because the stellar populations in objects such as rich clusters (where the masses can be determined) differ systematically from those in other regions.

19.4.3. *Gravitational lensing*:

A robust method for determining masses in cosmology is to use gravitational light deflection. Most systems can be treated as a geometrically thin gravitational lens, where the light bending is assumed to take place only at a single distance. Simple geometry then determines a mapping between the coordinates in the intrinsic source plane and the observed image plane:

$$\alpha(D_{\rm L}\theta_{\rm I}) = \frac{D_{\rm S}}{D_{\rm LS}}(\theta_{\rm I} - \theta_{\rm S}) \ , \tag{19.67}$$

where the angles $\theta_{\rm I}, \theta_{\rm S}$ and α are in general two-dimensional vectors on the sky. The distances $D_{\rm LS}$ etc. are given by an extension of the usual distance-redshift formula:

$$D_{\rm LS} = \frac{R_0 S_k(\chi_{\rm S} - \chi_{\rm L})}{1 + z_{\rm S}} \ . \tag{19.68}$$

This is the angular-diameter distance for objects on the source plane as perceived by an observer on the lens.

Solutions of this equation divide into weak lensing, where the mapping between source plane and image plane is one-to-one, and strong lensing, in which multiple imaging is possible. For circularly-symmetric lenses, an on-axis source is multiply imaged into a 'caustic' ring, whose radius is the Einstein radius:

$$\begin{aligned} \theta_{\rm E} &= \left(4GM\,\frac{D_{\rm LS}}{D_{\rm L} D_{\rm S}}\right)^{1/2} \\ &= \left(\frac{M}{10^{11.09} M_\odot}\right)^{1/2} \left(\frac{D_{\rm L} D_{\rm S}/D_{\rm LS}}{\rm Gpc}\right)^{-1/2} \quad {\rm arcsec} \end{aligned} \tag{19.69}$$

The observation of 'arcs' (segments of near-perfect Einstein rings) in rich clusters of galaxies has thus given very accurate masses for the central parts of clusters—generally in good agreement with other indicators, such as analysis of X-ray emission from the cluster IGM [59].

19.4.4. *Density Fluctuations*:

The overall properties of the Universe are very close to being homogeneous; and yet telescopes reveal a wealth of detail on scales varying from single galaxies to large-scale structures of size exceeding 100 Mpc. The existence of these structures must be telling us something important about the initial conditions of the Big Bang, and about the physical processes that have operated subsequently. This motivates the study of the density perturbation field, defined as

$$\delta(\mathbf{x}) \equiv \frac{\rho(\mathbf{x}) - \langle\rho\rangle}{\langle\rho\rangle} \ . \tag{19.70}$$

A critical feature of the δ field is that it inhabits a universe that is isotropic and homogeneous in its large-scale properties. This suggests that the statistical properties of δ should also be statistically homogeneous—*i.e.*, it is a stationary random process.

It is often convenient to describe δ as a Fourier superposition:

$$\delta(\mathbf{x}) = \sum \delta_{\mathbf{k}} e^{-i\mathbf{k}\cdot\mathbf{x}} \ . \tag{19.71}$$

We avoid difficulties with an infinite universe by applying periodic boundary conditions in a cube of some large volume V. The cross-terms vanish when we compute the variance in the field, which is just a sum over modes of the power spectrum

$$\langle\delta^2\rangle = \sum |\delta_{\mathbf{k}}|^2 \equiv \sum P(k) \ . \tag{19.72}$$

Note that the statistical nature of the fluctuations must be isotropic, so we write $P(k)$ rather than $P(\mathbf{k})$. The $\langle\ldots\rangle$ average here is a volume average. Cosmological density fields are an example of an ergodic process, in which the average over a large volume tends to the same answer as the average over a statistical ensemble.

The statistical properties of discrete objects sampled from the density field are often described in terms of N-point correlation functions, which represent the excess probability over random for finding one particle in each of N boxes in a given configuration. For the 2-point case, the correlation function is readily shown to be identical to the autocorrelation function of the δ field: $\xi(r) = \langle\delta(x)\delta(x+r)\rangle$.

The power spectrum and correlation function are Fourier conjugates, and thus are equivalent descriptions of the density field (similarly, k-space equivalents exist for the higher-order correlations). It is convenient to take the limit $V \to \infty$ and use k-space integrals, defining a dimensionless power spectrum as $\Delta^2(k) = d\langle\delta^2\rangle/d\ln k = Vk^3P(k)/2\pi^2$:

$$\xi(r) = \int \Delta^2(k)\,\frac{\sin kr}{kr}\,d\ln k; \quad \Delta^2(k) = \frac{2}{\pi}k^3\int_0^\infty \xi(r)\,\frac{\sin kr}{kr}\,r^2\,dr \ . \tag{19.73}$$

For many years, an adequate approximation to observational data on galaxies was $\xi = (r/r_0)^{-\gamma}$, with $\gamma \simeq 1.8$ and $r_0 \simeq 5\,h^{-1}$ Mpc. Modern surveys are now able to probe into the large-scale linear regime where traces of the curved primordial spectrum can be detected [60].

19.4.5. *Formation of cosmological structure*:

The simplest model for the generation of cosmological structure is gravitational instability acting on some small initial fluctuations (for the origin of which a theory such as inflation is required). If the perturbations are adiabatic (*i.e.*, fractionally perturb number densities of photons and matter equally), the linear growth law for matter perturbations is simple:

$$\delta \propto \begin{cases} a(t)^2 & \text{(radiation domination; } \Omega_{\rm r} = 1) \\ a(t) & \text{(matter domination; } \Omega_{\rm m} = 1) \end{cases} \tag{19.74}$$

For low density universes, the present-day amplitude is suppressed by a factor $g(\Omega)$, where

$$g(\Omega) \simeq \frac{5}{2}\Omega_m \left[\Omega_m^{4/7} - \Omega_v + (1 + \Omega_m/2)(1 + \frac{1}{70}\Omega_v)\right]^{-1} \ , \tag{19.75}$$

is an accurate fit for models with matter plus cosmological constant. The alternative perturbation mode is isocurvature: only the equation of state changes, and the total density is initially unperturbed. These modes perturb the total entropy density, and thus induce additional large-scale CMB anisotropies [61]. Although the character of perturbations in the simplest inflationary theories are purely adiabatic, correlated adiabatic and isocurvature modes are predicted in many models; the simplest example is the curvaton, which is a scalar field that decays to yield a perturbed radiation density. If the matter content already exists at this time, the overall perturbation field will have a significant isocurvature component. Such a prediction is inconsistent with current CMB data [62], and most analyses of CMB and LSS data assume the adiabatic case to hold exactly.

Linear evolution preserves the shape of the power spectrum. However, a variety of processes mean that growth actually depends on the matter content:

(1) Pressure opposes gravity effectively for wavelengths below the horizon length while the Universe is radiation dominated. The *comoving* horizon size at $z_{\rm eq}$ is therefore an important scale:

$$D_{\rm H}(z_{\rm eq}) = \frac{2(\sqrt{2}-1)}{(\Omega_m z_{\rm eq})^{1/2} H_0} = \frac{16.0}{\Omega_m h^2}\,{\rm Mpc} \tag{19.76}$$

(2) At early times, dark matter particles will undergo free streaming at the speed of light, and so erase all scales up to the horizon—a process that only ceases when the particles go nonrelativistic. For light massive neutrinos, this happens at $z_{\rm eq}$; all structure up to the horizon-scale power-spectrum break is in fact erased. Hot(cold) dark matter models are thus sometimes dubbed large(small)-scale damping models.

(3) A further important scale arises where photon diffusion can erase perturbations in the matter–radiation fluid; this process is named Silk damping.

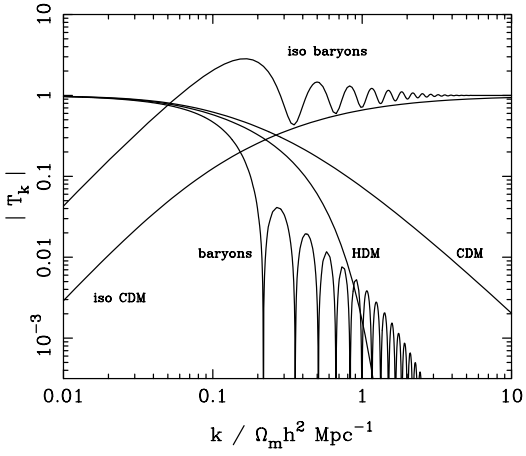

Figure 19.4: A plot of transfer functions for various models. For adiabatic models, $T_k \to 1$ at small k, whereas the opposite is true for isocurvature models. For dark-matter models, the characteristic wavenumber scales proportional to $\Omega_m h^2$. The scaling for baryonic models does not obey this exactly; the plotted cases correspond to $\Omega_m = 1$, $h = 0.5$.

The overall effect is encapsulated in the transfer function, which gives the ratio of the late-time amplitude of a mode to its initial value (see Fig. 19.4). The overall power spectrum is thus the primordial power-law, times the square of the transfer function:

$$P(k) \propto k^n T_k^2 \ . \tag{19.77}$$

The most generic power-law index is $n = 1$: the 'Zeldovich' or 'scale-invariant' spectrum. Inflationary models tend to predict a small 'tilt': $|n-1| \lesssim 0.03$ [13,14]. On the assumption that the dark matter is cold, the power spectrum then depends on 5 parameters: n, h, Ω_b, $\Omega_{\rm cdm}$ ($\equiv \Omega_m - \Omega_b$) and an overall amplitude. The latter is often specified as σ_8, the linear-theory fractional rms in density when a spherical filter of radius $8\,h^{-1}\,$Mpc is applied in linear theory. This scale can be probed directly via weak gravitational lensing, and also via its effect on the abundance of rich galaxy clusters. The favored value is approximately [63,64]

$$\sigma_8 = (0.7 \pm 15\%)(\Omega_m/0.3)^{-0.5} \ . \tag{19.78}$$

A direct measure of mass inhomogeneity is valuable, since the galaxies inevitably are biased with respect to the mass. This means that the fractional fluctuations in galaxy number, $\delta n/n$ may differ from the mass fluctuations, $\delta\rho/\rho$. It is commonly assumed that the two fields obey some proportionality on large scales where the fluctuations are small, $\delta n/n = b\delta\rho/\rho$, but even this is not guaranteed [65].

The main shape of the transfer function is a break around the horizon scale at $z_{\rm eq}$, which depends just on $\Omega_m h$ when wavenumbers are measured in observable units ($h\,$Mpc^{-1}). In principle, accurate data over a wide range of k could determine both Ωh and n, but in practice there is a strong degeneracy between these. For reasonable baryon content, weak oscillations in the transfer function may be visible, giving an alternative means of fixing the baryon content. Current data [60] favor $\Omega_m h \simeq 0.20$ and a baryon fraction of about 0.15 for $n = 1$ (see Fig. 19.5). In order to constrain n itself, it is necessary to examine data on anisotropies in the CMB.

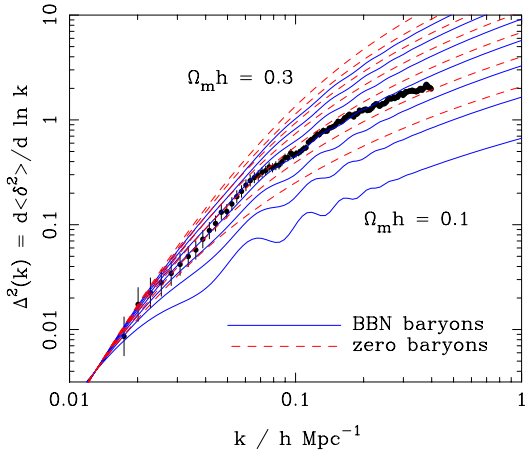

Figure 19.5: The galaxy power spectrum from the 2dFGRS, shown in dimensionless form, $\Delta^2(k) \propto k^3 P(k)$. The solid points with error bars show the power estimate. The window function correlates the results at different k values, and also distorts the large-scale shape of the power spectrum An approximate correction for the latter effect has been applied. The solid and dashed lines show various CDM models, all assuming $n = 1$. For the case with non-negligible baryon content, a big-bang nucleosynthesis value of $\Omega_b h^2 = 0.02$ is assumed, together with $h = 0.7$. A good fit is clearly obtained for $\Omega_m h \simeq 0.2$.

19.4.6. *CMB anisotropies*:

The CMB has a clear dipole anisotropy, of magnitude 1.23×10^{-3}. This is interpreted as being due to the Earth's motion, which is equivalent to a peculiar velocity for the Milky Way of

$$v_{\rm MW} \simeq 600\,{\rm km\,s^{-1}} \quad \text{towards} \quad (\ell, b) \simeq (270^\circ, 30^\circ) \ . \tag{19.79}$$

All higher-order multipole moments of the CMB are however much smaller (of order 10^{-5}), and interpreted as signatures of density fluctuations at last scattering ($\simeq 1100$). To analyze these, the sky is expanded in spherical harmonics as explained in the review on CBR–Sec. 23 of this *Review*. The dimensionless power per ln k or 'bandpower' for the CMB is defined as

$$\mathcal{T}^2(\ell) = \frac{\ell(\ell+1)}{2\pi} C_\ell \ . \tag{19.80}$$

This function encodes information from the three distinct mechanisms that cause CMB anisotropies:

(1) Gravitational (Sachs–Wolfe) perturbations. Photons from high-density regions at last scattering have to climb out of potential wells, and are thus redshifted.

(2) Intrinsic (adiabatic) perturbations. In high-density regions, the coupling of matter and radiation can compress the radiation also, giving a higher temperature.

(3) Velocity (Doppler) perturbations. The plasma has a non-zero velocity at recombination, which leads to Doppler shifts in frequency and hence shifts in brightness temperature.

Because the potential fluctuations obey Poisson's equation, $\nabla^2\Phi = 4\pi G\rho\delta$, and the velocity field satisfies the continuity equation $\nabla\cdot\mathbf{u} = -\dot{\delta}$, the resulting different powers of k ensure that the Sachs-Wolfe effect dominates on large scales and adiabatic effects on small scales.

The relation between angle and comoving distance on the last-scattering sphere requires the comoving angular-diameter distance to the last-scattering sphere; because of its high redshift, this is effectively identical to the horizon size at the present epoch, $D_{\rm H}$:

$$\begin{aligned} D_{\rm H} &= \frac{2}{\Omega_m H_0} \quad (\Omega_v = 0) \\ D_{\rm H} &\simeq \frac{2}{\Omega_m^{0.4} H_0} \quad ({\rm flat}: \Omega_m + \Omega_v = 1) \end{aligned} \tag{19.81}$$

These relations show how the CMB is strongly sensitive to curvature: the horizon length at last scattering is $\propto 1/\sqrt{\Omega_m}$, so that this subtends an angle that is virtually independent of Ω_m for a flat model. Observations of a peak in the CMB power spectrum at relatively large scales ($\ell \simeq 225$) are thus strongly inconsistent with zero-Λ models with low density: current CMB data require $\Omega_m + \Omega_v \simeq 1 \pm 0.05$. (See *e.g.*, Fig. 19.2).

In addition to curvature, the CMB encodes information about several other key cosmological parameters. Within the compass of simple adiabatic CDM models, there are 9 of these:

$$\omega_c,\ \omega_b,\ \Omega_t,\ h,\ \tau,\ n_s,\ n_t,\ r,\ Q\ . \tag{19.82}$$

The symbol ω denotes the physical density, Ωh^2: the transfer function depends only on the densities of CDM (ω_c) and baryons (ω_b). Transcribing the power spectrum at last scattering into an angular power spectrum brings in the total density parameter ($\Omega_t \equiv \Omega_m + \Omega_v = \Omega_c + \Omega_b + \Omega_v$) and h: there is an exact geometrical degeneracy [66] between these that keeps the angular-diameter distance to last scattering invariant, so that models with substantial spatial curvature and large vacuum energy cannot be ruled out without prior knowledge of the Hubble parameter. Alternatively, the CMB alone cannot measure the Hubble parameter.

The other main parameter degeneracy involves the tensor contribution to the CMB anisotropies. These are important at large scales (up to the horizon scales); for smaller scales, only scalar fluctuations (density perturbations) are important. Each of these components is characterized by a spectral index, n, and a ratio between the power spectra of tensors and scalars (r). Finally, the overall amplitude of the spectrum must be specified (Q), together with the optical depth to Compton scattering owing to recent reionization (τ). The tensor degeneracy operates as follows: the main effect of adding a large tensor contribution is to reduce the contrast between low ℓ and the peak at $\ell \simeq 225$ (because the tensor spectrum has no acoustic component). The required height of the peak can be recovered by increasing n_s to increase the small-scale power in the scalar component; this in turn over-predicts the power at $\ell \sim 1000$, but this effect can be counteracted by raising the baryon density [67]. In order to break this degeneracy, additional data are required. For example, an excellent fit to the CMB data is obtained with a scalar-only model with zero curvature and $\omega_b = 0.023$, $\omega_c = 0.134$, $h = 0.73$, $n_s = 0.97$ [28], but this is indistinguishable from a model where tensors dominate at $\ell \lesssim 100$, but we raise ω_b to 0.03 and n_s to 1.2. This baryon density is too high for nucleosynthesis, which disfavors the high-tensor solution [68].

The reason the tensor component is introduced, and why it is so important, is that it is the only non-generic prediction of inflation. Slow-roll models of inflation involve two dimensionless parameters:

$$\begin{aligned} \epsilon &\equiv \frac{M_{\rm P}^2}{16\pi}\,(V'/V)^2 \\ \eta &\equiv \frac{M_{\rm P}^2}{8\pi}\,(V''/V) \end{aligned}\ , \tag{19.83}$$

where V is the inflaton potential, and dashes denote derivatives with respect to the inflation field. In terms of these, the tensor-to-scalar ratio is $r \simeq 12\epsilon$, and the spectral indices are $n_s = 1 - 6\epsilon + 2\eta$ and $n_t = -2\epsilon$. The natural expectation of inflation is that the quasi-exponential phase ends once the slow-roll parameters become significantly non-zero, so that both $n_s \neq 1$ and a significant tensor component are expected. These prediction can be avoided in some models, but it is undeniable that observation of such features would be a great triumph for inflation. Much future effort in cosmology will therefore be directed towards the question of whether the Universe contains anything other than scale-invariant scalar fluctuations.

References:

1. V.M. Slipher, Pop. Astr. **23**, 21 (1915).
2. K. Lundmark, MNRAS **84**, 747 (1924).
3. E. Hubble and M.L. Humason, Ap. J. **74**, 43 (1931).
4. G. Gamow, Phys. Rev. **70**, 572 (1946).
5. R.A. Alpher, H. Bethe, and G. Gamow, Phys. Rev. **73**, 803 (1948).
6. R.A. Alpher and R.C. Herman, Phys. Rev. **74**, 1737 (1948).
7. R.A. Alpher and R.C. Herman, Phys. Rev. **75**, 1089 (1949).
8. A.A. Penzias and R.W. Wilson, Ap. J. **142**, 419 (1965).
9. S. Weinberg, *Gravitation and Cosmology*, John Wiley and Sons (1972).
10. P.J.E. Peebles, *Principles of Physical Cosmology* Princeton University Press (1993).
11. G. Börner, *The Early Universe: Facts and Fiction*, Springer-Verlag (1988).
12. E.W. Kolb and M.S. Turner, *The Early Universe*, Addison-Wesley (1990).
13. J.A. Peacock, *Cosmological Physics*, Cambridge University Press (1999).
14. A.R. Liddle and D. Lyth, *Cosmological Inflation and Large-Scale Structure*, Cambridge University Press (2000).
15. E.B. Gliner, Sov. Phys. JETP 22, 378 (1966).
16. Y.B. Zeldovich, (1967), Sov. Phys. Uspekhi, **11**, 381 (1968).
17. P.M. Garnavich *et al.*, Ap. J. **507**, 74 (1998).
18. S. Perlmutter *et al.*, Phys. Rev. Lett. **83**, 670 (1999).
19. I. Maor *et al.*, Phys. Rev. **D65**, 123003 (2002).
20. A.G. Riess *et al.*, A. J. **116**, 1009 (1998).
21. S. Perlmutter *et al.*, Ap. J. **517**, 565 (1999).
22. A.G. Riess, PASP, **112**, 1284 (2000).
23. J.L. Tonry *et al.*, `astro-ph/0305008` (2003).
24. W.L. Freedman *et al.*, ApJ **553**, 47 (2001).
25. J.A. Johnson and M. Bolte, ApJ **554**, 888 (2001).
26. R. Jimenez and P. Padoan, ApJ **498**, 704 (1998).
27. E. Carretta *et al.*, ApJ **533**, 215 (2000).
28. D.N. Spergel *et al.*, `astro-ph/0302209` (2003).
29. M. Srednicki, R. Watkins and K. A. Olive, Nucl. Phys. B **310**, 693 (1988).
30. G. Mangano *et al.*, Phys. Lett. **B534**, 8 (2002).
31. A. Linde, Phys. Rev. **D14**, 3345 (1976).
32. A. Linde, Rep. Prog. Phys. **42**, 389 (1979).
33. C.E. Vayonakis, Surveys High Energ. Phys. **5**, 87 (1986).
34. S.A. Bonometto and A. Masiero, Riv. Nuovo Cim. **9N5**, 1 (1986).
35. A. Linde, A.D. Linde, *Particle Physics And Inflationary Cosmology*, Harwood (1990).
36. K.A. Olive, Phys. Rep. **190**, 3345 (1990).
37. D. Lyth and A. Riotto, Phys. Rep. **314**, 1 (1999).
38. A.H. Guth, Phys. Rev. **D23**, 347 (1981).
39. A.D. Linde, Phys. Lett. **108B**, 389 (1982).
40. A. Albrecht and P.J. Steinhardt, Phys. Rev. Lett. **48**, 1220 (1982).
41. A.D. Sakharov, Sov. Phys. JETP Lett. **5**, 24 (1967).
42. S. Weinberg, Phys. Rev. Lett. **42**, 850 (1979).
43. D. Toussaint *et al.*, Phys. Rev. **D19**, 1036 (1979).
44. I. Affleck and M. Dine, Nucl. Phys. **B249**, 361 (1985).
45. V. Kuzmin, V. Rubakov, and M. Shaposhnikov, Phys. Lett. **B155**, 36 (1985).
46. M. Fukugita and T. Yanagida, Phys. Lett. **B174**, 45 (1986).
47. R.H. Cyburt, B.D. Fields, and K.A. Olive, Phys. Lett. **B567**, 227 (2003).
48. K.A. Olive, G. Steigman, and T.P. Walker, Phys. Rept. **333**, 389 (2000).
49. D. Kirkman *et al.*, `astro-ph/0302006` (2003).
50. D.J. Fixsen *et al.*, ApJ **473**, 576 (1996).
51. J.C. Mather *et al.*, ApJ **512**, 511 (1999).

52. S.M. Cole *et al.*, MNRAS **326**, 255 (2001).
53. R.H. Becker *et al.*, Astr. J. **122**, 2850 (2001).
54. S.D.M. White *et al.*, Nature **366**, 429 (1993).
55. S.W. Allen, R.W. Schmidt, A.C. Fabian, MNRAS, **334**, L11 (2002).
56. S. Folkes *et al.*, MNRAS **308**, 459 (1999).
57. M.L. Blanton *et al.*, Astr. J. **121**, 2358 (2001).
58. H. Hoekstra *et al.*, ApJ, **548**, L5 (2001).
59. S.W. Allen, MNRAS **296**, 392 (1998).
60. W.J. Percival *et al.*, MNRAS **327**, 1297 (2001).
61. G. Efstathiou and J.R. Bond, MNRAS **218**, 103 (1986).
62. C. Gordon and A. Lewis, Phys. Rev. **D67**, 123513 (2003).
63. M.L. Brown *et al.*, MNRAS, **341**, 1 (2003).
64. P.T.P. Viana, R.C. Nichol, A.R. Liddle, ApJ, **569**, L75 (2002).
65. A. Dekel and O. Lahav, ApJ **520**, 24 (1999).
66. G. Efstathiou and J.R. Bond, MNRAS, **304**, 75 (1999).
67. G.P. Efstathiou *et al.*, MNRAS **330**, L29 (2002).
68. G.P. Efstathiou, MNRAS **332**, 193 (2002).

20. BIG-BANG NUCLEOSYNTHESIS

Revised October 2003 by B.D. Fields (Univ. of Illinois) and S. Sarkar (Univ. of Oxford).

Big-bang nucleosynthesis (BBN) offers the deepest reliable probe of the early universe, being based on well-understood Standard Model physics [1]. Predictions of the abundances of the light elements, D, ^{3}He, ^{4}He, and ^{7}Li, synthesized at the end of the "first three minutes" are in good overall agreement with the primordial abundances inferred from observational data, thus validating the standard hot big-bang cosmology (see [5] for a recent review). This is particularly impressive given that these abundances span nine orders of magnitude — from $^4\mathrm{He/H} \sim 0.08$ down to $^7\mathrm{Li/H} \sim 10^{-10}$ (ratios by number). Thus BBN provides powerful constraints on possible deviations from the standard cosmology [2], and on new physics beyond the Standard Model [3].

20.1. Big-bang nucleosynthesis theory

The synthesis of the light elements is sensitive to physical conditions in the early radiation-dominated era at temperatures $T \lesssim 1$ MeV, corresponding to an age $t \gtrsim 1$ s. At higher temperatures, weak interactions were in thermal equilibrium, thus fixing the ratio of the neutron and proton number densities to be $n/p = \mathrm{e}^{-Q/T}$, where $Q = 1.293$ MeV is the neutron-proton mass difference. As the temperature dropped, the neutron-proton inter-conversion rate, $\Gamma_{n\leftrightarrow p} \sim G_\mathrm{F}^2 T^5$, fell faster than the Hubble expansion rate, $H \sim \sqrt{g_* G_\mathrm{N}}\, T^2$, where g_* counts the number of relativistic particle species determining the energy density in radiation. This resulted in departure from chemical equilibrium ("freeze-out") at $T_\mathrm{fr} \sim (g_* G_\mathrm{N}/G_F^4)^{1/6} \simeq 1$ MeV. The neutron fraction at this time, $n/p = \mathrm{e}^{-Q/T_\mathrm{fr}} \simeq 1/6$, is thus sensitive to every known physical interaction, since Q is determined by both strong and electromagnetic interactions while T_fr depends on the weak as well as gravitational interactions. Moreover the sensitivity to the Hubble expansion rate affords a probe of e.g. the number of relativistic neutrino species [6]. After freeze-out the neutrons were free to β-decay so the neutron fraction dropped to $\simeq 1/7$ by the time nuclear reactions began. A useful semi-analytic description of freeze-out has been given [7].

The rates of these reactions depend on the density of baryons (strictly speaking, nucleons), which is usually expressed normalized to the blackbody photon density as $\eta \equiv n_\mathrm{B}/n_\gamma$. As we shall see, all the light-element abundances can be explained with $\eta_{10} \equiv \eta \times 10^{10}$ in the range 3.4–6.9 (95% CL). Equivalently, this can be stated as the allowed range for the baryon mass density today, $\rho_\mathrm{B} = (2.3\text{–}4.7) \times 10^{-31}$ g cm^{-3}, or as the baryonic fraction of the critical density: $\Omega_\mathrm{B} = \rho_\mathrm{B}/\rho_\mathrm{crit} \simeq \eta_{10} h^{-2}/274 = (0.012\text{–}0.025) h^{-2}$, where $h \equiv H_0/100$ km s^{-1} Mpc$^{-1} = 0.72 \pm 0.08$ is the present Hubble parameter (see Cosmological Parameters review).

The nucleosynthesis chain begins with the formation of deuterium in the process $p(n,\gamma)$D. However, photo-dissociation by the high number density of photons delays production of deuterium (and other complex nuclei) well after T drops below the binding energy of deuterium, $\Delta_\mathrm{D} = 2.23$ MeV. The quantity $\eta^{-1}\mathrm{e}^{-\Delta_\mathrm{D}/T}$, i.e. the number of photons per baryon above the deuterium photo-dissociation threshold, falls below unity at $T \simeq 0.1$ MeV; nuclei can then begin to form without being immediately photo-dissociated again. Only 2-body reactions such as $\mathrm{D}(p,\gamma)^3\mathrm{He}$, $^3\mathrm{He}(\mathrm{D},p)^4\mathrm{He}$, are important because the density has become rather low by this time.

Nearly all the surviving neutrons when nucleosynthesis begins end up bound in the most stable light element ^{4}He. Heavier nuclei do not form in any significant quantity both because of the absence of stable nuclei with mass number 5 or 8 (which impedes nucleosynthesis via n^4He, p^4He or ^{4}He^{4}He reactions) and the large Coulomb barriers for reactions such as $\mathrm{T}(^4\mathrm{He},\gamma)^7$Li and $^3\mathrm{He}(^4\mathrm{He},\gamma)^7$Be. Hence the primordial mass fraction of ^{4}He, conventionally referred to as Y_p, can be estimated by the simple counting argument

$$Y_\mathrm{p} = \frac{2(n/p)}{1+n/p} \simeq 0.25\ . \qquad (20.1)$$

There is little sensitivity here to the actual nuclear reaction rates, which are however important in determining the other "left-over" abundances: D and ^{3}He at the level of a few times 10^{-5} by number relative to H, and ^{7}Li/H at the level of about 10^{-10} (when η_{10} is in the range 1–10). These values can be understood in terms of approximate analytic arguments [8]. The experimental parameter most important in determining Y_p is the neutron lifetime, τ_n, which normalizes (the inverse of) $\Gamma_{n\leftrightarrow p}$. (This is not fully determined by G_F alone since neutrons and protons also have strong interactions, the effects of which cannot be calculated very precisely.) The experimental uncertainty in τ_n used to be a source of concern but has recently been reduced substantially: $\tau_n = 885.7 \pm 0.8$ s.

The elemental abundances, calculated using the (publicly available [9]) Wagoner code [1,10], are shown in Fig. 20.1 as a function of η_{10}. The ^{4}He curve includes small corrections due to radiative processes at zero and finite temperature [11], non-equilibrium neutrino heating during $e^\pm$ annihilation [12], and finite nucleon mass effects [13]; the range reflects primarily the 1σ uncertainty in the neutron lifetime. The spread in the curves for D, ^{3}He and ^{7}Li corresponds to the 1σ uncertainties in nuclear cross sections estimated by Monte Carlo methods [14–15]. Recently the input nuclear data have been carefully reassessed [16–18], leading to improved precision in the abundance predictions. Polynomial fits to the predicted abundances and the error correlation matrix have been given [15,19]. The boxes in Fig. 20.1 show the observationally inferred primordial abundances with their associated uncertainties, as discussed below.

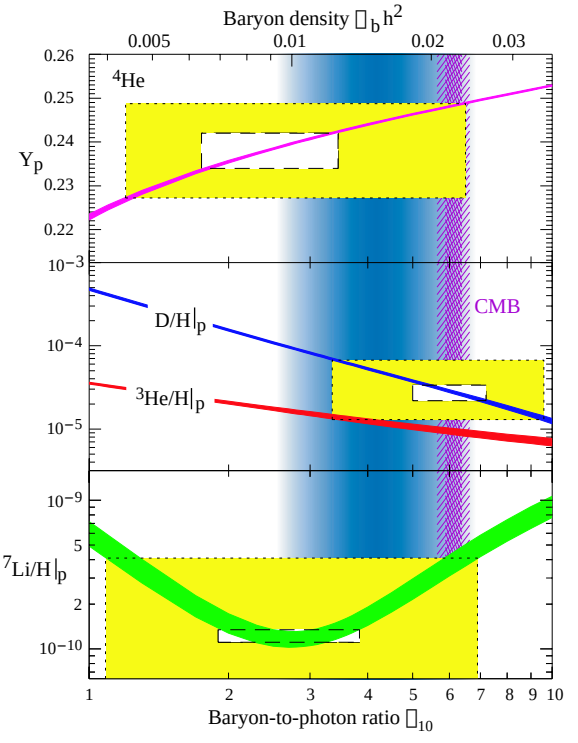

Figure 20.1: The abundances of ^{4}He, D, ^{3}He and ^{7}Li as predicted by the standard model of big-bang nucleosynthesis. Boxes indicate the observed light element abundances (smaller boxes: 2σ statistical errors; larger boxes: $\pm 2\sigma$ statistical and systematic errors added in quadrature). The narrow vertical band indicates the CMB measure of the cosmic baryon density. See full-color version on color pages at end of book.

20.2. Light Element Observations

BBN theory predicts the universal abundances of D, ^{3}He, ^{4}He, and ^{7}Li, which are essentially determined by $t \sim 180$ s. Abundances are however observed at much later epochs, after stellar nucleosynthesis has commenced. The ejected remains of this stellar processing can alter the light element abundances from their primordial values, but also produce heavy elements such as C, N, O, and Fe ("metals"). Thus one seeks astrophysical sites with low metal abundances, in order to measure light element abundances which are closer to primordial. For all of the light elements, systematic errors are an important and often dominant limitation to the precision with which primordial abundances can be inferred.

In recent years, high-resolution spectra have revealed the presence of D in high-redshift, low-metallicity quasar absorption systems (QAS), via its isotope-shifted Lyman-α absorption [20–24]. These are the first measurements of light element abundances at cosmological distances. It is believed that there are no astrophysical sources of deuterium [25], so any measurement of D/H provides a lower limit to primordial D/H and thus an upper limit on η; for example, the local interstellar value of $\mathrm{D/H} = (1.5 \pm 0.1) \times 10^{-5}$ [26] requires that $\eta_{10} \leq 9$. In fact, local interstellar D may have been depleted by a factor of 2 or more due to stellar processing; however, for the high-redshift systems, conventional models of galactic nucleosynthesis (chemical evolution) do not predict significant D/H depletion [27].

The 5 most precise observations of deuterium in QAS give $\mathrm{D/H} = (2.78 \pm 0.29) \times 10^{-5}$ [20–21], where the error is statistical only. However there remains concern over systematic errors, the dispersion between the values being much larger than is expected from the individual measurement errors ($\chi^2 = 12.4$ for 4 d.o.f.). Other lower values have been reported in different (damped Lyman-α) systems [22–23] and even the ISM value of D/H now shows unexpected scatter of a factor of 2 [28]. We thus conservatively bracket the observed values with an upper limit set by the non-detection of D in a high-redshift system, $\mathrm{D/H} < 6.7 \times 10^{-5}$ at 1σ [24], and a lower limit set by the local interstellar value [26]. These appear on Fig. 20.1, where it is clear that despite the observational uncertainties, the steep decrease of D/H with η makes it a sensitive probe of the baryon density. We are optimistic that a larger sample of D/H in high-redshift, low-redshift, and local systems will bring down systematic errors, and increase the precision with which η can be determined.

We observe ^{4}He in clouds of ionized hydrogen (H II regions), the most metal-poor of which are in dwarf galaxies. There is now a large body of data on ^{4}He and CNO in these systems [29]. These data confirm that the small stellar contribution to helium is positively correlated with metal production. Extrapolating to zero metallicity gives the primordial ^{4}He abundance [30] $Y_{\rm p} = 0.238 \pm 0.002 \pm 0.005$. Here the latter error is an estimate of the systematic uncertainty; this dominates, and is based on the scatter in different analyses of the physical properties of the H II regions [29,31]. Other extrapolations to zero metallicity give $Y_{\rm p} = 0.2443 \pm 0.0015$ [29], and $Y_{\rm p} = 0.2391 \pm 0.0020$ [32]. These are consistent (given the systematic errors) with the above estimate [30], which appears in Fig. 20.1.

The systems best suited for Li observations are metal-poor stars in the spheroid (Pop II) of our Galaxy, which have metallicities going down to at least 10^{-4} and perhaps 10^{-5} of the Solar value [33]. Observations have long shown [34–38] that Li does not vary significantly in Pop II stars with metallicities $\lesssim 1/30$ of Solar — the "Spite plateau" [34]. Recent precision data suggest a small but significant correlation between Li and Fe [35] which can be understood as the result of Li production from Galactic cosmic rays [36]. Extrapolating to zero metallicity one arrives at a primordial value [37] $\mathrm{Li/H}|_{\rm p} = (1.23 \pm 0.06) \times 10^{-10}$. One systematic error stems from the differences in techniques to determine the physical parameters (e.g., the temperature) of the stellar atmosphere in which the Li absorption line is formed. An alternative analysis [38] using a different set of stars (in a globular cluster) and a method that gives systematically higher temperatures yields $\mathrm{Li/H}|_{\rm p} = (2.19 \pm 0.28) \times 10^{-10}$; the difference with [37] indicates a systematic uncertainty of about a factor ~ 2. Another systematic error arises because it is possible that the Li in Pop II stars has been partially destroyed, due to mixing of the outer layers with the hotter interior [39]. Such processes can be constrained by the absence of significant scatter in Li-Fe [35], and by observations of the fragile isotope ^{6}Li [36]. Nevertheless, depletions by a factor as large as ~ 1.6 remain allowed [37,39]. Including these systematics, we estimate a primordial Li range of $\mathrm{Li/H}|_{\rm p} = (0.59 - 4.1) \times 10^{-10}$.

Finally, we turn to ^{3}He. Here, the only observations available are in the Solar system and (high-metallicity) H II regions in our Galaxy [40]. This makes inference of the primordial abundance difficult, a problem compounded by the fact that stellar nucleosynthesis models for ^{3}He are in conflict with observations [41]. Consequently, it is no longer appropriate to use ^{3}He as a cosmological probe; instead, one might hope to turn the problem around and constrain stellar astrophysics using the predicted primordial ^{3}He abundance [42].

20.3. Concordance, Dark Matter, and the CMB

We now use the observed light element abundances to assess the theory. We first consider standard BBN, which is based on Standard Model physics alone, so $N_\nu = 3$ and the only free parameter is the baryon-to-photon ratio η. (The implications of BBN for physics beyond the Standard Model will be considered below, §4). Thus, any abundance measurement determines η, while additional measurements overconstrain the theory and thereby provide a consistency check.

First we note that the overlap in the η ranges spanned by the larger boxes in Fig. 20.1 indicates overall concordance. More quantitatively, when we account for theoretical uncertainties as well as the statistical and systematic errors in observations, there is acceptable agreement among the abundances when

$$3.4 \leq \eta \leq 6.9 \ (95\%\ \mathrm{CL}). \tag{20.2}$$

However the agreement is much less satisfactory if we use only the quoted statistical errors in the observations. In particular, as seen in Fig. 20.1, ^{4}He and ^{7}Li are consistent with each other but favour a value of η which is lower by $\sim 2\sigma$ from that indicated by the D abundance. Additional studies are required to clarify if this discrepancy is real.

Even so the overall concordance is remarkable: using well-established microphysics we have extrapolated back to an age of ~ 1 s to correctly predict light element abundances spanning 9 orders of magnitude. This is a major success for the standard cosmology, and inspires confidence in extrapolation back to still earlier times.

This concordance provides a measure of the baryon content of the universe. With n_γ fixed by the present CMB temperature (see CMB Review), the baryon density is $\Omega_{\rm B} = 3.65 \times 10^{-3} h^{-2} \eta_{10}$, so that

$$0.012 \leq \Omega_{\rm B} h^2 \leq 0.025 \ (95\%\ \mathrm{CL}) \ , \tag{20.3}$$

a result that plays a key role in our understanding of the matter budget of the universe. First we note that $\Omega_{\rm B} \ll 1$, i.e., baryons cannot close the universe [43]. Furthermore, the cosmic density of (optically) luminous matter is $\Omega_{\rm lum} \simeq 0.0024 h^{-1}$ [44], so that $\Omega_{\rm B} \gg \Omega_{\rm lum}$: most baryons are optically dark, probably in the form of a $\sim 10^6$ K X-ray emitting intergalactic medium [45]. Finally, given that $\Omega_{\rm M} \sim 0.3$ (see Dark Matter, Cosmological Parameter Review), we infer that most matter in the universe is not only dark but also takes some non-baryonic (more precisely, non-nucleonic) form.

The BBN prediction for the cosmic baryon density can be tested through precision observations of CMB temperature fluctuations (see CMB Review). One can determine η from the amplitudes of the acoustic peaks in the CMB angular power spectrum, making it possible to compare two measures of η using very different physics, at two widely separated epochs [46]. In the standard cosmology, there is no change in η between BBN and CMB decoupling, thus, a comparison of $\eta_{\rm BBN}$ and $\eta_{\rm CMB}$ is a key test. Agreement would endorse the standard picture, and would open the way to sharper understanding of particle physics and astrophysics [54]. Disagreement could point to new physics during or between the BBN and CMB epochs.

The release of the first-year WMAP results are a landmark event in this test of BBN. As with other cosmological parameter determinations from CMB data, the derived $\eta_{\rm CMB}$ depends on the

adopted priors [47], in particular the form assumed for the power spectrum of primordial density fluctuations. If this is taken to be a scale-free power-law, the WMAP data implies $\Omega_{\rm B}h^2 = 0.024 \pm 0.001$ or $\eta_{10} = 6.58 \pm 0.27$, while allowing for a "running" spectral index lowers the value to $\Omega_{\rm B}h^2 = 0.0224 \pm 0.0009$ or $\eta_{10} = 6.14 \pm 0.25$ [48]; this latter range appears in Fig. 20.1. Other assumptions for the shape of the power spectrum can lead to baryon densities as low as $\Omega_{\rm B}h^2 = 0.019$ [49]. Thus outstanding uncertainties regarding priors are a source of systematic error which presently exceeds the statistical error in the prediction for η.

Even so, the CMB estimate of the baryon density is not inconsistent with the BBN range quoted in Eq. (20.3), and is in fact in good agreement with the value inferred from recent high-redshift D/H measurements [20]. However note that both ^{4}He and ^{7}Li are inconsistent with the CMB (as they are with D) given the error budgets we have quoted. The question then becomes more pressing as to whether this mismatch come from systematic errors in the observed abundances, and/or uncertainties in stellar astrophysics, or whether there might be new physics at work. Inhomogeneous nucleosynthesis can alter abundances for a given $\eta_{\rm BBN}$ but will overproduce ^{7}Li [50]. However a small excess of electron neutrinos over antineutrinos will lower the ^{4}He abundance below the standard BBN prediction without affecting the other elements [1]. Note that entropy generation by some non-standard process could have decreased η between the BBN era and CMB decoupling, however the lack of spectral distortions in the CMB rules out any significant energy injection upto a redshift $z \sim 10^7$ [51]. Interestingly, the CMB itself offers the promise of measuring ^{4}He [52] and possibly ^{7}Li [53] directly at $z \sim 300 - 1000$.

Bearing in mind the importance of priors, the promise of precision determinations of the baryon density using the CMB motivates using this value as an input to BBN calculations. Within the context of the Standard Model, BBN then becomes a zero-parameter theory, and the light element abundances are completely determined to within the uncertainties in $\eta_{\rm CMB}$ and the BBN theoretical errors. Comparison with the observed abundances then can be used to test the astrophysics of post-BBN light element evolution [54]. Alternatively, one can consider possible physics beyond the Standard Model (e.g., which might change the expansion rate during BBN) and then use all of the abundances to test such models; this is the subject of our final section.

20.4. Beyond the Standard Model

Given the simple physics underlying BBN, it is remarkable that it still provides the most effective test for the cosmological viability of ideas concerning physics beyond the Standard Model. Although baryogenesis and inflation must have occurred at higher temperatures in the early universe, we do not as yet have 'standard models' for these so BBN still marks the boundary between the established and the speculative in big bang cosmology. It might appear possible to push the boundary back to the quark-hadron transition at $T \sim \Lambda_{\rm QCD}$ or electroweak symmetry breaking at $T \sim 1/\sqrt{G_{\rm F}}$; however so far no observable relics of these epochs have been identified, either theoretically or observationally. Thus although the Standard Model provides a precise description of physics up to the Fermi scale, cosmology cannot be traced in detail before the BBN era.

Limits on particle physics beyond the Standard Model come mainly from the observational bounds on the ^{4}He abundance. This is proportional to the n/p ratio which is determined when the weak-interaction rates fall behind the Hubble expansion rate at $T_{\rm fr} \sim 1$ MeV. The presence of additional neutrino flavors (or of any other relativistic species) at this time increases g_*, hence the expansion rate, leading to a larger value of $T_{\rm fr}$, n/p, and therefore $Y_{\rm p}$ [6,55]. In the Standard Model, the number of relativistic particle species at 1 MeV is $g_* = 5.5 + \frac{7}{4}N_\nu$, where 5.5 accounts for photons and $e^\pm$, and N_ν is the number of (nearly massless) neutrino flavors (see Big Bang Cosmology Review). The helium curves in Fig. 20.1 were computed taking $N_\nu = 3$; the computed abundance scales as $\Delta\, Y_{\rm BBN} \simeq 0.013 \Delta N_\nu$ [7]. Clearly the central value for N_ν from BBN will depend on η, which is independently determined (with little sensitivity to N_ν) by the adopted D or ^{7}Li abundance. For example, if the best value for the observed primordial ^{4}He abundance is 0.238, then, for $\eta_{10} \sim 2$, the central value for N_ν is very close to 3. A maximum likelihood analysis on η and N_ν based on ^{4}He and ^{7}Li [56] finds the (correlated) 95% CL ranges to be $1.7 \leq \eta_{10} \leq 4.3$, and $1.4 \leq N_\nu \leq 4.9$. Similar results were obtained in another study [57] which presented a simpler method (FastBBN [9]) to extract such bounds based on χ^2 statistics, given a set of input abundances. Tighter bounds are obtained if less conservative assumptions are made concerning primordial abundances, e.g. adopting the 'low' D abundance [21] fixes $\eta_{10} = 5.6 \pm 0.6$ ($\Omega_{\rm B}h^2 = 0.02 \pm 0.002$) at 95% CL, and requires $N_\nu < 3.2$ [58] even if the 'high' ^{4}He abundance [29] is used. Using the CMB determination of η yields even tighter constraints, with $N_\nu = 3$ barely allowed at 2σ [59]! However if the discrepancy between the ^{4}He and D abundances is indeed due to a ν_e chemical potential, then N_ν can range up to 7.1 at 2σ [60].

It is clear that just as one can use the measured helium abundance to place limits on g_* [55], any changes in the strong, weak, electromagnetic, or gravitational coupling constants, arising e.g. from the dynamics of new dimensions, can be similarly constrained [61].

The limits on N_ν can be translated into limits on other types of particles or particle masses that would affect the expansion rate of the Universe during nucleosynthesis. For example consider 'sterile' neutrinos with only right-handed interactions of strength $G_{\rm R} < G_{\rm F}$. Such particles would decouple at higher temperature than (left-handed) neutrinos, so their number density ($\propto T^3$) relative to neutrinos would be reduced by any subsequent entropy release, e.g. due to annihilations of massive particles that become non-relativistic in between the two decoupling temperatures. Thus (relativistic) particles with less than full strength weak interactions contribute less to the energy density than particles that remain in equilibrium up to the time of nucleosynthesis [62]. If we impose $N_\nu < 4$ as an illustrative constraint, then the three right-handed neutrinos must have a temperature $3(T_{\nu_{\rm R}}/T_{\nu_{\rm L}})^4 < 1$. Since the temperature of the decoupled $\nu_{\rm R}$'s is determined by entropy conservation (see Big Bang Cosmology Review), $T_{\nu_{\rm R}}/T_{\nu_{\rm L}} = [(43/4)/g_*(T_{\rm d})]^{1/3} < 0.76$, where $T_{\rm d}$ is the decoupling temperature of the $\nu_{\rm R}$'s. This requires $g_*(T_{\rm d}) > 24$ so decoupling must have occurred at $T_{\rm d} > 140$ MeV. The decoupling temperature is related to $G_{\rm R}$ through $(G_{\rm R}/G_{\rm F})^2 \sim (T_{\rm d}/3\,{\rm MeV})^{-3}$, where 3 MeV is the decoupling temperature for $\nu_{\rm L}$s. This yields a limit $G_{\rm R} \lesssim 10^{-2} G_{\rm F}$. The above argument sets lower limits on the masses of new Z' gauge bosons in superstring models [63] or in extended technicolour models [64] to which such right-handed neutrinos would be coupled. Similarly a Dirac magnetic moment for neutrinos, which would allow the right-handed states to be produced through scattering and thus increase g_*, can be significantly constrained [65], as can any new interactions for neutrinos which have a similar effect [66]. Right-handed states can be populated directly by helicity-flip scattering if the neutrino mass is large enough and this can be used to used to infer e.g. a bound of $m_{\nu_\tau} \lesssim 1$ MeV taking $N_\nu < 4$ [67]. If there is mixing between active and sterile neutrinos then the effect on BBN is more complicated [68].

The limit on the expansion rate during BBN can also be translated into bounds on the mass/lifetime of particles which are non-relativistic during BBN resulting in an even faster speed-up rate; the subsequent decays of such particles will typically also change the entropy, leading to further constraints [69]. Even more stringent constraints come from requiring that the synthesized light element abundances are not excessively altered through photodissociations by the electromagnetic cascades triggered by the decays [70,71], or by the effects of hadrons in the cascades [80]. Such arguments have been applied to e.g. rule out a MeV mass ν_τ which decays during nucleosynthesis [73]; even if the decays are to non-interacting particles (and light neutrinos), bounds can be derived from considering their effects on BBN [74].

Such arguments have proved very effective in constraining supersymmetry. For example if the gravitino is light and contributes to g_*, the illustrative BBN limit $N_\nu < 4$ requires its mass to exceed ~ 1 eV [75]. In models where supersymmetry breaking is gravity mediated, the gravitino mass is usually much higher, of order the electroweak scale; such gravitinos would be unstable and decay after BBN. The constraints on unstable particles discussed above imply stringent bounds on the allowed abundance of such particles, which in turn impose powerful constraints on supersymmetric inflationary

cosmology [71,80]. These can be evaded only if the gravitino is massive enough to decay before BBN, i.e. $m_{3/2} \gtrsim 50$ TeV [76] which would be unnatural, or if it is in fact the LSP and thus stable [71,77]. Similar constraints apply to moduli — very weakly coupled fields in supergravity/string models which obtain an electroweak-scale mass from supersymmetry breaking [78].

Finally we mention that BBN places powerful constraints on the recently suggested possibility that there are new large dimensions in nature, perhaps enabling the scale of quantum gravity to be as low as the electroweak scale [79]. Thus Standard Model fields may be localized on a 'brane' while gravity alone propagates in the 'bulk'. It has been further noted that the new dimensions may be non-compact, even infinite [80] and the cosmology of such models has attracted considerable attention. The expansion rate in the early universe can be significantly modified so BBN is able to set interesting constraints on such possibilities [81].

References:

1. R.V. Wagoner *et al.*, Astrophys. J. **148**, 3 (1967).
2. R.A. Malaney and G.J. Mathews, Phys. Reports **229**, 145 (1993).
3. S. Sarkar, Rept. on Prog. in Phys. **59**, 1493 (1996).
4. D.N. Schramm and M.S. Turner, Rev. Mod. Phys. **70**, 303 (1998).
5. K.A. Olive *et al.*, Phys. Reports **333**, 389 (2000).
6. P.J.E. Peebles, Phys. Rev. Lett. **16**, 411 (1966).
7. J. Bernstein *et al.*, Rev. Mod. Phys. **61**, 25 (1989).
8. R. Esmailzadeh *et al.*, Astrophys. J. **378**, 504 (1991).
9. www-thphys.physics.ox.ac.uk/users/SubirSarkar/bbn.html.
10. L. Kawano, FERMILAB-PUB-92/04-A.
11. S. Esposito *et al.*, Nucl. Phys. **B568**, 421 (2000).
12. S. Dodelson and M.S. Turner, Phys. Rev. **D46**, 3372 (1992).
13. D. Seckel, hep-ph/9305311;
    R. Lopez and M.S. Turner, Phys. Rev. **D59**, 103502 (1999).
14. M.S. Smith *et al.*, Astrophys. J. Supp. **85**, 219 (1993).
15. G. Fiorentini *et al.*, Phys. Rev. **D58**, 063506 (1998).
16. K.M. Nollett and S. Burles, Phys. Rev. **D61**, 123505 (2000).
17. R.H. Cyburt *et al.*, New Astron. **6**, 215 (2001).
18. A. Coc *et al.*, astro-ph/0309480.
19. K.M. Nollett *et al.*, Astrophys. J. Lett. **552**, L1 (2001).
20. D. Kirkman *et al.*, astro-ph/0302006.
21. J.M. O'Meara *et al.*, Astrophys. J. **552**, 718 (2001).
22. S. D'Odorico *et al.*, Astron. & Astrophys. **368**, L21 (2001).
23. M. Pettini and D. Bowen, Astrophys. J. **560**, 41 (2001).
24. D. Kirkman *et al.*, Astrophys. J. **529**, 655 (2000).
25. R.I. Epstein *et al.*, Nature **263**, 198 (1976).
26. J. Linsky, Space Sci. Rev., **106**, 49 (2003).
27. B.D. Fields, Astrophys. J. **456**, 678 (1996).
28. G. Sonneborn *et al.*, Astrophys. J. **545**, 277 (2000).
29. Y.I. Izotov *et al.*, Astrophys. J. **527**, 757 (1999).
30. B.D. Fields and K.A. Olive, Astrophys. J. **506**, 177 (1998).
31. K.A. Olive and E. Skillman, New Astron. **6**, 119 (2001).
32. V. Luridiana *et al.*, Astrophys. J. **592**, 846 (2003).
33. N. Christlieb *et al.*, Nature **419**, 904 (2002).
34. M. Spite and F. Spite, Nature **297**, 483 (1982).
35. S.G. Ryan *et al.*, Astrophys. J. Lett. **530**, L57 (2000).
36. E. Vangioni-Flam *et al.*, New Astron. **4**, 245 (1999).
37. S.G. Ryan *et al.*, Astrophys. J. Lett. **530**, L57 (2000).
38. P. Bonifacio *et al.*, Astron. & Astrophys. **390**, 91 (2002).
39. M.H. Pinsonneault *et al.*, Astrophys. J. **574**, 389 (2002).
40. D.S. Balser *et al.*, Astrophys. J. **510**, 759 (1999).
41. K.A. Olive *et al.*, Astrophys. J. **479**, 752 (1997).
42. E. Vangioni-Flam *et al.*, Astrophys. J. **585**, 611 (2003).
43. H. Reeves *et al.*, Astrophys. J. **179**, 909 (1973).
44. M. Fukugita *et al.*, Astrophys. J. **503**, 518 (1998).
45. R. Cen and J.P. Ostriker, Astrophys. J. **514**, 1 (1999).
46. G. Jungman *et al.*, Phys. Rev. **D54**, 1332 (1996).
47. M. Tegmark *et al.*, Phys. Rev. **D63**, 043007 (2001).
48. D.N. Spergel *et al.*, Astrophys. J. Supp. **148**, 175 (2003).
49. A. Blanchard *et al.*, astro-ph/0304237;
    S. Bridle *et al.*, MNRAS **342**, L72 (2003).
50. K. Jedamzik and J.B. Rehm, Phys. Rev. **D64**, 023510 (2001).
51. D.J. Fixsen *et al.*, Astrophys. J. **473**, 576 (1996).
52. R. Trotta and S.H. Hansen, astro-ph/0306588.
53. P.C. Stancil *et al.*, Astrophys. J. **580**, 29 (2002).
54. R.H. Cyburt *et al.*, Phys. Lett. **B567**, 227 (2003).
55. G. Steigman *et al.*, Phys. Lett. **B66**, 202 (1977).
56. K.A. Olive and D. Thomas, Astropart. Phys. **11**, 403 (1999)..
57. E. Lisi *et al.*, Phys. Rev. **D59**, 123520 (1999).
58. S. Burles *et al.*, Phys. Rev. **D63**, 063512 (2001).
59. V. Barger *et al.*, Phys. Lett. **B566**, 8 (2003).
60. V. Barger *et al.*, Phys. Lett. **B569**, 123 (2003).
61. E.W. Kolb *et al.*, Phys. Rev. **D33**, 869 (1986);
    F.S. Accetta *et al.*, Phys. Lett. **B248**, 146 (1990);
    B.A. Campbell and K.A. Olive, Phys. Lett. **B345**, 429 (1995);
    K.M. Nollett and R. Lopez, Phys. Rev. **D66**, 063507 (2002).
62. K.A. Olive *et al.*, Nucl. Phys. **B180**, 497 (1981).
63. J. Ellis *et al.*, Phys. Lett. **B167**, 457 (1986).
64. L.M. Krauss *et al.*, Phys. Rev. Lett. **71**, 823 (1993).
65. J.A. Morgan, Phys. Lett. **B102**, 247 (1981).
66. E.W. Kolb *et al.*, Phys. Rev. **D34**, 2197 (1986);
    J.A. Grifols and E. Massó, Mod. Phys. Lett. **A2**, 205 (1987);
    K.S. Babu *et al.*, Phys. Rev. Lett. **67**, 545 (1991).
67. A.D. Dolgov *et al.*, Nucl. Phys. **B524**, 621 (1998).
68. K. Enqvist *et al.*, Nucl. Phys. **B373**, 498 (1992);
    A.D. Dolgov, Phys. Reports **370**, 333 (2002).
69. K. Sato and M. Kobayashi, Prog. Theor. Phys. **58**, 1775 (1977);
    D.A. Dicus *et al.*, Phys. Rev. **D17**, 1529 (1978);
    R.J. Scherrer and M.S. Turner, Astrophys. J. **331**, 19 (1988).
70. D. Lindley, MNRAS **188**, 15 (1979), Astrophys. J. **294**, 1 (1985).
71. J. Ellis *et al.*, Nucl. Phys. **B373**, 399 (1992);
    R.H. Cyburt *et al.*, Phys. Rev. **D67**, 103521 (2003).
72. M.H. Reno and D. Seckel, Phys. Rev. **D37**, 3441 (1988);
    S. Dimopoulos *et al.*, Nucl. Phys. **B311**, 699 (1989);
    K. Kohri, Phys. Rev. **D64**, 043515 (2001).
73. S. Sarkar and A.M. Cooper, Phys. Lett. **B148**, 347 (1984).
74. S. Dodelson *et al.*, Phys. Rev. **D49**, 5068 (1994).
75. J.A. Grifols *et al.*, Phys. Lett. **B400**, 124 (1997).
76. S. Weinberg, Phys. Rev. Lett. **48**, 1303 (1979).
77. M. Bolz *et al.*, Nucl. Phys. **B606**, 518 (2001).
78. G. Coughlan *et al.*, Phys. Lett. **B131**, 59 (1983).
79. N. Arkani-Hamed *et al.*, Phys. Rev. **D59**, 086004 (1999).
80. L. Randall and R. Sundrum, Phys. Rev. Lett. **83**, 3370 (1999);
    Phys. Rev. Lett. **83**, 4690 (1999).
81. J.M. Cline *et al.*, Phys. Rev. Lett. **83**, 4245 (1999);
    P. Binetruy *et al.*, Phys. Lett. **B477**, 285 (2000).

21. THE COSMOLOGICAL PARAMETERS

Written August 2003 by O. Lahav (University of Cambridge) and A.R. Liddle (University of Sussex).

21.1. Parametrizing the Universe

Rapid advances in observational cosmology are leading to the establishment of the first precision cosmological model, with many of the key cosmological parameters determined to one or two significant figure accuracy. Particularly prominent are measurements of cosmic microwave anisotropies, led by the first results from the Wilkinson Microwave Anisotropy Probe (WMAP) announced in February 2003 [1]. However the most accurate model of the Universe requires consideration of a wide range of different types of observation, with complementary probes providing consistency checks, lifting parameter degeneracies, and enabling the strongest constraints to be placed.

The term 'cosmological parameters' is forever increasing in its scope, and nowadays includes the parametrization of some functions, as well as simple numbers describing properties of the Universe. The original usage referred to the parameters describing the global dynamics of the Universe, such as its expansion rate and curvature. Also now of great interest is how the matter budget of the Universe is built up from its constituents: baryons, photons, neutrinos, dark matter, and dark energy. We are interested in describing the nature of perturbations in the Universe, through global statistical descriptions such as the matter and radiation power spectra. There may also be parameters describing the physical state of the Universe, most prominent being the ionization fraction as a function of time during the era since decoupling. Typical comparisons of cosmological models with observational data now feature about ten parameters.

21.1.1. *The global description of the Universe*:

Ordinarily, the Universe is taken to be a perturbed Robertson-Walker space-time with dynamics governed by Einstein's equations. This is described in detail by Olive and Peacock in this volume. Using the density parameters Ω_i for the various matter species and Ω_Λ for the cosmological constant, the Friedmann equation can be written

$$\sum_i \Omega_i + \Omega_\Lambda = \frac{k}{R^2 H^2}\,, \tag{21.1}$$

where the sum is over all the different species of matter in the Universe. This equation applies at any epoch, but later in this article we will use the symbols Ω_i and Ω_Λ to refer to the present values. A typical collection would be baryons, photons, neutrinos, and dark matter (given charge neutrality, the electron density is guaranteed to be too small to be worth considering separately).

The complete present state of the homogeneous Universe can be described by giving the present values of all the density parameters and the present Hubble parameter h, and indeed one of the density parameters can be eliminated using Eq. (21.1). These also allow us to track the history of the Universe back in time, at least until an epoch where interactions allow interchanges between the densities of the different species, which is believed to have last happened at neutrino decoupling shortly before nucleosynthesis. To probe further back into the Universe's history requires assumptions about particle interactions, and perhaps about the nature of physical laws themselves.

21.1.2. *Neutrinos*:

The standard neutrino sector has three flavors. For neutrinos of mass in the range 5×10^{-4} eV to 1 MeV, the density parameter in neutrinos is predicted to be

$$\Omega_\nu h^2 = \frac{\sum m_\nu}{94\,\mathrm{eV}}\,, \tag{21.2}$$

where the sum is over all families with mass in that range (higher masses need a more sophisticated calculation). We use units with $c = 1$ throughout. Recent results on atmospheric and solar neutrino oscillations [2] imply non-zero mass-squared differences between the three neutrino flavors. These oscillation experiments cannot tell us the absolute neutrino masses, but within the simple assumption of a mass hierarchy suggest a lower limit of $\Omega_\nu \approx 0.001$ on the neutrino mass density parameter.

For a total mass as small as 0.1 eV, this could have a potentially observable effect on the formation of structure, as neutrino free-streaming damps the growth of perturbations. Present cosmological observations have shown no convincing evidence of any effects from either neutrino masses or an otherwise non-standard neutrino sector, and impose quite stringent limits, which we summarize in Section 21.3.4. Consequently, the standard assumption at present is that the masses are too small to have a significant cosmological impact, but this may change in the near future.

The cosmological effect of neutrinos can also be modified if the neutrinos have decay channels, or if there is a large asymmetry in the lepton sector manifested as a different number density of neutrinos versus anti-neutrinos. This latter effect would need to be of order unity to be significant, rather than the 10^{-9} seen in the baryon sector, which may be in conflict with nucleosynthesis [3].

21.1.3. *Inflation and perturbations*:

A complete description of the Universe should include a description of deviations from homogeneity, at least in a statistical way. Indeed, some of the most powerful probes of the parameters described above come from studying the evolution of perturbations, so their study is naturally intertwined in the determination of cosmological parameters.

There are many different notations used to describe the perturbations, both in terms of the quantity used to describe the perturbations and the definition of the statistical measure. We use the dimensionless power spectrum Δ^2 as defined in Olive and Peacock (also denoted $\mathcal{P}$ in some of the literature). If the perturbations obey Gaussian statistics, the power spectrum provides a complete description of their properties.

From a theoretical perspective, a useful quantity to describe the perturbations is the curvature perturbation $\mathcal{R}$, which measures the spatial curvature of a comoving slicing of the space-time. A case of particular interest is the Harrison-Zel'dovich spectrum, which corresponds to a constant spectrum $\Delta^2_\mathcal{R}$. More generally, one can approximate the spectrum by a power-law, writing

$$\Delta^2_\mathcal{R}(k) = \Delta^2_\mathcal{R}(k_*) \left[\frac{k}{k_*}\right]^{n-1}\,, \tag{21.3}$$

where n is known as the spectral index, always defined so that $n = 1$ for the Harrison-Zel'dovich spectrum, and k_* is an arbitrarily chosen scale. The initial spectrum, defined at some early epoch of the Universe's history, is usually taken to have a simple form such as this power-law, and we will see that observations require n close to one, which corresponds to the perturbations in the curvature being independent of scale. Subsequent evolution will modify the spectrum from its initial form.

The simplest viable mechanism for generating the observed perturbations is the inflationary cosmology, which posits a period of accelerated expansion in the Universe's early stages [4]. It is a useful working hypothesis that this is the sole mechanism for generating perturbations. Commonly, it is further assumed to be the simplest class of inflationary model, where the dynamics are equivalent to that of a single scalar field ϕ slowly rolling on a potential $V(\phi)$. One aim of cosmology is to verify that this simple picture can match observations, and to determine the properties of $V(\phi)$ from the observational data.

Inflation generates perturbations through the amplification of quantum fluctuations, which are stretched to astrophysical scales by the rapid expansion. The simplest models generate two types, density perturbations which come from fluctuations in the scalar field and its corresponding scalar metric perturbation, and gravitational waves which are tensor metric fluctuations. The former experience gravitational instability and lead to structure formation, while the latter can influence the cosmic microwave background anisotropies. Defining slow-roll parameters, with primes indicating derivatives with respect to the scalar field, as

$$\epsilon = \frac{m_{\rm Pl}^2}{16\pi}\left(\frac{V'}{V}\right)^2 \quad ; \quad \eta = \frac{m_{\rm Pl}^2}{8\pi}\frac{V''}{V}\,, \tag{21.4}$$

which should satisfy $\epsilon, |\eta| \ll 1$, the spectra can be computed using the slow-roll approximation as

$$\Delta^2_{\mathcal{R}}(k) \simeq \frac{8}{3m_{\rm Pl}^4}\frac{V}{\epsilon}\bigg|_{k=aH} \quad ;$$
$$\Delta^2_{\rm grav}(k) \simeq \frac{128}{3m_{\rm Pl}^4} V\bigg|_{k=aH} . \qquad (21.5)$$

In each case, the expressions on the right-hand side are to be evaluated when the scale k is equal to the Hubble radius during inflation. The symbol '$\simeq$' indicates use of the slow-roll approximation, which is expected to be accurate to a few percent or better.

From these expressions, we can compute the spectral indices

$$n \simeq 1 - 6\epsilon + 2\eta \quad ; \quad n_{\rm grav} \simeq -2\epsilon . \qquad (21.6)$$

Another useful quantity is the ratio of the two spectra, defined by

$$r \equiv \frac{\Delta^2_{\rm grav}(k_*)}{\Delta^2_{\mathcal{R}}(k_*)} . \qquad (21.7)$$

The literature contains a number of definitions of r; this convention matches that of recent versions of CMBFAST [5] and of WMAP [6], while definitions based on the relative effect on the microwave background anisotropies typically differ by tens of percent. We have

$$r \simeq 16\epsilon \simeq -8 n_{\rm grav} , \qquad (21.8)$$

which is known as the consistency equation.

In general one could consider corrections to the power-law approximation, and indeed WMAP found some low-significance evidence that this might be needed, which we discuss later. However for now we make the working assumption that the spectra can be approximated by power laws. The consistency equation shows that r and $n_{\rm grav}$ are not independent parameters, and so the simplest inflation models give initial conditions described by three parameters, usually taken as $\Delta^2_{\mathcal{R}}$, n, and r, all to be evaluated at some scale k_*, usually the 'statistical centre' of the range explored by the data. Alternatively, one could use the parametrization V, ϵ, and η, all evaluated at a point on the putative inflationary potential.

After the perturbations are created in the early Universe, they undergo a complex evolution up until the time they are observed in the present Universe. While the perturbations are small, this can be accurately followed using a linear theory numerical code such as CMBFAST [5]. This works right up to the present for the cosmic microwave background, but for density perturbations on small scales non-linear evolution is important and can be addressed by a variety of semi-analytical and numerical techniques. However the analysis is made, the outcome of the evolution is in principle determined by the cosmological model, and by the parameters describing the initial perturbations, and hence can be used to determine them.

Of particular interest are cosmic microwave background anisotropies. Both the total intensity and two independent polarization modes are predicted to have anisotropies. These can be described by the radiation angular power spectra C_ℓ as defined in the article of Scott and Smoot in this volume, and again provide a complete description if the density perturbations are Gaussian.

21.1.4. *The standard cosmological model*:

We now have most of the ingredients in place to describe the cosmological model. Beyond those of the previous subsections, there is only one parameter which is essential, which is a measure of the ionization state of the Universe. The Universe is known to be highly ionized at low redshifts (otherwise radiation from distant quasars would be heavily absorbed in the ultra-violet), and the ionized electrons can scatter microwave photons altering the pattern of observed anisotropies. The most convenient parameter to describe this is the optical depth to scattering τ (i.e. the probability that a given photon scatters once); in the approximation of instantaneous and complete re-ionization, this could equivalently be described by the redshift of re-ionization $z_{\rm ion}$.

Table 21.1: The basic set of cosmological parameters. We give values as obtained using particular fit to a dataset known as WMAPext+2dF, described later. We cannot stress too much that the exact values and uncertainties depend on both the precise datasets used and the choice of parameters allowed to vary, and the effects of varying some assumptions will be shown later in Table 21.2. Limits on the cosmological constant depend on whether the Universe is assumed flat, while there is no established convention for specifying the density perturbation amplitude. Uncertainties are one-sigma/68% confidence unless otherwise stated.

Parameter	Symbol	Value
Hubble parameter	h	0.73 ± 0.03
Total matter density	$\Omega_{\rm m}$	$\Omega_{\rm m}h^2 = 0.134 \pm 0.006$
Baryon density	$\Omega_{\rm b}$	$\Omega_{\rm b}h^2 = 0.023 \pm 0.001$
Cosmological constant	Ω_Λ	See Ref. 7
Radiation density	$\Omega_{\rm r}$	$\Omega_{\rm r}h^2 = 2.47 \times 10^{-5}$
Neutrino density	Ω_ν	See Sec. 21.1.2
Density perturbation amplitude	$\Delta^2_{\mathcal{R}}(k_*)$	See Ref. 7
Density perturbation spectral index	n	$n = 0.97 \pm 0.03$
Tensor to scalar ratio	r	$r < 0.53$ (95% conf)
Ionization optical depth	τ	$\tau = 0.15 \pm 0.07$

The basic set of cosmological parameters is therefore as shown in Table 21.1. The spatial curvature does not appear in the list, because it can be determined from the other parameters using Eq. (21.1). The total present matter density $\Omega_{\rm m} = \Omega_{\rm dm} + \Omega_{\rm b}$ is usually used in place of the dark matter density.

As described in Sec. 21.4, models based on these ten parameters are able to give a good fit to the complete set of high-quality data available at present, and indeed some simplification is possible. Observations are consistent with spatial flatness, and indeed the inflation models so far described automatically generate spatial flatness, so we can set $k = 0$; the density parameters then must sum to one, and so one can be eliminated. The neutrino energy density is often not taken as an independent parameter. Provided the neutrino sector has the standard interactions the neutrino energy density while relativistic can be related to the photon density using thermal physics arguments, and it is currently difficult to see the effect of the neutrino mass although observations of large-scale structure have already placed interesting upper limits. This reduces the standard parameter set to eight. In addition, there is no observational evidence for the existence of tensor perturbations (though the upper limits are quite weak), and so r could be set to zero.* This leaves seven parameters, which is the smallest set that can usefully be compared to the present cosmological data set. This model is referred to by various names, including ΛCDM, the concordance cosmology, and the standard cosmological model.

Of these parameters, only $\Omega_{\rm r}$ is accurately measured directly. The radiation density is dominated by the energy in the cosmic microwave background, and the COBE FIRAS experiment has determined its temperature to be $T = 2.725 \pm 0.001$ Kelvin [8], corresponding to $\Omega_{\rm r} = 2.47 \times 10^{-5} h^{-2}$.

In addition to this minimal set, there is a range of other parameters which might prove important in future as the dataset further improves, but for which there is so far no direct evidence, allowing them to be set to a specific value. We discuss various speculative options in the next section. For completeness at this point, we mention one other interesting parameter, the helium fraction, which is a non-zero parameter that can affect the microwave anisotropies at a subtle level. Presently, big-bang nucleosynthesis provides the best measurement of this parameter, and it is usually fixed in microwave anisotropy studies, but the data are just reaching a level where allowing its variation may become mandatory.

* More controversially, one could argue that as no evidence against the Harrison-Zel'dovich spectrum has yet been seen, then n could be set to one. We will however allow it to vary.

21.1.5. ***Derived parameters*:**

The parameter list of the previous subsection is sufficient to give a complete description of cosmological models which agree with observational data. However, it is not a unique parametrization, and one could instead use parameters derived from that basic set. Parameters which can be derived from the set given above include the age of the Universe, the present horizon distance, the present microwave background and neutrino background temperatures, the epoch of matter-radiation equality, the epochs of recombination and decoupling, the epoch of transition to an accelerating Universe, the baryon-to-photon ratio, and the baryon to dark matter density ratio. The physical densities of the matter components, $\Omega_i h^2$, are often more useful than the density parameters. The density perturbation amplitude can be specified in many different ways other than the large-scale primordial amplitude, for instance, in terms of its effect on the cosmic microwave background, or by specifying a short-scale quantity, a common choice being the present linear-theory mass dispersion on a scale of $8\,h^{-1}$Mpc, known as σ_8.

Different types of observation are sensitive to different subsets of the full cosmological parameter set, and some are more naturally interpreted in terms of some of the derived parameters of this subsection than on the original base parameter set. In particular, most types of observation feature degeneracies whereby they are unable to separate the effects of simultaneously varying several of the base parameters, an example being the angular diameter/physical density degeneracy of cosmic microwave anisotropies.

21.2. Extensions to the standard model

This section discusses some ways in which the standard model could be extended. At present, there is no positive evidence in favor of any of these possibilities, which are becoming increasingly constrained by the data, though there always remains the possibility of trace effects at a level below present observational capability.

21.2.1. ***More general perturbations*:**

The standard cosmology assumes adiabatic, Gaussian perturbations. Adiabaticity means that all types of material in the Universe share a common perturbation, so that if the space-time is foliated by constant-density hypersurfaces, then all fluids and fields are homogeneous on those slices, with the perturbations completely described by the variation of the spatial curvature of the slices. Gaussianity means that the initial perturbations obey Gaussian statistics, with the amplitudes of waves of different wavenumbers being randomly drawn from a Gaussian distribution of width given by the power spectrum. Note that gravitational instability generates non-Gaussianity; in this context, Gaussianity refers to a property of the initial perturbations before they evolve significantly.

The simplest inflation models based on one dynamical field predict adiabatic fluctuations and a level of non-Gaussianity which is too small to be detected by any experiment so far conceived. For present data, the primordial spectra are usually assumed to be power laws.

21.2.1.1. *Non-power-law spectra:*

For typical inflation models, it is an approximation to take the spectra as power laws, albeit usually a good one. As data quality improves, one might expect this approximation to come under pressure, requiring a more accurate description of the initial spectra, particularly for the density perturbations. In general, one can write a Taylor expansion of $\ln \Delta^2_{\mathcal{R}}$ as

$$\ln \Delta^2_{\mathcal{R}}(k) = \ln \Delta^2_{\mathcal{R}}(k_*) + (n_* - 1) \ln \frac{k}{k_*} + \frac{1}{2} \left. \frac{dn}{d\ln k} \right|_* \ln^2 \frac{k}{k_*} + \cdots , \quad (21.9)$$

where the coefficients are all evaluated at some scale k_*. The term $dn/d\ln k|_*$ is often called the running of the spectral index [9], and has recently become topical due to a possible low-significance detection by WMAP. Once non-power-law spectra are allowed, it is necessary to specify the scale k_* at which quantities such as the spectral index are defined.

21.2.1.2. *Isocurvature perturbations:*

An isocurvature perturbation is one which leaves the total density unperturbed, while perturbing the relative amounts of different materials. If the Universe contains N fluids, there is one growing adiabatic mode and $N-1$ growing isocurvature modes. These can be excited, for example, in inflationary models where there are two or more fields which acquire dynamically important perturbations. If one field decays to form normal matter, while the second survives to become the dark matter, this will generate a cold dark matter isocurvature perturbation.

In general there are also correlations between the different modes, and so the full set of perturbations is described by a matrix giving the spectra and their correlations. Constraining such a general construct is challenging, though constraints on individual modes are beginning to become meaningful, with no evidence that any other than the adiabatic mode must be non-zero.

21.2.1.3. *Non-Gaussianity:*

Multi-field inflation models can also generate primordial non-Gaussianity. The extra fields can either be in the same sector of the underlying theory as the inflaton, or completely separate, an interesting example of the latter being the curvaton model [10]. Current upper limits on non-Gaussianity are becoming stringent, but there remains much scope to push down those limits and perhaps reveal trace non-Gaussianity in the data. If non-Gaussianity is observed, its nature may favor an inflationary origin, or a different one such as topological defects. A plausible possibility is non-Gaussianity caused by defects forming in a phase transition which ended inflation.

21.2.2. ***Dark matter properties*:**

Dark matter properties are discussed in the article by Drees and Gerbier in this volume. The simplest assumption concerning the dark matter is that it has no significant interactions with other matter, and that its particles have a negligible velocity. Such dark matter is described as 'cold,' and candidates include the lightest supersymmetric particle, the axion, and primordial black holes. As far as astrophysicists are concerned, a complete specification of the relevant cold dark matter properties is given by the density parameter $\Omega_{\rm cdm}$, though those seeking to directly detect it are as interested in its interaction properties.

Cold dark matter is the standard assumption and gives an excellent fit to observations, except possibly on the shortest scales where there remains some controversy concerning the structure of dwarf galaxies and possible substructure in galaxy halos. For all the dark matter to have a large velocity dispersion, so-called hot dark matter, has long been excluded as it does not permit galaxies to form; for thermal relics the mass must be above about 1 keV to satisfy this constraint, though relics produced non-thermally, such as the axion, need not obey this limit. However, there remains the possibility that further parameters might need to be introduced to describe dark matter properties relevant to astrophysical observations. Suggestions which have been made include a modest velocity dispersion (warm dark matter) and dark matter self-interactions. There remains the possibility that the dark matter comprises two separate components, *e.g.*, a cold one and a hot one, an example being if massive neutrinos have a non-negligible effect.

21.2.3. ***Dark energy*.**

While the standard cosmological model given above features a cosmological constant, in order to explain observations indicating that the Universe is presently accelerating, further possibilities exist under the general heading dark energy.† A particularly attractive possibility (usually called quintessence, though that word is used with various different meanings in the literature) is that a scalar field is responsible, with the mechanism mimicking that of early Universe inflation [11]. As described by Olive and Peacock, a fairly model-independent description of dark energy can be given just using the equation of state parameter w, with $w = -1$ corresponding to a cosmological constant.

† Unfortunately this is rather a misnomer, as it is the negative pressure of this material, rather than its energy, that is responsible for giving the acceleration.

In general, the function w could itself vary with redshift, though practical experiments devised so far would be sensitive primarily to some average value weighted over recent epochs. For high-precision predictions of microwave background anisotropies, it is better to use a scalar-field description in order to have a self-consistent evolution of the 'sound speed' associated with the dark energy perturbations.

Present observations are consistent with a cosmological constant, but it is quite common to see w kept as a free parameter to be added to the set described in the previous section. Most, but not all, researchers assume the weak energy condition $w \geq -1$. In the future it may be necessary to use a more sophisticated parametrization of the dark energy.

21.2.4. *Complex ionization history*:

The full ionization history of the Universe is given by specifying the ionization fraction as a function of redshift z. The simplest scenario takes the ionization to be zero from recombination up to some redshift $z_{\rm ion}$, at which point the Universe instantaneously re-ionizes completely. In that case, there is a one-to-one correspondence between τ and $z_{\rm ion}$ (that relation, however, also depending on other cosmological parameters).

While simple models of the re-ionization process suggest that rapid ionization is a good approximation, observational evidence is mixed, as it is difficult to reconcile the high optical depth inferred from the microwave background with absorption seen in some high-redshift quasar systems, and also perhaps with the temperature of the intergalactic medium at $z \simeq 3$. Accordingly, a more complex ionization history may need to be considered, and perhaps separate histories for hydrogen and helium, which will necessitate new parameters. Additionally, high-precision microwave anisotropy experiments may require consideration of the level of residual ionization left after recombination, which in principle is computable from the other cosmological parameters.

21.2.5. *Varying 'constants'*:

Variation of the fundamental constants of nature over cosmological times is another possible enhancement of the standard cosmology. There is a long history of study of variation of the gravitational constant G, and more recently attention has been drawn to the possibility of small fractional variations in the fine-structure constant. There is presently no observational evidence for the former, which is tightly constrained by a variety of measurements. Evidence for the latter has been claimed from studies of spectral line shifts in quasar spectra at redshifts of order two [12], but this is presently controversial and in need of further observational study.

21.2.6. *Cosmic topology*:

The usual hypothesis is that the Universe has the simplest topology consistent with its geometry, for example that a flat Universe extends forever. Observations cannot tell us whether that is true, but they can test the possibility of a non-trivial topology on scales up to roughly the present Hubble scale. Extra parameters would be needed to specify both the type and scale of the topology, for example, a cuboidal topology would need specification of the three principal axis lengths. At present, there is no direct evidence for cosmic topology, though the low values of the observed cosmic microwave quadrupole and octupole have been cited as a possible signature.

21.3. Probes

The goal of the observational cosmologist is to utilize astronomical objects to derive cosmological parameters. The transformation from the observables to the key parameters usually involves many assumptions about the nature of the objects, as well as about the nature of the dark matter. Below we outline the physical processes involved in each probe, and the main recent results. The first two subsections concern probes of the homogeneous Universe, while the remainder consider constraints from perturbations.

21.3.1. *Direct measures of the Hubble constant*:

In 1929 Edwin Hubble discovered the law of expansion of the Universe by measuring distances to nearby galaxies. The slope of the relation between the distance and recession velocity is defined to be the Hubble constant H_0. Astronomers argued for decades on the systematic uncertainties in various methods and derived values over the wide range, $40\,{\rm km\,s^{-1}\,Mpc^{-1}} \lesssim H_0 \lesssim 100\,{\rm km\,s^{-1}\,Mpc^{-1}}$.

One of the most reliable results on the Hubble constant comes from the Hubble Space Telescope Key Project [13]. The group has used the empirical period-luminosity relations for Cepheid variable stars to obtain distances to 31 galaxies, and calibrated a number of secondary distance indicators (Type Ia Supernovae, Tully-Fisher, surface brightness fluctuations and Type II Supernovae) measured over distances of 400 to 600 Mpc. They estimated $H_0 = 72 \pm 3\,({\rm statistical}) \pm 7\,({\rm systematic})\,{\rm km\,s^{-1}\,Mpc^{-1}}$.[‡] The major sources of uncertainty in this result are due to the metallicity of the Cepheids and the distance to the fiducial nearby galaxy (called the Large Magellanic Cloud) to which all Cepheid distances are measured relative to. Nevertheless, it is remarkable that this result is in such good agreement with the result derived from the WMAP CMB and large-scale structure measurements (see Table 21.2).

21.3.2. *Supernovae as cosmological probes*:

The relation between observed flux and the intrinsic luminosity of an object depends on the luminosity distance d_L, which in turn depends on cosmological parameters. More specifically

$$d_L = (1+z) r_e(z)\,, \tag{21.10}$$

where $r_e(z)$ is the coordinate distance. For example, in a flat Universe

$$r_e(z) = \int_0^z dz'/H(z')\,. \tag{21.11}$$

For a general dark energy equation of state $w(z) = p_Q(z)/\rho_Q(z)$, the Hubble parameter is, still considering only the flat case,

$$H^2(z)/H_0^2 = (1+z)^3\Omega_{\rm m} + \Omega_Q \exp[3X(z)]\,, \tag{21.12}$$

where

$$X(z) = \int_0^z [1+w(z')](1+z')^{-1} dz'\,, \tag{21.13}$$

and $\Omega_{\rm m}$ and Ω_Q are the present density parameters of matter and dark energy components. If a general equation of state is allowed, then one has to solve for $w(z)$ (parameterized, for example, as $w(z) = w = {\rm constant}$, or $w(z) = w_0 + w_1 z$) as well as for Ω_Q.

Empirically, the peak luminosity of supernova of Type Ia (SNe Ia) can be used as an efficient distance indicator (*e.g.*, Ref. 14). The favorite theoretical explanation for SNe Ia is the thermonuclear disruption of carbon-oxygen white dwarfs. Although not perfect 'standard candles', it has been demonstrated that by correcting for a relation between the light curve shape and the luminosity at maximum brightness, the dispersion of the measured luminosities can be greatly reduced. There are several possible systematic effects which may affect the accuracy of the SNe Ia as distance indicators, for example, evolution with redshift and interstellar extinction in the host galaxy and in the Milky Way, but there is no indication that any of these effects are significant for the cosmological constraints.

Two major studies, the 'Supernova Cosmology Project' and the 'High-z Supernova Search Team', found evidence for an accelerating Universe [15], interpreted as due to a cosmological constant, or to a more general 'dark energy' component. Recent results obtained by Tonry *et al.* [16] are shown in Fig. 21.1 (see also Ref. 17). The SNe Ia data alone can only constrain a combination of $\Omega_{\rm m}$ and Ω_Λ. When combined with the CMB data (which indicates flatness, *i.e.*, $\Omega_{\rm m} + \Omega_\Lambda \approx 1$), the best-fit values are $\Omega_{\rm m} \approx 0.3$ and $\Omega_\Lambda \approx 0.7$. Future experiments will aim to set constraints on the cosmic equation of state $w(z)$. However, given the integral relation between the luminosity distance and $w(z)$, it is not straightforward to recover $w(z)$ (*e.g.*, Ref. 18).

[‡] Unless stated otherwise, all quoted uncertainties in this article are one-sigma/68% confidence. It is common for cosmological parameters to have significantly non-Gaussian error distributions.

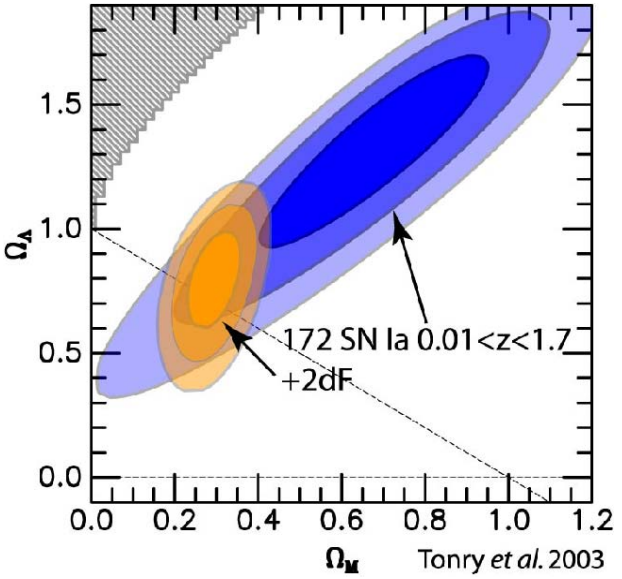

Figure 21.1: This shows the preferred region in the Ω_m–Ω_Λ plane from a study of 172 supernovae, and also how the constraints tighten when the 2dF galaxy redshift survey power spectrum is added as an additional constraint. [Reproduced with permission from Tonry *et al.* [16].] See full-color version on color pages at end of book.

21.3.3. *Cosmic microwave background*:

The physics of the cosmic microwave background (CMB) is described in detail by Scott and Smoot in this volume. Before recombination, the baryons and photons are tightly coupled, and the perturbations oscillate in the potential wells generated primarily by the dark matter perturbations. After decoupling, the baryons are free to collapse into those potential wells. The CMB carries a record of conditions at the time of decoupling, often called primary anisotropies. In addition, it is affected by various processes as it propagates towards us, including the effect of a time-varying gravitational potential (the integrated Sachs-Wolfe effect), gravitational lensing, and scattering from ionized gas at low redshift.

The primary anisotropies, the integrated Sachs-Wolfe effect, and scattering from a homogeneous distribution of ionized gas, can all be calculated using linear perturbation theory, a widely-used implementation being the CMBFAST code of Seljak and Zaldarriaga [5]. Gravitational lensing is also calculated in this code. Secondary effects such as inhomogeneities in the re-ionization process, and scattering from gravitationally-collapsed gas (the Sunyaev-Zel'dovich effect), require more complicated, and more uncertain, calculations.

The upshot is that the detailed pattern of anisotropies, quantified, for instance, by the angular power spectrum C_ℓ, depends on all of the cosmological parameters. In a typical cosmology, the anisotropy power spectrum [usually plotted as $\ell(\ell+1)C_\ell$] features a flat plateau at large angular scales (small ℓ), followed by a series of oscillatory features at higher angular scales, the first and most prominent being at around one degree ($\ell \simeq 200$). These features, known as acoustic peaks, represent the oscillations of the photon-baryon fluid around the time of decoupling. Some features can be closely related to specific parameters—for instance, the location of the first peak probes the spatial geometry, while the relative heights of the peaks probes the baryon density—but many other parameters combine to determine the overall shape.

The WMAP experiment [1] has provided the most accurate results to date on the spectrum of CMB fluctuations [19], with a precision determination of the temperature power spectrum up to $\ell \simeq 900$, shown in Fig. 21.2, and the first detailed measurement of the correlation spectrum between temperature and polarization [20] (the correlation having first been detected by DASI [21]). These are consistent with models based on the parameters we have described, and provide quite accurate determinations of many of them [7]. In this subsection, we will refer to results from WMAP alone, with the following section combining those with other observations. We note that as the parameter fitting is done in a multi-parameter space, one has to assume a 'prior' range for each of the parameters (*e.g.*, Hubble constant $0.5 < h < 1$), and there may be some dependence on these assumed priors.

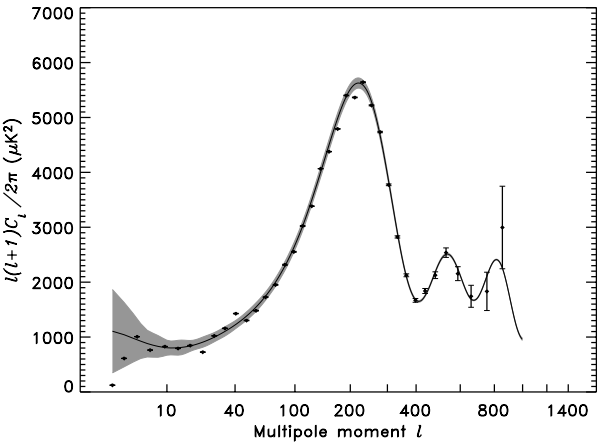

Figure 21.2: The angular power spectrum of the cosmic microwave background as measured by the WMAP satellite. The solid line shows the prediction from the best-fitting ΛCDM model [7]. The error bars on the data points (which are tiny for most of them) indicate the observational errors, while the shaded region indicates the statistical uncertainty from being able to observe only one microwave sky, known as cosmic variance, which is the dominant uncertainty on large angular scales. [Figure courtesy NASA/WMAP Science Team.]

WMAP provides an exquisite measurement of the location of the first acoustic peak, which directly probes the spatial geometry and yields a total density $\Omega_{\rm tot} \equiv \sum \Omega_i + \Omega_\Lambda$ of

$$\Omega_{\rm tot} = 1.02 \pm 0.02\,, \tag{21.14}$$

consistent with spatial flatness and completely excluding significantly curved Universes (this result does however assume a fairly strong prior on the Hubble parameter from other measurements; WMAP alone constrains it only weakly, and allows significantly closed Universes if h is small, e.g. $\Omega_{\rm tot} = 1.3$ for $h = 0.3$). It also gives a precision measurement of the age of the Universe. It gives a baryon density consistent with that coming from nucleosynthesis, and affirms the need for both dark matter and dark energy if the data are to be explained. For the spectral index of density perturbations, WMAP alone is consistent with a power-law spectrum, with spectral index $n = 0.99 \pm 0.04$, and in particular with a scale-invariant initial spectrum $n = 1$. It shows no evidence for dynamics of the dark energy, being consistent with a pure cosmological constant ($w = -1$).

One of the most interesting results, driven primarily by detection of large-angle polarization-temperature correlations, is the discovery of a high optical depth to re-ionization, $\tau \sim 0.17$, which roughly corresponds to a re-ionization redshift $z_{\rm ion} \sim 17$. This was higher than expected, though it appears it can be accommodated in models for development of the first structures which provide the ionizing flux.

In addition to WMAP, useful information comes from measurements of the CMB on small angular scales by, amongst others, the ACBAR and CBI experiments. Further, in 2002 the DASI experiment made the first measurement of the polarization anisotropies [21], again consistent with the standard cosmology, though not with sufficient accuracy to provide detailed constraints.

21.3.4. ***Galaxy clustering:***

The power spectrum of density perturbations depends on the nature of the dark matter. Within the Cold Dark Matter model, the shape of the power spectrum depends primarily on the primordial power spectrum and on the combination $\Omega_{\rm m}h$ which determines the horizon scale at matter-radiation equality, with a subdominant dependence on the baryon density. The matter distribution is most easily probed by observing the galaxy distribution, but this must be done with care as the galaxies do not perfectly trace the dark matter distribution. Rather, they are a 'biased' tracer of the dark matter. The need to allow for such bias is emphasized by the observation that different types of galaxies show bias with respect to each other. Further, the observed 3D galaxy distribution is in redshift space, *i.e.*, the observed redshift is the sum of the Hubble expansion and the line-of-sight peculiar velocity, leading to linear and non-linear dynamical effects which also depend on the cosmological parameters. On the largest length scales, the galaxies are expected to trace the location of the dark matter, except for a constant multiplier b to the power spectrum, known as the linear bias parameter. On scales smaller than 20 h^{-1} Mpc or so, the clustering pattern is 'squashed' in the radial direction due to coherent infall, which depends on the parameter $\beta \equiv \Omega_{\rm m}^{0.6}/b$ (on these shorter scales, more complicated forms of biasing are not excluded by the data). On scales of a few h^{-1} Mpc, there is an effect of elongation along the line of sight (colloquially known as the 'finger of God' effect) which depends on the galaxy velocity dispersion $\sigma_{\rm p}$.

21.3.4.1. *The galaxy power spectrum:*

The 2-degree Field (2dF) Galaxy Redshift Survey is now complete and publicly available, with nearly 230,000 redshifts.** Analyses of a subset of the full data (containing 160,000 redshifts) measured the power spectrum for $k > 0.02\,h\,{\rm Mpc}^{-1}$ with $\sim 10\%$ accuracy, shown in Fig. 21.3. The measured power spectrum is well fit by a CDM model with $\Omega_{\rm m}h = 0.18 \pm 0.02$, and a baryon fraction $\Omega_{\rm b}/\Omega_{\rm m} = 0.17 \pm 0.06$ [22]. The pattern of the galaxy clustering in redshift space is fitted by $\beta = 0.49 \pm 0.09$ and velocity dispersion $\sigma_{\rm p} = 506 \pm 52\,{\rm km\,s}^{-1}$ [23]; note that the two are strongly correlated. Combination of the 2dF data with the CMB indicates $b \sim 1$, in agreement with a 2dF-alone analysis of higher-order clustering statistics. Results for these parameters also depend on the length scale over which a fit is done, and the selection of the objects by luminosity, spectral type, or color. In particular, on scales smaller than 10 h^{-1}Mpc, different galaxy types are clustered differently. This 'biasing' introduces a systematic effect on the determination of cosmological parameters from redshift surveys. Prior knowledge from simulations of galaxy formation could help, but is model-dependent. We note that the present-epoch power spectrum is not sensitive to dark energy, so it is mainly a probe of the matter density.

The Sloan Digital Sky Survey (SDSS) is a project to image a quarter of the sky, and to obtain spectra of galaxies and quasars selected from the imaging data.†† A maximum likelihood analysis of early SDSS data by Szalay *et al.* [24] used the projected distribution of galaxies in a redshift bin around $z = 0.33$ to find $\Omega_{\rm m}h = 0.18 \pm 0.04$, assuming a flat ΛCDM model with $\Omega_{\rm m} = 1 - \Omega_\Lambda = 0.3$. The power spectrum of the latest version of SDSS redshift survey was published as this article was being finalized [25].

21.3.4.2. *Limits on neutrino mass from 2dFGRS:*

Large-scale structure data can put an upper limit on the ratio $\Omega_\nu/\Omega_{\rm m}$ due to the neutrino 'free streaming' effect [26]. By comparing the 2dF galaxy power spectrum with a four-component model (baryons, cold dark matter, a cosmological constant, and massive neutrinos), it was estimated that $\Omega_\nu/\Omega_{\rm m} < 0.13$ (95% confidence limit), giving $\Omega_\nu < 0.04$ if a concordance prior of $\Omega_{\rm m} = 0.3$ is imposed. The latter corresponds to an upper limit of about 2 eV on the total neutrino mass, assuming a prior of $h \approx 0.7$ [27]. The above analysis assumes that the primordial power spectrum is adiabatic, scale-invariant and Gaussian. Potential systematic effects include biasing of the galaxy distribution and non-linearities of the power spectrum. Additional cosmological data sets bring down this upper limit by a factor of two [28]. The analysis of WMAP+2dFGRS [7] derived $\Omega_\nu h^2 < 0.0067$ (95% CL).

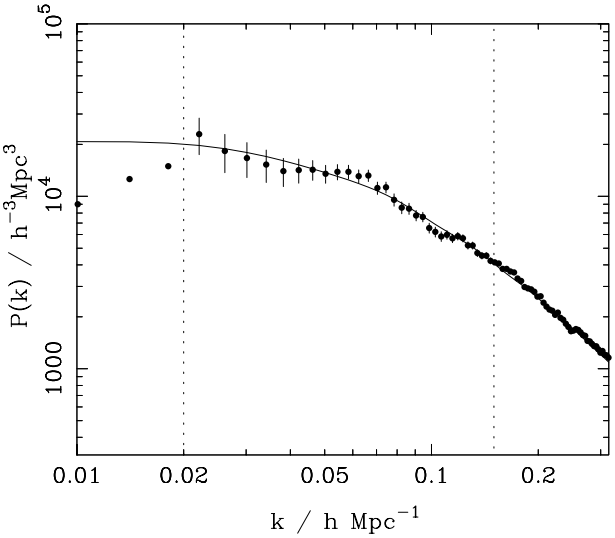

Figure 21.3: The galaxy power spectrum from the 2dF galaxy redshift survey as derived in Ref. 22. This plot shows $P(k) \propto \Delta^2(k)/k^3$, but with distances measured in redshift space and convolved with the survey geometry. The solid line shows a linear-theory ΛCDM fit (also convolved with the survey geometry) with $\Omega_{\rm m}h = 0.2$, $\Omega_{\rm b}/\Omega_{\rm m} = 0.15$, $h = 0.7$ and $n = 1$. Only the range $0.02\,h\,{\rm Mpc}^{-1} < k < 0.15\,h\,{\rm Mpc}^{-1}$, where perturbations are in the linear regime, was used to obtain that best fit. The error bars are correlated, but with known covariances. [Figure provided by Will Percival; see also Ref. 22.]

Laboratory limits on absolute neutrino masses from tritium beta decay and especially from neutrinoless double-beta decay should, within the next decade, push down towards (or perhaps even beyond) the 0.1 eV level that has cosmological significance.

21.3.5. ***Clusters of galaxies:***

A cluster of galaxies is a large collection of galaxies held together by their mutual gravitational attraction. The largest ones are around 10^{15} solar masses, and are the largest gravitationally-bound structures in the Universe. Even at the present epoch they are relatively rare, with only a few percent of galaxies being in clusters. They provide various ways to study the cosmological parameters; here we discuss constraints from the measurements of the cluster number density and the baryon fraction in clusters.

21.3.5.1. *Cluster number density:* The first objects of a given kind form at the rare high peaks of the density distribution, and if the primordial density perturbations are Gaussian-distributed, their number density is exponentially sensitive to the size of the perturbations, and hence can strongly constrain it. Clusters are an ideal application in the present Universe. They are usually used to constrain the amplitude σ_8, as a box of side $8\,h^{-1}\,{\rm Mpc}$ contains about the right amount of material to form a cluster. The most useful observations at present are of X-ray emission from hot gas lying within the cluster, whose temperature is typically a few keV, and which can be used to estimate the mass of the cluster. A theoretical prediction for the mass function of clusters can come either from semi-analytic arguments or from numerical simulations. At present, the main uncertainty is the relation between the observed gas temperature and the cluster mass, despite extensive study using simulations. A recent analysis [29] gives

$$\sigma_8 = 0.78^{+0.30}_{-0.06} \qquad (95\%{\rm CL}) \tag{21.15}$$

for $\Omega_{\rm m} = 0.35$, with highly non-Gaussian error bars, but different authors still find a spread of values. Scaling to lower $\Omega_{\rm m}$ increases σ_8

** See `http://www.mso.anu.edu.au/2dFGRS`

†† See `http://www.sdss.org`

somewhat, and the result above is consistent with values predicted in cosmologies compatible with WMAP.

The same approach can be adopted at high redshift (which for clusters means redshifts approaching one) to attempt to measure σ_8 at an earlier epoch. The evolution of σ_8 is primarily driven by the value of the matter density $\Omega_{\rm m}$, with a sub-dominant dependence on the dark energy density. It is generally recognized that such analyses favor a low matter density, though there is not complete consensus on this, and at present this technique for constraining the density is not competitive with the CMB.

21.3.5.2. *Cluster baryon fraction:* If clusters are representative of the mass distribution in the Universe, the fraction of the mass in baryons to the overall mass distribution would be $f_{\rm b} = \Omega_{\rm b}/\Omega_{\rm m}$. If $\Omega_{\rm b}$, the baryon density parameter, can be inferred from the primordial nucleosynthesis abundance of the light elements, the cluster baryon fraction $f_{\rm b}$ can then be used to constrain $\Omega_{\rm m}$ and h (*e.g.*, Ref. 30). The baryons in clusters are primarily in the form of X-ray-emitting gas that falls into the cluster, and secondarily in the form of stellar baryonic mass. Hence, the baryon fraction in clusters is estimated to be

$$f_{\rm b} = \frac{\Omega_{\rm b}}{\Omega_{\rm m}} \simeq f_{\rm gas} + f_{\rm gal}\,, \qquad (21.16)$$

where $f_{\rm b} = M_{\rm b}/M_{\rm grav}$, $f_{\rm gas} = M_{\rm gas}/M_{\rm grav}$, $f_{\rm gal} = M_{\rm gal}/M_{\rm grav}$, and $M_{\rm grav}$ is the total gravitating mass.

This can be used to obtain an approximate relation between $\Omega_{\rm m}$ and h:

$$\Omega_{\rm m} = \frac{\Omega_{\rm b}}{f_{\rm gas} + f_{\rm gal}} \simeq \frac{\Omega_{\rm b}}{0.08h^{-1.5} + 0.01h^{-1}}\,. \qquad (21.17)$$

Big Bang Nucleosynthesis gives $\Omega_{\rm b}h^2 \approx 0.02$, allowing the above relation to be approximated as $\Omega_{\rm m}h^{0.5} \approx 0.25$ (*e.g.*, Ref. 31). For example, Allen *et al.* [32] derived a density parameter consistent with $\Omega_{\rm m} = 0.3$ from Chandra observations.

21.3.6. ***Clustering in the inter-galactic medium*:**

It is commonly assumed, based on hydrodynamic simulations, that the neutral hydrogen in the inter-galactic medium (IGM) can be related to the underlying mass distribution. It is then possible to estimate the matter power spectrum on scales of a few megaparsecs from the absorption observed in quasar spectra, the so-called Lyman-alpha forest. The usual procedure is to measure the power spectrum of the transmitted flux, and then to infer the mass power spectrum. Photo-ionization heating by the ultraviolet background radiation and adiabatic cooling by the expansion of the Universe combine to give a simple power-law relation between the gas temperature and the baryon density. It also follows that there is a power-law relation between the optical depth τ and $\rho_{\rm b}$. Therefore, the observed flux $F = \exp(-\tau)$ is strongly correlated with $\rho_{\rm b}$, which itself traces the mass density. The matter and flux power-spectra can be related by

$$P_{\rm m}(k) = b^2(k)\; P_F(k)\,, \qquad (21.18)$$

where $b(k)$ is a bias function which is calibrated from simulations. Croft *et al.* [33] derived cosmological parameters from Keck Telescope observations of the Lyman-alpha forest at redshifts $z = 2 - 4$. Their derived power spectrum corresponds to that of a CDM model, which is in good agreement with the 2dF galaxy power spectrum. A recent study using VLT spectra [34] agrees with the flux power spectrum of Ref. 33.

This method depends on various assumptions. Seljak *et al.* [35] pointed out that errors are sensitive to the range of cosmological parameters explored in the simulations, and the treatment of the mean transmitted flux. Combination of the Lyman-alpha data with WMAP suggested deviation from the scale-invariant $n = 1$ power spectrum [7,6], but Seljak *et al.* [35] have argued that the combined data set is still compatible with $n = 1$ model.

21.3.7. ***Gravitational lensing*:**

Images of background galaxies get distorted due to the gravitational effect of mass fluctuations along the line of sight. Deep gravitational potential wells such as galaxy clusters generate 'strong lensing', *i.e.*, arcs and arclets, while more moderate fluctuations give rise to 'weak lensing'. Weak lensing is now widely used to measure the mass power spectrum in random regions of the sky (see Ref. 36 for recent reviews). As the signal is weak, the CCD frame of deformed galaxy shapes ('shear map') is analyzed statistically to measure the power spectrum, higher moments, and cosmological parameters.

The shear measurements are mainly sensitive to the combination of $\Omega_{\rm m}$ and the amplitude σ_8. There are various systematic effects in the interpretation of weak lensing, *e.g.*, due to atmospheric distortions during observations, the redshift distribution of the background galaxies, intrinsic correlation of galaxy shapes, and non-linear modeling uncertainties. Hoekstra *et al.* [37] derived the result $\sigma_8\Omega_{\rm m}^{0.52} = 0.46^{+0.05}_{-0.07}$ (95% confidence level), assuming a ΛCDM model. Other recent results are summarized in Ref. 36. For a $\Omega_{\rm m} = 0.3, \Omega_\Lambda = 0.7$ cosmology, different groups derived normalizations σ_8 over a wide range, indicating that the systematic errors are still larger than some of the quoted error bars.

21.3.8. ***Peculiar velocities*:**

Deviations from the Hubble flow directly probe the mass fluctuations in the Universe, and hence provide a powerful probe of the dark matter. Peculiar velocities are deduced from the difference between the redshift and the distance of a galaxy. The observational difficulty is in accurately measuring distances to galaxies. Even the best distance indicators (*e.g.*, the Tully-Fisher relation) give an error of 15% per galaxy, hence limiting the application of the method at large distances. Peculiar velocities are mainly sensitive to $\Omega_{\rm m}$, not to Ω_Λ or quintessence. Extensive analyses in the early 1990s (*e.g.*, Ref. 38) suggested a value of $\Omega_{\rm m}$ close to unity. A more recent analysis [39], which takes into account non-linear corrections, gives $\sigma_8\Omega_{\rm m}^{0.6} = 0.49 \pm 0.06$ and $\sigma_8\Omega_{\rm m}^{0.6} = 0.63 \pm 0.08$ (90% errors) for two independent data sets. While at present cosmological parameters derived from peculiar velocities are strongly affected by random and systematic errors, a new generation of surveys may improve their accuracy. Two promising approaches are the 6dF near-infrared survey of 15,000 peculiar velocities[‡‡] and the kinematic Sunyaev-Zel'dovich effect.

21.4. Bringing observations together

Although it contains two ingredients—dark matter and dark energy—which have not yet been verified by laboratory experiments, the ΛCDM model is almost universally accepted by cosmologists as the best description of present data. The basic ingredients are given by the parameters listed in Sec. 21.1.4, with approximate values of some of the key parameters being $\Omega_{\rm b} \approx 0.04$, $\Omega_{\rm dm} \approx 0.26$, $\Omega_\Lambda \approx 0.70$, and a Hubble constant $h \approx 0.7$. The spatial geometry is very close to flat (and often assumed to be precisely flat), and the initial perturbations Gaussian, adiabatic, and nearly scale-invariant.

The most powerful single experiment is WMAP, which on its own supports all these main tenets. Values for some parameters, as given in Spergel *et al.* [7], are reproduced in Table 21.2. This model presumes a flat Universe, and so Ω_Λ is a derived quantity in this analysis, with best-fit value $\Omega_\Lambda = 0.73$.

However, to obtain the most powerful constraints, other data sets need to be considered in addition to WMAP. A standard data compilation unites WMAP with shorter-scale CMB measurements from CBI and ACBAR, and the galaxy power spectrum from the 2dF survey. In our opinion, this combination of datasets offers the most reliable set of constraints at present. In addition, it is possible to add the Lyman-alpha forest power spectrum data, but this has proven more controversial as the interpretation of such data has not reached a secure level.

Using the extended data set without the Lyman-alpha constraints produces no surprises; as compared to WMAP alone, the best-fit values move around a little within the uncertainties, and the error bars

[‡‡] See `http://www.mso.anu.edu.au/6dFGS/`

Table 21.2: Parameter constraints reproduced from Spergel *et al.* [7], both from WMAP alone and from the preferred data compilation of WMAP+CBI+ACBAR (known as WMAPext) plus 2dFGRS. The first two columns assume a power-law initial spectrum, while the third allows a running of the spectral index (in this case n is defined at a particular scale, and its value cannot be directly compared with the power-law case). Spatial flatness is assumed in the parameter fit. The parameter A is a measure of the perturbation amplitude; see Ref. 7 for details. Uncertainties are shown at one sigma, and caution is needed in extrapolating them to higher significance levels due to non-Gaussian likelihoods and assumed priors.

	WMAP alone power-law	WMAPext + 2dFGRS power-law	WMAPext + 2dFGRS running
$\Omega_{\rm m}h^2$	0.14 ± 0.02	0.134 ± 0.006	0.136 ± 0.009
$\Omega_{\rm b}h^2$	0.024 ± 0.001	0.023 ± 0.001	0.022 ± 0.001
h	0.72 ± 0.05	0.73 ± 0.03	0.71 ± 0.04
n	0.99 ± 0.04	0.97 ± 0.03	$0.93^{+0.04}_{-0.05}$
τ	$0.17^{+0.08}_{-0.07}$	0.15 ± 0.07	0.17 ± 0.06
A	0.9 ± 0.1	0.8 ± 0.1	0.84 ± 0.09
$dn/d\ln k$	-	-	$-0.031^{+0.023}_{-0.025}$

improve somewhat, as seen in Table 21.2. In this table we also show the effect of allowing the spectral index to vary with scale ('running'): the running is found to be consistent with zero and there are small drifts in the values and uncertainties of the other parameters.¶

However, inclusion of the Lyman-alpha data suggests a more radical development, with the running weakly detected at around 95% confidence, the spectral index making a transition from $n > 1$ on large scales to $n < 1$ on small scales [7,6]. The significance of this measurement is not high, and the result rather unexpected on theoretical grounds (it suggests that the power spectrum has a maximum which just happens to lie in the rather narrow range of scales that observations are able to probe, and the running is much larger than in typical inflation models giving a spectral index close to one). In our view it is premature to read much significance into this observation, though if true, it should rapidly be firmed up by new data.

The baryon density Ω_b is now measured with quite high accuracy from the CMB and large-scale structure, and shows reasonable agreement with the determination from big bang nucleosynthesis; Fields and Sarkar in this volume quote the range $0.009 \geq \Omega_{\rm b}h^2 \geq 0.023$. Given the sensitivity of the measurement, it is important to note that it has significant dependence on both the datasets and parameter sets chosen, as seen in Table 21.2.

While Ω_Λ is measured to be non-zero with very high confidence, there is no evidence of evolution of the dark energy density. The WMAP team find the limit $w < -0.78$ at 95% confidence from a compilation of data including SNe Ia data, where they impose a prior $w \geq -1$, with the cosmological constant case $w = -1$ giving an excellent fit to the data.

As far as inflation is concerned, the data provide good news and bad news. The good news is that WMAP supports all the main predictions of the simplest inflation models: spatial flatness and adiabatic, Gaussian, nearly scale-invariant density perturbations. But it is disappointing that there is no sign of primordial gravitational waves, with WMAP providing only a weak upper limit $r < 0.53$ at 95% confidence [6] (this assumes no running, and weakens significantly if running is allowed), and especially that no convincing deviations from scale-invariance have been seen. It is perfectly possible for inflation models to give $n \simeq 1$ and $r \simeq 0$, but in that limit, the observations give no clues as to the dynamical processes driving inflation. Tests have been made for various types of non-Gaussianity, a particular example being a parameter $f_{\rm NL}$ which measures a quadratic contribution to the perturbations and is constrained to $-58 < f_{\rm NL} < 134$ at 95% confidence [41] (this looks weak, but prominent non-Gaussianity requires the product $f_{\rm NL}\Delta_{\mathcal{R}}$ to be large, and $\Delta_{\mathcal{R}}$ is of order 10^{-5}).

¶ As we were finalizing this article, an analysis of WMAP combined with the SDSS galaxy power spectrum appeared [40], giving results in good agreement with those discussed here.

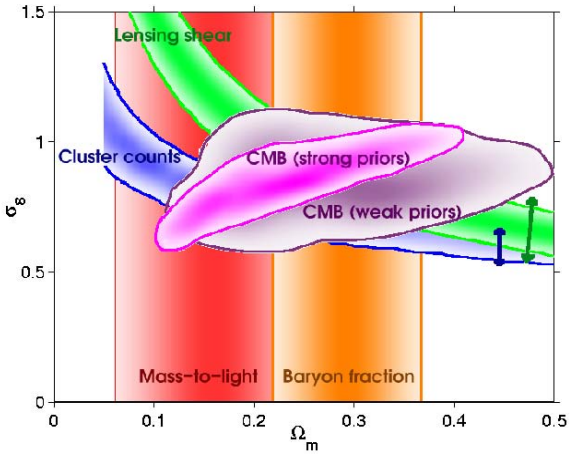

Figure 21.4: Various constraints shown in the $\Omega_{\rm m}$–σ_8 plane. [Figure provided by Sarah Bridle; see also Ref. 42.] See full-color version on color pages at end of book.

Two parameters which are still uncertain are $\Omega_{\rm m}$ and σ_8 (see Figure 21.4 and Ref. 42). The value of $\Omega_{\rm m}$ is beginning to be pinned down with some precision, with most observations indicating a value around 0.3, including the CMB anisotropies, the cluster number density, and gravitational lensing, though the latter two have a strong degeneracy with the amplitude of mass fluctuations σ_8. However, not all observations yet agree fully on this, for instance mass-to-light ratio measurements give $\Omega_{\rm m} \approx 0.15$ [43], and the fractional uncertainty remains significantly higher than one would like. Concerning σ_8, results from the cluster number density have varied quite a lot in recent years, spanning the range 0.6 to 1.0, primarily due to the uncertainties in the mass-temperature-luminosity relations used to connect the observables with theory. There is certainly scope for improving this calibration by comparison to mass measurements from strong gravitational lensing. The WMAP-alone measurements gives $\sigma_8 = 0.9 \pm 0.1$. However, this is not a direct constraint; WMAP only probes larger length scales, and the constraint comes from using WMAP to estimate all the parameters of the model needed to determine σ_8. As such, their constraint depends strongly on the assumed set of cosmological parameters being sufficient.

One parameter which is surprisingly robust is the age of the Universe. There is a useful coincidence that for a flat Universe the position of the first peak is strongly correlated with the age of the Universe. The WMAP-only result is 13.4 ± 0.3 Gyr (assuming a flat Universe). This is in good agreement with the ages of the oldest globular clusters [44] and radioactive dating [45].

21.5. Outlook for the future

The concordance model is now well established, and there seems little room left for any dramatic revision of this paradigm. A measure of the strength of that statement is how difficult it has proven to formulate convincing alternatives. For example, one corner of parameter space that has been explored is the possibility of abandoning the dark energy, and instead considering a mixed dark matter model with $\Omega_{\rm m} = 1$ and $\Omega_\nu = 0.2$. Such a model fits both the 2dF and WMAP data reasonably well, but only for a Hubble constant $h < 0.5$ [27,46]. However, this model is inconsistent with the HST key project value of h, the results from SNe Ia, cluster number density evolution, and baryon fraction in clusters.

Should there indeed be no major revision of the current paradigm, we can expect future developments to take one of two directions.

Either the existing parameter set will continue to prove sufficient to explain the data, with the parameters subject to ever-tightening constraints, or it will become necessary to deploy new parameters. The latter outcome would be very much the more interesting, offering a route towards understanding new physical processes relevant to the cosmological evolution. There are many possibilities on offer for striking discoveries, for example:

- The cosmological effects of a neutrino mass may be unambiguously detected, shedding light on fundamental neutrino properties;
- Detection of deviations from scale-invariance in the initial perturbations would indicate dynamical processes during perturbation generation, for instance, by inflation;
- Detection of primordial non-Gaussianities would indicate that non-linear processes influence the perturbation generation mechanism;
- Detection of variation in the dark energy density (*i.e.*, $w \neq -1$) would provide much-needed experimental input into the question of the properties of the dark energy.

These provide more than enough motivation for continued efforts to test the cosmological model and improve its precision.

Over the coming years, there are a wide range of new observations, which will bring further precision to cosmological studies. Indeed, there are far too many for us to be able to mention them all here, and so we will just highlight a few areas.

The cosmic microwave background observations will improve in several directions. The new frontier is the study of polarization, first detected in 2002. Data are imminent from balloon-based experiments including Maxipol and Boomerang, and with WMAP continuing to take data, they should be able to measure a polarization spectrum, as well as improve measures of the temperature-polarization cross-correlation (which is easier to measure as the temperature anisotropies are much larger). Dedicated ground-based polarization experiments, such as CBI and QUEST, promise powerful measures of the polarization spectrum in the next few years, and may be able to separately detect the two modes of polarization. Another area of development is pushing accurate power spectrum measurements to smaller angular scales, typically achieved by interferometry, which should allow measurements of secondary anisotropy effects, such as the Sunyaev-Zel'dovich effect, whose detection has already been tentatively claimed by CBI. Finally, we mention the Planck satellite, due to launch in 2007, which will make high-precision all-sky maps of temperature and polarization, utilizing a very wide frequency range for observations to improve understanding of foreground contaminants, and to compile a large sample of clusters via the Sunyaev-Zel'dovich effect.

Concerning galaxy clustering, the Sloan Digital Sky Survey is well underway, and currently expected to yield around 600,000 galaxy redshifts covering one quarter of the sky. Large samples of galaxy positions at high redshifts ($z \sim 1$) will begin to be obtained, for instance, by the DEEP2 survey using the Keck telescopes, and the VIRMOS survey on the VLT. The 6dF survey aims to take high-quality redshift and peculiar velocity data for a large sample of nearby galaxies, and has already taken around 40,000 of the planned 170,000 redshifts.

Still awaiting final approval is the SNAP satellite, which seeks to carry out a survey for Type Ia supernovae out to redshifts approaching two, which should in particular be a powerful probe of the dark energy. With large samples, it may be possible to detect evolution of the dark energy density, thus measuring its equation of state. SNAP is also able to carry out a large weak gravitational lensing survey, complementing those becoming possible with large-format CCDs on ground-based telescopes. Before SNAP, the ESSENCE project will significantly increase the size of the SNe Ia dataset.

The development of the first precision cosmological model is a major achievement. However, it is important not to lose sight of the motivation for developing such a model, which is to understand the underlying physical processes at work governing the Universe's evolution. On that side, progress has been much less dramatic. For instance, there are many proposals for the nature of the dark matter, but no consensus as to which is correct. The nature of the dark energy remains a mystery. Even the baryon density, now measured to an accuracy of a few percent, lacks an underlying theory able to predict it even within orders of magnitude. Precision cosmology may have arrived, but at present many key questions remain unanswered.

Acknowledgments:

ARL was supported in part by the Leverhulme Trust. We thank Sarah Bridle and Jochen Weller for useful comments on this article, and OL thanks members of the Cambridge Leverhulme Quantitative Cosmology and 2dFGRS Teams for helpful discussions.

References:

1. C.L. Bennett *et al.*, Astrophys. J. Supp. **148**, 1 (2003).
2. S. Fukuda *et al.*, Phys. Rev. Lett. **85**, 3999 (2000);
   Q. R. Ahmad *et al.*, Phys. Rev. Lett. **87**, 071301 (2001).
3. A.D. Dolgov *et al.*, Nucl. Phys. **B632**, 363 (2002).
4. For detailed accounts of inflation see E.W. Kolb and M.S. Turner, *The Early Universe*, Addison–Wesley (Redwood City, 1990);
   A.R. Liddle and D.H. Lyth, *Cosmological Inflation and Large-Scale Structure*, (Cambridge University Press, 2000).
5. U. Seljak and M. Zaldarriaga, Astrophys. J. **469**, 1 (1996).
6. H.V. Peiris *et al.*, Astrophys. J. Supp. **148**, 213 (2003).
7. D.N. Spergel *et al.*, Astrophys. J. Supp. **148**, 175 (2003).
8. J.C. Mather *et al.*, Astrophys. J. **512**, 511 (1999).
9. A. Kosowsky and M.S. Turner, Phys. Rev. **D52**, 1739 (1995).
10. D.H. Lyth and D. Wands, Phys. Lett. **B524**, 5 (2002);
    K. Enqvist and M.S. Sloth, Nucl. Phys. **B626**, 395 (2002);
    T. Moroi and T. Takahashi, Phys. Lett. **B522**, 215 (2001).
11. B. Ratra and P.J.E. Peebles, Phys. Rev. **D37**, 3406 (1988);
    C. Wetterich, Nucl. Phys. **B302**, 668 (1988);
    T. Padmanabhan, Phys. Rept. **380**, 235 (2003).
12. J.K. Webb *et al.*, Phys. Rev. Lett. **82**, 884 (1999);
    J.K. Webb *et al.*, Phys. Rev. Lett. **87**, 091301 (2001);
    J.K. Webb, M. Murphy, V. Flambaum, and S.J. Curran, Astrophys. Sp. Sci. **283**, 565 (2003).
13. W.L. Freedman *et al.*, Astrophys. J. **553**, 47 (2001).
14. A. Filippenko, `astro-ph/0307139`.
15. A.G. Riess *et al.*, Astron. J. **116**, 1009 (1998);
    P. Garnavich *et al.*, Astrophys. J. **509**, 74 (1998);
    S. Perlmutter *et al.*, Astrophys. J. **517**, 565 (1999).
16. J.L. Tonry *et al.*, Astrophys. J. **594**, 1 (2003).
17. R.A. Knop *et al.*, `astro-ph/0309368`.
18. I. Maor *et al.*, Phys. Rev. **D65**, 123003 (2002).
19. G. Hinshaw *et al.*, Astrophys. J. Supp. **148**, 135 (2003).
20. A. Kogut *et al.*, Astrophys. J. Supp. **148**, 161 (2003).
21. J. Kovac *et al.*, Nature **420**, 772 (2002).
22. W.J. Percival *et al.*, Mon. Not. Roy. Astr. Soc. **337**, 1068 (2002).
23. E. Hawkins *et al.*, in press, Mon. Not. Roy. Astr. Soc.
24. A.S. Szalay *et al.*, Astrophys. J. **591**, 1 (2003).
25. M. Tegmark *et al.*, `astro-ph/0310725`.
26. W. Hu, D. Eisenstein, and M. Tegmark, Phys. Rev. Lett. **80**, 5255 (1998).
27. O. Elgaroy and O. Lahav, JCAP **0304**, 004 (2003).
28. S. Hannestad, JCAP, **0305**, 004 (2003).
29. P.T.P. Viana *et al.*, Mon. Not. Roy. Astr. Soc., **346**, 319 (2003).
30. S.D.M. White *et al.*, Nature **366**, 429 (1993).
31. P. Erdogdu, S. Ettori, and O. Lahav, Mon. Not. Roy. Astr. Soc. **340**, 573 (2003).
32. S.W. Allen *et al.*, Mon. Not. Roy. Astr. Soc. **342**, 287 (2003).
33. R.A.C. Croft *et al.*, Astrophys. J. **581**, 20 (2002).
34. S. Kim *et al.*, `astro-ph/0308103`.

35. U. Seljak, P. McDonald, and A. Makarov, Mon. Not. Roy. Astr. Soc. **342**, L79 (2003).
36. P. Schneider, `astro-ph/0306465`;
A. Refregier, in press, Ann. Rev. Astron. Astrophys, `astro-ph/0307212`.
37. H. Hoekstra, H.K.C. Yee, and M. Gladders, Astrophys. J. **577**, 595 (2002).
38. A. Dekel, Ann. Rev. Astron. Astrophys. **32**, 371 (1994).
39. L. Silberman *et al.*, Astrophys. J. **557**, 102 (2001).
40. M. Tegmark *et al.*, `astro-ph/0310723`.
41. E. Komatsu *et al.*, Astrophys. J. Supp. **148**, 119 (2003).
42. S.L. Bridle *et al.*, Science **299**, 1532 (2003).
43. N. Bahcall *et al.*, Astrophys. J. **541**, 1 (2000).
44. B. Chaboyer and L.M. Krauss, Science **299**, 65 (2003).
45. R. Cayrel *et al.*, Nature **409**, 691 (2001).
46. A. Blanchard *et al.*, `astro-ph/0304237`.

22. DARK MATTER

Written September 2003 by M. Drees (Technical University, Munich) and G. Gerbier (Saclay, CEA).

22.1. Theory

22.1.1. *Evidence for Dark Matter*:

The existence of Dark (*i.e.*, non-luminous and non-absorbing) Matter (DM) is by now well established. The earliest [1], and perhaps still most convincing, evidence for DM came from the observation that various luminous objects (stars, gas clouds, globular clusters, or entire galaxies) move faster than one would expect if they only felt the gravitational attraction of other visible objects. An important example is the measurement of galactic rotation curves. The rotational velocity v of an object on a stable Keplerian orbit with radius r around a galaxy scales like $v(r) \propto \sqrt{M(r)/r}$, where $M(r)$ is the mass inside the orbit. If r lies outside the visible part of the galaxy and mass tracks light, one would expect $v(r) \propto 1/\sqrt{r}$. Instead, in most galaxies one finds that v becomes approximately constant out to the largest values of r where the rotation curve can be measured; in our own galaxy, $v \simeq 220$ km/s at the location of our solar system, with little change out to the largest observable radius. This implies the existence of a *dark halo*, with mass density $\rho(r) \propto 1/r^2$, *i.e.*, $M(r) \propto r$; at some point ρ will have to fall off faster (in order to keep the total mass of the galaxy finite), but we do not know at what radius this will happen. This leads to a lower bound on the DM mass density, $\Omega_{\rm DM} \gtrsim 0.1$, where $\Omega_X \equiv \rho_X/\rho_{\rm crit}$, $\rho_{\rm crit}$ being the critical mass density (*i.e.*, $\Omega_{\rm tot} = 1$ corresponds to a flat Universe).

The observation of clusters of galaxies tends to give somewhat larger values, $\Omega_{\rm DM} \simeq 0.2$ to 0.3. These observations include measurements of the peculiar velocities of galaxies in the cluster, which are a measure of their potential energy if the cluster is virialized; measurements of the *X-ray* temperature of hot gas in the cluster, which again correlates with the gravitational potential felt by the gas; and—most directly—studies of (weak) gravitational lensing of background galaxies on the cluster.

The currently most accurate, if somewhat indirect, determination of $\Omega_{\rm DM}$ comes from global fits of cosmological parameters to a variety of observations; see the Section on Cosmological Parameters for details. For example, using measurements of the anisotropy of the cosmic microwave background (CMB) and of the spatial distribution of galaxies, Ref. 2 finds a density of cold, non–baryonic matter

$$\Omega_{\rm nbm} h^2 = 0.111 \pm 0.006 \ , \tag{22.1}$$

where h is the Hubble constant in units of 100 km/(s·Mpc). Some part of the baryonic matter density [2],

$$\Omega_{\rm b} h^2 = 0.023 \pm 0.001 \ , \tag{22.2}$$

may well contribute to (baryonic) DM, *e.g.*, MACHOs [3] or cold molecular gas clouds [4].

The DM density in the "neighborhood" of our solar system is also of considerable interest. This was first estimated as early as 1922 by J.H. Jeans, who analyzed the motion of nearby stars transverse to the galactic plane [1]. He concluded that in our galactic neighborhood the average density of DM must be roughly equal to that of luminous matter (stars, gas, dust). Remarkably enough, the most recent estimates, based on a detailed model of our galaxy, find quite similar results [5]:

$$\rho_{\rm DM}^{\rm local} \simeq 0.3 \frac{\rm GeV}{\rm cm^3} \ ; \tag{22.3}$$

this value is known to within a factor of two or so.

22.1.2. *Candidates for Dark Matter*:

Analyses of structure formation in the Universe [6] indicate that most DM should be "cold", *i.e.*, should have been non-relativistic at the onset of galaxy formation (when there was a galactic mass inside the causal horizon). This agrees well with the upper bound [2] on the contribution of light neutrinos to Eq. (22.1),

$$\Omega_\nu h^2 \leq 0.0076 \quad 95\%\ {\rm CL} \tag{22.4}$$

Candidates for non-baryonic DM in Eq. (22.1) must satisfy several conditions: they must be stable on cosmological time scales (otherwise they would have decayed by now), they must interact very weakly with electromagnetic radiation (otherwise they wouldn't qualify as *dark* matter), and they must have the right relic density. Candidates include primordial black holes, axions, and weakly interacting massive particles (WIMPs).

Primordial black holes must have formed before the era of Big-Bang nucleosynthesis, since otherwise they would have been counted in Eq. (22.2) rather than Eq. (22.1). Such an early creation of a large number of black holes is possible only in certain somewhat contrived cosmological models [7].

The existence of axions [8] was first postulated to solve the strong *CP* problem of QCD; they also occur naturally in superstring theories. They are pseudo Nambu-Goldstone bosons associated with the (mostly) spontaneous breaking of a new global "Peccei-Quinn" (PQ) U(1) symmetry at scale f_a; see the Section on Axions in this *Review* for further details. Although very light, axions would constitute cold DM, since they were produced non-thermally. At temperatures well above the QCD phase transition, the axion is massless, and the axion field can take any value, parameterized by the "misalignment angle" θ_i. At $T \lesssim 1$ GeV the axion develops a mass m_a due to instanton effects. Unless the axion field happens to find itself at the minimum of its potential ($\theta_i = 0$), it will begin to oscillate once m_a becomes comparable to the Hubble parameter H. These coherent oscillations transform the energy originally stored in the axion field into physical axion quanta. The contribution of this mechanism to the present axion relic density is [8]

$$\Omega_a h^2 = \kappa_a \left(f_a/10^{12}\ {\rm GeV} \right)^{1.175} \theta_i^2 \ , \tag{22.5}$$

where the numerical factor κ_a lies roughly between 0.5 and a few. If $\theta_i \sim \mathcal{O}(1)$, Eq. (22.5) will saturate Eq. (22.1) for $f_a \sim 10^{11}$ GeV, comfortably above laboratory and astrophysical constraints [8]; this would correspond to an axion mass around 0.1 meV. However, if the post-inflationary reheat temperature $T_R > f_a$, cosmic strings will form during the PQ phase transition at $T \simeq f_a$. Their decay will give an additional contribution to Ω_a, which is often bigger than that in Eq. (22.5) [9], leading to a smaller preferred value of f_a, *i.e.*, larger m_a. On the other hand, values of f_a near the Planck scale become possible if θ_i is for some reason very small.

Weakly interacting massive particles (WIMPs) χ are particles with mass roughly between 10 GeV and a few TeV, and with cross sections of approximately weak strength. Their present relic density can be calculated reliably if the WIMPs were in thermal and chemical equilibrium with the hot "soup" of Standard Model (SM) particles after inflation. In this case their density would become exponentially (Boltzmann) suppressed at $T < m_\chi$. The WIMPs therefore drop out of thermal equilibrium ("freeze out") once the rate of reactions that change SM particles into WIMPs or vice versa, which is proportional to the product of the WIMP number density and the WIMP pair annihilation cross section into SM particles σ_A times velocity, becomes smaller than the Hubble expansion rate of the Universe. After freeze out, the co-moving WIMP density remains essentially constant. Their present relic density is then approximately given by (ignoring logarithmic corrections) [10]

$$\Omega_\chi h^2 \simeq const. \cdot \frac{T_0^3}{M_{\rm Pl}^3 \langle \sigma_A v \rangle} \simeq \frac{0.1\ {\rm pb} \cdot c}{\langle \sigma_A v \rangle} \ . \tag{22.6}$$

Here T_0 is the current CMB temperature, $M_{\rm Pl}$ is the Planck mass, c is the speed of light, σ_A is the total annihilation cross section of a pair of WIMPs into SM particles, v is the relative velocity between the two WIMPs in their cms system, and $\langle \ldots \rangle$ denotes thermal averaging. Freeze out happens at temperature $T_F \simeq m_\chi/20$ almost independently of the properties of the WIMP. This means that WIMPs are already non-relativistic when they decouple from the thermal plasma; it also implies that Eq. (22.6) is applicable if $T_R \gtrsim m_\chi/10$. Notice that the 0.1 pb in Eq. (22.6) contains factors of T_0 and $M_{\rm Pl}$; it is therefore quite intriguing that it "happens" to come out near the typical size of weak interaction cross sections.

The seemingly most obvious WIMP candidate is a heavy neutrino. However, an SU(2) doublet neutrino will have too small a relic density if its mass exceeds $M_Z/2$, as required by LEP data. One can suppress the annihilation cross section, and hence increase the relic density, by postulating mixing between a heavy SU(2) doublet and some "sterile" SU(2) $\times$ U(1)$_Y$ singlet neutrino. However, one also has to require the neutrino to be stable; it is not obvious why a massive neutrino should not be allowed to decay.

The currently best motivated WIMP candidate is therefore the lightest superparticle (LSP) in supersymmetric models [11] with exact R-parity (which guarantees the stability of the LSP). Searches for exotic isotopes [12] imply that a stable LSP has to be neutral. This leaves basically two candidates among the superpartners of ordinary particles, a sneutrino, and a neutralino. Sneutrinos again have quite large annihilation cross sections; their masses would have to exceed several hundred GeV for them to make good DM candidates. This is uncomfortably heavy for the lightest sparticle, in view of naturalness arguments. Moreover, the negative outcome of various WIMP searches (see below) rules out "ordinary" sneutrinos as primary component of the DM halo of our galaxy. (In models with gauge-mediated SUSY breaking the lightest "messenger sneutrino" could make a good WIMP [13].) The most widely studied WIMP is therefore the lightest neutralino. Detailed calculations [14] show that the lightest neutralino will have the desired thermal relic density Eq. (22.1) in at least four distinct regions of parameter space. χ could be (mostly) a bino or photino (the superpartner of the U(1)$_Y$ gauge boson and photon, respectively), if both χ and some sleptons have mass below $\sim$ 150 GeV, or if m_χ is close to the mass of some sfermion (so that its relic density is reduced through co-annihilation with this sfermion), or if $2m_\chi$ is close to the mass of the CP-odd Higgs boson present in supersymmetric models [15]. Finally, Eq. (22.1) can also be satisfied if χ has a large higgsino component.

Although WIMPs are attractive DM candidates because their thermal relic density naturally has at least the right order of magnitude, non-thermal production mechanisms have also been suggested, *e.g.*, LSP production from the decay of some moduli fields [16], from the decay of the inflaton [17], or from the decay of "Q–balls" (non-topological solitons) formed in the wake of Affleck-Dine baryogenesis [18]. Although LSPs from these sources are typically highly relativistic when produced, they quickly achieve kinetic (but not chemical) equilibrium if T_R exceeds a few MeV [19](but stays below $m_\chi/20$). They therefore also contribute to cold DM.

Primary black holes (as MACHOs), axions, and WIMPs are all (in principle) detectable with present or near-future technology (see below). There are also particle physics DM candidates which currently seem almost impossible to detect. These include the gravitino (the spin-3/2 superpartner of the graviton) [20], states from the "hidden sector" thought responsible for supersymmetry breaking [13], and the axino (the spin-1/2 superpartner of the axion) [21].

22.2. Experimental detection of Dark Matter

22.2.1. *The case of baryonic matter in our galaxy*:

The search for hidden galactic baryonic matter in the form of MAssive Compact Halo Objects (MACHOs) has been initiated following the suggestion that they may represent a large part of the galactic DM and could be detected through the microlensing effect [3]. The MACHO, EROS, and OGLE collaborations have performed a program of observation of such objects by monitoring the luminosity of millions of stars in the Large and Small Magellanic Clouds for several years. EROS concluded that MACHOs cannot contribute more than 20% to the mass of the galactic halo [22], while MACHO observed a signal at 0.4 solar mass and put an upper limit of 40%. Overall, this strengthens the need for non-baryonic DM, also supported by the arguments developed above.

22.2.2. *Axion searches*:

Axions can be detected by looking for $a \to \gamma$ conversion in a strong magnetic field [23]. Such a conversion proceeds through the loop-induced $a\gamma\gamma$ coupling, whose strength $g_{a\gamma\gamma}$ is an important parameter of axion models. Currently two experiments searching for axionic DM are taking data. They both employ high quality cavities. The cavity "Q factor" enhances the conversion rate on resonance, *i.e.*, for $m_a c^2 = \hbar\omega_{\rm res}$. One then needs to scan the resonance frequency in order to cover a significant range in m_a or, equivalently, f_a. The bigger of the two experiments, situated at the LLNL in California [24], started taking data in the first half of 1996. It uses very sophisticated "conventional" electronic amplifiers with very low noise temperature to enhance the conversion signal. Their first published results [25] exclude axions with mass between 2.9 and 3.3 μeV, corresponding to $f_a \simeq 4 \cdot 10^{13}$ GeV, as a major component of the dark halo of our galaxy, if $g_{a\gamma\gamma}$ is near the upper end of the theoretically expected range.

The smaller "CARRACK" experiment now under way in Kyoto, Japan [26] uses Rydberg atoms (atoms excited to a very high state, $n \simeq 230$) to detect the microwave photons that would result from axion conversion. This allows almost noise-free detection of single photons. Preliminary results of the CARRACK I experiment [27] exclude axions with mass in a narrow range around 10 μeV as major component of the galactic dark halo for some plausible range of $g_{a\gamma\gamma}$ values. This experiment is being upgraded to CARRACK II, which intends to probe the range between 2 and 50 μeV with sensitivity to all plausible axion models, if axions form most of DM [27].

22.2.3. *Basics of direct WIMP search*:

As stated above, WIMPs should be gravitationally trapped inside galaxies and should have the adequate density profile to account for the observed rotational curves. These two constraints determine the main features of experimental detection of WIMPs, which have been detailed in the reviews [28].

Their mean velocity inside our galaxy is expected to be similar to that of stars around the center of the galaxy, *i.e.*, a few hundred kilometers per second at the location of our solar system. For these velocities, WIMPs interact with ordinary matter through elastic scattering on nuclei. With expected WIMP masses in the range 10 GeV to 10 TeV, typical nuclear recoil energies are of order of 1 to 100 keV.

The shape of the nuclear recoil spectrum results from a convolution of the WIMP velocity distribution, usually taken as a shifted Maxwellian distribution, with the angular scattering distribution, which is isotropic to first approximation but forward-peaked for high nuclear mass (typically higher than Ge mass) due to the nuclear form factor. Overall, this results in a roughly exponential spectrum. The higher the WIMP mass, the higher the mean value of the exponential. This points to the need for low nuclear energy threshold detectors.

On the other hand, expected interaction rates depend on the product of the WIMP local flux and the interaction cross section. The first term is fixed by the local density of dark matter, taken as 0.3 GeV/cm^3 (see above), the mean WIMP velocity, typically 220 km/s, and the mass of the WIMP. The expected interaction rate then mainly depends on two unknowns, the mass and cross section of WIMP (with some uncertainty [5] due to the halo model). This is why the experimental observable, which is basically the scattering rate as a function of energy, is usually expressed as a contour in the WIMP mass—cross section plane.

The cross section depends on the nature of the couplings. For non-relativistic WIMPs one in general has to distinguish spin–independent and spin–dependent couplings. The former can involve scalar and vector WIMP and nucleon currents (vector currents are absent for Majorana WIMPs, e.g. the neutralino), while the latter involve axial vector currents (and obviously only exist if χ carries

spin). Due to coherence effects the spin–independent cross section scales approximately as the square of the mass of the nucleus, so higher mass nuclei, from Ge to Xe, are preferred for this search. For spin-dependent coupling, the cross section depends on the nuclear spin factor; the useful target nuclei are ^{19}F and ^{127}I.

Cross sections calculated in MSSM models induce rates of at most 1 evt day^{-1} kg^{-1} of detector, much lower than the usual radioactive backgrounds. This indicates the need for underground laboratories to protect against cosmic ray induced backgrounds, and for the selection of extremely radiopure materials.

The typical shape of exclusion contours can be anticipated from this discussion: at low WIMP mass, the sensitivity drops because of the detector energy threshold, whereas at high masses, the sensitivity also decreases because, for a fixed mass density, the WIMP flux decreases $\propto 1/m_\chi$. The sensitivity is best for WIMP masses near the mass of the recoiling nucleus.

22.2.4. *Status and prospects of direct WIMP searches*:

The first searches have been performed with ultra-pure semiconductors installed in pure lead and copper shields in underground environments [29]. Combining a priori excellent energy resolutions and very pure detector material, they produced the first limits on WIMP searches and until recently had the best performance (Heidelberg-Moscow, IGEX, COSME-II, HDMS) [29]. Without positive identification of nuclear recoil events, however, these experiments could only set limits, *e.g.*, excluding sneutrinos as major component of the galactic halo. Still, planned experiments using several tens of kgs to a ton of Germanium (many of which were designed for double-beta decay search)—GENIUS TF, GEDEON, MAJORANA—are based on only passive reduction of the external and internal electromagnetic, and neutron background by using segmented detectors, minimal detector housing, close electronics, and large liquid nitrogen shields.

To make further progress, active background rejection and signal identification questions have to be addressed. This has been the focus of many recent investigations and improvements. Active background rejection in detectors relies on the relatively small ionization in nuclear recoils due to their low velocity. This induces a reduction—quenching—of the ionization/scintillation signal for nuclear recoil signal events relative to e or γ induced backgrounds. Energies calibrated with gamma sources are then called "electron equivalent energies" (eee). This effects has been calculated and measured [29]. It is exploited in cryogenic detectors described later. In scintillation detectors, it induces in addition a difference in decay times of pulses induced by e/γ events vs nuclear recoils. Due to the limited resolution and discrimination power of this technique at low energies, this effect allows only a statistical background rejection. It has been used in NaI(Tl) (DAMA, NAIAD, Saclay NaI), in CsI(Tl)(KIMS), Xe (ZEPLIN) [29]. No observation of nuclear recoils has been reported by these experiments.

There are two experimental signatures of WIMP detection that would prove its astrophysical origin. One is the measurement of the strong daily forward/backward asymmetry of the nuclear recoil direction, due to the alternate sweeping of the WIMP cloud by the rotating Earth. Detection of this effect requires gaseous detectors or anisotropic response scintillators (stilbene). The second is the few percent annual modulation of the recoil rate due to the Earth speed adding to or subtracting from the speed of the Sun. This tiny effect can only be detected with large masses; nuclear recoil identification should also be performed, as the much larger background may also be subject to modulation.

The DAMA experiment operating 100 kg of NaI(Tl) in Gran Sasso has observed, with a statistical significance of 6.3 σ, an annually modulated signal with the expected phase, over a period of 7 years with a total exposure of around 100 000 kg·d , in the 2 to 6 keV (eee) energy interval [30]. This effect is attributed to a WIMP signal by the authors. If interpreted within the standard halo model described above, it would require a WIMP with $m_\chi \simeq 50$ GeV and $\sigma_{\chi p} \simeq 7 \cdot 10^{-6}$ pb (central values). This interpretation has however several unaddressed implications. In particular, the expected nuclear recoil rate from WIMPs should be of the order of 50% of the total measured rate in the 2–3 keV (eee) bin and 7% in the 4–6 keV (eee) bin. The rather large WIMP signal should be detectable by the pulse shape analysis. Moreover, the remaining, presumably e/γ induced, background would have to rise with energy; no explanation for this is given by the authors.

Annual modulation has also been searched for by NaI-32 (Zaragoza), DEMOS (Ge), ELEGANTS (NaI) [29]. No signal has been seen in these experiments, but their sensitivity is too low to contradict DAMA. The best current limit for a WIMP mass above 30 GeV has been produced in 2002 by Ge cryogenics detectors operated by EDELWEISS at 20 mK in the deep underground Fréjus lab [31]. They superseded the earlier CDMS results obtained at the much shallower Stanford site, with its large cosmic ray induced fast neutron flux [32]. The simultaneous measurement of the phonon signal and the ionization signal in such semiconductor detectors permits event by event discrimination between nuclear and electronic recoils down to 5 to 10 keV recoil energy. Assuming conventional WIMP halo parameters described above, EDELWEISS and CDMS exclude the DAMA signal at 99.8% CL. Varying the halo parameters, and/or including spin–dependent interactions compatible with the neutrino flux limit from the Sun, does not allow reconciliation of both results without finetuning [33]. The obtained sensitivity of $\sigma_{\chi p} \simeq 10^{-6}$ pb for the first time tests cross sections that can be accommodated in the MSSM [34].

Other cryogenic experiments like CRESST and ROSEBUD [35] use the scintillation of $CaWO_4$ as second variable for background discrimination, while CUORECINO will use TeO_2 in the purely thermal mode. In the coming years the cryogenic experimental programs of CDMS II, EDELWEISS II, CRESST II, CUORICINO, and ROSEBUD [35] intend to increase their sensitivity by a factor 100, by operating from few to 40 kg of detectors.

Liquid or two-phase Xenon detectors are rapidly coming on line. ZEPLIN has been operating 6 kg in the Boulby laboratory for about 1 year and announced a sensitivity close to that of EDELWEISS. With only 1.5 photoelectron/keV (eee), and a three-fold coincidence, searching for the WIMP signal in the 2–10 keV (eee) region is quite challenging. Neutron discrimination calibrations and trigger efficiency measurements will strengthen the reliability of this potentially powerful technique. With masses of 7 to 30 kg, ZEPLIN II and III aim at sensitivities down to 10^{-8} pb, while XMASS in Japan will soon operate 100 kg (ultimately 800 kg) at the SuperKamiokande site, using self-shielding and pulse shape analysis to lower the background [29]. XENON in US has approximately the same program.

On the other hand, the extended version of DAMA, LIBRA, starts operating 250 kg of NaI(Tl) in Gran Sasso, ANAIS will operate 107 kg of NaI(Tl) in Canfranc laboratory, KIMS, 80 kg of CsI(Tl)in Yang Yang lab in Korea, and ELEGANTS VI the large shield of 750 kg of NaI(Tl) [29].

There is also growing work in the development of low pressure Time Projection Chamber, the only convincing technique to measure the direction of nuclear recoils [36]. DRIFT, a 1m^3 volume detector is currently taking data. The small active mass of 200 g precludes competitive results. The sub-keV energy threshold gaseous detector MICROMEGAS is being investigated for WIMP search [36]. Other exotic techniques include the superheated droplet detectors SIMPLE, PICASSO, ORPHEUS, and ultra cold pure ^{3}He detector MacHe3 [29].

Sensitivities down to $\sigma_{\chi p}$ of 10^{-10} pb, as needed to probe large regions of MSSM parameter space [34], can be reached with detectors of typical masses of 1 ton [35], assuming nearly perfect background discrimination capabilities. Note that the expected WIMP rate is then 5 evts/ton/year for Ge. The ultimate neutron background will only be identified by its multiple interactions in a finely segmented or multiple interaction sensitive detector, and/or by operating detectors containing different target materials within the same set–up. Information on various neutron backgrounds calculations and measurements can be found in [37]. With intermediate mass of 10 to 30 kg and less efficient multiple interaction detection, a muon veto seems mandatory.

22.2.5. ***Status and prospects of indirect WIMP searches***:

WIMPs can annihilate and their annihilation products can be detected; these include neutrinos, gamma rays, positrons, antiprotons, and antinuclei [38]. These methods are complementary to direct detection and can explore higher masses and different coupling scenarios. "Smoking gun" signals for indirect detection are neutrinos coming from the center of the Sun or Earth, and monoenergetic photons from the halo.

WIMPs can be slowed down, captured, and trapped in celestial objects like the Earth or the Sun, thus enhancing their density and their probability of annihilation. This is a source of muon neutrinos which can interact in the Earth. Upward going muons can then be detected in large neutrino telescopes such as MACRO, BAKSAN, SuperKamiokande, Baikal, AMANDA, ANTARES, NESTOR, and the future large sensitive area IceCube [38]. The best upper limits, of $\simeq$ 3000 muons/km2/year, have been set by MACRO and BAKSAN [39]. However, at least in the framework of the MSSM, only the limits from the Sun are competitive with direct WIMP search limits. ANTARES (IceCube) will increase this sensitivity respectively by $\simeq$ one (two) order(s) of magnitude.

WIMP annihilation in the halo can give a continuous spectrum of gamma rays and (at one-loop level) also monoenergetic photon contributions from the $\gamma\gamma$ and γZ channels. The size of this signal depends very strongly on the halo model, but is expected to be most prominent towards the galactic center. Existing limits come from the EGRET satellite below 10 GeV, and from the WHIPPLE ground based telescope above 100 GeV [40]. However, only the planned space mission GLAST will be able to provide competitive SUSY sensitivities in both the continuous and γ line channels. Also, Atmospheric Cherenkov Telescopes like MAGIC, VERITAS, and HESS should be able to test some SUSY models, at large WIMP mass, for halo models showing a significant WIMP enhancement at the galactic center [38].

Diffuse continuum gammas could also give a signature due to their isotropic halo origin. The excess of GeV gamma-rays observed by EGRET [40] and attributed to a possible WIMP signal could however be due to classical sources.

The antiproton signal arises as another WIMP annihilation product in the halo. The signal is expected to be detectable above background only at very low energies. The BESS balloon-borne experiment indeed observed antiprotons below 1 GeV [41]. However, the uncertainties in the calculation of the expected signal and background energy spectra are too large to reach a firm conclusion. Precision measurements by the future experiments BESS, AMS2, and PAMELA may allow to disentangle signal and background [38].

A cosmic-ray positron flux excess at around 8 GeV measured by HEAT [42] has given rise to numerous calculations and conjectures concerning a possible SUSY interpretation. The need for an ad-hoc "boost" of expected flux to match the observed one and the failure to reproduce the energy shape by including a component from WIMP annihilation are illustrative of the difficulty to assign a Dark Matter origin to such measurements.

Last but not least, an antideuteron signal [43], as potentially observable by AMS2 or PAMELA, could constitute a signal for WIMP annihilation in the halo.

An interesting comparison of respective sensitivities to MSSM parameter space of future direct and various indirect searches has been performed with the DARKSUSY tool [44]. Searching for neutrinos from the Sun tests the spin-dependent WIMP couplings to matter, whereas direct searches are mostly sensitive to spin-independent couplings. Moreover, γ line searches are sensitive to higgsino-like neutralinos, whereas direct detection methods are more sensitive to gaugino-like neutralinos. However, it should be kept in mind that signals for WIMP annihilation in the halo strongly depend on various details of the halo model.

Numerous new experiments are in line to bring accurate measurements to constrain or discover Dark Matter.

References:

1. For a brief but delightful history of DM, see V. Trimble, in Proceedings of the *First International Symposium on Sources of Dark Matter in the Universe*, Bel Air, California, 1994; published by World Scientific, Singapore (ed. D.B. Cline).
2. See *Global cosmological parameters* in this *Review*.
3. B. Paczynski, Astrophys. J. **304**, 1 (1986);
   K. Griest, Astrophys. J. **366**, 412 (1991).
4. F. De Paolis *et al.*, Phys. Rev. Lett. **74**, 14 (1995).
5. M. Kamionkowski and A. Kinkhabwala, Phys. Rev. **D57**, 3256 (1998).
6. See *e.g.*, J.R. Primack, in the Proceedings of *Midrasha Mathematicae in Jerusalem: Winter School in Dynamical Systems*, Jerusalem, Israel, January 1997, `astro-ph/9707285` . There is currently some debate whether cold DM models correctly reproduce the DM density profile near the center of galactic haloes. See *e.g.*, R.A. Swaters *et al.*, Astrophys. J. **583**, 732 (2003).
7. B.J. Carr and S.W. Hawking, MNRAS **168**, 399 (1974).
8. See *Axions and other Very Light Bosons* in this *Review*.
9. R.A. Battye and E.P.S. Shellard, Phys. Rev. Lett. **73**, 2954 (1994);
   Erratum-ibid. **76**, 2203 (1996).
10. E.W. Kolb and M.E. Turner, *The Early Universe*, Addison-Wesley (1990).
11. For a review, see G. Jungman, M. Kamionkowski, and K. Griest, Phys. Reports **267**, 195 (1996).
12. See *Searches for WIMPs and other Particles* in this *Review*.
13. S. Dimopoulos, G.F. Giudice, and A. Pomarol, Phys. Lett. **B389**, 37 (1996).
14. See *e.g.*, J.R. Ellis *et al.*, Nucl. Phys. **B652**, 259 (2003);
    J.R. Ellis *et al.*, Phys. Lett. **B565**, 176 (2003);
    H. Baer *et al.*, JHEP **0306**, 054 (2003);
    A. Bottino *et al.*, `hep-ph/0304080` .
15. G. Griest and D. Seckel, Phys. Rev. **D43**, 3191 (1991).
16. T. Moroi and L. Randall, Nucl. Phys. **B570**, 455 (2000).
17. R. Allahverdi and M. Drees, Phys. Rev. Lett. **89**, 091302 (2002).
18. M. Fujii and T. Yanagida, Phys. Lett. **B542**, 80 (2002).
19. J. Hisano, K. Kohri, and M.M. Nojiri, Phys. Lett. **B505**, 169 (2001);
    X. Chen, M. Kamionkowski, and X. Zhang, Phys. Rev. **D64**, 021302 (2001).
20. M. Bolz, W. Buchmüller, and M. Plümacher, Phys. Lett. **B443**, 209 (1998).
21. L. Covi *et al.*, JHEP **0105**, 033 (2001).
22. MACHO Collab., C. Alcock *et al.*, Astrophys. J. **542**, 257 (2000);
    EROS Collab., AA 355, 39 (2000);
    OGLE Collab., AA 343, 10 (1999).
23. P. Sikivie, Phys. Rev. Lett. **51**, 1415 (1983), Erratum-ibid. **52**, 695 (1984).
24. H. Peng *et al.*, Nucl. Instrum. Methods **A444**, 569 (2000).
25. S. Asztalos *et al.*, Phys. Rev. **D64**, 092003 (2001).
26. M. Tada *et al.*, `physics/0101028` .
27. K. Yamamoto *et al.*, in *Heidelberg 2000, Dark matter in astro—and particle—physics*, `hep-ph/0101200` .
28. P.F. Smith and J.D. Lewin, Phys. Reports **187**, 203 (1990);
    J.R. Primack, D. Seckel, and B. Sadoulet, Ann. Rev. Nucl. Part. Sci. **38** 751 (1988).

29. For recent reviews on non cryogenic detectors, see *e.g.*, A. Morales in *Proceedings of IFMP2002*, Jaca (Spain) astro-ph/0211446;
Proceedings of Topics in Astroparticles and Underground Physics TAUP 2001, Nucl. Phys B (Proc. Suppl.) vol. 11 (2002);
TAUP 2003 Conference site:
http://int.phys.washington.edu/taup2003;
Proceedings of *Identification of Dark Matter*. IDM 2000, World Scientific, ed. N. Spooner and V. Kudryavtsev, (York, UK, 2000);
IDM 2002 Conference site:
http://www.shef.ac.uk/ phys/idm2002.html.
30. DAMA Collab., R. Bernabei *et al.*, Phys. Lett. **B480**, 23 (2000), and Riv. Nuovo Cimento **26**, 1 (2003).
31. EDELWEISS Collab., A. Benoit *et al.*, Phys. Lett. **B545**, 43 (2002).
32. CDMS Collab., D. Abrams *et al.*, Phys. Rev. **D66**, 122003 (2002);
CDMS Collab., D.S. Akerib *et al.*, Phys. Rev. **D68**, 082002 (2003).
33. C.J. Copi and L.M. Krauss, Phys. Rev. **67**, 103507 (2003);
A. Kurylov and M. Kamionkowski, hep-ph/0307185.
34. For a general introduction to SUSY, see the section devoted in this *Review of Particle Physics*. For a recent review on cross sections for direct detection, see J. Ellis *et al.*, Phys. Rev. **D67**, 123502 (2003).
35. For a recent review on cryogenic detectors, see *e.g.*, L. Mosca in Proceedings of IFMP2002. In addition to the TAUP and IDM Conference Proceedings, see also the Proceedings of *Int. Workshop on Low Temperature Detectors*, LTD9, AIP Conference Proceedings, Volume 605(2001).
36. Workshop on large TPC for low energy rare event detection, Paris, December 2002, http://www.unine.ch/phys/tpc.html.
37. These sites gather informations on neutrons from various underground labs:
http://www.physics.ucla.edu/wimps/nBG/nBG.html;
www.e15.physik.tu-muenchen.de/Tecnomusiq/Tecnomusiq.html.
38. L. Bergstrom, Rept. on Prog. in Phys. **63**, 793 (2000);
L. Bergstrom *et al.*, Phys. Rev. **D59**, 043506 (1999);
C. Tao, Phys. Scripta **T93**, 82 (2001).
39. MACRO Collab., M. Ambrosio *et al.*, Phys. Rev. **D60**, 082002 (1999);
BAKSAN Collab., M. M. Boliev *et al.*, Nucl. Phys. (Proc. Supp.) **B48**, 83 (1996).
40. EGRET Collab., D. Dixon *et al.*, New Astron. **3**, 539 (1998).
41. BESS Collab., S. Orito *et al.*, Phys. Rev. Lett. **84**, 1078 (2000).
42. HEAT Collab., S. W. Barwick *et al.*, Astrophys. J. **482**, L191 (2000).
43. F. Donato, N. Fornengo and P. Salati, Phys. Rev. **D62**, 043003 (2000).
44. DARKSUSY site: http://www.physto.se/ edsjo/darksusy/.

23. COSMIC MICROWAVE BACKGROUND

Revised September 2003 by D. Scott (University of British Columbia) and G.F. Smoot (UCB/LBNL).

23.1. Introduction

The energy content in radiation from beyond our Galaxy is dominated by the Cosmic Microwave Background (CMB), discovered in 1965 [1]. The spectrum of the CMB is well described by a blackbody function with $T = 2.725\,\mathrm{K}$. This spectral form is one of the main pillars of the hot Big Bang model for the early Universe. The lack of any observed deviations from a blackbody spectrum constrains physical processes over the history of the universe at redshifts $z \lesssim 10^7$ (see previous versions of this mini-review). However, at the moment, all viable cosmological models predict a very nearly Planckian spectrum, and so are not stringently limited.

Another observable quantity inherent in the CMB is the variation in temperature (or intensity) from one part of the microwave sky to another [2]. Since the first detection of these anisotropies by the *COBE* satellite [3], there has been intense activity to map the sky at increasing levels of sensitivity and angular resolution. A series of ground- and balloon-based measurements has recently been joined by the first results from NASA's Wilkinson Microwave Anisotropy Probe (*WMAP*) [4]. These observations have led to a stunning confirmation of the 'Standard Model of Cosmology.' In combination with other astrophysical data, the CMB anisotropy measurements place quite precise constraints on a number of cosmological parameters, and have launched us into an era of precision cosmology.

23.2. Description of CMB Anisotropies

Observations show that the CMB contains anisotropies at the 10^{-5} level, over a wide range of angular scales. These anisotropies are usually expressed by using a spherical harmonic expansion of the CMB sky:

$$T(\theta,\phi) = \sum_{\ell m} a_{\ell m}\, Y_{\ell m}(\theta,\phi).$$

The vast majority of the cosmological information is contained in the temperature 2 point function, *i.e.*, the variance as a function of separation θ. Equivalently, the power per unit $\ln\ell$ is $\ell\sum_m |a_{\ell m}|^2/4\pi$.

23.2.1. *The Monopole*:

The CMB has a mean temperature of $T_\gamma = 2.725 \pm 0.001\,\mathrm{K}\ (1\sigma)$ [5], which can be considered as the monopole component of CMB maps, a_{00}. Since all mapping experiments involve difference measurements, they are insensitive to this average level. Monopole measurements can only be made with absolute temperature devices, such as the FIRAS instrument on the *COBE* satellite [5]. Such measurements of the spectrum are consistent with a blackbody distribution over more than three decades in frequency. A blackbody of the measured temperature corresponds to $n_\gamma = (2\zeta(3)/\pi^2)\,T_\gamma^3 \simeq 411\,\mathrm{cm}^{-3}$ and $\rho_\gamma = (\pi^2/15)\,T_\gamma^4 \simeq 4.64\times10^{-34}\,\mathrm{g\,cm}^{-3} \simeq 0.260\,\mathrm{eV\,cm}^{-3}$.

23.2.2. *The Dipole*:

The largest anisotropy is in the $\ell = 1$ (dipole) first spherical harmonic, with amplitude $3.346 \pm 0.017\,\mathrm{mK}$ [4]. The dipole is interpreted to be the result of the Doppler shift caused by the solar system motion relative to the nearly isotropic blackbody field, as confirmed by measurements of the velocity field of local galaxies [6]. The motion of an observer with velocity $\beta = v/c$ relative to an isotropic Planckian radiation field of temperature T_0 produces a Doppler-shifted temperature pattern

$$\begin{aligned} T(\theta) &= T_0(1-\beta^2)^{1/2}/(1-\beta\cos\theta) \\ &\approx T_0\,\left(1+\beta\cos\theta+(\beta^2/2)\cos2\theta+O(\beta^3)\right). \end{aligned}$$

At every point in the sky one observes a blackbody spectrum, with temperature $T(\theta)$. The spectrum of the dipole is the differential of a blackbody spectrum, as confirmed by Ref. 7.

The implied velocity [8,4] for the solar system barycenter is $v = 368 \pm 2\,\mathrm{km\,s}^{-1}$, assuming a value $T_0 = T_\gamma$, towards $(\ell, b) = (263.85^\circ \pm 0.10^\circ, 48.25^\circ \pm 0.04^\circ)$. Such a solar system velocity implies a velocity for the Galaxy and the Local Group of galaxies relative to the CMB. The derived value is $v_{\rm LG} = 627 \pm 22\,\mathrm{km\,s}^{-1}$ toward $(\ell, b) = (276^\circ \pm 3^\circ, 30^\circ \pm 3^\circ)$, where most of the error comes from uncertainty in the velocity of the solar system relative to the Local Group.

The dipole is a frame dependent quantity, and one can thus determine the 'absolute rest frame' of the Universe as that in which the CMB dipole would be zero. Our velocity relative to the Local Group, as well as the velocity of the Earth around the Sun, and any velocity of the receiver relative to the Earth, is normally removed for the purposes of CMB anisotropy study.

23.2.3. *Higher-Order Multipoles*:

Excess variance in CMB maps at higher multipoles ($\ell \geq 2$) is interpreted as being the result of perturbations in the energy density of the early Universe, manifesting themselves at the epoch of the last scattering of the CMB photons. In the hot Big Bang picture, this happens at a redshift $z \simeq 1100$, with little dependence on the details of the model. The process by which the hydrogen and helium nuclei can hold onto their electrons is usually referred to as recombination [9]. Before this epoch, the CMB photons are tightly coupled to the baryons, while afterwards they can freely stream towards us.

Theoretical models generally predict that the $a_{\ell m}$ modes are Gaussian random fields, and all tests are consistent with this simplifying assumption [10]. With this assumption, and if there is no preferred axis, then it is the variance of the temperature field which carries the cosmological information, rather than the values of the individual $a_{\ell m}$s; in other words the power spectrum in ℓ fully characterizes the anisotropies. The power at each ℓ is $(2\ell+1)C_\ell/(4\pi)$, where $C_\ell \equiv \langle|a_{\ell m}|^2\rangle$, and a statistically isotropic sky means that all ms are equivalent. We use our estimators of the C_ℓs to constrain their expectation values, which are the quantities predicted by a theoretical model. For an idealized full-sky observation, the variance of each measured C_ℓ (the variance of the variance) is $[2/(2\ell+1)]C_\ell^2$. This sampling uncertainty (known as cosmic variance) comes about because each C_ℓ is χ^2 distributed with $(2\ell+1)$ degrees of freedom for our observable volume of the Universe. For partial sky coverage, $f_{\rm sky}$, this variance is increased by $1/f_{\rm sky}$ and the modes become partially correlated.

It is important to understand that theories predict the expectation value of the power spectrum, whereas our sky is a single realization. Hence the 'cosmic variance' is an unavoidable source of uncertainty when constraining models; it dominates the scatter at lower ℓs, while the effects of instrumental noise and resolution dominate at higher ℓs.

23.2.4. *Angular Resolution and Binning*:

There is no one-to-one conversion between the angle subtended by a particular wavevector projected on the sky and multipole ℓ. However, a single spherical harmonic $Y_{\ell m}$ corresponds to angular variations of $\theta \sim \pi/\ell$. CMB maps contain anisotropy information from the size of the map (or in practice some fraction of that size) down to the beam-size of the instrument, σ. One can think of the effect of a Gaussian beam as rolling off the power spectrum with the function $\mathrm{e}^{-\ell(\ell+1)\sigma^2}$.

For less than full sky coverage, the ℓ modes are correlated. Hence, experimental results are usually quoted as a series of 'band powers', defined as estimators of $\ell(\ell+1)C_\ell/2\pi$ over different ranges of ℓ. Because of the strong foreground signals in the Galactic Plane, even 'all-sky' surveys, such as *COBE* and *WMAP* involve a cut sky. The amount of binning required to obtain uncorrelated estimates of power also depends on the map size.

23.3. Cosmological Parameters

The current 'Standard Model' of cosmology contains around 10 free parameters (see the review on The Cosmological Parameters—Sec. 21 of this *Review*). The basic framework is the Friedmann-Robertson-Walker metric (*i.e.*, a universe that is approximately homogeneous and isotropic on large scales), with density perturbations laid down at early times and evolving into today's structures (see the review on Big-Bang Cosmology—Sec. 19 of this *Review*). These perturbations can be either 'adiabatic' (meaning that there is no change to the

entropy per particle for each species, *i.e.*, $\delta\rho/\rho$ for matter is $(3/4)\delta\rho/\rho$ for radiation) or 'isocurvature' (meaning that, for example, matter perturbations compensate radiation perturbations so that the total energy density remains unperturbed, *i.e.*, $\delta\rho$ for matter is $-\delta\rho$ for radiation). These different modes give rise to distinct phases during growth, and the adiabatic scenario is strongly preferred by the data. Models that generate mainly isocurvature type perturbations (such as most topological defect scenarios) are no longer considered to be viable.

Within the adiabatic family of models, there, is in principle, a free function describing how the comoving curvature perturbations, $\mathcal{R}$, vary with scale. In inflationary models, the Taylor series expansion of $\ln\mathcal{R}(\ln k)$ has terms of steadily decreasing size. For the simplest models, there are thus 2 parameters describing the initial conditions for density perturbations: the amplitude and slope of the power spectrum, $\left\langle|\mathcal{R}|^2\right\rangle \propto k^n$. This can be explicitly defined, for example, through:

$$\Delta^2_{\mathcal{R}} \equiv (k^3/2\pi^2)\left\langle|\mathcal{R}|^2\right\rangle,$$

and using $A^2 \equiv \Delta^2_{\mathcal{R}}(k_0)$ with $k_0 = 0.05\,\mathrm{Mpc}^{-1}$. There are many other equally valid definitions of the amplitude parameter (see also Sec. Olive & Peacock and Sec. Lahav & Liddle), and we caution that the relationships between some of them can be cosmology dependent. In 'slow roll' inflationary models this normalization is proportional to the combination $V^3/(V')^2$, for the inflationary potential $V(\phi)$. The slope n also involves V'', and so the combination of A and n can, in principle, constrain potentials.

Inflationary models can generate tensor (gravity wave) modes as well as scalar (density perturbation) modes. This fact introduces another parameter measuring the amplitude of a possible tensor component, or equivalently the ratio of the tensor to scalar contributions. The tensor amplitude $A_{\mathrm{T}} \propto V$, and thus one expects a larger gravity wave contribution in models where inflation happens at higher energies. The tensor power spectrum also has a slope, often denoted n_{T}, but since this seems likely to be extremely hard to measure, it is sufficient for now to focus only on the amplitude of the gravity wave component. It is most common to define the tensor contribution through r, the ratio of tensor to scalar perturbation spectra at large scales (say $k = 0.002\,\mathrm{Mpc}^{-1}$). There are other definitions in terms of the ratio of contributions to C_2, for example. Different inflationary potentials will lead to different predictions, e.g. for $\lambda\phi^4$ inflation, $r = 0.32$, while other models can have arbitrarily small values of r. In any case, whatever the specific definition, and whether they come from inflation or something else, the 'initial conditions' give rise to a minimum of 3 parameters: A, n, and r.

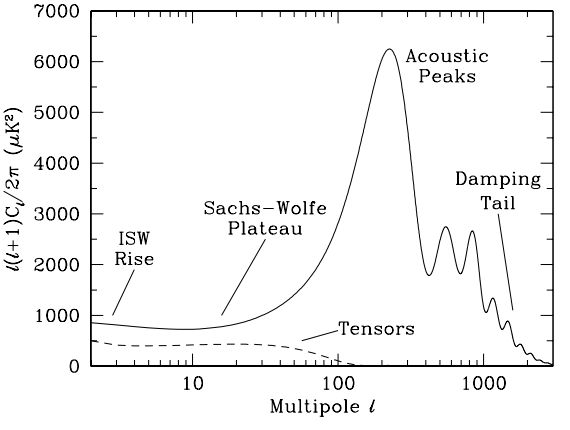

Figure 23.1: Plot of the theoretical CMB anisotropy power spectrum, using a standard ΛCDM model from `CMBFAST`. The x-axis is logarithmic here. The regions are labeled as in the text: the ISW Rise; Sachs-Wolfe Plateau; Acoustic Peaks; and Damping Tail. Also shown is the shape of the tensor (gravity wave) contribution, with an arbitrary normalization.

The background cosmology requires an expansion parameter (the Hubble Constant, H_0, often represented through $H_0 = 100\,h\,\mathrm{km\,s^{-1}Mpc^{-1}}$) and several parameters to describe the matter and energy content of the Universe. These are usually given in terms of the critical density, *i.e.*, for species 'x', $\Omega_{\mathrm{x}} = \rho_{\mathrm{x}}/\rho_{\mathrm{crit}}$, where $\rho_{\mathrm{crit}} = 3H_0^2/8\pi G$. Since physical densities $\rho_{\mathrm{x}} \propto \Omega_{\mathrm{x}}h^2 \equiv \omega_{\mathrm{x}}$ are what govern the physics of the CMB anisotropies, it is these ωs that are best constrained by CMB data. In particular CMB observations constrain $\Omega_{\mathrm{B}}h^2$ for baryons and $\Omega_{\mathrm{M}}h^2$ for baryons plus Cold Dark Matter.

The contribution of a cosmological constant Λ (or other form of Dark Energy) is usually included through a parameter which quantifies the curvature, $\Omega_{\mathrm{K}} \equiv 1 - \Omega_{\mathrm{tot}}$, where $\Omega_{\mathrm{tot}} = \Omega_{\mathrm{M}} + \Omega_\Lambda$. The radiation content, while in principle a free parameter, is precisely enough determined through the measurement of T_γ.

The main effect of astrophysical processes on the C_ℓs comes through reionization. The Universe became reionized at some redshift long after recombination, affecting the CMB through the integrated Thomson scattering optical depth:

$$\tau = \int_0^{z_{\mathrm{i}}} \sigma_{\mathrm{T}} n_{\mathrm{e}}(z)\frac{dt}{dz}dz,$$

where σ_{T} is the Thomson cross-section, $n_{\mathrm{e}}(z)$ is the number density of free electrons (which depends on astrophysics) and dt/dz is fixed by the background cosmology. In principle, τ can be determined from the small scale power spectrum together with the physics of structure formation and feedback processes. However, this is a sufficiently complicated calculation that τ needs to be considered as a free parameter.

Thus we have 8 basic cosmological parameters: A, n, r, h, $\Omega_{\mathrm{B}}h^2$, $\Omega_{\mathrm{M}}h^2$, Ω_{tot}, and τ. One can add additional parameters to this list, particularly when using the CMB in combination with other data sets. The next most relevant ones might be: $\Omega_\nu h^2$, the massive neutrino contribution; w ($\equiv p/\rho$), the equation of state parameter for the Dark Energy; and $dn/d\ln k$, measuring deviations from a constant spectral index. To these 11 one could of course add further parameters describing additional physics, such as details of the reionization process, features in the initial power spectrum, a sub-dominant contribution of isocurvature modes, *etc.*

As well as these underlying parameters, there are other quantities that can be derived from them. Such quantities include the actual Ωs of the various components (*e.g.*, Ω_{M}), the variance of density perturbations at particular scales (*e.g.*, σ_8), the age of the Universe today (t_0), the age of the Universe at recombination, reionization, *etc.*

23.4. Physics of Anisotropies

The cosmological parameters affect the anisotropies through the well understood physics of the evolution of linear perturbations within a background FRW cosmology. There are very effective, fast, and publicly-available software codes for computing the CMB anisotropy, polarization, and matter power spectra, *e.g.*, `CMBFAST` [12] and `CAMB` [13]. `CMBFAST` is the most extensively used code; it has been tested over a wide range of cosmological parameters and is considered to be accurate to better than the 1% level [14].

A description of the physics underlying the C_ℓs can be separated into 3 main regions, as shown in Fig. 23.1.

23.4.1. *The Sachs-Wolfe plateau:* $\ell \lesssim 100$:

The horizon scale (or more precisely, the angle subtended by the Hubble radius) at last scattering corresponds to $\ell \simeq 100$. Anisotropies at larger scales have not evolved significantly, and hence directly reflect the 'initial conditions.' The combination of gravitational redshift and intrinsic temperature fluctuations leads to $\delta T/T \simeq (1/3)\delta\phi/c^2$, where $\delta\phi$ is the perturbation to the gravitational potential. This is usually referred to as the 'Sachs-Wolfe' effect [15].

Assuming that a nearly scale-invariant spectrum of density perturbations was laid down at early times (*i.e.*, $n \simeq 1$, meaning equal power per decade in k), then $\ell(\ell+1)C_\ell \simeq$ constant at low ℓs. This effect is hard to see unless the multipole axis is plotted logarithmically (as in Fig. 23.1, but not Fig. 23.2).

Time variation in the potentials (*i.e.*, time-dependent metric perturbations) leads to an upturn in the C_ℓs in the lowest several

multipoles; any deviation from a total equation of state $w = 0$ has such an effect. So the dominance of the Dark Energy at low redshift makes the lowest ℓs rise above the plateau. This is sometimes called the 'integrated Sachs-Wolfe effect' (or ISW Rise), since it comes from the line integral of $\dot{\phi}$. It has been confirmed through correlations between the large-angle anisotropies and large-scale structure [16]. Specific models can also give additional contributions at low ℓ (*e.g.*, perturbations in the Dark Energy component itself [11]) but typically these are buried in the cosmic variance.

In principle, the mechanism that produces primordial perturbations would generate scalar, vector, and tensor modes. However, the vector (vorticity) modes decay with the expansion of the Universe. Tensors also decay when they enter the horizon, and so they contribute only to angular scales above about 1° (see Fig. 23.1). Hence some fraction of the low ℓ signal could be due to a gravity wave contribution, although small amounts of tensors are essentially impossible to discriminate from other effects that might raise the level of the plateau. However the tensors *can* be distinguished using polarization information (see Sec. 23.6).

23.4.2. *The acoustic peaks:* $100 \lesssim \ell \lesssim 1000$:

On sub-degree scales, the rich structure in the anisotropy spectrum is the consequence of gravity-driven acoustic oscillations occurring before the atoms in the universe became neutral. Perturbations inside the horizon at last scattering have been able to evolve causally and produce anisotropy at the last scattering epoch which reflects that evolution. The frozen-in phases of these sound waves imprint a dependence on the cosmological parameters, which gives CMB anisotropies their great constraining power.

The underlying physics can be understood as follows. When the proton-electron plasma was tightly coupled to the photons, these components behaved as a single 'photon-baryon fluid', with the photons providing most of the pressure and the baryons the inertia. Perturbations in the gravitational potential, dominated by the dark matter component, are steadily evolving. They drive oscillations in the photon-baryon fluid, with photon pressure providing the restoring force. The perturbations are quite small, $O(10^{-5})$, and so evolve linearly. That means each Fourier mode evolves independently and is described by a driven harmonic oscillator, with frequency determined by the sound speed in the fluid. Thus, there is an oscillation of the fluid density, with velocity $\pi/2$ out of phase and having amplitude reduced by the sound speed.

After the Universe recombined the baryons and radiation decoupled, and the radiation could travel freely towards us. At that point the phases of the oscillations were frozen-in, and projected on the sky as a harmonic series of peaks. The main peak is the mode that went through 1/4 of a period, reaching maximal compression. The even peaks are maximal *under*-densities, which are generally of smaller amplitude because the rebound has to fight against the baryon inertia. The troughs, which do not extend to zero power, are partially filled by the Doppler effect because they are at the velocity maxima.

An additional effect comes from geometrical projection. The scale associated with the peaks is the sound horizon at last scattering, which can be confidently calculated as a physical length scale. This scale is projected onto the sky, leading to an angular scale that depends on the background cosmology. Hence the angular position of the peaks is a sensitive probe of the spatial curvature of the Universe (*i.e.*, $\Omega_{\rm tot}$), with the peaks lying at higher ℓ in open universes and lower ℓ in closed geometry.

One last effect arises from reionization at redshift $z_{\rm i}$. A fraction of photons will be isotropically scattered at $z < z_{\rm i}$, partially erasing the anisotropies at angular scales smaller than those subtended by the Hubble radius at $z_{\rm i}$. This corresponds typically to ℓs above about a few 10s, depending on the specific reionization model. The acoustic peaks are therefore reduced by a factor $e^{-2\tau}$ relative to the plateau.

These acoustic peaks were a clear theoretical prediction going back to about 1970 [17]. Their empirical existence started to become clear around 1994 [18], and the emergence, over the following decade, of a coherent series of acoustic peaks and troughs is a triumph of modern cosmology. One can think of these peaks as a snapshot of stochastic standing waves. And, since the physics governing them is simple, then one can see how they encode information about the cosmological parameters.

23.4.3. *The damping tail:* $\ell \gtrsim 1000$:

The recombination process is not instantaneous, giving a thickness to the last scattering surface. This leads to a damping of the anisotropies at the highest ℓs, corresponding to scales smaller than that subtended by this thickness. One can also think of the photon-baryon fluid as having imperfect coupling, so that there is diffusion between the two components, and the oscillations have amplitudes that decrease with time. These effects lead to a damping of the C_ℓs, sometimes called Silk damping [19], which cuts off the anisotropies at multipoles above about 2000.

An extra effect at high ℓs comes from gravitational lensing, caused mainly by non-linear structures at low redshift. The C_ℓs are convolved with a smoothing function in a calculable way, partially flattening the peaks, generating a power-law tail at the highest multipoles, and complicating the polarization signal [20]. This is an example of a 'secondary effect', *i.e.*, the processing of anisotropies due to relatively nearby structures. Galaxies and clusters of galaxies give several such effects, but all are expected to be of low amplitude and are typically only important for the highest ℓs.

23.5. Current Anisotropy Data

There has been a steady improvement in the quality of CMB data that has led to the development of the present-day cosmological model. Probably the most robust constraints currently available come from the combination of the *WMAP* first year data [4] with smaller scale results from the CBI [21] and ACBAR [22] experiments. We plot these power spectrum estimates in Fig. 23.2. Other recent experiments, such as ARCHEOPS [23], BOOMERANG [24], DASI [25], MAXIMA [26], and VSA [27] also give powerful constraints, which are quite consistent with what we describe below. There have been some comparisons among data-sets [28], which indicate very good agreement, both in maps and in derived power spectra (up to systematic uncertainties in the overall calibration for some experiments). This makes it clear that systematic effects are largely under control. However, a fully self-consistent joint analysis of all the current data sets has not been attempted, one of the reasons being that it requires a careful treatment of the overlapping sky coverage.

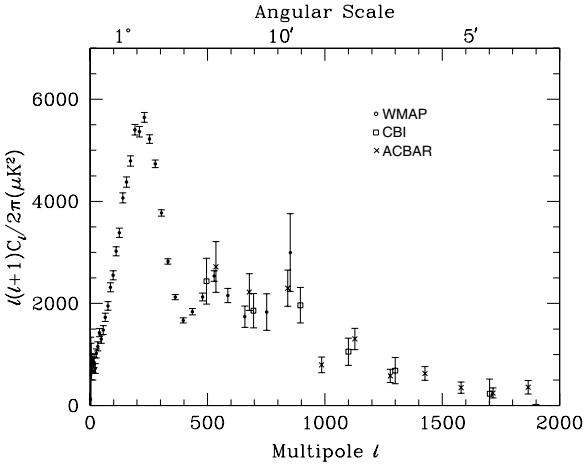

Figure 23.2: Band-power estimates from the *WMAP*, CBI, and ACBAR experiments. The *WMAP* data are the points, while squares are CBI and crosses ACBAR. We have shown only CBI and ACBAR data relevant for $\ell > 500$, and both experiments also probe to higher ℓ than shown. This plot represents only a fraction of experimental results, with several other data-sets being of similar quality. The multipole axis here is linear, so the Sachs-Wolfe plateau is hard to see. The acoustic peaks and damping region are very clearly observed, with no need for a theoretical curve to guide the eye.

Fig. 23.2 shows band-powers from the first year *WMAP* data [29], together with CBI and ACBAR data at higher ℓ. The points are in

very good agreement with a 'ΛCDM' type model, as described in the previous section, with several of the peaks and troughs quite apparent. For details of how these estimates were arrived at, the strength of any correlations between band-powers and other information required to properly interpret them, turn to the original papers [4,21,22].

23.6. CMB Polarization

Since Thomson scattering of an anisotropic radiation field also generates linear polarization, the CMB is predicted to be polarized at the roughly 5% level [30]. Polarization is a spin 2 field on the sky, and the algebra of the modes in ℓ-space is strongly analogous to spin-orbit coupling in quantum mechanics [31]. The linear polarization pattern can be decomposed in a number of ways, with two quantities required for each pixel in a map, often given as the Q and U Stokes parameters. However, the most intuitive and physical decomposition is a geometrical one, splitting the polarization pattern into a part that comes from a divergence (often referred to as the 'E-mode') and a part with a curl (called the 'B-mode') [32]. More explicitly, the modes are defined in terms of second derivatives of the polarization amplitude, with the Hessian for the E-modes having principle axes in the same sense as the polarization, while the B-mode pattern can be thought of simply as a 45° rotation of the E-mode pattern. Globally one sees that the E-modes have $(-1)^\ell$ parity (like the spherical harmonics), while the B-modes have $(-1)^{\ell+1}$ parity.

The existence of this linear polarization allows for 6 different cross power spectra to be determined from data that measure the full temperature and polarization anisotropy information. Parity considerations make 2 of these zero, and we are left with 4 potential observables: $C_\ell^{\rm TT}$, $C_\ell^{\rm TE}$, $C_\ell^{\rm EE}$, and $C_\ell^{\rm BB}$. Since scalar perturbations have no handedness, the B-mode power spectrum can only be generated by vectors or tensors. Hence, in the context of inflationary models, the determination of a non-zero B-mode signal is a way to measure the gravity wave contribution (and thus potentially derived the energy scale of inflation), even if it is rather weak. However, one must first eliminate the foreground contributions and other systematic effects down to very low levels.

The oscillating photon-baryon fluid also results in a series of acoustic peaks in the polarization power spectra. The main 'EE' power spectrum has peaks that are out of phase with those in the 'TT' spectrum, because the polarization anisotropies are sourced by the fluid velocity. The correlated component of the polarization and temperature patterns comes from correlations between density and velocity perturbations on the last scattering surface, which can be both positive and negative. There is no polarization 'Sachs-Wolfe' effect, and hence no large-angle plateau. However, scattering during a recent period of reionization can create a polarization 'bump' at large angular scales.

The strongest upper limits on polarization are at the roughly 10 μK level from the POLAR [33] experiment at large angular scales and the PIQUE [34] and COMPASS [35] experiments at smaller scales. The first measurement of a polarization signal came in 2002 from the DASI experiment [36], which provided a convincing detection, confirming the general paradigm, but of low enough significance that it lends little constraint to models. As well as the E-mode signal, DASI also made a statistical detection of the TE correlation.

More recently the *WMAP* experiment was able to measure the TE cross-correlation power spectrum with high precision [37]. The results are shown in Fig. 23.3, along with some estimates from the DASI experiment. The detected shape of the cross-correlation power spectrum provides supporting evidence of the adiabatic nature of the perturbations, as well as directly constraining the thickness of the last scattering surface. Since the polarization anisotropies are generated in this scattering surface, the existence of correlations at angles above about a degree demonstrate that there were super-Hubble fluctuations at the recombination epoch.

Perhaps the most intriguing result from the polarization measurements is at the largest angular scales ($\ell < 10$), where there is an excess signal compared to that expected from the temperature power spectrum alone. This is precisely the signal expected from an early period of reionization, arising from Doppler shifts during the partial scattering at $z < z_{\rm i}$. It seems to indicate that the first stars (presumably the source of the ionizing radiation) formed around $z = 20$.

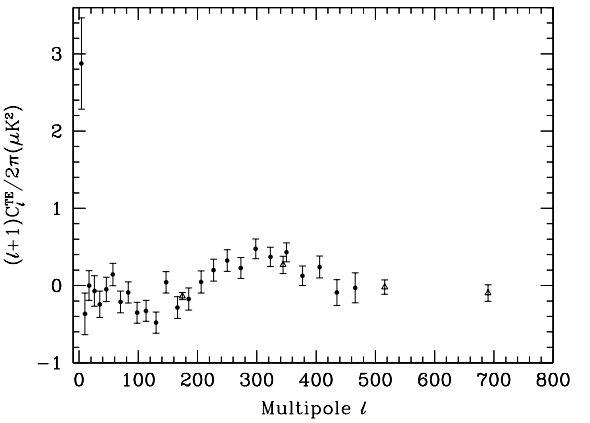

Figure 23.3: Cross power spectrum of the temperature anisotropies and E-mode polarization signal from *WMAP* (points), together with some estimates from DASI (triangles) which extend to higher ℓ. Note that the DASI bands are much wider in ℓ than those of *WMAP*. Also note that the y-axis is not multiplied by the additional ℓ, which helps to show both the large and small angular scale features.

23.7. Complications

There are a number of issues which complicate the interpretation of CMB anisotropy data, some of which we sketch out below.

23.7.1. *Foregrounds*:

The microwave sky contains significant emission from our Galaxy and from extra-galactic sources. Fortunately, the frequency dependence of these various sources are in general substantially different than the CMB anisotropy signals. The combination of Galactic synchrotron, bremsstrahlung and dust emission reaches a minimum at a wavelength of roughly 3 mm (or about 100 GHz). As one moves to greater angular resolution, the minimum moves to slightly higher frequencies, but becomes more sensitive to unresolved (point-like) sources.

At frequencies around 100 GHz and for portions of the sky away from the Galactic Plane the foregrounds are typically 1 to 10% of the CMB anisotropies. By making observations at multiple frequencies, it is relatively straightforward to separate the various components and determine the CMB signal to the few per cent level. For greater sensitivity it is necessary to improve the separation techniques by adding spatial information and statistical properties of the foregrounds compared to the CMB.

The foregrounds for CMB polarization are expected to follow a similar pattern, but are less well studied, and are intrinsically more complicated. Whether it is possible to achieve sufficient separation to detect B-mode CMB polarization is still an open question. However, for the time being, foreground contamination is not a major issue for CMB experiments.

23.7.2. *Secondary Anisotropies*:

With increasingly precise measurements of the primary anisotropies, there is growing theoretical and experimental interest in 'secondary anisotropies.' Effects which happen at $z \ll 1000$ become more important as experiments push to higher angular resolution and sensitivity.

These secondary effects include gravitational lensing, patchy reionization and the Sunyaev-Zel'dovich (SZ) effect [38]. This is Compton scattering ($\gamma e \to \gamma' e'$) of the CMB photons by a hot electron gas, which creates spectral distortions by transferring energy from the electrons to the photons. The effect is particularly important for clusters of galaxies, through which one observes a partially Comptonized spectrum, resulting in a decrement at radio wavelengths and an increment in the submillimeter. This can be used to find and study individual clusters and to obtain estimates of the Hubble

constant. There is also the potential to constrain the equation of state of the Dark Energy through counts of clusters as a function of redshift [39].

23.7.3. *Higher-order Statistics*:

Although most of the CMB anisotropy information is contained in the power spectra, there will also be weak signals present in higher-order statistics. These statistics will measure primordial non-Gaussianity in the perturbations, as well as non-linear growth of the fluctuations on small scales and other secondary effects (plus residual foreground contamination). Although there are an infinite variety of ways in which the CMB could be non-Gaussian, there is a generic form to consider for the initial conditions, where a quadratic contribution to the curvature perturbations is parameterized through a dimensionless number $f_{\rm NL}$. This weakly non-linear component can be constrained through measurements of the bispectrum or Minkowski functionals for example, and the result from *WMAP* is $-58 < f_{\rm NL} < 134$ (95% confidence region) [10].

23.8. Constraints on Cosmologies

The most important outcome of the newer experimental results is that the standard cosmological paradigm is in good shape. A large amount of high precision data on the power spectrum is adequately fit with fewer than 10 free parameters. The framework is that of Friedmann-Robertson-Walker models, which have nearly flat geometry, containing Dark Matter and Dark Energy, and with adiabatic perturbations having close to scale invariant initial conditions.

Within this framework, bounds can be placed on the values of the cosmological parameters. Of course, much more stringent constraints can be placed on models which cover a restricted number of parameters, e.g. assuming that $\Omega_{\rm tot} = 1$, $n = 1$ or $r = 0$. More generally, the constraints depend upon the adopted priors, even if they are implicit, for example by restricting the parameter freedom or the ranges of parameters (particularly where likelihoods peak near the boundaries), or by using different choices of other data in combination with the CMB. When the data become even more precise, these considerations will become less important, but for now we caution that restrictions on model space and choice of priors need to be kept in mind when adopting specific parameter values and uncertainties.

There are some combinations of parameters that fit the CMB anisotropies almost equivalently. For example, there is a nearly exact geometric degeneracy, where any combination of $\Omega_{\rm M}$ and Ω_Λ that gives the same angular diameter distance to last scattering will give nearly identical C_ℓs. There are also other near degeneracies among the parameters. Such degeneracies can be broken when using the CMB data in combination with other cosmological data sets. Particularly useful are complementary constraints from galaxy clustering, the abundance of galaxy clusters, weak gravitational lensing measurements, Type Ia supernova distances and the distribution of Lyman α forest clouds. For an overview of some of these other cosmological constraints, see the review on The Cosmological Parameters—Sec. 21 of this *Review*.

The combination of *WMAP*, CBI and ACBAR, together with weak priors (on h and $\Omega_{\rm B}h^2$ for example), and within the context of a 6 parameter family of models (which fixes $\Omega_{\rm tot} = 1$), yields the following results [40]: $A = 2.7(\pm 0.3) \times 10^{-9}$, $n = 0.97 \pm 0.03$, $h = 0.73 \pm 0.05$, $\Omega_{\rm B}h^2 = 0.023 \pm 0.001$, $\Omega_{\rm M}h^2 = 0.13 \pm 0.01$ and $\tau = 0.17 \pm 0.07$. Note that for h, the CMB data alone provide only a very weak constraint, unless spatial flatness or some other cosmological data are used. For $\Omega_{\rm B}h^2$ the precise value depends sensitively on how much freedom is allowed in the shape of the primordial power spectrum (see the review on Big-Bang nucleosynthesis—Sec. 20 of this *Review*). For the optical depth τ, the error bar is large enough that apparently quite different results can come from other combinations of data.

The best constraint on $\Omega_{\rm tot}$ is 1.02 ± 0.02. This comes from including priors from h and supernova data. Slightly different, but consistent results come from using different data combinations.

The 95% confidence upper limit on r is 0.53 (including some extra constraint from galaxy clustering). This limit is stronger if we restrict ourselves to $n < 1$ and weaker if we allow $dn/d\ln k \neq 0$.

There are also constraints on parameters over and above the basic 8 that we have described. But for such constraints it is necessary to include additional data in order to break the degeneracies. For example the addition of the Dark Energy equation of state, w adds the partial degeneracy of being able to fit a ridge in (w, h) space, extending to low values of both parameters. This degeneracy is broken when the CMB is used in combination with independent H_0 limits, for example [13], giving $w < -0.5$ at 95% confidence. Tighter limits can be placed using restrictive model-spaces and/or additional data.

For the optical depth τ, the error bar is large enough that apparently quite different results can come from other combinations of data. The constraint from the combined *WMAP* $C_\ell^{\rm TT}$ and $C_\ell^{\rm TE}$ data is $\tau = 0.17 \pm 0.04$, which corresponds (within reasonable models) to a reionization redshift $9 < z_{\rm i} < 30$ (95% CL) [37]. This is a little higher than some theoretical predictions and some suggestions from studies of absorption in high-z quasar spectra [42]. The excitement here is that we have direct information from CMB polarization which can be combined with other astrophysical measurements to understand when the first stars formed and brought about the end of the cosmic dark ages.

23.9. Particle Physics Constraints

CMB data are beginning to put limits on parameters which are directly relevant for particle physics models. For example there is a limit on the neutrino contribution $\Omega_\nu h^2 < 0.0076$ (95% confidence) from a combination of *WMAP* and galaxy clustering data from the 2dFGRS project [43]. This directly implies a limit on neutrino mass, assuming the usual number density of fermions which decoupled when they were relativistic.

A combination of the *WMAP* data with other data-sets gives some hint of a running spectral index, *i.e.*, $dn/d\ln k \neq 0$ [40]. Although this is still far from resolved [44], things will certainly improve as new data come in. A convincing measurement of a non-zero running of the index would be quite constraining for inflationary models [45].

One other hint of new physics lies in the fact that the quadrupole and some of the other low ℓ modes seem anomalously low compared with the best-fit ΛCDM model [29]. This is what might be expected in a universe which has a large scale cut-off to the power spectrum, or is topologically non-trivial. However, because of cosmic variance, possible foregrounds *etc.*, the significance of this feature is still a matter of debate [46].

In addition it is also possible to put limits on other pieces of physics [47], for example the neutrino chemical potentials, time variation of the fine-structure constant, or physics beyond general relativity. Further particle physics constraints will follow as the anisotropy measurements increase in precision.

Careful measurement of the CMB power spectra and non-Gaussianity can in principle put constraints on high energy physics, including ideas of string theory, extra dimensions, colliding branes, *etc.* At the moment any calculation of predictions appears to be far from definitive. However, there is a great deal of activity on implications of string theory for the early Universe, and hence a very real chance that there might be observational implications for specific scenarios.

23.10. Fundamental Lessons

More important than the precise values of parameters is what we have learned about the general features which describe our observable Universe. Beyond the basic hot Big Bang picture, the CMB has taught us that:

- The Universe recombined at $z \simeq 1100$ and started to become ionized again at $z \simeq 10$–30.
- The geometry of the Universe is close to flat.
- Both Dark Matter and Dark Energy are required.
- Gravitational instability is sufficient to grow all of the observed large structures in the Universe.
- Topological defects were not important for structure formation.
- There are 'synchronized' super-Hubble modes generated in the early Universe.
- The initial perturbations were adiabatic in nature.
- The perturbations had close to Gaussian (*i.e.*, maximally random) initial conditions.

It is very tempting to make an analogy between the status of the cosmological 'Standard Model' and that of particle physics. In cosmology there are about 10 free parameters, each of which is becoming well determined, and with a great deal of consistency between different measurements. However, none of these parameters can be calculated from a fundamental theory, and so hints of the bigger picture, 'physics beyond the Standard Model' are being searched for with ever more challenging experiments.

Despite this analogy, there are some basic differences. For one thing, many of the cosmological parameters change with cosmic epoch, and so the measured values are simply the ones determined today, and hence they are not 'constants', like particle masses for example (although they *are* deterministic, so that if one knows their values at one epoch, they can be calculated at another). Moreover, the number of parameters is not as fixed as it is in the particle physics Standard Model; different researchers will not necessarily agree on what the free parameters are, and new ones can be added as the quality of the data improves. In addition parameters like τ, which come from astrophysics, are in principle calculable from known physical processes, although this is currently impractical. On top of all this, other parameters might be 'stochastic' in that they may be fixed only in our observable patch of the Universe.

In a more general sense the cosmological 'Standard Model' is much further from the underlying 'fundamental theory' which will provide the values of the parameters from first principles. On the other hand, any genuinely complete 'theory of everything' must include an explanation for the values of these cosmological parameters as well as the parameters of the Standard Model.

23.11. Future Directions

With all the observational progress in the CMB and the tying down of cosmological parameters, what can we anticipate for the future? Of course there will be a steady improvement in the precision and confidence with which we can determine the appropriate cosmological model and its parameters. We can anticipate that the evolution from one year to four years of *WMAP* data will bring improvements from the increased statistical accuracy and from the more detailed treatment of calibration and systematic effects. Ground-based experiments operating at the smaller angular scales will also improve over the next few years, providing significantly tighter constraints on the damping tail. In addition, the next CMB satellite mission, *Planck*, is scheduled for launch in 2007, and there are even more ambitious projects currently being discussed.

Despite the increasing improvement in the results, it is also true that the addition of the latest experiments has not significantly changed the cosmological model (apart from a suggestion of higher reionization redshift perhaps). It is therefore appropriate to ask: what should we expect to come from *Planck* and from other more grandiose future experiments, including the proposed *Inflation Probe* or *CMBPol*? *Planck* certainly has the the advantage of high sensitivity and a full sky survey. A detailed measurement of the third acoustic peak provides a good determination of the matter density; this can only be done by measurements which are accurate relative to the first two peaks (which themselves constrained the curvature and the baryon density). A detailed measurement of the damping tail region will also significantly improve the determination of n and any running of the slope. *Planck* should also be capable of measuring $C_\ell^{\rm EE}$ quite well, providing both a strong check on the Standard Model and extra constraints that will improve parameter estimation.

A set of cosmological parameters are now known to roughly 10% accuracy, and that may seem sufficient for many people. However, we should certainly demand more of measurements which describe *the entire observable Universe*! Hence a lot of activity in the coming years will continue to focus on determining those parameters with increasing precision. This necessarily includes testing for consistency among different predictions of the Standard Model, and searching for signals which might require additional physics.

A second area of focus will be the smaller scale anisotropies and 'secondary effects.' There is a great deal of information about structure formation at $z \ll 1000$ encoded in the CMB sky. This may involve higher-order statistics as well as spectral signatures. Such investigations can also provide constraints on the Dark Energy equation of state, for example. *Planck*, as well as experiments aimed at the highest ℓs, should be able to make a lot of progress in this arena.

A third direction is increasingly sensitive searches for specific signatures of physics at the highest energies. The most promising of these may be the primordial gravitational wave signals in $C_\ell^{\rm BB}$, which could be a probe of the $\sim 10^{16}$ GeV energy range. Whether the amplitude of the effect coming from inflation will be detectable is unclear, but the prize makes the effort worthwhile.

Anisotropies in the CMB have proven to be the premier probe of cosmology and the early Universe. Theoretically the CMB involves well-understood physics in the linear regime, and is under very good calculational control. A substantial and improving set of observational data now exists. Systematics appear to be well understood and not a limiting factor. And so for the next few years we can expect an increasing amount of cosmological information to be gleaned from CMB anisotropies, with the prospect also of some genuine surprises.

References:

1. A.A. Penzias and R. Wilson, Astrophys. J. **142**, 419 (1965); R.H. Dicke *et al.*, Astrophys. J. **142**, 414 (1965).
2. M. White, D. Scott, and J. Silk, Ann. Rev. Astron. & Astrophys. **32**, 329 (1994); W. Hu and S. Dodelson, Ann. Rev. Astron. & Astrophys. **40**, 171 (2002).
3. G.F. Smoot *et al.*, Astrophys. J. **396**, L1 (1992).
4. C.L. Bennett *et al.*, Astrophys. J. Supp. **148**, 1 (2003).
5. J.C. Mather *et al.*, Astrophys. J. **512**, 511 (1999).
6. S. Courteau *et al.*, Astrophys. J. **544**, 636 (2000).
7. D.J. Fixsen *et al.*, Astrophys. J. **420**, 445 (1994).
8. D.J. Fixsen *et al.*, Astrophys. J. **473**, 576 (1996); A. Kogut *et al.*, Astrophys. J. **419**, 1 (1993).
9. S. Seager, D.D. Sasselov, and D. Scott, Astrophys. J. Supp. **128**, 407 (2000).
10. E. Komatsu *et al.*, Astrophys. J. Supp. **148**, 119 (2003).
11. W. Hu and D.J. Eisenstein, Phys. Rev. **D59**, 083509 (1999); W. Hu *et al.*, Phys. Rev. **D59**, 023512 (1999).
12. U. Seljak and M. Zaldarriaga, Astrophys. J. **469**, 437 (1996).
13. A. Lewis, A. Challinor, A. Lasenby, Astrophys. J. **538**, 473 (2000).
14. U. Seljak *et al.*, Physical Review D, in press, `astro-ph/0306052`.
15. R.K. Sachs and A.M. Wolfe, Astrophys. J. **147**, 73 (1967).
16. M.R. Nolta *et al.*, Astrophysical J., in press, `astro-ph/0305097`.
17. P.J.E. Peebles and J.T. Yu, Astrophys. J. **162**, 815 (1970); R.A. Sunyaev and Ya.B. Zel'dovich, Astrophysics & Space Science **7**, 3 (1970).
18. D. Scott, J. Silk, and M. White, Science **268**, 829 (1995).
19. J. Silk, Astrophys. J. **151**, 459 (1968).
20. M. Zaldarriaga and U. Seljak, Phys. Rev. **D58**, 023003 (1998).
21. T.J. Pearson *et al.*, Astrophys. J. **591**, 556 (2003).
22. C.L. Kuo *et al.*, Astrophysical J., in press, `astro-ph/0212289`.
23. A. Benoit *et al.*, Astronomy & Astrophysics **399**, L19 (2003).
24. J.E. Ruhl *et al.*, Astrophysical J., in press, `astro-ph/0212229`.
25. N.W. Halverson *et al.*, Astrophys. J. **568**, 38 (2002).
26. A.T. Lee *et al.*, Astrophys. J. **561**, L1 (2001).
27. P.F. Scott *et al.*, Monthly Not. Royal Astron. Soc. **341**, 1076 (2003).
28. M.E. Abroe *et al.*, Astrophysical J., in press, `astro-ph/0308355`.
29. G. Hinshaw *et al.*, Astrophys. J. Supp. **148**, 135 (2003).
30. W. Hu, M. White, New Astron. **2**, 323 (1997).
31. W. Hu, M. White, Phys. Rev. **D56**, 596 (1997).
32. M. Zaldarriaga and U. Seljak, Phys. Rev. **D55**, 1830 (1997); M. Kamionkowski, A. Kosowsky, and A. Stebbins, Phys. Rev. **D55**, 7368 (1997).

33. B.G. Keating *et al.*, Astrophysical J., in press, `astro-ph/0107013`.
34. M.M. Hedman *et al.*, Astrophys. J. **548**, L111 (2001).
35. P.C. Farese *et al.*, Astrophysical J., in press, `astro-ph/0308309`.
36. J. Kovac *et al.*, Nature, 420, 772 (2002).
37. A. Kogut *et al.*, Astrophys. J. Supp. **148**, 161 (2003).
38. R.A. Sunyaev and Ya.B. Zel'dovich, Ann. Rev. Astron. Astrophys. **18**, 537 (1980);
    M. Birkinshaw, Phys. Rep. **310**, 98 (1999).
39. J.E. Carlstrom, G.P. Holder, and E.D. Reese, Ann. Rev. Astron. & Astrophys. **40**, 643 (2002).
40. D.N. Spergel *et al.*, Astrophys. J. Supp. **148**, 175 (2003).
41. W.L. Freedman *et al.*, Astrophys. J. **553**, 47 (2001).
42. X. Fan *et al.*, Astrophys. J. **123**, 1247 (2002).
43. M. Colless *et al.*, Monthly Not. Royal Astron. Soc. **328**, 1039 (2001).
44. U. Seljak, P. McDonald, and A. Makarov, Monthly Not. Royal Astron. Soc. **342**, L79 (2003).
45. H.V. Peiris *et al.*, Astrophys. J. Supp. **148**, 213 (2003).
46. A. de Oliveira-Costa *et al.*, Physical Review D, in press, `astro-ph/0307282`;
    G. Efstathiou, Monthly Notices of the Royal Astronomical Society, in press, `astro-ph/0306431`.
47. M. Kamionkowski and A. Kosowsky, Ann. Rev. Nucl. Part. Sci. **49**, 77 (1999).

24. COSMIC RAYS

Revised March 2002 by T.K. Gaisser and T. Stanev (Bartol Research Inst., University of Delaware).

24.1. Primary spectra

The cosmic radiation incident at the top of the terrestrial atmosphere includes all stable charged particles and nuclei with lifetimes of order 10^6 years or longer. Technically, "primary" cosmic rays are those particles accelerated at astrophysical sources and "secondaries" are those particles produced in interaction of the primaries with interstellar gas. Thus electrons, protons and helium, as well as carbon, oxygen, iron, and other nuclei synthesized in stars, are primaries. Nuclei such as lithium, beryllium, and boron (which are not abundant end-products of stellar nucleosynthesis) are secondaries. Antiprotons and positrons are also in large part secondary. Whether a small fraction of these particles may be primary is a question of current interest.

Apart from particles associated with solar flares, the cosmic radiation comes from outside the solar system. The incoming charged particles are "modulated" by the solar wind, the expanding magnetized plasma generated by the Sun, which decelerates and partially excludes the lower energy galactic cosmic rays from the inner solar system. There is a significant anticorrelation between solar activity (which has an alternating eleven-year cycle) and the intensity of the cosmic rays with energies below about 10 GeV. In addition, the lower-energy cosmic rays are affected by the geomagnetic field, which they must penetrate to reach the top of the atmosphere. Thus the intensity of any component of the cosmic radiation in the GeV range depends both on the location and time.

There are four different ways to describe the spectra of the components of the cosmic radiation: (1) By particles per unit rigidity. Propagation (and probably also acceleration) through cosmic magnetic fields depends on gyroradius or *magnetic rigidity, R*, which is gyroradius multiplied by the magnetic field strength:

$$R = \frac{p\,c}{Z\,e} = r_L\,B\,. \qquad (24.1)$$

(2) By particles per energy-per-nucleon. Fragmentation of nuclei propagating through the interstellar gas depends on energy per nucleon, since that quantity is approximately conserved when a nucleus breaks up on interaction with the gas. (3) By nucleons per energy-per-nucleon. Production of secondary cosmic rays in the atmosphere depends on the intensity of nucleons per energy-per-nucleon, approximately independently of whether the incident nucleons are free protons or bound in nuclei. (4) By particles per energy-per-nucleus. Air shower experiments that use the atmosphere as a calorimeter generally measure a quantity that is related to total energy per particle.

The units of differential intensity I are $[\mathrm{cm}^{-2}\mathrm{s}^{-1}\mathrm{sr}^{-1}\mathcal{E}^{-1}]$, where $\mathcal{E}$ represents the units of one of the four variables listed above.

The intensity of primary nucleons in the energy range from several GeV to somewhat beyond 100 TeV is given approximately by

$$I_N(E) \;\approx\; 1.8\;E^{-\alpha}\;\frac{\text{nucleons}}{\mathrm{cm}^2\ \mathrm{s}\ \mathrm{sr}\ \mathrm{GeV}}\,, \qquad (24.2)$$

where E is the energy-per-nucleon (including rest mass energy) and $\alpha\ (\equiv \gamma + 1) = 2.7$ is the differential spectral index of the cosmic ray flux and γ is the integral spectral index. About 79% of the primary nucleons are free protons and about 70% of the rest are nucleons bound in helium nuclei. The fractions of the primary nuclei are nearly constant over this energy range (possibly with small but interesting variations). Fractions of both primary and secondary incident nuclei are listed in Table 24.1. Figure 24.1 [1] shows the major components as a function of energy at a particular epoch of the solar cycle. There has been a series of more precise measurements of the primary spectrum of protons and helium in the past decade [2–6].

The spectrum of electrons and positrons incident at the top of the atmosphere is steeper than the spectra of protons and nuclei,

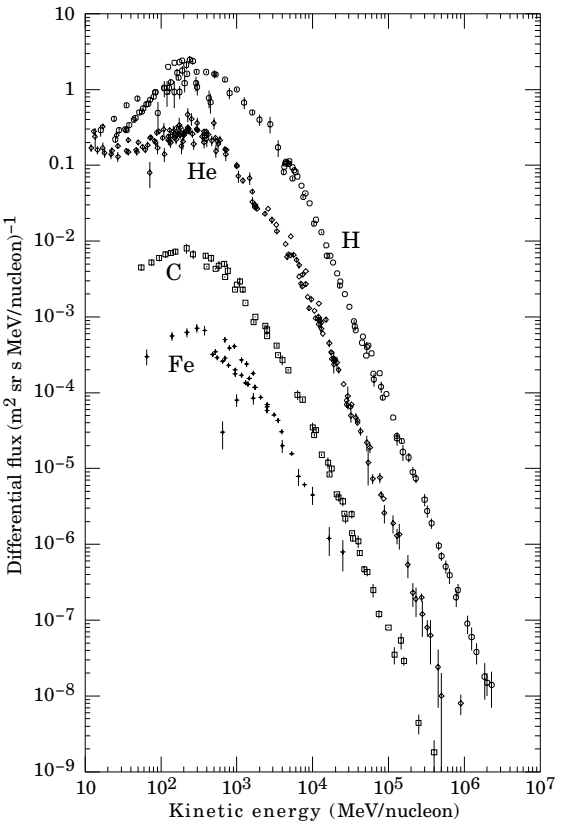

Figure 24.1: Major components of the primary cosmic radiation (from Ref. 1).

Table 24.1: Relative abundances F of cosmic-ray nuclei at 10.6 GeV/nucleon normalized to oxygen ($\equiv$ 1) [7]. The oxygen flux at kinetic energy of 10.6 GeV/nucleon is 3.26×10^{-6} cm^{-2} s^{-1} sr^{-1} (GeV/nucleon)$^{-1}$. Abundances of hydrogen and helium are from Ref. [5,6].

Z	Element	F	Z	Element	F
1	H	540	13–14	Al-Si	0.19
2	He	26	15–16	P-S	0.03
3–5	Li-B	0.40	17–18	Cl-Ar	0.01
6–8	C-O	2.20	19–20	K-Ca	0.02
9–10	F-Ne	0.30	21–25	Sc-Mn	0.05
11–12	Na-Mg	0.22	26–28	Fe-Ni	0.12

as shown in Fig. 24.2. The positron fraction decreases from ~ 0.2 below 1 GeV [9–11] to ~ 0.1 around 2 GeV and to ~ 0.05 in at the highest energies for which it is measured ($5 - 20$ GeV) [12]. This behavior refers to measurements made during solar cycles of positive magnetic polarity and at high geomagnetic latitude. Ref. 11 discusses the dependence of the positron fraction on solar cycle and Ref. 5 studies the geomagnetic effects.

The ratio of antiprotons to protons is $\sim 2 \times 10^{-4}$ [13,14] at around 10–20 GeV, and there is clear evidence [15–17] for the kinematic suppression at lower energy that is the signature of secondary antiprotons. The $\overline{p}/p$ ratio also shows a strong dependence on the phase and polarity of the solar cycle [18] in the opposite sense to

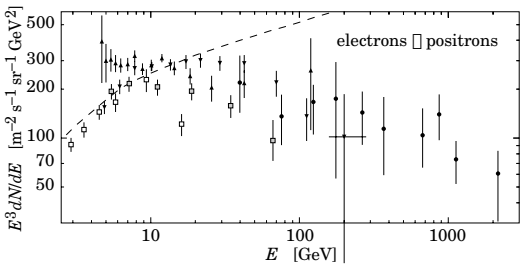

Figure 24.2: Differential spectrum of electrons plus positrons multiplied by E^3 (data summary from Ref. 8). The dashed line shows the proton spectrum multiplied by 0.01.

that of the positron fraction. There is at this time no evidence for a significant primary component either of positrons or of antiprotons.

24.2. Cosmic rays in the atmosphere

Figure 24.3 shows the vertical fluxes of the major cosmic ray components in the atmosphere in the energy region where the particles are most numerous (except for electrons, which are most numerous near their critical energy, which is about 81 MeV in air). Except for protons and electrons near the top of the atmosphere, all particles are produced in interactions of the primary cosmic rays in the air. Muons and neutrinos are products of the decay of charged mesons, while electrons and photons originate in decays of neutral mesons.

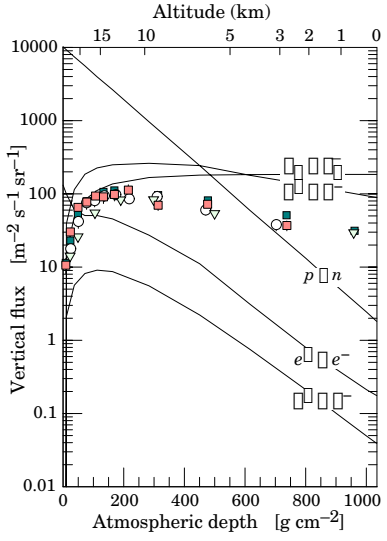

Figure 24.3: Vertical fluxes of cosmic rays in the atmosphere with $E > 1$ GeV estimated from the nucleon flux of Eq. (24.2). The points show measurements of negative muons with $E_\mu > 1$ GeV [4,19,20,21].

Most measurements are made at ground level or near the top of the atmosphere, but there are also measurements of muons and electrons from airplanes and balloons. Fig. 24.3 includes recent measurements of negative muons [4,19,20,21]. Since $\mu^+(\mu^-)$ are produced in association with $\nu_\mu(\overline{\nu}_\mu)$, the measurement of muons near the maximum of the intensity curve for the parent pions serves to calibrate the atmospheric ν_μ beam [22]. Because muons typically lose almost two GeV in passing through the atmosphere, the comparison near the production altitude is important for the sub-GeV range of $\nu_\mu(\overline{\nu}_\mu)$ energies.

The flux of cosmic rays through the atmosphere is described by a set of coupled cascade equations with boundary conditions at the top of the atmosphere to match the primary spectrum. Numerical or Monte Carlo calculations are needed to account accurately for decay and energy-loss processes, and for the energy-dependences of the cross sections and of the primary spectral index γ. Approximate analytic solutions are, however, useful in limited regions of energy [23]. For example, the vertical intensity of nucleons at depth X (g cm^{-2}) in the atmosphere is given by

$$I_N(E, X) \approx I_N(E, 0)\, e^{-X/\Lambda} , \qquad (24.3)$$

where Λ is the attenuation length of nucleons in air.

The corresponding expression for the vertical intensity of charged pions with energy $E_\pi \ll \epsilon_\pi = 115$ GeV is

$$I_\pi(E_\pi, X) \approx \frac{Z_{N\pi}}{\lambda_N} I_N(E_\pi, 0)\, e^{-X/\Lambda} \frac{X\, E_\pi}{\epsilon_\pi} . \qquad (24.4)$$

This expression has a maximum at $t = \Lambda \approx 120$ g cm^{-2}, which corresponds to an altitude of 15 kilometers. The quantity $Z_{N\pi}$ is the spectrum-weighted moment of the inclusive distribution of charged pions in interactions of nucleons with nuclei of the atmosphere. The intensity of low-energy pions is much less than that of nucleons because $Z_{N\pi} \approx 0.079$ is small and because most pions with energy much less than the critical energy ϵ_π decay rather than interact.

24.3. Cosmic rays at the surface

24.3.1. ***Muons***: Muons are the most numerous charged particles at sea level (see Fig. 24.3). Most muons are produced high in the atmosphere (typically 15 km) and lose about 2 GeV to ionization before reaching the ground. Their energy and angular distribution reflect a convolution of production spectrum, energy loss in the atmosphere, and decay. For example, 2.4 GeV muons have a decay length of 15 km, which is reduced to 8.7 km by energy loss. The mean energy of muons at the ground is ≈ 4 GeV. The energy spectrum is almost flat below 1 GeV, steepens gradually to reflect the primary spectrum in the 10–100 GeV range, and steepens further at higher energies because pions with $E_\pi > \epsilon_\pi \approx 115$ GeV tend to interact in the atmosphere before they decay. Asymptotically ($E_\mu \gg 1$ TeV), the energy spectrum of atmospheric muons is one power steeper than the primary spectrum. The integral intensity of vertical muons above 1 GeV/c at sea level is ≈ 70 m^{-2}s^{-1}sr^{-1} [24,25], with recent measurements [26–28] tending to give lower normalization by 10-15%. Experimentalists are familiar with this number in the form $I \approx 1$ cm^{-2} min^{-1} for horizontal detectors.

The overall angular distribution of muons at the ground is $\propto \cos^2\theta$, which is characteristic of muons with $E_\mu \sim 3$ GeV. At lower energy the angular distribution becomes increasingly steep, while at higher energy it flattens, approaching a $\sec\theta$ distribution for $E_\mu \gg \epsilon_\pi$ and $\theta < 70°$.

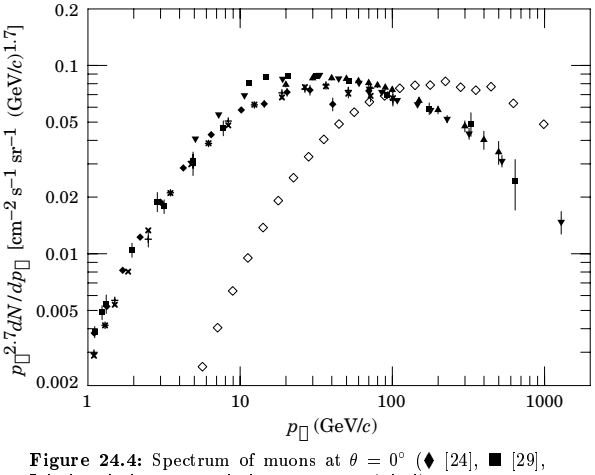

Figure 24.4: Spectrum of muons at $\theta = 0°$ (♦ [24], ■ [29], ▼ [30], ▲ [31], × and + [26], and $\theta = 75°$ ◊ [32]).

Figure 24.4 shows the muon energy spectrum at sea level for two angles. At large angles low energy muons decay before reaching the surface and high energy pions decay before they interact, thus the average muon energy increases. An approximate extrapolation formula valid when muon decay is negligible ($E_\mu > 100/\cos\theta$ GeV) and the curvature of the Earth can be neglected ($\theta < 70^\circ$) is

$$\frac{dN_\mu}{dE_\mu} \approx \frac{0.14\, E_\mu^{-2.7}}{\mathrm{cm^2\ s\ sr\ GeV}} \times \left\{ \frac{1}{1+\frac{1.1 E_\mu \cos\theta}{115\,\mathrm{GeV}}} + \frac{0.054}{1+\frac{1.1 E_\mu \cos\theta}{850\,\mathrm{GeV}}} \right\}, \qquad (24.5)$$

where the two terms give the contribution of pions and charged kaons. Eq. (24.5) neglects a small contribution from charm and heavier flavors which is negligible except at very high energy [33].

The muon charge ratio reflects the excess of π^+ over π^- in the forward fragmentation region of proton initiated interactions together with the fact that there are more protons than neutrons in the primary spectrum. The charge ratio is between 1.1 and 1.4 from 1 GeV to 100 GeV [24,26,27]. Below 1 GeV there is a systematic dependence on location due to geomagnetic effects [26,27].

24.3.2. ***Electromagnetic component***: At the ground, this component consists of electrons, positrons, and photons primarily from electromagnetic cascades initiated by decay of neutral and charged mesons. Muon decay is the dominant source of low-energy electrons at sea level. Decay of neutral pions is more important at high altitude or when the energy threshold is high. Knock-on electrons also make a small contribution at low energy [34]. The integral vertical intensity of electrons plus positrons is very approximately 30, 6, and 0.2 $\mathrm{m^{-2}s^{-1}sr^{-1}}$ above 10, 100, and 1000 MeV respectively [25,35], but the exact numbers depend sensitively on altitude, and the angular dependence is complex because of the different altitude dependence of the different sources of electrons [34,35,36]. The ratio of photons to electrons plus positrons is approximately 1.3 above a GeV and 1.7 below the critical energy [36].

24.3.3. ***Protons***: Nucleons above 1 GeV/c at ground level are degraded remnants of the primary cosmic radiation. The intensity is approximately represented by Eq. (24.3) with the replacement $t \to t/\cos\theta$ for $\theta < 70^\circ$ and an attenuation length $\Lambda = 123$ g cm^{-2}. At sea level, about 1/3 of the nucleons in the vertical direction are neutrons (up from $\approx 10\%$ at the top of the atmosphere as the n/p ratio approaches equilibrium). The integral intensity of vertical protons above 1 GeV/c at sea level is ≈ 0.9 $\mathrm{m^{-2}s^{-1}sr^{-1}}$ [25,37].

24.4. Cosmic rays underground

Only muons and neutrinos penetrate to significant depths underground. The muons produce tertiary fluxes of photons, electrons, and hadrons.

24.4.1. ***Muons***: As discussed in Section 27.6 of this *Review*, muons lose energy by ionization and by radiative processes: bremsstrahlung, direct production of e^+e^- pairs, and photonuclear interactions. The total muon energy loss may be expressed as a function of the amount of matter traversed as

$$-\frac{dE_\mu}{dX} = a + b\,E_\mu\ , \qquad (24.6)$$

where a is the ionization loss and b is the fractional energy loss by the three radiation processes. Both are slowly varying functions of energy. The quantity $\epsilon \equiv a/b$ (≈ 500 GeV in standard rock) defines a critical energy below which continuous ionization loss is more important than radiative losses. Table 24.2 shows a and b values for standard rock as a function of muon energy. The second column of Table 24.2 shows the muon range in standard rock ($A = 22$, $Z = 11$, $\rho = 2.65$ g cm^{-3}). These parameters are quite sensitive to the chemical composition of the rock, which must be evaluated for each experimental location.

Table 24.2: Average muon range R and energy loss parameters calculated for standard rock [38]. Range is given in km-water-equivalent, or 10^5 g cm^{-2}.

E_μ	R	a	b_{brems}	b_{pair}	b_{nucl}	$\sum b_i$
GeV	km.w.e.	MeV g^{-1} cm^2		10^{-6} g^{-1} cm^2		
10	0.05	2.17	0.70	0.70	0.50	1.90
100	0.41	2.44	1.10	1.53	0.41	3.04
1000	2.45	2.68	1.44	2.07	0.41	3.92
10000	6.09	2.93	1.62	2.27	0.46	4.35

The intensity of muons underground can be estimated from the muon intensity in the atmosphere and their rate of energy loss. To the extent that the mild energy dependence of a and b can be neglected, Eq. (24.6) can be integrated to provide the following relation between the energy $E_{\mu,0}$ of a muon at production in the atmosphere and its average energy E_μ after traversing a thickness X of rock (or ice or water):

$$E_\mu = (E_{\mu,0} + \epsilon)\, e^{-bX} - \epsilon\ . \qquad (24.7)$$

Especially at high energy, however, fluctuations are important and an accurate calculation requires a simulation that accounts for stochastic energy-loss processes [39].

There are two depth regimes for Eq. (24.7). For $X \ll b^{-1} \approx 2.5$ km water equivalent, $E_{\mu,0} \approx E_\mu(X) + aX$, while for $X \gg b^{-1}$ $E_{\mu,0} \approx (\epsilon + E_\mu(X))\exp(bX)$. Thus at shallow depths the differential muon energy spectrum is approximately constant for $E_\mu < aX$ and steepens to reflect the surface muon spectrum for $E_\mu > aX$, whereas for $X > 2.5$ km.w.e. the differential spectrum underground is again constant for small muon energies but steepens to reflect the surface muon spectrum for $E_\mu > \epsilon \approx 0.5$ TeV. In the deep regime the shape is independent of depth although the intensity decreases exponentially with depth. In general the muon spectrum at slant depth X is

$$\frac{dN_\mu(X)}{dE_\mu} = \frac{dN_\mu}{dE_{\mu,0}}\frac{dE_{\mu,0}}{dE_\mu} = \frac{dN_\mu}{dE_{\mu,0}}\, e^{bX}\ , \qquad (24.8)$$

where $E_{\mu,0}$ is the solution of Eq. (24.7) in the approximation neglecting fluctuations.

Fig. 24.5 shows the vertical muon intensity versus depth. In constructing this "depth-intensity curve," each group has taken account of the angular distribution of the muons in the atmosphere, the map of the overburden at each detector, and the properties of the local medium in connecting measurements at various slant depths and zenith angles to the vertical intensity. Use of data from a range of angles allows a fixed detector to cover a wide range of depths. The flat portion of the curve is due to muons produced locally by charged-current interactions of ν_μ.

24.4.2. ***Neutrinos***: Because neutrinos have small interaction cross sections, measurements of atmospheric neutrinos require a deep detector to avoid backgrounds. There are two types of measurements: contained (or semi-contained) events, in which the vertex is determined to originate inside the detector, and neutrino-induced muons. The latter are muons that enter the detector from zenith angles so large (*e.g.*, nearly horizontal or upward) that they cannot be muons produced in the atmosphere. In neither case is the neutrino flux measured directly. What is measured is a convolution of the neutrino flux and cross section with the properties of the detector (which includes the surrounding medium in the case of entering muons).

Contained and semi-contained events reflect neutrinos in the sub-GeV to multi-GeV region where the product of increasing cross section and decreasing flux is maximum. In the GeV region the neutrino flux and its angular distribution depend on the geomagnetic location of the detector and, to a lesser extent, on the phase of the solar cycle. Naively, we expect $\nu_\mu/\nu_e = 2$ from counting neutrinos of the two flavors coming from the chain of pion and muon decay. This ratio is only slightly modified by the details of the decay kinematics, but the fraction of electron neutrinos gradually decreases above a

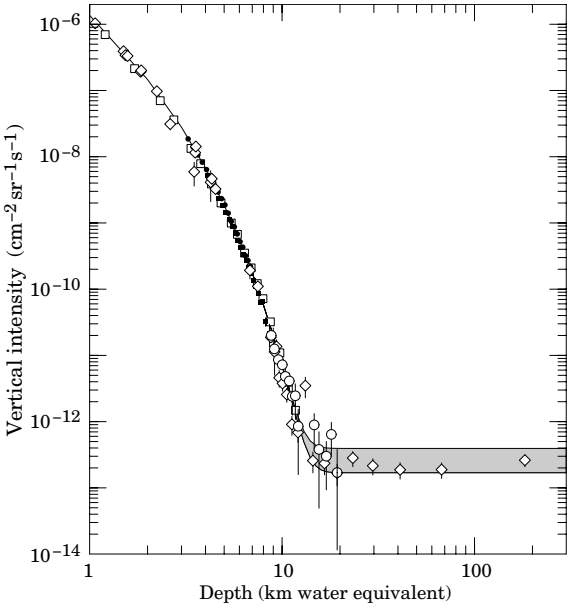

Figure 24.5: Vertical muon intensity vs depth (1 km.w.e. = 10^5 g cm^{-2} of standard rock). The experimental data are from: ◇: the compilations of Crouch [40], □: Baksan [41], ○: LVD [42], •: MACRO [43], ■: Frejus [44]. The shaded area at large depths represents neutrino-induced muons of energy above 2 GeV. The upper line is for horizontal neutrino-induced muons, the lower one for vertically upward muons.

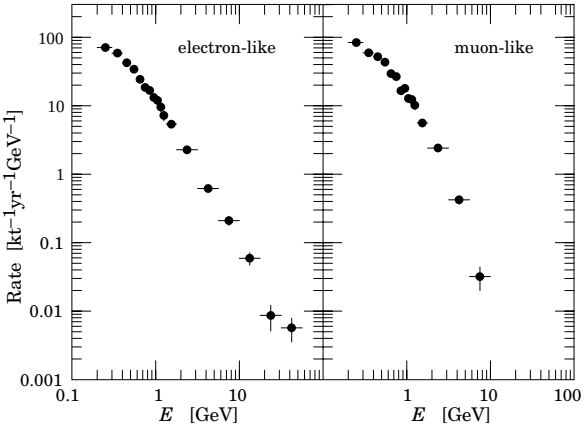

Figure 24.6: Sub-GeV and multi-GeV neutrino interactions from SuperKamiokande [45]. The plot shows the spectra of visible energy in the detector.

GeV as parent muons begin to reach the ground before decaying. Experimental measurements have to account for the ratio of $\overline{\nu}/\nu$, which have cross sections different by a factor of 3 in this energy range. In addition, detectors generally have different efficiencies for detecting muon neutrinos and electron neutrinos which need to be accounted for in comparing measurements with expectation. Fig. 24.6 shows the distributions of the visible energy in the Super-Kamiokande detector [45] for electron-like and muon-like charged current neutrino interactions. Contrary to expectation, the numbers of the two classes of events are similar rather than different by a factor of two. The exposure for the data sample shown here is 50 kiloton-years. The falloff of the muon-like events at high energy is a consequence of the poor containment for high energy muons. Corrections for detection efficiencies and backgrounds are, however, insufficient to account for the large difference from the expectation.

Two well-understood properties of atmospheric cosmic rays provide a standard for comparison of the measurements of atmospheric neutrinos. These are the "secθ effect" and the "east-west effect". The former refers originally to the enhancement of the flux of > 10 GeV muons (and neutrinos) at large zenith angles because the parent pions propagate more in the low density upper atmosphere where decay is enhanced relative to interaction. For neutrinos from muon decay, the enhancement near the horizontal becomes important for $E_\nu > 1$ GeV and arises mainly from the increased pathlength through the atmosphere for muon decay in flight. Fig. 24.7 from Ref. 46 shows a comparison between measurement and expectation for the zenith angle dependence of multi-GeV electron-like (mostly ν_e) and muon-like (mostly ν_μ) events separately. The ν_e show an enhancement near the horizontal and approximate equality for nearly upward ($\cos\theta \approx -1$) and nearly downward ($\cos\theta \approx 1$) events. There is, however, a very significant deficit of upward ($\cos\theta < 0$) ν_μ events, which have long pathlengths comparable to the radius of the Earth. This pattern has been interpreted as evidence for oscillations involving muon neutrinos [45]. (See the article on neutrino properties in this *Review*.) Including three dimensional effects in the calculation of atmospheric neutrinos may change somewhat the expected angular distributions of neutrinos at low energy [47], but it does not change the fundamental expectation of up-down symmetry, which is the basis of the evidence for oscillations.

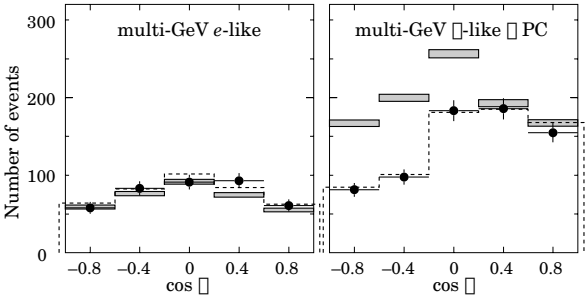

Figure 24.7: Zenith-angle dependence of multi-GeV neutrino interactions from SuperKamiokande [46]. The shaded boxes show the expectation in the absence of any oscillations. The lines show fits with some assumed oscillation parameters, as described in Ref. 46.

The east-west effect [48,49] is the enhancement, especially at low geomagnetic latitudes, of cosmic rays incident on the atmosphere from the west as compared to those from the east. This is a consequence of the fact that the cosmic rays are postively charged nuclei which are bent systematically in one sense in the geomagnetic field. Not all trajectories can reach the atmosphere from outside the geomagnetic field. The standard procedure to see which trajectories are allowed is to inject antiprotons outward from near the top of the atmosphere in various directions and see if they escape from the geomagnetic field without becoming trapped indefinitely or intersecting the surface of the Earth. Any direction in which an antiproton of a given momentum can escape is an allowed direction from which a proton of the opposite momentum can arrive. Since the geomagnetic field is oriented from south to north in the equatorial region, antiprotons injected toward the east are bent back towards the Earth. Thus there is a range of momenta and zenith angles for which positive particles cannot arrive from the east but can arrive from the west. This east-west asymmetry of the incident cosmic rays induces a similar asymmetry on the secondaries, including neutrinos. Since this is an azimuthal effect, the resulting asymmetry is independent of possible oscillations, which depend on pathlength (equivalently zenith angle), but not on azimuth. Fig. 24.8 (from Ref. 50) is a comparison of data and expectation for this effect, which serves as a consistency check of the measurement and analysis.

Muons that enter the detector from outside after production in charged-current interactions of neutrinos naturally reflect a higher

Table 24.3: Measured fluxes (10^{-13} cm^{-2} s^{-1} sr^{-1}) of neutrino-induced muons as a function of the effective minimum muon energy E_μ.

$E_\mu >$	1 GeV	1 GeV	1 GeV	2 GeV	3 GeV	3 GeV
Ref.	CWI [51]	Baksan [52]	MACRO [53]	IMB [54]	Kam [55]	SuperK [56]
F_μ	2.17±0.21	2.77±0.17	2.29 ± 0.15	2.26±0.11	1.94±0.12	1.74±0.07

energy portion of the neutrino spectrum than contained events because the muon range increases with energy as well as the cross section. The relevant energy range is $\sim 10 < E_\nu < 1000$ GeV, depending somewhat on angle. Neutrinos in this energy range show a $\sec\theta$ effect similar to muons (see Eq. (24.5)). This causes the flux of horizontal neutrino-induced muons to be approximately a factor two higher than the vertically upward flux. The upper and lower edges of the horizontal shaded region in Fig. 24.5 correspond to horizontal and vertical intensities of neutrino-induced muons. Table 24.3 gives the measured fluxes of upward-moving neutrino-induced muons averaged over the lower hemisphere. Generally the definition of minimum muon energy depends on where it passes through the detector. The tabulated effective minimum energy estimates the average over various accepted trajectories.

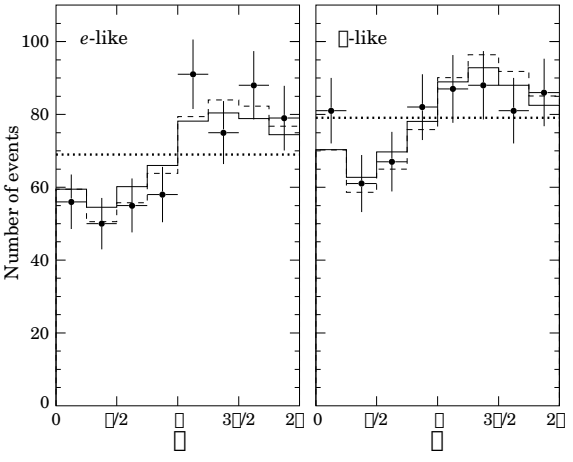

Figure 24.8: Azimuthal dependence of ∼GeV neutrino interactions from SuperKamiokande [50]. The cardinal points of the compass are S, E, N, W starting at 0. These are the direction from which the particles arrive. The lines show the expectation based on two different calculations, as described in Ref. 50.

24.5. Air showers

So far we have discussed inclusive or uncorrelated fluxes of various components of the cosmic radiation. An air shower is caused by a single cosmic ray with energy high enough for its cascade to be detectable at the ground. The shower has a hadronic core, which acts as a collimated source of electromagnetic subshowers, generated mostly from $\pi^0 \to \gamma\gamma$. The resulting electrons and positrons are the most numerous particles in the shower. The number of muons, produced by decays of charged mesons, is an order of magnitude lower.

Air showers spread over a large area on the ground, and arrays of detectors operated for long times are useful for studying cosmic rays with primary energy $E_0 > 100$ TeV, where the low flux makes measurements with small detectors in balloons and satellites difficult.

Greisen [57] gives the following approximate expressions for the numbers and lateral distributions of particles in showers at ground level. The total number of muons N_μ with energies above 1 GeV is

$$N_\mu(>1\ \mathrm{GeV}) \approx 0.95 \times 10^5 \left(N_e/10^6\right)^{3/4} , \qquad (24.9)$$

where N_e is the total number of charged particles in the shower (not just $e^\pm$). The number of muons per square meter, ρ_μ, as a function of the lateral distance r (in meters) from the center of the shower is

$$\rho_\mu = \frac{1.25\,N_\mu}{2\pi\ \Gamma(1.25)} \left(\frac{1}{320}\right)^{1.25} r^{-0.75} \left(1+\frac{r}{320}\right)^{-2.5} , \qquad (24.10)$$

where Γ is the gamma function. The number density of charged particles is

$$\rho_e = C_1(s,d,C_2)\, x^{(s-2)}(1+x)^{(s-4.5)}(1+C_2 x^d) . \qquad (24.11)$$

Here s, d, and C_2 are parameters in terms of which the overall normalization constant $C_1(s,d,C_2)$ is given by

$$C_1(s,d,C_2) = \frac{N_e}{2\pi r_1^2}\,[\,B(s,4.5-2s) + C_2\,B(s+d,\,4.5-d-2s)]^{-1} , \qquad (24.12)$$

where $B(m,n)$ is the beta function. The values of the parameters depend on shower size (N_e), depth in the atmosphere, identity of the primary nucleus, etc. For showers with $N_e \approx 10^6$ at sea level, Greisen uses $s = 1.25$, $d = 1$, and $C_2 = 0.088$. Finally, x is r/r_1, where r_1 is the Molière radius, which depends on the density of the atmosphere and hence on the altitude at which showers are detected. At sea level $r_1 \approx 78$ m. It increases with altitude.

The lateral spread of a shower is determined largely by Coulomb scattering of the many low-energy electrons and is characterized by the Molière radius. The lateral spread of the muons (ρ_μ) is larger and depends on the transverse momenta of the muons at production as well as multiple scattering.

There are large fluctuations in development from shower to shower, even for showers of the same energy and primary mass—especially for small showers, which are usually well past maximum development when observed at the ground. Thus the shower size N_e and primary energy E_0 are only related in an average sense, and even this relation depends on depth in the atmosphere. One estimate of the relation is [58]

$$E_0 \sim 3.9 \times 10^6\ \mathrm{GeV}\ (N_e/10^6)^{0.9} \qquad (24.13)$$

for vertical showers with $10^{14} < E < 10^{17}$ eV at 920 g cm^{-2} (965 m above sea level). Because of fluctuations, N_e as a function of E_0 is not the inverse of Eq. (24.13). As E_0 increases the shower maximum (on average) moves down into the atmosphere and the relation between N_e and E_0 changes. At the maximum of shower development, there are approximately 2/3 particles per GeV of primary energy.

Detailed simulations and cross-calibrations between different types of detectors are necessary to establish the primary energy spectrum from air-shower experiments [58,59]. Figure 24.9 shows the "all-particle" spectrum. The differential energy spectrum has been multiplied by $E^{2.7}$ in order to display the features of the steep spectrum that are otherwise difficult to discern. The steepening that occurs between 10^{15} and 10^{16} eV is known as the *knee* of the spectrum. The feature around 10^{19} eV is called the *ankle* of the spectrum.

Measurements with small air shower experiments in the knee region differ by as much as a factor of two, indicative of systematic uncertainties in interpretation of the data. (For a recent review see Ref. 60.) In establishing the spectrum shown in Fig. 24.9, efforts have been made to minimize the dependence of the analysis on the primary composition. Ref. 61 uses an unfolding procedure to obtain the spectra of the individual components, giving a result for the all-particle spectrum between 10^{15} and 10^{17} eV that lies toward the

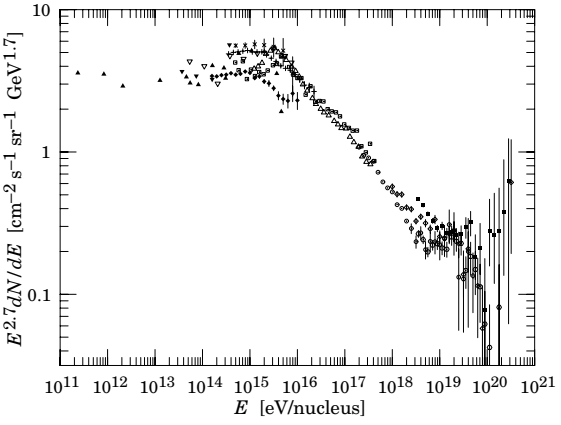

Figure 24.9: The all-particle spectrum: □ [58], ▲ [62], ▼ [63], ▽ [64], △ [65], + [66], × [67], ♦ [68]. References for the high energy portion of the spectrum are given in Fig. 24.10.

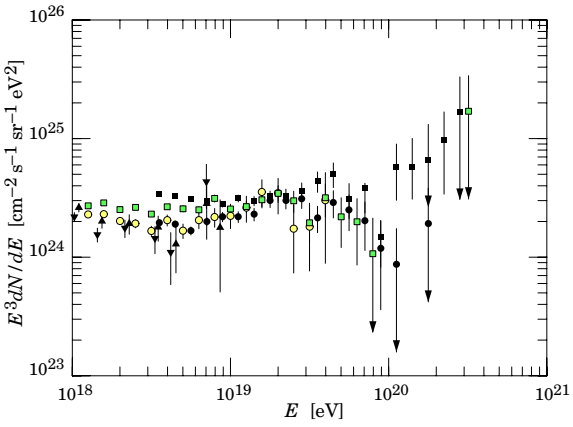

Figure 24.10: Expanded view of the highest energy portion of the cosmic-ray spectrum: o [69] (stereo), □ [69] (monocular) ■ [78], • [79](Hi-Res monocular, preliminary), ▲ [80](if protons) ▼ [80](if iron).

upper range of the data shown in Fig. 24.9. In the energy range above 10^{17} eV, the Fly's Eye technique [69] is particularly useful because it can establish the primary energy in a model-independent way by observing most of the longitudinal development of each shower, from which E_0 is obtained by integrating the energy deposition in the atmosphere.

If the cosmic ray spectrum below 10^{18} eV is of galactic origin, the *knee* could reflect the fact that some (but not all) cosmic accelerators have reached their maximum energy. Some types of expanding supernova remnants, for example, are estimated not to be able to accelerate particles above energies in the range of 10^{15} eV total energy per particle. Effects of propagation and confinement in the galaxy [70] also need to be considered.

The *ankle* has the classical characteristic shape [71] of a higher energy population of particles overtaking a lower energy population. A possible interpretation is that the higher energy population represents cosmic rays of extragalactic origin. If this is the case and if the cosmic rays are cosmological in origin, then there should be a cutoff around 5×10^{19} eV, resulting from interactions with the microwave background [72,73]. It is therefore of special interest that several events have been assigned energies above 10^{20} eV [74–77].

Figure 24.10 gives an expanded view of the high energy end of the spectrum. The differential flux is multiplied by E^3, a procedure that amplifies small systematic differences in energy assignments into sizeable differences in rate. Current discussion focuses on systematic effects with small data samples from a steep spectrum. At issue is whether or not the spectrum of the highest energy cosmic rays indeed continues well past the cutoff expected for a cosmological distribution of sources. If it does, the implication would be that some sources of the highest energy particles must be relatively nearby. For example, the attenuation length for protons at 2×10^{20} eV is 30 Mpc [81]. Both cosmic accelerators ("bottom-up") and massive cosmological relics ("top-down") have been suggested [82].

References:

1. J.A. Simpson, Ann. Rev. Nucl. and Part. Sci. **33**, 323 (1983).
2. M. Boezio *et al.*, Astrophys. J. **518**, 457 (1999).
3. W. Menn *et al.*, Astrophys. J. **533**, 281 (2000).
4. R. Bellotti *et al.*, Phys. Rev. **D60**, 052002 (1999).
5. AMS Collaboration, Phys. Lett. **B490**, 27 (2000).
6. T. Sanuki *et al.*, Astrophys. J. **545**, 1135 (2000).
7. J.J. Engelmann *et al.*, Astron. & Astrophys. **233**, 96 (1990); See also *Cosmic Abundances of Matter* (ed. C. Jake Waddington) A.I.P. Conf. Proceedings No. 183 (1988) p. 111.
8. S.W. Barwick *et al.*, Astrophys. J. **498**, 779 (1998).
9. M. Boezio *et al.*, Astrophys. J. **552**, 635 (2000).
10. J. Alcaraz *et al.*, Phys. Lett. **B484**, 10 (2000).
11. J.M. Clem & P.A. Evenson, Astrophys. J. **568**, 216 (2002).
12. M.A. DuVernois *et al.*, Astrophys. J. **559**, 296 (2000).
13. M. Hof *et al.*, Astrophys. J. **467**, L33 (1996) See also G. Basini *et al.*, *Proc. 26th Int. Cosmic Ray Conf.*, Salt Lake City, **3**, 101 (1999).
14. A.S. Beach *et al.*, Phys. Rev. Lett. **87**, 271101 (2001).
15. J.W. Mitchell *et al.*, Phys. Rev. Lett. **76**, 3057 (1996).
16. M. Boezio *et al.*, Astrophys. J. **487**, 415 (1997).
17. S. Orito *et al.*, Phys. Rev. Lett. **84**, 1078 (2000).
18. Y. Asaoka *et al.*, Phys. Rev. Lett. **88**, 51101 (2002).
19. R. Bellotti *et al.*, Phys. Rev. **D53**, 35 (1996).
20. M. Boezio *et al.*, Phys. Rev. **D62**, 032007 (2000).
21. S. Coutu *et al.*, Phys. Rev. **D62**, 032001 (2000).
22. D.H. Perkins, Astropart. Phys. **2**, 249 (1994).
23. T.K. Gaisser, *Cosmic Rays and Particle Physics*, Cambridge University Press (1990).
24. M.P. De Pascale *et al.*, J. Geophys. Res. **98**, 3501 (1993).
25. P.K.F. Grieder, *Cosmic Rays at Earth*, Elsevier Science (2001).
26. J. Kremer *et al.*, Phys. Rev. Lett. **83**, 4241 (1999).
27. M. Motoki *et al.*, Proc. 27th Int. Cosmic Ray Conf. (Hamburg) **3**, 927 (2001).
28. P. Le Coultre on behalf of the L3 Collaboration, Proc. 27th Int. Cosmic Ray Conf. (Hamburg) **3**, 974 (2001)..
29. O.C. Allkofer, K. Carstensen, and W.D. Dau, Phys. Lett. **B36**, 425 (1971).
30. B.C. Rastin, J. Phys. **G10**, 1609 (1984).
31. C.A. Ayre *et al.*, J. Phys. **G1**, 584 (1975).
32. H. Jokisch *et al.*, Phys. Rev. **D19**, 1368 (1979).
33. C.G.S. Costa, Astropart. Phys. **16**, 193 (2001).
34. S. Hayakawa, *Cosmic Ray Physics*, Wiley, Interscience, New York (1969).
35. R.R. Daniel and S.A. Stephens, Revs. Geophysics & Space Sci. **12**, 233 (1974).
36. K.P. Beuermann and G. Wibberenz, Can. J. Phys. **46**, S1034 (1968).
37. I.S. Diggory *et al.*, J. Phys. **A7**, 741 (1974).
38. D.E. Groom, N.V. Mokhov, and S.I. Striganov, "Muon stopping-power and range tables," Atomic Data and Nuclear Data Tables, 78, 183 (2001).
39. P. Lipari and T. Stanev, Phys. Rev. **D44**, 3543 (1991).

40. M. Crouch, in *Proc. 20th Int. Cosmic Ray Conf.*, Moscow, **6**, 165 (1987).
41. Yu.M. Andreev, V.I. Gurentzov, and I.M. Kogai, in *Proc. 20th Int. Cosmic Ray Conf.*, Moscow, **6**, 200 (1987).
42. M. Aglietta *et al.*, (LVD Collaboration), Astropart. Phys. **3**, 311 (1995).
43. M. Ambrosio *et al.*, (MACRO Collaboration), Phys. Rev. **D52**, 3793 (1995).
44. Ch. Berger *et al.*, (Frejus Collaboration), Phys. Rev. **D40**, 2163 (1989).
45. Y. Fukuda *et al.*, Phys. Rev. Lett. **81**, 1562 (1998).
46. K. Scholberg *et al.*, in *Proc. Eighth Int. Workshop on Neutrino Telescopes* (ed. Milla Baldo Ceolin, edizioni papergraf, Venezia, 1999) p. 183.
47. G. Battistoni *et al.*, Astropart. Phys. **12**, 315 (2000).
48. T.H. Johnson, Phys. Rev. **43**, 834 (1933). See also T.H. Johnson & E.C. Street, Phys. Rev. **44**, 125 (1933).
49. L.W. Alvarez and A.H. Compton, Phys. Rev. **43**, 835 (1933).
50. T. Futagami *et al.*, Phys. Rev. Lett. **82**, 5194 (1999).
51. F. Reines *et al.*, Phys. Rev. Lett. **15**, 429 (1965).
52. M.M. Boliev *et al.*, in *Proceedings 3rd Int. Workshop on Neutrino Telescopes*(ed. Milla Baldo Ceolin), 235 (1991).
53. M. Ambrosio *et al.*, (MACRO) Phys. Lett. **B434**, 451 (1998). The number quoted for MACRO is the average over 90% of the lower hemisphere, $\cos\theta < -0.1$; see F. Ronga *et al.*, `hep-ex/9905025`.
54. R. Becker-Szendy *et al.*, Phys. Rev. Lett. **69**, 1010 (1992); *Proc. 25th Int. Conf. High-Energy Physics*, Singapore (ed. K.K. Phua and Y. Yamaguchi, World Scientific, 1991) p. 662.
55. S. Hatakeyama *et al.*, Phys. Rev. Lett. **81**, 2016 (1998).
56. Y. Fukuda *et al.*, Phys. Rev. Lett. **82**, 2644 (1999).
57. K. Greisen, Ann. Rev. Nucl. Sci. **10**, 63 (1960).
58. M. Nagano *et al.*, J. Phys. **G10**, 1295 (1984).
59. M. Teshima *et al.*, J. Phys. **G12**, 1097 (1986).
60. S.P. Swordy *et al.*, astro-ph/0202159v1, Astropart. Phys. (to be published).
61. H. Ulrich *et al.*, *Proc. 27th Int. Cosmic Ray Conf.*, Hamburg, **1**, 97 (2001).
62. N.L. Grigorov *et al.*, Yad. Fiz. **11**, 1058 (1970) and *Proc. 12th Int. Cosmic Ray Conf.*, Hobart, **2**, 206 (1971).
63. K. Asakimori *et al.*, *Proc. 23rd Int. Cosmic Ray Conf.*, Calgary, **2**, 25 (1993); *Proc. 22nd Int. Cosmic Ray Conf.*, Dublin, **2**, 57 and 97 (1991).
64. T.V. Danilova *et al.*, *Proc. 15th Int. Cosmic Ray Conf.*, Plovdiv, **8**, 129 (1977).
65. Yu. A. Fomin *et al.*, *Proc. 22nd Int. Cosmic Ray Conf.*, Dublin, **2**, 85 (1991).
66. M. Amenomori *et al.*, Astrophys. J. **461**, 408 (1996).
67. F. Arqueros *et al.*, Astron. & Astrophys. **359**, 682 (2000).
68. M.A.K. Glasmacher *et al.*, Astropart. Phys. **10**, 291 (1999).
69. D.J. Bird *et al.*, Astrophys. J. **424**, 491 (1994).
70. V.S. Ptuskin *et al.*, Astron. & Astrophys. **268**, 726 (1993).
71. B. Peters, Nuovo Cimento **22**, 800 (1961).
72. K. Greisen, Phys. Rev. Lett. **16**, 748 (1966).
73. G.T. Zatsepin and V.A. Kuz'min, Sov. Phys. JETP Lett. **4**, 78 (1966).
74. J. Linsley, Phys. Rev. Lett. **10**, 146 (1963).
75. D.J. Bird *et al.*, Astrophys. J. **441**, 144 (1995).
76. N. Hayashima *et al.*, Phys. Rev. Lett. **73**, 3941 (1994).
77. M. Nagano & A.A. Watson, Rev. Mod. Phys. **72**, 689 (2000).
78. M. Takeda *et al.*, Phys. Rev. Lett. **81**, 1163 (1998) (as updated by M. Teshima, private communication).
79. P. Sokolsky, private communication.
80. M. Ave *et al.*, `astro-ph/0112253`.
81. V.S. Berezinskii *et al.*, *Astrophysics of Cosmic Rays*, North-Holland (1990).
82. P. Bhattacharjee & G. Sigl, Phys. Reports **327**, 109 (2000).

25. ACCELERATOR PHYSICS OF COLLIDERS

Revised August 2003 by K. Desler and D.A. Edwards (DESY).

25.1. Introduction

This article is intended to be a mini-introduction to accelerator physics, with emphasis on colliders. Essential data are summarized in the "Tables of Collider Parameters" (Sec. 26). Luminosity is the quantity of most immediate interest for HEP, and so we begin with its definition and a discussion of the various factors involved. Then we talk about some of the underlying beam dynamics. Finally, we comment on present limitations and possible future directions.

The focus is on colliders because they provide the highest c.m. energy, and therefore, the longest potential discovery reach. All present-day colliders are synchrotrons with the exception of the SLAC Linear Collider. In the pursuit of higher c.m. energy with electrons, synchrotron radiation presents a formidable barrier to energy beyond LEP. The LHC will be the first proton collider in which synchrotron radiation has significant design impact.

25.2. Luminosity

The event rate R in a collider is proportional to the interaction cross section $\sigma_{\rm int}$, and the factor of proportionality is called the *luminosity*:

$$R = \mathscr{L}\sigma_{\rm int} \ . \tag{25.1}$$

If two bunches containing n_1 and n_2 particles collide with frequency f, then the luminosity is approximately

$$\mathscr{L} = f\frac{n_1 n_2}{4\pi\sigma_x\sigma_y}, \tag{25.2}$$

where σ_x and σ_y characterize the Gaussian transverse beam profiles in the horizontal (bend) and vertical directions. Though the initial particle distribution at the source may be far from Gaussian, by the time the beam reaches high energy, the normal form is a very good approximation, thanks to the central limit theorem of probability and diminished importance of space charge effects. The qualifier "approximately" appears because this generic expression requires adaptation to particular cases. Discussion may be found in the article of Furman and Zisman in Sec. 3.1.1 of Ref. 1.

Luminosity is often expressed in units of $\mathrm{cm}^{-2}\mathrm{s}^{-1}$, and tends to be a large number. For example, KEK recently announced that its B factory had reached a peak luminosity in excess of 10^{34} cm^{-2} s^{-1}. The highest luminosity for protons achieved so far is 1.3×10^{32} $\mathrm{cm}^{-2}\mathrm{s}^{-1}$ at the now decommissioned ISR; a goal of the Tevatron run just getting underway as this is written is to challenge that record. The relevant quantity for HEP is the luminosity integrated over time, usually stated in the units normally used for cross sections, such as pb^{-1} or fb^{-1}. B-factory integrated luminosities are moving into the hundreds of fb^{-1} range.

The beam size can be expressed in terms of two quantities, one termed the *transverse emittance*, ϵ, and the other, the *amplitude function*, β. The transverse emittance is a beam quality concept reflecting the process of bunch preparation, extending all the way back to the source for hadrons and, in the case of electrons, mostly dependent on synchrotron radiation. The amplitude function is a beam optics quantity, and is determined by the accelerator magnet configuration.

The transverse emittance is a measure of the phase space area associated with either of the two transverse degrees of freedom, x and y. These coordinates represent the position of a particle with reference to some ideal design trajectory. Think of x as the "horizontal" displacement (in the bend plane for the case of a synchrotron), and y as the "vertical" displacement. The conjugate coordinates are the transverse momenta, which at constant energy are proportional to the angles of particle motion with respect to the design trajectory, x' and y'. Various conventions are in use to characterize the boundary of phase space. Beam sizes are usually given as the standard deviations characterizing Gaussian beam profiles in the two transverse degrees of freedom. In each degree of freedom, the one-σ contour in displacement and angle is frequently used, and we will follow this choice.

Suppose that at some location in the collider, the phase space boundary appears as an upright ellipse, where the coordinates are the displacement x (using the horizontal plane for instance), and the angle x' with respect to the beam axis. The choice of an elliptical contour will be justified under Beam Dynamics below. If σ and σ' are the ellipse semi-axes in the x and x' directions respectively, then the emittance may be defined by $\epsilon \equiv \pi\sigma\sigma'$. Transverse emittance is often stated in units of mm-mrad.

At either a minimum or maximum of the beam size of a beam circulating in equilibrium, the *amplitude function* β at those points is the aspect ratio σ/σ'. When expressed in terms of σ and β, the transverse emittance becomes

$$\epsilon = \pi\sigma^2/\beta \ . \tag{25.3}$$

Of particular significance is the value of the amplitude function at the interaction point, β^*. To achieve high luminosity, one wants β^* to be as small as possible; how small depends on the capability of the hardware to make a near-focus at the interaction point. For example, in the HERA proton ring, β^* at one of the major detectors is 1 m while elsewhere in the synchrotron, typical values of the amplitude function lie in the range 30–100 m. For e^+e^- colliders, $\beta_y^* \sim 1$ cm.

Eq. (25.2) can now be recast in terms of emittances and amplitude functions as

$$\mathscr{L} = f\frac{n_1 n_2}{4\sqrt{\epsilon_x\,\beta_x^*\,\epsilon_y\,\beta_y^*}} \ . \tag{25.4}$$

Thus, to achieve high luminosity, all one has to do is make high population bunches of low emittance collide at high frequency at locations where the beam optics provides as low values of the amplitude functions as possible.

Depending on the particular facility, there are other ways of stating the expression for the luminosity. In a multibunch collider, the various bunch populations will differ; in a facility such as HERA, the electron and proton bunches may differ in emittance, the variation of the beam size in the neighborhood of the interaction point may be significant, and so on.

25.3. Beam dynamics

A major concern of beam dynamics is stability: conservation of adequate beam properties over a sufficiently long time scale. Several time scales are involved, and the approximations used in writing the equations of motion reflect the time scale under consideration. For example, when, in Sec. 25.3.1 below, we write the equations for transverse stability, no terms associated with phase stability or synchrotron radiation appear; the time scale associated with the last two processes is much longer than that demanded by the need for transverse stability.

25.3.1. *Betatron oscillations*:

Present-day high-energy accelerators employ alternating gradient focussing provided by quadrupole magnetic fields [2]. The equations of motion of a particle undergoing oscillations with respect to the design trajectory are

$$x'' + K_x(s)\,x = 0 \ , \quad y'' + K_y(s)\,y = 0 \ , \tag{25.5}$$

with

$$x' \equiv dx/ds \ , \quad y' \equiv dy/ds \tag{25.6}$$

$$K_x \equiv B'/(B\rho) + \rho^{-2} \ , \quad K_y \equiv -B'/(B\rho) \tag{25.7}$$

$$B' \equiv \partial B_y/\partial x \ . \tag{25.8}$$

The independent variable s is path length along the design trajectory. This motion is called a *betatron* oscillation because it was initially studied in the context of that type of accelerator. The functions K_x and K_y reflect the transverse focussing—primarily due to quadrupole fields except for the radius of curvature, ρ, term in K_x for a synchrotron—so each equation of motion resembles that for a harmonic oscillator, but with spring constants that are a function of position. No terms relating to synchrotron oscillations appear,

because their time scale is much longer and, in this approximation, play no role.

These equations have the form of Hill's equation, and so the solution in one plane may be written as

$$x(s) = A\sqrt{\beta(s)}\,\cos(\psi(s)+\delta), \tag{25.9}$$

where A and δ are constants of integration and the phase advances according to $d\psi/ds = 1/\beta$. The dimension of A is the square root of length, reflecting the fact that the oscillation amplitude is modulated by the square root of the amplitude function. In addition to describing the envelope of the oscillation, β also plays the role of an 'instantaneous' λ. The wavelength of a betatron oscillation may be some tens of meters, and so typically values of the amplitude function are of the order of meters, rather than on the order of the beam size. The beam optics arrangement generally has some periodicity, and the amplitude function is chosen to reflect that periodicity. As noted above, a small value of the amplitude function is desired at the interaction point, and so the focussing optics is tailored in its neighborhood to provide a suitable β^*.

The number of betatron oscillations per turn in a synchrotron is called the *tune* and is given by

$$\nu = \frac{1}{2\pi}\oint\frac{ds}{\beta}\ . \tag{25.10}$$

Expressing the integration constant A in the solution above in terms of x, x' yields the *Courant-Snyder invariant*

$$A^2 = \gamma(s)\,x(s)^2 + 2\alpha(s)\,x(s)\,x'(s) + \beta(s)\,x'(s)^2$$

where

$$\alpha \equiv -\beta'/2,\ \ \gamma \equiv \frac{1+\alpha^2}{\beta}\ . \tag{25.11}$$

(The Courant-Snyder parameters α, β, and γ employ three Greek letters which have other meanings, and the significance at hand must often be recognized from context.) Because β is a function of position in the focussing structure, this ellipse changes orientation and aspect ratio from location to location, but the area πA^2 remains the same.

As noted above, the transverse emittance is a measure of the area in x, x' (or y, y') phase space occupied by an ensemble of particles. The definition used in Eq. (25.3) is the area that encloses 39% of a Gaussian beam.

For electron synchrotrons, the equilibrium emittance results from the balance between synchrotron radiation damping and excitation from quantum fluctuations in the radiation rate. The equilibrium is reached in a time which is small compared with the storage time.

For present-day hadron synchrotrons, synchrotron radiation does not play a similar role in determining the transverse emittance. Rather, the emittance during storage reflects the source properties and the abuse suffered by the particles throughout acceleration and storage. Nevertheless, it is useful to argue as follows: Though x' and x can serve as canonically conjugate variables at constant energy, this definition of the emittance would not be an adiabatic invariant when the energy changes during the acceleration cycle. However, $\gamma(v/c)x'$, where here γ is the Lorentz factor, is proportional to the transverse momentum, and so qualifies as a variable conjugate to x. So often one sees a normalized emittance defined according to

$$\epsilon_N = \gamma\,\frac{v}{c}\,\epsilon, \tag{25.12}$$

which is an approximate adiabatic invariant, *e.g.* during acceleration.

25.3.2. ***Phase stability***: The particles in a circular collider also undergo synchrotron oscillations. This is usually referred to as motion in the *longitudinal* degree-of-freedom because particles arrive at a particular position along the accelerator earlier or later than an ideal reference particle. This circumstance results in a finite bunch length, which is related to an energy spread.

For dynamical variables in longitudinal phase space, let us take ΔE and Δt, where these are the energy and time differences from that of the ideal particle. A positive Δt means a particle is behind the ideal particle. The equation of motion is the same as that for a physical pendulum, and therefore is nonlinear. But for small oscillations, it reduces to a simple harmonic oscillator:

$$\frac{d^2\Delta t}{dn^2} = -(2\pi\nu_s)^2\,\Delta t \tag{25.13}$$

where the independent variable n is the turn number, and ν_s is the number of synchrotron oscillations per turn, analogous to the betatron oscillation tune defined earlier. Implicit in this equation is the approximation that n is a continuous variable. This approximation is valid provided $\nu_s \ll 1$, which is usually well satisfied in practice.

In the high-energy limit, where $v/c \approx 1$,

$$\nu_s = \left[\frac{h\eta\,eV\,\cos\phi_s}{2\pi E}\right]^{1/2}\ . \tag{25.14}$$

There are four as yet undefined quantities in this expression: the harmonic number h, the slip factor η, the maximum energy eV gain per turn from the acceleration system, and the synchronous phase ϕ_s. The frequency of the RF system is normally a relatively high multiple, h, of the orbit frequency. The slip factor relates the fractional change in the orbit period τ to changes in energy according to

$$\frac{\Delta\tau}{\tau} = \eta\frac{\Delta E}{E}\ . \tag{25.15}$$

At sufficiently high energy, the slip factor just reflects the relationship between path length and energy, since the speed is a constant; η is positive for all the synchrotrons in the "Tables of Collider Parameters" (Sec. 26).

The synchronous phase is a measure of how far up on the RF wave the average particle must ride in order to maintain constant energy to counteract synchrotron radiation. That is, $\sin\phi_s$ is the ratio of the energy loss per turn to the maximum energy per turn that can be provided by the acceleration system. For hadron colliders built to date, $\sin\phi_s$ is effectively zero. This is not the case for electron storage rings; for example, the electron ring of HERA runs at a synchronous phase of 45°.

Now if one has a synchrotron oscillation with amplitudes $\widehat{\Delta t}$ and $\widehat{\Delta E}$,

$$\Delta t = \widehat{\Delta t}\,\sin(2\pi\nu_s n)\ ,\qquad \Delta E = \widehat{\Delta E}\,\cos(2\pi\nu_s n), \tag{25.16}$$

then the amplitudes are related according to

$$\widehat{\Delta E} = \frac{2\pi\nu_s E}{\eta\tau}\widehat{\Delta t}\ . \tag{25.17}$$

The longitudinal emittance ϵ_ℓ may be defined as the phase space area bounded by particles with amplitudes $\widehat{\Delta t}$ and $\widehat{\Delta E}$. In general, the longitudinal emittance for a given amplitude is found by numerical integration. For $\sin\phi_s = 0$, an analytical expression is:

$$\epsilon_\ell = \left[\frac{2\pi^3 EeVh}{\tau^2\eta}\right]^{1/2}(\widehat{\Delta t})^2. \tag{25.18}$$

Again, a Gaussian is a reasonable representation of the longitudinal profile of a well-behaved beam bunch; if $\sigma_{\Delta t}$ is the standard deviation of the time distribution, then the bunch length can be characterized by

$$\ell = c\,\sigma_{\Delta t}\ . \tag{25.19}$$

In the electron case, the longitudinal emittance is determined by the synchrotron radiation process just, as in the transverse degrees of freedom. For the hadron case, the history of acceleration plays a role, and because energy and time are conjugate coordinates, the longitudinal emittance is a quasi-invariant.

For HEP, bunch length is a significant quantity, because if the bunch length becomes larger than β^*, the luminosity is adversely affected. This is because β grows parabolically as one proceeds away from the IP, and so the beam size increases, thus lowering the contribution to the luminosity from such locations.

25.3.3. ***Synchrotron radiation*** [3]: A relativistic particle undergoing centripetal acceleration radiates at a rate given by the Larmor formula multiplied by the 4th power of the Lorentz factor:

$$P = \frac{1}{6\pi\epsilon_0}\frac{e^2a^2}{c^3}\gamma^4. \qquad (25.20)$$

Here, $a = v^2/\rho$ is the centripetal acceleration of a particle with speed v undergoing deflection with radius of curvature ρ. In a synchrotron that has a constant radius of curvature within bending magnets, the energy lost due to synchrotron radiation per turn is the above multiplied by the time spent in bending magnets, $2\pi\rho/v$. Expressed in familiar units, this result may be written

$$W = 8.85 \times 10^{-5} E^4/\rho \ \text{ MeV per turn} \qquad (25.21)$$

for electrons at sufficiently high energy that $v \approx c$. The energy E is in GeV and ρ is in kilometers. The radiation has a broad energy spectrum which falls off rapidly above the *critical energy*, $E_c = (3c/2\rho)\hbar\gamma^3$. Typically, E_c is in the hard x-ray region.

The characteristic time for synchrotron radiation processes is the time during which the energy must be replenished by the acceleration system. If f_0 is the orbit frequency, then the characteristic time is given by

$$\tau_0 = \frac{E}{f_0 W} \ . \qquad (25.22)$$

Oscillations in each of the three degrees of freedom either damp or antidamp depending on the design of the accelerator. For a simple separated-function alternating gradient synchrotron, all three modes damp. The damping time constants are related by Robinson's Theorem [4], which, expressed in terms of τ_0, is

$$\frac{1}{\tau_x} + \frac{1}{\tau_y} + \frac{1}{\tau_s} = 2\frac{1}{\tau_0} \ . \qquad (25.23)$$

Even though all three modes may damp, the emittances do not tend toward zero. Statistical fluctuations in the radiation rate excite synchrotron oscillations and radial betatron oscillations. Thus there is an equilibrium emittance at which the damping and excitation are in balance. The vertical emittance is non-zero due to horizontal-vertical coupling.

Polarization can develop from an initially unpolarized beam as a result of synchrotron radiation. A small fraction $\approx E_c/E$ of the radiated power flips the electron spin. Because the lower energy state is that in which the particle magnetic moment points in the same direction as the magnetic bend field, the transition rate toward this alignment is larger than the rate toward the reverse orientation. An equilibrium polarization of 92% is predicted, and despite a variety of depolarizing processes, polarization above 80% has been observed at a number of facilities.

The radiation rate for protons, is of, course down by a factor of the fourth power of the mass ratio, and is given by

$$W = 7.8 \times 10^{-3} E^4/\rho \ \text{ keV per turn} \qquad (25.24)$$

where E is now in TeV and ρ in km. For the LHC, synchrotron radiation presents a significant load to the cryogenic system, and impacts magnet design due to gas desorption and secondary electron emission from the wall of the cold beam tube. The critical energy for the LHC is 44 eV.

25.3.4. ***Beam-beam tune shift***: In a bunch-bunch collision, the particles of one bunch see the other bunch as a nonlinear lens. Therefore, the focussing properties of the ring are changed in a way that depends on the transverse oscillation amplitude. Hence, there is a spread in the frequency of betatron oscillations.

There is an extensive literature on the subject of how large this tune spread can be. In practice, the limiting value is hard to predict. It is consistently larger for electrons because of the beneficial effects of damping from synchrotron radiation.

In order that contributions to the total tune spread arise only at the detector locations, the beams in a multibunch collider are kept apart elsewhere in the collider by a variety of techniques. For equal energy particles of opposite charge circulating in the same vacuum chamber, electrostatic separators may be used assisted by a crossing angle if appropriate. For particles of equal energy and of the same charge, a crossing angle is needed not only for tune spread reasons, but also to steer the particles into two separate beam pipes. In HERA, because of the large ratio of proton to electron energy, separation can be achieved by bending magnets.

25.3.5. ***Luminosity lifetime***: In electron synchrotrons, the luminosity degrades during the store primarily due to particles leaving the phase stable region in longitudinal phase space, as a result of quantum fluctuations in the radiation rate and bremsstrahlung. For hadron colliders, the luminosity deteriorates due to emittance dilution resulting from a variety of processes. In practice, stores are intentionally terminated when the luminosity drops to the point where a refill will improve the integrated luminosity.

25.4. Status and prospects

Present facilities represent a balance among current technology, the desires of High Energy Physics, and public support. For a half century, beam optics has exploited the invention of alternating gradient focussing. This principle is employed in all colliders both linear and circular. Superconducting technology has grown dramatically in importance during the last two decades. Superconducting magnets are vital to the Tevatron, HERA, and to the future LHC. Superconducting accelerating structures are necessary to CESR, LEP, HERA, Jefferson Laboratory, the spallation neutron source, and other facilities requiring high-gradient long pulse length RF systems. Present room temperature accelerating structures produce very short pulses, but with gradients well in excess of the superconducting variety [1].

At present, the next facilities will include the LHC, and possibly an electron linear collider. The LHC is an approved project that will represent a major step forward in superconducting magnet technology. No linear collider project has been approved as yet, and the conventional and superconducting approaches compete for prominence.

In addition to the possibilities of the preceding paragraph, there are other synchrotron-based collider studies underway. Despite formidable R&D challenges, a muon-muon collider may become feasible. Proponents of a very large hadron collider at higher energy than the cancelled SSC project are exploring low-cost magnets and tunnels for a facility on the 100 TeV c.m. energy scale.

The approach to collider design sketched here—guidance and focussing provided by external magnetic fields, and acceleration produced by RF resonators—has led to ever larger and more costly facilities with increase of c.m. energy. Support for new HEP facilities has diminished as proposals have climbed into the multi-billion dollar range.

There is no shortage of ideas for departure from the current design paradigm. Wakefield accelerators, plasma-laser combinations, and related investigations may, if successful, deliver gradients far higher than any realized today in existing HEP facilities. However, staging and energy efficiency are major hurdles. These approaches are exceedingly challenging technologically, and require a strong R&D program if they are to succeed.

Other important references include Ref. [5–7], which are not cited in the text above.

References:

1. *Handbook of Accelerator Physics and Engineering*, eds. A.W. Chao and M. Tigner, World Scientific Publishing Co. (Singapore, 2nd printing, 2002).
2. E.D. Courant and H.S. Snyder, Ann. Phys. **3**, 1 (1958). This is the classic article on the alternating gradient synchrotron.
3. M. Sands, *The Physics of Electron Storage Rings—An Introduction*, SLAC Publication SLAC 121, UC-28 (ACC), 1970.
4. K. Robinson, Phys. Rev. **111**, 373 (1958).

5. D.A. Edwards and M.J. Syphers, *An Introduction to the Physics of High Energy Accelerators*, John Wiley & Sons, 1993. This is an elementary textbook on accelerator physics. The next two references are more advanced, and are cited here for readers who may wish to pursue beam physics in greater depth.

6. A. Wu Chao, *Physics of Collective Beam Instabilities in High Energy Accelerators*, John Wiley & Sons, 1993.

7. M. Reiser, *Theory and Design of Charged Particle Beams*, John Wiley & Sons, 1994.

HIGH-ENERGY COLLIDER PARAMETERS: e^+e^- Colliders (I)

The numbers here were received from representatives of the colliders in early 2004 (contact C.G. Wohl, LBNL). Many of the numbers of course change with time, and only the latest values (or estimates) are given here; those in brackets are for coming upgrades. Quantities are, where appropriate, r.m.s. H and V indicate horizontal and vertical directions. Parameters for the defunct SPEAR, DORIS, PETRA, PEP, SLC, TRISTAN, and VEPP-2M colliders may be found in our 1996 edition (Phys. Rev. **D54**, 1 July 1996, Part I).

	VEPP-2000 (Novosibirsk)	VEPP-4M (Novosibirsk)	BEPC (China)	BEPC-II (China)	DAΦNE (Frascati)
Physics start date	2005	1994	1989	2007	1999
Physics end date	—	—	—	—	∼2007
Maximum beam energy (GeV)	1.0	6	2.2	1.89 (2.1 max)	0.700
Luminosity (10^{30} cm^{-2}s^{-1})	100	20	10 at 1.843 GeV/beam 5 at 1.55 GeV/beam	1000	80 present 200 achievable
Time between collisions (μs)	0.04	0.6	0.8	0.008	0.0027
Crossing angle (μ rad)	0	0	0	1.1×10^4	$(2.5 \text{ to } 3.2)\times 10^4$
Energy spread (units 10^{-3})	0.64	1	0.58 at 2.2 GeV	0.52	0.40
Bunch length (cm)	4	5	≈ 5	1.3	1 low current 2 high current
Beam radius (10^{-6} m)	125 (round)	H: 1000 V: 30	H: 890 V: 37	H: 380 V: 5.7	H: 800 V: 4.8
Free space at interaction point (m)	±1	±2	±2.15	±1.009	±0.40
Luminosity lifetime (hr)	continuous	2	7–12	1.5	0.7
Filling time (min)	continuous	15	30	26	0.8 (topping up)
Acceleration period (s)	—	150	120	—	on energy
Injection energy (GeV)	0.2–1.0	1.8	1.55	1.89	on energy
Transverse emittance ($10^{-9}\pi$ rad-m)	H: 250 V: 250	H: 200 V: 20	H: 660 V: 28	H: 144 V: 3.1	H: 300 V: 1
β^*, amplitude function at interaction point (m)	H: 0.06 V: 0.06	H: 0.75 V: 0.05	H: 1.2 V: 0.05	H: 1.0 V: 0.015	H: 1.7 V: 0.025
Beam-beam tune shift per crossing (units 10^{-4})	H: 750 V: 750	500	350	400	250
RF frequency (MHz)	172	180	199.53	499.8	356
Particles per bunch (units 10^{10})	16	15	20 at 2 GeV 11 at 1.55 GeV	4.8	
Bunches per ring per species	1	2	1	93	110/120
Average beam current per species (mA)	300	80	40 at 2 GeV 22 at 1.55 GeV	910	1000 (goal 2000)
Circumference or length (km)	0.024	0.366	0.2404	0.23753	0.098
Interaction regions	2	1	2	1	2
Utility insertions	2	1	4	4	2
Magnetic length of dipole (m)	1.2	2	1.6	Outer ring 1.6 Inner ring 1.41	1
Length of standard cell (m)	12	7.2	6.6	Outer ring 6.6 Inner ring 6.2	12
Phase advance per cell (deg)	H: 738 V: 378	65	≈ 60	60–90 no standard cell	360
Dipoles in ring	8	78	40 + 4 weak	84 + 8 weak	8
Quadrupoles in ring	20	150	68	134+2 s.c.	48
Peak magnetic field (T)	2.4	0.6	0.9028 at 2.8 GeV	Outer ring 0.67712 Inner ring 0.76636	1.7

HIGH-ENERGY COLLIDER PARAMETERS: e^+e^- Colliders (II)

The numbers here were received from representatives of the colliders in early 2004. Many of the numbers of course change with time, and only the latest values (or estimates) are given here. Quantities are, where appropriate, r.m.s. H and V indicate horizontal and vertical directions; s.c. indicates superconducting.

	CESR (Cornell)	CESR-C (Cornell)	KEKB (KEK)	PEP-II (SLAC)	LEP (CERN)
Physics start date	1979	2002	1999	1999	1989
Physics end date	2002	—	—	—	2000
Maximum beam energy (GeV)	6	6	$e^- \times e^+$: 8 × 3.5	e^-: 7–12 (9.0 nominal) e^+: 2.5–4 (3.1 ") (nominal E_{cm} = 10.5 GeV)	101 in 1999 (105=max. foreseen
Luminosity (10^{30} cm^{-2}s^{-1})	1280 at 5.3 GeV/beam	35 at 1.9 GeV/beam	11305	6777	24 at Z^0 100 at > 90 GeV
Time between collisions (μs)	0.014 to 0.22	0.014 to 0.22	0.008	0.0042	22
Crossing angle (μ rad)	±2000	±4000	±11,000	0	0
Energy spread (units 10^{-3})	0.6 at 5.3 GeV/beam	0.8 at 1.9 GeV/beam	0.7	e^-/e^+: 0.61/0.77	0.7→1.5
Bunch length (cm)	1.8	1.2	0.65	e^-/e^+: 1.1/1.0	1.0
Beam radius (μm)	H: 460 V: 4	H: 300 V: 5.7	H: 110 V: 2.4	H: 157 V: 4.7	H: 200 → 300 V: 2.5 → 8
Free space at interaction point (m)	±2.2 (±0.6 to REC quads)	±2.2 (±0.3 to PM quads)	+0.75/−0.58 (+300/−500) mrad cone	±0.2, ±300 mrad cone	±3.5
Luminosity lifetime (hr)	2–3	2–3	continuous	3.5	20 at Z^0 10 at > 90 GeV
Filling time (min)	5 (topping up)	5 (topping up)	continuous	3 (topping up)	20 to setup 20 to accumulate
Acceleration period (s)	—	—	—	—	600
Injection energy (GeV)	1.8–6	1.5–6	e^-/e^+: 8/3.5	2.5–12	22
Transverse emittance (π rad-nm)	H: 210 V: 1	H: 150 V: 2.5	e^-: 24 (H), 0.82 (V) e^+: 18 (H), 1.0 (V)	e^-: 48 (H), 1.5 (V) e^+: 24 (H), 1.5 (V)	H: 20–45 V: 0.25 → 1
β^*, amplitude function at interaction point (m)	H: 1.0 V: 0.018	H: 0.60 V: 0.013	e^-: 0.63 (H), 0.0070 (V) e^+: 0.59 (H), 0.0058 (V)	e^-: 0.50 (H), 0.012 (V) e^+: 0.50 (H), 0.012 (V)	H: 1.5 V: 0.05
Beam-beam tune shift per crossing (units 10^{-4})	H: 250 V: 620	H: 175 V: 200	e^-: 710 (H), 510 (V) e^+: 1040 (H), 680 (V)	e^-: 400 (H), 400 (V) e^+: 990 (H), 800 (V)	830
RF frequency (MHz)	500	500	508.887	476	352.2
Particles per bunch (units 10^{10})	1.15	1.15	e^-/e^+: 5.5/7.3	e^-/e^+: 4.6/6.7	45 in collision 60 in single beam
Bunches per ring per species	9 trains of 5 bunches	8 trains of 5 bunches	1281	1230	4 trains of 1 or 2
Average beam current per species (mA)	340	55	e^-/e^+: 1130/1500	e^-/e^+: 1200/1800	4 at Z^0 4→6 at > 90 GeV
Beam polarization (%)	—	—	—	—	55 at 45 GeV 5 at 61 GeV
Circumference or length (km)	0.768	0.768	3.016	2.2	26.66
Interaction regions	1	1	1	1 (2 possible)	4
Utility insertions	3	3	3 per ring	5	4
Magnetic length of dipole (m)	1.6–6.6	1.6–6.6	e^-/e^+: 5.86/0.915	e^-/e^+: 5.4/0.45	11.66/pair
Length of standard cell (m)	16	16	e^-/e^+: 75.7/76.1	15.2	79
Phase advance per cell (deg)	45–90 (no standard cell)	45–90 (no standard cell)	450	e^-/e^+: 60/90	102/90
Dipoles in ring	86	84	e^-/e^+: 116/112	e^-/e^+: 192/192	3280+24 inj. + 64 weak
Quadrupoles in ring	101 + 4 s.c.	101 + 4 s.c.	e^-/e^+: 452/452	e^-/e^+: 290/326	520+288 + 8 s.c.
Peak magnetic field (T)	0.3 normal } at 8 0.8 high field } GeV	0.3 normal } at 8 0.8 high field } GeV 2.1 wigglers at 1.9 GeV	e^-/e^+: 0.25/0.72	e^-/e^+: 0.18/0.75	0.135

HIGH-ENERGY COLLIDER PARAMETERS: ep, $\overline{p}p$, and pp Colliders

The numbers here were received from representatives of the colliders in early 2004. Many of the numbers of course change with time, and only the latest values (or estimates) are given here. Quantities are, where appropriate, r.m.s. H, V, and, s.c. indicate horizontal and vertical directions, and superconducting. For existing colliders, the table shows achieved parameters.

	HERA (DESY)	TEVATRON (Fermilab)	RHIC (Brookhaven)			LHC (CERN)	
Physics start date	1992	1987	2000			2007	2008
Physics end date	—	—	—			—	
Particles collided	ep	$p\overline{p}$	pp (pol.)	Au Au	d Au	pp	Pb Pb
Maximum beam energy (TeV)	e: 0.030 p: 0.92	0.980	0.1 40% pol	0.1 TeV/u	0.1 TeV/u	7.0	2.76 TeV/u
Luminosity (10^{30} cm^{-2}s^{-1})	75	50	6	0.0004	0.07	1.0×10^4	0.001
Time between collisions (μs)	0.096	0.396	0.213			0.025	0.100
Crossing angle (μ rad)	0	0	0			300	≤ 100
Energy spread (units 10^{-3})	e: 0.91 p: 0.2	0.14	0.2	0.5	0.5	0.11	0.11
Bunch length (cm)	e: 0.83 p: 8.5	57	40	20	20	7.7	7.94
Beam radius (10^{-6} m)	e: 280(H), 50(V) p: 265(H), 50(V)	p: 39 $\bar{p}$: 31	175 (β^*=1 m)	150 (215 β^*=1 m)	(β^*=2 m)	16.7	15.9
Free space at interaction point (m)	± 2	± 6.5	16			38	38
Luminosity lifetime (hr)	10	11–13	10	3	6	14.9	7.3
Filling time (min)	e: 60 p: 120	30	15			7.5 (both beams)	20 (both beams)
Acceleration period (s)	e: 200 p: 1500	86	140	230	230	1200	
Injection energy (TeV)	e: 0.012 p: 0.040	0.15	0.023	0.011 TeV/u	0.012 TeV/u	0.450	0.1774 TeV/u
Transverse emittance ($10^{-9}\pi$ rad-m)	e: 20(H), 3.5(V) p: 5(H), 5(V)	p: 4.3 $\bar{p}$: 2.7	31	23	23	0.5	0.5
β^*, ampl. function at interaction point (m)	e: 0.6 (H), 0.26(V) p: 2.45(H), 0.18(V)	0.35	1–10	1–5	2–5	0.55	0.5
Beam-beam tune shift per crossing (units 10^{-4})	e: 190(H), 450(V) p: 12(H), 9(V)	p: 14 $\bar{p}$: 70	26	9	11	34	—
RF frequency (MHz)	e: 499.7 p: 208.2/52.05	53	accel: 28 store: 28	accel: 28 store: 197	accel: 28 store: 197	400.8	400.8
Particles per bunch (units 10^{10})	e: 3 p: 7	p: 24 $\bar{p}$: 3	7	0.06	d: 1.1 Au: 0.07	11.5	0.007
Bunches per ring per species	e: 189 p: 180	36	55			2808	592
Average beam current per species (mA)	e: 40 p: 90	p: 66 $\bar{p}$: 8.2	48	33	d: 7.7 Au: 38	584	6.12
Circumference (km)	6.336	6.28	3.834			26.659	
Interaction regions	2 collining beam 1 fixed target (e beam)	2 high $\mathscr{L}$	6			2 high $\mathscr{L}$ +1	1
Utility insertions	4	4	13/ring			4	
Magnetic length of dipole (m)	e: 9.185 p: 8.82	6.12	9.45			14.3	
Length of standard cell (m)	e: 23.5 p: 47	59.5	29.7			106.90	
Phase advance per cell (deg)	e: 60 p: 90	67.8	84			90	
Dipoles in ring	e: 396 p: 416	774	192 per ring + 12 common			1232 main dipoles	
Quadrupoles in ring	e: 580 p: 280	216	246 per ring			482 2-in-1 24 1-in-1	
Magnet type	e: C-shaped p: s.c., collared, cold iron	s.c. cosθ warm iron	s.c. cosθ cold iron			s.c. 2 in 1 cold iron	
Peak magnetic field (T)	e: 0.274 p: 5	4.4	3.5			8.3	
$\overline{p}$ source accum. rate (hr^{-1})	—	13.5×10^{10}	—			—	
Max. no. $\overline{p}$ in accum. ring	—	2.4×10^{12}	—			—	

27. PASSAGE OF PARTICLES THROUGH MATTER

Revised April 2002 by H. Bichsel (University of Washington), D.E. Groom (LBNL), and S.R. Klein (LBNL).

27.1. Notation

Table 27.1: Summary of variables used in this section. The kinematic variables β and γ have their usual meanings.

Symbol	Definition	Units or Value
α	Fine structure constant $(e^2/4\pi\epsilon_0\hbar c)$	1/137.035 999 11(46)
M	Incident particle mass	MeV/c^2
E	Incident particle energy γMc^2	MeV
T	Kinetic energy	MeV
$m_e c^2$	Electron mass $\times\ c^2$	0.510 998 918(44) MeV
r_e	Classical electron radius $e^2/4\pi\epsilon_0 m_e c^2$	2.817 940 325(28) fm
N_A	Avogadro's number	$6.022\,1415(10)\times10^{23}$ mol^{-1}
ze	Charge of incident particle	
Z	Atomic number of absorber	
A	Atomic mass of absorber	g mol^{-1}
K/A	$4\pi N_A r_e^2 m_e c^2/A$	0.307 075 MeV g^{-1} cm^2 for A = 1 g mol^{-1}
I	Mean excitation energy	eV (*Nota bene!*)
δ	Density effect correction to ionization energy loss	
$\hbar\omega_p$	Plasma energy $(\sqrt{4\pi N_e r_e^3}\ m_e c^2/\alpha)$	$28.816\sqrt{\rho\langle Z/A\rangle}$ eV[a]
N_c	Electron density	(units of r_e)$^{-3}$
w_j	Weight fraction of the jth element in a compound or mixture	
n_j	$\propto$ number of jth kind of atoms in a compound or mixture	
—	$4\alpha r_e^2 N_A/A$	(716.408 g cm^{-2})$^{-1}$ for $A = 1$ g mol^{-1}
X_0	Radiation length	g cm^{-2}
E_c	Critical energy for electrons	MeV
$E_{\mu c}$	Critical energy for muons	GeV
E_s	Scale energy $\sqrt{4\pi/\alpha}\ m_e c^2$	21.2052 MeV
R_M	Molière radius	g cm^{-2}

[a] For ρ in g cm^{-3}.

27.2. Electronic energy loss by heavy particles [1–5]

Moderately relativistic charged particles other than electrons lose energy in matter primarily by ionization and atomic excitation. The mean rate of energy loss (or stopping power) is given by the Bethe-Bloch equation,

$$-\frac{dE}{dx} = Kz^2\frac{Z}{A}\frac{1}{\beta^2}\left[\frac{1}{2}\ln\frac{2m_e c^2\beta^2\gamma^2 T_{\max}}{I^2} - \beta^2 - \frac{\delta}{2}\right] . \qquad (27.1)$$

Here $T_{\max}$ is the maximum kinetic energy which can be imparted to a free electron in a single collision, and the other variables are defined in Table 27.1. With K as defined in Table 27.1 and A in g mol^{-1}, the units are MeV g^{-1}cm^2.

In this form, the Bethe-Bloch equation describes the energy loss of pions in a material such as copper to about 1% accuracy for energies between about 6 MeV and 6 GeV (momenta between about 40 MeV/c and 6 GeV/c). At lower energies various corrections discussed in Sec. 27.2.1 must be made. At higher energies, radiative effects begin to be important. These limits of validity depend on both the effective atomic number of the absorber and the mass of the slowing particle.

The function as computed for muons on copper is shown by the solid curve in Fig. 27.1, and for pions on other materials in Fig. 27.3. A minor dependence on M at the highest energies is introduced through $T_{\max}$, but for all practical purposes in high-energy physics dE/dx in a given material is a function only of β. Except in hydrogen, particles of the same velocity have similar rates of energy loss in different materials; there is a slow decrease in the rate of energy loss with increasing Z. The qualitative difference in stopping power behavior at high energies between a gas (He) and the other materials shown in Fig. 27.3 is due to the density-effect correction, δ, discussed below. The stopping power functions are characterized by broad minima whose position drops from $\beta\gamma = 3.5$ to 3.0 as Z goes from 7 to 100. The values of minimum ionization as a function of atomic number are shown in Fig. 27.2.

In practical cases, most relativistic particles (*e.g.*, cosmic-ray muons) have mean energy loss rates close to the minimum, and are said to be minimum ionizing particles, or mip's.

As discussed below, the most probable energy loss in a detector is considerably below the mean given by the Bethe-Bloch equation.

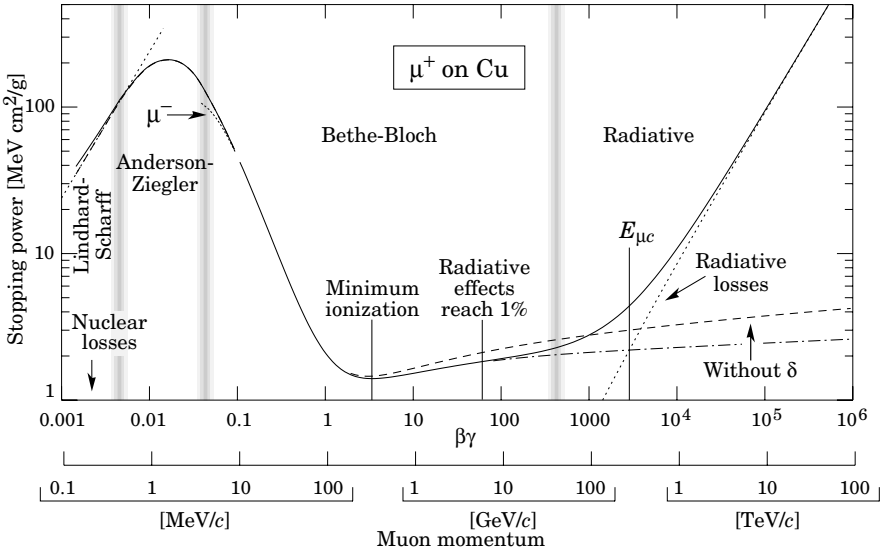

Fig. 27.1: Stopping power ($= \langle -dE/dx\rangle$) for positive muons in copper as a function of $\beta\gamma = p/Mc$ over nine orders of magnitude in momentum (12 orders of magnitude in kinetic energy). Solid curves indicate the total stopping power. Data below the break at $\beta\gamma \approx 0.1$ are taken from ICRU 49 [2], and data at higher energies are from Ref. 1. Vertical bands indicate boundaries between different approximations discussed in the text. The short dotted lines labeled "μ^-" illustrate the "Barkas effect," the dependence of stopping power on projectile charge at very low energies [6].

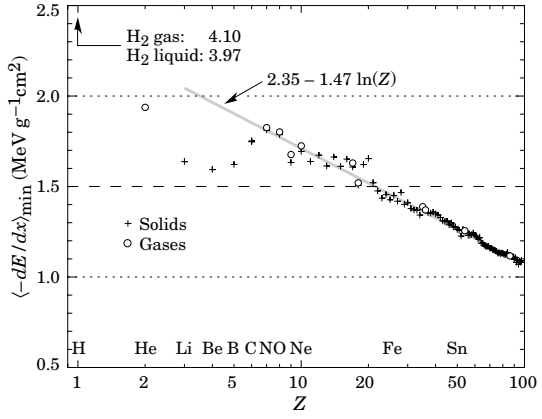

Figure 27.2: Stopping power at minimum ionization for the chemical elements. The straight line is fitted for $Z > 6$. A simple functional dependence on Z is not to be expected, since $\langle -dE/dx \rangle$ also depends on other variables.

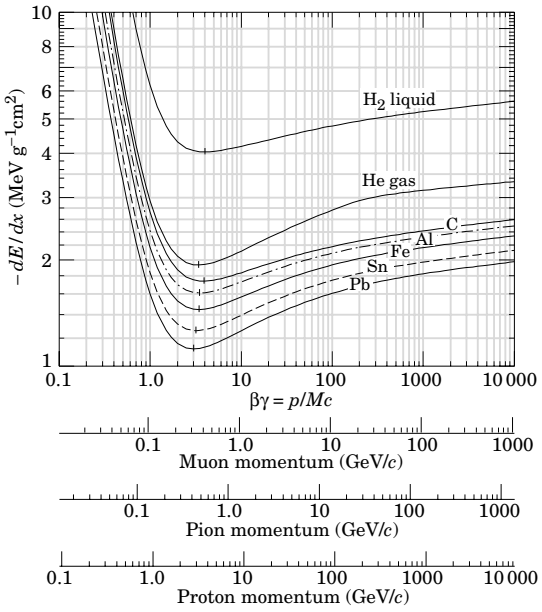

Figure 27.3: Mean energy loss rate in liquid (bubble chamber) hydrogen, gaseous helium, carbon, aluminum, iron, tin, and lead. Radiative effects, relevant for muons and pions, are not included. These become significant for muons in iron for $\beta\gamma \gtrsim 1000$, and at lower momenta for muons in higher-Z absorbers. See Fig. 27.20.

Eq. (27.1) may be integrated to find the total (or partial) "continuous slowing-down approximation" (CSDA) range R for a particle which loses energy only through ionization and atomic excitation. Since dE/dx depends only on β, R/M is a function of E/M or pc/M. In practice, range is a useful concept only for low-energy hadrons ($R \lesssim \lambda_I$, where λ_I is the nuclear interaction length), and for muons below a few hundred GeV (above which radiative effects dominate). R/M as a function of $\beta\gamma = p/Mc$ is shown for a variety of materials in Fig. 27.4.

The mass scaling of dE/dx and range is valid for the electronic losses described by the Bethe-Bloch equation, but not for radiative losses, relevant only for muons and pions.

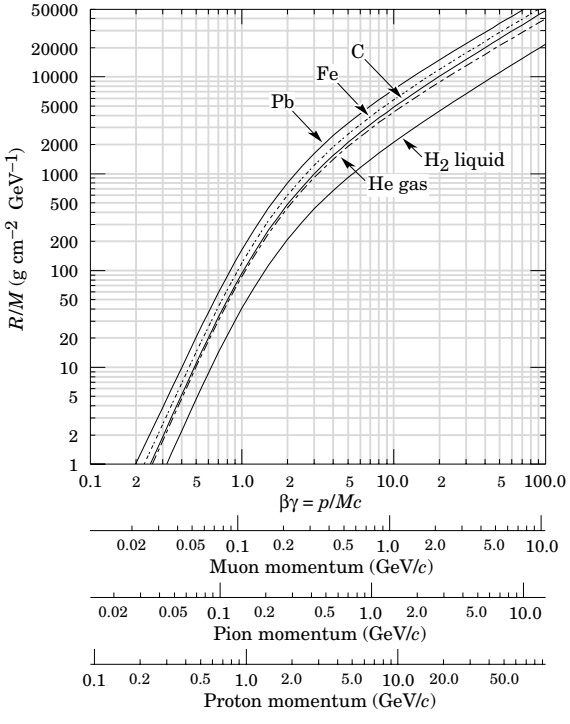

Figure 27.4: Range of heavy charged particles in liquid (bubble chamber) hydrogen, helium gas, carbon, iron, and lead. For example: For a K^+ whose momentum is 700 MeV/c, $\beta\gamma = 1.42$. For lead we read $R/M \approx 396$, and so the range is 195 g cm^{-2}.

For a particle with mass M and momentum $M\beta\gamma c$, $T_{\rm max}$ is given by

$$T_{\rm max} = \frac{2m_e c^2\,\beta^2\gamma^2}{1 + 2\gamma m_e/M + (m_e/M)^2}\ . \qquad (27.2)$$

In older references [3,4] the "low-energy" approximation $T_{\rm max} = 2m_e c^2\,\beta^2\gamma^2$, valid for $2\gamma m_e/M \ll 1$, is often implicit. For a pion in copper, the error thus introduced into dE/dx is greater than 6% at 100 GeV. The correct expression should be used.

At energies of order 100 GeV, the maximum 4-momentum transfer to the electron can exceed 1 GeV/c, where hadronic structure effects significantly modify the cross sections. This problem has been investigated by J.D. Jackson [7], who concluded that for hadrons (but not for large nuclei) corrections to dE/dx are negligible below energies where radiative effects dominate. While the cross section for rare hard collisions is modified, the average stopping power, dominated by many softer collisions, is almost unchanged.

"The determination of the mean excitation energy is the principal non-trivial task in the evaluation of the Bethe stopping-power formula" [8]. Recommended values have varied substantially with time. Estimates based on experimental stopping-power measurements for protons, deuterons, and alpha particles and on oscillator-strength distributions and dielectric-response functions were given in ICRU 37 [9]. These values, shown in Fig. 27.5, have since been widely used. Machine-readable versions can also be found [10]. These values are widely used.

27.2.1. ***Energy loss at low energies***: Shell corrections C/Z must be included in the square brackets of of Eq. (27.1) [2,9,11,12] to correct for atomic binding having been neglected in calculating some of the contributions to Eq. (27.1). The Barkas form [12] was used in generating Fig. 27.1. For copper it contributes about 1% at $\beta\gamma = 0.3$ (kinetic energy 6 MeV for a pion), and the correction decreases very rapidly with energy.

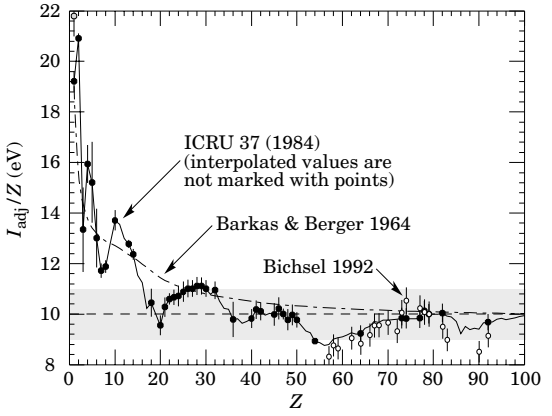

Figure 27.5: Mean excitation energies (divided by Z) as adopted by the ICRU [9]. Those based on experimental measurements are shown by symbols with error flags; the interpolated values are simply joined. The grey point is for liquid H_2; the black point at 19.2 eV is for H_2 gas. The open circles show more recent determinations by Bichsel [11]. The dotted curve is from the approximate formula of Barkas [12] used in early editions of this *Review*.

Eq. (27.1) is based on a first-order Born approximation. Higher-order corrections, again important only at lower energy, are normally included by adding a term $z^2 L_2(\beta)$ inside the square brackets.

An additional "Barkas correction" $zL_1(\beta)$ makes the stopping power for a negative particle somewhat larger than for a positive particle with the same mass and velocity. In a 1956 paper, Barkas *et al.* noted that negative pions had a longer range than positive pions [6]. The effect has been measured for a number of negative/positive particle pairs, most recently for antiprotons at the CERN LEAR facility [13].

A detailed discussion of low-energy corrections to the Bethe formula is given in ICRU Report 49 [2]. When the corrections are properly included, the accuracy of the Bethe-Bloch treatment is accurate to about 1% down to $\beta \approx 0.05$, or about 1 MeV for protons.

For $0.01 < \beta < 0.05$, there is no satisfactory theory. For protons, one usually relies on the phenomenological fitting formulae developed by Andersen and Ziegler [2,14]. For particles moving more slowly than $\approx 0.01c$ (more or less the velocity of the outer atomic electrons), Lindhard has been quite successful in describing electronic stopping power, which is proportional to β [15,16]. Finally, we note that at low energies, *e.g.*, for protons of less than several hundred eV, non-ionizing nuclear recoil energy loss dominates the total energy loss [2,16,17].

As shown in ICRU49 [2] (using data taken from Ref. 14), the nuclear plus electronic proton stopping power in copper is 113 MeV cm^2 g^{-1} at $T = 10$ keV, rises to a maximum of 210 MeV cm^2 g^{-1} at 100–150 keV, then falls to 120 MeV cm^2 g^{-1} at 1 MeV. Above 0.5–1.0 MeV the corrected Bethe-Bloch theory is adequate.

27.2.2. ***Density effect***: As the particle energy increases, its electric field flattens and extends, so that the distant-collision contribution to Eq. (27.1) increases as $\ln\beta\gamma$. However, real media become polarized, limiting the field extension and effectively truncating this part of the logarithmic rise [3–4,18–21]. At very high energies,

$$\delta/2 \to \ln(\hbar\omega_p/I) + \ln\beta\gamma - 1/2 \ , \tag{27.3}$$

where $\delta/2$ is the density effect correction introduced in Eq. (27.1) and $\hbar\omega_p$ is the plasma energy defined in Table 27.1. A comparison with Eq. (27.1) shows that $|dE/dx|$ then grows as $\ln\beta\gamma$ rather than $\ln\beta^2\gamma^2$, and that the mean excitation energy I is replaced by the plasma energy $\hbar\omega_p$. The ionization stopping power as calculated with and without the density effect correction is shown in Fig. 27.1. Since the plasma frequency scales as the square root of the electron density, the correction is much larger for a liquid or solid than for a gas, as is illustrated by the examples in Fig. 27.3.

The density effect correction is usually computed using Sternheimer's parameterization [18]:

$$\delta = \begin{cases} 2(\ln 10)x - \overline{C} & \text{if } x \geq x_1; \\ 2(\ln 10)x - \overline{C} + a(x_1 - x)^k & \text{if } x_0 \leq x < x_1; \\ 0 & \text{if } x < x_0 \text{ (nonconductors);} \\ \delta_0 10^{2(x-x_0)} & \text{if } x < x_0 \text{ (conductors)} \end{cases} \tag{27.4}$$

Here $x = \log_{10}\eta = \log_{10}(p/Mc)$. $\overline{C}$ (the negative of the C used in Ref. 18) is obtained by equating the high-energy case of Eq. (27.4) with the limit given in Eq. (27.3). The other parameters are adjusted to give a best fit to the results of detailed calculations for momenta below $Mc\exp(x_1)$. Parameters for elements and nearly 200 compounds and mixtures of interest are published in a variety of places, notably in Ref. 21. A recipe for finding the coefficients for nontabulated materials is given by Sternheimer and Peierls [19], and is summarized in Ref. 1.

The remaining relativistic rise comes from the $\beta^2\gamma^2$ growth of T_{max}, which in turn is due to (rare) large energy transfers to a few electrons. When these events are excluded, the energy deposit in an absorbing layer approaches a constant value, the Fermi plateau (see Sec. 27.2.4 below). At extreme energies (*e.g.*, > 332 GeV for muons in iron, and at a considerably higher energy for protons in iron), radiative effects are more important than ionization losses. These are especially relevant for high-energy muons, as discussed in Sec. 27.6.

27.2.3. ***Energetic knock-on electrons (δ rays)***: The distribution of secondary electrons with kinetic energies $T \gg I$ is given by [3]

$$\frac{d^2N}{dT\,dx} = \frac{1}{2}\,K z^2 \frac{Z}{A}\frac{1}{\beta^2}\frac{F(T)}{T^2} \tag{27.5}$$

for $I \ll T \leq T_{max}$, where T_{max} is given by Eq. (27.2). Here β is the velocity of the primary particle. The factor F is spin-dependent, but is about unity for $T \ll T_{max}$. For spin-0 particles $F(T) = (1 - \beta^2 T/T_{max})$; forms for spins 1/2 and 1 are also given by Rossi [3]. For incident electrons, the indistinguishability of projectile and target means that the range of T extends only to half the kinetic energy of the incident particle. Additional formulae are given in Ref. 22. Equation (27.5) is inaccurate for T close to I: for $2I \lesssim T \lesssim 10I$, the $1/T^2$ dependence above becomes approximately $T^{-\eta}$, with $3 \lesssim \eta \lesssim 5$ [23].

δ rays of appreciable energy are rare. For example, for a 500 MeV pion incident on a silicon detector with thickness $x = 300$ μm, one may integrate Eq. (27.5) from T_{cut} to T_{max} to find that $x(dN/dx) = 1$, or an average of one δ ray per particle crossing, for T_{cut} equal to only 12 keV. For $T_{cut} = 116$ keV (the mean minimum energy loss in 300 μm of silicon), $x(dN/dx) = 0.0475$—less than one particle in 20 produces a δ ray with kinetic energy greater than T_{cut}.*

A δ ray with kinetic energy T_e and corresponding momentum p_e is produced at an angle θ given by

$$\cos\theta = (T_e/p_e)(p_{max}/T_{max}) \ , \tag{27.6}$$

where p_{max} is the momentum of an electron with the maximum possible energy transfer T_{max}.

27.2.4. ***Restricted energy loss rates for relativistic ionizing particles***: Further insight can be obtained by examining the mean energy deposit by an ionizing particle when energy transfers are restricted to $T \leq T_{cut} \leq T_{max}$. The restricted energy loss rate is

$$-\left.\frac{dE}{dx}\right|_{T<T_{cut}} = K z^2 \frac{Z}{A}\frac{1}{\beta^2}\left[\frac{1}{2}\ln\frac{2m_e c^2\beta^2\gamma^2 T_{cut}}{I^2} - \frac{\beta^2}{2}\left(1 + \frac{T_{cut}}{T_{max}}\right) - \frac{\delta}{2}\right] . \tag{27.7}$$

This form approaches the normal Bethe-Bloch function (Eq. (27.1)) as $T_{cut} \to T_{max}$. It can be verified that the difference between Eq. (27.1) and Eq. (27.7) is equal to $\int_{T_{cut}}^{T_{max}} T(d^2N/dT\,dx)dT$, where $d^2N/dT\,dx$ is given by Eq. (27.5).

* These calculations assume a spin-0 incident particle and the validity of the Rutherford cross section used in Eq. (27.5).

Since $T_{\rm cut}$ replaces $T_{\rm max}$ in the argument of the logarithmic term of Eq. (27.1), the $\beta\gamma$ term producing the relativistic rise in the close-collision part of dE/dx is replaced by a constant, and $|dE/dx|_{T<T_{\rm cut}}$ approaches the constant "Fermi plateau." (The density effect correction δ eliminates the explicit $\beta\gamma$ dependence produced by the distant-collision contribution.)

27.2.5. ***Fluctuations in energy loss***: The mean energy loss per unit absorber thickness by charged particles in matter, as given by the Bethe-Bloch formula (Eq. (27.1)), is essentially useless in describing the behavior of a single particle because of the stochastic nature of the energy losses. Since the single-collision spectrum is highly skewed, the probability distribution function (pdf) describing the "straggling" is also highly skewed. The pdf $f(\Delta;\beta\gamma,x)$ describing the distribution of energy loss Δ in absorber thickness x is usually called the "Landau distribution [24]," although a careful reading of Rossi [3] shows that the matter is much more complicated. Examples of the distribution based on recent calculations by Bichsel [25–27] are shown in Fig. 27.6. The most probable loss Δ_p increases in a first approximation as $x\,(a+\ln x)$, and the ratio w/Δ_p decreases with increasing x (where w is the full width at half maximum, as indicated in the figure). For very thick absorbers, where the energy loss exceeds one half of the original energy, $f(\Delta)$ begins to approximate a Gaussian.

The most probable loss per unit thickness, normalized to the mean loss rate by a minimum ionizing particle, is shown in Fig. 27.7. These "Bichsel functions" rise by perhaps 10% from their minimum values as the energy increases, but reach a Fermi plateau for the same reasons that restricted energy loss does: The asymptotic $\ln\beta\gamma$ rise in the Bethe-Block formula comes from the hard-collision losses that create the tail.

The most probable loss is much more relevant to detector calibration than the mean energy loss, since the tail is often lost in background and in any case is difficult to define because of the weight of a few high-loss events. Note that the most probable loss is less than 70% of the mean for a typical silicon strip detector.

The function $f(\Delta;\beta\gamma,x)$ should be used in maximum likelihood fits to the signals produced by a single particle, as in the case of a track in a TPC.

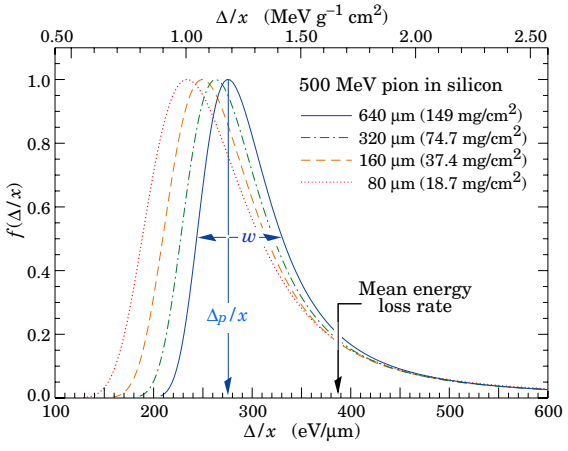

Figure 27.6: Straggling functions in silicon for 500 MeV pions, normalized to unity at the most probable value Δ_p/x. The width w is the full width at half maximum.

27.2.6. ***Energy loss in mixtures and compounds***: A mixture or compound can be thought of as made up of thin layers of pure elements in the right proportion (Bragg additivity). In this case,

$$\frac{dE}{dx} = \sum w_j \left.\frac{dE}{dx}\right|_j , \qquad (27.8)$$

where $dE/dx|_j$ is the mean rate of energy loss (in MeV g cm^{-2}) in the jth element. Eq. (27.1) can be inserted into Eq. (27.8) to find expressions for $\langle Z/A\rangle$, $\langle I\rangle$, and $\langle\delta\rangle$; for example, $\langle Z/A\rangle = \sum w_j Z_j/A_j = \sum n_j Z_j / \sum n_j A_j$. However, $\langle I\rangle$ as defined this way is an underestimate, because in a compound electrons are more tightly bound than in the free elements, and $\langle\delta\rangle$ as calculated this way has little relevance, because it is the electron density which matters. If possible, one uses the tables given in Refs. 21 and 28, which include effective excitation energies and interpolation coefficients for calculating the density effect correction for the chemical elements and nearly 200 mixtures and compounds. If a compound or mixture is not found, then one uses the recipe for δ given in Ref. 19 (repeated in Ref. 1), and calculates $\langle I\rangle$ according to the discussion in Ref. 8. (Note the "13%" rule!)

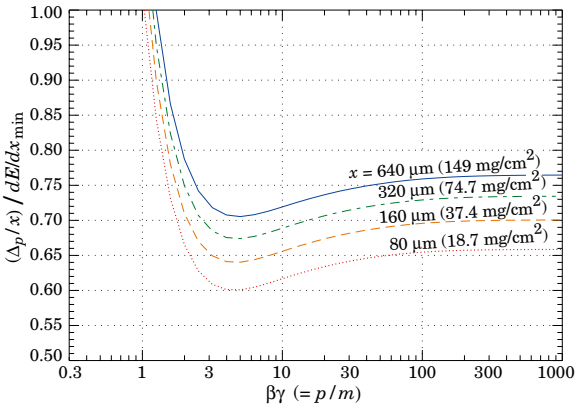

Figure 27.7: Most probable energy loss in silicon, scaled to the mean loss of a minimum ionizing particle, 388 eV/μm (1.66 MeV g^{-1}cm^2).

27.2.7. ***Ionization yields***: Physicists frequently relate total energy loss to the number of ion pairs produced near the particle's track. This relation becomes complicated for relativistic particles due to the wandering of energetic knock-on electrons whose ranges exceed the dimensions of the fiducial volume. For a qualitative appraisal of the nonlocality of energy deposition in various media by such modestly energetic knock-on electrons, see Ref. 29. The mean local energy dissipation per local ion pair produced, W, while essentially constant for relativistic particles, increases at slow particle speeds [30]. For gases, W can be surprisingly sensitive to trace amounts of various contaminants [30]. Furthermore, ionization yields in practical cases may be greatly influenced by such factors as subsequent recombination [31].

27.3. Multiple scattering through small angles

A charged particle traversing a medium is deflected by many small-angle scatters. Most of this deflection is due to Coulomb scattering from nuclei, and hence the effect is called multiple Coulomb scattering. (However, for hadronic projectiles, the strong interactions also contribute to multiple scattering.) The Coulomb scattering distribution is well represented by the theory of Molière [32]. It is roughly Gaussian for small deflection angles, but at larger angles (greater than a few θ_0, defined below) it behaves like Rutherford scattering, having larger tails than does a Gaussian distribution.

If we define

$$\theta_0 = \theta^{\rm rms}_{\rm plane} = \frac{1}{\sqrt{2}}\,\theta^{\rm rms}_{\rm space} . \qquad (27.9)$$

then it is sufficient for many applications to use a Gaussian approximation for the central 98% of the projected angular distribution, with a width given by [33,34]

$$\theta_0 = \frac{13.6\ {\rm MeV}}{\beta cp}\, z\,\sqrt{x/X_0}\Big[1 + 0.038\ln(x/X_0)\Big] . \qquad (27.10)$$

Here p, βc, and z are the momentum, velocity, and charge number of the incident particle, and x/X_0 is the thickness of the scattering medium in radiation lengths (defined below). This value of θ_0 is from a fit to Molière distribution [32] for singly charged particles with $\beta = 1$ for all Z, and is accurate to 11% or better for $10^{-3} < x/X_0 < 100$.

Eq. (27.10) describes scattering from a single material, while the usual problem involves the multiple scattering of a particle traversing many different layers and mixtures. Since it is from a fit to a Molière distribution, it is incorrect to add the individual θ_0 contributions in quadrature; the result is systematically too small. It is much more accurate to apply Eq. (27.10) once, after finding x and X_0 for the combined scatterer.

Lynch and Dahl have extended this phenomenological approach, fitting Gaussian distributions to a variable fraction of the Molière distribution for arbitrary scatterers [34], and achieve accuracies of 2% or better.

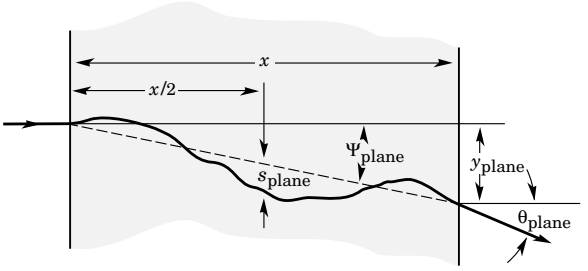

Figure 27.8: Quantities used to describe multiple Coulomb scattering. The particle is incident in the plane of the figure.

The nonprojected (space) and projected (plane) angular distributions are given approximately by [32]

$$\frac{1}{2\pi\,\theta_0^2}\,\exp\left(-\frac{\theta^2_{\rm space}}{2\theta_0^2}\right)\,d\Omega\ , \tag{27.11}$$

$$\frac{1}{\sqrt{2\pi}\,\theta_0}\,\exp\left(-\frac{\theta^2_{\rm plane}}{2\theta_0^2}\right)\,d\theta_{\rm plane}\ , \tag{27.12}$$

where θ is the deflection angle. In this approximation, $\theta^2_{\rm space} \approx (\theta^2_{{\rm plane},x} + \theta^2_{{\rm plane},y})$, where the x and y axes are orthogonal to the direction of motion, and $d\Omega \approx d\theta_{{\rm plane},x}\,d\theta_{{\rm plane},y}$. Deflections into $\theta_{{\rm plane},x}$ and $\theta_{{\rm plane},y}$ are independent and identically distributed.

Figure 27.8 shows these and other quantities sometimes used to describe multiple Coulomb scattering. They are

$$\psi^{\rm\ rms}_{\rm\ plane} = \frac{1}{\sqrt{3}}\,\theta^{\rm\ rms}_{\rm\ plane} = \frac{1}{\sqrt{3}}\,\theta_0\ , \tag{27.13}$$

$$y^{\rm\ rms}_{\rm\ plane} = \frac{1}{\sqrt{3}}\,x\,\theta^{\rm\ rms}_{\rm\ plane} = \frac{1}{\sqrt{3}}\,x\,\theta_0\ , \tag{27.14}$$

$$s^{\rm\ rms}_{\rm\ plane} = \frac{1}{4\sqrt{3}}\,x\,\theta^{\rm\ rms}_{\rm\ plane} = \frac{1}{4\sqrt{3}}\,x\,\theta_0\ . \tag{27.15}$$

All the quantitative estimates in this section apply only in the limit of small $\theta^{\rm\ rms}_{\rm\ plane}$ and in the absence of large-angle scatters. The random variables s, ψ, y, and θ in a given plane are distributed in a correlated fashion (see Sec. 31.1 of this *Review* for the definition of the correlation coefficient). Obviously, $y \approx x\psi$. In addition, y and θ have the correlation coefficient $\rho_{y\theta} = \sqrt{3}/2 \approx 0.87$. For Monte Carlo generation of a joint $(y_{\rm\ plane}, \theta_{\rm plane})$ distribution, or for other calculations, it may be most convenient to work with independent Gaussian random variables (z_1, z_2) with mean zero and variance one, and then set

$$\begin{aligned} y_{\rm plane} &= z_1\,x\,\theta_0(1-\rho^2_{y\theta})^{1/2}/\sqrt{3} + z_2\,\rho_{y\theta}\,x\,\theta_0/\sqrt{3} \\ &= z_1\,x\,\theta_0/\sqrt{12} + z_2\,x\,\theta_0/2\,; \end{aligned} \tag{27.16}$$

$$\theta_{\rm plane} = z_2\,\theta_0\ . \tag{27.17}$$

Note that the second term for $y_{\rm\ plane}$ equals $x\,\theta_{\rm plane}/2$ and represents the displacement that would have occurred had the deflection $\theta_{\rm plane}$ all occurred at the single point $x/2$.

For heavy ions the multiple Coulomb scattering has been measured and compared with various theoretical distributions [35].

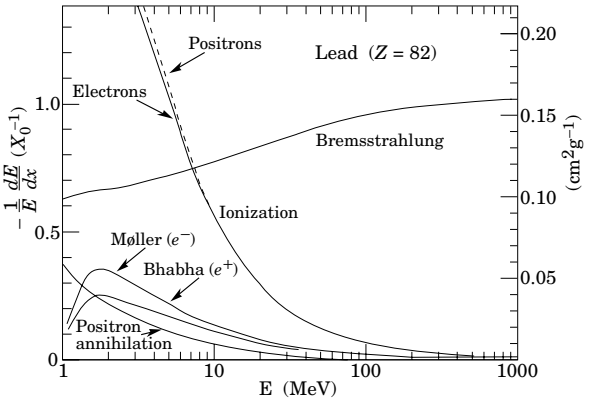

Figure 27.9: Fractional energy loss per radiation length in lead as a function of electron or positron energy. Electron (positron) scattering is considered as ionization when the energy loss per collision is below 0.255 MeV, and as Møller (Bhabha) scattering when it is above. Adapted from Fig. 3.2 from Messel and Crawford, *Electron-Photon Shower Distribution Function Tables for Lead, Copper, and Air Absorbers*, Pergamon Press, 1970. Messel and Crawford use X_0(Pb) = 5.82 g/cm^2, but we have modified the figures to reflect the value given in the Table of Atomic and Nuclear Properties of Materials (X_0(Pb) = 6.37 g/cm^2).

27.4. Photon and electron interactions in matter

27.4.1. ***Radiation length***: High-energy electrons predominantly lose energy in matter by bremsstrahlung, and high-energy photons by e^+e^- pair production. The characteristic amount of matter traversed for these related interactions is called the radiation length X_0, usually measured in g cm^{-2}. It is both (a) the mean distance over which a high-energy electron loses all but $1/e$ of its energy by bremsstrahlung, and (b) $\frac{7}{9}$ of the mean free path for pair production by a high-energy photon [36]. It is also the appropriate scale length for describing high-energy electromagnetic cascades. X_0 has been calculated and tabulated by Y.S. Tsai [37]:

$$\frac{1}{X_0} = 4\alpha r_e^2\,\frac{N_A}{A}\Big\{Z^2\big[L_{\rm rad} - f(Z)\big] + Z\,L'_{\rm rad}\Big\}\ . \tag{27.18}$$

For $A = 1$ g mol^{-1}, $4\alpha r_e^2 N_A/A = (716.408\ {\rm g\ cm^{-2}})^{-1}$. $L_{\rm rad}$ and $L'_{\rm rad}$ are given in Table 27.2. The function $f(Z)$ is an infinite sum, but for elements up to uranium can be represented to 4-place accuracy by

$$\begin{aligned} f(Z) = a^2\,&\big[(1+a^2)^{-1} + 0.20206 \\ &-0.0369\,a^2 + 0.0083\,a^4 - 0.002\,a^6\big]\ , \end{aligned} \tag{27.19}$$

where $a = \alpha Z$ [38].

Table 27.2: Tsai's $L_{\rm rad}$ and $L'_{\rm rad}$, for use in calculating the radiation length in an element using Eq. (27.18).

Element	Z	$L_{\rm rad}$	$L'_{\rm rad}$
H	1	5.31	6.144
He	2	4.79	5.621
Li	3	4.74	5.805
Be	4	4.71	5.924
Others	>4	$\ln(184.15\,Z^{-1/3})$	$\ln(1194\,Z^{-2/3})$

Although it is easy to use Eq. (27.18) to calculate X_0, the functional dependence on Z is somewhat hidden. Dahl provides a compact fit to the data [39]:

$$X_0 = \frac{716.4\ {\rm g\ cm^{-2}}\,A}{Z(Z+1)\ln(287/\sqrt{Z})}\ . \tag{27.20}$$

Results using this formula agree with Tsai's values to better than 2.5% for all elements except helium, where the result is about 5% low.

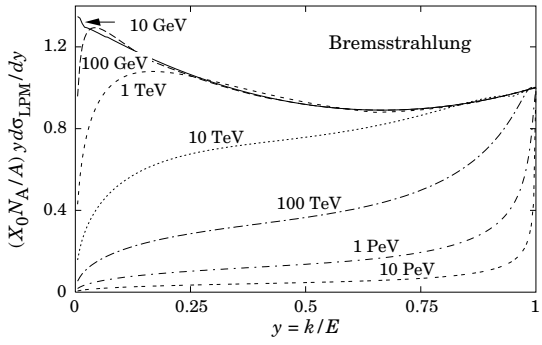

Figure 27.10: The normalized bremsstrahlung cross section $k\, d\sigma_{LPM}/dk$ in lead versus the fractional photon energy $y = k/E$. The vertical axis has units of photons per radiation length.

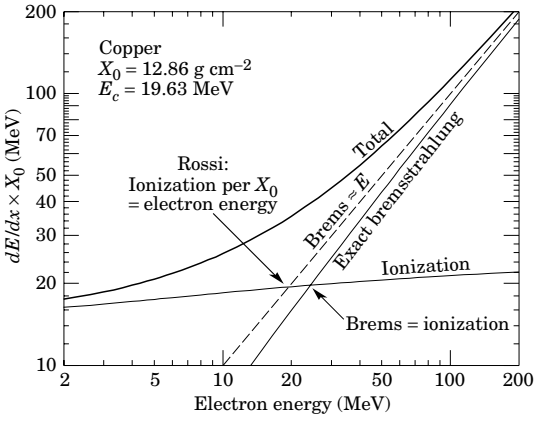

Figure 27.11: Two definitions of the critical energy E_c.

The radiation length in a mixture or compound may be approximated by

$$1/X_0 = \sum w_j/X_j \ , \tag{27.21}$$

where w_j and X_j are the fraction by weight and the radiation length for the jth element.

27.4.2. ***Energy loss by electrons***: At low energies electrons and positrons primarily lose energy by ionization, although other processes (Møller scattering, Bhabha scattering, e^+ annihilation) contribute, as shown in Fig. 27.9. While ionization loss rates rise logarithmically with energy, bremsstrahlung losses rise nearly linearly (fractional loss is nearly independent of energy), and dominates above a few tens of MeV in most materials

Ionization loss by electrons and positrons differs from loss by heavy particles because of the kinematics, spin, and the identity of the incident electron with the electrons which it ionizes. Complete discussions and tables can be found in Refs. 8, 9, and 28.

At very high energies and except at the high-energy tip of the bremsstrahlung spectrum, the cross section can be approximated in the "complete screening case" as [37]

$$d\sigma/dk = (1/k)4\alpha r_e^2 \{(\tfrac{4}{3} - \tfrac{4}{3}y + y^2)[Z^2(L_{\rm rad} - f(Z)) + Z\, L'_{\rm rad}] + \tfrac{1}{9}(1-y)(Z^2+Z)\} \ , \tag{27.22}$$

where $y = k/E$ is the fraction of the electron's energy transfered to the radiated photon. At small y (the "infrared limit") the term on the second line can reach 2.5%. If it is ignored and the first line simplified with the definition of X_0 given in Eq. (27.18), we have

$$\frac{d\sigma}{dk} = \frac{A}{X_0 N_A k}\left(\tfrac{4}{3} - \tfrac{4}{3}y + y^2\right) \ . \tag{27.23}$$

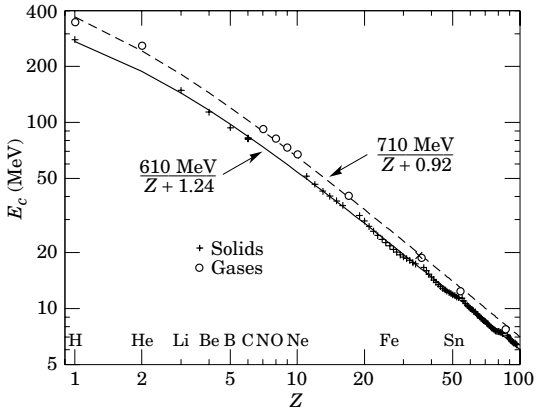

Figure 27.12: Electron critical energy for the chemical elements, using Rossi's definition [3]. The fits shown are for solids and liquids (solid line) and gases (dashed line). The rms deviation is 2.2% for the solids and 4.0% for the gases. (Computed with code supplied by A. Fassó.)

This cross section (times k) is shown by the top curve in Fig. 27.10.

This formula is accurate except in near $y = 1$, where screening may become incomplete, and near $y = 0$, where the infrared divergence is removed by the interference of bremsstrahlung amplitudes from nearby scattering centers (the LPM effect) [40,41] and dielectric supression [42,43]. These and other supression effects in bulk media are discussed in Sec. 27.4.5.

With decreasing energy ($E \lesssim 10$ GeV) the high-y cross section drops and the curves become rounded as $y \to 1$. Curves of this familar shape can be seen in Rossi [3] (Figs. 2.11.2,3); see also the review by Koch & Motz [44].

Except at these extremes, and still in the complete-screening approximation, the the number of photons with energies between $k_{\rm min}$ and $k_{\rm max}$ emitted by an electron travelling a distance $d \ll X_0$ is

$$N_\gamma = \frac{d}{X_0}\left[\frac{4}{3}\ln\left(\frac{k_{\rm max}}{k_{\rm min}}\right) - \frac{4(k_{\rm max} - k_{\rm min})}{3E} + \frac{(k_{\rm max} - k_{\rm min})^2}{2E^2}\right] \ . \tag{27.24}$$

27.4.3. ***Critical energy***: An electron loses energy by bremsstrahlung at a rate nearly proportional to its energy, while the ionization loss rate varies only logarithmically with the electron energy. The *critical energy* E_c is sometimes defined as the energy at which the two loss rates are equal [45]. Berger and Seltzer [45] also give the approximation $E_c = (800\ {\rm MeV})/(Z + 1.2)$. This formula has been widely quoted, and has been given in older editions of this *Review* [46]. Among alternate definitions is that of Rossi [3], who defines the critical energy as the energy at which the ionization loss per radiation length is equal to the electron energy. Equivalently, it is the same as the first definition with the approximation $|dE/dx|_{\rm brems} \approx E/X_0$. This form has been found to describe transverse electromagnetic shower development more accurately (see below). These definitions are illustrated in the case of copper in Fig. 27.11.

The accuracy of approximate forms for E_c has been limited by the failure to distinguish between gases and solid or liquids, where there is a substantial difference in ionization at the relevant energy because of the density effect. We distinguish these two cases in Fig. 27.12. Fits were also made with functions of the form $a/(Z+b)^\alpha$, but α was found to be essentially unity. Since E_c also depends on A, I, and other factors, such forms are at best approximate.

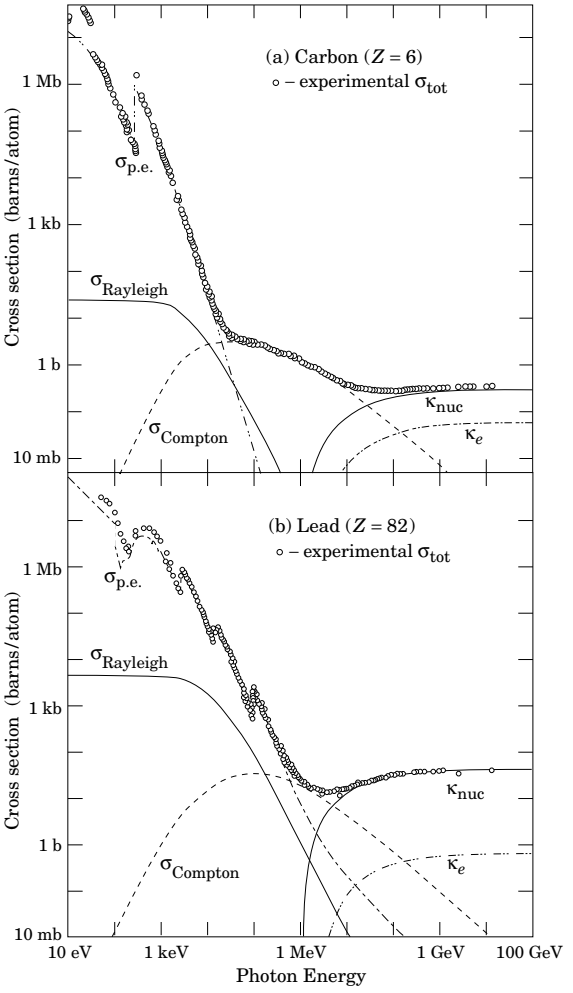

Figure 27.13: Photon total cross sections as a function of energy in carbon and lead, showing the contributions of different processes:

$\sigma_{\rm p.e.}$ = Atomic photoelectric effect (electron ejection, photon absorption)

$\sigma_{\rm Rayleigh}$ = Coherent scattering (Rayleigh scattering—atom neither ionized nor excited)

$\sigma_{\rm Compton}$ = Incoherent scattering (Compton scattering off an electron)

$\kappa_{\rm nuc}$ = Pair production, nuclear field

κ_e = Pair production, electron field

Data from Hubbell, Gimm, and Øverbø, J. Phys. Chem. Ref. Data **9**, 1023 (1980). Curves for these and other elements, compounds, and mixtures may be obtained from `http://physics.nist.gov/PhysRefData`. The photon total cross section is approximately flat for at least two decades beyond the energy range shown. Original figures courtesy J.H. Hubbell (NIST).

27.4.4. ***Energy loss by photons***: Contributions to the photon cross section in a light element (carbon) and a heavy element (lead) are shown in Fig. 27.13. At low energies it is seen that the photoelectric effect dominates, although Compton scattering, Rayleigh scattering, and photonuclear absorption also contribute. The photoelectric cross section is characterized by discontinuities (absorption edges) as thresholds for photoionization of various atomic levels are reached.

Photon attenuation lengths for a variety of elements are shown in Fig. 27.15, and data for 30 eV$< k <$100 GeV for all elements is available from the web pages given in the caption. Here k is the photon energy.

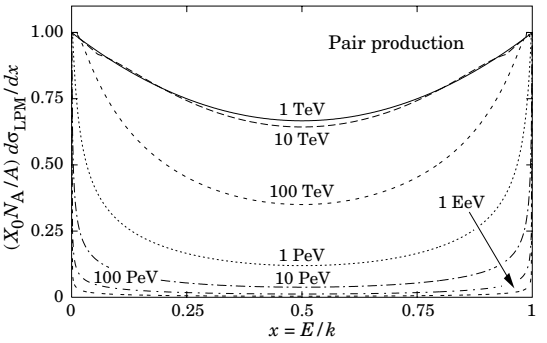

Figure 27.14: The normalized pair production cross section $d\sigma_{LPM}/dy$, versus fractional electron energy $x = E/k$.

The increasing domination of pair production as the energy increases is shown in Fig. 27.16. Using approximations similar to those used to obtain Eq. (27.23), Tsai's formula for the differential cross section [37] reduces to

$$\frac{d\sigma}{dE} = \frac{A}{X_0 N_A}\left[1 - \tfrac{4}{3}x(1-x)\right] \qquad (27.25)$$

in the complete-screening limit valid at high energies. Here $x = E/k$ is the fractional energy transfer to the pair-produced electron (or positron), and k is the incident photon energy. The cross section is very closely related to that for bremsstrahlung, since the Feynman diagrams are variants of one another. The cross section is of necessity symmetric between x and $1 - x$, as can be seen by the solid curve in Fig. 27.14. See the review by Motz, Olsen, & Koch for a more detailed treatment [47].

Eq. (27.25) may be integrated to find the high-energy limit for the total e^+e^- pair-production cross section:

$$\sigma = \tfrac{7}{9}(A/X_0 N_A)\ . \qquad (27.26)$$

Equation Eq. (27.26) is accurate to within a few percent down to energies as low as 1 GeV, particularly for high-Z materials.

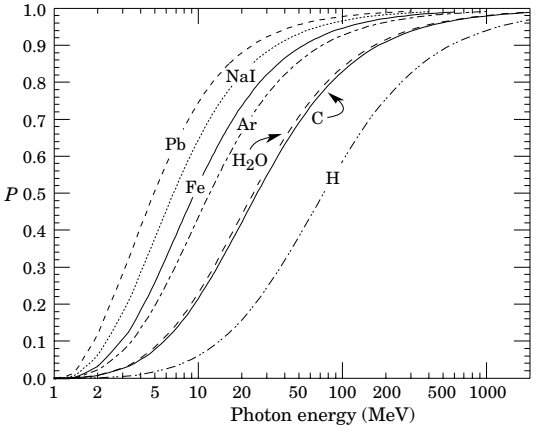

Figure 27.16: Probability P that a photon interaction will result in conversion to an e^+e^- pair. Except for a few-percent contribution from photonuclear absorption around 10 or 20 MeV, essentially all other interactions in this energy range result in Compton scattering off an atomic electron. For a photon attenuation length λ (Fig. 27.15), the probability that a given photon will produce an electron pair (without first Compton scattering) in thickness t of absorber is $P[1 - \exp(-t/\lambda)]$.

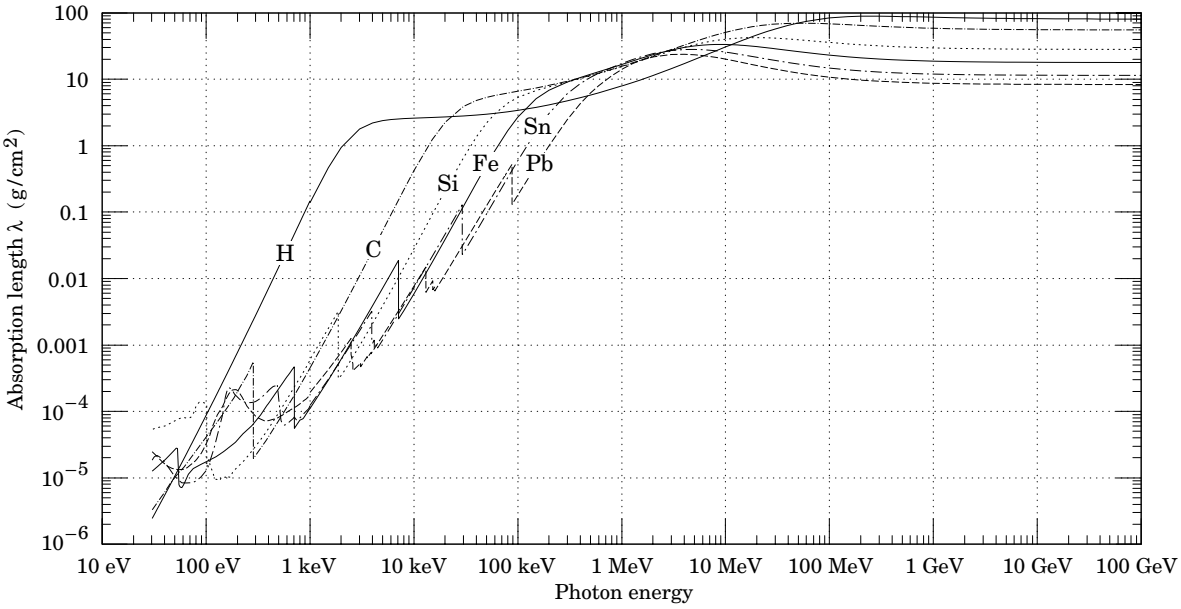

Fig. 27.15: The photon mass attenuation length (or mean free path) $\lambda = 1/(\mu/\rho)$ for various elemental absorbers as a function of photon energy. The mass attenuation coefficient is μ/ρ, where ρ is the density. The intensity I remaining after traversal of thickness t (in mass/unit area) is given by $I = I_0 \exp(-t/\lambda)$. The accuracy is a few percent. For a chemical compound or mixture, $1/\lambda_{\rm eff} \approx \sum_{\rm elements} w_Z/\lambda_Z$, where w_Z is the proportion by weight of the element with atomic number Z. The processes responsible for attenuation are given in not Fig. 27.9. Since coherent processes are included, not all these processes result in energy deposition. The data for 30 eV $< E <$ 1 keV are obtained from `http://www-cxro.lbl.gov/optical_constants` (courtesy of Eric M. Gullikson, LBNL). The data for 1 keV $< E <$ 100 GeV are from `http://physics.nist.gov/PhysRefData`, through the courtesy of John H. Hubbell (NIST).

27.4.5. ***Bremsstrahlung and pair production at very high energies:*** At ultrahigh energies, Eqns. 27.22–27.26 will fail because of quantum mechanical interference between amplitudes from different scattering centers. Since the longitudinal momentum transfer to a given center is small ($\propto k/E^2$, in the case of bremsstrahlung), the interaction is spread over a comparatively long distance called the formation length ($\propto E^2/k$) via the uncertainty principle. In alternate language, the formation length is the distance over which the highly relatistic electron and the photon "split apart." The interference is usually destructive. Calculations of the "Landau-Pomeranchuk-Migdal" (LPM) effect may be made semi-classically based on the average multiple scattering, or more rigorously using a quantum transport approach [40,41].

In amorphous media, bremsstrahlung is suppressed if the photon energy k is less than E^2/E_{LPM} [41], where*

$$E_{LPM} = \frac{(m_e c^2)^2 \alpha \rho X_0}{4\pi\hbar c} = (7.7 \text{ TeV/cm}) \times \rho X_0 \,. \qquad (27.27)$$

Since physical distances are involved, ρX_0, in cm, appears. The energy-weighted bremsstrahlung spectrum for lead, $k\, d\sigma_{LPM}/dk$, is shown in Fig. 27.10. With appropriate scaling by ρX_0, other materials behave similarly.

For photons, pair production is reduced for $E(k-E) > k\,E_{LPM}$. The pair-production cross sections for different photon energies are shown in Fig. 27.14.

If $k \ll E$, several additional mechanisms can also produce suppression. When the formation length is long, even weak factors can perturb the interaction. For example, the emitted photon can coherently forward scatter off of the electrons in the media. Because of this, for $k < \omega_p E/m_e \sim 10^{-4}$, bremsstrahlung is suppressed by a factor $(k m_e/\omega_p E)^2$ [43]. Magnetic fields can also suppress bremsstrahlung.

In crystalline media, the situation is more complicated, with coherent enhancement or suppression possible. The cross section depends on the electron and photon energies and the angles between the particle direction and the crystalline axes [41].

* This definition differs from that of Ref. 48 by a factor of two. E_{LPM} scales as the 4th power of the mass of the incident particle, so that $E_{LPM} = (1.4 \times 10^{10} \text{ TeV/cm}) \times \rho X_0$ for a muon.

27.5. Electromagnetic cascades

When a high-energy electron or photon is incident on a thick absorber, it initiates an electromagnetic cascade as pair production and bremsstrahlung generate more electrons and photons with lower energy. The longitudinal development is governed by the high-energy part of the cascade, and therefore scales as the radiation length in the material. Electron energies eventually fall below the critical energy, and then dissipate their energy by ionization and excitation rather than by the generation of more shower particles. In describing shower behavior, it is therefore convenient to introduce the scale variables

$$t = x/X_0 \,, \qquad y = E/E_c \,, \qquad (27.28)$$

so that distance is measured in units of radiation length and energy in units of critical energy.

Longitudinal profiles from an EGS4 [49] simulation of a 30 GeV electron-induced cascade in iron are shown in Fig. 27.17. The number of particles crossing a plane (very close to Rossi's Π function [3]) is sensitive to the cutoff energy, here chosen as a total energy of 1.5 MeV for both electrons and photons. The electron number falls off more quickly than energy deposition. This is because, with increasing depth, a larger fraction of the cascade energy is carried by photons. Exactly what a calorimeter measures depends on the device, but it is not likely to be exactly any of the profiles shown. In gas counters it may be very close to the electron number, but in glass Cherenkov detectors and other devices with "thick" sensitive regions it is closer to the energy deposition (total track length). In such detectors the signal is proportional to the "detectable" track length T_d, which is in general less than the total track length T. Practical devices are

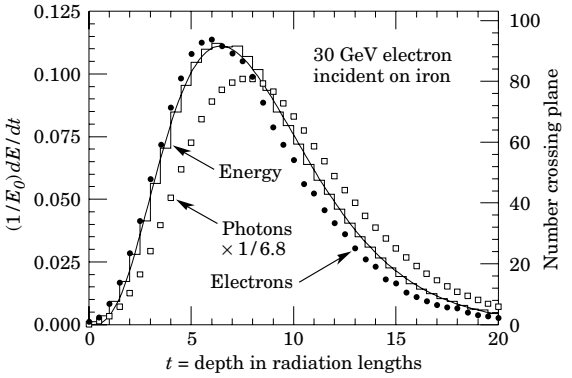

Figure 27.17: An EGS4 simulation of a 30 GeV electron-induced cascade in iron. The histogram shows fractional energy deposition per radiation length, and the curve is a gamma-function fit to the distribution. Circles indicate the number of electrons with total energy greater than 1.5 MeV crossing planes at $X_0/2$ intervals (scale on right) and the squares the number of photons with $E \geq 1.5$ MeV crossing the planes (scaled down to have same area as the electron distribution).

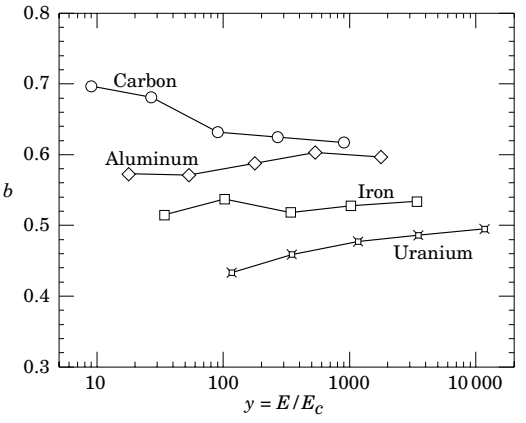

Figure 27.18: Fitted values of the scale factor b for energy deposition profiles obtained with EGS4 for a variety of elements for incident electrons with $1 \leq E_0 \leq 100$ GeV. Values obtained for incident photons are essentially the same.

sensitive to electrons with energy above some detection threshold E_d, and $T_d = T\,F(E_d/E_c)$. An analytic form for $F(E_d/E_c)$ obtained by Rossi [3] is given by Fabjan [50]; see also Amaldi [51].

The mean longitudinal profile of the energy deposition in an electromagnetic cascade is reasonably well described by a gamma distribution [52]:

$$\frac{dE}{dt} = E_0\, b\, \frac{(bt)^{a-1} e^{-bt}}{\Gamma(a)} \tag{27.29}$$

The maximum $t_{\max}$ occurs at $(a-1)/b$. We have made fits to shower profiles in elements ranging from carbon to uranium, at energies from 1 GeV to 100 GeV. The energy deposition profiles are well described by Eq. (27.29) with

$$t_{\max} = (a-1)/b = 1.0 \times (\ln y + C_j)\,, \qquad j = e, \gamma\,, \tag{27.30}$$

where $C_e = -0.5$ for electron-induced cascades and $C_\gamma = +0.5$ for photon-induced cascades. To use Eq. (27.29), one finds $(a-1)/b$ from Eq. (27.30) and Eq. (27.28), then finds a either by assuming $b \approx 0.5$ or by finding a more accurate value from Fig. 27.18. The results are very similar for the electron number profiles, but there is some dependence on the atomic number of the medium. A similar form for the electron number maximum was obtained by Rossi in the context of his "Approximation B," [3] (see Fabjan's review in Ref. 50), but with $C_e = -1.0$ and $C_\gamma = -0.5$; we regard this as superseded by the EGS4 result.

The "shower length" $X_s = X_0/b$ is less conveniently parameterized, since b depends upon both Z and incident energy, as shown in Fig. 27.18. As a corollary of this Z dependence, the number of electrons crossing a plane near shower maximum is underestimated using Rossi's approximation for carbon and seriously overestimated for uranium. Essentially the same b values are obtained for incident electrons and photons. For many purposes it is sufficient to take $b \approx 0.5$.

The gamma function distribution is very flat near the origin, while the EGS4 cascade (or a real cascade) increases more rapidly. As a result Eq. (27.29) fails badly for about the first two radiation lengths; it was necessary to exclude this region in making fits.

Because fluctuations are important, Eq. (27.29) should be used only in applications where average behavior is adequate. Grindhammer *et al.* have developed fast simulation algorithms in which the variance and correlation of a and b are obtained by fitting Eq. (27.29) to individually simulated cascades, then generating profiles for cascades using a and b chosen from the correlated distributions [53].

The transverse development of electromagnetic showers in different materials scales fairly accurately with the *Molière radius* R_M, given by [54,55]

$$R_M = X_0\, E_s/E_c\,, \tag{27.31}$$

where $E_s \approx 21$ MeV (Table 27.1), and the Rossi definition of E_c is used.

In a material containing a weight fraction w_j of the element with critical energy E_{cj} and radiation length X_j, the Molière radius is given by

$$\frac{1}{R_M} = \frac{1}{E_s} \sum \frac{w_j\, E_{cj}}{X_j}\,. \tag{27.32}$$

Measurements of the lateral distribution in electromagnetic cascades are shown in Refs. 54 and 55. On the average, only 10% of the energy lies outside the cylinder with radius R_M. About 99% is contained inside of $3.5R_M$, but at this radius and beyond composition effects become important and the scaling with R_M fails. The distributions are characterized by a narrow core, and broaden as the shower develops. They are often represented as the sum of two Gaussians, and Grindhammer [53] describes them with the function

$$f(r) = \frac{2r\,R^2}{(r^2 + R^2)^2}\,, \tag{27.33}$$

where R is a phenomenological function of x/X_0 and $\ln E$.

At high enough energies, the LPM effect (Sec. 27.4.5) reduces the cross sections for bremsstrahlung and pair production, and hence can cause significant enlongation of electromagnetic cascades [41].

27.6. Muon energy loss at high energy

At sufficiently high energies, radiative processes become more important than ionization for all charged particles. For muons and pions in materials such as iron, this "critical energy" occurs at several hundred GeV. (There is no simple scaling with particle mass, but for protons the "critical energy" is much, much higher.) Radiative effects dominate the energy loss of energetic muons found in cosmic rays or produced at the newest accelerators. These processes are characterized by small cross sections, hard spectra, large energy fluctuations, and the associated generation of electromagnetic and (in the case of photonuclear interactions) hadronic showers [56–64]. As a consequence, at these energies the treatment of energy loss as a uniform and continuous process is for many purposes inadequate.

It is convenient to write the average rate of muon energy loss as [65]

$$-dE/dx = a(E) + b(E)\,E\,. \tag{27.34}$$

Here $a(E)$ is the ionization energy loss given by Eq. (27.1), and $b(E)$ is the sum of e^+e^- pair production, bremsstrahlung, and photonuclear contributions. To the approximation that these slowly-varying functions are constant, the mean range x_0 of a muon with initial energy E_0 is given by

$$x_0 \approx (1/b) \ln(1 + E_0/E_{\mu c})\,, \tag{27.35}$$

where $E_{\mu c} = a/b$. Figure 27.19 shows contributions to $b(E)$ for iron. Since $a(E) \approx 0.002$ GeV g^{-1} cm^2, $b(E)E$ dominates the energy loss above several hundred GeV, where $b(E)$ is nearly constant. The rates of energy loss for muons in hydrogen, uranium, and iron are shown in Fig. 27.20 [1].

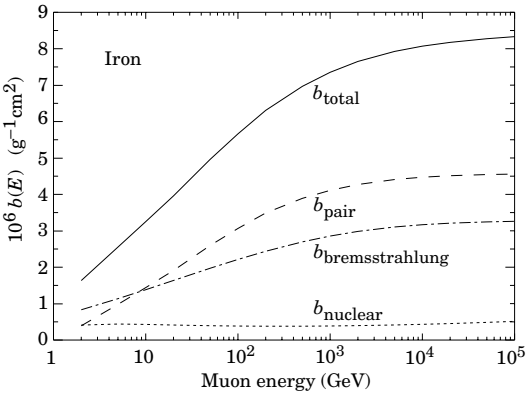

Figure 27.19: Contributions to the fractional energy loss by muons in iron due to e^+e^- pair production, bremsstrahlung, and photonuclear interactions, as obtained from Groom *et al.* [1] except for post-Born corrections to the cross section for direct pair production from atomic electrons.

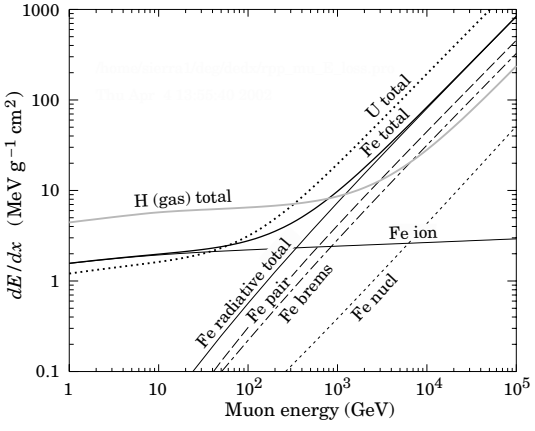

Figure 27.20: The average energy loss of a muon in hydrogen, iron, and uranium as a function of muon energy. Contributions to dE/dx in iron from ionization and the processes shown in Fig. 27.19 are also shown.

The "muon critical energy" $E_{\mu c}$ can be defined more exactly as the energy at which radiative and ionization losses are equal, and can be found by solving $E_{\mu c} = a(E_{\mu c})/b(E_{\mu c})$. This definition corresponds to the solid-line intersection in Fig. 27.11, and is different from the Rossi definition we used for electrons. It serves the same function: below $E_{\mu c}$ ionization losses dominate, and above $E_{\mu c}$ radiative effects dominate. The dependence of $E_{\mu c}$ on atomic number Z is shown in Fig. 27.21.

The radiative cross sections are expressed as functions of the fractional energy loss ν. The bremsstrahlung cross section goes roughly as $1/\nu$ over most of the range, while for the pair production case the distribution goes as ν^{-3} to ν^{-2} [66]. "Hard" losses are therefore more probable in bremsstrahlung, and in fact energy losses due to pair production may very nearly be treated as continuous. The simulated [64] momentum distribution of an incident 1 TeV/c muon beam after it crosses 3 m of iron is shown in Fig. 27.22.

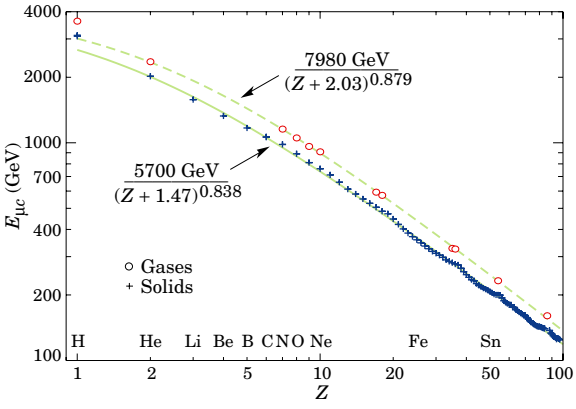

Figure 27.21: Muon critical energy for the chemical elements, defined as the energy at which radiative and ionization energy loss rates are equal [1]. The equality comes at a higher energy for gases than for solids or liquids with the same atomic number because of a smaller density effect reduction of the ionization losses. The fits shown in the figure exclude hydrogen. Alkali metals fall 3–4% above the fitted function, while most other solids are within 2% of the function. Among the gases the worst fit is for radon (2.7% high).

The most probable loss is 8 GeV, or 3.4 MeV g^{-1}cm^2. The full width at half maximum is 9 GeV/c, or 0.9%. The radiative tail is almost entirely due to bremsstrahlung, although most of the events in which more than 10% of the incident energy lost experienced relatively hard photonuclear interactions. The latter can exceed detector resolution [67], necessitating the reconstruction of lost energy. Tables [1] list the stopping power as 9.82 MeV g^{-1}cm^2 for a 1 TeV muon, so that the mean loss should be 23 MeV ($\approx$ 23 MeV/c), for a final momentum of 977 MeV/c, far below the peak. This agrees with the indicated mean calculated from the simulation. Electromagnetic and hadronic cascades in detector materials can obscure muon tracks in detector planes and reduce tracking efficiency [68].

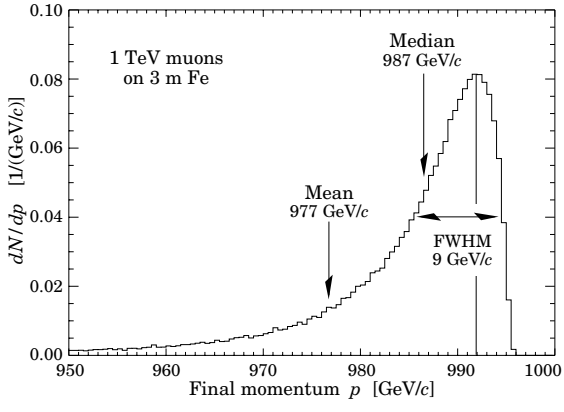

Figure 27.22: The momentum distribution of 1 TeV/c muons after traversing 3 m of iron as calculated withthe MARS14 Monte Carlo code [64] by S.I. Striganov [1].

27.7. Cherenkov and transition radiation [5,69,70]

A charged particle radiates if its velocity is greater than the local phase velocity of light (Cherenkov radiation) or if it crosses suddenly from one medium to another with different optical properties (transition radiation). Neither process is important for energy loss, but both are used in high-energy physics detectors.

Cherenkov Radiation. The half-angle θ_c of the Cherenkov cone for a particle with velocity βc in a medium with index of refraction n is

$$\theta_c = \arccos(1/n\beta) \approx \sqrt{2(1-1/n\beta)} \quad \text{for small } \theta_c, \textit{e.g.} \text{ in gases.} \tag{27.36}$$

The threshold velocity β_t is $1/n$, and $\gamma_t = 1/(1-\beta_t^2)^{1/2}$. Therefore, $\beta_t\gamma_t = 1/(2\delta+\delta^2)^{1/2}$, where $\delta = n-1$. Values of δ for various commonly used gases are given as a function of pressure and wavelength in Ref. 71. For values at atmospheric pressure, see Table 6.1. Data for other commonly used materials are given in Ref. 72.

The number of photons produced per unit path length of a particle with charge ze and per unit energy interval of the photons is

$$\frac{d^2N}{dEdx} = \frac{\alpha z^2}{\hbar c}\sin^2\theta_c = \frac{\alpha^2 z^2}{r_e\, m_e c^2}\left(1 - \frac{1}{\beta^2 n^2(E)}\right) \approx 370 \sin^2\theta_c(E)\ \text{eV}^{-1}\text{cm}^{-1} \qquad (z=1)\,, \tag{27.37}$$

or, equivalently,

$$\frac{d^2N}{dxd\lambda} = \frac{2\pi\alpha z^2}{\lambda^2}\left(1 - \frac{1}{\beta^2 n^2(\lambda)}\right)\,. \tag{27.38}$$

The index of refraction is a function of photon energy E, as is the sensitivity of the transducer used to detect the light. For practical use, Eq. (27.37) must be multiplied by the the transducer response function and integrated over the region for which $\beta\, n(E) > 1$. Further details are given in the discussion of Cherenkov detectors in the Detectors section (Sec. 28 of this *Review*).

Transition radiation. The energy radiated when a particle with charge ze crosses the boundary between vacuum and a medium with plasma frequency ω_p is

$$I = \alpha z^2 \gamma \hbar\omega_p/3\,, \tag{27.39}$$

where

$$\hbar\omega_p = \sqrt{4\pi N_e r_e^3}\, m_e c^2/\alpha = \sqrt{4\pi N_e a_\infty^3}\ 2\times 13.6\ \text{eV}\,. \tag{27.40}$$

Here N_e is the electron density in the medium, r_e is the classical electron radius, and a_∞ is the Bohr radius. For styrene and similar materials, $\sqrt{4\pi N_e a_\infty^3} \approx 0.8$, so that $\hbar\omega_p \approx 20$ eV. The typical emission angle is $1/\gamma$.

The radiation spectrum is logarithmically divergent at low energies and decreases rapidly for $\hbar\omega/\gamma\hbar\omega_p > 1$. About half the energy is emitted in the range $0.1 \le \hbar\omega/\gamma\hbar\omega_p \le 1$. For a particle with $\gamma = 10^3$, the radiated photons are in the soft x-ray range 2 to 20 keV. The γ dependence of the emitted energy thus comes from the hardening of the spectrum rather than from an increased quantum yield. For a typical radiated photon energy of $\gamma\hbar\omega_p/4$, the quantum yield is

$$N_\gamma \approx \frac{1}{2}\,\frac{\alpha z^2\gamma\hbar\omega_p}{3}\Big/\frac{\gamma\hbar\omega_p}{4} \approx \tfrac{2}{3}\alpha z^2 \approx 0.5\% \times z^2\,. \tag{27.41}$$

More precisely, the number of photons with energy $\hbar\omega > \hbar\omega_0$ is given by [5]

$$N_\gamma(\hbar\omega > \hbar\omega_0) = \frac{\alpha z^2}{\pi}\left[\left(\ln\frac{\gamma\hbar\omega_p}{\hbar\omega_0} - 1\right)^2 + \frac{\pi^2}{12}\right]\,, \tag{27.42}$$

within corrections of order $(\hbar\omega_0/\gamma\hbar\omega_p)^2$. The number of photons above a fixed energy $\hbar\omega_0 \ll \gamma\hbar\omega_p$ thus grows as $(\ln\gamma)^2$, but the number above a fixed fraction of $\gamma\hbar\omega_p$ (as in the example above) is constant. For example, for $\hbar\omega > \gamma\hbar\omega_p/10$, $N_\gamma = 2.519\,\alpha z^2/\pi = 0.59\% \times z^2$.

The yield can be increased by using a stack of plastic foils with gaps between. However, interference can be important, and the soft x rays are readily absorbed in the foils. The first problem can be overcome by choosing thicknesses and spacings large compared to the "formation length" $D = \gamma c/\omega_p$, which in practical situations is tens of μm. Other practical problems are discussed in Sec. 28.

References:

1. D.E. Groom, N.V. Mokhov, and S.I. Striganov, "Muon stopping-power and range tables: 10 MeV–100 TeV" Atomic Data and Nuclear Data Tables **78**, 183–356 (2001). Since submission of this paper it has become likely that post-Born corrections to the direct pair production cross section should be made. Code used to make Figs. 27.19, 27.20, and 27.11 included these corrections [D.Yu. Ivanov *et al.*, Phys. Lett. **B442**, 453 (1998)]. The effect is negligible for except at high Z. (It is less than 1% for iron);
   More extensive tables in printable and machine-readable formats are given at `http://pdg.lbl.gov/AtomicNuclearProperties/`.
2. "Stopping Powers and Ranges for Protons and Alpha Particles," ICRU Report No. 49 (1993);
   Tables and graphs of these data are available at `http://physics.nist.gov/PhysRefData/`.
3. B. Rossi, *High Energy Particles*, Prentice-Hall, Inc., Englewood Cliffs, NJ, 1952.
4. U. Fano, Ann. Rev. Nucl. Sci. **13**, 1 (1963).
5. J.D. Jackson, *Classical Electrodynamics*, 3rd edition, (John Wiley & Sons, New York, 1998).
6. W.H. Barkas, W. Birnbaum, and F.M. Smith, Phys. Rev. **101**, 778 (1956).
7. J. D. Jackson, Phys. Rev. **D59**, 017301 (1999).
8. S.M. Seltzer and M.J. Berger, Int. J. of Applied Rad. **33**, 1189 (1982).
9. "Stopping Powers for Electrons and Positrons," ICRU Report No. 37 (1984).
10. `http://physics.nist.gov/PhysRefData/XrayMassCoef/tab1.html`.
11. H. Bichsel, Phys. Rev. **A46**, 5761 (1992).
12. W.H. Barkas and M.J. Berger, *Tables of Energy Losses and Ranges of Heavy Charged Particles*, NASA-SP-3013 (1964).
13. M. Agnello *et al.*, Phys. Rev. Lett. **74**, 371 (1995).
14. H.H. Andersen and J.F. Ziegler, *Hydrogen: Stopping Powers and Ranges in All Elements*. Vol. 3 of *The Stopping and Ranges of Ions in Matter* (Pergamon Press 1977).
15. J. Lindhard, Kgl. Danske Videnskab. Selskab, Mat.-Fys. Medd. **28**, No. 8 (1954).
16. J. Lindhard, M. Scharff, and H.E. Schiøtt, Kgl. Danske Videnskab. Selskab, Mat.-Fys. Medd. **33**, No. 14 (1963).
17. J.F. Ziegler, J.F. Biersac, and U. Littmark, *The Stopping and Range of Ions in Solids*, Pergamon Press 1985.
18. R.M. Sternheimer, Phys. Rev. **88**, 851 (1952).
19. R.M. Sternheimer and R.F. Peierls, Phys. Rev. **B3**, 3681 (1971).
20. A. Crispin and G.N. Fowler, Rev. Mod. Phys. **42**, 290 (1970).
21. R.M. Sternheimer, S.M. Seltzer, and M.J. Berger, "The Density Effect for the Ionization Loss of Charged Particles in Various Substances," Atomic Data and Nuclear Data Tables **30**, 261 (1984). Minor errors are corrected in Ref. 1. Chemical composition for the tabulated materials is given in Ref. 8.
22. For unit-charge projectiles, see E.A. Uehling, Ann. Rev. Nucl. Sci. **4**, 315 (1954). For highly charged projectiles, see J.A. Doggett and L.V. Spencer, Phys. Rev. **103**, 1597 (1956). A Lorentz transformation is needed to convert these center-of-mass data to knock-on energy spectra.
23. N.F. Mott and H.S.W. Massey, *The Theory of Atomic Collisions*, Oxford Press, London, 1965.
24. L.D. Landau, J. Exp. Phys. (USSR) **8**, 201 (1944).
25. H. Bichsel, Rev. Mod. Phys. **60**, 663 (1988).
26. H. Bichsel, Nuc. Inst. Meth. **6 B 52**, 136 (1990).
27. H. Bichsel, Ch. 87 in the Atomic, Molecular and Optical Physics Handbook, G.W.F. Drake, editor (Am. Inst. Phys. Press, Woodbury NY, 1996).
28. S.M. Seltzer and M.J. Berger, Int. J. of Applied Rad. **35**, 665 (1984). This paper corrects and extends the results of Ref. 8.

29. L.V. Spencer "Energy Dissipation by Fast Electrons," Nat'l Bureau of Standards Monograph No. 1 (1959).
30. "Average Energy Required to Produce an Ion Pair," ICRU Report No. 31 (1979).
31. N. Hadley *et al.*, "List of Poisoning Times for Materials," Lawrence Berkeley Lab Report TPC-LBL-79-8 (1981).
32. H.A. Bethe, Phys. Rev. **89**, 1256 (1953). A thorough review of multiple scattering is given by W.T. Scott, Rev. Mod. Phys. **35**, 231 (1963). However, the data of Shen *et al.*, (Phys. Rev. **D20**, 1584 (1979)) show that Bethe's simpler method of including atomic electron effects agrees better with experiment that does Scott's treatment. For a thorough discussion of simple formulae for single scatters and methods of compounding these into multiple-scattering formulae, see W.T. Scott, Rev. Mod. Phys. **35**, 231 (1963). For detailed summaries of formulae for computing single scatters, see J.W. Motz, H. Olsen, and H.W. Koch, Rev. Mod. Phys. **36**, 881 (1964).
33. V.L. Highland, Nucl. Instrum. Methods **129**, 497 (1975), and Nucl. Instrum. Methods **161**, 171 (1979).
34. G.R. Lynch and O.I Dahl, Nucl. Instrum. Methods **B58**, 6 (1991).
35. M. Wong *et al.*, Med. Phys. **17**, 163 (1990).
36. E. Segré, *Nuclei and Particles*, New York, Benjamin (1964) p. 65 ff.
37. Y.S. Tsai, Rev. Mod. Phys. **46**, 815 (1974).
38. H. Davies, H.A. Bethe, and L.C. Maximon, Phys. Rev. **93**, 788 (1954).
39. O.I. Dahl, private communication.
40. L.D. Landau and I.J. Pomeranchuk, Dokl. Akad. Nauk. SSSR **92**, 535 (1953); **92**, 735 (1953). These papers are available in English in L. Landau, *The Collected Papers of L.D. Landau*, Pergamon Press, 1965; A.B. Migdal, Phys. Rev. **103**, 1811 (1956).
41. S. Klein, Rev. Mod. Phys. **71**, 1501 (1999).
42. M. L. Ter-Mikaelian, SSSR **94**, 1033 (1954);
    M. L. Ter-Mikaelian, *High Energy Electromagnetic Processes in Condensed Media* (John Wiley & Sons, New York, 1972).
43. P. Anthony *et al.*, Phys. Rev. Lett. **76**, 3550 (1996).
44. H. W. Koch and J. W. Motz, Rev. Mod. Phys. **31**, 920 (1959).
45. M.J. Berger and S.M. Seltzer, "Tables of Energy Losses and Ranges of Electrons and Positrons," National Aeronautics and Space Administration Report NASA-SP-3012 (Washington DC 1964).
46. K. Hikasa *et al.*, *Review of Particle Properties*, Phys. Rev. **D46** (1992) S1.
47. J. W. Motz, H. A. Olsen, and H. W. Koch, Rev. Mod. Phys. **41**, 581 (1969).
48. P. Anthony *et al.*, Phys. Rev. Lett. **75**, 1949 (1995).
49. W.R. Nelson, H. Hirayama, and D.W.O. Rogers, "The EGS4 Code System," SLAC-265, Stanford Linear Accelerator Center (Dec. 1985).
50. *Experimental Techniques in High Energy Physics*, ed. by T. Ferbel (Addision-Wesley, Menlo Park CA 1987).
51. U. Amaldi, Phys. Scripta **23**, 409 (1981).
52. E. Longo and I. Sestili, Nucl. Instrum. Methods **128**, 283 (1975).
53. G. Grindhammer *et al.*, in *Proceedings of the Workshop on Calorimetry for the Supercollider*, Tuscaloosa, AL, March 13–17, 1989, edited by R. Donaldson and M.G.D. Gilchriese (World Scientific, Teaneck, NJ, 1989), p. 151.
54. W.R. Nelson, T.M. Jenkins, R.C. McCall, and J.K. Cobb, Phys. Rev. **149**, 201 (1966).
55. G. Bathow *et al.*, Nucl. Phys. **B20**, 592 (1970).
56. H.A. Bethe and W. Heitler, *Proc. Roy. Soc.* **A146**, 83 (1934);
    H.A. Bethe, *Proc. Cambridge Phil. Soc.* **30**, 542 (1934).
57. A.A. Petrukhin and V.V. Shestakov, Can. J. Phys. **46**, S377 (1968).
58. V.M. Galitskii and S.R. Kel'ner, Sov. Phys. JETP **25**, 948 (1967).
59. S.R. Kel'ner and Yu.D. Kotov, Sov. J. Nucl. Phys. **7**, 237 (1968).
60. R.P. Kokoulin and A.A. Petrukhin, in *Proceedings of the International Conference on Cosmic Rays*, Hobart, Australia, August 16–25, 1971, Vol. **4**, p. 2436.
61. A.I. Nikishov, Sov. J. Nucl. Phys. **27**, 677 (1978).
62. Y.M. Andreev *et al.*, Phys. Atom. Nucl. **57**, 2066 (1994).
63. L.B. Bezrukov and E.V. Bugaev, Sov. J. Nucl. Phys. **33**, 635 (1981).
64. N.V. Mokhov, "The MARS Code System User's Guide," Fermilab-FN-628 (1995);
    N. V. Mokhov, S. I. Striganov, A. Van Ginneken, S. G. Mashnik, A. J. Sierk, J.Ranft, in *Proc. of the Fourth Workshop on Simulating Accelerator Radiation Environments* (SARE-4), Knoxville, TN, September 14-16, 1998, pp. 87–99, Fermilab-Conf-98/379 (1998), nucl-th/9812038-v2-16-Dec-1998;
    N. V. Mokhov, in *Proc. of ICRS-9 International Conference on Radiation Shielding*, (Tsukuba,Ibaraki, Japan, 1999), J. Nucl. Sci. Tech., **1** (2000), pp. 167–171, Fermilab-Conf-00/066 (2000);
    `http://www-ap.fnal.gov/MARS/`.
65. P.H. Barrett, L.M. Bollinger, G. Cocconi, Y. Eisenberg, and K. Greisen, Rev. Mod. Phys. **24**, 133 (1952).
66. A. Van Ginneken, Nucl. Instrum. Methods **A251**, 21 (1986).
67. U. Becker *et al.*, Nucl. Instrum. Methods **A253**, 15 (1986).
68. J.J. Eastman and S.C. Loken, in *Proceedings of the Workshop on Experiments, Detectors, and Experimental Areas for the Supercollider*, Berkeley, CA, July 7–17, 1987, edited by R. Donaldson and M.G.D. Gilchriese (World Scientific, Singapore, 1988), p. 542.
69. *Methods of Experimental Physics*, L.C.L. Yuan and C.-S. Wu, editors, Academic Press, 1961, Vol. 5A, p. 163.
70. W.W.M. Allison and P.R.S. Wright, "The Physics of Charged Particle Identification: dE/dx, Cherenkov Radiation, and Transition Radiation," p. 371 in *Experimental Techniques in High Energy Physics*, T. Ferbel, editor, (Addison-Wesley 1987).
71. E.R. Hayes, R.A. Schluter, and A. Tamosaitis, "Index and Dispersion of Some Cherenkov Counter Gases," ANL-6916 (1964).
72. T. Ypsilantis, "Particle Identification at Hadron Colliders", CERN-EP/89-150 (1989), or ECFA 89-124, **2** 661 (1989).

28. PARTICLE DETECTORS

Revised 2003 (see the various sections for authors).

In this section we give various parameters for common detector components. The quoted numbers are usually based on typical devices, and should be regarded only as rough approximations for new designs. More detailed discussions of detectors and their underlying physics can be found in books by Ferbel [1], Grupen [2], Kleinknecht [3], Knoll [4], and Green [5]. In Table 28.1 are given typical spatial and temporal resolutions of common detectors.

Table 28.1: Typical spatial and temporal resolutions of common detectors. Revised September 2003 by R. Kadel (LBNL).

Detector Type	Accuracy (rms)	Resolution Time	Dead Time
Bubble chamber	10–150 μm	1 ms	50 ms[a]
Streamer chamber	300 μm	2 μs	100 ms
Proportional chamber	50–300 μm[b,c,d]	2 ns	200 ns
Drift chamber	50–300 μm	2 ns[e]	100 ns
Scintillator	—	100 ps/n[f]	10 ns
Emulsion	1 μm	—	—
Liquid Argon Drift [Ref. 6]	$\sim$175–450 μm	$\sim$ 200 ns	$\sim$ 2 μs
Gas Micro Strip [Ref. 7]	30–40 μm	$<$ 10 ns	—
Resistive Plate chamber [Ref. 8]	$\lesssim$ 10 μm	1–2 ns	—
Silicon strip	pitch/(3 to 7)[g]	*h*	*h*
Silicon pixel	2 μm[i]	*h*	*h*

[a] Multiple pulsing time.
[b] 300 μm is for 1 mm pitch.
[c] Delay line cathode readout can give $\pm$150 μm parallel to anode wire.
[d] wirespacing/$\sqrt{12}$.
[e] For two chambers.
[f] n = index of refraction.
[g] The highest resolution ("7") is obtained for small-pitch detectors ($\lesssim$25 μm) with pulse-height-weighted center finding.
[h] Limited by the readout electronics [9]. (Time resolution of $\leq$ 25 ns is planned for the ATLAS SCT.)
[i] Analog readout of 34 μm pitch, monolithic pixel detectors.

28.1. Organic scintillators

Revised September 2001 by K.F. Johnson (FSU).

Organic scintillators are broadly classed into three types, crystalline, liquid, and plastic, all of which utilize the ionization produced by charged particles (see the section on "Passage of particles through matter" (Sec. 27.2) of this *Review*) to generate optical photons, usually in the blue to green wavelength regions [10]. Plastic scintillators are by far the most widely used. Crystal organic scintillators are practically unused in high-energy physics.

Densities range from 1.03 to 1.20 g cm^{-3}. Typical photon yields are about 1 photon per 100 eV of energy deposit [11]. A one-cm-thick scintillator traversed by a minimum-ionizing particle will therefore yield $\approx 2 \times 10^4$ photons. The resulting photoelectron signal will depend on the collection and transport efficiency of the optical package and the quantum efficiency of the photodetector.

Plastic scintillators do not respond linearly to the ionization density. Very dense ionization columns emit less light than expected on the basis of dE/dx for minimum-ionizing particles. A widely used semi-empirical model by Birks posits that recombination and quenching effects between the excited molecules reduce the light yield [12]. These effects are more pronounced the greater the density of the excited molecules. Birks' formula is

$$\frac{d\mathscr{L}}{dx} = \mathscr{L}_0 \frac{dE/dx}{1 + k_B\, dE/dx} ,$$

where $\mathscr{L}$ is the luminescence, $\mathscr{L}_0$ is the luminescence at low specific ionization density, and k_B is Birks' constant, which must be determined for each scintillator by measurement.

Decay times are in the ns range; rise times are much faster. The combination of high light yield and fast response time allows the possibility of sub-ns timing resolution [13]. The fraction of light emitted during the decay "tail" can depend on the exciting particle. This allows pulse shape discrimination as a technique to carry out particle identification. Because of the hydrogen content (carbon to hydrogen ratio $\approx$ 1) plastic scintillator is sensitive to proton recoils from neutrons. Ease of fabrication into desired shapes and low cost has made plastic scintillators a common detector component. Recently, plastic scintillators in the form of scintillating fibers have found widespread use in tracking and calorimetry [14].

28.1.1. *Scintillation mechanism* :

Scintillation: A charged particle traversing matter leaves behind it a wake of excited molecules. Certain types of molecules, however, will release a small fraction ($\approx$ 3%) of this energy as optical photons. This process, scintillation, is especially marked in those organic substances which contain aromatic rings, such as polystyrene (PS) and polyvinyltoluene (PVT). Liquids which scintillate include toluene and xylene.

Fluorescence: In fluorescence, the initial excitation takes place via the absorption of a photon, and de-excitation by emission of a longer wavelength photon. Fluors are used as "waveshifters" to shift scintillation light to a more convenient wavelength. Occurring in complex molecules, the absorption and emission are spread out over a wide band of photon energies, and have some overlap, that is, there is some fraction of the emitted light which can be re-absorbed [15]. This "self-absorption" is undesirable for detector applications because it causes a shortened attenuation length. The wavelength difference between the major absorption and emission peaks is called the Stokes' shift. It is usually the case that the greater the Stokes' shift, the smaller the self absorption—thus, a large Stokes' shift is a desirable property for a fluor (aka the "Better red than dead" strategy).

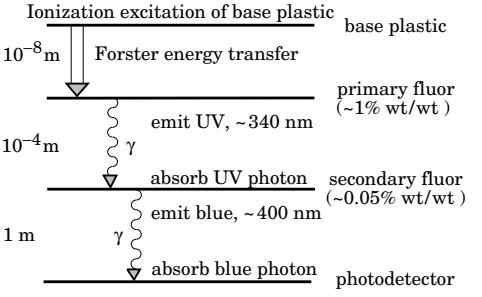

Figure 28.1: Cartoon of scintillation "ladder" depicting the operating mechanism of plastic scintillator. Approximate fluor concentrations and energy transfer distances for the separate sub-processes are shown.

Scintillators: The plastic scintillators used in high-energy physics are binary or ternary solutions of selected fluors in a plastic base containing aromatic rings. (See the appendix in Ref. 16 for a comprehensive list of components.) Virtually all plastic scintillators contain as a base either PVT or PS. PVT-based scintillator can be up to 50% brighter. The fluors must satisfy additional conditions besides being fluorescent. They must be sufficiently stable, soluble, chemically inert, fast, radiation tolerant, and efficient.

Ionization in the plastic base produces UV photons with short attenuation length (several mm). Longer attenuation lengths are obtained by dissolving a "primary" fluor in high concentration (1% by weight) into the base, which is selected to efficiently re-radiate absorbed energy at wavelengths where the base is more transparent.

The primary fluor has a second important function. The decay time of the scintillator base material can be quite long—in pure polystyrene it is 16 ns, for example. The addition of the primary fluor in high concentration can shorten the decay time by an order of magnitude and increase the total light yield. At the concentrations used (1% and greater), the average distance between a fluor molecule and an excited base unit is around 100 Å, much less than a wavelength of light. At these distances the predominant mode of energy transfer from base to fluor is not the radiation of a photon, but a resonant dipole-dipole interaction, first described by Foerster, which strongly couples the base and fluor [17]. The strong coupling sharply increases the speed and the light yield of the plastic scintillators.

Unfortunately, a fluor which fulfills other requirements is usually not completely adequate with respect to emission wavelength or attenuation length, so it is necessary to add yet another waveshifter (the "secondary" fluor), at fractional percent levels, and occasionally a third (not shown in Fig. 28.1).

External wavelength shifters: Light emitted from a plastic scintillator may be absorbed in a (nonscintillating) base doped with a wave-shifting fluor. Such wavelength shifters are widely used to aid light collection in complex geometries. The wavelength shifter must be insensitive to ionizing radiation and Cherenkov light. A typical wavelength shifter uses an acrylic base because of its good optical qualities, a single fluor to shift the light emerging from the plastic scintillator to the blue-green, and contains ultra-violet absorbing additives to deaden response to Cherenkov light.

28.1.2. ***Caveats and cautions***: Plastic scintillators are reliable, robust, and convenient. However, they possess quirks to which the experimenter must be alert.

Aging and Handling: Plastic scintillators are subject to aging which diminishes the light yield. Exposure to solvent vapors, high temperatures, mechanical flexing, irradiation, or rough handling will aggravate the process. A particularly fragile region is the surface which can 'craze"—develop microcracks—which rapidly destroy the capability of plastic scintillators to transmit light by total internal reflection. Crazing is particularly likely where oils, solvents, or *fingerprints* have contacted the surface.

Attenuation length: The Stokes' shift is not the only factor determining attenuation length. Others are the concentration of fluors (the higher the concentration of a fluor, the greater will be its self-absorption); the optical clarity and uniformity of the bulk material; the quality of the surface; and absorption by additives, such as stabilizers, which may be present.

Afterglow: Plastic scintillators have a long-lived luminescence which does not follow a simple exponential decay. Intensities at the 10^{-4} level of the initial fluorescence can persist for hundreds of ns [10,18].

Atmospheric quenching: Plastic scintillators will decrease their light yield with increasing partial pressure of oxygen. This can be a 10% effect in an artificial atmosphere [19]. It is not excluded that other gases may have similar quenching effects.

Magnetic field: The light yield of plastic scintillators may be changed by a magnetic field. The effect is very nonlinear and apparently not all types of plastic scintillators are so affected. Increases of $\approx 3\%$ at 0.45 T have been reported [20]. Data are sketchy and mechanisms are not understood.

Radiation damage: Irradiation of plastic scintillators creates color centers which absorb light more strongly in the UV and blue than at longer wavelengths. This poorly understood effect appears as a reduction both of light yield and attenuation length. Radiation damage depends not only on the integrated dose, but on the dose rate, atmosphere, and temperature, before, during and after irradiation, as well as the materials properties of the base such as glass transition temperature, polymer chain length, *etc.* Annealing also occurs, accelerated by the diffusion of atmospheric oxygen and elevated temperatures. The phenomena are complex, unpredictable, and not well understood [21]. Since color centers are less intrusive at longer wavelengths, the most reliable method of mitigating radiation damage is to shift emissions at every step to the longest practical wavelengths, *e.g.*, utilize fluors with large Stokes' shifts (aka the "Better red than dead" strategy).

28.1.3. ***Scintillating and wavelength-shifting fibers***:

The clad optical fiber is an incarnation of scintillator and wavelength shifter (WLS) which is particularly useful [22]. Since the initial demonstration of the scintillating fiber (SCIFI) calorimeter [23], SCIFI techniques have become mainstream. SCIFI calorimeters are found, for example, in the $g-2$ experiment at Brookhaven [24] and at KLOE; SCIFI trackers are found at CHORUS and DØ ; WLS readout is used in both ATLAS and CMS hadron calorimeters [25].

SCIFI calorimeters are fast, dense, radiation hard, and can have leadglass-like resolution. SCIFI trackers can handle high rates and are radiation tolerant, but the low photon yield at the end of a long fiber (see below) forces the use of very sophisticated photodetectors such as VLPC's, such as are used in DØ . WLS scintillator readout of a calorimeter allows a very high level of hermeticity since the solid angle blocked by the fiber on its way to the photodetector is very small. The sensitive region of scintillating fibers can be controlled by splicing them onto clear (non-scintillating/non-WLS) fibers.

A typical configuration would be fibers with a core of polystyrene-based scintillator or WLS (index of refraction $n = 1.59$), surrounded by a cladding of PMMA ($n = 1.49$) a few microns thick, or, for added light capture, with another cladding of fluorinated PMMA with $n = 1.42$, for an overall diameter of 0.5 to 1 mm. The fiber is drawn from a boule and great care is taken during production to ensure that the intersurface between the core and the cladding has the highest possible uniformity and quality, so that the signal transmission via total internal reflection has a low loss. The fraction of generated light which is transported down the optical pipe is denoted the capture fraction and is about 6% for the single-clad fiber and 10% for the double-clad fiber.

The number of photons from the fiber available at the photodetector is always smaller than desired, and increasing the light yield has proven difficult [26]. A minimum-ionizing particle traversing a high-quality 1 mm diameter fiber perpendicular to its axis will produce fewer than 2000 photons, of which about 200 are captured. Attenuation eliminates about 95% of these photons. DØ uses 0.775 mm diameter scintillating fibers in the tracker and obtains 9 photoelectrons with the VLPC reaching 85% quantum efficiency.

A scintillating or WLS fiber is often characterized by its "attenuation length," over which the signal is attenuated to $1/e$ of its original value. Many factors determine the attenuation length, including the importance of re-absorption of emitted photons by the polymer base or dissolved fluors, the level of crystallinity of the base polymer, and the quality of the total internal reflection boundary. Attenuation lengths of several meters are obtained by high quality fibers. However, it should be understood that the attenuation length is not necessarily a measure of fiber quality. Among other things, it is not constant with distance from the excitation source and it is wavelength dependent. So-called "cladding light" causes some of the distance dependence [27], but not all. The wavelength dependence is usually related to the higher re-absorption of shorter wavelength photons—once absorbed, re-emitted isotropically and lost with 90% probability—and to the lower absorption of longer wavelengths by polystyrene. Experimenters should be aware that measurements of attenuation length by a phototube with a bialkali photocathode, whose quantum efficiency drops below 10% at 480 nm, should not be naïvely compared to measurements utilizing a silicon photodiode, whose quantum efficiency is still rising at 600 nm.

28.2. Inorganic scintillators:

Revised September 2003 by C.L. Woody (BNL). and R.-Y. Zhu (California Inst. of Technology).

Inorganic crystals form a class of scintillating materials with much higher densities than organic plastic scintillators (typically $\sim$ 4–8 g/cm^3) with a variety of different properties for use as scintillation detectors. Due to their high density and high effective atomic number, they can be used in applications where high stopping power or

a high conversion efficiency for electrons or photons is required. These include total absorption electromagnetic calorimeters (see Sec. 28.10.1), which consist of a totally active absorber (as opposed to a sampling calorimeter), as well as serving as gamma ray detectors over a wide range of energies. Many of these crystals also have very high light output, and can therefore provide excellent energy resolution down to very low energies ($\sim$ few hundred keV).

Some crystals are intrinsic scintillators in which the luminescence is produced by a part of the crystal lattice itself. However, other crystals require the addition of a dopant, typically fluorescent ions such as thallium (Tl) or cerium (Ce) which is responsible for producing the scintillation light. However, in both cases, the scintillation mechanism is the same. Energy is deposited in the crystal by ionization, either directly by charged particles, or by the conversion of photons into electrons or positrons which subsequently produce ionization. This energy is transfered to the luminescent centers which then radiate scintillation photons. The efficiency η for the conversion of energy deposit in the crystal to scintillation light can be expressed by the relation [28]

$$\eta = \beta \cdot S \cdot Q \ . \tag{28.1}$$

where β is the efficiency of the energy conversion process, S is the efficiency of energy transfer to the luminescent center, and Q is the quantum efficiency of the luminescent center. The value of η ranges between 0.1 and $\sim$ 1 depending on the crystal, and is the main factor in determining the intrinsic light output of the scintillator. In addition, the scintillation decay time is primarily determined by the energy transfer and emission process. The decay time of the scintillator is mainly dominated by the decay time of the luminescent center. For example, in the case of thallium doped sodium iodide (NaI(Tl)), the value of η is $\sim$ 0.5, which results in a light output $\sim$ 40,000 photons per MeV of energy deposit. This high light output is largely due to the high quantum efficiency of the thallium ion (Q $\sim$ 1), but the decay time is rather slow ($\tau \sim 250$ ns).

Table 28.2 lists the basic properties of some commonly used inorganic crystal scintillators. NaI(Tl) is one of the most common and widely used scintillators, with an emission that is well matched to a bialkali photomultiplier tube, but it is highly hygroscopic and difficult to work with, and has a rather low density. CsI(Tl) has high light yield, an emission that is well matched to solid state photodiodes, and is mechanically robust (high plasticity and resistance to cracking). However, it needs careful surface treatment and is slightly hygroscopic. Compared with CsI(Tl), pure CsI has identical mechanical properties, but faster emission at shorter wavelengths and light output approximately an order of magnitude lower. BaF_2 has a fast component with a sub-nanosecond decay time, and is the fastest known scintillator. However, it also has a slow component with a much longer decay time ($\sim$ 630 ns). Bismuth gemanate ($Bi_4Ge_3O_{12}$ or BGO) has a very high density, and consequently a short radiation length X_0 and Molière radius R_M. BGO's emission is well-matched to the spectral sensitivity of photodiodes, and it is easy to handle and not hygroscopic. Lead tungstate ($PbWO_4$ or PWO) has a very high density, with a very short X_0 and R_M, but its intrinsic light yield is rather low. Both cerium doped lutetium oxyorthosilicate (Lu_2SiO_5:Ce, or LSO:Ce) [29] and cerium doped gadolinium orthosilicate (Gd_2SiO_5:Ce, or GSO:Ce) [30] are dense crystal scintillators which have a high light yield and a fast decay time.

Beside the crystals listed in Table 28.2, a number of new crystals are being developed that may have potenial applications in high energy or nuclear physics. Of particular interest is the family of yttrium and lutetium perovskites, which include YAP ($YAlO_3$:Ce) and LuAP ($LuAlO_3$:Ce) and their mixed compositions. These have been shown to be linear over a large energy range [31], and have the potential for providing extremely good intrinsic energy resolution. In addition, other fluoride crystals such as CeF_3 have been shown to provide excellent energy resolution in calorimeter applications.

Table 28.2 gives the light output of other crystals relative to NaI(Tl) as measured with a bialkalai photomultiplier tube. However, the useful signal produced by a scintillator is usually quoted in terms of the number of photoelectrons per MeV produced by a given photodetector. The relationship between the number of photons/MeV produced and photoelectrons/MeV detected involves the factors for the light collection efficiency L and the quantum efficiency QE of the photodetector:

$$N_{\mathrm{p.e.}}/\mathrm{MeV} = L \cdot QE \cdot N_\gamma/\mathrm{MeV} \tag{28.2}$$

L includes the transmission of scintillation light within the crystal (*i.e.*, the bulk attenuation length of the material), reflections and scattering from the surfaces, and the size and shape of the crystal. These factors can vary considerably depending on the sample, but can be in the range of $\sim$50–60%. However, the internal light transmission depends on the intrinsic properties of the material, as well as the number and type of impurites and defects that can produce internal absorption within the crystal, and can be highly affected by factors such as radiation damage, as discussed below.

The quantum efficiency depends on the type of photodetector used to detect the scintillation light, which is typically $\sim$15–20% for photomultiplier tubes and $\sim$70% for silicon photodiodes for visible wavelengths. The quantum efficiency of the detector is usually highly wavelength dependent and should be matched to the particular crystal of interest to give the highest quantum yield at the wavelength corresponding to the peak of the scintillation emission. The comparison of the light output given in Table 28.2 is for a standard photomultiplier tube with a bialkali photocathode. Results with different photodetectors can be significantly different. For example, the response of CsI(Tl) relative to NaI(Tl) with a silicon photodiode would be 140 rather than 45 due to its higher quantum efficiency at longer wavelengths. For scintillators which emit in the UV, a detector with a quartz window should be used.

One important issue related to the application of a crystal scintillator is its radiation hardness. Stability of its light output, or the ability to track and monitor the variation of its light output in a radiation environment, is required for high resolution and precision calibration [32]. All known crystal scintillators suffer from radiation damage. A common damage phenomenon is the appearance of radiation induced absorption caused by the formation of impurities or point defect related color centers. This radiation induced absorption reduces the light attenuation length in the crystal, and hence its light output. For crystals with high defect density, a severe reduction of light attenuation length may lead to a distortion of the light response uniformity, leading to a degradation of energy resolution. Additional radiation damage effects may include a reduced intrinsic scintillation light yield (damage to the luminescent centers) and an increased phosphorescence (afterglow). For crystals to be used in the construction a high precision calorimeter in a radiation environment, its scintillation mechanism must not be damaged and its light attenuation length in the expected radiation environment must be long enough so that its light response uniformity, and thus its energy resolution, does not change [33].

Most of the crystals listed in Table 28.2 have been used in high energy or nuclear physics experiments when the ultimate energy resolution for electrons and photons is desired. Examples are the Crystal Ball NaI(Tl) calorimeter at SPEAR, the L3 BGO calorimeter at LEP, the CLEO CsI(Tl) calorimeter at CESR, the KTeV CsI calorimeter at the Tevatron, and the BaBar and BELLE CsI(Tl) calorimeters at PEP-II and KEK. Because of its high density and low cost, PWO calorimeters are now being constructed by CMS and ALICE at LHC, by CLAS and PrimEx at CEBAF, and by BTeV at the Tevatron.

28.3. Cherenkov detectors

Written September 2003 by B.N. Ratcliff (SLAC).

Although devices using Cherenkov radiation are often thought of as particle identification (PID) detectors, in practice, they are widely used over a much broader range of applications; including (1) fast particle counters; (2) hadronic particle identification; and (3) tracking detectors performing complete event reconstruction. A few examples of specific applications from each category include; (1) the polarization detector of the SLD [34]; (2) the hadronic PID detectors at the B factory detectors (DIRC in BaBar [8] and the aerogel threshold Cherenkov in Belle [35]); and (3) large water Cherenkov counters

Table 28.2: Properties of several inorganic crystal scintillators. Most of the notation is defined in Sec. 6 of this *Review*.

Parameter:	ρ	MP	X_0	R_M	dE/dx	λ_I	$\tau_{\rm decay}$	$\lambda_{\rm max}$	n^*	Relative output†	Hygro-scopic?	d(LY)/dT
Units:	g/cm^3	°C	cm	cm	MeV/cm	cm	ns	nm				%/°C‡
NaI(Tl)	3.67	651	2.59	4.8	4.8	41.4	230	410	1.85	100	yes	∼0
BGO	7.13	1050	1.12	2.3	9.0	21.8	300	480	2.15	9	no	−1.6
BaF_2	4.89	1280	2.06	3.4	6.6	29.9	630^s	300^s	1.50	21^s	no	-2^s
							0.9^f	220^f		2.7^f		$\sim 0^f$
CsI(Tl)	4.51	621	1.85	3.5	5.6	37.0	1300	560	1.79	45	slight	0.3
CsI(pure)	4.51	621	1.85	3.5	5.6	37.0	35^s	420^s	1.95	5.6^s	slight	−0.6
							6^f	310^f		2.3^f		
$PbWO_4$	8.3	1123	0.9	2.0	10.2	18	50^s	560^s	2.20	0.1^s	no	−1.9
							10^f	420^f			0.6^f	
LSO(Ce)	7.40	2070	1.14	2.3	9.6	21	40	420	1.82	75	no	−0.3
GSO(Ce)	6.71	1950	1.37	2.4	8.9	22	600^s	430	1.85	3^s	no	−0.1
							56^f			30^f		

* Refractive index at the wavelength of the emission maximum.
† Relative light yield measured with a bi-alkali cathode PMT.
‡ Variation of light yield with temperature evalutated at room temperature.
f = fast component, s = slow component

such as Super-Kamiokande [36]. Cherenkov counters contain two main elements; (1) a radiator through which the charged particle passes, and (2) a photodetector. As Cherenkov radiation is a weak source of photons, light collection and detection must be as efficient as possible. The presence of the refractive index n and the path length of the particle in the radiator in the Cherenkov relations allows tuning these quantities for a particular experimental application.

Cherenkov detectors utilize one or more of the properties of Cherenkov radiation discussed in the Passages of Particles through Matter section (Sec. 27 of this *Review*): the prompt emission of a light pulse; the existence of a velocity threshold for radiation; and the dependence of the Cherenkov cone half-angle θ_c and the number of emitted photons on the velocity of the particle.

The number of photoelectrons ($N_{\rm p.e.}$) detected in a given device is

$$N_{\rm p.e.} = L\frac{\alpha^2 z^2}{r_e\, m_e c^2}\int \epsilon(E)\, \sin^2\theta_c(E) dE\,, \qquad (28.3)$$

where L is the path length in the radiator, ϵ(E) is the efficiency for collecting the Cherenkov light and transducing it in photoelectrons, and $\alpha^2/(r_e\, m_e c^2) = 370\ {\rm cm}^{-1}{\rm eV}^{-1}$.

The quantities ϵ and θ_c are functions of the photon energy E. However, since the typical energy dependent variation of the index of refraction is modest, a quantity called the *Cherenkov detector quality factor* N_0 can be defined as

$$N_0 = \frac{\alpha^2 z^2}{r_e\, m_e c^2}\int \epsilon\, dE\,, \qquad (28.4)$$

so that

$$N_{\rm p.e.} \approx L N_0 \langle \sin^2\theta_c\rangle\,. \qquad (28.5)$$

We take $z = 1$, the usual case in high-energy physics, in the following discussion.

This definition of the quality factor N_0 is not universal, nor, indeed, very useful for situations where the geometrical photon collection efficiency ($\epsilon_{\rm coll}$) varies substantially for different tracks. In this case, separate factors for photon collection and detection ($\epsilon_{\rm det}$), so that $\epsilon = \epsilon_{\rm coll}\epsilon_{\rm det}$, are sometimes included on the right hand side of the equation. A typical value of N_0 for a photomultiplier (PMT) detection system working in the visible and near UV, and collecting most of the Cherenkov light, is about 100 cm^{-1}. Practical counters, utilizing a variety of different photodetectors, have values ranging between about 30 and 180 cm^{-1}.

Radiators can be chosen from a variety of transparent materials (Sec. 27 of this *Review* and Table 6.1). In addition to refractive index, the choice requires consideration of factors such as material density, radiation length, transmission bandwidth, absorption length, chromatic dispersion, optical workability (for solids), availability, and cost. Long radiator lengths are required to obtain sufficient numbers of photons when the momenta of the particle species to be separated are high. Recently, the gap in refractive index that has traditionally existed between gases and liquid or solid materials has been partially closed with transparent *silica aerogels* with indices that range between about 1.007 and 1.13.

Cherenkov counters may be classified as either *imaging* or *threshold* types, depending on whether they do or do not make use of Cherenkov angle (θ_c) information. Imaging counters may be used to track particles as well as identify them.

28.3.1. ***Threshold counters:*** Threshold Cherenkov detectors [37], in their simplest form, make a yes/no decision based on whether the particle is above or below the Cherenkov threshold velocity $\beta_t = 1/n$. A straightforward enhancement of such detectors uses the number of observed photoelectrons (or a calibrated pulse height) to discriminate between species or to set probabilities for each particle species [38]. This strategy can increase the momentum range of particle separation by a modest amount (to a momentum some 20% above the threshold momentum of the heavier particle in a typical case).

Careful designs give $\langle\epsilon_{\rm coll}\rangle \gtrsim 90\%$. For a photomultiplier with a typical bialkali cathode, $\int \epsilon_{\rm det} dE \approx 0.27$, so that

$$N_{\rm p.e.}/L \approx 90\ {\rm cm}^{-1}\,\langle\sin^2\theta_c\rangle \quad (i.e.,\ N_0 = 90\ {\rm cm}^{-1})\,. \qquad (28.6)$$

Suppose, for example, that n is chosen so that the threshold for species a is p_t; that is, at this momentum species a has velocity $\beta_a = 1/n$. A second, lighter, species b with the same momentum has velocity β_b, so $\cos\theta_c = \beta_a/\beta_b$, and

$$N_{\rm p.e.}\, L \approx 90\ {\rm cm}^{-1}\,\frac{m_a^2 - m_b^2}{p_t^2 + m_a^2}\,. \qquad (28.7)$$

For K/π separation at $p = p_t = 1(5)$ GeV/c, $N_{\rm p.e.}/L \approx 16(0.8)$ cm^{-1} for π's and (by design) 0 for K's.

For limited path lengths $N_{\rm p.e.}$ can be small, and a minimum number is required to trigger external electronics. The overall efficiency of the device is controlled by Poisson fluctuations, which can be especially critical for separation of species where one particle type is dominant. The effective number of photoelectrons is often less than the average

number calculated above due to additional equivalent noise from the photodetector. It is common to design for at least 10 photoelectrons for the high velocity particle in order to obtain a robust counter. As rejection of the particle that is below threshold depends on *not* seeing a signal, electronic and other background noise can be important. Physics sources of light production for the below threshold particle, such as decay of the above threshold particle or the production of delta rays in the radiator, often limit the separation attainable, and need to be carefully considered. Well designed, modern multi-channel counters, such as the ACC at Belle [35], can attain good particle separation performance over a substantial momentum range for essentially the full solid angle of the spectrometer.

28.3.2. ***Imaging counters***: The most powerful use of the information available from the Cherenkov process comes from measuring the ring-correlated angles of emission of the individual Cherenkov photons. Since low-energy photon detectors can measure only the position (and, perhaps, a precise detection time) of the individual Cherenkov photons (not the angles directly), the photons must be "imaged" onto a detector so that their angles can be derived [39]. In most cases the optics map the Cherenkov cone onto (a portion of) a distorted circle at the photodetector. Though this imaging process is directly analogous to the familiar imaging techniques used in telescopes and other optical instruments, there is a somewhat bewildering variety of methods used in a wide variety of counter types with different names. Some of the imaging methods used include (1) focusing by a lens; (2) proximity focusing (i.e., focusing by limiting the emission region of the radiation); and (3) focusing through an aperture (a pinhole). In addition, the prompt Cherenkov emission coupled with the speed of modern photon detectors allows the use of time imaging, a method which is used much less frequently in conventional imaging technology. Finally, full tracking (and event reconstruction) can be performed in large water counters by combining the individual space position and time of each photon together with the constraint that Cherenkov photons are emitted from each track at a constant polar angle.

In a simple model of an imaging PID counter, the fractional error on the particle velocity (δ_β) is given by

$$\delta_\beta = \frac{\sigma_\beta}{\beta} = \tan\theta_c \sigma(\theta_c) \quad , \tag{28.8}$$

where

$$\sigma(\theta_c) = \frac{\langle\sigma(\theta_i)\rangle}{\sqrt{N_{\rm p.e.}}} \oplus C \ , \tag{28.9}$$

where $\langle\sigma(\theta_i)\rangle$ is the average single photoelectron resolution, as defined by the optics, detector resolution and the intrinsic chromaticity spread of the radiator index of refraction averaged over the photon detection bandwidth. C combines a number of other contributions to resolution including,(1) correlated terms such as tracking, alignment, and multiple scattering, (2) hit ambiguities, (3) background hits from random sources, and (4) hits coming from other tracks. In many practical cases, the resolution is limited by these effects.

For a $\beta \approx 1$ particle of momentum (p) well above threshold entering a radiator with index of refraction (n), the number of σ separation (N_σ) between particles of mass m_1 and m_2 is approximately

$$N_\sigma \approx \frac{|m_1^2 - m_2^2|}{2p^2\sigma(\theta_c)\sqrt{n^2-1}} \, . \tag{28.10}$$

In practical counters, the angular resolution term $\sigma(\theta_c)$ varies between about 0.1 and 5 mrad depending on the size, radiator, and photodetector type of the particular counter. The range of momenta over which a particular counter can separate particle species extends from the point at which the number of photons emitted becomes sufficient for the counter to operate efficiently as a threshold device ($\sim$20% above the threshold for the lighter species) to the value in the imaging region given by the equation above. For example, for $\sigma(\theta_c) = 2$mrad, a fused silica radiator($n = 1.474$), or a flourocarbon gas radiator (C_5F_{12}, $n = 1.0017$), would separate π/K's from the threshold region starting around 0.15(3) GeV/c through the imaging region up to about 4.2(18) GeV/c at better than 3σ.

Many different imaging counters have been built during the last several decades [42]. Among the earliest examples of this class of counters are the very limited acceptance Differential Cherenkov detectors, designed for particle selection in high momentum beam lines. These devices use optical focusing and/or geometrical masking to select particles having velocities in a specified region. With careful design, a velocity resolution of $\sigma_\beta/\beta \approx 10^{-4}$–$10^{-5}$ can be obtained [37].

Practical multi-track Ring-Imaging Cherenkov detectors (generically called RICH counters) are a more recent development. They have been built in small-aperture and 4π geometries both as PID counters and as stand-alone detectors with complete tracking and event reconstruction as discussed more fully below. PID RICH counters are sometimes further classified by 'generations' that differ based on performance, design, and photodetection techniques.

A typical example of a first generation RICH used at the Z factory e^+e^- colliders [40,41] has both liquid (C_6F_{14}, $n = 1.276$) and gas (C_5F_{12}, $n = 1.0017$) radiators, the former being proximity imaged using the small radiator thickness while the latter use mirrors. The phototransducers are a TPC/wire-chamber combination having charge division or pads. They are made sensitive to photons by doping the TPC gas (usually, ethane/methane) with $\sim 0.05\%$ TMAE (tetrakis(dimethylamino)ethylene). Great attention to detail is required, (1) to avoid absorbing the UV photons to which TMAE is sensitive, (2) to avoid absorbing the single photoelectrons as they drift in the long TPC, and (3) to keep the chemically active TMAE vapor from interacting with materials in the system. In spite of their unforgiving operational characteristics, these counters attained good $e/\pi/K/p$ separation over wide momentum ranges during several years of operation. In particular, their π/K separation range extends over momenta from about 0.25 to 20 GeV/c.

Second and third generation counters [42] generally must operate at much higher particle rates than the first generation detectors, and utilize different photon detection bandwidths, with higher readout channel counts, and faster, more forgiving photon detection technology than the TMAE doped TPCs just described. Radiator choices have broadened to include materials such as lithium flouride, fused silica, and aerogel. Vacuum based photodetection systems (*e.g.*, photomultiplier tubes (PMT) or hybrid photodiodes (HPD)) have become increasingly common. They handle very high rates, can be used in either single or multi anode versions, and allow a wide choice of radiators. Other fast detection systems that use solid cesium iodide (CSI) photocathodes or triethylamine (TEA) doping in proportional chambers are useful with certain radiator types and geometries.

A DIRC (Detector of Internally Reflected Cherenkov light) is a third generation subtype of a RICH first used in the BaBar detector [8]. It "inverts" the usual principle for use of light from the radiator of a RICH by collecting and imaging the total internally reflected light, rather than the transmitted light. A DIRC utilizes the optical material of the radiator in two ways, simultaneously; first as a Cherenkov radiator, and second, as a light pipe for the Cherenkov light trapped in the radiator by total internal reflection. The DIRC makes use of the fact that the magnitudes of angles are preserved during reflection from a flat surface. This fact, coupled with the high reflection coefficients of the total internal reflection process (> 0.9995 for higly polished SiO_2), and the long attenuation length for photons in high purity fused silica, allows the photons of the ring image to be transported to a detector outside the path of the particle where they may be imaged. The BaBar DIRC uses 144 fused silica radiator bars ($1.7 \times 3.5 \times 490$ cm) with the light being focused onto 11 000 conventional PMT's located about 120 cm from the end of the bars by the "pinhole" of the bar end. DIRC performance can be understood using the formula for (N_σ) discussed above. Typically, $N_{\rm p.e.}$ is rather large (between 15 and 60) and the Cherenkov polar angle is measured to about 2.5 mrad. The momentum range with good π/K separation extends up to about 4 GeV/c, matching the B decay momentum spectrum observed in BaBar.

28.4. Cherenkov tracking calorimeters

Written August 2003 by D. Casper (UC Irvine).

In addition to the specialized applications described in the previous section, Cherenkov radiation is also exploited in large, ring-imaging detectors with masses measured in kilotons or greater. Such devices are not subdetector components, but complete experiments with triggering, tracking, vertexing, particle identification and calorimetric capabilities, where the large mass of the transparent dielectric medium serves as an active target for neutrino interactions (or their secondary muons) and rare processes like nucleon decay.

For volumes of this scale, absorption and scattering of Cherenkov light are non-negligible, and a wavelength-dependent factor $e^{-d/L(\lambda)}$ (where d is the distance from emission to the sensor and $L(\lambda)$ is the attenuation length of the medium) must be included in the integral of Eq. (28.3) for the photoelectron yield. The choice of medium is therefore constrained by the refractive index and transparency in the region of photodetector sensitivity; highly-purified water is an inexpensive and effective choice; sea-water, mineral oil, polar ice, and D_2O are also used. Photo-multiplier tubes (PMTs) on either a volume or surface lattice measure the time of arrival and intensity of Cherenkov radiation. Hemispherical PMTs are favored for the widest angular acceptance, and sometimes mounted with reflectors or wavelength-shifting plates to increase the effective photosensitive area. Gains and calibration curves are measured with pulsed laser signals transmitted to each PMT individually via optical fiber or applied to the detector as a whole through one or more diffusing balls.

Volume instrumentation [43] is only cost-effective at low densities, with a spacing comparable to the attenuation (absorption and scattering) length of Cherenkov light in the medium (15–40 m for Antarctic ice and ∼45 m in the deep ocean). PMTs are deployed in vertical strings as modular units which include pressure housings, front-end electronics and calibration hardware. The effective photocathode coverage of such arrays is less than 1% but still adequate (using timing information and the Cherenkov angular constraint) to reconstruct the direction of TeV muons to 1° or better. The size of such "neutrino telescopes" is limited only by cost once the technical challenges of deployment, power, signal extraction and calibration in an inaccessible and inhospitable environment are addressed; arrays up to $(1\ \mathrm{km})^3$ in size are under study or development.

Surface instrumentation [44] allows the target volume to be viewed with higher photocathode density by a number of PMTs which scales like $(\mathrm{volume})^{2/3}$. To improve hermeticity and shielding, and to ensure that an outward-going particle's Cherenkov cone illuminates sufficient PMTs for reconstruction, a software-defined fiducial volume begins some distance (∼ 2 m) inside the photosensor surface. Events originating within the fiducial volume are classified as *fully-contained* if no particles exit the inner detector, or *partially-contained* otherwise. An outer (veto) detector, optically separated from the inner volume and instrumented at reduced density, greatly assists in making this determination and also simplifies the selection of contained events. The maximum size of a pure surface array is limited by the attenuation length (∼ 100 m has been achieved for large volumes using reverse-osmosis water purification), pressure tolerance of the PMTs (< 80 meters of water, without pressure housings) and structural integrity of the enclosing cavity, if underground. In practice, these limitations can be overcome by a segmented design involving multiple modules of the nominal maximum size; megaton-scale devices are under study.

Cherenkov detectors are excellent electromagnetic calorimeters, and the number of Cherenkov photons *produced* by an e/γ is nearly proportional to its kinetic energy. For massive particles, the number of photons produced is also related to the energy, but not linearly. For any type of particle, the *visible energy* E_{vis} is defined as the energy of an electron which would produce the same number of Cherenkov photons. The number of photoelectrons *collected* depends on a detector-specific scale factor, with event-by-event corrections for geometry and attenuation. For typical PMTs, in water $N_{\mathrm{p.e.}} \approx 15\,\xi\,E_{\mathrm{vis}}(\mathrm{MeV})$, where ξ is the effective fractional photosensor coverage; for other materials, the photoelectron yield scales with the ratio of $\sin^2\theta_c$ over density. At solar neutrino energies, the visible energy resolution ($\sim 30\%/\sqrt{\xi\,E_{\mathrm{vis}}(\mathrm{MeV})}$) is about 20% worse than photoelectron counting statistics would imply. For higher energies, multi-photoelectron hits are likely and the charge collected by each PMT (rather the number of PMTs firing) must be used; this degrades the energy resolution to approximately $2\%/\sqrt{\xi\,E_{\mathrm{vis}}(\mathrm{GeV})}$. In addition, the absolute energy scale must be determined with sources of known energy. Using an electron LINAC and/or nuclear sources, 0.5–1.5% has been achieved at solar neutrino energies; for higher energies, cosmic-ray muons, Michel electrons and π^0 from neutrino interactions allow ∼ 3% absolute energy calibration.

A trigger can be formed by the coincidence of PMTs within a window comparable to the detector's light crossing time; the coincidence level thus corresponds to a visible energy threshold. Physics analysis is usually not limited by the hardware trigger, but rather the ability to reconstruct events. The interaction vertex can be estimated using timing and refined by applying the Cherenkov angle constraint to identified ring edges. Multi-ring events are more strongly constrained, and their vertex resolution is 33–50% better than single rings. Vertex resolution depends on the photosensor density and detector size, with smaller detectors performing somewhat better than large ones (∼ 25 cm is typical for existing devices). Angular resolution is limited by multiple scattering at solar neutrino energies (25–30°) and improves to a few degrees around $E_{vis} = 1\,\mathrm{GeV}$.

A non-showering $(\mu, \pi^{\pm}, p)$ track produces a sharp ring with small contributions from delta rays and other radiated secondaries, while the more diffuse pattern of a showering (e, γ) particle is actually the superposition of many individual rings from charged shower products. Using maximum likelihood techniques and the Cherenkov angle constraint, these two topologies can be distinguished with an efficiency which depends on the photosensor density and detector size [45]. This particle identification capability has been confirmed by using cosmic-rays and Michel electrons, as well as charged-particle [46] and neutrino [47] beams. Large detectors perform somewhat better than smaller ones with identical photocathode coverage; a misidentification probability of $\sim 0.4\%/\xi$ in the sub-GeV range is consistent with the performance of several experiments for $4\% < \xi < 40\%$. Detection of a delayed coincidence from muon decay offers another, more indirect, means of particle identification; with suitable electronics, efficiency approaches 100% for μ^+ decays but is limited by nuclear absorption (22% probability in water) for μ^-.

Reconstruction of multiple Cherenkov rings presents a challenging pattern recognition problem, which must be attacked by some combination of heuristics, maximum likelihood fitting, Hough transforms and/or neural networks. The problem itself is somewhat ill-defined since, as noted, even a single showering primary produces many closely-overlapping rings. For $\pi^0 \to \gamma\gamma$ two-ring identification, performance falls off rapidly with increasing π^0 momentum, and selection criteria must be optimized with respect to the analysis-dependent cost-function for $e \leftrightarrow \pi^0$ mis-identification. Two representative cases for $\xi = 39\%$ will be illustrated. In an atmospheric neutrino experiment, where π^0 are relatively rare compared to $e^{\pm}$, one can isolate a $> 90\%$ pure 500 MeV/c π^0 sample with an efficiency of ∼ 40%. In a ν_e appearance experiment at $E_\nu \leq 1\,\mathrm{GeV}$, where $e^{\pm}$ are rare compared to π^0, a 99% pure 500 MeV/c electron sample can be identified with an efficiency of ∼ 70%. For constant ξ, a larger detector (with, perforce, a greater number of pixels to sample the light distribution) performs somewhat better at multi-ring separation than a smaller one. For a more detailed discussion of event reconstruction techniques, see Ref. 36.

28.5. Transition radiation detectors (TRD's)

Revised September 2003 by D. Froidevaux (CERN).

It is clear from the discussion in the section on "Passages of Particles Through Matter" (Sec. 27 of this *Review*) that transition radiation (TR) only becomes useful for particle detectors when the signal can be observed as x rays emitted along the particle direction for Lorentz factors γ larger than 1000. In practice, TRD's are therefore used to provide electron/pion separation for $0.5\ \mathrm{GeV}/c \lesssim p \lesssim 100\ \mathrm{GeV}/c$. The charged-particle momenta have usually been measured elsewhere in the detector in the past [57].

Table 28.3: Properties of Cherenkov tracking calorimeters. LSND was a hybrid scintillation/Cherenkov detector; the estimated ratio of isotropic to Cherenkov photoelectrons was about 5:1. MiniBooNE's light yield also includes a small scintillation component.

Detector	Fiducial mass (kton)	PMTs (diameter, cm)	ξ	p.e./ MeV	Dates
IMB-1 [48]	3.3 H_2O	2048 (12.5)	1%	0.25	1982–85
IMB-3 [49]	3.3 H_2O	2048 (20 +plate)	4.5%	1.1	1987–90
KAM I [50,51]	0.88/0.78 H_2O	1000/948 (50)	20%	3.4	1983–85
KAM II [52]	1.04 H_2O	948 (50)	20%	3.4	1986–90
LSND [53]	0.084 oil+scint.	1220 (20)	25%	33	1993–98
SK-1 [54]	22.5 H_2O	11146 (50)	39%	6	1997–2001
SK-2	22.5 H_2O	5182 (50)	18%	3	2002–
K2K [55]	0.025 H_2O	680 (50)	39%	6	1999–
SNO [56]	1.0 D_2O	9456 (20+cone)	55%	9	1999–
MiniBooNE	0.445 oil	1280 (20)	10%	3–4	2002–

Since soft x rays, in the useful energy range between 2 and 20 keV, are radiated with about 1% probability per boundary crossing, practical detectors use radiators with several hundred interfaces, *e.g.* foils or fibers of low-Z materials such as polypropylene (or, more rarely, lithium) in a gas. Absorption inside the radiator itself and in the inactive material of the x-ray detector is important and limits the usefulness of the softer x rays, but interference effects are even larger, and saturate the x-ray yield for electron energies above a few GeV [58,59].

A classical detector is composed of several similar modules, each consisting of a radiator and an x-ray detector, which is usually a wire chamber operated with a xenon-rich mixture, in order to efficiently absorb the x rays. The most prominent and recent examples of such detectors for large-scale experiments are the TRD detectors of NOMAD [60], ALICE [61], and PHENIX. Since transition-radiation photons are mostly emitted at very small angles with respect to the charged-particle direction, the x-ray detector most often detects the sum of the ionization loss (dE/dx) of the charged particle in the gas and energy deposition of the x rays. The discrimination between electrons and pions can be based on the charges measured in each detection module, on the number of energy clusters observed above an optimal threshold (usually in the 5 to 7 keV region), or on more sophisticated methods analyzing the pulse shape as a function of time. Once properly calibrated and optimized, most of these methods yield very similar results.

Development work over the past years for accelerator (ATLAS [62]) and space (AMS [63], PAMELA [64] applications has aimed at increasing the intrinsic quality of the TRD-performance by increasing the probability per detection module of observing a signal from TR-photons produced by electrons. This has been achieved experimentally by distributing small-diameter straw-tube detectors uniformly throughout the radiator material. This method has thereby also cured one of the major drawbacks of more classical TRD's, that is, their need to rely on another detector to measure the charged-particle trajectory. For example, in the ATLAS Transition Radiator Tracker [65] charged particles cross about 35 straw tubes embedded in the radiator material. Dedicated R&D work and detailed simulations have shown that the combination of charged-track measurement and particle identification in the same detector will provide a very powerful tool even at the highest LHC luminosity [66].

The major factor in the performance of any TRD is its overall length. This is illustrated in Fig. 28.2, which shows, for a variety of detectors, the measured (or predicted) pion efficiency at a fixed electron efficiency of 90% as a function of the overall detector length. The experimental data cover too wide a range of particle energies (from a few GeV to 40 GeV) to allow for a quantitative fit to a universal curve. Fig. 28.2 shows that an order of magnitude in rejection power against pions is gained each time the detector length is increased by ~ 20 cm.

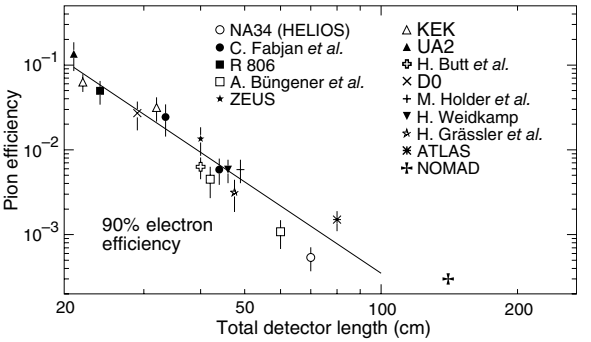

Figure 28.2: Pion efficiency measured (or predicted) for different TRDs as a function of the detector length for a fixed electron efficiency of 90%. The experimental data are directly taken or extrapolated from references [67–79,60](NA34 to NOMAD).

28.6. Wire chambers

Written October 1999 by A. Cattai and G. Rolandi (CERN).

A wire chamber relies on the detection of a large fraction of the charge created in a volume filled with an appropriate gas mixture. A charged particle traversing a gas layer of thickness Δ produces electron-ion pairs along its path (see Sec. 27.2). The yield $(1/\lambda)$ of ionization encounters for a minimum ionization particle (m.i.p.) (see Fig. 27.1) is given in Table 28.4.

Table 28.4: For various gases at STP: (a) yield of ionization encounters $(1/\lambda)$ for m.i.p. [80], (b) t_{99}: thickness of the gas layer for 99% efficiency, and (c) the average number of free electrons produced by a m.i.p. (calculated using data from Ref. 81).

	Encounters/cm	t_{99}(mm)	Free electrons/cm
He	5	9.2	16
Ne	12	3.8	42
Ar	25	1.8	103
Xe	46	1.0	340
CH_4	27	1.7	62
CO_2	35	1.3	107
C_2H_6	43	1.1	113

The probability to have at least one ionization encounter is $1-\exp(-\Delta/\lambda)$ and the thickness of the gas layer for 99% efficiency is $t_{99} = 4.6\lambda$. Depending on the gas, some 65–80% of the encounters result in the production of only one electron; the probability that a cluster has more than five electrons is smaller than 10%. However the tail of the distribution is very long and the yield of ionization electrons is 3–4 times that of the ionization encounters. The secondary ionization happens either in collisions of (primary) ionization electrons with atoms or through intermediate excited states. The process is non-linear and gas mixtures may have larger yields than each of their components. See also the discussion in Sec. 27.7.

Under the influence of electric and magnetic fields the ionization electrons drift inside the gas with velocity $\boldsymbol{u}$ given by:

$$\boldsymbol{u} = \mu|\boldsymbol{E}|\frac{1}{1+\omega^2\tau^2}\left(\widehat{\boldsymbol{E}} + \omega\tau(\widehat{\boldsymbol{E}}\times\widehat{\boldsymbol{B}}) + \omega^2\tau^2(\widehat{\boldsymbol{E}}\cdot\widehat{\boldsymbol{B}})\widehat{\boldsymbol{B}}\right) \qquad (28.11)$$

where $\widehat{\boldsymbol{E}}$ and $\widehat{\boldsymbol{B}}$ are unit vectors in the directions of the electric and magnetic fields respectively, μ is the electron mobility in the gas, ω is the cyclotron frequency eB/mc, and $\tau = \mu m/e$ is the mean time between collisions of the drifting electrons. The magnitude of the drift velocity depends on many parameters; typical values are in the range 1–8 cm/μs.

In a quite common geometry, the drift electric field is perpendicular to the magnetic field. In this case the electrons drift at an angle ψ with respect to the electric field direction such that $\tan\psi = \omega\tau$.

The ionization electrons are eventually collected by a thin (typically 10 μm radius) anode wire where a strong electric field—increasing as $1/r$—accelerates the electrons enough to produce secondary ionization and hence an avalanche. A quenching gas (organic molecules with large photo-absorption cross-section) absorbs the majority of the photons produced during the avalanche development, keeping the avalanche region localized. The gain achievable with a wire counter depends exponentially on the charge density on the wire, on the gas density ρ and—through it—on pressure and temperature: $dG/G \approx -K\,d\rho/\rho$, where the coefficient K ranges between 5 and 8 in practical cases. Gains larger than 10^4 can be obtained in proportional mode.

The electrons produced in the avalanche are collected by the wire in a few nanoseconds. The positive ions move away from the wire and generate a signal that can be detected with an amplifier. Depending on whether the wire is treated as a current source or a voltage source, the signal is described respectively by:

$$I(t) = q\frac{d}{dt}F(t)\ ; \qquad \Delta V(t) = \frac{q}{C}F(t)\ , \tag{28.12}$$

where q is the positive charge in the avalanche, C is the capacitance between the anode wire and the cathodes and $F(t) = \ln(1 + t/t_0)/\ln(1 + t_{\max}/t_0)$. The constant t_0 is of the order of one or few nanoseconds; the constant $t_{\max}$ (several microseconds) describes the time that it takes ions to reach the cathodes.

A sketch of the first multi-wire proportional chamber (MWPC) [82] is shown in Fig. 28.3. It consists of a plane of parallel sense wires with spacing s and length L inserted in a gap of thickness Δ. The potential distributions and fields in a proportional or drift chamber can usually be calculated with good accuracy from the exact formula for the potential around an array of parallel line charges q (coul/m) along z and located at $y = 0$, $x = 0$, $\pm s$, $\pm 2s$, ...,

$$V(x,y) = -\frac{q}{4\pi\,\epsilon_0}\ln\left\{4\left[\sin^2\left(\frac{\pi x}{s}\right) + \sinh^2\left(\frac{\pi y}{s}\right)\right]\right\}\ . \tag{28.13}$$

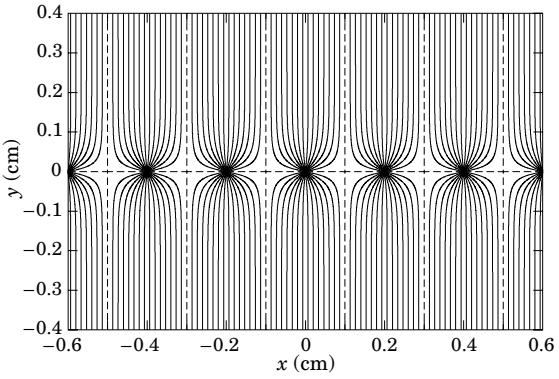

Figure 28.3: Electric field lines in a (MWPC) with an anode pitch of 2 mm as calculated with GARFIELD program [83].

With digital readout, the resolution in the direction perpendicular to the wire is $s/\sqrt{12}$, where s is typically 1–2 mm. Similar resolution can be achieved with a smaller channel density by measuring the difference in time between the arrival of electrons at the wire and the traversal of the particle, albeit with a longer response time. In the case of drift chambers, the spatial resolution is limited by the diffusion of ionization electrons during the drift and by the fluctuations of the ionization process. Depending on the gas mixture, the width of the diffusing cloud after 1 cm of drift is typically between 50 and 300 μm; small diffusion implies low drift velocity. With drift lengths up to 5 cm (1 μs), resolutions in the range 100–200 μm have been achieved in chambers with surface areas of several square meters [84]. The central detectors in many collider experiments are drift chambers with the wires parallel to the beam direction. Small volume chambers (0.1 m^3) have been used for vertex measurement achieving resolutions of 50 μm using high pressure (2–4 bar) and low diffusion gas mixtures [85]. Large volume chambers (5–40 m^3) with several thousand wires of length of 1–2 meters are operated with resolution between 100 and 200 μm [86].

The spatial resolution cannot be improved by arbitrarily reducing the spacing of the wires. In addition to the practical difficulties of precisely stringing wires at a pitch below 1 mm, there is a fundamental limitation: the electrostatic force between the wires is balanced by the mechanical tension, which cannot exceed a critical value. This gives the following approximate stability condition:

$$\frac{s}{L} \geq 1.5 \times 10^{-3} V(\mathrm{kV})\sqrt{\frac{20\ \mathrm{g}}{T}}\ , \tag{28.14}$$

where V is the voltage of the sense wire and T is the tension of the wire in grams-weight equivalent.

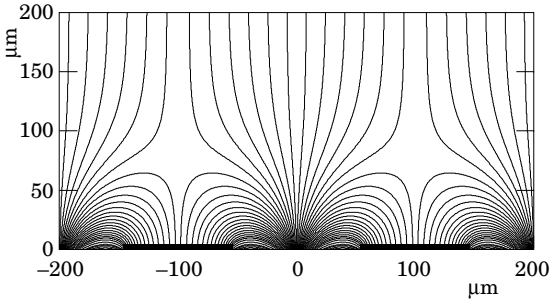

Figure 28.4: Electron drift lines in a micro-strip gas chamber with a pitch of 200 μm.

This limitation can be overcome by means of lithographic techniques [87]: a series of thin aluminum strips are precisely 0.2 μm engraved on an insulating support producing a miniaturized version of a MWPC (see Fig. 28.4). With this technique the spacing of the anodes can be reduced to 0.1–0.2 mm, reducing the drift time of the ions and improving on the spatial resolution and on the rate capability of the chamber.

In all these devices, since the avalanche is very localized along the anode, signals induced on nearby electrodes can be used to measure the coordinate along the anode direction (see Sec. 28.7).

A review of the principle of particle detection with drift chambers can be found in [88]. A compilation of the mobilities, diffusion coefficients and drift deflection angles as a function of $\boldsymbol{E}$ and $\boldsymbol{B}$ for several gas mixtures used in proportional chambers can be found in [89]. A review of micro-strip gas chambers (MSGC) can be found in [90].

28.7. Time-projection chambers

Written November 1997 by M.T Rownan; revised August 2003.

Detectors with long drift distances perpendicular to a multi-anode proportional plane provide three-dimensional information, with one being the time projection. A (typically strong) magnetic field parallel to the drift direction suppresses transverse diffusion ($\sigma = \sqrt{2Dt}$) by a factor

$$D(B)/D(0) = \frac{1}{1 + \omega^2\tau^2}\ , \tag{28.15}$$

where D is the diffusion coefficient, $\omega = eB/mc$ is the cyclotron frequency, and τ is the mean time between collisions. Multiple measurements of energy deposit along the particle trajectory combined with the measurement of momentum in the magnetic field allows excellent particle identification [91], as can be seen in Fig. 28.5.

A typical gas-filled TPC consists of a long uniform drift region (1–2 m) generated by a central high-voltage membrane and precision concentric cylindrical field cages within a uniform, parallel magnetic field [88]. Details of construction and electron trajectories near the anode end are shown in Fig. 28.6. Signal shaping and processing using analog storage devices or FADC's allows excellent pattern recognition,

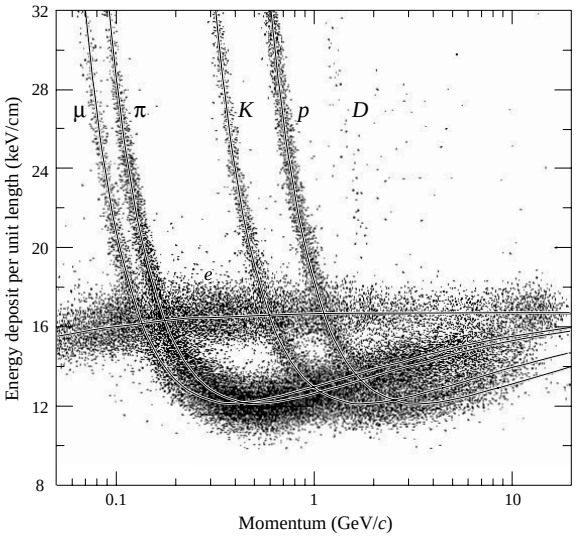

Figure 28.5: PEP4/9-TPC energy-deposit measurements (185 samples @8.5 atm Ar-CH_4 80–20%) in multihadron events. The electrons reach a Fermi plateau value of 1.4 times the most probably energy deposit at minimum ionization. Muons from pion decays are separated from pions at low momentum; π/K are separated over all momenta except in the cross-over region. (Low-momentum protons and deuterons originate from hadron-nucleus collisions in inner materials such as the beam pipe.)

track reconstruction, and particle identification within the same detector.

Typical values:	
Gas: Ar + (10–20%) CH_4	Pressure(P) = 1–8.5 atm.
E/P = 100–200 V/cm/atm	B = 1–1.5 Tesla
$v_{\rm drift}$ = 5–7 cm/μs	$\omega\tau$ = 1–8
$\sigma_{x\ {\rm or}\ y}$ = 100–200 μm	σ_z = 0.2–1 mm
σ_{Edep} = 2.5–5.5 %	

Truncated mean energy-deposit resolution depends on the number and size of samples, and gas pressure:

$$\sigma_{Edep} \propto N^{-0.43} \times (P\ell)^{-0.32} \ . \qquad (28.16)$$

Here N is the number of samples, ℓ is the sample size, and P is the pressure. Typical energy-deposit distributions are shown in Fig. 28.5. Good three-dimensional two-track resolutions of about 1–1.5 cm are routinely achieved.

$E \times B$ distortions arise from nonparallel E and B fields (see Eq. (28.11)), and from the curved drift of electrons to the anode wires in the amplification region. Position measurement errors include contributions from the anode-cathode geometry, the track crossing angle (α), $E \times B$ distortions, and from the drift diffusion of electrons

$$\sigma^2_{x\ {\rm or}\ y} = \sigma^2_0 + \sigma^2_D(1+\tan^2\alpha)L/L_{\rm max} + \sigma^2_\alpha(\tan\alpha - \tan\psi)^2 \qquad (28.17)$$

where σ is the coordinate resolution, σ_0 includes the anode-cathode geometry contribution, ψ is the Lorentz angle, and L is the drift distance.

Space-charge distortions arise in high-rate environments, especially for low values of $\omega\tau$. However, they are mitigated by an effective gating grid (Fig. 28.6). Field uniformities of

$$\int (E_\perp/E)\, dz \lesssim 0.5\text{–}1 \text{ mm} \ , \qquad (28.18)$$

over 10–40 m^3 volumes have been obtained. Laser tracks and calibration events allow mapping of any remnant drift non-uniformities.

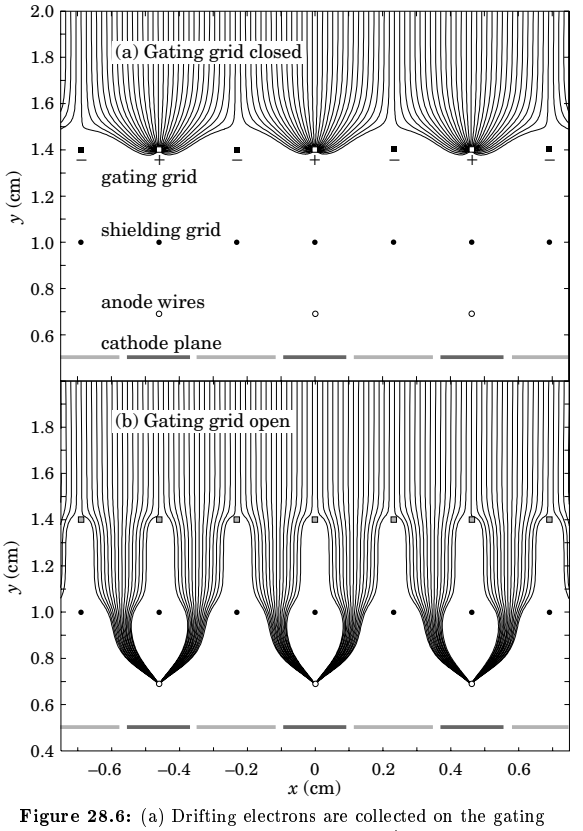

Figure 28.6: (a) Drifting electrons are collected on the gating grid until gated open by a triggering event. A shielding grid at ground potential is used to terminate the drift region. Electrons drifting through an open gating grid (b) pass through to the amplification region around the anode wires. Positive ions generated in the avalanche are detected on segmented cathode pads to provide precise measurements along the wire. The slow positive ions are blocked from entering the drift region by closing the gating grid after the electrons have drifted through.

28.8. Silicon semiconductor detectors

Updated August 2003 by H. Spieler (LBNL).

Semiconductor detectors are widely used in modern high-energy physics experiments. They are the key ingredient of high-resolution vertex and tracking detectors and are also used as photodetectors in scintillation calorimeters. The most commonly used material is silicon, but germanium, gallium-arsenide and diamond are also useful in some applications. Integrated circuit technology allows the formation of high-density micron-scale electrodes on large (10–15 cm diameter) wafers, providing excellent position resolution. Furthermore, the density of silicon and its small ionization energy result in adequate signals with active layers only 100–300 μm thick, so the signals are also fast (typically tens of ns). Semiconductor detectors depend crucially on low-noise electronics (see Sec. 28.9), so the detection sensitivity is determined by signal charge and capacitance. For a survey of recent developments see Ref. 92.

Silicon detectors are p-n junction diodes operated at reverse bias. This forms a sensitive region depleted of mobile charge and sets up an electric field that sweeps charge liberated by radiation to the electrodes. Detectors typically use an asymmetric structure, e.g. a highly doped p electrode and a lightly doped n region, so that the depletion region extends predominantly into the lightly doped volume.

The thickness of the depleted region is

$$W = \sqrt{2\epsilon(V + V_{bi})/Ne} = \sqrt{2\rho\mu\epsilon(V + V_{bi})}\,, \tag{28.19}$$

where $V =$ external bias voltage
$V_{bi} =$ "built-in" voltage (≈ 0.5 V for resistivities typically used in detectors)
$N =$ doping concentration
$e =$ electronic charge
$\epsilon =$ dielectric constant $= 11.9\ \epsilon_0 \approx 1$ pF/cm
$\rho =$ resistivity (typically 1–10 kΩ cm)
$\mu =$ charge carrier mobility
$= 1350$ cm^2 V^{-1} s^{-1} for electrons
$= 450$ cm^2 V^{-1} s^{-1} for holes

or

$$W = 0.5\ [\mu\text{m}/\sqrt{\Omega\text{-cm}\cdot\text{V}}] \times \sqrt{\rho(V + V_{bi})} \text{ for } n\text{-type material, and}$$

$$W = 0.3\ [\mu\text{m}/\sqrt{\Omega\text{-cm}\cdot\text{V}}] \times \sqrt{\rho(V + V_{bi})} \text{ for } p\text{-type material.}$$

The conductive p and n regions together with the depleted volume form a capacitor with the capacitance per unit area

$$C = \epsilon/W \approx 1\,[\text{pF/cm}]\,/W\ . \tag{28.20}$$

In strip and pixel detectors the capacitance is dominated by the fringing capacitance. For example, the strip-to-strip fringing capacitance is $\sim$ 1–1.5 pF cm^{-1} of strip length at a strip pitch of 25–50 μm.

For energetic particles and photons the energy required to create an electron-hole pair $E_i = 3.6$ eV (which is larger than the band gap because phonon excitation is required for momentum conservation). For minimum-ionizing particles, the most probable charge deposition in a 300 μm thick silicon detector is about 3.5 fC (22000 electrons). Since both electronic and lattice excitations are involved, the variance in the number of charge carriers $N = E/E_i$ produced by an absorbed energy E is reduced by the Fano factor F (about 0.1 in Si). Thus, $\sigma_N = \sqrt{FN}$ and the energy resolution $\sigma_E/E = \sqrt{FE_i/E}$. However, the measured signal fluctuations are usually dominated by electronic noise or energy loss fluctuations in the detector. Visible light can be detected with photon energies above the band gap. In optimized photodiodes quantum efficiencies $> 80\%$ for wavelengths between 400 nm and nearly 1 μm are achievable. UV-extended photodiodes have useful efficiency down to 200 nm.

Charge collection time decreases with increasing bias voltage, and can be reduced further by operating the detector with "overbias," *i.e.*, a bias voltage exceeding the value required to fully deplete the device. The collection time is limited by velocity saturation at high fields (approaching 10^7 cm/s at $E > 10^4$ V/cm); at an average field of 10^4 V/cm the collection time is about 15 ps/μm for electrons and 30 ps/μm for holes. In typical fully-depleted detectors 300 μm thick, electrons are collected within about 10 ns, and holes within about 25 ns.

Position resolution is limited by transverse diffusion during charge collection (typically 5 μm for 300 μm thickness) and by knock-on electrons. Resolutions of 2–4 μm (rms) have been obtained in beam tests. In magnetic fields, the Lorentz drift deflects the electron and hole trajectories and the detector must be tilted to reduce spatial spreading (see "Hall effect" in semiconductor textbooks).

Radiation damage occurs through two basic mechanisms:

1. Bulk damage due to displacement of atoms from their lattice sites. This leads to increased leakage current, carrier trapping, and build-up of space charge that changes the required operating voltage. Displacement damage depends on the nonionizing energy loss and the energy imparted to the recoil atoms, which can initiate a chain of subsequent displacements, *i.e.*, damage clusters. Hence, it is critical to consider both particle type and energy.
2. Surface damage due to charge build-up in surface layers, which leads to increased surface leakage currents. In strip detectors the inter-strip isolation is affected. The effects of charge build-up are strongly dependent on the device structure and on fabrication details. Since the damage is proportional to the absorbed energy (when ionization dominates), the dose can be specified in rad (or Gray) independent of particle type.

The increase in reverse bias current due to bulk damage is $\Delta I_r = \alpha\Phi$ per unit volume, where Φ is the particle fluence and α the damage coefficient ($\alpha \approx 3 \times 10^{-17}$ A/cm for minimum ionizing protons and pions after long-term annealing; $\alpha \approx 2 \times 10^{-17}$ A/cm for 1 MeV neutrons). The reverse bias current depends strongly on temperature

$$\frac{I_R(T_2)}{I_R(T_1)} = \left(\frac{T_2}{T_1}\right)^2 \exp\left[-\frac{E}{2k}\left(\frac{T_1 - T_2}{T_1 T_2}\right)\right] \tag{28.21}$$

where $E = 1.2$ eV, so rather modest cooling can reduce the current substantially ($\sim$ 6-fold current reduction in cooling from room temperature to 0°C).

The space-charge concentration in high-resistivity n-type Si changes approximately as

$$N = N_0 e^{-\delta\Phi} - \beta\Phi\ , \tag{28.22}$$

where N_0 is the initial donor concentration, $\delta \approx 6 \times 10^{-14}$ cm^2 determines donor removal, and $\beta \approx 0.03$ cm^{-1} describes acceptor creation. The acceptor states trap electrons, building up a negative space charge, which in turn requires an increase in the applied voltage to sweep signal charge through the detector thickness. This has the same effect as a change in resistivity, *i.e.*, the required voltage drops initially with fluence, until the positive and negative space charge balance and very little voltage is required to collect all signal charge. At larger fluences the negative space charge dominates, and the required operating voltage increases ($V \propto N$). The safe operating limit of depletion voltage ultimately limits the detector lifetime. Strip detectors specifically designed for high voltages have been operated at bias voltages >500V. Since the effect of radiation damage depends on the electronic activity of defects, various techniques have been applied to neutralize the damage sites. For example, additional doping with oxygen increases the allowable charged hadron fluence roughly three-fold [93]. The increase in leakage current with fluence, on the other hand, appears to be unaffected by resistivity and whether the material is n or p-type.

Strip and pixel detectors have remained functional at fluences beyond 10^{15} cm^{-2} for minimum ionizing protons. At this damage level, charge loss due to recombination and trapping also becomes significant and the high signal-to-noise ratio obtainable with low-capacitance pixel structures extends detector lifetime. The occupancy of the defect charge states is strongly temperature dependent; competing processes can increase or decrease the required operating voltage. It is critical to choose the operating temperature judiciously (-10 to 0°C in typical collider detectors) and limit warm-up periods during maintenance. For a more detailed summary see Ref. 94 and and the web-site of the ROSE collaboration at `http://RD48.web.cern.ch/rd48`.

Currently, the lifetime of detector systems is still limited by the detectors; in the electronics use of standard "deep submicron" CMOS fabrication processes with appropriately designed circuitry has increased the radiation resistance to fluences $> 10^{15}$ cm^{-2} of minimum ionizing protons or pions. For a comprehensive discussion of radiation effects see Ref. 95.

28.9. Low-noise electronics

Revised August 2003 by H. Spieler (LBNL).

Many detectors rely critically on low-noise electronics, either to improve energy resolution or to allow a low detection threshold. A typical detector front-end is shown in Fig. 28.7.

The detector is represented by a capacitance C_d, a relevant model for most detectors. Bias voltage is applied through resistor R_b and the signal is coupled to the preamplifier through a blocking capacitor C_c. The series resistance R_s represents the sum of all resistances present in the input signal path, *e.g.* the electrode resistance, any input protection networks, and parasitic resistances in the input transistor. The preamplifier provides gain and feeds a pulse shaper, which tailors

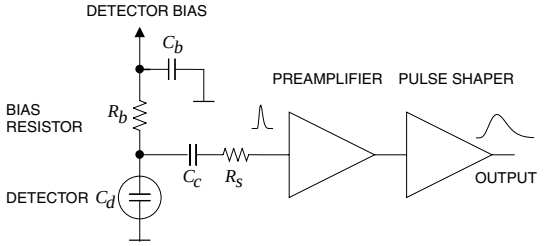

Figure 28.7: Typical detector front-end circuit.

the overall frequency response to optimize signal-to-noise ratio while limiting the duration of the signal pulse to accommodate the signal pulse rate. Even if not explicitly stated, all amplifiers provide some form of pulse shaping due to their limited frequency response.

The equivalent circuit for the noise analysis (Fig. 28.8) includes both current and voltage noise sources. The leakage current of a semiconductor detector, for example, fluctuates due to electron emission statistics. This "shot noise" i_{nd} is represented by a current noise generator in parallel with the detector. Resistors exhibit noise due to thermal velocity fluctuations of the charge carriers. This noise source can be modeled either as a voltage or current generator. Generally, resistors shunting the input act as noise current sources and resistors in series with the input act as noise voltage sources (which is why some in the detector community refer to current and voltage noise as "parallel" and "series" noise). Since the bias resistor effectively shunts the input, as the capacitor C_b passes current fluctuations to ground, it acts as a current generator i_{nb} and its noise current has the same effect as the shot noise current from the detector. Any other shunt resistances can be incorporated in the same way. Conversely, the series resistor R_s acts as a voltage generator. The electronic noise of the amplifier is described fully by a combination of voltage and current sources at its input, shown as e_{na} and i_{na}.

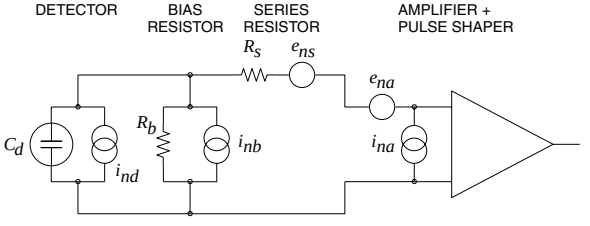

Figure 28.8: Equivalent circuit for noise analysis.

Shot noise and thermal noise have a "white" frequency distribution, *i.e.* the spectral power densities $dP_n/df \propto di_n^2/df \propto de_n^2/df$ are constant with the magnitudes

$$\begin{aligned} i_{nd}^2 &= 2eI_d \ , \\ i_{nb}^2 &= \frac{4kT}{R_b} \ , \\ e_{ns}^2 &= 4kTR_s \ , \end{aligned} \tag{28.23}$$

where e is the electronic charge, I_d the detector bias current, k the Boltzmann constant and T the temperature. Typical amplifier noise parameters e_{na} and i_{na} are of order $\mathrm{nV}/\sqrt{\mathrm{Hz}}$ and $\mathrm{pA}/\sqrt{\mathrm{Hz}}$. Trapping and detrapping processes in resistors, dielectrics and semiconductors can introduce additional fluctuations whose noise power frequently exhibits a $1/f$ spectrum. The spectral density of the $1/f$ noise voltage is

$$e_{nf}^2 = \frac{A_f}{f} \ , \tag{28.24}$$

where the noise coefficient A_f is device specific and of order 10^{-10}–$10^{-12}\,\mathrm{V}^2$.

A fraction of the noise current flows through the detector capacitance, resulting in a frequency-dependent noise voltage $i_n/(\omega C_d)$, which is added to the noise voltage in the input circuit. Since the individual noise contributions are random and uncorrelated, they add in quadrature. The total noise at the output of the pulse shaper is obtained by integrating over the full bandwidth of the system. Superimposed on repetitive detector signal pulses of constant magnitude, purely random noise produces a Gaussian signal distribution.

Since radiation detectors typically convert the deposited energy into charge, the system's noise level is conveniently expressed as an equivalent noise charge Q_n, which is equal to the detector signal that yields a signal-to-noise ratio of one. The equivalent noise charge is commonly expressed in Coulombs, the corresponding number of electrons, or the equivalent deposited energy (eV). For a capacitive sensor

$$Q_n^2 = i_n^2 F_i T_S + e_n^2 F_v \frac{C^2}{T_S} + F_{vf} A_f C^2 \ , \tag{28.25}$$

where C is the sum of all capacitances shunting the input, F_i, F_v, and F_{vf} depend on the shape of the pulse determined by the shaper and T_s is a characteristic time, for example, the peaking time of a semi-gaussian pulse or the sampling interval in a correlated double sampler. The form factors F_i, F_v are easily calculated

$$F_i = \frac{1}{2T_S} \int_{-\infty}^{\infty} [W(t)]^2 \, dt \ , \qquad F_v = \frac{T_S}{2} \int_{-\infty}^{\infty} \left[\frac{dW(t)}{dt} \right]^2 dt \ , \tag{28.26}$$

where for time-invariant pulse-shaping $W(t)$ is simply the system's impulse response (the output signal seen on an oscilloscope) with the peak output signal normalized to unity. For more details see Refs. [96–97].

A pulse shaper formed by a single differentiator and integrator with equal time constants has $F_i = F_v = 0.9$ and $F_{fv} = 4$, independent of the shaping time constant. The overall noise bandwidth, however, depends on the time constant, *i.e.* the characteristic time T_s. The contribution from noise currents increases with shaping time, *i.e.*, pulse duration, whereas the voltage noise decreases with increasing shaping time. Noise with a $1/f$ spectrum depends only on the ratio of upper to lower cutoff frequencies (integrator to differentiator time constants), so for a given shaper topology the $1/f$ contribution to Q_n is independent of T_s. Furthermore, the contribution of noise voltage sources to Q_n increases with detector capacitance. Pulse shapers can be designed to reduce the effect of current noise, *e.g.*, mitigate radiation damage. Increasing pulse symmetry tends to decrease F_i and increase F_v (*e.g.*, to 0.45 and 1.0 for a shaper with one CR differentiator and four cascaded integrators). For the circuit shown in Fig. 28.8,

$$\begin{aligned} Q_n^2 = &\left(2eI_d + 4kT/R_b + i_{na}^2 \right) F_i T_S \\ &+ \left(4kTR_s + e_{na}^2 \right) F_v C_d^2 / T_S + F_{vf} A_f C_d^2 \ . \end{aligned} \tag{28.27}$$

As the characteristic time T_S is changed, the total noise goes through a minimum, where the current and voltage contributions are equal. Fig. 28.9 shows a typical example. At short shaping times the voltage noise dominates, whereas at long shaping times the current noise takes over. The noise minimum is flattened by the presence of $1/f$ noise. Increasing the detector capacitance will increase the voltage noise and shift the noise minimum to longer shaping times.

For quick estimates, one can use the following equation, which assumes an FET amplifier (negligible i_{na}) and a simple CR–RC shaper with time constants τ (equal to the peaking time):

$$\begin{aligned} (Q_n/e)^2 = 12 &\left[\frac{1}{\mathrm{nA \cdot ns}} \right] I_d \tau + 6 \times 10^5 \left[\frac{\mathrm{k\Omega}}{\mathrm{ns}} \right] \frac{\tau}{R_b} \\ &+ 3.6 \times 10^4 \left[\frac{\mathrm{ns}}{(\mathrm{pF})^2 (\mathrm{nV})^2 / \mathrm{Hz}} \right] e_n^2 \frac{C^2}{\tau} \ . \end{aligned} \tag{28.28}$$

Noise is improved by reducing the detector capacitance and leakage current, judiciously selecting all resistances in the input circuit, and choosing the optimum shaping time constant.

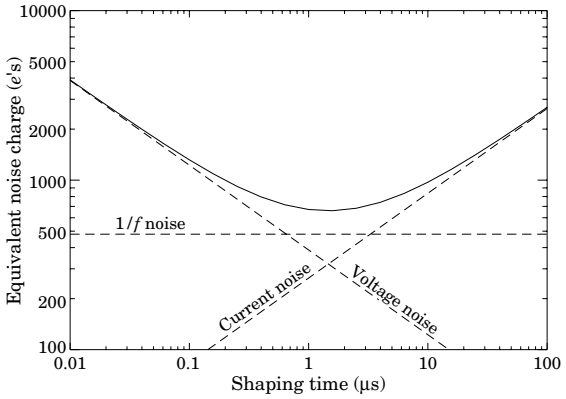

Figure 28.9: Equivalent noise charge vs shaping time.

The noise parameters of the amplifier depend primarily on the input device. In field effect transistors, the noise current contribution is very small, so reducing the detector leakage current and increasing the bias resistance will allow long shaping times with correspondingly lower noise. In bipolar transistors, the base current sets a lower bound on the noise current, so these devices are best at short shaping times. In special cases where the noise of a transistor scales with geometry, *i.e.*, decreasing noise voltage with increasing input capacitance, the lowest noise is obtained when the input capacitance of the transistor is equal to the detector capacitance, albeit at the expense of power dissipation. Capacitive matching is useful with field-effect transistors, but not bipolar transistors. In bipolar transistors, the minimum obtainable noise is independent of shaping time, but only at the optimum collector current I_C, which does depend on shaping time.

$$Q^2_{n,\min} = 4kT\frac{C}{\sqrt{\beta_{DC}}}\sqrt{F_i F_v} \quad \text{at} \quad I_c = \frac{kT}{e}C\sqrt{\beta_{DC}}\sqrt{\frac{F_v}{F_i}}\frac{1}{T_S}\,, \quad (28.29)$$

where β_{DC} is the DC current gain. For a CR–RC shaper and $\beta_{DC} = 100$,

$$Q_{n,\min}/e \approx 250\sqrt{C/\text{pF}}\,. \quad (28.30)$$

Practical noise levels range from $\sim 1e$ for CCDs at long shaping times to $\sim 10^4$ e in high-capacitance liquid argon calorimeters. Silicon strip detectors typically operate at $\sim 10^3$ e electrons, whereas pixel detectors with fast readout provide noise of several hundred electrons.

In timing measurements, the slope-to-noise ratio must be optimized, rather than the signal-to-noise ratio alone, so the rise time t_r of the pulse is important. The "jitter" σ_t of the timing distribution is

$$\sigma_t = \frac{\sigma_n}{(dS/dt)_{S_T}} \approx \frac{t_r}{S/N}\,, \quad (28.31)$$

where σ_n is the rms noise and the derivative of the signal dS/dt is evaluated at the trigger level S_T. To increase dS/dt without incurring excessive noise, the amplifier bandwidth should match the rise-time of the detector signal. The 10 to 90% rise time of an amplifier with bandwidth f_U is $0.35/f_U$. For example, an oscilloscope with 350 MHz bandwidth has a 1 ns rise time. When amplifiers are cascaded, which is invariably necessary, the individual rise times add in quadrature.

$$t_r \approx \sqrt{t_{r1}^2 + t_{r2}^2 + \ldots + t_{rn}^2}$$

Increasing signal-to-noise ratio also improves time resolution, so minimizing the total capacitance at the input is also important. At high signal-to-noise ratios, the time jitter can be much smaller than the rise time. The timing distribution may shift with signal level ("walk"), but this can be corrected by various means, either in hardware or software [9].

For a more detailed introduction to detector signal processing and electronics see Ref. 98.

28.10. Calorimeters

28.10.1. *Electromagnetic calorimeters*:

Written August 2003 by R.-Y. Zhu (California Inst. of Technology).

The development of electromagnetic showers is discussed in the section on "Passage of Particles Through Matter" (Sec. 27 of this *Review*).

Formulae are given which approximately describe average showers, but since the physics of electromagnetic showers is well understood, detailed and reliable Monte Carlo simulation is possible. EGS4 [99] and GEANT [100] have emerged as the standards.

There are homogeneous and sampling electromagnetic calorimeters. In a homogeneous calorimeter the entire volume is sensitive, *i.e.*, contributes signal. Homogeneous electromagnetic calorimeters may be built with inorganic heavy (high-Z) scintillating crystals such as BGO, CsI, NaI, and PWO, non-scintillating Cherenkov radiators such as lead glass and lead fluoride, or ionizing noble liquids. Properties of commonly used inorganic crystal scintillators can be found in Table 28.2. A sampling calorimeter consists of an active medium which generates signal and a passive medium which functions as an absorber. The active medium may be a scintillator, an ionizing noble liquid, a gas chamber, or a semiconductor. The passive medium is usually a material of high density, such as lead, iron, copper, or depleted uranium.

The energy resolution σ_E/E of a calorimeter can be parametrized as $a/\sqrt{E} \oplus b \oplus c/E$, where $\oplus$ represents addition in quadrature and E is in GeV. The stochastic term a represents statistics-related fluctuations such as intrinsic shower fluctuations, photoelectron statistics, dead material at the front of the calorimeter, and sampling fluctuations. For a fixed number of radiation lengths, the stochastic term a for a sampling calorimeter is expected to be proportional to $\sqrt{t/f}$, where t is plate thickness and f is sampling fraction [101,102]. While a is at a few percent level for a homogeneous calorimeter, it is typically 10% for sampling calorimeters. The main contributions to the systematic, or constant, term b are detector non-uniformity and calibration uncertainty. In the case of the hadronic cascades discussed below, non-compensation also contributes to the constant term. One additional contribution to the constant term for calorimeters built for modern high-energy physics experiments, operated in a high-beam intensity environment, is radiation damage of the active medium. This can be minimized by developing radiation-hard active media [33] and by frequent *in situ* calibration and monitoring [32,102]. With effort, the constant term b can be reduced to below one percent. The term c is due to electronic noise summed over readout channels within a few Molière radii. The best energy resolution for electromagnetic shower measurement is obtained in total absorption homogeneous calorimeters, *e.g.* calorimeters built with heavy crystal scintillators. These are used when ultimate performance is pursued.

The position resolution depends on the effective Molière radius and the transverse granularity of the calorimeter. Like the energy resolution, it can be factored as $a/\sqrt{E} \oplus b$, where a is a few to 20 mm and b can be as small as a fraction of mm for a dense calorimeter with fine granularity. Electromagnetic calorimeters may also provide direction measurement for electrons and photons. This is important for photon-related physics when there are uncertainties in event origin, since photons do not leave information in the particle tracking system. Typical photon angular resolution is about 45 $mrad/\sqrt{E}$, which can be provided by implementing longitudinal segmentation [103] for a sampling calorimeter or by adding a preshower detector [104] for a homogeneous calorimeter without longitudinal segmentation.

Novel technologies have been developed for electromagnetic calorimetry. New heavy crystal scintillators, such as PWO, LSO:Ce, and GSO:Ce (see Sec. 28.2), have attracted much attention for homogeneous calorimetry. In some cases, such as PWO, it has received broad applications in high-energy and nuclear physics experiments. The "spaghetti" structure has been developed for sampling calorimetry with scintillating fibers as the sensitive medium. The "accordion" structure has been developed for sampling calorimetry with ionizing noble liquid as the sensitive medium. Table 28.5 provides a brief description of typical electromagnetic calorimeters built recently for high-energy physics experiments. Also listed in this table are

calorimeter depths in radiation lengths (X_0) and the achieved energy resolution. Whenever possible, the performance of calorimeters *in situ* is quoted, which is usually in good agreement with prototype test beam results as well as EGS or GEANT simulations, provided that all systematic effects are properly included. Detailed references on detector design and performance can be found in Appendix C of reference [102] and Proceedings of the International Conference series on Calorimetry in Particle Physics.

Table 28.5: Resolution of typical electromagnetic calorimeters. E is in GeV.

Technology (Experiment)	Depth	Energy resolution	Date
NaI(Tl) (Crystal Ball)	$20X_0$	$2.7\%/\mathrm{E}^{1/4}$	1983
$Bi_4Ge_3O_{12}$ (BGO) (L3)	$22X_0$	$2\%/\sqrt{E} \oplus 0.7\%$	1993
CsI (KTeV)	$27X_0$	$2\%/\sqrt{E} \oplus 0.45\%$	1996
CsI(Tl) (BaBar)	16–$18X_0$	$2.3\%/E^{1/4} \oplus 1.4\%$	1999
CsI(Tl) (BELLE)	$16X_0$	1.7% for $E_\gamma > 3.5$ GeV	1998
$PbWO_4$ (PWO) (CMS)	$25X_0$	$3\%/\sqrt{E} \oplus 0.5\% \oplus 0.2/E$	1997
Lead glass (OPAL)	$20.5X_0$	$5\%/\sqrt{E}$	1990
Liquid Kr (NA48)	$27X_0$	$3.2\%/\sqrt{E} \oplus 0.42\% \oplus 0.09/E$	1998
Scintillator/depleted U (ZEUS)	20–$30X_0$	$18\%/\sqrt{E}$	1988
Scintillator/Pb (CDF)	$18X_0$	$13.5\%/\sqrt{E}$	1988
Scintillator fiber/Pb spaghetti (KLOE)	$15X_0$	$5.7\%/\sqrt{E} \oplus 0.6\%$	1995
Liquid Ar/Pb (NA31)	$27X_0$	$7.5\%/\sqrt{E} \oplus 0.5\% \oplus 0.1/E$	1988
Liquid Ar/Pb (SLD)	$21X_0$	$8\%/\sqrt{E}$	1993
Liquid Ar/Pb (H1)	20–$30X_0$	$12\%/\sqrt{E} \oplus 1\%$	1998
Liquid Ar/depl. U (DØ)	$20.5X_0$	$16\%/\sqrt{E} \oplus 0.3\% \oplus 0.3/E$	1993
Liquid Ar/Pb accordion (ATLAS)	$25X_0$	$10\%/\sqrt{E} \oplus 0.4\% \oplus 0.3/E$	1996

28.10.2. ***Hadronic calorimeters***: [102,105] The length scale appropriate for hadronic cascades is the nuclear interaction length, given very roughly by

$$\lambda_I \approx 35 \text{ g cm}^{-2} A^{1/3} . \tag{28.32}$$

Longitudinal energy deposition profiles are characterized by a sharp peak near the first interaction point (from the fairly local deposition of EM energy resulting from π^0's produced in the first interaction), followed by a more gradual development with a maximum at

$$x/\lambda_I \equiv t_{\max} \approx 0.2 \ln(E/1 \text{ GeV}) + 0.7 \tag{28.33}$$

as measured from the front of the detector.

The depth required for containment of a fixed fraction of the energy also increases logarithmically with incident particle energy. The thickness of iron required for 95% (99%) containment of cascades induced by single hadrons is shown in Fig. 28.10 [106]. Two of the sets of data are from large neutrino experiments, while the third is from a commonly-used parameterization. Depths as measured in nuclear interaction lengths presumably scale to other materials. From the same data it can be concluded that the requirement that 95% of the energy in 95% of the showers be contained requires 40 to 50 cm (2.4 to 3.0 λ_I) more material material than for an average 95% containment. The transverse dimensions of hadronic showers also scale as λ_I, although most of the energy is contained in a narrow core.

The energy deposit in a hadronic cascade consists of a prompt EM component due to π^0 production and a somewhat slower component mainly due to low-energy hadronic activity. An induction argument verified by Monte-Carlo simulations has shown that the

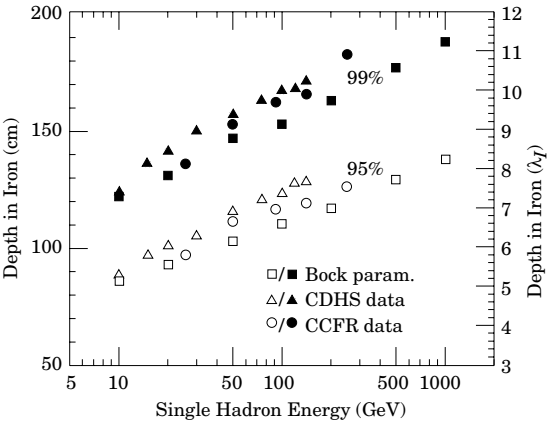

Figure 28.10: Required calorimeter thickness for 95% and 99% hadronic cascade containment in iron, on the basis of data from two large neutrino detectors and the parameterization of Bock *et al.* [106].

fraction of hadronic energy in a cascade is $(E/E_0)^{m-1}$, where $0.80 \lesssim m \lesssim 0.85$ [107]. E_0 is about 1 GeV for incident pions, and the power-law description is approximately valid for incident energy E greater than a few tens of GeV. In general, the electromagnetic and hadronic energy depositions are converted to electrical signals with different efficiencies. The ratio of the conversion efficiencies is usually called the intrinsic e/h ratio. It follows in the power-law approximation the ratio of the responses for incident pions and incident electrons is given by "π/e"$= 1 - (1 - h/e)(E/E_0)^{m-1}$. With or without the power-law approximation the response for pions is not a linear function of energy for $e/h \neq 1$. (But in any case, as the energy increases a larger and larger fraction of the energy is transferred to π^0's, and "π/e"$\to 1$.) If $e/h = 1.0$ the calorimeter is said to be *compensating*. If e/h differs from unity by more than 5% or 10%, detector performance is compromised because of fluctuations in the π^0 content of the cascades. This results in (a) a skewed signal distribution and (b) an almost-constant contribution to detector resolution which is proportional to the degree of noncompensation $|1 - h/e|$. The coefficient relating the size of the constant term to $|1 - h/e|$ is 14% according to FLUKA simulations [107], and 21% according to Wigmans' calculations [108]. (Wigmans now prefers a different approach to the "constant term" [102].)

The formula for "π/e" given above is valid for a large uniform calorimeter. Real calorimeters usually have an EM front structure which is different, and so modifications must be made in modeling the response.

In most cases e/h is greater than unity, particularly if little hydrogen is present or if the gate time is short. This is because much of the low-energy hadronic energy is "hidden" in nuclear binding energy release, low-energy spallation products, *etc.* Partial correction for these losses occurs in a sampling calorimeter with high-Z absorbers, because a disproportionate fraction of electromagnetic energy is deposited in the inactive region. For this reason, a fully sensitive detector such as scintillator or glass cannot be made compensating.

The average electromagnetic energy fraction in a high-energy cascade is smaller for incident protons than for pions; $E_0 \approx 2.6$ GeV rather than ≈ 1 GeV. As a result "π/e">"p/e" (if $e/h > 1$) in a noncompensating calorimeter [107]. This difference has now been measured [109].

Circa 1990 compensation was thought to be very important in hadronic calorimeter design. Motivated very much by the work of Wigmans [108], several calorimeters were built with $e/h \approx 1 \pm 0.02$. These include

- ZEUS [110] 2.6 cm thick scintillator sheets sandwiched between 3.3 mm depleted uranium plates; a resolution of $0.35/\sqrt{E}$ was obtained;

- ZEUS prototype study [111], with 10 mm lead plates and 2.5 mm scintillator sheets; $0.44/\sqrt{E}$;
- D0 [112], where the sandwich cell consists of a 4–6 mm thick depleted uranium plate, 2.3 mm LAr, a G-10 signal board, and another 2.3 mm LAr gap; $45\%/\sqrt{E}$.

Approximately Gaussian signal distributions were observed.

More recently, compensation has not been considered as important, and, in addition, the new generation of calorimeters for LHC experiments operate in a different energy regime and can tolerate poorer resolution in return for simpler, deeper structures. For example, the ATLAS endcaps consist of iron plates with scintillating fiber readout [113]. The fraction of the structure consisting of low-Z active region (scintillator in this case) is much smaller than would be necessary to achieve compensation. Test beam results with these modules show a resolution of $\approx 46\%/\sqrt{E}$, and $e/h = 1.5$–1.6.

28.10.3. ***Free electron drift velocities in liquid ionization sensors***: Velocities as a function of electric field strength are given in Refs. 114–117 and are plotted in Fig. 28.11. Recent precise measurements of the free electron drift velocity in LAr have been published by W. Walkowiak [118]. These measurements were motivated by the design of the ATLAS electromagnetic calorimeter and inconsistencies in the previous literature. Velocities are systematically higher than those shown in Fig. 28.11.

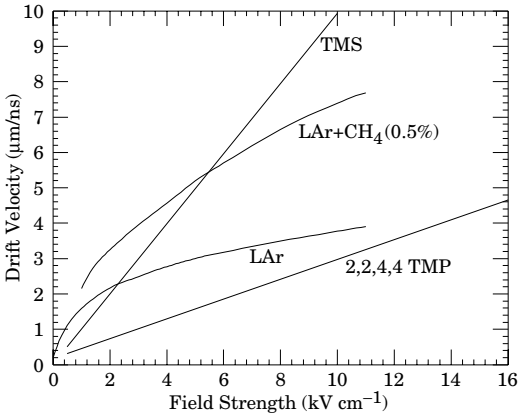

Figure 28.11: Electron drift velocity as a function of field strength for commonly used liquids.

28.11. Superconducting solenoids for collider detectors

Revised October 2001 by R.D. Kephart (FNAL).

28.11.1. ***Basic (approximate) equations***: In all cases SI units are assumed, so that B is in tesla, E is in joules, dimensions are in meters, and $\mu_0 = 4\pi \times 10^{-7}$.

Magnetic field: The magnetic field at the center of a solenoid of length L and radius R, having N total turns and a current I is

$$B(0,0) = \frac{\mu_0 NI}{\sqrt{L^2 + 4R^2}} \, . \tag{28.34}$$

Stored energy: The energy stored in the magnetic field of any magnet is calculated by integrating B^2 over all space:

$$E = \frac{1}{2\mu_0} \int B^2 dV \, . \tag{28.35}$$

For a solenoid with an iron flux return in which the magnetic field is $< 2T$, the field in the aperture is approximately uniform and equal to $\mu_0 NI/L$. If the thickness of the coil is small, (which is the case if it is superconducting), then

$$E \approx (\pi/2\mu_0) B^2 R^2 L \, . \tag{28.36}$$

Cost of a superconducting solenoid [119]:

$$\text{Cost (in M\$)} = 0.523 \, [E/(1 \text{ MJ})]^{0.662} \tag{28.37}$$

Magnetostatic computer programs: It is too difficult to solve the Biot-Savart equation for a magnetic circuit which includes iron components and so iterative computer programs are used. These include POISSON, TOSCA [120], and ANSYS [121].

28.11.2. ***Scaling laws for thin solenoids***: For a detector in which the calorimetry is outside the aperture of the solenoid, the coil must be thin in terms of radiation and absorption lengths. This usually means that the coil is superconducting and that the vacuum vessel encasing it is of minimum real thickness and fabricated of a material with long radiation length. There are two major contributers to the thickness of a thin solenoid:

1. The conductor, consisting of the current-carrying superconducting material (usually Cu/Nb-Ti) and the quench protecting stabilizer (usually aluminum), is wound on the inside of a structural support cylinder (usually aluminum also). This package typically represents about 60% of the total thickness in radiation lengths. The thickness scales approximately as B^2R.
2. Approximately another 25% of the thickness of the magnet comes from the outer cylindrical shell of the vacuum vessel. Since this shell is susceptible to buckling collapse, its thickness is determined by the diameter, length, and the modulus of the material of which it is fabricated. When designing this shell to a typical standard, the real thickness is

$$t = P_c D^{2.5} [(L/D) - 0.45(t/D)^{0.5}]/2.6Y^{0.4} \, , \tag{28.38}$$

where t = shell thickness (in), D = shell diameter (in), L = shell length (in), Y = modulus of elasticity (psi), and P_c = design collapse pressure (= 30 psi). For most large-diameter detector solenoids, the thickness to within a few percent is given by [122]

$$t = P_c D^{2.5} (L/D)/2.6Y^{0.4} \, . \tag{28.39}$$

28.11.3. ***Properties of collider detector solenoids***: The physical dimensions, central field, stored energy and thickness in radiation lengths normal to the beam line of the superconducting solenoids associated with the major colliders are given in Table 28.6.

Table 28.6: Properties of superconducting collider detector solenoids.

Experiment–Lab	Field (T)	Bore Dia (m)	Length (m)	Energy (MJ)	Thickness (X_0)
CDF–Fermilab	1.5	2.86	5.07	30	0.86
DØ –Fermilab	2.0	1.06	2.73	5.6	0.87
BaBar–SLAC	1.5	2.80	3.46	27.0	< 1.4
Topaz–KEK*	1.2	2.72	5.4	19.5	0.70
Venus–KEK*	0.75	3.4	5.64	12	0.52
Cleo II–Cornell	1.5	2.9	3.8	25	2.5
Aleph–CERN*	1.5	5.0	7.0	130	1.7
ATLAS–CERN†	2.0	2.5	5.3	700	0.66
CMS–CERN†	4.0	5.9	12.5	2700	‡
Delphi–CERN*	1.2	5.2	7.4	109	4.0
H1–DESY	1.2	5.2	5.75	120	1.2
Zeus–DESY	1.8	1.72	2.85	10.5	0.9

*No longer in service.
†Detectors under construction.
‡EM calorimeter inside solenoid, so small X_0 not a goal.

The ratio of stored energy to cold mass (E/M) is a useful performance measure. One would like the cold mass to be as small as possible to minimize the thickness, but temperature rise during a quench must also be minimized. Ratios as large as 12 kJ/kg may

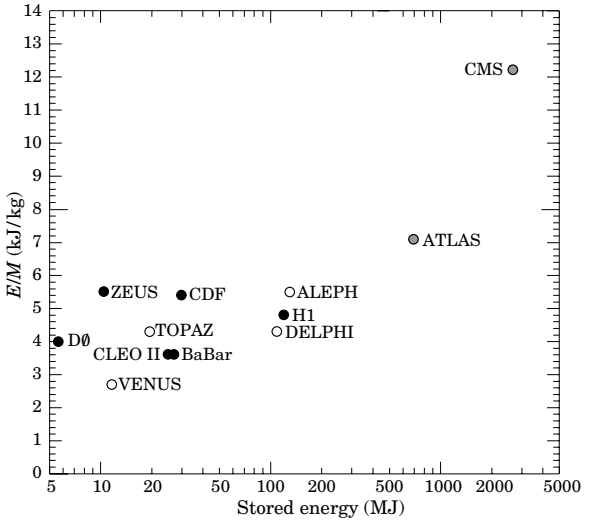

Figure 28.12: Ratio of stored energy to cold mass for existing thin detector solenoids. Solenoids in decommissioned detectors are indicated by open circles. Solenoids for detectors under construction are indicated by grey circles.

be used. The limit is set by the maximum temperature that the coil design can tolerate during a fast quench. This maximum temperature is usually limited to < 100 K so that thermal expansion effects in the coil are manageable. This quantity is shown as a function of total stored energy for some major collider detectors in Fig. 28.12.

28.12. Measurement of particle momenta in a uniform magnetic field [123,124]

The trajectory of a particle with momentum p (in GeV/c) and charge ze in a constant magnetic field $\vec{B}$ is a helix, with radius of curvature R and pitch angle λ. The radius of curvature and momentum component perpendicular to $\vec{B}$ are related by

$$p\cos\lambda = 0.3\, z\, B\, R\,, \tag{28.40}$$

where B is in tesla and R is in meters.

The distribution of measurements of the curvature $k \equiv 1/R$ is approximately Gaussian. The curvature error for a large number of uniformly spaced measurements on the trajectory of a charged particle in a uniform magnetic field can be approximated by

$$(\delta k)^2 = (\delta k_{\rm res})^2 + (\delta k_{\rm ms})^2\,, \tag{28.41}$$

where $\delta k =$ curvature error

$\delta k_{\rm res} =$ curvature error due to finite measurement resolution

$\delta k_{\rm ms} =$ curvature error due to multiple scattering.

If many (≥ 10) uniformly spaced position measurements are made along a trajectory in a uniform medium,

$$\delta k_{\rm res} = \frac{\epsilon}{L'^2}\sqrt{\frac{720}{N+4}}\,, \tag{28.42}$$

where $N =$ number of points measured along track

$L' =$ the projected length of the track onto the bending plane

$\epsilon =$ measurement error for each point, perpendicular to the trajectory.

If a vertex constraint is applied at the origin of the track, the coefficient under the radical becomes 320.

For arbitrary spacing of coordinates s_i measured along the projected trajectory and with variable measurement errors ϵ_i the curvature error $\delta k_{\rm res}$ is calculated from:

$$(\delta k_{\rm res})^2 = \frac{4}{w}\,\frac{V_{ss}}{V_{ss}V_{s^2s^2} - (V_{ss^2})^2}\,, \tag{28.43}$$

where V are covariances defined as $V_{s^m s^n} = \langle s^m s^n\rangle - \langle s^m\rangle\langle s^n\rangle$ with $\langle s^m\rangle = w^{-1}\sum(s_i{}^m/\epsilon_i{}^2)$ and $w = \sum \epsilon_i{}^{-2}$.

The contribution due to multiple Coulomb scattering is approximately

$$\delta k_{\rm ms} \approx \frac{(0.016)(\text{GeV}/c)z}{Lp\beta\cos^2\lambda}\sqrt{\frac{L}{X_0}}\,, \tag{28.44}$$

where $p =$ momentum (GeV/c)

$z =$ charge of incident particle in units of e

$L =$ the total track length

$X_0 =$ radiation length of the scattering medium (in units of length; the X_0 defined elsewhere must be multiplied by density)

$\beta =$ the kinematic variable v/c.

More accurate approximations for multiple scattering may be found in the section on Passage of Particles Through Matter (Sec. 27 of this *Review*). The contribution to the curvature error is given approximately by $\delta k_{\rm ms} \approx 8 s^{\rm rms}_{\rm plane}/L^2$, where $s^{\rm rms}_{\rm plane}$ is defined there.

References:

1. *Experimental Techniques in High Energy Physics*, T. Ferbel (ed.) (Addison-Wesley, Menlo Park, CA, 1987).
2. Claus Grupen, *Particle Detectors,* Cambridge Monographs on Particle Physics, Nuclear Physics and Cosmology, # 5, Cambridge University Press (1996).
3. K. Kleinknecht, *Detectors for Particle Radiation*, Cambridge University Press (1998).
4. G.F. Knoll, *Radiation Detection and Measurement*, 3nd edition, John Wiley & Sons, New York (1999).
5. Dan Green, *The Physics of Particle Detectors,* Cambridge Monographs on Particle Physics, Nuclear Physics and Cosmology, # 12, Cambridge University Press (2000).
6. [Icarus Collaboration], ICARUS-TM/2001-09; LGNS-EXP 13/89 add 2-01.
7. E. Albert *et al.*, Nucl. Instrum. Methods **A409**, 70 (1998).
8. B. Aubert *et al.*, [BaBar Collaboration], Nucl. Instrum. Methods **A479**, 1 (2002).
9. H. Spieler, IEEE Trans. Nucl. Sci. **NS-29**, 1142 (1982).
10. J.B. Birks, *The Theory and Practice of Scintillation Counting*(Pergamon, London, 1964).
11. D. Clark, Nucl. Instrum. Methods **117**, 295 (1974).
12. J.B. Birks, Proc. Phys. Soc. **A64**, 874 (1951).
13. B. Bengston and M. Moszynski, Nucl. Instrum. Methods **117**, 227 (1974);
    J. Bialkowski *et al.*, Nucl. Instrum. Methods **117**, 221 (1974).
14. *Proceedings of the Symposium on Detector Research and Development for the Superconducting Supercollider*, eds. T. Dombeck, V. Kelly, and G.P. Yost (World Scientific, Singapore, 1991).
15. I.B. Berlman, *Handbook of Fluorescence Spectra of Aromatic Molecules*, 2nd edition (Academic Press, New York, 1971).
16. C. Zorn, in *Instrumentation in High Energy Physics,* ed. F. Sauli, (1992, World Scientific, Singapore) pp. 218–279.
17. T. Foerster, Ann. Phys. **2**, 55 (1948).
18. J.M. Fluornoy, Conference on Radiation-Tolerant Plastic Scintillators and Detectors, K.F. Johnson and R.L. Clough editors, Rad. Phys. and Chem., **41** 389 (1993).
19. D. Horstman and U. Holm, *ibid,* 395.
20. D. Blomker *et al.*, Nucl. Instrum. Methods **A311**, 505 (1992);
    J. Mainusch *et al.*, Nucl. Instrum. Methods **A312**, 451 (1992).
21. Conference on Radiation-Tolerant Plastic Scintillators and Detectors, K.F. Johnson and R.L. Clough editors, Rad. Phys. and Chem., **41** (1993).
22. S.R. Borenstein and R.C. Strand, IEEE Trans. Nuc. Sci. **NS-31(1)**, 396 (1984).
23. P. Sonderegger, Nucl. Instrum. Methods **A257**, 523 (1987).

24. S.A. Sedykh *et al.*, Nucl. Instrum. Methods **A455**, 346 (2000).
25. SCIFI 97: Conference on Scintillating Fiber Detectors, 1997 University of Notre Dame, Indiana, eds. A. Bross, R. Ruchti, and M. Wayne.
26. K.F. Johnson, Nucl. Instrum. Methods **A344**, 432 (1994).
27. C.M. Hawkes *et al.*, Nucl. Instrum. Methods **A292**, 329 (1990).
28. A. Lempicki *et al.*, Nucl. Instrum. Methods **A333**, 304 (1993); G. Blasse, *Proceedings of the Crystal 2000 International Workshop on Heavy Scintillators for Scientific and Industrial Applications*, Chamonix, France, Sept. (1992), Edition Frontieres.
29. C. Melcher and J. Schweitzer, Nucl. Instrum. Methods **A314**, 212 (1992).
30. K. Takagi and T. Fakazawa, Appl. Phys. Lett. **42**, 43 (1983).
31. C. Kuntner *et al.*, Nucl. Instrum. Methods **A493**, 131 (2002).
32. G. Gratta, H. Newman, and R.Y. Zhu, Ann. Rev. Nucl. and Part. Sci. **44**, 453 (1994).
33. R.Y. Zhu, Nucl. Instrum. Methods **A413**, 297 (1998).
34. M. Woods *et al.*, SPIN96 (QCD161:S921:1996) 843.
35. A. Abashian *et al.*, Nucl. Instrum. Methods **A479**, 117 (2002).
36. M. Shiozawa, [Super-Kamiokande Collaboration], Nucl. Instrum. Methods **A433**, 240 (1999).
37. J. Litt and R. Meunier, Ann. Rev. Nucl. Sci. **23**, 1 (1973).
38. D. Bartlett *et al.*, Nucl. Instrum. Methods **A260**, 55 (1987).
39. B. Ratcliff, Nucl. Instrum. Methods **A502**, 211 (2003).
40. M. Cavalli-Sforza *et al.*, "Construction and Testing of the SLC Cherenkov Ring Imaging Detector," IEEE **37**, N3:1132 (1990).
41. E.G. Anassontzis *et al.*, "Recent Results from the DELPHI Barrel Ring Imaging Cherenkov Counter," IEEE **38**, N2:417 (1991).
42. See the RICH Workshop series: Nucl. Instrum. Methods **A343**, 1 (1993); Nucl. Instrum. Methods **A371**, 1 (1996); Nucl. Instrum. Methods **A433**, 1 (1999); Nucl. Instrum. Methods **A502**, 1 (2003).
43. H. Blood *et al.*, FERMILAB-PUB-76-051-EXP.
44. L. Sulak, HUEP-252 Presented at the Workshop on Proton Stability, Madison, Wisc. (1978).
45. K.S. Hirata *et al.*, Phys. Lett. **B205**, 416 (1988).
46. S. Kasuga *et al.*, Phys. Lett. **B374**, 238 (1996).
47. M.H. Ahn *et al.*, Phys. Rev. Lett. **90**, 041801 (2003).
48. R.M. Bionta *et al.*, Phys. Rev. Lett. **51**, 27 (1983); [Erratum-ibid. **51**, 522 (1983)].
49. R. Becker-Szendy *et al.*, Nucl. Instrum. Methods **A324**, 363 (1993).
50. H. Ikeda *et al.*, UTLICEPP-82-04.
51. K. Arisaka *et al.*, J. Phys. Soc. Jap. **54**, 3213 (1985).
52. K.S. Hirata *et al.*, Phys. Rev. **D38**, 448 (1988).
53. C. Athanassopoulos *et al.*, Nucl. Instrum. Methods **A388**, 149 (1997).
54. Y. Fukuda *et al.*, Nucl. Instrum. Methods **A501**, 418 (2003).
55. S.H. Ahn *et al.*, Phys. Lett. **B511**, 178 (2001).
56. J. Boger *et al.*, Nucl. Instrum. Methods **A449**, 172 (2000).
57. B. Dolgoshein Nucl. Instrum. Methods **A326**, 434 (1993).
58. X. Artru *et al.*, Phys. Rev. **D12**, 1289 (1975).
59. G.M. Garibian *et al.*, Nucl. Instrum. Methods **125**, 133 (1975).
60. G. Bassompierre *et al.*, Nucl. Instrum. Methods **411**, 63 (1998).
61. ALICE Collaboration, "Technical Design Report of the Transition Radiation Tracker," CERN/LHCC/ 2001-021 (2001).
62. RD6 Collaboration, CERN/DRDC 90-38 (1990); CERN/DRDC 91-47 (1991); CERN/DRDC 93-46 (1993).
63. T. Kirn et al., *Proceedings of TRDs for the 3rd millenium,* Workshop on advanced transition radiation detectors for accelerator and space applications, eds N. Giglietto and P. Spinelli, Frascati Physics Series, Vol. XXV, 161 (2002).
64. P. Spinelli et al., Proceedings of "TRDs for the 3rd millenium", Workshop on advanced transition radiation detectors for accelerator and space applications,"eds N. Giglietto and P. Spinelli, Frascati Physics Series, Vol. XXV, 177 (2002).
65. ATLAS Collaboration, ATLAS Inner Detector Technical Design Report, v 2, ATLAS TDR 5, CERN/LHCC/97-16 (30 April 1997).
66. ATLAS Collaboration, Detector and Physics Performance Technical Design Report, CERN/LHCC/99-14, 71 (1999).
67. B. Dolgoshein, Nucl. Instrum. Methods **252**, 137 (1986).
68. C.W. Fabjan *et al.*, Nucl. Instrum. Methods **185**, 119 (1981).
69. J. Cobb *et al.*, Nucl. Instrum. Methods **140**, 413 (1977).
70. A. Büngener *et al.*, Nucl. Instrum. Methods **214**, 261 (1983).
71. R.D. Appuhn *et al.*, Nucl. Instrum. Methods **263**, 309 (1988).
72. Y. Watase *et al.*, Nucl. Instrum. Methods **248**, 379 (1986).
73. R. Ansari *et al.*, Nucl. Instrum. Methods **263**, 51 (1988).
74. H.J. Butt *et al.*, Nucl. Instrum. Methods **252**, 483 (1986).
75. J.F. Detoeuf *et al.*, Nucl. Instrum. Methods **265**, 157 (1988).
76. M. Holder *et al.*, Nucl. Instrum. Methods **263**, 319 (1988).
77. H. Weidkamp, DiplomArbeit, Rhein-Westf. Tech. Hochschule Aachen (1984).
78. H. Grässler *et al.*, Proc. Vienna Wire Chamber Conference (1989).
79. T. Akesson *et al.*, Nucl. InstrumMethods A412, 200 (1998).
80. F.F. Rieke and W. Prepejchal, Phys. Rev. **A6**, 1507 (1972).
81. L.G. Christophorou, "Atomic and molecular radiation physics" (Wiley, London 1991).
82. G. Charpak *et al.*, Nucl. Instrum. Methods **62**, 262 (1968).
83. R. Veenhof, GARFIELD program: simulation of gaseous detectors, version 6.32, CERN Program Library Pool W999 (W5050).
84. As representative examples see: B. Adeva *et al.*, Nucl. Instrum. Methods **A287**, 35 (1990).
85. As representative example see: A. Alexander *et al.*, Nucl. Instrum. Methods **A276**, 42 (1989).
86. As representative examples see: F. Bedeschi *et al.*, Nucl. Instrum. Methods **A268**, 50 (1988); **Opal** Collaboration: Nucl. Instrum. Methods **A305**, 275 (1991).
87. A. Oed, Nucl. Instrum. Methods **A263**, 351 (1988).
88. W. Blum and G. Rolandi, *Particle Detection with Drift Chambers*, Springer-Verlag (1994).
89. A. Peisert and F. Sauli, CERN-84-08 (Jul 1984).
90. R. Bellazzini and A. M. Spezziga, Rivista del Nuovo Cimento **17**, 1 (1994).
91. D.R. Nygren and J.N. Marx, "The Time Projection Chamber," Phys. Today **31**, 46 (1978).
92. P. Weilhammer, Nucl. Instrum. Methods **A453**, 60 (2000).
93. G. Lindström *et al.*, Nucl. Instrum. Methods **A465**, 60 (2001).
94. G. Lindström *et al.*, Nucl. Instrum. Methods **A426**, 1 (1999).
95. A. Holmes-Siedle and L. Adams, *Handbook of Radiation Effects*, 2nd ed., Oxford 2002, ISBN 0-19-850733-X, QC474.H59 2001.
96. V. Radeka, IEEE Trans. Nucl. Sci. **NS-15/3**, 455 (1968); V. Radeka, IEEE Trans. Nucl. Sci. **NS-21**, 51 (1974).
97. F.S. Goulding, Nucl. Instrum. Methods **100**, 493 (1972); F.S. Goulding and D.A. Landis, IEEE Trans. Nucl. Sci. **NS-29**, 1125 (1982).
98. H. Spieler, Front-End Electronics and Signal Processing, in *Proceedings of the First ICFA School at the ICFA Instrumentation Center in Morelia*, AIP vol. 674, pp. 76 - 100, eds. L. Villaseñor, V. Villanueva, ISBN 0-7354-0141-1, LBNL-52914.
99. W.R. Nelson, H. Hirayama, and D.W.O. Rogers, "The EGS4 Code System," SLAC-265, Stanford Linear Accelerator Center (Dec. 1985).
100. R. Brun *et al.*, *GEANT3*, `CERN DD/EE/84-1` (1987).

101. D. Hitlin *et al.*, Nucl. Instrum. Methods **137**, 225 (1976). See also W. J. Willis and V. Radeka, Nucl. Instrum. Methods **120**, 221 (1974), for a more detailed discussion.
102. R. Wigmans, *Calorimetry: Energy Measurement in Particle Physics*, Clarendon, Oxford (2000).
103. ATLAS Collaboration, *The ATLAS Liquid Argon Calorimeter Technical Design Report*, CERN/LHCC 96-41 (1996).
104. CMS Collaboration, *The CMS Electromagnetic Calorimeter Technical Design Report*, CERN/LHCC 97-33 (1997).
105. C. Leroy and P.-G. Rancoita, Rep. Prog. Phys. **63**, 505 (2000).
106. D. Bintinger, in *Proceedings of the Workshop on Calorimetry for the Supercollider*, Tuscaloosa, AL, March 13–17, 1989, edited by R. Donaldson and M.G.D. Gilchriese (World Scientific, Teaneck, NJ, 1989), p. 91;
R.K. Bock, T. Hansl-Kozanecka, and T.P. Shah, Nucl. Instrum. Methods **186**, 533 (1981).
107. T.A. Gabriel, D.E. Groom, P.K. Job, N.V. Mokhov, and G.R. Stevenson, Nucl. Instrum. Methods **A338**, 336 (1994).
108. R. Wigmans, Nucl. Instrum. Methods **A259**, 389 (1987);
R. Wigmans, Nucl. Instrum. Methods **A265**, 273 (1988).
109. N. Akchurian *et al.*, Nucl. Instrum. Methods **A408**, 380 (1998).
110. U. Behrens *et al.*, Nucl. Instrum. Methods **A289**, 115 (1990);
A. Bernstein *et al.*, Nucl. Instrum. Methods **A336**, 23 (1993).
111. E. Bernardi *et al.*, Nucl. Instrum. Methods **A262**, 229 (1987).
112. S. Abachi *et al.*, Nucl. Instrum. Methods **A324**, 53 (1993).
113. F. Ariztizabal *et al.*, Nucl. Instrum. Methods **A349**, 384 (1994).
114. E. Shibamura *et al.*, Nucl. Instrum. Methods **131**, 249 (1975).
115. T.G. Ryan and G.R. Freeman, J. Chem. Phys. **68**, 5144 (1978).
116. W.F. Schmidt, "Electron Migration in Liquids and Gases," HMI B156 (1974).
117. A.O. Allen, "Drift Mobilities and Conduction Band Energies of Excess Electrons in Dielectric Liquids," NSRDS-NBS-58 (1976).
118. W. Walkowiak, Nucl. Instrum. Methods **A449**, 288 (2000).
119. M.A. Green, R.A. Byrns, and S.J. St. Lorant, "Estimating the cost of superconducting magnets and the refrigerators needed to keep them cold," in *Advances in Cryogenic Engineering*, Vol. 37, Plenum Press, New York (1992).
120. Vector Fields, Inc., 1700 N. Farnsworth Ave., Aurora, IL.
121. Swanson Analysis Systems, Inc., P.O. Box 65, Johnson Rd., Houston, PA.
122. CGA-341-1987, "Standard for insulated cargo tank specification for cryogenic liquids," Compressed Gas Association, Inc., Arlington, VA (1987).
123. R.L. Gluckstern, Nucl. Instrum. Methods **24**, 381 (1963).
124. V. Karimäki, Nucl. Instrum. Methods **A410**, 284 (1998).

29. RADIOACTIVITY AND RADIATION PROTECTION

Revised March 1998 by R.J. Donahue (LBNL) and A. Fassò (SLAC).

29.1. Definitions

The International Commission on Radiation Units and Measurements (ICRU) recommends the use of SI units. Therefore we list SI units first, followed by cgs (or other common) units in parentheses, where they differ.

• **Unit of activity** = becquerel (curie):

1 Bq = 1 disintegration s^{-1} [= $1/(3.7 \times 10^{10})$ Ci]

• **Unit of absorbed dose** = gray (rad):

1 Gy = 1 joule kg^{-1} (= 10^4 erg g^{-1} = 100 rad)

= 6.24×10^{12} MeV kg^{-1} deposited energy

• **Unit of exposure**, the quantity of x- or γ- radiation at a point in space integrated over time, in terms of charge of either sign produced by showering electrons in a small volume of air about the point:

= 1 coul kg^{-1} of air (roentgen; 1 $R = 2.58 \times 10^{-4}$ coul kg^{-1})

= 1 esu cm^{-3}(= 87.8 erg released energy per g of air)

Implicit in the definition is the assumption that the small test volume is embedded in a sufficiently large uniformly irradiated volume that the number of secondary electrons entering the volume equals the number leaving. This unit is somewhat historical, but appears on many measuring instruments.

• **Unit of equivalent dose** (for biological damage) = sievert [= 100 rem (**r**oentgen **e**quivalent for **m**an)]: Equivalent dose in Sv = absorbed dose in grays $\times\, w_R$, where w_R (radiation weighting factor, formerly the quality factor Q) expresses long-term risk (primarily cancer and leukemia) from low-level chronic exposure. It depends upon the type of radiation and other factors, as follows [2]:

Table 29.1: Radiation weighting factors.

Radiation	w_R
X- and γ-rays, all energies	1
Electrons and muons, all energies	1
Neutrons < 10 keV	5
10–100 keV	10
> 100 keV to 2 MeV	20
2–20 MeV	10
> 20 MeV	5
Protons (other than recoils) > 2 MeV	5
Alphas, fission fragments, & heavy nuclei	20

29.2. Radiation levels [3]

• **Natural annual background**, all sources: Most world areas, whole-body equivalent dose rate ≈ (0.4–4) mSv (40–400 millirems). Can range up to 50 mSv (5 rems) in certain areas. U.S. average ≈ 3.6 mSv, including ≈ 2 mSv (≈ 200 mrem) from inhaled natural radioactivity, mostly radon and radon daughters (0.1–0.2 mSv in open areas. Average is for a typical house and varies by more than an order of magnitude. It can be more than two orders of magnitude higher in poorly ventilated mines).

• **Cosmic ray background** in counters (Earth's surface): ∼ 1 min^{-1} cm^{-2} sr^{-1}. For more accurate estimates and details, see the Cosmic Rays section (Sec. 24 of this *Review*).

• **Fluxes** (per cm^2) to deposit one Gy, assuming uniform irradiation:

≈ (**charged particles**) $6.24 \times 10^9/(dE/dx)$, where dE/dx (MeV g^{-1} cm^2), the energy loss per unit length, may be obtained from the Mean Range and Energy Loss figures.

≈ 3.5×10^9 cm^{-2} minimum-ionizing singly-charged particles in carbon.

≈ (**photons**) $6.24 \times 10^9/[Ef/\lambda]$, for photons of energy E (MeV), attenuation length λ (g cm^{-2}) (see Photon Attenuation Length figure), and fraction $f \lesssim 1$ expressing the fraction of the photon's energy deposited in a small volume of thickness $\ll \lambda$ but large enough to contain the secondary electrons.

≈ 2×10^{11} photons cm^{-2} for 1 MeV photons on carbon ($f \approx 1/2$).

(Quoted fluxes are good to about a factor of 2 for all materials.)

• **Recommended limits to exposure of radiation workers (whole-body dose):***

CERN: 15 mSv yr^{-1}

U.K.: 15 mSv yr^{-1}

U.S.: 50 mSv yr^{-1} (5 rem yr^{-1})†

• **Lethal dose**: Whole-body dose from penetrating ionizing radiation resulting in 50% mortality in 30 days (assuming no medical treatment) 2.5–3.0 Gy (250–300 rads), as measured internally on body longitudinal center line. Surface dose varies due to variable body attenuation and may be a strong function of energy.

29.3. Prompt neutrons at accelerators

29.3.1. ***Electron beams***: At electron accelerators neutrons are generated via photonuclear reactions from bremsstrahlung photons. Neutron yields from semi-infinite targets per unit electron beam power are plotted in Fig. 29.1 as a function of electron beam energy [4]. In the photon energy range 10–30 MeV neutron production results from the giant photonuclear resonance mechanism. Neutrons are produced roughly isotropically (within a factor of 2) and with a Maxwellian energy distribution described as:

$$\frac{dN}{dE_n} = \frac{E_n}{T^2} e^{-E_n/T} \ , \qquad (29.1)$$

where T is the nuclear temperature characteristic of the target nucleus, generally in the range of T = 0.5–1.0 MeV. For higher energy photons the quasi-deuteron and photopion production mechanisms become important.

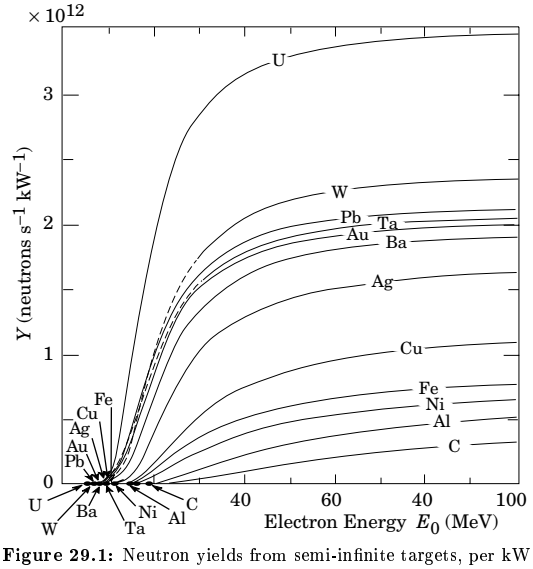

Figure 29.1: Neutron yields from semi-infinite targets, per kW of electron beam power, as a function of electron beam energy, disregarding target self-shielding.

29.3.2. ***Proton beams***: At proton accelerators neutron yields emitted per incident proton by different target materials are roughly independent [5] of proton energy between 20 MeV and 1 GeV and are given by the ratio C:Al:Cu-Fe:Sn:Ta-Pb = 0.3 : 0.6 : 1.0 : 1.5 : 1.7. Above 1 GeV neutron yield [6] is proportional to E^m, where $0.80 \leq m \leq 0.85$.

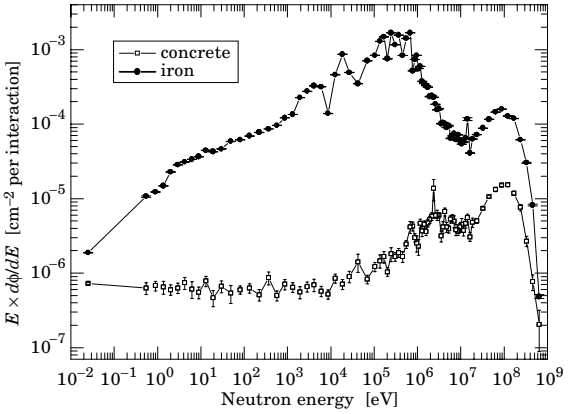

Figure 29.2: Calculated neutron spectrum from 205 GeV/c hadrons (2/3 protons and 1/3 π^+) on a thick copper target. Spectra are evaluated at 90° to beam and through 80 cm of normal density concrete or 40 cm of iron.

A typical neutron spectrum [7] outside a proton accelerator concrete shield is shown in Fig. 29.2. The shape of these spectra are generally characterized as having a thermal-energy peak which is very dependent on geometry and the presence of hydrogenic material, a low-energy evaporation peak around 2 MeV, and a high-energy spallation shoulder.

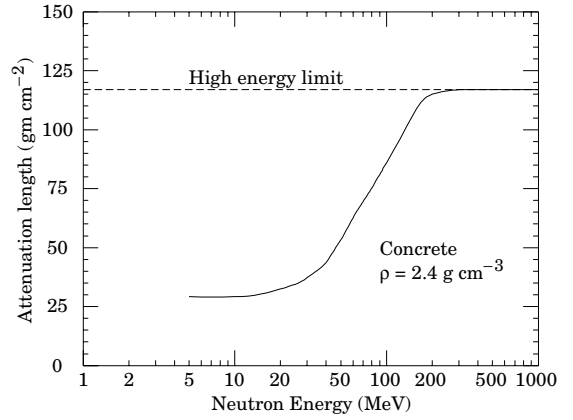

Figure 29.3: The variation of the attenuation length for monoenergetic neutrons in concrete as a function of neutron energy [5].

The neutron-attenuation length, λ, is shown in Fig. 29.3 for monoenergetic broad-beam conditions. These values give a satisfactory representation at depths greater than 1 m in concrete.

Letaw's [8] formula for the energy dependence of the inelastic proton cross-section (asymptotic values given in Table 6.1) for $E < 2$ GeV is:

$$\sigma(E) = \sigma_{\rm asympt}\left[1 - 0.62e^{-E/200}\sin(10.9E^{-0.28})\right] \ , \qquad (29.2)$$

and for $E > 2$ GeV:

$$\sigma_{\rm asympt} = 45A^{0.7}\left[1 + 0.016\sin(5.3 - 2.63\ln\ A)\right] \ , \qquad (29.3)$$

where σ is in mb, E is the proton energy in MeV and A is the mass number.

29.4. Dose conversion factors

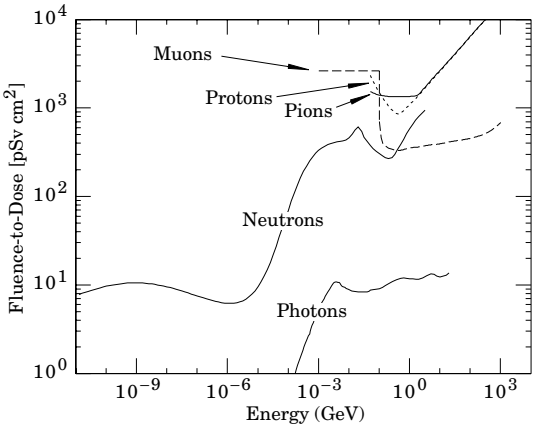

Figure 29.4: Fluence to dose equivalent conversion factors for various particles.

Fluence to dose equivalent factors are given in Fig. 29.4 for photons [9], neutrons [10], muons [11], protons and pions [12]. These factors can be used for converting particle fluence to dose for personnel protection purposes.

29.5. Accelerator-induced activity

The dose rate at 1 m due to spallation-induced activity by high energy hadrons in a 1 g medium atomic weight target can be estimated [13] from the following expression:

$$D = D_0\ \Phi\ \ln[(T + t)/t] \ , \qquad (29.4)$$

where T is the irradiation time, t is the decay time since irradiation, Φ is the flux of irradiating hadrons (hadrons cm^{-2} s^{-1}) and D_0 has a value of 5.2×10^{-17} [(Sv hr^{-1})/(hadron cm^{-2} s^{-1})]. This relation is essentially independent of hadron energy above 200 MeV.

Dose due to accelerator-produced induced activity can also be estimated with the use of "ω factors" [5]. These factors give the dose rate per unit star density (inelastic reaction for $E > 50$ MeV) after a 30-day irradiation and 1-day decay. The ω factor for steel or iron is $\simeq 3 \times 10^{-12}$ (Sv cm^3/star). This does not include possible contributions from thermal-neutron activation. Induced activity in concrete can vary widely depending on concrete composition, particularly with the concentration of trace quantities such as sodium. Additional information can be found in Barbier [14].

29.6. Photon sources

The dose rate from a gamma point source of C Curies emitting one photon of energy $0.07 < E < 4$ MeV per disintegration at a distance of 30 cm is 6CE (rem/hr), or 60CE (mSv/hr), ±20%.

The dose rate from a semi-infinite uniform photon source of specific activity C (μCi/g) and gamma energy E (MeV) is $1.07CE$ (rem/hr), or $10.7CE$ (mSv/hr).

Footnotes:

* The ICRP recomendation [2] is 20 mSv yr^{-1} averaged over 5 years, with the dose in any one year $\leq$ 50 mSv.

† Many laboratories in the U.S. and elsewhere set lower limits.

‡ *Dose* is the time integral of *dose rate*, and *fluence* is the time integral of *flux*.

References:

1. C. Birattari *et al.*, "Measurements and simulations in high energy neutron fields" Proceedings of the Second Shielding Aspects of Accelerators, Targets and Irradiation Facilities, in press (1995).
2. ICRP Publication 60, *1990 Recommendation of the International Commission on Radiological Protection* Pergamon Press (1991).
3. See E. Pochin, *Nuclear Radiation: Risks and Benefits* (Clarendon Press, Oxford, 1983).
4. W.P. Swanson, *Radiological Safety Aspects of the operation of Electron Linear Accelerators,* IAEA Technical Reports Series No. 188 (1979).
5. R.H. Thomas and G.R. Stevenson, *Radiological Safety Aspects of the Operation of Proton Accelerators,* IAEA Technical Report Series No. 283 (1988).
6. T.A. Gabriel *et al.*, "Energy Dependence of Hadronic Activity," Nucl. Instrum. Methods **A338**, 336 (1994).
7. A.V. Sannikov, "BON94 Code for Neutron Spectra Unfolding from Bonner Spectrometer Data," CERN/TIS-RP/IR/94-16 (1994).
8. Letaw, Silberberg, and Tsao, "Proton-nucleus Total Inelastic Cross Sections: An Empirical Formula for E > 10 MeV," *Astrophysical Journal Supplement Series,* **51**, 271 (1983);

   For improvements to this formula see Shen Qing-bang, "Systematics of intermediate energy proton nonelastic and neutron total cross section," International Nuclear Data Committee INDC(CPR)-020 (July 1991).
9. A. Ferrari and M. Pelliccioni, "On the Conversion Coefficients from Fluence to Ambient Dose Equivalent," Rad. Pro. Dosimetry 51, 251 (1994).
10. A.V. Sannikov and E.N. Savitskaya, "Ambient Dose and Ambient Dose Equivalent Conversion Factors for High-Energy neutrons," CERN/TIS-RP/93-14 (1993).
11. "Data for Use in Protection Against External Radiation," ICRP Publication 51 (1987).
12. G.R. Stevenson, "Dose Equivalent Per Star in Hadron Cascade Calculations," CERN TIS-RP/173 (1986).
13. A.H. Sullivan *A Guide To Radiation and Radioactivity Levels Near High Energy Particle Accelerators,* Nuclear Technology Publishing, Ashford, Kent, England (1992).
14. M. Barbier, *Induced Activity,* North-Holland, Amsterdam (1969).

30. COMMONLY USED RADIOACTIVE SOURCES

Table 30.1. Revised November 1993 by E. Browne (LBNL).

			Particle		Photon	
		Type of	Energy	Emission	Energy	Emission
Nuclide	Half-life	decay	(MeV)	prob.	(MeV)	prob.
$^{22}_{11}$Na	2.603 y	β^+, EC	0.545	90%	0.511	Annih.
					1.275	100%
$^{54}_{25}$Mn	0.855 y	EC			0.835	100%
					Cr K x rays 26%	
$^{55}_{26}$Fe	2.73 y	EC			Mn K x rays:	
					0.00590	24.4%
					0.00649	2.86%
$^{57}_{27}$Co	0.744 y	EC			0.014	9%
					0.122	86%
					0.136	11%
					Fe K x rays 58%	
$^{60}_{27}$Co	5.271 y	β^-	0.316	100%	1.173	100%
					1.333	100%
$^{68}_{32}$Ge	0.742 y	EC			Ga K x rays 44%	
$\rightarrow$ $^{68}_{31}$Ga		β^+, EC	1.899	90%	0.511	Annih.
					1.077	3%
$^{90}_{38}$Sr	28.5 y	β^-	0.546	100%		
$\rightarrow$ $^{90}_{39}$Y		β^-	2.283	100%		
$^{106}_{44}$Ru	1.020 y	β^-	0.039	100%		
$\rightarrow$ $^{106}_{45}$Rh		β^-	3.541	79%	0.512	21%
					0.622	10%
$^{109}_{48}$Cd	1.267 y	EC	0.063 e^-	41%	0.088	3.6%
			0.084 e^-	45%	Ag K x rays 100%	
			0.087 e^-	9%		
$^{113}_{50}$Sn	0.315 y	EC	0.364 e^-	29%	0.392	65%
			0.388 e^-	6%	In K x rays 97%	
$^{137}_{55}$Cs	30.2 y	β^-	0.514 e^-	94%	0.662	85%
			1.176 e^-	6%		
$^{133}_{56}$Ba	10.54 y	EC	0.045 e^-	50%	0.081	34%
			0.075 e^-	6%	0.356	62%
					Cs K x rays 121%	
$^{207}_{83}$Bi	31.8 y	EC	0.481 e^-	2%	0.569	98%
			0.975 e^-	7%	1.063	75%
			1.047 e^-	2%	1.770	7%
					Pb K x rays 78%	
$^{228}_{90}$Th	1.912 y	6α:	5.341 to 8.785		0.239	44%
		3β^-:	0.334 to 2.246		0.583	31%
					2.614	36%
($\rightarrow$ $^{224}_{88}$Ra	$\rightarrow$ $^{220}_{86}$Rn	$\rightarrow$ $^{216}_{84}$Po	$\rightarrow$ $^{212}_{82}$Pb	$\rightarrow$ $^{212}_{83}$Bi	$\rightarrow$ $^{212}_{84}$Po)	
$^{241}_{95}$Am	432.7 y	α	5.443	13%	0.060	36%
			5.486	85%	Np L x rays 38%	
$^{241}_{95}$Am/Be	432.2 y	6×10^{-5} neutrons (4–8 MeV) and				
		$4 \times 10^{-5}\gamma$'s (4.43 MeV) per Am decay				
$^{244}_{96}$Cm	18.11 y	α	5.763	24%	Pu L x rays $\sim$ 9%	
			5.805	76%		
$^{252}_{98}$Cf	2.645 y	α (97%)	6.076	15%		
			6.118	82%		
		Fission (3.1%)				
		$\approx$ 20 γ's/fission; 80% $<$ 1 MeV				
		$\approx$ 4 neutrons/fission; $\langle E_n \rangle$ = 2.14 MeV				

"Emission probability" is the probability per decay of a given emission; because of cascades these may total more than 100%. Only principal emissions are listed. EC means electron capture, and e^- means monoenergetic internal conversion (Auger) electron. The intensity of 0.511 MeV e^+e^- annihilation photons depends upon the number of stopped positrons. Endpoint $\beta^\pm$ energies are listed. In some cases when energies are closely spaced, the γ-ray values are approximate weighted averages. Radiation from short-lived daughter isotopes is included where relevant.

Half-lives, energies, and intensities are from E. Browne and R.B. Firestone, *Table of Radioactive Isotopes* (John Wiley & Sons, New York, 1986), recent *Nuclear Data Sheets*, and *X-ray and Gamma-ray Standards for Detector Calibration*, IAEA-TECDOC-619 (1991).

Neutron data are from *Neutron Sources for Basic Physics and Applications* (Pergamon Press, 1983).

31. PROBABILITY

Revised May 1996 by D.E. Groom (LBNL) and F. James (CERN), September 1999 by R. Cousins (UCLA), October 2001 and October 2003 by G. Cowan (RHUL).

31.1. General [1–8]

An abstract definition of probability can be given by considering a set S, called the sample space, and possible subsets $A, B, \ldots$, the interpretation of which is left open. The probability P is a real-valued function defined by the following axioms due to Kolmogorov [9]:

1. For every subset A in S, $P(A) \geq 0$.
2. For disjoint subsets (*i.e.*, $A \cap B = \emptyset$), $P(A \cup B) = P(A) + P(B)$.
3. $P(S) = 1$.

In addition one defines the conditional probability $P(A|B)$ (read P of A given B) as

$$P(A|B) = \frac{P(A \cap B)}{P(B)} \,. \tag{31.1}$$

From this definition and using the fact that $A \cap B$ and $B \cap A$ are the same, one obtains *Bayes' theorem*,

$$P(A|B) = \frac{P(B|A)P(A)}{P(B)} \,. \tag{31.2}$$

From the three axioms of probability and the definition of conditional probability, one obtains the *law of total probability*,

$$P(B) = \sum_i P(B|A_i)P(A_i) \,, \tag{31.3}$$

for any subset B and for disjoint A_i with $\cup_i A_i = S$. This can be combined with Bayes' theorem Eq. (31.2) to give

$$P(A|B) = \frac{P(B|A)P(A)}{\sum_i (B|A_i)P(A_i)} \,, \tag{31.4}$$

where the subset A could, for example, be one of the A_i.

The most commonly used interpretation of the subsets of the sample space are outcomes of a repeatable experiment. The probability $P(A)$ is assigned a value equal to the limiting frequency of occurrence of A. This interpretation forms the basis of *frequentist statistics*.

The subsets of the sample space can also be interpreted as *hypotheses*, *i.e.*, statements that are either true or false, such as 'The mass of the W boson lies between 80.3 and 80.5 GeV'. In the frequency interpretation, such statements are either always or never true, *i.e.*, the corresponding probabilities would be 0 or 1. Using *subjective probability*, however, $P(A)$ is interpreted as the degree of belief that the hypothesis A is true.

Subjective probability is used in *Bayesian* (as opposed to frequentist) statistics. Bayes' theorem can be written

$$P(\text{theory}|\text{data}) \propto P(\text{data}|\text{theory})P(\text{theory}) \,, \tag{31.5}$$

where 'theory' represents some hypothesis and 'data' is the outcome of the experiment. Here $P(\text{theory})$ is the *prior* probability for the theory, which reflects the experimenter's degree of belief before carrying out the measurement, and $P(\text{data}|\text{theory})$ is the probability to have gotten the data actually obtained, given the theory, which is also called the *likelihood*.

Bayesian statistics provides no fundamental rule for obtaining the prior probability; this is necessarily subjective and may depend on previous measurements, theoretical prejudices, etc. Once this has been specified, however, Eq. (31.5) tells how the probability for the theory must be modified in the light of the new data to give the *posterior* probability, $P(\text{theory}|\text{data})$. As Eq. (31.5) is stated as a proportionality, the probability must be normalized by summing (or integrating) over all possible hypotheses.

31.2. Random variables

A *random variable* is a numerical characteristic assigned to an element of the sample space. In the frequency interpretation of probability, it corresponds to an outcome of a repeatable experiment. Let x be a possible outcome of an observation. If x can take on any value from a continuous range, we write $f(x;\theta)dx$ as the probability that the measurement's outcome lies between x and $x + dx$. The function $f(x;\theta)$ is called the *probability density function* (p.d.f.), which may depend on one or more parameters θ. If x can take on only discrete values (*e.g.*, the non-negative integers), then $f(x;\theta)$ is itself a probability.

The p.d.f. is always normalized to unit area (unit sum, if discrete). Both x and θ may have multiple components and are then often written as vectors. If θ is unknown, we may wish to estimate its value from a given set of measurements of x; this is a central topic of *statistics* (see Sec. 32).

The *cumulative distribution function* $F(a)$ is the probability that $x \leq a$:

$$F(a) = \int_{-\infty}^{a} f(x)\,dx \,. \tag{31.6}$$

Here and below, if x is discrete-valued, the integral is replaced by a sum. The endpoint a is expressly included in the integral or sum. Then $0 \leq F(x) \leq 1$, $F(x)$ is nondecreasing, and $P(a < x \leq b) = F(b) - F(a)$. If x is discrete, $F(x)$ is flat except at allowed values of x, where it has discontinuous jumps equal to $f(x)$.

Any function of random variables is itself a random variable, with (in general) a different p.d.f. The *expectation value* of any function $u(x)$ is

$$E[u(x)] = \int_{-\infty}^{\infty} u(x)\,f(x)\,dx \,, \tag{31.7}$$

assuming the integral is finite. For $u(x)$ and $v(x)$ any two functions of x, $E[u+v] = E[u] + E[v]$. For c and k constants, $E[cu+k] = cE[u] + k$.

The n^{th} moment of a random variable is

$$\alpha_n \equiv E[x^n] = \int_{-\infty}^{\infty} x^n f(x)\,dx \,, \tag{31.8a}$$

and the n^{th} central moment of x (or moment about the mean, α_1) is

$$m_n \equiv E[(x-\alpha_1)^n] = \int_{-\infty}^{\infty} (x-\alpha_1)^n f(x)\,dx \,. \tag{31.8b}$$

The most commonly used moments are the mean μ and variance σ^2:

$$\mu \equiv \alpha_1 \,, \tag{31.9a}$$

$$\sigma^2 \equiv V[x] \equiv m_2 = \alpha_2 - \mu^2 \,. \tag{31.9b}$$

The mean is the location of the "center of mass" of the p.d.f., and the variance is a measure of the square of its width. Note that $V[cx+k] = c^2 V[x]$. It is often convenient to use the *standard deviation* of x, σ, defined as the square root of the variance.

Any odd moment about the mean is a measure of the skewness of the p.d.f. The simplest of these is the dimensionless coefficient of skewness $\gamma_1 = m_3/\sigma^3$.

The fourth central moment m_4 provides a convenient measure of the tails of a distribution. For the Gaussian distribution (see Sec. 31.4) one has $m_4 = 3\sigma^4$. The *kurtosis* is defined as $\gamma_2 = m_4/\sigma^4 - 3$, *i.e.*, it is zero for a Gaussian, positive for a *leptokurtic* distribution with longer tails, and negative for a *platykurtic* distribution with tails that die off more quickly than those of a Gaussian.

Besides the mean, another useful indicator of the "middle" of the probability distribution is the *median*, $x_{\rm med}$, defined by $F(x_{\rm med}) = 1/2$, *i.e.*, half the probability lies above and half lies below $x_{\rm med}$. (More rigorously, $x_{\rm med}$ is a median if $P(x \geq x_{\rm med}) \geq 1/2$ and $P(x \leq x_{\rm med}) \geq 1/2$. If only one value exists it is called 'the median'.)

Let x and y be two random variables with a *joint* p.d.f. $f(x,y)$. The *marginal* p.d.f. of x (the distribution of x with y unobserved) is

$$f_1(x) = \int_{-\infty}^{\infty} f(x,y)\,dy\ , \tag{31.10}$$

and similarly for the marginal p.d.f. $f_2(y)$. The *conditional* p.d.f. of y given fixed x (with $f_1(x) \neq 0$) is defined by $f_3(y|x) = f(x,y)/f_1(x)$ and similarly $f_4(x|y) = f(x,y)/f_2(y)$. From these we immediately obtain Bayes' theorem (see Eqs. (31.2) and (31.4)),

$$f_4(x|y) = \frac{f_3(y|x)f_1(x)}{f_2(y)} = \frac{f_3(y|x)f_1(x)}{\int f_3(y|x')f_1(x')\,dx'}\ . \tag{31.11}$$

The mean of x is

$$\mu_x = \int_{-\infty}^{\infty}\int_{-\infty}^{\infty} x\,f(x,y)\,dx\,dy = \int_{-\infty}^{\infty} x\,f_1(x)\,dx\ , \tag{31.12}$$

and similarly for y. The *covariance* of x and y is

$$\mathrm{cov}[x,y] = E[(x-\mu_x)(y-\mu_y)] = E[xy] - \mu_x\mu_y\ . \tag{31.13}$$

A dimensionless measure of the covariance of x and y is given by the *correlation coefficient*,

$$\rho_{xy} = \mathrm{cov}[x,y]/\sigma_x\sigma_y\ , \tag{31.14}$$

where σ_x and σ_y are the standard deviations of x and y. It can be shown that $-1 \leq \rho_{xy} \leq 1$.

Two random variables x and y are *independent* if and only if

$$f(x,y) = f_1(x)f_2(y)\ . \tag{31.15}$$

If x and y are independent then $\rho_{xy} = 0$; the converse is not necessarily true. If x and y are independent, $E[u(x)v(y)] = E[u(x)]E[v(y)]$, and $V[x+y] = V[x] + V[y]$; otherwise, $V[x+y] = V[x] + V[y] + 2\mathrm{cov}[x,y]$ and $E[uv]$ does not necessarily factorize.

Consider a set of n continuous random variables $\boldsymbol{x} = (x_1,\ldots,x_n)$ with joint p.d.f. $f(\boldsymbol{x})$ and a set of n new variables $\boldsymbol{y} = (y_1,\ldots,y_n)$, related to $\boldsymbol{x}$ by means of a function $\boldsymbol{y}(\boldsymbol{x})$ that is one-to-one, *i.e.*, the inverse $\boldsymbol{x}(\boldsymbol{y})$ exists. The joint p.d.f. for $\boldsymbol{y}$ is given by

$$g(\boldsymbol{y}) = f(\boldsymbol{x}(\boldsymbol{y}))|J|\ , \tag{31.16}$$

where $|J|$ is the absolute value of the determinant of the square matrix $J_{ij} = \partial x_i/\partial y_j$ (the Jacobian determinant). If the transformation from $\boldsymbol{x}$ to $\boldsymbol{y}$ is not one-to-one, the $\boldsymbol{x}$-space must be broken in to regions where the function $\boldsymbol{y}(\boldsymbol{x})$ can be inverted and the contributions to $g(\boldsymbol{y})$ from each region summed.

Given a set of functions $\boldsymbol{y} = (y_1,\ldots,y_m)$ with $m < n$, one can construct $n-m$ additional independent functions, apply the procedure above, then integrate the resulting $g(\boldsymbol{y})$ over the unwanted y_i to find the marginal distribution of those of interest.

To change variables for discrete random variables simply substitute; no Jacobian is necessary because now f is a probability rather than a probability density. If f depends on a set of parameters $\boldsymbol{\theta}$, a change to a different parameter set $\boldsymbol{\eta}(\boldsymbol{\theta})$ is made by simple substitution; no Jacobian is used.

31.3. Characteristic functions

The characteristic function $\phi(u)$ associated with the p.d.f. $f(x)$ is essentially its Fourier transform, or the expectation value of e^{iux}:

$$\phi(u) = E\left[e^{iux}\right] = \int_{-\infty}^{\infty} e^{iux} f(x)\,dx\ . \tag{31.17}$$

Once $\phi(u)$ is specified, the p.d.f. $f(x)$ is uniquely determined and vice versa; knowing one is equivalent to the other. Characteristic functions are useful in deriving a number of important results about moments and sums of random variables.

It follows from Eqs. (31.8a) and (31.17) that the n^{th} moment of a random variable x that follows $f(x)$ is given by

$$i^{-n}\left.\frac{d^n\phi}{du^n}\right|_{u=0} = \int_{-\infty}^{\infty} x^n f(x)\,dx = \alpha_n\ . \tag{31.18}$$

Thus it is often easy to calculate all the moments of a distribution defined by $\phi(u)$, even when $f(x)$ cannot be written down explicitly.

If the p.d.f.s $f_1(x)$ and $f_2(y)$ for independent random variables x and y have characteristic functions $\phi_1(u)$ and $\phi_2(u)$, then the characteristic function of the weighted sum $ax+by$ is $\phi_1(au)\phi_2(bu)$. The addition rules for several important distributions (*e.g.*, that the sum of two Gaussian distributed variables also follows a Gaussian distribution) easily follow from this observation.

Let the (partial) characteristic function corresponding to the conditional p.d.f. $f_2(x|z)$ be $\phi_2(u|z)$, and the p.d.f. of z be $f_1(z)$. The characteristic function after integration over the conditional value is

$$\phi(u) = \int \phi_2(u|z)f_1(z)\,dz\ . \tag{31.19}$$

Suppose we can write ϕ_2 in the form

$$\phi_2(u|z) = A(u)e^{ig(u)z}\ . \tag{31.20}$$

Then

$$\phi(u) = A(u)\phi_1(g(u))\ . \tag{31.21}$$

The semi-invariants κ_n are defined by

$$\phi(u) = \exp\left[\sum_{n=1}^{\infty}\frac{\kappa_n}{n!}(iu)^n\right] = \exp\left(i\kappa_1 u - \tfrac{1}{2}\kappa_2 u^2 + \ldots\right)\ . \tag{31.22}$$

The values κ_n are related to the moments α_n and m_n. The first few relations are

$$\begin{aligned}
&\kappa_1 = \alpha_1\ (=\mu,\ \text{the mean})\\
&\kappa_2 = m_2\ = \alpha_2 - \alpha_1^2\ (=\sigma^2,\ \text{the variance})\\
&\kappa_3 = m_3 = \alpha_3 - 3\alpha_1\alpha_2 + 2\alpha_1^2\ .
\end{aligned} \tag{31.23}$$

Table 31.1. Some common probability density functions, with corresponding characteristic functions and means and variances. In the Table, $\Gamma(k)$ is the gamma function, equal to $(k-1)!$ when k is an integer.

Distribution	Probability density function f (variable; parameters)	Characteristic function $\phi(u)$	Mean	Variance σ^2
Uniform	$f(x;a,b) = \begin{cases} 1/(b-a) & a \le x \le b \\ 0 & \text{otherwise} \end{cases}$	$\dfrac{e^{ibu} - e^{iau}}{(b-a)iu}$	$\dfrac{a+b}{2}$	$\dfrac{(b-a)^2}{12}$
Binomial	$f(r;N,p) = \dfrac{N!}{r!(N-r)!}\, p^r q^{N-r}$ $r = 0, 1, 2, \ldots, N\ ; \quad 0 \le p \le 1\ ; \quad q = 1-p$	$(q + pe^{iu})^N$	Np	Npq
Poisson	$f(n;\nu) = \dfrac{\nu^n e^{-\nu}}{n!}\ ; \quad n = 0, 1, 2, \ldots\ ; \quad \nu > 0$	$\exp[\nu(e^{iu} - 1)]$	ν	ν
Normal (Gaussian)	$f(x;\mu,\sigma^2) = \dfrac{1}{\sigma\sqrt{2\pi}}\ \exp(-(x-\mu)^2/2\sigma^2)$ $-\infty < x < \infty\ ; \quad -\infty < \mu < \infty\ ; \quad \sigma > 0$	$\exp(i\mu u - \frac{1}{2}\sigma^2 u^2)$	μ	σ^2
Multivariate Gaussian	$f(\boldsymbol{x};\boldsymbol{\mu},V) = \dfrac{1}{(2\pi)^{n/2}\sqrt{\lvert V\rvert}}$ $\times \exp\left[-\frac{1}{2}(\boldsymbol{x}-\boldsymbol{\mu})^T V^{-1}(\boldsymbol{x}-\boldsymbol{\mu})\right]$ $-\infty < x_j < \infty; \quad -\infty < \mu_j < \infty; \quad \det V > 0$	$\exp\left[i\boldsymbol{\mu}\cdot\boldsymbol{u} - \frac{1}{2}\boldsymbol{u}^T V \boldsymbol{u}\right]$	$\boldsymbol{\mu}$	V_{jk}
χ^2	$f(z;n) = \dfrac{z^{n/2-1}e^{-z/2}}{2^{n/2}\Gamma(n/2)}\ ; \quad z \ge 0$	$(1-2iu)^{-n/2}$	n	$2n$
Student's t	$f(t;n) = \dfrac{1}{\sqrt{n\pi}}\ \dfrac{\Gamma[(n+1)/2]}{\Gamma(n/2)}\left(1 + \dfrac{t^2}{n}\right)^{-(n+1)/2}$ $-\infty < t < \infty\ ; \quad n$ not required to be integer	—	0 for $n \ge 2$	$n/(n-2)$ for $n \ge 3$
Gamma	$f(x;\lambda,k) = \dfrac{x^{k-1}\lambda^k e^{-\lambda x}}{\Gamma(k)}\ ; \quad 0 < x < \infty\ ;$ k not required to be integer	$(1 - iu/\lambda)^{-k}$	k/λ	k/λ^2

31.4. Some probability distributions

Table 31.1 gives a number of common probability density functions and corresponding characteristic functions, means, and variances. Further information may be found in Refs. [1– 8] and [10]; Ref. [10] has particularly detailed tables. Monte Carlo techniques for generating each of them may be found in our Sec. 33.4. We comment below on all except the trivial uniform distribution.

31.4.1. *Binomial distribution*:

A random process with exactly two possible outcomes which occur with fixed probabilities is called a *Bernoulli* process. If the probability of obtaining a certain outcome (a "success") in each trail is p, then the probability of obtaining exactly r successes ($r = 0, 1, 2, \ldots, N$) in N independent trials, without regard to the order of the successes and failures, is given by the binomial distribution $f(r;N,p)$ in Table 31.1. If r and s are binomially distributed with parameters (N_r, p) and (N_s, p), then $t = r + s$ follows a binomial distribution with parameters $(N_r + N_s, p)$.

31.4.2. *Poisson distribution*:

The Poisson distribution $f(n;\nu)$ gives the probability of finding exactly n events in a given interval of x (*e.g.*, space and time) when the events occur independently of one another and of x at an average rate of ν per the given interval. The variance σ^2 equals ν. It is the limiting case $p \to 0$, $N \to \infty$, $Np = \nu$ of the binomial distribution. The Poisson distribution approaches the Gaussian distribution for large ν.

31.4.3. *Normal or Gaussian distribution*:

The normal (or Gaussian) probability density function $f(x;\mu,\sigma^2)$ given in Table 31.1 has mean $E[x] = \mu$ and variance $V[x] = \sigma^2$. Comparison of the characteristic function $\phi(u)$ given in Table 31.1 with Eq. (31.22) shows that all semi-invariants κ_n beyond κ_2 vanish; this is a unique property of the Gaussian distribution. Some other properties are:

$P(x \text{ in range } \mu \pm \sigma) = 0.6827,$

$P(x \text{ in range } \mu \pm 0.6745\sigma) = 0.5,$

$E[|x - \mu|] = \sqrt{2/\pi}\,\sigma = 0.7979\sigma,$

half-width at half maximum $= \sqrt{2\ln 2}\,\sigma = 1.177\sigma.$

For a Gaussian with $\mu = 0$ and $\sigma^2 = 1$ (the *standard* Gaussian), the cumulative distribution, Eq. (31.6), is related to the error function erf(y) by

$$F(x;0,1) = \tfrac{1}{2}\left[1 + \mathrm{erf}(x/\sqrt{2})\right]\ . \tag{31.24}$$

The error function and standard Gaussian are tabulated in many references (*e.g.*, Ref. [10]) and are available in libraries of computer routines such as CERNLIB. For a mean μ and variance σ^2, replace x by $(x-\mu)/\sigma$. The probability of x in a given range can be calculated with Eq. (32.43).

For x and y independent and normally distributed, $z = ax + by$ follows $f(z; a\mu_x + b\mu_y, a^2\sigma_x^2 + b^2\sigma_y^2)$; that is, the weighted means and variances add.

The Gaussian derives its importance in large part from the *central limit theorem*: If independent random variables $x_1, \ldots, x_n$ are distributed according to *any* p.d.f.s with finite means and variances, then the sum $y = \sum_{i=1}^{n} x_i$ will have a p.d.f. that approaches a Gaussian for large n. The mean and variance are given by the sums of corresponding terms from the individual x_i. Therefore the sum of a

large number of fluctuations x_i will be distributed as a Gaussian, even if the x_i themselves are not.

(Note that the *product* of a large number of random variables is not Gaussian, but its logarithm is. The p.d.f. of the product is *log-normal*. See Ref. [8] for details.)

For a set of n Gaussian random variables $\boldsymbol{x}$ with means $\boldsymbol{\mu}$ and corresponding Fourier variables $\boldsymbol{u}$, the characteristic function for a one-dimensional Gaussian is generalized to

$$\phi(\boldsymbol{u};\boldsymbol{\mu},V) = \exp\left[i\boldsymbol{\mu}\cdot\boldsymbol{u} - \tfrac{1}{2}\boldsymbol{u}^T V\boldsymbol{u}\right] . \tag{31.25}$$

From Eq. (31.18), the covariance of x_i and x_j is

$$E\left[(x_i-\mu_i)(x_j-\mu_j)\right] = V_{ij} . \tag{31.26}$$

If the components of $\boldsymbol{x}$ are independent, then $V_{ij} = \delta_{ij}\sigma_i^2$, and Eq. (31.25) is the product of the c.f.s of n Gaussians.

The covariance matrix V can be related to the correlation matrix defined by Eq. (31.14) (a sort of normalized covariance matrix) as $\rho_{ij} = V_{ij}/\sigma_i\sigma_j$. Note that by construction $\rho_{ii} = 1$, since $V_{ii} = \sigma_i^2$.

The characteristic function may be inverted to find the corresponding p.d.f.,

$$f(\boldsymbol{x};\boldsymbol{\mu},V) = \frac{1}{(2\pi)^{n/2}\sqrt{|V|}}\exp\left[-\tfrac{1}{2}(\boldsymbol{x}-\boldsymbol{\mu})^T V^{-1}(\boldsymbol{x}-\boldsymbol{\mu})\right] \tag{31.27}$$

where the determinant $|V|$ must be greater than 0. For diagonal V (independent variables), $f(\boldsymbol{x};\boldsymbol{\mu},V)$ is the product of the p.d.f.s of n Gaussian distributions.

For $n = 2$, $f(\boldsymbol{x};\boldsymbol{\mu},V)$ is

$$f(x_1,x_2;\ \mu_1,\mu_2,\sigma_1,\sigma_2,\rho) = \frac{1}{2\pi\sigma_1\sigma_2\sqrt{1-\rho^2}}$$
$$\times\ \exp\left\{\frac{-1}{2(1-\rho^2)}\left[\frac{(x_1-\mu_1)^2}{\sigma_1^2} - \frac{2\rho(x_1-\mu_1)(x_2-\mu_2)}{\sigma_1\sigma_2} + \frac{(x_2-\mu_2)^2}{\sigma_2^2}\right]\right\} . \tag{31.28}$$

The marginal distribution of any x_i is a Gaussian with mean μ_i and variance V_{ii}. V is $n\times n$, symmetric, and positive definite. Therefore for any vector $\boldsymbol{X}$, the quadratic form $\boldsymbol{X}^T V^{-1}\boldsymbol{X} = C$, where C is any positive number, traces an n-dimensional ellipsoid as $\boldsymbol{X}$ varies. If $X_i = x_i - \mu_i$, then C is a random variable obeying the χ^2 distribution with n degrees of freedom, discussed in the following section. The probability that $\boldsymbol{X}$ corresponding to a set of Gaussian random variables x_i lies outside the ellipsoid characterized by a given value of C $(= \chi^2)$ is given by $1 - F_{\chi^2}(C;n)$, where F_{χ^2} is the cumulative χ^2 distribution. This may be read from Fig. 32.1. For example, the "s-standard-deviation ellipsoid" occurs at $C = s^2$. For the two-variable case ($n = 2$), the point $\boldsymbol{X}$ lies outside the one-standard-deviation ellipsoid with 61% probability. The use of these ellipsoids as indicators of probable error is described in Sec. 32.3.2.3; the validity of those indicators assumes that $\boldsymbol{\mu}$ and V are correct.

31.4.4. χ^2 *distribution*:

If $x_1,\ldots,x_n$ are independent Gaussian random variables, the sum $z = \sum_{i=1}^n (x_i-\mu_i)^2/\sigma_i^2$ follows the χ^2 p.d.f. with n *degrees of freedom*, which we denote by $\chi^2(n)$. Under a linear transformation to n correlated Gaussian variables x_i', the value of z is invariant; then $z = \boldsymbol{X}'^T V^{-1}\boldsymbol{X}'$ as in the previous section. For a set of z_i, each of which follows $\chi^2(n_i)$, $\sum z_i$ follows $\chi^2(\sum n_i)$. For large n, the χ^2 p.d.f. approaches a Gaussian with mean $\mu = n$ and variance $\sigma^2 = 2n$.

The χ^2 p.d.f. is often used in evaluating the level of compatibility between observed data and a hypothesis for the p.d.f. that the data might follow. This is discussed further in Sec. 32.2.2 on tests of goodness-of-fit.

31.4.5. *Student's t distribution*:

Suppose that x and $x_1,\ldots,x_n$ are independent and Gaussian distributed with mean 0 and variance 1. We then define

$$z = \sum_{i=1}^n x_i^2 \quad\text{and}\quad t = \frac{x}{\sqrt{z/n}} . \tag{31.29}$$

The variable z thus follows a $\chi^2(n)$ distribution. Then t is distributed according to Student's t distribution with n degrees of freedom, $f(t;n)$, given in Table 31.1.

The Student's t distribution resembles a Gaussian with wide tails. As $n\to\infty$, the distribution approaches a Gaussian. If $n = 1$, it is a *Cauchy* or *Breit–Wigner* distribution. The mean is finite only for $n > 1$ and the variance is finite only for $n > 2$, so the central limit theorem is not applicable to sums of random variables following the t distribution for $n = 1$ or 2.

As an example, consider the *sample mean* $\overline{x} = \sum x_i/n$ and the *sample variance* $s^2 = \sum(x_i-\overline{x})^2/(n-1)$ for normally distributed x_i with unknown mean μ and variance σ^2. The sample mean has a Gaussian distribution with a variance σ^2/n, so the variable $(\overline{x}-\mu)/\sqrt{\sigma^2/n}$ is normal with mean 0 and variance 1. Similarly, $(n-1)s^2/\sigma^2$ is independent of this and follows $\chi^2(n-1)$. The ratio

$$t = \frac{(\overline{x}-\mu)/\sqrt{\sigma^2/n}}{\sqrt{(n-1)s^2/\sigma^2(n-1)}} = \frac{\overline{x}-\mu}{\sqrt{s^2/n}} \tag{31.30}$$

is distributed as $f(t;n-1)$. The unknown variance σ^2 cancels, and t can be used to test the probability that the true mean is some particular value μ.

In Table 31.1, n in $f(t;n)$ is not required to be an integer. A Student's t distribution with non-integral $n > 0$ is useful in certain applications.

31.4.6. *Gamma distribution*:

For a process that generates events as a function of x (*e.g.*, space or time) according to a Poisson distribution, the distance in x from an arbitrary starting point (which may be some particular event) to the k^{th} event follows a *gamma* distribution, $f(x;\lambda,k)$. The Poisson parameter μ is λ per unit x. The special case $k = 1$ (*i.e.*, $f(x;\lambda,1) = \lambda e^{-\lambda x}$) is called the *exponential* distribution. A sum of k' exponential random variables x_i is distributed as $f(\sum x_i;\lambda,k')$.

The parameter k is not required to be an integer. For $\lambda = 1/2$ and $k = n/2$, the gamma distribution reduces to the $\chi^2(n)$ distribution.

References:

1. H. Cramér, *Mathematical Methods of Statistics,* (Princeton Univ. Press, New Jersey, 1958).
2. A. Stuart and A.K. Ord, *Kendall's Advanced Theory of Statistics*, Vol. 1 *Distribution Theory* 5th Ed., (Oxford Univ. Press, New York, 1987), and earlier editions by Kendall and Stuart.
3. W.T. Eadie, D. Drijard, F.E. James, M. Roos, and B. Sadoulet, *Statistical Methods in Experimental Physics* (North Holland, Amsterdam, and London, 1971).
4. L. Lyons, *Statistics for Nuclear and Particle Physicists* (Cambridge University Press, New York, 1986).
5. B.R. Roe, *Probability and Statistics in Experimental Physics,* 2nd Ed., (Springer, New York, 2001).
6. R.J. Barlow, *Statistics: A Guide to the Use of Statistical Methods in the Physical Sciences* (John Wiley, New York, 1989).
7. S. Brandt, *Data Analysis*, 3rd Ed., (Springer, New York, 1999).
8. G. Cowan, *Statistical Data Analysis* (Oxford University Press, Oxford, 1998).
9. A.N. Kolmogorov, *Grundbegriffe der Wahrscheinlichkeitsrechnung* (Springer, Berlin 1933); *Foundations of the Theory of Probability*, 2nd Ed., (Chelsea, New York 1956).
10. M. Abramowitz and I. Stegun, eds., *Handbook of Mathematical Functions* (Dover, New York, 1972).

32. STATISTICS

Revised April 1998 by F. James (CERN); February 2000 by R. Cousins (UCLA); October 2001 and October 2003 by G. Cowan (RHUL).

This chapter gives an overview of statistical methods used in High Energy Physics. In statistics we are interested in using a given sample of data to make inferences about a probabilistic model, e.g., to assess the model's validity or to determine the values of its parameters. There are two main approaches to statistical inference, which we may call frequentist and Bayesian. In frequentist statistics, probability is interpreted as the frequency of the outcome of a repeatable experiment. The most important tools in this framework are parameter estimation, covered in Section 32.1, and statistical tests, discussed in Section 32.2. Frequentist confidence intervals, which are constructed so as to cover the true value of a parameter with a specified probability, are treated in Section 32.3.2. Note that in frequentist statistics one does not define a probability for a hypothesis or for a parameter.

Frequentist statistics provides the usual tools for reporting objectively the outcome of an experiment without needing to incorporate prior beliefs concerning the parameter being measured or the theory being tested. As such they are used for reporting essentially all measurements and their statistical uncertainties in High Energy Physics.

In Bayesian statistics, the interpretation of probability is more general and includes *degree of belief*. One can then speak of a probability density fundtion (p.d.f.) for a parameter, which expresses one's state of knowledge about where its true value lies. Bayesian methods allow for a natural way to input additional information such as physical boundaries and subjective information; in fact they *require* as input the *prior* p.d.f. for the parameters, *i.e.*, the degree of belief about the parameters' values before carrying out the measurement. Using Bayes' theorem Eq. (31.4), the prior degree of belief is updated by the data from the experiment. Bayesian methods for interval estimation are discussed in Sections 32.3.1 and 32.3.2.5

Bayesian techniques are often used to treat systematic uncertainties, where the author's subjective beliefs about, say, the accuracy of the measuring device may enter. Bayesian statistics also provides a useful framework for discussing the validity of different theoretical interpretations of the data. This aspect of a measurement, however, will usually be treated separately from the reporting of the result.

For many inference problems, the frequentist and Bayesian approaches give the same numerical answers, even though they are based on fundamentally different interpretations of probability. For small data samples, however, and for measurements of a parameter near a physical boundary, the different approaches may yield different results, so we are forced to make a choice. For a discussion of Bayesian vs. non-Bayesian methods, see References written by a statistician[1], by a physicist[2], or the more detailed comparison in Ref. [3].

Following common usage in physics, the word "error" is often used in this chapter to mean "uncertainty". More specifically it can indicate the size of an interval as in "the standard error" or "error propagation", where the term refers to the standard deviation of an estimator.

32.1. Parameter estimation

Here we review *point estimation* of parameters. An *estimator* $\widehat{\theta}$ (written with a hat) is a function of the data whose value, the *estimate*, is intended as a meaningful guess for the value of the parameter θ.

There is no fundamental rule dictating how an estimator must be constructed. One tries therefore to choose that estimator which has the best properties. The most important of these are (a) *consistency*, (b) *bias*, (c) *efficiency*, and (d) *robustness*.

(a) An estimator is said to be *consistent* if the estimate $\widehat{\theta}$ converges to the true value θ as the amount of data increases. This property is so important that it is possessed by all commonly used estimators.

(b) The *bias*, $b = E[\widehat{\theta}\,] - \theta$, is the difference between the expectation value of the estimator and the true value of the parameter. The expectation value is taken over a hypothetical set of similar experiments in which $\widehat{\theta}$ is constructed in the same way. When $b = 0$ the estimator is said to be unbiased. The bias depends on the chosen metric, *i.e.*, if $\widehat{\theta}$ is an unbiased estimator of θ, then $\widehat{\theta}^{\,2}$ is not in general an unbiased estimator for θ^2. If we have an estimate $\widehat{b}$ for the bias we can subtract it from $\widehat{\theta}$ to obtain a new $\widehat{\theta}\,' = \widehat{\theta} - \widehat{b}$. The estimate $\widehat{b}$ may, however, be subject to statistical or systematic uncertainties that are larger than the bias itself, so that the new estimator may not be better than the original.

(c) *Efficiency* is the inverse of the ratio of the variance $V[\widehat{\theta}\,]$ to its minimum possible value. Under rather general conditions, the minimum variance is given by the Rao-Cramér-Frechet bound,

$$\sigma^2_{\rm min} = \left(1 + \frac{\partial b}{\partial \theta}\right)^2 / I(\theta)\,, \tag{32.1}$$

where

$$I(\theta) = E\left[\left(\frac{\partial}{\partial\theta}\sum_i \ln f(x_i;\theta)\right)^2\right] \tag{32.2}$$

is the *Fisher information*. The sum is over all data, assumed independent and distributed according to the p.d.f. $f(x;\theta)$, b is the bias, if any, and the allowed range of x must not depend on θ.

The *mean-squared error*,

$$\mathrm{MSE} = E[(\widehat{\theta} - \theta)^2] = V[\widehat{\theta}\,] + b^2\,, \tag{32.3}$$

is a convenient quantity which combines the uncertainties in an estimate due to bias and variance.

(d) *Robustness* is the property of being insensitive to departures from assumptions in the p.d.f. owing to factors such as noise.

For some common estimators the properties above are known exactly. More generally, it is possible to evaluate them by Monte Carlo simulation. Note that they will often depend on the unknown θ.

32.1.1. *Estimators for mean, variance and median*:

Suppose we have a set of N independent measurements x_i assumed to be unbiased measurements of the same unknown quantity μ with a common, but unknown, variance σ^2. Then

$$\widehat{\mu} = \frac{1}{N}\sum_{i=1}^{N} x_i \tag{32.4}$$

$$\widehat{\sigma^2} = \frac{1}{N-1}\sum_{i=1}^{N}(x_i - \widehat{\mu})^2 \tag{32.5}$$

are unbiased estimators of μ and σ^2. The variance of $\widehat{\mu}$ is σ^2/N and the variance of $\widehat{\sigma^2}$ is

$$V\left[\widehat{\sigma^2}\right] = \frac{1}{N}\left(m_4 - \frac{N-3}{N-1}\sigma^4\right)\,, \tag{32.6}$$

where m_4 is the 4th central moment of x. For Gaussian distributed x_i this becomes $2\sigma^4/(N-1)$ for any $N \geq 2$, and for large N the standard deviation of $\widehat{\sigma}$ (the "error of the error") is $\sigma/\sqrt{2N}$. Again if the x_i are Gaussian, $\widehat{\mu}$ is an efficient estimator for μ and the estimators $\widehat{\mu}$ and $\widehat{\sigma^2}$ are uncorrelated. Otherwise the arithmetic mean (32.4) is not necessarily the most efficient estimator; this is discussed in more detail in [4] Sec. 8.7

If σ^2 is known, it does not improve the estimate $\widehat{\mu}$, as can be seen from Eq. (32.4); however, if μ is known, substitute it for $\widehat{\mu}$ in Eq. (32.5) and replace $N-1$ by N to obtain a somewhat better estimator of σ^2.

If the x_i have different, known variances σ_i^2, then the weighted average

$$\widehat{\mu} = \frac{1}{w}\sum_{i=1}^{N} w_i x_i \qquad (32.7)$$

is an unbiased estimator for μ with a smaller variance than an unweighted average; here $w_i = 1/\sigma_i^2$ and $w = \sum_i w_i$. The standard deviation of $\widehat{\mu}$ is $1/\sqrt{w}$.

As an estimator for the median $x_{\rm med}$ one can use the value $\widehat{x}_{\rm med}$ such that half the x_i are below and half above (the sample median). If the sample median lies between two observed values, it is set by convention halfway between them. If the p.d.f. of x has the form $f(x-\mu)$ and μ is both mean and median, then for large N the variance of the sample median approaches $1/[4Nf^2(0)]$, provided $f(0) > 0$. Although estimating the median can often be more difficult computationally than the mean, the resulting estimator is generally more robust, as it is insensitive to the exact shape of the tails of a distribution.

32.1.2. *The method of maximum likelihood*:

"From a theoretical point of view, the most important general method of estimation so far known is the *method of maximum likelihood*" [5]. We suppose that a set of N independently measured quantities x_i came from a p.d.f. $f(x;\boldsymbol{\theta})$, where $\boldsymbol{\theta} = (\theta_1, \ldots, \theta_n)$ is set of n parameters whose values are unknown. The method of maximum likelihood takes the estimators $\widehat{\boldsymbol{\theta}}$ to be those values of $\boldsymbol{\theta}$ that maximize the *likelihood function*,

$$L(\boldsymbol{\theta}) = \prod_{i=1}^{N} f(x_i;\boldsymbol{\theta}) \, . \qquad (32.8)$$

The likelihood function is the joint p.d.f. for the data, evaluated with the data obtained in the experiment and regarded as a function of the parameters. Note that the likelihood function is *not* a p.d.f. for the parameters $\boldsymbol{\theta}$; in frequentist statistics this is not defined. In Bayesian statistics one can obtain from the likelihood the posterior p.d.f. for $\boldsymbol{\theta}$, but this requires multiplying by a prior p.d.f. (see Sec. 32.3.1).

It is usually easier to work with $\ln L$, and since both are maximized for the same parameter values $\boldsymbol{\theta}$, the maximum likelihood (ML) estimators can be found by solving the *likelihood equations*,

$$\frac{\partial \ln L}{\partial \theta_i} = 0 \, , \qquad i = 1, \ldots, n \, . \qquad (32.9)$$

Maximum likelihood estimators are important because they are approximately unbiased and efficient for large data samples, under quite general conditions, and the method has a wide range of applicability.

In evaluating the likelihood function, it is important that any normalization factors in the p.d.f. that involve $\boldsymbol{\theta}$ be included. However, we will only be interested in the maximum of L and in ratios of L at different values of the parameters; hence any multiplicative factors that do not involve the parameters that we want to estimate may be dropped, including factors that depend on the data but not on $\boldsymbol{\theta}$.

Under a one-to-one change of parameters from $\boldsymbol{\theta}$ to $\boldsymbol{\eta}$, the ML estimators $\widehat{\boldsymbol{\theta}}$ transform to $\boldsymbol{\eta}(\widehat{\boldsymbol{\theta}})$. That is, the ML solution is invariant under change of parameter. However, other properties of ML estimators, in particular the bias, are not invariant under change of parameter.

The inverse V^{-1} of the covariance matrix $V_{ij} = \mathrm{cov}[\widehat{\theta}_i, \widehat{\theta}_j]$ for a set of ML estimators can be estimated by using

$$(\widehat{V}^{-1})_{ij} = -\left.\frac{\partial^2 \ln L}{\partial\theta_i \partial\theta_j}\right|_{\widehat{\theta}} \, . \qquad (32.10)$$

For finite samples, however, Eq. (32.10) can result in an underestimate of the variances. In the large sample limit (or in a linear model with Gaussian errors), L has a Gaussian form and $\ln L$ is (hyper)parabolic. In this case it can be seen that a numerically equivalent way of determining s-standard-deviation errors is from the contour given by the $\boldsymbol{\theta}'$ such that

$$\ln L(\boldsymbol{\theta}') = \ln L_{\rm max} - s^2/2 \, , \qquad (32.11)$$

where $\ln L_{\rm max}$ is the value of $\ln L$ at the solution point (compare with Eq. (32.46)). The extreme limits of this contour on the θ_i axis give an approximate s-standard-deviation confidence interval for θ_i (see Section 32.3.2.3).

In the case where the size n of the data sample $x_1, \ldots, x_n$ is small, the unbinned maximum likelihood method, i.e., use of equation (32.8), is preferred since binning can only result in a loss of information and hence larger statistical errors for the parameter estimates. The sample size n can be regarded as fixed or the user can choose to treat it as a Poisson-distributed variable; this latter option is sometimes called "extended maximum likelihood" (see, *e.g.*, [6, 7, 8]). If the sample is large it can be convenient to bin the values in a histogram, so that one obtains a vector of data $\boldsymbol{n} = (n_1, \ldots, n_N)$ with expectation values $\boldsymbol{\nu} = E[\boldsymbol{n}]$ and probabilities $f(\boldsymbol{n};\boldsymbol{\nu})$. Then one may maximize the likelihood function based on the contents of the bins (so i labels bins). This is equivalent to maximizing the likelihood ratio $\lambda(\boldsymbol{\theta}) = f(\boldsymbol{n};\boldsymbol{\nu}(\boldsymbol{\theta}))/f(\boldsymbol{n};\boldsymbol{n})$, or to minimizing the quantity [9]

$$-2\ln\lambda(\boldsymbol{\theta}) = 2\sum_{i=1}^{N}\left[\nu_i(\boldsymbol{\theta}) - n_i + n_i \ln\frac{n_i}{\nu_i(\boldsymbol{\theta})}\right] \, , \qquad (32.12)$$

where in bins where $n_i = 0$, the last term in (32.12) is zero. In the limit of zero bin width, maximizing (32.12) is equivalent to maximizing the unbinned likelihood function (32.8).

A benefit of binning is that it allows for a goodness-of-fit test (see Sec. 32.2.2). The minimum of $-2\ln\lambda$ as defined by Eq. (32.12) follows a χ^2 distribution in the large sample limit. If there are N bins and m fitted parameters, then the number of degrees of freedom for the χ^2 distribution is $N - m - 1$ if the data are treated as multinomially distributed and $N - m$ if the n_i are Poisson variables with $\nu_{\rm tot} = \sum_i \nu_i$ fixed. If the n_i are Poisson distributed and $\nu_{\rm tot}$ is also fitted, then by minimizing Eq. (32.12) one obtains that the area under the fitted function is equal to the sum of the histogram contents, *i.e.*, $\sum_i \nu_i = \sum_i n_i$. This is not the case for parameter estimation methods based on a least-squares procedure with traditional weights (see, *e.g.*, Ref. [8]).

32.1.3. *The method of least squares*:

The *method of least squares* (LS) coincides with the method of maximum likelihood in the following special case. Consider a set of N independent measurements y_i at known points x_i. The measurement y_i is assumed to be Gaussian distributed with mean $F(x_i;\boldsymbol{\theta})$ and known variance σ_i^2. The goal is to construct estimators for the unknown parameters $\boldsymbol{\theta}$. The likelihood function contains the sum of squares

$$\chi^2(\boldsymbol{\theta}) = -2\ln L(\boldsymbol{\theta}) + \text{ constant } = \sum_{i=1}^{N}\frac{(y_i - F(x_i;\boldsymbol{\theta}))^2}{\sigma_i^2} \, . \qquad (32.13)$$

The set of parameters $\boldsymbol{\theta}$ which maximize L is the same as those which minimize χ^2.

The minimum of Equation (32.13) defines the least-squares estimators $\widehat{\boldsymbol{\theta}}$ for the more general case where the y_i are not Gaussian distributed as long as they are independent. If they are not independent but rather have a covariance matrix $V_{ij} = \mathrm{cov}[y_i, y_j]$, then the LS estimators are determined by the minimum of

$$\chi^2(\boldsymbol{\theta}) = (\boldsymbol{y} - \boldsymbol{F}(\boldsymbol{\theta}))^T V^{-1} (\boldsymbol{y} - \boldsymbol{F}(\boldsymbol{\theta})) \, , \qquad (32.14)$$

where $\boldsymbol{y} = (y_1, \ldots, y_N)$ is the vector of measurements, $\boldsymbol{F}(\boldsymbol{\theta})$ is the corresponding vector of predicted values (understood as a column vector in (32.14)), and the superscript T denotes transposed (*i.e.*, row) vector.

In many practical cases one further restricts the problem to the situation where $F(x_i;\boldsymbol{\theta})$ is a linear function of the parameters, *i.e.*,

$$F(x_i;\boldsymbol{\theta}) = \sum_{j=1}^{m} \theta_j h_j(x_i) \; . \tag{32.15}$$

Here the $h_j(x)$ are m linearly independent functions, *e.g.*, $1, x, x^2, \ldots, x^{m-1}$, or Legendre polynomials. We require $m < N$ and at least m of the x_i must be distinct.

Minimizing χ^2 in this case with m parameters reduces to solving a system of m linear equations. Defining $H_{ij} = h_j(x_i)$ and minimizing χ^2 by setting its derivatives with respect to the θ_i equal to zero gives the LS estimators,

$$\widehat{\boldsymbol{\theta}} = (H^T V^{-1} H)^{-1} H^T V^{-1} \boldsymbol{y} \equiv D\boldsymbol{y} \; . \tag{32.16}$$

The covariance matrix for the estimators $U_{ij} = \mathrm{cov}[\widehat{\theta}_i, \widehat{\theta}_j]$ is given by

$$U = DVD^T = (H^T V^{-1} H)^{-1} \; , \tag{32.17}$$

or equivalently, its inverse U^{-1} can be found from

$$(U^{-1})_{ij} = \frac{1}{2} \frac{\partial^2 \chi^2}{\partial\theta_i \partial\theta_j}\bigg|_{\theta=\widehat{\theta}} = \sum_{k,l=1}^{N} h_i(x_k)(V^{-1})_{kl} h_j(x_l) \; . \tag{32.18}$$

The LS estimators can also be found from the expression

$$\widehat{\boldsymbol{\theta}} = U\boldsymbol{g} \; , \tag{32.19}$$

where the vector $\boldsymbol{g}$ is defined by

$$g_i = \sum_{j,k=1}^{N} y_j h_i(x_k)(V^{-1})_{jk} \; . \tag{32.20}$$

For the case of uncorrelated y_i, for example, one can use (32.19) with

$$(U^{-1})_{ij} = \sum_{k=1}^{N} \frac{h_i(x_k) h_j(x_k)}{\sigma_k^2} \; , \tag{32.21}$$

$$g_i = \sum_{k=1}^{N} \frac{y_k h_i(x_k)}{\sigma_k^2} \; . \tag{32.22}$$

Expanding $\chi^2(\boldsymbol{\theta})$ about $\widehat{\boldsymbol{\theta}}$, one finds that the contour in parameter space defined by

$$\chi^2(\boldsymbol{\theta}) = \chi^2(\widehat{\boldsymbol{\theta}}) + 1 = \chi^2_{\min} + 1 \tag{32.23}$$

has tangent planes located at plus or minus one standard deviation $\sigma_{\widehat{\theta}}$ from the LS estimates $\widehat{\boldsymbol{\theta}}$.

In constructing the quantity $\chi^2(\boldsymbol{\theta})$, one requires the variances or, in the case of correlated measurements, the covariance matrix. Often these quantities are not known *a priori* and must be estimated from the data; an important example is where the measured value y_i represents a counted number of events in the bin of a histogram. If, for example, y_i represents a Poisson variable, for which the variance is equal to the mean, then one can either estimate the variance from the predicted value, $F(x_i;\boldsymbol{\theta})$, or from the observed number itself, y_i. In the first option, the variances become functions of the fitted parameters, which may lead to calculational difficulties. The second option can be undefined if y_i is zero, and in both cases for small y_i the variance will be poorly estimated. In either case one should constrain the normalization of the fitted curve to the correct value, *e.g.*, one should determine the area under the fitted curve directly from the number of entries in the histogram (see [8] Section 7.4). A further alternative is to use the method of maximum likelihood; for binned data this can be done by minimizing Eq. (32.12)

As the minimum value of the χ^2 represents the level of agreement between the measurements and the fitted function, it can be used for assessing the goodness-of-fit; this is discussed further in Section 32.2.2.

32.1.4. ***Propagation of errors***:

Consider a set of n quantities $\boldsymbol{\theta} = (\theta_1, \ldots, \theta_n)$ and a set of m functions $\boldsymbol{\eta}(\boldsymbol{\theta}) = (\eta_1(\boldsymbol{\theta}), \ldots, \eta_m(\boldsymbol{\theta}))$. Suppose we have estimates $\widehat{\boldsymbol{\theta}} = (\widehat{\theta}_1, \ldots, \widehat{\theta}_n)$, using, say, maximum likelihood or least squares, and we also know or have estimated the covariance matrix $V_{ij} = \mathrm{cov}[\widehat{\theta}_i, \widehat{\theta}_j]$. The goal of *error propagation* is to determine the covariance matrix for the functions, $U_{ij} = \mathrm{cov}[\widehat{\eta}_i, \widehat{\eta}_j]$, where $\widehat{\boldsymbol{\eta}} = \boldsymbol{\eta}(\widehat{\boldsymbol{\theta}})$. In particular, the diagonal elements $U_{ii} = V[\widehat{\eta}_i]$ give the variances. The new covariance matrix can be found by expanding the functions $\boldsymbol{\eta}(\boldsymbol{\theta})$ about the estimates $\widehat{\boldsymbol{\theta}}$ to first order in a Taylor series. Using this one finds

$$U_{ij} \approx \sum_{k,l} \frac{\partial\eta_i}{\partial\theta_k} \frac{\partial\eta_j}{\partial\theta_l}\bigg|_{\widehat{\theta}} V_{kl} \; . \tag{32.24}$$

This can be written in matrix notation as $U \approx AVA^T$ where the matrix of derivatives A is

$$A_{ij} = \frac{\partial\eta_i}{\partial\theta_j}\bigg|_{\widehat{\theta}} \tag{32.25}$$

and A^T is its transpose. The approximation is exact if $\boldsymbol{\eta}(\boldsymbol{\theta})$ is linear (it holds, for example, in equation (32.17)). If this is not the case the approximation can break down if, for example, $\boldsymbol{\eta}(\boldsymbol{\theta})$ is significantly nonlinear close to $\widehat{\boldsymbol{\theta}}$ in a region of a size comparable to the standard deviations of $\widehat{\boldsymbol{\theta}}$.

32.2. Statistical tests

In addition to estimating parameters, one often wants to assess the validity of certain statements concerning the data's underlying distribution. *Hypothesis tests* provide a rule for accepting or rejecting hypotheses depending on the outcome of a measurement. In *goodness-of-fit tests* one gives the probability to obtain a level of incompatibility with a certain hypothesis that is greater than or equal to the level observed with the actual data.

32.2.1. ***Hypothesis tests***:

Consider an experiment whose outcome is characterized by a vector of data $\boldsymbol{x}$. A *hypothesis* is a statement about the distribution of $\boldsymbol{x}$. It could, for example, define completely the p.d.f. for the data (a simple hypothesis) or it could specify only the functional form of the p.d.f., with the values of one or more parameters left open (a composite hypothesis).

A *statistical test* is a rule that states for which values of $\boldsymbol{x}$ a given hypothesis (often called the null hypothesis, H_0) should be rejected. This is done by defining a region of $\boldsymbol{x}$-space called the critical region; if the outcome if the experiment lands in this region, H_0 is rejected. Equivalently one can say that the hypothesis is accepted if $\boldsymbol{x}$ is observed in the acceptance region, *i.e.*, the complement of the critical region. Here 'accepted' is understood to mean simply that the test did not reject H_0.

Rejecting H_0 if it is true is called an error of the first kind. The probability for this to occur is called the *significance level* of the test, α, which is often chosen to be equal to some pre-specified value. It can also happen that H_0 is false and the true hypothesis is given by some alternative, H_1. If H_0 is accepted in such a case, this is called an error of the second kind. The probability for this to occur, β, depends on the alternative hypothesis, say, H_1, and $1-\beta$ is called the *power* of the test to reject H_1.

In High Energy Physics the components of $\boldsymbol{x}$ might represent the measured properties of candidate events, and the acceptance region is defined by the cuts that one imposes in order to select events of a certain desired type. That is, H_0 could represent the signal hypothesis, and various alternatives, H_1, H_2, etc., could represent background processes.

Often rather than using the full data sample $\boldsymbol{x}$ it is convenient to define a *test statistic*, t, which can be a single number or in any case a vector with fewer components than $\boldsymbol{x}$. Each hypothesis for the distribution of $\boldsymbol{x}$ will determine a distribution for t, and the acceptance region in $\boldsymbol{x}$-space will correspond to a specific range of values of t.

In constructing t one attempts to reduce the volume of data without losing the ability to discriminate between different hypotheses.

In particle physics terminology, the probability to accept the signal hypothesis, H_0, is the selection efficiency, *i.e.*, one minus the significance level. The efficiencies for the various background processes are given by one minus the power. Often one tries to construct a test to minimize the background efficiency for a given signal efficiency. The *Neyman–Pearson lemma* states that this is done by defining the acceptance region such that, for $\boldsymbol{x}$ in that region, the ratio of p.d.f.s for the hypotheses H_0 and H_1,

$$\lambda(\boldsymbol{x}) = \frac{f(\boldsymbol{x}|H_0)}{f(\boldsymbol{x}|H_1)}\,, \tag{32.26}$$

is greater than a given constant, the value of which is chosen to give the desired signal efficiency. This is equivalent to the statement that (32.26) represents the test statistic with which one may obtain the highest purity sample for a given signal efficiency. It can be difficult in practice, however, to determine $\lambda(\boldsymbol{x})$, since this requires knowledge of the joint p.d.f.s $f(\boldsymbol{x}|H_0)$ and $f(\boldsymbol{x}|H_1)$. Instead, test statistics based on *neural networks* or *Fisher discriminants* are often used (see [10]).

32.2.2. *Goodness-of-fit tests*:

Often one wants to quantify the level of agreement between the data and a hypothesis without explicit reference to alternative hypotheses. This can be done by defining a *goodness-of-fit statistic*, t, which is a function of the data whose value reflects in some way the level of agreement between the data and the hypothesis. The user must decide what values of the statistic correspond to better or worse levels of agreement with the hypothesis in question; for many goodness-of-fit statistics there is an obvious choice.

The hypothesis in question, say, H_0, will determine the p.d.f. $g(t|H_0)$ for the statistic. The goodness-of-fit is quantified by giving the p-value, defined as the probability to find t in the region of equal or lesser compatibility with H_0 than the level of compatibility observed with the actual data. For example, if t is defined such that large values correspond to poor agreement with the hypothesis, then the p-value would be

$$p = \int_{t_{\rm obs}}^{\infty} g(t|H_0)\,dt\,, \tag{32.27}$$

where $t_{\rm obs}$ is the value of the statistic obtained in the actual experiment. The p-value should not be confused with the significance level of a test or the confidence level of a confidence interval (Section 32.3), both of which are pre-specified constants.

The p-value is a function of the data and is therefore itself a random variable. If the hypothesis used to compute the p-value is true, then for continuous data, p will be uniformly distributed between zero and one. Note that the p-value is not the probability for the hypothesis; in frequentist statistics this is not defined. Rather, the p-value is the probability, under the assumption of a hypothesis H_0, of obtaining data at least as incompatible with H_0 as the data actually observed.

When estimating parameters using the method of least squares, one obtains the minimum value of the quantity χ^2 (32.13), which can be used as a goodness-of-fit statistic. It may also happen that no parameters are estimated from the data, but that one simply wants to compare a histogram, *e.g.*, a vector of Poisson distributed numbers $\boldsymbol{n} = (n_1, \ldots, n_N)$, with a hypothesis for their expectation values $\nu_i = E[n_i]$. As the distribution is Poisson with variances $\sigma_i^2 = \nu_i$, the χ^2 (32.13) becomes *Pearson's* χ^2 *statistic*,

$$\chi^2 = \sum_{i=1}^{N} \frac{(n_i - \nu_i)^2}{\nu_i}\,. \tag{32.28}$$

If the hypothesis $\boldsymbol{\nu} = (\nu_1, \ldots, \nu_N)$ is correct and if the measured values n_i in (32.28) are sufficiently large (in practice, this will be a good approximation if all $n_i > 5$), then the χ^2 statistic will follow the χ^2 p.d.f. with the number of degrees of freedom equal to the number of measurements N minus the number of fitted parameters. The same holds for the minimized χ^2 from Eq. (32.13) if the y_i are Gaussian.

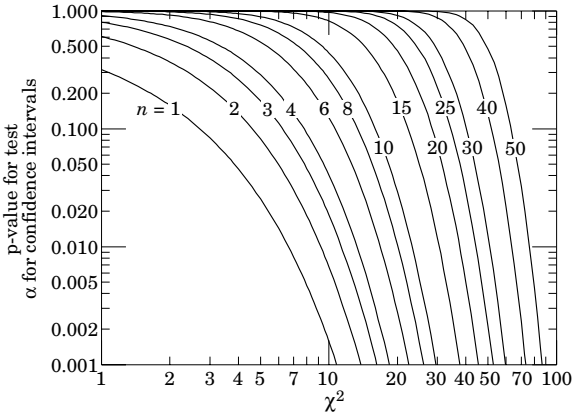

Figure 32.1: One minus the χ^2 cumulative distribution, $1 - F(\chi^2; n)$, for n degrees of freedom. This gives the p-value for the χ^2 goodness-of-fit test as well as one minus the coverage probability for confidence regions (see Sec. 32.3.2.3).

Alternatively one may fit parameters and evaluate goodness-of-fit by minimizing $-2\ln\lambda$ from Eq. (32.12). One finds that the distribution of this statistic approaches the asymptotic limit faster than does Pearson's χ^2 and thus computing the p-value with the χ^2 p.d.f. will in general be better justified (see [9] and references therein).

Assuming the goodness-of-fit statistic follows a χ^2 p.d.f., the p-value for the hypothesis is then

$$p = \int_{\chi^2}^{\infty} f(z; n_{\rm d})\,dz\,, \tag{32.29}$$

where $f(z; n_{\rm d})$ is the χ^2 p.d.f. and $n_{\rm d}$ is the appropriate number of degrees of freedom. Values can be obtained from Fig. 32.1 or from the CERNLIB routine `PROB`. If the conditions for using the χ^2 p.d.f. do not hold, the statistic can still be defined as before, but its p.d.f. must be determined by other means in order to obtain the p-value, *e.g.*, using a Monte Carlo calculation.

Since the mean of the χ^2 distribution is equal to $n_{\rm d}$, one expects in a "reasonable" experiment to obtain $\chi^2 \approx n_{\rm d}$. Hence the quantity $\chi^2/n_{\rm d}$ is sometimes reported. Since the p.d.f. of $\chi^2/n_{\rm d}$ depends on $n_{\rm d}$, however, one must report $n_{\rm d}$ as well in order to make a meaningful statement. The p-values obtained for different values of $\chi^2/n_{\rm d}$ are shown in Fig. 32.2.

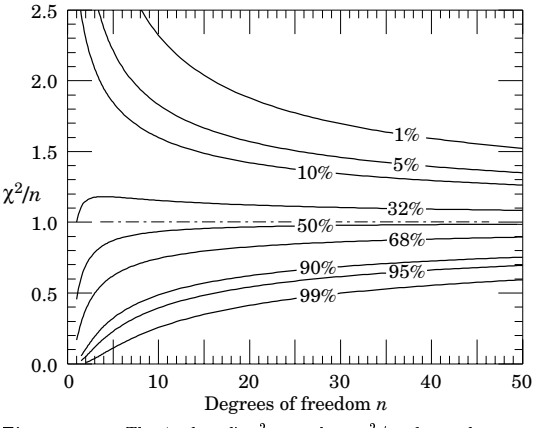

Figure 32.2: The 'reduced' χ^2, equal to χ^2/n, for n degrees of freedom. The curves show as a function of n the χ^2/n that corresponds to a given p-value.

32.3. Confidence intervals and limits

When the goal of an experiment is to determine a parameter θ, the result is usually expressed by quoting, in addition to the point estimate, some sort of interval which reflects the statistical precision of the measurement. In the simplest case this can be given by the parameter's estimated value $\widehat{\theta}$ plus or minus an estimate of the standard deviation of $\widehat{\theta}$, $\sigma_{\widehat{\theta}}$. If, however, the p.d.f. of the estimator is not Gaussian or if there are physical boundaries on the possible values of the parameter, then one usually quotes instead an interval according to one of the procedures described below.

In reporting an interval or limit, the experimenter may wish to

- communicate as objectively as possible the result of the experiment;
- provide an interval that is constructed to cover the true value of the parameter with a specified probability;
- provide the information needed by the consumer of the result to draw conclusions about the parameter or to make a particular decision;
- draw conclusions about the parameter that incorporate stated prior beliefs.

With a sufficiently large data sample, the point estimate and standard deviation (or for the multiparameter case, the parameter estimates and covariance matrix) satisfy essentially all of these goals. For finite data samples, no single method for quoting an interval will achieve all of them. In particular, drawing conclusions about the parameter in the framework of Bayesian statistics necessarily requires subjective input.

In addition to the goals listed above, the choice of method may be influenced by practical considerations such as ease of producing an interval from the results of several measurements. Of course the experimenter is not restricted to quoting a single interval or limit; one may choose, for example, first to communicate the result with a confidence interval having certain frequentist properties, and then in addition to draw conclusions about a parameter using Bayesian statistics. It is recommended, however, that there be a clear separation between these two aspects of reporting a result. In the remainder of this section we assess the extent to which various types of intervals achieve the goals stated here.

32.3.1. *The Bayesian approach*:

Suppose the outcome of the experiment is characterized by a vector of data $\boldsymbol{x}$, whose probability distribution depends on an unknown parameter (or parameters) $\boldsymbol{\theta}$ that we wish to determine. In Bayesian statistics, all knowledge about $\boldsymbol{\theta}$ is summarized by the posterior p.d.f. $p(\boldsymbol{\theta}|\boldsymbol{x})$, which gives the degree of belief for $\boldsymbol{\theta}$ to take on values in a certain region given the data $\boldsymbol{x}$. It is obtained by using Bayes' theorem,

$$p(\boldsymbol{\theta}|\boldsymbol{x}) = \frac{L(\boldsymbol{x}|\boldsymbol{\theta})\pi(\boldsymbol{\theta})}{\int L(\boldsymbol{x}|\boldsymbol{\theta}')\pi(\boldsymbol{\theta}')\,d\boldsymbol{\theta}'}\,, \tag{32.30}$$

where $L(\boldsymbol{x}|\boldsymbol{\theta})$ is the likelihood function, *i.e.*, the joint p.d.f. for the data given a certain value of $\boldsymbol{\theta}$, evaluated with the data actually obtained in the experiment, and $\pi(\boldsymbol{\theta})$ is the prior p.d.f. for $\boldsymbol{\theta}$. Note that the denominator in (32.30) serves simply to normalize the posterior p.d.f. to unity.

Bayesian statistics supplies no fundamental rule for determining $\pi(\boldsymbol{\theta})$; this reflects the experimenter's subjective degree of belief about $\boldsymbol{\theta}$ before the measurement was carried out. By itself, therefore, the posterior p.d.f. is not a good way to report objectively the result of an observation, since it contains both the result (through the likelihood function) and the experimenter's prior beliefs. Without the likelihood function, someone with different prior beliefs would be unable to substitute these to determine his or her own posterior p.d.f. This is an important reason, therefore, to publish wherever possible the likelihood function or an appropriate summary of it. Often this can be achieved by reporting the ML estimate and one or several low order derivatives of L evaluated at the estimate.

In the single parameter case, for example, an interval (called a Bayesian or credible interval) $[\theta_{\rm lo}, \theta_{\rm up}]$ can be determined which contains a given fraction $1-\alpha$ of the probability, *i.e.*,

$$1-\alpha = \int_{\theta_{\rm lo}}^{\theta_{\rm up}} p(\theta|\boldsymbol{x})\,d\theta\,. \tag{32.31}$$

Sometimes an upper or lower limit is desired, *i.e.*, $\theta_{\rm lo}$ can be set to zero or $\theta_{\rm up}$ to infinity. In other cases one might choose $\theta_{\rm lo}$ and $\theta_{\rm up}$ such that $p(\theta|\boldsymbol{x})$ is higher everywhere inside the interval than outside; these are called *highest posterior density* (HPD) intervals. Note that HPD intervals are not invariant under a nonlinear transformation of the parameter.

The main difficulty with Bayesian intervals is in quantifying the prior beliefs. Sometimes one attempts to construct $\pi(\boldsymbol{\theta})$ to represent complete ignorance about the parameters by setting it equal to a constant. A problem here is that if the prior p.d.f. is flat in $\boldsymbol{\theta}$, then it is not flat for a nonlinear function of $\boldsymbol{\theta}$, and so a different parametrization of the problem would lead in general to a different posterior p.d.f. In fact, one rarely chooses a flat prior as a true expression of degree of belief about a parameter; rather, it is used as a recipe to construct an interval, which in the end will have certain frequentist properties.

If a parameter is constrained to be non-negative, then the prior p.d.f. can simply be set to zero for negative values. An important example is the case of a Poisson variable n which counts signal events with unknown mean s as well as background with mean b, assumed known. For the signal mean s one often uses the prior

$$\pi(s) = \begin{cases} 0 & s < 0 \\ 1 & s \geq 0 \end{cases}\,. \tag{32.32}$$

As mentioned above, this is regarded as providing an interval whose frequentist properties can be studied, rather than as representing a degree of belief. In the absence of a clear discovery, (*e.g.*, if $n = 0$ or if in any case n is compatible with the expected background), one usually wishes to place an upper limit on s. Using the likelihood function for Poisson distributed n,

$$L(n|s) = \frac{(s+b)^n}{n!}e^{-(s+b)}\,, \tag{32.33}$$

along with the prior (32.32) in (32.30) gives the posterior density for s. An upper limit $s_{\rm up}$ at confidence level $1-\alpha$ can be obtained by requiring

$$1-\alpha = \int_{-\infty}^{s_{\rm up}} p(s|n)ds = \frac{\int_{-\infty}^{s_{\rm up}} L(n|s)\,\pi(s)\,ds}{\int_{-\infty}^{\infty} L(n|s)\,\pi(s)\,ds}\,, \tag{32.34}$$

where the lower limit of integration is effectively zero because of the cut-off in $\pi(s)$. By relating the integrals in Eq. (32.34) to incomplete gamma functions, the equation reduces to

$$\alpha = e^{-s_{\rm up}}\frac{\sum_{m=0}^{n}(s_{\rm up}+b)^m/m!}{\sum_{m=0}^{n} b^m/m!}\,. \tag{32.35}$$

This must be solved numerically for the limit $s_{\rm up}$. For the special case of $b = 0$, the sums can be related to the *quantile* $F_{\chi^2}^{-1}$ of the χ^2 distribution (inverse of the cumulative distribution) to give

$$s_{\rm up} = \tfrac{1}{2}F_{\chi^2}^{-1}(1-\alpha; n_{\rm d})\,, \tag{32.36}$$

where the number of degrees of freedom is $n_{\rm d} = 2(n+1)$. The quantile of the χ^2 distribution can be obtained using the CERNLIB routine `CHISIN`. It so happens that for the case of $b = 0$, the upper limits from Eq. (32.36) coincide numerically with the values of the frequentist upper limits discussed in Section 32.3.2.4. Values for $1-\alpha = 0.9$ and 0.95 are given by the values $\nu_{\rm up}$ in Table 32.3. The frequentist properties of confidence intervals for the Poisson mean obtained in this way are discussed in Refs. [2] and [11].

Bayesian statistics provides a framework for incorporating systematic uncertainties into a result. Suppose, for example, that a model depends not only on parameters of interest $\boldsymbol{\theta}$ but on *nuisance parameters* $\boldsymbol{\nu}$, whose values are known with some limited accuracy. For a single nuisance parameter ν, for example, one might have a p.d.f. centered about its nominal value with a certain standard deviation σ_ν. Often a Gaussian p.d.f. provides a reasonable model for one's degree of belief about a nuisance parameter; in other cases more complicated shapes may be appropriate. The likelihood function, prior and posterior p.d.f.s then all depend on both $\boldsymbol{\theta}$ and $\boldsymbol{\nu}$ and are related by Bayes' theorem as usual. One can obtain the posterior p.d.f. for $\boldsymbol{\theta}$ alone by integrating over the nuisance parameters, *i.e.*,

$$p(\boldsymbol{\theta}|\boldsymbol{x}) = \int p(\boldsymbol{\theta}, \boldsymbol{\nu}|\boldsymbol{x})\, d\boldsymbol{\nu}\ . \tag{32.37}$$

If the prior joint p.d.f. for $\boldsymbol{\theta}$ and $\boldsymbol{\nu}$ factorizes, then integrating the posterior p.d.f. over $\boldsymbol{\nu}$ is equivalent to replacing the likelihood function by (see Ref. [12]),

$$L'(\boldsymbol{x}|\boldsymbol{\theta}) = \int L(\boldsymbol{x}|\boldsymbol{\theta}, \boldsymbol{\nu})\pi(\boldsymbol{\nu})\, d\boldsymbol{\nu}\ . \tag{32.38}$$

The function $L'(\boldsymbol{x}|\boldsymbol{\theta})$ can also be used together with frequentist methods that employ the likelihood function such as ML estimation of parameters. The results then have a mixed frequentist/Bayesian character, where the systematic uncertainty due to limited knowledge of the nuisance parameters is built in. Although this may make it more difficult to disentangle statistical from systematic effects, such a hybrid approach may satisfy the objective of reporting the result in a convenient way.

Even if the subjective Bayesian approach is not used explicitly, Bayes' theorem represents the way that people evaluate the impact of a new result on their beliefs. One of the criteria in choosing a method for reporting a measurement, therefore, should be the ease and convenience with which the consumer of the result can carry out this exercise.

32.3.2. *Frequentist confidence intervals*:

The unqualified phrase "confidence intervals" refers to frequentist intervals obtained with a procedure due to Neyman [13], described below. These are intervals (or in the multiparameter case, regions) constructed so as to include the true value of the parameter with a probability greater than or equal to a specified level, called the *coverage probability*. In this section we discuss several techniques for producing intervals that have, at least approximately, this property.

32.3.2.1. *The Neyman construction for confidence intervals:*

Consider a p.d.f. $f(x;\theta)$ where x represents the outcome of the experiment and θ is the unknown parameter for which we want to construct a confidence interval. The variable x could (and often does) represent an estimator for θ. Using $f(x;\theta)$ we can find for a pre-specified probability $1-\alpha$ and for every value of θ a set of values $x_1(\theta,\alpha)$ and $x_2(\theta,\alpha)$ such that

$$P(x_1 < x < x_2; \theta) = 1-\alpha = \int_{x_1}^{x_2} f(x;\theta)\, dx\ . \tag{32.39}$$

This is illustrated in Fig. 32.3: a horizontal line segment $[x_1(\theta,\alpha), x_2(\theta,\alpha)]$ is drawn for representative values of θ. The union of such intervals for all values of θ, designated in the figure as $D(\alpha)$, is known as the *confidence belt*. Typically the curves $x_1(\theta,\alpha)$ and $x_2(\theta,\alpha)$ are monotonic functions of θ, which we assume for this discussion.

Upon performing an experiment to measure x and obtaining a value x_0, one draws a vertical line through x_0. The confidence interval for θ is the set of all values of θ for which the corresponding line segment $[x_1(\theta,\alpha), x_2(\theta,\alpha)]$ is intercepted by this vertical line. Such confidence intervals are said to have a *confidence level* (CL) equal to $1-\alpha$.

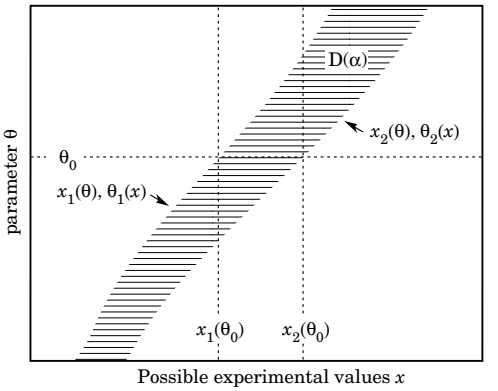

Figure 32.3: Construction of the confidence belt (see text).

Now suppose that the true value of θ is θ_0, indicated in the figure. We see from the figure that θ_0 lies between $\theta_1(x)$ and $\theta_2(x)$ if and only if x lies between $x_1(\theta_0)$ and $x_2(\theta_0)$. The two events thus have the same probability, and since this is true for any value θ_0, we can drop the subscript 0 and obtain

$$1-\alpha = P(x_1(\theta) < x < x_2(\theta)) = P(\theta_2(x) < \theta < \theta_1(x))\ . \tag{32.40}$$

In this probability statement $\theta_1(x)$ and $\theta_2(x)$, *i.e.*, the endpoints of the interval, are the random variables and θ is an unknown constant. If the experiment were to be repeated a large number of times, the interval $[\theta_1, \theta_2]$ would vary, covering the fixed value θ in a fraction $1-\alpha$ of the experiments.

The condition of coverage Eq. (32.39) does not determine x_1 and x_2 uniquely and additional criteria are needed. The most common criterion is to choose *central intervals* such that the probabilities excluded below x_1 and above x_2 are each $\alpha/2$. In other cases one may want to report only an upper or lower limit, in which case the probability excluded below x_1 or above x_2 can be set to zero. Another principle based on *likelihood ratio ordering* for determining which values of x should be included in the confidence belt is discussed in Sec. 32.3.2.2

When the observed random variable x is continuous, the coverage probability obtained with the Neyman construction is $1-\alpha$, regardless of the true value of the parameter. If x is discrete, however, it is not possible to find segments $[x_1(\theta,\alpha), x_2(\theta,\alpha)]$ that satisfy (32.39) exactly for all values of θ. By convention one constructs the confidence belt requiring the probability $P(x_1 < x < x_2)$ to be *greater than or equal to* $1-\alpha$. This gives confidence intervals that include the true parameter with a probability greater than or equal to $1-\alpha$.

32.3.2.2. *Relationship between intervals and tests:*

An equivalent method of constructing confidence intervals is to consider a test (see Sec. 32.2) of the hypothesis that the parameter's true value is θ. One then excludes all values of θ where the hypothesis would be rejected at a significance level less than α. The remaining values constitute the confidence interval at confidence level $1-\alpha$.

In this procedure one is still free to choose the test to be used; this corresponds to the freedom in the Neyman construction as to which values of the data are included in the confidence belt. One possibility is use a test statistic based on the *likelihood ratio*,

$$\lambda = \frac{f(x;\theta)}{f(x;\widehat{\theta}\,)}\ , \tag{32.41}$$

where $\widehat{\theta}$ is the value of the parameter which, out of all allowed values, maximizes $f(x;\theta)$. This results in the intervals described in [14] by Feldman and Cousins. The same intervals can be obtained from the Neyman construction described in the previous section by including in the confidence belt those values of x which give the greatest values of λ.

Table 32.1: Area of the tails α outside $\pm\delta$ from the mean of a Gaussian distribution.

α (%)	δ	α (%)	δ
31.73	1σ	20	1.28σ
4.55	2σ	10	1.64σ
0.27	3σ	5	1.96σ
6.3×10^{-3}	4σ	1	2.58σ
5.7×10^{-5}	5σ	0.1	3.29σ
2.0×10^{-7}	6σ	0.01	3.89σ

Another technique that can be formulated in the language of statistical tests has been used to set limits on the Higgs mass from measurements at LEP [15,16]. For each value of the Higgs mass, a statistic called $\mathrm{CL_s}$ is determined from the ratio

$$\mathrm{CL_s} = \frac{p\text{-value of signal plus background hypothesis}}{1 - p\text{-value of hypothesis of background only}} \,. \qquad (32.42)$$

The p-values in (32.42) are themselves based on a goodness-of-fit statistic which depends in general on the signal being tested, *i.e.*, on the hypothesized Higgs mass. Smaller $\mathrm{CL_s}$ corresponds to a lesser level of agreement with the signal hypothesis.

In the usual procedure for constructing confidence intervals, one would exclude the signal hypothesis if the probability to obtain a value of $\mathrm{CL_s}$ less than the one actually observed is less than α. The LEP Higgs group has in fact followed a more conservative approach and excludes the signal at a confidence level $1-\alpha$ if $\mathrm{CL_s}$ itself (not the probability to obtain a lower $\mathrm{CL_s}$ value) is less than α. This results in a coverage probability that is in general greater than $1-\alpha$. The interpretation of such intervals is discussed in [15,16].

32.3.2.3. *Gaussian distributed measurements:*

An important example of constructing a confidence interval is when the data consists of a single random variable x that follows a Gaussian distribution; this is often the case when x represents an estimator for a parameter and one has a sufficiently large data sample. If there is more than one parameter being estimated, the multivariate Gaussian is used. For the univariate case with known σ,

$$1-\alpha = \frac{1}{\sqrt{2\pi}\sigma}\int_{\mu-\delta}^{\mu+\delta} e^{-(x-\mu)^2/2\sigma^2}\,dx = \mathrm{erf}\left(\frac{\delta}{\sqrt{2}\,\sigma}\right) \qquad (32.43)$$

is the probability that the measured value x will fall within $\pm\delta$ of the true value μ. From the symmetry of the Gaussian with respect to x and μ, this is also the probability for the interval $x \pm \delta$ to include μ. Fig. 32.4 shows a $\delta = 1.64\sigma$ confidence interval unshaded. The choice $\delta = \sigma$ gives an interval called the *standard error* which has $1-\alpha = 68.27\%$ if σ is known. Values of α for other frequently used choices of δ are given in Table 32.1.

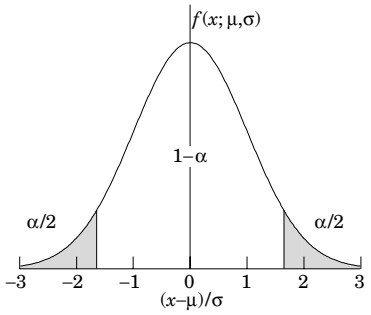

Figure 32.4: Illustration of a symmetric 90% confidence interval (unshaded) for a measurement of a single quantity with Gaussian errors. Integrated probabilities, defined by α, are as shown.

We can set a one-sided (upper or lower) limit by excluding above $x+\delta$ (or below $x-\delta$). The values of α for such limits are half the values in Table 32.1.

In addition to Eq. (32.43), α and δ are also related by the cumulative distribution function for the χ^2 distribution,

$$\alpha = 1 - F(\chi^2; n) \,, \qquad (32.44)$$

for $\chi^2 = (\delta/\sigma)^2$ and $n = 1$ degree of freedom. This can be obtained from Fig. 32.1 on the $n = 1$ curve or by using the CERNLIB routine `PROB`.

For multivariate measurements of, say, n parameter estimates $\widehat{\boldsymbol{\theta}} = (\widehat{\theta}_1, \ldots, \widehat{\theta}_n)$, one requires the full covariance matrix $V_{ij} = \mathrm{cov}[\widehat{\theta}_i, \widehat{\theta}_j]$, which can be estimated as described in Sections 32.1.2 and 32.1.3. Under fairly general conditions with the methods of maximum-likelihood or least-squares in the large sample limit, the estimators will be distributed according to a multivariate Gaussian centered about the true (unknown) values $\boldsymbol{\theta}$, and furthermore the likelihood function itself takes on a Gaussian shape.

The standard error ellipse for the pair $(\widehat{\theta}_i, \widehat{\theta}_j)$ is shown in Fig. 32.5, corresponding to a contour $\chi^2 = \chi^2_{\mathrm{min}} + 1$ or $\ln L = \ln L_{\mathrm{max}} - 1/2$. The ellipse is centered about the estimated values $\widehat{\boldsymbol{\theta}}$, and the tangents to the ellipse give the standard deviations of the estimators, σ_i and σ_j. The angle of the major axis of the ellipse is given by

$$\tan 2\phi = \frac{2\rho_{ij}\sigma_i\sigma_j}{\sigma_i^2 - \sigma_j^2} \,, \qquad (32.45)$$

where $\rho_{ij} = \mathrm{cov}[\widehat{\theta}_i, \widehat{\theta}_j]/\sigma_i\sigma_j$ is the correlation coefficient.

The correlation coefficient can be visualized as the fraction of the distance σ_i from the ellipse's horizontal centerline at which the ellipse becomes tangent to vertical, *i.e.* at the distance $\rho_{ij}\sigma_i$ below the centerline as shown. As ρ_{ij} goes to $+1$ or -1, the ellipse thins to a diagonal line.

It could happen that one of the parameters, say, θ_j, is known from previous measurements to a precision much better than σ_j so that the current measurement contributes almost nothing to the knowledge of θ_j. However, the current measurement of of θ_i and its dependence on θ_j may still be important. In this case, instead of quoting both parameter estimates and their correlation, one sometimes reports the value of θ_i which minimizes χ^2 at a fixed value of θ_j, such as the PDG best value. This θ_i value lies along the dotted line between the points where the ellipse becomes tangent to vertical, and has statistical error σ_{inner} as shown on the figure, where $\sigma_{\mathrm{inner}} = (1-\rho_{ij}^2)^{1/2}\sigma_i$. Instead of the correlation ρ_{ij}, one reports the dependency $d\widehat{\theta}_i/d\theta_j$ which is the slope of the dotted line. This slope is related to the correlation coefficient by $d\widehat{\theta}_i/d\theta_j = \rho_{ij} \times \frac{\sigma_i}{\sigma_j}$.

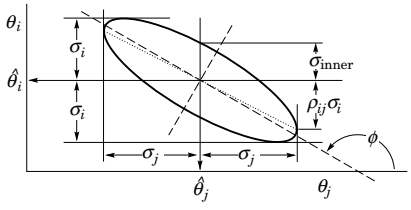

Figure 32.5: Standard error ellipse for the estimators $\widehat{\theta}_i$ and $\widehat{\theta}_j$. In this case the correlation is negative.

As in the single-variable case, because of the symmetry of the Gaussian function between $\boldsymbol{\theta}$ and $\widehat{\boldsymbol{\theta}}$, one finds that contours of constant $\ln L$ or χ^2 cover the true values with a certain, fixed probability. That is, the confidence region is determined by

$$\ln L(\boldsymbol{\theta}) \geq \ln L_{\mathrm{max}} - \Delta \ln L \,, \qquad (32.46)$$

Table 32.2: $\Delta\chi^2$ or $2\Delta\ln L$ corresponding to a coverage probability $1-\alpha$ in the large data sample limit, for joint estimation of m parameters.

$(1-\alpha)$ (%)	$m=1$	$m=2$	$m=3$
68.27	1.00	2.30	3.53
90.	2.71	4.61	6.25
95.	3.84	5.99	7.82
95.45	4.00	6.18	8.03
99.	6.63	9.21	11.34
99.73	9.00	11.83	14.16

or where a χ^2 has been defined for use with the method of least squares,

$$\chi^2(\boldsymbol{\theta}) \leq \chi^2_{\rm min} + \Delta\chi^2 \,. \tag{32.47}$$

Values of $\Delta\chi^2$ or $2\Delta\ln L$ are given in Table 32.2 for several values of the coverage probability and number of fitted parameters.

For finite data samples, the probability for the regions determined by Equations (32.46) or (32.47) to cover the true value of $\boldsymbol{\theta}$ will depend on $\boldsymbol{\theta}$, so these are not exact confidence regions according to our previous definition. Nevertheless, they can still have a coverage probability only weakly dependent on the true parameter and approximately as given in Table 32.2. In any case the coverage probability of the intervals or regions obtained according to this procedure can in principle be determined as a function of the true parameter(s), for example, using a Monte Carlo calculation.

One of the practical advantages of intervals that can be constructed from the log-likelihood function or χ^2 is that it is relatively simple to produce the interval for the combination of several experiments. If N independent measurements result in log-likelihood functions $\ln L_i(\boldsymbol{\theta})$, then the combined log-likelihood function is simply the sum,

$$\ln L(\boldsymbol{\theta}) = \sum_{i=1}^{N} \ln L_i(\boldsymbol{\theta}) \,. \tag{32.48}$$

This can then be used to determine an approximate confidence interval or region with Equation (32.46), just as with a single experiment.

32.3.2.4. *Poisson or binomial data:*

Another important class of measurements consists of counting a certain number of events n. In this section we will assume these are all events of the desired type, *i.e.*, there is no background. If n represents the number of events produced in a reaction with cross section σ, say, in a fixed integrated luminosity $\mathcal{L}$, then it follows a Poisson distribution with mean $\nu = \sigma\mathcal{L}$. If, on the other hand, one has selected a larger sample of N events and found n of them to have a particular property, then n follows a binomial distribution where the parameter p gives the probability for the event to possess the property in question. This is appropriate, *e.g.*, for estimates of branching ratios or selection efficiencies based on a given total number of events.

For the case of Poisson distributed n, the upper and lower limits on the mean value ν can be found from the Neyman procedure to be

$$\nu_{\rm lo} = \tfrac{1}{2} F^{-1}_{\chi^2}(\alpha_{\rm lo}; 2n) \,, \tag{32.49a}$$

$$\nu_{\rm up} = \tfrac{1}{2} F^{-1}_{\chi^2}(1-\alpha_{\rm up}; 2(n+1)) \,, \tag{32.49b}$$

where the upper and lower limits are at confidence levels of $1-\alpha_{\rm lo}$ and $1-\alpha_{\rm up}$, respectively, and $F^{-1}_{\chi^2}$ is the *quantile* of the χ^2 distribution (inverse of the cumulative distribution). The quantiles $F^{-1}_{\chi^2}$ can be obtained from standard tables or from the CERNLIB routine `CHISIN`. For central confidence intervals at confidence level $1-\alpha$, set $\alpha_{\rm lo} = \alpha_{\rm up} = \alpha/2$.

It happens that the upper limit from (32.49a) coincides numerically with the Bayesian upper limit for a Poisson parameter using a uniform prior p.d.f. for ν. Values for confidence levels of 90% and 95% are shown in Table 32.3.

Table 32.3: Lower and upper (one-sided) limits for the mean ν of a Poisson variable given n observed events in the absence of background, for confidence levels of 90% and 95%.

	$1-\alpha$ =90%		$1-\alpha$ =95%	
n	$\nu_{\rm lo}$	$\nu_{\rm up}$	$\nu_{\rm lo}$	$\nu_{\rm up}$
0	–	2.30	–	3.00
1	0.105	3.89	0.051	4.74
2	0.532	5.32	0.355	6.30
3	1.10	6.68	0.818	7.75
4	1.74	7.99	1.37	9.15
5	2.43	9.27	1.97	10.51
6	3.15	10.53	2.61	11.84
7	3.89	11.77	3.29	13.15
8	4.66	12.99	3.98	14.43
9	5.43	14.21	4.70	15.71
10	6.22	15.41	5.43	16.96

For the case of binomially distributed n successes out of N trials with probability of success p, the upper and lower limits on p are found to be

$$p_{\rm lo} = \frac{nF^{-1}_F[\alpha_{\rm lo}; 2n, 2(N-n+1)]}{N-n+1+nF^{-1}_F[\alpha_{\rm lo}; 2n, 2(N-n+1)]} \,, \tag{32.50a}$$

$$p_{\rm up} = \frac{(n+1)F^{-1}_F[1-\alpha_{\rm up}; 2(n+1), 2(N-n)]}{(N-n)+(n+1)F^{-1}_F[1-\alpha_{\rm up}; 2(n+1), 2(N-n)]} \,. \tag{32.50b}$$

Here F^{-1}_F is the quantile of the F distribution (also called the Fisher–Snedecor distribution; see Ref. [4]).

32.3.2.5. *Difficulties with intervals near a boundary:*

A number of issues arise in the construction and interpretation of confidence intervals when the parameter can only take on values in a restricted range. An important example is where the mean of a Gaussian variable is constrained on physical grounds to be non-negative. This arises, for example, when the square of the neutrino mass is estimated from $\widehat{m}^2 = \widehat{E}^2 - \widehat{p}^2$, where $\widehat{E}$ and $\widehat{p}$ are independent, Gaussian distributed estimates of the energy and momentum. Although the true m^2 is constrained to be positive, random errors in $\widehat{E}$ and $\widehat{p}$ can easily lead to negative values for the estimate $\widehat{m}^2$.

If one uses the prescription given above for Gaussian distributed measurements, which says to construct the interval by taking the estimate plus or minus one standard deviation, then this can give intervals that are partially or entirely in the unphysical region. In fact, by following strictly the Neyman construction for the central confidence interval, one finds that the interval is truncated below zero; nevertheless an extremely small or even a zero-length interval can result.

An additional important example is where the experiment consists of counting a certain number of events, n, which is assumed to be Poisson distributed. Suppose the expectation value $E[n] = \nu$ is equal to $s+b$, where s and b are the means for signal and background processes, and assume further that b is a known constant. Then $\widehat{s} = n - b$ is an unbiased estimator for s. Depending on true magnitudes of s and b, the estimate $\widehat{s}$ can easily fall in the negative region. Similar to the Gaussian case with the positive mean, the central confidence interval or even the upper limit for s may be of zero length.

The confidence interval is in fact designed not to cover the parameter with a probability of at most α, and if a zero-length interval results, then this is evidently one of those experiments. So

although the construction is behaving as it should, a null interval is an unsatisfying result to report and several solutions to this type of problem are possible.

An additional difficulty arises when a parameter estimate is not significantly far away from the boundary, in which case it is natural to report a one-sided confidence interval (often an upper limit). It is straightforward to force the Neyman prescription to produce only an upper limit by setting $x_2 = \infty$ in Eq. 32.39. Then x_1 is uniquely determined and the upper limit can be obtained. If, however, the data come out such that the parameter estimate is not so close to the boundary, one might wish to report a central (*i.e.*, two-sided) confidence interval. As pointed out by Feldman and Cousins [14], however, if the decision to report an upper limit or two-sided interval is made by looking at the data ("flip-flopping"), then the resulting intervals will not in general cover the parameter with the probability $1 - \alpha$.

With the confidence intervals suggested in [14], the prescription determines whether the interval is one- or two-sided in a way which preserves the coverage probability. Intervals with this property are said to be *unified*. Furthermore, the Feldman–Cousins prescription is such that null intervals do not occur. For a given choice of $1 - \alpha$, if the parameter estimate is sufficiently close to the boundary, then the method gives a one-sided limit. In the case of a Poisson variable in the presence of background, for example, this would occur if the number of observed events is compatible with the expected background. For parameter estimates increasingly far away from the boundary, i.e., for increasing signal significance, the interval makes a smooth transition from one- to two-sided, and far away from the boundary one obtains a central interval.

The intervals according to this method for the mean of Poisson variable in the absence of background are given in Table 32.4. (Note that α in [14] is defined following Neyman [13] as the coverage probability; this is opposite the modern convention used here in which the coverage probability is $1 - \alpha$.) The values of $1 - \alpha$ given here refer to the coverage of the true parameter by the whole interval $[\nu_1, \nu_2]$. In Table 32.3 for the one-sided upper and lower limits, however, $1 - \alpha$ refers to the probability to have individually $\nu_{\rm up} \geq \nu$ or $\nu_{\rm lo} \leq \nu$.

Table 32.4: Unified confidence intervals $[\nu_1, \nu_2]$ for a the mean of a Poisson variable given n observed events in the absence of background, for confidence levels of 90% and 95%.

	$1-\alpha$ =90%		$1-\alpha$ =95%	
n	ν_1	ν_2	ν_1	ν_2
0	0.00	2.44	0.00	3.09
1	0.11	4.36	0.05	5.14
2	0.53	5.91	0.36	6.72
3	1.10	7.42	0.82	8.25
4	1.47	8.60	1.37	9.76
5	1.84	9.99	1.84	11.26
6	2.21	11.47	2.21	12.75
7	3.56	12.53	2.58	13.81
8	3.96	13.99	2.94	15.29
9	4.36	15.30	4.36	16.77
10	5.50	16.50	4.75	17.82

A potential difficulty with unified intervals arises if, for example, one constructs such an interval for a Poisson parameter s of some yet to be discovered signal process with, say, $1 - \alpha = 0.9$. If the true signal parameter is zero, or in any case much less than the expected background, one will usually obtain a one-sided upper limit on s. In a certain fraction of the experiments, however, a two-sided interval for s will result. Since, however, one typically chooses $1 - \alpha$ to be only 0.9 or 0.95 when searching for a new effect, the value $s = 0$ may be excluded from the interval before the existence of the effect is well established. It must then be communicated carefully that in excluding $s = 0$ from the interval, one is not necessarily claiming to have discovered the effect.

The intervals constructed according to the unified procedure in [14] for a Poisson variable n consisting of signal and background have the property that for $n = 0$ observed events, the upper limit decreases for increasing expected background. This is counter-intuitive, since it is known that if $n = 0$ for the experiment in question, then no background was observed, and therefore one may argue that the expected background should not be relevant. The extent to which one should regard this feature as a drawback is a subject of some controversy (see, *e.g.*, Ref. [18]).

Another possibility is to construct a Bayesian interval as described in Section 32.3.1. The presence of the boundary can be incorporated simply by setting the prior density to zero in the unphysical region. Priors based on invariance principles (rather than subjective degree of belief) for the Poisson mean are rarely used in high energy physics; they diverge for the case of zero events observed, and they give upper limits which undercover when evaluated by the frequentist definition of coverage [2]. Rather, priors uniform in the Poisson mean have been used, although as previously mentioned, this is generally not done to reflect the experimenter's degree of belief but rather as a procedure for obtaining an interval with certain frequentist properties. The resulting upper limits have a coverage probability that depends on the true value of the Poisson parameter and is everywhere greater than the stated probability content. Lower limits and two-sided intervals for the Poisson mean based on flat priors undercover, however, for some values of the parameter, although to an extent that in practical cases may not be too severe [2, 11]. Intervals constructed in this way have the advantage of being easy to derive; if several independent measurements are to be combined then one simply multiplies the likelihood functions (cf. Eq. (32.48)).

An additional alternative is presented by the intervals found from the likelihood function or χ^2 using the prescription of Equations (32.46) or (32.47). As in the case of the Bayesian intervals, the coverage probability is not, in general, independent of the true parameter. Furthermore, these intervals can for some parameter values undercover. The coverage probability can of course be determined with some extra effort and reported with the result.

Also as in the Bayesian case, intervals derived from the value of the likelihood function from a combination of independent experiments can be determined simply by multiplying the likelihood functions. These intervals are also invariant under transformation of the parameter; this is not true for Bayesian intervals with a conventional flat prior, because a uniform distribution in, say, θ will not be uniform if transformed to θ^2. Use of the likelihood function to determine approximate confidence intervals is discussed further in [17].

In any case it is important always to report sufficient information so that the result can be combined with other measurements. Often this means giving an unbiased estimator and its standard deviation, even if the estimated value is in the unphysical region.

Regardless of the type of interval reported, the consumer of that result will almost certainly use it to derive some impression about the value of the parameter. This will inevitably be done, either explicitly or intuitively, with Bayes' theorem,

$$p(\theta|\text{result}) \propto L(\text{result}|\theta)\pi(\theta)\ , \tag{32.51}$$

where the reader supplies his or her own prior beliefs $\pi(\theta)$ about the parameter, and the 'result' is whatever sort of interval or other information the author has reported. For all of the intervals discussed, therefore, it is not sufficient to know the result; one must also know the probability to have obtained this result as a function of the parameter, *i.e.*, the likelihood. Contours of constant likelihood, for example, provide this information, and so an interval obtained from $\ln L = \ln L_{\rm max} - \Delta \ln L$ already takes one step in this direction.

It can also be useful with a frequentist interval to calculate its subjective probability content using the posterior p.d.f. based on one or several reasonable guesses for the prior p.d.f. If it turns out to be significantly less than the stated confidence level, this warns that

it would be particularly misleading to draw conclusions about the parameter's value without further information from the likelihood.

References:

1. B. Efron, Am. Stat. **40**, 11 (1986).
2. R.D. Cousins, Am. J. Phys. **63**, 398 (1995).
3. A. Stuart, A.K. Ord, and Arnold, *Kendall's Advanced Theory of Statistics*, Vol. 2 *Classical Inference and Relationship* 6th Ed., (Oxford Univ. Press, 1998), and earlier editions by Kendall and Stuart. The likelihood-ratio ordering principle is described at the beginning of Ch. 23. Chapter 26 compares different schools of statistical inference.
4. W.T. Eadie, D. Drijard, F.E. James, M. Roos, and B. Sadoulet, *Statistical Methods in Experimental Physics* (North Holland, Amsterdam and London, 1971).
5. H. Cramér, *Mathematical Methods of Statistics,* Princeton Univ. Press, New Jersey (1958).
6. L. Lyons, *Statistics for Nuclear and Particle Physicists* (Cambridge University Press, New York, 1986).
7. R. Barlow, Nucl. Inst. Meth. A **297**, 496 (1990).
8. G. Cowan, *Statistical Data Analysis* (Oxford University Press, Oxford, 1998).
9. For a review, see S. Baker and R. Cousins, Nucl. Instrum. Methods **221**, 437 (1984).
10. For information on neural networks and related topics, see *e.g.* C.M. Bishop, *Neural Networks for Pattern Recognition*, Clarendon Press, Oxford (1995); C. Peterson and T. Rögnvaldsson, An Introduction to Artificial Neural Networks, in *Proceedings of the 1991 CERN School of Computing*, C. Verkerk (ed.), CERN 92-02 (1992).
11. Byron P. Roe and Michael B. Woodroofe, Phys. Rev. **D63**, 13009 (2001).
12. Paul H. Garthwaite, Ian T. Jolliffe and Byron Jones, *Statistical Inference* (Prentice Hall, 1995).
13. J. Neyman, Phil. Trans. Royal Soc. London, Series A, **236**, 333 (1937), reprinted in *A Selection of Early Statistical Papers on J. Neyman* (University of California Press, Berkeley, 1967).
14. G.J. Feldman and R.D. Cousins, Phys. Rev. **D57**, 3873 (1998). This paper does not specify what to do if the ordering principle gives equal rank to some values of x. Eq. 23.6 of Ref. 3 gives the rule: all such points are included in the acceptance region (the domain $D(\alpha)$). Some authors have assumed the contrary, and shown that one can then obtain null intervals.
15. T. Junk, Nucl. Inst. Meth. A **434**, 435 (1999).
16. A.L. Read, *Modified frequentist analysis of search results (the CL_s method)*, in F. James, L. Lyons and Y. Perrin (eds.), *Workshop on Confidence Limits*, CERN Yellow Report 2000-005, available through `weblib.cern.ch`.
17. F. Porter, Nucl. Inst. Meth. A **368**, 793 (1996).
18. Workshop on Confidence Limits, CERN, 17-18 Jan. 2000, `www.cern.ch/CERN/Divisions/EP/Events/CLW/`. The proceedings, F. James, L. Lyons, and Y. Perrin (eds.), CERN Yellow Report 2000-005, are available through `weblib.cern.ch`. See also the later Fermilab workshop linked to the CERN web page.

33. MONTE CARLO TECHNIQUES

Revised July 1995 by S. Youssef (SCRI, Florida State University). Updated February 2000 by R. Cousins (UCLA) in consultation with F. James (CERN); October 2003 by G. Cowan (RHUL) and R. Miquel (LBNL)

Monte Carlo techniques are often the only practical way to evaluate difficult integrals or to sample random variables governed by complicated probability density functions. Here we describe an assortment of methods for sampling some commonly occurring probability density functions.

33.1. Sampling the uniform distribution

Most Monte Carlo sampling or integration techniques assume a "random number generator" which generates uniform statistically independent values on the half open interval $[0, 1)$. There is a long history of problems with various generators on a finite digital computer, but recently, the RANLUX generator [1] has emerged with a solid theoretical basis in chaos theory. Based on the method of Lüscher, it allows the user to select different quality levels, trading off quality with speed.

Other generators are also available which pass extensive batteries of tests for statistical independence and which have periods which are so long that, for practical purposes, values from these generators can be considered to be uniform and statistically independent. In particular, the lagged-Fibonacci based generator introduced by Marsaglia, Zaman, and Tsang [2] is efficient, has a period of approximately 10^{43}, produces identical sequences on a wide variety of computers and, passes the extensive "DIEHARD" battery of tests [3]. Many commonly available congruential generators fail these tests and often have sequences (typically with periods less than 2^{32}) which can be easily exhausted on modern computers and should therefore be avoided [4].

33.2. Inverse transform method

If the desired probability density function is $f(x)$ on the range $-\infty < x < \infty$, its cumulative distribution function (expressing the probability that $x \leq a$) is given by Eq. (31.6). If a is chosen with probability density $f(a)$, then the integrated probability up to point a, $F(a)$, is itself a random variable which will occur with uniform probability density on $[0, 1]$. If x can take on any value, and ignoring the endpoints, we can then find a unique x chosen from the p.d.f. $f(s)$ for a given u if we set

$$u = F(x) \, , \tag{33.1}$$

provided we can find an inverse of F, defined by

$$x = F^{-1}(u) \, . \tag{33.2}$$

This method is shown in Fig. 33.1a. It is most convenient when one can calculate by hand the inverse function of the indefinite integral of f. This is the case for some common functions $f(x)$ such as $\exp(x)$, $(1-x)^n$, and $1/(1+x^2)$ (Cauchy or Breit-Wigner), although it does not necessarily produce the fastest generator. CERNLIB contains routines to implement this method numerically, working from functions or histograms.

For a discrete distribution, $F(x)$ will have a discontinuous jump of size $f(x_k)$ at each allowed x_k, $k = 1, 2, \cdots$. Choose u from a uniform distribution on (0,1) as before. Find x_k such that

$$F(x_{k-1}) < u \leq F(x_k) \equiv \text{Prob}\,(x \leq x_k) = \sum_{i=1}^{k} f(x_i) \, ; \tag{33.3}$$

then x_k is the value we seek (note: $F(x_0) \equiv 0$). This algorithm is illustrated in Fig. 33.1b.

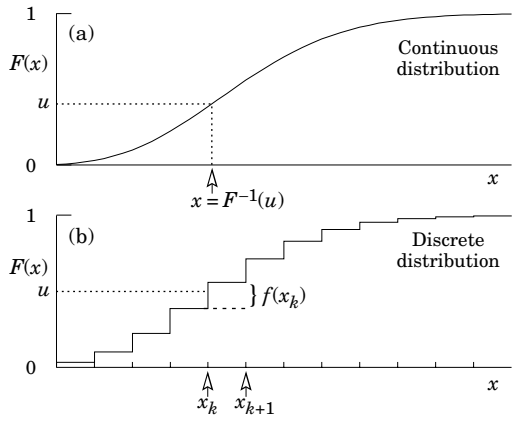

Figure 33.1: Use of a random number u chosen from a uniform distribution (0,1) to find a random number x from a distribution with cumulative distribution function $F(x)$.

33.3. Acceptance-rejection method (Von Neumann)

Very commonly an analytic form for $F(x)$ is unknown or too complex to work with, so that obtaining an inverse as in Eq. (33.2) is impractical. We suppose that for any given value of x the probability density function $f(x)$ can be computed and further that enough is known about $f(x)$ that we can enclose it entirely inside a shape which is C times an easily generated distribution $h(x)$ as illustrated in Fig. 33.2.

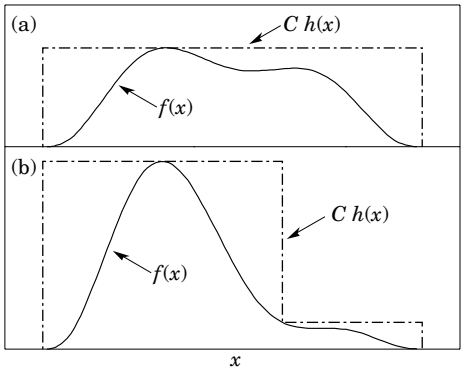

Figure 33.2: Illustration of the acceptance-rejection method. Random points are chosen inside the upper bounding figure, and rejected if the ordinate exceeds $f(x)$. Lower figure illustrates importance sampling.

Frequently $h(x)$ is uniform or is a normalized sum of uniform distributions. Note that both $f(x)$ and $h(x)$ must be normalized to unit area and therefore the proportionality constant $C > 1$. To generate $f(x)$, first generate a candidate x according to $h(x)$. Calculate $f(x)$ and the height of the envelope $C\,h(x)$; generate u and test if $uC\,h(x) \leq f(x)$. If so, accept x; if not reject x and try again. If we regard x and $uC\,h(x)$ as the abscissa and ordinate of a point in a two-dimensional plot, these points will populate the entire area $C\,h(x)$ in a smooth manner; then we accept those which fall under $f(x)$. The efficiency is the ratio of areas, which must equal $1/C$; therefore we must keep C as close as possible to 1.0. Therefore we try to choose $C\,h(x)$ to be as close to $f(x)$ as convenience dictates, as in the lower part of Fig. 33.2. This practice is called importance sampling, because we generate more trial values of x in the region where $f(x)$ is most important.

33.4. Algorithms

Algorithms for generating random numbers belonging to many different distributions are given by Press [5], Ahrens and Dieter [6], Rubinstein [7], Everett and Cashwell [8], Devroye [9], and Walck [10]. For many distributions alternative algorithms exist, varying in complexity, speed, and accuracy. For time-critical applications, these algorithms may be coded in-line to remove the significant overhead often encountered in making function calls. Variables named "u" are assumed to be independent and uniform on [0,1). (Hence, u must be verified to be non-zero where relevant.)

In the examples given below, we use the notation for the variables and parameters given in Table 31.1.

33.4.1. *Exponential decay*:

This is a common application of the inverse transform method, also using the fact that $(1-u)$ is uniform if u is uniform. To generate decays between times t_1 and t_2 according to $f(t) = \exp(-t/\tau)$: let $r_2 = \exp(-t_2/\tau)$ and $r_1 = \exp(-t_1/\tau)$; generate u and let

$$t = -\tau \ln(r_2 + u(r_1 - r_2)). \tag{33.4}$$

For $(t_1, t_2) = (0, \infty)$, we have simply $t = -\tau \ln u$. (See also Sec. 33.4.6.)

33.4.2. *Isotropic direction in 3D*:

Isotropy means the density is proportional to solid angle, the differential element of which is $d\Omega = d(\cos\theta)d\phi$. Hence $\cos\theta$ is uniform $(2u_1 - 1)$ and ϕ is uniform $(2\pi u_2)$. For alternative generation of $\sin\phi$ and $\cos\phi$, see the next subsection.

33.4.3. *Sine and cosine of random angle in 2D*:

Generate u_1 and u_2. Then $v_1 = 2u_1 - 1$ is uniform on $(-1,1)$, and $v_2 = u_2$ is uniform on (0,1). Calculate $r^2 = v_1^2 + v_2^2$. If $r^2 > 1$, start over. Otherwise, the sine (S) and cosine (C) of a random angle are given by

$$S = 2v_1v_2/r^2 \quad \text{and} \quad C = (v_1^2 - v_2^2)/r^2 \ . \tag{33.5}$$

33.4.4. *Gaussian distribution*:

If u_1 and u_2 are uniform on (0,1), then

$$z_1 = \sin 2\pi u_1 \sqrt{-2\ln u_2} \quad \text{and} \quad z_2 = \cos 2\pi u_1 \sqrt{-2\ln u_2} \tag{33.6}$$

are independent and Gaussian distributed with mean 0 and $\sigma = 1$.

There are many faster variants of this basic algorithm. For example, construct $v_1 = 2u_1 - 1$ and $v_2 = 2u_2 - 1$, which are uniform on $(-1,1)$. Calculate $r^2 = v_1^2 + v_2^2$, and if $r^2 > 1$ start over. If $r^2 < 1$, it is uniform on (0,1). Then

$$z_1 = v_1\sqrt{\frac{-2\ln r^2}{r^2}} \quad \text{and} \quad z_2 = v_2\sqrt{\frac{-2\ln r^2}{r^2}} \tag{33.7}$$

are independent numbers chosen from a normal distribution with mean 0 and variance 1. $z_i' = \mu + \sigma z_i$ distributes with mean μ and variance σ^2. A recent implementation of the fast algorithm of Leva Ref. 11 is in CERNLIB.

For a multivariate Gaussian with an $n \times n$ covariance matrix V, one can start by generating n independent Gaussian variables, $\{\eta_j\}$, with mean 0 and variance 1 as above. Then the new set $\{x_i\}$ is obtained as $x_i = \mu_i + \sum_j L_{ij}\eta_j$, where μ_i is the mean of x_i, and L_{ij} are the components of L, the unique lower triangular matrix that fulfils $V = LL^T$. The matrix L can be easily computed by the following recursive relation (Cholesky's method):

$$L_{jj} = \left(V_{jj} - \sum_{k=1}^{j-1} L_{jk}^2 \right)^{1/2} \ , \tag{33.8a}$$

$$L_{ij} = \frac{V_{ij} - \sum_{k=1}^{j-1} L_{ik}L_{jk}}{L_{jj}} \ , \ j = 1, ..., n \ ; \ i = j+1, ..., n \ , \tag{33.8b}$$

where $V_{ij} = \rho_{ij}\sigma_i\sigma_j$ are the components of V. For $n = 2$ one has

$$L = \begin{pmatrix} \sigma_1 & 0 \\ \rho\sigma_2 & \sqrt{1-\rho^2}\,\sigma_2 \end{pmatrix} \ , \tag{33.9}$$

and therefore the correlated Gaussian variables are generated as $x_1 = \mu_1 + \sigma_1\eta_1$, $x_2 = \mu_2 + \rho\sigma_2\eta_1 + \sqrt{1-\rho^2}\,\sigma_2\eta_2$.

33.4.5. $\chi^2(n)$ distribution:

For n even, generate $n/2$ uniform numbers u_i; then

$$y = -2\ln\left(\prod_{i=1}^{n/2} u_i\right) \quad \text{is} \quad \chi^2(n) \ . \tag{33.10}$$

For n odd, generate $(n-1)/2$ uniform numbers u_i and one Gaussian z as in Sec. 33.4.4; then

$$y = -2\ln\left(\prod_{i=1}^{(n-1)/2} u_i\right) + z^2 \quad \text{is} \quad \chi^2(n) \ . \tag{33.11}$$

For $n \gtrsim 30$ the much faster Gaussian approximation for the χ^2 may be preferable: generate z as in Sec. 33.4.4 and use $y = \left[z + \sqrt{2n-1}\right]^2/2$; if $z < -\sqrt{2n-1}$ reject and start over.

33.4.6. *Gamma distribution*:

All of the following algorithms are given for $\lambda = 1$. For $\lambda \neq 1$, divide the resulting random number x by λ.

- If $k = 1$ (the *exponential* distribution), accept $x = -(\ln u)$. (See also Sec. 33.4.1.)

- If $0 < k < 1$, initialize with $v_1 = (e+k)/e$ (with $e = 2.71828...$ being the natural log base). Generate u_1, u_2. Define $v_2 = v_1u_1$.

  Case 1: $v_2 \leq 1$. Define $x = v_2^{1/k}$. If $u_2 \leq e^{-x}$, accept x and stop, else restart by generating new u_1, u_2.
  Case 2: $v_2 > 1$. Define $x = -\ln([v_1 - v_2]/k)$. If $u_2 \leq x^{k-1}$, accept x and stop, else restart by generating new u_1, u_2. Note that, for $k < 1$, the probability density has a pole at $x = 0$, so that return values of zero due to underflow must be accepted or otherwise dealt with.

- Otherwise, if $k > 1$, initialize with $c = 3k - 0.75$. Generate u_1 and compute $v_1 = u_1(1-u_1)$ and $v_2 = (u_1 - 0.5)\sqrt{c/v_1}$. If $x = k + v_2 - 1 \leq 0$, go back and generate new u_1; otherwise generate u_2 and compute $v_3 = 64v_1^3u_2^2$. If $v_3 \leq 1 - 2v_2^2/x$ **or** if $\ln v_3 \leq 2\{[k-1]\ln[x/(k-1)] - v_2\}$, accept x and stop; otherwise go back and generate new u_1.

33.4.7. *Binomial distribution*:

Begin with $k = 0$ and generate u uniform in $[0,1)$. Compute $P_k = (1-p)^n$ and store P_k into B. If $u \leq B$ accept $r_k = k$ and stop. Otherwise, increment k by one; compute the next P_k as $P_k \cdot (p/(1-p)) \cdot (n-k)/(k+1)$; add this to B. Again if $u \leq B$ accept $r_k = k$ and stop, otherwise iterate until a value is accepted. If $p > 1/2$ it will be more efficient to generate r from $f(r; n, q)$, *i.e.*, with p and q interchanged, and then set $r_k = n - r$.

33.4.8. *Poisson distribution*:

Iterate until a successful choice is made: Begin with $k = 1$ and set $A = 1$ to start. Generate u. Replace A with uA; if now $A < \exp(-\mu)$, where μ is the Poisson parameter, accept $n_k = k - 1$ and stop. Otherwise increment k by 1, generate a new u and repeat, always starting with the value of A left from the previous try. For large $\mu(\gtrsim 10)$ it may be satisfactory (and much faster) to approximate the Poisson distribution by a Gaussian distribution (see our Probability chapter, Sec. 31.4.3) and generate z from $f(z;0,1)$; then accept $x = \max(0, [\mu + z\sqrt{\mu} + 0.5])$ where [ ] signifies the greatest integer $\leq$ the expression. [12]

33.4.9. *Student's t* distribution:

For $n > 0$ degrees of freedom (n not necessarily integer), generate x from a Gaussian with mean 0 and $\sigma^2 = 1$ according to the method of 33.4.4. Next generate y, an independent gamma random variate with $k = n/2$ degrees of freedom. Then $z = x\sqrt{2n}/\sqrt{y}$ is distributed as a t with n degrees of freedom.

For the special case $n = 1$, the Breit-Wigner distribution, generate u_1 and u_2; set $v_1 = 2u_1 - 1$ and $v_2 = 2u_2 - 1$. If $v_1^2 + v_2^2 \leq 1$ accept $z = v_1/v_2$ as a Breit-Wigner distribution with unit area, center at 0.0, and FWHM 2.0. Otherwise start over. For center M_0 and FWHM Γ, use $W = z\Gamma/2 + M_0$.

References:

1. F. James, Comp. Phys. Comm. **79** 111 (1994), based on M. Lüscher, Comp. Phys. Comm. **79** 100 (1994). This generator is available as the CERNLIB routine V115, RANLUX.
2. G. Marsaglia, A. Zaman, and W.W. Tsang, *Towards a Universal Random Number Generator*, Supercomputer Computations Research Institute, Florida State University technical report FSU-SCRI-87-50 (1987). This generator is available as the CERNLIB routine V113, RANMAR, by F. Carminati and F. James.
3. Much of DIEHARD is described in: G. Marsaglia, *A Current View of Random Number Generators*, keynote address, *Computer Science and Statistics: 16th Symposium on the Interface*, Elsevier (1985).
4. Newer generators with periods even longer than the lagged-Fibonacci based generator are described in G. Marsaglia and A. Zaman, *Some Portable Very-Long-Period Random Number Generators*, Compt. Phys. **8**, 117 (1994). The Numerical Recipes generator **ran2** [W.H. Press and S.A. Teukolsky, *Portable Random Number Generators*, Compt. Phys. **6**, 521 (1992)] is also known to pass the DIEHARD tests.
5. W.H. Press *et al.*, *Numerical Recipes* (Cambridge University Press, New York, 1986).
6. J.H. Ahrens and U. Dieter, Computing **12**, 223 (1974).
7. R.Y. Rubinstein, *Simulation and the Monte Carlo Method* (John Wiley and Sons, Inc., New York, 1981).
8. C.J. Everett and E.D. Cashwell, *A Third Monte Carlo Sampler*, Los Alamos report LA-9721-MS (1983).
9. L. Devroye, *Non-Uniform Random Variate Generation* (Springer-Verlag, New York, 1986).
10. Ch. Walck, *Random Number Generation*, University of Stockholm Physics Department Report 1987-10-20 (Vers. 3.0).
11. J.L. Leva, ACM Trans. Math. Softw. **18** 449 (1992). This generator has been implemented by F. James in the CERNLIB routine V120, RNORML.
12. This generator has been implemented by D. Drijard and K. Kölbig in the CERNLIB routine V136, RNPSSN.

34. MONTE CARLO PARTICLE NUMBERING SCHEME

Revised March 2004 by L. Garren (Fermilab), I.G. Knowles (Edinburgh U.), S. Navas (U. Granada), T. Sjöstrand (Lund U.), and T. Trippe (LBNL).

The Monte Carlo particle numbering scheme presented here is intended to facilitate interfacing between event generators, detector simulators, and analysis packages used in particle physics. The numbering scheme was introduced in 1988 [1] and a revised version [2,3] was adopted in 1998 in order to allow systematic inclusion of quark model states which are as yet undiscovered and hypothetical particles such as SUSY particles. The numbering scheme is used in several event generators, *e.g.* HERWIG and PYTHIA/JETSET, and in the `/HEPEVT/` [4] standard interface.

The general form is a 7–digit number:

$$\pm n\ n_r\, n_L\, n_{q_1}\, n_{q_2}\, n_{q_3}\, n_J\ .$$

This encodes information about the particle's spin, flavor content, and internal quantum numbers. The details are as follows:

1. Particles are given positive numbers, antiparticles negative numbers. The PDG convention for mesons is used, so that K^+ and B^+ are particles.
2. Quarks and leptons are numbered consecutively starting from 1 and 11 respectively; to do this they are first ordered by family and within families by weak isospin.
3. In composite quark systems (diquarks, mesons, and baryons) $n_{q_{1-3}}$ are quark numbers used to specify the quark content, while the rightmost digit $n_J = 2J+1$ gives the system's spin (except for the K^0_S and K^0_L). The scheme does not cover particles of spin $J > 4$.
4. Diquarks have 4-digit numbers with $n_{q_1} \geq n_{q_2}$ and $n_{q_3} = 0$.
5. The numbering of mesons is guided by the nonrelativistic (L–S decoupled) quark model, as listed in Tables 14.2 and 14.3.
   a. The numbers specifying the meson's quark content conform to the convention $n_{q_1} = 0$ and $n_{q_2} \geq n_{q_3}$. The special case K^0_L is the sole exception to this rule.
   b. The quark numbers of flavorless, light (u, d, s) mesons are: 11 for the member of the isotriplet ($\pi^0, \rho^0, \ldots$), 22 for the lighter isosinglet ($\eta, \omega, \ldots$), and 33 for the heavier isosinglet ($\eta', \phi, \ldots$). Since isosinglet mesons are often large mixtures of $u\overline{u} + d\overline{d}$ and $s\overline{s}$ states, 22 and 33 are assigned by mass and do not necessarily specify the dominant quark composition.
   c. The special numbers 310 and 130 are given to the K^0_S and K^0_L respectively.
   d. The fifth digit n_L is reserved to distinguish mesons of the same total (J) but different spin (S) and orbital (L) angular momentum quantum numbers. For $J > 0$ the numbers are: $(L, S) = (J-1, 1)\ n_L = 0$, $(J, 0)\ n_L = 1$, $(J, 1)\ n_L = 2$ and $(J+1, 1)\ n_L = 3$. For the exceptional case $J = 0$ the numbers are $(0, 0)\ n_L = 0$ and $(1, 1)\ n_L = 1$ (*i.e.* $n_L = L$). See Table 34.1.

Table 34.1: Meson numbering logic. Here qq stands for $n_{q2}\, n_{q3}$.

	$L = J-1$, $S = 1$			$L = J$, $S = 0$			$L = J$, $S = 1$			$L = J+1$, $S = 1$		
J	code	J^{PC}	L	code	J^{PC}	L	code	J^{PC}	L	code	J^{PC}	L
0	—	—	—	$00qq1$	0^{-+}	0	—	—	—	$10qq1$	0^{++}	1
1	$00qq3$	1^{--}	0	$10qq3$	1^{+-}	1	$20qq3$	1^{++}	1	$30qq3$	1^{--}	2
2	$00qq5$	2^{++}	1	$10qq5$	2^{-+}	2	$20qq5$	2^{--}	2	$30qq5$	2^{++}	3
3	$00qq7$	3^{--}	2	$10qq7$	3^{+-}	3	$20qq7$	3^{++}	3	$30qq7$	3^{--}	4
4	$00qq9$	4^{++}	3	$10qq9$	4^{-+}	4	$20qq9$	4^{--}	4	$30qq9$	4^{++}	5

   e. If a set of physical mesons correspond to a (non-negligible) mixture of basis states, differing in their internal quantum numbers, then the lightest physical state gets the smallest basis state number. For example the $K_1(1270)$ is numbered 10313 ($1^1P_1\ K_{1B}$) and the $K_1(1400)$ is numbered 20313 ($1^3P_1\ K_{1A}$).
   f. The sixth digit n_r is used to label mesons radially excited above the ground state.
   g. Numbers have been assigned for complete $n_r = 0$ S- and P-wave multiplets, even where states remain to be identified.
   h. In some instances assignments within the $q\bar{q}$ meson model are only tentative; here best guess assignments are made.
   i. Many states appearing in the Meson Listings are not yet assigned within the $q\bar{q}$ model. Here $n_{q_{2-3}}$ and n_J are assigned according to the state's likely flavors and spin; all such unassigned light isoscalar states are given the flavor code 22. Within these groups $n_L = 0, 1, 2, \ldots$ is used to distinguish states of increasing mass. These states are flagged using $n = 9$. It is to be expected that these numbers will evolve as the nature of the states are elucidated.
6. The numbering of baryons is again guided by the nonrelativistic quark model, see Table 14.5.
   a. The numbers specifying a baryon's quark content are such that in general $n_{q_1} \geq n_{q_2} \geq n_{q_3}$.
   b. Two states exist for $J = 1/2$ baryons containing 3 different types of quarks. In the lighter baryon ($\Lambda, \Xi, \Omega, \ldots$) the light quarks are in an antisymmetric ($J = 0$) state while for the heavier baryon ($\Sigma^0, \Xi', \Omega', \ldots$) they are in a symmetric ($J = 1$) state. In this situation n_{q_2} and n_{q_3} are reversed for the lighter state, so that the smaller number corresponds to the lighter baryon.
   c. At present most Monte Carlos do not include excited baryons and no systematic scheme has been developed to denote them, though one is foreseen. In the meantime, use of the PDG 96 [5] numbers for excited baryons is recommended.
   d. For pentaquark states $n = 9$, $n_r n_L n_{q_1} n_{q_2}$ gives the four quark numbers in order $n_r \geq n_L \geq n_{q_1} \geq n_{q_2}$, n_{q_3} gives the antiquark number, and $n_J = 2J+1$, with the assumption that $J = 1/2$ for the states currently reported.
7. The gluon, when considered as a gauge boson, has official number 21. In codes for glueballs, however, 9 is used to allow a notation in close analogy with that of hadrons.
8. The pomeron and odderon trajectories and a generic reggeon trajectory of states in QCD are assigned codes 990, 9990, and 110 respectively, where the final 0 indicates the indeterminate nature of the spin, and the other digits reflect the expected "valence" flavor content. We do not attempt a complete classification of all reggeon trajectories, since there is currently no need to distinguish a specific such trajectory from its lowest-lying member.
9. Two-digit numbers in the range 21–30 are provided for the Standard Model gauge bosons and Higgs.
10. Codes 81–100 are reserved for generator-specific pseudoparticles and concepts.
11. The search for physics beyond the Standard Model is an active area, so these codes are also standardized as far as possible.
    a. A standard fourth generation of fermions is included by analogy with the first three.
    b. The graviton and the boson content of a two-Higgs-doublet scenario and of additional SU(2)×U(1) groups are found in the range 31–40.
    c. "One-of-a-kind" exotic particles are assigned numbers in the range 41–80.
    d. Fundamental supersymmetric particles are identified by adding a nonzero n to the particle number. The superpartner of a boson or a left-handed fermion has $n = 1$ while the superpartner of a right-handed fermion has $n = 2$. When mixing occurs, such as between the winos and charged Higgsinos to give charginos, or between left and right sfermions, the lighter physical state is given the smaller basis state number.
    e. Technicolor states have $n = 3$, with technifermions treated like ordinary fermions. States which are ordinary color singlets have $n_r = 0$. Color octets have $n_r = 1$. If a state has non-trivial quantum numbers under the topcolor groups $\mathrm{SU}(3)_1 \times \mathrm{SU}(3)_2$, the quantum numbers are specified by tech,ij, where i and j are 1 or 2. n_L is then $2i + j$. The coloron, V_8, is a heavy gluon color octet and thus is 3100021.

f. Excited (composite) quarks and leptons are identified by setting $n = 4$.

12. Occasionally program authors add their own states. To avoid confusion, these should be flagged by setting $nn_r = 99$.
13. Concerning the non-99 numbers, it may be noted that only quarks, excited quarks, squarks, and diquarks have $n_{q3} = 0$; only diquarks, baryons (including pentaquarks), and the odderon have $n_{q_1} \neq 0$; and only mesons, the reggeon, and the pomeron have $n_{q_1} = 0$ and $n_{q_2} \neq 0$. Concerning mesons (not antimesons), if n_{q_1} is odd then it labels a quark and an antiquark if even.

This text and lists of particle numbers can be found on the WWW [6]. The StdHep Monte Carlo standardization project [7] maintains the list of PDG particle numbers, as well as numbering schemes from most event generators and software to convert between the different schemes.

References:

1. G.P. Yost *et al.*, Particle Data Group, Phys. Lett. **B204**, 1 (1988).
2. I. G. Knowles *et al.*, in *"Physics at LEP2"*, CERN 96-01, vol. 2, p. 103.
3. C. Caso *et al.*, Particle Data Group, Eur. Phys. J. **C3**, 1 (1998).
4. T. Sjöstrand *et al.*, in *"Z physics at LEP1"*, CERN 89-08, vol. 3, p. 327.
5. R.M. Barnett *et al.*, PDG, Phys. Rev. **D54**, 1 (1996).
6. `http://pdg.lbl.gov/mc_particle_id_contents.html`.
7. L. Garren, StdHep, *Monte Carlo Standardization at FNAL*, Fermilab PM0091 and StdHep WWW site: `http://cepa.fnal.gov/psm/stdhep/`.
8. K. Hagiwara *et al.*, PDG, Phys. Rev. **D66**, 010001-1 (2002).

QUARKS

d	1
u	2
s	3
c	4
b	5
t	6
b'	7
t'	8

LEPTONS

e^-	11
ν_e	12
μ^-	13
ν_μ	14
τ^-	15
ν_τ	16
τ'^-	17
$\nu_{\tau'}$	18

EXCITED PARTICLES

d^*	4000001
u^*	4000002
e^*	4000011
ν_e^*	4000012

GAUGE AND HIGGS BOSONS

g	(9) 21
γ	22
Z^0	23
W^+	24
h^0/H_1^0	25
Z'/Z_2^0	32
Z''/Z_3^0	33
W'/W_2^+	34
H^0/H_2^0	35
A^0/H_3^0	36
H^+	37

DIQUARKS

$(dd)_1$	1103
$(ud)_0$	2101
$(ud)_1$	2103
$(uu)_1$	2203
$(sd)_0$	3101
$(sd)_1$	3103
$(su)_0$	3201
$(su)_1$	3203
$(ss)_1$	3303
$(cd)_0$	4101
$(cd)_1$	4103
$(cu)_0$	4201
$(cu)_1$	4203
$(cs)_0$	4301
$(cs)_1$	4303
$(cc)_1$	4403
$(bd)_0$	5101
$(bd)_1$	5103
$(bu)_0$	5201
$(bu)_1$	5203
$(bs)_0$	5301
$(bs)_1$	5303
$(bc)_0$	5401
$(bc)_1$	5403
$(bb)_1$	5503

TECHNICOLOR PARTICLES

$\pi^0_{\rm tech}$	3000111
$\pi^+_{\rm tech}$	3000211
$\pi'^0_{\rm tech}$	3000221
$\eta^0_{\rm tech}$	3100221
$\rho^0_{\rm tech}$	3000113
$\rho^+_{\rm tech}$	3000213
$\omega^0_{\rm tech}$	3000223
V_8	3100021
$\pi^1_{\rm tech,22}$	3060111
$\pi^8_{\rm tech,22}$	3160111
$\rho_{\rm tech,11}$	3130113
$\rho_{\rm tech,12}$	3140113
$\rho_{\rm tech,21}$	3150113
$\rho_{\rm tech,22}$	3160113

SUSY PARTICLES

$\widetilde{d}_L$	1000001
$\widetilde{u}_L$	1000002
$\widetilde{s}_L$	1000003
$\widetilde{c}_L$	1000004
$\widetilde{b}_1$	1000005[a]
$\widetilde{t}_1$	1000006[a]
$\widetilde{e}^-_L$	1000011
$\widetilde{\nu}_{eL}$	1000012
$\widetilde{\mu}^-_L$	1000013
$\widetilde{\nu}_{\mu L}$	1000014
$\widetilde{\tau}^-_1$	1000015[a]
$\widetilde{\nu}_{\tau L}$	1000016
$\widetilde{d}_R$	2000001
$\widetilde{u}_R$	2000002
$\widetilde{s}_R$	2000003
$\widetilde{c}_R$	2000004
$\widetilde{b}_2$	2000005[a]
$\widetilde{t}_2$	2000006[a]
$\widetilde{e}^-_R$	2000011
$\widetilde{\mu}^-_R$	2000013
$\widetilde{\tau}^-_2$	2000015[a]
$\widetilde{g}$	1000021
$\widetilde{\chi}^0_1$	1000022[b]
$\widetilde{\chi}^0_2$	1000023[b]
$\widetilde{\chi}^+_1$	1000024[b]
$\widetilde{\chi}^0_3$	1000025[b]
$\widetilde{\chi}^0_4$	1000035[b]
$\widetilde{\chi}^+_2$	1000037[b]
$\widetilde{G}$	1000039

SPECIAL PARTICLES

G (graviton)	39
R^0	41
LQ^c	42
reggeon	110
pomeron	990
odderon	9990

for MC internal use 81–100

LIGHT $I = 1$ MESONS

π^0	111
π^+	211
$a_0(980)^0$	9000111
$a_0(980)^+$	9000211
$\pi(1300)^0$	100111
$\pi(1300)^+$	100211
$a_0(1450)^0$	10111
$a_0(1450)^+$	10211
$\pi(1800)^0$	**9010111**[*]
$\pi(1800)^+$	**9010211**[*]
$\rho(770)^0$	113
$\rho(770)^+$	213
$b_1(1235)^0$	10113
$b_1(1235)^+$	10213
$a_1(1260)^0$	20113
$a_1(1260)^+$	20213
$\pi_1(1400)^0$	9000113
$\pi_1(1400)^+$	9000213
$\rho(1450)^0$	100113
$\rho(1450)^+$	100213
$\pi_1(1600)^0$	9010113
$\pi_1(1600)^+$	9010213
$\rho(1700)^0$	30113
$\rho(1700)^+$	30213
$\rho(1900)^0$	**9020113**[*]
$\rho(1900)^+$	**9020213**[*]
$\rho(2150)^0$	**9030113**[*]
$\rho(2150)^+$	**9030213**[*]
$a_2(1320)^0$	115
$a_2(1320)^+$	215
$\pi_2(1670)^0$	10115
$\pi_2(1670)^+$	10215
$\pi_2(2100)^0$	9000115
$\pi_2(2100)^+$	9000215
$\rho_3(1690)^0$	117
$\rho_3(1690)^+$	217
$\rho_3(1990)^0$	9000117
$\rho_3(1990)^+$	9000217
$\rho_3(2250)^0$	9010117
$\rho_3(2250)^+$	9010217
$a_4(2040)^0$	119
$a_4(2040)^+$	219

LIGHT $I = 0$ MESONS

($u\overline{u}$, $d\overline{d}$, and $s\overline{s}$ Admixtures)

η	221
$\eta'(958)$	331
$f_0(600)$	9000221
$f_0(980)$	9010221
$\eta(1295)$	100221
$f_0(1370)$	10221
$\eta(1405)$	**9020221**[*]
$\eta(1475)$	100331
$f_0(1500)$	**9030221**[*]
$f_0(1710)$	10331
$f_0(2020)$	**9040221**[*]
$f_0(2100)$	**9050221**[*]
$f_0(2200)$	**9060221**[*]
$f_0(2330)$	9070221
$\omega(782)$	223
$\phi(1020)$	333
$h_1(1170)$	10223
$f_1(1285)$	20223
$h_1(1380)$	10333
$f_1(1420)$	20333
$\omega(1420)$	100223
$f_1(1510)$	9000223
$\omega(1650)$	30223
$\phi(1680)$	100333
$f_2(1270)$	225
$f_2(1430)$	9000225
$f_2'(1525)$	335
$f_2(1565)$	9010225
$f_2(1640)$	9020225
$\eta_2(1645)$	10225
$f_2(1810)$	9030225
$\eta_2(1870)$	10335
$f_2(1910)$	9040225
$f_2(1950)$	**9050225**[*]
$f_2(2010)$	**9060225**[*]
$f_2(2150)$	**9070225**[*]
$f_2(2300)$	**9080225**[*]
$f_2(2340)$	**9090225**[*]
$\omega_3(1670)$	227
$\phi_3(1850)$	337
$f_4(2050)$	229
$f_J(2220)$	**9000229**[*]
$f_4(2300)$	**9010229**[*]

STRANGE MESONS

K_L^0	130
K_S^0	310
K^0	311
K^+	321
$\boldsymbol{K_0^*(800)^0}$	**9000311***
$\boldsymbol{K_0^*(800)^+}$	**9000321***
$K_0^*(1430)^0$	10311
$K_0^*(1430)^+$	10321
$K(1460)^0$	100311
$K(1460)^+$	100321
$K_0^*(1950)^0$	**9010311***
$K_0^*(1950)^+$	**9010321***
$K^*(892)^0$	313
$K^*(892)^+$	323
$K_1(1270)^0$	10313
$K_1(1270)^+$	10323
$K_1(1400)^0$	20313
$K_1(1400)^+$	20323
$K^*(1410)^0$	100313
$K^*(1410)^+$	100323
$K^*(1680)^0$	30313
$K^*(1680)^+$	30323
$K_2^*(1430)^0$	315
$K_2^*(1430)^+$	325
$K_2(1580)^0$	9000315
$K_2(1580)^+$	9000325
$K_2(1770)^0$	10315
$K_2(1770)^+$	10325
$K_2(1820)^0$	20315
$K_2(1820)^+$	20325
$K_2(2250)^0$	9010315
$K_2(2250)^+$	9010325
$K_3^*(1780)^0$	317
$K_3^*(1780)^+$	327
$K_3(2320)^0$	9010317
$K_3(2320)^+$	9010327
$K_4^*(2045)^0$	319
$K_4^*(2045)^+$	329
$K_4(2500)^0$	9000319
$K_4(2500)^+$	9000329

CHARMED MESONS

D^+	411
D^0	421
D_0^{*+}	10411
D_0^{*0}	10421
$D^*(2010)^+$	413
$D^*(2007)^0$	423
$D_1(2420)^+$	10413
$D_1(2420)^0$	10423
$D_1(H)^+$	20413
$D_1(H)^0$	20423
$D_2^*(2460)^+$	415
$D_2^*(2460)^0$	425
D_s^+	431
$\boldsymbol{D_{s0}^*(2317)^+}$	10431
D_s^{*+}	433
$D_{s1}(2536)^+$	10433
$\boldsymbol{D_{s1}(2460)^+}$	20433
$\boldsymbol{D_{s2}^*(2573)^+}$	435

BOTTOM MESONS

B^0	511
B^+	521
B_0^{*0}	10511
B_0^{*+}	10521
B^{*0}	513
B^{*+}	523
$B_1(L)^0$	10513
$B_1(L)^+$	10523
$B_1(H)^0$	20513
$B_1(H)^+$	20523
B_2^{*0}	515
B_2^{*+}	525
B_s^0	531
B_{s0}^{*0}	10531
B_s^{*0}	533
$B_{s1}(L)^0$	10533
$B_{s1}(H)^0$	20533
B_{s2}^{*0}	535
B_c^+	541
B_{c0}^{*+}	10541
B_c^{*+}	543
$B_{c1}(L)^+$	10543
$B_{c1}(H)^+$	20543
B_{c2}^{*+}	545

$c\bar{c}$ MESONS

$\eta_c(1S)$	441
$\chi_{c0}(1P)$	10441
$\eta_c(2S)$	100441
$J/\psi(1S)$	443
$h_c(1P)$	10443
$\chi_{c1}(1P)$	20443
$\psi(2S)$	100443
$\psi(3770)$	30443
$\psi(4040)$	9000443
$\psi(4160)$	9010443
$\psi(4415)$	9020443
$\chi_{c2}(1P)$	445
$\psi(3836)$	9000445

$b\bar{b}$ MESONS

$\eta_b(1S)$	551
$\chi_{b0}(1P)$	10551
$\eta_b(2S)$	100551
$\chi_{b0}(2P)$	110551
$\eta_b(3S)$	200551
$\chi_{b0}(3P)$	210551
$\Upsilon(1S)$	553
$h_b(1P)$	10553
$\chi_{b1}(1P)$	20553
$\Upsilon_1(1D)$	30553
$\Upsilon(2S)$	100553
$h_b(2P)$	110553
$\chi_{b1}(2P)$	120553
$\Upsilon_1(2D)$	130553
$\Upsilon(3S)$	200553
$h_b(3P)$	210553
$\chi_{b1}(3P)$	220553
$\Upsilon(4S)$	300553
$\Upsilon(10860)$	9000553
$\Upsilon(11020)$	9010553
$\chi_{b2}(1P)$	555
$\eta_{b2}(1D)$	10555
$\Upsilon_2(1D)$	20555
$\chi_{b2}(2P)$	100555
$\eta_{b2}(2D)$	110555
$\Upsilon_2(2D)$	120555
$\chi_{b2}(3P)$	200555
$\Upsilon_3(1D)$	557
$\Upsilon_3(2D)$	100557

LIGHT BARYONS

p	2212
n	2112
Δ^{++}	2224
Δ^+	2214
Δ^0	2114
Δ^-	1114

STRANGE BARYONS

Λ	3122
Σ^+	3222
Σ^0	3212
Σ^-	3112
Σ^{*+}	3224^d
Σ^{*0}	3214^d
Σ^{*-}	3114^d
Ξ^0	3322
Ξ^-	3312
Ξ^{*0}	3324^d
Ξ^{*-}	3314^d
Ω^-	3334

CHARMED BARYONS

Λ_c^+	4122
Σ_c^{++}	4222
Σ_c^+	4212
Σ_c^0	4112
Σ_c^{*++}	4224
Σ_c^{*+}	4214
Σ_c^{*0}	4114
Ξ_c^+	4232
Ξ_c^0	4132
$\Xi_c'^+$	4322
$\Xi_c'^0$	4312
Ξ_c^{*+}	4324
Ξ_c^{*0}	4314
Ω_c^0	4332
Ω_c^{*0}	4334
Ξ_{cc}^+	4412
Ξ_{cc}^{++}	4422
Ξ_{cc}^{*+}	4414
Ξ_{cc}^{*++}	4424
Ω_{cc}^+	4432
Ω_{cc}^{*+}	4434
Ω_{ccc}^{++}	4444

PENTAQUARKS

$\boldsymbol{\Theta^+}$	**9221132***
$\boldsymbol{\Phi^{--}}$	**9331122***

BOTTOM BARYONS

Λ_b^0	5122
Σ_b^-	5112
Σ_b^0	5212
Σ_b^+	5222
Σ_b^{*-}	5114
Σ_b^{*0}	5214
Σ_b^{*+}	5224
Ξ_b^-	5132
Ξ_b^0	5232
$\Xi_b'^-$	5312
$\Xi_b'^0$	5322
Ξ_b^{*-}	5314
Ξ_b^{*0}	5324
Ω_b^-	5332
Ω_b^{*-}	5334
Ξ_{bc}^0	5142
Ξ_{bc}^+	5242
$\Xi_{bc}'^0$	5412
$\Xi_{bc}'^+$	5422
Ξ_{bc}^{*0}	5414
Ξ_{bc}^{*+}	5424
Ω_{bc}^0	5342
$\Omega_{bc}'^0$	5432
Ω_{bc}^{*0}	5434
Ω_{bcc}^+	5442
Ω_{bcc}^{*+}	5444
Ξ_{bb}^-	5512
Ξ_{bb}^0	5522
Ξ_{bb}^{*-}	5514
Ξ_{bb}^{*0}	5524
Ω_{bb}^-	5532
Ω_{bb}^{*-}	5534
Ω_{bbc}^0	5542
Ω_{bbc}^{*0}	5544
Ω_{bbb}^-	5554

Footnotes to the Tables:

*) Numbers or names in bold face are new or have changed since the 2002 *Review* [8].

a) Particulary in the third generation, the left and right sfermion states may mix, as shown. The lighter mixed state is given the smaller number.

b) The physical $\widetilde{\chi}$ states are admixtures of the pure $\widetilde{\gamma}$, $\widetilde{Z}^0$, $\widetilde{W}^+$, $\widetilde{H}_1^0$, $\widetilde{H}_2^0$, and $\widetilde{H}^+$ states.

c) In this draft we have only provided one generic leptoquark code. More general classifications according to spin, weak isospin and flavor content would lead to a host of states, that could be added as the need arises.

d) Σ^* and Ξ^* are alternate names for $\Sigma(1385)$ and $\Xi(1530)$.

35. CLEBSCH-GORDAN COEFFICIENTS, SPHERICAL HARMONICS, AND d FUNCTIONS

Note: A square-root sign is to be understood over *every* coefficient, *e.g.*, for $-8/15$ read $-\sqrt{8/15}$.

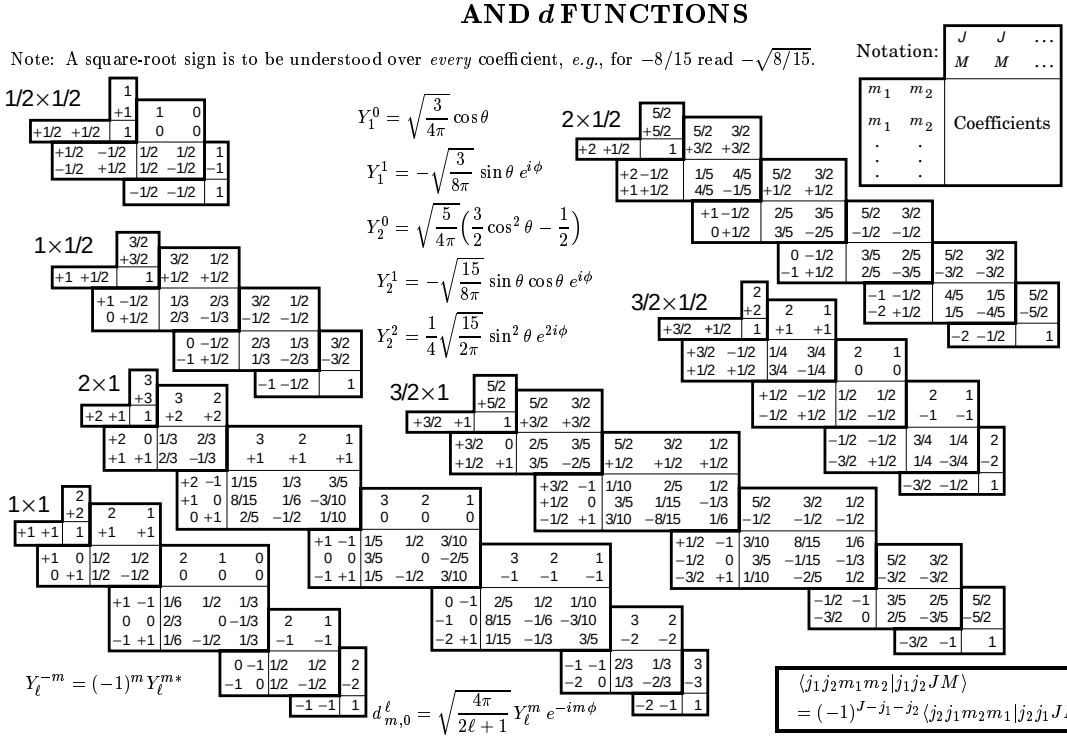

$$Y_1^0 = \sqrt{\frac{3}{4\pi}}\cos\theta \qquad Y_1^1 = -\sqrt{\frac{3}{8\pi}}\sin\theta\, e^{i\phi}$$

$$Y_2^0 = \sqrt{\frac{5}{4\pi}}\left(\frac{3}{2}\cos^2\theta - \frac{1}{2}\right) \qquad Y_2^1 = -\sqrt{\frac{15}{8\pi}}\sin\theta\cos\theta\, e^{i\phi}$$

$$Y_2^2 = \frac{1}{4}\sqrt{\frac{15}{2\pi}}\sin^2\theta\, e^{2i\phi}$$

$$Y_\ell^{-m} = (-1)^m Y_\ell^{m*} \qquad d^{\,\ell}_{m,0} = \sqrt{\frac{4\pi}{2\ell+1}}\, Y_\ell^m\, e^{-im\phi}$$

$$\langle j_1 j_2 m_1 m_2 | j_1 j_2 J M\rangle = (-1)^{J-j_1-j_2}\langle j_2 j_1 m_2 m_1 | j_2 j_1 J M\rangle$$

$$d^{\,j}_{m',m} = (-1)^{m-m'} d^{\,j}_{m,m'} = d^{\,j}_{-m,-m'}$$

$$d^{\,0}_{0,0} = \cos\theta \qquad d^{\,1/2}_{1/2,1/2} = \cos\frac{\theta}{2} \qquad d^{\,1/2}_{1/2,-1/2} = -\sin\frac{\theta}{2}$$

$$d^{\,1}_{1,1} = \frac{1+\cos\theta}{2} \qquad d^{\,1}_{1,0} = -\frac{\sin\theta}{\sqrt{2}} \qquad d^{\,1}_{1,-1} = \frac{1-\cos\theta}{2}$$

$$d^{\,3/2}_{3/2,3/2} = \frac{1+\cos\theta}{2}\cos\frac{\theta}{2}$$

$$d^{\,3/2}_{3/2,1/2} = -\sqrt{3}\frac{1+\cos\theta}{2}\sin\frac{\theta}{2} \qquad d^{\,2}_{2,2} = \left(\frac{1+\cos\theta}{2}\right)^2$$

$$d^{\,3/2}_{3/2,-1/2} = \sqrt{3}\frac{1-\cos\theta}{2}\cos\frac{\theta}{2} \qquad d^{\,2}_{2,1} = -\frac{1+\cos\theta}{2}\sin\theta$$

$$d^{\,3/2}_{3/2,-3/2} = -\frac{1-\cos\theta}{2}\sin\frac{\theta}{2} \qquad d^{\,2}_{2,0} = \frac{\sqrt{6}}{4}\sin^2\theta \qquad d^{\,2}_{1,1} = \frac{1+\cos\theta}{2}(2\cos\theta - 1)$$

$$d^{\,3/2}_{1/2,1/2} = \frac{3\cos\theta - 1}{2}\cos\frac{\theta}{2} \qquad d^{\,2}_{2,-1} = -\frac{1-\cos\theta}{2}\sin\theta \qquad d^{\,2}_{1,0} = -\sqrt{\frac{3}{2}}\sin\theta\cos\theta$$

$$d^{\,3/2}_{1/2,-1/2} = -\frac{3\cos\theta + 1}{2}\sin\frac{\theta}{2} \qquad d^{\,2}_{2,-2} = \left(\frac{1-\cos\theta}{2}\right)^2 \qquad d^{\,2}_{1,-1} = \frac{1-\cos\theta}{2}(2\cos\theta + 1) \qquad d^{\,2}_{0,0} = \left(\frac{3}{2}\cos^2\theta - \frac{1}{2}\right)$$

Figure 35.1: The sign convention is that of Wigner (*Group Theory*, Academic Press, New York, 1959), also used by Condon and Shortley (*The Theory of Atomic Spectra*, Cambridge Univ. Press, New York, 1953), Rose (*Elementary Theory of Angular Momentum*, Wiley, New York, 1957), and Cohen (*Tables of the Clebsch-Gordan Coefficients*, North American Rockwell Science Center, Thousand Oaks, Calif., 1974). The coefficients here have been calculated using computer programs written independently by Cohen and at LBNL.

36. SU(3) ISOSCALAR FACTORS AND REPRESENTATION MATRICES

Written by R.L. Kelly (LBNL).

The most commonly used SU(3) isoscalar factors, corresponding to the singlet, octet, and decuplet content of $8 \otimes 8$ and $10 \otimes 8$, are shown at the right. The notation uses particle names to identify the coefficients, so that the pattern of relative couplings may be seen at a glance. We illustrate the use of the coefficients below. See J.J de Swart, Rev. Mod. Phys. **35**, 916 (1963) for detailed explanations and phase conventions.

A $\sqrt{\ }$ is to be understood over every integer in the matrices; the exponent 1/2 on each matrix is a reminder of this. For example, the $\Xi \to \Omega K$ element of the $10 \to 10 \otimes 8$ matrix is $-\sqrt{6}/\sqrt{24} = -1/2$.

Intramultiplet relative decay strengths may be read directly from the matrices. For example, in decuplet $\to$ octet + octet decays, the ratio of $\Omega^* \to \Xi\overline{K}$ and $\Delta \to N\pi$ partial widths is, from the $10 \to 8 \times 8$ matrix,

$$\frac{\Gamma\,(\Omega^* \to \Xi\overline{K})}{\Gamma\,(\Delta \to N\pi)} = \frac{12}{6} \times \text{ (phase space factors)}\,. \tag{36.1}$$

Including isospin Clebsch-Gordan coefficients, we obtain, *e.g.*,

$$\frac{\Gamma(\Omega^{*-} \to \Xi^0 K^-)}{\Gamma(\Delta^+ \to p\,\pi^0)} = \frac{1/2}{2/3} \times \frac{12}{6} \times p.s.f. = \frac{3}{2} \times p.s.f. \tag{36.2}$$

Partial widths for $8 \to 8 \otimes 8$ involve a linear superposition of 8_1 (symmetric) and 8_2 (antisymmetric) couplings. For example,

$$\Gamma(\Xi^* \to \Xi\pi) \sim \left(-\sqrt{\frac{9}{20}}\, g_1 + \sqrt{\frac{3}{12}}\, g_2\right)^2 . \tag{36.3}$$

The relations between g_1 and g_2 (with de Swart's normalization) and the standard D and F couplings that appear in the interaction Lagrangian,

$$\mathscr{L} = -\sqrt{2}\, D\, Tr\,(\{\overline{B}, B\}M) + \sqrt{2}\, F\, Tr\,([\overline{B}, B]\, M)\ , \tag{36.4}$$

where $[\overline{B}, B] \equiv \overline{B}B - B\overline{B}$ and $\{\overline{B}, B\} \equiv \overline{B}B + B\overline{B}$, are

$$D = \frac{\sqrt{30}}{40}\, g_1\ , \qquad F = \frac{\sqrt{6}}{24}\, g_2\ . \tag{36.5}$$

Thus, for example,

$$\Gamma(\Xi^* \to \Xi\pi) \sim (F - D)^2 \sim (1 - 2\alpha)^2\ , \tag{36.6}$$

where $\alpha \equiv F/(D + F)$. (This definition of α is de Swart's. The alternative $D/(D + F)$, due to Gell-Mann, is also used.)

The generators of SU(3) transformations, λ_a ($a = 1, 8$), are 3×3 matrices that obey the following commutation and anticommutation relationships:

$$[\lambda_a,\ \lambda_b] \equiv \lambda_a\lambda_b - \lambda_b\lambda_a = 2i\, f_{abc}\lambda_c \tag{36.7}$$

$$\{\lambda_a,\ \lambda_b\} \equiv \lambda_a\lambda_b + \lambda_b\lambda_a = \frac{4}{3}\delta_{ab} I + 2 d_{abc}\lambda_c\ , \tag{36.8}$$

where I is the 3×3 identity matrix, and δ_{ab} is the Kronecker delta symbol. The f_{abc} are odd under the permutation of any pair of indices, while the d_{abc} are even. The nonzero values are

$1 \to 8 \otimes 8$

$$(\,\Lambda\,) \quad \to (\,N\overline{K}\ \ \Sigma\pi\ \ \ \Lambda\eta\ \ \ \Xi K\,) \qquad = \frac{1}{\sqrt{8}}\ (2\ \ \ 3\ \ \ -1\ \ \ -2)^{1/2}$$

$8_1 \to 8 \otimes 8$

$$\begin{pmatrix} N \\ \Sigma \\ \Lambda \\ \Xi \end{pmatrix} \to \begin{pmatrix} N\pi & N\eta & \Sigma K & \Lambda K \\ N\overline{K} & \Sigma\pi & \Lambda\pi & \Sigma\eta & \Xi K \\ & N\overline{K} & \Sigma\pi & \Lambda\eta & \Xi K \\ & & \Sigma\overline{K} & \Lambda\overline{K} & \Xi\pi & \Xi\eta \end{pmatrix} = \frac{1}{\sqrt{20}} \begin{pmatrix} 9 & -1 & -9 & -1 \\ -6 & 0 & 4 & 4 & -6 \\ 2 & -12 & -4 & -2 \\ 9 & -1 & -9 & -1 \end{pmatrix}^{1/2}$$

$8_2 \to 8 \otimes 8$

$$\begin{pmatrix} N \\ \Sigma \\ \Lambda \\ \Xi \end{pmatrix} \to \begin{pmatrix} N\pi & N\eta & \Sigma K & \Lambda K \\ N\overline{K} & \Sigma\pi & \Lambda\pi & \Sigma\eta & \Xi K \\ & N\overline{K} & \Sigma\pi & \Lambda\eta & \Xi K \\ & & \Sigma\overline{K} & \Lambda\overline{K} & \Xi\pi & \Xi\eta \end{pmatrix} = \frac{1}{\sqrt{12}} \begin{pmatrix} 3 & 3 & 3 & -3 \\ 2 & 8 & 0 & 0 & -2 \\ & 6 & 0 & 0 & 6 \\ & 3 & 3 & 3 & -3 \end{pmatrix}^{1/2}$$

$10 \to 8 \otimes 8$

$$\begin{pmatrix} \Delta \\ \Sigma \\ \Xi \\ \Omega \end{pmatrix} \to \begin{pmatrix} N\pi & \Sigma K \\ N\overline{K} & \Sigma\pi & \Lambda\pi & \Sigma\eta & \Xi K \\ & \Sigma\overline{K} & \Lambda\overline{K} & \Xi\pi & \Xi\eta \\ & & \Xi\overline{K} \end{pmatrix} = \frac{1}{\sqrt{12}} \begin{pmatrix} -6 & 6 \\ -2 & 2 & -3 & 3 & 2 \\ & 3 & -3 & 3 & 3 \\ & & 12 \end{pmatrix}^{1/2}$$

$8 \to 10 \otimes 8$

$$\begin{pmatrix} N \\ \Sigma \\ \Lambda \\ \Xi \end{pmatrix} \to \begin{pmatrix} \Delta\pi & \Sigma K \\ \Delta\overline{K} & \Sigma\pi & \Sigma\eta & \Xi K \\ & \Sigma\pi & \Xi K \\ \Sigma\overline{K} & \Xi\pi & \Xi\eta & \Omega K \end{pmatrix} = \frac{1}{\sqrt{15}} \begin{pmatrix} -12 & 3 \\ 8 & -2 & -3 & 2 \\ & -9 & 6 \\ 3 & -3 & -3 & 6 \end{pmatrix}^{1/2}$$

$10 \to 10 \otimes 8$

$$\begin{pmatrix} \Delta \\ \Sigma \\ \Xi \\ \Omega \end{pmatrix} \to \begin{pmatrix} \Delta\pi & \Delta\eta & \Sigma K \\ \Delta\overline{K} & \Sigma\pi & \Sigma\eta & \Xi K \\ \Sigma\overline{K} & \Xi\pi & \Xi\eta & \Omega K \\ & \Xi\overline{K} & \Omega\eta \end{pmatrix} = \frac{1}{\sqrt{24}} \begin{pmatrix} 15 & 3 & -6 \\ 8 & 8 & 0 & -8 \\ 12 & 3 & -3 & -6 \\ & 12 & -12 \end{pmatrix}^{1/2}$$

abc	f_{abc}
123	1
147	1/2
156	−1/2
246	1/2
257	1/2
345	1/2
367	−1/2
458	$\sqrt{3}/2$
678	$\sqrt{3}/2$

abc	d_{abc}
118	$1/\sqrt{3}$
146	1/2
157	1/2
228	$1/\sqrt{3}$
247	−1/2
256	1/2
338	$1/\sqrt{3}$
344	1/2

abc	d_{abc}
355	1/2
366	−1/2
377	−1/2
448	$-1/(2\sqrt{3})$
558	$-1/(2\sqrt{3})$
668	$-1/(2\sqrt{3})$
778	$-1/(2\sqrt{3})$
888	$-1/\sqrt{3}$

The λ_a's are

$$\lambda_1 = \begin{pmatrix} 0 & 1 & 0 \\ 1 & 0 & 0 \\ 0 & 0 & 0 \end{pmatrix} \quad \lambda_2 = \begin{pmatrix} 0 & -i & 0 \\ i & 0 & 0 \\ 0 & 0 & 0 \end{pmatrix} \quad \lambda_3 = \begin{pmatrix} 1 & 0 & 0 \\ 0 & -1 & 0 \\ 0 & 0 & 0 \end{pmatrix}$$

$$\lambda_4 = \begin{pmatrix} 0 & 0 & 1 \\ 0 & 0 & 0 \\ 1 & 0 & 0 \end{pmatrix} \quad \lambda_5 = \begin{pmatrix} 0 & 0 & -i \\ 0 & 0 & 0 \\ i & 0 & 0 \end{pmatrix} \quad \lambda_6 = \begin{pmatrix} 0 & 0 & 0 \\ 0 & 0 & 1 \\ 0 & 1 & 0 \end{pmatrix}$$

$$\lambda_7 = \begin{pmatrix} 0 & 0 & 0 \\ 0 & 0 & -i \\ 0 & i & 0 \end{pmatrix} \quad \lambda_8 = \frac{1}{\sqrt{3}} \begin{pmatrix} 1 & 0 & 0 \\ 0 & 1 & 0 \\ 0 & 0 & -2 \end{pmatrix}$$

Equation (36.7) defines the Lie algebra of SU(3). A general d-dimensional representation is given by a set of $d \times d$ matrices satisfying Eq. (36.7) with the f_{abc} given above. Equation (36.8) is specific to the defining 3-dimensional representation.

37. SU(n) MULTIPLETS AND YOUNG DIAGRAMS

Written by C.G. Wohl (LBNL).

This note tells (1) how SU(n) particle multiplets are identified or labeled, (2) how to find the number of particles in a multiplet from its label, (3) how to draw the Young diagram for a multiplet, and (4) how to use Young diagrams to determine the overall multiplet structure of a composite system, such as a 3-quark or a meson-baryon system.

In much of the literature, the word "representation" is used where we use "multiplet," and "tableau" is used where we use "diagram."

37.1. Multiplet labels

An SU(n) multiplet is uniquely identified by a string of $(n-1)$ nonnegative integers: $(\alpha, \beta, \gamma, \ldots)$. Any such set of integers specifies a multiplet. For an SU(2) multiplet such as an isospin multiplet, the single integer α is the number of *steps* from one end of the multiplet to the other (*i.e.*, it is one fewer than the number of particles in the multiplet). In SU(3), the two integers α and β are the numbers of steps across the top and bottom levels of the multiplet diagram. Thus the labels for the SU(3) octet and decuplet

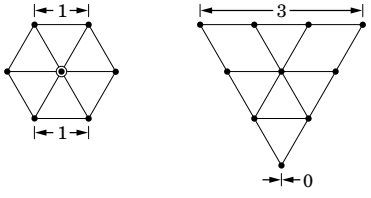

are (1,1) and (3,0). For larger n, the interpretation of the integers in terms of the geometry of the multiplets, which exist in an $(n-1)$-dimensional space, is not so readily apparent.

The label for the SU(n) singlet is $(0, 0, \ldots, 0)$. In a flavor SU(n), the n quarks together form a $(1, 0, \ldots, 0)$ multiplet, and the n antiquarks belong to a $(0, \ldots, 0, 1)$ multiplet. These two multiplets are *conjugate* to one another, which means their labels are related by $(\alpha, \beta, \ldots) \leftrightarrow (\ldots, \beta, \alpha)$.

37.2. Number of particles

The number of particles in a multiplet, $N = N(\alpha, \beta, \ldots)$, is given as follows (note the pattern of the equations).

In SU(2), $N = N(\alpha)$ is

$$N = \frac{(\alpha+1)}{1} \,. \tag{37.1}$$

In SU(3), $N = N(\alpha, \beta)$ is

$$N = \frac{(\alpha+1)}{1} \cdot \frac{(\beta+1)}{1} \cdot \frac{(\alpha+\beta+2)}{2} \,. \tag{37.2}$$

In SU(4), $N = N(\alpha, \beta, \gamma)$ is

$$N = \frac{(\alpha+1)}{1} \cdot \frac{(\beta+1)}{1} \cdot \frac{(\gamma+1)}{1} \cdot \frac{(\alpha+\beta+2)}{2} \cdot \frac{(\beta+\gamma+2)}{2} \cdot \frac{(\alpha+\beta+\gamma+3)}{3} \,. \tag{37.3}$$

Note that in Eq. (37.3) there is no factor with $(\alpha+\gamma+2)$: only a *consecutive* sequence of the label integers appears in any factor. One more example should make the pattern clear for any SU(n). In SU(5), $N = N(\alpha, \beta, \gamma, \delta)$ is

$$N = \frac{(\alpha+1)}{1} \cdot \frac{(\beta+1)}{1} \cdot \frac{(\gamma+1)}{1} \cdot \frac{(\delta+1)}{1} \cdot \frac{(\alpha+\beta+2)}{2} \cdot \frac{(\beta+\gamma+2)}{2} \times \frac{(\gamma+\delta+2)}{2} \cdot \frac{(\alpha+\beta+\gamma+3)}{3} \cdot \frac{(\beta+\gamma+\delta+3)}{3} \cdot \frac{(\alpha+\beta+\gamma+\delta+4)}{4} \tag{37.4}$$

From the symmetry of these equations, it is clear that multiplets that are conjugate to one another have the same number of particles, but so can other multiplets. For example, the SU(4) multiplets (3,0,0) and (1,1,0) each have 20 particles. Try the equations and see.

37.3. Young diagrams

A Young diagram consists of an array of boxes (or some other symbol) arranged in one or more *left-justified* rows, with each row being *at least as long* as the row beneath. The correspondence between a diagram and a multiplet label is: The top row juts out α boxes to the right past the end of the second row, the second row juts out β boxes to the right past the end of the third row, *etc.* A diagram in SU(n) has at most n rows. There can be any number of "completed" columns of n boxes buttressing the left of a diagram; these don't affect the label. Thus in SU(3) the diagrams

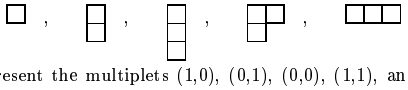

represent the multiplets (1,0), (0,1), (0,0), (1,1), and (3,0). In any SU(n), the quark multiplet is represented by a single box, the antiquark multiplet by a column of $(n-1)$ boxes, and a singlet by a completed column of n boxes.

37.4. Coupling multiplets together

The following recipe tells how to find the multiplets that occur in coupling two multiplets together. To couple together more than two multiplets, first couple two, then couple a third with each of the multiplets obtained from the first two, *etc.*

First a definition: A sequence of the letters $a, b, c, \ldots$ is *admissible* if at any point in the sequence at least as many a's have occurred as b's, at least as many b's have occurred as c's, *etc.* Thus *abcd* and *aabcb* are admissible sequences and *abb* and *acb* are not. Now the recipe:

(a) Draw the Young diagrams for the two multiplets, but in one of the diagrams replace the boxes in the first row with a's, the boxes in the second row with b's, *etc.* Thus, to couple two SU(3) octets (such as the π-meson octet and the baryon octet), we start with  and  . The *unlettered* diagram forms the *upper left-hand corner* of all the enlarged diagrams constructed below.

(b) Add the a's from the lettered diagram to the right-hand ends of the rows of the unlettered diagram to form all possible legitimate Young diagrams that have no more than one a per column. In general, there will be several distinct diagrams, and all the a's appear in each diagram. At this stage, for the coupling of the two SU(3) octets, we have:

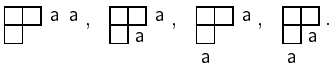

(c) Use the b's to further enlarge the diagrams already obtained, subject to the same rules. Then throw away any diagram in which the full sequence of letters formed by reading *right to left* in the first row, then the second row, *etc.*, is not admissible.

(d) Proceed as in (c) with the c's (if any), *etc.*

The final result of the coupling of the two SU(3) octets is:

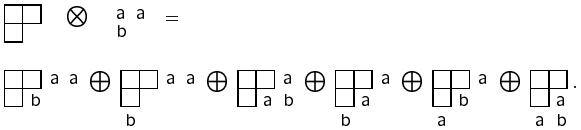

Here only the diagrams with admissible sequences of a's and b's and with fewer than four rows (since $n = 3$) have been kept. In terms of multiplet labels, the above may be written

$$(1,1) \otimes (1,1) = (2,2) \oplus (3,0) \oplus (0,3) \oplus (1,1) \oplus (1,1) \oplus (0,0) \,.$$

In terms of numbers of particles, it may be written

$$\mathbf{8} \otimes \mathbf{8} = \mathbf{27} \oplus \mathbf{10} \oplus \overline{\mathbf{10}} \oplus \mathbf{8} \oplus \mathbf{8} \oplus \mathbf{1} \,.$$

The product of the numbers on the left here is equal to the sum on the right, a useful check. (See also Sec. 14 on the Quark Model.)

38. KINEMATICS

Revised January 2000 by J.D. Jackson (LBNL).

Throughout this section units are used in which $\hbar = c = 1$. The following conversions are useful: $\hbar c = 197.3$ MeV fm, $(\hbar c)^2 = 0.3894$ (GeV)^2 mb.

38.1. Lorentz transformations

The energy E and 3-momentum $\boldsymbol{p}$ of a particle of mass m form a 4-vector $p = (E, \boldsymbol{p})$ whose square $p^2 \equiv E^2 - |\boldsymbol{p}|^2 = m^2$. The velocity of the particle is $\boldsymbol{\beta} = \boldsymbol{p}/E$. The energy and momentum $(E^*, \boldsymbol{p}^*)$ viewed from a frame moving with velocity $\boldsymbol{\beta}_f$ are given by

$$\begin{pmatrix} E^* \\ p_\parallel^* \end{pmatrix} = \begin{pmatrix} \gamma_f & -\gamma_f \beta_f \\ -\gamma_f \beta_f & \gamma_f \end{pmatrix} \begin{pmatrix} E \\ p_\parallel \end{pmatrix} , \quad p_T^* = p_T , \tag{38.1}$$

where $\gamma_f = (1 - \beta_f^2)^{-1/2}$ and p_T ($p_\parallel$) are the components of $\boldsymbol{p}$ perpendicular (parallel) to $\boldsymbol{\beta}_f$. Other 4-vectors, such as the space-time coordinates of events, of course transform in the same way. The scalar product of two 4-momenta $p_1 \cdot p_2 = E_1 E_2 - \boldsymbol{p}_1 \cdot \boldsymbol{p}_2$ is invariant (frame independent).

38.2. Center-of-mass energy and momentum

In the collision of two particles of masses m_1 and m_2 the total center-of-mass energy can be expressed in the Lorentz-invariant form

$$\begin{aligned} E_{\rm cm} &= \left[(E_1 + E_2)^2 - (\boldsymbol{p}_1 + \boldsymbol{p}_2)^2 \right]^{1/2} , \\ &= \left[m_1^2 + m_2^2 + 2E_1 E_2 (1 - \beta_1 \beta_2 \cos\theta) \right]^{1/2} , \end{aligned} \tag{38.2}$$

where θ is the angle between the particles. In the frame where one particle (of mass m_2) is at rest (lab frame),

$$E_{\rm cm} = (m_1^2 + m_2^2 + 2E_{1\,\rm lab}\, m_2)^{1/2} . \tag{38.3}$$

The velocity of the center-of-mass in the lab frame is

$$\boldsymbol{\beta}_{\rm cm} = \boldsymbol{p}_{\rm lab}/(E_{1\,\rm lab} + m_2) , \tag{38.4}$$

where $\boldsymbol{p}_{\rm lab} \equiv \boldsymbol{p}_{1\,\rm lab}$ and

$$\gamma_{\rm cm} = (E_{1\,\rm lab} + m_2)/E_{\rm cm} . \tag{38.5}$$

The c.m. momenta of particles 1 and 2 are of magnitude

$$p_{\rm cm} = p_{\rm lab} \frac{m_2}{E_{\rm cm}} . \tag{38.6}$$

For example, if a 0.80 GeV/c kaon beam is incident on a proton target, the center of mass energy is 1.699 GeV and the center of mass momentum of either particle is 0.442 GeV/c. It is also useful to note that

$$E_{\rm cm}\, dE_{\rm cm} = m_2\, dE_{1\,\rm lab} = m_2\, \beta_{1\,\rm lab}\, dp_{\rm lab} . \tag{38.7}$$

38.3. Lorentz-invariant amplitudes

The matrix elements for a scattering or decay process are written in terms of an invariant amplitude $-i\mathscr{M}$. As an example, the S-matrix for $2 \to 2$ scattering is related to $\mathscr{M}$ by

$$\begin{aligned} \langle p_1' p_2' \,|S|\, p_1 p_2 \rangle &= I - i(2\pi)^4\, \delta^4(p_1 + p_2 - p_1' - p_2') \\ &\times \frac{\mathscr{M}(p_1,\, p_2;\, p_1',\, p_2')}{(2E_1)^{1/2}\,(2E_2)^{1/2}\,(2E_1')^{1/2}\,(2E_2')^{1/2}} . \end{aligned} \tag{38.8}$$

The state normalization is such that

$$\langle p' | p \rangle = (2\pi)^3 \delta^3(\boldsymbol{p} - \boldsymbol{p}') . \tag{38.9}$$

38.4. Particle decays

The partial decay rate of a particle of mass M into n bodies in its rest frame is given in terms of the Lorentz-invariant matrix element $\mathscr{M}$ by

$$d\Gamma = \frac{(2\pi)^4}{2M} |\mathscr{M}|^2\, d\Phi_n\, (P;\, p_1, \ldots, p_n), \tag{38.10}$$

where $d\Phi_n$ is an element of n-body phase space given by

$$d\Phi_n(P;\, p_1, \ldots, p_n) = \delta^4\, (P - \sum_{i=1}^{n} p_i) \prod_{i=1}^{n} \frac{d^3 p_i}{(2\pi)^3 2E_i} . \tag{38.11}$$

This phase space can be generated recursively, viz.

$$\begin{aligned} d\Phi_n(P;\, p_1, \ldots, p_n) &= d\Phi_j(q;\, p_1, \ldots, p_j) \\ &\times\, d\Phi_{n-j+1}\,(P;\, q, p_{i+1}, \ldots, p_n)(2\pi)^3 dq^2 , \end{aligned} \tag{38.12}$$

where $q^2 = (\sum_{i=1}^{j} E_i)^2 - \left| \sum_{i=1}^{j} \boldsymbol{p}_i \right|^2$. This form is particularly useful in the case where a particle decays into another particle that subsequently decays.

38.4.1. ***Survival probability.*** If a particle of mass M has mean proper lifetime τ ($= 1/\Gamma$) and has momentum $(E, \boldsymbol{p})$, then the probability that it lives for a time t_0 or greater before decaying is given by

$$P(t_0) = e^{-t_0\, \Gamma/\gamma} = e^{-Mt_0\, \Gamma/E} , \tag{38.13}$$

and the probability that it travels a distance x_0 or greater is

$$P(x_0) = e^{-Mx_0\, \Gamma/|\boldsymbol{p}|} . \tag{38.14}$$

38.4.2. ***Two-body decays***:

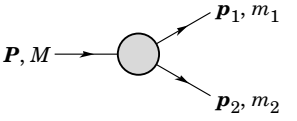

Figure 38.1: Definitions of variables for two-body decays.

In the rest frame of a particle of mass M, decaying into 2 particles labeled 1 and 2,

$$E_1 = \frac{M^2 - m_2^2 + m_1^2}{2M} , \tag{38.15}$$

$$\begin{aligned} |\boldsymbol{p}_1| &= |\boldsymbol{p}_2| \\ &= \frac{\left[\left(M^2 - (m_1 + m_2)^2\right) \left(M^2 - (m_1 - m_2)^2\right) \right]^{1/2}}{2M} , \end{aligned} \tag{38.16}$$

and

$$d\Gamma = \frac{1}{32\pi^2} |\mathscr{M}|^2\, \frac{|\boldsymbol{p}_1|}{M^2}\, d\Omega , \tag{38.17}$$

where $d\Omega = d\phi_1 d(\cos\theta_1)$ is the solid angle of particle 1.

38.4.3. ***Three-body decays***:

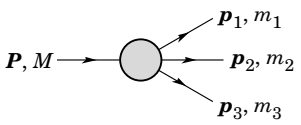

Figure 38.2: Definitions of variables for three-body decays.

Defining $p_{ij} = p_i + p_j$ and $m_{ij}^2 = p_{ij}^2$, then $m_{12}^2 + m_{23}^2 + m_{13}^2 = M^2 + m_1^2 + m_2^2 + m_3^2$ and $m_{12}^2 = (P - p_3)^2 = M^2 + m_3^2 - 2ME_3$, where E_3 is the energy of particle 3 in the rest frame of M. In that frame, the momenta of the three decay particles lie in a plane. The relative orientation of these three momenta is fixed if their energies are known. The momenta can therefore be specified in space by giving three Euler angles (α, β, γ) that specify the orientation of the final system relative to the initial particle [1]. Then

$$d\Gamma = \frac{1}{(2\pi)^5} \frac{1}{16M} \, |\mathscr{M}|^2 \, dE_1 \, dE_2 \, d\alpha \, d(\cos\beta) \, d\gamma \; . \tag{38.18}$$

Alternatively

$$d\Gamma = \frac{1}{(2\pi)^5} \frac{1}{16M^2} \, |\mathscr{M}|^2 \, |\boldsymbol{p}_1^*| \, |\boldsymbol{p}_3| \, dm_{12} \, d\Omega_1^* \, d\Omega_3 \; , \tag{38.19}$$

where $(|\boldsymbol{p}_1^*|, \Omega_1^*)$ is the momentum of particle 1 in the rest frame of 1 and 2, and Ω_3 is the angle of particle 3 in the rest frame of the decaying particle. $|\boldsymbol{p}_1^*|$ and $|\boldsymbol{p}_3|$ are given by

$$|\boldsymbol{p}_1^*| = \frac{\left[(m_{12}^2 - (m_1 + m_2)^2) \, (m_{12}^2 - (m_1 - m_2)^2)\right]^{1/2}}{2m_{12}} \; , \tag{38.20a}$$

and

$$|\boldsymbol{p}_3| = \frac{\left[(M^2 - (m_{12} + m_3)^2) \, (M^2 - (m_{12} - m_3)^2)\right]^{1/2}}{2M} \; . \tag{38.20b}$$

[Compare with Eq. (38.16).]

If the decaying particle is a scalar or we average over its spin states, then integration over the angles in Eq. (38.18) gives

$$d\Gamma = \frac{1}{(2\pi)^3} \frac{1}{8M} \, \overline{|\mathscr{M}|^2} \, dE_1 \, dE_2$$

$$= \frac{1}{(2\pi)^3} \frac{1}{32M^3} \, \overline{|\mathscr{M}|^2} \, dm_{12}^2 \, dm_{23}^2 \; . \tag{38.21}$$

This is the standard form for the Dalitz plot.

38.4.3.1. *Dalitz plot:* For a given value of m_{12}^2, the range of m_{23}^2 is determined by its values when $\boldsymbol{p}_2$ is parallel or antiparallel to $\boldsymbol{p}_3$:

$$(m_{23}^2)_{\rm max} =$$

$$(E_2^* + E_3^*)^2 - \left(\sqrt{E_2^{*2} - m_2^2} - \sqrt{E_3^{*2} - m_3^2}\right)^2 \; , \tag{38.22a}$$

$$(m_{23}^2)_{\rm min} =$$

$$(E_2^* + E_3^*)^2 - \left(\sqrt{E_2^{*2} - m_2^2} + \sqrt{E_3^{*2} - m_3^2}\right)^2 \; . \tag{38.22b}$$

Here $E_2^* = (m_{12}^2 - m_1^2 + m_2^2)/2m_{12}$ and $E_3^* = (M^2 - m_{12}^2 - m_3^2)/2m_{12}$ are the energies of particles 2 and 3 in the m_{12} rest frame. The scatter plot in m_{12}^2 and m_{23}^2 is called a Dalitz plot. If $\overline{|\mathscr{M}|^2}$ is constant, the allowed region of the plot will be uniformly populated with events [see Eq. (38.21)]. A nonuniformity in the plot gives immediate information on $|\mathscr{M}|^2$. For example, in the case of $D \to K\pi\pi$, bands appear when $m_{(K\pi)} = m_{K^*(892)}$, reflecting the appearance of the decay chain $D \to K^*(892)\pi \to K\pi\pi$.

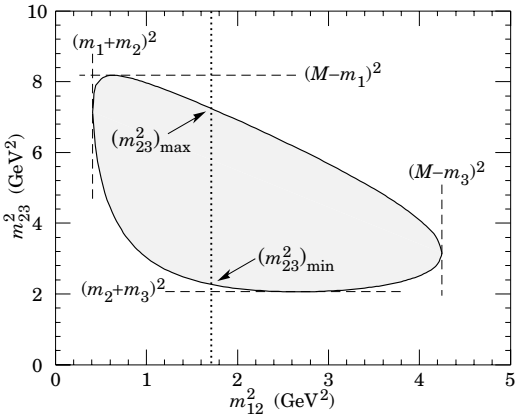

Figure 38.3: Dalitz plot for a three-body final state. In this example, the state is $\pi^+\overline{K}{}^0 p$ at 3 GeV. Four-momentum conservation restricts events to the shaded region.

38.4.4. ***Kinematic limits***: In a three-body decay the maximum of $|\boldsymbol{p}_3|$, [given by Eq. (38.20)], is achieved when $m_{12} = m_1 + m_2$, *i.e.*, particles 1 and 2 have the same vector velocity in the rest frame of the decaying particle. If, in addition, $m_3 > m_1, m_2$, then $|\boldsymbol{p}_3|_{\rm max} > |\boldsymbol{p}_1|_{\rm max}$, $|\boldsymbol{p}_2|_{\rm max}$.

38.4.5. ***Multibody decays***: The above results may be generalized to final states containing any number of particles by combining some of the particles into "effective particles" and treating the final states as 2 or 3 "effective particle" states. Thus, if $p_{ijk\ldots} = p_i + p_j + p_k + \ldots$, then

$$m_{ijk\ldots} = \sqrt{p^2_{ijk\ldots}} \; , \tag{38.23}$$

and $m_{ijk\ldots}$ may be used in place of *e.g.*, m_{12} in the relations in Sec. 38.4.3 or 38.4.3.1 above.

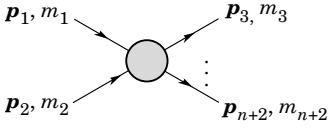

Figure 38.4: Definitions of variables for production of an n-body final state.

38.5. Cross sections

The differential cross section is given by

$$d\sigma = \frac{(2\pi)^4 \, |\mathscr{M}|^2}{4\sqrt{(p_1 \cdot p_2)^2 - m_1^2 m_2^2}}$$

$$\times \; d\Phi_n(p_1 + p_2;\, p_3, \ldots, p_{n+2}) \; . \tag{38.24}$$

[See Eq. (38.11).] In the rest frame of m_2(lab),

$$\sqrt{(p_1 \cdot p_2)^2 - m_1^2 m_2^2} = m_2 p_{1\,\rm lab} \; ; \tag{38.25a}$$

while in the center-of-mass frame

$$\sqrt{(p_1 \cdot p_2)^2 - m_1^2 m_2^2} = p_{1\rm cm}\sqrt{s} \; . \tag{38.25b}$$

38.5.1. ***Two-body reactions***:

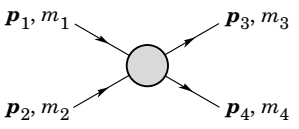

Figure 38.5: Definitions of variables for a two-body final state.

Two particles of momenta p_1 and p_2 and masses m_1 and m_2 scatter to particles of momenta p_3 and p_4 and masses m_3 and m_4; the Lorentz-invariant Mandelstam variables are defined by

$$\begin{aligned} s &= (p_1+p_2)^2 = (p_3+p_4)^2 \\ &= m_1^2 + 2E_1E_2 - 2\boldsymbol{p}_1\cdot\boldsymbol{p}_2 + m_2^2 \,, \end{aligned} \tag{38.26}$$

$$\begin{aligned} t &= (p_1-p_3)^2 = (p_2-p_4)^2 \\ &= m_1^2 - 2E_1E_3 + 2\boldsymbol{p}_1\cdot\boldsymbol{p}_3 + m_3^2 \,, \end{aligned} \tag{38.27}$$

$$\begin{aligned} u &= (p_1-p_4)^2 = (p_2-p_3)^2 \\ &= m_1^2 - 2E_1E_4 + 2\boldsymbol{p}_1\cdot\boldsymbol{p}_4 + m_4^2 \,, \end{aligned} \tag{38.28}$$

and they satisfy

$$s + t + u = m_1^2 + m_2^2 + m_3^2 + m_4^2 \,. \tag{38.29}$$

The two-body cross section may be written as

$$\frac{d\sigma}{dt} = \frac{1}{64\pi s}\,\frac{1}{|\boldsymbol{p}_{1\mathrm{cm}}|^2}\,|\mathscr{M}|^2 \,. \tag{38.30}$$

In the center-of-mass frame

$$\begin{aligned} t = (E_{1\mathrm{cm}} - E_{3\mathrm{cm}})^2 - (p_{1\mathrm{cm}} - p_{3\mathrm{cm}})^2 \qquad & - 4p_{1\mathrm{cm}}\,p_{3\mathrm{cm}}\,\sin^2(\theta_{\mathrm{cm}}/2) \\ = t_0 - 4p_{1\mathrm{cm}}\,p_{3\mathrm{cm}}\,\sin^2(\theta_{\mathrm{cm}}/2) \,, & \end{aligned} \tag{38.31}$$

where θ_{cm} is the angle between particle 1 and 3. The limiting values t_0 ($\theta_{\mathrm{cm}} = 0$) and t_1 ($\theta_{\mathrm{cm}} = \pi$) for $2 \to 2$ scattering are

$$t_0(t_1) = \left[\frac{m_1^2 - m_3^2 - m_2^2 + m_4^2}{2\sqrt{s}}\right]^2 - (p_{1\,\mathrm{cm}} \mp p_{3\,\mathrm{cm}})^2 \,. \tag{38.32}$$

In the literature the notation t_{min} (t_{max}) for t_0 (t_1) is sometimes used, which should be discouraged since $t_0 > t_1$. The center-of-mass energies and momenta of the incoming particles are

$$E_{1\mathrm{cm}} = \frac{s + m_1^2 - m_2^2}{2\sqrt{s}} \,, \qquad E_{2\mathrm{cm}} = \frac{s + m_2^2 - m_1^2}{2\sqrt{s}} \,, \tag{38.33}$$

For $E_{3\mathrm{cm}}$ and $E_{4\mathrm{cm}}$, change m_1 to m_3 and m_2 to m_4. Then

$$p_{i\,\mathrm{cm}} = \sqrt{E_{i\,\mathrm{cm}}^2 - m_i^2} \text{ and } p_{1\mathrm{cm}} = \frac{p_{1\,\mathrm{lab}}\,m_2}{\sqrt{s}} \,. \tag{38.34}$$

Here the subscript lab refers to the frame where particle 2 is at rest. [For other relations see Eqs. (38.2)–(38.4).]

38.5.2. ***Inclusive reactions***: Choose some direction (usually the beam direction) for the z-axis; then the energy and momentum of a particle can be written as

$$E = m_T \cosh y \;,\; p_x \;,\; p_y \;,\; p_z = m_T \sinh y \,, \tag{38.35}$$

where m_T is the transverse mass

$$m_T^2 = m^2 + p_x^2 + p_y^2 \,, \tag{38.36}$$

and the rapidity y is defined by

$$y = \frac{1}{2}\ln\left(\frac{E+p_z}{E-p_z}\right)$$

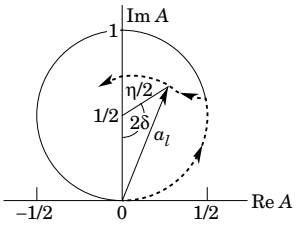

Figure 38.6: Argand plot showing a partial-wave amplitude a_ℓ as a function of energy. The amplitude leaves the unitary circle where inelasticity sets in ($\eta_\ell < 1$).

$$= \ln\left(\frac{E+p_z}{m_T}\right) = \tanh^{-1}\left(\frac{p_z}{E}\right) \,. \tag{38.37}$$

Under a boost in the z-direction to a frame with velocity β, $y \to y - \tanh^{-1}\beta$. Hence the shape of the rapidity distribution dN/dy is invariant. The invariant cross section may also be rewritten

$$E\frac{d^3\sigma}{d^3p} = \frac{d^3\sigma}{d\phi\,dy\,p_T\,dp_T} \Longrightarrow \frac{d^2\sigma}{\pi\,dy\,d(p_T^2)} \,. \tag{38.38}$$

The second form is obtained using the identity $dy/dp_z = 1/E$, and the third form represents the average over ϕ.

Feynman's x variable is given by

$$x = \frac{p_z}{p_{z\,\mathrm{max}}} \approx \frac{E+p_z}{(E+p_z)_{\mathrm{max}}} \quad (p_T \ll |p_z|) \,. \tag{38.39}$$

In the c.m. frame,

$$x \approx \frac{2p_{z\,\mathrm{cm}}}{\sqrt{s}} = \frac{2m_T\sinh y_{\mathrm{cm}}}{\sqrt{s}} \tag{38.40}$$

and

$$= (y_{\mathrm{cm}})_{\mathrm{max}} = \ln(\sqrt{s}/m) \,. \tag{38.41}$$

For $p \gg m$, the rapidity [Eq. (38.37)] may be expanded to obtain

$$\begin{aligned} y &= \frac{1}{2}\ln\frac{\cos^2(\theta/2) + m^2/4p^2 + \ldots}{\sin^2(\theta/2) + m^2/4p^2 + \ldots} \\ &\approx -\ln\tan(\theta/2) \equiv \eta \end{aligned} \tag{38.42}$$

where $\cos\theta = p_z/p$. The pseudorapidity η defined by the second line is approximately equal to the rapidity y for $p \gg m$ and $\theta \gg 1/\gamma$, and in any case can be measured when the mass and momentum of the particle is unknown. From the definition one can obtain the identities

$$\sinh\eta = \cot\theta \;,\quad \cosh\eta = 1/\sin\theta \;,\quad \tanh\eta = \cos\theta \,. \tag{38.43}$$

38.5.3. ***Partial waves***: The amplitude in the center of mass for elastic scattering of spinless particles may be expanded in Legendre polynomials

$$f(k,\theta) = \frac{1}{k}\sum_\ell (2\ell+1)a_\ell P_\ell(\cos\theta) \,, \tag{38.44}$$

where k is the c.m. momentum, θ is the c.m. scattering angle, $a_\ell = (\eta_\ell e^{2i\delta_\ell} - 1)/2i$, $0 \le \eta_\ell \le 1$, and δ_ℓ is the phase shift of the ℓ^{th} partial wave. For purely elastic scattering, $\eta_\ell = 1$. The differential cross section is

$$\frac{d\sigma}{d\Omega} = |f(k,\theta)|^2 \,. \tag{38.45}$$

The optical theorem states that

$$\sigma_{\mathrm{tot}} = \frac{4\pi}{k}\mathrm{Im}\,f(k,0) \,, \tag{38.46}$$

and the cross section in the ℓ^{th} partial wave is therefore bounded:

$$\sigma_\ell = \frac{4\pi}{k^2}(2\ell+1)|a_\ell|^2 \le \frac{4\pi(2\ell+1)}{k^2} \,. \tag{38.47}$$

The evolution with energy of a partial-wave amplitude a_ℓ can be displayed as a trajectory in an Argand plot, as shown in Fig. 38.6.

The usual Lorentz-invariant matrix element $\mathscr{M}$ (see Sec. 38.3 above) for the elastic process is related to $f(k,\theta)$ by

$$\mathscr{M} = -8\pi\sqrt{s}\, f(k,\theta)\,, \tag{38.48}$$

so

$$\sigma_{\rm tot} = -\frac{1}{2p_{\rm lab}\, m_2}\,{\rm Im}\,\mathscr{M}(t=0)\,, \tag{38.49}$$

where s and t are the center-of-mass energy squared and momentum transfer squared, respectively (see Sec. 38.4.1).

38.5.3.1. *Resonances:* The Breit-Wigner (nonrelativistic) form for an elastic amplitude a_ℓ with a resonance at c.m. energy E_R, elastic width $\Gamma_{\rm el}$, and total width $\Gamma_{\rm tot}$ is

$$a_\ell = \frac{\Gamma_{\rm el}/2}{E_R - E - i\Gamma_{\rm tot}/2}\,, \tag{38.50}$$

where E is the c.m. energy. As shown in Fig. 38.7, in the absence of background the elastic amplitude traces a counterclockwise circle with center $ix_{\rm el}/2$ and radius $x_{\rm el}/2$, where the elasticity $x_{\rm el} = \Gamma_{\rm el}/\Gamma_{\rm tot}$. The amplitude has a pole at $E = E_R - i\Gamma_{\rm tot}/2$.

The spin-averaged Breit-Wigner cross section for a spin-J resonance produced in the collision of particles of spin S_1 and S_2 is

$$\sigma_{BW}(E) = \frac{(2J+1)}{(2S_1+1)(2S_2+1)}\,\frac{\pi}{k^2}\,\frac{B_{\rm in}B_{\rm out}\Gamma_{\rm tot}^2}{(E-E_R)^2+\Gamma_{\rm tot}^2/4}\,, \tag{38.51}$$

where k is the c.m. momentum, E is the c.m. energy, and $B_{\rm in}$ and $B_{\rm out}$ are the branching fractions of the resonance into the entrance and exit channels. The $2S+1$ factors are the multiplicities of the incident spin states, and are replaced by 2 for photons. This expression is valid only for an isolated state. If the width is not small, $\Gamma_{\rm tot}$ cannot be treated as a constant independent of E. There are many other forms for σ_{BW}, all of which are equivalent to the one given here in the narrow-width case. Some of these forms may be more appropriate if the resonance is broad.

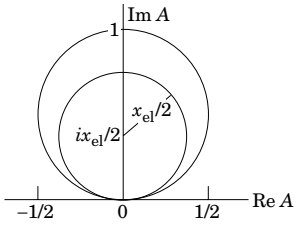

Figure 38.7: Argand plot for a resonance.

The relativistic Breit-Wigner form corresponding to Eq. (38.50) is:

$$a_\ell = \frac{-m\Gamma_{\rm el}}{s - m^2 + im\Gamma_{\rm tot}}\,. \tag{38.52}$$

A better form incorporates the known kinematic dependences, replacing $m\Gamma_{\rm tot}$ by $\sqrt{s}\,\Gamma_{\rm tot}(s)$, where $\Gamma_{\rm tot}(s)$ is the width the resonance particle would have if its mass were $\sqrt{s}$, and correspondingly $m\Gamma_{\rm el}$ by $\sqrt{s}\,\Gamma_{\rm el}(s)$ where $\Gamma_{\rm el}(s)$ is the partial width in the incident channel for a mass $\sqrt{s}$:

$$a_\ell = \frac{-\sqrt{s}\,\Gamma_{\rm el}(s)}{s - m^2 + i\sqrt{s}\,\Gamma_{\rm tot}(s)}\,. \tag{38.53}$$

For the Z boson, all the decays are to particles whose masses are small enough to be ignored, so on dimensional grounds $\Gamma_{\rm tot}(s) = \sqrt{s}\,\Gamma_0/m_Z$, where Γ_0 defines the width of the Z, and $\Gamma_{\rm el}(s)/\Gamma_{\rm tot}(s)$ is constant. A full treatment of the line shape requires consideration of dynamics, not just kinematics. For the Z this is done by calculating the radiative corrections in the Standard Model.

References:

1. See, for example, J.J. Sakurai, *Modern Quantum Mechnaics*, Addison-Wesley (1985), p. 172, or D.M. Brink and G.R. Satchler, *Angular Momentum*, 2nd ed., Oxford University Press (1968), p. 20.

39. CROSS-SECTION FORMULAE FOR SPECIFIC PROCESSES

Revised October 2001 by R.N. Cahn (LBNL).

39.1. Leptoproduction

See section on Structure Functions (Sec. 16 of this *Review*).

39.2. e^+e^- annihilation

For pointlike, spin-1/2 fermions, the differential cross section in the c.m. for $e^+e^- \to f\overline{f}$ via single photon annihilation is (θ is the angle between the incident electron and the produced fermion; $N_c = 1$ if f is a lepton and $N_c = 3$ if f is a quark).

$$\frac{d\sigma}{d\Omega} = N_c \frac{\alpha^2}{4s}\beta\left[1 + \cos^2\theta + (1-\beta^2)\sin^2\theta\right]Q_f^2 \ , \qquad (39.1)$$

where β is the velocity of the final state fermion in the c.m. and Q_f is the charge of the fermion in units of the proton charge. For $\beta \to 1$,

$$\sigma = N_c \frac{4\pi\alpha^2}{3s}Q_f^2 = N_c \frac{86.8 Q_f^2 \ nb}{s} \ . \qquad (39.2)$$

where s is in GeV^2 units.

At higher energies, the Z^0 (mass M_Z and width Γ_Z) must be included. If the mass of a fermion f is much less than the mass of the Z^0, then the differential cross section for $e^+e^- \to f\overline{f}$ is

$$\begin{aligned}\frac{d\sigma}{d\Omega} = \ & N_c \frac{\alpha^2}{4s}\Big\{(1+\cos^2\theta)\left[Q_f^2 - 2\chi_1 v_e v_f Q_f + \chi_2(a_e^2+v_e^2)(a_f^2+v_f^2)\right] \\ & + 2\cos\theta\left[-2\chi_1 a_e a_f Q_f + 4\chi_2 a_e a_f v_e v_f\right]\Big\} \qquad (39.3)\end{aligned}$$

where

$$\begin{aligned}\chi_1 = \ & \frac{1}{16\sin^2\theta_W\cos^2\theta_W}\frac{s(s-M_Z^2)}{(s-M_Z^2)^2+M_Z^2\Gamma_Z^2} \ , \\ \chi_2 = \ & \frac{1}{256\sin^4\theta_W\cos^4\theta_W}\frac{s^2}{(s-M_Z^2)^2+M_Z^2\Gamma_Z^2} \ , \\ a_e = \ & -1 \ , \\ v_e = \ & -1 + 4\sin^2\theta_W \ , \\ a_f = \ & 2T_{3f} \ , \\ v_f = \ & 2T_{3f} - 4Q_f\sin^2\theta_W \ , \qquad (39.4)\end{aligned}$$

where $T_{3f} = 1/2$ for u, c and neutrinos, while $T_{3f} = -1/2$ for d, s, b, and negatively charged leptons.

At LEP II it may be possible to produce the orthodox Higgs boson, H, (see the mini-review on Higgs bosons) in the reaction $e^+e^- \to HZ^0$, which proceeds dominantly through a virtual Z^0. The Standard Model prediction for the cross section [3] is

$$\sigma(e^+e^- \to HZ^0) = \frac{\pi\alpha^2}{24}\cdot\frac{2K}{\sqrt{s}}\cdot\frac{K^2+3M_Z^2}{(s-M_Z^2)^2}\cdot\frac{1-4\sin^2\theta_W+8\sin^4\theta_W}{\sin^4\theta_W\cos^4\theta_W} \ . \qquad (39.5)$$

where K is the c.m. momentum of the produced H or Z^0. Near the production threshold, this formula needs to be corrected for the finite width of the Z^0.

39.3. Two-photon process at e^+e^- colliders

When an e^+ and an e^- collide with energies E_1 and E_2, they emit dn_1 and dn_2 virtual photons with energies ω_1 and ω_2 and 4-momenta q_1 and q_2. In the equivalent photon approximation, the cross section for $e^+e^- \to e^+e^-X$ is related to the cross section for $\gamma\gamma \to X$ by (Ref. 1)

$$d\sigma_{e^+e^-\to e^+e^-X}(s) = dn_1\, dn_2\, d\sigma_{\gamma\gamma\to X}(W^2) \qquad (39.6)$$

where $s = 4E_1E_2$, $W^2 = 4\omega_1\omega_2$ and

$$dn_i = \frac{\alpha}{\pi}\left[1 - \frac{\omega_i}{E_i} + \frac{\omega_i^2}{2E_i^2} - \frac{m_e^2\omega_i^2}{(-q_i^2)E_i^2}\right]\frac{d\omega_i}{\omega_i}\frac{d(-q_i^2)}{(-q_i^2)} \ . \qquad (39.7)$$

After integration (including that over q_i^2 in the region $m_e^2\omega_i^2/E_i(E_i-\omega_i) \le -q_i^2 \le (-q^2)_{\max}$), the cross section is

$$\begin{aligned}\sigma_{e^+e^-\to e^+e^-X}(s) = & \frac{\alpha^2}{\pi^2}\int_{z_{th}}^1 \frac{dz}{z}\left[f(z)\left(\ln\frac{(-q^2)_{\max}}{m_e^2 z} - 1\right)^2\right. \\ & \left. - \tfrac{1}{3}\left(\ln\frac{1}{z}\right)^3\right]\sigma_{\gamma\gamma\to X}(zs) \ ; \\ f(z) = & \left(1+\tfrac{1}{2}z\right)^2\ln\frac{1}{z} - \tfrac{1}{2}(1-z)(3+z) \ ; \\ z = & \frac{W^2}{s} \ . \qquad (39.8)\end{aligned}$$

The quantity $(-q^2)_{\max}$ depends on properties of the produced system X, in particular, $(-q^2)_{\max} \sim m_\rho^2$ for hadron production ($X = h$) and $(-q^2)_{\max} \sim W^2$ for lepton pair production ($X = \ell^+\ell^-$, $\ell = e, \mu, \tau$).

For production of a resonance of mass m_R and spin $J \neq 1$

$$\begin{aligned}\sigma_{e^+e^-\to e^+e^-R}(s) = & (2J+1)\frac{8\alpha^2\Gamma_{R\to\gamma\gamma}}{m_R^3} \\ & \times\left[f(m_R^2/s)\left(\ln\frac{sm_V^2}{m_e^2m_R^2} - 1\right)^2 - \frac{1}{3}\left(\ln\frac{s}{m_R^2}\right)^3\right] \qquad (39.9)\end{aligned}$$

where m_V is the mass that enters into the form factor of the $\gamma\gamma \to R$ transition: $m_V \sim m_\rho$ for $R = \pi^0$, η, $f_2(1270)$, ..., $m_V \sim m_R$ for $R = c\overline{c}$ or $b\overline{b}$ resonances.

39.4. Inclusive hadronic reactions

One-particle inclusive cross sections $Ed^3\sigma/d^3p$ for the production of a particle of momentum p are conveniently expressed in terms of rapidity (see above) and the momentum p_T transverse to the beam direction (defined in the center-of-mass frame)

$$E\frac{d^3\sigma}{d^3p} = \frac{d^3\sigma}{d\phi\, dy\, p_T\, dp_T} \ . \qquad (39.10)$$

In the case of processes where p_T is large or the mass of the produced particle is large (here large means greater than 10 GeV), the parton model can be used to calculate the rate. Symbolically

$$\sigma_{\rm hadronic} = \sum_{ij}\int f_i(x_1,\, Q^2)\ f_j(x_2,\, Q^2)\ dx_1\ dx_2\ \widehat{\sigma}_{\rm partonic} \ , \qquad (39.11)$$

where $f_i(x, Q^2)$ is the parton distribution introduced above and Q is a typical momentum transfer in the partonic process and $\widehat{\sigma}$ is the partonic cross section. Some examples will help to clarify. The production of a W^+ in pp reactions at rapidity y in the center-of-mass frame is given by

$$\begin{aligned}\frac{d\sigma}{dy} = & \frac{G_F\,\pi\sqrt{2}}{3}\times\tau\left[\cos^2\theta_c\left(u(x_1\ ,\ M_W^2)\ \overline{d}\ (x_2, M_W^2)\right.\right. \\ & \left. + u(x_2\ ,\ M_W^2)\ \overline{d}\ (x_1, M_W^2)\right) \\ & + \sin^2\theta_c\left(u(x_1\ ,\ M_W^2)\ \overline{s}\ (x_2\ ,\ M_W^2)\right. \\ & \left.\left. + s(x_2, M_W^2)\ \overline{u}\ (x_1, M_W^2)\right)\right] \ , \qquad (39.12)\end{aligned}$$

where $x_1 = \sqrt{\tau}\ e^y$, $x_2 = \sqrt{\tau}\ e^{-y}$, and $\tau = M_W^2/s$. Similarly the production of a jet in pp (or $p\overline{p}$) collisions is given by

$$\begin{aligned}\frac{d^3\sigma}{d^2p_T\, dy} = & \sum_{ij}\int f_i(x_1\ ,\ p_T^2)\ f_j(x_2, p_T^2) \\ & \times\left[\widehat{s}\ \frac{d\widehat{\sigma}}{d\widehat{t}}\right]_{ij} dx_1\ dx_2\ \delta(\widehat{s}+\widehat{t}+\widehat{u}) \ , \qquad (39.13)\end{aligned}$$

where the summation is over quarks, gluons, and antiquarks. Here

$$s = (p_1 + p_2)^2 \,, \tag{39.14}$$

$$t = (p_1 - p_{\rm jet})^2 \,, \tag{39.15}$$

$$u = (p_2 - p_{\rm jet})^2 \,, \tag{39.16}$$

p_1 and p_2 are the momenta of the incoming p and p (or $\overline{p}$) and $\hat{s}$, $\hat{t}$, and $\hat{u}$ are s, t, and u with $p_1 \to x_1 p_1$ and $p_2 \to x_2\, p_2$. The partonic cross section $\hat{s}[(d\hat{\sigma})/(d\hat{t})]$ can be found in Ref. 2. Example: for the process $gg \to q\overline{q}$,

$$\hat{s}\,\frac{d\sigma}{dt} = 3\alpha_s^2\,\frac{(\hat{t}^{\,2}+\hat{u}^2)}{8\hat{s}}\,\left[\frac{4}{9\,\hat{t}\,\hat{u}} - \frac{1}{\hat{s}^{\,2}}\right] \,. \tag{39.17}$$

The prediction of Eq. (39.13) is compared to data from the UA1 and UA2 collaborations in Fig. 40.1 in the Plots of Cross Sections and Related Quantities section of this *Review*.

The associated production of a Higgs boson and a gauge boson is analogous to the process $e^+e^- \to HZ^0$ in Sec. 39.2. The required parton-level cross sections [4], averaged over initial quark colors, are

$$\sigma(q_i\overline{q}_j \to W^\pm H) = \frac{\pi\alpha^2|V_{ij}|^2}{36\sin^4\theta_W}\cdot\frac{2K}{\sqrt{s}}\cdot\frac{K^2+3M_W^2}{(s-M_W^2)^2}$$

$$\sigma(q\overline{q} \to Z^0 H) = \frac{\pi\alpha^2(a_q^2+v_q^2)}{144\sin^4\theta_W\cos^4\theta_W}\cdot\frac{2K}{\sqrt{s}}\cdot\frac{K^2+3M_Z^2}{(s-M_Z^2)^2} \,.$$

Here V_{ij} is the appropriate element of the Kobayashi-Maskawa matrix and K is the c.m. momentum of the produced H. The axial and vector couplings are defined as in Sec. 39.2.

39.5. One-particle inclusive distributions

In order to describe one-particle inclusive production in e^+e^- annihilation or deep inelastic scattering, it is convenient to introduce a fragmentation function $D_i^h\,(z,Q^2)$ where $D_i^h\,(z,Q^2)$ is the number of hadrons of type h and momentum between zp and $(z+dz)p$ produced in the fragmentation of a parton of type i. The Q^2 evolution is predicted by QCD and is similar to that of the parton distribution functions [see section on Quantum Chromodynamics (Sec. 9 of this *Review*)]. The $D_i^h(z,Q^2)$ are normalized so that

$$\sum_h \int z D_i^h\,(z,Q^2)dz = 1 \,. \tag{39.18}$$

If the contributions of the Z boson and three-jet events are neglected, the cross section for producing a hadron h in e^+e^- annihilation is given by

$$\frac{1}{\sigma_{\rm had}}\frac{d\sigma}{dz} = \frac{\sum_i e_i^2\; D_i^h\,(z,Q^2)}{\sum_i e_i^2} \,, \tag{39.19}$$

where e_i is the charge of quark-type i, $\sigma_{\rm had}$ is the total hadronic cross section, and the momentum of the hadron is $zE_{\rm cm}/2$.

In the case of deep inelastic muon scattering, the cross section for producing a hadron of energy E_h is given by

$$\frac{1}{\sigma_{\rm tot}}\frac{d\sigma}{dz} = \frac{\sum_i e_i^2\; q_i(x,Q^2)\; D_i^h(z,Q^2)}{\sum_i e_i^2\; q_i(x,Q^2)} \,, \tag{39.20}$$

where $E_h = \nu z$. (For the kinematics of deep inelastic scattering, see Sec. 38.4.2 of the Kinematics section of this *Review*.) The fragmentation functions for light and heavy quarks have a different z dependence; the former peak near $z = 0$. They are illustrated in Figs. 17.5a and 17.5b in the section on "Fragmentation Functions in e^+e^- Annihilation" (Sec. 17 of this *Review*).

References:

1. V.M. Budnev, I.F. Ginzburg, G.V. Meledin, and V.G. Serbo,Phys. Reports **15C**, 181 (1975);
   See also S. Brodsky, T. Kinoshita, and H. Terazawa, Phys. Rev. **D4**, 1532 (1971).
2. G.F. Owens, F. Reya, and M. Glück, Phys. Rev. **D18**, 1501 (1978).
3. B.W. Lee, C. Quigg, and B. Thacker, Phys. Rev. **D16**, 1519 (1977).
4. E. Eichten, I. Hinchliffe, K. Lane, and C. Quigg, Rev. Mod. Phys. **56**, 579 (1984).

40. PLOTS OF CROSS SECTIONS AND RELATED QUANTITIES

Jet Production in pp and $\overline{p}p$ Interactions

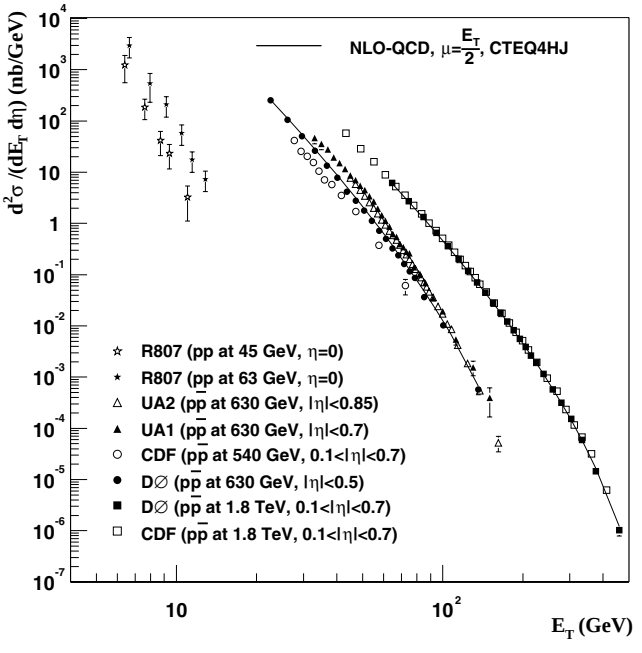

Figure 40.1: Transverse energy dependence of the inclusive differential jet cross sections in the central pseudorapidity region. The error bars are either statistical (DØ), statistical and p_T dependent (UA2), statistical and energy dependent from unsmearing (UA1), uncorrelated (CDF), or total (R806) uncertainties. Comparison of the different experimental results is not straight forward, since the different experiments used different jet reconstruction algorithms. For instance, DØ and CDF used a fixed cone algorithm with a size $\mathcal{R}$=0.7 for all their measurements, compared to a cone size of 1.3 for UA2. **DØ**: Phys. Rev. **D64**, 032003 (2001); **CDF**: Phys. Rev. **D64**, 032001 (2001); **UA1**: Phys. Lett. **B172**, 461 (1986); **UA2**: Phys. Lett. **B257**, 232 (1991); **R807**: Phys. Lett. **B123**, 133 (1983). Next-to-Leading order QCD predictions, using CTEQ4HJ pdfs and $\mu_{R,F} = E_T/2$, are shown for $p\overline{p}$ at 630 GeV and 1.8 TeV. (Courtesy of V.D. Elvira, Fermilab, 2001)

Direct γ Production in $\overline{p}p$ Interactions

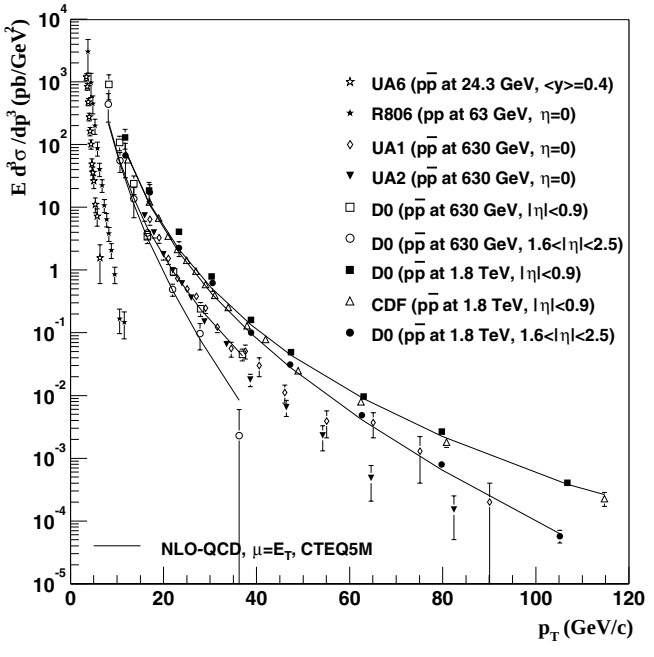

Figure 40.2: Transverse energy dependence of isolated photon cross sections. The error bars are either statistical (CDF), uncorrelated (DØ), or total (UA1, UA2, R806) uncertainties. **DØ**: Phys. Rev. Lett. **87**, 251805 (2001); **CDF**: Phys. Rev. **D73**, 2662 (1994); **UA6**: Phys. Lett. **B206**, 163 (1988); **UA1**: Phys. Lett. **B209**, 385 (1988); **UA2**: Phys. Lett. **B288**, 386 (1992); **R806**: Z. Phys. **C13**, 277 (1982). Next-to-Leading order QCD predictions are shown for $p\overline{p}$ at 630 GeV and 1.8 TeV. (Courtesy of V.D. Elvira, Fermilab, 2001)

Differential Cross Section for W and Z Boson Production

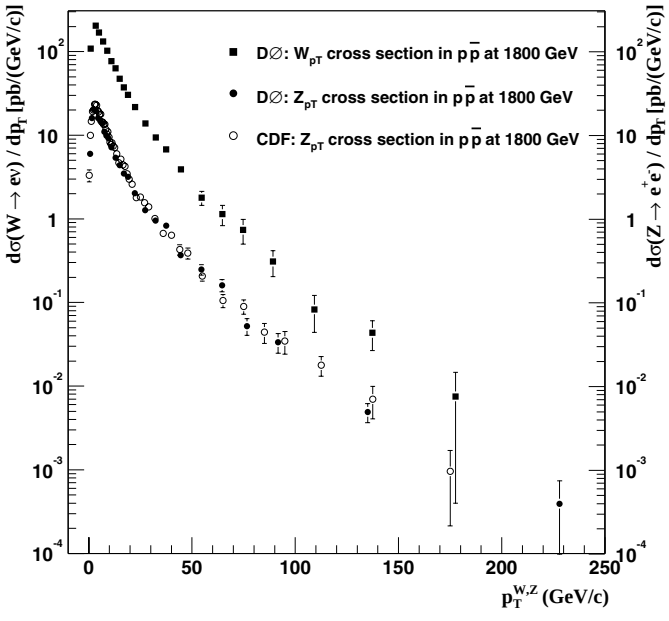

Figure 40.3: Differential cross section for W and Z boson production. The error bars are total errors, excluding the DØ (CDF) 4.4% (3.9%) luminosity uncertainty. **DØ**: Phys. Lett. **B513**, 292 (2001), Phys. Rev. Lett. **84**, 2792 (2000). **CDF**: Phys. Rev. Lett. **84**, 845 (2000). (Courtesy of V.D. Elvira, Fermilab, 2001)

Pseudorapidity Distributions in $\overline{p}p$ Interactions

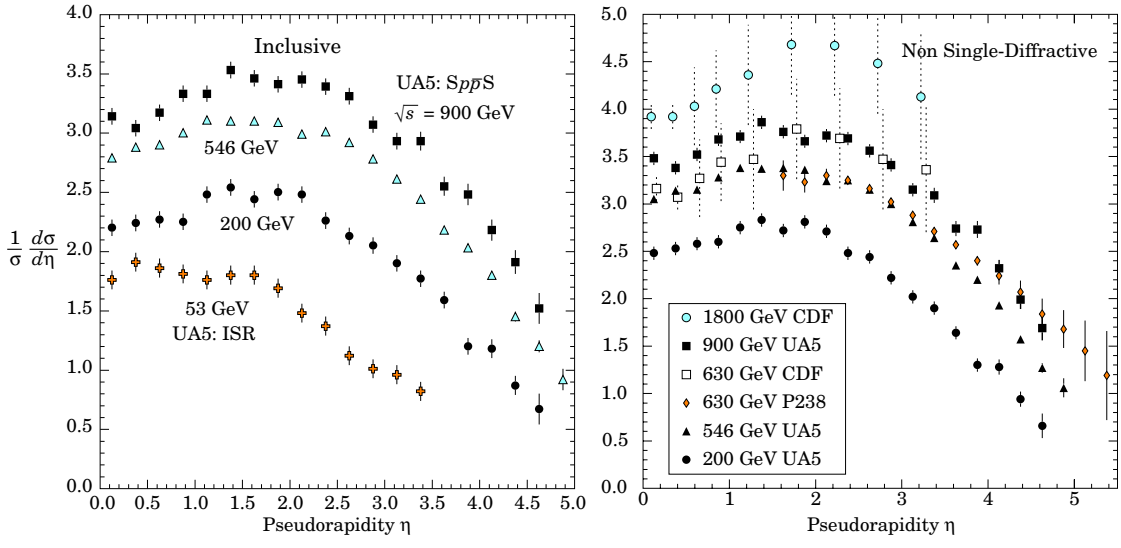

Figure 40.4: Charged particle pseudorapidity distributions in $p\overline{p}$ collisions for 53 GeV $\leq \sqrt{s} \leq$ 1800 GeV. UA5 data from the S$p\overline{p}$S are taken from G.J. Alner *et al.*, Z. Phys. **C33**, 1 (1986), and from the ISR from K. Alpgøard *et al.*, Phys. Lett. **112B**, 193 (1982). The UA5 data are shown for both the full inelastic cross-section and with singly diffractive events excluded. Additional non single-diffractive measurements are available from CDF at the Tevatron, F. Abe *et al.*, Phys. Rev. **D41**, 2330 (1990) and Experiment P238 at the S$p\overline{p}$S, R. Harr *et al.*, Phys. Lett. **B401**, 176 (1997). (Courtesy of D.R. Ward, Cambridge Univ., 1999.)

Average Hadron Multiplicities in Hadronic e^+e^- Annihilation Events

Table 40.1: Average hadron multiplicities per hadronic e^+e^- annihilation event at $\sqrt{s} \approx 10$, 29–35, 91, and 130–200 GeV. The rates given include decay products from resonances with $c\tau < 10$ cm, and include the corresponding anti-particle state. Correlations of the systemaic uncertainties were considered for the calculation of the averages. (Updated July 2003 by O. Biebel, LMU, Munich.)

Particle	$\sqrt{s} \approx 10$ GeV	$\sqrt{s} = 29$–35 GeV	$\sqrt{s} = 91$ GeV	$\sqrt{s} = 130$–200 GeV
Pseudoscalar mesons:				
π^+	6.6 ± 0.2	10.3 ± 0.4	16.99 ± 0.27	21.24 ± 0.39
π^0	3.2 ± 0.3	5.83 ± 0.28	9.42 ± 0.32	
K^+	0.90 ± 0.04	1.48 ± 0.09	2.242 ± 0.063	2.81 ± 0.19
K^0	0.91 ± 0.05	1.48 ± 0.07	2.049 ± 0.026	2.10 ± 0.12
η	0.20 ± 0.04	0.61 ± 0.07	1.049 ± 0.080	
$\eta'(958)$	0.03 ± 0.01	0.26 ± 0.10	0.152 ± 0.020	
D^+	$0.16 \pm 0.03^{(k)}$	0.17 ± 0.03	0.175 ± 0.016	
D^0	$0.37 \pm 0.06^{(k)}$	0.45 ± 0.07	0.454 ± 0.030	
D_s^+	$0.13 \pm 0.02^{(k)}$	$0.45 \pm 0.20^{(a)}$	0.131 ± 0.021	
B^+, B_d^0	—	—	$0.165 \pm 0.026^{(b)}$	
B_s^0	—	—	$0.057 \pm 0.013^{(b)}$	
Scalar mesons:				
$f_0(980)$	0.024 ± 0.006	$0.05 \pm 0.02^{(c)}$	0.146 ± 0.012	
$a_0(980)^\pm$	—	—	$0.27 \pm 0.11^{(d)}$	
Vector mesons:				
$\rho(770)^0$	0.35 ± 0.04	0.81 ± 0.08	1.231 ± 0.098	
$\rho(770)^\pm$	—	—	$2.40 \pm 0.43^{(d)}$	
$\omega(782)$	0.30 ± 0.08	—	1.016 ± 0.065	
$K^*(892)^+$	0.27 ± 0.03	0.64 ± 0.05	0.715 ± 0.059	
$K^*(892)^0$	0.29 ± 0.03	0.56 ± 0.06	0.738 ± 0.024	
$\phi(1020)$	0.044 ± 0.003	0.085 ± 0.011	0.0963 ± 0.0032	
$D^*(2010)^+$	$0.22 \pm 0.04^{(k)}$	0.43 ± 0.07	$0.1937 \pm 0.0057^{(j)}$	
$D^*(2007)^0$	$0.23 \pm 0.06^{(k)}$	0.27 ± 0.11	—	
$D_s^*(2112)^+$	—	—	$0.101 \pm 0.048^{(f)}$	
$B^{*\ (g)}$	—	—	0.288 ± 0.026	
$J/\psi(1S)$	$0.00050 \pm 0.00005^{(k)}$	—	$0.0052 \pm 0.0004^{(h)}$	
$\psi(2S)$	—	—	$0.0023 \pm 0.0004^{(h)}$	
$\Upsilon(1S)$	—	—	$0.00014 \pm 0.00007^{(h)}$	
Pseudovector mesons:				
$\chi_{c1}(3510)$	—	—	$0.0041 \pm 0.0011^{(h)}$	
Tensor mesons:				
$f_2(1270)$	0.09 ± 0.02	0.14 ± 0.04	0.166 ± 0.020	
$f_2'(1525)$	—	—	0.012 ± 0.006	
$K_2^*(1430)^+$	—	0.09 ± 0.03	—	
$K_2^*(1430)^0$	—	0.12 ± 0.06	$0.084 \pm 0.022^{(h)}$	
$B^{**\ (i)}$	—	—	0.118 ± 0.024	
$D_{s1}^\pm$	—	—	$0.0052 \pm 0.0011^{(\ell)}$	
$D_{s2}^{*\pm}$	—	—	$0.0083 \pm 0.0031^{(\ell)}$	
Baryons:				
p	0.253 ± 0.016	0.640 ± 0.050	1.048 ± 0.045	1.41 ± 0.18
Λ	0.080 ± 0.007	0.205 ± 0.010	0.3915 ± 0.0065	0.39 ± 0.03
Σ^0	0.023 ± 0.008	—	0.076 ± 0.011	
Σ^-	—	—	0.081 ± 0.010	
Σ^+	—	—	0.107 ± 0.011	
$\Sigma^\pm$	—	—	0.174 ± 0.009	
Ξ^-	0.0059 ± 0.0007	0.0176 ± 0.0027	0.0258 ± 0.0010	
$\Delta(1232)^{++}$	0.040 ± 0.010	—	0.085 ± 0.014	
$\Sigma(1385)^-$	0.006 ± 0.002	0.017 ± 0.004	0.0240 ± 0.0017	
$\Sigma(1385)^+$	0.005 ± 0.001	0.017 ± 0.004	0.0239 ± 0.0015	
$\Sigma(1385)^\pm$	0.0106 ± 0.0020	0.033 ± 0.008	0.0462 ± 0.0028	
$\Xi(1530)^0$	0.0015 ± 0.0006	—	0.0055 ± 0.0005	
Ω^-	0.0007 ± 0.0004	0.014 ± 0.007	0.0016 ± 0.0003	
Λ_c^+	$0.100 \pm 0.030^{(j)}$	0.110 ± 0.050	0.078 ± 0.017	
Λ_b^0	—	—	0.031 ± 0.016	
Σ_c^{++}, Σ_c^0	0.014 ± 0.007	—	—	
$\Lambda(1520)$	0.008 ± 0.002	—	0.0222 ± 0.0027	

Notes for Table 40.1:

(*a*) B($D_s \to \eta\pi,\ \eta'\pi$) was used (RPP1994).

(*b*) The Standard Model B($Z \to b\overline{b}$) = 0.217 was used.

(*c*) $x_p = p/p_{\rm beam} > 0.1$ only.

(*d*) Both charge states.

(*e*) B($D^*(2010)^+ \to D^0\pi^+$) × B($D^0 \to K^-\pi^+$) has been used (RPP2000).

(*f*) B($D_s^* \to D_S^+\gamma$), B($D_s^+ \to \phi\pi^+$), B($\phi \to K^+K^-$) have been used (RPP1998).

(*g*) Any charge state (*i.e.*, B_d^*, B_u^*, or B_s^*).

(*h*) B($Z \to$ hadrons) = 0.699 was used (RPP1994).

(*i*) Any charge state (*i.e.*, B_d^{**}, B_u^{**}, or B_s^{**}).

(*j*) The value was derived from the cross section of $\Lambda_c^+ \to p\pi K$, assuming the branching fraction to be (3.2 ± 0.7)% (RPP1992).

(*k*) $\sigma_{\rm had} = 3.33 \pm 0.05 \pm 0.21$ nb (**CLEO**: Phys. Rev. **D29**, 1254 (1984)) has been used in converting the measured cross sections to average hadron multiplicities.

(*ℓ*) Assumes B($D_{s1}^+ \to D^{*+}K^0 + D^{*0}K+$) = 100% and B($D_{s2}^+ \to D^0K^+$) = 45%.

References for Table 40.1:

RPP1992: Phys. Rev. **D45** (1992) and references therein.

RPP1994: Phys. Rev. **D50**, 1173 (1994) and references therein.

RPP1996: Phys. Rev. **D54**, 1 (1996) and references therein.

RPP1998: Eur. Phys. J. **C3**, 1 (1998) and references therein.

RPP2000: Eur. Phys. J. **C15**, 1 (2000) and references therein.

RPP2002: Phys. Rev. **D66**, 010001 (2002) and references therein.

R. Marshall, Rep. Prog. Phys. **52**, 1329 (1989)

A. De Angelis, J. Phys. **G19**, 1233 (1993) and references therein.

ALEPH: D. Buskulic *et al.*: Phys. Lett. **B295**, 396 (1992); Z. Phys. **C64**, 361 (1994); **C69**, 15 (1996); **C69**, 379 (1996); **C73**, 409 (1997); and
R. Barate *et al.*: Z. Phys. **C74**, 451 (1997); Phys. Reports **294**, 1 (1998); Eur. Phys. J. **C5**, 205 (1998); **C16**, 597 (2000); **C16**, 613 (2000); and
A. Heister *et al.*: Phys. Lett. **B526**, 34 (2002); **B528**, 19 (2002).

ARGUS: H. Albrecht *et al.*: Phys. Lett. **230B**, 169 (1989); Z. Phys. **C44**, 547 (1989); **C46**, 15 (1990); **C54**, 1 (1992); **C58**, 199 (1993); **C61**, 1 (1994); Phys. Rep. **276**, 223 (1996).

BaBar: B. Aubert *et al.*: Phys. Rev. Lett. **87**, 162002 (2001).

Belle: K. Abe *et al.*: Phys. Rev. Lett. **88**, 052001 (2002).

CELLO: H.J. Behrend *et al.*: Z. Phys. **C46**, 397 (1990); **C47**, 1 (1990).

CLEO: D. Bortoletto *et al.*, Phys. Rev. **D37**, 1719 (1988).

Crystal Ball: Ch. Bieler *et al.*, Z. Phys. **C49**, 225 (1991).

DELPHI: P. Abreu *et al.*: Z. Phys. **C57**, 181 (1993); **C59**, 533 (1993); **C61**, 40 7(1994); **C65**, 587 (1995); **C67**, 543 (1995); **C68**, 353 (1995); **C73**, 61 (1996); Nucl. Phys. **B444**, 3 (1995); Phys. Lett. **B341**, 109 (1994); **B345**, 598 (1995); **B361**, 207 (1995); **B372**, 172 (1996); **B379**, 309 (1996); **B416**, 233 (1998); **B449**, 364 (1999); **B475**, 429 (2000); Eur. Phys. J. **C6**, 19 (1999); **C5**, 585 (1998); **C18**, 203 (2000).

HRS: S. Abachi *et al.*, Phys. Rev. Lett. **57**, 1990 (1986); and
M. Derrick *et al.*, Phys. Rev. **D35**, 2639 (1987).

L3: M. Acciarri *et al.*: Phys. Lett. **B328**, 223 (1994); **B345**, 589 (1995); **B371**, 126 (1996); **B371**, 137 (1996); **B393**, 465 (1997); **B404**, 390 (1997); **B407**, 351 (1997); **B407**, 389 (1997), erratum ibid. **B427**, 409 (1998); **B453**, 94 (1999); **B479**, 79 (2000).

MARK II: H. Schellman *et al.*, Phys. Rev. **D31**, 3013 (1985); and
G. Wormser *et al.*, Phys. Rev. Lett. **61**, 1057 (1988).

JADE: W. Bartel *et al.*, Z. Phys. **C20**, 187 (1983); andD.D. Pietzl *et al.*, Z. Phys. **C46**, 1 (1990).

OPAL: R. Akers *et al.*: Z. Phys. **C63**, 181 (1994); **C66**, 555 (1995); **C67**, 389 (1995); **C68**, 1 (1995); and
G. Alexander *et al.*: Phys. Lett. **B358**, 162 (1995); Z. Phys. **C70**, 197 (1996); **C72**, 1 (1996); **C72**, 191 (1996); **C73**, 569 (1997); **C73**, 587 (1997); Phys. Lett. **B370**, 185 (1996); and
K. Ackerstaff *et al.*: Z. Phys. **C75**, 192 (1997); Phys. Lett. **B412**, 210 (1997); Eur. Phys. J. **C1**, 439 (1998); **C4**, 19 (1998); **C5**, 1 (1998); **C5**, 411 (1998); and
G. Abbiendi *et al.*: Eur. Phys. J. **C16**, 185 (2000); **C16**, 185 (2000).

PLUTO: Ch. Berger *et al.*, Phys. Lett. **104B**, 79 (1981).

SLD: K. Abe, Phys. Rev. **D59**, 052001 (1999).

TASSO: H. Aihara *et al.*, Z. Phys. **C27**, 27 (1985).

TPC: H. Aihara *et al.*, Phys. Rev. Lett. **53**, 2378 (1984).

Average e^+e^-, pp, and $\overline{p}p$ Multiplicity

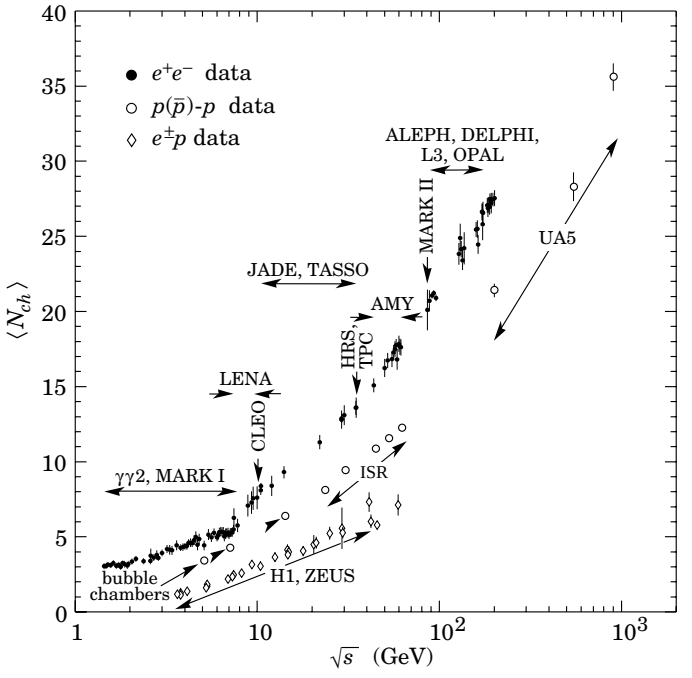

Figure 40.5: Average multiplicity as a function of $\sqrt{s}$ for e^+e^- and $p\overline{p}$ annihilations, and pp and ep collisions. The indicated errors are statistical and systematic errors added in quadrature, except when no systematic errors are given. Files of the data shown in this figure are given in `http://home.cern.ch/b/biebel/www/RPP02`

—

e^+e^-: Most e^+e^- measurements include contributions from K^0_S and Λ decays. The $\gamma\gamma$2 and MARK I measurements contain a systematic 5% error. Points at identical energies have been spread horizontally for clarity:

ALEPH: D. Buskulic *et al.*, Z. Phys. **C69**, 15 (1995); and Z. Phys. **C73**, 409 (1997).

ARGUS: H. Albrecht *et al.*, Z. Phys. **C54**, 13 (1992).

DELPHI: P. Abreu *et al.*, Eur. Phys. J. **C6**, 19 (1999); Phys. Lett. **B372**, 172 (1996); Phys. Lett. **B416**, 233 (1998); and Eur. Phys. J. **C18**, 203 (2000).

L3: M. Acciarri *et al.*, Phys. Lett. **B371**, 137 (1996); Phys. Lett. **B404**, 390 (1997); and Phys. Lett. **B444**, 569 (1998).

OPAL: G. Abbiendi *et al.*, Eur. Phys. J. **C16**, 185 (2000);
K. Ackerstaff *et al.*, Z. Phys. **C75**, 193 (1997);
P.D. Acton *et al.*, Z. Phys. **C53**, 539 (1992) and references therein;
R. Akers *et al.*, Z. Phys. **C68**, 203 (1995).

TOPAZ: K. Nakabayashi *et al.*, Phys. Lett. **B413**, 447 (1997).

VENUS: K. Okabe *et al.*, Phys. Lett. **B423**, 407 (1998).

—

$e^{\pm}p$: Multiplicities have been measured in the current fragmentation region of the Breit frame:

H1: C. Adloff *et al.*, Nucl. Phys. **B504**, 3 (1997).

ZEUS: J. Breitweg *et al.*, Eur. Phys. J. **C11**, 251 (1999);
S. Chekanov *et al.*, Phys. Lett. **B510**, 36 (2001).

—

$p(\overline{p})$: The errors of the $p(\overline{p})$ measurements are the quadratically added statistical and systematic errors, except for the bubble chamber measurements for which only statistical errors are given in the references. The values measured by UA5 exclude single diffractive dissociation:

—

bubble chamber: J. Benecke *et al.*, Nucl. Phys. **B76**, 29 (1976); W.M. Morse *et al.*, Phys. Rev. **D15**, 66 (1977).

ISR: A. Breakstone *et al.*, Phys. Rev. **D30**, 528 (1984).

UA5: G.J. Alner *et al.*, Phys. Lett. **167B**, 476 (1986);
R.E. Ansorge *et al.*, Z. Phys. **C43**, 357 (1989).

(Courtesy of O. Biebel, MPI München, 2001.)

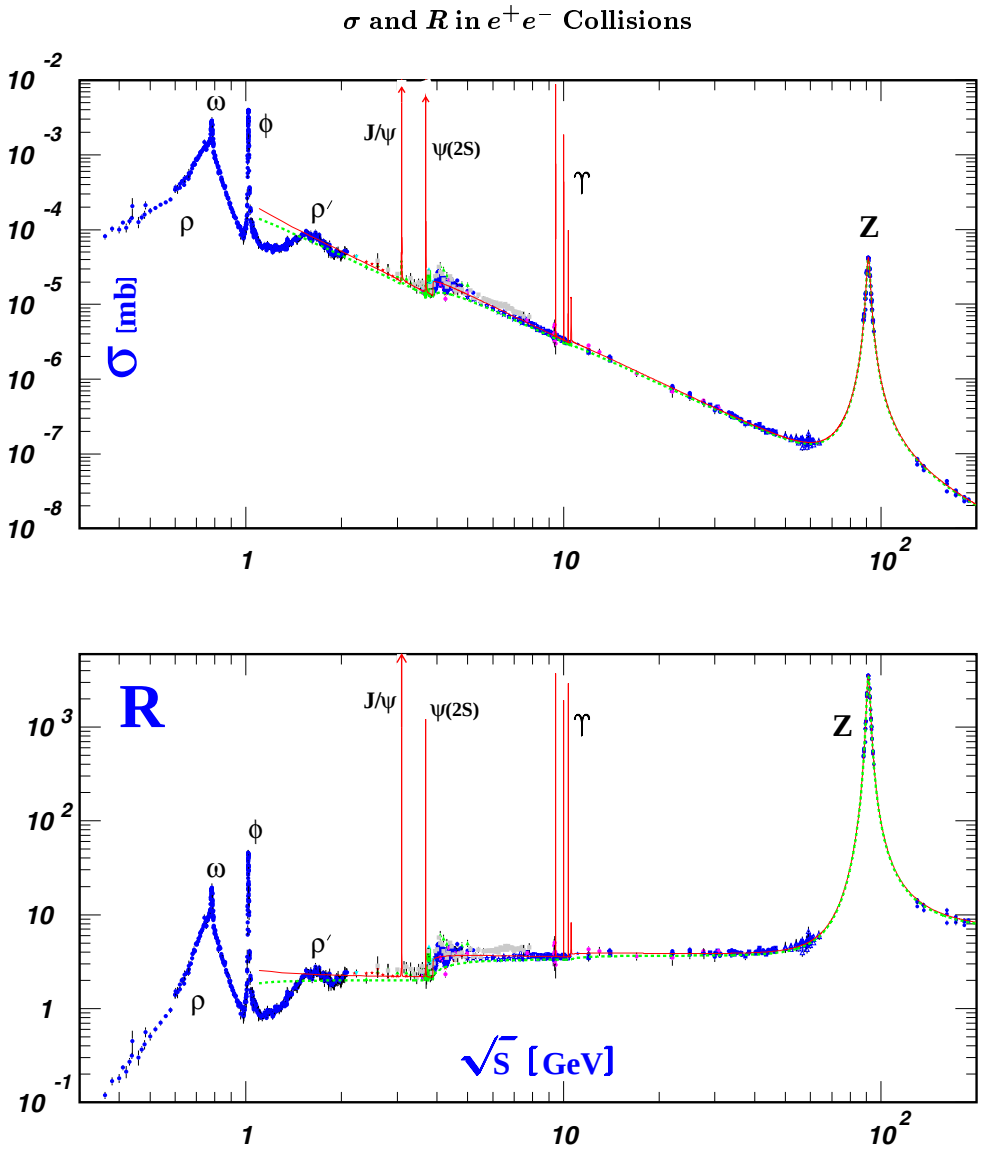

Figure 40.6: World data on the total cross section of $e^+e^- \to hadrons$ and the ratio $R(s) = \sigma(e^+e^- \to hadrons, s)/\sigma(e^+e^- \to \mu^+\mu^-, s)$. $\sigma(e^+e^- \to hadrons, s)$ is the experimental cross section corrected for initial state radiation and electron-positron vertex loops, $\sigma(e^+e^- \to \mu^+\mu^-, s) = 4\pi\alpha^2(s)/3s$. Data errors are total below 2 GeV and statistical above 2 GeV. The curves are an educative guide: the broken one is a naive quark-parton model prediction and the solid one is 3-loop pQCD prediction (see "Quantum Chromodynamics" section of this *Review*, Eq. (9.12) or, for more details, K. G. Chetyrkin et al., `hep-ph/0005139`, p.3, Eqs. (1)-(3)). Breit-Wigner parameterizations of J/ψ, $\psi(2S)$, and $\Upsilon(nS), n = 1..4$ are also shown. **Note:** The experimental shapes of these resonances are dominated by machine energy spread and are not shown. The full list of references to the original data and the details of the R ratio extraction from them can be found in `hep-ph/0312114`. Corresponding computer-readable data files are available at `http://pdg.ihep.su/xsect/contents.html`. (Courtesy of the COMPAS(Protvino) and HEPDATA(Durham) Groups, March 2004. Corrections by P. Janot (CERN) and M. Schmitt (Northwestern U.))

R in Light-Flavor, Charm, and Beauty Threshold Regions

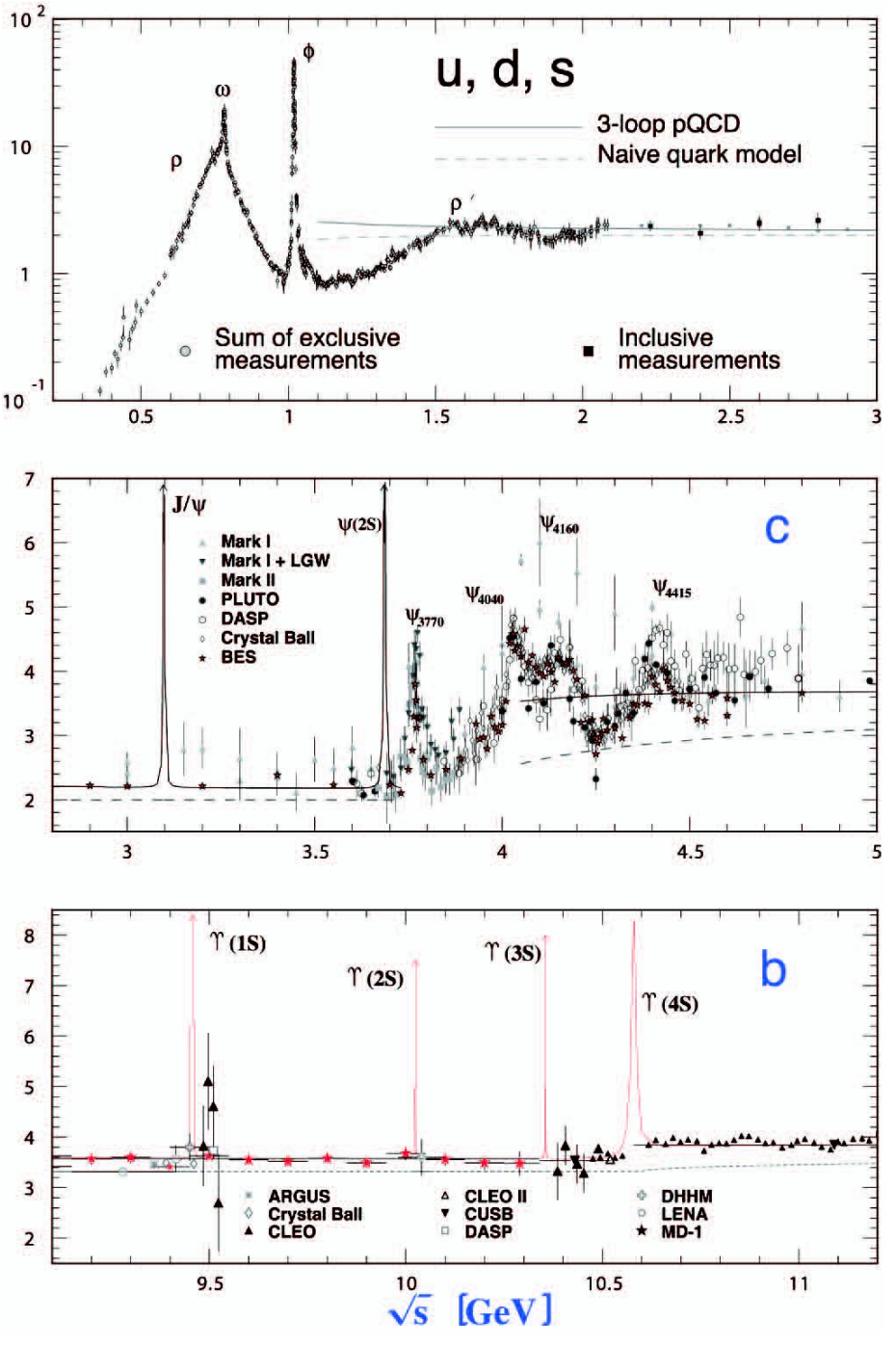

Figure 40.7: *R* in the light-flavor, charm, and beauty threshold regions. Data errors are total below 2 GeV and statistical above 2 GeV. The curves are the same as in Fig. 40.6. **Note:** CLEO data above $\Upsilon(4S)$ were not fully corrected for radiative effects, and we retain them on the plot only for illustrative purposes with a normalization factor of 0.8. The full list of references to the original data and the details of the *R* ratio extraction from them can be found in `hep-ph/0312114`. The computer-readable data are available at `http://pdg.ihep.su/xsect/contents.html` (Courtesy of the COMPAS (Protvino) and HEPDATA (Durham) Groups, March 2004.)

Annihilation Cross Section Near M_Z

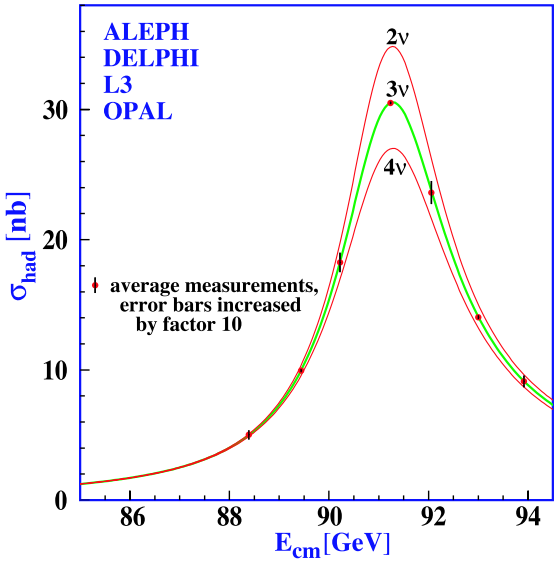

Figure 40.8: Combined data from the ALEPH, DELPHI, L3, and OPAL Collaborations for the cross section in e^+e^- annihilation into hadronic final states as a function of the center-of-mass energy near the Z pole. The curves show the predictions of the Standard Model with two, three, and four species of light neutrinos. The asymmetry of the curve is produced by initial-state radiation. Note that the error bars have been increased by a factor ten for display purposes. References:

ALEPH: R. Barate *et al.*, Eur. Phys. J. **C14**, 1 (2000).
DELPHI: P. Abreu *et al.*, Eur. Phys. J. **C16**, 371 (2000).
L3: M. Acciarri *et al.*, Eur. Phys. J. **C16**, 1 (2000).
OPAL: G. Abbiendi *et al.*, Eur. Phys. J. **C19**, 587 (2001).
Combination: The Four LEP Collaborations (ALEPH, DELPHI, L3, OPAL) and the Lineshape Sub-group of the LEP Electroweak Working Group, `hep-ph/0101027`.

(Courtesy of M. Grünewald and the LEP Electroweak Working Group, 2003)

Muon Neutrino and Anti-Neutrino Charged-Current Total Cross Section

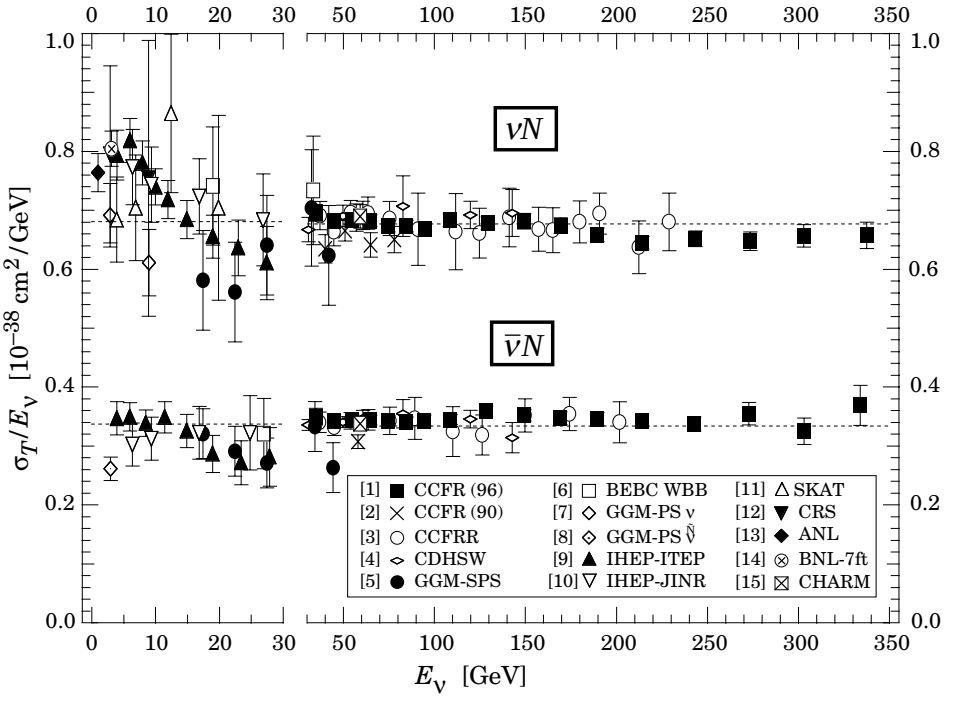

Figure 40.9: σ_T/E_ν, for the muon neutrino and anti-neutrino charged-current total cross section as a function of neutrino energy. The error bars include both statistical and systematic errors. The straight lines are the averaged values over all energies as measured by the experiments in Refs. [1–4]: $= 0.677 \pm 0.014$ $(0.334 \pm 0.008) \times 10^{-38}$ cm^2/GeV. Note the change in the energy scale at 30 GeV. (Courtesy W. Seligman and M.H. Shaevitz, Columbia University, 2001.)

[1] W. Seligman, Ph.D. Thesis, Nevis Report 292 (1996);
[2] P.S. Auchincloss *et al.*, Z. Phys. **C48**, 411 (1990);
[3] D.B. MacFarlane *et al.*, Z. Phys. **C26**, 1 (1984);
[4] P. Berge *et al.*, Z. Phys. **C35**, 443 (1987);
[5] J. Morfin *et al.*, Phys. Lett. **104B**, 235 (1981);
[6] D.C. Colley *et al.*, Z. Phys. **C2**, 187 (1979);
[7] S. Campolillo *et al.*, Phys. Lett. **84B**, 281 (1979);
[8] O. Erriquez *et al.*, Phys. Lett. **80B**, 309 (1979);
[9] V.B. Anikeev *et al.*, Z. Phys. **C70**, 39 (1996);
[10] A.S. Vovenko *et al.*, Sov. J. Nucl. Phys. **30**, 527 (1979);
[11] D.S. Baranov *et al.*, Phys. Lett. **81B**, 255 (1979);
[12] C. Baltay *et al.*, Phys. Rev. Lett. **44**, 916 (1980);
[13] S.J. Barish *et al.*, Phys. Rev. **D19**, 2521 (1979);
[14] N.J. Baker *et al.*, Phys. Rev. **D25**, 617 (1982);
[15] J.V. Allaby *et al.*, Z. Phys. **C38**, 403 (1988).

Table 40.2: Total hadronic cross section. Analytic S-matrix and Regge theory suggest a variety of parameterizations of total cross sections at high energies with different areas of applicability and fits quality.

A ranking procedure, based on measures of different aspects of the quality of the fits to the current evaluated experimental database, allows one to single out the following parameterization of highest rank[1]

$$\sigma^{ab} = Z^{ab} + B\log^2(s/s_0) + Y_1^{ab}(s_1/s)^{\eta_1} - Y_2^{ab}(s_1/s)^{\eta_2}\ , \qquad \sigma^{\overline{a}b} = Z^{ab} + B\log^2(s/s_0) + Y_1^{ab}(s_1/s)^{\eta_1} + Y_2^{ab}(s_1/s)^{\eta_2}$$

where Z^{ab}, B, Y_i^{ab} are in mb, s, s_1, and s_0 are in GeV^2. The scales s_0, s_1, the rate of universal rise of the cross sections B, and exponents η_1 and η_2 are independent of the colliding particles. The scale s_1 is fixed at 1 GeV^2. Terms $Z^{ab} + B\log^2(s/s_0)$ represent the pomerons. The exponents η_1 and η_2 represent lower-lying C-even and C-odd exchanges, respectively. Requiring $\eta_1 = \eta_2$ results in somewhat poorer fits. In addition to total cross sections σ, the measured ratios of the real-to-imaginary parts of the forward scattering amplitudes $\rho = \mathrm{Re}(T)/\mathrm{Im}(T)$ were included in the fits by using s to u crossing symmetry and differential dispersion relations. Global fits were made to the 2003-updated data for $\overline{p}(p)p$, $\Sigma^- p$, $\pi^\pm p$, $K^\pm p$, γp, and $\gamma\gamma$ collisions. Exact factorisation hypothesis was used for both Z^{ab} and $\log^2(s/s_0)$ to extend the universal rise of the total hadronic cross sections to the $\gamma p \to hadrons$ and $\gamma\gamma \to hadrons$ collisions. This resulted in reducing the number of adjusted parameters from 21 used for the 2002 edition to 19, and in the higher quality rank of the parameterization. The asymptotic parameters thus obtained were then fixed and used as inputs to a fit to a larger data sample that included cross sections on deuterons (d) and neutrons (n). All fits were produced to data above $\sqrt{s_{\min}} = 5$ GeV.

Fits to $\overline{p}(p)\,p$, $\Sigma^- p$, $\pi^\pm p$, $K^\pm p$, γp, $\gamma\gamma$			Beam/	Fits to groups				χ^2/dof
Z	Y_1	Y_2	Target	Z	Y_1	Y_2	B	by groups
35.45(48)	42.53(1.35)	33.34(1.04)	$\overline{p}(p)/p$	35.45(48)	42.53(23)	33.34(33)	0.308(10)	
			$\overline{p}(p)n$	35.80(16)	40.15(1.59)	30.00(96)	0.308(10)	1.029
35.20(1.46)	−199(102)	−264(126)	Σ^-/p	35.20(1.41)	−199(86)	−264(112)	0.308(10)	0.565
20.86(40)	19.24(1.22)	6.03(19)	$\pi^\pm/p$	20.86(3)	19.24(18)	6.03(9)	0.308(10)	0.955
17.91(36)	7.1(1.5)	13.45(40)	$K^\pm/p$	17.91(3)	7.14(25)	13.45(13)	0.308(10)	
			$K^\pm/n$	17.87(6)	5.17(50)	7.23(28)	0.308(10)	0.669
0.0317(6)			γ/p	0.0320(40)			0.308(10)	
−0.61(62)E−3			γ/γ	−0.58(61)E−3			0.308(10)	0.766
$\chi^2/dof = 0.971$, $B = 0.308(10)$ mb,			$\overline{p}(p)/d$	64.35(38)	130(3)	85.5(1.3)	0.537(31)	1.432
$\eta_1 = 0.458(17)$, $\eta_2 = 0.545(7)$			$\pi^\pm/d$	38.62(21)	59.62(1.53)	1.60(41)	0.461(14)	0.735
$\delta = 0.00308(2)$, $\sqrt{s_0} = 5.38(50)$ GeV			$K^\pm/d$	33.41(20)	23.66(1.45)	28.70(37)	0.449(14)	0.814

The fitted functions are shown in the following figures, along with one-standard-deviation error bands. When the reduced χ^2 is greater than one, a scale factor has been included to evaluate the parameter values, and to draw the error bands. Where appropriate, statistical and systematic errors were combined quadratically in constructing weights for all fits. On the plots, only statistical error bars are shown. Vertical arrows indicate lower limits on the $p_{\rm lab}$ or $E_{\rm cm}$ range used in the fits.

One can find the details of the global fits (all data on proton target and $\gamma\gamma$ fitted simultaneously) and ranking procedure, as well as the exact parameterizations of the total cross sections, and corresponding ratios of the real to imaginary parts of the forward-scattering amplitudes in the recent paper of COMPETE Collab. [1]. Database used in the fits now includes the recent OPAL and L3 (LEP) $\gamma\gamma$ data, highest energy data for $\pi^- p$ and $\Sigma^- p$ from SELEX(FNAL) experiment, γp from ZEUS(DESY), cosmic ray pp data from the Fly's Eye and AKENO(Agasa), and γp data from Baksan experiments. The numerical experimental data were extracted from the PPDS accessible at `http://wwwppds.ihep.su:8001/ppds.html`. Computer-readable data files are also available at `http://pdg.lbl.gov`. (Courtesy of the COMPAS group, IHEP, Protvino, August 2003.) On-line "Predictor" to calculate σ and ρ for any energy from five high rank models is also available at `http://nuclth02.phys.ulg.ac.be/compete/predictor.html/`.

References:

1. J.R. Cudell *et al.* (COMPETE Collab.), Phys. Rev. **D65**, 074024 (2002).
2. G. Abbiendi *et al.* (OPAL Collab.), Eur. Phys. J. **C14**, 199 (2000).
3. M. Acciarri *et al.* (L3 Collab.), Phys. Lett. **B519**, 33 (2001).
4. U. Dersch *et al.* (SELEX Collab.), Nucl. Phys. **B579**, 277 (2000).
5. S. Chekanov *et al.* (ZEUS Collab.), Nucl. Phys. **B627**, 3 (2002).
6. R.M. Baltrusaitis *et al.* (Fly's Eye Collab.), Phys. Rev. Lett. **52**, 1380 (1984).
7. M. Honda *et al.* (Akeno Collab.), Phys. Rev. Lett. **70**, 525 (1993).
8. G.M. Vereshkov *et al.* (Baksan Collab.), Phys. Atom. Nucl. **66**, 565 (2003) [Yad. Fiz. **66**, 591 (2003)].

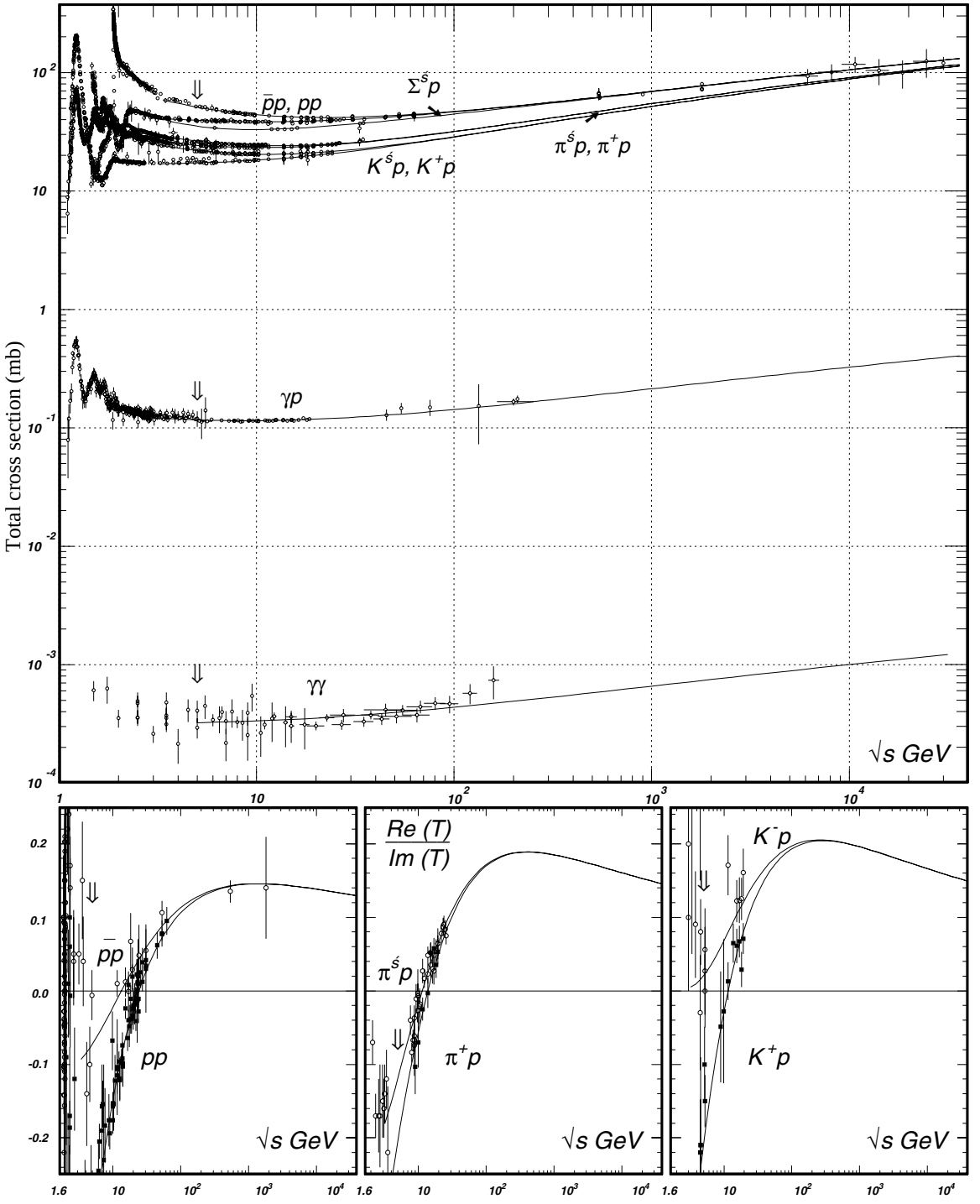

Figure 40.10: Summary of hadronic, γp, and $\gamma\gamma$ total cross sections, and ratio of the real to imaginary parts of the forward hadronic amplitudes. Corresponding computer-readable data files may be found at `http://pdg.lbl.gov/xsect/contents.html`. (Courtesy of the COMPAS group, IHEP, Protvino, August 2003.)

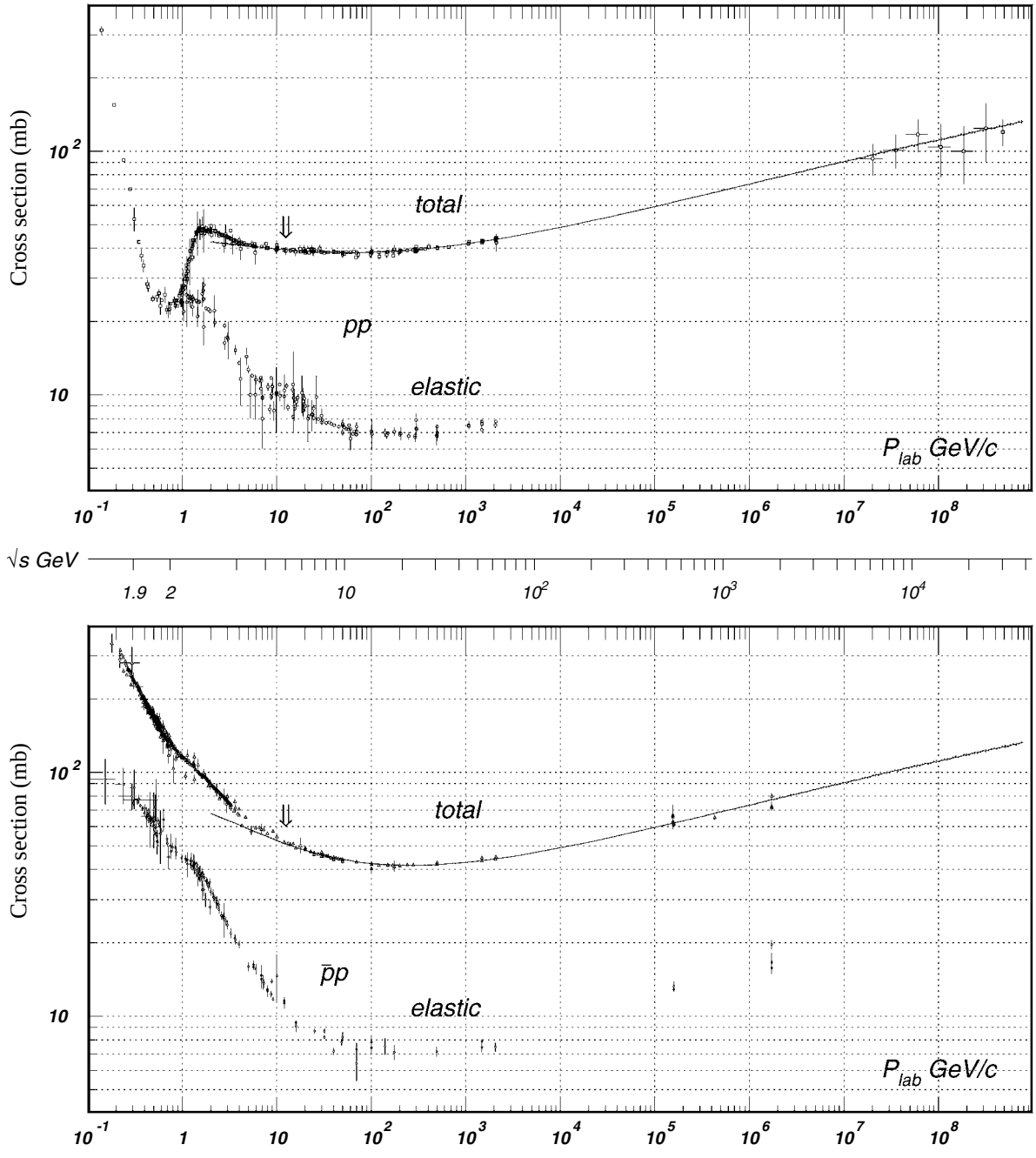

Figure 40.11: Total and elastic cross sections for pp and $\overline{p}p$ collisions as a function of laboratory beam momentum and total center-of-mass energy. Corresponding computer-readable data files may be found at `http://pdg.lbl.gov/xsect/contents.html`. (Courtesy of the COMPAS group, IHEP, Protvino, August 2003.)

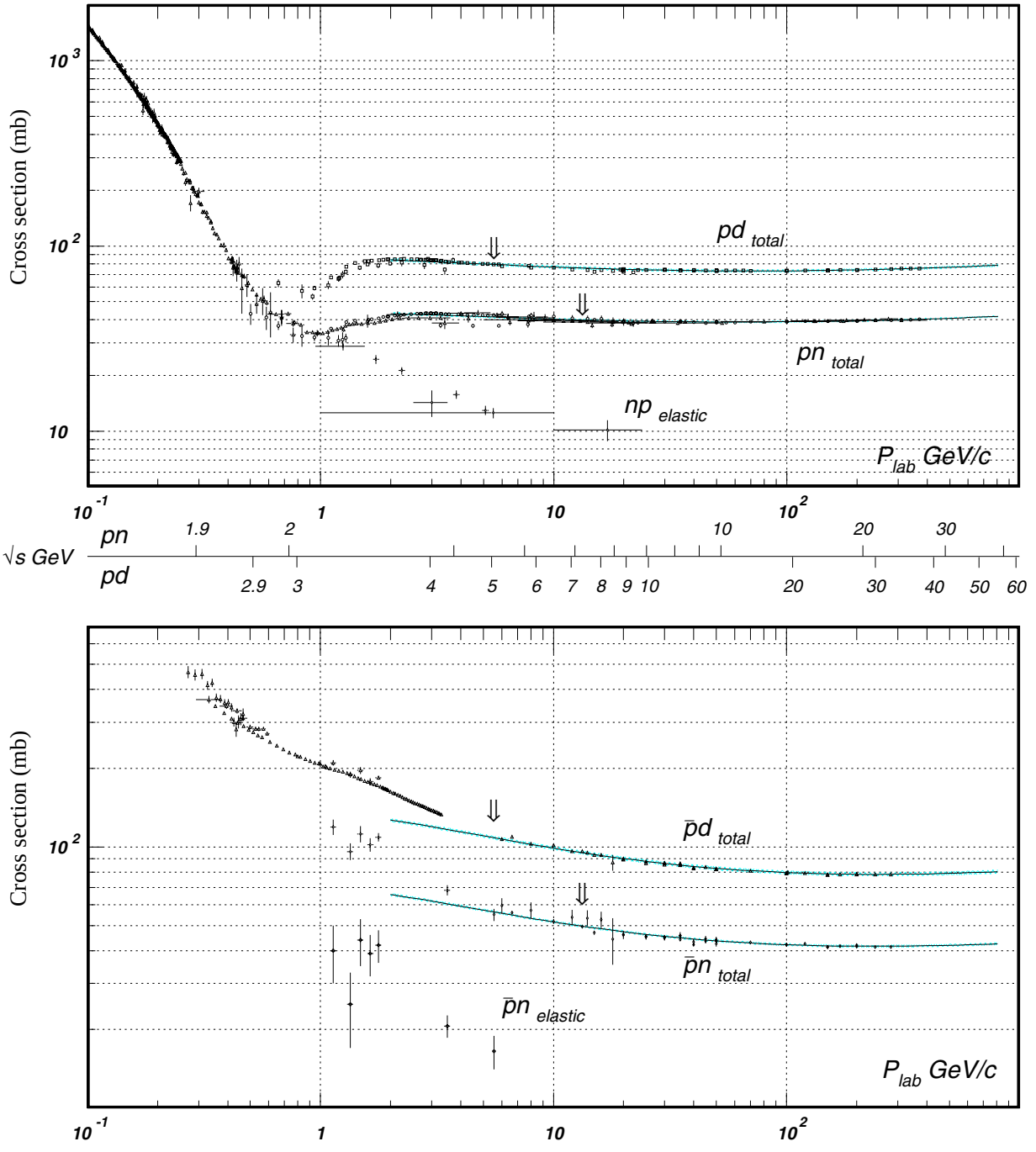

Figure 40.12: Total and elastic cross sections for pd (total only), np, $\overline{p}d$ (total only), and $\overline{p}n$ collisions as a function of laboratory beam momentum and total center-of-mass energy. Corresponding computer-readable data files may be found at `http://pdg.lbl.gov/xsect/contents.html`. (Courtesy of the COMPAS Group, IHEP, Protvino, August 2003.)

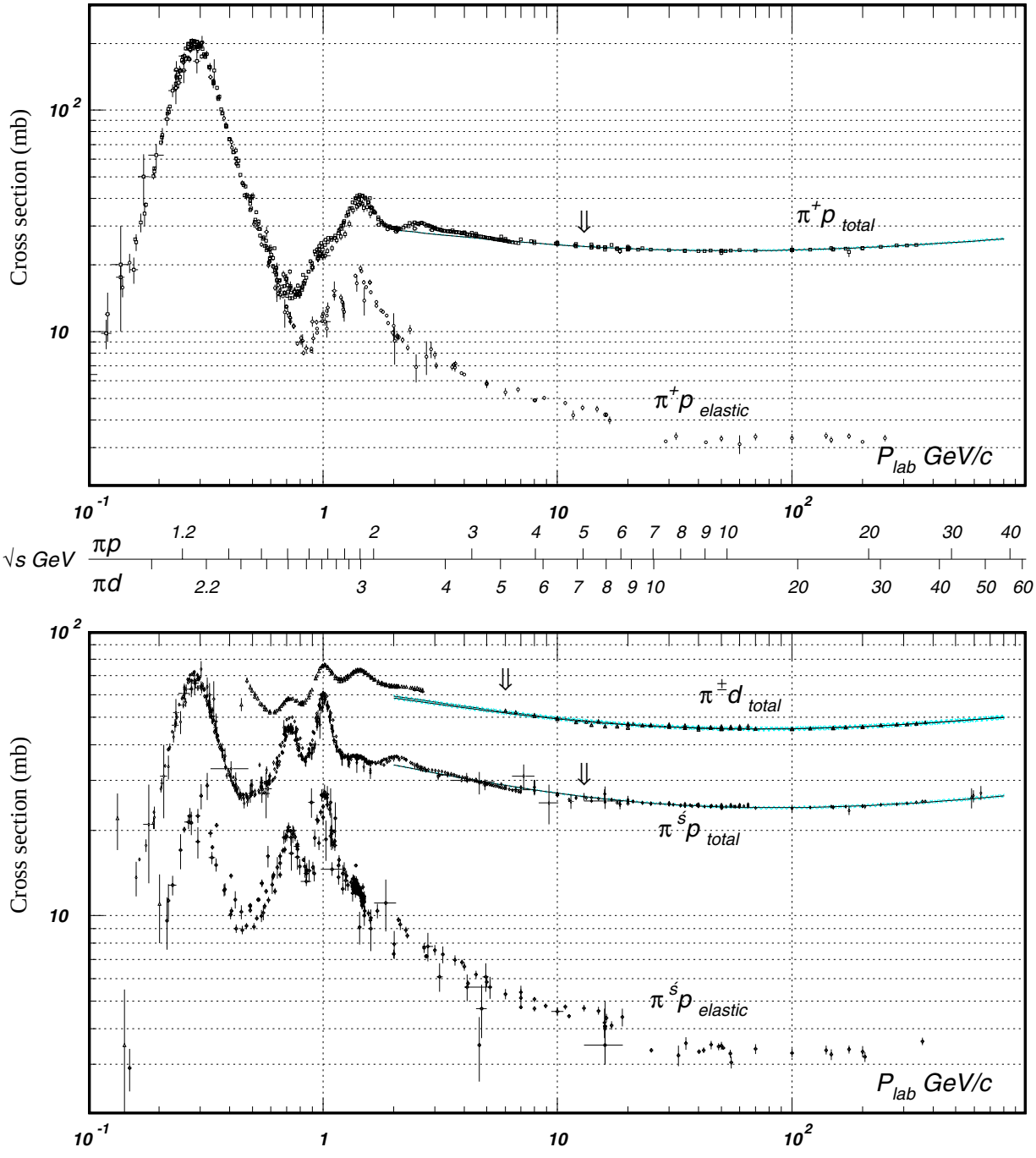

Figure 40.13: Total and elastic cross sections for $\pi^\pm p$ and $\pi^\pm d$ (total only) collisions as a function of laboratory beam momentum and total center-of-mass energy. Corresponding computer-readable data files may be found at `http://pdg.lbl.gov/xsect/contents.html`. (Courtesy of the COMPAS Group, IHEP, Protvino, August 2003.)

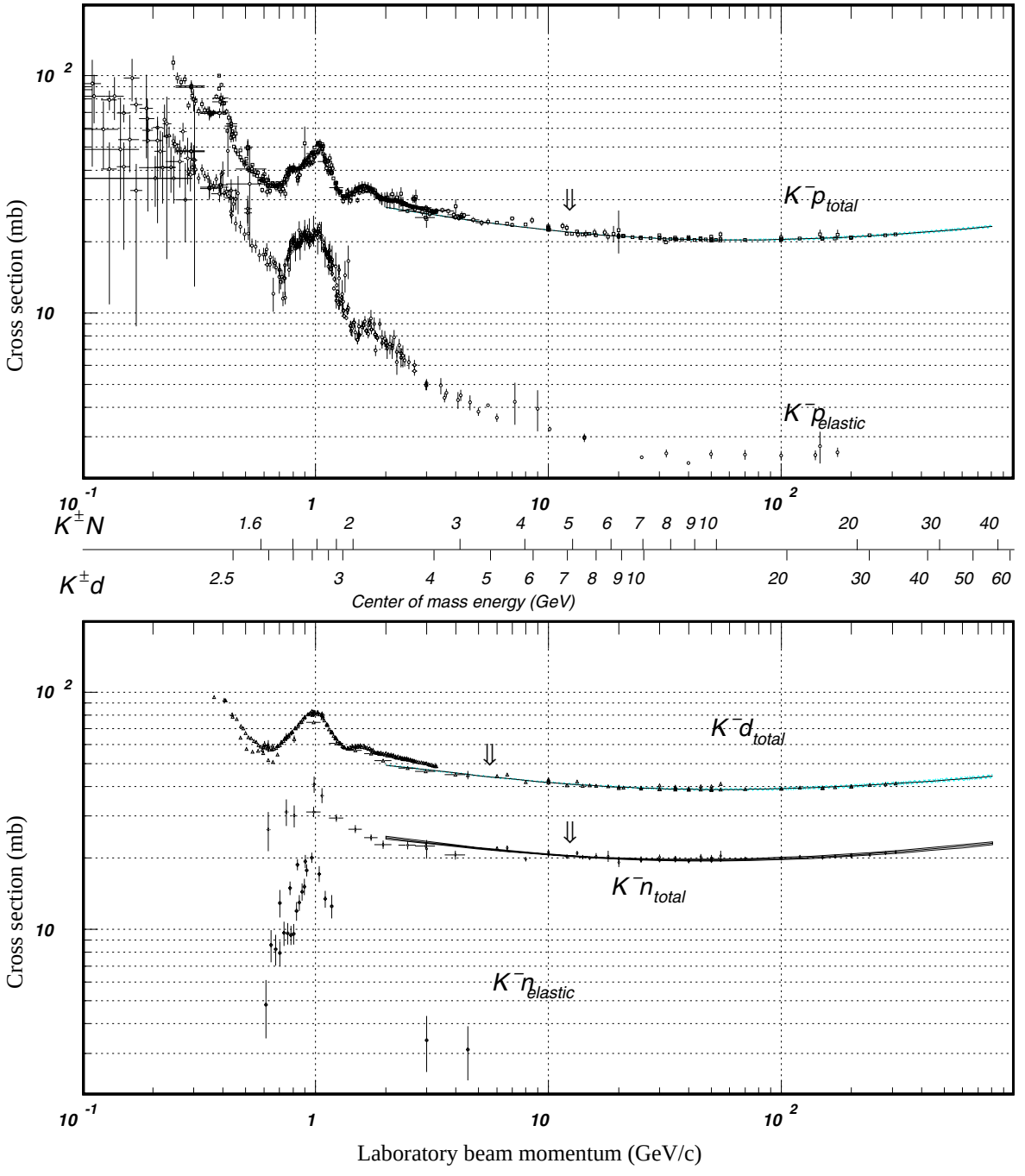

Figure 40.14: Total and elastic cross sections for $K^- p$ and $K^- d$ (total only), and $K^- n$ collisions as a function of laboratory beam momentum and total center-of-mass energy. Corresponding computer-readable data files may be found at `http://pdg.lbl.gov/xsect/contents.html`. (Courtesy of the COMPAS Group, IHEP, Protvino, August 2003.)

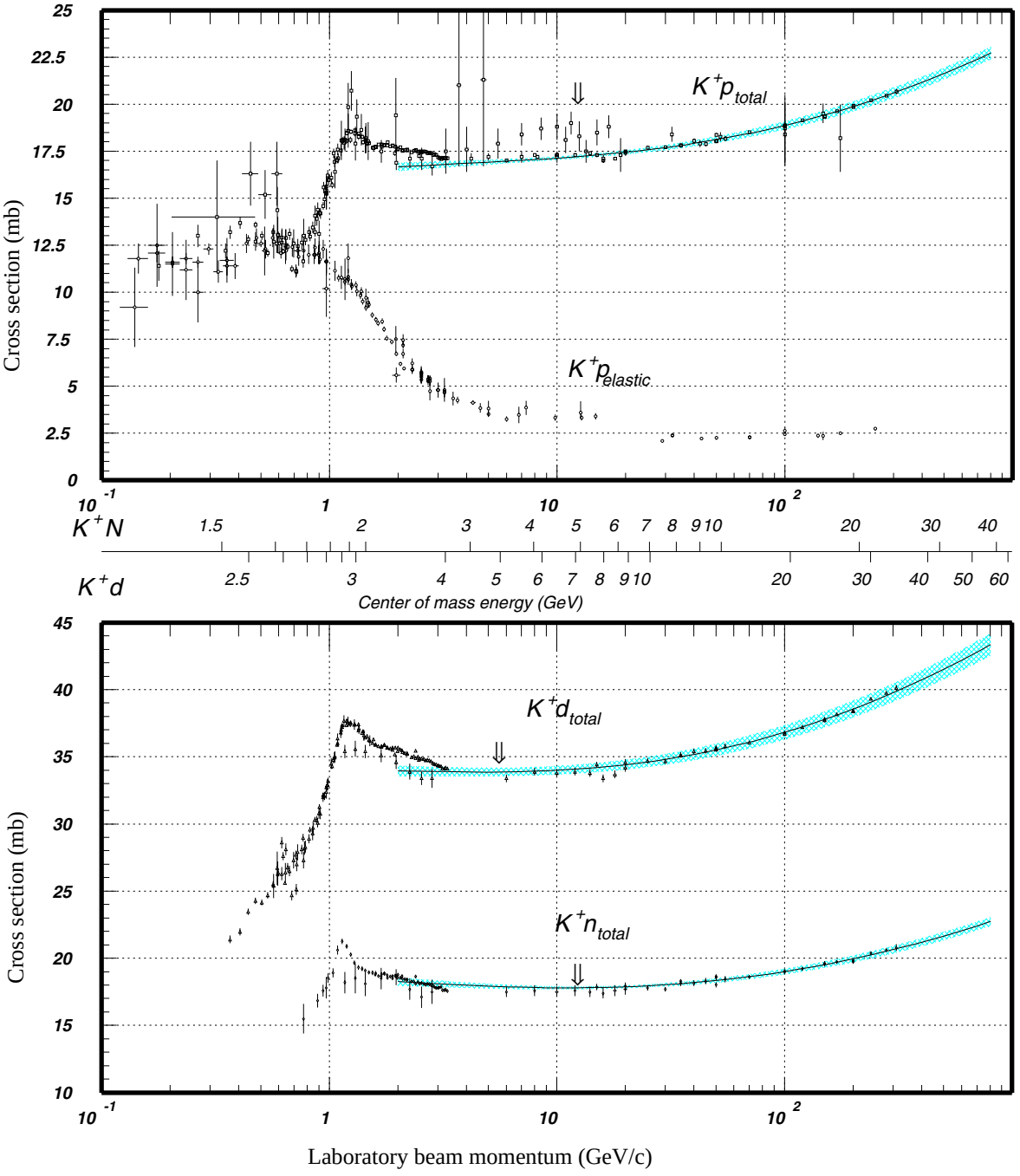

Figure 40.15: Total and elastic cross sections for K^+p and total cross sections for K^+d and K^+n collisions as a function of laboratory beam momentum and total center-of-mass energy. Corresponding computer-readable data files may be found at `http://pdg.lbl.gov/xsect/contents.html`. (Courtesy of the COMPAS Group, IHEP, Protvino, August 2003.)

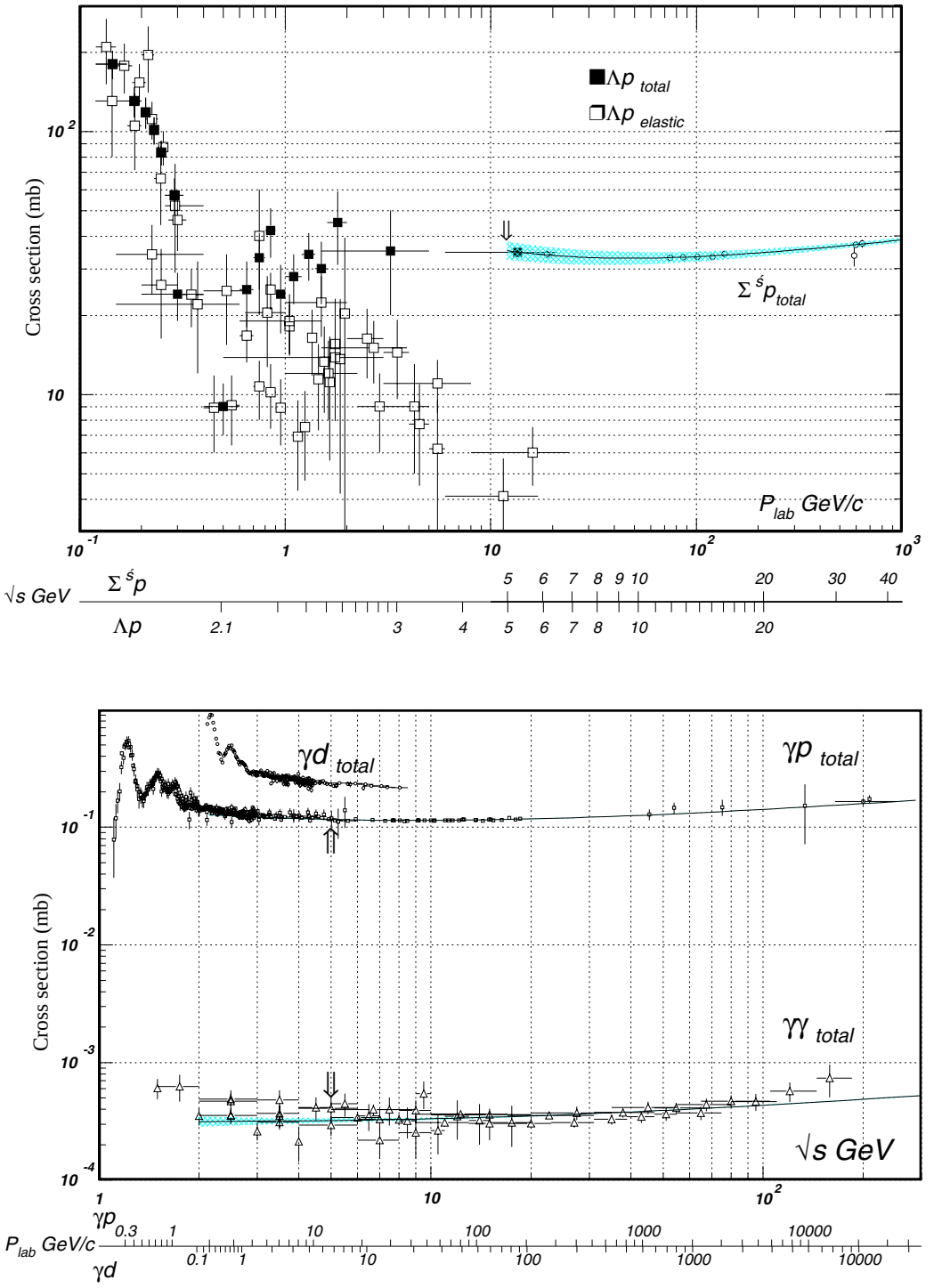

Figure 40.16: Total and elastic cross sections for Λp, total cross section for $\Sigma^- p$, and total hadronic cross sections for γd, γp, and $\gamma\gamma$ collisions as a function of laboratory beam momentum and the total center-of-mass energy. Corresponding computer-readable data files may be found at `http://pdg.lbl.gov/xsect/contents.html`. (Courtesy of the COMPAS group, IHEP, Protvino, August 2003.)

INTRODUCTION TO THE PARTICLE LISTINGS

Illustrative Key to the Particle Listings

Name of particle. "Old" name used before 1986 renaming scheme also given if different. See the section "Naming Scheme for Hadrons" for details.

Particle quantum numbers (where known).

Indicates particle omitted from Particle Physics Summary Table, implying particle's existence is not confirmed.

Quantity tabulated below.

General comments on particle.

Top line gives our best value (and error) of quantity tabulated here, based on weighted average of measurements used. Could also be from fit, best limit, estimate, or other evaluation. See next page for details.

"Document id" for this result; full reference given below.

Footnote number linking measurement to text of footnote.

Measurement technique. (See abbreviations on next page.)

Number of events *above background*.

Scale factor > 1 indicates possibly inconsistent data.

Measured value used in averages, fits, limits, etc.

Reaction producing particle, or general comments.

Error in measured value (often statistical only; followed by systematic if separately known; the two are combined in quadrature for averaging and fitting.)

"Change bar" indicates result added or changed since previous edition.

Measured value *not used* in averages, fits, limits, etc. See the Introductory Text for explanations.

Charge(s) of particle(s) detected.

Arrow points to weighted average.

Ideogram to display possibly inconsistent data. Curve is sum of Gaussians, one for each experiment (area of Gaussian = 1/error; width of Gaussian = ±error). See Introductory Text for discussion.

Shaded pattern extends $\pm 1\sigma$ (scaled by "scale factor" S) from weighted average.

Value and error for each experiment.

Contribution of experiment to χ^2 (if no entry present, experiment not used in calculating χ^2 or scale factor because of very large error).

Partial decay mode (labeled by Γ_i).

Our best value for branching fraction as determined from data averaging, fitting, evaluating, limit selection, etc. This list is basically a compact summary of results in the Branching Ratio section below.

Branching ratio.

Our best value (and error) of quantity tabulated, as determined from constrained fit (using *all significant* measured branching ratios for this particle).

Weighted average of measurements of this ratio only.

Footnote (referring to LYNCH 81).

Branching ratio in terms of partial decay mode(s) Γ_i above.

Confidence level for measured upper limit.

References, ordered inversely by year, then author.

Partial list of author(s) in addition to first author.

"Document id" used on data entries above.

Quantum number determinations in this reference.

Journal, report, preprint, etc. (See abbreviations on next page.)

Institution(s) of author(s). (See abbreviations on next page.)

$a_0(1200)$

$I^G(J^{PC}) = 1^-(0^{++})$

OMITTED FROM SUMMARY TABLE

Evidence not compelling, may be a kinematic effect.

$a_0(1200)$ MASS

VALUE (MeV)	EVTS	DOCUMENT ID		TECN	CHG	COMMENT
1206 ± 7 OUR AVERAGE						
1210 ± 8 ± 9	3000	FENNER	87	MMS	–	3.5 $\pi^- p$
1198 ± 10		PIERCE	83	ASPK	+	2.1 $K^- p$
1216 ± 11 ± 9	1500	[1] MERRILL	81	HBC	0	3.2 $K^- p$
• • • We do not use the following data for averages, fits, limits, etc. • • •						
1192 ± 16	200	LYNCH	81	HBC	±	2.7 $\pi^- p$

[1] Systematic error was added quadratically by us in our 1986 edition.

$a_0(1200)$ WIDTH

VALUE (MeV)	EVTS	DOCUMENT ID		TECN	CHG	COMMENT
41 ± 11 OUR AVERAGE Error includes scale factor of 1.8. See the ideogram below.						
50 ± 8		PIERCE	83	ASPK	+	2.1 $K^- p$
70^{+30}_{-20}	200	LYNCH	81	HBC	±	2.7 $\pi^- p$
25 ± 5 ± 7		MERRILL	81	HBC	0	3.2 $K^- p$
• • • We do not use the following data for averages, fits, limits, etc. • • •						
< 60		FENNER	87	MMS	–	3.5 $\pi^- p$

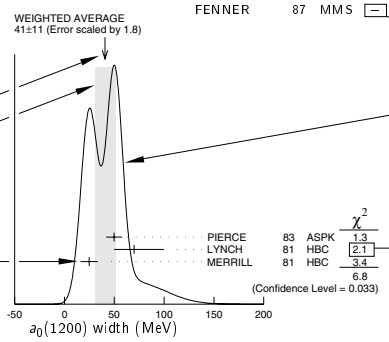

$a_0(1200)$ DECAY MODES

Mode		Fraction (Γ_i/Γ)		Scale factor/ Confidence level
Γ_1	3π			
Γ_2	$K\overline{K}$	(65.2 ± 1.3) %		S=1.7
Γ_3	$\eta\pi^\pm$	(34.8 ± 1.3) %		S=1.7
		< 4.9	$\times 10^{-4}$	CL=95%

$a_0(1200)$ BRANCHING RATIOS

$\Gamma(3\pi)/\Gamma_{total}$ Γ_1/Γ

VALUE	DOCUMENT ID		TECN	CHG	COMMENT
0.652 ± 0.013 OUR FIT Error includes scale factor of 1.7.					
0.643 ± 0.010 OUR AVERAGE					
0.64 ± 0.01	PIERCE	83	ASPK	+	2.1 $K^- p$
0.74 ± 0.06	MERRILL	81	HBC	0	3.2 $K^- p$
• • • We do not use the following data for averages, fits, limits, etc. • • •					
0.48 ± 0.15	[2] LYNCH	81	HBC	±	2.7 $\pi^- p$

[2] Data has questionable background subtraction.

$\Gamma(K\overline{K})/\Gamma_{total}$ Γ_2/Γ

VALUE	DOCUMENT ID	TECN	CHG	COMMENT
0.348 ± 0.013 OUR FIT Error includes scale factor of 1.7.				
0.35 ± 0.05	PIERCE 83	ASPK	+	2.1 $K^- p$

$\Gamma(K\overline{K})/\Gamma(3\pi)$ Γ_2/Γ_1

VALUE	DOCUMENT ID	TECN	CHG	COMMENT
0.535 ± 0.030 OUR FIT Error includes scale factor of 1.7.				
0.50 ± 0.03	MERRILL 81	HBC	0	3.2 $K^- p$

$\Gamma(\eta(\text{neutral decay})\pi^\pm)/\Gamma_{total}$ $0.71\Gamma_3/\Gamma$

VALUE (units 10^{-4})	CL%	DOCUMENT ID	TECN	CHG	COMMENT
< 3.5	95	PIERCE 83	ASPK	+	2.1 $K^- p$

$a_0(1200)$ REFERENCES

FENNER	87	PRL 55 14	H. Fenner *et al.*	(SLAC) (FNAL)	UP
PIERCE	83	PL 123B 230	J.H. Pierce		
LYNCH	81	PR D24 610	G.R. Lynch *et al.*	(CLEO Collab.)	
MERRILL	81	PRL 47 143	D.W. Merrill *et al.*	(SACL, CERN)	

Abbreviations Used in the Particle Listings

Indicator of Procedure Used to Obtain Our Result

OUR AVERAGE	From a weighted average of selected data.
OUR FIT	From a constrained or overdetermined multiparameter fit of selected data.
OUR EVALUATION	Not from a direct measurement, but evaluated from measurements of other quantities.
OUR ESTIMATE	Based on the observed range of the data. Not from a formal statistical procedure.
OUR LIMIT	For special cases where the limit is evaluated by us from measured ratios or other data. Not from a direct measurement.

Measurement Techniques (i.e., Detectors and Methods of Analysis)

ACCM	ACCMOR Collaboration
AEMS	Argonne effective mass spectrometer
ALEP	ALEPH – CERN LEP detector
AMY	AMY detector at KEK-TRISTAN
APEX	FNAL APEX Collab.
ARG	ARGUS detector at DORIS
ARGD	Fit to semicircular amplitude path on Argand diagram
ASP	Anomalous single-photon detector
ASPK	Automatic spark chambers
ASTE	ASTERIX detector at LEAR
ASTR	Astronomy
B787	BNL experiment 787 detector
B791	BNL experiment 791 detector
B845	BNL experiment 845 detector
B865	BNL E865 Collab.
B871	BNL experiment 871 detector
BABR	BaBar Collab.
BAKS	Baksan underground scintillation telescope
BC	Bubble chamber
BDMP	Beam dump
BEAT	CERN BEATRICE Collab.
BEBC	Big European bubble chamber at CERN
BELL	Belle Collab.
BES	BES Beijing Spectrometer at Beijing Electron-Positron Collider
BES2	BES Beijing Spectrometer at Beijing Electron-Positron Collider
BIS2	BIS-2 spectrometer at Serpukhov
BKEI	BENKEI spectrometer system at KEK Proton Synchroton
BOLO	Bolometer, a cryogenic thermal detector
BONA	Bonanza nonmagnetic detector at DORIS
BORX	BOREXINO
BPWA	Barrelet-zero partial-wave analysis
CALO	Calorimeter
CBAL	Crystal Ball detector at SLAC-SPEAR or DORIS
CBAR	Crystal Barrel detector at CERN-LEAR
CBOX	Crystal Box at LAMPF
CC	Cloud chamber
CCFR	Columbia-Chicago-Fermilab-Rochester detector
CDF	Collider detector at Fermilab
CDF2	CDF-II Collab.
CDHS	CDHS neutrino detector at CERN
CDMS	CDMS Collab.
CELL	CELLO detector at DESY
CHER	Cherenkov detector
CHM2	CHARM-II neutrino detector (glass) at CERN
CHOZ	Nuclear Power Station near Chooz, France
CHRM	CHARM neutrino detector (marble) at CERN
CHRS	CHORUS Collaboration – CERNS SPS
CIBS	CERN-IHEP boson spectrometer
CLAS	Jefferson CLAS Collab.
CLE2	CLEO II detector at CESR
CLE3	CLEO III detector at CESR
CLEO	Cornell magnetic detector at CESR
CMD	Cryogenic magnetic detector at VEPP-2M, Novosibirsk
CMD2	Cryogenic magnetic detector 2 at VEPP-2M, Novosibirsk
CNTR	Counters
COSM	Cosmology and astrophysics
CPLR	CPLEAR Collaboration
CRES	CRESST cryogenic detector
CRYB	Crystal Ball at BNL
CSB2	Columbia U. - Stony Brook BGO calorimeter inserted in NaI array
CSME	COSME Collaboration
CUSB	Columbia U. - Stony Brook segmented NaI detector at CESR
D0	D0 detector at Fermilab Tevatron Collider
DAMA	DAMA, dark matter detector at Gran Sasso National Lab.
DASP	DESY double-arm spectrometer
DBC	Deuterium bubble chamber
DLCO	DELCO detector at SLAC-SPEAR or SLAC-PEP
DLPH	DELPHI detector at LEP
DM1	Magnetic detector no. 1 at Orsay DCI collider
DM2	Magnetic detector no. 2 at Orsay DCI collider
DONU	DONUT Collab.
DPWA	Energy-dependent partial-wave analysis
E621	Fermilab E621 detector
E653	Fermilab E653 detector
E665	Fermilab E665 detector
E687	Fermilab E687 detector
E691	Fermilab E691 detector
E705	Fermilab E705 Spectrometer-Calorimeter
E731	Fermilab E731 Spectrometer-Calorimeter
E756	Fermilab E756 detector
E760	Fermilab E760 detector
E761	Fermilab E761 detector
E771	Fermilab E771 detector
E773	Fermilab E773 Spectrometer-Calorimeter
E789	Fermilab E789 detector
E791	Fermilab E791 detector
E799	Fermilab E799 Spectrometer-Calorimeter
E835	Fermilab E835 detector
E852	BNL E-852
EDEL	EDELWEISS Collab. .
EHS	Four-pi detector at CERN
ELEC	Electronic combination
EMC	European muon collaboration detector at CERN
EMUL	Emulsions
FBC	Freon bubble chamber
FENI	FENICE (at the ADONE collider of Frascati)
FIT	Fit to previously existing data
FMPS	Fermilab Multiparticle Spectrometer
FOCS	FNAL E831 FOCUS Collab.
FRAB	ADONE $B\overline{B}$ group detector
FRAG	ADONE $\gamma\gamma$ group detector
FRAM	ADONE MEA group detector
FREJ	FREJUS Collaboration – modular flash chamber detector (calorimeter)
GA24	Hodoscope Cherenkov γ calorimeter (IHEP GAMS-2000) (CERN GAMS-4000)
GALX	GALLEX solar neutrino detector in the Gran Sasso Underground Lab.
GAM2	IHEP hodoscope Cherenkov γ calorimeter GAMS-2000
GAM4	CERN hodoscope Cherenkov γ calorimeter GAMS-4000
GNO	Gallium Neutrino Observatory in the Gran Sasso Underground Lab.
GOLI	CERN Goliath spectrometer
H1	H1 detector at DESY/HERA
HBC	Hydrogen bubble chamber
HDBC	Hydrogen and deuterium bubble chambers
HDMO	Heidelberg-Moscow Experiment
HDMS	Heidelberg Dark Matter Search Experiment
HEBC	Helium bubble chamber
HEPT	Helium proportional tubes
HLBC	Heavy-liquid bubble chamber
HOME	Homestake underground scintillation detector
HPW	Harvard-Pennsylvania-Wisconsin detector
HRS	SLAC high-resolution spectrometer
HYBR	Hybrid: bubble chamber + electronics
HYCP	HyperCP Collab. (FNAL E-871)
IGEX	IGEX Collab.
IMB	Irvine-Michigan-Brookhaven underground Cherenkov detector
IMB3	Irvine-Michigan-Brookhaven underground Cherenkov detector
INDU	Magnetic induction
IPWA	Energy-independent partial-wave analysis
ISTR	IHEP ISTRA+ spectrometer-calorimeter
JADE	JADE detector at DESY
K246	KEK E246 detector with polarimeter
K2K	KEK to Super-Kamiokande
K470	KEK-E470 Stopping K detector
KAM2	KAMIOKANDE-II underground Cherenkov detector
KAMI	KAMIOKANDE underground Cherenkov detector
KAR2	KARMEN2 calorimeter at the ISIS neutron spallation source at Rutherford
KARM	KARMEN calorimeter at the ISIS neutron spallation source at Rutherford

Abbreviations Used in the Particle Listings

KEDR detector operating at VEPP-4M collider (Novosibirsk)
KLND KamLand Collab. (Japan)
KLOE KLOE detector at DAFNE (the Frascati e+e- collider Italy)
KOLR Kolar Gold Field underground detector
KTEV KTeV Collaboration
L3 L3 detector at LEP
LASS Large-angle superconducting solenoid spectrometer at SLAC
LATT Lattice calculations
LEBC Little European bubble chamber at CERN
LEGS BNL LEGS Collab.
LENA Nonmagnetic lead-glass NaI detector at DORIS
LEP From combination of all 4 LEP experiments: ALEPH, DELPHI, L3, OPAL
LEPS Low-Energy Pion Spectrometer at the Paul Scherrer Institute
LSND Liquid Scintillator Neutrino Detector
MAC MAC detector at PEP/SLAC
MBR Molecular beam resonance technique
MCRO MACRO detector in Gran Sasso
MD1 Magnetic detector at VEPP-4, Novosibirsk
MDRP Millikan drop measurement
MICA Underground mica deposits
MIRA MIRABELLE Liquid-hydrogen bubble chamber
MLEV Magnetic levitation
MMS Missing mass spectrometer
MPS Multiparticle spectrometer at BNL
MPS2 Multiparticle spectrometer upgrade at BNL
MPSF Multiparticle spectrometer at Fermilab
MPWA Model-dependent partial-wave analysis
MRK1 SLAC Mark-I detector
MRK2 SLAC Mark-II detector
MRK3 SLAC Mark-III detector
MRKJ Mark-J detector at DESY
MRS Magnetic resonance spectrometer
MUG2 MUON(g-2)
MWPC Multi-Wire Proportional Chamber
NA14 CERN NA14
NA31 CERN NA31 Spectrometer-Calorimeter
NA32 CERN NA32 Spectrometer
NA48 CERN NA48 Collaboration
NA49 CERN NA49
NAIA NAIAD (NaI Advanced Detector) experiment
ND NaI detector at VEPP-2M, Novosibirsk
NICE Serpukhov nonmagnetic precision spectrometer
NMR Nuclear magnetic resonance
NOMD NOMAD Collaboration, CERN SPS
NTEV NuTeV Collab. at Fermilab
NUSX Mont Blanc NUSEX underground detector
OBLX OBELIX detector at LEAR
OLYA Detector at VEPP-2M and VEPP-4, Novosibirsk
OMEG CERN OMEGA spectrometer
OPAL OPAL detector at LEP
OSPK Optical spark chamber
PLAS Plastic detector
PLUT DESY PLUTO detector
PWA Partial-wave analysis
REDE Resonance depolarization
RVUE Review of previous data
SAGE US - Russian Gallium Experiment
SELX FNAL SELEX Collab.
SFM CERN split-field magnet
SHF SLAC Hybrid Facility Photon Collaboration
SIGM Serpukhov CERN-IHEP magnetic spectrometer (SIGMA)
SILI Silicon detector
SKAM Super-Kamiokande Collab.
SLAX Solar Axion Experiment in Canfranc Underground Laboratory
SLD SLC Large Detector for e^+e^- colliding beams at SLAC
SMPL SIMPLE superheated droplet detector.
SND Novosibirisk Spherical neutral detector at VEPP-2M
SNO SNO Collaboration (Sudbury Neutrino Observatory)
SOU2 Soudan 2 underground detector
SOUD Soudan underground detector
SPEC Spectrometer
SPED From maximum of speed plot or resonant amplitude
SPHR Bonn SAPHIR Collab.
SPRK Spark chamber
SQID SQUID device
STRC Streamer chamber
TASS DESY TASSO detector
THEO Theoretical or heavily model-dependent result
TOF Time-of-flight
TOPZ TOPAZ detector at KEK-TRISTAN
TPC TPC detector at PEP/SLAC
TPS Tagged photon spectrometer at Fermilab
TRAP Penning trap
UA1 UA1 detector at CERN
UA2 UA2 detector at CERN
UA5 UA5 detector at CERN
UKDM UK Dark Matter Collab.
VES Vertex Spectrometer Facility at 70 GeV IHEP accelerator
VNS VENUS detector at KEK-TRISTAN
WA75 CERN WA75 experiment
WA82 CERN WA82 experiment
WA89 CERN WA89 experiment
WIRE Wire chamber
XEBC Xenon bubble chamber
ZEUS ZEUS detector at DESY/HERA

Conferences

Conferences are generally referred to by the location at which they were held (e.g., HAMBURG, TORONTO, CORNELL, BRIGHTON, etc.).

Journals

AA Astronomy and Astrophysics
ADVP Advances in Physics
AFIS Anales de Fisica
AJP American Journal of Physics
ANP Annals of Physics
ANPL Annals of Physics (Leipzig)
ANYAS Annals of the New York Academy of Sciences
AP Atomic Physics
APAH Acta Physica Academiae Scientiarum Hungaricae
APJ Astrophysical Journal
APJS Astrophysical Journal Suppl.
APP Acta Physica Polonica
APS Acta Physica Slovaca
ARNPS Annual Review of Nuclear and Particle Science
ARNS Annual Review of Nuclear Science
ASP Astroparticle Physics
BAPS Bulletin of the American Physical Society
BASUP Bulletin of the Academy of Science, USSR (Physics)
CJNP Chinese Journal of Nuclear Physics
CJP Canadian Journal of Physics
CNPP Comments on Nuclear and Particle Physics
CZJP Czechoslovak Journal of Physics
DANS Doklady Akademii nauk SSSR
EPJ The European Physical Journal
EPL Europhysics Letters
FECAY Fizika Elementarnykh Chastits i Atomnogo Yadra
HADJ Hadronic Journal
IJMP International Journal of Modern Physics
JAP Journal of Applied Physics
JCAP Journal of Cosmology and Astroparticle Physics
JETP English Translation of Soviet Physics ZETF
JETPL English Translation of Soviet Physics ZETF Letters
JHEP Journal of High Energy Physics
JINR Joint Inst. for Nuclear Research
JINRRC JINR Rapid Communications
JPA Journal of Physics, A
JPB Journal of Physics, B
JPCRD Journal of Physical and Chemical Reference Data
JPG Journal of Physics, G
JPSJ Journal of the Physical Society of Japan
LNC Lettere Nuovo Cimento
MNRAS Monthly Notices of the Royal Astronomical Society
MPL Modern Physics Letters
NAT Nature
NC Nuovo Cimento
NIM Nuclear Instruments and Methods
NJP New Journal of Physics
NP Nuclear Physics
NPBPS Nuclear Physics B Proceedings Supplement
PAN Physics of Atomic Nuclei (formerly SJNP)
PD Physics Doklady (Magazine)

Abbreviations Used in the Particle Listings

PDAT	Physik Daten
PL	Physics Letters
PN	Particles and Nuclei
PPCF	Plasma Physics Control Fusion
PPN	Physics of Particles and Nuclei (formerly SJPN)
PPNL	Physics of Particles and Nuclei Letters
PPNP	Progress in Particles and Nuclear Physics
PPSL	Proc. of the Physical Society of London
PR	Physical Review
PRAM	Pramana
PRL	Physical Review Letters
PRPL	Physics Reports (Physics Letters C)
PRSE	Proc. of the Royal Society of Edinburgh
PRSL	Proc. of the Royal Society of London, Section A
PS	Physica Scripta
PTP	Progress of Theoretical Physics
PTRSL	Phil. Trans. Royal Society of London
RA	Radiochimica Acta
RMP	Reviews of Modern Physics
RNC	La Rivista del Nuovo Cimento
RPP	Reports on Progress in Physics
RRP	Revue Roumaine de Physique
SCI	Science
SJNP	Soviet Journal of Nuclear Physics
SJPN	Soviet Journal of Particles and Nuclei
SPD	Soviet Physics Doklady (Magazine)
SPU	Soviet Physics - Uspekhi
UFN	Usp. Fiz. Nauk – Russian version of SPU
YAF	Yadernaya Fizika
ZETF	Zhurnal Eksperimental'noi i Teoreticheskoi Fiziki
ZETFP	Zhurnal Eksperimental'noi i Teoreticheskoi Fiziki, Pis'ma v Redakts
ZNAT	Zeitschrift fur Naturforschung
ZPHY	Zeitschrift fur Physik

Institutions

AACH	Phys. Inst. der Techn. Hochschule **Aachen** (Historical, use for general Inst. der Techn. Hochschule)	Aachen, Germany
AACH1	I Phys. Inst. RWTH **Aachen** Ib	Aachen, Germany
AACH3	III Phys. Inst. der Techn. Hochschule **Aachen**	Aachen, Germany
AACHT	Institut für Theoretische Physik E	**Aachen**, Germany
AARH	Univ. of **Aarhus**	Aarhus C, Denmark
ABO	**Åbo** Akademi	Abo, Finland
ADEL	**Adelphi** Univ.	Garden City, NY, USA
ADLD	The Univ. of **Adelaide**; Dept. of Physics & Math. Physics; Centre for Subatomic Structure of Matter (CSSM)	Adelaide, SA, Australia
AERE	Atomic Energy Research Estab.	Didcot, United Kingdom
AFRR	**Armed Forces** Radiobiology Res. Inst.	Bethesda, MD, USA
AHMED	Physical Research Lab.	**Ahmedabad**, Gujarat, India
AICH	**Aichi** Univ. of Education	Aichi, Japan
AKIT	**Akita** Univ.	Akita, Japan
ALAH	Univ. of **Alabama (Huntsville)**	Huntsville, AL, USA
ALAT	Univ. of **Alabama (Tuscaloosa)**	Tuscaloosa, AL, USA
ALBA	**SUNY at Albany**	Albany, NY, USA
ALBE	Univ. of **Alberta**	Edmonton, AB, Canada
AMES	**Ames Lab.**	Ames, IA, USA
AMHT	**Amherst** College	Amherst, MA, USA
AMST	Univ. van **Amsterdam**	Amsterdam, The Netherlands
ANIK	NIKHEF	**Amsterdam**, The Netherlands
ANKA	**Middle East** Technical Univ.; Dept. of Physics; Experimental HEP Lab	Ankara, Turkey
ANL	**Argonne** National Lab.; High Energy Physics Division, Bldg. 362; Physics Division, Bldg. 203	Argonne, IL, USA
ANSM	**St. Anselm** Coll.	Manchester, NH, USA
ARCBO	**Arecibo** Observatory	Arecibo, PR, USA
ARIZ	Univ. of **Arizona**	Tucson, AZ, USA
ARZS	**Arizona State** Univ.	Tempe, AZ, USA
ASCI	Russian Academy of Sciences	**Moscow**, Russian Federation
AST	**Inst. of Phys.**	Nankang, Taipei, The Republic of China (Taiwan)
ATEN	NCSR **"Demokritos"**	**Aghia** Paraskevi Attikis, Greece
ATHU	Univ. of **Athens**	Athens, Greece
AUCK	Univ. of **Auckland**	Auckland, New Zealand
BAKU	**Azerbaijan Academy of Sciences**, Inst. of Physics	**Baku**, Azerbaijan
BANGB	**Bangabasi** College	Calcutta, India
BARC	Univ. Autónoma de **Barcelona**	Bellaterra (Barcelona), Spain
BARI	Univ. di **Bari**	Bari, Italy
BART	Univ. of **Delaware**; **Bartol** Research Inst.	Newark, DE, USA
BASL	Inst. für Physik der Univ. **Basel**	Basel, Switzerland
BAYR	Univ. **Bayreuth**	Bayreuth, Germany
BCEN	Centre d'Etudes Nucleaires de **Bordeaux-Gradignan**	Gradignan, France
BEIJ	**Beijing** Univ.	Beijing, The People's Republic of China
BEIJT	**Inst. of Theoretical Physics**	**Beijing**, The People's Republic of China
BELG	Inter-University Inst. for High Energies (ULB-VUB)	**Brussel**, Belgium
BELL	AT & T **Bell** Labs	Murray Hill, NJ, USA
BERG	Univ. of **Bergen**	Bergen, Norway
BERL	**DESY Zeuthen**	**Zeuthen**, Germany
BERN	Univ. of **Berne**	Berne, Switzerland
BGNA	Univ. di **Bologna**, & INFN, Sezione di Bologna; Viale C. Berti Pichat, n. 6/2; Via Irnerio, 46, I-40126 Bologna	Bologna, Italy
BHAB	**Bhabha Atomic** Research Center	Trombay, Bombay, India
BHEP	**Inst. of High Energy Physics**	**Beijing**, The People's Republic of China
BIEL	Univ. **Bielefeld**	Bielefeld, Germany
BING	**SUNY at Binghamton**	Binghamton, NY, USA
BIRK	**Birkbeck** College, Univ. of London	London, United Kingdom
BIRM	Univ. of **Birmingham**	Edgbaston, Birmingham, United Kingdom
BLSU	**Bloomsburg** Univ.	Bloomsburg, PA, USA
BNL	**Brookhaven National Lab.**	Upton, NY, USA
BOCH	**Ruhr** Univ. **Bochum**	Bochum, Germany
BOHR	**Niels Bohr Inst.**	Copenhagen Ø, Denmark
BOIS	**Boise** State Univ.	Boise, ID, USA
BOMB	Univ. of **Bombay**	Bombay, India
BONN	**Rheinische Friedr.-Wilhelms-Univ. Bonn**	Bonn, Germany
BORD	Univ. de **Bordeaux** I	Gradignan, France
BOSE	S.N. **Bose** National Centre for Basis Sciences	Calcutta, India
BOSK	**"Rudjer Bošković"** Inst.	Zagreb, Croatia
BOST	**Boston** Univ.	Boston, MA, USA
BRAN	**Brandeis** Univ.	Waltham, MA, USA
BRCO	Univ. of **British Columbia**	Vancouver, BC, Canada
BRIS	Univ. of **Bristol**	Bristol, United Kingdom
BROW	**Brown** Univ.	Providence, RI, USA
BRUN	**Brunel** Univ.	Uxbridge, Middlesex, United Kingdom
BRUX	Univ. Libre de **Bruxelles**; Service de Physique des Particules Elémentaires	Bruxelles, Belgium
BRUXT	Univ. Libre de **Bruxelles**; Physique Théorique	Bruxelles, Belgium
BUCH	Univ. of **Bucharest**	Bucharest-Mágurele, Romania
BUDA	KFKI Research Inst. for Particle & Nuclear Physics	**Budapest**, Hungary
BUFF	**SUNY at Buffalo**	Buffalo, NY, USA
BURE	Inst. des Hautes Etudes Scientifiques	**Bures-sur-Yvette**, France
CAEN	Lab. de Physique Corpusculaire, **ISMRA**	**Caen**, France
CAGL	Univ. degli Studi di **Cagliari**	Monserrato (CA), Italy

Abbreviations Used in the Particle Listings

CAIR	**Cairo** University	Orman, Giza, Cairo, Egypt
CAIW	**Carnegie Inst.** of Washington	Washington, DC, USA
CALC	Univ. of **Calcutta**	Calcutta, India
CAMB	**DAMTP**	Cambridge, United Kingdom
CAMP	Univ. de **Campinas**	**Campinas**, SP, Brasil
CANB	**Australian National Univ.**	Canberra, ACT, Australia
CAPE	University of **Capetown**	Rondebosch, Cape, South Africa
CARA	Univ. Central de **Venezuela**	Caracas, Venezuela
CARL	**Carleton** Univ.	Ottawa, ON, Canada
CARLC	**Carleton** College	Northfield, MN, USA
CASE	**Case** Western Reserve Univ.	Cleveland, OH, USA
CAST	**China** Center of Advanced Science and Technology	Beijing, The People's Republic of China
CATA	Univ. di **Catania**	Catania, Italy
CATH	**Catholic** Univ. of America	Washington, DC, USA
CAVE	**Cavendish** Lab.	Cambridge, United Kingdom
CBNM	CBNM	**Geel**, Belgium
CCAC	**Allegheny** College	Meadville, PA, USA
CDEF	**Collège de France**	Paris, France
CEA	Cambridge Electron Accelerator (Historical in *Review*)	**Cambridge, MA**, USA
CEBAF	**Jefferson Lab—Thomas Jefferson National Accelerator Facility**	**Newport News**, VA, USA
CENG	Centre d'Etudes Nucleaires	**Grenoble**, France
CERN	**CERN**, European Organization for Nuclear Research	Genève, Switzerland
CFPA	Univ. of **California, (Berkeley)**	Berkeley, CA, USA
CHIC	Univ. of **Chicago**	Chicago, IL, USA
CIAE	**China Institute of Atomic Energy**	**Beijing**, The People's Republic of China
CINC	Univ. of **Cincinnati**	Cincinnati, OH, USA
CINV	CINVESTAV-IPN, Centro de Investigacion y de Estudios Avanzados del IPN	**México**, DF, Mexico
CIT	**California Inst. of Tech.**	Pasadena, CA, USA
CLER	Univ. de **Clermont-Ferrand**	Aubière, France
CLEV	**Cleveland** State Univ.	Cleveland, OH, USA
CMNS	**Comenius** Univ.	**Bratislava**, Slovakia
CMU	**Carnegie Mellon** Univ.	Pittsburgh, PA, USA
CNEA	**Comisión Nacional de Energía Atómica**	Buenos Aires, Argentina
CNRC	Centre for Research in Particle Physics	Ottawa, ON, Canada
COLO	Univ. of **Colorado**	Boulder, CO, USA
COLU	**Columbia** Univ.	New York, NY, USA
CONC	**Concordia** University	Montreal, PQ, Canada
CORN	**Cornell** Univ.	Ithaca, NY, USA
COSU	**Colorado State** Univ.	Fort Collins, CO, USA
CPPM	Centre National de la Recherche Scientifique, Luminy	**Marseille**, France
CRAC	**Kraków** Inst. of Nuclear Physics	Kraków, Poland
CRNL	**Chalk River** Labs.	Chalk River, ON, Canada
CSOK	**Oklahoma** Central State Univ.	Edmond, OK, USA
CST	Univ. of **Science and Technology** of China	**Hefei**, Anhui 230027, The People's Republic of China
CSULB	**California** State Univ.	Long Beach, CA, USA
CUNY	**City College** of **New York**	New York, NY, USA
CURIN	**Univ. Pierre et Marie Curie** (Paris VI), LPNHE	Paris, France
CURIT	**Univ. Pierre et Marie Curie** (Paris VI), LPTHE	Paris, France
DALH	**Dalhousie** Univ.	Halifax, NS, Canada
DARE	**Daresbury** Lab	Cheshire, United Kingdom
DARM	Tech. Hochschule **Darmstadt**	Darmstadt, Germany
DELA	Univ. of **Delaware**; Dept. of Physics & Astronomy	Newark, DE, USA
DELH	Univ. of **Delhi**	Delhi, India
DESY	**DESY**, Deutsches Elektronen-Synchrotron	**Hamburg**, Germany
DFAB	Escuela de Ingenieros	**Bilbao**, Spain
DOE	**Department of Energy**	Washington, DC, USA
DORT	Univ. **Dortmund**	Dortmund, Germany
DUKE	**Duke** Univ.	Durham, NC, USA
DURH	Univ. of **Durham**	Durham , United Kingdom
DUUC	**University** College Dublin	Dublin, Ireland
EDIN	Univ. of **Edinburgh**	Edinburgh, United Kingdom
EFI	**Enrico Fermi Inst.**	**Chicago**, IL, USA
ELMT	**Elmhurst** College	Elmhurst, IL, USA
ENSP	**l'Ecole Normale Supérieure**	**Paris**, France
EOTV	**Eötvös** University	Budapest, Hungary
EPOL	**École Polytechnique**	**Palaiseau**, France
ERLA	Univ. **Erlangen-Nurnberg**	Erlangen, Germany
ETH	**Univ. Zürich**	Zürich, Switzerland
FERR	Univ. di **Ferrara**	Ferrara, Italy
FIRZ	Univ. di **Firenze**	Sesto Fiorentino, Italy
FISK	**Fisk** Univ.	Nashville, TN, USA
FLOR	Univ. of **Florida**	Gainesville, FL, USA
FNAL	**Fermilab**	Batavia, IL, USA
FOM	**FOM**, Stichting voor Fundamenteel Onderzoek der Materie	JP **Utrecht**, The Netherlands
FRAN	Univ. **Frankfurt**	Frankfurt am Main, Germany
FRAS	Lab. Nazionali di **Frascati** dell'INFN	Frascati (Roma), Italy
FREIB	**Albert-Ludwigs** Univ.	**Freiburg**, Germany
FREIE	**Freie Univ. Berlin**	Berlin, Germany
FRIB	Univ. de **Fribourg**	Fribourg, Switzerland
FSU	**Florida State** University	Tallahassee, FL, USA
FSUSC	**Florida State** Univ.	Tallahassee, FL, USA
FUKI	**Fukui** Univ.	Fukui, Japan
FUKU	**Fukushima** Univ.	Fukushima, Japan
GENO	Univ. di **Genova**	Genova, Italy
GEOR	**Georgian Academy of Sciences**	Tbilisi, Republic of Georgia
GESC	**General Electric** Co.	Schenectady, NY, USA
GEVA	Univ. de **Genève**	Genève, Switzerland
GIES	Univ. **Giessen**	Giessen, Germany
GIFU	**Gifu** Univ.	Gifu, Japan
GLAS	Univ. of **Glasgow**	Glasgow, United Kingdom
GMAS	**George Mason** Univ.	Fairfax, VA, USA
GOET	Univ. **Göttingen**	Göttingen, Germany
GRAN	Univ. de **Granada**	Granada, Spain
GRAZ	Univ. **Graz**	Graz, Austria
GRON	Univ. of **Groningen**	Groningen, The Netherlands
GSCO	**Geological Survey of Canada**	Ottawa, ON, Canada
GSI	**Darmstadt Gesellschaft** fur Schwerionenforschung	Darmstadt, Germany
GUEL	Univ. of **Guelph**	Guelph, ON, Canada
GWU	**George Washington** Univ.	Washington, DC, USA
HAHN	**Hahn-Meitner** Inst. Berlin GmbH	Berlin, Germany
HAIF	**Technion** – Israel Inst. of Tech.	Technion, Haifa, Israel
HAMB	Univ. **Hamburg**	Hamburg, Germany
HANN	Univ. **Hannover**	Hannover, Germany
HARC	**Houston Advanced Research Ctr.**	The Woodlands, TX, USA
HARV	**Harvard** Univ.	Cambridge, MA, USA
HAWA	Univ. of **Hawai'i**	Honolulu, HI, USA
HEBR	**Hebrew** Univ.	Jerusalem, Israel
HEID	Univ. **Heidelberg**; (unspecified division) (Historical in *Review*)	Heidelberg, Germany
HEIDH	Ruprecht-Karls Univ. **Heidelberg**	Heidelberg, Germany
HEIDP	Univ. **Heidelberg**; Physik Inst.	Heidelberg, Germany
HEIDT	Univ. **Heidelberg**; Inst. für Theoretische Physik	Heidelberg, Germany
HELS	Univ. of **Helsinki**; Dept. of Phys. Sci., High Energy Phys. Div. (SEFO); Dept. of Phys. Sci., Theor. Phys. Div. (TFO); Helsinki Institute of Physics (HIP)	University of Helsinki, Finland
HIRO	**Hiroshima** Univ.	Higashi-Hiroshima, Japan
HOUS	Univ. of **Houston**	Houston, TX, USA
HPC	**Hewlett-Packard** Corp.	Cupertino, CA, USA

Abbreviations Used in the Particle Listings

HSCA	**Harvard-Smithsonian** Center for Astrophysics	Cambridge, MA, USA
IAS	**Inst. for Advanced Study**	Princeton, NJ, USA
IASD	**Dublin** Inst. for Advanced Studies	Dublin, Ireland
IBAR	**Ibaraki** Univ.	Ibaraki, Japan
IBM	**IBM** Corp.	Palo Alto, CA, USA
IBMY	**IBM**	Yorktown Heights, NY, USA
IBS	Inst. for **Boson Studies**	Pasadena, CA, USA
ICEPP	Univ. of **Tokyo**; Int. Center for Elementary Particle Physics (ICEPP)	Tokyo, Japan
ICRR	Univ. of **Tokyo**	Chiba, Japan
ICTP	Abdus Salam International Centre for Theoretical Physics	**Trieste**, Italy
IFIC	**IFIC** (Instituto de Física Corpuscular)	**Valencia**, Spain
IFRJ	Univ. Federal do **Rio de Janeiro**	Rio de Janeiro, RJ, Brasil
IIT	**Illinois Inst. of Tech.**	Chicago, IL, USA
ILL	Univ. of **Illinois at Urbana-Champaign**	Urbana, IL, USA
ILLC	Univ. of **Illinois at Chicago**	Chicago, IL, USA
ILLG	Inst. **Laue-Langevin**	Grenoble, France
IND	**Indiana** Univ.	Bloomington, IN, USA
INEL	E G and G **Idaho**, Inc.	Idaho Falls, ID, USA
INFN	Ist. Nazionale di Fisica Nuclear (Generic INFN, unknown location)	Various places, Italy
INNS	**Leopold-Franzens** Univ.	**Innsbruck**, Austria
INPK	Inst. of Nuclear Physics	**Kraków**, Poland
INRM	**INR**, Inst. for Nucl. Research	**Moscow**, Russian Federation
INUS	**KEK**, High Energy Accelerator Research Organization	Tokyo, Japan
IOAN	Univ. of **Ioannina**	Ioannina, Greece
IOFF	A.F. **Ioffe** Phys. Tech. Inst.	St. **Petersburg**, Russian Federation
IOWA	Univ. of **Iowa**	Iowa City, IA, USA
IPN	**IPN**, Inst. de Phys. Nucl.	**Orsay**, France
IPNP	Univ. Pierre et Marie Curie (**Paris** VI)	Paris, France
IRAD	Inst. du Radium (Historical)	**Paris**, France
ISNG	Lab. de Physique Subatomique et de Cosmologie (**LPSC**)	**Grenoble**, France
ISU	**Iowa State** Univ.	Ames, IA, USA
ITEP	**ITEP**, Inst. of Theor. and Exp. Physics	**Moscow**, Russian Federation
ITHA	**Ithaca** College	Ithaca, NY, USA
IUPU	**Indiana** Univ., **Purdue** Univ. **Indianapolis**	Indianapolis, IN, USA
JADA	**Jadavpur** Univ.	Calcutta, India
JAGL	**Jagiellonian** Univ.	Kraków, Poland
JHU	**Johns Hopkins** Univ.	Baltimore, MD, USA
JINR	**JINR**, Joint Inst. for Nucl. Research	**Dubna**, Russian Federation
JULI	**Julich**, Forschungszentrum	Julich, Germany
JYV	Univ. of **Jyväskylä**	Jyväskylä, Finland
KAGO	Univ. of **Kagoshima**	Kagoshima-shi, Japan
KANS	Univ. of **Kansas**	Lawrence, KS, USA
KARL	Univ. **Karlsruhe**; (unspecified division) (Historical in *Review*)	Karlsruhe, Germany
KARLE	Univ. **Karlsruhe**; Inst. für Experimentelle Kernphysik	Karlsruhe, Germany
KARLK	Forschungszentrum **Karlsruhe**	Karlsruhe, Germany
KARLT	Univ. **Karlsruhe**; Inst. für Theoretische Teilchenphysik	Karlsruhe, Germany
KAZA	**Kazakh** Inst. of High Energy Physics	Alma Ata, Kazakhstan
KEK	**KEK**, High Energy Accelerator Research Organization	Ibaraki-ken, Japan
KENT	Univ. of **Kent**	Canterbury, United Kingdom
KEYN	**Open** Univ.	Milton Keynes, United Kingdom
KFTI	**Kharkov** Inst. of Physics and Tech. (KFTI)	Kharkov, Ukraine
KIAE	The Russian Research Center, **Kurchatov** Inst.	**Moscow**, Russian Federation
KIAM	**Keldysh** Inst. of Applied Math., Acad. Sci., Russia	Moscow, Russian Federation
KIDR	**Vinča Inst. of Nuclear Sciences**	Belgrade, Serbia and Montenegro
KIEV	**Institute for Nuclear Research**	**Kiev**, Ukraine
KINK	**Kinki** Univ.	Osaka, Japan
KNTY	Univ. of **Kentucky**	Lexington, KY, USA
KOBE	**Kobe** Univ.	Kobe, Japan
KOMAB	Univ. of **Tokyo, Komaba**	Tokyo, Japan
KONAN	**Konan** Univ.	Kobe, Japan
KOSI	Inst. of Experimental Physics	**Košice**, Slovakia
KYOT	**Kyoto** Univ.; Dept. of Physics, Graduate School of Science	Kyoto, Japan
KYOTU	**Kyoto** Univ.; **Yukawa** Inst. for Theor. Physics	Kyoto, Japan
KYUN	**Kyungpook** National Univ.	Taegu, Republic of Korea
KYUSH	**Kyushu** Univ.	Fukuoka, Japan
LALO	**LAL**, Laboratoire de l'Accélérateur Linéaire	**Orsay**, France
LANC	**Lancaster** Univ.	Lancaster, United Kingdom
LANL	**Los Alamos National Lab.** (LANL)	Los Alamos, NM, USA
LAPP	**LAPP**, Lab. d'Annecy-le-Vieux de Phys. des Particules	**Annecy-le-Vieux**, France
LASL	U.C. **Los Alamos Scientific** Lab. (Old name for LANL)	Los Alamos, NM, USA
LATV	**Latvian** State Univ.	Riga, Latvia
LAUS	EPFL **Lausanne**	Lausanne, Switzerland
LAVL	Univ. **Laval**	Quebec, QC, Canada
LBL	**Lawrence Berkeley National Lab.**	Berkeley, CA, USA
LCGT	Univ. di **Torino**	Turin, Italy
LEBD	**Lebedev** Physical Inst.	**Moscow**, Russian Federation
LECE	Univ. di **Lecce**	Lecce, Italy
LEED	Univ. of **Leeds**	Leeds, United Kingdom
LEHI	**Lehigh** Univ.	Bethlehem, PA, USA
LEHM	**Lehman** College of CUNY	Bronx, NY, USA
LEID	Univ. **Leiden**	Leiden, The Netherlands
LEMO	**Le Moyne** Coll.	Syracuse, NY, USA
LEUV	Katholieke Univ. **Leuven**	Leuven, Belgium
LINZ	Univ. **Linz**	Linz, Austria
LISB	Inst. Nacional de Investigacion Cientifica	**Lisboa** CODEX, Portugal
LISBT	Univ. Técnica de Lisboa, Inst. Superior Técnico	**Lisboa**, Portugal
LIVP	Univ. of **Liverpool**	Liverpool, United Kingdom
LLL	**Lawrence Livermore Lab.** (Old name for LLNL)	Livermore, CA, USA
LLNL	**Lawrence Livermore National Lab.**	Livermore, CA, USA
LOCK	**Lockheed** Palo Alto Res. Lab	Palo Alto, CA, USA
LOIC	**Imperial** College of Science Tech. & Medicine	London, United Kingdom
LOQM	Queen Mary, **Univ. of London**	London, United Kingdom
LOUC	**University College** London	London, United Kingdom
LOUV	Univ. Catholique de **Louvain**	Louvain-la-Neuve, Belgium
LOWC	**Westfield** College (Historical, see LOQM (Queen Mary and Westfield joined))	London, United Kingdom
LRL	U.C. Lawrence Radiation Lab. (Old name for LBL)	**Berkeley**, CA, USA
LSU	**Louisiana** State Univ.	Baton Rouge, LA, USA
LUND	Univ. of **Lund**	Lund, Sweden
LUND	**Fysiska Institutionen**	**Lund**, Sweden
LYON	Institute de Physique Nucléaire de **Lyon** (IPN)	Villeurbanne, France
MADE	**CSIC**, Inst. de Estructura de la Materia	**Madrid**, Spain
MADR	**C.I.E.M.A.T**	**Madrid**, Spain
MADU	Univ. Autónoma de **Madrid**	Madrid, Spain
MANI	Univ. of **Manitoba**	Winnipeg, MB, Canada
MANZ	**Johannes-Gutenberg-Univ.**	**Mainz**, Germany
MARB	Univ. **Marburg**	Marburg, Germany

Abbreviations Used in the Particle Listings

MARS	Centre de Physique des Particules de **Marseille**	Marseille, France
MASA	Univ. of **Massachusetts** Amherst	**Amherst**, MA, USA
MASB	Univ. of **Massachusetts** Boston	**Boston**, MA, USA
MASD	Univ. of **Massachusetts** Dartmouth	N. **Dartmouth**, MA, USA
MCGI	**McGill** Univ.	Montreal, QC, Canada
MCHS	Univ. of **Manchester**	Manchester, United Kingdom
MCMS	**McMaster** Univ.	Hamilton, ON, Canada
MEHTA	**Harish-Chandra** Research Inst.	Allahabad, India
MEIS	**Meisei** Univ.	Tokyo, Japan
MELB	Univ. of **Melbourne**	Victoria, Australia
MEUD	Observatoire de **Meudon**	Meudon, France
MICH	Univ. of **Michigan**	Ann Arbor, MI, USA
MILA	Univ. di **Milano**	Milano, Italy
MILAI	INFN, Sez. di **Milano**	Milano, Italy
MINN	Univ. of **Minnesota**	Minneapolis, MN, USA
MISS	Univ. of **Mississippi**	University, MS, USA
MISSR	Univ. of **Missouri**	Rolla, MO, USA
MIT	**MIT Massachusetts Inst. of Technology**	Cambridge, MA, USA
MIU	**Maharishi** International Univ.	Fairfield, IA, USA
MIYA	**Miyazaki** Univ.	Miyazaki-shi, Japan
MONP	Univ. de **Montpellier** II	Montpellier, France
MONS	Univ. de **Mons-Hainaut**	**Mons**, Belgium
MONT	Univ. de **Montréal**; Laboratoire René-J.-A.-Lévesque	Montréal, PQ, Canada
MONTC	Univ. de **Montréal**; Centre de recherches mathématiques	Montréal, PQ, Canada
MOSU	**Skobeltsyn** Inst. of Nuclear Physics, Moscow State Univ.	**Moscow**, Russian Federation
MPCM	Max Planck Inst. fur Chemie	**Mainz**, Germany
MPEI	**Moscow Physical Engineering** Inst.	Moscow, Russian Federation
MPIA	**Max-Planck**-Institute für Astrophysik	Garching, Germany
MPIH	**Max-Planck-Inst.** für Kernphysik	**Heidelberg**, Germany
MPIM	**Max-Planck-Inst.** für Physik	**München**, Germany
MSU	**Michigan State** Univ.	East Lansing, MI, USA
MTHO	**Mount Holyoke** College	South Hadley, MA, USA
MULH	Centre Univ. du **Haut-Rhin**	Mulhouse, France
MUNI	**Ludwig-Maximilians-Univ. München**	Garching, Germany
MUNT	Tech. Univ. **München**	Garching, Germany
MURA	**Midwestern** Univ. Research Assoc. (Historical in *Review*)	Stroughton, WI, USA
NAAS	North Americal Aviation Science Center (Historical in *Review*)	Thousand Oaks, CA, USA
NAGO	**Nagoya** Univ.	Nagoya, Japan
NAPL	Univ. di **Napoli**	Napoli, Italy
NASA	**NASA**	Greenbelt, MD, USA
NBS	U.S **National Bureau of Standards** (Old name for NIST)	Gaithersburg, MD, USA
NBSB	**National Inst. Standards Tech.**	Boulder, CO, USA
NCAR	**National Center for Atmospheric Research**	Boulder, CO, USA
NCARO	**North Carolina** State Univ.	**Raleigh**, NC, USA
NDAM	Univ. of **Notre Dame**	Notre Dame, IN, USA
NEAS	**Northeastern** Univ.	Boston, MA, USA
NEUC	Univ. de **Neuchâtel**	Neuchâtel, Switzerland
NICEA	Univ. de **Nice**	Nice, France
NICEO	Observatoire de **Nice**	Nice, France
NIHO	**Nihon** Univ.	Tokyo, Japan
NIIG	**Niigata** Univ.	Niigata, Japan
NIJM	Univ. of **Nijmegen**	ED NIJMEGEN, The Netherlands
NIRS	Nat. Inst. Radiological Sciences	**Chiba**, Japan
NIST	**National Institute of Standards & Technology**	Gaithersburg, MD, USA
NIU	**Northern Illinois** Univ.	De Kalb, IL, USA
NMSU	**New Mexico** State Univ.; Dept. of Physics; Part. & Nucl. Phys. Group, Box 30001/Dept. MSC 3D	Las Cruces, NM, USA
NORD	**Nordita**	Copenhagen Ø, Denmark
NOTT	Univ. of **Nottingham**	Nottingham, United Kingdom
NOVM	Inst. of Mathematics	**Novosibirsk**, Russian Federation
NOVO	BINP, **Budker** Inst. of Nuclear Physics	**Novosibirsk**, Russian Federation
NPOL	Polytechnic of **North London**	London, United Kingdom
NRL	**Naval Research** Lab	Washington, DC, USA
NSF	**National Science Foundation**	Arlington, VA, USA
NTHU	**National Tsing Hua** Univ.	Hsinchu, The Republic of China (Taiwan)
NTUA	**National Tech. Univ. of Athens**	Athens, Greece
NWES	**Northwestern** Univ.	Evanston, IL, USA
NYU	**New York** Univ.	New York, NY, USA
OBER	**Oberlin** College	Oberlin, OH, USA
OCH	**Ochanomizu** Univ.	Tokyo, Japan
OHIO	**Ohio** Univ.	Athens, OH, USA
OKAY	**Okayama** Univ.	Okayama, Japan
OKLA	Univ. of **Oklahoma**	Norman, OK, USA
OKSU	**Oklahoma State** Univ.	Stillwater, OK, USA
OREG	Univ. of **Oregon**; Inst. of Theor. Science; U.O. Center for High Energy Physics	Eugene, OR, USA
ORNL	**Oak Ridge** National Laboratory	Oak Ridge, TN, USA
ORSAY	Univ. de **Paris Sud**	**Orsay** CEDEX, France
ORST	**Oregon State** Univ.	Corvallis, OR, USA
OSAK	**Osaka** Univ.	Osaka, Japan
OSKC	**Osaka City** Univ.	Osaka-shi, Japan
OSLO	Univ. of **Oslo**	Oslo, Norway
OSU	**Ohio State** Univ.	Columbus, OH, USA
OTTA	Univ. of **Ottawa**	Ottawa, ON, Canada
OXF	University of **Oxford**	Oxford, United Kingdom
OXFTP	Univ. of **Oxford**	Oxford, United Kingdom
PADO	Univ. degli Studi di **Padova**	Padova, Italy
PARIN	**Univ. Paris VI et Paris VII**, IN^2P^3/CNRS	Paris, France
PARIS	Univ. de Paris (Historical)	**Paris**, France
PARIT	**Univ. Paris VII**, LPTHE	Paris, France
PARM	Univ. di **Parma**	Parma, Italy
PAST	Institut **Pasteur**	**Paris**, France
PATR	Univ. of **Patras**	Patras, Greece
PAVI	Univ. di **Pavia**	Pavia, Italy
PENN	Univ. of **Pennsylvania**	Philadelphia, PA, USA
PGIA	INFN, Sezione di **Perugia**	Perugia, Italy
PISA	Univ. di **Pisa**	Pisa, Italy
PISAI	**INFN, Sez. di Pisa**	Pisa, Italy
PITT	Univ. of **Pittsburgh**	Pittsburgh, PA, USA
PLAT	**SUNY at Plattsburgh**	Plattsburgh, NY, USA
PLRM	Univ. di **Palermo**	Palermo, Italy
PNL	**Battelle Memorial** Inst.	Richland, WA, USA
PNPI	**Petersburg** Nuclear Physics Inst. of Russian Academy of Sciences	Gatchina, Russian Federation
PPA	Princeton-Penn. Proton Accelerator (Historical in *Review*)	Princeton, NJ, USA
PRAG	Inst. of Physics, **ASCR**	**Prague**, Czech Republic
PRIN	**Princeton** Univ.	Princeton, NJ, USA
PSI	Paul Scherrer Inst.	**Villigen** PSI, Switzerland
PSLL	**Physical Science Lab**	Las Cruces, NM, USA
PSU	**Penn State** Univ.	University Park, PA, USA
PUCB	**Pontifícia Univ. Católica do Rio de Janeiro**	Rio de Janeiro, RJ, Brasil
PUEB	Univ. Autonoma de **Puebla**	**Puebla**, Pue, Mexico
PURD	**Purdue** Univ.	West Lafayette, IN, USA
QUKI	**Queen's** Univ.	Kingston, ON, Canada
RAL	**Rutherford Appleton** Lab.	Chilton, Didcot, Oxon., United Kingdom
REGE	Univ. **Regensburg**	Regensburg, Germany
REHO	**Weizmann** Inst. of Science	Rehovot, Israel

Abbreviations Used in the Particle Listings

RHBL	**Royal Holloway, Univ. of London**	Egham, Surrey, United Kingdom
RHEL	**Rutherford** High Energy Lab (Old name for RAL)	Chilton, Didcot, Oxon., United Kingdom
RICE	**Rice** Univ.	Houston, TX, USA
RIKEN	**Riken** Accelerator Research Facility (RARF), Cyclotron Lab	Saitama, Japan
RIKK	**Rikkyo** Univ.	Tokyo, Japan
RIS	**Rowland** Inst. for Science	Cambridge, MA, USA
RISC	**Rockwell** International	Thousand Oaks, CA, USA
RISL	**Universities Research Reactor**	**Risley**, Warrington, United Kingdom
RISO	**Riso** National Laboratory	Roskilde, Denmark
RL	**Rutherford** High Energy Lab (Old name for RAL)	Chilton, Didcot, Oxon., United Kingdom
RMCS	**Royal Military** Coll. of Science	Swindon, Wilts., United Kingdom
ROCH	Univ. of **Rochester**	Rochester, NY, USA
ROCK	**Rockefeller** Univ.	New York, NY, USA
ROMA	Univ. di **Roma** (Historical)	**Roma**, Italy
ROMA2	Univ. di **Roma**, "Tor Vergata"	Roma, Italy
ROMAI	**INFN, Sez. di Roma**	Roma, Italy
ROSE	**Rose-Hulman** Inst. of Technology	Terre Haute IN, USA
RPI	**Rensselaer Polytechnic** Inst.	Troy, NY, USA
RUTG	**Rutgers**, the State Univ. of New Jersey	Piscataway, NJ, USA
SACL	**CE Saclay**, DAPNIA	Gif-sur-Yvette, France
SACL	**CEA Saclay**, DAPNIA	Gif-sur-Yvette, France
SACL	**CEA/Saclay** – SPhT	Gif-sur-Yvette, France
SACLD	**CEA Saclay**, DAPNIA; Direction	Gif-sur-Yvette, France
SAGA	**Saga** Univ.	Saga-shi, Japan
SAHA	**Saha** Inst. of Nuclear Physics	Bidhannagar, Calcutta, India
SANG	**Kyoto Sangyo** Univ.	Kyoto-shi, Japan
SANI	Physics Lab., Ist. Superiore di Sanità	**Roma**, Italy
SASK	Univ. of **Saskatchewan**	Saskatoon, SK, Canada
SASSO	Lab. Naz. del **Gran Sasso** dell'INFN	**Assergi** (L'Aquila), Italy
SAVO	Univ. de **Savoie**	Chambery, France
SBER	**California** State Univ.	**San Bernardino**, CA, USA
SCHAF	W.J. **Schafer** Assoc.	Livermore, DA, USA
SCIT	**Science** Univ. of **Tokyo**	Tokyo, Japan
SCOT	**Scottish** Univ. Research and Reactor Ctr.	Glasgow, United Kingdom
SCUC	Univ. of **South Carolina**	Columbia, SC, USA
SEAT	**Seattle Pacific** Coll.	Seattle, WA, USA
SEIB	Austrian Research Center, **Seibersdorf** LTD.	Seibersdorf, Austria
SEOU	**Korea** Univ.; Dept. of Physics; HEP Group	Seoul, Republic of Korea
SEOUL	**Seoul** National Univ.; Dept. of Physics, Coll. of Natural Sciences; Center for Theoretical Physics	Seoul, Republic of Korea
SERP	**IHEP**, Inst. for High Energy Physics (Also known as Serpukhov)	Protvino, Russian Federation
SETO	**Seton Hall** Univ.	South Orange, NJ, USA
SFLA	Univ. of **South Florida**	Tampa, FL, USA
SFRA	**Simon Fraser University**	Burnaby, BC, Canada
SFSU	**California** State Univ.	**San Francisco**, CA, USA
SHAMS	**Ain Shams** University	Abbassia, Cairo, Egypt
SHEF	Univ. of **Sheffield**	Sheffield, United Kingdom
SHMP	Univ. of **Southampton**	Southampton, United Kingdom
SIEG	Univ. **Siegen**	Siegen, Germany
SILES	Univ. of **Silesia**	Katowice, Poland
SIN	Swiss Inst. of Nuclear Research (Old name for VILL)	**Villigen**, Switzerland
SING	**National Univ.** of Singapore	Kent Ridge, Singapore
SISSA	Scuola Internazionale Superiore di Studi Avanzati	**Trieste**, Italy
SLAC	**Stanford Linear Accelerator Center**	Menlo Park, CA, USA
SLOV	Inst. of Physics, Slovak Acad. of Sciences	**Bratislava**, Slovakia
SMU	**Southern Methodist** Univ.	Dallas, TX, USA
SNSP	**Scuola Normale Superiore**	**Pisa**, Italy
SOFI	Inst. for Nuclear Research and Nuclear Energy	**Sofia**, Bulgaria
SOFU	Univ. of **Sofia** "St. Kliment Ohridski"	Sofia, Bulgaria
SPAUL	Univ. de **São Paulo**	São Paulo, SP, Brasil
SPIFT	Inst. de Física Teórica (**IFT**)	**São Paulo**, SP, Brasil
SSL	Univ. of **California (Berkeley)**; Space Sciences Lab	Berkeley, CA, USA
STAN	**Stanford** Univ.	Stanford, CA, USA
STEV	**Stevens** Inst. of Tech.	Hoboken, NJ, USA
STLO	**St. Louis** Univ.	St. Louis, MO, USA
STOH	**Stockholm** Univ.	Stockholm, Sweden
STON	**SUNY at Stony Brook**	Stony Brook, NY, USA
STRB	**IReS**, Inst. de Recherches Subatomiques	**Strasbourg**, France
STUT	Univ. **Stuttgart**	Stuttgart, Germany
STUTM	Max-Planck-Inst.	**Stuttgart**, Germany
SUGI	**Sugiyama Jogakuen** Univ.	Aichi, Japan
SURR	Univ. of **Surrey**	Guildford, Surrey, United Kingdom
SUSS	Univ. of **Sussex**	Brighton, United Kingdom
SVR	**Savannah** River Labs.	Aiken, SC, USA
SYDN	Univ. of **Sydney**	Sydney, NSW, Australia
SYRA	**Syracuse** Univ.	Syracuse, NY, USA
TAJK	Acad. Sci., Tadzhik SSR	**Dushanbe**, Tadzhikstan
TAMU	**Texas A&M** Univ.	College Station, TX, USA
TATA	**Tata** Inst. of Fundamental Research	Bombay, India
TBIL	**Tbilisi State University**	Tbilisi, Republic of Georgia
TELA	**Tel-Aviv** Univ.	Tel Aviv, Israel
TELE	**Teledyne Brown** Engineering	Huntsville, AL, USA
TEMP	**Temple** Univ.	Philadelphia, PA, USA
TENN	Univ. of **Tennessee**	Knoxville, TN, USA
TEXA	Univ. of **Texas** at **Austin**	Austin, TX, USA
TGAK	**Tokyo Gakugei** Univ.	Tokyo, Japan
TGU	**Tohoku Gakuin** Univ.	Miyagi, Japan
THES	Aristotle Univ. of **Thessaloniki** (AUTh)	Thessaloniki, Greece
TINT	**Tokyo Inst. of Technology**	Tokyo, Japan
TISA	**Sagamihara** Inst. of Space & Astronautical Sci.	Kanagawa, Japan
TMSK	Inst. Nuclear Physics	**Tomsk**, Russian Federation
TMTC	**Tokyo Metropolitan** Coll. Tech.	Tokyo, Japan
TMU	**Tokyo Metropolitan Univ.**	Tokyo, Japan
TNTO	Univ. of **Toronto**	Toronto, ON, Canada
TOHO	**Toho** Univ.	Chiba, Japan
TOHOK	**Tohoku** Univ.	Sendai, Japan
TOKA	**Tokai** Univ.	Shimizu, Japan
TOKAH	**Tokai** Univ.	Hiratsuka, Japan
TOKMS	Univ. of **Tokyo**; Meson Science Laboratory	Tokyo, Japan
TOKU	Univ. of **Tokushima**	Tokushima-shi, Japan
TOKY	Univ. of **Tokyo**; High-Energy Physics Theory Group	Tokyo, Japan
TOKYC	Univ. of **Tokyo**; Dept. of Chemistry	Tokyo, Japan
TORI	Univ. degli Studi di **Torino**	Torino, Italy
TPTI	Lab. of High Energy Phys.	**Tashkent**, Republic of Uzbekistan
TRIN	Univ. of **Dublin**, Trinity College	**Dublin**, Ireland
TRIU	**TRIUMF**	Vancouver, BC, Canada
TRST	Univ. di **Trieste**	Trieste, Italy
TRSTI	INFN, Sez. di **Trieste**	Trieste, Italy
TRSTT	Univ. di **Trieste**	**Trieste**, Italy
TSUK	Univ. of **Tsukuba**	Ibaraki-ken, Japan
TTAM	**Tamagawa** Univ.	Tokyo, Japan
TUAT	**Tokyo** Univ. of Agriculture Tech.	Tokyo, Japan
TUBIN	Univ. **Tübingen**	Tübingen, Germany
TUFTS	**Tufts** Univ.	Medford, MA, USA
TUW	**Technische** Univ. **Wien**	Vienna, Austria
TUZL	**Tuzla** Univ.	Tuzla, Argentina

Abbreviations Used in the Particle Listings

UCB	Univ. of **California (Berkeley)**; Dept. of Physics	Berkeley, CA, USA
UCD	Univ. of **California (Davis)**	Davis, CA, USA
UCI	Univ. of **California (Irvine)**	Irvine, CA, USA
UCLA	Univ. of **California (Los Angeles)**	Los Angeles, CA, USA
UCND	**Union Carbide** Corp.	Oak Ridge, TN, USA
UCR	Univ. of **California (Riverside)**	Riverside, CA, USA
UCSB	Univ. of **California (Santa Barbara)**; Physics Dept.	Santa Barbara, CA, USA
UCSBT	Univ. of **California (Santa Barbara)**; **Kavli Inst. for Theoretical Physics**	Santa Barbara, CA, USA
UCSC	Univ. of **California (Santa Cruz)**	Santa Cruz, CA, USA
UCSD	Univ. of **California (San Diego)**	La Jolla, CA, USA
UMD	Univ. of **Maryland**	College Park, MD, USA
UNC	Univ. of **North Carolina**	Greensboro, NC, USA
UNCCH	Univ. of **North Carolina** at **Chapel Hill**	Chapel Hill, NC, USA
UNCS	**Union** College	Schenectady, NY, USA
UNH	Univ. of **New Hampshire**	Durham, NH, USA
UNM	Univ. of **New Mexico**	Albuquerque, NM, USA
UOEH	Univ. of Occupational and Environmental Health	**Kitakyushu**, Japan
UPNJ	**Upsala** College	East Orange, NJ, USA
UPPS	**Uppsala** Univ.	**Uppsala**, Sweden
UPR	Univ. of **Puerto Rico**	**Rio Piedras**, PR, USA
URI	Univ. of **Rhode Island**	Kingston, RI, USA
USC	Univ. of **Southern California**	Los Angeles, CA, USA
USF	Univ. of **San Francisco**	San Francisco, CA, USA
UTAH	Univ. of **Utah**; Dept. of Physics; High-Energy Astrophysics Inst.	Salt Lake City, UT, USA
UTRE	Univ. of **Utrecht**	Utrecht, The Netherlands
UTRO	**Norwegian Univ. of Science & Technology**	Trondheim, Norway
UZINR	Acad. Sci., **Ukrainian** SSR	**Uzhgorod**, Ukraine
VALE	Univ. de **Valencia**	Burjassot, **Valencia**, Spain
VALP	**Valparaiso** Univ.	Valparaiso, IN, USA
VAND	**Vanderbilt** Univ.	Nashville, TN, USA
VASS	**Vassar** College	Poughkeepsie, NY, USA
VICT	Univ. of **Victoria**	Victoria, BC, Canada
VIEN	Inst. für Hochenergiephysik (HEPHY)	**Vienna**, Austria
VILL	Inst. for Particle Physics of ETH Zürich	**Zürich**, Switzerland
VIRG	Univ. of **Virginia**	Charlottesville, VA, USA
VPI	**Virginia Tech.**	Blacksburg, VA, USA
VRIJ	**Vrije** Univ.	HV **Amsterdam**, The Netherlands
WABRN	Eidgenossisches Amt für Messwesen	**Waber**, Switzerland
WARS	**Warsaw** Univ.	Warsaw, Poland
WASCR	**Waseda** Univ.; Cosmic Ray Division	Tokyo, Japan
WASH	Univ. of **Washington**; Elem. Particle Experiment (EPE); Particle Astrophysics (PA)	Seattle, WA, USA
WASU	**Waseda** Univ.; Dept. of Physics, High Energy Physics Group	Tokyo, Japan
WAYN	**Wayne** State Univ.	Detroit, MI, USA
WESL	**Wesleyan** Univ.	Middletown, CT, USA
WIEN	Univ. **Wien**	Vienna, Austria
WILL	Coll. of **William and Mary**	Williamsburg, VA, USA
WINR	Andrzej **Soltan** Inst. for Nuclear Studies	**Warsaw**, Poland
WISC	Univ. of **Wisconsin**	Madison, WI, USA
WITW	Univ. of the **Witwatersrand**	Wits, South Africa
WMIU	**Western Michigan** Univ.	Kalamazoo, MI, USA
WONT	The Univ. of **Western Ontario**	London, ON, Canada
WOOD	**Woodstock** College (No longer in existence)	Woodstock, MD, USA
WUPP	**Bergische** Univ.	**Wuppertal**, Germany
WURZ	Univ. **Würzburg**	Würzburg, Germany
WUSL	**Washington** Univ.	St. Louis, MO, USA
WYOM	Univ. of **Wyoming**	Laramie, WY, USA
YALE	**Yale** Univ.	New Haven, CT, USA
YARO	**Yaroslavl** State Univ.	Yaroslavl, Russian Federation
YCC	**Yokohama** Coll. of Commerce	Yokohama, Japan
YERE	**Yerevan** Physics Inst.	Yerevan, Armenia
YOKO	**Yokohama National** Univ.	Yokohama-shi, Japan
YORKC	**York** Univ.	Toronto, Canada
ZAGR	**Zagreb** Univ.	Zagreb, Croatia
ZARA	Univ. de **Zaragoza**	Zaragoza, Spain
ZEEM	Univ. van **Amsterdam**	TV Amsterdam, The Netherlands
ZURI	Univ. **Zürich**	Zürich, Switzerland

GAUGE AND HIGGS BOSONS

Notes in the Gauge and Higgs Boson Listings

GAUGE AND HIGGS BOSONS

γ

$I(J^{PC}) = 0,1(1^{--})$

γ MASS

For a review of the photon mass, see BYRNE 77.

VALUE (eV)		CL%	DOCUMENT ID		TECN	COMMENT
< 6	**$\times 10^{-17}$**		[1] RYUTOV	97		MHD of solar wind
• • • We do not use the following data for averages, fits, limits, etc. • • •						
< 7	$\times 10^{-19}$		[2] LUO	03		Modulation torsion balance
< 1	$\times 10^{-17}$		[3] LAKES	98		Torque on toroid balance
< 9	$\times 10^{-16}$	90	[4] FISCHBACH	94		Earth magnetic field
$< (4.73 \pm 0.45)$	$\times 10^{-12}$		[5] CHERNIKOV	92	SQID	Ampere-law null test
$< (9.0 \pm 8.1)$	$\times 10^{-10}$		[6] RYAN	85		Coulomb-law null test
< 3	$\times 10^{-27}$		[7] CHIBISOV	76		Galactic magnetic field
< 6	$\times 10^{-16}$	99.7	DAVIS	75		Jupiter magnetic field
< 7.3	$\times 10^{-16}$		HOLLWEG	74		Alfven waves
< 6	$\times 10^{-17}$		[8] FRANKEN	71		Low freq. res. cir.
< 1	$\times 10^{-14}$		WILLIAMS	71	CNTR	Tests Gauss law
< 2.3	$\times 10^{-15}$		GOLDHABER	68		Satellite data
< 6	$\times 10^{-15}$		[8] PATEL	65		Satellite data
< 6	$\times 10^{-15}$		GINTSBURG	64		Satellite data

[1] RYUTOV 97 uses a magnetohydrodynamics argument concerning survival of the Sun's field to the radius of the Earth's orbit. "To reconcile observations to theory, one has to reduce [the photon mass] by approximately an order of magnitude compared with" DAVIS 75.

[2] LUO 03 determine a limit on $\mu^2 \boldsymbol{A} < 1.1 \times 10^{-11}$ T m/m^2 (with μ^{-1}=characteristic length for photon mass; $\boldsymbol{A}$=ambient vector potential) — similar to the LAKES 98 technique. Unlike LAKES 98 who used static, the authors used dynamic torsion balance. Assuming $\boldsymbol{A}$ to be 10^{12} T m, they obtain $\mu < 1.2 \times 10^{-51}$ g, equivalent to 6.7×10^{-19} eV. The rotating modified Cavendish balance removes dependence on the direction of $\boldsymbol{A}$. GOLDHABER 03 argue that because plasma current effects are neglected, the LUO 03 limit does not provide the best available limit on $\mu^2 \boldsymbol{A}$ nor a reliable limit at all on μ. The reason is that the $\boldsymbol{A}$ associated with cluster magnetic fields could become arbitrarily small in plasma voids, whose existence would be compatible with present knowledge. LUO 03B reply that fields of distant clusters are not accurately mapped, but assert that a zero $\boldsymbol{A}$ is unlikely given what we know about the magnetic field in our galaxy.

[3] LAKES 98 reports limits on torque on a toroid Cavendish balance, obtaining a limit on $\mu^2 \boldsymbol{A} < 2 \times 10^{-9}$ Tm/m^2 via the Maxwell-Proca equations, where μ^{-1} is the characteristic length associated with the photon mass and $\boldsymbol{A}$ is the ambient vector potential in the Lorentz gauge. Assuming $\boldsymbol{A} \approx 1 \times 10^{12}$ Tm due to cluster fields he obtains $\mu^{-1} > 2 \times 10^{10}$ m, corresponding to $\mu < 1 \times 10^{-17}$ eV. A more conservative limit, using $\boldsymbol{A} \approx (1\ \mu\text{G}) \times (600\ \text{pc})$ based on the galactic field, is $\mu^{-1} > 1 \times 10^{9}$ m or $\mu < 2 \times 10^{-16}$ eV.

[4] FISCHBACH 94 report $< 8 \times 10^{-16}$ with unknown CL. We report Bayesian CL used elsewhere in these Listings and described in the Statistics section.

[5] CHERNIKOV 92 measures the photon mass at 1.24 K, following a theoretical suggestion that electromagnetic gauge invariance might break down at some low critical temperature. See the erratum for a correction, included here, to the published result.

[6] RYAN 85 measures the photon mass at 1.36 K (see the footnote to CHERNIKOV 92).

[7] CHIBISOV 76 depends in critical way on assumptions such as applicability of virial theorem. Some of the arguments given only in unpublished references.

[8] See criticism questioning the validity of these results in GOLDHABER 71, PARK 71 and KROLL 71. See also review GOLDHABER 71B.

γ CHARGE

VALUE (e)		DOCUMENT ID		TECN	COMMENT
<5	**$\times 10^{-30}$**	[9] RAFFELT	94	TOF	Pulsar $f_1 - f_2$
• • • We do not use the following data for averages, fits, limits, etc. • • •					
$< 8.5 \times 10^{-17}$		[10] SEMERTZIDIS	03		Laser light deflection in B-field
$< 2 \times 10^{-28}$		[11] COCCONI	92		VLBA radio telescope resolution
$< 2 \times 10^{-32}$		COCCONI	88	TOF	Pulsar $f_1 - f_2$ TOF

[9] RAFFELT 94 notes that COCCONI 88 neglects the fact that the time delay due to dispersion by free electrons in the interstellar medium has the same photon energy dependence as that due to bending of a charged photon in the magnetic field. His limit is based on the assumption that the entire observed dispersion is due to photon charge. It is a factor of 200 less stringent than the COCCONI 88 limit.

[10] SEMERTZIDIS 03 reports the first laboratory limit on the photon charge in the last 30 years. Straightforward improvements in the apparatus could attain a sensitivity of 10^{-20} e.

[11] See COCCONI 92 for less stringent limits in other frequency ranges. Also see RAFFELT 94 note.

γ REFERENCES

GOLDHABER	03	PRL 91 149101	A.S. Goldhaber, M.M. Nieto	
LUO	03	PRL 90 081801	J. Luo *et al.*	
LUO	03B	PRL 91 149102	J. Luo *et al.*	
SEMERTZIDIS	03	PR D67 017701	Y.K. Semertzidis, G.T. Danby, D.M. Lazarus	
LAKES	98	PRL 80 1826	R. Lakes	(WISC)
RYUTOV	97	PPCF 39 A73	D.D. Ryutov	(LLNL)
FISCHBACH	94	PRL 73 514	E. Fischbach *et al.*	(PURD, JHU+)
RAFFELT	94	PR D50 7729	G. Raffelt	(MPIM)
CHERNIKOV	92	PRL 68 3383	M.A. Chernikov *et al.*	(ETH)
Also	92B	PRL 69 2999 (erratum)	M.A. Chernikov *et al.*	(ETH)
COCCONI	92	AJP 60 750	G. Cocconi	(CERN)
COCCONI	88	PL B206 705	G. Cocconi	(CERN)
RYAN	85	PR D32 802	J.J. Ryan, F. Accetta, R.H. Austin	(PRIN)
BYRNE	77	Ast.Sp.Sci. 46 115	J. Byrne	(LOIC)
CHIBISOV	76	SPU 19 624	G.V. Chibisov	(LEBD)
DAVIS	75	PRL 35 1402	L. Davis, A.S. Goldhaber, M.M. Nieto	(CIT, STON+)
HOLLWEG	74	PRL 32 961	J.V. Hollweg	(NCAR)
FRANKEN	71	PRL 26 115	P.A. Franken, G.W. Ampulski	(MICH)
GOLDHABER	71	PRL 26 1390	A.S. Goldhaber, M.M. Nieto	(STON, BOHR, UCSB)
GOLDHABER	71B	RMP 43 277	A.S. Goldhaber, M.M. Nieto	(STON, BOHR, UCSB)
KROLL	71	PRL 26 1395	N.M. Kroll	(SLAC)
PARK	71	PRL 26 1393	D. Park, E.R. Williams	(WILC)
WILLIAMS	71	PRL 26 721	E.R. Williams, J.E. Faller, H.A. Hill	(WESL)
GOLDHABER	68	PRL 21 567	A.S. Goldhaber, M.M. Nieto	(STON)
PATEL	65	PL 14 105	V.L. Patel	(DUKE)
GINTSBURG	64	Sov. Astr. AJ7 536	M.A. Gintsburg	(ASCI)

g or gluon

$I(J^P) = 0(1^-)$

SU(3) color octet

Mass $m = 0$. Theoretical value. A mass as large as a few MeV may not be precluded, see YNDURAIN 95.

VALUE	DOCUMENT ID		TECN	COMMENT
• • • We do not use the following data for averages, fits, limits, etc. • • •				
	ABREU	92E	DLPH	Spin 1, not 0
	ALEXANDER	91H	OPAL	Spin 1, not 0
	BEHREND	82D	CELL	Spin 1, not 0
	BERGER	80D	PLUT	Spin 1, not 0
	BRANDELIK	80C	TASS	Spin 1, not 0

gluon REFERENCES

YNDURAIN	95	PL B345 524	F.J. Yndurain	(MADU)
ABREU	92E	PL B274 498	P. Abreu *et al.*	(DELPHI Collab.)
ALEXANDER	91H	ZPHY C52 543	G. Alexander *et al.*	(OPAL Collab.)
BEHREND	82D	PL B110 329	H.J. Behrend *et al.*	(CELLO Collab.)
BERGER	80D	PL B97 459	C. Berger *et al.*	(PLUTO Collab.)
BRANDELIK	80C	PL B97 453	R. Brandelik *et al.*	(TASSO Collab.)

graviton

$J = 2$

OMITTED FROM SUMMARY TABLE

graviton MASS

All of the following limits are obtained assuming Yukawa potential in weak field limit. VANDAM 70 argue that a massive field cannot approach general relativity in the zero-mass limit; however, see GOLDHABER 74 and references therein. h_0 is the Hubble constant in units of 100 km s^{-1} Mpc^{-1}.

VALUE (eV)	DOCUMENT ID		COMMENT
• • • We do not use the following data for averages, fits, limits, etc. • • •			
$< 7.6 \times 10^{-20}$	[1] FINN	02	Binary Pulsars
	[2] DAMOUR	91	Binary pulsar PSR 1913+16
$< 2 \times 10^{-29}\ h_0^{-1}$	GOLDHABER	74	Rich clusters
$< 7 \times 10^{-28}$	HARE	73	Galaxy
$< 8 \times 10^{4}$	HARE	73	2γ decay

[1] FINN 02 analyze the orbital decay rates of PSR B1913+16 and PSR B1534+12 with a possible graviton mass as a parameter. The combined frequentist mass limit is at 90%CL.

[2] DAMOUR 91 is an analysis of the orbital period change in binary pulsar PSR 1913+16, and confirms the general relativity prediction to 0.8%. "The theoretical importance of the [rate of orbital period decay] measurement has long been recognized as a direct confirmation that the gravitational interaction propagates with velocity c (which is the immediate cause of the appearance of a damping force in the binary pulsar system) and thereby as a test of the existence of gravitational radiation and of its quadrupolar nature." TAYLOR 93 adds that orbital parameter studies now agree with general relativity to 0.5%, and set limits on the level of scalar contribution in the context of a family of tensor [spin 2]-biscalar theories.

graviton REFERENCES

FINN	02	PR D65 044022	L.S. Finn, P.J. Sutton	
TAYLOR	93	NAT 355 132	J.N. Taylor *et al.*	(PRIN, ARCBO, BURE+) J
DAMOUR	91	APJ 366 501	T. Damour, J.H. Taylor	(BURE, MEUD, PRIN)
GOLDHABER	74	PR D9 1119	A.S. Goldhaber, M.M. Nieto	(LANL, STON)
HARE	73	CJP 51 431	M.G. Hare	(SASK)
VANDAM	70	NP B22 397	H. van Dam, M. Veltman	(UTRE)

W

$J = 1$

THE MASS OF THE *W* BOSON

Revised November 2003 by C. Caso (University of Genova) and A. Gurtu (Tata Institute).

Till 1995 the production and study of the W boson was the exclusive domain of the $\overline{p}p$ colliders at CERN and FNAL. W production in these hadron colliders is tagged by a high p_T lepton from W decay. Owing to unknown parton–parton effective energy and missing energy in the longitudinal direction, the experiments reconstruct only the transverse mass of the W and derive the W mass from comparing the transverse mass distribution with Monte Carlo predictions as a function of M_W.

Beginning 1996 the energy of LEP increased to above 161 GeV, the threshold for W–pair production. A precise knowledge of the e^+e^- center-of-mass energy enables one to reconstruct the W mass even if one of them decays leptonically. At LEP two methods have been used to obtain the W mass. In the first method the measured W–pair production cross sections, $\sigma(e^+e^- \to W^+W^-)$, have been used to determine the W mass using the predicted dependence of this cross section on M_W (see Fig. 1). At 161 GeV, which is just above the W–pair production threshold, this dependence is a much more sensitive function of the W mass than at the higher energies (172 to 208 GeV) at which LEP has run during 1996–2000. In the second method, which is used at the higher energies, the W mass has been determined by directly reconstructing the W from its decay products.

Each LEP experiment has combined their own mass values properly taking into account the common systematic errors. In order to compute the LEP average W mass each experiment has provided its measured W mass for the $qqqq$ and $qq\ell\nu$ channels at each center-of-mass energy along with a detailed break-up of errors (statistical and uncorrelated, partially correlated and fully correlated systematics [1]). These have been properly combined to obtain a *preliminary* LEP W mass = 80.412±0.042 GeV [2]. Errors due uncertainties in LEP energy (17 MeV) and possible effect of color reconnection (CR) and Bose–Einstein (BE) correlations between quarks from different W's are included. The mass difference between $qqqq$ and $qq\ell\nu$ final states (due to possible CR and BE effects) is $+22 \pm 43$ MeV.

The two Tevatron experiments have also carried out the exercise of identifying common systematic errors and averaging with CERN UA2 data obtain an average W mass [2]= 80.454±0.059 GeV.

Combining the above W mass values from LEP and hadron colliders, which are based on all published and unpublished results, and assuming no common systematics between them, yields an average W mass of 80.426 ± 0.034 GeV.

Finally a fit to this directly determined W mass together with measurements on the ratio of W to Z mass (M_W/M_Z) and on their mass difference ($M_Z - M_W$) yields a world average W-boson mass of 80.425 ± 0.033 GeV.

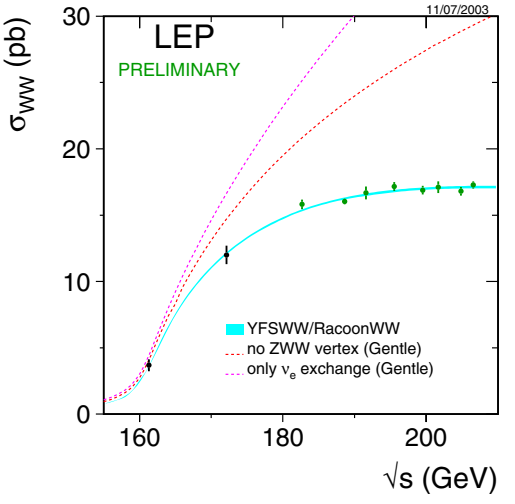

Figure 1: The W–pair cross section as a function of the center–of–mass energy. The data points are the LEP averages. The solid lines are predictions from different models of WW production. For comparison the figure contains also the cross section if the ZWW coupling did not exist (dashed line), or if only the t–channel ν_e exchange diagram existed (dotted-dashed line). (Figure from `http://lepewwg.web.cern.ch/LEPEWWG/lepww/4f/Summer03/wwxsec_nocouplings_2003.eps`)
See full-color version on color pages at end of book.

The Standard Model prediction from the electroweak fit, using Z-pole data plus $m_{\rm top}$ measurement, gives a W–boson mass of 80.378 ± 0.023 GeV [2].

OUR FIT in the listing below is obtained by combining only published LEP and p–$\overline{p}$ Collider results using the same procedure as above.

References

1. The LEP Collaborations: ALEPH, DELPHI, L3, OPAL, the LEP Electroweak Working Group, and the SLD Heavy Flavour Group, CERN-EP-2002-091, `hep-ex/0212036` (17 December 2002).
2. P. Wells, "Experimental Tests of the Standard Model," Int. Europhysics Conference on High-Energy Physics (Aachen, Germany, 17–23 July 2003).

W MASS

To obtain the world average, common systematics between experiments are properly taken into account. The procedure for averaging the LEP data is given in the note LEPEWWG/MASS/2002-01 (March 11, 2002), accessible at http://lepewwg.web.cern.ch/LEPEWWG/lepww/mw/pdg_2002/. The LEP average W mass based on published results is 80.400 ± 0.056 GeV. The combined $p\overline{p}$ collider data yields an average W mass of 80.454 ± 0.059 GeV (KOTWAL 02).

OUR FIT uses these average LEP and $p\overline{p}$ collider W mass values together with the Z mass, the W to Z mass ratio, and mass difference measurements.

VALUE (GeV)	*EVTS*	*DOCUMENT ID*		*TECN*	*COMMENT*
80.425 ± 0.038 OUR FIT					
80.41 ± 0.41 ± 0.13	1101	[1] ABBIENDI	03C	OPAL	E_{cm}^{ee} = 183–207 GeV
80.483 ± 0.084	49247	[2] ABAZOV	02D	D0	$E_{cm}^{p\overline{p}}$ = 1.8 TeV
80.432 ± 0.066 ± 0.045	2789	[3] ABBIENDI	01F	OPAL	E_{cm}^{ee} = 161+172+183 +189 GeV
80.359 ± 0.074 ± 0.049	3077	[4] ABREU	01K	DLPH	E_{cm}^{ee} = 161+172+183 +189 GeV
80.433 ± 0.079	53841	[5] AFFOLDER	01E	CDF	$E_{cm}^{p\overline{p}}$ = 1.8 TeV
80.418 ± 0.061 ± 0.047	2977	[6] BARATE	00T	ALEP	E_{cm}^{ee} = 161+172+183 +189 GeV
80.61 ± 0.15	801	[7] ACCIARRI	99	L3	E_{cm}^{ee} = 161+172+ 183 GeV
• • • We do not use the following data for averages, fits, limits, etc. • • •					
80.3 ± 2.1 ± 1.2 ± 1.0	645	[8] CHEKANOV	02C	ZEUS	$e^- p \to \nu_e X$, $\sqrt{s}$ = 318 GeV
79.9 ± 2.2 ± 2.3	700	[9] ADLOFF	01A	H1	$e^- p \to \nu_e X$, $\sqrt{s} \approx$ 320 GeV
80.482 ± 0.091	45394	[10] ABBOTT	00	D0	Repl. by ABAZOV 02D
80.9 ± 3.7 ± 3.7	700	[11] ADLOFF	00B	H1	$e^+ p \to \overline{\nu}_e X$, $\sqrt{s} \approx$ 300 GeV
$81.4^{+2.7}_{-2.6} \pm 2.0^{+3.3}_{-3.0}$	1086	[12] BREITWEG	00D	ZEUS	$e^+ p \to \overline{\nu}_e X$, $\sqrt{s} \approx$ 300 GeV
80.38 ± 0.12 ± 0.05	701	[13] ABBIENDI	99C	OPAL	Repl. by ABBIENDI 01F
80.270 ± 0.137 ± 0.048	809	[14] ABREU	99T	DLPH	Repl. by ABREU 01K
80.423 ± 0.112 ± 0.054	812	[15] BARATE	99	ALEP	Repl. by BARATE 00T
$80.80 \pm {}^{0.48}_{0.42} \pm 0.03$	20	[16] ACCIARRI	97	L3	Repl. by ACCIARRI 99
$80.5 \pm {}^{1.4}_{2.4} \pm 0.3$	94	[17] ACCIARRI	97M	L3	Repl. by ACCIARRI 99
$80.71 \pm {}^{0.34}_{0.35} \pm 0.09$	101	[18] ACCIARRI	97S	L3	Repl. by ACCIARRI 99
80.41 ± 0.18	8986	[19] ABE	95P	CDF	Repl. by AFFOLDER 01E
80.84 ± 0.22 ± 0.83	2065	[20] ALITTI	92B	UA2	See W/Z ratio below
80.79 ± 0.31 ± 0.84		[21] ALITTI	90B	UA2	$E_{cm}^{p\overline{p}}$ = 546,630 GeV
80.0 ± 3.3 ± 2.4	22	[22] ABE	89I	CDF	$E_{cm}^{p\overline{p}}$ = 1.8 TeV
82.7 ± 1.0 ± 2.7	149	[23] ALBAJAR	89	UA1	$E_{cm}^{p\overline{p}}$ = 546,630 GeV
$81.8 \pm {}^{6.0}_{5.3} \pm 2.6$	46	[24] ALBAJAR	89	UA1	$E_{cm}^{p\overline{p}}$ = 546,630 GeV
89 ± 3 ± 6	32	[25] ALBAJAR	89	UA1	$E_{cm}^{p\overline{p}}$ = 546,630 GeV
81. ± 5.	6	ARNISON	83	UA1	E_{cm}^{ee} = 546 GeV
$80. \pm {}^{10.}_{6.}$	4	BANNER	83B	UA2	Repl. by ALITTI 90B

[1] ABBIENDI 03C determine the mass of the W boson using fully leptonic decays $W^+W^- \to \ell\nu_\ell \ell'\nu_{\ell'}$. They use the measured energies of the charged leptons and an approximate kinematic reconstruction of the event (both neutrinos are assumed in the same plane as the charged leptons) to get a W pseudo-mass. All these variables are combined in a simultaneous maximum likelihood fit. The systematic error is dominated by the uncertainty on the lepton energy.

[2] ABAZOV 02D improve the measurement of the W-boson mass including $W \to e\nu_e$ events in which the electron is close to a boundary of a central electromagnetic calorimeter module. Properly combining the results obtained by fitting $m_T(W)$, $p_T(e)$, and $p_T(\nu)$, this sample provides a mass value of 80.574 ± 0.405 GeV. The value reported here is a combination of this measurement with all previous DØ W-boson mass measurements.

[3] ABBIENDI 01F obtain this value properly combining results obtained from a direct W mass reconstruction at 172, 183, and 189 GeV with that from measurement of the W-pair production cross section at 161 GeV. The systematic error includes ±0.017 GeV due to LEP energy uncertainty and ±0.028 GeV due to possible color reconnection and Bose-Einstein effects in the purely hadronic final state.

[4] ABREU 01K obtain this value properly combining results obtained from a direct W mass reconstruction at 172, 183, and 189 GeV with those from measurements of W-pair production cross sections at 161, 172, and 183 GeV. The systematic error includes ±0.017 GeV due to the beam energy uncertainty and ±0.033 GeV due to possible color reconnection and Bose-Einstein effects in the purely hadronic final state.

[5] AFFOLDER 01E fit the transverse mass spectrum of 30115 $W \to e\nu_e$ events (M_W = 80.473 ± 0.065 ± 0.092 GeV) and of 14740 $W \to \mu\nu_\mu$ events (M_W = 80.465 ± 0.100 ± 0.103 GeV) obtained in the run IB (1994-95). Combining the electron and muon results, accounting for correlated uncertainties, yields M_W = 80.470 ± 0.089 GeV. They combine this value with their measurement of ABE 95P reported in run IA (1992-93) to obtain the quoted value.

[6] BARATE 00T obtain this value properly combining results obtained from a direct W mass reconstruction at 172, 183, and 189 GeV with those from measurements of W-pair production cross sections at 161 and 172 GeV. The systematic error includes ±0.017 GeV due to LEP energy uncertainty and ±0.019 GeV due to possible color reconnection and Bose-Einstein effects in the purely hadronic final state.

[7] ACCIARRI 99 obtain this value properly combining results obtained from a direct W mass reconstruction at 172 and 183 GeV with those from the measurements of the total W-pair production cross sections at 161 and 172 GeV. The value of the mass obtained from the direct reconstruction at 172 and 183 GeV is $M(W)$ = 80.58 ± 0.14 ± 0.08 GeV.

[8] CHEKANOV 02C fit the Q^2 dependence (200 < Q^2 < 60000 GeV^2) of the charged-current differential cross sections with a propagator mass fit. The last error is due to the uncertainty on the probability density functions.

[9] ADLOFF 01A fit the Q^2 dependence (150 < Q^2 < 30000 GeV^2) of the charged-current double-differential cross sections with a propagator mass fit. The second error includes 2.1 GeV due to the theoretical uncertainties.

[10] ABBOTT 00 use $W \to e\nu_e$ events to measure the W mass with a fit to the transverse mass distribution. The result quoted here corresponds to electrons detected both in the forward and in the central calorimeters for the data recorded in 1992–1995. For the large rapidity electrons recorded in 1994–1995, the analysis combines results obtained from m_T, $p_T(e)$, and $p_T(\nu)$.

[11] ADLOFF 00B fit the Q^2 dependence (300 < Q^2 < 15000 GeV^2) of the charged-current double-differential cross sections with a propagator mass fit. The second error is due to the theoretical uncertainties.

[12] BREITWEG 00D fit the Q^2 dependence (200 < Q^2 < 22500 GeV^2) of the charged-current differential cross sections with a propagator mass fit. The last error is due to the uncertainty on the probability density functions.

[13] ABBIENDI 99C obtain this value properly combining results from a direct W mass reconstruction at 172 and 183 GeV with that from the measurement of the total W-pair production cross section at 161 GeV. The systematic error includes an uncertainty of ±0.02 GeV due to the possible color-reconnection and Bose-Einstein effects in the purely hadronic final states and an uncertainty of ±0.02 GeV due to the beam energy.

[14] ABREU 99T obtain this value properly combining results obtained from a direct W mass reconstruction at 172 and 183 GeV with those from measurement of W-pair production cross sections at 161, 172, and 183 GeV. The systematic error includes ±0.021 GeV due to the beam energy uncertainty and ±0.030 GeV due to possible color reconnection and Bose-Einstein effects in the purely hadronic final state.

[15] BARATE 99 obtain this value properly combining results from a direct W mass reconstruction at 172 and 183 GeV with those from the measurements of the total W-pair production cross sections at 161 and 172 GeV. The systematic error includes ±0.023 GeV due to LEP energy uncertainty and ±0.021 GeV due to theory uncertainty on account of possible color reconnection and Bose-Einstein correlations.

[16] ACCIARRI 97 derive this value from their measured W-W production cross section $\sigma_{WW} = 2.89^{+0.81}_{-0.70} \pm 0.14$ pb using the Standard Model dependence of σ_{WW} on M_W at the given c.m. energy. Statistical and systematic errors are added in quadrature and the last error of ±0.03 GeV arises from the beam energy uncertainty. The same result is given by a fit of the production cross sections to the data.

[17] ACCIARRI 97M derive this value from their measured WW production cross section $\sigma_{WW} = 12.27^{+1.41}_{-1.32} \pm 0.23$ pb using the Standard Model dependence of σ_{WW} on M_W at the given c.m. energy. Combining with ACCIARRI 97 authors find $M(W) = 80.78^{+0.45}_{-0.41} \pm 0.03$ GeV where the last error is due to beam energy uncertainty.

[18] ACCIARRI 97S obtain this value from a fit to the reconstructed W mass distribution. The W width was taken as its Standard Model value at the fitted W mass. When both W mass and width are varied they obtain $M(W) = 80.72^{+0.31}_{-0.33} \pm 0.09$ GeV. The systematic error includes ±0.03 GeV due to the beam energy uncertainty and ±0.05 GeV due to the possible color reconnection and Bose-Einstein effects in the purely hadronic final state. Combining with ACCIARRI 97 and ACCIARRI 97M authors find: $M(W) = 80.75^{+0.26}_{-0.27} \pm 0.03$ (LEP) GeV.

[19] ABE 95P use 3268 $W \to \mu\nu_\mu$ events to find M = 80.310 ± 0.205 ± 0.130 GeV and 5718 $W \to e\nu_e$ events to find M = 80.490 ± 0.145 ± 0.175 GeV. The result given here combines these while accounting for correlated uncertainties.

[20] ALITTI 92B result has two contributions to the systematic error (±0.83); one (±0.81) cancels in m_W/m_Z and one (±0.17) is noncancelling. These were added in quadrature. We choose the ALITTI 92B value without using the LEP m_Z value, because we perform our own combined fit.

[21] There are two contributions to the systematic error (±0.84): one (±0.81) which cancels in m_W/m_Z and one (±0.21) which is non-cancelling. These were added in quadrature.

[22] ABE 89I systematic error dominated by the uncertainty in the absolute energy scale.

[23] ALBAJAR 89 result is from a total sample of 299 $W \to e\nu$ events.

[24] ALBAJAR 89 result is from a total sample of 67 $W \to \mu\nu$ events.

[25] ALBAJAR 89 result is from $W \to \tau\nu$ events.

W/Z MASS RATIO

The fit uses the W and Z mass, mass difference, and mass ratio measurements.

VALUE	*EVTS*	*DOCUMENT ID*		*TECN*	*COMMENT*
0.88197 ± 0.00042 OUR FIT					
0.8821 ± 0.0011 ± 0.0008	28323	[26] ABBOTT	98N	D0	$E_{cm}^{p\overline{p}}$ = 1.8 TeV
0.88114 ± 0.00154 ± 0.00252	5982	[27] ABBOTT	98P	D0	$E_{cm}^{p\overline{p}}$ = 1.8 TeV
0.8813 ± 0.0036 ± 0.0019	156	[28] ALITTI	92B	UA2	$E_{cm}^{p\overline{p}}$ = 630 GeV

[26] ABBOTT 98N obtain this from a study of 28323 $W \to e\nu_e$ and 3294 $Z \to e^+e^-$ decays. Of this latter sample, 2179 events are used to calibrate the electron energy scale.

[27] ABBOTT 98P obtain this from a study of 5982 $W \to e\nu_e$ events. The systematic error includes an uncertainty of ±0.00175 due to the electron energy scale.

[28] Scale error cancels in this ratio.

$m_Z - m_W$

The fit uses the W and Z mass, mass difference, and mass ratio measurements.

VALUE (GeV)	*DOCUMENT ID*		*TECN*	*COMMENT*
10.763 ± 0.038 OUR FIT				
10.4 ± 1.4 ± 0.8	ALBAJAR	89	UA1	$E_{cm}^{p\overline{p}}$ = 546,630 GeV
• • • We do not use the following data for averages, fits, limits, etc. • • •				
11.3 ± 1.3 ± 0.9	ANSARI	87	UA2	$E_{cm}^{p\overline{p}}$ = 546,630 GeV

$m_{W^+} - m_{W^-}$

Test of CPT invariance.

VALUE (GeV)	EVTS	DOCUMENT ID		TECN	COMMENT
−0.19±0.58	1722	ABE	90G	CDF	$E_{cm}^{p\overline{p}}$= 1.8 TeV

W WIDTH

The CDF and DØ widths labelled "extracted value" are obtained by measuring $R = [\sigma(W)/\sigma(Z)]\,[\Gamma(W \to \ell\nu_\ell)]/(B(Z \to \ell\ell)\Gamma(W))$ where the bracketed quantities can be calculated with plausible reliability. $\Gamma(W)$ is then extracted by using a value of $B(Z \to \ell\ell)$ measured at LEP. The UA1 and UA2 widths used $R = [\sigma(W)/\sigma(Z)]\,[\Gamma(W \to \ell\nu_\ell)/\Gamma(Z \to \ell\ell)]\,\Gamma(Z)/\Gamma(W)$ and the measured value of $\Gamma(Z)$. The Standard Model prediction is 2.0921 ± 0.0025 GeV (see Review on "Electroweak model and constraints on new physics" in this Edition).

To obtain OUR FIT,the correlation between systematics for the Direct Measurements is properly taken into account. The following notes may be consulted for details as well as the respective average values: for the LEP experiments the note LEPEWWG/MASS/2002-01 (http://lepewwg.web.cern.ch/LEPEWWG/lepww/mw/pdg_2002/) of 11 March 2002 and for the Tevatron experiments the note FERMILAB-FN-716 of 1 July 2002 (KOTWAL 02). The respective average values (2.17 ± 0.12 GeV from LEP and 2.115 ± 0.105 GeV from Tevatron) yield an average W width of 2.139 ± 0.079 GeV coming from direct measurements. Combined with the Extracted Values one obtains the quoted value.

VALUE (GeV)	CL%	EVTS	DOCUMENT ID		TECN	COMMENT
2.124±0.041 OUR FIT						
$2.23\ ^{+0.15}_{-0.14}\ \pm0.10$		294	[29] ABAZOV	02E	D0	Direct meas.
2.04 ±0.16 ±0.09		2756	[30] ABBIENDI	01F	OPAL	E_{cm}^{ee}= 172+183 +189 GeV
2.266±0.176±0.076		3005	[31] ABREU	01K	DLPH	E_{cm}^{ee}= 183+189 GeV
2.152±0.066		79176	[32] ABBOTT	00B	D0	Extracted value
2.05 ±0.10 ±0.08		662	[33] AFFOLDER	00M	CDF	Direct meas.
2.24 ±0.20 ±0.13		1711	[34] BARATE	00T	ALEP	E_{cm}^{ee}= 189 GeV
1.97 ±0.34 ±0.17		687	[35] ACCIARRI	99	L3	E_{cm}^{ee}= 172+183 GeV
2.064±0.060±0.059			[36] ABE	95W	CDF	Extracted value
$2.10\ ^{+0.14}_{-0.13}\ \pm0.09$		3559	[37] ALITTI	92	UA2	Extracted value
$2.18\ ^{+0.26}_{-0.24}\ \pm0.04$			[38] ALBAJAR	91	UA1	Extracted value
• • • We do not use the following data for averages, fits, limits, etc. • • •						
1.84 ±0.32 ±0.20		674	[39] ABBIENDI	99C	OPAL	Repl. by ABBIENDI 01F
2.044±0.097		11858	[40] ABBOTT	99H	D0	Repl. by ABBOTT 00B
2.48 ±0.40 ±0.10		737	[41] ABREU	99T	DLPH	Repl. by ABREU 01K
$2.126\ ^{+0.052}_{-0.048}\pm0.035$			[42] BARATE	99I	ALEP	E_{cm}^{ee}= 161+172+183 GeV
$1.74\ ^{+0.88}_{-0.78}\ \pm0.25$		101	[43] ACCIARRI	97S	L3	Repl. by ACCIARRI 99
2.11 ±0.28 ±0.16		58	[44] ABE	95C	CDF	Repl. by AFFOLDER 00M
2.30 ±0.19 ±0.06			[45] ALITTI	90C	UA2	Extracted value
$2.8\ ^{+1.4}_{-1.5}\ \pm1.3$		149	[46] ALBAJAR	89	UA1	$E_{cm}^{p\overline{p}}$= 546,630 GeV
<7	90	119	APPEL	86	UA2	$E_{cm}^{p\overline{p}}$= 546,630 GeV
<6.5	90	86	[47] ARNISON	86	UA1	$E_{cm}^{p\overline{p}}$= 546,630 GeV

[29] ABAZOV 02E obtain this result fitting the high-end tail (90–200 GeV) of the transverse-mass spectrum in semileptonic $W \to e\nu_e$ decays.

[30] ABBIENDI 01F obtain this value from a fit to the reconstructed W mass distribution using data at 172, 183, and 189 GeV. The systematic error includes ±0.010 GeV due to LEP energy uncertainty and ±0.078 GeV due to possible color reconnection and Bose-Einstein effects in the purely hadronic final state.

[31] ABREU 01K obtain this value properly combining results obtained at 183 and 189 GeV using $WW \to \ell\overline{\nu}_\ell q\overline{q}$ and $WW \to q\overline{q}q\overline{q}$ decays. The systematic error includes an uncertainty of ±0.052 GeV due to possible color reconnection and Bose-Einstein effects in the purely hadronic final state.

[32] ABBOTT 00B measure $R = 10.43 \pm 0.27$ for the $W \to e\nu_e$ decay channel. They use the SM theoretical predictions for $\sigma(W)/\sigma(Z)$ and $\Gamma(W \to e\nu_e)$ and the world average for $B(Z \to ee)$. The value quoted here is obtained combining this result (2.169 ± 0.070 GeV) with that of ABBOTT 99H.

[33] AFFOLDER 00M fit the high transverse mass (100–200 GeV) $W \to e\nu_e$ and $W \to \mu\nu_\mu$ events to obtain $\Gamma(W)$= 2.04 ± 0.11(stat)±0.09(syst) GeV. This is combined with the earlier CDF measurement (ABE 95C) to obtain the quoted result.

[34] BARATE 00T obtain this value using $WW \to q\overline{q}q\overline{q}$, $WW \to e\nu_e q\overline{q}$, and $WW \to \mu\nu_\mu q\overline{q}$ decays. The systematic error includes ±0.015 GeV due to LEP energy uncertainty and ±0.080 GeV due to possible color reconnection and Bose-Einstein effects in the purely hadronic final state.

[35] ACCIARRI 99 obtain this value from a fit to the reconstructed W mass distribution using data at 172 and 183 GeV.

[36] ABE 95W measured $R = 10.90 \pm 0.32 \pm 0.29$. They use m_W=80.23 ± 0.18 GeV, $\sigma(W)/\sigma(Z) = 3.35 \pm 0.03$, $\Gamma(W \to e\nu) = 225.9 \pm 0.9$ MeV, $\Gamma(Z \to e^+e^-) = 83.98 \pm 0.18$ MeV, and $\Gamma(Z) = 2.4969 \pm 0.0038$ GeV.

[37] ALITTI 92 measured $R = 10.4\ ^{+0.7}_{-0.6} \pm 0.3$. The values of $\sigma(Z)$ and $\sigma(W)$ come from $O(\alpha_s^2)$ calculations using $m_W = 80.14 \pm 0.27$ GeV, and $m_Z = 91.175 \pm 0.021$ GeV along with the corresponding value of $\sin^2\theta_W = 0.2274$. They use $\sigma(W)/\sigma(Z) = 3.26 \pm 0.07 \pm 0.05$ and $\Gamma(Z) = 2.487 \pm 0.010$ GeV.

[38] ALBAJAR 91 measured $R = 9.5\ ^{+1.1}_{-1.0}$ (stat. + syst.). $\sigma(W)/\sigma(Z)$ is calculated in QCD at the parton level using $m_W = 80.18 \pm 0.28$ GeV and $m_Z = 91.172 \pm 0.031$ GeV along with $\sin^2\theta_W = 0.2322 \pm 0.0014$. They use $\sigma(W)/\sigma(Z) = 3.23 \pm 0.05$ and $\Gamma(Z) = 2.498 \pm 0.020$ GeV. This measurement is obtained combining both the electron and muon channels.

[39] ABBIENDI 99C obtain this value from a fit to the reconstructed W mass distribution using data at 172 and 183 GeV. The systematic error includes an uncertainty of ±0.12 GeV due to the possible color-reconnection and Bose-Einstein effects in the purely hadronic final states and an uncertainty of ±0.01 GeV due to the beam energy.

[40] ABBOTT 99H measure R= 10.90 ± 0.52 combining electron and muon channels. They use $M_W = 80.39 \pm 0.06$ GeV and the SM theoretical predictions for $\sigma(W)/\sigma(Z)$, $B(Z \to \ell\ell)$, and $\Gamma(W \to \ell\nu_\ell)$.

[41] ABREU 99T obtain this value using $WW \to \ell\overline{\nu}_\ell q\overline{q}$ and $WW \to q\overline{q}q\overline{q}$ events. The systematic error includes an uncertainty of ±0.080 GeV due to possible color reconnection and Bose-Einstein effects in the purely hadronic final state.

[42] BARATE 99I obtain this result with a fit to the WW measured cross sections at 161, 172, and 183 GeV. The theoretical prediction takes into account the sensitivity to the W total width.

[43] ACCIARRI 97S obtain this value from a fit to the reconstructed W mass distribution.

[44] ABE 95C use the tail of the transverse mass distribution of $W \to e\nu_e$ decays.

[45] ALITTI 90C used the same technique as described for ABE 90. They measured $R = 9.38\ ^{+0.82}_{-0.72} \pm 0.25$, obtained $\Gamma(W)/\Gamma(Z) = 0.902 \pm 0.074 \pm 0.024$. Using $\Gamma(Z) = 2.546 \pm 0.032$ GeV, they obtained the $\Gamma(W)$ value quoted above and the limits $\Gamma(W) < 2.56$ (2.64) GeV at the 90% (95%) CL. $E_{cm}^{p\overline{p}} = 546,630$ GeV.

[46] ALBAJAR 89 result is from a total sample of 299 $W \to e\nu$ events.

[47] If systematic error is neglected, result is $2.7\ ^{+1.4}_{-1.5}$ GeV. This is enhanced subsample of 172 total events.

W^+ DECAY MODES

W^- modes are charge conjugates of the modes below.

	Mode		Fraction (Γ_i/Γ)		Confidence level
Γ_1	$\ell^+\nu$	[a]	(10.68± 0.12) %		
Γ_2	$e^+\nu$		(10.72± 0.16) %		
Γ_3	$\mu^+\nu$		(10.57± 0.22) %		
Γ_4	$\tau^+\nu$		(10.74± 0.27) %		
Γ_5	hadrons		(67.96± 0.35) %		
Γ_6	$\pi^+\gamma$		< 8	$\times10^{-5}$	95%
Γ_7	$D_s^+\gamma$		< 1.3	$\times10^{-3}$	95%
Γ_8	cX		(33.6 ± 2.7) %		
Γ_9	$c\overline{s}$		(31 $^{+13}_{-11}$) %		
Γ_{10}	invisible	[b]	(1.4 ± 2.8) %		

[a] ℓ indicates each type of lepton (e, μ, and τ), not sum over them.

[b] This represents the width for the decay of the W boson into a charged particle with momentum below detectability, p< 200 MeV.

W PARTIAL WIDTHS

Γ(invisible) Γ10

This represents the width for the decay of the W boson into a charged particle with momentum below detectability, p< 200 MeV.

VALUE (MeV)	DOCUMENT ID		TECN	COMMENT
30 $^{+52}_{-48}$ ±33	[48] BARATE	99I	ALEP	E_{cm}^{ee}= 161+172+183 GeV
• • • We do not use the following data for averages, fits, limits, etc. • • •				
	[49] BARATE	99L	ALEP	E_{cm}^{ee}= 161+172+183 GeV

[48] BARATE 99I measure this quantity using the dependence of the total cross section σ_{WW} upon a change in the total width. The fit is performed to the WW measured cross sections at 161, 172, and 183 GeV. This partial width is < 139 MeV at 95%CL.

[49] BARATE 99L use W-pair production to search for effectively invisible W decays, tagging with the decay of the other W boson to Standard Model particles. The partial width for effectively invisible decay is < 27 MeV at 95%CL.

W BRANCHING RATIOS

Overall fits are performed to determine the branching ratios of the W. For each LEP experiment the correlation matrix of the leptonic branching ratios is used and the common systematic errors among LEP experiments are properly taken into account (see LEP Electroweak Working Group note LEPEWWG/XSEC/2001-02, 30 March 2001, accessible at http://lepewwg.web.cern.ch/LEPEWWG/lepww/4f/PDG01). A first fit determines three individual leptonic branching ratios, $B(W \to e\nu_e)$, $B(W \to \mu\nu_\mu)$, and $B(W \to \tau\nu_\tau)$. This fit has a $\chi^2 = 11.0$ for 22 degrees of freedom. A second fit assumes lepton universality and determines the leptonic branching ratio $B(W \to \ell\nu_\ell)$ and the hadronic branching ratio is derived as $B(W \to \text{hadrons}) = 1 - 3\,B(W \to \ell\nu)$. This fit has a χ^2=11.4 for 24 degrees of freedom.

The LEP $W \to \ell\nu$ data are obtained by the Collaborations using individual leptonic channels and are, therefore, not included in the overall fits to avoid double counting.

$\Gamma(\ell^+\nu)/\Gamma_{\text{total}}$ Γ_1/Γ

ℓ indicates average over e, μ, and τ modes, not sum over modes.

VALUE	EVTS	DOCUMENT ID		TECN	COMMENT
0.1068±0.0012 OUR FIT					
0.1056±0.0020±0.0009	5778	ABBIENDI,G	00	OPAL	$E^{ee}_{\rm cm}$= 161+172+183 +189 GeV
0.1071±0.0024±0.0014	4843	ABREU	00K	DLPH	$E^{ee}_{\rm cm}$= 161+172+183 +189 GeV
0.1060±0.0023±0.0011	5328	ACCIARRI	00V	L3	$E^{ee}_{\rm cm}$= 161+172+183 +189 GeV
0.1101±0.0022±0.0011	5258	BARATE	00J	ALEP	$E^{ee}_{\rm cm}$= 161+172+183 +189 GeV
0.1102±0.0052	11858	[50] ABBOTT	99H	D0	$E^{p\overline{p}}_{\rm cm}$= 1.8 TeV
0.104 ±0.008	3642	[51] ABE	92I	CDF	$E^{p\overline{p}}_{\rm cm}$= 1.8 TeV
• • • We do not use the following data for averages, fits, limits, etc. • • •					
0.107 ±0.004 ±0.002	1440	ABBIENDI	99D	OPAL	Repl. by ABBIENDI,G 00
0.1085±0.0048±0.0017	1336	ABREU	99K	DLPH	Repl. by ABREU 00K
0.1036±0.0040±0.0017	1322	BARATE	99I	ALEP	Repl. by BARATE 00J
0.100 ±0.004 ±0.001	1434	ACCIARRI	98P	L3	Repl. by ACCIARRI 00V

[50] ABBOTT 99H measure $R \equiv [\sigma_W \text{B}(W \to \ell\nu_\ell)]/[\sigma_Z \text{B}(Z \to \ell\ell)] = 10.90 \pm 0.52$ combining electron and muon channels. They use $M_W = 80.39 \pm 0.06$ GeV and the SM theoretical predictions for $\sigma(W)/\sigma(Z)$ and $\text{B}(Z \to \ell\ell)$.

[51] $1216 \pm 38^{+27}_{-31}$ $W \to \mu\nu$ events from ABE 92I and 2426 $W \to e\nu$ events of ABE 91C. ABE 92I give the inverse quantity as 9.6 ± 0.7 and we have inverted.

$\Gamma(e^+\nu)/\Gamma_{\text{total}}$ Γ_2/Γ

VALUE	EVTS	DOCUMENT ID		TECN	COMMENT
0.1072±0.0016 OUR FIT					
0.1046±0.0042±0.0014	801	ABBIENDI,G	00	OPAL	$E^{ee}_{\rm cm}$= 161+172+183 +189 GeV
0.1044±0.0015±0.0028	67318	[52] ABBOTT	00B	D0	$E^{p\overline{p}}_{\rm cm}$= 1.8 TeV
0.1018±0.0054±0.0026	527	ABREU	00K	DLPH	$E^{ee}_{\rm cm}$= 161+172+183 +189 GeV
0.1077±0.0045±0.0016	715	ACCIARRI	00V	L3	$E^{ee}_{\rm cm}$= 161+172+183 +189 GeV
0.1135±0.0046±0.0017	720	BARATE	00J	ALEP	$E^{ee}_{\rm cm}$= 161+172+183 +189 GeV
0.1094±0.0033±0.0031		[53] ABE	95W	CDF	$E^{p\overline{p}}_{\rm cm}$= 1.8 TeV
0.10 ±0.014 $^{+0.02}_{-0.03}$	248	[54] ANSARI	87C	UA2	$E^{p\overline{p}}_{\rm cm}$= 546,630 GeV
• • • We do not use the following data for averages, fits, limits, etc. • • •					
0.117 ±0.009 ±0.002	224	ABBIENDI	99D	OPAL	Repl. by ABBIENDI,G 00
0.1012±0.0107±0.0028	150	ABREU	99K	DLPH	Repl. by ABREU 00K
0.1115±0.0085±0.0024	192	BARATE	99I	ALEP	Repl. by BARATE 00J
0.105 ±0.009 ±0.002	173	ACCIARRI	98P	L3	Repl. by ACCIARRI 00V
seen	119	APPEL	86	UA2	$E^{p\overline{p}}_{\rm cm}$= 546,630 GeV
seen	172	ARNISON	86	UA1	$E^{p\overline{p}}_{\rm cm}$= 546,630 GeV

[52] ABBOTT 00B measure $R \equiv [\sigma_W \text{B}(W \to e\nu_e)]/[\sigma_Z \text{B}(Z \to ee)] = 10.43 \pm 0.27$ for the $W \to e\nu_e$ decay channel. They use the SM theoretical prediction for $\sigma(W)/\sigma(Z)$ and the world average for $\text{B}(Z \to ee)$.

[53] ABE 95W result is from a measurement of $\sigma\text{B}(W \to e\nu)/\sigma\text{B}(Z \to e^+e^-) = 10.90 \pm 0.32 \pm 0.29$, the theoretical prediction for the cross section ratio, the experimental knowledge of $\Gamma(Z \to e^+e^-) = 83.98 \pm 0.18$ MeV, and $\Gamma(Z) = 2.4969 \pm 0.0038$ GeV.

[54] The first error was obtained by adding the statistical and systematic experimental uncertainties in quadrature. The second error reflects the dependence on theoretical prediction of total W cross section: $\sigma(546\text{ GeV}) = 4.7^{+1.4}_{-0.7}$ nb and $\sigma(630\text{ GeV}) = 5.8^{+1.8}_{-1.0}$ nb. See ALTARELLI 85B.

$\Gamma(\mu^+\nu)/\Gamma_{\text{total}}$ Γ_3/Γ

VALUE	EVTS	DOCUMENT ID		TECN	COMMENT
0.1057±0.0022 OUR FIT					
0.1050±0.0041±0.0012	803	ABBIENDI,G	00	OPAL	$E^{ee}_{\rm cm}$= 161+172+183 +189 GeV
0.1092±0.0048±0.0012	649	ABREU	00K	DLPH	$E^{ee}_{\rm cm}$= 161+172+183 +189 GeV
0.0990±0.0046±0.0015	617	ACCIARRI	00V	L3	$E^{ee}_{\rm cm}$= 161+172+183 +189 GeV
0.1110±0.0044±0.0016	710	BARATE	00J	ALEP	$E^{ee}_{\rm cm}$= 161+172+183 +189 GeV
0.10 ±0.01	1216	[55] ABE	92I	CDF	$E^{p\overline{p}}_{\rm cm}$= 1.8 TeV
• • • We do not use the following data for averages, fits, limits, etc. • • •					
0.102 ±0.008 ±0.002	193	ABBIENDI	99D	OPAL	Repl. by ABBIENDI,G 00
0.1139±0.0096±0.0023	186	ABREU	99K	DLPH	Repl. by ABREU 00K
0.1006±0.0078±0.0021	179	BARATE	99I	ALEP	Repl. by BARATE 00J
0.102 ±0.009 ±0.002	160	ACCIARRI	98P	L3	Repl. by ACCIARRI 00V

[55] ABE 92I quote the inverse quantity as 9.9 ± 1.2 which we have inverted.

$\Gamma(\tau^+\nu)/\Gamma_{\text{total}}$ Γ_4/Γ

VALUE	EVTS	DOCUMENT ID		TECN	COMMENT
0.1074±0.0027 OUR FIT					
0.1075±0.0052±0.0021	794	ABBIENDI,G	00	OPAL	$E^{ee}_{\rm cm}$= 161+172+183 +189 GeV
0.1105±0.0075±0.0032	579	ABREU	00K	DLPH	$E^{ee}_{\rm cm}$= 161+172+183 +189 GeV
0.1124±0.0062±0.0022	536	ACCIARRI	00V	L3	$E^{ee}_{\rm cm}$= 161+172+183 +189 GeV
0.1051±0.0055±0.0022	607	BARATE	00J	ALEP	$E^{ee}_{\rm cm}$= 161+172+183 +189 GeV
• • • We do not use the following data for averages, fits, limits, etc. • • •					
0.101 ±0.010 ±0.003	183	ABBIENDI	99D	OPAL	Repl. by ABBIENDI,G 00
0.1095±0.0149±0.0041	142	ABREU	99K	DLPH	Repl. by ABREU 00K
0.0976±0.0101±0.0033	160	BARATE	99I	ALEP	Repl. by BARATE 00J
0.090 ±0.012 ±0.003	123	ACCIARRI	98P	L3	Repl. by ACCIARRI 00V

$\Gamma(\text{hadrons})/\Gamma_{\text{total}}$ Γ_5/Γ

OUR FIT value is obtained by a fit to the lepton branching ratio data assuming lepton universality.

VALUE	EVTS	DOCUMENT ID		TECN	COMMENT
0.6796±0.0035 OUR FIT					
0.679 ±0.004 OUR AVERAGE					
0.6832±0.0061±0.0028	5778	ABBIENDI,G	00	OPAL	$E^{ee}_{\rm cm}$= 161+172+183 +189 GeV
0.6789±0.0073±0.0043	4843	ABREU	00K	DLPH	$E^{ee}_{\rm cm}$= 161+172+183 +189 GeV
0.6820±0.0068±0.0033	5328	ACCIARRI	00V	L3	$E^{ee}_{\rm cm}$= 161+172+183 +189 GeV
0.6697±0.0065±0.0032	5258	BARATE	00J	ALEP	$E^{ee}_{\rm cm}$= 161+172+183 +189 GeV
• • • We do not use the following data for averages, fits, limits, etc. • • •					
0.679 ±0.012 ±0.005	1440	ABBIENDI	99D	OPAL	Repl. by ABBIENDI,G 00
0.6746±0.0143±0.0052	1336	ABREU	99K	DLPH	Repl. by ABREU 00K
0.6893±0.0121±0.0051	1322	BARATE	99I	ALEP	Repl. by BARATE 00J
0.701 ±0.013 ±0.004	1434	ACCIARRI	98P	L3	Repl. by ACCIARRI 00V

$\Gamma(\mu^+\nu)/\Gamma(e^+\nu)$ Γ_3/Γ_2

VALUE	EVTS	DOCUMENT ID		TECN	COMMENT
0.986±0.024 OUR FIT					
0.89 ±0.10	13k	[56] ABACHI	95D	D0	$E^{p\overline{p}}_{\rm cm}$= 1.8 TeV
1.02 ±0.08	1216	[57] ABE	92I	CDF	$E^{p\overline{p}}_{\rm cm}$= 1.8 TeV
1.00 ±0.14 ±0.08	67	ALBAJAR	89	UA1	$E^{p\overline{p}}_{\rm cm}$= 546,630 GeV
• • • We do not use the following data for averages, fits, limits, etc. • • •					
1.24 $^{+0.6}_{-0.4}$	14	ARNISON	84D	UA1	Repl. by ALBAJAR 89

[56] ABACHI 95D obtain this result from the measured $\sigma_W \text{B}(W \to \mu\nu) = 2.09 \pm 0.23 \pm 0.11$ nb and $\sigma_W \text{B}(W \to e\nu) = 2.36 \pm 0.07 \pm 0.13$ nb in which the first error is the combined statistical and systematic uncertainty, the second reflects the uncertainty in the luminosity.

[57] ABE 92I obtain $\sigma_W \text{B}(W \to \mu\nu) = 2.21 \pm 0.07 \pm 0.21$ and combine with ABE 91C $\sigma_W \text{B}((W \to e\nu))$ to give a ratio of the couplings from which we derive this measurement.

$\Gamma(\tau^+\nu)/\Gamma(e^+\nu)$ Γ_4/Γ_2

VALUE	EVTS	DOCUMENT ID		TECN	COMMENT
1.002±0.029 OUR FIT					
0.961±0.061	980	[58] ABBOTT	00D	D0	$E^{p\overline{p}}_{\rm cm}$= 1.8 TeV
0.94 ±0.14	179	[59] ABE	92E	CDF	$E^{p\overline{p}}_{\rm cm}$= 1.8 TeV
1.04 ±0.08 ±0.08	754	[60] ALITTI	92F	UA2	$E^{p\overline{p}}_{\rm cm}$= 630 GeV
1.02 ±0.20 ±0.12	32	ALBAJAR	89	UA1	$E^{p\overline{p}}_{\rm cm}$= 546,630 GeV
• • • We do not use the following data for averages, fits, limits, etc. • • •					
0.995±0.112±0.083	198	ALITTI	91C	UA2	Repl. by ALITTI 92F
1.02 ±0.20 ±0.10	32	ALBAJAR	87	UA1	Repl. by ALBAJAR 89

[58] ABBOTT 00D measure $\sigma_W \times \text{B}(W \to \tau\nu_\tau) = 2.22 \pm 0.09 \pm 0.10 \pm 0.10$ nb. Using the ABBOTT 00B result $\sigma_W \times \text{B}(W \to e\nu_e) = 2.31 \pm 0.01 \pm 0.05 \pm 0.10$ nb, they quote the ratio of the couplings from which we derive this measurement.

[59] ABE 92E use two procedures for selecting $W \to \tau\nu_\tau$ events. The missing E_T trigger leads to $132 \pm 14 \pm 8$ events and the τ trigger to $47 \pm 9 \pm 4$ events. Proper statistical and systematic correlations are taken into account to arrive at $\sigma\text{B}(W \to \tau\nu) = 2.05 \pm 0.27$ nb. Combined with ABE 91C result on $\sigma\text{B}(W \to e\nu)$, ABE 92E quote a ratio of the couplings from which we derive this measurement.

[60] This measurement is derived by us from the ratio of the couplings of ALITTI 92F.

$\Gamma(\pi^+\gamma)/\Gamma(e^+\nu)$ Γ_6/Γ_2

VALUE	CL%	DOCUMENT ID		TECN	COMMENT
< 7 ×10^{-4}	95	ABE	98H	CDF	$E^{p\overline{p}}_{\rm cm}$= 1.8 TeV
< 4.9 ×10^{-3}	95	[61] ALITTI	92D	UA2	$E^{p\overline{p}}_{\rm cm}$= 630 GeV
<58 ×10^{-3}	95	[62] ALBAJAR	90	UA1	$E^{p\overline{p}}_{\rm cm}$= 546, 630 GeV

[61] ALITTI 92D limit is 3.8×10^{-3} at 90%CL.

[62] ALBAJAR 90 obtain < 0.048 at 90%CL.

$\Gamma(D_s^+\gamma)/\Gamma(e^+\nu)$ Γ_7/Γ_2

VALUE	CL%	DOCUMENT ID		TECN	COMMENT
$<1.2\times10^{-2}$	95	ABE	98P	CDF	$E_{\rm cm}^{p\overline{p}}$= 1.8 TeV

$\Gamma(cX)/\Gamma(\text{hadrons})$ Γ_8/Γ_5

VALUE	EVTS	DOCUMENT ID		TECN	COMMENT
0.49 ±0.04 OUR AVERAGE					
0.481±0.042±0.032	3005	[63] ABBIENDI	00V	OPAL	$E_{\rm cm}^{ee}$= 183 + 189 GeV
0.51 ±0.05 ±0.03	746	[64] BARATE	99M	ALEP	$E_{\rm cm}^{ee}$= 172 + 183 GeV

[63] ABBIENDI 00V tag $W \to cX$ decays using measured jet properties, lifetime information, and leptons produced in charm decays. From this result, and using the additional measurements of $\Gamma(W)$ and $B(W \to \text{hadrons})$, $|V_{cs}|$ is determined to be 0.969 ± 0.045 ± 0.036.

[64] BARATE 99M tag c jets using a neural network algorithm. From this measurement $|V_{cs}|$ is determined to be 1.00 ± 0.11 ± 0.07.

$R_{cs} = \Gamma(c\overline{s})/\Gamma(\text{hadrons})$ Γ_9/Γ_5

VALUE	DOCUMENT ID		TECN	COMMENT
$0.46^{+0.18}_{-0.14}\pm0.07$	[65] ABREU	98N	DLPH	$E_{\rm cm}^{ee}$= 161+172 GeV

[65] ABREU 98N tag c and s jets by identifying a charged kaon as the highest momentum particle in a hadronic jet. They also use a lifetime tag to independently identify a c jet, based on the impact parameter distribution of charged particles in a jet. From this measurement $|V_{cs}|$ is determined to be $0.94^{+0.32}_{-0.26}$ ± 0.13.

AVERAGE PARTICLE MULTIPLICITIES IN HADRONIC *W* DECAY

Summed over particle and antiparticle, when appropriate.

$\langle N_{\pi^\pm}\rangle$

VALUE	DOCUMENT ID		TECN	COMMENT
15.70±0.35	[66] ABREU,P	00F	DLPH	$E_{\rm cm}^{ee}$= 189 GeV

[66] ABREU,P 00F measure $\langle N_{\pi^\pm}\rangle$ = 31.65 ± 0.48 ± 0.76 and 15.51 ± 0.38 ± 0.40 in the fully hadronic and semileptonic final states respectively. The value quoted is a weighted average without assuming any correlations.

$\langle N_{K^\pm}\rangle$

VALUE	DOCUMENT ID		TECN	COMMENT
2.20±0.19	[67] ABREU,P	00F	DLPH	$E_{\rm cm}^{ee}$= 189 GeV

[67] ABREU,P 00F measure $\langle N_{K^\pm}\rangle$ = 4.38 ± 0.42 ± 0.12 and 2.23 ± 0.32 ± 0.17 in the fully hadronic and semileptonic final states respectively. The value quoted is a weighted average without assuming any correlations.

$\langle N_p\rangle$

VALUE	DOCUMENT ID		TECN	COMMENT
0.92±0.14	[68] ABREU,P	00F	DLPH	$E_{\rm cm}^{ee}$= 189 GeV

[68] ABREU,P 00F measure $\langle N_p\rangle$ = 1.82 ± 0.29 ± 0.16 and 0.94 ± 0.23 ± 0.06 in the fully hadronic and semileptonic final states respectively. The value quoted is a weighted average without assuming any correlations.

$\langle N_{\rm charged}\rangle$

VALUE	DOCUMENT ID		TECN	COMMENT
19.41±0.15 OUR AVERAGE				
19.44±0.17	[69] ABREU,P	00F	DLPH	$E_{\rm cm}^{ee}$= 183+189 GeV
19.3 ±0.3 ±0.3	[70] ABBIENDI	99N	OPAL	$E_{\rm cm}^{ee}$= 183 GeV
19.23±0.74	[71] ABREU	98C	DLPH	$E_{\rm cm}^{ee}$= 172 GeV

[69] ABREU,P 00F measure $\langle N_{\rm charged}\rangle$ = 39.12 ± 0.33 ± 0.36 and 38.11 ± 0.57 ± 0.44 in the fully hadronic final states at 189 and 183 GeV respectively, and $\langle N_{\rm charged}\rangle$ = 19.49 ± 0.31 ± 0.27 and 19.78 ± 0.49 ± 0.43 in the semileptonic final states. The value quoted is a weighted average without assuming any correlations.

[70] ABBIENDI 99N use the final states $W^+W^- \to q\overline{q}\ell\overline{\nu}_\ell$ to derive this value.

[71] ABREU 98C combine results from both the fully hadronic as well semileptonic WW final states after demonstrating that the W decay charged multiplicity is independent of the topology within errors.

TRIPLE GAUGE COUPLINGS (TGC'S)

Revised February 2002 by C. Caso (University of Genova) and A. Gurtu (Tata Institute).

Fourteen independent couplings, 7 each for ZWW and γWW, completely describe the VWW vertices within the most general framework of the electroweak Standard Model (SM) consistent with Lorentz invariance and U(1) gauge invariance. Of each of the 7 TGC's, 3 conserve C and P individually, 3 violate CP, and one TGC violates C and P individually while conserving CP. Assumption of C and P conservation and electromagnetic gauge invariance reduces the independent VWW couplings to five: one common set [1,2] is $(\Delta\kappa_\gamma, \Delta\kappa_Z, \lambda_\gamma, \lambda_Z, \Delta g_1^Z)$, where $\Delta\kappa_\gamma = \Delta\kappa_Z = \Delta g_1^Z = 0$ and $\lambda_\gamma = \lambda_Z = 0$ in the Standard Model at the tree level. The W magnetic dipole moment, μ_W, and the W electric quadrupole moment, q_W, are expressed as $\mu_W = e\,(1+\kappa_\gamma+\lambda_\gamma)/2M_W$ and $q_W = -e\,(\kappa_\gamma-\lambda_\gamma)/M_W^2$.

Precision measurements of suitable observables at LEP1 has already led to an exploration of much of the TGC parameter space. For LEP2 data, the LEP Collaborations have agreed to express their results in terms of the parameters Δg_1^Z, $\Delta\kappa_\gamma$ and λ_γ (λ_Z and $\Delta\kappa_Z$ are related to these by gauge invariance).

At LEP2 the VWW coupling arises in W-pair production via s-channel exchange or in single W production via the radiation of a virtual photon off the incident e^+ or e^-. At the TEVATRON hard photon bremstrahlung off a produced W or Z signals the presence of a triple gauge vertex. In order to extract the value of one TGC the others are generally kept fixed to their SM values.

References

1. K. Hagiwara *et al.*, Nucl. Phys. **B282**, 253 (1987).
2. G. Gounaris *et al.*, CERN 96-01 525.

Δg_1^Z

Combining published and unpublished LEP results (as of Summer 2003), a single-parameter fit yields $\Delta g_1^Z = -0.009^{+0.022}_{-0.021}$, where the other two parameters, $\Delta\kappa_\gamma$ and λ_γ, were kept fixed to their Standard Model values.

(See EP Preprint Summer 2003: CERN-EP/2003-091 and hep-ex/0312023, December 2003, on http://lepewwg.web.cern.ch/LEPEWWG/stanmod/)

VALUE	EVTS	DOCUMENT ID		TECN	COMMENT
$\mathbf{-0.013^{+0.034}_{-0.033}}$	9800	[72] ABBIENDI	04D	OPAL	$E_{\rm cm}^{ee}$= 183–209 GeV
• • • We do not use the following data for averages, fits, limits, etc. • • •					
−0.02 ±0.07 ±0.01	2114	[73] ABREU	01I	DLPH	$E_{\rm cm}^{ee}$= 183+189 GeV
$0.023^{+0.059}_{-0.055}$	3586	[74] HEISTER	01C	ALEP	$E_{\rm cm}^{ee}$= 161–189 GeV
	331	[75] ABBOTT	99I	D0	$E_{\rm cm}^{p\overline{p}}$= 1.8 TeV
$0.11\ ^{+0.19}_{-0.18}\pm0.10$	1154	[76] ACCIARRI	99Q	L3	$E_{\rm cm}^{ee}$= 161+172+ 183 GeV

[72] ABBIENDI 04D combine results from W^+W^- in all decay channels. Only CP-conserving couplings are considered and each parameter is determined from a single-parameter fit in which the other parameters assume their Standard Model values. The 95% confidence interval is $-0.077 < \Delta g_1^Z < 0.054$.

[73] ABREU 01I combine results from e^+e^- interactions at 189 GeV leading to W^+W^- and $We\nu_e$ final states with results from ABREU 99L at 183 GeV. The 95% confidence interval is $-0.16 < \Delta g_1^Z < 0.13$.

[74] HEISTER 01C study W-pair, single-W, and single photon events and combine with earlier results from BARATE,R 98, BARATE 98Y, and BARATE 99L to obtain the quoted value, fixing $\Delta\kappa_\gamma$ and λ_γ to their Standard Model values. The 95% confidence interval is $-0.087 < \Delta g_1^Z < 0.141$. When all three couplings Δg_1^Z, $\Delta\kappa_\gamma$, and λ_γ are floated freely in the fit, one obtains $\Delta g_1^Z = 0.013^{+0.066}_{-0.068}$.

[75] ABBOTT 99I perform a simultaneous fit to the $W\gamma$, $WW \to$ dilepton, $WW/WZ \to e\nu jj$, $WW/WZ \to \mu\nu jj$, and $WZ \to$ trilepton data samples. For Λ = 2.0 TeV, the 95%CL limits are $-0.37 < \Delta g_1^Z < 0.57$, fixing λ_Z=$\Delta\kappa_Z$ =0 and assuming Standard Model values for the $WW\gamma$ couplings.

[76] ACCIARRI 99Q study W-pair, single-W, and single photon events.

$\Delta\kappa_\gamma$

Combining published and unpublished LEP results (as of Summer 2003), a single-parameter fit yields $\Delta\kappa_\gamma = -0.016^{+0.042}_{-0.047}$, where the other two parameters, Δg_1^Z and λ_γ, were kept fixed to their Standard Model values.

(See EP Preprint Summer 2003: CERN-EP/2003-091 and hep-ex/0312023, December 2003, on http://lepewwg.web.cern.ch/LEPEWWG/stanmod/)

VALUE	EVTS	DOCUMENT ID		TECN	COMMENT
$\mathbf{-0.12\ ^{+0.09}_{-0.08}}$	9800	[77] ABBIENDI	04D	OPAL	$E_{\rm cm}^{ee}$= 183–209 GeV

• • • We do not use the following data for averages, fits, limits, etc. • • •

$0.116^{+0.082}_{-0.086}\pm0.068$	315	[78] ACHARD	02I L3	E^{ee}_{cm}= 161–209 GeV	
$0.25\ ^{+0.21}_{-0.20}\pm0.06$	2298	[79] ABREU	01I DLPH	E^{ee}_{cm}= 183+189 GeV	
$0.022^{+0.119}_{-0.115}$	3586	[80] HEISTER	01C ALEP	E^{ee}_{cm}= 161–189 GeV	
		[81] BREITWEG	00 ZEUS	$e^+p\rightarrow\ e^+W^\pm X$, $\sqrt{s}\approx$ 300 GeV	
$-0.08\ \pm0.34$	331	[82] ABBOTT	99I D0	$E^{p\overline{p}}_{cm}$= 1.8 TeV	
$0.11\ \pm0.25\ \pm0.17$	1154	[83] ACCIARRI	99Q L3	E^{ee}_{cm}= 161+172+ 183 GeV	

[77] ABBIENDI 04D combine results from W^+W^- in all decay channels. Only *CP*-conserving couplings are considered and each parameter is determined from a single-parameter fit in which the other parameters assume their Standard Model values. The 95% confidence interval is $-0.27<\Delta\kappa_\gamma<0.07$.

[78] ACHARD 02I study single W production in e^+e^- interactions from 192 to 209 GeV. The result quoted here is obtained including data from 161 to 189 GeV, ACCIARRI 00N. The 95% C.L. limits are $-0.10<\Delta\kappa_\gamma<0.32$ (for λ_γ=0). When both couplings λ_γ and κ_γ are floated freely in the fit one obtains $\Delta\kappa_\gamma=0.07\pm0.10\pm0.07$.

[79] ABREU 01I combine results from e^+e^- interactions at 189 GeV leading to W^+W^-, $We\nu_e$, and $\nu\overline{\nu}\gamma$ final states with results from ABREU 99L at 183 GeV. The 95% confidence interval is $-0.13<\Delta\kappa_\gamma<0.68$.

[80] HEISTER 01C study W-pair, single-W, and single photon events and combine with earlier results from BARATE,R 98, BARATE 98Y, and BARATE 99L to obtain the quoted value, fixing Δg_1^Z and λ_γ to their Standard Model values. The 95% confidence interval is $-0.200<\Delta\kappa_\gamma<0.258$. When all three couplings Δg_1^Z, $\Delta\kappa_\gamma$, and λ_γ are floated freely in the fit, one obtains $\Delta\kappa_\gamma=0.043\pm0.110$.

[81] BREITWEG 00 search for W production in events with large hadronic p_T. For $p_T>20$ GeV, the upper limit on the cross section gives the 95%CL limit $-4.7<\Delta\kappa_\gamma<1.5$ (for λ_γ=0).

[82] ABBOTT 99I perform a simultaneous fit to the $W\gamma$, $WW\rightarrow$ dilepton, $WW/WZ\rightarrow e\nu jj$, $WW/WZ\rightarrow\mu\nu jj$, and $WZ\rightarrow$ trilepton data samples. For $\Lambda=2.0$ TeV, the 95%CL limits are $-0.25<\Delta\kappa_\gamma<0.39$.

[83] ACCIARRI 99Q study W-pair, single-W, and single photon events.

λ_γ

Combining published and unpublished LEP results (as of Summer 2003), a single-parameter fit yields $\lambda_\gamma=-0.016^{+0.021}_{-0.023}$, where the other two parameters, Δg_1^Z and $\Delta\kappa_\gamma$, were kept fixed to their Standard Model values.

(See EP Preprint Summer 2003: CERN-EP/2003-091 and hep-ex/0312023, December 2003, on http://lepewwg.web.cern.ch/LEPEWWG/stanmod/)

VALUE	EVTS	DOCUMENT ID		TECN	COMMENT
$-0.060^{+0.034}_{-0.033}$	9800	[84] ABBIENDI	04D OPAL		E^{ee}_{cm}= 183–209 GeV

• • • We do not use the following data for averages, fits, limits, etc. • • •

$0.35\ ^{+0.10}_{-0.13}\pm0.08$	315	[85] ACHARD	02I L3	E^{ee}_{cm}= 161–209 GeV	
$0.05\ \pm0.09\ \pm0.01$	2298	[86] ABREU	01I DLPH	E^{ee}_{cm}= 183+189 GeV	
$0.040^{+0.054}_{-0.052}$	3586	[87] HEISTER	01C ALEP	E^{ee}_{cm}= 161–189 GeV	
		[88] BREITWEG	00 ZEUS	$e^+p\rightarrow\ e^+W^\pm X$, $\sqrt{s}\approx$ 300 GeV	
$0.00\ ^{+0.10}_{-0.09}$	331	[89] ABBOTT	99I D0	$E^{p\overline{p}}_{cm}$= 1.8 TeV	
$0.10\ ^{+0.22}_{-0.20}\pm0.10$	1154	[90] ACCIARRI	99Q L3	E^{ee}_{cm}= 161+172+ 183 GeV	

[84] ABBIENDI 04D combine results from W^+W^- in all decay channels. Only *CP*-conserving couplings are considered and each parameter is determined from a single-parameter fit in which the other parameters assume their Standard Model values. The 95% confidence interval is $-0.13<\lambda_\gamma<0.01$.

[85] ACHARD 02I study single W production in e^+e^- interactions from 192 to 209 GeV. The result quoted here is obtained including data from 161 to 189 GeV, ACCIARRI 00N. The 95% C.L. limits are $-0.37<\lambda_\gamma<0.61$ (for κ_γ=1). When both couplings λ_γ and κ_γ are floated freely in the fit one obtains $\lambda_\gamma=0.31^{+0.12}_{-0.20}\pm0.07$.

[86] ABREU 01I combine results from e^+e^- interactions at 189 GeV leading to W^+W^-, $We\nu_e$, and $\nu\overline{\nu}\gamma$ final states with results from ABREU 99L at 183 GeV. The 95% confidence interval is $-0.11<\lambda_\gamma<0.23$.

[87] HEISTER 01C study W-pair, single-W, and single photon events and combine with earlier results from BARATE,R 98, BARATE 98Y, and BARATE 99L to obtain the quoted value, fixing Δg_1^Z and $\Delta\kappa_\gamma$ to their Standard Model values. The 95% confidence interval is $-0.062<\lambda_\gamma<0.147$. When all three couplings Δg_1^Z, $\Delta\kappa_\gamma$, and λ_γ are floated freely in the fit, one obtains $\lambda_\gamma=0.023^{+0.074}_{-0.077}$.

[88] BREITWEG 00 search for W production in events with large hadronic p_T. For $p_T>20$ GeV, the upper limit on the cross section gives the 95%CL limit $-3.2<\lambda_\gamma<3.2$ (for $\Delta\kappa_\gamma$=0).

[89] ABBOTT 99I perform a simultaneous fit to the $W\gamma$, $WW\rightarrow$ dilepton, $WW/WZ\rightarrow e\nu jj$, $WW/WZ\rightarrow\mu\nu jj$, and $WZ\rightarrow$ trilepton data samples. For $\Lambda=2.0$ TeV, the 95%CL limits are $-0.18<\lambda_\gamma<0.19$.

[90] ACCIARRI 99Q study W-pair, single-W, and single photon events.

Δg_5^Z

This coupling is *CP*-conserving but *C*- and *P*-violating.

VALUE	EVTS	DOCUMENT ID		TECN	COMMENT
-0.11 ± 0.16 OUR AVERAGE		Error includes scale factor of 1.4.			
$-0.04^{+0.13}_{-0.12}$	9800	[91] ABBIENDI	04D OPAL		E^{ee}_{cm}= 183–209 GeV
$-0.44^{+0.23}_{-0.22}\pm0.12$	1154	[92] ACCIARRI	99Q L3		E^{ee}_{cm}= 161+172+ 183 GeV

• • • We do not use the following data for averages, fits, limits, etc. • • •

-0.16 ± 0.23	[93] EBOLI	00	THEO	LEP1, SLC+ Tevatron

[91] ABBIENDI 04D combine results from W^+W^- in all decay channels. Only *CP*-conserving couplings are considered and each parameter is determined from a single-parameter fit in which the other parameters assume their Standard Model values. The 95% confidence interval is $-0.28<\Delta g_5^Z<0.21$.

[92] ACCIARRI 99Q study W-pair, single-W, and single photon events.

[93] EBOLI 00 extract this indirect value of the coupling studying the non-universal one-loop contributions to the experimental value of the $Z\rightarrow\ b\overline{b}$ width (Λ=1 TeV is assumed).

g_4^Z

This coupling is *CP*-violating (*C*-violating and *P*-conserving).

VALUE	EVTS	DOCUMENT ID		TECN	COMMENT
$-0.02^{+0.32}_{-0.33}$	1065	[94] ABBIENDI	01H OPAL		E^{ee}_{cm}= 189 GeV

[94] ABBIENDI 01H study W-pair events, with one leptonically and one hadronically decaying W. The coupling is extracted using information from the W production angle together with decay angles from the leptonically decaying W.

$\tilde{\kappa}_Z$

This coupling is *CP*-violating (*C*-conserving and *P*-violating).

VALUE	EVTS	DOCUMENT ID		TECN	COMMENT
$-0.20^{+0.10}_{-0.07}$	1065	[95] ABBIENDI	01H OPAL		E^{ee}_{cm}= 189 GeV

[95] ABBIENDI 01H study W-pair events, with one leptonically and one hadronically decaying W. The coupling is extracted using information from the W production angle together with decay angles from the leptonically decaying W.

$\tilde{\lambda}_Z$

This coupling is *CP*-violating (*C*-conserving and *P*-violating).

VALUE	EVTS	DOCUMENT ID		TECN	COMMENT
$-0.18^{+0.24}_{-0.16}$	1065	[96] ABBIENDI	01H OPAL		E^{ee}_{cm}= 189 GeV

[96] ABBIENDI 01H study W-pair events, with one leptonically and one hadronically decaying W. The coupling is extracted using information from the W production angle together with decay angles from the leptonically decaying W.

W ANOMALOUS MAGNETIC MOMENT

The full magnetic moment is given by $\mu_W=e(1+\kappa+\lambda)/2m_W$. In the Standard Model, at tree level, $\kappa=1$ and $\lambda=0$. Some papers have defined $\Delta\kappa=1-\kappa$ and assume that $\lambda=0$. Note that the electric quadrupole moment is given by $-e(\kappa-\lambda)/m_W^2$. A description of the parameterization of these moments and additional references can be found in HAGIWARA 87 and BAUR 88. The parameter Λ appearing in the theoretical limits below is a regularization cutoff which roughly corresponds to the energy scale where the structure of the W boson becomes manifest.

VALUE ($e/2m_W$)	EVTS	DOCUMENT ID		TECN	COMMENT
$2.22^{+0.20}_{-0.19}$	2298	[97] ABREU	01I DLPH		E^{ee}_{cm}= 183+189 GeV

• • • We do not use the following data for averages, fits, limits, etc. • • •

[98] ABE	95G CDF		
[99] ALITTI	92C UA2		
[100] SAMUEL	92	THEO	
[101] SAMUEL	91	THEO	
[102] GRIFOLS	88	THEO	
[103] GROTCH	87	THEO	
[104] VANDERBIJ	87	THEO	
[105] GRAU	85	THEO	
[106] SUZUKI	85	THEO	
[107] HERZOG	84	THEO	

[97] ABREU 01I combine results from e^+e^- interactions at 189 GeV leading to W^+W^-, $We\nu_e$, and $\nu\overline{\nu}\gamma$ final states with results from ABREU 99L at 183 GeV to determine Δg_1^Z, $\Delta\kappa_\gamma$, and λ_γ. $\Delta\kappa_\gamma$ and λ_γ are simultaneously floated in the fit to determine μ_W.

[98] ABE 95G report $-1.3<\kappa<3.2$ for λ=0 and $-0.7<\lambda<0.7$ for κ=1 in $p\overline{p}\rightarrow\ e\nu_e\gamma X$ and $\mu\nu_\mu\gamma X$ at $\sqrt{s}=1.8$ TeV.

[99] ALITTI 92C measure $\kappa=1\ ^{+2.6}_{-2.2}$ and $\lambda=0\ ^{+1.7}_{-1.8}$ in $p\overline{p}\rightarrow\ e\nu\gamma+X$ at $\sqrt{s}=630$ GeV. At 95%CL they report $-3.5<\kappa<5.9$ and $-3.6<\lambda<3.5$.

[100] SAMUEL 92 use preliminary CDF and UA2 data and find $-2.4<\kappa<3.7$ at 96%CL and $-3.1<\kappa<4.2$ at 95%CL respectively. They use data for $W\gamma$ production and radiative W decay.

[101] SAMUEL 91 use preliminary CDF data for $p\overline{p}\rightarrow\ W\gamma X$ to obtain $-11.3\ \leq\ \Delta\kappa\ \leq\ 10.9$. Note that their $\kappa=1-\Delta\kappa$.

[102] GRIFOLS 88 uses deviation from ρ parameter to set limit $\Delta\kappa\lesssim 65\ (M_W^2/\Lambda^2)$.

[103] GROTCH 87 finds the limit $-37\ <\ \Delta\kappa\ <73.5$ (90% CL) from the experimental limits on $e^+e^-\ \rightarrow\ \nu\overline{\nu}\gamma$ assuming three neutrino generations and $-19.5\ <\ \Delta\kappa\ <56$ for four generations. Note their $\Delta\kappa$ has the opposite sign as our definition.

[104] VANDERBIJ 87 uses existing limits to the photon structure to obtain $|\Delta\kappa| < 33$ (m_W/Λ). In addition VANDERBIJ 87 discusses problems with using the ρ parameter of the Standard Model to determine $\Delta\kappa$.

[105] GRAU 85 uses the muon anomaly to derive a coupled limit on the anomalous magnetic dipole and electric quadrupole (λ) moments $1.05 > \Delta\kappa \ln(\Lambda/m_W) + \lambda/2 > -2.77$. In the Standard Model $\lambda = 0$.

[106] SUZUKI 85 uses partial-wave unitarity at high energies to obtain $|\Delta\kappa| \lesssim 190$ $(m_W/\Lambda)^2$. From the anomalous magnetic moment of the muon, SUZUKI 85 obtains $|\Delta\kappa| \lesssim 2.2/\ln(\Lambda/m_W)$. Finally SUZUKI 85 uses deviations from the ρ parameter and obtains a very qualitative, order-of-magnitude limit $|\Delta\kappa| \lesssim 150\ (m_W/\Lambda)^4$ if $|\Delta\kappa| \ll 1$.

[107] HERZOG 84 consider the contribution of W-boson to muon magnetic moment including anomalous coupling of $WW\gamma$. Obtain a limit $-1 < \Delta\kappa < 3$ for $\Lambda \gtrsim 1$ TeV.

ANOMALOUS W/Z QUARTIC COUPLINGS

Revised November 2003 by C. Caso (University of Genova) and A. Gurtu (Tata Institute).

The Standard Model predictions for $WWWW$, $WWZZ$, $WWZ\gamma$, $WW\gamma\gamma$, and $ZZ\gamma\gamma$ couplings are small at LEP, but expected to become important at a TeV Linear Collider. Outside the Standard Model framework such possible couplings, a_0, a_c, a_n, are expressed in terms of the following dimension-6 operators [1,2];

$$L_6^0 = -\frac{e^2}{16\Lambda^2}\, a_0\, F^{\mu\nu}\, F_{\mu\nu} \vec{W}^\alpha \cdot \vec{W}_\alpha$$
$$L_6^c = -\frac{e^2}{16\Lambda^2}\, a_c\, F^{\mu\alpha}\, F_{\mu\beta} \vec{W}^\beta \cdot \vec{W}_\alpha$$
$$L_6^n = -i\frac{e^2}{16\Lambda^2}\, a_n \epsilon_{ijk}\, W_{\mu\alpha}^{(i)}\, W_\nu^{(j)}\, W^{(k)\alpha} F^{\mu\nu}$$
$$\widetilde{L}_6^0 = -\frac{e^2}{16\Lambda^2}\, \widetilde{a}_0\, F^{\mu\nu}\, \widetilde{F}_{\mu\nu} \vec{W}^\alpha \cdot \vec{W}_\alpha$$
$$\widetilde{L}_6^n = -i\frac{e^2}{16\Lambda^2}\, \widetilde{a}_n \epsilon_{ijk}\, W_{\mu\alpha}^{(i)}\, W_\nu^{(j)}\, W^{(k)\alpha} \widetilde{F}^{\mu\nu}$$

where F,W are photon and W fields, L_6^0 and L_6^c conserve C, P separately ($\widetilde{L}_6^0$ conserves only C) and generate anomalous $W^+W^-\gamma\gamma$ and $ZZ\gamma\gamma$ couplings, L_6^n violates CP ($\widetilde{L}_6^n$ violates both C and P) and generates an anomalous $W^+W^-Z\gamma$ coupling, and Λ is a scale for new physics. For the $ZZ\gamma\gamma$ coupling the CP-violating term represented by L_6^n does not contribute. These couplings are assumed to be real and to vanish at tree level in the Standard Model.

Within the same framework as above, a more recent description of the quartic couplings [3] treats the anomalous parts of the $WW\gamma\gamma$ and $ZZ\gamma\gamma$ couplings separately leading to two sets parameterized as a_0^V/Λ^2 and a_c^V/Λ^2, where $V = W$ or Z.

At LEP the processes studied in search of these quartic couplings are $e^+e^- \to WW\gamma$, $e^+e^- \to \gamma\gamma\nu\overline{\nu}$, and $e^+e^- \to Z\gamma\gamma$ and limits are set on the quantities $a_0^W/\Lambda^2, a_c^W/\Lambda^2, a_n/\Lambda^2$. The characteristics of the first process depend on all the three couplings whereas those of the latter two depend only on the two CP-conserving couplings. The sensitive measured variables are the cross sections for these processes as well as the energy and angular distributions of the photon and recoil mass to the photon pair.

References

1. G. Belanger and F. Boudjema, Phys. Lett. **B288**, 201 (1992).
2. J.W. Stirling and A. Werthenbach, Eur. Phys. J. **C14**, 103 (2000);
   J.W. Stirling and A. Werthenbach, Phys. Lett. **B466**, 369 (1999);
   A. Denner *et al.*, Eur. Phys. J. **C20**, 201 (2001);
   G. Montagna *et al.*, Phys. Lett. **B515**, 197 (2001).
3. G. Belanger *et al.*, Eur. Phys. J. **C13**, 103 (2000).

a_0/Λ^2, a_c/Λ^2, a_n/Λ^2

Using the $WW\gamma$ final state, the LEP combined 95% CL limits on the anomalous contributions to the $WW\gamma\gamma$ and $WWZ\gamma$ vertices (as of summer 2003) are given below:

(See P. Wells, "Experimental Tests of the Standard Model," Int. Europhysics Conference on High-Energy Physics, Aachen, Germany, 17–23 July 2003)

$$-0.02 < a_0^W/\Lambda^2 < 0.02\ \text{GeV}^{-2},$$
$$-0.05 < a_c^W/\Lambda^2 < 0.03\ \text{GeV}^{-2},$$
$$-0.15 < a_n/\Lambda^2 < 0.15\ \text{GeV}^{-2}.$$

VALUE	DOCUMENT ID	TECN
• • • We do not use the following data for averages, fits, limits, etc. • • •		
	[108] ABBIENDI 04B	OPAL
	[109] ABDALLAH 03I	DLPH
	[110] ACHARD 02F	L3

[108] ABBIENDI 04B select 187 $e^+e^- \to W^+W^-\gamma$ events in the C.M. energy range 180–209 GeV, where $E_\gamma > 2.5$ GeV, the photon has a polar angle $|\cos\theta_\gamma| < 0.975$ and is well isolated from the nearest jet and charged lepton, and the effective masses of both fermion-antifermion systems agree with the W mass within $3\,\Gamma_W$. The measured differential cross section as a function of the photon energy and photon polar angle is used to extract the 95% CL limits: $-0.020\ \text{GeV}^{-2} < a_0/\Lambda^2 < 0.020\ \text{GeV}^{-2}$, $-0.053\ \text{GeV}^{-2} < a_c/\Lambda^2 < 0.037\ \text{GeV}^{-2}$ and $-0.16\ \text{GeV}^{-2} < a_n/\Lambda^2 < 0.15\ \text{GeV}^{-2}$.

[109] ABDALLAH 03I select 122 $e^+e^- \to W^+W^-\gamma$ events in the C.M. energy range 189–209 GeV, where $E_\gamma > 5$ GeV, the photon has a polar angle $|\cos\theta_\gamma| < 0.95$ and is well isolated from the nearest charged fermion. A fit to the photon energy spectra yields $a_c/\Lambda^2 = 0.000^{+0.019}_{-0.040}\ \text{GeV}^{-2}$, $a_0/\Lambda^2 = -0.004^{+0.018}_{-0.010}\ \text{GeV}^{-2}$, $\tilde{a}_0/\Lambda^2 = -0.007^{+0.019}_{-0.008}\ \text{GeV}^{-2}$, $a_n/\Lambda^2 = -0.09^{+0.16}_{-0.05}\ \text{GeV}^{-2}$, and $\tilde{a}_n/\Lambda^2 = +0.05^{+0.07}_{-0.15}\ \text{GeV}^{-2}$, keeping the other parameters fixed to their Standard Model values (0). The 95% CL limits are: $-0.063\ \text{GeV}^{-2} < a_c/\Lambda^2 < +0.032\ \text{GeV}^{-2}$, $-0.020\ \text{GeV}^{-2} < a_0/\Lambda^2 < +0.020\ \text{GeV}^{-2}$, $-0.020\ \text{GeV}^{-2} < \tilde{a}_0/\Lambda^2 < +0.020\ \text{GeV}^{-2}$, $-0.18\ \text{GeV}^{-2} < a_n/\Lambda^2 < +0.14\ \text{GeV}^{-2}$, $-0.16\ \text{GeV}^{-2} < \tilde{a}_n/\Lambda^2 < +0.17\ \text{GeV}^{-2}$.

[110] ACHARD 02F select 86 $e^+e^- \to W^+W^-\gamma$ events at 192–207 GeV, where $E_\gamma > 5$ GeV and the photon is well isolated. They also select 43 acoplanar $e^+e^- \to \nu\overline{\nu}\gamma\gamma$ events in this energy range, where the photon energies are >5 GeV and >1 GeV and the photon polar angles are between 14° and 166°. All these 43 events are in the recoil mass region corresponding to the Z (75–110 GeV). Using the shape and normalization of the photon spectra in the $W^+W^-\gamma$ events, and combining with the 42 event sample from 189 GeV data (ACCIARRI 00T), they obtain: $a_0/\Lambda^2 = 0.000 \pm 0.010\ \text{GeV}^{-2}$, $a_c/\Lambda^2 = -0.013 \pm 0.023\ \text{GeV}^{-2}$, and $a_n/\Lambda^2 = -0.002 \pm 0.076\ \text{GeV}^{-2}$. Further combining the analyses of $W^+W^-\gamma$ events with the low recoil mass region of $\nu\overline{\nu}\gamma\gamma$ events (including samples collected at $183 + 189$ GeV), they obtain the following one-parameter 95% CL limits: $-0.015\ \text{GeV}^{-2} < a_0/\Lambda^2 < 0.015\ \text{GeV}^{-2}$, $-0.048\ \text{GeV}^{-2} < a_c/\Lambda^2 < 0.026\ \text{GeV}^{-2}$, and $-0.14\ \text{GeV}^{-2} < a_n/\Lambda^2 < 0.13\ \text{GeV}^{-2}$.

W REFERENCES

ABBIENDI	04B	PL B580 17	G. Abbiendi *et al.*	(OPAL Collab.)
ABBIENDI	04D	EPJ C33 463	G. Abbiendi *et al.*	(OPAL Collab.)
ABBIENDI	03C	EPJ C26 321	G. Abbiendi *et al.*	(OPAL Collab.)
ABDALLAH	03I	EPJ C31 139	J. Abdallah *et al.*	(DELPHI Collab.)
ABAZOV	02D	PR D66 012001	V.M. Abazov *et al.*	(D0 Collab.)
ABAZOV	02E	PR D66 032008	V.M. Abazov *et al.*	(D0 Collab.)
ACHARD	02F	PL B527 29	P. Achard *et al.*	(L3 Collab.)
ACHARD	02I	PL B547 151	P. Achard *et al.*	(L3 Collab.)
CHEKANOV	02C	PL B539 197	S. Chekanov *et al.*	(ZEUS Collab.)
KOTWAL	02	FERMILAB-FN-0716	A. Kotwal *et al.*	
ABBIENDI	01F	PL B507 29	G. Abbiendi *et al.*	(OPAL Collab.)
ABBIENDI	01H	EPJ C19 229	G. Abbiendi *et al.*	(OPAL Collab.)
ABREU	01I	PL B502 9	P. Abreu *et al.*	(DELPHI Collab.)
ABREU	01K	PL B511 159	P. Abreu *et al.*	(DELPHI Collab.)
ADLOFF	01A	EPJ C19 269	C. Adloff *et al.*	(H1 Collab.)
AFFOLDER	01E	PR D64 052001	T. Affolder *et al.*	(CDF Collab.)
HEISTER	01C	EPJ C21 423	A. Heister *et al.*	(ALEPH Collab.)
ABBIENDI	00V	PL B490 71	G. Abbiendi *et al.*	(OPAL Collab.)
ABBIENDI,G	00	PL B493 249	G. Abbiendi *et al.*	(OPAL Collab.)
ABBOTT	00	PRL 84 222	B. Abbott *et al.*	(D0 Collab.)
ABBOTT	00B	PR D61 072001	B. Abbott *et al.*	(D0 Collab.)
ABBOTT	00D	PRL 84 5710	B. Abbott *et al.*	(D0 Collab.)
ABREU	00K	PL B479 89	P. Abreu *et al.*	(DELPHI Collab.)
ABREU,P	00F	EPJ C18 203	P. Abreu *et al.*	(DELPHI Collab.)
Also	02	EPJ C25 493 (erratum)	P. Abreu *et al.*	(DELPHI Collab.)
ACCIARRI	00N	PL B487 229	M. Acciarri *et al.*	(L3 Collab.)
ACCIARRI	00T	PL B490 187	M. Acciarri *et al.*	(L3 Collab.)
ACCIARRI	00V	PL B496 19	M. Acciarri *et al.*	(L3 Collab.)
ADLOFF	00B	EPJ C13 609	C. Adloff *et al.*	(H1 Collab.)
AFFOLDER	00M	PRL 85 3347	T. Affolder *et al.*	(CDF Collab.)
BARATE	00J	PL B484 205	R. Barate *et al.*	(ALEPH Collab.)
BARATE	00T	EPJ C17 241	R. Barate *et al.*	(ALEPH Collab.)
BREITWEG	00	PL B471 411	J. Breitweg *et al.*	(ZEUS Collab.)
BREITWEG	00D	EPJ C12 411	J. Breitweg *et al.*	(ZEUS Collab.)
EBOLI	00	MPL A15 1	O. Eboli, M. Gonzalez-Garcia, S. Novaes	
ABBIENDI	99C	PL B453 138	G. Abbiendi *et al.*	(OPAL Collab.)
ABBIENDI	99D	EPJ C8 191	G. Abbiendi *et al.*	(OPAL Collab.)
ABBIENDI	99N	PL B453 153	G. Abbiendi *et al.*	(OPAL Collab.)
ABBOTT	99H	PR D60 052003	B. Abbott *et al.*	(D0 Collab.)
ABBOTT	99I	PR D60 072002	B. Abbott *et al.*	(D0 Collab.)
ABREU	99K	PL B456 310	P. Abreu *et al.*	(DELPHI Collab.)
ABREU	99L	PL B459 382	P. Abreu *et al.*	(DELPHI Collab.)
ABREU	99T	PL B462 410	P. Abreu *et al.*	(DELPHI Collab.)
ACCIARRI	99	PL B454 386	M. Acciarri *et al.*	(L3 Collab.)
ACCIARRI	99Q	PL B467 171	M. Acciarri *et al.*	(L3 Collab.)
BARATE	99	PL B453 121	R. Barate *et al.*	(ALEPH Collab.)
BARATE	99I	PL B453 107	R. Barate *et al.*	(ALEPH Collab.)
BARATE	99L	PL B462 389	R. Barate *et al.*	(ALEPH Collab.)
BARATE	99M	PL B465 349	R. Barate *et al.*	(ALEPH Collab.)
ABBOTT	98N	PR D58 092003	B. Abbott *et al.*	(D0 Collab.)
ABBOTT	98P	PR D58 012002	B. Abbott *et al.*	(D0 Collab.)
ABE	98H	PR D58 031101	F. Abe *et al.*	(CDF Collab.)

ABE	98P	PR D58 091101	F. Abe *et al.*	(CDF Collab.)
ABREU	98C	PL B416 233	P. Abreu *et al.*	(DELPHI Collab.)
ABREU	98N	PL B439 209	P. Abreu *et al.*	(DELPHI Collab.)
ACCIARRI	98P	PL B436 437	M. Acciarri *et al.*	(L3 Collab.)
BARATE	98Y	PL B422 369	R. Barate *et al.*	(ALEPH Collab.)
BARATE,R	98	PL B445 239	R. Barate *et al.*	(ALEPH Collab.)
ACCIARRI	97	PL B398 223	M. Acciarri *et al.*	(L3 Collab.)
ACCIARRI	97M	PL B407 419	M. Acciarri *et al.*	(L3 Collab.)
ACCIARRI	97S	PL B413 176	M. Acciarri *et al.*	(L3 Collab.)
ABACHI	95D	PRL 75 1456	S. Abachi *et al.*	(D0 Collab.)
ABE	95C	PRL 74 341	F. Abe *et al.*	(CDF Collab.)
ABE	95G	PRL 74 1936	F. Abe *et al.*	(CDF Collab.)
ABE	95P	PRL 75 11	F. Abe *et al.*	(CDF Collab.)
Also	95Q	PR D52 4784	F. Abe *et al.*	(CDF Collab.)
ABE	95W	PR D52 2624	F. Abe *et al.*	(CDF Collab.)
Also	94B	PRL 73 220	F. Abe *et al.*	(CDF Collab.)
ABE	92E	PRL 68 3398	F. Abe *et al.*	(CDF Collab.)
ABE	92I	PRL 69 28	F. Abe *et al.*	(CDF Collab.)
ALITTI	92	PL B276 365	J. Alitti *et al.*	(UA2 Collab.)
ALITTI	92B	PL B276 354	J. Alitti *et al.*	(UA2 Collab.)
ALITTI	92C	PL B277 194	J. Alitti *et al.*	(UA2 Collab.)
ALITTI	92D	PL B277 203	J. Alitti *et al.*	(UA2 Collab.)
ALITTI	92F	PL B280 137	J. Alitti *et al.*	(UA2 Collab.)
SAMUEL	92	PL B280 124	M.A. Samuel *et al.*	(OKSU, CARL)
ABE	91C	PR D44 29	F. Abe *et al.*	(CDF Collab.)
ALBAJAR	91	PL B253 503	C. Albajar *et al.*	(UA1 Collab.)
ALITTI	91C	ZPHY C52 209	J. Alitti *et al.*	(UA2 Collab.)
SAMUEL	91	PRL 67 9	M.A. Samuel *et al.*	(OKSU, CARL)
Also	91C	PRL 67 2920 erratum	M.A. Samuel *et al.*	
ABE	90	PRL 64 152	F. Abe *et al.*	(CDF Collab.)
Also	91C	PR D44 29	F. Abe *et al.*	(CDF Collab.)
ABE	90G	PRL 65 2243	F. Abe *et al.*	(CDF Collab.)
Also	91B	PR D43 2070	F. Abe *et al.*	(CDF Collab.)
ALBAJAR	90	PL B241 283	C. Albajar *et al.*	(UA1 Collab.)
ALITTI	90B	PL B241 150	J. Alitti *et al.*	(UA2 Collab.)
ALITTI	90C	ZPHY C47 11	J. Alitti *et al.*	(UA2 Collab.)
ABE	89I	PRL 62 1005	F. Abe *et al.*	(CDF Collab.)
ALBAJAR	89	ZPHY C44 15	C. Albajar *et al.*	(UA1 Collab.)
BAUR	88	NP B308 127	U. Baur, D. Zeppenfeld	(FSU, WISC)
GRIFOLS	88	IJMP A3 225	J.A. Grifols, S. Peris, J. Sola	(BARC, DESY)
Also	87	PL B197 437	J.A. Grifols, S. Peris, J. Sola	(BARC, DESY)
ALBAJAR	87	PL B185 233	C. Albajar *et al.*	(UA1 Collab.)
ANSARI	87	PL B186 440	R. Ansari *et al.*	(UA2 Collab.)
ANSARI	87C	PL B194 158	R. Ansari *et al.*	(UA2 Collab.)
GROTCH	87	PR D36 2153	H. Grotch, R.W. Robinett	(PSU)
HAGIWARA	87	NP B282 253	K. Hagiwara *et al.*	(KEK, UCLA, FSU)
VANDERBIJ	87	PR D35 1088	J.J. van der Bij	(FNAL)
APPEL	86	ZPHY C30 1	J.A. Appel *et al.*	(UA2 Collab.)
ARNISON	86	PL 166B 484	G.T.J. Arnison *et al.*	(UA1 Collab.) J
ALTARELLI	85B	ZPHY C27 617	G. Altarelli, R.K. Ellis, G. Martinelli	(CERN+)
GRAU	85	PL 154B 283	A. Grau, J.A. Grifols	(BARC)
SUZUKI	85	PL 153B 289	M. Suzuki	(LBL)
ARNISON	84D	PL 134B 469	G.T.J. Arnison *et al.*	(UA1 Collab.)
HERZOG	84	PL 148B 355	F. Herzog	(WISC)
Also	84B	PL 155B 468 erratum	F. Herzog	(WISC)
ARNISON	83	PL 122B 103	G.T.J. Arnison *et al.*	(UA1 Collab.)
BANNER	83B	PL 122B 476	M. Banner *et al.*	(UA2 Collab.)

Z $J = 1$

THE Z BOSON

Revised November 2003 by C. Caso (University of Genova) and A. Gurtu (Tata Institute).

Precision measurements at the Z-boson resonance using electron–positron colliding beams began in 1989 at the SLC and at LEP. During 1989–95, the four CERN experiments made high-statistics studies of the Z. The availability of longitudinally polarized electron beams at the SLC since 1993 enabled a precision determination of the effective electroweak mixing angle $\sin^2\overline{\theta}_W$ that is competitive with the CERN results on this parameter.

The Z-boson properties reported in this section may broadly be categorized as:

- The standard 'lineshape' parameters of the Z consisting of its mass, M_Z, its total width, Γ_Z, and its partial decay widths, Γ(hadrons), and $\Gamma(\ell\overline{\ell})$ where $\ell = e, \mu, \tau, \nu$;
- Z asymmetries in leptonic decays and extraction of Z couplings to charged and neutral leptons;
- The b- and c-quark-related partial widths and charge asymmetries which require special techniques;
- Determination of Z decay modes and the search for modes that violate known conservation laws;
- Average particle multiplicities in hadronic Z decay;
- Z anomalous couplings.

Details on Z-parameter determination and the study of $Z \to b\overline{b}, c\overline{c}$ at LEP and SLC are given in this note.

The standard 'lineshape' parameters of the Z are determined from an analysis of the production cross sections of these final states in e^+e^- collisions. The $Z \to \nu\overline{\nu}(\gamma)$ state is identified directly by detecting single photon production and indirectly by subtracting the visible partial widths from the total width. Inclusion in this analysis of the forward-backward asymmetry of charged leptons, $A_{FB}^{(0,\ell)}$, of the τ polarization, $P(\tau)$, and its forward-backward asymmetry, $P(\tau)^{fb}$, enables the separate determination of the effective vector ($\overline{g}_V$) and axial vector ($\overline{g}_A$) couplings of the Z to these leptons and the ratio ($\overline{g}_V/\overline{g}_A$) which is related to the effective electroweak mixing angle $\sin^2\overline{\theta}_W$ (see the "Electroweak Model and Constraints on New Physics" Review).

Determination of the b- and c-quark-related partial widths and charge asymmetries involves tagging the b and c quarks. Traditionally this was done by requiring the presence of a prompt lepton in the event with high momentum and high transverse momentum (with respect to the accompanying jet). Precision vertex measurement with high-resolution detectors enabled one to do impact parameter and lifetime tagging. Neural-network techniques have also been used to classify events as b or non-b on a statistical basis using event–shape variables. Finally, the presence of a charmed meson (D/D^*) has been used to tag heavy quarks.

Z-parameter determination

LEP was run at energy points on and around the Z mass (88–94 GeV) constituting an energy 'scan.' The shape of the cross-section variation around the Z peak can be described by a Breit-Wigner *ansatz* with an energy-dependent total width [1–3]. The **three** main properties of this distribution, viz., the **position** of the peak, the **width** of the distribution, and the **height** of the peak, determine respectively the values of M_Z, Γ_Z, and $\Gamma(e^+e^-) \times \Gamma(f\overline{f})$, where $\Gamma(e^+e^-)$ and $\Gamma(f\overline{f})$ are the electron and fermion partial widths of the Z. The quantitative determination of these parameters is done by writing analytic expressions for these cross sections in terms of the parameters and fitting the calculated cross sections to the measured ones by varying these parameters, taking properly into account all the errors. Single-photon exchange (σ_γ^0) and γ-Z interference ($\sigma_{\gamma Z}^0$) are included, and the large ($\sim$25 %) initial-state radiation (ISR) effects are taken into account by convoluting the analytic expressions over a 'Radiator Function' [1–5] $H(s, s')$. Thus for the process $e^+e^- \to f\overline{f}$:

$$\sigma_f(s) = \int H(s, s')\ \sigma_f^0(s')\ ds' \tag{1}$$

$$\sigma_f^0(s) = \sigma_Z^0 + \sigma_\gamma^0 + \sigma_{\gamma Z}^0 \tag{2}$$

$$\sigma_Z^0 = \frac{12\pi}{M_Z^2}\ \frac{\Gamma(e^+e^-)\Gamma(f\overline{f})}{\Gamma_Z^2}\ \frac{s\ \Gamma_Z^2}{(s - M_Z^2)^2\ +\ s^2\Gamma_Z^2/M_Z^2} \tag{3}$$

$$\sigma_\gamma^0 = \frac{4\pi\alpha^2(s)}{3s}\ Q_f^2 N_c^f \tag{4}$$

$$\sigma^0_{\gamma Z} = -\frac{2\sqrt{2}\alpha(s)}{3}\ (Q_f G_F N_c^f \mathcal{G}_V^e \mathcal{G}_V^f) \times \frac{(s-M_Z^2)M_Z^2}{(s-M_Z^2)^2 + s^2\Gamma_Z^2/M_Z^2} \quad (5)$$

where Q_f is the charge of the fermion, $N_c^f = 3(1)$ for quark (lepton) and $\mathcal{G}_V^f$ is the neutral vector coupling of the Z to the fermion-antifermion pair $f\overline{f}$.

Since $\sigma^0_{\gamma Z}$ is expected to be much less than σ^0_Z, the LEP Collaborations have generally calculated the interference term in the framework of the Standard Model. This fixing of $\sigma^0_{\gamma Z}$ leads to a tighter constraint on M_Z and consequently a smaller error on its fitted value.

In the above framework, the QED radiative corrections have been explicitly taken into account by convoluting over the ISR and allowing the electromagnetic coupling constant to run [9]: $\alpha(s) = \alpha/(1-\Delta\alpha)$. On the other hand, weak radiative corrections that depend upon the assumptions of the electroweak theory and on the values of $M_{\rm top}$ and $M_{\rm Higgs}$ are accounted for by **absorbing them into the couplings**, which are then called the *effective* couplings $\mathcal{G}_V$ and $\mathcal{G}_A$ (or alternatively the effective parameters of the $\star$ scheme of Kennedy and Lynn [10]).

$\mathcal{G}_V^f$ and $\mathcal{G}_A^f$ are complex numbers with a small imaginary part. As experimental data does not allow simultaneous extraction of both real and imaginary parts of the effective couplings, the convention $g_A^f = {\rm Re}(\mathcal{G}_A^f)$ and $g_V^f = {\rm Re}(\mathcal{G}_V^f)$ is used and the imaginary parts are added in the fitting code [4].

Defining

$$A_f = 2\frac{g_V^f \cdot g_A^f}{(g_V^f)^2 + (g_A^f)^2} \quad (6)$$

the lowest-order expressions for the various lepton-related asymmetries on the Z pole are [6–8] $A_{FB}^{(0,\ell)} = (3/4)A_e A_f$, $P(\tau) = -A_\tau$, $P(\tau)^{fb} = -(3/4)A_e$, $A_{LR} = A_e$. The full analysis takes into account the energy dependence of the asymmetries. Experimentally A_{LR} is defined as $(\sigma_L - \sigma_R)/(\sigma_L + \sigma_R)$ where $\sigma_{L(R)}$ are the $e^+e^- \to Z$ production cross sections with left-(right)-handed electrons.

The definition of the partial decay width of the Z to $f\overline{f}$ includes the effects of QED and QCD final state corrections as well as the contribution due to the imaginary parts of the couplings:

$$\Gamma(f\overline{f}) = \frac{G_F M_Z^3}{6\sqrt{2}\pi}\ N_c^f\left(\left|\mathcal{G}_A^f\right|^2 R_A^f + \left|\mathcal{G}_V^f\right|^2 R_V^f\right) + \Delta_{ew/{\rm QCD}} \quad (7)$$

where R_V^f and R_A^f are radiator factors to account for final state QED and QCD corrections as well as effects due to nonzero fermion masses, and $\Delta_{ew/{\rm QCD}}$ represents the non-factorizable electroweak/QCD corrections.

S-matrix approach to the Z

While practically all experimental analyses of LEP/SLC data have followed the 'Breit-Wigner' approach described above, an alternative S-matrix-based analysis is also possible. The Z, like all unstable particles, is associated with a complex pole in the S matrix. The pole position is process independent and gauge invariant. The mass, $\overline{M}_Z$, and width, $\overline{\Gamma}_Z$, can be defined in terms of the pole in the energy plane via [11–14]

$$\overline{s} = \overline{M}_Z^2 - i\overline{M}_Z\overline{\Gamma}_Z \quad (8)$$

leading to the relations

$$\overline{M}_Z = M_Z/\sqrt{1+\Gamma_Z^2/M_Z^2} \approx M_Z\ -34.1\ {\rm MeV} \quad (9)$$

$$\overline{\Gamma}_Z = \Gamma_Z/\sqrt{1+\Gamma_Z^2/M_Z^2} \approx \Gamma_Z\ -0.9\ {\rm MeV}\ . \quad (10)$$

Some authors [15] choose to define the Z mass and width via

$$\overline{s} = (\overline{M}_Z - \frac{i}{2}\overline{\Gamma}_Z)^2 \quad (11)$$

which yields $\overline{M}_Z \approx M_Z - 26$ MeV, $\overline{\Gamma}_Z \approx \Gamma_Z - 1.2$ MeV.

The L3 and OPAL Collaborations at LEP (ACCIARRI 00Q and ACKERSTAFF 97C) have analyzed their data using the S–matrix approach as defined in Eq. (8), in addition to the conventional one. They observe a downward shift in the Z mass as expected.

Handling the large-angle e^+e^- final state

Unlike other $f\overline{f}$ decay final states of the Z, the e^+e^- final state has a contribution not only from the s-channel but also from the t-channel and s-t interference. The full amplitude is not amenable to fast calculation, which is essential if one has to carry out minimization fits within reasonable computer time. The usual procedure is to calculate the non-s channel part of the cross section separately using the Standard Model programs ALIBABA [16] or TOPAZ0 [17] with the measured value of $M_{\rm top}$, and $M_{\rm Higgs} = 150$ GeV and add it to the s-channel cross section calculated as for other channels. This leads to two additional sources of error in the analysis: firstly, the theoretical calculation in ALIBABA itself is known to be accurate to $\sim 0.5\%$, and secondly, there is uncertainty due to the error on $M_{\rm top}$ and the unknown value of $M_{\rm Higgs}$ (100–1000 GeV). These errors are propagated into the analysis by including them in the systematic error on the e^+e^- final state. As these errors are common to the four LEP experiments, this is taken into account when performing the LEP average.

Errors due to uncertainty in LEP energy determination [18–23]

The systematic errors related to the LEP energy measurement can be classified as:

- The absolute energy scale error;
- Energy-point-to-energy-point errors due to the non-linear response of the magnets to the exciting currents;
- Energy-point-to-energy-point errors due to possible higher-order effects in the relationship between the dipole field and beam energy;
- Energy reproducibility errors due to various unknown uncertainties in temperatures, tidal effects, corrector settings, RF status, *etc.*

Precise energy calibration was done outside normal data taking using the resonant depolarization technique. Run-time energies were determined every 10 minutes by measuring the relevant machine parameters and using a model which takes into account all the known effects, including leakage currents produced by trains in the Geneva area and the tidal effects due to gravitational forces of the Sun and the Moon. The LEP Energy Working Group has provided a covariance matrix from the determination of LEP energies for the different running periods during 1993–1995 [18].

Choice of fit parameters

The LEP Collaborations have chosen the following primary set of parameters for fitting: M_Z, Γ_Z, $\sigma^0_{\rm hadron}$, R(lepton), $A^{(0,\ell)}_{FB}$, where R(lepton) = Γ(hadrons)/Γ(lepton), $\sigma^0_{\rm hadron} = 12\pi\Gamma(e^+e^-)\Gamma({\rm hadrons})/M_Z^2\Gamma_Z^2$. With a knowledge of these fitted parameters and their covariance matrix, any other parameter can be derived. The main advantage of these parameters is that they form the **least correlated** set of parameters, so that it becomes easy to combine results from the different LEP experiments.

Thus, the most general fit carried out to cross section and asymmetry data determines the **nine parameters**: M_Z, Γ_Z, $\sigma^0_{\rm hadron}$, $R(e)$, $R(\mu)$, $R(\tau)$, $A^{(0,e)}_{FB}$, $A^{(0,\mu)}_{FB}$, $A^{(0,\tau)}_{FB}$. Assumption of lepton universality leads to a **five-parameter fit** determining M_Z, Γ_Z, $\sigma^0_{\rm hadron}$, R(lepton), $A^{(0,\ell)}_{FB}$.

Combining results from LEP and SLC experiments

With steady increase in statistics over the years and improved understanding of the common systematic errors between LEP experiments, the procedures for combining results have evolved continuously [24]. The Line Shape Sub-group of the LEP Electroweak Working Group investigated the effects of these common errors and devised a combination procedure for the precise determination of the Z parameters from LEP experiments [25]. Using these procedures this note also gives the results after combining the final parameter sets from the four experiments and these are the results quoted as the fit results in the Z listings below. Transformation of variables leads to values of derived parameters like partial decay widths and branching ratios to hadrons and leptons. Finally, transforming the LEP combined nine parameter set to (M_Z, Γ_Z, $\sigma^\circ_{\rm hadron}$, g^f_A, g^f_V, $f = e, \mu, \tau$) using the average values of lepton asymmetry parameters (A_e, A_μ, A_τ) as constraints, leads to the best fitted values of the vector and axial-vector couplings (g_V, g_A) of the charged leptons to the Z.

Brief remarks on the handling of common errors and their magnitudes are given below. The identified common errors are those coming from

(a) LEP energy calibration uncertainties, and

(b) the theoretical uncertainties in (i) the luminosity determination using small angle Bhabha scattering, (ii) estimating the non-s channel contribution to large angle Bhabha scattering, (iii) the calculation of QED radiative effects, and (iv) the parametrization of the cross section in terms of the parameter set used.

Common LEP energy errors

All the collaborations incorporate in their fit the full LEP energy error matrix as provided by the LEP energy group for their intersection region [18]. The effect of these errors is separated out from that of other errors by carrying out fits with energy errors scaled up and down by $\sim 10\%$ and redoing the fits. From the observed changes in the overall error matrix the covariance matrix of the common energy errors is determined. Common LEP energy errors lead to uncertainties on M_Z, Γ_Z, and $\sigma^\circ_{\rm hadron}$ of 1.7, 1.2 MeV, and 0.011 nb respectively.

Common luminosity errors

BHLUMI 4.04 [26] is used by all LEP collaborations for small angle Bhabha scattering leading to a common uncertainty in their measured cross sections of 0.061% [27]. BHLUMI does not include a correction for production of light fermion pairs. OPAL explicitly correct for this effect and reduce their luminosity uncertainty to 0.054% which is taken fully correlated with the other experiments. The other three experiments among themselves have a common uncertainty of 0.061%.

Common non-s channel uncertainties

The same standard model programs ALIBABA [16] and TOPAZ0 [17] are used to calculate the non-s channel contribution to the large angle Bhabha scattering [28]. As this contribution is a function of the Z mass, which itself is a variable in the fit, it is parametrized as a function of M_Z by each collaboration to properly track this contribution as M_Z varies in the fit. The common errors on R_e and $A^{0,e}_{FB}$ are 0.024 and 0.0014 respectively and are correlated between them.

Common theoretical uncertainties: QED

There are large initial state photon and fermion pair radiation effects near the Z resonance for which the best currently available evaluations include contributions up to $\mathcal{O}(\alpha^3)$. To estimate the remaining uncertainties different schemes are incorporated in the standard model programs ZFITTER [5], TOPAZ0 [17] and MIZA [29]. Comparing the different options leads to error estimates of 0.3 and 0.2 MeV on M_Z and Γ_Z respectively and of 0.02% on $\sigma^\circ_{\rm hadron}$.

Common theoretical uncertainties: parametrization of lineshape and asymmetries

To estimate uncertainties arising from ambiguities in the model-independent parametrization of the differential cross-section near the Z resonance, results from TOPAZ0 and ZFITTER were compared by using ZFITTER to fit the cross sections and asymmetries calculated using TOPAZ0. The resulting uncertainties on M_Z, Γ_Z, $\sigma^\circ_{\rm hadron}$, R(lepton) and $A^{0,\ell}_{FB}$ are 0.1 MeV, 0.1 MeV, 0.001 nb, 0.004, and 0.0001 respectively.

Thus the overall theoretical errors on M_Z, Γ_Z, $\sigma^\circ_{\rm hadron}$ are 0.3 MeV, 0.2 MeV, and 0.008 nb respectively; on each R(lepton) is 0.004 and on each $A^{0,\ell}_{FB}$ is 0.0001. Within the set of three

R(lepton)'s and the set of three $A_{FB}^{0,\ell}$'s the respective errors are fully correlated.

All the theory related errors mentioned above utilize standard model programs which need the Higgs mass and running electromagnetic coupling constant as inputs; uncertainties on these inputs will also lead to common errors. All LEP collaborations used the same set of inputs for standard model calculations: $M_Z = 91.187$ GeV, the Fermi constant $G_F = (1.16637 \pm 0.00001) \times 10^{-5}$ GeV^{-2} [30], $\alpha^{(5)}(M_Z) = 1/128.877 \pm 0.090$ [31], $\alpha_s(M_Z) = 0.119$ [32], $M_{\rm top} = 174.3 \pm 5.1$ GeV [32] and $M_{\rm Higgs} = 150$ GeV. The only observable effect, on M_Z, is due to the variation of $M_{\rm Higgs}$ between 100–1000 GeV (due to the variation of the γ/Z interference term which is taken from the standard model): M_Z changes by +0.23 MeV per unit change in $\log_{10} M_{\rm Higgs}/{\rm GeV}$, which is not an error but a correction to be applied once $M_{\rm Higgs}$ is determined. The effect is much smaller than the error on M_Z ($\pm$2.1 MeV).

Methodology of combining the LEP experimental results

The LEP experimental results actually used for combination are slightly modified from those published by the experiments (which are given in the Listings below). This has been done in order to facilitate the procedure by making the inputs more consistent. These modified results are given explicitly in [25]. The main differences compared to the published results are

(a) consistent use of ZFITTER 6.23 and TOPAZ0. The published ALEPH results used ZFITTER 6.10. (b) use of the combined energy error matrix which makes a difference of 0.1 MeV on the M_Z and Γ_Z for L3 only as at that intersection the RF modeling uncertainties are the largest.

Thus, nine-parameter sets from all four experiments with their covariance matrices are used together with all the common errors correlations. A grand covariance matrix, V, is constructed and a combined nine-parameter set is obtained by minimizing $\chi^2 = \Delta^T V^{-1} \Delta$, where Δ is the vector of residuals of the combined parameter set to the results of individual experiments.

Study of $Z \to b\overline{b}$ and $Z \to c\overline{c}$

In the sector of c- and b-physics the LEP experiments have measured the ratios of partial widths $R_b = \Gamma(Z \to b\overline{b})/\Gamma(Z \to$ hadrons) and $R_c = \Gamma(Z \to c\overline{c})/\Gamma(Z \to$ hadrons) and the forward-backward (charge) asymmetries $A_{FB}^{b\overline{b}}$ and $A_{FB}^{c\overline{c}}$. The final state coupling parameters A_b and A_c have been obtained from the left-right forward-backward asymmetry at SLD. Several of the analyses have also determined other quantities, in particular the semileptonic branching ratios, B($b \to \ell^-$), B($b \to c \to \ell^+$), and B($c \to \ell^+$), the average $B^0\overline{B}^0$ mixing parameter $\overline{\chi}$ and the probabilities for a c–quark to fragment into a D^+, a D_s, a D^{*+} , or a charmed baryon. The latter measurements do not concern properties of the Z boson and hence they do not appear in the listing below. However, for completeness, we will report at the end of this minireview their values as obtained fitting the data contained in the Z section. All these quantities are correlated with the electroweak parameters, and since the mixture of b hadrons is different from the one at the $\Upsilon(4S)$, their values might differ from those measured at the $\Upsilon(4S)$.

All the above quantities are correlated to each other since:

- Several analyses (for example the lepton fits) determine more than one parameter simultaneously;
- Some of the electroweak parameters depend explicitly on the values of other parameters (for example R_b depends on R_c);
- Common tagging and analysis techniques produce common systematic uncertainties.

The LEP Electroweak Heavy Flavour Working Group has developed [33] a procedure for combining the measurements taking into account known sources of correlation. The combining procedure determines twelve parameters: the four parameters of interest in the electroweak sector, R_b, R_c, $A_{FB}^{b\overline{b}}$, and $A_{FB}^{c\overline{c}}$ and, in addition, B($b \to \ell^-$), B($b \to c \to \ell^+$), B($c \to \ell^+$), $\overline{\chi}$, $f(D^+)$, $f(D_s)$, $f(c_{\rm baryon})$ and $P(c \to D^{*+}) \times$ B($D^{*+} \to \pi^+ D^0$), to take into account their correlations with the electroweak parameters. Before the fit both the peak and off-peak asymmetries are translated to the common energy $\sqrt{s} = 91.26$ GeV using the predicted energy dependence from ZFITTER [5].

Summary of the measurements and of the various kinds of analysis

The measurements of R_b and R_c fall into two classes. In the first, named single-tag measurement, a method for selecting b and c events is applied and the number of tagged events is counted. The second technique, named double-tag measurement, is based on the following principle: if the number of events with a single hemisphere tagged is N_t and with both hemispheres tagged is N_{tt}, then given a total number of $N_{\rm had}$ hadronic Z decays one has:

$$\frac{N_t}{2N_{\rm had}} = \varepsilon_b R_b + \varepsilon_c R_c + \varepsilon_{uds}(1 - R_b - R_c) \qquad (12)$$

$$\frac{N_{tt}}{N_{\rm had}} = \mathcal{C}_b \varepsilon_b^2 R_b + \mathcal{C}_c \varepsilon_c^2 R_c + \mathcal{C}_{uds} \varepsilon_{uds}^2 (1 - R_b - R_c) \qquad (13)$$

where ε_b, ε_c, and ε_{uds} are the tagging efficiencies per hemisphere for b, c, and light quark events, and $\mathcal{C}_q \neq 1$ accounts for the fact that the tagging efficiencies between the hemispheres may be correlated. In tagging the b one has $\varepsilon_b \gg \varepsilon_c \gg \varepsilon_{uds}$, $C_b \approx 1$. Neglecting the c and uds background and the hemisphere correlations, these equations give:

$$\varepsilon_b = 2N_{tt}/N_t \qquad (14)$$

$$R_b = N_t^2/(4N_{tt}N_{\rm had}) \ . \qquad (15)$$

The double-tagging method has thus the great advantage that the tagging efficiency is directly derived from the data, reducing the systematic error of the measurement. The backgrounds, dominated by $c\overline{c}$ events, obviously complicate this simple picture, and their level must still be inferred by other

means. The rate of charm background in these analyses depends explicitly on the value of R_c. The correlations in the tagging efficiencies between the hemispheres (due for instance to correlations in momentum between the b hadrons in the two hemispheres) are small but nevertheless lead to further systematic uncertainties.

The measurements in the b- and c-sector can be essentially grouped in the following categories:

- Lifetime (and lepton) double-tagging measurements of R_b. These are the most precise measurements of R_b and obviously dominate the combined result. The main sources of systematics come from the charm contamination and from estimating the hemisphere b-tagging efficiency correlation. The charm rejection has been improved (and hence the systematic errors reduced) by using either the information of the secondary vertex invariant mass or the information from the energy of all particles at the secondary vertex and their rapidity;
- Analyses with $D/D^{*\pm}$ to measure R_c. These measurements make use of several different tagging techniques (inclusive/exclusive double tag, exclusive double tag, reconstruction of all weakly decaying charmed states) and no assumptions are made on the energy dependence of charm fragmentation;
- Lepton fits which use hadronic events with one or more leptons in the final state to measure $A_{FB}^{b\overline{b}}$ and $A_{FB}^{c\overline{c}}$. Each analysis usually gives several other electroweak parameters. The dominant sources of systematics are due to lepton identification, to other semileptonic branching ratios and to the modeling of the semileptonic decay;
- Measurements of $A_{FB}^{b\overline{b}}$ using lifetime tagged events with a hemisphere charge measurement. Their contribution to the combined result has roughly the same weight as the lepton fits;
- Analyses with $D/D^{*\pm}$ to measure $A_{FB}^{c\overline{c}}$ or simultaneously $A_{FB}^{b\overline{b}}$ and $A_{FB}^{c\overline{c}}$;
- Measurements of A_b and A_c from SLD, using several tagging methods (lepton, kaon, D/D^*, and vertex mass). These quantities are directly extracted from a measurement of the left–right forward–backward asymmetry in $c\overline{c}$ and $b\overline{b}$ production using a polarized electron beam.

Averaging procedure

All the measurements are provided by the LEP Collaborations in the form of tables with a detailed breakdown of the systematic errors of each measurement and its dependence on other electroweak parameters.

The averaging proceeds via the following steps:

- Define and propagate a consistent set of external inputs such as branching ratios, hadron lifetimes, fragmentation models *etc.* All the measurements are also consistently checked to ensure that all use a common set of assumptions (for instance since the QCD corrections for the forward–backward asymmetries are strongly dependent on the experimental conditions, the data are corrected before combining);
- Form the full (statistical and systematic) covariance matrix of the measurements. The systematic correlations between different analyses are calculated from the detailed error breakdown in the measurement tables. The correlations relating several measurements made by the same analysis are also used;
- Take into account any explicit dependence of a measurement on the other electroweak parameters. As an example of this dependence we illustrate the case of the double-tag measurement of R_b, where c-quarks constitute the main background. The normalization of the charm contribution is not usually fixed by the data and the measurement of R_b depends on the assumed value of R_c, which can be written as:

$$R_b = R_b^{\rm meas} + a(R_c)\frac{(R_c - R_c^{\rm used})}{R_c}\ , \qquad (16)$$

  where $R_b^{\rm meas}$ is the result of the analysis which assumed a value of $R_c = R_c^{\rm used}$ and $a(R_c)$ is the constant which gives the dependence on R_c;
- Perform a χ^2 minimization with respect to the combined electroweak parameters.

After the fit the average peak asymmetries $A_{FB}^{c\overline{c}}$ and $A_{FB}^{b\overline{b}}$ are corrected for the energy shift from 91.26 GeV to M_Z and for QED (initial state radiation), γ exchange, and γZ interference effects to obtain the corresponding pole asymmetries $A_{FB}^{0,c}$ and $A_{FB}^{0,b}$.

This averaging procedure, using the fourteen parameters described above and applied to the data contained in the Z particle listing below, gives the following results:

$$\begin{aligned}
R_b^0 &= 0.21643 \pm 0.00072 \\
R_c^0 &= 0.1689 \pm 0.0047 \\
A_{FB}^{0,b} &= 0.1001 \pm 0.0017 \\
A_{FB}^{0,c} &= 0.0704 \pm 0.0036 \\
A_b &= 0.926 \pm 0.024 \\
A_c &= 0.666 \pm 0.036 \\
B(b \to \ell^-) &= 0.1069 \pm 0.0021 \\
\mathrm{B}(b \to c \to \ell^+) &= 0.0801 \pm 0.0018
\end{aligned}$$

$B(c \to \ell^+) = 0.0980 \pm 0.0033$

$\overline{\chi} = 0.1251 \pm 0.0040$

$f(D^+) = 0.237 \pm 0.016$

$f(D_s) = 0.119 \pm 0.025$

$f(c_{\rm baryon}) = 0.090 \pm 0.022$

$P(c \to D^{*+}) \times {\rm B}(D^{*+} \to \pi^+ D^0) = 0.1648 \pm 0.0056$

References

1. R.N. Cahn, Phys. Rev. **D36**, 2666 (1987).
2. F.A. Berends *et al.*, "*Z* Physics at LEP 1", CERN Report 89-08 (1989), Vol. 1, eds. G. Altarelli, R. Kleiss, and C. Verzegnassi, p. 89.
3. A. Borrelli *et al.*, Nucl. Phys. **B333**, 357 (1990).
4. D. Bardin and G. Passarino, "Upgrading of Precision Calculations for Electroweak Observables," hep-ph/9803425; D. Bardin, G. Passarino, and M. Grünewald, "Precision Calculation Project Report," hep-ph/9902452.
5. D. Bardin *et al.*, Z. Phys. **C44**, 493 (1989); Comp. Phys. Comm. **59**, 303 (1990); D. Bardin *et al.*, Nucl. Phys. **B351**, 1 (1991); Phys. Lett. **B255**, 290 (1991) and CERN-TH/6443/92 (1992); Comp. Phys. Comm. **133**, 229 (2001).
6. M. Consoli *et al.*, "*Z* Physics at LEP 1", CERN Report 89-08 (1989), Vol. 1, eds. G. Altarelli, R. Kleiss, and C. Verzegnassi, p. 7.
7. M. Bohm *et al.*, *ibid*, p. 203.
8. S. Jadach *et al.*, *ibid*, p. 235.
9. G. Burgers *et al.*, *ibid*, p. 55.
10. D.C. Kennedy and B.W. Lynn, SLAC-PUB 4039 (1986, revised 1988).
11. R. Stuart, Phys. Lett. **B262**, 113 (1991).
12. A. Sirlin, Phys. Rev. Lett. **67**, 2127 (1991).
13. A. Leike, T. Riemann, and J. Rose, Phys. Lett. **B273**, 513 (1991).
14. See also D. Bardin *et al.*, Phys. Lett. **B206**, 539 (1988).
15. S. Willenbrock and G. Valencia, Phys. Lett. **B259**, 373 (1991).
16. W. Beenakker, F.A. Berends, and S.C. van der Marck, Nucl. Phys. **B349**, 323 (1991).
17. G. Montagna *et al.*, Nucl. Phys. **B401**, 3 (1993); Comp. Phys. Comm. **76**, 328 (1993); Comp. Phys. Comm. **93**, 120 (1996); G. Montagna *et al.*, Comp. Phys. Comm. **117**, 278 (1999).
18. R. Assmann *et al.* (Working Group on LEP Energy), Eur. Phys. J. **C6**, 187 (1999).
19. R. Assmann *et al.* (Working Group on LEP Energy), Z. Phys. **C66**, 567 (1995).
20. L. Arnaudon *et al.* (Working Group on LEP Energy and LEP Collaborations), Phys. Lett. **B307**, 187 (1993).
21. L. Arnaudon *et al.* (Working Group on LEP Energy), CERN-PPE/92-125 (1992).
22. L. Arnaudon *et al.*, Phys. Lett. **B284**, 431 (1992).
23. R. Bailey *et al.*, 'LEP Energy Calibration' CERN-SL-90-95-AP, Proceedings of the "2^{nd} European Particle Accelerator Conference," Nice, France, 12–16 June 1990, pp. 1765-1767.
24. The LEP Collaborations: ALEPH, DELPHI, L3, OPAL, the LEP Electroweak Working Group, and the SLD Heavy Flavour Group: CERN-EP/2002-091 (2002); CERN-EP/2001-098 (2001); CERN-EP/2001-021 (2001); CERN-EP/2000-016 (1999); CERN-EP/99-15 (1998); CERN-PPE/97-154 (1997); CERN-PPE/96-183 (1996); CERN-PPE/95-172 (1995); CERN-PPE/94-187 (1994); CERN-PPE/93-157 (1993).
25. The LEP Collaborations ALEPH, DELPHI, L3, OPAL, and the Line Shape Sub-group of the LEP Electroweak Working Group: CERN-EP/2000-153, hep-ex/0101027 (to be published as part of a review in Physics Reports).
26. S. Jadach *et al.*, BHLUMI 4.04, Comp. Phys. Comm. **102**, 229 (1997); S. Jadach and O. Nicrosini, Event generators for Bhabha scattering, in Physics at LEP2, CERN-96-01 Vol. 2, February 1996.
27. B.F.L. Ward *et al.*, Phys. Lett. **B450**, 262 (1999).
28. W. Beenakker and G. Passarino, Phys. Lett. **B425**, 199 (1998).
29. L. Garrido *et al.*, Z. Phys. **C49**, 645 (1991); M. Martinez and F. Teubert, Z. Phys. **C65**, 267 (1995), updated with results summarized in S. Jadach, B. Pietrzyk and M. Skrzypek, Phys. Lett. **B456**, 77 (1999) and Reports of the working group on precision calculations for the *Z* resonance, CERN 95-03, ed. D. Bardin, W. Hollik, and G. Passarino, and references therein.
30. T. van Ritbergen, R. Stuart, Phys. Lett. **B437**, 201 (1998); Phys. Rev. Lett. **81**, 488 (1999).
31. S. Eidelman and F. Jegerlehner, Z. Phys. **C67**, 585 (1995); M. Steinhauser, Phys. Lett. **B249**, 158 (1998).
32. Particle Data Group (D.E. Groom *et al.*), Eur. Phys. J. **C15**, 1 (2000).
33. The LEP Experiments: ALEPH, DELPHI, L3, and OPAL Nucl. Instrum. Methods **A378**, 101 (1996).

Z MASS

OUR FIT is obtained using the fit procedure and correlations as determined by the LEP Electroweak Working Group (see the "Note on the *Z* boson"). The fit is performed using the *Z* mass and width, the *Z* hadronic pole cross section, the ratios of hadronic to leptonic partial widths, and the *Z* pole forward-backward lepton asymmetries. This set is believed to be most free of correlations.

The *Z*-boson mass listed here corresponds to a Breit-Wigner resonance parameter. The value is 34 MeV greater than the real part of the position of the pole (in the energy-squared plane) in the *Z*-boson propagator. Also the LEP experiments have generally assumed a fixed value of the $\gamma - Z$ interferences term based on the standard model. Keeping this term as free parameter leads to a somewhat larger error on the fitted *Z* mass. See ACCIARRI 00Q and ACKERSTAFF 97C for a detailed investigation of both these issues.

VALUE (GeV)			*EVTS*	*DOCUMENT ID*		*TECN*	*COMMENT*
91.1876 ± 0.0021 OUR FIT							
91.1852	± 0.0030		4.57M	[1] ABBIENDI	01A	OPAL	$E_{\rm cm}^{ee}$= 88–94 GeV
91.1863	± 0.0028		4.08M	[2] ABREU	00F	DLPH	$E_{\rm cm}^{ee}$= 88–94 GeV
91.1898	± 0.0031		3.96M	[3] ACCIARRI	00C	L3	$E_{\rm cm}^{ee}$= 88–94 GeV
91.1885	± 0.0031		4.57M	[4] BARATE	00C	ALEP	$E_{\rm cm}^{ee}$= 88–94 GeV
• • • We do not use the following data for averages, fits, limits, etc. • • •							
91.1875	± 0.0039		3.97M	[5] ACCIARRI	00Q	L3	$E_{\rm cm}^{ee}$= LEP1 + 130–189 GeV
91.185	± 0.010			[6] ACKERSTAFF	97C	OPAL	$E_{\rm cm}^{ee}$= LEP1 + 130–136 GeV + 161 GeV
91.151	± 0.008			[7] MIYABAYASHI	95	TOPZ	$E_{\rm cm}^{ee}$= 57.8 GeV
91.187	± 0.007	± 0.006	1.16M	[8] ABREU	94	DLPH	Repl. by ABREU 00F
91.195	± 0.006	± 0.007	1.19M	[8] ACCIARRI	94	L3	Repl. by ACCIARRI 00C
91.182	± 0.007	± 0.006	1.33M	[8] AKERS	94	OPAL	Repl. by ABBIENDI 01A
91.187	± 0.007	± 0.006	1.27M	[8] BUSKULIC	94	ALEP	Repl. by BARATE 00C
91.74	± 0.28	± 0.93	156	[9] ALITTI	92B	UA2	$E_{\rm cm}^{p\overline{p}}$= 630 GeV
90.9	± 0.3	± 0.2	188	[10] ABE	89C	CDF	$E_{\rm cm}^{p\overline{p}}$= 1.8 TeV
91.14	± 0.12		480	[11] ABRAMS	89B	MRK2	$E_{\rm cm}^{ee}$= 89–93 GeV
93.1	± 1.0	± 3.0	24	[12] ALBAJAR	89	UA1	$E_{\rm cm}^{p\overline{p}}$= 546,630 GeV

[1] ABBIENDI 01A error includes approximately 2.3 MeV due to statistics and 1.8 MeV due to LEP energy uncertainty.
[2] The error includes 1.6 MeV due to LEP energy uncertainty.
[3] The error includes 1.8 MeV due to LEP energy uncertainty.
[4] BARATE 00C error includes approximately 2.4 MeV due to statistics, 0.2 MeV due to experimental systematics, and 1.7 MeV due to LEP energy uncertainty.
[5] ACCIARRI 00Q interpret the s-dependence of the cross sections and lepton forward-backward asymmetries in the framework of the S-matrix formalism. They fit to their cross section and asymmetry data at high energies, using the results of S-matrix fits to Z-peak data (ACCIARRI 00C) as constraints. The 130–189 GeV data constrains the γ/Z interference term. The authors have corrected the measurement for the 34.1 MeV shift with respect to the Breit-Wigner fits. The error contains a contribution of ± 2.3 MeV due to the uncertainty on the γZ interference.
[6] ACKERSTAFF 97C obtain this using the S-matrix formalism for a combined fit to their cross-section and asymmetry data at the Z peak (AKERS 94) and their data at 130, 136, and 161 GeV. The authors have corrected the measurement for the 34 MeV shift with respect to the Breit-Wigner fits.
[7] MIYABAYASHI 95 combine their low energy total hadronic cross-section measurement with the ACTON 93D data and perform a fit using an S-matrix formalism. As expected, this result is below the mass values obtained with the standard Breit-Wigner parametrization.
[8] The second error of 6.3 MeV is due to a common LEP energy uncertainty.
[9] Enters fit through W/Z mass ratio given in the W Particle Listings. The ALITTI 92B systematic error (± 0.93) has two contributions: one (± 0.92) cancels in m_W/m_Z and one (± 0.12) is noncancelling. These were added in quadrature.
[10] First error of ABE 89 is combination of statistical and systematic contributions; second is mass scale uncertainty.
[11] ABRAMS 89B uncertainty includes 35 MeV due to the absolute energy measurement.
[12] ALBAJAR 89 result is from a total sample of 33 $Z \to e^+e^-$ events.

Z WIDTH

OUR FIT is obtained using the fit procedure and correlations as determined by the LEP Electroweak Working Group (see the "Note on the Z boson").

VALUE (GeV)	*EVTS*	*DOCUMENT ID*		*TECN*	*COMMENT*
2.4952 ± 0.0023 OUR FIT					
2.4948 ± 0.0041	4.57M	[13] ABBIENDI	01A	OPAL	E_{cm}^{ee} = 88–94 GeV
2.4876 ± 0.0041	4.08M	[14] ABREU	00F	DLPH	E_{cm}^{ee} = 88–94 GeV
2.5024 ± 0.0042	3.96M	[15] ACCIARRI	00C	L3	E_{cm}^{ee} = 88–94 GeV
2.4951 ± 0.0043	4.57M	[16] BARATE	00C	ALEP	E_{cm}^{ee} = 88–94 GeV
• • • We do not use the following data for averages, fits, limits, etc. • • •					
2.5025 ± 0.0041	3.97M	[17] ACCIARRI	00Q	L3	E_{cm}^{ee} = LEP1 + 130–189 GeV
2.50 ± 0.21 ± 0.06		[18] ABREU	96R	DLPH	E_{cm}^{ee} = 91.2 GeV
2.483 ± 0.011 ± 0.0045	1.16M	[19] ABREU	94	DLPH	Repl. by ABREU 00F
2.494 ± 0.009 ± 0.0045	1.19M	[19] ACCIARRI	94	L3	Repl. by ACCIARRI 00C
2.483 ± 0.011 ± 0.0045	1.33M	[19] AKERS	94	OPAL	Repl. by ABBIENDI 01A
2.501 ± 0.011 ± 0.0045	1.27M	[19] BUSKULIC	94	ALEP	Repl. by BARATE 00C
3.8 ± 0.8 ± 1.0	188	ABE	89C	CDF	$E_{cm}^{p\overline{p}}$ = 1.8 TeV
$2.42\ ^{+0.45}_{-0.35}$	480	[20] ABRAMS	89B	MRK2	E_{cm}^{ee} = 89–93 GeV
$2.7\ ^{+1.2}_{-1.0} \pm 1.3$	24	[21] ALBAJAR	89	UA1	$E_{cm}^{p\overline{p}}$ = 546,630 GeV
2.7 ± 2.0 ± 1.0	25	[22] ANSARI	87	UA2	$E_{cm}^{p\overline{p}}$ = 546,630 GeV

[13] ABBIENDI 01A error includes approximately 3.6 MeV due to statistics, 1 MeV due to event selection systematics, and 1.3 MeV due to LEP energy uncertainty.
[14] The error includes 1.2 MeV due to LEP energy uncertainty.
[15] The error includes 1.3 MeV due to LEP energy uncertainty.
[16] BARATE 00C error includes approximately 3.8 MeV due to statistics, 0.9 MeV due to experimental systematics, and 1.3 MeV due to LEP energy uncertainty.
[17] ACCIARRI 00Q interpret the s-dependence of the cross sections and lepton forward-backward asymmetries in the framework of the S-matrix formalism. They fit to their cross section and asymmetry data at high energies, using the results of S-matrix fits to Z-peak data (ACCIARRI 00C) as constraints. The 130–189 GeV data constrains the γ/Z interference term. The authors have corrected the measurement for the 0.9 MeV shift with respect to the Breit-Wigner fits.
[18] ABREU 96R obtain this value from a study of the interference between initial and final state radiation in the process $e^+e^- \to Z \to \mu^+\mu^-$.
[19] The second error of 4.5 MeV is due to a common LEP energy uncertainty.
[20] ABRAMS 89B uncertainty includes 50 MeV due to the miniSAM background subtraction error.
[21] ALBAJAR 89 result is from a total sample of 33 $Z \to e^+e^-$ events.
[22] Quoted values of ANSARI 87 are from direct fit. Ratio of Z and W production gives either $\Gamma(Z) < (1.09 \pm 0.07) \times \Gamma(W)$, CL = 90% or $\Gamma(Z) = (0.82\ ^{+0.19}_{-0.14} \pm 0.06) \times \Gamma(W)$. Assuming Standard-Model value $\Gamma(W) = 2.65$ GeV then gives $\Gamma(Z) < 2.89 \pm 0.19$ or $= 2.17\ ^{+0.50}_{-0.37} \pm 0.16$.

Z DECAY MODES

	Mode		Fraction (Γ_i/Γ)		Scale factor/ Confidence level
Γ_1	e^+e^-		(3.363 ± 0.004) %		
Γ_2	$\mu^+\mu^-$		(3.366 ± 0.007) %		
Γ_3	$\tau^+\tau^-$		(3.370 ± 0.008) %		
Γ_4	$\ell^+\ell^-$	[a]	(3.3658 ± 0.0023) %		
Γ_5	invisible		(20.00 ± 0.06) %		
Γ_6	hadrons		(69.91 ± 0.06) %		
Γ_7	$(u\overline{u}+c\overline{c})/2$		(10.1 ± 1.1) %		
Γ_8	$(d\overline{d}+s\overline{s}+b\overline{b})/3$		(16.6 ± 0.6) %		
Γ_9	$c\overline{c}$		(11.81 ± 0.33) %		
Γ_{10}	$b\overline{b}$		(15.13 ± 0.05) %		
Γ_{11}	$b\overline{b}b\overline{b}$		(3.6 ± 1.3) $\times 10^{-4}$		
Γ_{12}	ggg		< 1.1	%	CL=95%
Γ_{13}	$\pi^0\gamma$		< 5.2	$\times 10^{-5}$	CL=95%
Γ_{14}	$\eta\gamma$		< 5.1	$\times 10^{-5}$	CL=95%
Γ_{15}	$\omega\gamma$		< 6.5	$\times 10^{-4}$	CL=95%
Γ_{16}	$\eta'(958)\gamma$		< 4.2	$\times 10^{-5}$	CL=95%
Γ_{17}	$\gamma\gamma$		< 5.2	$\times 10^{-5}$	CL=95%
Γ_{18}	$\gamma\gamma\gamma$		< 1.0	$\times 10^{-5}$	CL=95%
Γ_{19}	$\pi^\pm W^\mp$	[b]	< 7	$\times 10^{-5}$	CL=95%
Γ_{20}	$\rho^\pm W^\mp$	[b]	< 8.3	$\times 10^{-5}$	CL=95%
Γ_{21}	$J/\psi(1S)$X		(3.51 $^{+0.23}_{-0.25}$) $\times 10^{-3}$		S=1.1
Γ_{22}	$\psi(2S)$X		(1.60 ± 0.29) $\times 10^{-3}$		
Γ_{23}	$\chi_{c1}(1P)$X		(2.9 ± 0.7) $\times 10^{-3}$		
Γ_{24}	$\chi_{c2}(1P)$X		< 3.2	$\times 10^{-3}$	CL=90%
Γ_{25}	$\Upsilon(1S)$ X + $\Upsilon(2S)$ X + $\Upsilon(3S)$ X		(1.0 ± 0.5) $\times 10^{-4}$		
Γ_{26}	$\Upsilon(1S)$X		< 4.4	$\times 10^{-5}$	CL=95%
Γ_{27}	$\Upsilon(2S)$X		< 1.39	$\times 10^{-4}$	CL=95%
Γ_{28}	$\Upsilon(3S)$X		< 9.4	$\times 10^{-5}$	CL=95%
Γ_{29}	$(D^0/\overline{D}^0)$ X		(20.7 ± 2.0) %		
Γ_{30}	$D^\pm$X		(12.2 ± 1.7) %		
Γ_{31}	$D^*(2010)^\pm$X	[b]	(11.4 ± 1.3) %		
Γ_{32}	$D_{s1}(2536)^\pm$X		(3.6 ± 0.8) $\times 10^{-3}$		
Γ_{33}	$D_{sJ}(2573)^\pm$X		(5.8 ± 2.2) $\times 10^{-3}$		
Γ_{34}	$D^{*\prime}(2629)^\pm$X		searched for		
Γ_{35}	$B\overline{B}$X				
Γ_{36}	$B^*\overline{B}$X				
Γ_{37}	$B_s^0\overline{B}_s^0$X		seen		
Γ_{38}	B_c^+X		searched for		
Γ_{39}	anomalous γ + hadrons	[c]	< 3.2	$\times 10^{-3}$	CL=95%
Γ_{40}	$e^+e^-\gamma$	[c]	< 5.2	$\times 10^{-4}$	CL=95%
Γ_{41}	$\mu^+\mu^-\gamma$	[c]	< 5.6	$\times 10^{-4}$	CL=95%
Γ_{42}	$\tau^+\tau^-\gamma$	[c]	< 7.3	$\times 10^{-4}$	CL=95%
Γ_{43}	$\ell^+\ell^-\gamma\gamma$	[d]	< 6.8	$\times 10^{-6}$	CL=95%
Γ_{44}	$q\overline{q}\gamma\gamma$	[d]	< 5.5	$\times 10^{-6}$	CL=95%
Γ_{45}	$\nu\overline{\nu}\gamma\gamma$	[d]	< 3.1	$\times 10^{-6}$	CL=95%
Γ_{46}	$e^\pm\mu^\mp$	LF [b]	< 1.7	$\times 10^{-6}$	CL=95%
Γ_{47}	$e^\pm\tau^\mp$	LF [b]	< 9.8	$\times 10^{-6}$	CL=95%
Γ_{48}	$\mu^\pm\tau^\mp$	LF [b]	< 1.2	$\times 10^{-5}$	CL=95%
Γ_{49}	pe	L,B	< 1.8	$\times 10^{-6}$	CL=95%
Γ_{50}	$p\mu$	L,B	< 1.8	$\times 10^{-6}$	CL=95%

[a] ℓ indicates each type of lepton (e, μ, and τ), not sum over them.
[b] The value is for the sum of the charge states or particle/antiparticle states indicated.
[c] See the Particle Listings below for the γ energy range used in this measurement.
[d] For $m_{\gamma\gamma} = (60 \pm 5)$ GeV.

Z PARTIAL WIDTHS

$\Gamma(e^+e^-)$ Γ_1

For the LEP experiments, this parameter is not directly used in the overall fit but is derived using the fit results; see the 'Note on the Z Boson.'

VALUE (MeV)	*EVTS*	*DOCUMENT ID*		*TECN*	*COMMENT*
83.91 ± 0.12 OUR FIT					
83.66 ± 0.20	137.0K	ABBIENDI	01A	OPAL	E_{cm}^{ee} = 88–94 GeV
83.54 ± 0.27	117.8k	ABREU	00F	DLPH	E_{cm}^{ee} = 88–94 GeV
84.16 ± 0.22	124.4k	ACCIARRI	00C	L3	E_{cm}^{ee} = 88–94 GeV
83.88 ± 0.19		BARATE	00C	ALEP	E_{cm}^{ee} = 88–94 GeV
82.89 ± 1.20 ± 0.89		[23] ABE	95J	SLD	E_{cm}^{ee} = 91.31 GeV

[23] ABE 95J obtain this measurement from Bhabha events in a restricted fiducial region to improve systematics. They use the values 91.187 and 2.489 GeV for the Z mass and total decay width to extract this partial width.

$\Gamma(\mu^+\mu^-)$ Γ_2

This parameter is not directly used in the overall fit but is derived using the fit results; see the 'Note on the Z Boson.'

VALUE (MeV)	EVTS	DOCUMENT ID		TECN	COMMENT
83.99±0.18 OUR FIT					
84.03±0.30	182.8K	ABBIENDI	01A	OPAL	E_{cm}^{ee}= 88–94 GeV
84.48±0.40	157.6k	ABREU	00F	DLPH	E_{cm}^{ee}= 88–94 GeV
83.95±0.44	113.4k	ACCIARRI	00C	L3	E_{cm}^{ee}= 88–94 GeV
84.02±0.28		BARATE	00C	ALEP	E_{cm}^{ee}= 88–94 GeV

$\Gamma(\tau^+\tau^-)$ Γ_3

This parameter is not directly used in the overall fit but is derived using the fit results; see the 'Note on the Z Boson.'

VALUE (MeV)	EVTS	DOCUMENT ID		TECN	COMMENT
84.08±0.22 OUR FIT					
83.94±0.41	151.5K	ABBIENDI	01A	OPAL	E_{cm}^{ee}= 88–94 GeV
83.71±0.58	104.0k	ABREU	00F	DLPH	E_{cm}^{ee}= 88–94 GeV
84.23±0.58	103.0k	ACCIARRI	00C	L3	E_{cm}^{ee}= 88–94 GeV
84.38±0.31		BARATE	00C	ALEP	E_{cm}^{ee}= 88–94 GeV

$\Gamma(\ell^+\ell^-)$ Γ_4

In our fit $\Gamma(\ell^+\ell^-)$ is defined as the partial Z width for the decay into a pair of massless charged leptons. This parameter is not directly used in the 5-parameter fit assuming lepton universality but is derived using the fit results. See the 'Note on the Z Boson.'

VALUE (MeV)	EVTS	DOCUMENT ID		TECN	COMMENT
83.984±0.086 OUR FIT					
83.82 ±0.15	471.3K	ABBIENDI	01A	OPAL	E_{cm}^{ee}= 88–94 GeV
83.85 ±0.17	379.4k	ABREU	00F	DLPH	E_{cm}^{ee}= 88–94 GeV
84.14 ±0.17	340.8k	ACCIARRI	00C	L3	E_{cm}^{ee}= 88–94 GeV
84.02 ±0.15	500k	BARATE	00C	ALEP	E_{cm}^{ee}= 88–94 GeV

Γ(invisible) Γ_5

We use only direct measurements of the invisible partial width using the single photon channel to obtain the average value quoted below. OUR FIT value is obtained as a difference between the total and the observed partial widths assuming lepton universality.

VALUE (MeV)	EVTS	DOCUMENT ID		TECN	COMMENT
499.0± 1.5 OUR FIT					
503 ±16 OUR AVERAGE Error includes scale factor of 1.2.					
498 ±12 ±12	1791	ACCIARRI	98G	L3	E_{cm}^{ee}= 88–94 GeV
539 ±26 ±17	410	AKERS	95C	OPAL	E_{cm}^{ee}= 88–94 GeV
450 ±34 ±34	258	BUSKULIC	93L	ALEP	E_{cm}^{ee}= 88–94 GeV
540 ±80 ±40	52	ADEVA	92	L3	E_{cm}^{ee}= 88–94 GeV
• • • We do not use the following data for averages, fits, limits, etc. • • •					
498.1± 2.6		[24] ABBIENDI	01A	OPAL	E_{cm}^{ee}= 88–94 GeV
498.1± 3.2		[24] ABREU	00F	DLPH	E_{cm}^{ee}= 88–94 GeV
499.1± 2.9		[24] ACCIARRI	00C	L3	E_{cm}^{ee}= 88–94 GeV
499.1± 2.5		[24] BARATE	00C	ALEP	E_{cm}^{ee}= 88–94 GeV

[24] This is an indirect determination of Γ(invisible) from a fit to the visible Z decay modes.

Γ(hadrons) Γ_6

This parameter is not directly used in the 5-parameter fit assuming lepton universality, but is derived using the fit results. See the 'Note on the Z Boson.'

VALUE (MeV)	EVTS	DOCUMENT ID		TECN	COMMENT
1744.4±2.0 OUR FIT					
1745.4±3.5	4.10M	ABBIENDI	01A	OPAL	E_{cm}^{ee}= 88–94 GeV
1738.1±4.0	3.70M	ABREU	00F	DLPH	E_{cm}^{ee}= 88–94 GeV
1751.1±3.8	3.54M	ACCIARRI	00C	L3	E_{cm}^{ee}= 88–94 GeV
1744.0±3.4	4.07M	BARATE	00C	ALEP	E_{cm}^{ee}= 88–94 GeV

Z BRANCHING RATIOS

OUR FIT is obtained using the fit procedure and correlations as determined by the LEP Electroweak Working Group (see the "Note on the Z boson").

$\Gamma(\text{hadrons})/\Gamma(e^+e^-)$ Γ_6/Γ_1

VALUE	EVTS	DOCUMENT ID		TECN	COMMENT
20.804± 0.050 OUR FIT					
20.902± 0.084	137.0K	[25] ABBIENDI	01A	OPAL	E_{cm}^{ee}= 88–94 GeV
20.88 ± 0.12	117.8k	ABREU	00F	DLPH	E_{cm}^{ee}= 88–94 GeV
20.816± 0.089	124.4k	ACCIARRI	00C	L3	E_{cm}^{ee}= 88–94 GeV
20.677± 0.075		[26] BARATE	00C	ALEP	E_{cm}^{ee}= 88–94 GeV
• • • We do not use the following data for averages, fits, limits, etc. • • •					
20.74 ± 0.18	31.4k	ABREU	94	DLPH	Repl. by ABREU 00F
20.96 ± 0.15	38k	ACCIARRI	94	L3	Repl. by ACCIARRI 00C
20.83 ± 0.16	42k	AKERS	94	OPAL	Repl. by ABBIENDI 01A
20.59 ± 0.15	45.8k	BUSKULIC	94	ALEP	Repl. by BARATE 00C
27.0 $^{+11.7}_{-8.8}$	12	[27] ABRAMS	89D	MRK2	E_{cm}^{ee}= 89–93 GeV

[25] ABBIENDI 01A error includes approximately 0.067 due to statistics, 0.040 due to event selection systematics, 0.027 due to the theoretical uncertainty in t-channel prediction, and 0.014 due to LEP energy uncertainty.

[26] BARATE 00C error includes approximately 0.062 due to statistics, 0.033 due to experimental systematics, and 0.026 due to the theoretical uncertainty in t-channel prediction.

[27] ABRAMS 89D have included both statistical and systematic uncertainties in their quoted errors.

$\Gamma(\text{hadrons})/\Gamma(\mu^+\mu^-)$ Γ_6/Γ_2

OUR FIT is obtained using the fit procedure and correlations as determined by the LEP Electroweak Working Group (see the "Note on the Z boson").

VALUE	EVTS	DOCUMENT ID		TECN	COMMENT
20.785±0.033 OUR FIT					
20.811±0.058	182.8K	[28] ABBIENDI	01A	OPAL	E_{cm}^{ee}= 88–94 GeV
20.65 ±0.08	157.6k	ABREU	00F	DLPH	E_{cm}^{ee}= 88–94 GeV
20.861±0.097	113.4k	ACCIARRI	00C	L3	E_{cm}^{ee}= 88–94 GeV
20.799±0.056		[29] BARATE	00C	ALEP	E_{cm}^{ee}= 88–94 GeV
• • • We do not use the following data for averages, fits, limits, etc. • • •					
20.54 ±0.14	45.6k	ABREU	94	DLPH	Repl. by ABREU 00F
21.02 ±0.16	34k	ACCIARRI	94	L3	Repl. by ACCIARRI 00C
20.78 ±0.11	57k	AKERS	94	OPAL	Repl. by ABBIENDI 01A
20.83 ±0.15	46.4k	BUSKULIC	94	ALEP	Repl. by BARATE 00C
18.9 $^{+7.1}_{-5.3}$	13	[30] ABRAMS	89D	MRK2	E_{cm}^{ee}= 89–93 GeV

[28] ABBIENDI 01A error includes approximately 0.050 due to statistics and 0.027 due to event selection systematics.

[29] BARATE 00C error includes approximately 0.053 due to statistics and 0.021 due to experimental systematics.

[30] ABRAMS 89D have included both statistical and systematic uncertainties in their quoted errors.

$\Gamma(\text{hadrons})/\Gamma(\tau^+\tau^-)$ Γ_6/Γ_3

OUR FIT is obtained using the fit procedure and correlations as determined by the LEP Electroweak Working Group (see the "Note on the Z boson").

VALUE	EVTS	DOCUMENT ID		TECN	COMMENT
20.764±0.045 OUR FIT					
20.832±0.091	151.5K	[31] ABBIENDI	01A	OPAL	E_{cm}^{ee}= 88–94 GeV
20.84 ±0.13	104.0k	ABREU	00F	DLPH	E_{cm}^{ee}= 88–94 GeV
20.792±0.133	103.0k	ACCIARRI	00C	L3	E_{cm}^{ee}= 88–94 GeV
20.707±0.062		[32] BARATE	00C	ALEP	E_{cm}^{ee}= 88–94 GeV
• • • We do not use the following data for averages, fits, limits, etc. • • •					
20.68 ±0.18	25k	ABREU	94	DLPH	Repl. by ABREU 00F
20.80 ±0.20	25k	ACCIARRI	94	L3	Repl. by ACCIARRI 00C
21.01 ±0.15	47k	AKERS	94	OPAL	Repl. by ABBIENDI 01A
20.70 ±0.16	45.1k	BUSKULIC	94	ALEP	Repl. by BARATE 00C
15.2 $^{+4.8}_{-3.9}$	21	[33] ABRAMS	89D	MRK2	E_{cm}^{ee}= 89–93 GeV

[31] ABBIENDI 01A error includes approximately 0.055 due to statistics and 0.071 due to event selection systematics.

[32] BARATE 00C error includes approximately 0.054 due to statistics and 0.033 due to experimental systematics.

[33] ABRAMS 89D have included both statistical and systematic uncertainties in their quoted errors.

$\Gamma(\text{hadrons})/\Gamma(\ell^+\ell^-)$ Γ_6/Γ_4

ℓ indicates each type of lepton (e, μ, and τ), not sum over them.

Our fit result is obtained requiring lepton universality.

VALUE	EVTS	DOCUMENT ID		TECN	COMMENT
20.767±0.025 OUR FIT					
20.823±0.044	471.3K	[34] ABBIENDI	01A	OPAL	E_{cm}^{ee}= 88–94 GeV
20.730±0.060	379.4k	ABREU	00F	DLPH	E_{cm}^{ee}= 88–94 GeV
20.810±0.060	340.8k	ACCIARRI	00C	L3	E_{cm}^{ee}= 88–94 GeV
20.725±0.039	500k	[35] BARATE	00C	ALEP	E_{cm}^{ee}= 88–94 GeV
• • • We do not use the following data for averages, fits, limits, etc. • • •					
20.62 ±0.10	102k	ABREU	94	DLPH	Repl. by ABREU 00F
20.93 ±0.10	97k	ACCIARRI	94	L3	Repl. by ACCIARRI 00C
20.835±0.086	146k	AKERS	94	OPAL	Repl. by ABBIENDI 01A
20.69 ±0.09	137.3k	BUSKULIC	94	ALEP	Repl. by BARATE 00C
18.9 $^{+3.6}_{-3.2}$	46	ABRAMS	89B	MRK2	E_{cm}^{ee}= 89–93 GeV

[34] ABBIENDI 01A error includes approximately 0.034 due to statistics and 0.027 due to event selection systematics.

[35] BARATE 00C error includes approximately 0.033 due to statistics, 0.020 due to experimental systematics, and 0.005 due to the theoretical uncertainty in t-channel prediction.

$\Gamma(\text{hadrons})/\Gamma_{\text{total}}$ Γ_6/Γ

This parameter is not directly used in the overall fit but is derived using the fit results; see the 'Note on the Z Boson.'

VALUE (%)	DOCUMENT ID
69.911 ± 0.056 OUR FIT	

$\Gamma(e^+e^-)/\Gamma_{\text{total}}$ Γ_1/Γ

This parameter is not directly used in the overall fit but is derived using the fit results; see the 'Note on the Z Boson.'

VALUE (%)	DOCUMENT ID
3.3632 ± 0.0042 OUR FIT	

$\Gamma(\mu^+\mu^-)/\Gamma_{\text{total}}$ Γ_2/Γ

This parameter is not directly used in the overall fit but is derived using the fit results; see the 'Note on the Z Boson.'

VALUE (%)	DOCUMENT ID
3.3662 ± 0.0066 OUR FIT	

$\Gamma(\tau^+\tau^-)/\Gamma_{\text{total}}$ Γ_3/Γ

This parameter is not directly used in the overall fit but is derived using the fit results; see the 'Note on the Z Boson.'

VALUE (%)	DOCUMENT ID
3.3696 ± 0.0083 OUR FIT	

$\Gamma(\ell^+\ell^-)/\Gamma_{\text{total}}$ Γ_4/Γ

ℓ indicates each type of lepton (e, μ, and τ), not sum over them.

Our fit result assumes lepton universality.

This parameter is not directly used in the overall fit but is derived using the fit results; see the 'Note on the Z Boson.'

VALUE (%)	DOCUMENT ID
3.3658 ± 0.0023 OUR FIT	

$\Gamma(\text{invisible})/\Gamma_{\text{total}}$ Γ_5/Γ

See the data, the note, and the fit result for the partial width, Γ_5, above.

VALUE (%)	DOCUMENT ID
20.000 ± 0.055 OUR FIT	

$\Gamma(\mu^+\mu^-)/\Gamma(e^+e^-)$ Γ_2/Γ_1

This parameter is not directly used in the overall fit but is derived using the fit results; see the 'Note on the Z Boson.'

VALUE	DOCUMENT ID
1.0009 ± 0.0028 OUR FIT	

$\Gamma(\tau^+\tau^-)/\Gamma(e^+e^-)$ Γ_3/Γ_1

This parameter is not directly used in the overall fit but is derived using the fit results; see the 'Note on the Z Boson.'

VALUE	DOCUMENT ID
1.0019 ± 0.0032 OUR FIT	

$\Gamma((u\overline{u}+c\overline{c})/2)/\Gamma(\text{hadrons})$ Γ_7/Γ_6

This quantity is the branching ratio of $Z \to$ "up-type" quarks to $Z \to$ hadrons. Except ACKERSTAFF 97T the values of $Z \to$ "up-type" and $Z \to$ "down-type" branchings are extracted from measurements of Γ(hadrons), and $\Gamma(Z \to \gamma +$ jets) where γ is a high-energy (>5 GeV) isolated photon. As the experiments use different procedures and slightly different values of M_Z, Γ(hadrons) and α_s in their extraction procedures, our average has to be taken with caution.

VALUE	DOCUMENT ID		TECN	COMMENT
0.145 ± 0.015 OUR AVERAGE				
0.160 ± 0.019 ± 0.019	[36] ACKERSTAFF	97T	OPAL	E_{cm}^{ee} = 88–94 GeV
$0.137^{+0.038}_{-0.054}$	[37] ABREU	95X	DLPH	E_{cm}^{ee} = 88–94 GeV
0.139 ± 0.026	[38] ACTON	93F	OPAL	E_{cm}^{ee} = 88–94 GeV
0.137 ± 0.033	[39] ADRIANI	93	L3	E_{cm}^{ee} = 91.2 GeV

[36] ACKERSTAFF 97T measure $\Gamma_{u\overline{u}}/(\Gamma_{d\overline{d}}+\Gamma_{u\overline{u}}+\Gamma_{s\overline{s}}) = 0.258 \pm 0.031 \pm 0.032$. To obtain this branching ratio authors use $R_c+R_b = 0.380 \pm 0.010$. This measurement is fully negatively correlated with the measurement of $\Gamma_{d\overline{d},s\overline{s}}/(\Gamma_{d\overline{d}}+\Gamma_{u\overline{u}}+\Gamma_{s\overline{s}})$ given in the next data block.

[37] ABREU 95X use $M_Z = 91.187 \pm 0.009$ GeV, Γ(hadrons) = 1725 ± 12 MeV and $\alpha_s = 0.123 \pm 0.005$. To obtain this branching ratio we divide their value of $C_{2/3} = 0.91^{+0.25}_{-0.36}$ by their value of $(3C_{1/3} + 2C_{2/3}) = 6.66 \pm 0.05$.

[38] ACTON 93F use the LEP 92 value of Γ(hadrons) = 1740 ± 12 MeV and $\alpha_s = 0.122^{+0.006}_{-0.005}$.

[39] ADRIANI 93 use $M_Z = 91.181 \pm 0.022$ GeV, Γ(hadrons) = 1742 ± 19 MeV and $\alpha_s = 0.125 \pm 0.009$. To obtain this branching ratio we divide their value of $C_{2/3} = 0.92 \pm 0.22$ by their value of $(3C_{1/3} + 2C_{2/3}) = 6.720 \pm 0.076$.

$\Gamma((d\overline{d}+s\overline{s}+b\overline{b})/3)/\Gamma(\text{hadrons})$ Γ_8/Γ_6

This quantity is the branching ratio of $Z \to$ "down-type" quarks to $Z \to$ hadrons. Except ACKERSTAFF 97T the values of $Z \to$ "up-type" and $Z \to$ "down-type" branchings are extracted from measurements of Γ(hadrons), and $\Gamma(Z \to \gamma +$ jets) where γ is a high-energy (>5 GeV) isolated photon. As the experiments use different procedures and slightly different values of M_Z, Γ(hadrons) and α_s in their extraction procedures, our average has to be taken with caution.

VALUE	DOCUMENT ID		TECN	COMMENT
0.237 ± 0.009 OUR AVERAGE				
0.230 ± 0.010 ± 0.010	[40] ACKERSTAFF	97T	OPAL	E_{cm}^{ee} = 88–94 GeV
$0.243^{+0.036}_{-0.026}$	[41] ABREU	95X	DLPH	E_{cm}^{ee} = 88–94 GeV
0.241 ± 0.017	[42] ACTON	93F	OPAL	E_{cm}^{ee} = 88–94 GeV
0.243 ± 0.022	[43] ADRIANI	93	L3	E_{cm}^{ee} = 91.2 GeV

[40] ACKERSTAFF 97T measure $\Gamma_{d\overline{d},s\overline{s}}/(\Gamma_{d\overline{d}}+\Gamma_{u\overline{u}}+\Gamma_{s\overline{s}}) = 0.371 \pm 0.016 \pm 0.016$. To obtain this branching ratio authors use $R_c+R_b = 0.380 \pm 0.010$. This measurement is fully negatively correlated with the measurement of $\Gamma_{u\overline{u}}/(\Gamma_{d\overline{d}}+\Gamma_{u\overline{u}}+\Gamma_{s\overline{s}})$ presented in the previous data block.

[41] ABREU 95X use $M_Z = 91.187 \pm 0.009$ GeV, Γ(hadrons) = 1725 ± 12 MeV and $\alpha_s = 0.123 \pm 0.005$. To obtain this branching ratio we divide their value of $C_{1/3} = 1.62^{+0.24}_{-0.17}$ by their value of $(3C_{1/3} + 2C_{2/3}) = 6.66 \pm 0.05$.

[42] ACTON 93F use the LEP 92 value of Γ(hadrons) = 1740 ± 12 MeV and $\alpha_s = 0.122^{+0.006}_{-0.005}$.

[43] ADRIANI 93 use $M_Z = 91.181 \pm 0.022$ GeV, Γ(hadrons) = 1742 ± 19 MeV and $\alpha_s = 0.125 \pm 0.009$. To obtain this branching ratio we divide their value of $C_{1/3} = 1.63 \pm 0.15$ by their value of $(3C_{1/3} + 2C_{2/3}) = 6.720 \pm 0.076$.

$R_c = \Gamma(c\overline{c})/\Gamma(\text{hadrons})$ Γ_9/Γ_6

OUR FIT is obtained by a simultaneous fit to several c- and b-quark measurements as explained in the "Note on the Z boson." As a cross check we have also performed a weighted average of the R_c measurements. Taking into account the various common systematic errors, we obtain $R_c = 0.1679 \pm 0.0059$.

The Standard Model predicts $R_c = 0.1723$ for $m_t = 174.3$ GeV and $M_H = 150$ GeV.

VALUE	DOCUMENT ID		TECN	COMMENT
0.1689 ± 0.0047 OUR FIT				
0.1665 ± 0.0051 ± 0.0081	[44] ABREU	00	DLPH	E_{cm}^{ee} = 88–94 GeV
0.1698 ± 0.0069	[45] BARATE	00B	ALEP	E_{cm}^{ee} = 88–94 GeV
0.180 ± 0.011 ± 0.013	[46] ACKERSTAFF	98E	OPAL	E_{cm}^{ee} = 88–94 GeV
0.167 ± 0.011 ± 0.012	[47] ALEXANDER	96R	OPAL	E_{cm}^{ee} = 88–94 GeV
• • • We do not use the following data for averages, fits, limits, etc. • • •				
0.1675 ± 0.0062 ± 0.0103	[48] BARATE	98T	ALEP	Repl. by BARATE 00B
0.1689 ± 0.0095 ± 0.0068	[49] BARATE	98T	ALEP	Repl. by BARATE 00B
0.1623 ± 0.0085 ± 0.0209	[50] ABREU	95D	DLPH	E_{cm}^{ee} = 88–94 GeV
0.142 ± 0.008 ± 0.014	[51] AKERS	95O	OPAL	Repl. by ACKERSTAFF 98E
0.165 ± 0.005 ± 0.020	[52] BUSKULIC	94G	ALEP	Repl. by BARATE 00B

[44] ABREU 00 obtain this result properly combining the measurement from the D^{*+} production rate (R_c = 0.1610 ± 0.0104 ± 0.0077 ± 0.0043 (BR)) with that from the overall charm counting (R_c = 0.1692 ± 0.0047 ± 0.0063 ± 0.0074 (BR)) in $c\overline{c}$ events. The systematic error includes an uncertainty of ±0.0054 due to the uncertainty on the charmed hadron branching fractions.

[45] BARATE 00B use exclusive decay modes to independently determine the quantities $R_c \times f(c \to X)$, X=D^0, D^+, D_s^+, and Λ_c. Estimating $R_c \times f(c \to \Xi_c/\Omega_c)$= 0.0034, they simply sum over all the charm decays to obtain R_c = 0.1738 ± 0.0047 ± 0.0088 ± 0.0075(BR). This is combined with all previous ALEPH measurements (BARATE 98T and BUSKULIC 94G, R_c = 0.1681 ± 0.0054 ± 0.0062) to obtain the quoted value.

[46] ACKERSTAFF 98E use an inclusive/exclusive double tag. In one jet $D^{*\pm}$ mesons are exclusively reconstructed in several decay channels and in the opposite jet a slow pion (opposite charge inclusive $D^{*\pm}$) tag is used. The b content of this sample is measured by the simultaneous detection of a lepton in one jet and an inclusively reconstructed $D^{*\pm}$ meson in the opposite jet. The systematic error includes an uncertainty of ±0.006 due to the external branching ratios.

[47] ALEXANDER 96R obtain this value via direct charm counting, summing the partial contributions from D^0, D^+, D_s^+, and Λ_c^+, and assuming that strange-charmed baryons account for the 15% of the Λ_c^+ production. An uncertainty of ±0.005 due to the uncertainties in the charm hadron branching ratios is included in the overall systematics.

[48] BARATE 98T perform a simultaneous fit to the p and p_T spectra of electrons from hadronic Z decays. The semileptonic branching ratio B($c \to e$) is taken as 0.098 ± 0.005 and the systematic error includes an uncertainty of ±0.0084 due to this.

[49] BARATE 98T obtain this result combining two double-tagging techniques. Searching for a D meson in each hemisphere by full reconstruction in an exclusive decay mode gives R_c = 0.173 ± 0.014 ± 0.0009. The same tag in combination with inclusive identification using the slow pion from the $D^{*+} \to D^0\pi^+$ decay in the opposite hemisphere yields R_c = 0.166 ± 0.012 ± 0.009. The R_b dependence is given by R_c = 0.1689−0.023×(R_b−0.2159). The three measurements of BARATE 98T are combined with BUSKULIC 94G to give the average R_c = 0.1681 ± 0.0054 ± 0.0062.

[50] ABREU 95D perform a maximum likelihood fit to the combined p and p_T distributions of single and dilepton samples. The second error includes an uncertainty of ±0.0124 due to models and branching ratios.

[51] AKERS 95O use the presence of a $D^{*\pm}$ to tag $Z \to c\overline{c}$ with $D^* \to D^0\pi$ and $D^0 \to K\pi$. They measure $P_c * \Gamma(c\overline{c})/\Gamma$(hadrons) to be $(1.006 \pm 0.055 \pm 0.061) \times 10^{-3}$, where P_c is the product branching ratio B($c \to D^*$)B($D^* \to D^0\pi$)B($D^0 \to K\pi$). Assuming that P_c remains unchanged with energy, they use its value $(7.1 \pm 0.5) \times 10^{-3}$ determined at CESR/PETRA to obtain $\Gamma(c\overline{c})/\Gamma$(hadrons). The second error of AKERS 95O includes an uncertainty of ±0.011 from the uncertainty on P_c.

[52] BUSKULIC 94G perform a simultaneous fit to the p and p_T spectra of both single and dilepton events.

$R_b = \Gamma(b\overline{b})/\Gamma(\text{hadrons})$ Γ_{10}/Γ_6

OUR FIT is obtained by a simultaneous fit to several c- and b-quark measurements as explained in the "Note on the Z boson." As a cross check we have also performed a weighted average of the R_b measurements taking into account the various common systematic errors. For R_c = 0.1689 (as given by OUR FIT above), we obtain R_b = 0.21622 ± 0.00076. For an expected Standard Model value of R_c = 0.1723, our weighted average gives R_b = 0.21614 ± 0.00076.

The Standard Model predicts $R_b = 0.21581$ for $m_t = 174.3$ GeV and $M_H = 150$ GeV.

VALUE			DOCUMENT ID		TECN	COMMENT
0.21643 ± 0.00072 OUR FIT						
0.2174	± 0.0015	± 0.0028	[53] ACCIARRI	00	L3	E_{cm}^{ee} = 89–93 GeV
0.2178	± 0.0011	± 0.0013	[54] ABBIENDI	99B	OPAL	E_{cm}^{ee} = 88–94 GeV
0.21634	± 0.00067	± 0.00060	[55] ABREU	99B	DLPH	E_{cm}^{ee} = 88–94 GeV
0.2142	± 0.0034	± 0.0015	[56] ABE	98D	SLD	E_{cm}^{ee} = 91.2 GeV
0.2159	± 0.0009	± 0.0011	[57] BARATE	97F	ALEP	E_{cm}^{ee} = 88–94 GeV
• • • We do not use the following data for averages, fits, limits, etc. • • •						
0.2175	± 0.0014	± 0.0017	[58] ACKERSTAFF	97K	OPAL	Repl. by ABBIENDI 99B
0.2167	± 0.0011	± 0.0013	[59] BARATE	97E	ALEP	E_{cm}^{ee} = 88–94 GeV
0.229	± 0.011		[60] ABE	96E	SLD	Repl. by ABE 98D
0.2216	± 0.0016	± 0.0021	[61] ABREU	96	DLPH	Repl. by ABREU 99B
0.2145	± 0.0089	± 0.0067	[62] ABREU	95D	DLPH	E_{cm}^{ee} = 88–94 GeV
0.219	± 0.006	± 0.005	[63] BUSKULIC	94G	ALEP	E_{cm}^{ee} = 88–94 GeV
0.251	± 0.049	± 0.030	[64] JACOBSEN	91	MRK2	E_{cm}^{ee} = 91 GeV

[53] ACCIARRI 00 obtain this result using a double-tagging technique, with a high p_T lepton tag and an impact parameter tag in opposite hemispheres.

[54] ABBIENDI 99B tag $Z \to b\overline{b}$ decays using leptons and/or separated decay vertices. The b-tagging efficiency is measured directly from the data using a double-tagging technique.

[55] ABREU 99B obtain this result combining in a multivariate analysis several tagging methods (impact parameter and secondary vertex reconstruction, complemented by event shape variables). For R_c different from its Standard Model value of 0.172, R_b varies as $-0.024\times(R_c-0.172)$.

[56] ABE 98D use a double tag based on 3D impact parameter with reconstruction of secondary vertices. The charm background is reduced by requiring the invariant mass at the secondary vertex to be above 2 GeV. The systematic error includes an uncertainty of ± 0.0002 due to the uncertainty on R_c.

[57] BARATE 97F combine the lifetime-mass hemisphere tag (BARATE 97E) with event shape information and lepton tag to identify $Z \to b\overline{b}$ candidates. They further use c- and uds-selection tags to identify the background. For R_c different from its Standard Model value of 0.172, R_b varies as $-0.019\times(R_c-0.172)$.

[58] ACKERSTAFF 97K use lepton and/or separated decay vertex to tag independently each hemisphere. Comparing the numbers of single- and double-tagged events, they determine the b-tagging efficiency directly from the data.

[59] BARATE 97E combine a lifetime tag with a mass cut based on the mass difference between c hadrons and b hadrons. Included in BARATE 97F.

[60] ABE 96E obtain this value by combining results from three different b-tagging methods (2D impact parameter, 3D impact parameter, and 3D displaced vertex).

[61] ABREU 96 obtain this result combining several analyses (double lifetime tag, mixed tag and multivariate analysis). This value is obtained assuming $R_c = \Gamma(c\overline{c})/\Gamma(\text{hadrons}) = 0.172$. For a value of R_c different from this by an amount ΔR_c the change in the value is given by $-0.087\cdot\Delta R_c$.

[62] ABREU 95D perform a maximum likelihood fit to the combined p and p_T distributions of single and dilepton samples. The second error includes an uncertainty of ± 0.0023 due to models and branching ratios.

[63] BUSKULIC 94G perform a simultaneous fit to the p and p_T spectra of both single and dilepton events.

[64] JACOBSEN 91 tagged $b\overline{b}$ events by requiring coincidence of ≥ 3 tracks with significant impact parameters using vertex detector. Systematic error includes lifetime and decay uncertainties (± 0.014).

$\Gamma(b\overline{b}b\overline{b})/\Gamma(\text{hadrons})$ Γ_{11}/Γ_6

VALUE (units 10^{-4})		DOCUMENT ID		TECN	COMMENT
5.2 ± 1.9 OUR AVERAGE					
3.6 ± 1.7 ± 2.7		[65] ABBIENDI	01G	OPAL	E_{cm}^{ee} = 88–94 GeV
6.0 ± 1.9 ± 1.4		[66] ABREU	99U	DLPH	E_{cm}^{ee} = 88–94 GeV

[65] ABBIENDI 01G use a sample of four-jet events from hadronic Z decays. To enhance the $b\overline{b}b\overline{b}$ signal, at least three of the four jets are required to have a significantly detached secondary vertex.

[66] ABREU 99U force hadronic Z decays into 3 jets to use all the available phase space and require a b tag for every jet. This decay mode includes primary and secondary $4b$ production, *e.g.*, from gluon splitting to $b\overline{b}$.

$\Gamma(ggg)/\Gamma(\text{hadrons})$ Γ_{12}/Γ_6

VALUE	CL%	DOCUMENT ID		TECN	COMMENT
< 1.6 × 10⁻²	95	[67] ABREU	96S	DLPH	E_{cm}^{ee} = 88–94 GeV

[67] This branching ratio is slightly dependent on the jet-finder algorithm. The value we quote is obtained using the JADE algorithm, while using the DURHAM algorithm ABREU 96S obtain an upper limit of 1.5×10^{-2}.

$\Gamma(\pi^0\gamma)/\Gamma_{\text{total}}$ Γ_{13}/Γ

VALUE	CL%	DOCUMENT ID		TECN	COMMENT
< 5.2 × 10⁻⁵	95	[68] ACCIARRI	95G	L3	E_{cm}^{ee} = 88–94 GeV
< 5.5 × 10⁻⁵	95	ABREU	94B	DLPH	E_{cm}^{ee} = 88–94 GeV
< 2.1 × 10⁻⁴	95	DECAMP	92	ALEP	E_{cm}^{ee} = 88–94 GeV
< 1.4 × 10⁻⁴	95	AKRAWY	91F	OPAL	E_{cm}^{ee} = 88–94 GeV

[68] This limit is for both decay modes $Z \to \pi^0\gamma/\gamma\gamma$ which are indistinguishable in ACCIARRI 95G.

$\Gamma(\eta\gamma)/\Gamma_{\text{total}}$ Γ_{14}/Γ

VALUE	CL%	DOCUMENT ID		TECN	COMMENT
< 7.6 × 10⁻⁵	95	ACCIARRI	95G	L3	E_{cm}^{ee} = 88–94 GeV
< 8.0 × 10⁻⁵	95	ABREU	94B	DLPH	E_{cm}^{ee} = 88–94 GeV
< 5.1 × 10⁻⁵	95	DECAMP	92	ALEP	E_{cm}^{ee} = 88–94 GeV
< 2.0 × 10⁻⁴	95	AKRAWY	91F	OPAL	E_{cm}^{ee} = 88–94 GeV

$\Gamma(\omega\gamma)/\Gamma_{\text{total}}$ Γ_{15}/Γ

VALUE	CL%	DOCUMENT ID		TECN	COMMENT
< 6.5 × 10⁻⁴	95	ABREU	94B	DLPH	E_{cm}^{ee} = 88–94 GeV

$\Gamma(\eta'(958)\gamma)/\Gamma_{\text{total}}$ Γ_{16}/Γ

VALUE	CL%	DOCUMENT ID		TECN	COMMENT
< 4.2 × 10⁻⁵	95	DECAMP	92	ALEP	E_{cm}^{ee} = 88–94 GeV

$\Gamma(\gamma\gamma)/\Gamma_{\text{total}}$ Γ_{17}/Γ

This decay would violate the Landau-Yang theorem.

VALUE	CL%	DOCUMENT ID		TECN	COMMENT
< 5.2 × 10⁻⁵	95	[69] ACCIARRI	95G	L3	E_{cm}^{ee} = 88–94 GeV
< 5.5 × 10⁻⁵	95	ABREU	94B	DLPH	E_{cm}^{ee} = 88–94 GeV
< 1.4 × 10⁻⁴	95	AKRAWY	91F	OPAL	E_{cm}^{ee} = 88–94 GeV

[69] This limit is for both decay modes $Z \to \pi^0\gamma/\gamma\gamma$ which are indistinguishable in ACCIARRI 95G.

$\Gamma(\gamma\gamma\gamma)/\Gamma_{\text{total}}$ Γ_{18}/Γ

VALUE	CL%	DOCUMENT ID		TECN	COMMENT
< 1.0 × 10⁻⁵	95	[70] ACCIARRI	95C	L3	E_{cm}^{ee} = 88–94 GeV
< 1.7 × 10⁻⁵	95	[70] ABREU	94B	DLPH	E_{cm}^{ee} = 88–94 GeV
< 6.6 × 10⁻⁵	95	AKRAWY	91F	OPAL	E_{cm}^{ee} = 88–94 GeV

[70] Limit derived in the context of composite Z model.

$\Gamma(\pi^\pm W^\mp)/\Gamma_{\text{total}}$ Γ_{19}/Γ

The value is for the sum of the charge states indicated.

VALUE	CL%	DOCUMENT ID		TECN	COMMENT
< 7 × 10⁻⁵	95	DECAMP	92	ALEP	E_{cm}^{ee} = 88–94 GeV

$\Gamma(\rho^\pm W^\mp)/\Gamma_{\text{total}}$ Γ_{20}/Γ

The value is for the sum of the charge states indicated.

VALUE	CL%	DOCUMENT ID		TECN	COMMENT
< 8.3 × 10⁻⁵	95	DECAMP	92	ALEP	E_{cm}^{ee} = 88–94 GeV

$\Gamma(J/\psi(1S)X)/\Gamma_{\text{total}}$ Γ_{21}/Γ

VALUE (units 10^{-3})	EVTS	DOCUMENT ID		TECN	COMMENT
$3.51^{+0.23}_{-0.25}$ OUR AVERAGE Error includes scale factor of 1.1.					
$3.21\pm0.21^{+0.19}_{-0.28}$	553	[71] ACCIARRI	99F	L3	E_{cm}^{ee} = 88–94 GeV
3.9 ± 0.2 ± 0.3	511	[72] ALEXANDER	96B	OPAL	E_{cm}^{ee} = 88–94 GeV
3.73 ± 0.39 ± 0.36	153	[73] ABREU	94P	DLPH	E_{cm}^{ee} = 88–94 GeV
• • • We do not use the following data for averages, fits, limits, etc. • • •					
3.40 ± 0.23 ± 0.27	441	[74] ACCIARRI	97J	L3	Repl. by ACCIARRI 99F

[71] ACCIARRI 99F combine $\mu^+\mu^-$ and e^+e^- $J/\psi(1S)$ decay channels. The branching ratio for prompt $J/\psi(1S)$ production is measured to be $(2.1\pm0.6\pm0.4^{+0.4}_{-0.2}(\text{theor.}))\times10^{-4}$.

[72] ALEXANDER 96B identify $J/\psi(1S)$ from the decays into lepton pairs. (4.8 ± 2.4)% of this branching ratio is due to prompt $J/\psi(1S)$ production (ALEXANDER 96N).

[73] Combining $\mu^+\mu^-$ and e^+e^- channels and taking into account the common systematic errors. $(7.7^{+6.3}_{-5.4})$% of this branching ratio is due to prompt $J/\psi(1S)$ production.

[74] ACCIARRI 97J combine $\mu^+\mu^-$ and e^+e^- $J/\psi(1S)$ decay channels and take into account the common systematic error.

$\Gamma(\psi(2S)X)/\Gamma_{\text{total}}$ Γ_{22}/Γ

VALUE (units 10^{-3})	EVTS	DOCUMENT ID		TECN	COMMENT
1.60 ± 0.29 OUR AVERAGE					
1.6 ± 0.5 ± 0.3	39	[75] ACCIARRI	97J	L3	E_{cm}^{ee} = 88–94 GeV
1.6 ± 0.3 ± 0.2	46.9	[76] ALEXANDER	96B	OPAL	E_{cm}^{ee} = 88–94 GeV
1.60 ± 0.73 ± 0.33	5.4	[77] ABREU	94P	DLPH	E_{cm}^{ee} = 88–94 GeV

[75] ACCIARRI 97J measure this branching ratio via the decay channel $\psi(2S) \to \ell^+\ell^-$ ($\ell = \mu, e$).

[76] ALEXANDER 96B measure this branching ratio via the decay channel $\psi(2S) \to J/\psi\pi^+\pi^-$, with $J/\psi \to \ell^+\ell^-$.

[77] ABREU 94P measure this branching ratio via decay channel $\psi(2S) \to J/\psi\pi^+\pi^-$, with $J/\psi \to \mu^+\mu^-$.

$\Gamma(\chi_{c1}(1P)X)/\Gamma_{\text{total}}$ Γ_{23}/Γ

VALUE (units 10^{-3})	EVTS	DOCUMENT ID		TECN	COMMENT
2.9 ± 0.7 OUR AVERAGE					
2.7 ± 0.6 ± 0.5	33	[78] ACCIARRI	97J	L3	E_{cm}^{ee} = 88–94 GeV
$5.0\pm2.1^{+1.5}_{-0.9}$	6.4	[79] ABREU	94P	DLPH	E_{cm}^{ee} = 88–94 GeV

[78] ACCIARRI 97J measure this branching ratio via the decay channel $\chi_{c1} \to J/\psi + \gamma$, with $J/\psi \to \ell^+\ell^-$ ($\ell = \mu, e$). The $M(\ell^+\ell^-\gamma)$–$M(\ell^+\ell^-)$ mass difference spectrum is fitted with two gaussian shapes for χ_{c1} and χ_{c2}.

[79] This branching ratio is measured via the decay channel $\chi_{c1} \to J/\psi + \gamma$, with $J/\psi \to \mu^+\mu^-$.

$\Gamma(\chi_{c2}(1P)X)/\Gamma_{total}$ Γ_{24}/Γ

VALUE	CL%	DOCUMENT ID		TECN	COMMENT
$<3.2\times10^{-3}$	90	[80] ACCIARRI	97J	L3	E_{cm}^{ee}= 88–94 GeV

[80] ACCIARRI 97J derive this limit via the decay channel $\chi_{c2}\to J/\psi+\gamma$, with $J/\psi\to\ell^+\ell^-$ ($\ell=\mu, e$). The $M(\ell^+\ell^-\gamma)$–$M(\ell^+\ell^-)$ mass difference spectrum is fitted with two gaussian shapes for χ_{c1} and χ_{c2}.

$\Gamma(\Upsilon(1S)X+\Upsilon(2S)X+\Upsilon(3S)X)/\Gamma_{total}$ $\Gamma_{25}/\Gamma=(\Gamma_{26}+\Gamma_{27}+\Gamma_{28})/\Gamma$

VALUE (units 10^{-4})	EVTS	DOCUMENT ID		TECN	COMMENT
$1.0\pm0.4\pm0.22$	6.4	[81] ALEXANDER	96F	OPAL	E_{cm}^{ee}= 88–94 GeV

[81] ALEXANDER 96F identify the Υ (which refers to any of the three lowest bound states) through its decay into e^+e^- and $\mu^+\mu^-$. The systematic error includes an uncertainty of ±0.2 due to the production mechanism.

$\Gamma(\Upsilon(1S)X)/\Gamma_{total}$ Γ_{26}/Γ

VALUE	CL%	DOCUMENT ID		TECN	COMMENT
$<4.4\times10^{-5}$	95	[82] ACCIARRI	99F	L3	E_{cm}^{ee}= 88–94 GeV

[82] ACCIARRI 99F search for $\Upsilon(1S)$ through its decay into $\ell^+\ell^-$ ($\ell=e$ or μ).

$\Gamma(\Upsilon(2S)X)/\Gamma_{total}$ Γ_{27}/Γ

VALUE	CL%	DOCUMENT ID		TECN	COMMENT
$<13.9\times10^{-5}$	95	[83] ACCIARRI	97R	L3	E_{cm}^{ee}= 88–94 GeV

[83] ACCIARRI 97R search for $\Upsilon(2S)$ through its decay into $\ell^+\ell^-$ ($\ell=e$ or μ).

$\Gamma(\Upsilon(3S)X)/\Gamma_{total}$ Γ_{28}/Γ

VALUE	CL%	DOCUMENT ID		TECN	COMMENT
$<9.4\times10^{-5}$	95	[84] ACCIARRI	97R	L3	E_{cm}^{ee}= 88–94 GeV

[84] ACCIARRI 97R search for $\Upsilon(3S)$ through its decay into $\ell^+\ell^-$ ($\ell=e$ or μ).

$\Gamma((D^0/\overline{D}^0)X)/\Gamma(\text{hadrons})$ Γ_{29}/Γ_6

VALUE	EVTS	DOCUMENT ID		TECN	COMMENT
$0.296\pm0.019\pm0.021$	369	[85] ABREU	93I	DLPH	E_{cm}^{ee}= 88–94 GeV

[85] The $(D^0/\overline{D}^0)$ states in ABREU 93I are detected by the $K\pi$ decay mode. This is a corrected result (see the erratum of ABREU 93I).

$\Gamma(D^{\pm}X)/\Gamma(\text{hadrons})$ Γ_{30}/Γ_6

VALUE	EVTS	DOCUMENT ID		TECN	COMMENT
$0.174\pm0.016\pm0.018$	539	[86] ABREU	93I	DLPH	E_{cm}^{ee}= 88–94 GeV

[86] The $D^{\pm}$ states in ABREU 93I are detected by the $K\pi\pi$ decay mode. This is a corrected result (see the erratum of ABREU 93I).

$\Gamma(D^*(2010)^{\pm}X)/\Gamma(\text{hadrons})$ Γ_{31}/Γ_6

The value is for the sum of the charge states indicated.

VALUE	EVTS	DOCUMENT ID		TECN	COMMENT
0.163 ± 0.019 OUR AVERAGE		Error includes scale factor of 1.3.			
$0.155\pm0.010\pm0.013$	358	[87] ABREU	93I	DLPH	E_{cm}^{ee}= 88–94 GeV
$0.21\ \pm0.04$	362	[88] DECAMP	91J	ALEP	E_{cm}^{ee}= 88–94 GeV

[87] $D^*(2010)^{\pm}$ in ABREU 93I are reconstructed from $D^0\pi^{\pm}$, with $D^0\to K^-\pi^+$. The new CLEO II measurement of $B(D^{*\pm}\to D^0\pi^{\pm})=(68.1\pm1.6)$ % is used. This is a corrected result (see the erratum of ABREU 93I).

[88] DECAMP 91J report $B(D^*(2010)^+\to D^0\pi^+)\ B(D^0\to K^-\pi^+)\ \Gamma(D^*(2010)^{\pm}X)/\Gamma(\text{hadrons})=(5.11\pm0.34)\times10^{-3}$. They obtained the above number assuming $B(D^0\to K^-\pi^+)=(3.62\pm0.34\pm0.44)$% and $B(D^*(2010)^+\to D^0\pi^+)=(55\pm4)$%. We have rescaled their original result of 0.26 ± 0.05 taking into account the new CLEO II branching ratio $B(D^*(2010)^+\to D^0\pi^+)=(68.1\pm1.6)$%.

$\Gamma(D_{s1}(2536)^{\pm}X)/\Gamma(\text{hadrons})$ Γ_{32}/Γ_6

$D_{s1}(2536)^{\pm}$ is an expected orbitally-excited state of the D_s meson.

VALUE (%)	EVTS	DOCUMENT ID		TECN	COMMENT
$0.52\pm0.09\pm0.06$	92	[89] HEISTER	02B	ALEP	E_{cm}^{ee}= 88–94 GeV

[89] HEISTER 02B reconstruct this meson in the decay modes $D_{s1}(2536)^{\pm}\to D^{*\pm}K^0$ and $D_{s1}(2536)^{\pm}\to D^{*0}K^{\pm}$. The quoted branching ratio assumes that the decay width of the $D_{s1}(2536)$ is saturated by the two measured decay modes.

$\Gamma(D_{sJ}(2573)^{\pm}X)/\Gamma(\text{hadrons})$ Γ_{33}/Γ_6

$D_{sJ}(2573)^{\pm}$ is an expected orbitally-excited state of the D_s meson.

VALUE (%)	EVTS	DOCUMENT ID		TECN	COMMENT
$0.83\pm0.29^{+0.07}_{-0.13}$	64	[90] HEISTER	02B	ALEP	E_{cm}^{ee}= 88–94 GeV

[90] HEISTER 02B reconstruct this meson in the decay mode $D_{s2}(2573)^{\pm}\to D^0K^{\pm}$. The quoted branching ratio assumes that the detected decay mode represents 45% of the full decay width.

$\Gamma(D^{*\prime}(2629)^{\pm}X)/\Gamma(\text{hadrons})$ Γ_{34}/Γ_6

$D^{*\prime}(2629)^{\pm}$ is a predicted radial excitation of the $D^*(2010)^{\pm}$ meson.

VALUE	DOCUMENT ID		TECN	COMMENT
searched for	[91] ABBIENDI	01N	OPAL	E_{cm}^{ee}= 88–94 GeV

[91] ABBIENDI 01N searched for the decay mode $D^{*\prime}(2629)^{\pm}\to D^{*\pm}\pi^+\pi^-$ with $D^{*+}\to D^0\pi^+$, and $D^0\to K^-\pi^+$. They quote a 95% CL limit for $Z\to D^{*\prime}(2629)^{\pm}\times B(D^{*\prime}(2629)^+\to D^{*+}\pi^+\pi^-)<3.1\times10^{-3}$.

$\Gamma(B_s^0X)/\Gamma(\text{hadrons})$ Γ_{37}/Γ_6

VALUE	DOCUMENT ID		TECN	COMMENT
seen	[92] ABREU	92M	DLPH	E_{cm}^{ee}= 88–94 GeV
seen	[93] ACTON	92N	OPAL	E_{cm}^{ee}= 88–94 GeV
seen	[94] BUSKULIC	92E	ALEP	E_{cm}^{ee}= 88–94 GeV

[92] ABREU 92M reported value is $\Gamma(B_s^0X)*B(B_s^0\to D_s\mu\nu_{\mu}X)*B(D_s\to\phi\pi)/\Gamma(\text{hadrons})=(18\pm8)\times10^{-5}$.

[93] ACTON 92N find evidence for B_s^0 production using D_s-ℓ correlations, with $D_s^+\to\phi\pi^+$ and $K^*(892)K^+$. Assuming R_b from the Standard Model and averaging over the e and μ channels, authors measure the product branching fraction to be $f(\overline{b}\to B_s^0)\times B(B_s^0\to D_s^-\ell^+\nu_{\ell}X)\times B(D_s^-\to\phi\pi^-)=(3.9\pm1.1\pm0.8)\times10^{-4}$.

[94] BUSKULIC 92E find evidence for B_s^0 production using D_s-ℓ correlations, with $D_s^+\to\phi\pi^+$ and $K^*(892)K^+$. Using $B(D_s^+\to\phi\pi^+)=(2.7\pm0.7)$% and summing up the e and μ channels, the weighted average product branching fraction is measured to be $B(\overline{b}\to B_s^0)\times B(B_s^0\to D_s^-\ell^+\nu_{\ell}X)=0.040\pm0.011^{+0.010}_{-0.012}$.

$\Gamma(B_c^+X)/\Gamma(\text{hadrons})$ Γ_{38}/Γ_6

VALUE	DOCUMENT ID		TECN	COMMENT
searched for	[95] ACKERSTAFF	98O	OPAL	E_{cm}^{ee}= 88–94 GeV
searched for	[96] ABREU	97E	DLPH	E_{cm}^{ee}= 88–94 GeV
searched for	[97] BARATE	97H	ALEP	E_{cm}^{ee}= 88–94 GeV

[95] ACKERSTAFF 98O searched for the decay modes $B_c\to J/\psi\pi^+$, $J/\psi a_1^+$, and $J/\psi\ell^+\nu_{\ell}$, with $J/\psi\to\ell^+\ell^-$, $\ell=e,\mu$. The number of candidates (background) for the three decay modes is 2 (0.63 ± 0.2), 0 (1.10 ± 0.22), and 1 (0.82 ± 0.19) respectively. Interpreting the $2\ B_c\to J/\psi\pi^+$ candidates as signal, they report $\Gamma(B_c^+X)\times B(B_c\to J/\psi\pi^+)/\Gamma(\text{hadrons})=(3.8^{+5.0}_{-2.4}\pm0.5)\times10^{-5}$. Interpreted as background, the 90% CL bounds are $\Gamma(B_c^+X)*B(B_c\to J/\psi\pi^+)/\Gamma(\text{hadrons})<1.06\times10^{-4}$, $\Gamma(B_c^+X)*B(B_c\to J/\psi a_1^+)/\Gamma(\text{hadrons})<5.29\times10^{-4}$, $\Gamma(B_c^+X)*B(B_c\to J/\psi\ell^+\nu_{\ell})/\Gamma(\text{hadrons})<6.96\times10^{-5}$.

[96] ABREU 97E searched for the decay modes $B_c\to J/\psi\pi^+$, $J/\psi\ell^+\nu_{\ell}$, and $J/\psi(3\pi)^+$, with $J/\psi\to\ell^+\ell^-$, $\ell=e,\mu$. The number of candidates (background) for the three decay modes is 1 (1.7), 0 (0.3), and 1 (2.3) respectively. They report the following 90% CL limits: $\Gamma(B_c^+X)*B(B_c\to J/\psi\pi^+)/\Gamma(\text{hadrons})<(1.05\text{–}0.84)\times10^{-4}$, $\Gamma(B_c^+X)*B(B_c\to J/\psi\ell\nu_{\ell})/\Gamma(\text{hadrons})<(5.8\text{–}5.0)\times10^{-5}$, $\Gamma(B_c^+X)*B(B_c\to J/\psi(3\pi)^+)/\Gamma(\text{hadrons})<1.75\times10^{-4}$, where the ranges are due to the predicted B_c lifetime (0.4–1.4) ps.

[97] BARATE 97H searched for the decay modes $B_c\to J/\psi\pi^+$ and $J/\psi\ell^+\nu_{\ell}$ with $J/\psi\to\ell^+\ell^-$, $\ell=e,\mu$. The number of candidates (background) for the two decay modes is 0 (0.44) and 2 (0.81) respectively. They report the following 90% CL limits: $\Gamma(B_c^+X)*B(B_c\to J/\psi\pi^+)/\Gamma(\text{hadrons})<3.6\times10^{-5}$ and $\Gamma(B_c^+X)*B(B_c\to J/\psi\ell^+\nu_{\ell})/\Gamma(\text{hadrons})<5.2\times10^{-5}$.

$\Gamma(B^*X)/[\Gamma(BX)+\Gamma(B^*X)]$ $\Gamma_{36}/(\Gamma_{35}+\Gamma_{36})$

As the experiments assume different values of the b-baryon contribution, our average should be taken with caution. If we assume a common baryon production fraction of (11.8 ± 2.0)% as given in the 2002 edition of this *Review* OUR AVERAGE becomes 0.75 ± 0.04.

VALUE	EVTS	DOCUMENT ID		TECN	COMMENT
0.75 ±0.04 OUR AVERAGE					
$0.760\pm0.036\pm0.083$		[98] ACKERSTAFF	97M	OPAL	E_{cm}^{ee}= 88–94 GeV
$0.771\pm0.026\pm0.070$		[99] BUSKULIC	96D	ALEP	E_{cm}^{ee}= 88–94 GeV
$0.72\ \pm0.03\ \pm0.06$		[100] ABREU	95R	DLPH	E_{cm}^{ee}= 88–94 GeV
$0.76\ \pm0.08\ \pm0.06$	1378	[101] ACCIARRI	95B	L3	E_{cm}^{ee}= 88–94 GeV

[98] ACKERSTAFF 97M use an inclusive B reconstruction method and assume a (13.2 ± 4.1)% b-baryon contribution. The value refers to a b-flavored meson mixture of B_u, B_d, and B_s.

[99] BUSKULIC 96D use an inclusive reconstruction of B hadrons and assume a (12.2 ± 4.3)% b-baryon contribution. The value refers to a b-flavored mixture of B_u, B_d, and B_s.

[100] ABREU 95R use an inclusive B-reconstruction method and assume a (10 ± 4)% b-baryon contribution. The value refers to a b-flavored meson mixture of B_u, B_d, and B_s.

[101] ACCIARRI 95B assume a 9.4% b-baryon contribution. The value refers to a b-flavored mixture of B_u, B_d, and B_s.

$\Gamma(\text{anomalous }\gamma+\text{hadrons})/\Gamma_{total}$ Γ_{39}/Γ

Limits on additional sources of prompt photons beyond expectations for final-state bremsstrahlung.

VALUE	CL%	DOCUMENT ID		TECN	COMMENT
$<3.2\times10^{-3}$	95	[102] AKRAWY	90J	OPAL	E_{cm}^{ee}= 88–94 GeV

[102] AKRAWY 90J report $\Gamma(\gamma X)<8.2$ MeV at 95%CL. They assume a three-body $\gamma q\overline{q}$ distribution and use $E(\gamma)>10$ GeV.

$\Gamma(e^+e^-\gamma)/\Gamma_{total}$ Γ_{40}/Γ

VALUE	CL%	DOCUMENT ID		TECN	COMMENT
$<5.2\times10^{-4}$	95	[103] ACTON	91B	OPAL	E_{cm}^{ee}= 91.2 GeV

[103] ACTON 91B looked for isolated photons with $E>2$% of beam energy (>0.9 GeV).

$\Gamma(\mu^+\mu^-\gamma)/\Gamma_{total}$ Γ_{41}/Γ

VALUE	CL%	DOCUMENT ID		TECN	COMMENT
$<5.6\times10^{-4}$	95	[104] ACTON	91B	OPAL	E_{cm}^{ee}= 91.2 GeV

[104] ACTON 91B looked for isolated photons with $E>2\%$ of beam energy ($>$ 0.9 GeV).

$\Gamma(\tau^+\tau^-\gamma)/\Gamma_{total}$ Γ_{42}/Γ

VALUE	CL%	DOCUMENT ID		TECN	COMMENT
$<7.3\times10^{-4}$	95	[105] ACTON	91B	OPAL	E_{cm}^{ee}= 91.2 GeV

[105] ACTON 91B looked for isolated photons with $E>2\%$ of beam energy ($>$ 0.9 GeV).

$\Gamma(\ell^+\ell^-\gamma\gamma)/\Gamma_{total}$ Γ_{43}/Γ

The value is the sum over $\ell = e, \mu, \tau$.

VALUE	CL%	DOCUMENT ID		TECN	COMMENT
$<6.8\times10^{-6}$	95	[106] ACTON	93E	OPAL	E_{cm}^{ee}= 88–94 GeV

[106] For $m_{\gamma\gamma} = 60 \pm 5$ GeV.

$\Gamma(q\bar{q}\gamma\gamma)/\Gamma_{total}$ Γ_{44}/Γ

VALUE	CL%	DOCUMENT ID		TECN	COMMENT
$<5.5\times10^{-6}$	95	[107] ACTON	93E	OPAL	E_{cm}^{ee}= 88–94 GeV

[107] For $m_{\gamma\gamma} = 60 \pm 5$ GeV.

$\Gamma(\nu\bar{\nu}\gamma\gamma)/\Gamma_{total}$ Γ_{45}/Γ

VALUE	CL%	DOCUMENT ID		TECN	COMMENT
$<3.1\times10^{-6}$	95	[108] ACTON	93E	OPAL	E_{cm}^{ee}= 88–94 GeV

[108] For $m_{\gamma\gamma} = 60 \pm 5$ GeV.

$\Gamma(e^\pm\mu^\mp)/\Gamma(e^+e^-)$ Γ_{46}/Γ_1

Test of lepton family number conservation. The value is for the sum of the charge states indicated.

VALUE	CL%	DOCUMENT ID		TECN	COMMENT
<0.07	90	ALBAJAR	89	UA1	$E_{cm}^{p\bar{p}}$= 546,630 GeV

$\Gamma(e^\pm\mu^\mp)/\Gamma_{total}$ Γ_{46}/Γ

Test of lepton family number conservation. The value is for the sum of the charge states indicated.

VALUE	CL%	DOCUMENT ID		TECN	COMMENT
$<2.5\times10^{-6}$	95	ABREU	97C	DLPH	E_{cm}^{ee}= 88–94 GeV
$<1.7\times10^{-6}$	95	AKERS	95W	OPAL	E_{cm}^{ee}= 88–94 GeV
$<0.6\times10^{-5}$	95	ADRIANI	93I	L3	E_{cm}^{ee}= 88–94 GeV
$<2.6\times10^{-5}$	95	DECAMP	92	ALEP	E_{cm}^{ee}= 88–94 GeV

$\Gamma(e^\pm\tau^\mp)/\Gamma_{total}$ Γ_{47}/Γ

Test of lepton family number conservation. The value is for the sum of the charge states indicated.

VALUE	CL%	DOCUMENT ID		TECN	COMMENT
$<2.2\times10^{-5}$	95	ABREU	97C	DLPH	E_{cm}^{ee}= 88–94 GeV
$<9.8\times10^{-6}$	95	AKERS	95W	OPAL	E_{cm}^{ee}= 88–94 GeV
$<1.3\times10^{-5}$	95	ADRIANI	93I	L3	E_{cm}^{ee}= 88–94 GeV
$<1.2\times10^{-4}$	95	DECAMP	92	ALEP	E_{cm}^{ee}= 88–94 GeV

$\Gamma(\mu^\pm\tau^\mp)/\Gamma_{total}$ Γ_{48}/Γ

Test of lepton family number conservation. The value is for the sum of the charge states indicated.

VALUE	CL%	DOCUMENT ID		TECN	COMMENT
$<1.2\times10^{-5}$	95	ABREU	97C	DLPH	E_{cm}^{ee}= 88–94 GeV
$<1.7\times10^{-5}$	95	AKERS	95W	OPAL	E_{cm}^{ee}= 88–94 GeV
$<1.9\times10^{-5}$	95	ADRIANI	93I	L3	E_{cm}^{ee}= 88–94 GeV
$<1.0\times10^{-4}$	95	DECAMP	92	ALEP	E_{cm}^{ee}= 88–94 GeV

$\Gamma(pe)/\Gamma_{total}$ Γ_{49}/Γ

Test of baryon number and lepton number conservations. Charge conjugate states are implied.

VALUE	CL%	DOCUMENT ID		TECN	COMMENT
$<1.8\times10^{-6}$	95	[109] ABBIENDI	99I	OPAL	E_{cm}^{ee}= 88–94 GeV

[109] ABBIENDI 99I give the 95%CL limit on the partial width $\Gamma(Z^0 \rightarrow pe) < 4.6$ KeV and we have transformed it into a branching ratio.

$\Gamma(p\mu)/\Gamma_{total}$ Γ_{50}/Γ

Test of baryon number and lepton number conservations. Charge conjugate states are implied.

VALUE	CL%	DOCUMENT ID		TECN	COMMENT
$<1.8\times10^{-6}$	95	[110] ABBIENDI	99I	OPAL	E_{cm}^{ee}= 88–94 GeV

[110] ABBIENDI 99I give the 95%CL limit on the partial width $\Gamma(Z^0 \rightarrow p\mu) < 4.4$ KeV and we have transformed it into a branching ratio.

AVERAGE PARTICLE MULTIPLICITIES IN HADRONIC Z DECAY

Summed over particle and antiparticle, when appropriate.

$\langle N_\gamma \rangle$

VALUE	DOCUMENT ID		TECN	COMMENT
$20.97\pm0.02\pm1.15$	ACKERSTAFF	98A	OPAL	E_{cm}^{ee}= 91.2 GeV

$\langle N_{\pi^\pm} \rangle$

VALUE	DOCUMENT ID		TECN	COMMENT
16.99 ± 0.20 OUR AVERAGE				
16.84 ± 0.37	ABE	99E	SLD	E_{cm}^{ee}= 91.2 GeV
$17.26\pm0.10\pm0.88$	ABREU	98L	DLPH	E_{cm}^{ee}= 91.2 GeV
17.04 ± 0.31	BARATE	98V	ALEP	E_{cm}^{ee}= 91.2 GeV
17.05 ± 0.43	AKERS	94P	OPAL	E_{cm}^{ee}= 91.2 GeV

$\langle N_{\pi^0} \rangle$

VALUE	DOCUMENT ID		TECN	COMMENT
9.76 ± 0.26 OUR AVERAGE				
$9.55\pm0.06\pm0.75$	ACKERSTAFF	98A	OPAL	E_{cm}^{ee}= 91.2 GeV
$9.63\pm0.13\pm0.63$	BARATE	97J	ALEP	E_{cm}^{ee}= 91.2 GeV
$9.90\pm0.02\pm0.33$	ACCIARRI	96	L3	E_{cm}^{ee}= 91.2 GeV
$9.2\ \pm0.2\ \pm1.0$	ADAM	96	DLPH	E_{cm}^{ee}= 91.2 GeV

$\langle N_\eta \rangle$

VALUE	DOCUMENT ID		TECN	COMMENT
1.01 ± 0.08 OUR AVERAGE Error includes scale factor of 1.3. See the ideogram below.				
$1.20\pm0.04\pm0.11$	HEISTER	02C	ALEP	E_{cm}^{ee}= 91.2 GeV
$0.97\pm0.03\pm0.11$	ACKERSTAFF	98A	OPAL	E_{cm}^{ee}= 91.2 GeV
$0.93\pm0.01\pm0.09$	ACCIARRI	96	L3	E_{cm}^{ee}= 91.2 GeV

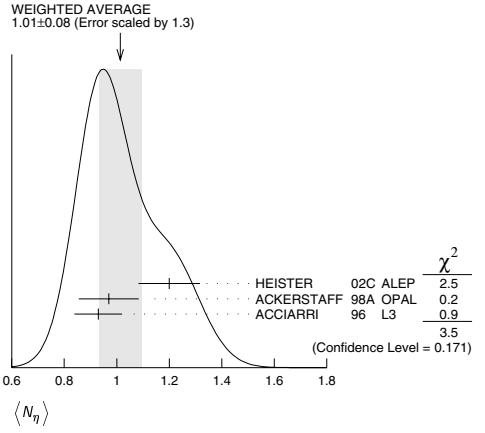

$\langle N_{\rho^\pm} \rangle$

VALUE	DOCUMENT ID		TECN	COMMENT
$2.40\pm0.06\pm0.43$	ACKERSTAFF	98A	OPAL	E_{cm}^{ee}= 91.2 GeV

$\langle N_{\rho^0} \rangle$

VALUE	DOCUMENT ID		TECN	COMMENT
1.24 ± 0.10 OUR AVERAGE Error includes scale factor of 1.1.				
1.19 ± 0.10	ABREU	99J	DLPH	E_{cm}^{ee}= 91.2 GeV
$1.45\pm0.06\pm0.20$	BUSKULIC	96H	ALEP	E_{cm}^{ee}= 91.2 GeV

$\langle N_\omega \rangle$

VALUE	DOCUMENT ID		TECN	COMMENT
1.02 ± 0.06 OUR AVERAGE				
$1.00\pm0.03\pm0.06$	HEISTER	02C	ALEP	E_{cm}^{ee}= 91.2 GeV
$1.04\pm0.04\pm0.14$	ACKERSTAFF	98A	OPAL	E_{cm}^{ee}= 91.2 GeV
$1.17\pm0.09\pm0.15$	ACCIARRI	97D	L3	E_{cm}^{ee}= 91.2 GeV

$\langle N_{\eta'} \rangle$

VALUE	DOCUMENT ID		TECN	COMMENT
$0.17\ \pm0.05$ OUR AVERAGE Error includes scale factor of 2.4.				
$0.14\ \pm0.01\ \pm0.02$	ACKERSTAFF	98A	OPAL	E_{cm}^{ee}= 91.2 GeV
$0.25\ \pm0.04$	[111] ACCIARRI	97D	L3	E_{cm}^{ee}= 91.2 GeV
• • • We do not use the following data for averages, fits, limits, etc. • • •				
$0.068\pm0.018\pm0.016$	[112] BUSKULIC	92D	ALEP	E_{cm}^{ee}= 91.2 GeV

[111] ACCIARRI 97D obtain this value averaging over the two decay channels $\eta' \rightarrow \pi^+\pi^-\eta$ and $\eta' \rightarrow \rho^0\gamma$.

[112] BUSKULIC 92D obtain this value for $x > 0.1$.

$\langle N_{f_0(980)} \rangle$

VALUE	DOCUMENT ID		TECN	COMMENT
0.147 ± 0.011 OUR AVERAGE				
0.164 ± 0.021	ABREU	99J	DLPH	E_{cm}^{ee}= 91.2 GeV
$0.141\pm0.007\pm0.011$	ACKERSTAFF	98Q	OPAL	E_{cm}^{ee}= 91.2 GeV

$\langle N_{a_0(980)^\pm} \rangle$

VALUE	DOCUMENT ID		TECN	COMMENT
0.27 ± 0.04 ± 0.10	ACKERSTAFF	98A	OPAL	E_{cm}^{ee} = 91.2 GeV

$\langle N_\phi \rangle$

VALUE	DOCUMENT ID		TECN	COMMENT
0.098 ± 0.006 OUR AVERAGE	Error includes scale factor of 2.0. See the ideogram below.			
0.105 ± 0.008	ABE	99E	SLD	E_{cm}^{ee} = 91.2 GeV
0.091 ± 0.002 ± 0.003	ACKERSTAFF	98Q	OPAL	E_{cm}^{ee} = 91.2 GeV
0.104 ± 0.003 ± 0.007	ABREU	96U	DLPH	E_{cm}^{ee} = 91.2 GeV
0.122 ± 0.004 ± 0.008	BUSKULIC	96H	ALEP	E_{cm}^{ee} = 91.2 GeV

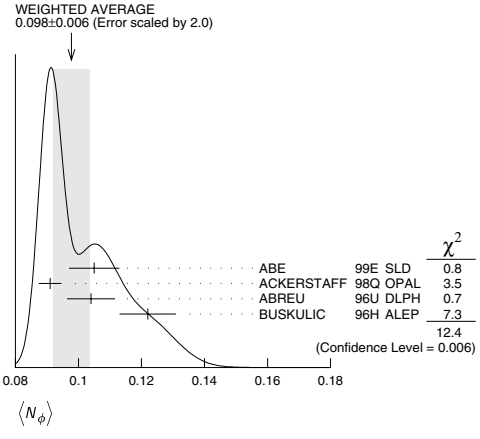

$\langle N_{f_2(1270)} \rangle$

VALUE	DOCUMENT ID		TECN	COMMENT
0.169 ± 0.025 OUR AVERAGE	Error includes scale factor of 1.4.			
0.214 ± 0.038	ABREU	99J	DLPH	E_{cm}^{ee} = 91.2 GeV
0.155 ± 0.011 ± 0.018	ACKERSTAFF	98Q	OPAL	E_{cm}^{ee} = 91.2 GeV

$\langle N_{f_1(1285)} \rangle$

VALUE	DOCUMENT ID		TECN	COMMENT
0.165 ± 0.051	[113] ABDALLAH	03H	DLPH	E_{cm}^{ee} = 91.2 GeV

[113] ABDALLAH 03H assume a $K\overline{K}\pi$ branching ratio of (9.0 ± 0.4)%.

$\langle N_{f_1(1420)} \rangle$

VALUE	DOCUMENT ID		TECN	COMMENT
0.056 ± 0.012	[114] ABDALLAH	03H	DLPH	E_{cm}^{ee} = 91.2 GeV

[114] ABDALLAH 03H assume a $K\overline{K}\pi$ branching ratio of 100%.

$\langle N_{f_2'(1525)} \rangle$

VALUE	DOCUMENT ID		TECN	COMMENT
0.012 ± 0.006	ABREU	99J	DLPH	E_{cm}^{ee} = 91.2 GeV

$\langle N_{K^\pm} \rangle$

VALUE	DOCUMENT ID		TECN	COMMENT
2.25 ± 0.05 OUR AVERAGE				
2.22 ± 0.16	ABE	99E	SLD	E_{cm}^{ee} = 91.2 GeV
2.21 ± 0.05 ± 0.05	ABREU	98L	DLPH	E_{cm}^{ee} = 91.2 GeV
2.26 ± 0.12	BARATE	98V	ALEP	E_{cm}^{ee} = 91.2 GeV
2.42 ± 0.13	AKERS	94P	OPAL	E_{cm}^{ee} = 91.2 GeV

$\langle N_{K^0} \rangle$

VALUE	DOCUMENT ID		TECN	COMMENT
2.039 ± 0.025 OUR AVERAGE	Error includes scale factor of 1.3. See the ideogram below.			
2.093 ± 0.004 ± 0.029	BARATE	00O	ALEP	E_{cm}^{ee} = 91.2 GeV
2.01 ± 0.08	ABE	99E	SLD	E_{cm}^{ee} = 91.2 GeV
2.024 ± 0.006 ± 0.042	ACCIARRI	97L	L3	E_{cm}^{ee} = 91.2 GeV
1.962 ± 0.022 ± 0.056	ABREU	95L	DLPH	E_{cm}^{ee} = 91.2 GeV
1.99 ± 0.01 ± 0.04	AKERS	95U	OPAL	E_{cm}^{ee} = 91.2 GeV

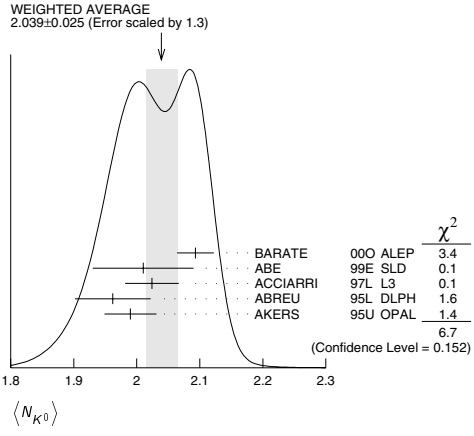

$\langle N_{K^*(892)^\pm} \rangle$

VALUE	DOCUMENT ID		TECN	COMMENT
0.72 ± 0.05 OUR AVERAGE				
0.712 ± 0.031 ± 0.059	ABREU	95L	DLPH	E_{cm}^{ee} = 91.2 GeV
0.72 ± 0.02 ± 0.08	ACTON	93	OPAL	E_{cm}^{ee} = 91.2 GeV

$\langle N_{K^*(892)^0} \rangle$

VALUE	DOCUMENT ID		TECN	COMMENT
0.739 ± 0.022 OUR AVERAGE				
0.707 ± 0.041	ABE	99E	SLD	E_{cm}^{ee} = 91.2 GeV
0.74 ± 0.02 ± 0.02	ACKERSTAFF	97S	OPAL	E_{cm}^{ee} = 91.2 GeV
0.77 ± 0.02 ± 0.07	ABREU	96U	DLPH	E_{cm}^{ee} = 91.2 GeV
0.83 ± 0.01 ± 0.09	BUSKULIC	96H	ALEP	E_{cm}^{ee} = 91.2 GeV
0.97 ± 0.18 ± 0.31	ABREU	93	DLPH	E_{cm}^{ee} = 91.2 GeV

$\langle N_{K_2^*(1430)} \rangle$

VALUE	DOCUMENT ID		TECN	COMMENT
0.073 ± 0.023	ABREU	99J	DLPH	E_{cm}^{ee} = 91.2 GeV
• • • We do not use the following data for averages, fits, limits, etc. • • •				
0.19 ± 0.04 ± 0.06	[115] AKERS	95X	OPAL	E_{cm}^{ee} = 91.2 GeV

[115] AKERS 95X obtain this value for $x < 0.3$.

$\langle N_{D^\pm} \rangle$

VALUE	DOCUMENT ID		TECN	COMMENT
0.187 ± 0.020 OUR AVERAGE	Error includes scale factor of 1.5. See the ideogram below.			
0.170 ± 0.009 ± 0.014	ALEXANDER	96R	OPAL	E_{cm}^{ee} = 91.2 GeV
0.251 ± 0.026 ± 0.025	BUSKULIC	94J	ALEP	E_{cm}^{ee} = 91.2 GeV
0.199 ± 0.019 ± 0.024	[116] ABREU	93I	DLPH	E_{cm}^{ee} = 91.2 GeV

[116] See ABREU 95 (erratum).

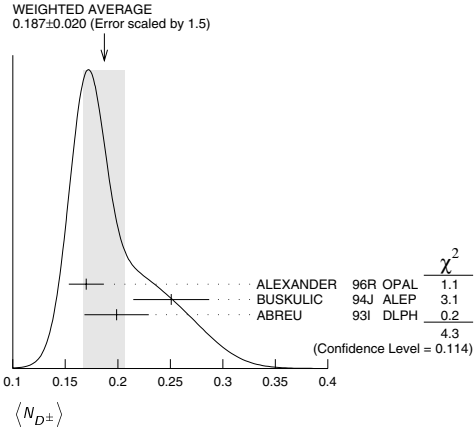

$\langle N_{D^0} \rangle$

VALUE	DOCUMENT ID		TECN	COMMENT
0.462 ± 0.026 OUR AVERAGE				
0.465 ± 0.017 ± 0.027	ALEXANDER	96R	OPAL	E_{cm}^{ee} = 91.2 GeV
0.518 ± 0.052 ± 0.035	BUSKULIC	94J	ALEP	E_{cm}^{ee} = 91.2 GeV
0.403 ± 0.038 ± 0.044	[117] ABREU	93I	DLPH	E_{cm}^{ee} = 91.2 GeV

[117] See ABREU 95 (erratum).

$\langle N_{D_s^\pm} \rangle$

VALUE	DOCUMENT ID		TECN	COMMENT
0.131 ± 0.010 ± 0.018	ALEXANDER	96R	OPAL	E_{cm}^{ee} = 91.2 GeV

$\langle N_{D^*(2010)^\pm} \rangle$

VALUE	DOCUMENT ID		TECN	COMMENT
0.183 ± 0.008 OUR AVERAGE				
0.1854 ± 0.0041 ± 0.0091	[118] ACKERSTAFF	98E	OPAL	E_{cm}^{ee} = 91.2 GeV
0.187 ± 0.015 ± 0.013	BUSKULIC	94J	ALEP	E_{cm}^{ee} = 91.2 GeV
0.171 ± 0.012 ± 0.016	[119] ABREU	93I	DLPH	E_{cm}^{ee} = 91.2 GeV

[118] ACKERSTAFF 98E systematic error includes an uncertainty of ±0.0069 due to the branching ratios $B(D^{*+} \to D^0\pi^+) = 0.683 \pm 0.014$ and $B(D^0 \to K^-\pi^+) = 0.0383 \pm 0.0012$.

[119] See ABREU 95 (erratum).

$\langle N_{D_{s1}(2536)^+} \rangle$

VALUE (units 10^{-3})	DOCUMENT ID		TECN	COMMENT
• • • We do not use the following data for averages, fits, limits, etc. • • •				
$2.9^{+0.7}_{-0.6} \pm 0.2$	[120] ACKERSTAFF	97W	OPAL	E_{cm}^{ee} = 91.2 GeV

[120] ACKERSTAFF 97W obtain this value for $x > 0.6$ and with the assumption that its decay width is saturated by the D^*K final states.

$\langle N_{B^*} \rangle$

VALUE	DOCUMENT ID		TECN	COMMENT
0.28 ± 0.01 ± 0.03	[121] ABREU	95R	DLPH	E_{cm}^{ee} = 91.2 GeV

[121] ABREU 95R quote this value for a flavor-averaged excited state.

$\langle N_{J/\psi(1S)} \rangle$

VALUE	DOCUMENT ID		TECN	COMMENT
0.0056 ± 0.0003 ± 0.0004	[122] ALEXANDER	96B	OPAL	E_{cm}^{ee} = 91.2 GeV

[122] ALEXANDER 96B identify $J/\psi(1S)$ from the decays into lepton pairs.

$\langle N_{\psi(2S)} \rangle$

VALUE	DOCUMENT ID		TECN	COMMENT
0.0023 ± 0.0004 ± 0.0003	ALEXANDER	96B	OPAL	E_{cm}^{ee} = 91.2 GeV

$\langle N_p \rangle$

VALUE	DOCUMENT ID		TECN	COMMENT
1.04 ± 0.04 OUR AVERAGE				
1.03 ± 0.13	ABE	99E	SLD	E_{cm}^{ee} = 91.2 GeV
1.08 ± 0.04 ± 0.03	ABREU	98L	DLPH	E_{cm}^{ee} = 91.2 GeV
1.00 ± 0.07	BARATE	98V	ALEP	E_{cm}^{ee} = 91.2 GeV
0.92 ± 0.11	AKERS	94P	OPAL	E_{cm}^{ee} = 91.2 GeV

$\langle N_{\Delta(1232)^{++}} \rangle$

VALUE	DOCUMENT ID		TECN	COMMENT
0.087 ± 0.033 OUR AVERAGE	Error includes scale factor of 2.4.			
0.079 ± 0.009 ± 0.011	ABREU	95W	DLPH	E_{cm}^{ee} = 91.2 GeV
0.22 ± 0.04 ± 0.04	ALEXANDER	95D	OPAL	E_{cm}^{ee} = 91.2 GeV

$\langle N_\Lambda \rangle$

VALUE	DOCUMENT ID		TECN	COMMENT
0.388 ± 0.009 OUR AVERAGE	Error includes scale factor of 1.7. See the ideogram below.			
0.404 ± 0.002 ± 0.007	BARATE	00O	ALEP	E_{cm}^{ee} = 91.2 GeV
0.395 ± 0.022	ABE	99E	SLD	E_{cm}^{ee} = 91.2 GeV
0.364 ± 0.004 ± 0.017	ACCIARRI	97L	L3	E_{cm}^{ee} = 91.2 GeV
0.374 ± 0.002 ± 0.010	ALEXANDER	97D	OPAL	E_{cm}^{ee} = 91.2 GeV
0.357 ± 0.003 ± 0.017	ABREU	93L	DLPH	E_{cm}^{ee} = 91.2 GeV

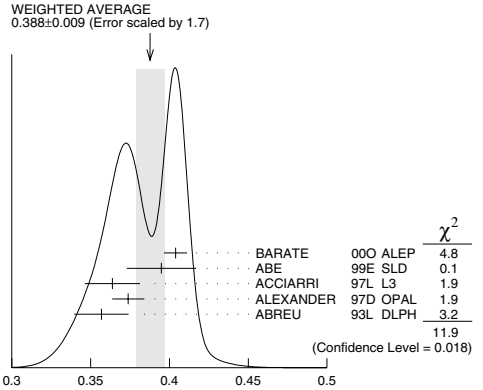

$\langle N_{\Lambda(1520)} \rangle$

VALUE	DOCUMENT ID		TECN	COMMENT
0.0224 ± 0.0027 OUR AVERAGE				
0.029 ± 0.005 ± 0.005	ABREU	00P	DLPH	E_{cm}^{ee} = 91.2 GeV
0.0213 ± 0.0021 ± 0.0019	ALEXANDER	97D	OPAL	E_{cm}^{ee} = 91.2 GeV

$\langle N_{\Sigma^+} \rangle$

VALUE	DOCUMENT ID		TECN	COMMENT
0.107 ± 0.010 OUR AVERAGE				
0.114 ± 0.011 ± 0.009	ACCIARRI	00J	L3	E_{cm}^{ee} = 91.2 GeV
0.099 ± 0.008 ± 0.013	ALEXANDER	97E	OPAL	E_{cm}^{ee} = 91.2 GeV

$\langle N_{\Sigma^-} \rangle$

VALUE	DOCUMENT ID		TECN	COMMENT
0.082 ± 0.007 OUR AVERAGE				
0.081 ± 0.002 ± 0.010	ABREU	00P	DLPH	E_{cm}^{ee} = 91.2 GeV
0.083 ± 0.006 ± 0.009	ALEXANDER	97E	OPAL	E_{cm}^{ee} = 91.2 GeV

$\langle N_{\Sigma^+ + \Sigma^-} \rangle$

VALUE	DOCUMENT ID		TECN	COMMENT
0.181 ± 0.018 OUR AVERAGE				
0.182 ± 0.010 ± 0.016	[123] ALEXANDER	97E	OPAL	E_{cm}^{ee} = 91.2 GeV
0.170 ± 0.014 ± 0.061	ABREU	95O	DLPH	E_{cm}^{ee} = 91.2 GeV

[123] We have combined the values of $\langle N_{\Sigma^+} \rangle$ and $\langle N_{\Sigma^-} \rangle$ from ALEXANDER 97E adding the statistical and systematic errors of the two final states separately in quadrature. If isospin symmetry is assumed this value becomes 0.174 ± 0.010 ± 0.015.

$\langle N_{\Sigma^0} \rangle$

VALUE	DOCUMENT ID		TECN	COMMENT
0.076 ± 0.010 OUR AVERAGE				
0.095 ± 0.015 ± 0.013	ACCIARRI	00J	L3	E_{cm}^{ee} = 91.2 GeV
0.071 ± 0.012 ± 0.013	ALEXANDER	97E	OPAL	E_{cm}^{ee} = 91.2 GeV
0.070 ± 0.010 ± 0.010	ADAM	96B	DLPH	E_{cm}^{ee} = 91.2 GeV

$\langle N_{(\Sigma^+ + \Sigma^- + \Sigma^0)/3} \rangle$

VALUE	DOCUMENT ID		TECN	COMMENT
0.084 ± 0.005 ± 0.008	ALEXANDER	97E	OPAL	E_{cm}^{ee} = 91.2 GeV

$\langle N_{\Sigma(1385)^+} \rangle$

VALUE	DOCUMENT ID		TECN	COMMENT
0.0239 ± 0.0009 ± 0.0012	ALEXANDER	97D	OPAL	E_{cm}^{ee} = 91.2 GeV

$\langle N_{\Sigma(1385)^-} \rangle$

VALUE	DOCUMENT ID		TECN	COMMENT
0.0240 ± 0.0010 ± 0.0014	ALEXANDER	97D	OPAL	E_{cm}^{ee} = 91.2 GeV

$\langle N_{\Sigma(1385)^+ + \Sigma(1385)^-} \rangle$

VALUE	DOCUMENT ID		TECN	COMMENT
0.046 ± 0.004 OUR AVERAGE	Error includes scale factor of 1.6.			
0.0479 ± 0.0013 ± 0.0026	ALEXANDER	97D	OPAL	E_{cm}^{ee} = 91.2 GeV
0.0382 ± 0.0028 ± 0.0045	ABREU	95O	DLPH	E_{cm}^{ee} = 91.2 GeV

$\langle N_{\Xi^-} \rangle$

VALUE	DOCUMENT ID		TECN	COMMENT
0.0258 ± 0.0009 OUR AVERAGE				
0.0259 ± 0.0004 ± 0.0009	ALEXANDER	97D	OPAL	E_{cm}^{ee} = 91.2 GeV
0.0250 ± 0.0009 ± 0.0021	ABREU	95O	DLPH	E_{cm}^{ee} = 91.2 GeV

$\langle N_{\Xi(1530)^0} \rangle$

VALUE	DOCUMENT ID		TECN	COMMENT
0.0053 ± 0.0013 OUR AVERAGE	Error includes scale factor of 3.2.			
0.0068 ± 0.0005 ± 0.0004	ALEXANDER	97D	OPAL	E_{cm}^{ee} = 91.2 GeV
0.0041 ± 0.0004 ± 0.0004	ABREU	95O	DLPH	E_{cm}^{ee} = 91.2 GeV

$\langle N_{\Omega^-} \rangle$

VALUE	DOCUMENT ID		TECN	COMMENT
0.00164 ± 0.00028 OUR AVERAGE				
0.0018 ± 0.0003 ± 0.0002	ALEXANDER	97D	OPAL	E_{cm}^{ee} = 91.2 GeV
0.0014 ± 0.0002 ± 0.0004	ADAM	96B	DLPH	E_{cm}^{ee} = 91.2 GeV

$\langle N_{\Lambda_c^+} \rangle$

VALUE	DOCUMENT ID		TECN	COMMENT
0.078 ± 0.012 ± 0.012	ALEXANDER	96R	OPAL	E_{cm}^{ee} = 91.2 GeV

$\langle N_{charged} \rangle$

VALUE	DOCUMENT ID		TECN	COMMENT
21.07 ± 0.11 OUR AVERAGE				
21.21 ± 0.01 ± 0.20	ABREU	99	DLPH	E_{cm}^{ee} = 91.2 GeV
21.05 ± 0.20	AKERS	95Z	OPAL	E_{cm}^{ee} = 91.2 GeV
20.91 ± 0.03 ± 0.22	BUSKULIC	95R	ALEP	E_{cm}^{ee} = 91.2 GeV
21.40 ± 0.43	ACTON	92B	OPAL	E_{cm}^{ee} = 91.2 GeV
20.71 ± 0.04 ± 0.77	ABREU	91H	DLPH	E_{cm}^{ee} = 91.2 GeV
20.7 ± 0.7	ADEVA	91I	L3	E_{cm}^{ee} = 91.2 GeV
20.1 ± 1.0 ± 0.9	ABRAMS	90	MRK2	E_{cm}^{ee} = 91.1 GeV

Z HADRONIC POLE CROSS SECTION

OUR FIT is obtained using the fit procedure and correlations as determined by the LEP Electroweak Working Group (see the "Note on the Z boson"). This quantity is defined as

$$\sigma_h^0 = \frac{12\pi}{M_Z^2} \frac{\Gamma(e^+e^-)\Gamma(\text{hadrons})}{\Gamma_Z^2}$$

It is one of the parameters used in the Z lineshape fit.

VALUE (nb)	EVTS	DOCUMENT ID		TECN	COMMENT
41.541 ± 0.037 OUR FIT					
41.501 ± 0.055	4.10M	[124] ABBIENDI	01A	OPAL	E_{cm}^{ee} = 88–94 GeV
41.578 ± 0.069	3.70M	ABREU	00F	DLPH	E_{cm}^{ee} = 88–94 GeV
41.535 ± 0.055	3.54M	ACCIARRI	00C	L3	E_{cm}^{ee} = 88–94 GeV
41.559 ± 0.058	4.07M	[125] BARATE	00C	ALEP	E_{cm}^{ee} = 88–94 GeV
• • • We do not use the following data for averages, fits, limits, etc. • • •					
41.23 ± 0.20	1.05M	ABREU	94	DLPH	Repl. by ABREU 00F
41.39 ± 0.26	1.09M	ACCIARRI	94	L3	Repl. by ACCIARRI 00C
41.70 ± 0.23	1.19M	AKERS	94	OPAL	Repl. by ABBIENDI 01A
41.60 ± 0.16	1.27M	BUSKULIC	94	ALEP	Repl. by BARATE 00C
42 ± 4	450	ABRAMS	89B	MRK2	E_{cm}^{ee} = 89.2–93.0 GeV

[124] ABBIENDI 01A error includes approximately 0.031 due to statistics, 0.033 due to event selection systematics, 0.029 due to uncertainty in luminosity measurement, and 0.011 due to LEP energy uncertainty.

[125] BARATE 00C error includes approximately 0.030 due to statistics, 0.026 due to experimental systematics, and 0.025 due to uncertainty in luminosity measurement.

Z VECTOR COUPLINGS TO CHARGED LEPTONS

These quantities are the effective vector couplings of the Z to charged leptons. Their magnitude is derived from a measurement of the Z lineshape and the forward-backward lepton asymmetries as a function of energy around the Z mass. The relative sign among the vector to axial-vector couplings is obtained from a measurement of the Z asymmetry parameters, A_e, A_μ, and A_τ. By convention the sign of g_A^e is fixed to be negative (and opposite to that of g^{ν_e} obtained using ν_e scattering measurements). The fit values quoted below correspond to global nine- or five-parameter fits to lineshape, lepton forward-backward asymmetry, and A_e, A_μ, and A_τ measurements. See "Note on the Z boson" for details.

g_V^e

VALUE	EVTS	DOCUMENT ID		TECN	COMMENT
−0.03816 ± 0.00047 OUR FIT					
−0.0346 ± 0.0023	137.0K	[126] ABBIENDI	01O	OPAL	E_{cm}^{ee} = 88–94 GeV
−0.0412 ± 0.0027	124.4k	[127] ACCIARRI	00C	L3	E_{cm}^{ee} = 88–94 GeV
−0.0400 ± 0.0037		BARATE	00C	ALEP	E_{cm}^{ee} = 88–94 GeV
−0.0414 ± 0.0020		[128] ABE	95J	SLD	E_{cm}^{ee} = 91.31 GeV

[126] ABBIENDI 01O use their measurement of the τ polarization in addition to the lineshape and forward-backward lepton asymmetries.

[127] ACCIARRI 00C use their measurement of the τ polarization in addition to forward-backward lepton asymmetries.

[128] ABE 95J obtain this result combining polarized Bhabha results with the A_{LR} measurement of ABE 94C. The Bhabha results alone give $-0.0507 \pm 0.0096 \pm 0.0020$.

g_V^μ

VALUE	EVTS	DOCUMENT ID		TECN	COMMENT
−0.0367 ± 0.0023 OUR FIT					
$-0.0388^{+0.0060}_{-0.0064}$	182.8K	[129] ABBIENDI	01O	OPAL	E_{cm}^{ee} = 88–94 GeV
−0.0386 ± 0.0073	113.4k	[130] ACCIARRI	00C	L3	E_{cm}^{ee} = 88–94 GeV
−0.0362 ± 0.0061		BARATE	00C	ALEP	E_{cm}^{ee} = 88–94 GeV
• • • We do not use the following data for averages, fits, limits, etc. • • •					
−0.0413 ± 0.0060	66143	[131] ABBIENDI	01K	OPAL	E_{cm}^{ee} = 89–93 GeV

[129] ABBIENDI 01O use their measurement of the τ polarization in addition to the lineshape and forward-backward lepton asymmetries.

[130] ACCIARRI 00C use their measurement of the τ polarization in addition to forward-backward lepton asymmetries.

[131] ABBIENDI 01K obtain this from an angular analysis of the muon pair asymmetry which takes into account effects of initial state radiation on an event by event basis and of initial-final state interference.

g_V^τ

VALUE	EVTS	DOCUMENT ID		TECN	COMMENT
−0.0366 ± 0.0010 OUR FIT					
−0.0365 ± 0.0023	151.5K	[132] ABBIENDI	01O	OPAL	E_{cm}^{ee} = 88–94 GeV
−0.0384 ± 0.0026	103.0k	[133] ACCIARRI	00C	L3	E_{cm}^{ee} = 88–94 GeV
−0.0361 ± 0.0068		BARATE	00C	ALEP	E_{cm}^{ee} = 88–94 GeV

[132] ABBIENDI 01O use their measurement of the τ polarization in addition to the lineshape and forward-backward lepton asymmetries.

[133] ACCIARRI 00C use their measurement of the τ polarization in addition to forward-backward lepton asymmetries.

g_V^ℓ

VALUE	EVTS	DOCUMENT ID		TECN	COMMENT
−0.03783 ± 0.00041 OUR FIT					
−0.0358 ± 0.0014	471.3K	[134] ABBIENDI	01O	OPAL	E_{cm}^{ee} = 88–94 GeV
−0.0397 ± 0.0020	379.4k	[135] ABREU	00F	DLPH	E_{cm}^{ee} = 88–94 GeV
−0.0397 ± 0.0017	340.8k	[136] ACCIARRI	00C	L3	E_{cm}^{ee} = 88–94 GeV
−0.0383 ± 0.0018	500k	BARATE	00C	ALEP	E_{cm}^{ee} = 88–94 GeV

[134] ABBIENDI 01O use their measurement of the τ polarization in addition to the lineshape and forward-backward lepton asymmetries.

[135] Using forward-backward lepton asymmetries.

[136] ACCIARRI 00C use their measurement of the τ polarization in addition to forward-backward lepton asymmetries.

Z AXIAL-VECTOR COUPLINGS TO CHARGED LEPTONS

These quantities are the effective axial-vector couplings of the Z to charged leptons. Their magnitude is derived from a measurement of the Z lineshape and the forward-backward lepton asymmetries as a function of energy around the Z mass. The relative sign among the vector to axial-vector couplings is obtained from a measurement of the Z asymmetry parameters, A_e, A_μ, and A_τ. By convention the sign of g_A^e is fixed to be negative (and opposite to that of g^{ν_e} obtained using ν_e scattering measurements). The fit values quoted below correspond to global nine- or five-parameter fits to lineshape, lepton forward-backward asymmetry, and A_e, A_μ, and A_τ measurements. See "Note on the Z boson" for details.

g_A^e

VALUE	EVTS	DOCUMENT ID		TECN	COMMENT
−0.50111 ± 0.00035 OUR FIT					
−0.50062 ± 0.00062	137.0K	[137] ABBIENDI	01O	OPAL	E_{cm}^{ee} = 88–94 GeV
−0.5015 ± 0.0007	124.4k	[138] ACCIARRI	00C	L3	E_{cm}^{ee} = 88–94 GeV
−0.50166 ± 0.00057		BARATE	00C	ALEP	E_{cm}^{ee} = 88–94 GeV
−0.4977 ± 0.0045		[139] ABE	95J	SLD	E_{cm}^{ee} = 91.31 GeV

[137] ABBIENDI 01O use their measurement of the τ polarization in addition to the lineshape and forward-backward lepton asymmetries.

[138] ACCIARRI 00C use their measurement of the τ polarization in addition to forward-backward lepton asymmetries.

[139] ABE 95J obtain this result combining polarized Bhabha results with the A_{LR} measurement of ABE 94C. The Bhabha results alone give $-0.4968 \pm 0.0039 \pm 0.0027$.

g_A^μ

VALUE	EVTS	DOCUMENT ID		TECN	COMMENT
−0.50120±0.00054 OUR FIT					
−0.50117±0.00099	182.8K	[140] ABBIENDI	01O	OPAL	E_{cm}^{ee} = 88–94 GeV
−0.5009 ±0.0014	113.4k	[141] ACCIARRI	00C	L3	E_{cm}^{ee} = 88–94 GeV
−0.50046±0.00093		BARATE	00C	ALEP	E_{cm}^{ee} = 88–94 GeV
• • • We do not use the following data for averages, fits, limits, etc. • • •					
−0.520 ±0.015	66143	[142] ABBIENDI	01K	OPAL	E_{cm}^{ee} = 89–93 GeV

[140] ABBIENDI 01O use their measurement of the τ polarization in addition to the lineshape and forward-backward lepton asymmetries.
[141] ACCIARRI 00C use their measurement of the τ polarization in addition to forward-backward lepton asymmetries.
[142] ABBIENDI 01K obtain this from an angular analysis of the muon pair asymmetry which takes into account effects of initial state radiation on an event by event basis and of initial-final state interference.

g_A^τ

VALUE	EVTS	DOCUMENT ID		TECN	COMMENT
−0.50204±0.00064 OUR FIT					
−0.50165±0.00124	151.5K	[143] ABBIENDI	01O	OPAL	E_{cm}^{ee} = 88–94 GeV
−0.5023 ±0.0017	103.0k	[144] ACCIARRI	00C	L3	E_{cm}^{ee} = 88–94 GeV
−0.50216±0.00100		BARATE	00C	ALEP	E_{cm}^{ee} = 88–94 GeV

[143] ABBIENDI 01O use their measurement of the τ polarization in addition to the lineshape and forward-backward lepton asymmetries.
[144] ACCIARRI 00C use their measurement of the τ polarization in addition to forward-backward lepton asymmetries.

g_A^ℓ

VALUE	EVTS	DOCUMENT ID		TECN	COMMENT
−0.50123±0.00026 OUR FIT					
−0.50089±0.00045	471.3K	[145] ABBIENDI	01O	OPAL	E_{cm}^{ee} = 88–94 GeV
−0.5007 ±0.0005	379.4k	ABREU	00F	DLPH	E_{cm}^{ee} = 88–94 GeV
−0.50153±0.00053	340.8k	[146] ACCIARRI	00C	L3	E_{cm}^{ee} = 88–94 GeV
−0.50150±0.00046	500k	BARATE	00C	ALEP	E_{cm}^{ee} = 88–94 GeV

[145] ABBIENDI 01O use their measurement of the τ polarization in addition to the lineshape and forward-backward lepton asymmetries.
[146] ACCIARRI 00C use their measurement of the τ polarization in addition to forward-backward lepton asymmetries.

Z COUPLINGS TO NEUTRAL LEPTONS

These quantities are the effective couplings of the Z to neutral leptons. $\nu_e e$ and $\nu_\mu e$ scattering results are combined with g_A^e and g_V^e measurements at the Z mass to obtain g^{ν_e} and g^{ν_μ} following NOVIKOV 93C.

g^{ν_e}

VALUE	DOCUMENT ID			TECN	COMMENT
0.528±0.085	[147] VILAIN	94		CHM2	From $\nu_\mu e$ and $\nu_e e$ scattering

[147] VILAIN 94 derive this value from their value of g^{ν_μ} and their ratio $g^{\nu_e}/g^{\nu_\mu} = 1.05^{+0.15}_{-0.18}$.

g^{ν_μ}

VALUE	DOCUMENT ID			TECN	COMMENT
0.502±0.017	[148] VILAIN	94		CHM2	From $\nu_\mu e$ scattering

[148] VILAIN 94 derive this value from their measurement of the couplings $g_A^{e\nu_\mu} = -0.503 \pm 0.017$ and $g_V^{e\nu_\mu} = -0.035 \pm 0.017$ obtained from $\nu_\mu e$ scattering. We have re-evaluated this value using the current PDG values for g_A^e and g_V^e.

Z ASYMMETRY PARAMETERS

For each fermion-antifermion pair coupling to the Z these quantities are defined as

$$A_f = \frac{2 g_V^f g_A^f}{(g_V^f)^2 + (g_A^f)^2}$$

where g_V^f and g_A^f are the effective vector and axial-vector couplings. For their relation to the various lepton asymmetries see the 'Note on the Z Boson.'

A_e

Using polarized beams, this quantity can also be measured as $(\sigma_L - \sigma_R)/(\sigma_L + \sigma_R)$, where σ_L and σ_R are the e^+e^- production cross sections for Z bosons produced with left-handed and right-handed electrons respectively.

VALUE		EVTS	DOCUMENT ID		TECN	COMMENT
0.1515 ±0.0019 OUR AVERAGE						
0.1454 ±0.0108	±0.0036	144810	[149] ABBIENDI	01O	OPAL	E_{cm}^{ee} = 88–94 GeV
0.1516 ±0.0021		559000	[150] ABE	01B	SLD	E_{cm}^{ee} = 91.24 GeV
0.1504 ±0.0068	±0.0008		[151] HEISTER	01	ALEP	E_{cm}^{ee} = 88–94 GeV
0.1382 ±0.0116	±0.0005	105000	[152] ABREU	00E	DLPH	E_{cm}^{ee} = 88–94 GeV
0.1678 ±0.0127	±0.0030	137092	[153] ACCIARRI	98H	L3	E_{cm}^{ee} = 88–94 GeV
0.162 ±0.041	±0.014	89838	[154] ABE	97	SLD	E_{cm}^{ee} = 91.27 GeV
0.202 ±0.038	±0.008		[155] ABE	95J	SLD	E_{cm}^{ee} = 91.31 GeV
• • • We do not use the following data for averages, fits, limits, etc. • • •						
0.15138±0.00216		537000	[156] ABE	00B	SLD	Repl. by ABE 01B
0.152 ±0.012		4527	[157] ABE	97N	SLD	Repl. by ABE 01B
0.129 ±0.014	±0.005	89075	[158] ALEXANDER	96U	OPAL	Repl. by ABBIENDI 01O
0.136 ±0.027	±0.003		[153] ABREU	95I	DLPH	Repl. by ABREU 00E
0.129 ±0.016	±0.005	33000	[159] BUSKULIC	95Q	ALEP	Repl. by HEISTER 01
0.157 ±0.020	±0.005	86000	[153] ACCIARRI	94E	L3	Repl. by ACCIARRI 98H

[149] ABBIENDI 01O fit for A_e and A_τ from measurements of the τ polarization at varying τ production angles. The correlation between A_e and A_τ is less than 0.03.
[150] ABE 01B use the left-right production and left-right forward-backward decay asymmetries in leptonic Z decays to obtain a value of 0.1544 ± 0.0060. This is combined with left-right production asymmetry measurement using hadronic Z decays (ABE 00B) to obtain the quoted value.
[151] HEISTER 01 obtain this result fitting the τ polarization as a function of the polar production angle of the τ.
[152] ABREU 00E obtain this result fitting the τ polarization as a function of the polar τ production angle. This measurement is a combination of different analyses (exclusive τ decay modes, inclusive hadronic 1-prong reconstruction, and a neural network analysis).
[153] Derived from the measurement of forward-backward τ polarization asymmetry.
[154] ABE 97 obtain this result from a measurement of the observed left-right charge asymmetry, $A_Q^{obs} = 0.225 \pm 0.056 \pm 0.019$, in hadronic Z decays. If they combine this value of A_Q^{obs} with their earlier measurement of A_{LR}^{obs} they determine A_e to be $0.1574 \pm 0.0197 \pm 0.0067$ independent of the beam polarization.
[155] ABE 95J obtain this result from polarized Bhabha scattering.
[156] ABE 00B obtain this value measuring the left-right Z boson cross-section asymmetry. This is equivalent to an effective weak mixing angle of $\sin^2\theta_W^{eff} = 0.23097 \pm 0.00027$.
[157] ABE 97N obtain this direct measurement using the left-right cross section asymmetry and the left-right forward-backward asymmetry in leptonic decays of the Z boson obtained with a polarized electron beam.
[158] ALEXANDER 96U measure the τ-lepton polarization and the forward-backward polarization asymmetry.
[159] BUSKULIC 95Q obtain this result fitting the τ polarization as a function of the polar τ production angle.

A_μ

This quantity is directly extracted from a measurement of the left-right forward-backward asymmetry in $\mu^+\mu^-$ production at SLC using a polarized electron beam. This double asymmetry eliminates the dependence on the Z-e-e coupling parameter A_e.

VALUE	EVTS	DOCUMENT ID		TECN	COMMENT
0.142±0.015	16844	[160] ABE	01B	SLD	E_{cm}^{ee} = 91.24 GeV
• • • We do not use the following data for averages, fits, limits, etc. • • •					
0.102±0.034	3788	[161] ABE	97N	SLD	Repl. by ABE 01B

[160] ABE 01B obtain this direct measurement using the left-right production and left-right forward-backward polar angle asymmetries in $\mu^+\mu^-$ decays of the Z boson obtained with a polarized electron beam.
[161] ABE 97N obtain this direct measurement using the left-right cross section asymmetry and the left-right forward-backward asymmetry in $\mu^+\mu^-$ decays of the Z boson obtained with a polarized electron beam.

A_τ

The LEP Collaborations derive this quantity from the measurement of the τ polarization in $Z \to \tau^+\tau^-$. The SLD Collaboration directly extracts this quantity from its measured left-right forward-backward asymmetry in $Z \to \tau^+\tau^-$ produced using a polarized e^- beam. This double asymmetry eliminates the dependence on the Z-e-e coupling parameter A_e.

VALUE	EVTS	DOCUMENT ID		TECN	COMMENT
0.143 ±0.004 OUR AVERAGE					
0.1456±0.0076±0.0057	144810	[162] ABBIENDI	01O	OPAL	E_{cm}^{ee} = 88–94 GeV
0.136 ±0.015	16083	[163] ABE	01B	SLD	E_{cm}^{ee} = 91.24 GeV
0.1451±0.0052±0.0029		[164] HEISTER	01	ALEP	E_{cm}^{ee} = 88–94 GeV
0.1359±0.0079±0.0055	105000	[165] ABREU	00E	DLPH	E_{cm}^{ee} = 88–94 GeV
0.1476±0.0088±0.0062	137092	ACCIARRI	98H	L3	E_{cm}^{ee} = 88–94 GeV
• • • We do not use the following data for averages, fits, limits, etc. • • •					
0.195 ±0.034	3748	[166] ABE	97N	SLD	Repl. by ABE 01B
0.134 ±0.009 ±0.010	89075	[167] ALEXANDER	96U	OPAL	Repl. by ABBIENDI 01O
0.148 ±0.017 ±0.014		ABREU	95I	DLPH	Repl. by ABREU 00E
0.136 ±0.012 ±0.009	33000	[168] BUSKULIC	95Q	ALEP	Repl. by HEISTER 01
0.150 ±0.013 ±0.009	86000	ACCIARRI	94E	L3	Repl. by ACCIARRI 98H

[162] ABBIENDI 01O fit for A_e and A_τ from measurements of the τ polarization at varying τ production angles. The correlation between A_e and A_τ is less than 0.03.
[163] ABE 01B obtain this direct measurement using the left-right production and left-right forward-backward polar angle asymmetries in $\tau^+\tau^-$ decays of the Z boson obtained with a polarized electron beam.
[164] HEISTER 01 obtain this result fitting the τ polarization as a function of the polar production angle of the τ.
[165] ABREU 00E obtain this result fitting the τ polarization as a function of the polar τ production angle. This measurement is a combination of different analyses (exclusive τ decay modes, inclusive hadronic 1-prong reconstruction, and a neural network analysis).
[166] ABE 97N obtain this direct measurement using the left-right cross section asymmetry and the left-right forward-backward asymmetry in $\tau^+\tau^-$ decays of the Z boson obtained with a polarized electron beam.

[167] ALEXANDER 96U measure the τ-lepton polarization and the forward-backward polarization asymmetry.

[168] BUSKULIC 95Q obtain this result fitting the τ polarization as a function of the polar τ production angle.

A_s

The SLD Collaboration directly extracts this quantity by a simultaneous fit to four measured s-quark polar angle distributions corresponding to two states of e^- polarization (positive and negative) and to the K^+K^- and $K^\pm K^0_S$ strange particle tagging modes in the hadronic final states.

VALUE	EVTS	DOCUMENT ID		TECN	COMMENT
0.895 ± 0.066 ± 0.062	2870	[169] ABE	00D	SLD	E^{ee}_{cm} = 91.2 GeV

[169] ABE 00D tag $Z \to s\overline{s}$ events by an absence of B or D hadrons and the presence in each hemisphere of a high momentum $K^\pm$ or K^0_S.

A_c

This quantity is directly extracted from a measurement of the left-right forward-backward asymmetry in $c\overline{c}$ production at SLC using polarized electron beam. This double asymmetry eliminates the dependence on the Z-e-e coupling parameter A_e. OUR FIT is obtained by a simultaneous fit to several c- and b-quark measurements as explained in the note "The Z Boson."

VALUE	DOCUMENT ID		TECN	COMMENT
0.666 ± 0.036 OUR FIT				
0.583 ± 0.055 ± 0.055	[170] ABE	02G	SLD	E^{ee}_{cm} = 91.24 GeV
0.688 ± 0.041	[171] ABE	01C	SLD	E^{ee}_{cm} = 91.25 GeV
• • • We do not use the following data for averages, fits, limits, etc. • • •				
0.642 ± 0.110 ± 0.063	[172] ABE	99O	SLD	Repl. by ABE 02G
0.73 ± 0.22 ± 0.10	[173] ABE,K	95	SLD	Repl. by ABE 01C

[170] ABE 02G tag b and c quarks through their semileptonic decays into electrons and muons. A maximum likelihood fit is performed to extract simultaneously A_b and A_c.

[171] ABE 01C tag $Z \to c\overline{c}$ events using two techniques: exclusive reconstruction of D^{*+}, D^+ and D^0 mesons and the soft pion tag for $D^{*+} \to D^0\pi^+$. The large background from D mesons produced in $b\overline{b}$ events is separated efficiently from the signal using precision vertex information. When combining the A_c values from these two samples, care is taken to avoid double counting of events common to the two samples, and common systematic errors are properly taken into account.

[172] ABE 99O tag b and c quarks through their semileptonic decays into electrons and muons. A maximum likelihood fit is performed to extract simultaneously A_b and A_c.

[173] ABE,K 95 tag $Z \to c\overline{c}$ events using D^{*+} and D^+ meson production. To take care of the $b\overline{b}$ contamination in their analysis they use $A^D_b = 0.64 \pm 0.11$ (which is A_b from D^*/D tagging). This is obtained by starting with a Standard Model value of 0.935, assigning it an estimated error of ± 0.105 to cover LEP and SLD measurements, and finally taking into account B-$\overline{B}$ mixing ($1-2\chi_{\rm mix} = 0.72 \pm 0.09$).

A_b

This quantity is directly extracted from a measurement of the left-right forward-backward asymmetry in $b\overline{b}$ production at SLC using polarized electron beam. This double asymmetry eliminates the dependence on the Z-e-e coupling parameter A_e. OUR FIT is obtained by a simultaneous fit to several c- and b-quark measurements as explained in the note "The Z Boson."

VALUE	EVTS	DOCUMENT ID		TECN	COMMENT
0.926 ± 0.024 OUR FIT					
0.907 ± 0.020 ± 0.024	48028	[174] ABE	03F	SLD	E^{ee}_{cm} = 91.24 GeV
0.919 ± 0.030 ± 0.024		[175] ABE	02G	SLD	E^{ee}_{cm} = 91.24 GeV
0.855 ± 0.088 ± 0.102	7473	[176] ABE	99L	SLD	E^{ee}_{cm} = 91.27 GeV
• • • We do not use the following data for averages, fits, limits, etc. • • •					
0.910 ± 0.068 ± 0.037		[177] ABE	99O	SLD	Repl. by ABE 02G
0.911 ± 0.045 ± 0.045	11092	[178] ABE	98I	SLD	Repl. by ABE 03F

[174] ABE 03F obtain an enriched sample of $b\overline{b}$ events tagging on the invariant mass of a 3-dimensional topologically reconstructed secondary decay. The charge of the underlying b quark is obtained using a self-calibrating track-charge method. For the 1996–1998 data sample they measure $A_b = 0.906 \pm 0.022 \pm 0.023$. The value quoted here is obtained combining the above with the result of ABE 98I (1993–1995 data sample).

[175] ABE 02G tag b and c quarks through their semileptonic decays into electrons and muons. A maximum likelihood fit is performed to extract simultaneously A_b and A_c.

[176] ABE 99L obtain an enriched sample of $b\overline{b}$ events tagging with an inclusive vertex mass cut. For distinguishing b and $\overline{b}$ quarks they use the charge of identified $K^\pm$.

[177] ABE 99O tag b and c quarks through their semileptonic decays into electrons and muons. A maximum likelihood fit is performed to extract simultaneously A_b and A_c.

[178] ABE 98I obtain an enriched sample of $b\overline{b}$ events tagging with an inclusive vertex mass cut. A momentum-weighted track charge is used to identify the sign of the charge of the underlying b quark.

TRANSVERSE SPIN CORRELATIONS IN $Z \to \tau^+\tau^-$

The correlations between the transverse spin components of $\tau^+\tau^-$ produced in Z decays may be expressed in terms of the vector and axial-vector couplings:

$$C_{TT} = \frac{|g^\tau_A|^2 - |g^\tau_V|^2}{|g^\tau_A|^2 + |g^\tau_V|^2}$$

$$C_{TN} = -2\frac{|g^\tau_A||g^\tau_V|}{|g^\tau_A|^2 + |g^\tau_V|^2}\sin(\Phi_{g^\tau_V} - \Phi_{g^\tau_A})$$

C_{TT} refers to the transverse-transverse (within the collision plane) spin correlation and C_{TN} refers to the transverse-normal (to the collision plane) spin correlation.

The longitudinal τ polarization P_τ $(= -A_\tau)$ is given by:

$$P_\tau = -2\frac{|g^\tau_A||g^\tau_V|}{|g^\tau_A|^2 + |g^\tau_V|^2}\cos(\Phi_{g^\tau_V} - \Phi_{g^\tau_A})$$

Here Φ is the phase and the phase difference $\Phi_{g^\tau_V} - \Phi_{g^\tau_A}$ can be obtained using both the measurements of C_{TN} and P_τ.

C_{TT}

VALUE	EVTS	DOCUMENT ID		TECN	COMMENT
1.01 ± 0.12 OUR AVERAGE					
$0.87 \pm 0.20^{+0.10}_{-0.12}$	9.1k	ABREU	97G	DLPH	E^{ee}_{cm} = 91.2 GeV
1.06 ± 0.13 ± 0.05	120k	BARATE	97D	ALEP	E^{ee}_{cm} = 91.2 GeV

C_{TN}

VALUE	EVTS	DOCUMENT ID		TECN	COMMENT
0.08 ± 0.13 ± 0.04	120k	[179] BARATE	97D	ALEP	E^{ee}_{cm} = 91.2 GeV

[179] BARATE 97D combine their value of C_{TN} with the world average $P_\tau = -0.140 \pm 0.007$ to obtain $\tan(\Phi_{g^\tau_V} - \Phi_{g^\tau_A}) = -0.57 \pm 0.97$.

FORWARD-BACKWARD $e^+e^- \to f\overline{f}$ CHARGE ASYMMETRIES

These asymmetries are experimentally determined by tagging the respective lepton or quark flavor in e^+e^- interactions. Details of heavy flavor (c- or b-quark) tagging at LEP are described in the note on "The Z Boson." The Standard Model predictions for LEP data have been (re)computed using the ZFITTER package (version 6.36) with input parameters M_Z=91.187 GeV, $M_{\rm top}$=174.3 GeV, $M_{\rm Higgs}$=150 GeV, α_s=0.119, $\alpha^{(5)}(M_Z) = 1/128.877$ and the Fermi constant $G_F = 1.16637 \times 10^{-5}$ GeV^{-2} (see the note on "The Z Boson" for references). For non-LEP data the Standard Model predictions are as given by the authors of the respective publications.

$A^{(0,e)}_{FB}$ CHARGE ASYMMETRY IN $e^+e^- \to e^+e^-$

OUR FIT is obtained using the fit procedure and correlations as determined by the LEP Electroweak Working Group (see the "Note on the Z boson"). For the Z peak, we report the pole asymmetry defined by $(3/4)A^2_e$ as determined by the nine-parameter fit to cross-section and lepton forward-backward asymmetry data.

ASYMMETRY (%)	STD. MODEL	$\sqrt{s}$ (GeV)	DOCUMENT ID		TECN
1.45 ± 0.25 OUR FIT					
0.89 ± 0.44	1.57	91.2	[180] ABBIENDI	01A	OPAL
1.71 ± 0.49	1.57	91.2	ABREU	00F	DLPH
1.06 ± 0.58	1.57	91.2	ACCIARRI	00C	L3
1.88 ± 0.34	1.57	91.2	[181] BARATE	00C	ALEP
• • • We do not use the following data for averages, fits, limits, etc. • • •					
2.5 ± 0.9	1.57	91.2	ABREU	94	DLPH
1.04 ± 0.92	1.57	91.2	ACCIARRI	94	L3
0.62 ± 0.80	1.57	91.2	AKERS	94	OPAL
1.85 ± 0.66	1.57	91.2	BUSKULIC	94	ALEP

[180] ABBIENDI 01A error includes approximately 0.38 due to statistics, 0.16 due to event selection systematics, and 0.18 due to the theoretical uncertainty in t-channel prediction.

[181] BARATE 00C error includes approximately 0.31 due to statistics, 0.06 due to experimental systematics, and 0.13 due to the theoretical uncertainty in t-channel prediction.

$A^{(0,\mu)}_{FB}$ CHARGE ASYMMETRY IN $e^+e^- \to \mu^+\mu^-$

OUR FIT is obtained using the fit procedure and correlations as determined by the LEP Electroweak Working Group (see the "Note on the Z boson"). For the Z peak, we report the pole asymmetry defined by $(3/4)A_eA_\mu$ as determined by the nine-parameter fit to cross-section and lepton forward-backward asymmetry data.

ASYMMETRY (%)	STD. MODEL	$\sqrt{s}$ (GeV)	DOCUMENT ID		TECN
1.69 ± 0.13 OUR FIT					
1.59 ± 0.23	1.57	91.2	[182] ABBIENDI	01A	OPAL
1.65 ± 0.25	1.57	91.2	ABREU	00F	DLPH
1.88 ± 0.33	1.57	91.2	ACCIARRI	00C	L3
1.71 ± 0.24	1.57	91.2	[183] BARATE	00C	ALEP
• • • We do not use the following data for averages, fits, limits, etc. • • •					
9 ±30	−1.3	20	[184] ABREU	95M	DLPH
7 ±26	−8.3	40	[184] ABREU	95M	DLPH
−11 ±33	−24.1	57	[184] ABREU	95M	DLPH
−62 ±17	−44.6	69	[184] ABREU	95M	DLPH
−56 ±10	−63.5	79	[184] ABREU	95M	DLPH
−13 ± 5	−34.4	87.5	[184] ABREU	95M	DLPH
1.4 ± 0.5	1.57	91.2	ABREU	94	DLPH
1.79 ± 0.61	1.57	91.2	ACCIARRI	94	L3
0.99 ± 0.42	1.57	91.2	AKERS	94	OPAL
1.46 ± 0.48	1.57	91.2	BUSKULIC	94	ALEP
$-29.0\ ^{+5.0}_{-4.8} \pm 0.5$	−32.1	56.9	[185] ABE	90I	VNS
− 9.9 ± 1.5 ±0.5	−9.2	35	HEGNER	90	JADE
0.05 ± 0.22	0.026	91.14	[186] ABRAMS	89D	MRK2
−43.4 ±17.0	−24.9	52.0	[187] BACALA	89	AMY

−11.0	±16.5	−29.4	55.0	[187] BACALA	89	AMY
−30.0	±12.4	−31.2	56.0	[187] BACALA	89	AMY
−46.2	±14.9	−33.0	57.0	[187] BACALA	89	AMY
−29	±13	−25.9	53.3	ADACHI	88C	TOPZ
+ 5.3	± 5.0 ±0.5	−1.2	14.0	ADEVA	88	MRKJ
−10.4	± 1.3 ±0.5	−8.6	34.8	ADEVA	88	MRKJ
−12.3	± 5.3 ±0.5	−10.7	38.3	ADEVA	88	MRKJ
−15.6	± 3.0 ±0.5	−14.9	43.8	ADEVA	88	MRKJ
− 1.0	± 6.0	−1.2	13.9	BRAUNSCH...	88D	TASS
− 9.1	± 2.3 ±0.5	−8.6	34.5	BRAUNSCH...	88D	TASS
−10.6	$^{+\ 2.2}_{-\ 2.3}$ ±0.5	−8.9	35.0	BRAUNSCH...	88D	TASS
−17.6	$^{+\ 4.4}_{-\ 4.3}$ ±0.5	−15.2	43.6	BRAUNSCH...	88D	TASS
− 4.8	± 6.5 ±1.0	−11.5	39	BEHREND	87C	CELL
−18.8	± 4.5 ±1.0	−15.5	44	BEHREND	87C	CELL
+ 2.7	± 4.9	−1.2	13.9	BARTEL	86C	JADE
−11.1	± 1.8 ±1.0	−8.6	34.4	BARTEL	86C	JADE
−17.3	± 4.8 ±1.0	−13.7	41.5	BARTEL	86C	JADE
−22.8	± 5.1 ±1.0	−16.6	44.8	BARTEL	86C	JADE
− 6.3	± 0.8 ±0.2	−6.3	29	ASH	85	MAC
− 4.9	± 1.5 ±0.5	−5.9	29	DERRICK	85	HRS
− 7.1	± 1.7	−5.7	29	LEVI	83	MRK2
−16.1	± 3.2	−9.2	34.2	BRANDELIK	82C	TASS

[182] ABBIENDI 01A error is almost entirely on account of statistics.
[183] BARATE 00C error is almost entirely on account of statistics.
[184] ABREU 95M perform this measurement using radiative muon-pair events associated with high-energy isolated photons.
[185] ABE 90I measurements in the range $50 \leq \sqrt{s} \leq 60.8$ GeV.
[186] ABRAMS 89D asymmetry includes both 9 $\mu^+\mu^-$ and 15 $\tau^+\tau^-$ events.
[187] BACALA 89 systematic error is about 5%.

$A_{FB}^{(0,\tau)}$ CHARGE ASYMMETRY IN $e^+e^- \to \tau^+\tau^-$

OUR FIT is obtained using the fit procedure and correlations as determined by the LEP Electroweak Working Group (see the "Note on the Z boson"). For the Z peak, we report the pole asymmetry defined by $(3/4)A_eA_\tau$ as determined by the nine-parameter fit to cross-section and lepton forward-backward asymmetry data.

ASYMMETRY (%)	STD. MODEL	$\sqrt{s}$ (GeV)	DOCUMENT ID		TECN
1.88± 0.17 OUR FIT					
1.45± 0.30	1.57	91.2	[188] ABBIENDI	01A	OPAL
2.41± 0.37	1.57	91.2	ABREU	00F	DLPH
2.60± 0.47	1.57	91.2	ACCIARRI	00C	L3
1.70± 0.28	1.57	91.2	[189] BARATE	00C	ALEP
• • • We do not use the following data for averages, fits, limits, etc. • • •					
2.2 ± 0.7	1.57	91.2	ABREU	94	DLPH
2.65± 0.88	1.57	91.2	ACCIARRI	94	L3
2.05± 0.52	1.57	91.2	AKERS	94	OPAL
1.97± 0.56	1.57	91.2	BUSKULIC	94	ALEP
−32.8 $^{+\ 6.4}_{-\ 6.2}$ ±1.5	−32.1	56.9	[190] ABE	90I	VNS
− 8.1 ± 2.0 ±0.6	−9.2	35	HEGNER	90	JADE
−18.4 ±19.2	−24.9	52.0	[191] BACALA	89	AMY
−17.7 ±26.1	−29.4	55.0	[191] BACALA	89	AMY
−45.9 ±16.6	−31.2	56.0	[191] BACALA	89	AMY
−49.5 ±18.0	−33.0	57.0	[191] BACALA	89	AMY
−20 ±14	−25.9	53.3	ADACHI	88C	TOPZ
−10.6 ± 3.1 ±1.5	−8.5	34.7	ADEVA	88	MRKJ
− 8.5 ± 6.6 ±1.5	−15.4	43.8	ADEVA	88	MRKJ
− 6.0 ± 2.5 ±1.0	8.8	34.6	BARTEL	85F	JADE
−11.8 ± 4.6 ±1.0	14.8	43.0	BARTEL	85F	JADE
− 5.5 ± 1.2 ±0.5	−0.063	29.0	FERNANDEZ	85	MAC
− 4.2 ± 2.0	0.057	29	LEVI	83	MRK2
−10.3 ± 5.2	−9.2	34.2	BEHREND	82	CELL
− 0.4 ± 6.6	−9.1	34.2	BRANDELIK	82C	TASS

[188] ABBIENDI 01A error includes approximately 0.26 due to statistics and 0.14 due to event selection systematics.
[189] BARATE 00C error includes approximately 0.26 due to statistics and 0.11 due to experimental systematics.
[190] ABE 90I measurements in the range $50 \leq \sqrt{s} \leq 60.8$ GeV.
[191] BACALA 89 systematic error is about 5%.

$A_{FB}^{(0,\ell)}$ CHARGE ASYMMETRY IN $e^+e^- \to \ell^+\ell^-$

For the Z peak, we report the pole asymmetry defined by $(3/4)A_\ell^2$ as determined by the five-parameter fit to cross-section and lepton forward-backward asymmetry data assuming lepton universality. For details see the "Note on the Z boson."

ASYMMETRY (%)	STD. MODEL	$\sqrt{s}$ (GeV)	DOCUMENT ID		TECN
1.71±0.10 OUR FIT					
1.45±0.17	1.57	91.2	[192] ABBIENDI	01A	OPAL
1.87±0.19	1.57	91.2	ABREU	00F	DLPH
1.92±0.24	1.57	91.2	ACCIARRI	00C	L3
1.73±0.16	1.57	91.2	[193] BARATE	00C	ALEP
• • • We do not use the following data for averages, fits, limits, etc. • • •					
1.77±0.37	1.57	91.2	ABREU	94	DLPH
1.84±0.45	1.57	91.2	ACCIARRI	94	L3
1.28±0.30	1.57	91.2	AKERS	94	OPAL
1.71±0.33	1.57	91.2	BUSKULIC	94	ALEP

[192] ABBIENDI 01A error includes approximately 0.15 due to statistics, 0.06 due to event selection systematics, and 0.03 due to the theoretical uncertainty in t-channel prediction.
[193] BARATE 00C error includes approximately 0.15 due to statistics, 0.04 due to experimental systematics, and 0.02 due to the theoretical uncertainty in t-channel prediction.

$A_{FB}^{(0,u)}$ CHARGE ASYMMETRY IN $e^+e^- \to u\overline{u}$

ASYMMETRY (%)	STD. MODEL	$\sqrt{s}$ (GeV)	DOCUMENT ID		TECN
4.0±6.7±2.8	**7.2**	**91.2**	[194] ACKERSTAFF	97T	OPAL

[194] ACKERSTAFF 97T measure the forward-backward asymmetry of various fast hadrons made of light quarks. Then using SU(2) isospin symmetry and flavor independence for down and strange quarks authors solve for the different quark types.

$A_{FB}^{(0,s)}$ CHARGE ASYMMETRY IN $e^+e^- \to s\overline{s}$

The s-quark asymmetry is derived from measurements of the forward-backward asymmetry of fast hadrons containing an s quark.

ASYMMETRY (%)	STD. MODEL	$\sqrt{s}$ (GeV)	DOCUMENT ID		TECN
9.8 ±1.1 OUR AVERAGE					
10.08±1.13±0.40	10.1	91.2	[195] ABREU	00B	DLPH
6.8 ±3.5 ±1.1	10.1	91.2	[196] ACKERSTAFF	97T	OPAL
• • • We do not use the following data for averages, fits, limits, etc. • • •					
13.1 ±3.5 ±1.3	10.1	91.2	[197] ABREU	95G	DLPH

[195] ABREU 00B tag the presence of an s quark requiring a high-momentum-identified charged kaon. The s-quark pole asymmetry is extracted from the charged-kaon asymmetry taking the expected d- and u-quark asymmetries from the Standard Model and using the measured values for the c- and b-quark asymmetries.
[196] ACKERSTAFF 97T measure the forward-backward asymmetry of various fast hadrons made of light quarks. Then using SU(2) isospin symmetry and flavor independence for down and strange quarks authors solve for the different quark types. The value reported here corresponds then to the forward-backward asymmetry for "down-type" quarks.
[197] ABREU 95G require the presence of a high-momentum charged kaon or Λ^0 to tag the s quark. An unresolved s- and d-quark asymmetry of $(11.2 \pm 3.1 \pm 5.4)\%$ is obtained by tagging the presence of a high-energy neutron or neutral kaon in the hadron calorimeter. Superseded by ABREU 00B.

$A_{FB}^{(0,c)}$ CHARGE ASYMMETRY IN $e^+e^- \to c\overline{c}$

OUR FIT, which is obtained by a simultaneous fit to several c- and b-quark measurements as explained in the "Note on the Z boson," refers to the **Z pole** asymmetry. The experimental values, on the other hand, correspond to the measurements carried out at the respective energies. As a cross check we have also performed a weighted average of the "near peak" measurements taking into account the various common systematic errors. Applying to this combined "peak" measurement QED and energy-dependence corrections, our weighted average gives a pole asymmetry of $(6.98 \pm 0.42)\%$, the Standard Model prediction being 7.25%.

ASYMMETRY (%)	STD. MODEL	$\sqrt{s}$ (GeV)	DOCUMENT ID		TECN
7.04± 0.36 OUR FIT					
5.68± 0.54±0.39	6.3	91.25	[198] ABBIENDI	03P	OPAL
6.45± 0.57±0.37	6.10	91.21	[199] HEISTER	02H	ALEP
6.59± 0.94±0.35	6.2	91.235	[200] ABREU	99Y	DLPH
6.3 ± 0.9 ±0.3	6.1	91.22	[201] BARATE	98O	ALEP
6.3 ± 1.2 ±0.6	6.1	91.22	[202] ALEXANDER	97C	OPAL
8.3 ± 2.2 ±1.6	6.4	91.27	[203] ABREU	95K	DLPH
8.3 ± 3.8 ±2.7	6.2	91.24	[204] ADRIANI	92D	L3
• • • We do not use the following data for averages, fits, limits, etc. • • •					
− 6.8 ± 2.5 ±0.9	−3.0	89.51	[198] ABBIENDI	03P	OPAL
14.6 ± 2.0 ±0.8	12.2	92.95	[198] ABBIENDI	03P	OPAL
−12.4 ±15.9 ±2.0	−9.6	88.38	[199] HEISTER	02H	ALEP
− 2.3 ± 2.6 ±0.2	−3.8	89.38	[199] HEISTER	02H	ALEP
− 0.3 ± 8.3 ±0.6	0.9	90.21	[199] HEISTER	02H	ALEP
10.6 ± 7.7 ±0.7	9.6	92.05	[199] HEISTER	02H	ALEP
11.9 ± 2.1 ±0.6	12.2	92.94	[199] HEISTER	02H	ALEP
12.1 ±11.0 ±1.0	14.2	93.90	[199] HEISTER	02H	ALEP
− 4.96± 3.68±0.53	−3.5	89.434	[200] ABREU	99Y	DLPH
11.80± 3.18±0.62	12.3	92.990	[200] ABREU	99Y	DLPH
− 1.0 ± 4.3 ±1.0	−3.9	89.37	[201] BARATE	98O	ALEP
11.0 ± 3.3 ±0.8	12.3	92.96	[201] BARATE	98O	ALEP
3.9 ± 5.1 ±0.9	−3.4	89.45	[202] ALEXANDER	97C	OPAL
15.8 ± 4.1 ±1.1	12.4	93.00	[202] ALEXANDER	97C	OPAL
−12.9 ± 7.8 ±5.5	−13.6	35	BEHREND	90D	CELL
7.7 ±13.4 ±5.0	−22.1	43	BEHREND	90D	CELL
−12.8 ± 4.4 ±4.1	−13.6	35	ELSEN	90	JADE
−10.9 ±12.9 ±4.6	−23.2	44	ELSEN	90	JADE
−14.9 ± 6.7	−13.3	35	OULD-SAADA	89	JADE

[198] ABBIENDI 03P tag heavy flavors using events with one or two identified leptons. This allows the simultaneous fitting of the b and c quark forward-backward asymmetries as well as the average B^0-$\overline{B}^0$ mixing.

[199] HEISTER 02H measure simultaneously b and c quark forward-backward asymmetries using their semileptonic decays to tag the quark charge. The flavor separation is obtained with a discriminating multivariate analysis.

[200] ABREU 99Y tag $Z \to b\overline{b}$ and $Z \to c\overline{c}$ events by an exclusive reconstruction of several D meson decay modes (D^{*+}, D^0, and D^+ with their charge-conjugate states).

[201] BARATE 98O tag $Z \to c\overline{c}$ events requiring the presence of high-momentum reconstructed D^{*+}, D^+, or D^0 mesons.

[202] ALEXANDER 97C identify the b and c events using a D/D^* tag.

[203] ABREU 95K identify c and b quarks using both electron and muon semileptonic decays.

[204] ADRIANI 92D use both electron and muon semileptonic decays.

$A_{FB}^{(0,b)}$ CHARGE ASYMMETRY IN $e^+e^- \to b\overline{b}$

OUR FIT, which is obtained by a simultaneous fit to several c- and b-quark measurements as explained in the "Note on the Z boson," refers to the ***Z* pole** asymmetry. The experimental values, on the other hand, correspond to the measurements carried out at the respective energies. As a cross check we have also performed a weighted average of the "near peak" measurements taking into account the various common systematic errors. Applying to this combined "peak" measurement QED and energy-dependence corrections, our weighted average gives a pole asymmetry of (10.14 ± 0.18)%, the Standard Model prediction being 10.15%. For the jet-charge measurements (where the QCD effects are included since they represent an inherent part of the analysis), we use the corrections given by the authors.

ASYMMETRY (%)	STD. MODEL	$\sqrt{s}$ (GeV)	DOCUMENT ID		TECN
10.01 ± 0.17 OUR FIT					
9.72 ± 0.42 ± 0.15	9.67	91.25	[205] ABBIENDI	03P	OPAL
9.77 ± 0.36 ± 0.18	9.69	91.26	[206] ABBIENDI	02I	OPAL
9.52 ± 0.41 ± 0.17	9.59	91.21	[207] HEISTER	02H	ALEP
10.00 ± 0.27 ± 0.11	9.63	91.232	[208] HEISTER	01D	ALEP
9.82 ± 0.47 ± 0.16	9.69	91.26	[209] ABREU	99M	DLPH
7.62 ± 1.94 ± 0.85	9.64	91.235	[210] ABREU	99Y	DLPH
9.60 ± 0.66 ± 0.33	9.69	91.26	[211] ACCIARRI	99D	L3
9.31 ± 1.01 ± 0.55	9.65	91.24	[212] ACCIARRI	98U	L3
9.4 ± 2.7 ± 2.2	9.61	91.22	[213] ALEXANDER	97C	OPAL
10.4 ± 1.3 ± 0.5	9.70	91.27	[214] ABREU	95K	DLPH
• • • We do not use the following data for averages, fits, limits, etc. • • •					
4.7 ± 1.8 ± 0.1	5.9	89.51	[205] ABBIENDI	03P	OPAL
10.3 ± 1.5 ± 0.2	12.0	92.95	[205] ABBIENDI	03P	OPAL
5.82 ± 1.53 ± 0.12	5.9	89.50	[206] ABBIENDI	02I	OPAL
12.21 ± 1.23 ± 0.25	12.0	92.91	[206] ABBIENDI	02I	OPAL
−13.1 ±13.5 ± 1.0	3.2	88.38	[207] HEISTER	02H	ALEP
5.5 ± 1.9 ± 0.1	5.6	89.38	[207] HEISTER	02H	ALEP
− 0.4 ± 6.7 ± 0.8	7.5	90.21	[207] HEISTER	02H	ALEP
11.1 ± 6.4 ± 0.5	11.0	92.05	[207] HEISTER	02H	ALEP
10.4 ± 1.5 ± 0.3	12.0	92.94	[207] HEISTER	02H	ALEP
13.8 ± 9.3 ± 1.1	12.9	93.90	[207] HEISTER	02H	ALEP
4.36 ± 1.19 ± 0.11	5.8	89.472	[208] HEISTER	01D	ALEP
11.72 ± 0.97 ± 0.11	12.0	92.950	[208] HEISTER	01D	ALEP
6.8 ± 1.8 ± 0.13	6.0	89.55	[209] ABREU	99M	DLPH
12.3 ± 1.6 ± 0.27	12.0	92.94	[209] ABREU	99M	DLPH
5.67 ± 7.56 ± 1.17	5.7	89.434	[210] ABREU	99Y	DLPH
8.82 ± 6.33 ± 1.22	12.1	92.990	[210] ABREU	99Y	DLPH
6.11 ± 2.93 ± 0.43	5.9	89.50	[211] ACCIARRI	99D	L3
13.71 ± 2.40 ± 0.44	12.2	93.10	[211] ACCIARRI	99D	L3
4.95 ± 5.23 ± 0.40	5.8	89.45	[212] ACCIARRI	98U	L3
11.37 ± 3.99 ± 0.65	12.1	92.99	[212] ACCIARRI	98U	L3
− 8.6 ±10.8 ± 2.9	5.8	89.45	[213] ALEXANDER	97C	OPAL
− 2.1 ± 9.0 ± 2.6	12.1	93.00	[213] ALEXANDER	97C	OPAL
$-71 \pm 34 \; {}^{+\,7}_{-\,8}$	−58	58.3	SHIMONAKA	91	TOPZ
−22.2 ± 7.7 ± 3.5	−26.0	35	BEHREND	90D	CELL
−49.1 ±16.0 ± 5.0	−39.7	43	BEHREND	90D	CELL
−28 ±11	−23	35	BRAUNSCH...	90	TASS
−16.6 ± 7.7 ± 4.8	−24.3	35	ELSEN	90	JADE
−33.6 ±22.2 ± 5.2	−39.9	44	ELSEN	90	JADE
3.4 ± 7.0 ± 3.5	−16.0	29.0	BAND	89	MAC
−72 ±28 ±13	−56	55.2	SAGAWA	89	AMY

[205] ABBIENDI 03P tag heavy flavors using events with one or two identified leptons. This allows the simultaneous fitting of the b and c quark forward-backward asymmetries as well as the average B^0-$\overline{B}^0$ mixing.

[206] ABBIENDI 02I tag $Z^0 \to b\overline{b}$ decays using a combination of secondary vertex and lepton tags. The sign of the b-quark charge is determined using an inclusive tag based on jet, vertex, and kaon charges.

[207] HEISTER 02H measure simultaneously b and c quark forward-backward asymmetries using their semileptonic decays to tag the quark charge. The flavor separation is obtained with a discriminating multivariate analysis.

[208] HEISTER 01D tag $Z \to b\overline{b}$ events using the impact parameters of charged tracks complemented with information from displaced vertices, event shape variables, and lepton identification. The b-quark direction and charge is determined using the hemisphere charge method along with information from fast kaon tagging and charge estimators of primary and secondary vertices. The change in the quoted value due to variation of A_{FB}^c and R_b is given as $+0.103\,(A_{FB}^c - 0.0651) - 0.440\,(R_b - 0.21585)$.

[209] ABREU 99M tag $Z \to b\overline{b}$ events using lifetime and vertex charge. The original quark charge is obtained from the charge flow, the difference between the forward and backward hemisphere charges.

[210] ABREU 99Y tag $Z \to b\overline{b}$ and $Z \to c\overline{c}$ events by an exclusive reconstruction of several D meson decay modes (D^{*+}, D^0, and D^+ with their charge-conjugate states).

[211] ACCIARRI 99D tag $Z \to b\overline{b}$ events using high p and p_T leptons. The analysis determines simultaneously a mixing parameter $\chi_b = 0.1192 \pm 0.0068 \pm 0.0051$ which is used to correct the observed asymmetry.

[212] ACCIARRI 98U tag $Z \to b\overline{b}$ events using lifetime and measure the jet charge using the hemisphere charge.

[213] ALEXANDER 97C identify the b and c events using a D/D^* tag.

[214] ABREU 95K identify c and b quarks using both electron and muon semileptonic decays. The systematic error includes an uncertainty of ±0.3 due to the mixing correction ($\chi = 0.115 \pm 0.011$).

CHARGE ASYMMETRY IN $e^+e^- \to q\overline{q}$

Summed over five lighter flavors.

Experimental and Standard Model values are somewhat event-selection dependent. Standard Model expectations contain some assumptions on B^0-$\overline{B}^0$ mixing and on other electroweak parameters.

ASYMMETRY (%)	STD. MODEL	$\sqrt{s}$ (GeV)	DOCUMENT ID		TECN
• • • We do not use the following data for averages, fits, limits, etc. • • •					
− 0.76 ± 0.12 ± 0.15		91.2	[215] ABREU	92I	DLPH
4.0 ± 0.4 ± 0.63	4.0	91.3	[216] ACTON	92L	OPAL
9.1 ± 1.4 ± 1.6	9.0	57.9	ADACHI	91	TOPZ
− 0.84 ± 0.15 ± 0.04		91	DECAMP	91B	ALEP
8.3 ± 2.9 ± 1.9	8.7	56.6	STUART	90	AMY
11.4 ± 2.2 ± 2.1	8.7	57.6	ABE	89L	VNS
6.0 ± 1.3	5.0	34.8	GREENSHAW	89	JADE
8.2 ± 2.9	8.5	43.6	GREENSHAW	89	JADE

[215] ABREU 92I has 0.14 systematic error due to uncertainty of quark fragmentation.

[216] ACTON 92L use the weight function method on 259k selected $Z \to$ hadrons events. The systematic error includes a contribution of 0.2 due to B^0-$\overline{B}^0$ mixing effect, 0.4 due to Monte Carlo (MC) fragmentation uncertainties and 0.3 due to MC statistics. ACTON 92L derive a value of $\sin^2\theta_W^{\rm eff}$ to be 0.2321 ± 0.0017 ± 0.0028.

CHARGE ASYMMETRY IN $p\overline{p} \to Z \to e^+e^-$

ASYMMETRY (%)	STD. MODEL	$\sqrt{s}$ (GeV)	DOCUMENT ID		TECN
• • • We do not use the following data for averages, fits, limits, etc. • • •					
5.2 ± 5.9 ± 0.4		91	ABE	91E	CDF

ANOMALOUS $ZZ\gamma$, $Z\gamma\gamma$, AND ZZV COUPLINGS

Revised February 2002 by C. Caso (University of Genova) and A. Gurtu (Tata Institute).

In the reaction $e^+e^- \to Z\gamma$, deviations from the Standard Model for the $Z\gamma\gamma^*$ and $Z\gamma Z^*$ couplings may be described in terms of 8 parameters, h_i^V $(i = 1, 4;\ V = \gamma, Z)$ [1]. The parameters h_i^γ describe the $Z\gamma\gamma^*$ couplings and the parameters h_i^Z the $Z\gamma Z^*$ couplings. In this formalism h_1^V and h_2^V lead to CP-violating and h_3^V and h_4^V to CP-conserving effects. All these anomalous contributions to the cross section increase rapidly with center-of-mass energy. In order to ensure unitarity, these parameters are usually described by a form-factor representation, $h_i^V(s) = h_{i0}^V/(1 + s/\Lambda^2)^n$, where Λ is the energy scale for the manifestation of a new phenomenon and n is a sufficiently large power. By convention one uses $n = 3$ for $h_{1,3}^V$ and $n = 4$ for $h_{2,4}^V$. Usually limits on h_i^V's are put assuming some value of Λ (sometimes ∞).

Above the $e^+e^- \to ZZ$ threshold, deviations from the Standard Model for the $ZZ\gamma^*$ and ZZZ^* couplings may be described by means of four anomalous couplings f_i^V $(i = 4, 5;\ V = \gamma, Z)$ [2]. As above, the parameters f_i^γ describe the $Z\gamma\gamma^*$ couplings and the parameters f_i^Z the ZZZ^* couplings. The anomalous couplings f_5^V lead to violation of C and P symmetries while f_4^V introduces CP violation.

All these couplings h_i^V and f_i^V are zero at tree level in the Standard Model.

References

1. U. Baur and E.L. Berger Phys. Rev. **D47**, 4889 (1993).
2. K. Hagiwara *et al.*, Nucl. Phys. **B282**, 253 (1987).

h_i^V

Combining the LEP results properly taking into account the correlations the following 95% CL limits are derived:

(See EP Preprint Summer 2003: CERN-EP/2003-091 and hep-ex/0312023, December 2003, on http://lepewwg.web.cern.ch/LEPEWWG/stanmod/)

$-0.13 < h_1^Z < +0.13$, $-0.078 < h_2^Z < +0.071$,
$-0.20 < h_3^Z < +0.07$, $-0.05 < h_4^Z < +0.12$,
$-0.056 < h_1^\gamma < +0.055$, $-0.045 < h_2^\gamma < +0.025$,
$-0.049 < h_3^\gamma < -0.008$, $-0.002 < h_4^\gamma < +0.034$.

VALUE	DOCUMENT ID		TECN
• • • We do not use the following data for averages, fits, limits, etc. • • •			
	[217] ABBIENDI,G	00C	OPAL
	[218] ACCIARRI	00O	L3
	[219] ABBOTT	98M	D0
	[220] ABREU	98K	DLPH

[217] ABBIENDI,G 00C study $e^+e^- \to Z\gamma$ events (with $Z \to q\overline{q}$ and $Z \to \nu\overline{\nu}$) at 189 GeV to obtain the central values (and 95% CL limits) of these couplings: $h_1^Z = 0.000 \pm 0.100$ $(-0.190, 0.190)$, $h_2^Z = 0.000 \pm 0.068$ $(-0.128, 0.128)$, $h_3^Z = -0.074^{+0.102}_{-0.103}$ $(-0.269, 0.119)$, $h_4^Z = 0.046 \pm 0.068$ $(-0.084, 0.175)$, $h_1^\gamma = 0.000 \pm 0.061$ $(-0.115, 0.115)$, $h_2^\gamma = 0.000 \pm 0.041$ $(-0.077, 0.077)$, $h_3^\gamma = -0.080^{+0.039}_{-0.041}$ $(-0.164, -0.006)$, $h_4^\gamma = 0.064^{+0.033}_{-0.030}$ $(+0.007, +0.134)$. The results are derived assuming that only one coupling at a time is different from zero.

[218] ACCIARRI 00O study 189 GeV $e^+e^- \to q\overline{q}\gamma$ and $e^+e^- \to \nu\overline{\nu}\gamma$ events to derive 95% CL limits on h_i^V. For deriving each limit the others are fixed at zero. They report: $-0.26 < h_1^Z < 0.09$, $-0.10 < h_2^Z < 0.16$, $-0.26 < h_3^Z < 0.21$, $-0.11 < h_4^Z < 0.19$, $-0.20 < h_1^\gamma < 0.08$, $-0.11 < h_2^\gamma < 0.11$, $-0.11 < h_3^\gamma < 0.03$, $-0.02 < h_4^\gamma < 0.10$.

[219] ABBOTT 98M study $p\overline{p} \to Z\gamma + X$, with $Z \to e^+e^-$, $\mu^+\mu^-$, $\overline{\nu}\nu$ at 1.8 TeV, to obtain 95% CL limits at $\Lambda = 750$ GeV: $|h_{30}^Z| < 0.36$, $|h_{40}^Z| < 0.05$ (keeping $|h_{30}^\gamma| < 0.37$, $|h_{40}^\gamma| < 0.05$ (keeping $h_i^Z = 0$). Limits on the CP-violating couplings are $|h_{10}^Z| < 0.36$, $|h_{20}^Z| < 0.05$ (keeping $h_i^\gamma = 0$), and $|h_{10}^\gamma| < 0.37$, $|h_{20}^\gamma| < 0.05$ (keeping $h_i^Z = 0$).

[220] ABREU 98K determine a 95% CL upper limit on $\sigma(e^+e^- \to \gamma +$ invisible particles$) <$ 2.5 pb using 161 and 172 GeV data. This is used to set 95% CL limits on $|h_{30}^\gamma| < 0.8$ and $|h_{30}^Z| < 1.3$, derived at a scale $\Lambda = 1$ TeV and with $n = 3$ in the form factor representation.

f_i^V

Combining the LEP results properly taking into account the correlations the following 95% CL limits are derived:

(See EP Preprint Summer 2003: CERN-EP/2003-091 and hep-ex/0312023, December 2003, on http://lepewwg.web.cern.ch/LEPEWWG/stanmod/)

$-0.30 < f_4^Z < +0.30$, $-0.34 < f_5^Z < +0.38$,
$-0.17 < f_4^\gamma < +0.19$, $-0.32 < f_5^\gamma < +0.36$.

VALUE	DOCUMENT ID		TECN
• • • We do not use the following data for averages, fits, limits, etc. • • •			
	[221] ABBIENDI	04C	OPAL
	[222] ACHARD	03D	L3

[221] ABBIENDI 04C study ZZ production in e^+e^- collisions in the C.M. energy range 190–209 GeV. They select 340 events with an expected background of 180 events. Including the ABBIENDI 00N data at 183 and 189 GeV (118 events with an expected background of 65 events) they report the following 95% CL limits: $-0.45 < f_4^Z < 0.58$, $-0.94 < f_5^Z < 0.25$, $-0.32 < f_4^\gamma < 0.33$, and $-0.71 < f_5^\gamma < 0.59$.

[222] ACHARD 03D study Z-boson pair production in e^+e^- collisions in the C.M. energy range 200–209 GeV. They select 549 events with an expected background of 432 events. Including the ACCIARRI 99G and ACCIARRI 99O data (183 and 189 GeV respectively, 286 events with an expected background of 241 events) and the 192–202 GeV ACCIARRI 01I results (656 events, expected background of 512 events), they report the following 95% CL limits: $-0.48 \le f_4^Z \le 0.46$, $-0.36 \le f_5^Z \le 1.03$, $-0.28 \le f_4^\gamma \le 0.28$, and $-0.40 \le f_5^\gamma \le 0.47$.

ANOMALOUS WW/ZZ QUARTIC COUPLINGS

Revised November 2003 by C. Caso (University of Genova) and A. Gurtu (Tata Institute).

The Standard Model predictions for $WWWW$, $WWZZ$, $WWZ\gamma$, $WW\gamma\gamma$, and $ZZ\gamma\gamma$ couplings are small at LEP, but expected to become important at a TeV Linear Collider. Outside the Standard Model framework such possible couplings, a_0, a_c, a_n, are expressed in terms of the following dimension-6 operators [1,2];

$$L_6^0 = -\frac{e^2}{16\Lambda^2}\, a_0\, F^{\mu\nu}\, F_{\mu\nu}\vec{W}^\alpha \cdot \vec{W}_\alpha$$
$$L_6^c = -\frac{e^2}{16\Lambda^2}\, a_c\, F^{\mu\alpha}\, F_{\mu\beta}\vec{W}^\beta \cdot \vec{W}_\alpha$$
$$L_6^n = -i\frac{e^2}{16\Lambda^2}\, a_n \epsilon_{ijk}\, W_{\mu\alpha}^{(i)}\, W_\nu^{(j)}\, W^{(k)\alpha} F^{\mu\nu}$$
$$\widetilde{L}_6^0 = -\frac{e^2}{16\Lambda^2}\, \widetilde{a}_0\, F^{\mu\nu}\, \widetilde{F}_{\mu\nu}\vec{W}^\alpha \cdot \vec{W}_\alpha$$
$$\widetilde{L}_6^n = -i\frac{e^2}{16\Lambda^2}\, \widetilde{a}_n \epsilon_{ijk}\, W_{\mu\alpha}^{(i)}\, W_\nu^{(j)}\, W^{(k)\alpha} \widetilde{F}^{\mu\nu}$$

where F, W are photon and W fields, L_6^0 and L_6^c conserve C, P separately ($\widetilde{L}_6^0$ conserves only C) and generate anomalous $W^+W^-\gamma\gamma$ and $ZZ\gamma\gamma$ couplings, L_6^n violates CP ($\widetilde{L}_6^n$ violates both C and P) and generates an anomalous $W^+W^-Z\gamma$ coupling, and Λ is a scale for new physics. For the $ZZ\gamma\gamma$ coupling the CP-violating term represented by L_6^n does not contribute. These couplings are assumed to be real and to vanish at tree level in the Standard Model.

Within the same framework as above, a more recent description of the quartic couplings [3] treats the anomalous parts of the $WW\gamma\gamma$ and $ZZ\gamma\gamma$ couplings separately leading to two sets parameterized as a_0^V/Λ^2 and a_c^V/Λ^2, where $V = W$ or Z.

At LEP the processes studied in search of these quartic couplings are $e^+e^- \to WW\gamma$, $e^+e^- \to \gamma\gamma\nu\overline{\nu}$, and $e^+e^- \to Z\gamma\gamma$ and limits are set on the quantities $a_0^W/\Lambda^2, a_c^W/\Lambda^2, a_n/\Lambda^2$. The characteristics of the first process depend on all the three couplings whereas those of the latter two depend only on the two CP-conserving couplings. The sensitive measured variables are the cross sections for these processes as well as the energy and angular distributions of the photon and recoil mass to the photon pair.

References

1. G. Belanger and F. Boudjema, Phys. Lett. **B288**, 201 (1992).
2. J.W. Stirling and A. Werthenbach, Eur. Phys. J. **C14**, 103 (2000);
   J.W. Stirling and A. Werthenbach, Phys. Lett. **B466**, 369 (1999);
   A. Denner *et al.*, Eur. Phys. J. **C20**, 201 (2001);
   G. Montagna *et al.*, Phys. Lett. **B515**, 197 (2001).
3. G. Belanger *et al.*, Eur. Phys. J. **C13**, 103 (2000).

a_0/Λ^2, a_c/Λ^2

Combining published and unpublished preliminary LEP results the following 95% CL intervals for the QGCs associated with the $ZZ\gamma\gamma$ vertex are derived:

(See EP Preprint Summer 2003: CERN-EP/2003-091 and hep-ex/0312023, December 2003, on http://lepewwg.web.cern.ch/LEPEWWG/stanmod/)

$-0.008 < a_0^Z/\Lambda^2 < +0.021$
$-0.029 < a_c^Z/\Lambda^2 < +0.039$

VALUE	DOCUMENT ID	TECN

• • • We do not use the following data for averages, fits, limits, etc. • • •

^{223} ACHARD 02G L3

^{223} ACHARD 02G study $e^+e^- \to Z\gamma\gamma \to q\bar{q}\gamma\gamma$ events using data at center-of-mass energies from 200 to 209 GeV. The photons are required to be isolated, each with energy >5 GeV and $|\cos\theta| < 0.97$, and the di-jet invariant mass to be compatible with that of the Z boson (74–111 GeV). Cuts on Z velocity ($\beta < 0.73$) and on the energy of the most energetic photon reduce the backgrounds due to non-resonant production of the $q\bar{q}\gamma\gamma$ state and due to ISR respectively, yielding a total of 40 candidate events of which 8.6 are expected to be due to background. The energy spectra of the least energetic photon are fitted for all ten center-of-mass energy values from 130 GeV to 209 GeV (as obtained adding to the present analysis 130–202 GeV data of ACCIARRI 01E, for a total of 137 events with an expected background of 34.1 events) to obtain the fitted values $a_0/\Lambda^2 = 0.00^{+0.02}_{-0.01}$ GeV^{-2} and $a_C/\Lambda^2 = 0.03^{+0.01}_{-0.02}$ GeV^{-2}, where the other parameter is kept fixed to its Standard Model value (0). A simultaneous fit to both parameters yields the 95% CL limits -0.02 GeV$^{-2} < a_0/\Lambda^2 < 0.03$ GeV^{-2} and -0.07 GeV$^{-2} < a_C/\Lambda^2 < 0.05$ GeV^{-2}.

Z REFERENCES

ABBIENDI 04C EPJ C32 303 G. Abbiendi *et al.* (OPAL Collab.)
ABBIENDI 03P PL B577 18 G. Abbiendi *et al.* (OPAL Collab.)
ABDALLAH 03H PL B569 129 J. Abdallah *et al.* (DELPHI Collab.)
ABE 03F PRL 90 141804 K. Abe *et al.* (SLD Collab.)
ACHARD 03D PL B572 133 P. Achard *et al.* (L3 Collab.)
ABBIENDI 02I PL B546 29 G. Abbiendi *et al.* (OPAL Collab.)
ABE 02G PRL 88 151801 K. Abe *et al.* (SLD Collab.)
ACHARD 02G PL B540 43 P. Achard *et al.* (L3 Collab.)
HEISTER 02B PL B526 34 A. Heister *et al.* (ALEPH Collab.)
HEISTER 02C PL B528 19 A. Heister *et al.* (ALEPH Collab.)
HEISTER 02H EPJ C24 177 A. Heister *et al.* (ALEPH Collab.)
ABBIENDI 01A EPJ C19 587 G. Abbiendi *et al.* (OPAL Collab.)
ABBIENDI 01G EPJ C18 447 G. Abbiendi *et al.* (OPAL Collab.)
ABBIENDI 01K PL B516 1 G. Abbiendi *et al.* (OPAL Collab.)
ABBIENDI 01N EPJ C20 445 G. Abbiendi *et al.* (OPAL Collab.)
ABBIENDI 01O EPJ C21 1 G. Abbiendi *et al.* (OPAL Collab.)
ABE 01B PRL 86 1162 K. Abe *et al.* (SLD Collab.)
ABE 01C PR D63 032005 K. Abe *et al.* (SLD Collab.)
ACCIARRI 01E PL B505 47 M. Acciarri *et al.* (L3 Collab.)
ACCIARRI 01I PL B497 23 M. Acciarri *et al.* (L3 Collab.)
HEISTER 01 EPJ C20 401 A. Heister *et al.* (ALEPH Collab.)
HEISTER 01D EPJ C22 201 A. Heister *et al.* (ALEPH Collab.)
ABBIENDI 00N PL B476 256 G. Abbiendi *et al.* (OPAL Collab.)
ABBIENDI,G 00C EPJ C17 553 G. Abbiendi *et al.* (OPAL Collab.)
ABE 00B PRL 84 5945 K. Abe *et al.* (SLD Collab.)
ABE 00D PRL 85 5059 K. Abe *et al.* (SLD Collab.)
ABREU 00 EPJ C12 225 P. Abreu *et al.* (DELPHI Collab.)
ABREU 00B EPJ C14 613 P. Abreu *et al.* (DELPHI Collab.)
ABREU 00E EPJ C14 585 P. Abreu *et al.* (DELPHI Collab.)
ABREU 00F EPJ C16 371 P. Abreu *et al.* (DELPHI Collab.)
ABREU 00P PL B475 429 P. Abreu *et al.* (DELPHI Collab.)
ACCIARRI 00 EPJ C13 47 M. Acciarri *et al.* (L3 Collab.)
ACCIARRI 00C EPJ C16 1 M. Acciarri *et al.* (L3 Collab.)
ACCIARRI 00J PL B479 79 M. Acciarri *et al.* (L3 Collab.)
ACCIARRI 00O PL B489 55 M. Acciarri *et al.* (L3 Collab.)
ACCIARRI 00Q PL B489 93 M. Acciarri *et al.* (L3 Collab.)
BARATE 00B EPJ C16 597 R. Barate *et al.* (ALEPH Collab.)
BARATE 00C EPJ C14 1 R. Barate *et al.* (ALEPH Collab.)
BARATE 00O EPJ C16 613 R. Barate *et al.* (ALEPH Collab.)
ABBIENDI 99B EPJ C8 217 G. Abbiendi *et al.* (OPAL Collab.)
ABBIENDI 99I PL B447 157 G. Abbiendi *et al.* (OPAL Collab.)
ABE 99E PR D59 052001 K. Abe *et al.* (SLD Collab.)
ABE 99L PRL 83 1902 K. Abe *et al.* (SLD Collab.)
ABE 99O PRL 83 3384 K. Abe *et al.* (SLD Collab.)
ABREU 99 EPJ C6 19 P. Abreu *et al.* (DELPHI Collab.)
ABREU 99B EPJ C10 415 P. Abreu *et al.* (DELPHI Collab.)
ABREU 99J PL B449 364 P. Abreu *et al.* (DELPHI Collab.)
ABREU 99M EPJ C9 367 P. Abreu *et al.* (DELPHI Collab.)
ABREU 99U PL B462 425 P. Abreu *et al.* (DELPHI Collab.)
ABREU 99Y EPJ C10 219 P. Abreu *et al.* (DELPHI Collab.)
ACCIARRI 99D PL B448 152 M. Acciarri *et al.* (L3 Collab.)
ACCIARRI 99F PL B453 94 M. Acciarri *et al.* (L3 Collab.)
ACCIARRI 99G PL B450 281 M. Acciarri *et al.* (L3 Collab.)
ACCIARRI 99O PL B465 363 M. Acciarri *et al.* (L3 Collab.)
ABBOTT 98M PR D57 R3817 B. Abbott *et al.* (D0 Collab.)
ABE 98D PRL 80 660 K. Abe *et al.* (SLD Collab.)
ABE 98I PRL 81 942 K. Abe *et al.* (SLD Collab.)
ABREU 98K PL B423 194 P. Abreu *et al.* (DELPHI Collab.)
ABREU 98L EPJ C5 585 P. Abreu *et al.* (DELPHI Collab.)
ACCIARRI 98G PL B431 199 M. Acciarri *et al.* (L3 Collab.)
ACCIARRI 98H PL B429 387 M. Acciarri *et al.* (L3 Collab.)
ACCIARRI 98U PL B439 225 M. Acciarri *et al.* (L3 Collab.)
ACKERSTAFF 98A EPJ C5 411 K. Ackerstaff *et al.* (OPAL Collab.)
ACKERSTAFF 98E EPJ C1 439 K. Ackerstaff *et al.* (OPAL Collab.)
ACKERSTAFF 98O PL B420 157 K. Ackerstaff *et al.* (OPAL Collab.)
ACKERSTAFF 98Q EPJ C4 19 K. Ackerstaff *et al.* (OPAL Collab.)
BARATE 98O PL B434 415 R. Barate *et al.* (ALEPH Collab.)
BARATE 98T EPJ C4 557 R. Barate *et al.* (ALEPH Collab.)
BARATE 98V EPJ C5 205 R. Barate *et al.* (ALEPH Collab.)
ABE 97 PRL 78 17 K. Abe *et al.* (SLD Collab.)
ABE 97N PRL 79 804 K. Abe *et al.* (SLD Collab.)
ABREU 97C ZPHY C73 243 P. Abreu *et al.* (DELPHI Collab.)
ABREU 97E PL B398 207 P. Abreu *et al.* (DELPHI Collab.)
ABREU 97G PL B404 194 P. Abreu *et al.* (DELPHI Collab.)
ACCIARRI 97D PL B393 465 M. Acciarri *et al.* (L3 Collab.)
ACCIARRI 97J PL B407 351 M. Acciarri *et al.* (L3 Collab.)
ACCIARRI 97L PL B407 389 M. Acciarri *et al.* (L3 Collab.)
ACCIARRI 97R PL B413 167 M. Acciarri *et al.* (L3 Collab.)
ACKERSTAFF 97C PL B391 221 K. Ackerstaff *et al.* (OPAL Collab.)
ACKERSTAFF 97K ZPHY C74 1 K. Ackerstaff *et al.* (OPAL Collab.)
ACKERSTAFF 97M ZPHY C74 413 K. Ackerstaff *et al.* (OPAL Collab.)
ACKERSTAFF 97S PL B412 210 K. Ackerstaff *et al.* (OPAL Collab.)
ACKERSTAFF 97T ZPHY C76 387 K. Ackerstaff *et al.* (OPAL Collab.)
ACKERSTAFF 97W ZPHY C76 425 K. Ackerstaff *et al.* (OPAL Collab.)
ALEXANDER 97C ZPHY C73 379 G. Alexander *et al.* (OPAL Collab.)
ALEXANDER 97D ZPHY C73 569 G. Alexander *et al.* (OPAL Collab.)
ALEXANDER 97E ZPHY C73 587 G. Alexander *et al.* (OPAL Collab.)
BARATE 97D PL B405 191 R. Barate *et al.* (ALEPH Collab.)
BARATE 97E PL B401 150 R. Barate *et al.* (ALEPH Collab.)
BARATE 97F PL B401 163 R. Barate *et al.* (ALEPH Collab.)
BARATE 97H PL B402 213 R. Barate *et al.* (ALEPH Collab.)
BARATE 97J ZPHY C74 451 R. Barate *et al.* (ALEPH Collab.)
ABE 96E PR D53 1023 K. Abe *et al.* (SLD Collab.)
ABREU 96 ZPHY C70 531 P. Abreu *et al.* (DELPHI Collab.)
ABREU 96R ZPHY C72 31 P. Abreu *et al.* (DELPHI Collab.)
ABREU 96S PL B389 405 P. Abreu *et al.* (DELPHI Collab.)
ABREU 96U ZPHY C73 61 P. Abreu *et al.* (DELPHI Collab.)
ACCIARRI 96 PL B371 126 M. Acciarri *et al.* (L3 Collab.)
ADAM 96 ZPHY C69 561 W. Adam *et al.* (DELPHI Collab.)
ADAM 96B ZPHY C70 371 W. Adam *et al.* (DELPHI Collab.)
ALEXANDER 96B ZPHY C70 197 G. Alexander *et al.* (OPAL Collab.)
ALEXANDER 96F PL B370 185 G. Alexander *et al.* (OPAL Collab.)
ALEXANDER 96N PL B384 343 G. Alexander *et al.* (OPAL Collab.)
ALEXANDER 96R ZPHY C72 1 G. Alexander *et al.* (OPAL Collab.)
ALEXANDER 96U ZPHY C72 365 G. Alexander *et al.* (OPAL Collab.)
BUSKULIC 96D ZPHY C69 393 D. Buskulic *et al.* (ALEPH Collab.)
BUSKULIC 96H ZPHY C69 379 D. Buskulic *et al.* (ALEPH Collab.)
ABE 95J PRL 74 2880 K. Abe *et al.* (SLD Collab.)
ABE,K 95 PRL 75 3609 K. Abe *et al.* (SLD Collab.)
ABREU 95 ZPHY C65 709 erratum P. Abreu *et al.* (DELPHI Collab.)
ABREU 95D ZPHY C66 323 P. Abreu *et al.* (DELPHI Collab.)
ABREU 95G ZPHY C67 1 P. Abreu *et al.* (DELPHI Collab.)
ABREU 95I ZPHY C67 183 P. Abreu *et al.* (DELPHI Collab.)
ABREU 95K ZPHY C65 569 P. Abreu *et al.* (DELPHI Collab.)
ABREU 95L ZPHY C65 587 P. Abreu *et al.* (DELPHI Collab.)
ABREU 95M ZPHY C65 603 P. Abreu *et al.* (DELPHI Collab.)
ABREU 95O ZPHY C67 543 P. Abreu *et al.* (DELPHI Collab.)
ABREU 95R ZPHY C68 353 P. Abreu *et al.* (DELPHI Collab.)
ABREU 95W PL B361 207 P. Abreu *et al.* (DELPHI Collab.)
ABREU 95X ZPHY C69 1 P. Abreu *et al.* (DELPHI Collab.)
ACCIARRI 95B PL B345 589 M. Acciarri *et al.* (L3 Collab.)
ACCIARRI 95C PL B345 609 M. Acciarri *et al.* (L3 Collab.)
ACCIARRI 95G PL B353 136 M. Acciarri *et al.* (L3 Collab.)
AKERS 95C ZPHY C65 47 R. Akers *et al.* (OPAL Collab.)
AKERS 95O ZPHY C67 27 R. Akers *et al.* (OPAL Collab.)
AKERS 95U ZPHY C67 389 R. Akers *et al.* (OPAL Collab.)
AKERS 95W ZPHY C67 555 R. Akers *et al.* (OPAL Collab.)
AKERS 95X ZPHY C68 1 R. Akers *et al.* (OPAL Collab.)
AKERS 95Z ZPHY C68 203 R. Akers *et al.* (OPAL Collab.)
ALEXANDER 95D PL B358 162 G. Alexander *et al.* (OPAL Collab.)
BUSKULIC 95Q ZPHY C69 183 D. Buskulic *et al.* (ALEPH Collab.)
BUSKULIC 95R ZPHY C69 15 D. Buskulic *et al.* (ALEPH Collab.)
MIYABAYASHI 95 PL B347 171 K. Miyabayashi *et al.* (TOPAZ Collab.)
ABE 94C PRL 73 25 K. Abe *et al.* (SLD Collab.)
ABREU 94 NP B418 403 P. Abreu *et al.* (DELPHI Collab.)
ABREU 94B PL B327 386 P. Abreu *et al.* (DELPHI Collab.)
ABREU 94P PL B341 109 P. Abreu *et al.* (DELPHI Collab.)
ACCIARRI 94 ZPHY C62 551 M. Acciarri *et al.* (L3 Collab.)
ACCIARRI 94E PL B341 245 M. Acciarri *et al.* (L3 Collab.)
AKERS 94 ZPHY C61 19 R. Akers *et al.* (OPAL Collab.)
AKERS 94P ZPHY C63 181 R. Akers *et al.* (OPAL Collab.)
BUSKULIC 94 ZPHY C62 539 D. Buskulic *et al.* (ALEPH Collab.)
BUSKULIC 94G ZPHY C62 179 D. Buskulic *et al.* (ALEPH Collab.)
BUSKULIC 94J ZPHY C62 1 D. Buskulic *et al.* (ALEPH Collab.)
VILAIN 94 PL B320 203 P. Vilain *et al.* (CHARM II Collab.)
ABREU 93 PL B298 236 P. Abreu *et al.* (DELPHI Collab.)
ABREU 93I ZPHY C59 533 P. Abreu *et al.* (DELPHI Collab.)
Also 95 ZPHY C65 709 erratum P. Abreu *et al.* (DELPHI Collab.)
ABREU 93L PL B318 249 P. Abreu *et al.* (DELPHI Collab.)
ACTON 93 PL B305 407 P.D. Acton *et al.* (OPAL Collab.)
ACTON 93D ZPHY C58 219 P.D. Acton *et al.* (OPAL Collab.)
ACTON 93E PL B311 391 P.D. Acton *et al.* (OPAL Collab.)
ACTON 93F ZPHY C58 405 P.D. Acton *et al.* (OPAL Collab.)
ADRIANI 93 PL B301 136 O. Adriani *et al.* (L3 Collab.)
ADRIANI 93I PL B316 427 O. Adriani *et al.* (L3 Collab.)
BUSKULIC 93L PL B313 520 D. Buskulic *et al.* (ALEPH Collab.)
NOVIKOV 93C PL B298 453 V.A. Novikov, L.B. Okun, M.I. Vysotsky (ITEP)
ABREU 92I PL B277 371 P. Abreu *et al.* (DELPHI Collab.)
ABREU 92M PL B289 199 P. Abreu *et al.* (DELPHI Collab.)
ACTON 92B ZPHY C53 539 P.D. Acton *et al.* (OPAL Collab.)
ACTON 92L PL B294 436 P.D. Acton *et al.* (OPAL Collab.)
ACTON 92N PL B295 357 P.D. Acton *et al.* (OPAL Collab.)
ADEVA 92 PL B275 209 B. Adeva *et al.* (L3 Collab.)
ADRIANI 92D PL B292 454 O. Adriani *et al.* (L3 Collab.)
ALITTI 92B PL B276 354 J. Alitti *et al.* (UA2 Collab.)
BUSKULIC 92D PL B292 210 D. Buskulic *et al.* (ALEPH Collab.)
BUSKULIC 92E PL B294 145 D. Buskulic *et al.* (ALEPH Collab.)
DECAMP 92 PRPL 216 253 D. Decamp *et al.* (ALEPH Collab.)
LEP 92 PL B276 247 LEP Collabs. (LEP, ALEPH, DELPHI, L3, OPAL)
ABE 91E PRL 67 1502 F. Abe *et al.* (CDF Collab.)
ABREU 91H ZPHY C50 185 P. Abreu *et al.* (DELPHI Collab.)
ACTON 91B PL B273 338 D.P. Acton *et al.* (OPAL Collab.)
ADACHI 91 PL B255 613 I. Adachi *et al.* (TOPAZ Collab.)
ADEVA 91I PL B259 199 B. Adeva *et al.* (L3 Collab.)
AKRAWY 91F PL B257 531 M.Z. Akrawy *et al.* (OPAL Collab.)
DECAMP 91B PL B259 377 D. Decamp *et al.* (ALEPH Collab.)
DECAMP 91J PL B266 218 D. Decamp *et al.* (ALEPH Collab.)
JACOBSEN 91 PRL 67 3347 R.G. Jacobsen *et al.* (Mark II Collab.)
SHIMONAKA 91 PL B268 457 A. Shimonaka *et al.* (TOPAZ Collab.)
ABE 90I ZPHY C48 13 K. Abe *et al.* (VENUS Collab.)
ABRAMS 90 PRL 64 1334 G.S. Abrams *et al.* (Mark II Collab.)
AKRAWY 90J PL B246 285 M.Z. Akrawy *et al.* (OPAL Collab.)
BEHREND 90D ZPHY C47 333 H.J. Behrend *et al.* (CELLO Collab.)
BRAUNSCH... 90 ZPHY C48 433 W. Braunschweig *et al.* (TASSO Collab.)
ELSEN 90 ZPHY C46 349 E. Elsen *et al.* (JADE Collab.)
HEGNER 90 ZPHY C46 547 S. Hegner *et al.* (JADE Collab.)
STUART 90 PRL 64 983 D. Stuart *et al.* (AMY Collab.)
ABE 89 PRL 62 613 F. Abe *et al.* (CDF Collab.)
ABE 89C PRL 63 720 F. Abe *et al.* (CDF Collab.)
ABE 89L PL B232 425 K. Abe *et al.* (VENUS Collab.)
ABRAMS 89B PRL 63 2173 G.S. Abrams *et al.* (Mark II Collab.)
ABRAMS 89D PRL 63 2780 G.S. Abrams *et al.* (Mark II Collab.)
ALBAJAR 89 ZPHY C44 15 C. Albajar *et al.* (UA1 Collab.)
BACALA 89 PL B218 112 A. Bacala *et al.* (AMY Collab.)
BAND 89 PL B218 369 H.R. Band *et al.* (MAC Collab.)
GREENSHAW 89 ZPHY C42 1 T. Greenshaw *et al.* (JADE Collab.)
OULD-SAADA 89 ZPHY C44 567 F. Ould-Saada *et al.* (JADE Collab.)
SAGAWA 89 PRL 63 2341 H. Sagawa *et al.* (AMY Collab.)
ADACHI 88C PL B208 319 I. Adachi *et al.* (TOPAZ Collab.)
ADEVA 88 PR D38 2665 B. Adeva *et al.* (Mark-J Collab.)
BRAUNSCH... 88D ZPHY C40 163 W. Braunschweig *et al.* (TASSO Collab.)
ANSARI 87 PL B186 440 R. Ansari *et al.* (UA2 Collab.)
BEHREND 87C PL B191 209 H.J. Behrend *et al.* (CELLO Collab.)
BARTEL 86C ZPHY C30 371 W. Bartel *et al.* (JADE Collab.)
Also 85B ZPHY C26 507 W. Bartel *et al.* (JADE Collab.)
Also 82 PL 108B 140 W. Bartel *et al.* (JADE Collab.)
ASH 85 PRL 55 1831 W.W. Ash *et al.* (MAC Collab.)
BARTEL 85F PL 161B 188 W. Bartel *et al.* (JADE Collab.)
DERRICK 85 PR D31 2352 M. Derrick *et al.* (HRS Collab.)
FERNANDEZ 85 PRL 54 1624 E. Fernandez *et al.* (MAC Collab.)
LEVI 83 PRL 51 1941 M.E. Levi *et al.* (Mark II Collab.)
BEHREND 82 PL 114B 282 H.J. Behrend *et al.* (CELLO Collab.)
BRANDELIK 82C PL 110B 173 R. Brandelik *et al.* (TASSO Collab.)

Higgs Bosons — H^0 and $H^\pm$, Searches for

SEARCHES FOR HIGGS BOSONS

Updated October 2003 by P. Igo-Kemenes
(Physikalisches Institut, Heidelberg, Germany).

I. Introduction

One of the main challenges in high-energy physics is to understand electroweak symmetry breaking and the origin of mass. In the Standard Model (SM) [1], the electroweak interaction is described by a gauge field theory based on the $SU(2)_L \times U(1)_Y$ symmetry group. Masses can be introduced by the Higgs mechanism [2]. In the simplest form of this mechanism, which is implemented in the SM, fundamental scalar "Higgs" fields interact with each other such that they acquire non-zero vacuum expectation values, and the $SU(2)_L \times U(1)_Y$ symmetry is spontaneously broken down to the electromagnetic $U(1)_{EM}$ symmetry. Gauge bosons and fermions obtain their masses by interacting with the vacuum Higgs fields. Associated with this description is the existence of massive scalar particles, Higgs bosons.

The minimal SM requires one Higgs field doublet and predicts a single neutral Higgs boson. Beyond the SM, supersymmetric (SUSY) extensions [3] are of interest, since they provide a consistent framework for the unification of the gauge interactions at a high-energy scale, $\Lambda_{GUT} \approx 10^{16}$ GeV, and an explanation for the stability of the electroweak energy scale in the presence of quantum corrections (the "scale hierarchy problem"). Moreover, their predictions are compatible with existing high-precision data.

The Minimal Supersymmetric Standard Model (MSSM) (reviewed *e.g.*, in Ref. 4) is the SUSY extension of the SM with minimal new particle content. It introduces two Higgs field doublets, which is the minimal Higgs structure required to keep the theory free of anomalies and to provide masses to all charged fermions. The MSSM predicts three neutral and two charged Higgs bosons. The lightest of the neutral Higgs bosons is predicted to have its mass close to the electroweak energy scale ($\approx M_W$) [5,6].

Prior to 1989, when the e^+e^- collider LEP at CERN came into operation, the searches for Higgs bosons were sensitive to masses below a few GeV only (see Ref. 7 for a review). From 1989 to 1994 (the LEP1 phase) the LEP collider was operating at a center-of-mass energy $\sqrt{s} \approx M_Z$. After 1994 (the LEP2 phase), the center-of-mass energy increased each year, reaching 209 GeV in the year 2000 before the final shutdown. The combined data of the four LEP experiments, ALEPH, DELPHI, L3, and OPAL, are sensitive to neutral Higgs boson masses up to about 117 GeV.

Higgs boson searches have also been carried out at the Tevatron $p\overline{p}$ collider. With the currently analyzed data samples, the sensitivity of the two experiments, CDF and DØ, is rather limited, but with increasing energy and sample sizes, the range of sensitivity should eventually exceed the LEP range [8]. The searches will continue later at the LHC pp collider, covering masses up to about 1 TeV [9]. If Higgs bosons are indeed discovered, the Higgs mechanism could be studied in great detail at future e^+e^- [10,11] and $\mu^+\mu^-$ colliders [12].

In order to keep this review up-to-date, some recent but unpublished results are also quoted. These are marked with (*) in the reference list and can be accessed conveniently from the public web page `http://lephiggs.web.cern.ch/LEPHIGGS/pdg2004/index.html`.

II. The Standard Model Higgs boson

The mass of the SM Higgs boson H^0 is given by $m_{H^0} = \sqrt{2\lambda}\, v$. While the vacuum expectation value of the Higgs field, $v = 247$ GeV, is fixed by the Fermi coupling, the quartic Higgs self-coupling λ is a free parameter; thus, the mass m_{H^0} is not predicted. However, arguments of self-consistency of the theory can be used to place approximate upper and lower bounds upon the mass [13]. Since for large Higgs boson masses the running coupling λ rises with energy, the theory would eventually become non-perturbative. The requirement that this does not occur below a given energy scale Λ defines an upper bound for the Higgs mass. A lower bound is obtained from the study of quantum corrections to the SM and requiring the effective potential to be positive definite. These theoretical bounds imply that if the SM is to be self-consistent up to $\Lambda_{GUT} \approx 10^{16}$ GeV, the Higgs boson mass should be within about 130 and 190 GeV. In other terms, the discovery of a Higgs boson with mass below 130 GeV would suggest the onset of new physics at a scale below Λ_{GUT}.

Indirect experimental bounds for the SM Higgs boson mass are obtained from fits to precision measurements of electroweak observables, and to the measured top and $W^\pm$ masses. These measurements are sensitive to $\log(m_{H^0})$ through radiative corrections. The current best fit value is $m_{H^0} = 96^{+60}_{-38}$ GeV, or $m_{H^0} < 219$ GeV at the 95% confidence level (CL) [14], which is consistent with the SM being valid up to the GUT scale.

Production processes

The principal mechanism for producing the SM Higgs particle in e^+e^- collisions at LEP energies is Higgs-strahlung in the s-channel [15], $e^+e^- \to H^0Z^0$. The Z^0 boson in the final state is either virtual (LEP1), or on mass shell (LEP2). The cross section [16] σ^{SM}_{HZ} is shown in Fig. 1 (top) for the LEP energy range, together with those of the dominant background processes, $e^+e^- \to$ fermion pairs, W^+W^-, and Z^0Z^0. The SM Higgs boson can also be produced by W^+W^- and Z^0Z^0 fusion in the t-channel [17], but at LEP energies these processes have small cross sections.

At hadron colliders, the most important Higgs production processes are [18]: gluon fusion ($gg \to H^0$), Higgs production in association with a vector boson (WH^0 or ZH^0) or with a top quark pair ($t\bar{t}H^0$), and the WW fusion process giving (ppH^0 or $p\overline{p}H^0$). At the Tevatron and for masses less than

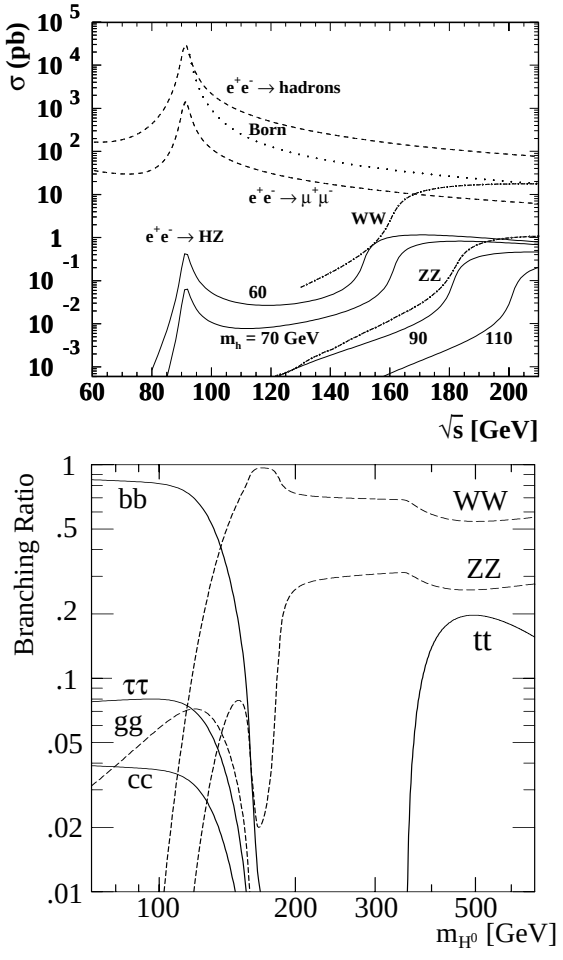

Figure 1: Cross sections, as a function of $\sqrt{s}$, for the Higgs-strahlung process in the SM for fixed values of m_{H^0} (full lines) and for other SM processes which contribute to the background; Bottom: Branching ratios for the main decay modes of the SM Higgs boson (from Ref. 10).

about 140 GeV (where the Higgs boson mainly decays to $b\bar{b}$), the most promising discovery channels are WH^0 and ZH^0 with $H^0 \to b\bar{b}$ ($H^0 \to W^*W$ is also contributing). At the future pp collider LHC, the gluon fusion channels $gg \to H^0 \to \gamma\gamma$, WW, ZZ, the associated production channel $t\bar{t}H^0 \to t\bar{t}b\bar{b}$ and the WW fusion channel $qqH^0 \to qq\tau^+\tau^-$ are all expected to contribute. Their relative sensitivity as well as the relevance of the WH^0 and ZH^0 channels strongly depend upon the precise value of the Higgs boson mass.

Decay of the SM Higgs boson

The most relevant decays of the SM Higgs boson [16,19] are summarized in Fig. 1 (bottom). For masses below about 140 GeV, decays to fermion pairs dominate, of which the decay $H^0 \to b\bar{b}$ has the largest branching ratio. Decays to $\tau^+\tau^-$, $c\bar{c}$, and gluon pairs (via loops) contribute less than 10%. For such low masses, the decay width is less than 10 MeV. For larger masses, the W^+W^- and Z^0Z^0 final states dominate, and the decay width rises rapidly, reaching about 1 GeV at m_{H^0}=200 GeV, and even 100 GeV at m_{H^0}=500 GeV.

Searches for the SM Higgs boson

During the LEP1 phase, the experiments ALEPH, DELPHI, L3, and OPAL analyzed over 17 million Z^0 decays, and have set lower bounds of approximately 65 GeV on the mass of the SM Higgs boson [20]. Substantial data samples have also been collected during the LEP2 phase at energies up to 209 GeV, including more than 40,000 $e^+e^- \to W^+W^-$ events. At LEP2, the composition of the background is more complex than at LEP1, due to the four-fermion processes $e^+e^- \to W^+W^-$ and Z^0Z^0, in addition to the two-fermion processes known from LEP1 (see Fig. 1 (top)). These have kinematic properties similar to the signal process (especially for $m_{H^0} \approx M_W$, M_Z), but since at LEP2 the Z^0 boson is on mass shell, constrained kinematic fits yield additional separation power. Furthermore, jets with b flavor, such as occurring in Higgs boson decays, are identified in high-precision silicon microvertex detectors.

The following final states provide good sensitivity for the SM Higgs boson. (a) The most abundant, four-jet, topology is produced in the $e^+e^- \to (H^0 \to b\bar{b})(Z^0 \to q\bar{q})$ process, and occurs with a branching ratio of about 60% for a Higgs boson with 115 GeV mass. The invariant mass of two jets is close to M_Z, while the other two jets contain b flavor. (b) The missing energy topology is produced mainly in the $e^+e^- \to (H^0 \to b\bar{b})(Z^0 \to \nu\bar{\nu})$ process, and occurs with a branching ratio of about 17%. The signal has two b jets, substantial missing transverse momentum, and missing mass compatible with M_Z. (c) In the leptonic final states, $e^+e^- \to (H^0 \to b\bar{b})(Z^0 \to e^+e^-, \mu^+\mu^-)$, the two leptons reconstruct to M_Z, and the two jets have b flavor. Although the branching ratio is small (only about 6%), this channel adds significantly to the overall search sensitivity, since it has low background. (d) Final states with tau leptons are produced in the processes $e^+e^- \to (H^0 \to \tau^+\tau^-)(Z^0 \to q\bar{q})$ and $(H^0 \to q\bar{q})(Z^0 \to \tau^+\tau^-)$; they occur with a branching ratio of about 10% in total. At LEP1, only the missing energy (b) and leptonic (c) final states could be used in the search for the SM Higgs boson, because of prohibitive backgrounds in the other channels; at LEP2 all four search topologies could be exploited.

The overall sensitivity of the searches is improved by combining statistically the data of the four LEP experiments in different decay channels, and at different LEP energies. After preselection, the combined data configuration (distribution in several discriminating variables) is compared in a frequentist approach to Monte-Carlo simulated configurations for two hypotheses: the background "b" hypothesis, and the signal plus background "$s + b$" hypothesis; in the latter case a SM Higgs boson of hypothetical mass (test-mass), m_H, is assumed in addition to the background.

The ratio $Q = \mathcal{L}_{s+b}/\mathcal{L}_b$ of the corresponding likelihoods is used as test statistic. The predicted, normalized, distributions of Q (probability density functions) are integrated to obtain the p-values $1 - CL_b = 1 - \mathcal{P}_b(Q \leq Q_{\rm observed})$ and $CL_{s+b} = \mathcal{P}_{s+b}(Q \leq Q_{\rm observed})$, which measure the compatibility of the observed data configuration with the two hypotheses [21].

The searches carried out at LEP prior to the year 2000, and their combinations [22], did not reveal any evidence for the production of a SM Higgs boson. However, in the data of the year 2000, mostly at energies $\sqrt{s} > 205$ GeV, ALEPH reported an excess of about three standard deviations beyond the background prediction [23], arising mainly from a few four-jet candidates with clean b tags and kinematic properties suggesting a SM Higgs boson with mass in the vicinity of 115 GeV. The data of DELPHI [24], L3 [25], and OPAL [26] do not show evidence for such an excess, but do not, however, exclude a 115 GeV Higgs boson. When the data of the four experiments are combined [27], the overall significance decreases to about 1.7 standard deviations. Figure 2 shows the test statistic $-2\ln Q$ for the ALEPH data and for the LEP data combined. For a test-mass $m_H = 115$ GeV, one calculates the p-values $1 - CL_b = 0.09$ for the background hypothesis and $CL_{s+b} = 0.15$ for the signal-plus-background hypothesis. From the same combination, a 95% CL lower bound of 114.4 GeV is obtained for the mass of the SM Higgs boson.

At the Tevatron, the currently published results of the CDF collaboration [28] are based on the Run I data sample of about 100 pb^{-1}. The searches concentrate on the associated production of a Higgs boson with a vector boson, $p\overline{p} \to VH^0$ ($V \equiv Z^0$, $W^\pm$), where the vector boson decays into the leptonic and hadronic channels and the Higgs boson into a $b\overline{b}$ pair. The main source of background is from QCD processes with genuine $b\overline{b}$ pairs. The Run I data sample is too small for a discovery, but allows model-independent upper bounds to be set on the cross section for such Higgs-like event topologies. These are currently higher by an order of magnitude than the SM predictions. However, Run II started in the year 2001, and with the projected data samples, the search sensitivity will increase considerably [8]. First results from the DØ collaboration, searching for the $H^0 \to W^*W$ channel and using Run II data of about 118 pb^{-1}, have been reported [29].

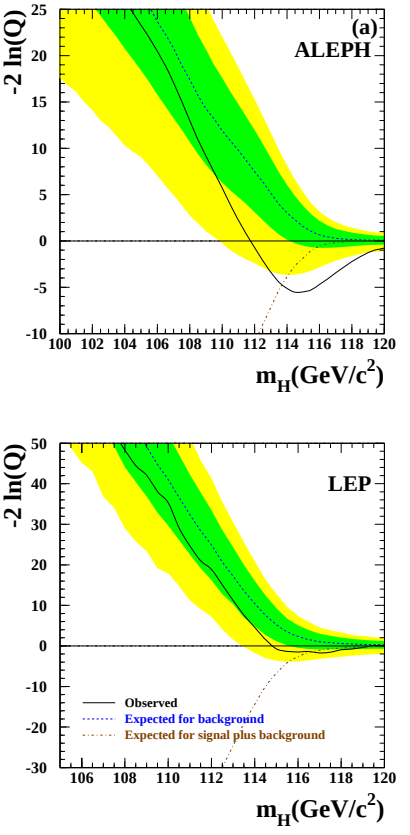

Figure 2: Observed (solid line), and expected behaviors of the test statistic $-2\ln Q$ for the background (dashed line), and the signal + background hypothesis (dash-dotted line) as a function of the test mass m_H. Top: ALEPH data alone; bottom: LEP data combined [27]. The dark and light shaded areas represent the 68% and 95% probability bands about the background expectation. See full-color version on color pages at end of book.

III. Higgs bosons in the MSSM

Most of the experimental investigations carried out so far assume CP invariance in the MSSM Higgs sector, in which case the three neutral Higgs bosons are CP eigenstates [4–6]. However, CP-violating (CPV) phases in the mechanism of soft SUSY breaking can lead to sizeable CP violation in the MSSM Higgs sector [30,31]. Such scenarios are theoretically appealing, since they provide one of the ingredients needed to explain the observed cosmic matter-antimatter asymmetry. In such models, the three neutral Higgs mass eigenstates are mixtures of CP-even and CP-odd fields. Consequently, their production and decay properties are different, and the experimental limits obtained for CP conserving (CPC) scenarios may thus be invalidated by CP-violating effects.

An important prediction of the MSSM, both CPC and CPV, is the relatively small mass of the lightest neutral scalar boson, less than about 130 GeV after radiative corrections. This prediction strongly motivated the investigations at LEP and supports future searches.

1. The CP-conserving MSSM scenario

Assuming CP invariance, the spectrum of MSSM Higgs bosons consists of two CP-even neutral scalars h^0 and H^0 (h^0 is defined to be the lighter of the two), one CP-odd neutral scalar A^0, and one pair of charged Higgs bosons $H^\pm$. At tree level, two parameters are required (beyond known parameters of the SM fermion and gauge sectors) to fix all Higgs boson masses and couplings. A convenient choice is the mass m_{A^0} of the CP-odd scalar A^0 and the ratio $\tan\beta = v_2/v_1$ of the vacuum expectation values associated to the neutral components of the two Higgs fields (v_2 and v_1 couple to up and down fermions, respectively). Often the mixing angle α is used, which diagonalizes the CP-even Higgs mass matrix (α can also be expressed in terms of m_{A^0} and $\tan\beta$).

The following ordering of masses is valid at tree level: $m_{h^0} < (M_Z,\ m_{A^0}) < m_{H^0}$ and $M_W < m_{H^\pm}$. These relations are modified by radiative corrections [32,33], with the largest contribution arising from the incomplete cancelation between top and scalar-top (stop) loops. The corrections affect mainly the masses in the neutral Higgs sector; they depend strongly on the top quark mass ($\sim m_t^4$), and logarithmically on the scalar-top (stop) masses. Furthermore, they involve a detailed parametrization of soft SUSY breaking and the mixing between the SUSY partners of left- and right-handed top quarks (stop mixing).

Production of neutral MSSM Higgs bosons

In e^+e^- collisions, the main production mechanisms of the neutral MSSM Higgs bosons are the Higgs-strahlung processes $e^+e^- \to h^0Z^0$, H^0Z^0 and the pair production processes $e^+e^- \to h^0A^0$, H^0A^0. Fusion processes play a marginal role at LEP energies. The cross sections for these processes can be expressed in terms of the SM Higgs boson cross section $\sigma^{\rm SM}_{HZ}$ and the parameters α and β introduced before. For the light CP-even Higgs boson h^0 the following expressions hold

$$\sigma_{\rm h^0 Z^0} = \sin^2(\beta-\alpha)\ \ \sigma^{\rm SM}_{HZ} \qquad (1)$$

$$\sigma_{\rm h^0 A^0} = \cos^2(\beta-\alpha)\overline{\lambda}\ \ \sigma^{\rm SM}_{HZ} \qquad (2)$$

with the kinematic factor

$$\overline{\lambda} = \lambda^{3/2}_{A^0{\rm h}^0} / \left[\lambda^{1/2}_{Z^0{\rm h}^0}(12M_Z^2/s + \lambda_{Z^0{\rm h}^0})\right] \qquad (3)$$

and $\lambda_{ij} = [1-(m_i+m_j)^2/s][1-(m_i-m_j)^2/s]$. These Higgs-strahlung and pair production cross sections are complementary, obeying the sum rule $\sin^2(\beta-\alpha)+\cos^2(\beta-\alpha)=1$. Typically, the process $e^+e^- \to h^0Z^0$ is more abundant at small $\tan\beta$ and $e^+e^- \to h^0A^0$ at large $\tan\beta$, unless the latter is suppressed by the kinematic factor $\overline{\lambda}$. The cross sections for the heavy scalar boson H^0 are obtained by interchanging $\sin^2(\beta-\alpha)$ by $\cos^2(\beta-\alpha)$ in Eqs. 1 and 2, and replacing the index h^0 by H^0 in Eq. 3.

At the Tevatron, and over most of the MSSM parameter space, one of the CP-even neutral Higgs bosons (h^0 or H^0) couples to the vector bosons with SM-like strength. The associated production $p\overline{p} \to (h^0$ or $H^0)V$ (with $V \equiv W^\pm, Z^0$), and the Yukawa process $p\overline{p} \to h^0b\overline{b}$ are the most promising search mechanisms. The gluon fusion processes $gg \to h^0$, H^0, A^0 have the highest cross section, but in these cases, only the Higgs to $\tau^+\tau^-$ decay mode is promising, since the $b\overline{b}$ decay mode is overwhelmed by QCD background.

Decay properties of neutral MSSM Higgs bosons

In the MSSM, the couplings of the neutral Higgs bosons to quarks, leptons, and gauge bosons are modified with respect to the SM couplings by factors which depend upon the angles α and β. These factors, valid at tree level, are summarized in Table 1.

Table 1: Factors relating the MSSM Higgs couplings to the couplings in the SM.

	"Up" fermions	"Down" fermions	Vector bosons
SM-Higgs:	1	1	1
MSSM h^0:	$\cos\alpha/\sin\beta$	$-\sin\alpha/\cos\beta$	$\sin(\beta-\alpha)$
H^0:	$\sin\alpha/\sin\beta$	$\cos\alpha/\cos\beta$	$\cos(\beta-\alpha)$
A^0:	$1/\tan\beta$	$\tan\beta$	0

The following decay features are relevant to the MSSM. The h^0 boson will decay mainly to fermion pairs, since the mass is smaller than about 130 GeV. The A^0 boson also decays predominantly to fermion pairs, independently of its mass, since its coupling to vector bosons is zero at leading order (see Table 1). For $\tan\beta > 1$, decays of h^0 and A^0 to $b\overline{b}$ and $\tau^+\tau^-$ pairs are preferred, with branching ratios of about 90% and 8%, while the decays to $c\overline{c}$ and gluon pairs are suppressed. Decays to $c\overline{c}$ may become important for $\tan\beta < 1$. The decay $h^0 \to A^0A^0$ may be dominant if it is kinematically allowed. Other decays could imply SUSY particles such as sfermions, charginos, or invisible neutralinos, thus requiring special search strategies.

Searches for neutral Higgs bosons (CPC scenario)

The searches at LEP address the Higgs-strahlung process $e^+e^- \to h^0Z^0$ and the pair production process $e^+e^- \to h^0A^0$, and exploit the complementarity of the two cross sections. The results for h^0Z^0 are obtained by re-interpreting the SM Higgs searches, taking into account the MSSM reduction factor $\sin^2(\beta-\alpha)$. Those for h^0A^0 are obtained from specific searches for $(b\overline{b})(b\overline{b})$ and $(\tau^+\tau^-)(q\overline{q})$ final states.

The search results are interpreted in a constrained MSSM model where universal soft SUSY breaking masses, $M_{\rm SUSY}$ and M_2, are assumed for the electroweak scale for sfermions and SU(2)×U(1) gauginos, respectively. Besides the tree-level parameters m_{A^0} and $\tan\beta$, the Higgs mixing parameter μ and trilinear Higgs-fermion coupling A_t also enter at the loop level. Most results assume a top quark mass of 174.3 GeV [34]. Furthermore, the gluino mass, entering at the two-loop level, is fixed at 800 GeV. The widths of the Higgs bosons are taken to

be small compared to the experimental mass resolution, which is a valid assumption for $\tan\beta$ less than about 50.

Most interpretations are limited to specific "benchmark" scenarios [33], where some of the parameters have fixed values: $M_{\rm SUSY} = 1$ TeV, $M_2 = 200$ GeV, and $\mu = -200$ GeV. In the *no-mixing* benchmark scenario, stop mixing is put to zero by choosing $X_t \equiv A_t - \mu\cot\beta = 0$, while in the m_{h^0}-*max* benchmark scenario, $X_t = 2M_{\rm SUSY}$ is chosen. The m_{h^0}-*max* scenario is designed to maximize the allowed parameter space in the (m_{h^0}, $\tan\beta$) projection, and therefore yields the most conservative exclusion limits.

The limits from the four LEP experiments are described in Refs. [23,35,36]. Preliminary combined LEP limits [37] are shown in Fig. 3 for the m_{h^0}-*max* scenario (in the *no mixing* scenario, the unexcluded region is much smaller). The current 95% CL mass bounds are: $m_{h^0} > 91.0$ GeV, $m_{A^0} > 91.9$ GeV. Furthermore, values of $\tan\beta$ from 0.5 to 2.4 are excluded, but this exclusion can be smaller if, for example, the top mass turns out to be higher than assumed, or if $\mathcal{O}(\alpha_t^2 m_t^2)$ corrections to $(m_{h^0})^2$ are included in the model calculation.

The neutral Higgs bosons may also be produced by Yukawa processes $e^+e^- \to f\overline{f}\phi$ with $\phi \equiv h^0$, H^0, A^0, where the Higgs particles are radiated off a massive fermion ($f \equiv b$ or $\tau^\pm$). These processes can be dominant where the "standard" processes, $e^+e^- \to h^0Z^0$ and h^0A^0, are suppressed. The corresponding enhancement factors (ratios of the $f\overline{f}h^0$ and $f\overline{f}A^0$ couplings to the SM $f\overline{f}H^0$ coupling) are $\sin\alpha/\cos\beta$ and $\tan\beta$, respectively. The LEP data have been analyzed searching specifically for $b\overline{b}b\overline{b}$, $b\overline{b}\tau^+\tau^-$, and $\tau^+\tau^-\tau^+\tau^-$ final states [38]. Regions of low mass and high enhancement factors are excluded by these searches. The CDF collaboration has searched for the Yukawa process $p\overline{p} \to b\overline{b}\ \phi \to b\overline{b}b\overline{b}$ [39]; the domains excluded, at large $\tan\beta$, are indicated in Fig. 3 along with the limits from LEP.

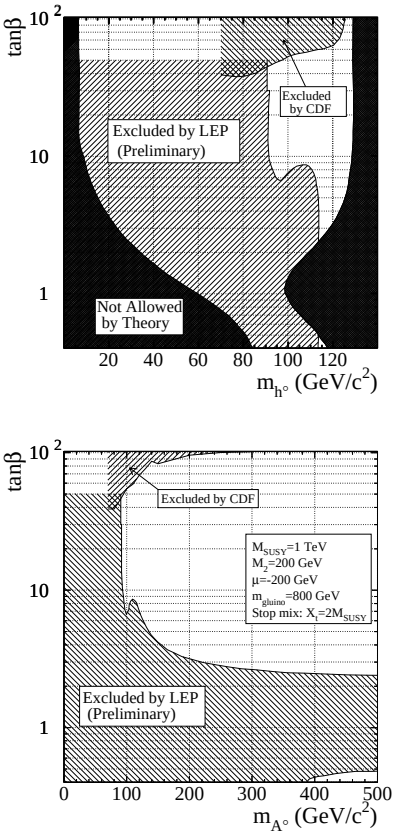

Figure 3: The 95% CL bounds on m_{h^0}, m_{A^0} and $\tan\beta$ for the m_{h^0}-*max* benchmark scenario, from LEP [37]. The exclusions at large $\tan\beta$ from CDF [39] are also indicated.

2. The CP-violating MSSM scenario

Within the SM, the size of CP violation is insufficient to drive the cosmological baryon asymmetry. In the MSSM, however, while the Higgs potential is invariant under the CP transformation at tree level, CP symmetry could be broken substantially by radiative corrections, especially by contributions from third generation scalar-quarks [31]. Such a scenario has recently been investigated by the OPAL Collaboration [36].

In the CPV MSSM scenario, the three neutral Higgs eigenstates H_i $(i = 1,2,3)$ do not have well defined CP quantum numbers; each of them can thus be produced by Higgs-strahlung, $e^+e^- \to H_iZ^0$, and in pairs, $e^+e^- \to H_iH_j$ $(i \neq j)$. For wide ranges of the model parameters, the lightest neutral Higgs boson H_1 has a predicted mass that is accessible at LEP, but it may decouple from the Z^0 boson. On the other hand, the second- and third-lightest Higgs bosons H_2 and H_3 may be either out of reach, or may also have small cross sections. Thus, the searches in the CPV MSSM scenario are experimentally more challenging than in the CPC scenario.

The cross section for the Higgs-strahlung and pair production processes are given by [31]

$$\sigma_{H_iZ^0} = g^2_{H_iZZ}\ \sigma^{\rm SM}_{HZ} \tag{4}$$

$$\sigma_{H_iH_j} = g^2_{H_iH_jZ}\ \overline{\lambda}\ \sigma^{\rm SM}_{HZ} \tag{5}$$

(in the expression of $\overline{\lambda}$, Eq. 3, the indices h^0 and A^0 have to be replaced by H_1 and H_2). The couplings

$$g_{H_iZZ} = \cos\beta\mathcal{O}_{1i} + \sin\beta\mathcal{O}_{2i} \tag{6}$$

$$g_{H_iH_jZ} = \mathcal{O}_{3i}(\cos\beta\mathcal{O}_{2j} - \sin\beta\mathcal{O}_{1j}) - \mathcal{O}_{3j}(\cos\beta\mathcal{O}_{2i} - \sin\beta\mathcal{O}_{1i}) \tag{7}$$

obey sum rules which, similarly to the CPC case, express the complementarity of the two cross sections. The orthogonal matrix $\mathcal{O}_{ij}$ $(i,j = 1,2,3)$ relating the weak CP eigenstates to the mass eigenstates has non-zero off-diagonal elements,

$$\mathcal{M}^2_{ij} \sim m_t^4 \cdot {\rm Im}(\mu A_t)/M^2_{\rm SUSY}\ ; \tag{8}$$

their size is a measure for CP-violating effects in the production processes.

Regarding the decay properties, the lightest mass eigenstate, H_1, predominantly decays to $b\overline{b}$ if kinematically allowed, with only a small fraction decaying to $\tau^+\tau^-$. The second-lightest Higgs boson, H_2, decays predominantly to H_1H_1 when kinematically allowed, otherwise preferentially to $b\overline{b}$.

The OPAL search [36] is performed for a number of variants of the CPX benchmark scenario [40], where the parameters are chosen in such a way as to maximize the off-diagonal elements $\mathcal{M}^2_{ij}$, and thereby enhance the phenomenological differences with respect to the CPC scenario. This is obtained typically for small $M_{\rm SUSY}$ (*e.g.*, 500 GeV) and large μ (up to 4 TeV), and when the CPV phases related to $A_{t,b}$ and $m_{\tilde{g}}$ are put to their maximal values. The precise choice of the top quark mass is also an issue. Figure 4 shows the preliminary OPAL exclusions in the $(m_{H_1}, \tan\beta)$ plane [36]. Values of $\tan\beta$ less than about 3 are excluded at the 95% CL, but no absolute limit can be set today for the mass of H_1 .

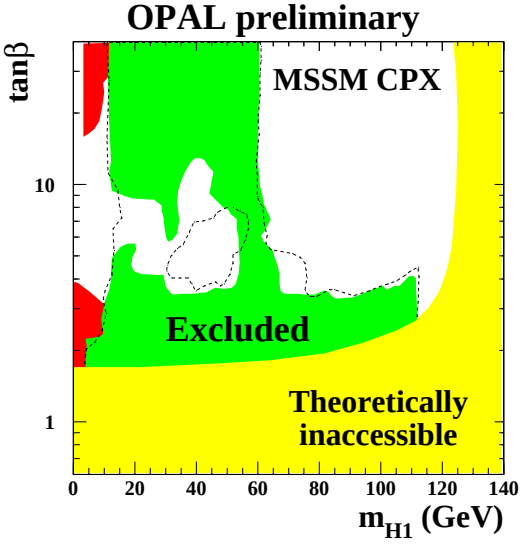

Figure 4: The 95% CL bounds on m_{H_1} and $\tan\beta$ in the CPX MSSM scenario with μ = 2 TeV and $M_{\rm SUSY}$ = 500 GeV, from a preliminary OPAL analysis [36]. The shaded areas are excluded either by the model or by the experiment. The areas delimited by the dashed lines are expected to be excluded on the basis of Monte Carlo simulations. The top mass is fixed to 174.3 GeV. See full-color version on color pages at end of book.

IV. Charged Higgs bosons

Charged Higgs bosons are predicted in models with two Higgs field doublets (2HDM), thus also in the MSSM [4,5]. While in the MSSM, the mass of the charged Higgs boson is restricted essentially to $m_{H^\pm} > M_W$, such a restriction does not exist in the general 2HDM case. The searches conducted at LEP and at the Tevatron are, therefore, interpreted primarily in the general 2HDM framework.

Searches for charged Higgs bosons at LEP

In e^+e^- collisions, charged Higgs bosons are expected to be pair-produced via s-channel exchange of a photon or a Z^0 boson [5,19]. In the 2HDM framework, the couplings are specified by the electric charge and the weak mixing angle θ_W, and the cross section only depends on the mass $m_{H^\pm}$ at tree level. Charged Higgs bosons decay preferentially to heavy particles, but the precise branching ratios are model dependent. In 2HDM of "type 2,"* and for masses which are accessible at LEP energies, the decays $H^+ \to c\overline{s}$ and $\tau^+\nu$ dominate. The final states $H^+H^- \to (c\overline{s})(\overline{c}s)$, $(\tau^+\nu_\tau)(\tau^-\overline{\nu}_\tau)$, and $(c\overline{s})(\tau^-\overline{\nu}_\tau)+(\overline{c}s)(\tau^+\nu_\tau)$ are therefore considered, and the results are presented with the $H^+ \to \tau^+\nu$ decay branching ratio as a free parameter.

At LEP2 energies, the background process $e^+e^- \to W^+W^-$ constrains the search sensitivity essentially to $m_{H^\pm}$ less than M_W. The searches of the four LEP experiments are described in Ref. 41. A preliminary combination [42] resulted in a general 2HDM ("type 2") bound of $m_{H^\pm}$ >78.6 GeV (95% CL), which is valid for arbitrary $H^+ \to \tau^+\nu$ branching ratio.

In the 2HDM of "type 1" [43], and if the CP-odd neutral Higgs boson A^0 is light (which is not excluded in the general 2HDM case), the decay $H^\pm \to W^{(\pm *)}A^0$ may be predominant for masses of interest at LEP. To cover this eventuality, the search of the DELPHI Collaboration is extended to this decay mode [44].

Searches for charged Higgs bosons at the Tevatron

In $p\overline{p}$ collisions at Tevatron energies, charged Higgs bosons with mass less than $m_t - m_b$ can be produced in the decay of the top quark. The decay $t \to bH^+$ would then compete with the SM process $t \to bW^+$, and the relative rate would depend on the value of $\tan\beta$. In the 2HDM of "type 2," the decay to charged Higgs bosons could have a detectable rate for $\tan\beta$ larger than 30, or for $\tan\beta$ less than one.

The DØ Collaboration adopted an indirect "disappearance technique" optimized for the detection of $t \to bW^+$, and a direct search for $t \to bH^+ \to b\tau^+\nu_\tau$ [45]. The CDF Collaboration also reported an indirect approach [46], in which the rate of dileptons and lepton+jets in top quark decays was compared to the SM prediction, and on a direct search for $t \to bH^+$ [47]. The results

* In the 2HDM of "type 2," the two Higgs fields couple separately to "up" and "down" type fermions; in the 2HDM of "type 1," one field couples to all fermions while the other field is decoupled.

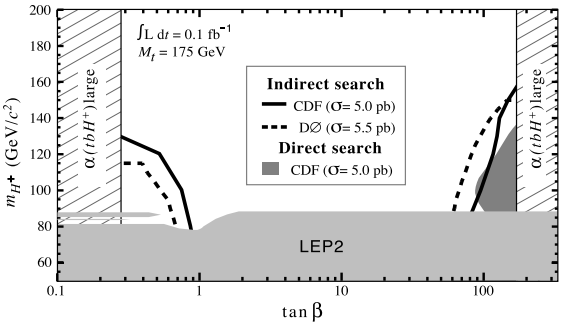

Figure 5: Summary of the 95% CL exclusions in the (m_{H^+}, $\tan\beta$) plane from DØ [45] and CDF [47], using various indirect and direct observation techniques (the regions below the curves are excluded). The two experiments use slightly different theoretical $t\bar{t}$ cross sections, as indicated. The shaded domains at extreme values of $\tan\beta$ are not considered in these searches, since there the tbH^+ coupling becomes large and perturbative calculations do not apply. The dark region labeled LEP2 is excluded by LEP [42]. See full-color version on color pages at end of book.

from the Tevatron are summarized in Fig. 5, together with the exclusion obtained at LEP. The Tevatron limits are subject to potentially large theoretical uncertainties [48].

Indirect limits in the ($m_{H^\pm}$, $\tan\beta$) plane can be derived by comparing the measured rate of the flavor-changing neutral-current process $b \to s\gamma$ to the SM prediction. In the SM, this process is mediated by virtual W exchange [49], while in the 2HDM of "type 2," the branching ratio is altered by contributions from the exchange of charged Higgs bosons [50]. The current experimental value, obtained from combining the measurements of CLEO, BELLE, and ALEPH [51], is in agreement with the SM prediction. From the comparison, the bound $m_{H^\pm} > 316$ GeV (95% CL) is obtained, which is much stronger than the current bounds from direct searches. However, these indirect bounds may be invalidated by anomalous couplings or, in SUSY models, by sparticle loops.

Doubly-charged Higgs bosons

Higgs bosons with double electric charge, $H^{\pm\pm}$, are predicted, for example, by models with additional triplet scalar fields or left-right symmetric models [5,52]. It has been emphasized that the see-saw mechanism could lead to doubly-charged Higgs bosons with masses accessible to current and future colliders [53]. Searches were performed at LEP for the pair-production process $Z^0 \to H^{++}H^{--}$ with four prompt leptons in the final state [54–56]. Lower mass bounds between 95 GeV and 100 GeV were obtained for left-right symmetric models (the exact limits depend on the lepton flavors). Doubly-charged Higgs bosons were also searched in single production [57]. Furthermore, if such particles existed, they would affect the Bhabha scattering cross-section and forward-backward asymmetry via t-channel exchange. The absence of a significant deviation from the SM prediction puts constraints on the Yukawa coupling of $H^{\pm\pm}$ to electrons for Higgs masses which reach into the TeV range [56,57].

V. Model extensions

The addition of a singlet scalar field to the CP-conserving MSSM [58] gives rise to two additional neutral scalars, one CP-even and one CP-odd. The radiative corrections to the masses are similar to those in the MSSM, and arguments of perturbative continuation to the GUT scale lead to an upper bound of about 135-140 GeV for the mass of the lightest neutral CP-even scalar. DELPHI has reinterpreted their searches for neutral Higgs bosons to constrain such models [59].

Decays into invisible (weakly interacting neutral) particles may occur, for example in the MSSM, if the Higgs bosons decay to pairs of neutralinos. In a different context, Higgs bosons might also decay into pairs of massless Goldstone bosons or Majorons [60]. In the process $e^+e^- \to h^0Z^0$, the mass of the invisible Higgs boson can be inferred from the reconstructed Z^0 boson using the beam energy constraint. Results from the LEP experiments can be found in Refs. [23,61]. Some LEP results have recently been combined and yield a 95% CL lower bound of 114.4 GeV for the mass of a Higgs boson with SM production rate, and decaying exclusively into invisible final states [62].

Most of the searches for the processes $e^+e^- \to h^0Z^0$ and h^0A^0, which have been discussed in the context of the CPC MSSM, rely on the experimental signature of Higgs bosons decaying into $b\bar{b}$. However, in the general 2HDM case, decays to non-$b\bar{b}$ final states may be strongly enhanced. Recently flavor-independent searches have been reported at LEP which do not require b tagging [63], and a preliminary combination has been performed [64]. In conjunction with the b-flavor sensitive searches, large domains of the general 2HDM parameter space of "type 2" could be excluded [65].

Photonic final states from the processes $e^+e^- \to Z^0/\gamma^* \to H^0\gamma$ and $H^0 \to \gamma\gamma$, do not occur in the SM at tree level, but may have a low rate due to $W^\pm$ and top quark loops [66]. Additional loops, for example, from SUSY particles, would increase the rates only slightly [67], but models with anomalous couplings predict enhancements by orders of magnitude. Searches for the processes $e^+e^- \to (H^0 \to b\bar{b})\gamma$, $(H^0 \to \gamma\gamma)q\bar{q}$, and $(H^0 \to \gamma\gamma)\gamma$ have been used to set model-independent limits on such anomalous couplings, and to constrain the very specific "fermiophobic" 2HDM of "type 1" [68], which also predicts an enhanced $h^0 \to \gamma\gamma$ rate. The LEP searches are described in Ref. 69. In a preliminary combination [70], a fermiophobic Higgs boson with mass less than 108.2 GeV (95% CL) has been excluded. Limits of about 80 GeV are obtained at the Tevatron [71]. Along with the photonic decay, the 2HDM of "type 1" also predicts an enhanced rate for the decays $h^0 \to W^*W$ and $Z^{0*}Z^0$. This possibility has been addressed by the L3 Collaboration [72].

The OPAL Collaboration has performed a decay-mode independent search for the Bjorken process $e^+e^- \to S^0Z^0$ [73], where S^0 denotes a generic scalar particle. The search is based on studies of the recoil mass spectrum in events with $Z^0 \to e^+e^-$ and $Z^0 \to \mu^+\mu^-$ decays, and on the final states ($Z^0 \to \nu\overline{\nu}$)($S^0 \to e^+e^-$ or photons), and produces upper bounds for the cross section for a broad range of S^0 masses between 10^{-6} GeV to 100 GeV.

VI. Prospects

The LEP collider stopped producing data in November 2000. At the Tevatron, Run II started in 2001. Performance studies suggest [8] that collecting data samples in excess of 2 fb^{-1} per experiment would extend the combined sensitivity of CDF and DØ beyond the LEP reach; with 4 fb^{-1} (9 fb^{-1}) per experiment, the Tevatron should be able to exclude (detect at the 3σ level) the Higgs boson up to about 130 GeV mass. Such data samples would also provide sensitivity to MSSM Higgs bosons in large domains of the parameter space.

The Large Hadron Collider (LHC) should deliver proton-proton collisions at 14 TeV in the year 2007. The ATLAS and CMS detectors have been optimized for Higgs boson searches [9]. The discovery of the SM Higgs boson will be possible over the mass range between about 100 GeV and 1 TeV. This broad range is covered by a variety of production and decay processes. The LHC experiments will provide full coverage of the MSSM parameter space by direct searches for the h^0, H^0, A^0, and $H^\pm$ bosons, and by detecting the h^0 boson in cascade decays of SUSY particles. The discovery of several of the Higgs bosons is possible over extended domains of the parameter space. Decay branching fractions can be determined and masses measured with statistical accuracies between 10^{-3} (at 400 GeV mass) and 10^{-2} (at 700 GeV mass).

A high-energy e^+e^- linear collider could be realized after the year 2010, running initially at energies up to 500 GeV and at 1 TeV or more at a later stage [11]. One of the prime goals would be to extend the precision measurements, which are typical of e^+e^- colliders, to the Higgs sector. At such a collider the Higgs couplings to fermions and vector bosons can be measured with precisions of a few percent. The MSSM parameters can be studied in great detail. At the highest collider energies and luminosities, the self-coupling of the Higgs fields can be studied directly through final states with two Higgs bosons [74]. At a future $\mu^+\mu^-$ collider, the Higgs bosons can be generated as s-channel resonances [12]. Mass measurements with precisions of a few MeV would be possible and the widths could be obtained directly from Breit-Wigner scans. The heavy CP-even and CP-odd bosons, H^0 and A^0, degenerate over most of the MSSM parameter space, could be disentangled experimentally.

Models are emerging which propose solutions to the electroweak scale hierarchy problem without introducing SUSY. The "little Higgs model" [75] proposes an additional set of heavy gauge bosons with Higgs-gauge couplings tuned in such a way that the quadratic divergences induced by the SM gauge boson loops are cancelled. Among the strong signatures of this model, there are the new gauge bosons, but there is also a doubly charged Higgs boson with mass in the TeV range, decaying to W^+W^+. These predictions can be tested at future colliders. Alternatively, models with extra space dimensions [76] propose a natural way for avoiding the scale hierarchy problem. In this class of models, the Planck scale looses its fundamental character and becomes merely an effective scale in 3-dimensional space. The model predicts a light Higgs-like particle, the radion, which differs from the Higgs boson in that it couples more strongly to gluons. A first search for the radion in LEP data, conducted by OPAL, gave negative results [77].

Finally, if Higgs bosons are not discovered at the TeV scale, both the LHC and the future lepton colliders will be in a position to test alternative theories of electroweak symmetry breaking, such as those with strongly interacting vector bosons [78] expected in theories with dynamical symmetry breaking [79].

References

1. S.L. Glashow, Nucl. Phys. **20**, 579 (1961); S. Weinberg, Phys. Rev. Lett. **19**, 1264 (1967); A. Salam, *Elementary Particle Theory*, eds.: N. Svartholm, Almquist, and Wiksells, Stockholm, 1968; S. Glashow, J. Iliopoulos, and L. Maiani, Phys. Rev. **D2**, 1285 (1970).
2. P.W. Higgs, Phys. Rev. Lett. **12**, 132 (1964); *idem* Phys. Rev. **145**, 1156 (1966); F. Englert and R. Brout, Phys. Rev. Lett. **13**, 321 (1964); G.S. Guralnik, C.R. Hagen, and T.W. Kibble, Phys. Rev. Lett. **13**, 585 (1964).
3. J. Wess and B. Zumino, Nucl. Phys. **B70**, 39 (1974); *idem*, Phys. Lett. **49B**, 52 (1974); P. Fayet, Phys. Lett. **69B**, 489 (1977); *ibid.* **84B**, 421 (1979), *ibid.* **86B**, 272 (1979).
4. H.E. Haber and G.L. Kane, Phys. Rev. **C117**, 75 (1985).
5. J.F. Gunion, H.E. Haber, G.L. Kane, and S. Dawson, *The Higgs Hunter's Guide* (Addison-Wesley) 1990.
6. H.E. Haber and M. Schmitt, *Supersymmetry*, in this volume.
7. P.J. Franzini and P. Taxil, in *Z physics at LEP 1*, CERN 89-08 (1989).
8. *Results of the Tevatron Higgs Sensitivity Study,* `http://www-d0.fnal.gov/Run2Physics/Higgs_sensitivity_study.html`.
9. ATLAS TDR on Physics performance, Vol. II, Chap. 19, *Higgs Bosons* (1999); CMS TP, CERN/LHC 94-38 (1994).
10. E. Accomando *et al.*, Physics Reports **299**, 1–78 (1998).
11. J.A. Aguilar-Saavedra *et al.*, TESLA Technical Design Report, Part III: *Physics at an e^+e^- Linear Collider*, `hep-ph/0106315`; T. Abe *et al.*, SLAC-R-570 (2001), `hep-ph/0109166`; M. Battaglia, `hep-ph/0103338`.
12. B. Autin, A. Blondel, and J. Ellis (eds.), CERN 99-02; C.M. Ankenbrandt *et al.*, Phys. Rev. ST Acc. Beams **2**, 081001 (1999).
13. N. Cabibbo *et al.*, Nucl. Phys. **B158**, 295 (1979);

T. Hambye and K. Riesselmann, Phys. Rev. **D55**, 7255 (1997);
G. Isidori, G. Ridolfi, and A. Strumia, Nucl. Phys. **B609**, 387 (2001).

14. LEP Electroweak Working Group, status of July 2003, http://lepewwg.web.cern.ch/LEPEWWG/.
15. J. Ellis, M.K. Gaillard, and D.V. Nanopoulos, Nucl. Phys. **B106**, 292 (1976);
B.L. Ioffe and V.A. Khoze, Sov. J. Nucl. Phys. **9**, 50 (1978).
16. E. Gross, B.A. Kniehl, and G. Wolf, Z. Phys. **C63**, 417 (1994); Erratum: *ibid.* **C66**, 32 (1995).
17. D.R.T. Jones and S.T. Petcov, Phys. Lett. **84B**, 440 (1979);
R.N. Cahn and S. Dawson, Phys. Lett. **136B**, 96 (1984); *ibid.* **138B**, 464 (1984);
W. Kilian, M. Krämer, and P.M. Zerwas, Phys. Lett. **B373**, 135 (1996).
18. S.L. Glashow, D.V. Nanopoulos, and A. Yildiz, Phys. Rev. **D18**, 1724 (1978);
A. Stange, W. Marciano, and S. Willenbrock, Phys. Rev. **D49**, 1354 (1994); *ibid.* **D50**, 4491 (1994).
19. A. Djouadi, M. Spira, and P.M. Zerwas, Z. Phys. **C70**, 675 (1996).
20. P. Janot, *Searching for Higgs Bosons at LEP 1 and LEP 2*, in Perspectives in Higgs Physics II, World Scientific, ed. G.L. Kane (1998).
21. K. Hagiwara *et al.*, Phys. Rev. **D66**, 010001-1 (2002), Review No. 31 on *Statistics*, p. 229.
22. ALEPH, DELPHI, L3, OPAL, The LEP Working Group for Higgs Boson Searches, CERN-EP/2000-055.
23. ALEPH Collab., Phys. Lett. **B526**, 191 (2002).
24. DELPHI Collab., CERN-EP/2003-008, to be published in Eur. Phys. J. **C**.
25. L3 Collab., Phys. Lett. **B517**, 319 (2001).
26. OPAL Collab., Eur. Phys. J. **C26**, 479 (2003).
27. ALEPH, DELPHI, L3, OPAL, The LEP Working Group for Higgs Boson Searches, Phys. Lett. **B565**, 61 (2003).
28. CDF Collab., Phys. Rev. Lett. **79**, 3819 (1997); *ibid*, **81**, 5748 (1998).
29. M. Schmitt, *Higgs and Susy Searches*, Lepton Photon Conference 2003, http://conferences.fnal.gov/lp2003/program/index.html.
30. A. D. Sakharov, JETP Lett. **5**, 24 (1967).
31. M. Carena *et al.*, Nucl. Phys. **B599**, 158 (2001).
32. Y. Okada, M. Yamaguchi, and T. Yanagida, Theor. Phys. **85**, 1 (1991);
H. Haber and R. Hempfling, Phys. Rev. Lett. **66**, 1815 (1991);
J. Ellis, G. Ridolfi, and F. Zwirner, Phys. Lett. **B257**, 83 (1991);
M. Carena, M. Quiros, and C.E.M. Wagner, Nucl. Phys. **B461**, 407 (1996);
S. Heinemeyer, W. Hollik, and G. Weiglein, Phys. Lett. **B455**, 179 (1999);
idem, Eur. Phys. J. **C9**, 343 (1999);
J. R. Espinosa and R.-J. Zhang, Nucl. Phys. **B586**, 3 (2000);
A. Brignole, G. Degrassi, P. Slavich, and F. Zwirner, hep-ph/0112177.
33. M. Carena, S. Heinemeyer, C.E.M. Wagner, and G. Weiglein, hep-ph/9912223, *idem*, hep-ph/0202167.
34. D.E. Groom *et al.*, Eur. Phys. J. **C15**, 1 (2000).
35. DELPHI Collab., CERN-EP/2003-008;
L3 Collab., Phys. Lett. **B545**, 30 (2002).
36. (*)OPAL Physics Note PN524 (2003).
37. (*)LHWG Note 2001-04.
38. (*)DELPHI 1999-76 CONF-263;
(*)DELPHI 2002-037 CONF-571;
OPAL Collab., Eur. Phys. J. **C23**, 397 (2002).
39. CDF Collab., Phys. Rev. Lett. **86**, 4472 (2001).
40. M. Carena *et al.*, Phys. Lett. **B495**, 155 (2000).
41. ALEPH Collab., Phys. Lett. **B543**, 1 (2002);
DELPHI Collab., Phys. Lett. **B525**, 17 (2002);
L3 Collab., CERN-EP/2003-054;
OPAL Collab., Eur. Phys. J. **C7**, 407 (1999).
42. (*)LHWG Note/2001-05.
43. A. G. Akeroyd *et al.*, Eur. Phys. J. **C20**, 51 (2001).
44. DELPHI Collab., CERN-EP/2003-064.
45. DØ Collab., Phys. Rev. Lett. **82**, 4975 (1999); *idem*, **88**, 151803 (2002).
46. CDF Collab., Phys. Rev. **D62**, 012004 (2000).
47. CDF Collab., Phys. Rev. Lett. **79**, 357 (1997).
48. J.A. Coarasa, J. Guasch, J. Solá, and W. Hollik, Phys. Lett. **B442**, 326 (1998);
J.A. Coarasa, J. Guasch, and J. Solá, hep-ph/9903212;
F.M. Borzumati and A. Djouadi, hep-ph/9806301.
49. P. Gambino and M. Misiak, Nucl. Phys. **B611**, 338 (2001).
50. R. Ellis *et al.*, Phys. Lett. **B179**, 119 (1986);
V. Barger, J. Hewett, and R. Phillips, Phys. Rev. **D41**, 3421 (1990).
51. S. Chen *et al.*, CLEO Collab., hep-ex/0108032;
G. Taylor, BELLE Collab., XXXVIth Rencontres de Moriond, March 2001;
ALEPH Collab., Phys. Lett. **B429**, 169 (1998).
52. G.B. Gelmini and M. Roncadelli, Phys. Lett. **B99**, 411 (1981);
R.N. Mohapatra and J.D. Vergados, Phys. Rev. Lett. **47**, 1713 (1981);
V. Barger *et al.*, Phys. Rev. **D26**, 218 (1982).
53. B. Dutta and R.N. Mohapatra, Phys. Rev. **D59**, 015018-1 (1999).
54. OPAL Collab., Phys. Lett. **B295**, 347 (1992); *idem*, **B526**, 221 (2002).
55. DELPHI Collab., Phys. Lett. **B552**, 127 (2003).
56. L3 Collab., CERN-EP/2003-060.
57. OPAL Collab., CERN-EP/2003-041.
58. P. Fayet, Nucl. Phys. **B90**, 104 (1975);
S.F. King and P.L. White, Phys. Rev. **D53**, 4049 (1996).
59. (*)DELPHI 1999-97 CONF 284.
60. Y. Chikashige, R.N. Mohapatra, and P.D. Peccei, Phys. Lett. **98B**, 265 (1981);
A.S. Joshipura and S.D. Rindani, Phys. Rev. Lett. **69**, 3269 (1992);
F. de Campos *et al.*, Phys. Rev. **D55**, 1316 (1997).
61. ALEPH Collab., Phys. Lett. **B526**, 191 (2002);
DELPHI Collab., CERN-EP/2003-046;
(*)L3 Note 2690 (2001);
OPAL Collab., Phys. Lett. **B377**, 273 (1996).
62. (*)LHWG-Note/2001-06.

63. ALEPH Collab., Phys. Lett. **B544**, 25 (2002);
(*)DELPHI 2001-070 CONF 498;
(*)DELPHI 2003-005 CONF 628;
(*)L3 Note 2806 (2003);
(*)OPAL Physics Note 525 (2003).

64. (*)LHWG Note 2001-07.

65. OPAL Collab., Eur. Phys. J. **C18**, 425 (2001);
(*)OPAL Physics Note 475 (2001);
(*)DELPHI 2001-068 CONF 496.

66. J. Ellis, M.K. Gaillard, and D.V. Nanopoulos, Nucl. Phys. **B106**, 292 (1976);
A. Abbasabadi *et al.*, Phys. Rev. **D52**, 3919 (1995);
R.N. Cahn, M.S. Chanowitz, and N. Fleishon, Phys. Lett. **B82**, 113 (1997).

67. G. Gamberini, G.F. Giudice, and G. Ridolfi, Nucl. Phys. **B292**, 237 (1987);
R. Bates, J.N. Ng, and P. Kalyniak, Phys. Rev. **D34**, 172 (1986);
K. Hagiwara, R. Szalapski, and D. Zeppenfeld, Phys. Lett. **B318**, 155 (1993);
O.J.P. Éboli *et al.*, Phys. Lett. **B434**, 340 (1998).

68. A. G. Akeroyd, Phys. Lett. **B368**, 89 (1996);
H.Haber, G. Kane, and T. Stirling, Nucl. Phys. **B161**, 493 (1979).

69. ALEPH Collab., Phys. Lett. **B544**, 16 (2002);
(*)DELPHI 2003-004 CONF 627;
L3 Collab., Phys. Lett. **B534**, 28 (2002);
OPAL Collab., Phys. Lett. **B544**, 44 (2002).

70. (*)LHWG Note/2002-02.

71. DØ Collab., Phys. Rev. Lett. **82**, 2244 (1999);
CDF Collab., Phys. Rev. **D64**, 092002 (2001).

72. L3 Collab., CERN-EP/2002-080.

73. OPAL Collab., CERN-EP/2002-032.

74. G.J. Gounaris, F. Renard, and D. Schildknecht, Phys. Lett. **B83**, 191 (1979);
V. Barger, T. Han, and R.J.N. Phillips, Phys. Rev. **D38**, 2766 (1988);
F. Boudjema and E. Chopin, Z. Phys. **C37**, 85 (1996);
A. Djouadi *et al.*, Eur. Phys. J. **C10**, 27 (1999).

75. N. Arkani-Hamed *et al.*, Phys. Lett. **B513**, 232 (2001);
I. Low *et al.*, Phys. Rev. **D66**, 072001 (2002);
M. Schmaltz, hep-ph/0210415;
T. Han *et al.*, hep-ph/0301040.

76. L. Randall and R. Sundrum, Phys. Rev. Lett. **83**, 3370 (1999);
idem **84**, 4690 (1999);
G.F. Giudice, R. Rattazzi, and J.D. Wells, Nucl. Phys. **B544**, 3 (1999);
C. Csáki, M.L. Graesser, and G.D. Kribs, Phys. Rev. **D63**, 065002 (2001).

77. (*)OPAL Physics-Note 526 (2003).

78. B.W. Lee, C. Quigg, and H.B. Thacker, Phys. Rev. **D16**, 1519 (1977);
R.S. Chivukula *et al.*, hep-ph/9503202;
C. Yuan, hep-ph/9712513;
M. Chanowitz, hep-ph/9812215.

79. S. Weinberg, Phys. Rev. **D13**, 974 (1976); *ibid.* **D19**, 1277 (1979);
L. Susskind, Phys. Rev. **D20**, 2619 (1979).

STANDARD MODEL H^0 (Higgs Boson) MASS LIMITS

These limits apply to the Higgs boson of the three-generation Standard Model with the minimal Higgs sector. For a review and a bibliography, see the above Note on 'Searches for Higgs Bosons' by P. Igo-Kemenes.

Limits from Coupling to $Z/W^\pm$

Limits on the Standard Model Higgs obtained from the study of Z^0 decays rule out conclusively its existence in the whole mass region $m_{H^0} \lesssim 60$ GeV. These limits, as well as stronger limits obtained from e^+e^- collisions at LEP at energies up to 202 GeV, and weaker limits obtained from other sources, have been superseded by the most recent data of LEP. They have been removed from this compilation, and are documented in previous editions of this Review of Particle Physics.

In this Section, unless otherwise stated, limits from the four LEP experiments (ALEPH, DELPHI, L3, and OPAL) are obtained from the study of the $e^+e^- \to H^0Z$ process, at center-of-mass energies reported in the comment lines.

VALUE (GeV)	*CL%*	*DOCUMENT ID*		*TECN*	*COMMENT*
>114.1	95	[1] ABDALLAH	04	DLPH	$E_{cm} \leq 209$ GeV
>112.7	95	[1] ABBIENDI	03B	OPAL	$E_{cm} \leq 209$ GeV
>114.4	95	[1,2] HEISTER	03D	LEP	$E_{cm} \leq 209$ GeV
>111.5	95	[1,3] HEISTER	02	ALEP	$E_{cm} \leq 209$ GeV
>112.0	95	[1] ACHARD	01C	L3	$E_{cm} \leq 209$ GeV
• • • We do not use the following data for averages, fits, limits, etc. • • •					
		[4] ABAZOV	01E	D0	$p\overline{p} \to H^0WX$, H^0ZX
		[5] ABE	98T	CDF	$p\overline{p} \to H^0WX$, H^0ZX

[1] Search for $e^+e^- \to H^0Z$ in the final states $H^0 \to b\overline{b}$ with $Z \to \ell\overline{\ell}$, $\nu\overline{\nu}$, $q\overline{q}$, $\tau^+\tau^-$ and $H^0 \to \tau^+\tau^-$ with $Z \to q\overline{q}$.

[2] Combination of the results of all LEP experiments.

[3] A 3σ excess of candidate events compatible with m_{H^0} near 114 GeV is observed in the combined channels $q\overline{q}q\overline{q}$, $q\overline{q}\ell\overline{\ell}$, $q\overline{q}\tau^+\tau^-$.

[4] ABAZOV 01E search for associated H^0W and H^0Z production in $p\overline{p}$ collisions at E_{cm}= 1.8 TeV. The limits of $\sigma(H^0W)\times B(W \to e\nu)\times B(H^0 \to q\overline{q}) < 2.0$ pb (95%CL) and $\sigma(H^0Z)\times B(Z \to e^+e^-)\times B(H^0 \to q\overline{q}) < 0.8$ pb (95%CL) are given for m_H=115 GeV.

[5] ABE 98T search for associated H^0W and H^0Z production in $p\overline{p}$ collisions at $\sqrt{s}$= 1.8 TeV with $W(Z) \to q\overline{q}^{(\prime)}$, $H^0 \to b\overline{b}$. The results are combined with the search in ABE 97W, resulting in the cross-section limit $\sigma(H^0+W/Z)\cdot B(H^0 \to b\overline{b})$<(23–17) pb (95%CL) for m_H= 70–140 GeV. This limit is one to two orders of magnitude larger than the expected cross section in the Standard Model.

H^0 Indirect Mass Limits from Electroweak Analysis

For limits obtained before the direct measurement of the top quark mass, see the 1996 (Physical Review **D54** 1 (1996)) Edition of this Review. Other studies based on data available prior to 1996 can be found in the 1998 Edition (The European Physical Journal **C3** 1 (1998)) of this Review. For indirect limits obtained from other considerations of theoretical nature, see the Note on "Searches for Higgs Bosons."

Because of the high current interest, we mention here the following unpublished result (LEP 02,) although we do not include it in the Listings or Tables: $m_H = 81^{+52}_{-33}$ GeV. This is obtained from a fit to LEP, SLD, W mass, top mass, and neutrino scattering data available in the Summer of 2002, with $\Delta\alpha^{(5)}_{had}(m_Z)$= 0.0276 ± 0.0036. The 95%CL limit is 193 GeV.

VALUE (GeV)	*CL%*	*DOCUMENT ID*		*TECN*	*COMMENT*
• • • We do not use the following data for averages, fits, limits, etc. • • •					
		[6] CHANOWITZ	02	RVUE	
390^{+750}_{-280}		[7] ABBIENDI	01A	OPAL	
		[8] CHANOWITZ	99	RVUE	
<290	95	[9] D'AGOSTINI	99	RVUE	
<211	95	[10] FIELD	99	RVUE	
		[11] CHANOWITZ	98	RVUE	
170^{+150}_{-90}		[12] HAGIWARA	98B	RVUE	
141^{+140}_{-77}		[13] DEBOER	97B	RVUE	
127^{+143}_{-71}		[14] DEGRASSI	97	RVUE	$\sin^2\theta_W$(eff,lept)
158^{+148}_{-84}		[15] DITTMAIER	97	RVUE	
149^{+148}_{-82}		[16] RENTON	97	RVUE	
145^{+164}_{-77}		[17] ELLIS	96C	RVUE	
185^{+251}_{-134}		[18] GURTU	96	RVUE	

[6] CHANOWITZ 02 studies the impact for the prediction of the Higgs mass of two 3σ anomalies in the SM fits to electroweak data. It argues that the Higgs mass limit should not be trusted whether the anomalies originate from new physics or from systematic effects.

[7] ABBIENDI 01A make Standard Model fits to OPAL's measurements of Z-lineshape parameters and lepton forward-backward asymmetries, using m_t=174.3 ± 5.1 GeV and $1/\alpha(m_Z)$ = 128.90 ± 0.09. The fit also yields $\alpha_s(m_Z)$=0.127 ± 0.005. If the external value of $\alpha_s(m_Z)$=0.1184 ± 0.0031 is added to the fit, the result changes to $m_{H^0} = 190^{+335}_{-165}$ GeV.

[8] CHANOWITZ 99 studies LEP/SLD data on 9 observables related $\sin^2\theta^\ell_{\rm eff}$, available in the Spring of 1998. A scale factor method is introduced to perform a global fit, in view of the conflicting data. m_H as large as 750 GeV is allowed at 95% CL.

[9] D'AGOSTINI 99 use m_t, m_W, and effective $\sin^2\theta_W$ from LEP/SLD available in the Fall 1998 and combine with direct Higgs search constraints from LEP2 at E_{cm}=183 GeV. $\alpha(m_Z)$ given by DAVIER 98.

[10] FIELD 99 studies the data on b asymmetries from $Z^0 \to b\overline{b}$ decays at LEP and SLD (from LEP 99). The limit uses $1/\alpha(M_Z)$= 128.90 ± 0.09, the variation in the fitted top quark mass, m_t=171.2$^{+3.7}_{-3.8}$ GeV, and excludes b-asymmetry data. It is argued that exclusion of these data, which deviate from the Standard Model expectation, from the electroweak fits reduces significantly the upper limit on m_H. Including the b-asymmetry data gives instead the 95%CL limit $m_H < 284$ GeV. See also FIELD 00.

[11] CHANOWITZ 98 fits LEP and SLD Z-decay-asymmetry data (as reported in ABBANEO 97), and explores the sensitivity of the fit to the weight ascribed to measurements that are individually in significant contradiction with the direct-search limits. Various prescriptions are discussed, and significant variations of the 95%CL Higgs-mass upper limits are found. The Higgs-mass central value varies from 100 to 250 GeV and the 95%CL upper limit from 340 GeV to the TeV scale.

[12] HAGIWARA 98B fit to LEP, SLD, W mass, and neutrino scattering data as reported in ALCARAZ 96, with m_t = 175 ± 6 GeV, $1/\alpha(m_Z)$= 128.90 ± 0.09 and $\alpha_s(m_Z)$= 0.118 ± 0.003. Strong dependence on m_t is found.

[13] DEBOER 97B fit to LEP and SLD data (as reported in ALCARAZ 96), as well as m_W and m_t from CDF/DØ and CLEO $b \to s\gamma$ data (ALAM 95). $1/\alpha(m_Z)$ = 128.90 ± 0.09 and $\alpha_s(m_Z)$ = 0.120 ± 0.003 are used. Exclusion of SLC data yields m_H=241$^{+218}_{-123}$ GeV. $\sin^2\theta_{\rm eff}$ from SLC (0.23061 ± 0.00047) would give m_H=16$^{+16}_{-9}$ GeV.

[14] DEGRASSI 97 is a two-loop calculation of M_W and $\sin^2\theta^{\rm lept}_{\rm eff}$ as a function of m_H, using $\sin^2\theta^{\rm lept}_{\rm eff}$ 0.23165(24) as reported in ALCARAZ 96, m_t = 175 ± 6 GeV, and $1/\alpha(m_Z)$=128.90 ± 0.09.

[15] DITTMAIER 97 fit to m_W and LEP/SLC data as reported in ALCARAZ 96, with m_t = 175 ± 6 GeV, $1/\alpha(m_Z^2)$ = 128.89 ± 0.09. Exclusion of the SLD data gives m_H = 261$^{+224}_{-128}$ GeV. Taking only the data on m_t, m_W, $\sin^2\theta^{\rm lept}_{\rm eff}$, and $\Gamma^{\rm lept}_Z$, the authors get m_H = 190$^{+174}_{-102}$ GeV and m_H = 296$^{+243}_{-143}$ GeV, with and without SLD data, respectively. The 95% CL upper limit is given by 550 GeV (800 GeV removing the SLD data).

[16] RENTON 97 fit to LEP and SLD data (as reported in ALCARAZ 96), as well as m_W and m_t from $p\overline{p}$, and low-energy νN data available in early 1997. $1/\alpha(m_Z)$ = 128.90 ± 0.09 is used.

[17] ELLIS 96C fit to LEP, SLD, m_W, neutral-current data available in the summer of 1996, plus m_t = 175 ± 6 GeV from CDF/DØ . The fit yields m_t = 172 ± 6 GeV.

[18] GURTU 96 studies the effect of the mutually incompatible SLD and LEP asymmetry data on the determination of m_H; Use is made of data available in the Summer of 1996. The quoted value is obtained by increasing the errors *à la* PDG. A fit ignoring the SLD data yields 267$^{+242}_{-135}$ GeV.

MASS LIMITS FOR NEUTRAL HIGGS BOSONS IN SUPERSYMMETRIC MODELS

The minimal supersymmetric model has two complex doublets of Higgs bosons. The resulting physical states are two scalars [H^0_1 and H^0_2, where we define $m_{H^0_1} < m_{H^0_2}$], a pseudoscalar (A^0), and a charged Higgs pair ($H^\pm$). H^0_1 and H^0_2 are also called h and H in the literature. There are two free parameters in the theory which can be chosen to be m_{A^0} and $\tan\beta = v_2/v_1$, the ratio of vacuum expectation values of the two Higgs doublets. Tree-level Higgs masses are constrained by the model to be $m_{H^0_1} \leq m_Z$, $m_{H^0_2} \geq m_Z$, $m_{A^0} \geq m_{H^0_1}$, and $m_{H^\pm} \geq m_W$. However, as described in the Review on Supersymmetry in this Volume these relations are violated by radiative corrections.

Unless otherwise noted, the experiments in e^+e^- collisions search for the processes $e^+e^- \to H^0_1 Z^0$ in the channels used for the Standard Model Higgs searches and $e^+e^- \to H^0_1 A^0$ in the final states $b\overline{b}b\overline{b}$ and $b\overline{b}\tau^+\tau^-$. Limits on the A^0 mass arise from these direct searches, as well as from the relations valid in the minimal supersymmetric model between m_{A^0} and $m_{H^0_1}$. As discussed in the minireview on Supersymmetry, in this volume, these relations depend on the masses of the t quark and $\tilde{t}$ squark. The limits are weaker for larger t and $\tilde{t}$ masses, while they increase with the inclusion of two-loop radiative corrections. To include the radiative corrections to the Higgs masses, unless otherwise stated, the listed papers use the two-loop results with m_t = 175 GeV, the universal scalar mass of 1 TeV, SU(2) gaugino mass of 200 GeV, and the Higgsino mass parameter $\mu = -200$ GeV, and examine the two scenarios of no scalar top mixing and 'maximal' stop mixing (which maximizes the effect of the radiative correction).

The mass region $m_{H^0_1} \lesssim 45$ GeV has been by now entirely ruled out by measurements at the Z pole. The relative limits, as well as other by now obsolete limits from different techniques, have been removed from this compilation, and can be found in earlier editions of this Review. Unless otherwise stated, the following results assume no invisible H^0_1 or A^0 decays.

H^0_1 (Higgs Boson) MASS LIMITS in Supersymmetric Models

VALUE (GeV)	CL%	DOCUMENT ID		TECN	COMMENT
> 89.7	95	[19,20] ABDALLAH	04	DLPH	$E_{cm} \leq 209$ GeV, $\tan\beta > 0.4$
> 86.0	95	[19,21] ACHARD	02H	L3	$E_{cm} \leq 209$ GeV, $\tan\beta > 0.4$
> 89.8	95	[19,22] HEISTER	02	ALEP	$E_{cm} \leq 209$ GeV, $\tan\beta > 0.5$
>100	95	[23] AFFOLDER	01D	CDF	$p\overline{p} \to b\overline{b}H^0_1$, $\tan\beta \gtrsim 55$
> 74.8	95	[24] ABBIENDI	00F	OPAL	$E_{cm} \leq 189$ GeV, $\tan\beta > 1$
• • • We do not use the following data for averages, fits, limits, etc. • • •					
		[25] ABBIENDI	03G	OPAL	$H^0_1 \to A^0A^0$

[19] Search for $e^+e^- \to H^0_1 A^0$ in the final states $b\overline{b}b\overline{b}$ and $b\overline{b}\tau^+\tau^-$, and $e^+e^- \to H^0_1 Z$. Universal scalar mass of 1 TeV, SU(2) gaugino mass of 200 GeV, and $\mu = -200$ GeV are assumed, and two-loop radiative corrections incorporated. The limits hold for m_t=175 GeV, and for the so-called "m_h-max scenario" (CARENA 99B).

[20] This limit applies also in the no-mixing scenario. Furthermore, ABDALLAH 04 excludes the range $0.54 < \tan\beta < 2.36$. The limit improves in the region $\tan\beta < 6$ (see Fig. 28). Limits for $\mu = 1$ TeV are given in Fig. 30.

[21] ACHARD 02H also search for the final state $H^0_1 Z \to 2A^0 q\overline{q}$, $A^0 \to q\overline{q}$. In addition, the MSSM parameter set in the "large-μ" and "no-mixing" scenarios are examined.

[22] HEISTER 02 excludes the range $0.7 < \tan\beta < 2.3$. A wider range is excluded with different stop mixing assumptions. Updates BARATE 01C.

[23] AFFOLDER 01D search for final states with 3 or more b-tagged jets. See Figs. 2 and 3 for Higgs mass limits as a function of $\tan\beta$, and for different stop mixing scenarios. Stronger limits are obtained at larger $\tan\beta$ values.

[24] ABBIENDI 00F search for $e^+e^- \to H^0_1 A^0$ in the final states $b\overline{b}b\overline{b}$, $b\overline{b}\tau^+\tau^-$, and $A^0A^0A^0 \to b\overline{b}b\overline{b}b\overline{b}$, and $e^+e^- \to H^0_1 Z$. Universal scalar mass of 1 TeV, SU(2) gaugino mass parameter $\mu = -0.1$ TeV are assumed. m_t=175 GeV is used. The cases of maximal and no-stop mixing are examined. Limits obtained from scans of the Supersymmetric parameter space can be found in the paper. Updates the results of ABBIENDI 99E.

[25] ABBIENDI 03G search for $e^+e^- \to H^0_1 Z$ followed by $H^0_1 \to A^0A^0$, $A^0 \to c\overline{c}$, gg, or $\tau^+\tau^-$. In the no-mixing scenario, the region $m_{H^0_1}$ = 45-85 GeV and m_{A^0} = 2-9.5 GeV is excluded at 95% CL.

A^0 (Pseudoscalar Higgs Boson) MASS LIMITS in Supersymmetric Models

VALUE (GeV)	CL%	DOCUMENT ID		TECN	COMMENT
> 90.4	95	[26,27] ABDALLAH	04	DLPH	$E_{cm} \leq 209$ GeV, $\tan\beta > 0.4$
> 86.5	95	[26,28] ACHARD	02H	L3	$E_{cm} \leq 209$ GeV, $\tan\beta > 0.4$
> 90.1	95	[26,29] HEISTER	02	ALEP	$E_{cm} \leq 209$ GeV, $\tan\beta > 0.5$
>100	95	[30] AFFOLDER	01D	CDF	$p\overline{p} \to b\overline{b}A^0$, $\tan\beta \gtrsim 55$
> 76.5	95	[31] ABBIENDI	00F	OPAL	$E_{cm} \leq 189$ GeV, $\tan\beta > 1$
• • • We do not use the following data for averages, fits, limits, etc. • • •					
		[32] ABBIENDI	03G	OPAL	$H^0_1 \to A^0A^0$
		[33] AKEROYD	02	RVUE	

[26] Search for $e^+e^- \to H^0_1 A^0$ in the final states $b\overline{b}b\overline{b}$ and $b\overline{b}\tau^+\tau^-$, and $e^+e^- \to H^0_1 Z$. Universal scalar mass of 1 TeV, SU(2) gaugino mass of 200 GeV, and $\mu = -200$ GeV are assumed, and two-loop radiative corrections incorporated. The limits hold for m_t=175 GeV, and for the so-called "m_h-max scenario" (CARENA 99B).

[27] This limit applies also in the no-mixing scenario. Furthermore, ABDALLAH 04 excludes the range $0.54 < \tan\beta < 2.36$. The limit improves in the region $\tan\beta < 6$ (see Fig. 28). Limits for $\mu = 1$ TeV are given in Fig. 30.

[28] ACHARD 02H also search for the final state $H^0_1 Z \to 2A^0 q\overline{q}$, $A^0 \to q\overline{q}$. In addition, the MSSM parameter set in the "large-μ" and "no-mixing" scenarios are examined.

[29] HEISTER 02 excludes the range $0.7 < \tan\beta < 2.3$. A wider range is excluded with different stop mixing assumptions. Updates BARATE 01C.

[30] AFFOLDER 01D search for final states with 3 or more b-tagged jets. See Figs. 2 and 3 for Higgs mass limits as a function of $\tan\beta$, and for different stop mixing scenarios. Stronger limits are obtained at larger $\tan\beta$ values.

[31] ABBIENDI 00F search for $e^+e^- \to H^0_1 A^0$ in the final states $b\overline{b}b\overline{b}$, $b\overline{b}\tau^+\tau^-$, and $A^0A^0A^0 \to b\overline{b}b\overline{b}b\overline{b}$, and $e^+e^- \to H^0_1 Z$. Universal scalar mass of 1 TeV, SU(2) gaugino mass of 1.63 TeV and Higgsino mass parameter $\mu = -0.1$ TeV are assumed. m_t=175 GeV is used. The cases of maximal and no-stop mixing are examined. Limits obtained from scans of the Supersymmetric parameter space can be found in the paper. Updates the results of ABBIENDI 99E.

[32] ABBIENDI 03G search for $e^+e^- \to H^0_1 Z$ followed by $H^0_1 \to A^0A^0$, $A^0 \to c\overline{c}$, gg, or $\tau^+\tau^-$. In the no-mixing scenario, the region $m_{H^0_1}$ = 45-85 GeV and m_{A^0} = 2-9.5 GeV is excluded at 95% CL.

[33] AKEROYD 02 examine the possibility of a light A^0 with $\tan\beta < 1$. Electroweak measurements are found to be inconsistent with such a scenario.

H^0 (Higgs Boson) MASS LIMITS in Extended Higgs Models

This Section covers models which do not fit into either the Standard Model or its simplest minimal Supersymmetric extension (MSSM), leading to anomalous production rates, or nonstandard final states and branching ratios. In particular, this Section covers limits which may apply to generic two-Higgs-doublet models (2HDM), or to special regions of the MSSM parameter space where decays to invisible particles or to photon pairs are dominant (see the Note on 'Searches for Higgs Bosons' at the beginning of this Chapter). See the footnotes or the comment lines for details on the nature of the models to which the limits apply.

VALUE (GeV)	CL%	DOCUMENT ID		TECN	COMMENT
• • • We do not use the following data for averages, fits, limits, etc. • • •					
		[34] ABDALLAH	04	DLPH	H^0VV couplings
		[35] ABBIENDI	03F	OPAL	$e^+e^- \to H^0Z$, $H^0 \to$ any
		[36] ABBIENDI	03G	OPAL	$H^0_1 \to A^0A^0$

>107	95	[37] ACHARD	03C L3	$H^0 \to WW^*, ZZ^*, \gamma\gamma$	
		[38] ABBIENDI	02D OPAL	$e^+e^- \to b\overline{b}H$	
>105.5	95	[39,40] ABBIENDI	02F OPAL	$H_1^0 \to \gamma\gamma$	
>105.4	95	[41] ACHARD	02C L3	$H_1^0 \to \gamma\gamma$	
>114.1	95	[42] HEISTER	02 ALEP	Invisible H^0, $E_{cm} \leq 209$ GeV	
>105.4	95	[39,43] HEISTER	02L ALEP	$H_1^0 \to \gamma\gamma$	
>109.1	95	[44] HEISTER	02M ALEP	$H^0 \to$ 2 jets or $\tau^+\tau^-$	
none 1–44	95	[45] ABBIENDI	01E OPAL	H_1^0, Type-II model	
none 12–56	95	[45] ABBIENDI	01E OPAL	A^0, Type-II model	
>107	95	[46] ABREU	01F DLPH	$H_1^0 \to \gamma\gamma$	
> 98	95	[47] AFFOLDER	01H CDF	$p\overline{p} \to H^0 W/Z$, $H^0 \to \gamma\gamma$	
>106.4	95	[42] BARATE	01C ALEP	Invisible H^0, $E_{cm} \leq$ 202 GeV	
> 89.2	95	[48] ACCIARRI	00M L3	Invisible H^0	
		[49] ACCIARRI	00R L3	$e^+e^- \to H^0\gamma$ and/or $H^0 \to \gamma\gamma$	
		[50] ACCIARRI	00R L3	$e^+e^- \to e^+e^- H^0$	
> 94.9	95	[51] ACCIARRI	00S L3	$e^+e^- \to H^0 Z$, $H^0 \to \gamma\gamma$	
>100.7	95	[52] BARATE	00L ALEP	$e^+e^- \to H^0 Z$, $H^0 \to \gamma\gamma$	
> 68.0	95	[53] ABBIENDI	99E OPAL	$\tan\beta > 1$	
> 96.2	95	[54] ABBIENDI	99O OPAL	$e^+e^- \to H^0 Z$, $H^0 \to \gamma\gamma$	
> 78.5	95	[55] ABBOTT	99B D0	$p\overline{p} \to H^0 W/Z$, $H^0 \to \gamma\gamma$	
		[56] ABREU	99P DLPH	$e^+e^- \to H^0\gamma$ and/or $H^0 \to \gamma\gamma$	
> 76.1	95	[57] ABREU	99Q DLPH	Invisible H^0	
		[58] GONZALEZ-G..	98B RVUE	Anomalous coupling	
		[59] KRAWCZYK	97 RVUE	$(g-2)_\mu$	
		[60] ALEXANDER	96H OPAL	$Z \to H^0\gamma$	
		[61] ABREU	95H DLPH	$Z \to H^0 Z^*$, $H^0 A^0$	
		[62] PICH	92 RVUE	Very light Higgs	

[34] ABDALLAH 04 consider the full combined LEP and LEP2 datasets to set limits on the Higgs coupling to W or Z bosons, assuming SM decays of the Higgs. Results in Fig. 26.

[35] ABBIENDI 03F search for $H^0 \to$ anything in $e^+e^- \to H^0 Z$, using the recoil mass spectrum of $Z \to e^+e^-$ or $\mu^+\mu^-$. In addition, it searched for $Z \to \nu\overline{\nu}$ and $H^0 \to e^+e^-$ or photons. Scenarios with large width or continuum H^0 mass distribution are considered. See their Figs. 11–14 for the results.

[36] ABBIENDI 03G search for $e^+e^- \to H_1^0 Z$ followed by $H_1^0 \to A^0A^0$, $A^0 \to c\overline{c}$, gg, or $\tau^+\tau^-$ in the region $m_{H_1^0}$ = 45-86 GeV and m_{A^0} = 2-11 GeV. See their Fig. 7 for the limits.

[37] ACHARD 03C search for $e^+e^- \to ZH^0$ followed by $H^0 \to WW^*$ or ZZ^* at E_{cm}= 200-209 GeV and combine with the ACHARD 02C result. The limit is for a H^0 with SM production cross section and B($H^0 \to f\overline{f}$) = 0 for all f. For B($H^0 \to WW^*$) + B($H^0 \to ZZ^*$) = 1, $m_{H^0} > 108.1$ GeV is obtained. See fig. 6 for the limits under different BR assumptions.

[38] ABBIENDI 02D search for $Z \to b\overline{b}H_1^0$ and $b\overline{b}A^0$ with $H_1^0/A^0 \to \tau^+\tau^-$, in the range $4 < m_H < 12$ GeV. See their Fig. 8 for limits on the Yukawa coupling.

[39] Search for associated production of a $\gamma\gamma$ resonance with a Z boson, followed by $Z \to q\overline{q}$, $\ell^+\ell^-$, or $\nu\overline{\nu}$, at $E_{cm} \leq 209$ GeV. The limit is for a H^0 with SM production cross section and B($H^0 \to f\overline{f}$)=0 for all fermions f.

[40] For B($H^0 \to \gamma\gamma$)=1, $m_{H^0} >$117 GeV is obtained.

[41] ACHARD 02C search for associated production of a $\gamma\gamma$ resonance with a Z boson, followed by $Z \to q\overline{q}$, $\ell^+\ell^-$, or $\nu\overline{\nu}$, at $E_{cm} \leq 209$ GeV. The limit is for a H^0 with SM production cross section and B($H^0 \to f\overline{f}$)=0 for all fermions f. For B($H^0 \to \gamma\gamma$)=1, $m_{H^0} >$114 GeV is obtained.

[42] HEISTER 02 and BARATE 01C search for $e^+e^- \to H^0 Z$ with H^0 decaying invisibly. The limit assumes SM production cross section and B($H^0 \to$ invisible) = 1.

[43] For B($H^0 \to \gamma\gamma$)=1, $m_{H^0} > 113.1$ GeV is obtained.

[44] HEISTER 02M search for $e^+e^- \to H^0 Z$, assuming that H^0 decays to $q\overline{q}$, gg, or $\tau^+\tau^-$ only. The limit assumes SM production cross section.

[45] ABBIENDI 01E search for neutral Higgs bosons in general Type-II two-doublet models, at $E_{cm} \leq 189$ GeV. In addition to usual final states, the decays $H_1^0, A^0 \to q\overline{q}$, gg are searched for. See their Figs. 15,16 for excluded regions.

[46] ABREU 01F search for neutral, fermiophobic Higgs bosons in Type-I two-doublet models, at $E_{cm} \leq 202$ GeV. The limit is from $e^+e^- \to H^0 Z$ with the SM cross section and B($H^0 \to \gamma\gamma$)=1. The process $e^+e^- \to H^0A^0$ with $H^0 \to \gamma\gamma$ is also searched for in the modes $A^0 \to b\overline{b}$, $H^0 Z$ and long-lived A^0. See their Figs. 4–6 for the excluded regions.

[47] AFFOLDER 01H search for associated production of a $\gamma\gamma$ resonance and a W or Z (tagged by two jets, an isolated lepton, or missing E_T). The limit assumes Standard Model values for the production cross section and for the couplings of the H^0 to W and Z bosons. See their Fig. 11 for limits with B($H^0 \to \gamma\gamma$)< 1.

[48] ACCIARRI 00M search for $e^+e^- \to ZH^0$ with H^0 decaying invisibly at E_{cm}=183–189 GeV. The limit assumes SM production cross section and B($H^0 \to$ invisible)=1. See their Fig. 6 for limits for smaller branching ratios.

[49] ACCIARRI 00R search for $e^+e^- \to H^0\gamma$ with $H^0 \to b\overline{b}$, $Z\gamma$, or $\gamma\gamma$. See their Fig. 3 for limits on $\sigma \cdot$ B. Explicit limits within an effective interaction framework are also given, for which the Standard Model Higgs search results are used in addition.

[50] ACCIARRI 00R search for the two-photon type processes $e^+e^- \to e^+e^- H^0$ with $H^0 \to b\overline{b}$ or $\gamma\gamma$. See their Fig. 4 for limits on $\Gamma(H^0 \to \gamma\gamma)\cdot$B($H^0 \to \gamma\gamma$or $b\overline{b}$) for m_{H^0}=70–170 GeV.

[51] ACCIARRI 00S search for associated production of a $\gamma\gamma$ resonance with a $q\overline{q}$, $\nu\overline{\nu}$, or $\ell^+\ell^-$ pair in e^+e^- collisions at E_{cm}= 189 GeV. The limit is for a H^0 with SM production cross section and B($H^0 \to f\overline{f}$)=0 for all fermions f. For B($H^0 \to \gamma\gamma$)=1, $m_{H^0} > 98$ GeV is obtained. See their Fig. 5 for limits on B($H \to \gamma\gamma$)$\cdot\sigma(e^+e^- \to Hf\overline{f})/\sigma(e^+e^- \to Hf\overline{f})$ (SM).

[52] BARATE 00L search for associated production of a $\gamma\gamma$ resonance with a $q\overline{q}$, $\nu\overline{\nu}$, or $\ell^+\ell^-$ pair in e^+e^- collisions at E_{cm}= 88–202 GeV. The limit is for a H^0 with SM production cross section and B($H^0 \to f\overline{f}$)=0 for all fermions f. For B($H^0 \to \gamma\gamma$)=1, $m_{H^0} > 109$ GeV is obtained. See their Fig. 3 for limits on B($H \to \gamma\gamma$)$\cdot\sigma(e^+e^- \to Hf\overline{f})/\sigma(e^+e^- \to Hf\overline{f})$ (SM).

[53] ABBIENDI 99E search for $e^+e^- \to H^0A^0$ and H^0Z at $E_{cm} = 183$ GeV. The limit is with m_H=m_A in general two Higgs-doublet models. See their Fig. 18 for the exclusion limit in the m_H–m_A plane. Updates the results of ACKERSTAFF 98S.

[54] ABBIENDI 99O search for associated production of a $\gamma\gamma$ resonance with a $q\overline{q}$, $\nu\overline{\nu}$, or $\ell^+\ell^-$ pair in e^+e^- collisions at 189 GeV. The limit is for a H^0 with SM production cross section and B($H^0 \to f\overline{f}$)=0, for all fermions f. See their Fig. 4 for limits on $\sigma(e^+e^- \to H^0Z^0)\times$B($H^0 \to \gamma\gamma$)×B($X^0 \to f\overline{f}$) for various masses. Updates the results of ACKERSTAFF 98Y.

[55] ABBOTT 99B search for associated production of a $\gamma\gamma$ resonance and a dijet pair. The limit assumes Standard Model values for the production cross section and for the couplings of the H^0 to W and Z bosons. Limits in the range of $\sigma(H^0 + Z/W)\cdot$B($H^0 \to \gamma\gamma$)= 0.80–0.34 pb are obtained in the mass range m_{H^0}= 65–150 GeV.

[56] ABREU 99P search for $e^+e^- \to H^0\gamma$ with $H^0 \to b\overline{b}$ or $\gamma\gamma$, and $e^+e^- \to H^0q\overline{q}$ with $H^0 \to \gamma\gamma$. See their Fig. 4 for limits on $\sigma\times$B. Explicit limits within an effective interaction framework are also given.

[57] ABREU 99Q search for $e^+e^- \to H^0Z$ with H^0 decaying invisibly at E_{cm} between 161 and 183 GeV. The limit assumes SM production cross section, and holds for any B($H^0 \to$ invisible). In the case of invisible decays in the MSSM, the excluded region of the (M_2, tanβ) plane overlaps the exclusion region from direct searches for charginos and neutralinos (ABREU 99E in the Supersymmetry Listings). See their Fig. 6(d) for limits on a Majoron model.

[58] GONZALEZ-GARCIA 98B use DØ limit for $\gamma\gamma$ events with missing E_T in $p\overline{p}$ collisions (ABBOTT 98) to constrain possible ZH or WH production followed by unconventional $H \to \gamma\gamma$ decay which is induced by higher-dimensional operators. See their Figs. 1 and 2 for limits on the anomalous couplings.

[59] KRAWCZYK 97 analyse the muon anomalous magnetic moment in a two-doublet Higgs model (with type II Yukawa couplings) assuming no H_1^0ZZ coupling and obtain $m_{H_1^0} \gtrsim$ 5 GeV or $m_{A^0} \gtrsim$ 5 GeV for tan$\beta > 50$. Other Higgs bosons are assumed to be much heavier.

[60] ALEXANDER 96H give B($Z \to H^0\gamma$)×B($H^0 \to q\overline{q}$) < $1\text{–}4 \times 10^{-5}$ (95%CL) and B($Z \to H^0\gamma$)×B($H^0 \to b\overline{b}$) < $0.7\text{–}2 \times 10^{-5}$ (95%CL) in the range $20 < m_{H^0} < 80$ GeV.

[61] See Fig. 4 of ABREU 95H for the excluded region in the $m_{H^0} - m_{A^0}$ plane for general two-doublet models. For tan$\beta > 1$, the region $m_{H^0}+m_{A^0} \lesssim 87$ GeV, $m_{H^0} < 47$ GeV is excluded at 95% CL.

[62] PICH 92 analyse H^0 with $m_{H^0} < 2m_\mu$ in general two-doublet models. Excluded regions in the space of mass-mixing angles from LEP, beam dump, and $\pi^\pm$, η rare decays are shown in Figs. 3,4. The considered mass region is not totally excluded.

$H^\pm$ (Charged Higgs) MASS LIMITS

Unless otherwise stated, the limits below assume B($H^+ \to \tau^+\nu$)+B($H^+ \to c\overline{s}$)=1, and hold for all values of B($H^+ \to \tau^+\nu_\tau$), and assume H^+ weak isospin of T_3=+1/2. In the following, tanβ is the ratio of the two vacuum expectation values in two-doublet models (2HDM).

The limits are also applicable to point-like technipions. For a discussion of technipar-ticles, see the Review of Dynamical Electroweak Symmetry Breaking in this Review.

For limits obtained in hadronic collisions before the observation of the top quark, and based on the top mass values inconsistent with the current measurements, see the 1996 (Physical Review **D54** 1 (1996)) Edition of this Review.

Searches in e^+e^- collisions at and above the Z pole have conclusively ruled out the existence of a charged Higgs in the region $m_{H^+} \lesssim 45$ GeV, and are now superseded by the most recent searches in higher energy e^+e^- collisions at LEP. Results by now obsolete are therefore not included in this compilation, and can be found in the previous Edition (The European Physical Journal **C15** 1 (2000)) of this Review.

In the following, and unless otherwise stated, results from the LEP experiments (ALEPH, DELPHI, L3, and OPAL) are assumed to derive from the study of the $e^+e^- \to H^+H^-$ process. Limits from $b \to s\gamma$ decays are usually stronger in generic 2HDM models than in Supersymmetric models.

A recent combination (LEP 00B) of preliminary, unpublished results relative to data taken at LEP in the Summer of 1999 at energies up to 202 GeV gives the limit $m_{H_1^\pm} > 78.6$ GeV.

VALUE (GeV)	*CL%*	*DOCUMENT ID*		*TECN*	*COMMENT*
> 71.5	95	ABDALLAH	02	DLPH	$E_{cm} \leq 202$ GeV
> 79.3	95	HEISTER	02P	ALEP	$E_{cm} \leq 209$ GeV
> 67.4	95	ACCIARRI	00W	L3	$E_{cm} \leq 202$ GeV
> 59.5	95	ABBIENDI	99E	OPAL	$E_{cm} \leq 183$ GeV
• • • We do not use the following data for averages, fits, limits, etc. • • •					
		[63] ABBIENDI	03	OPAL	$t \to \mu\overline{\nu}\nu$, $e\overline{\nu}\nu$
		[64] ABAZOV	02B	D0	$t \to bH^+$, $H \to \tau\nu$
		[65] BORZUMATI	02	RVUE	
		[66] ABBIENDI	01Q	OPAL	$B \to \tau\nu_\tau X$
		[67] BARATE	01E	ALEP	$B \to \tau\nu_\tau$
>315	99	[68] GAMBINO	01	RVUE	$b \to s\gamma$
> 82.8	95	ABBIENDI	00G	OPAL	$E_{cm} \leq 189$ GeV, B($\tau\nu$) = 1
		[69] AFFOLDER	00I	CDF	$t \to bH^+$, $H \to \tau\nu$
		[70] ABBOTT	99E	D0	$t \to bH^+$

> 56.3	95	ABREU	99R	DLPH	$E_{cm} \leq 183$ GeV
		[71] ACKERSTAFF	99D	OPAL	$\tau \to e\nu\nu$, $\mu\nu\nu$
		[72] ACCIARRI	97F	L3	$B \to \tau\nu_\tau$
		[73] AMMAR	97B	CLEO	$\tau \to \mu\nu\nu$
		[74] COARASA	97	RVUE	$B \to \tau\nu_\tau X$
		[75] GUCHAIT	97	RVUE	$t \to bH^+$, $H \to \tau\nu$
		[76] MANGANO	97	RVUE	$B_{u(c)} \to \tau\nu_\tau$
		[77] STAHL	97	RVUE	$\tau \to \mu\nu\nu$
>244	95	[78] ALAM	95	CLE2	$b \to s\gamma$
		[79] BUSKULIC	95	ALEP	$b \to \tau\nu_\tau X$

[63] ABBIENDI 03 give a limit $m_{H^+} > 1.28 \tan\beta$ GeV (95%CL) in Type II two-doublet models.

[64] ABAZOV 02B search for a charged Higgs boson in top decays with $H^+ \to \tau^+\nu$ at E_{cm}=1.8 TeV. For m_{H^+}=75 GeV, the region $\tan\beta > 32.0$ is excluded at 95%CL. The excluded mass region extends to over 140 GeV for $\tan\beta$ values above 100.

[65] BORZUMATI 02 point out that the decay modes such as $b\overline{b}W$, A^0W, and supersymmetric ones can have substantial branching fractions in the mass range explored at LEP II and Tevatron.

[66] ABBIENDI 01Q give a limit $\tan\beta/m_{H^+} < 0.53$ GeV^{-1} (95%CL) in Type II two-doublet models.

[67] BARATE 01E give a limit $\tan\beta/m_{H^+} < 0.40$ GeV^{-1} (90%CL) in Type II two-doublet models. An independent measurement of $B \to \tau\nu_\tau X$ gives $\tan\beta/m_{H^+} < 0.49$ GeV^{-1} (90%CL).

[68] GAMBINO 01 use the world average data in the summer of 2001 $B(b \to s\gamma) = (3.23 \pm 0.42) \times 10^{-4}$. The limit applies for Type-II two-doublet models.

[69] AFFOLDER 00I search for a charged Higgs boson in top decays with $H^+ \to \tau^+\nu$ in $p\overline{p}$ collisions at E_{cm}=1.8 TeV. The excluded mass region extends to over 120 GeV for $\tan\beta$ values above 100 and $B(\tau\nu)$=1. If $B(t \to bH^+) \gtrsim 0.6$, m_{H^+} up to 160 GeV is excluded. Updates ABE 97L.

[70] ABBOTT 99E search for a charged Higgs boson in top decays in $p\overline{p}$ collisions at E_{cm}=1.8 TeV, by comparing the observed $t\overline{t}$ cross section (extracted from the data assuming the dominant decay $t \to bW^+$) with theoretical expectation. The search is sensitive to regions of the domains $\tan\beta \lesssim 1$, $50 < m_{H^+}$(GeV) $\lesssim 120$ and $\tan\beta \gtrsim 40$, $50 < m_{H^+}$(GeV) $\lesssim 160$. See Fig. 3 for the details of the excluded region.

[71] ACKERSTAFF 99D measure the Michel parameters ρ, ξ, η, and $\xi\delta$ in leptonic τ decays from $Z \to \tau\tau$. Assuming e-μ universality, the limit $m_{H^+} > 0.97 \tan\beta$ GeV (95%CL) is obtained for two-doublet models in which only one doublet couples to leptons.

[72] ACCIARRI 97F give a limit $m_{H^+} > 2.6 \tan\beta$ GeV (90%CL) from their limit on the exclusive $B \to \tau\nu_\tau$ branching ratio.

[73] AMMAR 97B measure the Michel parameter ρ from $\tau \to e\nu\nu$ decays and assumes e/μ universality to extract the Michel η parameter from $\tau \to \mu\nu\nu$ decays. The measurement is translated to a lower limit on m_{H^+} in a two-doublet model $m_{H^+} > 0.97 \tan\beta$ GeV (90% CL).

[74] COARASA 97 reanalyzed the constraint on the ($m_{H^\pm}$,$\tan\beta$) plane derived from the inclusive $B \to \tau\nu_\tau X$ branching ratio in GROSSMAN 95B and BUSKULIC 95. They show that the constraint is quite sensitive to supersymmetric one-loop effects.

[75] GUCHAIT 97 studies the constraints on m_{H^+} set by Tevatron data on $\ell\tau$ final states in $t\overline{t} \to (Wb)(Hb)$, $W \to \ell\nu$, $H \to \tau\nu_\tau$. See Fig. 2 for the excluded region.

[76] MANGANO 97 reconsiders the limit in ACCIARRI 97F including the effect of the potentially large $B_c \to \tau\nu_\tau$ background to $B_u \to \tau\nu_\tau$ decays. Stronger limits are obtained.

[77] STAHL 97 fit τ lifetime, leptonic branching ratios, and the Michel parameters and derive limit $m_{H^+} > 1.5 \tan\beta$ GeV (90% CL) for a two-doublet model. See also STAHL 94.

[78] ALAM 95 measure the inclusive $b \to s\gamma$ branching ratio at $\Upsilon(4S)$ and give $B(b \to s\gamma) < 4.2 \times 10^{-4}$ (95% CL), which translates to the limit $m_{H^+} > [244 + 63/(\tan\beta)^{1.3}]$ GeV in the Type II two-doublet model. Light supersymmetric particles can invalidate this bound.

[79] BUSKULIC 95 give a limit $m_{H^+} > 1.9 \tan\beta$ GeV (90%CL) for Type-II models from $b \to \tau\nu_\tau X$ branching ratio, as proposed in GROSSMAN 94.

MASS LIMITS for $H^{\pm\pm}$ (doubly-charged Higgs boson)

VALUE (GeV)	CL%	DOCUMENT ID		TECN	COMMENT
>97.3	95	[80] ABDALLAH	03	DLPH	$E_{cm} \leq 209$ GeV
>98.5	95	[81] ABBIENDI	02C	OPAL	$E_{cm} \leq 209$ GeV
• • • We do not use the following data for averages, fits, limits, etc. • • •					
		[82] ABBIENDI	03Q	OPAL	$E_{cm} \leq 209$ GeV, single $H^{\pm\pm}$
		[83] GORDEEV	97	SPEC	muonium conversion
		[84] ASAKA	95	THEO	
>45.6	95	[85] ACTON	92M	OPAL	
>30.4	95	[86] ACTON	92M	OPAL	$T_3(H^{++}) = +1$
>25.5	95	[86] ACTON	92M	OPAL	$T_3(H^{++}) = 0$
none 6.5–36.6	95	[87] SWARTZ	90	MRK2	$T_3(H^{++}) = +1$
none 7.3–34.3	95	[87] SWARTZ	90	MRK2	$T_3(H^{++}) = 0$

[80] ABDALLAH 03 search for $H^{++}H^{--}$ pair production either followed by $H^{++} \to \tau^+\tau^+$, or decaying outside the detector. The limit is for weak single H^{++}. The limit for weak triplet is 98.1 GeV.

[81] ABBIENDI 02C searches for pair production of $H^{++}H^{--}$, with $H^{\pm\pm} \to \ell^\pm\ell^\pm$ ($\ell,\ell' = e,\mu,\tau$). The limit holds for ℓ=ℓ'=τ, and becomes stronger for other combinations of leptonic final states. To ensure the decay within the detector, the limit only applies for $g(H\ell\ell) \gtrsim 10^{-7}$.

[82] ABBIENDI 03Q searches for single $H^{\pm\pm}$ via direct production in $e^+e^- \to e^\pm e^\pm H^\mp\mp$, and via t-channel exchange in $e^+e^- \to e^+e^-$. In the direct case, and assuming $B(H^{\pm\pm} \to \ell^\pm\ell^\pm) = 1$, a 95% CL limit on $h_{ee} < 0.071$ is set for $m_{H^{\pm\pm}} < 160$ GeV (see Fig. 6). In the second case, indirect limits on h_{ee} are set for $m_{H^{\pm\pm}} < 2$ TeV (see Fig. 8).

[83] GORDEEV 97 search for muonium-antimuonium conversion and find $G_{M\overline{M}}/G_F < 0.14$ (90% CL), where $G_{M\overline{M}}$ is the lepton-flavor violating effective four-fermion coupling. This limit may be converted to $m_{H^{++}} > 210$ GeV if the Yukawa couplings of H^{++} to ee and $\mu\mu$ are as large as the weak gauge coupling. For similar limits on muonium-antimuonium conversion, see the muon Particle Listings.

[84] ASAKA 95 point out that H^{++} decays dominantly to four fermions in a large region of parameter space where the limit of ACTON 92M from the search of dilepton modes does not apply.

[85] ACTON 92M limit assumes $H^{\pm\pm} \to \ell^\pm\ell^\pm$ or $H^{\pm\pm}$ does not decay in the detector. Thus the region $g\ell\ell \approx 10^{-7}$ is not excluded.

[86] ACTON 92M from $\Delta\Gamma_Z < 40$ MeV.

[87] SWARTZ 90 assume $H^{\pm\pm} \to \ell^\pm\ell^\pm$ (any flavor). The limits are valid for the Higgs-lepton coupling $g(H\ell\ell) \gtrsim 7.4 \times 10^{-7}/[m_H/\text{GeV}]^{1/2}$. The limits improve somewhat for ee and $\mu\mu$ decay modes.

H^0 and $H^\pm$ REFERENCES

ABDALLAH	04	EPJ C32 145	J. Abdallah *et al.* (DELPHI Collab.)
ABBIENDI	03	PL B551 35	G. Abbiendi *et al.* (OPAL Collab.)
ABBIENDI	03B	EPJ C26 479	G. Abbiendi *et al.* (OPAL Collab.)
ABBIENDI	03F	EPJ C27 311	G. Abbiendi *et al.* (OPAL Collab.)
ABBIENDI	03G	EPJ C27 483	G. Abbiendi *et al.* (OPAL Collab.)
ABBIENDI	03Q	PL B577 93	G. Abbiendi *et al.* (OPAL Collab.)
ABDALLAH	03	PL B552 127	J. Abdallah *et al.* (DELPHI Collab.)
ACHARD	03C	PL B568 191	P. Achard *et al.* (L3 Collab.)
HEISTER	03D	PL B565 61	A. Heister *et al.* (ALEPH, DELPHI, L3+)
ALEPH, DELPHI, L3, OPAL, LEP Higgs Working Group			
ABAZOV	02B	PRL 88 151803	V.M. Abazov *et al.* (D0 Collab.)
ABBIENDI	02C	PL B544 221	G. Abbiendi *et al.* (OPAL Collab.)
ABBIENDI	02D	EPJ C23 397	G. Abbiendi *et al.* (OPAL Collab.)
ABBIENDI	02F	PL B544 44	G. Abbiendi *et al.* (OPAL Collab.)
ABDALLAH	02	PL B525 17	J. Abdallah *et al.* (DELPHI Collab.)
ACHARD	02C	PL B534 28	P. Achard *et al.* (L3 Collab.)
ACHARD	02H	PL B545 30	P. Achard *et al.* (L3 Collab.)
AKEROYD	02	PR D66 037702	A.G. Akeroyd *et al.*
BORZUMATI	02	PL B549 170	F.M. Borzumati, A. Djouadi
CHANOWITZ	02	PR D66 073002	M.S. Chanowitz
HEISTER	02	PL B526 191	A. Heister *et al.* (ALEPH Collab.)
HEISTER	02L	PL B544 16	A. Heister *et al.* (ALEPH Collab.)
HEISTER	02M	PL B544 25	A. Heister *et al.* (ALEPH Collab.)
HEISTER	02P	PL B543 1	A. Heister *et al.* (ALEPH Collab.)
LEP	02	CERN-EP/2002-091	LEP Collabs.
ALEPH, DELPHI, L3, OPAL, the LEP Electroweak Working Group, and the SLD Heavy Flavor Group			
ABAZOV	01E	PRL 87 231801	V.M. Abazov *et al.* (D0 Collab.)
ABBIENDI	01A	EPJ C19 587	G. Abbiendi *et al.* (OPAL Collab.)
ABBIENDI	01E	EPJ C18 425	G. Abbiendi *et al.* (OPAL Collab.)
ABBIENDI	01Q	PL B520 1	G. Abbiendi *et al.* (OPAL Collab.)
ABREU	01F	PL B507 89	P. Abreu *et al.* (DELPHI Collab.)
ACHARD	01C	PL B517 319	P. Achard *et al.* (L3 Collab.)
AFFOLDER	01D	PRL 86 4472	T. Affolder *et al.* (CDF Collab.)
AFFOLDER	01H	PR D64 092002	T. Affolder *et al.* (CDF Collab.)
BARATE	01C	PL B499 53	R. Barate *et al.* (ALEPH Collab.)
BARATE	01E	EPJ C19 213	R. Barate *et al.* (ALEPH Collab.)
GAMBINO	01	NP B611 338	P. Gambino, M. Misiak
ABBIENDI	00F	EPJ C12 567	G. Abbiendi *et al.* (OPAL Collab.)
ABBIENDI	00G	EPJ C14 51	G. Abbiendi *et al.* (OPAL Collab.)
ACCIARRI	00M	PL B485 85	M. Acciarri *et al.* (L3 Collab.)
ACCIARRI	00R	PL B489 102	M. Acciarri *et al.* (L3 Collab.)
ACCIARRI	00S	PL B489 115	M. Acciarri *et al.* (L3 Collab.)
ACCIARRI	00W	PL B496 34	M. Acciarri *et al.* (L3 Collab.)
AFFOLDER	00I	PR D62 012004	T. Affolder *et al.* (CDF Collab.)
BARATE	00L	PL B487 241	R. Barate *et al.* (ALEPH Collab.)
FIELD	00	PR D61 013010	J.H. Field
LEP	00B	CERN-EP-2000-055	LEP Collabs.
PDG	00	EPJ C15 1	D.E. Groom *et al.*
ABBIENDI	99E	EPJ C7 407	G. Abbiendi *et al.* (OPAL Collab.)
ABBIENDI	99O	PL B464 311	G. Abbiendi *et al.* (OPAL Collab.)
ABBOTT	99B	PRL 82 2244	B. Abbott *et al.* (D0 Collab.)
ABBOTT	99E	PRL 82 4975	B. Abbott *et al.* (D0 Collab.)
ABREU	99E	PL B446 75	P. Abreu *et al.* (DELPHI Collab.)
Also	99N	PL B451 447 (erratum)	P. Abreu *et al.* (DELPHI Collab.)
ABREU	99P	PL B458 431	P. Abreu *et al.* (DELPHI Collab.)
ABREU	99Q	PL B459 367	P. Abreu *et al.* (DELPHI Collab.)
ABREU	99R	PL B460 484	P. Abreu *et al.* (DELPHI Collab.)
ACKERSTAFF	99D	EPJ C8 3	K. Ackerstaff *et al.* (OPAL Collab.)
CARENA	99B	hep-ph/9912223 CERN-TH/99-374	M. Carena *et al.*
CHANOWITZ	99	PR D59 073005	M.S. Chanowitz
D'AGOSTINI	99	EPJ C10 663	G. D'Agostini, G. Degrassi
FIELD	99	MPL A14 1815	J.H. Field
LEP	99	CERN-EP/99-015	LEP Collabs. (ALEPH, DELPHI, L3, OPAL, LEP EWWG+)
ABBOTT	98	PRL 80 442	B. Abbott *et al.* (D0 Collab.)
ABE	98T	PRL 81 5748	F. Abe *et al.* (CDF Collab.)
ACKERSTAFF	98S	EPJ C5 19	K. Ackerstaff *et al.* (OPAL Collab.)
ACKERSTAFF	98Y	PL B437 218	K. Ackerstaff *et al.* (OPAL Collab.)
CHANOWITZ	98	PRL 80 2521	M. Chanowitz
DAVIER	98	PL B435 427	M. Davier, A. Hoecker
GONZALEZ-G...	98B	PR D57 7045	M.C. Gonzalez-Garcia, S.M. Lietti, S.F. Novaes
HAGIWARA	98B	EPJ C2 95	K. Hagiwara, D. Haidt, S. Matsumoto
PDG	98	EPJ C3 1	C. Caso *et al.*
ABBANEO	97	CERN-PPE/97-154	D. Abbaneo *et al.*
ALEPH, DELPHI, L3, OPAL, and SLD Collaborations, and the LEP Electroweak Working Group.			
ABE	97L	PRL 79 357	F. Abe *et al.* (CDF Collab.)
ABE	97W	PRL 79 3819	F. Abe *et al.* (CDF Collab.)
ACCIARRI	97F	PL B396 327	M. Acciarri *et al.* (L3 Collab.)
AMMAR	97B	PRL 78 4686	R. Ammar *et al.* (CLEO Collab.)
COARASA	97	PL B406 337	J.A. Coarasa, R.A. Jimenez, J. Sola
DEBOER	97B	ZPHY C75 627	W. de Boer *et al.*
DEGRASSI	97	PL B394 188	G. Degrassi, P. Gambino, A. Sirlin (MPIM, NYU)
DITTMAIER	97	PL B391 420	S. Dittmaier, D. Schildknecht (BIEL)
GORDEEV	97	PAN 60 1164 Translated from YAF 60 1291.	V.A. Gordeev *et al.* (PNPI)
GUCHAIT	97	PR D55 7263	M. Guchait, D.P. Roy (TATA)
KRAWCZYK	97	PR D55 6968	M. Krawczyk, J. Zochowski (WARS)
MANGANO	97	PL B410 299	M. Mangano, S. Slabospitsky
RENTON	97	IJMP A12 4109	P.B. Renton
STAHL	97	ZPHY C74 73	A. Stahl, H. Voss (BONN)
ALCARAZ	96	CERN-PPE/96-183	J. Alcaraz *et al.*
The ALEPH, DELPHI, L3, OPAL, and SLD Collaborations and the LEP Electroweak Working Group			
ALEXANDER	96H	ZPHY C71 1	G. Alexander *et al.* (OPAL Collab.)
ELLIS	96C	PL B389 321	J. Ellis, G.L. Fogli, E. Lisi (CERN, BARI)
GURTU	96	PL B385 415	A. Gurtu (TATA)
PDG	96	PR D54 1	R. M. Barnett *et al.*
ABREU	95H	ZPHY C67 69	P. Abreu *et al.* (DELPHI Collab.)
ALAM	95	PRL 74 2885	M.S. Alam *et al.* (CLEO Collab.)

ASAKA	95	PL B345 36	T. Asaka, K.I. Hikasa	(TOHOK)
BUSKULIC	95	PL B343 444	D. Buskulic *et al.*	(ALEPH Collab.)
GROSSMAN	95B	PL B357 630	Y. Grossman, H. Haber, Y. Nir	
GROSSMAN	94	PL B332 373	Y. Grossman, Z. Ligeti	
STAHL	94	PL B324 121	A. Stahl	(BONN)
ACTON	92M	PL B295 347	P.D. Acton *et al.*	(OPAL Collab.)
PICH	92	NP B388 31	A. Pich, J. Prades, P. Yepes	(CERN, CPPM)
SWARTZ	90	PRL 64 2877	M.L. Swartz *et al.*	(Mark II Collab.)

Heavy Bosons Other Than Higgs Bosons, Searches for

We list here various limits on charged and neutral heavy vector bosons (other than W's and Z's), heavy scalar bosons (other than Higgs bosons), vector or scalar leptoquarks, and axigluons.

THE W' SEARCHES

Written October 1997 by K.S. Babu (Oklahoma State University), C. Kolda (Notre Dame University), and J. March-Russell (CERN).

Any electrically charged gauge boson outside of the Standard Model is generically denoted W'. A W' always couples to two different flavors of fermions, similar to the W boson. In particular, if a W' couples quarks to leptons it is a leptoquark gauge boson.

The most attractive candidate for W' is the W_R gauge boson associated with the left-right symmetric models [1]. These models seek to provide a spontaneous origin for parity violation in weak interactions. Here the gauge group is extended to $\mathrm{SU}(3)_C \times \mathrm{SU}(2)_L \times \mathrm{SU}(2)_R \times \mathrm{U}(1)_{B-L}$ with the Standard Model hypercharge identified as $Y = T_{3R} + (B\text{–}L)/2$, T_{3R} being the third component of $\mathrm{SU}(2)_R$. The fermions transform under the gauge group in a left-right symmetric fashion: $q_L(3,2,1,1/3) + q_R(3,1,2,1/3)$ for quarks and $\ell_L(1,2,1,-1) + \ell_R(1,1,2,-1)$ for leptons. Note that the model requires the introduction of right-handed neutrinos, which can facilitate the see-saw mechanism for explaining the smallness of the ordinary neutrino masses. A Higgs bidoublet $\Phi(1,2,2,0)$ is usually employed to generate quark and lepton masses and to participate in the electroweak symmetry breaking. Under left-right (or parity) symmetry, $q_L \leftrightarrow q_R$, $\ell_L \leftrightarrow \ell_R$, $W_L \leftrightarrow W_R$ and $\Phi \leftrightarrow \Phi^\dagger$.

After spontaneous symmetry breaking, the two W bosons of the model, W_L and W_R, will mix. The physical mass eigenstates are denoted as

$$W_1 = \cos\zeta\, W_L + \sin\zeta\, W_R, \qquad W_2 = -\sin\zeta\, W_L + \cos\zeta\, W_R \quad (1)$$

with W_1 identified as the observed W boson. The most general Lagrangian that describes the interactions of the $W_{1,2}$ with the quarks can be written as [2]

$$\mathcal{L} = -\frac{1}{\sqrt{2}}\overline{u}\gamma_\mu \left[\left(g_L \cos\zeta\, V^L P_L - g_R e^{i\omega} \sin\zeta\, V^R P_R\right) W_1^\mu + \left(g_L \sin\zeta\, V^L P_L + g_R e^{i\omega} \cos\zeta\, V^R P_R\right) W_2^\mu\right] d + h.c. \quad (2)$$

where $g_{L,R}$ are the $\mathrm{SU}(2)_{L,R}$ gauge couplings, $P_{L,R} = (1 \mp \gamma_5)/2$ and $V^{L,R}$ are the left- and right-handed CKM matrices in the quark sector. The phase ω reflects a possible complex mixing parameter in the W_L–W_R mass-squared matrix. Note that there is CP violation in the model arising from the right-handed currents even with only two generations. The Lagrangian for leptons is identical to that for quarks, with the replacements $u \to \nu$, $d \to e$ and the identification of $V^{L,R}$ with the CKM matrices in the leptonic sector.

If parity invariance is imposed on the Lagrangian, then $g_L = g_R$. Furthermore, the Yukawa coupling matrices that arise from coupling to the Higgs bidoublet Φ will be Hermitian. If in addition the vacuum expectation values of Φ are assumed to be real, the quark and lepton mass matrices will also be Hermitian, leading to the relation $V^L = V^R$. Such models are called *manifest* left-right symmetric models and are approximately realized with a minimal Higgs sector [3]. If instead parity and CP are both imposed on the Lagrangian, then the Yukawa coupling matrices will be real symmetric and, after spontaneous CP violation, the mass matrices will be complex symmetric. In this case, which is known in the literature as *pseudo-manifest* left-right symmetry, $V^L = (V^R)^*$.

Indirect constraints: In minimal version of manifest or pseudo-manifest left-right symmetric models with $\omega = 0$ or π, there are only two free parameters, ζ and M_{W_2}, and they can be constrained from low energy processes. In the large M_{W_2} limit, stringent bounds on the angle ζ arise from three processes. (i) Nonleptonic K decays: The decays $K \to 3\pi$ and $K \to 2\pi$ are sensitive to small admixtures of right-handed currents. Assuming the validity of PCAC relations in the Standard Model it has been argued in Ref. 4 that the success in the $K \to 3\pi$ prediction will be spoiled unless $|\zeta| \leq 4 \times 10^{-3}$. (ii) $b \to s\gamma$: The amplitude for this process has an enhancement factor m_t/m_b relative to the Standard Model and thus can be used to constrain ζ yielding the limit $-0.01 \leq \zeta \leq 0.003$ [5]. (iii) Universality in weak decays: If the right-handed neutrinos are heavy, the right-handed admixture in the charged current will contribute to β decay and K decay, but not to the μ decay. This will modify the extracted values of V_{ud}^L and V_{us}^L. Demanding that the difference not upset the three generation unitarity of the CKM matrix, a bound $|\zeta| \leq 10^{-3}$ has been derived [6].

If the ν_R are heavy, leptonic and semileptonic processes do not constrain ζ since the emission of ν_R will not be kinematically allowed. However, if the ν_R is light enough to be emitted in μ decay and β decay, stringent limits on ζ do arise. For example, $|\zeta| \leq 0.039$ can be obtained from polarized μ decay [7] in the large M_{W_2} limit of the manifest left-right model. Alternatively, in the $\zeta = 0$ limit, there is a constraint $M_{W_2} \geq 484$ GeV from direct W_2 exchange. For the constraint on the case in which M_{W_2} is not taken to be heavy, see Ref. 2. There are also cosmological and astrophysical constraints on M_{W_2} and ζ in scenarios with a light ν_R. During nucleosynthesis the process $e^+e^- \to \nu_R\overline{\nu}_R$, proceeding via W_2 exchange, will keep the ν_R in equilibrium leading to an overproduction of ^{4}He unless M_{W_2} is greater than about 1 TeV [8]. Likewise the ν_{eR} produced via $e_R^- p \to n\nu_R$ inside a supernova must not drain too much of its energy, leading to limits $M_{W_2} > 16$ TeV and $|\zeta| \leq 3 \times 10^{-5}$ [9]. Note that models with light ν_R do not

have a see-saw mechanism for explaining the smallness of the neutrino masses, though other mechanisms may arise in variant models [10].

The mass of W_2 is severely constrained (independent of the value of ζ) from K_L–K_S mass-splitting. The box diagram with exchange of one W_L and one W_R has an anomalous enhancement and yields the bound $M_{W_2} \geq 1.6$ TeV [11] for the case of manifest or pseudo-manifest left-right symmetry. If the ν_R have Majorana masses, another constraint arises from neutrinoless double β decay. Combining the experimental limit from ^{76}Ge decay with arguments of vacuum stability, a limit of $M_{W_2} \geq 1.1$ TeV has been obtained [12].

Direct search limits: Limits on M_{W_2} from direct searches depend on the available decay channels of W_2. If ν_R is heavier than W_2, the decay $W_2^+ \to \ell_R^+ \nu_R$ will be forbidden kinematically. Assuming that ζ is small, the dominant decay of W_2 will be into dijets. UA2 [13] has excluded a W_2 in the mass range of 100 to 251 GeV in this channel. DØ excludes the mass range of 340 to 680 GeV [14], while CDF excludes the mass range of 300 to 420 GeV for such a W_2 [15]. If ν_R is lighter than W_2, the decay $W_2^+ \to e_R^+ \nu_R$ is allowed. The ν_R can then decay into $e_R W_R^*$, leading to an $eejj$ signature. DØ has a limit of $M_{W_2} > 720$ GeV if $m_{\nu_R} \ll M_{W_2}$; the bound weakens, for example, to 650 GeV for $m_{\nu_R} = M_{W_2}/2$ [16]. CDF finds $M_{W_2} > 652$ GeV if ν_R is stable and much lighter than W_2 [17]. All of these limits assume manifest or pseudo-manifest left-right symmetry. See [16] for some variations in the limits if the assumption of left-right symmetry is relaxed.

Alternative models: W' gauge bosons can also arise in other models. We shall briefly mention some such popular models, but for details we refer the reader to the original literature. The *alternate* left-right model [18] is based on the same gauge group as the left-right model, but arises in the following way: In E_6 unification, there is an option to identify the right-handed down quarks as $\mathrm{SU}(2)_R$ singlets or doublets. If they are $\mathrm{SU}(2)_R$ doublets, one recovers the conventional left-right model; if they are singlets it leads to the alternate left-right model. A similar ambiguity exists in the assignment of left-handed leptons; the alternate left-right model assigns them to a $(1,2,2,0)$ multiplet. As a consequence, the ordinary neutrino remains exactly massless in the model. One important difference from the usual left-right model is that the limit from the K_L–K_S mass difference is no longer applicable, since the d_R do not couple to the W_R. There is also no limit from polarized μ decay, since the $\mathrm{SU}(2)_R$ partner of e_R can receive a large Majorana mass. Other W' models include the un-unified Standard Model of Ref. 19 where there are two different SU(2) gauge groups, one each for the quarks and leptons; models with separate SU(2) gauge factors for each generation [20]; and the $\mathrm{SU}(3)_C \times \mathrm{SU}(3)_L \times \mathrm{U}(1)$ model of Ref. 21.

Leptoquark gauge bosons: The $\mathrm{SU}(3)_C \times \mathrm{U}(1)_{B-L}$ part of the gauge symmetry discussed above can be embedded into a simple $\mathrm{SU}(4)_C$ gauge group [22]. The model then will contain leptoquark gauge boson as well, with couplings of the type $\{(\overline{e}_L \gamma_\mu d_L + \overline{\nu}_L \gamma_\mu u_L) W'^\mu + (L \to R)\}$. The best limit on such leptoquark W' comes from nonobservation of $K_L \to \mu e$, which requires $M_{W'} \geq 1400$ TeV; for the corresponding limits on less conventional leptoquark flavor structures, see Ref. 23. Thus such a W' is inaccessible to direct searches with present machines which are sensitive to vector leptoquark masses of order 300 GeV only.

References

1. J.C. Pati and A. Salam, Phys. Rev. **D10**, 275 (1974); R.N. Mohapatra and J.C. Pati, Phys. Rev. **D11**, 566 (1975); *ibid.* Phys. Rev. **D11**, 2558 (1975); G. Senjanovic and R.N. Mohapatra, Phys. Rev. **D12**, 1502 (1975).
2. P. Langacker and S. Uma Sankar, Phys. Rev. **D40**, 1569 (1989).
3. A. Masiero, R.N. Mohapatra, and R. Peccei, Nucl. Phys. **B192**, 66 (1981); J. Basecq, *et al.*, Nucl. Phys. **B272**, 145 (1986).
4. J. Donoghue and B. Holstein, Phys. Lett. **113B**, 383 (1982).
5. K.S. Babu, K. Fujikawa, and A. Yamada, Phys. Lett. **B333**, 196 (1994); P. Cho and M. Misiak, Phys. Rev. **D49**, 5894 (1994); T.G. Rizzo, Phys. Rev. **D50**, 3303 (1994).
6. L. Wolfenstein, Phys. Rev. **D29**, 2130 (1984).
7. P. Herczeg, Phys. Rev. **D34**, 3449 (1986).
8. G. Steigman, K.A. Olive, and D. Schramm, Nucl. Phys. **B180**, 497 (1981).
9. R. Barbieri and R.N. Mohapatra, Phys. Rev. **D39**, 1229 (1989); G. Raffelt and D. Seckel, Phys. Rev. Lett. **60**, 1793 (1988).
10. D. Chang and R.N. Mohapatra, Phys. Rev. Lett. **58**, 1600 (1987); K.S. Babu and X.G. He, Mod. Phys. Lett. **A4**, 61 (1989).
11. G. Beall, M. Bender, and A. Soni, Phys. Rev. Lett. **48**, 848 (1982).
12. R.N. Mohapatra, Phys. Rev. **D34**, 909 (1986).
13. J. Alitti, *et al.* (UA2 Collaboration), Nucl. Phys. **B400**, 3 (1993).
14. B. Abbott, *et al.* (DØ Collaboration), International Europhysics Conference on High Energy Physics, August 19-26, 1997, Jerusalem, Israel.
15. F. Abe, *et al.* (CDF Collaboration), Phys. Rev. **D55**, R5263 (1997).
16. S. Abachi, *et al.* (DØ Collaboration), Phys. Rev. Lett. **76**, 3271 (1996).
17. F. Abe, *et al.* (CDF Collaboration), Phys. Rev. Lett. **74**, 2900 (1995).
18. E. Ma, Phys. Rev. **D36**, 274 (1987); K.S. Babu, X-G. He and E. Ma, Phys. Rev. **D36**, 878 (1987).
19. H. Georgi and E. Jenkins, Phys. Rev. Lett. **62**, 2789 (1989); Nucl. Phys. **B331**, 541 (1990).
20. X. Li and E. Ma, Phys. Rev. Lett. **47**, 1788 (1981); R.S. Chivukula, E.H. Simmons, and J. Terning, Phys. Lett. **B331**, 383 (1994); D.J. Muller and S. Nandi, Phys. Lett. **B383**, 345 (1996).

21. F. Pisano, V. Pleitez, Phys. Rev. **D46**, 410 (1992); P. Frampton, Phys. Rev. Lett. **69**, 2889 (1992).

22. J.C. Pati and A. Salam, Phys. Rev. **D10**, 275 (1974).

23. A. Kuznetsov and N. Mikheev, Phys. Lett. **B329**, 295 (1994); G. Valencia and S. Willenbrock, Phys. Rev. **D50**, 6843 (1994).

MASS LIMITS for W' (Heavy Charged Vector Boson Other Than W) in Hadron Collider Experiments

Couplings of W' to quarks and leptons are taken to be identical with those of W. The following limits are obtained from $p\overline{p} \rightarrow W'X$ with W' decaying to the mode indicated in the comments. New decay channels (*e.g.*, $W' \rightarrow WZ$) are assumed to be suppressed. UA1 and UA2 experiments assume that the $t\overline{b}$ channel is not open.

VALUE (GeV)	CL%	DOCUMENT ID		TECN	COMMENT
>786	95	[1] AFFOLDER	01I	CDF	$W' \rightarrow e\nu, \mu\nu$
• • • We do not use the following data for averages, fits, limits, etc. • • •					
225–536	95	[2] ACOSTA	03B	CDF	$W' \rightarrow tb$
none 200–480	95	[3] AFFOLDER	02C	CDF	$W' \rightarrow WZ$
>660	95	[4] ABE	00	CDF	$W' \rightarrow \mu\nu$
none 300–420	95	[5] ABE	97G	CDF	$W' \rightarrow q\overline{q}$
>720	95	[6] ABACHI	96C	D0	$W' \rightarrow e\nu$
>610	95	[7] ABACHI	95E	D0	$W' \rightarrow e\nu, \tau\nu$
>652	95	[8] ABE	95M	CDF	$W' \rightarrow e\nu$
>251	90	[9] ALITTI	93	UA2	$W' \rightarrow q\overline{q}$
none 260–600	95	[10] RIZZO	93	RVUE	$W' \rightarrow q\overline{q}$
>220	90	[11] ALBAJAR	89	UA1	$W' \rightarrow e\nu$
>209	90	[12] ANSARI	87D	UA2	$W' \rightarrow e\nu$

[1] AFFOLDER 01I combine a new bound on $W' \rightarrow e\nu$ of 754 GeV with the bound of ABE 00 on $W' \rightarrow \mu\nu$ to obtain quoted bound.

[2] The ACOSTA 03B quoted limit is for $M_{W'} \gg M_{\nu_R}$. For $M_{W'} < M_{\nu_R}$, $M_{W'}$ between 225 and 566 GeV is excluded.

[3] The quoted limit is obtained assuming $W'WZ$ coupling strength is the same as the ordinary WWZ coupling strength in the Standard Model. See their Fig. 2 for the limits on the production cross sections as a function of the W' width.

[4] ABE 00 assume that the neutrino from W' decay is stable and has a mass significantly less than $m_{W'}$.

[5] ABE 97G search for new particle decaying to dijets.

[6] For bounds on W_R with nonzero right-handed mass, see Fig. 5 from ABACHI 96C.

[7] ABACHI 95E assume that the decay $W' \rightarrow WZ$ is suppressed and that the neutrino from W' decay is stable and has a mass significantly less $m_{W'}$.

[8] ABE 95M assume that the decay $W' \rightarrow WZ$ is suppressed and the (right-handed) neutrino is light, noninteracting, and stable. If m_ν=60 GeV, for example, the effect on the mass limit is negligible.

[9] ALITTI 93 search for resonances in the two-jet invariant mass. The limit assumes $\Gamma(W')/m_{W'} = \Gamma(W)/m_W$ and $B(W' \rightarrow jj) = 2/3$. This corresponds to W_R with $m_{\nu_R} > m_{W_R}$ (no leptonic decay) and $W_R \rightarrow t\overline{b}$ allowed. See their Fig. 4 for limits in the $m_{W'}$–$B(q\overline{q})$ plane.

[10] RIZZO 93 analyses CDF limit on possible two-jet resonances. The limit is sensitive to the inclusion of the assumed K factor.

[11] ALBAJAR 89 cross section limit at 630 GeV is $\sigma(W')\ B(e\nu) < 4.1$ pb (90% CL).

[12] See Fig. 5 of ANSARI 87D for the excluded region in the $m_{W'}$–$[(g_{W'q})^2\ B(W' \rightarrow e\overline{\nu})]$ plane. Note that the quantity $(g_{W'q})^2\ B(W' \rightarrow e\overline{\nu})$ is normalized to unity for the standard W couplings.

W_R (Right-Handed W Boson) MASS LIMITS

Assuming a light right-handed neutrino, except for BEALL 82, LANGACKER 89B, and COLANGELO 91. $g_R = g_L$ assumed. [Limits in the section MASS LIMITS for W' below are also valid for W_R if $m_{\nu_R} \ll m_{W_R}$.] Some limits assume manifest left-right symmetry, *i.e.*, the equality of left- and right Cabibbo-Kobayashi-Maskawa matrices. For a comprehensive review, see LANGACKER 89B. Limits on the W_L-W_R mixing angle ζ are found in the next section. Values in brackets are from cosmological and astrophysical considerations and assume a light right-handed neutrino.

VALUE (GeV)	CL%	DOCUMENT ID		TECN	COMMENT
> 715	90	[13] CZAKON	99	RVUE	Electroweak
• • • We do not use the following data for averages, fits, limits, etc. • • •					
> 310	90	[14] THOMAS	01	CNTR	β^+ decay
> 137	95	[15] ACKERSTAFF	99D	OPAL	τ decay
>1400	68	[16] BARENBOIM	98	RVUE	Electroweak, Z-Z' mixing
> 549	68	[17] BARENBOIM	97	RVUE	μ decay
> 220	95	[18] STAHL	97	RVUE	τ decay
> 220	90	[19] ALLET	96	CNTR	β^+ decay
> 281	90	[20] KUZNETSOV	95	CNTR	Polarized neutron decay
> 282	90	[21] KUZNETSOV	94B	CNTR	Polarized neutron decay
> 439	90	[22] BHATTACH...	93	RVUE	Z-Z' mixing
> 250	90	[23] SEVERIJNS	93	CNTR	β^+ decay
		[24] IMAZATO	92	CNTR	K^+ decay
> 475	90	[25] POLAK	92B	RVUE	μ decay
> 240	90	[26] AQUINO	91	RVUE	Neutron decay
> 496	90	[26] AQUINO	91	RVUE	Neutron and muon decay
> 700		[27] COLANGELO	91	THEO	$m_{K^0_L} - m_{K^0_S}$
> 477	90	[28] POLAK	91	RVUE	μ decay
[none 540–23000]		[29] BARBIERI	89B	ASTR	SN 1987A; light ν_R
> 300	90	[30] LANGACKER	89B	RVUE	General
> 160	90	[31] BALKE	88	CNTR	$\mu \rightarrow e\nu\overline{\nu}$
> 406	90	[32] JODIDIO	86	ELEC	Any ζ
> 482	90	[32] JODIDIO	86	ELEC	$\zeta = 0$
> 800		MOHAPATRA	86	RVUE	$SU(2)_L \times SU(2)_R \times U(1)$
> 400	95	[33] STOKER	85	ELEC	Any ζ
> 475	95	[33] STOKER	85	ELEC	$\zeta < 0.041$
		[34] BERGSMA	83	CHRM	$\nu_\mu e \rightarrow \mu\nu_e$
> 380	90	[35] CARR	83	ELEC	μ^+ decay
>1600		[36] BEALL	82	THEO	$m_{K^0_L} - m_{K^0_S}$
[> 4000]		STEIGMAN	79	COSM	Nucleosynthesis; light ν_R

[13] CZAKON 99 perform a simultaneous fit to charged and neutral sectors.

[14] THOMAS 01 limit is from measurement of β^+ polarization in decay of polarized ^{12}N. The listed limit assumes no mixing.

[15] ACKERSTAFF 99D limit is from τ decay parameters. Limit increase to 145 GeV for zero mixing.

[16] BARENBOIM 98 assumes minimal left-right model with Higgs of $SU(2)_R$ in $SU(2)_L$ doublet. For Higgs in $SU(2)_L$ triplet, $m_{W_R} > 1100$ GeV. Bound calculated from effect of corresponding Z_{LR} on electroweak data through Z–Z_{LR} mixing.

[17] The quoted limit is from μ decay parameters. BARENBOIM 97 also evaluate limit from K_L-K_S mass difference.

[18] STAHL 97 limit is from fit to τ-decay parameters.

[19] ALLET 96 measured polarization-asymmetry correlation in ^{12}N β^+ decay. The listed limit assumes zero L-R mixing.

[20] KUZNETSOV 95 limit is from measurements of the asymmetry $\langle \vec{p}_\nu \cdot \sigma_n \rangle$ in the β decay of polarized neutrons. Zero mixing assumed. See also KUZNETSOV 94B.

[21] KUZNETSOV 94B limit is from measurements of the asymmetry $\langle \vec{p}_\nu \cdot \sigma_n \rangle$ in the β decay of polarized neutrons. Zero mixing assumed.

[22] BHATTACHARYYA 93 uses Z-Z' mixing limit from LEP '90 data, assuming a specific Higgs sector of $SU(2)_L \times SU(2)_R \times U(1)$ gauge model. The limit is for m_t=200 GeV and slightly improves for smaller m_t.

[23] SEVERIJNS 93 measured polarization-asymmetry correlation in ^{107}In β^+ decay. The listed limit assumes zero L-R mixing. Value quoted here is from SEVERIJNS 94 erratum.

[24] IMAZATO 92 measure positron asymmetry in $K^+ \rightarrow \mu^+\nu_\mu$ decay and obtain $\xi P_\mu > 0.990$ (90%CL). If W_R couples to $u\overline{s}$ with full weak strength (V^R_{us}=1), the result corresponds to $m_{W_R} > 653$ GeV. See their Fig. 4 for m_{W_R} limits for general $|V^R_{us}|^2 = 1 - |V^R_{ud}|^2$.

[25] POLAK 92B limit is from fit to muon decay parameters and is essentially determined by JODIDIO 86 data assuming ζ=0. Supersedes POLAK 91.

[26] AQUINO 91 limits obtained from neutron lifetime and asymmetries together with unitarity of the CKM matrix. Manifest left-right symmetry assumed. Stronger of the two limits also includes muon decay results.

[27] COLANGELO 91 limit uses hadronic matrix elements evaluated by QCD sum rule and is less restrictive than BEALL 82 limit which uses vacuum saturation approximation. Manifest left-right symmetry assumed.

[28] POLAK 91 limit is from fit to muon decay parameters and is essentially determined by JODIDIO 86 data assuming ζ=0. Superseded by POLAK 92B.

[29] BARBIERI 89B limit holds for $m_{\nu_R} \leq 10$ MeV.

[30] LANGACKER 89B limit is for any ν_R mass (either Dirac or Majorana) and for a general class of right-handed quark mixing matrices.

[31] BALKE 88 limit is for $m_{\nu_{eR}} = 0$ and $m_{\nu_{\mu R}} \leq 50$ MeV. Limits come from precise measurements of the muon decay asymmetry as a function of the positron energy.

[32] JODIDIO 86 is the same TRIUMF experiment as STOKER 85 (and CARR 83); however, it uses a different technique. The results given here are combined results of the two techniques. The technique here involves precise measurement of the end-point e^+ spectrum in the decay of the highly polarized μ^+.

[33] STOKER 85 is same TRIUMF experiment as CARR 83. Here they measure the decay e^+ spectrum asymmetry above 46 MeV/c using a muon-spin-rotation technique. Assumed a light right-handed neutrino. Quoted limits are from combining with CARR 83.

[34] BERGSMA 83 set limit $m_{W_2}/m_{W_1} > 1.9$ at CL = 90%.

[35] CARR 83 is TRIUMF experiment with a highly polarized μ^+ beam. Looked for deviation from $V-A$ at the high momentum end of the decay e^+ energy spectrum. Limit from previous world-average muon polarization parameter is $m_{W_R} > 240$ GeV. Assumes a light right-handed neutrino.

[36] BEALL 82 limit is obtained assuming that W_R contribution to K^0_L–K^0_S mass difference is smaller than the standard one, neglecting the top quark contributions. Manifest left-right symmetry assumed.

Limit on W_L-W_R Mixing Angle ζ

Lighter mass eigenstate $W_1 = W_L \cos\zeta - W_R \sin\zeta$. Light ν_R assumed unless noted. Values in brackets are from cosmological and astrophysical considerations.

VALUE	CL%	DOCUMENT ID		TECN	COMMENT
• • • We do not use the following data for averages, fits, limits, etc. • • •					
< 0.12	95	[37] ACKERSTAFF	99D	OPAL	τ decay
< 0.013	90	[38] CZAKON	99	RVUE	Electroweak
< 0.0333		[39] BARENBOIM	97	RVUE	μ decay
< 0.04	90	[40] MISHRA	92	CCFR	νN scattering
−0.0006 to 0.0028	90	[41] AQUINO	91	RVUE	
[none 0.00001–0.02]		[42] BARBIERI	89B	ASTR	SN 1987A
< 0.040	90	[43] JODIDIO	86	ELEC	μ decay
−0.056 to 0.040	90	[43] JODIDIO	86	ELEC	μ decay

[37] ACKERSTAFF 99D limit is from τ decay parameters.
[38] CZAKON 99 perform a simultaneous fit to charged and neutral sectors.
[39] The quoted limit is from μ decay parameters. BARENBOIM 97 also evaluate limit from K_L-K_S mass difference.
[40] MISHRA 92 limit is from the absence of extra large-x, large-y $\overline{\nu}_\mu N \to \overline{\nu}_\mu X$ events at Tevatron, assuming left-handed ν and right-handed $\overline{\nu}$ in the neutrino beam. The result gives $\zeta^2(1-2m^2_{W_1}/m^2_{W_2}) < 0.0015$. The limit is independent of ν_R mass.
[41] AQUINO 91 limits obtained from neutron lifetime and asymmetries together with unitarity of the CKM matrix. Manifest left-right asymmetry is assumed.
[42] BARBIERI 89B limit holds for $m_{\nu_R} \leq 10$ MeV.
[43] First JODIDIO 86 result assumes $m_{W_R}=\infty$, second is for unconstrained m_{W_R}.

THE Z' SEARCHES

Revised March 2002 by K.S. Babu (Oklahoma State University) and C. Kolda (Notre Dame University).

New massive and electrically neutral gauge bosons are a common feature of physics beyond the Standard Model. They are present in most extensions of the Standard Model gauge group, including models in which the Standard Model is embedded into a unifying group. They can also arise in certain classes of theories with extra dimensions. Whatever the source, such a gauge boson is called a Z'. While current theories suggest that there may be a multitude of such states at or just below the Planck scale, there exist many models in which the Z' sits at or near the weak scale. Models with extra neutral gauge bosons often contain charged gauge bosons as well; these are discussed in the review of W' physics.

The Lagrangian describing a single Z' and its interactions with the fields of the Standard Model is [1,2,3]:

$$\mathcal{L}_{Z'} = -\frac{1}{4}F'_{\mu\nu}F'^{\mu\nu} - \frac{\sin\chi}{2}F'_{\mu\nu}F^{\mu\nu} + M^2_{Z'}Z'_\mu Z'^\mu + \delta M^2\, Z'_\mu Z^\mu - \frac{e}{2c_W s_W}\sum_i \overline{\psi}_i\gamma^\mu(f^i_V - f^i_A\gamma^5)\psi_i Z'_\mu \tag{1}$$

where c_W, s_W are the cosine and sine of the weak angle, $F_{\mu\nu}$, $F'_{\mu\nu}$ are the field strength tensors for the hypercharge and the Z' gauge bosons respectively, ψ_i are the matter fields with Z' vector and axial charges f^i_V and f^i_A, and Z_μ is the electroweak Z-boson. (The overall Z' coupling strength has been normalized to that of the usual Z.) The mass terms are assumed to come from spontaneous symmetry breaking via scalar expectation values; the δM^2 term is generated by Higgs bosons that are charged under both the Standard Model and the extra gauge symmetry, and can have either sign. The above Lagrangian is general to all abelian and non-abelian extensions; however, for the non-abelian case, $F'_{\mu\nu}$ is not gauge invariant and so the kinetic mixing parameter $\chi = 0$. Most analyses take $\chi = 0$, even for the abelian case, and so we do likewise here; see Ref. 3 for a discussion of observables with $\chi \neq 0$.

Strictly speaking, the Z' defined in the Lagrangian above is not a mass eigenstate since it can mix with the usual Z boson. The mixing angle is given by

$$\xi \simeq \frac{\delta M^2}{M^2_Z - M^2_{Z'}}\,. \tag{2}$$

This mixing can alter a large number of the Z-pole observables, including the T-parameter which receives a contribution

$$\alpha T_{\rm new} = \xi^2\left(\frac{M^2_{Z'}}{M^2_Z} - 1\right) \tag{3}$$

to leading order in small ξ. (For $\chi \neq 0$, both S and T receive additional contributions [4,3].) However, the oblique parameters do not encode all the effects generated by $Z - Z'$ mixing; the mixing also alters the couplings of the Z itself, shifting its vector and axial couplings to $T^i_3 - 2Q^i s^2_W + \xi f^i_V$ and $T^i_3 + \xi f^i_A$ respectively.

If the Z' charges are generation-dependent, tree-level flavor-changing neutral currents will generically arise. There exist severe constraints in the first two generations coming from precision measurements such as the $K_L - K_S$ mass splitting and $B(\mu \to 3e)$; constraints on a Z' which couples differently only to the third generation are somewhat weaker. If the Z' interactions commute with the Standard Model gauge group, then per generation, there are only five independent $Z'\bar{\psi}\psi$ couplings; one can choose them to be $f^u_V, f^u_A, f^d_V, f^e_V, f^e_A$. All other couplings can be determined in terms of these, *e.g.*, $f^\nu_V = (f^e_V + f^e_A)/2$.

Experimental Constraints: There are four primary sets of constraints on the existence of a Z' which will be considered here: precision measurements of neutral current processes at low energies, Z-pole constraints on $Z - Z'$ mixing, indirect constraints from precision electroweak measurements off the Z-pole, and direct search constraints from production at very high energies. In principle, one should expect other new states to appear at the same scale as the Z', including its symmetry-breaking sector and any additional fermions necessary for anomaly cancellation. Because these states are highly model-dependent, searches for these states, or for Z' decays into them, are not included in the Listings.

Low-energy Constraints: After the gauge symmetry of the Z' and the electroweak symmetry are both broken, the Z of the Standard Model can mix with the Z', with mixing angle ξ defined above. As already discussed, this $Z - Z'$ mixing implies a shift in the usual oblique parameters. Current bounds on T (and S) translate into stringent constraints on the mixing angle, ξ, requiring $\xi \ll 1$; similar constraints on ξ arise from the LEP Z-pole data. Thus, we will only consider the small-ξ limit henceforth.

Whether or not the new gauge interactions are parity violating, stringent constraints can arise from atomic parity violation (APV) and polarized electron-nucleon scattering experiments [5]. At low energies, the effective neutral current Lagrangian is conventionally written:

$$\mathcal{L}_{\rm NC} = \frac{G_F}{\sqrt{2}}\sum_{q=u,d}\left\{C_{1q}(\bar{e}\gamma_\mu\gamma^5 e)(\bar{q}\gamma^\mu q) + C_{2q}(\bar{e}\gamma_\mu e)(\bar{q}\gamma^\mu\gamma^5 q)\right\}. \tag{4}$$

APV experiments are sensitive only to C_{1u} and C_{1d} through the "weak charge" $Q_W = -2\,[C_{1u}(2Z+N) + C_{1d}(Z+2N)]$, where

$$C_{1q} = 2(1+\alpha T)(g_A^e + \xi f_A^e)(g_V^q + \xi f_V^q) + 2r(f_A^e f_V^q) \qquad (5)$$

with $r = M_Z^2/M_{Z'}^2$. (Terms $\mathcal{O}(r\xi)$ are dropped.) The r-dependent terms arise from Z' exchange and can interfere constructively or destructively with the Z contribution. In the limit $\xi = r = 0$, this reduces to the Standard Model expression. Polarized electron scattering is sensitive to both the C_{1q} and C_{2q} couplings, again as discussed in the Standard Model review. The C_{2q} can be derived from the expression for C_{1q} with the complete interchange $V \leftrightarrow A$.

Stringent limits also arise from neutrino-hadron scattering. One usually expresses experimental results in terms of the effective 4-fermion operators $(\bar{\nu}\gamma_\mu\nu)(\bar{q}_{L,R}\gamma^\mu q_{L,R})$ with coefficients $(2\sqrt{2}G_F)\epsilon_{L,R}(q)$. (Again, see the Standard Model review.) In the presence of the Z and Z', the $\epsilon_{L,R}(q)$ are given by:

$$\epsilon_{L,R}(q) = \frac{1+\alpha T}{2}\left\{(g_V^q \pm g_A^q)[1 + \xi(f_V^\nu \pm f_A^\nu)] + \xi(f_V^q \pm f_A^q)\right\} + \frac{r}{2}(f_V^q \pm f_A^q)(f_V^\nu \pm f_A^\nu)\ . \qquad (6)$$

Again, the r-dependent terms arise from Z'-exchange.

Z-pole Constraints: Electroweak measurements made at LEP and SLC while sitting on the Z-resonance are generally sensitive to Z' physics only through the mixing with the Z, unless the Z and Z' are very nearly degenerate. Constraints on the allowed mixing angle and Z' couplings arise by fitting all data simultaneously to the *ansatz* of $Z-Z'$ mixing. A number of such fits are included in the Listings. If the listed analysis uses data only from the Z resonance, it is marked with a comment "Z parameters" while it is commented as "Electroweak" if low-energy data is also included in the fits. Both types of fits place simultaneous limits on the Z' mass and on ξ.

High-energy Indirect Constraints: At $\sqrt{s} < M_{Z'}$, but off the Z-pole, strong constraints on new Z' physics arise by comparing measurements of asymmetries and leptonic and hadronic cross-sections with their Standard Model predictions. These processes are sensitive not only to $Z-Z'$ mixing, but also to direct Z' exchange primarily through $\gamma - Z'$ and $Z-Z'$ interference; therefore, information on the Z' couplings and mass can be extracted that is not accessible via $Z-Z'$ mixing alone.

Far below the Z' mass scale, experiments at a given $\sqrt{s}$ are only sensitive to the scaled Z' couplings $\sqrt{s}f_{V,A}^i/M_{Z'}$. However, the Z' mass and overall magnitude of the couplings can be separately extracted if measurements are made at more than one energy. As $\sqrt{s}$ approaches $M_{Z'}$ the Z' exchange can no longer be approximated by a contact interaction and the mass and couplings can be simultaneously extracted.

Z' studies done before LEP relied heavily on this approach; see, for example, Ref. 6. LEP has also done similar work using data collected above the Z-peak; see, for example, Ref. 7. For indirect Z' searches at future facilities, see, for example, Refs. 8,9. At a hadron collider the possibility of measuring leptonic forward-backward asymmetries has been suggested [10] and used [11] in searches for a Z' below its threshold.

Direct Search Constraints: Finally, high-energy experiments have searched for on-shell Z' production and decay. Searches can be classified by the initial state off of which the Z' is produced, and the final state into which the Z' decays; exotic decays of a Z' are not included in the listings. Experiments to date have been sensitive to Z' production via their coupling to quarks ($p\bar{p}$ colliders), to electrons (e^+e^-), or to both (ep).

For a heavy Z' ($M_{Z'} \gg M_Z$), the best limits come from $p\bar{p}$ machines via Drell-Yan production and subsequent decay to charged leptons. For $M_{Z'} > 600\,\text{GeV}$, CDF [12] quotes limits on $\sigma(p\bar{p} \to Z'X) \cdot B(Z' \to \ell^+\ell^-) < 0.04\,\text{pb}$ at 95% C.L. for $\ell = e+\mu$ combined; DØ [13] quotes $\sigma \cdot B < 0.06\,\text{pb}$ for $\ell = e$ and $M_{Z'} > 500\,\text{GeV}$. For smaller masses, the bounds can be found in the original literature. For studies of the search capabilities of future facilities, see, for example, Ref. 8.

If the Z' has suppressed, or no, couplings to leptons (*i.e.*, it is leptophobic), then experimental sensitivities are much weaker. Searches for a Z' via hadronic decays at CDF [14] are unable to rule out a Z' with quark couplings identical to those of the Z in any mass region. UA2 [15] does find $\sigma \cdot B(Z' \to jj) < 11.7\,\text{pb}$ at 90% C.L. for $M_{Z'} > 200\,\text{GeV}$, with more complicated bounds in the range $130\,\text{GeV} < M_{Z'} < 200\,\text{GeV}$.

For a light Z' ($M_{Z'} < M_Z$), direct searches in e^+e^- colliders have ruled out any Z', unless it has extremely weak couplings to leptons. For a combined analysis of the various pre-LEP experiments see Ref. 6.

Canonical Models: One of the prime motivations for an additional Z' has come from string theory, in which certain compactifications lead naturally to an E_6 gauge group, or one of its subgroups. E_6 contains two U(1) factors beyond the Standard Model, a basis for which is formed by the two groups $\mathrm{U}(1)_\chi$ and $\mathrm{U}(1)_\psi$, defined via the decompositions $E_6 \to \mathrm{SO}(10) \times \mathrm{U}(1)_\psi$ and $\mathrm{SO}(10) \to \mathrm{SU}(5) \times \mathrm{U}(1)_\chi$; one special case often encountered is $\mathrm{U}(1)_\eta$, where $Q_\eta = \sqrt{\frac{3}{8}}Q_\chi - \sqrt{\frac{5}{8}}Q_\psi$. The charges of the SM fermions under these U(1)'s can be found in Table 1, and a discussion of their experimental signatures can be found in Ref. 16. A separate listing appears for each of the canonical models, with direct and indirect constraints combined.

It is also common to express experimental bounds in terms of a toy Z', usually denoted Z'_{SM}. This Z'_{SM}, of arbitrary mass, couples to the SM fermions identically to the usual Z. Almost all analyses of Z' physics have worked with one of these canonical models and have assumed zero kinetic mixing at the weak scale.

Extra Dimensions: A new motivation for Z' searches comes from recent work on extensions of the Standard Model into extra

Table 1: Charges of Standard Model fermions in canonical Z' models.

	Y	T_{3R}	$B-L$	$\sqrt{24}Q_\chi$	$\sqrt{\frac{72}{5}}Q_\psi$	Q_η
ν_L, e_L	$-\frac{1}{2}$	0	-1	$+3$	$+1$	$+\frac{1}{6}$
ν_R	0	$+\frac{1}{2}$	-1	$+5$	-1	$+\frac{5}{6}$
e_R	-1	$-\frac{1}{2}$	-1	$+1$	-1	$+\frac{1}{3}$
u_L, d_L	$+\frac{1}{6}$	0	$+\frac{1}{3}$	-1	$+1$	$-\frac{1}{3}$
u_R	$+\frac{2}{3}$	$+\frac{1}{2}$	$+\frac{1}{3}$	$+1$	-1	$+\frac{1}{3}$
d_R	$-\frac{1}{3}$	$-\frac{1}{2}$	$+\frac{1}{3}$	-3	-1	$-\frac{1}{6}$

dimensions. (See the "Review of Extra Dimensions" for many details not included here.) In some classes of these models, the gauge bosons of the Standard Model can inhabit these new directions [17]. When compactified down to the usual (3+1) dimensions, the extra degrees of freedom that were present in the higher-dimensional theory (associated with propagation in the extra dimensions) appear as a tower of massive gauge bosons, called Kaluza-Klein (KK) states. The simplest case is the compactification of a $(4+d)$-dimensional space on a d-torus (T^d) of uniform radius R in all d directions. Then a tower of massive gauge bosons are present with masses

$$M^2_{V_{\vec{n}}} = M^2_{V_{\vec{0}}} + \frac{\vec{n}\cdot\vec{n}}{R^2}\,, \qquad (7)$$

where V represents any of the gauge fields of the Standard Model and $\vec{n}$ is a d-vector whose components are semi-positive integers; the vector $\vec{n} = (0, 0, \ldots 0)$ corresponds to the "zero-mode" gauge boson, which is nothing more than the usual gauge boson of the Standard Model, with mass $M_{V_{\vec{0}}} = M_V$. Compactifications on either non-factorizable or asymmetric manifolds can significantly alter the KK mass formula, but a tower of states will nonetheless persist. All bounds cited in the Listings assume the maximally symmetric spectrum given above for simplicity.

The KK mass formula, coupled with the absence of any observational evidence for W' or Z' states below the weak scale, implies that the extra dimensions in which gauge bosons can propagate must have inverse radii greater than at least a few hundred GeV. If any extra dimensions are larger than this, gravity alone may propagate in them.

Though the gauge principle guarantees that the usual Standard Model gauge fields couple with universal strength (or gauge coupling) to all charged matter, the coupling of KK bosons to ordinary matter is highly model-dependent. In the simplest case, all Standard Model fields are localized at the same point in the d-dimensional subspace; in the parlance of the field, they all live on the same 3-brane. Then the couplings of KK bosons are identical to those of the usual gauge fields, but enhanced: $g_{KK} = \sqrt{2}\,g$. However, in many models, particularly those which naturally suppress proton decay [18], it is common to find ordinary fermions living on different, parallel branes in the extra dimensions. In such cases, different fermions experience very different coupling strengths for the KK states; the effective coupling varies fermion by fermion, and also KK mode by KK mode. In the particular case that fermions of different generations with identical quantum numbers are placed on different branes, large flavor-changing neutral currents can occur unless the mass scale of the KK states is very heavy: $R^{-1} \gtrsim 1000$ TeV [19]. In the Listings, all bounds assume that Standard Model fermions live on a single 3-brane. (The case of the Higgs field is again complicated; see the footnotes on the individual listings.)

In some sense, searches for KK bosons are no different than searches for any other Z' or W'; in fact, bounds on the artificially defined $Z'_{\rm SM}$ are almost precisely bounds on the first KK mode of the Z^0, modulo the $\sqrt{2}$ enhancement in the coupling strength. To date, no experiment has examined direct production of KK Z^0 bosons, but an approximate bound of 820 GeV [20] can be inferred from the CDF bound on Z'_{SM} [12].

Indirect bounds have a very different behavior for KK gauge bosons than for canonical Z' bosons; a number of indirect bounds are given in the Listings. Indirect bounds arise from virtual boson exchange and require a summation over the entire tower of KK states. For $d > 1$, this summation diverges, a remnant of the non-renormalizability of the underlying $(4+d)$-dimensional field theory. In a fully consistent theory, such as a string theory, the summation would be regularized and finite. However, this procedure cannot be uniquely defined within the confines of our present knowledge, and so most authors choose to terminate the sum with an explicit cut-off, Λ_{KK}, set equal to the "Planck scale" of the D-dimensional theory, M_D [21]. Reasonable arguments exist that this cut-off could be very different and could vary by process, and so these bounds should be regarded merely as indicative [22].

References

1. B. Holdom, Phys. Lett. **166B**, 196 (1986).
2. F. del Aguila, Acta Phys. Polon. **B25**, 1317 (1994); F. del Aguila, M. Cvetič, and P. Langacker, Phys. Rev. **D52**, 37 (1995).
3. K.S. Babu, C. Kolda, and J. March-Russell, Phys. Rev. **D54**, 4635 (1996); *ibid.*, **D57**, 6788 (1998).
4. B. Holdom, Phys. Lett. **B259**, 329 (1991).
5. J. Kim *et al.*, Rev. Mod. Phys. **53**, 211 (1981); U. Amaldi *et al.*, Phys. Rev. **D36**, 1385 (1987); W. Marciano and J. Rosner, Phys. Rev. Lett. **65**, 2963 (1990) (*Erratum:* **68**, 898 (1992)); K. Mahanthappa and P. Mohapatra, Phys. Rev. **D43**, 3093 (1991) (*Erratum:* **D44**, 1616 (1991)); P. Langacker and M. Luo, Phys. Rev. **D45**, 278 (1992); P. Langacker, M. Luo, and A. Mann, Rev. Mod. Phys. **64**, 87 (1992).
6. L. Durkin and P. Langacker, Phys. Lett. **166B**, 436 (1986).
7. P. Abreu *et al.*, (DELPHI Collaboration), Eur. Phys. J. **C11**, 383 (1999); R. Barate *et al.*, (ALEPH Collaboration) Eur. Phys. J. **C12**, 183 (1999).

8. M. Cvetič and S. Godfrey, in *Electroweak Symmetry Breaking and New Physics at the TeV Scale*, eds. T. Barklow *et al.*, (World Scientific 1996), p. 383 [hep-ph/9504216].
9. T. Rizzo, Phys. Rev. **D55**, 5483 (1997).
10. J. L. Rosner, Phys. Rev. **D54**, 1078 (1996).
11. T. Affolder *et al.*, (CDF Collaboration), Phys. Rev. Lett. **87**, 131802 (2001).
12. F. Abe *et al.*, (CDF Collaboration), Phys. Rev. Lett. **79**, 2191 (1997).
13. V. Abazov *et al.*, (D0 Collaboration), Phys. Rev. Lett. **87**, 061802 (2001).
14. F. Abe *et al.*, (CDF Collaboration), Phys. Rev. **D55**, 5263R (1997) and Phys. Rev. Lett. **82**, 2038 (1999).
15. J. Alitti *et al.*, (UA2 Collaboration), Nucl. Phys. **B400**, 3 (1993).
16. J. Hewett and T. Rizzo, Phys. Rept. **183**, 193 (1989).
17. I. Antoniadis, Phys. Lett. **B246**, 377 (1990); I. Antoniadis, K. Benakli, and M. Quiros, Phys. Lett. **B331**, 313 (1994); K. Dienes, E. Dudas, and T. Gherghetta, Phys. Lett. B **436**, 55 (1998); A. Pomarol and M. Quiros, Phys. Lett. **B438**, 255 (1998).
18. N. Arkani-Hamed and M. Schmaltz, Phys. Rev. **D61**, 033005 (2000).
19. A. Delgado, A. Pomarol, and M. Quiros, JHEP **0001**, 030 (2000).
20. M. Masip and A. Pomarol, Phys. Rev. **D60**, 096005 (1999).
21. G. Giudice, R. Rattazzi, and J. Wells, Nucl. Phys. **B544**, 3 (1999); T. Han, J. Lykken, and R. Zhang, Phys. Rev. **D59**, 105006 (1999); J. Hewett, Phys. Rev. Lett. **82**, 4765 (1999).
22. See for example: M. Bando *et al.*, Phys. Rev. Lett. **83**, 3601 (1999); T. Rizzo and J. Wells, Phys. Rev. **D61**, 016007 (2000); S. Cullen, M. Perelstein, and M. Peskin, Phys. Rev. **D62**, 055012 (2000).

MASS LIMITS for Z' (Heavy Neutral Vector Boson Other Than Z)

Limits for Z'_{SM}

Z'_{SM} is assumed to have couplings with quarks and leptons which are identical to those of Z, and decays only to known fermions.

VALUE (GeV)	CL%	DOCUMENT ID		TECN	COMMENT
>1500	95	[44] CHEUNG	01B	RVUE	Electroweak
> 690	95	[45] ABE	97S	CDF	$p\overline{p}$; $Z'_{SM} \rightarrow e^+e^-$, $\mu^+\mu^-$
• • • We do not use the following data for averages, fits, limits, etc. • • •					
> 670	95	[46] ABAZOV	01B	D0	$p\overline{p}$; $Z'_{SM} \rightarrow e^+e^-$
> 710	95	[47] ABREU	00S	DLPH	e^+e^-
> 898	95	[48] BARATE	00I	ALEP	e^+e^-
> 809	95	[49] ERLER	99	RVUE	Electroweak
> 490	95	ABACHI	96D	D0	$p\overline{p}$; $Z'_{SM} \rightarrow e^+e^-$
> 398	95	[50] VILAIN	94B	CHM2	$\nu_\mu e \rightarrow \nu_\mu e$ and $\overline{\nu}_\mu e \rightarrow \overline{\nu}_\mu e$
> 237	90	[51] ALITTI	93	UA2	$p\overline{p}$; $Z'_{SM} \rightarrow q\overline{q}$
none 260–600	95	[52] RIZZO	93	RVUE	$p\overline{p}$; $Z'_{SM} \rightarrow q\overline{q}$
> 426	90	[53] ABE	90F	VNS	e^+e^-

[44] CHEUNG 01B limit is derived from bounds on contact interactions in a global electroweak analysis.
[45] ABE 97S find $\sigma(Z')\times B(e^+e^-,\mu^+\mu^-) < 40$ fb for $m_{Z'} > 600$ GeV at $\sqrt{s}$= 1.8 TeV.
[46] ABAZOV 01B search for resonances in $p\overline{p} \rightarrow e^+e^-$ at $\sqrt{s}$=1.8 TeV. They find $\sigma \cdot B(Z' \rightarrow ee) < 0.06$ pb for $M_{Z'} > 500$ GeV.
[47] ABREU 00S uses LEP data at $\sqrt{s}$=90 to 189 GeV.
[48] BARATE 00I search for deviations in cross section and asymmetries in $e^+e^- \rightarrow$ fermions at $\sqrt{s}$=90 to 183 GeV. Assume θ=0. Bounds in the mass-mixing plane are shown in their Figure 18.
[49] ERLER 99 give 90%CL limit on the Z-Z' mixing $-0.0041 < \theta < 0.0003$. ρ_0=1 is assumed.
[50] VILAIN 94B assume m_t = 150 GeV.
[51] ALITTI 93 search for resonances in the two-jet invariant mass. The limit assumes $B(Z' \rightarrow q\overline{q})$=0.7. See their Fig. 5 for limits in the $m_{Z'}$–$B(q\overline{q})$ plane.
[52] RIZZO 93 analyses CDF limit on possible two-jet resonances.
[53] ABE 90F use data for R, $R_{\ell\ell}$, and $A_{\ell\ell}$. They fix $m_W = 80.49 \pm 0.43 \pm 0.24$ GeV and $m_Z = 91.13 \pm 0.03$ GeV.

Limits for Z_{LR}

Z_{LR} is the extra neutral boson in left-right symmetric models. $g_L = g_R$ is assumed unless noted. Values in parentheses assume stronger constraint on the Higgs sector, usually motivated by specific left-right symmetric models (see the Note on the W'). Values in brackets are from cosmological and astrophysical considerations and assume a light right-handed neutrino. Direct search bounds assume decays to Standard Model fermions only, unless noted.

VALUE (GeV)	CL%	DOCUMENT ID		TECN	COMMENT
>860	95	[54] CHEUNG	01B	RVUE	Electroweak
>630	95	[55] ABE	97S	CDF	$p\overline{p}$; $Z'_{LR} \rightarrow e^+e^-$, $\mu^+\mu^-$
• • • We do not use the following data for averages, fits, limits, etc. • • •					
>380	95	[56] ABREU	00S	DLPH	e^+e^-
>436	95	[57] BARATE	00I	ALEP	e^+e^-
>550	95	[58] CHAY	00	RVUE	Electroweak
		[59] ERLER	00	RVUE	Cs
		[60] CASALBUONI	99	RVUE	Cs
(> 1205)	90	[61] CZAKON	99	RVUE	Electroweak
>564	95	[62] ERLER	99	RVUE	Electroweak
(> 1673)	95	[63] ERLER	99	RVUE	Electroweak
(> 1700)	68	[64] BARENBOIM	98	RVUE	Electroweak
>244	95	[65] CONRAD	98	RVUE	$\nu_\mu N$ scattering
>253	95	[66] VILAIN	94B	CHM2	$\nu_\mu e \rightarrow \nu_\mu e$ and $\overline{\nu}_\mu e \rightarrow \overline{\nu}_\mu e$
none 200–600	95	[67] RIZZO	93	RVUE	$p\overline{p}$; $Z_{LR} \rightarrow q\overline{q}$
[> 2000]		WALKER	91	COSM	Nucleosynthesis; light ν_R
none 200–500		[68] GRIFOLS	90	ASTR	SN 1987A; light ν_R
none 350–2400		[69] BARBIERI	89B	ASTR	SN 1987A; light ν_R

[54] CHEUNG 01B limit is derived from bounds on contact interactions in a global electroweak analysis.
[55] ABE 97S find $\sigma(Z')\times B(e^+e^-,\mu^+\mu^-) < 40$ fb for $m_{Z'} > 600$ GeV at $\sqrt{s}$= 1.8 TeV.
[56] ABREU 00S give 95%CL limit on Z-Z' mixing $|\theta| < 0.0018$. See their Fig. 6 for the limit contour in the mass-mixing plane. $\sqrt{s}$=90 to 189 GeV.
[57] BARATE 00I search for deviations in cross section and asymmetries in $e^+e^- \rightarrow$ fermions at $\sqrt{s}$=90 to 183 GeV. Assume θ=0. Bounds in the mass-mixing plane are shown in their Figure 18.
[58] CHAY 00 also find $-0.0003 < \theta < 0.0019$. For g_R free, $m_{Z'} > 430$ GeV.
[59] ERLER 00 discuss the possibility that a discrepancy between the observed and predicted values of Q_W(Cs) is due to the exchange of Z'. The data are better described in a certain class of the Z' models including Z_{LR} and Z_χ.
[60] CASALBUONI 99 discuss the discrepancy between the observed and predicted values of Q_W(Cs). It is shown that the data are better described in a class of models including the Z_{LR} model.
[61] CZAKON 99 perform a simultaneous fit to charged and neutral sectors. Assumes manifest left-right symmetric model. Finds $|\theta| < 0.0042$.
[62] ERLER 99 give 90%CL limit on the Z-Z' mixing $-0.0009 < \theta < 0.0017$.
[63] ERLER 99 assumes 2 Higgs doublets, transforming as 10 of SO(10), embedded in E_6.
[64] BARENBOIM 98 also gives 68% CL limits on the Z-Z' mixing $-0.0005 < \theta < 0.0033$. Assumes Higgs sector of minimal left-right model.
[65] CONRAD 98 limit is from measurements at CCFR, assuming no Z-Z' mixing.
[66] VILAIN 94B assume m_t = 150 GeV and θ=0. See Fig. 2 for limit contours in the mass-mixing plane.
[67] RIZZO 93 analyses CDF limit on possible two-jet resonances.
[68] GRIFOLS 90 limit holds for $m_{\nu_R} \lesssim 1$ MeV. A specific Higgs sector is assumed. See also GRIFOLS 90D, RIZZO 91.
[69] BARBIERI 89B limit holds for $m_{\nu_R} \leq 10$ MeV. Bounds depend on assumed supernova core temperature.

Limits for Z_χ

Z_χ is the extra neutral boson in SO(10) $\rightarrow$ SU(5) $\times$ U(1)$_\chi$. $g_\chi = e/\cos\theta_W$ is assumed unless otherwise stated. We list limits with the assumption $\rho = 1$ but with no further constraints on the Higgs sector. Values in parentheses assume stronger constraint on the Higgs sector motivated by superstring models. Values in brackets are from cosmological and astrophysical considerations and assume a light right-handed neutrino.

VALUE (GeV)	CL%	DOCUMENT ID		TECN	COMMENT
> 680	95	[70] CHEUNG	01B	RVUE	Electroweak
> 595	95	[71] ABE	97S	CDF	$p\overline{p}$; $Z'_\chi \rightarrow e^+e^-$, $\mu^+\mu^-$
• • • We do not use the following data for averages, fits, limits, etc. • • •					
>2100		[72] BARGER	03B	COSM	Nucleosynthesis; light ν_R
> 440	95	[73] ABREU	00S	DLPH	e^+e^-
> 533	95	[74] BARATE	00I	ALEP	e^+e^-
> 554	95	[75] CHO	00	RVUE	Electroweak
		[76] ERLER	00	RVUE	Cs
		[77] ROSNER	00	RVUE	Cs
> 545	95	[78] ERLER	99	RVUE	Electroweak
(> 1368)	95	[79] ERLER	99	RVUE	Electroweak

> 215	95	[80] CONRAD	98	RVUE	$\nu_\mu N$ scattering
> 190	95	[81] ARIMA	97	VNS	Bhabha scattering
> 262	95	[82] VILAIN	94B	CHM2	$\nu_\mu e \to \nu_\mu e$ and $\overline{\nu}_\mu e \to \overline{\nu}_\mu e$
[>1470]		[83] FARAGGI	91	COSM	Nucleosynthesis; light ν_R
> 231	90	[84] ABE	90F	VNS	e^+e^-
[> 1140]		[85] GONZALEZ-G..90D		COSM	Nucleosynthesis; light ν_R
[> 2100]		[86] GRIFOLS	90	ASTR	SN 1987A; light ν_R

[70] CHEUNG 01B limit is derived from bounds on contact interactions in a global electroweak analysis.

[71] ABE 97S find $\sigma(Z')\times B(e^+e^-,\mu^+\mu^-) < 40$ fb for $m_{Z'} > 600$ GeV at $\sqrt{s} = 1.8$ TeV.

[72] BARGER 03B limit is from the nucleosynthesis bound on the effective number of light neutrino $\delta N_\nu < 1$. The quark-hadron transition temperature T_c=150 MeV is assumed. The limit with T_c=400 MeV is >4300 GeV.

[73] ABREU 00S give 95%CL limit on Z-Z' mixing $|\theta| < 0.0017$. See their Fig. 6 for the limit contour in the mass-mixing plane. $\sqrt{s}$=90 to 189 GeV.

[74] BARATE 00I search for deviations in cross section and asymmetries in $e^+e^- \to$ fermions at $\sqrt{s}$=90 to 183 GeV. Assume θ=0. Bounds in the mass-mixing plane are shown in their Figure 18.

[75] CHO 00 use various electroweak data to constrain Z' models assuming m_H=100 GeV. See Fig. 3 for limits in the mass-mixing plane.

[76] ERLER 00 discuss the possibility that a discrepancy between the observed and predicted values of Q_W(Cs) is due to the exchange of Z'. The data are better described in a certain class of the Z' models including Z_{LR} and Z_χ.

[77] ROSNER 00 discusses the possibility that a discrepancy between the observed and predicted values of Q_W(Cs) is due to the exchange of Z'. The data are better described in a certain class of the Z' models including Z_χ.

[78] ERLER 99 give 90%CL limit on the Z-Z' mixing $-0.0020 < \theta < 0.0015$.

[79] ERLER 99 assumes 2 Higgs doublets, transforming as 10 of SO(10), embedded in E_6.

[80] CONRAD 98 limit is from measurements at CCFR, assuming no Z-Z' mixing.

[81] Z-Z' mixing is assumed to be zero. $\sqrt{s}$= 57.77 GeV.

[82] VILAIN 94B assume m_t = 150 GeV and θ=0. See Fig. 2 for limit contours in the mass-mixing plane.

[83] FARAGGI 91 limit assumes the nucleosynthesis bound on the effective number of neutrinos $\Delta N_\nu < 0.5$ and is valid for $m_{\nu_R} < 1$ MeV.

[84] ABE 90F use data for R, $R_{\ell\ell}$, and $A_{\ell\ell}$. ABE 90F fix $m_W = 80.49 \pm 0.43 \pm 0.24$ GeV and $m_Z = 91.13 \pm 0.03$ GeV.

[85] Assumes the nucleosynthesis bound on the effective number of light neutrinos ($\delta N_\nu < 1$) and that ν_R is light ($\lesssim 1$ MeV).

[86] GRIFOLS 90 limit holds for $m_{\nu_R} \lesssim 1$ MeV. See also GRIFOLS 90D, RIZZO 91.

Limits for Z_ψ

Z_ψ is the extra neutral boson in $E_6 \to SO(10) \times U(1)_\psi$. $g_\psi = e/\cos\theta_W$ is assumed unless otherwise stated. We list limits with the assumption $\rho = 1$ but with no further constraints on the Higgs sector. Values in brackets are from cosmological and astrophysical considerations and assume a light right-handed neutrino.

VALUE (GeV)	CL%	DOCUMENT ID		TECN	COMMENT
>350	95	[87] ABREU	00S	DLPH	e^+e^-
>590	95	[88] ABE	97S	CDF	$p\overline{p}$; $Z'_\psi \to e^+e^-, \mu^+\mu^-$
• • • We do not use the following data for averages, fits, limits, etc. • • •					
>600		[89] BARGER	03B	COSM	Nucleosynthesis; light ν_R
>294	95	[90] BARATE	00I	ALEP	e^+e^-
>137	95	[91] CHO	00	RVUE	Electroweak
>146	95	[92] ERLER	99	RVUE	Electroweak
> 54	95	[93] CONRAD	98	RVUE	$\nu_\mu N$ scattering
>135	95	[94] VILAIN	94B	CHM2	$\nu_\mu e \to \nu_\mu e$ and $\overline{\nu}_\mu e \to \overline{\nu}_\mu e$
>105	90	[95] ABE	90F	VNS	e^+e^-
[> 160]		[96] GONZALEZ-G..90D		COSM	Nucleosynthesis; light ν_R
[> 2000]		[97] GRIFOLS	90D	ASTR	SN 1987A; light ν_R

[87] ABREU 00S give 95%CL limit on Z-Z' mixing $|\theta| < 0.0018$. See their Fig. 6 for the limit contour in the mass-mixing plane. $\sqrt{s}$=90 to 189 GeV.

[88] ABE 97S find $\sigma(Z')\times B(e^+e^-,\mu^+\mu^-) < 40$ fb for $m_{Z'} > 600$ GeV at $\sqrt{s}$= 1.8 TeV.

[89] BARGER 03B limit is from the nucleosynthesis bound on the effective number of light neutrino $\delta N_\nu < 1$. The quark-hadron transition temperature T_c=150 MeV is assumed. The limit with T_c=400 MeV is >1100 GeV.

[90] BARATE 00I search for deviations in cross section and asymmetries in $e^+e^- \to$ fermions at $\sqrt{s}$=90 to 183 GeV. Assume θ=0. Bounds in the mass-mixing plane are shown in their Figure 18.

[91] CHO 00 use various electroweak data to constrain Z' models assuming m_H=100 GeV. See Fig. 3 for limits in the mass-mixing plane.

[92] ERLER 99 give 90%CL limit on the Z-Z' mixing $-0.0013 < \theta < 0.0024$.

[93] CONRAD 98 limit is from measurements at CCFR, assuming no Z-Z' mixing.

[94] VILAIN 94B assume m_t = 150 GeV and θ=0. See Fig. 2 for limit contours in the mass-mixing plane.

[95] ABE 90F use data for R, $R_{\ell\ell}$, and $A_{\ell\ell}$. ABE 90F fix $m_W = 80.49 \pm 0.43 \pm 0.24$ GeV and $m_Z = 91.13 \pm 0.03$ GeV.

[96] Assumes the nucleosynthesis bound on the effective number of light neutrinos ($\delta N_\nu < 1$) and that ν_R is light ($\lesssim 1$ MeV).

[97] GRIFOLS 90D limit holds for $m_{\nu_R} \lesssim 1$ MeV. See also RIZZO 91.

Limits for Z_η

Z_η is the extra neutral boson in E_6 models, corresponding to $Q_\eta = \sqrt{3/8}\, Q_\chi - \sqrt{5/8}\, Q_\psi$. $g_\eta = e/\cos\theta_W$ is assumed unless otherwise stated. We list limits with the assumption $\rho = 1$ but with no further constraints on the Higgs sector. Values in parentheses assume stronger constraint on the Higgs sector motivated by superstring models. Values in brackets are from cosmological and astrophysical considerations and assume a light right-handed neutrino.

VALUE (GeV)	CL%	DOCUMENT ID		TECN	COMMENT
> 619	95	[98] CHO	00	RVUE	Electroweak
> 620	95	[99] ABE	97S	CDF	$p\overline{p}$; $Z'_\eta \to e^+e^-, \mu^+\mu^-$
• • • We do not use the following data for averages, fits, limits, etc. • • •					
>1600		[100] BARGER	03B	COSM	Nucleosynthesis; light ν_R
> 310	95	[101] ABREU	00S	DLPH	e^+e^-
> 329	95	[102] BARATE	00I	ALEP	e^+e^-
> 365	95	[103] ERLER	99	RVUE	Electroweak
> 87	95	[104] CONRAD	98	RVUE	$\nu_\mu N$ scattering
> 100	95	[105] VILAIN	94B	CHM2	$\nu_\mu e \to \nu_\mu e$ and $\overline{\nu}_\mu e \to \overline{\nu}_\mu e$
> 125	90	[106] ABE	90F	VNS	e^+e^-
[> 820]		[107] GONZALEZ-G..90D		COSM	Nucleosynthesis; light ν_R
[> 3300]		[108] GRIFOLS	90	ASTR	SN 1987A; light ν_R
[> 1040]		[107] LOPEZ	90	COSM	Nucleosynthesis; light ν_R

[98] CHO 00 use various electroweak data to constrain Z' models assuming m_H=100 GeV. See Fig. 3 for limits in the mass-mixing plane.

[99] ABE 97S find $\sigma(Z')\times B(e^+e^-,\mu^+\mu^-) < 40$ fb for $m_{Z'} > 600$ GeV at $\sqrt{s}$= 1.8 TeV.

[100] BARGER 03B limit is from the nucleosynthesis bound on the effective number of light neutrino $\delta N_\nu < 1$. The quark-hadron transition temperature T_c=150 MeV is assumed. The limit with T_c=400 MeV is >3300 GeV.

[101] ABREU 00S give 95%CL limit on Z-Z' mixing $|\theta| < 0.0024$. See their Fig. 6 for the limit contour in the mass-mixing plane. $\sqrt{s}$=90 to 189 GeV.

[102] BARATE 00I search for deviations in cross section and asymmetries in $e^+e^- \to$ fermions at $\sqrt{s}$=90 to 183 GeV. Assume θ=0. Bounds in the mass-mixing plane are shown in their Figure 18.

[103] ERLER 99 give 90%CL limit on the Z-Z' mixing $-0.0062 < \theta < 0.0011$.

[104] CONRAD 98 limit is from measurements at CCFR, assuming no Z-Z' mixing.

[105] VILAIN 94B assume m_t = 150 GeV and θ=0. See Fig. 2 for limit contours in the mass-mixing plane.

[106] ABE 90F use data for R, $R_{\ell\ell}$, and $A_{\ell\ell}$. ABE 90F fix $m_W = 80.49 \pm 0.43 \pm 0.24$ GeV and $m_Z = 91.13 \pm 0.03$ GeV.

[107] These authors claim that the nucleosynthesis bound on the effective number of light neutrinos ($\delta N_\nu < 1$) constrains Z' masses if ν_R is light ($\lesssim 1$ MeV).

[108] GRIFOLS 90 limit holds for $m_{\nu_R} \lesssim 1$ MeV. See also GRIFOLS 90D, RIZZO 91.

Limits for other Z'

VALUE (GeV)	DOCUMENT ID		TECN	COMMENT
• • • We do not use the following data for averages, fits, limits, etc. • • •				
	[109] BARGER	03B	COSM	Nucleosynthesis; light ν_R
	[110] CHO	00	RVUE	E_6-motivated
	[111] CHO	98	RVUE	E_6-motivated
	[112] ABE	97G	CDF	$Z' \to \overline{q}q$

[109] BARGER 03B use the nucleosynthesis bound on the effective number of light neutrino δN_ν. See their Figs. 4–5 for limits in general E_6 motivated models.

[110] CHO 00 use various electroweak data to constrain Z' models assuming m_H=100 GeV. See Fig. 2 for limits in general E_6-motivated models.

[111] CHO 98 study constraints on four-Fermi contact interactions obtained from low-energy electroweak experiments, assuming no Z-Z' mixing.

[112] Search for Z' decaying to dijets at $\sqrt{s}$=1.8 TeV. For Z' with electromagnetic strength coupling, no bound is obtained.

Indirect Constraints on Kaluza-Klein Gauge Bosons

Bounds on a Kaluza-Klein excitation of the Z boson or photon in d=1 extra dimension. These bounds can also be interpreted as a lower bound on $1/R$, the size of the extra dimension. Unless otherwise stated, bounds assume all fermions live on a single brane and all gauge fields occupy the $4+d$-dimensional bulk. See also the section on "Extra Dimensions" in the "Searches" Listings in this *Review*.

VALUE (TeV)	CL%	DOCUMENT ID		TECN	COMMENT
• • • We do not use the following data for averages, fits, limits, etc. • • •					
> 4.7		[113] MUECK	02	RVUE	Electroweak
> 3.3	95	[114] CORNET	00	RVUE	$e\nu\, qq'$
>5000		[115] DELGADO	00	RVUE	ϵ_K
> 2.6	95	[116] DELGADO	00	RVUE	Electroweak
> 3.3	95	[117] RIZZO	00	RVUE	Electroweak
> 2.9	95	[118] MARCIANO	99	RVUE	Electroweak
> 2.5	95	[119] MASIP	99	RVUE	Electroweak
> 1.6	90	[120] NATH	99	RVUE	Electroweak
> 3.4	95	[121] STRUMIA	99	RVUE	Electroweak

[113] MUECK 02 limit is 2σ and is from global electroweak fit ignoring correlations among observables. Higgs is assumed to be confined on the brane and its mass is fixed. For scenarios of bulk Higgs, of brane-SU(2)$_L$, bulk-U(1)$_Y$, and of bulk-SU(2)$_L$, brane-U(1)$_Y$, the corresponding limits are > 4.6 TeV, > 4.3 TeV and > 3.0 TeV, respectively.

[114] Bound is derived from limits on $e\nu qq'$ contact interaction, using data from HERA and the Tevatron.

[115] Bound holds only if first two generations of quarks lives on separate branes. If quark mixing is not complex, then bound lowers to 400 TeV from Δm_K.

[116] See Figs. 1 and 2 of DELGADO 00 for several model variations. Special boundary conditions can be found which permit KK states down to 950 GeV and that agree with the measurement of Q_W(Cs). Quoted bound assumes all Higgs bosons confined to brane; placing one Higgs doublet in the bulk lowers bound to 2.3 TeV.

[117] Bound is derived from global electroweak analysis assuming the Higgs field is trapped on the matter brane. If the Higgs propagates in the bulk, the bound increases to 3.8 TeV.

[118] Bound is derived from global electroweak analysis but considering only presence of the KK W bosons.

[119] Global electroweak analysis used to obtain bound independent of position of Higgs on brane or in bulk.

[120] Bounds from effect of KK states on G_F, α, M_W, and M_Z. Hard cutoff at string scale determined using gauge coupling unification. Limits for d=2,3,4 rise to 3.5, 5.7, and 7.8 TeV.

[121] Bound obtained for Higgs confined to the matter brane with m_H=500 GeV. For Higgs in the bulk, the bound increases to 3.5 TeV.

LEPTOQUARK QUANTUM NUMBERS

Revised September 2001 by M. Tanabashi (Tohoku University).

Leptoquarks are particles carrying both baryon number (B) and lepton number (L). They are expected to exist in various extensions of the Standard Model (SM). The possible quantum numbers of leptoquark states can be restricted by assuming that their direct interactions with the ordinary SM fermions are dimensionless and invariant under the SM gauge group. Table 1 shows the list of all possible quantum numbers with this assumption [1]. The columns of SU(3)$_C$, SU(2)$_W$, and U(1)$_Y$ in Table 1 indicate the QCD representation, the weak isospin representation, and the weak hypercharge, respectively. The spin of a leptoquark state is taken to be 1 (vector leptoquark) or 0 (scalar leptoquark).

Table 1: Possible leptoquarks and their quantum numbers.

Spin	$3B+L$	SU(3)$_c$	SU(2)$_W$	U(1)$_Y$	Allowed coupling
0	-2	$\bar{3}$	1	1/3	$\bar{q}^c_L \ell_L$ or $\bar{u}^c_R e_R$
0	-2	$\bar{3}$	1	4/3	$\bar{d}^c_R e_R$
0	-2	$\bar{3}$	3	1/3	$\bar{q}^c_L \ell_L$
1	-2	$\bar{3}$	2	5/6	$\bar{q}^c_L \gamma^\mu e_R$ or $\bar{d}^c_R \gamma^\mu \ell_L$
1	-2	$\bar{3}$	2	$-1/6$	$\bar{u}^c_R \gamma^\mu \ell_L$
0	0	3	2	7/6	$\bar{q}_L e_R$ or $\bar{u}_R \ell_L$
0	0	3	2	1/6	$\bar{d}_R \ell_L$
1	0	3	1	2/3	$\bar{q}_L \gamma^\mu \ell_L$ or $\bar{d}_R \gamma^\mu e_R$
1	0	3	1	5/3	$\bar{u}_R \gamma^\mu e_R$
1	0	3	3	2/3	$\bar{q}_L \gamma^\mu \ell_L$

If we do not require leptoquark states to couple directly with SM fermions, different assignments of quantum numbers become possible.

The Pati-Salam model [2] is an example predicting the existence of a leptoquark state. In this model a vector leptoquark appears at the scale where the Pati-Salam SU(4) "color" gauge group breaks into the familiar QCD SU(3)$_C$ group (or SU(3)$_C$ $\times$ U(1)$_{B-L}$). The Pati-Salam leptoquark is a weak isosinglet and its hypercharge is 2/3. The coupling strength of the Pati-Salam leptoquark is given by the QCD coupling at the Pati-Salam symmetry breaking scale.

Bounds on leptoquark states are obtained both directly and indirectly. Direct limits are from their production cross sections at colliders, while indirect limits are calculated from the bounds on the leptoquark induced four-fermion interactions which are obtained from low energy experiments.

The pair production cross sections of leptoquarks are evaluated from their interactions with gauge bosons. The gauge couplings of a scalar leptoquark are determined uniquely according to its quantum numbers in Table 1. The magnetic-dipole-type and the electric-quadrupole-type interactions of a vector leptoquark are, however, not determined even if we fix its gauge quantum numbers as listed in the table [3]. We need extra assumptions about these interactions to evaluate the pair production cross section for a vector leptoquark.

If a leptoquark couples to fermions of more than a single generation in the mass eigenbasis of the SM fermions, it can induce four-fermion interactions causing flavor-changing-neutral-currents and lepton-family-number violations. Non-chiral leptoquarks, which couple simultaneously to both left- and right-handed quarks, cause four-fermion interactions affecting the $(\pi \to e\nu)/(\pi \to \mu\nu)$ ratio [4]. Indirect limits provide stringent constraints on these leptoquarks. Since the Pati-Salam leptoquark has non-chiral coupling with both e and μ, indirect limits from the bounds on $K_L \to \mu e$ lead to severe bounds on the Pati-Salam leptoquark mass. For detailed bounds obtained in this way, see the Boson Particle Listings for "Indirect Limits for Leptoquarks" and its references.

It is therefore often assumed that a leptoquark state couples only to a single generation in a chiral interaction, where indirect limits become much weaker. This assumption gives strong constraints on concrete models of leptoquarks, however. Leptoquark states which couple only to left- or right-handed quarks are called chiral leptoquarks. Leptoquark states which couple only to the first (second, third) generation are referred as the first (second, third) generation leptoquarks in this section.

Reference

1. W. Buchmüller, R. Rückl, and D. Wyler, Phys. Lett. **B191**, 442 (1987).
2. J.C. Pati and A. Salam, Phys. Rev. **D10**, 275 (1974).
3. J. Blümlein, E. Boos, and A. Kryukov, Z. Phys. **C76**, 137 (1997).
4. O. Shanker, Nucl. Phys. **B204**, 375 (1982).

MASS LIMITS for Leptoquarks from Pair Production

These limits rely only on the color or electroweak charge of the leptoquark.

VALUE (GeV)	CL%	EVTS	DOCUMENT ID		TECN	COMMENT
>200	95		[122] ABBOTT	00C	D0	Second generation
>148	95		[123] AFFOLDER	00K	CDF	Third generation
>202	95		[124] ABE	98S	CDF	Second generation
>242	95		[125] GROSS-PILCH..	98		First generation

• • • We do not use the following data for averages, fits, limits, etc. • • •

> 98	95		[126] ABAZOV	02	D0	All generatrions
>225	95		[127] ABAZOV	01D	D0	First generation
> 85.8	95		[128] ABBIENDI	00M	OPAL	First generation
> 85.5	95		[128] ABBIENDI	00M	OPAL	Second generation
> 82.7	95		[128] ABBIENDI	00M	OPAL	Third generation
>123	95		[129] AFFOLDER	00K	CDF	Second generation
>160	95		[130] ABBOTT	99J	D0	Second generation
>225	95		[131] ABBOTT	98E	D0	First generation
> 94	95		[132] ABBOTT	98J	D0	Third generation
> 99	95		[133] ABE	97F	CDF	Third generation
>213	95		[134] ABE	97X	CDF	First generation
> 45.5	95	[135,136]	ABREU	93J	DLPH	First + second generation
> 44.4	95		[137] ADRIANI	93M	L3	First generation
> 44.5	95		[137] ADRIANI	93M	L3	Second generation
> 45	95		[137] DECAMP	92	ALEP	Third generation
none 8.9–22.6	95		[138] KIM	90	AMY	First generation
none 10.2–23.2	95		[138] KIM	90	AMY	Second generation
none 5–20.8	95		[139] BARTEL	87B	JADE	
none 7–20.5	95	2	[140] BEHREND	86B	CELL	

[122] ABBOTT 00C search for scalar leptoquarks using $\mu\mu jj$, $\mu\nu jj$, and $\nu\nu jj$ events in $p\overline{p}$ collisions at E_{cm}=1.8 TeV. The limit above assumes B(μq)=1. For B(μq)=0.5 and 0, the bound becomes 180 and 79 GeV respectively. Bounds for vector leptoquarks are also given.

[123] AFFOLDER 00K search for scalar leptoquark using $\nu\nu bb$ events in $p\overline{p}$ collisions at E_{cm}=1.8 TeV. The quoted limit assumes B(νb)=1. Bounds for vector leptoquarks are also given.

[124] ABE 98S search for scalar leptoquarks using $\mu\mu jj$ events in $p\overline{p}$ collisions at E_{cm}= 1.8 TeV. The limit is for B(μq)= 1. For B(μq)=B(νq)=0.5, the limit is > 160 GeV.

[125] GROSS-PILCHER 98 is the combined limit of the CDF and DØ Collaborations as determined by a joint CDF/DØ working group and reported in this FNAL Technical Memo. Original data published in ABE 97X and ABBOTT 98E.

[126] ABAZOV 02 search for scalar leptoquarks using $\nu\nu jj$ events in $\overline{p}p$ collisions at E_{cm}=1.8 TeV. The bound holds for all leptoquark generations. Vector leptoquarks are likewise constrained to lie above 200 GeV.

[127] ABAZOV 01D search for scalar leptoquarks using $e\nu jj$, $eejj$, and $\nu\nu jj$ events in $p\overline{p}$ collisions at E_{cm}=1.8 TeV. The limit above assumes B(eq)=1. For B(eq)=0.5 and 0, the bound becomes 204 and 79 GeV, respectively. Bounds for vector leptoquarks are also given. Supersedes ABBOTT 98E.

[128] ABBIENDI 00M search for scalar/vector leptoquarks in e^+e^- collisions at $\sqrt{s}$=183 GeV. The quoted limits are for charge $-4/3$ isospin 0 scalar-leptoquarks with B(ℓq)=1. See their Table 8 and Figs. 6–9 for other cases.

[129] AFFOLDER 00K search for scalar leptoquark using $\nu\nu cc$ events in $p\overline{p}$ collisions at E_{cm}=1.8 TeV. The quoted limit assumes B(νc)=1. Bounds for vector leptoquarks are also given.

[130] ABBOTT 99J search for leptoquarks using $\mu\nu jj$ events in $p\overline{p}$ collisions at E_{cm}= 1.8TeV. The quoted limit is for a scalar leptoquark with B(μq) = B(νq) = 0.5. Limits on vector leptoquarks range from 240 to 290 GeV.

[131] ABBOTT 98E search for scalar leptoquarks using $e\nu jj$, $eejj$, and $\nu\nu jj$ events in $p\overline{p}$ collisions at E_{cm}=1.8 TeV. The limit above assumes B(eq)=1. For B(eq)=0.5 and 0, the bound becomes 204 and 79 GeV, respectively.

[132] ABBOTT 98J search for charge $-1/3$ third generation scalar and vector leptoquarks in $p\overline{p}$ collisions at E_{cm}= 1.8 TeV. The quoted limit is for scalar leptoquark with B(νb)=1.

[133] ABE 97F search for third generation scalar and vector leptoquarks in $p\overline{p}$ collisions at E_{cm} = 1.8 TeV. The quoted limit is for scalar leptoquark with B(τb) = 1.

[134] ABE 97X search for scalar leptoquarks using $eejj$ events in $p\overline{p}$ collisions at E_{cm}=1.8 TeV. The limit is for B(eq)=1.

[135] Limit is for charge $-1/3$ isospin-0 leptoquark with B(ℓq) = 2/3.

[136] First and second generation leptoquarks are assumed to be degenerate. The limit is slightly lower for each generation.

[137] Limits are for charge $-1/3$, isospin-0 scalar leptoquarks decaying to $\ell^- q$ or νq with any branching ratio. See paper for limits for other charge-isospin assignments of leptoquarks.

[138] KIM 90 assume pair production of charge 2/3 scalar-leptoquark via photon exchange. The decay of the first (second) generation leptoquark is assumed to be any mixture of de^+ and $u\overline{\nu}$ ($s\mu^+$ and $c\overline{\nu}$). See paper for limits for specific branching ratios.

[139] BARTEL 87B limit is valid when a pair of charge 2/3 spinless leptoquarks X is produced with point coupling, and when they decay under the constraint B(X → $c\overline{\nu}_\mu$) + B(X → $s\mu^+$) = 1.

[140] BEHREND 86B assumed that a charge 2/3 spinless leptoquark, χ, decays either into $s\mu^+$ or $c\overline{\nu}$: B(χ → $s\mu^+$) + B(χ → $c\overline{\nu}$) = 1.

MASS LIMITS for Leptoquarks from Single Production

These limits depend on the q-ℓ-leptoquark coupling g_{LQ}. It is often assumed that $g^2_{LQ}/4\pi$=1/137. Limits shown are for a scalar, weak isoscalar, charge $-1/3$ leptoquark.

VALUE (GeV)	CL%		DOCUMENT ID		TECN	COMMENT
• • • We do not use the following data for averages, fits, limits, etc. • • •						
>298	95	[141]	CHEKANOV	03B	ZEUS	First generation
>197	95	[142]	ABBIENDI	02B	OPAL	First generation
		[143]	CHEKANOV	02	ZEUS	Lepton-flavor violation
>290	95	[144]	ADLOFF	01C	H1	First generation
>204	95	[145]	BREITWEG	01	ZEUS	First generation
		[146]	BREITWEG	00E	ZEUS	First generation
>161	95	[147]	ABREU	99G	DLPH	First generation
>200	95	[148]	ADLOFF	99	H1	First generation
		[149]	DERRICK	97	ZEUS	Lepton-flavor violation
> 73	95	[150]	ABREU	93J	DLPH	Second generation
>168	95	[151]	DERRICK	93	ZEUS	First generation

[141] CHEKANOV 03B limit is for a scalar, weak isoscalar, charge $-1/3$ leptoquark coupled with e_R. See their Figs. 11–12 and Table 5 for limits on states with different quantum numbers.

[142] For limits on states with different quantum numbers and the limits in the mass-coupling plane, see their Fig. 4 and Fig. 5.

[143] CHEKANOV 02 search for various leptoquarks with lepton-flavor violating couplings. See their Figs. 6–7 and Tables 5–6 for detailed limits.

[144] For limits on states with different quantum numbers and the limits in the mass-coupling plane, see their Fig. 3.

[145] See their Fig. 14 for limits in the mass-coupling plane.

[146] BREITWEG 00E search for F=0 leptoquarks in e^+p collisions. For limits in mass-coupling plane, see their Fig. 11.

[147] ABREU 99G limit obtained from process $e\gamma \to LQ+q$. For limits on vector and scalar states with different quantum numbers and the limits in the coupling-mass plane, see their Fig. 4 and Table 2.

[148] For limits on states with different quantum numbers and the limits in the mass-coupling plane, see their Fig. 13 and Fig. 14. ADLOFF 99 also search for leptoquarks with lepton-flavor violating couplings. ADLOFF 99 supersedes AID 96B.

[149] DERRICK 97 search for various leptoquarks with lepton-flavor violating couplings. See their Figs. 5–8 and Table 1 for detailed limits.

[150] Limit from single production in Z decay. The limit is for a leptoquark coupling of electromagnetic strength and assumes B(ℓq) = 2/3. The limit is 77 GeV if first and second leptoquarks are degenerate.

[151] DERRICK 93 search for single leptoquark production in ep collisions with the decay eq and νq. The limit is for leptoquark coupling of electromagnetic strength and assumes B(eq) = B(νq) = 1/2. The limit for B(eq) = 1 is 176 GeV. For limits on states with different quantum numbers, see their Table 3.

Indirect Limits for Leptoquarks

VALUE (TeV)	CL%		DOCUMENT ID		TECN	COMMENT
• • • We do not use the following data for averages, fits, limits, etc. • • •						
> 1.7	96	[152]	ADLOFF	03	H1	First generation
		[153]	CHEKANOV	02	ZEUS	Lepton-flavor violation
> 1.7	95	[154]	CHEUNG	01B	RVUE	First generation
> 0.39	95	[155]	ACCIARRI	00P	L3	$e^+e^- \to qq$
> 1.5	95	[156]	ADLOFF	00	H1	First generation
> 0.2	95	[157]	BARATE	00I	ALEP	e^+e^-
		[158]	BARGER	00	RVUE	Cs
		[159]	GABRIELLI	00	RVUE	Lepton flavor violation
> 0.74	95	[160]	ZARNECKI	00	RVUE	S_1 leptoquark
		[161]	ABBIENDI	99	OPAL	
> 19.3	95	[162]	ABE	98V	CDF	$B_s \to e^\pm\mu^\mp$, Pati-Salam type
		[163]	ACCIARRI	98J	L3	$e^+e^- \to q\overline{q}$
		[164]	ACKERSTAFF	98V	OPAL	$e^+e^- \to q\overline{q}$, $e^+e^- \to b\overline{b}$
> 0.76	95	[165]	DEANDREA	97	RVUE	$\tilde{R}_2$ leptoquark
		[166]	DERRICK	97	ZEUS	Lepton-flavor violation
		[167]	GROSSMAN	97	RVUE	$B \to \tau^+\tau^-$(X)
		[168]	JADACH	97	RVUE	$e^+e^- \to q\overline{q}$
>1200		[169]	KUZNETSOV	95B	RVUE	Pati-Salam type
		[170]	MIZUKOSHI	95	RVUE	Third generation scalar leptoquark
> 0.3	95	[171]	BHATTACH...	94	RVUE	Spin-0 leptoquark coupled to $\overline{e}_R t_L$
		[172]	DAVIDSON	94	RVUE	
> 18		[173]	KUZNETSOV	94	RVUE	Pati-Salam type
> 0.43	95	[174]	LEURER	94	RVUE	First generation spin-1 leptoquark
> 0.44	95	[174]	LEURER	94B	RVUE	First generation spin-0 leptoquark
		[175]	MAHANTA	94	RVUE	P and T violation
> 1		[176]	SHANKER	82	RVUE	Nonchiral spin-0 leptoquark
> 125		[176]	SHANKER	82	RVUE	Nonchiral spin-1 leptoquark

[152] ADLOFF 03 limit is for the weak isotriplet spin-0 leptoquark at strong coupling λ=$\sqrt{4\pi}$. For the limits of leptoquarks with different quantum numbers, see their Table 3. Limits are derived from bounds on $e^\pm q$ contact interactions.

[153] CHEKANOV 02 search for lepton-flavor violation in ep collisions. See their Tables 1–4 for limits on lepton-flavor violating and four-fermion interactions induced by various leptoquarks.

[154] CHEUNG 01B quoted limit is for a scalar, weak isoscalar, charge $-1/3$ leptoquark with a coupling of electromagnetic strength. The limit is derived from bounds on contact interactions in a global electroweak analysis. For the limits of leptoquarks with different quantum numbers, see Table 5.

[155] ACCIARRI 00P limit is for the weak isoscalar spin-0 leptoquark with the coupling of electromagnetic strength. For the limits of leptoquarks with different quantum numbers, see their Table 4.

[156] ADLOFF 00 limit is for the weak isotriplet spin-0 leptoquark at strong coupling, λ=$\sqrt{4\pi}$. For the limits of leptoquarks with different quantum numbers, see their Table 2. ADLOFF 00 limits are from the Q^2 spectrum measurement of $e^+p \to e^+$X.

[157] BARATE 00I search for deviations in cross section and jet-charge asymmetry in $e^+e^- \to \overline{q}q$ due to t-channel exchange of a leptoquark at $\sqrt{s}$=130 to 183 GeV. Limits for other scalar and vector leptoquarks are also given in their Table 22.

[158] BARGER 00 explain the deviation of atomic parity violation in cesium atoms from prediction is explained by scalar leptoquark exchange.

[159] GABRIELLI 00 calculate various process with lepton flavor violation in leptoquark models.

[160] ZARNECKI 00 limit is derived from data of HERA, LEP, and Tevatron and from various low-energy data including atomic parity violation. Leptoquark coupling with electromagnetic strength is assumed.

[161] ABBIENDI 99 limits are from $e^+e^- \to q\overline{q}$ cross section at 130–136, 161–172, 183 GeV. See their Fig. 8 and Fig. 9 for limits in mass-coupling plane.

[162] ABE 98V quoted limit is from $B(B_s \to e^\pm\mu^\mp) < 8.2\times10^{-6}$. ABE 98V also obtain a similar limit on $M_{LQ} > 20.4$ TeV from $B(B_d \to e^\pm\mu^\mp) < 4.5\times10^{-6}$. Both bounds assume the non-canonical association of the b quark with electrons or muons under SU(4).

[163] ACCIARRI 98J limit is from $e^+e^- \to q\overline{q}$ cross section at $\sqrt{s}$= 130–172 GeV which can be affected by the t- and u-channel exchanges of leptoquarks. See their Fig. 4 and Fig. 5 for limits in the mass-coupling plane.

[164] ACKERSTAFF 98V limits are from $e^+e^- \to q\overline{q}$ and $e^+e^- \to b\overline{b}$ cross sections at $\sqrt{s}$ = 130–172 GeV, which can be affected by the t- and u-channel exchanges of leptoquarks. See their Fig. 21 and Fig. 22 for limits of leptoquarks in mass-coupling plane.

[165] DEANDREA 97 limit is for $\tilde{R}_2$ leptoquark obtained from atomic parity violation (APV). The coupling of leptoquark is assumed to be electromagnetic strength. See Table 2 for limits of the four-fermion interactions induced by various scalar leptoquark exchange. DEANDREA 97 combines APV limit and limits from Tevatron and HERA. See Fig. 1–4 for combined limits of leptoquark in mass-coupling plane.

[166] DERRICK 97 search for lepton-flavor violation in ep collision. See their Tables 2–5 for limits on lepton-flavor violating four-fermion interactions induced by various leptoquarks.

[167] GROSSMAN 97 estimate the upper bounds on the branching fraction $B \to \tau^+\tau^-(X)$ from the absence of the B decay with large missing energy. These bounds can be used to constrain leptoquark induced four-fermion interactions.

[168] JADACH 97 limit is from $e^+e^- \to q\overline{q}$ cross section at $\sqrt{s}$=172.3 GeV which can be affected by the t- and u-channel exchanges of leptoquarks. See their Fig. 1 for limits on vector leptoquarks in mass-coupling plane.

[169] KUZNETSOV 95B use π, K, B, τ decays and μe conversion and give a list of bounds on the leptoquark mass and the fermion mixing matrix in the Pati-Salam model. The quoted limit is from $K_L \to \mu e$ decay assuming zero mixing.

[170] MIZUKOSHI 95 calculate the one-loop radiative correction to the Z-physics parameters in various scalar leptoquark models. See their Fig. 4 for the exclusion plot of third generation leptoquark models in mass-coupling plane.

[171] BHATTACHARYYA 94 limit is from one-loop radiative correction to the leptonic decay width of the Z. m_H=250 GeV, $\alpha_s(m_Z)$=0.12, m_t=180 GeV, and the electroweak strength of leptoquark coupling are assumed. For leptoquark coupled to $\overline{e}_L t_R$, $\overline{\mu}t$, and $\overline{\tau}t$, see Fig. 2 in BHATTACHARYYA 94B erratum and Fig. 3.

[172] DAVIDSON 94 gives an extensive list of the bounds on leptoquark-induced four-fermion interactions from π, K, D, B, μ, τ decays and meson mixings, *etc.* See Table 15 of DAVIDSON 94 for detail.

[173] KUZNETSOV 94 gives mixing independent bound of the Pati-Salam leptoquark from the cosmological limit on $\pi^0 \to \overline{\nu}\nu$.

[174] LEURER 94, LEURER 94B limits are obtained from atomic parity violation and apply to any chiral leptoquark which couples to the first generation with electromagnetic strength. For a nonchiral leptoquark, universality in $\pi_{\ell 2}$ decay provides a much more stringent bound.

[175] MAHANTA 94 gives bounds of P- and T-violating scalar-leptoquark couplings from atomic and molecular experiments.

[176] From $(\pi \to e\nu)/(\pi \to \mu\nu)$ ratio. SHANKER 82 assumes the leptoquark induced four-fermion coupling $4g^2/M^2\ (\overline{\nu}_{eL}\ u_R)\ (\overline{d}_L\ e_R)$ with g=0.004 for spin-0 leptoquark and $g^2/M^2\ (\overline{\nu}_{eL}\ \gamma_\mu\ u_L)\ (\overline{d}_R\ \gamma^\mu\ e_R)$ with $g\simeq$ 0.6 for spin-1 leptoquark.

MASS LIMITS for Diquarks

VALUE (GeV)	CL%	DOCUMENT ID		TECN	COMMENT
• • • We do not use the following data for averages, fits, limits, etc. • • •					
none 290–420	95	[177] ABE	97G	CDF	E_6 diquark
none 15–31.7	95	[178] ABREU	94O	DLPH	SUSY E_6 diquark

[177] ABE 97G search for new particle decaying to dijets.

[178] ABREU 94O limit is from $e^+e^- \to \overline{c}s\,c\,s$. Range extends up to 43 GeV if diquarks are degenerate in mass.

MASS LIMITS for g_A (axigluon)

Axigluons are massive color-octet gauge bosons in chiral color models and have axial-vector coupling to quarks with the same coupling strength as gluons.

VALUE (GeV)	CL%	DOCUMENT ID		TECN	COMMENT
• • • We do not use the following data for averages, fits, limits, etc. • • •					
>365	95	[179] DONCHESKI	98	RVUE	$\Gamma(Z \to$ hadron)
none 200–980	95	[180] ABE	97G	CDF	$p\overline{p} \to g_A X$, X → 2 jets
none 200–870	95	[181] ABE	95N	CDF	$p\overline{p} \to g_A X$, $g_A \to q\overline{q}$
none 240–640	95	[182] ABE	93G	CDF	$p\overline{p} \to g_A X$, $g_A \to$ 2jets
> 50	95	[183] CUYPERS	91	RVUE	$\sigma(e^+e^- \to$ hadrons)
none 120–210	95	[184] ABE	90H	CDF	$p\overline{p} \to g_A X$, $g_A \to$ 2jets
> 29		[185] ROBINETT	89	THEO	Partial-wave unitarity
none 150–310	95	[186] ALBAJAR	88B	UA1	$p\overline{p} \to g_A X$, $g_A \to$ 2jets
> 20		BERGSTROM	88	RVUE	$p\overline{p} \to \Upsilon X$ via $g_A g$
> 9		[187] CUYPERS	88	RVUE	Υ decay
> 25		[188] DONCHESKI	88B	RVUE	Υ decay

[179] DONCHESKI 98 compare α_s derived from low-energy data and that from $\Gamma(Z \to$ hadrons$)/\Gamma(Z \to$ leptons).

[180] ABE 97G search for new particle decaying to dijets.

[181] ABE 95N assume axigluons decaying to quarks in the Standard Model only.

[182] ABE 93G assume $\Gamma(g_A) = N\alpha_s m_{g_A}/6$ with N = 10.

[183] CUYPERS 91 compare α_s measured in Υ decay and that from R at PEP/PETRA energies.

[184] ABE 90H assumes $\Gamma(g_A) = N\alpha_s m_{g_A}/6$ with N = 5 ($\Gamma(g_A) = 0.09 m_{g_A}$). For N = 10, the excluded region is reduced to 120–150 GeV.

[185] ROBINETT 89 result demands partial-wave unitarity of J = 0 $t\overline{t} \to t\overline{t}$ scattering amplitude and derives a limit $m_{g_A} > 0.5\ m_t$. Assumes $m_t > 56$ GeV.

[186] ALBAJAR 88B result is from the nonobservation of a peak in two-jet invariant mass distribution. $\Gamma(g_A) < 0.4\ m_{g_A}$ assumed. See also BAGGER 88.

[187] CUYPERS 88 requires $\Gamma(\Upsilon \to gg g_A) < \Gamma(\Upsilon \to ggg)$. A similar result is obtained by DONCHESKI 88.

[188] DONCHESKI 88B requires $\Gamma(\Upsilon \to g\,q\overline{q})/\Gamma(\Upsilon \to ggg) < 0.25$, where the former decay proceeds via axigluon exchange. A more conservative estimate of < 0.5 leads to $m_{g_A} > 21$ GeV.

X^0 (Heavy Boson) Searches in Z Decays

Searches for radiative transition of Z to a lighter spin-0 state X^0 decaying to hadrons, a lepton pair, a photon pair, or invisible particles as shown in the comments. The limits are for the product of branching ratios.

VALUE	CL%	DOCUMENT ID		TECN	COMMENT
• • • We do not use the following data for averages, fits, limits, etc. • • •					
		[189] BARATE	98U	ALEP	$X^0 \to \ell\overline{\ell}$, $q\overline{q}$, gg, $\gamma\gamma$, $\nu\overline{\nu}$
		[190] ACCIARRI	97Q	L3	$X^0 \to$ invisible particle(s)
		[191] ACTON	93E	OPAL	$X^0 \to \gamma\gamma$
		[192] ABREU	92D	DLPH	$X^0 \to$ hadrons
		[193] ADRIANI	92F	L3	$X^0 \to$ hadrons
		[194] ACTON	91	OPAL	$X^0 \to$ anything
$<1.1\times10^{-4}$	95	[195] ACTON	91B	OPAL	$X^0 \to e^+e^-$
$<9\ \times10^{-5}$	95	[195] ACTON	91B	OPAL	$X^0 \to \mu^+\mu^-$
$<1.1\times10^{-4}$	95	[195] ACTON	91B	OPAL	$X^0 \to \tau^+\tau^-$
$<2.8\times10^{-4}$	95	[196] ADEVA	91D	L3	$X^0 \to e^+e^-$
$<2.3\times10^{-4}$	95	[196] ADEVA	91D	L3	$X^0 \to \mu^+\mu^-$
$<4.7\times10^{-4}$	95	[197] ADEVA	91D	L3	$X^0 \to$ hadrons
$<8\ \times10^{-4}$	95	[198] AKRAWY	90J	OPAL	$X^0 \to$ hadrons

[189] BARATE 98U obtain limits on $B(Z \to \gamma X^0)B(X^0 \to \ell\overline{\ell}, q\overline{q}, gg, \gamma\gamma, \nu\overline{\nu})$. See their Fig. 17.

[190] See Fig. 4 of ACCIARRI 97Q for the upper limit on $B(Z \to \gamma X^0;\ E_\gamma > E_{\min})$ as a function of $E_{\min}$.

[191] ACTON 93E give $\sigma(e^+e^- \to X^0\gamma)\cdot B(X^0 \to \gamma\gamma) < 0.4$ pb (95%CL) for m_{X^0}=60 ± 2.5 GeV. If the process occurs via s-channel γ exchange, the limit translates to $\Gamma(X^0)\cdot B(X^0 \to \gamma\gamma)^2 < 20$ MeV for $m_{X^0} = 60 \pm 1$ GeV.

[192] ABREU 92D give $\sigma_Z \cdot B(Z \to \gamma X^0) \cdot B(X^0 \to$ hadrons) <(3–10) pb for m_{X^0} = 10–78 GeV. A very similar limit is obtained for spin-1 X^0.

[193] ADRIANI 92F search for isolated γ in hadronic Z decays. The limit $\sigma_Z \cdot B(Z \to \gamma X^0) \cdot B(X^0 \to$ hadrons) <(2–10) pb (95%CL) is given for m_{X^0} = 25–85 GeV.

[194] ACTON 91 searches for $Z \to Z^* X^0$, $Z^* \to e^+e^-$, $\mu^+\mu^-$, or $\nu\overline{\nu}$. Excludes any new scalar X^0 with $m_{X^0} < 9.5$ GeV/c if it has the same coupling to ZZ^* as the MSM Higgs boson.

[195] ACTON 91B limits are for m_{X^0} = 60–85 GeV.

[196] ADEVA 91D limits are for m_{X^0} = 30–89 GeV.

[197] ADEVA 91D limits are for m_{X^0} = 30–86 GeV.

[198] AKRAWY 90J give $\Gamma(Z \to \gamma X^0)\cdot B(X^0 \to$ hadrons) < 1.9 MeV (95%CL) for m_{X^0} = 32–80 GeV. We divide by $\Gamma(Z)$ = 2.5 GeV to get product of branching ratios. For nonresonant transitions, the limit is $B(Z \to \gamma q\overline{q}) < 8.2$ MeV assuming three-body phase space distribution.

MASS LIMITS for a Heavy Neutral Boson Coupling to e^+e^-

VALUE (GeV)	CL%	DOCUMENT ID		TECN	COMMENT
• • • We do not use the following data for averages, fits, limits, etc. • • •					
none 55–61		[199] ODAKA	89	VNS	$\Gamma(X^0 \to e^+e^-)\cdot B(X^0 \to$ hadrons) $\gtrsim$ 0.2 MeV
>45	95	[200] DERRICK	86	HRS	$\Gamma(X^0 \to e^+e^-)$=6 MeV
>46.6	95	[201] ADEVA	85	MRKJ	$\Gamma(X^0 \to e^+e^-)$=10 keV
>48	95	[201] ADEVA	85	MRKJ	$\Gamma(X^0 \to e^+e^-)$=4 MeV
		[202] BERGER	85B	PLUT	
none 39.8–45.5		[203] ADEVA	84	MRKJ	$\Gamma(X^0 \to e^+e^-)$=10 keV
>47.8	95	[203] ADEVA	84	MRKJ	$\Gamma(X^0 \to e^+e^-)$=4 MeV
none 39.8–45.2		[203] BEHREND	84C	CELL	
>47	95	[203] BEHREND	84C	CELL	$\Gamma(X^0 \to e^+e^-)$=4 MeV

[199] ODAKA 89 looked for a narrow or wide scalar resonance in $e^+e^- \to$ hadrons at $E_{\rm cm}$ = 55.0–60.8 GeV.

[200] DERRICK 86 found no deviation from the Standard Model Bhabha scattering at $E_{\rm cm}$= 29 GeV and set limits on the possible scalar boson e^+e^- coupling. See their figure 4 for excluded region in the $\Gamma(X^0 \to e^+e^-)$-m_{X^0} plane. Electronic chiral invariance requires a parity doublet of X^0, in which case the limit applies for $\Gamma(X^0 \to e^+e^-)$ = 3 MeV.

[201] ADEVA 85 first limit is from 2γ, $\mu^+\mu^-$, hadrons assuming X^0 is a scalar. Second limit is from e^+e^- channel. $E_{\rm cm}$ = 40–47 GeV. Supersedes ADEVA 84.

[202] BERGER 85B looked for effect of spin-0 boson exchange in $e^+e^- \to e^+e^-$ and $\mu^+\mu^-$ at $E_{\rm cm}$ = 34.7 GeV. See Fig. 5 for excluded region in the $m_{X^0} - \Gamma(X^0)$ plane.

[203] ADEVA 84 and BEHREND 84C have $E_{\rm cm}$ = 39.8–45.5 GeV. MARK-J searched X^0 in $e^+e^- \to$ hadrons, 2γ, $\mu^+\mu^-$, e^+e^- and CELLO in the same channels plus τ pair. No narrow or broad X^0 is found in the energy range. They also searched for the effect of

X^0 with $m_X > E_{cm}$. The second limits are from Bhabha data and for spin-0 singlet. The same limits apply for $\Gamma(X^0 \to e^+e^-) = 2$ MeV if X^0 is a spin-0 doublet. The second limit of BEHREND 84C was read off from their figure 2. The original papers also list limits in other channels.

Search for X^0 Resonance in e^+e^- Collisions

The limit is for $\Gamma(X^0 \to e^+e^-) \cdot B(X^0 \to f)$, where f is the specified final state. Spin 0 is assumed for X^0.

VALUE (keV)	CL%	DOCUMENT ID		TECN	COMMENT
• • • We do not use the following data for averages, fits, limits, etc. • • •					
$<10^3$	95	[204] ABE		93C VNS	$\Gamma(ee)$
<(0.4–10)	95	[205] ABE		93C VNS	$f = \gamma\gamma$
<(0.3–5)	95	[206,207] ABE		93D TOPZ	$f = \gamma\gamma$
<(2–12)	95	[206,207] ABE		93D TOPZ	f = hadrons
<(4–200)	95	[207,208] ABE		93D TOPZ	$f = ee$
<(0.1–6)	95	[207,208] ABE		93D TOPZ	$f = \mu\mu$
<(0.5–8)	90	[209] STERNER		93 AMY	$f = \gamma\gamma$

[204] Limit is for $\Gamma(X^0 \to e^+e^-)\ m_{X^0} = 56$–63.5 GeV for $\Gamma(X^0) = 0.5$ GeV.

[205] Limit is for $m_{X^0} = 56$–61.5 GeV and is valid for $\Gamma(X^0) \ll 100$ MeV. See their Fig. 5 for limits for $\Gamma = 1,2$ GeV.

[206] Limit is for $m_{X^0} = 57.2$–60 GeV.

[207] Limit is valid for $\Gamma(X^0) \ll 100$ MeV. See paper for limits for $\Gamma = 1$ GeV and those for $J = 2$ resonances.

[208] Limit is for $m_{X^0} = 56.6$–60 GeV.

[209] STERNER 93 limit is for $m_{X^0} = 57$–59.6 GeV and is valid for $\Gamma(X^0)$<100 MeV. See their Fig. 2 for limits for $\Gamma = 1,3$ GeV.

Search for X^0 Resonance in ep Collisions

VALUE	DOCUMENT ID		TECN	COMMENT
• • • We do not use the following data for averages, fits, limits, etc. • • •				
	[210] CHEKANOV	02B ZEUS		$X \to jj$

[210] CHEKANOV 02B search for photoproduction of X decaying into dijets in ep collisions. See their Fig. 5 for the limit on the photoproduction cross section.

Search for X^0 Resonance in Two-Photon Process

The limit is for $\Gamma(X^0) \cdot B(X^0 \to \gamma\gamma)^2$. Spin 0 is assumed for X^0.

VALUE (MeV)	CL%	DOCUMENT ID		TECN	COMMENT
• • • We do not use the following data for averages, fits, limits, etc. • • •					
<2.6	95	[211] ACTON		93E OPAL	m_{X^0}=60 ± 1 GeV
<2.9	95	BUSKULIC		93F ALEP	$m_{X^0} \sim 60$ GeV

[211] ACTON 93E limit for a $J = 2$ resonance is 0.8 MeV.

Search for X^0 Resonance in $e^+e^- \to X^0\gamma$

VALUE (GeV)	DOCUMENT ID		TECN	COMMENT
• • • We do not use the following data for averages, fits, limits, etc. • • •				
	[212] ABBIENDI	03D OPAL		$X^0 \to \gamma\gamma$
	[213] ABREU	00Z DLPH		X^0 decaying invisibly
	[214] ADAM	96C DLPH		X^0 decaying invisibly

[212] ABBIENDI 03D measure the $e^+e^- \to \gamma\gamma\gamma$ cross section at $\sqrt{s}$=181–209 GeV. The upper bound on the production cross section, $\sigma(e^+e^- \to X^0\gamma)$ times the branching ratio for $X^0 \to \gamma\gamma$, is less than 0.03 pb at 95%CL for X^0 masses between 20 and 180 GeV. See their Fig. 9b for the limits in the mass-cross section plane.

[213] ABREU 00Z is from the single photon cross section at $\sqrt{s}$=183, 189 GeV. The production cross section upper limit is less than 0.3 pb for X^0 mass between 40 and 160 GeV. See their Fig. 4 for the limit in mass-cross section plane.

[214] ADAM 96C is from the single photon production cross at $\sqrt{s}$=130, 136 GeV. The upper bound is less than 3 pb for X^0 masses between 60 and 130 GeV. See their Fig. 5 for the exact bound on the cross section $\sigma(e^+e^- \to \gamma X^0)$.

Search for X^0 Resonance in $Z \to f\bar{f}X^0$

The limit is for $B(Z \to f\bar{f}X^0) \cdot B(X^0 \to F)$ where f is a fermion and F is the specified final state. Spin 0 is assumed for X^0.

VALUE	CL%	DOCUMENT ID		TECN	COMMENT
• • • We do not use the following data for averages, fits, limits, etc. • • •					
		[215] ABREU	96T DLPH		f=e,μ,τ; F=$\gamma\gamma$
$<3.7 \times 10^{-6}$	95	[216] ABREU	96T DLPH		f=ν; F=$\gamma\gamma$
		[217] ABREU	96T DLPH		f=q; F=$\gamma\gamma$
$<6.8 \times 10^{-6}$	95	[216] ACTON	93E OPAL		f=e,μ,τ; F=$\gamma\gamma$
$<5.5 \times 10^{-6}$	95	[216] ACTON	93E OPAL		f=q; F=$\gamma\gamma$
$<3.1 \times 10^{-6}$	95	[216] ACTON	93E OPAL		f=ν; F=$\gamma\gamma$
$<6.5 \times 10^{-6}$	95	[216] ACTON	93E OPAL		f=e,μ; F=$\ell\bar{\ell}$, $q\bar{q}$, $\nu\bar{\nu}$
$<7.1 \times 10^{-6}$	95	[216] BUSKULIC	93F ALEP		f=e,μ; F=$\ell\bar{\ell}$, $q\bar{q}$, $\nu\bar{\nu}$
		[218] ADRIANI	92F L3		f=q; F=$\gamma\gamma$

[215] ABREU 96T obtain limit as a function of m_{X^0}. See their Fig. 6.

[216] Limit is for m_{X^0} around 60 GeV.

[217] ABREU 96T obtain limit as a function of m_{X^0}. See their Fig. 15.

[218] ADRIANI 92F give $\sigma_Z \cdot B(Z \to q\bar{q}X^0) \cdot B(X^0 \to \gamma\gamma)$<(0.75–1.5) pb (95%CL) for m_{X^0} = 10–70 GeV. The limit is 1 pb at 60 GeV.

Search for X^0 Resonance in $p\bar{p} \to WX^0$

VALUE (MeV)	DOCUMENT ID		TECN	COMMENT
• • • We do not use the following data for averages, fits, limits, etc. • • •				
	[219] ABE	97W CDF		$X^0 \to b\bar{b}$

[219] ABE 97W search for X^0 production associated with W in $p\bar{p}$ collisions at E_{cm}=1.8 TeV. The 95%CL upper limit on the production cross section times the branching ratio for $X^0 \to b\bar{b}$ ranges from 14 to 19 pb for X^0 mass between 70 and 120 GeV. See their Fig. 3 for upper limits of the production cross section as a function of m_{X^0}.

Heavy Particle Production in Quarkonium Decays

Limits are for branching ratios to modes shown.

VALUE	CL%	DOCUMENT ID		TECN	COMMENT
• • • We do not use the following data for averages, fits, limits, etc. • • •					
$<1.5 \times 10^{-5}$	90	[220] BALEST	95	CLE2	$\Upsilon(1S) \to X^0\gamma$, $m_{X^0} < 5$ GeV
$< 3 \times 10^{-5}$–6×10^{-3}	90	[221] BALEST	95	CLE2	$\Upsilon(1S) \to X^0\overline{X}^0\gamma$, $m_{X^0} < 3.9$ GeV
$<5.6 \times 10^{-5}$	90	[222] ANTREASYAN	90C	CBAL	$\Upsilon(1S) \to X^0\gamma$, $m_{X^0} < 7.2$ GeV
		[223] ALBRECHT	89	ARG	

[220] BALEST 95 two-body limit is for pseudoscalar X^0. The limit becomes $< 10^{-4}$ for $m_{X^0} < 7.7$ GeV.

[221] BALEST 95 three-body limit is for phase-space photon energy distribution and angular distribution same as for $\Upsilon \to gg\gamma$.

[222] ANTREASYAN 90C assume that X^0 does not decay in the detector.

[223] ALBRECHT 89 give limits for $B(\Upsilon(1S), \Upsilon(2S) \to X^0\gamma) \cdot B(X^0 \to \pi^+\pi^-, K^+K^-, p\bar{p})$ for $m_{X^0} < 3.5$ GeV.

REFERENCES FOR Searches for Heavy Bosons Other Than Higgs Bosons

ABBIENDI	03D	EPJ C26 331	G. Abbiendi *et al.* (OPAL Collab.)
ACOSTA	03B	PRL 90 081802	D. Acosta *et al.* (CDF Collab.)
ADLOFF	03	PL B568 35	C. Adloff *et al.* (H1 Collab.)
BARGER	03B	PR D67 075009	V. Barger, P. Langacker, H. Lee
CHEKANOV	03B	PR D68 052004	S. Chekanov *et al.* (ZEUS Collab.)
ABAZOV	02	PRL 88 191801	V.M. Abazov *et al.* (D0 Collab.)
ABBIENDI	02B	PL B526 233	G. Abbiendi *et al.* (OPAL Collab.)
AFFOLDER	02C	PRL 88 071806	T. Affolder *et al.* (CDF Collab.)
CHEKANOV	02	PR D65 092004	S. Chekanov *et al.* (ZEUS Collab.)
CHEKANOV	02B	PL B531 9	S. Chekanov *et al.* (ZEUS Collab.)
MUECK	02	PR D65 085037	A. Mueck, A. Pilaftsis, R. Rueckl
ABAZOV	01B	PRL 87 061802	V.M. Abazov *et al.* (D0 Collab.)
ABAZOV	01D	PR D64 092004	V.M. Abazov *et al.* (D0 Collab.)
ADLOFF	01C	PL B523 234	C. Adloff *et al.* (H1 Collab.)
AFFOLDER	01I	PRL 87 231803	T. Affolder *et al.* (CDF Collab.)
BREITWEG	01	PR D63 052002	J. Breitweg *et al.* (ZEUS Collab.)
CHEUNG	01B	PL B517 167	K. Cheung
THOMAS	01	NP A694 559	E. Thomas *et al.*
ABBIENDI	00M	EPJ C13 15	G. Abbiendi *et al.* (OPAL Collab.)
ABBOTT	00C	PRL 84 2088	B. Abbott *et al.* (D0 Collab.)
ABE	00	PRL 84 5716	F. Abe *et al.* (CDF Collab.)
ABREU	00S	PL B485 45	P. Abreu *et al.* (DELPHI Collab.)
ABREU	00Z	EPJ C17 53	P. Abreu *et al.* (DELPHI Collab.)
ACCIARRI	00P	PL B489 81	M. Acciarri *et al.* (L3 Collab.)
ADLOFF	00	PL B479 358	C. Adloff *et al.* (H1 Collab.)
AFFOLDER	00K	PRL 85 2056	T. Affolder *et al.* (CDF Collab.)
BARATE	00I	EPJ C12 183	R. Barate *et al.* (ALEPH Collab.)
BARGER	00	PL B480 149	V. Barger, K. Cheung
BREITWEG	00E	EPJ C16 253	J. Breitweg *et al.* (ZEUS Collab.)
CHAY	00	PR D61 035002	J. Chay, K.Y. Lee, S. Nam
CHO	00	MPL A15 311	G. Cho
CORNET	00	PR D61 037701	F. Cornet, M. Relano, J. Rico
DELGADO	00	JHEP 0001 030	A. Delgado, A. Pomarol, M. Quiros
ERLER	00	PRL 84 212	J. Erler, P. Langacker
GABRIELLI	00	PR D62 055009	E. Gabrielli
RIZZO	00	PR D61 016007	T.G. Rizzo, J.D. Wells
ROSNER	00	PR D61 016006	J.L. Rosner
ZARNECKI	00	EPJ C17 695	A. Zarnecki
ABBIENDI	99	EPJ C6 1	G. Abbiendi *et al.* (OPAL Collab.)
ABBOTT	99J	PRL 83 2896	B. Abbott *et al.* (D0 Collab.)
ABREU	99G	PL B446 62	P. Abreu *et al.* (DELPHI Collab.)
ACKERSTAFF	99D	EPJ C8 3	K. Ackerstaff *et al.* (OPAL Collab.)
ADLOFF	99	EPJ C11 447	C. Adloff *et al.* (H1 Collab.)
Also	00C	EPJ C14 553 errata	C. Adloff *et al.* (H1 Collab.)
CASALBUONI	99	PL B460 135	R. Casalbuoni *et al.*
CZAKON	99	PL B458 355	M. Czakon, J. Gluza, M. Zralek
ERLER	99	PL B456 68	J. Erler, P. Langacker
MARCIANO	99	PR D60 093006	W. Marciano
MASIP	99	PR D60 096005	M. Masip, A. Pomarol
NATH	99	PR D60 116004	P. Nath, M. Yamaguchi
STRUMIA	99	PL B466 107	A. Strumia
ABBOTT	98E	PRL 80 2051	B. Abbott *et al.* (D0 Collab.)
ABBOTT	98J	PRL 81 38	B. Abbott *et al.* (D0 Collab.)
ABE	98S	PRL 81 4806	F. Abe *et al.* (CDF Collab.)
ABE	98V	PRL 81 5742	F. Abe *et al.* (CDF Collab.)
ACCIARRI	98J	PL B433 163	M. Acciarri *et al.* (L3 Collab.)
ACKERSTAFF	98V	EPJ C2 441	K. Ackerstaff *et al.* (OPAL Collab.)
BARATE	98U	EPJ C4 571	R. Barate *et al.* (ALEPH Collab.)
BARENBOIM	98	EPJ C1 369	G. Barenboim
CHO	98	EPJ C5 155	G. Cho, K. Hagiwara, S. Matsumoto
CONRAD	98	RMP 70 1341	J.M. Conrad, M.H. Shaevitz, T. Bolton
DONCHESKI	98	PR D58 097702	M.A. Doncheski, R.W. Robinett
GROSS-PILCH...98		hep-ex/9810015	C. Grosso-Pilcher, G. Landsberg, M. Paterno
ABE	97F	PRL 78 2906	F. Abe *et al.* (CDF Collab.)
ABE	97G	PR D55 R5263	F. Abe *et al.* (CDF Collab.)

ABE	97S	PRL 79 2192	F. Abe *et al.*	(CDF Collab.)
ABE	97W	PRL 79 3819	F. Abe *et al.*	(CDF Collab.)
ABE	97X	PRL 79 4327	F. Abe *et al.*	(CDF Collab.)
ACCIARRI	97Q	PL B412 201	M. Acciarri *et al.*	(L3 Collab.)
ARIMA	97	PR D55 19	T. Arima *et al.*	(VENUS Collab.)
BARENBOIM	97	PR D55 4213	G. Barenboim *et al.*	(VALE, IFIC)
DEANDREA	97	PL B409 277	A. Deandrea	(MARS)
DERRICK	97	ZPHY C73 613	M. Derrick *et al.*	(ZEUS Collab.)
GROSSMAN	97	PR D55 2768	Y. Grossman, Z. Ligeti, E. Nardi	(REHO, CIT)
JADACH	97	PL B408 281	S. Jadach, B.F.L. Ward, Z. Was	(CERN, INPK+)
STAHL	97	ZPHY C74 73	A. Stahl, H. Voss	(BONN)
ABACHI	96C	PRL 76 3271	S. Abachi *et al.*	(D0 Collab.)
ABACHI	96D	PL B385 471	S. Abachi *et al.*	(D0 Collab.)
ABREU	96T	ZPHY C72 179	P. Abreu *et al.*	(DELPHI Collab.)
ADAM	96C	PL B380 471	W. Adam *et al.*	(DELPHI Collab.)
AID	96B	PL B369 173	S. Aid *et al.*	(H1 Collab.)
ALLET	96	PL B383 139	M. Allet *et al.*	(VILL, LEUV, LOUV, WISC)
ABACHI	95E	PL B358 405	S. Abachi *et al.*	(D0 Collab.)
ABE	95M	PRL 74 2900	F. Abe *et al.*	(CDF Collab.)
ABE	95N	PRL 74 3538	F. Abe *et al.*	(CDF Collab.)
BALEST	95	PR D51 2053	R. Balest *et al.*	(CLEO Collab.)
KUZNETSOV	95	PRL 75 794	I.A. Kuznetsov *et al.*	(PNPI, KIAE, HARV+)
KUZNETSOV	95B	PAN 58 2113	A.V. Kuznetsov, N.V. Mikheev	(YARO)
		Translated from YAF 58 2228.		
MIZUKOSHI	95	NP B443 20	J.K. Mizukoshi, O.J.P. Eboli, M.C. Gonzalez-Garcia	
ABREU	94O	ZPHY C64 183	P. Abreu *et al.*	(DELPHI Collab.)
BHATTACH...	94	PL B336 100	G. Bhattacharyya, J. Ellis, K. Sridhar	(CERN)
Also	94B	PL B338 522 (erratum)	G. Bhattacharyya, J. Ellis, K. Sridhar	(CERN)
BHATTACH...	94B	PL B338 522 (erratum)	G. Bhattacharyya, J. Ellis, K. Sridhar	(CERN)
DAVIDSON	94	ZPHY C61 613	S. Davidson, D. Bailey, B.A. Campbell	(CFPA+)
KUZNETSOV	94	PL B329 295	A.V. Kuznetsov, N.V. Mikheev	(YARO)
KUZNETSOV	94B	JETPL 60 315	I.A. Kuznetsov *et al.*	(PNPI, KIAE, HARV+)
		Translated from ZETFP 60 311.		
LEURER	94	PR D50 536	M. Leurer	(REHO)
LEURER	94B	PR D49 333	M. Leurer	(REHO)
Also	93	PRL 71 1324	M. Leurer	(REHO)
MAHANTA	94	PL B337 128	U. Mahanta	(MEHTA)
SEVERIJNS	94	PRL 73 611 (erratum)	N. Severijns *et al.*	(LOUV, WISC, LEUV+)
VILAIN	94B	PL B332 465	P. Vilain *et al.*	(CHARM II Collab.)
ABE	93C	PL B302 119	K. Abe *et al.*	(VENUS Collab.)
ABE	93D	PL B304 373	T. Abe *et al.*	(TOPAZ Collab.)
ABE	93G	PRL 71 2542	F. Abe *et al.*	(CDF Collab.)
ABREU	93J	PL B316 620	P. Abreu *et al.*	(DELPHI Collab.)
ACTON	93E	PL B311 391	P.D. Acton *et al.*	(OPAL Collab.)
ADRIANI	93M	PRPL 236 1	O. Adriani *et al.*	(L3 Collab.)
ALITTI	93	NP B400 3	J. Alitti *et al.*	(UA2 Collab.)
BHATTACH...	93	PR D47 R3693	G. Bhattacharyya *et al.*	(CALC, JADA, ICTP+)
BUSKULIC	93F	PL B308 425	D. Buskulic *et al.*	(ALEPH Collab.)
DERRICK	93	PL B306 173	M. Derrick *et al.*	(ZEUS Collab.)
RIZZO	93	PR D48 4470	T.G. Rizzo	(ANL)
SEVERIJNS	93	PRL 70 4047	N. Severijns *et al.*	(LOUV, WISC, LEUV+)
Also	94	PRL 73 611 (erratum)	N. Severijns *et al.*	(LOUV, WISC, LEUV+)
STERNER	93	PL B303 385	K.L. Sterner *et al.*	(AMY Collab.)
ABREU	92D	ZPHY C53 555	P. Abreu *et al.*	(DELPHI Collab.)
ADRIANI	92F	PL B292 472	O. Adriani *et al.*	(L3 Collab.)
DECAMP	92	PRPL 216 253	D. Decamp *et al.*	(ALEPH Collab.)
IMAZATO	92	PRL 69 877	J. Imazato *et al.*	(KEK, INUS, TOKY+)
MISHRA	92	PRL 68 3499	S.R. Mishra *et al.*	(COLU, CHIC, FNAL+)
POLAK	92B	PR D46 3871	J. Polak, M. Zralek	(SILES)
ACTON	91	PL B268 122	D.P. Acton *et al.*	(OPAL Collab.)
ACTON	91B	PL B273 338	D.P. Acton *et al.*	(OPAL Collab.)
ADEVA	91D	PL B262 155	B. Adeva *et al.*	(L3 Collab.)
AQUINO	91	PL B261 280	M. Aquino, A. Fernandez, A. Garcia	(CINV, PUEB)
COLANGELO	91	PL B253 154	P. Colangelo, G. Nardulli	(BARI)
CUYPERS	91	PL B259 173	F. Cuypers, A.F. Falk, P.H. Frampton	(DURH, HARV+)
FARAGGI	91	MPL A6 61	A.E. Faraggi, D.V. Nanopoulos	(TAMU)
POLAK	91	NP B363 385	J. Polak, M. Zralek	(SILES)
RIZZO	91	PR D44 202	T.G. Rizzo	(WISC, ISU)
WALKER	91	APJ 376 51	T.P. Walker *et al.*	(HSCA, OSU, CHIC+)
ABE	90F	PL B246 297	K. Abe *et al.*	(VENUS Collab.)
ABE	90H	PR D41 1722	F. Abe *et al.*	(CDF Collab.)
AKRAWY	90J	PL B246 285	M.Z. Akrawy *et al.*	(OPAL Collab.)
ANTREASYAN	90C	PL B251 204	D. Antreasyan *et al.*	(Crystal Ball Collab.)
GONZALEZ-G...	90D	PL B240 163	M.C. Gonzalez-Garcia, J.W.F. Valle	(VALE)
GRIFOLS	90	NP B331 244	J.A. Grifols, E. Masso	(BARC)
GRIFOLS	90D	PR D42 3293	J.A. Grifols, E. Masso, T.G. Rizzo	(BARC, CERN+)
KIM	90	PL B240 243	G.N. Kim *et al.*	(AMY Collab.)
LOPEZ	90	PL B241 392	J.L. Lopez, D.V. Nanopoulos	(TAMU)
ALBAJAR	89	ZPHY C44 15	C. Albajar *et al.*	(UA1 Collab.)
ALBRECHT	89	ZPHY C42 349	H. Albrecht *et al.*	(ARGUS Collab.)
BARBIERI	89B	PR D39 1229	R. Barbieri, R.N. Mohapatra	(PISA, UMD)
LANGACKER	89B	PR D40 1569	P. Langacker, S. Uma Sankar	(PENN)
ODAKA	89	JPSJ 58 3037	S. Odaka *et al.*	(VENUS Collab.)
ROBINETT	89	PR D39 834	R.W. Robinett	(PSU)
ALBAJAR	88B	PL B209 127	C. Albajar *et al.*	(UA1 Collab.)
BAGGER	88	PR D37 1188	J. Bagger, C. Schmidt, S. King	(HARV, BOST)
BALKE	88	PR D37 587	B. Balke *et al.*	(LBL, UCB, COLO, NWES+)
BERGSTROM	88	PL B212 386	L. Bergstrom	(STOH)
CUYPERS	88	PRL 60 1237	F. Cuypers, P.H. Frampton	(UNCCH)
DONCHESKI	88	PL B206 137	M.A. Doncheski, H. Grotch, R. Robinett	(PSU)
DONCHESKI	88B	PR D38 412	M.A. Doncheski, H. Grotch, R.W. Robinett	(PSU)
ANSARI	87D	PL B195 613	R. Ansari *et al.*	(UA2 Collab.)
BARTEL	87B	ZPHY C36 15	W. Bartel *et al.*	(JADE Collab.)
BEHREND	86B	PL B178 452	H.J. Behrend *et al.*	(CELLO Collab.)
DERRICK	86	PL 166B 463	M. Derrick *et al.*	(HRS Collab.)
Also	86B	PR D34 3286	M. Derrick *et al.*	(HRS Collab.)
JODIDIO	86	PR D34 1967	A. Jodidio *et al.*	(LBL, NWES, TRIU)
Also	88	PR D37 237 erratum	A. Jodidio *et al.*	(LBL, NWES, TRIU)
MOHAPATRA	86	PR D34 909	R.N. Mohapatra	(UMD)
ADEVA	85	PRL 152B 439	B. Adeva *et al.*	(Mark-J Collab.)
BERGER	85B	ZPHY C27 341	C. Berger *et al.*	(PLUTO Collab.)
STOKER	85	PRL 54 1887	D.P. Stoker *et al.*	(LBL, NWES, TRIU)
ADEVA	84	PRL 53 134	B. Adeva *et al.*	(Mark-J Collab.)
BEHREND	84C	PL 140B 130	H.J. Behrend *et al.*	(CELLO Collab.)
BERGSMA	83	PL 122B 465	F. Bergsma *et al.*	(CHARM Collab.)
CARR	83	PRL 51 627	J. Carr *et al.*	(LBL, NWES, TRIU)
BEALL	82	PRL 48 848	G. Beall, M. Bander, A. Soni	(UCI, UCLA)
SHANKER	82	NP B204 375	O. Shanker	(TRIU)
STEIGMAN	79	PRL 43 239	G. Steigman, K.A. Olive, D.N. Schramm	(BART+)

Axions (A^0) and Other Very Light Bosons, Searches for

AXIONS AND OTHER VERY LIGHT BOSONS

Written October 1997 by H. Murayama (University of California, Berkeley) Part I; April 1998 by G. Raffelt (Max-Planck Institute, München) Part II; and April 1998 by C. Hagmann, K. van Bibber (Lawrence Livermore National Laboratory), and L.J. Rosenberg (Massachusetts Institute of Technology) Part III.

This review is divided into three parts:

Part I (Theory)
Part II (Astrophysical Constraints)
Part III (Experimental Limits)

AXIONS AND OTHER VERY LIGHT BOSONS, PART I (THEORY)

(by H. Murayama)

In this section we list limits for very light neutral (pseudo) scalar bosons that couple weakly to stable matter. They arise if there is a global continuous symmetry in the theory that is spontaneously broken in the vacuum. If the symmetry is exact, it results in a massless Nambu–Goldstone (NG) boson. If there is a small explicit breaking of the symmetry, either already in the Lagrangian or due to quantum mechanical effects such as anomalies, the would-be NG boson acquires a finite mass; then it is called a pseudo-NG boson. Typical examples are axions (A^0) [1], familons [2], and Majorons [3,4], associated, respectively, with spontaneously broken Peccei-Quinn [5], family, and lepton-number symmetries. This Review provides brief descriptions of each of them and their motivations.

One common characteristic for all these particles is that their coupling to the Standard Model particles are suppressed by the energy scale of symmetry breaking, *i.e.* the decay constant f, where the interaction is described by the Lagrangian

$$\mathcal{L} = \frac{1}{f}(\partial_\mu \phi) J^\mu, \qquad (1)$$

where J^μ is the Noether current of the spontaneously broken global symmetry.

An axion gives a natural solution to the strong CP problem: why the effective θ-parameter in the QCD Lagrangian $\mathcal{L}_\theta = \theta_{eff} \frac{\alpha_s}{8\pi} F^{\mu\nu a} \widetilde{F}^a_{\mu\nu}$ is so small ($\theta_{eff} \lesssim 10^{-9}$) as required by the current limits on the neutron electric dipole moment, even though $\theta_{eff} \sim O(1)$ is perfectly allowed by the QCD gauge invariance. Here, θ_{eff} is the effective θ parameter after the diagonalization of the quark masses, and $F^{\mu\nu a}$ is the gluon field strength and $\widetilde{F}^a_{\mu\nu} = \frac{1}{2}\epsilon_{\mu\nu\rho\sigma} F^{\rho\sigma a}$. An axion is a pseudo-NG boson of a spontaneously broken Peccei–Quinn symmetry, which is an exact symmetry at the classical level, but is broken quantum mechanically due to the triangle anomaly with the gluons. The definition of the Peccei–Quinn symmetry is model dependent. As a result of the triangle anomaly, the axion acquires an effective coupling to gluons

$$\mathcal{L} = \left(\theta_{eff} - \frac{\phi_A}{f_A}\right) \frac{\alpha_s}{8\pi} F^{\mu\nu a} \widetilde{F}^a_{\mu\nu}, \qquad (2)$$

where ϕ_A is the axion field. It is often convenient to *define* the axion decay constant f_A with this Lagrangian [6]. The QCD nonperturbative effect induces a potential for ϕ_A whose minimum is at $\phi_A = \theta_{eff} f_A$ cancelling θ_{eff} and solving the strong CP problem. The mass of the axion is inversely proportional to f_A as

$$m_A = 0.62 \times 10^{-3}\text{eV} \times (10^{10}\text{GeV}/f_A) \ . \qquad (3)$$

The original axion model [1,5] assumes $f_A \sim v$, where $v = (\sqrt{2}G_F)^{-1/2} = 247$ GeV is the scale of the electroweak symmetry breaking, and has two Higgs doublets as minimal ingredients. By requiring tree-level flavor conservation, the axion mass and its couplings are completely fixed in terms of one parameter ($\tan\beta$): the ratio of the vacuum expectation values of two Higgs fields. This model is excluded after extensive experimental searches for such an axion [7]. Observation of a narrow-peak structure in positron spectra from heavy ion collisions [8] suggested a particle of mass 1.8 MeV that decays into e^+e^-. Variants of the original axion model, which keep $f_A \sim v$, but drop the constraints of tree-level flavor conservation, were proposed [9]. Extensive searches for this particle, $A^0(1.8\text{ MeV})$, ended up with another negative result [10].

The popular way to save the Peccei-Quinn idea is to introduce a new scale $f_A \gg v$. Then the A^0 coupling becomes weaker, thus one can easily avoid all the existing experimental limits; such models are called invisible axion models [11,12]. Two classes of models are discussed commonly in the literature. One introduces new heavy quarks which carry Peccei–Quinn charge while the usual quarks and leptons do not (KSVZ axion or "hadronic axion") [11]. The other does not need additional quarks but requires two Higgs doublets, and all quarks and leptons carry Peccei–Quinn charges (DFSZ axion or "GUT-axion") [12]. All models contain at least one electroweak singlet scalar boson which acquires an expectation value and breaks Peccei–Quinn symmetry. The invisible axion with a large decay constant $f_A \sim 10^{12}$ GeV was found to be a good candidate of the cold dark matter component of the Universe [13](see Dark Matter review). The energy density is stored in the low-momentum modes of the axion field which are highly occupied and thus represent essentially classical field oscillations.

The constraints on the invisible axion from astrophysics are derived from interactions of the axion with either photons, electrons or nucleons. The strengths of the interactions are model dependent (*i.e.*, not a function of f_A only), and hence one needs to specify a model in order to place lower bounds on f_A. Such constraints will be discussed in Part II. Serious experimental searches for an invisible axion are underway; they typically rely on axion-photon coupling, and some of them assume that the axion is the dominant component of our galactic halo density. Part III will discuss experimental techniques and limits.

Familons arise when there is a global family symmetry broken spontaneously. A family symmetry interchanges generations or acts on different generations differently. Such a symmetry may explain the structure of quark and lepton masses and their mixings. A familon could be either a scalar or a pseudoscalar. For instance, an SU(3) family symmetry among three generations is non-anomalous and hence the familons are exactly massless. In this case, familons are scalars. If one has larger family symmetries with separate groups of left-handed and right-handed fields, one also has pseudoscalar familons. Some of them have flavor-off-diagonal couplings such as $\partial_\mu\phi_F\bar{d}\gamma^\mu s/F_{ds}$ or $\partial_\mu\phi_F\bar{e}\gamma^\mu\mu/F_{\mu e}$, and the decay constant F can be different for individual operators. The decay constants have lower bounds constrained by flavor-changing processes. For instance, $\text{B}(K^+ \to \pi^+\phi_F) < 3 \times 10^{-10}$ [14] gives $F_{ds} > 3.4\times10^{11}$ GeV [15]. The constraints on familons primarily coupled to third generation are quite weak [15].

If there is a global lepton-number symmetry and if it breaks spontaneously, there is a Majoron. The triplet Majoron model [4] has a weak-triplet Higgs boson, and Majoron couples to Z. It is now excluded by the Z invisible-decay width. The model is viable if there is an additional singlet Higgs boson and if the Majoron is mainly a singlet [16]. In the singlet Majoron model [3], lepton-number symmetry is broken by a weak-singlet scalar field, and there are right-handed neutrinos which acquire Majorana masses. The left-handed neutrino masses are generated by a "seesaw" mechanism [17]. The scale of lepton number breaking can be much higher than the electroweak scale in this case. Astrophysical constraints require the decay constant to be $\gtrsim 10^9$ GeV [18].

There is revived interest in a long-lived neutrino, to improve Big-Bang Nucleosynthesis [19] or large scale structure formation theories [20]. Since a decay of neutrinos into electrons or photons is severely constrained, these scenarios require a familon (Majoron) mode $\nu_1 \to \nu_2\phi_F$ (see, *e.g.*, Ref. 15 and references therein).

Other light bosons (scalar, pseudoscalar, or vector) are constrained by "fifth force" experiments. For a compilation of constraints, see Ref. 21.

It has been widely argued that a fundamental theory will not possess global symmetries; gravity, for example, is expected to violate them. Global symmetries such as baryon number arise by accident, typically as a consequence of gauge symmetries. It has been noted [22] that the Peccei-Quinn symmetry, from this perspective, must also arise by accident and must hold to an extraordinary degree of accuracy in order to solve the strong CP problem. Possible resolutions to this problem, however, have been discussed [22,23]. String theory also provides sufficiently good symmetries, especially using a large compactification radius motivated by recent developments in M-theory [24].

References

1. S. Weinberg, Phys. Rev. Lett. **40**, 223 (1978);

F. Wilczek, Phys. Rev. Lett. **40**, 279 (1978).
2. F. Wilczek, Phys. Rev. Lett. **49**, 1549 (1982).
3. Y. Chikashige, R.N. Mohapatra, and R.D. Peccei, Phys. Lett. **98B**, 265 (1981).
4. G.B. Gelmini and M. Roncadelli, Phys. Lett. **99B**, 411 (1981).
5. R.D. Peccei and H. Quinn, Phys. Rev. Lett. **38**, 1440 (1977); also Phys. Rev. **D16**, 1791 (1977).
6. Our normalization here is the same as f_a used in G.G. Raffelt, Phys. Reports **198**, 1 (1990). See this *Review* for the relation to other conventions in the literature.
7. T.W. Donnelly *et al.*, Phys. Rev. **D18**, 1607 (1978);
S. Barshay *et al.*, Phys. Rev. Lett. **46**, 1361 (1981);
A. Barroso and N.C. Mukhopadhyay, Phys. Lett. **106B**, 91 (1981);
R.D. Peccei, in *Proceedings of Neutrino '81*, Honolulu, Hawaii, Vol. 1, p. 149 (1981);
L.M. Krauss and F. Wilczek, Phys. Lett. **B173**, 189 (1986).
8. J. Schweppe *et al.*, Phys. Rev. Lett. **51**, 2261 (1983);
T. Cowan *et al.*, Phys. Rev. Lett. **54**, 1761 (1985).
9. R.D. Peccei, T.T. Wu, and T. Yanagida, Phys. Lett. **B172**, 435 (1986).
10. W.A. Bardeen, R.D. Peccei, and T. Yanagida, Nucl. Phys. **B279**, 401 (1987).
11. J.E. Kim, Phys. Rev. Lett. **43**, 103 (1979);
M.A. Shifman, A.I. Vainstein, and V.I. Zakharov, Nucl. Phys. **B166**, 493 (1980).
12. A.R. Zhitnitsky, Sov. J. Nucl. Phys. **31**, 260 (1980);
M. Dine and W. Fischler, Phys. Lett. **120B**, 137 (1983).
13. J. Preskill, M. Wise, F. Wilczek, Phys. Lett. **120B**, 127 (1983);
L. Abbott and P. Sikivie, Phys. Lett. **120B**, 133 (1983);
M. Dine and W. Fischler, Phys. Lett. **120B**, 137 (1983);
M.S. Turner, Phys. Rev. **D33**, 889 (1986).
14. S. Adler *et al.*, Phys. Rev. Lett. **79**, 2204 (1997).
15. J. Feng, T. Moroi, H. Murayama, and E. Schnapka, UCB-PTH-97/47.
16. K. Choi and A. Santamaria, Phys. Lett. **B267**, 504 (1991).
17. T. Yanagida, in *Proceedings of Workshop on the Unified Theory and the Baryon Number in the Universe*, Tsukuba, Japan, 1979, edited by A. Sawada and A. Sugamoto (KEK, Tsukuba, 1979), p. 95;
M. Gell-Mann, P. Ramond, and R. Slansky, in *Supergravity*, Proceedings of the Workshop, Stony Brook, New York, 1979, edited by P. Van Nieuwenhuizen and D.Z. Freedman (North-Holland, Amsterdam, 1979), p. 315.
18. For a recent analysis of the astrophysical bound on axion-electron coupling, see G. Raffelt and A. Weiss, Phys. Rev. **D51**, 1495 (1995). A bound on Majoron decay constant can be inferred from the same analysis..
19. M. Kawasaki, P. Kernan, H.-S. Kang, R.J. Scherrer, G. Steigman, and T.P. Walker, Nucl. Phys. **B419**, 105 (1994);
S. Dodelson, G. Gyuk, and M.S. Turner, Phys. Rev. **D49**, 5068 (1994);
J.R. Rehm, G. Raffelt, and A. Weiss, Astron. Astrophys. **327**, 443 (1997);
M. Kawasaki, K. Kohri, and K. Sato, Phys. Lett. **B430**, 132 (1998).
20. M. White, G. Gelmini, and J. Silk, Phys. Rev. **D51**, 2669 (1995);
S. Bharadwaj and S.K. Kethi, Astrophys. J. Supp. **114**, 37 (1998).
21. E.G. Adelberger, B.R. Heckel, C.W. Stubbs, and W.F. Rogers, Ann. Rev. Nucl. and Part. Sci. **41**, 269 (1991).
22. M. Kamionkowski and J. March-Russell, Phys. Lett. **B282**, 137 (1992);
R. Holman *et al.*, Phys. Lett. **B282**, 132 (1992).
23. R. Kallosh, A. Linde, D. Linde, and L. Susskind, Phys. Rev. **D52**, 912 (1995).
24. See, for instance, T. Banks and M. Dine, Nucl. Phys. **B479**, 173 (1996); Nucl. Phys. **B505**, 445 (1997).

AXIONS AND OTHER VERY LIGHT BOSONS: PART II (ASTROPHYSICAL CONSTRAINTS)

(by G.G. Raffelt)

Low-mass weakly-interacting particles (neutrinos, gravitons, axions, baryonic or leptonic gauge bosons, *etc.*) are produced in hot plasmas and thus represent an energy-loss channel for stars. The strength of the interaction with photons, electrons, and nucleons can be constrained from the requirement that stellar-evolution time scales are not modified beyond observational limits. For detailed reviews see Refs. [1,2].

The energy-loss rates are steeply increasing functions of temperature T and density ρ. Because the new channel has to compete with the standard neutrino losses which tend to increase even faster, the best limits arise from low-mass stars, notably from horizontal-branch (HB) stars which have a helium-burning core of about 0.5 solar masses at $\langle\rho\rangle \approx 0.6\times10^4\,\mathrm{g\,cm^{-3}}$ and $\langle T\rangle \approx 0.7\times10^8\,\mathrm{K}$. The new energy-loss rate must not exceed about $10\,\mathrm{ergs\,g^{-1}\,s^{-1}}$ to avoid a conflict with the observed number ratio of HB stars in globular clusters. Likewise the ignition of helium in the degenerate cores of the preceding red-giant phase is delayed too much unless the same constraint holds at $\langle\rho\rangle \approx 2\times10^5\,\mathrm{g\,cm^{-3}}$ and $\langle T\rangle \approx 1\times10^8\,\mathrm{K}$. The white-dwarf luminosity function also yields useful bounds.

The new bosons X^0 interact with electrons and nucleons with a dimensionless strength g. For scalars it is a Yukawa coupling, for new gauge bosons (*e.g.*, from a baryonic or leptonic gauge symmetry) a gauge coupling. Axion-like pseudoscalars couple derivatively as $f^{-1}\bar\psi\gamma_\mu\gamma_5\psi\,\partial^\mu\phi_X$ with f an energy scale. Usually this is equivalent to $(2m/f)\bar\psi\gamma_5\psi\,\phi_X$ with m the mass of the fermion ψ so that $g = 2m/f$. For the coupling to electrons, globular-cluster stars yield the constraint

$$g_{Xe} \lesssim \begin{cases} 0.5\times10^{-12} & \text{for pseudoscalars [3]} \\ 1.3\times10^{-14} & \text{for scalars [4]} \end{cases}, \qquad (1)$$

if $m_X \lesssim 10\,\mathrm{keV}$. The Compton process $\gamma + {}^4\mathrm{He} \to {}^4\mathrm{He} + X^0$ limits the coupling to nucleons to $g_{XN} \lesssim 0.4\times10^{-10}$ [4].

Scalar and vector bosons mediate long-range forces which are severely constrained by "fifth-force" experiments [5]. In the massless case the best limits come from tests of the equivalence principle in the solar system, leading to

$$g_{B,L} \lesssim 10^{-23} \qquad (2)$$

for a baryonic or leptonic gauge coupling [6].

In analogy to neutral pions, axions A^0 couple to photons as $g_{A\gamma}\mathbf{E}\cdot\mathbf{B}\,\phi_A$ which allows for the Primakoff conversion $\gamma \leftrightarrow A^0$ in external electromagnetic fields. The most restrictive limit arises from globular-cluster stars [2]

$$g_{A\gamma} \lesssim 0.6 \times 10^{-10}\,\mathrm{GeV}^{-1}\ . \tag{3}$$

The often-quoted "red-giant limit" [7] is slightly weaker.

The duration of the SN 1987A neutrino signal of a few seconds proves that the newborn neutron star cooled mostly by neutrinos rather than through an "invisible channel" such as right-handed (sterile) neutrinos or axions [8]. Therefore,

$$3 \times 10^{-10} \lesssim g_{AN} \lesssim 3 \times 10^{-7} \tag{4}$$

is excluded for the pseudoscalar Yukawa coupling to nucleons [2]. The "strong" coupling side is allowed because axions then escape only by diffusion, quenching their efficiency as an energy-loss channel [9]. Even then the range

$$10^{-6} \lesssim g_{AN} \lesssim 10^{-3} \tag{5}$$

is excluded to avoid excess counts in the water Cherenkov detectors which registered the SN 1987A neutrino signal [11].

In terms of the Peccei-Quinn scale f_A, the axion couplings to nucleons and photons are $g_{AN} = C_N m_N/f_A$ ($N = n$ or p) and $g_{A\gamma} = (\alpha/2\pi f_A)\,(E/N - 1.92)$ where C_N and E/N are model-dependent numerical parameters of order unity. With $m_A = 0.62\,\mathrm{eV}\,(10^7\,\mathrm{GeV}/f_A)$, Eq. (3) yields $m_A \lesssim 0.4\,\mathrm{eV}$ for $E/N = 8/3$ as in GUT models or the DFSZ model. The SN 1987A limit is $m_A \lesssim 0.008\,\mathrm{eV}$ for KSVZ axions while it varies between about 0.004 and 0.012 eV for DFSZ axions, depending on the angle β which measures the ratio of two Higgs vacuum expectation values [10]. In view of the large uncertainties it is good enough to remember $m_A \lesssim 0.01\,\mathrm{eV}$ as a generic limit (Fig. 1).

In the early universe, axions come into thermal equilibrium only if $f_A \lesssim 10^8\,\mathrm{GeV}$ [12]. Some fraction of the relic axions end up in galaxies and galaxy clusters. Their decay $a \to 2\gamma$ contributes to the cosmic extragalactic background light and to line emissions from galactic dark-matter haloes and galaxy clusters. An unsuccessful "telescope search" for such features yields $m_a < 3.5\,\mathrm{eV}$ [13]. For $m_a \gtrsim 30\,\mathrm{eV}$, the axion lifetime is shorter than the age of the universe.

For $f_A \gtrsim 10^8\,\mathrm{GeV}$ cosmic axions are produced nonthermally. If inflation occurred after the Peccei-Quinn symmetry breaking or if $T_{\mathrm{reheat}} < f_A$, the "misalignment mechanism" [14] leads to a contribution to the cosmic critical density of

$$\Omega_A h^2 \approx 1.9 \times 3^{\pm 1}\,(1\,\mu\mathrm{eV}/m_A)^{1.175}\,\Theta_{\mathrm{i}}^2 F(\Theta_{\mathrm{i}}) \tag{6}$$

where h is the Hubble constant in units of $100\,\mathrm{km\,s^{-1}\,Mpc^{-1}}$. The stated range reflects recognized uncertainties of the cosmic conditions at the QCD phase transition and of the temperature-dependent axion mass. The function $F(\Theta)$ with $F(0) = 1$ and $F(\pi) = \infty$ accounts for anharmonic corrections to the axion potential. Because the initial misalignment angle Θ_{i} can be very small or very close to π, there is no real prediction for the mass of dark-matter axions even though one would expect $\Theta_{\mathrm{i}}^2 F(\Theta_{\mathrm{i}}) \sim 1$ to avoid fine-tuning the initial conditions.

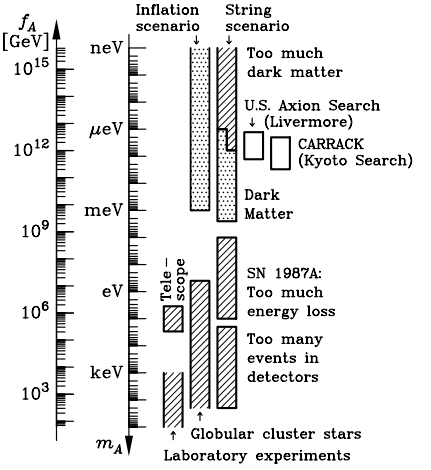

Figure 1: Astrophysical and cosmological exclusion regions (hatched) for the axion mass m_A or equivalently, the Peccei-Quinn scale f_A. An "open end" of an exclusion bar means that it represents a rough estimate; its exact location has not been established or it depends on detailed model assumptions. The globular cluster limit depends on the axion-photon coupling; it was assumed that $E/N = 8/3$ as in GUT models or the DFSZ model. The SN 1987A limits depend on the axion-nucleon couplings; the shown case corresponds to the KSVZ model and approximately to the DFSZ model. The dotted "inclusion regions" indicate where axions could plausibly be the cosmic dark matter. Most of the allowed range in the inflation scenario requires fine-tuned initial conditions. In the string scenario the plausible dark-matter range is controversial as indicated by the step in the low-mass end of the "inclusion bar" (see main text for a discussion). Also shown is the projected sensitivity range of the search experiments for galactic dark-matter axions.

A possible fine-tuning of Θ_{i} is limited by inflation-induced quantum fluctuations which in turn lead to temperature fluctuations of the cosmic microwave background [15,16]. In a broad class of inflationary models one thus finds an upper limit to m_A where axions could be the dark matter. According to the most recent discussion [16] it is about 10^{-3} eV (Fig. 1).

If inflation did not occur at all or if it occurred before the Peccei-Quinn symmetry breaking with $T_{\mathrm{reheat}} > f_A$, cosmic axion strings form by the Kibble mechanism [17]. Their motion is damped primarily by axion emission rather than gravitational waves. After axions acquire a mass at the QCD phase transition they quickly become nonrelativistic and thus form a cold dark matter component. Battye and Shellard [18] found that the

dominant source of axion radiation are string loops rather than long strings. At a cosmic time t the average loop creation size is parametrized as $\langle \ell \rangle = \alpha t$ while the radiation power is $P = \kappa \mu$ with μ the renormalized string tension. The loop contribution to the cosmic axion density is [18]

$$\Omega_A h^2 \approx 88 \times 3^{\pm 1} \left[(1 + \alpha/\kappa)^{3/2} - 1 \right] \, (1\,\mu\mathrm{eV}/m_A)^{1.175} \ , \quad (7)$$

where the stated nominal uncertainty has the same source as in Eq. (6). The values of α and κ are not known, but probably $0.1 < \alpha/\kappa < 1.0$ [18], taking the expression in square brackets to 0.15–1.83. If axions are the dark matter, we have

$$0.05 \lesssim \Omega_A h^2 \lesssim 0.50 \ , \quad (8)$$

where it was assumed that the universe is older than 10 Gyr, that the dark-matter density is dominated by axions with $\Omega_A \gtrsim 0.2$, and that $h \gtrsim 0.5$. This implies $m_A = 6$–2500 μeV for the plausible mass range of dark-matter axions (Fig. 1).

Contrary to Ref. 18, Sikivie *et al.* [19] find that the motion of global strings is strongly damped, leading to a flat axion spectrum. In Battye and Shellard's treatment the axion radiation is strongly peaked at wavelengths of order the loop size. In Sikivie *et al.*'s picture more of the string radiation goes into kinetic axion energy which is redshifted so that ultimately there are fewer axions. In this scenario the contributions from string decay and vacuum realignment are of the same order of magnitude; they are both given by Eq. (6) with Θ_i of order one. As a consequence, Sikivie *et al.* allow for a plausible range of dark-matter axions which reaches to smaller masses as indicated in Fig. 1.

The work of both groups implies that the low-mass end of the plausible mass interval in the string scenario overlaps with the projected sensitivity range of the U.S. search experiment for galactic dark-matter axions (Livermore) [20] and of the Kyoto search experiment CARRACK [21] as indicated in Fig. 1. (See also Part III of this Review by Hagmann, van Bibber, and Rosenberg.)

In summary, a variety of robust astrophysical arguments and laboratory experiments (Fig. 1) indicate that $m_A \lesssim 10^{-2}$ eV. The exact value of this limit may change with a more sophisticated treatment of supernova physics and/or the observation of the neutrino signal from a future galactic supernova, but a dramatic modification is not expected unless someone puts forth a completely new argument. The stellar-evolution limits shown in Fig. 1 depend on the axion couplings to various particles and thus can be irrelevant in fine-tuned models where, for example, the axion-photon coupling strictly vanishes. For nearly any m_A in the range generically allowed by stellar evolution, axions could be the cosmic dark matter, depending on the cosmological scenario realized in nature. It appears that our only practical chance to discover these "invisible" particles rests with the ongoing or future search experiments for galactic dark-matter.

References

1. M.S. Turner, Phys. Reports **197**, 67 (1990); G.G. Raffelt, Phys. Reports **198**, 1 (1990).
2. G.G. Raffelt, Stars as Laboratories for Fundamental Physics (Univ. of Chicago Press, Chicago, 1996).
3. D.A. Dicus, E.W. Kolb, V.L. Teplitz, and R.V. Wagoner, Phys. Rev. **D18**, 1829 (1978); G.G. Raffelt and A. Weiss, Phys. Rev. **D51**, 1495 (1995).
4. J.A. Grifols and E. Massó, Phys. Lett. **B173**, 237 (1986); J.A. Grifols, E. Massó, and S. Peris, Mod. Phys. Lett. **A4**, 311 (1989).
5. E. Fischbach and C. Talmadge, Nature **356**, 207 (1992).
6. L.B. Okun, Yad. Fiz. **10**, 358 (1969) [Sov. J. Nucl. Phys. **10**, 206 (1969)]; S.I. Blinnikov *et al.*, Nucl. Phys. **B458**, 52 (1996).
7. G.G. Raffelt, Phys. Rev. **D33**, 897 (1986); G.G. Raffelt and D. Dearborn, *ibid.* **36**, 2211 (1987).
8. J. Ellis and K.A. Olive, Phys. Lett. **B193**, 525 (1987); G.G. Raffelt and D. Seckel, Phys. Rev. Lett. **60**, 1793 (1988).
9. M.S. Turner, Phys. Rev. Lett. **60**, 1797 (1988); A. Burrows, T. Ressel, and M. Turner, Phys. Rev. **D42**, 3297 (1990).
10. H.-T. Janka, W. Keil, G. Raffelt, and D. Seckel, Phys. Rev. Lett. **76**, 2621 (1996); W. Keil *et al.*, Phys. Rev. **D56**, 2419 (1997).
11. J. Engel, D. Seckel, and A.C. Hayes, Phys. Rev. Lett. **65**, 960 (1990).
12. M.S. Turner, Phys. Rev. Lett. **59**, 2489 (1987).
13. M.A. Bershady, M.T. Ressell, and M.S. Turner, Phys. Rev. Lett. **66**, 1398 (1991); M.T. Ressell, Phys. Rev. **D44**, 3001 (1991); J.M. Overduin and P.S. Wesson, Astrophys. J. **414**, 449 (1993).
14. J. Preskill, M. Wise, and F. Wilczek, Phys. Lett. **B120**, 127 (1983); L. Abbott and P. Sikivie, *ibid.* 133; M. Dine and W. Fischler, *ibid.* 137; M.S. Turner, Phys. Rev. **D33**, 889 (1986).
15. D.H. Lyth, Phys. Lett. **B236**, 408 (1990); M.S. Turner and F. Wilczek, Phys. Rev. Lett. **66**, 5 (1991); A. Linde, Phys. Lett. **B259**, 38 (1991).
16. E.P.S. Shellard and R.A. Battye, "Inflationary axion cosmology revisited", in preparation (1998); The main results can be found in: E.P.S. Shellard and R.A. Battye, `astro-ph/9802216`.
17. R.L. Davis, Phys. Lett. **B180**, 225 (1986); R.L. Davis and E.P.S. Shellard, Nucl. Phys. **B324**, 167 (1989).
18. R.A. Battye and E.P.S. Shellard, Nucl. Phys. **B423**, 260 (1994); Phys. Rev. Lett. **73**, 2954 (1994) (E) *ibid.* **76**, 2203 (1996); `astro-ph/9706014`, to be published in: Proceedings Dark Matter 96, Heidelberg, ed. by H.V. Klapdor-Kleingrothaus and Y. Ramacher.
19. D. Harari and P. Sikivie, Phys. Lett. **B195**, 361 (1987); C. Hagmann and P. Sikivie, Nucl. Phys. **B363**, 247 (1991).
20. C. Hagmann *et al.*, Phys. Rev. Lett. **80**, 2043 (1998).
21. I. Ogawa, S. Matsuki, and K. Yamamoto, Phys. Rev. **D53**, R1740 (1996).

AXIONS AND OTHER VERY LIGHT BOSONS, PART III (EXPERIMENTAL LIMITS)

(Revised November 2003 by C. Hagmann, K. van Bibber, and L.J. Rosenberg, LLNL)

In this section we review the experimental methodology and limits on light axions and light pseudoscalars in general. (A comprehensive overview of axion theory is given by H. Murayama in the Part I of this Review, whose notation we follow [1].) Within its scope are purely laboratory experiments, searches where the axion is assumed to be halo dark matter, and searches where the Sun is presumed to be a source of axions. We restrict the discussion to axions of mass $m_A < O(\mathrm{eV})$, as the allowed range for the axion mass is nominally $10^{-6} < m_A < 10^{-2}$ eV. Experimental work in this range predominantly has been through the axion-to-two-photon coupling $g_{A\gamma}$, to which the present review is largely confined. As discussed in Part II of this Review by G. Raffelt, the lower bound to the axion mass derives from a cosmological overclosure argument, and the upper bound most restrictively from SN1987A [2]. Limits from stellar evolution overlap seamlessly above that, connecting with accelerator-based limits that ruled out the original axion. There, it was assumed that the Peccei-Quinn symmetry-breaking scale was the electroweak scale, *i.e.,* $f_A \sim 250$ GeV, implying axions of mass $m_A \sim O(100\,\mathrm{keV})$. These earlier limits from nuclear transitions, particle decays, *etc.,* while not discussed here, are included in the Listings.

While the axion mass is well-determined by the Peccei-Quinn scale, *i.e.,* $m_A = 0.62\,\mathrm{eV}(10^7\,\mathrm{GeV}/f_A)$, the axion-photon coupling $g_{A\gamma}$ is not: $g_{A\gamma} = (\alpha/\pi f_A)g_\gamma$, with $g_\gamma = (E/N - 1.92)/2$, and where E/N is a model-dependent number. It is noteworthy, however, that quite distinct models lead to axion-photon couplings that are not very different. For example, in the case of axions imbedded in Grand Unified Theories, the DFSZ axion [3], $g_\gamma = 0.37$, whereas in one popular implementation of the "hadronic" class of axions, the KSVZ axion [4], $g_\gamma = -0.96$. Hence, between these two models, rates for axion-photon processes $\sim g_{A\gamma}^2$ differ by less than a factor of 10. The Lagrangian $\mathcal{L} = g_{A\gamma}\mathbf{E}\cdot\mathbf{B}\phi_A$, with ϕ_A the axion field, permits the conversion of an axion into a single real photon in an external electromagnetic field, *i.e.,* a Primakoff interaction. In the case of relativistic axions, $k_\gamma - k_A \sim m_A^2/2\omega$, pertinent to several experiments below, coherent axion-photon mixing in long magnetic fields results in significant conversion probability even for very weakly coupled axions [5]. This mixing of photons and axions has been posited to explain dimming from distant supernovae and the apparent long interstellar attenuation length of the most energetic cosmic rays [6].

Below are discussed several experimental techniques constraining $g_{A\gamma}$, and their results. Also included are recent unpublished results, and projected sensitivities of experiments soon to be upgraded or made operational. Recent reviews describe these experiments in greater detail [7].

III.1. Microwave cavity experiments: Perhaps the most promising avenue to the discovery of the axion presumes that axions constitute a significant fraction of the local dark matter halo in our galaxy. An estimate for the Cold Dark matter (CDM) component of our local galactic halo is $\rho_{\mathrm{CDM}} = 7.5\times10^{-25}\mathrm{g/cm}^3$ $(450\,\mathrm{MeV/cm}^3)$ [8]. That the CDM halo is in fact made of axions (rather than, *e.g.,* WIMPs) is in principle an independent assumption. However should very light axions exist, they would almost necessarily be cosmologically abundant [2]. As shown by Sikivie [9] and Krauss *et al.* [10], halo axions may be detected by their resonant conversion into a quasi-monochromatic microwave signal in a high-Q cavity permeated by a strong static magnetic field. The cavity is tunable and the signal is maximum when the frequency $\nu = m_A(1 + O(10^{-6}))$, the width of the peak representing the virial distribution of thermalized axions in the galactic gravitational potential. The signal may possess finer structure due to axions recently fallen into the galaxy and not yet thermalized [11]. The feasibility of the technique was established in early experiments of small sensitive volume, $V = O(1\,\mathrm{liter})$ [12] with HFET amplifiers, setting limits in the mass range $4.5 < m_A < 16.3$ μeV, but lacking by 2–3 orders of magnitude the sensitivity to detect KSVZ and DFSZ axions (the conversion power $P_{A\to\gamma} \propto g_{A\gamma}^2$). ADMX, a later experiment ($B \sim 7.8$ T, $V \sim 200$ liter) has achieved sensitivity to KSVZ axions over the mass range 1.9–3.3 μeV, and continues to operate [13]. The exclusion regions shown in Figure 1 for Refs. 12,13 are all normalized to the CDM density $\rho_{\mathrm{CDM}} = 7.5\times10^{-25}\mathrm{g/cm}^3$ $(450\,\mathrm{MeV/cm}^3)$ and 90% CL. A near quantum-limited low noise DC SQUID amplifier [14] is being installed in the upgraded ADMX experiment. A Rydberg atom single-quantum detector [15] is being commissioned in a new RF cavity axion search [16]. These new technologies promise dramatic improvements in experimental sensitivity, which should enable rapid scanning of the axion mass range at or better than the sensitivity required to detect DFSZ axions. The search region of the microwave cavity experiments is shown in detail in Figure 1.

III.2 Optical and Radio Telescope searches: For axions of mass greater than about 10^{-1} eV, their cosmological abundance is no longer dominated by vacuum misalignment of string radiation mechanisms, but rather by thermal emission. Their contribution to critical density is small $\Omega \sim 0.01(m_A/\mathrm{eV})$. However, the spontaneous-decay lifetime of axions, $\tau(A \to 2\gamma) \sim 10^{25}\mathrm{sec}(m_A/\mathrm{eV})^{-5}$ while irrelevant for μeV axions, is short enough to afford a powerful constraint on such thermally produced axions in the eV mass range, by looking for a quasi-monochromatic photon line from galactic clusters. This line, corrected for Doppler shift, would be at half the axion mass and its width would be consistent with the observed virial motion, typically $\Delta\lambda/\lambda \sim 10^{-2}$. The expected line intensity would be of the order $I_A \sim 10^{-17}(m_A/3\,\mathrm{eV})^7\mathrm{erg\,cm}^{-2}\mathrm{arcsec}^{-2}\mathrm{\AA}^{-1}\mathrm{sec}^{-1}$ for DFSZ axions, comparable to the continuum night emission.

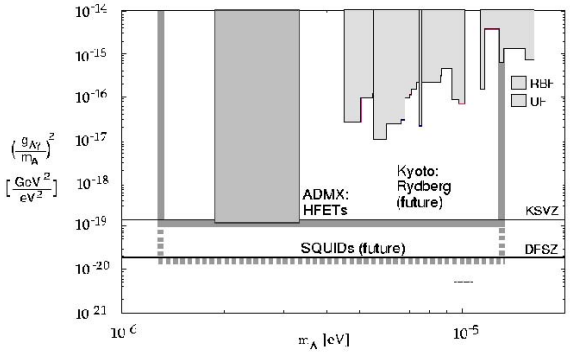

Figure 1: Exclusion region from the microwave cavity experiments, where the plot is flattened by presenting $(g_{A\gamma}/m_A)^2$ versus m_A. The first-generation experiments ("RBF" and "UF" [12]) and in-progress "ADMX" [13] are all HFET-based. Shown also is the full mass range to be covered by the latter experiment (shaded line), and the improved sensitivity when upgraded with DC SQUID amplifiers [14] (shaded dashed line). The expected sensitivity of "CARRACK II" based on a Rydberg single-quantum receiver (dotted line) is also shown in Ref. 16.

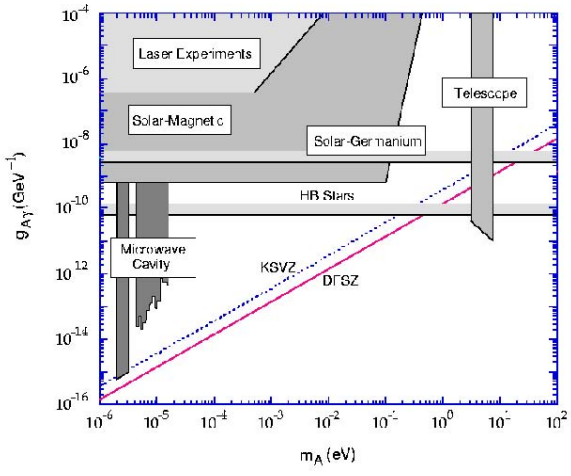

Figure 2: Exclusion region in mass versus axion-photon coupling $(m_A, g_{A\gamma})$ for various experiments. The limit set by globular cluster Horizontal Branch Stars ("HB Stars") is shown in Ref. 2.

The conservative assumption is made that the relative density of thermal axions fallen into the cluster gravitational potential reflects their overall cosmological abundance. A search for thermal axions in three rich Abell clusters was carried out at Kitt Peak National Laboratory [17]; no such line was observed between 3100–8300 Å (m_A = 3–8 eV) after on-off field subtraction of the atmospheric molecular background spectra. A limit everywhere stronger than $g_{A\gamma} < 10^{-10}\text{GeV}^{-1}$ is set, which is seen from Fig. 2 to easily exclude DFSZ axions throughout the mass range.

Similar in principle to the optical telescope search, microwave photons from spontaneous axion decay in halos of astrophysical objects may be searched for with a radio telescope. One group [18] aimed the Haystack radio dish at several nearby dwarf galaxies. The expected signal is a narrow spectral line with the expected virial width, Doppler shift, and intensity distribution about the center of the galaxies. They reported limits of $g_{A\gamma} < 1.0 \times 10^{-9}\text{GeV}^{-1}$ for $m_A \sim$ few$\times 100$ μeV. They propose an interferometric radio telescope search with sensitivity near $g_{A\gamma}$ of 10^{-10}GeV^{-1}.

III.3 A search for solar axions: As with the telescope search for thermally produced axions, the search for solar axions was stimulated by the possibility of there being a "1 eV window" for hadronic axions (*i.e.,* axions with no tree-level coupling to leptons), a "window" subsequently closed by an improved understanding of the evolution of globular cluster stars and SN1987A [2]. Hadronic axions would be copiously produced within our Sun's interior by a Primakoff process. Their flux at the Earth of $\sim 10^{12}\text{cm}^{-2}\text{sec}^{-1}(m_A/\text{eV})^2$, which is independent of the details of the solar model, is sufficient for a definitive test via the axion reconversion into photons in a large magnetic field. However, their average energy is $\sim$ 4 keV, implying an oscillation length in the vacuum of $2\pi(m_A^2/2\omega)^{-1} \sim O(\text{mm})$, precluding the mixing from achieving its theoretically maximum value in any practical magnet. It was recognized that one could endow the photon with an effective mass in the gas, $m_\gamma = \omega_{\text{pl}}$, thus permitting the axion and photon dispersion relations to be matched [5]. A first simple implementation of this proposal was carried out using a conventional dipole magnet with a conversion volume of variable-pressure gas and a xenon proportional chamber as the x-ray detector [19]. The magnet was fixed in orientation to take data for $\sim$ 1000 sec/day. Axions were excluded for $g_{A\gamma} < 3.6 \times 10^{-9}\text{GeV}^{-1}$ for $m_A < 0.03$ eV, and $g_{A\gamma} < 7.7 \times 10^{-9}\text{GeV}^{-1}$ for $0.03 < m_A < 0.11$ eV (95% CL). A more sensitive experiment (Tokyo axion helioscope) has been completed, using a superconducting magnet on a telescope mount to track the sun continuously. This gives an exclusion limit of $g_{A\gamma} < 6 \times 10^{-10}\text{GeV}^{-1}$ for $m_A < 0.3$ eV [20]. A new experiment CAST (CERN Axion Solar Telescope), using a decommissioned LHC dipole magnet, is taking first data [21]. The projected sensitivity $g_{A\gamma} < 10^{-10}\text{GeV}^{-1}$ for $m_A < 1$ eV, is about that of the globular cluster bounds.

Other searches for solar axions have been carried out using crystal germanium detectors. These exploit the coherent conversion of axions into photons when their angle of incidence satisfies a Bragg condition with a crystalline plane. Analysis of 1.94 kg-yr of data from a 1 kg germanium detector yields a bound of $g_{A\gamma} < 2.7 \times 10^{-9}\text{GeV}^{-1}$ (95% CL) independent

of mass up to $m_A \sim 1$ keV [22]. Analysis of 0.2 kg-yr of data from a 0.234 kg germanium detector yields a bound of $g_{A\gamma} < 2.8 \times 10^{-9}\text{GeV}^{-1}$ (95% CL) [23]. A general study of sensitivities [24] concludes these crystal detectors are unlikely to compete with axion bounds arising from globular clusters [25] or helioseismology [26].

III.4 Photon regeneration ("invisible light shining through walls"): Photons propagating through a transverse field (with $\mathbf{E}\|\mathbf{B}$ may convert into axions. For light axions with $m_A^2 l/2\omega \ll 2\pi$, where l is the length of the magnetic field, the axion beam produced is colinear and coherent with the photon beam, and the conversion probability Π is given by $\Pi \sim (1/4)(g_{A\gamma}Bl)^2$. An ideal implementation for this limit is a laser beam propagating down a long, superconducting dipole magnet like those for high-energy physics accelerators. If another such dipole magnet is set up in line with the first, with an optical barrier interposed between them, then photons may be regenerated from the pure axion beam in the second magnet and detected [27]. The overall probability $P(\gamma \to A \to \gamma) = \Pi^2$. such an experiment has been carried our, utilizing two magnets of length $l = 4.4$ m and $B = 3.7$ T. Axions with mass $m_A < 10^{-3}$ eV, and $g_{A\gamma} > 6.7 \times 10^{-7}\text{GeV}^{-1}$ were excluded at 95% CL [28]. With sufficient effort, limits comparable to those from stellar evolution would be achievable. Due to the $g_{A\gamma}^4$ rate suppression, however, it does not seem feasible to reach standard axion couplings.

III.5 Polarization experiments: The existence of axions can affect the polarization of light propagating through a transverse magnetic field in two ways [29]. First, as the $\mathbf{E}_\|$ component, but not the $\mathbf{E}_\perp$ component will be depleted by the production of real axions, there will be in general a small rotation of the polarization vector of linearly polarized light. This effect will be constant for all sufficiently light m_A such that the oscillation length is much longer than the magnet $m_A^2 l/2\omega \ll 2\pi$. For heavier axions, the effect oscillates and diminishes with increasing m_A, and vanishes for $m_A > \omega$. The second effect is birefringence of the vacuum, again because there could be a mixing of virtual axions in the $\mathbf{E}_\|$ state, but not for the $\mathbf{E}_\perp$ state. This will lead to light that is initially linearly polarized becoming elliptically polarized. Higher-order QED also induces vacuum birefringence, and is much stronger than the contribution due to axions. A search for both polarization-rotation and induced ellipticity has been carried out with the same dipole magnets described above [30]. As in the case of photon regeneration, the observables are boosted linearly by the number of passes of the laser beam in the optical cavity within the magnet. The polarization-rotation resulted in a stronger limit than that from ellipticity, $g_{A\gamma} < 3.6 \times 10^{-7}\text{GeV}^{-1}$ (95% CL) for $m_A < 5 \times 10^{-4}$ eV. The limits from ellipticity are better at higher masses, as they fall off smoothly and do not terminate at m_A. Current experiments with greatly improved sensitivity that, while still far from being able to detect standard axions, have measured the QED "light-by-light" contribution for the first time [31]. The overall envelope for limits from the laser-based experiments is shown schematically in Fig. 2.

III.6 Non-Newtonian monopole-dipole couplings: Axions mediate a CP violating monopole-dipole Yukawa-type gravitational interaction potential ($g_s g_p \hat{\sigma}\cdot\hat{r}\, e^{-r/\lambda}$) between spin and matter [32] where $g_s g_p$ is the product of couplings at the scalar and polarized vertices and λ is the range of the force. Two experiments placed upper limits on the product coupling $g_s g_p$ in a system of magnetized media and test masses. One experiment [33] had peak sensitivity near 100 mm (2 μeV axion mass) another [34] had peak sensitivity near 10 mm (20 μeV axion mass). Both lacked sensitivity by 10 orders of magnitude of the sensitivity required to detect couplings implied by the existing limits on a neutron EDM.

References

1. H. Murayama, Part I (Theory) of this Review.
2. G. Raffelt, Part II (Astrophysical Constraints) of this Review.
3. M. Dine *et al.*, Phys. Lett. **B104**, 199 (1981); A. Zhitnitsky, Sov. J. Nucl. Phys. **31**, 260 (1980).
4. J. Kim, Phys. Rev. Lett. **43**, 103 (1979); M. Shifman *et al.*, Nucl. Phys. **B166**, 493 (1980).
5. G. Raffelt and L. Stodolsky, Phys. Rev. **D37**, 1237 (1988).
6. See, *e.g.*, C. Csaki, N. Kaloper and J. Terning, Phys. Rev. Lett. **88**, 161302 (2002); E. Mörtsell, L. Bergström, and A. Goobar, Phys. Rev. **D66**, 047702 (2002); D.S. Gorbunov, G.G. Raffelt, and D.V. Semikoz, Phys. Rev. **D64**, 096005 (2001); C. Csaki, N. Kaloper, M. Peloso and J. Terning, JCAP **0305**, 005 (2003).
7. L.J. Rosenberg and K.A. van Bibber, Phys. Reports **325**, 1 (2000); R. Bradley *et al.*, Rev. Mod. Phys. **75**, 777 (2003).
8. E. Gates *et al.*, Ap. J. **499**, 123 (1995).
9. P. Sikivie, Phys. Rev. Lett. **51**, 1415 (1983); **52(E)**, 695 (1984); Phys. Rev. **D32**, 2988 (1985).
10. L. Krauss *et al.*, Phys. Rev. Lett. **55**, 1797 (1985).
11. P. Sikivie and J. Ipser, Phys. Lett. **B291**, 288 (1992); P. Sikivie *et al.*, Phys. Rev. Lett. **75**, 2911 (1995).
12. S. DePanfilis *et al.*, Phys. Rev. Lett. **59**, 839 (1987); W. Wuensch *et al.*, Phys. Rev. **D40**, 3153 (1989); C. Hagmann *et al.*, Phys. Rev. **D40**, 3153 (1989).
13. C. Hagmann *et al.*, Phys. Rev. Lett. **80**, 2043 (1998); S. J. Asztalos *et al.*, Astrophys. J. **571**, L27 (2002); H. Peng at al., Nucl. Instrum. Methods **A444**, 569 (2000); S. Asztalos *et al.*, Phys. Rev. **D64**, 092003 (2003).
14. M. Mück, J.B. Kycia, and J. Clarke, Appl. Phys. Lett. **78**, 967 (2001).
15. I. Ogawa, S. Matsuki, and K. Yamamoto, Phys. Rev. **D53**, 1740 (1996).
16. S. Matsuki *et al.*, Nucl. Phys. **51B** (Proc. Suppl.) 213, (1996).
17. M. Bershady *et al.*, Phys. Rev. Lett. **66**, 1398 (1991); M. Ressell, Phys. Rev. **D44**, 3001 (1991).
18. B.D. Blout *et al.*, Astrophys. J. **546**, 825 (2001).
19. D. Lazarus *et al.*, Phys. Rev. Lett. **69**, 2333 (1992).

20. S. Moriyama *et al.*, Phys. Lett. **B434**, 147 (1998); Y. Inoue *et al.*, Phys. Lett. **B536**, 18 (2002).
21. K. Zioutas *et al.*, Nucl. Instrum. Methods **A425**, 480 (1999); J.I. Collar *et al.*. [CAST Collaboration], "CAST: A search for solar axions at CERN," hep-ex/0304024.
22. F.T. Avignone III *et al.*, Phys. Rev. Lett. **81**, 5068 (1998).
23. I.G. Irastorza *et al.*, Nucl. Phys. **87** (Proc. Suppl.) 111, (2000).
24. S. Cebrián *et al.*, Astropart. Phys. **10**, 397 (1999).
25. G. Raffelt, "Stars as Laboratories for Fundamental Physics," University of Chicago Press, Chicago (1996).
26. H. Schlattl, A. Weiss, and G. Raffelt, Astropart. Phys. **10**, 353 (1999).
27. K. van Bibber *et al.*, Phys. Rev. Lett. **59**, 759 (1987); A similar proposal has been made for exactly massless pseudoscalars: A. Ansel'm, Sov. J. Nucl. Phys. **42**, 936 (1985).
28. G. Ruoso *et al.*, Z. Phys. **C56**, 505 (1992); R. Cameron *et al.*, Phys. Rev. **D47**, 3707 (1993).
29. L. Maiani *et al.*, Phys. Lett. **B175**, 359 (1986).
30. See Ref. 28 and Y. Semertzadis *et al.*, Phys. Rev. Lett. **64**, 2988 (1990).
31. D. Bakalov *et al.*, Quantum Semiclass. Opt. **10**, 239(1998).
32. J.E. Moody and F. Wilczek, Phys. Rev. **D30**, 130 (1984).
33. A.N. Youdin *et al.*, Phys. Rev. Lett. **77**, 2170 (1996).
34. Wei-Tou Ni *et al.*, Phys. Rev. Lett. **82**, 2439 (1999).

A^0 (Axion) MASS LIMITS from Astrophysics and Cosmology

These bounds depend on model-dependent assumptions (i.e. — on a combination of axion parameters).

VALUE (MeV)	DOCUMENT ID		TECN	COMMENT
• • • We do not use the following data for averages, fits, limits, etc. • • •				
>0.2	BARROSO	82	ASTR	Standard Axion
>0.25	[1] RAFFELT	82	ASTR	Standard Axion
>0.2	[2] DICUS	78C	ASTR	Standard Axion
	MIKAELIAN	78	ASTR	Stellar emission
>0.3	[2] SATO	78	ASTR	Standard Axion
>0.2	VYSOTSKII	78	ASTR	Standard Axion

[1] Lower bound from 5.5 MeV γ-ray line from the sun.
[2] Lower bound from requiring the red giants' stellar evolution not be disrupted by axion emission.

A^0 (Axion) and Other Light Boson (X^0) Searches in Meson Decays

Limits are for branching ratios.

VALUE	CL%	EVTS	DOCUMENT ID		TECN	COMMENT
• • • We do not use the following data for averages, fits, limits, etc. • • •						
$<4.5 \times 10^{-11}$	90		[3] ADLER	02C	B787	$K^+ \to \pi^+ A^0$
$<4.9 \times 10^{-5}$	90		AMMAR	01B	CLEO	$B^\pm \to \pi^\pm(K^\pm)X^0$
$<5.3 \times 10^{-5}$	90		AMMAR	01B	CLEO	$B^0 \to K^0_S X^0$
$<1.1 \times 10^{-10}$	90		[4] ADLER	00	B787	$K^+ \to \pi^+ A^0$
$<3.3 \times 10^{-5}$	90		[5] ALTEGOER	98	NOMD	$\pi^0 \to \gamma X^0$, $m_{X^0} < 120$ MeV
$<5.0 \times 10^{-8}$	90		[6] KITCHING	97	B787	$K^+ \to \pi^+ A^0$ $(A^0 \to \gamma\gamma)$
$<5.2 \times 10^{-10}$	90		[7] ADLER	96	B787	$K^+ \to \pi^+ A^0$
$<2.8 \times 10^{-4}$	90		[8] AMSLER	96B	CBAR	$\pi^0 \to \gamma X^0$, $m_{X^0} < 65$ MeV
$<3 \times 10^{-4}$	90		[8] AMSLER	96B	CBAR	$\eta \to \gamma X^0$, $m_{X^0}=$ 50–200 MeV
$<4 \times 10^{-5}$	90		[8] AMSLER	96B	CBAR	$\eta' \to \gamma X^0$, $m_{X^0}=$ 50–925 MeV
$<6 \times 10^{-5}$	90		[8] AMSLER	94B	CBAR	$\pi^0 \to \gamma X^0$, $m_{X^0}=$65–125 MeV
$<6 \times 10^{-5}$	90		[8] AMSLER	94B	CBAR	$\eta \to \gamma X^0$, $m_{X^0}=$200–525 MeV
<0.007	90		[9] MEIJERDREES	94	CNTR	$\pi^0 \to \gamma X^0$, $m_{X^0}=25$ MeV
<0.002	90		[9] MEIJERDREES	94	CNTR	$\pi^0 \to \gamma X^0$, $m_{X^0}=100$ MeV
$<2 \times 10^{-7}$	90		[10] ATIYA	93B	B787	$K^+ \to \pi^+ A^0$
$<3 \times 10^{-13}$			[11] NG	93	COSM	$\pi^0 \to \gamma X^0$
$<1.1 \times 10^{-8}$	90		[12] ALLIEGRO	92	SPEC	$K^+ \to \pi^+ A^0$ $(A^0 \to e^+e^-)$
$<5 \times 10^{-4}$	90		[13] ATIYA	92	B787	$\pi^0 \to \gamma X^0$
$<4 \times 10^{-6}$	90		[14] MEIJERDREES	92	SPEC	$\pi^0 \to \gamma X^0$, $X^0 \to e^+e^-$, $m_{X^0}=$ 100 MeV
$<1 \times 10^{-7}$	90		[15] ATIYA	90B	B787	Sup. by KITCHING 97
$<1.3 \times 10^{-8}$	90		[16] KORENCHE...	87	SPEC	$\pi^+ \to e^+\nu A^0$ $(A^0 \to e^+e^-)$
$<1 \times 10^{-9}$	90	0	[17] EICHLER	86	SPEC	Stopped $\pi^+ \to e^+\nu A^0$
$<2 \times 10^{-5}$	90		[18] YAMAZAKI	84	SPEC	For 160<m<260 MeV
$<(1.5\text{–}4) \times 10^{-6}$	90		[18] YAMAZAKI	84	SPEC	K decay, $m_{A^0} \ll$ 100 MeV
		0	[19] ASANO	82	CNTR	Stopped $K^+ \to \pi^+ A^0$
		0	[20] ASANO	81B	CNTR	Stopped $K^+ \to \pi^+ A^0$
			[21] ZHITNITSKII	79		Heavy axion

[3] ADLER 02C bound is for $m_{A^0} < 60$ MeV. See Fig. 2 for limits at higher masses.
[4] ADLER 00 bound is for massless A^0.
[5] ALTEGOER 98 looked for X^0 from π^0 decay which penetrate the shielding and convert to π^0 in the external Coulomb field of a nucleus.
[6] KITCHING 97 limit is for $B(K^+ \to \pi^+ A^0)\cdot B(A^0 \to \gamma\gamma)$ and applies for $m_{A^0} \simeq 50$ MeV, $\tau_{A^0} < 10^{-10}$ s. Limits are provided for $0 < m_{A^0} < 100$ MeV, $\tau_{A^0} < 10^{-8}$ s.
[7] ADLER 96 looked for a peak in missing-mass distribution. This work is an update of ATIYA 93. The limit is for massless stable A^0 particles and extends to $m_{A^0}=80$ MeV at the same level. See paper for dependence on finite lifetime.
[8] AMSLER 94B and AMSLER 96B looked for a peak in missing-mass distribution.
[9] The MEIJERDREES 94 limit is based on inclusive photon spectrum and is independent of X^0 decay modes. It applies to $\tau(X^0) > 10^{-23}$ sec.
[10] ATIYA 93B looked for a peak in missing mass distribution. The bound applies for stable A^0 of $m_{A^0}=150$–250 MeV, and the limit becomes stronger (10^{-8}) for $m_{A^0}=180$–240 MeV.
[11] NG 93 studied the production of X^0 via $\gamma\gamma \to \pi^0 \to \gamma X^0$ in the early universe at $T \simeq 1$ MeV. The bound on extra neutrinos from nucleosynthesis $\Delta N_\nu < 0.3$ (WALKER 91) is employed. It applies to $m_{X^0} \ll 1$ MeV in order to be relativistic down to nucleosynthesis temperature. See paper for heavier X^0.
[12] ALLIEGRO 92 limit applies for $m_{A^0}=150$–340 MeV and is the branching ratio times the decay probability. Limit is $< 1.5 \times 10^{-8}$ at 99%CL.
[13] ATIYA 92 looked for a peak in missing mass distribution. The limit applies to $m_{X^0}=0$–130 MeV in the narrow resonance limit. See paper for the dependence on lifetime. Covariance requires X^0 to be a vector particle.
[14] MEIJERDREES 92 limit applies for $\tau_{X^0} = 10^{-23}$–10^{-11} sec. Limits between 2×10^{-4} and 4×10^{-6} are obtained for $m_{X^0} = 25$–120 MeV. Angular momentum conservation requires that X^0 has spin ≥ 1.
[15] ATIYA 90B limit is for $B(K^+ \to \pi^+ A^0)\cdot B(A^0 \to \gamma\gamma)$ and applies for $m_{A^0} = 50$ MeV, $\tau_{A^0} < 10^{-10}$ s. Limits are also provided for $0 < m_{A^0} < 100$ MeV, $\tau_{A^0} < 10^{-8}$ s.
[16] KORENCHENKO 87 limit assumes $m_{A^0} = 1.7$ MeV, $\tau_{A^0} \lesssim 10^{-12}$ s, and $B(A^0 \to e^+e^-) = 1$.
[17] EICHLER 86 looked for $\pi^+ \to e^+\nu A^0$ followed by $A^0 \to e^+e^-$. Limits on the branching fraction depend on the mass and and lifetime of A^0. The quoted limits are valid when $\tau(A^0) \gtrsim 3. \times 10^{-10}$s if the decays are kinematically allowed.
[18] YAMAZAKI 84 looked for a discrete line in $K^+ \to \pi^+ X$. Sensitive to wide mass range (5–300 MeV), independent of whether X decays promptly or not.
[19] ASANO 82 at KEK set limits for $B(K^+ \to \pi^+ A^0)$ for $m_{A^0} < 100$ MeV as BR $< 4. \times 10^{-8}$ for $\tau(A^0 \to n\gamma\text{'s}) > 1. \times 10^{-9}$ s, BR $< 1.4 \times 10^{-6}$ for $\tau < 1. \times 10^{-9}$s.
[20] ASANO 81B is KEK experiment. Set $B(K^+ \to \pi^+ A^0) < 3.8 \times 10^{-8}$ at CL = 90%.
[21] ZHITNITSKII 79 argue that a heavy axion predicted by YANG 78 ($3 < m < 40$ MeV) contradicts experimental muon anomalous magnetic moments.

A^0 (Axion) Searches in Quarkonium Decays

Decay or transition of quarkonium. Limits are for branching ratio.

VALUE	CL%	EVTS	DOCUMENT ID		TECN	COMMENT
• • • We do not use the following data for averages, fits, limits, etc. • • •						
$<1.3 \times 10^{-5}$	90		[22] BALEST	95	CLEO	$\Upsilon(1S) \to A^0\gamma$
$<4.0 \times 10^{-5}$	90		ANTREASYAN	90C	CBAL	$\Upsilon(1S) \to A^0\gamma$
			[23] ANTREASYAN	90C	RVUE	
$<5 \times 10^{-5}$	90		[24] DRUZHININ	87	ND	$\phi \to A^0\gamma$ $(A^0 \to e^+e^-)$
$<2 \times 10^{-3}$	90		[25] DRUZHININ	87	ND	$\phi \to A^0\gamma$ $(A^0 \to \gamma\gamma)$
$<7 \times 10^{-6}$	90		[26] DRUZHININ	87	ND	$\phi \to A^0\gamma$ $(A^0 \to$ missing)
$<3.1 \times 10^{-4}$	90	0	[27] ALBRECHT	86D	ARG	$\Upsilon(1S) \to A^0\gamma$ $(A^0 \to e^+e^-)$
$<4 \times 10^{-4}$	90	0	[27] ALBRECHT	86D	ARG	$\Upsilon(1S) \to A^0\gamma$ $(A^0 \to \mu^+\mu^-, \pi^+\pi^-, K^+K^-)$

$<8 \times 10^{-4}$	90	1	[28] ALBRECHT	86D	ARG	$\Upsilon(1S) \to A^0\gamma$	
$<1.3 \times 10^{-3}$	90	0	[29] ALBRECHT	86D	ARG	$\Upsilon(1S) \to A^0\gamma$ ($A^0 \to e^+e^-, \gamma\gamma$)	
$<2. \times 10^{-3}$	90		[30] BOWCOCK	86	CLEO	$\Upsilon(2S) \to \Upsilon(1S) \to A^0$	
$<5. \times 10^{-3}$	90		[31] MAGERAS	86	CUSB	$\Upsilon(1S) \to A^0\gamma$	
$<3. \times 10^{-4}$	90		[32] ALAM	83	CLEO	$\Upsilon(1S) \to A^0\gamma$	
$<9.1 \times 10^{-4}$	90		[33] NICZYPORUK	83	LENA	$\Upsilon(1S) \to A^0\gamma$	
$<1.4 \times 10^{-5}$	90		[34] EDWARDS	82	CBAL	$J/\psi \to A^0\gamma$	
$<3.5 \times 10^{-4}$	90		[35] SIVERTZ	82	CUSB	$\Upsilon(1S) \to A^0\gamma$	
$<1.2 \times 10^{-4}$	90		[35] SIVERTZ	82	CUSB	$\Upsilon(3S) \to A^0\gamma$	

[22] BALEST 95 looked for a monochromatic γ from $\Upsilon(1S)$ decay. The bound is for $m_{A^0} <$ 5.0 GeV. See Fig. 7 in the paper for bounds for heavier m_{A^0}. They also quote a bound on branching ratios 10^{-3}–10^{-5} of three-body decay $\gamma X\overline{X}$ for $0 < m_X < 3.1$ GeV.

[23] The combined limit of ANTREASYAN 90C and EDWARDS 82 excludes standard axion with $m_{A^0} < 2m_e$ at 90% CL as long as $C_\Upsilon C_{J/\psi} > 0.09$, where C_V ($V = \Upsilon, J/\psi$) is the reduction factor for $\Gamma(V \to A^0\gamma)$ due to QCD and/or relativistic corrections. The same data excludes $0.02 < x < 260$ (90% CL) if $C_\Upsilon = C_{J/\psi} = 0.5$, and further combining with ALBRECHT 86D result excludes $5 \times 10^{-5} < x < 260$. x is the ratio of the vacuum expectation values of the two Higgs fields. These limits use conventional assumption $\Gamma(A^0 \to ee) \propto x^{-2}$. The alternative assumption $\Gamma(A^0 \to ee) \propto x^2$ gives a somewhat different excluded region $0.00075 < x < 44$.

[24] The first DRUZHININ 87 limit is valid when $\tau_{A^0}/m_{A^0} < 3 \times 10^{-13}$ s/MeV and $m_{A^0} < 20$ MeV.

[25] The second DRUZHININ 87 limit is valid when $\tau_{A^0}/m_{A^0} < 5 \times 10^{-13}$ s/MeV and $m_{A^0} < 20$ MeV.

[26] The third DRUZHININ 87 limit is valid when $\tau_{A^0}/m_{A^0} > 7 \times 10^{-12}$ s/MeV and $m_{A^0} < 200$ MeV.

[27] $\tau_{A^0} < 1 \times 10^{-13}$ s and $m_{A^0} < 1.5$ GeV. Applies for $A^0 \to \gamma\gamma$ when $m_{A^0} < 100$ MeV.

[28] $\tau_{A^0} > 1 \times 10^{-7}$ s.

[29] Independent of τ_{A^0}.

[30] BOWCOCK 86 looked for A^0 that decays into e^+e^- in the cascade decay $\Upsilon(2S) \to \Upsilon(1S)\pi^+\pi^-$ followed by $\Upsilon(1S) \to A^0\gamma$. The limit for $B(\Upsilon(1S) \to A^0\gamma)B(A^0 \to e^+e^-)$ depends on m_{A^0} and τ_{A^0}. The quoted limit for m_{A^0}=1.8 MeV is at $\tau_{A^0} \sim 2. \times 10^{-12}$s, where the limit is the worst. The same limit $2. \times 10^{-3}$ applies for all lifetimes for masses $2m_e < m_{A^0} < 2m_\mu$ when the results of this experiment are combined with the results of ALAM 83.

[31] MAGERAS 86 looked for $\Upsilon(1S) \to \gamma A^0$ ($A^0 \to e^+e^-$). The quoted branching fraction limit is for $m_{A^0} = 1.7$ MeV, at $\tau(A^0) \sim 4. \times 10^{-13}$s where the limit is the worst.

[32] ALAM 83 is at CESR. This limit combined with limit for $B(J/\psi \to A^0\gamma)$ (EDWARDS 82) excludes standard axion.

[33] NICZYPORUK 83 is DESY-DORIS experiment. This limit together with lower limit 9.2×10^{-4} of $B(\Upsilon \to A^0\gamma)$ derived from $B(J/\psi(1S) \to A^0\gamma)$ limit (EDWARDS 82) excludes standard axion.

[34] EDWARDS 82 looked for $J/\psi \to \gamma A^0$ decays by looking for events with a single γ [of energy $\sim 1/2$ the $J/\psi(1S)$ mass], plus nothing else in the detector. The limit is inconsistent with the axion interpretation of the FAISSNER 81B result.

[35] SIVERTZ 82 is CESR experiment. Looked for $\Upsilon \to \gamma A^0$, A^0 undetected. Limit for $1S$ ($3S$) is valid for $m_{A^0} <$7 GeV (4 GeV).

A^0 (Axion) Searches in Positronium Decays

Decay or transition of positronium. Limits are for branching ratio.

VALUE	CL%	DOCUMENT ID		TECN	COMMENT
• • • We do not use the following data for averages, fits, limits, etc. • • •					
$<4.4 \times 10^{-5}$	90	[36] BADERT...	02	CNTR	o-Ps $\to \gamma X_1 X_2$, $m_{X_1}+m_{X_2} \leq 900$ keV
$<2 \times 10^{-4}$	90	MAENO	95	CNTR	o-Ps $\to A^0\gamma$ m_{A^0}=850–1013 keV
$<3.0 \times 10^{-3}$	90	[37] ASAI	94	CNTR	o-Ps $\to A^0\gamma$ m_{A^0}=30–500 keV
$<2.8 \times 10^{-5}$	90	[38] AKOPYAN	91	CNTR	o-Ps $\to A^0\gamma$ ($A^0 \to \gamma\gamma$), $m_{A^0} < 30$ keV
$<1.1 \times 10^{-6}$	90	[39] ASAI	91	CNTR	o-Ps $\to A^0\gamma$, $m_{A^0} < 800$ keV
$<3.8 \times 10^{-4}$	90	GNINENKO	90	CNTR	o-Ps $\to A^0\gamma$, $m_{A^0} <$ 30 keV
$<(1–5) \times 10^{-4}$	95	[40] TSUCHIAKI	90	CNTR	o-Ps $\to A^0\gamma$, m_{A^0} = 300–900 keV
$<6.4 \times 10^{-5}$	90	[41] ORITO	89	CNTR	o-Ps $\to A^0\gamma$, $m_{A^0} < 30$ keV
		[42] AMALDI	85	CNTR	Ortho-positronium
		[43] CARBONI	83	CNTR	Ortho-positronium

[36] BADERTSCHER 02 looked for a three-body decay of ortho-positronium into a photon and two penetrating (neutral or milli-charged) particles.

[37] The ASAI 94 limit is based on inclusive photon spectrum and is independent of A^0 decay modes.

[38] The AKOPYAN 91 limit applies for a short-lived A^0 with $\tau_{A^0} < 10^{-13}\ m_{A^0}$ [keV] s.

[39] ASAI 91 limit translates to $g^2_{A^0 e^+e^-}/4\pi < 1.1 \times 10^{-11}$ (90%CL) for $m_{A^0} < 800$ keV.

[40] The TSUCHIAKI 90 limit is based on inclusive photon spectrum and is independent of A^0 decay modes.

[41] ORITO 89 limit translates to $g^2_{A^0 ee}/4\pi < 6.2 \times 10^{-10}$. Somewhat more sensitive limits are obtained for larger m_{A^0}: $B < 7.6 \times 10^{-6}$ at 100 keV.

[42] AMALDI 85 set limits $B(A^0\gamma) / B(\gamma\gamma) <$ (1–5) $\times 10^{-6}$ for m_{A^0} = 900–100 keV which are about 1/10 of the CARBONI 83 limits.

[43] CARBONI 83 looked for orthopositronium $\to A^0\gamma$. Set limit for A^0 electron coupling squared, $g(ee\,A^0)^2/(4\pi) < 6. \times 10^{-10}$–$7. \times 10^{-9}$ for m_{A^0} from 150–900 keV (CL = 99.7%). This is about 1/10 of the bound from $g-2$ experiments.

A^0 (Axion) Search in Photoproduction

VALUE	DOCUMENT ID	COMMENT
• • • We do not use the following data for averages, fits, limits, etc. • • •		
	[44] BASSOMPIE... 95	$m_{A^0} = 1.8 \pm 0.2$ MeV

[44] BASSOMPIERRE 95 is an extension of BASSOMPIERRE 93. They looked for a peak in the invariant mass of e^+e^- pairs in the region $m_{e^+e^-} = 1.8 \pm 0.2$ MeV. They obtained bounds on the production rate A^0 for $\tau(A^0) = 10^{-18}$–10^{-9} sec. They also found an excess of events in the range $m_{e^+e^-} = 2.1$–3.5 MeV.

A^0 (Axion) Production in Hadron Collisions

Limits are for $\sigma(A^0) / \sigma(\pi^0)$.

VALUE	CL%	EVTS	DOCUMENT ID		TECN	COMMENT
• • • We do not use the following data for averages, fits, limits, etc. • • •						
			[45] AHMAD	97	SPEC	e^+ production
			[46] LEINBERGER	97	SPEC	$A^0 \to e^+e^-$
			[47] GANZ	96	SPEC	$A^0 \to e^+e^-$
			[48] KAMEL	96	EMUL	^{32}S emulsion, $A^0 \to e^+e^-$
			[49] BLUEMLEIN	92	BDMP	$A^0 N_Z \to \ell^+\ell^- N_Z$
			[50] MEIJERDREES	92	SPEC	$\pi^- p \to nA^0$, $A^0 \to e^+e^-$
			[51] BLUEMLEIN	91	BDMP	$A^0 \to e^+e^-$, 2γ
			[52] FAISSNER	89	OSPK	Beam dump, $A^0 \to e^+e^-$
			[53] DEBOER	88	RVUE	$A^0 \to e^+e^-$
			[54] EL-NADI	88	EMUL	$A^0 \to e^+e^-$
			[55] FAISSNER	88	OSPK	Beam dump, $A^0 \to 2\gamma$
			[56] BADIER	86	BDMP	$A^0 \to e^+e^-$
$<2. \times 10^{-11}$	90	0	[57] BERGSMA	85	CHRM	CERN beam dump
$<1. \times 10^{-13}$	90	0	[57] BERGSMA	85	CHRM	CERN beam dump
		24	[58] FAISSNER	83	OSPK	Beam dump, $A^0 \to 2\gamma$
			[59] FAISSNER	83B	RVUE	LAMPF beam dump
			[60] FRANK	83B	RVUE	LAMPF beam dump
			[61] HOFFMAN	83	CNTR	$\pi p \to nA^0$ ($A^0 \to e^+e^-$)
			[62] FETSCHER	82	RVUE	See FAISSNER 81B
		12	[63] FAISSNER	81	OSPK	CERN PS ν wideband
		15	[64] FAISSNER	81B	OSPK	Beam dump, $A^0 \to 2\gamma$
		8	[65] KIM	81	OSPK	26 GeV $pN \to A^0$X
		0	[66] FAISSNER	80	OSPK	Beam dump, $A^0 \to e^+e^-$
$<1. \times 10^{-8}$	90		[67] JACQUES	80	HLBC	28 GeV protons
$<1. \times 10^{-14}$	90		[67] JACQUES	80	HLBC	Beam dump
			[68] SOUKAS	80	CALO	28 GeV p beam dump
			[69] BECHIS	79	CNTR	
$<1. \times 10^{-8}$	90		[70] COTEUS	79	OSPK	Beam dump
$<1. \times 10^{-3}$	95		[71] DISHAW	79	CALO	400 GeV pp
$<1. \times 10^{-8}$	90		ALIBRAN	78	HYBR	Beam dump
$<6. \times 10^{-9}$	95		ASRATYAN	78B	CALO	Beam dump
$<1.5 \times 10^{-8}$	90		[72] BELLOTTI	78	HLBC	Beam dump
$<5.4 \times 10^{-14}$	90		[72] BELLOTTI	78	HLBC	m_{A^0}=1.5 MeV
$<4.1 \times 10^{-9}$	90		[72] BELLOTTI	78	HLBC	m_{A^0}=1 MeV
$<1. \times 10^{-8}$	90		[73] BOSETTI	78B	HYBR	Beam dump
			[74] DONNELLY	78		
$<0.5 \times 10^{-8}$	90		HANSL	78D	WIRE	Beam dump
			[75] MICELMAC...	78		
			[76] VYSOTSKII	78		

[45] AHMAD 97 reports a result of APEX Collaboration which studied positron production in ^{238}U+^{232}Ta and ^{238}U+^{181}Ta collisions, without requiring a coincident electron. No narrow lines were found for $250 < E_{e^+} < 750$ keV.

[46] LEINBERGER 97 (ORANGE Collaboration) at GSI looked for a narrow sum-energy e^+e^--line at $\sim$ 635 keV in ^{238}U+^{181}Ta collision. Limits on the production probability for a narrow sum-energy e^+e^- line are set. See their Table 2.

[47] GANZ 96 (EPos II Collaboration) has placed upper bounds on the production cross section of e^+e^- pairs from ^{238}U+^{181}Ta and ^{238}U+^{232}Th collisions at GSI. See Table 2 for limits both for back-to-back and isotropic configurations of e^+e^- pairs. These limits rule out the existence of peaks in the e^+e^- sum-energy distribution, reported by an earlier version of this experiment.

[48] KAMEL 96 looked for e^+e^- pairs from the collision of ^{32}S (200 GeV/nucleon) and emulsion. No evidence of mass peaks is found in the region of sensitivity $m_{ee} > 2$ MeV.

[49] BLUEMLEIN 92 is a proton beam dump experiment at Serpukhov with a secondary target to induce Bethe-Heitler production of e^+e^- or $\mu^+\mu^-$ from the produce A^0.

See Fig. 5 for the excluded region in m_{A^0}-x plane. For the standard axion, $0.3 < x < 25$ is excluded at 95% CL. If combined with BLUEMLEIN 91, $0.008 < x < 32$ is excluded.

[50] MEIJERDREES 92 give $\Gamma(\pi^- p \to n A^0)\cdot B(A^0 \to e^+e^-)/\Gamma(\pi^- p \to \text{all}) < 10^{-5}$ (90% CL) for $m_{A^0} = 100$ MeV, $\tau_{A^0} = 10^{-11}$–10^{-23} sec. Limits ranging from 2.5×10^{-3} to 10^{-7} are given for $m_{A^0} = 25$–136 MeV.

[51] BLUEMLEIN 91 is a proton beam dump experiment at Serpukhov. No candidate event for $A^0 \to e^+e^-$, 2γ are found. Fig. 6 gives the excluded region in m_{A^0}-x plane ($x = \tan\beta = v_2/v_1$). Standard axion is excluded for $0.2 < m_{A^0} < 3.2$ MeV for most $x > 1$, 0.2–11 MeV for most $x < 1$.

[52] FAISSNER 89 searched for $A^0 \to e^+e^-$ in a proton beam dump experiment at SIN. No excess of events was observed over the background. A standard axion with mass $2m_e$–20 MeV is excluded. Lower limit on f_{A^0} of $\simeq 10^4$ GeV is given for $m_{A^0} = 2m_e$–20 MeV.

[53] DEBOER 88 reanalyze EL-NADI 88 data and claim evidence for three distinct states with mass ~ 1.1, ~ 2.1, and ~ 9 MeV, lifetimes 10^{-16}–10^{-15} s decaying to e^+e^- and note the similarity of the data with those of a cosmic-ray experiment by Bristol group (B.M. Anand, Proc. of the Royal Society of London, Section A **A22** 183 (1953)). For a criticism see PERKINS 89, who suggests that the events are compatible with π^0 Dalitz decay. DEBOER 89B is a reply which contests the criticism.

[54] EL-NADI 88 claim the existence of a neutral particle decaying into e^+e^- with mass 1.60 ± 0.59 MeV, lifetime $(0.15 \pm 0.01) \times 10^{-14}$ s, which is produced in heavy ion interactions with emulsion nuclei at ~ 4 GeV/c/nucleon.

[55] FAISSNER 88 is a proton beam dump experiment at SIN. They found no candidate event for $A^0 \to \gamma\gamma$. A standard axion decaying to 2γ is excluded except for a region $x \simeq 1$. Lower limit on f_{A^0} of 10^2–10^3 GeV is given for $m_{A^0} = 0.1$–1 MeV.

[56] BADIER 86 did not find long-lived A^0 in 300 GeV π^- Beam Dump Experiment that decays into e^+e^- in the mass range $m_{A^0} = (20$–$200)$ MeV, which excludes the A^0 decay constant $f(A^0)$ in the interval (60–600) GeV. See their figure 6 for excluded region on $f(A^0)$-m_{A^0} plane.

[57] BERGSMA 85 look for $A^0 \to 2\gamma$, e^+e^-, $\mu^+\mu^-$. First limit above is for $m_{A^0} = 1$ MeV; second is for 200 MeV. See their figure 4 for excluded region on f_{A^0}–m_{A^0} plane, where f_{A^0} is A^0 decay constant. For Peccei-Quinn PECCEI 77 A^0, $m_{A^0} < 180$ keV and $\tau > 0.037$ s. (CL = 90%). For the axion of FAISSNER 81B at 250 keV, BERGSMA 85 expect 15 events but observe zero.

[58] FAISSNER 83 observed 19 1-γ and 12 2-γ events where a background of 4.8 and 2.3 respectively is expected. A small-angle peak is observed even if iron wall is set in front of the decay region.

[59] FAISSNER 83B extrapolate SIN γ signal to LAMPF ν experimental condition. Resulting 370 γ's are not at variance with LAMPF upper limit of 450 γ's. Derived from LAMPF limit that $[d\sigma(A^0)/d\omega$ at $90^\circ] m_{A^0}/\tau_{A^0} < 14 \times 10^{-35}$ cm^2 sr^{-1} MeV ms^{-1}. See comment on FRANK 83B.

[60] FRANK 83B stress the importance of LAMPF data bins with negative net signal. By statistical analysis say that LAMPF and SIN-A0 are at variance when extrapolation by phase-space model is done. They find LAMPF upper limit is 248 not 450 γ's. See comment on FAISSNER 83B.

[61] HOFFMAN 83 set CL = 90% limit $d\sigma/dt\ B(e^+e^-) < 3.5 \times 10^{-32}$ cm^2/GeV^2 for $140 < m_{A^0} < 160$ MeV. Limit assumes $\tau(A^0) < 10^{-9}$ s.

[62] FETSCHER 82 reanalyzes SIN beam-dump data of FAISSNER 81. Claims no evidence for axion since 2-γ peak rate remarkably decreases if iron wall is set in front of the decay region.

[63] FAISSNER 81 see excess μe events. Suggest axion interactions.

[64] FAISSNER 81B is SIN 590 MeV proton beam dump. Observed 14.5 ± 5.0 events of 2γ decay of long-lived neutral penetrating particle with $m_{2\gamma} \lesssim 1$ MeV. Axion interpretation with η-A^0 mixing gives $m_{A^0} = 250 \pm 25$ keV, $\tau_{(2\gamma)} = (7.3 \pm 3.7) \times 10^{-3}$ s from above rate. See critical remarks below in comments of FETSCHER 82, FAISSNER 83, FAISSNER 83B, FRANK 83B, and BERGSMA 85. Also see in the next subsection ALEKSEEV 82, CAVAIGNAC 83, and ANANEV 85.

[65] KIM 81 analyzed 8 candidates for $A^0 \to 2\gamma$ obtained by Aachen-Padova experiment at CERN with 26 GeV protons on Be. Estimated axion mass is about 300 keV and lifetime is $(0.86 \sim 5.6) \times 10^{-3}$ s depending on models. Faissner (private communication), says axion production underestimated and mass overestimated. Correct value around 200 keV.

[66] FAISSNER 80 is SIN beam dump experiment with 590 MeV protons looking for $A^0 \to e^+e^-$ decay. Assuming $A^0/\pi^0 = 5.5 \times 10^{-7}$, obtained decay rate limit $20/(A^0$ mass) MeV/s (CL = 90%), which is about 10^{-7} below theory and interpreted as upper limit to $m_{A^0} < 2m_{e^-}$.

[67] JACQUES 80 is a BNL beam dump experiment. First limit above comes from nonobservation of excess neutral-current-type events $[\sigma(\text{production})\sigma(\text{interaction}) < 7. \times 10^{-68}$ cm^4, CL = 90%$]$. Second limit is from nonobservation of axion decays into 2γ's or e^+e^-, and for axion mass a few MeV.

[68] SOUKAS 80 at BNL observed no excess of neutral-current-type events in beam dump.

[69] BECHIS 79 looked for the axion production in low energy electron Bremsstrahlung and the subsequent decay into either 2γ or e^+e^-. No signal found. CL = 90% limits for model parameter(s) are given.

[70] COTEUS 79 is a beam dump experiment at BNL.

[71] DISHAW 79 is a calorimetric experiment and looks for low energy tail of energy distributions due to energy lost to weakly interacting particles.

[72] BELLOTTI 78 first value comes from search for $A^0 \to e^+e^-$. Second value comes from search for $A^0 \to 2\gamma$, assuming mass $< 2m_{e^-}$. For any mass satisfying this, limit is above value$\times$(mass^{-4}). Third value uses data of PL 60B 401 and quotes $\sigma(\text{production})\sigma(\text{interaction}) < 10^{-67}$ cm^4.

[73] BOSETTI 78B quotes $\sigma(\text{production})\sigma(\text{interaction}) < 2. \times 10^{-67}$ cm^4.

[74] DONNELLY 78 examines data from reactor neutrino experiments of REINES 76 and GURR 74 as well as SLAC beam dump experiment. Evidence is negative.

[75] MICELMACHER 78 finds no evidence of axion existence in reactor experiments of REINES 76 and GURR 74. (See reference under DONNELLY 78 below).

[76] VYSOTSKII 78 derived lower limit for the axion mass 25 keV from luminosity of the sun and 200 keV from red supergiants.

A^0 (Axion) Searches in Reactor Experiments

VALUE		DOCUMENT ID		TECN	COMMENT
• • • We do not use the following data for averages, fits, limits, etc. • • •					
		[77] ALTMANN	95	CNTR	Reactor; $A^0 \to e^+e^-$
		[78] KETOV	86	SPEC	Reactor, $A^0 \to \gamma\gamma$
		[79] KOCH	86	SPEC	Reactor; $A^0 \to \gamma\gamma$
		[80] DATAR	82	CNTR	Light water reactor
		[81] VUILLEUMIER	81	CNTR	Reactor, $A^0 \to 2\gamma$

[77] ALTMANN 95 looked for A^0 decaying into e^+e^- from the Bugey5 nuclear reactor. They obtain an upper limit on the A^0 production rate of $\omega(A^0)/\omega(\gamma) \times B(A^0 \to e^+e^-) < 10^{-16}$ for $m_{A^0} = 1.5$ MeV at 90% CL. The limit is weaker for heavier A^0. In the case of a standard axion, this limit excludes a mass in the range $2m_e < m_{A^0} < 4.8$ MeV at 90% CL. See Fig. 5 of their paper for exclusion limits of axion-like resonances Z^0 in the (m_{X^0}, f_{X^0}) plane.

[78] KETOV 86 searched for A^0 at the Rovno nuclear power plant. They found an upper limit on the A^0 production probability of $0.8\ [100\text{ keV}/m_{A^0}]^6 \times 10^{-6}$ per fission. In the standard axion model, this corresponds to $m_{A^0} > 150$ keV. Not valid for $m_{A^0} \gtrsim 1$ MeV.

[79] KOCH 86 searched for $A^0 \to \gamma\gamma$ at nuclear power reactor Biblis A. They found an upper limit on the A^0 production rate of $\omega(A^0)/\omega(\gamma(M1)) < 1.5 \times 10^{-10}$ (CL=95%). Standard axion with $m_{A^0} = 250$ keV gives 10^{-5} for the ratio. Not valid for $m_{A^0} > 1022$ keV.

[80] DATAR 82 looked for $A^0 \to 2\gamma$ in neutron capture ($np \to dA^0$) at Tarapur 500 MW reactor. Sensitive to sum of $I = 0$ and $I = 1$ amplitudes. With ZEHNDER 81 $[(I = 0) - (I = 1)]$ result, assert nonexistence of standard A^0.

[81] VUILLEUMIER 81 is at Grenoble reactor. Set limit $m_{A^0} < 280$ keV.

A^0 (Axion) and Other Light Boson (X^0) Searches in Nuclear Transitions

Limits are for branching ratio.

VALUE	CL%	EVTS	DOCUMENT ID		TECN	COMMENT
• • • We do not use the following data for averages, fits, limits, etc. • • •						
$< 8.5 \times 10^{-6}$	90		[82] DERBIN	02	CNTR	^{125m}Te decay
			[83] DEBOER	97C	RVUE	M1 transitions
$< 5.5 \times 10^{-10}$	95		[84] TSUNODA	95	CNTR	^{252}Cf fission, $A^0 \to ee$
$< 1.2 \times 10^{-6}$	95		[85] MINOWA	93	CNTR	^{139}La* $\to$ ^{139}LaA^0
$< 2 \times 10^{-4}$	90		[86] HICKS	92	CNTR	^{35}S decay, $A^0 \to \gamma\gamma$
$< 1.5 \times 10^{-9}$	95		[87] ASANUMA	90	CNTR	^{241}Am decay
$< (0.4$–$10) \times 10^{-3}$	95		[88] DEBOER	90	CNTR	^{8}Be* $\to$ ^{8}BeA^0, $A^0 \to e^+e^-$
$< (0.2$–$1) \times 10^{-3}$	90		[89] BINI	89	CNTR	$^{16}O^* \to {}^{16}OX^0$, $X^0 \to e^+e^-$
			[90] AVIGNONE	88	CNTR	Cu* $\to$ CuA^0 ($A^0 \to 2\gamma$, $A^0 e \to \gamma e$, $A^0 Z \to \gamma Z$)
$< 1.5 \times 10^{-4}$	90		[91] DATAR	88	CNTR	$^{12}C^* \to {}^{12}CA^0$, $A^0 \to e^+e^-$
$< 5 \times 10^{-3}$	90		[92] DEBOER	88C	CNTR	$^{16}O^* \to {}^{16}OX^0$, $X^0 \to e^+e^-$
$< 3.4 \times 10^{-5}$	95		[93] DOEHNER	88	SPEC	^{2}H*, $A^0 \to e^+e^-$
$< 4 \times 10^{-4}$	95		[94] SAVAGE	88	CNTR	Nuclear decay (isovector)
$< 3 \times 10^{-3}$	95		[94] SAVAGE	88	CNTR	Nuclear decay (isoscalar)
< 0.106	90		[95] HALLIN	86	SPEC	^{6}Li isovector decay
< 10.8	90		[95] HALLIN	86	SPEC	^{10}B isoscalar decays
< 2.2	90		[95] HALLIN	86	SPEC	^{14}N isoscalar decays
$< 4 \times 10^{-4}$	90	0	[96] SAVAGE	86B	CNTR	^{14}N*
			[97] ANANEV	85	CNTR	Li*, deut* $A^0 \to 2\gamma$
			[98] CAVAIGNAC	83	CNTR	^{97}Nb*, deut* transition $A^0 \to 2\gamma$
			[99] ALEKSEEV	82B	CNTR	Li*, deut* transition $A^0 \to 2\gamma$
			[100] LEHMANN	82	CNTR	Cu* $\to$ CuA^0 ($A^0 \to 2\gamma$)
		0	[101] ZEHNDER	82	CNTR	Li*, Nb* decay, n-capt.
		0	[102] ZEHNDER	81	CNTR	Ba* $\to$ BaA^0 ($A^0 \to 2\gamma$)
			[103] CALAPRICE	79		Carbon

[82] DERBIN 02 looked for the axion emission in an M1 transition in ^{125m}Te decay. They looked for a possible presence of a shifted energy spectrum in gamma rays due to the undetected axion.

[83] DEBOER 97C reanalyzed the existent data on Nuclear M1 transitions and find that a 9 MeV boson decaying into e^+e^- would explain the excess of events with large opening angles. See also DEBOER 01 for follow-up experiments.

[84] TSUNODA 95 looked for axion emission when ^{252}Cf undergoes a spontaneous fission, with the axion decaying into e^+e^-. The bound is for m_{A^0}=40 MeV. It improves to 2.5×10^{-5} for m_{A^0}=200 MeV.

[85] MINOWA 93 studied chain process, ^{139}Ce $\to$ ^{139}La* by electron capture and M1 transition of ^{139}La* to the ground state. It does not assume decay modes of A^0. The bound applies for $m_{A^0} < 166$ keV.

[86] HICKS 92 bound is applicable for $\tau_{X^0} < 4 \times 10^{-11}$ sec.

[87] The ASANUMA 90 limit is for the branching fraction of X^0 emission per ^{241}Am α decay and valid for $\tau_{X^0} < 3 \times 10^{-11}$ s.

[88] The DEBOER 90 limit is for the branching ratio ^{8}Be* (18.15 MeV, 1^+) $\to$ ^{8}BeA^0, $A^0 \to e^+e^-$ for the mass range $m_{A^0} = 4$–15 MeV.

[89] The BINI 89 limit is for the branching fraction of $^{16}O^*(6.05\ MeV, 0^+) \to {}^{16}O X^0$, $X^0 \to e^+e^-$ for $m_X = 1.5$–3.1 MeV. $\tau_{X^0} \lesssim 10^{-11}$ s is assumed. The spin-parity of X is restricted to 0^+ or 1^-.

[90] AVIGNONE 88 looked for the 1115 keV transition $C^* \to C u A^0$, either from $A^0 \to 2\gamma$ in-flight decay or from the secondary A^0 interactions by Compton and by Primakoff processes. Limits for axion parameters are obtained for $m_{A^0} < 1.1$ MeV.

[91] DATAR 88 rule out light pseudoscalar particle emission through its decay $A^0 \to e^+e^-$ in the mass range 1.02–2.5 MeV and lifetime range 10^{-13}–10^{-8} s. The above limit is for $\tau = 5 \times 10^{-13}$ s and $m = 1.7$ MeV; see the paper for the τ-m dependence of the limit.

[92] The limit is for the branching fraction of $^{16}O^*(6.05\ MeV, 0^+) \to {}^{16}O X^0$, $X^0 \to e^+e^-$ against internal pair conversion for $m_{X^0} = 1.7$ MeV and $\tau_{X^0} < 10^{-11}$ s. Similar limits are obtained for $m_{X^0} = 1.3$–3.2 MeV. The spin parity of X^0 must be either 0^+ or 1^-. The limit at 1.7 MeV is translated into a limit for the X^0-nucleon coupling constant: $g^2_{X^0NN}/4\pi < 2.3 \times 10^{-9}$.

[93] The DOEHNER 88 limit is for $m_{A^0} = 1.7$ MeV, $\tau(A^0) < 10^{-10}$ s. Limits less than 10^{-4} are obtained for $m_{A^0} = 1.2$–2.2 MeV.

[94] SAVAGE 88 looked for A^0 that decays into e^+e^- in the decay of the 9.17 MeV $J^P = 2^+$ state in ^{14}N, 17.64 MeV state $J^P = 1^+$ in ^8Be, and the 18.15 MeV state $J^P = 1^+$ in ^8Be. This experiment constrains the isovector coupling of A^0 to hadrons, if $m_{A^0} = (1.1 \to 2.2)$ MeV and the isoscalar coupling of A^0 to hadrons, if $m_{A^0} = (1.1 \to 2.6)$ MeV. Both limits are valid only if $\tau(A^0) \lesssim 1 \times 10^{-11}$ s.

[95] Limits are for $\Gamma(A^0(1.8\ MeV))/\Gamma(\pi M1)$; i.e., for 1.8 MeV axion emission normalized to the rate for internal emission of e^+e^- pairs. Valid for $\tau_{A^0} < 2 \times 10^{-11}$s. ^6Li isovector decay data strongly disfavor PECCEI 86 model I, whereas the ^{10}B and ^{14}N isoscalar decay data strongly reject PECCEI 86 model II and III.

[96] SAVAGE 86B looked for A^0 that decays into e^+e^- in the decay of the 9.17 MeV $J^P = 2^+$ state in ^{14}N. Limit on the branching fraction is valid if $\tau_{A^0} \lesssim 1. \times 10^{-11}$s for $m_{A^0} = (1.1$–$1.7)$ MeV. This experiment constrains the iso-vector coupling of A^0 to hadrons.

[97] ANANEV 85 with IBR-2 pulsed reactor exclude standard A^0 at CL = 95% masses below 470 keV (Li* decay) and below $2m_e$ for deuteron* decay.

[98] CAVAIGNAC 83 at Bugey reactor exclude axion at any $m_{^{97}Nb^*decay}$ and axion with m_{A^0} between 275 and 288 keV (deuteron* decay).

[99] ALEKSEEV 82 with IBR-2 pulsed reactor exclude standard A^0 at CL = 95% mass-ranges $m_{A^0} < 400$ keV (Li* decay) and 330 keV $< m_{A^0} < 2.2$ MeV. (deuteron* decay).

[100] LEHMANN 82 obtained $A^0 \to 2\gamma$ rate $< 6.2 \times 10^{-5}$/s (CL = 95%) excluding m_{A^0} between 100 and 1000 keV.

[101] ZEHNDER 82 used Goesgen 2.8GW light-water reactor to check A^0 production. No 2γ peak in Li*, Nb* decay (both single p transition) nor in n capture (combined with previous Ba* negative result) rules out standard A^0. Set limit $m_{A^0} < 60$ keV for any A^0.

[102] ZEHNDER 81 looked for $Ba^* \to A^0 Ba$ transition with $A^0 \to 2\gamma$. Obtained 2γ coincidence rate $< 2.2 \times 10^{-5}$/s (CL = 95%) excluding $m_{A^0} > 160$ keV (or 200 keV depending on Higgs mixing). However, see BARROSO 81.

[103] CALAPRICE 79 saw no axion emission from excited states of carbon. Sensitive to axion mass between 1 and 15 MeV.

A^0 (Axion) Limits from Its Electron Coupling

Limits are for $\tau(A^0 \to e^+e^-)$.

VALUE (s)	CL%	DOCUMENT ID		TECN	COMMENT
• • • We do not use the following data for averages, fits, limits, etc. • • •					
none 4×10^{-16}–4.5×10^{-12}	90	[104] BROSS	91	BDMP	$eN \to eA^0N$ ($A^0 \to ee$)
		[105] GUO	90	BDMP	$eN \to eA^0N$ ($A^0 \to ee$)
		[106] BJORKEN	88	CALO	$A \to e^+e^-$ or 2γ
		[107] BLINOV	88	MD1	$ee \to eeA^0$ ($A^0 \to ee$)
none 1×10^{-14}–1×10^{-10}	90	[108] RIORDAN	87	BDMP	$eN \to eA^0N$ ($A^0 \to ee$)
none 1×10^{-14}–1×10^{-11}	90	[109] BROWN	86	BDMP	$eN \to eA^0N$ ($A^0 \to ee$)
none 6×10^{-14}–9×10^{-11}	95	[110] DAVIER	86	BDMP	$eN \to eA^0N$ ($A^0 \to ee$)
none 3×10^{-13}–1×10^{-7}	90	[111] KONAKA	86	BDMP	$eN \to eA^0N$ ($A^0 \to ee$)

[104] The listed BROSS 91 limit is for $m_{A^0} = 1.14$ MeV. $B(A^0 \to e^+e^-) = 1$ assumed. Excluded domain in the τ_{A^0}–m_{A^0} plane extends up to $m_{A^0} \approx 7$ MeV (see Fig. 5). Combining with electron $g-2$ constraint, axions coupling only to e^+e^- ruled out for $m_{A^0} < 4.8$ MeV (90%CL).

[105] GUO 90 use the same apparatus as BROWN 86 and improve the previous limit in the shorter lifetime region. Combined with $g-2$ constraint, axions coupling only to e^+e^- are ruled out for $m_{A^0} < 2.7$ MeV (90% CL).

[106] BJORKEN 88 reports limits on axion parameters (f_A, m_A, τ_A) for $m_{A^0} < 200$ MeV from electron beam-dump experiment with production via Primakoff photoproduction, bremsstrahlung from electrons, and resonant annihilation of positrons on atomic electrons.

[107] BLINOV 88 assume zero spin, $m = 1.8$ MeV and lifetime $< 5 \times 10^{-12}$ s and find $\Gamma(A^0 \to \gamma\gamma)B(A^0 \to e^+e^-) < 2$ eV (CL=90%).

[108] Assumes $A^0\gamma\gamma$ coupling is small and hence Primakoff production is small. Their figure 2 shows limits on axions for $m_{A^0} < 15$ MeV.

[109] Uses electrons in hadronic showers from an incident 800 GeV proton beam. Limits for $m_{A^0} < 15$ MeV are shown in their figure 3.

[110] $m_{A^0} = 1.8$ MeV assumed. The excluded domain in the τ_{A^0}–m_{A^0} plane extends up to $m_{A^0} \approx 14$ MeV, see their figure 4.

[111] The limits are obtained from their figure 3. Also given is the limit on the $A^0\gamma\gamma$–$A^0e^+e^-$ coupling plane by assuming Primakoff production.

Search for A^0 (Axion) Resonance in Bhabha Scattering

The limit is for $\Gamma(A^0)[B(A^0 \to e^+e^-)]^2$.

VALUE (10^{-3} eV)	CL%	DOCUMENT ID		TECN	COMMENT
• • • We do not use the following data for averages, fits, limits, etc. • • •					
< 1.3	97	[112] HALLIN	92	CNTR	$m_{A^0} = 1.75$–1.88 MeV
none 0.0016–0.47	90	[113] HENDERSON	92C	CNTR	$m_{A^0} = 1.5$–1.86 MeV
< 2.0	90	[114] WU	92	CNTR	$m_{A^0} = 1.56$–1.86 MeV
< 0.013	95	TSERTOS	91	CNTR	$m_{A^0} = 1.832$ MeV
none 0.19–3.3	95	[115] WIDMANN	91	CNTR	$m_{A^0} = 1.78$–1.92 MeV
< 5	97	BAUER	90	CNTR	$m_{A^0} = 1.832$ MeV
none 0.09–1.5	95	[116] JUDGE	90	CNTR	$m_{A^0} = 1.832$ MeV, elastic
< 1.9	97	[117] TSERTOS	89	CNTR	$m_{A^0} = 1.82$ MeV
< (10–40)	97	[117] TSERTOS	89	CNTR	$m_{A^0} = 1.51$–1.65 MeV
< (1–2.5)	97	[117] TSERTOS	89	CNTR	$m_{A^0} = 1.80$–1.86 MeV
< 31	95	LORENZ	88	CNTR	$m_{A^0} = 1.646$ MeV
< 94	95	LORENZ	88	CNTR	$m_{A^0} = 1.726$ MeV
< 23	95	LORENZ	88	CNTR	$m_{A^0} = 1.782$ MeV
< 19	95	LORENZ	88	CNTR	$m_{A^0} = 1.837$ MeV
< 3.8	97	[118] TSERTOS	88	CNTR	$m_{A^0} = 1.832$ MeV
		[119] VANKLINKEN	88	CNTR	
		[120] MAIER	87	CNTR	
< 2500	90	MILLS	87	CNTR	$m_{A^0} = 1.8$ MeV
		[121] VONWIMMER..	87	CNTR	

[112] HALLIN 92 quote limits on lifetime, $8 \times 10^{-14} - 5 \times 10^{-13}$ sec depending on mass, assuming $B(A^0 \to e^+e^-) = 100\%$. They say that TSERTOS 91 overstated their sensitivity by a factor of 3.

[113] HENDERSON 92C exclude axion with lifetime $\tau_{A^0} = 1.4 \times 10^{-12} - 4.0 \times 10^{-10}$ s, assuming $B(A^0 \to e^+e^-) = 100\%$. HENDERSON 92C also exclude a vector boson with $\tau = 1.4 \times 10^{-12} - 6.0 \times 10^{-10}$ s.

[114] WU 92 quote limits on lifetime $> 3.3 \times 10^{-13}$ s assuming $B(A^0 \to e^+e^-) = 100\%$. They say that TSERTOS 89 overestimate the limit by a factor of $\pi/2$. WU 92 also quote a bound for vector boson, $\tau > 8.2 \times 10^{-13}$ s.

[115] WIDMANN 91 bound applies exclusively to the case $B(A^0 \to e^+e^-) = 1$, since the detection efficiency varies substantially as $\Gamma(A^0)_{total}$ changes. See their Fig. 6.

[116] JUDGE 90 excludes an elastic pseudoscalar e^+e^- resonance for 4.5×10^{-13} s $< \tau(A^0) < 7.5 \times 10^{-12}$ s (95% CL) at $m_{A^0} = 1.832$ MeV. Comparable limits can be set for $m_{A^0} = 1.776$–1.856 MeV.

[117] See also TSERTOS 88B in references.

[118] The upper limit listed in TSERTOS 88 is too large by a factor of 4. See TSERTOS 88B, footnote 3.

[119] VANKLINKEN 88 looked for relatively long-lived resonance ($\tau = 10^{-10}$–10^{-12} s). The sensitivity is not sufficient to exclude such a narrow resonance.

[120] MAIER 87 obtained limits $R\Gamma \lesssim 60$ eV (100 eV) at $m_{A^0} \simeq 1.64$ MeV (1.83 MeV) for energy resolution $\Delta E_{cm} \simeq 3$ keV, where R is the resonance cross section normalized to that of Bhabha scattering, and $\Gamma = \Gamma^2_{ee}/\Gamma_{total}$. For a discussion implying that $\Delta E_{cm} \simeq 10$ keV, see TSERTOS 89.

[121] VONWIMMERSPERG 87 measured Bhabha scattering for $E_{cm} = 1.37$–1.86 MeV and found a possible peak at 1.73 with $\int \sigma dE_{cm} = 14.5 \pm 6.8$ keV·b. For a comment and a reply, see VANKLINKEN 88B and VONWIMMERSPERG 88. Also see CONNELL 88.

Search for A^0 (Axion) Resonance in $e^+e^- \to \gamma\gamma$

The limit is for $\Gamma(A^0 \to e^+e^-)\cdot\Gamma(A^0 \to \gamma\gamma)/\Gamma_{total}$

VALUE (10^{-3} eV)	CL%	DOCUMENT ID		TECN	COMMENT
• • • We do not use the following data for averages, fits, limits, etc. • • •					
< 0.18	95	VO	94	CNTR	m_{A^0}=1.1 MeV
< 1.5	95	VO	94	CNTR	m_{A^0}=1.4 MeV
<12	95	VO	94	CNTR	m_{A^0}=1.7 MeV
< 6.6	95	[122] TRZASKA	91	CNTR	$m_{A^0} = 1.8$ MeV
< 4.4	95	WIDMANN	91	CNTR	$m_{A^0} = 1.78$–1.92 MeV
		[123] FOX	89	CNTR	
< 0.11	95	[124] MINOWA	89	CNTR	$m_{A^0} = 1.062$ MeV
<33	97	CONNELL	88	CNTR	$m_{A^0} = 1.580$ MeV
<42	97	CONNELL	88	CNTR	$m_{A^0} = 1.642$ MeV
<73	97	CONNELL	88	CNTR	$m_{A^0} = 1.782$ MeV
<79	97	CONNELL	88	CNTR	$m_{A^0} = 1.832$ MeV

[122] TRZASKA 91 also give limits in the range (6.6–30) $\times 10^{-3}$ eV (95%CL) for m_{A^0} = 1.6–2.0 MeV.

[123] FOX 89 measured positron annihilation with an electron in the source material into two photons and found no signal at 1.062 MeV ($< 9\times10^{-5}$ of two-photon annihilation at rest).

[124] Similar limits are obtained for m_{A^0} = 1.045–1.085 MeV.

Search for X^0 (Light Boson) Resonance in $e^+e^- \to \gamma\gamma\gamma$

The limit is for $\Gamma(X^0 \to e^+e^-)\cdot\Gamma(X^0 \to \gamma\gamma\gamma)/\Gamma_{\rm total}$. C invariance forbids spin-0 X^0 coupling to both e^+e^- and $\gamma\gamma\gamma$.

VALUE (10^{-3} eV)	CL%	DOCUMENT ID		TECN	COMMENT
• • • We do not use the following data for averages, fits, limits, etc. • • •					
< 0.2	95	[125] VO	94	CNTR	m_{X^0}=1.1–1.9 MeV
< 1.0	95	[126] VO	94	CNTR	m_{X^0}=1.1 MeV
< 2.5	95	[126] VO	94	CNTR	m_{X^0}=1.4 MeV
<120	95	[126] VO	94	CNTR	m_{X^0}=1.7 MeV
< 3.8	95	[127] SKALSEY	92	CNTR	m_{X^0}= 1.5 MeV

[125] VO 94 looked for $X^0 \to \gamma\gamma\gamma$ decaying at rest. The precise limits depend on m_{X^0}. See Fig. 2(b) in paper.

[126] VO 94 looked for $X^0 \to \gamma\gamma\gamma$ decaying in flight.

[127] SKALSEY 92 also give limits 4.3 for m_{X^0} = 1.54 and 7.5 for 1.64 MeV. The spin of X^0 is assumed to be one.

Light Boson (X^0) Search in Nonresonant e^+e^- Annihilation at Rest

Limits are for the ratio of $n\gamma + X^0$ production relative to $\gamma\gamma$.

VALUE (units 10^{-6})	CL%	DOCUMENT ID		TECN	COMMENT
• • • We do not use the following data for averages, fits, limits, etc. • • •					
< 4.2	90	[128] MITSUI	96	CNTR	γX^0
< 4	68	[129] SKALSEY	95	CNTR	γX^0
<40	68	[130] SKALSEY	95	RVUE	γX^0
< 0.18	90	[131] ADACHI	94	CNTR	$\gamma\gamma X^0$, $X^0 \to \gamma\gamma$
< 0.26	90	[132] ADACHI	94	CNTR	$\gamma\gamma X^0$, $X^0 \to \gamma\gamma$
< 0.33	90	[133] ADACHI	94	CNTR	γX^0, $X^0 \to \gamma\gamma\gamma$

[128] MITSUI 96 looked for a monochromatic γ. The bound applies for a vector X^0 with $C=-1$ and m_{X^0} <200 keV. They derive an upper bound on $ee X^0$ coupling and hence on the branching ratio B(o-Ps $\to \gamma\gamma X^0$)< 6.2×10^{-6}. The bounds weaken for heavier X^0.

[129] SKALSEY 95 looked for a monochromatic γ without an accompanying γ in e^+e^- annihilation. The bound applies for scalar and vector X^0 with $C=-1$ and m_{X^0} = 100–1000 keV.

[130] SKALSEY 95 reinterpreted the bound on γA^0 decay of o-Ps by ASAI 91 where 3% of delayed annihilations are not from $^3S_1$ states. The bound applies for scalar and vector X^0 with $C=-1$ and m_{X^0} = 0–800 keV.

[131] ADACHI 94 looked for a peak in the $\gamma\gamma$ invariant mass distribution in $\gamma\gamma\gamma\gamma$ production from e^+e^- annihilation. The bound applies for m_{X^0} = 70–800 keV.

[132] ADACHI 94 looked for a peak in the missing-mass mass distribution in $\gamma\gamma$ channel, using $\gamma\gamma\gamma\gamma$ production from e^+e^- annihilation. The bound applies for m_{X^0} <800 keV.

[133] ADACHI 94 looked for a peak in the missing mass distribution in $\gamma\gamma\gamma$ channel, using $\gamma\gamma\gamma\gamma$ production from e^+e^- annihilation. The bound applies for m_{X^0} = 200–900 keV.

Searches for Goldstone Bosons (X^0)

(Including Horizontal Bosons and Majorons.) Limits are for branching ratios.

VALUE	CL%	EVTS	DOCUMENT ID		TECN	COMMENT
• • • We do not use the following data for averages, fits, limits, etc. • • •						
			[134] DIAZ	98	THEO	$H^0 \to X^0X^0$, $A^0 \to X^0X^0X^0$, Majoron
			[135] BOBRAKOV	91		Electron quasi-magnetic interaction
$<3.3\times10^{-2}$	95		[136] ALBRECHT	90E	ARG	$\tau \to \mu X^0$. Familon
$<1.8\times10^{-2}$	95		[136] ALBRECHT	90E	ARG	$\tau \to e X^0$. Familon
$<6.4\times10^{-9}$	90		[137] ATIYA	90	B787	$K^+ \to \pi^+ X^0$. Familon
$<1.1\times10^{-9}$	90		[138] BOLTON	88	CBOX	$\mu^+ \to e^+\gamma X^0$. Familon
			[139] CHANDA	88	ASTR	Sun, Majoron
			[140] CHOI	88	ASTR	Majoron, SN 1987A
$<5\times10^{-6}$	90		[141] PICCIOTTO	88	CNTR	$\pi \to e\nu X^0$, Majoron
$<1.3\times10^{-9}$	90		[142] GOLDMAN	87	CNTR	$\mu \to e\gamma X^0$. Familon
$<3\times10^{-4}$	90		[143] BRYMAN	86B	RVUE	$\mu \to e X^0$. Familon
$<1.\times10^{-10}$	90	0	[144] EICHLER	86	SPEC	$\mu^+ \to e^+X^0$. Familon
$<2.6\times10^{-6}$	90		[145] JODIDIO	86	SPEC	$\mu^+ \to e^+X^0$. Familon
			[146] BALTRUSAIT...85		MRK3	$\tau \to \ell X^0$. Familon
			[147] DICUS	83	COSM	ν(hvy) $\to \nu$(light)X^0

[134] DIAZ 98 studied models of spontaneously broken lepton number with both singlet and triplet Higgses. They obtain limits on the parameter space from invisible decay $Z \to H^0A^0 \to X^0X^0X^0X^0X^0$ and $e^+e^- \to ZH^0$ with $H^0 \to X^0X^0$.

[135] BOBRAKOV 91 searched for anomalous magnetic interactions between polarized electrons expected from the exchange of a massless pseudoscalar boson (arion). A limit $x_e^2 < 2\times10^{-4}$ (95%CL) is found for the effective anomalous magneton parametrized as $x_e(G_F/8\pi\sqrt{2})^{1/2}$.

[136] ALBRECHT 90E limits are for B($\tau \to \ell X^0$)/B($\tau \to \ell\nu\overline{\nu}$). Valid for $m_{X^0} < 100$ MeV. The limits rise to 7.1% (for μ), 5.0% (for e) for m_{X^0} = 500 MeV.

[137] ATIYA 90 limit is for $m_{X^0} = 0$. The limit B $< 1\times10^{-8}$ holds for $m_{X^0} < 95$ MeV. For the reduction of the limit due to finite lifetime of X^0, see their Fig. 3.

[138] BOLTON 88 limit corresponds to $F > 3.1\times10^9$ GeV, which does not depend on the chirality property of the coupling.

[139] CHANDA 88 find $v_T < 10$ MeV for the weak-triplet Higgs vacuum expectation value in Gelmini-Roncadelli model, and $v_S > 5.8\times10^6$ GeV in the singlet Majoron model.

[140] CHOI 88 used the observed neutrino flux from the supernova SN 1987A to exclude the neutrino Majoron Yukawa coupling h in the range $2\times10^{-5} < h < 3\times10^{-4}$ for the interaction $L_{\rm int} = \frac{1}{2}ih\overline{\psi^c_\nu}\gamma_5\psi_\nu\phi_X$. For several families of neutrinos, the limit applies for $(\Sigma h_i^4)^{1/4}$.

[141] PICCIOTTO 88 limit applies when $m_{X^0} < 55$ MeV and $\tau_{X^0} > 2$ns, and it decreases to 4×10^{-7} at $m_{X^0} = 125$ MeV, beyond which no limit is obtained.

[142] GOLDMAN 87 limit corresponds to $F > 2.9\times10^9$ GeV for the family symmetry breaking scale from the Lagrangian $L_{\rm int} = (1/F)\overline{\psi}_\mu\gamma^\mu(a+b\gamma_5)\psi_e\partial_\mu\phi_{X^0}$ with $a^2+b^2=1$. This is not as sensitive as the limit $F > 9.9\times10^9$ GeV derived from the search for $\mu^+ \to e^+X^0$ by JODIDIO 86, but does not depend on the chirality property of the coupling.

[143] Limits are for $\Gamma(\mu \to eX^0)/\Gamma(\mu \to e\nu\overline{\nu})$. Valid when m_{X^0} = 0–93.4, 98.1–103.5 MeV.

[144] EICHLER 86 looked for $\mu^+ \to e^+X^0$ followed by $X^0 \to e^+e^-$. Limits on the branching fraction depend on the mass and and lifetime of X^0. The quoted limits are valid when $\tau_{X^0} \lesssim 3.\times10^{-10}$ s if the decays are kinematically allowed.

[145] JODIDIO 86 corresponds to $F > 9.9\times10^9$ GeV for the family symmetry breaking scale with the parity-conserving effective Lagrangian $L_{\rm int} = (1/F)\,\overline{\psi}_\mu\gamma^\mu\psi_e\partial^\mu\phi_{X^0}$.

[146] BALTRUSAITIS 85 search for light Goldstone boson(X^0) of broken U(1). CL = 95% limits are B($\tau \to \mu^+X^0$)/B($\tau \to \mu^+\nu\nu$) <0.125 and B($\tau \to e^+X^0$)/B($\tau \to e^+\nu\nu$) <0.04. Inferred limit for the symmetry breaking scale is m >3000 TeV.

[147] The primordial heavy neutrino must decay into ν and familon, f_A, early so that the red-shifted decay products are below critical density, see their table. In addition, $K \to \pi f_A$ and $\mu \to e f_A$ are unseen. Combining these excludes $m_{{\rm heavy}\nu}$ between 5×10^{-5} and 5×10^{-4} MeV (μ decay) and $m_{{\rm heavy}\nu}$ between 5×10^{-5} and 0.1 MeV (K-decay).

Majoron Searches in Neutrinoless Double β Decay

Limits are for the half-life of neutrinoless $\beta\beta$ decay with a Majoron emission.
No experiment currently claims any such evidence. Only the best or comparable limits for each isotope are reported. Also see the reviews ZUBER 98 and FAESSLER 98B.

$t_{1/2}(10^{21}$ yr)	CL%	ISOTOPE	TRANSITION	METHOD		DOCUMENT ID	
>7200	**90**	**^{128}Te**		**CNTR**	[148]	BERNATOW...	92
• • • We do not use the following data for averages, fits, limits, etc. • • •							
> 2.2	90	^{130}Te	$0\nu1\chi$	Cryog. det.	[149]	ARNABOLDI	03
> 0.9	90	^{130}Te	$0\nu2\chi$	Cryog. det.	[150]	ARNABOLDI	03
> 8	90	^{116}Cd	$0\nu1\chi$	$CdWO_4$ scint.	[151]	DANEVICH	03
> 0.8	90	^{116}Cd	$0\nu2\chi$	$CdWO_4$ scint.	[152]	DANEVICH	03
> 500	90	^{136}Xe	$0\nu\chi$	Liquid Xe Scint.	[153]	BERNABEI	02D
> 5.8	90	^{100}Mo	$0\nu\chi$	ELEGANT V	[154]	FUSHIMI	02
> 0.32	90	^{100}Mo	$0\nu\chi$	Liq. Ar ioniz.	[155]	ASHITKOV	01
> 0.0035	90	^{160}Gd	$0\nu\chi$	$^{160}Gd_2SiO_5$:Ce	[156]	DANEVICH	01
> 0.013	90	^{160}Gd	$0\nu2\chi$	$^{160}Gd_2SiO_5$:Ce	[157]	DANEVICH	01
> 2.3	90	^{82}Se	$0\nu\chi$	NEMO 2	[158]	ARNOLD	00
> 0.31	90	^{96}Zr	$0\nu\chi$	NEMO 2	[159]	ARNOLD	00
> 0.63	90	^{82}Se	$0\nu2\chi$	NEMO 2	[160]	ARNOLD	00
> 0.063	90	^{96}Zr	$0\nu2\chi$	NEMO 2	[160]	ARNOLD	00
> 0.16	90	^{100}Mo	$0\nu2\chi$	NEMO 2	[160]	ARNOLD	00
> 2.4	90	^{82}Se	$0\nu\chi$	NEMO 2	[161]	ARNOLD	98
> 7.2	90	^{136}Xe	$0\nu2\chi$	TPC	[162]	LUESCHER	98
> 7.91	90	^{76}Ge		SPEC	[163]	GUENTHER	96
> 17	90	^{76}Ge		CNTR		BECK	93

[148] BERNATOWICZ 92 studied double-β decays of ^{128}Te and ^{130}Te, and found the ratio $\tau(^{130}{\rm Te})/\tau(^{128}{\rm Te}) = (3.52\pm0.11)\times10^{-4}$ in agreement with relatively stable theoretical predictions. The bound is based on the requirement that Majoron-emitting decay cannot be larger than the observed double-beta rate of ^{128}Te of $(7.7\pm0.4)\times10^{24}$ year. We calculated 90% CL limit as $(7.7-1.28\times0.4=7.2)\times10^{24}$.

[149] Supersedes ALESSANDRELLO 00. Array of TeO_2 crystals in high resolution cryogenic calorimeter. Some enriched in ^{130}Te. Derive $\langle g_{\nu\chi}\rangle < 17$–$33\times10^{-5}$ depending on matrix element.

[150] Supersedes ALESSANDRELLO 00. Cryogenic calorimeter search.

[151] Limit for the $0\nu\chi$ decay with Majoron emission of ^{116}Cd using enriched $CdWO_4$ scintillators. $\langle g_{\nu\chi}\rangle < 4.6$–$8.1\times10^{-5}$ depending on the matrix element. Supersedes DANEVICH 00.

[152] Limit for the $0\nu2\chi$ decay of ^{116}Cd. Supersedes DANEVICH 00.

[153] BERNABEI 02D obtain limit for $0\nu\chi$ decay with Majoron emission of ^{136}Xe using liquid Xe scintillation detector. They derive $\langle g_{\nu\chi}\rangle < 2.0$–$3.0\times10^{-5}$ with several nuclear matrix elements.

[154] Replaces TANAKA 93. FUSHIMI 02 derive half-life limit for the $0\nu\chi$ decay by means of tracking calorimeter ELEGANT V. Considering various matrix element calculations, a range of limits for the Majoron-neutrino coupling is given: $\langle g_{\nu\chi}\rangle < (6.3\text{–}360)\times10^{-5}$.

[155] ASHITKOV 01 result for $0\nu\chi$ of ^{100}Mo is less stringent than ARNOLD 00.

[156] DANEVICH 01 obtain limit for the $0\nu\chi$ decay with Majoron emission of ^{160}Gd using Gd_2SiO_5:Ce crystal scintillators.

[157] DANEVICH 01 obtain limit for the $0\nu2\chi$ decay with 2 Majoron emission of ^{160}Gd.

[158] ARNOLD 00 reports limit for the $0\nu\chi$ decay with Majoron emission derived from tracking calorimeter NEMO 2. Using ^{82}Se source: $\langle g_{\nu\chi}\rangle < 1.6\times10^{-4}$. Matrix element from GUENTHER 96.

[159] Using ^{96}Zr source: $\langle g_{\nu\chi}\rangle < 2.6\times10^{-4}$. Matrix element from ARNOLD 99.

[160] ARNOLD 00 reports limit for the $0\nu2\chi$ decay with two Majoron emission derived from tracking calorimeter NEMO 2.

[161] ARNOLD 98 determine the limit for $0\nu\chi$ decay with Majoron emission of ^{82}Se using the NEMO-2 tracking detector. They derive $\langle g_{\nu_x}\rangle < 2.3\text{–}4.3\times10^{-4}$ with several nuclear matrix elements.

[162] LUESCHER 98 report a limit for the 0ν decay with Majoron emission of ^{136}Xe using Xe TPC. This result is more stringent than BARABASH 89. Using the matrix elements of ENGEL 88, they obtain a limit on $\langle g_{\nu\chi}\rangle$ of 2.0×10^{-4}.

[163] See Table 1 in GUENTHER 96 for limits on the Majoron coupling in different models.

Invisible A^0 (Axion) MASS LIMITS from Astrophysics and Cosmology

$v_1 = v_2$ is usually assumed (v_i = vacuum expectation values). For a review of these limits, see RAFFELT 90C and TURNER 90. In the comment lines below, D and K refer to DFSZ and KSVZ axion types, discussed in the above minireview.

VALUE (eV)		DOCUMENT ID		TECN	COMMENT
• • • We do not use the following data for averages, fits, limits, etc. • • •					
3 to 20	[164]	MOROI	98	COSM	K, hot dark matter
< 0.007	[165]	BORISOV	97	ASTR	D, neutron star
< 4	[166]	KACHELRIESS	97	ASTR	D, neutron star cooling
$<(0.5\text{–}6)\times10^{-3}$	[167]	KEIL	97	ASTR	SN 1987A
< 0.018	[168]	RAFFELT	95	ASTR	D, red giant
< 0.010	[169]	ALTHERR	94	ASTR	D, red giants, white dwarfs
	[170]	CHANG	93	ASTR	K, SN 1987A
< 0.01		WANG	92	ASTR	D, white dwarf
< 0.03		WANG	92C	ASTR	D, C-O burning
none 3–8	[171]	BERSHADY	91	ASTR	D, K, intergalactic light
<10	[172]	KIM	91C	COSM	D, K, mass density of the universe, super-symmetry
	[173]	RAFFELT	91B	ASTR	D,K, SN 1987A
$< 1 \times10^{-3}$	[174]	RESSELL	91	ASTR	K, intergalactic light
none 10^{-3}–3		BURROWS	90	ASTR	D,K, SN 1987A
	[175]	ENGEL	90	ASTR	D,K, SN 1987A
< 0.02	[176]	RAFFELT	90D	ASTR	D, red giant
$< 1 \times10^{-3}$	[177]	BURROWS	89	ASTR	D,K, SN 1987A
$<(1.4\text{–}10)\times10^{-3}$	[178]	ERICSON	89	ASTR	D,K, SN 1987A
$< 3.6 \times10^{-4}$	[179]	MAYLE	89	ASTR	D,K, SN 1987A
<12		CHANDA	88	ASTR	D, Sun
$< 1 \times10^{-3}$		RAFFELT	88	ASTR	D,K, SN 1987A
	[180]	RAFFELT	88B	ASTR	red giant
< 0.07		FRIEMAN	87	ASTR	D, red giant
< 0.7	[181]	RAFFELT	87	ASTR	K, red giant
$< 2\text{–}5$		TURNER	87	COSM	K, thermal production
< 0.01	[182]	DEARBORN	86	ASTR	D, red giant
< 0.06		RAFFELT	86	ASTR	D, red giant
< 0.7	[183]	RAFFELT	86	ASTR	K, red giant
< 0.03		RAFFELT	86B	ASTR	D, white dwarf
< 1	[184]	KAPLAN	85	ASTR	K, red giant
$< 0.003\text{–}0.02$		IWAMOTO	84	ASTR	D, K, neutron star
$> 1 \times10^{-5}$		ABBOTT	83	COSM	D,K, mass density of the universe
$> 1 \times10^{-5}$		DINE	83	COSM	D,K, mass density of the universe
< 0.04		ELLIS	83B	ASTR	D, red giant
$> 1 \times10^{-5}$		PRESKILL	83	COSM	D,K, mass density of the universe
< 0.1		BARROSO	82	ASTR	D, red giant
< 1	[185]	FUKUGITA	82	ASTR	D, stellar cooling
< 0.07		FUKUGITA	82B	ASTR	D, red giant

[164] MOROI 98 points out that a KSVZ axion of this mass range (see CHANG 93) can be a viable hot dark matter of Universe, as long as the model-dependent $g_{A\gamma}$ is accidentally small enough as originally emphasized by KAPLAN 85; see Fig. 1.

[165] BORISOV 97 bound is on the axion-electron coupling $g_{ae} < 1\times10^{-13}$ from the photo-production of axions off of magnetic fields in the outer layers of neutron stars.

[166] KACHELRIESS 97 bound is on the axion-electron coupling $g_{ae} < 1\times10^{-10}$ from the production of axions in strongly magnetized neutron stars. The authors also quote a stronger limit, $g_{ae} < 9\times10^{-13}$ which is strongly dependent on the strength of the magnetic field in white dwarfs.

[167] KEIL 97 uses new measurements of the axial-vector coupling strength of nucleons, as well as a reanalysis of many-body effects and pion-emission processes in the core of the neutron star, to update limits on the invisible-axion mass.

[168] RAFFELT 95 reexamined the constraints on axion emission from red giants due to the axion-electron coupling. They improve on DEARBORN 86 by taking into proper account degeneracy effects in the bremsstrahlung rate. The limit comes from requiring the red giant core mass at helium ignition not to exceed its standard value by more than 5% (0.025 solar masses).

[169] ALTHERR 94 bound is on the axion-electron coupling $g_{ae} < 1.5\times10^{-13}$, from energy loss via axion emission.

[170] CHANG 93 updates ENGEL 90 bound with the Kaplan-Manohar ambiguity in $z = m_u/m_d$ (see the Note on the Quark Masses in the Quark Particle Listings). It leaves the window $f_A = 3\times10^5 - 3\times10^6$ GeV open. The constraint from Big-Bang Nucleosynthesis is satisfied in this window as well.

[171] BERSHADY 91 searched for a line at wave length from 3100–8300 Å expected from 2γ decays of relic thermal axions in intergalactic light of three rich clusters of galaxies.

[172] KIM 91C argues that the bound from the mass density of the universe will change drastically for the supersymmetric models due to the entropy production of saxion (scalar component in the axionic chiral multiplet) decay. Note that it is an *upperbound* rather than a lowerbound.

[173] RAFFELT 91B argue that previous SN 1987A bounds must be relaxed due to corrections to nucleon bremsstrahlung processes.

[174] RESSELL 91 uses absence of any intracluster line emission to set limit.

[175] ENGEL 90 rule out $10^{-10} \lesssim g_{AN} \lesssim 10^{-3}$, which for a hadronic axion with EMC motivated axion-nucleon couplings corresponds to 2.5×10^{-3} eV $\lesssim m_{A^0} \lesssim 2.5\times10^4$ eV. The constraint is loose in the middle of the range, i.e. for $g_{AN} \sim 10^{-6}$.

[176] RAFFELT 90D is a re-analysis of DEARBORN 86.

[177] The region $m_{A^0} \gtrsim 2$ eV is also allowed.

[178] ERICSON 89 considered various nuclear corrections to axion emission in a supernova core, and found a reduction of the previous limit (MAYLE 88) by a large factor.

[179] MAYLE 89 limit based on naive quark model couplings of axion to nucleons. Limit based on couplings motivated by EMC measurements is 2–4 times weaker. The limit from axion-electron coupling is weak: see HATSUDA 88B.

[180] RAFFELT 88B derives a limit for the energy generation rate by exotic processes in helium-burning stars $\epsilon < 100$ erg g^{-1} s^{-1}, which gives a firmer basis for the axion limits based on red giant cooling.

[181] RAFFELT 87 also gives a limit $g_{A\gamma} < 1\times10^{-10}$ GeV^{-1}.

[182] DEARBORN 86 also gives a limit $g_{A\gamma} < 1.4\times10^{-11}$ GeV^{-1}.

[183] RAFFELT 86 gives a limit $g_{A\gamma} < 1.1\times10^{-10}$ GeV^{-1} from red giants and $< 2.4\times10^{-9}$ GeV^{-1} from the sun.

[184] KAPLAN 85 says $m_{A^0} < 23$ eV is allowed for a special choice of model parameters.

[185] FUKUGITA 82 gives a limit $g_{A\gamma} < 2.3\times10^{-10}$ GeV^{-1}.

Search for Relic Invisible Axions

Limits are for $[G_{A\gamma\gamma}/m_{A^0}]^2\rho_A$ where $G_{A\gamma\gamma}$ denotes the axion two-photon coupling, $L_{\rm int} = \frac{G_{A\gamma\gamma}}{4}\phi_A F_{\mu\nu}\tilde{F}^{\mu\nu} = G_{A\gamma\gamma}\phi_A \mathbf{E}\cdot\mathbf{B}$, and ρ_A is the axion energy density near the earth.

VALUE	CL%	DOCUMENT ID		TECN	COMMENT
• • • We do not use the following data for averages, fits, limits, etc. • • •					
$<5.5\times10^{-43}$	95	[186] HAGMANN	98	CNTR	$m_{A^0} = 2.9\text{–}3.3\times10^{-6}$ eV
		[187] KIM	98	THEO	
$<2 \times10^{-41}$		[188] HAGMANN	90	CNTR	$m_{A^0} = (5.4\text{–}5.9)10^{-6}$ eV
$<1.3\times10^{-42}$	95	[189] WUENSCH	89	CNTR	$m_{A^0} = (4.5\text{–}10.2)10^{-6}$ eV
$<2 \times10^{-41}$	95	[189] WUENSCH	89	CNTR	$m_{A^0} = (11.3\text{–}16.3)10^{-6}$ eV

[186] Based on the conversion of halo axions to microwave photons. Limit assumes $\rho_A = 0.45$ GeV cm^{-3}. At 90%CL this result excludes a version of KSVZ axions as dark matter in the halo of our Galaxy, for the quoted axion mass range. See ASZTALOS 01 for more details.

[187] KIM 98 calculated the axion-to-photon couplings for various axion models and compared them to the HAGMANN 90 bounds. This analysis demonstrates a strong model dependence of $G_{A\gamma\gamma}$ and hence the bound from relic axion search.

[188] HAGMANN 90 experiment is based on the proposal of SIKIVIE 83.

[189] WUENSCH 89 looks for condensed axions near the earth that could be converted to photons in the presence of an intense electromagnetic field via the Primakoff effect, following the proposal of SIKIVIE 83. The theoretical prediction with $[G_{A\gamma\gamma}/m_{A^0}]^2 = 2\times10^{-14}$ MeV^{-4} (the three generation DFSZ model) and $\rho_A = 300$ MeV/cm^3 that makes up galactic halos gives $(G_{A\gamma\gamma}/m_{A^0})^2\,\rho_A = 4\times10^{-44}$. Note that our definition of $G_{A\gamma\gamma}$ is $(1/4\pi)$ smaller than that of WUENSCH 89.

Invisible A^0 (Axion) Limits from Photon Coupling

Limits are for the axion-two-photon coupling $G_{A\gamma\gamma}$ defined by $L = G_{A\gamma\gamma}\phi_A \mathbf{E}\cdot\mathbf{B}$. Related limits from astrophysics can be found in the "Invisible A^0 (Axion) Mass Limits from Astrophysics and Cosmology" section.

VALUE (GeV^{-1})	CL%	DOCUMENT ID		TECN	COMMENT
• • • We do not use the following data for averages, fits, limits, etc. • • •					
$<1.1 \times10^{-9}$	95	[190] INOUE	02		$m_{A^0} = 0.05\text{–}0.27$ eV
$<2.78\times10^{-9}$	95	[191] MORALES	02B		$m_{A^0} < 1$ keV
$<1.7 \times10^{-9}$	90	[192] BERNABEI	01B		$m_{A^0} < 100$ eV
$<1.5 \times10^{-4}$	90	[193] ASTIER	00B	NOMD	$m_{A^0} < 40$ eV
		[194] MASSO	00	THEO	induced photon coupling
$<2.7 \times10^{-9}$	95	[195] AVIGNONE	98	SLAX	$m_{A^0} < 1$ keV
$<6.0 \times10^{-10}$	95	[196] MORIYAMA	98		$m_{A^0} < 0.03$ eV
$<3.6 \times10^{-7}$	95	[197] CAMERON	93		$m_{A^0} < 10^{-3}$ eV, optical rotation
$<6.7 \times10^{-7}$	95	[198] CAMERON	93		$m_{A^0} < 10^{-3}$ eV, photon regeneration
$<3.6 \times10^{-9}$	99.7	[199] LAZARUS	92		$m_{A^0} < 0.03$ eV
$<7.7 \times10^{-9}$	99.7	[199] LAZARUS	92		$m_{A^0} = 0.03\text{–}0.11$ eV
$<7.7 \times10^{-7}$	99	[200] RUOSO	92		$m_{A^0} < 10^{-3}$ eV
$<2.5 \times10^{-6}$		[201] SEMERTZIDIS	90		$m_{A^0} < 7\times10^{-4}$ eV

[190] INOUE 02 looked for Primakoff conversion of solar axions in 4T superconducting magnet into X ray.

[191] MORALES 02B looked for the coherent conversion of solar axions to photons via the Primakoff effect in Germanium detector.

[192] BERNABEI 01B looked for Primakoff coherent conversion of solar axions into photons via Bragg scattering in NaI crystal in DAMA dark matter detector.

[193] ASTIER 00B looked for production of axions from the interaction of high-energy photons with the horn magnetic field and their subsequent re-conversion to photons via the interaction with the NOMAD dipole magnetic field.

[194] MASSO 00 studied limits on axion-proton coupling using the induced axion-photon coupling through the proton loop and CAMERON 93 bound on the axion-photon coupling using optical rotation. They obtained the bound $g_p^2/4\pi < 1.7\times10^{-9}$ for the coupling $g_p\overline{p}\gamma_5 p\phi_A$.

[195] AVIGNONE 98 result is based on the coherent conversion of solar axions to photons via the Primakoff effect in a single crystal germanium detector.

[196] Based on the conversion of solar axions to X-rays in a strong laboratory magnetic field.

[197] Experiment based on proposal by MAIANI 86.

[198] Experiment based on proposal by VANBIBBER 87.

[199] LAZARUS 92 experiment is based on proposal found in VANBIBBER 89.

[200] RUOSO 92 experiment is based on the proposal by VANBIBBER 87.

[201] SEMERTZIDIS 90 experiment is based on the proposal of MAIANI 86. The limit is obtained by taking the noise amplitude as the upper limit. Limits extend to $m_{A^0} = 4\times10^{-3}$ where $G_{A\gamma\gamma} < 1\times10^{-4}$ GeV^{-1}.

Limit on Invisible A^0 (Axion) Electron Coupling

The limit is for $G_{Aee}\partial_\mu\phi_A\overline{e}\gamma^\mu\gamma_5 e$ in GeV^{-1}, or equivalently, the dipole-dipole potential $\frac{G_{Aee}^2}{4\pi}((\boldsymbol{\sigma}_1\cdot\boldsymbol{\sigma}_2)-3(\boldsymbol{\sigma}_1\cdot\boldsymbol{n})(\boldsymbol{\sigma}_2\cdot\boldsymbol{n}))/r^3$ where $\boldsymbol{n}=\boldsymbol{r}/r$.

The limits below apply to invisible axion of $m_A \le 10^{-6}$ eV.

VALUE (GeV^{-1})	CL%	DOCUMENT ID		TECN	COMMENT
• • • We do not use the following data for averages, fits, limits, etc. • • •					
$<5.3\times10^{-5}$	66	[202] NI	94		Induced magnetism
$<6.7\times10^{-5}$	66	[202] CHUI	93		Induced magnetism
$<3.6\times10^{-4}$	66	[203] PAN	92		Torsion pendulum
$<2.7\times10^{-5}$	95	[202] BOBRAKOV	91		Induced magnetism
$<1.9\times10^{-3}$	66	[204] WINELAND	91	NMR	
$<8.9\times10^{-4}$	66	[203] RITTER	90		Torsion pendulum
$<6.6\times10^{-5}$	95	[202] VOROBYOV	88		Induced magnetism

[202] These experiments measured induced magnetization of a bulk material by the spin-dependent potential generated from other bulk material with aligned electron spins, where the magnetic field is shielded with superconductor.

[203] These experiments used a torsion pendulum to measure the potential between two bulk matter objects where the spins are polarized but without a net magnetic field in either of them.

[204] WINELAND 91 looked for an effect of bulk matter with aligned electron spins on atomic hyperfine splitting using nuclear magnetic resonance.

Invisible A^0 (Axion) Limits from Nucleon Coupling

Limits are for the axion mass in eV.

VALUE (eV)	CL%	DOCUMENT ID		TECN	COMMENT
• • • We do not use the following data for averages, fits, limits, etc. • • •					
$< 3.2\times10^4$	95	[205] KRCMAR	01	CNTR	Solar axion
<745	90	[206] KRCMAR	98	CNTR	Solar axion

[205] KRCMAR 01 looked for solar axions emitted by the M1 transition of ^{7}Li after the electron capture by ^{7}Be and the emission of 384 keV line neutrino, using their resonant capture on ^{7}Li in the laboratory. The mass bound assumes $m_u/m_d = 0.56$ and the flavor-singlet axial-vector matrix element S=0.4.

[206] KRCMAR 98 looked for solar axions emitted by the M1 transition of thermally excited ^{57}Fe nuclei in the Sun, using their possible resonant capture on ^{57}Fe in the laboratory, following MORIYAMA 95B. The mass bound assumes m_u/m_d=0.56 and the flavor-singlet axial-vector matrix element $S=3F-D\simeq 0.5$.

Axion Limits from T-violating Medium-Range Forces

The limit is for the coupling g in a T-violating potential between nucleons or nucleon and electron of the form $V = \frac{g\hbar^2}{8\pi m_p}(\boldsymbol{\sigma}\cdot\hat{\boldsymbol{r}})\left(\frac{1}{r^2}+\frac{m_A c}{\hbar r}\right)e^{-m_A cr/\hbar}$

VALUE	DOCUMENT ID		TECN	COMMENT
• • • We do not use the following data for averages, fits, limits, etc. • • •				
	[207] NI	99		paramagnetic Tb F_3
	[208] POSPELOV	98	THEO	neutron EDM
	[209] YOUDIN	96		
	[210] RITTER	93		torsion pendulum
	[211] VENEMA	92		nuclear spin-precession frequencies
	[212] WINELAND	91	NMR	

[207] NI 99 searched for a T-violating medium-range force acting on paramagnetic Tb F_3 salt. See their Fig. 1 for the result.

[208] POSPELOV 98 studied the possible contribution of T-violating Medium-Range Force to the neutron electric dipole moment, which is possible when axion interactions violate CP. The size of the force among nucleons must be smaller than gravity by a factor of 2×10^{-10} $(1\,\mathrm{cm}/\lambda_A)$, where $\lambda_A=\hbar/m_A c$.

[209] YOUDIN 96 compared the precession frequencies of atomic ^{199}Hg and Cs when a large mass is positioned near the cells, relative to an applied magnetic field. See Fig. 3 for their limits.

[210] RITTER 93 used a torsion pendulum to study the influence of bulk mass with polarized electrons on the pendulum.

[211] VENEMA 92 looked for an effect of Earth's gravity on nuclear spin-precession frequencies of ^{199}Hg and ^{201}Hg atoms.

[212] WINELAND 91 looked for an effect of bulk matter with aligned electron spins on atomic hyperfine resonances in stored ^{9}Be$^+$ ions using nuclear magnetic resonance.

REFERENCES FOR Searches for Axions (A^0) and Other Very Light Bosons

ARNABOLDI	03	PL B557 167	C. Arnaboldi *et al.*	
DANEVICH	03	PR C68 035501	F.A. Danevich *et al.*	
ADLER	02C	PL B537 211	S. Adler *et al.*	(BNL E787 Collab.)
BADERT...	02	PL B542 29	A. Badertscher *et al.*	
BERNABEI	02D	PL B546 23	R. Bernabei *et al.*	(DAMA Collab.)
DERBIN	02	PAN 65 1302	A.V. Derbin *et al.*	
		Translated from YAF 65 1335.		
FUSHIMI	02	PL B531 190	K. Fushimi *et al.*	(ELEGANT V Collab.)
INOUE	02	PL B536 18	Y. Inoue *et al.*	
MORALES	02B	ASP 16 325	A. Morales *et al.*	(COSME Collab.)
AMMAR	01B	PRL 87 271801	R. Ammar *et al.*	(CLEO Collab.)
ASHITKOV	01	JETPL 74 529	V.D. Ashitkov *et al.*	
		Translated from ZETFP 74 601.		
ASZTALOS	01	PR D64 092003	S. Asztalos *et al.*	
BERNABEI	01B	PL B515 6	R. Bernabei *et al.*	(DAMA Collab.)
DANEVICH	01	NP A694 375	F.A. Danevich *et al.*	
DEBOER	01	JPG 27 L29	F.W.N. de Boer *et al.*	
KRCMAR	01	PR D64 115016	M. Krcmar *et al.*	
ADLER	00	PRL 84 3768	S. Adler *et al.*	(BNL E787 Collab.)
ALESSAND...	00	PL B486 13	A. Alessandrello *et al.*	
ARNOLD	00	NP A678 341	R. Arnold *et al.*	
ASTIER	00B	PL B479 371	P. Astier *et al.*	(NOMAD Collab.)
DANEVICH	00	PR C62 045501	F.A. Danevich *et al.*	
MASSO	00	PR D61 011701R	E. Masso	
ARNOLD	99	NP A658 299	R. Arnold *et al.*	(NEMO Collab.)
NI	99	PRL 82 2439	W.-T. Ni *et al.*	
ALTEGOER	98	PL B428 197	J. Altegoer *et al.*	
ARNOLD	98	NP A636 209	R. Arnold *et al.*	(NEMO-2 Collab.)
AVIGNONE	98	PRL 81 5068	F.T. Avignone *et al.*	(Solar Axion Experiment)
DIAZ	98	NP B527 44	M.A. Diaz *et al.*	
FAESSLER	98B	JPG 24 2139	A. Faessler, F. Simkovic	
HAGMANN	98	PRL 80 2043	C. Hagmann *et al.*	
KIM	98	PR D58 055006	J.E. Kim	
KRCMAR	98	PL B442 38	M. Krcmar *et al.*	
LUESCHER	98	PL B434 407	R. Luescher *et al.*	
MORIYAMA	98	PL B434 147	S. Moriyama *et al.*	
MOROI	98	PL B440 69	T. Moroi, H. Murayama	
POSPELOV	98	PR D58 097703	M. Pospelov	
ZUBER	98	PRPL 305 295	K. Zuber	
AHMAD	97	PRL 78 618	I. Ahmad *et al.*	(APEX Collab.)
BORISOV	97	JETP 83 868	A.V. Borisov, V.Y. Grishinia	(MOSU)
DEBOER	97C	JPG 23 L85	F.W.N. de Boer *et al.*	
KACHELRIESS	97	PR D56 1313	M. Kachelriess, C. Wilke, G. Wunner	(BOCH)
KEIL	97	PR D56 2419	W. Keil *et al.*	
KITCHING	97	PRL 79 4079	P. Kitching *et al.*	(BNL E787 Collab.)
LEINBERGER	97	PL B394 16	U. Leinberger *et al.*	(ORANGE Collab.)
ADLER	96	PRL 76 1421	S. Adler *et al.*	(BNL E787 Collab.)
AMSLER	96B	ZPHY C70 219	C. Amsler *et al.*	(Crystal Barrel Collab.)
GANZ	96	PL B389 4	R. Ganz *et al.*	(GSI, HEID, FRAN, JAGL+)
GUENTHER	96	PR D54 3641	M. Gunther *et al.*	(MPIH, SASSO)
KAMEL	96	PL B368 291	S. Kamel	(SHAMS)
MITSUI	96	EPL 33 111	T. Mitsui *et al.*	(TOKY)
YOUDIN	96	PRL 77 2170	A.N. Youdin *et al.*	(AMHT, WASH)
ALTMANN	95	ZPHY C68 221	M. Altmann *et al.*	(MUNT, LAPP, CPPM)
BALEST	95	PR D51 2053	R. Balest *et al.*	(CLEO Collab.)
BASSOMPIE...	95	PL B355 584	G. Bassompierre *et al.*	(LAPP, LCGT, LYON)
MAENO	95	PL B351 574	T. Maeno *et al.*	(TOKY)
MORIYAMA	95B	PRL 75 3222	S. Moriyama	
RAFFELT	95	PR D51 1495	G. Raffelt, A. Weiss	(MPIM, MPIA)
SKALSEY	95	PR D51 6292	M. Skalsey, R.S. Conti	(MICH)
TSUNODA	95	EPL 30 273	T. Tsunoda *et al.*	(TOKY)
ADACHI	94	PR A49 3201	S. Adachi *et al.*	(TMU)
ALTHERR	94	ASP 2 175	T. Altherr, E. Petitgirard, T. del Rio Gaztelurrutia	
AMSLER	94B	PL B333 271	C. Amsler *et al.*	(Crystal Barrel Collab.)
ASAI	94	PL B323 90	S. Asai *et al.*	(TOKY)
MEIJERDREES	94	PR D49 4937	M.R. Drees *et al.*	(BRCO, OREG, TRIU)
NI	94	Physica B194 153	W.T. Ni *et al.*	(NTHU)
VO	94	PR C49 1551	D.T. Vo *et al.*	(ISU, LBL, LLNL, UCD)
ATIYA	93	PRL 70 2521	M.S. Atiya *et al.*	(BNL E787 Collab.)
Also	93C	PRL 71 305 (erratum)	M.S. Atiya *et al.*	(BNL E787 Collab.)
ATIYA	93B	PR D48 R1	M.S. Atiya *et al.*	(BNL E787 Collab.)
BASSOMPIE...	93	EPL 22 239	G. Bassompierre *et al.*	(LAPP, TORI, LYON)
BECK	93	PRL 70 2853	M. Beck *et al.*	(MPIH, KIAE, SASSO)
CAMERON	93	PR D47 3707	R.E. Cameron *et al.*	(ROCH, BNL, FNAL+)
CHANG	93	PL B316 51	S. Chang, K. Choi	
CHUI	93	PRL 71 3247	T.C.P. Chui, W.T. Ni	(NTHU)
MINOWA	93	PRL 71 4120	M. Minowa *et al.*	(TOKY)
NG	93	PR D48 2941	K.W. Ng	(AST)
RITTER	93	PRL 70 701	R.C. Ritter *et al.*	
TANAKA	93	PR D48 5412	J. Tanaka, H. Ejiri	(OSAK)
ALLIEGRO	92	PRL 68 278	C. Allegro *et al.*	(BNL, FNAL, PSI+)
ATIYA	92	PRL 69 733	M.S. Atiya *et al.*	(BNL, LANL, PRIN+)
BERNATOW...	92	PRL 69 2341	T. Bernatowicz *et al.*	(WUSL, TATA)
BLUEMLEIN	92	IJMP A7 3835	J. Blumlein *et al.*	(BERL, BUDA, JINR+)
HALLIN	92	PR D45 3955	A.L. Hallin *et al.*	(PRIN)
HENDERSON	92C	PRL 69 1733	S.D. Henderson *et al.*	(YALE, BNL)
HICKS	92	PL B276 423	K.H. Hicks, D.E. Alburger	(OHIO, BNL)
LAZARUS	92	PRL 69 2333	D.M. Lazarus *et al.*	(BNL, ROCH, FNAL)
MEIJERDREES	92	PRL 68 3845	R. Meijer Drees *et al.*	(SINDRUM I Collab.)
PAN	92	MPL A7 1287	S.S. Pan, W.T. Ni, S.C. Chen	(NTHU)
RUOSO	92	ZPHY C56 505	G. Ruoso *et al.*	(ROCH, BNL, FNAL, TRST)
SKALSEY	92	PRL 68 456	M. Skalsey, J.J. Kolata	(MICH, NDAM)
VENEMA	92	PRL 68 135	B.J. Venema *et al.*	
WANG	92	MPL A7 1497	J. Wang	(ILL)
WANG	92C	PL B291 97	J. Wang	(ILL)
WU	92	PRL 69 1729	X.Y. Wu *et al.*	(BNL, YALE, CUNY)
AKOPYAN	91	PL B272 443	M.V. Akopyan *et al.*	(INRM)
ASAI	91	PRL 66 2440	S. Asai *et al.*	(ICEPP)

Gauge & Higgs Boson Particle Listings

Axions (A^0) and Other Very Light Bosons

BERSHADY 91 PRL 66 1398 M.A. Bershady, M.T. Ressell, M.S. Turner (CHIC+)
BLUEMLEIN 91 ZPHY C51 341 J. Blumlein *et al.* (BERL, BUDA, JINR+)
BOBRAKOV 91 JETPL 53 294 V.F. Bobrakov *et al.* (PNPI)
Translated from ZETFP 53 283.
BROSS 91 PRL 67 2942 A.D. Bross *et al.* (FNAL, ILL)
KIM 91C PRL 67 3465 J.E. Kim (SEOUL)
RAFFELT 91B PRL 67 2605 G. Raffelt, D. Seckel (MPIM, BART)
RESSELL 91 PR D44 3001 M.T. Ressell (CHIC, FNAL)
TRZASKA 91 PL B269 54 W.H. Trzaska *et al.* (TAMU)
TSERTOS 91 PL B266 259 H. Tsertos *et al.* (ILLG, GSI)
WALKER 91 APJ 376 51 T.P. Walker *et al.* (HSCA, OSU, CHIC+)
WIDMANN 91 ZPHY A340 209 E. Widmann *et al.* (STUT, GSI, STUTM)
WINELAND 91 PRL 67 1735 D.J. Wineland *et al.* (NBSB)
ALBRECHT 90E PL B246 278 H. Albrecht *et al.* (ARGUS Collab.)
ANTREASYAN 90C PL B251 204 D. Antreasyan *et al.* (Crystal Ball Collab.)
ASANUMA 90 PL B237 588 T. Asanuma *et al.* (TOKY)
ATIYA 90 PRL 64 21 M.S. Atiya *et al.* (BNL E787 Collab.)
ATIYA 90B PRL 65 1188 M.S. Atiya *et al.* (BNL E787 Collab.)
BAUER 90 NIM B50 300 W. Bauer *et al.* (STUT, VILL, GSI)
BURROWS 90 PR D42 3297 A. Burrows, M.T. Ressell, M.S. Turner (ARIZ+)
DEBOER 90 JPG 16 L1 F.W.N. de Boer, J. Lehmann, J. Steyaert (LOUV)
ENGEL 90 PRL 65 960 J. Engel, D. Seckel, A.C. Hayes (BART, LANL)
GNINENKO 90 PL B237 287 S.N. Gninenko *et al.* (INRM)
GUO 90 PR D41 2924 R. Guo *et al.* (NIU, LANL, FNAL, CASE+)
HAGMANN 90 PR D42 1297 C. Hagmann *et al.* (FLOR)
JUDGE 90 PRL 65 972 S.M. Judge *et al.* (ILLG, GSI)
RAFFELT 90C PRPL 198 1 G.G. Raffelt (MPIM)
RAFFELT 90D PR D41 1324 G.G. Raffelt (MPIM)
RITTER 90 PR D42 977 R.C. Ritter *et al.* (VIRG)
SEMERTZIDIS 90 PRL 64 2988 Y.K. Semertzidis *et al.* (ROCH, BNL, FNAL+)
TSUCHIAKI 90 PL B236 81 M. Tsuchiaki *et al.* (ICEPP)
TURNER 90 PRPL 197 67 M.S. Turner (FNAL)
BARABASH 89 PL B223 273 A.S. Barabash *et al.* (ITEP, INRM)
BINI 89 PL B221 99 M. Bini *et al.* (FIRZ, CERN, AARH)
BURROWS 89 PR D39 1020 A. Burrows, M.S. Turner, R.P. Brinkmann (ARIZ+)
Also 88 PRL 60 1797 M.S. Turner (FNAL, EFI)
DEBOER 89B PRL 62 2639 F.W.N. de Boer, R. van Dantzig (ANIK)
ERICSON 89 PL B219 507 T.E.O. Ericson, J.F. Mathiot (CERN, IPN)
FAISSNER 89 ZPHY C44 557 H. Faissner *et al.* (AACH3, BERL, PSI)
FOX 89 PR C39 288 J.D. Fox *et al.* (FSU)
MAYLE 89 PL B219 515 R. Mayle *et al.* (LLL, CERN, MINN, FNAL+)
Also 88 PL B203 188 R. Mayle *et al.* (LLL, CERN, MINN, FNAL+)
MINOWA 89 PRL 62 1091 H. Minowa *et al.* (ICEPP)
ORITO 89 PRL 63 597 S. Orito *et al.* (ICEPP)
PERKINS 89 PRL 62 2638 D.H. Perkins (OXF)
TSERTOS 89 PR D40 1397 H. Tsertos *et al.* (GSI, ILLG)
VANBIBBER 89 PR D39 2089 K. van Bibber *et al.* (LLL, TAMU, LBL)
WUENSCH 89 PR D40 3153 W.U. Wuensch *et al.* (ROCH, BNL, FNAL)
Also 87 PRL 59 839 S. de Panfilis *et al.* (ROCH, BNL, FNAL)
AVIGNONE 88 PR D37 618 F.T. Avignone *et al.* (PRIN, SCUC, ORNL+)
BJORKEN 88 PR D38 3375 J.D. Bjorken *et al.* (FNAL, SLAC, VPI)
BLINOV 88 SJNP 47 563 A.E. Blinov *et al.* (NOVO)
Translated from YAF 47 889.
BOLTON 88 PR D38 2077 R.D. Bolton *et al.* (LANL, STAN, CHIC+)
Also 86 PRL 56 2461 R.D. Bolton *et al.* (LANL, STAN, CHIC+)
Also 86 PRL 57 3241 D. Grosnick *et al.* (CHIC, LANL, STAN+)
CHANDA 88 PR D37 2714 R. Chanda, J.F. Nieves, P.B. Pal (UMD, UPR+)
CHOI 88 PR D37 3225 K. Choi *et al.* (JHU)
CONNELL 88 PRL 60 2242 S.H. Connell *et al.* (WITW)
DATAR 88 PR C37 250 V.M. Datar *et al.* (IPN)
DEBOER 88 PRL 61 1274 F.W.N. de Boer, R. van Dantzig (ANIK)
Also 89 PRL 62 2644 erratum F.W.N. de Boer, R. van Dantzig (ANIK)
Also 89 PRL 62 2638 D.H. Perkins (OXF)
Also 89B PRL 62 2639 F.W.N. de Boer, R. van Dantzig (ANIK)
DEBOER 88C JPG 14 L131 F.W.N. de Boer *et al.* (LOUV)
DOEHNER 88 PR D38 2722 J. Dohner *et al.* (HEIDP, ANL, ILG)
EL-NADI 88 PRL 61 1271 M. el Nadi, O.E. Badawy (CAIR)
ENGEL 88 PR C37 731 J. Engel, P. Vogel, M.R. Zirnbauer
FAISSNER 88 ZPHY C37 231 H. Faissner *et al.* (AACH3, BERL, SIN)
HATSUDA 88B PL B203 469 T. Hatsuda, M. Yoshimura (KEK)
LORENZ 88 PL B214 10 E. Lorenz *et al.* (MPIM, PSI)
MAYLE 88 PL B203 188 R. Mayle *et al.* (LLL, CERN, MINN, FNAL+)
PICCIOTTO 88 PR D37 1131 C.E. Picciotto *et al.* (TRIU, CNRC)
RAFFELT 88 PRL 60 1793 G. Raffelt, D. Seckel (UCB, LLL, UCSC)
RAFFELT 88B PR D37 549 G.G. Raffelt, D.S.P. Dearborn (UCB, LLL)
SAVAGE 88 PR D37 1134 M.J. Savage, B.W. Filippone, L.W. Mitchell (CIT)
TSERTOS 88 PL B207 273 A. Tsertos *et al.* (GSI, ILLG)
TSERTOS 88B ZPHY A331 103 A. Tsertos *et al.* (GSI, ILLG)
VANKLINKEN 88 PL B205 223 J. van Klinken *et al.* (GRON, GSI)
VANKLINKEN 88B PRL 60 2442 J. van Klinken (GRON)
VONWIMMER...88 PRL 60 2443 U. von Wimmersperg (BNL)
VOROBYOV 88 PL B208 146 P.V. Vorobiev, Y.I. Gitarts (NOVO)
DRUZHININ 87 ZPHY C37 1 V.P. Druzhinin *et al.* (NOVO)
FRIEMAN 87 PR D36 2201 J.A. Frieman, S. Dimopoulos, M.S. Turner (SLAC+)
GOLDMAN 87 PR D36 1543 T. Goldman *et al.* (LANL, CHIC, STAN+)
KORENCHE... 87 SJNP 46 192 S.M. Korenchenko *et al.* (JINR)
Translated from YAF 46 313.
MAIER 87 ZPHY A326 527 K. Maier *et al.* (STUT, GSI)
MILLS 87 PR D36 707 A.P. Mills, J. Levy (BELL)
RAFFELT 87 PR D36 2211 G.G. Raffelt, D.S.P. Dearborn (LLL, UCB)
RIORDAN 87 PRL 59 755 E.M. Riordan *et al.* (ROCH, CIT+)
TURNER 87 PRL 59 2489 M.S. Turner (FNAL, EFI)
VANBIBBER 87 PRL 59 759 K. van Bibber *et al.* (LLL, CIT, MIT+)
VONWIMMER...87 PRL 59 266 U. von Wimmersperg *et al.* (WITW)
ALBRECHT 86D PL B179 403 H. Albrecht *et al.* (ARGUS Collab.)
BADIER 86 ZPHY C31 21 J. Badier *et al.* (NA3 Collab.)
BOWCOCK 86 PRL 56 2676 T.J.V. Bowcock *et al.* (CLEO Collab.)
BROWN 86 PRL 57 2101 C.N. Brown *et al.* (FNAL, WASH, KYOT+)
BRYMAN 86B PRL 57 2787 D.A. Bryman, E.T.H. Clifford (TRIU)
DAVIER 86 PL B180 295 M. Davier, J. Jeanjean, H. Nguyen Ngoc (LALO)
DEARBORN 86 PRL 56 26 D.S.P. Dearborn, D.N. Schramm, G. Steigman (LLL+)
EICHLER 86 PL B175 101 R.A. Eichler *et al.* (SINDRUM Collab.)
HALLIN 86 PRL 57 2105 A.L. Hallin *et al.* (PRIN)
JODIDIO 86 PR D34 1967 A. Jodidio *et al.* (LBL, NWES, TRIU)
Also 88 PR D37 237 erratum A. Jodidio *et al.* (LBL, NWES, TRIU)
KETOV 86 JETPL 44 146 S.N. Ketov *et al.* (KIAE)
Translated from ZETFP 44 114.
KOCH 86 NC 96A 182 H.R. Koch, O.W.B. Schult (JULI)
KONAKA 86 PRL 57 659 A. Konaka *et al.* (KYOT, KEK)
MAGERAS 86 PRL 56 2672 G. Mageras *et al.* (MPIM, COLU, STON)
MAIANI 86 PL B175 359 L. Maiani, R. Petronzio, E. Zavattini (CERN)
PECCEI 86 PL B172 435 R.D. Peccei, T.T. Wu, T. Yanagida (DESY)
RAFFELT 86 PR D33 897 G.G. Raffelt (MPIM)
RAFFELT 86B PL 166B 402 G.G. Raffelt (MPIM)
SAVAGE 86B PRL 57 178 M.J. Savage *et al.* (CIT)
AMALDI 85 PL 153B 444 U. Amaldi *et al.* (CERN)
ANANEV 85 SJNP 41 585 V.D. Ananev *et al.* (JINR)
Translated from YAF 41 912.
BALTRUSAIT...85 PRL 55 1842 R.M. Baltrusaitis *et al.* (Mark III Collab.)
BERGSMA 85 PL 157B 458 F. Bergsma *et al.* (CHARM Collab.)
KAPLAN 85 NP B260 215 D.B. Kaplan (HARV)
IWAMOTO 84 PRL 53 1198 N. Iwamoto (UCSB, WUSL)
YAMAZAKI 84 PRL 52 1089 T. Yamazaki *et al.* (INUS, KEK)
ABBOTT 83 PL 120B 133 L.F. Abbott, P. Sikivie (BRAN, FLOR)
ALAM 83 PR D27 1665 M.S. Alam *et al.* (VAND, CORN, ITHA, HARV+)
CARBONI 83 PL 123B 349 G. Carboni, W. Dahme (CERN, MUNI)
CAVAIGNAC 83 PL 121B 193 J.F. Cavaignac *et al.* (ISNG, LAPP)
DICUS 83 PR D28 1778 D.A. Dicus, V.L. Teplitz (TEXA, UMD)
DINE 83 PL 120B 137 M. Dine, W. Fischler (IAS, PENN)
ELLIS 83B NP B223 252 J. Ellis, K.A. Olive (CERN)
FAISSNER 83 PR D28 1198 H. Faissner *et al.* (AACH)
FAISSNER 83B PR D28 1787 H. Faissner *et al.* (AACH3)
FRANK 83B PR D28 1790 J.S. Frank *et al.* (LANL, YALE, LBL+)
HOFFMAN 83 PR D28 660 C.M. Hoffman *et al.* (LANL, ARZS)
NICZYPORUK 83 ZPHY C17 197 B. Niczyporuk *et al.* (LENA Collab.)
PRESKILL 83 PL 120B 127 J. Preskill, M.B. Wise, F. Wilczek (HARV, UCSBT)
SIKIVIE 83 PRL 51 1415 P. Sikivie (FLOR)
Also 84 PRL 52 695 erratum P. Sikivie (FLOR)
ALEKSEEV 82 JETP 55 591 E.A. Alekseeva *et al.* (KIAE)
Translated from ZETF 82 1007.
ALEKSEEV 82B JETPL 36 116 G.D. Alekseev *et al.* (MOSU, JINR)
Translated from ZETFP 36 94.
ASANO 82 PL 113B 195 Y. Asano *et al.* (KEK, TOKY, INUS, OSAK)
BARROSO 82 PL 116B 247 A. Barroso, G.C. Branco (LISB)
DATAR 82 PL 114B 63 V.M. Datar *et al.* (BHAB)
EDWARDS 82 PRL 48 903 C. Edwards *et al.* (Crystal Ball Collab.)
FETSCHER 82 JPG 8 L147 W. Fetscher (ETH)
FUKUGITA 82 PRL 48 1522 M. Fukugita, S. Watamura, M. Yoshimura (KEK)
FUKUGITA 82B PR D26 1840 M. Fukugita, S. Watamura, M. Yoshimura (KEK)
LEHMANN 82 PL 115B 270 P. Lehmann *et al.* (SACL)
RAFFELT 82 PL 119B 323 G. Raffelt, L. Stodolsky (MPIM)
SIVERTZ 82 PR D26 717 J.M. Sivertz *et al.* (CUSB Collab.)
ZEHNDER 82 PL 110B 419 A. Zehnder, K. Gabathuler, J.L. Vuilleumier (ETH+)
ASANO 81B PL 107B 159 Y. Asano *et al.* (KEK, TOKY, INUS, OSAK)
BARROSO 81 PL 106B 91 A. Barroso, N.C. Mukhopadhyay (SIN)
FAISSNER 81 ZPHY C10 95 H. Faissner *et al.* (AACH3)
FAISSNER 81B PL 103B 234 H. Faissner *et al.* (AACH3)
KIM 81 PL 105B 55 B.R. Kim, C. Stamm (AACH3)
VUILLEUMIER 81 PL 101B 341 J.L. Vuilleumier *et al.* (CIT, MUNI)
ZEHNDER 81 PL 104B 494 A. Zehnder (ETH)
FAISSNER 80 PL 96B 201 H. Faissner *et al.* (AACH3)
JACQUES 80 PR D21 1206 P.F. Jacques *et al.* (RUTG, STEV, COLU)
SOUKAS 80 PRL 44 564 A. Soukas *et al.* (BNL, HARV, ORNL, PENN)
BECHIS 79 PRL 42 1511 D.J. Bechis *et al.* (UMD, COLU, AFRR)
CALAPRICE 79 PR D20 2708 F.P. Calaprice *et al.* (PRIN)
COTEUS 79 PRL 42 1438 P. Coteus *et al.* (COLU, ILL, BNL)
DISHAW 79 PL 85B 142 J.P. Dishaw *et al.* (SLAC, CIT)
ZHITNITSKII 79 SJNP 29 517 A.R. Zhitnitsky, Y.I. Skovpen (NOVO)
Translated from YAF 29 1001.
ALIBRAN 78 PL 74B 134 P. Alibran *et al.* (Gargamelle Collab.)
ASRATYAN 78B PL 79B 497 A.E. Asratyan *et al.* (ITEP, SERP)
BELLOTTI 78 PL 76B 223 E. Bellotti, E. Fiorini, L. Zanotti (MILA)
BOSETTI 78B PL 74B 143 P.C. Bosetti *et al.* (BEBC Collab.)
DICUS 78C PR D18 1829 D.A. Dicus *et al.* (TEXA, VPI, STAN)
DONNELLY 78 PR D18 1607 T.W. Donnelly *et al.* (STAN)
Also 76 PRL 37 315 F. Reines, H.S. Gurr, H.W. Sobel (UCI)
Also 74 PRL 33 179 H.S. Gurr, F. Reines, H.W. Sobel (UCI)
HANSL 78D PL 74B 139 T. Hansl *et al.* (CDHS Collab.)
MICELMAC... 78 LNC 21 441 G.V. Mitselmakher, B. Pontecorvo (JINR)
MIKAELIAN 78 PR D18 3605 K.O. Mikaelian (FNAL, NWES)
SATO 78 PTP 60 1942 K. Sato (KYOT)
VYSOTSKII 78 JETPL 27 502 M.I. Vysotsky *et al.* (ASCI)
Translated from ZETFP 27 533.
YANG 78 PRL 41 523 T.C. Yang (MASA)
PECCEI 77 PR D16 1791 R.D. Peccei, H.R. Quinn (STAN, SLAC)
Also 77B PRL 38 1440 R.D. Peccei, H.R. Quinn (STAN, SLAC)
REINES 76 PRL 37 315 F. Reines, H.S. Gurr, H.W. Sobel (UCI)
GURR 74 PRL 33 179 H.S. Gurr, F. Reines, H.W. Sobel (UCI)
ANAND 53 PRSL A22 183 B.M. Anand

OTHER RELATED PAPERS

SREDNICKI 85 NP B260 689 M. Srednicki (UCSB)
BARDEEN 78 PL 74B 229 W.A. Bardeen, S.-H.H. Tye (FNAL)

LEPTONS

Notes in the Lepton Listings

LEPTONS

e

$J = \frac{1}{2}$

e MASS (atomic mass units u)

The primary determination of an electron's mass comes from measuring the ratio of the mass to that of a nucleus, so that the result is obtained in u (atomic mass units). The conversion factor to MeV is more uncertain than the mass of the electron in u; indeed, the recent improvements in the mass determination are not evident when the result is given in MeV. In this datablock we give the result in u, and the following datablock in MeV.

VALUE (10^{-6} u)		DOCUMENT ID		TECN	COMMENT
548.57990945 ± 0.00000024		MOHR	04	RVUE	2002 CODATA value
• • • We do not use the following data for averages, fits, limits, etc. • • •					
548.5799092 ± 0.0000004	[1]	BEIER	02	CNTR	Penning trap
548.5799110 ± 0.0000012		MOHR	99	RVUE	1998 CODATA value
548.5799111 ± 0.0000012	[2]	FARNHAM	95	CNTR	Penning trap
548.579903 ± 0.000013		COHEN	87	RVUE	1986 CODATA value

[1] BEIER 02 compares Larmor frequency of the electron bound in a $^{12}C^{5+}$ ion with the cyclotron frequency of a single trapped $^{12}C^{5+}$ ion.

[2] FARNHAM 95 compares cyclotron frequency of trapped electrons with that of a single trapped $^{12}C^{6+}$ ion.

e MASS

2002 CODATA gives the conversion factor from u (atomic mass units, see the above datablock) as 931.494 043 (80). Earlier values use the then-current conversion factor. The conversion error dominates the masses given below.

VALUE (MeV)		DOCUMENT ID		TECN	COMMENT
0.510998918 ± 0.000000044		MOHR	04	RVUE	2002 CODATA value
• • • We do not use the following data for averages, fits, limits, etc. • • •					
0.510998901 ± 0.000000020	[3,4]	BEIER	02	CNTR	Penning trap
0.510998902 ± 0.000000021		MOHR	99	RVUE	1998 CODATA value
0.510998903 ± 0.000000020	[3,5]	FARNHAM	95	CNTR	Penning trap
0.510998895 ± 0.000000024	[3]	COHEN	87	RVUE	1986 CODATA value
0.5110034 ± 0.0000014		COHEN	73	RVUE	1973 CODATA value

[3] Converted to MeV using the 1998 CODATA value of the conversion constant, 931.494013 ± 0.0000037 MeV/u.

[4] BEIER 02 compares Larmor frequency of the electron bound in a $^{12}C^{5+}$ ion with the cyclotron frequency of a single trapped $^{12}C^{5+}$ ion.

[5] FARNHAM 95 compares cyclotron frequency of trapped electrons with that of a single trapped $^{12}C^{6+}$ ion.

$(m_{e^+} - m_{e^-}) / m_{average}$

A test of *CPT* invariance.

VALUE	CL%	DOCUMENT ID		TECN	COMMENT
$< 8 \times 10^{-9}$	90	[6] FEE	93	CNTR	Positronium spectroscopy
• • • We do not use the following data for averages, fits, limits, etc. • • •					
$< 4 \times 10^{-8}$	90	CHU	84	CNTR	Positronium spectroscopy

[6] FEE 93 value is obtained under the assumption that the positronium Rydberg constant is exactly half the hydrogen one.

$|q_{e^+} + q_{e^-}|/e$

A test of *CPT* invariance. See also similar tests involving the proton.

VALUE	DOCUMENT ID		TECN	COMMENT
$< 4 \times 10^{-8}$	[7] HUGHES	92	RVUE	
• • • We do not use the following data for averages, fits, limits, etc. • • •				
$< 2 \times 10^{-18}$	[8] SCHAEFER	95	THEO	Vacuum polarization
$< 1 \times 10^{-18}$	[9] MUELLER	92	THEO	Vacuum polarization

[7] HUGHES 92 uses recent measurements of Rydberg-energy and cyclotron-frequency ratios.

[8] SCHAEFER 95 removes model dependency of MUELLER 92.

[9] MUELLER 92 argues that an inequality of the charge magnitudes would, through higher-order vacuum polarization, contribute to the net charge of atoms.

e MAGNETIC MOMENT ANOMALY

$\mu_e/\mu_B - 1 = (g-2)/2$

The CODATA value assumes the $g/2$ values for e^+ and e^- are equal, as required by *CPT*.

VALUE (units 10^{-6})	DOCUMENT ID		TECN	CHG	COMMENT
1159.6521859 ± 0.0000038	MOHR	04	RVUE		2002 CODATA value
• • • We do not use the following data for averages, fits, limits, etc. • • •					
1159.6521869 ± 0.0000041	MOHR	99	RVUE		1998 CODATA value
1159.652193 ± 0.000010	COHEN	87	RVUE		1986 CODATA value
1159.6521884 ± 0.0000043	VANDYCK	87	MRS	−	Single electron
1159.6521879 ± 0.0000043	VANDYCK	87	MRS	+	Single positron

$(g_{e^+} - g_{e^-}) / g_{average}$

A test of *CPT* invariance.

VALUE (units 10^{-12})	CL%	DOCUMENT ID		TECN	COMMENT
− 0.5 ± 2.1		[10] VANDYCK	87	MRS	Penning trap
• • • We do not use the following data for averages, fits, limits, etc. • • •					
< 12	95	[11] VASSERMAN	87	CNTR	Assumes $m_{e^+} = m_{e^-}$
22 ± 64		SCHWINBERG	81	MRS	Penning trap

[10] VANDYCK 87 measured $(g_-/g_+) - 1$ and we converted it.

[11] VASSERMAN 87 measured $(g_+ - g_-)/(g-2)$. We multiplied by $(g-2)/g = 1.2 \times 10^{-3}$.

e ELECTRIC DIPOLE MOMENT

A nonzero value is forbidden by both *T* invariance and *P* invariance.

VALUE (10^{-26} e cm)	CL%	DOCUMENT ID		TECN	COMMENT
0.069 ± 0.074		REGAN	02	MRS	[205]Tl beams
• • • We do not use the following data for averages, fits, limits, etc. • • •					
0.18 ± 0.12 ± 0.10		[12] COMMINS	94	MRS	[205]Tl beams
− 0.27 ± 0.83		[12] ABDULLAH	90	MRS	[205]Tl beams
− 14 ± 24		CHO	89	NMR	Tl F molecules
− 1.5 ± 5.5 ± 1.5		MURTHY	89		Cesium, no *B* field
− 50 ± 110		LAMOREAUX	87	NMR	[199]Hg
190 ± 340	90	SANDARS	75	MRS	Thallium
70 ± 220	90	PLAYER	70	MRS	Xenon
< 300	90	WEISSKOPF	68	MRS	Cesium

[12] ABDULLAH 90, COMMINS 94, and REGAN 02 use the relativistic enhancement of a valence electron's electric dipole moment in a high-Z atom.

e^- MEAN LIFE / BRANCHING FRACTION

A test of charge conservation. See the "Note on Testing Charge Conservation and the Pauli Exclusion Principle" following this section in our 1992 edition (Physical Review **D45,** 1 June, Part II (1992), p. VI.10).

Most of these experiments are one of three kinds: Attempts to observe (a) the 255.5 keV gamma ray produced in $e^- \to \nu_e \gamma$, (b) the (K) shell x ray produced when an electron decays without additional energy deposit, e.g., $e^- \to \nu_e \bar{\nu}_e \nu_e$ ("disappearance" experiments), and (c) nuclear de-excitation gamma rays after the electron disappears from an atomic shell and the nucleus is left in an excited state. The last can include both weak boson and photon mediating processes. We use the best $e^- \to \nu_e \gamma$ limit for the Summary Tables.

Note that we use the mean life rather than the half life, which is often reported.

$e \to \nu_e \gamma$ and astrophysical limits

VALUE (yr)	CL%	DOCUMENT ID		TECN	COMMENT
$> 4.6 \times 10^{26}$	90	BACK	02	BORX	$e^- \to \nu\gamma$
• • • We do not use the following data for averages, fits, limits, etc. • • •					
$> 3.4 \times 10^{26}$	68	BELLI	00B	DAMA	$e^- \to \nu\gamma$, liquid Xe
$> 3.7 \times 10^{25}$	68	AHARONOV	95B	CNTR	$e^- \to \nu\gamma$
$> 2.35 \times 10^{25}$	68	BALYSH	93	CNTR	$e^- \to \nu\gamma$, [76]Ge detector
$> 1.5 \times 10^{25}$	68	AVIGNONE	86	CNTR	$e^- \to \nu\gamma$
$> 1 \times 10^{39}$		[13] ORITO	85	ASTR	Astrophysical argument
$> 3 \times 10^{23}$	68	BELLOTTI	83B	CNTR	$e^- \to \nu\gamma$

[13] ORITO 85 assumes that electromagnetic forces extend out to large enough distances and that the age of our galaxy is 10^{10} years.

Disappearance and nuclear-de-excitation experiments

VALUE (yr)	CL%	DOCUMENT ID		TECN	COMMENT
$> 6.4 \times 10^{24}$	68	[14] BELLI	99B	DAMA	De-excitation of [129]Xe
• • • We do not use the following data for averages, fits, limits, etc. • • •					
$> 4.2 \times 10^{24}$	68	BELLI	99	DAMA	Iodine L-shell disappearance
$> 2.4 \times 10^{23}$	90	[15] BELLI	99D	DAMA	De-excitation of [127]I (in NaI)
$> 4.3 \times 10^{23}$	68	AHARONOV	95B	CNTR	Ge K-shell disappearance
$> 2.7 \times 10^{23}$	68	REUSSER	91	CNTR	Ge K-shell disappearance
$> 2 \times 10^{22}$	68	BELLOTTI	83B	CNTR	Ge K-shell disappearance

[14] BELLI 99B limit on charge nonconserving e^- capture involving excitation of the 236.1 keV nuclear state of ^{129}Xe; the 90% CL limit is 3.7×10^{24} yr. Less stringent limits for other states are also given.

[15] BELLI 99D limit on charge nonconserving e^- capture involving excitation of the 57.6 keV nuclear state of ^{127}I. Less stringent limits for the other states and for the state of ^{23}Na are also given.

e REFERENCES

MOHR	04	RMP (to be publ.)	P.J. Mohr, B.N. Taylor	(NIST)
physics.nist.gov/constants				
BACK	02	PL B525 29	H.O. Back *et al.*	(BOREXINO/SASSO Collab.)
BEIER	02	PRL 88 011603	T. Beier *et al.*	
REGAN	02	PRL 88 071805	B.C. Regan *et al.*	
BELLI	00B	PR D61 117301	P. Belli *et al.*	(DAMA Collab.)
BELLI	99	PL B460 236	P. Belli *et al.*	(DAMA Collab.)
BELLI	99B	PL B465 315	P. Belli *et al.*	(DAMA Collab.)
BELLI	99D	PR C60 065501	P. Belli *et al.*	(DAMA Collab.)
MOHR	99	JPCRD 28 1713	P.J. Mohr, B.N. Taylor	(NIST)
Also	00	RMP 72 351	P.J. Mohr, B.N. Taylor	(NIST)
AHARONOV	95B	PR D52 3785	Y. Aharonov *et al.*	(SCUC, PNL, ZARA+)
Also	95	PL B353 168	Y. Aharonov *et al.*	(SCUC, PNL, ZARA+)
FARNHAM	95	PRL 75 3598	D.L. Farnham, R.S. van Dyck, P.B. Schwinberg	(WASH)
SCHAEFER	95	PR A51 838	A. Schaefer, J. Reinhardt	(FRAN)
COMMINS	94	PR A50 2960	E.D. Commins *et al.*	
BALYSH	93	PL B298 278	A. Balysh *et al.*	(KIAE, MPIH, SASSO)
FEE	93	PR A48 192	M.S. Fee *et al.*	
HUGHES	92	PRL 69 578	R.J. Hughes, B.I. Deutch	(LANL, AARH)
MUELLER	92	PRL 69 3432	B. Muller, M.H. Thoma	(DUKE)
PDG	92	PR D45, 1 June, Part II	K. Hikasa *et al.*	(KEK, LBL, BOST+)
REUSSER	91	PL B255 143	D. Reusser *et al.*	(NEUC, CIT, PSI)
ABDULLAH	90	PRL 65 2347	K. Abdullah *et al.*	(LBL, UCB)
CHO	89	PRL 63 2559	D. Cho, K. Sangster, E.A. Hinds	(YALE)
MURTHY	89	PRL 63 965	S.A. Murthy *et al.*	(AMHT)
COHEN	87	RMP 59 1121	E.R. Cohen, B.N. Taylor	(RISC, NBS)
LAMOREAUX	87	PRL 59 2275	S.K. Lamoreaux *et al.*	(WASH)
VANDYCK	87	PRL 59 26	R.S. van Dyck, P.B. Schwinberg, H.G. Dehmelt	(WASH)
VASSERMAN	87	PL B198 302	I.B. Vasserman *et al.*	(NOVO)
Also	87B	PL B187 172	I.B. Vasserman *et al.*	(NOVO)
AVIGNONE	86	PR D34 97	F.T. Avignone *et al.*	(PNL, SCUC)
ORITO	85	PRL 54 2457	S. Orito, M. Yoshimura	(TOKY, KEK)
CHU	84	PRL 52 1689	S. Chu, A.P. Mills, J.L. Hall	(BELL, NBS, COLO)
BELLOTTI	83B	PL 124B 435	E. Bellotti *et al.*	(MILA)
SCHWINBERG	81	PRL 47 1679	P.B. Schwinberg, R.S. van Dyck, H.G. Dehmelt	(WASH)
SANDARS	75	PR A11 473	P.G.H. Sandars, D.M. Sternheimer	(OXF, BNL)
COHEN	73	JPCRD 2 664	E.R. Cohen, B.N. Taylor	(RISC, NBS)
PLAYER	70	JPB 3 1620	M.A. Player, P.G.H. Sandars	(OXF)
WEISSKOPF	68	PRL 21 1645	M.C. Weisskopf *et al.*	(BRAN)

μ $J = \frac{1}{2}$

μ MASS (atomic mass units u)

The primary determination of a muon's mass comes from measuring the ratio of the mass to that of a nucleus, so that the result is obtained in u (atomic mass units). The conversion factor to MeV is more uncertain than the mass of the muon in u. In this datablock we give the result in u, and in the following datablock in MeV.

VALUE (u)	DOCUMENT ID		TECN	COMMENT
0.1134289264 ± 0.0000000030	MOHR	04	RVUE	2002 CODATA value
• • • We do not use the following data for averages, fits, limits, etc. • • •				
0.1134289168 ± 0.0000000034	[1] MOHR	99	RVUE	1998 CODATA value
0.113428913 ± 0.000000017	[2] COHEN	87	RVUE	1986 CODATA value

[1] MOHR 99 make use of other 1998 CODATA entries below.
[2] COHEN 87 make use of other 1986 CODATA entries below.

μ MASS

2002 CODATA gives the conversion factor from u (atomic mass units, see the above datablock) as 931.494 043 (80). Earlier values use the then-current conversion factor. The conversion error dominates the masses given below.

VALUE (MeV)	DOCUMENT ID		TECN	CHG	COMMENT
105.6583692 ± 0.0000094	MOHR	04	RVUE		2002 CODATA value
• • • We do not use the following data for averages, fits, limits, etc. • • •					
105.6583568 ± 0.0000052	MOHR	99	RVUE		1998 CODATA value
105.658353 ± 0.000016	[3] COHEN	87	RVUE		1986 CODATA value
105.658386 ± 0.000044	[4] MARIAM	82	CNTR	+	
105.65836 ± 0.00026	[5] CROWE	72	CNTR		
105.65865 ± 0.00044	[6] CRANE	71	CNTR		

[3] Converted to MeV using the 1998 CODATA value of the conversion constant, 931.494013 ± 0.0000037 MeV/u.
[4] MARIAM 82 give $m_\mu/m_e = 206.768259(62)$.
[5] CROWE 72 give $m_\mu/m_e = 206.7682(5)$.
[6] CRANE 71 give $m_\mu/m_e = 206.76878(85)$.

μ MEAN LIFE τ

Measurements with an error $> 0.001 \times 10^{-6}$ s have been omitted.

VALUE (10^{-6} s)	DOCUMENT ID		TECN	CHG
2.19703 ± 0.00004 OUR AVERAGE				
2.197078 ± 0.000073	BARDIN	84	CNTR	+
2.197025 ± 0.000155	BARDIN	84	CNTR	−
2.19695 ± 0.00006	GIOVANETTI	84	CNTR	+
2.19711 ± 0.00008	BALANDIN	74	CNTR	+
2.1973 ± 0.0003	DUCLOS	73	CNTR	+

$\tau_{\mu^+}/\tau_{\mu^-}$ MEAN LIFE RATIO

A test of CPT invariance.

VALUE	DOCUMENT ID		TECN	COMMENT
1.000024 ± 0.000078	BARDIN	84	CNTR	
• • • We do not use the following data for averages, fits, limits, etc. • • •				
1.0008 ± 0.0010	BAILEY	79	CNTR	Storage ring
1.000 ± 0.001	MEYER	63	CNTR	Mean life μ^+/μ^-

$(\tau_{\mu^+} - \tau_{\mu^-}) / \tau_{\text{average}}$

A test of CPT invariance. Calculated from the mean-life ratio, above.

VALUE	DOCUMENT ID
(2 ± 8) × 10^{-5} OUR EVALUATION	

μ/p MAGNETIC MOMENT RATIO

This ratio is used to obtain a precise value of the muon mass and to reduce experimental muon Larmor frequency measurements to the muon magnetic moment anomaly. Measurements with an error > 0.00001 have been omitted. By covention, the minus sign on this ratio is omitted. CODATA values were fitted using their selection of data, plus other data from multiparameter fits.

VALUE	DOCUMENT ID		TECN	CHG	COMMENT
3.183345118 ± 0.000000089	MOHR	04	RVUE		2002 CODATA value
• • • We do not use the following data for averages, fits, limits, etc. • • •					
3.18334513 ± 0.00000039	LIU	99	CNTR	+	HFS in muonium
3.18334539 ± 0.00000010	MOHR	99	RVUE		1998 CODATA value
3.18334547 ± 0.00000047	COHEN	87	RVUE		1986 CODATA value
3.1833441 ± 0.0000017	KLEMPT	82	CNTR	+	Precession strob
3.1833461 ± 0.0000011	MARIAM	82	CNTR	+	HFS splitting
3.1833448 ± 0.0000029	CAMANI	78	CNTR	+	See KLEMPT 82
3.1833403 ± 0.0000044	CASPERSON	77	CNTR	+	HFS splitting
3.1833402 ± 0.0000072	COHEN	73	RVUE		1973 CODATA value
3.1833467 ± 0.0000082	CROWE	72	CNTR	+	Precession phase

μ MAGNETIC MOMENT ANOMALY

The parity-violating decay of muons in a storage ring is observed. The difference frequency ω_a between the muon spin precision and the orbital angular frequency $(e/m_\mu c)\langle B \rangle$ is measured, as is the free proton NMR frequency ω_p, thus determining the ratio $R = \omega_a/\omega_p$. Given the magnetic moment ratio $\lambda = \mu_\mu/\mu_p$ (from hyperfine structure in muonium), $(g-2)/2 = R/(\lambda - R)$.

The new precision results from the Brookhaven MUG2 Collaboration have inspired reevaluation of the theoretical value. Most of the problem concerns the hadronic contributions. Examples of the present uncertainty in this changing field are two theoretical values presented by A. Nyffeler in his theory review at a March 2003 Moriond Conference: 11659167.4 ± 7.5 (had) ±4.0 (light-by-light scattering) ±0.35 (QED + EW) using experimental input from e^+e^- around the ρ (CMD-2), and 11659192.6 ± 5.9 ± 4.0 ± 0.35 from precision τ decay studies (ALEPH).

$\mu_\mu/(e\hbar/2m_\mu) - 1 = (g_\mu - 2)/2$

VALUE (units 10^{-10})	DOCUMENT ID		TECN	CHG	COMMENT
11659203 ± 7 OUR AVERAGE					
11659204 ± 7 ± 5	BENNETT	02	MUG2	+	Storage ring
11659202 ± 14 ± 6	BROWN	01	MUG2	+	Storage ring
11659191 ± 59	BROWN	00	MUG2	+	
• • • We do not use the following data for averages, fits, limits, etc. • • •					
11659100 ± 110	[7] BAILEY	79	CNTR	+	Storage ring
11659360 ± 120	[7] BAILEY	79	CNTR	−	Storage ring
11659230 ± 85	[7] BAILEY	79	CNTR	±	Storage ring
11620000 ± 5000	CHARPAK	62	CNTR	+	

[7] BAILEY 79 values recalculated by HUGHES 99 using the COHEN 87 μ/p magnetic moment. The improved MOHR 99 value does not change the result.

$(g_{\mu^+} - g_{\mu^-}) / g_{\text{average}}$

A test of CPT invariance.

VALUE (units 10^{-8})	DOCUMENT ID		
-2.6 ± 1.6	BAILEY	79	

μ ELECTRIC DIPOLE MOMENT

A nonzero value is forbidden by both T invariance and P invariance.

VALUE (10^{-19} ecm)	DOCUMENT ID		TECN	CHG	COMMENT
3.7 ± 3.4	[8] BAILEY	78	CNTR	$\pm$	Storage ring
• • • We do not use the following data for averages, fits, limits, etc. • • •					
8.6 ± 4.5	BAILEY	78	CNTR	+	Storage rings
0.8 ± 4.3	BAILEY	78	CNTR	−	Storage rings

[8] This is the combination of the two BAILEY 78 results given below.

MUON-ELECTRON CHARGE RATIO ANOMALY $q_{\mu^+}/q_{e^-} + 1$

VALUE	DOCUMENT ID		TECN	CHG	COMMENT
$(1.1 \pm 2.1) \times 10^{-9}$	[9] MEYER	00	CNTR	+	1s–2s muonium interval

[9] MEYER 00 measure the 1s–2s muonium interval, and then interpret the result in terms of muon-electron charge ratio q_{μ^+}/q_{e^-}.

μ^- DECAY MODES

μ^+ modes are charge conjugates of the modes below.

	Mode		Fraction (Γ_i/Γ)	Confidence level
Γ_1	$e^- \overline{\nu}_e \nu_\mu$		$\approx 100\%$	
Γ_2	$e^- \overline{\nu}_e \nu_\mu \gamma$	[a]	$(1.4 \pm 0.4)\ \%$	
Γ_3	$e^- \overline{\nu}_e \nu_\mu e^+ e^-$	[b]	$(3.4 \pm 0.4) \times 10^{-5}$	
	Lepton Family number (LF) violating modes			
Γ_4	$e^- \nu_e \overline{\nu}_\mu$	LF [c]	< 1.2 %	90%
Γ_5	$e^- \gamma$	LF	$< 1.2 \times 10^{-11}$	90%
Γ_6	$e^- e^+ e^-$	LF	$< 1.0 \times 10^{-12}$	90%
Γ_7	$e^- 2\gamma$	LF	$< 7.2 \times 10^{-11}$	90%

[a] This only includes events with the γ energy > 10 MeV. Since the $e^- \overline{\nu}_e \nu_\mu$ and $e^- \overline{\nu}_e \nu_\mu \gamma$ modes cannot be clearly separated, we regard the latter mode as a subset of the former.

[b] See the Particle Listings below for the energy limits used in this measurement.

[c] A test of additive vs. multiplicative lepton family number conservation.

μ^- BRANCHING RATIOS

$\Gamma(e^- \overline{\nu}_e \nu_\mu \gamma)/\Gamma_{\text{total}}$ Γ_2/Γ

VALUE	EVTS	DOCUMENT ID		TECN	COMMENT
0.014 ± 0.004		CRITTENDEN	61	CNTR	γ KE > 10 MeV
• • • We do not use the following data for averages, fits, limits, etc. • • •					
	862	BOGART	67	CNTR	γ KE > 14.5 MeV
0.0033 ± 0.0013		CRITTENDEN	61	CNTR	γ KE > 20 MeV
	27	ASHKIN	59	CNTR	

$\Gamma(e^- \overline{\nu}_e \nu_\mu e^+ e^-)/\Gamma_{\text{total}}$ Γ_3/Γ

VALUE (units 10^{-5})	EVTS	DOCUMENT ID		TECN	CHG	COMMENT
$3.4 \pm 0.2 \pm 0.3$	7443	[10] BERTL	85	SPEC	+	SINDRUM
• • • We do not use the following data for averages, fits, limits, etc. • • •						
2.2 ± 1.5	7	[11] CRITTENDEN	61	HLBC	+	$E(e^+ e^-) > 10$ MeV
2	1	[12] GUREVICH	60	EMUL	+	
1.5 ± 1.0	3	[13] LEE	59	HBC	+	

[10] BERTL 85 has transverse momentum cut $p_T > 17$ MeV/c. Systematic error was increased by us.

[11] CRITTENDEN 61 count only those decays where total energy of either (e^+, e^-) combination is >10 MeV.

[12] GUREVICH 60 interpret their event as either virtual or real photon conversion. e^+ and e^- energies not measured.

[13] In the three LEE 59 events, the sum of energies $E(e^+) + E(e^-) + E(e^+)$ was 51 MeV, 55 MeV, and 33 MeV.

$\Gamma(e^- \overline{\nu}_e \overline{\nu}_\mu)/\Gamma_{\text{total}}$ Γ_4/Γ

Forbidden by the additive conservation law for lepton family number. A multiplicative law predicts this branching ratio to be 1/2. For a review see NEMETHY 81.

VALUE	CL%	DOCUMENT ID		TECN	CHG	COMMENT
< 0.012	90	[14] FREEDMAN	93	CNTR	+	ν oscillation search
• • • We do not use the following data for averages, fits, limits, etc. • • •						
< 0.018	90	KRAKAUER	91B	CALO	+	
< 0.05	90	[15] BERGSMA	83	CALO		$\overline{\nu}_\mu e \to \mu^- \overline{\nu}_e$
< 0.09	90	JONKER	80	CALO		See BERGSMA 83
-0.001 ± 0.061		WILLIS	80	CNTR	+	
0.13 ± 0.15		BLIETSCHAU	78	HLBC	$\pm$	Avg. of 4 values
< 0.25	90	EICHTEN	73	HLBC	+	

[14] FREEDMAN 93 limit on $\overline{\nu}_e$ observation is here interpreted as a limit on lepton family number violation.

[15] BERGSMA 83 gives a limit on the inverse muon decay cross-section ratio $\sigma(\overline{\nu}_\mu e^- \to \mu^- \overline{\nu}_e)/\sigma(\nu_\mu e^- \to \mu^- \nu_e)$, which is essentially equivalent to $\Gamma(e^- \nu_e \overline{\nu}_\mu)/\Gamma_{\text{total}}$ for small values like that quoted.

$\Gamma(e^- \gamma)/\Gamma_{\text{total}}$ Γ_5/Γ

Forbidden by lepton family number conservation.

VALUE (units 10^{-11})	CL%	DOCUMENT ID		TECN	CHG	COMMENT
< 1.2	90	BROOKS	99	SPEC	+	LAMPF
• • • We do not use the following data for averages, fits, limits, etc. • • •						
< 1.2	90	AHMED	02	SPEC	+	MEGA
< 4.9	90	BOLTON	88	CBOX	+	LAMPF
<100	90	AZUELOS	83	CNTR	+	TRIUMF
< 17	90	KINNISON	82	SPEC	+	LAMPF
<100	90	SCHAAF	80	ELEC	+	SIN

$\Gamma(e^- e^+ e^-)/\Gamma_{\text{total}}$ Γ_6/Γ

Forbidden by lepton family number conservation.

VALUE (units 10^{-12})	CL%	DOCUMENT ID		TECN	CHG	COMMENT
< 1.0	90	[16] BELLGARDT	88	SPEC	+	SINDRUM
• • • We do not use the following data for averages, fits, limits, etc. • • •						
< 36	90	BARANOV	91	SPEC	+	ARES
< 35	90	BOLTON	88	CBOX	+	LAMPF
< 2.4	90	[16] BERTL	85	SPEC	+	SINDRUM
<160	90	[16] BERTL	84	SPEC	+	SINDRUM
<130	90	[16] BOLTON	84	CNTR		LAMPF

[16] These experiments assume a constant matrix element.

$\Gamma(e^- 2\gamma)/\Gamma_{\text{total}}$ Γ_7/Γ

Forbidden by lepton family number conservation.

VALUE (units 10^{-11})	CL%	DOCUMENT ID		TECN	CHG	COMMENT
< 7.2	90	BOLTON	88	CBOX	+	LAMPF
• • • We do not use the following data for averages, fits, limits, etc. • • •						
< 840	90	[17] AZUELOS	83	CNTR	+	TRIUMF
<5000	90	[18] BOWMAN	78	CNTR		DEPOMMIER 77 data

[17] AZUELOS 83 uses the phase space distribution of BOWMAN 78.

[18] BOWMAN 78 assumes an interaction Lagrangian local on the scale of the inverse μ mass.

LIMIT ON $\mu^- \to e^-$ CONVERSION

Forbidden by lepton family number conservation.

$\sigma(\mu^- {}^{32}\text{S} \to e^- {}^{32}\text{S}) / \sigma(\mu^- {}^{32}\text{S} \to \nu_\mu {}^{32}\text{P}^*)$

VALUE	CL%	DOCUMENT ID		TECN	COMMENT
$< 7 \times 10^{-11}$	90	BADERT...	80	STRC	SIN
• • • We do not use the following data for averages, fits, limits, etc. • • •					
$< 4 \times 10^{-10}$	90	BADERT...	77	STRC	SIN

$\sigma(\mu^- \text{Cu} \to e^- \text{Cu}) / \sigma(\mu^- \text{Cu} \to \text{capture})$

VALUE	CL%	DOCUMENT ID	TECN
• • • We do not use the following data for averages, fits, limits, etc. • • •			
$< 1.6 \times 10^{-8}$	90	BRYMAN	72 SPEC

$\sigma(\mu^- \text{Ti} \to e^- \text{Ti}) / \sigma(\mu^- \text{Ti} \to \text{capture})$

VALUE	CL%	DOCUMENT ID		TECN	COMMENT
$< 4.3 \times 10^{-12}$	90	[19] DOHMEN	93	SPEC	SINDRUM II
• • • We do not use the following data for averages, fits, limits, etc. • • •					
$< 4.6 \times 10^{-12}$	90	AHMAD	88	TPC	TRIUMF
$< 1.6 \times 10^{-11}$	90	BRYMAN	85	TPC	TRIUMF

[19] DOHMEN 93 assumes $\mu^- \to e^-$ conversion leaves the nucleus in its ground state, a process enhanced by coherence and expected to dominate.

$\sigma(\mu^- \text{Pb} \to e^- \text{Pb}) / \sigma(\mu^- \text{Pb} \to \text{capture})$

VALUE	CL%	DOCUMENT ID		TECN	COMMENT
$< 4.6 \times 10^{-11}$	90	HONECKER	96	SPEC	SINDRUM II
• • • We do not use the following data for averages, fits, limits, etc. • • •					
$< 4.9 \times 10^{-10}$	90	AHMAD	88	TPC	TRIUMF

LIMIT ON $\mu^- \to e^+$ CONVERSION

Forbidden by total lepton number conservation.

$\sigma(\mu^- {}^{32}S \to e^+ {}^{32}Si^*) / \sigma(\mu^- {}^{32}S \to \nu_\mu {}^{32}P^*)$

VALUE	CL%	DOCUMENT ID		TECN	COMMENT
<9 $\times 10^{-10}$	90	BADERT...	80	STRC	SIN
• • • We do not use the following data for averages, fits, limits, etc. • • •					
$<1.5 \times 10^{-9}$	90	BADERT...	78	STRC	SIN

$\sigma(\mu^- {}^{127}I \to e^+ {}^{127}Sb^*) / \sigma(\mu^- {}^{127}I \to$ anything)

VALUE	CL%	DOCUMENT ID		TECN	COMMENT
<3 $\times 10^{-10}$	90	[20] ABELA	80	CNTR	Radiochemical tech.

[20] ABELA 80 is upper limit for $\mu^- e^+$ conversion leading to particle-stable states of ^{127}Sb. Limit for total conversion rate is higher by a factor less than 4 (G. Backenstoss, private communication).

$\sigma(\mu^- Cu \to e^+ Co) / \sigma(\mu^- Cu \to \nu_\mu Ni)$

VALUE	CL%	DOCUMENT ID		TECN
• • • We do not use the following data for averages, fits, limits, etc. • • •				
$<2.6 \times 10^{-8}$	90	BRYMAN	72	SPEC
$<2.2 \times 10^{-7}$	90	CONFORTO	62	OSPK

$\sigma(\mu^- Ti \to e^+ Ca) / \sigma(\mu^- Ti \to$ capture)

VALUE	CL%	EVTS	DOCUMENT ID		TECN	CHG	COMMENT
<3.6 $\times 10^{-11}$	90	1	[21,22] KAULARD	98	SPEC	–	SINDRUM II
• • • We do not use the following data for averages, fits, limits, etc. • • •							
$<1.7 \times 10^{-12}$	90	1	[22,23] KAULARD	98	SPEC	–	SINDRUM II
$<4.3 \times 10^{-12}$	90		[23] DOHMEN	93	SPEC		SINDRUM II
$<8.9 \times 10^{-11}$	90		[21] DOHMEN	93	SPEC		SINDRUM II
$<1.7 \times 10^{-10}$	90		[24] AHMAD	88	TPC		TRIUMF

[21] This limit assumes a giant resonance excitation of the daughter Ca nucleus (mean energy and width both 20 MeV).
[22] KAULARD 98 obtained these same limits using the unified classical analysis of FELDMAN 98.
[23] This limit assumes the daughter Ca nucleus is left in the ground state. However, the probability of this is unknown.
[24] Assuming a giant-resonance-excitation model.

LIMIT ON MUONIUM → ANTIMUONIUM CONVERSION

Forbidden by lepton family number conservation.

$R_g = G_C / G_F$

The effective Lagrangian for the $\mu^+ e^- \to \mu^- e^+$ conversion is assumed to be

$$\mathcal{L} = 2^{-1/2}\, G_C\, [\overline{\psi}_\mu \gamma_\lambda\, (1-\gamma_5)\, \psi_e]\, [\overline{\psi}_\mu \gamma_\lambda\, (1-\gamma_5)\, \psi_e] + \text{h.c.}$$

The experimental result is then an upper limit on G_C/G_F, where G_F is the Fermi coupling constant.

VALUE	CL%	EVTS	DOCUMENT ID		TECN	CHG	COMMENT
< 0.0030	90	1	[25] WILLMANN	99	SPEC	+	μ^+ at 26 GeV/c
• • • We do not use the following data for averages, fits, limits, etc. • • •							
< 0.14	90	1	[26] GORDEEV	97	SPEC	+	JINR phasotron
< 0.018	90	0	[27] ABELA	96	SPEC	+	μ^+ at 24 MeV
< 6.9	90		NI	93	CBOX		LAMPF
< 0.16	90		MATTHIAS	91	SPEC		LAMPF
< 0.29	90		HUBER	90B	CNTR		TRIUMF
<20	95		BEER	86	CNTR		TRIUMF
<42	95		MARSHALL	82	CNTR		

[25] WILLMANN 99 quote both probability $P_{M\overline{M}} < 8.3 \times 10^{-11}$ at 90%CL in a 0.1 T field and $R_g = G_C/G_F$.
[26] GORDEEV 97 quote limits on both $f = G_{MM}/GF$ and the probability $W_{MM} < 4.7 \times 10^{-7}$ (90%CL).
[27] ABELA 96 quote both probability $P_{M\overline{M}} < 8 \times 10^{-9}$ at 90% CL and $R_g = G_C/G_F$.

MUON DECAY PARAMETERS

Revised September 2001 by W. Fetscher and H.-J. Gerber (ETH Zürich).

Introduction: All measurements in direct muon decay, $\mu^- \to e^- + 2$ neutrals, and its inverse, $\nu_\mu + e^- \to \mu^-$ + neutral, are successfully described by the "V-A interaction", which is a particular case of a local, derivative-free, lepton-number-conserving, four fermion interaction [1]. As shown below, within this framework, the Standard Model assumptions, such as the V-A form and the nature of the neutrals (ν_μ and $\bar{\nu}_e$), and hence the doublet assignments $(\nu_e\ e^-)_L$ and $(\nu_\mu\ \mu^-)_L$, have been determined from experiments [2,3]. All considerations on muon decay are valid for the leptonic tau decays $\tau \to \ell + \nu_\tau + \bar{\nu}_e$ with the replacements $m_\mu \to m_\tau$, $m_e \to m_\ell$.

Parameters: The differential decay probability to obtain an $e^\pm$ with (reduced) energy between x and $x + dx$, emitted in the direction $\widehat{\boldsymbol{x}}_3$ at an angle between ϑ and $\vartheta + d\vartheta$ with respect to the muon polarization vector $\boldsymbol{P}_\mu$, and with its spin parallel to the arbitrary direction $\widehat{\boldsymbol{\zeta}}$, neglecting radiative corrections, is given by

$$\begin{aligned}\frac{d^2\Gamma}{dx\ d\cos\vartheta} =& \frac{m_\mu}{4\pi^3}\, W_{e\mu}^4\, G_F^2\, \sqrt{x^2 - x_0^2} \\ & \times (F_{\rm IS}(x) \pm P_\mu \cos\vartheta\ F_{\rm AS}(x)) \\ & \times \left[1 + \widehat{\boldsymbol{\zeta}} \cdot \boldsymbol{P}_e(x,\vartheta)\right] \ . \end{aligned} \tag{1}$$

Here, $W_{e\mu} = \max(E_e) = (m_\mu^2 + m_e^2)/2m_\mu$ is the maximum $e^\pm$ energy, $x = E_e/W_{e\mu}$ is the reduced energy, $x_0 = m_e/W_{e\mu} = 9.67 \times 10^{-3}$, and $P_\mu = |\boldsymbol{P}_\mu|$ is the degree of muon polarization. $\widehat{\boldsymbol{\zeta}}$ is the direction in which a perfect polarization-sensitive electron detector is most sensitive. The isotropic part of the spectrum, $F_{\rm IS}(x)$, the anisotropic part $F_{\rm AS}(x)$ and the electron polarization, $\boldsymbol{P}_e(x,\vartheta)$, may be parametrized by the Michel parameters [1,4] ρ, η, ξ, δ, *etc.* These are bilinear combinations of the coupling constants $g_{\epsilon\mu}^\gamma$, which occur in the matrix element (given below).

If the masses of the neutrinos as well as x_0^2 are neglected, the energy and angular distribution of the electron in the rest frame of a muon ($\mu^\pm$) measured by a polarization insensitive detector, is given by

$$\begin{aligned}\frac{d^2\Gamma}{dx\ d\cos\vartheta} \sim x^2 \cdot \Bigg\{ & 3(1-x) + \frac{2\rho}{3}(4x-3) + 3\eta\, x_0(1-x)/x \\ & \pm P_\mu \cdot \xi \cdot \cos\vartheta \left[1 - x + \frac{2\delta}{3}(4x-3)\right] \Bigg\} \ . \end{aligned} \tag{2}$$

Here, ϑ is the angle between the electron momentum and the muon spin, and $x \equiv 2E_e/m_\mu$. For the Standard Model coupling, we obtain $\rho = \xi\delta = 3/4$, $\xi = 1$, $\eta = 0$ and the differential decay rate is

$$\frac{d^2\Gamma}{dx\ d\cos\vartheta} = \frac{G_F^2 m_\mu^5}{192\pi^3}\ [3 - 2x \pm P_\mu \cos\vartheta(2x-1)]\ x^2 \quad . \tag{3}$$

The coefficient in front of the square bracket is the total decay rate.

If only the neutrino masses are neglected, and if the $e^\pm$ polarization is detected, then the functions in Eq. (1) become

$$\begin{aligned} F_{\rm IS}(x) &= x(1-x) + \tfrac{2}{9}\,\rho(4x^2 - 3x - x_0^2) + \eta \cdot x_0(1-x) \\ F_{\rm AS}(x) &= \tfrac{1}{3}\xi\, \sqrt{x^2 - x_0^2} \\ &\quad \times \left[1 - x + \tfrac{2}{3}\delta\Big(4x - 3 + \Big(\sqrt{1 - x_0^2} - 1\Big)\Big)\right] \\ \boldsymbol{P}_e(x,\vartheta) &= P_{\rm T_1} \cdot \widehat{\boldsymbol{x}}_1 + P_{\rm T_2} \cdot \widehat{\boldsymbol{x}}_2 + P_L \cdot \widehat{\boldsymbol{x}}_3 \ . \end{aligned} \tag{4}$$

Here $\widehat{\boldsymbol{x}}_1$, $\widehat{\boldsymbol{x}}_2$, and $\widehat{\boldsymbol{x}}_3$ are orthogonal unit vectors defined as follows:

$$\begin{aligned}
\widehat{\boldsymbol{x}}_3 &\text{ is along the } e \text{ momentum } \boldsymbol{p}_e \\
\frac{\widehat{\boldsymbol{x}}_3 \times \boldsymbol{P}_\mu}{|\widehat{\boldsymbol{x}}_2 \times \boldsymbol{P}_\mu|} = \widehat{\boldsymbol{x}}_2 &\text{ is transverse to } \boldsymbol{p}_e \text{ and perpendicular to the "decay plane"} \\
\widehat{\boldsymbol{x}}_2 \times \widehat{\boldsymbol{x}}_3 = \widehat{\boldsymbol{x}}_1 &\text{ is transverse to the } \boldsymbol{p}_e \text{ and in the "decay plane."}
\end{aligned}$$

The components of $\boldsymbol{P}_e$ then are given by

$$\begin{aligned}
P_{\mathrm{T}_1}(x,\vartheta) &= P_\mu \sin\vartheta \cdot F_{\mathrm{T}_1}(x)/\left(F_{\mathrm{IS}}(x) \pm P_\mu \cos\vartheta \cdot F_{\mathrm{AS}}(x)\right) \\
P_{\mathrm{T}_2}(x,\vartheta) &= P_\mu \sin\vartheta \cdot F_{\mathrm{T}_2}(x)/\left(F_{\mathrm{IS}}(x) \pm P_\mu \cos\vartheta \cdot F_{\mathrm{AS}}(x)\right) \\
P_L(x,\vartheta) &= \Big(\pm F_{\mathrm{IP}}(x) + P_\mu \cos\vartheta \\
&\quad \times F_{\mathrm{AP}}(x)\Big)/\left(F_{\mathrm{IS}}(x) \pm P_\mu \cos\vartheta \cdot F_{\mathrm{AS}}(x)\right) \ ,
\end{aligned}$$

where

$$\begin{aligned}
F_{\mathrm{T}_1}(x) &= \tfrac{1}{12}\Big\{-2\left[\xi'' + 12(\rho - \tfrac{3}{4})\right](1-x)x_0 \\
&\quad -3\eta(x^2 - x_0^2) + \eta''(-3x^2 + 4x - x_0^2)\Big\} \\
F_{\mathrm{T}_2}(x) &= \tfrac{1}{3}\sqrt{x^2 - x_0^2}\Big\{3\frac{\alpha'}{A}(1-x) + 2\frac{\beta'}{A}\sqrt{1-x_0^2}\Big\} \\
F_{\mathrm{IP}}(x) &= \tfrac{1}{54}\sqrt{x^2 - x_0^2}\Big\{9\xi'\left(-2x + 2 + \sqrt{1-x_0^2}\right) \\
&\quad + 4\xi(\delta - \tfrac{3}{4})(4x - 4 + \sqrt{1-x_0^2})\Big\} \\
F_{\mathrm{AP}}(x) &= \tfrac{1}{6}\Big\{\xi''(2x^2 - x - x_0^2) + 4(\rho - \tfrac{3}{4})\left(4x^2 - 3x - x_0^2\right) \\
&\quad + 2\eta''(1-x)x_0\Big\} \ . \qquad (5)
\end{aligned}$$

For the experimental values of the parameters ρ, ξ, ξ', ξ'', δ, η, η'', α/A, β/A, α'/A, β'/A, which are not all independent, see the Data Listings below. Experiments in the past have also been analyzed using the parameters a, b, c, a', b', c', α/A, β/A, α'/A, β'/A (and $\eta = (\alpha - 2\beta)/2A$), as defined by Kinoshita and Sirlin [5]. They serve as a model-independent summary of all possible measurements on the decay electron (see Listings below). The relations between the two sets of parameters are

$$\begin{aligned}
\rho - \tfrac{3}{4} &= \tfrac{3}{4}(-a + 2c)/A \ , \\
\eta &= (\alpha - 2\beta)/A \ , \\
\eta'' &= (3\alpha + 2\beta)/A \ , \\
\delta - \tfrac{3}{4} &= \tfrac{9}{4} \cdot \frac{(a' - 2c')/A}{1 - [a + 3a' + 4(b+b') + 6c - 14c']/A} \ , \\
1 - \xi\frac{\delta}{\rho} &= 4\,\frac{[(b+b') + 2(c-c')]/A}{1 - (a - 2c)/A} \ , \\
1 - \xi' &= [(a+a') + 4(b+b') + 6(c+c')]/A \ , \\
1 - \xi'' &= (-2a + 20c)/A \ ,
\end{aligned}$$

where

$$A = a + 4b + 6c \ . \qquad (6)$$

The differential decay probability to obtain a *left-handed* ν_e with (reduced) energy between y and $y + dy$, neglecting radiative corrections as well as the masses of the electron and of the neutrinos, is given by [6]

$$\frac{d\Gamma}{dy} = \frac{m_\mu^5\, G_F^2}{16\pi^3} \cdot Q_L^{\nu_e} \cdot y^2\Big\{(1-y) - \omega_L \cdot (y - \tfrac{3}{4})\Big\} \ . \qquad (7)$$

Here, $y = 2\ E_{\nu_e}/m_\mu$. $Q_L^{\nu_e}$ and ω_L are parameters. ω_L is the neutrino analog of the spectral shape parameter ρ of Michel. Since in the Standard Model, $Q_L^{\nu_e} = 1$, $\omega_L = 0$, the measurement of $d\Gamma/dy$ has allowed a null-test of the Standard Model (see Listings below).

Matrix element: All results in direct muon decay (energy spectra of the electron and of the neutrinos, polarizations, and angular distributions) and in inverse muon decay (the reaction cross section) at energies well below $m_W c^2$ may be parametrized in terms of amplitudes $g^\gamma_{\varepsilon\mu}$ and the Fermi coupling constant G_F, using the matrix element

$$\frac{4G_F}{\sqrt{2}} \sum_{\substack{\gamma=S,V,T \\ \varepsilon,\mu=R,L}} g^\gamma_{\varepsilon\mu} \langle \bar{e}_\varepsilon | \Gamma^\gamma | (\nu_e)_n \rangle \langle (\bar{\nu}_\mu)_m | \Gamma_\gamma | \mu_\mu \rangle . \qquad (8)$$

We use the notation of Fetscher *et al.* [2], who in turn use the sign conventions and definitions of Scheck [7]. Here, $\gamma = S, V, T$ indicates a scalar, vector, or tensor interaction; and $\varepsilon, \mu = R, L$ indicate a right- or left-handed chirality of the electron or muon. The chiralities n and m of the ν_e and $\bar{\nu}_\mu$ are then determined by the values of γ, ε, and μ. The particles are represented by fields of definite chirality [8].

As shown by Langacker and London [9], explicit lepton-number nonconservation still leads to a matrix element equivalent to Eq. (8). They conclude that it is not possible, even in principle, to test lepton-number conservation in (leptonic) muon decay if the final neutrinos are massless and are not observed.

The ten complex amplitudes $g^\gamma_{\varepsilon\mu}$ (g^T_{RR} and g^T_{LL} are identically zero) and G_F constitute 19 independent (real) parameters to be determined by experiment. The Standard Model interaction corresponds to one single amplitude g^V_{LL} being unity and all the others being zero.

The (direct) muon decay experiments are compatible with an arbitrary mix of the scalar and vector amplitudes g^S_{LL} and g^V_{LL} – in the extreme even with purely scalar $g^S_{LL} = 2$, $g^V_{LL} = 0$. The decision in favour of the Standard Model comes from the quantitative observation of inverse muon decay, which would be forbidden for pure g^S_{LL} [2].

Experimental determination of V–A: In order to determine the amplitudes $g^\gamma_{\varepsilon\mu}$ uniquely from experiment, the following set of equations, where the left-hand sides represent experimental results, has to be solved.

$$\begin{aligned}
a &= 16(|g^V_{RL}|^2 + |g^V_{LR}|^2) + |g^S_{RL} + 6g^T_{RL}|^2 + |g^S_{LR} + 6g^T_{LR}|^2 \\
a' &= 16(|g^V_{RL}|^2 - |g^V_{LR}|^2) + |g^S_{RL} + 6g^T_{RL}|^2 - |g^S_{LR} + 6g^T_{LR}|^2 \\
\alpha &= 8\mathrm{Re}\Big\{g^V_{RL}(g^{S*}_{LR} + 6g^{T*}_{LR}) + g^V_{LR}(g^{S*}_{RL} + 6g^{T*}_{RL})\Big\}
\end{aligned}$$

$$\alpha' = 8\mathrm{Im}\left\{g_{LR}^{V}(g_{RL}^{S*}+6g_{RL}^{T*})-g_{RL}^{V}(g_{LR}^{S*}+6g_{LR}^{T*})\right\}$$
$$b = 4(|g_{RR}^{V}|^2+|g_{LL}^{V}|^2)+|g_{RR}^{S}|^2+|g_{LL}^{S}|^2$$
$$b' = 4(|g_{RR}^{V}|^2-|g_{LL}^{V}|^2)+|g_{RR}^{S}|^2-|g_{LL}^{S}|^2$$
$$\beta = -4\mathrm{Re}\left\{g_{RR}^{V}g_{LL}^{S*}+g_{LL}^{V}g_{RR}^{S*}\right\}$$
$$\beta' = 4\mathrm{Im}\left\{g_{RR}^{V}g_{LL}^{S*}-g_{LL}^{V}g_{RR}^{S*}\right\}$$
$$c = \tfrac{1}{2}\left\{|g_{RL}^{S}-2g_{RL}^{T}|^2+|g_{LR}^{S}-2g_{LR}^{T}|^2\right\}$$
$$c' = \tfrac{1}{2}\left\{|g_{RL}^{S}-2g_{RL}^{T}|^2-|g_{LR}^{S}-2g_{LR}^{T}|^2\right\}$$

and

$$Q_L^{\nu_e} = 1-\left\{\tfrac{1}{4}|g_{LR}^{S}|^2+\tfrac{1}{4}|g_{LL}^{S}|^2+|g_{RR}^{V}|^2+|g_{RL}^{V}|^2+3|g_{LR}^{T}|^2\right\}$$
$$\omega_L = \tfrac{3}{4}\,\frac{\{|g_{RR}^{S}|^2+4|g_{LR}^{V}|^2+|g_{RL}^{S}+2g_{RL}^{T}|^2\}}{|g_{RL}^{S}|^2+|g_{RR}^{S}|^2+4|g_{LL}^{V}|^2+4|g_{LR}^{V}|^2+12|g_{RL}^{T}|^2\}}\ .$$

It has been noted earlier by C. Jarlskog [10], that certain experiments observing the decay electron are especially informative if they yield the V-A values. The complete solution is now found as follows. Fetscher *et al.* [2] introduced four probabilities $Q_{\varepsilon\mu}(\varepsilon,\mu=R,L)$ for the decay of a μ-handed muon into an ε-handed electron and showed that there exist upper bounds on Q_{RR}, Q_{LR}, and Q_{RL}, and a lower bound on Q_{LL}. These probabilities are given in terms of the $g_{\varepsilon\mu}^{\gamma}$'s by

$$Q_{\varepsilon\mu} = \tfrac{1}{4}|g_{\varepsilon\mu}^{S}|^2+|g_{\varepsilon\mu}^{V}|^2+3(1-\delta_{\varepsilon\mu})|g_{\varepsilon\mu}^{T}|^2\ , \qquad (9)$$

where $\delta_{\varepsilon\mu}=1$ for $\varepsilon=\mu$, and $\delta_{\varepsilon\mu}=0$ for $\varepsilon\neq\mu$. They are related to the parameters a, b, c, a', b', and c' by

$$Q_{RR} = 2(b+b')/A\ ,$$
$$Q_{LR} = [(a-a')+6(c-c')]/2A\ ,$$
$$Q_{RL} = [(a+a')+6(c+c')]/2A\ ,$$
$$Q_{LL} = 2(b-b')/A\ , \qquad (10)$$

with $A=16$. In the Standard Model, $Q_{LL}=1$ and the others are zero.

Since the upper bounds on Q_{RR}, Q_{LR}, and Q_{RL} are found to be small, and since the helicity of the ν_μ in pion decay is known from experiment [11,12] to very high precision to be -1 [13], the cross section S of *inverse* muon decay, normalized to the V-A value, yields [2]

$$|g_{LL}^{S}|^2 \le 4(1-S) \qquad (11)$$

and

$$|g_{LL}^{V}|^2 \;=\; S\ . \qquad (12)$$

Thus the Standard Model assumption of a pure V-A leptonic charged weak interaction of e and μ is derived (within errors) from experiments at energies far below mass of the $W^{\pm}$: Eq. (12) gives a lower limit for V-A, and Eqs. (9) and (11) give upper limits for the other four-fermion interactions. The existence of such upper limits may also be seen from $Q_{RR}+Q_{RL}=(1-\xi')/2$ and $Q_{RR}+Q_{LR}=\frac{1}{2}(1+\xi/3-16\ \xi\delta/9)$. Table 1 gives the current experimental limits on the magnitudes of the $g_{\varepsilon\mu}^{\gamma}$'s.

Limits on the "charge retention" coordinates, as used in the older literature (*e.g.*, Ref. 16), are given by Burkard *et al.* [17].

Table 1. Coupling constants $g_{\varepsilon\mu}^{\gamma}$. Ninety-percent confidence level experimental limits. The limits on $|g_{LL}^{S}|$ and $|g_{LL}^{V}|$ are from Ref. 14, and the others are from Ref. 15. The experimental uncertainty on the muon polarization in pion decay is included. Note that, by definition, $|g_{\varepsilon\mu}^{S}|\le 2$, $|g_{\varepsilon\mu}^{V}|\le 1$ and $|g_{\varepsilon\mu}^{T}|\le 1/\sqrt{3}$.

$\lvert g_{RR}^{S}\rvert < 0.066$	$\lvert g_{RR}^{V}\rvert < 0.033$	$\lvert g_{RR}^{T}\rvert \equiv 0$
$\lvert g_{LR}^{S}\rvert < 0.125$	$\lvert g_{LR}^{V}\rvert < 0.060$	$\lvert g_{LR}^{T}\rvert < 0.036$
$\lvert g_{RL}^{S}\rvert < 0.424$	$\lvert g_{RL}^{V}\rvert < 0.110$	$\lvert g_{RL}^{T}\rvert < 0.122$
$\lvert g_{LL}^{S}\rvert < 0.550$	$\lvert g_{LL}^{V}\rvert > 0.960$	$\lvert g_{LL}^{T}\rvert \equiv 0$

References

1. L. Michel, Proc. Phys. Soc. **A63**, 514 (1950).
2. W. Fetscher, H.-J. Gerber, and K.F. Johnson, Phys. Lett. **B173**, 102 (1986).
3. P. Langacker, Comm. Nucl. Part. Phys. **19**, 1 (1989).
4. C. Bouchiat and L. Michel, Phys. Rev. **106**, 170 (1957).
5. T. Kinoshita and A. Sirlin, Phys. Rev. **108**, 844 (1957).
6. W. Fetscher, Phys. Rev. **D49**, 5945 (1994).
7. F. Scheck, in *Electroweak and Strong Interactions* (Springer Verlag, 1996).
8. K. Mursula and F. Scheck, Nucl. Phys. **B253**, 189 (1985).
9. P. Langacker and D. London, Phys. Rev. **D39**, 266 (1989).
10. C. Jarlskog, Nucl. Phys. **75**, 659 (1966).
11. A. Jodidio *et al.*, Phys. Rev. **D34**, 1967 (1986); A. Jodidio *et al.*, Phys. Rev. **D37**, 237 (1988).
12. L.Ph. Roesch *et al.*, Helv. Phys. Acta **55**, 74 (1982).
13. W. Fetscher, Phys. Lett. **140B**, 117 (1984).
14. S.R. Mishra *et al.*, Phys. Lett. **B252**, 170 (1990); S.R. Mishra, private communication; See also P. Vilain *et al.*, Phys. Lett. **B364**, 121 (1995).
15. B. Balke *et al.*, Phys. Rev. **D37**, 587 (1988).
16. S.E. Derenzo, Phys. Rev. **181**, 1854 (1969).
17. H. Burkard *et al.*, Phys. Lett. **160B**, 343 (1985).

μ DECAY PARAMETERS

ρ PARAMETER

($V-A$) theory predicts $\rho = 0.75$.

VALUE	EVTS	DOCUMENT ID		TECN	CHG	COMMENT
0.7518 ± 0.0026		DERENZO	69	RVUE		
• • • We do not use the following data for averages, fits, limits, etc. • • •						
0.762 ± 0.008	170k	[28] FRYBERGER	68	ASPK	+	25–53 MeV e^+
0.760 ± 0.009	280k	[28] SHERWOOD	67	ASPK	+	25–53 MeV e^+
0.7503 ± 0.0026	800k	[28] PEOPLES	66	ASPK	+	20–53 MeV e^+

[28] η constrained = 0. These values incorporated into a two parameter fit to ρ and η by DERENZO 69.

η PARAMETER

($V-A$) theory predicts $\eta = 0$.

VALUE	EVTS	DOCUMENT ID		TECN	CHG	COMMENT
−0.007 ± 0.013 OUR AVERAGE						
−0.007 ± 0.013	5.3M	[29] BURKARD	85B	FIT	+	9–53 MeV e^+
−0.12 ± 0.21	6346	DERENZO	69	HBC	+	1.6–6.8 MeV e^+

• • • We do not use the following data for averages, fits, limits, etc. • • •

$-0.012\pm0.015\pm0.003$	5.3M	[30]	BURKARD	85B	CNTR	+	9–53 MeV e^+
$0.011\pm0.081\pm0.026$	5.3M		BURKARD	85B	CNTR	+	9–53 MeV e^+
$-0.7\ \pm0.5$	170k	[31]	FRYBERGER	68	ASPK	+	25–53 MeV e^+
$-0.7\ \pm0.6$	280k	[31]	SHERWOOD	67	ASPK	+	25–53 MeV e^+
$0.05\ \pm0.5$	800k	[31]	PEOPLES	66	ASPK	+	20–53 MeV e^+
$-2.0\ \pm0.9$	9213	[32]	PLANO	60	HBC	+	Whole spectrum

[29] Global fit to all measured parameters. Correlation coefficients are given in BURKARD 85B.
[30] $\alpha = \alpha' = 0$ assumed.
[31] ρ constrained $= 0.75$.
[32] Two parameter fit to ρ and η; PLANO 60 discounts value for η.

δ PARAMETER

($V-A$) theory predicts $\delta = 0.75$.

VALUE	EVTS	DOCUMENT ID		TECN	CHG	COMMENT
0.7486±0.0026±0.0028		[33] BALKE	88	SPEC	+	Surface μ^+'s
• • • We do not use the following data for averages, fits, limits, etc. • • •						
		[34] VOSSLER	69			
$0.752\ \pm0.009$	490k	FRYBERGER	68	ASPK	+	25–53 MeV e^+
$0.782\ \pm0.031$		KRUGER	61			
$0.78\ \pm0.05$	8354	PLANO	60	HBC	+	Whole spectrum

[33] BALKE 88 uses $\rho = 0.752 \pm 0.003$.
[34] VOSSLER 69 has measured the asymmetry below 10 MeV. See comments about radiative corrections in VOSSLER 69.

$|(\xi$ PARAMETER)×(μ LONGITUDINAL POLARIZATION)|

($V-A$) theory predicts $\xi = 1$, longitudinal polarization $= 1$.

VALUE	EVTS	DOCUMENT ID		TECN	CHG	COMMENT
1.0027±0.0079±0.0030		BELTRAMI	87	CNTR		SIN, π decay in flight
• • • We do not use the following data for averages, fits, limits, etc. • • •						
$1.0013\pm0.0030\pm0.0053$		[35] IMAZATO	92	SPEC	+	$K^+ \to \mu^+\nu_\mu$
$0.975\ \pm0.015$		AKHMANOV	68	EMUL		140 kG
$0.975\ \pm0.030$	66k	GUREVICH	64	EMUL		See AKHMANOV 68
$0.903\ \pm0.027$		[36] ALI-ZADE	61	EMUL	+	27 kG
$0.93\ \pm0.06$	8354	PLANO	60	HBC	+	8.8 kG
$0.97\ \pm0.05$	9k	BARDON	59	CNTR		Bromoform target

[35] The corresponding 90% confidence limit from IMAZATO 92 is $|\xi P_\mu| > 0.990$. This measurement is of K^+ decay, not π^+ decay, so we do not include it in an average, nor do we yet set up a separate data block for K results.
[36] Depolarization by medium not known sufficiently well.

ξ × (μ LONGITUDINAL POLARIZATION) × δ / ρ

VALUE	CL%	DOCUMENT ID		TECN	CHG	COMMENT
>0.99682	90	[37] JODIDIO	86	SPEC	+	TRIUMF
• • • We do not use the following data for averages, fits, limits, etc. • • •						
>0.9966	90	[38] STOKER	85	SPEC	+	μ-spin rotation
>0.9959	90	CARR	83	SPEC	+	11 kG

[37] JODIDIO 86 includes data from CARR 83 and STOKER 85. The value here is from the erratum.
[38] STOKER 85 find $(\xi P_\mu \delta/\rho) > 0.9955$ and > 0.9966, where the first limit is from new μ spin-rotation data and the second is from combination with CARR 83 data. In $V-A$ theory, $(\delta/\rho) = 1.0$.

ξ' = LONGITUDINAL POLARIZATION OF e^+

($V-A$) theory predicts the longitudinal polarization $= \pm1$ for $e^\pm$, respectively. We have flipped the sign for e^- so our programs can average.

VALUE	EVTS	DOCUMENT ID		TECN	CHG	COMMENT
1.00 ±0.04 OUR AVERAGE						
0.998 ± 0.045	1M	BURKARD	85	CNTR	+	Bhabha + annihil
$0.89\ \pm0.28$	29k	SCHWARTZ	67	OSPK	−	Moller scattering
$0.94\ \pm0.38$		BLOOM	64	CNTR	+	Brems. transmiss.
$1.04\ \pm0.18$		DUCLOS	64	CNTR	+	Bhabha scattering
$1.05\ \pm0.30$		BUHLER	63	CNTR	+	Annihilation

ξ'' PARAMETER

VALUE	EVTS	DOCUMENT ID		TECN	CHG	COMMENT
0.65±0.36	326k	[39] BURKARD	85	CNTR	+	Bhabha + annihil

[39] BURKARD 85 measure $(\xi'' - \xi\xi')/\xi$ and ξ' and set $\xi = 1$.

TRANSVERSE e^+ POLARIZATION IN PLANE OF μ SPIN, e^+ MOMENTUM

VALUE	EVTS	DOCUMENT ID		TECN	CHG	COMMENT
• • • We do not use the following data for averages, fits, limits, etc. • • •						
$0.016\pm0.021\pm0.01$	5.3M	BURKARD	85B	CNTR	+	Annihil 9–53 MeV

TRANSVERSE e^+ POLARIZATION NORMAL TO PLANE OF μ SPIN, e^+ MOMENTUM

Zero if T invariance holds.

VALUE	EVTS	DOCUMENT ID		TECN	CHG	COMMENT
0.007±0.022±0.007	5.3M	BURKARD	85B	CNTR	+	Annihil 9–53 MeV

α/A

VALUE (units 10^{-3})	EVTS	DOCUMENT ID		TECN	CHG	COMMENT
0.4± 4.3		[40] BURKARD	85B	FIT		
• • • We do not use the following data for averages, fits, limits, etc. • • •						
$15\ \pm50\ \pm14$	5.3M	BURKARD	85B	CNTR	+	9–53 MeV e^+

[40] Global fit to all measured parameters. Correlation coefficients are given in BURKARD 85B.

α'/A

Zero if T invariance holds.

VALUE (units 10^{-3})	EVTS	DOCUMENT ID		TECN	CHG	COMMENT
− 0.2± 4.3		[41] BURKARD	85B	FIT		
• • • We do not use the following data for averages, fits, limits, etc. • • •						
$-47\ \pm50\ \pm14$	5.3M	[42] BURKARD	85B	CNTR	+	9–53 MeV e^+

[41] Global fit to all measured parameters. Correlation coefficients are given in BURKARD 85B.
[42] BURKARD 85B measure e^+ polarizations P_{T_1} and P_{T_2} versus e^+ energy.

β/A

VALUE (units 10^{-3})	EVTS	DOCUMENT ID		TECN	CHG	COMMENT
3.9± 6.2		[43] BURKARD	85B	FIT		
• • • We do not use the following data for averages, fits, limits, etc. • • •						
$2\ \pm17\ \pm6$	5.3M	BURKARD	85B	CNTR	+	9–53 MeV e^+

[43] Global fit to all measured parameters. Correlation coefficients are given in BURKARD 85B.

β'/A

Zero if T invariance holds.

VALUE (units 10^{-3})	EVTS	DOCUMENT ID		TECN	CHG	COMMENT
1.5± 6.3		[44] BURKARD	85B	FIT		
• • • We do not use the following data for averages, fits, limits, etc. • • •						
$17\ \pm17\ \pm6$	5.3M	[45] BURKARD	85B	CNTR	+	9–53 MeV e^+

[44] Global fit to all measured parameters. Correlation coefficients are given in BURKARD 85B.
[45] BURKARD 85B measure e^+ polarizations P_{T_1} and P_{T_2} versus e^+ energy.

a/A

This comes from an alternative parameterization to that used in the Summary Table (see the "Note on Muon Decay Parameters" above).

VALUE (units 10^{-3})	CL%	DOCUMENT ID		TECN
• • • We do not use the following data for averages, fits, limits, etc. • • •				
<15.9	90	[46] BURKARD	85B	FIT

[46] Global fit to all measured parameters. Correlation coefficients are given in BURKARD 85B.

a'/A

This comes from an alternative parameterization to that used in the Summary Table (see the "Note on Muon Decay Parameters" above).

VALUE (units 10^{-3})	DOCUMENT ID		TECN
• • • We do not use the following data for averages, fits, limits, etc. • • •			
5.3 ± 4.1	[47] BURKARD	85B	FIT

[47] Global fit to all measured parameters. Correlation coefficients are given in BURKARD 85B.

$(b'+b)/A$

This comes from an alternative parameterization to that used in the Summary Table (see the "Note on Muon Decay Parameters" above).

VALUE (units 10^{-3})	CL%	DOCUMENT ID		TECN
• • • We do not use the following data for averages, fits, limits, etc. • • •				
<1.04	90	[48] BURKARD	85B	FIT

[48] Global fit to all measured parameters. Correlation coefficients are given in BURKARD 85B.

c/A

This comes from an alternative parameterization to that used in the Summary Table (see the "Note on Muon Decay Parameters" above).

VALUE (units 10^{-3})	CL%	DOCUMENT ID		TECN
• • • We do not use the following data for averages, fits, limits, etc. • • •				
<6.4	90	[49] BURKARD	85B	FIT

[49] Global fit to all measured parameters. Correlation coefficients are given in BURKARD 85B.

c'/A

This comes from an alternative parameterization to that used in the Summary Table (see the "Note on Muon Decay Parameters" above).

VALUE (units 10^{-3})	DOCUMENT ID		TECN
• • • We do not use the following data for averages, fits, limits, etc. • • •			
3.5 ± 2.0	[50] BURKARD	85B	FIT

[50] Global fit to all measured parameters. Correlation coefficients are given in BURKARD 85B.

Lepton Particle Listings

μ, τ

$\overline{\eta}$ PARAMETER

$(V-A)$ theory predicts $\overline{\eta} = 0$. $\overline{\eta}$ affects spectrum of radiative muon decay.

VALUE	DOCUMENT ID		TECN	CHG	COMMENT
0.02 ±0.08 OUR AVERAGE					
−0.014±0.090	EICHENBER...	84	ELEC	+	ρ free
+0.09 ±0.14	BOGART	67	CNTR	+	
• • • We do not use the following data for averages, fits, limits, etc. • • •					
−0.035±0.098	EICHENBER...	84	ELEC	+	ρ=0.75 assumed

μ REFERENCES

MOHR	04	RMP (to be publ.)	P.J. Mohr, B.N. Taylor	(NIST)
physics.nist.gov/constants				
AHMED	02	PR D65 112002	M. Ahmed *et al.*	(MEGA Collab.)
BENNETT	02	PRL 89 101804	G.W. Bennett *et al.*	(Muon(g-2) Collab.)
BROWN	01	PRL 86 2227	H.N. Brown *et al.*	(Muon(g-2) Collab.)
BROWN	00	PR D62 091101R	H.N. Brown *et al.*	(BNL/G-2 Collab.)
MEYER	00	PRL 84 1136	V. Meyer *et al.*	
BROOKS	99	PRL 83 1521	M.L. Brooks *et al.*	(MEGA/LAMPF Collab.)
HUGHES	99	RMP 71 S133	V.W. Hughes, T. Kinoshita	
LIU	99	PRL 82 711	W. Liu *et al.*	(LAMPF Collab.)
MOHR	99	JPCRD 28 1713	P.J. Mohr, B.N. Taylor	(NIST)
Also	00	RMP 72 351	P.J. Mohr, B.N. Taylor	(NIST)
WILLMANN	99	PRL 82 49	L. Willmann *et al.*	
FELDMAN	98	PR D57 3873	G.J. Feldman, R.D. Cousins	
KAULARD	98	PL B422 334	J. Kaulard *et al.*	(SINDRUM-II Collab.)
GORDEEV	97	PAN 60 1164	V.A. Gordeev *et al.*	(PNPI)
		Translated from YAF 60 1291.		
ABELA	96	PRL 77 1950	R. Abela *et al.*	(PSI, ZURI, HEIDH, TBIL+)
HONECKER	96	PRL 76 200	W. Honecker *et al.*	(SINDRUM II Collab.)
DOHMEN	93	PL B317 631	C. Dohmen *et al.*	(PSI SINDRUM-II Collab.)
FREEDMAN	93	PR D47 811	S.J. Freedman *et al.*	(LAMPF E645 Collab.)
NI	93	PR D48 1976	B. Ni *et al.*	(LAMPF Crystal-Box Collab.)
IMAZATO	92	PRL 69 877	J. Imazato *et al.*	(KEK, INUS, TOKY+)
BARANOV	91	SJNP 53 802	V.A. Baranov *et al.*	(JINR)
		Translated from YAF 53 1302.		
KRAKAUER	91B	PL B263 534	D.A. Krakauer *et al.*	(UMD, UCI, LANL)
MATTHIAS	91	PRL 66 2716	B.E. Matthias *et al.*	(YALE, HEIDP, WILL+)
Also	91B	PRL 67 932 erratum	B.E. Matthias *et al.*	(YALE, HEIDP, WILL+)
HUBER	90B	PR D41 2709	T.M. Huber *et al.*	(WYOM, VICT, ARIZ+)
AHMAD	88	PR D38 2102	S. Ahmad *et al.*	(TRIU, VICT, VPI, BRCO+)
Also	87	PRL 59 970	S. Ahmad *et al.*	(TRIU, VPI, VICT, BRCO+)
BALKE	88	PR D37 587	B. Balke *et al.*	(LBL, UCB, COLO, NWES+)
BELLGARDT	88	NP B299 1	U. Bellgardt *et al.*	(SINDRUM Collab.)
BOLTON	88	PR D38 2077	R.D. Bolton *et al.*	(LANL, STAN, CHIC+)
	86	PRL 56 2461	R.D. Bolton *et al.*	(LANL, STAN, CHIC+)
Also	86	PRL 57 3241	D. Grosnick *et al.*	(CHIC, LANL, STAN+)
BELTRAMI	87	PL B194 326	I. Beltrami *et al.*	(ETH, SIN, MANZ)
COHEN	87	RMP 59 1121	E.R. Cohen, B.N. Taylor	(RISC, NBS)
BEER	86	PRL 57 671	G.A. Beer *et al.*	(VICT, TRIU, WYOM)
JODIDIO	86	PR D34 1967	A. Jodidio *et al.*	(LBL, NWES, TRIU)
Also	88	PR D37 237 erratum	A. Jodidio *et al.*	(LBL, NWES, TRIU)
BERTL	85	NP B260 1	W. Bertl *et al.*	(SINDRUM Collab.)
BRYMAN	85	PRL 55 465	D.A. Bryman *et al.*	(TRIU, CNRC, BRCO+)
BURKARD	85	PL 150B 242	H. Burkhardt *et al.*	(ETH, SIN, MANZ)
BURKARD	85B	PL 160B 343	H. Burkhardt *et al.*	(ETH, SIN, MANZ)
Also	81B	PR D23 2004	F. Corriveau *et al.*	(ETH, SIN, MANZ)
Also	83B	PL 129B 260	F. Corriveau *et al.*	(ETH, SIN, MANZ)
STOKER	85	PRL 54 1887	D.P. Stoker *et al.*	(LBL, NWES, TRIU)
BARDIN	84	PL 137B 135	G. Bardin *et al.*	(SACL, CERN, BGNA, FIRZ)
BERTL	84	PL 140B 299	W. Bertl *et al.*	(SINDRUM Collab.)
BOLTON	84	PRL 53 1415	R.D. Bolton *et al.*	(LANL, CHIC, STAN+)
EICHENBER...	84	NP A412 523	W. Eichenberger, R. Engfer, A. van der Schaff	
GIOVANETTI	84	PR D29 343	K.L. Giovanetti *et al.*	(WILL)
AZUELOS	83	PRL 51 164	G. Azuelos *et al.*	(MONT, TRIU, BRCO)
Also	77	PRL 39 1113	P. Depommier *et al.*	(MONT, BRCO, TRIU+)
BERGSMA	83	PL 122B 465	F. Bergsma *et al.*	(CHARM Collab.)
CARR	83	PRL 51 627	J. Carr *et al.*	(LBL, NWES, TRIU)
KINNISON	82	PR D25 2846	W.W. Kinnison *et al.*	(EFI, STAN, LANL)
Also	79	PRL 42 556	J.D. Bowman *et al.*	(LASL, EFI, STAN)
KLEMPT	82	PR D25 652	E. Klempt *et al.*	(MANZ, ETH)
MARIAM	82	PRL 49 993	F.G. Mariam *et al.*	(YALE, HEIDH, BERN)
MARSHALL	82	PR D25 1174	G.M. Marshall *et al.*	(BRCO)
NEMETHY	81	CNPP 10 147	P. Nemethy, V.W. Hughes	(LBL, YALE)
ABELA	80	PL 95B 318	R. Abela *et al.*	(BASL, KARLK, KARLE)
BADERT...	80	LNC 28 401	A. Badertscher *et al.*	(BERN)
Also	82	NP A377 406	A. Badertscher *et al.*	(BERN)
JONKER	80	PL 93B 203	M. Jonker *et al.*	(CHARM Collab.)
SCHAAF	80	NP A340 249	A. van der Schaaf *et al.*	(ZURI, ETH+)
Also	77	PL 72B 183	H.P. Povel *et al.*	(ZURI, ETH, SIN)
WILLIS	80	PRL 44 522	S.E. Willis *et al.*	(YALE, LBL, LASL+)
Also	80B	PRL 45 1370	S.E. Willis *et al.*	(YALE, LBL, LASL+)
BAILEY	79	NP B150 1	J.M. Bailey	(CERN, DARE, MANZ)
BADERT...	78	PL 79B 371	A. Badertscher *et al.*	(BERN)
BAILEY	78	JPG 4 345	J.M. Bailey (DARE, BERN, SHEF, MANZ, RMCS+)	
Also	79	NP B150 1	J.M. Bailey	(CERN, DARE, MANZ)
BLIETSCHAU	78	NP B133 205	J. Bletschau *et al.*	(Gargamelle Collab.)
BOWMAN	78	PRL 41 442	J.D. Bowman *et al.*	(LASL, IAS, CMU+)
CAMANI	78	PL 77B 326	M. Camani *et al.*	(ETH, MANZ)
BADERT...	77	PRL 39 1385	A. Badertscher *et al.*	(BERN)
CASPERSON	77	PRL 38 956	D.E. Casperson *et al.*	(BERN, HEIDH, LASL+)
DEPOMMIER	77	PRL 39 1113	P. Depommier *et al.*	(MONT, BRCO, TRIU+)
BALANDIN	74	JETP 40 811	M.P. Balandin *et al.*	(JINR)
		Translated from ZETF 67 1631.		
COHEN	73	JPCRD 2 664	E.R. Cohen, B.N. Taylor	(RISC, NBS)
DUCLOS	73	PL 47B 491	J. Duclos, A. Magnon, J. Picard	(SACL)
EICHTEN	73	PL 46B 281	T. Eichten *et al.*	(Gargamelle Collab.)
BRYMAN	72	PRL 28 1469	D.A. Bryman *et al.*	(VPI)
CROWE	72	PR D5 2145	K.M. Crowe *et al.*	(LBL, WASH)
CRANE	71	PRL 27 474	T. Crane *et al.*	(YALE)
DERENZO	69	PR 181 1854	S.E. Derenzo	(EFI)
VOSSLER	69	NC 63A 423	C. Vossler	(EFI)
AKHMANOV	68	SJNP 6 230	V.V. Akhmanov *et al.*	(KIAE)
		Translated from YAF 6 316.		
FRYBERGER	68	PR 166 1379	D. Fryberger	(EFI)
BOGART	67	PR 156 1405	E. Bogart *et al.*	(COLU)
SCHWARTZ	67	PR 162 1306	D.M. Schwartz	(EFI)
SHERWOOD	67	PR 156 1475	B.A. Sherwood	(EFI)
PEOPLES	66	Nevis 147 unpub.	J. Peoples	(COLU)
BLOOM	64	PL 8 87	S. Bloom *et al.*	(CERN)
DUCLOS	64	PL 9 62	J. Duclos *et al.*	(CERN)
GUREVICH	64	PL 11 185	I.I. Gurevich *et al.*	(KIAE)
BUHLER	63	PL 7 368	A. Buhler-Broglin *et al.*	(CERN)
MEYER	63	PR 132 2693	S.L. Meyer *et al.*	(COLU)
CHARPAK	62	PL 1 16	G. Charpak *et al.*	(CERN)
CONFORTO	62	NC 26 261	G. Conforto *et al.*	(INFN, ROMA, CERN)
ALI-ZADE	61	JETP 13 313	S.A. Ali-Zade, I.I. Gurevich, B.A. Nikolsky	
		Translated from ZETF 40 452.		
CRITTENDEN	61	PR 121 1823	R.R. Crittenden, W.D. Walker, J. Ballam	(WISC+)
KRUGER	61	UCRL 9322 unpub.	H. Kruger	(LRL)
GUREVICH	60	JETP 10 225	I.I. Gurevich, B.A. Nikolsky, L.V. Surkova	(ITEP)
		Translated from ZETF 37 318.		
PLANO	60	PR 119 1400	R.J. Plano	(COLU)
ASHKIN	59	NC 14 1266	J. Ashkin *et al.*	(CERN)
BARDON	59	PRL 2 56	M. Bardon, D. Berley, L.M. Lederman	(COLU)
LEE	59	PRL 3 55	J. Lee, N.P. Samios	(COLU)

τ

$J = \frac{1}{2}$

τ discovery paper was PERL 75. $e^+e^- \to \tau^+\tau^-$ cross-section threshold behavior and magnitude are consistent with pointlike spin-1/2 Dirac particle. BRANDELIK 78 ruled out pointlike spin-0 or spin-1 particle. FELDMAN 78 ruled out $J = 3/2$. KIRKBY 79 also ruled out J=integer, $J = 3/2$.

τ MASS

VALUE (MeV)	EVTS	DOCUMENT ID		TECN	COMMENT
1776.99 $^{+0.29}_{-0.26}$ OUR AVERAGE					
1775.1 ±1.6 ±1.0	13.3k	[1] ABBIENDI	00A	OPAL	1990–1995 LEP runs
1778.2 ±0.8 ±1.2		ANASTASSOV	97	CLEO	$E^{ee}_{\rm cm}$= 10.6 GeV
1776.96 $^{+0.18+0.25}_{-0.21-0.17}$	65	[2] BAI	96	BES	$E^{ee}_{\rm cm}$= 3.54–3.57 GeV
1776.3 ±2.4 ±1.4	11k	[3] ALBRECHT	92M	ARG	$E^{ee}_{\rm cm}$= 9.4–10.6 GeV
1783 $^{+3}_{-4}$	692	[4] BACINO	78B	DLCO	$E^{ee}_{\rm cm}$= 3.1–7.4 GeV
• • • We do not use the following data for averages, fits, limits, etc. • • •					
1777.8 ±0.7 ±1.7	35k	[5] BALEST	93	CLEO	Repl. by ANASTASSOV 97
1776.9 $^{+0.4}_{-0.5}$ ±0.2	14	[6] BAI	92	BES	Repl. by BAI 96

[1] ABBIENDI 00A fit τ pseudomass spectrum in $\tau \to \pi^\pm \le 2\pi^0\nu_\tau$ and $\tau \to \pi^\pm\pi^+\pi^- \le 1\pi^0\nu_\tau$ decays. Result assumes m_{ν_τ}=0.

[2] BAI 96 fit $\sigma(e^+e^- \to \tau^+\tau^-)$ at different energies near threshold.

[3] ALBRECHT 92M fit τ pseudomass spectrum in $\tau^- \to 2\pi^-\pi^+\nu_\tau$ decays. Result assumes m_{ν_τ}=0.

[4] BACINO 78B value comes from $e^\pm X^\mp$ threshold. Published mass 1782 MeV increased by 1 MeV using the high precision $\psi(2S)$ mass measurement of ZHOLENTZ 80 to eliminate the absolute SPEAR energy calibration uncertainty.

[5] BALEST 93 fit spectra of minimum kinematically allowed τ mass in events of the type $e^+e^- \to \tau^+\tau^- \to (\pi^+ n\pi^0\nu_\tau)(\pi^- m\pi^0\nu_\tau)$ $n \le 2$, $m \le 2$, $1 \le n+m \le 3$. If $m_{\nu_\tau} \neq 0$, result increases by $(m^2_{\nu_\tau}/1100$ MeV).

[6] BAI 92 fit $\sigma(e^+e^- \to \tau^+\tau^-)$ near threshold using $e\mu$ events.

$(m_{\tau^+} - m_{\tau^-})/m_{\rm average}$

A test of *CPT* invariance.

VALUE	CL%	DOCUMENT ID		TECN	COMMENT
$< 3.0 \times 10^{-3}$	90	ABBIENDI	00A	OPAL	1990–1995 LEP runs

τ MEAN LIFE

VALUE (10^{-15} s)	EVTS	DOCUMENT ID		TECN	COMMENT
290.6 ± 1.1 OUR AVERAGE					
293.2 ± 2.0 ± 1.5		ACCIARRI	00B	L3	1991–1995 LEP runs
290.1 ± 1.5 ± 1.1		BARATE	97R	ALEP	1989–1994 LEP runs
291.4 ± 3.0		ABREU	96B	DLPH	1991–1993 LEP runs
289.2 ± 1.7 ± 1.2		ALEXANDER	96E	OPAL	1990–1994 LEP runs
289.0 ± 2.8 ± 4.0	57.4k	BALEST	96	CLEO	$E^{ee}_{\rm cm}$= 10.6 GeV
• • • We do not use the following data for averages, fits, limits, etc. • • •					
291.2 ± 2.0 ± 1.2		BARATE	97I	ALEP	Repl. by BARATE 97R
290.1 ± 4.0	34k	ACCIARRI	96K	L3	Repl. by ACCIARRI 00B
297 ± 9 ± 5	1671	ABE	95Y	SLD	1992–1993 SLC runs
304 ± 14 ± 7	4100	BATTLE	92	CLEO	$E^{ee}_{\rm cm}$= 10.6 GeV
301 ± 29	3780	KLEINWORT	89	JADE	$E^{ee}_{\rm cm}$= 35–46 GeV
288 ± 16 ±17	807	AMIDEI	88	MRK2	$E^{ee}_{\rm cm}$= 29 GeV
306 ± 20 ±14	695	BRAUNSCH...	88C	TASS	$E^{ee}_{\rm cm}$= 36 GeV
299 ± 15 ±10	1311	ABACHI	87C	HRS	$E^{ee}_{\rm cm}$= 29 GeV
295 ± 14 ±11	5696	ALBRECHT	87P	ARG	$E^{ee}_{\rm cm}$= 9.3–10.6 GeV
309 ± 17 ± 7	3788	BAND	87B	MAC	$E^{ee}_{\rm cm}$= 29 GeV
325 ± 14 ±18	8470	BEBEK	87C	CLEO	$E^{ee}_{\rm cm}$= 10.5 GeV
460 ±190	102	FELDMAN	82	MRK2	$E^{ee}_{\rm cm}$= 29 GeV

τ MAGNETIC MOMENT ANOMALY

The q^2 dependence is expected to be small providing no thresholds are nearby.

$\mu_\tau/(e\hbar/2m_\tau)-1 = (g_\tau-2)/2$

For a theoretical calculation [$(g_\tau-2)/2 = 11773(3)\times10^{-7}$], see SAMUEL 91B.

VALUE	CL%	DOCUMENT ID		TECN	COMMENT
> -0.052 and < 0.058 (CL = 95%) OUR LIMIT					
> -0.052 and < 0.058	95	ACCIARRI	98E	L3	1991–1995 LEP runs
• • • We do not use the following data for averages, fits, limits, etc. • • •					
> -0.007 and < 0.005	95	[7] GONZALEZ-S..00		RVUE	$e^+e^- \to \tau^+\tau^-$ and $W \to \tau\nu_\tau$
> -0.068 and < 0.065	95	[8] ACKERSTAFF	98N	OPAL	1990–1995 LEP runs
> -0.004 and < 0.006	95	[9] ESCRIBANO	97	RVUE	$Z \to \tau^+\tau^-$ at LEP
< 0.01	95	[10] ESCRIBANO	93	RVUE	$Z \to \tau^+\tau^-$ at LEP
< 0.12	90	GRIFOLS	91	RVUE	$Z \to \tau\tau\gamma$ at LEP
< 0.023	95	[11] SILVERMAN	83	RVUE	$e^+e^- \to \tau^+\tau^-$ at PETRA

[7] GONZALEZ-SPRINBERG 00 use data on tau lepton production at LEP1, SLC, and LEP2, and data from colliders and LEP2 to determine limits. Assume imaginary component is zero.
[8] ACKERSTAFF 98N use $Z \to \tau^+\tau^-\gamma$ events. The limit applies to an average of the form factor for off-shell τ's having p^2 ranging from m_τ^2 to $(M_Z-m_\tau)^2$.
[9] ESCRIBANO 97 use preliminary experimental results.
[10] ESCRIBANO 93 limit derived from $\Gamma(Z \to \tau^+\tau^-)$, and is on the absolute value of the magnetic moment anomaly.
[11] SILVERMAN 83 limit is derived from $e^+e^- \to \tau^+\tau^-$ total cross-section measurements for q^2 up to $(37\ \text{GeV})^2$.

τ ELECTRIC DIPOLE MOMENT (d_τ)

A nonzero value is forbidden by both T invariance and P invariance.

The q^2 dependence is expected to be small providing no thresholds are nearby.

Re(d_τ)

VALUE (10^{-16} ecm)	CL%	DOCUMENT ID		TECN	COMMENT
-0.22 to 0.45	95	[12] INAMI	03	BELL	$E_{\rm cm}^{ee}$= 10.6 GeV
• • • We do not use the following data for averages, fits, limits, etc. • • •					
< 4.6	95	[13] ALBRECHT	00	ARG	$E_{\rm cm}^{ee}$= 10.4 GeV
> -3.1 and < 3.1	95	ACCIARRI	98E	L3	1991–1995 LEP runs
> -3.8 and < 3.6	95	[14] ACKERSTAFF	98N	OPAL	1990–1995 LEP runs
< 0.11	95	[15,16] ESCRIBANO	97	RVUE	$Z \to \tau^+\tau^-$ at LEP
< 0.5	95	[17] ESCRIBANO	93	RVUE	$Z \to \tau^+\tau^-$ at LEP
< 7	90	GRIFOLS	91	RVUE	$Z \to \tau\tau\gamma$ at LEP
< 1.6	90	DELAGUILA	90	RVUE	$e^+e^- \to \tau^+\tau^-$ $E_{\rm cm}^{ee}$= 35 GeV

[12] INAMI 03 use $e^+e^- \to \tau^+\tau^-$ events.
[13] ALBRECHT 00 use $e^+e^- \to \tau^+\tau^-$ events. Limit is on the absolute value of Re(d_τ).
[14] ACKERSTAFF 98N use $Z \to \tau^+\tau^-\gamma$ events. The limit applies to an average of the form factor for off-shell τ's having p^2 ranging from m_τ^2 to $(M_Z-m_\tau)^2$.
[15] ESCRIBANO 97 derive the relationship $|d_\tau| = \cot\theta_W\,|d_\tau^W|$ using effective Lagrangian methods, and use a conference result $|d_\tau^W| < 5.8\times10^{-18}\ e$ cm at 95% CL (L. Silvestris, ICHEP96) to obtain this result.
[16] ESCRIBANO 97 use preliminary experimental results.
[17] ESCRIBANO 93 limit derived from $\Gamma(Z \to \tau^+\tau^-)$, and is on the absolute value of the electric dipole moment.

Im(d_τ)

VALUE (10^{-16} ecm)	CL%	DOCUMENT ID		TECN	COMMENT
-0.25 to 0.008	95	[18] INAMI	03	BELL	$E_{\rm cm}^{ee}$= 10.6 GeV
• • • We do not use the following data for averages, fits, limits, etc. • • •					
< 1.8	95	[19] ALBRECHT	00	ARG	$E_{\rm cm}^{ee}$= 10.4 GeV

[18] INAMI 03 use $e^+e^- \to \tau^+\tau^-$ events.
[19] ALBRECHT 00 use $e^+e^- \to \tau^+\tau^-$ events. Limit is on the absolute value of Im(d_τ).

τ WEAK DIPOLE MOMENT (d_τ^W)

A nonzero value is forbidden by CP invariance.

The q^2 dependence is expected to be small providing no thresholds are nearby.

Re(d_τ^W)

VALUE (10^{-17} ecm)	CL%	DOCUMENT ID		TECN	COMMENT
< 0.50	95	[20] HEISTER	03F	ALEP	1990–1995 LEP runs
• • • We do not use the following data for averages, fits, limits, etc. • • •					
< 3.0	90	[20] ACCIARRI	98C	L3	1991–1995 LEP runs
< 0.56	95	ACKERSTAFF	97L	OPAL	1991–1995 LEP runs
< 0.78	95	[21] AKERS	95F	OPAL	Repl. by ACKERSTAFF 97L
< 1.5	95	[21] BUSKULIC	95C	ALEP	Repl. by HEISTER 03F
< 7.0	95	[21] ACTON	92F	OPAL	$Z \to \tau^+\tau^-$ at LEP
< 3.7	95	[21] BUSKULIC	92J	ALEP	Repl. by BUSKULIC 95C

[20] Limit is on the absolute value of the real part of the weak dipole moment.
[21] Limit is on the absolute value of the real part of the weak dipole moment, and applies for $q^2 = m_Z^2$.

Im(d_τ^W)

VALUE (10^{-17} ecm)	CL%	DOCUMENT ID		TECN	COMMENT
< 1.1	95	[22] HEISTER	03F	ALEP	1990–1995 LEP runs
• • • We do not use the following data for averages, fits, limits, etc. • • •					
< 1.5	95	ACKERSTAFF	97L	OPAL	1991–1995 LEP runs
< 4.5	95	[23] AKERS	95F	OPAL	Repl. by ACKERSTAFF 97L

[22] HEISTER 03F limit is on the absolute value of the imaginary part of the weak dipole moment.
[23] Limit is on the absolute value of the imaginary part of the weak dipole moment, and applies for $q^2 = m_Z^2$.

τ WEAK ANOMALOUS MAGNETIC DIPOLE MOMENT (α_τ^W)

Electroweak radiative corrections are expected to contribute at the 10^{-6} level. See BERNABEU 95.

The q^2 dependence is expected to be small providing no thresholds are nearby.

Re(α_τ^W)

VALUE	CL%	DOCUMENT ID		TECN	COMMENT
$< 1.1\times10^{-3}$	95	[24] HEISTER	03F	ALEP	1990–1995 LEP runs
• • • We do not use the following data for averages, fits, limits, etc. • • •					
> -0.0024 and < 0.0025	95	[25] GONZALEZ-S..00		RVUE	$e^+e^- \to \tau^+\tau^-$ and $W \to \tau\nu_\tau$
$< 4.5\times10^{-3}$	90	[24] ACCIARRI	98C	L3	1991–1995 LEP runs

[24] Limit is on the absolute value of the real part of the weak anomalous magnetic dipole moment.
[25] GONZALEZ-SPRINBERG 00 use data on tau lepton production at LEP1, SLC, and LEP2, and data from colliders and LEP2 to determine limits. Assume imaginary component is zero.

Im(α_τ^W)

VALUE	CL%	DOCUMENT ID		TECN	COMMENT
$< 2.7\times10^{-3}$	95	[26] HEISTER	03F	ALEP	1990–1995 LEP runs
• • • We do not use the following data for averages, fits, limits, etc. • • •					
$< 9.9\times10^{-3}$	90	[26] ACCIARRI	98C	L3	1991–1995 LEP runs

[26] Limit is on the absolute value of the imaginary part of the weak anomalous magnetic dipole moment.

τ^- DECAY MODES

τ^+ modes are charge conjugates of the modes below. "$h^\pm$" stands for $\pi^\pm$ or $K^\pm$. "ℓ" stands for e or μ. "Neutrals" stands for γ's and/or π^0's.

	Mode	Fraction (Γ_i/Γ)		Scale factor/ Confidence level
	Modes with one charged particle			
Γ_1	particle$^- \geq 0$ neutrals $\geq 0K^0\nu_\tau$ ("1-prong")	(85.35 ± 0.07) %		S=1.1
Γ_2	particle$^- \geq 0$ neutrals $\geq 0K_L^0\nu_\tau$	(84.72 ± 0.07) %		S=1.1
Γ_3	$\mu^-\overline{\nu}_\mu\nu_\tau$	(17.36 ± 0.06) %	[a]	
Γ_4	$\mu^-\overline{\nu}_\mu\nu_\tau\gamma$	(3.6 ± 0.4) $\times10^{-3}$	[b]	
Γ_5	$e^-\overline{\nu}_e\nu_\tau$	(17.84 ± 0.06) %	[a]	
Γ_6	$e^-\overline{\nu}_e\nu_\tau\gamma$	(1.75 ± 0.18) %	[b]	
Γ_7	$h^- \geq 0K_L^0\nu_\tau$	(12.30 ± 0.11) %		S=1.4
Γ_8	$h^-\nu_\tau$	(11.75 ± 0.11) %		S=1.4
Γ_9	$\pi^-\nu_\tau$	(11.06 ± 0.11) %	[a]	S=1.4
Γ_{10}	$K^-\nu_\tau$	(6.86 ± 0.23) $\times10^{-3}$	[a]	
Γ_{11}	$h^- \geq 1$ neutralν_τ	(36.92 ± 0.14) %		S=1.1
Γ_{12}	$h^-\pi^0\nu_\tau$	(25.87 ± 0.13) %		S=1.1
Γ_{13}	$\pi^-\pi^0\nu_\tau$	(25.42 ± 0.14) %	[a]	S=1.1
Γ_{14}	$\pi^-\pi^0$ non-$\rho(770)\nu_\tau$	(3.0 ± 3.2) $\times10^{-3}$		
Γ_{15}	$K^-\pi^0\nu_\tau$	(4.50 ± 0.30) $\times10^{-3}$	[a]	
Γ_{16}	$h^- \geq 2\pi^0\nu_\tau$	(10.77 ± 0.15) %		S=1.1
Γ_{17}	$h^-2\pi^0\nu_\tau$	(9.39 ± 0.14) %		S=1.1

Γ_{18}	$h^- 2\pi^0 \nu_\tau$ (ex. K^0)		(9.23 ± 0.14) %		S=1.1
Γ_{19}	$\pi^- 2\pi^0 \nu_\tau$ (ex. K^0)	[a]	(9.17 ± 0.14) %		S=1.1
Γ_{20}	$\pi^- 2\pi^0 \nu_\tau$ (ex. K^0), scalar	<	9	$\times 10^{-3}$	CL=95%
Γ_{21}	$\pi^- 2\pi^0 \nu_\tau$ (ex. K^0), vector	<	7	$\times 10^{-3}$	CL=95%
Γ_{22}	$K^- 2\pi^0 \nu_\tau$ (ex. K^0)	[a]	(5.8 ± 2.3)	$\times 10^{-4}$	
Γ_{23}	$h^- \geq 3\pi^0 \nu_\tau$		(1.37 ± 0.11) %		S=1.1
Γ_{24}	$h^- 3\pi^0 \nu_\tau$		(1.21 ± 0.10) %		
Γ_{25}	$\pi^- 3\pi^0 \nu_\tau$ (ex. K^0)	[a]	(1.08 ± 0.10) %		
Γ_{26}	$K^- 3\pi^0 \nu_\tau$ (ex. K^0, η)	[a]	($3.8\ ^{+2.2}_{-2.0}$)	$\times 10^{-4}$	
Γ_{27}	$h^- 4\pi^0 \nu_\tau$ (ex. K^0)		(1.6 ± 0.6)	$\times 10^{-3}$	
Γ_{28}	$h^- 4\pi^0 \nu_\tau$ (ex. K^0, η)	[a]	($1.0\ ^{+0.6}_{-0.5}$)	$\times 10^{-3}$	
Γ_{29}	$K^- \geq 0\pi^0 \geq 0K^0 \geq 0\gamma\ \nu_\tau$		(1.56 ± 0.04) %		
Γ_{30}	$K^- \geq 1$ (π^0 or K^0 or γ) ν_τ		(8.74 ± 0.35)	$\times 10^{-3}$	

Modes with K^0's

Γ_{31}	K^0_S(particles)$^- \nu_\tau$		(9.2 ± 0.4)	$\times 10^{-3}$	S=1.1
Γ_{32}	$h^- \overline{K}^0 \nu_\tau$		(1.05 ± 0.04) %		S=1.1
Γ_{33}	$\pi^- \overline{K}^0 \nu_\tau$	[a]	(8.9 ± 0.4)	$\times 10^{-3}$	S=1.1
Γ_{34}	$\pi^- \overline{K}^0$(non-$K^*(892)^-$)ν_τ	<	1.7	$\times 10^{-3}$	CL=95%
Γ_{35}	$K^- K^0 \nu_\tau$	[a]	(1.54 ± 0.16)	$\times 10^{-3}$	
Γ_{36}	$K^- K^0 \geq 0\pi^0 \nu_\tau$		(3.09 ± 0.24)	$\times 10^{-3}$	
Γ_{37}	$h^- \overline{K}^0 \pi^0 \nu_\tau$		(5.2 ± 0.4)	$\times 10^{-3}$	
Γ_{38}	$\pi^- \overline{K}^0 \pi^0 \nu_\tau$	[a]	(3.7 ± 0.4)	$\times 10^{-3}$	
Γ_{39}	$\overline{K}^0 \rho^- \nu_\tau$		(2.2 ± 0.5)	$\times 10^{-3}$	
Γ_{40}	$K^- K^0 \pi^0 \nu_\tau$	[a]	(1.55 ± 0.20)	$\times 10^{-3}$	
Γ_{41}	$\pi^- \overline{K}^0 \geq 1\pi^0 \nu_\tau$		(3.2 ± 1.0)	$\times 10^{-3}$	
Γ_{42}	$\pi^- \overline{K}^0 \pi^0 \pi^0 \nu_\tau$		(2.6 ± 2.4)	$\times 10^{-4}$	
Γ_{43}	$K^- K^0 \pi^0 \pi^0 \nu_\tau$	<	1.6	$\times 10^{-4}$	CL=95%
Γ_{44}	$\pi^- K^0 \overline{K}^0 \nu_\tau$		(1.59 ± 0.29)	$\times 10^{-3}$	S=1.1
Γ_{45}	$\pi^- K^0_S K^0_S \nu_\tau$	[a]	(2.4 ± 0.5)	$\times 10^{-4}$	
Γ_{46}	$\pi^- K^0_S K^0_L \nu_\tau$	[a]	(1.10 ± 0.28)	$\times 10^{-3}$	S=1.1
Γ_{47}	$\pi^- K^0 \overline{K}^0 \pi^0 \nu_\tau$		(3.1 ± 2.3)	$\times 10^{-4}$	
Γ_{48}	$\pi^- K^0_S K^0_S \pi^0 \nu_\tau$	<	2.0	$\times 10^{-4}$	CL=95%
Γ_{49}	$\pi^- K^0_S K^0_L \pi^0 \nu_\tau$		(3.1 ± 1.2)	$\times 10^{-4}$	
Γ_{50}	$K^0 h^+ h^- h^- \geq 0$ neutrals ν_τ	<	1.7	$\times 10^{-3}$	CL=95%
Γ_{51}	$K^0 h^+ h^- h^- \nu_\tau$		(2.3 ± 2.0)	$\times 10^{-4}$	

Modes with three charged particles

Γ_{52}	$h^- h^- h^+ \geq 0$ neutrals $\geq 0K^0_L \nu_\tau$		(15.19 ± 0.07) %		S=1.1
Γ_{53}	$h^- h^- h^+ \geq 0$ neutrals ν_τ (ex. $K^0_S \to \pi^+\pi^-$) ("3-prong")		(14.57 ± 0.07) %		S=1.1
Γ_{54}	$h^- h^- h^+ \nu_\tau$		(10.01 ± 0.09) %		S=1.2
Γ_{55}	$h^- h^- h^+ \nu_\tau$ (ex. K^0)		(9.65 ± 0.09) %		S=1.2
Γ_{56}	$h^- h^- h^+ \nu_\tau$ (ex. K^0,ω)		(9.60 ± 0.09) %		S=1.2
Γ_{57}	$\pi^- \pi^+ \pi^- \nu_\tau$		(9.47 ± 0.10) %		S=1.2
Γ_{58}	$\pi^- \pi^+ \pi^- \nu_\tau$ (ex. K^0)		(9.16 ± 0.10) %		S=1.2
Γ_{59}	$\pi^- \pi^+ \pi^- \nu_\tau$ (ex. K^0), non-axial vector	<	2.4	%	CL=95%
Γ_{60}	$\pi^- \pi^+ \pi^- \nu_\tau$ (ex. K^0,ω)	[a]	(9.12 ± 0.10) %		S=1.2
Γ_{61}	$h^- h^- h^+ \geq 1$ neutrals ν_τ		(5.19 ± 0.10) %		S=1.3
Γ_{62}	$h^- h^- h^+ \geq 1$ neutrals ν_τ (ex. $K^0_S \to \pi^+\pi^-$)		(4.92 ± 0.09) %		S=1.3
Γ_{63}	$h^- h^- h^+ \pi^0 \nu_\tau$		(4.53 ± 0.09) %		S=1.3
Γ_{64}	$h^- h^- h^+ \pi^0 \nu_\tau$ (ex. K^0)		(4.35 ± 0.09) %		S=1.3
Γ_{65}	$h^- h^- h^+ \pi^0 \nu_\tau$ (ex. K^0, ω)		(2.62 ± 0.09) %		S=1.2
Γ_{66}	$\pi^- \pi^+ \pi^- \pi^0 \nu_\tau$		(4.37 ± 0.09) %		S=1.3
Γ_{67}	$\pi^- \pi^+ \pi^- \pi^0 \nu_\tau$ (ex. K^0)		(4.25 ± 0.09) %		S=1.3
Γ_{68}	$\pi^- \pi^+ \pi^- \pi^0 \nu_\tau$ (ex. K^0,ω)	[a]	(2.51 ± 0.09) %		S=1.2
Γ_{69}	$h^- \rho\pi^0 \nu_\tau$				
Γ_{70}	$h^- \rho^+ h^- \nu_\tau$				
Γ_{71}	$h^- \rho^- h^+ \nu_\tau$				
Γ_{72}	$h^- h^- h^+ 2\pi^0 \nu_\tau$		(5.5 ± 0.4)	$\times 10^{-3}$	
Γ_{73}	$h^- h^- h^+ 2\pi^0 \nu_\tau$ (ex. K^0)		(5.4 ± 0.4)	$\times 10^{-3}$	
Γ_{74}	$h^- h^- h^+ 2\pi^0 \nu_\tau$ (ex. K^0,ω,η)	[a]	(1.1 ± 0.4)	$\times 10^{-3}$	
Γ_{75}	$h^- h^- h^+ 3\pi^0 \nu_\tau$	[a]	(2.3 ± 0.8)	$\times 10^{-4}$	S=1.5
Γ_{76}	$K^- h^+ h^- \geq 0$ neutrals ν_τ		(6.9 ± 0.4)	$\times 10^{-3}$	S=1.3
Γ_{77}	$K^- h^+ \pi^- \nu_\tau$ (ex. K^0)		(4.8 ± 0.4)	$\times 10^{-3}$	S=1.5
Γ_{78}	$K^- h^+ \pi^- \pi^0 \nu_\tau$ (ex. K^0)		(1.07 ± 0.22)	$\times 10^{-3}$	
Γ_{79}	$K^- \pi^+ \pi^- \geq 0$ neutrals ν_τ		(5.0 ± 0.4)	$\times 10^{-3}$	S=1.3
Γ_{80}	$K^- \pi^+ \pi^- \geq 0\pi^0 \nu_\tau$ (ex. K^0)		(3.9 ± 0.4)	$\times 10^{-3}$	S=1.3
Γ_{81}	$K^- \pi^+ \pi^- \nu_\tau$		(3.8 ± 0.4)	$\times 10^{-3}$	S=1.6
Γ_{82}	$K^- \pi^+ \pi^- \nu_\tau$ (ex. K^0)	[a]	(3.3 ± 0.4)	$\times 10^{-3}$	S=1.6
Γ_{83}	$K^- \rho^0 \nu_\tau \to K^- \pi^+ \pi^- \nu_\tau$		(1.6 ± 0.6)	$\times 10^{-3}$	
Γ_{84}	$K^- \pi^+ \pi^- \pi^0 \nu_\tau$		(1.18 ± 0.25)	$\times 10^{-3}$	
Γ_{85}	$K^- \pi^+ \pi^- \pi^0 \nu_\tau$ (ex. K^0)		(6.5 ± 2.4)	$\times 10^{-4}$	
Γ_{86}	$K^- \pi^+ \pi^- \pi^0 \nu_\tau$ (ex. K^0,η)	[a]	(5.9 ± 2.4)	$\times 10^{-4}$	
Γ_{87}	$K^- \pi^+ K^- \geq 0$ neut. ν_τ	<	9	$\times 10^{-4}$	CL=95%
Γ_{88}	$K^- K^+ \pi^- \geq 0$ neut. ν_τ		(1.97 ± 0.18)	$\times 10^{-3}$	S=1.1
Γ_{89}	$K^- K^+ \pi^- \nu_\tau$	[a]	(1.55 ± 0.07)	$\times 10^{-3}$	
Γ_{90}	$K^- K^+ \pi^- \pi^0 \nu_\tau$	[a]	(4.2 ± 1.6)	$\times 10^{-4}$	S=1.1
Γ_{91}	$K^- K^+ K^- \geq 0$ neut. ν_τ	<	2.1	$\times 10^{-3}$	CL=95%
Γ_{92}	$K^- K^+ K^- \nu_\tau$	<	3.7	$\times 10^{-5}$	CL=90%
Γ_{93}	$\pi^- K^+ \pi^- \geq 0$ neut. ν_τ	<	2.5	$\times 10^{-3}$	CL=95%
Γ_{94}	$e^- e^- e^+ \overline{\nu}_e \nu_\tau$		(2.8 ± 1.5)	$\times 10^{-5}$	
Γ_{95}	$\mu^- e^- e^+ \overline{\nu}_\mu \nu_\tau$	<	3.6	$\times 10^{-5}$	CL=90%

Modes with five charged particles

Γ_{96}	$3h^- 2h^+ \geq 0$ neutrals ν_τ (ex. $K^0_S \to \pi^-\pi^+$) ("5-prong")		(1.00 ± 0.06)	$\times 10^{-3}$	
Γ_{97}	$3h^- 2h^+ \nu_\tau$ (ex. K^0)	[a]	(8.2 ± 0.6)	$\times 10^{-4}$	
Γ_{98}	$3h^- 2h^+ \pi^0 \nu_\tau$ (ex. K^0)	[a]	(1.81 ± 0.27)	$\times 10^{-4}$	
Γ_{99}	$3h^- 2h^+ 2\pi^0 \nu_\tau$	<	1.1	$\times 10^{-4}$	CL=90%

Miscellaneous other allowed modes

Γ_{100}	$(5\pi)^- \nu_\tau$		(8.0 ± 0.7)	$\times 10^{-3}$	
Γ_{101}	$4h^- 3h^+ \geq 0$ neutrals ν_τ ("7-prong")	<	2.4	$\times 10^{-6}$	CL=90%
Γ_{102}	$X^-(S=-1)\nu_\tau$		(2.91 ± 0.08) %		S=1.1
Γ_{103}	$K^*(892)^- \geq 0$ neutrals $\geq 0K^0_L \nu_\tau$		(1.42 ± 0.18) %		S=1.4
Γ_{104}	$K^*(892)^- \nu_\tau$		(1.29 ± 0.05) %		
Γ_{105}	$K^*(892)^0 K^- \geq 0$ neutrals ν_τ		(3.2 ± 1.4)	$\times 10^{-3}$	
Γ_{106}	$K^*(892)^0 K^- \nu_\tau$		(2.1 ± 0.4)	$\times 10^{-3}$	
Γ_{107}	$\overline{K}^*(892)^0 \pi^- \geq 0$ neutrals ν_τ		(3.8 ± 1.7)	$\times 10^{-3}$	
Γ_{108}	$\overline{K}^*(892)^0 \pi^- \nu_\tau$		(2.2 ± 0.5)	$\times 10^{-3}$	
Γ_{109}	$(\overline{K}^*(892)\pi)^- \nu_\tau \to \pi^- \overline{K}^0 \pi^0 \nu_\tau$		(1.0 ± 0.4)	$\times 10^{-3}$	
Γ_{110}	$K_1(1270)^- \nu_\tau$		(4.7 ± 1.1)	$\times 10^{-3}$	
Γ_{111}	$K_1(1400)^- \nu_\tau$		(1.7 ± 2.6)	$\times 10^{-3}$	S=1.7
Γ_{112}	$K^*(1410)^- \nu_\tau$		($1.5\ ^{+1.4}_{-1.0}$)	$\times 10^{-3}$	
Γ_{113}	$K^*_0(1430)^- \nu_\tau$	<	5	$\times 10^{-4}$	CL=95%
Γ_{114}	$K^*_2(1430)^- \nu_\tau$	<	3	$\times 10^{-3}$	CL=95%
Γ_{115}	$a_0(980)^- \geq 0$ neutrals ν_τ				
Γ_{116}	$\eta \pi^- \nu_\tau$	<	1.4	$\times 10^{-4}$	CL=95%
Γ_{117}	$\eta \pi^- \pi^0 \nu_\tau$	[a]	(1.74 ± 0.24)	$\times 10^{-3}$	
Γ_{118}	$\eta \pi^- \pi^0 \pi^0 \nu_\tau$		(1.5 ± 0.5)	$\times 10^{-4}$	
Γ_{119}	$\eta K^- \nu_\tau$	[a]	(2.7 ± 0.6)	$\times 10^{-4}$	
Γ_{120}	$\eta K^*(892)^- \nu_\tau$		(2.9 ± 0.9)	$\times 10^{-4}$	
Γ_{121}	$\eta K^- \pi^0 \nu_\tau$		(1.8 ± 0.9)	$\times 10^{-4}$	
Γ_{122}	$\eta \overline{K}^0 \pi^- \nu_\tau$		(2.2 ± 0.7)	$\times 10^{-4}$	
Γ_{123}	$\eta \pi^+ \pi^- \pi^- \geq 0$ neutrals ν_τ	<	3	$\times 10^{-3}$	CL=90%
Γ_{124}	$\eta \pi^- \pi^+ \pi^- \nu_\tau$		(2.3 ± 0.5)	$\times 10^{-4}$	
Γ_{125}	$\eta\, a_1(1260)^- \nu_\tau \to \eta \pi^- \rho^0 \nu_\tau$	<	3.9	$\times 10^{-4}$	CL=90%
Γ_{126}	$\eta \eta \pi^- \nu_\tau$	<	1.1	$\times 10^{-4}$	CL=95%
Γ_{127}	$\eta \eta \pi^- \pi^0 \nu_\tau$	<	2.0	$\times 10^{-4}$	CL=95%
Γ_{128}	$\eta'(958) \pi^- \nu_\tau$	<	7.4	$\times 10^{-5}$	CL=90%
Γ_{129}	$\eta'(958) \pi^- \pi^0 \nu_\tau$	<	8.0	$\times 10^{-5}$	CL=90%
Γ_{130}	$\phi \pi^- \nu_\tau$	<	2.0	$\times 10^{-4}$	CL=90%
Γ_{131}	$\phi K^- \nu_\tau$	<	6.7	$\times 10^{-5}$	CL=90%
Γ_{132}	$f_1(1285) \pi^- \nu_\tau$		(5.8 ± 2.3)	$\times 10^{-4}$	
Γ_{133}	$f_1(1285) \pi^- \nu_\tau \to \eta \pi^- \pi^+ \pi^- \nu_\tau$		(1.3 ± 0.4)	$\times 10^{-4}$	
Γ_{134}	$\pi(1300)^- \nu_\tau \to (\rho\pi)^- \nu_\tau \to (3\pi)^- \nu_\tau$	<	1.0	$\times 10^{-4}$	CL=90%
Γ_{135}	$\pi(1300)^- \nu_\tau \to ((\pi\pi)_{S-\text{wave}}\, \pi)^- \nu_\tau \to (3\pi)^- \nu_\tau$	<	1.9	$\times 10^{-4}$	CL=90%
Γ_{136}	$h^- \omega \geq 0$ neutrals ν_τ		(2.38 ± 0.08) %		
Γ_{137}	$h^- \omega \nu_\tau$	[a]	(1.94 ± 0.07) %		
Γ_{138}	$h^- \omega \pi^0 \nu_\tau$	[a]	(4.4 ± 0.5)	$\times 10^{-3}$	
Γ_{139}	$h^- \omega 2\pi^0 \nu_\tau$		(1.4 ± 0.5)	$\times 10^{-4}$	
Γ_{140}	$2h^- h^+ \omega \nu_\tau$		(1.20 ± 0.22)	$\times 10^{-4}$	

Lepton Family number (LF), Lepton number (L), or Baryon number (B) violating modes

L means lepton number violation (*e.g.* $\tau^- \to e^+\pi^-\pi^-$). Following common usage, LF means lepton family violation *and not* lepton number violation (*e.g.* $\tau^- \to e^-\pi^+\pi^-$). B means baryon number violation.

Γ_{141}	$e^-\gamma$	LF	$<$	2.7	$\times 10^{-6}$	CL=90%
Γ_{142}	$\mu^-\gamma$	LF	$<$	1.1	$\times 10^{-6}$	CL=90%
Γ_{143}	$e^-\pi^0$	LF	$<$	3.7	$\times 10^{-6}$	CL=90%
Γ_{144}	$\mu^-\pi^0$	LF	$<$	4.0	$\times 10^{-6}$	CL=90%
Γ_{145}	$e^- K^0_S$	LF	$<$	9.1	$\times 10^{-7}$	CL=90%
Γ_{146}	$\mu^- K^0_S$	LF	$<$	9.5	$\times 10^{-7}$	CL=90%
Γ_{147}	$e^-\eta$	LF	$<$	8.2	$\times 10^{-6}$	CL=90%
Γ_{148}	$\mu^-\eta$	LF	$<$	9.6	$\times 10^{-6}$	CL=90%
Γ_{149}	$e^-\rho^0$	LF	$<$	2.0	$\times 10^{-6}$	CL=90%
Γ_{150}	$\mu^-\rho^0$	LF	$<$	6.3	$\times 10^{-6}$	CL=90%
Γ_{151}	$e^- K^*(892)^0$	LF	$<$	5.1	$\times 10^{-6}$	CL=90%
Γ_{152}	$\mu^- K^*(892)^0$	LF	$<$	7.5	$\times 10^{-6}$	CL=90%
Γ_{153}	$e^- \overline{K}^*(892)^0$	LF	$<$	7.4	$\times 10^{-6}$	CL=90%
Γ_{154}	$\mu^- \overline{K}^*(892)^0$	LF	$<$	7.5	$\times 10^{-6}$	CL=90%
Γ_{155}	$e^-\phi$	LF	$<$	6.9	$\times 10^{-6}$	CL=90%
Γ_{156}	$\mu^-\phi$	LF	$<$	7.0	$\times 10^{-6}$	CL=90%
Γ_{157}	$e^- e^+ e^-$	LF	$<$	2.9	$\times 10^{-6}$	CL=90%
Γ_{158}	$e^-\mu^+\mu^-$	LF	$<$	1.8	$\times 10^{-6}$	CL=90%
Γ_{159}	$e^+\mu^-\mu^-$	LF	$<$	1.5	$\times 10^{-6}$	CL=90%
Γ_{160}	$\mu^- e^+ e^-$	LF	$<$	1.7	$\times 10^{-6}$	CL=90%
Γ_{161}	$\mu^+ e^- e^-$	LF	$<$	1.5	$\times 10^{-6}$	CL=90%
Γ_{162}	$\mu^-\mu^+\mu^-$	LF	$<$	1.9	$\times 10^{-6}$	CL=90%
Γ_{163}	$e^-\pi^+\pi^-$	LF	$<$	2.2	$\times 10^{-6}$	CL=90%
Γ_{164}	$e^+\pi^-\pi^-$	L	$<$	1.9	$\times 10^{-6}$	CL=90%
Γ_{165}	$\mu^-\pi^+\pi^-$	LF	$<$	8.2	$\times 10^{-6}$	CL=90%
Γ_{166}	$\mu^+\pi^-\pi^-$	L	$<$	3.4	$\times 10^{-6}$	CL=90%
Γ_{167}	$e^-\pi^+ K^-$	LF	$<$	6.4	$\times 10^{-6}$	CL=90%
Γ_{168}	$e^-\pi^- K^+$	LF	$<$	3.8	$\times 10^{-6}$	CL=90%
Γ_{169}	$e^+\pi^- K^-$	L	$<$	2.1	$\times 10^{-6}$	CL=90%
Γ_{170}	$e^- K^0_S K^0_S$	LF	$<$	2.2	$\times 10^{-6}$	CL=90%
Γ_{171}	$e^- K^+ K^-$	LF	$<$	6.0	$\times 10^{-6}$	CL=90%
Γ_{172}	$e^+ K^- K^-$	L	$<$	3.8	$\times 10^{-6}$	CL=90%
Γ_{173}	$\mu^-\pi^+ K^-$	LF	$<$	7.5	$\times 10^{-6}$	CL=90%
Γ_{174}	$\mu^-\pi^- K^+$	LF	$<$	7.4	$\times 10^{-6}$	CL=90%
Γ_{175}	$\mu^+\pi^- K^-$	L	$<$	7.0	$\times 10^{-6}$	CL=90%
Γ_{176}	$\mu^- K^0_S K^0_S$	LF	$<$	3.4	$\times 10^{-6}$	CL=90%
Γ_{177}	$\mu^- K^+ K^-$	LF	$<$	1.5	$\times 10^{-5}$	CL=90%
Γ_{178}	$\mu^+ K^- K^-$	L	$<$	6.0	$\times 10^{-6}$	CL=90%
Γ_{179}	$e^-\pi^0\pi^0$	LF	$<$	6.5	$\times 10^{-6}$	CL=90%
Γ_{180}	$\mu^-\pi^0\pi^0$	LF	$<$	1.4	$\times 10^{-5}$	CL=90%
Γ_{181}	$e^-\eta\eta$	LF	$<$	3.5	$\times 10^{-5}$	CL=90%
Γ_{182}	$\mu^-\eta\eta$	LF	$<$	6.0	$\times 10^{-5}$	CL=90%
Γ_{183}	$e^-\pi^0\eta$	LF	$<$	2.4	$\times 10^{-5}$	CL=90%
Γ_{184}	$\mu^-\pi^0\eta$	LF	$<$	2.2	$\times 10^{-5}$	CL=90%
Γ_{185}	$\overline{p}\gamma$	L,B	$<$	3.5	$\times 10^{-6}$	CL=90%
Γ_{186}	$\overline{p}\pi^0$	L,B	$<$	1.5	$\times 10^{-5}$	CL=90%
Γ_{187}	$\overline{p}2\pi^0$	L,B	$<$	3.3	$\times 10^{-5}$	CL=90%
Γ_{188}	$\overline{p}\eta$	L,B	$<$	8.9	$\times 10^{-6}$	CL=90%
Γ_{189}	$\overline{p}\pi^0\eta$	L,B	$<$	2.7	$\times 10^{-5}$	CL=90%
Γ_{190}	e^- light boson	LF	$<$	2.7	$\times 10^{-3}$	CL=95%
Γ_{191}	μ^- light boson	LF	$<$	5	$\times 10^{-3}$	CL=95%

[*a*] Basis mode for the τ.

[*b*] See the Particle Listings below for the energy limits used in this measurement.

CONSTRAINED FIT INFORMATION

An overall fit to 65 branching ratios uses 128 measurements and one constraint to determine 31 parameters. The overall fit has a $\chi^2 = 62.5$ for 98 degrees of freedom.

The following *off-diagonal* array elements are the correlation coefficients $\langle \delta x_i \delta x_j \rangle / (\delta x_i \cdot \delta x_j)$, in percent, from the fit to the branching fractions, $x_i \equiv \Gamma_i/\Gamma_{\rm total}$. The fit constrains the x_i whose labels appear in this array to sum to one.

	x_3	x_5	x_9	x_{10}	x_{13}	x_{15}	x_{19}	x_{22}	x_{25}	x_{26}
x_5	3									
x_9	−5	−5								
x_{10}	0	0	−20							
x_{13}	−13	−13	−25	1						
x_{15}	0	0	1	−3	−22					
x_{19}	−13	−14	−25	0	−36	4				
x_{22}	0	0	1	−2	5	−21	−16			
x_{25}	−8	−8	−15	0	−18	5	−24	3		
x_{26}	0	0	1	−2	5	−19	3	−13	−22	
x_{28}	−4	−4	−7	0	−10	0	−12	0	−7	0
x_{33}	−1	−2	−13	0	−3	1	−8	1	−1	1
x_{35}	0	0	−4	−1	2	−12	−1	−8	2	−8
x_{38}	−2	−2	−2	0	−5	3	−5	2	−9	2
x_{40}	−1	−1	0	−1	2	−16	1	−11	−1	−10
x_{45}	0	0	−2	0	0	0	0	0	0	0
x_{46}	−2	−2	−2	0	−4	1	−4	1	−2	1
x_{60}	−1	−1	−2	0	−4	0	−3	0	−2	0
x_{68}	−1	−1	−3	0	−3	0	−4	0	−2	0
x_{74}	0	0	0	0	0	0	0	0	0	0
x_{75}	0	0	0	0	0	0	0	0	0	0
x_{82}	0	0	0	0	0	0	0	0	0	0
x_{86}	0	0	0	0	0	0	0	0	0	0
x_{89}	0	0	0	0	0	0	0	0	0	0
x_{90}	0	0	0	0	0	0	0	0	0	0
x_{97}	0	0	−1	0	−1	0	−1	0	0	0
x_{98}	0	0	0	0	0	0	0	0	0	0
x_{117}	−1	−1	−1	0	−2	0	−2	0	−1	0
x_{119}	0	0	0	0	0	−3	0	−2	−2	−2
x_{137}	−1	−1	−2	0	−3	0	−3	0	−1	0
x_{138}	−1	−1	−1	0	−2	0	−2	0	−1	0

	x_{28}	x_{33}	x_{35}	x_{38}	x_{40}	x_{45}	x_{46}	x_{60}	x_{68}	x_{74}
x_{33}	−1									
x_{35}	0	−5								
x_{38}	−1	−7	0							
x_{40}	0	−2	−15	−19						
x_{45}	0	−2	−1	−2	0					
x_{46}	−1	−12	−4	−10	−3	−3				
x_{60}	−1	−7	−3	3	2	0	0			
x_{68}	−1	4	2	−5	−2	0	0	−47		
x_{74}	2	1	0	1	0	0	0	−8	−7	
x_{75}	0	0	0	0	0	0	0	−3	−3	0
x_{82}	0	−1	0	0	0	0	0	−31	−1	0
x_{86}	0	0	0	0	0	0	0	2	−14	0
x_{89}	0	0	0	0	0	0	0	−3	−1	0
x_{90}	0	0	0	0	0	0	0	−6	−1	−1
x_{97}	0	0	0	0	0	0	0	−1	−1	0
x_{98}	0	0	0	0	0	0	0	0	0	0
x_{117}	−14	0	0	0	0	0	0	−1	−1	−14
x_{119}	0	0	−1	0	−2	0	0	0	0	0
x_{137}	−1	1	1	−3	−1	0	0	−23	−29	−3
x_{138}	−1	1	0	1	0	0	0	−9	−10	−44

	x_{75}	x_{82}	x_{86}	x_{89}	x_{90}	x_{97}	x_{98}	x_{117}	x_{119}	x_{137}
x_{82}	0									
x_{86}	0	−14								
x_{89}	0	−11	1							
x_{90}	0	6	−47	−1						
x_{97}	0	0	0	0	0					
x_{98}	0	0	0	0	0	−19				
x_{117}	0	0	0	0	0	0	0			
x_{119}	0	0	−6	0	0	0	0	0		
x_{137}	−1	−2	2	0	2	0	0	0	0	
x_{138}	−1	−1	0	0	−1	0	0	0	0	−4

τ BRANCHING FRACTIONS

Revised April 2004 by K.G. Hayes (Hillsdale College).

The constrained fit to τ branching fractions: The Lepton Summary Table and the List of τ-Decay Modes contain branching fractions for 109 conventional τ-decay modes and upper limits on the branching fractions for 27 other conventional τ-decay modes. Of the 109 modes with branching fractions, 79 are derived from a constrained fit to τ branching fraction data. The goal of the constrained fit is to make optimal use of the experimental data to determine τ branching fractions. For example, the branching fractions for the decay modes $\tau^- \to \pi^-\pi^+\pi^-\nu_\tau$ and $\tau^- \to \pi^-\pi^+\pi^-\pi^0\nu_\tau$ are determined mostly from experimental measurements of the branching fractions for $\tau^- \to h^-h^-h^+\nu_\tau$ and $\tau^- \to h^-h^-h^+\pi^0\nu_\tau$ and recent measurements of exclusive branching fractions for 3-prong modes containing charged kaons and 0 or 1 π^0's.

Branching fractions from the constrained fit are derived from a set of basis modes. The basis modes form an exclusive set whose branching fractions are constrained to sum exactly to one. The set of selected basis modes expands as branching fraction measurements for new τ-decay modes are published. The number of basis modes has expanded from 12 in the year 1994 fit to 31 in the 2002 and 2004 fits. The 31 basis modes selected for the 2004 fit are listed in Table 1. See the 1996 edition of this *Review* [1] for a complete description of our notation for naming τ-decay modes and the selection of the basis modes. For each edition since the 1996 edition, the changes in the selected basis modes from the previous edition are described in the τ Branching Fractions Review.

In selecting the basis modes, assumptions and choices must be made. For example, we assume the decays $\tau^- \to \pi^-K^+\pi^- \geq 0\pi^0\nu_\tau$ and $\tau^- \to \pi^+K^-K^- \geq 0\pi^0\nu\tau$ have negligible branching fractions. This is consistent with standard model predictions for τ decay, although the experimental limits for these branching fractions are not very stringent. The 95% confidence level upper limits for these branching fractions in the current Listings are $\mathrm{B}(\tau^- \to \pi^-K^+\pi^- \geq 0\pi^0\nu_\tau) < 0.25\%$ and $\mathrm{B}(\tau^- \to \pi^+K^-K^- \geq 0\pi^0\nu_\tau) < 0.09\%$, values not so different from measured branching fractions for allowed 3-prong modes containing charged kaons. Although our usual goal is to impose as few theoretical constraints as possible so that the world averages and fit results can be used to test the theoretical constraints (*i.e.*, we do not make use of the theoretical constraint from lepton universality on the ratio of the τ-leptonic branching fractions $\mathrm{B}(\tau^- \to \mu^-\overline{\nu}_\mu\nu_\tau)/\ \mathrm{B}(\tau^- \to e^-\overline{\nu}_e\nu_\tau) = 0.9726$), the experimental challenge to identify charged prongs in 3-prong τ decays is sufficiently difficult that experimenters have been forced to make these assumptions when measuring the branching fractions of the allowed decays.

Table 1: Basis modes for the 2004 fit to τ branching fraction data.

$e^-\overline{\nu}_e\nu_\tau$	$K^-K^0\pi^0\nu_\tau$
$\mu^-\overline{\nu}_\mu\nu_\tau$	$\pi^-\pi^+\pi^-\nu_\tau$ (ex. K^0, ω)
$\pi^-\nu_\tau$	$\pi^-\pi^+\pi^-\pi^0\nu_\tau$ (ex. K^0, ω)
$\pi^-\pi^0\nu_\tau$	$K^-\pi^+\pi^-\nu_\tau$ (ex. K^0)
$\pi^-2\pi^0\nu_\tau$ (ex. K^0)	$K^-\pi^+\pi^-\pi^0\nu_\tau$ (ex. K^0, η)
$\pi^-3\pi^0\nu_\tau$ (ex. K^0)	$K^-K^+\pi^-\nu_\tau$
$h^-4\pi^0\nu_\tau$ (ex. K^0, η)	$K^-K^+\pi^-\pi^0\nu_\tau$
$K^-\nu_\tau$	$h^-h^-h^+2\pi^0\nu_\tau$ (ex. K^0, ω, η)
$K^-\pi^0\nu_\tau$	$h^-h^-h^+3\pi^0\nu_\tau$
$K^-2\pi^0\nu_\tau$ (ex. K^0)	$3h^-2h^+\nu_\tau$ (ex. K^0)
$K^-3\pi^0\nu_\tau$ (ex. K^0, η)	$3h^-2h^+\pi^0\nu_\tau$ (ex. K^0)
$\pi^-\overline{K}^0\nu_\tau$	$h^-\omega\nu_\tau$
$\pi^-\overline{K}^0\pi^0\nu_\tau$	$h^-\omega\pi^0\nu_\tau$
$\pi^-K^0_SK^0_S\nu_\tau$	$\eta\pi^-\pi^0\nu_\tau$
$\pi^-K^0_SK^0_L\nu_\tau$	$\eta K^-\nu_\tau$
$K^-K^0\nu_\tau$	

There are several recently measured modes with small but well-measured (> 2.5 sigma from zero) branching fractions [2] which cannot be expressed in terms of the selected basis modes and are therefore left out of the fit:

$$\begin{aligned}
\mathrm{B}(\tau^- \to \pi^-K^0_SK^0_L\pi^0\nu_\tau) &= (3.1 \pm 1.2) \times 10^{-4} \\
\mathrm{B}(\tau^- \to h^-\omega\pi^0\pi^0\nu_\tau) &= (1.4 \pm 0.5) \times 10^{-4} \\
\mathrm{B}(\tau^- \to 2h^-h^+\omega\nu_\tau) &= (1.20 \pm 0.22) \times 10^{-4}
\end{aligned}$$

plus the $\eta \to \gamma\gamma$ and $\eta \to \pi^+\pi^-\gamma$ components of the branching fractions

$$\begin{aligned}
\mathrm{B}(\tau^- \to \eta\pi^-\pi^+\pi^-\nu_\tau) &= (2.3 \pm 0.5) \times 10^{-4}\ , \\
\mathrm{B}(\tau^- \to \eta\pi^-\pi^0\pi^0\nu_\tau) &= (1.5 \pm 0.5) \times 10^{-4}\ , \\
\mathrm{B}(\tau^- \to \eta\overline{K}^0\pi^-\nu_\tau) &= (2.2 \pm 0.7) \times 10^{-4}\ .
\end{aligned}$$

The sum of these excluded branching fractions is $(0.08 \pm 0.01)\%$. This is near our goal of 0.1% for the internal consistency of the τ Listings for this edition, and thus for simplicity we do not include these small branching fraction decay modes in the basis set.

Begininng with the 2002 edition, the fit algorithm has been improved to allow for correlations between branching fraction measurements used in the fit. In this edition, correlations between measurements contained in Refs. [3,4,5,6] have been included. In the τ Listings, the correlation coefficients are listed in the footnote for each measurement. Sometimes experimental papers contain correlation coefficients between measurements using only statistical errors without including systematic errors. We usually cannot make use of these correlation coefficients.

The constrained fit has a χ^2 of 62.5 for 99 degrees of freedom. Only one of the year 2004 basis mode branching fractions shifted by more than 1 sigma from its 2002 value: $B(\tau^- \to K^-\pi^+\pi^-\nu_\tau(\text{ex. } K^0))$ changed from $(0.28 \pm 0.05)\%$ to $(0.33 \pm 0.04)\%$.

Overconsistency of Leptonic Branching Fraction Measurements: To minimize the effects of older experiments which often have larger systematic errors and sometimes make assumptions that have later been shown to be invalid, we exclude old measurements in decay modes which contain at least several newer data of much higher precision. As a rule, we exclude those experiments with large errors which together would contribute no more than 5% of the weight in the average. This procedure leaves six measurements for $B_e \equiv B(\tau^- \to e^-\overline{\nu}_e\nu_\tau)$ and five measurements for $B_\mu \equiv B(\tau^- \to \mu^-\overline{\nu}_\mu\nu_\tau)$. For both B_e and B_μ, the six measurements are considerably more consistent with each other than should be expected from the quoted errors on the individual measurements. The χ^2 from the calculation of the average of the selected measurements is 0.49 for B_e and 0.09 for B_μ.

References

1. R.M. Barnett *et al.* (Particle Data Group), *Review of Particle Physics*, Phys. Rev. **D54**, 1 (1996).
2. See the τ Listings for references.
3. P. Abreu *et al.* (**DELPHI** Collaboration), Eur. Phys. J. **C20**, 617 (2001).
4. P. Achard *et al.* (**L3** Collaboration), Phys. Lett. **B519**, 189 (2001).
5. A. Anastassov *et al.* (**CLEO** Collaboration), Phys. Rev. **D55**, 2559 (1997) and Phys. Rev. **D58**, 119903 (1998) (erratum).
6. M. Acciarri *et al.* (**L3** Collaboration), Phys. Lett. **B507**, 47 (2001).

τ^- BRANCHING RATIOS

$\Gamma(\text{particle}^- \geq 0 \text{ neutrals} \geq 0K^0\nu_\tau(\text{"1-prong"}))/\Gamma_{\text{total}}$ Γ_1/Γ

$\Gamma_1/\Gamma = (\Gamma_3+\Gamma_5+\Gamma_9+\Gamma_{10}+\Gamma_{13}+\Gamma_{15}+\Gamma_{19}+\Gamma_{22}+\Gamma_{25}+\Gamma_{26}+\Gamma_{28}+\Gamma_{33}+\Gamma_{35}+\Gamma_{38}+\Gamma_{40}+2\Gamma_{45}+\Gamma_{46}+0.708\Gamma_{117}+0.715\Gamma_{119}+0.09\Gamma_{137}+0.09\Gamma_{138})/\Gamma$

The charged particle here can be e, μ, or hadron. In many analyses, the sum of the topological branching fractions (1, 3, and 5 prongs) is constrained to be unity. Since the 5-prong fraction is very small, the measured 1-prong and 3-prong fractions are highly correlated and cannot be treated as independent quantities in our overall fit. We arbitrarily choose to use the 3-prong fraction in our fit, and leave the 1-prong fraction out. We do, however, use these 1-prong measurements in our average below. The measurements used only for the average are marked "avg," whereas "f&a" marks a result used for the fit and the average.

VALUE (%)		EVTS	DOCUMENT ID		TECN	COMMENT
85.35 ±0.07 OUR FIT	Error includes scale factor of 1.1.					
85.26 ±0.13 OUR AVERAGE	Error includes scale factor of 1.6. See the ideogram below.					
85.316 ±0.093 ±0.049	avg	78k	[27] ABREU	01M DLPH		1992–1995 LEP runs
85.274 ±0.105 ±0.073	avg		[28] ACHARD	01D L3		1992–1995 LEP runs
84.48 ±0.27 ±0.23	avg		ACTON	92H OPAL		1990–1991 LEP runs
85.45 $^{+0.69}_{-0.73}$ ±0.65	f&a		DECAMP	92C ALEP		1989–1990 LEP runs

[27] The correlation coefficients between this measurement and the ABREU 01M measurements of $B(\tau \to$ 3-prong) and $B(\tau \to$ 5-prong) are -0.98 and -0.08 respectively.

[28] The correlation coefficients between this measurement and the ACHARD 01D measurements of $B(\tau \to$ "3-prong") and $B(\tau \to$ "5-prong") are -0.978 and -0.082 respectively.

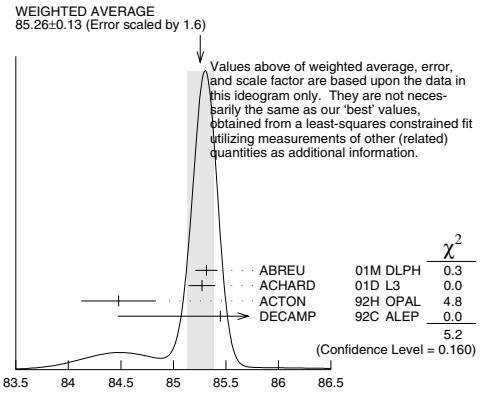

$\Gamma(\text{particle}^- \geq 0 \text{ neutrals} \geq 0K^0\nu_\tau(\text{"1-prong"}))/\Gamma_{\text{total}}$

$\Gamma(\text{particle}^- \geq 0 \text{ neutrals} \geq 0K^0_L\nu_\tau)/\Gamma_{\text{total}}$ Γ_2/Γ

$\Gamma_2/\Gamma = (\Gamma_3+\Gamma_5+\Gamma_9+\Gamma_{10}+\Gamma_{13}+\Gamma_{15}+\Gamma_{19}+\Gamma_{22}+\Gamma_{25}+\Gamma_{26}+\Gamma_{28}+0.6569\Gamma_{33}+0.6569\Gamma_{35}+0.6569\Gamma_{38}+0.6569\Gamma_{40}+1.0985\Gamma_{45}+0.3139\Gamma_{46}+0.708\Gamma_{117}+0.715\Gamma_{119}+0.09\Gamma_{137}+0.09\Gamma_{138})/\Gamma$

VALUE (%)		EVTS	DOCUMENT ID		TECN	COMMENT
84.72±0.07 OUR FIT	Error includes scale factor of 1.1.					
85.1 ±0.4 OUR AVERAGE						
85.6 ±0.6 ±0.3	avg	3300	[29] ADEVA	91F L3		E^{ee}_{cm}= 88.3–94.3 GeV
84.9 ±0.4 ±0.3	avg		BEHREND	89B CELL		E^{ee}_{cm}= 14–47 GeV
84.7 ±0.8 ±0.6	avg		[30] AIHARA	87B TPC		E^{ee}_{cm}= 29 GeV
• • • We do not use the following data for averages, fits, limits, etc. • • •						
86.4 ±0.3 ±0.3			ABACHI	89B HRS		E^{ee}_{cm}= 29 GeV
87.1 ±1.0 ±0.7			[31] BURCHAT	87 MRK2		E^{ee}_{cm}= 29 GeV
87.2 ±0.5 ±0.8			SCHMIDKE	86 MRK2		E^{ee}_{cm}= 29 GeV
84.7 ±1.1 $^{+1.6}_{-1.3}$		169	[32] ALTHOFF	85 TASS		E^{ee}_{cm}= 34.5 GeV
86.1 ±0.5 ±0.9			BARTEL	85F JADE		E^{ee}_{cm}= 34.6 GeV
87.8 ±1.3 ±3.9			[33] BERGER	85 PLUT		E^{ee}_{cm}= 34.6 GeV
86.7 ±0.3 ±0.6			FERNANDEZ	85 MAC		E^{ee}_{cm}= 29 GeV

[29] Not independent of ADEVA 91F $\Gamma(h^-h^-h^+ \geq 0 \text{ neutrals} \geq 0K^0_L\nu_\tau)/\Gamma_{\text{total}}$ value.

[30] Not independent of AIHARA 87B $\Gamma(\mu^-\overline{\nu}_\mu\nu_\tau)/\Gamma_{\text{total}}$, $\Gamma(e^-\overline{\nu}_e\nu_\tau)/\Gamma_{\text{total}}$, and $/\Gamma_{\text{total}}$ values.

[31] Not independent of SCHMIDKE 86 value (also not independent of BURCHAT 87 value for $\Gamma(h^-h^-h^+ \geq 0 \text{ neutrals} \geq 0K^0_L\nu_\tau)/\Gamma_{\text{total}}$.

[32] Not independent of ALTHOFF 85 $\Gamma(\mu^-\overline{\nu}_\mu\nu_\tau)/\Gamma_{\text{total}}$, $\Gamma(e^-\overline{\nu}_e\nu_\tau)/\Gamma_{\text{total}}$, $/\Gamma_{\text{total}}$, and $\Gamma(h^-h^-h^+ \geq 0 \text{ neutrals} \geq 0K^0_L\nu_\tau)/\Gamma_{\text{total}}$ values.

[33] Not independent of (1-prong + $\geq 0\pi^0$) and (1-prong + $\geq 1\pi^0$) values.

$\Gamma(\mu^-\overline{\nu}_\mu\nu_\tau)/\Gamma_{\text{total}}$ Γ_3/Γ

Data marked "avg" are highly correlated with data appearing elsewhere in the Listings, and are therefore used for the average given below but not in the overall fits. "f&a" marks results used for the fit and the average.

To minimize the effect of experiments with large systematic errors, we exclude experiments which together would contribute 5% of the weight in the average.

VALUE (%)		EVTS	DOCUMENT ID		TECN	COMMENT
17.36 ±0.06 OUR FIT						
17.33 ±0.06 OUR AVERAGE						
17.34 ±0.09 ±0.06	f&a	31.4k	ABBIENDI	03 OPAL		1990–1995 LEP runs
17.342 ±0.110 ±0.067	f&a	21.5k	[34] ACCIARRI	01F L3		1991–1995 LEP runs
17.325 ±0.095 ±0.077	f&a	27.7k	ABREU	99X DLPH		1991–1995 LEP runs
17.37 ±0.08 ±0.18	avg		[35] ANASTASSOV	97 CLEO		E^{ee}_{cm}= 10.6 GeV
17.31 ±0.11 ±0.05	f&a	20.7k	BUSKULIC	96C ALEP		1991–1993 LEP runs
• • • We do not use the following data for averages, fits, limits, etc. • • •						
17.02 ±0.19 ±0.24		6586	ABREU	95T DLPH		Repl.. by ABREU 99X
17.36 ±0.27		7941	AKERS	95I OPAL		Repl. by ABBIENDI 03
17.6 ±0.4 ±0.4		2148	ADRIANI	93M L3		Repl. by ACCIARRI 01F
17.4 ±0.3 ±0.5			[36] ALBRECHT	93G ARG		E^{ee}_{cm}= 9.4–10.6 GeV
17.35 ±0.41 ±0.37	f&a		DECAMP	92C ALEP		1989–1990 LEP runs
17.7 ±0.8 ±0.4		568	BEHREND	90 CELL		E^{ee}_{cm}= 35 GeV
17.4 ±1.0		2197	ADEVA	88 MRKJ		E^{ee}_{cm}= 14–16 GeV
17.7 ±1.2 ±0.7			AIHARA	87B TPC		E^{ee}_{cm}= 29 GeV

18.3	±0.9	±0.8			BURCHAT	87 MRK2	E_{cm}^{ee}= 29 GeV
18.6	±0.8	±0.7	558	[37]	BARTEL	86D JADE	E_{cm}^{ee}= 34.6 GeV
12.9	±1.7	$^{+0.7}_{-0.5}$			ALTHOFF	85 TASS	E_{cm}^{ee}= 34.5 GeV
18.0	±0.9	±0.5	473	[37]	ASH	85B MAC	E_{cm}^{ee}= 29 GeV
18.0	±1.0	±0.6		[38]	BALTRUSAIT...85	MRK3	E_{cm}^{ee}= 3.77 GeV
19.4	±1.6	±1.7	153		BERGER	85 PLUT	E_{cm}^{ee}= 34.6 GeV
17.6	±2.6	±2.1	47		BEHREND	83C CELL	E_{cm}^{ee}= 34 GeV
17.8	±2.0	±1.8			BERGER	81B PLUT	E_{cm}^{ee}= 9–32 GeV

[34] The correlation coefficient between this measurement and the ACCIARRI 01F measurement of $B(\tau^- \to e^- \overline{\nu}_e \nu_\tau)$ is 0.08.

[35] The correlation coefficients between this measurement and the ANASTASSOV 97 measurements of $B(e\overline{\nu}_e\nu_\tau)$, $B(\mu\overline{\nu}_\mu\nu_\tau)/B(e\overline{\nu}_e\nu_\tau)$, $B(h^-\nu_\tau)$, and $B(h^-\nu_\tau)/B(e\overline{\nu}_e\nu_\tau)$ are 0.50, 0.58, 0.50, and 0.08 respectively.

[36] Not independent of ALBRECHT 92D $\Gamma(\mu^-\overline{\nu}_\mu\nu_\tau)/\Gamma(e^-\overline{\nu}_e\nu_\tau)$ and ALBRECHT 93G $\Gamma(\mu^-\overline{\nu}_\mu\nu_\tau)\times\Gamma(e^-\overline{\nu}_e\nu_\tau)/\Gamma^2_{\rm total}$ values.

[37] Modified using $B(e^-\overline{\nu}_e\nu_\tau)/B(\text{"1 prong"})$ and B("1 prong") $=0.855$.

[38] Error correlated with BALTRUSAITIS 85 $e\nu\overline{\nu}$ value.

$\Gamma(\mu^-\overline{\nu}_\mu\nu_\tau\gamma)/\Gamma_{\rm total}$ Γ_4/Γ

VALUE (%)	EVTS	DOCUMENT ID		TECN	COMMENT
0.361±0.016±0.035		[39] BERGFELD	00	CLEO	E_{cm}^{ee}= 10.6 GeV
• • • We do not use the following data for averages, fits, limits, etc. • • •					
0.30 ±0.04 ±0.05	116	[40] ALEXANDER	96S	OPAL	1991–1994 LEP runs
0.23 ±0.10	10	[41] WU	90	MRK2	E_{cm}^{ee}= 29 GeV

[39] BERGFELD 00 impose requirements on detected γ's corresponding to a τ-rest-frame energy cutoff $E^*_\gamma > 10$ MeV. For $E^*_\gamma > 20$ MeV, they quote $(3.04\pm0.14\pm0.30)\times10^{-3}$.

[40] ALEXANDER 96S impose requirements on detected γ's corresponding to a τ-rest-frame energy cutoff $E_\gamma > 20$ MeV.

[41] WU 90 reports $\Gamma(\mu^-\overline{\nu}_\mu\nu_\tau\gamma)/\Gamma(\mu^-\overline{\nu}_\mu\nu_\tau) = 0.013 \pm 0.006$, which is converted to $\Gamma(\mu^-\overline{\nu}_\mu\nu_\tau\gamma)/\Gamma_{\rm total}$ using $\Gamma(\mu^-\overline{\nu}_\mu\nu_\tau\gamma)/\Gamma_{\rm total} = 17.35\%$. Requirements on detected γ's correspond to a τ rest frame energy cutoff $E_\gamma > 37$ MeV.

$\Gamma(e^-\overline{\nu}_e\nu_\tau)/\Gamma_{\rm total}$ Γ_5/Γ

To minimize the effect of experiments with large systematic errors, we exclude experiments which together would contribute 5% of the weight in the average.

VALUE (%)	EVTS	DOCUMENT ID		TECN	COMMENT
17.84 ±0.06 OUR FIT					
17.81 ±0.06 OUR AVERAGE					
17.806±0.104±0.076	24.7k	[42] ACCIARRI	01F	L3	1991–1995 LEP runs
17.81 ±0.09 ±0.06	33.1k	ABBIENDI	99H	OPAL	1991–1995 LEP runs
17.877±0.109±0.110	23.3k	ABREU	99X	DLPH	1991–1995 LEP runs
17.76 ±0.06 ±0.17		[43] ANASTASSOV	97	CLEO	E_{cm}^{ee}= 10.6 GeV
17.79 ±0.12 ±0.06	20.6k	BUSKULIC	96C	ALEP	1991–1993 LEP runs
18.09 ±0.45 ±0.45		DECAMP	92C	ALEP	1989–1990 LEP runs
• • • We do not use the following data for averages, fits, limits, etc. • • •					
17.78 ±0.10 ±0.09	25.3k	ALEXANDER	96D	OPAL	Repl. by ABBIENDI 99H
17.51 ±0.23 ±0.31	5059	ABREU	95T	DLPH	Repl.. by ABREU 99X
17.9 ±0.4 ±0.4	2892	ADRIANI	93M	L3	Repl. by ACCIARRI 01F
17.5 ±0.3 ±0.5		[44] ALBRECHT	93G	ARG	E_{cm}^{ee}= 9.4–10.6 GeV
17.97 ±0.14 ±0.23	3970	AKERIB	92	CLEO	E_{cm}^{ee}= 10.5–10.9 GeV
19.1 ±0.4 ±0.6	2960	[45] AMMAR	92	CLEO	Repl. by ANASTASSOV 97
17.0 ±0.5 ±0.6	1.7k	ABACHI	90	HRS	E_{cm}^{ee}= 29 GeV
18.4 ±0.8 ±0.4	644	BEHREND	90	CELL	E_{cm}^{ee}= 35 GeV
16.3 ±0.3 ±3.2		JANSSEN	89	CBAL	E_{cm}^{ee}= 9.4–10.6 GeV
18.4 ±1.2 ±1.0		AIHARA	87B	TPC	E_{cm}^{ee}= 29 GeV
19.1 ±0.8 ±1.1		BURCHAT	87	MRK2	E_{cm}^{ee}= 29 GeV
16.8 ±0.7 ±0.9	515	[45] BARTEL	86D	JADE	E_{cm}^{ee}= 34.6 GeV
20.4 ±3.0 $^{+1.4}_{-0.9}$		ALTHOFF	85	TASS	E_{cm}^{ee}= 34.5 GeV
17.8 ±0.9 ±0.6	390	[45] ASH	85B	MAC	E_{cm}^{ee}= 29 GeV
18.2 ±0.7 ±0.5		[46] BALTRUSAIT...85		MRK3	E_{cm}^{ee}= 3.77 GeV
13.0 ±1.9 ±2.9		BERGER	85	PLUT	E_{cm}^{ee}= 34.6 GeV
18.3 ±2.4 ±1.9	60	BEHREND	83C	CELL	E_{cm}^{ee}= 34 GeV
16.0 ±1.3	459	[47] BACINO	78B	DLCO	E_{cm}^{ee}= 3.1–7.4 GeV

[42] The correlation coefficient between this measurement and the ACCIARRI 01F measurement of $B(\tau^- \to \mu^- \overline{\nu}_\mu \nu_\tau)$ is 0.08.

[43] The correlation coefficients between this measurement and the ANASTASSOV 97 measurements of $B(\mu\overline{\nu}_\mu\nu_\tau)$, $B(\mu\overline{\nu}_\mu\nu_\tau)/B(e\overline{\nu}_e\nu_\tau)$, $B(h^-\nu_\tau)$, and $B(h^-\nu_\tau)/B(e\overline{\nu}_e\nu_\tau)$ are 0.50, −0.42, 0.48, and −0.39 respectively.

[44] Not independent of ALBRECHT 92D $\Gamma(\mu^-\overline{\nu}_\mu\nu_\tau)/\Gamma(e^-\overline{\nu}_e\nu_\tau)$ and ALBRECHT 93G $\Gamma(\mu^-\overline{\nu}_\mu\nu_\tau)\times\Gamma(e^-\overline{\nu}_e\nu_\tau)/\Gamma^2_{\rm total}$ values.

[45] Modified using $B(e^-\overline{\nu}_e\nu_\tau)/B(\text{"1 prong"})$ and B("1 prong") $=0.855$.

[46] Error correlated with BALTRUSAITIS 85 $\Gamma(\mu^-\overline{\nu}_\mu\nu_\tau)/\Gamma_{\rm total}$.

[47] BACINO 78B value comes from fit to events with $e^\pm$ and one other nonelectron charged prong.

$\Gamma(e^-\overline{\nu}_e\nu_\tau\gamma)/\Gamma_{\rm total}$ Γ_6/Γ

VALUE (%)	DOCUMENT ID		TECN	COMMENT
1.75±0.06±0.17	[48] BERGFELD	00	CLEO	E_{cm}^{ee}= 10.6 GeV

[48] BERGFELD 00 impose requirements on detected γ's corresponding to a τ-rest-frame energy cutoff $E^*_\gamma > 10$ MeV.

$\Gamma(\mu^-\overline{\nu}_\mu\nu_\tau)/\Gamma(e^-\overline{\nu}_e\nu_\tau)$ Γ_3/Γ_5

Standard Model prediction including mass effects is 0.9726.

Data marked "avg" are highly correlated with data appearing elsewhere in the Listings, and are therefore used for the average given below but not in the overall fits. "f&a" marks results used for the fit and the average.

VALUE		DOCUMENT ID		TECN	COMMENT
0.974 ±0.004 OUR FIT					
0.978 ±0.011 OUR AVERAGE					
0.9777±0.0063±0.0087	f&a	[49] ANASTASSOV	97	CLEO	E_{cm}^{ee}= 10.6 GeV
0.997 ±0.035 ±0.040	f&a	ALBRECHT	92D	ARG	E_{cm}^{ee}= 9.4–10.6 GeV

[49] The correlation coefficients between this measurement and the ANASTASSOV 97 measurements of $B(\mu\overline{\nu}_\mu\nu_\tau)$, $B(e\overline{\nu}_e\nu_\tau)$, $B(h^-\nu_\tau)$, and $B(h^-\nu_\tau)/B(e\overline{\nu}_e\nu_\tau)$ are 0.58, −0.42, 0.07, and 0.45 respectively.

$\Gamma(h^-\geq 0K^0_L\nu_\tau)/\Gamma_{\rm total}$ Γ_7/Γ

$\Gamma_7/\Gamma = (\Gamma_9+\Gamma_{10}+\frac{1}{2}\Gamma_{33}+\frac{1}{2}\Gamma_{35}+\Gamma_{45})/\Gamma$

Data marked "avg" are highly correlated with data appearing elsewhere in the Listings, and are therefore used for the average given below but not in the overall fits. "f&a" marks results used for the fit and the average.

VALUE (%)		EVTS	DOCUMENT ID		TECN	COMMENT
12.30±0.11 OUR FIT Error includes scale factor of 1.4.						
12.44±0.14 OUR AVERAGE						
12.44±0.11±0.11	f&a	15k	[50] BUSKULIC	96	ALEP	1991–1993 LEP run
12.47±0.26±0.43	f&a	2967	[51] ACCIARRI	95	L3	1992 LEP run
12.4 ±0.7 ±0.7	f&a	283	[52] ABREU	92N	DLPH	1990 LEP run
12.98±0.44±0.33	f&a		[53] DECAMP	92C	ALEP	1989–1990 LEP runs
12.1 ±0.7 ±0.5	f&a	309	ALEXANDER	91D	OPAL	1990 LEP run
11.3 ±0.5 ±0.8	avg	798	[54] FORD	87	MAC	E_{cm}^{ee}= 29 GeV
• • • We do not use the following data for averages, fits, limits, etc. • • •						
11.7 ±0.6 ±0.8			[55] ALBRECHT	92D	ARG	E_{cm}^{ee}= 9.4–10.6 GeV
12.3 ±0.9 ±0.5		1338	BEHREND	90	CELL	E_{cm}^{ee}= 35 GeV
11.1 ±1.1 ±1.4			[56] BURCHAT	87	MRK2	E_{cm}^{ee}= 29 GeV
12.3 ±0.6 ±1.1		328	[57] BARTEL	86D	JADE	E_{cm}^{ee}= 34.6 GeV
13.0 ±2.0 ±4.0			BERGER	85	PLUT	E_{cm}^{ee}= 34.6 GeV
11.2 ±1.7 ±1.2		34	[58] BEHREND	83C	CELL	E_{cm}^{ee}= 34 GeV

[50] BUSKULIC 96 quote 11.78 ± 0.11 ± 0.13 We add 0.66 to undo their correction for unseen K^0_L and modify the systematic error accordingly.

[51] ACCIARRI 95 with 0.65% added to remove their correction for $\pi^- K^0_L$ backgrounds.

[52] ABREU 92N with 0.5% added to remove their correction for $K^*(892)^-$ backgrounds.

[53] DECAMP 92C quote $B(h^- \geq 0K^0_L \geq 0\,(K^0_S \to \pi^+\pi^-)\,\nu_\tau) = 13.32 \pm 0.44 \pm 0.33$. We subtract 0.35 to correct for their inclusion of the K^0_S decays.

[54] FORD 87 result for $B(\pi^-\nu_\tau)$ with 0.67% added to remove their K^- correction and adjusted for 1992 B("1 prong").

[55] Not independent of ALBRECHT 92D $\Gamma(\mu^-\overline{\nu}_\mu\nu_\tau)/\Gamma(e^-\overline{\nu}_e\nu_\tau)$, $\Gamma(\mu^-\overline{\nu}_\mu\nu_\tau)\times\Gamma(e^-\overline{\nu}_e\nu_\tau)$, and $\Gamma(h^-\geq 0K^0_L\nu_\tau)/\Gamma(e^-\overline{\nu}_e\nu_\tau)$ values.

[56] BURCHAT 87 with 1.1% added to remove their correction for K^- and $K^*(892)^-$ backgrounds.

[57] BARTEL 86D result for $B(\pi^-\nu_\tau)$ with 0.59% added to remove their K^- correction and adjusted for 1992 B("1 prong").

[58] BEHREND 83C quote $B(\pi^-\nu_\tau) = 9.9 \pm 1.7 \pm 1.3$ after subtracting 1.3 ± 0.5 to correct for $B(K^-\nu_\tau)$.

$\Gamma(h^-\nu_\tau)/\Gamma_{\rm total}$ $\Gamma_8/\Gamma = (\Gamma_9+\Gamma_{10})/\Gamma$

Data marked "avg" are highly correlated with data appearing elsewhere in the Listings, and are therefore used for the average given below but not in the overall fits. "f&a" marks results used for the fit and the average.

VALUE (%)		DOCUMENT ID		TECN	COMMENT
11.75±0.11 OUR FIT Error includes scale factor of 1.4.					
11.65±0.21 OUR AVERAGE Error includes scale factor of 1.9.					
11.98±0.13±0.16	f&a	ACKERSTAFF	98M	OPAL	1991–1995 LEP runs
11.52±0.05±0.12	f&a	[59] ANASTASSOV	97	CLEO	E_{cm}^{ee}= 10.6 GeV

[59] The correlation coefficients between this measurement and the ANASTASSOV 97 measurements of $B(\mu\overline{\nu}_\mu\nu_\tau)$, $B(e\overline{\nu}_e\nu_\tau)$, $B(\mu\overline{\nu}_\mu\nu_\tau)/B(e\overline{\nu}_e\nu_\tau)$, and $B(h^-\nu_\tau)/B(e\overline{\nu}_e\nu_\tau)$ are 0.50, 0.48, 0.07, and 0.63 respectively.

$\Gamma(h^-\nu_\tau)/\Gamma(e^-\overline{\nu}_e\nu_\tau)$ $\Gamma_8/\Gamma_5 = (\Gamma_9+\Gamma_{10})/\Gamma_5$

Data marked "avg" are highly correlated with data appearing elsewhere in the Listings, and are therefore used for the average given below but not in the overall fits. "f&a" marks results used for the fit and the average.

VALUE		DOCUMENT ID		TECN	COMMENT
0.659 ±0.007 OUR FIT Error includes scale factor of 1.4.					
0.6484±0.0041±0.0060 avg		[60] ANASTASSOV	97	CLEO	E_{cm}^{ee}= 10.6 GeV

[60] The correlation coefficients between this measurement and the ANASTASSOV 97 measurements of $B(\mu\overline{\nu}_\mu\nu_\tau)$, $B(e\overline{\nu}_e\nu_\tau)$, $B(\mu\overline{\nu}_\mu\nu_\tau)/B(e\overline{\nu}_e\nu_\tau)$, and $B(h^-\nu_\tau)$ are 0.08, −0.39, 0.45, and 0.63 respectively.

$\Gamma(\pi^-\nu_\tau)/\Gamma_{\rm total}$ Γ_9/Γ

Data marked "avg" are highly correlated with data appearing elsewhere in the Listings, and are therefore used for the average given below but not in the overall fits. "f&a" marks results used for the fit and the average.

VALUE (%)		EVTS	DOCUMENT ID		TECN	COMMENT
11.06±0.11 OUR FIT	Error includes scale factor of 1.4.					
11.07±0.18 OUR AVERAGE						
11.06±0.11±0.14	avg		[61] BUSKULIC	96	ALEP	LEP 1991–1993 data
11.7 ±0.4 ±1.8	f&a	1138	BLOCKER	82D	MRK2	$E^{ee}_{\rm cm}$= 3.5–6.7 GeV

[61] Not independent of BUSKULIC 96 B($h^-\nu_\tau$) and B($K^-\nu_\tau$) values.

$\Gamma(K^-\nu_\tau)/\Gamma_{\rm total}$ Γ_{10}/Γ

VALUE (%)	EVTS	DOCUMENT ID		TECN	COMMENT
0.686±0.023 OUR FIT					
0.685±0.023 OUR AVERAGE					
0.658±0.027±0.029		[62] ABBIENDI	01J	OPAL	1990–1995 LEP runs
0.696±0.025±0.014	2032	BARATE	99K	ALEP	1991–1995 LEP runs
0.85 ±0.18	27	ABREU	94K	DLPH	LEP 1992 Z data
0.66 ±0.07 ±0.09	99	BATTLE	94	CLEO	$E^{ee}_{\rm cm}\approx$ 10.6 GeV
• • • We do not use the following data for averages, fits, limits, etc. • • •					
0.72 ±0.04 ±0.04	728	BUSKULIC	96	ALEP	Repl. by BARATE 99K
0.59 ±0.18	16	MILLS	84	DLCO	$E^{ee}_{\rm cm}$= 29 GeV
1.3 ±0.5	15	BLOCKER	82B	MRK2	$E^{ee}_{\rm cm}$= 3.9–6.7 GeV

[62] The correlation coefficient between this measurement and the ABBIENDI 01J B($\tau^-\to K^-\geq 0\pi^0\geq 0K^0\geq 0\gamma\ \nu_\tau$) is 0.60.

$\Gamma(h^-\geq 1\ \text{neutrals}\ \nu_\tau)/\Gamma_{\rm total}$ Γ_{11}/Γ

$\Gamma_{11}/\Gamma=(\Gamma_{13}+\Gamma_{15}+\Gamma_{19}+\Gamma_{22}+\Gamma_{25}+\Gamma_{26}+\Gamma_{28}+0.157\Gamma_{33}+0.157\Gamma_{35}+0.157\Gamma_{38}+0.157\Gamma_{40}+0.0985\Gamma_{45}+0.708\Gamma_{117}+0.715\Gamma_{119}+0.09\Gamma_{137}+0.09\Gamma_{138})/\Gamma$

VALUE (%)	DOCUMENT ID		TECN	COMMENT
36.92±0.14 OUR FIT	Error includes scale factor of 1.1.			
• • • We do not use the following data for averages, fits, limits, etc. • • •				
36.14±0.33±0.58	[63] AKERS	94E	OPAL	1991–1992 LEP runs
38.4 ±1.2 ±1.0	[64] BURCHAT	87	MRK2	$E^{ee}_{\rm cm}$= 29 GeV
42.7 ±2.0 ±2.9	BERGER	85	PLUT	$E^{ee}_{\rm cm}$= 34.6 GeV

[63] Not independent of ACKERSTAFF 98M B($h^-\pi^0\nu_\tau$) and B($h^-\geq 2\pi^0\nu_\tau$) values.

[64] BURCHAT 87 quote for B($\pi^\pm\geq 1$ neutral ν_τ) = 0.378 ± 0.012 ± 0.010. We add 0.006 to account for contribution from ($K^{*-}\nu_\tau$) which they fixed at BR = 0.013.

$\Gamma(h^-\pi^0\nu_\tau)/\Gamma_{\rm total}$ $\Gamma_{12}/\Gamma=(\Gamma_{13}+\Gamma_{15})/\Gamma$

VALUE (%)	EVTS	DOCUMENT ID		TECN	COMMENT
25.87±0.13 OUR FIT	Error includes scale factor of 1.1.				
25.76±0.15 OUR AVERAGE					
25.89±0.17±0.29		ACKERSTAFF	98M	OPAL	1991–1995 LEP runs
25.76±0.15±0.13	31k	BUSKULIC	96	ALEP	LEP 1991–1993 data
25.05±0.35±0.50	6613	ACCIARRI	95	L3	1992 LEP run
25.87±0.12±0.42	51k	[65] ARTUSO	94	CLEO	$E^{ee}_{\rm cm}$= 10.6 GeV
• • • We do not use the following data for averages, fits, limits, etc. • • •					
25.98±0.36±0.52		[66] AKERS	94E	OPAL	Repl. by ACKERSTAFF 98M
22.9 ±0.8 ±1.3	283	[67] ABREU	92N	DLPH	$E^{ee}_{\rm cm}$= 88.2–94.2 GeV
23.1 ±0.4 ±0.9	1249	[68] ALBRECHT	92Q	ARG	$E^{ee}_{\rm cm}$= 10 GeV
25.02±0.64±0.88	1849	DECAMP	92C	ALEP	1989–1990 LEP runs
22.0 ±0.8 ±1.9	779	ANTREASYAN	91	CBAL	$E^{ee}_{\rm cm}$= 9.4–10.6 GeV
22.6 ±1.5 ±0.7	1101	BEHREND	90	CELL	$E^{ee}_{\rm cm}$= 35 GeV
23.1 ±1.9 ±1.6		BEHREND	84	CELL	$E^{ee}_{\rm cm}$= 14,22 GeV

[65] ARTUSO 94 reports the combined result from three independent methods, one of which (23% of the $\tau^-\to h^-\pi^0\nu_\tau$) is normalized to the inclusive one-prong branching fraction, taken as 0.854 ± 0.004. Renormalization to the present value causes negligible change.

[66] AKERS 94E quote $(26.25\pm0.36\pm0.52)\times10^{-2}$; we subtract 0.27% from their number to correct for $\tau^-\to h^-K^0_L\nu_\tau$.

[67] ABREU 92N with 0.5% added to remove their correction for $K^*(892)^-$ backgrounds.

[68] ALBRECHT 92Q with 0.5% added to remove their correction for $\tau^-\to K^*(892)^-\nu_\tau$ background.

$\Gamma(\pi^-\pi^0\nu_\tau)/\Gamma_{\rm total}$ Γ_{13}/Γ

Data marked "avg" are highly correlated with data appearing elsewhere in the Listings, and are therefore used for the average given below but not in the overall fits. "f&a" marks results used for the fit and the average.

VALUE (%)		EVTS	DOCUMENT ID		TECN	COMMENT
25.42±0.14 OUR FIT	Error includes scale factor of 1.1.					
25.31±0.18 OUR AVERAGE						
25.30±0.15±0.13	avg		[69] BUSKULIC	96	ALEP	LEP 1991–1993 data
25.36±0.44	avg		[70] ARTUSO	94	CLEO	$E^{ee}_{\rm cm}$= 10.6 GeV
• • • We do not use the following data for averages, fits, limits, etc. • • •						
21.5 ±0.4 ±1.9		4400	[71,72] ALBRECHT	88L	ARG	$E^{ee}_{\rm cm}$= 10 GeV
23.0 ±1.3 ±1.7		582	ADLER	87B	MRK3	$E^{ee}_{\rm cm}$= 3.77 GeV
25.8 ±1.7 ±2.5			[73] BURCHAT	87	MRK2	$E^{ee}_{\rm cm}$= 29 GeV
22.3 ±0.6 ±1.4		629	[72] YELTON	86	MRK2	$E^{ee}_{\rm cm}$= 29 GeV

[69] Not independent of BUSKULIC 96 B($h^-\pi^0\nu_\tau$) and B($K^-\pi^0\nu_\tau$) values.

[70] Not independent of ARTUSO 94 B($h^-\pi^0\nu_\tau$) and BATTLE 94 B($K^-\pi^0\nu_\tau$) values.

[71] The authors divide by ($\Gamma_3+\Gamma_5+\Gamma_9+\Gamma_{10}$)/Γ = 0.467 to obtain this result.

[72] Experiment had no hadron identification. Kaon corrections were made, but insufficient information is given to permit their removal.

[73] BURCHAT 87 value is not independent of YELTON 86 value. Nonresonant decays included.

$\Gamma(\pi^-\pi^0\,\text{non-}\rho(770)\,\nu_\tau)/\Gamma_{\rm total}$ Γ_{14}/Γ

VALUE (%)	DOCUMENT ID		TECN	COMMENT
0.3 ±0.1 ±0.3	[74] BEHREND	84	CELL	$E^{ee}_{\rm cm}$= 14,22 GeV

[74] BEHREND 84 assume a flat nonresonant mass distribution down to the $\rho(770)$ mass, using events with mass above 1300 to set the level.

$\Gamma(K^-\pi^0\nu_\tau)/\Gamma_{\rm total}$ Γ_{15}/Γ

VALUE (%)	EVTS	DOCUMENT ID		TECN	COMMENT
0.450±0.030 OUR FIT					
0.449±0.034 OUR AVERAGE					
0.444±0.026±0.024	923	BARATE	99K	ALEP	1991–1995 LEP runs
0.51 ±0.10 ±0.07	37	BATTLE	94	CLEO	$E^{ee}_{\rm cm}\approx$ 10.6 GeV
• • • We do not use the following data for averages, fits, limits, etc. • • •					
0.52 ±0.04 ±0.05	395	BUSKULIC	96	ALEP	Repl. by BARATE 99K

$\Gamma(h^-\geq 2\pi^0\nu_\tau)/\Gamma_{\rm total}$ Γ_{16}/Γ

$\Gamma_{16}/\Gamma=(\Gamma_{19}+\Gamma_{22}+\Gamma_{25}+\Gamma_{26}+\Gamma_{28}+0.157\Gamma_{33}+0.157\Gamma_{35}+0.157\Gamma_{38}+0.157\Gamma_{40}+0.0985\Gamma_{45}+0.319\Gamma_{117}+0.322\Gamma_{119})/\Gamma$

Data marked "avg" are highly correlated with data appearing elsewhere in the Listings, and are therefore used for the average given below but not in the overall fits. "f&a" marks results used for the fit and the average.

VALUE (%)		EVTS	DOCUMENT ID		TECN	COMMENT
10.77±0.15 OUR FIT	Error includes scale factor of 1.1.					
10.0 ±0.4 OUR AVERAGE						
9.91±0.31±0.27	f&a		ACKERSTAFF	98M	OPAL	1991–1995 LEP runs
12.0 ±1.4 ±2.5	f&a		[75] BURCHAT	87	MRK2	$E^{ee}_{\rm cm}$= 29 GeV
• • • We do not use the following data for averages, fits, limits, etc. • • •						
9.89±0.34±0.55			[76] AKERS	94E	OPAL	Repl. by ACKERSTAFF 98M
14.0 ±1.2 ±0.6		938	[77] BEHREND	90	CELL	$E^{ee}_{\rm cm}$= 35 GeV
13.9 ±2.0 $^{+1.9}_{-2.2}$			[78] AIHARA	86E	TPC	$E^{ee}_{\rm cm}$= 29 GeV

[75] Error correlated with BURCHAT 87 $\Gamma(\rho^-\nu_e)/\Gamma$(total) value.

[76] AKERS 94E not independent of AKERS 94E B($h^-\geq 1\pi^0\nu_\tau$) and B($h^-\pi^0\nu_\tau$) measurements.

[77] No independent of BEHREND 90 $\Gamma(h^-2\pi^0\nu_\tau$ (exp. K^0)) and $\Gamma(h^-\geq 3\pi^0\nu_\tau)$.

[78] AIHARA 86E (TPC) quote B($2\pi^0\pi^-\nu_\tau$) + 1.6B($3\pi^0\pi^-\nu_\tau$) + 1.1B($\pi^0\eta\pi^-\nu_\tau$).

$\Gamma(h^-2\pi^0\nu_\tau)/\Gamma_{\rm total}$ Γ_{17}/Γ

$\Gamma_{17}/\Gamma=(\Gamma_{19}+\Gamma_{22}+0.157\Gamma_{33}+0.157\Gamma_{35})/\Gamma$

VALUE (%)	EVTS	DOCUMENT ID		TECN	COMMENT
9.39±0.14 OUR FIT	Error includes scale factor of 1.1.				
9.48±0.13±0.10	12k	[79] BUSKULIC	96	ALEP	LEP 1991–1993 data

[79] BUSKULIC 96 quote 9.29 ± 0.13 ± 0.10. We add 0.19 to undo their correction for $\tau^-\to h^-K^0\nu_\tau$.

$\Gamma(h^-2\pi^0\nu_\tau(\text{ex.}\,K^0))/\Gamma_{\rm total}$ Γ_{18}/Γ

$\Gamma_{18}/\Gamma=(\Gamma_{19}+\Gamma_{22})/\Gamma$

Data marked "avg" are highly correlated with data appearing elsewhere in the Listings, and are therefore used for the average given below but not in the overall fits. f&a marks results used for the fit and the average.

VALUE (%)		EVTS	DOCUMENT ID		TECN	COMMENT
9.23±0.14 OUR FIT	Error includes scale factor of 1.1.					
9.08±0.34 OUR AVERAGE						
8.88±0.37±0.42	f&a	1060	ACCIARRI	95	L3	1992 LEP run
8.96±0.16±0.44	avg		[80] PROCARIO	93	CLEO	$E^{ee}_{\rm cm}\approx$ 10.6 GeV
10.38±0.66±0.82	f&a	809	[81] DECAMP	92C	ALEP	1989–1990 LEP runs
• • • We do not use the following data for averages, fits, limits, etc. • • •						
5.7 ±0.5 $^{+1.7}_{-1.0}$		133	[82] ANTREASYAN	91	CBAL	$E^{ee}_{\rm cm}$= 9.4–10.6 GeV
10.0 ±1.5 ±1.1		333	[83] BEHREND	90	CELL	$E^{ee}_{\rm cm}$= 35 GeV
8.7 ±0.4 ±1.1		815	[84] BAND	87	MAC	$E^{ee}_{\rm cm}$= 29 GeV
6.2 ±0.6 ±1.2			[85] GAN	87	MRK2	$E^{ee}_{\rm cm}$= 29 GeV
6.0 ±3.0 ±1.8			BEHREND	84	CELL	$E^{ee}_{\rm cm}$= 14,22 GeV

[80] PROCARIO 93 entry is obtained from B($h^-2\pi^0\nu_\tau$)/B($h^-\pi^0\nu_\tau$) using ARTUSO 94 result for B($h^-\pi^0\nu_\tau$).

[81] We subtract 0.0015 to account for $\tau^-\to K^*(892)^-\nu_\tau$ contribution.

[82] ANTREASYAN 91 subtract 0.001 to account for the $\tau^-\to K^*(892)^-\nu_\tau$ contribution.

[83] BEHREND 90 subtract 0.002 to account for the $\tau^-\to K^*(892)^-\nu_\tau$ contribution.

[84] BAND 87 assume B($\pi^-3\pi^0\nu_\tau$) = 0.01 and B($\pi^-\pi^0\eta\nu_\tau$) = 0.005.

[85] GAN 87 analysis use photon multiplicity distribution.

$\Gamma(h^-2\pi^0\nu_\tau(\text{ex. }K^0))/\Gamma(h^-\pi^0\nu_\tau)$ Γ_{18}/Γ_{12}

$\Gamma_{18}/\Gamma_{12}=(\Gamma_{19}+\Gamma_{22})/(\Gamma_{13}+\Gamma_{15})$

VALUE	DOCUMENT ID		TECN	COMMENT
0.357 ± 0.006 OUR FIT	Error includes scale factor of 1.1.			
0.342 ± 0.006 ± 0.016	[86] PROCARIO	93	CLEO	$E^{ee}_{cm}\approx 10.6$ GeV

[86] PROCARIO 93 quote 0.345 ± 0.006 ± 0.016 after correction for 2 kaon backgrounds assuming $B(K^{*-}\nu_\tau)=1.42\pm0.18\%$ and $B(h^-K^0\pi^0\nu_\tau)=0.48\pm0.48\%$. We multiply by 0.990 ± 0.010 to remove these corrections to $B(h^-\pi^0\nu_\tau)$.

$\Gamma(\pi^-2\pi^0\nu_\tau(\text{ex. }K^0))/\Gamma_{\text{total}}$ Γ_{19}/Γ

Data marked "avg" are highly correlated with data appearing elsewhere in the Listings, and are therefore used for the average given below but not in the overall fits. "f&a" marks results used for the fit and the average.

VALUE (%)		DOCUMENT ID		TECN	COMMENT
9.17 ± 0.14 OUR FIT	Error includes scale factor of 1.1.				
9.21 ± 0.13 ± 0.11	**avg**	[87] BUSKULIC	96	ALEP	LEP 1991–1993 data

[87] Not independent of BUSKULIC 96 $B(h^-2\pi^0\nu_\tau(\text{ex. }K^0))$ and $B(K^-2\pi^0\nu_\tau(\text{ex. }K^0))$ values.

$\Gamma(\pi^-2\pi^0\nu_\tau(\text{ex. }K^0),\text{scalar})/\Gamma(\pi^-2\pi^0\nu_\tau(\text{ex. }K^0))$ Γ_{20}/Γ_{19}

VALUE	CL%	DOCUMENT ID		TECN	COMMENT
< 0.094	95	[88] BROWDER	00	CLEO	4.7 fb^{-1} E^{ee}_{cm}= 10.6 GeV

[88] Model-independent limit from structure function analysis on contribution to $B(\tau^-\to\pi^-2\pi^0\nu_\tau(\text{ex. }K^0))$ from scalars.

$\Gamma(\pi^-2\pi^0\nu_\tau(\text{ex. }K^0),\text{vector})/\Gamma(\pi^-2\pi^0\nu_\tau(\text{ex. }K^0))$ Γ_{21}/Γ_{19}

VALUE	CL%	DOCUMENT ID		TECN	COMMENT
< 0.073	95	[89] BROWDER	00	CLEO	4.7 fb^{-1} E^{ee}_{cm}= 10.6 GeV

[89] Model-independent limit from structure function analysis on contribution to $B(\tau^-\to\pi^-2\pi^0\nu_\tau(\text{ex. }K^0))$ from vectors.

$\Gamma(K^-2\pi^0\nu_\tau(\text{ex. }K^0))/\Gamma_{\text{total}}$ Γ_{22}/Γ

VALUE (%)	EVTS	DOCUMENT ID		TECN	COMMENT
0.058 ± 0.023 OUR FIT					
0.058 ± 0.024 OUR AVERAGE					
0.056 ± 0.020 ± 0.015	131	BARATE	99K	ALEP	1991–1995 LEP runs
0.09 ± 0.10 ± 0.03	3	[90] BATTLE	94	CLEO	$E^{ee}_{cm}\approx 10.6$ GeV
• • • We do not use the following data for averages, fits, limits, etc. • • •					
0.08 ± 0.02 ± 0.02	59	BUSKULIC	96	ALEP	Repl. by BARATE 99K

[90] BATTLE 94 quote 0.14 ± 0.10 ± 0.03 or < 0.3% at 90% CL. We subtract (0.05 ± 0.02)% to account for $\tau^-\to K^-(K^0\to\pi^0\pi^0)\nu_\tau$ background.

$\Gamma(h^-\geq 3\pi^0\nu_\tau)/\Gamma_{\text{total}}$ Γ_{23}/Γ

$\Gamma_{23}/\Gamma=(\Gamma_{25}+\Gamma_{26}+\Gamma_{28}+0.157\Gamma_{38}+0.157\Gamma_{40}+0.0985\Gamma_{45}+0.319\Gamma_{117}+0.322\Gamma_{119})/\Gamma$

VALUE (%)	EVTS	DOCUMENT ID		TECN	COMMENT
1.37 ± 0.11 OUR FIT	Error includes scale factor of 1.1.				
1.53 ± 0.40 ± 0.46	186	DECAMP	92C	ALEP	1989–1990 LEP runs
• • • We do not use the following data for averages, fits, limits, etc. • • •					
3.2 ± 1.0 ± 1.0		BEHREND	90	CELL	E^{ee}_{cm}= 35 GeV

$\Gamma(h^-3\pi^0\nu_\tau)/\Gamma_{\text{total}}$ Γ_{24}/Γ

$\Gamma_{24}/\Gamma=(\Gamma_{25}+\Gamma_{26}+0.157\Gamma_{38}+0.157\Gamma_{40}+0.322\Gamma_{119})/\Gamma$

Data marked "avg" are highly correlated with data appearing elsewhere in the Listings, and are therefore used for the average given below but not in the overall fits. "f&a" marks results used for the fit and the average.

VALUE (%)	EVTS	DOCUMENT ID		TECN	COMMENT
1.21 ± 0.10 OUR FIT					
1.22 ± 0.10 OUR AVERAGE					
1.24 ± 0.09 ± 0.11	f&a 2.3k	[91] BUSKULIC	96	ALEP	LEP 1991–1993 data
1.70 ± 0.24 ± 0.38	f&a 293	ACCIARRI	95	L3	1992 LEP run
1.15 ± 0.08 ± 0.13	avg	[92] PROCARIO	93	CLEO	$E^{ee}_{cm}\approx 10.6$ GeV
• • • We do not use the following data for averages, fits, limits, etc. • • •					
$0.0\ ^{+1.4}_{-0.1}\ ^{+1.1}_{-0.1}$		[93] GAN	87	MRK2	E^{ee}_{cm}= 29 GeV

[91] BUSKULIC 96 quote $B(h^-3\pi^0\nu_\tau(\text{ex. }K^0))=1.17\pm0.09\pm0.11$. We add 0.07 to remove their correction for K^0 backgrounds.

[92] PROCARIO 93 entry is obtained from $B(h^-3\pi^0\nu_\tau)/B(h^-\pi^0\nu_\tau)$ using ARTUSO 94 result for $B(h^-\pi^0\nu_\tau)$.

[93] Highly correlated with GAN 87 $\Gamma(\eta\pi^-\pi^0\nu_\tau)/\Gamma_{\text{total}}$ value. Authors quote $B(\pi^\pm3\pi^0\nu_\tau)+0.67B(\pi^\pm\eta\pi^0\nu_\tau)=0.047\pm0.010\pm0.011$.

$\Gamma(h^-3\pi^0\nu_\tau)/\Gamma(h^-\pi^0\nu_\tau)$ Γ_{24}/Γ_{12}

$\Gamma_{24}/\Gamma_{12}=(\Gamma_{25}+\Gamma_{26}+0.157\Gamma_{38}+0.157\Gamma_{40}+0.322\Gamma_{119})/(\Gamma_{13}+\Gamma_{15})$

VALUE	DOCUMENT ID		TECN	COMMENT
0.047 ± 0.004 OUR FIT	Error includes scale factor of 1.1.			
0.044 ± 0.003 ± 0.005	[94] PROCARIO	93	CLEO	$E^{ee}_{cm}\approx 10.6$ GeV

[94] PROCARIO 93 quote 0.041 ± 0.003 ± 0.005 after correction for 2 kaon backgrounds assuming $B(K^{*-}\nu_\tau)=1.42\pm0.18\%$ and $B(h^-K^0\pi^0\nu_\tau)=0.48\pm0.48\%$. We add 0.003 ± 0.003 and multiply the sum by 0.990 ± 0.010 to remove these corrections.

$\Gamma(\pi^-3\pi^0\nu_\tau(\text{ex. }K^0))/\Gamma_{\text{total}}$ Γ_{25}/Γ

VALUE (%)	DOCUMENT ID
1.08 ± 0.10 OUR FIT	

$\Gamma(K^-3\pi^0\nu_\tau(\text{ex. }K^0,\eta))/\Gamma_{\text{total}}$ Γ_{26}/Γ

VALUE (%)	EVTS	DOCUMENT ID		TECN	COMMENT
$0.038\ ^{+0.022}_{-0.020}$ OUR FIT					
0.037 ± 0.021 ± 0.011	22	BARATE	99K	ALEP	1991–1995 LEP runs
• • • We do not use the following data for averages, fits, limits, etc. • • •					
0.05 ± 0.13		[95] BUSKULIC	94E	ALEP	Repl. by BARATE 99K

[95] BUSKULIC 94E quote $B(K^-\geq0\pi^0\geq0K^0\nu_\tau)-[B(K^-\nu_\tau)+B(K^-\pi^0\nu_\tau)+B(K^-K^0\nu_\tau)+B(K^-\pi^0\pi^0\nu_\tau)+B(K^-\pi^0K^0\nu_\tau)]=0.05\pm0.13\%$ accounting for common systematic errors in BUSKULIC 94E and BUSKULIC 94F measurements of these modes. We assume $B(K^-\geq2K^0\nu_\tau)$ and $B(K^-\geq4\pi^0\nu_\tau)$ are negligible.

$\Gamma(h^-4\pi^0\nu_\tau(\text{ex. }K^0))/\Gamma_{\text{total}}$ Γ_{27}/Γ

$\Gamma_{27}/\Gamma=(\Gamma_{28}+0.319\Gamma_{117})/\Gamma$

VALUE (%)	EVTS	DOCUMENT ID		TECN	COMMENT
0.16 ± 0.06 OUR FIT					
0.16 ± 0.06 OUR AVERAGE					
0.16 ± 0.04 ± 0.09	232	[96] BUSKULIC	96	ALEP	LEP 1991–1993 data
0.16 ± 0.05 ± 0.05		[97] PROCARIO	93	CLEO	$E^{ee}_{cm}\approx 10.6$ GeV

[96] BUSKULIC 96 quote result for $\tau^-\to h^-\geq4\pi^0\nu_\tau$. We assume $B(h^-\geq5\pi^0\nu_\tau)$ is negligible.

[97] PROCARIO 93 quotes $B(h^-4\pi^0\nu_\tau)/B(h^-\pi^0\nu_\tau)=0.006\pm0.002\pm0.002$. We multiply by the ARTUSO 94 result for $B(h^-\pi^0\nu_\tau)$ to obtain $B(h^-4\pi^0\nu_\tau)$. PROCARIO 93 assume $B(h^-\geq5\ \pi^0\nu_\tau)$ is small and do not correct for it.

$\Gamma(h^-4\pi^0\nu_\tau(\text{ex. }K^0,\eta))/\Gamma_{\text{total}}$ Γ_{28}/Γ

VALUE (%)	DOCUMENT ID
$0.10\ ^{+0.06}_{-0.05}$ OUR FIT	

$\Gamma(K^-\geq0\pi^0\geq0K^0\geq0\gamma\nu_\tau)/\Gamma_{\text{total}}$ Γ_{29}/Γ

$\Gamma_{29}/\Gamma=(\Gamma_{10}+\Gamma_{15}+\Gamma_{22}+\Gamma_{26}+\Gamma_{35}+\Gamma_{40}+0.715\Gamma_{119})/\Gamma$

Data marked "avg" are highly correlated with data appearing elsewhere in the Listings, and are therefore used for the average given below but not in the overall fits. "f&a" marks results used for the fit and the average.

VALUE (%)	EVTS	DOCUMENT ID		TECN	COMMENT
1.56 ± 0.04 OUR FIT					
1.53 ± 0.04 OUR AVERAGE					
1.528 ± 0.039 ± 0.040	f&a	[98] ABBIENDI	01J	OPAL	1990–1995 LEP runs
1.520 ± 0.040 ± 0.041	avg 4006	[99] BARATE	99K	ALEP	1991–1995 LEP runs
1.54 ± 0.24	f&a	ABREU	94K	DLPH	LEP 1992 Z data
1.70 ± 0.12 ± 0.19	f&a 202	[100] BATTLE	94	CLEO	$E^{ee}_{cm}\approx 10.6$ GeV
1.6 ± 0.4 ± 0.2	f&a 35	AIHARA	87B	TPC	E^{ee}_{cm}= 29 GeV
1.71 ± 0.29	f&a 53	MILLS	84	DLCO	E^{ee}_{cm}= 29 GeV
• • • We do not use the following data for averages, fits, limits, etc. • • •					
1.70 ± 0.05 ± 0.06	1610	[101] BUSKULIC	96	ALEP	Repl. by BARATE 99K

[98] The correlation coefficient between this measurement and the ABBIENDI 01J $B(\tau^-\to K^-\nu_\tau)$ is 0.60.

[99] Not independent of BARATE 99K $B(K^-\nu_\tau)$, $B(K^-\pi^0\nu_\tau)$, $B(K^-2\pi^0\nu_\tau(\text{ex. }K^0))$, $B(K^-3\pi^0\nu_\tau(\text{ex. }K^0))$, $B(K^-K^0\nu_\tau)$, and $B(K^-K^0\pi^0\nu_\tau)$ values.

[100] BATTLE 94 quote 1.60 ± 0.12 ± 0.19. We add 0.10 ± 0.02 to correct for their rejection of $K^0_S\to\pi^+\pi^-$ decays.

[101] Not independent of BUSKULIC 96 $B(K^-\nu_\tau)$, $B(K^-\pi^0\nu_\tau)$, $B(K^-2\pi^0\nu_\tau)$, $B(K^-K^0\nu_\tau)$, and $B(K^-K^0\pi^0\nu_\tau)$ values.

$\Gamma(K^-\geq1(\pi^0\text{ or }K^0\text{ or }\gamma)\nu_\tau)/\Gamma_{\text{total}}$ Γ_{30}/Γ

$\Gamma_{30}/\Gamma=(\Gamma_{15}+\Gamma_{22}+\Gamma_{26}+\Gamma_{35}+\Gamma_{40}+0.715\Gamma_{119})/\Gamma$

Data marked "avg" are highly correlated with data appearing elsewhere in the Listings, and are therefore used for the average given below but not in the overall fits. "f&a" marks results used for the fit and the average.

VALUE (%)	EVTS	DOCUMENT ID		TECN	COMMENT
0.874 ± 0.035 OUR FIT					
0.86 ± 0.05 OUR AVERAGE					
0.869 ± 0.031 ± 0.034	avg	[102] ABBIENDI	01J	OPAL	1990–1995 LEP runs
0.69 ± 0.25	avg	[103] ABREU	94K	DLPH	LEP 1992 Z data
$1.2\ \pm0.5\ ^{+0.2}_{-0.4}$	f&a 9	AIHARA	87B	TPC	E^{ee}_{cm}= 29 GeV

[102] Not independent of ABBIENDI 01J $B(\tau^-\to K^-\nu_\tau)$ and $B(\tau^-\to K^-\geq0\pi^0\geq0K^0\geq0\gamma\nu_\tau)$ values.

[103] Not independent of ABREU 94K $B(K^-\nu_\tau)$ and $B(K^-\geq0\text{ neutrals}\,\nu_\tau)$ measurements.

$\Gamma(K^0_S(\text{particles})^-\nu_\tau)/\Gamma_{\text{total}}$ Γ_{31}/Γ

$\Gamma_{31}/\Gamma=(\frac{1}{2}\Gamma_{33}+\frac{1}{2}\Gamma_{35}+\frac{1}{2}\Gamma_{38}+\frac{1}{2}\Gamma_{40}+\Gamma_{45}+\Gamma_{46})/\Gamma$

VALUE (%)	EVTS	DOCUMENT ID		TECN	COMMENT
0.92 ± 0.04 OUR FIT	Error includes scale factor of 1.1.				
0.97 ± 0.07 OUR AVERAGE					
0.970 ± 0.058 ± 0.062	929	BARATE	98E	ALEP	1991–1995 LEP runs
0.97 ± 0.09 ± 0.06	141	AKERS	94G	OPAL	E^{ee}_{cm}= 88–94 GeV

$\Gamma(h^-\overline{K}^0\nu_\tau)/\Gamma_{total}$ $\Gamma_{32}/\Gamma=(\Gamma_{33}+\Gamma_{35})/\Gamma$

Data marked "avg" are highly correlated with data appearing elsewhere in the Listings, and are therefore used for the average given below but not in the overall fits. "f&a" marks results used for the fit and the average.

VALUE (%)		EVTS	DOCUMENT ID		TECN	COMMENT
1.05 ±0.04	**OUR FIT**	Error includes scale factor of 1.1.				
0.90 ±0.07	**OUR AVERAGE**					
1.01 ±0.11 ±0.07	avg	555	[104] BARATE	98E	ALEP	1991–1995 LEP runs
0.855±0.036±0.073	f&a	1242	COAN	96	CLEO	$E^{ee}_{cm}\approx$ 10.6 GeV

[104] Not independent of BARATE 98E B($\tau^-\to\pi^-\overline{K}^0\nu_\tau$) and B($\tau^-\to K^-K^0\nu_\tau$) values.

$\Gamma(\pi^-\overline{K}^0\nu_\tau)/\Gamma_{total}$ Γ_{33}/Γ

Data marked "avg" are highly correlated with data appearing elsewhere in the Listings, and are therefore used for the average given below but not in the overall fits. "f&a" marks results used for the fit and the average.

VALUE (%)		EVTS	DOCUMENT ID		TECN	COMMENT
0.89 ±0.04	**OUR FIT**	Error includes scale factor of 1.1.				
0.88 ±0.05	**OUR AVERAGE**	Error includes scale factor of 1.2.				
0.933±0.068±0.049	f&a	377	ABBIENDI	00C	OPAL	1991–1995 LEP runs
0.928±0.045±0.034	f&a	937	[105] BARATE	99K	ALEP	1991–1995 LEP runs
0.855±0.117±0.066	avg	509	[106] BARATE	98E	ALEP	1991–1995 LEP runs
0.704±0.041±0.072	avg		[107] COAN	96	CLEO	$E^{ee}_{cm}\approx$ 10.6 GeV
0.95 ±0.15 ±0.06	f&a		[108] ACCIARRI	95F	L3	1991–1993 LEP runs
• • • We do not use the following data for averages, fits, limits, etc. • • •						
0.79 ±0.10 ±0.09		98	[109] BUSKULIC	96	ALEP	Repl. by BARATE 99K

[105] BARATE 99K measure K^0's by detecting K^0_L's in their hadron calorimeter.

[106] BARATE 98E reconstruct K^0's using $K^0_S\to\pi^+\pi^-$ decays. Not independent of BARATE 98E B(K^0 particles$^-\nu_\tau$) value.

[107] Not independent of COAN 96 B($h^-K^0\nu_\tau$) and B($K^-K^0\nu_\tau$) measurements.

[108] ACCIARRI 95F do not identify π^-/K^- and assume B($K^-K^0\nu_\tau$) = (0.29 ± 0.12)%.

[109] BUSKULIC 96 measure K^0's by detecting K^0_L's in their hadron calorimeter.

$\Gamma(\pi^-\overline{K}^0(\text{non-}K^*(892)^-)\nu_\tau)/\Gamma_{total}$ Γ_{34}/Γ

VALUE (%)	CL%	DOCUMENT ID		TECN	COMMENT
<0.17	95	ACCIARRI	95F	L3	1991–1993 LEP runs

$\Gamma(K^-K^0\nu_\tau)/\Gamma_{total}$ Γ_{35}/Γ

VALUE (%)	EVTS	DOCUMENT ID		TECN	COMMENT
0.154±0.016 OUR FIT					
0.158±0.017 OUR AVERAGE					
0.162±0.021±0.011	150	[110] BARATE	99K	ALEP	1991–1995 LEP runs
0.158±0.042±0.017	46	[111] BARATE	98E	ALEP	1991–1995 LEP runs
0.151±0.021±0.022	111	COAN	96	CLEO	$E^{ee}_{cm}\approx$ 10.6 GeV
• • • We do not use the following data for averages, fits, limits, etc. • • •					
0.26 ±0.09 ±0.02	13	[112] BUSKULIC	96	ALEP	Repl. by BARATE 99K

[110] BARATE 99K measure K^0's by detecting K^0_L's in their hadron calorimeter.

[111] BARATE 98E reconstruct K^0's using $K^0_S\to\pi^+\pi^-$ decays.

[112] BUSKULIC 96 measure K^0's by detecting K^0_L's in their hadron calorimeter.

$\Gamma(K^-K^0\geq 0\pi^0\nu_\tau)/\Gamma_{total}$ $\Gamma_{36}/\Gamma=(\Gamma_{35}+\Gamma_{40})/\Gamma$

VALUE (%)	EVTS	DOCUMENT ID		TECN	COMMENT
0.309±0.024 OUR FIT					
0.330±0.055±0.039	124	ABBIENDI	00C	OPAL	1991–1995 LEP runs

$\Gamma(h^-\overline{K}^0\pi^0\nu_\tau)/\Gamma_{total}$ $\Gamma_{37}/\Gamma=(\Gamma_{38}+\Gamma_{40})/\Gamma$

Data marked "avg" are highly correlated with data appearing elsewhere in the Listings, and are therefore used for the average given below but not in the overall fits. "f&a" marks results used for the fit and the average.

VALUE (%)		EVTS	DOCUMENT ID		TECN	COMMENT
0.52 ±0.04	**OUR FIT**					
0.50 ±0.06	**OUR AVERAGE**	Error includes scale factor of 1.2.				
0.446±0.052±0.046	avg	157	[113] BARATE	98E	ALEP	1991–1995 LEP runs
0.562±0.050±0.048	f&a	264	COAN	96	CLEO	$E^{ee}_{cm}\approx$ 10.6 GeV

[113] Not independent of BARATE 98E B($\tau^-\to\pi^-\overline{K}^0\pi^0\tau$) and B($\tau^-\to K^-K^0\pi^0\nu_\tau$) values.

$\Gamma(\pi^-\overline{K}^0\pi^0\nu_\tau)/\Gamma_{total}$ Γ_{38}/Γ

Data marked "avg" are highly correlated with data appearing elsewhere in the Listings, and are therefore used for the average given below but not in the overall fits. "f&a" marks results used for the fit and the average.

VALUE (%)		EVTS	DOCUMENT ID		TECN	COMMENT
0.37 ±0.04	**OUR FIT**					
0.36 ±0.04	**OUR AVERAGE**					
0.347±0.053±0.037	f&a	299	[114] BARATE	99K	ALEP	1991–1995 LEP runs
0.294±0.073±0.037	f&a	142	[115] BARATE	98E	ALEP	1991–1995 LEP runs
0.417±0.058±0.044	avg		[116] COAN	96	CLEO	$E^{ee}_{cm}\approx$ 10.6 GeV
0.41 ±0.12 ±0.03	f&a		[117] ACCIARRI	95F	L3	1991–1993 LEP runs
• • • We do not use the following data for averages, fits, limits, etc. • • •						
0.32 ±0.11 ±0.05		23	[118] BUSKULIC	96	ALEP	Repl. by BARATE 99K

[114] BARATE 99K measure K^0's by detecting K^0_L's in their hadron calorimeter.

[115] BARATE 98E reconstruct K^0's using $K^0_S\to\pi^+\pi^-$ decays.

[116] Not independent of COAN 96 B($h^-K^0\pi^0\nu_\tau$) and B($K^-K^0\pi^0\nu_\tau$) measurements.

[117] ACCIARRI 95F do not identify π^-/K^- and assume B($K^-K^0\pi^0\nu_\tau$) = (0.05 ± 0.05)%.

[118] BUSKULIC 96 measure K^0's by detecting K^0_L's in their hadron calorimeter.

$\Gamma(\overline{K}^0\rho^-\nu_\tau)/\Gamma_{total}$ Γ_{39}/Γ

VALUE (%)		DOCUMENT ID		TECN	COMMENT
0.22 ±0.05	**OUR AVERAGE**				
0.250±0.057±0.044		[119] BARATE	99K	ALEP	1991–1995 LEP runs
0.188±0.054±0.038		[120] BARATE	98E	ALEP	1991–1995 LEP runs

[119] BARATE 99K measure K^0's by detecting K^0_L's in hadron calorimeter. They determine the $\overline{K}^0\rho^-$ fraction in $\tau^-\to\pi^-\overline{K}^0\pi^0\nu_\tau$ decays to be (0.72 ± 0.12 ± 0.10) and multiply their B($\pi^-\overline{K}^0\pi^0\nu_\tau$) measurement by this fraction to obtain the quoted result.

[120] BARATE 98E reconstruct K^0's using $K^0_S\to\pi^+\pi^-$ decays. They determine the $\overline{K}^0\rho^-$ fraction in $\tau^-\to\pi^-\overline{K}^0\pi^0\nu_\tau$ decays to be (0.64 ± 0.09 ± 0.10) and multiply their B($\pi^-\overline{K}^0\pi^0\nu_\tau$) measurement by this fraction to obtain the quoted result.

$\Gamma(K^-K^0\pi^0\nu_\tau)/\Gamma_{total}$ Γ_{40}/Γ

VALUE (%)	EVTS	DOCUMENT ID		TECN	COMMENT
0.155±0.020 OUR FIT					
0.144±0.023 OUR AVERAGE					
0.143±0.025±0.015	78	[121] BARATE	99K	ALEP	1991–1995 LEP runs
0.152±0.076±0.021	15	[122] BARATE	98E	ALEP	1991–1995 LEP runs
0.145±0.036±0.020	32	COAN	96	CLEO	$E^{ee}_{cm}\approx$ 10.6 GeV
• • • We do not use the following data for averages, fits, limits, etc. • • •					
0.10 ±0.05 ±0.03	5	[123] BUSKULIC	96	ALEP	Repl. by BARATE 99K

[121] BARATE 99K measure K^0's by detecting K^0_L's in their hadron calorimeter.

[122] BARATE 98E reconstruct K^0's using $K^0_S\to\pi^+\pi^-$ decays.

[123] BUSKULIC 96 measure K^0's by detecting K^0_L's in their hadron calorimeter.

$\Gamma(\pi^-\overline{K}^0\geq 1\pi^0\nu_\tau)/\Gamma_{total}$ $\Gamma_{41}/\Gamma=(\Gamma_{38}+\Gamma_{42})/\Gamma$

VALUE (%)	EVTS	DOCUMENT ID		TECN	COMMENT
0.324±0.074±0.066	148	ABBIENDI	00C	OPAL	1991–1995 LEP runs

$\Gamma(\pi^-\overline{K}^0\pi^0\pi^0\nu_\tau)/\Gamma_{total}$ Γ_{42}/Γ

VALUE (units 10^{-3})	CL%	EVTS	DOCUMENT ID		TECN	COMMENT
0.26±0.24			[124] BARATE	99R	ALEP	1991–1995 LEP runs
• • • We do not use the following data for averages, fits, limits, etc. • • •						
<0.66	95	17	[125] BARATE	99K	ALEP	1991–1995 LEP runs
0.58±0.33±0.14		5	[126] BARATE	98E	ALEP	1991–1995 LEP runs

[124] BARATE 99R combine the BARATE 98E and BARATE 99K measurements to obtain this value.

[125] BARATE 99K measure K^0's by detecting K^0_L's in their hadron calorimeter.

[126] BARATE 98E reconstruct K^0's using $K^0_S\to\pi^+\pi^-$ decays.

$\Gamma(K^-K^0\pi^0\pi^0\nu_\tau)/\Gamma_{total}$ Γ_{43}/Γ

VALUE	CL%	DOCUMENT ID		TECN	COMMENT
<0.16 × 10^{-3}	95	[127] BARATE	99R	ALEP	1991–1995 LEP runs
• • • We do not use the following data for averages, fits, limits, etc. • • •					
<0.18 × 10^{-3}	95	[128] BARATE	99K	ALEP	1991–1995 LEP runs
<0.39 × 10^{-3}	95	[129] BARATE	98E	ALEP	1991–1995 LEP runs

[127] BARATE 99R combine the BARATE 98E and BARATE 99K bounds to obtain this value.

[128] BARATE 99K measure K^0's by detecting K^0_L's in hadron calorimeter.

[129] BARATE 98E reconstruct K^0's by using $K^0_S\to\pi^+\pi^-$ decays.

$\Gamma(\pi^-K^0\overline{K}^0\nu_\tau)/\Gamma_{total}$ $\Gamma_{44}/\Gamma=(2\Gamma_{45}+\Gamma_{46})/\Gamma$

Data marked "avg" are highly correlated with data appearing elsewhere in the Listings, and are therefore used for the average given below but not in the overall fits. "f&a" marks results used for the fit and the average.

VALUE (%)		EVTS	DOCUMENT ID		TECN	COMMENT
0.159±0.029 OUR FIT	Error includes scale factor of 1.1.					
0.153±0.030±0.016	**avg**	74	[130] BARATE	98E	ALEP	1991–1995 LEP runs
• • • We do not use the following data for averages, fits, limits, etc. • • •						
0.31 ±0.12 ±0.04			[131] ACCIARRI	95F	L3	1991–1993 LEP runs

[130] BARATE 98E obtain this value by adding twice their B($\pi^-K^0_SK^0_S\nu_\tau$) value to their B($\pi^-K^0_SK^0_L\nu_\tau$) value.

[131] ACCIARRI 95F assume B($\pi^-K^0_SK^0_S\nu$)= B($\pi^-K^0_SK^0_L\nu$) = 1/2B($\pi^-K^0_SK^0_L\nu$).

$\Gamma(\pi^-K^0_SK^0_S\nu_\tau)/\Gamma_{total}$ Γ_{45}/Γ

Bose-Einstein correlations might make the mixing fraction different than 1/4.

VALUE (%)	EVTS	DOCUMENT ID		TECN	COMMENT
0.024±0.005 OUR FIT					
0.024±0.005 OUR AVERAGE					
0.026±0.010±0.005	6	BARATE	98E	ALEP	1991–1995 LEP runs
0.023±0.005±0.003	42	COAN	96	CLEO	$E^{ee}_{cm}\approx$ 10.6 GeV

$\Gamma(\pi^- K^0_S K^0_L \nu_\tau)/\Gamma_{total}$ Γ_{46}/Γ

VALUE (%)	EVTS	DOCUMENT ID	TECN	COMMENT
0.110±0.028 OUR FIT	Error includes scale factor of 1.1.			
0.101±0.023±0.013	68	BARATE	98E ALEP	1991–1995 LEP runs

$\Gamma(\pi^- K^0 \overline{K}^0 \pi^0 \nu_\tau)/\Gamma_{total}$ Γ_{47}/Γ

VALUE	DOCUMENT ID	TECN	COMMENT
$(0.31\pm0.23)\times10^{-3}$	[132] BARATE 99R	ALEP	1991–1995 LEP runs

[132] BARATE 99R combine BARATE 98E $\Gamma(\pi^- K^0_S K^0_S \pi^0 \nu_\tau)/\Gamma_{total}$ and $\Gamma(\pi^- K^0_S K^0_L \pi^0 \nu_\tau)/\Gamma_{total}$ measurements to obtain this value.

$\Gamma(\pi^- K^0_S K^0_S \pi^0 \nu_\tau)/\Gamma_{total}$ Γ_{48}/Γ

VALUE (%)	CL%	DOCUMENT ID	TECN	COMMENT
<0.020	95	BARATE	98E ALEP	1991–1995 LEP runs

$\Gamma(\pi^- K^0_S K^0_L \pi^0 \nu_\tau)/\Gamma_{total}$ Γ_{49}/Γ

VALUE (%)	EVTS	DOCUMENT ID	TECN	COMMENT
0.031±0.011±0.005	11	BARATE	98E ALEP	1991–1995 LEP runs

$\Gamma(K^0 h^+ h^- h^- \geq 0 \text{ neutrals } \nu_\tau)/\Gamma_{total}$ Γ_{50}/Γ

VALUE (%)	CL%	DOCUMENT ID	TECN	COMMENT
<0.17	95	TSCHIRHART 88	HRS	E^{ee}_{cm}= 29 GeV
• • • We do not use the following data for averages, fits, limits, etc. • • •				
<0.27	90	BELTRAMI 85	HRS	E^{ee}_{cm}= 29 GeV

$\Gamma(K^0 h^+ h^- h^- \nu_\tau)/\Gamma_{total}$ Γ_{51}/Γ

VALUE (%)	EVTS	DOCUMENT ID	TECN	COMMENT
0.023±0.019±0.007	6	[133] BARATE 98E	ALEP	1991–1995 LEP runs

[133] BARATE 98E reconstruct K^0's using $K^0_S \to \pi^+\pi^-$ decays.

$\Gamma(h^- h^- h^+ \geq 0 \text{ neutrals } \geq 0 K^0_L \nu_\tau)/\Gamma_{total}$ Γ_{52}/Γ

$\Gamma_{52}/\Gamma = (0.3431\Gamma_{33}+0.3431\Gamma_{35}+0.3431\Gamma_{38}+0.3431\Gamma_{40}+0.4307\Gamma_{45}+0.6861\Gamma_{46}+\Gamma_{60}+\Gamma_{68}+\Gamma_{74}+\Gamma_{75}+\Gamma_{82}+\Gamma_{86}+\Gamma_{89}+\Gamma_{90}+0.285\Gamma_{117}+0.285\Gamma_{119}+0.9101\Gamma_{137}+0.9101\Gamma_{138})/\Gamma$

VALUE (%)	EVTS	DOCUMENT ID	TECN	COMMENT
15.19± 0.07 OUR FIT	Error includes scale factor of 1.1.			
14.8 ± 0.4 OUR AVERAGE				
14.4 ± 0.6 ±0.3		ADEVA 91F	L3	E^{ee}_{cm}= 88.3–94.3 GeV
15.0 ± 0.4 ±0.3		BEHREND 89B	CELL	E^{ee}_{cm}= 14–47 GeV
15.1 ± 0.8 ±0.6		AIHARA 87B	TPC	E^{ee}_{cm}= 29 GeV
• • • We do not use the following data for averages, fits, limits, etc. • • •				
13.5 ± 0.3 ±0.3		ABACHI 89B	HRS	E^{ee}_{cm}= 29 GeV
12.8 ± 1.0 ±0.7		[134] BURCHAT 87	MRK2	E^{ee}_{cm}= 29 GeV
12.1 ± 0.5 ±1.2		RUCKSTUHL 86	DLCO	E^{ee}_{cm}= 29 GeV
12.8 ± 0.5 ±0.8	1420	SCHMIDKE 86	MRK2	E^{ee}_{cm}= 29 GeV
15.3 ± 1.1 $^{+1.3}_{-1.6}$	367	ALTHOFF 85	TASS	E^{ee}_{cm}= 34.5 GeV
13.6 ± 0.5 ±0.8		BARTEL 85F	JADE	E^{ee}_{cm}= 34.6 GeV
12.2 ± 1.3 ±3.9		[135] BERGER 85	PLUT	E^{ee}_{cm}= 34.6 GeV
13.3 ± 0.3 ±0.6		FERNANDEZ 85	MAC	E^{ee}_{cm}= 29 GeV
24 ± 6	35	BRANDELIK 80	TASS	E^{ee}_{cm}= 30 GeV
32 ± 5	692	[136] BACINO 78B	DLCO	E^{ee}_{cm}= 3.1–7.4 GeV
35 ±11		[136] BRANDELIK 78	DASP	Assumes $V-A$ decay
18 ± 6.5	33	[136] JAROS 78	MRK1	$E^{ee}_{cm} > 6$ GeV

[134] BURCHAT 87 value is not independent of SCHMIDKE 86 value.

[135] Not independent of BERGER 85 $\Gamma(\mu^- \overline{\nu}_\mu \nu_\tau)/\Gamma_{total}$, $\Gamma(e^- \overline{\nu}_e \nu_\tau)/\Gamma_{total}$, $\Gamma(h^- \geq 1 \text{ neutrals } \nu_\tau)/\Gamma_{total}$, and $\Gamma(h^- \geq 0 K^0_L \nu_\tau)/\Gamma_{total}$, and therefore not used in the fit.

[136] Low energy experiments are not in average or fit because the systematic errors in background subtraction are judged to be large.

$\Gamma(h^- h^- h^+ \geq 0 \text{ neutrals } \nu_\tau(\text{ex. } K^0_S \to \pi^+\pi^-)(\text{"3-prong"}))/\Gamma_{total}$ Γ_{53}/Γ

$\Gamma_{53}/\Gamma = (\Gamma_{60}+\Gamma_{68}+\Gamma_{74}+\Gamma_{75}+\Gamma_{82}+\Gamma_{86}+\Gamma_{89}+\Gamma_{90}+0.285\Gamma_{117}+0.285\Gamma_{119}+0.9101\Gamma_{137}+0.9101\Gamma_{138})/\Gamma$

Data marked "avg" are highly correlated with data appearing elsewhere in the Listings, and are therefore used for the average given below but not in the overall fits. "f&a" marks results used for the fit and the average.

VALUE (%)		EVTS	DOCUMENT ID		TECN	COMMENT
14.57 ±0.07 OUR FIT	Error includes scale factor of 1.1.					
14.59 ±0.08 OUR AVERAGE	Error includes scale factor of 1.1.					
14.569±0.093±0.048	f&a	23k	[137] ABREU	01M	DLPH	1992–1995 LEP runs
14.556±0.105±0.076	f&a		[138] ACHARD	01D	L3	1992–1995 LEP runs
14.96 ±0.09 ±0.22	f&a	10.4k	AKERS	95Y	OPAL	1991–1994 LEP runs
14.22 ±0.10 ±0.37	avg		[139] BALEST	95C	CLEO	$E^{ee}_{cm} \approx$ 10.6 GeV
• • • We do not use the following data for averages, fits, limits, etc. • • •						
15.26 ±0.26 ±0.22			ACTON	92H	OPAL	Repl. by AKERS 95Y
13.3 ±0.3 ±0.8			[140] ALBRECHT	92D	ARG	E^{ee}_{cm}= 9.4–10.6 GeV
14.35 $^{+0.40}_{-0.45}$ ±0.24			DECAMP	92C	ALEP	1989–1990 LEP runs

[137] The correlation coefficients between this measurement and the ABREU 01M measurements of B($\tau \to$ 1-prong) and B($\tau \to$ 5-prong) are -0.98 and -0.08 respectively.

[138] The correlation coefficients between this measurement and the ACHARD 01D measurements of B($\tau \to$ "1-prong") and B($\tau \to$ "5-prong") are -0.978 and -0.19 respectively.

[139] Not independent of BALEST 95C B($h^- h^- h^+ \nu_\tau$) and B($h^- h^- h^+ \pi^0 \nu_\tau$) values, and BORTOLETTO 93 B($h^- h^- h^+ 2\pi^0 \nu_\tau$)/B($h^- h^- h^+ \geq 0$ neutrals ν_τ) value.

[140] This ALBRECHT 92D value is not independent of their $\Gamma(\mu^- \overline{\nu}_\mu \nu_\tau)\Gamma(e^- \overline{\nu}_e \nu_\tau)/\Gamma^2_{total}$ value.

$\Gamma(h^- h^- h^+ \nu_\tau)/\Gamma_{total}$ Γ_{54}/Γ

$\Gamma_{54}/\Gamma = (0.3431\Gamma_{33}+0.3431\Gamma_{35}+\Gamma_{60}+\Gamma_{82}+\Gamma_{89}+0.0221\Gamma_{137})/\Gamma$

Data marked "avg" are highly correlated with data appearing elsewhere in the Listings, and are therefore used for the average given below but not in the overall fits. "f&a" marks results used for the fit and the average.

VALUE (%)		EVTS	DOCUMENT ID		TECN	COMMENT
10.01±0.09 OUR FIT	Error includes scale factor of 1.2.					
9.8 ±0.6 OUR AVERAGE	Error includes scale factor of 4.4. See the ideogram below.					
7.6 ±0.1 ±0.5	avg	7.5k	[141] ALBRECHT	96E	ARG	E^{ee}_{cm}= 9.4–10.6 GeV
9.92±0.10±0.09	f&a	11.2k	[142] BUSKULIC	96	ALEP	LEP 1991–1993 data
9.49±0.36±0.63	f&a		DECAMP	92C	ALEP	1989–1990 LEP runs
• • • We do not use the following data for averages, fits, limits, etc. • • •						
8.7 ±0.7 ±0.3		694	[143] BEHREND	90	CELL	E^{ee}_{cm}= 35 GeV
7.0 ±0.3 ±0.7		1566	[144] BAND	87	MAC	E^{ee}_{cm}= 29 GeV
6.7 ±0.8 ±0.9			[145] BURCHAT	87	MRK2	E^{ee}_{cm}= 29 GeV
6.4 ±0.4 ±0.9			[146] RUCKSTUHL	86	DLCO	E^{ee}_{cm}= 29 GeV
7.8 ±0.5 ±0.8		890	SCHMIDKE	86	MRK2	E^{ee}_{cm}= 29 GeV
8.4 ±0.4 ±0.7		1255	[146] FERNANDEZ	85	MAC	E^{ee}_{cm}= 29 GeV
9.7 ±2.0 ±1.3			BEHREND	84	CELL	E^{ee}_{cm}= 14,22 GeV

[141] ALBRECHT 96E not independent of ALBRECHT 93C $\Gamma(h^- h^- h^+ \nu_\tau(\text{ex. } K^0)) \times \Gamma(\text{particle}^- \geq 0 \text{ neutrals } \geq 0 K^0_L \nu_\tau)/\Gamma^2_{total}$ value.

[142] BUSKULIC 96 quote B($h^- h^- h^+ \nu_\tau$(ex. K^0)) = 9.50 ± 0.10 ± 0.11. We add 0.42 to remove their K^0 correction and reduce the systematic error accordingly.

[143] BEHREND 90 subtract 0.3% to account for the $\tau^- \to K^*(892)^- \nu_\tau$ contribution to measured events.

[144] BAND 87 subtract for charged kaon modes; not independent of FERNANDEZ 85 value.

[145] BURCHAT 87 value is not independent of SCHMIDKE 86 value.

[146] Value obtained by multiplying paper's $R = B(h^- h^- h^+ \nu_\tau)/B(3\text{-prong})$ by B(3-prong) = 0.143 and subtracting 0.3% for $K^*(892)$ background.

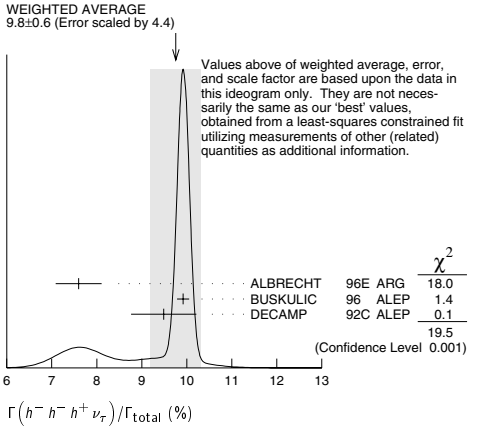

$\Gamma(h^- h^- h^+ \nu_\tau(\text{ex. } K^0))/\Gamma_{total}$ Γ_{55}/Γ

$\Gamma_{55}/\Gamma = (\Gamma_{60}+\Gamma_{82}+\Gamma_{89}+0.0221\Gamma_{137})/\Gamma$

Data marked "avg" are highly correlated with data appearing elsewhere in the Listings, and are therefore used for the average given below but not in the overall fits. "f&a" marks results used for the fit and the average.

VALUE (%)		EVTS	DOCUMENT ID		TECN	COMMENT
9.65±0.09 OUR FIT	Error includes scale factor of 1.2.					
9.57±0.11 OUR AVERAGE						
9.50±0.10±0.11	avg	11.2k	[147] BUSKULIC	96	ALEP	LEP 1991–1993 data
9.87±0.10±0.24	avg		[148] AKERS	95Y	OPAL	1991–1994 LEP runs
9.51±0.07±0.20	f&a	37.7k	BALEST	95C	CLEO	$E^{ee}_{cm} \approx$ 10.6 GeV

[147] Not independent of BUSKULIC 96 B($h^- h^- h^+ \nu_\tau$) value.

[148] Not independent of AKERS 95Y B($h^- h^- h^+ \geq 0$ neutrals ν_τ(ex. $K^0_S \to \pi^+\pi^-$)) and B($h^- h^- h^+ \nu_\tau$(ex. K^0))/B($h^- h^- h^+ \geq 0$ neutrals ν_τ(ex. $K^0_S \to \pi^+\pi^-$)) values.

$\Gamma(h^-h^-h^+\nu_\tau(\text{ex. }K^0))/\Gamma(h^-h^-h^+\geq 0\text{ neutrals }\nu_\tau(\text{ex. }K^0_S\to\pi^+\pi^-)(\text{"3-prong"}))$ Γ_{55}/Γ_{53}

$\Gamma_{55}/\Gamma_{53}=(\Gamma_{60}+\Gamma_{82}+\Gamma_{89}+0.0221\Gamma_{137})/(\Gamma_{60}+\Gamma_{68}+\Gamma_{74}+\Gamma_{75}+\Gamma_{82}+\Gamma_{86}+\Gamma_{89}+\Gamma_{90}+0.285\Gamma_{117}+0.285\Gamma_{119}+0.9101\Gamma_{137}+0.9101\Gamma_{138})$

VALUE	DOCUMENT ID	TECN	COMMENT
0.662±0.006 OUR FIT	Error includes scale factor of 1.3.		
0.660±0.004±0.014	AKERS 95Y	OPAL	1991–1994 LEP runs

$\Gamma(h^-h^-h^+\nu_\tau(\text{ex. }K^0,\omega))/\Gamma_{\text{total}}$ $\Gamma_{56}/\Gamma=(\Gamma_{60}+\Gamma_{82}+\Gamma_{89})/\Gamma$

VALUE (%)	DOCUMENT ID
9.60±0.09 OUR FIT	Error includes scale factor of 1.2.

$\Gamma(\pi^-\pi^+\pi^-\nu_\tau)/\Gamma_{\text{total}}$ $\Gamma_{57}/\Gamma=(0.3431\Gamma_{33}+\Gamma_{60}+0.0221\Gamma_{137})/\Gamma$

VALUE (%)	DOCUMENT ID
9.47±0.10 OUR FIT	Error includes scale factor of 1.2.

$\Gamma(\pi^-\pi^+\pi^-\nu_\tau(\text{ex. }K^0))/\Gamma_{\text{total}}$ $\Gamma_{58}/\Gamma=(\Gamma_{60}+0.0221\Gamma_{137})/\Gamma$

VALUE (%)	EVTS	DOCUMENT ID	TECN	COMMENT
9.16±0.10 OUR FIT	Error includes scale factor of 1.2.			
9.13±0.05±0.46	43k	[149] BRIERE 03	CLE3	E^{ee}_{cm}= 10.6 GeV

[149] 47% correlated with BRIERE 03 $\tau^-\to K^-\pi^+\pi^-\nu_\tau$ and 71% correlated with $\tau^-\to K^-K^+\pi^-\nu_\tau$ because of a common 5% normalization error.

$\Gamma(\pi^-\pi^+\pi^-\nu_\tau(\text{ex. }K^0)\text{, non-axial vector})/\Gamma(\pi^-\pi^+\pi^-\nu_\tau(\text{ex. }K^0))$ $\Gamma_{59}/\Gamma_{58}=\Gamma_{59}/(\Gamma_{60}+0.0221\Gamma_{137})$

VALUE	CL%	DOCUMENT ID	TECN	COMMENT
<0.261	95	[150] ACKERSTAFF 97R	OPAL	1992–1994 LEP runs

[150] Model-independent limit from structure function analysis on contribution to $B(\tau^-\to\pi^-\pi^+\pi^-\nu_\tau(\text{ex. }K^0))$ from non-axial vectors.

$\Gamma(\pi^-\pi^+\pi^-\nu_\tau(\text{ex. }K^0,\omega))/\Gamma_{\text{total}}$ Γ_{60}/Γ

VALUE (%)	DOCUMENT ID
9.12±0.10 OUR FIT	Error includes scale factor of 1.2.

$\Gamma(h^-h^-h^+\geq 1\text{ neutrals }\nu_\tau)/\Gamma_{\text{total}}$ Γ_{61}/Γ

$\Gamma_{61}/\Gamma=(0.3431\Gamma_{38}+0.3431\Gamma_{40}+0.4307\Gamma_{45}+0.6861\Gamma_{46}+\Gamma_{68}+\Gamma_{74}+\Gamma_{75}+\Gamma_{86}+\Gamma_{90}+0.285\Gamma_{117}+0.285\Gamma_{119}+0.888\Gamma_{137}+0.9101\Gamma_{138})/\Gamma$

VALUE (%)	EVTS	DOCUMENT ID	TECN	COMMENT
5.19±0.10 OUR FIT	Error includes scale factor of 1.3.			
• • • We do not use the following data for averages, fits, limits, etc. • • •				
5.6 ±0.7 ±0.3	352	[151] BEHREND 90	CELL	E^{ee}_{cm}= 35 GeV
4.2 ±0.5 ±0.9	203	[152] ALBRECHT 87L	ARG	E^{ee}_{cm}= 10 GeV
6.1 ±0.8 ±0.9		[153] BURCHAT 87	MRK2	E^{ee}_{cm}= 29 GeV
7.6 ±0.4 ±0.9		[154,155] RUCKSTUHL 86	DLCO	E^{ee}_{cm}= 29 GeV
4.7 ±0.5 ±0.8	530	[156] SCHMIDKE 86	MRK2	E^{ee}_{cm}= 29 GeV
5.6 ±0.4 ±0.7		[155] FERNANDEZ 85	MAC	E^{ee}_{cm}= 29 GeV
6.2 ±2.3 ±1.7		BEHREND 84	CELL	E^{ee}_{cm}= 14,22 GeV

[151] BEHREND 90 value is not independent of BEHREND 90 $B(3h\nu_\tau\geq 1\text{ neutrals})+B(5\text{-prong})$.

[152] ALBRECHT 87L measure the product of branching ratios $B(3\pi^\pm\pi^0\nu_\tau)\,B((e\,\overline{\nu}\text{ or }\mu\,\overline{\nu}\text{ or }\pi\text{ or }K\text{ or }\rho)\,\nu_\tau)=0.029$ and use the PDG 86 values for the second branching ratio which sum to 0.69 ± 0.03 to get the quoted value.

[153] BURCHAT 87 value is not independent of SCHMIDKE 86 value.

[154] Contributions from kaons and from $>1\pi^0$ are subtracted. Not independent of (3-prong + $0\pi^0$) and (3-prong + $\geq 0\pi^0$) values.

[155] Value obtained using paper's $R=B(h^-h^-h^+\nu_\tau)/B(3\text{-prong})$ and current B(3-prong) = 0.143.

[156] Not independent of SCHMIDKE 86 $h^-h^-h^+\nu_\tau$ and $h^-h^-h^+(\geq 0\pi^0)\nu_\tau$ values.

$\Gamma(h^-h^-h^+\geq 1\text{ neutrals }\nu_\tau(\text{ex. }K^0_S\to\pi^+\pi^-))/\Gamma_{\text{total}}$ Γ_{62}/Γ

$\Gamma_{62}/\Gamma=(\Gamma_{68}+\Gamma_{74}+\Gamma_{75}+\Gamma_{86}+\Gamma_{90}+0.285\Gamma_{117}+0.285\Gamma_{119}+0.888\Gamma_{137}+0.9101\Gamma_{138})/\Gamma$

Data marked "avg" are highly correlated with data appearing elsewhere in the Listings, and are therefore used for the average given below but not in the overall fits. "f&a" marks results used for the fit and the average.

VALUE (%)	EVTS	DOCUMENT ID	TECN	COMMENT
4.92±0.09 OUR FIT	Error includes scale factor of 1.3.			
5.07±0.24 OUR AVERAGE				
5.09±0.10±0.23	avg	[157] AKERS 95Y	OPAL	1991–1994 LEP runs
4.95±0.29±0.65	f&a 570	DECAMP 92C	ALEP	1989–1990 LEP runs

[157] Not independent of AKERS 95Y $B(h^-h^-h^+\geq 0\text{ neutrals }\nu_\tau(\text{ex. }K^0_S\to\pi^+\pi^-))$ and $B(h^-h^-h^+\geq 0\text{ neutrals }\nu_\tau(\text{ex. }K^0))/B(h^-h^-h^+\geq 0\text{ neutrals }\nu_\tau(\text{ex. }K^0_S\to\pi^+\pi^-))$ values.

$\Gamma(h^-h^-h^+\pi^0\nu_\tau)/\Gamma_{\text{total}}$ Γ_{63}/Γ

$\Gamma_{63}/\Gamma=(0.3431\Gamma_{38}+0.3431\Gamma_{40}+\Gamma_{68}+\Gamma_{86}+\Gamma_{90}+0.231\Gamma_{119}+0.888\Gamma_{137}+0.0221\Gamma_{138})/\Gamma$

VALUE (%)	EVTS	DOCUMENT ID	TECN	COMMENT
4.53±0.09 OUR FIT	Error includes scale factor of 1.3.			
4.45±0.09±0.07	6.1k	[158] BUSKULIC 96	ALEP	LEP 1991–1993 data

[158] BUSKULIC 96 quote $B(h^-h^-h^+\pi^0\nu_\tau(\text{ex. }K^0))=4.30\pm0.09\pm0.09$. We add 0.15 to remove their K^0 correction and reduce the systematic error accordingly.

$\Gamma(h^-h^-h^+\pi^0\nu_\tau(\text{ex. }K^0))/\Gamma_{\text{total}}$ Γ_{64}/Γ

$\Gamma_{64}/\Gamma=(\Gamma_{68}+\Gamma_{86}+\Gamma_{90}+0.231\Gamma_{119}+0.888\Gamma_{137}+0.0221\Gamma_{138})/\Gamma$

VALUE (%)	EVTS	DOCUMENT ID	TECN	COMMENT
4.35±0.09 OUR FIT	Error includes scale factor of 1.3.			
4.23±0.06±0.22	7.2k	BALEST 95C	CLEO	$E^{ee}_{\text{cm}}\approx$ 10.6 GeV

$\Gamma(h^-h^-h^+\pi^0\nu_\tau(\text{ex. }K^0,\omega))/\Gamma_{\text{total}}$ $\Gamma_{65}/\Gamma=(\Gamma_{68}+\Gamma_{86}+\Gamma_{90}+0.231\Gamma_{119})/\Gamma$

VALUE (%)	DOCUMENT ID
2.62±0.09 OUR FIT	Error includes scale factor of 1.2.

$\Gamma(\pi^-\pi^+\pi^-\pi^0\nu_\tau)/\Gamma_{\text{total}}$ $\Gamma_{66}/\Gamma=(0.3431\Gamma_{38}+\Gamma_{68}+0.888\Gamma_{137}+0.0221\Gamma_{138})/\Gamma$

VALUE (%)	DOCUMENT ID
4.37±0.09 OUR FIT	Error includes scale factor of 1.3.

$\Gamma(\pi^-\pi^+\pi^-\pi^0\nu_\tau(\text{ex. }K^0))/\Gamma_{\text{total}}$ $\Gamma_{67}/\Gamma=(\Gamma_{68}+0.888\Gamma_{137}+0.0221\Gamma_{138})/\Gamma$

VALUE (%)	DOCUMENT ID	TECN	COMMENT
4.25±0.09 OUR FIT	Error includes scale factor of 1.3.		
4.19±0.10±0.21	[159] EDWARDS 00A	CLEO	4.7 fb^{-1} E^{ee}_{cm}= 10.6 GeV

[159] EDWARDS 00A quote $(4.19\pm0.10)\times10^{-2}$ with a 5% systematic error.

$\Gamma(\pi^-\pi^+\pi^-\pi^0\nu_\tau(\text{ex. }K^0,\omega))/\Gamma_{\text{total}}$ Γ_{68}/Γ

VALUE (%)	DOCUMENT ID
2.51±0.09 OUR FIT	Error includes scale factor of 1.2.

$\Gamma(h^-\rho\pi^0\nu_\tau)/\Gamma(h^-h^-h^+\pi^0\nu_\tau)$ Γ_{69}/Γ_{63}

VALUE	EVTS	DOCUMENT ID	TECN	COMMENT
• • • We do not use the following data for averages, fits, limits, etc. • • •				
0.30±0.04±0.02	393	ALBRECHT 91D	ARG	E^{ee}_{cm}= 9.4–10.6 GeV

$\Gamma(h^-\rho^+h^-\nu_\tau)/\Gamma(h^-h^-h^+\pi^0\nu_\tau)$ Γ_{70}/Γ_{63}

VALUE	EVTS	DOCUMENT ID	TECN	COMMENT
• • • We do not use the following data for averages, fits, limits, etc. • • •				
0.10±0.03±0.04	142	ALBRECHT 91D	ARG	E^{ee}_{cm}= 9.4–10.6 GeV

$\Gamma(h^-\rho^-h^+\nu_\tau)/\Gamma(h^-h^-h^+\pi^0\nu_\tau)$ Γ_{71}/Γ_{63}

VALUE	EVTS	DOCUMENT ID	TECN	COMMENT
• • • We do not use the following data for averages, fits, limits, etc. • • •				
0.26±0.05±0.01	370	ALBRECHT 91D	ARG	E^{ee}_{cm}= 9.4–10.6 GeV

$\Gamma(h^-h^-h^+2\pi^0\nu_\tau)/\Gamma_{\text{total}}$ Γ_{72}/Γ

$\Gamma_{72}/\Gamma=(0.4307\Gamma_{45}+\Gamma_{74}+0.236\Gamma_{117}+0.888\Gamma_{138})/\Gamma$

VALUE (%)	DOCUMENT ID
0.55±0.04 OUR FIT	

$\Gamma(h^-h^-h^+2\pi^0\nu_\tau(\text{ex. }K^0))/\Gamma_{\text{total}}$ Γ_{73}/Γ

$\Gamma_{73}/\Gamma=(\Gamma_{74}+0.236\Gamma_{117}+0.888\Gamma_{138})/\Gamma$

VALUE (%)	EVTS	DOCUMENT ID	TECN	COMMENT
0.54±0.04 OUR FIT				
0.50±0.07±0.07	1.8k	BUSKULIC 96	ALEP	LEP 1991–1993 data

$\Gamma(h^-h^-h^+2\pi^0\nu_\tau(\text{ex. }K^0))/\Gamma(h^-h^-h^+\geq 0\text{ neutrals }\geq 0K^0_L\nu_\tau)$ Γ_{73}/Γ_{52}

$\Gamma_{73}/\Gamma_{52}=(\Gamma_{74}+0.236\Gamma_{117}+0.888\Gamma_{138})/(0.3431\Gamma_{33}+0.3431\Gamma_{35}+0.3431\Gamma_{38}+0.3431\Gamma_{40}+0.4307\Gamma_{45}+0.6861\Gamma_{46}+\Gamma_{60}+\Gamma_{68}+\Gamma_{74}+\Gamma_{75}+\Gamma_{82}+\Gamma_{86}+\Gamma_{89}+\Gamma_{90}+0.285\Gamma_{117}+0.285\Gamma_{119}+0.9101\Gamma_{137}+0.9101\Gamma_{138})$

VALUE	EVTS	DOCUMENT ID	TECN	COMMENT
0.0355±0.0028 OUR FIT				
0.034 ±0.002 ±0.003	668	BORTOLETTO 93	CLEO	$E^{ee}_{\text{cm}}\approx$ 10.6 GeV

$\Gamma(h^-h^-h^+2\pi^0\nu_\tau(\text{ex. }K^0,\omega,\eta))/\Gamma_{\text{total}}$ Γ_{74}/Γ

VALUE (%)	DOCUMENT ID
0.11±0.04 OUR FIT	

$\Gamma(h^-h^-h^+3\pi^0\nu_\tau)/\Gamma_{\text{total}}$ Γ_{75}/Γ

VALUE (%)	EVTS	DOCUMENT ID	TECN	COMMENT
0.023 ±0.008 OUR FIT	Error includes scale factor of 1.5.			
0.023 ±0.005 OUR AVERAGE				
0.022 ±0.003 ±0.004	139	ANASTASSOV 01	CLEO	E^{ee}_{cm}= 10.6 GeV
0.11 ±0.04 ±0.05	440	[160] BUSKULIC 96	ALEP	LEP 1991–1993 data
• • • We do not use the following data for averages, fits, limits, etc. • • •				
0.0285±0.0056±0.0051	57	ANDERSON 97	CLEO	Repl. by ANASTASSOV 01

[160] BUSKULIC 96 state their measurement is for $B(h^-h^-h^+\geq 3\pi^0\nu_\tau)$. We assume that $B(h^-h^-h^+\geq 4\pi^0\nu_\tau)$ is very small.

$\Gamma(K^-h^+h^-\geq 0\text{ neutrals }\nu_\tau)/\Gamma_{\text{total}}$ $\Gamma_{76}/\Gamma=(0.3431\Gamma_{35}+0.3431\Gamma_{40}+\Gamma_{82}+\Gamma_{86}+\Gamma_{89}+\Gamma_{90}+0.285\Gamma_{119})/\Gamma$

VALUE (%)	CL%	DOCUMENT ID	TECN	COMMENT
0.69±0.04 OUR FIT	Error includes scale factor of 1.3.			
<0.6	90	AIHARA 84C	TPC	E^{ee}_{cm}= 29 GeV

$\Gamma(K^- h^+ \pi^- \nu_\tau (\text{ex.}\, K^0))/\Gamma_{\text{total}}$ $\Gamma_{77}/\Gamma = (\Gamma_{82}+\Gamma_{89})/\Gamma$

VALUE (%)	DOCUMENT ID
0.48 ± 0.04 OUR FIT Error includes scale factor of 1.5.	

$\Gamma(K^- h^+ \pi^- \nu_\tau (\text{ex.}\, K^0))/\Gamma(\pi^- \pi^+ \pi^- \nu_\tau (\text{ex.}\, K^0))$ $\Gamma_{77}/\Gamma_{58} = (\Gamma_{82}+\Gamma_{89})/(\Gamma_{60}+0.0221\Gamma_{137})$

VALUE (%)	EVTS	DOCUMENT ID		TECN	COMMENT
5.2 ± 0.4 OUR FIT Error includes scale factor of 1.6.					
5.44 ± 0.21 ± 0.53	7.9k	RICHICHI	99	CLEO	E_{cm}^{ee} = 10.6 GeV

$\Gamma(K^- h^+ \pi^- \pi^0 \nu_\tau (\text{ex.}\, K^0))/\Gamma_{\text{total}}$ $\Gamma_{78}/\Gamma = (\Gamma_{86}+\Gamma_{90}+0.231\Gamma_{119})/\Gamma$

VALUE (%)	DOCUMENT ID
0.107 ± 0.022 OUR FIT	

$\Gamma(K^- h^+ \pi^- \pi^0 \nu_\tau (\text{ex.}\, K^0))/\Gamma(\pi^- \pi^+ \pi^- \pi^0 \nu_\tau (\text{ex.}\, K^0))$ $\Gamma_{78}/\Gamma_{67} = (\Gamma_{86}+\Gamma_{90}+0.231\Gamma_{119})/(\Gamma_{68}+0.888\Gamma_{137}+0.0221\Gamma_{138})$

VALUE (%)	EVTS	DOCUMENT ID		TECN	COMMENT
2.5 ± 0.5 OUR FIT					
2.61 ± 0.45 ± 0.42	719	RICHICHI	99	CLEO	E_{cm}^{ee} = 10.6 GeV

$\Gamma(K^- \pi^+ \pi^- \geq 0 \text{ neutrals } \nu_\tau)/\Gamma_{\text{total}}$ $\Gamma_{79}/\Gamma = (0.3431\Gamma_{35}+0.3431\Gamma_{40}+\Gamma_{82}+\Gamma_{86}+0.285\Gamma_{119})/\Gamma$

VALUE (%)	EVTS	DOCUMENT ID		TECN	COMMENT
0.50 ± 0.04 OUR FIT Error includes scale factor of 1.3.					
$0.58^{+0.15}_{-0.13} \pm 0.12$	20	[161] BAUER	94	TPC	E_{cm}^{ee} = 29 GeV
• • • We do not use the following data for averages, fits, limits, etc. • • •					
$0.22^{+0.16}_{-0.13} \pm 0.05$	9	[162] MILLS	85	DLCO	E_{cm}^{ee} = 29 GeV

[161] We multiply 0.58% by 0.20, the relative systematic error quoted by BAUER 94, to obtain the systematic error.

[162] Error correlated with MILLS 85 ($K K \pi \nu$) value. We multiply 0.22% by 0.23, the relative systematic error quoted by MILLS 85, to obtain obtain the systematic error.

$\Gamma(K^- \pi^+ \pi^- \geq 0 \pi^0 \nu_\tau (\text{ex.}\, K^0))/\Gamma_{\text{total}}$ $\Gamma_{80}/\Gamma = (\Gamma_{82}+\Gamma_{86}+0.231\Gamma_{119})/\Gamma$

Data marked "avg" are highly correlated with data appearing elsewhere in the Listings, and are therefore used for the average given below but not in the overall fits. "f&a" marks results used for the fit and the average.

VALUE (%)		DOCUMENT ID		TECN	COMMENT
0.39 ± 0.04 OUR FIT Error includes scale factor of 1.3.					
0.30 ± 0.05 OUR AVERAGE					
0.343 ± 0.073 ± 0.031	f&a	ABBIENDI	00D	OPAL	1990–1995 LEP runs
0.275 ± 0.064	avg	[163] BARATE	98	ALEP	1991–1995 LEP runs

[163] Not independent of BARATE 98 $\Gamma(\tau^- \to K^- \pi^+ \pi^- \nu_\tau)/\Gamma_{\text{total}}$ and $\Gamma(\tau^- \to K^- \pi^+ \pi^- \pi^0 \nu_\tau)/\Gamma_{\text{total}}$ values.

$\Gamma(K^- \pi^+ \pi^- \nu_\tau)/\Gamma_{\text{total}}$ $\Gamma_{81}/\Gamma = (0.3431\Gamma_{35}+\Gamma_{82})/\Gamma$

VALUE (%)	DOCUMENT ID
0.38 ± 0.04 OUR FIT Error includes scale factor of 1.6.	

$\Gamma(K^- \pi^+ \pi^- \nu_\tau (\text{ex.}\, K^0))/\Gamma_{\text{total}}$ Γ_{82}/Γ

Data marked "avg" are highly correlated with data appearing elsewhere in the Listings, and are therefore used for the average given below but not in the overall fits. "f&a" marks results used for the fit and the average.

VALUE (%)		EVTS	DOCUMENT ID		TECN	COMMENT
0.33 ± 0.04 OUR FIT Error includes scale factor of 1.6.						
0.32 ± 0.04 OUR AVERAGE Error includes scale factor of 1.6. See the ideogram below.						
0.384 ± 0.014 ± 0.038	f&a	3.5k	[164] BRIERE	03	CLE3	E_{cm}^{ee} = 10.6 GeV
0.360 ± 0.082 ± 0.048	avg		ABBIENDI	00D	OPAL	1990–1995 LEP runs
0.346 ± 0.023 ± 0.056	avg	158	[165] RICHICHI	99	CLEO	E_{cm}^{ee} = 10.6 GeV
0.214 ± 0.037 ± 0.029	f&a		BARATE	98	ALEP	1991–1995 LEP runs

[164] 47% correlated with BRIERE 03 $\tau^- \to \pi^- \pi^+ \pi^- \nu_\tau$ and 34% correlated with $\tau^- \to K^- K^+ \pi^- \nu_\tau$ because of a common 5% normalization error.

[165] Not independent of RICHICHI 99 $\Gamma(\tau^- \to K^- h^+ \pi^- \nu_\tau (\text{ex.}\, K^0))/\Gamma(\tau^- \to \pi^- \pi^+ \pi^- \nu_\tau (\text{ex.}\, K^0))$, $\Gamma(\tau^- \to K^- K^+ \pi^- \nu_\tau)/\Gamma(\tau^- \to \pi^- \pi^+ \pi^- \nu_\tau (\text{ex.}\, K^0))$ and BALEST 95C $\Gamma(\tau^- \to h^- h^- h^+ \nu_\tau (\text{ex.}\, K^0))/\Gamma_{\text{total}}$ values.

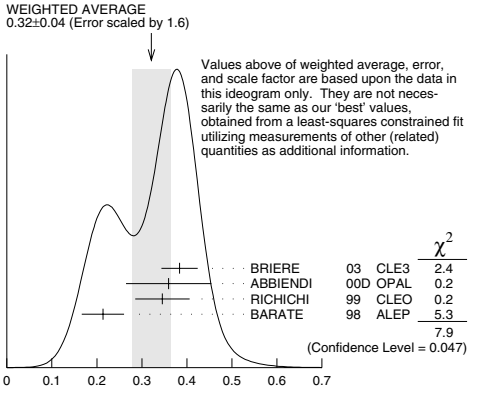

$\Gamma(K^- \rho^0 \nu_\tau \to K^- \pi^+ \pi^- \nu_\tau)/\Gamma(K^- \pi^+ \pi^- \nu_\tau (\text{ex.}\, K^0))$ Γ_{83}/Γ_{82}

VALUE	DOCUMENT ID		TECN	COMMENT
0.48 ± 0.14 ± 0.10	[166] ASNER	00B	CLEO	E_{cm}^{ee} = 10.6 GeV
• • • We do not use the following data for averages, fits, limits, etc. • • •				
0.39 ± 0.14	[167] BARATE	99R	ALEP	1991–1995 LEP runs

[166] ASNER 00B assume $\tau^- \to K^- \pi^+ \pi^- \nu_\tau$ (ex. K^0) decays proceed only through $K\rho$ and $K^*\pi$ intermediate states. They assume the resonance structure of $\tau^- \to K^- \pi^+ \pi^- \nu_\tau$ (ex. K^0) decays is dominated by $K_1(1270)^-$ and $K_1(1400)^-$ resonances, and assume $B(K_1(1270) \to K^*(892)\pi) = (16 \pm 5)\%$, $B(K_1(1270) \to K\rho) = (42 \pm 6)\%$, and $B(K_1(1400) \to K\rho) = 0$.

[167] BARATE 99R assume $\tau^- \to K^- \pi^+ \pi^- \nu_\tau$ (ex. K^0) decays proceed only through $K\rho$ and $K^*\pi$ intermediate states. The quoted error is statistical only.

$\Gamma(K^- \pi^+ \pi^- \pi^0 \nu_\tau)/\Gamma_{\text{total}}$ $\Gamma_{84}/\Gamma = (0.3431\Gamma_{40}+\Gamma_{86}+0.231\Gamma_{119})/\Gamma$

VALUE (units 10^{-4})	DOCUMENT ID
11.8 ± 2.5 OUR FIT	

$\Gamma(K^- \pi^+ \pi^- \pi^0 \nu_\tau (\text{ex.}\, K^0))/\Gamma_{\text{total}}$ $\Gamma_{85}/\Gamma = (\Gamma_{86}+0.231\Gamma_{119})/\Gamma$

Data marked "avg" are highly correlated with data appearing elsewhere in the Listings, and are therefore used for the average given below but not in the overall fits. "f&a" marks results used for the fit and the average.

VALUE (units 10^{-4})		CL%	DOCUMENT ID		TECN	COMMENT
6.5 ± 2.4 OUR FIT						
7.0 ± 2.5 OUR AVERAGE						
7.5 ± 2.6 ± 1.8	avg		[168] RICHICHI	99	CLEO	E_{cm}^{ee} = 10.6 GeV
6.1 ± 3.9 ± 1.8	f&a		BARATE	98	ALEP	1991–1995 LEP runs
• • • We do not use the following data for averages, fits, limits, etc. • • •						
< 17		95	ABBIENDI	00D	OPAL	1990–1995 LEP runs

[168] Not independent of RICHICHI 99 $\Gamma(\tau^- \to K^- h^+ \pi^- \nu_\tau (\text{ex.}\, K^0))/\Gamma(\tau^- \to \pi^- \pi^+ \pi^- \nu_\tau (\text{ex.}\, K^0))$, $\Gamma(\tau^- \to K^- K^+ \pi^- \nu_\tau)/\Gamma(\tau^- \to \pi^- \pi^+ \pi^- \nu_\tau (\text{ex.}\, K^0))$ and BALEST 95C $\Gamma(\tau^- \to h^- h^- h^+ \nu_\tau (\text{ex.}\, K^0))/\Gamma_{\text{total}}$ values.

$\Gamma(K^- \pi^+ \pi^- \pi^0 \nu_\tau (\text{ex.}\, K^0, \eta))/\Gamma_{\text{total}}$ Γ_{86}/Γ

Test of lepton family number conservation.

VALUE (units 10^{-4})	DOCUMENT ID
5.9 ± 2.4 OUR FIT	

$\Gamma(K^- \pi^+ K^- \geq 0 \text{ neut. } \nu_\tau)/\Gamma_{\text{total}}$ Γ_{87}/Γ

VALUE (%)	CL%	DOCUMENT ID		TECN	COMMENT
< 0.09	95	BAUER	94	TPC	E_{cm}^{ee} = 29 GeV

$\Gamma(K^- K^+ \pi^- \geq 0 \text{ neut. } \nu_\tau)/\Gamma_{\text{total}}$ $\Gamma_{88}/\Gamma = (\Gamma_{89}+\Gamma_{90})/\Gamma$

Data marked "avg" are highly correlated with data appearing elsewhere in the Listings, and are therefore used for the average given below but not in the overall fits. "f&a" marks results used for the fit and the average.

VALUE (%)		EVTS	DOCUMENT ID		TECN	COMMENT
0.197 ± 0.018 OUR FIT Error includes scale factor of 1.1.						
0.203 ± 0.031 OUR AVERAGE						
0.159 ± 0.053 ± 0.020	f&a		ABBIENDI	00D	OPAL	1990–1995 LEP runs
0.238 ± 0.042	avg		[169] BARATE	98	ALEP	1991–1995 LEP runs
$0.15\ ^{+0.09}_{-0.07} \pm 0.03$	f&a	4	[170] BAUER	94	TPC	E_{cm}^{ee} = 29 GeV

[169] Not independent of BARATE 98 $\Gamma(\tau^- \to K^- K^+ \pi^- \nu_\tau)/\Gamma_{\text{total}}$ and $\Gamma(\tau^- \to K^- K^+ \pi^- \pi^0 \nu_\tau)/\Gamma_{\text{total}}$ values.

[170] We multiply 0.15% by 0.20, the relative systematic error quoted by BAUER 94, to obtain the systematic error.

$\Gamma(K^- K^+ \pi^- \nu_\tau)/\Gamma_{total}$ Γ_{89}/Γ

Data marked "avg" are highly correlated with data appearing elsewhere in the Listings, and are therefore used for the average given below but not in the overall fits. "f&a" marks results used for the fit and the average.

VALUE (%)		EVTS	DOCUMENT ID		TECN	COMMENT
0.155 ± 0.007 OUR FIT						
0.154 ± 0.009 OUR AVERAGE						
0.155 ± 0.006 ± 0.009	f&a	932	[171] BRIERE	03	CLE3	E_{cm}^{ee} = 10.6 GeV
0.087 ± 0.056 ± 0.040	avg		ABBIENDI	00D	OPAL	1990–1995 LEP runs
0.145 ± 0.013 ± 0.028	avg	2.3k	[172] RICHICHI	99	CLEO	E_{cm}^{ee} = 10.6 GeV
0.163 ± 0.021 ± 0.017	f&a		BARATE	98	ALEP	1991–1995 LEP runs
0.22 $^{+0.17}_{-0.11}$ ± 0.05	f&a	9	[173] MILLS	85	DLCO	E_{cm}^{ee} = 29 GeV

[171] 71% correlated with BRIERE 03 $\tau^- \to \pi^-\pi^+\pi^-\nu_\tau$ and 34% correlated with $\tau \to K^-\pi^+\pi^-\nu_\tau$ because of a common 5% normalization error.

[172] Not independent of RICHICHI 99 $\Gamma(\tau^- \to K^- K^+ \pi^- \nu_\tau)/\Gamma(\tau^- \to \pi^-\pi^+\pi^-\nu_\tau (\text{ex.} K^0))$ and BALEST 95C $\Gamma(\tau^- \to h^- h^+ \nu_\tau (\text{ex.} K^0))/\Gamma_{total}$ values.

[173] Error correlated with MILLS 85 ($K\pi\pi\pi^0\nu$) value. We multiply 0.22% by 0.23, the relative systematic error quoted by MILLS 85, to obtain obtain the systematic error.

$\Gamma(K^- K^+ \pi^- \nu_\tau)/\Gamma(\pi^-\pi^+\pi^-\nu_\tau (\text{ex.} K^0))$ $\Gamma_{89}/\Gamma_{58} = \Gamma_{89}/(\Gamma_{60}+0.0221\Gamma_{137})$

VALUE (%)	EVTS	DOCUMENT ID		TECN	COMMENT
1.69 ± 0.08 OUR FIT	Error includes scale factor of 1.1.				
1.60 ± 0.15 ± 0.30	2.3k	RICHICHI	99	CLEO	E_{cm}^{ee} = 10.6 GeV

$\Gamma(K^- K^+ \pi^- \pi^0 \nu_\tau)/\Gamma_{total}$ Γ_{90}/Γ

Data marked "avg" are highly correlated with data appearing elsewhere in the Listings, and are therefore used for the average given below but not in the overall fits. "f&a" marks results used for the fit and the average.

VALUE (units 10^{-4})		CL%	EVTS	DOCUMENT ID		TECN	COMMENT
4.2 ± 1.6 OUR FIT	Error includes scale factor of 1.1.						
4.4 ± 1.8 OUR AVERAGE	Error includes scale factor of 1.1.						
3.3 ± 1.8 ± 0.7	avg		158	[174] RICHICHI	99	CLEO	E_{cm}^{ee} = 10.6 GeV
7.5 ± 2.9 ± 1.5	f&a			BARATE	98	ALEP	1991–1995 LEP runs
• • • We do not use the following data for averages, fits, limits, etc. • • •							
< 27		95		ABBIENDI	00D	OPAL	1990–1995 LEP runs

[174] Not independent of RICHICHI 99 $\Gamma(\tau^- \to K^- K^+ \pi^- \nu_\tau)/\Gamma(\tau^- \to \pi^-\pi^+\pi^-\nu_\tau (\text{ex.} K^0))$ and BALEST 95C $\Gamma(\tau^- \to h^- h^- h^+ \nu_\tau (\text{ex.} K^0))/\Gamma_{total}$ values.

$\Gamma(K^- K^+ \pi^- \pi^0 \nu_\tau)/\Gamma(\pi^-\pi^+\pi^-\pi^0\nu_\tau (\text{ex.} K^0))$ $\Gamma_{90}/\Gamma_{67} = \Gamma_{90}/(\Gamma_{68}+0.888\Gamma_{137}+0.0221\Gamma_{138})$

VALUE (%)	EVTS	DOCUMENT ID		TECN	COMMENT
1.0 ± 0.4 OUR FIT	Error includes scale factor of 1.1.				
0.79 ± 0.44 ± 0.16	158	[175] RICHICHI	99	CLEO	E_{cm}^{ee} = 10.6 GeV

[175] RICHICHI 99 also quote a 95%CL upper limit of 0.0157 for this measurement.

$\Gamma(K^- K^+ K^- \geq 0 \text{ neut. } \nu_\tau)/\Gamma_{total}$ Γ_{91}/Γ

VALUE (%)	CL%	DOCUMENT ID		TECN	COMMENT
< 0.21	95	BAUER	94	TPC	E_{cm}^{ee} = 29 GeV

$\Gamma(K^- K^+ K^- \nu_\tau)/\Gamma_{total}$ Γ_{92}/Γ

VALUE	CL%	DOCUMENT ID		TECN	COMMENT
< 3.7 × 10^{-5}	90	BRIERE	03	CLE3	E_{cm}^{ee} = 10.6 GeV
< 1.9 × 10^{-4}	90	BARATE	98	ALEP	1991–1995 LEP runs

$\Gamma(\pi^- K^+ \pi^- \geq 0 \text{ neut. } \nu_\tau)/\Gamma_{total}$ Γ_{93}/Γ

VALUE (%)	CL%	DOCUMENT ID		TECN	COMMENT
< 0.25	95	BAUER	94	TPC	E_{cm}^{ee} = 29 GeV

$\Gamma(e^- e^- e^+ \bar{\nu}_e \nu_\tau)/\Gamma_{total}$ Γ_{94}/Γ

VALUE (units 10^{-5})	EVTS	DOCUMENT ID		TECN	COMMENT
2.8 ± 1.4 ± 0.4	5	ALAM	96	CLEO	E_{cm}^{ee} = 10.6 GeV

$\Gamma(\mu^- e^- e^+ \bar{\nu}_\mu \nu_\tau)/\Gamma_{total}$ Γ_{95}/Γ

VALUE (units 10^{-5})	CL%	DOCUMENT ID		TECN	COMMENT
< 3.6	90	ALAM	96	CLEO	E_{cm}^{ee} = 10.6 GeV

$\Gamma(3h^- 2h^+ \geq 0 \text{ neutrals } \nu_\tau (\text{ex. } K_S^0 \to \pi^-\pi^+)(\text{"5-prong"}))/\Gamma_{total}$ Γ_{96}/Γ

Data marked "avg" are highly correlated with data appearing elsewhere in the Listings, and are therefore used for the average given below but not in the overall fits. "f&a" marks results used for the fit and the average. $\Gamma_{96}/\Gamma = (\Gamma_{97}+\Gamma_{98})/\Gamma$

VALUE (%)		EVTS	DOCUMENT ID		TECN	COMMENT
0.100 ± 0.006 OUR FIT						
0.111 ± 0.008 OUR AVERAGE	Error includes scale factor of 1.1.					
0.115 ± 0.013 ± 0.006	f&a	112	[176] ABREU	01M	DLPH	1992–1995 LEP runs
0.170 ± 0.022 ± 0.026	f&a		[177] ACHARD	01D	L3	1992–1995 LEP runs
0.119 ± 0.013 ± 0.008	avg	119	[178] ACKERSTAFF	99E	OPAL	1991–1995 LEP runs
0.097 ± 0.005 ± 0.011	f&a	419	GIBAUT	94B	CLEO	E_{cm}^{ee} = 10.6 GeV
0.102 ± 0.029	f&a	13	BYLSMA	87	HRS	E_{cm}^{ee} = 29 GeV
• • • We do not use the following data for averages, fits, limits, etc. • • •						
0.26 ± 0.06 ± 0.05			ACTON	92H	OPAL	E_{cm}^{ee} = 88.2–94.2 GeV
0.10 $^{+0.05}_{-0.04}$ ± 0.03			DECAMP	92C	ALEP	1989–1990 LEP runs
0.16 ± 0.13 ± 0.04			BEHREND	89B	CELL	E_{cm}^{ee} = 14–47 GeV
0.3 ± 0.1 ± 0.2			BARTEL	85F	JADE	E_{cm}^{ee} = 34.6 GeV
0.13 ± 0.04		10	BELTRAMI	85	HRS	Repl. by BYLSMA 87
0.16 ± 0.08 ± 0.04		4	BURCHAT	85	MRK2	E_{cm}^{ee} = 29 GeV
1.0 ± 0.4		10	BEHREND	82	CELL	Repl. by BEHREND 89B

[176] The correlation coefficients between this measurement and the ABREU 01M measurements of B($\tau \to$ 1-prong) and B($\tau \to$ 3-prong) are − 0.08 and − 0.08 respectively.

[177] The correlation coefficients between this measurement and the ACHARD 01D measurements of B($\tau \to$ "1-prong") and B($\tau \to$ "3-prong") are − 0.082 and − 0.19 respectively.

[178] Not independent of ACKERSTAFF 99E B($\tau^- \to 3h^- 2h^+ \nu_\tau$ (ex. K^0)) and B($\tau^- \to 3h^- 2h^+ \pi^0 \nu_\tau$ (ex. K^0)) measurements.

$\Gamma(3h^- 2h^+ \nu_\tau (\text{ex.} K^0))/\Gamma_{total}$ Γ_{97}/Γ

VALUE (%)	EVTS	DOCUMENT ID		TECN	COMMENT
0.082 ± 0.006 OUR FIT					
0.076 ± 0.007 OUR AVERAGE					
0.091 ± 0.014 ± 0.006	97	ACKERSTAFF	99E	OPAL	1991–1995 LEP runs
0.080 ± 0.011 ± 0.013	58	BUSKULIC	96	ALEP	LEP 1991–1993 data
0.077 ± 0.005 ± 0.009	295	GIBAUT	94B	CLEO	E_{cm}^{ee} = 10.6 GeV
0.064 ± 0.023 ± 0.01	12	ALBRECHT	88B	ARG	E_{cm}^{ee} = 10 GeV
0.051 ± 0.020	7	BYLSMA	87	HRS	E_{cm}^{ee} = 29 GeV
• • • We do not use the following data for averages, fits, limits, etc. • • •					
0.067 ± 0.030	5	[179] BELTRAMI	85	HRS	Repl. by BYLSMA 87

[179] The error quoted is statistical only.

$\Gamma(3h^- 2h^+ \pi^0 \nu_\tau (\text{ex.} K^0))/\Gamma_{total}$ Γ_{98}/Γ

VALUE (%)	EVTS	DOCUMENT ID		TECN	COMMENT
0.0181 ± 0.0027 OUR FIT					
0.0172 ± 0.0027 OUR AVERAGE					
0.017 ± 0.002 ± 0.002	231	ANASTASSOV 01		CLEO	E_{cm}^{ee} = 10.6 GeV
0.027 ± 0.018 ± 0.009	23	ACKERSTAFF	99E	OPAL	1991–1995 LEP runs
0.018 ± 0.007 ± 0.012	18	BUSKULIC	96	ALEP	LEP 1991–1993 data
• • • We do not use the following data for averages, fits, limits, etc. • • •					
0.019 ± 0.004 ± 0.004	31	GIBAUT	94B	CLEO	Repl. by ANASTASSOV 01
0.051 ± 0.022	6	BYLSMA	87	HRS	E_{cm}^{ee} = 29 GeV
0.067 ± 0.030	5	[180] BELTRAMI	85	HRS	Repl. by BYLSMA 87

[180] The error quoted is statistical only.

$\Gamma(3h^- 2h^+ 2\pi^0 \nu_\tau)/\Gamma_{total}$ Γ_{99}/Γ

VALUE (%)	CL%	DOCUMENT ID		TECN	COMMENT
< 0.011	90	GIBAUT	94B	CLEO	E_{cm}^{ee} = 10.6 GeV

$\Gamma((5\pi)^- \nu_\tau)/\Gamma_{total}$ Γ_{100}/Γ

$\Gamma_{100}/\Gamma = (\Gamma_{28}+\Gamma_{45}+\Gamma_{74}+\Gamma_{97}+0.553\Gamma_{117}+0.888\Gamma_{138})/\Gamma$

Data marked "avg" are highly correlated with data appearing elsewhere in the Listings, and are therefore used for the average given below but not in the overall fits. "f&a" marks results used for the fit and the average.

VALUE (%)		DOCUMENT ID		TECN	COMMENT
0.80 ± 0.07 OUR FIT					
0.61 ± 0.06 ± 0.08	**avg**	[181] GIBAUT	94B	CLEO	E_{cm}^{ee} = 10.6 GeV

[181] Not independent of GIBAUT 94B B($3h^- 2h^+ \nu_\tau$), PROCARIO 93 B($h^- 4\pi^0 \nu_\tau$), and BORTOLETTO 93 B($2h^- h^+ 2\pi^0 \nu_\tau$)/B("3prong") measurements. Result is corrected for η contributions.

$\Gamma(4h^- 3h^+ \geq 0 \text{ neutrals } \nu_\tau (\text{"7-prong"}))/\Gamma_{total}$ Γ_{101}/Γ

VALUE	CL%	DOCUMENT ID		TECN	COMMENT
< 2.4 × 10^{-6}	90	EDWARDS	97B	CLEO	E_{cm}^{ee} = 10.6 GeV
• • • We do not use the following data for averages, fits, limits, etc. • • •					
< 1.8 × 10^{-5}	95	ACKERSTAFF	97J	OPAL	1990–1995 LEP runs
< 2.9 × 10^{-4}	90	BYLSMA	87	HRS	E_{cm}^{ee} = 29 GeV

$\Gamma(X^-(S=-1)\nu_\tau)/\Gamma_{total}$

$\Gamma_{102}/\Gamma = (\Gamma_{10}+\Gamma_{15}+\Gamma_{22}+\Gamma_{26}+\Gamma_{33}+\Gamma_{38}+\Gamma_{82}+\Gamma_{86}+\Gamma_{119})/\Gamma$

Data marked "avg" are highly correlated with data appearing elsewhere in the Listings, and are therefore used for the average given below but not in the overall fits. "f&a" marks results used for the fit and the average.

VALUE (%)		DOCUMENT ID		TECN	COMMENT
2.91 ± 0.08 OUR FIT		Error includes scale factor of 1.1.			
2.87 ± 0.12	**avg**	[182] BARATE	99R	ALEP	1991–1995 LEP runs

[182] BARATE 99R perform a combined analysis of all ALEPH LEP1 data on τ branching fraction measurements for decay modes having total strangeness equal to -1.

$\Gamma(K^*(892)^- \geq 0\,\text{neutrals} \geq 0 K_L^0 \nu_\tau)/\Gamma_{total}$ Γ_{103}/Γ

VALUE (%)	EVTS	DOCUMENT ID		TECN	COMMENT
1.42 ± 0.18 OUR AVERAGE		Error includes scale factor of 1.4. See the ideogram below.			
$1.19 \pm 0.15 \pm {}^{0.13}_{0.18}$	104	ALBRECHT	95H	ARG	E^{ee}_{cm} = 9.4–10.6 GeV
$1.94 \pm 0.27 \pm 0.15$	74	[183] AKERS	94G	OPAL	E^{ee}_{cm} = 88–94 GeV
$1.43 \pm 0.11 \pm 0.13$	475	[184] GOLDBERG	90	CLEO	E^{ee}_{cm} = 9.4–10.9 GeV

[183] AKERS 94G reject events in which a K^0_S accompanies the $K^*(892)^-$. We do not correct for them.

[184] GOLDBERG 90 estimates that 10% of observed $K^*(892)$ are accompanied by a π^0.

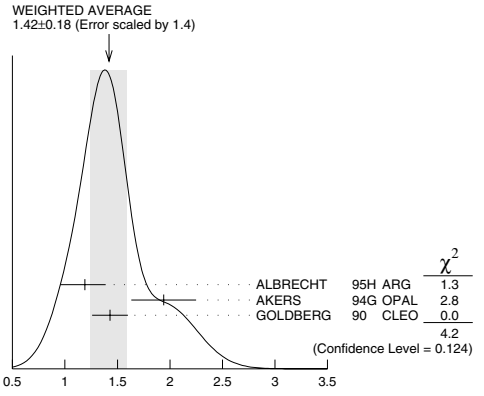

$\Gamma(K^*(892)^- \geq 0\,\text{neutrals} \geq 0 K_L^0 \nu_\tau)/\Gamma_{total}$ Γ_{103}/Γ

$\Gamma(K^*(892)^- \nu_\tau)/\Gamma_{total}$ Γ_{104}/Γ

VALUE (%)		EVTS	DOCUMENT ID		TECN	COMMENT
1.29 ± 0.05 OUR AVERAGE						
1.326 ± 0.063			BARATE	99R	ALEP	1991–1995 LEP runs
1.11 ± 0.12			[185] COAN	96	CLEO	$E^{ee}_{cm} \approx 10.6$ GeV
$1.42 \pm 0.22 \pm 0.09$			[186] ACCIARRI	95F	L3	1991–1993 LEP runs
$1.23 \pm 0.21 \pm {}^{0.11}_{0.21}$		54	[187] ALBRECHT	88L	ARG	E^{ee}_{cm} = 10 GeV
$1.9 \pm 0.3 \pm 0.4$		44	[188] TSCHIRHART	88	HRS	E^{ee}_{cm} = 29 GeV
$1.5 \pm 0.4 \pm 0.4$		15	[189] AIHARA	87C	TPC	E^{ee}_{cm} = 29 GeV
$1.3 \pm 0.3 \pm 0.3$		31	YELTON	86	MRK2	E^{ee}_{cm} = 29 GeV
• • • We do not use the following data for averages, fits, limits, etc. • • •						
$1.39 \pm 0.09 \pm 0.10$			[190] BUSKULIC	96	ALEP	Repl. by BARATE 99R
$1.45 \pm 0.13 \pm 0.11$		273	[191] BUSKULIC	94F	ALEP	Repl. by BUSKULIC 96
1.7 ± 0.7		11	DORFAN	81	MRK2	E^{ee}_{cm} = 4.2–6.7 GeV

[185] Not independent of COAN 96 $B(\pi^- \overline{K}^0 \nu_\tau)$ and BATTLE 94 $B(K^- \pi^0 \nu_\tau)$ measurements. $K\pi$ final states are consistent with and assumed to originate from $K^*(892)^-$ production.

[186] This result is obtained from their $B(\pi^- \overline{K}^0 \nu_\tau)$ assuming all those decays originate in $K^*(892)^-$ decays.

[187] The authors divide by $\Gamma_2/\Gamma = 0.865$ to obtain this result.

[188] Not independent of TSCHIRHART 88 $\Gamma(\tau^- \to h^- \overline{K}^0 \geq 0\,\text{neutrals} \geq 0 K_L^0 \nu_\tau)/\Gamma(\text{total})$.

[189] Decay π^- identified in this experiment, is assumed in the others.

[190] Not independent of BUSKULIC 96 $B(\pi^- \overline{K}^0 \nu_\tau)$ and $B(K^- \pi^0 \nu_\tau)$ measurements.

[191] BUSKULIC 94F obtain this result from BUSKULIC 94F $B(\overline{K}^0 \pi^- \nu_\tau)$ and BUSKULIC 94E $B(K^- \pi^0 \nu_\tau)$ assuming all of those decays originate in $K^*(892)^-$ decays.

$\Gamma(K^*(892)^- \nu_\tau)/\Gamma(\pi^- \pi^0 \nu_\tau)$ Γ_{104}/Γ_{13}

VALUE	DOCUMENT ID		TECN	COMMENT
0.075 ± 0.027	[192] ABREU	94K	DLPH	LEP 1992 Z data

[192] ABREU 94K quote $B(\tau^- \to K^*(892)^- \nu_\tau) B(K^*(892)^- \to K^- \pi^0)/B(\tau^- \to \rho^- \nu_\tau) = 0.025 \pm 0.009$. We divide by $B(K^*(892)^- \to K^- \pi^0) = 0.333$ to obtain this result.

$\Gamma(K^*(892)^0 K^- \geq 0\,\text{neutrals}\, \nu_\tau)/\Gamma_{total}$ Γ_{105}/Γ

VALUE (%)	EVTS	DOCUMENT ID		TECN	COMMENT
0.32 ± 0.08 ± 0.12	119	GOLDBERG	90	CLEO	E^{ee}_{cm} = 9.4–10.9 GeV

$\Gamma(K^*(892)^0 K^- \nu_\tau)/\Gamma_{total}$ Γ_{106}/Γ

VALUE (%)	EVTS	DOCUMENT ID		TECN	COMMENT
0.21 ± 0.04 OUR AVERAGE					
0.213 ± 0.048		[193] BARATE	98	ALEP	1991–1995 LEP runs
$0.20 \pm 0.05 \pm 0.04$	47	ALBRECHT	95H	ARG	E^{ee}_{cm} = 9.4–10.6 GeV

[193] BARATE 98 measure the K^- ($\rho^0 \to \pi^+ \pi^-$) fraction in $\tau^- \to K^- \pi^+ \pi^- \nu_\tau$ decays to be (35 ± 11)% and derive this result from their measurement of $\Gamma(\tau^- \to K^- \pi^+ \pi^- \nu_\tau)/\Gamma_{total}$ assuming the intermediate states are all $K^-\rho$ and $K^- K^*(892)^0$.

$\Gamma(\overline{K}^*(892)^0 \pi^- \geq 0\,\text{neutrals}\, \nu_\tau)/\Gamma_{total}$ Γ_{107}/Γ

VALUE (%)	EVTS	DOCUMENT ID		TECN	COMMENT
0.38 ± 0.11 ± 0.13	105	GOLDBERG	90	CLEO	E^{ee}_{cm} = 9.4–10.9 GeV

$\Gamma(\overline{K}^*(892)^0 \pi^- \nu_\tau)/\Gamma_{total}$ Γ_{108}/Γ

VALUE (%)	EVTS	DOCUMENT ID		TECN	COMMENT
0.22 ± 0.05 OUR AVERAGE					
0.209 ± 0.058		[194] BARATE	98	ALEP	1991–1995 LEP runs
$0.25 \pm 0.10 \pm 0.05$	27	ALBRECHT	95H	ARG	E^{ee}_{cm} = 9.4–10.6 GeV

[194] BARATE 98 measure the $K^- K^*(892)^0$ fraction in $\tau^- \to K^- K^+ \pi^- \nu_\tau$ decays to be (87 ± 13)% and derive this result from their measurement of $\Gamma(\tau^- \to K^- K^+ \pi^- \nu_\tau)/\Gamma_{total}$.

$\Gamma((\overline{K}^*(892)\pi)^- \nu_\tau \to \pi^- \overline{K}^0 \pi^0 \nu_\tau)/\Gamma_{total}$ Γ_{109}/Γ

VALUE (%)	DOCUMENT ID		TECN	COMMENT
0.10 ± 0.04 OUR AVERAGE				
$0.097 \pm 0.044 \pm 0.036$	[195] BARATE	99K	ALEP	1991–1995 LEP runs
$0.106 \pm 0.037 \pm 0.032$	[196] BARATE	98E	ALEP	1991–1995 LEP runs

[195] BARATE 99K measure K^0's by detecting K^0_L's in their hadron calorimeter. They determine the $\overline{K}^0 \rho^-$ fraction in $\tau^- \to \pi^- \overline{K}^0 \pi^0 \nu_\tau$ decays to be (0.72 ± 0.12 ± 0.10) and multiply their $B(\pi^- \overline{K}^0 \pi^0 \nu_\tau)$ measurement by one minus this fraction to obtain the quoted result.

[196] BARATE 98E reconstruct K^0's using $K^0_S \to \pi^+ \pi^-$ decays. They determine the $\overline{K}^0 \rho^-$ fraction in $\tau^- \to \pi^- \overline{K}^0 \pi^0 \nu_\tau$ decays to be (0.64 ± 0.09 ± 0.10) and multiply their $B(\pi^- \overline{K}^0 \pi^0 \nu_\tau)$ measurement by one minus this fraction to obtain the quoted result.

$\Gamma(K_1(1270)^- \nu_\tau)/\Gamma_{total}$ Γ_{110}/Γ

VALUE (%)	EVTS	DOCUMENT ID		TECN	COMMENT
0.47 ± 0.11 OUR AVERAGE					
0.48 ± 0.11		BARATE	99R	ALEP	1991–1995 LEP runs
$0.41 \pm {}^{0.41}_{0.35} \pm 0.10$	5	[197] BAUER	94	TPC	E^{ee}_{cm} = 29 GeV

[197] We multiply 0.41% by 0.25, the relative systematic error quoted by BAUER 94, to obtain the systematic error.

$\Gamma(K_1(1400)^- \nu_\tau)/\Gamma_{total}$ Γ_{111}/Γ

VALUE (%)	EVTS	DOCUMENT ID		TECN	COMMENT
0.17 ± 0.26 OUR AVERAGE	Error includes scale factor of 1.7.				
0.05 ± 0.17		BARATE	99R	ALEP	1991–1995 LEP runs
$0.76 \pm {}^{0.40}_{0.33} \pm 0.20$	11	[198] BAUER	94	TPC	E^{ee}_{cm} = 29 GeV

[198] We multiply 0.76% by 0.25, the relative systematic error quoted by BAUER 94, to obtain the systematic error.

$[\Gamma(K_1(1270)^- \nu_\tau) + \Gamma(K_1(1400)^- \nu_\tau)]/\Gamma_{total}$ $(\Gamma_{110}+\Gamma_{111})/\Gamma$

VALUE (%)	EVTS	DOCUMENT ID		TECN	COMMENT
1.17 ± 0.41 ± 0.29	16	[199] BAUER	94	TPC	E^{ee}_{cm} = 29 GeV

[199] We multiply 1.17% by 0.25, the relative systematic error quoted by BAUER 94, to obtain the systematic error. Not independent of BAUER 94 $B(K_1(1270)^- \nu_\tau)$ and BAUER 94 $B(K_1(1400)^- \nu_\tau)$ measurements.

$\Gamma(K_1(1270)^- \nu_\tau)/[\Gamma(K_1(1270)^- \nu_\tau) + \Gamma(K_1(1400)^- \nu_\tau)]$ $\Gamma_{110}/(\Gamma_{110}+\Gamma_{111})$

VALUE	DOCUMENT ID		TECN	COMMENT
0.69 ± 0.15 OUR AVERAGE				
$0.71 \pm 0.16 \pm 0.11$	[200] ABBIENDI	00D	OPAL	1990–1995 LEP runs
$0.66 \pm 0.19 \pm 0.13$	[201] ASNER	00B	CLEO	E^{ee}_{cm} = 10.6 GeV

[200] ABBIENDI 00D assume the resonance structure of $\tau^- \to K^- \pi^+ \pi^- \nu_\tau$ decays is dominated by the $K_1(1270)^-$ and $K_1(1400)^-$ resonances.

[201] ASNER 00B assume the resonance structure of $\tau^- \to K^- \pi^+ \pi^- \nu_\tau$ (ex. K^0) decays is dominated by $K_1(1270)^-$ and $K_1(1400)^-$ resonances.

$\Gamma(K^*(1410)^- \nu_\tau)/\Gamma_{total}$ Γ_{112}/Γ

VALUE (units 10^{-3})	DOCUMENT ID		TECN	COMMENT
1.5 ${}^{+1.4}_{-1.0}$	BARATE	99R	ALEP	1991–1995 LEP runs

$\Gamma(K_0^*(1430)^- \nu_\tau)/\Gamma_{total}$ Γ_{113}/Γ

VALUE (units 10^{-3})	CL%	DOCUMENT ID		TECN	COMMENT
< 0.5	95	BARATE	99R	ALEP	1991–1995 LEP runs

$\Gamma(K_2^*(1430)^-\nu_\tau)/\Gamma_{total}$ Γ_{114}/Γ

VALUE (%)	CL%	EVTS	DOCUMENT ID		TECN	COMMENT
< 0.3	95		TSCHIRHART	88	HRS	E_{cm}^{ee} = 29 GeV
• • • We do not use the following data for averages, fits, limits, etc. • • •						
< 0.33	95		[202] ACCIARRI	95F	L3	1991–1993 LEP runs
< 0.9	95	0	DORFAN	81	MRK2	E_{cm}^{ee} = 4.2–6.7 GeV

[202] ACCIARRI 95F quote $B(\tau^- \to K^*(1430)^- \to \pi^- \overline{K}^0 \nu_\tau) < 0.11\%$. We divide by $B(K^*(1430)^- \to \pi^- \overline{K}^0) = 0.33$ to obtain the limit shown.

$\Gamma(a_0(980)^- \geq 0 \text{ neutrals } \nu_\tau)/\Gamma_{total} \times B(a_0(980) \to K^0 K^-)$ $\Gamma_{115}/\Gamma \times B$

VALUE (units 10^{-4})	CL%	DOCUMENT ID		TECN	COMMENT
< 2.8	90	GOLDBERG	90	CLEO	E_{cm}^{ee} = 9.4–10.9 GeV

$\Gamma(\eta\pi^-\nu_\tau)/\Gamma_{total}$ Γ_{116}/Γ

VALUE (units 10^{-4})	CL%	EVTS	DOCUMENT ID		TECN	COMMENT
< 1.4	95	0	BARTELT	96	CLEO	$E_{cm}^{ee} \approx$ 10.6 GeV
• • • We do not use the following data for averages, fits, limits, etc. • • •						
< 6.2	95		BUSKULIC	97C	ALEP	1991–1994 LEP runs
< 3.4	95		ARTUSO	92	CLEO	$E_{cm}^{ee} \approx$ 10.6 GeV
< 90	95		ALBRECHT	88M	ARG	$E_{cm}^{ee} \approx$ 10 GeV
<140	90		BEHREND	88	CELL	E_{cm}^{ee} = 14–46.8 GeV
<180	95		BARINGER	87	CLEO	E_{cm}^{ee} = 10.5 GeV
<250	90	0	COFFMAN	87	MRK3	E_{cm}^{ee} = 3.77 GeV
510 ±100±120		65	DERRICK	87	HRS	E_{cm}^{ee} = 29 GeV
<100	95		GAN	87B	MRK2	E_{cm}^{ee} = 29 GeV

$\Gamma(\eta\pi^-\pi^0\nu_\tau)/\Gamma_{total}$ Γ_{117}/Γ

VALUE (%)	CL%	EVTS	DOCUMENT ID		TECN	COMMENT
0.174±0.024 OUR FIT						
0.173±0.024 OUR AVERAGE						
0.18 ±0.04 ±0.02			BUSKULIC	97C	ALEP	1991–1994 LEP runs
0.17 ±0.02 ±0.02		125	ARTUSO	92	CLEO	$E_{cm}^{ee} \approx$ 10.6 GeV
• • • We do not use the following data for averages, fits, limits, etc. • • •						
<1.10	95		ALBRECHT	88M	ARG	$E_{cm}^{ee} \approx$ 10 GeV
<2.10	95		BARINGER	87	CLEO	E_{cm}^{ee} = 10.5 GeV
$4.20\ ^{+0.70}_{-1.20}$ ±1.60			[203] GAN	87	MRK2	E_{cm}^{ee} = 29 GeV

[203] Highly correlated with GAN 87 $\Gamma(\pi^- 3\pi^0\nu_\tau)/\Gamma(\text{total})$ value.

$\Gamma(\eta\pi^-\pi^0\pi^0\nu_\tau)/\Gamma_{total}$ Γ_{118}/Γ

VALUE (units 10^{-4})	CL%	EVTS	DOCUMENT ID		TECN	COMMENT
1.5±0.5		30	[204] ANASTASSOV	01	CLEO	E_{cm}^{ee} = 10.6 GeV
• • • We do not use the following data for averages, fits, limits, etc. • • •						
1.4±0.6±0.3		15	[205] BERGFELD	97	CLEO	Repl. by ANASTASSOV 01
< 4.3	95		ARTUSO	92	CLEO	$E_{cm}^{ee} \approx$ 10.6 GeV
<120	95		ALBRECHT	88M	ARG	$E_{cm}^{ee} \approx$ 10 GeV

[204] Weighted average of BERGFELD 97 and ANASTASSOV 01 value of $(1.5 \pm 0.6 \pm 0.3) \times 10^{-4}$ obtained using η's reconstructed from $\eta \to \pi^+\pi^-\pi^0$ decays.
[205] BERGFELD 97 reconstruct η's using $\eta \to \gamma\gamma$ decays.

$\Gamma(\eta K^-\nu_\tau)/\Gamma_{total}$ Γ_{119}/Γ

VALUE (units 10^{-4})	CL%	EVTS	DOCUMENT ID		TECN	COMMENT
2.7±0.6 OUR FIT						
2.7±0.6 OUR AVERAGE						
$2.9^{+1.3}_{-1.2}$±0.7			BUSKULIC	97C	ALEP	1991–1994 LEP runs
2.6±0.5±0.5		85	BARTELT	96	CLEO	$E_{cm}^{ee} \approx$ 10.6 GeV
• • • We do not use the following data for averages, fits, limits, etc. • • •						
<4.7	95		ARTUSO	92	CLEO	$E_{cm}^{ee} \approx$ 10.6 GeV

$\Gamma(\eta K^*(892)^-\nu_\tau)/\Gamma_{total}$ Γ_{120}/Γ

VALUE (units 10^{-4})	EVTS	DOCUMENT ID		TECN	COMMENT
2.90±0.80±0.42	25	BISHAI	99	CLEO	E_{cm}^{ee} = 10.6 GeV

$\Gamma(\eta K^-\pi^0\nu_\tau)/\Gamma_{total}$ Γ_{121}/Γ

VALUE (units 10^{-4})	EVTS	DOCUMENT ID		TECN	COMMENT
1.77±0.56±0.71	36	BISHAI	99	CLEO	E_{cm}^{ee} = 10.6 GeV

$\Gamma(\eta\overline{K}^0\pi^-\nu_\tau)/\Gamma_{total}$ Γ_{122}/Γ

VALUE (units 10^{-4})	EVTS	DOCUMENT ID		TECN	COMMENT
2.20±0.70±0.22	15	[206] BISHAI	99	CLEO	E_{cm}^{ee} = 10.6 GeV

[206] We multiply the BISHAI 99 measurement $B(\tau^- \to \eta K_S^0 \pi^-\nu_\tau) = (1.10 \pm 0.35 \pm 0.11) \times 10^{-4}$ by 2 to obtain the listed value.

$\Gamma(\eta\pi^+\pi^-\pi^-\geq 0 \text{ neutrals } \nu_\tau)/\Gamma_{total}$ Γ_{123}/Γ

VALUE (%)	CL%	DOCUMENT ID		TECN	COMMENT
< 0.3	90	ABACHI	87B	HRS	E_{cm}^{ee} = 29 GeV

$\Gamma(\eta\pi^-\pi^+\pi^-\nu_\tau)/\Gamma_{total}$ Γ_{124}/Γ

VALUE (units 10^{-4})	EVTS	DOCUMENT ID		TECN	COMMENT
2.3±0.5	170	[207] ANASTASSOV	01	CLEO	E_{cm}^{ee} = 10.6 GeV
• • • We do not use the following data for averages, fits, limits, etc. • • •					
$3.4^{+0.6}_{-0.5}$ ±0.6	89	[208] BERGFELD	97	CLEO	Repl. by ANASTASSOV 01

[207] Weighted average of BERGFELD 97 and ANASTASSOV 01 measurements using η's reconstructed from $\eta \to \pi^+\pi^-\pi^0$ and $\eta \to 3\pi^0$ decays.
[208] BERGFELD 97 reconstruct η's using $\eta \to \gamma\gamma$ and $\eta \to 3\pi^0$ decays.

$\Gamma(\eta a_1(1260)^-\nu_\tau \to \eta\pi^-\rho^0\nu_\tau)/\Gamma_{total}$ Γ_{125}/Γ

VALUE	CL%	DOCUMENT ID		TECN	COMMENT
<3.9 × 10⁻⁴	90	BERGFELD	97	CLEO	E_{cm}^{ee} = 10.6 GeV

$\Gamma(\eta\eta\pi^-\nu_\tau)/\Gamma_{total}$ Γ_{126}/Γ

VALUE (units 10^{-4})	CL%	DOCUMENT ID		TECN	COMMENT
< 1.1	95	ARTUSO	92	CLEO	$E_{cm}^{ee} \approx$ 10.6 GeV
• • • We do not use the following data for averages, fits, limits, etc. • • •					
<83	95	ALBRECHT	88M	ARG	$E_{cm}^{ee} \approx$ 10 GeV

$\Gamma(\eta\eta\pi^-\pi^0\nu_\tau)/\Gamma_{total}$ Γ_{127}/Γ

VALUE (units 10^{-4})	CL%	DOCUMENT ID		TECN	COMMENT
< 2.0	95	ARTUSO	92	CLEO	$E_{cm}^{ee} \approx$ 10.6 GeV
• • • We do not use the following data for averages, fits, limits, etc. • • •					
<90	95	ALBRECHT	88M	ARG	$E_{cm}^{ee} \approx$ 10 GeV

$\Gamma(\eta'(958)\pi^-\nu_\tau)/\Gamma_{total}$ Γ_{128}/Γ

VALUE	CL%	DOCUMENT ID		TECN	COMMENT
<7.4 × 10⁻⁵	90	BERGFELD	97	CLEO	E_{cm}^{ee} = 10.6 GeV

$\Gamma(\eta'(958)\pi^-\pi^0\nu_\tau)/\Gamma_{total}$ Γ_{129}/Γ

VALUE	CL%	DOCUMENT ID		TECN	COMMENT
<8.0 × 10⁻⁵	90	BERGFELD	97	CLEO	E_{cm}^{ee} = 10.6 GeV

$\Gamma(\phi\pi^-\nu_\tau)/\Gamma_{total}$ Γ_{130}/Γ

VALUE	CL%	DOCUMENT ID		TECN	COMMENT
<2.0 × 10⁻⁴	90	[209] AVERY	97	CLEO	E_{cm}^{ee} = 10.6 GeV
• • • We do not use the following data for averages, fits, limits, etc. • • •					
<3.5 × 10⁻⁴	90	ALBRECHT	95H	ARG	E_{cm}^{ee} = 9.4–10.6 GeV

[209] AVERY 97 limit varies from $(1.2–2.0) \times 10^{-4}$ depending on decay model assumptions.

$\Gamma(\phi K^-\nu_\tau)/\Gamma_{total}$ Γ_{131}/Γ

VALUE	CL%	DOCUMENT ID		TECN	COMMENT
<6.7 × 10⁻⁵	90	[210] AVERY	97	CLEO	E_{cm}^{ee} = 10.6 GeV

[210] AVERY 97 limit varies from $(5.4–6.7) \times 10^{-5}$ depending on decay model assumptions.

$\Gamma(f_1(1285)\pi^-\nu_\tau)/\Gamma_{total}$ Γ_{132}/Γ

VALUE (units 10^{-4})	EVTS	DOCUMENT ID		TECN	COMMENT
$5.8^{+1.4}_{-1.3}$±1.8	54	BERGFELD	97	CLEO	E_{cm}^{ee} = 10.6 GeV

$\Gamma(f_1(1285)\pi^-\nu_\tau \to \eta\pi^-\pi^+\pi^-\nu_\tau)/\Gamma(\eta\pi^-\pi^+\pi^-\nu_\tau)$ $\Gamma_{133}/\Gamma_{124}$

VALUE	DOCUMENT ID		TECN	COMMENT
0.55±0.14	BERGFELD	97	CLEO	E_{cm}^{ee} = 10.6 GeV

$\Gamma(\pi(1300)^-\nu_\tau \to (\rho\pi)^-\nu_\tau \to (3\pi)^-\nu_\tau)/\Gamma_{total}$ Γ_{134}/Γ

VALUE	CL%	DOCUMENT ID		TECN	COMMENT
<1.0 × 10⁻⁴	90	ASNER	00	CLEO	E_{cm}^{ee} = 10.6 GeV

$\Gamma(\pi(1300)^-\nu_\tau \to ((\pi\pi)_{S-wave}\pi)^-\nu_\tau \to (3\pi)^-\nu_\tau)/\Gamma_{total}$ Γ_{135}/Γ

VALUE	CL%	DOCUMENT ID		TECN	COMMENT
<1.9 × 10⁻⁴	90	ASNER	00	CLEO	E_{cm}^{ee} = 10.6 GeV

$\Gamma(h^-\omega \geq 0 \text{ neutrals } \nu_\tau)/\Gamma_{total}$ Γ_{136}/Γ

$\Gamma_{136}/\Gamma = (\Gamma_{137}+\Gamma_{138})/\Gamma$

Data marked "avg" are highly correlated with data appearing elsewhere in the Listings, and are therefore used for the average given below but not in the overall fits. "f&a" marks results used for the fit and the average.

VALUE (%)		EVTS	DOCUMENT ID		TECN	COMMENT
2.38±0.08 OUR FIT						
1.65±0.3 ±0.2	**avg**	1513	ALBRECHT	88M	ARG	$E_{cm}^{ee} \approx$ 10 GeV

$\Gamma(h^-\omega\nu_\tau)/\Gamma_{\rm total}$ Γ_{137}/Γ

Data marked "avg" are highly correlated with data appearing elsewhere in the Listings, and are therefore used for the average given below but not in the overall fits. "f&a" marks results used for the fit and the average.

VALUE (%)		EVTS	DOCUMENT ID		TECN	COMMENT
1.94±0.07 OUR FIT						
1.92±0.07 OUR AVERAGE						
1.91±0.07±0.06	f&a	5803	BUSKULIC	97C	ALEP	1991–1994 LEP runs
1.95±0.07±0.11	avg	2223	[211] BALEST	95C	CLEO	$E^{ee}_{\rm cm}\approx$ 10.6 GeV
1.60±0.27±0.41	f&a	139	BARINGER	87	CLEO	$E^{ee}_{\rm cm}$= 10.5 GeV

[211] Not independent of BALEST 95C $B(\tau^-\to h^-\omega\nu_\tau)/B(\tau^-\to h^-h^-h^+\pi^0\nu_\tau)$ value.

$\Gamma(h^-\omega\nu_\tau)/\Gamma(h^-h^-h^+\pi^0\nu_\tau({\rm ex.}\,K^0))$ Γ_{137}/Γ_{64}

$\Gamma_{137}/\Gamma_{64}=\Gamma_{137}/(\Gamma_{68}+\Gamma_{86}+\Gamma_{90}+0.231\Gamma_{119}+0.888\Gamma_{137}+0.0221\Gamma_{138})$

VALUE	EVTS	DOCUMENT ID		TECN	COMMENT
0.446±0.015 OUR FIT					
0.453±0.019 OUR AVERAGE					
0.431±0.033	2350	[212] BUSKULIC	96	ALEP	LEP 1991–1993 data
0.464±0.016±0.017	2223	[213] BALEST	95C	CLEO	$E^{ee}_{\rm cm}\approx$ 10.6 GeV
• • • We do not use the following data for averages, fits, limits, etc. • • •					
0.37 ±0.05 ±0.02	458	[214] ALBRECHT	91D	ARG	$E^{ee}_{\rm cm}$= 9.4–10.6 GeV

[212] BUSKULIC 96 quote the fraction of $\tau\to h^-h^-h^+\pi^0\nu_\tau$ (ex. K^0) decays which originate in a $h^-\omega$ final state = 0.383 ± 0.029. We divide this by the $\omega(782)\to\pi^+\pi^-\pi^0$ branching fraction (0.888).

[213] BALEST 95C quote the fraction of $\tau^-\to h^-h^-h^+\pi^0\nu_\tau$ (ex. K^0) decays which originate in a $h^-\omega$ final state equals 0.412 ± 0.014 ± 0.015. We divide this by the $\omega(782)\to\pi^+\pi^-\pi^0$ branching fraction (0.888).

[214] ALBRECHT 91D quote the fraction of $\tau^-\to h^-h^-h^+\pi^0\nu_\tau$ decays which originate in a $\pi^-\omega$ final state equals 0.33 ± 0.04 ± 0.02. We divide this by the $\omega(782)\to\pi^+\pi^-\pi^0$ branching fraction (0.888).

$\Gamma(h^-\omega\pi^0\nu_\tau)/\Gamma_{\rm total}$ Γ_{138}/Γ

VALUE (%)	EVTS	DOCUMENT ID		TECN	COMMENT
0.44±0.05 OUR FIT					
0.43±0.06±0.05	7283	BUSKULIC	97C	ALEP	1991–1994 LEP runs

$\Gamma(h^-\omega2\pi^0\nu_\tau)/\Gamma_{\rm total}$ Γ_{139}/Γ

VALUE (units 10^{-4})	EVTS	DOCUMENT ID		TECN	COMMENT
1.4 ±0.4 ±0.3	53	ANASTASSOV	01	CLEO	$E^{ee}_{\rm cm}$= 10.6 GeV
• • • We do not use the following data for averages, fits, limits, etc. • • •					
$1.89^{+0.74}_{-0.67}\pm0.40$	19	ANDERSON	97	CLEO	Repl. by ANASTASSOV 01

$\Gamma(h^-\omega\pi^0\nu_\tau)/\Gamma(h^-h^-h^+\geq0\,{\rm neutrals}\geq0K^0_L\nu_\tau)$ Γ_{138}/Γ_{52}

$\Gamma_{138}/\Gamma_{52}=\Gamma_{138}/(0.3431\Gamma_{33}+0.3431\Gamma_{35}+0.3431\Gamma_{38}+0.3431\Gamma_{40}+0.4307\Gamma_{45}+0.6861\Gamma_{46}+\Gamma_{60}+\Gamma_{68}+\Gamma_{74}+\Gamma_{75}+\Gamma_{82}+\Gamma_{86}+\Gamma_{89}+\Gamma_{90}+0.285\Gamma_{117}+0.285\Gamma_{119}+0.9101\Gamma_{137}+0.9101\Gamma_{138})$

Data marked "avg" are highly correlated with data appearing elsewhere in the Listings, and are therefore used for the average given below but not in the overall fits. "f&a" marks results used for the fit and the average.

VALUE		EVTS	DOCUMENT ID		TECN	COMMENT
0.0286±0.0031 OUR FIT						
0.028 ±0.003 ±0.003	**avg**	430	[215] BORTOLETTO	93	CLEO	$E^{ee}_{\rm cm}\approx$ 10.6 GeV

[215] Not independent of BORTOLETTO 93 $\Gamma(\tau^-\to h^-\omega\pi^0\nu_\tau)/\Gamma(\tau^-\to h^-h^-h^+2\pi^0\nu_\tau({\rm ex.}\,K^0))$ value.

$\Gamma(h^-\omega\pi^0\nu_\tau)/\Gamma(h^-h^-h^+2\pi^0\nu_\tau({\rm ex.}\,K^0))$ Γ_{138}/Γ_{73}

$\Gamma_{138}/\Gamma_{73}=\Gamma_{138}/(\Gamma_{74}+0.236\Gamma_{117}+0.888\Gamma_{138})$

VALUE	DOCUMENT ID		TECN	COMMENT
0.81±0.08 OUR FIT				
0.81±0.06±0.06	BORTOLETTO	93	CLEO	$E^{ee}_{\rm cm}\approx$ 10.6 GeV

$\Gamma(2h^-h^+\omega\nu_\tau)/\Gamma_{\rm total}$ Γ_{140}/Γ

VALUE (units 10^{-4})	EVTS	DOCUMENT ID		TECN	COMMENT
1.2 ±0.2 ±0.1	110	ANASTASSOV	01	CLEO	$E^{ee}_{\rm cm}$= 10.6 GeV

$\Gamma(e^-\gamma)/\Gamma_{\rm total}$ Γ_{141}/Γ

Test of lepton family number conservation.

VALUE	CL%	DOCUMENT ID		TECN	COMMENT
<2.7 × 10⁻⁶	90	EDWARDS	97	CLEO	
• • • We do not use the following data for averages, fits, limits, etc. • • •					
$<1.1\times10^{-4}$	90	ABREU	95U	DLPH	1990–1993 LEP runs
$<1.2\times10^{-4}$	90	ALBRECHT	92K	ARG	$E^{ee}_{\rm cm}$= 10 GeV
$<2.0\times10^{-4}$	90	KEH	88	CBAL	$E^{ee}_{\rm cm}$= 10 GeV
$<6.4\times10^{-4}$	90	HAYES	82	MRK2	$E^{ee}_{\rm cm}$= 3.8–6.8 GeV

$\Gamma(\mu^-\gamma)/\Gamma_{\rm total}$ Γ_{142}/Γ

Test of lepton family number conservation.

VALUE	CL%	DOCUMENT ID		TECN	COMMENT
< 1.1 × 10⁻⁶	90	AHMED	00	CLEO	$E^{ee}_{\rm cm}$= 10.6 GeV
• • • We do not use the following data for averages, fits, limits, etc. • • •					
$<3.0\times10^{-6}$	90	EDWARDS	97	CLEO	
$<6.2\times10^{-5}$	90	ABREU	95U	DLPH	1990–1993 LEP runs
$<0.42\times10^{-5}$	90	BEAN	93	CLEO	$E^{ee}_{\rm cm}$= 10.6 GeV
$<3.4\times10^{-5}$	90	ALBRECHT	92K	ARG	$E^{ee}_{\rm cm}$= 10 GeV
$<55\times10^{-5}$	90	HAYES	82	MRK2	$E^{ee}_{\rm cm}$= 3.8–6.8 GeV

$\Gamma(e^-\pi^0)/\Gamma_{\rm total}$ Γ_{143}/Γ

Test of lepton family number conservation.

VALUE	CL%	DOCUMENT ID		TECN	COMMENT
< 3.7 × 10⁻⁶	90	BONVICINI	97	CLEO	$E^{ee}_{\rm cm}$= 10.6 GeV
• • • We do not use the following data for averages, fits, limits, etc. • • •					
$<17\times10^{-5}$	90	ALBRECHT	92K	ARG	$E^{ee}_{\rm cm}$= 10 GeV
$<14\times10^{-5}$	90	KEH	88	CBAL	$E^{ee}_{\rm cm}$= 10 GeV
$<210\times10^{-5}$	90	HAYES	82	MRK2	$E^{ee}_{\rm cm}$= 3.8–6.8 GeV

$\Gamma(\mu^-\pi^0)/\Gamma_{\rm total}$ Γ_{144}/Γ

Test of lepton family number conservation.

VALUE	CL%	DOCUMENT ID		TECN	COMMENT
< 4.0 × 10⁻⁶	90	BONVICINI	97	CLEO	$E^{ee}_{\rm cm}$= 10.6 GeV
• • • We do not use the following data for averages, fits, limits, etc. • • •					
$<4.4\times10^{-5}$	90	ALBRECHT	92K	ARG	$E^{ee}_{\rm cm}$= 10 GeV
$<82\times10^{-5}$	90	HAYES	82	MRK2	$E^{ee}_{\rm cm}$= 3.8–6.8 GeV

$\Gamma(e^-K^0_S)/\Gamma_{\rm total}$ Γ_{145}/Γ

Test of lepton family number conservation.

VALUE	CL%	DOCUMENT ID		TECN	COMMENT
<9.1 × 10⁻⁷	90	CHEN	02C	CLEO	$E^{ee}_{\rm cm}$= 10.6 GeV
• • • We do not use the following data for averages, fits, limits, etc. • • •					
$<1.3\times10^{-3}$	90	HAYES	82	MRK2	$E^{ee}_{\rm cm}$= 3.8–6.8 GeV

$\Gamma(\mu^-K^0_S)/\Gamma_{\rm total}$ Γ_{146}/Γ

Test of lepton family number conservation.

VALUE	CL%	DOCUMENT ID		TECN	COMMENT
<9.5 × 10⁻⁷	90	CHEN	02C	CLEO	$E^{ee}_{\rm cm}$= 10.6 GeV
• • • We do not use the following data for averages, fits, limits, etc. • • •					
$<1.0\times10^{-3}$	90	HAYES	82	MRK2	$E^{ee}_{\rm cm}$= 3.8–6.8 GeV

$\Gamma(e^-\eta)/\Gamma_{\rm total}$ Γ_{147}/Γ

Test of lepton family number conservation.

VALUE	CL%	DOCUMENT ID		TECN	COMMENT
< 8.2 × 10⁻⁶	90	BONVICINI	97	CLEO	$E^{ee}_{\rm cm}$= 10.6 GeV
• • • We do not use the following data for averages, fits, limits, etc. • • •					
$<6.3\times10^{-5}$	90	ALBRECHT	92K	ARG	$E^{ee}_{\rm cm}$= 10 GeV
$<24\times10^{-5}$	90	KEH	88	CBAL	$E^{ee}_{\rm cm}$= 10 GeV

$\Gamma(\mu^-\eta)/\Gamma_{\rm total}$ Γ_{148}/Γ

Test of lepton family number conservation.

VALUE	CL%	DOCUMENT ID		TECN	COMMENT
<9.6 × 10⁻⁶	90	BONVICINI	97	CLEO	$E^{ee}_{\rm cm}$= 10.6 GeV
• • • We do not use the following data for averages, fits, limits, etc. • • •					
$<7.3\times10^{-5}$	90	ALBRECHT	92K	ARG	$E^{ee}_{\rm cm}$= 10 GeV

$\Gamma(e^-\rho^0)/\Gamma_{\rm total}$ Γ_{149}/Γ

Test of lepton family number conservation.

VALUE	CL%	DOCUMENT ID		TECN	COMMENT
< 2.0 × 10⁻⁶	90	BLISS	98	CLEO	$E^{ee}_{\rm cm}$= 10.6 GeV
• • • We do not use the following data for averages, fits, limits, etc. • • •					
$<0.42\times10^{-5}$	90	[216] BARTELT	94	CLEO	Repl. by BLISS 98
$<1.9\times10^{-5}$	90	ALBRECHT	92K	ARG	$E^{ee}_{\rm cm}$= 10 GeV
$<37\times10^{-5}$	90	HAYES	82	MRK2	$E^{ee}_{\rm cm}$= 3.8–6.8 GeV

[216] BARTELT 94 assume phase space decays.

$\Gamma(\mu^-\rho^0)/\Gamma_{\rm total}$ Γ_{150}/Γ

Test of lepton family number conservation.

VALUE	CL%	DOCUMENT ID		TECN	COMMENT
< 6.3 × 10⁻⁶	90	BLISS	98	CLEO	$E^{ee}_{\rm cm}$= 10.6 GeV
• • • We do not use the following data for averages, fits, limits, etc. • • •					
$<0.57\times10^{-5}$	90	[217] BARTELT	94	CLEO	Repl. by BLISS 98
$<2.9\times10^{-5}$	90	ALBRECHT	92K	ARG	$E^{ee}_{\rm cm}$= 10 GeV
$<44\times10^{-5}$	90	HAYES	82	MRK2	$E^{ee}_{\rm cm}$= 3.8–6.8 GeV

[217] BARTELT 94 assume phase space decays.

$\Gamma(e^- K^*(892)^0)/\Gamma_{total}$ Γ_{151}/Γ

Test of lepton family number conservation.

VALUE	CL%	DOCUMENT ID		TECN	COMMENT
<5.1 $\times 10^{-6}$	90	BLISS	98	CLEO	E_{cm}^{ee}= 10.6 GeV
• • • We do not use the following data for averages, fits, limits, etc. • • •					
$<0.63\times10^{-5}$	90	[218] BARTELT	94	CLEO	Repl. by BLISS 98
$<3.8\times10^{-5}$	90	ALBRECHT	92K	ARG	E_{cm}^{ee}= 10 GeV

[218] BARTELT 94 assume phase space decays.

$\Gamma(\mu^- K^*(892)^0)/\Gamma_{total}$ Γ_{152}/Γ

Test of lepton family number conservation.

VALUE	CL%	DOCUMENT ID		TECN	COMMENT
<7.5 $\times 10^{-6}$	90	BLISS	98	CLEO	E_{cm}^{ee}= 10.6 GeV
• • • We do not use the following data for averages, fits, limits, etc. • • •					
$<0.94\times10^{-5}$	90	[219] BARTELT	94	CLEO	Repl. by BLISS 98
$<4.5\times10^{-5}$	90	ALBRECHT	92K	ARG	E_{cm}^{ee}= 10 GeV

[219] BARTELT 94 assume phase space decays.

$\Gamma(e^- \overline{K}^*(892)^0)/\Gamma_{total}$ Γ_{153}/Γ

Test of lepton family number conservation.

VALUE	CL%	DOCUMENT ID		TECN	COMMENT
<7.4 $\times 10^{-6}$	90	BLISS	98	CLEO	E_{cm}^{ee}= 10.6 GeV
• • • We do not use the following data for averages, fits, limits, etc. • • •					
$<1.1\times10^{-5}$	90	[220] BARTELT	94	CLEO	Repl. by BLISS 98

[220] BARTELT 94 assume phase space decays.

$\Gamma(\mu^- \overline{K}^*(892)^0)/\Gamma_{total}$ Γ_{154}/Γ

Test of lepton family number conservation.

VALUE	CL%	DOCUMENT ID		TECN	COMMENT
<7.5 $\times 10^{-6}$	90	BLISS	98	CLEO	E_{cm}^{ee}= 10.6 GeV
• • • We do not use the following data for averages, fits, limits, etc. • • •					
$<0.87\times10^{-5}$	90	[221] BARTELT	94	CLEO	Repl. by BLISS 98

[221] BARTELT 94 assume phase space decays.

$\Gamma(e^- \phi)/\Gamma_{total}$ Γ_{155}/Γ

Test of lepton family number conservation.

VALUE	CL%	DOCUMENT ID		TECN	COMMENT
<6.9 $\times 10^{-6}$	90	BLISS	98	CLEO	E_{cm}^{ee}= 10.6 GeV

$\Gamma(\mu^- \phi)/\Gamma_{total}$ Γ_{156}/Γ

Test of lepton family number conservation.

VALUE	CL%	DOCUMENT ID		TECN	COMMENT
<7.0 $\times 10^{-6}$	90	BLISS	98	CLEO	E_{cm}^{ee}= 10.6 GeV

$\Gamma(e^- e^+ e^-)/\Gamma_{total}$ Γ_{157}/Γ

Test of lepton family number conservation.

VALUE	CL%	DOCUMENT ID		TECN	COMMENT
< 2.9 $\times 10^{-6}$	90	BLISS	98	CLEO	E_{cm}^{ee}= 10.6 GeV
• • • We do not use the following data for averages, fits, limits, etc. • • •					
$<0.33\times10^{-5}$	90	[222] BARTELT	94	CLEO	Repl. by BLISS 98
$<1.3\times10^{-5}$	90	ALBRECHT	92K	ARG	E_{cm}^{ee}= 10 GeV
$<2.7\times10^{-5}$	90	BOWCOCK	90	CLEO	E_{cm}^{ee}= 10.4–10.9
$<40\times10^{-5}$	90	HAYES	82	MRK2	E_{cm}^{ee}= 3.8–6.8 GeV

[222] BARTELT 94 assume phase space decays.

$\Gamma(e^- \mu^+ \mu^-)/\Gamma_{total}$ Γ_{158}/Γ

Test of lepton family number conservation.

VALUE	CL%	DOCUMENT ID		TECN	COMMENT
< 1.8 $\times 10^{-6}$	90	BLISS	98	CLEO	E_{cm}^{ee}= 10.6 GeV
• • • We do not use the following data for averages, fits, limits, etc. • • •					
$<0.36\times10^{-5}$	90	[223] BARTELT	94	CLEO	Repl. by BLISS 98
$<1.9\times10^{-5}$	90	ALBRECHT	92K	ARG	E_{cm}^{ee}= 10 GeV
$<2.7\times10^{-5}$	90	BOWCOCK	90	CLEO	E_{cm}^{ee}= 10.4–10.9
$<33\times10^{-5}$	90	HAYES	82	MRK2	E_{cm}^{ee}= 3.8–6.8 GeV

[223] BARTELT 94 assume phase space decays.

$\Gamma(e^+ \mu^- \mu^-)/\Gamma_{total}$ Γ_{159}/Γ

Test of lepton family number conservation.

VALUE	CL%	DOCUMENT ID		TECN	COMMENT
<1.5 $\times 10^{-6}$	90	BLISS	98	CLEO	E_{cm}^{ee}= 10.6 GeV
• • • We do not use the following data for averages, fits, limits, etc. • • •					
$<0.35\times10^{-5}$	90	[224] BARTELT	94	CLEO	Repl. by BLISS 98
$<1.8\times10^{-5}$	90	ALBRECHT	92K	ARG	E_{cm}^{ee}= 10 GeV
$<1.6\times10^{-5}$	90	BOWCOCK	90	CLEO	E_{cm}^{ee}= 10.4–10.9

[224] BARTELT 94 assume phase space decays.

$\Gamma(\mu^- e^+ e^-)/\Gamma_{total}$ Γ_{160}/Γ

Test of lepton family number conservation.

VALUE	CL%	DOCUMENT ID		TECN	COMMENT
< 1.7 $\times 10^{-6}$	90	BLISS	98	CLEO	E_{cm}^{ee}= 10.6 GeV
• • • We do not use the following data for averages, fits, limits, etc. • • •					
$<0.34\times10^{-5}$	90	[225] BARTELT	94	CLEO	Repl. by BLISS 98
$<1.4\times10^{-5}$	90	ALBRECHT	92K	ARG	E_{cm}^{ee}= 10 GeV
$<2.7\times10^{-5}$	90	BOWCOCK	90	CLEO	E_{cm}^{ee}= 10.4–10.9
$<44\times10^{-5}$	90	HAYES	82	MRK2	E_{cm}^{ee}= 3.8–6.8 GeV

[225] BARTELT 94 assume phase space decays.

$\Gamma(\mu^+ e^- e^-)/\Gamma_{total}$ Γ_{161}/Γ

Test of lepton family number conservation.

VALUE	CL%	DOCUMENT ID		TECN	COMMENT
<1.5 $\times 10^{-6}$	90	BLISS	98	CLEO	E_{cm}^{ee}= 10.6 GeV
• • • We do not use the following data for averages, fits, limits, etc. • • •					
$<0.34\times10^{-5}$	90	[226] BARTELT	94	CLEO	Repl. by BLISS 98
$<1.4\times10^{-5}$	90	ALBRECHT	92K	ARG	E_{cm}^{ee}= 10 GeV
$<1.6\times10^{-5}$	90	BOWCOCK	90	CLEO	E_{cm}^{ee}= 10.4–10.9

[226] BARTELT 94 assume phase space decays.

$\Gamma(\mu^- \mu^+ \mu^-)/\Gamma_{total}$ Γ_{162}/Γ

Test of lepton family number conservation.

VALUE	CL%	DOCUMENT ID		TECN	COMMENT
< 1.9 $\times 10^{-6}$	90	BLISS	98	CLEO	E_{cm}^{ee}= 10.6 GeV
• • • We do not use the following data for averages, fits, limits, etc. • • •					
$<0.43\times10^{-5}$	90	[227] BARTELT	94	CLEO	Repl. by BLISS 98
$<1.9\times10^{-5}$	90	ALBRECHT	92K	ARG	E_{cm}^{ee}= 10 GeV
$<1.7\times10^{-5}$	90	BOWCOCK	90	CLEO	E_{cm}^{ee}= 10.4–10.9
$<49\times10^{-5}$	90	HAYES	82	MRK2	E_{cm}^{ee}= 3.8–6.8 GeV

[227] BARTELT 94 assume phase space decays.

$\Gamma(e^- \pi^+ \pi^-)/\Gamma_{total}$ Γ_{163}/Γ

Test of lepton family number conservation.

VALUE	CL%	DOCUMENT ID		TECN	COMMENT
<2.2 $\times 10^{-6}$	90	BLISS	98	CLEO	E_{cm}^{ee}= 10.6 GeV
• • • We do not use the following data for averages, fits, limits, etc. • • •					
$<0.44\times10^{-5}$	90	[228] BARTELT	94	CLEO	Repl. by BLISS 98
$<2.7\times10^{-5}$	90	ALBRECHT	92K	ARG	E_{cm}^{ee}= 10 GeV
$<6.0\times10^{-5}$	90	BOWCOCK	90	CLEO	E_{cm}^{ee}= 10.4–10.9

[228] BARTELT 94 assume phase space decays.

$\Gamma(e^+ \pi^- \pi^-)/\Gamma_{total}$ Γ_{164}/Γ

Test of lepton number conservation.

VALUE	CL%	DOCUMENT ID		TECN	COMMENT
<1.9 $\times 10^{-6}$	90	BLISS	98	CLEO	E_{cm}^{ee}= 10.6 GeV
• • • We do not use the following data for averages, fits, limits, etc. • • •					
$<0.44\times10^{-5}$	90	[229] BARTELT	94	CLEO	Repl. by BLISS 98
$<1.8\times10^{-5}$	90	ALBRECHT	92K	ARG	E_{cm}^{ee}= 10 GeV
$<1.7\times10^{-5}$	90	BOWCOCK	90	CLEO	E_{cm}^{ee}= 10.4–10.9

[229] BARTELT 94 assume phase space decays.

$\Gamma(\mu^- \pi^+ \pi^-)/\Gamma_{total}$ Γ_{165}/Γ

Test of lepton family number conservation.

VALUE	CL%	DOCUMENT ID		TECN	COMMENT
<8.2 $\times 10^{-6}$	90	BLISS	98	CLEO	E_{cm}^{ee}= 10.6 GeV
• • • We do not use the following data for averages, fits, limits, etc. • • •					
$<0.74\times10^{-5}$	90	[230] BARTELT	94	CLEO	Repl. by BLISS 98
$<3.6\times10^{-5}$	90	ALBRECHT	92K	ARG	E_{cm}^{ee}= 10 GeV
$<3.9\times10^{-5}$	90	BOWCOCK	90	CLEO	E_{cm}^{ee}= 10.4–10.9

[230] BARTELT 94 assume phase space decays.

$\Gamma(\mu^+ \pi^- \pi^-)/\Gamma_{total}$ Γ_{166}/Γ

Test of lepton number conservation.

VALUE	CL%	DOCUMENT ID		TECN	COMMENT
<3.4 $\times 10^{-6}$	90	BLISS	98	CLEO	E_{cm}^{ee}= 10.6 GeV
• • • We do not use the following data for averages, fits, limits, etc. • • •					
$<0.69\times10^{-5}$	90	[231] BARTELT	94	CLEO	Repl. by BLISS 98
$<6.3\times10^{-5}$	90	ALBRECHT	92K	ARG	E_{cm}^{ee}= 10 GeV
$<3.9\times10^{-5}$	90	BOWCOCK	90	CLEO	E_{cm}^{ee}= 10.4–10.9

[231] BARTELT 94 assume phase space decays.

$\Gamma(e^- \pi^+ K^-)/\Gamma_{total}$ Γ_{167}/Γ

Test of lepton family number conservation.

VALUE	CL%	DOCUMENT ID		TECN	COMMENT
<6.4 $\times 10^{-6}$	90	BLISS	98	CLEO	E_{cm}^{ee}= 10.6 GeV
• • • We do not use the following data for averages, fits, limits, etc. • • •					
$<0.77\times10^{-5}$	90	[232] BARTELT	94	CLEO	Repl. by BLISS 98
$<2.9\times10^{-5}$	90	ALBRECHT	92K	ARG	E_{cm}^{ee}= 10 GeV
$<5.8\times10^{-5}$	90	BOWCOCK	90	CLEO	E_{cm}^{ee}= 10.4–10.9

[232] BARTELT 94 assume phase space decays.

$\Gamma(e^-\pi^-K^+)/\Gamma_{total}$ Γ_{168}/Γ

Test of lepton family number conservation.

VALUE	CL%	DOCUMENT ID		TECN	COMMENT
$<3.8\times10^{-6}$	90	BLISS	98	CLEO	$E_{cm}^{ee}=10.6$ GeV
• • • We do not use the following data for averages, fits, limits, etc. • • •					
$<0.46\times10^{-5}$	90	[233] BARTELT	94	CLEO	Repl. by BLISS 98
$<5.8\times10^{-5}$	90	BOWCOCK	90	CLEO	$E_{cm}^{ee}=10.4$–10.9

[233] BARTELT 94 assume phase space decays.

$\Gamma(e^+\pi^-K^-)/\Gamma_{total}$ Γ_{169}/Γ

Test of lepton number conservation.

VALUE	CL%	DOCUMENT ID		TECN	COMMENT
$<2.1\times10^{-6}$	90	BLISS	98	CLEO	$E_{cm}^{ee}=10.6$ GeV
• • • We do not use the following data for averages, fits, limits, etc. • • •					
$<0.45\times10^{-5}$	90	[234] BARTELT	94	CLEO	Repl. by BLISS 98
$<2.0\times10^{-5}$	90	ALBRECHT	92K	ARG	$E_{cm}^{ee}=10$ GeV
$<4.9\times10^{-5}$	90	BOWCOCK	90	CLEO	$E_{cm}^{ee}=10.4$–10.9

[234] BARTELT 94 assume phase space decays.

$\Gamma(e^-K_S^0K_S^0)/\Gamma_{total}$ Γ_{170}/Γ

Test of lepton family number conservation.

VALUE	CL%	DOCUMENT ID		TECN	COMMENT
$<2.2\times10^{-6}$	90	CHEN	02C	CLEO	$E_{cm}^{ee}=10.6$ GeV

$\Gamma(e^-K^+K^-)/\Gamma_{total}$ Γ_{171}/Γ

Test of lepton family number conservation.

VALUE	CL%	DOCUMENT ID		TECN	COMMENT
$<6.0\times10^{-6}$	90	BLISS	98	CLEO	$E_{cm}^{ee}=10.6$ GeV

$\Gamma(e^+K^-K^-)/\Gamma_{total}$ Γ_{172}/Γ

Test of lepton number conservation.

VALUE	CL%	DOCUMENT ID		TECN	COMMENT
$<3.8\times10^{-6}$	90	BLISS	98	CLEO	$E_{cm}^{ee}=10.6$ GeV

$\Gamma(\mu^-\pi^+K^-)/\Gamma_{total}$ Γ_{173}/Γ

Test of lepton family number conservation.

VALUE	CL%	DOCUMENT ID		TECN	COMMENT
$<7.5\times10^{-6}$	90	BLISS	98	CLEO	$E_{cm}^{ee}=10.6$ GeV
• • • We do not use the following data for averages, fits, limits, etc. • • •					
$<0.87\times10^{-5}$	90	[235] BARTELT	94	CLEO	Repl. by BLISS 98
$<11\times10^{-5}$	90	ALBRECHT	92K	ARG	$E_{cm}^{ee}=10$ GeV
$<7.7\times10^{-5}$	90	BOWCOCK	90	CLEO	$E_{cm}^{ee}=10.4$–10.9

[235] BARTELT 94 assume phase space decays.

$\Gamma(\mu^-\pi^-K^+)/\Gamma_{total}$ Γ_{174}/Γ

Test of lepton family number conservation.

VALUE	CL%	DOCUMENT ID		TECN	COMMENT
$<7.4\times10^{-6}$	90	BLISS	98	CLEO	$E_{cm}^{ee}=10.6$ GeV
• • • We do not use the following data for averages, fits, limits, etc. • • •					
$<1.5\times10^{-5}$	90	[236] BARTELT	94	CLEO	Repl. by BLISS 98
$<7.7\times10^{-5}$	90	BOWCOCK	90	CLEO	$E_{cm}^{ee}=10.4$–10.9

[236] BARTELT 94 assume phase space decays.

$\Gamma(\mu^+\pi^-K^-)/\Gamma_{total}$ Γ_{175}/Γ

Test of lepton number conservation.

VALUE	CL%	DOCUMENT ID		TECN	COMMENT
$<7.0\times10^{-6}$	90	BLISS	98	CLEO	$E_{cm}^{ee}=10.6$ GeV
• • • We do not use the following data for averages, fits, limits, etc. • • •					
$<2.0\times10^{-5}$	90	[237] BARTELT	94	CLEO	Repl. by BLISS 98
$<5.8\times10^{-5}$	90	ALBRECHT	92K	ARG	$E_{cm}^{ee}=10$ GeV
$<4.0\times10^{-5}$	90	BOWCOCK	90	CLEO	$E_{cm}^{ee}=10.4$–10.9

[237] BARTELT 94 assume phase space decays.

$\Gamma(\mu^-K_S^0K_S^0)/\Gamma_{total}$ Γ_{176}/Γ

VALUE	CL%	DOCUMENT ID		TECN	COMMENT
$<3.4\times10^{-6}$	90	CHEN	02C	CLEO	$E_{cm}^{ee}=10.6$ GeV

$\Gamma(\mu^-K^+K^-)/\Gamma_{total}$ Γ_{177}/Γ

Test of lepton family number conservation.

VALUE	CL%	DOCUMENT ID		TECN	COMMENT
$<15\times10^{-6}$	90	BLISS	98	CLEO	$E_{cm}^{ee}=10.6$ GeV

$\Gamma(\mu^+K^-K^-)/\Gamma_{total}$ Γ_{178}/Γ

Test of lepton number conservation.

VALUE	CL%	DOCUMENT ID		TECN	COMMENT
$<6.0\times10^{-6}$	90	BLISS	98	CLEO	$E_{cm}^{ee}=10.6$ GeV

$\Gamma(e^-\pi^0\pi^0)/\Gamma_{total}$ Γ_{179}/Γ

Test of lepton family number conservation.

VALUE	CL%	DOCUMENT ID		TECN	COMMENT
$<6.5\times10^{-6}$	90	BONVICINI	97	CLEO	$E_{cm}^{ee}=10.6$ GeV

$\Gamma(\mu^-\pi^0\pi^0)/\Gamma_{total}$ Γ_{180}/Γ

Test of lepton family number conservation.

VALUE	CL%	DOCUMENT ID		TECN	COMMENT
$<14\times10^{-6}$	90	BONVICINI	97	CLEO	$E_{cm}^{ee}=10.6$ GeV

$\Gamma(e^-\eta\eta)/\Gamma_{total}$ Γ_{181}/Γ

Test of lepton family number conservation.

VALUE	CL%	DOCUMENT ID		TECN	COMMENT
$<35\times10^{-6}$	90	BONVICINI	97	CLEO	$E_{cm}^{ee}=10.6$ GeV

$\Gamma(\mu^-\eta\eta)/\Gamma_{total}$ Γ_{182}/Γ

Test of lepton family number conservation.

VALUE	CL%	DOCUMENT ID		TECN	COMMENT
$<60\times10^{-6}$	90	BONVICINI	97	CLEO	$E_{cm}^{ee}=10.6$ GeV

$\Gamma(e^-\pi^0\eta)/\Gamma_{total}$ Γ_{183}/Γ

Test of lepton family number conservation.

VALUE	CL%	DOCUMENT ID		TECN	COMMENT
$<24\times10^{-6}$	90	BONVICINI	97	CLEO	$E_{cm}^{ee}=10.6$ GeV

$\Gamma(\mu^-\pi^0\eta)/\Gamma_{total}$ Γ_{184}/Γ

Test of lepton family number conservation.

VALUE	CL%	DOCUMENT ID		TECN	COMMENT
$<22\times10^{-6}$	90	BONVICINI	97	CLEO	$E_{cm}^{ee}=10.6$ GeV

$\Gamma(\overline{p}\gamma)/\Gamma_{total}$ Γ_{185}/Γ

Test of lepton number and baryon number conservation.

VALUE	CL%	DOCUMENT ID		TECN	COMMENT
$<3.5\times10^{-6}$	90	GODANG	99	CLEO	$E_{cm}^{ee}=10.6$ GeV
• • • We do not use the following data for averages, fits, limits, etc. • • •					
$<29\times10^{-5}$	90	ALBRECHT	92K	ARG	$E_{cm}^{ee}=10$ GeV

$\Gamma(\overline{p}\pi^0)/\Gamma_{total}$ Γ_{186}/Γ

Test of lepton number and baryon number conservation.

VALUE	CL%	DOCUMENT ID		TECN	COMMENT
$<15\times10^{-6}$	90	GODANG	99	CLEO	$E_{cm}^{ee}=10.6$ GeV
• • • We do not use the following data for averages, fits, limits, etc. • • •					
$<66\times10^{-5}$	90	ALBRECHT	92K	ARG	$E_{cm}^{ee}=10$ GeV

$\Gamma(\overline{p}2\pi^0)/\Gamma_{total}$ Γ_{187}/Γ

Test of lepton number and baryon number conservation.

VALUE	CL%	DOCUMENT ID		TECN	COMMENT
$<33\times10^{-6}$	90	GODANG	99	CLEO	$E_{cm}^{ee}=10.6$ GeV

$\Gamma(\overline{p}\eta)/\Gamma_{total}$ Γ_{188}/Γ

Test of lepton number and baryon number conservation.

VALUE	CL%	DOCUMENT ID		TECN	COMMENT
$<8.9\times10^{-6}$	90	GODANG	99	CLEO	$E_{cm}^{ee}=10.6$ GeV
• • • We do not use the following data for averages, fits, limits, etc. • • •					
$<130\times10^{-5}$	90	ALBRECHT	92K	ARG	$E_{cm}^{ee}=10$ GeV

$\Gamma(\overline{p}\pi^0\eta)/\Gamma_{total}$ Γ_{189}/Γ

Test of lepton number and baryon number conservation.

VALUE	CL%	DOCUMENT ID		TECN	COMMENT
$<27\times10^{-6}$	90	GODANG	99	CLEO	$E_{cm}^{ee}=10.6$ GeV

$\Gamma(e^-\text{light boson})/\Gamma(e^-\overline{\nu}_e\nu_\tau)$ Γ_{190}/Γ_5

Test of lepton family number conservation.

VALUE	CL%	DOCUMENT ID		TECN	COMMENT
<0.015	95	[238] ALBRECHT	95G	ARG	$E_{cm}^{ee}=9.4$–10.6 GeV
• • • We do not use the following data for averages, fits, limits, etc. • • •					
<0.018	95	[239] ALBRECHT	90E	ARG	$E_{cm}^{ee}=9.4$–10.6 GeV
<0.040	95	[240] BALTRUSAIT...85		MRK3	$E_{cm}^{ee}=3.77$ GeV

[238] ALBRECHT 95G limit holds for bosons with mass <0.4 GeV. The limit rises to 0.036 for a mass of 1.0 GeV, then falls to 0.006 at the upper mass limit of 1.6 GeV.

[239] ALBRECHT 90E limit applies for spinless boson with mass <100 MeV, and rises to 0.050 for mass $=500$ MeV.

[240] BALTRUSAITIS 85 limit applies for spinless boson with mass <100 MeV.

$\Gamma(\mu^-\text{light boson})/\Gamma(e^-\overline{\nu}_e\nu_\tau)$ Γ_{191}/Γ_5

Test of lepton family number conservation.

VALUE	CL%	DOCUMENT ID		TECN	COMMENT
<0.026	95	[241] ALBRECHT	95G	ARG	$E_{cm}^{ee}=9.4$–10.6 GeV
• • • We do not use the following data for averages, fits, limits, etc. • • •					
<0.033	95	[242] ALBRECHT	90E	ARG	$E_{cm}^{ee}=9.4$–10.6 GeV
<0.125	95	[243] BALTRUSAIT...85		MRK3	$E_{cm}^{ee}=3.77$ GeV

[241] ALBRECHT 95G limit holds for bosons with mass <1.3 GeV. The limit rises to 0.034 for a mass of 1.4 GeV, then falls to 0.003 at the upper mass limit of 1.6 GeV.

[242] ALBRECHT 90E limit applies for spinless boson with mass <100 MeV, and rises to 0.071 for mass $=500$ MeV.

[243] BALTRUSAITIS 85 limit applies for spinless boson with mass <100 MeV.

τ-DECAY PARAMETERS

τ-LEPTON DECAY PARAMETERS

Written April 2002 by A. Stahl (DESY).

The purpose of the measurements of the decay parameters (*i.e.,* Michel parameters) of the τ is to determine the structure (spin and chirality) of the current mediating its decays.

Leptonic Decays: The Michel parameters are extracted from the energy spectrum of the charged daughter lepton $\ell = e, \mu$ in the decays $\tau \to \ell\nu_\ell\nu_\tau$. Ignoring radiative corrections, neglecting terms of order $(m_\ell/m_\tau)^2$ and $(m_\tau/\sqrt{s})^2$, and setting the neutrino masses to zero, the spectrum in the laboratory frame reads

$$\frac{d\Gamma}{dx} = \frac{G_{\tau\ell}^2}{192}\frac{m_\tau^5}{\pi^3} \times \left\{ f_0(x) + \rho f_1(x) + \eta\frac{m_\ell}{m_\tau} f_2(x) - P_\tau\left[\xi g_1(x) + \xi\delta g_2(x)\right] \right\} , \quad (1)$$

with

$$f_0(x) = 2 - 6x^2 + 4x^3$$
$$f_1(x) = -\frac{4}{9} + 4x^2 - \frac{32}{9}x^3 \qquad g_1(x) = -\frac{2}{3} + 4x - 6x^2 + \frac{8}{3}x^3$$
$$f_2(x) = 12(1-x)^2 \qquad g_2(x) = \frac{4}{9} - \frac{16}{3}x + 12x^2 - \frac{64}{9}x^3 .$$

The integrated decay width is given by

$$\Gamma = \frac{G_{\tau\ell}^2}{192}\frac{m_\tau^5}{\pi^3}\left(1 + 4\eta\,\frac{m_\ell}{m_\tau}\right) . \quad (2)$$

The situation is similar to muon decays $\mu \to e\nu_e\nu_\mu$. The generalized matrix element with the couplings $g_{\varepsilon\mu}^\gamma$ and their relations to the Michel parameters ρ, η, ξ, and δ have been described in the "Note on Muon Decay Parameters". The Standard Model expectations are 3/4, 0, 1, and 3/4, respectively. For more details, see Ref. 1.

Hadronic Decays: In the case of hadronic decays $\tau \to h\nu_\tau$, with $h = \pi$, ρ, or a_1, the ansatz is restricted to purely vectorial currents. The matrix element is

$$\frac{G_{\tau h}}{\sqrt{2}} \sum_{\lambda=R,L} g_\lambda \langle\ \overline{\Psi}_\omega(\nu_\tau)\ |\ \gamma^\mu\ |\ \Psi_\lambda(\tau)\ \rangle\ \ J_\mu^h \quad (3)$$

with the hadronic current J_μ^h. The neutrino chirality ω is uniquely determined from λ. The spectrum depends only on a single parameter ξ_h

$$\frac{d\Gamma}{d\vec{x}} = f(\vec{x}) + \xi_h P_\tau g(\vec{x}) , \quad (4)$$

with f and g being channel-dependent functions of the observables $\vec{x}$ (see Ref. 2). The parameter ξ_h is related to the couplings through

$$\xi_h = |g_L|^2 - |g_R|^2 . \quad (5)$$

ξ_h is the negative of the chirality of the τ neutrino in these decays. In the Standard Model, $\xi_h = 1$. Also included are measurements of the neutrino helicity which coincide with ξ_h, if the neutrino is massless (ASNER 00, ACKERSTAFF 97R, AKERS 95P, ALBRECHT 93C, and ALBRECHT 90I).

Combination of Measurements: The individual measurements are combined, taking into account the correlations between the parameters. There is one fit, assuming universality between the two leptonic decays, and between all hadronic decays and a second fit without these assumptions. These are the values labeled 'OUR FIT' in the tables. The measurements show good agreement with the Standard Model. The χ^2 values with respect to the Standard model predictions are 24.1 for 41 degrees of freedom and 26.8 for 56 degrees of freedom, respectively. The correlations are reduced through this combination to less than 20%, with the exception of ρ and η which are correlated by +23%, for the fit with universality and by +70% for $\tau \to \mu\nu_\mu\nu_\tau$.

Model-independent Analysis: From the Michel parameters, limits can be derived on the couplings $g_{\varepsilon\lambda}^\kappa$ without further module assumptions. In the Standard model $g_{LL}^V = 1$ (leptonic decays), and $g_L = 1$ (hadronic decays) and all other couplings vanish. First, the partial decay widths have to be compared to the Standard Model predictions to derive limits on the normalization of the couplings $A_x = G_{\tau x}^2/G_F^2$ with Fermi's constant G_F:

$$A_e = 1.0012 \pm 0.0053 ,$$
$$A_\mu = 0.981 \pm 0.018 ,$$
$$A_\pi = 1.018 \pm 0.012 . \quad (6)$$

Then limits on the couplings (95% CL) can be extracted (see Ref. 3 and Ref. 4). Without the assumption of universality, the limits given in Table 1 are derived.

Model-dependent Interpretation: More stringent limits can be derived assuming specific models. For example, in the framework of a two Higgs doublet model, the measurements correspond to a limit of $m_{H^\pm} > 1.9$ GeV $\times \tan\beta$ on the mass of the charged Higgs boson, or a limit of 253 GeV on the mass of the second W boson in left-right symmetric models for arbitrary mixing (both 95% CL). See Ref. 4 and Ref. 5.

Footnotes and References

1. F. Scheck, Phys. Reports **44**, 187 (1978);
W. Fetscher and H.J. Gerber in *Precision Tests of the Standard Model*, edited by P. Langacker, World Scientific, 1993;
A. Stahl, *Physics with τ Leptons*, Springer Tracts in Modern Physics.
2. M. Davier, L. Duflot, F. Le-Diberder, and A. Rougé Phys. Lett. **B306**, 411 (1993).
3. OPAL Collab., K. Ackerstaff *et al.*, Eur. Phys. J. **C8**, 3 (1999).
4. A. Stahl, Nucl. Phys. (Proc. Supp.) **B76**, 173 (1999).
5. M.-T. Dova *et al.*, Phys. Rev. **D58**, 015005 (1998);
T. Hebbeker and W. Lohmann, Z. Phys. **C74**, 399 (1997);
A. Pich and J.P. Silva, Phys. Rev. **D52**, 4006 (1995).

Table 1: Coupling constants $g^{\gamma}_{\varepsilon\mu}$. 95% confidence level experimental limits. The limits include the quoted values of A_e, A_μ, and A_π and assume $A_\rho = A_{a_1} = 1$.

$\tau \to e\nu_e\nu_\tau$		
$\lvert g^S_{RR}\rvert < 0.70$	$\lvert g^V_{RR}\rvert < 0.17$	$\lvert g^T_{RR}\rvert \equiv 0$
$\lvert g^S_{LR}\rvert < 0.99$	$\lvert g^V_{LR}\rvert < 0.13$	$\lvert g^T_{LR}\rvert < 0.082$
$\lvert g^S_{RL}\rvert < 2.01$	$\lvert g^V_{RL}\rvert < 0.52$	$\lvert g^T_{RL}\rvert < 0.51$
$\lvert g^S_{LL}\rvert < 2.01$	$\lvert g^V_{LL}\rvert < 1.005$	$\lvert g^T_{LL}\rvert \equiv 0$
$\tau \to \mu\nu_\mu\nu_\tau$		
$\lvert g^S_{RR}\rvert < 0.72$	$\lvert g^V_{RR}\rvert < 0.18$	$\lvert g^T_{RR}\rvert \equiv 0$
$\lvert g^S_{LR}\rvert < 0.95$	$\lvert g^V_{LR}\rvert < 0.12$	$\lvert g^T_{LR}\rvert < 0.079$
$\lvert g^S_{RL}\rvert < 2.01$	$\lvert g^V_{RL}\rvert < 0.52$	$\lvert g^T_{RL}\rvert < 0.51$
$\lvert g^S_{LL}\rvert < 2.01$	$\lvert g^V_{LL}\rvert < 1.005$	$\lvert g^T_{LL}\rvert \equiv 0$
$\tau \to \pi\nu_\tau$		
$\lvert g^V_R\rvert < 0.15$	$\lvert g^V_L\rvert > 0.992$	
$\tau \to \rho\nu_\tau$		
$\lvert g^V_R\rvert < 0.10$	$\lvert g^V_L\rvert > 0.995$	
$\tau \to a_1\nu_\tau$		
$\lvert g^V_R\rvert < 0.16$	$\lvert g^V_L\rvert > 0.987$	

$\rho^\tau(e$ or $\mu)$ PARAMETER

($V-A$) theory predicts $\rho = 0.75$.

VALUE	EVTS	DOCUMENT ID		TECN	COMMENT
0.745±0.008 OUR FIT					
0.749±0.008 OUR AVERAGE					
0.742±0.014±0.006	81k	HEISTER	01E	ALEP	1991–1995 LEP runs
0.775±0.023±0.020	36k	ABREU	00L	DLPH	1992–1995 runs
0.781±0.028±0.018	46k	ACKERSTAFF	99D	OPAL	1990–1995 LEP runs
0.762±0.035	54k	ACCIARRI	98R	L3	1991–1995 LEP runs
0.731±0.031		[244] ALBRECHT	98	ARG	$E^{ee}_{\rm cm}$= 9.5–10.6 GeV
0.72 ±0.09 ±0.03		[245] ABE	97O	SLD	1993–1995 SLC runs
0.747±0.010±0.006	55k	ALEXANDER	97F	CLEO	$E^{ee}_{\rm cm}$= 10.6 GeV
0.79 ±0.10 ±0.10	3732	FORD	87B	MAC	$E^{ee}_{\rm cm}$= 29 GeV
0.71 ±0.09 ±0.03	1426	BEHRENDS	85	CLEO	e^+e^- near $\Upsilon(4S)$
• • • We do not use the following data for averages, fits, limits, etc. • • •					
0.735±0.013±0.008	31k	AMMAR	97B	CLEO	Repl. by ALEXANDER 97F
0.794±0.039±0.031	18k	ACCIARRI	96H	L3	Repl. by ACCIARRI 98R
0.732±0.034±0.020	8.2k	[246] ALBRECHT	95	ARG	$E^{ee}_{\rm cm}$= 9.5–10.6 GeV
0.738±0.038		[247] ALBRECHT	95C	ARG	Repl. by ALBRECHT 98
0.751±0.039±0.022		BUSKULIC	95D	ALEP	Repl. by HEISTER 01E
0.742±0.035±0.020	8000	ALBRECHT	90E	ARG	$E^{ee}_{\rm cm}$= 9.4–10.6 GeV

[244] Combined fit to ARGUS tau decay parameter measurements in ALBRECHT 98, ALBRECHT 95C, ALBRECHT 93G, and ALBRECHT 94E. ALBRECHT 98 use tau pair events of the type $\tau^-\tau^+ \to (\ell^-\overline{\nu}_\ell\nu_\tau)(\pi^+\pi^0\overline{\nu}_\tau)$, and their charged conjugates.

[245] ABE 97O assume $\eta^\tau = 0$ in their fit. Letting η^τ vary in the fit gives a ρ^τ value of $0.69 \pm 0.13 \pm 0.05$.

[246] Value is from a simultaneous fit for the ρ^τ and η^τ decay parameters to the lepton energy spectrum. Not independent of ALBRECHT 90E $\rho^\tau(e$ or $\mu)$ value which assumes η^τ=0. Result is strongly correlated with ALBRECHT 95C.

[247] Combined fit to ARGUS tau decay parameter measurements in ALBRECHT 95C, ALBRECHT 93G, and ALBRECHT 94E.

$\rho^\tau(e)$ PARAMETER

($V-A$) theory predicts $\rho = 0.75$.

VALUE	EVTS	DOCUMENT ID		TECN	COMMENT
0.747±0.010 OUR FIT					
0.744±0.010 OUR AVERAGE					
0.747±0.019±0.014	44k	HEISTER	01E	ALEP	1991–1995 LEP runs
0.744±0.036±0.037	17k	ABREU	00L	DLPH	1992–1995 runs
0.779±0.047±0.029	25k	ACKERSTAFF	99D	OPAL	1990–1995 LEP runs
0.68 ±0.04 ±0.07		[248] ALBRECHT	98	ARG	$E^{ee}_{\rm cm}$= 9.5–10.6 GeV
0.71 ±0.14 ±0.05		ABE	97O	SLD	1993–1995 SLC runs
0.747±0.012±0.004	34k	ALEXANDER	97F	CLEO	$E^{ee}_{\rm cm}$= 10.6 GeV
0.735±0.036±0.020	4.7k	[249] ALBRECHT	95	ARG	$E^{ee}_{\rm cm}$= 9.5–10.6 GeV
0.79 ±0.08 ±0.06	3230	[250] ALBRECHT	93G	ARG	$E^{ee}_{\rm cm}$= 9.4–10.6 GeV
0.64 ±0.06 ±0.07	2753	JANSSEN	89	CBAL	$E^{ee}_{\rm cm}$= 9.4–10.6 GeV
0.62 ±0.17 ±0.14	1823	FORD	87B	MAC	$E^{ee}_{\rm cm}$= 29 GeV
0.60 ±0.13	699	BEHRENDS	85	CLEO	e^+e^- near $\Upsilon(4S)$
0.72 ±0.10 ±0.11	594	BACINO	79B	DLCO	$E^{ee}_{\rm cm}$= 3.5–7.4 GeV
• • • We do not use the following data for averages, fits, limits, etc. • • •					
0.732±0.014±0.009	19k	AMMAR	97B	CLEO	Repl. by ALEXANDER 97F
0.793±0.050±0.025		BUSKULIC	95D	ALEP	Repl. by HEISTER 01E
0.747±0.045±0.028	5106	ALBRECHT	90E	ARG	Repl. by ALBRECHT 95

[248] ALBRECHT 98 use tau pair events of the type $\tau^-\tau^+ \to (\ell^-\overline{\nu}_\ell\nu_\tau)(\pi^+\pi^0\overline{\nu}_\tau)$, and their charged conjugates.

[249] ALBRECHT 95 use tau pair events of the type $\tau^-\tau^+ \to (\ell^-\overline{\nu}_\ell\nu_\tau)(h^+h^-h^+(\pi^0)\overline{\nu}_\tau)$ and their charged conjugates.

[250] ALBRECHT 93G use tau pair events of the type $\tau^-\tau^+ \to (\mu^-\overline{\nu}_\mu\nu_\tau)(e^+\nu_e\overline{\nu}_\tau)$ and their charged conjugates.

$\rho^\tau(\mu)$ PARAMETER

($V-A$) theory predicts $\rho = 0.75$.

VALUE	EVTS	DOCUMENT ID		TECN	COMMENT
0.763±0.020 OUR FIT					
0.770±0.022 OUR AVERAGE					
0.776±0.045±0.019	46k	HEISTER	01E	ALEP	1991–1995 LEP runs
0.999±0.098±0.045	22k	ABREU	00L	DLPH	1992–1995 runs
0.777±0.044±0.016	27k	ACKERSTAFF	99D	OPAL	1990–1995 LEP runs
0.69 ±0.06 ±0.06		[251] ALBRECHT	98	ARG	$E^{ee}_{\rm cm}$= 9.5–10.6 GeV
0.54 ±0.28 ±0.14		ABE	97O	SLD	1993–1995 SLC runs
0.750±0.017±0.045	22k	ALEXANDER	97F	CLEO	$E^{ee}_{\rm cm}$= 10.6 GeV
0.76 ±0.07 ±0.08	3230	ALBRECHT	93G	ARG	$E^{ee}_{\rm cm}$= 9.4–10.6 GeV
0.734±0.055±0.027	3041	ALBRECHT	90E	ARG	$E^{ee}_{\rm cm}$= 9.4–10.6 GeV
0.89 ±0.14 ±0.08	1909	FORD	87B	MAC	$E^{ee}_{\rm cm}$= 29 GeV
0.81 ±0.13	727	BEHRENDS	85	CLEO	e^+e^- near $\Upsilon(4S)$
• • • We do not use the following data for averages, fits, limits, etc. • • •					
0.747±0.048±0.044	13k	AMMAR	97B	CLEO	Repl. by ALEXANDER 97F
0.693±0.057±0.028		BUSKULIC	95D	ALEP	Repl. by HEISTER 01E

[251] ALBRECHT 98 use tau pair events of the type $\tau^-\tau^+ \to (\ell^-\overline{\nu}_\ell\nu_\tau)(\pi^+\pi^0\overline{\nu}_\tau)$, and their charged conjugates.

$\xi^\tau(e$ or $\mu)$ PARAMETER

($V-A$) theory predicts $\xi = 1$.

VALUE	EVTS	DOCUMENT ID		TECN	COMMENT
0.985±0.030 OUR FIT					
0.981±0.031 OUR AVERAGE					
0.986±0.068±0.031	81k	HEISTER	01E	ALEP	1991–1995 LEP runs
0.929±0.070±0.030	36k	ABREU	00L	DLPH	1992–1995 runs
0.98 ±0.22 ±0.10	46k	ACKERSTAFF	99D	OPAL	1990–1995 LEP runs
0.70 ±0.16	54k	ACCIARRI	98R	L3	1991–1995 LEP runs
1.03 ±0.11		[252] ALBRECHT	98	ARG	$E^{ee}_{\rm cm}$= 9.5–10.6 GeV
1.05 ±0.35 ±0.04		[253] ABE	97O	SLD	1993–1995 SLC runs
1.007±0.040±0.015	55k	ALEXANDER	97F	CLEO	$E^{ee}_{\rm cm}$= 10.6 GeV
• • • We do not use the following data for averages, fits, limits, etc. • • •					
0.94 ±0.21 ±0.07	18k	ACCIARRI	96H	L3	Repl. by ACCIARRI 98R
0.97 ±0.14		[254] ALBRECHT	95C	ARG	Repl. by ALBRECHT 98
1.18 ±0.15 ±0.16		BUSKULIC	95D	ALEP	Repl. by HEISTER 01E
0.90 ±0.15 ±0.10	3230	[255] ALBRECHT	93G	ARG	$E^{ee}_{\rm cm}$= 9.4–10.6 GeV

[252] Combined fit to ARGUS tau decay parameter measurements in ALBRECHT 98, ALBRECHT 95C, ALBRECHT 93G, and ALBRECHT 94E. ALBRECHT 98 use tau pair events of the type $\tau^-\tau^+ \to (\ell^-\overline{\nu}_\ell\nu_\tau)(\pi^+\pi^0\overline{\nu}_\tau)$, and their charged conjugates.

[253] ABE 97O assume $\eta^\tau = 0$ in their fit. Letting η^τ vary in the fit gives a ξ^τ value of $1.02 \pm 0.36 \pm 0.05$.

[254] Combined fit to ARGUS tau decay parameter measurements in ALBRECHT 95C, ALBRECHT 93G, and ALBRECHT 94E. ALBRECHT 95C uses events of the type $\tau^-\tau^+ \to (\ell^-\overline{\nu}_\ell\nu_\tau)(h^+h^-h^+\overline{\nu}_\tau)$ and their charged conjugates.

[255] ALBRECHT 93G measurement determines $\lvert\xi^\tau\rvert$ for the case $\xi^\tau(e) = \xi^\tau(\mu)$, but the authors point out that other LEP experiments determine the sign to be positive.

$\xi^\tau(e)$ PARAMETER

($V-A$) theory predicts $\xi = 1$.

VALUE	EVTS	DOCUMENT ID		TECN	COMMENT
0.994±0.040 OUR FIT					
1.00 ±0.04 OUR AVERAGE					
1.011±0.094±0.038	44k	HEISTER	01E	ALEP	1991–1995 LEP runs
1.01 ±0.12 ±0.05	17k	ABREU	00L	DLPH	1992–1995 runs
1.13 ±0.39 ±0.14	25k	ACKERSTAFF	99D	OPAL	1990–1995 LEP runs
1.11 ±0.20 ±0.08		[256] ALBRECHT	98	ARG	$E^{ee}_{\rm cm}$= 9.5–10.6 GeV
1.16 ±0.52 ±0.06		ABE	97O	SLD	1993–1995 SLC runs
0.979±0.048±0.016	34k	ALEXANDER	97F	CLEO	$E^{ee}_{\rm cm}$= 10.6 GeV
• • • We do not use the following data for averages, fits, limits, etc. • • •					
1.03 ±0.23 ±0.09		BUSKULIC	95D	ALEP	Repl. by HEISTER 01E

[256] ALBRECHT 98 use tau pair events of the type $\tau^-\tau^+ \to (\ell^-\overline{\nu}_\ell\nu_\tau)(\pi^+\pi^0\overline{\nu}_\tau)$, and their charged conjugates.

$\xi^\tau(\mu)$ PARAMETER

($V-A$) theory predicts $\xi = 1$.

VALUE	EVTS	DOCUMENT ID		TECN	COMMENT
1.030±0.059 OUR FIT					
1.06 ±0.06 OUR AVERAGE					
1.030±0.120±0.050	46k	HEISTER	01E	ALEP	1991–1995 LEP runs
1.16 ±0.19 ±0.06	22k	ABREU	00L	DLPH	1992–1995 runs
0.79 ±0.41 ±0.09	27k	ACKERSTAFF	99D	OPAL	1990–1995 LEP runs
1.26 ±0.27 ±0.14	[257]	ALBRECHT	98	ARG	$E^{ee}_{\rm cm}$= 9.5–10.6 GeV
0.75 ±0.50 ±0.14		ABE	97O	SLD	1993–1995 SLC runs
1.054±0.069±0.047	22k	ALEXANDER	97F	CLEO	$E^{ee}_{\rm cm}$= 10.6 GeV
• • • We do not use the following data for averages, fits, limits, etc. • • •					
1.23 ±0.22 ±0.10		BUSKULIC	95D	ALEP	Repl. by HEISTER 01E

[257] ALBRECHT 98 use tau pair events of the type $\tau^-\tau^+ \to (\ell^-\overline{\nu}_\ell\nu_\tau)(\pi^+\pi^0\overline{\nu}_\tau)$, and their charged conjugates.

$\eta^\tau(e$ or $\mu)$ PARAMETER

($V-A$) theory predicts $\eta = 0$.

VALUE	EVTS	DOCUMENT ID		TECN	COMMENT
0.013±0.020 OUR FIT					
0.015±0.021 OUR AVERAGE					
0.012±0.026±0.004	81k	HEISTER	01E	ALEP	1991–1995 LEP runs
−0.005±0.036±0.037		ABREU	00L	DLPH	1992–1995 runs
0.027±0.055±0.005	46k	ACKERSTAFF	99D	OPAL	1990–1995 LEP runs
0.27 ±0.14	54k	ACCIARRI	98R	L3	1991–1995 LEP runs
−0.13 ±0.47 ±0.15		ABE	97O	SLD	1993–1995 SLC runs
−0.015±0.061±0.062	31k	AMMAR	97B	CLEO	$E^{ee}_{\rm cm}$= 10.6 GeV
0.03 ±0.18 ±0.12	8.2k	ALBRECHT	95	ARG	$E^{ee}_{\rm cm}$= 9.5–10.6 GeV
• • • We do not use the following data for averages, fits, limits, etc. • • •					
0.25 ±0.17 ±0.11	18k	ACCIARRI	96H	L3	Repl. by ACCIARRI 98R
−0.04 ±0.15 ±0.11		BUSKULIC	95D	ALEP	Repl. by HEISTER 01E

$\eta^\tau(\mu)$ PARAMETER

($V-A$) theory predicts $\eta = 0$.

VALUE	EVTS	DOCUMENT ID		TECN	COMMENT
0.094±0.073 OUR FIT					
0.17 ±0.15 OUR AVERAGE		Error includes scale factor of 1.2.			
0.160±0.150±0.060	46k	HEISTER	01E	ALEP	1991–1995 LEP runs
0.72 ±0.32 ±0.15		ABREU	00L	DLPH	1992–1995 runs
−0.59 ±0.82 ±0.45	[258]	ABE	97O	SLD	1993–1995 SLC runs
0.010±0.149±0.171	13k	[259] AMMAR	97B	CLEO	$E^{ee}_{\rm cm}$= 10.6 GeV
• • • We do not use the following data for averages, fits, limits, etc. • • •					
0.010±0.065±0.001	27k	[260] ACKERSTAFF	99D	OPAL	1990–1995 LEP runs
−0.24 ±0.23 ±0.18		BUSKULIC	95D	ALEP	Repl. by HEISTER 01E

[258] Highly correlated (corr. = 0.92) with ABE 97O $\rho^\tau(\mu)$ measurement.

[259] Highly correlated (corr. = 0.949) with AMMAR 97B $\rho^\tau(\mu)$ value.

[260] ACKERSTAFF 99D result is dominated by a constraint on η^τ from the OPAL measurements of the τ lifetime and B($\tau^- \to \mu^-\overline{\nu}_\mu\nu_\tau$) assuming lepton universality for the total coupling strength.

$(\delta\xi)^\tau(e$ or $\mu)$ PARAMETER

($V-A$) theory predicts $(\delta\xi) = 0.75$.

VALUE	EVTS	DOCUMENT ID		TECN	COMMENT
0.746±0.021 OUR FIT					
0.744±0.022 OUR AVERAGE					
0.776±0.045±0.024	81k	HEISTER	01E	ALEP	1991–1995 LEP runs
0.779±0.070±0.028	36k	ABREU	00L	DLPH	1992–1995 runs
0.65 ±0.14 ±0.07	46k	ACKERSTAFF	99D	OPAL	1990–1995 LEP runs
0.70 ±0.11	54k	ACCIARRI	98R	L3	1991–1995 LEP runs
0.63 ±0.09	[261]	ALBRECHT	98	ARG	$E^{ee}_{\rm cm}$= 9.5–10.6 GeV
0.88 ±0.27 ±0.04	[262]	ABE	97O	SLD	1993–1995 SLC runs
0.745±0.026±0.009	55k	ALEXANDER	97F	CLEO	$E^{ee}_{\rm cm}$= 10.6 GeV
• • • We do not use the following data for averages, fits, limits, etc. • • •					
0.81 ±0.14 ±0.06	18k	ACCIARRI	96H	L3	Repl. by ACCIARRI 98R
0.65 ±0.12	[263]	ALBRECHT	95C	ARG	Repl. by ALBRECHT 98
0.88 ±0.11 ±0.07		BUSKULIC	95D	ALEP	Repl. by HEISTER 01E

[261] Combined fit to ARGUS tau decay parameter measurements in ALBRECHT 98, ALBRECHT 95C, ALBRECHT 93G, and ALBRECHT 94E. ALBRECHT 98 use tau pair events of the type $\tau^-\tau^+ \to (\ell^-\overline{\nu}_\ell\nu_\tau)(\pi^+\pi^0\overline{\nu}_\tau)$, and their charged conjugates.

[262] ABE 97O assume $\eta^\tau = 0$ in their fit. Letting η^τ vary in the fit gives a $(\rho\xi)^\tau$ value of 0.87 ± 0.27 ± 0.04.

[263] Combined fit to ARGUS tau decay parameter measurements in ALBRECHT 95C, ALBRECHT 93G, and ALBRECHT 94E. ALBRECHT 95C uses events of the type $\tau^-\tau^+ \to (\ell^-\overline{\nu}_\ell\nu_\tau)\,(h^+h^-h^+\overline{\nu}_\tau)$ and their charged conjugates.

$(\delta\xi)^\tau(e)$ PARAMETER

($V-A$) theory predicts $(\delta\xi) = 0.75$.

VALUE	EVTS	DOCUMENT ID		TECN	COMMENT
0.734±0.028 OUR FIT					
0.731±0.029 OUR AVERAGE					
0.778±0.066±0.024	44k	HEISTER	01E	ALEP	1991–1995 LEP runs
0.85 ±0.12 ±0.04	17k	ABREU	00L	DLPH	1992–1995 runs
0.72 ±0.31 ±0.14	25k	ACKERSTAFF	99D	OPAL	1990–1995 LEP runs
0.56 ±0.14 ±0.06	[264]	ALBRECHT	98	ARG	$E^{ee}_{\rm cm}$= 9.5–10.6 GeV
0.85 ±0.43 ±0.08		ABE	97O	SLD	1993–1995 SLC runs
0.720±0.032±0.010	34k	ALEXANDER	97F	CLEO	$E^{ee}_{\rm cm}$= 10.6 GeV
• • • We do not use the following data for averages, fits, limits, etc. • • •					
1.11 ±0.17 ±0.07		BUSKULIC	95D	ALEP	Repl. by HEISTER 01E

[264] ALBRECHT 98 use tau pair events of the type $\tau^-\tau^+ \to (\ell^-\overline{\nu}_\ell\nu_\tau)(\pi^+\pi^0\overline{\nu}_\tau)$, and their charged conjugates.

$(\delta\xi)^\tau(\mu)$ PARAMETER

($V-A$) theory predicts $(\delta\xi) = 0.75$.

VALUE	EVTS	DOCUMENT ID		TECN	COMMENT
0.778±0.037 OUR FIT					
0.79 ±0.04 OUR AVERAGE					
0.786±0.066±0.028	46k	HEISTER	01E	ALEP	1991–1995 LEP runs
0.86 ±0.13 ±0.04	22k	ABREU	00L	DLPH	1992–1995 runs
0.63 ±0.23 ±0.05	27k	ACKERSTAFF	99D	OPAL	1990–1995 LEP runs
0.73 ±0.18 ±0.10	[265]	ALBRECHT	98	ARG	$E^{ee}_{\rm cm}$= 9.5–10.6 GeV
0.82 ±0.32 ±0.07		ABE	97O	SLD	1993–1995 SLC runs
0.786±0.041±0.032	22k	ALEXANDER	97F	CLEO	$E^{ee}_{\rm cm}$= 10.6 GeV
• • • We do not use the following data for averages, fits, limits, etc. • • •					
0.71 ±0.14 ±0.06		BUSKULIC	95D	ALEP	Repl. by HEISTER 01E

[265] ALBRECHT 98 use tau pair events of the type $\tau^-\tau^+ \to (\ell^-\overline{\nu}_\ell\nu_\tau)(\pi^+\pi^0\overline{\nu}_\tau)$, and their charged conjugates.

$\xi^\tau(\pi)$ PARAMETER

($V-A$) theory predicts $\xi^\tau(\pi) = 1$.

VALUE	EVTS	DOCUMENT ID		TECN	COMMENT
0.993±0.022 OUR FIT					
0.994±0.023 OUR AVERAGE					
0.994±0.020±0.014	27k	HEISTER	01E	ALEP	1991–1995 LEP runs
0.81 ±0.17 ±0.02		ABE	97O	SLD	1993–1995 SLC runs
1.03 ±0.06 ±0.04	2.0k	COAN	97	CLEO	$E^{ee}_{\rm cm}$= 10.6 GeV
• • • We do not use the following data for averages, fits, limits, etc. • • •					
0.987±0.057±0.027		BUSKULIC	95D	ALEP	Repl. by HEISTER 01E
0.95 ±0.11 ±0.05	[266]	BUSKULIC	94D	ALEP	1990+1991 LEP run

[266] Superseded by BUSKULIC 95D.

$\xi^\tau(\rho)$ PARAMETER

($V-A$) theory predicts $\xi^\tau(\rho) = 1$.

VALUE	EVTS	DOCUMENT ID		TECN	COMMENT
0.994±0.008 OUR FIT					
0.994±0.009 OUR AVERAGE					
0.987±0.012±0.011	59k	HEISTER	01E	ALEP	1991–1995 LEP runs
0.99 ±0.12 ±0.04		ABE	97O	SLD	1993–1995 SLC runs
0.995±0.010±0.003	66k	ALEXANDER	97F	CLEO	$E^{ee}_{\rm cm}$= 10.6 GeV
1.022±0.028±0.030	1.7k	[267] ALBRECHT	94E	ARG	$E^{ee}_{\rm cm}$= 9.4–10.6 GeV
• • • We do not use the following data for averages, fits, limits, etc. • • •					
1.045±0.058±0.032		BUSKULIC	95D	ALEP	Repl. by HEISTER 01E
1.03 ±0.11 ±0.05	[268]	BUSKULIC	94D	ALEP	1990+1991 LEP run

[267] ALBRECHT 94E measure the square of this quantity and use the sign determined by ALBRECHT 90I to obtain the quoted result.

[268] Superseded by BUSKULIC 95D.

$\xi^\tau(a_1)$ PARAMETER

($V-A$) theory predicts $\xi^\tau(a_1) = 1$.

VALUE	EVTS	DOCUMENT ID		TECN	COMMENT
1.001±0.027 OUR FIT					
1.002±0.028 OUR AVERAGE					
1.000±0.016±0.024	35k	[269] HEISTER	01E	ALEP	1991–1995 LEP runs
1.02 ±0.13 ±0.03	17.2k	ASNER	00	CLEO	$E^{ee}_{\rm cm}$= 10.6 GeV
1.29 ±0.26 ±0.11	7.4k	[270] ACKERSTAFF	97R	OPAL	1992–1994 LEP runs
0.85 $^{+0.15}_{-0.17}$ ±0.05		ALBRECHT	95C	ARG	$E^{ee}_{\rm cm}$= 9.5–10.6 GeV
1.25 ±0.23 $^{+0.15}_{-0.08}$	7.5k	ALBRECHT	93C	ARG	$E^{ee}_{\rm cm}$= 9.4–10.6 GeV
• • • We do not use the following data for averages, fits, limits, etc. • • •					
1.08 $^{+0.46}_{-0.41}$ $^{+0.14}_{-0.25}$	2.6k	[271] AKERS	95P	OPAL	Repl. by ACKERSTAFF 97R
0.937±0.116±0.064		BUSKULIC	95D	ALEP	Repl. by HEISTER 01E

[269] HEISTER 01E quote 1.000 ± 0.016 ± 0.013 ± 0.020 where the errors are statistical, systematic, and an uncertainty due to the final state model. We combine the systematic error and model uncertainty.

[270] ACKERSTAFF 97R obtain this result with a model independent fit to the hadronic structure functions. Fitting with the model of Kuhn and Santamaria (ZPHY **C48**, 445 (1990)) gives 0.87 ± 0.16 ± 0.04, and with the model of of Isgur *et al.* (PR **D39**,1357 (1989)) they obtain 1.20 ± 0.21 ± 0.14.

[271] AKERS 95P obtain this result with a model independent fit to the hadronic structure functions. Fitting with the model of Kuhn and Santamaria (ZPHY **C48**, 445 (1990)) gives 0.87 ± 0.27 $^{+0.05}_{-0.06}$, and with the model of of Isgur *et al.* (PR **D39**,1357 (1989)) they obtain 1.10 ± 0.31 $^{+0.13}_{-0.14}$.

ξ^τ (all hadronic modes) PARAMETER

$(V-A)$ theory predicts $\xi^\tau = 1$.

VALUE	EVTS	DOCUMENT ID		TECN	COMMENT
0.995 ± 0.007 OUR FIT					
0.997 ± 0.007 OUR AVERAGE					
0.992 ± 0.007 ± 0.008	102k	[272] HEISTER	01E	ALEP	1991–1995 LEP runs
0.997 ± 0.027 ± 0.011	39k	[273] ABREU	00L	DLPH	1992–1995 runs
1.02 ± 0.13 ± 0.03	17.2k	[274] ASNER	00	CLEO	$E^{ee}_{\rm cm}$ = 10.6 GeV
1.032 ± 0.031	37k	[275] ACCIARRI	98R	L3	1991–1995 LEP runs
0.93 ± 0.10 ± 0.04		ABE	97O	SLD	1993–1995 SLC runs
1.29 ± 0.26 ± 0.11	7.4k	[276] ACKERSTAFF	97R	OPAL	1992–1994 LEP runs
0.995 ± 0.010 ± 0.003	66k	[277] ALEXANDER	97F	CLEO	$E^{ee}_{\rm cm}$ = 10.6 GeV
1.03 ± 0.06 ± 0.04	2.0k	[278] COAN	97	CLEO	$E^{ee}_{\rm cm}$ = 10.6 GeV
1.017 ± 0.039		[279] ALBRECHT	95C	ARG	$E^{ee}_{\rm cm}$ = 9.5–10.6 GeV
1.25 ± 0.23 $^{+0.15}_{-0.08}$	7.5k	[280] ALBRECHT	93C	ARG	$E^{ee}_{\rm cm}$ = 9.4–10.6 GeV
• • • We do not use the following data for averages, fits, limits, etc. • • •					
0.970 ± 0.053 ± 0.011	14k	[281] ACCIARRI	96H	L3	Repl. by ACCIARRI 98R
1.08 $^{+0.46}_{-0.41}$ $^{+0.14}_{-0.25}$	2.6k	[282] AKERS	95P	OPAL	Repl. by ACKERSTAFF 97R
1.006 ± 0.032 ± 0.019		[283] BUSKULIC	95D	ALEP	Repl. by HEISTER 01E
1.022 ± 0.028 ± 0.030	1.7k	[284] ALBRECHT	94E	ARG	$E^{ee}_{\rm cm}$ = 9.4–10.6 GeV
0.99 ± 0.07 ± 0.04		[285] BUSKULIC	94D	ALEP	1990+1991 LEP run

[272] HEISTER 01E quote 0.992 ± 0.007 ± 0.006 ± 0.005 where the errors are statistical, systematic, and an uncertainty due to the final state model. We combine the systematic error and model uncertainty. They use $\tau \to \pi\nu_\tau$, $\tau \to K\nu_\tau$, $\tau \to \rho\nu_\tau$, and $\tau \to a_1\nu_\tau$ decays.

[273] ABREU 00L use $\tau^- \to h^- \geq 0\pi^0\nu_\tau$ decays.

[274] ASNER 00 use $\tau^- \to \pi^- 2\pi^0\nu_\tau$ decays.

[275] ACCIARRI 98R use $\tau \to \pi\nu_\tau$, $\tau \to K\nu_\tau$, and $\tau \to \rho\nu_\tau$ decays.

[276] ACKERSTAFF 97R use $\tau \to a_1\nu_\tau$ decays.

[277] ALEXANDER 97F use $\tau \to \rho\nu_\tau$ decays.

[278] COAN 97 use h^+h^- energy correlations.

[279] Combined fit to ARGUS tau decay parameter measurements in ALBRECHT 95C, ALBRECHT 93G, and ALBRECHT 94E.

[280] Uses $\tau \to a_1\nu_\tau$ decays. Replaced by ALBRECHT 95C.

[281] ACCIARRI 96H use $\tau \to \pi\nu_\tau$, $\tau \to K\nu_\tau$, and $\tau \to \rho\nu_\tau$ decays.

[282] AKERS 95P use $\tau \to a_1\nu_\tau$ decays.

[283] BUSKULIC 95D use $\tau \to \pi\nu_\tau$, $\tau \to \rho\nu_\tau$, and $\tau \to a_1\nu_\tau$ decays.

[284] ALBRECHT 94E measure the square of this quantity and use the sign determined by ALBRECHT 90I to obtain the quoted result. Uses $\tau \to a_1\nu_\tau$ decays. Replaced by ALBRECHT 95C.

[285] BUSKULIC 94D use $\tau \to \pi\nu_\tau$ and $\tau \to \rho\nu_\tau$ decays. Superseded by BUSKULIC 95D.

τ REFERENCES

ABBIENDI 03 PL B551 35 G. Abbiendi *et al.* (OPAL Collab.)
BRIERE 03 PRL 90 181802 R. A. Briere *et al.* (CLEO Collab.)
HEISTER 03F EPJ C30 291 A. Heister *et al.* (ALEPH Collab.)
INAMI 03 PL B551 16 K. Inami *et al.* (BELLE Collab.)
CHEN 02C PR D66 071101R S. Chen *et al.* (CLEO Collab.)
ABBIENDI 01J EPJ C19 653 G. Abbiendi *et al.* (OPAL Collab.)
ABREU 01M EPJ C20 617 P. Abreu *et al.* (DELPHI Collab.)
ACCIARRI 01F PL B507 47 M. Acciarri *et al.* (L3 Collab.)
ACHARD 01D PL B519 189 P. Achard *et al.* (L3 Collab.)
ANASTASSOV 01 PRL 86 4467 A. Anastassov *et al.* (CLEO Collab.)
HEISTER 01E EPJ C22 217 A. Heister *et al.* (ALEPH Collab.)
ABBIENDI 00A PL B492 23 G. Abbiendi *et al.* (OPAL Collab.)
ABBIENDI 00C EPJ C13 213 G. Abbiendi *et al.* (OPAL Collab.)
ABBIENDI 00D EPJ C13 197 G. Abbiendi *et al.* (OPAL Collab.)
ABREU 00L EPJ C16 229 P. Abreu *et al.* (DELPHI Collab.)
ACCIARRI 00B PL B479 67 M. Acciarri *et al.* (L3 Collab.)
AHMED 00 PR D61 071101R S. Ahmed *et al.* (CLEO Collab.)
ALBRECHT 00 PL B485 37 H. Albrecht *et al.* (ARGUS Collab.)
ASNER 00 PR D61 012002 D.M. Asner *et al.* (CLEO Collab.)
ASNER 00B PR D62 072006 D.M. Asner *et al.* (CLEO Collab.)
BERGFELD 00 PRL 84 830 T. Bergfeld *et al.* (CLEO Collab.)
BROWDER 00 PR D61 052004 T.E. Browder *et al.* (CLEO Collab.)
EDWARDS 00A PR D61 072003 K.W. Edwards *et al.* (CLEO Collab.)
GONZALEZ-S... 00 NP B582 3 G.A. Gonzalez-Sprinberg *et al.*
ABBIENDI 99H PL B447 134 G. Abbiendi *et al.* (OPAL Collab.)
ABREU 99X EPJ C10 201 P. Abreu *et al.* (DELPHI Collab.)
ACKERSTAFF 99D EPJ C8 3 K. Ackerstaff *et al.* (OPAL Collab.)
ACKERSTAFF 99E EPJ C8 183 K. Ackerstaff *et al.* (OPAL Collab.)
BARATE 99K EPJ C10 1 R. Barate *et al.* (ALEPH Collab.)
BARATE 99R EPJ C11 599 R. Barate *et al.* (ALEPH Collab.)
BISHAI 99 PRL 82 281 M. Bishai *et al.* (CLEO Collab.)
GODANG 99 PR D59 091303 R. Godang *et al.* (CLEO Collab.)
RICHICHI 99 PR D60 112002 S.J. Richichi *et al.* (CLEO Collab.)
ACCIARRI 98C PL B426 207 M. Acciarri *et al.* (L3 Collab.)
ACCIARRI 98E PL B434 169 M. Aciarri *et al.* (L3 Collab.)
ACCIARRI 98R PL B438 405 M. Acciarri *et al.* (L3 Collab.)
ACKERSTAFF 98M EPJ C4 193 K. Ackerstaff *et al.* (OPAL Collab.)
ACKERSTAFF 98N PL B431 188 K. Ackerstaff *et al.* (OPAL Collab.)
ALBRECHT 98 PL B431 179 H. Albrecht *et al.* (ARGUS Collab.)
BARATE 98 EPJ C1 65 R. Barate *et al.* (ALEPH Collab.)
BARATE 98E EPJ C4 29 R. Barate *et al.* (ALEPH Collab.)
BLISS 98 PR D57 5903 D.W. Bliss *et al.* (CLEO Collab.)
ABE 97O PRL 78 4691 K. Abe *et al.* (SLD Collab.)
ACKERSTAFF 97J PL B404 213 K. Ackerstaff *et al.* (OPAL Collab.)
ACKERSTAFF 97L ZPHY C74 403 K. Ackerstaff *et al.* (OPAL Collab.)
ACKERSTAFF 97R ZPHY C75 593 K. Ackerstaff *et al.* (OPAL Collab.)
ALEXANDER 97F PR D56 5320 J.P. Alexander *et al.* (CLEO Collab.)
AMMAR 97B PRL 78 4686 R. Ammar *et al.* (CLEO Collab.)
ANASTASSOV 97 PR D55 2559 A. Anastassov *et al.* (CLEO Collab.)
Also 98B PR D58 119903 (erratum) A. Anastassov *et al.* (CLEO Collab.)
ANDERSON 97 PRL 79 3814 S. Anderson *et al.* (CLEO Collab.)
AVERY 97 PR D55 R1119 P. Avery *et al.* (CLEO Collab.)
BARATE 97I ZPHY C74 387 R. Barate *et al.* (ALEPH Collab.)
BARATE 97R PL B414 362 R. Barate *et al.* (ALEPH Collab.)
BERGFELD 97 PRL 79 2406 T. Bergfeld *et al.* (CLEO Collab.)
BONVICINI 97 PRL 79 1221 G. Bonvicini *et al.* (CLEO Collab.)
BUSKULIC 97C ZPHY C74 263 D. Buskulic *et al.* (ALEPH Collab.)
COAN 97 PR D55 7291 T.E. Coan *et al.* (CLEO Collab.)
EDWARDS 97 PR D55 R3919 K.W. Edwards *et al.* (CLEO Collab.)
EDWARDS 97B PR D56 R5297 K.W. Edwards *et al.* (CLEO Collab.)
ESCRIBANO 97 PL B395 369 R. Escribano, E. Masso (BARC, PARIT)
ABREU 96B PL B365 448 P. Abreu *et al.* (DELPHI Collab.)
ACCIARRI 96H PL B377 313 M. Acciarri *et al.* (L3 Collab.)
ACCIARRI 96K PL B389 187 M. Acciarri *et al.* (L3 Collab.)
ALAM 96 PRL 76 2637 M.S. Alam *et al.* (CLEO Collab.)
ALBRECHT 96E PRPL 276 223 H. Albrecht *et al.* (ARGUS Collab.)
ALEXANDER 96D PL B369 163 G. Alexander *et al.* (OPAL Collab.)
ALEXANDER 96E PL B374 341 G. Alexander *et al.* (OPAL Collab.)
ALEXANDER 96S PL B388 437 G. Alexander *et al.* (OPAL Collab.)
BAI 96 PR D53 20 J.Z. Bai *et al.* (BES Collab.)
BALEST 96 PL B388 402 R. Balest *et al.* (CLEO Collab.)
BARTELT 96 PRL 76 4119 J.E. Bartelt *et al.* (CLEO Collab.)
BUSKULIC 96 ZPHY C70 579 D. Buskulic *et al.* (ALEPH Collab.)
BUSKULIC 96C ZPHY C70 561 D. Buskulic *et al.* (ALEPH Collab.)
COAN 96 PR D53 6037 T.E. Coan *et al.* (CLEO Collab.)
ABE 95Y PR D52 4828 K. Abe *et al.* (SLD Collab.)
ABREU 95T PL B357 715 P. Abreu *et al.* (DELPHI Collab.)
ABREU 95U PL B359 411 P. Abreu *et al.* (DELPHI Collab.)
ACCIARRI 95 PL B345 93 M. Acciarri *et al.* (L3 Collab.)
ACCIARRI 95F PL B352 487 M. Acciarri *et al.* (L3 Collab.)
AKERS 95F ZPHY C66 31 R. Akers *et al.* (OPAL Collab.)
AKERS 95I ZPHY C66 543 R. Akers *et al.* (OPAL Collab.)
AKERS 95P ZPHY C67 45 R. Akers *et al.* (OPAL Collab.)
AKERS 95Y ZPHY C68 555 R. Akers *et al.* (OPAL Collab.)
ALBRECHT 95 PL B341 441 H. Albrecht *et al.* (ARGUS Collab.)
ALBRECHT 95C PL B349 576 H. Albrecht *et al.* (ARGUS Collab.)
ALBRECHT 95G ZPHY C68 25 H. Albrecht *et al.* (ARGUS Collab.)
ALBRECHT 95H ZPHY C68 215 H. Albrecht *et al.* (ARGUS Collab.)
BALEST 95C PRL 75 3809 R. Balest *et al.* (CLEO Collab.)
BERNABEU 95 NP B436 474 J. Bernabeu *et al.*
BUSKULIC 95C PL B346 371 D. Buskulic *et al.* (ALEPH Collab.)
BUSKULIC 95D PL B346 379 D. Buskulic *et al.* (ALEPH Collab.)
Also 95P PL B363 265 erratum D. Buskulic *et al.* (ALEPH Collab.)
ABREU 94K PL B334 435 P. Abreu *et al.* (DELPHI Collab.)
AKERS 94E PL B328 207 R. Akers *et al.* (OPAL Collab.)
AKERS 94G PL B339 278 R. Akers *et al.* (OPAL Collab.)
ALBRECHT 94E PL B337 383 H. Albrecht *et al.* (ARGUS Collab.)
ARTUSO 94 PRL 72 3762 M. Artuso *et al.* (CLEO Collab.)
BARTELT 94 PRL 73 1890 J.E. Bartelt *et al.* (CLEO Collab.)
BATTLE 94 PRL 73 1079 M. Battle *et al.* (CLEO Collab.)
BAUER 94 PR D50 R13 D.A. Bauer *et al.* (TPC/2gamma Collab.)
BUSKULIC 94D PL B321 168 D. Buskulic *et al.* (ALEPH Collab.)
BUSKULIC 94E PL B332 209 D. Buskulic *et al.* (ALEPH Collab.)
BUSKULIC 94F PL B332 219 D. Buskulic *et al.* (ALEPH Collab.)
GIBAUT 94B PRL 73 934 D. Gibaut *et al.* (CLEO Collab.)
ADRIANI 93M PRPL 236 1 O. Adriani *et al.* (L3 Collab.)
ALBRECHT 93C ZPHY C58 61 H. Albrecht *et al.* (ARGUS Collab.)
ALBRECHT 93G PL B316 608 H. Albrecht *et al.* (ARGUS Collab.)
BALEST 93 PR D47 R3671 R. Balest *et al.* (CLEO Collab.)
BEAN 93 PRL 70 138 A. Bean *et al.* (CLEO Collab.)
BORTOLETTO 93 PRL 71 1791 D. Bortoletto *et al.* (CLEO Collab.)
ESCRIBANO 93 PL B301 419 R. Escribano, E. Masso (BARC)
PROCARIO 93 PRL 70 1207 M. Procario *et al.* (CLEO Collab.)
ABREU 92N ZPHY C55 555 P. Abreu *et al.* (DELPHI Collab.)
ACTON 92F PL B281 405 D.P. Acton *et al.* (OPAL Collab.)
ACTON 92H PL B288 373 P.D. Acton *et al.* (OPAL Collab.)
AKERIB 92 PRL 69 3610 D.S. Akerib *et al.* (CLEO Collab.)
Also 93B PRL 71 3395 (erratum) D.S. Akerib *et al.* (CLEO Collab.)
ALBRECHT 92D ZPHY C53 367 H. Albrecht *et al.* (ARGUS Collab.)
ALBRECHT 92K ZPHY C55 179 H. Albrecht *et al.* (ARGUS Collab.)
ALBRECHT 92M PL B292 221 H. Albrecht *et al.* (ARGUS Collab.)
ALBRECHT 92Q ZPHY C56 339 H. Albrecht *et al.* (ARGUS Collab.)
AMMAR 92 PR D45 3976 R. Ammar *et al.* (CLEO Collab.)
ARTUSO 92 PRL 69 3278 M. Artuso *et al.* (CLEO Collab.)
BAI 92 PRL 69 3021 J.Z. Bai *et al.* (BES Collab.)
BATTLE 92 PL B291 488 M. Battle *et al.* (CLEO Collab.)
BUSKULIC 92J PL B297 459 D. Buskulic *et al.* (ALEPH Collab.)
DECAMP 92C ZPHY C54 211 D. Decamp *et al.* (ALEPH Collab.)
ADEVA 91F PL B265 451 B. Adeva *et al.* (L3 Collab.)
ALBRECHT 91D PL B260 259 H. Albrecht *et al.* (ARGUS Collab.)
ALEXANDER 91D PL B266 201 G. Alexander *et al.* (OPAL Collab.)
ANTREASYAN 91 PL B259 216 D. Antreasyan *et al.* (Crystal Ball Collab.)
GRIFOLS 91 PL B255 611 J.A. Grifols, A. Mendez (BARC)
SAMUEL 91B PRL 67 668 M.A. Samuel, G.W. Li, R. Mendel (OKSU, WONT)
Also 92B PRL 69 995 M.A. Samuel, G.W. Li, R. Mendel (OKSU, WONT)
Erratum.
ABACHI 90 PR D41 1414 S. Abachi *et al.* (HRS Collab.)
ALBRECHT 90E PL B246 278 H. Albrecht *et al.* (ARGUS Collab.)
ALBRECHT 90I PL B250 164 H. Albrecht *et al.* (ARGUS Collab.)
BEHREND 90 ZPHY C46 537 H.J. Behrend *et al.* (CELLO Collab.)
BOWCOCK 90 PR D41 805 T.J.V. Bowcock *et al.* (CLEO Collab.)
DELAGUILA 90 PL B252 116 F. del Aguila, M. Sher (BARC, WILL)
GOLDBERG 90 PL B251 223 M. Goldberg *et al.* (CLEO Collab.)
WU 90 PR D41 2339 D.Y. Wu *et al.* (Mark II Collab.)
ABACHI 89B PR D40 902 S. Abachi *et al.* (HRS Collab.)
BEHREND 89B PL B222 163 H.J. Behrend *et al.* (CELLO Collab.)
JANSSEN 89 PL B228 273 H. Janssen *et al.* (Crystal Ball Collab.)
KLEINWORT 89 ZPHY C42 7 C. Kleinwort *et al.* (JADE Collab.)
ADEVA 88 PR D38 2665 B. Adeva *et al.* (Mark-J Collab.)
ALBRECHT 88B PL B202 149 H. Albrecht *et al.* (ARGUS Collab.)
ALBRECHT 88L ZPHY C41 1 H. Albrecht *et al.* (ARGUS Collab.)
ALBRECHT 88M ZPHY C41 405 H. Albrecht *et al.* (ARGUS Collab.)
AMIDEI 88 PR D37 1750 D. Amidei *et al.* (Mark II Collab.)
BEHREND 88 PL B200 226 H.J. Behrend *et al.* (CELLO Collab.)
BRAUNSCH... 88C ZPHY C39 331 W. Braunschweig *et al.* (TASSO Collab.)
KEH 88 PL B212 123 S. Keh *et al.* (Crystal Ball Collab.)
TSCHIRHART 88 PL B205 407 R. Tschirhart *et al.* (HRS Collab.)
ABACHI 87B PL B197 291 S. Abachi *et al.* (HRS Collab.)
ABACHI 87C PRL 59 2519 S. Abachi *et al.* (HRS Collab.)
ADLER 87B PRL 59 1527 J. Adler *et al.* (Mark III Collab.)
AIHARA 87B PR D35 1553 H. Aihara *et al.* (TPC Collab.)
AIHARA 87C PRL 59 751 H. Aihara *et al.* (TPC Collab.)
ALBRECHT 87L PL B185 223 H. Albrecht *et al.* (ARGUS Collab.)
ALBRECHT 87P PL B199 580 H. Albrecht *et al.* (ARGUS Collab.)
BAND 87 PL B198 297 H.R. Band *et al.* (MAC Collab.)
BAND 87B PRL 59 415 H.R. Band *et al.* (MAC Collab.)
BARINGER 87 PRL 59 1993 P. Baringer *et al.* (CLEO Collab.)
BEBEK 87C PR D36 690 C. Bebek *et al.* (CLEO Collab.)
BURCHAT 87 PR D35 27 P.R. Burchat *et al.* (Mark II Collab.)
BYLSMA 87 PR D35 2269 B.G. Bylsma *et al.* (HRS Collab.)
COFFMAN 87 PR D36 2185 D.M. Coffman *et al.* (Mark III Collab.)
DERRICK 87 PL B189 260 M. Derrick *et al.* (HRS Collab.)
FORD 87 PR D35 408 W.T. Ford *et al.* (MAC Collab.)
FORD 87B PR D36 1971 W.T. Ford *et al.* (MAC Collab.)
GAN 87 PRL 59 411 K.K. Gan *et al.* (Mark II Collab.)
GAN 87B PL B197 561 K.K. Gan *et al.* (Mark II Collab.)
AIHARA 86E PRL 57 1836 H. Aihara *et al.* (TPC Collab.)
BARTEL 86D PL B182 216 W. Bartel *et al.* (JADE Collab.)
PDG 86 PL 170B M. Aguilar-Benitez *et al.* (CERN, CIT+)

RUCKSTUHL	86	PRL 56 2132	W. Ruckstuhl *et al.*	(DELCO Collab.)
SCHMIDKE	86	PRL 57 527	W.B. Schmidke *et al.*	(Mark II Collab.)
YELTON	86	PRL 56 812	J.M. Yelton *et al.*	(Mark II Collab.)
ALTHOFF	85	ZPHY C26 521	M. Althoff *et al.*	(TASSO Collab.)
ASH	85B	PRL 55 2118	W.W. Ash *et al.*	(MAC Collab.)
BALTRUSAIT...	85	PRL 55 1842	R.M. Baltrusaitis *et al.*	(Mark III Collab.)
BARTEL	85F	PL 161B 188	W. Bartel *et al.*	(JADE Collab.)
BEHRENDS	85	PR D32 2468	S. Behrends *et al.*	(CLEO Collab.)
BELTRAMI	85	PRL 54 1775	I. Beltrami *et al.*	(HRS Collab.)
BERGER	85	ZPHY C28 1	C. Berger *et al.*	(PLUTO Collab.)
BURCHAT	85	PRL 54 2489	P.R. Burchat *et al.*	(Mark II Collab.)
FERNANDEZ	85	PRL 54 1624	E. Fernandez *et al.*	(MAC Collab.)
MILLS	85	PRL 54 624	G.B. Mills *et al.*	(DELCO Collab.)
AIHARA	84C	PR D30 2436	H. Aihara *et al.*	(TPC Collab.)
BEHREND	84	ZPHY C23 103	H.J. Behrend *et al.*	(CELLO Collab.)
MILLS	84	PRL 52 1944	G.B. Mills *et al.*	(DELCO Collab.)
BEHREND	83C	PL 127B 270	H.J. Behrend *et al.*	(CELLO Collab.)
SILVERMAN	83	PR D27 1196	D.J. Silverman, G.L. Shaw	(UCI)
BEHREND	82	PL 114B 282	H.J. Behrend *et al.*	(CELLO Collab.)
BLOCKER	82B	PRL 48 1586	C.A. Blocker *et al.*	(Mark II Collab.)
BLOCKER	82D	PL 109B 119	C.A. Blocker *et al.*	(Mark II Collab.) J
FELDMAN	82	PRL 48 66	G.J. Feldman *et al.*	(Mark II Collab.)
HAYES	82	PR D25 2869	K.G. Hayes *et al.*	(Mark II Collab.)
BERGER	81B	PL 99B 489	C. Berger *et al.*	(PLUTO Collab.)
DORFAN	81	PRL 46 215	J.M. Dorfan *et al.*	(Mark II Collab.)
BRANDELIK	80	PL 92B 199	R. Brandelik *et al.*	(TASSO Collab.)
ZHOLENTZ	80	PL 96B 214	A.A. Zholents *et al.*	(NOVO)
Also	81	SJNP 34 814 Translated from YAF 34 1471.	A.A. Zholents *et al.*	(NOVO)
BACINO	79B	PRL 42 749	W.J. Bacino *et al.*	(DELCO Collab.)
KIRKBY	79	SLAC-PUB-2419 Batavia Lepton Photon Conference.	J. Kirkby	(SLAC) J
BACINO	78B	PRL 41 13	W.J. Bacino *et al.*	(DELCO Collab.) J
Also	78	Tokyo Conf. 249	J. Kirz	(STON)
Also	80	PL 96B 214	A.A. Zholents *et al.*	(NOVO)
BRANDELIK	78	PL 73B 109	R. Brandelik *et al.*	(DASP Collab.) J
FELDMAN	78	Tokyo Conf. 777	G.J. Feldman	(SLAC) J
JAROS	78	PRL 40 1120	J. Jaros *et al.*	(SLAC, LBL, NWES, HAWA)
PERL	75	PRL 35 1489	M.L. Perl *et al.*	(LBL, SLAC)

OTHER RELATED PAPERS

RAHAL-CAL...	98	IJMP A13 695	G. Rahal-Callot	(ETH)
GENTILE	96	PRPL 274 287	S. Gentile, M. Pohl	(ROMAI, ETH)
WEINSTEIN	93	ARNPS 43 457	A.J. Weinstein, R. Stroynowski	(CIT, SMU)
PERL	92	RPP 55 653	M.L. Perl	(SLAC)
PICH	90	MPL A5 1995	A. Pich	(VALE)
BARISH	88	PRPL 157 1	B.C. Barish, R. Stroynowski	(CIT)
GAN	88	IJMP A3 531	K.K. Gan, M.L. Perl	(SLAC)
HAYES	88	PR D38 3351	K.G. Hayes, M.L. Perl	(SLAC)
PERL	80	ARNPS 30 299	M.L. Perl	(SLAC)

Heavy Charged Lepton Searches

Charged Heavy Lepton MASS LIMITS

Sequential Charged Heavy Lepton ($L^{\pm}$) MASS LIMITS

These experiments assumed that a fourth generation $L^{\pm}$ decayed to a fourth generation ν_L (or L^0) where ν_L was stable, or that $L^{\pm}$ decays to a light ν_ℓ via mixing.

See the "Quark and Lepton Compositeness, Searches for" Listings for limits on radiatively decaying excited leptons, *i.e.* $\ell^* \to \ell\gamma$. See the "WIMPs and other Particle Searches" section for heavy charged particle search limits in which the charged particle could be a lepton.

VALUE (GeV)	*CL%*	*DOCUMENT ID*		*TECN*	*COMMENT*
>100.8	95	ACHARD	01B	L3	Decay to νW
>101.9	95	ACHARD	01B	L3	$m_L - m_{L^0} > 15$ GeV
• • • We do not use the following data for averages, fits, limits, etc. • • •					
> 81.5	95	ACKERSTAFF	98C	OPAL	Assumed $m_{L^\pm} - m_{L^0} > 8.4$ GeV
> 80.2	95	ACKERSTAFF	98C	OPAL	$m_{L^0} > m_{L^\pm}$ and $L^\pm \to \nu W$
< 48 or > 61	95	[1] ACCIARRI	96G	L3	
> 63.9	95	ALEXANDER	96P	OPAL	Decay to massless ν's
> 63.5	95	BUSKULIC	96S	ALEP	$m_L - m_{L^0} > 7$ GeV
> 65	95	BUSKULIC	96S	ALEP	Decay to massless ν's
none 10–225		[2] AHMED	94	CNTR	H1 Collab. at HERA
none 12.6–29.6	95	KIM	91B	AMY	Massless ν assumed
> 44.3	95	AKRAWY	90G	OPAL	
none 0.5–10	95	[3] RILES	90	MRK2	For $(m_{L^0}$-$m_{L^0})$> 0.25–0.4GeV
> 8		[4] STOKER	89	MRK2	For $(m_{L^+} - m_{L^0}) = 0.4$ GeV
> 12		[4] STOKER	89	MRK2	For m_{L^0}=0.9 GeV
none 18.4–27.6	95	[5] ABE	88	VNS	
> 25.5	95	[6] ADACHI	88B	TOPZ	
none 1.5–22.0	95	BEHREND	88C	CELL	
> 41	90	[7] ALBAJAR	87B	UA1	
> 22.5	95	[8] ADEVA	85	MRKJ	
> 18.0	95	[9] BARTEL	83	JADE	
none 4–14.5	95	[10] BERGER	81B	PLUT	
> 15.5	95	[11] BRANDELIK	81	TASS	
> 13.		[12] AZIMOV	80		
> 16.	95	[13] BARBER	80B	CNTR	
> 0.490		[14] ROTHE	69	RVUE	

[1] ACCIARRI 96G assumes LEP result that the associated neutral heavy lepton mass > 40 GeV.

[2] The AHMED 94 limits are from a search for neutral and charged sequential heavy leptons at HERA via the decay channels $L^- \to e\gamma$, $L^- \to \nu W^-$, $L^- \to eZ$; and $L^0 \to \nu\gamma$, $L^0 \to e^- W^+$, $L^- \to \nu Z$, where the W decays to $\ell\nu_\ell$, or to jets, and Z decays to $\ell^+\ell^-$ or jets.

[3] RILES 90 limits were the result of a special analysis of the data in the case where the mass difference $m_{L^-} - m_{L^0}$ was allowed to be quite small, where L^0 denotes the neutrino into which the sequential charged lepton decays. With a slightly reduced $m_{L^\pm}$ range, the mass difference extends to about 4 GeV.

[4] STOKER 89 (Mark II at PEP) gives bounds on charged heavy lepton (L^+) mass for the generalized case in which the corresponding neutral heavy lepton (L^0) in the SU(2) doublet is not of negligible mass.

[5] ABE 88 search for L^+ and L^- → hadrons looking for acoplanar jets. The bound is valid for $m_\nu < 10$ GeV.

[6] ADACHI 88B search for hadronic decays giving acoplanar events with large missing energy. $E_{\rm cm}{}^{ee} = 52$ GeV.

[7] Assumes associated neutrino is approximately massless.

[8] ADEVA 85 analyze one-isolated-muon data and sensitive to τ <10 nanosec. Assume B(lepton) = 0.30. $E_{\rm cm} = 40$–47 GeV.

[9] BARTEL 83 limit is from PETRA e^+e^- experiment with average $E_{\rm cm} = 34.2$ GeV.

[10] BERGER 81B is DESY DORIS and PETRA experiment. Looking for $e^+e^- \to L^+L^-$.

[11] BRANDELIK 81 is DESY-PETRA experiment. Looking for $e^+e^- \to L^+L^-$.

[12] AZIMOV 80 estimated probabilities for $M + N$ type events in $e^+e^- \to L^+L^-$ deducing semi-hadronic decay multiplicities of L from e^+e^- annihilation data at $E_{\rm cm} = (2/3)m_L$. Obtained above limit comparing these with e^+e^- data (BRANDELIK 80).

[13] BARBER 80B looked for $e^+e^- \to L^+L^-$, $L \to \nu_L^+ X$ with MARK-J at DESY-PETRA.

[14] ROTHE 69 examines previous data on μ pair production and π and K decays.

Stable Charged Heavy Lepton ($L^{\pm}$) MASS LIMITS

VALUE (GeV)	*CL%*	*DOCUMENT ID*		*TECN*
>102.6	95	ACHARD	01B	L3
• • • We do not use the following data for averages, fits, limits, etc. • • •				
> 28.2	95	[15] ADACHI	90C	TOPZ
none 18.5–42.8	95	AKRAWY	90O	OPAL
> 26.5	95	DECAMP	90F	ALEP
none m_μ–36.3	95	SODERSTROM	90	MRK2

[15] ADACHI 90C put lower limits on the mass of stable charged particles with electric charge Q satisfying $2/3 < Q/e < 4/3$ and with spin 0 or 1/2. We list here the special case for a stable charged heavy lepton.

Charged Long-Lived Heavy Lepton MASS LIMITS

VALUE (GeV)	*CL%*	*EVTS*	*DOCUMENT ID*		*TECN*	*CHG*	*COMMENT*
• • • We do not use the following data for averages, fits, limits, etc. • • •							
>102.0	95		ABBIENDI	03L	OPAL		pair produced in e^+e^-
> 0.1		0	[16] ANSORGE	73B	HBC	–	Long-lived
none 0.55–4.5			[17] BUSHNIN	73	CNTR	–	Long-lived
none 0.2–0.92			[18] BARNA	68	CNTR	–	Long-lived
none 0.97–1.03			[18] BARNA	68	CNTR	–	Long-lived

[16] ANSORGE 73B looks for electron pair production and electron-like Bremsstrahlung.

[17] BUSHNIN 73 is SERPUKHOV 70 GeV p experiment. Masses assume mean life above 7×10^{-10} and 3×10^{-8} respectively. Calculated from cross section (see "Charged Quasi-Stable Lepton Production Differential Cross Section" below) and 30 GeV muon pair production data.

[18] BARNA 68 is SLAC photoproduction experiment.

Doubly-Charged Heavy Lepton MASS LIMITS

VALUE (GeV)	*CL%*	*DOCUMENT ID*		*TECN*	*CHG*
• • • We do not use the following data for averages, fits, limits, etc. • • •					
none 1–9 GeV	90	[19] CLARK	81	SPEC	++

[19] CLARK 81 is FNAL experiment with 209 GeV muons. Bounds apply to μ_P which couples with full weak strength to muon. See also section on "Doubly-Charged Lepton Production Cross Section."

Doubly-Charged Lepton Production Cross Section (μN Scattering)

VALUE (cm^2)	*EVTS*	*DOCUMENT ID*		*TECN*	*CHG*
• • • We do not use the following data for averages, fits, limits, etc. • • •					
$<6. \times 10^{-38}$	0	[20] CLARK	81	SPEC	++

[20] CLARK 81 is FNAL experiment with 209 GeV muon. Looked for μ^+ nucleon → $\overline{\mu}_P^0$ X, $\overline{\mu}_P^0 \to \mu^+\mu^-\overline{\nu}_\mu$ and $\mu^+ n \to \mu_P^{++}$X, $\mu_P^{++} \to 2\mu^+\nu_\mu$. Above limits are for $\sigma \times$BR taken from their mass-dependence plot figure 2.

REFERENCES FOR Heavy Charged Lepton Searches

ABBIENDI	03L	PL B572 8	G. Abbiendi *et al.*	(OPAL Collab.)
ACHARD	01B	PL B517 75	P. Achard *et al.*	(L3 Collab.)
ACKERSTAFF	98C	EPJ C1 45	K. Ackerstaff *et al.*	(OPAL Collab.)
ACCIARRI	96G	PL B377 304	M. Acciarri *et al.*	(L3 Collab.)
ALEXANDER	96P	PL B385 433	G. Alexander *et al.*	(OPAL Collab.)
BUSKULIC	96S	PL B384 439	D. Buskulic *et al.*	(ALEPH Collab.)
AHMED	94	PL B340 205	T. Ahmed *et al.*	(H1 Collab.)
KIM	91B	IJMP A6 2583	G.N. Kim *et al.*	(AMY Collab.)
ADACHI	90C	PL B244 352	I. Adachi *et al.*	(TOPAZ Collab.)
AKRAWY	90G	PL B240 250	M.Z. Akrawy *et al.*	(OPAL Collab.)
AKRAWY	90O	PL B252 290	M.Z. Akrawy *et al.*	(OPAL Collab.)
DECAMP	90F	PL B236 511	D. Decamp *et al.*	(ALEPH Collab.)
RILES	90	PR D42 1	K. Riles *et al.*	(Mark II Collab.)
SODERSTROM	90	PRL 64 2980	E. Soderstrom *et al.*	(Mark II Collab.)
STOKER	89	PR D39 1811	D.P. Stoker *et al.*	(Mark II Collab.)
ABE	88	PRL 61 915	K. Abe *et al.*	(VENUS Collab.)
ADACHI	88B	PR D37 1339	I. Adachi *et al.*	(TOPAZ Collab.)
BEHREND	88C	ZPHY C41 7	H.J. Behrend *et al.*	(CELLO Collab.)
ALBAJAR	87B	PL B185 241	C. Albajar *et al.*	(UA1 Collab.)
ADEVA	85	PL 152B 439	B. Adeva *et al.*	(Mark-J Collab.)
Also	84C	PRPL 109 131	B. Adeva *et al.*	(Mark-J Collab.)
BARTEL	83	PL 123B 353	W. Bartel *et al.*	(JADE Collab.)
BERGER	81B	PL 99B 489	C. Berger *et al.*	(PLUTO Collab.)
BRANDELIK	81	PL 99B 163	R. Brandelik *et al.*	(TASSO Collab.)
CLARK	81	PRL 46 299	A.R. Clark *et al.*	(UCB, LBL, FNAL+)
Also	82	PR D25 2762	W.H. Smith *et al.*	(LBL, FNAL, PRIN)
AZIMOV	80	JETPL 32 664	Y.I. Azimov, V.A. Khoze	(PNPI)
		Translated from ZETFP 32 677.		
BARBER	80B	PRL 45 1904	D.P. Barber *et al.*	(Mark-J Collab.)
BRANDELIK	80	PL 92B 199	R. Brandelik *et al.*	(TASSO Collab.)
ANSORGE	73B	PR D7 26	R.E. Ansorge *et al.*	(CAVE)
BUSHNIN	73	NP B58 476	Y.B. Bushnin *et al.*	(SERP)
Also	72	PL 42B 136	S.V. Golovkin *et al.*	(SERP)
ROTHE	69	NP B10 241	K.W. Rothe, A.M. Wolsky	(PENN)
BARNA	68	PR 173 1391	A. Barna *et al.*	(SLAC, STAN)

OTHER RELATED PAPERS

PERL	81	SLAC-PUB-2752	M.L. Perl	(SLAC)
		Physics in Collision Conference.		

Neutrinos

OMITTED FROM SUMMARY TABLE

ELECTRON, MUON, AND TAU NEUTRINO LISTINGS

Revised July 2003 by P. Vogel (Caltech) and
A. Piepke (University of Alabama).

The following Listings concern measurements of the properties of neutrinos produced in association with $e^{\pm}$, $\mu^{\pm}$, and $\tau^{\pm}$. Nearly all of the measurements, all of which so far are upper limits, actually concern superpositions of the mass eigenstates ν_i, which are in turn related to the weak eigenstates ν_ℓ, via the neutrino mixing matrix

$$|\nu_\ell\rangle = \sum_i U_{\ell i}\,|\nu_i\rangle \quad . \tag{1}$$

In the analogous case of quark mixing via the CKM matrix, the smallness of the off-diagonal terms (small mixing angles) permits a "dominant eigenstate" approximation. Previous editions of this Review have assumed that the dominant eigenstate paradigm applies to neutrinos as well. However, the present results of neutrino oscillation searches suggest that the mixing matrix contains two large mixing angles. We can therefore no longer associate any particular state $|\nu_i\rangle$ with any particular lepton label e, μ, or τ. Nevertheless, neutrinos are produced in weak decays with a definite lepton flavor, and are typically detected by the charged current weak interaction again associated with a specific lepton flavor. The listings that follow are separated into the three associated charged lepton categories.

Measured quantities (mass-squared, magnetic moments, mean lifetimes, *etc.*) all depend upon the mixing parameters $|U_{\ell i}|^2$, but to some extent also on experimental conditions (energy resolution). Most of these observables, in particular mass-squared, cannot distinguish between Dirac and Majorana neutrinos and are unaffected by CP phases.

Direct neutrino mass measurements are usually based on the analysis of the kinematics of charged particles (leptons, pions) emitted together with neutrinos (flavor states) in various weak decays. The most sensitive neutrino mass measurement to date, involving electron type neutrinos, is based on fitting the shape of the beta spectrum. The quantity $m^{2(\mathrm{eff})}_{\nu_e} = \sum_i |U_{ei}|^2 m^2_{\nu_i}$ is determined or constrained, where the sum is over all mass eigenvalues m_{ν_i} that are too close together to be resolved experimentally. If the energy resolution is better than $\Delta m^2_{ij} \equiv m^2_{\nu_i} - m^2_{\nu_j}$, the corresponding heavier m_{ν_i} and mixing parameter could be determined by fitting the resulting spectral anomaly (step or kink).

A limit on $m^{2(\mathrm{eff})}_{\nu_e}$ implies an *upper* limit on the *minimum* value $m^2_{\nu_{\min}}$ of $m^2_{\nu_i}$, independent of the mixing parameters U_{ei}: $m^2_{\nu_{\min}} \leq m^{2(\mathrm{eff})}_{\nu_e}$. However, if and when the study of neutrino oscillations provides us with the values of *all* neutrino mass-squared differences Δm^2_{ij} and the mixing parameters $|U_{ei}|^2$, then the individual neutrino mass squares $m^2_{\nu_j} = m^{2(\mathrm{eff})}_{\nu_e} - \sum_i |U_{ei}|^2 \Delta m^2_{ij}$ can be determined. If only the $|\Delta m^2_{ij}|$ are known, a limit on $m^{(\mathrm{eff})}_{\nu_e}$ from beta decay may be used to define an *upper* limit on the *maximum* value $m_{\nu_{\max}}$ of m_{ν_i}: $m^2_{\nu_{\max}} \leq m^{2(\mathrm{eff})}_{\nu_e} + \sum_{i<j} |\Delta m^2_{ij}|$.

The analysis of the low energy beta decay of tritium yields the most stringent limit on $m^{(\mathrm{eff})}_{\nu_e}$ to date (where $m^{(\mathrm{eff})}_{\nu_e} \equiv \sqrt{m^{2(\mathrm{eff})}_{\nu_e}}$) . Unphysical negative $m^{2(\mathrm{eff})}_{\nu_e}$ fits, caused by an as yet not understood event excess near the spectrum endpoint, are sometimes encountered. In Ref. 1 two analyses which either exclude the spectral anomaly by choice of the analysis energy window or by using one of four data sets yield an acceptable $m^{2(\mathrm{eff})}_{\nu_e}$ fit and a $m^{(\mathrm{eff})}_{\nu_e}$ limit of 2.8 eV. Ref. 2 reports a $m^{(\mathrm{eff})}_{\nu_e}$ limit of 2.5 eV by introducing an *a priori* chosen parameterization of the anomalous near-endpoint events into the spectral analysis.

In analogous way, by measuring the muon momentum in the pion decay $\pi^+ \to \mu^+ + \nu_\mu$ one constrains the quantity $m^{2(\mathrm{eff})}_{\nu_\mu} = \sum_i |U_{\mu i}|^2 m^2_{\nu_i}$, where the sum is again over all m_{ν_i} that cannot be resolved experimentally. Obviously, the true $m^{2(\mathrm{eff})}_{\nu_\mu}$ cannot be larger than the *maximum* value of $m^2_{\nu_i}$. As pointed out above, this maximum could be restricted by the tritium beta decay, provided *all* neutrino mass-squared differences $|\Delta m^2_{ij}|$ are known. The most sensitive measurement is $m^{(\mathrm{eff})}_{\nu_\mu} < 170$ keV [3], more than four orders of magnitude less stringent than the tritium experiments.

Similar remarks can be made about $m^{2(\mathrm{eff})}_{\nu_\tau}$ constrained by the shape of the spectrum of decay products of the τ lepton. Again, the true $m^{2(\mathrm{eff})}_{\nu_\tau}$ cannot exceed the *maximum* $m^2_{\nu_i}$ value, which could be constrained by *both* $m^{2(\mathrm{eff})}_{\nu_e}$ and $m^{2(\mathrm{eff})}_{\nu_\mu}$ values or limits, provided the corresponding $|\Delta m^2_{ij}|$ are known. The most stringent limit on $m^{(\mathrm{eff})}_{\nu_\tau}$, 18.2 MeV [4], is yet another two orders of magnitude less sensitive than the $m^{(\mathrm{eff})}_{\nu_\mu}$ limit. The different sensitivities of the current experiments regarding $m^{(\mathrm{eff})}_{\nu_\tau}$, $m^{(\mathrm{eff})}_{\nu_\mu}$, and $m^{(\mathrm{eff})}_{\nu_e}$ are relevant, however, only if the oscillation searches, reported below, can be regarded as an reliable source of all $|\Delta m^2_{ij}|$ values.

The spread of arrival times of the neutrinos from SN1987A, coupled with the measured neutrino energies, provides a time-of-flight limit on a quantity similar to $m^{(\mathrm{eff})}_{\nu_e}$. This statement, clothed in various degrees of sophistication, has been the basis for a very large number of papers. The resulting limits, however, are no longer competitive with the limits from the tritium beta decay.

Another constraint has been obtained recently from the analysis of the cosmic microwave background anisotropy ([5]), combined with the galaxy redshift surveys and other data. The constrained quantity is the sum of the neutrino masses, $\sum_i m_{\nu_i} \leq 0.7$ eV. Discussion concerning the model dependence of this limit is continuing.

References

1. Ch. Weinheimer *et al.*, Phys. Lett. **B460**, 219 (1999); Phys. Lett. **B464**, 352 (1999) (*erratum*).
2. M. Lobashev *et al.*, Phys. Lett. **B460**, 227 (1999).
3. K.A. Assamagan *et al.*, Phys. Rev. **D53**, 6065 (1996).
4. R. Barate *et al.*, Eur. Phys. J. **C2**, 395 (1998).
5. N. Spergel *et al.*, Astrophys. J. Supp. **148**, 175 (2003).

ν_e $J = \frac{1}{2}$

The following results are obtained using neutrinos associated with e^+ or e^-. See Note on "Electron, muon, and tau neutrino listings."

$\overline{\nu}$ MASS

Those limits given below for $\overline{\nu}$ mass that come from the kinematics of $^3\mathrm{H}\beta^-\overline{\nu}$ decay are the square roots of limits for $m^{2(\mathrm{eff})}_{\nu_e}$. These are obtained from the measurements reported in the Listings for "$\overline{\nu}$ Mass Squared," below.

VALUE (eV)	CL%	DOCUMENT ID		TECN	COMMENT
< 3 OUR EVALUATION					
< 5.7	95	[1] LOREDO	02	ASTR	SN1987A
< 2.5	95	[2] LOBASHEV	99	SPEC	^{3}H β decay
< 2.8	95	[3] WEINHEIMER	99	SPEC	^{3}H β decay
• • • We do not use the following data for averages, fits, limits, etc. • • •					
< 4.35	95	[4] BELESEV	95	SPEC	^{3}H β decay
<12.4	95	[5] CHING	95	SPEC	^{3}H β decay
<92	95	[6] HIDDEMANN	95	SPEC	^{3}H β decay
$15\ ^{+32}_{-15}$		HIDDEMANN	95	SPEC	^{3}H β decay
<19.6	95	KERNAN	95	ASTR	SN 1987A
< 7.0	95	[7] STOEFFL	95	SPEC	^{3}H β decay
< 7.2	95	[8] WEINHEIMER	93	SPEC	^{3}H β decay
<11.7	95	[9] HOLZSCHUH	92B	SPEC	^{3}H β decay
<13.1	95	[10] KAWAKAMI	91	SPEC	^{3}H β decay
< 9.3	95	[11] ROBERTSON	91	SPEC	^{3}H β decay
<14	95	AVIGNONE	90	ASTR	SN 1987A
<16		SPERGEL	88	ASTR	SN 1987A
17 to 40		[12] BORIS	87	SPEC	^{3}H β decay

[1] LOREDO 02 updates LOREDO 89.

[2] LOBASHEV 99 report a new measurement which continues the work reported in BELESEV 95. This limit depends on phenomenological fit parameters used to derive their best fit to m^2_ν, making unambiguous interpretation difficult. See the footnote under "$\overline{\nu}$ Mass Squared."

[3] WEINHEIMER 99 presents two analyses which exclude the spectral anomaly and result in an acceptable m^2_ν. We report the most conservative limit, but the other (< 2.7 eV) is nearly the same. See the footnote under "$\overline{\nu}$ Mass Squared."

[4] BELESEV 95 (Moscow) use an integral electrostatic spectrometer with adiabatic magnetic collimation and a gaseous tritium sources. A fit to a normal Kurie plot above 18300–18350 eV (to avoid a low-energy anomaly) plus a monochromatic line 7–15 eV below the endpoint yields $m^2_\nu = -4.1 \pm 10.9$ eV^2, leading to this Bayesian limit.

[5] CHING 95 quotes results previously given by SUN 93; no experimental details are given. A possible explanation for consistently negative values of m^2_ν is given.

[6] HIDDEMANN 95 (Munich) experiment uses atomic tritium embedded in a metal-dioxide lattice. Bayesian limit calculated from the weighted mean $m^2_\nu = 221 \pm 4244$ eV^2 from the two runs listed below.

[7] STOEFFL 95 (LLNL) result is the Bayesian limit obtained from the m^2_ν errors given below but with m^2_ν set equal to 0. The anomalous endpoint accumulation leads to a value of m^2_ν which is negative by more than 5 standard deviations.

[8] WEINHEIMER 93 (Mainz) is a measurement of the endpoint of the tritium β spectrum using an electrostatic spectrometer with a magnetic guiding field. The source is molecular tritium frozen onto an aluminum substrate.

[9] HOLZSCHUH 92B (Zurich) result is obtained from the measurement $m^2_\nu = -24 \pm 48 \pm 61$ (1σ errors), in eV^2, using the PDG prescription for conversion to a limit in m_ν.

[10] KAWAKAMI 91 (Tokyo) experiment uses tritium-labeled arachidic acid. This result is the Bayesian limit obtained from the m^2_ν limit with the errors combined in quadrature. This was also done in ROBERTSON 91, although the authors report a different procedure.

[11] ROBERTSON 91 (LANL) experiment uses gaseous molecular tritium. The result is in strong disagreement with the earlier claims by the ITEP group [LUBIMOV 80, BORIS 87 (+ BORIS 88 erratum)] that m_ν lies between 17 and 40 eV. However, the probability of a positive m^2 is only 3% if statistical and systematic error are combined in quadrature.

[12] See also comment in BORIS 87B and erratum in BORIS 88.

$\overline{\nu}$ MASS SQUARED

Given troubling systematics which result in improbably negative estimators of $m^{2(\mathrm{eff})}_{\nu_e}$ in many experiments, we use only WEINHEIMER 99 and LOBASHEV 99 for our average, as discussed above in the Note on the "Electron, muon, and tau neutrino listings."

VALUE (eV^2)	CL%	DOCUMENT ID		TECN	COMMENT
– 2.5 ± 3.3 OUR AVERAGE					
– 1.9 ± 3.4 ± 2.2		[13] LOBASHEV	99	SPEC	^{3}H β decay
– 3.7 ± 5.3 ± 2.1		[14] WEINHEIMER	99	SPEC	^{3}H β decay
• • • We do not use the following data for averages, fits, limits, etc. • • •					
– 22 ± 4.8		[15] BELESEV	95	SPEC	^{3}H β decay
129 ±6010		[16] HIDDEMANN	95	SPEC	^{3}H β decay
313 ±5994		[16] HIDDEMANN	95	SPEC	^{3}H β decay
–130 ± 20 ±15	95	[17] STOEFFL	95	SPEC	^{3}H β decay
– 31 ± 75 ±48		[18] SUN	93	SPEC	^{3}Hβ decay
– 39 ± 34 ±15		[19] WEINHEIMER	93	SPEC	^{3}H β decay
– 24 ± 48 ±61		[20] HOLZSCHUH	92B	SPEC	^{3}H β decay
– 65 ± 85 ±65		[21] KAWAKAMI	91	SPEC	^{3}H β decay
–147 ± 68 ±41		[22] ROBERTSON	91	SPEC	^{3}H β decay

[13] LOBASHEV 99 report a new measurement which continues the work reported in BELESEV 95. The data were corrected for electron trapping effects in the source, eliminating the dependence of the fitted neutrino mass on the fit interval. The analysis assuming a pure beta spectrum yields significantly negative fitted $m^2_\nu \approx -(20\text{–}10)$ eV^2. This problem is attributed to a discrete spectral anomaly of about 6×10^{-11} intensity with a time-dependent energy of 5–15 eV below the endpoint. The data analysis accounts for this anomaly by introducing two extra phenomenological fit parameters resulting in a best fit of $m^2_\nu = -1.9 \pm 3.4 \pm 2.2$ eV^2 which is used to derive a neutrino mass limit. However, the introduction of phenomenological fit parameters which are correlated with the derived m^2_ν limit makes unambiguous interpretation of this result difficult.

[14] WEINHEIMER 99 is a continuation of the work reported in WEINHEIMER 93 . Using a lower temperature of the frozen tritium source eliminated the dewetting of the T_2 film, which introduced a dependence of the fitted neutrino mass on the fit interval in the earlier work. An indication for a spectral anomaly reported in LOBASHEV 99 has been seen, but its time dependence does not agree with LOBASHEV 99. Two analyses, which exclude the spectral anomaly either by choice of the analysis interval or by using a particular data set which does not exhibit the anomaly, result in acceptable m^2_ν fits and are used to derive the neutrino mass limit published by the authors. We list the most conservative of the two.

[15] BELESEV 95 (Moscow) use an integral electrostatic spectrometer with adiabatic magnetic collimation and a gaseous tritium sources. This value comes from a fit to a normal Kurie plot above 18300–18350 eV (to avoid a low-energy anomaly), including the effects of an apparent peak 7–15 eV below the endpoint.

[16] HIDDEMANN 95 (Munich) experiment uses atomic tritium embedded in a metal-dioxide lattice. They quote measurements from two data sets.

[17] STOEFFL 95 (LLNL) uses a gaseous source of molecular tritium. An anomalous pileup of events at the endpoint leads to the negative value for m^2_ν. The authors acknowledge that "the negative value for the best fit of m^2_ν has no physical meaning" and discuss possible explanations for this effect.

[18] SUN 93 uses a tritiated hydrocarbon source. See also CHING 95.

[19] WEINHEIMER 93 (Mainz) is a measurement of the endpoint of the tritium β spectrum using an electrostatic spectrometer with a magnetic guiding field. The source is molecular tritium frozen onto an aluminum substrate.

[20] HOLZSCHUH 92B (Zurich) source is a monolayer of tritiated hydrocarbon.

[21] KAWAKAMI 91 (Tokyo) experiment uses tritium-labeled arachidic acid.

[22] ROBERTSON 91 (LANL) experiment uses gaseous molecular tritium. The result is in strong disagreement with the earlier claims by the ITEP group [LUBIMOV 80, BORIS 87 (+ BORIS 88 erratum)] that m_ν lies between 17 and 40 eV. However, the probability of a positive m^2_ν is only 3% if statistical and systematic error are combined in quadrature.

Lepton Particle Listings

ν_e

ν MASS

These are measurement of m_ν (in contrast to $m_{\overline{\nu}}$, given above). The masses can be different for a Dirac neutrino in the absence of CPT invariance. The possible distinction between ν and $\overline{\nu}$ properties is usually ignored elsewhere in these Listings.

VALUE (eV)	CL%	DOCUMENT ID		TECN	COMMENT
< 460	68	YASUMI	94	CNTR	^{163}Ho decay
< 225	95	SPRINGER	87	CNTR	^{163}Ho decay
• • • We do not use the following data for averages, fits, limits, etc. • • •					
$< 4.5 \times 10^5$	90	CLARK	74	ASPK	$K_{\ell 3}$ decay
< 4100	67	BECK	68	CNTR	^{22}Na decay

ν CHARGE

VALUE (units: electron charge)	DOCUMENT ID		TECN	COMMENT
• • • We do not use the following data for averages, fits, limits, etc. • • •				
$< 2 \times 10^{-14}$	[23] RAFFELT	99	ASTR	Red giant luminosity
$< 6 \times 10^{-14}$	[24] RAFFELT	99	ASTR	Solar cooling
$< 2 \times 10^{-15}$	[25] BARBIELLINI	87	ASTR	SN 1987A
$< 1 \times 10^{-13}$	BERNSTEIN	63	ASTR	Solar energy losses

[23] This RAFFELT 99 limit applies to all neutrino flavors which are light enough (<5 keV) to be emitted from globular-cluster red giants.

[24] This RAFFELT 99 limit is derived from the helioseismological limit on a new energy-loss channel of the Sun, and applies to all neutrino flavors which are light enough (<1 keV) to be emitted from the sun.

[25] Precise BARBIELLINI 87 limit depends on assumptions about the intergalactic or galactic magnetic fields and about the direct distance and time through the field.

ν MEAN LIFE

Measures $\left[\sum |U_{\ell j}|^2 \, \Gamma_j\right]^{-1}$, where the sum is over mass eigenstates which cannot be resolved experimentally. In most cases the limit pertains to any decaying neutrino. See footnotes for qualifications and exceptions.

VALUE (s)	CL%	DOCUMENT ID		TECN	COMMENT
• • • We do not use the following data for averages, fits, limits, etc. • • •					
		[26] BILLER	98	ASTR	$m_\nu = 0.05$–1 eV
		[27] COWSIK	89	ASTR	$m_\nu = 1$–50 MeV
		[28] RAFFELT	89	RVUE	$\overline{\nu}$ (Dirac, Majorana)
		[29] RAFFELT	89B	ASTR	
> 278	90	[30] LOSECCO	87B	IMB	
$> 1.1 \times 10^{25}$		[31] HENRY	81	ASTR	$m_\nu = 16$–20 eV
$> 10^{22}$–10^{23}		[32] KIMBLE	81	ASTR	$m_\nu = 10$–100 eV

[26] BILLER 98 use the observed TeV γ-ray spectra to set limits on the mean life of any radiatively decaying neutrino between 0.05 and 1 eV. Curve shows $\tau_\nu/B_\gamma > 0.15 \times 10^{21}$ s at 0.05 eV, $> 1.2 \times 10^{21}$ s at 0.17 eV, $> 3 \times 10^{21}$ s at 1 eV, where B_γ is the branching ratio to photons.

[27] COWSIK 89 use observations of supernova SN 1987A to set the limit for the lifetime of a neutrino with $1 < m < 50$ MeV decaying through $\nu_H \to \nu e e$ to be $\tau > 4 \times 10^{15} \exp(-m/5 \text{ MeV})$ s.

[28] RAFFELT 89 uses KYULDJIEV 84 to obtain $\tau m^3 > 3 \times 10^{18}$ s eV^3 (based on $\overline{\nu} e^-$ cross sections). The bound is not valid if electric and magnetic transition moments are equal for Dirac neutrinos.

[29] RAFFELT 89B analyze stellar evolution and exclude the region $3 \times 10^{12} < \tau m^3 < 3 \times 10^{21}$ s eV^3.

[30] LOSECCO 87B assumes observed rate of 2.1 SNU (solar neutrino units) comes from sun while 7.0 ± 3.0 is theory.

[31] HENRY 81 uses UV flux from clusters of galaxies to find limit for radiative decay.

[32] KIMBLE 81 uses extreme UV flux limits.

ν (MEAN LIFE) / MASS

Measures $\left[\sum |U_{ej}|^2 \, \Gamma_j \, m_j\right]^{-1}$, where the sum is over mass eigenstates which cannot be resolved experimentally. For many of the ASTR papers (RAFFELT 85 excepted), the limit applies to any ν in the indicated mass range.

VALUE (s/eV)	CL%	DOCUMENT ID		TECN	COMMENT
$> 7 \times 10^9$		[33] RAFFELT	85	ASTR	
> 300	90	[34] REINES	74	CNTR	$\overline{\nu}$
• • • We do not use the following data for averages, fits, limits, etc. • • •					
$> 8.7 \times 10^{-5}$	99	[35] BANDYOPA...	03	FIT	nonradiative decay
≥ 4200	90	[36] DERBIN	02B	CNTR	Solar pp and Be ν
$> 2.8 \times 10^{-5}$	99	[37] JOSHIPURA	02B	FIT	nonradiative decay
$> 2.8 \times 10^{15}$		[38,39] BLUDMAN	92	ASTR	$m_\nu < 50$ eV
> 6.4	90	[40] KRAKAUER	91	CNTR	ν at LAMPF
$> 6.3 \times 10^{15}$		[39,41] CHUPP	89	ASTR	$m_\nu < 20$ eV
$> 1.7 \times 10^{15}$		[39] KOLB	89	ASTR	$m_\nu < 20$ eV
$> 8.3 \times 10^{14}$		[42] VONFEILIT...	88	ASTR	
> 22	68	[43] OBERAUER	87		$\overline{\nu}_R$ (Dirac)
> 38	68	[43] OBERAUER	87		$\overline{\nu}$ (Majorana)
> 59	68	[43] OBERAUER	87		$\overline{\nu}_L$ (Dirac)
> 30	68	KETOV	86	CNTR	$\overline{\nu}$ (Dirac)
> 20	68	KETOV	86	CNTR	$\overline{\nu}$ (Majorana)
$> 2 \times 10^{21}$		[44] STECKER	80	ASTR	$m_\nu = 10$–100 eV

[33] RAFFELT 85 limit is from solar x- and γ-ray fluxes. Limit depends on ν flux from pp, now established from GALLEX and SAGE to be > 0.5 of expectation.

[34] REINES 74 looked for ν of nonzero mass decaying to a neutral of lesser mass + γ. Used liquid scintillator detector near fission reactor. Finds lab lifetime 6×10^7 s or more. Above value of (mean life)/mass assumes average effective neutrino energy of 0.2 MeV. To obtain the limit 6×10^7 s REINES 74 assumed that the full $\overline{\nu}$ reactor flux could be responsible for yielding decays with photon energies in the interval 0.1 MeV – 0.5 MeV. This represents some overestimate so their lower limit is an over-estimate of the lab lifetime (VOGEL 84). If so, OBERAUER 87 may be comparable or better.

[35] The ratio of the lifetime over the mass derived by BANDYOPADHYAY 03 is for ν_2. They obtained this result using the following solar-neutrino data: total rates measured in Cl and Ga experiments, the Super-Kamiokande's zenith-angle spectra, and SNO's day and night spectra. They assumed that ν_1 is the lowest mass, stable or nearly stable neutrino state and ν_2 decays through nonradiative Majoron emission process, $\nu_2 \to \overline{\nu}_1 + J$, or through nonradiative process with all the final state particles being sterile. The best fit is obtained in the region of the LMA solution.

[36] DERBIN 02B (also BACK 03B) obtained this bound from the results of background measurements with Counting Test Facility (the prototype of the Borexino detector). The laboratory gamma spectrum is given as $dN_\gamma/d\cos\theta = (1/2)(1 + \alpha\cos\theta)$ with $\alpha = 0$ for a Majorana neutrino, and α varying to -1 to 1 for a Dirac neutrino. The listed bound is for the case of $\alpha = 0$. The most conservative bound 1.5×10^3 s eV^{-1} is obtained for the case of $\alpha = -1$.

[37] The ratio of the lifetime over the mass derived by JOSHIPURA 02B is for ν_2. They obtained this result from the total rates measured in all solar neutrino experiments. They assumed that ν_1 is the lowest mass, stable or nearly stable neutrino state and ν_2 decays through nonradiative process like Majoron emission decay, $\nu_2 \to \nu_1' + J$ where ν_1' state is sterile. The exact limit depends on the specific solution of the solar neutrino problem. The quoted limit is for the LMA solution.

[38] BLUDMAN 92 sets additional limits by this method for higher mass ranges. Cosmological limits are also obtained.

[39] Nonobservation of γ's in coincidence with ν's from SN 1987A.

[40] KRAKAUER 91 quotes the limit $\tau/m_\nu > (0.3a^2 + 9.8a + 15.9)$ s/eV, where a is a parameter describing the asymmetry in the neutrino decay defined as $dN_\gamma/d\cos\theta = (1/2)(1 + a\cos\theta)$ $a = 0$ for a Majorana neutrino, but can vary from -1 to 1 for a Dirac neutrino. The bound given by the authors is the most conservative (which applies for $a = -1$).

[41] CHUPP 89 should be multiplied by a branching ratio (about 1) and a detection efficiency (about 1/4), and pertains to radiative decay of any neutrino to a lighter or sterile neutrino.

[42] Model-dependent theoretical analysis of SN 1987A neutrinos.

[43] OBERAUER 87 bounds are from comparison of observed and expected rate of reactor neutrinos.

[44] STECKER 80 limit based on UV background; result given is $\tau > 4 \times 10^{22}$ s at $m_\nu = 20$ eV.

$|(v - c)/c|$ ($v \equiv \nu$ VELOCITY)

Expected to be zero for massless neutrino, but tests also whether photons and neutrinos have the same limiting velocity in vacuum.

VALUE (units 10^{-8})	EVTS	DOCUMENT ID		TECN	COMMENT
< 1	17	[45] STODOLSKY	88	ASTR	SN 1987A
< 0.2		[46] LONGO	87	ASTR	SN 1987A

[45] STODOLSKY 88 result based on <10 hr between $\overline{\nu}$ detection in IMB and KAMI detectors and beginning of light signal. Inclusion of the problematic 5 neutrino events from Mont Blanc (four hours later) does not change the result.

[46] LONGO 87 argues that uncertainty between light and neutrino transit times is ± 3 hr, ignoring Mont Blanc events.

ν MAGNETIC MOMENT

Must vanish for a purely chiral massless Dirac neutrino. A massive Dirac or Majorana neutrino can have a transition magnetic moment connecting one mass eigenstate to another one. The experimental limits below usually cannot distinguish between the true (diagonal, in mass) magnetic moment and a transition magnetic moment. The value of the magnetic moment for the standard SU(2)×U(1) electroweak theory extended to include massive neutrinos (see FUJIKAWA 80) is $\mu_\nu = 3eG_F m_\nu/(8\pi^2\sqrt{2}) = (3.20 \times 10^{-19}) m_\nu \mu_B$ where m_ν is in eV and $\mu_B = e\hbar/2m_e$ is the Bohr magneton. Given the upper bound $m_\nu < 3$ eV, it follows that for the extended standard electroweak theory, $\mu_\nu < 1 \times 10^{-18} \mu_B$. Current experiments are not yet challenging this limit. There is considerable controversy over the validity of many of the claimed upper limits on the magnetic moment from the astrophysical data. For example, VOLOSHIN 90 states that "in connection with the astrophysical limits on μ_ν, ... there is by now a general consensus that contrary to the initial claims (BARBIERI 88, LATTIMER 88, GOLDMAN 88, NOTZOLD 88), essentially no better than quoted limits (from previous constraints) can be derived from detection of the neutrino flux from the supernova SN1987A." See VOLOSHIN 88 and VOLOSHIN 88C.

VALUE (10^{-10} μ_B)	CL%	DOCUMENT ID		TECN	COMMENT
< 1.0	90	[47] DARAKTCH...	03		Reactor $\overline{\nu}_e$
• • • We do not use the following data for averages, fits, limits, etc. • • •					
< 5.5	90	[48] BACK	03B	CNTR	Solar pp and Be ν
< 1.3	90	[49] LI	03B	CNTR	Reactor $\overline{\nu}_e$

< 2	90	[50] GRIMUS	02	FIT	solar + reactor (Majorana ν)
< 0.01–0.04		[51] AYALA	99	ASTR	$\nu_L \to \nu_R$ in SN 1987A
< 1.5	90	[52] BEACOM	99	SKAM	ν spectrum shape
< 0.03		[53] RAFFELT	99	ASTR	Red giant luminosity
< 4		[54] RAFFELT	99	ASTR	Solar cooling
< 0.62		[55] ELMFORS	97	COSM	Depolarization in early universe plasma
< 1.9	95	[56] DERBIN	93	CNTR	Reactor $\overline{\nu}e \to \overline{\nu}e$
< 2.4	90	[57] VIDYAKIN	92	CNTR	Reactor $\overline{\nu}e \to \overline{\nu}e$
< 10.8	90	[58] KRAKAUER	90	CNTR	LAMPF $\nu e \to \nu e$
< 0.02		[59] RAFFELT	90	ASTR	Red giant luminosity
< 0.1		[60] RAFFELT	89B	ASTR	Cooling helium stars
		[61] FUKUGITA	88	COSM	Primordial magn. fields
$\leq .3$		[60] RAFFELT	88B	ASTR	He burning stars
< 0.11		[60] FUKUGITA	87	ASTR	Cooling helium stars
< 0.1–0.2		MORGAN	81	COSM	^{4}He abundance
< 0.85		BEG	78	ASTR	Stellar plasmons
< 0.6		[62] SUTHERLAND	76	ASTR	Red giants + degenerate dwarfs
< 1		BERNSTEIN	63	ASTR	Solar cooling
< 14		COWAN	57	CNTR	Reactor $\overline{\nu}$

[47] Search for non-standard $\overline{\nu}_e$-e scattering component at Bugey nuclear reactor. Full kinematical event reconstruction by use of TPC. Most stringent laboratory limit on magnetic moment.

[48] BACK 03B obtained this bound from the results of background measurements with Counting Test Facility (the prototype of the Borexino detector). Standard Solar Model flux was assumed. This μ_ν can be different from the reactor μ_ν in certain oscillation scenarios (see BEACOM 99).

[49] LI 03B used Ge detector in active shield near nuclear reactor to test for nonstandard $\overline{\nu}_e$-e scattering.

[50] GRIMUS 02 obtain stringent bounds on all Majorana neutrino transition moments from a simultaneous fit of LMA-MSW oscillation parameters and transition moments to global solar neutrino data + reactor data. Using only solar neutrino data, a 90% CL bound of $6.3 \times 10^{-10} \mu_B$ is obtained.

[51] AYALA 99 improves the limit of BARBIERI 88.

[52] BEACOM 99 obtain the limit using the shape, but not the absolute magnitude which is affected by oscillations, of the solar neutrino spectrum obtained by Superkamiokande (825 days). This μ_ν can be different from the reactor μ_ν in certain oscillation scenarios.

[53] RAFFELT 99 is an update of RAFFELT 90. This limit applies to all neutrino flavors which are light enough (< 5 keV) to be emitted from globular-cluster red giants. This limit pertains equally to electric dipole moments and magnetic transition moments, and it applies to both Dirac and Majorana neutrinos.

[54] RAFFELT 99 is essentially an update of BERNSTEIN 63, but is derived from the helioseismological limit on a new energy-loss channel of the Sun. This limit applies to all neutrino flavors which are light enough (<1 keV) to be emitted from the Sun. This limit pertains equally to electric dipole and magnetic transition moments, and it applies to both Dirac and Majorana neutrinos.

[55] ELMFORS 97 calculate the rate of depolarization in a plasma for neutrinos with a magnetic moment and use the constraints from a big-bang nucleosynthesis on additional degrees of freedom.

[56] DERBIN 93 determine the cross section for 0.6–2.0 MeV electron energy as $(1.28 \pm 0.63) \times \sigma_{weak}$. However, the (reactor on − reactor off)/(reactor off) is only $\sim 1/100$.

[57] VIDYAKIN 92 limit is from a $e\overline{\nu}_e$ elastic scattering experiment. No experimental details are given except for the cross section from which this limit is derived. Signal/noise was 1/10. The limit uses $\sin^2\theta_W = 0.23$ as input.

[58] KRAKAUER 90 experiment fully reported in ALLEN 93.

[59] RAFFELT 90 limit applies for a diagonal magnetic moment of a Dirac neutrino, or for a transition magnetic moment of a Majorana neutrino. In the latter case, the same analysis gives $< 1.4 \times 10^{-12}$. Limit at 95%CL obtained from δM_c.

[60] Significant dependence on details of stellar models.

[61] FUKUGITA 88 find magnetic dipole moments of any two neutrino species are bounded by $\mu < 10^{-16}\ [10^{-9}\ G/B_0]$ where B_0 is the present-day intergalactic field strength.

[62] We obtain above limit from SUTHERLAND 76 using their limit $f < 1/3$.

NONSTANDARD CONTRIBUTIONS TO NEUTRINO SCATTERING

We report limits on the so-called neutrino charge radius squared. While the straight-forward definition of a neutrino charge radius has been proven to be gauge-dependent and, hence, unphysical (LEE 77C), there have been recent attempts to define a physically observable neutrino charge radius (BERNABEU 00, BERNABEU 02). The issue is still controversial (FUJIKAWA 03, BERNABEU 03). A more general interpretation of the experimental results is that they are limits on certain nonstandard contributions to neutrino scattering.

VALUE (10^{-32} cm^2)	*CL%*	*DOCUMENT ID*		*TECN*	*COMMENT*
-2.97 to 4.14	90	[63] AUERBACH	01	LSND	$\nu_e e \to \nu_e e$
• • • We do not use the following data for averages, fits, limits, etc. • • •					
0.9 ± 2.7		ALLEN	93	CNTR	LAMPF $\nu e \to \nu e$
< 2.3	95	MOURAO	92	ASTR	HOME/KAM2 ν rates
< 7.3	90	[64] VIDYAKIN	92	CNTR	Reactor $\overline{\nu}e \to \overline{\nu}e$
1.1 ± 2.3		ALLEN	91	CNTR	Repl. by ALLEN 93
		[65] GRIFOLS	89B	ASTR	SN 1987A

[63] AUERBACH 01 measure $\nu_e e$ elastic scattering with LSND detector. The cross section agrees with the Standard Model expectation, including the charge and neutral current interference. The 90% CL applies to the range shown.

[64] VIDYAKIN 92 limit is from a $e\overline{\nu}$ elastic scattering experiment. No experimental details are given except for the cross section from which this limit is derived. Signal/noise was 1/10. The limit uses $\sin^2\theta_W = 0.23$ as input.

[65] GRIFOLS 89B sets a limit of $\langle r^2 \rangle < 0.2 \times 10^{-32}$ cm^2 for right-handed neutrinos.

ν_e REFERENCES

BACK	03B	PL B563 35	H.O. Back *et al.* (Borexino Collab.)
BANDYOPA...	03	PL B555 33	A. Bandyopadhyay, S. Choubey, S. Goswami (SAHA+)
BERNABEU	03	hep-ph/0303202	J. Bernabeu, J. Papavassiliou, J. Vidal
DARAKTCH...	03	PL B564 190	Z. Daraktchieva *et al.* (MUNU Collab.)
FUJIKAWA	03	hep-ph/0303188	K. Fujikawa, R. Shrock
LI	03B	PRL 90 131802	H.B. Li *et al.* (TEXONO Collab.)
BERNABEU	02	PRL 89 101802	J. Bernabeu, J. Papavassiliou, J. Vidal
Also	02B	PRL 89 229902 (erratum)	J. Bernabeu, J. Papavassiliou, J. Vidal
DERBIN	02B	JETPL 76 409	A.V. Derbin, O.Ju. Smirnov
		Translated from ZETFP 76 483.	
GRIMUS	02	NP B648 376	W. Grimus *et al.*
JOSHIPURA	02B	PR D66 113008	A.S. Joshipura, E. Masso, S. Mohanty
LOREDO	02	PR D65 063002	T.J. Loredo, D.Q. Lamb
AUERBACH	01	PR D63 112001	L.B. Auerbach *et al.* (LSND Collab.)
BERNABEU	00	PR D62 113012	J. Bernabeu *et al.*
AYALA	99	PR D59 111901	A. Ayala, J.C. D'Olivo, M. Torres
BEACOM	99	PRL 83 5222	J.F. Beacom, P. Vogel
LOBASHEV	99	PL B460 227	V.M. Lobashev *et al.*
RAFFELT	99	PRPL 320 319	G.G. Raffelt
WEINHEIMER	99	PL B460 219	Ch. Weinheimer *et al.*
BILLER	98	PRL 80 2992	S.D. Biller *et al.* (WHIPPLE Collab.)
ELMFORS	97	NP B503 3	P. Elmfors *et al.*
BELESEV	95	PL B350 263	A.I. Belesev *et al.* (INRM, KIAE)
CHING	95	UMP A10 2841	C.R. Ching *et al.* (CST, BEUT, CIAE)
HIDDEMANN	95	JPG 21 639	K.H. Hiddemann, H. Daniel, O. Schwentker (MUNT)
KERNAN	95	NP B437 243	P.J. Kernan, L.M. Krauss (CASE)
STOEFFL	95	PRL 75 3237	W. Stoeffl, D.J. Decman (LLNL)
YASUMI	94	PL B334 229	S. Yasumi *et al.* (KEK, TSUK, KYOT+)
ALLEN	93	PR D47 11	R.C. Allen *et al.* (UCI, LANL, ANL+)
DERBIN	93	JETPL 57 768	A.V. Derbin *et al.* (PNPI)
		Translated from ZETFP 57 755.	
SUN	93	CJNP 15 261	H.C. Sun *et al.* (CIAE, CST, BEUT)
WEINHEIMER	93	PL B300 210	C. Weinheimer *et al.* (MANZ)
BLUDMAN	92	PR D45 4720	S.A. Bludman (CFPA)
HOLZSCHUH	92B	PL B287 381	E. Holzschuh, M. Fritschi, W. Kundig (ZURI)
MOURAO	92	PL B285 364	A.M. Mourao, J. Pulido, J.P. Ralston (LISB, LISBT+)
VIDYAKIN	92	JETPL 55 206	G.S. Vidyakin *et al.* (KIAE)
		Translated from ZETFP 55 212.	
ALLEN	91	PR D43 R1	R.C. Allen *et al.* (UCI, LANL, UMD)
KAWAKAMI	91	PL B256 105	H. Kawakami *et al.* (INUS, TOHOK, TINT+)
KRAKAUER	91	PR D44 R6	D.A. Krakauer *et al.* (LAMPF E225 Collab.)
ROBERTSON	91	PRL 67 957	R.G.H. Robertson *et al.* (LASL, LLL)
AVIGNONE	90	PR D41 682	F.T. Avignone, J.I. Collar (SCUC)
KRAKAUER	90	PL B252 177	D.A. Krakauer *et al.* (LAMPF E225 Collab.)
RAFFELT	90	PRL 64 2856	G.G. Raffelt (MPIM)
VOLOSHIN	90	NPBPS 19 433	M. Voloshin (ITEP)
Neutrino 90 Conference			
CHUPP	89	PRL 62 505	E.L. Chupp, W.T. Vestrand, C. Reppin (UNH, MPIM)
COWSIK	89	PL B218 91	R. Cowsik, D.N. Schramm, P. Hoflich (WUSL, TATA+)
GRIFOLS	89B	PR D40 3819	J.A. Grifols, E. Masso (BARC)
KOLB	89	PRL 62 509	E.W. Kolb, M.S. Turner (CHIC, FNAL)
LOREDO	89	ANYAS 571 601	T.J. Loredo, D.Q. Lamb (CHIC)
RAFFELT	89	PR D39 2066	G.G. Raffelt (PRIN, UCB)
RAFFELT	89B	APJ 336 61	G. Raffelt, D. Dearborn, J. Silk (UCB, LLL)
BARBIERI	88	PRL 61 27	R. Barbieri, R.N. Mohapatra (PISA, UMD)
BORIS	88	PRL 61 245 erratum	S.D. Boris *et al.* (ITEP, ASCI)
FUKUGITA	88	PRL 60 879	M. Fukugita *et al.* (KYOTU, MPIM, UCB)
GOLDMAN	88	PRL 60 1789	I. Goldman *et al.* (TELA)
LATTIMER	88	PRL 61 23	J.M. Lattimer, J. Cooperstein (STON, BNL)
Also	88B	PRL 61 2633 erratum	J.M. Lattimer, J. Cooperstein (STON, BNL)
NOTZOLD	88	PR D38 1658	D. Notzold (MPIM)
RAFFELT	88B	PR D37 549	G.G. Raffelt, D.S.P. Dearborn (UCB, LLL)
SPERGEL	88	PL B200 366	D.N. Spergel, J.N. Bahcall (IAS)
STODOLSKY	88	PL B201 353	L. Stodolsky (MPIM)
VOLOSHIN	88	PL B209 360	M.B. Voloshin (ITEP)
Also	88B	JETPL 47 501	M.B. Voloshin (ITEP)
		Translated from ZETFP 47 421.	
VOLOSHIN	88C	JETPL 68 690	M.B. Voloshin (ITEP)
VONFEILIT...	88	PL B200 580	M. von Feilitzsch, L. Oberauer (MUNT)
BARBIELLINI	87	NAT 329 21	G. Barbiellini, G. Cocconi (CERN)
BORIS	87	PRL 58 2019	S.D. Boris *et al.* (ITEP, ASCI)
Also	88	PRL 61 245 erratum	S.D. Boris *et al.* (ITEP, ASCI)
BORIS	87B	JETPL 45 333	S.D. Boris *et al.* (ITEP)
		Translated from ZETFP 45 267.	
FUKUGITA	87	PR D36 3817	M. Fukugita, S. Yazaki (KYOTU, TOKY)
LONGO	87	PR D36 3276	M.J. Longo (MICH)
LOSECCO	87B	PR D35 2073	J.M. LoSecco *et al.* (IMB Collab.)
OBERAUER	87	PL B198 113	L.F. Oberauer, F. von Feilitzsch, R.L. Mossbauer
SPRINGER	87	PR A35 679	P.T. Springer *et al.* (LLNL)
KETOV	86	JETPL 44 146	S.N. Ketov *et al.* (KIAE)
		Translated from ZETFP 44 114.	
RAFFELT	85	PR D31 3002	G.G. Raffelt (MPIM)
KYULDJIEV	84	NP B243 387	A.V. Kyuldjiev (SOFI)
VOGEL	84	PR D30 1505	P. Vogel
HENRY	81	PRL 47 618	R.C. Henry, P.D. Feldman (JHU)
KIMBLE	81	PRL 46 80	R. Kimble, S. Bowyer, P. Jakobsen (UCB)
MORGAN	81	PL 102B 247	J.A. Morgan (SUSS)
FUJIKAWA	80	PRL 45 963	K. Fujikawa, R. Shrock (STON)
LUBIMOV	80	PL 94B 266	V.A. Lyubimov *et al.* (ITEP)
Also	80	SJNP 32 154	V.S. Kozik *et al.* (ITEP)
		Translated from YAF 32 301.	
Also	81	JETP 54 616	V.A. Lyubimov *et al.* (ITEP)
		Translated from ZETF 81 1158.	
STECKER	80	PRL 45 1460	F.W. Stecker (NASA)
BEG	78	PR D17 1395	M.A.B. Beg, W.J. Marciano, M. Ruderman (ROCK+)
LEE	77C	PR D16 1444	B.W. Lee, R.E. Shrock (STON)
SUTHERLAND	76	PR D13 2700	P. Sutherland *et al.* (PENN, COLU, NYU)
CLARK	74	PR D9 533	A.R. Clark *et al.* (LBL)
REINES	74	PRL 32 180	F. Reines, H.W. Sobel, H.S. Gurr (UCI)
Also	78	Private Comm.	V.E. Barnes (PURD)
BECK	68	ZPHY 216 229	E. Beck, H. Daniel (MPIH)
BERNSTEIN	63	PR 132 1227	J. Bernstein, M. Ruderman, G. Feinberg (NYU+)
COWAN	57	PR 107 528	C.L. Cowan, F. Reines (LANL)

ν_μ

$J = \frac{1}{2}$

The following results are obtained using neutrinos associated with μ^+ or μ^-. See Note on "Electron, muon, and tau neutrino listings."

ν MASS

In the context of some models, it is possible that this weighted sum over mass eigenstates is the same as for the neutrinos produced in τ decay.

In some of the ASTR and COSM papers listed below, the authors did not distinguish between weak and mass eigenstates.

OUR EVALUATION is based on OUR AVERAGE for the $\pi^\pm$ mass and the ASSAMAGAN 96 value for the muon momentum for the π^+ decay at rest. The limit is calculated using the unified classical analysis of FELDMAN 98 for a Gaussian distribution near a physical boundary. WARNING: since $m^{2(\text{eff})}_{\nu_\mu}$ is calculated from the differences of large numbers, it and the corresponding limits are extraordinarily sensitive to small changes in the pion mass, the decay muon momentum, and their errors. For example, the limits obtained using the JECKELMANN 94, LENZ 98, and the weighted averages are 0.15, 0.29, and 0.19 MeV, respectively.

VALUE (MeV)	CL%	DOCUMENT ID		TECN	COMMENT
<0.19 (CL = 90%) OUR EVALUATION					
<0.17	90	[1] ASSAMAGAN	96	SPEC	$m^2_\nu = -0.016 \pm 0.023$
• • • We do not use the following data for averages, fits, limits, etc. • • •					
<0.15		[2] DOLGOV	95	COSM	Nucleosynthesis
<0.48		[3] ENQVIST	93	COSM	Nucleosynthesis
<0.3		[4] FULLER	91	COSM	Nucleosynthesis
<0.42		[4] LAM	91	COSM	Nucleosynthesis
<0.50	90	[5] ANDERHUB	82	SPEC	$m^2_\nu = -0.14 \pm 0.20$
<0.65	90	CLARK	74	ASPK	$K_{\mu 3}$ decay

[1] ASSAMAGAN 96 measurement of p_μ from $\pi^+ \to \mu^+\nu$ at rest combined with JECKELMANN 94 Solution B pion mass yields $m^2_\nu = -0.016 \pm 0.023$ with corresponding Bayesian limit listed above. If Solution A is used, $m^2_\nu = -0.143 \pm 0.024$ MeV^2. Replaces ASSAMAGAN 94.

[2] DOLGOV 95 removes earlier assumptions (DOLGOV 93) about thermal equilibrium below T_{QCD} for wrong-helicity Dirac neutrinos (ENQVIST 93, FULLER 91) to set more stringent limits.

[3] ENQVIST 93 bases limit on the fact that thermalized wrong-helicity Dirac neutrinos would speed up expansion of early universe, thus reducing the primordial abundance. FULLER 91 exploits the same mechanism but in the older calculation obtains a larger production rate for these states, and hence a lower limit. Neutrino lifetime assumed to exceed nucleosynthesis time, ~ 1 s.

[4] Assumes neutrino lifetime >1 s. For Dirac neutrinos only. See also ENQVIST 93.

[5] ANDERHUB 82 kinematics is insensitive to the pion mass.

$m_\nu - m_{\overline{\nu}}$

Test of CPT for a Dirac neutrino. (Not a very strong test.)

VALUE (MeV)	CL%	DOCUMENT ID		TECN	COMMENT
• • • We do not use the following data for averages, fits, limits, etc. • • •					
<0.45	90	CLARK	74	ASPK	$K_{\mu 3}$ decay

ν (MEAN LIFE) / MASS

Measures $\left[\sum |U_{\ell j}|^2 \Gamma_j m_j\right]^{-1}$, where the sum is over mass eigenstates which cannot be resolved experimentally. Most of these limits apply to any ν within the indicated mass range.

VALUE (s/eV)	CL%	EVTS	DOCUMENT ID		TECN	COMMENT
>15.4	90		[6] KRAKAUER	91	CNTR	$\nu_\mu, \overline{\nu}_\mu$ at LAMPF
• • • We do not use the following data for averages, fits, limits, etc. • • •						
			[7] BILLER	98	ASTR	$m_\nu = 0.05$–1 eV
$> 2.8 \times 10^{15}$			[8,9] BLUDMAN	92	ASTR	$m_\nu < 50$ eV
none $10^{-12} - 5 \times 10^4$			[10] DODELSON	92	ASTR	m_ν=1–300 keV
$> 6.3 \times 10^{15}$			[9,11] CHUPP	89	ASTR	$m_\nu < 20$ eV
$> 1.7 \times 10^{15}$			[9] KOLB	89	ASTR	$m_\nu < 20$ eV
$> 3.3 \times 10^{14}$			[12,13] VONFEILIT...	88	ASTR	
> 0.11	90	0	[14] FRANK	81	CNTR	$\nu\overline{\nu}$ LAMPF
			[15] HENRY	81	ASTR	$m_\nu = 16$–20 eV
			[16] KIMBLE	81	ASTR	$m_\nu = 10$–100 eV
			[17] REPHAELI	81	ASTR	$m_\nu = 30$–150 eV
			[18] DERUJULA	80	ASTR	$m_\nu = 10$–100 eV
			[19] STECKER	80	ASTR	$m_\nu = 10$–100 eV
$> 2 \times 10^{21}$			[14] BLIETSCHAU	78	HLBC	ν_μ, CERN GGM
$> 1.0 \times 10^{-2}$	90	0	[14] BLIETSCHAU	78	HLBC	$\overline{\nu}_\mu$, CERN GGM
$> 1.7 \times 10^{-2}$	90	0	[14] BARNES	77	DBC	ν, ANL 12-ft
$> 2.2 \times 10^{-3}$	90	0	[14] BELLOTTI	76	HLBC	ν, CERN GGM
$> 3. \times 10^{-3}$	90	0	[14] BELLOTTI	76	HLBC	$\overline{\nu}$, CERN GGM
$> 1.3 \times 10^{-2}$	90	1				

[6] KRAKAUER 91 quotes the limit $\tau/m_{\nu_1} > (0.75a^2 + 21.65a + 26.3)$ s/eV, where a is a parameter describing the asymmetry in the neutrino decay defined as $dN_\gamma/d\cos\theta = (1/2)(1 + a\cos\theta)$ The parameter $a = 0$ for a Majorana neutrino, but can vary from -1 to 1 for a Dirac neutrino. The bound given by the authors is the most conservative (which applies for $a = -1$).

[7] BILLER 98 use the observed TeV γ-ray spectra to set limits on the mean life of a radiatively decaying neutrino between 0.05 and 1 eV. Curve shows $\tau_\nu/B_\gamma > 0.15 \times 10^{21}$ s at 0.05 eV, $> 1.2 \times 10^{21}$ s at 0.17 eV, $> 3 \times 10^{21}$ s at 1 eV, where B_γ is the branching ratio to photons.

[8] BLUDMAN 92 sets additional limits by this method for higher mass ranges. Cosmological limits are also obtained.

[9] Nonobservation of γ's in coincidence with ν's from SN 1987A. Results should be divided by the $\nu \to \gamma X$ branching ratio.

[10] DODELSON 92 range is for wrong-helicity keV mass Dirac ν's from the core of neutron star in SN 1987A decaying to ν's that would have interacted in KAM2 or IMB detectors.

[11] CHUPP 89 should be multiplied by a branching ratio (about 1) and a detection efficiency (about 1/4), and pertains to radiative decay of any neutrino to a lighter or sterile neutrino.

[12] Model-dependent theoretical analysis of SN 1987A neutrinos.

[13] Limit applies to ν_τ also.

[14] These experiments look for $\nu_k \to \nu_j\gamma$ or $\overline{\nu}_k \to \overline{\nu}_j\gamma$.

[15] HENRY 81 uses UV flux from clusters of galaxies to find $\tau > 1.1 \times 10^{25}$ s for radiative decay.

[16] KIMBLE 81 uses extreme UV flux limits to find $\tau > 10^{22}$–10^{23} s.

[17] REPHAELI 81 consider the effect of radiative neutrino decay on neutral H in early universe based on M31 HI. They conclude $\tau > 10^{24}$ s.

[18] DERUJULA 80 finds $\tau > 3 \times 10^{23}$ s based on CDM neutrino decay contribution to UV background.

[19] STECKER 80 limit based on UV background; result given is $\tau > 4 \times 10^{22}$ s at $m_\nu = 20$ eV.

ν CHARGE

VALUE (units: electron charge)	DOCUMENT ID		TECN	COMMENT
• • • We do not use the following data for averages, fits, limits, etc. • • •				
$<2 \times 10^{-14}$	[20] RAFFELT	99	ASTR	Red giant luminosity
$<6 \times 10^{-14}$	[21] RAFFELT	99	ASTR	Solar cooling

[20] This RAFFELT 99 limit applies to all neutrinos which are light enough (<5 keV) to be emitted from globular-cluster red giants.

[21] This RAFFELT 99 limit is derived from the helioseismological limit on a new energy-loss channel of the Sun, and applies to all neutrinos which are light enough (<1 keV) to be emitted from the sun.

$|(v - c)/c|$ ($v \equiv \nu$ VELOCITY)

Expected to be zero for massless neutrino, but also tests whether photons and neutrinos have the same limiting velocity in vacuum.

VALUE (units 10^{-4})	CL%	EVTS	DOCUMENT ID		TECN	CHG	COMMENT
• • • We do not use the following data for averages, fits, limits, etc. • • •							
<0.4	95	9800	KALBFLEISCH	79	SPEC		
<2.0	99	77	ALSPECTOR	76	SPEC	0	>5 GeV ν
<4.0	99	26	ALSPECTOR	76	SPEC	0	<5 GeV ν

ν MAGNETIC MOMENT

Must vanish for a purely chiral massless Dirac neutrino. A massive Dirac or Majorana neutrino can have a transition magnetic moment connecting one mass eigenstate to another one. The experimental limits below usually cannot distinguish between the true (diagonal, in mass) magnetic moment and a transition magnetic moment. The value of the magnetic moment for the standard SU(2)×U(1) electroweak theory extended to include massive neutrinos (see FUJIKAWA 80) is $\mu_\nu = 3eG_F m_\nu/(8\pi^2\sqrt{2}) = (3.2 \times 10^{-19}) m_\nu \mu_B$ where m_ν is in eV and $\mu_B = e\hbar/2m_e$ is the Bohr magneton. Given the upper bound $m_\nu < 0.19$ MeV, it follows that for the extended standard electroweak theory, $\mu_\nu < 6 \times 10^{-14}\,\mu_B$.

VALUE ($10^{-10}\,\mu_B$)	CL%	DOCUMENT ID		TECN	COMMENT
< 6.8	90	[22] AUERBACH	01	LSND	$\nu_e e$ scatt.
• • • We do not use the following data for averages, fits, limits, etc. • • •					
< 2	90	[23] GRIMUS	02	FIT	solar + reactor (Majorana ν)
< 0.03		[24] RAFFELT	99	ASTR	Red giant luminosity
< 4		[25] RAFFELT	99	ASTR	Solar cooling
< 0.62		[26] ELMFORS	97	COSM	Depolarization in early universe plasma
< 30	90	VILAIN	95B	CHM2	$\nu_\mu e \to \nu_\mu e$
<100	95	[27] DORENBOS...	91	CHRM	$\nu_\mu e \to \nu_\mu e$
< 8.5	90	AHRENS	90	CNTR	$\nu_\mu e \to \nu_\mu e$
< 7.4	90	[28] KRAKAUER	90	CNTR	LAMPF ($\nu_\mu, \overline{\nu}_\mu$) e elast.
< 0.02		[29] RAFFELT	90	ASTR	Red giant luminosity
< 0.1		[30] RAFFELT	89B	ASTR	Cooling helium stars
< 0.11		[30,31] FUKUGITA	87	ASTR	Cooling helium stars
< 0.0006		[32] NUSSINOV	87	ASTR	Cosmic EM backgrounds
< 0.85		[31] BEG	78	ASTR	Stellar plasmons
< 81		[33] KIM	74	RVUE	$\overline{\nu}_\mu e \to \overline{\nu}_\mu e$
< 1		[34] BERNSTEIN	63	ASTR	Solar cooling

[22] AUERBACH 01 limit is based on the LSND ν_e and ν_μ electron scattering measurements. The limit is slightly more stringent than KRAKAUER 90.

[23] GRIMUS 02 obtain stringent bounds on all Majorana neutrino transition moments from a simultaneous fit of LMA-MSW oscillation parameters and transition moments to global solar neutrino data + reactor data. Using only solar neutrino data, a 90% CL bound of $6.3 \times 10^{-10} \mu_B$ is obtained.

[24] RAFFELT 99 is an update of RAFFELT 90. This limit applies to all neutrino flavors which are light enough (< 5 keV) to be emitted from globular-cluster red giants. This limit pertains equally to electric dipole moments and magnetic transition moments, and it applies to both Dirac and Majorana neutrinos.

[25] RAFFELT 99 is essentially an update of BERNSTEIN 63, but is derived from the helioseismological limit on a new energy-loss channel of the Sun. This limit applies to all neutrino flavors which are light enough (<1 keV) to be emitted from the Sun. This limit pertains equally to electric dipole and magnetic transition moments, and it applies to both Dirac and Majorana neutrinos.

[26] ELMFORS 97 calculate the rate of depolarization in a plasma for neutrinos with a magnetic moment and use the constraints from a big-bang nucleosynthesis on additional degrees of freedom.

[27] DORENBOSCH 91 corrects an incorrect statement in DORENBOSCH 89 that the ν magnetic moment is $< 1 \times 10^{-9}$ at the 95%CL. DORENBOSCH 89 measures both $\nu_\mu e$ and $\overline{\nu} e$ elastic scattering and assume $\mu(\nu) = \mu(\overline{\nu})$.

[28] KRAKAUER 90 experiment fully reported in ALLEN 93.

[29] RAFFELT 90 limit applies for a diagonal magnetic moment of a Dirac neutrino, or for a transition magnetic moment of a Majorana neutrino. In the latter case, the same analysis gives $< 1.4 \times 10^{-12}$. Limit at 95%CL obtained from δM_C.

[30] Significant dependence on details of stellar properties.

[31] If $m_\nu < 10$ keV.

[32] For m_ν = 8–200 eV. NUSSINOV 87 examines transition magnetic moments for $\nu_\mu \to \nu_e$ and obtain $< 3 \times 10^{-15}$ for $m_\nu > 16$ eV and $< 6 \times 10^{-14}$ for $m_\nu > 4$ eV.

[33] KIM 74 is a theoretical analysis of $\overline{\nu}_\mu$ reaction data.

[34] If $m_\nu < 1$ keV.

NONSTANDARD CONTRIBUTIONS TO NEUTRINO SCATTERING

We report limits on the so-called neutrino charge radius squared. While the straight-forward definition of a neutrino charge radius has been proven to be gauge-dependent and, hence, unphysical (LEE 77C), there have been recent attempts to define a physically observable neutrino charge radius (BERNABEU 00, BERNABEU 02). The issue is still controversial (FUJIKAWA 03, BERNABEU 03). A more general interpretation of the experimental results is that they are limits on certain nonstandard contributions to neutrino scattering.

VALUE (10^{-32} cm^2)	CL%	DOCUMENT ID		TECN	COMMENT
• • • We do not use the following data for averages, fits, limits, etc. • • •					
$<0.68, > -0.53$	90	[35] HIRSCH	03		νe scat.
$< \lvert 0.6 \rvert$	90	VILAIN	95B	CHM2	νe elastic scat.
-1.1 ± 1.0		[36] AHRENS	90	CNTR	νe elastic scat.
-0.3 ± 1.5		[36] DORENBOS...	89	CHRM	νe elastic scat.

[35] Based on analysis of CCFR 98 results. Limit is on $\langle r_V^2 \rangle + \langle r_A^2 \rangle$. The CHARM II and E734 at BNL results are reanalyzed, and weaker bounds on the charge radius squared than previously published are obtained. The NuTeV result is discussed; when tentatively interpreted as ν_μ charge radius it implies $\langle r_V^2 \rangle + \langle r_A^2 \rangle = (4.20 \pm 1.64) \times 10^{-33}$ cm^2.

[36] Result is obtained from reanalysis given in ALLEN 91, followed by our reduction to obtain 1σ errors.

ν_μ REFERENCES

BERNABEU	03	hep-ph/0303202	J. Bernabeu, J. Papavassiliou, J. Vidal	
FUJIKAWA	03	hep-ph/0303188	K. Fujikawa, R. Shrock	
HIRSCH	03	PR D67 033005	M. Hirsch *et al.*	
BERNABEU	02	PRL 89 101802	J. Bernabeu, J. Papavassiliou, J. Vidal	
Also	02B	PRL 89 229902 (erratum)	J. Bernabeu, J. Papavassiliou, J. Vidal	
GRIMUS	02	NP B648 376	W. Grimus *et al.*	
AUERBACH	01	PR D63 112001	L.B. Auerbach *et al.*	(LSND Collab.)
BERNABEU	00	PR D62 113012	J. Bernabeu *et al.*	
RAFFELT	99	PRPL 320 319	G.G. Raffelt	
BILLER	98	PRL 80 2992	S.D. Biller *et al.*	(WHIPPLE Collab.)
FELDMAN	98	PR D57 3873	G.J. Feldman, R.D. Cousins	
LENZ	98	PL B416 50	S. Lenz *et al.*	
ELMFORS	97	NP B503 3	P. Elmfors *et al.*	
ASSAMAGAN	96	PR D53 6065	K.A. Assamagan *et al.*	(PSI, ZURI, VILL+)
DOLGOV	95	PR D51 4129	A.D. Dolgov, K. Kainulainen, I.Z. Rothstein	(MICH+)
VILAIN	95B	PL B345 115	P. Vilain *et al.*	(CHARM II Collab.)
ASSAMAGAN	94	PL B335 231	K.A. Assamagan *et al.*	(PSI, ZURI, VILL+)
JECKELMANN	94	PL B335 326	B. Jeckelmann, P.F.A. Goudsmit, H.J. Leisi	(WABRN+)
ALLEN	93	PR D47 11	R.C. Allen *et al.*	(UCI, LANL, ANL+)
DOLGOV	93	PRL 71 476	A.D. Dolgov, I.Z. Rothstein	(MICH)
ENQVIST	93	PL B301 376	K. Enqvist, H. Uibo	(NORD)
BLUDMAN	92	PR D45 4720	S.A. Bludman	(CFPA)
DODELSON	92	PRL 68 2572	S. Dodelson, J.A. Frieman, M.S. Turner	(FNAL+)
ALLEN	91	PR D43 R1	R.C. Allen *et al.*	(UCI, LANL, UMD)
DORENBOS...	91	ZPHY C51 142	J. Dorenbosch *et al.*	(CHARM Collab.)
FULLER	91	PR D43 3136	G.M. Fuller, R.A. Malaney	(UCSD)
KRAKAUER	91	PR D44 R6	D.A. Krakauer *et al.*	(LAMPF E225 Collab.)
LAM	91	PR D44 3345	W.P. Lam, K.W. Ng	(AST)
AHRENS	90	PR D41 3297	L.A. Ahrens *et al.*	(BNL, BROW, HIRO+)
KRAKAUER	90	PL B252 177	D.A. Krakauer *et al.*	(LAMPF E225 Collab.)
RAFFELT	90	PRL 64 2856	G.G. Raffelt	(MPIM)
CHUPP	89	PR 62 505	E.L. Chupp, W.T. Vestrand, C. Reppin	(UNH, MPIM)
DORENBOS...	89	ZPHY C41 567	J. Dorenbosch *et al.*	(CHARM Collab.)
KOLB	89	PRL 62 509	E.W. Kolb, M.S. Turner	(CHIC, FNAL)
RAFFELT	89B	APJ 336 61	G. Raffelt, D. Dearborn, J. Silk	(UCB, LLL)
VONFEILIT...	88	PL B200 580	F. von Feilitzsch, L. Oberauer	(MUNT)
FUKUGITA	87	PR D36 3817	M. Fukugita, S. Yazaki	(KYOTU, TOKY)
NUSSINOV	87	PR D36 2278	S. Nussinov, Y. Rephaeli	(TELA)
ANDERHUB	82	PL 114B 76	H.B. Anderhub *et al.*	(ETH, SIN)
FRANK	81	PR D24 2001	J.S. Frank *et al.*	(LASL, YALE, MIT+)
HENRY	81	PRL 47 618	R.C. Henry, P.D. Feldman	(JHU)
KIMBLE	81	PRL 46 80	R. Kimble, S. Bowyer, P. Jakobsen	(UCB)
REPHAELI	81	PL 106B 73	Y. Rephaeli, A.S. Szalay	(UCSB, CHIC)
DERUJULA	80	PRL 45 942	A. De Rujula, S.L. Glashow	(MIT, HARV)
FUJIKAWA	80	PRL 45 963	K. Fujikawa, R. Shrock	(STON)
STECKER	80	PRL 45 1460	F.W. Stecker	(NASA)
KALBFLEISCH	79	PRL 43 1361	G.R. Kalbfleisch *et al.*	(FNAL, PURD, BELL)
BEG	78	PR D17 1395	M.A.B. Beg, W.J. Marciano, M. Ruderman	(ROCK+)
BLIETSCHAU	78	NP B133 205	J. Blietschau *et al.*	(Gargamelle Collab.)
BARNES	77	PRL 38 1049	V.E. Barnes *et al.*	(PURD, ANL)
LEE	77C	PR D16 1444	B.W. Lee, R.E. Shrock	(STON)
ALSPECTOR	76	PRL 36 837	J. Alspector *et al.*	(BNL, PURD, CIT+)
BELLOTTI	76	LNC 17 553	E. Bellotti *et al.*	(MILA)
CLARK	74	PR D9 533	A.R. Clark *et al.*	(LBL)
KIM	74	PR D9 3050	J.E. Kim, V.S. Mathur, S. Okubo	(ROCH)
BERNSTEIN	63	PR 132 1227	J. Bernstein, M. Ruderman, G. Feinberg	(NYU+)

ν_τ

$J = \frac{1}{2}$

The following results are obtained using neutrinos associated with τ^+ or τ^-. See Note on "Electron, muon, and tau neutrino listings."

The ν_τ was directly observed by the DONUT Collaboration (KODAMA 01). Existence indirectly established from τ decay data combined with ν reaction data. See for example FELDMAN 81. ALBRECHT 92Q rules out $J = 3/2$ by establishing that the ρ^- is not in a pure H_ρ=−1 helicity state in $\tau^- \to \rho^- \nu_\tau$.

ν MASS

In the context of some models, it is possible that this weighted sum over mass eigenstates is the same as for the neutrinos produced in μ decay.

In some of the ASTR and COSM papers listed below, the authors did not distinguish between weak and mass eigenstates.

VALUE (MeV)	CL%	EVTS	DOCUMENT ID		TECN	COMMENT
< 18.2	95		[1] BARATE	98F	ALEP	1991–1995 LEP runs
• • • We do not use the following data for averages, fits, limits, etc. • • •						
< 28	95		[2] ATHANAS	00	CLEO	$E_{\rm cm}^{ee} = 10.6$ GeV
< 27.6	95		[3] ACKERSTAFF	98T	OPAL	1990–1995 LEP runs
< 30	95	473	[4] AMMAR	98	CLEO	$E_{\rm cm}^{ee} = 10.6$ GeV
< 60	95		[5] ANASTASSOV	97	CLEO	$E_{\rm cm}^{ee} = 10.6$ GeV
< 0.37 or >22			[6] FIELDS	97	COSM	Nucleosynthesis
< 68	95		[7] SWAIN	97	THEO	m_τ, τ_τ, τ partial widths
< 29.9	95		[8] ALEXANDER	96M	OPAL	1990–1994 LEP runs
<149			[9] BOTTINO	96	THEO	π, μ, τ leptonic decays
<1 or >25			[10] HANNESTAD	96C	COSM	Nucleosynthesis
< 71	95		[11] SOBIE	96	THEO	m_τ, τ_τ, B($\tau^- \to e^- \overline{\nu}_e \nu_\tau$)
< 24	95	25	[12] BUSKULIC	95H	ALEP	1991–1993 LEP runs
< 0.19			[13] DOLGOV	95	COSM	Nucleosynthesis
< 3			[14] SIGL	95	ASTR	SN 1987A
< 0.4 or > 30			[15] DODELSON	94	COSM	Nucleosynthesis
< 0.1 or > 50			[16] KAWASAKI	94	COSM	Nucleosynthesis
155–225			[17] PERES	94	THEO	π, K, μ, τ weak decays
< 32.6	95	113	[18] CINABRO	93	CLEO	$E_{\rm cm}^{ee} \approx 10.6$ GeV
< 0.3 or > 35			[19] DOLGOV	93	COSM	Nucleosynthesis
< 0.74			[20] ENQVIST	93	COSM	Nucleosynthesis
< 31	95	19	[21] ALBRECHT	92M	ARG	$E_{\rm cm}^{ee} = 9.4$–10.6 GeV
< 0.3			[22] FULLER	91	COSM	Nucleosynthesis
< 0.5 or > 25			[23] KOLB	91	COSM	Nucleosynthesis
< 0.42			[22] LAM	91	COSM	Nucleosynthesis

[1] BARATE 98F result based on kinematics of 2939 $\tau^- \to 2\pi^- \pi^+ \nu_\tau$ and 52 $\tau^- \to 3\pi^- 2\pi^+ (\pi^0) \nu_\tau$ decays. If possible 2.5% excited a_1 decay is included in 3-prong sample analysis, limit increases to 19.2 MeV.

[2] ATHANAS 00 bound comes from analysis of $\tau^- \to \pi^- \pi^+ \pi^- \pi^0 \nu_\tau$ decays.

[3] ACKERSTAFF 98T use $\tau \to 5\pi^\pm \nu_\tau$ decays to obtain a limit of 43.2 MeV (95%CL). They combine this with ALEXANDER 96M value using $\tau \to 3h^\pm \nu_\tau$ decays to obtain quoted limit.

[4] AMMAR 98 limit comes from analysis of $\tau^- \to 3\pi^- 2\pi^+ \nu_\tau$ and $\tau^- \to 2\pi^- \pi^+ 2\pi^0 \nu_\tau$ decay modes.

[5] ANASTASSOV 97 derive limit by comparing their m_τ measurement (which depends on m_{ν_τ}) to BAI 96 m_τ threshold measurement.

[6] FIELDS 97 limit for a Dirac neutrino. For a Majorana neutrino the mass region < 0.93 or >31 MeV is excluded. These bounds assume $N_\nu < 4$ from nucleosynthesis; a wider excluded region occurs with a smaller N_ν upper limit.

[7] SWAIN 97 derive their limit from the Standard Model relationships between the tau mass, lifetime, branching fractions for $\tau^- \to e^- \overline{\nu}_e \nu_\tau$, $\tau^- \to \mu^- \overline{\nu}_\mu \nu_\tau$, $\tau^- \to \pi^- \nu_\tau$, and $\tau^- \to K^- \nu_\tau$, and the muon mass and lifetime by assuming lepton universality and using world average values. Limit is reduced to 48 MeV when the CLEO τ mass measurement (BALEST 93) is included; see CLEO's more recent m_{ν_τ} limit (ANASTASSOV 97). Consideration of mixing with a fourth generation heavy neutrino yields $\sin^2\theta_L < 0.016$ (95%CL).

[8] ALEXANDER 96M bound comes from analyses of $\tau^- \to 3\pi^- 2\pi^+ \nu_\tau$ and $\tau^- \to h^- h^- h^+ \nu_\tau$ decays.

[9] BOTTINO 96 assumes three generations of neutrinos with mixing, finds consistency with massless neutrinos with no mixing based on 1995 data for masses, lifetimes, and leptonic partial widths.

[10] HANNESTAD 96C limit is on the mass of a Majorana neutrino. This bound assumes $N_\nu < 4$ from nucleosynthesis. A wider excluded region occurs with a smaller N_ν upper limit. This paper is the corrected version of HANNESTAD 96; see the erratum: HANNESTAD 96B.

[11] SOBIE 96 derive their limit from the Standard Model relationship between the tau mass, lifetime, and leptonic branching fraction, and the muon mass and lifetime, by assuming lepton universality and using world average values.

[12] BUSKULIC 95H bound comes from a two-dimensional fit of the visible energy and invariant mass distribution of $\tau \to 5\pi(\pi^0)\nu_\tau$ decays. Replaced by BARATE 98F.

[13] DOLGOV 95 removes earlier assumptions (DOLGOV 93) about thermal equilibrium below T_{QCD} for wrong-helicity Dirac neutrinos (ENQVIST 93, FULLER 91) to set more stringent limits. DOLGOV 96 argues that a possible window near 20 MeV is excluded.

[14] SIGL 95 exclude massive Dirac or Majorana neutrinos with lifetimes between 10^{-3} and 10^8 seconds if the decay products are predominantly γ or e^+e^-.

[15] DODELSON 94 calculate constraints on ν_τ mass and lifetime from nucleosynthesis for 4 generic decay modes. Limits depend strongly on decay mode. Quoted limit is valid for all decay modes of Majorana neutrinos with lifetime greater than about 300 s. For Dirac neutrinos limits change to < 0.3 or > 33.

[16] KAWASAKI 94 excluded region is for Majorana neutrino with lifetime >1000 s. Other limits are given as a function of ν_τ lifetime for decays of the type $\nu_\tau \to \nu_\mu \phi$ where ϕ is a Nambu-Goldstone boson.

[17] PERES 94 used PDG 92 values for parameters to obtain a value consistent with mixing. Reexamination by BOTTINO 96 which included radiative corrections and 1995 PDG parameters resulted in two allowed regions, $m_3 < 70$ MeV and 140 MeV $m_3 < 149$ MeV.

[18] CINABRO 93 bound comes from analysis of $\tau^- \to 3\pi^- 2\pi^+ \nu_\tau$ and $\tau^- \to 2\pi^- \pi^+ 2\pi^0 \nu_\tau$ decay modes.

[19] DOLGOV 93 assumes neutrino lifetime >100 s. For Majorana neutrinos, the low mass limit is 0.5 MeV. KAWANO 92 points out that these bounds can be overcome for a Dirac neutrino if it possesses a magnetic moment. See also DOLGOV 96.

[20] ENQVIST 93 bases limit on the fact that thermalized wrong-helicity Dirac neutrinos would speed up expansion of early universe, thus reducing the primordial abundance. FULLER 91 exploits the same mechanism but in the older calculation obtains a larger production rate for these states, and hence a lower limit. Neutrino lifetime assumed to exceed nucleosynthesis time, ~ 1 s.

[21] ALBRECHT 92M reports measurement of a slightly lower τ mass, which has the effect of reducing the ν_τ mass reported in ALBRECHT 88B. Bound is from analysis of $\tau^- \to 3\pi^- 2\pi^+ \nu_\tau$ mode.

[22] Assumes neutrino lifetime >1 s. For Dirac neutrinos. See also ENQVIST 93.

[23] KOLB 91 exclusion region is for Dirac neutrino with lifetime >1 s; other limits are given.

ν (MEAN LIFE) / MASS

Measures $\left[\sum |U_{\ell j}|^2 \Gamma_j m_j\right]^{-1}$, where the sum is over mass eigenstates which cannot be resolved experimentally. Most of these limits apply to any ν within the indicated mass range.

VALUE (s/eV)		DOCUMENT ID		TECN	COMMENT
• • • We do not use the following data for averages, fits, limits, etc. • • •					
		[24] DOLGOV	99	COSM	
		[25] BILLER	98	ASTR	m_ν= 0.05–1 eV
$>1 \times 10^{14}$		[26] SIGL	95	ASTR	$m_\nu >$ few MeV
$>2.8 \times 10^{15}$		[27,28] BLUDMAN	92	ASTR	$m_\nu < 50$ eV
$< 10^{-12}$ or $> 5 \times 10^4$		[29] DODELSON	92	ASTR	m_ν=1–300 keV
		[30] GRANEK	91	COSM	Decaying L^0
		[31] WALKER	90	ASTR	m_ν= 0.03 – $\sim$ 2 MeV
$>6.3 \times 10^{15}$		[28,32] CHUPP	89	ASTR	$m_\nu < 20$ eV
$>1.7 \times 10^{15}$		[28] KOLB	89	ASTR	$m_\nu < 20$ eV
		[33] TERASAWA	88	COSM	m_μ= 30–70 MeV
		[34] KAWASAKI	86	COSM	$m_\nu >$10 MeV
		[35] LINDLEY	85	COSM	$m_\nu > 10$ MeV
		[36] BINETRUY	84	COSM	$m_\nu \sim$ 1 MeV
		[37] SARKAR	84	COSM	m_ν= 10–100 MeV
		[38] HENRY	81	ASTR	m_ν= 16–20 eV
		[39] KIMBLE	81	ASTR	m_ν= 10–100 eV
		[40] REPHAELI	81	ASTR	m_ν= 30–150 eV
		[41] DERUJULA	80	ASTR	m_ν= 10–100 eV
$>2 \times 10^{21}$		[42] STECKER	80	ASTR	m_ν= 10–100 eV
		[43] DICUS	78	COSM	m_ν= 0.5–30 MeV
$<3 \times 10^{-11}$		[44] FALK	78	ASTR	$m_\nu <$10 MeV
		[45] COWSIK	77	ASTR	

[24] DOLGOV 99 places limits in the (Majorana) τ-associated ν mass-lifetime plane based on nucleosynthesis. Results would be considerably modified if neutrino oscillations exist.

[25] BILLER 98 use the observed TeV γ-ray spectra to set limits on the mean life of a radiatively decaying neutrino between 0.05 and 1 eV. Curve shows $\tau_\nu/B_\gamma > 0.15 \times 10^{21}$ s at 0.05 eV, $> 1.2 \times 10^{21}$ s at 0.17 eV, $> 3 \times 10^{21}$ s at 1 eV, where B_γ is the branching ratio to photons.

[26] SIGL 95 exclude 1 s $\lesssim \tau \lesssim 10^8$ s for MeV-mass τ neutrinos from SN 1987A decaying radiatively, and eliminates the lower limit using other published results.

[27] BLUDMAN 92 sets additional limits by this method for higher mass ranges. Cosmological limits are also obtained.

[28] Nonobservation of γ's in coincidence with ν's from SN 1987A. Results should be divided by the $\nu \to \gamma X$ branching ratio.

[29] DODELSON 92 range is for wrong-helicity keV mass Dirac ν's from the core of neutron star in SN 1987A decaying to ν's that would have interacted in KAM2 or IMB detectors.

[30] GRANEK 91 considers heavy neutrino decays to $\gamma\nu_L$ and $3\nu_L$, where $m_{\nu_L} <$100 keV. Lifetime is calculated as a function of heavy neutrino mass, branching ratio into $\gamma\nu_L$, and m_{ν_L}.

[31] WALKER 90 uses SN 1987A γ flux limits after 289 days to find $\langle m/\tau \rangle > 1.1 \times 10^{15}$ eV s.

[32] CHUPP 89 should be multiplied by a branching ratio (about 1) and a detection efficiency (about 1/4), and pertains to radiative decay of any neutrino to a lighter or sterile neutrino.

[33] TERASAWA 88 finds only $10^2 < \tau < 10^4$ allowed for 30–70 MeV ν's from primordial nucleosynthesis.

[34] KAWASAKI 86 concludes that light elements in primordial nucleosynthesis would be destroyed by radiative decay of neutrinos with 10 MeV$< m_\nu <$1 GeV unless $\tau \lesssim 10^4$ s.

[35] LINDLEY 85 considers destruction of cosmologically-produced light elements, and finds $\tau < 2 \times 10^3$ s for 10 MeV $< m_\nu <$100 MeV. See also LINDLEY 79.

[36] BINETRUY 84 finds $\tau < 10^8$ s for neutrinos in a radiation-dominated universe.

[37] SARKAR 84 finds $\tau <$ 20 s at m_ν=10 MeV, with higher limits for other m_ν, and claims that all masses between 1 MeV and 50 MeV are ruled out.

[38] HENRY 81 uses UV flux from clusters of galaxies to find $\tau > 1.1 \times 10^{25}$ s for radiative decay.

[39] KIMBLE 81 uses extreme UV flux limits to find $\tau > 10^{22}$–10^{23} s.

[40] REPHAELI 81 consider ν decay γ effect on neutral H in early universe; based on M31 HI concludes $\tau > 10^{24}$ s.

[41] DERUJULA 80 finds $\tau > 3 \times 10^{23}$ s based on CDM neutrino decay contribution to UV background.

[42] STECKER 80 limit based on UV background; result given is $\tau > 4 \times 10^{22}$ s at $m = 20$ eV.

[43] DICUS 78 considers effect of ν decay photons on light-element production, and finds lifetime must be less than "hours." See also DICUS 77.

[44] FALK 78 finds lifetime constraints based on supernova energetics.

[45] COWSIK 77 considers variety of scenarios. For neutrinos produced in the big bang, present limits on optical photon flux require $\tau > 10^{23}$ s for $m_\nu \sim 1$ eV. See also COWSIK 79 and GOLDMAN 79.

ν MAGNETIC MOMENT

Must vanish for a purely chiral massless Dirac neutrino. A massive Dirac or Majorana neutrino can have a transition magnetic moment connecting one mass eigenstate to another one. The experimental limits below usually cannot distinguish between the true (diagonal, in mass) magnetic moment and a transition magnetic moment.

The value of the magnetic moment for the standard SU(2)×U(1) electroweak theory extended to include massive neutrinos (see FUJIKAWA 80) is $\mu_\nu = 3eG_F m_\nu/(8\pi^2\sqrt{2}) = (3.20 \times 10^{-19}) m_\nu \mu_B$ where m_ν is in eV and $\mu_B = e\hbar/2m_e$ is the Bohr magneton. Given the upper bound $m_\nu <$ 18 MeV, it follows that for the extended standard electroweak theory, $\mu_\nu < 6 \times 10^{-12}\ \mu_B$.

Most of the astrophysical limits pertain to any neutrino.

VALUE (μ_B)	CL%	DOCUMENT ID		TECN	COMMENT
$<3.9 \times 10^{-7}$	90	[46] SCHWIENHO...01		DONU	$\nu_\tau e^- \to \nu_\tau e^-$
• • • We do not use the following data for averages, fits, limits, etc. • • •					
$<2 \times 10^{-10}$	90	[47] GRIMUS	02	FIT	solar + reactor (Majorana ν)
$<8.0 \times 10^{-6}$	90	[48] TANIMOTO	00	RVUE	$e^+e^- \to \nu\overline{\nu}\gamma$
$<3 \times 10^{-12}$		[49] RAFFELT	99	ASTR	Red giant luminosity
$<4 \times 10^{-10}$		[50] RAFFELT	99	ASTR	Solar cooling
$<4.4 \times 10^{-6}$	90	ABREU	97J	DLPH	$e^+e^- \to \nu\overline{\nu}\gamma$ at LEP
$<3.3 \times 10^{-6}$	90	[51] ACCIARRI	97Q	L3	$e^+e^- \to \nu\overline{\nu}\gamma$ at LEP
$<6.2 \times 10^{-11}$		[52] ELMFORS	97	COSM	Depolarization in early universe plasma
$<2.7 \times 10^{-6}$	95	[53] ESCRIBANO	97	RVUE	$\Gamma(Z \to \nu\nu)$ at LEP
$<5.5 \times 10^{-6}$	90	GOULD	94	RVUE	$e^+e^- \to \nu\overline{\nu}\gamma$ at LEP
$<5.4 \times 10^{-7}$	90	[54] COOPER-...	92	BEBC	$\nu_\tau e^- \to \nu_\tau e^-$
$\gtrsim 10^{-8}$		[55] KAWANO	92	ASTR	Primodial ^{4}He abundance
$<5.6 \times 10^{-6}$	90	DESHPANDE	91	RVUE	$e^+e^- \to \nu\overline{\nu}\gamma$
$<2 \times 10^{-12}$		[56] RAFFELT	90	ASTR	Red giant luminosity
$<1 \times 10^{-11}$		[57] RAFFELT	89B	ASTR	Cooling helium stars
$<4. \times 10^{-6}$	90	[58] GROTCH	88	RVUE	$e^+e^- \to \nu\overline{\nu}\gamma$
$<1.1 \times 10^{-11}$		[57,59] FUKUGITA	87	ASTR	Cooling helium stars
$<6 \times 10^{-14}$		[60] NUSSINOV	87	ASTR	Cosmic EM backgrounds
$<8.5 \times 10^{-11}$		[59] BEG	78	ASTR	Stellar plasmons

[46] SCHWIENHORST 01 quote an experimental sensitivity of 4.9×10^{-7}.

[47] GRIMUS 02 obtain stringent bounds on all Majorana neutrino transition moments from a simultaneous fit of LMA-MSW oscillation parameters and transition moments to global solar neutrino data + reactor data. Using only solar neutrino data, a 90% CL bound of $6.3 \times 10^{-10} \mu_B$ is obtained.

[48] TANIMOTO 00 combined $e^+e^- \to \nu\overline{\nu}\gamma$ data from VENUS, TOPAZ, and AMY.

[49] RAFFELT 99 is an update of RAFFELT 90. This limit applies to all neutrino flavors which are light enough ($<$ 5 keV) to be emitted from globular-cluster red giants. This limit pertains equally to electric dipole moments and magnetic transition moments, and it applies to both Dirac and Majorana neutrinos.

[50] RAFFELT 99 is derived from the helioseismological limit on a new energy-loss channel of the Sun. This limit applies to all neutrino flavors which are light enough ($<$1 keV) to be emitted from the Sun. This limit pertains equally to electric dipole and magnetic transition moments, and it applies to both Dirac and Majorana neutrinos.

[51] ACCIARRI 97Q result applies to both direct and transition magnetic moments and for q^2=0.

[52] ELMFORS 97 calculate the rate of depolarization in a plasma for neutrinos with a magnetic moment and use the constraints from a big-bang nucleosynthesis on additional degrees of freedom.

[53] Applies to absolute value of magnetic moment.

[54] COOPER-SARKAR 92 assume $f_{D_s}/f_\pi = 2$ and D_s, $\overline{D}_s$ production cross section = 2.6 μb to calculate ν flux.

[55] KAWANO 92 lower limit is that needed to circumvent ^{4}He production if m_ν is between 5 and ~ 30 MeV/c^2.

[56] RAFFELT 90 limit valid if $m_\nu < 5$ keV. It applies for a diagonal magnetic moment of a Dirac neutrino, or for a transition magnetic moment of a Majorana neutrino. In the latter case, the same analysis gives $< 1.4\times10^{-12}$. Limit at 95%CL obtained from δM_c.

[57] Significant dependence on details of stellar properties.

[58] GROTCH 88 combined data from MAC, ASP, CELLO, and Mark J.

[59] If $m_\nu < 10$ keV.

[60] For $m_\nu = 8$–200 eV. NUSSINOV 87 examines transition magnetic moments for $\nu_\tau \to \nu_e$ and obtain $< 3\times10^{-15}$ for $m_\nu < 16$ eV and $< 6\times10^{-14}$ for $m_\nu > 4$ eV.

ν ELECTRIC DIPOLE MOMENT

VALUE (ecm)	CL%	DOCUMENT ID		TECN	COMMENT
$<5.2\times10^{-17}$	95	[61] ESCRIBANO	97	RVUE	$\Gamma(Z \to \nu\nu)$ at LEP

[61] Applies to absolute value of electric dipole moment.

ν CHARGE

VALUE (units: electron charge)	DOCUMENT ID		TECN	COMMENT
• • • We do not use the following data for averages, fits, limits, etc. • • •				
$<2\times10^{-14}$	[62] RAFFELT	99	ASTR	Red giant luminosity
$<6\times10^{-14}$	[63] RAFFELT	99	ASTR	Solar cooling
$<4\times10^{-4}$	[64] BABU	94	RVUE	BEBC beam dump
$<3\times10^{-4}$	[65] DAVIDSON	91	RVUE	SLAC electron beam dump

[62] This RAFFELT 99 limit applies to all neutrino flavors which are light enough (<5 keV) to be emitted from globular-cluster red giants.

[63] This RAFFELT 99 limit is derived from the helioseismological limit on a new energy-loss channel of the Sun, and applies to all neutrino flavors which are light enough (<1 keV) to be emitted from the sun.

[64] BABU 94 use COOPER-SARKAR 92 limit on ν magnetic moment to derive quoted result.

[65] DAVIDSON 91 use data from early SLAC electron beam dump experiment to derive charge limit as a function of neutrino mass.

NONSTANDARD CONTRIBUTIONS TO NEUTRINO SCATTERING

We report limits on the so-called neutrino charge radius squared. While the straight-forward definition of a neutrino charge radius has been proven to be gauge-dependent and, hence, unphysical (LEE 77C), there have been recent attempts to define a physically observable neutrino charge radius (BERNABEU 00, BERNABEU 02). The issue is still controversial (FUJIKAWA 03, BERNABEU 03). A more general interpretation of the experimental results is that they are limits on certain nonstandard contributions to neutrino scattering.

VALUE (10^{-32} cm^2)	CL%	DOCUMENT ID		COMMENT
• • • We do not use the following data for averages, fits, limits, etc. • • •				
<9.9 and >-8.2	90	[66] HIRSCH	03	anomalous $e^+e^- \to \nu\overline{\nu}\gamma$

[66] Results of LEP-2 are interpreted as limits on the axial-vector charge radius squared of a Majorana ν_τ. Slightly weaker limits for both vector and axial-vector charge radius squared are obtained for the Dirac case, and somewhat weaker limits are obtained from the analysis of lower energy data (LEP-1.5 and TRISTAN).

ν_τ REFERENCES

BERNABEU	03	hep-ph/0303202	J. Bernabeu, J. Papavassiliou, J. Vidal	
FUJIKAWA	03	hep-ph/0303188	K. Fujikawa, R. Shrock	
HIRSCH	03	PR D67 033005	M. Hirsch *et al.*	
BERNABEU	02	PRL 89 101802	J. Bernabeu, J. Papavassiliou, J. Vidal	
Also	02B	PRL 89 229902 (erratum)	J. Bernabeu, J. Papavassiliou, J. Vidal	
GRIMUS	02	NP B648 376	W. Grimus *et al.*	
KODAMA	01	PL B504 218	K. Kodama *et al.*	(DONUT Collab.)
SCHWIENHO...	01	PL B513 23	R. Schwienhorst *et al.*	(DONUT Collab.)
ATHANAS	00	PR D61 052002	M. Athanas *et al.*	(CLEO Collab.)
BERNABEU	00	PR D62 113012	J. Bernabeu *et al.*	
TANIMOTO	00	PL B478 1	N. Tanimoto *et al.*	
DOLGOV	99	NP B548 385	A.D. Dolgov *et al.*	
RAFFELT	99	PRPL 320 319	G.G. Raffelt	
ACKERSTAFF	98T	EPJ C5 229	K. Ackerstaff *et al.*	(OPAL Collab.)
AMMAR	98	PL B431 209	R. Ammar *et al.*	(CLEO Collab.)
BARATE	98F	EPJ C2 395	R. Barate *et al.*	(ALEPH Collab.)
BILLER	98	PRL 80 2992	S.D. Biller *et al.*	(WHIPPLE Collab.)
ABREU	97J	ZPHY C74 577	P. Abreu *et al.*	(DELPHI Collab.)
ACCIARRI	97Q	PL B412 201	M. Acciarri *et al.*	(L3 Collab.)
ANASTASSOV	97	PR D55 2559	A. Anastassov *et al.*	(CLEO Collab.)
Also	98B	PR D58 119903 (erratum)	A. Anastassov *et al.*	(CLEO Collab.)
ELMFORS	97	NP B503 3	P. Elmfors *et al.*	
ESCRIBANO	97	PL B395 369	R. Escribano, E. Masso	(BARC, PARIT)
FIELDS	97	ASP 6 169	B.D. Fields, K. Kainulainen, K.A. Olive	(NDAM+)
SWAIN	97	PR D55 R1	J. Swain, L. Taylor	(NEAS)
ALEXANDER	96M	ZPHY C72 231	G. Alexander *et al.*	(OPAL Collab.)
BAI	96	PR D53 20	J.Z. Bai *et al.*	(BES Collab.)
BOTTINO	96	PR D53 6361	A. Bottino *et al.*	
DOLGOV	96	PL B383 193	A.D. Dolgov, S. Pastor, J.W.F. Valle	(IFIC, VALE)
HANNESTAD	96	PRL 76 2848	S. Hannestad, J. Madsen	(AARH)
HANNESTAD	96B	PRL 77 5148 (erratum)	S. Hannestad, J. Madsen	(AARH)
HANNESTAD	96C	PR D54 7894	S. Hannestad, J. Madsen	(AARH)
SOBIE	96	ZPHY C70 383	R.J. Sobie, R.K. Keeler, I. Lawson	(VICT)
BUSKULIC	95H	PL B349 585	D. Buskulic *et al.*	(ALEPH Collab.)
DOLGOV	95	PR D51 4129	A.D. Dolgov, K. Kainulainen, I.Z. Rothstein	(MICH+)
SIGL	95	PR D51 1499	G. Sigl, M.S. Turner	(FNAL, EFI)
BABU	94	PL B321 140	K.S. Babu, T.M. Gould, I.Z. Rothstein	(BART+)
DODELSON	94	PR D49 5068	S. Dodelson, G. Gyuk, M.S. Turner	(FNAL, CHIC+)
GOULD	94	PL B333 545	T.M. Gould, I.Z. Rothstein	(JHU, MICH)
KAWASAKI	94	NP B419 105	M. Kawasaki *et al.*	(OSU)
PERES	94	PR D50 513	O.L.G. Peres, V. Pleitez, R. Zukanovich Funchal	
BALEST	93	PR D47 R3671	R. Balest *et al.*	(CLEO Collab.)
CINABRO	93	PRL 70 3700	D. Cinabro *et al.*	(CLEO Collab.)
DOLGOV	93	PRL 71 476	A.D. Dolgov, I.Z. Rothstein	(MICH)
ENQVIST	93	PL B301 376	K. Enqvist, H. Uibo	(NORD)
ALBRECHT	92M	PL B292 221	H. Albrecht *et al.*	(ARGUS Collab.)
ALBRECHT	92Q	ZPHY C56 339	H. Albrecht *et al.*	(ARGUS Collab.)
BLUDMAN	92	PR D45 4720	S.A. Bludman	(CFPA)
COOPER-...	92	PL B280 153	A.M. Cooper-Sarkar *et al.*	(BEBC WA66 Collab.)
DODELSON	92	PRL 68 2572	S. Dodelson, J.A. Frieman, M.S. Turner	(FNAL+)
KAWANO	92	PL B275 487	L.H. Kawano *et al.*	(CIT, UCSD, LLL+)
PDG	92	PR D45, 1 June, Part II	K. Hikasa *et al.*	(KEK, LBL, BOST+)
DAVIDSON	91	PR D43 2314	S. Davidson, B.A. Campbell, D. Bailey	(ALBE+)
DESHPANDE	91	PR D43 943	N.G. Deshpande, K.V.L. Sarma	(OREG, TATA)
FULLER	91	PR D43 3136	G.M. Fuller, R.A. Malaney	(UCSD)
GRANEK	91	IJMP A6 2387	H. Granek, B.H.J. McKellar	(MELB)
KOLB	91	PRL 67 533	E.W. Kolb *et al.*	(FNAL, CHIC)
LAM	91	PR D44 3345	W.P. Lam, K.W. Ng	(AST)
RAFFELT	90	PRL 64 2856	G.G. Raffelt	(MPIM)
WALKER	90	PR D41 689	T.P. Walker	(HARV)
CHUPP	89	PRL 62 505	E.L. Chupp, W.T. Vestrand, C. Reppin	(UNH, MPIM)
KOLB	89	PRL 62 509	E.W. Kolb, M.S. Turner	(CHIC, FNAL)
RAFFELT	89B	APJ 336 61	G. Raffelt, D. Dearborn, J. Silk	(UCB, LLL)
ALBRECHT	88B	PL B202 149	H. Albrecht *et al.*	(ARGUS Collab.)
GROTCH	88	ZPHY C39 553	H. Grotch, R.W. Robinett	(PSU)
TERASAWA	88	NP B302 697	N. Terasawa, M. Kawasaki, K. Sato	(TOKY)
FUKUGITA	87	PR D36 3817	M. Fukugita, S. Yazaki	(KYOTU, TOKY)
NUSSINOV	87	PR D36 2278	S. Nussinov, Y. Rephaeli	(TELA)
KAWASAKI	86	PL B178 71	M. Kawasaki, N. Terasawa, K. Sato	(TOKY)
LINDLEY	85	APJ 294 1	D. Lindley	(FNAL)
BINETRUY	84	PL 134B 174	P. Binetruy, G. Girardi, P. Salati	(LAPP)
SARKAR	84	PL 148B 347	S. Sarkar, A.M. Cooper	(OXF, CERN)
FELDMAN	81	SLAC-PUB-2839 Santa Cruz APS.	G.J. Feldman	(SLAC, STAN)
HENRY	81	PRL 47 618	R.C. Henry, P.D. Feldman	(JHU)
KIMBLE	81	PRL 46 80	R. Kimble, S. Bowyer, P. Jakobsen	(UCB)
REPHAELI	81	PL 106B 73	Y. Rephaeli, A.S. Szalay	(UCSB, CHIC)
DERUJULA	80	PRL 45 942	A. De Rujula, S.L. Glashow	(MIT, HARV)
FUJIKAWA	80	PRL 45 963	K. Fujikawa, R. Shrock	(STON)
STECKER	80	PRL 45 1460	F.W. Stecker	(NASA)
COWSIK	79	PR D19 2219	R. Cowsik	(TATA)
GOLDMAN	79	PR D19 2215	T. Goldman, G.J. Stephenson	(LASL)
LINDLEY	79	MNRAS 188 15P	D. Lindley	(SUSS)
BEG	78	PR D17 1395	M.A.B. Beg, W.J. Marciano, M. Ruderman	(ROCK+)
DICUS	78	PR D17 1529	D.A. Dicus *et al.*	(TEXA, VPI, STAN)
FALK	78	PL 79B 511	S.W. Falk, D.N. Schramm	(CHIC)
COWSIK	77	PRL 39 784	R. Cowsik	(MPIM, TATA)
DICUS	77	PRL 39 168	D.A. Dicus, E.W. Kolb, V.L. Teplitz	(TEXA, VPI)
LEE	77C	PR D16 1444	B.W. Lee, R.E. Shrock	(STON)

OTHER RELATED PAPERS

WEINSTEIN	93	ARNPS 43 457	A.J. Weinstein, R. Stroynowski	(CIT, SMU)

Number of Neutrino Types and Sum of Neutrino Masses

The neutrinos referred to in this section are those of the Standard SU(2)×U(1) Electroweak Model possibly extended to allow nonzero neutrino masses. Light neutrinos are those with $m < m_Z/2$. The limits are on the number of neutrino mass eigenstates, including ν_1, ν_2, and ν_3.

THE NUMBER OF LIGHT NEUTRINO TYPES FROM COLLIDER EXPERIMENTS

Revised August 2001 by D. Karlen (Carleton University).

The most precise measurements of the number of light neutrino types, N_ν, come from studies of Z production in e^+e^- collisions. The invisible partial width, $\Gamma_{\rm inv}$, is determined by subtracting the measured visible partial widths, corresponding to Z decays into quarks and charged leptons, from the total Z width. The invisible width is assumed to be due to N_ν light neutrino species each contributing the neutrino partial width Γ_ν as given by the Standard Model. In order to reduce the model dependence, the Standard Model value for the ratio of the neutrino to charged leptonic partial widths, $(\Gamma_\nu/\Gamma_\ell)_{\rm SM} = 1.991\pm0.001$, is used instead of $(\Gamma_\nu)_{\rm SM}$ to determine the number of light neutrino types:

$$N_\nu = \frac{\Gamma_{\rm inv}}{\Gamma_\ell}\left(\frac{\Gamma_\ell}{\Gamma_\nu}\right)_{\rm SM} \quad . \tag{1}$$

The combined result from the four LEP experiments is $N_\nu = 2.984 \pm 0.008$ [1].

In the past, when only small samples of Z decays had been recorded by the LEP experiments and by the Mark II at SLC,

the uncertainty in N_ν was reduced by using Standard Model fits to the measured hadronic cross sections at several center-of-mass energies near the Z resonance. Since this method is much more dependent on the Standard Model, the approach described above is favored.

Before the advent of the SLC and LEP, limits on the number of neutrino generations were placed by experiments at lower-energy e^+e^- colliders by measuring the cross section of the process $e^+e^- \to \nu\overline{\nu}\gamma$. The ASP, CELLO, MAC, MARK J, and VENUS experiments observed a total of 3.9 events above background [2], leading to a 95% CL limit of $N_\nu < 4.8$. This process has a much larger cross section at center-of-mass energies near the Z mass and has been measured at LEP by the ALEPH, DELPHI, L3, and OPAL experiments [3]. These experiments have observed several thousand such events, and the combined result is $N_\nu = 3.00 \pm 0.08$. The same process has also been measured by the LEP experiments at much higher center-of-mass energies, between 130 and 208 GeV, in searches for new physics [4]. Combined, the measured cross section is 0.982 ± 0.012 (stat) of that expected for three light neutrino generations [5].

Experiments at $p\overline{p}$ colliders also placed limits on N_ν by determining the total Z width from the observed ratio of $W^\pm \to \ell^\pm\nu$ to $Z \to \ell^+\ell^-$ events [6]. This involved a calculation that assumed Standard Model values for the total W width and the ratio of W and Z leptonic partial widths, and used an estimate of the ratio of Z to W production cross sections. Now that the Z width is very precisely known from the LEP experiments, the approach is now one of those used to determine the W width.

References

1. The LEP Collaborations and the LEP Electroweak Working Group, as reported by J. Dress at the *XX International Symposium on Lepton and Photon Interactions at High Energy*, Rome, Italy (July 2001).
2. VENUS: K. Abe *et al.*, Phys. Lett. **B232**, 431 (1989); ASP: C. Hearty *et al.*, Phys. Rev. **D39**, 3207 (1989); CELLO: H.J. Behrend *et al.*, Phys. Lett. **B215**, 186 (1988); MAC: W.T. Ford *et al.*, Phys. Rev. **D33**, 3472 (1986); MARK J: H. Wu, Ph.D. Thesis, Univ. Hamburg (1986).
3. L3: M. Acciarri *et al.*, Phys. Lett. **B431**, 199 (1998); DELPHI: P. Abreu *et al.*, Z. Phys. **C74**, 577 (1997); OPAL: R. Akers *et al.*, Z. Phys. **C65**, 47 (1995); ALEPH: D. Buskulic *et al.*, Phys. Lett. **B313**, 520 (1993).
4. OPAL: G. Abbiendi *et al.*, Eur. Phys. J. **C18**, 253 (2000); DELPHI: P. Abreu *et al.*, Eur. Phys. J. **C17**, 53 (2000); L3: M. Acciarri *et al.*, Phys. Lett. **B470**, 268 (1999); ALEPH: R. Barate *et al.*, Phys. Lett. **B429**, 201 (1998).
5. The LEP Collaborations and the LEP SUSY Working Group, LEPSUSYWG/01-05.1.
6. UA1: C. Albajar *et al.*, Phys. Lett. **B198**, 271 (1987); UA2: R. Ansari *et al.*, Phys. Lett. **B186**, 440 (1987).

Number from e^+e^- Colliders

Number of Light ν Types

Our evaluation uses the invisible and leptonic widths of the Z boson from our combined fit shown in the Particle Listings for the Z Boson, and the Standard Model value $\Gamma_\nu/\Gamma_\ell = 1.9908 \pm 0.0015$.

VALUE	DOCUMENT ID	TECN	
2.994±0.012 OUR EVALUATION	Combined fit to all LEP data.		
• • • We do not use the following data for averages, fits, limits, etc. • • •			
3.00 ±0.05	[1] LEP	92	RVUE

[1] Simultaneous fits to all measured cross section data from all four LEP experiments.

Number of Light ν Types from Direct Measurement of Invisible Z Width

In the following, the invisible Z width is obtained from studies of single-photon events from the reaction $e^+e^- \to \nu\overline{\nu}\gamma$. All are obtained from LEP runs in the $E^{ee}_{\rm cm}$ range 88–209 GeV.

VALUE	DOCUMENT ID	TECN	COMMENT
2.92±0.07 OUR AVERAGE			
2.86 ± 0.09	HEISTER	03C ALEP	$\sqrt{s}$=189–209 GeV
2.69±0.13±0.11	ABBIENDI,G	00D OPAL	1998 LEP run
2.84±0.15±0.14	ABREU	00Z DLPH	1997–1998 LEP runs
3.01±0.08	ACCIARRI	99R L3	1991–1998 LEP runs
2.89±0.32±0.19	ABREU	97J DLPH	1993–1994 LEP runs
2.68±0.20±0.20	BUSKULIC	93L ALEP	1990–1991 LEP runs
• • • We do not use the following data for averages, fits, limits, etc. • • •			
3.1 ±0.6 ±0.1	ADAM	96C DLPH	$\sqrt{s}$ = 130, 136 GeV

Limits from Astrophysics and Cosmology

Number of Light ν Types

("light" means < about 1 MeV). See also OLIVE 81. For a review of limits based on Nucleosynthesis, Supernovae, and also on terrestial experiments, see DENEGRI 90. Also see "Big-Bang Nucleosynthesis" in this *Review*.

VALUE	DOCUMENT ID	TECN	COMMENT
• • • We do not use the following data for averages, fits, limits, etc. • • •			
< 3.3	[2] BARGER	03C COSM	
$1.4 < N_\nu < 6.8$	[3] CROTTY	03 COSM	
< 3.6	[4] CYBURT	03 COSM	
$1.9 < N_\nu < 7.0$	[5] HANNESTAD	03B COSM	
$1.9 < N_\nu < 6.6$	[3] PIERPAOLI	03 COSM	
$2 < N_\nu < 4$	LISI	99	BBN
< 4.3	OLIVE	99	BBN
< 4.9	COPI	97	Cosmology
< 3.6	HATA	97B	High D/H quasar abs.
< 4.0	OLIVE	97	BBN; high ^{4}He and ^{7}Li
< 4.7	CARDALL	96B	Cosmology, High D/H quasar abs.
< 3.9	FIELDS	96	Cosmology, BBN; high ^{4}He and ^{7}Li
< 4.5	KERNAN	96	Cosmology, High D/H quasar abs.
< 3.6	OLIVE	95	BBN; $\geq$ 3 massless ν
< 3.3	WALKER	91	Cosmology
< 3.4	OLIVE	90	Cosmology
< 4	YANG	84	Cosmology
< 4	YANG	79	Cosmology
< 7	STEIGMAN	77	Cosmology
	PEEBLES	71	Cosmology
<16	[6] SHVARTSMAN	69	Cosmology
	HOYLE	64	Cosmology

[2] Limit on the number of neutrino types based on combination of WMAP data and big-bang nucleosynthesis. The limit from WMAP data alone is 8.3. See also KNELLER 01. $N_\nu \geq 3$ is assumed to compute the limit.

[3] 95% confidence level range on the number of neutrino flavors from WMAP data combined with other CMB measurements, the 2dfGRS data, and HST data.

[4] Limit on the number of neutrino types based on ^{4}He abundance assuming a baryon density fixed by the WMAP data. Limit relaxes to 5.2 if D/H is used instead of ^{4}He. See also CYBURT 01. $N_\nu \geq 3$ is assumed to compute the limit.

[5] 95% confidence level range on the number of neutrino flavors from WMAP data combined with other CMB measurements, the 2dfGRS data, HST data, and SN1a data.

[6] SHVARTSMAN 69 limit inferred from his equations.

Number Coupling with Less Than Full Weak Strength

VALUE	DOCUMENT ID	TECN	
• • • We do not use the following data for averages, fits, limits, etc. • • •			
<20	[7] OLIVE	81C COSM	
<20	[7] STEIGMAN	79 COSM	

[7] Limit varies with strength of coupling. See also WALKER 91.

Revised April 1998 by K.A. Olive (University of Minnesota).

The limits on low mass ($m_\nu \lesssim$ 1 MeV) neutrinos apply to $m_{\rm tot}$ given by

$$m_{\rm tot} = \sum_\nu (g_\nu/2) m_\nu \ ,$$

where g_ν is the number of spin degrees of freedom for ν plus $\overline{\nu}$: $g_\nu = 4$ for neutrinos with Dirac masses; $g_\nu = 2$ for Majorana neutrinos. Stable neutrinos in this mass range make a contribution to the total energy density of the Universe which is given by

$$\rho_\nu = m_{\rm tot} n_\nu = m_{\rm tot}(3/11) n_\gamma \ ,$$

where the factor 3/11 is the ratio of (light) neutrinos to photons. Writing $\Omega_\nu = \rho_\nu/\rho_c$, where ρ_c is the critical energy density of the Universe, and using $n_\gamma = 412\ {\rm cm}^{-3}$, we have

$$\Omega_\nu h^2 = m_{\rm tot}/(94\ {\rm eV}) \ .$$

Therefore, a limit on $\Omega_\nu h^2$ such as $\Omega_\nu h^2 < 0.25$ gives the limit

$$m_{\rm tot} < 24\ {\rm eV} \ .$$

The limits on high mass ($m_\nu > 1$ MeV) neutrinos apply separately to each neutrino type.

Limit on Total ν MASS, $m_{\rm tot}$

(Defined in the above note), of effectively stable neutrinos (i.e., those with mean lives greater than or equal to the age of the universe). These papers assumed Dirac neutrinos. When necessary, we have generalized the results reported so they apply to $m_{\rm tot}$. For other limits, see SZALAY 76, VYSOTSKY 77, BERNSTEIN 81, FREESE 84, SCHRAMM 84, and COWSIK 85.

VALUE (eV)		DOCUMENT ID		TECN	COMMENT
• • • We do not use the following data for averages, fits, limits, etc. • • •					
< 1.0	[8]	HANNESTAD	03B	COSM	
< 0.7	[9]	SPERGEL	03	COSM	WMAP
< 1.8	[10]	ELGAROY	02	ASTR	2dF Galaxy Redshift Survey
< 0.9	[11]	LEWIS	02	COSM	
< 4.2	[12]	WANG	02	COSM	CMB
< 2.7	[13]	FUKUGITA	00	COSM	
< 5.5	[14]	CROFT	99	ASTR	Ly α power spec
<180		SZALAY	74	COSM	
<132		COWSIK	72	COSM	
<280		MARX	72	COSM	
<400		GERSHTEIN	66	COSM	

[8] Constrains the fractional contribution of neutrinos to the total matter density in the Universe from WMAP data combined with other CMB measurements, the 2dfGRS data, HST data, and SN1a data.

[9] Constrains the fractional contribution of neutrinos to the total matter density in the Universe from WMAP data combined with other CMB measurements, the 2dfGRS data, and Lyman α data. The limit does not noticeably change if the Lyman α data are not used.

[10] ELGAROY 02 constrains the fractional contribution of neutrinos to the total matter density in the Universe from the power spectrum of fluctuations derived from the 2 Degree Field Galaxy Redshift Survey. Assumes $\Omega_{\rm matter} < 0.5$ and a spectral index of 1.0. Limit softens to $m_\nu < 2.2$ eV for n=1.0 $\pm$ 0.1.

[11] LEWIS 02 constrains the total mass of neutrinos from the power spectrum of fluctuations derived from the CMB, HST Key project, 2dF galaxy redshift survey, supernovae type Ia, and BBN.

[12] WANG 02 constrains the total mass of neutrinos from the power spectrum of fluctuations derived from the CMB and other cosmological data sets such as galaxy clustering and the Lyman α forest.

[13] FUKUGITA 00 is a limit on neutrino masses from structure formation. The constraint is based on the clustering scale σ_8 and the COBE normalization and leads to a conservative limit of 0.9 eV assuming 3 nearly degenerate neutrinos. The quoted limit is on the sum of the light neutrino masses.

[14] CROFT 99 result based on the power spectrum of the Ly α forest. If $\Omega_{\rm matter} < 0.5$, the limit is improved to $m_\nu < 2.4\ (\Omega_{\rm matter}/0.17\text{–}1)$ eV.

Limits on MASSES of Light Stable Right-Handed ν (with necessarily suppressed interaction strengths)

VALUE (eV)		DOCUMENT ID		TECN	COMMENT
• • • We do not use the following data for averages, fits, limits, etc. • • •					
<100–200	[15]	OLIVE	82	COSM	Dirac ν
<200–2000	[15]	OLIVE	82	COSM	Majorana ν

[15] Depending on interaction strength G_R where $G_R < G_F$.

Limits on MASSES of Heavy Stable Right-Handed ν (with necessarily suppressed interaction strengths)

VALUE (GeV)		DOCUMENT ID		TECN	COMMENT
• • • We do not use the following data for averages, fits, limits, etc. • • •					
> 10	[16]	OLIVE	82	COSM	G_R/G_F <0.1
>100	[16]	OLIVE	82	COSM	G_R/G_F <0.01

[16] These results apply to heavy Majorana neutrinos and are summarized by the equation: m_ν >1.2 GeV (G_F/G_R). The bound saturates, and if G_R is too small no mass range is allowed.

REFERENCES FOR Limits on Number of Neutrino Types and Sum of Neutrino Masses

BARGER	03C	PL B566 8	V. Barger *et al.*	
CROTTY	03	PR D67 123005	P. Crotty, J. Lesgourgues, S. Pastor	
CYBURT	03	PL B567 227	R.H. Cyburt, B.D. Fields, K.A. Olive	
HANNESTAD	03B	JCAP 0305 004	S. Hannestad	
HEISTER	03C	EPJ C28 1	A. Heister *et al.*	(ALEPH Collab.)
PIERPAOLI	03	MNRAS 342 L63	E. Pierpaoli	
SPERGEL	03	APJS 148 175	D.N. Spergel *et al.*	
ELGAROY	02	PRL 89 061301	O. Elgaroy *et al.*	
LEWIS	02	PR D66 103511	A. Lewis, S. Bridle	
WANG	02	PR D65 123001	X. Wang, M. Tegmark, M. Zaldarriaga	
CYBURT	01	ASP 17 87	R.H. Cyburt, B.D. Fields, K.A. Olive	
KNELLER	01	PR D64 123506	J.P. Kneller *et al.*	
ABBIENDI,G	00D	EPJ C18 253	G. Abbiendi *et al.*	(OPAL Collab.)
ABREU	00Z	EPJ C17 53	P. Abreu *et al.*	(DELPHI Collab.)
FUKUGITA	00	PRL 84 1082	M. Fukugita, G.C. Liu, N. Sugiyama	
ACCIARRI	99R	PL B470 268	M. Acciarri *et al.*	(L3 Collab.)
CROFT	99	PRL 83 1092	R.A.C. Croft, W. Hu, R. Dave	
LISI	99	PR D59 123520	E. Lisi, S. Sarkar, F.L. Villante	
OLIVE	99	ASP 11 403	K.A. Olive, D. Thomas	
ABREU	97J	ZPHY C74 577	P. Abreu *et al.*	(DELPHI Collab.)
COPI	97	PR D55 3389	C.J. Copi, D.N. Schramm, M.S. Turner	(CHIC)
HATA	97B	PR D55 540	N. Hata *et al.*	(OSU, PENN)
OLIVE	97	ASP 7 27	K.A. Olive, D. Thomas	(MINN, FLOR)
ADAM	96C	PL B380 471	W. Adam *et al.*	(DELPHI Collab.)
CARDALL	96B	APJ 472 435	C.Y. Cardall, G.M. Fuller	(UCSD)
FIELDS	96	New Ast 1 77	B.D. Fields *et al.*	(NDAM, CERN, MINN+)
KERNAN	96	PR D54 3681	P.S. Kernan, S. Sarkar	(CASE, OXFTP)
OLIVE	95	PL B354 357	K.A. Olive, G. Steigman	(MINN, OSU)
BUSKULIC	93L	PL B313 520	D. Buskulic *et al.*	(ALEPH Collab.)
LEP	92	PL B276 247	LEP Collabs.	(LEP, ALEPH, DELPHI, L3, OPAL)
WALKER	91	APJ 376 51	T.P. Walker *et al.*	(HSCA, OSU, CHIC+)
DENEGRI	90	RMP 62 1	D. Denegri, B. Sadoulet, M. Spiro	(CERN, UCB+)
OLIVE	90	PL B236 454	K.A. Olive *et al.*	(MINN, CHIC, OSU+)
COWSIK	85	PL 151B 62	R. Cowsik	(TATA)
FREESE	84	NP B233 167	K. Freese, D.N. Schramm	(CHIC, FNAL)
SCHRAMM	84	PL 141B 337	D.N. Schramm, G. Steigman	(FNAL, BART)
YANG	84	APJ 281 493	J. Yang *et al.*	(CHIC, BART)
OLIVE	82	PR D25 213	K.A. Olive, M.S. Turner	(CHIC, UCSB)
BERNSTEIN	81	PL 101B 39	J. Bernstein, G. Feinberg	(STEV, COLU)
OLIVE	81	APJ 246 557	K.A. Olive *et al.*	(CHIC, BART)
OLIVE	81C	NP B180 497	K.A. Olive, D.N. Schramm, G. Steigman	(EFI+)
STEIGMAN	79	PRL 43 239	G. Steigman, K.A. Olive, D.N. Schramm	(BART+)
YANG	79	APJ 227 697	J. Yang *et al.*	(CHIC, YALE, VIRG)
STEIGMAN	77	PL 66B 202	G. Steigman, D.N. Schramm, J.E. Gunn	(YALE, CHIC+)
VYSOTSKY	77	JETPL 26 188 Translated from ZETFP 26 200.	M.I. Vysotsky, A.D. Dolgov, Y.B. Zeldovich	(ITEP)
SZALAY	76	AA 49 437	A.S. Szalay, G. Marx	(EOTV)
SZALAY	74	APAH 35 8	A.S. Szalay, G. Marx	(EOTV)
COWSIK	72	PRL 29 669	R. Cowsik, J. McClelland	(UCB)
MARX	72	Nu Conf. Budapest	G. Marx, A.S. Szalay	(EOTV)
PEEBLES	71	Physical Cosmology Princeton Univ. Press (1971)	P.Z. Peebles	(PRIN)
SHVARTSMAN	69	JETPL 9 184 Translated from ZETFP 9 315.	V.F. Shvartsman	(MOSU)
GERSHTEIN	66	JETPL 4 120 Translated from ZETFP 4 189.	S.S. Gershtein, Y.B. Zeldovich	(KIAM)
HOYLE	64	NAT 203 1108	F. Hoyle, R.J. Tayler	(CAMB)

Double-β Decay

OMITTED FROM SUMMARY TABLE

LIMITS FROM NEUTRINOLESS DOUBLE-β DECAY

Revised September 2003 by P. Vogel (Caltech) and A. Piepke (University of Alabama).

Neutrinoless double-beta ($0\nu\beta\beta$) decay, if observed, would signal violation of the total lepton number conservation. The process can be mediated by an exchange of a light Majorana neutrino, or by an exchange of other particles. However, the existence of $0\nu\beta\beta$-decay requires Majorana neutrino mass, no matter what the actual mechanism is. As long as only a limit on the lifetime is available, limits on the effective Majorana neutrino mass, and on the lepton-number violating right-handed current can be obtained, independently on the actual mechanism. These limits are listed in the next three tables. In the following we *assume* that the exchange of light Majorana neutrinos ($m_{\nu_i} \leq \mathcal{O}(10\ {\rm MeV})$) contributes dominantly to the decay rate.

Besides a dependence on the phase space ($G^{0\nu}$) and the nuclear matrix element ($M^{0\nu}$), the observable $0\nu\beta\beta$-decay rate is proportional to the square of the effective Majorana mass ($\langle m_{\beta\beta}\rangle$), $(T^{0\nu}_{1/2})^{-1} = G^{0\nu} \cdot |M^{0\nu}|^2 \cdot |\langle m_{\beta\beta}\rangle|^2$, with $\langle m_{\beta\beta}\rangle = \sum_i U^2_{ei} m_{\nu_i}$. The sum contains, in general, complex CP phases in U^2_{ei}, i.e., cancelations may occur. For three neutrino flavors there are three physical phases for Majorana neutrinos and one for Dirac neutrinos. The two additional Majorana phases affect only total lepton number violating processes. Given the general 3×3 mixing matrix for Majorana neutrinos, one can construct other analogous lepton number violating quantities, $\sum_i U_{li} U_{l'i} m_{\nu_i}$. However, these are currently much less constrained than $\langle m_{\beta\beta}\rangle$.

Nuclear structure calculations are needed to deduce $\langle m_{\beta\beta}\rangle$ from the decay rate. While $G^{0\nu}$ can be calculated reliably, the computation of $M^{0\nu}$ is subject to considerable uncertainty. If the spread among different ways of evaluating the nuclear matrix elements is taken as a measure of error, then there is a factor of $\sim$3 uncertainty in the derived $\langle m_{\beta\beta}\rangle$ values.

The particle physics quantities to be determined are thus nuclear model-dependent, so the half-life measurements are listed first. Where possible, we reference the nuclear matrix elements used in the subsequent analysis. Since rates for the more conventional $2\nu\beta\beta$ decay serve to calibrate the nuclear theory, results for this process are also given.

Neutrino oscillation experiments yield strong evidence that at least some neutrinos are massive. However, these findings shed no light on the mass hierarchy, the absolute neutrino mass values or the properties of neutrinos under CP conjugation (Dirac or Majorana). The atmospheric neutrino anomaly implies $\Delta m^2_{atm} \sim (2-3) \times 10^{-3}$ eV^2 and a large mixing angle $\sin^2\theta_{atm} \approx \sin^2\theta_{23} \approx 0.5$. Oscillations of solar ν_e and reactor $\bar{\nu}_e$ neutrinos lead to the unique 'LMA solution' with $\Delta m^2_{sol} \sim 7 \times 10^{-5}$ eV^2 and $\sin^2\theta_{sol} \approx \sin^2\theta_{12} \approx 0.3$. The investigation of reactor $\bar{\nu}_e$ at 1 km baseline indicates that electron type neutrinos couple only weakly to the third mass eigenstate with $\sin^2\theta_{13} < 0.03$. The so called 'LSND evidence' for oscillations at short baseline requires $\Delta m^2 \sim 0.2 - 2$ eV^2 and small mixing.

Based on these results (and neglecting the not yet confirmed LSND signal): $|\langle m_{\beta\beta}\rangle|^2 \approx |\cos^2\theta_{sol}\ m_1 + e^{i\alpha_1}\ \sin^2\theta_{sol}\ m_2 + e^{i\alpha_2}\ \sin^2\theta_{13}\ m_3|^2$, with α_1, α_2 denoting CP phases. The apparent smallness of $\sin^2\theta_{13}$ thus effectively shields $\langle m_{\beta\beta}\rangle$ from one of the CP phases. Given the present knowledge of the neutrino oscillation parameters, both of the Δm^2 values and of the mixing angles, one can derive the relation between the effective Majorana mass and the mass of the lightest neutrino, as illustrated in Fig. 1. The contribution of possible sterile neutrinos has been neglected.

If the neutrinoless double-beta decay is observed, it will be possible to fix a *range* of absolute values of the masses m_{ν_i}. However, if direct neutrino mass measurements, e.g. using beta decay (which is sensitive to $m^{2(\mathrm{eff})}_{\nu_e} = \sum_i |U_{ei}|^2 m^2_{\nu_i}$), also yield positive results, we may learn something about the otherwise

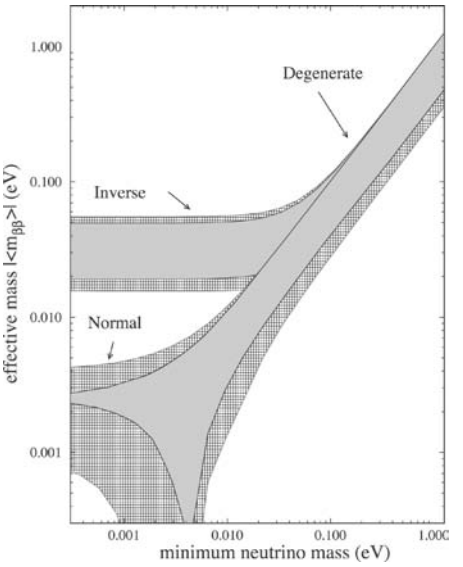

Figure 1: Dependence of the effective Majorana mass $\langle m_{\beta\beta}\rangle$ derived from the rate of neutrinoless double-beta decay ($1/T^{0\nu}_{1/2} \sim \left|\langle m_{\beta\beta}\rangle\right|^2$) on the absolute mass of the lightest neutrino. The arrows indicate the three possible neutrino mass patterns or "hierarchies." The curves are based on the 'LMA solution,' $\Delta m^2_{sol} = 7 \times 10^{-5}$ eV^2, $\sin^2\theta_{sol} = 0.3$, and $\Delta m^2_{atm} = 2.4 \times 10^{-3}$ eV^2, $\theta_{13} = 0$. The cross-hatched region is covered if one σ errors on these oscillation parameters are included.

inaccessible CP phases. To do so we have to assume that the Majorana mass is responsible for the decay and that the calculations of $M^{0\nu}$ will be improved. Unlike the direct neutrino mass measurements, however, a limit on $\langle m_{\beta\beta}\rangle$ does not allow one to constrain the individual mass values m_{ν_i} even when the mass differences Δm^2 are known.

Depending on the pattern of neutrino mass, $0\nu\beta\beta$-decay may be driven by the small Δm^2_{sol}, "normal hierarchy" in Fig. 1 ($\langle m_{\beta\beta}\rangle \sim \sin^2\theta_{sol}\sqrt{\Delta m^2_{sol}} \sim 5$ meV), or by the larger Δm^2_{atm}, "inverse hierarchy" in Fig. 1 ($\langle m_{\beta\beta}\rangle \sim \sqrt{\Delta m^2_{atm}} \sim 50$ meV). In the so called "degenerate" scenario an overall mass offset exists and $\langle m_{\beta\beta}\rangle$ is relatively large.

Neutrino oscillation data imply the existence of a *lower limit* for the Majorana neutrino mass for some of the mass patterns. Several new double-beta searches have been proposed to probe the interesting $\langle m_{\beta\beta}\rangle$ mass range.

If lepton-number violating right-handed current weak interactions exist, the $0\nu\beta\beta$ decay rate also depends on the quantities $\langle\eta\rangle = \eta\sum_i U_{ei}V_{ei}$ and $\langle\lambda\rangle = \lambda\sum_i U_{ei}V_{ei}$, where V_{lj} is a matrix analogous to U_{lj} but describing the mixing with

the hypothetical right-handed neutrinos and the coupling constants η and λ characterize the strength of the corresponding right-right and right-left weak interactions. The $\langle\eta\rangle$ and $\langle\lambda\rangle$ vanish for massless or unmixed neutrinos due to the unitarity of the generalized mixing matrix containing both the U and V matrices. The limits on $\langle\eta\rangle$ are of order 10^{-8}, while the limits on $\langle\lambda\rangle$ are of order 10^{-6}. The reader is cautioned that a number of earlier experiments did not distinguish between η and λ. In addition, see the section on Majoron searches for additional limits set by these experiments.

Half-life Measurements and Limits for Double-β Decay

In all cases of double-beta decay, (Z,A) $\rightarrow$ (Z+2,A) $+2e^-$ + (0 or 2)$\overline{\nu}_e$. In the following Listings, only best or comparable limits or lifetimes for each isotope are reported. For 2ν decay, which is well established, only measured half-lives are reported.

$t_{1/2}(10^{21}$ yr)	CL%	ISOTOPE	TRANSITION	METHOD	DOCUMENT ID
• • • We do not use the following data for averages, fits, limits, etc. • • •					
> 210	90	^{130}Te 0ν		Cryog. det.	[1] ARNABOLDI 03
> 31	90	^{130}Te 0ν	$0^+ \rightarrow 2^+$	Cryog. det.	[2] ARNABOLDI 03
$0.61 \pm 0.14^{+0.29}_{-0.35}$	90	^{130}Te 2ν		Cryog. det.	[3] ARNABOLDI 03
> 110	90	^{128}Te 0ν		Cryog. det.	[4] ARNABOLDI 03
$(0.029^{+0.004}_{-0.003})$		^{116}Cd 2ν		$^{116}CdWO_4$ scint.	[5] DANEVICH 03
> 170	90	^{116}Cd 0ν		$^{116}CdWO_4$ scint.	[6] DANEVICH 03
> 29	90	^{116}Cd 0ν	$0^+ \rightarrow 2^+$	$^{116}CdWO_4$ scint.	[7] DANEVICH 03
> 14	90	^{116}Cd 0ν	$0^+ \rightarrow 0^+_1$	$^{116}CdWO_4$ scint.	[8] DANEVICH 03
> 6	90	^{116}Cd 0ν	$0^+ \rightarrow 0^+_2$	$^{116}CdWO_4$ scint.	[9] DANEVICH 03
>15700	90	^{76}Ge 0ν		Enriched HPGe	[10] AALSETH 02B
> 58	90	^{134}Xe 0ν		Liquid Xe Scint.	[11] BERNABEI 02D
> 1200	90	^{136}Xe 0ν		Liquid Xe Scint.	[12] BERNABEI 02D
$15000^{+168000}_{-7500}$		^{76}Ge 0ν		Enriched HPGe	[13] KLAPDOR-K... 02D
$(7.2 \pm 0.9 \pm 1.8)$E-3		^{100}Mo 2ν		Liq. Ar ioniz.	[14] ASHITKOV 01
> 4.9	90	^{100}Mo 0ν		Liq. Ar ioniz.	[15] ASHITKOV 01
> 1.3	90	^{160}Gd 0ν		Gd_2SiO_5:Ce	[16] DANEVICH 01
> 1.3	90	^{160}Gd 0ν	$0^+ \rightarrow 2^+$	Gd_2SiO_5:Ce	[17] DANEVICH 01
$0.59^{+0.17}_{-0.11} \pm 0.06$		^{100}Mo $0\nu+2\nu$	$0^+ \rightarrow 0^+_1$	Ge coinc.	[18] DEBRAECKEL.01
> 55	90	^{100}Mo $0\nu,\langle m_\nu\rangle$		ELEGANT V	[19] EJIRI 01
> 42	90	^{100}Mo $0\nu,\langle\lambda\rangle$		ELEGANT V	[19] EJIRI 01
> 49	90	^{100}Mo $0\nu,\langle\eta\rangle$		ELEGANT V	[19] EJIRI 01
>19000	90	^{76}Ge 0ν		Enriched HPGe	[20] KLAPDOR-K... 01
$1.55 \pm 0.001^{+0.19}_{-0.15}$	90	^{76}Ge 2ν		Enriched HPGe	[21] KLAPDOR-K... 01
(9.4 ± 3.2)E-3	90	^{96}Zr $0\nu+2\nu$		Geochem	[22] WIESER 01
$0.042^{+0.033}_{-0.013}$		^{48}Ca 2ν		Ge spectrometer	[23] BRUDANIN 00
$0.021^{+0.008}_{-0.004} \pm 0.002$		^{96}Zr 2ν		NEMO-2	[24] ARNOLD 99
> 1.0	90	^{96}Zr 0ν		NEMO-2	[24] ARNOLD 99
$(8.3 \pm 1.0 \pm 0.7)$E-2		^{82}Se 2ν		NEMO-2	[25] ARNOLD 98
> 9.5	90	^{82}Se 0ν		NEMO-2	[26] ARNOLD 98
> 2.8	90	^{82}Se 0ν	$0^+ \rightarrow 2^+$	NEMO-2	[27] ARNOLD 98
$(7.6^{+2.2}_{-1.4})$E-3		^{100}Mo 2ν		Si(Li)	[28] ALSTON-... 97
$(6.82^{+0.38}_{-0.53} \pm 0.68)$E-3		^{100}Mo 2ν		TPC	[29] DESILVA 97
$(6.75^{+0.37}_{-0.42} \pm 0.68)$E-3		^{150}Nd 2ν		TPC	[30] DESILVA 97
> 1.2	90	^{150}Nd 0ν		TPC	[31] DESILVA 97
$1.77 \pm 0.01^{+0.13}_{-0.11}$		^{76}Ge 2ν		Enriched HPGe	[32] GUENTHER 97
$(3.75 \pm 0.35 \pm 0.21)$E-2		^{116}Cd 2ν	$0^+ \rightarrow 0^+$	NEMO 2	[33] ARNOLD 96
$0.043^{+0.024}_{-0.011} \pm 0.014$		^{48}Ca 2ν		TPC	[34] BALYSH 96
0.79 ± 0.10		^{130}Te $0\nu+2\nu$		Geochem	[35] TAKAOKA 96
$0.61^{+0.18}_{-0.11}$		^{100}Mo $0\nu+2\nu$	$0^+ \rightarrow 0^+_1$	γ in HPGe	[36] BARABASH 95
$(9.5 \pm 0.4 \pm 0.9)$E-3		^{100}Mo 2ν		NEMO 2	DASSIE 95
> 0.6	90	^{100}Mo 0ν	$0^+ \rightarrow 0^+_1$	NEMO 2	DASSIE 95
$0.026^{+0.009}_{-0.005}$		^{116}Cd 2ν	$0^+ \rightarrow 0^+$	ELEGANT IV	EJIRI 95
$0.017^{+0.010}_{-0.005} \pm 0.0035$		^{150}Nd 2ν	$0^+ \rightarrow 0^+$	TPC	ARTEMEV 93
0.039 ± 0.009		^{96}Zr $0\nu+2\nu$		Geochem	KAWASHIMA 93
2.7 ± 0.1		^{130}Te $0\nu+2\nu$		Geochem	BERNATOW... 92
7200 ± 400		^{128}Te $0\nu+2\nu$		Geochem	[37] BERNATOW... 92
> 27	68	^{82}Se 0ν	$0^+ \rightarrow 0^+$	TPC	ELLIOTT 92
$0.108^{+0.026}_{-0.006}$		^{82}Se 2ν	$0^+ \rightarrow 0^+$	TPC	ELLIOTT 92
2.0 ± 0.6		^{238}U $0\nu+2\nu$		Radiochem	[38] TURKEVICH 91
> 9.5	76	^{48}Ca 0ν		CaF_2 scint.	YOU 91
$0.12 \pm 0.01 \pm 0.04$	68	^{82}Se $0\nu+2\nu$		Geochem.	[39] LIN 88
$0.75 \pm 0.03 \pm 0.23$	68	^{130}Te $0\nu+2\nu$		Geochem.	[40] LIN 88
1800 ± 700	68	^{128}Te $0\nu+2\nu$		Geochem.	[41] LIN 88B
2.60 ± 0.28		^{130}Te $0\nu+2\nu$		Geochem	[42] KIRSTEN 83

[1] Supersedes ALESSANDRELLO 00. Array of TeO_2 crystals in high resolution cryogenic calorimeter. Some enriched in ^{130}Te. Ground state to ground state decay.

[2] Decay into first excited state of daughter nucleus.

[3] Two neutrino decay into ground state. Relatively large error mainly due to uncertainties in background determination. Reported value is shorter than the geochemical measurements of KIRSTEN 83 and BERNATOWICZ 92 but in agreement with LIN 88 and TAKAOKA 96.

[4] Supersedes ALESSANDRELLO 00. Array of TeO_2 crystals in high resolution cryogenic calorimeter. Some enriched in ^{128}Te. Ground state to ground state decay.

[5] Calorimetric measurement of 2ν ground state decay of ^{116}Cd using enriched $CdWO_4$ scintillators. Agrees with EJIRI 95 and ARNOLD 96. Supersedes DANEVICH 00.

[6] Limit on 0ν decay of ^{116}Cd using enriched $CdWO_4$ scintillators. Supersedes DANEVICH 00.

[7] Limit on 0ν decay of ^{116}Cd into first excited 2^+ state of daughter nucleus using enriched $CdWO_4$ scintillators. Supersedes DANEVICH 00.

[8] Limit on 0ν decay of ^{116}Cd into first excited 0^+ state of daughter nucleus using enriched $CdWO_4$ scintillators. Supersedes DANEVICH 00.

[9] Limit on 0ν decay of ^{116}Cd into second excited 0^+ state of daughter nucleus using enriched $CdWO_4$ scintillators. Supersedes DANEVICH 00.

[10] AALSETH 02B limit is based on 117 mol·yr of data using enriched Ge detectors. Background reduction by means of pulse shape analysis is applied to part of the data set. Reported limit is slightly less restrictive than that in KLAPDOR-KLEINGROTHAUS 01 However, it excludes part of the allowed half-life range reported in KLAPDOR-KLEINGROTHAUS 01B for the same nuclide.

[11] BERNABEI 02D report a limit for the 0ν, $0^+ \rightarrow 0^+$ decay of ^{134}Xe, present in the source at 17%, by considering the maximum number of events for this mode compatible with the fitted smooth background.

[12] BERNABEI 02D report a limit for the 0ν, $0^+ \rightarrow 0^+$ decay of ^{136}Xe, by considering the maximum number of events for this mode compatible with the fitted smooth background. The quoted sensitivity is 450×10^{21} yr. The Feldman and Cousins method is used to obtain the quoted limit.

[13] KLAPDOR-KLEINGROTHAUS 02D is an expanded version of KLAPDOR-KLEINGROTHAUS 01B. The authors re-evaluate the data collected by the Heidelberg-Moscow experiment (KLAPDOR-KLEINGROTHAUS 01) and present a more detailed description of their analysis of an excess of counts at the energy expected for neutrinoless double-beta decay. They interpret this excess, which has a significance of 2.2 to 3.1 σ depending on the data analysis, as evidence for the observation of Lepton Number violation and violation of Baryon minus Lepton Number. The analysis has been criticized by AALSETH 02 and others. The criticisms have been addressed in KLAPDOR-KLEINGROTHAUS 02. See also KLAPDOR-KLEINGROTHAUS 02B.

[14] ASHITKOV 01 result for 2ν of ^{100}Mo is in agreement with other determinations of that halflife.

[15] ASHITKOV 01 result for 0ν of ^{100}Mo is less stringent than EJIRI 01.

[16] DANEVICH 01 place limit on 0ν decay of ^{160}Gd using Gd_2SiO_5:Ce crystal scintillators. The limit is more stringent than KOBAYASHI 95.

[17] DANEVICH 01 place limits on 0ν decay of ^{160}Gd into excited 2^+ state of daughter nucleus using Gd_2SiO_5:Ce crystal scintillators.

[18] DEBRAECKELEER 01 performed an inclusive measurement of the $\beta\beta$ decay into the second excited state of the daughter nucleus. A novel coincidence technique counting the de-excitation photons is employed. The result agrees with BARABASH 95.

[19] EJIRI 01 uses tracking calorimeter and isotopically enriched passive source. Efficiencies were calculated assuming $\langle m_\nu\rangle$, $\langle\lambda\rangle$, or $\langle\eta\rangle$ driven decay. This is a continuation of EJIRI 96 which it supersedes.

[20] KLAPDOR-KLEINGROTHAUS 01 is a continuation of the work published in BAUDIS 99. Isotopically enriched Ge detectors are used in calorimetric measurement. The most stringent bound is derived from the data set in which pulse-shape analysis has been used to reduce background. Exposure time is 35.5 kg·y. Supersedes BAUDIS 99 as most stringent result.

[21] KLAPDOR-KLEINGROTHAUS 01 is a measurement of the $\beta\beta2\nu$-decay rate with higher statistics than GUENTHER 97. The reported value has a worse systematic error than their previous result.

[22] WIESER 01 reports an inclusive geochemical measurement of ^{96}Zr $\beta\beta$ half life. Their result agrees within 2σ with ARNOLD 99 but only marginally, within 3σ, with KAWASHIMA 93.

[23] BRUDANIN 00 determine the 2ν halflife of ^{48}Ca. Their value is less accurate than BALYSH 96.

[24] ARNOLD 99 measure directly the 2ν decay of Zr for the first time, using the NEMO-2 tracking detector and an isotopically enriched source. The lifetime is more accurate than the geochemical result of KAWASHIMA 93.

[25] ARNOLD 98 measure the 2ν decay of ^{82}Se by comparing the spectra in an enriched and natural selenium source using the NEMO-2 tracking detector. The measured half-life is in agreement, perhaps slightly shorter, than ELLIOTT 92.

[26] ARNOLD 98 determine the limit for 0ν decay to the ground state of ^{82}Se using the NEMO-2 tracking detector. The half-life limit is in agreement, but less stringent, than ELLIOTT 92.

[27] ARNOLD 98 determine the limit for 0ν decay to the excited 2^+ state of ^{82}Se using the NEMO-2 tracking detector.

[28] ALSTON-GARNJOST 97 report evidence for 2ν decay of ^{100}Mo. This decay has been also observed by EJIRI 91, DASSIE 95, and DESILVA 97.

[29] DESILVA 97 result for 2ν decay of ^{100}Mo is in agreement with ALSTON-GARNJOST 97 and DASSIE 95. This measurement has the smallest errors.

[30] DESILVA 97 result for 2ν decay of ^{150}Nd is in marginal agreement with ARTEMEV 93. It has smaller errors.

[31] DESILVA 97 do not explain whether their efficiency for 0ν decay of ^{150}Nd was calculated under the assumption of a $\langle m_\nu\rangle$, $\langle\lambda\rangle$, or $\langle\eta\rangle$ driven decay.

[32] GUENTHER 97 half-life for the 2ν decay of ^{76}Ge is not in good agreement with the previous measurements of BALYSH 94, AVIGNONE 91, and MILEY 90.

[33] ARNOLD 96 measure the 2ν decay of ^{116}Cd. This result is in agreement with EJIRI 95, but has smaller errors. Supersedes ARNOLD 95.

[34] BALYSH 96 measure the 2ν decay of ^{48}Ca, using a passive source of enriched ^{48}Ca in a TPC.

[35] TAKAOKA 96 measure the geochemical half-life of ^{130}Te. Their value is in disagreement with the quoted values of BERNATOWICZ 92 and KIRSTEN 83; but agrees with several other unquoted determinations, e.g., MANUEL 91.

[36] BARABASH 95 cannot distinguish 0ν and 2ν, but it is inferred indirectly that the 0ν mode accounts for less than 0.026% of their event sample. They also note that their result disagrees with the previous experiment by the NEMO group (BLUM 92).

[37] BERNATOWICZ 92 finds ^{128}Te/^{130}Te activity ratio from slope of ^{128}Xe/^{132}Xe vs ^{130}Xe/^{132}Xe ratios during extraction, and normalizes to lead-dated ages for the ^{130}Te lifetime. The authors state that their results imply that "(a) the double beta decay of ^{128}Te has been firmly established and its half-life has been determined ... without any ambiguity due to trapped Xe interferences... (b) Theoretical calculations ... underestimate the [long half-lives of ^{128}Te ^{130}Te] by 1 or 2 orders of magnitude, pointing to a real suppression in the 2ν decay rate of these isotopes. (c) Despite [this], most $\beta\beta$-models predict a *ratio* of 2ν decay widths ... in fair agreement with observation." Further details of the experiment are given in BERNATOWICZ 93. Our listed half-life has been revised downward from the published value by the authors, on the basis of reevaluated cosmic-ray ^{128}Xe production corrections.

[38] TURKEVICH 91 observes activity in old U sample. The authors compare their results with theoretical calculations. They state "Using the phase-space factors of Boehm and Vogel (BOEHM 87) leads to matrix element values for the ^{238}U transition in the same range as deduced for ^{130}Te and ^{76}Ge. On the other hand, the latest theoretical estimates (STAUDT 90) give an upper limit that is 10 times lower. This large discrepancy implies either a defect in the calculations or the presence of a faster path than the standard two-neutrino mode in this case." See BOEHM 87 and STAUDT 90.

[39] Result agrees with direct determination of ELLIOTT 92.

[40] Inclusive half life inferred from mass spectroscopic determination of abundance of $\beta\beta$-decay product ^{130}Te in mineral kitkaite (NiTeSe). Systematic uncertainty reflects variations in U-Xe gas-retention-age derived from different uranite samples. Agrees with geochemical determination of TAKAOKA 96 and direct measurement of ARNABOLDI 03. Inconsistent with results of KIRSTEN 83 and BERNATOWICZ 92.

[41] Ratio of inclusive double beta half lives of ^{128}Te and ^{130}Te determined from minerals melonite ($NiTe_2$) and altaite (PbTe) by means of mass spectroscopic measurement of abundance of $\beta\beta$-decay products. As gas-retention-age could not be determined the authors use half life of ^{130}Te (LIN 88) to infer the half life of ^{128}Te. No estimate of the systematic uncertainty of this method is given. The directly determined half life ratio agrees with BERNATOWICZ 92. However, the inferred ^{128}Te half life disagrees with KIRSTEN 83 and BERNATOWICZ 92.

[42] KIRSTEN 83 reports "2σ" error. References are given to earlier determinations of the ^{130}Te lifetime.

$\langle m_\nu \rangle$, The Effective Weighted Sum of Majorana Neutrino Masses Contributing to Neutrinoless Double-β Decay

$\langle m_\nu \rangle = |\sum U_{1j}^2 m_{\nu_j}|$, where the sum goes from 1 to n and where n = number of neutrino generations, and ν_j is a Majorana neutrino. Note that U_{ej}^2, not $|U_{ej}|^2$, occurs in the sum. The possibility of cancellations has been stressed. In the following Listings, only best or comparable limits or lifetimes for each isotope are reported.

VALUE (eV)	CL%	ISOTOPE	TRANSITION	METHOD	DOCUMENT ID	
• • • We do not use the following data for averages, fits, limits, etc. • • •						
< 1.1–2.6	90	^{130}Te		Cryo. det.	[43] ARNABOLDI	03
< 1.5–1.7	90	^{116}Cd	0ν	$^{116}CdWO_4$ scint.	[44] DANEVICH	03
< 0.33–1.35	90			Enriched HPGe	[45] AALSETH	02B
< 2.9	90	^{136}Xe	0ν	Liquid Xe Scint.	[46] BERNABEI	02D
$0.39^{+0.17}_{-0.28}$		^{76}Ge	0ν	Enriched HPGe	[47] KLAPDOR-K...	02D
< 2.1–4.8	90	^{100}Mo	0ν	ELEGANT V	[48] EJIRI	01
< 0.35	90	^{76}Ge		Enriched HPGe	[49] KLAPDOR-K...	01
< 23	90	^{96}Zr		NEMO-2	[50] ARNOLD	99
< 1.1–1.5		^{128}Te		Geochem	[51] BERNATOW...	92
< 5	68	^{82}Se		TPC	[52] ELLIOTT	92
< 8.3	76	^{48}Ca	0ν	CaF_2 scint.	YOU	91

[43] Supersedes ALESSANDRELLO 00. Cryogenic calorimeter search. Reported a range reflecting uncertainty in nuclear matrix element calculations.

[44] Limit for $\langle m_\nu \rangle$ is based on the nuclear matrix elements of STAUDT 90 and ARNOLD 96. Supersedes DANEVICH 00.

[45] AALSETH 02B reported range of limits on $\langle m_\nu \rangle$ reflects the spread of theoretical nuclear matrix elements. Excludes part of allowed mass range reported in KLAPDOR-KLEINGROTHAUS 01B.

[46] BERNABEI 02D limit is based on the matrix elements of SIMKOVIC 02. The range of neutrino masses based on a variety of matrix elements is 1.1–2.9 eV.

[47] KLAPDOR-KLEINGROTHAUS 02D is a detailed description of the analysis of the data collected by the Heidelberg-Moscow experiment, previously presented in KLAPDOR-KLEINGROTHAUS 01B. Matrix elements in STAUDT 90 have been used. See the footnote in the preceding table for further details. See also KLAPDOR-KLEINGROTHAUS 02B.

[48] The range of the reported $\langle m_\nu \rangle$ values reflects the spread of the nuclear matrix elements. On axis value assuming $\langle \lambda \rangle = \langle \eta \rangle = 0$.

[49] KLAPDOR-KLEINGROTHAUS 01 uses the calculation by STAUDT 90. Using several other models in the literature could worsen the limit up to 1.2 eV. This is the most stringent experimental bound on m_ν. It supersedes BAUDIS 99B.

[50] ARNOLD 99 limit based on the nuclear matrix elements of STAUDT 90.

[51] BERNATOWICZ 92 finds these majorana neutrino mass limits assuming that the measured geochemical decay width is a limit on the 0ν decay width. The range is the range found using matrix elements from HAXTON 84, TOMODA 87, and SUHONEN 91. Further details of the experiment are given in BERNATOWICZ 93.

[52] ELLIOTT 92 uses the matrix elements of HAXTON 84.

Limits on Lepton-Number Violating ($V+A$) Current Admixture

For reasons given in the discussion at the beginning of this section, we list only results from 1989 and later. $\langle \lambda \rangle = \lambda \sum U_{ej} V_{ej}$ and $\langle \eta \rangle = \eta \sum U_{ej} V_{ej}$, where the sum is over the number of neutrino generations. This sum vanishes for massless or unmixed neutrinos. In the following Listings, only best or comparable limits or lifetimes for each isotope are reported.

$\langle \lambda \rangle$ (10^{-6})	CL%	$\langle \eta \rangle$ (10^{-8})	CL%	ISOTOPE	METHOD	DOCUMENT ID	
• • • We do not use the following data for averages, fits, limits, etc. • • •							
< 1.6–2.4	90	< 0.9–5.3	90	^{130}Te	Cryo. det.	[53] ARNABOLDI	03
< 2.2	90	< 2.5	90	^{116}Cd	$^{116}CdWO_4$ scint.	[54] DANEVICH	03
< 3.2–4.7	90	< 2.4–2.7	90	^{100}Mo	ELEGANT V	[55] EJIRI	01
< 1.1	90	< 0.64	90	^{76}Ge	Enriched HPGe	[56] GUENTHER	97
< 4.4	90	< 2.3	90	^{136}Xe	TPC	[57] VUILLEUMIER	93
		< 5.3		^{128}Te	Geochem	[58] BERNATOW...	92

[53] Supersedes ALESSANDRELLO 00. Cryogenic calorimeter search. Reported a range reflecting uncertainty in nuclear matrix element calculations.

[54] Limits for $\langle \lambda \rangle$ and $\langle \eta \rangle$ are based on nuclear matrix elements of STAUDT 90. Supersedes DANEVICH 00.

[55] The range of the reported $\langle \lambda \rangle$ and $\langle \eta \rangle$ values reflects the spread of the nuclear matrix elements. On axis value assuming $\langle m_\nu \rangle = 0$ and $\langle \lambda \rangle = \langle \eta \rangle = 0$, respectively.

[56] GUENTHER 97 limits use the matrix elements of STAUDT 90. Supersedes BALYSH 95 and BALYSH 92.

[57] VUILLEUMIER 93 uses the matrix elements of MUTO 89. Based on a half-life limit 2.6×10^{23} y at 90%CL.

[58] BERNATOWICZ 92 takes the measured geochemical decay width as a limit on the 0ν width, and uses the SUHONEN 91 coefficients to obtain the least restrictive limit on η. Further details of the experiment are given in BERNATOWICZ 93.

Double-β Decay REFERENCES

ARNABOLDI	03	PL B557 167	C. Arnaboldi *et al.*
DANEVICH	03	PR C68 035501	F.A. Danevich *et al.*
AALSETH	02	MPL A17 1475	C.E. Aalseth *et al.*
AALSETH	02B	PR D65 092007	C.E. Aalseth *et al.* (IGEX Collab.)
BERNABEI	02D	PL B546 23	R. Bernabei *et al.* (DAMA Collab.)
KLAPDOR-K...	02	hep-ph/0205228	H.V. Klapdor-Kleingrothaus
KLAPDOR-K...	02B	JINRRC 110 57	H.V. Klapdor-Kleingrothaus, A. Dietz, I.V. Krivosheina
KLAPDOR-K...	02D	FP 32 1181	H.V. Klapdor-Kleingrothaus, A. Dietz, I.V. Krivosheina
SIMKOVIC	02	hep-ph/0204278	F. Simkovic, P. Domin, A. Faessler
ASHITKOV	01	JETPL 74 529 Translated from ZETFP 74 601.	V.D. Ashitkov *et al.*
DANEVICH	01	NP A694 375	F.A. Danevich *et al.*
DEBRAECKEL...	01	PRL 86 3510	L. De Braeckeleer *et al.*
EJIRI	01	PR C63 065501	H. Ejiri *et al.*
KLAPDOR-K...	01	EPJ A12 147	H.V. Klapdor-Kleingrothaus *et al.*
KLAPDOR-K...	01B	MPL A16 2409	H.V. Klapdor-Kleingrothaus *et al.*
WIESER	01	PR C64 024308	M.E. Wieser, J.R. De Laeter
ALESSAND...	00	PL B486 13	A. Alessandrello *et al.*
BRUDANIN	00	PL B495 63	V.B. Brudanin *et al.*
DANEVICH	00	PR C62 045501	F.A. Danevich *et al.*
ARNOLD	99	NP A658 299	R. Arnold *et al.* (NEMO Collab.)
BAUDIS	99	PR D59 022001	L. Baudis *et al.* (Heidelberg-Moscow Collab.)
BAUDIS	99B	PRL 83 41	L. Baudis *et al.* (Heidelberg-Moscow Collab.)
ARNOLD	98	NP A636 209	R. Arnold *et al.* (NEMO-2 Collab.)
ALSTON-...	97	PR C55 474	M. Alston-Garnjost *et al.* (LBL, MTHO+)
DESILVA	97	PR C56 2451	A. de Silva *et al.* (UCI)
GUENTHER	97	PR D55 54	M. Gunther *et al.* (Heidelberg-Moscow Collab.)
ARNOLD	96	ZPHY C72 239	R. Arnold *et al.* (BCEN, CAEN, JINR+)
BALYSH	96	PRL 77 5186	A. Balysh *et al.* (KIAE, UCI, CIT)
EJIRI	96	NP A611 85	H. Ejiri *et al.* (OSAK)
TAKAOKA	96	PR C53 1557	N. Takaoka, Y. Motomura, K. Nagao (KYUSH, OKAY)
ARNOLD	95	JETPL 61 170 Translated from ZETFP 61 168.	R.G. Arnold *et al.* (NEMO Collab.)
BALYSH	95	PL B356 450	A. Balysh *et al.* (Heidelberg-Moscow Collab.)
BARABASH	95	PL B345 408	A.S. Barabash *et al.* (ITEP, SCUC, PNL+)
DASSIE	95	PR D51 2090	D. Dassie *et al.* (NEMO Collab.)
EJIRI	95	JPSJ 64 339	H. Ejiri *et al.* (OSAK, KIEV)
KOBAYASHI	95	NP A586 457	M. Kobayashi, M. Kobayashi (KEK, SAGA)
BALYSH	94	PL B322 176	A. Balysh *et al.* (Heidelberg-Moscow Collab.)
ARTEMEV	93	JETPL 58 262 Translated from ZETFP 58 256.	V.A. Artemiev *et al.* (ITEP, INRM)
BERNATOW...	93	PR C47 806	T. Bernatowicz *et al.* (WUSL, TATA)
KAWASHIMA	93	PR C47 R2452	A. Kawashima, K. Takahashi, A. Masuda (TOKYC+)
VUILLEUMIER	93	PR D48 1009	J.C. Vuilleumier *et al.* (NEUC, CIT, VILL)
BALYSH	92	PL B283 32	A. Balysh *et al.* (MPIH, KIAE, SASSO)
BERNATOW...	92	PRL 69 2341	T. Bernatowicz *et al.* (WUSL, TATA)
BLUM	92	PL B275 506	D. Blum *et al.* (NEMO Collab.)
ELLIOTT	92	PR C46 1535	S.R. Elliott *et al.* (UCI)
AVIGNONE	91	PL B256 559	F.T. Avignone *et al.* (SCUC, PNL, ITEP+)
EJIRI	91	PL B258 17	H. Ejiri *et al.* (OSAK)
MANUEL	91	JPG 17 S221	O.K. Manuel (MISSR)
SUHONEN	91	NP A535 509	J. Suhonen, S.B. Khadkikar, A. Faessler (JYV+)
TURKEVICH	91	PRL 67 3211	A. Turkevich, T.E. Economou, G.A. Cowan (CHIC+)
YOU	91	PL B265 53	K. You *et al.* (BHEP, CAST+)
MILEY	90	PRL 65 3092	H.S. Miley *et al.* (SCUC, PNL)
STAUDT	90	EPL 13 31	A. Staudt, K. Muto, H.V. Klapdor-Kleingrothaus
MUTO	89	ZPHY A334 187	K. Muto, E. Bender, H.V. Klapdor (TINT, MPIH)
LIN	88	NP A481 477	W.J. Lin *et al.*
LIN	88B	NP A481 484	W.J. Lin *et al.*
BOEHM	87	Massive Neutrinos Cambridge Univ. Press, Cambridge	F. Boehm, P. Vogel (CIT)
TOMODA	87	PL B199 475	T. Tomoda, A. Faessler (TUBIN)
HAXTON	84	PPNP 12 409	W.C. Haxton, G.J. Stevenson
KIRSTEN	83	PRL 50 474	T. Kirsten, H. Richter, E. Jessberger (MPIH)

See key on page 323

UNDERSTANDING TWO-FLAVOR OSCILLATION PARAMETERS AND LIMITS

Revised March 2002 by D.E. Groom (LBNL).

As discussed in Boris Kayser's Review "Neutrino Mass, Mixing, and Flavor Change," there are several conditions under which the two-neutrino mixing approximation is valid. Many results have been published with this assumption, whether it is valid or not. In this context, and in the context of vacuum oscillations, the probability that a neutrino with original flavor ℓ, for example, oscillates into a flavor ℓ' over a distance L in vacuum is given by

$$P(\nu_\ell \to \nu_{\ell'}) = \sin^2 2\theta \sin^2(\Delta m^2_{ij} L/4\hbar cE) = \sin^2 2\theta \sin^2(1.27\Delta m^2_{ij}(\mathrm{eV}^2)\, L(\mathrm{km})/E(\mathrm{GeV})) \quad (1)$$

where we assume that mass eigenstates i and j are involved. Although this equation is frequently quoted and is used in Monte Carlo calculations, the function is badly behaved for arguments larger than about one, where it oscillates more and more rapidly between $\sin^2 2\theta = P$ and $\sin^2 2\theta = 0$ as the argument increases. It is difficult to relate this function to the exclusion curves in the literature.

In a real experiment, E, and sometimes L, have some spread due to various effects, but in a subset of these experiments there is a well-defined $\langle L/E\rangle$ about which the events distribute. It is instructive to make a toy model in which $b \equiv 1.27L/E$ has a Gaussian distribution with standard deviation σ_b about a central value b_0. The convolution of this Gaussian with P as given in Eq. (1) is analytic, with the result

$$\langle P\rangle = \tfrac{1}{2}\sin^2 2\theta[1 - \cos(2b_0\Delta m^2_{ij})\exp(-2\sigma_b^2(\Delta m^2_{ij})^2)]\ . \quad (2)$$

The value of $\langle P\rangle$ is set by the experiment. For example, if 230 interactions of the expected flavor are detected and none of the wrong flavor are seen, then $P = 0.010$ at the 90% CL (slightly subject to one's way of calculating the CL). Then with fixed $\langle P\rangle$ we can find $\sin^2 2\theta$ as a function of Δm^2_{ij}. This function is shown in Fig. 1(a) and (c) for particular parameter choices. The resulting parameter exclusion region boundary has the following features:

(1) For large Δm^2_{ij} the fast oscillations are completely washed out by the resolution, and $\sin^2 2\theta = 2\langle P\rangle$ in this limit;

(2) the maximum excursion of the curve to the left is to $\sin^2 2\theta = \langle P\rangle$ if the resolution is very good, and somewhat smaller if it is not. This "bump" to the left occurs at $\Delta m^2_{ij} = \pi/2b_0$;

(3) For large $\sin^2 2\theta$, $\Delta m^2_{ij} \approx \sqrt{\langle P\rangle}/(b_0\sqrt{\sin^2 2\theta})$; and, consequently,

  (a) the nearly straight-line segment at the bottom is described by $\Delta m^2_{ij} \approx \langle P\rangle/b_0\sqrt{\sin^2 2\theta}$

  (b) the intercept at $\sin^2 2\theta = 1$ is at $\Delta m^2_{ij} = \sqrt{\langle P\rangle}/b_0 = \sqrt{\langle P\rangle}/1.27\langle L/E\rangle$.

The intercept for large Δm^2_{ij} is a measure of running time and backgrounds, while the intercept at $\sin^2 2\theta = 1$ also depends upon $\langle L/E\rangle$. The wiggles depend upon the experimental features such as the size of the source, the neutrino energy distribution, detector resolution (L and E), and analysis details. Aside from such details, the two intercepts completely describe the exclusion region: For large Δm^2_{ij}, $\sin^2 2\theta$ is constant and equal to $2\langle P\rangle$, and for large $\sin^2 2\theta$ the slope and intercept are known. For these reasons, it is (nearly) sufficient to summarize the results of an experiment by stating the two intercepts, as is done in our Listings in cases where two-neutrino analyses of this sort have been published.

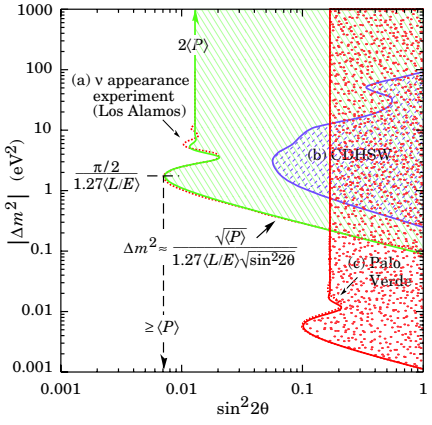

Figure 1: Neutrino oscillation parameter ranges excluded by three experiments. The dotted line in (a) is from an older Los Alamos appearance experiment (DURKIN 88), while the solid line is obtained from Eq. (2) using the parameters $\langle P\rangle = 0.0065$, $\Delta m^2 = 0.095$ eV^2 at $\sin^2 2\theta = 1$, and $\sigma_b/b_0 = 0.23$; (b) is a disappearance experiment with the flux obtained from the data in a long detector (DYDAK 84); and for (c) the Palo Verde reactor experiment result (BOEHM 01) is shown by the dotted line. In this experiment the flux at production is known. The solid line is calculated from Eq. (2) using $\langle P\rangle = 0.084$, $\Delta m^2 = 0.0011$ eV^2 at $\sin^2 2\theta = 1$, and $\sigma_b/b_0 = 0.3$. The experiments have been chosen for illustrative purposes, and none represents a current best limit. See full-color version on color pages at end of book.

While there is no reason for such a naïve 3-parameter function to describe all real experiments, the function actually does give a remarkably good description of *some* experimental results, underscoring the usefulness of the way we report results in the Listings. In example (a) in Fig. 1, the dotted curve shows the result obtained in an old Los Alamos appearance experiment (DURKIN 88). DURKIN 88 reports $\Delta m^2 = 0.11$ eV^2 for maximal mixing and $\sin^2 2\theta = 2 \times 0.070$ for large Δm^2. The solid curve is obtained using Eq. (2), with parameters $\langle P\rangle = 0.0065$, $\Delta m^2 = 0.095$ eV^2 at $\sin^2 2\theta = 1$, and $\sigma_b/b_0 = 0.23$.

If a positive effect is claimed, then the excluded region is replaced by an allowed band. However, in a real experiment there is usually other information, such as estimators of L and E for each event. The likelihood function is formed using this

event-by-event information. The CL is not uniform along the allowed band, resulting in "islands" of high confidence.

In a "disappearance" experiment, one looks for the attenuation of the initial lepton eigenstate ν_ℓ beam in transit to a detector, where the ν_ℓ flux is measured. (We label such experiments as $\nu_\ell \not\to \nu_\ell$.) In the two-neutrino mixing approximation, the probability that a lepton eigenstate remains unscathed from the production point to the detector is given by

$$P(\nu_\ell \to \nu_\ell) = 1 - P(\nu_\ell \to \nu_{\ell'}) \ , \qquad (3)$$

where mixing occurs between the ν_ℓ and $\nu_{\ell'}$, with $P(\nu_\ell \to \nu_{\ell'})$ given by Eq. (1) or Eq. (2).

The disappearance of a small fraction of the "right-flavor" neutrinos in such an experiment can go unobserved because of statistical fluctuations—if 100 events are expected and 95 events are observed, nothing is proven.* For this reason, disappearance experiments usually cannot establish small-probability (small $\sin^2 2\theta$) mixing.

Disappearance experiments fall into several classes:

(1) Those in which attenuation or oscillation of the beam neutrino flux is measured in the apparatus itself (two detectors, or a "long" detector). Above some minimum Δm^2_{ij} the equilibrium is established upstream, and there is no change in intensity over the length of the apparatus. As a result, sensitivity is lost at high Δm^2_{ij}, as can be seen by the CDHSW curve, Fig. 1(b) (DYDAK 84). Such experiments have not been competitive for a long time. However, a new generation of long-baseline experiments will use this strategy to advantage.

(2) Accelerator and reactor experiments in which the beam neutrino flux is known, from theory or from other measurements. Although such experiments cannot establish very small $\sin^2 2\theta$ mixing, they can establish small limits on Δm^2_{ij} for large $\sin^2 2\theta$ because L/E can be very large. Results of the Palo Verde experiment (BOEHM 01) are shown by the dotted curve (c) in Fig. 1. The solid curve has been calculated via Eq. (2), with parameters $\langle P \rangle = 0.084$, $\Delta m^2 = 0.0011$ eV^2 at $\sin^2 2\theta = 1$ (very nearly the values reported in BOEHM 01), and $\sigma_b/b_0 = 0.3$.

(3) Atmospheric neutrino experiments, in which ν_e and ν_μ are detected over a large range of L (the diameter of the earth). This is a subset of (1) above, and the resulting curves, in this case showing a positive effect, are similar.

This discussion has so far been limited to "vacuum oscillations," where the mixing probability is described Eq. (1). In the solar neutrino case it is likely that interactions between the neutrinos and solar electrons affect the oscillation probability ("matter oscillations," the MSW effect). This effect is described in the Review "Neutrino Mass, Mixing, and Flavor Change," by Boris Kayser. In this situation the formalism discussed above is not applicable.

* In contrast, if 5 golden "wrong-flavor" events are seen among 100 "right-flavor" events, a great deal is learned.

Eq. (1) depends on the mixing angle only through $\sin^2 2\theta$, giving the false impression that physically distinct possibilities map one-to-one onto the interval [0,1] in $\sin^2 2\theta$.† The relationship between mass eigenstates, *e.g.*, ν_1, ν_2, and weak eigenstates, *e.g.*, ν_e, ν_μ, is given by

$$\begin{pmatrix} |\nu_1\rangle \\ |\nu_2\rangle \end{pmatrix} = \begin{pmatrix} \cos\theta & -\sin\theta \\ \sin\theta & \cos\theta \end{pmatrix} \begin{pmatrix} |\nu_e\rangle \\ |\nu_\mu\rangle \end{pmatrix} \ . \qquad (4)$$

By convention, we can take ν_2 always heavier than ν_1, *i.e.*, $\Delta m^2_{21} = m^2_2 - m^2_1 > 0$, without a loss of generality. The $\theta \to 0$ limit is relevant when there is no mixing and ν_e is lighter, while $\theta \to \pi/2$ is needed to describe the possibility where ν_e is heavier with no mixing. Therefore, θ needs to be varied between 0 and $\pi/2$, which makes $\sin^2 2\theta$ fold at 1 back down to 0. In the case of oscillation in vacuum, θ and $\pi/2 - \theta$ happen to give identical oscillation probabilities, even though they are physically inequivalent. In this case, the use of $\sin^2 2\theta$ is misleading, but acceptable from practical point of view. In presence of matter effects, even the oscillation probabilities are different, and $\sin^2 2\theta$ is not an appropriate parameter in oscillation parameter plots. One common choice is $\tan^2\theta$, because it can cover the whole range of $0 \le \theta \le \pi/2$, while showing the same probabilities for $\theta \leftrightarrow \pi/2 - \theta$ in the absence of matter effects as a reflection symmetry around $\tan^2\theta = 1$ if plotted on log scale.‡

Neutrino Mixing

INTRODUCTION TO NEUTRINO MIXING LISTINGS

Based on the discussion in the previous review "Understanding Two-Flavor Oscillation Parameters and Limits" by Don Groom, most results in the neutrino mixing listings are presented as Δm^2 limits (or ranges) for $\sin^2 2\theta = 1$, and $\sin^2 2\theta$ limits (or ranges) for large Δm^2. Together, they summarize most of the information contained in the usual Δm^2 vs $\sin^2 2\theta$ plots in the experiments' papers. The neutrino mixing listings are divided into four sub-sections:

(A) Accelerator neutrino experiments: shows Δm^2 and $\sin^2 2\theta$ limits for, successively, $\nu_e \to \nu_\tau$ and $\overline{\nu}_e \to \overline{\nu}_\tau$ appearance, $\nu_e \not\to \nu_e$ disappearance, $\nu_\mu \to \nu_e$, $\overline{\nu}_\mu \to \overline{\nu}_e$, $\nu_\mu \to \nu_\tau$ and $\overline{\nu}_\mu \to \overline{\nu}_\tau$ appearance, and $\nu_\mu \not\to \nu_\mu$ and $\overline{\nu}_\mu \not\to \overline{\nu}_\mu$ disappearance. They are all limits, except for the positive $\nu_\mu \not\to \nu_\mu$ signal from the K2K collaboration reported in AHN 03.

(B) Reactor $\overline{\nu}_e$ disappearance experiments: has Δm^2 and $\sin^2 2\theta$ limits for $\overline{\nu}_e \not\to \overline{\nu}_e$ disappearance, together with the ratios of measured to expected rates of events. It also contains

† For example, see G.L. Fogli, E. Lisi, and D. Montanino, Phys. Rev. **D54**, 2048 (1996), and A. de Gouvêa, A. Friedland, and H. Murayama, Phys. Lett. **B490**, 125 (2000)

‡ This discussion of the $\pi/4 \le \theta \le \pi/2$ region was contributed by H. Murayama.

the positive signal from the KamLAND collaboration (EGUCHI 03).

(C) Atmospheric neutrino observations: lists the ratio of measured to expect ν_μ rate, the double ratio of measured ν_μ/ν_e rates over expected, and the up/down ratio of measured over expected for both ν_μ and ν_e. It also gives Δm^2 and $\sin^2 2\theta$ limits for $\nu_e \leftrightarrow \nu_\mu$ and $\overline{\nu}_e \leftrightarrow \overline{\nu}_\mu$, as well as the Kamiokande, SuperKamiokande and MACRO measurements of both $\sin^2 2\theta$ and Δm^2 for $\nu_\mu \leftrightarrow \nu_\tau$ oscillations, together with limits on ν_μ oscillations to a sterile neutrino.

(D) Solar ν experiments: is organized differently, showing first the results from radiochemical experiments and moving then to results of ^{8}B fluxes from elastic scattering, charged current and neutral current. From these, the solar fluxes for all three neutrino flavors combined and for only ν_μ and ν_τ are derived and listed. The day/night asymmetry for ^{8}B is also listed. Finally, the Kamiokande limit on the "hep" ν_e flux from the sun as measured in elastic scattering is given.

(A) Accelerator neutrino experiments

$\nu_e \rightarrow \nu_\tau$

$\Delta(m^2)$ for $\sin^2(2\theta) = 1$

VALUE (eV^2)	CL%	DOCUMENT ID		TECN	COMMENT
< 0.77	90	[1] ARMBRUSTER	98	KARM	
• • • We do not use the following data for averages, fits, limits, etc. • • •					
< 5.9	90	[2] ASTIER	01B	NOMD	CERN SPS
< 7.5	90	[3] ESKUT	01	CHRS	CERN SPS
<17	90	NAPLES	99	CCFR	FNAL
<44	90	TALEBZADEH	87	HLBC	BEBC
< 9	90	USHIDA	86C	EMUL	FNAL

[1] ARMBRUSTER 98 use KARMEN detector with ν_e from muon decay at rest and observe $^{12}C(\nu_e,e^-)^{12}N_{gs}$. This is a disappearance experiment which is almost insensitive to $\nu_e \rightarrow \nu_\mu$ oscillation. Results are presented as limits to $\nu_e \rightarrow \nu_\tau$ oscillation, although the (non)oscillation could be to a non-visible flavor. A three-flavor analysis is also presented.

[2] ASTIER 01B searches for the appearance of ν_τ with the NOMAD detector at CERN's SPS. The limit is based on an oscillation probability $< 0.74 \times 10^{-2}$, whereas the quoted sensitivity was 1.1×10^{-2}. The limit was obtained following the statistical prescriptions of FELDMAN 98. See also the footnote to ESKUT 01.

[3] ESKUT 01 searches for the appearance of the ν_τ with the CHORUS detector at CERN's SPS. The limit is obtained following the statistical prescriptions in JUNK 99. The limit would have been 6 eV^2 if the prescriptions in FELDMAN 98 had been followed, as they were in ASTIER 01B.

$\sin^2(2\theta)$ for "Large" $\Delta(m^2)$

VALUE	CL%	DOCUMENT ID		TECN	COMMENT
<0.015	90	[4] ASTIER	01B	NOMD	CERN SPS
• • • We do not use the following data for averages, fits, limits, etc. • • •					
<0.052	90	[5] ESKUT	01	CHRS	CERN SPS
<0.21	90	NAPLES	99	CCFR	FNAL
<0.338	90	[6] ARMBRUSTER	98	KARM	
<0.36	90	TALEBZADEH	87	HLBC	BEBC
<0.25	90	[7] USHIDA	86C	EMUL	FNAL

[4] ASTIER 01B limit is based on an oscillation probability $< 0.74 \times 10^{-2}$, whereas the quoted sensitivity was 1.1×10^{-2}. The limit was obtained following the statistical prescriptions of FELDMAN 98. See also the footnote to ESKUT 01.

[5] ESKUT 01 limit obtained following the statistical prescriptions in JUNK 99. The limit would have been 0.03 if the prescriptions in FELDMAN 98 had been followed, as they were in ASTIER 01B.

[6] See footnote in preceding table (ARMBRUSTER 98) for further details, and see the paper for a plot showing allowed regions. A three-flavor analysis is also presented here.

[7] USHIDA 86C published result is $\sin^2 2\theta < 0.12$. The quoted result is corrected for a numerical mistake incurred in calculating the expected number of ν_e CC events, normalized to the total number of neutrino interactions (3886) rather than to the total number of ν_μ CC events (1870).

$\overline{\nu}_e \rightarrow \overline{\nu}_\tau$

$\sin^2(2\theta)$ for "Large" $\Delta(m^2)$

VALUE	CL%	DOCUMENT ID		TECN	COMMENT
<0.7	90	[8] FRITZE	80	HYBR	BEBC CERN SPS

[8] Authors give $P(\nu_e \rightarrow \nu_\tau) < 0.35$, equivalent to above limit.

$\nu_e \not\rightarrow \nu_e$

$\Delta(m^2)$ for $\sin^2(2\theta) = 1$

VALUE (eV^2)	CL%	DOCUMENT ID		TECN	COMMENT
< 0.18	90	[9] HAMPEL	98	GALX	^{51}Cr source
• • • We do not use the following data for averages, fits, limits, etc. • • •					
<40	90	[10] BORISOV	96	CNTR	IHEP-JINR detector
<14.9	90	BRUCKER	86	HLBC	15-ft FNAL
< 8	90	BAKER	81	HLBC	15-ft FNAL
<56	90	DEDEN	81	HLBC	BEBC CERN SPS
<10	90	ERRIQUEZ	81	HLBC	BEBC CERN SPS
<2.3 OR >8	90	NEMETHY	81B	CNTR	LAMPF

[9] HAMPEL 98 analyzed the GALLEX calibration results with ^{51}Cr neutrino sources and updates the BAHCALL 95 analysis result. They also gave 95% and 99% CL limits of < 0.2 and < 0.22, respectively.

[10] BORISOV 96 exclusion curve extrapolated to obtain this value; however, it does not have the right curvature in this region.

$\sin^2(2\theta)$ for "Large" $\Delta(m^2)$

VALUE	CL%	DOCUMENT ID		TECN	COMMENT
<7 $\times 10^{-2}$	90	[11] ERRIQUEZ	81	HLBC	BEBC CERN SPS
• • • We do not use the following data for averages, fits, limits, etc. • • •					
<0.4	90	[12] HAMPEL	98	GALX	^{51}Cr source
<0.115	90	[13] BORISOV	96	CNTR	$\Delta(m^2) = 175$ eV^2
<0.54	90	BRUCKER	86	HLBC	15-ft FNAL
<0.6	90	BAKER	81	HLBC	15-ft FNAL
<0.3	90	[11] DEDEN	81	HLBC	BEBC CERN SPS

[11] Obtained from a Gaussian centered in the unphysical region.

[12] HAMPEL 98 analyzed the GALLEX calibration results with ^{51}Cr neutrino sources and updates the BAHCALL 95 analysis result. They also gave 95% and 99% CL limits of < 0.45 and < 0.56, respectively.

[13] BORISOV 96 sets less stringent limits at large $\Delta(m^2)$, but exclusion curve does not have clear asymptotic behavior.

$\nu_e \rightarrow (\overline{\nu}_e)_L$

This is a limit on lepton family-number violation and total lepton-number violation. $(\overline{\nu}_e)_L$ denotes a hypothetical left-handed $\overline{\nu}_e$. The bound is quoted in terms of $\Delta(m^2)$, $\sin(2\theta)$, and α, where α denotes the fractional admixture of $(V+A)$ charged current.

$\alpha\Delta(m^2)$ for $\sin^2(2\theta) = 1$

VALUE (eV^2)	CL%	DOCUMENT ID		TECN	COMMENT
<0.14	90	[14] FREEDMAN	93	CNTR	LAMPF
• • • We do not use the following data for averages, fits, limits, etc. • • •					
<7	90	[15] COOPER	82	HLBC	BEBC CERN SPS

[14] FREEDMAN 93 is a search at LAMPF for $\overline{\nu}_e$ generated from any of the three neutrino types ν_μ, $\overline{\nu}_\mu$, and ν_e which come from the beam stop. The $\overline{\nu}_e$'s would be detected by the reaction $\overline{\nu}_e p \rightarrow e^+ n$.

[15] COOPER 82 states that existing bounds on V+A currents require α to be small.

$\alpha^2\sin^2(2\theta)$ for "Large" $\Delta(m^2)$

VALUE	CL%	DOCUMENT ID		TECN	COMMENT
<0.032	90	[16] FREEDMAN	93	CNTR	LAMPF
• • • We do not use the following data for averages, fits, limits, etc. • • •					
<0.05	90	[17] COOPER	82	HLBC	BEBC CERN SPS

[16] FREEDMAN 93 is a search at LAMPF for $\overline{\nu}_e$ generated from any of the three neutrino types ν_μ, $\overline{\nu}_\mu$, and ν_e which come from the beam stop. The $\overline{\nu}_e$'s would be detected by the reaction $\overline{\nu}_e p \rightarrow e^+ n$.

[17] COOPER 82 states that existing bounds on V+A currents require α to be small.

$\nu_\mu \rightarrow \nu_e$

$\Delta(m^2)$ for $\sin^2(2\theta) = 1$

VALUE (eV^2)	CL%	DOCUMENT ID		TECN	COMMENT
<0.09	90	ANGELINI	86	HLBC	BEBC CERN PS
• • • We do not use the following data for averages, fits, limits, etc. • • •					
<0.4	90	ASTIER	03	NOMD	CERN SPS
<2.4	90	AVVAKUNOV	02	NTEV	NUTEV FNAL
		[18] AGUILAR	01	LSND	$\nu_\mu \rightarrow \nu_e$ osc.prob.
0.03 to 0.3	95	[19] ATHANASSO...98		LSND	$\nu_\mu \rightarrow \nu_e$
<2.3	90	[20] LOVERRE	96		CHARM/CDHS
<0.9	90	VILAIN	94C	CHM2	CERN SPS
<0.1	90	BLUMENFELD	89	CNTR	
<1.3	90	AMMOSOV	88	HLBC	SKAT at Serpukhov
<0.19	90	BERGSMA	88	CHRM	
		[21] LOVERRE	88	RVUE	
<2.4	90	AHRENS	87	CNTR	BNL AGS
<1.8	90	BOFILL	87	CNTR	FNAL
<2.2	90	[22] BRUCKER	86	HLBC	15-ft FNAL
<0.43	90	AHRENS	85	CNTR	BNL AGS E734
<0.20	90	BERGSMA	84	CHRM	
<1.7	90	ARMENISE	81	HLBC	GGM CERN PS
<0.6	90	BAKER	81	HLBC	15-ft FNAL
<1.7	90	ERRIQUEZ	81	HLBC	BEBC CERN PS
<1.2	95	BLIETSCHAU	78	HLBC	GGM CERN PS
<1.2	95	BELLOTTI	76	HLBC	GGM CERN PS

[18] AGUILAR 01 is the final analysis of the LSND full data set. Search is made for the $\nu_\mu \rightarrow \nu_e$ oscillations using ν_μ from π^+ decay in flight by observing beam-on electron events from $\nu_e C \rightarrow e^- X$. Present analysis results in $8.1 \pm 12.2 \pm 1.7$ excess events in the $60 < E_e < 200$ MeV energy range, corresponding to oscillation probability of $0.10 \pm 0.16 \pm 0.04\%$. This is consistent, though less significant, with the previous result of ATHANASSOPOULOS 98, which it supersedes. The present analysis uses selection criteria developed for the decay at rest region, and is less effective in removing the background above 60 MeV than ATHANASSOPOULOS 98.

[19] ATHANASSOPOULOS 98 is a search for the $\nu_\mu \rightarrow \nu_e$ oscillations using ν_μ from π^+ decay in flight. The 40 observed beam-on electron events are consistent with $\nu_e C \rightarrow e^- X$; the expected background is 21.9 ± 2.1. Authors interpret this excess as evidence for an oscillation signal corresponding to oscillations with probability $(0.26 \pm 0.10 \pm 0.05)\%$. Although the significance is only 2.3σ, this measurement is an important and consistent cross check of ATHANASSOPOULOS 96 who reported evidence for $\overline{\nu}_\mu \rightarrow \overline{\nu}_e$ oscillations from μ^+ decay at rest. See also ATHANASSOPOULOS 98B.

[20] LOVERRE 96 uses the charged-current to neutral-current ratio from the combined CHARM (ALLABY 86) and CDHS (ABRAMOWICZ 86) data from 1986.

[21] LOVERRE 88 reports a less stringent, indirect limit based on theoretical analysis of neutral to charged current ratios.

[22] 15ft bubble chamber at FNAL.

$\sin^2(2\theta)$ for "Large" $\Delta(m^2)$

VALUE (units 10^{-3})	CL%	DOCUMENT ID		TECN	COMMENT
< 1.4	90	ASTIER	03	NOMD	CERN SPS
• • • We do not use the following data for averages, fits, limits, etc. • • •					
< 1.6	90	AVVAKUNOV	02	NTEV	NUTEV FNAL
		[23] AGUILAR	01	LSND	$\nu\mu \rightarrow \nu_e$ osc.prob.
0.5 to 30	95	[24] ATHANASSO...	98	LSND	$\nu_\mu \rightarrow \nu_e$
< 3.0	90	[25] LOVERRE	96		CHARM/CDHS
< 9.4	90	VILAIN	94C	CHM2	CERN SPS
< 5.6	90	[26] VILAIN	94C	CHM2	CERN SPS
< 16	90	BLUMENFELD	89	CNTR	
< 2.5	90	AMMOSOV	88	HLBC	SKAT at Serpukhov
< 8	90	BERGSMA	88	CHRM	$\Delta(m^2) \geq 30$ eV^2
		[27] LOVERRE	88	RVUE	
< 10	90	AHRENS	87	CNTR	BNL AGS
< 15	90	BOFILL	87	CNTR	FNAL
< 20	90	[28] ANGELINI	86	HLBC	BEBC CERN PS
20 to 40		[29] BERNARDI	86B	CNTR	$\Delta(m^2)$=5–10
< 11	90	[30] BRUCKER	86	HLBC	15-ft FNAL
< 3.4	90	AHRENS	85	CNTR	BNL AGS E734
< 240	90	BERGSMA	84	CHRM	
< 10	90	ARMENISE	81	HLBC	GGM CERN PS
< 6	90	BAKER	81	HLBC	15-ft FNAL
< 10	90	ERRIQUEZ	81	HLBC	BEBC CERN PS
< 4	95	BLIETSCHAU	78	HLBC	GGM CERN PS
< 10	95	BELLOTTI	76	HLBC	GGM CERN PS

[23] AGUILAR 01 is the final analysis of the LSND full data set of the search for the $\nu_\mu \rightarrow \nu_e$ oscillations. See footnote in preceding table for further details.

[24] ATHANASSOPOULOS 98 report $(0.26 \pm 0.10 \pm 0.05)\%$ for the oscillation probability; the value of $\sin^2 2\theta$ for large Δm^2 is deduced from this probability. See footnote in preceding table for further details, and see the paper for a plot showing allowed regions. If effect is due to oscillation, it is most likely to be intermediate $\sin^2 2\theta$ and Δm^2. See also ATHANASSOPOULOS 98B.

[25] LOVERRE 96 uses the charged-current to neutral-current ratio from the combined CHARM (ALLABY 86) and CDHS (ABRAMOWICZ 86) data from 1986.

[26] VILAIN 94C limit derived by combining the ν_μ and $\overline{\nu}_\mu$ data assuming *CP* conservation.

[27] LOVERRE 88 reports a less stringent, indirect limit based on theoretical analysis of neutral to charged current ratios.

[28] ANGELINI 86 limit reaches 13×10^{-3} at $\Delta(m^2) \approx 2$ eV^2.

[29] BERNARDI 86B is a typical fit to the data, assuming mixing between two species. As the authors state, this result is in conflict with earlier upper bounds on this type of neutrino oscillations.

[30] 15ft bubble chamber at FNAL.

$\overline{\nu}_\mu \rightarrow \overline{\nu}_e$

$\Delta(m^2)$ for $\sin^2(2\theta) = 1$

VALUE (eV^2)	CL%	DOCUMENT ID		TECN	COMMENT
< 0.055	90	[31] ARMBRUSTER	02	KAR2	Liquid Sci. calor.
• • • We do not use the following data for averages, fits, limits, etc. • • •					
< 2.6	90	AVVAKUNOV	02	NTEV	NUTEV FNAL
0.03–0.05		[32] AGUILAR	01	LSND	LAMPF
0.05–0.08	90	[33] ATHANASSO...	96	LSND	LAMPF
0.048–0.090	80	[34] ATHANASSO...	95		
< 0.07	90	[35] HILL	95		
< 0.9	90	VILAIN	94C	CHM2	CERN SPS
< 0.14	90	[36] FREEDMAN	93	CNTR	LAMPF
< 3.1	90	BOFILL	87	CNTR	FNAL
< 2.4	90	TAYLOR	83	HLBC	15-ft FNAL
< 0.91	90	[37] NEMETHY	81B	CNTR	LAMPF
< 1	95	BLIETSCHAU	78	HLBC	GGM CERN PS

[31] ARMBRUSTER 02 is the final analysis of the KARMEN 2 data for 17.7 m distance from the ISIS stopped pion and muon neutrino source. It is a search for $\overline{\nu}_e$, detected by the inverse β-decay reaction on protons and ^{12}C. 15 candidate events are observed, and 15.8 ± 0.5 background events are expected, hence no oscillation signal is detected. The results exclude large regions of the parameter area favored by the LSND experiment.

[32] AGUILAR 01 is the final analysis of the LSND full data set. It is a search for $\overline{\nu}_e$ 30 m from LAMPF beam stop. Neutrinos originate mainly for π^+ decay at rest. $\overline{\nu}_e$ are detected through $\overline{\nu}_e p \rightarrow e^+ n$ ($20 < E_{e^+} < 60$ MeV) in delayed coincidence with $np \rightarrow d\gamma$. AUthors observe $87.9 \pm 22.4 \pm 6.0$ total excess events. The observation is attributed to $\overline{\nu}_\mu \rightarrow \overline{\nu}_e$ oscillations with the oscillation probability of $0.264 \pm 0.067 \pm 0.045\%$, consistent with the previously published result. Taking into account all constraints, the most favored allowed region of oscillation parameters is a band of $\Delta(m^2)$ from 0.2–2.0 eV^2. Supersedes ATHANASSOPOULOS 95, ATHANASSOPOULOS 96, and ATHANASSOPOULOS 98.

[33] ATHANASSOPOULOS 96 is a search for $\overline{\nu}_e$ 30 m from LAMPF beam stop. Neutrinos originate mainly from π^+ decay at rest. $\overline{\nu}_e$ could come from either $\overline{\nu}_\mu \rightarrow \overline{\nu}_e$ or $\nu_e \rightarrow \overline{\nu}_e$; our entry assumes the first interpretation. They are detected through $\overline{\nu}_e p \rightarrow e^+ n$ (20 MeV $< E_{e^+} <$ 60 MeV) in delayed coincidence with $np \rightarrow d\gamma$. Authors observe $51 \pm 20 \pm 8$ total excess events over an estimated background 12.5 ± 2.9. ATHANASSOPOULOS 96B is a shorter version of this paper.

[34] ATHANASSOPOULOS 95 error corresponds to the 1.6σ band in the plot. The expected background is 2.7 ± 0.4 events. Corresponds to an oscillation probability of $(0.34^{+0.20}_{-0.18} \pm 0.07)\%$. For a different interpretation, see HILL 95. Replaced by ATHANASSOPOULOS 96.

[35] HILL 95 is a report by one member of the LSND Collaboration, reporting a different conclusion from the analysis of the data of this experiment (see ATHANASSOPOULOS 95). Contrary to the rest of the LSND Collaboration, Hill finds no evidence for the neutrino oscillation $\overline{\nu}_\mu \rightarrow \overline{\nu}_e$ and obtains only upper limits.

[36] FREEDMAN 93 is a search at LAMPF for $\overline{\nu}_e$ generated from any of the three neutrino types ν_μ, $\overline{\nu}_\mu$, and ν_e which come from the beam stop. The $\overline{\nu}_e$'s would be detected by the reaction $\overline{\nu}_e p \rightarrow e^+ n$. FREEDMAN 93 replaces DURKIN 88.

[37] In reaction $\overline{\nu}_e p \rightarrow e^+ n$.

$\sin^2(2\theta)$ for "Large" $\Delta(m^2)$

VALUE	CL%	DOCUMENT ID		TECN	COMMENT
< 0.0011	90	AVVAKUNOV	02	NTEV	NUTEV FNAL
• • • We do not use the following data for averages, fits, limits, etc. • • •					
< 0.0017	90	[38] ARMBRUSTER	02	KAR2	Liquid Sci. calor.
$0.0053 \pm 0.0013 \pm 0.009$		[39] AGUILAR	01	LSND	LAMPF
$0.0062 \pm 0.0024 \pm 0.0010$		[40] ATHANASSO...	96	LSND	LAMPF
0.003–0.012	80	[41] ATHANASSO...	95		
< 0.006	90	[42] HILL	95		
< 4.8	90	VILAIN	94C	CHM2	CERN SPS
< 5.6	90	[43] VILAIN	94C	CHM2	CERN SPS
< 0.024	90	[44] FREEDMAN	93	CNTR	LAMPF
< 0.04	90	BOFILL	87	CNTR	FNAL
< 0.013	90	TAYLOR	83	HLBC	15-ft FNAL
< 0.2	90	[45] NEMETHY	81B	CNTR	LAMPF
< 0.004	95	BLIETSCHAU	78	HLBC	GGM CERN PS

[38] ARMBRUSTER 02 is the final analysis of the KARMEN 2 data. See footnote in the preceding table for further details, and the paper for the exclusion plot.

[39] AGUILAR 01 is the final analysis of the LSND full data set. The deduced oscillation probability is $0.264 \pm 0.067 \pm 0.045\%$; the value of $\sin^2 2\theta$ for large $\Delta(m^2)$ is twice this probability (although these values are excluded by other constraints). See footnote in preceding table for further details, and the paper for a plot showing allowed regions. Supersedes ATHANASSOPOULOS 95, ATHANASSOPOULOS 96, and ATHANASSOPOULOS 98.

[40] ATHANASSOPOULOS 96 reports $(0.31 \pm 0.12 \pm 0.05)\%$ for the oscillation probability; the value of $\sin^2 2\theta$ for large $\Delta(m^2)$ should be twice this probability. See footnote in preceding table for further details, and see the paper for a plot showing allowed regions.

[41] ATHANASSOPOULOS 95 error corresponds to the 1.6σ band in the plot. The expected background is 2.7 ± 0.4 events. Corresponds to an oscillation probability of $(0.34^{+0.20}_{-0.18} \pm 0.07)\%$. For a different interpretation, see HILL 95. Replaced by ATHANASSOPOULOS 96.

[42] HILL 95 is a report by one member of the LSND Collaboration, reporting a different conclusion from the analysis of the data of this experiment (see ATHANASSOPOULOS 95). Contrary to the rest of the LSND Collaboration, Hill finds no evidence for the neutrino oscillation $\overline{\nu}_\mu \rightarrow \overline{\nu}_e$ and obtains only upper limits.

[43] VILAIN 94C limit derived by combining the ν_μ and $\overline{\nu}_\mu$ data assuming *CP* conservation.

[44] FREEDMAN 93 is a search at LAMPF for $\overline{\nu}_e$ generated from any of the three neutrino types ν_μ, $\overline{\nu}_\mu$, and ν_e which come from the beam stop. The $\overline{\nu}_e$'s would be detected by the reaction $\overline{\nu}_e p \rightarrow e^+ n$. FREEDMAN 93 replaces DURKIN 88.

[45] In reaction $\overline{\nu}_e p \rightarrow e^+ n$.

$\nu_\mu(\overline{\nu}_\mu) \rightarrow \nu_e(\overline{\nu}_e)$

$\Delta(m^2)$ for $\sin^2(2\theta) = 1$

VALUE (eV^2)	CL%	DOCUMENT ID		TECN	COMMENT
< 0.075	90	BORODOV...	92	CNTR	BNL E776
• • • We do not use the following data for averages, fits, limits, etc. • • •					
< 1.6	90	[46] ROMOSAN	97	CCFR	FNAL

[46] ROMOSAN 97 uses wideband beam with a 0.5 km decay region.

$\sin^2(2\theta)$ for "Large" $\Delta(m^2)$

VALUE (units 10^{-3})	CL%	DOCUMENT ID		TECN	COMMENT
<1.8	90	[47] ROMOSAN	97	CCFR	FNAL
• • • We do not use the following data for averages, fits, limits, etc. • • •					
<3.8	90	[48] MCFARLAND	95	CCFR	FNAL
<3	90	BORODOV...	92	CNTR	BNL E776

[47] ROMOSAN 97 uses wideband beam with a 0.5 km decay region.

[48] MCFARLAND 95 state that "This result is the most stringent to date for 250< $\Delta(m^2)$ <450 eV^2 and also excludes at 90%CL much of the high $\Delta(m^2)$ region favored by the recent LSND observation." See ATHANASSOPOULOS 95 and ATHANASSOPOULOS 96.

$\nu_\mu \rightarrow \nu_\tau$

$\Delta(m^2)$ for $\sin^2(2\theta) = 1$

VALUE (eV^2)	CL%	DOCUMENT ID		TECN	COMMENT
< 0.6	90	[49] ESKUT	01	CHRS	CERN SPS
• • • We do not use the following data for averages, fits, limits, etc. • • •					
< 0.7	90	[50] ASTIER	01B	NOMD	CERN SPS
< 1.4	90	[51] ALTEGOER	98B	NOMD	CERN SPS
< 1.5	90	[52] ESKUT	98	CHRS	CERN SPS
< 1.1	90	[53] ESKUT	98B	CHRS	CERN SPS
< 3.3	90	[54] LOVERRE	96		CHARM/CDHS
< 1.4	90	MCFARLAND	95	CCFR	FNAL
< 4.5	90	BATUSOV	90B	EMUL	FNAL
<10.2	90	BOFILL	87	CNTR	FNAL
< 6.3	90	BRUCKER	86	HLBC	15-ft FNAL
< 0.9	90	USHIDA	86C	EMUL	FNAL
< 4.6	90	ARMENISE	81	HLBC	GGM CERN SPS
< 3	90	BAKER	81	HLBC	15-ft FNAL
< 6	90	ERRIQUEZ	81	HLBC	BEBC CERN SPS
< 3	90	USHIDA	81	EMUL	FNAL

[49] ESKUT 01 limit obtained following the statistical prescriptions in JUNK 99. The limit would have been 0.5 eV^2 if the prescriptions in FELDMAN 98 had been followed, as they were in ASTIER 01B.

[50] ASTIER 01B limit is based on an oscillation probability $< 1.63 \times 10^{-4}$, whereas the quoted sensitivity was 2.5×10^{-4}. The limit was obtained following the statistical prescriptions of FELDMAN 98. See also the footnote to ESKUT 01.

[51] ALTEGOER 98B is the NOMAD 1995 data sample result, searching for events with $\tau^- \rightarrow e^- \nu_\tau \overline{\nu}_e$, hadron$^-$ ν_τ, or $\pi^- \pi^+ \pi^-$ decay modes using classical CL approach of FELDMAN 98.

[52] ESKUT 98 search for events with one μ^- with indication of a kink from τ^- decay in the nuclear emulsion. No candidates were found in a 31,423 event subsample.

[53] ESKUT 98B search for $\tau^- \rightarrow \mu^- \nu_\tau \overline{\nu}_\mu$ or $h^- \nu_\tau \overline{\nu}_\mu$, where h^- is a negatively charged hadron. The μ^- sample is somewhat larger than in ESKUT 98, which this result supersedes. Bayesian limit.

[54] LOVERRE 96 uses the charged-current to neutral-current ratio from the combined CHARM (ALLABY 86) and CDHS (ABRAMOWICZ 86) data from 1986.

$\sin^2(2\theta)$ for "Large" $\Delta(m^2)$

VALUE	CL%	DOCUMENT ID		TECN	COMMENT
<0.00033	90	[55] ASTIER	01B	NOMD	CERN SPS
• • • We do not use the following data for averages, fits, limits, etc. • • •					
<0.00068	90	[56] ESKUT	01	CHRS	CERN SPS
<0.0042	90	[57] ALTEGOER	98B	NOMD	CERN SPS
<0.0035	90	[58] ESKUT	98	CHRS	CERN SPS
<0.0018	90	[59] ESKUT	98B	CHRS	CERN SPS
<0.006	90	[60] LOVERRE	96		CHARM/CDHS
<0.0081	90	MCFARLAND	95	CCFR	FNAL
<0.06	90	BATUSOV	90B	EMUL	FNAL
<0.34	90	BOFILL	87	CNTR	FNAL
<0.088	90	BRUCKER	86	HLBC	15-ft FNAL
<0.004	90	USHIDA	86C	EMUL	FNAL
<0.11	90	BALLAGH	84	HLBC	15-ft FNAL
<0.017	90	ARMENISE	81	HLBC	GGM CERN SPS
<0.06	90	BAKER	81	HLBC	15-ft FNAL
<0.05	90	ERRIQUEZ	81	HLBC	BEBC CERN SPS
<0.013	90	USHIDA	81	EMUL	FNAL

[55] ASTIER 01B limit is based on an oscillation probability $< 1.63 \times 10^{-4}$, whereas the quoted sensitivity was 2.5×10^{-4}. The limit was obtained following the statistical prescriptions of FELDMAN 98. See also the footnote to ESKUT 01.

[56] ESKUT 01 limit obtained following the statistical prescriptions in JUNK 99. The limit would have been 0.00040 if the prescriptions in FELDMAN 98 had been followed, as they were in ASTIER 01B.

[57] ALTEGOER 98B is the NOMAD 1995 data sample result, searching for events with $\tau^- \rightarrow e^- \nu_\tau \overline{\nu}_e$, hadron$^-$ ν_τ, or $\pi^- \pi^+ \pi^-$ decay modes using classical CL approach of FELDMAN 98.

[58] ESKUT 98 search for events with one μ^- with indication of a kink from τ^- decay in the nuclear emulsion. No candidates were found in a 31,423 event subsample.

[59] ESKUT 98B search for $\tau^- \rightarrow \mu^- \nu_\tau \overline{\nu}_\mu$ or $h^- \nu_\tau \overline{\nu}_\mu$, where h^- is a negatively charged hadron. The μ^- sample is somewhat larger than in ESKUT 98, which this result supersedes. Bayesian limit.

[60] LOVERRE 96 uses the charged-current to neutral-current ratio from the combined CHARM (ALLABY 86) and CDHS (ABRAMOWICZ 86) data from 1986.

$\overline{\nu}_\mu \rightarrow \overline{\nu}_\tau$

$\Delta(m^2)$ for $\sin^2(2\theta) = 1$

VALUE (eV^2)	CL%	DOCUMENT ID		TECN	COMMENT
<2.2	90	ASRATYAN	81	HLBC	FNAL
• • • We do not use the following data for averages, fits, limits, etc. • • •					
<1.4	90	MCFARLAND	95	CCFR	FNAL
<6.5	90	BOFILL	87	CNTR	FNAL
<7.4	90	TAYLOR	83	HLBC	15-ft FNAL

$\sin^2(2\theta)$ for "Large" $\Delta(m^2)$

VALUE	CL%	DOCUMENT ID	TECN	COMMENT
<4.4 $\times 10^{-2}$	90	ASRATYAN 81	HLBC	FNAL
• • • We do not use the following data for averages, fits, limits, etc. • • •				
<0.0081	90	MCFARLAND 95	CCFR	FNAL
<0.15	90	BOFILL 87	CNTR	FNAL
<8.8 $\times 10^{-2}$	90	TAYLOR 83	HLBC	15-ft FNAL

$\nu_\mu(\overline{\nu}_\mu) \rightarrow \nu_\tau(\overline{\nu}_\tau)$

$\Delta(m^2)$ for $\sin^2(2\theta) = 1$

VALUE (eV^2)	CL%	DOCUMENT ID		TECN	COMMENT
<1.5	90	[61] GRUWE	93	CHM2	CERN SPS

[61] GRUWE 93 is a search using the CHARM II detector in the CERN SPS wide-band neutrino beam for $\nu_\mu \rightarrow \nu_\tau$ and $\overline{\nu}_\mu \rightarrow \overline{\nu}_\tau$ oscillations signalled by quasi-elastic ν_τ and $\overline{\nu}_\tau$ interactions followed by the decay $\tau \rightarrow \nu_\tau \pi$. The maximum sensitivity in $\sin^2 2\theta$ ($< 6.4 \times 10^{-3}$ at the 90% CL) is reached for $\Delta(m^2) \simeq 50$ eV^2.

$\sin^2(2\theta)$ for "Large" $\Delta(m^2)$

VALUE (units 10^{-3})	CL%	DOCUMENT ID		TECN	COMMENT
<8	90	[62] GRUWE	93	CHM2	CERN SPS

[62] GRUWE 93 is a search using the CHARM II detector in the CERN SPS wide-band neutrino beam for $\nu_\mu \rightarrow \nu_\tau$ and $\overline{\nu}_\mu \rightarrow \overline{\nu}_\tau$ oscillations signalled by quasi-elastic ν_τ and $\overline{\nu}_\tau$ interactions followed by the decay $\tau \rightarrow \nu_\tau \pi$. The maximum sensitivity in $\sin^2 2\theta$ ($< 6.4 \times 10^{-3}$ at the 90% CL) is reached for $\Delta(m^2) \simeq 50$ eV^2.

$\nu_\mu \not\rightarrow \nu_\mu$

$\Delta(m^2)$ for $\sin^2(2\theta) = 1$

VALUE (eV^2)	CL%	DOCUMENT ID		TECN	COMMENT
>0.0015 AND < 0.0039	90	[63] AHN	03	K2K	KEK to Super-K
• • • We do not use the following data for averages, fits, limits, etc. • • •					
< 0.29 OR >22	90	BERGSMA	88	CHRM	
<7	90	BELIKOV	85	CNTR	Serpukhov
<8.0 OR >1250	90	STOCKDALE	85	CNTR	
<0.29 OR >22	90	BERGSMA	84	CHRM	
<0.23 OR >100	90	DYDAK	84	CNTR	
<13 OR >1500	90	STOCKDALE	84	CNTR	
<8.0	90	BELIKOV	83	CNTR	

[63] K2K is a 250 km long-baseline disappearance experiment. The result indicates neutrino oscillations. The measured oscillation parameters are consistent with the ones suggested by atmospheric neutrino observations.

$\sin^2(2\theta)$ for $\Delta(m^2) = 0.003$ eV^2

VALUE	CL%	DOCUMENT ID		TECN	COMMENT
• • • We do not use the following data for averages, fits, limits, etc. • • •					
> 0.35	90	[64] AHN	03	K2K	KEK to Super-K

[64] K2K is a 250 km long-baseline disappearance experiment. The result indicates neutrino oscillations. The measured oscillation parameters are consistent with the ones suggested by atmospheric neutrino observations.

$\sin^2(2\theta)$ for $\Delta(m^2) = 100$eV^2

VALUE	CL%	DOCUMENT ID		TECN	COMMENT
<0.02	90	[65] STOCKDALE	85	CNTR	FNAL
• • • We do not use the following data for averages, fits, limits, etc. • • •					
<0.17	90	[66] BERGSMA	88	CHRM	
<0.07	90	[67] BELIKOV	85	CNTR	Serpukhov
<0.27	90	[66] BERGSMA	84	CHRM	CERN PS
<0.1	90	[68] DYDAK	84	CNTR	CERN PS
<0.02	90	[69] STOCKDALE	84	CNTR	FNAL
<0.1	90	[70] BELIKOV	83	CNTR	Serpukhov

[65] This bound applies for $\Delta(m^2) = 100$ eV^2. Less stringent bounds apply for other $\Delta(m^2)$; these are nontrivial for $8 < \Delta(m^2) < 1250$ eV^2.

[66] This bound applies for $\Delta(m^2) = 0.7$–9. eV^2. Less stringent bounds apply for other $\Delta(m^2)$; these are nontrivial for $0.28 < \Delta(m^2) < 22$ eV^2.

[67] This bound applies for a wide range of $\Delta(m^2) > 7$ eV^2. For some values of $\Delta(m^2)$, the value is less stringent; the least restrictive, nontrivial bound occurs approximately at $\Delta(m^2) = 300$ eV^2 where $\sin^2(2\theta) < 0.13$ at CL = 90%.

[68] This bound applies for $\Delta(m^2) = 1.$–10. eV^2. Less stringent bounds apply for other $\Delta(m^2)$; these are nontrivial for $0.23 < \Delta(m^2) < 90$ eV^2.

[69] This bound applies for $\Delta(m^2) = 110$ eV^2. Less stringent bounds apply for other $\Delta(m^2)$; these are nontrivial for $13 < \Delta(m^2) < 1500$ eV^2.

[70] Bound holds for $\Delta(m^2) = 20$–1000 eV^2.

$\overline{\nu}_\mu \not\to \overline{\nu}_\mu$

$\Delta(m^2)$ for $\sin^2(2\theta) = 1$

VALUE (eV^2)	CL%	DOCUMENT ID		TECN
<7 OR >1200 OUR LIMIT				
<7 OR >1200	90	STOCKDALE	85	CNTR

$\sin^2(2\theta)$ for 190 $eV^2 < \Delta(m^2) <$ 320 eV^2

VALUE	CL%	DOCUMENT ID		TECN	COMMENT
<0.02	90	[71] STOCKDALE	85	CNTR	FNAL

[71] This bound applies for $\Delta(m^2)$ between 190 and 320 or = 530 eV^2. Less stringent bounds apply for other $\Delta(m^2)$; these are nontrivial for $7 < \Delta(m^2) < 1200$ eV^2.

$\nu_\mu \to (\overline{\nu}_e)_L$

See note above for $\nu_e \to (\overline{\nu}_e)_L$ limit

$\alpha\Delta(m^2)$ for $\sin^2(2\theta) = 1$

VALUE (eV^2)	CL%	DOCUMENT ID		TECN	COMMENT
<0.16	90	[72] FREEDMAN	93	CNTR	LAMPF
• • • We do not use the following data for averages, fits, limits, etc. • • •					
<0.7	90	[73] COOPER	82	HLBC	BEBC CERN SPS

[72] FREEDMAN 93 is a search at LAMPF for $\overline{\nu}_e$ generated from any of the three neutrino types ν_μ, $\overline{\nu}_\mu$, and ν_e which come from the beam stop. The $\overline{\nu}_e$'s would be detected by the reaction $\overline{\nu}_e p \to e^+ n$. The limit on $\Delta(m^2)$ is better than the CERN BEBC experiment, but the limit on $\sin^2\theta$ is almost a factor of 100 less sensitive.

[73] COOPER 82 states that existing bounds on V+A currents require α to be small.

$\alpha^2\sin^2(2\theta)$ for "Large" $\Delta(m^2)$

VALUE	CL%	DOCUMENT ID		TECN	COMMENT
<0.001	90	[74] COOPER	82	HLBC	BEBC CERN SPS
• • • We do not use the following data for averages, fits, limits, etc. • • •					
<0.07	90	[75] FREEDMAN	93	CNTR	LAMPF

[74] COOPER 82 states that existing bounds on V+A currents require α to be small.

[75] FREEDMAN 93 is a search at LAMPF for $\overline{\nu}_e$ generated from any of the three neutrino types ν_μ, $\overline{\nu}_\mu$, and ν_e which come from the beam stop. The $\overline{\nu}_e$'s would be detected by the reaction $\overline{\nu}_e p \to e^+ n$. The limit on $\Delta(m^2)$ is better than the CERN BEBC experiment, but the limit on $\sin^2\theta$

(B) Reactor $\overline{\nu}_e$ disappearance experiments

In most cases, the reaction $\overline{\nu}_e p \to e^+ n$ is observed at different distances from one or more reactors in a complex.

Events (Observed/Expected) from Reactor $\overline{\nu}_e$ Experiments

VALUE	DOCUMENT ID		TECN	COMMENT
• • • We do not use the following data for averages, fits, limits, etc. • • •				
$0.611 \pm 0.085 \pm 0.041$	[76] EGUCHI	03	KLND	Japanese react ~ 180 km
$1.01 \pm 0.024 \pm 0.053$	[77] BOEHM	01		Palo Verde react. 0.75–0.89 km
$1.04 \pm 0.03 \pm 0.08$	[78] BOEHM	00C		Palo Verde react. 0.75–0.89 km
$1.01 \pm 0.028 \pm 0.027$	[79] APOLLONIO	99	CHOZ	Chooz reactors 1 km
$0.987 \pm 0.006 \pm 0.037$	[80] GREENWOOD	96		Savannah River, 18.2 m
$0.988 \pm 0.004 \pm 0.05$	ACHKAR	95	CNTR	Bugey reactor, 15 m
$0.994 \pm 0.010 \pm 0.05$	ACHKAR	95	CNTR	Bugey reactor, 40 m
$0.915 \pm 0.132 \pm 0.05$	ACHKAR	95	CNTR	Bugey reactor, 95 m
$0.987 \pm 0.014 \pm 0.027$	[81] DECLAIS	94	CNTR	Bugey reactor, 15 m
$0.985 \pm 0.018 \pm 0.034$	KUVSHINN...	91	CNTR	Rovno reactor
$1.05 \pm 0.02 \pm 0.05$	VUILLEUMIER	82		Gösgen reactor
$0.955 \pm 0.035 \pm 0.110$	[82] KWON	81		$\overline{\nu}_e p \to e^+ n$
0.89 ± 0.15	[82] BOEHM	80		$\overline{\nu}_e p \to e^+ n$
0.38 ± 0.21	[83,84] REINES	80		
0.40 ± 0.22	[83,84] REINES	80		

[76] EGUCHI 03 observe reactor neutrino disappearance at ~ 180 km baseline to various Japanese nuclear power reactors. See the footnote in the following table for further details, and the paper for the inclusion/exclusion plot.

[77] BOEHM 01 search for neutrino oscillations at 0.75 and 0.89 km distance from the Palo Verde reactors.

[78] BOEHM 00C search for neutrino oscillations at 0.75 and 0.89 km distance from the Palo Verde reactors.

[79] APOLLONIO 99, APOLLONIO 98 search for neutrino oscillations at 1.1 km fixed distance from Chooz reactors. They use $\overline{\nu}_e p \to e^+ n$ in Gd-loaded scintillator target. APOLLONIO 99 supersedes APOLLONIO 98. See also APOLLONIO 03 for detailed description.

[80] GREENWOOD 96 search for neutrino oscillations at 18 m and 24 m from the reactor at Savannah River.

[81] DECLAIS 94 result based on integral measurement of neutrons only. Result is ratio of measured cross section to that expected in standard *V-A* theory. Replaced by ACHKAR 95.

[82] KWON 81 represents an analysis of a larger set of data from the same experiment as BOEHM 80.

[83] REINES 80 involves comparison of neutral- and charged-current reactions $\overline{\nu}_e d \to np\overline{\nu}_e$ and $\overline{\nu}_e d \to nne^+$ respectively. Combined analysis of reactor $\overline{\nu}_e$ experiments was performed by SILVERMAN 81.

[84] The two REINES 80 values correspond to the calculated $\overline{\nu}_e$ fluxes of AVIGNONE 80 and DAVIS 79 respectively.

$\overline{\nu}_e \not\to \overline{\nu}_e$

$\Delta(m^2)$ for $\sin^2(2\theta) = 1$

VALUE (eV^2)	CL%	DOCUMENT ID		TECN	COMMENT
>8 $\times 10^{-6}$	95	[85] EGUCHI	03	KLND	Japanese react ~ 180 km
• • • We do not use the following data for averages, fits, limits, etc. • • •					
<0.0011	90	[86] BOEHM	01		Palo Verde react. 0.75–0.89 km
<0.0011	90	[87] BOEHM	00		Palo Verde react. 0.8 km
<0.0007	90	[88] APOLLONIO	99	CHOZ	Chooz reactors 1 km
<0.01	90	[89] ACHKAR	95	CNTR	Bugey reactor
<0.0075	90	[90] VIDYAKIN	94		Krasnoyarsk reactors
<0.04	90	[91] AFONIN	88	CNTR	Rovno reactor
<0.014	68	[92] VIDYAKIN	87		$\overline{\nu}_e p \to e^+ n$
<0.019	90	[93] ZACEK	86		Gösgen reactor

[85] EGUCHI 03 observe reactor neutrino disappearance at ~ 180 km baseline to various Japanese nuclear power reactors. This is the lower limit on the mass difference spread, unlike all other entries in this table. Observation is consistent with neutrino oscillations, with mass-mixing and mixing-angle parameters in the Large Mixing Angle Solution region of the solar neutrino problem.

[86] BOEHM 01, a continuation of BOEHM 00, is a disappearance search for neutrino oscillations at 0.75 and 0.89 km distance from the Palo Verde reactors. Result is less restrictive than APOLLONIO 99.

[87] BOEHM 00 is a disappearance search for neutrino oscillations at 0.75 and 0.89 km distance from Palo Verde reactors. The detection reaction is $\overline{\nu}_e p \to e^+ n$ in a segmented Gd loaded scintillator target. Result is less restrictive than APOLLONIO 99.

[88] APOLLONIO 99 search for neutrino oscillations at 1.1 km fixed distance from Chooz reactors. They use $\overline{\nu}_e p \to e^+ n$ in Gd-loaded scintillator target. APOLLONIO 99 supersedes APOLLONIO 98. This is the most sensitive search in terms of $\Delta(m^2)$ for $\overline{\nu}_e$ disappearance. See also APOLLONIO 03 for detailed description.

[89] ACHKAR 95 bound is for L=15, 40, and 95 m.

[90] VIDYAKIN 94 bound is for L=57.0 m, 57.6 m, and 231.4 m. Supersedes VIDYAKIN 90.

[91] AFONIN 86 and AFONIN 87 also give limits on $\sin^2(2\theta)$ for intermediate values of $\Delta(m^2)$. (See also KETOV 92). Supersedes AFONIN 87, AFONIN 86, AFONIN 85, AFONIN 83, and BELENKII 83.

[92] VIDYAKIN 87 bound is for L = 32.8 and 92.3 m distance from two reactors.

[93] This bound is from data for L=37.9 m, 45.9 m, and 64.7 m.

$\sin^2(2\theta)$ for "Large" $\Delta(m^2)$

VALUE	CL%	DOCUMENT ID		TECN	COMMENT
>0.4	95	[94] EGUCHI	03	KLND	Japanese react ~ 180 km
• • • We do not use the following data for averages, fits, limits, etc. • • •					
<0.17	90	[95] BOEHM	01		Palo Verde react. 0.75–0.89 km
<0.21	90	[96] BOEHM	00		Palo Verde react. 0.8 km
<0.10	90	[97] APOLLONIO	99	CHOZ	Chooz reactors 1 km
<0.24	90	[98] GREENWOOD	96		
<0.04	90	[98] GREENWOOD	96		For $\Delta(m^2) = 1.0$ eV^2
<0.02	90	[99] ACHKAR	95	CNTR	For $\Delta(m^2) = 0.6$ eV^2
<0.087	68	[100] VYRODOV	95	CNTR	For $\Delta(m^2) > 2$ eV^2
<0.15	90	[101] VIDYAKIN	94		For $\Delta(m^2) > 5.0 \times 10^{-2}$ eV^2
<0.2	90	[102] AFONIN	88	CNTR	$\overline{\nu}_e p \to e^+ n$
<0.14	68	[103] VIDYAKIN	87		$\overline{\nu}_e p \to e^+ n$
<0.21	90	[104] ZACEK	86		$\overline{\nu}_e p \to e^+ n$
<0.19	90	[105] ZACEK	85		Gösgen reactor
<0.16	90	[106] GABATHULER	84		$\overline{\nu}_e p \to e^+ n$

[94] EGUCHI 03 observe reactor neutrino disappearance at ~ 180 km baseline to various Japanese nuclear power reactors. This is the lower limit on $\sin^2 2\theta$, unlike all other entries in this table. It is based on the observed rate only; consideration of the spectrum shape results in somewhat more restrictive limit. Observation is consistent with neutrino oscillations, with mass-mixing and mixing-angle parameters in the Large Mixing Angle Solution region of the solar neutrino problem.

[95] BOEHM 01 search for neutrino oscillations at 0.75 and 0.89 km distance from the Palo Verde reactors. Continuation of BOEHM 00.

[96] BOEHM 00 search for neutrino oscillations at 0.75 and 0.89 km distance from Palo Verde reactors.

[97] APOLLONIO 99 search for neutrino oscillations at 1.1 km fixed distance from Chooz reactors. See also APOLLONIO 03 for detailed description.

[98] GREENWOOD 96 search for neutrino oscillations at 18 m and 24 m from the reactor at Savannah River by observing $\overline{\nu}_e p \to e^+ n$ in a Gd loaded scintillator target. Their region of sensitivity in $\Delta(m^2)$ and $\sin^2 2\theta$ is already excluded by ACHKAR 95.

[99] ACHKAR 95 bound is from data for L=15, 40, and 95 m distance from the Bugey reactor.

[100] The VYRODOV 95 bound is from data for L=15 m distance from the Bugey-5 reactor.

[101] The VIDYAKIN 94 bound is from data for L=57.0 m, 57.6 m, and 231.4 m from three reactors in the Krasnoyarsk Reactor complex.

[102] Several different methods of data analysis are used in AFONIN 88. We quote the most stringent limits. Different upper limits on $\sin^2 2\theta$ apply at intermediate values of $\Delta(m^2)$. Supersedes AFONIN 87, AFONIN 85, and BELENKII 83.

[103] VIDYAKIN 87 bound is for L = 32.8 and 92.3 m distance from two reactors.

[104] This bound is from data for L=37.9 m, 45.9 m, and 64.7 m distance from Gosgen reactor.

[105] ZACEK 85 gives two sets of bounds depending on what assumptions are used in the data analysis. The bounds in figure 3(a) of ZACEK 85 are progressively poorer for large $\Delta(m^2)$ whereas those of figure 3(b) approach a constant. We list the latter. Both sets of bounds use combination of data from 37.9, 45.9, and 64.7m distance from reactor. ZACEK 85 states "Our experiment excludes this area (the oscillation parameter region allowed by the Bugey data, CAVAIGNAC 84) almost completely, thus disproving the indications of neutrino oscillations of CAVAIGNAC 84 with a high degree of confidence."

[106] This bound comes from a combination of the VUILLEUMIER 82 data at distance 37.9m from Gosgen reactor and new data at 45.9m.

(C) Atmospheric neutrino observations

Neutrinos and antineutrinos produced in the atmosphere induce μ-like and e-like events in underground detectors. The ratio of the numbers of the two kinds of events is defined as μ/e. It has the advantage that systematic effects, such as flux uncertainty, tend to cancel, for both experimental and theoretical values of the ratio. The "ratio of the ratios" of experimental to theoretical μ/e, $R(\mu/e)$, or that of experimental to theoretical μ/total, $R(\mu/\text{total})$ with total $= \mu+e$, is reported below. If the actual value is not unity, the value obtained in a given experiment may depend on the experimental conditions.

R(μ/e) = (Measured Ratio μ/e) / (Expected Ratio μ/e)

VALUE	DOCUMENT ID		TECN	COMMENT
• • • We do not use the following data for averages, fits, limits, etc. • • •				
$0.64 \pm 0.11 \pm 0.06$	[107] ALLISON	99	SOU2	Calorimeter
$0.61 \pm 0.03 \pm 0.05$	[108] FUKUDA	98	SKAM	sub-GeV
$0.66 \pm 0.06 \pm 0.08$	[109] FUKUDA	98E	SKAM	multi-GeV
	[110] FUKUDA	96B	KAMI	Water Cherenkov
$1.00 \pm 0.15 \pm 0.08$	[111] DAUM	95	FREJ	Calorimeter
$0.60^{+0.06}_{-0.05} \pm 0.05$	[112] FUKUDA	94	KAMI	sub-GeV
$0.57^{+0.08}_{-0.07} \pm 0.07$	[113] FUKUDA	94	KAMI	multi-Gev
	[114] BECKER-SZ...	92B	IMB	Water Cherenkov

[107] ALLISON 99 result is based on an exposure of 3.9 kton yr, 2.6 times the exposure reported in ALLISON 97, and replaces that result.

[108] FUKUDA 98 result is based on an exposure of 25.5 kton yr. The analyzed data sample consists of fully-contained e-like events with $0.1\ \text{GeV}/c < p_e$ and μ-like events with $0.2\ \text{GeV}/c < p_\mu$, both having a visible energy < 1.33 GeV. These criteria match the definition used by FUKUDA 94.

[109] FUKUDA 98E result is based on an exposure of 25.5 kton yr. The analyzed data sample consists of fully-contained single-ring events with visible energy > 1.33 GeV and partially contained events. All partially contained events are classified as μ-like.

[110] FUKUDA 96B studied neutron background in the atmospheric neutrino sample observed in the Kamiokande detector. No evidence for the background contamination was found.

[111] DAUM 95 results are based on an exposure of 2.0 kton yr which includes the data used by BERGER 90B. This ratio is for the contained and semicontained events. DAUM 95 also report $R(\mu/e) = 0.99 \pm 0.13 \pm 0.08$ for the total neutrino induced data sample which includes upward going stopping muons and horizontal muons in addition to the contained and semicontained events.

[112] FUKUDA 94 result is based on an exposure of 7.7 kton yr and updates the HIRATA 92 result. The analyzed data sample consists of fully-contained e-like events with $0.1 < p_e < 1.33\ \text{GeV}/c$ and fully-contained μ-like events with $0.2 < p_\mu < 1.5\ \text{GeV}/c$.

[113] FUKUDA 94 analyzed the data sample consisting of fully contained events with visible energy > 1.33 GeV and partially contained μ-like events.

[114] BECKER-SZENDY 92B reports the fraction of nonshowering events (mostly muons from atmospheric neutrinos) as $0.36 \pm 0.02 \pm 0.02$, as compared with expected fraction $0.51 \pm 0.01 \pm 0.05$. After cutting the energy range to the Kamiokande limits, BEIER 92 finds $R(\mu/e)$ very close to the Kamiokande value.

R(ν_μ) = (Measured Flux of ν_μ) / (Expected Flux of ν_μ)

VALUE	DOCUMENT ID		TECN	COMMENT
• • • We do not use the following data for averages, fits, limits, etc. • • •				
$0.72 \pm 0.026 \pm 0.13$	[115] AMBROSIO	01	MCRO	upward through-going
$0.57 \pm 0.05 \pm 0.15$	[116] AMBROSIO	00	MCRO	upgoing partially contained
$0.71 \pm 0.05 \pm 0.19$	[117] AMBROSIO	00	MCRO	downgoing partially contained + upgoing stopping
$0.74 \pm 0.036 \pm 0.046$	[118] AMBROSIO	98	MCRO	Streamer tubes
	[119] CASPER	91	IMB	Water Cherenkov
	[120] AGLIETTA	89	NUSX	
0.95 ± 0.22	[121] BOLIEV	81		Baksan
0.62 ± 0.17	CROUCH	78		Case Western/UCI

[115] AMBROSIO 01 result is based on the upward through-going muon tracks with $E_\mu > 1$ GeV. The data came from three different detector configurations, but the statistics is largely dominated by the full detector run, from May 1994 to December 2000. The total live time, normalized to the full detector configuration, is 6.17 years. The first error is the statistical error, the second is the systematic error, dominated by the theoretical error in the predicted flux.

[116] AMBROSIO 00 result is based on the upgoing partially contained event sample. It came from 4.1 live years of data taking with the full detector, from April 1994 to February 1999. The average energy of atmospheric muon neutrinos corresponding to this sample is 4 GeV. The first error is statistical, the second is the systematic error, dominated by the 25% theoretical error in the rate (20% in the flux and 15% in the cross section, added in quadrature). Within statistics, the observed deficit is uniform over the zenith angle.

[117] AMBROSIO 00 result is based on the combined samples of downgoing partially contained events and upgoing stopping events. These two subsamples could not be distinguished due to the lack of timing information. The result came from 4.1 live years of data taking with the full detector, from April 1994 to February 1999. The average energy of atmospheric muon neutrinos corresponding to this sample is 4 GeV. The first error is statistical, the second is the systematic error, dominated by the 25% theoretical error in the rate (20% in the flux and 15% in the cross section, added in quadrature). Within statistics, the observed deficit is uniform over the zenith angle.

[118] AMBROSIO 98 result is for all nadir angles and updates AHLEN 95 result. The lower cutoff on the muon energy is 1 GeV. In addition to the statistical and systematic errors, there is a Monte Carlo flux error (theoretical error) of ± 0.13. With a neutrino oscillation hypothesis, the fit either to the flux or zenith distribution independently yields $\sin^2 2\theta = 1.0$ and $\Delta(m^2) \sim$ a few times $10^{-3}\ \text{eV}^2$. However, the fit to the observed zenith distribution gives a maximum probability for χ^2 of only 5% for the best oscillation hypothesis.

[119] CASPER 91 correlates showering/nonshowering signature of single-ring events with parent atmospheric-neutrino flavor. They find nonshowering ($\approx \nu_\mu$ induced) fraction is $0.41 \pm 0.03 \pm 0.02$, as compared with expected 0.51 ± 0.05 (syst).

[120] AGLIETTA 89 finds no evidence for any anomaly in the neutrino flux. They define ρ = (measured number of ν_e's)/(measured number of ν_μ's). They report $\rho(\text{measured}) = \rho(\text{expected}) = 0.96^{+0.32}_{-0.28}$.

[121] From this data BOLIEV 81 obtain the limit $\Delta(m^2) \leq 6 \times 10^{-3}\ \text{eV}^2$ for maximal mixing, $\nu_\mu \not\to \nu_\mu$ type oscillation.

R(μ/total) = (Measured Ratio μ/total) / (Expected Ratio μ/total)

VALUE	DOCUMENT ID		TECN	COMMENT
• • • We do not use the following data for averages, fits, limits, etc. • • •				
$1.1^{+0.07}_{-0.12} \pm 0.11$	[122] CLARK	97	IMB	multi-GeV

[122] CLARK 97 obtained this result by an analysis of fully contained and partially contained events in the IMB water-Cherenkov detector with visible energy > 0.95 GeV.

$N_{up}(\mu)/N_{down}(\mu)$

VALUE	DOCUMENT ID		TECN	COMMENT
• • • We do not use the following data for averages, fits, limits, etc. • • •				
$0.52^{+0.07}_{-0.06} \pm 0.01$	[123] FUKUDA	98E	SKAM	multi-GeV

[123] FUKUDA 98E result is based on an exposure of 25.5 kton yr. The analyzed data sample consists of fully-contained single-ring μ-like events with visible energy > 1.33 GeV and partially contained events. All partially contained events are classified as μ-like. Upward-going events are those with $-1 < \cos$ (zenith angle) < -0.2 and downward-going events with those with $0.2 < \cos$ (zenith angle) < 1. FUKUDA 98E result strongly deviates from an expected value of $0.98 \pm 0.03 \pm 0.02$.

$N_{up}(e)/N_{down}(e)$

VALUE	DOCUMENT ID		TECN	COMMENT
• • • We do not use the following data for averages, fits, limits, etc. • • •				
$0.84^{+0.14}_{-0.12} \pm 0.02$	[124] FUKUDA	98E	SKAM	multi-GeV

[124] FUKUDA 98E result is based on an exposure of 25.5 kton yr. The analyzed data sample consists of fully-contained single-ring e-like events with visible energy > 1.33 GeV. Upward-going events are those with $-1 < \cos$ (zenith angle) < -0.2 and downward-going events are those with $0.2 < \cos$ (zenith angle) < 1. FUKUDA 98E result is compared to an expected value of $1.01 \pm 0.06 \pm 0.03$.

$\sin^2(2\theta)$ for given $\Delta(m^2)$ ($\nu_e \leftrightarrow \nu_\mu$)

For a review see BAHCALL 89.

VALUE	CL%	DOCUMENT ID		TECN	COMMENT
• • • We do not use the following data for averages, fits, limits, etc. • • •					
< 0.6	90	[125] OYAMA	98	KAMI	$\Delta(m^2) > 0.1\ \text{eV}^2$
< 0.5		[126] CLARK	97	IMB	$\Delta(m^2) > 0.1\ \text{eV}^2$
> 0.55	90	[127] FUKUDA	94	KAMI	$\Delta(m^2) = 0.007$–$0.08\ \text{eV}^2$
< 0.47	90	[128] BERGER	90B	FREJ	$\Delta(m^2) > 1\ \text{eV}^2$
< 0.14	90	LOSECCO	87	IMB	$\Delta(m^2) = 0.00011\ \text{eV}^2$

[125] OYAMA 98 obtained this result by an analysis of upward-going muons in Kamiokande. The data sample used is essentially the same as that used by HATAKEYAMA 98.

[126] CLARK 97 obtained this result by an analysis of fully contained and partially contained events in the IMB water-Cherenkov detector with visible energy > 0.95 GeV.

[127] FUKUDA 94 obtained this result by a combined analysis of sub- and multi-GeV atmospheric neutrino events in Kamiokande.

[128] BERGER 90B uses the Frejus detector to search for oscillations of atmospheric neutrinos. Bounds are for both neutrino and antineutrino oscillations.

$\Delta(m^2)$ for $\sin^2(2\theta) = 1$ ($\nu_e \leftrightarrow \nu_\mu$)

VALUE ($10^{-5}\ \text{eV}^2$)	CL%	DOCUMENT ID		TECN
• • • We do not use the following data for averages, fits, limits, etc. • • •				
< 560	90	[129] OYAMA	98	KAMI
< 980		[130] CLARK	97	IMB
$700 < \Delta(m^2) < 7000$	90	[131] FUKUDA	94	KAMI
< 150	90	[132] BERGER	90B	FREJ

[129] OYAMA 98 obtained this result by an analysis of upward-going muons in Kamiokande. The data sample used is essentially the same as that used by HATAKEYAMA 98.

[130] CLARK 97 obtained this result by an analysis of fully contained and partially contained events in the IMB water-Cherenkov detector with visible energy > 0.95 GeV.

[131] FUKUDA 94 obtained this result by a combined analysis of sub- and multi-GeV atmospheric neutrino events in Kamiokande.

[132] BERGER 90B uses the Frejus detector to search for oscillations of atmospheric neutrinos. Bounds are for both neutrino and antineutrino oscillations.

$\sin^2(2\theta)$ for given $\Delta(m^2)$ ($\overline{\nu}_e \leftrightarrow \overline{\nu}_\mu$)

VALUE ($10^{-5}\ \text{eV}^2$)	CL%	DOCUMENT ID		TECN	COMMENT
• • • We do not use the following data for averages, fits, limits, etc. • • •					
< 0.9	99	[133] SMIRNOV	94	THEO	$\Delta(m^2) > 3 \times 10^{-4}\ \text{eV}^2$
< 0.7	99	[133] SMIRNOV	94	THEO	$\Delta(m^2) < 10^{-11}\ \text{eV}^2$

[133] SMIRNOV 94 analyzed the data from SN 1987A using stellar-collapse models. They also give less stringent upper limits on $\sin^2 2\theta$ for $10^{-11} < \Delta(m^2) < 3 \times 10^{-7}\ \text{eV}^2$ and $10^{-5} < \Delta(m^2) < 3 \times 10^{-4}\ \text{eV}^2$. The same results apply to $\overline{\nu}_e \leftrightarrow \overline{\nu}_\tau$, ν_μ, and ν_τ.

$\sin^2(2\theta)$ for given $\Delta(m^2)$ ($\nu_\mu \leftrightarrow \nu_\tau$)

VALUE	CL%	DOCUMENT ID		TECN	COMMENT
• • • We do not use the following data for averages, fits, limits, etc. • • •					
>0.45	90	[134] AMBROSIO	03	MCRO	$\Delta(m^2)$= 0.00025–0.009 eV^2
>0.77	90	[135] AMBROSIO	03	MCRO	$\Delta(m^2)$= 0.0006–0.007 eV^2
>0.8	90	[136] AMBROSIO	01	MCRO	$\Delta(m^2)$= 0.0006–0.015 eV^2
>0.82	90	[137] AMBROSIO	01	MCRO	$\Delta(m^2)$= 0.001–0.006 ev^2
>0.25	90	[138] AMBROSIO	00	MCRO	$\Delta(m^2) > 3\times10^{-4}$ eV^2
>0.4	90	[139] FUKUDA	99C	SKAM	$\Delta(m^2)$= 0.001–0.1 eV^2
>0.7	90	[140] FUKUDA	99D	SKAM	$\Delta(m^2)$= 0.0015–0.015 eV^2
>0.82	90	[141] AMBROSIO	98	MCRO	$\Delta(m^2) \sim 0.0025$ eV^2
>0.82	90	[142] FUKUDA	98C	SKAM	$\Delta(m^2)$ = 0.0005–0.006 eV^2
>0.3	90	[143] HATAKEYAMA	98	KAMI	$\Delta(m^2)$= 0.00055–0.14 eV^2
>0.73	90	[144] HATAKEYAMA	98	KAMI	$\Delta(m^2)$= 0.004–0.025 eV^2
<0.7		[145] CLARK	97	IMB	$\Delta(m^2) >$ 0.1 eV^2
>0.65	90	[146] FUKUDA	94	KAMI	$\Delta(m^2)$ = 0.005–0.03 eV^2
<0.5	90	[147] BECKER-SZ...	92	IMB	$\Delta(m^2)$= 1–2 $\times10^{-4}$ eV^2
<0.6	90	[148] BERGER	90B	FREJ	$\Delta(m^2) >$ 1 eV^2

[134] AMBROSIO 03 obtained this result on the basis of the ratio $R=N_{\rm low}/N_{\rm high}$, where $N_{\rm low}$ and $N_{\rm high}$ are the number of upward through-going muon events with reconstructed neutrino energy <30 GeV and >130 GeV, respectively. The data came from the full detector run started in 1994. The method of FELDMAN 98 is used to obtain the limits.

[135] AMBROSIO 03 obtained this result by using the ratio R and the angular distribution of the upward through-going muons. R is given by $N_{\rm low}/N_{\rm high}$, where $N_{\rm low}$ and $N_{\rm high}$ are the number of events with reconstructed neutrino energy <30 and >130 GeV, respectively. The angular distribution is reported in AMBROSIO 01. The method of FELDMAN 98 is used to obtain the limits.

[136] AMBROSIO 01 result is based on the angular distribution of upward through-going muon tracks with $E_\mu > 1$ GeV. The data came from three different detector configurations, but the statistics is largely dominated by the full detector run, from May 1994 to December 2000. The total live time, normalized to the full detector configuration, is 6.17 years. The best fit is obtained outside the physical region. The method of FELDMAN 98 is used to obtain the limits.

[137] AMBROSIO 01 result is based on the angular distribution and normalization of upward through-going muon tracks with $E_\mu > 1$ GeV. The best fit is obtained outside the physical region. The method of FELDMAN 98 is used to obtain the limits. See the previous footnote.

[138] AMBROSIO 00 obtained this result by using the upgoing partially contained event sample and the combined samples of downgoing partially contained events and upgoing stopping events. These data came from 4.1 live years of data taking with the full detector, from April 1994 to February 1999. The average energy of atmospheric muon neutrinos corresponding to these samples is 4 GeV. The maximum of the χ^2 probability (97%) occurs at maximal mixing and $\Delta(m^2)=(1\sim 20)\times10^{-3}$ eV^2.

[139] FUKUDA 99C obtained this result from a total of 537 live days of upward through-going muon data in Super-Kamiokande between April 1996 to January 1998. With a threshold of $E_\mu > 1.6$ GeV, the observed flux of upward through-going muons is $(1.74 \pm 0.07 \pm 0.02)\times10^{-13}$ cm^{-2} s^{-1} sr^{-1}. The zenith-angle dependence of the flux does not agree with no-oscillation predictions. For the $\nu_\mu \rightarrow \nu_\tau$ hypothesis, FUKUDA 99C obtained the best fit at $\sin^2 2\theta$=0.95 and $\Delta(m^2)$=5.9 $\times10^{-3}$ eV^2. FUKUDA 99C also reports 68% and 99% confidence-level allowed regions for the same hypothesis.

[140] FUKUDA 99D obtained this result from a simultaneous fitting to zenith angle distributions of upward-stopping and through-going muons. The flux of upward-stopping muons of minimum energy of 1.6 GeV measured between April 1996 and January 1998 is $(0.39 \pm 0.04 \pm 0.02)\times10^{-13}$ cm^{-2} s^{-1} sr^{-1}. This is compared to the expected flux of $(0.73 \pm 0.16$ (theoretical error)$)\times10^{-13}$ cm^{-2} s^{-1} sr^{-1}. The flux of upward through-going muons is taken from FUKUDA 99C. For the $\nu_\mu \rightarrow \nu_\tau$ hypothesis, FUKUDA 99D obtained the best fit in the physical region at $\sin^2 2\theta$=1.0 and $\Delta(m^2)$=3.9 $\times10^{-3}$ eV^2. FUKUDA 99D also reports 68% and 99% confidence-level allowed regions for the same hypothesis. FUKUDA 99D further reports the result of the oscillation analysis using the zenith-angle dependence of upward-stopping/through-going flux ratio. The best fit in the physical region is obtained at $\sin^2 2\theta$=1.0 and $\Delta(m^2)$=3.1 $\times10^{-3}$ eV^2.

[141] AMBROSIO 98 result is only 17% probable at maximum because of relatively low flux for $\cos\theta < -0.8$.

[142] FUKUDA 98C obtained this result by an analysis of 33.0 kton yr atmospheric-neutrino data which include the 25.5 kton yr data used by FUKUDA 98 (sub-GeV) and FUKUDA 98E (multi-GeV). Inside the physical region, the best fit was obtained at $\sin^2 2\theta$=1.0 and $\Delta(m^2)$=2.2$\times10^{-3}$ eV^2. In addition, FUKUDA 98C gave the 99% confidence interval, $\sin^2 2\theta > 0.73$ and $3\times10^{-4} < \Delta(m^2) < 8.5\times10^{-3}$ eV^2. FUKUDA 98C also tested the $\nu_\mu \rightarrow \nu_e$ hypothesis, and concluded that it is not favored.

[143] HATAKEYAMA 98 obtained this result from a total of 2456 live days of upward-going muon data in Kamiokande between December 1985 and May 1995. With a threshold of $E_\mu > 1.6$ GeV, the observed flux of upward through-going muon is $(1.94 \pm 0.10^{+0.07}_{-0.06})\times10^{-13}$ cm^{-2} s^{-1} sr^{-1}. This is compared to the expected flux of $(2.46 \pm 0.54$ (theoretical error)$)\times10^{-13}$ cm^{-2} s^{-1} sr^{-1}. For the $\nu_\mu \rightarrow \nu_\tau$ hypothesis, the best fit inside the physical region was obtained at $\sin^2 2\theta$=1.0 and $\Delta(m^2)$=3.2 $\times10^{-3}$ eV^2.

[144] HATAKEYAMA 98 obtained this result from a combined analysis of Kamiokande's contained events (FUKUDA 94) and upward-going muon events. The best fit was obtained at $\sin^2 2\theta$=0.95 and $\Delta(m^2)$=1.3 $\times10^{-2}$ eV^2.

[145] CLARK 97 obtained this result by an analysis of fully contained and partially contained events in the IMB water-Cherenkov detector with visible energy > 0.95 GeV.

[146] FUKUDA 94 obtained this result by a combined analysis of sub-and multi-GeV atmospheric neutrino events in Kamiokande.

[147] BECKER-SZENDY 92 uses upward-going muons to search for atmospheric ν_μ oscillations. The fraction of muons which stop in the detector is used to search for deviations in the expected spectrum. No evidence for oscillations is found.

[148] BERGER 90B uses the Frejus detector to search for oscillations of atmospheric neutrinos. Bounds are for both neutrino and antineutrino oscillations.

$\Delta(m^2)$ for $\sin^2(2\theta) = 1$ ($\nu_\mu \leftrightarrow \nu_\tau$)

VALUE (10^{-5} eV^2)	CL%	DOCUMENT ID		TECN
• • • We do not use the following data for averages, fits, limits, etc. • • •				
$25< \Delta(m^2) <900$	90	[149] AMBROSIO	03	MCRO
$60< \Delta(m^2) <700$	90	[150] AMBROSIO	03	MCRO
$60< \Delta(m^2) <1500$	90	[151] AMBROSIO	01	MCRO
$100< \Delta(m^2) <600$	90	[152] AMBROSIO	01	MCRO
> 35	90	[153] AMBROSIO	00	MCRO
$100< \Delta(m^2) < 5000$	90	[154] FUKUDA	99C	SKAM
$150< \Delta(m^2) < 1500$	90	[155] FUKUDA	99D	SKAM
$50< \Delta(m^2) < 600$	90	[156] AMBROSIO	98	MCRO
$50< \Delta(m^2) < 600$	90	[157] FUKUDA	98C	SKAM
$55< \Delta(m^2) < 5000$	90	[158] HATAKEYAMA	98	KAMI
$400< \Delta(m^2) < 2300$	90	[159] HATAKEYAMA	98	KAMI
<1500		[160] CLARK	97	IMB
$500 < \Delta(m^2) < 2500$	90	[161] FUKUDA	94	KAMI
< 350	90	[162] BERGER	90B	FREJ

[149] AMBROSIO 03 obtained this result on the basis of the ratio $R=N_{\rm low}/N_{\rm high}$, where $N_{\rm low}$ and $N_{\rm high}$ are the number of upward through-going muon events with reconstructed neutrino energy <30 GeV and >130 GeV, respectively. The data came from the full detector run started in 1994. The method of FELDMAN 98 is used to obtain the limits.

[150] AMBROSIO 03 obtained this result by using the ratio R and the angular distribution of the upward through-going muons. R is given by $N_{\rm low}/N_{\rm high}$, where $N_{\rm low}$ and $N_{\rm high}$ are the number of events with reconstructed neutrino energy <30 and >130 GeV, respectively. The angular distribution is reported in AMBROSIO 01. The method of FELDMAN 98 is used to obtain the limits.

[151] AMBROSIO 01 result is based on the angular distribution of upward through-going muon tracks with $E_\mu > 1$ GeV. The data came from three different detector configurations, but the statistics is largely dominated by the full detector run, from May 1994 to December 2000. The total live time, normalized to the full detector configuration, is 6.17 years. The best fit is obtained outside the physical region. The method of FELDMAN 98 is used to obtain the limits.

[152] AMBROSIO 01 result is based on the angular distribution and normalization of upward through-going muon tracks with $E_\mu > 1$ GeV. The best fit is obtained outside the physical region. The method of FELDMAN 98 is used to obtain the limits. See the previous footnote.

[153] AMBROSIO 00 obtained this result by using the upgoing partially contained event sample and the combined samples of downgoing partially contained events and upgoing stopping events. These data came from 4.1 live years of data taking with the full detector, from April 1994 to February 1999. The average energy of atmospheric muon neutrinos corresponding to these samples is 4 GeV. The maximum of the χ^2 probability (97%) occurs at maximal mixing and $\Delta(m^2)=(1\sim 20)\times10^{-3}$ eV^2.

[154] FUKUDA 99C obtained this result from a total of 537 live days of upward through-going muon data in Super-Kamiokande between April 1996 to January 1998. With a threshold of $E_\mu > 1.6$ GeV, the observed flux of upward through-going muon is $(1.74 \pm 0.07 \pm 0.02)\times10^{-13}$ cm^{-2} s^{-1} sr^{-1}. The zenith-angle dependence of the flux does not agree with no-oscillation predictions. For the $\nu_\mu \rightarrow \nu_\tau$ hypothesis, FUKUDA 99C obtained the best fit at $\sin^2 2\theta$=0.95 and $\Delta(m^2)$=5.9 $\times10^{-3}$ eV^2. FUKUDA 99C also reports 68% and 99% confidence-level allowed regions for the same hypothesis.

[155] FUKUDA 99D obtained this result from a simultaneous fitting to zenith angle distributions of upward-stopping and through-going muons. The flux of upward-stopping muons of minimum energy of 1.6 GeV measured between April 1996 and January 1998 is $(0.39 \pm 0.04 \pm 0.02)\times10^{-13}$ cm^{-2} s^{-1} sr^{-1}. This is compared to the expected flux of $(0.73 \pm 0.16$ (theoretical error)$)\times10^{-13}$ cm^{-2} s^{-1} sr^{-1}. The flux of upward through-going muons is taken from FUKUDA 99C. For the $\nu_\mu \rightarrow \nu_\tau$ hypothesis, FUKUDA 99D obtained the best fit in the physical region at $\sin^2 2\theta$=1.0 and $\Delta(m^2)$=3.9 $\times10^{-3}$ eV^2. FUKUDA 99D also reports 68% and 99% confidence-level allowed regions for the same hypothesis. FUKUDA 99D further reports the result of the oscillation analysis using the zenith-angle dependence of upward-stopping/through-going flux ratio. The best fit in the physical region is obtained at $\sin^2 2\theta$=1.0 and $\Delta(m^2)$=3.1 $\times10^{-3}$ eV^2.

[156] AMBROSIO 98 result is only 17% probable at maximum because of relatively low flux for $\cos\theta < -0.8$.

[157] FUKUDA 98C obtained this result by an analysis of 33.0 kton yr atmospheric-neutrino data which include the 25.5 kton yr data used by FUKUDA 98 (sub-GeV) and FUKUDA 98E (multi-GeV). Inside the physical region, the best fit was obtained at $\sin^2 2\theta$=1.0 and $\Delta(m^2)$=2.2$\times10^{-3}$ eV^2. In addition, FUKUDA 98C gave the 99% confidence interval, $\sin^2 2\theta > 0.73$ and $3\times10^{-4} < \Delta(m^2) < 8.5\times10^{-3}$ eV^2. FUKUDA 98C also tested the $\nu_\mu \rightarrow \nu_e$ hypothesis, and concluded that it is not favored.

[158] HATAKEYAMA 98 obtained this result from a total of 2456 live days of upward-going muon data in Kamiokande between December 1985 and May 1995. With a threshold of $E_\mu > 1.6$ GeV, the observed flux of upward through-going muon is $(1.94 \pm 0.10^{+0.07}_{-0.06})\times10^{-13}$ cm^{-2} s^{-1} sr^{-1}. This is compared to the expected flux of $(2.46 \pm 0.54$ (theoretical error)$)\times10^{-13}$ cm^{-2} s^{-1} sr^{-1}. For the $\nu_\mu \rightarrow \nu_\tau$ hypothesis, the best fit inside the physical region was obtained at $\sin^2 2\theta$=1.0 and $\Delta(m^2)$=3.2 $\times10^{-3}$ eV^2.

[159] HATAKEYAMA 98 obtained this result from a combined analysis of Kamiokande's contained events (FUKUDA 94) and upward-going muon events. The best fit was obtained at $\sin^2 2\theta$=0.95 and $\Delta(m^2)$=1.3 $\times10^{-2}$ eV^2.

[160] CLARK 97 obtained this result by an analysis of fully contained and partially contained events in the IMB water-Cherenkov detector with visible energy > 0.95 GeV.

[161] FUKUDA 94 obtained this result by a combined analysis of sub-and multi-GeV atmospheric neutrino events in Kamiokande.

[162] BERGER 90B uses the Frejus detector to search for oscillations of atmospheric neutrinos. Bounds are for both neutrino and antineutrino oscillations.

$\Delta(m^2)$ for $\sin^2(2\theta) = 1$ ($\nu_\mu \rightarrow \nu_s$)

ν_s means ν_τ or any sterile (noninteracting) ν.

VALUE (10^{-5} eV^2)	CL%	DOCUMENT ID		TECN	COMMENT
• • • We do not use the following data for averages, fits, limits, etc. • • •					
<3000 (or <550)	90	[163] OYAMA	89	KAMI	Water Cherenkov
< 4.2 or > 54.	90	BIONTA	88	IMB	Flux has ν_μ, $\overline{\nu}_\mu$, ν_e, and $\overline{\nu}_e$

[163] OYAMA 89 gives a range of limits, depending on assumptions in their analysis. They argue that the region $\Delta(m^2) = (100\text{–}1000) \times 10^{-5}$ eV^2 is not ruled out by any data for large mixing.

Search for $\nu_\mu \rightarrow \nu_s$

VALUE	DOCUMENT ID		TECN	COMMENT
• • • We do not use the following data for averages, fits, limits, etc. • • •				
	[164] AMBROSIO	01	MCRO	matter effects
	[165] FUKUDA	00	SKAM	neutral currents + matter effects

[164] AMBROSIO 01 tested the pure 2-flavor $\nu_\mu \rightarrow \nu_s$ hypothesis using matter effects which change the shape of the zenith-angle distribution of upward through-going muons. With maximum mixing and $\Delta(m^2)$ around 0.0024 eV^2, the $\nu_\mu \rightarrow \nu_s$ oscillation is disfavored with 99% confidence level with respect to the $\nu_\mu \rightarrow \nu_\tau$ hypothesis.

[165] FUKUDA 00 tested the pure 2-flavor $\nu_\mu \rightarrow \nu_s$ hypothesis using three complementary atmospheric-neutrino data samples. With this hypothesis, zenith-angle distributions are expected to show characteristic behavior due to neutral currents and matter effects. In the $\Delta(m^2)$ and $\sin^2 2\theta$ region preferred by the Super-Kamiokande data, the $\nu_\mu \rightarrow \nu_s$ hypothesis is rejected at the 99% confidence level, while the $\nu_\mu \rightarrow \nu_\tau$ hypothesis consistently fits all of the data sample.

(D) Solar ν Experiments

SOLAR NEUTRINOS

Revised November 2003 by K. Nakamura (KEK, High Energy Accelerator Research Organization, Japan).

1. Introduction

The Sun is a main-sequence star at a stage of stable hydrogen burning. It produces an intense flux of electron neutrinos as a consequence of nuclear fusion reactions whose combined effect is

$$4p \rightarrow {}^4\mathrm{He} + 2e^+ + 2\nu_e. \qquad (1)$$

Positrons annihilate with electrons. Therefore, when considering the solar thermal energy generation, a relevant expression is

$$4p + 2e^- \rightarrow {}^4\mathrm{He} + 2\nu_e + 26.73\ \mathrm{MeV} - E_\nu\ , \qquad (2)$$

where E_ν represents the energy taken away by neutrinos, with an average value being $\langle E_\nu \rangle \sim 0.6$ MeV. The neutrino-producing reactions which are at work inside the Sun are enumerated in the first column in Table 1. The second column in Table 1 shows abbreviation of these reactions. The energy spectrum of each reaction is shown in Fig. 1.

Observation of solar neutrinos directly addresses the theory of stellar structure and evolution, which is the basis of the standard solar model (SSM). The Sun as a well-defined neutrino source also provides extremely important opportunities to investigate nontrivial neutrino properties such as nonzero mass and mixing, because of the wide range of matter density and the great distance from the Sun to the Earth.

A pioneering solar neutrino experiment by Davis and collaborators using ^{37}Cl started in the late 1960's. From the very beginning of the solar-neutrino observation [1], it was recognized that the observed flux was significantly smaller than the SSM prediction, provided nothing happens to the electron neutrinos after they are created in the solar interior. This deficit has been called "the solar-neutrino problem."

In spite of the challenges by the chlorine and gallium radiochemical experiments (GALLEX, SAGE, and GNO) and water-Cherenkov experiments (Kamiokande and Super-Kamiokande), the solar-neutrino problem had persisted for more than 30 years. However, there have been remarkable developments in the past few years and now the solar-neutrino problem has been finally solved.

In 2001, the initial result from SNO (Sudbury Neutrino Observatory) [2], a water Cherenkov detector with heavy water, on the solar-neutrino flux measured via charged-current (CC) reaction, $\nu_e d \rightarrow e^- pp$, combined with the Super-Kamiokande's high-statistics flux measurement via νe elastic scattering [3], provided direct evidence for flavor conversion of solar neutrinos [2]. Later in 2002, SNO's measurement of the neutral-current (NC) rate, $\nu d \rightarrow \nu pn$, and the updated CC result further strengthened this conclusion [4].

The most probable explanation which can also solve the solar-neutrino problem is neutrino oscillation. At this stage, the LMA (large mixing angle) solution was the most promising. However, at 3σ confidence level, LOW (low probability or low mass) and/or VAC (vacuum) solutions were allowed depending on the method of analysis (see Sec. 3.6). LMA and LOW are solutions of neutrino oscillation in matter [5,6] and VAC is a solution of neutrino oscillation in vacuum. Subsequently, experiments have excluded vacuum oscillations and there exists strong evidence that matter effects are required in the solution to the solar-neutrino problem.

In December 2002, KamLAND (Kamioka Liquid Scintillator Anti-Neutrino Detector), a terrestrial $\overline{\nu}_e$ disappearance experiment using reactor neutrinos, observed clear evidence of neutrino oscillation with the allowed parameter region overlapping with the parameter region of the LMA solution [7]. Assuming CPT invariance, this result directly implies that the true solution of the solar ν_e oscillation has been determined to be LMA. A combined analysis of all the solar-neutrino data and KamLAND data significantly constrained the allowed parameter region. Inside the LMA region, the allowed region splits into two bands with higher Δm^2 and lower Δm^2.

More recently, in September, 2003, SNO reported [8] results on solar-neutrino fluxes observed with NaCl added in heavy water: this improved the sensitivity for the detection of the NC reaction. A global analysis of all the solar neutrino data combined with the KamLAND data further reduced the allowed region to the lower Δm^2 band with the best fit point of $\Delta m^2 = 7.1 \times 10^{-5}$ eV^2 and $\theta = 32.5$ degrees [8].

2. Solar Model Predictions

A standard solar model is based on the standard theory of stellar evolution. A variety of input information is needed in the evolutionary calculations. The most elaborate SSM, BP2000 [9], is presented by Bahcall *et al.* who define their SSM as the solar model which is constructed with the best available physics and input data. Though they used no helioseismological constraints in defining the SSM, the calculated sound speed as a function

of the solar radius shows an excellent agreement with the helioseismologically determined sound speed to a precision of 0.1% rms throughout essentially the entire Sun. This greatly strengthens the confidence in the solar model. The BP2000 predictions [9] for the flux and contributions to the event rates in chlorine and gallium solar-neutrino experiments from each neutrino-producing reaction are listed in Table 1. The solar-neutrino spectra shown in Fig. 1 also resulted from the BP2000 calculations [9].

Other recent solar-model predictions for solar-neutrino fluxes were given by Turck-Chieze *et al.* [10] Their model is based on the standard theory of stellar evolution where the best physics available is adopted, but some fundamental inputs such as the *pp* reaction rate and the heavy-element abundance in the Sun are seismically adjusted within the commonly estimated errors aiming at reducing the residual differences between the helioseismologically-determined and the model-calculated sound speeds. Their predictions for the event rates in chlorine and gallium solar-neutrino experiments as well as ^{8}B solar-neutrino flux are shown in the last line in Table 2, where the BP2000 predictions [9] are also shown in the same format. As is apparent from this table, the predictions of the two models are remarkably consistent.

The SSM predicted ^{8}B solar-neutrino flux is proportional to the low-energy cross section factor $S_{17}(0)$ for the ^{7}Be(p,γ)^{8}B reaction. The BP2000 [9] and Turck-Chieze *et al.* [10] models adopted $S_{17}(0) = 19^{+4}_{-2}$ eV·b. Inspired by the recent precise measurement of the low-energy cross section for the ^{7}Be(p,γ)^{8}B reaction by Junghans *et al.* [11], Bahcall *et al.* [12] calculated the (BP2000 + New ^{8}B) SSM predictions using $S_{17}(0) = (22.3 \pm 0.9)$ eV·b. The results are: a ^{8}B solar-neutrino flux of $5.93(1.00^{+0.14}_{-0.15}) \times 10^6$ cm^{-2} s^{-1}, a chlorine capture rate of $8.59^{+1.1}_{-1.2}$ SNU, and a gallium capture rate of 130^{+9}_{-7} SNU.

Table 1: Neutrino-producing reactions in the Sun (first column) and their abbreviations (second column). The neutrino fluxes and event rates in chlorine and gallium solar-neutrino experiments predicted by Bahcall, Pinsonneault and Basu [9] are listed in the third, fourth, and fifth columns respectively.

		BP2000 [9]		
Reaction	Abbr.	Flux (cm^{-2} s^{-1})	Cl (SNU*)	Ga (SNU*)
$pp \to d\,e^+\,\nu$	*pp*	$5.95(1.00^{+0.01}_{-0.01}) \times 10^{10}$	—	69.7
$pe^-p \to d\,\nu$	*pep*	$1.40(1.00^{+0.015}_{-0.015}) \times 10^8$	0.22	2.8
^{3}He $p \to {}^4$He $e^+\nu$	*hep*	9.3×10^3	0.04	0.1
^{7}Be $e^- \to {}^7$Li $\nu + (\gamma)$	^{7}Be	$4.77(1.00^{+0.10}_{-0.10}) \times 10^9$	1.15	34.2
^{8}B $\to {}^8$Be* $e^+\nu$	^{8}B	$5.05(1.00^{+0.20}_{-0.16}) \times 10^6$	5.76	12.1
^{13}N $\to {}^{13}$C $e^+\nu$	^{13}N	$5.48(1.00^{+0.21}_{-0.17}) \times 10^8$	0.09	3.4
^{15}O $\to {}^{15}$N $e^+\nu$	^{15}O	$4.80(1.00^{+0.25}_{-0.19}) \times 10^8$	0.33	5.5
^{17}F $\to {}^{17}$O $e^+\nu$	^{17}F	$5.63(1.00^{+0.25}_{-0.25}) \times 10^6$	0.0	0.1
Total			$7.6^{+1.3}_{-1.1}$	128^{+9}_{-7}

* 1 SNU (Solar Neutrino Unit) = 10^{-36} captures per atom per second.

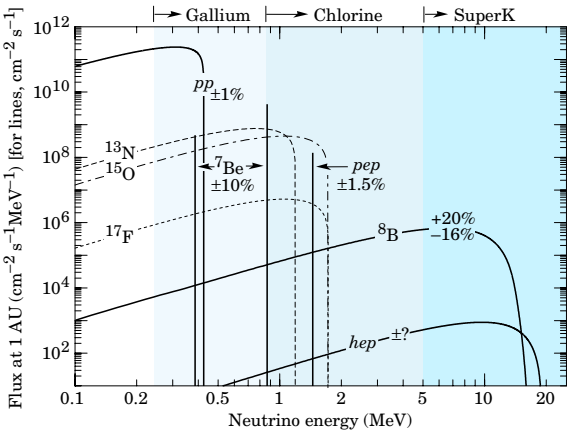

Figure 1: The solar neutrino spectrum predicted by the standard solar model. The neutrino fluxes from continuum sources are given in units of number cm^{-2}s^{-1}MeV^{-1} at one astronomical unit, and the line fluxes are given in number cm^{-2}s^{-1}. Spectra for the *pp* chain, shown by the solid curves, are courtesy of J.N. Bahcall (2001). Spectra for the CNO chain are shown by the dotted curves, and are also courtesy of J.N. Bahcall (1995). See full-color version on color pages at end of book.

3. Solar Neutrino Experiments

So far, seven solar-neutrino experiments have published results. The most recent published results on the average event rates or flux from these experiments are listed in Table 2 and compared to the two recent solar-model predictions.

3.1. Radiochemical Experiments

Radiochemical experiments exploit electron neutrino absorption on nuclei followed by their decay through orbital electron capture. Produced Auger electrons are counted.

The Homestake chlorine experiment in USA uses the reaction

$$^{37}\mathrm{Cl} + \nu_e \to {}^{37}\mathrm{Ar} + e^- \quad \text{(threshold 814 keV)}. \qquad (3)$$

Three gallium experiments (GALLEX and GNO at Gran Sasso in Italy and SAGE at Baksan in Russia) use the reaction

$$^{71}\mathrm{Ga} + \nu_e \to {}^{71}\mathrm{Ge} + e^- \quad \text{(threshold 233 keV)}. \qquad (4)$$

The produced ^{37}Ar and ^{71}Ge atoms are both radioactive, with half lives ($\tau_{1/2}$) of 34.8 days and 11.43 days, respectively. After an exposure of the detector for two to three times $\tau_{1/2}$, the reaction products are chemically extracted and introduced into a low-background proportional counter, where they are counted for a sufficiently long period to determine the exponentially decaying signal and a constant background.

Solar-model calculations predict that the dominant contribution in the chlorine experiment comes from ^{8}B neutrinos, but

See key on page 323

Table 2: Recent results from the seven solar-neutrino experiments and a comparison with standard solar-model predictions. Solar model calculations are also presented. The first and the second errors in the experimental results are the statistical and systematic errors, respectively.

	^{37}Cl→^{37}Ar (SNU)	^{71}Ga→^{71}Ge (SNU)	^{8}B ν flux (10^6cm^{-2}s^{-1})
Homestake			
(CLEVELAND 98)[13]	$2.56 \pm 0.16 \pm 0.16$	—	—
GALLEX			
(HAMPEL 99)[14]	—	$77.5 \pm 6.2^{+4.3}_{-4.7}$	—
GNO			
(ALTMANN 00)[15]	—	$65.8^{+10.2+3.4}_{-\ 9.6-3.6}$	—
SAGE			
(ABDURASHI...02)[16]	—	$70.8^{+5.3+3.7}_{-5.2-3.2}$	—
Kamiokande			
(FUKUDA 96)[17]	—	—	$2.80 \pm 0.19 \pm 0.33^{\dagger}$
Super-Kamiokande			
(FUKUDA 02)[18]	—	—	$2.35 \pm 0.03^{+0.07}_{-0.06}{}^{\dagger}$
SNO (pure D_2O)			
(AHMAD 02)[4]	—	—	$1.76^{+0.06}_{-0.05} \pm 0.09^{\ddagger}$
	—	—	$2.39^{+0.24}_{-0.23} \pm 0.12^{\dagger}$
	—	—	$5.09^{+0.44+0.46}_{-0.43-0.43}{}^{*}$
SNO (NaCl in D_2O)			
(AHMED 03)[8]	—	—	$1.59^{+0.08+0.06}_{-0.07-0.08}{}^{\ddagger}$
	—	—	$2.21^{+0.31}_{-0.26} \pm 0.10^{\dagger}$
	—	—	$5.21 \pm 0.27 \pm 0.38^{*}$
(BAHCALL 01)[9]	$7.6^{+1.3}_{-1.1}$	128^{+9}_{-7}	$5.05(1.00^{+0.20}_{-0.16})$
(TURCK-CHIEZE 01)[10]	7.44 ± 0.96	127.8 ± 8.6	4.95 ± 0.72

* Flux measured via the neutral-current reaction.

† Flux measured via νe elastic scattering.

‡ Flux measured via the charged-current reaction.

^{7}Be, *pep*, ^{13}N, and ^{15}O neutrinos also contribute. At present, the most abundant *pp* neutrinos can be detected only in gallium experiments. Even so, according to the solar-model calculations, almost half of the capture rate in the gallium experiments is due to other solar neutrinos.

The Homestake chlorine experiment was the first to attempt the observation of solar neutrinos. Initial results obtained in 1968 showed no events above background with upper limit for the solar-neutrino flux of 3 SNU [1]. After introduction of an improved electronics system which discriminates signal from background by measuring the rise time of the pulses from proportional counters, a finite solar-neutrino flux has been observed since 1970. The solar-neutrino capture rate shown in Table 2 is a combined result of 108 runs between 1970 and 1994 [13]. It is only about 1/3 of the BP2000 prediction [9].

GALLEX presented the first evidence of *pp* solar-neutrino observation in 1992 [19]. Here also, the observed capture rate is significantly less than the SSM prediction. SAGE initially reported very low capture rate, $20^{+15}_{-20} \pm 32$ SNU, with a 90% confidence-level upper limit of 79 SNU [20]. Later, SAGE observed similar capture rate to that of GALLEX [21]. Both GALLEX and SAGE groups tested the overall detector response with intense man-made ^{51}Cr neutrino sources, and observed good agreement between the measured ^{71}Ge production rate and that predicted from the source activity, demonstrating the reliability of these experiments. The GALLEX Collaboration formally finished observations in early 1997. Since April, 1998, a newly defined collaboration, GNO (Gallium Neutrino Observatory) resumed the observations.

3.2 Kamiokande and Super-Kamiokande

Kamiokande and Super-Kamiokande in Japan are real-time experiments utilizing νe scattering

$$\nu_x + e^- \rightarrow \nu_x + e^- \qquad (5)$$

in a large water-Cherenkov detector. It should be noted that the reaction Eq. (5) is sensitive to all active neutrinos, $x = e$, μ, and τ. However, the sensitivity to ν_μ and ν_τ is much smaller than the sensitivity to ν_e, $\sigma(\nu_{\mu,\tau}e) \approx 0.16\,\sigma(\nu_e e)$. The solar-neutrino flux measured via νe scattering is deduced assuming no neutrino oscillations.

These experiments take advantage of the directional correlation between the incoming neutrino and the recoil electron. This feature greatly helps the clear separation of the solar-neutrino signal from the background. Due to the high thresholds (7 MeV in Kamiokande and 5 MeV at present in Super-Kamiokande) the experiments observe pure ^{8}B solar neutrinos because *hep* neutrinos contribute negligibly according to the SSM.

The Kamiokande-II Collaboration started observing ^{8}B solar neutrinos at the beginning of 1987. Because of the strong directional correlation of νe scattering, this result gave the first direct evidence that the Sun emits neutrinos [22] (no directional information is available in radiochemical solar-neutrino experiments). The observed solar-neutrino flux was also significantly less than the SSM prediction. In addition, Kamiokande-II obtained the energy spectrum of recoil electrons and the fluxes separately measured in the daytime and nighttime. The Kamiokande-II experiment came to an end at the beginning of 1995.

Super-Kamiokande is a 50-kton second-generation solar-neutrino detector, which is characterized by a significantly larger counting rate than the first-generation experiments. This experiment started observation in April 1996. The solar-neutrino flux was measured as a function of zenith angle and recoil-electron energy [18]. The average solar-neutrino flux was smaller than, but consistent with, the Kamiokande-II result [17]. The observed day-night asymmetry was $A_{\rm DN} = \dfrac{\rm Day - Night}{0.5(\rm Day + Night)} = -0.021 \pm 0.020^{+0.013}_{-0.012}$. No indication of spectral distortion was observed.

In November 2001, Super-Kamiokande suffered from an accident in which substantial number of photomultiplier tubes were lost. The detector was rebuilt within a year with about half of the original number of photomultiplier tubes. The experiment

with the detector before the accident is now called Super-Kamiokande-I, and that after the accident is called Super-Kamiokande-II.

3.3 SNO

In 1999, a new real time solar-neutrino experiment, SNO, in Canada started observation. This experiment uses 1000 tons of ultra-pure heavy water (D_2O) contained in a spherical acrylic vessel, surrounded by an ultra-pure H_2O shield. SNO measures ^{8}B solar neutrinos via the reactions

$$\nu_e + d \rightarrow e^- + p + p \qquad (6)$$

and

$$\nu_x + d \rightarrow \nu_x + p + n, \qquad (7)$$

as well as νe scattering, Eq. (5). The CC reaction, Eq. (6), is sensitive only to electron neutrinos, while the NC reaction, Eq. (7), is sensitive to all active neutrinos.

The Q-value of the CC reaction is -1.4 MeV and the electron energy is strongly correlated with the neutrino energy. Thus, the CC reaction provides an accurate measure of the shape of the ^{8}B solar-neutrino spectrum. The contributions from the CC reaction and νe scattering can be distinguished by using different cos $\theta_\odot$ distributions where $\theta_\odot$ is the angle of the electron momentum with respect to the direction from the Sun to the Earth. While the νe scattering events have a strong forward peak, CC events have an approximate angular distribution of $1 - 1/3\ \cos\theta_\odot$.

The threshold of the NC reaction is 2.2 MeV. In the pure D_2O, the signal of the NC reaction is neutron capture in deuterium, producing a 6.25-MeV γ-ray. In this case, the capture efficiency is low and the deposited energy is close to the detection threshold of 5 MeV. In order to enhance both the capture efficiency and the total γ-ray energy (8.6 MeV), 2 tons of NaCl were added to the heavy water in the second phase of the experiment. In addition, installation of discrete ^{3}He neutron counters is planned for the NC measurement in the third phase.

In 2001, SNO published the initial results on the measurement of the ^{8}B solar-neutrino flux via CC reaction [2]. The electron energy spectrum and the $\cos\theta_\odot$ distribution were also measured. The spectral shape of the electron energy was consistent with the expectations for an undistorted ^{8}B solar-neutrino spectrum.

SNO also measured the ^{8}B solar-neutrino flux via νe scattering. Though the latter result had poor statistics, it was consistent with the high-statistics Super-Kamiokande result. Thus, the SNO group compared their CC result with Super-Kamiokande's νe scattering result, and obtained evidence of an active non-ν_e component in the solar-neutrino flux, as further described in Sec. 3.5.

Later, in April, 2002, SNO reported the first result on the ^{8}B solar-neutrino flux measurement via NC reaction [4]. The total flux measured via NC reaction was consistent with the solar-model predictions (see Table 2). Also, the SNO's CC and νe scattering results were updated [4]. These results were consistent with the earlier results [2].

Further, the day and night energy spectra were measured and the day-night asymmetry of the ν_e flux measured with CC events was presented [23]. Assuming an undistorted ^{8}B spectrum, the asymmetry was $A_{\rm DN} = \dfrac{\rm Day - Night}{0.5({\rm Day + Night})} = -0.140 \pm 0.063^{+0.015}_{-0.014}$. With an additional constraint of no asymmetry for the total flux of active neutrinos, the asymmetry was found to be $-0.070 \pm 0.049^{+0.013}_{-0.012}$.

The SNO Collaboration made a global analysis (see Sect. 3.6) of the SNO's day and night energy spectra together with the data from other solar-neutrino experiments. The results strongly favored the LMA solution, with the LOW solution allowed at 99.5% confidence level [23]. (In most of the similar global analyses, the VAC solution was also allowed at 99.9 $\sim$ 99.73% confidence level, see Sect. 3.6.) For the LMA solution (and also for the LOW solution), the maximal mixing was excluded at $> 3\sigma$.

Recently, in September, 2003, SNO has released the results of solar-neutrino flux measurements with dissolved NaCl in the heavy water. The results from the "salt phase" are described in Sect. 5.

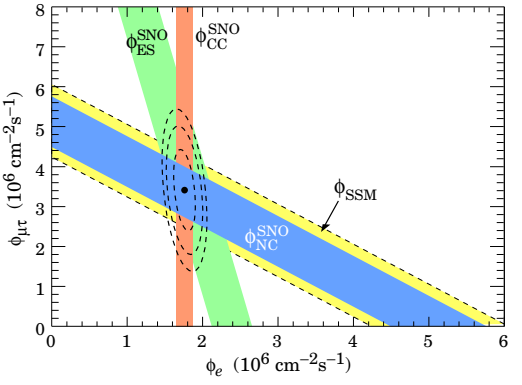

Figure 2: Fluxes of ^{8}B solar neutrinos, $\phi(\nu_e)$, and $\phi(\nu_{\mu\ {\rm or}\ \tau})$, deduced from the SNO's charged-current (CC), ν_e elastic scattering (ES), and neutral-current (NC) results for pure D_2O. The standard solar model prediction [9] is also shown. The bands represent the 1σ error. The contours show the 68%, 95%, and 99% joint probability for $\phi(\nu_e)$ and $\phi(\nu_{\mu\ {\rm or}\ \tau})$. This figure is courtesy of K.T. Lesko (LBNL). See full-color version on color pages at end of book.

3.4 Comparison of Experimental Results with Solar-Model Predictions

It is clear from Table 2 that the results from all the solar-neutrino experiments, except the SNO's NC result, indicate

significantly less flux than expected from the BP2000 SSM [9] and the Turck-Chieze *et al.* solar model [10].

There has been a consensus that a consistent explanation of all the results of solar-neutrino observations is unlikely within the framework of astrophysics using the solar-neutrino spectra given by the standard electroweak model. Many authors made solar model-independent analyses constrained by the observed solar luminosity [24–28], where they attempted to fit the measured solar-neutrino capture rates and ^{8}B flux with normalization-free, undistorted energy spectra. All these attempts only obtained solutions with very low probabilities.

The data therefore suggest that the solution to the solar-neutrino problem requires nontrivial neutrino properties.

3.5 Evidence for Solar Neutrino Oscillations

Denoting the ^{8}B solar-neutrino flux obtained by the SNO's CC measurement as $\phi^{\rm CC}_{\rm SNO}(\nu_e)$ and that obtained by the Super-Kamiokande νe scattering as $\phi^{\rm ES}_{\rm SK}(\nu_x)$, $\phi^{\rm CC}_{\rm SNO}(\nu_e) = \phi^{\rm ES}_{\rm SK}(\nu_x)$ is expected for the standard neutrino physics. However, SNO's initial data [2] indicated

$$\phi^{\rm ES}_{\rm SK}(\nu_x) - \phi^{\rm CC}_{\rm SNO}(\nu_e) = (0.57 \pm 0.17) \times 10^6 \ \ {\rm cm}^{-2}{\rm s}^{-1}. \qquad (8)$$

The significance of the difference was $> 3\sigma$, implying direct evidence for the existence of a non-ν_e active neutrino flavor component in the solar-neutrino flux. A natural and most probable explanation of neutrino flavor conversion is neutrino oscillation. Note that both the SNO [2] and Super-Kamiokande [3] flux results were obtained by assuming the standard ^{8}B neutrino spectrum shape. This assumption was justified by the measured energy spectra in both of the experiments.

The SNO's results for pure D_2O, reported in 2002 [4], provided stronger evidence for neutrino oscillation than Eq. (8). The fluxes measured with CC, ES and NC events were

$$\phi^{\rm CC}_{\rm SNO}(\nu_e) = (1.76^{+0.06}_{-0.05} \pm 0.09) \times 10^6 {\rm cm}^{-2}{\rm s}^{-1} \ , \qquad (9)$$

$$\phi^{\rm ES}_{\rm SNO}(\nu_x) = (2.39^{+0.24}_{-0.23} \pm 0.12) \times 10^6 {\rm cm}^{-2}{\rm s}^{-1} \ , \qquad (10)$$

$$\phi^{\rm NC}_{\rm SNO}(\nu_x) = (5.09^{+0.44+0.46}_{-0.43-0.43}) \times 10^6 {\rm cm}^{-2}{\rm s}^{-1} \ . \qquad (11)$$

Eq. (11) is a mixing-independent result and therefore tests solar models. It shows very good agreement with the ^{8}B solar-neutrino flux predicted by the BP2000 SSM [9] and that predicted by Turck-Chieze *et al.* model [10]. The fluxes $\phi(\nu_e)$ and $\phi(\nu_{\mu \text{ or } \tau})$ deduced from these results were remarkably consistent as can be seen in Fig. 2. The resultant flux of non-ν_e active neutrinos, $\phi(\nu_{\mu \text{ or } \tau})$, was

$$\phi(\nu_{\mu \text{ or } \tau}) = \left(3.41^{+0.66}_{-0.64}\right) \times 10^6 {\rm cm}^{-2}{\rm s}^{-1} \qquad (12)$$

where the statistical and systematic errors were added in quadrature. This $\phi(\nu_{\mu \text{ or } \tau})$ was 5.3 σ above 0.

3.6. Pre-KamLAND Global Analyses of the Solar Neutrino Data

A global analysis of the solar-neutrino data essentially uses all the independent solar-neutrino data that are available when the analysis is made to determine the globally allowed regions in terms of two neutrino oscillations either in vacuum or in matter. A number of pre-SNO global analyses of the solar-neutrino data yielded various solutions. (For example, see Ref. [29].) With the SNO's CC and NC measurements, various global analyses [30–36] showed that LMA was the most favored solution, but either or both of the two other solutions, LOW (low probability or low mass) and VAC (vacuum), were marginally allowed at $99.9 \sim 99.73\%$ confidence level. These global analyses mostly differ in the statistical treatment of the data.

Typical parameter values [34] corresponding to these solutions are

- LMA: $\Delta m^2 = 5.5 \times 10^{-5}$ eV^2, $\tan^2\theta = 0.42$
- LOW: $\Delta m^2 = 7.3 \times 10^{-8}$ eV^2, $\tan^2\theta = 0.67$
- VAC: $\Delta m^2 = 6.5 \times 10^{-10}$ eV^2, $\tan^2\theta = 1.33$.

It should be noted that all these solutions have large mixing angles. SMA (small mixing angle) solution (typical parameter values [34] are $\Delta m^2 = 5.2 \times 10^{-6}$ eV^2 and $\tan^2\theta = 1.1 \times 10^{-3}$) was once favored, but after SNO it was excluded at $> 3\sigma$ [30–36].

4. KamLAND and Combined Oscillation Analysis

KamLAND is a 1-kton ultra-pure liquid scintillator detector located at the old Kamiokande's site in Japan. Although the ultimate goal of KamLAND is observation of ^{7}Be solar neutrinos with much lower energy threshold, the initial phase of the experiment is a long baseline (flux-weighted average distance of $\sim$ 180 km) neutrino oscillation experiment using $\bar{\nu}_e$'s emitted from power reactors. The reaction $\bar{\nu}_e + p \rightarrow e^+ + n$ is used to detect reactor $\bar{\nu}_e$'s and delayed coincidence with 2.2 MeV γ-ray from neutron capture on a proton is used to reduce the backgrounds.

With the reactor $\bar{\nu}_e$'s energy spectrum (< 8 MeV) and an analysis threshold of 2.6 MeV, this experiment has a sensitive Δm^2 range down to $\sim 10^{-5}$ eV^2. Therefore, if the LMA solution is the real solution of the solar neutrino problem, KamLAND should observe reactor $\bar{\nu}_e$ disappearance, assuming CPT invariance.

The first KamLAND results [7] with live time of 145 days were reported in December 2002. The ratio of observed to expected (assuming no neutrino oscillation) number of events was

$$\frac{N_{\rm obs} - N_{\rm BG}}{N_{\rm NoOsc}} = 0.611 \pm 0.085 \pm 0.041. \qquad (13)$$

with obvious notation. This result shows clear evidence of event deficit expected from neutrino oscillation. The 95% confidence level allowed regions shown in Fig. 3 are obtained from the oscillation analysis with the observed event rates and positron spectrum shape. In this figure, the allowed region for the LMA solution from a global analysis [34] of the solar-neutrino data is also shown. There are two bands of regions allowed by both solar and KamLAND data. The LOW and VAC solutions are excluded by the KamLAND results.

A combined global solar and KamLAND analysis shows that the LMA is a unique solution to the solar neutrino problem with $> 5\sigma$ confidence level [37]. The 99% confidence

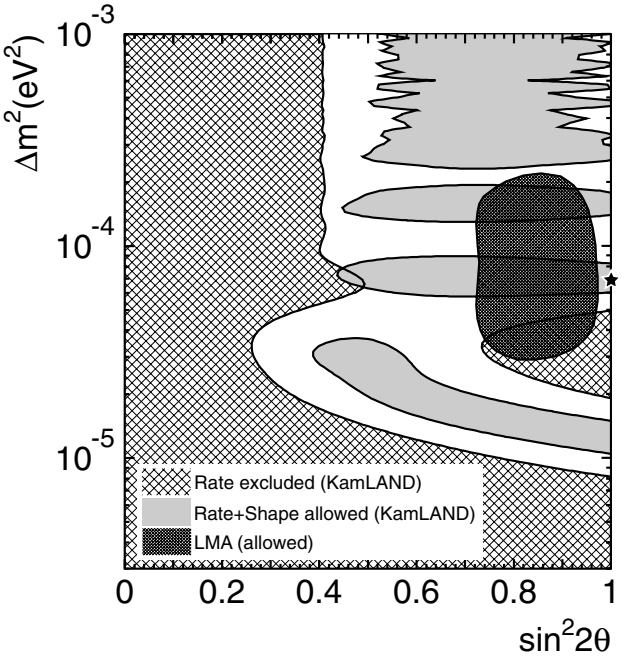

Figure 3: Excluded regions of neutrino oscillation parameters for the rate analysis and allowed regions for the combined rate and shape analysis from KamLAND at 95% confidence level. The 95% confidence-level allowed region of the LMA solution taken from a global analysis by Fogli *et al.* [34] is also shown. The star shows the best fit to the KamLAND data in the physical region: $\sin^2 2\theta = 1.0$ and $\Delta m^2 = 6.9 \times 10^{-5}$ eV^2. All regions look identical under $\theta \leftrightarrow (\pi/2 - \theta)$ except for the LMA region from solar-neutrino experiments. This figure is courtesy of K. Inoue (Tohoku University).

level allowed region from combined analyses [37–45] splits into two subregions. At $> 3\sigma$ these subregions become connected.

5. SNO Salt Phase Results

The SNO Collaboration recently reported the total ^{8}B solar-neutrino flux measured via NC reaction with NaCl dissolved in the detector heavy water [8]. The accuracy in the flux measurement has improved compared to the previous measurements thanks to the enhanced sensitivity to NC reactions (see Table 2). These results further constrain the allowed region of the LMA solution (see Fig. 4). A global analysis of the solar-neutrino data combined with the KamLAND data has shrunk the allowed region to the lower Δm^2 band at 99% confidence level with the best fit point at $\Delta m^2 = 7.1^{+1.2}_{-0.6} \times 10^{-5}$ eV^2 and $\theta = 32.5^{+2.4}_{-2.3}$ degrees [8]. The maximal mixing is now excluded at $> 5\sigma$ confidence level [8]. Other combined analyses give consistent results [46–51].

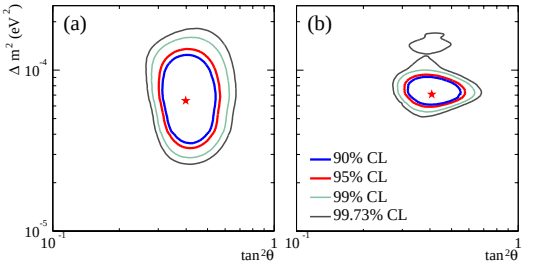

Figure 4: Global neutrino oscillation contours given by the SNO Collaboration assuming that the ^{8}B neutrino flux is free and the *hep* neutrino flux is fixed. (a) Solar global analysis. (b) Solar global + KamLAND. For details, see Ref. [8]. See full-color version on color pages at end of book.

6. Future Prospects

Now that the solar-neutrino problem has been essentially solved, what are the future prospects of the solar-neutrino experiments?

From the particle-physics point of view, precise determination of the oscillation parameters and search for non-standard physics such as a small admixture of a sterile component in the solar-neutrino flux will be still of interest. To determine Δm^2 more precisely, further KamLAND exposure to the reactor neutrinos will be most powerful [46,53]. More precise NC measurements by SNO will contribute in reducing the uncertainty of the mixing angle [51,53]. Measurements of the pp flux to an accuracy comparable to the quoted accuracy ($\pm 1\%$) of the SSM calculation will significantly improve the precision of the mixing angle [46,53].

An important task of the future solar neutrino experiments is further tests of the SSM by measuring monochromatic ^{7}Be neutrinos and fundamental *pp* neutrinos. The ^{7}Be neutrino flux will be measured by a new experiment, Borexino, at Gran Sasso via νe scattering in 300 tons of ultra-pure liquid scintillator with a detection threshold as low as 250 keV. KamLAND will also observe ^{7}Be neutrinos if the detection threshold can be lowered to a level similar to that of Borexino.

For the detection of *pp* neutrinos, various ideas for the detection scheme have been presented. However, no experiments have been approved yet, and extensive R&D efforts are still needed for any of these ideas to prove its feasibility.

References

1. D. Davis, Jr., D.S. Harmer, and K.C. Hoffman, Phys. Rev. Lett. **20**, 1205 (1968).
2. Q.R. Ahmad *et al.*, Phys. Rev. Lett. **87**, 071301 (2001).
3. Y. Fukuda *et al.*, Phys. Rev. Lett. **86**, 5651 (2001).
4. Q.R. Ahmad *et al.*, Phys. Rev. Lett. **89**, 011301 (2002).
5. L. Wolfenstein, Phys. Rev. **D17**, 2369 (1978).

6. S.P. Mikheyev and A. Yu. Smirnov, Sov. J. Nucl. Phys. **42**, 913 (1985).
7. K. Eguchi *et al.*, Phys. Rev. Lett. **90**, 021802 (2003).
8. S.N. Ahmed *et al.*, nucl-ex/03090034.
9. J.N. Bahcall, M.H. Pinsonneault, and S. Basu, Astrophys. J. **555**, 990 (2001).
10. S. Turck-Chieze *et al.*, Astrophys. J. **555**, L69 (2001).
11. A.R. Junghans *et al.*, Phys. Rev. Lett. **88**, 041101 (2002).
12. J.N. Bahcall, M.C. Gonzalez-Garcia, and C. Peña-Garay, JHEP **04**, 007 (2002).
13. B.T. Cleveland *et al.*, Ap. J. **496**, 505 (1998).
14. W. Hampel *et al.*, Phys. Lett. **B447**, 127 (1999).
15. M. Altmann *et al.*, Phys. Lett. **B490**, 16 (2000).
16. J.N. Abdurashitov *et al.*, Sov. Phys. JETP **95**, 181 (2002).
17. Y. Fukuda *et al.*, Phys. Rev. Lett. **77**, 1683 (1996).
18. Y. Fukuda *et al.*, Phys. Lett. **B539**, 179 (2002).
19. P. Anselmann *et al.*, Phys. Lett. **B285**, 376 (1994).
20. A.I. Abazov *et al.*, Phys. Rev. Lett. **67**, 3332 (1991).
21. J.N. Abdurashitov *et al.*, Phys. Lett. **B328**, 234 (1994).
22. K.S. Hirata *et al.*, Phys. Rev. Lett. **63**, 16 (1989).
23. Q.R. Ahmad *et al.*, Phys. Rev. Lett. **89**, 011302 (2002).
24. N. Hata, S. Bludman, and P. Langacker, Phys. Rev. **D49**, 3622 (1994).
25. N. Hata and P. Langacker, Phys. Rev. **D52**, 420 (1995).
26. N. Hata and P. Langacker, Phys. Rev. **D56**, 6107 (1997).
27. S. Parke, Phys. Rev. Lett. **74**, 839 (1995).
28. K.M. Heeger and R.G.H. Robertson, Phys. Rev. Lett. **77**, 3720 (1996).
29. J.N. Bahcall, P.I. Krastev, and A.Yu. Smirnov, JHEP, 05, 015 (2001).
30. V. Barger *et al.*, Phys. Lett. **B537**, 179 (2002).
31. A. Bandyopadhyay *et al.*, Phys. Lett. **B540**, 14 (2002).
32. J.N. Bahcall, C.M. Gonzalez-Garcia, and C. Peña-Garay, JHEP 07, 054 (2002).
33. A. Strumia *et al.*, Phys. Lett. **B541**, 327 (2002).
34. G.L. Fogli *et al.*, Phys. Rev. **D66**, 053010 (2002).
35. P.C. de Holanda and A. Yu Smirnov, Phys. Rev. **D66**, 113005 (2002).
36. M. Maltoni *et al.*, Phys. Rev. **D67**, 013011 (2003).
37. J.N. Bahcall, M.C. Gonzalez-Garcia, and C. Peña-Garay, JHEP 02, 009 (2003).
38. G.L. Fogli *et al.*, Phys. Rev. **D67**, 073002 (2003).
39. V. Barger and D. Marfatia Phys. Lett. **B555**, 144 (2003).
40. M. Maltoni *et al.*, Phys. Rev. **D67**, 093003 (2003).
41. A. Bandyopadhyay *et al.*, Phys. Lett. **B559**, 121 (2003).
42. P.C. de Holanda and A. Yu Smirnov, JCAP 02, 001 (2003).
43. A.B. Balantekin and H. Yüksel, J. Phys. **G29**, 665 (2003).
44. H. Nunokawa, W.J.C. Tevas, and R. Zukanovich Funchal, Phys. Lett. **B562**, 28 (2003).
45. P. Aliani *et al.*, hep-ph/0212212.
46. J.N. Bahcall and C. Peña-Garay, hep-ph/0305159.
47. A.B. Balantekin and H. Yüksel, hep-ph/0309079.
48. G.L. Fogli *et al.*, hep-ph/0309100.
49. M. Maltoni *et al.*, hep-ph/0309130.
50. P. Aliani *et al.*, hep-ph/0309156.
51. A. Bandyopadhyay *et al.*, hep-ph/0309174.
52. P.C. de Holanda and A. Yu Smirnov, hep-ph/0309299.
53. A. Bandyopadhyay, S. Choubey, and S. Goswami, Phys. Rev. **D67**, 113011 (2003).

ν_e Capture Rates from Radiochemical Experiments

1 SNU (Solar Neutrino Unit) = 10^{-36} captures per atom per second.

VALUE (SNU)	DOCUMENT ID		TECN	COMMENT
$70.8\ ^{+\ 5.3}_{-\ 5.2}\ ^{+3.7}_{-3.2}$	[166] ABDURASHI...	02	SAGE	^{71}Ga → ^{71}Ge
$65.8\ ^{+10.2}_{-\ 9.6}\ ^{+3.4}_{-3.6}$	[167] ALTMANN	00	GNO	^{71}Ga → ^{71}Ge
$74.1\ ^{+\ 6.7}_{-\ 6.8}$	[168] ALTMANN	00	GNO	GNO + GALX combined
$77.5\ \pm\ 6.2\ ^{+4.3}_{-4.7}$	[169] HAMPEL	99	GALX	^{71}Ga → ^{71}Ge
$2.56 \pm 0.16 \pm 0.16$	[170] CLEVELAND	98	HOME	^{37}Cl → ^{37}Ar

[166] ABDURASHITOV 02 report a combined analysis of 92 runs of the SAGE solar-neutrino experiment during the period January 1990 through December 2001, and updates the ABDURASHITOV 99B result. A total of 406.4 ^{71}Ge events were observed. No evidence was found for temporal variations of the neutrino capture rate over the entire observation period.

[167] ALTMANN 00 report the first result from the GNO solar-neutrino experiment (GNO I), which is the successor project of GALLEX. Experimental technique of GNO is essentially the same as that of GALLEX. The run data cover the period 20 May 1998 through 12 January 2000.

[168] Combined result of GALLEX I+II+III+IV (HAMPEL 99) and GNO I. The indicated errors include systematic errors.

[169] HAMPEL 99 report the combined result for GALLEX I+II+III+IV (65 runs in total), which update the HAMPEL 96 result. The GALLEX IV result (12 runs) is $118.4 \pm 17.8 \pm 6.6$ SNU. (HAMPEL 99 discuss the consistency of partial results with the mean.) The GALLEX experimental program has been completed with these runs. The total run data cover the period 14 May 1991 through 23 January 1997. A total of 300 ^{71}Ge events were observed.

[170] CLEVELAND 98 is a detailed report of the ^{37}Cl experiment at the Homestake Mine. The average solar neutrino-induced ^{37}Ar production rate from 108 runs between 1970 and 1994 updates the DAVIS 89 result.

ϕ_{ES} (^{8}B)

^{8}B solar-neutrino flux measured via νe elastic scattering. This process is sensitive to all active neutrino flavors, but with reduced sensitivity to ν_μ, ν_τ due to the cross-section difference, $\sigma(\nu_{\mu,\tau} e) \sim 0.16\sigma(\nu_e e)$. If the ^{8}B solar-neutrino flux involves nonelectron flavor active neutrinos, their contribution to the flux is ~ 0.16 times of ν_e.

VALUE (10^6 cm^{-2}s^{-1})	DOCUMENT ID		TECN	COMMENT
$2.35\ ^{+0.07}_{-0.06}$ OUR AVERAGE				
$2.39\ ^{+0.24}_{-0.23} \pm 0.12$	[171] AHMAD	02	SNO	average flux
$2.35 \pm 0.03\ ^{+0.07}_{-0.06}$	[172] FUKUDA	02	SKAM	average flux
• • • We do not use the following data for averages, fits, limits, etc. • • •				
$2.39 \pm 0.34\ ^{+0.16}_{-0.14}$	[173] AHMAD	01	SNO	average flux
$2.80 \pm 0.19 \pm 0.33$	[174] FUKUDA	96	KAMI	average flux
2.70 ± 0.27	[174] FUKUDA	96	KAMI	day flux
$2.87\ ^{+0.27}_{-0.26}$	[174] FUKUDA	96	KAMI	night flux

[171] AHMAD 02 reports the ^{8}B solar-neutrino flux measured via νe elastic scattering above the kinetic energy threshold of 5 MeV. The data correspond to 306.4 live days with SNO between November 2, 1999 and May 28, 2001, and updates AHMAD 01 results.

[172] FUKUDA 02 results are for 1496 live days with Super-Kamiokande between May 31, 1996 and July 15, 2002, and replace FUKUDA 01 results. The analysis threshold is 5 MeV except for the first 280 live days (6.5 MeV).

[173] AHMAD 01 reports the ^{8}B solar-neutrino flux measured via νe elastic scattering above the kinetic energy threshold of 6.75 MeV. The data correspond to 241 live days with SNO between November 2, 1999 and January 15, 2001.

[174] FUKUDA 96 results are for a total of 2079 live days with Kamiokande II and III from January 1987 through February 1995, covering the entire solar cycle 22, with threshold $E_e > 9.3$ MeV (first 449 days), > 7.5 MeV (middle 794 days), and > 7.0 MeV (last 836 days). These results update the HIRATA 90 result for the average ^{8}B solar-neutrino flux and HIRATA 91 result for the day-night variation in the ^{8}B solar-neutrino flux. The total data sample was also analyzed for short-term variations: within experimental errors, no strong correlation of the solar-neutrino flux with the sunspot numbers was found.

ϕ_{CC} (^{8}B)

^{8}B solar-neutrino flux measured with charged-current reaction which is sensitive exclusively to ν_e.

VALUE (10^6 cm^{-2}s^{-1})	DOCUMENT ID		TECN	COMMENT
$1.76\ ^{+0.06}_{-0.05} \pm 0.09$	[175] AHMAD	02	SNO	average flux
• • • We do not use the following data for averages, fits, limits, etc. • • •				
$1.75 \pm 0.07\ ^{+0.12}_{-0.11} \pm 0.05$	[176] AHMAD	01	SNO	average flux

[175] AHMAD 02 reports the SNO result of the ^{8}B solar-neutrino flux measured with charged-current reaction on deuterium, $\nu_e d \rightarrow pp e^-$, above the kinetic energy threshold of 5 MeV. The data correspond to 306.4 live days with SNO between November 2, 1999 and May 28, 2001, and updates AHMAD 01 results.

[176] AHMAD 01 reports the first SNO result of the ^{8}B solar-neutrino flux measured with the charged-current reaction on deuterium, $\nu_e d \rightarrow pp e^-$, above the kinetic energy threshold of 6.75 MeV. The data correspond to 241 live days with SNO between November 2, 1999 and January 15, 2001.

ϕ_{NC} (^{8}B)

^{8}B solar neutrino flux measured with neutral-current reaction, which is equally sensitive to ν_e, ν_μ, and ν_τ.

VALUE (10^6 cm^{-2}s^{-1})	DOCUMENT ID		TECN	COMMENT
$5.09^{+0.44}_{-0.43}{}^{+0.46}_{-0.43}$	[177] AHMAD	02	SNO	average flux

[177] AHMAD 02 reports the first SNO result of the ^{8}B solar-neutrino flux measured with the neutral-current reaction on deuterium, $\nu_\ell d \rightarrow np\nu_\ell$, above the neutral-current reaction threshold of 2.2 MeV. The data correspond to 306.4 live days with SNO between November 2, 1999 and May 28, 2001.

$\phi_{\nu_\mu+\nu_\tau}$ (^{8}B)

Nonelectron-flavor active neutrino component (ν_μ and ν_τ) in the ^{8}B solar-neutrino flux.

VALUE (10^6 cm^{-2}s^{-1})	DOCUMENT ID		TECN	COMMENT
$3.41 \pm 0.45^{+0.48}_{-0.45}$	[178] AHMAD	02	SNO	Derived from SNO ϕ_{CC}, ϕ_{ES}, and ϕ_{NC}
• • • We do not use the following data for averages, fits, limits, etc. • • •				
3.69 ± 1.13	[179] AHMAD	01		Derived from SNO+SuperKam, water Cherenkov

[178] AHMAD 02 deduced the nonelectron-flavor active neutrino component (ν_μ and ν_τ) in the ^{8}B solar-neutrino flux, by combining the charged-current result, the νe elastic-scattering result and the neutral-current result.

[179] AHMAD 01 deduced the nonelectron-flavor active neutrino component (ν_μ and ν_τ) in the ^{8}B solar-neutrino flux, by combining the SNO charged-current result (AHMAD 01) and the Super-Kamiokande νe elastic-scattering result (FUKUDA 01).

Total Flux of Active ^{8}B Solar Neutrinos

Total flux of active neutrinos (ν_e, ν_μ, and ν_τ).

VALUE (10^6 cm^{-2}s^{-1})	DOCUMENT ID		TECN	COMMENT
$5.09^{+0.44}_{-0.43}{}^{+0.46}_{-0.43}$	[180] AHMAD	02	SNO	Direct measurement from ϕ_{NC}
5.44 ± 0.99	[181] AHMAD	01		Derived from SNO+SuperKam, water Cherenkov

[180] AHMAD 02 determined the total flux of active ^{8}B solar neutrinos by directly measuring the neutral-current reaction, $\nu_\ell d \rightarrow np\nu_\ell$, which is equally sensitive to ν_e, ν_μ, and ν_τ.

[181] AHMAD 01 deduced the total flux of active ^{8}B solar neutrinos by combining the SNO charged-current result (AHMAD 01) and the Super-Kamiokande νe elastic-scattering result (FUKUDA 01).

Day-Night Asymmetry (^{8}B)

$A = (\phi_{\rm night} - \phi_{\rm day}) / \phi_{\rm average}$

VALUE	DOCUMENT ID		TECN	COMMENT
$0.14 \pm 0.063^{+0.015}_{-0.014}$	[182] AHMAD	02B	SNO	Derived from SNO ϕ_{CC}
$0.07 \pm 0.049^{+0.013}_{-0.012}$	[183] AHMAD	02B	SNO	Constraint of no ϕ_{NC} asymmetry
$0.021 \pm 0.020^{+0.013}_{-0.012}$	[184] FUKUDA	02	SKAM	Based on ϕ_{ES}

[182] AHMAD 02B results are based on the charged-current interactions recorded between November 2, 1999 and May 28, 2001, with the day and night live times of 128.5 and 177.9 days, respectively.

[183] AHMAD 02B results are derived from the charged-current interactions, neutral-current interactions, and νe elastic scattering, with the total flux of active neutrinos constrained to have no asymmetry. The data were recorded between November 2, 1999 and May 28, 2001, with the day and night live times of 128.5 and 177.9 days, respectively.

[184] FUKUDA 02 results are for 1496 live days with Super-Kamiokande between May 31, 1996 and July 15, 2002, and replace FUKUDA 01 results. The analysis threshold is 5 MeV except for the first 280 live days (6.5 MeV).

ϕ_{ES} (hep)

hep solar-neutrino flux measured via νe elastic scattering. This process is sensitive to all active neutrino flavors, but with reduced sensitivity to ν_μ, ν_τ due to the cross-section difference, $\sigma(\nu_{\mu,\tau} e) \sim 0.16\sigma(\nu_e e)$. If the hep solar-neutrino flux involves nonelectron flavor active neutrinos, their contribution to the flux is ~ 0.16 times of ν_e.

VALUE (10^3 cm^{-2}s^{-1})	CL%	DOCUMENT ID		TECN
<40	90	[185] FUKUDA	01	SKAM

[185] FUKUDA 01 result is obtained from the recoil electron energy window of 18–21 MeV, and the obtained 90% confidence level upper limit is 4.3 times the BP2000 Standard-Solar-Model prediction.

REFERENCES FOR Neutrino Mixing

AHN	03	PRL 90 041801	M.H. Ahn *et al.* (K2K Collab.)
AMBROSIO	03	PL B566 35	M. Ambrosio *et al.* (MACRO Collab.)
APOLLONIO	03	EPJ C27 331	M. Apollonio *et al.* (CHOOZ Collab.)
ASTIER	03	PL B570 19	P. Astier *et al.* (NOMAD Collab.)
EGUCHI	03	PRL 90 021802	K. Eguchi *et al.* (KamLAND Collab.)
ABDURASHI...	02	JETP 95 181	J.N. Abdurashitov *et al.* (SAGE Collab.)
		Translated from ZETF 122 211.	
AHMAD	02	PRL 89 011301	Q.R. Ahmad *et al.* (SNO Collab.)
AHMAD	02B	PRL 89 011302	Q.R. Ahmad *et al.* (SNO Collab.)
ARMBRUSTER	02	PR D65 112001	B. Armbruster *et al.* (KARMEN 2 Collab.)
AVVAKUNOV	02	PRL 89 011804	S. Avvakumov *et al.* (NuTeV Collab.)
FUKUDA	02	PL B539 179	S. Fukuda *et al.* (Super-Kamiokande Collab.)
AGUILAR	01	PR D64 112007	A. Aguilar *et al.* (LSND Collab.)
AHMAD	01	PRL 87 071301	Q.R. Ahmad *et al.* (SNO Collab.)
AMBROSIO	01	PL B517 59	M. Ambrosio *et al.* (MACRO Collab.)
ASTIER	01B	NP B611 3	P. Astier *et al.* (NOMAD Collab.)
BOEHM	01	PR D64 112001	F. Boehm *et al.*
ESKUT	01	PL B497 8	E. Eskut *et al.* (CHORUS Collab.)
FUKUDA	01	PRL 86 5651	S. Fukuda *et al.* (Super-Kamiokande Collab.)
ALTMANN	00	PL B490 16	M. Altmann *et al.* (GNO Collab.)
AMBROSIO	00	PL B478 5	M. Ambrosio *et al.* (MACRO Collab.)
BOEHM	00	PRL 84 3764	F. Boehm *et al.*
BOEHM	00C	PR D62 072002	F. Boehm *et al.*
FUKUDA	00	PRL 85 3999	S. Fukuda *et al.* (Super-Kamiokande Collab.)
ABDURASHI...	99B	PR C60 055801	J.N. Abdurashitov *et al.* (SAGE Collab.)
ALLISON	99	PL B449 137	W.W.M. Allison *et al.* (Soudan 2 Collab.)
APOLLONIO	99	PL B466 415	M. Apollonio *et al.* (CHOOZ Collab.)
Also	00	PL B472 434 erratum	M. Apollonio *et al.* (CHOOZ Collab.)
FUKUDA	99C	PRL 82 2644	Y. Fukuda *et al.* (Super-Kamiokande Collab.)
FUKUDA	99D	PL B467 185	Y. Fukuda *et al.* (Super-Kamiokande Collab.)
HAMPEL	99	PL B447 127	W. Hampel *et al.* (GALLEX Collab.)
JUNK	99	NIM A434 435	T. Junk
NAPLES	99	PR D59 031101	D. Naples *et al.* (CCFR Collab.)
ALTEGOER	98B	PL B431 219	S. Altegoer *et al.* (NOMAD Collab.)
AMBROSIO	98	PL B434 451	M. Ambrosio *et al.* (MACRO Collab.)
APOLLONIO	98	PL B420 397	M. Apollonio *et al.* (CHOOZ Collab.)
ARMBRUSTER	98	PR C57 3414	B. Armbruster *et al.* (KARMEN Collab.)
ATHANASSO...	98	PRL 81 1774	C. Athanassopoulos *et al.* (LSND Collab.)
ATHANASSO...	98B	PR C58 2489	C. Athanassopoulos *et al.* (LSND Collab.)
CLEVELAND	98	APJ 496 505	B.T. Cleveland *et al.* (Homestake Collab.)
ESKUT	98	PL B424 202	E. Eskut *et al.* (CHORUS Collab.)
ESKUT	98B	PL B434 205	E. Eskut *et al.* (CHORUS Collab.)
FELDMAN	98	PR D57 3873	G.J. Feldman, R.D. Cousins
FUKUDA	98	PL B433 9	Y. Fukuda *et al.* (Super-Kamiokande Collab.)
FUKUDA	98C	PRL 81 1562	Y. Fukuda *et al.* (Super-Kamiokande Collab.)
FUKUDA	98E	PL B436 33	Y. Fukuda *et al.* (Super-Kamiokande Collab.)
HAMPEL	98	PL B420 114	W. Hampel *et al.* (GALLEX Collab.)
HATAKEYAMA	98	PRL 81 2016	S. Hatakeyama *et al.* (Kamiokande Collab.)
OYAMA	98	PR D57 R6594	Y. Oyama
ALLISON	97	PL B391 491	W.W.M. Allison *et al.* (Soudan 2 Collab.)
CLARK	97	PRL 79 345	R. Clark *et al.* (IMB Collab.)
ROMOSAN	97	PRL 78 2912	A. Romosan *et al.* (CCFR Collab.)
ATHANASSO...	96	PR C54 2685	C. Athanassopoulos *et al.* (LSND Collab.)
ATHANASSO...	96B	PRL 77 3082	C. Athanassopoulos *et al.* (LSND Collab.)
BORISOV	96	PL B369 39	A.A. Borisov *et al.* (SERP, JINR)
FUKUDA	96	PRL 77 1683	Y. Fukuda *et al.* (Kamiokande Collab.)
FUKUDA	96B	PL B388 397	Y. Fukuda *et al.* (Kamiokande Collab.)
GREENWOOD	96	PR D53 6054	Z.D. Greenwood *et al.* (UCI SVR, SCUC)
HAMPEL	96	PL B388 384	W. Hampel *et al.* (GALLEX Collab.)
LOVERRE	96	PL B370 156	P.F. Loverre
ACHKAR	95	NP B434 503	B. Achkar *et al.* (SING, SACLD, CPPM, CDEF+)
AHLEN	95	PL B357 481	S.P. Ahlen *et al.* (MACRO Collab.)
ATHANASSO...	95	PRL 75 2650	C. Athanassopoulos *et al.* (LSND Collab.)
BAHCALL	95	PL B348 121	J.N. Bahcall, P.I. Krastev, E. Lisi (IAS)
DAUM	95	ZPHY C66 417	K. Daum *et al.* (FREJUS Collab.)
HILL	95	PRL 75 2654	J.E. Hill (PENN)
MCFARLAND	95	PRL 75 3993	K.S. McFarland *et al.* (CCFR Collab.)
VYRODOV	95	JETPL 61 163	V.N. Vyrodov *et al.* (KIAE, LAPP, CDEF)
		Translated from ZETFP 61 161.	
DECLAIS	94	PL B338 383	Y. Declais *et al.*
FUKUDA	94	PL B335 237	Y. Fukuda *et al.* (Kamiokande Collab.)
SMIRNOV	94	PR D49 1389	A.Y. Smirnov, D.N. Spergel, J.N. Bahcall (IAS+)
VIDYAKIN	94	JETPL 59 390	G.S. Vidyakin *et al.* (KIAE)
		Translated from ZETFP 59 364.	
VILAIN	94C	ZPHY C64 539	P. Vilain *et al.* (CHARM II Collab.)
FREEDMAN	93	PR D47 811	S.J. Freedman *et al.* (LAMPF E645 Collab.)
GRUWE	93	PL B309 463	M. Gruwe *et al.* (CHARM II Collab.)
BECKER-SZ...	92	PRL 69 1010	R.A. Becker-Szendy *et al.* (IMB Collab.)
BECKER-SZ...	92B	PR D46 3720	R.A. Becker-Szendy *et al.* (IMB Collab.)
BEIER	92	PL B283 446	E.W. Beier *et al.* (KAM2 Collab.)
Also	94	PTRSL A346 63	E.W. Beier, E.D. Frank (PENN)
BORODOV...	92	PRL 68 274	L. Borodovsky *et al.* (COLU, JHU, ILL)
HIRATA	92	PL B280 146	K.S. Hirata *et al.* (Kamiokande II Collab.)
KETOV	92	JETPL 55 564	S.N. Ketov *et al.* (KIAE)
		Translated from ZETFP 55 544.	
CASPER	91	PRL 66 2561	D. Casper *et al.* (IMB Collab.)
HIRATA	91	PRL 66 9	K.S. Hirata *et al.* (Kamiokande II Collab.)
KUVSHINN...	91	JETPL 54 253	A.A. Kuvshinnikov *et al.* (KIAE)
BATUSOV	90B	ZPHY C48 209	Y.A. Batusov *et al.* (JINR, ITEP, SERP)
BERGER	90B	PL B245 305	C. Berger *et al.* (FREJUS Collab.)
HIRATA	90	PRL 65 1297	K.S. Hirata *et al.* (Kamiokande II Collab.)
VIDYAKIN	90	JETP 71 424	G.S. Vidyakin *et al.* (KIAE)
		Translated from ZETF 98 764.	
AGLIETTA	89	EPL 8 611	M. Aglietta *et al.* (FREJUS Collab.)
BAHCALL	89	Neutrino Astrophysics Cambridge University Press	J.N. Bahcall (IAS)
BLUMENFELD	89	PRL 62 2237	B.J. Blumenfeld *et al.* (COLU, ILL, JHU)
DAVIS	89	ARNPS 39 467	R. Davis, A.K. Mann, L. Wolfenstein (BNL, PENN+)
OYAMA	89	PR D39 1481	Y. Oyama *et al.* (Kamiokande II Collab.)
AFONIN	88	JETP 67 213	A.I. Afonin *et al.* (KIAE)
		Translated from ZETF 94 1, issue 2.	
AMMOSOV	88	ZPHY C40 487	V.V. Ammosov *et al.* (SKAT Collab.)
BERGSMA	88	ZPHY C40 171	F. Bergsma *et al.* (CHARM Collab.)
BIONTA	88	PR D38 768	R.M. Bionta *et al.* (IMB Collab.)
DURKIN	88	PRL 61 1811	L.S. Durkin *et al.* (OSU, ANL, CIT+)
LOVERRE	88	PL B206 711	P.F. Loverre (INFN)
AFONIN	87	JETPL 45 247	A.I. Afonin *et al.* (KIAE)
		Translated from ZETFP 45 201.	
AHRENS	87	PR D36 702	L.A. Ahrens *et al.* (BNL, BROW, UCI+)
BOFILL	87	PR D36 3309	J. Bofill *et al.* (MIT, FNAL, MSU)
LOSECCO	87	PL B184 305	J.M. LoSecco *et al.* (IMB Collab.)
TALEBZADEH	87	NP B291 503	M. Talebzadeh *et al.* (BEBC WA66 Collab.)
VIDYAKIN	87	JETP 66 243	G.S. Vidyakin *et al.* (KIAE)
		Translated from ZETF 93 424.	
ABRAMOWICZ	86	PRL 57 298	H. Abramowicz *et al.* (CDHS Collab.)
AFONIN	86	JETPL 44 142	A.I. Afonin *et al.* (KIAE)
		Translated from ZETFP 44 111.	

ALLABY 86 PL B177 446 J.V. Allaby *et al.* (CHARM Collab.)
ANGELINI 86 PL B179 307 C. Angelini *et al.* (PISA, ATHU, PADO+)
BERNARDI 86B PL B181 173 G. Bernardi *et al.* (CURIN, INFN, CDEF+)
BRUCKER 86 PR D34 2183 E.B. Brucker *et al.* (RUTG, BNL, COLU)
USHIDA 86C PRL 57 2897 N. Ushida *et al.* (FNAL E531 Collab.)
ZACEK 86 PR D34 2621 G. Zacek *et al.* (CIT-SIN-TUM Collab.)
AFONIN 85 JETPL 41 435 A.I. Afonin *et al.* (KIAE)
Translated from ZETFP 41 355.
Also 85B JETPL 42 285 A.I. Afonin *et al.* (KIAE)
Translated from ZETFP 42 230.
AHRENS 85 PR D31 2732 L.A. Ahrens *et al.* (BNL, BROW, KEK+)
BELIKOV 85 SJNP 41 589 S.V. Belikov *et al.* (SERP)
Translated from YAF 41 919.
STOCKDALE 85 ZPHY C27 53 I.E. Stockdale *et al.* (ROCH, CHIC, COLU+)
ZACEK 85 PR D32 1664 V. Zacek *et al.* (MUNI, CIT, SIN)
BALLAGH 84 PR D30 2271 H.C. Ballagh *et al.* (UCB, LBL, FNAL+)
BERGSMA 84 PL 142B 103 F. Bergsma *et al.* (CHARM Collab.)
CAVAIGNAC 84 PL 148B 387 J.F. Cavaignac *et al.* (ISNG, LAPP)
DYDAK 84 PL 134B 281 F. Dydak *et al.* (CERN, DORT, HEIDH, SACL+)
GABATHULER 84 PL 138B 449 K. Gabathuler *et al.* (CIT, SIN, MUNI)
STOCKDALE 84 PRL 52 1384 I.E. Stockdale *et al.* (ROCH, CHIC, COLU+)
AFONIN 83 JETPL 38 436 A.I. Afonin *et al.* (KIAE)
Translated from ZETFP 38 361.
BELENKII 83 JETPL 38 498 S.N. Belenky *et al.* (KIAE)
Translated from ZETFP 38 406.
BELIKOV 83 JETPL 38 661 S.V. Belikov *et al.* (SERP)
Translated from ZETFP 38 547.
TAYLOR 83 PR D28 2705 G.N. Taylor *et al.* (HAWA, LBL, FNAL)
COOPER 82 PL 112B 97 A.M. Cooper *et al.* (RL)
VUILLEUMIER 82 PL 114B 298 J.L. Vuilleumier *et al.* (CIT, SIN, MUNI)
ARMENISE 81 PL 100B 182 N. Armenise *et al.* (BARI, CERN, MILA+)
ASRATYAN 81 PL 105B 301 A.E. Asratyan *et al.* (ITEP, FNAL, SERP+)
BAKER 81 PRL 47 1576 N.J. Baker *et al.* (BNL, COLU)
Also 78 PRL 40 144 A.M. Cnops *et al.* (BNL, COLU)
BOLIEV 81 SJNP 34 787 M.M. Boliev *et al.* (INRM)
Translated from YAF 34 1418.
DEDEN 81 PL 98B 310 H. Deden *et al.* (BEBC Collab.)
ERRIQUEZ 81 PL 102B 73 O. Erriquez *et al.* (BARI, BIRM, BRUX+)
KWON 81 PR D24 1097 H. Kwon *et al.* (CIT, ISNG, MUNI)
NEMETHY 81B PR D23 262 P. Nemethy *et al.* (YALE, LBL, LASL+)
SILVERMAN 81 PRL 46 467 D. Silverman, A. Soni (UCI, UCLA)
USHIDA 81 PRL 47 1694 N. Ushida *et al.* (AICH, FNAL, KOBE, SEOU+)
AVIGNONE 80 PR C22 594 F.T. Avignone, Z.D. Greenwood (SCUC)
BOEHM 80 PL 97B 310 F. Boehm *et al.* (ILLG, CIT, ISNG, MUNI)
FRITZE 80 PL 96B 427 P. Fritze (AACH3, BONN, CERN, LOIC, OXF+)
REINES 80 PRL 45 1307 F. Reines, H.W. Sobel, E. Pasierb (UCI)
Also 59 PR 113 273 F. Reines, C.L. Cowan (LASL)
Also 66 PR 142 852 F.A. Nezrick, F. Reines (CASE)
Also 76 PRL 37 315 F. Reines, H.S. Gurr, H.W. Sobel (UCI)
DAVIS 79 PR C19 2259 R. Davis *et al.* (CIT)
BLIETSCHAU 78 NP B133 205 J. Blietschau *et al.* (Gargamelle Collab.)
CROUCH 78 PR D18 2239 M.F. Crouch *et al.* (CASE, UCI, WITW)
BELLOTTI 76 LNC 17 553 E. Bellotti *et al.* (MILA)

Heavy Neutral Leptons, Searches for

(A) Heavy Neutral Leptons

Stable Neutral Heavy Lepton MASS LIMITS

Note that LEP results in combination with REUSSER 91 exclude a fourth stable neutrino with $m <$ 2400 GeV.

VALUE (GeV)	CL%	DOCUMENT ID		TECN	COMMENT
>45.0	95	ABREU	92B	DLPH	Dirac
>39.5	95	ABREU	92B	DLPH	Majorana
>44.1	95	ALEXANDER	91F	OPAL	Dirac
>37.2	95	ALEXANDER	91F	OPAL	Majorana
none 3–100	90	SATO	91	KAM2	Kamiokande II
>42.8	95	[1] ADEVA	90S	L3	Dirac
>34.8	95	[1] ADEVA	90S	L3	Majorana
>42.7	95	DECAMP	90F	ALEP	Dirac

[1] ADEVA 90S limits for the heavy neutrino apply if the mixing with the charged leptons satisfies $|U_{1j}|^2 + |U_{2j}|^2 > 6.2\times10^{-8}$ at $m_{L^0} = 20$ GeV and $> 5.1\times10^{-10}$ for $m_{L^0} = 40$ GeV.

Heavy Neutral Lepton MASS LIMITS

Limits apply only to heavy lepton type given in comment at right of data Listings. See review above for description of types.

See the "Quark and Lepton Compositeness, Searches for" Listings for limits on radiatively decaying excited neutral leptons, *i.e.* $\nu^* \to \nu\gamma$.

VALUE (GeV)	CL%	DOCUMENT ID		TECN	COMMENT
>101.3	95	ACHARD	01B	L3	Dirac coupling to e
>101.5	95	ACHARD	01B	L3	Dirac coupling to μ
> 90.3	95	ACHARD	01B	L3	Dirac coupling to τ
> 89.5	95	ACHARD	01B	L3	Majorana coupling to e
> 90.7	95	ACHARD	01B	L3	Majorana coupling to μ
> 80.5	95	ACHARD	01B	L3	Majorana coupling to τ
• • • We do not use the following data for averages, fits, limits, etc. • • •					
> 76.0	95	ABBIENDI	00I	OPAL	Majorana, coupling to e
> 88.0	95	ABBIENDI	00I	OPAL	Dirac, coupling to e
> 76.0	95	ABBIENDI	00I	OPAL	Majorana, coupling to μ
> 88.1	95	ABBIENDI	00I	OPAL	Dirac, coupling to μ
> 53.8	95	ABBIENDI	00I	OPAL	Majorana, coupling to τ
> 71.1	95	ABBIENDI	00I	OPAL	Dirac, coupling to τ
> 76.5	95	ABREU	99O	DLPH	Dirac coupling to e
> 79.5	95	ABREU	99O	DLPH	Dirac coupling to μ
> 60.5	95	ABREU	99O	DLPH	Dirac coupling to τ
> 63	95	[2,3] BUSKULIC	96S	ALEP	Dirac
> 54.3	95	[2,4] BUSKULIC	96S	ALEP	Majorana

[2] BUSKULIC 96S requires the decay length of the heavy lepton to be < 1 cm, limiting the square of the mixing angle $|U_{\ell j}|^2$ to 10^{-10}.

[3] BUSKULIC 96S limit for mixing with τ. Mass is > 63.6 GeV for mixing with e or μ.

[4] BUSKULIC 96S limit for mixing with τ. Mass is > 55.2 GeV for mixing with e or μ.

Astrophysical Limits on Neutrino MASS for $m_\nu > 1$ GeV

VALUE (GeV)	CL%	DOCUMENT ID		TECN	COMMENT
• • • We do not use the following data for averages, fits, limits, etc. • • •					
none 60–115		[5] FARGION	95	ASTR	Dirac
none 9.2–2000		[6] GARCIA	95	COSM	Nucleosynthesis
none 26–4700		[6] BECK	94	COSM	Dirac
none 6 – hundreds		[7,8] MORI	92B	KAM2	Dirac neutrino
none 24 – hundreds		[7,8] MORI	92B	KAM2	Majorana neutrino
none 10–2400	90	[9] REUSSER	91	CNTR	HPGe search
none 3–100	90	SATO	91	KAM2	Kamiokande II
		[10] ENQVIST	89	COSM	
none 12–1400		[6] CALDWELL	88	COSM	Dirac ν
none 4–16	90	[6,7] OLIVE	88	COSM	Dirac ν
none 4–35	90	OLIVE	88	COSM	Majorana ν
>4.2 to 4.7		SREDNICKI	88	COSM	Dirac ν
>5.3 to 7.4		SREDNICKI	88	COSM	Majorana ν
none 20–1000	95	[6] AHLEN	87	COSM	Dirac ν
>4.1		GRIEST	87	COSM	Dirac ν

[5] FARGION 95 bound is sensitive to assumed ν concentration in the Galaxy. See also KONOPLICH 94.

[6] These results assume that neutrinos make up dark matter in the galactic halo.

[7] Limits based on annihilations in the sun and are due to an absence of high energy neutrinos detected in underground experiments.

[8] MORI 92B results assume that neutrinos make up dark matter in the galactic halo. Limits based on annihilations in earth are also given.

[9] REUSSER 91 uses existing $\beta\beta$ detector (see FISHER 89) to search for CDM Dirac neutrinos.

[10] ENQVIST 89 argue that there is no cosmological upper bound on heavy neutrinos.

(B) Other Bounds from Nuclear and Particle Decays

Limits on $|U_{ex}|^2$ as Function of m_{ν_x}

Peak and kink search tests

Limits on $|U_{ex}|^2$ as function of m_{ν_j}

VALUE	CL%	DOCUMENT ID		TECN	COMMENT
<1 $\times 10^{-7}$	90	[11] BRITTON	92B	CNTR	50 MeV $< m_{\nu_x} <$ 130 MeV
• • • We do not use the following data for averages, fits, limits, etc. • • •					
<5 $\times 10^{-6}$	90	DELEENER-...	91		m_{ν_x}=20 MeV
<5 $\times 10^{-7}$	90	DELEENER-...	91		m_{ν_x}=40 MeV
<3 $\times 10^{-7}$	90	DELEENER-...	91		m_{ν_x}=60 MeV
<1 $\times 10^{-6}$	90	DELEENER-...	91		m_{ν_x}=80 MeV
<1 $\times 10^{-6}$	90	DELEENER-...	91		m_{ν_x}=100 MeV
<5 $\times 10^{-7}$	90	AZUELOS	86	CNTR	m_{ν_x}=60 MeV
<2 $\times 10^{-7}$	90	AZUELOS	86	CNTR	m_{ν_x}=80 MeV
<3 $\times 10^{-7}$	90	AZUELOS	86	CNTR	m_{ν_x}=100 MeV
<1 $\times 10^{-6}$	90	AZUELOS	86	CNTR	m_{ν_x}=120 MeV
<2 $\times 10^{-7}$	90	AZUELOS	86	CNTR	m_{ν_x}=130 MeV
<1 $\times 10^{-4}$	90	[12] BRYMAN	83B	CNTR	m_{ν_x}=5 MeV
<1.5 $\times 10^{-6}$	90	BRYMAN	83B	CNTR	m_{ν_x}=53 MeV
<1 $\times 10^{-5}$	90	BRYMAN	83B	CNTR	m_{ν_x}=70 MeV
<1 $\times 10^{-4}$	90	BRYMAN	83B	CNTR	m_{ν_x}=130 MeV
<1 $\times 10^{-4}$	68	[13] SHROCK	81	THEO	m_{ν_x}=10 MeV
<5 $\times 10^{-6}$	68	[13] SHROCK	81	THEO	m_{ν_x}=60 MeV
<1 $\times 10^{-5}$	68	[14] SHROCK	80	THEO	m_{ν_x}=80 MeV
<3 $\times 10^{-6}$	68	[14] SHROCK	80	THEO	m_{ν_x}=160 MeV

[11] BRITTON 92B is from a search for additional peaks in the e^+ spectrum from $\pi^+ \to e^+\nu_e$ decay at TRIUMF. See also BRITTON 92.

[12] BRYMAN 83B obtain upper limits from both direct peak search and analysis of $B(\pi \to e\nu)/B(\pi \to \mu\nu)$. Latter limits are not listed, except for this entry (i.e. — we list the most stringent limits for given mass).

[13] Analysis of $(\pi^+ \to e^+\nu_e)/(\pi^+ \to \mu^+\nu_\mu)$ and $(K^+ \to e^+\nu_e)/(K^+ \to \mu^+\nu_\mu)$ decay ratios.

[14] Analysis of $(K^+ \to e^+\nu_e)$ spectrum.

Kink search in nuclear β decay

High-sensitivity follow-up experiments show that indications for a neutrino with mass 17 keV (Simpson, Hime, and others) were not valid. Accordingly, we no longer list the experiments by these authors and some others which made positive claims of 17 keV neutrino emission. Complete listings are given in the 1994 edition (Physical Review **D50** 1173 (1994)) and in the 1998 edition (The European Physical Journal **C3** 1 (1998)). We list below only the best limits on $|U_{ex}|^2$ for each m_{ν_x}. See WIETFELDT 96 for a comprehensive review.

VALUE (units 10^{-3})	CL%	m_{ν_j} (keV)	ISOTOPE	METHOD	DOCUMENT ID

• • • We do not use the following data for averages, fits, limits, etc. • • •

< 4–20	90	700–3500	^{38m}K	Trap	[15] TRINCZEK 03
< 9–116	95	1–0.1	^{187}Re	cryog.	[16] GALEAZZI 01
< 1	95	10–90	^{35}S	Mag spect	[17] HOLZSCHUH 00
< 4	95	14–17	^{241}Pu	Electrostatic spec	[18] DRAGOUN 99
< 1	95	4–30	^{63}Ni	Mag spect	[19] HOLZSCHUH 99
< 10–40	90	370–640	^{37}Ar	EC ion recoil	[20] HINDI 98
< 10	95	1	^{3}H	SPEC	[21] HIDDEMANN 95
< 6	95	2	^{3}H	SPEC	[21] HIDDEMANN 95
< 2	95	3	^{3}H	SPEC	[21] HIDDEMANN 95
< 0.7	99	16.3–16.6	^{3}H	Prop chamber	[22] KALBFLEISCH 93
< 2	95	13–40	^{35}S	Si(Li)	[23] MORTARA 93
< 0.73	95	17	^{63}Ni	Mag spect	OHSHIMA 93
< 1.0	95	10–24	^{63}Ni	Mag spect	KAWAKAMI 92
< 0.9–2.5	90	1200–6800	^{20}F	beta spectrum	[24] DEUTSCH 90
< 8	90	80	^{35}S	Mag spect	[25] APALIKOV 85
< 1.5	90	60	^{35}S	Mag spect	APALIKOV 85
< 3.0	90	5–50		Mag spect	MARKEY 85
< 0.62	90	48	^{35}S	Si(Li)	OHI 85
< 0.90	90	30	^{35}S	Si(Li)	OHI 85
< 4	90	140	^{64}Cu	Mag spect	[26] SCHRECK... 83
< 8	90	440	^{64}Cu	Mag spect	[26] SCHRECK... 83
< 100	90	0.1–3000		THEO	[27] SHROCK 80
< 0.1	68	80		THEO	[28] SHROCK 80

[15] TRINCZEK 03 is a search for admixture of heavy neutrino to ν_e, in contrast to $\overline{\nu}_e$ used in many other searches. Full kinematic reconstruction of the neutrino momentum by use of a magneto optical trap.

[16] GALEAZZI 01 use an cryogenic microcalorimeter to search for mass 50–1000 eV neutrino admixtures using the ^{187}Re beta spectrum with 2.4 keV endpoint. They derive limits for the admixture of heavy neutrinos, ranging from 9×10^{-3} for mass 1 keV to 0.116 for mass 100 eV. This is a significant improvement with respect to HIDDEMANN 95, especially for masses below $\sim$ 500 MeV, where the limit is about a factor of $\sim$ 2 higher.

[17] HOLZSCHUH 00 use an iron-free β spectrometer to measure the ^{35}S β decay spectrum. An analysis of the spectrum in the energy range 56–173 keV is used to derive limits for the admixture of heavy neutrinos. This extends the range of neutrino masses explored in HOLZSCHUH 99.

[18] DRAGOUN 99 analyze the β decay spectrum of ^{241}Pu in the energy range 0.2–9.2 keV to derive limits for the admixture of heavy neutrinos. It is not competitive with HOLZSCHUH 99.

[19] HOLZSCHUH 99 use an iron-free β spectrometer to measure the ^{63}Ni β decay spectrum. An analysis of the spectrum in the energy rage 33–67.8 keV is used to derive limits for the admixture of heavy neutrinos.

[20] HINDI 98 obtain a limit on heavy neutrino admixture from EC decay of ^{37}Ar by measuring the time-of-flight distribution of the recoiling ions in coincidence with x-rays or Auger electrons. The authors report upper limit for $|U_{ex}|^2$ of $\approx$ 3% for m_{ν_x}=500 keV, 1% for m_{ν_x}=550 keV, 2% for m_{ν_x}=600 keV, and 4% for m_x=650 keV. Their reported limits for $m_{\nu_x} \leq$ 450 keV are inferior to the limits of SCHRECKENBACH 83.

[21] In the beta spectrum from tritium β decay nonvanishing or mixed $m_{\overline{\nu}_1}$ state in the mass region 0.01–4 keV. For m_{ν_x} <1 keV, their upper limit on $|U_{ex}|^2$ becomes less

[22] KALBFLEISCH 93 extends the 17 keV neutrino search of BAHRAN 92, using an improved proportional chamber to which a small amount of ^{3}H is added. Systematics are significantly reduced, allowing for an improved upper limit. The authors give a 99% confidence limit on $|U_{ex}|^2$ as a function of m_{ν_x} in the range from 13.5 keV to 17.5 keV. See also the related papers BAHRAN 93, BAHRAN 93B, and BAHRAN 95 on theoretical aspects of beta spectra and fitting methods for heavy neutrinos.

[23] MORTARA 93 limit is from study using a high-resolution solid-state detector with a superconducting solenoid. The authors note that "The sensitivity to neutrino mass is verified by measurement with a mixed source of ^{35}S and ^{14}C, which artificially produces a distortion in the beta spectrum similar to that expected from the massive neutrino."

[24] DEUTSCH 90 search for emission of heavy $\overline{\nu}_e$ in super-allowed beta decay of ^{20}F by spectral analysis of the electrons.

[25] This limit was taken from the figure 3 of APALIKOV 85; the text gives a more restrictive limit of 1.7×10^{-3} at CL = 90%.

[26] SCHRECKENBACH 83 is a combined measurement of the β^+ and β^- spectrum.

[27] SHROCK 80 was a retroactive analysis of data on several superallowed β decays to search for kinks in the Kurie plot.

[28] Application of test to search for kinks in β decay Kurie plots.

Searches for Decays of Massive ν

Limits on $|U_{ex}|^2$ as function of m_{ν_x}

VALUE	CL%	DOCUMENT ID		TECN	COMMENT
• • • We do not use the following data for averages, fits, limits, etc. • • •					
$<1.5 \times 10^{-3}$	95	ACHARD	01	L3	m_{ν_x}=80 GeV
$<2 \times 10^{-2}$	95	ACHARD	01	L3	m_{ν_x}=175 GeV
<0.3	95	ACHARD	01	L3	m_{ν_x}=200 GeV
$<4 \times 10^{-3}$	95	ACCIARRI	99K	L3	m_{ν_x}=80 GeV
$<5 \times 10^{-2}$	95	ACCIARRI	99K	L3	m_{ν_x}= 175 GeV
$<2 \times 10^{-5}$	95	[29] ABREU	97I	DLPH	m_{ν_x}=6 GeV
$<3 \times 10^{-5}$	95	[29] ABREU	97I	DLPH	m_{ν_x}=50 GeV
$<1.8 \times 10^{-3}$	90	[30] HAGNER	95	MWPC	m_{ν_h} = 1.5 MeV
$<2.5 \times 10^{-4}$	90	[30] HAGNER	95	MWPC	m_{ν_h} = 4 MeV
$<4.2 \times 10^{-3}$	90	[30] HAGNER	95	MWPC	m_{ν_h} = 9 MeV
$<1 \times 10^{-5}$	90	[31] BARANOV	93		m_{ν_x}=100 MeV
$<1 \times 10^{-6}$	90	[31] BARANOV	93		m_{ν_x}= 200 MeV
$<3 \times 10^{-7}$	90	[31] BARANOV	93		m_{ν_x}= 300 MeV
$<2 \times 10^{-7}$	90	[31] BARANOV	93		m_{ν_x}=400 MeV
$<6.2 \times 10^{-8}$	95	ADEVA	90S	L3	m_{ν_x}=20 GeV
$<5.1 \times 10^{-10}$	95	ADEVA	90S	L3	m_{ν_x}=40 GeV
all values ruled out	95	[32] BURCHAT	90	MRK2	m_{ν_x} < 19.6 GeV
$<1 \times 10^{-10}$	95	[32] BURCHAT	90	MRK2	m_{ν_x} = 22 GeV
$<1 \times 10^{-11}$	95	[32] BURCHAT	90	MRK2	m_{ν_x} = 41 GeV
all values ruled out	95	DECAMP	90F	ALEP	m_{ν_x} = 25.0–42.7 GeV
$<1 \times 10^{-13}$	95	DECAMP	90F	ALEP	m_{ν_x} = 42.7–45.7 GeV
$<5 \times 10^{-3}$	90	AKERLOF	88	HRS	m_{ν_x}=1.8 GeV
$<2 \times 10^{-5}$	90	AKERLOF	88	HRS	m_{ν_x}=4 GeV
$<3 \times 10^{-6}$	90	AKERLOF	88	HRS	m_{ν_x}=6 GeV
$<1.2 \times 10^{-7}$	90	BERNARDI	88	CNTR	m_{ν_x}=100 MeV
$<1 \times 10^{-8}$	90	BERNARDI	88	CNTR	m_{ν_x}=200 MeV
$<2.4 \times 10^{-9}$	90	BERNARDI	88	CNTR	m_{ν_x}=300 MeV
$<2.1 \times 10^{-9}$	90	BERNARDI	88	CNTR	m_{ν_x}=400 MeV
$<2 \times 10^{-2}$	68	[33] OBERAUER	87		m_{ν_x}=1.5 MeV
$<8 \times 10^{-4}$	68	[33] OBERAUER	87		m_{ν_x}=4.0 MeV
$<8 \times 10^{-3}$	90	BADIER	86	CNTR	m_{ν_x}=400 MeV
$<8 \times 10^{-5}$	90	BADIER	86	CNTR	m_{ν_x}=1.7 GeV
$<8 \times 10^{-8}$	90	BERNARDI	86	CNTR	m_{ν_x}=100 MeV
$<4 \times 10^{-8}$	90	BERNARDI	86	CNTR	m_{ν_x}=200 MeV
$<6 \times 10^{-9}$	90	BERNARDI	86	CNTR	m_{ν_x}=400 MeV
$<3 \times 10^{-5}$	90	DORENBOS...	86	CNTR	m_{ν_x}=150 MeV
$<1 \times 10^{-6}$	90	DORENBOS...	86	CNTR	m_{ν_x}=500 MeV
$<1 \times 10^{-7}$	90	DORENBOS...	86	CNTR	m_{ν_x}=1.6 GeV
$<7 \times 10^{-7}$	90	[34] COOPER-...	85	HLBC	m_{ν_x}=0.4 GeV
$<8 \times 10^{-8}$	90	[34] COOPER-...	85	HLBC	m_{ν_x}=1.5 GeV
$<1 \times 10^{-2}$	90	[35] BERGSMA	83B	CNTR	m_{ν_x}=10 MeV
$<1 \times 10^{-5}$	90	[35] BERGSMA	83B	CNTR	m_{ν_x}=110 MeV
$<6 \times 10^{-7}$	90	[35] BERGSMA	83B	CNTR	m_{ν_x}=410 MeV
$<1 \times 10^{-5}$	90	GRONAU	83		m_{ν_x}=160 MeV
$<1 \times 10^{-6}$	90	GRONAU	83		m_{ν_x}=480 MeV

[29] ABREU 97I long-lived ν_x analysis. Short-lived analysis extends limit to lower masses with decreasing sensitivity except at 3.5 GeV, where the limit is the same as at 6 GeV.

[30] HAGNER 95 obtain limits on heavy neutrino admixture from the decay $\nu_h \rightarrow \nu_e e^+ e^-$ at a nuclear reactor for the ν_h mass range 2–9 MeV.

[31] BARANOV 93 is a search for neutrino decays into $e^+ e^- \nu_e$ using a beam dump experiment at the 70 GeV Serpukhov proton synchrotron. The limits are not as good as those achieved earlier by BERGSMA 83 and BERNARDI 86, BERNARDI 88.

[32] BURCHAT 90 includes the analyses reported in JUNG 90, ABRAMS 89C, and WENDT 87.

[33] OBERAUER 87 bounds from search for $\nu \rightarrow \nu' e e$ decay mode using reactor (anti)neutrinos.

[34] COOPER-SARKAR 85 also give limits based on model-dependent assumptions for ν_τ flux. We do not list these. Note that for this bound to be nontrivial, x is not equal to 3, i.e. ν_x cannot be the dominant mass eigenstate in ν_τ since m_{ν_3} <70 MeV (ALBRECHT 85I). Also, of course, x is not equal to 1 or 2, so a fourth generation would be required for this bound to be nontrivial.

[35] BERGSMA 83B also quote limits on $|U_{e3}|^2$ where the index 3 refers to the mass eigenstate dominantly coupled to the τ. Those limits were based on assumptions about the D_s mass and $D_s \rightarrow \tau \nu_\tau$ branching ratio which are no longer valid. See COOPER-SARKAR 85.

Limits on Coupling of μ to ν_x as Function of m_{ν_x}

Peak search test

Limits on B(π (or K) $\rightarrow \mu \nu_x$).

VALUE	CL%	EVTS	DOCUMENT ID		TECN	COMMENT
• • • We do not use the following data for averages, fits, limits, etc. • • •						
			[36] ASTIER	02	NOMD	$\pi \rightarrow \mu X$ for m_X=33.9 MeV
$<6.0 \times 10^{-10}$	95	0	[37] DAUM	00	CNTR	$\pi \rightarrow \mu x$, for m_x=33.905 MeV
			[38] FORMAGGIO	00	CNTR	$\pi \rightarrow \mu x$, for m_x=33.905 MeV
<0.22	90		[39] ASSAMAGAN	98	SILI	m_{ν_x} = 0.53 MeV
<0.029	90		[39] ASSAMAGAN	98	SILI	m_{ν_x} = 0.75 MeV
<0.016	90		[39] ASSAMAGAN	98	SILI	m_{ν_x} = 1.0 MeV
$< 4–6 \times 10^{-5}$			[40] BRYMAN	96	CNTR	m_{ν_x} = 30–33.91 MeV
$\sim 1 \times 10^{-16}$			[41] ARMBRUSTER	95	KARM	m_{ν_x} = 33.9 MeV
$<4 \times 10^{-7}$	95		[42] BILGER	95	LEPS	$m_{\overline{\nu}_x}$ = 33.9 MeV
$<7 \times 10^{-8}$	95		[42] BILGER	95	LEPS	m_{ν_x} = 33.9 MeV
$<2.6 \times 10^{-8}$	95		[42] DAUM	95B	TOF	m_{ν_x} = 33.9 MeV
$<2 \times 10^{-2}$	90		DAUM	87		m_{ν_x}=1 MeV
$<1 \times 10^{-3}$	90		DAUM	87		m_{ν_x}=2 MeV
$<6 \times 10^{-5}$	90		DAUM	87		3 MeV < m_{ν_x} < 19.5 MeV

<3	$\times 10^{-2}$	90	[43] MINEHART	84	m_{ν_X}=2 MeV
<1	$\times 10^{-3}$	90	[43] MINEHART	84	m_{ν_X}=4 MeV
<3	$\times 10^{-4}$	90	[43] MINEHART	84	m_{ν_X}=10 GeV
<5	$\times 10^{-6}$	90	[44] HAYANO	82	m_{ν_X}=330 MeV
<1	$\times 10^{-4}$	90	[44] HAYANO	82	m_{ν_X}=70 MeV
<9	$\times 10^{-7}$	90	[44] HAYANO	82	m_{ν_X}=250 MeV
<1	$\times 10^{-1}$	90	[43] ABELA	81	m_{ν_X}=4 MeV
<7	$\times 10^{-5}$	90	[43] ABELA	81	m_{ν_X}=10.5 MeV
<2	$\times 10^{-4}$	90	[43] ABELA	81	m_{ν_X}=11.5 MeV
<2	$\times 10^{-5}$	90	[43] ABELA	81	m_{ν_X}=16–30 MeV

[36] ASTIER 02 search for anomalous pion decay into a 33.9 MeV neutral particle. No evidence was found and the sensitivity to the branching ratio $B(\pi \rightarrow \mu X)\cdot B(X \rightarrow \nu e^+ e^-)$ is as low as 3.7×10^{-15}, depending on the X lifetime.

[37] DAUM 00 search for anomalous pion decay into a 33.9 MeV neutral particle that might be responsible for the time-distribution anomaly observed by the KARMEN Collaboration.

[38] FORMAGGIO 00 search for anomalous pion decay into a 33.9 MeV neutral particle Q^0 that might be responsible for the time-distribution anomaly observed by the KARMEN Collaboration. In the E815 (NuTeV) experiment at Fermilab no evidence was found, with sensitivity for the pion branching ratio $B(\pi \rightarrow \mu Q^0)\cdot B(Q^0 \rightarrow$ visible) as low as 10^{-13}.

[39] ASSAMAGAN 98 obtain a limit on heavy neutrino admixture from π^+ decay essentially at rest, by measuring with good resolution the momentum distribution of the muons. However, the search uses an ad hoc shape correction. The authors report upper limit for $|U_{\mu X}|^2$ of 0.22 for m_ν = 0.53 MeV, 0.029 for m_ν = 0.75 MeV, and 0.016 for m_ν = 1.0 MeV at 90%CL.

[40] BRYMAN 96 search for massive unconventional neutrinos of mass m_{ν_X} in π^+ decay.

[41] ARMBRUSTER 95 study the reactions $^{12}C(\nu_e,e^-)\,^{12}N$ and $^{12}C(\nu,\nu')\,^{12}C^*$ induced by neutrinos from π^+ and μ^+ decay at the ISIS neutron spallation source at the Rutherford-Appleton laboratory. An anomaly in the time distribution can be interpreted as the decay $\pi^+ \rightarrow \mu^+ \nu_X$, where ν_X is a neutral weakly interacting particle with mass $\approx$ 33.9 MeV and spin 1/2. The lower limit to the branching ratio is a function of the lifetime of the new massive neutral particle, and reaches a minimum of a few $\times 10^{-16}$ for $\tau_X \sim 5$ s.

[42] From experiments of π^+ and π^- decay in flight at PSI, to check the claim of the KARMEN Collaboration quoted above (ARMBRUSTER 95).

[43] $\pi^+ \rightarrow \mu^+ \nu_\mu$ peak search experiment.

[44] $K^+ \rightarrow \mu^+ \nu_\mu$ peak search experiment.

Peak search test

Limits on $|U_{\mu X}|^2$ as function of m_{ν_X}

VALUE	CL%	DOCUMENT ID		TECN	COMMENT
• • • We do not use the following data for averages, fits, limits, etc. • • •					
<1–10×10^{-4}		[45] BRYMAN	96	CNTR	m_{ν_X} = 30–33.91 MeV
$<2\times10^{-5}$	95	[46] ASANO	81		m_{ν_X}=70 MeV
$<3\times10^{-6}$	95	[46] ASANO	81		m_{ν_X}=210 MeV
$<3\times10^{-6}$	95	[46] ASANO	81		m_{ν_X}=230 MeV
$<6\times10^{-6}$	95	[47] ASANO	81		m_{ν_X}=240 MeV
$<5\times10^{-7}$	95	[47] ASANO	81		m_{ν_X}=280 MeV
$<6\times10^{-6}$	95	[47] ASANO	81		m_{ν_X}=300 MeV
$<1\times10^{-2}$	95	CALAPRICE	81		m_{ν_X}=7 MeV
$<3\times10^{-3}$	95	[48] CALAPRICE	81		m_{ν_X}=33 MeV
$<1\times10^{-4}$	68	[49] SHROCK	81	THEO	m_{ν_X}=13 MeV
$<3\times10^{-5}$	68	[49] SHROCK	81	THEO	m_{ν_X}=33 MeV
$<6\times10^{-3}$	68	[50] SHROCK	81	THEO	m_{ν_X}=80 MeV
$<5\times10^{-3}$	68	[50] SHROCK	81	THEO	m_{ν_X}=120 MeV

[45] BRYMAN 96 search for massive unconventional neutrinos of mass m_{ν_X} in π^+ decay. They interpret the result as an upper limit for the admixture of a heavy sterile or otherwise

[46] $K^+ \rightarrow \mu^+ \nu_\mu$ peak search experiment.

[47] Analysis of experiment on $K^+ \rightarrow \mu^+ \nu_\mu \nu_X \overline{\nu}_X$ decay.

[48] $\pi^+ \rightarrow \mu^+ \nu_\mu$ peak search experiment.

[49] Analysis of magnetic spectrometer experiment, bubble chamber experiment, and emulsion experiment on $\pi^+ \rightarrow \mu^+ \nu_\mu$ decay.

[50] Analysis of magnetic spectrometer experiment on $K \rightarrow \mu, \nu_\mu$ decay.

Peak Search in Muon Capture

Limits on $|U_{\mu X}|^2$ as function of m_{ν_X}

VALUE	DOCUMENT ID		COMMENT
• • • We do not use the following data for averages, fits, limits, etc. • • •			
$<1\times10^{-1}$	DEUTSCH	83	m_{ν_X}=45 MeV
$<7\times10^{-3}$	DEUTSCH	83	m_{ν_X}=70 MeV
$<1\times10^{-1}$	DEUTSCH	83	m_{ν_X}=85 MeV

Searches for Decays of Massive ν

Limits on $|U_{\mu X}|^2$ as function of m_{ν_X}

VALUE	CL%	DOCUMENT ID		TECN	COMMENT
• • • We do not use the following data for averages, fits, limits, etc. • • •					
$<5\times10^{-7}$	90	[51] VAITAITIS	99	CCFR	m_{ν_X}=0.28 GeV
$<8\times10^{-8}$	90	[51] VAITAITIS	99	CCFR	m_{ν_X}=0.37 GeV
$<5\times10^{-7}$	90	[51] VAITAITIS	99	CCFR	m_{ν_X} = 0.50 GeV
$<6\times10^{-8}$	90	[51] VAITAITIS	99	CCFR	m_{ν_X} = 1.50 GeV
$<2\times10^{-5}$	95	[52] ABREU	97I	DLPH	m_{ν_X}=6 GeV
$<3\times10^{-5}$	95	[52] ABREU	97I	DLPH	m_{ν_X}=50 GeV
$<3\times10^{-6}$	90	GALLAS	95	CNTR	m_{ν_X} = 1 GeV
$<3\times10^{-5}$	90	[53] VILAIN	95C	CHM2	m_{ν_X} = 2 GeV
$<6.2\times10^{-8}$	95	ADEVA	90S	L3	m_{ν_X}=20 GeV
$<5.1\times10^{-10}$	95	ADEVA	90S	L3	m_{ν_X}=40 GeV
all values ruled out	95	[54] BURCHAT	90	MRK2	m_{ν_X} < 19.6 GeV
$<1\times10^{-10}$	95	[54] BURCHAT	90	MRK2	m_{ν_X} = 22 GeV
$<1\times10^{-11}$	95	[54] BURCHAT	90	MRK2	m_{ν_X} = 41 GeV
all values ruled out	95	DECAMP	90F	ALEP	m_{ν_X} = 25.0–42.7 GeV
$<1\times10^{-13}$	95	DECAMP	90F	ALEP	m_{ν_X} = 42.7–45.7 GeV
$<5\times10^{-3}$	90	AKERLOF	88	HRS	m_{ν_X}=1.8 GeV
$<2\times10^{-5}$	90	AKERLOF	88	HRS	m_{ν_X}=4 GeV
$<3\times10^{-6}$	90	AKERLOF	88	HRS	m_{ν_X}=6 GeV
$<1\times10^{-7}$	90	BERNARDI	88	CNTR	m_{ν_X}=200 MeV
$<3\times10^{-9}$	90	BERNARDI	88	CNTR	m_{ν_X}=300 MeV
$<4\times10^{-4}$	90	[55] MISHRA	87	CNTR	m_{ν_X}=1.5 GeV
$<4\times10^{-3}$	90	[55] MISHRA	87	CNTR	m_{ν_X}=2.5 GeV
$<0.9\times10^{-2}$	90	[55] MISHRA	87	CNTR	m_{ν_X}=5 GeV
<0.1	90	[55] MISHRA	87	CNTR	m_{ν_X}=10 GeV
$<8\times10^{-4}$	90	BADIER	86	CNTR	m_{ν_X}=600 MeV
$<1.2\times10^{-5}$	90	BADIER	86	CNTR	m_{ν_X}=1.7 GeV
$<3\times10^{-8}$	90	BERNARDI	86	CNTR	m_{ν_X}=200 MeV
$<6\times10^{-9}$	90	BERNARDI	86	CNTR	m_{ν_X}=350 MeV
$<1\times10^{-6}$	90	DORENBOS...	86	CNTR	m_{ν_X}=500 MeV
$<1\times10^{-7}$	90	DORENBOS...	86	CNTR	m_{ν_X}=1600 MeV
$<0.8\times10^{-5}$	90	[56] COOPER-...	85	HLBC	m_{ν_X}=0.4 GeV
$<1.0\times10^{-7}$	90	[56] COOPER-...	85	HLBC	m_{ν_X}=1.5 GeV

[51] VAITAITIS 99 search for $L^0_\mu \rightarrow \mu X$. See paper for rather complicated limit as function of m_{ν_X}.

[52] ABREU 97I long-lived ν_X analysis. Short-lived analysis extends limit to lower masses with decreasing sensitivity except at 3.5 GeV, where the limit is the same as at 6 GeV.

[53] VILAIN 95C is a search for the decays of heavy isosinglet neutrinos produced by neutral current neutrino interactions. Limits were quoted for masses in the range from 0.3 to 24 GeV. The best limit is listed above.

[54] BURCHAT 90 includes the analyses reported in JUNG 90, ABRAMS 89C, and WENDT 87.

[55] See also limits on $|U_{3x}|$ from WENDT 87.

[56] COOPER-SARKAR 85 also give limits based on model-dependent assumptions for ν_τ flux. We do not list these. Note that for this bound to be nontrivial, x is not equal to 3, i.e. ν_X cannot be the dominant mass eigenstate in ν_τ since m_{ν_3} <70 MeV (ALBRECHT 85I). Also, of course, x is not equal to 1 or 2, so a fourth generation would be required for this bound to be nontrivial.

Limits on $|U_{\tau X}|^2$ as a Function of m_{ν_X}

VALUE	CL%	DOCUMENT ID		TECN	COMMENT
• • • We do not use the following data for averages, fits, limits, etc. • • •					
$<1\times10^{-2}$	90	[57] ORLOFF	02	CHRM	m_{ν_X}=45 MeV
$<1.4\times10^{-4}$	90	[57] ORLOFF	02	CHRM	m_{ν_X}=180 MeV
<0.025	90	ASTIER	01		m_{ν_X}=45 MeV
<0.002	90	ASTIER	01		m_{ν_X}=140 MeV
$<2\times10^{-5}$	95	[58] ABREU	97I	DLPH	m_{ν_X}=6 GeV
$<3\times10^{-5}$	95	[58] ABREU	97I	DLPH	m_{ν_X}=50 GeV
$<6.2\times10^{-8}$	95	ADEVA	90S	L3	m_{ν_X}=20 GeV
$<5.1\times10^{-10}$	95	ADEVA	90S	L3	m_{ν_X}=40 GeV
all values ruled out	95	[59] BURCHAT	90	MRK2	m_{ν_X} < 19.6 GeV
$<1\times10^{-10}$	95	[59] BURCHAT	90	MRK2	m_{ν_X} = 22 GeV
$<1\times10^{-11}$	95	[59] BURCHAT	90	MRK2	m_{ν_X} = 41 GeV
all values ruled out	95	DECAMP	90F	ALEP	m_{ν_X} = 25.0–42.7 GeV
$<1\times10^{-13}$	95	DECAMP	90F	ALEP	m_{ν_X} = 42.7–45.7 GeV
$<5\times10^{-2}$	80	AKERLOF	88	HRS	m_{ν_X}=2.5 GeV
$<9\times10^{-5}$	80	AKERLOF	88	HRS	m_{ν_X}=4.5 GeV

[57] ORLOFF 02 use the negative result of a search for neutral particles decaying into two electrons performed by CHARM to get these limits for a mostly isosinglet heavy neutrino.

[58] ABREU 97I long-lived ν_X analysis. Short-lived analysis extends limit to lower masses with decreasing sensitivity.

[59] BURCHAT 90 includes the analyses reported in JUNG 90, ABRAMS 89C, and WENDT 87.

Limits on $|U_{ax}|^2$

Where $a = e$, μ from ρ parameter in μ decay.

VALUE	CL%	DOCUMENT ID		TECN	COMMENT
• • • We do not use the following data for averages, fits, limits, etc. • • •					
$<1\times10^{-2}$	68	SHROCK	81B	THEO	m_{ν_x}=10 GeV
$<2\times10^{-3}$	68	SHROCK	81B	THEO	m_{ν_x}=40 MeV
$<4\times10^{-2}$	68	SHROCK	81B	THEO	m_{ν_x}=70 MeV

Limits on $|U_{1j}\times U_{2j}|$ as Function of m_{ν_j}

VALUE	CL%	DOCUMENT ID		TECN	COMMENT
• • • We do not use the following data for averages, fits, limits, etc. • • •					
$<3\times10^{-5}$	90	[60] BARANOV	93		m_{ν_j}= 80 MeV
$<3\times10^{-6}$	90	[60] BARANOV	93		m_{ν_j}= 160 MeV
$<6\times10^{-7}$	90	[60] BARANOV	93		m_{ν_j}= 240 MeV
$<2\times10^{-7}$	90	[60] BARANOV	93		m_{ν_j}= 320 MeV
$<9\times10^{-5}$	90	BERNARDI	86	CNTR	m_{ν_j}=25 MeV
$<3.6\times10^{-7}$	90	BERNARDI	86	CNTR	m_{ν_j}=100 MeV
$<3\times10^{-8}$	90	BERNARDI	86	CNTR	m_{ν_j}=200 MeV
$<6\times10^{-9}$	90	BERNARDI	86	CNTR	m_{ν_j}=350 MeV
$<1\times10^{-2}$	90	BERGSMA	83B	CNTR	m_{ν_j}=10 MeV
$<1\times10^{-5}$	90	BERGSMA	83B	CNTR	m_{ν_j}=140 MeV
$<7\times10^{-7}$	90	BERGSMA	83B	CNTR	m_{ν_j}=370 MeV

[60] BARANOV 93 is a search for neutrino decays into $e^+e^-\nu_e$ using a beam dump experiment at the 70 GeV Serpukhov proton synchrotron.

REFERENCES FOR Heavy Neutral Leptons, Searches for

TRINCZEK	03	PRL 90 012501	M. Trinczek *et al.*	
ASTIER	02	PL B527 23	P. Astier *et al.*	(NOMAD Collab.)
ORLOFF	02	PL B550 8	J. Orloff *et al.*	
ACHARD	01	PL B517 67	P. Achard *et al.*	(L3 Collab.)
ACHARD	01B	PL B517 75	P. Achard *et al.*	(L3 Collab.)
ASTIER	01	PL B506 27	P. Astier *et al.*	(NOMAD Collab.)
GALEAZZI	01	PRL 86 1978	M. Galeazzi *et al.*	
ABBIENDI	00I	EPJ C14 73	G. Abbiendi *et al.*	(OPAL Collab.)
DAUM	00	PRL 85 1815	M. Daum *et al.*	
FORMAGGIO	00	PRL 84 4043	J.A. Formaggio *et al.*	
HOLZSCHUH	00	PL B482 1	E. Holzschuh *et al.*	
ABREU	99Q	EPJ C8 41	P. Abreu *et al.*	(DELPHI Collab.)
ACCIARRI	99K	PL B461 397	M. Acciarri *et al.*	(L3 Collab.)
DRAGOUN	99	JPG 25 1839	O. Dragoun *et al.*	
HOLZSCHUH	99	PL B451 247	E. Holzschuh *et al.*	
VAITAITIS	99	PRL 83 4943	A. Vaitaitis *et al.*	(CCFR Collab.)
ASSAMAGAN	98	PL B434 158	K. Assamagan *et al.*	
HINDI	98	PR C58 2512	M.M. Hindi *et al.*	
PDG	98	EPJ C3 1	C. Caso *et al.*	
ABREU	97I	ZPHY C74 57	P. Abreu *et al.*	(DELPHI Collab.)
Also	97L	ZPHY C75 580 erratum	P. Abreu *et al.*	(DELPHI Collab.)
BRYMAN	96	PR D53 558	D.A. Bryman, T. Numao	(TRIU)
BUSKULIC	96S	PL B384 439	D. Buskulic *et al.*	(ALEPH Collab.)
WIETFELDT	96	PRPL 273 149	F.E. Wietfeldt, E.B. Norman	(LBL)
ARMBRUSTER	95	PL B348 19	B. Armbruster *et al.*	(KARMEN Collab.)
BAHRAN	95	PL B354 481	M.Y. Bahran, G.R. Kalbfleisch	(OKLA)
BILGER	95	PL B363 41	R. Bilger *et al.*	(TUBIN, KARLE, PSI)
DAUM	95B	PL B361 179	M. Daum *et al.*	(PSI, VIRG)
FARGION	95	PR D52 1828	D. Fargion *et al.*	(ROMA, KIAM, MPEI)
GALLAS	95	PR D52 6	E. Gallas *et al.*	(MSU, FNAL, MIT, FLOR)
GARCIA	95	PR D51 1458	E. Garcia *et al.*	(ZARA, SCUC, PNL)
HAGNER	95	PR D52 1343	C. Hagner *et al.*	(MUNT, LAPP, CPPM)
HIDDEMANN	95	JPG 21 639	K.H. Hiddemann, H. Daniel, O. Schwentker	(MUNT)
VILAIN	95C	PL B351 387	P. Vilain *et al.*	(CHARM II Collab.)
Also	95	PL B343 453	P. Vilain *et al.*	(CHARM II Collab.)
BECK	94	PL B336 141	M. Beck *et al.*	(MPIH, KIAE, SASSO)
KONOPLICH	94	PAN 57 425	R.V. Konoplich, M.Y. Khlopov	(MPEI)
PDG	94	PR D50 1173	L. Montanet *et al.*	(CERN, LBL, BOST+)
BAHRAN	93	PR D47 R754	M. Bahran, G.R. Kalbfleisch	(OKLA)
BAHRAN	93B	PR D47 R759	M. Bahran, G.R. Kalbfleisch	(OKLA)
BARANOV	93	PL B302 336	S.A. Baranov *et al.*	(JINR, SERP, BUDA)
KALBFLEISCH	93	PL B303 355	G.R. Kalbfleisch, M.Y. Bahran	(OKLA)
MORTARA	93	PRL 70 394	J.L. Mortara *et al.*	(ANL, LBL, UCB)
OHSHIMA	93	PR D47 4840	T. Ohshima *et al.*	(KEK, TUAT, RIKEN+)
ABREU	92B	PL B274 230	P. Abreu *et al.*	(DELPHI Collab.)
BAHRAN	92	PL B291 336	M.Y. Bahran, G.R. Kalbfleisch	(OKLA)
BRITTON	92	PRL 68 3000	D.I. Britton *et al.*	(TRIU, CARL)
Also	94	PR D49 28	D.I. Britton *et al.*	(TRIU, CARL)
BRITTON	92B	PR D46 R885	D.I. Britton *et al.*	(TRIU, CARL)
KAWAKAMI	92	PL B287 45	H. Kawakami *et al.*	(INUS, KEK, SCUC+)
MORI	92B	PL B289 463	M. Mori *et al.*	(KAM2 Collab.)
ALEXANDER	91F	ZPHY C52 175	G. Alexander *et al.*	(OPAL Collab.)
DELEENER-...	91	PR D43 3611	N. de Leener-Rosier *et al.*	(LOUV, ZURI+)
REUSSER	91	PL B255 143	D. Reusser *et al.*	(NEUC, CIT, PSI)
SATO	91	PR D44 2220	N. Sato *et al.*	(Kamiokande Collab.)
ADEVA	90S	PL B251 321	B. Adeva *et al.*	(L3 Collab.)
BURCHAT	90	PR D41 3542	P.R. Burchat *et al.*	(Mark II Collab.)
DECAMP	90F	PL B236 511	D. Decamp *et al.*	(ALEPH Collab.)
DEUTSCH	90	NP A518 149	J. Deutsch, M. Lebrun, R. Prieels	
JUNG	90	PRL 64 1091	C. Jung *et al.*	(Mark II Collab.)
ABRAMS	89C	PRL 63 2447	G.S. Abrams *et al.*	(Mark II Collab.)
ENQVIST	89	NP B317 647	K. Enqvist, K. Kainulainen, J. Maalampi	(HELS)
FISHER	89	PL B218 257	P.H. Fisher *et al.*	(CIT, NEUC, PSI)
AKERLOF	88	PR D37 577	C.W. Akerlof *et al.*	(HRS Collab.)
BERNARDI	88	PL B203 332	G. Bernardi *et al.*	(PARIN, CERN, INFN+)
CALDWELL	88	PRL 61 510	D.O. Caldwell *et al.*	(UCSB, UCB, LBL)
OLIVE	88	PL B205 553	K.A. Olive, M. Srednicki	(MINN, UCSB)
SREDNICKI	88	NP B310 693	M. Srednicki, R. Watkins, K.A. Olive	(MINN, UCSB)
AHLEN	87	PL B195 603	S.P. Ahlen *et al.*	(BOST, SCUC, HARV+)
DAUM	87	PR D36 2624	M. Daum *et al.*	(SIN, VIRG)
GRIEST	87	NP B283 681	K. Griest, D. Seckel	(UCSC, CERN)
Also	88	NP B296 1034 erratum	K. Griest, D. Seckel	(UCSC, CERN)
MISHRA	87	PRL 59 1397	S.R. Mishra *et al.*	(COLU, CIT, FNAL+)
OBERAUER	87	PL B198 113	L.F. Oberauer, F. von Feilitzsch, R.L. Mossbauer	
WENDT	87	PRL 58 1810	C. Wendt *et al.*	(Mark II Collab.)
AZUELOS	86	PRL 56 2241	G. Azuelos *et al.*	(TRIU, CNRC)
BADIER	86	ZPHY C31 21	J. Badier *et al.*	(NA3 Collab.)
BERNARDI	86	PL 166B 479	G. Bernardi *et al.*	(CURIN, INFN, CDEF+)
DORENBOS...	86	PL 166B 473	J. Dorenbosch *et al.*	(CHARM Collab.)
ALBRECHT	85I	PL 163B 404	H. Albrecht *et al.*	(ARGUS Collab.)
APALIKOV	85	JETPL 42 289 Translated from ZETFP 42 233.	A.M. Apalikov *et al.*	(ITEP)
COOPER-...	85	PL 160B 207	A.M. Cooper-Sarkar *et al.*	(CERN, LOIC+)
MARKEY	85	PR C32 2215	J. Markey, F. Boehm	(CIT)
OHI	85	PL 160B 322	T. Ohi *et al.*	(TOKY, INUS, KEK)
MINEHART	84	PRL 52 804	R.C. Minehart *et al.*	(VIRG, SIN)
BERGSMA	83	PL 122B 465	F. Bergsma *et al.*	(CHARM Collab.)
BERGSMA	83B	PL 128B 361	F. Bergsma *et al.*	(CHARM Collab.)
BRYMAN	83B	PRL 50 1546	D.A. Bryman *et al.*	(TRIU, CNRC)
DEUTSCH	83	PR D27 1644	J.P. Deutsch, M. Lebrun, R. Prieels	(LOUV)
GRONAU	83	PR D28 2762	M. Gronau	(HAIF)
SCHRECK...	83	PL 129B 265	K. Schreckenbach *et al.*	(ISNG, ILLG)
HAYANO	82	PRL 49 1305	R.S. Hayano *et al.*	(TOKY, KEK, TSUK)
ABELA	81	PL 105B 263	R. Abela *et al.*	(SIN)
ASANO	81	PL 104B 84	Y. Asano *et al.*	(KEK, TOKY, INUS, OSAK)
CALAPRICE	81	PL 106B 175	F.P. Calaprice *et al.*	(PRIN, IND)
SHROCK	81	PR D24 1232	R.E. Shrock	(STON)
SHROCK	81B	PR D24 1275	R.E. Shrock	(STON)
SHROCK	80	PL 96B 159	R.E. Shrock	(STON)

QUARKS

Notes in the Quark Listings

QUARKS

QUARK MASSES

Revised April 2002 by A.V. Manohar (University of California, San Diego) and C.T. Sachrajda (University of Southampton).

A. Introduction:

This note discusses some of the theoretical issues relevant to the determination of quark masses, which are fundamental parameters of the Standard Model of particle physics. Unlike the leptons, quarks are confined inside hadrons and are not observed as physical particles. Quark masses, therefore, cannot be measured directly, but must be determined indirectly through their influence on hadronic properties. Although one often speaks loosely of quark masses as one would of the mass of the electron or muon, any quantitative statement about the value of a quark mass must make careful reference to the particular theoretical framework that is used to define it. It is important to keep this *scheme dependence* in mind when using the quark mass values tabulated in the data Listings.

Historically, the first determinations of quark masses were performed using quark models. The resulting masses only make sense in the limited context of a particular quark model, and cannot be related to the quark mass parameters of the Standard Model. In order to discuss quark masses at a fundamental level, definitions based on quantum field theory must be used, and the purpose of this note is to discuss these definitions and the corresponding determinations of the values of the masses.

B. Mass parameters and the QCD Lagrangian:

The QCD [1] Lagrangian for N_F quark flavors is

$$\mathcal{L} = \sum_{k=1}^{N_F} \overline{q}_k \left(i \not{\mathcal{D}} - m_k \right) q_k - \tfrac{1}{4} G_{\mu\nu} G^{\mu\nu} \ , \qquad (1)$$

where $\not{\mathcal{D}} = (\partial_\mu - igA_\mu)\gamma^\mu$ is the gauge covariant derivative, A_μ is the gluon field, $G_{\mu\nu}$ is the gluon field strength, m_k is the mass parameter of the k^{th} quark, and q_k is the quark Dirac field. After renormalization, the QCD Lagrangian Eq. (1) gives finite values for physical quantities, such as scattering amplitudes. Renormalization is a procedure that invokes a subtraction scheme to render the amplitudes finite, and requires the introduction of a dimensionful scale parameter μ. The mass parameters in the QCD Lagrangian Eq. (1) depend on the renormalization scheme used to define the theory, and also on the scale parameter μ. The most commonly used renormalization scheme for QCD perturbation theory is the $\overline{\text{MS}}$ scheme.

The QCD Lagrangian has a chiral symmetry in the limit that the quark masses vanish. This symmetry is spontaneously broken by dynamical chiral symmetry breaking, and explicitly broken by the quark masses. The nonperturbative scale of dynamical chiral symmetry breaking, Λ_χ, is around 1 GeV [2]. It is conventional to call quarks heavy if $m > \Lambda_\chi$, so that explicit chiral symmetry breaking dominates (c, b, and t quarks are heavy), and light if $m < \Lambda_\chi$, so that spontaneous chiral symmetry breaking dominates (u, d, and s quarks are light). The determination of light- and heavy-quark masses is considered separately in sections ***D*** and ***E*** below.

At high energies or short distances, nonperturbative effects, such as chiral symmetry breaking, become small, and one can, in principle, determine quark masses by analyzing mass-dependent effects using QCD perturbation theory. Such computations are conventionally performed using the $\overline{\text{MS}}$ scheme at a scale $\mu \gg \Lambda_\chi$, and give the $\overline{\text{MS}}$ "running" mass $\overline{m}(\mu)$. We use the $\overline{\text{MS}}$ scheme when reporting quark masses; one can readily convert these values into other schemes using perturbation theory.

The μ dependence of $\overline{m}(\mu)$ at short distances can be calculated using the renormalization group equation,

$$\mu^2 \frac{\mathrm{d}\overline{m}(\mu)}{\mathrm{d}\mu^2} = -\gamma(\overline{\alpha}_s(\mu))\, \overline{m}(\mu) \,, \qquad (2)$$

where γ is the anomalous dimension which is now known to four-loop order in perturbation theory [3,4]. $\overline{\alpha}_s$ is the coupling constant in the $\overline{\text{MS}}$ scheme. Defining the expansion coefficients γ_r by

$$\gamma(\overline{\alpha}_s) \equiv \sum_{r=1}^{\infty} \gamma_r \left(\frac{\overline{\alpha}_s}{4\pi} \right)^r ,$$

the first four coefficients are given by

$$\gamma_1 = 4,$$

$$\gamma_2 = \frac{202}{3} - \frac{20 N_L}{9},$$

$$\gamma_3 = 1249 + \left(-\frac{2216}{27} - \frac{160}{3}\zeta(3) \right) N_L - \frac{140}{81} N_L^2,$$

$$\begin{aligned} \gamma_4 = {} & \frac{4603055}{162} + \frac{135680}{27}\zeta(3) - 8800\zeta(5) \\ & + \left(-\frac{91723}{27} - \frac{34192}{9}\zeta(3) + 880\zeta(4) + \frac{18400}{9}\zeta(5) \right) N_L \\ & + \left(\frac{5242}{243} + \frac{800}{9}\zeta(3) - \frac{160}{3}\zeta(4) \right) N_L^2 \\ & + \left(-\frac{332}{243} + \frac{64}{27}\zeta(3) \right) N_L^3, \end{aligned}$$

where N_L is the number of active light quark flavors at the scale μ, *i.e.*, flavors with masses $< \mu$, and ζ is the Riemann zeta function ($\zeta(3) \simeq 1.2020569$, $\zeta(4) \simeq 1.0823232$, and $\zeta(5) \simeq 1.0369278$).

C. Lattice Gauge Theory:

The use of the lattice simulations for *ab initio* determinations of the fundamental parameters of QCD, including the coupling constant and quark masses (except for the top-quark mass), is a very active area of research, with the current emphasis being on the reduction and control of the systematic uncertainties. We now briefly review some of the features of

lattice QCD. In this approach, space-time is approximated by a finite, discrete *lattice* of points, and multi-local correlation functions are computed by the numerical evaluation of the corresponding functional integrals. To determine quark masses, one computes a convenient and appropriate set of physical quantities (frequently chosen to be a set of hadronic masses) using lattice QCD for a variety of input values of the quark masses. The true (physical) values of the quark masses are those which correctly reproduce the set of physical quantities being used for calibration.

The values of the quark masses obtained directly in lattice simulations are bare quark masses, with the lattice spacing a as the ultraviolet cut-off. In order for the lattice results to be useful in phenomenology, it is, therefore, necessary to relate the bare quark masses in a lattice formulation of QCD to renormalized masses in some standard renormalization scheme such as $\overline{\rm MS}$. Provided that both the ultraviolet cut-off a^{-1} and the renormalization scale are much greater than $\Lambda_{\rm QCD}$, the bare and renormalized masses can be related in perturbation theory (this is frequently facilitated by the use of chiral Ward identities). However, the coefficients in lattice perturbation theory are often found to be large, and our ignorance of higher-order terms is generally a significant source of systematic uncertainty (although techniques exist which help to resum some of the large higher-order effects). Increasingly, non-perturbative renormalization is used to calculate the relation between the bare and renormalized masses, circumventing the need for lattice perturbation theory.

The precision with which quark masses can be determined in lattice simulations is limited by the available computing resources. There are a number of sources of systematic uncertainty, and there has been considerable progress in recent years in reducing a number of these. Currently, the difficulty of performing a standard error analysis for lattice simulations is due predominantly to two sources of systematic uncertainty:

Quenching: Until recently most of the simulations have been performed in the "quenched" approximation, in which quark vacuum polarization effects are neglected. It is not possible, in general, to quantify the effects of quenching, although there is a folklore that they are of the order of 10 – 15%. Such an estimate is based on a comparison of results from quenched simulations, with experimental measurements for those quantities where this is possible, and with some (partially) unquenched calculations.

Extrapolation towards the Chiral Limit: Increasingly unquenched simulations are being performed, most often with two flavors of sea quarks. The difficulty, however, is that the masses of the u and d quarks (both valence and sea) used in these simulations are much larger than their physical values. The lattice results have, therefore, to be extrapolated as functions of m_u and m_d. Ideally such an extrapolation would be guided by the predictions of chiral perturbation theory, and there are some indications that this may be possible before too long. In general, however, it is likely that the values of m_u and m_d currently used in simulations are too large for the predictions of chiral perturbation theory to be useful. The results quoted below were obtained assuming there will be no major surprises when m_u and m_d are reduced.

In addition, one has to consider the uncertainties due to the fact that the lattice spacing is non-zero (lattice artifacts), and that the volume is not infinite. The former are studied by observing the stability of the results as a is varied, or by using "improved" formulations of lattice QCD. By varying the volume of the lattice one checks that finite-volume effects are indeed small.

D. Light quarks:

For light quarks, one can use the techniques of chiral perturbation theory to extract quark mass ratios. The mass term for light quarks is

$$\overline{\Psi} M \Psi = \overline{\Psi}_L M \Psi_R + \overline{\Psi}_R M \Psi_L, \tag{3}$$

where M is the light quark mass matrix M,

$$M = \begin{pmatrix} m_u & 0 & 0 \\ 0 & m_d & 0 \\ 0 & 0 & m_s \end{pmatrix}, \tag{4}$$

and $\Psi = (u, d, s)$. The mass term $\overline{\Psi} M \Psi$ is the only term in the QCD Lagrangian that mixes left- and right-handed quarks. In the limit $M \to 0$, there is an independent $\mathrm{SU}(3) \times \mathrm{U}(1)$ flavor symmetry for the left- and right-handed quarks. The vector U(1) symmetry is baryon number; the axial U(1) symmetry of the classical theory is broken in the quantum theory, due to the anomaly. The remaining $G_\chi = \mathrm{SU}(3)_L \times \mathrm{SU}(3)_R$ chiral symmetry of the QCD Lagrangian is spontaneously broken to $\mathrm{SU}(3)_V$, which, in the limit $M \to 0$, leads to eight massless Goldstone bosons, the π's, K's, and η.

The symmetry G_χ is only an approximate symmetry, since it is explicitly broken by the quark mass matrix M. The Goldstone bosons acquire masses which can be computed in a systematic expansion in M, in terms of certain unknown nonperturbative parameters of the theory. For example, to first order in M, one finds that [5]

$$\begin{aligned} m^2_{\pi^0} &= B\,(m_u + m_d)\ , \\ m^2_{\pi^\pm} &= B\,(m_u + m_d) + \Delta_{\rm em}\ , \\ m^2_{K^0} = m^2_{\overline{K}^0} &= B\,(m_d + m_s)\ , \\ m^2_{K^\pm} &= B\,(m_u + m_s) + \Delta_{\rm em}\ , \\ m^2_\eta &= \frac{1}{3} B\,(m_u + m_d + 4m_s)\ , \end{aligned} \tag{5}$$

with two unknown parameters B and $\Delta_{\rm em}$, the electromagnetic mass difference. From Eq. (5), one can determine the quark mass ratios [5]

$$\begin{aligned} \frac{m_u}{m_d} &= \frac{2m^2_{\pi^0} - m^2_{\pi^+} + m^2_{K^+} - m^2_{K^0}}{m^2_{K^0} - m^2_{K^+} + m^2_{\pi^+}} = 0.56\ , \\ \frac{m_s}{m_d} &= \frac{m^2_{K^0} + m^2_{K^+} - m^2_{\pi^+}}{m^2_{K^0} + m^2_{\pi^+} - m^2_{K^+}} = 20.1\ , \end{aligned} \tag{6}$$

to lowest order in chiral perturbation theory, with an error which will be estimated below. Since the mass ratios extracted using chiral perturbation theory use the symmetry transformation property of M under the chiral symmetry G_χ, it is important to use a renormalization scheme for QCD that does not change this transformation law. Any mass-independent subtraction scheme, such as $\overline{\rm MS}$, is suitable. The ratios of quark masses are scale-independent in such a scheme, and Eq. (6) can be taken to be the ratio of $\overline{\rm MS}$ masses. Chiral perturbation theory cannot determine the overall scale of the quark masses, since it uses only the symmetry properties of M, and any multiple of M has the same G_χ transformation law as M.

The second-order quark-mass term [9]

$$\left(M^\dagger\right)^{-1} \det M^\dagger \tag{7}$$

(which can be generated by instantons) transforms in the same way under G_χ as M. Chiral perturbation theory cannot distinguish between M and $\left(M^\dagger\right)^{-1} \det M^\dagger$; one can make the replacement $M \to M(\lambda) = M + \lambda M \left(M^\dagger M\right)^{-1} \det M^\dagger$ in the chiral Lagrangian,

$$\begin{aligned} M(\lambda) &= \mathrm{diag}\left(m_u(\lambda)\,,\ m_d(\lambda)\,,\ m_s(\lambda)\right) \\ &= \mathrm{diag}\left(m_u + \lambda m_d m_s\,,\ m_d + \lambda m_u m_s\,,\ m_s + \lambda m_u m_d\right), \end{aligned} \tag{8}$$

and leave all observables unchanged.

The combination

$$\left(\frac{m_u}{m_d}\right)^2 + \frac{1}{Q^2}\left(\frac{m_s}{m_d}\right)^2 = 1 \tag{9}$$

where

$$Q^2 = \frac{m_s^2 - \widehat{m}^2}{m_d^2 - m_u^2}, \qquad \widehat{m} = \frac{1}{2}\left(m_u + m_d\right),$$

is insensitive to the transformation in Eq. (8). Eq. (9) gives an ellipse in the $m_u/m_d - m_s/m_d$ plane. The ellipse is well-determined by chiral perturbation theory, but the exact location on the ellipse, and the absolute normalization of the quark masses, has larger uncertainties. Q is determined to be in the range 21–25 from $\eta \to 3\pi$ decay and the electromagnetic contribution to the K^+–K^0 and π^+–π^0 mass differences [10].

Chiral perturbation theory is a systematic expansion in powers of the light quark masses. The typical expansion parameter is $m_K^2/\Lambda_\chi^2 \sim 0.25$ if one uses SU(3) chiral symmetry, and $m_\pi^2/\Lambda_\chi^2 \sim 0.02$ if one uses SU(2) chiral symmetry. Electromagnetic effects at the few percent level also break SU(2) and SU(3) symmetry. The mass formulæ Eq. (5) were derived using SU(3) chiral symmetry, and are expected to have a 25% uncertainty due to second-order corrections.

It is particularly important to determine the quark mass ratio m_u/m_d, since there is no strong CP problem if $m_u = 0$. The chiral symmetry G_χ of the QCD Lagrangian is not enhanced even if $m_u = 0$. [The possible additional axial u-quark number symmetry is anomalous. The only additional symmetry when $m_u = 0$ is CP.] As a result, $m_u = 0$ is not a special value for chiral perturbation theory. One can try and extend the chiral perturbation expansion Eq. (5) to second order in the quark masses M, to get a more accurate determination of the quark mass ratios. However, as we have seen, due to the ambiguity Eq. (8) at second order, one cannot accurately determine m_u/m_d, only the combination Eq. (9).

The absolute normalization of the quark masses can be determined by using methods that go beyond chiral perturbation theory, such as spectral function sum rules for hadronic correlation functions or lattice simulations. In the former approach, one computes a hadron spectral function using QCD perturbation theory, and compares the result with the experimental data. The comparison must necessarily take place at large q^2, where QCD perturbation theory is valid. Quark mass effects are of order m/q, so that the spectral functions are not very sensitive to m at large q^2. The extraction of the absolute value of quark masses is very sensitive to theoretical and experimental uncertainties. The strange quark mass has been extracted from hadronic tau decays using this procedure, since the relevant scale m_τ is large enough for perturbation theory to be valid [11].

Lattice simulations allow for detailed studies of the behavior of hadronic masses and matrix elements as functions of the quark masses. Moreover, the quark masses do not have to take their physical values, but can be varied freely, and chiral perturbation theory applies also for unphysical masses, provided that they are sufficiently light. From such recent studies of pseudoscalar masses and decay constants, the relevant higher-order couplings in the chiral Lagrangian have been estimated, strongly suggesting that $m_u \neq 0$ [6–8]. In order to make this evidence conclusive, the lattice systematic errors must be reduced; in particular, the range of light quark masses should be increased, and the validity of chiral perturbation theory for this range established.

There have been numerous quenched-lattice determinations of the light quark masses, using a variety of formulations of lattice QCD (see, for example, the recent set of results in Refs. [12–22]). Given the different systematic errors in these determinations (*e.g.*, the different lattice formulations of QCD, the use of perturbative and non-perturbative renormalization), the level of agreement is satisfying. There have also been a number of unquenched studies with two flavors of sea quarks, Refs. [16,23,24,25] and results from the APE and MILC Collaborations cited in the review article Ref. 26.

In current lattice simulations, it is the combination $(m_u + m_d)/2$ which can be determined. In the evaluation of m_s, one gets a result which is about 20–25% larger if the ϕ meson is used as input rather than the K meson. This is evidence that the errors due to quenching are significant. It is reassuring that this difference is eliminated or reduced significantly in the cited unquenched studies.

The quark masses for light quarks discussed so far are often referred to as current quark masses. Nonrelativistic quark models use constituent quark masses, which are of order 350 MeV for the u and d quarks. Constituent quark masses

model the effects of dynamical chiral symmetry breaking, and are not related to the quark mass parameters m_k of the QCD Lagrangian Eq. (1). Constituent masses are only defined in the context of a particular hadronic model.

E. Heavy quarks:

The masses and decay rates of hadrons containing a single heavy quark, such as the B and D mesons, can be determined using the heavy quark effective theory (HQET) [37]. The theoretical calculations involve radiative corrections computed in perturbation theory with an expansion in $\alpha_s(m_Q)$, and non-perturbative corrections with an expansion in powers of $\Lambda_{\rm QCD}/m_Q$. Due to the asymptotic nature of the QCD perturbation series, the two kinds of corrections are intimately related; renormalon effects in the perturbative expansion are an example of this, which are associated with non-perturbative corrections.

Systems containing two heavy quarks, such as the Υ or J/ψ, are treated using NRQCD [38]. The typical momentum and energy transfers in these systems are $\alpha_s m_Q$, and $\alpha_s^2 m_Q$, respectively, so these bound states are sensitive to scales much smaller than m_Q. However, smeared observables, such as the cross-section for $e^+e^- \to \overline{b}b$, averaged over some range of s that includes several bound state energy levels, are better behaved and only sensitive to scales near m_Q. For this reason, most determinations of the b quark mass using perturbative calculations compare smeared observables with experiment [39,40,41].

Lattice simulations of heavy-quark systems have been performed using effective theories, including HQET and NRQCD, as well as directly in QCD. The systematic uncertainties in the two cases are different, so both approaches contribute to the final results. Simulating the effective theory requires lattice spacings to be fine enough to resolve the size of the hadron, whereas simulating QCD requires much finer lattice spacings, of order the inverse quark mass. For this reason, and because available computing resources limit the lattice spacings which can be used ($a^{-1} \simeq 2-3\,\text{GeV}$), simulations for the b quark using the QCD action are currently done at quark mass values near the c quark, and then extrapolated to the physical b-quark mass. On the other hand, in effective theories, when evaluating non-leading terms in $1/m_b$, one encounters power divergences in $1/a$ which have to be subtracted.

For an observable particle such as the electron, the position of the pole in the propagator is the definition of the particle mass. In QCD, this definition of the quark mass is known as the pole mass. It is known that the on-shell quark propagator has no infrared divergences in perturbation theory [27,28], so this provides a perturbative definition of the quark mass. The pole mass cannot be used to arbitrarily high accuracy because of nonperturbative infrared effects in QCD. The full quark propagator has no pole because the quarks are confined, so that the pole mass cannot be defined outside of perturbation theory.

The relation between the pole mass m_Q and the $\overline{\rm MS}$ mass $\overline{m}_Q$ is known to three loops [29–33]

$$m_Q = \overline{m}_Q(\overline{m}_Q)\Bigg\{1 + \frac{4\overline{\alpha}_s(\overline{m}_Q)}{3\pi} + \left[-1.0414\sum_k\left(1 - \frac{4}{3}\frac{\overline{m}_{Q_k}}{\overline{m}_Q}\right) + 13.4434\right]\left[\frac{\overline{\alpha}_s(\overline{m}_Q)}{\pi}\right]^2 + \left[0.6527N_L^2 - 26.655N_L + 190.595\right]\left[\frac{\overline{\alpha}_s(\overline{m}_Q)}{\pi}\right]^3\Bigg\}, \quad (10)$$

where $\overline{\alpha}_s(\mu)$ is the strong interaction coupling constants in the $\overline{\rm MS}$ scheme, and the sum over k extends over the N_L flavors Q_k lighter than Q. The complete mass dependence of the α_s^2 term can be found in Ref. 29; the mass dependence of the α_s^3 term is not known. For the b quark, Eq. (10) reads

$$m_b = \overline{m}_b\,(\overline{m}_b)\,[1 + 0.09 + 0.05 + 0.03]\,, \quad (11)$$

where the contributions from the different orders in α_s are shown explicitly. The two- and three-loop corrections are comparable in size, and have the same sign as the one-loop term. This is a signal of the asymptotic nature of the perturbation series [there is a renormalon in the pole mass]. Such a badly behaved perturbation expansion can be avoided by directly extracting the $\overline{\rm MS}$ mass from data without extracting the pole mass as an intermediate step.

F. Numerical values and caveats:

The quark masses in the Particle Data Group's Listings have been obtained by using a wide variety of methods. Each method involves its own set of approximations and errors. In most cases, the errors are a best guess at the size of neglected higher-order corrections or other uncertainties. The expansion parameters for some of the approximations are not very small (for example, they are $m_K^2/\Lambda_\chi^2 \sim 0.25$ for the chiral expansion, and $\Lambda_{\rm QCD}/m_b \sim 0.1$ for the heavy-quark expansion), so an unexpectedly large coefficient in a neglected higher-order term could significantly alter the results. It is also important to note that the quark mass values can be significantly different in the different schemes.

The heavy quark masses obtained using HQET, QCD sum rules, or lattice gauge theory are consistent with each other if they are all converted into the same scheme. When using the data listings, it is important to remember that the numerical value for a quark mass is meaningless without specifying the particular scheme in which it was obtained.

We have specified all masses in the $\overline{\rm MS}$ scheme. For light quarks, the renormalization scale has been chosen to be $\mu = 2\,\text{GeV}$, and for heavy quarks, the quark mass itself (*i.e.*, we quote $\overline{m}(\mu = \overline{m})$). If necessary, we have converted the values in the original papers using the two-loop formulæ. The light quark masses at 1 GeV are significantly different from those at 2 GeV, $\overline{m}(1\,\text{GeV})/\overline{m}(2\,\text{GeV}) = 1.35$.

From the spread of results, and taking into account the treatment of systematic errors in each of the lattice simulations, we quote as the current best results for the quark masses renormalized in the $\overline{\rm MS}$ scheme at a scale of 2 GeV:

$$\frac{1}{2}\left(\overline{m}_u + \overline{m}_d\right)\Big|_{\mu=2\ \rm GeV} = (4.2 \pm 1.0)\ \rm MeV \quad [Lattice\ only],$$

and

$$\overline{m}_s\Big|_{\mu=2\ \rm GeV} = (105 \pm 25)\ \rm MeV \quad [Lattice\ only].$$

It should be noted that recent results from simulations with two flavors of sea quarks suggest that the light-quark masses may be in the lower parts of the ranges quoted above (for example Refs. [16,25] find that $m_s \sim 90$ MeV, with an error of about 7 MeV, and $(m_u + m_d)/2 \sim 3.5$ MeV, with an error of perhaps 0.3 MeV). As such studies become more widespread, and use a variety of approaches to study and reduce systematic uncertainties, we can confidently expect that the errors quoted above for the best results will decrease significantly.

Continuum determinations of the absolute values of light quark masses have significant systematic uncertainties. The values are consistent with the lattice extractions above. The u- and d-quark masses are in the range

$$1.5\ \rm MeV \le \overline{m}_u\Big|_{\mu=2\ \rm GeV} \le 5\ \rm MeV \quad [Excluding\ lattice],$$

$$5\ \rm MeV \le m_d\Big|_{\mu=2\ \rm GeV} \le 9\ \rm MeV \quad [Excluding\ lattice].$$

The s-quark mass in more recent determinations tends to be smaller than in older extractions. The newer calculations use both better experimental data and perturbative calculations, which tend to reduce m_s. The continuum extractions give

$$80\ \rm MeV \le \overline{m}_s\Big|_{\mu=2\ \rm GeV} \le 155\ \rm MeV \quad [Excluding\ lattice].$$

Using the continuum determinations of the c-quark mass, we quote

$$1\ \rm GeV \le \overline{m}_c\left(\overline{m}_c\right) \le 1.4\ \rm GeV \quad [Excluding\ lattice]$$

as a best value. Recent determinations include at least two-loop corrections, and give values consistent with this range. The value $\overline{m}_c\left(\overline{m}_c\right)$ is sensitive to higher-order perturbative corrections, since α_s starts to get large below the charm quark scale.

There are rather few lattice determinations of m_c, as the charm quark is too light for comfortable use of HQET, and yet heavy enough that one must be careful about lattice artifacts. All the results are from quenched simulations, and most are still preliminary. For the best result, we take

$$\overline{m}_c\left(\overline{m}_c\right) = (1.26 \pm 0.13 \pm 0.20)\ \rm GeV \quad [Lattice\ only],$$

which is consistent with continuum extractions. The second error of 15% is our estimate of possible quenching effects.

There has been much recent work on the b-quark mass. As a best value from continuum extractions, we quote

$$4\ \rm GeV \le \overline{m}_b\left(\overline{m}_b\right) \le 4.5\ \rm GeV \quad [Excluding\ lattice],$$

which is consistent with continuum extractions. The dominant uncertainties in the b-quark mass are the non-perturbative corrections in the B and Υ systems.

As the current best lattice result for $\overline{m}_b$ we take:

$$\overline{m}_b\left(\overline{m}_b\right) = (4.26 \pm 0.15 \pm 0.15)\ \rm GeV \quad [Lattice\ only].$$

The second error is our estimate of possible quenching effects (15% on $M_B - \overline{m}_b$).

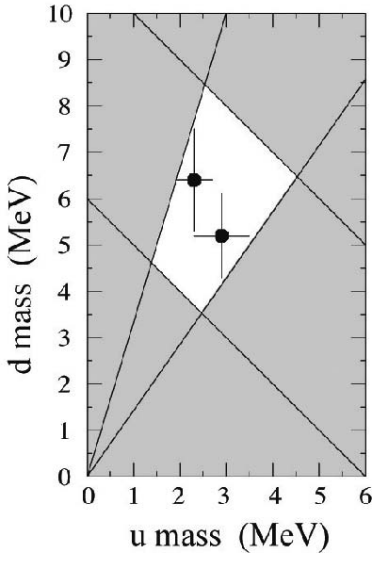

Figure 1: The allowed region (shown in white) for up quark and down quark masses. This region was determined in part from papers reporting values for m_u and m_d (data points shown), and in part from analysis of the allowed ranges of other mass parameters (see Fig. 2). The parameter $(m_u + m_d)/2$ yields the two downward-sloping lines, while m_u/m_d yields the two rising lines originating at (0,0).

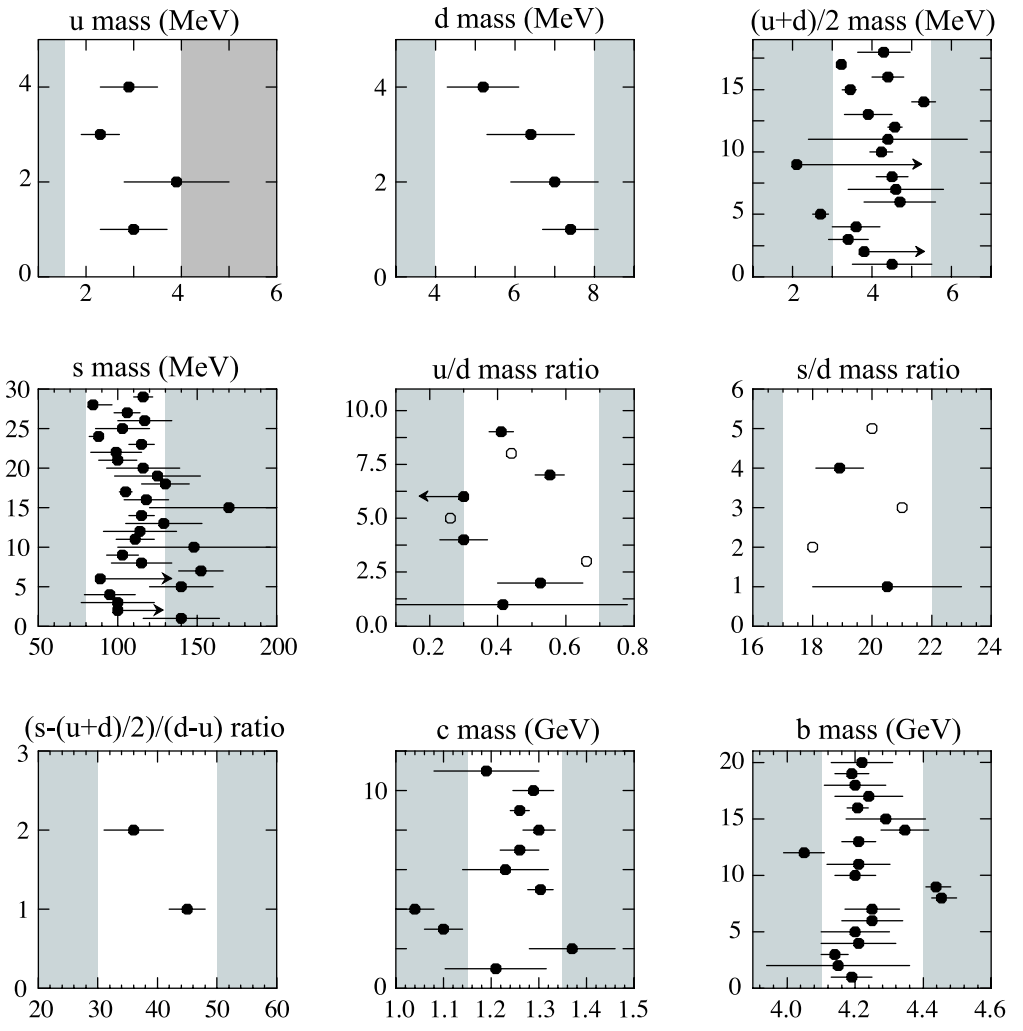

Figure 2. The values of each quark mass parameter taken from the 2004 Data Listings. The most recent data points are at the top of each plot. Points from papers reporting no error bars are open circles. Arrows indicate limits reported. The grey regions indicate values excluded by our evaluations; some regions were determined in part through examination of Fig. 1.

References

1. See the review on "Quantum chromodynamics" by I. Hinchliffe in this *Review*.
2. A.V. Manohar and H. Georgi, Nucl. Phys. **B234**, 189 (1984).
3. J.A.M. Vermaseren, S.A. Larin, and T. van Ritbergen, Phys. Lett. **B405**, 327 (1997).
4. K.G. Chetyrkin, B.A. Kniehl, and M. Steinhauser, Nucl. Phys. **B510**, 61 (1998).
5. S. Weinberg, Trans. N.Y. Acad. Sci. **38**, 185 (1977).
6. J. Heitger, R. Sommer, and H. Wittig (Alpha Collab.), Nucl. Phys. **B588**, 377 (2000).
7. A.C. Irving *et al.* (UKQCD Collab.), hep-lat/0107023 (2001).
8. D.R. Nelson, G.T. Fleming, and G.W. Kilcup, Phys. Lett. **B518**, 243 (2001).
9. D.B. Kaplan and A.V. Manohar, Phys. Rev. Lett. **56**, 2004 (1986).
10. H. Leutwyler, Phys. Lett. **B374**, 163 (1996).
11. E. Braaten, S. Narison, and A. Pich, Nucl. Phys. **B373**, 581 (1992).
12. D. Becirevic *et al.*, Phys. Rev. **D61**, 114507 (2000).
13. D. Becirevic *et al.*, Phys. Lett. **B444**, 401 (1998).
14. J. Garden *et al.*, Nucl. Phys. **B571**, 237 (2000).
15. S. Aoki *et al.* (CP-PACS Collab.), Phys. Rev. Lett. **84**, 238 (2000).
16. A. Ali Khan *et al.* (CP-PACS Collab.), Phys. Rev. Lett. **85**, 4674 (2000).
17. S. Aoki *et al.* (CP-PACS Collab.), Phys. Rev. Lett. **82**, 4392 (1999).
18. M. Göckeler *et al.*, Phys. Rev. **D62**, 054504 (2000).
19. M. Wingate *et al.* (RBC Collab.), Nucl. Phys. B. Proc. Suppl. **94**, 277 (2001).
20. A. Ali Khan *et al.* (CP-PACS Collab.), Phys. Rev. **D64**, 114506 (2001).
21. L. Giusti, C. Hoelbling, and C. Rebbi, Phys. Rev. **D64**, 114508 (2001).
22. S-J. Dong *et al.*, Nucl. Phys. Proc. Supp. **106**, 275 (2002).
23. S. Aoki *et al.* (JLQCD Collab.), Nucl. Phys. B. Proc. Suppl. **94**, 233 (2001).
24. N. Eicker *et al.* (SESAM/T_χL Collab.), Phys. Lett. **B407**, 290 (1997); Phys. Rev. **D59**, 014509 (1998).
25. D. Pleiter *et al.* (QCDSF and UKQCD Collabs.), Nucl. Phys. B. Proc. Suppl. **94**, 265 (2001).
26. V. Lubicz, Nucl. Phys. B. Proc. Suppl. **94**, 116 (2001).
27. R. Tarrach, Nucl. Phys. **B183**, 384 (1981).
28. A. Kronfeld, Phys. Rev. **D58**, 051501 (1998).
29. N. Gray *et al.*, Z. Phys. **C48**, 673 (1990).
30. D.J. Broadhurst, N. Gray, and K. Schilcher, Z. Phys. **C52**, 111 (1991).
31. K.G. Chetyrkin and M. Steinhauser, Nucl. Phys. **B573**, 617 (2000).
32. K.G. Chetyrkin and M. Steinhauser, Phys. Rev. Lett. **83**, 4001 (1999).
33. K. Melnikov and T. van Ritbergen, Phys. Lett. **B482**, 99 (2000).
34. V. Giménez *et al.*, J. High Energy Phys. **0003**, 018 (2000).
35. K. Hornbostel *et al.* (NRQCD Collab.), Nucl. Phys. B. Proc. Suppl. **73**, 339 (1999).
36. S. Collins, hep-lat/0009040.
37. N. Isgur and M.B. Wise, Phys. Lett. **B232**, 113 (1989), and *ibid*, **B237**, 527 (1990).
38. G.T. Bodwin, E. Braaten, and G.P. Lepage, Phys. Rev. **D51**, 1125 (1995).
39. A.H. Hoang, Phys. Rev. **D61**, 034005 (2000).
40. K. Melnikov and A. Yelkhovsky, Phys. Rev. **D59**, 114009 (1999).
41. M. Beneke and A. Signer, Phys. Lett. **B471**, 233 (1999).

u

$I(J^P) = \frac{1}{2}(\frac{1}{2}^+)$

Mass m = 1.5 to 4.0 MeV Charge = $\frac{2}{3}$ e $I_z = +\frac{1}{2}$

m_u/m_d = 0.3 to 0.7

d

$I(J^P) = \frac{1}{2}(\frac{1}{2}^+)$

Mass m = 4 to 8 MeV Charge = $-\frac{1}{3}$ e $I_z = -\frac{1}{2}$

m_s/m_d = 17 to 22

$\overline{m} = (m_u + m_d)/2$ = 3.0 to 5.5 MeV

s

$I(J^P) = 0(\frac{1}{2}^+)$

Mass m = 80 to 130 MeV Charge = $-\frac{1}{3}$ e Strangeness = -1

$(m_s - (m_u + m_d)/2)/(m_d - m_u)$ = 30 to 50

LIGHT QUARKS (u, d, s)

OMITTED FROM SUMMARY TABLE

u-QUARK MASS

The u-, d-, and s-quark masses are estimates of so-called "current-quark masses," in a mass- independent subtraction scheme such as $\overline{\text{MS}}$. The ratios m_u/m_d and m_s/m_d are extracted from pion and kaon masses using chiral symmetry. The estimates of d and u masses are not without controversy and remain under active investigation. Within the literature there are even suggestions that the u quark could be essentially massless. The s-quark mass is estimated from SU(3) splittings in hadron masses.

We have normalized the $\overline{\text{MS}}$ masses at a renormalization scale of $\mu = 2$ GeV. Results quoted in the literature at $\mu = 1$ GeV have been rescaled by dividing by 1.35. The values of "Our Evaluation" were determined in part via Figures 1 and 2.

VALUE (MeV)	DOCUMENT ID		TECN	COMMENT
1.5 to 4.0 OUR EVALUATION				
• • • We do not use the following data for averages, fits, limits, etc. • • •				
2.9±0.6	[1] JAMIN	02	THEO	$\overline{\text{MS}}$ scheme
2.3±0.4	[2] NARISON	99	THEO	$\overline{\text{MS}}$ scheme
3.9±1.1	[3] JAMIN	95	THEO	$\overline{\text{MS}}$ scheme
3.0±0.7	[4] NARISON	95C	THEO	$\overline{\text{MS}}$ scheme

[1] JAMIN 02 first calculates the strange quark mass from QCD sum rules using the scalar channel, and then combines with the quark mass ratios obtained from chiral perturbation theory to obtain m_u.

[2] NARISON 99 uses sum rules to order α_s^3 for ϕ meson decays to get m_s, and finds m_u by combining with sum rule estimates of m_u+m_d and Dashen's formula.

[3] JAMIN 95 uses QCD sum rules at next-to-leading order. We have rescaled $m_u(1\text{ GeV}) = 5.3 \pm 1.5$ to $\mu = 2$ GeV.

[4] For NARISON 95C, we have rescaled $m_u(1\text{ GeV}) = 4 \pm 1$ to $\mu = 2$ GeV.

d-QUARK MASS

See the comment for the u quark above.

We have normalized the $\overline{\text{MS}}$ masses at a renormalization scale of $\mu = 2$ GeV. Results quoted in the literature at $\mu = 1$ GeV have been rescaled by dividing by 1.35. The values of "Our Evaluation" were determined in part via Figures 1 and 2.

VALUE (MeV)	DOCUMENT ID		TECN	COMMENT
4 to 8 OUR EVALUATION				
• • • We do not use the following data for averages, fits, limits, etc. • • •				
5.2±0.9	[5] JAMIN	02	THEO	$\overline{\text{MS}}$ scheme
6.4±1.1	[6] NARISON	99	THEO	$\overline{\text{MS}}$ scheme
7.0±1.1	[7] JAMIN	95	THEO	$\overline{\text{MS}}$ scheme
7.4±0.7	[8] NARISON	95C	THEO	$\overline{\text{MS}}$ scheme

[5] JAMIN 02 first calculates the strange quark mass from QCD sum rules using the scalar channel, and then combines with the quark mass ratios obtained from chiral perturbation theory to obtain m_d.

[6] NARISON 99 uses sum rules to order α_s^3 for ϕ meson decays to get m_s, and finds m_d by combining with sum rule estimates of m_u+m_d and Dashen's formula.

[7] JAMIN 95 uses QCD sum rules at next-to-leading order. We have rescaled $m_d(1\ \text{GeV}) = 9.4 \pm 1.5$ to $\mu = 2$ GeV.

[8] For NARISON 95C, we have rescaled $m_d(1\ \text{GeV}) = 10 \pm 1$ to $\mu = 2$ GeV.

$\overline{m} = (m_u+m_d)/2$

See the comments for the u quark above.

We have normalized the $\overline{\text{MS}}$ masses at a renormalization scale of $\mu = 2$ GeV. Results quoted in the literature at $\mu = 1$ GeV have been rescaled by dividing by 1.35. The values of "Our Evaluation" were determined in part via Figures 1 and 2.

VALUE (MeV)		DOCUMENT ID		TECN	COMMENT
3.0 to 5.5 OUR EVALUATION					
• • • We do not use the following data for averages, fits, limits, etc. • • •					
4.29	$\pm 0.14 \pm 0.65$	[9] AOKI	03	LATT	$\overline{\text{MS}}$ scheme
$3.223^{+0.046}_{-0.069}$		[10] AOKI	03B	LATT	$\overline{\text{MS}}$ scheme
4.4	$\pm 0.1 \pm 0.4$	[11] BECIREVIC	03	LATT	$\overline{\text{MS}}$ scheme
$3.45^{+0.14}_{-0.20}$		[12] ALIKHAN	02	LATT	$\overline{\text{MS}}$ scheme
5.3	± 0.3	[13] CHIU	02	LATT	$\overline{\text{MS}}$ scheme
3.9	± 0.6	[14] MALTMAN	02	THEO	$\overline{\text{MS}}$ scheme
3.9	± 0.6	[15] MALTMAN	01	THEO	$\overline{\text{MS}}$ scheme
4.57	± 0.18	[16] AOKI	00	LATT	$\overline{\text{MS}}$ scheme
4.4	± 2	[17] GOECKELER	00	LATT	$\overline{\text{MS}}$ scheme
4.23	± 0.29	[18] AOKI	99	LATT	$\overline{\text{MS}}$ scheme
≥ 2.1		[19] STEELE	99	THEO	$\overline{\text{MS}}$ scheme
4.5	± 0.4	[20] BECIREVIC	98	LATT	$\overline{\text{MS}}$ scheme
4.6	± 1.2	[21] DOSCH	98	THEO	$\overline{\text{MS}}$ scheme
4.7	± 0.9	[22] PRADES	98	THEO	$\overline{\text{MS}}$ scheme
2.7	± 0.2	[23] EICKER	97	LATT	$\overline{\text{MS}}$ scheme
3.6	± 0.6	[24] GOUGH	97	LATT	$\overline{\text{MS}}$ scheme
3.4	$\pm 0.4 \pm 0.3$	[25] GUPTA	97	LATT	$\overline{\text{MS}}$ scheme
>3.8		[26] LELLOUCH	97	THEO	$\overline{\text{MS}}$ scheme
4.5	± 1.0	[27] BIJNENS	95	THEO	$\overline{\text{MS}}$ scheme

[9] AOKI 03 uses quenched lattice simulation of the meson and baryon masses with degenerate light quarks. The extrapolations are done using quenched chiral perturbation theory.

[10] AOKI 03B uses lattice simulation of the meson and baryon masses with two dynamical light quarks. Simulations are performed using the $\mathcal{O}(a)$ improved Wilson action.

[11] BECIREVIC 03 perform quenched lattice computation using the vector and axial Ward identities. Uses $\mathcal{O}(a)$ improved Wilson action and nonperturbative renormalization.

[12] ALIKHAN 02 uses lattice simulation of the meson and baryon masses with two dynamical flavors and degenerate light quarks.

[13] CHIU 02 extracts the average light quark mass from quenched lattice simulations using quenched chiral perturbation theory.

[14] MALTMAN 02 uses finite energy sum rules in the ud and us pseudoscalar channels. Other mass values are also obtained by similar methods.

[15] MALTMAN 01 uses Borel transformed and finite energy sum rules.

[16] AOKI 00 obtain the light quark masses from a quenched lattice simulation of the meson and baryon spectrum with the Wilson quark action.

[17] GOECKELER 00 obtained from a quenched lattice computation of the pseudoscalar meson masses using $\mathcal{O}(a)$ improved Wilson fermions and nonperturbative renormalization.

[18] AOKI 99 obtain the light quark masses from a quenched lattice simulation of the meson spectrum with the staggered quark action employing the regularization independent scheme.

[19] STEELE 99 obtain a bound on the light quark masses by applying the Holder inequality to a sum rule. We have converted their bound of $(m_u+m_d)/2 \geq 3$ MeV at μ=1 GeV to μ=2 GeV.

[20] BECIREVIC 98 compute the quark mass using the Alpha action in the quenched approximation. The conversion from the regularization independent scheme to the $\overline{\text{MS}}$ scheme is at NNLO.

[21] DOSCH 98 use sum rule determinations of the quark condensate and chiral perturbation theory to obtain $9.4 \leq (m_u+m_d)(1\ \text{GeV}) \leq 15.7$ MeV. We have converted to result to μ=2 GeV.

[22] PRADES 98 uses finite energy sum rules for the axial current correlator.

[23] EICKER 97 use lattice gauge computations with two dynamical light flavors.

[24] GOUGH 97 use lattice gauge computations in the quenched approximation. Correcting for quenching gives $2.1 < \overline{m} < 3.5$ MeV at μ=2 GeV.

[25] GUPTA 97 use Lattice Monte Carlo computations in the quenched approximation. The value for two light dynamic flavors at $\mu = 2$ GeV is $2.7 \pm 0.3 \pm 0.3$ MeV.

[26] LELLOUCH 97 obtain lower bounds on quark masses using hadronic spectral functions.

[27] BIJNENS 95 determines m_u+m_d (1 GeV) = 12 ± 2.5 MeV using finite energy sum rules. We have rescaled this to 2 GeV.

s-QUARK MASS

See the comment for the u quark above.

We have normalized the $\overline{\text{MS}}$ masses at a renormalization scale of $\mu = 2$ GeV. Results quoted in the literature at $\mu = 1$ GeV have been rescaled by dividing by 1.35.

VALUE (MeV)		DOCUMENT ID		TECN	COMMENT
80 to 130 OUR EVALUATION					
• • • We do not use the following data for averages, fits, limits, etc. • • •					
116	$\pm 6 \pm 0.65$	[28] AOKI	03	LATT	$\overline{\text{MS}}$ scheme
$84.5^{+12}_{-1.7}$		[29] AOKI	03B	LATT	$\overline{\text{MS}}$ scheme
106	$\pm 2 \pm 8$	[30] BECIREVIC	03	LATT	$\overline{\text{MS}}$ scheme
117	± 17	[31] GAMIZ	03	THEO	$\overline{\text{MS}}$ scheme
103	± 17	[32] GAMIZ	03	THEO	$\overline{\text{MS}}$ scheme
88	$^{+3}_{-6}$	[33] ALIKHAN	02	LATT	$\overline{\text{MS}}$ scheme
115	± 8	[34] CHIU	02	LATT	$\overline{\text{MS}}$ scheme
99	± 16	[35] JAMIN	02	THEO	$\overline{\text{MS}}$ scheme
100	± 12	[36] MALTMAN	02	THEO	$\overline{\text{MS}}$ scheme
116	$^{+20}_{-25}$	[37] CHEN	01B	THEO	$\overline{\text{MS}}$ scheme
125	± 27	[38] KOERNER	01	THEO	$\overline{\text{MS}}$ scheme
130	± 15	[39] AOKI	00	LATT	$\overline{\text{MS}}$ scheme
105	± 4	[40] GOECKELER	00	LATT	$\overline{\text{MS}}$ scheme
118	± 14	[41] AOKI	99	LATT	$\overline{\text{MS}}$ scheme
170	$^{+44}_{-55}$	[42] BARATE	99R	ALEP	$\overline{\text{MS}}$ scheme
115	± 8	[43] MALTMAN	99	THEO	$\overline{\text{MS}}$ scheme
129	± 24	[44] NARISON	99	THEO	$\overline{\text{MS}}$ scheme
114	± 23	[45] PICH	99	THEO	$\overline{\text{MS}}$ scheme
111	± 12	[46] BECIREVIC	98	LATT	$\overline{\text{MS}}$ scheme
148	± 48	[47] CHETYRKIN	98	THEO	$\overline{\text{MS}}$ scheme
103	± 10	[48] CUCCHIERI	98	LATT	$\overline{\text{MS}}$ scheme
115	± 19	[49] DOMINGUEZ	98	THEO	$\overline{\text{MS}}$ scheme
152.4 ± 14.1		[50] CHETYRKIN	97	THEO	$\overline{\text{MS}}$ scheme
≥ 89		[51] COLANGELO	97	THEO	$\overline{\text{MS}}$ scheme
140	± 20	[52] EICKER	97	LATT	$\overline{\text{MS}}$ scheme
95	± 16	[53] GOUGH	97	LATT	$\overline{\text{MS}}$ scheme
100	$\pm 21 \pm 10$	[54] GUPTA	97	LATT	$\overline{\text{MS}}$ scheme
>100		[55] LELLOUCH	97	THEO	$\overline{\text{MS}}$ scheme
140	± 24	[56] JAMIN	95	THEO	$\overline{\text{MS}}$ scheme

[28] AOKI 03 uses quenched lattice simulation of the meson and baryon masses with degenerate light quarks. The extrapolations are done using quenched chiral perturbation theory. Determines $m_s = 113.8 \pm 2.3^{+5.8}_{-2.9}$ using K mass as input and $m_s = 142.3 \pm 5.8^{+22}_{-0}$ using ϕ mass as input. We have performed a weighted average of these values.

[29] AOKI 03B uses lattice simulation of the meson and baryon masses with two dynamical light quarks. Simulations are performed using the $\mathcal{O}(a)$ improved Wilson action.

[30] BECIREVIC 03 perform quenched lattice computation using the vector and axial Ward identities. Uses $\mathcal{O}(a)$ improved Wilson action and nonperturbative renormalization. They also quote $\overline{m}/m_s = 24.3 \pm 0.2 \pm 0.6$.

[31] GAMIZ 03 determines m_s from SU(3) breaking in the τ hadronic width. The value of V_{us} is chosen to satisfy CKM unitarity.

[32] GAMIZ 03 determines m_s from SU(3) breaking in the τ hadronic width. The value of V_{us} is taken from the PDG.

[33] ALIKHAN 02 uses lattice simulation of the meson and baryon masses with two dynamical flavors and degenerate light quarks. The above value uses the K-meson mass to determine m_s. If the ϕ meson is used, the number changes to 90^{+5}_{-10}.

[34] CHIU 02 extracts the strange quark mass from quenched lattice simulations using quenched chiral perturbation theory.

[35] JAMIN 02 calculates the strange quark mass from QCD sum rules using the scalar channel.

[36] MALTMAN 02 uses finite energy sum rules in the ud and us pseudoscalar channels. Other mass values are also obtained by similar methods.

[37] CHEN 01B uses an analysis of the hadronic spectral function in τ decay.

[38] KOERNER 01 obtain the s quark mass of $m_s(m_\tau) = 130 \pm 27(\text{exp}) \pm 9(\text{thy})$ MeV from an analysis of Cabibbo suppressed τ decays. We have converted this to $\mu = 2$ GeV.

[39] AOKI 00 obtain the light quark masses from a quenched lattice simulation of the meson and baryon spectrum with the Wilson quark action. We have averaged their results of $m_s = 115.6 \pm 2.3$ and $m_s = 143.7 \pm 5.8$ obtained using m_K and m_ϕ, respectively, to normalize the spectrum.

[40] GOECKELER 00 obtained from a quenched lattice computation of the pseudoscalar meson masses using $\mathcal{O}(a)$ improved Wilson fermions and nonperturbative renormalization.

[41] AOKI 99 obtain the light quark masses from a quenched lattice simulation of the meson spectrum with the Staggered quark action employing the regularization independent scheme. We have averaged their results of $m_s = 106.0 \pm 7.1$ and $m_s = 129 \pm 12$ obtained using m_K and m_ϕ, respectively, to normalize the spectrum.

[42] BARATE 99R obtain the strange quark mass from an analysis of the observed mass spectra in τ decay. We have converted their value of $m_s(m_\tau) = 176^{+46}_{-57}$ MeV to μ=2 GeV.

[43] MALTMAN 99 determines the strange quark mass using finite energy sum rules.

[44] NARISON 99 uses sum rules to order α_s^3 for ϕ meson decays.

[45] PICH 99 obtain the s-quark mass from an analysis of the moments of the invariant mass distribution in τ decays.

[46] BECIREVIC 98 compute the quark mass using the Alpha action in the quenched approximation. The conversion from the regularization independent scheme to the $\overline{\text{MS}}$ scheme is at NNLO.

[47] CHETYRKIN 98 uses spectral moments of hadronic τ decays to determine $m_s(1\ \text{GeV}) = 200 \pm 70$ MeV. We have rescaled the result to μ=2 GeV.

[48] CUCCHIERI 98 obtains the quark mass using a quenched lattice computation of the hadronic spectrum.

[49] DOMINGUEZ 98 uses hadronic spectral function sum rules (to four loops, and including dimension six operators) to determine $m_s(1\ \text{GeV}) < 155 \pm 25$ MeV. We have rescaled the result to μ=2 GeV.

[50] CHETYRKIN 97 obtains 205.5 $\pm$ 19.1 MeV at μ=1 GeV from QCD sum rules including fourth-order QCD corrections. We have rescaled the result to 2 GeV.

[51] COLANGELO 97 is QCD sum rule computation. We have rescaled $m_s(1\ \text{GeV}) > 120$ to $\mu = 2$ GeV.

[52] EICKER 97 use lattice gauge computations with two dynamical light flavors.

[53] GOUGH 97 use lattice gauge computations in the quenched approximation. Correcting for quenching gives $54 < m_s < 92$ MeV at μ=2 GeV.

[54] GUPTA 97 use Lattice Monte Carlo computations in the quenched approximation. The value for two light dynamical flavors at $\mu = 2$ GeV is 68 $\pm$ 12 $\pm$ 7 MeV.

[55] LELLOUCH 97 obtain lower bounds on quark masses using hadronic spectral functions.

[56] JAMIN 95 uses QCD sum rules at next-to-leading order. We have rescaled $m_s(1\ \text{GeV}) = 189 \pm 32$ to $\mu = 2$ GeV.

LIGHT QUARK MASS RATIOS

u/d MASS RATIO

VALUE		DOCUMENT ID		TECN	COMMENT
0.3 to 0.7 OUR EVALUATION					
• • • We do not use the following data for averages, fits, limits, etc. • • •					
0.410 $\pm$ 0.036		[57] NELSON	03	LATT	$\overline{\text{MS}}$ scheme
0.44		[58] GAO	97	THEO	$\overline{\text{MS}}$ scheme
0.553 $\pm$ 0.043		[59] LEUTWYLER	96	THEO	Compilation
< 0.3		[60] CHOI	92	THEO	
0.26		[61] DONOGHUE	92	THEO	
0.30	$\pm$ 0.07	[62] DONOGHUE	92B	THEO	
0.66		[63] GERARD	90	THEO	
0.4	to 0.65	[64] LEUTWYLER	90B	THEO	
0.05	to 0.78	[65] MALTMAN	90	THEO	

[57] NELSON 03 computes coefficients in the order p^4 chiral Lagrangian using a lattice calculation with three dynamical flavors. The ratio m_u/m_d is obtained by combining this with the chiral perturbation theory computation of the meson masses to order p^4.

[58] GAO 97 uses electromagnetic mass splittings of light mesons.

[59] LEUTWYLER 96 uses a combined fit to $\eta \to 3\pi$ and $\psi' \to J/\psi\ (\pi,\eta)$ decay rates, and the electromagnetic mass differences of the π and K.

[60] CHOI 92 result obtained from the decays $\psi(2S) \to J/\psi(1S)\pi$ and $\psi(2S) \to J/\psi(1S)\eta$, and a dilute instanton gas estimate of some unknown matrix elements.

[61] DONOGHUE 92 result is from a combined analysis of meson masses, $\eta \to 3\pi$ using second-order chiral perturbation theory including nonanalytic terms, and $(\psi(2S) \to J/\psi(1S)\pi)/(\psi(2S) \to J/\psi(1S)\eta)$.

[62] DONOGHUE 92B computes quark mass ratios using $(\psi(2S) \to J/\psi(1S)\pi)/(\psi(2S) \to J/\psi(1S)\eta)$, and an estimate of L_{14} using Weinberg sum rules.

[63] GERARD 90 uses large N and η-η' mixing.

[64] LEUTWYLER 90B determines quark mass ratios using second-order chiral perturbation theory for the meson and baryon masses, including nonanalytic corrections. Also uses Weinberg sum rules to determine L_7.

[65] MALTMAN 90 uses second-order chiral perturbation theory including nonanalytic terms for the meson masses. Uses a criterion of "maximum reasonableness" that certain coefficients which are expected to be of order one are ≤ 3.

s/d MASS RATIO

VALUE		DOCUMENT ID		TECN	COMMENT
17 to 22 OUR EVALUATION					
• • • We do not use the following data for averages, fits, limits, etc. • • •					
20.0		[66] GAO	97	THEO	$\overline{\text{MS}}$ scheme
18.9 $\pm$ 0.8		[67] LEUTWYLER	96	THEO	Compilation
21		[68] DONOGHUE	92	THEO	
18		[69] GERARD	90	THEO	
18	to 23	[70] LEUTWYLER	90B	THEO	

[66] GAO 97 uses electromagnetic mass splittings of light mesons.

[67] LEUTWYLER 96 uses a combined fit to $\eta \to 3\pi$ and $\psi' \to J/\psi\ (\pi,\eta)$ decay rates, and the electromagnetic mass differences of the π and K.

[68] DONOGHUE 92 result is from a combined analysis of meson masses, $\eta \to 3\pi$ using second-order chiral perturbation theory including nonanalytic terms, and $(\psi(2S) \to J/\psi(1S)\pi)/(\psi(2S) \to J/\psi(1S)\eta)$.

[69] GERARD 90 uses large N and η-η' mixing.

[70] LEUTWYLER 90B determines quark mass ratios using second-order chiral perturbation theory for the meson and baryon masses, including nonanalytic corrections. Also uses Weinberg sum rules to determine L_7.

$(m_s - \overline{m})/(m_d - m_u)$ MASS RATIO

$\overline{m} \equiv (m_u + m_d)/2$

VALUE	DOCUMENT ID		TECN
30 to 50 OUR EVALUATION			
• • • We do not use the following data for averages, fits, limits, etc. • • •			
	[71] ANISOVICH	96	THEO
36 $\pm$ 5	[72] NEFKENS	92	THEO
45 $\pm$ 3	[73] NEFKENS	92	THEO

[71] ANISOVICH 96 find Q=22.7 $\pm$ 0.8 with $Q^2 \equiv (m_s^2 - \overline{m}^2)/(m_d^2 - m_s^2)$ from $\eta \to \pi^+\pi^-\pi^0$ decay using dispersion relations and chiral perturbation theory.

[72] NEFKENS 92 result is from an analysis of meson masses, mixing, and decay.

[73] NEFKENS 92 result is from an analysis of of baryon masses.

LIGHT QUARKS (u, d, s) REFERENCES

AOKI	03	PR D67 034503	S. Aoki *et al.*	(CP-PACS Collab.)
AOKI	03B	PR D68 054502	S. Aoki *et al.*	(CP-PACS Collab.)
BECIREVIC	03	PL B558 69	D. Becirevic, V. Lubicz, C. Tarantino	
GAMIZ	03	JHEP 0301 060	E. Gamiz *et al.*	
NELSON	03	PRL 90 021601	D. Nelson, G.T. Fleming, G.W. Kilcup	
ALIKHAN	02	PR D65 054505	A. Ali Khan *et al.*	(CP-PACS Collab.)
Also	03	PR D67 059901 (erratum)	A. Ali Khan *et al.*	(CP-PACS Collab.)
CHIU	02	PL B538 298	T.-W. Chiu, T.-H. Hsieh	
JAMIN	02	EPJ C24 237	M. Jamin, J.A. Oller, A. Pich	
MALTMAN	02	PR D65 074013	K. Maltman, J. Kambor	
CHEN	01B	EPJ C22 31	S. Chen *et al.*	
KOERNER	01	EPJ C20 259	J.G. Koerner, F. Krajewski, A.A. Pivovarov	
MALTMAN	01	PL B517 332	K. Maltman, J. Kambor	
AOKI	00	PRL 84 238	S. Aoki *et al.*	(CP-PACS Collab.)
GOECKELER	00	PR D62 054504	M. Goeckeler *et al.*	
AOKI	99	PRL 82 4392	S. Aoki *et al.*	(JLQCD Collab.)
BARATE	99R	EPJ C11 599	R. Barate *et al.*	(ALEPH Collab.)
MALTMAN	99	PL B462 195	K. Maltman	
NARISON	99	PL B466 345	S. Narison	
PICH	99	JHEP 9910 004	A. Pich, J. Prades	
STEELE	99	PL B451 201	T.G. Steele, K. Kostuik, J. Kwan	
BECIREVIC	98	PL B444 401	D. Becirevic *et al.*	
CHETYRKIN	98	NP B533 473	K.G. Chetyrkin, J.H. Kuehn, A.A. Pivovarov	
CUCCHIERI	98	PL B422 212	A. Chucchieri *et al.*	
DOMINGUEZ	98	PL B425 193	C.A. Dominguez, L. Pirovano, K. Schilcher	
DOSCH	98	PL B417 173	H.G. Dosch, S. Narison	
PRADES	98	NPBPS 64 253	J. Prades	
CHETYRKIN	97	PL B404 337	K.G. Chetyrkin, D. Pirjol, K. Schilcher	
COLANGELO	97	PL B408 340	P. Colangelo *et al.*	
EICKER	97	PL B407 290	N. Eicker *et al.*	(SESAM Collab.)
GAO	97	PR D56 4115	D.-N. Gao, B.A. Li, M.-L. Yan	
GOUGH	97	PRL 79 1622	B. Gough *et al.*	
GUPTA	97	PR D55 7203	R. Gupta, T. Bhattacharya	
LELLOUCH	97	PL B414 195	L. Lellouch, E. de Rafael, J. Taron	
ANISOVICH	96	PL B375 335	A.V. Anisovich, H. Leutwyler	
LEUTWYLER	96	PL B378 313	H. Leutwyler	
BIJNENS	95	PL B348 226	J. Bijnens, J. Prades, E. de Rafael	(NORD, BOHR+)
JAMIN	95	ZPHY C66 633	M. Jamin, M. Munz	(HEIDT, MUNT)
NARISON	95C	PL B358 113	S. Narison	(MONP)
CHOI	92	PL B292 159	K.W. Choi	(UCSD)
DONOGHUE	92	PRL 69 3444	J.F. Donoghue, B.R. Holstein, D. Wyler	(MASA+)
DONOGHUE	92B	PR D45 892	J.F. Donoghue, D. Wyler	(MASA, ZURI, UCSBT)
NEFKENS	92	CNPP 20 221	B.M.K. Nefkens, G.A. Miller, I. Slaus	(UCLA+)
GERARD	90	MPL A5 391	J.M. Gerard	(MPIM)
LEUTWYLER	90B	NP B337 108	H. Leutwyler	(BERN)
MALTMAN	90	PL B234 158	K. Maltman, T. Goldman, Stephenson Jr.	(YORKC+)

c

$I(J^P) = 0(\frac{1}{2}^+)$

Charge = $\frac{2}{3}$ e Charm = +1

c-QUARK MASS

The c-quark mass corresponds to the "running" mass m_c ($\mu = m_c$) in the $\overline{\text{MS}}$ scheme. We have converted masses in other schemes to the $\overline{\text{MS}}$ scheme using two-loop QCD perturbation theory with $\alpha_s(\mu{=}m_c) = 0.39$. The range 1.0–1.4 GeV for the $\overline{\text{MS}}$ mass corresponds to 1.47–1.83 GeV for the pole mass (see the "Note on Quark Masses").

VALUE (GeV)	DOCUMENT ID		TECN	COMMENT
1.15 to 1.35 OUR EVALUATION				
• • • We do not use the following data for averages, fits, limits, etc. • • •				
1.19 $\pm$ 0.11	[1] EIDEMULLER	03	THEO	$\overline{\text{MS}}$ scheme
1.289 $\pm$ 0.043	[2] ERLER	03	THEO	$\overline{\text{MS}}$ scheme
1.26 $\pm$ 0.02	[3] ZYABLYUK	03	THEO	$\overline{\text{MS}}$ scheme
1.26 $\pm$ 0.04 $\pm$ 0.12	[4] BECIREVIC	02	LATT	$\overline{\text{MS}}$ scheme
1.301 $\pm$ 0.034	[5] ROLF	02	LATT	$\overline{\text{MS}}$ scheme
1.23 $\pm$ 0.09	[6] EIDEMULLER	01	THEO	$\overline{\text{MS}}$ scheme
1.304 $\pm$ 0.027	[7] KUHN	01	THEO	$\overline{\text{MS}}$ scheme
1.04 $\pm$ 0.04	[8] MARTIN	01	THEO	$\overline{\text{MS}}$ scheme
1.1 $\pm$ 0.04	[9] NARISON	01B	THEO	$\overline{\text{MS}}$ scheme
1.37 $\pm$ 0.09	[10] PENARROCHA	01	THEO	$\overline{\text{MS}}$ scheme
1.210 $\pm$ 0.070 $\pm$ 0.080	[11] PINEDA	01	THEO	$\overline{\text{MS}}$ scheme
1.3 $\pm$ 0.3 $\pm$ 0.3	[12] ASTIER	00D	NOMD	
1.79 $\pm$ 0.38	[13] VILAIN	99	THEO	$\overline{\text{MS}}$ scheme

[1] EIDEMULLER 03 determines m_b and m_c using QCD sum rules.

[2] ERLER 03 determines m_b and m_c using QCD sum rules. Includes recent BES data.

[3] ZYABLYUK 03 determines m_c by using QCD sum rules in the pseudoscalar channel and comparing with the η_c mass.

[4] BECIREVIC 02 uses Monte-Carlo calculations of lattice Ward identities and the D_s mass. The authors estimate an error of about 5% for use of the quenched approximation, not included in systematic error of 0.12.

[5] ROLF 02 determines m_c from a quenched lattice calculation of the D_s mass. The error estimate is for all systematics except the quenched approximation, including lattice spacing effects, finite volume effects, excited states contamination, rounding errors, and the scale uncertainty. The authors estimate the uncertainty due to the quenched approximation may be about 3%.

[6] EIDEMULLER 01 result is QCD sum rule analysis of charmonium using NRQCD at next-to-next-to-leading order.

[7] KUHN 01 uses an analysis of the e^+e^- total cross section to hadrons.

[8] MARTIN 01 obtain a pole mass of 1.33–1.4 GeV from an analysis of R, the rate for $e^+e^- \to$ hadrons. We have converted this to the $\overline{\text{MS}}$ scheme using the two-loop formula.

[9] NARISON 01B uses pseudoscalar sum rules in the B and D meson channels.

[10] PENARROCHA 01 result is from an analysis of the BES-II e^+e^- data using finite energy sum rules.

[11] PINEDA 01 uses the $\Upsilon(1S)$ system and the B-D mass difference to determine m_c. The errors are due to theory, and the uncertainty in λ_1 and m_b.

[12] Study of opposite sign dimuon events.

[13] VILAIN 99 obtain the charm quark mass from an analysis of charm production in neutrino scattering.

c-QUARK REFERENCES

EIDEMULLER	03	PR D67 113002	M. Eidemuller	
ERLER	03	PL B558 125	J. Erler, M. Luo	
ZYABLYUK	03	JHEP 0301 081	K.N. Zyablyuk	(ITEP)
BECIREVIC	02	PL B524 115	D. Becirevic, V. Lubicz, G. Martinelli	
ROLF	02	JHEP 0212 007	J. Rolf, S. Sint	
EIDEMULLER	01	PL B498 203	M. Eidemueller, M. Jamin	
KUHN	01	NP B619 588	J.H. Kuhn, M. Steinhauser	
MARTIN	01	EPJ C19 681	A.D. Martin, J. Outhwaite, M.G. Ryskin	
NARISON	01B	PL B520 115	S. Narison	
PENARROCHA	01	PL B515 291	J. Penarrocha, K. Schilcher	
PINEDA	01	JHEP 0106 022	A. Pineda	
ASTIER	00D	PL B486 35	P. Astier *et al.*	(CERN NOMAD Collab.)
VILAIN	99	EPJ C11 19	P. Vilain *et al.*	(CHARM II Collab.)

b

$I(J^P) = 0(\frac{1}{2}^+)$

Charge $= -\frac{1}{3}\,e$ Bottom $= -1$

b-QUARK MASS

The first value is the "running mass" $\overline{m}_b(\mu = \overline{m}_b)$ in the $\overline{\text{MS}}$ scheme, and the second value is the $1S$ mass, which is half the mass of the $\Upsilon(1S)$ in perturbation theory. For a review of different quark mass definitions and their properties, see EL-KHADRA 02. The $1S$ mass is better suited for use in analyzing B decays than the $\overline{\text{MS}}$ mass because it gives a stable perturbative expansion. We have converted masses in other schemes to the $\overline{\text{MS}}$ mass and $1S$ mass using two-loop QCD perturbation theory with $\alpha_s(\mu = \overline{m}_b) = 0.22$. The range 4.1–4.4 for the $\overline{\text{MS}}$ mass corresponds to 4.6–4.9 for the $1S$ mass and 4.7–5.0 GeV for the pole mass.

$\overline{\text{MS}}$ MASS (GeV)	1S MASS (GeV)	DOCUMENT ID		TECN
4.1 to 4.4 OUR EVALUATION	of $\overline{\text{MS}}$ Mass			
4.6 to 4.9 OUR EVALUATION	of $1S$ Mass			
• • • We do not use the following data for averages, fits, limits, etc. • • •				
4.22 ±0.09	4.74 ± 0.10	[1] BAUER	03	THEO
4.19 ±0.05	4.66 ± 0.05	[2] BORDES	03	THEO
4.20 ±0.09	4.67 ± 0.10	[3] CORCELLA	03	THEO
4.24 ±0.10	4.72 ± 0.11	[4] EIDEMULLER	03	THEO
4.207±0.031	4.682 ± 0.035	[5] ERLER	03	THEO
4.33 ±0.06 ±0.10	4.82 ± 0.07 ± 0.11	[6] MAHMOOD	03	THEO
4.346±0.070	4.837 ± 0.078	[7] PENIN	02	THEO
3.95 ±0.57	4.40 ± 0.63	[8] ABBIENDI	01S	OPAL
4.21 ±0.05	4.69 ± 0.06	[9] KUHN	01	THEO
4.05 ±0.06	4.51 ± 0.07	[10] NARISON	01B	THEO
4.210±0.090±0.025	4.69 ± 0.100 ± 0.028	[11] PINEDA	01	THEO
4.7 ±0.74	5.23 ± 0.82	[12] BARATE	00V	ALEP
4.20 ±0.06	4.71 ± 0.03	[13] HOANG	00	THEO
$4.437^{+0.045}_{-0.029}$	$4.938^{+0.050}_{-0.032}$	[14] LUCHA	00	THEO
$4.454^{+0.045}_{-0.029}$	$4.957^{+0.050}_{-0.032}$	[14] PINEDA	00	THEO
4.25 ±0.08	4.73 ± 0.09	[15] BENEKE	99	THEO
$3.8\ ^{+0.77}_{-2.0}$	$4.23^{+0.86}_{-2.0}$	[16] BRANDENB...	99	
4.25 ±0.09	4.73 ± 0.10	[17] HOANG	99	THEO
4.2 ±0.1	4.67 ± 0.11	[18] MELNIKOV	99	THEO
4.21 ±0.11	4.69 ± 0.12	[19] PENIN	99	THEO
3.91 ±0.67	4.35 ± 0.75	[20] ABREU	98I	DLPH
4.14 ±0.04	4.61 ± 0.05	[21] KUEHN	98	THEO
4.15 ±0.05 ±0.20	4.62 ± 0.06 ± 0.22	[22] GIMENEZ	97	LATT
4.19 ±0.06	4.66 ± 0.07	[23] JAMIN	97	THEO
4.16 ±0.32 ±0.60	4.63 ± 0.36 ± 0.67	[24] RODRIGO	97	THEO

[1] BAUER 03 determine the b quark mass by a global fit to B decay observables. The experimental data includes lepton energy and hadron invariant mass moments in semileptonic $B \to X_c \ell \nu_\ell$ decay, and the inclusive photon spectrum in $B \to X_s \gamma$ decay. The theoretical expressions used are of order $1/m^3$, and $\alpha_s^2\beta_0$.

[2] BORDES 03 determines m_b using QCD finite energy sum rules to order α_s^2.

[3] CORCELLA 03 determines $\overline{m}_b$ using sum rules computed to order α_s^2. Includes charm quark mass effects.

[4] EIDEMULLER 03 determines $\overline{m}_b$ and $\overline{m}_c$ using QCD sum rules.

[5] ERLER 03 determines $\overline{m}_b$ and $\overline{m}_c$ using QCD sum rules. Includes recent BES data.

[6] MAHMOOD 03 determines m_b^{1S} by a fit to the lepton energy moments in $B \to X_c \ell \nu_\ell$ decay. The theoretical expressions used are of order $1/m^3$ and $\alpha_s^2\beta_0$. We have converted their result to the $\overline{\text{MS}}$ scheme.

[7] PENIN 02 determines $\overline{m}_b$ from the spectrum of the Υ system.

[8] ABBIENDI 01S find $\overline{m}_b$ (M_Z) to be 2.67 ± 0.4 GeV from an analysis of $Z \to b$ decays.

[9] KUHN 01 uses an analysis of the e^+e^- total cross section to hadrons.

[10] NARISON 01B uses pseudoscalar sum rules in the B and D meson channels.

[11] PINEDA 01 uses the $\Upsilon(1S)$ system to determine the quark mass. The errors are due to theory, and the uncertainty in α_s.

[12] BARATE 00V obtain the b quark mass $\overline{m}_b(M_Z) = 3.27 \pm 0.22(\text{stat}) \pm 0.22(\text{exp}) \pm 0.38(\text{had}) \pm 0.16(\text{thy})$ from an analysis of event shape variables in Z decays. We have converted this to $\mu = \overline{m}_b$.

[13] HOANG 00 uses a NNLO calculation of the vacuum polarization function to determine spectral moments of the masses and electronic decay widths of the Υ mesons.

[14] LUCHA 00, PINEDA 00 obtain the b-quark mass from a perturbative calculation of the Υ spectrum and decay widths to order α_s^4.

[15] BENEKE 99 uses a calculation of the $b\overline{b}$ production cross section and the mass of the Υ meson at NNLO.

[16] BRANDENBURG 99 obtain a b-quark mass of $\overline{m}_b(M_Z) = 2.56 \pm 0.27^{+0.28}_{-0.38} {}^{+0.49}_{-1.48}$ from a study of three-jet events at the Z. We have converted this to $\mu = \overline{m}_b$.

[17] HOANG 99 uses a NNLO calculation of the vacuum polarization function to determine spectral moments of the masses and electronic decay widths of the Υ mesons.

[18] MELNIKOV 99 compute the quark mass using Υ sum rules at NNLO.

[19] PENIN 99 compute the quark mass using Υ sum rules at NNLO.

[20] ABREU 98I determines the $\overline{\text{MS}}$ mass $\overline{m}_b = 2.67 \pm 0.25 \pm 0.34 \pm 0.27$ GeV at $\mu = M_Z$ from three jet heavy quark production at LEP. ABREU 98I have rescaled the result to $\mu = \overline{m}_b$ using $\alpha_s = 0.118 \pm 0.003$.

[21] KUEHN 98 uses a calculation of the vacuum polarization function, including resumming threshold effects, to determine spectral moments of the masses of the Υ mesons. We have converted their extracted value of 4.75 ± 0.04 for the pole mass to the $\overline{\text{MS}}$ scheme.

[22] GIMENEZ 97 uses lattice computations of the B-meson propagator and the B-meson binding energy $\overline{\Lambda}$ in the HQET. Their systematic (second) error for the $\overline{\text{MS}}$ mass is an estimate of the effects of higher-order corrections in the matching of the HQET operators (renormalon effects).

[23] JAMIN 97 apply the QCD moment method to the Υ system. They also find a pole mass of 4.60 ± 0.02.

[24] RODRIGO 97 determines the $\overline{\text{MS}}$ mass $\overline{m}_b = 2.85 \pm 0.22 \pm 0.20 \pm 0.36$ GeV at $\mu = M_Z$ from three jet heavy quark production at LEP. We have rescaled the result.

b-QUARK REFERENCES

BAUER	03	PR D67 054012	C.W. Bauer *et al.*	
BORDES	03	PL B562 81	J. Bordes, J. Penarrocha, K. Schilcher	
CORCELLA	03	PL B554 133	G. Corcella, A.H. Hoang	
EIDEMULLER	03	PR D67 113002	M. Eidemuller	
ERLER	03	PL B558 125	J. Erler, M. Luo	
MAHMOOD	03	PR D67 072001	A.H. Mahmood *et al.*	(CLEO Collab.)
EL-KHADRA	02	ARNPS 52 201	A.X. El-Khadra, M. Luke	
PENIN	02	PL B538 335	A. Penin, M. Steinhauser	
ABBIENDI	01S	EPJ C21 411	G. Abbiendi *et al.*	(OPAL Collab.)
KUHN	01	NP B619 588	J.H. Kuhn, M. Steinhauser	
NARISON	01B	PL B520 115	S. Narison	
PINEDA	01	JHEP 0106 022	A. Pineda	
BARATE	00V	EPJ C18 1	R. Barate *et al.*	(ALEPH Collab.)
HOANG	00	PR D61 034005	A.H .Hoang	
LUCHA	00	PR D62 097501	W. Lucha, F.F. Schoeberl	
PINEDA	00	PR D61 077505	A. Pineda, F.J. Yndurain	
BENEKE	99	PL B471 233	M. Beneke, A. Signer	
BRANDENB...	99	PL B468 168	A. Brandenburg *et al.*	
HOANG	99	PR D59 014039	A.H. Hoang	
MELNIKOV	99	PR D59 114009	K. Melnikov, A. Yelkhovsky	
PENIN	99	NP B549 217	A.A. Penin, A.A. Pivovarov	
ABREU	98I	PL B418 430	P. Abreu *et al.*	(DELPHI Collab.)
KUEHN	98	NP B534 356	J.H. Kuehn, A.A. Penin, A.A. Pivovarov	
GIMENEZ	97	PL B393 124	V. Gimenez, G. Martinelli, C.T. Sachrajda	
JAMIN	97	NP B507 334	M. Jamin, A. Pich	
RODRIGO	97	PRL 79 193	G. Rodrigo, A. Santamaria, M.S. Bilenky	

t

$I(J^P) = 0(\frac{1}{2}^+)$

Charge $= \frac{2}{3}\,e$ Top $= +1$

THE TOP QUARK

Updated January 2004 by M. Mangano (CERN) and T. Trippe (LBNL).

A. Introduction: The top quark is the $Q = 2/3$, $T_3 = +1/2$ member of the weak-isospin doublet containing the bottom quark (see our review on the "Standard Model of Electroweak Interactions" for more information). This note summarizes its currently measured properties, and provides a discussion of the experimental and theoretical issues involved in the determination of its parameters (mass, production cross section, decay branching ratios, *etc.*).

B. Top quark production at the Tevatron: All direct measurements of top quark production and decay have been made by the CDF and DØ experiments at the Fermilab Tevatron collider in $p\overline{p}$ collisions. The first observations and studies have been performed during the so-called run I, at $\sqrt{s} = 1.8$ TeV, completed in 1996. Most of the results in this note refer to analyses of these data. A new period of data-taking, the run II, started in 2001 at $\sqrt{s} = 1.96$ TeV. All analyses from run II are still only preliminary and yet unpublished [1]. The main body of this note will therefore only quote results relative to the run I data, with some highlights of current run II results included in an Appendix.

In hadron collisions, top quarks are produced dominantly in pairs from the QCD processes $q\overline{q} \to t\overline{t}$ and $gg \to t\overline{t}$. At 1.8 TeV (1.96 TeV), the production cross section [2] in these channels is expected to be approximately 5 pb (6.5 pb) for $m_t = 175$ GeV/c^2, with a 90% (85%) contribution from $q\overline{q}$ annihilation. Smaller contributions are expected from electroweak single-top production mechanisms, namely $q\overline{q'} \to W^* \to t\overline{b}$ and $qg \to q't\overline{b}$, the latter mediated by virtual-W exchange ("W-gluon fusion"). The combined rate of these processes at 1.8 TeV is approximately 2.5 pb at $m_t = 175$ GeV/c^2 (see Ref. 3 and references therein). The expected contribution of these channels is further reduced relative to the dominant pair-production mechanisms because of larger backgrounds and poor detection efficiency.

With a mass above the Wb threshold, the decay width of the top quark is expected to be dominated by the two-body channel $t \to Wb$. Neglecting terms of order m_b^2/m_t^2, α_s^2 and those of order $(\alpha_s/\pi)m_W^2/m_t^2$, this is predicted in the Standard Model to be [4]:

$$\Gamma_t = \frac{G_F m_t^3}{8\pi\sqrt{2}} \left(1 - \frac{M_W^2}{m_t^2}\right)^2 \left(1 + 2\frac{M_W^2}{m_t^2}\right) \left[1 - \frac{2\alpha_s}{3\pi}\left(\frac{2\pi^2}{3} - \frac{5}{2}\right)\right]. \quad (1)$$

The use of G_F in this equation accounts for the largest part of the one-loop electroweak radiative corrections, providing an expression accurate to better than 2%. The width increases with mass, going for example from 1.02 GeV/c^2 at $m_t = 160$ GeV/c^2 to 1.56 GeV/c^2 at $m_t = 180$ GeV/c^2 (we used $\alpha_S(\mathrm{M_Z}) = 0.118$). With such a correspondingly short lifetime, the top quark is expected to decay before top-flavored hadrons or $t\overline{t}$-quarkonium bound states can form [5]. The order α_s^2 QCD corrections to Γ_t have also been calculated [6], thereby improving the overall theoretical accuracy to better than 1%.

In top decay, the Ws and Wd final states are expected to be suppressed relative to Wb by the square of the CKM matrix elements V_{ts} and V_{td}, whose values can be estimated under the assumption of unitarity of the three-generation CKM matrix to be less than 0.043 and 0.014, respectively (see our review "The Cabibbo-Kobayashi-Maskawa Mixing Matrix" in the current edition for more information). Typical final states for the leading pair-production process therefore belong to three classes:

A. $t\overline{t} \to W\,b\,W\,\overline{b} \to q\,\overline{q'}\,b\,q''\,\overline{q'''}\,\overline{b}$,

B. $t\overline{t} \to W\,b\,W\,\overline{b} \to q\,\overline{q'}\,b\,\ell\,\overline{\nu}_\ell\,\overline{b} + \overline{\ell}\,\nu_\ell\,b\,q\,\overline{q'}\,\overline{b}$,

C. $t\overline{t} \to W\,b\,W\,\overline{b} \to \overline{\ell}\,\nu_\ell\,b\,\ell'\,\overline{\nu}_{\ell'}\,\overline{b}$,

where A, B, and C are referred to as the all-jets, lepton + jets, and dilepton channels, respectively. While ℓ in the above processes refers to e, μ, or τ, throughout the rest of this article, the meaning of ℓ is restricted to an observed e or μ.

The final state quarks can emit radiation and will eventually evolve into jets of hadrons. The precise number of jets reconstructed by the detectors varies event by event, as it depends on the decay kinematics, as well as on the precise definition of jet used in the analysis. (Additional gluon radiation can also be emitted from the initial states.) The transverse momenta of the neutrinos are reconstructed via the large imbalance in detected transverse momentum of the event (missing E_T).

The observation of $t\overline{t}$ pairs has been reported in all of the above decay modes. As discussed below, the production and decay properties of the top quark extracted from the above three decay channels are all consistent with each other within experimental uncertainty. In particular, the $t \to Wb$ decay mode is supported through the reconstruction of the $W \to jj$ invariant mass in the $\ell\nu_\ell b\overline{b}jj$ final state [7].

The extraction of top-quark properties from Tevatron data requires a good understanding of the production and decay mechanisms of the top, as well as of the large background processes. Because only leading order QCD calculations are available for most of the relevant processes (W+3 and 4 jets, or WW+2 jets), theoretical estimates of the backgrounds have large uncertainties. While this limitation affects estimates of the overall $t\overline{t}$ production rates, it is believed that the LO determination of the event kinematics and of the fraction of W + multi-jet events containing b quarks is relatively accurate. In particular, for the background one expects the E_T spectrum of jets to fall rather steeply, the jet direction to peak at small angles to the beams, and the fraction of events with b quarks to be of the order of a few percent. On the contrary, for the top signal, the b fraction is $\sim 100\%$ and the jets are rather energetic, since they come from the decay of a massive object. It is therefore possible to improve the S/B ratio either by requiring the presence of a b quark, or by selecting very energetic and central kinematic configurations.

A detailed study of control samples with features similar to those of the relevant backgrounds, but free from possible top contamination, is required to provide a reliable check on background estimates.

C. Measured top properties: Current measurements of top properties based on the run I data use an integrated luminosity of 109 pb^{-1} for CDF and 125 pb^{-1} for DØ. DØ and CDF determine the $t\overline{t}$ cross section $\sigma_{t\overline{t}}$ from their number of observed top candidates, estimated background, $t\overline{t}$ acceptance, and integrated luminosity, assuming the Standard-Model decay $t \to Wb$ with unity branching ratio. Table 1 shows the measured cross sections from DØ and CDF along with the range of theoretical expectations, evaluated at the m_t values used by the experiments in calculating their acceptances. The DØ values we quote [9] reflect the final analysis of the run I data, and are adjusted to the current DØ value of the top mass. The agreement of both DØ and CDF $t\overline{t}$ cross sections with theory supports the hypothesis that the excess of events over background in all of these channels can be attributed to $t\overline{t}$ production.

More precise measurements of the top production cross section will test current understanding of the production mechanisms.This is important for the extrapolation to higher energies of colliders such as the LHC, where the larger expected cross section will permit more extensive studies [15]. The results

Table 1: Cross section for $t\bar{t}$ production in $p\bar{p}$ collisions at $\sqrt{s} = 1.8$ TeV from DØ ($m_t = 172.1$ GeV/c^2), CDF ($m_t = 175$ GeV/c^2), and theory.

$\sigma_{t\bar{t}}(pb)$	Source	Ref.	Method
2.8 ± 2.1	DØ	[8,9]	e + jets/topological
5.6 ± 3.7	DØ	[8,9]	μ + jets/topological
6.0 ± 3.6	DØ	[8,9]	e + jets/soft μ b-tag
11.3 ± 6.6	DØ	[8,9]	μ + jets/soft μ b-tag
5.1 ± 1.9	DØ	[8,9]	all ℓ + jets combined
6.0 ± 3.2	DØ	[8,9]	$\ell\ell + e\nu$
7.3 ± 3.2	DØ	[9,10]	all jets
5.7 ± 1.6	DØ	[9,10]	all combined
$5.2 - 6.2$	Theory	[2]	$m_t = 172.1$ GeV/c^2
5.1 ± 1.5	CDF	[11,14]	ℓ + jets/vtx b-tag
9.2 ± 4.3	CDF	[11,14]	ℓ + jets/soft ℓ b-tag
$8.4^{+4.5}_{-3.5}$	CDF	[12,14]	$\ell\ell$
$7.6^{+3.5}_{-2.7}$	CDF	[13,14]	all jets
$6.5^{+1.7}_{-1.4}$	CDF	[14]	all combined
$4.5 - 5.7$	Theory	[2]	$m_t = 175$ GeV/c^2

of preliminary analyses of the run II data are given in the Appendix: the current statistical and systematic uncertainties are still too large to draw any conclusion. With the expected improvements once larger samples have been collected, discrepancies in rate between theory and data would be quite exciting, and might indicate the presence of exotic production or decay channels, as predicted in certain models. Such new sources of top would lead to a modification of kinematic distributions such as the invariant mass of the top pair or the transverse momentum of the top quark. Studies by CDF of the former [16] and of the latter [17] distributions, show no deviation from expected QCD behavior. DØ [18] also finds these kinematic distributions consistent with Standard Model expectations.

The top mass has been measured in the lepton + jets and dilepton channels by both DØ and CDF, and in the all-jets channel by CDF. At present, the most precise measurements come from the lepton + jets channel, with four or more jets and large missing E_T. In this channel, each event is subjected to a two-constraint kinematic fit to the hypothesis $t\bar{t} \to W^+ b W^- \bar{b} \to \ell \nu_\ell q \bar{q}' b \bar{b}$, assuming that the four highest E_T jets are the quarks from $t\bar{t}$ decay. The shape of the distribution of fitted top masses from these events is compared to templates expected from a mixture of background and signal distributions for a series of assumed top masses. This comparison yields values of the likelihood as a function of top mass, from which a best value of the top mass and its uncertainty can be obtained. The results are shown in Table 2. The systematic uncertainty (second uncertainty shown) is comparable to the statistical uncertainty, and is primarily due to uncertainties in the jet energy scale and in the Monte Carlo modeling.

Less precise determinations of the top mass come from the dilepton channel with two or more jets and large missing E_T, and from the all-jets channel. In the dilepton channel, a kinematically constrained fit is not possible because there are two missing neutrinos, so experiments must use other mass estimators than the reconstructed top mass. In principle, any quantity which is correlated with the top mass can be used as such an estimator. The DØ method uses the fact that if a value for m_t is assumed, the $t\bar{t}$ system can be reconstructed (up to a four-fold ambiguity). They compare the resulting kinematic configurations to expectations from $t\bar{t}$ production, and obtain an m_t-dependent weight curve for each event, which they histogram in five bins to obtain four shape-sensitive quantities as their multidimensional mass estimator. This method yields a significant increase in precision over one-dimensional estimators. CDF has employed a similar method, thereby reducing their previous systematic uncertainty in the $\ell\ell$ + jets channel by a factor of two. DØ and CDF obtain the top mass and uncertainty from these mass estimators using the same type of template likelihood method as for the lepton + jets channel. CDF also measures the mass in the all-jets channel using events with six or more jets, at least one of which is tagged as a b jet through the detection of a secondary vertex.

Table 2: Top mass measurements from DØ and CDF.

m_t (GeV/c^2)	Source	Ref.	Method
$173.3 \pm 5.6 \pm 5.5$	DØ	[18]	ℓ + jets
$(180.1 \pm 3.6 \pm 4.0)$ †	DØ	[19]	ℓ + jets
$168.4 \pm 12.3 \pm 3.6$	DØ	[20]	$\ell\ell$
$172.1 \pm 5.2 \pm 4.9$	DØ	[18]	DØ comb.
$176.1 \pm 5.1 \pm 5.3$	CDF	[21–23]	ℓ + jets
$167.4 \pm 10.3 \pm 4.8$	CDF	[21]	$\ell\ell$
$186.0 \pm 10.0 \pm 5.7$	CDF	[13,21]	all jets
176.1 ± 6.6	CDF	[21,23]	CDF comb.
$174.3 \pm 3.2 \pm 4.0$ *	DØ & CDF	[24]	PDG best

† DØ finds a significantly improved preliminary result for the mass, using the same data as for the Ref. 18 result, but analyzed using a method similar to that of their dilepton analysis. This value is not used in the "DØ combined" mass of 172.1 GeV/c^2, nor in the "PDG best" (DØ & CDF combined) mass.

* PDG uses this Top Averaging Group result as its best value. In spite of the new ℓ+jets CDF result [23], this average, given in Ref. 24, still applies within rounding errors.

As seen in Table 2, all results are in good agreement with a unique mass for the top quark, giving further support to the hypothesis that these events are due to $t\bar{t}$ production. The Top Averaging Group, a joint CDF/DØ working group, produced the combined CDF/DØ average top mass in Table 2, taking

into account correlations between systematic uncertainties in different measurements. They assume that the uncertainty in jet energy scale is completely correlated within CDF and within DØ but uncorrelated between the two experiments, and that the signal model and Monte Carlo generator uncertainties are completely correlated between all measurements. The uncertainties from uranium noise and multiple interactions relate only to DØ and are assumed completely correlated between their two measurements. The uncertainty on the background model is taken to be completely correlated between the CDF and the DØ ℓ+jets measurements, and similarly for the $\ell\ell$ measurements. The Particle Data Group uses this combined top mass, $m_t = 174.3 \pm 5.1$ GeV/c^2 (statistical and systematic uncertainties combined in quadrature), as our PDG best value.

Given the experimental technique used to extract the top mass, these mass values should be taken as representing the top *pole mass* (see our review "Note on Quark Masses" in the current edition for more information).

With a smaller uncertainty on the top mass, and with improved measurements of other electroweak parameters, it will be possible to get important constraints on the value of the Higgs mass. Current global fits performed within the Standard Model and its minimal supersymmetric extension provide indications for a relatively light Higgs (see the review "H^0 Indirect Mass Limits from Electroweak Analysis" in the Particle Listings of the current edition for more information).

Other properties of top decays are being studied. CDF reports a direct measurement of the $t \to Wb$ branching ratio [25]. Their result, obtained by comparing the number of events with 0, 1 and 2 tagged b jets and using the known b-tagging efficiency, is: $R = \mathrm{B}(t \to Wb)/\sum_{q=d,s,b} \mathrm{B}(t \to Wq) = 0.94^{+0.31}_{-0.24}$, or as a lower limit, $R > 0.56$ at 95% CL. Assuming that non-W decays of top can be neglected, that only three generations of fermions exist, and that the CKM matrix is unitary, they extract a CKM matrix-element $|V_{tb}| = 0.97^{+0.16}_{-0.12}$ or $|V_{tb}| > 0.75$ at 95% CL. A more direct measurement of the Wtb coupling constant will be possible when enough data are accumulated to detect the less frequent single-top production processes, such as $q\overline{q}' \to W^* \to t\overline{b}$ (a.k.a. s-channel W exchange) and $qb \to q't$ via W exchange (a.k.a. Wg fusion). The cross sections for these processes are proportional to $|V_{tb}|^2$, and there is no assumption needed on the number of families or the unitarity of the CKM matrix in the extraction of $|V_{tb}|$. CDF [26] gives 95% CL limits of 15.8 and 15.4 pb for the single-top production rates in the s-channel and Wg-fusion channels, respectively, while DØ [27] gives 17 and 22 pb, respectively. Comparison with the expected Standard Model rates of 0.73 ± 0.10 pb and 1.70 ± 0.30 pb, respectively, shows that far better statistics will be required before significant measurements can be achieved. For the prospects of these measurements at the LHC, see [15].

Both CDF and DØ have searched for non-Standard Model top decays [28,29], particularly those expected in supersymmetric models. These studies search for $t \to H^+b$, followed by $H^+ \to \tau\nu$ or $c\overline{s}$. The $t \to H^+b$ branching ratio is a minimum at $\tan\beta = \sqrt{m_t/m_b} \simeq 6$ and is large in the region of either $\tan\beta \ll 6$ or $\tan\beta \gg 6$. In the former range $H^+ \to c\overline{s}$ is the dominant decay, while $H^+ \to \tau\nu$ dominates in the latter range. These studies are based either on direct searches for these final states, or on top disappearance. In the standard lepton + jets or dilepton cross section analyses, the charged Higgs decays are not detected as efficiently as $t \to W^\pm b$, primarily because the selection criteria are optimized for the standard decays, and because of the absence of energetic isolated leptons in the Higgs decays. With a significant $t \to H^+b$ contribution, this would give rise to measured cross sections lower than the prediction from the Standard Model (assuming that non-Standard contributions to $t\overline{t}$ production are negligible). More details, and the results of these studies, can be found in the review "Search for Higgs bosons" and in the "H^+ Mass Limits" section of the Higgs Particle Listings of the current edition.

CDF reports a search for flavor changing neutral current (FCNC) decays of the top quark $t \to q\gamma$ and $t \to qZ$ [30], for which the Standard Model predicts such small rates that their observation here would indicate new physics. They assume that one top decays via FCNC while the other decays via Wb. For the $t \to q\gamma$ search, they examine two signatures, depending on whether the W decays leptonically or hadronically. For leptonic W decay, the signature is $\gamma\ell$ and missing E_T and two or more jets, while for hadronic W decay, it is γ plus four or more jets, one with a secondary vertex b tag. They observe one event ($\mu\gamma$) with an expected background of less than half an event, giving an upper limit on the top branching ratio of $\mathrm{B}(t \to q\gamma) < 3.2\%$ at 95% CL.

For the $t \to qZ$ FCNC search, they look for $Z \to \mu\mu$ or ee and $W \to$ hadrons, giving a Z + four jets signature. They observe one $\mu\mu$ event with an expected background of 1.2 events, giving an upper limit on the top branching ratio of $\mathrm{B}(t \to qZ) < 33\%$ at 95% CL. Both the γ and Z limits are non-background subtracted (i.e. conservative) estimates.

Indirect constraints on FCNC couplings of the top quark can be obtained from single-top production in e^+e^- collisions, via the process $e^+e^- \to \gamma, Z^* \to t\overline{q}$ and its charge-conjugate ($q = u, c$). Limits on the cross section for this reaction have been updated by ALEPH [31] and OPAL [32]. When interpreted in terms of top decay branching ratios [15,33], these limits lead to bounds of $\mathrm{B}(t \to qZ) < 0.17$ and < 0.137, respectively, which are stronger than the direct CDF limit.

Studies of the decay angular distributions allow a direct analysis of the V–A nature of the Wtb coupling, and provide information on the relative coupling of longitudinal and transverse W bosons to the top quark. In the Standard Model, the fraction of decays to longitudinally polarized W bosons is expected to be $\mathcal{F}_0^{\mathrm{SM}} = x/(1+x)$, $x = m_t^2/2M_W^2$ ($\mathcal{F}_0^{\mathrm{SM}} \sim 70\%$ for $m_t = 175$ GeV/c^2). Deviations from this value would bring into question the validity of the Higgs mechanism of spontaneous symmetry breaking. CDF has recently measured $\mathcal{F}_0^{\mathrm{SM}} = 0.91 \pm 0.37_{\mathrm{stat}} \pm 0.13_{\mathrm{syst}}$ [34], in agreement with the expectations.

DØ has studied $t\bar{t}$ spin correlation [35]. Top quark pairs produced at the Tevatron are expected to be unpolarized but to have correlated spins. Since top quarks decay before hadronizing, their spins are transmitted to their decay daughters. Spin correlation is studied by analyzing the joint decay angular distribution of one t daughter and one $\bar{t}$ daughter. The sensitivity to top spin is greatest when the daughters are charged leptons or d-type quarks, in which case, the joint distribution is

$$\frac{1}{\sigma}\frac{d^2\sigma}{d(cos\theta_+)d(cos\theta_-)} = \frac{1+\kappa cos\theta_+ cos\theta_-}{4}, \qquad (2)$$

where θ_+ and θ_- are the angles of the daughters in the top rest frames with respect to a particular quantization axis, the optimal off-diagonal basis [36]. In this basis, the Standard Model predicts maximum correlation with $\kappa = 0.88$ at the Tevatron. DØ analyzes their six dilepton events and obtains a likelihood as a function of κ which weakly favors the Standard Model ($\kappa = 0.88$) over no correlation ($\kappa = 0$) or anticorrelation ($\kappa = -1$, as would be expected for $t\bar{t}$ produced via an intermediate scalar). They quote a limit $\kappa > -0.25$ at 68% CL. With improved statistics, an observation of $t\bar{t}$ spin correlation could yield a lower limit on $|V_{tb}|$, independent of the assumption of three quark families [37].

Appendix. First Results from run II: Preliminary measurements of the top properties determined from run II data have been reported at several Conferences [1]. First results for the top mass have been shown by CDF. In the lepton plus four jets channel with at least one secondary vertex b-tagged jet CDF obtains a value of $m_t = 177.5^{+12.7}_{-9.4}(stat) \pm 7.1(syst)\,\mathrm{GeV/c^2}$ (22 candidate events). In the dilepton channel, CDF found a preliminary value of $m_t = 175.0^{+17.4}_{-16.9}(stat) \pm 7.9(syst)\,\mathrm{GeV/c^2}$ (6 candidate events). Results for the production cross-section have been given by both experiments, and are collected in Table Table 3. The uncertainties are still rather large when compared to those achieved in run I, and the rates are consistent both with the measurements at lower energy, and with the theoretical predictions [2].

Table 3: Cross section for $t\bar{t}$ production in $p\bar{p}$ collisions at $\sqrt{s} = 1.96$ TeV from DØ ($m_t = 172.1$ GeV/c^2), CDF ($m_t = 175$ GeV/c^2), and theory. CSIP refers to a "counted signed-impact-parameter" determination of secondary vertices. The first uncertainty is statistical, the second systematical, and the third uncertainty quoted by DØ reflects the luminosity uncertainty (included in CDF's systematics). Luminosities quoted in pb^{-1}.

$\sigma_{t\bar{t}}(pb)$	Source	Lum.	Method
$8.7\ ^{+6.4}_{-4.7}\ ^{+2.7}_{-2.0} \pm 0.9$	DØ	90–107	$\ell\ell$
$7.4\ ^{+4.4}_{-3.6}\ ^{+2.1}_{-1.6} \pm 0.7$	DØ	45	ℓ+jets, CSIP
$10.8\ ^{+4.9}_{-4.0}\ ^{+2.1}_{-2.0} \pm 1.1$	DØ	45	ℓ+jets/vtx b-tag
$4.6\ ^{+3.1}_{-2.7}\ ^{+2.1}_{-2.0} \pm 0.5$	DØ	92	ℓ+jets/topological
$11.4\ ^{+4.1}_{-3.5}\ ^{+2.0}_{-1.8} \pm 1.1$	DØ	92	ℓ+jets/soft μ b-tag
$8.0\ ^{+2.4}_{-2.1}\ ^{+1.7}_{-1.5} \pm 0.8$	DØ	92	ℓ+jets combined
$8.1\ ^{+2.2}_{-2.0}\ ^{+1.6}_{-1.4} \pm 0.8$	DØ	90–107	Dilepton and ℓ+jets combined
$7.6\ ^{+3.8}_{-3.1}\ ^{+1.5}_{-1.9}$	CDF	126	$\ell\ell$
$7.3 \pm 3.4 \pm 1.7$	CDF	126	ℓ+track
$5.3 \pm 1.9 \pm 0.9$	CDF	57	ℓ+jets/vtx b-tag
$5.1 \pm 1.8 \pm 2.1$	CDF	126	ℓ+jets/H_T
$5.8 - 7.4$	Theory [2]		$m_t = 175$ GeV/c^2

References

1. P. Azzi, to appear in the Proceedings of Lepton-Photon 2003, Fermilab, Batavia (IL), August 2003, arXiv:hep-ex/0312052;
   E. Shabalina, FERMILAB-CONF-03-317-E *To appear in the proceedings of International Europhysics Conference on High-Energy Physics (HEP 2003)*, Aachen, Germany, 17-23 July 2003.
2. M. Cacciari, S. Frixione, M. L. Mangano, P. Nason and G. Ridolfi, arXiv:hep-ph/0303085;
   N. Kidonakis and R. Vogt, Phys. Rev. **D68**, 114014 (2003).
3. T. Stelzer, Z. Sullivan, and S. Willenbrock, Phys. Rev. **D56**, 5919 (1997).
4. M. Jeżabek and J.H. Kühn, Nucl. Phys. **B314**, 1 (1989).
5. I.I.Y. Bigi *et al.*, Phys. Lett. **B181**, 157 (1986).
6. A. Czarnecki and K. Melnikov, Nucl. Phys. **B544**, 520 (1999);
   K.G. Chetyrkin *et al.*, Phys. Rev. **D60**, 114015 (1999).
7. F. Abe *et al.*, CDF Collab., Phys. Rev. Lett. **80**, 5720 (1998).
8. S. Abachi *et al.*, DØ Collab., Phys. Rev. Lett. **79**, 1203 (1997).
9. V.M. Abazov *et al.*, DØ Collab., Phys. Rev. **D67**, 012004 (2003).
10. B. Abbott *et al.*, DØ Collab., Phys. Rev. Lett. **83**, 1908 (1999);
    B. Abbott *et al.*, DØ Collab., Phys. Rev. **D60**, 012001 (1999).
11. F. Abe *et al.*, CDF Collab., Phys. Rev. Lett. **80**, 2773 (1998).
12. F. Abe *et al.*, CDF Collab., Phys. Rev. Lett. **80**, 2779 (1998).
13. F. Abe *et al.*, CDF Collab., Phys. Rev. Lett. **79**, 1992 (1997).
14. T. Affolder *et al.*, CDF Collab., Phys. Rev. **D64**, 032002 (2001).
15. M. Beneke, I. Efthymiopoulos, M.L. Mangano, J. Womersley *et al.*, `hep-ph/0003033`, in *Proceedings of 1999 CERN Workshop on Standard Model Physics (and more) at the LHC*, G. Altarelli and M.L. Mangano eds.
16. T. Affolder *et al.*, CDF Collab., Phys. Rev. Lett. **85**, 2062 (2000).
17. T. Affolder *et al.*, CDF Collab., Phys. Rev. Lett. **87**, 102001 (2001).
18. B. Abbott *et al.*, DØ Collab., Phys. Rev. **D58**, 052001 (1998);
    S. Abachi *et al.*, DØ Collab., Phys. Rev. Lett. **79**, 1197 (1997).

19. M. Warsinsky, *Proceedings of the International Europhysics Conference on High Energy Physics* , 17-23 July 2003, Europhysics Journal, to be publ.
20. B. Abbott *et al.*, DØ Collab., Phys. Rev. **D60**, 052001 (1999);
B. Abbott *et al.*, DØ Collab., Phys. Rev. Lett. **80**, 2063 (1998).
21. F. Abe *et al.*, CDF Collab., Phys. Rev. Lett. **82**, 271 (1999).
22. F. Abe *et al.*, CDF Collab.,Phys. Rev. Lett. **80**, 2767 (1998).
23. T. Affolder *et al.*, CDF Collab., Phys. Rev. **D63**, 032003 (2001).
24. L. Demortier *et al.*, The Top Averaging Group, For the CDF and DØ Collaborations, FERMILAB-TM-2084, September, 1999.
25. T. Affolder *et al.*, CDF Collab., Phys. Rev. Lett. **86**, 3233 (2001).
26. D. Acosta *et al.*, CDF Collab., Phys. Rev. **D65**, 091102 (2002).
27. V.M. Abazov *et al.*, DØ Collab., Phys. Lett. **B517**, 282 (2001).
28. F. Abe *et al.*, CDF Collab., Phys. Rev. Lett. **79**, 357 (1997);
B. Bevensee, for the CDF Collab., FERMILAB-CONF-98/155-E;
T. Affolder *et al.*, CDF Collab., Phys. Rev. **D62**, 012004 (2000).
29. B. Abbott *et al.*, Phys. Rev. Lett. **82**, 4975 (1999);
V.M Abazov *et al.*, DØ Collab., Phys. Rev. Lett. **88**, 151803 (2001).
30. F. Abe *et al.*, CDF Collab., Phys. Rev. Lett. **80**, 2525 (1998).
31. S. Barate *et al.*, ALEPH Collab., Phys. Lett. **B494**, 33 (2000).
32. G. Abbiendi *et al.*, OPAL Collab., Phys. Lett. **B521**, 181 (2001).
33. V.F. Obraztsov, S.R. Slabospitsky, and O.P. Yushchenko, Phys. Lett. **B426**, 393 (1998).
34. T. Affolder *et al.*, CDF Collab.,Phys. Rev. Lett. **84**, 216 (2000).
35. B. Abbott *et al.*, DØ Collab., Phys. Rev. Lett. **85**, 256 (2000).
36. G. Mahlon and S. Parke, Phys. Rev. **D53**, 4886 (1996);
G. Mahlon and S. Parke, Phys. Lett. **B411**, 173 (1997).
37. T. Stelzer and S. Willenbrock, Phys. Lett. **B374**, 169 (1996).

t-Quark Mass in $p\overline{p}$ Collisions

The t quark has been observed. Its mass is sufficiently high that decay is expected to occur before hadronization. OUR EVALUATION is an AVERAGE which incorporates correlations between systematic errors of the five different measurements. The average was done by a joint CDF/DØ working group and is reported in DEMORTIER 99, an FNAL Technical Memo. They report $174.3 \pm 3.2 \pm 4.0$ GeV, which yields "OUR EVALUATION" when statistical and systematic errors are combined. When the most recent CDF lepton + jets result is combined with the other CDF and DØ results, the combined result given as "OUR EVALUATION" is unchanged from the DEMORTIER 99 result after rounding.

For earlier search limits see the *Review of Particle Physics*, Phys. Rev. **D54**,1 (1996).

VALUE (GeV)		*DOCUMENT ID*		*TECN*	*COMMENT*
174.3± 5.1 OUR EVALUATION					
176.1± 5.1± 5.3		[1] AFFOLDER	01	CDF	lepton + jets
167.4±10.3± 4.8		[2,3] ABE	99B	CDF	dilepton
168.4±12.3± 3.6		[4] ABBOTT	98D	DØ	dilepton
173.3± 5.6± 5.5		[4] ABBOTT	98F	DØ	lepton + jets
186 ±10 ± 5.7		[2,5] ABE	97R	CDF	6 or more jets
• • • We do not use the following data for averages, fits, limits, etc. • • •					
176.1± 6.6		[6] AFFOLDER	01	CDF	lepton + jets, dileptons, all-jets
172.1± 5.2± 4.9		[7] ABBOTT	99G	DØ	di-lepton, lepton+jets
176.0± 6.5		[3,8] ABE	99B	CDF	dilepton, lepton+jets, and all jets
175.9± 4.8± 5.3		[2,9] ABE	98E	CDF	lepton + jets
161 ±17 ±10		[2] ABE	98F	CDF	dilepton
172.1± 5.2± 4.9		[10] BHAT	98B	RVUE	dilepton and lepton+jets
173.8± 5.0		[11] BHAT	98B	RVUE	dilepton, lepton+jets, and all jets
173.3± 5.6± 6.2		[4] ABACHI	97E	DØ	lepton + jets
199 $^{+19}_{-21}$ ±22		ABACHI	95	DØ	lepton + jets
176 ± 8 ±10		ABE	95F	CDF	lepton + b-jet
174 ±10 $^{+13}_{-12}$		ABE	94E	CDF	lepton + b-jet

[1] AFFOLDER 01 result uses lepton + jets topology. It is based on $\sim 106\,\text{pb}^{-1}$ of data at $\sqrt{s}$= 1.8 TeV.
[2] Result is based on $109 \pm 7\,\text{pb}^{-1}$ of data at $\sqrt{s} = 1.8$ TeV.
[3] See AFFOLDER 01 for details of systematic error re-evaluation.
[4] Result is based on $125 \pm 7\,\text{pb}^{-1}$ of data at $\sqrt{s} = 1.8$ TeV.
[5] ABE 97R result is based on the first observation of all hadronic decays of $t\overline{t}$ pairs. Single b-quark tagging with jet-shape variable constraints was used to select signal enriched multi-jet events. The updated systematic error is listed. See AFFOLDER 01, appendix C.
[6] AFFOLDER 01 is obtained by combining the measurements in the lepton + jets [AFFOLDER 01], all-jets [ABE 97R, ABE 99B], and dilepton [ABE 99B] decay topologies.
[7] ABBOTT 99G result is obtained by combining the D0 result m_t (GeV) $= 168.4 \pm 12.3 \pm 3.6$ from 6 di-lepton events (see also ABBOTT 98D) and m_t (GeV) $= 173.3 \pm 5.6 \pm 5.5$ from lepton+jet events (ABBOTT 98F).
[8] ABE 99B result is obtained by combining the CDF results of m_t (GeV)=$167.4 \pm 10.3 \pm 4.8$ from 8 dilepton events, m_t (GeV)=$175.9 \pm 4.8 \pm 5.3$ from lepton+jet events (ABE 98E), and m_t (GeV)=$186.0 \pm 10.0 \pm 5.7$ from all-jet events (ABE 97R). The systematic errors in the latter two measurements are changed in this paper.
[9] The updated systematic error is listed. See AFFOLDER 01, appendix C.
[10] BHAT 98B result is obtained by combining the DØ results of m_t(GeV)=$168.4 \pm 12.3 \pm 3.6$ from 6 dilepton events and m_t(GeV)=$173.3 \pm 5.6 \pm 5.5$ from 77 lepton+jet events.
[11] BHAT 98B result is obtained by combining the DØ results from dilepton and lepton+jet events, and the CDF results (ABE 99B) from dilepton, lepton+jet events, and all-jet events.

Indirect t-Quark Mass from Standard Model Electroweak Fit

"OUR EVALUATION" below is from the fit to electroweak data described in the "Electroweak Model and Constraints on New Physics" section of this Review. This fit result does not include direct measurements of m_t.

The RVUE values are based on the data described in the footnotes. RVUE's published before 1994 and superseded analyses are now omitted. For more complete listings of earlier results, see the 1994 edition (Physical Review **D50** 1173 (1994)).

VALUE (GeV)	*DOCUMENT ID*		*TECN*	*COMMENT*
178.1 $^{+10.4}_{-8.3}$ OUR EVALUATION				
• • • We do not use the following data for averages, fits, limits, etc. • • •				
162 ±15 $^{+25}_{-5}$	[12] ABBIENDI	01A	OPAL	Z parameters
170.7± 3.8	[13] FIELD	00	RVUE	Z parameters without b-jet + Direct
171.2 $^{+3.7}_{-3.8}$	[14] FIELD	99	RVUE	Z parameters without b jet + Direct
172.0 $^{+5.8}_{-5.7}$	[15] DEBOER	97B	RVUE	Electroweak + Direct
157 $^{+16}_{-12}$	[16] ELLIS	96C	RVUE	Z parameters, m_W, low energy
175 ±11 $^{+17}_{-19}$	[17] ERLER	95	RVUE	Z parameters, m_W, low energy
180 ± 9 $^{+19}_{-21}$ ∓ 2.6 ± 4.8	[18] MATSUMOTO	95	RVUE	
157 $^{+36}_{-48}$ $^{+19}_{-20}$	[19] ABREU	94	DLPH	Z parameters
158 $^{+32}_{-40}$ ±19	[20] ACCIARRI	94	L3	Z parameters
190 $^{+39}_{-48}$ $^{+12}_{-14}$	[21] ARROYO	94	CCFR	ν_μ iron scattering
184 $^{+25}_{-29}$ $^{+17}_{-18}$	[22] BUSKULIC	94	ALEP	Z parameters
153 ±15	[23] ELLIS	94B	RVUE	Electroweak
177 ± 9 $^{+16}_{-20}$	[24] GURTU	94	RVUE	Electroweak
174 $^{+11}_{-13}$ $^{+17}_{-18}$	[25] MONTAGNA	94	RVUE	Electroweak
171 ±12 $^{+15}_{-21}$	[26] NOVIKOV	94B	RVUE	Electroweak
160 $^{+50}_{-60}$	[27] ALITTI	92B	UA2	m_W, m_Z

[12] ABBIENDI 01A result is from fit with free α_s when m_H is fixed to 150 GeV. The second errors are for m_H= 90 GeV (lower) and 1000 GeV (upper). The fit also finds $\alpha_s = 0.125 \pm 0.005 \,^{+0.004}_{-0.001}$.
[13] FIELD 00 result updates FIELD 99 by using the 1998 EW data (CERN-EP/99-15). Only the lepton asymmetry data are used together with the direct measurement constraint m_t=173.8 ± 5.0 GeV, $\alpha_s(m_Z) = 0.12$, and $1/\alpha(m_Z) = 128.896$. The result is from a two parameter fit with free m_t and m_H, yielding also m_H=$38.0\,^{+30.5}_{-19.8}$ GeV.

[14] FIELD 99 result is from the two-parameter fit with free m_t and m_H, yielding also $m_H = 47.2^{+29.8}_{-24.5}$ GeV. Only the lepton and charm-jet asymmetry data are used together with the direct measurement constraint $m_t = 173.8 \pm 5.0$ GeV, and $1/\alpha(m_Z) = 128.896$.

[15] DEBOER 97B result is from the five-parameter fit which varies m_Z, m_t, m_H, α_s, and $\alpha(m_Z)$ under the constraints: m_t=175 ± 6 GeV, $1/\alpha(m_Z)$=128.896 ± 0.09. They found $m_H = 141^{+140}_{-77}$ GeV and $\alpha_s(m_Z)$=0.1197 ± 0.0031.

[16] ELLIS 96C result is a the two-parameter fit with free m_t and m_H, yielding also $m_H = 65^{+117}_{-37}$ GeV.

[17] ERLER 95 result is from fit with free m_t and $\alpha_s(m_Z)$, yielding $\alpha_s(m_Z) = 0.127(5)(2)$.

[18] MATSUMOTO 95 result is from fit with free m_t to Z parameters, M_W, and low-energy neutral-current data. The second error is for $m_H = 300^{+700}_{-240}$ GeV, the third error is for $\alpha_s(m_Z) = 0.116 \pm 0.005$, the fourth error is for $\delta\alpha_{\rm had} = 0.0283 \pm 0.0007$.

[19] ABREU 94 value is for $\alpha_s(m_Z)$ constrained to 0.123 ± 0.005. The second error corresponds to $m_H = 300^{+700}_{-240}$ GeV.

[20] ACCIARRI 94 value is for $\alpha_s(m_Z)$ constrained to 0.124 ± 0.006. The second error corresponds to $m_H = 300^{+700}_{-240}$ GeV.

[21] ARROYO 94 measures the ratio of the neutral-current and charged-current deep inelastic scattering of ν_μ on an iron target. By assuming the SM electroweak correction, they obtain $1 - m_W^2/m_Z^2 = 0.2218 \pm 0.0059$, yielding the quoted m_t value. The second error corresponds to $m_H = 300^{+700}_{-240}$ GeV.

[22] BUSKULIC 94 result is from fit with free α_s. The second error is from $m_H = 300^{+700}_{-240}$ GeV.

[23] ELLIS 94B result is fit to electroweak data available in spring 1994, including the 1994 A_{LR} data from SLD. m_t and m_H are two free parameters of the fit for $\alpha_s(m_Z) = 0.118 \pm 0.007$ yielding m_t above, and $m_H = 35^{+70}_{-22}$ GeV. ELLIS 94B also give results for fits including constraints from CDF's direct measurement of m_t and CDF's and DØ 's production cross-section measurements. Fits excluding the A_{LR} data from SLD are also given.

[24] GURTU 94 result is from fit with free m_t and $\alpha_s(m_Z)$, yielding m_t above and $\alpha_s(m_Z) = 0.125 \pm 0.005 \pm 0.003$. The second errors correspond to $m_H = 300^{+700}_{-240}$ GeV. Uses LEP, M_W, νN, and SLD electroweak data available in spring 1994.

[25] MONTAGNA 94 result is from fit with free m_t and $\alpha_s(m_Z)$, yielding m_t above and $\alpha_s(m_Z) = 0.124$. The second errors correspond to $m_H = 300^{+700}_{-240}$ GeV. Errors in $\alpha(m_Z)$ and m_b are taken into account in the fit. Uses LEP, SLC, and M_W/M_Z data available in spring 1994.

[26] NOVIKOV 94B result is from fit with free m_t and $\alpha_s(m_Z)$, yielding m_t above and $\alpha_s(m_Z) = 0.125 \pm 0.005 \pm 0.002$. The second errors correspond to $m_H = 300^{+700}_{-240}$ GeV. Uses LEP and CDF electroweak data available in spring 1994.

[27] ALITTI 92B assume $m_H = 100$ GeV. The 95%CL limit is $m_t < 250$ GeV for $m_H < 1$ TeV.

t DECAY MODES

	Mode	Fraction (Γ_i/Γ)	Confidence level
Γ_1	$Wq\,(q = b, s, d)$		
Γ_2	Wb		
Γ_3	$\ell\nu_\ell$ anything	[a,b] (9.4±2.4) %	
Γ_4	$\tau\nu_\tau b$		
Γ_5	$\gamma q (q{=}u,c)$	[c] < 5.9 $\times 10^{-3}$	95%

$\Delta T = 1$ weak neutral current ($T1$) modes

Γ_6	$Zq(q{=}u,c)$	$T1$	[d] < 13.7 %	95%

[a] ℓ means e or μ decay mode, not the sum over them.

[b] Assumes lepton universality and W-decay acceptance.

[c] This limit is for $\Gamma(t \to \gamma q)/\Gamma(t \to Wb)$.

[d] This limit is for $\Gamma(t \to Zq)/\Gamma(t \to Wb)$.

t BRANCHING RATIOS

$\Gamma(Wb)/\Gamma(Wq\,(q = b, s, d))$ Γ_2/Γ_1

VALUE	DOCUMENT ID	TECN
$\mathbf{0.94^{+0.26}_{-0.21}{}^{+0.17}_{-0.12}}$	[28] AFFOLDER 01C	CDF

[28] AFFOLDER 01C measures the top-quark decay width ratio $R = \Gamma(Wb)/\Gamma(Wq)$, where q is a d, s, or b quark, by using the number of events with multiple b tags. The first error is statistical and the second systematic. A numerical integration of the likelihood function gives $R > 0.61$ (0.56) at 90% (95%) CL. By assuming three generation unitarity, $|V_{tb}| = 0.97^{+0.16}_{-0.12}$ or $|V_{tb}| > 0.78$ (0.75) at 90% (95%) CL is obtained. The result is based on 109 pb^{-1} of data at $\sqrt{s}$= 1.8 TeV.

$\Gamma(\ell\nu_\ell \text{ anything})/\Gamma_{\rm total}$ Γ_3/Γ

VALUE	DOCUMENT ID	TECN
0.094±0.024	[29] ABE 98X	CDF

[29] ℓ means e or μ decay mode, not the sum. Assumes lepton universality and W-decay acceptance.

$\Gamma(\tau\nu_\tau b)/\Gamma_{\rm total}$ Γ_4/Γ

VALUE	DOCUMENT ID	TECN	COMMENT
• • • We do not use the following data for averages, fits, limits, etc. • • •			
	[30] ABE 97V	CDF	$\ell\tau$ + jets

[30] ABE 97V searched for $t\bar{t} \to (\ell\nu_\ell)(\tau\nu_\tau)b\bar{b}$ events in 109 pb^{-1} of $p\bar{p}$ collisions at $\sqrt{s} = 1.8$ TeV. They observed 4 candidate events where one expects ∼ 1 signal and ∼ 2 background events. Three of the four observed events have jets identified as b candidates.

$\Gamma(\gamma q(q{=}u,c))/\Gamma_{\rm total}$ Γ_5/Γ

VALUE	CL%	DOCUMENT ID	TECN	COMMENT
<0.0059	95	[31] CHEKANOV 03	ZEUS	B($t \to \gamma u$)
• • • We do not use the following data for averages, fits, limits, etc. • • •				
<0.041	95	[32] ACHARD 02J L3		B($t \to \gamma c$ or γu)
<0.032	95	[33] ABE 98G CDF		$t\bar{t} \to (Wb)(\gamma c$ or $\gamma u)$

[31] CHEKANOV 03 looked for single top production via FCNC in the reaction $e^\pm p \to e^\pm$ (t or $\bar{t}$) X in 130.1 pb^{-1} of data at $\sqrt{s}$=300–318 GeV. No evidence for top production and its decay into bW was found. The result is obtained for m_t=175 GeV when B(γc)=B(Zq)=0, where q is a u or c quark. Bounds on the effective t-u-γ and t-u-Z couplings are found in their Fig. 4. The conversion to the constraint listed is from private communication, E. Gallo, January 2004.

[32] ACHARD 02J looked for single top production via FCNC in the reaction $e^+e^- \to \bar{t}c$ or $\bar{t}u$ in 634 pb^{-1} of data at $\sqrt{s}$= 189–209 GeV. No deviation from the SM is found, which leads to a bound on the top-quark decay branching fraction B(γq), where q is a u or c quark. The bound assumes B(Zq)=0 and is for m_t= 175 GeV; bounds for m_t=170 GeV and 180 GeV and B(Zq) ≠ 0 are given in Fig. 5 and Table 7.

[33] ABE 98G looked for $t\bar{t}$ events where one t decays into $q\gamma$ while the other decays into bW. The quoted bound is for $\Gamma(\gamma q)/\Gamma(Wb)$.

$\Gamma(Zq(q{=}u,c))/\Gamma_{\rm total}$ Γ_6/Γ

Test for ΔT=1 weak neutral current. Allowed by higher-order electroweak interaction.

VALUE	CL%	DOCUMENT ID	TECN	COMMENT
<0.137	95	[34] ACHARD 02J	L3	$e^+e^- \to \bar{t}c$ or $\bar{t}u$
<0.14	95	[35] HEISTER 02Q	ALEP	$e^+e^- \to \bar{t}c$ or $\bar{t}u$
<0.137	95	[36] ABBIENDI 01T	OPAL	$e^+e^- \to \bar{t}c$ or $\bar{t}u$
• • • We do not use the following data for averages, fits, limits, etc. • • •				
<0.17	95	[37] BARATE 00S	ALEP	$e^+e^- \to \bar{t}c$ or $\bar{t}u$
<0.33	95	[38] ABE 98G	CDF	$t\bar{t} \to (Wb)(Zc$ or $Zu)$

[34] ACHARD 02J looked for single top production via FCNC in the reaction $e^+e^- \to \bar{t}c$ or $\bar{t}u$ in 634 pb^{-1} of data at $\sqrt{s}$= 189–209 GeV. No deviation from the SM is found, which leads to a bound on the top-quark decay branching fraction B(Zq), where q is a u or c quark. The bound assumes B(γq)=0 and is for m_t= 175 GeV; bounds for m_t=170 GeV and 180 GeV and B(γq) ≠0 are given in Fig. 5 and Table 7. Table 6 gives constraints on t-c-e-e four-fermi contact interactions.

[35] HEISTER 02Q looked for single top production via FCNC in the reaction $e^+e^- \to \bar{t}c$ or $\bar{t}u$ in 214 pb^{-1} of data at $\sqrt{s}$= 204–209 GeV. No deviation from the SM is found, which leads to a bound on the branching fraction B(Zq), where q is a u or c quark. The bound assumes B(γq)=0 and is for m_t= 174 GeV. Bounds on the effective t- (c or u)-γ and t- (c or u)- Z couplings are given in their Fig. 2.

[36] ABBIENDI 01T looked for single top production via FCNC in the reaction $e^+e^- \to \bar{t}c$ or $\bar{t}u$ in 600 pb^{-1} of data at $\sqrt{s}$= 189–209 GeV. No deviation from the SM is found, which leads to bounds on the branching fractions B(Zq) and B(γq), where q is a u or c quark. The result is obtained for m_t= 174 GeV. The upper bound becomes 9.7% (20.6%))) for m_t= 169 (179) GeV. Bounds on the effective t- (c or u)-γ and t- (c or u)-Z couplings are given in their Fig. 4.

[37] BARATE 00S looked for single top production via FCNC in the reaction $e^+e^- \to \bar{t}c$ or $\bar{t}u$ in 411 pb^{-1} of data at c.m. energies between 189 and 202 GeV. No deviation from the SM is found, which leads to a bound on the branching fraction. The bound assumes B(γq)=0. Bounds on the effective t- (c or u)-γ and t- (c or u)-Z couplings are given in their Fig. 4.

[38] ABE 98G looked for $t\bar{t}$ events where one t decays into three jets and the other decays into qZ with $Z \to \ell\ell$. The quoted bound is for $\Gamma(Zq)/\Gamma(Wb)$.

t Decay Vertices

VALUE	DOCUMENT ID	TECN	COMMENT
• • • We do not use the following data for averages, fits, limits, etc. • • •			
0.91±0.37±0.13	[39] AFFOLDER 00B	CDF	$F_0 = W_L/(W_L+W_T)$
0.11±0.15	[39] AFFOLDER 00B	CDF	B($t \to W_+ b$)

[39] AFFOLDER 00B studied the angular distribution of leptonic decays of W bosons in $t \to Wb$ events. The ratio F_0 is the fraction of the helicity zero (longitudinal) W bosons in the decaying top quark rest frame. The first error is statistical and the second systematic. B($t \to W_+ b$) is the fraction of positive helicity (right-handed) positive charge W bosons in the top quark decays. It is obtained by assuming the Standard Model value of F_0.

Single t-Quark Production Cross Section in $p\bar{p}$ Collisions

Direct probes of the tbW coupling and possible new physics

VALUE (pb)	CL%	DOCUMENT ID	TECN	COMMENT
• • • We do not use the following data for averages, fits, limits, etc. • • •				
<18	95	[40] ACOSTA 02	CDF	$p\bar{p} \to tb + X$
<13	95	[41] ACOSTA 02	CDF	$p\bar{p} \to tqb + X$
<17	95	[42,43] ABAZOV 01C	D0	$p\bar{p} \to tb + X$
<22	95	[43,44] ABAZOV 01C	D0	$p\bar{p} \to tqb + X$
<39	95	[42] ABBOTT 01B	D0	$p\bar{p} \to tb + X$
<58	95	[44] ABBOTT 01B	D0	$p\bar{p} \to tqb + X$

[40] ACOSTA 02 bounds the cross section for single top-quark production via the s-channel W-exchange process, $q'\overline{q} \rightarrow t\overline{b}$. It is based on $\sim 106\ \mathrm{pb}^{-1}$ of data at $\sqrt{s}$=1.8 TeV.

[41] ACOSTA 02 bounds the cross section for single top-quark production via the t-channel W-exchange process, $q'g \rightarrow qt\overline{b}$. It is based on $\sim 106\ \mathrm{pb}^{-1}$ of data at $\sqrt{s}$=1.8 TeV.

[42] Result bounds the cross section for single top-quark production via the s-channel process $q'\overline{q} \rightarrow W' \rightarrow tb$. It is based on $\sim 90\ \mathrm{pb}^{-1}$ of data at $\sqrt{s}$= 1.8 TeV.

[43] ABAZOV 01C results updates those of ABBOTT 01B by making use of arrays of neural networks to separate signals from backgrounds.

[44] Result bounds the cross section for single top-quark production via the t-channel W-exchange process $q'g \rightarrow qtb$. It is based on $\sim 90\ \mathrm{pb}^{-1}$ of data at $\sqrt{s}$= 1.8 TeV.

t-Quark REFERENCES

CHEKANOV	03	PL B559 153	S. Chekanov *et al.*	(ZEUS Collab.)
ACHARD	02J	PL B549 290	P. Achard *et al.*	(L3 Collab.)
ACOSTA	02	PR D65 091102	D. Acosta *et al.*	(CDF Collab.)
HEISTER	02Q	PL B543 173	A. Heister *et al.*	(ALEPH Collab.)
ABAZOV	01C	PL B517 282	V.M. Abazov *et al.*	(D0 Collab.)
ABBIENDI	01A	EPJ C19 587	G. Abbiendi *et al.*	(OPAL Collab.)
ABBIENDI	01T	PL B521 181	G. Abbiendi *et al.*	(OPAL Collab.)
ABBOTT	01B	PR D63 031101	B. Abbott *et al.*	(D0 Collab.)
AFFOLDER	01	PR D63 032003	T. Affolder *et al.*	(CDF Collab.)
AFFOLDER	01C	PRL 86 3233	T. Affolder *et al.*	(CDF Collab.)
AFFOLDER	00B	PRL 84 216	T. Affolder *et al.*	(CDF Collab.)
BARATE	00S	PL B494 33	S. Barate *et al.*	(ALEPH Collab.)
FIELD	00	PR D61 013010	J.H. Field	
ABBOTT	99G	PR D60 052001	B. Abbott *et al.*	(D0 Collab.)
ABE	99B	PRL 82 271	F. Abe *et al.*	(CDF Collab.)
Also	99G	PRL 82 2808 (erratum)	F. Abe *et al.*	(CDF Collab.)
DEMORTIER	99	FNAL-TM-2084	L. Demortier *et al.*	(CDF/D0 Working Group)
FIELD	99	MPL A14 1815	J.H. Field	
ABBOTT	98D	PRL 80 2063	B. Abbott *et al.*	(D0 Collab.)
ABBOTT	98F	PR D58 052001	B. Abbott *et al.*	(D0 Collab.)
ABE	98E	PRL 80 2767	F. Abe *et al.*	(CDF Collab.)
ABE	98F	PRL 80 2779	F. Abe *et al.*	(CDF Collab.)
ABE	98G	PRL 80 2525	F. Abe *et al.*	(CDF Collab.)
ABE	98X	PRL 80 2773	F. Abe *et al.*	(CDF Collab.)
BHAT	98B	IJMP A13 5113	P.C. Bhat, H.B. Prosper, S.S. Snyder	
ABACHI	97E	PRL 79 1197	S. Abachi *et al.*	(D0 Collab.)
ABE	97R	PRL 79 1992	F. Abe *et al.*	(CDF Collab.)
ABE	97V	PRL 79 3585	F. Abe *et al.*	(CDF Collab.)
DEBOER	97B	ZPHY C75 627	W. de Boer *et al.*	
ELLIS	96C	PL B389 321	J. Ellis, G.L. Fogli, E. Lisi	(CERN, BARI)
ABACHI	95	PRL 74 2632	S. Abachi *et al.*	(D0 Collab.)
ABE	95F	PRL 74 2626	F. Abe *et al.*	(CDF Collab.)
ERLER	95	PR D52 441	J. Erler, P. Langacker	(PENN)
MATSUMOTO	95	MPL A10 2553	S. Matsumoto	(KEK)
ABE	94E	PR D50 2966	F. Abe *et al.*	(CDF Collab.)
Also	94F	PRL 73 225	F. Abe *et al.*	(CDF Collab.)
ABREU	94	NP B418 403	P. Abreu *et al.*	(DELPHI Collab.)
ACCIARRI	94	ZPHY C62 551	M. Acciarri *et al.*	(L3 Collab.)
ARROYO	94	PRL 72 3452	C.G. Arroyo *et al.*	(COLU, CHIC, FNAL+)
BUSKULIC	94	ZPHY C62 539	D. Buskulic *et al.*	(ALEPH Collab.)
ELLIS	94B	PL B333 118	J. Ellis, G.L. Fogli, E. Lisi	(CERN, BARI)
GURTU	94	MPL A9 3301	A. Gurtu	(TATA)
MONTAGNA	94	PL B335 484	G. Montagna *et al.*	(INFN, PAVI, CERN+)
NOVIKOV	94B	MPL A9 2641	V.A. Novikov *et al.*	(GUEL, CERN, ITEP)
PDG	94	PR D50 1173	L. Montanet *et al.*	(CERN, LBL, BOST+)
ALITTI	92B	PL B276 354	J. Alitti *et al.*	(UA2 Collab.)

b' (4^{th} Generation) Quark, Searches for

MASS LIMITS for b' (4^{th} Generation) Quark or Hadron in $p\overline{p}$ Collisions

VALUE (GeV)	CL%	DOCUMENT ID		TECN	COMMENT
>190	95	[1] ACOSTA	03	CDF	quasi-stable b'
>199	95	[2] AFFOLDER	00	CDF	NC: $b' \rightarrow bZ$
>128	95	[3] ABACHI	95F	D0	$\ell\ell$ + jets, ℓ + jets
• • • We do not use the following data for averages, fits, limits, etc. • • •					
>148	95	[4] ABE	98N	CDF	NC: $b' \rightarrow bZ$ +decay vertex
> 96	95	[5] ABACHI	97D	D0	NC: $b' \rightarrow b\gamma$
> 75	95	[6] MUKHOPAD...	93	RVUE	NC: $b' \rightarrow b\ell\ell$
> 85	95	[7] ABE	92	CDF	CC: $\ell\ell$
> 72	95	[8] ABE	90B	CDF	CC: e + μ
> 54	95	[9] AKESSON	90	UA2	CC: e + jets + missing E_T
> 43	95	[10] ALBAJAR	90B	UA1	CC: μ + jets
> 34	95	[11] ALBAJAR	88	UA1	CC: e or μ + jets

[1] ACOSTA 03 looked for long-lived fourth generation quarks in the data sample of 90 pb^{-1} of $\sqrt{s}$=1.8 TeV $p\overline{p}$ collisions by using the muon-like penetration and anomalously high ionization energy loss signature. The corresponding lower mass bound for the charge (2/3)e quark (t') is 220 GeV. The t' bound is higher than the b' bound because t' is more likely to produce charged hadrons than b'. The 95% CL upper bounds for the production cross sections are given in their Fig. 3.

[2] AFFOLDER 00 looked for b' that decays in to b+Z. The signal searched for is $bbZZ$ events where one Z decays into e^+e^- or $\mu^+\mu^-$ and the other Z decays hadronically. The bound assumes B($b' \rightarrow bZ$)= 100%. Between 100 GeV and 199 GeV, the 95%CL upper bound on $\sigma(b' \rightarrow \overline{b'})\times B^2(b' \rightarrow bZ)$ is also given (see their Fig. 2).

[3] ABACHI 95F bound on the top-quark also applies to b' and t' quarks that decay predominantly into W. See FROGGATT 97.

[4] ABE 98N looked for $Z \rightarrow e^+e^-$ decays with displaced vertices. Quoted limit assumes B($b' \rightarrow bZ$)=1 and $c\tau_{b'}$=1 cm. The limit is lower than m_Z+m_b ($\sim$ 96 GeV) if $c\tau >$ 22 cm or $c\tau <$ 0.009 cm. See their Fig. 4.

[5] ABACHI 97D searched for b' that decays mainly via FCNC. They obtained 95%CL upper bounds on B($b'\overline{b'} \rightarrow \gamma$+ 3 jets) and B($b'\overline{b'} \rightarrow 2\gamma$+ 2 jets), which can be interpreted as the lower mass bound $m_{b'} > m_Z+m_b$.

[6] MUKHOPADHYAYA 93 analyze CDF dilepton data of ABE 92G in terms of a new quark decaying via flavor-changing neutral current. The above limit assumes B($b' \rightarrow b\ell^+\ell^-$)=1%. For an exotic quark decaying only via virtual Z [B($b\ell^+\ell^-$) = 3%], the limit is 85 GeV.

[7] ABE 92 dilepton analysis limit of >85 GeV at CL=95% also applies to b' quarks, as discussed in ABE 90B.

[8] ABE 90B exclude the region 28–72 GeV.

[9] AKESSON 90 searched for events having an electron with $p_T > 12$ GeV, missing momentum > 15 GeV, and a jet with $E_T > 10$ GeV, $|\eta| < 2.2$, and excluded $m_{b'}$ between 30 and 69 GeV.

[10] For the reduction of the limit due to non-charged-current decay modes, see Fig. 19 of ALBAJAR 90B.

[11] ALBAJAR 88 study events at E_{cm} = 546 and 630 GeV with a muon or isolated electron, accompanied by one or more jets and find agreement with Monte Carlo predictions for the production of charm and bottom, without the need for a new quark. The lower mass limit is obtained by using a conservative estimate for the $b'\overline{b'}$ production cross section and by assuming that it cannot be produced in W decays. The value quoted here is revised using the full $O(\alpha_s^3)$ cross section of ALTARELLI 88.

MASS LIMITS for b' (4^{th} Generation) Quark or Hadron in e^+e^- Collisions

Search for hadrons containing a fourth-generation $-1/3$ quark denoted b'.

The last column specifies the assumption for the decay mode (CC denotes the conventional charged-current decay) and the event signature which is looked for.

VALUE (GeV)	CL%	DOCUMENT ID		TECN	COMMENT
>46.0	95	[12] DECAMP	90F	ALEP	any decay
• • • We do not use the following data for averages, fits, limits, etc. • • •					
		[13] ADRIANI	93G	L3	Quarkonium
>44.7	95	ADRIANI	93M	L3	$\Gamma(Z)$
>45	95	ABREU	91F	DLPH	$\Gamma(Z)$
none 19.4–28.2	95	ABE	90D	VNS	Any decay; event shape
>45.0	95	ABREU	90D	DLPH	B(CC) = 1; event shape
>44.5	95	[14] ABREU	90D	DLPH	$b' \rightarrow cH^-$, $H^- \rightarrow \overline{c}s$, $\tau^-\nu$
>40.5	95	[15] ABREU	90D	DLPH	$\Gamma(Z \rightarrow$ hadrons)
>28.3	95	ADACHI	90	TOPZ	B(FCNC)=100%; isol. γ or 4 jets
>41.4	95	[16] AKRAWY	90B	OPAL	Any decay; acoplanarity
>45.2	95	[16] AKRAWY	90B	OPAL	B(CC) = 1; acoplanarity
>46	95	[17] AKRAWY	90J	OPAL	$b' \rightarrow \gamma$ + any
>27.5	95	[18] ABE	89E	VNS	B(CC) =1; μ, e
none 11.4–27.3	95	[19] ABE	89G	VNS	B($b' \rightarrow b\gamma$) > 10%; isolated γ
>44.7	95	[20] ABRAMS	89C	MRK2	B(CC)= 100%; isol. track
>42.7	95	[20] ABRAMS	89C	MRK2	B(bg)= 100%; event shape
>42.0	95	[20] ABRAMS	89C	MRK2	Any decay; event shape
>28.4	95	[21,22] ADACHI	89C	TOPZ	B(CC) =1; μ
>28.8	95	[23] ENO	89	AMY	B(CC) $\gtrsim$ 90%; μ, e
>27.2	95	[23,24] ENO	89	AMY	any decay; event shape
>29.0	95	[23] ENO	89	AMY	B($b' \rightarrow bg$) $\gtrsim$ 85%; event shape
>24.4	95	[25] IGARASHI	88	AMY	μ,e
>23.8	95	[26] SAGAWA	88	AMY	event shape
>22.7	95	[27] ADEVA	86	MRKJ	μ
>21		[28] ALTHOFF	84C	TASS	R, event shape
>19		[29] ALTHOFF	84I	TASS	Aplanarity

[12] DECAMP 90F looked for isolated charged particles, for isolated photons, and for four-jet final states. The modes $b' \rightarrow bg$ for B($b' \rightarrow bg$) > 65% $b' \rightarrow b\gamma$ for B($b' \rightarrow b\gamma$) > 5% are excluded. Charged Higgs decay were not discussed.

[13] ADRIANI 93G search for vector quarkonium states near Z and give limit on quarkonium-Z mixing parameter $\delta m^2 <$(10–30) GeV^2 (95%CL) for the mass 88–94.5 GeV. Using Richardson potential, a 1S ($b'\overline{b'}$) state is excluded for the mass range 87.7–94.7 GeV. This range depends on the potential choice.

[14] ABREU 90D assumed $m_{H^-} < m_{b'} - 3$ GeV.

[15] Superseded by ABREU 91F.

[16] AKRAWY 90B search was restricted to data near the Z peak at E_{cm} = 91.26 GeV at LEP. The excluded region is between 23.6 and 41.4 GeV if no H^+ decays exist. For charged Higgs decays the excluded regions are between (m_{H^+} + 1.5 GeV) and 45.5 GeV.

[17] AKRAWY 90J search for isolated photons in hadronic Z decay and derive B($Z \rightarrow b'\overline{b'}$)·B($b' \rightarrow \gamma$X)/B($Z \rightarrow$ hadrons) < 2.2×10^{-3}. Mass limit assumes B($b' \rightarrow \gamma$X) > 10%.

[18] ABE 89E search at E_{cm} = 56–57 GeV at TRISTAN for multihadron events with a spherical shape (using thrust and acoplanarity) or containing isolated leptons.

[19] ABE 89G search was at E_{cm} = 55–60.8 GeV at TRISTAN.

[20] If the photonic decay mode is large (B($b' \rightarrow b\gamma$) > 25%), the ABRAMS 89C limit is 45.4 GeV. The limit for for Higgs decay ($b' \rightarrow cH^-$, $H^- \rightarrow \overline{c}s$) is 45.2 GeV.

[21] ADACHI 89C search was at E_{cm} = 56.5–60.8 GeV at TRISTAN using multi-hadron events accompanying muons.

[22] ADACHI 89C also gives limits for any mixture of CC and bg decays.

[23] ENO 89 search at E_{cm} = 50–60.8 at TRISTAN.

[24] ENO 89 considers arbitrary mixture of the charged current, bg, and $b\gamma$ decays.

[25] IGARASHI 88 searches for leptons in low-thrust events and gives $\Delta R(b') <$ 0.26 (95% CL) assuming charged current decay, which translates to $m_{b'} >$ 24.4 GeV.

[26] SAGAWA 88 set limit σ(top) < 6.1 pb at CL=95% for top-flavored hadron production from event shape analyses at E_{cm} = 52 GeV. By using the quark parton model cross-section formula near threshold, the above limit leads to lower mass bounds of 23.8 GeV for charge $-1/3$ quarks.

[27] ADEVA 86 give 95%CL upper bound on an excess of the normalized cross section, ΔR, as a function of the minimum c.m. energy (see their figure 3). Production of a pair of 1/3 charge quarks is excluded up to $E_{cm} = 45.4$ GeV.

[28] ALTHOFF 84C narrow state search sets limit $\Gamma(e^+e^-)B(\text{hadrons}) < 2.4$ keV CL = 95% and heavy charge 1/3 quark pair production $m > 21$ GeV, CL = 95%.

[29] ALTHOFF 84I exclude heavy quark pair production for $7 < m < 19$ GeV (1/3 charge) using aplanarity distributions (CL = 95%).

REFERENCES FOR Searches for (Fourth Generation) b' Quark

ACOSTA	03	PRL 90 131801	D. Acosta *et al.*	(CDF Collab.)
AFFOLDER	00	PRL 84 835	A. Affolder *et al.*	(CDF Collab.)
ABE	98N	PR D58 051102	F. Abe *et al.*	(CDF Collab.)
ABACHI	97D	PRL 78 3818	S. Abachi *et al.*	(D0 Collab.)
FROGGATT	97	ZPHY C73 333	C.D. Froggatt, D.J. Smith, H.B. Nielsen	(GLAS+)
ABACHI	95F	PR D52 4877	S. Abachi *et al.*	(D0 Collab.)
ADRIANI	93G	PL B313 326	O. Adriani *et al.*	(L3 Collab.)
ADRIANI	93M	PRPL 236 1	O. Adriani *et al.*	(L3 Collab.)
MUKHOPAD...	93	PR D48 2105	B. Mukhopadhyaya, D.P. Roy	(TATA)
ABE	92	PRL 68 447	F. Abe *et al.*	(CDF Collab.)
Also	92G	PR D45 3921	F. Abe *et al.*	(CDF Collab.)
ABE	92G	PR D45 3921	F. Abe *et al.*	(CDF Collab.)
ABREU	91F	NP B367 511	P. Abreu *et al.*	(DELPHI Collab.)
ABE	90B	PRL 64 147	F. Abe *et al.*	(CDF Collab.)
ABE	90D	PL B234 382	K. Abe *et al.*	(VENUS Collab.)
ABREU	90D	PL B242 536	P. Abreu *et al.*	(DELPHI Collab.)
ADACHI	90	PL B234 197	I. Adachi *et al.*	(TOPAZ Collab.)
AKESSON	90	ZPHY C46 179	T. Akesson *et al.*	(UA2 Collab.)
AKRAWY	90B	PL B236 364	M.Z. Akrawy *et al.*	(OPAL Collab.)
AKRAWY	90J	PL B246 285	M.Z. Akrawy *et al.*	(OPAL Collab.)
ALBAJAR	90B	ZPHY C48 1	C. Albajar *et al.*	(UA1 Collab.)
DECAMP	90F	PL B236 511	D. Decamp *et al.*	(ALEPH Collab.)
ABE	89E	PR D39 3524	K. Abe *et al.*	(VENUS Collab.)
ABE	89G	PRL 63 1776	K. Abe *et al.*	(VENUS Collab.)
ABRAMS	89C	PRL 63 2447	G.S. Abrams *et al.*	(Mark II Collab.)
ADACHI	89C	PL B229 427	I. Adachi *et al.*	(TOPAZ Collab.)
ENO	89	PRL 63 1910	S. Eno *et al.*	(AMY Collab.)
ALBAJAR	88	ZPHY C37 505	C. Albajar *et al.*	(UA1 Collab.)
ALTARELLI	88	NP B308 724	G. Altarelli *et al.*	(CERN, ROMA, ETH)
IGARASHI	88	PRL 60 2359	S. Igarashi *et al.*	(AMY Collab.)
SAGAWA	88	PRL 60 93	H. Sagawa *et al.*	(AMY Collab.)
ADEVA	86	PR D34 681	B. Adeva *et al.*	(Mark-J Collab.)
ALTHOFF	84C	PL 138B 441	M. Althoff *et al.*	(TASSO Collab.)
ALTHOFF	84I	ZPHY C22 307	M. Althoff *et al.*	(TASSO Collab.)

Free Quark Searches

FREE QUARK SEARCHES

The basis for much of the theory of particle scattering and hadron spectroscopy is the construction of the hadrons from a set of fractionally charged constituents (quarks). A central but unproven hypothesis of this theory, Quantum Chromodynamics, is that quarks cannot be observed as free particles but are confined to mesons and baryons.

Experiments show that it is at best difficult to "unglue" quarks. Accelerator searches at increasing energies have produced no evidence for free quarks, while only a few cosmic-ray and matter searches have produced uncorroborated events.

This compilation is only a guide to the literature, since the quoted experimental limits are often only indicative. Reviews can be found in Refs. 1–3.

References

1. P.F. Smith, Ann. Rev. Nucl. and Part. Sci. **39**, 73 (1989).
2. L. Lyons, Phys. Reports **129**, 225 (1985).
3. M. Marinelli and G. Morpurgo, Phys. Reports **85**, 161 (1982).

Quark Production Cross Section — Accelerator Searches

X-SECT (cm^2)	CHG (e/3)	MASS (GeV)	ENERGY (GeV)	BEAM	EVTS	DOCUMENT ID		TECN
$<1.3E-36$	±2	45–84	130–172	e^+e^-	0	ABREU	97D	DLPH
$<2.E-35$	$+2$	250	1800	$p\overline{p}$	0	[1] ABE	92J	CDF
$<1.E-35$	$+4$	250	1800	$p\overline{p}$	0	[1] ABE	92J	CDF
$<3.8E-28$			14.5A	^{28}Si–Pb	0	[2] HE	91	PLAS
$<3.2E-28$			14.5A	^{28}Si–Cu	0	[2] HE	91	PLAS
$<1.E-40$	$\pm1,2$	<10		$p,\nu,\overline{\nu}$	0	BERGSMA	84B	CHRM
$<1.E-36$	$\pm1,2$	<9	200	μ	0	AUBERT	83C	SPEC
$<2.E-10$	$\pm2,4$	1–3	200	p	0	[3] BUSSIERE	80	CNTR
$<5.E-38$	$+1,2$	>5	300	p	0	[4,5] STEVENSON	79	CNTR
$<1.E-33$	±1	<20	52	pp	0	BASILE	78	SPEC
$<9.E-39$	$\pm1,2$	<6	400	p	0	[4] ANTREASYAN	77	SPEC
$<8.E-35$	$+1,2$	<20	52	pp	0	[6] FABJAN	75	CNTR
$<5.E-38$	$-1,2$	4–9	200	p	0	NASH	74	CNTR
$<1.E-32$	$+2,4$	4–24	52	pp	0	ALPER	73	SPEC
$<5.E-31$	$+1,2,4$	<12	300	p	0	LEIPUNER	73	CNTR
$<6.E-34$	$\pm1,2$	<13	52	pp	0	BOTT	72	CNTR
$<1.E-36$	-4	4	70	p	0	ANTIPOV	71	CNTR
$<1.E-35$	$\pm1,2$	2	28	p	0	[7] ALLABY	69B	CNTR
$<4.E-37$	-2	<5	70	p	0	[3] ANTIPOV	69	CNTR
$<3.E-37$	$-1,2$	2–5	70	p	0	[7] ANTIPOV	69B	CNTR
$<1.E-35$	$+1,2$	<7	30	p	0	DORFAN	65	CNTR
$<2.E-35$	-2	$<2.5-5$	30	p	0	[8] FRANZINI	65B	CNTR
$<5.E-35$	$+1,2$	<2.2	21	p	0	BINGHAM	64	HLBC
$<1.E-32$	$+1,2$	<4.0	28	p	0	BLUM	64	HBC
$<1.E-35$	$+1,2$	<2.5	31	p	0	[8] HAGOPIAN	64	HBC
$<1.E-34$	$+1$	<2	28	p	0	LEIPUNER	64	CNTR
$<1.E-33$	$+1,2$	<2.4	24	p	0	MORRISON	64	HBC

[1] ABE 92J flux limits decrease as the mass increases from 50 to 500 GeV.
[2] HE 91 limits are for charges of the form $N\pm1/3$ from 23/3 to 38/3.
[3] Hadronic or leptonic quarks.
[4] Cross section cm^2/GeV^2.
[5] 3×10^{-5} $<$ lifetime $<1\times10^{-3}$ s.
[6] Includes BOTT 72 results.
[7] Assumes isotropic cm production.
[8] Cross section inferred from flux.

Quark Differential Production Cross Section — Accelerator Searches

X-SECT (cm^{2}sr^{-1}GeV^{-1})	CHG e/3	MASS (GeV)	ENERGY (GeV)	BEAM	EVTS	DOCUMENT ID		TECN
$<4.E-36$	$-2,4$	1.5–6	70	p	0	BALDIN	76	CNTR
$<2.E-33$	±4	5–20	52	pp	0	ALBROW	75	SPEC
$<5.E-34$	<7	7–15	44	pp	0	JOVANOV...	75	CNTR
$<5.E-35$			20	γ	0	[9] GALIK	74	CNTR
$<9.E-35$	$-1,2$		200	p	0	NASH	74	CNTR
$<4.E-36$	-4	2.3–2.7	70	p	0	ANTIPOV	71	CNTR
$<3.E-35$	$\pm1,2$	<2.7	27	p	0	ALLABY	69B	CNTR
$<7.E-38$	$-1,2$	<2.5	70	p	0	ANTIPOV	69B	CNTR

[9] Cross section in cm^2/sr/equivalent quanta.

Quark Flux — Accelerator Searches

The definition of FLUX depends on the experiment

(a) is the ratio of measured free quarks to predicted free quarks if there is no "confinement."
(b) is the probability of fractional charge on nuclear fragments. Energy is in GeV/nucleon.
(c) is the 90%CL upper limit on fractionally-charged particles produced per interaction.
(d) is quarks per collision.
(e) is inclusive quark-production cross-section ratio to $\sigma(e^+e^- \to \mu^+\mu^-)$.
(f) is quark flux per charged particle.
(g) is the flux per ν-event.
(h) is quark yield per π^- yield.
(i) is 2-body exclusive quark-production cross-section ratio to $\sigma(e^+e^- \to \mu^+\mu^-)$.

FLUX		CHG [e/3]	MASS (GeV)	ENRGY (GeV)	BEAM	EVTS	DOCUMENT ID		TECN
$<1.6E-3$	b	see note		200	^{32}S–Pb	0	[10] HUENTRUP	96	PLAS
$<6.2E-4$	b	see note		10.6	^{32}S–Pb	0	[10] HUENTRUP	96	PLAS
$<0.94E-4$	e	±2	2–30	88–94	e^+e^-	0	AKERS	95R	OPAL
$<1.7E-4$	e	±2	30–40	88–94	e^+e^-	0	AKERS	95R	OPAL
$<3.6E-4$	e	±4	5–30	88–94	e^+e^-	0	AKERS	95R	OPAL
$<1.9E-4$	e	±4	30–45	88–94	e^+e^-	0	AKERS	95R	OPAL
$<2.E-3$	e	$+1$	5–40	88–94	e^+e^-	0	[11] BUSKULIC	93C	ALEP
$<6.E-4$	e	$+2$	5–30	88–94	e^+e^-	0	[11] BUSKULIC	93C	ALEP
$<1.2E-3$	e	$+4$	15–40	88–94	e^+e^-	0	[11] BUSKULIC	93C	ALEP
$<3.6E-4$	i	$+4$	5.0–10.2	88–94	e^+e^-	0	BUSKULIC	93C	ALEP
$<3.6E-4$	i	$+4$	16.5–26.0	88–94	e^+e^-	0	BUSKULIC	93C	ALEP
$<6.9E-4$	i	$+4$	26.0–33.3	88–94	e^+e^-	0	BUSKULIC	93C	ALEP
$<9.1E-4$	i	$+4$	33.3–38.6	88–94	e^+e^-	0	BUSKULIC	93C	ALEP
$<1.1E-3$	i	$+4$	38.6–44.9	88–94	e^+e^-	0	BUSKULIC	93C	ALEP
$<1.6E-4$	b	see note		see note		0	[12] CECCHINI	93	PLAS
	b	4,5,7,8		2.1A	^{16}O	0,2,0,6	[13] GHOSH	92	EMUL
$<6.4E-5$	g	1			$\nu,\overline{\nu}$	1	[14] BASILE	91	CNTR
$<3.7E-5$	g	2			$\nu,\overline{\nu}$	0	[14] BASILE	91	CNTR
$<3.9E-5$	g	1			$\nu,\overline{\nu}$	1	[15] BASILE	91	CNTR
$<2.8E-5$	g	2			$\nu,\overline{\nu}$	0	[15] BASILE	91	CNTR
$<1.9E-4$	c			14.5A	^{28}Si–Pb	0	[16] HE	91	PLAS
$<3.9E-4$	c			14.5A	^{28}Si–Cu	0	[16] HE	91	PLAS
$<1.E-9$	c	$\pm1,2,4$		14.5A	^{16}O–Ar	0	MATIS	91	MDRP
$<5.1E-10$	c	$\pm1,2,4$		14.5A	^{16}O–Hg	0	MATIS	91	MDRP
$<8.1E-9$	c	$\pm1,2,4$		14.5A	Si–Hg	0	MATIS	91	MDRP
$<1.7E-6$	c	$\pm1,2,4$		60A	^{16}O–Hg	0	MATIS	91	MDRP
$<3.5E-7$	c	$\pm1,2,4$		200A	^{16}O–Hg	0	MATIS	91	MDRP
$<1.3E-6$	c	$\pm1,2,4$		200A	S–Hg	0	MATIS	91	MDRP
$<5E-2$	e	2	19–27	52–60	e^+e^-	0	ADACHI	90C	TOPZ
$<5E-2$	e	4	<24	52–60	e^+e^-	0	ADACHI	90C	TOPZ

<1.E−4	e	+2	<3.5	10	e^+e^-	0	BOWCOCK	89B	CLEO
<1.E−6	d	±1,2		60	^{16}O–Hg	0	CALLOWAY	89	MDRP
<3.5E−7	d	±1,2		200	^{16}O–Hg	0	CALLOWAY	89	MDRP
<1.3E−6	d	±1,2		200	S–Hg	0	CALLOWAY	89	MDRP
<1.2E−10	d	±1	1	800	p–Hg	0	MATIS	89	MDRP
<1.1E−10	d	±2	1	800	p–Hg	0	MATIS	89	MDRP
<1.2E−10	d	±1	1	800	p–N_2	0	MATIS	89	MDRP
<7.7E−11	d	±2	1	800	p–N_2	0	MATIS	89	MDRP
<6.E−9	h	−5	0.9–2.3	12	p	0	NAKAMURA	89	SPEC
<5.E−5	g	1,2	<0.5		$\nu,\overline{\nu}d$	0	ALLASIA	88	BEBC
<3.E−4	b	See note		14.5	^{16}O–Pb	0	[17] HOFFMANN	88	PLAS
<2.E−4	b	See note		200	^{16}O–Pb	0	[18] HOFFMANN	88	PLAS
<8E−5	b	19,20,22,23		200*A*			GERBIER	87	PLAS
<2.E−4	a	±1,2	<300	320	$\overline{p}p$	0	LYONS	87	MLEV
<1.E−9	c	±1,2,4,5		14.5	^{16}O–Hg	0	SHAW	87	MDRP
<3.E−3	d	−1,2,3,4,6	<5	2	Si–Si	0	[19] ABACHI	86C	CNTR
<1.E−4	e	±1,2,4	<4	10	e^+e^-	0	ALBRECHT	85G	ARG
<6.E−5	b	±1,2	1	540	$p\overline{p}$	0	BANNER	85	UA2
<5.E−3	e	−4	1–8	29	e^+e^-	0	AIHARA	84	TPC
<1.E−2	e	±1,2	1–13	29	e^+e^-	0	AIHARA	84B	TPC
<2.E−4	b	±1		72	^{40}Ar	0	[20] BARWICK	84	CNTR
<1.E−4	e	±2	<0.4	1.4	e^+e^-	0	BONDAR	84	OLYA
<5.E−1	e	±1,2	<13	29	e^+e^-	0	GURYN	84	CNTR
<3.E−3	b	±1,2	<2	540	$p\overline{p}$	0	BANNER	83	CNTR
<1.E−4	b	±1,2		106	^{56}Fe	0	LINDGREN	83	CNTR
<3.E−3	b	$> \lvert \pm 0.1 \rvert$		74	^{40}Ar	0	[20] PRICE	83	PLAS
<1.E−2	e	±1,2	<14	29	e^+e^-	0	MARINI	82B	CNTR
<8.E−2	e	±1,2	<12	29	e^+e^-	0	ROSS	82	CNTR
<3.E−4	e	±2	1.8–2	7	e^+e^-	0	WEISS	81	MRK2
<5.E−2	e	+1,2,4,5	2–12	27	e^+e^-	0	BARTEL	80	JADE
<2.E−5	g	1,2			ν	0	[14,15] BASILE	80	CNTR
<3.E−10	f	±2,4	1–3	200	p	0	[21] BOZZOLI	79	CNTR
<6.E−11	f	±1	<21	52	pp	0	BASILE	78	SPEC
<5.E−3	g				ν_μ	0	BASILE	78B	CNTR
<2.E−9	f	±1	<26	62	pp	0	BASILE	77	SPEC
<7.E−10	f	+1,2	<20	52	p	0	[22] FABJAN	75	CNTR
		+1,2	>4.5		γ	0	[14,15] GALIK	74	CNTR
		+1,2	>1.5	12	e^-	0	[14,15] BELLAMY	68	CNTR
		+1,2	>0.9		γ	0	[15] BATHOW	67	CNTR
		+1,2	>0.9	6	γ	0	[15] FOSS	67	CNTR

[10] HUENTRUP 96 quote 95% CL limits for production of fragments with charge differing by as much as ±1/3 (in units of e) for charge $6 \leq Z \leq 10$.

[11] BUSKULIC 93C limits for inclusive quark production are more conservative if the ALEPH hadronic fragmentation function is assumed.

[12] CECCHINI 93 limit at 90%CL for $23/3 \leq Z \leq 40/3$, for 16*A* GeV O, 14.5*A* Si, and 200*A* S incident on Cu target. Other limits are 2.3×10^{-4} for $17/3 \leq Z \leq 20/3$ and 1.2×10^{-4} for $20/3 \leq Z \leq 23/3$.

[13] GHOSH 92 reports measurement of spallation fragment charge based on ionization in emulsion. Out of 650 measured tracks, 2 were consistent with charge $5e/3$, and 4 with $7e/3$.

[14] Hadronic quark.

[15] Leptonic quark.

[16] HE 91 limits are for charges of the form $N \pm 1/3$ from 23/3 to 38/3, and correspond to cross-section limits of 380μb (Pb) and 320μb (Cu).

[17] The limits apply to projectile fragment charges of 17, 19, 20, 22, 23 in units of $e/3$.

[18] The limits apply to projectile fragment charges of 16, 17, 19, 20, 22, 23 in units of $e/3$.

[19] Flux limits and mass range depend on charge.

[20] Bound to nuclei.

[21] Quark lifetimes $> 1 \times 10^{-8}$ s.

[22] One candidate $m < 0.17$ GeV.

Quark Flux — Cosmic Ray Searches

Shielding values followed with an asterisk indicate altitude in km. Shielding values not followed with an asterisk indicate sea level in kg/cm^2.

FLUX (cm^{-2}sr^{-1}s^{-1})	CHG (*e*/3)	MASS (GeV)	SHIELDING	EVTS	DOCUMENT ID		TECN
< 9.2E−15	±1		3800	0	[23] AMBROSIO	00C	MCRO
<2.1E−15	±1			0	MORI	91	KAM2
<2.3E−15	±2			0	MORI	91	KAM2
<2.E−10	±1,2		0.3	0	WADA	88	CNTR
	±4		0.3	12	[24] WADA	88	CNTR
	±4		0.3	9	[25] WADA	86	CNTR
<1.E−12	±2,3/2		−70.	0	[26] KAWAGOE	84B	PLAS
<9.E−10	±1,2		0.3	0	WADA	84B	CNTR
<4.E−9	±4		0.3	7	WADA	84B	CNTR
<2.E−12	±1,2,3		−0.3 *	0	MASHIMO	83	CNTR
<3.E−10	±1,2		0.3	0	MARINI	82	CNTR
<2.E−11	±1,2			0	MASHIMO	82	CNTR
<8.E−10	±1,2		0.3	0	[26] NAPOLITANO	82	CNTR
				3	[27] YOCK	78	CNTR
<1.E−9				0	[28] BRIATORE	76	ELEC
<2.E−11	+1			0	[29] HAZEN	75	CC
<2.E−10	+1,2			0	KRISOR	75	CNTR
<1.E−7	+1,2			0	[29,30] CLARK	74B	CC
<3.E−10	+1	>20		0	KIFUNE	74	CNTR
<8.E−11	+1			0	[29] ASHTON	73	CNTR
<2.E−8	+1,2			0	HICKS	73B	CNTR
<5.E−10	+4		2.8 *	0	BEAUCHAMP	72	CNTR
<1.E−10	+1,2			0	[29] BOHM	72B	CNTR
<1.E−10	+1,2		2.8 *	0	COX	72	ELEC
<3.E−10	+2			0	CROUCH	72	CNTR
<3.E−8			7	0	[28] DARDO	72	CNTR
<4.E−9	+1			0	[29] EVANS	72	CC
<2.E−9		>10		0	[28] TONWAR	72	CNTR
<2.E−10	+1		2.8 *	0	CHIN	71	CNTR
<3.E−10	+1,2			0	[29] CLARK	71B	CC
<1.E−10	+1,2			0	[29] HAZEN	71	CC
<5.E−10	+1,2		3.5 *	0	BOSIA	70	CNTR
	+1,2	<6.5		1	[29] CHU	70	HLBC
<2.E−9	+1			0	FAISSNER	70B	CNTR
<2.E−10	+1,2		0.8 *	0	KRIDER	70	CNTR
<5.E−11	+2			4	CAIRNS	69	CC
<8.E−10	+1,2	<10		0	FUKUSHIMA	69	CNTR
	+2			1	[29,31] MCCUSKER	69	CC
<1.E−10		>5	1.7,3.6	0	[28] BJORNBOE	68	CNTR
<1.E−8	±1,2,4		6.3,.2 *	0	[26] BRIATORE	68	CNTR
<3.E−8		>2		0	FRANZINI	68	CNTR
<9.E−11	±1,2			0	GARMIRE	68	CNTR
<4.E−10	±1			0	HANAYAMA	68	CNTR
<3.E−8		>15		0	KASHA	68	OSPK
<2.E−10	+2			0	KASHA	68B	CNTR
<2.E−10	+4			0	KASHA	68C	CNTR
<2.E−10	+2		6	0	BARTON	67	CNTR
<2.E−7	+4		0.008,0.5 *	0	BUHLER	67	CNTR
<5.E−10	1,2		0.008,0.5 *	0	BUHLER	67B	CNTR
<4.E−10	+1,2			0	GOMEZ	67	CNTR
<2.E−9	+2			0	KASHA	67	CNTR
<2.E−10	+2		220	0	BARTON	66	CNTR
<2.E−9	+1,2		0.5 *	0	BUHLER	66	CNTR
<3.E−9	+1,2			0	KASHA	66	CNTR
<2.E−9	+1,2			0	LAMB	66	CNTR
<2.E−8	+1,2	>7	2.8 *	0	DELISE	65	CNTR
<5.E−8	+2	>2.5	0.5 *	0	MASSAM	65	CNTR
<2.E−8	+1		2.5 *	0	BOWEN	64	CNTR
<2.E−7	+1		0.8	0	SUNYAR	64	CNTR

[23] AMBROSIO 00C limit is below 11×10^{-15} for $0.25 < q/e < 0.5$, and is changing rapidly near $q/e = 2/3$, where it is 2×10^{-14}.

[24] Distribution in celestial sphere was described as anisotropic.

[25] With telescope axis at zenith angle 40° to the south.

[26] Leptonic quarks.

[27] Lifetime $> 10^{-8}$ s; charge ±0.70, 0.68, 0.42; and mass >4.4, 4.8, and 20 GeV, respectively.

[28] Time delayed air shower search.

[29] Prompt air shower search.

[30] Also $e/4$ and $e/6$ charges.

[31] No events in subsequent experiments.

Quark Density — Matter Searches

For a review, see SMITH 89.

QUARKS/ NUCLEON	CHG (*e*/3)	MASS (GeV)	MATERIAL/METHOD	EVTS	DOCUMENT ID		
<4.7E−21	±1,2		silicone oil drops	0	MAR	96	
<8.E−22	+2		Si/infrared photoionization	0	PERERA	93	
<5.E−27	±1,2		sea water/levitation	0	HOMER	92	
<4.E−20	±1,2		meteorites/mag. levitation	0	JONES	89	
<1.E−19	±1,2		various/spectrometer	0	MILNER	87	
<5.E−22	±1,2		W/levitation	0	SMITH	87	
<3.E−20	+1,2		org liq/droplet tower	0	VANPOLEN	87	
<6.E−20	−1,2		org liq/droplet tower	0	VANPOLEN	87	
<3.E−21	±1		Hg drops-untreated	0	SAVAGE	86	
<3.E−22	±1,2		levitated niobium	0	SMITH	86	
<2.E−26	±1,2		^{4}He/levitation	0	SMITH	86B	
<2.E−20	>±1	0.2–250	niobium+tungs/ion	0	MILNER	85	
<1.E−21	±1		levitated niobium	0	SMITH	85	
	+1,2	<100	niobium/mass spec	0	KUTSCHERA	84	
<5.E−22			levitated steel	0	MARINELLI	84	
<9.E−20	± <13		water/oil drop	0	JOYCE	83	
<2.E−21	$> \lvert \pm 1/2 \rvert$		levitated steel	0	LIEBOWITZ	83	
<1.E−19	±1,2		photo ion spec	0	VANDESTEEG	83	
<2.E−20			mercury/oil drop	0	[32] HODGES	81	
1.E−20	+1		levitated niobium	4	[33] LARUE	81	
1.E−20	−1		levitated niobium	4	[33] LARUE	81	
<1.E−21			levitated steel	0	MARINELLI	80B	
<6.E−16			helium/mass spec	0	BOYD	79	
1.E−20	+1		levitated niobium	2	[33] LARUE	79	
<4.E−28			earth+/ion beam	0	OGOROD...	79	
<5.E−15	+1		tungs./mass spec	0	BOYD	78	
<5.E−16	+3	<1.7	hydrogen/mass spec	0	BOYD	78B	
<1.E−21	±2,4		water/ion beam	0	LUND	78	
<6.E−15	>1/2		levitated tungsten	0	PUTT	78	
<1.E−22			metals/mass spec	0	SCHIFFER	78	
<5.E−15			levitated tungsten ox	0	BLAND	77	
<3.E−21			levitated iron	0	GALLINARO	77	

Quark Particle Listings

Free Quark Searches

2.E−21	−1		levitated niobium	1	[33] LARUE	77
4.E−21	+1		levitated niobium	2	[33] LARUE	77
<1.E−13	+3	<7.7	hydrogen/mass spec	0	MULLER	77
<5.E−27			water+/ion beam	0	OGOROD...	77
<1.E−21			lunar+/ion spec	0	STEVENS	76
<1.E−15	+1	<60	oxygen+/ion spec	0	ELBERT	70
<5.E−19			levitated graphite	0	MORPURGO	70
<5.E−23			water+/atom beam	0	COOK	69
<1.E−17	±1,2		levitated graphite	0	BRAGINSK	68
<1.E−17			water+/uv spec	0	RANK	68
<3.E−19	±1		levitated iron	0	STOVER	67
<1.E−10			sun/uv spec	0	[34] BENNETT	66
<1.E−17	+1,2		meteorites+/ion beam	0	CHUPKA	66
<1.E−16	±1		levitated graphite	0	GALLINARO	66
<1.E−22			argon/electrometer	0	HILLAS	59
	−2		levitated oil	0	MILLIKAN	10

[32] Also set limits for $Q = \pm e/6$.

[33] Note that in PHILLIPS 88 these authors report a subtle magnetic effect which could account for the apparent fractional charges.

[34] Limit inferred by JONES 77B.

REFERENCES FOR Free Quark Searches

AMBROSIO 00C PR D62 052003 M. Ambrosio *et al.* (MACRO Collab.)
ABREU 97D PL B396 315 P. Abreu *et al.* (DELPHI Collab.)
HUENTRUP 96 PR C53 358 G. Huentrup *et al.* (SIEG)
MAR 96 PR D53 6017 N.M. Mar *et al.* (SLAC, SCHAF, LANL, UCI)
AKERS 95R ZPHY C67 203 R. Akers *et al.* (OPAL Collab.)
BUSKULIC 93C PL B303 198 D. Buskulic *et al.* (ALEPH Collab.)
CECCHINI 93 ASP 1 369 S. Cecchini *et al.*
PERERA 93 PRL 70 1053 A.G.U. Perera *et al.* (PITT)
ABE 92J PR D46 R1889 F. Abe *et al.* (CDF Collab.)
GHOSH 92 NC 105A 99 D. Ghosh *et al.* (JADA, BANGB)
HOMER 92 ZPHY C55 549 G.J. Homer *et al.* (RAL, SHMP, LOQM)
BASILE 91 NC 104A 405 M. Basile *et al.* (BGNA, INFN, CERN, PLRM+)
HE 91 PR C44 1672 Y.B. He, P.B. Price (UCB)
MATIS 91 NP A525 513c H.S. Matis *et al.* (LBL, SFSU, UCI+)
MORI 91 PR D43 2843 M. Mori *et al.* (Kamiokande II Collab.)
ADACHI 90C PL B244 352 I. Adachi *et al.* (TOPAZ Collab.)
BOWCOCK 89B PR D40 263 T.J.V. Bowcock *et al.* (CLEO Collab.)
CALLOWAY 89 PL B232 549 D. Calloway *et al.* (SFSU, UCI, LBL+)
JONES 89 ZPHY C43 349 W.G. Jones *et al.* (LOIC, RAL)
MATIS 89 PR D39 1851 H.S. Matis *et al.* (LBL, SFSU, UCI+)
NAKAMURA 89 PR D39 1261 T.T. Nakamura *et al.* (KYOT, TMTC)
SMITH 89 ARNPS 39 73 P.F. Smith (RAL)
ALLASIA 88 PR D37 219 D. Allasia *et al.* (WA25 Collab.)
HOFFMANN 88 PL B200 583 A. Hofmann *et al.* (SIEG, USF)
PHILLIPS 88 NIM A264 125 J.D. Phillips, W.M. Fairbank, J. Navarro (STAN)
WADA 88 NC 11C 229 T. Wada, Y. Yamashita, I. Yamamoto (OKAY)
GERBIER 87 PRL 59 2535 G. Gerbier *et al.* (UCB, CERN)
LYONS 87 ZPHY C36 363 L. Lyons *et al.* (OXF, RAL, LOIC)
MILNER 87 PR D36 37 R.E. Milner *et al.* (CIT)
SHAW 87 PR D36 3533 G.L. Shaw *et al.* (UCI, LBL, LANL, SFSU)
SMITH 87 PL B197 447 P.F. Smith *et al.* (RAL, LOIC)
VANPOLEN 87 PR D36 1983 J. van Polen, R.T. Hagstrom, G. Hirsch (ANL+)
ABACHI 86C PR D33 2733 S. Abachi *et al.* (UCLA, LBL, UCD)
SAVAGE 86 PL 167B 481 M.L. Savage *et al.* (SFSU)
SMITH 86 PL B171 129 P.F. Smith *et al.* (RAL, LOIC)
SMITH 86B PL B181 407 P.F. Smith *et al.* (RAL, LOIC)
WADA 86 NC 9C 358 T. Wada (OKAY)
ALBRECHT 85G PL 156B 134 H. Albrecht *et al.* (ARGUS Collab.)
BANNER 85 PL 156B 129 M. Banner *et al.* (UA2 Collab.)
MILNER 85 PRL 54 1472 R.E. Milner *et al.* (CIT)
SMITH 85 PL 153B 188 P.F. Smith *et al.* (RAL, LOIC)
AIHARA 84 PRL 52 168 H. Aihara *et al.* (TPC Collab.)
AIHARA 84B PRL 52 2332 H. Aihara *et al.* (TPC Collab.)
BARWICK 84 PR D30 691 S.W. Barwick, J.A. Musser, J.D. Stevenson (UCB)
BERGSMA 84B ZPHY C24 217 F. Bergsma *et al.* (CHARM Collab.)
BONDAR 84 JETPL 40 1265 A.E. Bondar *et al.* (NOVO)
Translated from ZETFP 40 440.
GURYN 84 PL 139B 313 W. Guryn *et al.* (FRAS, LBL, NWES, STAN+)
KAWAGOE 84B LNC 41 604 K. Kawagoe *et al.* (TOKY)
KUTSCHERA 84 PR D29 791 W. Kutschera *et al.* (ANL, FNAL)
MARINELLI 84 PL 137B 439 M. Marinelli, G. Morpurgo (GENO)
WADA 84B LNC 40 329 T. Wada, Y. Yamashita, I. Yamamoto (OKAY)
AUBERT 83C PL 133B 461 J.J. Aubert *et al.* (EMC Collab.)
BANNER 83 PL 121B 187 M. Banner *et al.* (UA2 Collab.)
JOYCE 83 PRL 51 731 D.C. Joyce *et al.* (SFSU)
LIEBOWITZ 83 PRL 50 1640 D. Liebowitz, M. Binder, K.O.H. Ziock (VIRG)
LINDGREN 83 PRL 51 1621 M.A. Lindgren *et al.* (SFSU, UCR, UCI+)
MASHIMO 83 PL 128B 327 T. Mashimo *et al.* (ICEPP)
PRICE 83 PRL 50 566 P.B. Price *et al.* (UCB)
VANDESTEEG 83 PRL 50 1234 M.J.H. van de Steeg, H.W.H.M. Jongbloets, P. Wyder
MARINI 82 PR D26 1777 A. Marini *et al.* (FRAS, LBL, NWES, STAN+)
MARINI 82B PRL 48 1649 A. Marini *et al.* (FRAS, LBL, NWES, STAN+)
MASHIMO 82 JPSJ 51 3067 T. Mashimo, K. Kawagoe, M. Koshiba (INUS)
NAPOLITANO 82 PR D25 2837 J. Napolitano *et al.* (STAN, FRAS, LBL+)
ROSS 82 PL 118B 199 M.C. Ross *et al.* (FRAS, LBL, NWES, STAN+)
HODGES 81 PRL 47 1651 C.L. Hodges *et al.* (UCR, SFSU)
LARUE 81 PRL 46 967 G.S. Larue, J.D. Phillips, W.M. Fairbank (STAN)
WEISS 81 PL 101B 439 J.M. Weiss *et al.* (SLAC, LBL, UCB)
BARTEL 80 ZPHY C6 295 W. Bartel *et al.* (JADE Collab.)
BASILE 80 LNC 29 251 M. Basile *et al.* (BGNA, CERN, FRAS, ROMA+)
BUSSIERE 80 NP B174 1 A. Bussiere *et al.* (BGNA, SACL, LAPP)
MARINELLI 80B PL 94B 433 M. Marinelli, G. Morpurgo (GENO)
Also 80 PL 94B 427 M. Marinelli, G. Morpurgo (GENO)
BOYD 79 PRL 43 1288 R.N. Boyd *et al.* (OSU)
BOZZOLI 79 NP B159 363 W. Bozzoli *et al.* (BGNA, LAPP, SACL+)
LARUE 79 PRL 42 142 G.S. Larue, W.M. Fairbank, J.D. Phillips (STAN)
Also 79B PRL 42 1019 G.S. Larue, W.M. Fairbank, J.D. Phillips
OGOROD... 79 JETP 49 953 D.D. Ogorodnikov, I.M. Samoilov, A.M. Soltntsev
Translated from ZETF 76 1881.
STEVENSON 79 PR D20 82 M.L. Stevenson (LBL)
BASILE 78 NC 45A 171 M. Basile *et al.* (CERN, BGNA)
BASILE 78B NC 45A 281 M. Basile *et al.* (CERN, BGNA)
BOYD 78 PRL 40 216 R.N. Boyd *et al.* (ROCH)
BOYD 78B PL 72B 484 R.N. Boyd *et al.* (ROCH)
LUND 78 RA 25 75 T. Lund, R. Brandt, Y. Fares (MARB)
PUTT 78 PR D17 1466 G.D. Putt, P.C.M. Yock (AUCK)
SCHIFFER 78 PR D17 2241 J.P. Schiffer *et al.* (CHIC, ANL)
YOCK 78 PR D18 641 P.C.M. Yock (AUCK)
ANTREASYAN 77 PRL 39 513 D. Antreasyan *et al.* (EFI, PRIN)
BASILE 77 NC 40A 41 M. Basile *et al.* (CERN, BGNA)
BLAND 77 PRL 39 369 R.W. Bland *et al.* (SFSU)
GALLINARO 77 PRL 38 1255 G. Gallinaro, M. Marinelli, G. Morpurgo (GENO)
JONES 77B RMP 49 717 L.W. Jones
LARUE 77 PRL 38 1011 G.S. Larue, W.M. Fairbank, A.F. Hebard (STAN)
MULLER 77 Science 196 521 R.A. Muller *et al.* (LBL)
OGOROD... 77 JETP 45 857 D.D. Ogorodnikov, I.M. Samoilov, A.M. Soltntsev
Translated from ZETF 72 1633.
BALDIN 76 SJNP 22 264 B.Y. Baldin *et al.* (JINR)
Translated from YAF 22 512.
BRIATORE 76 NC 31A 553 L. Briatore *et al.* (LCGT, FRAS, FREIB)
STEVENS 76 PR D14 716 C.M. Stevens, J.P. Schiffer, W. Chupka (ANL)
ALBROW 75 NP B97 189 M.G. Albrow *et al.* (CERN, DARE, FOM+)
FABJAN 75 NP B101 349 C.W. Fabjan *et al.* (CERN, MPIM)
HAZEN 75 NP B95 189 W.E. Hazen *et al.* (MICH, LEED)
JOVANOV... 75 PL 56B 105 J.V. Jovanovich *et al.* (MANI, AACH, CERN+)
KRISOR 75 NC 27A 132 K. Krisor (AACH3)
CLARK 74B PR D10 2721 A.F. Clark *et al.* (LLL)
GALIK 74 PR D9 1856 R.S. Galik *et al.* (SLAC, FNAL)
KIFUNE 74 JPSJ 36 629 T. Kifune *et al.* (TOKY, KEK)
NASH 74 PRL 32 858 T. Nash *et al.* (FNAL, CORN, NYU)
ALPER 73 PL 46B 265 B. Alper *et al.* (CERN, LIVP, LUND, BOHR+)
ASHTON 73 JPA 6 577 F. Ashton *et al.* (DURH)
HICKS 73B NC 14A 65 R.B. Hicks, R.W. Flint, S. Standil (MANI)
LEIPUNER 73 PRL 31 1226 L.B. Leipuner *et al.* (BNL, YALE)
BEAUCHAMP 72 PR D6 1211 W.T. Beauchamp *et al.* (ARIZ)
BOHM 72B PRL 28 326 A. Bohm *et al.* (AACH)
BOTT 72 PL 40B 693 M. Bott-Bodenhausen *et al.* (CERN, MPIM)
COX 72 PR D6 1203 A.J. Cox *et al.* (ARIZ)
CROUCH 72 PR D5 2667 M.F. Crouch, K. Mori, G.R. Smith (CASE)
DARDO 72 NC 9A 319 M. Dardo *et al.* (TORI)
EVANS 72 PRSE A70 143 G.R. Evans *et al.* (EDIN, LEED)
TONWAR 72 JPA 5 569 S.C. Tonwar, S. Naranan, B.V. Sreekantan (TATA)
ANTIPOV 71 NP B27 374 Y.M. Antipov *et al.* (SERP)
CHIN 71 NC 2A 419 S. Chin *et al.* (OSAK)
CLARK 71B PRL 27 51 A.F. Clark *et al.* (LLL, LBL)
HAZEN 71 PRL 26 582 W.E. Hazen (MICH)
BOSIA 70 NC 66A 167 G.F. Bosia, L. Briatore (TORI)
CHU 70 PRL 24 917 W.T. Chu *et al.* (OSU, ROSE, KANS)
Also 70B PRL 25 550 W.W.M. Allison *et al.* (ANL)
ELBERT 70 NP B20 217 J.W. Elbert *et al.* (WISC)
FAISSNER 70B PRL 24 1357 H. Faissner *et al.* (AACH3)
KRIDER 70 PR D1 835 E.P. Krider, T. Bowen, R.M. Kalbach (ARIZ)
MORPURGO 70 NIM 79 95 G. Morpurgo, G. Gallinaro, G. Palmieri (GENO)
ALLABY 69B NC 64A 75 J.V. Allaby *et al.* (CERN)
ANTIPOV 69 PL 29B 245 Y.M. Antipov *et al.* (SERP)
ANTIPOV 69B PL 30B 576 Y.M. Antipov *et al.* (SERP)
CAIRNS 69 PR 186 1394 I. Cairns *et al.* (SYDN)
COOK 69 PR 188 2092 D.D. Cook *et al.* (ILL)
FUKUSHIMA 69 PR 178 2058 Y. Fukushima *et al.* (TOKY)
MCCUSKER 69 PRL 23 658 C.B.A. McCusker, I. Cairns (SYDN)
BELLAMY 68 PR 166 1391 E.H. Bellamy *et al.* (STAN, SLAC)
BJORNBOE 68 NC B53 241 J. Bjornboe *et al.* (BOHR, TATA, BERN+)
BRAGINSK 68 JETP 27 51 V.B. Braginsky *et al.* (MOSU)
Translated from ZETF 54 91.
BRIATORE 68 NC 57A 850 L. Briatore *et al.* (TORI, CERN, BGNA)
FRANZINI 68 PRL 21 1013 P. Franzini, S. Shulman (COLU)
GARMIRE 68 PR 166 166 G. Garmire, C. Leong, V. Sreekantan (MIT)
HANAYAMA 68 CJP 46 S734 Y. Hanayama *et al.* (OSAK)
KASHA 68 PR 172 1297 H. Kasha, R.J. Stefanski (BNL, YALE)
KASHA 68B PRL 20 217 H. Kasha *et al.* (BNL, YALE)
KASHA 68C CJP 46 S730 H. Kasha *et al.* (BNL, YALE)
RANK 68 PR 176 1635 D. Rank (MICH)
BARTON 67 PRSL 90 87 J.C. Barton (NPOL)
BATHOW 67 PL 25B 163 G. Bathow *et al.* (DESY)
BUHLER 67 NC 49A 209 A. Buhler-Broglin *et al.* (CERN, BGNA)
BUHLER 67B NC 51A 837 A. Buhler-Broglin *et al.* (CERN, BGNA+)
FOSS 67 PL 25B 166 J. Foss *et al.* (MIT)
GOMEZ 67 PRL 18 1022 R. Gomez *et al.* (CIT)
KASHA 67 PR 154 1263 H. Kasha *et al.* (BNL, YALE)
STOVER 67 PR 164 1599 R.W. Stover, T.I. Moran, J.W. Trischka (SYRA)
BARTON 66 PL 21 360 J.C. Barton, C.T. Stockel (NPOL)
BENNETT 66 PRL 17 1196 W.R. Bennett (YALE)
BUHLER 66 NC 45A 520 A. Buhler-Broglin *et al.* (CERN, BGNA+)
CHUPKA 66 PRL 17 60 W.A. Chupka, J.P. Schiffer, C.M. Stevens (ANL)
GALLINARO 66 PL 23 609 G. Gallinaro, G. Morpurgo (GENO)
KASHA 66 PR 150 1140 H. Kasha, L.B. Leipuner, R.K. Adair (BNL, YALE)
LAMB 66 PRL 17 1068 R.C. Lamb *et al.* (ANL)
DELISE 65 PR 140B 458 D.A. de Lise, T. Bowen (ARIZ)
DORFAN 65 PRL 14 999 D.E. Dorfan *et al.* (COLU)
FRANZINI 65B PRL 14 196 P. Franzini *et al.* (BNL, COLU)
MASSAM 65 NC 40A 589 T. Massam, T. Muller, A. Zichichi (CERN)
BINGHAM 64 PL 9 201 H.H. Bingham *et al.* (CERN, EPOL)
BLUM 64 PRL 13 353A W. Blum *et al.* (CERN)
BOWEN 64 PRL 13 728 T. Bowen *et al.* (ARIZ)
HAGOPIAN 64 PRL 13 280 V. Hagopian *et al.* (PENN, BNL)
LEIPUNER 64 PRL 12 423 L.B. Leipuner *et al.* (BNL, YALE)
MORRISON 64 PL 9 199 D.R.O. Morrison (CERN)
SUNYAR 64 PR 136B 1157 A.W. Sunyar, A.Z. Schwarzschild, P.I. Connors (BNL)
HILLAS 59 NAT 184 B92 A.M. Hillas, T.E. Cranshaw (AERE)
MILLIKAN 10 Phil Mag 19 209 R.A. Millikan (CHIC)

OTHER RELATED PAPERS

LYONS 85 PRPL C129 225 L. Lyons (OXF)
Review
MARINELLI 82 PRPL 85 161 M. Marinelli, G. Morpurgo (GENO)
Review

(continued on the next page)

• Indicates the particle is in the Meson Summary Table

• Indicates the particle is in the Meson Summary Table

LIGHT UNFLAVORED MESONS ($S = C = B = 0$)

For $I = 1$ (π, b, ρ, a): $u\overline{d}$, $(u\overline{u}-d\overline{d})/\sqrt{2}$, $d\overline{u}$;
for $I = 0$ (η, η', h, h', ω, ϕ, f, f'): $c_1(u\overline{u}+d\overline{d}) + c_2(s\overline{s})$

PSEUDOSCALAR-MESON DECAY CONSTANTS

Revised October 2003 by M. Suzuki (LBNL).

Charged mesons

The decay constant f_P for a charged pseudoscalar meson P is defined by

$$\langle 0|A_\mu(0)|P(\mathbf{q})\rangle = i f_P\, q_\mu \ , \tag{1}$$

where A_μ is the axial-vector part of the charged weak current after a Cabibbo-Kobayashi-Maskawa mixing-matrix element $V_{qq'}$ has been removed. The state vector is normalized by $\langle P(\mathbf{q})|P(\mathbf{q}')\rangle = (2\pi)^3\, 2E_q\, \delta(\mathbf{q}-\mathbf{q}')$, and its phase is chosen to make f_P real and positive. Note, however, that in many theoretical papers our $f_P/\sqrt{2}$ is denoted by f_P.

In determining f_P experimentally, radiative corrections must be taken into account. Since the photon-loop correction introduces an infrared divergence that is canceled by soft-photon emission, we can determine f_P only from the combined rate for $P^\pm \to \ell^\pm\nu_\ell$ and $P^\pm \to \ell^\pm\nu_\ell\gamma$. This rate is given by

$$\Gamma\,(P \to \ell\nu_\ell + \ell\nu_\ell\gamma) = \frac{G_F^2|V_{qq'}{}^2|}{8\pi} f_P^2\, m_\ell^2\, m_P \left(1-\frac{m_\ell^2}{m_P^2}\right)^2 [1+\mathcal{O}(\alpha)] \ . \tag{2}$$

Here m_ℓ and m_P are the masses of the lepton and meson. Radiative corrections include inner bremsstrahlung, which is independent of the structure of the meson [1–3], and also a structure-dependent term [4,5]. After radiative corrections are made, there are ambiguities in extracting f_P from experimental measurements. In fact, the definition of f_P is no longer unique.

It is desirable to define f_P such that it depends only on the properties of the pseudoscalar meson, not on the final decay products. The short-distance corrections to the fundamental electroweak constants like $G_F|V_{qq'}|$ should be separated out. Following Marciano and Sirlin [6], we define f_P with the following form for the $\mathcal{O}(\alpha)$ corrections:

$$1+\mathcal{O}(\alpha) = \left[1+\frac{2\alpha}{\pi}\ln\!\left(\frac{m_Z}{m_\rho}\right)\right]\left[1+\frac{\alpha}{\pi}F(x)\right] \times\left\{1-\frac{\alpha}{\pi}\left[\frac{3}{2}\ln\!\left(\frac{m_\rho}{m_P}\right)+C_1+C_2\frac{m_\ell^2}{m_\rho^2}\ln\!\left(\frac{m_\rho^2}{m_\ell^2}\right)+C_3\frac{m_\ell^2}{m_\rho^2}+\ldots\right]\right\} , \tag{3}$$

where m_ρ and m_Z are the masses of the ρ meson and Z boson. Here

$$F(x) = 3\ln x + \frac{13-19x^2}{8(1-x^2)} - \frac{8-5x^2}{2(1-x^2)^2}\, x^2\ln x - 2\left(\frac{1+x^2}{1-x^2}\ln x+1\right)\ln(1-x^2) + 2\left(\frac{1+x^2}{1-x^2}\right)L(1-x^2) \ ,$$

with

$$x \equiv m_\ell/m_P \ , \qquad L(z) \equiv \int_0^z \frac{\ln(1-t)}{t}\, dt \ . \tag{4}$$

The first bracket in the expression for $1+\mathcal{O}(\alpha)$ is the short-distance electroweak correction. A quarter of $(2\alpha/\pi)\,\ln(m_Z/m_\rho)$ is subject to the QCD correction $(1-\alpha_s/\pi)$, which leads to a reduction of the total short-distance correction of 0.00033 from the electroweak contribution alone [6]. The second bracket together with the term $-(3\alpha/2\pi)\ln(m_\rho/m_P)$ in the third bracket corresponds to the radiative corrections to the point-like pion decay ($\Lambda_{\rm cutoff} \approx m_\rho$) [2]. The rest of the corrections in the third bracket are expanded in powers of m_ℓ/m_ρ. The expansion coefficients C_1, C_2, and C_3 depend on the hadronic structure of the pseudoscalar meson and in most cases cannot be computed accurately. In particular, C_1 absorbs the uncertainty in the matching energy scale between short- and long-distance strong interactions and thus is the main source of uncertainty in determining f_{π^+} accurately.

With the experimental value for the decay $\pi^+ \to \mu^+\nu_\mu + \mu^+\nu_\mu\gamma$, one obtains

$$f_{\pi^+} = 130.7 \pm 0.1 \pm 0.36 \text{ MeV} \ , \tag{5}$$

where the first error comes from the experimental uncertainty on $|V_{ud}|$ and the second comes from the uncertainty on C_1 ($= 0 \pm 0.24$) [6]. Similarly, one obtains from the decay $K^+ \to \mu^+\nu_\mu + \mu^+\nu_\mu\gamma$ the decay constant

$$f_{K^+} = 159.8 \pm 1.4 \pm 0.44 \text{ MeV} \ , \tag{6}$$

where the first error is due to the uncertainty on $|V_{us}|$.

For the heavy pseudoscalar mesons, uncertainties in the experimental values for the decay rates are much larger than the radiative corrections. For the D^+, a value (as opposed to an upper limit) has been obtained for the first time:

$$f_{D^+} = 300^{+180+80}_{-150-40} \text{ MeV} \ , \tag{7}$$

but it is based on only one $D^+ \to \mu^+\nu_\mu$ event [7]. The D_s^+ decay constant is discussed in a separate note in the D_s^+ Data Listings. The value obtained there is

$$f_{D_s^+} = 266 \pm 32 \text{ MeV} \ . \tag{8}$$

There have been many attempts to extract f_P from spectroscopy and nonleptonic decays using theoretical models. Since it is difficult to estimate uncertainties for them, we have listed here only values of decay constants that are obtained directly from the observation of $P^\pm \to \ell^\pm\nu_\ell$.

Light neutral mesons

The decay constants for the light neutral pseudoscalar mesons π^0, η, and η' are defined by

$$\sqrt{2}\ \langle 0|A_\mu^a(0)|P(q)\rangle = i\, f_P^a\, q_\mu \tag{9}$$

where A_μ^a is a neutral axial-vector current [8,9]. Restricting ourselves to the three light flavors, the index $a = 0, 3, 8$ refers

to the usual set of Gell-Mann matrices, including the flavor singlet. In case of exact isospin symmetry (which is for most applications a very good approximation) we have only one decay constant for the π^0 meson ($f^3_{\pi^0} \equiv f_{\pi^0}$) and two decay constants each for η and η' (f^8_η, f^0_η, and $f^8_{\eta'}$, $f^0_{\eta'}$).

In the limit of $m_P \to 0$, the Adler-Bell-Jackiw anomaly [10,11] determines the matrix elements of the two-photon decay $P \to \gamma\gamma$ through the decay constants f^a_P. In the case of f_{π^0}, the extrapolation to $m_\pi \neq 0$ gives only a tiny effect, and the value of f_{π^0} can be extracted from the $\pi^0 \to \gamma\gamma$ decay width. The experimental uncertainty in the π^0 lifetime dominates in the uncertainty of f_{π^0}:

$$f_{\pi^0} = 130 \pm 5 \text{ MeV} . \qquad (10)$$

This value is compatible with $f_{\pi^\pm}$, as it is expected from isospin symmetry.

The four decay constants of the η-η' system cannot be extracted from the two-photon decay widths alone. Also, the extrapolation to $m_{\eta(\eta')} \neq 0$ may give a larger effect here, and therefore the dominance of the Adler-Bell-Jackiw anomaly is perhaps questionable. Thus, an assessment of the values of the η and η' decay constants requires additional theoretical and phenomenological input about flavor symmetry breaking and η-η' mixing; see Ref. 12 for a review. Most analyses find similar values for the octet decay constants: $f^8_\eta \simeq 1.2\, f_\pi$ and $f^8_{\eta'} \simeq -0.45\, f_\pi$. The situation concerning the singlet decay constants, f^0_P, is less clear.

References

1. S. Berman, Phys. Rev. Lett. **1**, 468 (1958).
2. T. Kinoshita, Phys. Rev. Lett. **2**, 477 (1959).
3. A. Sirlin, Phys. Rev. **D5**, 436 (1972).
4. M.V. Terent'ev, Yad. Fiz. **18**, 870 (1973) [Sov. J. Nucl. Phys. **18**, 449 (1974)].
5. T. Goldman and W.J. Wilson, Phys. Rev. **D15**, 709 (1977).
6. W.J. Marciano and A. Sirlin, Phys. Rev. Lett. **71**, 3629 (1993).
7. J.Z. Bai *et al.*, Phys. Lett. **B429**, 188 (1998).
8. J. Gasser and H. Leutwyler, Nucl. Phys. **B250**, 465 (1985).
9. H. Leutwyler, Nucl. Phys. Proc. Suppl. **64**, 223 (1998).
10. S.L. Adler, Phys. Rev. **177**, 2426 (1969).
11. J.S. Bell and R. Jackiw, Nuovo Cimento **60A**, 46 (1969).
12. T. Feldmann, Int. J. Mod. Phys. **A15**, 159 (2000).

$\pi^{\pm}$

$I^G(J^P) = 1^-(0^-)$

We have omitted some results that have been superseded by later experiments. The omitted results may be found in our 1988 edition Physics Letters **B204** (1988).

$\pi^{\pm}$ MASS

The most accurate charged pion mass measurements are based upon x-ray wavelength measurements for transitions in π^--mesonic atoms. The observed line is the blend of three components, corresponding to different K-shell occupancies. JECKELMANN 94 revisits the occupancy question, with the conclusion that two sets of occupancy ratios, resulting in two different pion masses (Solutions A and B), are equally probable. We choose the higher Solution B since only this solution is consistent with a positive mass-squared for the muon neutrino, given the precise muon momentum measurements now available (DAUM 91, ASSAMAGAN 94, and ASSAMAGAN 96) for the decay of pions at rest. Earlier mass determinations with pi-mesonic atoms may have used incorrect K-shell screening corrections.

Measurements with an error of > 0.005 MeV have been omitted from this Listing.

VALUE (MeV)		DOCUMENT ID		TECN	CHG	COMMENT
139.57018±0.00035 OUR FIT Error includes scale factor of 1.2.						
139.57018±0.00035 OUR AVERAGE Error includes scale factor of 1.2.						
139.57071±0.00053	[1]	LENZ	98	CNTR	–	pionic N2-atoms gas target
139.56995±0.00035	[2]	JECKELMANN	94	CNTR	–	π^- atom, Soln. B
• • • We do not use the following data for averages, fits, limits, etc. • • •						
139.57022±0.00014	[3]	ASSAMAGAN	96	SPEC	+	$\pi^+ \to \mu^+\nu_\mu$
139.56782±0.00037	[4]	JECKELMANN	94	CNTR	–	π^- atom, Soln. A
139.56996±0.00067	[5]	DAUM	91	SPEC	+	$\pi^+ \to \mu^+\nu$
139.56752±0.00037	[6]	JECKELMANN	86B	CNTR	–	Mesonic atoms
139.5704 ±0.0011	[5]	ABELA	84	SPEC	+	See DAUM 91
139.5664 ±0.0009	[7]	LU	80	CNTR	–	Mesonic atoms
139.5686 ±0.0020		CARTER	76	CNTR	–	Mesonic atoms
139.5660 ±0.0024	[7,8]	MARUSHEN...	76	CNTR	–	Mesonic atoms

[1] LENZ 98 result does not suffer K-electron configuration uncertainties as does JECKELMANN 94.

[2] JECKELMANN 94 Solution B (dominant 2-electron K-shell occupancy), chosen for consistency with positive $m^2_{\nu_\mu}$.

[3] ASSAMAGAN 96 measures the μ^+ momentum p_μ in $\pi^+ \to \mu^+\nu_\mu$ decay at rest to be 29.79200 ± 0.00011 MeV/c. Combined with the μ^+ mass and the assumption $m_{\nu_\mu} = 0$, this gives the π^+ mass above; if $m_{\nu_\mu} > 0$, m_{π^+} given above is a lower limit. Combined instead with m_μ and (assuming CPT) the π^- mass of JECKELMANN 94, p_μ gives an upper limit on m_{ν_μ} (see the ν_μ).

[4] JECKELMANN 94 Solution A (small 2-electron K-shell occupancy) in combination with either the DAUM 91 or ASSAMAGAN 94 pion decay muon momentum measurement yields a significantly negative $m^2_{\nu_\mu}$. It is accordingly not used in our fits.

[5] The DAUM 91 value includes the ABELA 84 result. The value is based on a measurement of the μ^+ momentum for π^+ decay at rest, $p_\mu = 29.79179 \pm 0.00053$ MeV, uses $m_\mu = 105.658389 \pm 0.000034$ MeV, and assumes that $m_{\nu_\mu} = 0$. The last assumption means that in fact the value is a lower limit.

[6] JECKELMANN 86B gives $m_\pi/m_e = 273.12677(71)$. We use $m_e = 0.51099906(15)$ MeV from COHEN 87. The authors note that two solutions for the probability distribution of K-shell occupancy fit equally well, and use other data to choose the lower of the two possible $\pi^\pm$ masses.

[7] These values are scaled with a new wavelength-energy conversion factor $V\lambda = 1.23984244(37) \times 10^{-6}$ eV m from COHEN 87. The LU 80 screening correction relies upon a theoretical calculation of inner-shell refilling rates.

[8] This MARUSHENKO 76 value used at the authors' request to use the accepted set of calibration γ energies. Error increased from 0.0017 MeV to include QED calculation error of 0.0017 MeV (12 ppm).

$m_{\pi^+} - m_{\mu^+}$

Measurements with an error > 0.05 MeV have been omitted from this Listing.

VALUE (MeV)	EVTS	DOCUMENT ID		TECN	CHG	COMMENT
• • • We do not use the following data for averages, fits, limits, etc. • • •						
33.91157±0.00067		[9] DAUM	91	SPEC	+	$\pi^+ \to \mu^+\nu$
33.9111 ±0.0011		ABELA	84	SPEC		See DAUM 91
33.925 ±0.025		BOOTH	70	CNTR	+	Magnetic spect.
33.881 ±0.035	145	HYMAN	67	HEBC	+	K^- He

[9] The DAUM 91 value assumes that $m_{\nu_\mu} = 0$ and uses our $m_\mu = 105.658389 \pm 0.000034$ MeV.

$(m_{\pi^+} - m_{\pi^-}) / m_{\text{average}}$

A test of *CPT* invariance.

VALUE (units 10^{-4})	DOCUMENT ID		TECN
2±5	AYRES	71	CNTR

$\pi^{\pm}$ MEAN LIFE

Measurements with an error $> 0.02 \times 10^{-8}$ s have been omitted.

VALUE (10^{-8} s)	DOCUMENT ID		TECN	CHG	COMMENT
2.6033 ±0.0005 OUR AVERAGE	Error includes scale factor of 1.2.				
2.60361 ± 0.00052	[10] KOPTEV	95	SPEC	+	Surface μ^+'s
2.60231 ± 0.00050 ± 0.00084	NUMAO	95	SPEC	+	Surface μ^+'s
2.609 ± 0.008	DUNAITSEV	73	CNTR	+	
2.602 ± 0.004	AYRES	71	CNTR	±	
2.604 ± 0.005	NORDBERG	67	CNTR	+	
2.602 ± 0.004	ECKHAUSE	65	CNTR	+	
• • • We do not use the following data for averages, fits, limits, etc. • • •					
2.640 ± 0.008	[11] KINSEY	66	CNTR	+	

[10] KOPTEV 95 combines the statistical and systematic errors; the statistical error dominates.
[11] Systematic errors in the calibration of this experiment are discussed by NORDBERG 67.

$(\tau_{\pi^+} - \tau_{\pi^-}) / \tau_{\text{average}}$

A test of *CPT* invariance.

VALUE (units 10^{-4})	DOCUMENT ID		TECN
5.5 ± 7.1	AYRES	71	CNTR
• • • We do not use the following data for averages, fits, limits, etc. • • •			
−14 ±29	PETRUKHIN	68	CNTR
40 ±70	BARDON	66	CNTR
23 ±40	[12] LOBKOWICZ	66	CNTR

[12] This is the most conservative value given by LOBKOWICZ 66.

π^+ DECAY MODES

π^- modes are charge conjugates of the modes below.

For decay limits to particles which are not established, see the appropriate Search setions (Massive Neutrino Peak Search Test, A^0 (axion), and Other Light Boson (X^0) Searches, etc.).

	Mode		Fraction (Γ_i/Γ)			Confidence level
Γ_1	$\mu^+\nu_\mu$	[a]	(99.98770 ± 0.00004) %			
Γ_2	$\mu^+\nu_\mu\gamma$	[b]	(2.00	±0.25	) $\times 10^{-4}$	
Γ_3	$e^+\nu_e$	[a]	(1.230	±0.004	) $\times 10^{-4}$	
Γ_4	$e^+\nu_e\gamma$	[b]	(1.61	±0.23	) $\times 10^{-7}$	
Γ_5	$e^+\nu_e\pi^0$		(1.025	±0.034	) $\times 10^{-8}$	
Γ_6	$e^+\nu_e e^+ e^-$		(3.2	±0.5	) $\times 10^{-9}$	
Γ_7	$e^+\nu_e\nu\overline{\nu}$		< 5		$\times 10^{-6}$	90%
Lepton Family number (LF) or Lepton number (L) violating modes						
Γ_8	$\mu^+\overline{\nu}_e$	L	[c] < 1.5		$\times 10^{-3}$	90%
Γ_9	$\mu^+\nu_e$	LF	[c] < 8.0		$\times 10^{-3}$	90%
Γ_{10}	$\mu^- e^+ e^+ \nu$	LF	< 1.6		$\times 10^{-6}$	90%

[a] Measurements of $\Gamma(e^+\nu_e)/\Gamma(\mu^+\nu_\mu)$ always include decays with γ's, and measurements of $\Gamma(e^+\nu_e\gamma)$ and $\Gamma(\mu^+\nu_\mu\gamma)$ never include low-energy γ's. Therefore, since no clean separation is possible, we consider the modes with γ's to be subreactions of the modes without them, and let $[\Gamma(e^+\nu_e) + \Gamma(\mu^+\nu_\mu)]/\Gamma_{\text{total}} = 100\%$.

[b] See the Particle Listings below for the energy limits used in this measurement; low-energy γ's are not included.

[c] Derived from an analysis of neutrino-oscillation experiments.

π^+ BRANCHING RATIOS

$\Gamma(e^+\nu_e)/\Gamma_{\text{total}}$ Γ_3/Γ

See note [a] in the list of π^+ decay modes just above, and see also the next block of data.

VALUE (units 10^{-4})	DOCUMENT ID
1.230±0.004 OUR EVALUATION	

$[\Gamma(e^+\nu_e) + \Gamma(e^+\nu_e\gamma)]/[\Gamma(\mu^+\nu_\mu) + \Gamma(\mu^+\nu_\mu\gamma)]$ $(\Gamma_3+\Gamma_4)/(\Gamma_1+\Gamma_2)$

See note [a] in the list of π^+ decay modes above. See NUMAO 92 for a discussion of e-μ universality.

VALUE (units 10^{-4})	EVTS	DOCUMENT ID		TECN	COMMENT
1.230 ±0.004 OUR AVERAGE					
1.2346 ± 0.0035 ± 0.0036	120k	CZAPEK	93	CALO	Stopping π^+
1.2265 ± 0.0034 ± 0.0044	190k	BRITTON	92	CNTR	Stopping π^+
1.218 ±0.014	32k	BRYMAN	86	CNTR	Stopping π^+
• • • We do not use the following data for averages, fits, limits, etc. • • •					
1.273 ±0.028	11k	[13] DICAPUA	64	CNTR	
1.21 ±0.07		ANDERSON	60	SPEC	

[13] DICAPUA 64 has been updated using the current mean life.

$\Gamma(\mu^+\nu_\mu\gamma)/\Gamma_{\text{total}}$ Γ_2/Γ

Note that measurements here do not cover the full kinematic range.

VALUE (units 10^{-4})	EVTS	DOCUMENT ID		TECN	CHG	COMMENT
2.0 ±0.24±0.08		[14] BRESSI	98	CALO	+	Stopping π^+
• • • We do not use the following data for averages, fits, limits, etc. • • •						
1.24 ± 0.25	26	CASTAGNOLI	58	EMUL		$KE_\mu < 3.38$ MeV

[14] BRESSI 98 result is given for $E_\gamma > 1$ MeV only. Result agrees with QED expectation, 2.283×10^{-4} and does not confirm discrepancy of earlier experiment CASTAGNOLI 58.

$\Gamma(e^+\nu_e\gamma)/\Gamma_{\text{total}}$ Γ_4/Γ

Note that measurements here do not cover the full kinematic range.

VALUE (units 10^{-8})	EVTS	DOCUMENT ID		TECN	COMMENT
16.1±2.3		[15] BOLOTOV	90B	SPEC	17 GeV $\pi^- \to e^-\overline{\nu}_e\gamma$
• • • We do not use the following data for averages, fits, limits, etc. • • •					
5.6±0.7	226	[16] STETZ	78	SPEC	$P_e > 56$ MeV/c
3.0	143	DEPOMMIER	63B	CNTR	$(KE)_{e^+\gamma} > 48$ MeV

[15] BOLOTOV 90B is for $E_\gamma > 21$ MeV, $E_e > 70 - 0.8\,E_\gamma$.
[16] STETZ 78 is for an $e^-\gamma$ opening angle $> 132°$. Obtains 3.7 when using same cutoffs as DEPOMMIER 63B.

$\Gamma(e^+\nu_e\pi^0)/\Gamma_{\text{total}}$ Γ_5/Γ

VALUE (units 10^{-8})	EVTS	DOCUMENT ID		TECN	CHG	COMMENT
1.025±0.034 OUR AVERAGE						
1.026 ± 0.039	1224	[17] MCFARLANE	85	CNTR	+	Decay in flight
$1.00\ ^{+0.08}_{-0.10}$	332	DEPOMMIER	68	CNTR	+	
1.07 ±0.21	38	[18] BACASTOW	65	OSPK	+	
1.10 ±0.26		[18] BERTRAM	65	OSPK	+	
1.1 ±0.2	43	[18] DUNAITSEV	65	CNTR	+	
0.97 ±0.20	36	[18] BARTLETT	64	OSPK	+	
• • • We do not use the following data for averages, fits, limits, etc. • • •						
1.15 ±0.22	52	[18] DEPOMMIER	63	CNTR	+	See DEPOMMIER 68

[17] MCFARLANE 85 combines a measured rate (0.394 ± 0.015)/s with 1982 PDG mean life.
[18] DEPOMMIER 68 says the result of DEPOMMIER 63 is at least 10% too large because of a systematic error in the π^0 detection efficiency, and that this may be true of all the previous measurements (also V. Soergel, private communication, 1972).

$\Gamma(e^+\nu_e e^+e^-)/\Gamma(\mu^+\nu_\mu)$ Γ_6/Γ_1

VALUE (units 10^{-9})	CL%	EVTS	DOCUMENT ID		TECN	COMMENT
3.2 ±0.5 ±0.2		98	EGLI	89	SPEC	Uses $R_{PCAC} = 0.068 \pm 0.004$
• • • We do not use the following data for averages, fits, limits, etc. • • •						
0.46 ± 0.16 ± 0.07		7	[19] BARANOV	92	SPEC	Stopped π^+
< 4.8	90		KORENCHE...	76B	SPEC	
<34	90		KORENCHE...	71	OSPK	

[19] This measurement by BARANOV 92 is of the structure-dependent part of the decay. The value depends on values assumed for ratios of form factors.

$\Gamma(e^+\nu_e\nu\overline{\nu})/\Gamma_{\text{total}}$ Γ_7/Γ

VALUE (units 10^{-6})	CL%	DOCUMENT ID		TECN
<5	90	PICCIOTTO	88	SPEC

$\Gamma(\mu^+\overline{\nu}_e)/\Gamma_{\text{total}}$ Γ_8/Γ

Forbidden by total lepton number conservation.

VALUE (units 10^{-3})	CL%	DOCUMENT ID		TECN	COMMENT
<1.5	90	[20] COOPER	82	HLBC	Wideband ν beam

[20] COOPER 82 limit on $\overline{\nu}_e$ observation is here interpreted as a limit on lepton number violation.

$\Gamma(\mu^+\nu_e)/\Gamma_{\text{total}}$ Γ_9/Γ

Forbidden by lepton family number conservation.

VALUE (units 10^{-3})	CL%	DOCUMENT ID		TECN	COMMENT
<8.0	90	[21] COOPER	82	HLBC	Wideband ν beam

[21] COOPER 82 limit on ν_e observation is here interpreted as a limit on lepton family number violation.

$\Gamma(\mu^- e^+ e^+ \nu)/\Gamma_{\text{total}}$ Γ_{10}/Γ

Forbidden by lepton family number conservation.

VALUE (units 10^{-6})	CL%	DOCUMENT ID		TECN	CHG
<1.6	90	BARANOV	91B	SPEC	+
• • • We do not use the following data for averages, fits, limits, etc. • • •					
<7.7	90	KORENCHE...	87	SPEC	+

π^+ — POLARIZATION OF EMITTED μ^+

$\pi^+ \to \mu^+ \nu$

Tests the Lorentz structure of leptonic charged weak interactions.

VALUE	CL%	DOCUMENT ID		TECN	CHG	COMMENT
• • • We do not use the following data for averages, fits, limits, etc. • • •						
$<(-0.9959)$	90	[22] FETSCHER	84	RVUE	+	
-0.99 ± 0.16		[23] ABELA	83	SPEC	−	μ X-rays

[22] FETSCHER 84 uses only the measurement of CARR 83.
[23] Sign of measurement reversed in ABELA 83 to compare with μ^+ measurements.

$\pi^\pm \to \ell^\pm \nu\gamma$ AND $K^\pm \to \ell^\pm \nu\gamma$ FORM FACTORS

Written by H.S. Pruys (Zürich University).

In the radiative decays $\pi^\pm \to \ell^\pm \nu\gamma$ and $K^\pm \to \ell^\pm \nu\gamma$, where ℓ is an e or a μ and γ is a real or virtual photon (e^+e^- pair), both the vector and the axial-vector weak hadronic currents contribute to the decay amplitude. Each current gives a structure-dependent term (SD_V and SD_A) from virtual hadronic states, and the axial-vector current also gives a contribution from inner bremsstrahlung (IB) from the lepton and meson. The IB amplitudes are determined by the meson decay constants f_π and f_K [1]. The SD_V and SD_A amplitudes are parameterized in terms of the vector form factor F_V and the axial-vector form factors F_A and R [1–4]:

$$M(\mathrm{SD}_V) = \frac{-eG_F V_{qq'}}{\sqrt{2}\, m_P} \epsilon^\mu \ell^\nu F_V \epsilon_{\mu\nu\sigma\tau} k^\sigma q^\tau ,$$

$$M(\mathrm{SD}_A) = \frac{-ie\, G_F V_{qq'}}{\sqrt{2}\, m_P} \epsilon^\mu \ell^\nu \{F_A [(s-t) g_{\mu\nu} - q_\mu k_\nu] + R\, t\, g_{\mu\nu}\} . \quad (1)$$

Here $V_{qq'}$ is the Cabibbo-Kobayashi-Maskawa mixing-matrix element; ϵ^μ is the polarization vector of the photon (or the effective vertex, $\epsilon^\mu = (e/t)\overline{u}(p_-)\gamma^\mu v(p_+)$, of the e^+e^- pair); $\ell^\nu = \overline{u}(p_\nu)\gamma^\nu(1-\gamma_5)v(p_\ell)$ is the lepton-neutrino current; q and k are the meson and photon four-momenta, with $s = q\cdot k$ and $t = k^2 (= (p_+ + p_-)^2)$; and P stands for π or K. In the analysis of data, the s and t dependence of the form factors is neglected, which is a good approximation for pions [2] but not for kaons [4]. The pion vector form factor F_V^π is related via CVC to the π^0 lifetime, $|F_V^\pi| = (1/\alpha)\sqrt{2\Gamma_{\pi^0}/\pi m_{\pi^0}}$ [1]. PCAC relates R to the electromagnetic radius of the meson [2,4], $R^P = \frac{1}{3} m_P f_P \langle r_P^2 \rangle$. The calculation of the other form factors, F_A^π, F_V^K, and F_A^K, is model dependent [1,4].

When the photon is real, the partial decay rate can be given analytically [1,5]:

$$\frac{d^2\Gamma_{P\to\ell\nu\gamma}}{dxdy} = \frac{d^2(\Gamma_{\mathrm{IB}} + \Gamma_{\mathrm{SD}} + \Gamma_{\mathrm{INT}})}{dxdy} , \quad (2)$$

where $\Gamma_{\mathrm{IB}}, \Gamma_{\mathrm{SD}}$, and Γ_{INT} are the contributions from inner bremsstrahlung, structure-dependent radiation, and their interference, and the Γ_{SD} term is given by

$$\frac{d^2\Gamma_{\mathrm{SD}}}{dxdy} = \frac{\alpha}{8\pi}\Gamma_{P\to\ell\nu} \frac{1}{r(1-r)^2} \left(\frac{m_P}{f_P}\right)^2 \times \left[(F_V + F_A)^2\, \mathrm{SD}^+ + (F_V - F_A)^2\, \mathrm{SD}^-\right] . \quad (3)$$

Here

$$\mathrm{SD}^+ = (x + y - 1 - r)\,[(x+y-1)(1-x) - r] ,$$

$$\mathrm{SD}^- = (1 - y + r)\,[(1-x)(1-y) + r] , \quad (4)$$

where $x = 2E_\gamma/m_P$, $y = 2E_\ell/m_P$, and $r = (m_\ell/m_P)^2$.

In $\pi^\pm \to e^\pm\nu\gamma$ and $K^\pm \to e^\pm\nu\gamma$ decays, the interference terms are small, and thus only the absolute values $|F_A + F_V|$ and $|F_A - F_V|$ can be obtained. In $K^\pm \to \mu^\pm\nu\gamma$ decay, the interference term is important, and thus the signs of F_V and F_A can be obtained. In $\pi^\pm \to \mu^\pm\nu\gamma$ decay, bremsstrahlung completely dominates. In $\pi^\pm \to e^\pm\nu e^+e^-$ and $K^\pm \to \ell^\pm\nu e^+e^-$ decays, all three form factors, F_V, F_A, and R, can be determined.

We give the $\pi^\pm$ form factors F_V, F_A, and R in the Listings below. In the $K^\pm$ Listings, we give the sum $F_A + F_V$ and difference $F_A - F_V$.

The electroweak decays of the pseudoscalar mesons are investigated to learn something about the unknown hadronic structure of these mesons, assuming a standard $V-A$ structure of the weak leptonic current. The experiments are quite difficult, and it is not meaningful to analyse the results using parameters for both the hadronic structure (decay constants, form factors) and the leptonic weak current (*e.g.*, to add pseudoscalar or tensor couplings to the $V-A$ coupling). Deviations from the $V-A$ interactions are much better studied in purely leptonic systems such as muon decay.

References

1. D.A. Bryman *et al.*, Phys. Reports **88**, 151 (1982). See also our note on "Pseudoscalar-Meson Decay Constants," above.
2. A. Kersch and F. Scheck, Nucl. Phys. **B263**, 475 (1986).
3. W.T. Chu *et al.*, Phys. Rev. **166**, 1577 (1968).
4. D.Yu. Bardin and E.A. Ivanov, Sov. J. Part. Nucl. **7**, 286 (1976).
5. S.G. Brown and S.A. Bludman, Phys. Rev. **136**, B1160 (1964).

$\pi^\pm$ FORM FACTORS

F_V, VECTOR FORM FACTOR

VALUE	EVTS	DOCUMENT ID		TECN	COMMENT
0.017 ± 0.008 OUR AVERAGE					
0.014 ± 0.009		[24] BOLOTOV	90B	SPEC	17 GeV $\pi^- \to e^- \overline{\nu}_e \gamma$
$0.023^{+0.015}_{-0.013}$	98	EGLI	89	SPEC	$\pi^+ \to e^+ \nu_e e^+ e^-$

[24] BOLOTOV 90B only determines the absolute value.

F_A, AXIAL-VECTOR FORM FACTOR

VALUE	EVTS	DOCUMENT ID		TECN	COMMENT
0.0116 ± 0.0016 OUR AVERAGE		Error includes scale factor of 1.3. See the ideogram below.			
0.0106 ± 0.0060		[25] BOLOTOV	90B	SPEC	17 GeV $\pi^- \to e^- \overline{\nu}_e \gamma$
0.0135 ± 0.0016		[25] BAY	86	SPEC	$\pi^+ \to e^+ \nu\gamma$
0.006 ± 0.003		[25] PIILONEN	86	SPEC	$\pi^+ \to e^+ \nu\gamma$
0.011 ± 0.003		[25,26] STETZ	78	SPEC	$\pi^+ \to e^+ \nu\gamma$
• • • We do not use the following data for averages, fits, limits, etc. • • •					
$0.021\ ^{+0.011}_{-0.013}$	98	EGLI	89	SPEC	$\pi^+ \to e^+ \nu_e e^+ e^-$

[25] Using the vector form factor from CVC prediction $F_V = 0.0259 \pm 0.0005$. Only the absolute value of F_A is determined.

[26] The result of STETZ 78 has a two-fold ambiguity. We take the solution compatible with later determinations.

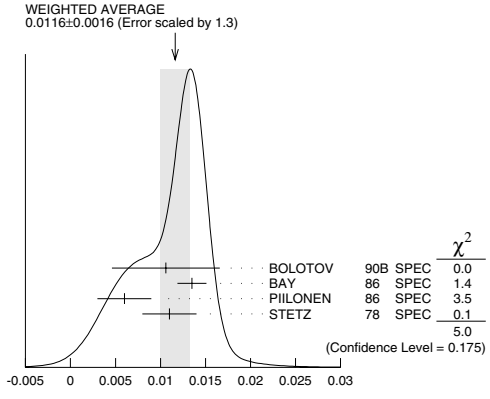

$\pi^{\pm}$ axial-vector form factor

R, SECOND AXIAL-VECTOR FORM FACTOR

VALUE	EVTS	DOCUMENT ID		TECN	COMMENT
$0.059^{+0.009}_{-0.008}$	98	EGLI	89	SPEC	$\pi^+ \to e^+ \nu_e e^+ e^-$

$\pi^{\pm}$ CHARGE RADIUS

VALUE (fm)	DOCUMENT ID		TECN	COMMENT
0.672±0.008 OUR AVERAGE	Error includes scale factor of 1.7. See the ideogram below.			
0.65 ±0.05 ±0.06	ESCHRICH	01	CNTR	$\pi e \to \pi e$
0.740±0.031	LIESENFELD	99	CNTR	$ep \to e\pi^+ n$
0.663±0.006	AMENDOLIA	86	CNTR	$\pi e \to \pi e$
0.663±0.023	DALLY	82	CNTR	$\pi e \to \pi e$
0.711±0.009±0.016	BEBEK	78	CNTR	$eN \to e\pi N$
0.678±0.004±0.008	QUENZER	78	CNTR	$e^+e^- \to \pi^+\pi^-$
• • • We do not use the following data for averages, fits, limits, etc. • • •				
0.661±0.012	[27] BIJNENS	98	CNTR	χPT extraction
0.660±0.024	AMENDOLIA	84	CNTR	$\pi e \to \pi e$
0.78 $^{+0.09}_{-0.10}$	ADYLOV	77	CNTR	$\pi e \to \pi e$
0.74 $^{+0.11}_{-0.13}$	BARDIN	77	CNTR	$ep \to e\pi^+ n$
0.56 ±0.04	DALLY	77	CNTR	$\pi e \to \pi e$

[27] BIJNENS 98 fits existing data.

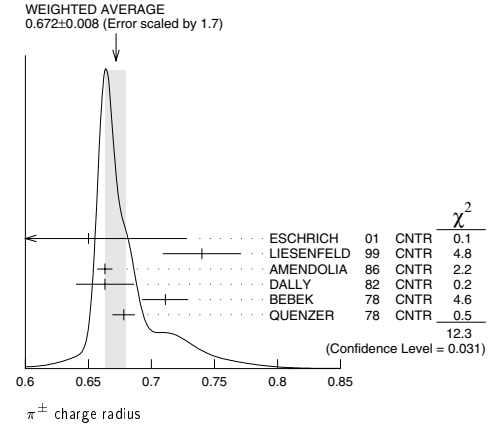

$\pi^{\pm}$ charge radius

$\pi^{\pm}$ REFERENCES

We have omitted some papers that have been superseded by later experiments. The omitted papers may be found in our 1988 edition Physics Letters **B204** (1988).

ESCHRICH	01	PL B522 233	I. Eschrich *et al.* (FNAL SELEX Collab.)
LIESENFELD	99	PL B468 20	A. Liesenfeld *et al.*
BIJNENS	98	JHEP 05 014	J. Bijnens *et al.*
BRESSI	98	NP B513 555	G. Bressi *et al.*
LENZ	98	PL B416 50	S. Lenz *et al.*
ASSAMAGAN	96	PR D53 6065	K.A. Assamagan *et al.* (PSI, ZURI, VILL+)
KOPTEV	95	JETPL 61 877	V.P. Koptev *et al.* (PNPI)
		Translated from ZETFP 61 865.	
NUMAO	95	PR D52 4855	T. Numao *et al.* (TRIU, BRCO)
ASSAMAGAN	94	PL B335 231	K.A. Assamagan *et al.* (PSI, ZURI, VILL+)
JECKELMANN	94	PL B335 326	B. Jeckelmann, P.F.A. Goudsmit, H.J. Leisi (WABRN+)
CZAPEK	93	PRL 70 17	G. Czapek *et al.* (BERN, VILL)
BARANOV	92	SJNP 55 1644	V.A. Baranov *et al.* (JINR)
		Translated from YAF 55 2940.	
BRITTON	92	PRL 68 3000	D.I. Britton *et al.* (TRIU, CARL)
Also	94	PR D49 28	D.I. Britton *et al.* (TRIU, CARL)
NUMAO	92	MPL A7 3357	T. Numao (TRIU)
BARANOV	91B	SJNP 54 790	V.A. Baranov *et al.* (JINR)
		Translated from YAF 54 1298.	
DAUM	91	PL B265 425	M. Daum *et al.* (VILL)
BOLOTOV	90B	PL B243 308	V.N. Bolotov *et al.* (INRM)
EGLI	89	PL B222 533	S. Egli *et al.* (SINDRUM Collab.)
Also	86	PL B175 97	S. Egli *et al.* (AACH3, ETH, SIN, ZURI)
PDG	88	PL B204	G.P. Yost *et al.* (LBL+)
PICCIOTTO	88	PR D37 1131	C.E. Picciotto *et al.* (TRIU, CNRC)
COHEN	87	RMP 59 1121	E.R. Cohen, B.N. Taylor (RISC, NBS)
KORENCHE...	87	SJNP 46 192	S.M. Korenchenko *et al.* (JINR)
		Translated from YAF 46 313.	
AMENDOLIA	86	NP B277 168	S.R. Amendolia *et al.* (CERN NA7 Collab.)
BAY	86	PL B174 445	A. Bay *et al.* (LAUS, ZURI)
BRYMAN	86	PR D33 1211	D.A. Bryman *et al.* (TRIU, CNRC)
Also	83	PRL 50 7	D.A. Bryman *et al.* (TRIU, CNRC)
JECKELMANN	86B	NP A457 709	B. Jeckelmann *et al.* (ETH, FRIB)
Also	86	PRL 56 1444	B. Jeckelmann *et al.* (ETH, FRIB)
PIILONEN	86	PRL 57 1402	L.E. Piilonen *et al.* (LANL, TEMP, CHIC)
MCFARLANE	85	PR D32 547	W.K. McFarlane *et al.* (TEMP, LANL)
ABELA	84	PL 146B 431	R. Abela *et al.* (SIN)
Also	78	PL 74B 126	M. Daum *et al.* (SIN)
Also	79	PR D20 2692	M. Daum *et al.* (SIN)
AMENDOLIA	84	PL 146B 116	S.R. Amendolia *et al.* (CERN NA7 Collab.)
FETSCHER	84	PL 140B 117	W. Fetscher (ETH)
ABELA	83	NP A395 413	R. Abela *et al.* (BASL, KARLK, KARLE)
CARR	83	PRL 51 627	J. Carr *et al.* (LBL, NWES, TRIU)
COOPER	82	PL 112B 97	A.M. Cooper *et al.* (RL)
DALLY	82	PRL 48 375	E.B. Dally *et al.*
LU	80	PRL 45 1066	D.C. Lu *et al.* (YALE, COLU, JHU)
BEBEK	78	PR D17 1693	C.J. Bebek *et al.*
QUENZER	78	PL 76B 512	A. Quenzer *et al.* (LALO)
STETZ	78	NP B138 285	A.W. Stetz *et al.* (LBL, UCLA)
ADYLOV	77	NP B128 461	G.T. Adylov *et al.*
BARDIN	77	NP B120 45	G. Bardin *et al.*
DALLY	77	PRL 39 1176	E.B. Dally *et al.*
CARTER	76	PRL 37 1380	A.L. Carter *et al.* (CARL, CNRC, CHIC+)
KORENCHE...	76B	JETP 44 35	S.M. Korenchenko *et al.* (JINR)
		Translated from ZETF 71 69.	
MARUSHEN...	76	JETPL 23 72	V.I. Marushenko *et al.* (PNPI)
		Translated from ZETFP 23 80.	
Also	76	Private Comm.	R.E. Shafer (FNAL)
Also	78	Private Comm.	A. Smirnov (PNPI)
DUNAITSEV	73	SJNP 16 292	A.F. Dunaitsev *et al.* (SERP)
		Translated from YAF 16 524.	
AYRES	71	PR D3 1051	D.S. Ayres *et al.* (LRL, UCSB)
Also	67	PR 157 1288	D.S. Ayres *et al.* (LRL)
Also	68	PRL 21 261	D.S. Ayres *et al.* (LRL, UCSB)
Also	69	Thesis UCRL 18369	D.S. Ayres (LRL)
Also	69	PRL 23 1267	A.J. Greenberg *et al.* (LRL, UCSB)
KORENCHE...	71	SJNP 13 189	S.M. Korenchenko *et al.* (JINR)
		Translated from YAF 13 339.	
BOOTH	70	PL 32B 723	P.S.L. Booth *et al.* (LIVP)
DEPOMMIER	68	NP B4 189	P. Depommier *et al.* (CERN)
PETRUKHIN	68	JINR P1 3862	V.I. Petrukhin *et al.* (JINR)
HYMAN	67	PL 25B 376	L.G. Hyman *et al.* (ANL, CMU, NWES)
NORDBERG	67	PL 24B 594	M.E. Nordberg, F. Lobkowicz, R.L. Burman (ROCH)
BARDON	66	PRL 16 775	M. Bardon *et al.* (COLU)
KINSEY	66	PR 144 1132	K.F. Kinsey, F. Lobkowicz, M.E. Nordberg (ROCH)
LOBKOWICZ	66	PRL 17 548	F. Lobkowicz *et al.* (ROCH, BNL)
BACASTOW	65	PR 139B 407	R.B. Bacastow *et al.* (LRL, SLAC)
BERTRAM	65	PR 139B 617	W.K. Bertram *et al.* (MICH, CMU)
DUNAITSEV	65	JETP 20 58	A.F. Dunaitsev *et al.* (JINR)
		Translated from ZETF 47 84.	
ECKHAUSE	65	PL 19 348	M. Eckhause *et al.* (WILL)
BARTLETT	64	PR 136B 1452	D. Bartlett *et al.* (COLU)
DICAPUA	64	PR 133B 1333	M. di Capua *et al.* (COLU)
Also	86	Private Comm.	L. Pondrom (WISC)
DEPOMMIER	63	PL 5 61	P. Depommier *et al.* (CERN)
DEPOMMIER	63B	PL 7 285	P. Depommier *et al.* (CERN)
ANDERSON	60	PR 119 2050	H.L. Anderson *et al.* (EFI)
CASTAGNOLI	58	PR 112 1779	C. Castagnoli, M. Muchnik (ROMA)

π^0

$I^G(J^{PC}) = 1^-(0^{-+})$

We have omitted some results that have been superseded by later experiments. The omitted results may be found in our 1988 edition Physics Letters **B204** (1988).

π^0 MASS

The value is calculated from $m_{\pi^\pm}$ and $(m_{\pi^\pm} - m_{\pi^0})$. See notes under the $\pi^\pm$ Mass Listings concerning recent revision of the charged pion mass.

VALUE (MeV)	DOCUMENT ID	
134.9766±0.0006 OUR FIT	Error includes scale factor of 1.1.	

Meson Particle Listings

π^0

$m_{\pi^\pm} - m_{\pi^0}$

Measurements with an error > 0.01 MeV have been omitted.

VALUE (MeV)	DOCUMENT ID		TECN	COMMENT
4.5936 ±0.0005 OUR FIT				
4.5936 ±0.0005 OUR AVERAGE				
4.59364 ± 0.00048	CRAWFORD	91	CNTR	$\pi^- p \to \pi^0 n$, n TOF
4.5930 ± 0.0013	CRAWFORD	86	CNTR	$\pi^- p \to \pi^0 n$, n TOF
• • • We do not use the following data for averages, fits, limits, etc. • • •				
4.59366 ± 0.00048	CRAWFORD	88B	CNTR	See CRAWFORD 91
4.6034 ± 0.0052	VASILEVSKY	66	CNTR	
4.6056 ± 0.0055	CZIRR	63	CNTR	

π^0 MEAN LIFE

Measurements with an error $> 1 \times 10^{-17}$ s have been omitted.

VALUE (10^{-17} s)	EVTS	DOCUMENT ID		TECN	COMMENT
8.4 ±0.6 OUR AVERAGE Error includes scale factor of 3.0. See the ideogram below.					
8.97 ± 0.22 ± 0.17		ATHERTON	85	CNTR	
8.2 ± 0.4		[1] BROWMAN	74	CNTR	Primakoff effect
5.6 ± 0.6		BELLETTINI	70	CNTR	Primakoff effect
9 ± 0.68		KRYSHKIN	70	CNTR	Primakoff effect
• • • We do not use the following data for averages, fits, limits, etc. • • •					
8.4 ± 0.5 ± 0.5	1182	[2] WILLIAMS	88	CBAL	$e^+e^- \to e^+e^-\pi^0$

[1] BROWMAN 74 gives a π^0 width $\Gamma = 8.02 \pm 0.42$ eV. The mean life is $\hbar/\Gamma$.
[2] WILLIAMS 88 gives $\Gamma(\gamma\gamma) = 7.7 \pm 0.5 \pm 0.5$ eV. We give here $\tau = \hbar/\Gamma$(total).

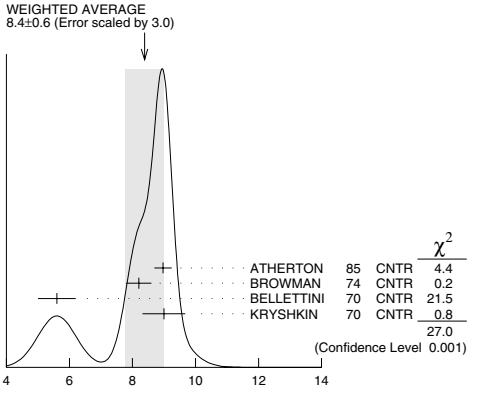

π^0 DECAY MODES

For decay limits to particles which are not established, see the appropriate Search setions (A^0 (axion), and Other Light Boson (X^0) Searches, etc.).

	Mode	Fraction (Γ_j/Γ)		Scale factor/ Confidence level
Γ_1	2γ	(98.798 ± 0.032) %		S=1.1
Γ_2	$e^+e^-\gamma$	(1.198 ± 0.032) %		S=1.1
Γ_3	γ positronium	(1.82 ± 0.29)	$\times 10^{-9}$	
Γ_4	$e^+e^+e^-e^-$	(3.14 ± 0.30)	$\times 10^{-5}$	
Γ_5	e^+e^-	(6.2 ± 0.5)	$\times 10^{-8}$	
Γ_6	4γ	< 2	$\times 10^{-8}$	CL=90%
Γ_7	$\nu\overline{\nu}$	[a] < 8.3	$\times 10^{-7}$	CL=90%
Γ_8	$\nu_e\overline{\nu}_e$	< 1.7	$\times 10^{-6}$	CL=90%
Γ_9	$\nu_\mu\overline{\nu}_\mu$	< 3.1	$\times 10^{-6}$	CL=90%
Γ_{10}	$\nu_\tau\overline{\nu}_\tau$	< 2.1	$\times 10^{-6}$	CL=90%
Γ_{11}	$\gamma\nu\overline{\nu}$	< 6	$\times 10^{-4}$	CL=90%
	Charge conjugation (C) or Lepton Family number (LF) violating modes			
Γ_{12}	3γ	C < 3.1	$\times 10^{-8}$	CL=90%
Γ_{13}	μ^+e^-	LF < 3.8	$\times 10^{-10}$	CL=90%
Γ_{14}	μ^-e^+	LF < 3.4	$\times 10^{-9}$	CL=90%
Γ_{15}	$\mu^+e^- + \mu^-e^+$	LF < 1.72	$\times 10^{-8}$	CL=90%

[a] Astrophysical and cosmological arguments give limits of order 10^{-13}; see the Particle Listings below.

CONSTRAINED FIT INFORMATION

An overall fit to 2 branching ratios uses 4 measurements and one constraint to determine 3 parameters. The overall fit has a $\chi^2 = 1.9$ for 2 degrees of freedom.

The following *off-diagonal* array elements are the correlation coefficients $\langle \delta x_i \delta x_j \rangle / (\delta x_i \cdot \delta x_j)$, in percent, from the fit to the branching fractions, $x_i \equiv \Gamma_i/\Gamma_{\rm total}$. The fit constrains the x_i whose labels appear in this array to sum to one.

x_2	−100	
x_4	−1	0
	x_1	x_2

π^0 BRANCHING RATIOS

$\Gamma(e^+e^-\gamma)/\Gamma(2\gamma)$ Γ_2/Γ_1

VALUE (%)	EVTS	DOCUMENT ID		TECN	COMMENT
1.213 ± 0.033 OUR FIT Error includes scale factor of 1.1.					
1.213 ± 0.030 OUR AVERAGE					
1.25 ± 0.04		SCHARDT	81	SPEC	$\pi^- p \to n\pi^0$
1.166 ± 0.047	3071	[3] SAMIOS	61	HBC	$\pi^- p \to n\pi^0$
1.17 ± 0.15	27	BUDAGOV	60	HBC	
• • • We do not use the following data for averages, fits, limits, etc. • • •					
1.196		JOSEPH	60	THEO	QED calculation

[3] SAMIOS 61 value uses a Panofsky ratio = 1.62.

$\Gamma(\gamma\,\text{positronium})/\Gamma(2\gamma)$ Γ_3/Γ_1

VALUE (units 10^{-9})	EVTS	DOCUMENT ID	TECN	COMMENT
1.84 ± 0.29	277	AFANASYEV	90 CNTR	pC 70 GeV

$\Gamma(e^+e^+e^-e^-)/\Gamma(2\gamma)$ Γ_4/Γ_1

VALUE (units 10^{-5})	EVTS	DOCUMENT ID		TECN
3.18 ± 0.30 OUR FIT				
3.18 ± 0.30	146	[4] SAMIOS	62B	HBC

[4] SAMIOS 62B value uses a Panofsky ratio = 1.62.

$\Gamma(e^+e^-)/\Gamma_{\rm total}$ Γ_5/Γ

Experimental results are listed; branching ratios corrected for radiative effects are given in the footnotes. BERMAN 60 found $B(\pi^0 \to e^+e^-) \geq 4.69 \times 10^{-8}$ via an exact QED calculation.

VALUE (units 10^{-8})	EVTS	DOCUMENT ID		TECN	CHG	COMMENT
6.2 ±0.5 OUR AVERAGE						
6.09 ± 0.40 ± 0.24	275	[5] ALAVI-HARATI	99C	SPEC	0	$K_L^0 \to 3\pi^0$ in flight
6.9 ± 2.3 ± 0.6	21	[6] DESHPANDE	93	SPEC		$K^+ \to \pi^+\pi^0$
7.6 $^{+2.9}_{-2.8}$ ± 0.5	8	[7] MCFARLAND	93	SPEC		$K_L^0 \to 3\pi^0$ in flight

[5] ALAVI-HARATI 99C quote result for $B[\pi^0 \to e^+e^-, (m_{e^+e^-}/m_{\pi^0})^2 > 0.95]$ to minimize radiative contributions from $\pi^0 \to e^+e^-\gamma$. After radiative corrections they obtain $(7.04 \pm 0.46 \pm 0.28) \times 10^{-8}$.
[6] The DESHPANDE 93 result with bremsstrahlung radiative corrections is $(8.0 \pm 2.6 \pm 0.6) \times 10^{-8}$.
[7] The MCFARLAND 93 result is for $B[\pi^0 \to e^+e^-, (m_{e^+e^-}/m_{\pi^0})^2 > 0.95]$. With radiative corrections it becomes $(8.8^{+4.5}_{-3.2} \pm 0.6) \times 10^{-8}$.

$\Gamma(e^+e^-)/\Gamma(2\gamma)$ Γ_5/Γ_1

VALUE (units 10^{-7})	CL%	EVTS	DOCUMENT ID		TECN	COMMENT
• • • We do not use the following data for averages, fits, limits, etc. • • •						
<1.3	90		NIEBUHR	89	SPEC	$\pi^- p \to \pi^0 n$ at rest
<5.3	90		ZEPHAT	87	SPEC	$\pi^- p \to \pi^0 n$ 0.3 GeV/c
1.7 ± 0.6 ± 0.3		59	FRANK	83	SPEC	$\pi^- p \to n\pi^0$
1.8 ± 0.6		58	MISCHKE	82	SPEC	See FRANK 83
2.23 $^{+2.40}_{-1.10}$	90	8	FISCHER	78B	SPRK	$K^+ \to \pi^+\pi^0$

$\Gamma(4\gamma)/\Gamma_{\rm total}$ Γ_6/Γ

VALUE (units 10^{-8})	CL%	EVTS	DOCUMENT ID	TECN	COMMENT
< 2	90		MCDONOUGH 88	CBOX	$\pi^- p$ at rest
• • • We do not use the following data for averages, fits, limits, etc. • • •					
<160	90		BOLOTOV	86C CALO	
<440	90	0	AUERBACH	80 CNTR	

$\Gamma(\nu\overline{\nu})/\Gamma_{\rm total}$ Γ_7/Γ

The astrophysical and cosmological limits are many orders of magnitude lower, but we use the best laboratory limit for the Summary Tables.

VALUE (units 10^{-6})	CL%	EVTS	DOCUMENT ID		TECN	COMMENT
< 0.83	90		[8] ATIYA	91	B787	$K^+ \to \pi^+\nu\nu'$

• • • We do not use the following data for averages, fits, limits, etc. • • •

$< 2.9 \times 10^{-7}$			[9] LAM	91		Cosmological limit
$< 3.2 \times 10^{-7}$			[10] NATALE	91		SN 1987A
< 6.5	90		DORENBOS...	88	CHRM	Beam dump, prompt ν
< 24	90	0	[8] HERCZEG	81	RVUE	$K^+ \to \pi^+ \nu\nu'$

[8] This limit applies to all possible $\nu\nu'$ states as well as to other massless, weakly interacting states.

[9] LAM 91 considers the production of right-handed neutrinos produced from the cosmic thermal background at the temperature of about the pion mass through the reaction $\gamma\gamma \to \pi^0 \to \nu\overline{\nu}$.

[10] NATALE 91 considers the excess energy-loss rate from SN 1987A if the process $\gamma\gamma \to \pi^0 \to \nu\overline{\nu}$ occurs, permitted if the neutrinos have a right-handed component. As pointed out in LAM 91 (and confirmed by Natale), there is a factor 4 error in the NATALE 91 published result (0.8×10^{-7}).

$\Gamma(\nu_e \overline{\nu}_e)/\Gamma_{total}$ Γ_8/Γ

VALUE (units 10^{-6})	CL%	DOCUMENT ID		TECN	COMMENT
<1.7	90	DORENBOS...	88	CHRM	Beam dump, prompt ν
• • • We do not use the following data for averages, fits, limits, etc. • • •					
<3.1	90	[11] HOFFMAN	88	RVUE	Beam dump, prompt ν

[11] HOFFMAN 88 analyzes data from a 400-GeV BEBC beam-dump experiment.

$\Gamma(\nu_\mu \overline{\nu}_\mu)/\Gamma_{total}$ Γ_9/Γ

VALUE (units 10^{-6})	CL%	DOCUMENT ID		TECN	COMMENT
<3.1	90	[12] HOFFMAN	88	RVUE	Beam dump, prompt ν
• • • We do not use the following data for averages, fits, limits, etc. • • •					
<7.8	90	DORENBOS...	88	CHRM	Beam dump, prompt ν

[12] HOFFMAN 88 analyzes data from a 400-GeV BEBC beam-dump experiment.

$\Gamma(\nu_\tau \overline{\nu}_\tau)/\Gamma_{total}$ Γ_{10}/Γ

VALUE (units 10^{-6})	CL%	DOCUMENT ID		TECN	COMMENT
<2.1	90	[13] HOFFMAN	88	RVUE	Beam dump, prompt ν
• • • We do not use the following data for averages, fits, limits, etc. • • •					
<4.1	90	DORENBOS...	88	CHRM	Beam dump, prompt ν

[13] HOFFMAN 88 analyzes data from a 400-GeV BEBC beam-dump experiment.

$\Gamma(\gamma\nu\overline{\nu})/\Gamma_{total}$ Γ_{11}/Γ

Standard Model prediction is 6×10^{-18}.

VALUE	CL%	DOCUMENT ID		TECN	COMMENT
$< 6 \times 10^{-4}$	90	ATIYA	92	CNTR	$K^+ \to \gamma\nu\overline{\nu}\pi^+$

$\Gamma(3\gamma)/\Gamma_{total}$ Γ_{12}/Γ

Forbidden by C invariance.

VALUE (units 10^{-8})	CL%	EVTS	DOCUMENT ID		TECN	COMMENT
< 3.1	90		MCDONOUGH	88	CBOX	$\pi^- p$ at rest
• • • We do not use the following data for averages, fits, limits, etc. • • •						
< 38	90	0	HIGHLAND	80	CNTR	
<150	90	0	AUERBACH	78	CNTR	
<490	90	0	[14] DUCLOS	65	CNTR	
<490	90		[14] KUTIN	65	CNTR	

[14] These experiments give $B(3\gamma/2\gamma) < 5.0 \times 10^{-6}$.

$\Gamma(\mu^+ e^-)/\Gamma_{total}$ Γ_{13}/Γ

Forbidden by lepton family number conservation.

VALUE (units 10^{-9})	CL%	EVTS	DOCUMENT ID		TECN	COMMENT
< 0.38	90	0	APPEL	00	SPEC	$K^+ \to \pi^+ \mu^+ e^-$
• • • We do not use the following data for averages, fits, limits, etc. • • •						
<16	90		LEE	90	SPEC	$K^+ \to \pi^+ \mu^+ e^-$
<78	90		CAMPAGNARI	88	SPEC	See LEE 90

$\Gamma(\mu^- e^+)/\Gamma_{total}$ Γ_{14}/Γ

Forbidden by lepton family number conservation.

VALUE (units 10^{-9})	CL%	EVTS	DOCUMENT ID		TECN	CHG	COMMENT
<3.4	90	0	APPEL	00B	B865	0	$K^+ \to \pi^+ e^+ \mu^-$

$[\Gamma(\mu^+ e^-) + \Gamma(\mu^- e^+)]/\Gamma_{total}$ Γ_{15}/Γ

Forbidden by lepton family number conservation.

VALUE (units 10^{-9})	CL%	DOCUMENT ID		TECN	COMMENT
< 17.2	90	KROLAK	94	E799	In $K_L^0 \to 3\pi^0$
• • • We do not use the following data for averages, fits, limits, etc. • • •					
<140		HERCZEG	84	RVUE	$K^+ \to \pi^+ \mu e$
$< 2 \times 10^{-6}$		HERCZEG	84	THEO	$\mu^- \to e^-$ conversion
< 70	90	BRYMAN	82	RVUE	$K^+ \to \pi^+ \mu e$

π^0 ELECTROMAGNETIC FORM FACTOR

The amplitude for the process $\pi^0 \to e^+ e^- \gamma$ contains a form factor $F(x)$ at the $\pi^0 \gamma\gamma$ vertex, where $x = [m_{e^+e^-}/m_{\pi^0}]^2$. The parameter a in the linear expansion $F(x) = 1 + ax$ is listed below.

All the measurements except that of BEHREND 91 are in the time-like region of momentum transfer.

LINEAR COEFFICIENT OF π^0 ELECTROMAGNETIC FORM FACTOR

VALUE			EVTS	DOCUMENT ID		TECN	COMMENT
0.032	**±0.004**	**OUR AVERAGE**					
+0.026	±0.024	±0.048	7548	FARZANPAY	92	SPEC	$\pi^- p \to \pi^0 n$ at rest
+0.025	±0.014	±0.026	54k	MEIJERDREES	92B	SPEC	$\pi^- p \to \pi^0 n$ at rest
+0.0326	±0.0026	±0.0026	127	[15] BEHREND	91	CELL	$e^+e^- \to e^+e^-\pi^0$
−0.11	±0.03	±0.08	32k	FONVIEILLE	89	SPEC	Radiation corr.
• • • We do not use the following data for averages, fits, limits, etc. • • •							
0.12	$^{+0.05}_{-0.04}$			[16] TUPPER	83	THEO	FISCHER 78 data
+0.10	±0.03		31k	[17] FISCHER	78	SPEC	Radiation corr.
+0.01	±0.11		2200	DEVONS	69	OSPK	No radiation corr.
−0.15	±0.10		7676	KOBRAK	61	HBC	No radiation corr.
−0.24	±0.16		3071	SAMIOS	61	HBC	No radiation corr.

[15] BEHREND 91 estimates that their systematic error is of the same order of magnitude as their statistical error, and so we have included a systematic error of this magnitude. The value of a is obtained by extrapolation from the region of large space-like momentum transfer assuming vector dominance.

[16] TUPPER 83 is a theoretical analysis of FISCHER 78 including 2-photon exchange in the corrections.

[17] The FISCHER 78 error is statistical only. The result without radiation corrections is $+0.05 \pm 0.03$.

π^0 REFERENCES

We have omitted some papers that have been superseded by later experiments. The omitted papers may be found in our 1988 edition Physics Letters **B204** (1988).

APPEL	00	PRL 85 2450	R. Appel *et al.*	(BNL 865 Collab.)
Also	97	Thesis, Yale Univ.	D.R. Bergman	
Also	97	Thesis, Univ. Zurich	S. Pislak	
APPEL	00B	PRL 85 2877	R. Appel *et al.*	(BNL 865 Collab.)
ALAVI-HARATI	99C	PRL 83 922	A. Alavi-Harati *et al.*	(FNAL KTeV Collab.)
KROLAK	94	PL B320 407	P. Krolak *et al.*	(EFI, UCLA, COLO, ELMT+)
DESHPANDE	93	PRL 71 27	A. Deshpande *et al.*	(BNL E851 Collab.)
MCFARLAND	93	PRL 71 31	K.S. McFarland *et al.*	(EFI, UCLA, COLO+)
ATIYA	92	PRL 69 733	M.S. Atiya *et al.*	(BNL, LANL, PRIN+)
FARZANPAY	92	PL B278 413	F. Farzanpay *et al.*	(ORST, TRIU, BRCO+)
MEIJERDREES	92B	PR D45 1439	R. Meijer Drees *et al.*	(PSI SINDRUM-I Collab.)
ATIYA	91	PRL 66 2189	M.S. Atiya *et al.*	(BNL, LANL, PRIN+)
BEHREND	91	ZPHY C49 401	H.J. Behrend *et al.*	(CELLO Collab.)
CRAWFORD	91	PR D43 46	J.F. Crawford *et al.*	(VILL, VIRG)
LAM	91	PR D44 3345	W.P. Lam, K.W. Ng	(AST)
NATALE	91	PL B258 227	A.A. Natale	(SPIFT)
AFANASYEV	90	PL B236 116	L.G. Afanasyev *et al.*	(JINR, MOSU, SERP)
Also	90B	SJNP 51 664	L.G. Afanasyev *et al.*	(JINR)
		Translated from YAF 51 1040.		
LEE	90	PRL 64 165	A.M. Lee *et al.*	(BNL, FNAL, VILL, WASH+)
FONVIEILLE	89	PL B233 65	H. Fonvieille *et al.*	(CLER, LYON, SACL)
NIEBUHR	89	PR D40 2796	C. Niebuhr *et al.*	(SINDRUM Collab.)
CAMPAGNARI	88	PRL 61 2062	C. Campagnari *et al.*	(BNL, FNAL, PSI+)
CRAWFORD	88B	PL B213 391	J.F. Crawford *et al.*	(PSI, VIRG)
DORENBOS...	88	ZPHY C40 497	J. Dorenbosch *et al.*	(CHARM Collab.)
HOFFMAN	88	PL B208 149	C.M. Hoffman	(LANL)
MCDONOUGH	88	PR D38 2121	J.M. McDonough *et al.*	(TEMP, LANL, CHIC)
PDG	88	PL B204	G.P. Yost *et al.*	(LBL+)
WILLIAMS	88	PR D38 1365	D.A. Williams *et al.*	(Crystal Ball Collab.)
ZEPHAT	87	JPG 13 1375	A.G. Zephat *et al.*	(OMICRON Collab.)
BOLOTOV	86C	JETPL 43 520	V.N. Bolotov *et al.*	(INRM)
		Translated from ZETFP 43 405.		
CRAWFORD	86	PRL 56 1043	J.F. Crawford *et al.*	(SIN, VIRG)
ATHERTON	85	PL 158B 81	H.W. Atherton *et al.*	(CERN, ISU, LUND+)
HERCZEG	84	PR D29 1954	P. Herczeg, C.M. Hoffman	(LANL)
FRANK	83	PR D28 423	J.S. Frank *et al.*	(LANL, ARZS)
TUPPER	83	PR D28 2905	G.B. Tupper, T.R. Grose, M.A. Samuel	(OKSU)
BRYMAN	82	PR D26 2538	D.A. Bryman	(TRIU)
MISCHKE	82	PRL 48 1153	R.E. Mischke *et al.*	(LANL, ARZS)
HERCZEG	81	PL 100B 347	P. Herczeg, C.M. Hoffman	(LANL)
SCHARDT	81	PR D23 639	M.A. Schardt *et al.*	(ARZS, LANL)
AUERBACH	80	PL 90B 317	L.B. Auerbach *et al.*	(TEMP, LASL)
HIGHLAND	80	PRL 44 628	V.L. Highland *et al.*	(TEMP, LASL)
AUERBACH	78	PRL 41 275	L.B. Auerbach *et al.*	(TEMP, LASL)
FISCHER	78	PL 73B 359	J. Fischer *et al.*	(GEVA, SACL)
FISCHER	78B	PL 73B 364	J. Fischer *et al.*	(GEVA, SACL)
BROWMAN	74	PRL 33 1400	A. Browman *et al.*	(CORN, BING)
BELLETTINI	70	NC 66A 243	G. Bellettini *et al.*	(PISA, BONN)
KRYSHKIN	70	JETP 30 1037	V.I. Kryshkin, A.G. Sterligov, Y.P. Usov	(TMSK)
		Translated from ZETF 57 1917.		
DEVONS	69	PR 184 1356	S. Devons *et al.*	(COLU, ROMA)
VASILEVSKY	66	PL 23 281	I.M. Vasilevsky *et al.*	(JINR)
DUCLOS	65	PL 19 253	J. Duclos *et al.*	(CERN, HEID)
KUTIN	65	JETPL 2 243	V.M. Kutjin, V.I. Petrukhin, Y.D. Prokoshkin	(JINR)
		Translated from ZETFP 2 387.		
CZIRR	63	PR 130 341	J.B. Czirr	(LRL)
SAMIOS	62B	PR 126 1844	N.P. Samios *et al.*	(COLU, BNL)
KOBRAK	61	NC 20 1115	H. Kobrak	(EFI)
SAMIOS	61	PR 121 275	N.P. Samios	(COLU, BNL)
BERMAN	60	NC XVIII 1192	S. Berman, D. Geffen	
BUDAGOV	60	JETP 11 755	Y.A. Budagov *et al.*	(JINR)
		Translated from ZETF 38 1047.		
JOSEPH	60	NC 16 997	D.W. Joseph	(EFI)

η

$I^G(J^{PC}) = 0^+(0^{-+})$

We have omitted some results that have been superseded by later experiments. The omitted results may be found in our 1988 edition Physics Letters **B204** (1988).

η MASS

We no longer use the bubble-chamber measurements from the 1960's, which seem to have been systematically high by about 1 MeV. (However, note that the latest measurement is midway between those old values and the newer ones.) Some early results have been omitted altogether.

VALUE (MeV)	EVTS	DOCUMENT ID		TECN	COMMENT
547.75 ±0.12 OUR AVERAGE		Error includes scale factor of 2.6. See the ideogram below.			
547.843 ± 0.030 ± 0.041	1134	LAI	02	NA48	$\eta \to 3\pi^0$
547.12 ±0.06 ±0.25		KRUSCHE	95D	SPEC	$\gamma p \to \eta p$, threshold
547.30 ±0.15		PLOUIN	92	SPEC	$dp \to \eta\, ^3$He
547.45 ±0.25		DUANE	74	SPEC	$\pi^- p \to n$ neutrals
• • • We do not use the following data for averages, fits, limits, etc. • • •					
548.2 ±0.65		FOSTER	65C	HBC	
549.0 ±0.7	148	FOELSCHE	64	HBC	
548.0 ±1.0	91	ALFF-...	62	HBC	
549.0 ±1.2	53	BASTIEN	62	HBC	

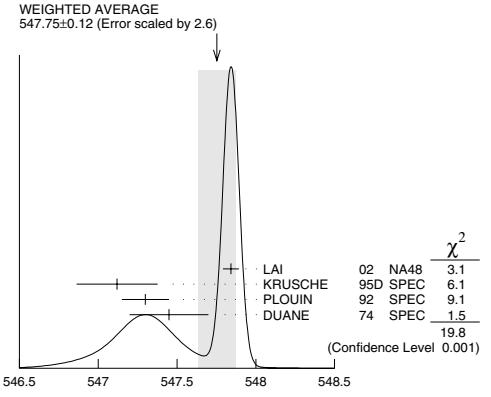

η WIDTH

This is the partial decay rate $\Gamma(\eta \to \gamma\gamma)$ divided by the fitted branching fraction for that mode. See the note at the start of the $\Gamma(2\gamma)$ data block, next below.

VALUE (keV)	DOCUMENT ID
1.29 ± 0.07 OUR FIT	

η DECAY MODES

	Mode	Fraction (Γ_i/Γ)	Scale factor/ Confidence level
	Neutral modes		
Γ_1	neutral modes	(72.0 ± 0.5) %	S=1.3
Γ_2	2γ	[a] (39.43 ± 0.26) %	S=1.2
Γ_3	$3\pi^0$	(32.51 ± 0.29) %	S=1.2
Γ_4	$\pi^0 2\gamma$	(7.2 ± 1.4) $\times 10^{-4}$	
Γ_5	other neutral modes	< 2.8 %	CL=90%
	Charged modes		
Γ_6	charged modes	(28.0 ± 0.5) %	S=1.3
Γ_7	$\pi^+\pi^-\pi^0$	(22.6 ± 0.4) %	S=1.3
Γ_8	$\pi^+\pi^-\gamma$	(4.68 ± 0.11) %	S=1.2
Γ_9	$e^+e^-\gamma$	(6.0 ± 0.8) $\times 10^{-3}$	S=1.4
Γ_{10}	$\mu^+\mu^-\gamma$	(3.1 ± 0.4) $\times 10^{-4}$	
Γ_{11}	e^+e^-	< 7.7 $\times 10^{-5}$	CL=90%
Γ_{12}	$\mu^+\mu^-$	(5.8 ± 0.8) $\times 10^{-6}$	
Γ_{13}	$e^+e^-e^+e^-$	< 6.9 $\times 10^{-5}$	CL=90%
Γ_{14}	$\pi^+\pi^-e^+e^-$	(4.0 $^{+14.0}_{-2.7}$) $\times 10^{-4}$	S=5.8
Γ_{15}	$\pi^+\pi^-2\gamma$	< 2.0 $\times 10^{-3}$	
Γ_{16}	$\pi^+\pi^-\pi^0\gamma$	< 5 $\times 10^{-4}$	CL=90%
Γ_{17}	$\pi^0\mu^+\mu^-\gamma$	< 3 $\times 10^{-6}$	CL=90%

Charge conjugation (C), Parity (P), Charge conjugation × Parity (CP), or Lepton Family number (LF) violating modes

Γ_{18}	$\pi^+\pi^-$	P,CP	<	3.3	$\times 10^{-4}$	CL=90%
Γ_{19}	$\pi^0\pi^0$	P,CP	<	4.3	$\times 10^{-4}$	CL=90%
Γ_{20}	3γ	C	<	5	$\times 10^{-4}$	CL=95%
Γ_{21}	$4\pi^0$	P,CP	<	6.9	$\times 10^{-7}$	CL=90%
Γ_{22}	$\pi^0 e^+e^-$	C [b]	<	4	$\times 10^{-5}$	CL=90%
Γ_{23}	$\pi^0\mu^+\mu^-$	C [b]	<	5	$\times 10^{-6}$	CL=90%
Γ_{24}	$\mu^+e^- + \mu^-e^+$	LF	<	6	$\times 10^{-6}$	CL=90%

[a] Due to removing an old measurement from the average, this is 0.11 keV larger than the width we gave in our 2002 edition, 1.18 ± 0.11 keV. See the $\Gamma(2\gamma)$ data block in the Data Listings.

[b] C parity forbids this to occur as a single-photon process.

CONSTRAINED FIT INFORMATION

An overall fit to a decay rate and 18 branching ratios uses 41 measurements and one constraint to determine 9 parameters. The overall fit has a $\chi^2 = 17.3$ for 33 degrees of freedom.

The following *off-diagonal* array elements are the correlation coefficients $\langle \delta x_i \delta x_j \rangle / (\delta x_i \cdot \delta x_j)$, in percent, from the fit to the branching fractions, $x_i \equiv \Gamma_i/\Gamma_{\rm total}$. The fit constrains the x_i whose labels appear in this array to sum to one.

	x_2	x_3	x_4	x_7	x_8	x_9	x_{10}	x_{14}
x_3	46							
x_4	2	2						
x_7	−79	−82	−5					
x_8	−63	−66	−4	68				
x_9	−8	−8	0	−7	−6			
x_{10}	0	0	0	−1	0	0		
x_{14}	−7	−8	0	−17	−13	−1	0	
Γ	−13	−6	0	10	8	1	0	1

	Mode	Rate (keV)	Scale factor
Γ_2	2γ	[a] 0.510 ±0.026	
Γ_3	$3\pi^0$	0.421 ±0.022	
Γ_4	$\pi^0 2\gamma$	(9.3 ±1.9) $\times 10^{-4}$	
Γ_7	$\pi^+\pi^-\pi^0$	0.293 ±0.016	
Γ_8	$\pi^+\pi^-\gamma$	0.0606 ±0.0035	
Γ_9	$e^+e^-\gamma$	0.0078 ±0.0011	1.3
Γ_{10}	$\mu^+\mu^-\gamma$	(4.0 ±0.6) $\times 10^{-4}$	
Γ_{14}	$\pi^+\pi^-e^+e^-$	(0.52 $^{+1.90}_{-0.35}$) $\times 10^{-3}$	5.8

η DECAY RATES

$\Gamma(2\gamma)$ Γ_2

See the table immediately above giving the fitted decay rates. Following the advice of NEFKENS 02, we have removed the Primakoff-effect measurement from the average. See also the "Note on the Decay Width $\Gamma(\eta \to \gamma\gamma)$," in our 1994 edition, Phys. Rev. **D50**, 1 August 1994, Part I, p. 1451, for a discussion of the various measurements.

VALUE (keV)	EVTS	DOCUMENT ID		TECN	COMMENT
0.510 ± 0.026 OUR FIT					
0.510 ± 0.026 OUR AVERAGE					
0.51 ±0.12 ±0.05	36	BARU	90	MD1	$e^+e^- \to e^+e^-\eta$
0.490 ± 0.010 ± 0.048	2287	ROE	90	ASP	$e^+e^- \to e^+e^-\eta$
0.514 ± 0.017 ± 0.035	1295	WILLIAMS	88	CBAL	$e^+e^- \to e^+e^-\eta$
0.53 ±0.04 ±0.04		BARTEL	85E	JADE	$e^+e^- \to e^+e^-\eta$
• • • We do not use the following data for averages, fits, limits, etc. • • •					
0.64 ±0.14 ±0.13		AIHARA	86	TPC	$e^+e^- \to e^+e^-\eta$
0.56 ±0.16	56	WEINSTEIN	83	CBAL	$e^+e^- \to e^+e^-\eta$
0.324 ± 0.046		BROWMAN	74B	CNTR	Primakoff effect
1.00 ±0.22	[1]	BEMPORAD	67	CNTR	Primakoff effect

[1] BEMPORAD 67 gives $\Gamma(2\gamma) = 1.21 \pm 0.26$ keV assuming $\Gamma(2\gamma)/\Gamma(\text{total}) = 0.314$. Bemporad private communication gives $\Gamma(2\gamma)^2/\Gamma(\text{total}) = 0.380 \pm 0.083$. We evaluate this using $\Gamma(2\gamma)/\Gamma(\text{total}) = 0.38 \pm 0.01$. Not included in average because the uncertainty resulting from the separation of the coulomb and nuclear amplitudes has apparently been underestimated.

η BRANCHING RATIOS

Neutral modes

Γ(neutral modes)/Γ_{total} $\Gamma_1/\Gamma = (\Gamma_2+\Gamma_3+\Gamma_4)/\Gamma$

VALUE	EVTS	DOCUMENT ID		TECN	COMMENT
0.720±0.005 OUR FIT		Error includes scale factor of 1.3.			
0.705±0.008	16k	BASILE	71D	CNTR	MM spectrometer
• • • We do not use the following data for averages, fits, limits, etc. • • •					
0.79 ±0.08		BUNIATOV	67	OSPK	

$\Gamma(2\gamma)/\Gamma_{total}$ Γ_2/Γ

VALUE	EVTS	DOCUMENT ID		TECN	COMMENT
0.3943±0.0026 OUR FIT		Error includes scale factor of 1.2.			
0.3949±0.0017±0.0030	65k	ABEGG	96	SPEC	$pd \to {}^3\mathrm{He}\eta$

$\Gamma(2\gamma)/\Gamma$(neutral modes) $\Gamma_2/\Gamma_1 = \Gamma_2/(\Gamma_2+\Gamma_3+\Gamma_4)$

VALUE	EVTS	DOCUMENT ID		TECN	COMMENT
0.5475±0.0021 OUR FIT		Error includes scale factor of 1.1.			
0.549 ±0.004 OUR AVERAGE					
0.549 ±0.004		ALDE	84	GAM2	
0.535 ±0.018		BUTTRAM	70	OSPK	
0.59 ±0.033		BUNIATOV	67	OSPK	
• • • We do not use the following data for averages, fits, limits, etc. • • •					
0.52 ±0.09	88	ABROSIMOV	80	HLBC	
0.60 ±0.14	113	KENDALL	74	OSPK	
0.57 ±0.09		STRUGALSKI	71	HLBC	
0.579 ±0.052		FELDMAN	67	OSPK	
0.416 ±0.044		DIGIUGNO	66	CNTR	Error doubled
0.44 ±0.07		GRUNHAUS	66	OSPK	
0.39 ±0.06		[2] JONES	66	CNTR	

[2] This result from combining cross sections from two different experiments.

$\Gamma(3\pi^0)/\Gamma$(neutral modes) $\Gamma_3/\Gamma_1 = \Gamma_3/(\Gamma_2+\Gamma_3+\Gamma_4)$

VALUE	EVTS	DOCUMENT ID		TECN	COMMENT
0.4515±0.0021 OUR FIT		Error includes scale factor of 1.1.			
0.450 ±0.004 OUR AVERAGE					
0.450 ±0.004		ALDE	84	GAM2	
0.439 ±0.024		BUTTRAM	70	OSPK	
• • • We do not use the following data for averages, fits, limits, etc. • • •					
0.44 ±0.08	75	ABROSIMOV	80	HLBC	
0.32 ±0.09		STRUGALSKI	71	HLBC	
0.41 ±0.033		BUNIATOV	67	OSPK	Not indep. of $\Gamma(2\gamma)$/ Γ(neutral modes)
0.177 ±0.035		FELDMAN	67	OSPK	
0.209 ±0.054		DIGIUGNO	66	CNTR	Error doubled
0.29 ±0.10		GRUNHAUS	66	OSPK	

$\Gamma(3\pi^0)/\Gamma(2\gamma)$ Γ_3/Γ_2

VALUE	DOCUMENT ID		TECN	COMMENT
0.825±0.007 OUR FIT	Error includes scale factor of 1.1.			
0.832±0.011 OUR AVERAGE				
0.826±0.024	ACHASOV	00D	SND	$e^+e^- \to \phi \to \eta\gamma$
0.832±0.005±0.012	KRUSCHE	95D	SPEC	$\gamma p \to \eta p$, threshold
0.841±0.034	AMSLER	93	CBAR	$\bar{p}p \to \pi^+\pi^-\eta$ at rest
• • • We do not use the following data for averages, fits, limits, etc. • • •				
0.796±0.016±0.016	ACHASOV	00	SND	See ACHASOV 00D
0.822±0.009	[3] ALDE	84	GAM2	
0.91 ±0.14	COX	70B	HBC	
0.75 ±0.09	DEVONS	70	OSPK	
0.88 ±0.16	BALTAY	67D	DBC	
1.1 ±0.2	CENCE	67	OSPK	
1.25 ±0.39	BACCI	63	CNTR	Inverse BR reported

[3] This result is not independent of other ALDE 84 results in this Listing, and so is omitted from the fit and average.

$\Gamma(\pi^0 2\gamma)/\Gamma$(neutral modes) $\Gamma_4/\Gamma_1 = \Gamma_4/(\Gamma_2+\Gamma_3+\Gamma_4)$

VALUE (units 10^{-3})	DOCUMENT ID		TECN
1.00±0.20 OUR FIT			
1.0 ±0.2	ALDE	84	GAM2

$\Gamma(\pi^0 2\gamma)/\Gamma_{total}$ Γ_4/Γ

Early results are summarized in the review by LANDSBERG 85.

VALUE (units 10^{-4})	CL%	EVTS	DOCUMENT ID		TECN	COMMENT
7.2±1.4 OUR FIT						
• • • We do not use the following data for averages, fits, limits, etc. • • •						
< 8.4	90	7	ACHASOV	01D	SND	$e^+e^- \to \phi \to \eta\gamma$
9.5 ±2.3		70	BINON	82	GAM2	See ALDE 84
<30	90	0	DAVYDOV	81	GAM2	$\pi^- p \to \eta n$

Γ(neutral modes)/$[\Gamma(\pi^+\pi^-\pi^0)+\Gamma(\pi^+\pi^-\gamma)+\Gamma(e^+e^-\gamma)]$ $\Gamma_1/(\Gamma_7+\Gamma_8+\Gamma_9) = (\Gamma_2+\Gamma_3+\Gamma_4)/(\Gamma_7+\Gamma_8+\Gamma_9)$

VALUE	EVTS	DOCUMENT ID		TECN
2.58±0.06 OUR FIT	Error includes scale factor of 1.3.			
2.64±0.23		BALTAY	67B	DBC
• • • We do not use the following data for averages, fits, limits, etc. • • •				
4.5 ±1.0	280	[4] JAMES	66	HBC
3.20±1.26	53	[4] BASTIEN	62	HBC
2.5 ±1.0	10	[4] PICKUP	62	HBC

[4] These experiments are not used in the averages as they do not separate clearly $\eta \to \pi^+\pi^-\pi^0$ and $\eta \to \pi^+\pi^-\gamma$ from each other. The reported values thus probably contain some unknown fraction of $\eta \to \pi^+\pi^-\gamma$.

Γ(neutral modes)/$\Gamma(\pi^+\pi^-\pi^0)$ $\Gamma_1/\Gamma_7 = (\Gamma_2+\Gamma_3+\Gamma_4)/\Gamma_7$

VALUE	EVTS	DOCUMENT ID		TECN
3.18±0.08 OUR FIT	Error includes scale factor of 1.3.			
3.26±0.30 OUR AVERAGE				
2.54±1.89	74	KENDALL	74	OSPK
3.4 ±1.1	29	AGUILAR-...	72B	HBC
2.83±0.80	70	[5] BLOODWO...	72B	HBC
3.6 ±0.6	244	FLATTE	67B	HBC
2.89±0.56		ALFF-...	66	HBC
3.6 ±0.8	50	KRAEMER	64	DBC
3.8 ±1.1		PAULI	64	DBC

[5] Error increased from published value 0.5 by Bloodworth (private communication).

$\Gamma(2\gamma)/[\Gamma(\pi^+\pi^-\pi^0)+\Gamma(\pi^+\pi^-\gamma)+\Gamma(e^+e^-\gamma)]$ $\Gamma_2/(\Gamma_7+\Gamma_8+\Gamma_9)$

VALUE	EVTS	DOCUMENT ID		TECN
1.412±0.033 OUR FIT	Error includes scale factor of 1.3.			
1.1 ±0.4 OUR AVERAGE				
1.51 ±0.93	75	KENDALL	74	OSPK
0.99 ±0.48		CRAWFORD	63	HBC

$\Gamma(2\gamma)/\Gamma(\pi^+\pi^-\pi^0)$ Γ_2/Γ_7

VALUE	EVTS	DOCUMENT ID		TECN	COMMENT
1.74±0.04 OUR FIT	Error includes scale factor of 1.3.				
1.75±0.13 OUR AVERAGE					
1.78±0.10±0.13	1077	AMSLER	95	CBAR	$\bar{p}p \to \pi^+\pi^-\eta$ at rest
1.72±0.25	401	BAGLIN	69	HLBC	
1.61±0.39		FOSTER	65	HBC	

$\Gamma(3\pi^0)/\Gamma(\pi^+\pi^-\pi^0)$ Γ_3/Γ_7

VALUE	EVTS	DOCUMENT ID		TECN	COMMENT
1.44±0.04 OUR FIT	Error includes scale factor of 1.3.				
1.49±0.06 OUR AVERAGE					
1.52±0.04±0.08	23k	[6] AKHMETSHIN	01B	CMD2	$e^+e^- \to \phi \to \eta\gamma$
1.44±0.09±0.10	1627	AMSLER	95	CBAR	$\bar{p}p \to \pi^+\pi^-\eta$ at rest
$1.50^{+0.15}_{-0.29}$	199	BAGLIN	69	HLBC	
$1.47^{+0.20}_{-0.17}$		BULLOCK	68	HLBC	
• • • We do not use the following data for averages, fits, limits, etc. • • •					
1.3 ±0.4		BAGLIN	67B	HLBC	
0.90±0.24		FOSTER	65	HBC	
2.0 ±1.0		FOELSCHE	64	HBC	
0.83±0.32		CRAWFORD	63	HBC	

[6] AKHMETSHIN 01B uses results from AKHMETSHIN 99F.

Γ(other neutral modes)/Γ_{total} Γ_5/Γ

These are neutral modes other than $\gamma\gamma$, $3\pi^0$, and $\pi^0\gamma\gamma$. Nearly any such mode one can think of would violate P, or C, or both.

VALUE	CL%	DOCUMENT ID		TECN	COMMENT
<0.028	90	ABEGG	96	SPEC	$pd \to {}^3\mathrm{He}\eta$

Charged modes

$\Gamma(\pi^+\pi^-\pi^0)/[\Gamma(2\gamma)+\Gamma(3\pi^0)]$ $\Gamma_7/(\Gamma_2+\Gamma_3)$

VALUE	DOCUMENT ID		TECN	COMMENT
0.315 ±0.007 OUR FIT	Error includes scale factor of 1.3.			
0.304 ±0.012	ACHASOV	00D	SND	$e^+e^- \to \phi \to \eta\gamma$
• • • We do not use the following data for averages, fits, limits, etc. • • •				
0.3141±0.0081±0.0058	ACHASOV	00B	SND	See ACHASOV 00D

$\Gamma(\pi^+\pi^-\gamma)/\Gamma(\pi^+\pi^-\pi^0)$ Γ_8/Γ_7

VALUE	EVTS	DOCUMENT ID		TECN
0.207±0.004 OUR FIT	Error includes scale factor of 1.1.			
0.207±0.004 OUR AVERAGE	Error includes scale factor of 1.1.			
0.209±0.004	18k	THALER	73	ASPK
0.201±0.006	7250	GORMLEY	70	ASPK
• • • We do not use the following data for averages, fits, limits, etc. • • •				
0.28 ±0.04		BALTAY	67B	DBC
0.25 ±0.035		LITCHFIELD	67	DBC
0.30 ±0.06		CRAWFORD	66	HBC
0.196±0.041		FOSTER	65C	HBC

$\Gamma(e^+e^-\gamma)/\Gamma_{\text{total}}$ Γ_9/Γ

VALUE (units 10^{-3})	EVTS	DOCUMENT ID		TECN	COMMENT
6.0 ±0.8 OUR FIT Error includes scale factor of 1.4.					
6.3 ±1.0 OUR AVERAGE Error includes scale factor of 1.6.					
5.15 ± 0.62 ± 0.74	283	ACHASOV	01B	SND	$e^+e^- \to \phi \to \eta\gamma$
7.10 ± 0.64 ± 0.46	323	AKHMETSHIN	01	CMD2	$e^+e^- \to \phi \to \eta\gamma$

$\Gamma(e^+e^-\gamma)/\Gamma(\pi^+\pi^-\pi^0)$ Γ_9/Γ_7

VALUE (units 10^{-2})	EVTS	DOCUMENT ID		TECN	COMMENT
2.65 ± 0.35 OUR FIT Error includes scale factor of 1.5.					
2.1 ±0.5	80	JANE	75B	OSPK	See the erratum

$\Gamma(\mu^+\mu^-\gamma)/\Gamma_{\text{total}}$ Γ_{10}/Γ

VALUE (units 10^{-4})	EVTS	DOCUMENT ID		TECN	COMMENT
3.1 ± 0.4 OUR FIT					
3.1 ± 0.4	600	DZHELYADIN	80	SPEC	$\pi^- p \to \eta n$
• • • We do not use the following data for averages, fits, limits, etc. • • •					
1.5 ± 0.75	100	BUSHNIN	78	SPEC	See DZHELYADIN 80

$\Gamma(e^+e^-)/\Gamma_{\text{total}}$ Γ_{11}/Γ

VALUE (units 10^{-4})	CL%	DOCUMENT ID		TECN	COMMENT
< 0.77	90	BROWDER	97B	CLE2	$e^+e^- \simeq 10.5$ GeV
• • • We do not use the following data for averages, fits, limits, etc. • • •					
< 2	90	WHITE	96	SPEC	$pd \to \eta\,^3$He
< 3	90	DAVIES	74	RVUE	Uses ESTEN 67

$\Gamma(\mu^+\mu^-)/\Gamma_{\text{total}}$ Γ_{12}/Γ

VALUE (units 10^{-6})	CL%	EVTS	DOCUMENT ID		TECN	COMMENT
5.8 ± 0.8 OUR AVERAGE						
5.7 ± 0.7 ± 0.5		114	ABEGG	94	SPEC	$pd \to \eta\,^3$He
6.5 ± 2.1		27	DZHELYADIN	80B	SPEC	$\pi^- p \to \eta n$
• • • We do not use the following data for averages, fits, limits, etc. • • •						
$5.6^{+0.6}_{-0.7} \pm 0.5$		100	KESSLER	93	SPEC	See ABEGG 94
< 20	95	0	WEHMANN	68	OSPK	

$\Gamma(\mu^+\mu^-)/\Gamma(2\gamma)$ Γ_{12}/Γ_2

VALUE (units 10^{-5})	DOCUMENT ID		TECN
• • • We do not use the following data for averages, fits, limits, etc. • • •			
5.9 ± 2.2	HYAMS	69	OSPK

$\Gamma(e^+e^-e^+e^-)/\Gamma_{\text{total}}$ Γ_{13}/Γ

VALUE (units 10^{-5})	CL%	DOCUMENT ID		TECN	COMMENT
< 6.9	90	AKHMETSHIN	01	CMD2	$e^+e^- \to \phi \to \eta\gamma$

$\Gamma(\pi^+\pi^-e^+e^-)/\Gamma(\pi^+\pi^-\gamma)$ Γ_{14}/Γ_8

VALUE (units 10^{-2})	EVTS	DOCUMENT ID		TECN
$\mathbf{0.9^{+3.1}_{-0.6}}$ **OUR FIT** Error includes scale factor of 5.9.				
2.6 ± 2.6	1	GROSSMAN	66	HBC

$\Gamma(\pi^+\pi^-e^+e^-)/\Gamma_{\text{total}}$ Γ_{14}/Γ

VALUE (units 10^{-4})	EVTS	DOCUMENT ID		TECN	COMMENT
$\mathbf{4.0^{+14.0}_{-2.7}}$ **OUR FIT** Error includes scale factor of 5.8.					
$\mathbf{3.7^{+2.5}_{-1.8} \pm 0.3}$	4	AKHMETSHIN	01	CMD2	$e^+e^- \to \phi \to \eta\gamma$

$\Gamma(\pi^+\pi^-2\gamma)/\Gamma(\pi^+\pi^-\pi^0)$ Γ_{15}/Γ_7

VALUE	CL%	DOCUMENT ID		TECN
< 0.009		PRICE	67	HBC
• • • We do not use the following data for averages, fits, limits, etc. • • •				
< 0.016	95	BALTAY	67B	DBC

$\Gamma(\pi^+\pi^-\pi^0\gamma)/\Gamma(\pi^+\pi^-\pi^0)$ Γ_{16}/Γ_7

VALUE (units 10^{-2})	CL%	EVTS	DOCUMENT ID		TECN
< 0.24	90	0	THALER	73	ASPK
• • • We do not use the following data for averages, fits, limits, etc. • • •					
< 1.7	90		ARNOLD	68	HLBC
< 1.6	95		BALTAY	67B	DBC
< 7.0			FLATTE	67	HBC
< 0.9			PRICE	67	HBC

$\Gamma(\pi^0\mu^+\mu^-\gamma)/\Gamma_{\text{total}}$ Γ_{17}/Γ

VALUE (units 10^{-6})	CL%	DOCUMENT ID		TECN	COMMENT
< 3	90	DZHELYADIN	81	SPEC	$\pi^- p \to \eta n$

Rare or forbidden modes

$\Gamma(\pi^+\pi^-)/\Gamma_{\text{total}}$ Γ_{18}/Γ

Forbidden by P and CP invariance.

VALUE (units 10^{-4})	CL%	EVTS	DOCUMENT ID		TECN	COMMENT
< 3.3	90		AKHMETSHIN	99B	CMD2	$e^+e^- \to \phi \to \eta\gamma$
• • • We do not use the following data for averages, fits, limits, etc. • • •						
< 9	90		AKHMETSHIN	97C	CMD2	See AKHMETSHIN 99B
<15		0	THALER	73	ASPK	

$\Gamma(\pi^0\pi^0)/\Gamma_{\text{total}}$ Γ_{19}/Γ

Forbidden by P and CP invariance.

VALUE (units 10^{-4})	CL%	DOCUMENT ID		TECN	COMMENT
<4.3	90	AKHMETSHIN	99C	CMD2	$e^+e^- \to \phi \to \eta\gamma$
• • • We do not use the following data for averages, fits, limits, etc. • • •					
<6	90	[7] ACHASOV	98	SND	$e^+e^- \to \phi \to \eta\gamma$

[7] ACHASOV 98 observes one event in a $\pm 3\sigma$ region around the η mass, while a Monte Carlo calculation gives 10 ± 5 events. The limit here is the Poisson upper limit for one observed event and no background.

$\Gamma(4\pi^0)/\Gamma_{\text{total}}$ Γ_{21}/Γ

Forbidden by P and CP invariance.

VALUE (units 10^{-7})	CL%	DOCUMENT ID		TECN	COMMENT
<6.9	90	PRAKHOV	00	CRYB	$\pi^- p \to n\eta$, 720 MeV/c

$\Gamma(3\gamma)/\Gamma(\text{neutral modes})$ $\Gamma_{20}/\Gamma_1 = \Gamma_{20}/(\Gamma_2+\Gamma_3+\Gamma_4)$

Forbidden by C invariance.

VALUE (units 10^{-4})	CL%	DOCUMENT ID		TECN
<7	95	ALDE	84	GAM2

$\Gamma(\pi^0e^+e^-)/\Gamma(\pi^+\pi^-\pi^0)$ Γ_{22}/Γ_7

C parity forbids this to occur as a single-photon process.

VALUE (units 10^{-4})	EVTS	DOCUMENT ID		TECN
< 1.9	90	JANE	75	OSPK
• • • We do not use the following data for averages, fits, limits, etc. • • •				
< 42	90	BAGLIN	67	HLBC
< 16	90 0	BILLING	67	HLBC
< 77	0	FOSTER	65B	HBC
<110		PRICE	65	HBC

$\Gamma(\pi^0e^+e^-)/\Gamma_{\text{total}}$ Γ_{22}/Γ

C parity forbids this to occur as a single-photon process.

VALUE (units 10^{-2})	CL%	EVTS	DOCUMENT ID		TECN
• • • We do not use the following data for averages, fits, limits, etc. • • •					
<0.016	90	0	MARTYNOV	76	HLBC
<0.084	90		BAZIN	68	DBC
<0.7			RITTENBERG	65	HBC

$\Gamma(\pi^0\mu^+\mu^-)/\Gamma_{\text{total}}$ Γ_{23}/Γ

C parity forbids this to occur as a single-photon process.

VALUE (units 10^{-4})	CL%	DOCUMENT ID		TECN	COMMENT
<0.05	90	DZHELYADIN	81	SPEC	$\pi^- p \to \eta n$
• • • We do not use the following data for averages, fits, limits, etc. • • •					
<5		WEHMANN	68	OSPK	

$[\Gamma(\mu^+e^-)+\Gamma(\mu^-e^+)]/\Gamma_{\text{total}}$ Γ_{24}/Γ

Forbidden by lepton family number conservation.

VALUE (units 10^{-6})	CL%	DOCUMENT ID		TECN	COMMENT
<6	90	WHITE	96	SPEC	$pd \to \eta\,^3$He

η C-NONCONSERVING DECAY PARAMETERS

$\pi^+\pi^-\pi^0$ LEFT-RIGHT ASYMMETRY PARAMETER

Measurements with an error $> 1.0 \times 10^{-2}$ have been omitted.

VALUE (units 10^{-2})	EVTS	DOCUMENT ID		TECN
0.09 ± 0.17 OUR AVERAGE				
0.28 ± 0.26	165k	JANE	74	OSPK
−0.05 ± 0.22	220k	LAYTER	72	ASPK
• • • We do not use the following data for averages, fits, limits, etc. • • •				
1.5 ± 0.5	37k	[8] GORMLEY	68C	ASPK

[8] The GORMLEY 68C asymmetry is probably due to unmeasured ($\mathbf{E} \times \mathbf{B}$) spark chamber effects. New experiments with ($\mathbf{E} \times \mathbf{B}$) controls don't observe an asymmetry.

$\pi^+\pi^-\pi^0$ SEXTANT ASYMMETRY PARAMETER

Measurements with an error $> 2.0 \times 10^{-2}$ have been omitted.

VALUE (units 10^{-2})	EVTS	DOCUMENT ID		TECN
0.18 ± 0.16 OUR AVERAGE				
0.20 ± 0.25	165k	JANE	74	OSPK
0.10 ± 0.22	220k	LAYTER	72	ASPK
0.5 ± 0.5	37k	GORMLEY	68C	WIRE

$\pi^+\pi^-\pi^0$ QUADRANT ASYMMETRY PARAMETER

VALUE (units 10^{-2})	EVTS	DOCUMENT ID		TECN
-0.17 ± 0.17 OUR AVERAGE				
-0.30 ± 0.25	165k	JANE	74	OSPK
-0.07 ± 0.22	220k	LAYTER	72	ASPK

$\pi^+\pi^-\gamma$ LEFT-RIGHT ASYMMETRY PARAMETER

Measurements with an error $> 2.0\times10^{-2}$ have been omitted.

VALUE (units 10^{-2})	EVTS	DOCUMENT ID		TECN
0.9 ±0.4 OUR AVERAGE				
1.2 ±0.6	35k	JANE	74B	OSPK
0.5 ±0.6	36k	THALER	72	ASPK
1.22±1.56	7257	GORMLEY	70	ASPK

$\pi^+\pi^-\gamma$ PARAMETER β (D-wave)

Sensitive to a D-wave contribution: $dN/d\cos\theta = \sin^2\theta\ (1+\beta\ \cos^2\theta)$.

VALUE	EVTS	DOCUMENT ID		TECN
-0.02 ±0.07 OUR AVERAGE	Error includes scale factor of 1.3.			
0.11 ±0.11	35k	JANE	74B	OSPK
-0.060 ± 0.065	7250	GORMLEY	70	WIRE
• • • We do not use the following data for averages, fits, limits, etc. • • •				
0.12 ±0.06	[9]	THALER	72	ASPK

[9] The authors don't believe this indicates D-wave because the dependence of β on the γ energy is inconsistent with the theoretical prediction. A $\cos^2\theta$ dependence can also come from P- and F-wave interference.

ENERGY DEPENDENCE OF $\eta \to 3\pi$ DALITZ PLOTS

PARAMETERS FOR $\eta \to \pi^+\pi^-\pi^0$

See the "Note on η Decay Parameters" in our 1994 edition, Phys. Rev. **D50**, 1 August 1994, Part I, p. 1454. The following experiments fit to one or more of the coefficients a, b, c, d, or e for $|\text{matrix element}|^2 = 1 + ay + by^2 + cx + dx^2 + exy$.

VALUE	EVTS	DOCUMENT ID		TECN	COMMENT
• • • We do not use the following data for averages, fits, limits, etc. • • •					
	3230	[10] ABELE	98D	CBAR	$\overline{p}p \to \pi^0\pi^0\eta$ at rest
	1077	[11] AMSLER	95	CBAR	$\overline{p}p \to \pi^+\pi^-\eta$ at rest
	81k	LAYTER	73	ASPK	
	220k	LAYTER	72	ASPK	
	1138	CARPENTER	70	HBC	
	349	DANBURG	70	DBC	
	7250	GORMLEY	70	WIRE	
	526	BAGLIN	69	HLBC	
	7170	CNOPS	68	OSPK	
	37k	GORMLEY	68C	WIRE	
	1300	CLPWY	66	HBC	
	705	LARRIBE	66	HBC	

[10] ABELE 98D obtains $a=-1.22\pm0.07$ and $b=0.22\pm0.11$ when c (our d) is fixed at 0.06.

[11] AMSLER 95 fits to $(1+ay+by^2)$ and obtains $a=-0.94\pm0.15$ and $b=0.11\pm0.27$.

α PARAMETER FOR $\eta \to 3\pi^0$

See the "Note on η Decay Parameters" in our 1994 edition, Phys. Rev. **D50**, 1 August 1994, Part I, p. 1454. The value here is of α in $|\text{matrix element}|^2 = 1 + 2\alpha z$.

VALUE	EVTS	DOCUMENT ID		TECN	COMMENT
-0.031 ± 0.004 OUR AVERAGE	Error includes scale factor of 1.1.				
$-0.010\pm0.021\pm0.010$	12k	ACHASOV	01C	SND	$e^+e^- \to \phi \to \eta\gamma$
-0.031 ± 0.004	1M	TIPPENS	01	CRYB	$\pi^- p \to n\eta$, 720 MeV/c
$-0.052\pm0.017\pm0.010$	98k	ABELE	98C	CBAR	$\overline{p}p \to 5\pi^0$
-0.022 ± 0.023	50k	ALDE	84	GAM2	
• • • We do not use the following data for averages, fits, limits, etc. • • •					
-0.32 ±0.37	192	BAGLIN	70	HLBC	

η REFERENCES

LAI	02	PL B533 196	A. Lai *et al.*	(CERN NA48 Collab.)
NEFKENS	02	PS T99 114	B.M.K. Nefkens, J.W. Price	(UCLA)
ACHASOV	01B	PL B504 275	M.N. Achasov *et al.*	(Novosibirsk SND Collab.)
ACHASOV	01C	JETPL 73 451 Translated from ZETFP 73 511.	M.N. Achasov *et al.*	(Novosibirsk SND Collab.)
ACHASOV	01D	NP B600 3	M.N. Achasov *et al.*	(Novosibirsk SND Collab.)
AKHMETSHIN	01	PL B501 191	R.R. Akhmetshin *et al.*	(Novosibirsk CMD-2 Collab.)
AKHMETSHIN	01B	PL B509 217	R.R. Akhmetshin *et al.*	(Novosibirsk CMD-2 Collab.)
TIPPENS	01	PRL 87 192001	W.B. Tippens *et al.*	(BNL Crystal Ball Collab.)
ACHASOV	00	EPJ C12 25	M.N. Achasov *et al.*	(Novosibirsk SND Collab.)
ACHASOV	00B	JETP 90 17 Translated from ZETF 117 22.	M.N. Achasov *et al.*	(Novosibirsk SND Collab.)
ACHASOV	00D	JETPL 72 282 Translated from ZETFP 72 411.	M.N. Achasov *et al.*	(Novosibirsk SND Collab.)
PRAKHOV	00	PRL 84 4802	S. Prakhov *et al.*	(BNL Crystal Ball Collab.)
AKHMETSHIN	99B	PL B462 371	R.R. Akhmetshin *et al.*	(Novosibirsk CMD-2 Collab.)
AKHMETSHIN	99C	PL B462 380	R.R. Akhmetshin *et al.*	(Novosibirsk CMD-2 Collab.)
AKHMETSHIN	99F	PL B460 242	R.R. Akhmetshin *et al.*	(Novosibirsk CMD-2 Collab.)
ABELE	98C	PL B417 193	A. Abele *et al.*	(Crystal Barrel Collab.)
ABELE	98D	PL B417 197	A. Abele *et al.*	(Crystal Barrel Collab.)
ACHASOV	98	PL B425 388	M.N. Achasov *et al.*	(Novosibirsk SND Collab.)
AKHMETSHIN	97C	PL B415 452	R.R. Akhmetshin *et al.*	(Novosibirsk CMD-2 Collab.)
BROWDER	97B	PR D56 5359	T.E. Browder *et al.*	(CLEO Collab.)
ABEGG	96	PR D53 11	R. Abegg *et al.*	(Saturne SPES2 Collab.)
WHITE	96	PR D53 6658	D.B. White *et al.*	(Saturne SPES2 Collab.)
AMSLER	95	PL B346 203	C. Amsler *et al.*	(Crystal Barrel Collab.)
KRUSCHE	95D	ZPHY A351 237	B. Krusche *et al.*	(TAPS + A2 Collab.)
ABEGG	94	PR D50 92	R. Abegg *et al.*	(Saturne SPES2 Collab.)
AMSLER	93	ZPHY C58 175	C. Amsler *et al.*	(Crystal Barrel Collab.)
KESSLER	93	PRL 70 892	R.S. Kessler *et al.*	(Saturne SPES2 Collab.)
PLOUIN	92	PL B276 526	F. Plouin *et al.*	(Saturne SPES4 Collab.)
BARU	90	ZPHY C48 581	S.E. Baru *et al.*	(MD-1 Collab.)
ROE	90	PR D41 17	N.A. Roe *et al.*	(ASP Collab.)
WILLIAMS	88	PR D38 1365	D.A. Williams *et al.*	(Crystal Ball Collab.)
AIHARA	86	PR D33 844	H. Aihara *et al.*	(TPC-2γ Collab.)
BARTEL	85E	PL 160B 421	W. Bartel *et al.*	(JADE Collab.)
LANDSBERG	85	PRPL 128 310	L.G. Landsberg	(SERP)
ALDE	84	ZPHY C25 225	D.M. Alde *et al.*	(SERP, BELG, LAPP)
Also	84B	SJNP 40 918 Translated from YAF 40 1447.	D.M. Alde *et al.*	(SERP, BELG, LAPP)
WEINSTEIN	83	PR D28 2896	A.J. Weinstein *et al.*	(Crystal Ball Collab.)
BINON	82	SJNP 36 391 Translated from YAF 36 670.	F.G. Binon *et al.*	(SERP, BELG, LAPP+)
Also	82B	NC 71A 497	F.G. Binon *et al.*	(SERP, BELG, LAPP+)
DAVYDOV	81	LNC 32 45	V.A. Davydov *et al.*	(SERP, BELG, LAPP+)
Also	81B	SJNP 33 825 Translated from YAF 33 1534.	V.A. Davydov *et al.*	(SERP, BELG, LAPP+)
DZHELYADIN	81	PL 105B 239	R.I. Dzhelyadin *et al.*	(SERP)
Also	81C	SJNP 33 822 Translated from YAF 33 1529.	R.I. Dzhelyadin *et al.*	(SERP)
ABROSIMOV	80	SJNP 31 195 Translated from YAF 31 371.	A.T. Abrosimov *et al.*	(JINR)
DZHELYADIN	80	PL 94B 548	R.I. Dzhelyadin *et al.*	(SERP)
Also	80C	SJNP 32 516 Translated from YAF 32 998.	R.I. Dzhelyadin *et al.*	(SERP)
DZHELYADIN	80B	PL 97B 471	R.I. Dzhelyadin *et al.*	(SERP)
Also	80D	SJNP 32 518 Translated from YAF 32 1002.	R.I. Dzhelyadin *et al.*	(SERP)
BUSHNIN	78	PL 79B 147	Y.B. Bushnin *et al.*	(SERP)
Also	78B	SJNP 28 775 Translated from YAF 28 1507.	Y.B. Bushnin *et al.*	(SERP)
MARTYNOV	76	SJNP 23 48 Translated from YAF 23 93.	A.S. Martynov *et al.*	(JINR)
JANE	75	PL 59B 99	M.R. Jane *et al.*	(RHEL, LOWC)
JANE	75B	PL 59B 103	M.R. Jane *et al.*	(RHEL, LOWC)
Also	78B	PL 73B 503 Erratum in private communication.	M.R. Jane	
BROWMAN	74B	PRL 32 1067	A. Browman *et al.*	(CORN, BING)
DAVIES	74	NC 24A 324	J.D. Davies, J.G. Guy, R.K.P. Zia	(BIRM, RHEL+)
DUANE	74	PRL 32 425	A. Duane *et al.*	(LOIC, SHMP)
JANE	74	PL 48B 260	M.R. Jane *et al.*	(RHEL, LOWC, SUSS)
JANE	74B	PL 48B 265	M.R. Jane *et al.*	(RHEL, LOWC, SUSS)
KENDALL	74	NC 21A 387	B.N. Kendall *et al.*	(BROW, BARI, MIT)
LAYTER	73	PR D7 2565	J.G. Layter *et al.*	(COLU)
THALER	73	PR D7 2569	J.J. Thaler *et al.*	(COLU)
AGUILAR-...	72B	PR D6 29	M. Aguilar-Benitez *et al.*	(BNL)
BLOODWO...	72B	NP B39 525	I.J. Bloodworth *et al.*	(TNTO)
LAYTER	72	PRL 29 316	J.G. Layter *et al.*	(COLU)
THALER	72	PRL 29 313	J.J. Thaler *et al.*	(COLU)
BASILE	71D	NC 3A 796	M. Basile *et al.*	(CERN, BGNA, STRB)
STRUGALSKI	71	NP B27 429	Z.S. Strugalski *et al.*	(JINR)
BAGLIN	70	NP B22 66	C. Baglin *et al.*	(EPOL, MADR, STRB)
BUTTRAM	70	PRL 25 1358	M.T. Buttram, M.N. Kreisler, R.E. Mischke	(PRIN)
CARPENTER	70	PR D1 1303	D.W. Carpenter *et al.*	(DUKE)
COX	70B	PRL 24 534	B. Cox, L. Fortney, J.P. Golson	(DUKE)
DANBURG	70	PR D2 2564	J.S. Danburg *et al.*	(LRL)
DEVONS	70	PR D1 1936	S. Devons *et al.*	(COLU, SYRA)
GORMLEY	70	PR D2 501	M. Gormley *et al.*	(COLU, BNL)
Also	70B	Thesis Nevis 181	M. Gormley	(COLU)
BAGLIN	69	PL 29B 445	C. Baglin *et al.*	(EPOL, UCB, MADR, STRB)
Also	70	NP B22 66	C. Baglin *et al.*	(EPOL, MADR, STRB)
HYAMS	69	PL 29B 128	B.D. Hyams *et al.*	(CERN, MPIM)
ARNOLD	68	PL 27B 466	R.G. Arnold *et al.*	(STRB, MADR, EPOL+)
BAZIN	68	PRL 20 895	M.J. Bazin *et al.*	(PRIN, QUIN)
BULLOCK	68	PL 27B 402	F.W. Bullock *et al.*	(LOUC)
CNOPS	68	PRL 21 1609	A.M. Cnops *et al.*	(BNL, ORNL, UCND+)
GORMLEY	68C	PRL 21 402	M. Gormley *et al.*	(COLU, BNL)
WEHMANN	68	PRL 20 748	A.W. Wehmann *et al.*	(HARV, CASE, SLAC+)
BAGLIN	67	PL 24B 637	C. Baglin *et al.*	(EPOL, UCB)
BAGLIN	67B	BAPS 12 567	C. Baglin *et al.*	(EPOL, UCB)
BALTAY	67B	PRL 19 1498	C. Baltay *et al.*	(COLU, STON)
BALTAY	67D	PRL 19 1495	C. Baltay *et al.*	(COLU, BRAN)
BEMPORAD	67	PL 25B 380	C. Bemporad *et al.*	(PISA, BONN)
Also	67	Private Comm.	I. Ion	
BILLING	67	PL 25B 435	K.D. Billing *et al.*	(LOUC, OXF)
BUNIATOV	67	PL 25B 560	S.A. Bunyatov *et al.*	(CERN, KARL)
CENCE	67	PRL 19 1393	R.J. Cence *et al.*	(HAWA, LRL)
ESTEN	67	PL 24B 115	M.J. Esten *et al.*	(LOUC, OXF)
FELDMAN	67	PRL 18 868	M. Feldman *et al.*	(PENN)
FLATTE	67	PRL 18 976	S.M. Flatte	(LRL)
FLATTE	67B	PR 163 1441	S.M. Flatte, C.G. Wohl	(LRL)
LITCHFIELD	67	PL 24B 486	P.J. Litchfield *et al.*	(RHEL, SACL)
PRICE	67	PRL 18 1207	L.R. Price, F.S. Crawford	(LRL)
ALFF-...	66	PR 145 1072	C. Alff-Steinberger *et al.*	(COLU, RUTG)
CLPWY	66	PR 149 1044	C. Baltay	(SCUC, LRL, PURD, WISC, YALE)
CRAWFORD	66	PRL 16 333	F.S. Crawford, L.R. Price	(LRL)
DIGIUGNO	66	PRL 16 767	G. di Giugno *et al.*	(NAPL, TRST, FRAS)
GROSSMAN	66	PR 146 993	R.A. Grossman, L.R. Price, F.S. Crawford	(LRL)
GRUNHAUS	66	Thesis	J. Grunhaus	(COLU)
JAMES	66	PR 142 896	F.E. James, H.L. Kraybill	(YALE, BNL)
JONES	66	PL 23 597	W.G. Jones *et al.*	(LOIC, RHEL)
LARRIBE	66	PL 23 600	A. Larribe *et al.*	(SACL, RHEL)
FOSTER	65	PR 138B 652	M. Foster *et al.*	(WISC, PURD)
FOSTER	65B	Athens Conf.	M. Foster, M. Good, M. Meer	(WISC)
FOSTER	65C	Thesis	M. Foster	(WISC)
PRICE	65	PRL 15 123	L.R. Price, F.S. Crawford	(LRL)
RITTENBERG	65	PRL 15 556	A. Rittenberg, G.R. Kalbfleisch	(LRL, BNL)
FOELSCHE	64	PR 134B 1138	H.W.J. Foelsche, H.L. Kraybill	(YALE)
KRAEMER	64	PR 136B 496	R.W. Kraemer *et al.*	(JHU, NWES, WOOD)
PAULI	64	PL 13 351	E. Pauli, A. Muller	(SACL)
BACCI	63	PRL 11 37	C. Bacci *et al.*	(ROMA, FRAS)
CRAWFORD	63	PRL 10 546	F.S.Jr. Crawford, L.J. Lloyd, E.C. Fowler	(LRL+)
Also	66B	PRL 16 907	F.S. Crawford, L.J. Lloyd, E.C. Fowler	(LRL+)
ALFF-...	62	PRL 9 322	C. Alff-Steinberger *et al.*	(COLU, RUTG)
BASTIEN	62	PRL 8 114	P.L. Bastien *et al.*	(LRL)
PICKUP	62	PRL 8 329	E. Pickup, D.K. Robinson, E.O. Salant	(CNRC+)

$f_0(600)$ or σ

$I^G(J^{PC}) = 0^+(0^{++})$

NOTE ON SCALAR MESONS

Updated October 2003 by S. Spanier (University of Tennessee) and N.A. Törnqvist (Helsinki).

I. Introduction: In contrast to the vector and tensor mesons, the identification of the scalar mesons is a long-standing puzzle. Scalar resonances are difficult to resolve because of their large decay widths, which cause a strong overlap between resonances and background, and also because several decay channels open up within a short mass interval. In addition, the $\overline{K}K$ and $\eta\eta$ thresholds produce sharp cusps in the energy dependence of the resonant amplitude. Furthermore, one expects non-$\overline{q}q$ scalar objects, like glueballs and multiquark states in the mass range below 1800 MeV. The number of experimental and theoretical publications since our last issue indicates great activity in this field.

Scalars are produced, for example, in πN scattering on polarized/unpolarized targets, $\overline{p}p$ annihilation, central hadronic production, J/ψ, B-, D-, and K-meson decays, $\gamma\gamma$ formation, and ϕ radiative decays. Experiments are accompanied by the development of theoretical models for the reaction amplitudes, which are based on common fundamental principles of two-body unitarity, analyticity, Lorentz invariance, and chiral- and flavor-symmetry using different techniques (K-matrix formalism, N/D-method, Dalitz Tuan ansatz, unitarized quark models with coupled channels, effective chiral field theories like the linear sigma model, *etc.*).

The mass and width of a resonance are found from the position of the nearest pole in the T-matrix (or equivalently, in the S matrix) at an unphysical sheet of the complex energy plane: $(E - i\frac{\Gamma}{2})$. It is important to realize that only in the case of narrow well-separated resonances, far away from the opening of decay channels, does the naive Breit-Wigner parameterization (K-matrix pole parameterization) agree with the T-matrix pole position in the amplitude.

In this note, we discuss all light scalars organized in the listings under the entries ($I = 1/2$) a possible $K_0^*(800)$ (or κ), which need to be confirmed, the $K_0^*(1430)$, ($I = 1$) $a_0(980)$, $a_0(1450)$, and ($I = 0$) $f_0(600)$ or σ, $f_0(980)$, $f_0(1370)$, and $f_0(1500)$. This list is minimal and does not necessarily exhaust the list of actual resonances. The ($I = 2$) $\pi\pi$ and ($I = 3/2$) $K\pi$ phase shifts do not exhibit any resonant behavior. See also our notes in previous issues for further comments on *e.g.*, scattering lengths and older papers.

II. The I = 1/2 States The $K_0^*(1430)$ (ASTON 88) is perhaps the least controversial of the light scalar mesons. The $K\pi$ S-wave scattering has two possible isospin channels, $I = 1/2$ and $I = 3/2$. The $I = 3/2$ wave is elastic and repulsive up to 1.7 GeV (ESTABROOKS 78) and contains no known resonances. The $I = 1/2$ $K\pi$ phase shift, measured from about 100 MeV above threshold on, rises smoothly, passes 90° at 1350 MeV, and continues to rise to about 170° at 1600 MeV. The first important inelastic threshold is $K\eta'(958)$. In the inelastic region, the continuation of the amplitude is uncertain since the partial-wave decomposition has several solutions. The data are extrapolated towards the $K\pi$ threshold using effective range type formulas (ASTON 88, ABELE 98), or chiral perturbation predictions (JAMIN 00, CHERRY 01). In analyses using unitarized amplitudes, there is agreement on the presence of a resonance pole around 1410 MeV having a width of about 300 MeV. In recent years, there has been controversy about the existence of a light and very broad "κ" meson in the 700–900 MeV region (*e.g.*, D-meson decay analyses LINK 02E, AITALA 02). Some authors find this pole in their phenomenological analysis (see *e.g.*, ISHIDA 97B,03, BLACK 01 03, DELBOURGO 98, OLLER 99,99C, ANISOVICH 97C, JAMIN 00, SHAKIN 01, SCADRON 03), while others do not (*e.g.*, CHERRY 01, KOPP 01). Since it appears to be a very wide object ($\Gamma \approx 400$ MeV) near threshold, its presence and properties are difficult to establish on data.

III. The I = 1 States Two isovector states are known, the established $a_0(980)$ and the $a_0(1450)$. Independent of any model, the $\overline{K}K$ component in the $a_0(980)$ wave function must be large: it lies just below the opening of the $\overline{K}K$ channel to which it couples strongly. This gives an important cusp-like behavior in the resonant amplitude. Hence, its mass and width parameters are strongly distorted. To reveal its true coupling constants, a coupled channel model with energy-dependent widths and mass shift contributions is necessary. In all measurements in our listings, the mass position agrees on a value near 984 MeV, but the width takes values between 50 and 300 MeV, mostly due to the different models. For example, the analysis of the $\overline{p}p$-annihilation data using an unitary K-matrix description finds a width as determined from the T-matrix pole of 92 ± 8 MeV, while the observed width of the peak in the $\pi\eta$ mass spectrum is about 45 MeV.

The relative coupling $\overline{K}K/\pi\eta$ is determined indirectly from $f_1(1285)$ (BARBERIS 98C, CORDEN 78, DEFOIX 72), or $\eta(1410)$ decays (BAI 90C, BOLTON 92B, AMSLER 95C), from the line shape observed in the $\pi\eta$ decay mode (FLATTE 76, AMSLER 94D, BUGG 94, JANSSEN 95), or from the coupled-channel analysis of $\pi\pi\eta$ and $\overline{K}K\pi$ final states of $\overline{p}p$ annihilation at rest (ABELE 98).

The $a_0(1450)$ is seen in $\overline{p}p$ annihilation experiments with stopped and higher momenta $\overline{p}$, with a mass of about 1450 MeV, or close to the $a_2(1320)$ meson, which is typically a dominant feature. The relative couplings to the final states $\pi\eta$, $\overline{K}K$, and $\pi\eta'(958)$ are close to SU(3)-flavor predictions for an ordinary $\overline{q}q$ meson. The broad structure at about 1300 MeV observed in $\pi N \to \overline{K}KN$ reactions needs further confirmation in its existence and isospin assignment.

IV. The I = 0 States The $I = 0\, J^{PC} = 0^{++}$ sector is the most complex one, both experimentally and theoretically. The data have been obtained from $\pi\pi$, $\overline{K}K$, $\eta\eta$, 4π, and $\eta\eta'(958)$ systems produced in S-wave. Analyses based on several different production processes conclude that probably four poles are needed in the mass range from $\pi\pi$ threshold to about

1600 MeV. The claimed isoscalar resonances are found under separate entries σ or $f_0(600)$, $f_0(980)$, $f_0(1370)$, and $f_0(1500)$.

Below 1100 MeV, the important data come from the $\pi\pi$ and $\overline{K}K$ final states. Information on the $\pi\pi$ S-wave phase shift $\delta^I_J = \delta^0_0$ was already extracted more than 25 years ago from the πN scattering with unpolarized (GRAYER 74) and polarized targets (BECKER 79), and near threshold from the K_{e4}-decay (ROSSELET 77). The $\pi\pi$ S-wave inelasticity is not accurately known, and the reported $\pi\pi \to \overline{K}K$ cross sections (WETZEL 76, POLYCHRONAKOS 79, COHEN 80, and ETKIN 82B) may have large uncertainties. The πN data (GRAYER 74, BECKER 79) have been analyzed in combination with high-statistics data from $\overline{p}p$ annihilation at rest (see entries labeled as RVUE for re-analyses of the data). The re-analysis (KAMINSKI 97, see also KAMINSKI 02, 03) finds two out of four relevant solutions, with the S-wave phase shift rising slower than the P-wave [$\rho(770)$], which is used as a reference. One of these corresponds to the well-known "down" solution of GRAYER 74. The other "up" solution shows a decrease of the modulus in the mass interval between 800–980 MeV. Both solutions exhibit a sudden drop in the modulus and inelasticity at 1 GeV, due to the appearance of $f_0(980)$ which is very close to the opening of the $\overline{K}K$-threshold. The phase shift δ^0_0 rises smoothly up to this point, where it jumps by 120^o (in the "up") or 140^o (in the "down") solution to reach 230^o, and then both continue to rise slowly.

The suggestion (SVEC 97) of the existence of a narrow f_0 state near 750 MeV, with a small width of 100 to 200 MeV, is excluded by unitarity as shown by (KAMINSKI 97, 00, 02, 03), using both the π- and $a_1(1260)$-exchange in the reaction amplitudes. Also, the $2\pi^0$ invariant mass spectra of the $\overline{p}p$ annihilation at rest (AMSLER 95D, ABELE 96), and the central collision (ALDE 97), do not show a distinct resonance structure below 900 MeV, and these data are consistently described with the standard "down" solution, which allows for the existence of the broad ($\Gamma \approx 500$ MeV) resonance called σ. The σ pole is difficult to establish because of its large width, and can certainly not be modelled by a naive Breit-Wigner resonance. It can be distorted by a large destructive background required by chiral symmetry, and from crossed channel exchanges, the $f_0(1370)$, and other dynamical features. However, most analyses listed in our issue under $f_0(600)$ agree on a pole position near $500 - i\,250$ MeV.

The $f_0(980)$ overlaps strongly with the σ and the above mentioned broad background. This can lead to a dip in the $\pi\pi$ spectrum at the $\overline{K}K$ threshold. It changes from a dip into a peak structure in the $\pi^0\pi^0$ invariant mass spectrum of the reaction $\pi^- p \to \pi^0\pi^0 n$ (ACHASOV 98E), with increasing four-momentum transfer to the $\pi^0\pi^0$ system, which means increasing the a_1-exchange contribution in the amplitude, while the π-exchange decreases.

A meson resonance that is very well studied experimentally is the $f_0(1500)$, seen by the Crystal Barrel experiment in five decay modes: $\pi\pi$, $\overline{K}K$, $\eta\eta$, $\eta\eta'(958)$, and 4π (AMSLER 95D, ABELE 96, and ABELE 98). Due to its interference with the $f_0(1370)$ (and $f_0(1700)$), the peak attributed to $f_0(1500)$ can appear shifted in invariant mass spectra. Therefore, the application of simple Breit-Wigner forms arrive at slightly different resonance masses for $f_0(1500)$. Analyses of central-production data of the likewise five decay modes (BABERIS 99D, BABERIS 00E) agree on the description of the S wave with the one above. The $\overline{p}p$, $\overline{n}p/\overline{p}n$ (GASPERO 93, ADAMO 93, AMSLER 94, ABELE 96) show a single enhancement at 1400 MeV in the invariant 4π mass spectra, which is resolved into $f_0(1370)$ and $f_0(1500)$ (ABELE 01, ABELE 01B). The data on 4π from central production (BABERIS 00C) require both resonances, too, but disagree on the relative content of $\rho\rho$ and $\sigma\sigma$ in 4π. All investigations agree that the 4π decay mode represents about half of the $f_0(1500)$ decay width, and is dominant for $f_0(1370)$.

The determination of the $\pi\pi$ coupling of $f_0(1370)$ is aggravated by the strong overlap with the broad $f_0(600)$ and $f_0(1500)$. Since it does not show up prominently in the 2π spectra, its mass and width are difficult to determine. The three-channel approach (KAMINSKI 99) supports the findings in $\overline{p}p$ annihilation, and yields a broad $f_0(1370)$ with a mass around 1400 MeV and a narrow $f_0(1500)$. Here, the $f_0(1370)$ couples more strongly to $\pi\pi$ than to $\overline{K}K$. The $f_0(1370)$ is identified as $\eta\eta$ resonance in the $\pi^0\eta\eta$ final state of the $\overline{p}p$ annihilation at rest (AMSLER 95D).

V. Interpretation What is the nature of the light scalars? In the literature, many suggestions are discussed in the literature such as $q\overline{q}$, $q\overline{q}q\overline{q}$ or meson-meson bound states supplemented with a scalar glueball. In reality, they are superpositions of these components, and one depends on models to determine the dominant component. Although we have seen progress in recent years, this question remains open. Here, we mention some of the present conclusions.

Almost every model on scalar states agrees that the $K^*_0(1430)$ is predominantly the quark model $s\overline{u}$ or $s\overline{d}$ state.

If one uses the naive quark model (which may be too naive because of lack of chiral symmetry constraints), it is natural to assume the $f_0(1370)$, $a_0(1450)$, and the $K^*_0(1430)$ are in the same SU(3) flavor nonet being the $(\overline{u}u + \overline{d}d)$, $u\overline{d}$ and $u\overline{s}$ state, respectively. In this picture, the choice of the ninth member of the nonet is ambiguous. The controversially discussed candidates are $f_0(1500)$ and $f_J(1720)$ (assuming $J = 0$). Compared to the above states, the $f_0(1500)$ is very narrow. Thus, it is unlikely to be their isoscalar partner. It is also too light to be the first radial excitation. Assuming the three f_0's in the 1300–1700 MeV region to be mixtures between an $\overline{u}u$, $\overline{s}s$, and a gluonium state, one can arrive at an arrangement of these states, although different analyses (CLOSE 01B, LI 01) do not agree in detail. See our note on non-$\overline{q}q$ states.

The $f_0(980)$ and $a_0(980)$ are often interpreted as multi-quark states (JAFFE 77, ALFORD 00) or $\overline{K}K$ bound states (WEINSTEIN 90). The insight into their internal structure using two-photon widths (BARNES 85, LI 91, DELBOURGO 99, LUCIO 99, ACHASOV 00H) is not conclusive. Based on D_s decays (DEANDREA 01), suggests that the $f_0(980)$ is mainly $\overline{s}s$

surrounded by a virtual $\overline{K}K$ cloud. Recent data on radiative decays ($\phi \to f_0\gamma$ and $\phi \to a_0\gamma$) from SND (ACHASOV 00F, ACHASOV 00H), CMD2 (AKHETSHIN 99C), and KLOE (ALOISIO 02C, ALOISIO 02D) favor a 4-quark picture of the $f_0(980)$ and $a_0(980)$. (This conclusion may, however, be due to an oversimplified model for the radiative decays (BOGLIONE 03, OLLER 03B).) But it remains quite possible that the states $f_0(980)$ and $a_0(980)$, together with the $f_0(600)$ and the κ, may form a new nonet of predominantly four-quark states. This light scalar nonet has also been suggested (CLOSE02B) to consist of a central core of mainly four quarks, like those suggested by JAFFE 77, to make up a flavour nonet composed of four quarks in a particular colour configuration. At larger distances, the quarks would recombine into a pair of color singlet $q\overline{q}$'s, forming finally two pseudoscalars mesons and a meson cloud at the periphery.

Attempts have been made to start directly from chiral Lagrangians (SCADRON 99, OLLER 99, ISHIDA 99, and TORNQVIST 99, OLLER 03B), which predict the existence of the σ meson near 500 MeV. Hence, *e.g.*, in the chiral linear sigma model with 3 flavors, the σ, $a_0(980)$, $f_0(980)$, and κ would form a nonet (not necessarily $\overline{q}q$), while the lightest pseudoscalars would be their chiral partners. In the approach of (OLLER 99), the above resonances are generated starting from chiral perturbation theory predictions near the first open channel, and then by extending the predictions to the resonance regions using unitarity.

In unitarized quark models with coupled $q\overline{q}$ and meson-meson channels, the light scalars can be understood as additional manifestations of bare $q\overline{q}$ confinement states, originally in the 1.3–1.5 GeV region, but very distorted and shifted due to the strong $^3P_0$ coupling to S-wave two-meson decay channels (TORNQVIST 95,96, BEVEREN 86,99,01B). Thus, the light scalar nonet comprising the $f_0(600)$ (σ), $f_0(980)$, $K_0^*(800)$ (κ), and $a_0(980)$, as well as the regular nonet consisting of the $f_0(1370)$, $f_0(1500)$ (or $f_0(1710)$), $K_0^*(1430)$, and $a_0(1450)$, respectively, are two manifestations of the same bare input states (see also BOGLIONE 02).

Other models with different groupings of the observed resonances do of course exist. See *e.g.*, earlier versions of this review and papers listed as other related papers below.

References

References may be found at the end of the $f_0(600)$ listing.

$f_0(600)$ T-MATRIX POLE $\sqrt{s}$

Note that $\Gamma \approx 2\,\mathrm{Im}(\sqrt{s_{\mathrm{pole}}})$.

VALUE (MeV)	DOCUMENT ID		TECN	COMMENT
(400–1200)$-i$(300–500) OUR ESTIMATE				
• • • We do not use the following data for averages, fits, limits, etc. • • •				
$(533 \pm 25) - i(247 \pm 25)$	[1] BUGG	03	RVUE	
$532 - i272$	BLACK	01	RVUE	$\pi^0\pi^0 \to \pi^0\pi^0$
$(470 \pm 30) - i(295 \pm 20)$	[2] COLANGELO	01	RVUE	$\pi\pi \to \pi\pi$
$(535^{+48}_{-36}) - i(155^{+76}_{-53})$	[3] ISHIDA	01		$\Upsilon(3S) \to \Upsilon\pi\pi$
$610 \pm 14 - i620 \pm 26$	[4] SUROVTSEV	01	RVUE	$\pi\pi \to \pi\pi,\ K\overline{K}$
$(558^{+34}_{-27}) - i(196^{+32}_{-41})$	ISHIDA	00B		$p\overline{p} \to \pi^0\pi^0\pi^0$
$445 - i235$	HANNAH	99	RVUE	π scalar form factor
$(523 \pm 12) - i(259 \pm 7)$	KAMINSKI	99	RVUE	$\pi\pi \to \pi\pi,\ K\overline{K},\ \sigma\sigma$
$442 - i\ 227$	OLLER	99	RVUE	$\pi\pi \to \pi\pi,\ K\overline{K}$
$469 - i203$	OLLER	99B	RVUE	$\pi\pi \to \pi\pi,\ K\overline{K}$
$445 - i221$	OLLER	99C	RVUE	$\pi\pi \to \pi\pi,\ K\overline{K},\ \eta\eta$
$(1530^{+\ 90}_{-250}) - i(560 \pm 40)$	ANISOVICH	98B	RVUE	Compilation
$420 - i\ 212$	LOCHER	98	RVUE	$\pi\pi \to \pi\pi\ ,\ K\overline{K}$
$(602 \pm 26) - i(196 \pm 27)$	[5] ISHIDA	97		$\pi\pi \to \pi\pi$
$(537 \pm 20) - i(250 \pm 17)$	[6] KAMINSKI	97B	RVUE	$\pi\pi \to \pi\pi,\ K\overline{K},\ 4\pi$
$470 - i250$	[7,8] TORNQVIST	96	RVUE	$\pi\pi \to \pi\pi,\ K\overline{K},\ K\pi,\ \eta\pi$
$\sim (1100 - i300)$	AMSLER	95B	CBAR	$\overline{p}p \to 3\pi^0$
$400 - i500$	[8,9] AMSLER	95D	CBAR	$\overline{p}p \to 3\pi^0$
$1100 - i137$	[8,10] AMSLER	95D	CBAR	$\overline{p}p \to 3\pi^0$
$387 - i305$	[8,11] JANSSEN	95	RVUE	$\pi\pi \to \pi\pi,\ K\overline{K}$
$525 - i269$	[12] ACHASOV	94	RVUE	$\pi\pi \to \pi\pi$
$(506 \pm 10) - i(247 \pm 3)$	KAMINSKI	94	RVUE	$\pi\pi \to \pi\pi,\ K\overline{K}$
$370 - i356$	[13] ZOU	94B	RVUE	$\pi\pi \to \pi\pi,\ K\overline{K}$
$408 - i342$	[8,13] ZOU	93	RVUE	$\pi\pi \to \pi\pi,\ K\overline{K}$
$870 - i370$	[8,14] AU	87	RVUE	$\pi\pi \to \pi\pi,\ K\overline{K}$
$470 - i208$	[15] BEVEREN	86	RVUE	$\pi\pi \to \pi\pi,\ K\overline{K},\ \eta\eta,\ \ldots$
$(750 \pm 50) - i(450 \pm 50)$	[16] ESTABROOKS	79	RVUE	$\pi\pi \to \pi\pi,\ K\overline{K}$
$(660 \pm 100) - i(320 \pm 70)$	PROTOPOP...	73	HBC	$\pi\pi \to \pi\pi,\ K\overline{K}$
$650 - i370$	[17] BASDEVANT	72	RVUE	$\pi\pi \to \pi\pi$

[1] From a combined analysis of HYAMS 73, AUGUSTIN 89, AITALA 01B, and PISLAK 01.
[2] From a phase-shift analysis of HYAMS 73 and PROTOPOPESCU 73 data.
[3] A similar analysis (KOMADA 01) finds $(580^{+79}_{-30}) - i(190^{+107}_{-\ 49})$ MeV.
[4] Coupled channel reanalysis of BATON 70, BENSINGER 71, BAILLON 72, HYAMS 73, HYAMS 75, ROSSELET 77, COHEN 80, and ETKIN 82B using the uniformizing variable.
[5] Reanalysis of data from HYAMS 73, GRAYER 74, SRINIVASAN 75, and ROSSELET 77 using the interfering amplitude method.
[6] Average and spread of 4 variants ("up" and "down") of KAMINSKI 97B 3-channel model.
[7] Uses data from BEIER 72B, OCHS 73, HYAMS 73, GRAYER 74, ROSSELET 77, CASON 83, ASTON 88, and ARMSTRONG 91B. Coupled channel analysis with flavor symmetry and all light two-pseudoscalars systems.
[8] Demonstrates explicitly that $f_0(600)$ and $f_0(1370)$ are two different poles.
[9] Coupled channel analysis of $\overline{p}p \to 3\pi^0$, $\pi^0\eta\eta$ and $\pi^0\pi^0\eta$ on sheet II.
[10] Coupled channel analysis of $\overline{p}p \to 3\pi^0$, $\pi^0\eta\eta$ and $\pi^0\pi^0\eta$ on sheet III.
[11] Analysis of data from FALVARD 88.
[12] Analysis of data from OCHS 73, ESTABROOKS 75, ROSSELET 77, and MUKHIN 80.
[13] Analysis of data from OCHS 73, GRAYER 74, and ROSSELET 77.
[14] Analysis of data from OCHS 73, GRAYER 74, BECKER 79, and CASON 83.
[15] Coupled-channel analysis using data from PROTOPOPESCU 73, HYAMS 73, HYAMS 75, GRAYER 74, ESTABROOKS 74, ESTABROOKS 75, FROGGATT 77, CORDEN 79, BISWAS 81.
[16] Analysis of data from APEL 73, GRAYER 74, CASON 76, PAWLICKI 77. Includes spread and errors of 4 solutions.
[17] Analysis of data from BATON 70, BENSINGER 71, COLTON 71, BAILLON 72,PROTOPOPESCU 73, and WALKER 67.

$f_0(600)$ BREIT-WIGNER MASS OR K-MATRIX POLE PARAMETERS

VALUE (MeV)	DOCUMENT ID		TECN	COMMENT
(400–1200) OUR ESTIMATE				
• • • We do not use the following data for averages, fits, limits, etc. • • •				
513 ± 32	[18] MURAMATSU	02	CLEO	$D^0 \to K^0_S\pi^+\pi^-$
$478^{+24}_{-23} \pm 17$	AITALA	01B	E791	$D^+ \to \pi^-\pi^+\pi^+$
$563 \pm\ ^{+58}_{-20}$	[19] ISHIDA	01		$\Upsilon(3S) \to \Upsilon\pi\pi$
555	[20] ASNER	00	CLE2	$\tau^- \to \pi^-\pi^0\pi^0\nu_\tau$
540 ± 36	ISHIDA	00B		$p\overline{p} \to \pi^0\pi^0\pi^0$
750 ± 4	ALEKSEEV	99	SPEC	$1.78\,\pi^-\,p_{\mathrm{polar}} \to \pi^-\pi^+n$
744 ± 5	ALEKSEEV	98	SPEC	$1.78\,\pi^-\,p_{\mathrm{polar}} \to \pi^-\pi^+n$
759 ± 5	[21] TROYAN	98		$5.2\,np \to np\pi^+\pi^-$
780 ± 30	ALDE	97	GAM2	$450\,pp \to pp\pi^0\pi^0$
585 ± 20	[22] ISHIDA	97		$\pi\pi \to \pi\pi$
761 ± 12	[23] SVEC	96	RVUE	6–$17\,\pi N_{\mathrm{polar}} \to \pi^+\pi^-N$
~ 860	[24,25] TORNQVIST	96	RVUE	$\pi\pi \to \pi\pi,\ K\overline{K},\ K\pi,\ \eta\pi$
1165 ± 50	[26,27] ANISOVICH	95	RVUE	$\pi^-p \to \pi^0\pi^0n,\ \overline{p}p \to \pi^0\pi^0\pi^0,\ \pi^0\pi^0\eta,\ \pi^0\eta\eta$
~ 1000	[28] ACHASOV	94	RVUE	$\pi\pi \to \pi\pi$
414 ± 20	[23] AUGUSTIN	89	DM2	

[18] Statistical uncertainty only.
[19] A similar analysis (KOMADA 01) finds 526^{+48}_{-37} MeV.
[20] From the best fit of the Dalitz plot.
[21] 6σ effect, no PWA.
[22] Reanalysis of data from HYAMS 73, GRAYER 74, SRINIVASAN 75, and ROSSELET 77 using the interfering amplitude method.
[23] Breit-Wigner fit to S-wave intensity measured in $\pi N \to \pi^-\pi^+N$ on polarized targets. The fit does not include $f_0(980)$.
[24] Uses data from ASTON 88, OCHS 73, HYAMS 73, ARMSTRONG 91B, GRAYER 74, CASON 83, ROSSELET 77, and BEIER 72B. Coupled channel analysis with flavor symmetry and all light two-pseudoscalars systems.
[25] Also observed by ASNER 00 in $\tau^- \to \pi^-\pi^0\pi^0\nu_\tau$ decays.
[26] Uses $\pi^0\pi^0$ data from ANISOVICH 94, AMSLER 94D, and ALDE 95B, $\pi^+\pi^-$ data from OCHS 73, GRAYER 74 and ROSSELET 77, and $\eta\eta$ data fromANISOVICH 94.
[27] The pole is on Sheet III. Demonstrates explicitly that $f_0(600)$ and $f_0(1370)$ are two different poles.
[28] Analysis of data from OCHS 73, ESTABROOKS 75, ROSSELET 77, and MUKHIN 80.

$f_0(600)$ BREIT-WIGNER WIDTH

VALUE (MeV)	DOCUMENT ID		TECN	COMMENT
(600–1000) OUR ESTIMATE				
• • • We do not use the following data for averages, fits, limits, etc. • • •				
335 ± 67	[29] MURAMATSU	02	CLEO	$D^0 \to K^0_S \pi^+ \pi^-$
$324^{+42}_{-40} \pm 21$	AITALA	01B	E791	$D^+ \to \pi^- \pi^+ \pi^+$
$372 \pm {}^{+229}_{-95}$	[30] ISHIDA	01		$\Upsilon(3S) \to \Upsilon \pi\pi$
540	[31] ASNER	00	CLE2	$\tau^- \to \pi^- \pi^0 \pi^0 \nu_\tau$
372 ± 80	ISHIDA	00B		$p\overline{p} \to \pi^0 \pi^0 \pi^0$
119 ± 13	ALEKSEEV	99	SPEC	$1.78\ \pi^-\ p_{\rm polar} \to \pi^- \pi^+ n$
77 ± 22	ALEKSEEV	98	SPEC	$1.78\ \pi^-\ p_{\rm polar} \to \pi^- \pi^+ n$
35 ± 12	[32] TROYAN	98		$5.2\ np \to np\pi^+\pi^-$
780 ± 60	ALDE	97	GAM2	$450\ pp \to pp\pi^0\pi^0$
385 ± 70	[33] ISHIDA	97		$\pi\pi \to \pi\pi$
290 ± 54	[34] SVEC	96	RVUE	6–$17\ \pi N_{\rm polar} \to \pi^+\pi^- N$
~ 880	[35,36] TORNQVIST	96	RVUE	$\pi\pi \to \pi\pi,\ K\overline{K},\ K\pi,\ \eta\pi$
460 ± 40	[37,38] ANISOVICH	95	RVUE	$\pi^- p \to \pi^0\pi^0 n,$ $\overline{p}p \to \pi^0\pi^0\pi^0,\ \pi^0\pi^0\eta,\ \pi^0\eta\eta$
~ 3200	[39] ACHASOV	94	RVUE	$\pi\pi \to \pi\pi$
494 ± 58	[34] AUGUSTIN	89	DM2	

[29] Statistical uncertainty only.

[30] A similar analysis (KOMADA 01) finds 301^{+145}_{-100} MeV.

[31] From the best fit of the Dalitz plot.

[32] 6σ effect, no PWA.

[33] Reanalysis of data from HYAMS 73, GRAYER 74, SRINIVASAN 75, and ROSSELET 77 using the interfering amplitude method.

[34] Breit-Wigner fit to S-wave intensity measured in $\pi N \to \pi^-\pi^+ N$ on polarized targets. The fit does not include $f_0(980)$.

[35] Uses data from ASTON 88, OCHS 73, HYAMS 73, ARMSTRONG 91B, GRAYER 74, CASON 83, ROSSELET 77, and BEIER 72B. Coupled channel analysis with flavor symmetry and all light two-pseudoscalars systems.

[36] Also observed by ASNER 00 in $\tau^- \to \pi^-\pi^0\pi^0\nu_\tau$ decays.

[37] Uses $\pi^0\pi^0$ data from ANISOVICH 94, AMSLER 94D, and ALDE 95B, $\pi^+\pi^-$ data from OCHS 73, GRAYER 74 and ROSSELET 77, and $\eta\eta$ data from ANISOVICH 94.

[38] The pole is on Sheet III. Demonstrates explicitly that $f_0(600)$ and $f_0(1370)$ are two different poles.

[39] Analysis of data from OCHS 73, ESTABROOKS 75, ROSSELET 77, and MUKHIN 80.

$f_0(600)$ DECAY MODES

	Mode	Fraction (Γ_i/Γ)
Γ_1	$\pi\pi$	dominant
Γ_2	$\gamma\gamma$	seen

$f_0(600)$ PARTIAL WIDTHS

$\Gamma(\gamma\gamma)$ Γ_2

VALUE (keV)	DOCUMENT ID		TECN	COMMENT
• • • We do not use the following data for averages, fits, limits, etc. • • •				
3.8 ± 1.5	[40,41] BOGLIONE	99	RVUE	$\gamma\gamma \to \pi^+\pi^-,\ \pi^0\pi^0$
5.4 ± 2.3	[40] MORGAN	90	RVUE	$\gamma\gamma \to \pi^+\pi^-,\ \pi^0\pi^0$
10 ± 6	COURAU	86	DM1	$e^+e^- \to \pi^+\pi^- e^+ e^-$

[40] This width could equally well be assigned to the $f_0(1370)$. The authors analyse data from BOYER 90 and MARSISKE 90 and report strong correlation with $\gamma\gamma$ width of $f_2(1270)$.

[41] Supersedes MORGAN 90.

$f_0(600)$ REFERENCES

BUGG	03	PL B572 1	D.V. Bugg	
MURAMATSU	02	PRL 89 251802	H. Muramatsu *et al.*	(CLEO Collab.)
Also	03	PRL 90 059901 (erratum)	H. Muramatsu *et al.*	(CLEO Collab.)
AITALA	01B	PRL 86 770	E.M. Aitala *et al.*	(FNAL E791 Collab.)
BLACK	01	PR D64 014031	D. Black *et al.*	
COLANGELO	01	NP B603 125	G. Colangelo, J. Gasser, H. Leytwyler	
ISHIDA	01	PL B518 47	M. Ishida *et al.*	
KOMADA	01	PL B508 31	T. Komada *et al.*	
PISLAK	01	PRL 87 221801	S. Pislak *et al.*	(BNL E865 Collab.)
Also	03	PR D67 072004	S. Pislak *et al.*	(BNL E865 Collab.)
SUROVTSEV	01	PR D63 054024	Y.S. Surovtsev, D. Krupa, M. Nagy	
ASNER	00	PR D61 012002	D.M. Asner *et al.*	(CLEO Collab.)
ISHIDA	00B	PTP 104 203	M. Ishida *et al.*	
ALEKSEEV	99	NP B541 3	I.G. Alekseev *et al.*	
BOGLIONE	99	EPJ C9 11	M. Boglione, M.R. Pennington	
HANNAH	99	PR D60 017502	T. Hannah	
KAMINSKI	99	EPJ C9 141	R. Kaminski, L. Lesniak, B. Loiseau	(CRAC, PARIN)
OLLER	99	PR D60 099906 (erratum)	J.A. Oller *et al.*	
OLLER	99B	NP A652 407 (erratum)	J.A. Oller, E. Oset	
OLLER	99C	PR D60 074023	J.A. Oller, E. Oset	
ALEKSEEV	98	PAN 61 174	I.G. Alekseev *et al.*	
ANISOVICH	98B	UFN 41 419	V.V. Anisovich *et al.*	
LOCHER	98	EPJ C4 317	M.P. Locher *et al.*	(PSI)
TROYAN	98	JINRRC 5-91 33	Yu. Troyan *et al.*	
ALDE	97	PL B397 350	D.M. Alde *et al.*	(GAMS Collab.)
ISHIDA	97	PTP 98 1005	S. Ishida *et al.*	(TOKY, MIYA, KEK)
KAMINSKI	97B	PL B413 130	R. Kaminski, L. Lesniak, B. Loiseau	(CRAC, IPN)
Also	96	PTP 95 745	S. Ishida *et al.*	(TOKY, MIYA, KEK)
SVEC	96	PR D53 2343	M. Svec	(MCGI)
TORNQVIST	96	PRL 76 1575	N.A. Tornqvist, M. Roos	(HELS)
ALDE	95B	ZPHY C66 375	D.M. Alde *et al.*	(GAMS Collab.)
AMSLER	95B	PL B342 433	C. Amsler *et al.*	(Crystal Barrel Collab.)
AMSLER	95D	PL B355 425	C. Amsler *et al.*	(Crystal Barrel Collab.)
ANISOVICH	95	PL B355 363	V.V. Anisovich *et al.*	(PNPI, SERP)
JANSSEN	95	PR D52 2690	G. Janssen *et al.*	(STON, ADLD, JULI)
ACHASOV	94	PR D49 5779	N.N. Achasov, G.N. Shestakov	(NOVM)
AMSLER	94D	PL B333 277	C. Amsler *et al.*	(Crystal Barrel Collab.)
ANISOVICH	94	PL B323 233	V.V. Anisovich *et al.*	(Crystal Barrel Collab.)
KAMINSKI	94	PR D50 3145	R. Kaminski, L. Lesniak, J.P. Maillet	(CRAC+)
ZOU	94B	PR D50 591	B.S. Zou, D.V. Bugg	(LOQM)
ZOU	93	PR D48 R3948	B.S. Zou, D.V. Bugg	(LOQM)
ARMSTRONG	91B	ZPHY C52 389	T.A. Armstrong *et al.*	(ATHU, BARI, BIRM+)
BOYER	90	PR D42 1350	J. Boyer *et al.*	(Mark II Collab.)
MARSISKE	90	PR D41 3324	H. Marsiske *et al.*	(Crystal Ball Collab.)
MORGAN	90	ZPHY C48 623	D. Morgan, M.R. Pennington	(RAL, DURH)
AUGUSTIN	89	NP B320 1	J.E. Augustin, G. Cosme	(DM2 Collab.)
ASTON	88	NP B296 493	D. Aston *et al.*	(SLAC, NAGO, CINC, INUS)
FALVARD	88	PR D38 2706	A. Falvard *et al.*	(CLER, FRAS, LALO+)
AU	87	PR D35 1633	K.L. Au, D. Morgan, M.R. Pennington	(DURH, RAL)
BEVEREN	86	ZPHY C30 615	E. van Beveren *et al.*	(NIJM, BIEL)
COURAU	86	NP B271 1	A. Courau *et al.*	(CLER, LALO)
CASON	83	PR D28 1586	N.M. Cason *et al.*	(NDAM, ANL)
ETKIN	82B	PR D25 1786	A. Etkin *et al.*	(BNL, CUNY, TUFTS, VAND)
BISWAS	81	PRL 47 1378	N.N. Biswas *et al.*	(NDAM, ANL)
COHEN	80	PR D22 2595	D. Cohen *et al.*	(ANL) IJP
MUKHIN	80	JETPL 32 601 Translated from ZETFP 32 616.	K.N. Mukhin *et al.*	(KIAE)
BECKER	79	NP B151 46	H. Becker *et al.*	(MPIM, CERN, ZEEM, CRAC)
CORDEN	79	NP B157 250	M.J. Corden *et al.*	(BIRM, RHEL, TELA+) JP
ESTABROOKS	79	PR D19 2678	P. Estabrooks	(CARL)
FROGGATT	77	NP B129 89	C.D. Froggatt, J.L. Petersen	(GLAS, NORD)
PAWLICKI	77	PR D15 3196	A.J. Pawlicki *et al.*	(ANL) IJ
ROSSELET	77	PR D15 574	L. Rosselet *et al.*	(GEVA, SACL)
CASON	76	PRL 36 1485	N.M. Cason *et al.*	(NDAM, ANL) IJ
ESTABROOKS	75	NP B95 322	P.G. Estabrooks, A.D. Martin	(DURH)
HYAMS	75	NP B100 205	B.D. Hyams *et al.*	(CERN, MPIM)
SRINIVASAN	75	PR D12 681	V. Srinivasan *et al.*	(NDAM, ANL)
ESTABROOKS	74	NP B79 301	P.G. Estabrooks, A.D. Martin	(DURH)
GRAYER	74	NP B75 189	G. Grayer *et al.*	(CERN, MPIM)
APEL	73	PL 41B 542	W.D. Apel *et al.*	(KARL, PISA)
HYAMS	73	NP B64 134	B.D. Hyams *et al.*	(CERN, MPIM)
OCHS	73	Thesis	W. Ochs	(MPIM, MUNI)
PROTOPOP...	73	PR D7 1279	S.D. Protopopescu *et al.*	(LBL)
BAILLON	72	PL 38B 555	P.H. Baillon *et al.*	(SLAC)
BASDEVANT	72	PL 41B 178	J.L. Basdevant, C.D. Froggatt, J.L. Petersen	(CERN)
BEIER	72B	PRL 29 511	E.W. Beier *et al.*	(PENN)
BENSINGER	71	PL 36B 134	J.R. Bensinger *et al.*	(WISC)
COLTON	71	PR D3 2028	E.P. Colton *et al.*	(LBL, FNAL, UCLA+)
BATON	70	PL 33B 528	J.P. Baton, G. Laurens, J. Reignier	(SACL)
WALKER	67	RMP 39 695	W.D. Walker	(WISC)

OTHER RELATED PAPERS

ABDEL-REHIM	03	PR D67 054001	A. Abdel-Rehim *et al.*	
ABDEL-REHIM	03B	PR D68 013008	A. Abdel-Rehim *et al.*	
ISHIDA	03	PTPS 149 190	M. Ishida	
KAMINSKI	03	PL B551 241	R. Kaminski, L. Lesniak, B. Loiseau	
OLLER	03B	NP A714 161	J.A. Oller *et al.*	
SCADRON	03	NP A724 391	M.D. Scadron *et al.*	
SEMENOV	03	PAN 66 526 Translated from YAF 66 553.	S.V. Semenov	
AITALA	02	PRL 89 121801	E.M. Aitala *et al.*	(FNAL E791 Collab.)
BEVEREN	02	MPL A17 1673	E. van Beveren *et al.*	
BLACK	02	PRL 88 181603	D. Black, M. Harada, J. Schechter	
BOGLIONE	02	PR D65 114010	M. Boglione, M.R. Pennington	
BRAMON	02	EPJ C26 253	A. Bramon *et al.*	
CLOSE	02B	JPG 28 R249	F.E. Close, N. Tornqvist	
HE	02	PL B536 59	J. He, Z.G. Xiao, H.Q. Zheng	
HERNANDEZ	02	PR C66 065201	E. Hernandez, E. Oset, M.J. Vicente Vacas	
ISHIDA	02	PL B539 249	S. Ishida, M. Ishida	
KAMINSKI	02	EPJ Direct C4 1	R. Kaminski, L. Lesniak, K. Rybicki	
LINK	02E	PL B535 43	J.M. Link *et al.*	(FNAL FOCUS Collab.)
TESHIMA	02	JPG 28 1391	T. Teshima, I. Kitamura, N. Morisita	
ABELE	01	EPJ C19 667	A. Abele *et al.*	(Crystal Barrel Collab.)
ABELE	01B	EPJ C21 261	A. Abele *et al.*	(Crystal Barrel Collab.)
BEVEREN	01B	EPJ C22 493	E. van Beveren	
CHERRY	01	NP A688 823	S.N. Cherry, M.R. Pennington	
DEANDREA	01	PL B502 79	A. Deandrea *et al.*	
FAZIO	01	PL B521 15	F. De Fazio, M.R. Pennington	
GOKALP	01	PR D64 053017	A. Gokalp, O. Yilmaz	
NARISON	01C	NPBPS 96 244	S. Narison	
XIAO	01	NP A695 273	Z. Xiao, H. Zheng	
ACHASOV	00H	PL B485 349	M.N. Achasov *et al.*	(Novosibirsk SND Collab.)
ALFORD	00	NP B578 367	M. Alford, R.L. Jaffe	
BLACK	00B	PR D61 074030	D. Black, A. Fariborz, J. Schechter	
FANG	00	NP A671 416	Fang Shi *et al.*	
JAMIN	00	NP B587 331	M. Jamin *et al.*	
MONTANET	00	NPBPS 86 381	L. Montanet	
ABREU	99J	PL B449 364	P. Abreu *et al.*	(DELPHI Collab.)
BLACK	99	PR D59 074026	D. Black *et al.*	
DELBOURGO	99	PL B446 332	R. Delbourgo, D. Liu, M. Scadron	
IGI	99	PR D59 034005	K. Igi, K. Hikasa	
LUCIO	99	PL B454 365	J.L. Lucio, M. Napsuciale	
MINKOWSKI	99	EPJ C9 283	P. Minkowski, W. Ochs	
SCADRON	99	EPJ C6 141	M. Scadron	
TAKAMATSU	99	PAN 62 435	K. Takamatsu	
ACKERSTAFF	98A	EPJ C5 411	K. Ackerstaff *et al.*	(OPAL Collab.)
ANISOVICH	98	PL B437 209	V.V. Anisovich *et al.*	
DELBOURGO	98	IJMP A13 657	R. Delbourgo *et al.*	
OLLER	98	PRL 80 3452	J.A. Oller *et al.*	
ANISOVICH	97	PL B395 123	A.V. Anisovich, A.V. Sarantsev	(PNPI)
ANISOVICH	97D	ZPHY A359 173	A.V. Anisovich, V.V. Anisovich, A.V. Sarantsev	
HARADA	97	PRL 78 1603	M. Harada, F. Sannino, J. Schechter	
ISHIDA	97B	PTP 98 621	S. Ishida *et al.*	
KAMINSKI	97	ZPHY C74 79	R. Kaminski, L. Lesniak, K. Rybicki	(CRAC)
MALTMAN	97	PL B393 19	K. Maltman, C.E. Wolfe	(YORKC)
OLLER	97	NP A620 438	J.A. Oller *et al.*	(VALE)
SVEC	97	PR D55 4355	M. Svec	
SVEC	97B	PR D55 5727	M. Svec	(MCGI)
AMSLER	96	PR D53 295	C. Amsler, F.E. Close	(ZURI, RAL)
BIJNENS	96	PL B374 210	J. Bijnens *et al.*	(NORD, BERN, WIEN+)
BONUTTI	96	PRL 77 603	F. Bonutti *et al.*	(TRSTI, TRSTT, TRIU)
BUGG	96	NP B471 59	D.V. Bugg, A.V. Sarantsev, B.S. Zou	(LOQM, PNPI)
HARADA	96	PR D54 1991	M. Harada *et al.*	(SYRA)
ISHIDA	96	PTP 95 745	S. Ishida *et al.*	(TOKY, MIYA, KEK)
ANTINORI	95	PL B353 589	F. Antinori *et al.*	(ATHU, BARI, BIRM+)
GASPERO	95	NP A588 861	M. Gaspero	(ROMA)
TORNQVIST	95	ZPHY C68 647	N.A. Tornqvist	(HELS)
AMSLER	94	PL B322 431	C. Amsler *et al.*	(Crystal Barrel Collab.)
BUGG	94	PR D50 4412	D.V. Bugg *et al.*	(LOQM)
ADAMO	93	NP A558 13C	A. Adamo *et al.*	(OBELIX Collab.)
GASPERO	93	NP A562 407	M. Gaspero	(ROMA)

MORGAN	93	PR D48 1185	D. Morgan, M.R. Pennington	(RAL, DURH)
Also	93C	NC A Conf. Suppl.	D. Morgan	(RAL)
BOLTON	92B	PRL 69 1328	T. Bolton *et al.*	(Mark III Collab.)
SVEC	92	PR D45 55	M. Svec, A. de Lesquen, L. van Rossum	(MCGI+)
SVEC	92B	PR D45 1518	M. Svec, A. de Lesquen, L. van Rossum	(MCGI+)
SVEC	92C	PR D46 949	M. Svec, A. de Lesquen, L. van Rossum	(MCGI+)
RIGGENBACH	91	PR D43 127	C. Riggenbach *et al.*	(BERN, CERN, MASA)
BAI	90C	PRL 65 2507	Z. Bai *et al.*	(Mark III Collab.)
WEINSTEIN	90	PR D41 2236	J. Weinstein, N. Isgur	(TNTO)
ASTON	88D	NP B301 525	D. Aston *et al.*	(SLAC, NAGO, CINC, INUS)
ACHASOV	84	ZPHY C22 53	N.N. Achasov, S.A. Devyanin, G.N. Shestakov	(NOVM)
GASSER	84	ANP 158 142	J. Gasser, H. Leutwyler	
TORNQVIST	82	PRL 49 624	N.A. Tornqvist	(HELS)
COSTA	80	NP B175 402	G. Costa *et al.*	(BARI, BONN, CERN, GLAS+)
BECKER	79B	NP B150 301	H. Becker *et al.*	(MPIM, CERN, ZEEM, CRAC)
NAGELS	79	PR D20 1633	M.M. Nagels, T.A. Rijken, J.J. de Swart	(NIJM)
POLYCHRO...	79	PR D19 1317	V.A. Polychronakos *et al.*	(NDAM, ANL) IJP
CORDEN	78	NP B144 253	M.J. Corden *et al.*	(BIRM, RHEL, TELA+)
JAFFE	77	PR D15 267,281	R. Jaffe	(MIT)
FLATTE	76	PL 63B 224	S.M. Flatte	(CERN)
WETZEL	76	NP B115 208	W. Wetzel *et al.*	(ETH, CERN, LOIC)
DEFOIX	72	NP B44 125	C. Defoix *et al.*	(CDEF, CERN)

$\rho(770)$

$I^G(J^{PC}) = 1^+(1^{--})$

THE $\rho(770)$

Updated December 2003 by S. Eidelman (Novosibirsk).

The determination of the parameters of the $\rho(770)$ is beset with many difficulties because of its large width. In physical region fits, the line shape does not correspond to a relativistic Breit-Wigner function with a P-wave width, but requires some additional shape parameter. This dependence on parameterization was demonstrated long ago by PISUT 68. Bose-Einstein correlations are another source of shifts in the $\rho(770)$ line shape, particularly in multiparticle final state systems (LAFFERTY 93).

The same model dependence afflicts any other source of resonance parameters, such as the energy dependence of the phase shift δ_1^1, or the pole position. It is, therefore, not surprising that a study of $\rho(770)$ dominance in the decays of the η and η' reveals the need for specific dynamical effects, in addition to the $\rho(770)$ pole (ABELE 97B, BENAYOUN 03B).

The cleanest determination of the $\rho(770)$ mass and width comes from the e^+e^- annihilation and τ-lepton decays. BARATE 97M showed that the charged $\rho(770)$ parameters measured from τ-lepton decays are consistent with those of the neutral one determined from e^+e^- data of BARKOV 85. This conclusion is qualitatively supported by the high statistics study of ANDERSON 00A. However, model-independent comparison of the two-pion mass spectrum in τ decays and the $e^+e^- \to \pi^+\pi^-$ cross section gave indications of discrepancies between the overall normalization: τ data are about 3% higher than e^+e^- data (ANDERSON 00A, EIDELMAN 99). A detailed analysis using such two-pion mass spectra from τ decays measured by OPAL (ACKERSTAFF 99F), CLEO (ANDERSON 00A), and ALEPH (DAVIER 02) as well as recent pion form factor measurements in e^+e^- annihilation by CMD-2 (AKHMETSHIN 02, AKHMETSHIN 04) showed that the discrepancy can be as high as 10% above the ρ meson (DAVIER 03, DAVIER 03B) and is not accounted for by isospin breaking (ALEMANY 98, CZYZ 01, CIRIGLIANO 01, CIRIGLIANO 02). GHOZZI 03 suggested that this effect can be explained if the charged ρ mass were higher than that of the neutral one by a few MeV. Existing theoretical models of the possible mass difference predict either a much smaller value (BIJNENS 96B), or a heavier neutral ρ meson (ACHASOV 99F). Experimental accuracy is not yet sufficient for unambiguous conclusions.

$\rho(770)$ MASS

We no longer list S-wave Breit-Wigner fits, or data with high combinatorial background.

NEUTRAL ONLY, e^+e^-

VALUE (MeV)	EVTS	DOCUMENT ID		TECN	CHG	COMMENT
775.8 ±0.5 OUR AVERAGE						
775.65 ± 0.64 ± 0.50	114k	[1,2] AKHMETSHIN	04	CMD2		$e^+e^- \to \pi^+\pi^-$
775.9 ± 0.5 ± 0.5	1.98M	[3] ALOISIO	03	KLOE		1.02 $e^+e^- \to \pi^+\pi^-\pi^0$
775.8 ± 0.9 ± 2.0	500k	[3] ACHASOV	02	SND		1.02 $e^+e^- \to \pi^+\pi^-\pi^0$
775.9 ± 1.1		[4] BARKOV	85	OLYA	0	$e^+e^- \to \pi^+\pi^-$
• • • We do not use the following data for averages, fits, limits, etc. • • •						
775.8 ± 0.5 ± 0.3	1.98M	[5] ALOISIO	03	KLOE		1.02 $e^+e^- \to \pi^+\pi^-\pi^0$
775.9 ± 0.6 ± 0.5	1.98M	[6] ALOISIO	03	KLOE		1.02 $e^+e^- \to \pi^+\pi^-\pi^0$
775.0 ± 0.6 ± 1.1	500k	[7] ACHASOV	02	SND		1.02 $e^+e^- \to \pi^+\pi^-\pi^0$
775.1 ± 0.7 ± 5.3		[8] BENAYOUN	98	RVUE		$e^+e^- \to \pi^+\pi^-$, $\mu^+\mu^-$
770.5 ± 1.9 ± 5.1		[9] GARDNER	98	RVUE		0.28–0.92 $e^+e^- \to \pi^+\pi^-$
764.1 ± 0.7		[10] O'CONNELL	97	RVUE		$e^+e^- \to \pi^+\pi^-$
757.5 ± 1.5		[11] BERNICHA	94	RVUE		$e^+e^- \to \pi^+\pi^-$
768 ± 1		[12] GESHKEN...	89	RVUE		$e^+e^- \to \pi^+\pi^-$

CHARGED ONLY, τ DECAYS and e^+e^-

VALUE (MeV)	EVTS	DOCUMENT ID		TECN	CHG	COMMENT
The data in this block is included in the average printed for a previous datablock.						
775.5 ±0.5 OUR AVERAGE						
775.5 ± 0.5 ± 0.4	1.98M	[3] ALOISIO	03	KLOE		1.02 $e^+e^- \to \pi^+\pi^-\pi^0$
775.1 ± 1.1 ± 0.5	87k	[13,14] ANDERSON	00A	CLE2		$\tau^- \to \pi^-\pi^0\nu_\tau$
776.4 ± 0.9 ± 1.5		[14] BARATE	97M	ALEP		$\tau^- \to \pi^-\pi^0\nu_\tau$
• • • We do not use the following data for averages, fits, limits, etc. • • •						
774.8 ± 0.6 ± 0.4	1.98M	[6] ALOISIO	03	KLOE	–	1.02 $e^+e^- \to \pi^+\pi^-\pi^0$
776.3 ± 0.6 ± 0.7	1.98M	[6] ALOISIO	03	KLOE	+	1.02 $e^+e^- \to \pi^+\pi^-\pi^0$
$773.9 \pm 2.0^{+0.3}_{-1.0}$		[15] SANZ-CILLERO	03	RVUE		$\tau^- \to \pi^-\pi^0\nu_\tau$
774.5 ± 0.7 ± 1.5	500k	[3] ACHASOV	02	SND	±	1.02 $e^+e^- \to \pi^+\pi^-\pi^0$
775.1 ± 0.5		[16] PICH	01	RVUE		$\tau^- \to \pi^-\pi^0\nu_\tau$

MIXED CHARGES, OTHER REACTIONS

VALUE (MeV)	EVTS	DOCUMENT ID		TECN	CHG	COMMENT
763.0 ± 0.3 ± 1.2	600k	[17] ABELE	99E	CBAR	0±	0.0 $\overline{p}p \to \pi^+\pi^-\pi^0$

CHARGED ONLY, HADROPRODUCED

VALUE (MeV)	EVTS	DOCUMENT ID		TECN	CHG	COMMENT
766.5 ±1.1 OUR AVERAGE						
763.7 ± 3.2		ABELE	97	CBAR		$\overline{p}n \to \pi^-\pi^0\pi^0$
768 ± 9		AGUILAR-...	91	EHS		400 pp
767 ± 3	2935	[18] CAPRARO	87	SPEC	–	200 π^- Cu $\to \pi^-\pi^0$ Cu
761 ± 5	967	[18] CAPRARO	87	SPEC	–	200 π^- Pb $\to \pi^-\pi^0$ Pb
771 ± 4		HUSTON	86	SPEC	+	202 π^+ A $\to \pi^+\pi^0$ A
766 ± 7	6500	[19] BYERLY	73	OSPK	–	5 π^-p
766.8 ± 1.5	9650	[20] PISUT	68	RVUE	–	1.7–3.2 π^-p, $t < 10$
767 ± 6	900	[18] EISNER	67	HBC	–	4.2 π^-p, $t < 10$

NEUTRAL ONLY, PHOTOPRODUCED

VALUE (MeV)	EVTS	DOCUMENT ID		TECN	CHG	COMMENT
768.5 ± 1.1 OUR AVERAGE						
770 ± 2 ± 1	79k	[21] BREITWEG	98B	ZEUS	0	50–100 γp
767.6 ± 2.7		BARTALUCCI	78	CNTR	0	$\gamma p \to e^+e^-p$
775 ± 5		GLADDING	73	CNTR	0	2.9–4.7 γp
767 ± 4	1930	BALLAM	72	HBC	0	2.8 γp
770 ± 4	2430	BALLAM	72	HBC	0	4.7 γp
765 ± 10		ALVENSLEB...	70	CNTR	0	γA, $t < 0.01$
767.7 ± 1.9	140k	BIGGS	70	CNTR	0	<4.1 γC $\to \pi^+\pi^-$C
765 ± 5	4000	ASBURY	67B	CNTR	0	γ + Pb
• • • We do not use the following data for averages, fits, limits, etc. • • •						
771 ± 2	79k	[22] BREITWEG	98B	ZEUS	0	50–100 γp

NEUTRAL ONLY, OTHER REACTIONS

VALUE (MeV)	EVTS	DOCUMENT ID		TECN	CHG	COMMENT
769.0±0.9 OUR AVERAGE		Error includes scale factor of 1.4. See the ideogram below.				
765 ±6		BERTIN	97C	OBLX		0.0 $\overline{p}p \rightarrow \pi^+\pi^-\pi^0$
773 ±1.6		WEIDENAUER	93	ASTE		$\overline{p}p \rightarrow \pi^+\pi^-\omega$
762.6±2.6		AGUILAR-...	91	EHS		400 pp
770 ±2		[23] HEYN	81	RVUE		Pion form factor
768 ±4		[24,25] BOHACIK	80	RVUE	0	
769 ±3		[19] WICKLUND	78	ASPK	0	3,4,6 $\pi^\pm N$
768 ±1	76000	DEUTSCH...	76	HBC	0	16 $\pi^+ p$
767 ±4	4100	ENGLER	74	DBC	0	6 $\pi^+ n \rightarrow \pi^+\pi^- p$
775 ±4	32000	[24] PROTOPOP...	73	HBC	0	7.1 $\pi^+ p$, $t < 0.4$
764 ±3	6800	RATCLIFF	72	ASPK	0	15 $\pi^- p$, $t < 0.3$
774 ±3	1700	REYNOLDS	69	HBC	0	2.26 $\pi^- p$
769.2±1.5	13300	[26] PISUT	68	RVUE	0	1.7–3.2 $\pi^- p$, $t < 10$
• • • We do not use the following data for averages, fits, limits, etc. • • •						
773.5±2.5		[27] COLANGELO	01	RVUE		$\pi\pi \rightarrow \pi\pi$
762.3±0.5±1.2	600k	[28] ABELE	99E	CBAR	0	0.0 $\overline{p}p \rightarrow \pi^+\pi^-\pi^0$
777 ±2	4943	[29] ADAMS	97	E665		470 $\mu p \rightarrow \mu X B$
770 ±2		[30] BOGOLYUB...	97	MIRA		32 $\overline{p}p \rightarrow \pi^+\pi^- X$
768 ±8		[30] BOGOLYUB...	97	MIRA		32 $pp \rightarrow \pi^+\pi^- X$
761.1±2.9		DUBNICKA	89	RVUE		π form factor
777.4±2.0		[31] CHABAUD	83	ASPK	0	17 $\pi^- p$ polarized
769.5±0.7		[24,25] LANG	79	RVUE	0	
770 ±9		[25] ESTABROOKS	74	RVUE	0	17 $\pi^- p \rightarrow \pi^+\pi^- n$
773.5±1.7	11200	[18] JACOBS	72	HBC	0	2.8 $\pi^- p$
775 ±3	2250	HYAMS	68	OSPK	0	11.2 $\pi^- p$

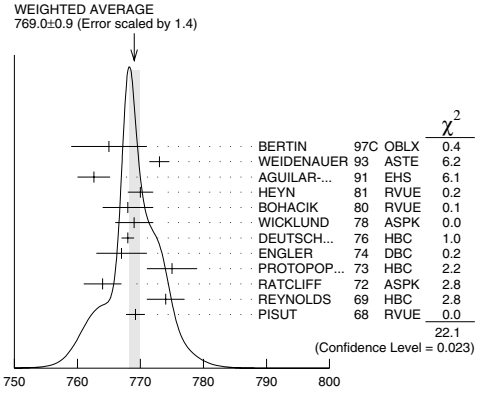

[1] Using the GOUNARIS 68 parametrization with the complex phase of the ρ-ω interference.
[2] Update of AKHMETSHIN 02.
[3] Assuming $m_{\rho^+} = m_{\rho^-}$, $\Gamma_{\rho^+} = \Gamma_{\rho^-}$.
[4] From the GOUNARIS 68 parametrization of the pion form factor.
[5] Assuming $m_{\rho^+} = m_{\rho^-} = m_{\rho^0}$, $\Gamma_{\rho^+} = \Gamma_{\rho^-} = \Gamma_{\rho^0}$.
[6] Without limitations on masses and widths.
[7] Assuming $m_{\rho^0} = m_{\rho^\pm}$, $g_{\rho^0\pi\pi} = g_{\rho^\pm\pi\pi}$.
[8] Using the data of BARKOV 85 in the hidden local symmetry model.
[9] From the fit to $e^+e^- \rightarrow \pi^+\pi^-$ data from the compilations of HEYN 81 and BARKOV 85, including the GOUNARIS 68 parametrization of the pion form factor.
[10] A fit of BARKOV 85 data assuming the direct $\omega\pi\pi$ coupling.
[11] Applying the S-matrix formalism to the BARKOV 85 data.
[12] Includes BARKOV 85 data. Model-dependent width definition.
[13] $\rho(1700)$ mass and width fixed at 1700 MeV and 235 MeV respectively.
[14] From the GOUNARIS 68 parametrization of the pion form factor. The second error is a model error taking into account different parametrizations of the pion form factor.
[15] Using the data of BARATE 97M and the effective chiral Lagrangian.
[16] From a fit of the model-independent parameterization of the pion form factor to the data of BARATE 97M.
[17] Assuming the equality of ρ^+ and ρ^- masses and widths.
[18] Mass errors enlarged by us to $\Gamma/\sqrt{N}$; see the note with the $K^*(892)$ mass.
[19] Phase shift analysis. Systematic errors added corresponding to spread of different fits.
[20] From fit of 3-parameter relativistic P-wave Breit-Wigner to total mass distribution. Includes BATON 68, MILLER 67B, ALFF-STEINBERGER 66, HAGOPIAN 66, HAGOPIAN 66B, JACOBS 66B, JAMES 66, WEST 66, BLIEDEN 65 and CARMONY 64.
[21] From the parametrization according to SOEDING 66.
[22] From the parametrization according to ROSS 66.
[23] HEYN 81 includes all spacelike and timelike F_π values until 1978.
[24] From pole extrapolation.
[25] From phase shift analysis of GRAYER 74 data.
[26] Includes MALAMUD 69, ARMENISE 68, BACON 67, HUWE 67, MILLER 67B, ALFF-STEINBERGER 66, HAGOPIAN 66, HAGOPIAN 66B, JACOBS 66B, JAMES 66, WEST 66, GOLDHABER 64, ABOLINS 63.
[27] Breit-Wigner mass from a phase-shift analysis of HYAMS 73 and PROTOPOPESCU 73 data.
[28] Using relativistic Breit-Wigner and taking into account ρ-ω interference.
[29] Systematic errors not evaluated.
[30] Systematic effects not studied.
[31] From fit of 3-parameter relativistic Breit-Wigner to helicity-zero part of P-wave intensity. CHABAUD 83 includes data of GRAYER 74.

$m_{\rho(770)^0} - m_{\rho(770)^\pm}$

VALUE (MeV)	EVTS	DOCUMENT ID		TECN	CHG	COMMENT
0.7±0.7 OUR AVERAGE						
0.4±0.7±0.6	1.98M	[32] ALOISIO	03	KLOE		1.02 $e^+e^- \rightarrow \pi^+\pi^-\pi^0$
1.3±1.1±2.0	500k	[32] ACHASOV	02	SND		1.02 $e^+e^- \rightarrow \pi^+\pi^-\pi^0$
1.6±0.6±1.7	600k	ABELE	99E	CBAR	0±	0.0 $\overline{p}p \rightarrow \pi^+\pi^-\pi^0$
−4 ±4	3000	[33] REYNOLDS	69	HBC	−0	2.26 $\pi^- p$
−5 ±5	3600	[33] FOSTER	68	HBC	±0	0.0 $\overline{p}p$
2.4±2.1	22950	[34] PISUT	68	RVUE		$\pi N \rightarrow \rho N$
• • • We do not use the following data for averages, fits, limits, etc. • • •						
0.0±1.0		[35] BARATE	97M	ALEP		$\tau^- \rightarrow \pi^-\pi^0\nu_\tau$

[32] Assuming $m_{\rho^+} = m_{\rho^-}$, $\Gamma_{\rho^+} = \Gamma_{\rho^-}$.
[33] From quoted masses of charged and neutral modes.
[34] Includes MALAMUD 69, ARMENISE 68, BATON 68, BACON 67, HUWE 67, MILLER 67B, ALFF-STEINBERGER 66, HAGOPIAN 66, HAGOPIAN 66B, JACOBS 66B, JAMES 66, WEST 66, BLIEDEN 65, CARMONY 64, GOLDHABER 64, ABOLINS 63.
[35] Using the compilation of e^+e^- data from BARKOV 85.

$m_{\rho(770)^+} - m_{\rho(770)^-}$

VALUE (MeV)	EVTS	DOCUMENT ID		TECN	COMMENT
• • • We do not use the following data for averages, fits, limits, etc. • • •					
1.5±0.8±0.7	1.98M	[36] ALOISIO	03	KLOE	1.02 $e^+e^- \rightarrow \pi^+\pi^-\pi^0$

[36] Without limitations on masses and widths.

$\rho(770)$ RANGE PARAMETER

The range parameter R enters an energy-dependent correction to the width, of the form $(1 + q_r^2\ R^2) / (1 + q^2\ R^2)$, where q is the momentum of one of the pions in the $\pi\pi$ rest system. At resonance, $q = q_r$.

VALUE (GeV^{-1})	DOCUMENT ID		TECN	CHG	COMMENT
$5.3^{+0.9}_{-0.7}$	CHABAUD	83	ASPK	0	17 $\pi^- p$ polarized

$\rho(770)$ WIDTH

We no longer list S-wave Breit-Wigner fits, or data with high combinatorial background.

NEUTRAL ONLY, e^+e^-

VALUE (MeV)	EVTS	DOCUMENT ID		TECN	CHG	COMMENT
146.4 ±1.5 OUR AVERAGE		Error includes scale factor of 1.4. See the ideogram below.				
143.85±1.33±0.80	114k	[39,40] AKHMETSHIN	04	CMD2		$e^+e^- \rightarrow \pi^+\pi^-$
147.3 ±1.5 ±0.7	1.98M	[37] ALOISIO	03	KLOE		1.02 $e^+e^- \rightarrow \pi^+\pi^-\pi^0$
151.1 ±2.6 ±3.0	500k	[37] ACHASOV	02	SND	0	1.02 $e^+e^- \rightarrow \pi^+\pi^-\pi^0$
150.5 ±3.0		[41] BARKOV	85	OLYA	0	$e^+e^- \rightarrow \pi^+\pi^-$
• • • We do not use the following data for averages, fits, limits, etc. • • •						
143.9 ±1.3 ±1.1	1.98M	[42] ALOISIO	03	KLOE		1.02 $e^+e^- \rightarrow \pi^+\pi^-\pi^0$
147.4 ±1.5 ±0.7	1.98M	[43] ALOISIO	03	KLOE		1.02 $e^+e^- \rightarrow \pi^+\pi^-\pi^0$
149.8 ±2.2 ±2.0	500k	[38] ACHASOV	02	SND		1.02 $e^+e^- \rightarrow \pi^+\pi^-\pi^0$
147.9 ±1.5 ±7.5		[44] BENAYOUN	98	RVUE		$e^+e^- \rightarrow \pi^+\pi^-$, $\mu^+\mu^-$
153.5 ±1.3 ±4.6		[45] GARDNER	98	RVUE		0.28–0.92 $e^+e^- \rightarrow \pi^+\pi^-$
145.0 ±1.7		[46] O'CONNELL	97	RVUE		$e^+e^- \rightarrow \pi^+\pi^-$
142.5 ±3.5		[47] BERNICHA	94	RVUE		$e^+e^- \rightarrow \pi^+\pi^-$
138 ±1		[48] GESHKEN...	89	RVUE		$e^+e^- \rightarrow \pi^+\pi^-$

[37] Assuming $m_{\rho^+} = m_{\rho^-}$, $\Gamma_{\rho^+} = \Gamma_{\rho^-}$.
[38] Assuming $m_{\rho^0} = m_{\rho^\pm}$, $g_{\rho^0\pi\pi} = g_{\rho^\pm\pi\pi}$.

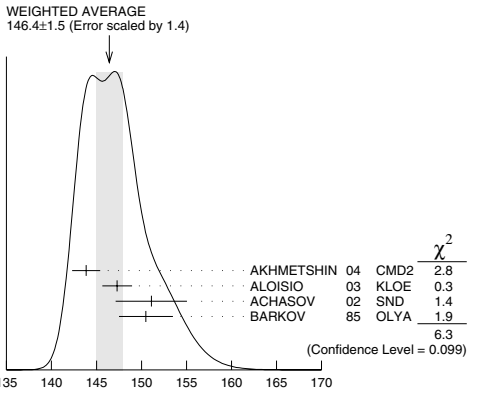

Neutral only, e^+e^-

CHARGED ONLY, τ DECAYS and e^+e^-

VALUE (MeV)	EVTS	DOCUMENT ID		TECN	CHG	COMMENT
The data in this block is included in the average printed for a previous datablock.						
150.3±1.6 OUR FIT						
150.3±1.6 OUR AVERAGE						
149.9±2.3±2.0	500k	[37] ACHASOV	02	SND	±	1.02 $e^+e^- \to \pi^+\pi^-\pi^0$
150.4±1.4±1.4	87k	[49,50] ANDERSON	00A	CLE2		$\tau^- \to \pi^-\pi^0\nu_\tau$
150.5±1.6±6.3		[50] BARATE	97M	ALEP		$\tau^- \to \pi^-\pi^0\nu_\tau$
• • • We do not use the following data for averages, fits, limits, etc. • • •						
143.7±1.3±1.2	1.98M	[37] ALOISIO	03	KLOE	±	1.02 $e^+e^- \to \pi^+\pi^-\pi^0$
142.9±1.3±1.4	1.98M	[43] ALOISIO	03	KLOE	−	1.02 $e^+e^- \to \pi^+\pi^-\pi^0$
144.7±1.4±1.2	1.98M	[43] ALOISIO	03	KLOE	+	1.02 $e^+e^- \to \pi^+\pi^-\pi^0$
$150.2\pm2.0^{+0.7}_{-1.6}$		[51] SANZ-CILLERO	03	RVUE		$\tau^- \to \pi^-\pi^0\nu_\tau$
150.9±2.2±2.0	500k	[38] ACHASOV	02	SND		1.02 $e^+e^- \to \pi^+\pi^-\pi^0$

MIXED CHARGES, OTHER REACTIONS

VALUE (MeV)	EVTS	DOCUMENT ID		TECN	CHG	COMMENT
149.5±1.3	600k	[52] ABELE	99E	CBAR	0±	0.0 $\overline{p}p \to \pi^+\pi^-\pi^0$

CHARGED ONLY, HADROPRODUCED

VALUE (MeV)	EVTS	DOCUMENT ID		TECN	CHG	COMMENT
150.2± 2.4 OUR FIT						
150.2± 2.4 OUR AVERAGE						
152.8± 4.3		ABELE	97	CBAR		$\overline{p}n \to \pi^-\pi^0\pi^0$
155 ±11	2935	[53] CAPRARO	87	SPEC	−	200 π^- Cu → $\pi^-\pi^0$ Cu
154 ±20	967	[53] CAPRARO	87	SPEC	−	200 π^- Pb → $\pi^-\pi^0$ Pb
150 ± 5		HUSTON	86	SPEC	+	202 π^+ A → $\pi^+\pi^0$ A
146 ±12	6500	[54] BYERLY	73	OSPK	−	5 π^-p
148.2± 4.1	9650	[55] PISUT	68	RVUE	−	1.7–3.2 π^-p, $t<10$
146 ±13	900	EISNER	67	HBC	−	4.2 π^-p, $t<10$

NEUTRAL ONLY, PHOTOPRODUCED

VALUE (MeV)	EVTS	DOCUMENT ID		TECN	CHG	COMMENT
150.7± 2.9 OUR AVERAGE						
146 ± 3 ±13	79k	[56] BREITWEG	98B	ZEUS	0	50–100 γp
150.9± 3.0		BARTALUCCI	78	CNTR	0	$\gamma p \to e^+e^-p$
• • • We do not use the following data for averages, fits, limits, etc. • • •						
138 ± 3	79k	[57] BREITWEG	98B	ZEUS	0	50–100 γp
147 ±11		GLADDING	73	CNTR	0	2.9–4.7 γp
155 ±12	2430	BALLAM	72	HBC	0	4.7 γp
145 ±13	1930	BALLAM	72	HBC	0	2.8 γp
140 ± 5		ALVENSLEB...	70	CNTR	0	γA, $t<0.01$
146.1± 2.9	140k	BIGGS	70	CNTR	0	<4.1 γ C → $\pi^+\pi^-$ C
160 ±10		LANZEROTTI	68	CNTR	0	γp
130 ± 5	4000	ASBURY	67B	CNTR	0	γ + Pb

NEUTRAL ONLY, OTHER REACTIONS

VALUE (MeV)	EVTS	DOCUMENT ID		TECN	CHG	COMMENT
150.9± 1.7 OUR AVERAGE	Error includes scale factor of 1.1.					
122 ±20		BERTIN	97C	OBLX		0.0 $\overline{p}p \to \pi^+\pi^-\pi^0$
145.7± 5.3		WEIDENAUER	93	ASTE		$\overline{p}p \to \pi^+\pi^-\omega$
144.9± 3.7		DUBNICKA	89	RVUE		π form factor
148 ± 6		[58,59] BOHACIK	80	RVUE	0	
152 ± 9		[54] WICKLUND	78	ASPK	0	3,4,6 $\pi^\pm pN$
154 ± 2	76000	DEUTSCH...	76	HBC	0	16 π^+p
157 ± 8	6800	RATCLIFF	72	ASPK	0	15 π^-p, $t<0.3$
143 ± 8	1700	REYNOLDS	69	HBC	0	2.26 π^-p
• • • We do not use the following data for averages, fits, limits, etc. • • •						
147.0± 2.5	600k	[60] ABELE	99E	CBAR	0	0.0 $\overline{p}p \to \pi^+\pi^-\pi^0$
146 ± 3	4943	[61] ADAMS	97	E665		470 $\mu p \to \mu XB$
$160.0^{+4.1}_{-4.0}$		[62] CHABAUD	83	ASPK	0	17 π^-p polarized
155 ± 1		[63] HEYN	81	RVUE	0	π form factor
148.0± 1.3		[58,59] LANG	79	RVUE	0	
146 ±14	4100	ENGLER	74	DBC	0	6 $\pi^+n \to \pi^+\pi^-p$
143 ±13		[59] ESTABROOKS	74	RVUE	0	17 $\pi^-p \to \pi^+\pi^-n$
160 ±10	32000	[58] PROTOPOP...	73	HBC	0	7.1 π^+p, $t<0.4$
145 ±12	2250	[53] HYAMS	68	OSPK	0	11.2 π^-p
163 ±15	13300	[64] PISUT	68	RVUE	0	1.7–3.2 π^-p, $t<10$

[39] Using the GOUNARIS 68 parametrization with the complex phase of the ρ-ω interference.
[40] From a fit in the energy range 0.61 to 0.96 GeV. Update of AKHMETSHIN 02.
[41] From the GOUNARIS 68 parametrization of the pion form factor.
[42] Assuming $m_{\rho^+} = m_{\rho^-} = m_{\rho^0}$, $\Gamma_{\rho^+} = \Gamma_{\rho^-} = \Gamma_{\rho^0}$.
[43] Without limitations on masses and widths.
[44] Using the data of BARKOV 85 in the hidden local symmetry model.
[45] From the fit to $e^+e^- \to \pi^+\pi^-$ data from the compilations of HEYN 81 and BARKOV 85, including the GOUNARIS 68 parametrization of the pion form factor.
[46] A fit of BARKOV 85 data assuming the direct $\omega\pi\pi$ coupling.
[47] Applying the S-matrix formalism to the BARKOV 85 data.
[48] Includes BARKOV 85 data. Model-dependent width definition.
[49] $\rho(1700)$ mass and width fixed at 1700 MeV and 235 MeV respectively.
[50] From the GOUNARIS 68 parametrization of the pion form factor. The second error is a model error taking into account different parametrizations of the pion form factor.
[51] Using the data of BARATE 97M and the effective chiral Lagrangian.
[52] Assuming the equality of ρ^+ and ρ^- masses and widths.
[53] Width errors enlarged by us to $4\Gamma/\sqrt{N}$; see the note with the $K^*(892)$ mass.
[54] Phase shift analysis. Systematic errors added corresponding to spread of different fits.
[55] From fit of 3-parameter relativistic P-wave Breit-Wigner to total mass distribution. Includes BATON 68, MILLER 67B, ALFF-STEINBERGER 66, HAGOPIAN 66, HAGOPIAN 66B, JACOBS 66B, JAMES 66, WEST 66, BLIEDEN 65 and CARMONY 64.
[56] From the parametrization according to SOEDING 66.
[57] From the parametrization according to ROSS 66.
[58] From pole extrapolation.
[59] From phase shift analysis of GRAYER 74 data.
[60] Using relativistic Breit-Wigner and taking into account ρ-ω interference.
[61] Systematic errors not evaluated.
[62] From fit of 3-parameter relativistic Breit-Wigner to helicity-zero part of P-wave intensity. CHABAUD 83 includes data of GRAYER 74.
[63] HEYN 81 includes all spacelike and timelike F_π values until 1978.
[64] Includes MALAMUD 69, ARMENISE 68, BACON 67, HUWE 67, MILLER 67B, ALFF-STEINBERGER 66, HAGOPIAN 66, HAGOPIAN 66B, JACOBS 66B, JAMES 66, WEST 66, GOLDHABER 64, ABOLINS 63.

$\Gamma_{\rho(770)^0} - \Gamma_{\rho(770)^\pm}$

VALUE	EVTS	DOCUMENT ID		TECN	COMMENT
3.6±1.8±1.7	1.98M	[37] ALOISIO	03	KLOE	1.02 $e^+e^- \to \pi^+\pi^-\pi^0$
• • • We do not use the following data for averages, fits, limits, etc. • • •					
−0.1±1.9		[65] BARATE	97M	ALEP	$\tau^- \to \pi^-\pi^0\nu_\tau$

$\Gamma_{\rho(770)^+} - \Gamma_{\rho(770)^-}$

VALUE	EVTS	DOCUMENT ID		TECN	COMMENT
1.8±2.0±0.5	1.98M	[43] ALOISIO	03	KLOE	1.02 $e^+e^- \to \pi^+\pi^-\pi^0$

[65] Using the compilation of e^+e^- data from BARKOV 85.

$\rho(770)$ DECAY MODES

	Mode	Fraction (Γ_i/Γ)		Scale factor/ Confidence level
Γ_1	$\pi\pi$	~ 100	%	
	$\rho(770)^\pm$ decays			
Γ_2	$\pi^\pm\pi^0$	~ 100	%	
Γ_3	$\pi^\pm\gamma$	(4.5 ±0.5)	$\times 10^{-4}$	S=2.2
Γ_4	$\pi^\pm\eta$	< 6	$\times 10^{-3}$	CL=84%
Γ_5	$\pi^\pm\pi^+\pi^-\pi^0$	< 2.0	$\times 10^{-3}$	CL=84%
	$\rho(770)^0$ decays			
Γ_6	$\pi^+\pi^-$	~ 100	%	
Γ_7	$\pi^+\pi^-\gamma$	(9.9 ±1.6)	$\times 10^{-3}$	
Γ_8	$\pi^0\gamma$	(6.0 ±1.3)	$\times 10^{-4}$	S=1.1
Γ_9	$\eta\gamma$	(3.0 ±0.4)	$\times 10^{-4}$	S=1.4
Γ_{10}	$\pi^0\pi^0\gamma$	(4.5 ±0.8)	$\times 10^{-5}$	
Γ_{11}	$\mu^+\mu^-$	[a] (4.55±0.28)	$\times 10^{-5}$	
Γ_{12}	e^+e^-	[a] (4.67±0.09)	$\times 10^{-5}$	
Γ_{13}	$\pi^+\pi^-\pi^0$	$(1.01^{+0.54}_{-0.36} \pm 0.34)$	$\times 10^{-4}$	
Γ_{14}	$\pi^+\pi^-\pi^+\pi^-$	(1.8 ±0.9)	$\times 10^{-5}$	
Γ_{15}	$\pi^+\pi^-\pi^0\pi^0$	< 4	$\times 10^{-5}$	CL=90%

[a] The $\omega\rho$ interference is then due to $\omega\rho$ mixing only, and is expected to be small. If $e\mu$ universality holds, $\Gamma(\rho^0 \to \mu^+\mu^-) = \Gamma(\rho^0 \to e^+e^-) \times 0.99785$.

CONSTRAINED FIT INFORMATION

An overall fit to the total width and a partial width uses 10 measurements and one constraint to determine 3 parameters. The overall fit has a $\chi^2 = 10.7$ for 8 degrees of freedom.

The following *off-diagonal* array elements are the correlation coefficients $\langle \delta p_i \delta p_j \rangle / (\delta p_i \cdot \delta p_j)$, in percent, from the fit to parameters p_i, including the branching fractions, $x_i \equiv \Gamma_i / \Gamma_{\text{total}}$. The fit constrains the x_i whose labels appear in this array to sum to one.

x_3	−100		
Γ	15	−15	
	x_2	x_3	

	Mode	Rate (MeV)	Scale factor
Γ_2	$\pi^\pm\pi^0$	150.2 ±2.4	
Γ_3	$\pi^\pm\gamma$	0.068±0.007	2.3

CONSTRAINED FIT INFORMATION

An overall fit to the total width, a partial width, and 7 branching ratios uses 16 measurements and one constraint to determine 9 parameters. The overall fit has a $\chi^2 = 6.3$ for 8 degrees of freedom.

The following *off-diagonal* array elements are the correlation coefficients $\langle \delta p_i \delta p_j \rangle / (\delta p_i \cdot \delta p_j)$, in percent, from the fit to parameters p_i, including the branching fractions, $x_i \equiv \Gamma_i / \Gamma_{\text{total}}$. The fit constrains the x_i whose labels appear in this array to sum to one.

x_7	−100							
x_8	−8	0						
x_9	−2	0	1					
x_{10}	−1	0	0	0				
x_{11}	2	−3	0	0	0			
x_{12}	1	0	−9	−16	0	0		
x_{14}	−1	0	0	0	0	0	0	
Γ	−1	0	5	9	0	0	−55	0
	x_6	x_7	x_8	x_9	x_{10}	x_{11}	x_{12}	x_{14}

	Mode		Rate (MeV)		Scale factor
Γ_6	$\pi^+\pi^-$		148.7	±1.6	
Γ_7	$\pi^+\pi^-\gamma$		1.49	±0.24	
Γ_8	$\pi^0\gamma$		0.089	±0.019	1.1
Γ_9	$\eta\gamma$		0.044	±0.005	1.4
Γ_{10}	$\pi^0\pi^0\gamma$		0.0067	±0.0013	
Γ_{11}	$\mu^+\mu^-$	[a]	0.0068	±0.0004	
Γ_{12}	e^+e^-	[a]	0.00702	±0.00011	
Γ_{14}	$\pi^+\pi^-\pi^+\pi^-$		0.0027	±0.0014	

$\rho(770)$ PARTIAL WIDTHS

$\Gamma(\pi^\pm\gamma)$ Γ_3

VALUE (keV)		DOCUMENT ID		TECN	CHG	COMMENT
68	**±7**	**OUR FIT**	Error includes scale factor of 2.3.			
68	**±7**	**OUR AVERAGE**	Error includes scale factor of 2.2. See the ideogram below.			
81	±4 ±4	CAPRARO	87	SPEC	−	200 π^-A → $\pi^-\pi^0$A
59.8±4.0		HUSTON	86	SPEC	+	202 π^+A → $\pi^+\pi^0$A
71	±7	JENSEN	83	SPEC	−	156–260 π^-A → $\pi^-\pi^0$A

WEIGHTED AVERAGE
68±7 (Error scaled by 2.2)

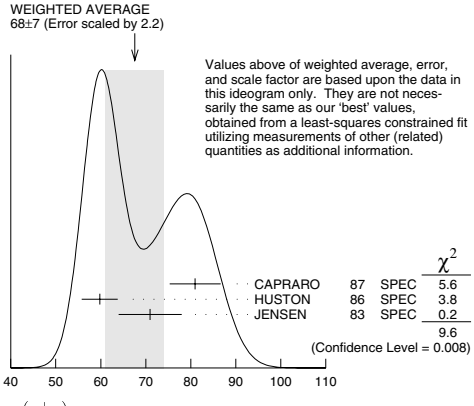

$\Gamma(e^+e^-)$ Γ_{12}

VALUE (keV)	EVTS	DOCUMENT ID		TECN	COMMENT
7.02±0.11 OUR FIT					
7.02±0.11 OUR AVERAGE					
7.06±0.11±0.05	114k	[66,67] AKHMETSHIN	04	CMD2	$e^+e^- \to \pi^+\pi^-$
6.77±0.10±0.30		BARKOV	85	OLYA	$e^+e^- \to \pi^+\pi^-$
• • • We do not use the following data for averages, fits, limits, etc. • • •					
6.3 ±0.1		[68] BENAYOUN	98	RVUE	$e^+e^- \to \pi^+\pi^-$, $\mu^+\mu^-$

$\Gamma(\pi^0\gamma)$ Γ_8

VALUE (keV)	EVTS	DOCUMENT ID		TECN	COMMENT
• • • We do not use the following data for averages, fits, limits, etc. • • •					
77±17±11	36500	[69] ACHASOV	03	SND	0.60–0.97 $e^+e^- \to \pi^0\gamma$
121±31		DOLINSKY	89	ND	$e^+e^- \to \pi^0\gamma$

$\Gamma(\eta\gamma)$ Γ_9

VALUE (keV)	DOCUMENT ID		TECN	COMMENT
• • • We do not use the following data for averages, fits, limits, etc. • • •				
62±17	[70] DOLINSKY	89	ND	$e^+e^- \to \eta\gamma$

$\Gamma(\pi^+\pi^-\pi^+\pi^-)$ Γ_{14}

VALUE (keV)	EVTS	DOCUMENT ID		TECN	COMMENT
• • • We do not use the following data for averages, fits, limits, etc. • • •					
2.8±1.4±0.5	153	AKHMETSHIN	00	CMD2	0.6–0.97 $e^+e^- \to \pi^+\pi^-\pi^+\pi^-$

[66] Using the GOUNARIS 68 parametrization with the complex phase of the ρ-ω interference.
[67] From a fit in the energy range 0.61 to 0.96 GeV. Update of AKHMETSHIN 02.
[68] Using the data of BARKOV 85 in the hidden local symmetry model.
[69] Using Γ_{total}= 147.9 ± 1.3 MeV and B($\rho \to \pi^0\gamma$) from ACHASOV 03.
[70] Solution corresponding to constructive ω-ρ interference.

$\rho(770)$ $\Gamma(i)\Gamma(e^+e^-)/\Gamma^2(\text{total})$

$\Gamma(e^+e^-) \times \Gamma(\eta\gamma)/\Gamma^2_{\text{total}}$ $\Gamma_{12}\Gamma_9/\Gamma^2$

VALUE (units 10^{-8})	EVTS	DOCUMENT ID		TECN	COMMENT
1.38±0.17 OUR FIT	Error includes scale factor of 1.4.				
1.36±0.15 OUR AVERAGE	Error includes scale factor of 1.3. See the ideogram below.				
1.61±0.20±0.11	23k	[73,74] AKHMETSHIN	01B	CMD2	$e^+e^- \to \eta\gamma$
1.21±0.14±0.04	312	[75] ACHASOV	00D	SND	$e^+e^- \to \eta\gamma$
1.85±0.49		[76] DOLINSKY	89	ND	$e^+e^- \to \eta\gamma$

Meson Particle Listings

$\rho(770)$

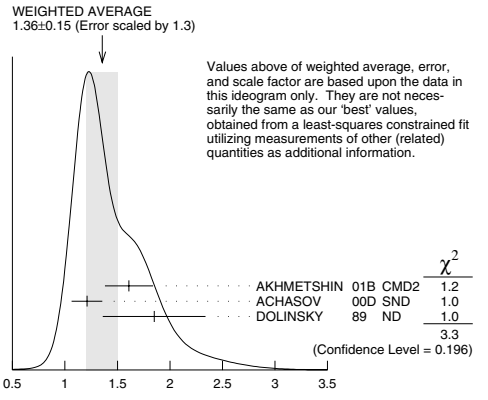

$\Gamma(e^+e^-) \times \Gamma(\eta\gamma)/\Gamma^2_{\rm total}$ $\Gamma_{12}\Gamma_9/\Gamma^2$

$\Gamma(e^+e^-) \times \Gamma(\pi^0\gamma)/\Gamma^2_{\rm total}$ $\Gamma_{12}\Gamma_8/\Gamma^2$

VALUE (units 10^{-8})	EVTS	DOCUMENT ID		TECN	COMMENT
2.8 ±0.6 OUR FIT Error includes scale factor of 1.1.					
2.8 ±0.6 OUR AVERAGE Error includes scale factor of 1.1.					
2.37±0.53±0.33	36500	[71] ACHASOV	03	SND	0.60–0.97 $e^+e^- \to \pi^0\gamma$
3.61±0.74±0.49	10625	[76] DOLINSKY	89	ND	$e^+e^- \to \pi^0\gamma$

[71] Using $\sigma_\phi \to \pi^0\gamma$ from ACHASOV 00 and m_ρ = 775.97 MeV in the model with the energy-independent phase of ρ-ω interference equal to $(-10.2 \pm 7.0)^\circ$.

$\Gamma(e^+e^-) \times \Gamma(\pi^+\pi^-\pi^0)/\Gamma^2_{\rm total}$ $\Gamma_{12}\Gamma_{13}/\Gamma^2$

VALUE (units 10^{-9})	EVTS	DOCUMENT ID		TECN	COMMENT
• • • We do not use the following data for averages, fits, limits, etc. • • •					
$4.58^{+2.46}_{-1.64}\pm1.56$	1.2M	[72] ACHASOV	03D	RVUE	0.44–2.00 $e^+e^- \to \pi^+\pi^-\pi^0$

[72] Statistical significance in less than 3σ.

[73] From the $\eta \to 3\pi^0$ decay and using $B(\eta \to 3\pi^0) = (32.24 \pm 0.29) \times 10^{-2}$.

[74] The combined fit from 600 to 1380 MeV taking into account $\rho(770)$, $\omega(782)$, $\phi(1020)$, and $\rho(1450)$ (mass and width fixed at 1450 MeV and 310 MeV respectively).

[75] From the $\eta \to 3\pi^0$ decay and using $B(\eta \to 3\pi^0) = (32.2 \pm 0.4) \times 10^{-2}$.

[76] Recalculated by us from the cross section in the peak.

$\rho(770)$ BRANCHING RATIOS

$\Gamma(\pi^\pm\eta)/\Gamma(\pi\pi)$ Γ_4/Γ_1

VALUE (units 10^{-4})	CL%	DOCUMENT ID		TECN	CHG	COMMENT
<60	84	FERBEL	66	HBC	±	$\pi^\pm p$ above 2.5

$\Gamma(\pi^\pm\pi^+\pi^-\pi^0)/\Gamma(\pi\pi)$ Γ_5/Γ_1

VALUE (units 10^{-4})	CL%	DOCUMENT ID		TECN	CHG	COMMENT
<20	84	FERBEL	66	HBC	±	$\pi^\pm p$ above 2.5
• • • We do not use the following data for averages, fits, limits, etc. • • •						
35 ±40		JAMES	66	HBC	+	2.1 $\pi^+ p$

$\Gamma(\mu^+\mu^-)/\Gamma(\pi^+\pi^-)$ Γ_{11}/Γ_6

VALUE (units 10^{-5})	DOCUMENT ID		TECN	COMMENT
4.60±0.28 OUR FIT				
4.6 ±0.2 ±0.2	ANTIPOV	89	SIGM	π^- Cu $\to \mu^+\mu^-\pi^-$ Cu
• • • We do not use the following data for averages, fits, limits, etc. • • •				
$8.2\ ^{+1.6}_{-3.6}$	[77] ROTHWELL	69	CNTR	Photoproduction
5.6 ±1.5	[78] WEHMANN	69	OSPK	12 π^- C, Fe
$9.7\ ^{+3.1}_{-3.3}$	[79] HYAMS	67	OSPK	11 π^- Li, H

$\Gamma(e^+e^-)/\Gamma(\pi\pi)$ Γ_{12}/Γ_1

VALUE (units 10^{-4})	DOCUMENT ID		TECN	COMMENT
• • • We do not use the following data for averages, fits, limits, etc. • • •				
0.40±0.05	[80] BENAKSAS	72	OSPK	$e^+e^- \to \pi^+\pi^-$

$\Gamma(\eta\gamma)/\Gamma_{\rm total}$ Γ_9/Γ

VALUE (units 10^{-4})	EVTS	DOCUMENT ID		TECN	CHG	COMMENT
3.0 ±0.4 OUR FIT Error includes scale factor of 1.4.						
3.6 ±0.9		[81] ANDREWS	77	CNTR	0	6.7–10 γ Cu
• • • We do not use the following data for averages, fits, limits, etc. • • •						
3.39±0.42±0.23		[81,82,83] AKHMETSHIN	01B	CMD2		$e^+e^- \to \eta\gamma$
2.69±0.32±0.16	312	[84] ACHASOV	00D	SND		$e^+e^- \to \eta\gamma$
$1.9\ ^{+0.6}_{-0.8}$		[85] BENAYOUN	96	RVUE		0.54-1.04 $e^+e^- \to \eta\gamma$
4.0 ±1.1		[81,86] DOLINSKY	89	ND		$e^+e^- \to \eta\gamma$

$\Gamma(\pi^+\pi^-\pi^+\pi^-)/\Gamma_{\rm total}$ Γ_{14}/Γ

VALUE (units 10^{-5})	CL%	EVTS	DOCUMENT ID		TECN	COMMENT
1.8±0.9 OUR FIT						
1.8±0.9±0.3		153	AKHMETSHIN	00	CMD2	0.6–0.97 $e^+e^- \to \pi^+\pi^-\pi^+\pi^-$
• • • We do not use the following data for averages, fits, limits, etc. • • •						
<20	90		KURDADZE	88	OLYA	$e^+e^- \to \pi^+\pi^-\pi^+\pi^-$

$\Gamma(\pi^+\pi^-\pi^+\pi^-)/\Gamma(\pi\pi)$ Γ_{14}/Γ_1

VALUE (units 10^{-4})	CL%	DOCUMENT ID		TECN	CHG	COMMENT
• • • We do not use the following data for averages, fits, limits, etc. • • •						
<15	90	ERBE	69	HBC	0	2.5–5.8 γp
<20		CHUNG	68	HBC	0	3.2,4.2 $\pi^- p$
<20	90	HUSON	68	HLBC	0	16.0 $\pi^- p$
<80		JAMES	66	HBC	0	2.1 $\pi^+ p$

$\Gamma(\pi^+\pi^-\pi^0)/\Gamma_{\rm total}$ Γ_{13}/Γ

VALUE (units 10^{-4})	CL%	EVTS	DOCUMENT ID		TECN	COMMENT
• • • We do not use the following data for averages, fits, limits, etc. • • •						
$1.01^{+0.54}_{-0.36}\pm0.34$	1.2M		[87] ACHASOV	03D	RVUE	0.44–2.00 $e^+e^- \to \pi^+\pi^-\pi^0$
<1.2	90		VASSERMAN	88B	ND	$e^+e^- \to \pi^+\pi^-\pi^0$

$\Gamma(\pi^+\pi^-\pi^0)/\Gamma(\pi\pi)$ Γ_{13}/Γ_1

VALUE	CL%	DOCUMENT ID		TECN	CHG	COMMENT
• • • We do not use the following data for averages, fits, limits, etc. • • •						
~ 0.01		BRAMON	86	RVUE	0	$J/\psi \to \omega\pi^0$
<0.01	84	[88] ABRAMS	71	HBC	0	3.7 $\pi^+ p$

$\Gamma(\pi^+\pi^-\pi^0\pi^0)/\Gamma_{\rm total}$ Γ_{15}/Γ

VALUE (units 10^{-4})	CL%	DOCUMENT ID		TECN	CHG	COMMENT
<0.4	90	AULCHENKO	87C	ND	0	$e^+e^- \to \pi^+\pi^-\pi^0\pi^0$
• • • We do not use the following data for averages, fits, limits, etc. • • •						
<2	90	KURDADZE	86	OLYA	0	$e^+e^- \to \pi^+\pi^-\pi^0\pi^0$

$\Gamma(\pi^+\pi^-\gamma)/\Gamma_{\rm total}$ Γ_7/Γ

VALUE	CL%	DOCUMENT ID		TECN	COMMENT
0.0099±0.0016 OUR FIT					
0.0099±0.0016		[89] DOLINSKY	91	ND	$e^+e^- \to \pi^+\pi^-\gamma$
• • • We do not use the following data for averages, fits, limits, etc. • • •					
0.0111±0.0014		[90] VASSERMAN	88	ND	$e^+e^- \to \pi^+\pi^-\gamma$
<0.005	90	[91] VASSERMAN	88	ND	$e^+e^- \to \pi^+\pi^-\gamma$

$\Gamma(\pi^0\gamma)/\Gamma_{\rm total}$ Γ_8/Γ

VALUE (units 10^{-4})	EVTS	DOCUMENT ID		TECN	COMMENT
• • • We do not use the following data for averages, fits, limits, etc. • • •					
5.22±1.17±0.75	36500	[92,93] ACHASOV	03	SND	0.60–0.97 $e^+e^- \to \pi^0\gamma$
6.8 ±1.7		[94] BENAYOUN	96	RVUE	0.54-1.04 $e^+e^- \to \pi^0\gamma$
7.9 ±2.0		[93] DOLINSKY	89	ND	$e^+e^- \to \pi^0\gamma$

$\Gamma(\pi^0\pi^0\gamma)/\Gamma_{\rm total}$ Γ_{10}/Γ

VALUE (units 10^{-5})	EVTS	DOCUMENT ID		TECN	COMMENT
4.5±0.8 OUR FIT					
$4.5^{+0.9}_{-0.8}$ OUR AVERAGE					
$5.2^{+1.5}_{-1.3}\pm0.6$	190	[95] AKHMETSHIN	04B	CMD2	0.6–0.97 $e^+e^- \to \pi^0\pi^0\gamma$
$4.1^{+1.0}_{-0.9}\pm0.3$	295	[96] ACHASOV	02F	SND	0.36–0.97 $e^+e^- \to \pi^0\pi^0\gamma$
• • • We do not use the following data for averages, fits, limits, etc. • • •					
$4.8^{+3.4}_{-1.8}\pm0.5$	63	[97] ACHASOV	00G	SND	$e^+e^- \to \pi^0\pi^0\gamma$

[77] Possibly large ρ-ω interference leads us to increase the minus error.

[78] Result contains 11 ± 11% correction using SU(3) for central value. The error on the correction takes account of possible ρ-ω interference and the upper limit agrees with the upper limit of $\omega \to \mu^+\mu^-$ from this experiment.

[79] HYAMS 67's mass resolution is 20 MeV. The ω region was excluded.

[80] The ρ' contribution is not taken into account.

[81] Solution corresponding to constructive ω-ρ interference.

[82] The combined fit from 600 to 1380 MeV taking into account $\rho(770)$, $\omega(782)$, $\phi(1020)$, and $\rho(1450)$ (mass and width fixed at 1450 MeV and 310 MeV respectively).

[83] Using $B(\rho \to e^+e^-) = (4.75 \pm 0.10) \times 10^{-5}$ from AKHMETSHIN 02 and $B(\eta \to 3\pi^0) = (32.24 \pm 0.29) \times 10^{-2}$.

[84] Using $B(\rho \to e^+e^-) = (4.49 \pm 0.22) \times 10^{-5}$ and $B(\eta \to 3\pi^0) = (32.2 \pm 0.4) \times 10^{-2}$.

[85] Reanalysis of DRUZHININ 84, DOLINSKY 89, and DOLINSKY 91 taking into account a triangle anomaly contribution. Constructive ρ-ω interference solution.

[86] Not independent of the corresponding $\Gamma(e^+e^-) \times \Gamma(\eta\gamma)/\Gamma^2_{\rm total}$.

[87] Statistical significance is less than 3σ.

[88] Model dependent, assumes I = 1, 2, or 3 for the 3π system.

[89] Bremsstrahlung from a decay pion and for photon energy above 50 MeV.
[90] Superseded by DOLINSKY 91.
[91] Structure radiation due to quark rearrangement in the decay.
[92] Using $B(\rho \to e^+e^-) = (4.54 \pm 0.10) \times 10^{-5}$.
[93] Not independent of the corresponding $\Gamma(e^+e^-) \times \Gamma(\pi^0\gamma)/\Gamma^2_{\text{total}}$.
[94] Reanalysis of DRUZHININ 84, DOLINSKY 89, and DOLINSKY 91 taking into account a triangle anomaly contribution.
[95] This branching ratio includes the conventional VMD mechanism $\rho \to \omega\pi^0$, $\omega \to \pi^0\gamma$, and the new decay mode $\rho \to f_0(600)\gamma$, $f_0(600) \to \pi^0\pi^0$ with a branching ratio $(2.0^{+1.1}_{-0.9} \pm 0.3) \times 10^{-5}$ differing from zero by 2.0 standard deviations.
[96] This branching ratio includes the conventional VMD mechanism $\rho \to \omega\pi^0$, $\omega \to \pi^0\gamma$ and the new decay mode $\rho \to f_0(600)\gamma$, $f_0(600) \to \pi^0\pi^0$ with a branching ratio $(1.9^{+0.9}_{-0.8} \pm 0.4) \times 10^{-5}$ differing from zero by 2.4 standard deviations. Supersedes ACHASOV 00G.
[97] Superseded by ACHASOV 02F.

$\rho(770)$ REFERENCES

AKHMETSHIN	04	PL B578 285	R.R. Akhmetshin *et al.*	(Novosibirsk CMD-2 Collab.)
AKHMETSHIN	04B	PL B580 119	R.R. Akhmetshin *et al.*	(Novosibirsk CMD-2 Collab.)
ACHASOV	03	PL B559 171	M.N. Achasov *et al.*	(Novosibirsk SND Collab.)
ACHASOV	03D	PR D68 052006	M.N. Achasov *et al.*	(Novosibirsk SND Collab.)
ALOISIO	03	PL B561 55	A. Aloisio *et al.*	(KLOE Collab.)
SANZ-CILLERO	03	EPJ C27 587	J.J. Sanz-Cillero, A. Pich	
ACHASOV	02	PR D65 032002	M.N. Achasov *et al.*	(Novosibirsk SND Collab.)
ACHASOV	02F	PL B537 201	M.N. Achasov *et al.*	(Novosibirsk SND Collab.)
AKHMETSHIN	02	PL B527 161	R.R. Akhmetshin *et al.*	(Novosibirsk CMD-2 Collab.)
AKHMETSHIN	01B	PL B509 217	R.R. Akhmetshin *et al.*	(Novosibirsk CMD-2 Collab.)
COLANGELO	01	NP B603 125	G. Colangelo, J. Gasser, H. Leytwyler	
PICH	01	PR D63 093005	A. Pich, J. Portoles	
ACHASOV	00	EPJ C12 25	M.N. Achasov *et al.*	(Novosibirsk SND Collab.)
ACHASOV	00D	JETPL 72 282 Translated from ZETFP 72 411.	M.N. Achasov *et al.*	(Novosibirsk SND Collab.)
ACHASOV	00G	JETPL 71 355 Translated from ZETFP 71 519.	M.N. Achasov *et al.*	(Novosibirsk SND Collab.)
AKHMETSHIN	00	PL B475 190	R.R. Akhmetshin *et al.*	(Novosibirsk CMD-2 Collab.)
ANDERSON	00A	PR D61 112002	S. Anderson *et al.*	(CLEO Collab.)
ABELE	99E	PL B469 270	A. Abele *et al.*	(Crystal Barrel Collab.)
BENAYOUN	98	EPJ C2 269	M. Benayoun *et al.*	(IPNP, NOVO, ADLD+)
BREITWEG	98B	EPJ C2 247	J. Breitweg *et al.*	(ZEUS Collab.)
GARDNER	98	PR D57 2716	S. Gardner, H.B. O'Connell	
Also	00A	PR D62 019903 (errata)	S. Gardner, H.B. O'Connell	
ABELE	97	PL B391 191	A. Abele *et al.*	(Crystal Barrel Collab.)
ADAMS	97	ZPHY C74 237	M.R. Adams *et al.*	(E665 Collab.)
BARATE	97M	ZPHY C76 15	R. Barate *et al.*	(ALEPH Collab.)
BERTIN	97C	PL B408 476	A. Bertin *et al.*	(OBELIX Collab.)
BOGOLYUB...	97	PAN 60 46 Translated from YAF 60 53.	M.Y. Bogolyubsky *et al.*	(MOSU, SERP)
O'CONNELL	97	NP A623 559	H.B. O'Connell *et al.*	(ADLD)
BENAYOUN	96	ZPHY C72 221	M. Benayoun *et al.*	(IPNP, NOVO)
BERNICHA	94	PR D50 4454	A. Bernicha, G. Lopez Castro, J. Pestieau	(LOUV+)
WEIDENAUER	93	ZPHY C59 387	P. Weidenauer *et al.*	(ASTERIX Collab.)
AGUILAR-...	91	ZPHY C50 405	M. Aguilar-Benitez *et al.*	(LEBC-EHS Collab.)
DOLINSKY	91	PRPL 202 99	S.I. Dolinsky *et al.*	(NOVO)
ANTIPOV	89	ZPHY C42 185	Y.M. Antipov *et al.*	(SERP, JINR, BGNA+)
DOLINSKY	89	ZPHY C42 511	S.I. Dolinsky *et al.*	(NOVO)
DUBNICKA	89	JPG 15 1349	S. Dubnicka *et al.*	(JINR, SLOV)
GESHKEN...	89	ZPHY C45 351	B.V. Geshkenbein	(ITEP)
KURDADZE	88	JETPL 47 512 Translated from ZETFP 47 432.	L.M. Kurdadze *et al.*	(NOVO)
VASSERMAN	88	SJNP 47 1035 Translated from YAF 47 1635.	I.B. Vasserman *et al.*	(NOVO)
VASSERMAN	88B	SJNP 48 480 Translated from YAF 48 753.	I.B. Vasserman *et al.*	(NOVO)
AULCHENKO	87C	IYF 87-90 Preprint	V.M. Aulchenko *et al.*	(NOVO)
CAPRARO	87	NP B288 659	L. Capraro *et al.*	(CLER, FRAS, MILA+)
BRAMON	86	PL B173 97	A. Bramon, J. Casulleras	(BARC)
HUSTON	86	PR 33 3199	J. Huston *et al.*	(ROCH, FNAL, MINN)
KURDADZE	86	JETPL 43 643 Translated from ZETFP 43 497.	L.M. Kurdadze *et al.*	(NOVO)
BARKOV	85	NP B256 365	L.M. Barkov *et al.*	(NOVO)
DRUZHININ	84	PL 144B 136	V.P. Druzhinin *et al.*	(NOVO)
CHABAUD	83	NP B223 1	V. Chabaud *et al.*	(CERN, CRAC, MPIM)
JENSEN	83	PR D27 26	T. Jensen *et al.*	(ROCH, FNAL, MINN)
HEYN	81	ZPHY C7 169	M.F. Heyn, C.B. Lang	(GRAZ)
BOHACIK	80	PR D21 1342	J. Bohacik, H. Kuhnelt	(SLOV, WIEN)
LANG	79	PR D19 956	C.B. Lang, A. Mas-Parareda	(GRAZ)
BARTALUCCI	78	NC 44A 587	S. Bartalucci *et al.*	(DESY, FRAS)
WICKLUND	78	PR D17 1197	A.B. Wicklund *et al.*	(ANL)
ANDREWS	77	PRL 38 198	D.E. Andrews *et al.*	(ROCH)
DEUTSCH...	76	NP B103 426	M. Deutschmann *et al.*	(AACH3, BERL, BONN+)
ENGLER	74	PR D10 2070	A. Engler *et al.*	(CMU, CASE)
ESTABROOKS	74	NP B79 301	P.G. Estabrooks, A.D. Martin	(DURH)
GRAYER	74	NP B75 189	G. Grayer *et al.*	(CERN, MPIM)
BYERLY	73	PR D7 637	W.L. Byerly *et al.*	(MICH)
GLADDING	73	PR D8 3721	G.E. Gladding *et al.*	(HARV)
HYAMS	73	NP B64 134	B.D. Hyams *et al.*	(CERN, MPIM)
PROTOPOP...	73	PR D7 1279	S.D. Protopopescu *et al.*	(LBL)
BALLAM	72	PR D5 545	J. Ballam *et al.*	(SLAC, LBL, TUFTS)
BENAKSAS	72	PL 39B 289	D. Benaksas *et al.*	(ORSAY)
JACOBS	72	PR D6 1291	L.D. Jacobs	(SACL)
RATCLIFF	72	PL 38B 345	B.N. Ratcliff *et al.*	(SLAC)
ABRAMS	71	PR D4 653	G.S. Abrams *et al.*	(LBL)
ALVENSLEB...	70	PRL 24 786	H. Alvensleben *et al.*	(DESY)
BIGGS	70	PRL 24 1197	P.J. Biggs *et al.*	(DARE)
ERBE	69	PR 188 2060	R. Erbe *et al.*	(German Bubble Chamber Collab.)
MALAMUD	69	Argonne Conf. 93	E.I. Malamud, P.E. Schlein	(UCLA)
REYNOLDS	69	PR 184 1424	B.G. Reynolds *et al.*	(FSU)
ROTHWELL	69	PRL 23 1521	P.L. Rothwell *et al.*	(NEAS)
WEHMANN	69	PR 178 2095	A.A. Wehmann *et al.*	(HARV, CASE, SLAC+)
ARMENISE	68	NC 54A 999	N. Armenise *et al.*	(BARI, BGNA, FIRZ+)
BATON	68	PR 176 1574	J.P. Baton, G. Laurens	(SACL)
CHUNG	68	PR 165 1491	S.U. Chung *et al.*	(LRL)
FOSTER	68	NP B6 107	M. Foster *et al.*	(CERN, CDEF)
GOUNARIS	68	PRL 21 244	G.J. Gounaris, J.J. Sakurai	
HUSON	68	PL 28B 208	R. Huson *et al.*	(ORSAY, MILA, UCLA)
HYAMS	68	NP B7 1	B.D. Hyams *et al.*	(CERN, MPIM)
LANZEROTTI	68	PR 166 1365	L.J. Lanzerotti *et al.*	(HARV)
PISUT	68	NP B6 325	J. Pisut, M. Roos	(CERN)
ASBURY	67B	PRL 19 865	J.G. Asbury *et al.*	(DESY, COLU)
BACON	67	PR 157 1263	T.C. Bacon *et al.*	(BNL)
EISNER	67	PR 164 1699	R.L. Eisner *et al.*	(PURD)
HUWE	67	PL 24B 252	D.O. Huwe *et al.*	(COLU)
HYAMS	67	PL 24B 634	B.D. Hyams *et al.*	(CERN, MPIM)
MILLER	67B	PR 153 1423	D.H. Miller *et al.*	(PURD)
ALFF-...	66	PR 145 1072	C. Alff-Steinberger *et al.*	(COLU, RUTG)
FERBEL	66	PL 21 111	T. Ferbel	(ROCH)
HAGOPIAN	66	PR 145 1128	V. Hagopian *et al.*	(PENN, SACL)
HAGOPIAN	66B	PR 152 1183	V. Hagopian, Y.L. Pan	(PENN, LRL)
JACOBS	66B	UCRL 16877	L.D. Jacobs	(LRL)
JAMES	66	PR 142 896	F.E. James, H.L. Kraybill	(YALE, BNL)
ROSS	66	PR 149 1172	M. Ross, L. Stodolsky	
SOEDING	66	PL B19 702	P. Soeding	
WEST	66	PR 149 1089	E. West *et al.*	(WISC)
BLIEDEN	65	PL 19 444	H.R. Blieden *et al.*	
CARMONY	64	PRL 12 254	D.D. Carmony *et al.*	(UCB)
GOLDHABER	64	PRL 12 336	G. Goldhaber *et al.*	(LRL, UCB)
ABOLINS	63	PRL 11 381	M.A. Abolins *et al.*	(UCSD)

OTHER RELATED PAPERS

GHOZZI	04	PL B583 222	S. Ghozzi, F. Jegerlehner	
ACHASOV	03C	JETP 96 789 Translated from ZETF 123 899.	M.N. Achasov *et al.*	(Novosibirsk SND Collab.)
AZIMOV	03	EPJ A16 209	Ya.I. Azimov	
BENAYOUN	03	EPJ C29 397	M. Benayoun *et al.*	
BENAYOUN	03B	EPJ C31 525	M. Benayoun *et al.*	
DAVIER	03	EPJ C27 497	M. Davier *et al.*	
DAVIER	03B	EPJ C31 503	M. Davier *et al.*	
DAVIER	02	hep-ex/0211057	M. Davier *et al.*	
BENAYOUN	01	EPJ C22 503	M. Benayoun, H.B. O'Connell	
CIRIGLIANO	01	PL B513 361	V. Cirigliano, G. Ecker, H. Neufeld	
CZYZ	01	EPJ C18 497	H. Czyz, J.J. Kuhn	
EIDELMAN	01	NPBPS 98 281	S. Eidelman	
FEUILLAT	01	PL B501 37	M. Feuillat, J.L. Lucio, M.J. Pestieau	
GOKALP	01B	EPJ C22 327	A. Gokalp, Y. Sarac, O. Yilmaz	
MELNIKOV	01	IJMP A16 4591	K. Melnikov	
ADLOFF	00F	EPJ C13 371	C. Adloff *et al.*	(H1 Collab.)
ACHASOV	99F	JETPL 69 7	M.N. Achasov, N.N. Achasov	
ACKERSTAFF	99F	EPJ C7 571	K. Ackerstaff *et al.*	
BENAYOUN	99	PR D59 074020	M. Benayoun *et al.*	
EIDELMAN	99	NPBPS 76 319	S. Eidelman, V. Ivanchenko	
MARCO	99	PL B470 20	E. Marco *et al.*	
ROOS	99	APS 49 N2 vii	M. Roos	
ALEMANY	98	EPJ C2 123	R. Alemany *et al.*	
ABELE	97B	PL B402 195	A. Abele *et al.*	(Crystal Barrel Collab.)
ABELE	97F	PL B411 354	A. Abele *et al.*	(Crystal Barrel Collab.)
BIJNENS	96	PL B374 210	J. Bijnens *et al.*	(NORD, BERN, WIEN+)
BENAYOUN	93	ZPHY C58 31	M. Benayoun *et al.*	(CDEF, CERN, BARI)
LAFFERTY	93	ZPHY C60 659	G.D. Lafferty	(MCHS)
KAMAL	92	PL B284 421	A.N. Kamal, Q.P. Xu	(ALBE)
KUHN	90	ZPHY C48 445	J.H. Kuhn *et al.*	(MPIM)
ERKAL	85	ZPHY C29 485	C. Erkal, M.G. Olsson	(WISC)
RYBICKI	85	ZPHY C28 65	K. Rybicki, I. Sakrejda	(CRAC)
KURDADZE	83	JETPL 37 733 Translated from ZETFP 37 613.	L.M. Kurdadze *et al.*	(NOVO)
ALEKSEEV	82	JETP 55 591 Translated from ZETF 82 1007.	E.A. Alekseeva *et al.*	(KIAE)
KENNEY	62	PR 126 736	V.P. Kenney, W.D. Shephard, C.D. Gall	(KNTY)
SAMIOS	62	PRL 9 139	N.P. Samios *et al.*	(BNL, CUNY, COLU+)
XUONG	62	PR 128 1849	H. Nguyen Ngoc, G.R. Lynch	(LRL)
ANDERSON	61	PRL 6 365	J.A. Anderson *et al.*	(LRL)
ERWIN	61	PRL 6 628	A.R. Erwin *et al.*	(WISC)

$\omega(782)$

$I^G(J^{PC}) = 0^-(1^{--})$

$\omega(782)$ MASS

VALUE (MeV)	*EVTS*	*DOCUMENT ID*		*TECN*	*COMMENT*
782.59±0.11 OUR AVERAGE		Error includes scale factor of 1.7. See the ideogram below.			
782.68±0.09±0.04	11200	[1] AKHMETSHIN	04	CMD2	$e^+e^- \to \pi^+\pi^-\pi^0$
782.79±0.08±0.09	1.2M	[2] ACHASOV	03D	RVUE	0.44–2.00 $e^+e^- \to \pi^+\pi^-\pi^0$
782.7 ±0.1 ±1.5	19500	WURZINGER	95	SPEC	1.33 $pd \to {}^3\text{He}\omega$
781.96±0.17±0.80	11k	[3] AMSLER	94C	CBAR	0.0 $\overline{p}p \to \omega\eta\pi^0$
782.08±0.36±0.82	3463	[4] AMSLER	94C	CBAR	0.0 $\overline{p}p \to \omega\eta\pi^0$
781.96±0.13±0.17	15k	AMSLER	93B	CBAR	0.0 $\overline{p}p \to \omega\pi^0\pi^0$
782.4 ±0.2	270k	WEIDENAUER	93	ASTE	$\overline{p}p \to 2\pi^+2\pi^-\pi^0$
782.2 ±0.4	1488	KURDADZE	83B	OLYA	$e^+e^- \to \pi^+\pi^-\pi^0$
782.4 ±0.5	7000	[5] KEYNE	76	CNTR	$\pi^- p \to \omega n$
• • • We do not use the following data for averages, fits, limits, etc. • • •					
781.78±0.10		[6] BARKOV	87	CMD	$e^+e^- \to \pi^+\pi^-\pi^0$
783.3 ±0.4	433	CORDIER	80	DM1	$e^+e^- \to \pi^+\pi^-\pi^0$
782.5 ±0.8	33260	ROOS	80	RVUE	0.0–3.6 $\overline{p}p$
782.6 ±0.8	3000	BENKHEIRI	79	OMEG	9–12 π^+p
781.8 ±0.6	1430	COOPER	78B	HBC	0.7–0.8 $\overline{p}p \to 5\pi$
782.7 ±0.9	535	VANAPEL...	78	HBC	7.2 $\overline{p}p \to \overline{p}p\omega$
783.5 ±0.8	2100	GESSAROLI	77	HBC	11 $\pi^- p \to \omega n$
782.5 ±0.8	418	AGUILAR-...	72B	HBC	3.9,4.6 $K^- p$
783.4 ±1.0	248	BIZZARRI	71	HBC	0.0 $p\overline{p} \to K^+K^-\omega$
781.0 ±0.6	510	BIZZARRI	71	HBC	0.0 $p\overline{p} \to K_1K_1\omega$
783.7 ±1.0	3583	[7] COYNE	71	HBC	3.7 $\pi^+p \to p\pi^+\pi^+\pi^-\pi^0$
784.1 ±1.2	750	ABRAMOVI...	70	HBC	3.9 $\pi^- p$
783.2 ±1.6		[8] BIGGS	70B	CNTR	$<4.1\ \gamma C \to \pi^+\pi^- C$
782.4 ±0.5	2400	BIZZARRI	69	HBC	0.0 $\overline{p}p$

[1] Update of AKHMETSHIN 00C.
[2] From the combined fit of ANTONELLI 92, ACHASOV 01E, ACHASOV 02E, and ACHASOV 03D data on the $\pi^+\pi^-\pi^0$ and ANTONELLI 92 on the $\omega\pi^+\pi^-$ final states. Supersedes ACHASOV 99E and ACHASOV 02E.
[3] From the $\eta \to \gamma\gamma$ decay.
[4] From the $\eta \to 3\pi^0$ decay.
[5] Observed by threshold-crossing technique. Mass resolution = 4.8 MeV FWHM.
[6] Systematic uncertainties underestimated.
[7] From best-resolution sample of COYNE 71.
[8] From ω-ρ interference in the $\pi^+\pi^-$ mass spectrum assuming ω width 12.6 MeV.

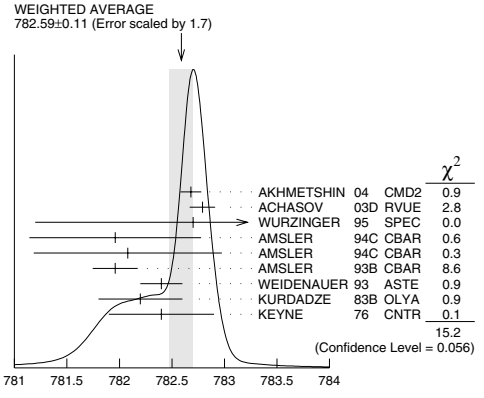

ω(782) WIDTH

VALUE (MeV)	EVTS	DOCUMENT ID		TECN	COMMENT
8.49±0.08 OUR AVERAGE					
8.68±0.23±0.10	11200	[9] AKHMETSHIN	04 CMD2		$e^+e^- \to \pi^+\pi^-\pi^0$
8.68±0.04±0.15	1.2M	[10] ACHASOV	03D RVUE		0.44–2.00 $e^+e^- \to \pi^+\pi^-\pi^0$
8.2 ±0.3	19500	WURZINGER	95 SPEC		1.33 $pd \to {}^3\mathrm{He}\omega$
8.4 ±0.1		[11] AULCHENKO	87 ND		$e^+e^- \to \pi^+\pi^-\pi^0$
8.30±0.40		BARKOV	87 CMD		$e^+e^- \to \pi^+\pi^-\pi^0$
9.8 ±0.9	1488	KURDADZE	83B OLYA		$e^+e^- \to \pi^+\pi^-\pi^0$
9.0 ±0.8	433	CORDIER	80 DM1		$e^+e^- \to \pi^+\pi^-\pi^0$
9.1 ±0.8	451	BENAKSAS	72B OSPK		$e^+e^- \to \pi^+\pi^-\pi^0$
• • • We do not use the following data for averages, fits, limits, etc. • • •					
12 ±2	1430	COOPER	78B HBC		0.7–0.8 $\bar{p}p \to 5\pi$
9.4 ±2.5	2100	GESSAROLI	77 HBC		11 $\pi^- p \to \omega n$
10.22±0.43	20000	[12] KEYNE	76 CNTR		$\pi^- p \to \omega n$
13.3 ±2	418	AGUILAR-...	72B HBC		3.9,4.6 $K^- p$
10.5 ±1.5		BORENSTEIN	72 HBC		2.18 $K^- p$
7.70±0.9 ±1.15	940	BROWN	72 MMS		2.5 $\pi^- p \to n\mathrm{MM}$
10.3 ±1.4	510	BIZZARRI	71 HBC		0.0 $p\bar{p} \to K_1 K_1 \omega$
12.8 ±3.0	248	BIZZARRI	71 HBC		0.0 $p\bar{p} \to K^+K^-\omega$
9.5 ±1.0	3583	COYNE	71 HBC		3.7 $\pi^+ p \to p\pi^+\pi^+\pi^-\pi^0$

[9] Update of AKHMETSHIN 00C.
[10] From the combined fit of ANTONELLI 92, ACHASOV 01E, ACHASOV 02E, and ACHASOV 03D data on the $\pi^+\pi^-\pi^0$ and ANTONELLI 92 on the $\omega\pi^+\pi^-$ final states. Supersedes ACHASOV 99E and ACHASOV 02E.
[11] Relativistic Breit-Wigner includes radiative corrections.
[12] Observed by threshold-crossing technique. Mass resolution = 4.8 MeV FWHM.

ω(782) DECAY MODES

	Mode	Fraction (Γ_j/Γ)	Scale factor/ Confidence level
Γ_1	$\pi^+\pi^-\pi^0$	(89.1 ±0.7) %	S=1.1
Γ_2	$\pi^0\gamma$	($8.92^{+0.28}_{-0.24}$) %	S=1.1
Γ_3	$\pi^+\pi^-$	(1.70±0.27) %	S=1.4
Γ_4	neutrals (excluding $\pi^0\gamma$)	($1.4^{+7.0}_{-0.9}$) $\times 10^{-3}$	
Γ_5	$\eta\gamma$	(4.9 ±0.5) $\times 10^{-4}$	
Γ_6	$\pi^0 e^+e^-$	(5.9 ±1.9) $\times 10^{-4}$	
Γ_7	$\pi^0\mu^+\mu^-$	(9.6 ±2.3) $\times 10^{-5}$	
Γ_8	e^+e^-	(7.14±0.13) $\times 10^{-5}$	S=1.1
Γ_9	$\pi^+\pi^-\pi^0\pi^0$	< 2 %	CL=90%
Γ_{10}	$\pi^+\pi^-\gamma$	< 3.6 $\times 10^{-3}$	CL=95%
Γ_{11}	$\pi^+\pi^-\pi^+\pi^-$	< 1 $\times 10^{-3}$	CL=90%
Γ_{12}	$\pi^0\pi^0\gamma$	(6.7 ±1.1) $\times 10^{-5}$	
Γ_{13}	$\eta\pi^0\gamma$	< 3.3 $\times 10^{-5}$	CL=90%
Γ_{14}	$\mu^+\mu^-$	(9.0 ±3.1) $\times 10^{-5}$	
Γ_{15}	3γ	< 1.9 $\times 10^{-4}$	CL=95%

Charge conjugation (C) violating modes

Γ_{16}	$\eta\pi^0$	C	< 1	$\times 10^{-3}$	CL=90%
Γ_{17}	$3\pi^0$	C	< 3	$\times 10^{-4}$	CL=90%

CONSTRAINED FIT INFORMATION

An overall fit to 15 branching ratios uses 43 measurements and one constraint to determine 10 parameters. The overall fit has a $\chi^2 = 30.7$ for 34 degrees of freedom.

The following *off-diagonal* array elements are the correlation coefficients $\langle \delta x_i \delta x_j \rangle / (\delta x_i \cdot \delta x_j)$, in percent, from the fit to the branching fractions, $x_i \equiv \Gamma_i/\Gamma_{\mathrm{total}}$. The fit constrains the x_i whose labels appear in this array to sum to one.

	x_1	x_2	x_3	x_4	x_5	x_6	x_7	x_8	x_{12}
x_2	27								
x_3	−36	−10							
x_4	−88	−56	1						
x_5	6	7	−2	−8					
x_6	−3	−1	0	0	0				
x_7	0	0	0	0	0	0			
x_8	−43	−50	16	52	−15	1	0		
x_{12}	1	3	0	−2	0	0	0	−2	
x_{14}	0	0	0	0	0	0	0	0	0

ω(782) PARTIAL WIDTHS

$\Gamma(e^+e^-)$ Γ_8

VALUE (keV)	EVTS	DOCUMENT ID		TECN	COMMENT
0.60 ±0.02 OUR EVALUATION					
• • • We do not use the following data for averages, fits, limits, etc. • • •					
0.591±0.015	11200	[13,14] AKHMETSHIN	04 CMD2		$e^+e^- \to \pi^+\pi^-\pi^0$
0.653±0.003±0.021	1.2M	[15] ACHASOV	03D RVUE		0.44–2.00 $e^+e^- \to \pi^+\pi^-\pi^0$
0.600±0.031	10625	DOLINSKY	89 ND		$e^+e^- \to \pi^0\gamma$

[13] Using $B(\omega \to \pi^+\pi^-\pi^0) = 0.891 \pm 0.007$ and $\Gamma_{\mathrm{total}} = 8.44 \pm 0.09$ MeV.
[14] Update of AKHMETSHIN 00C.
[15] Using ACHASOV 03, ACHASOV 03D and $B(\omega \to \pi^+\pi^-) = (1.70 \pm 0.28)\%$.

$\Gamma(\pi^0\gamma)$ Γ_2

VALUE (keV)	EVTS	DOCUMENT ID		TECN	COMMENT
• • • We do not use the following data for averages, fits, limits, etc. • • •					
788±12±27	36500	[16] ACHASOV	03 SND		0.60–0.97 $e^+e^- \to \pi^0\gamma$
764±51	10625	DOLINSKY	89 ND		$e^+e^- \to \pi^0\gamma$

[16] Using $\Gamma_\omega = 8.44 \pm 0.09$ MeV and $B(\omega \to \pi^0\gamma)$ from ACHASOV 03.

$\Gamma(\eta\gamma)$ Γ_5

VALUE (keV)	DOCUMENT ID		TECN	COMMENT
• • • We do not use the following data for averages, fits, limits, etc. • • •				
6.1±2.5	[17] DOLINSKY	89 ND		$e^+e^- \to \eta\gamma$

[17] Using $\Gamma_\omega = 8.4 \pm 0.1$ MeV and $B(\omega \to \eta\gamma)$ from DOLINSKY 89.

ω(782) Γ(i)Γ(e⁺e⁻)/Γ²(total)

$\Gamma(e^+e^-) \times \Gamma(\pi^+\pi^-\pi^0)/\Gamma^2_{\mathrm{total}}$ $\Gamma_8\Gamma_1/\Gamma^2$

VALUE (units 10^{-5})	EVTS	DOCUMENT ID		TECN	COMMENT
6.36±0.10 OUR FIT Error includes scale factor of 1.1.					
6.35±0.10 OUR AVERAGE Error includes scale factor of 1.1.					
6.24±0.11±0.08	11200	[18] AKHMETSHIN	04 CMD2		$e^+e^- \to \pi^+\pi^-\pi^0$
6.74±0.04±0.24	1.2M	[19,20] ACHASOV	03D RVUE		0.44–2.00 $e^+e^- \to \pi^+\pi^-\pi^0$
6.37±0.35		[19] DOLINSKY	89 ND		$e^+e^- \to \pi^+\pi^-\pi^0$
6.45±0.24		[19] BARKOV	87 CMD		$e^+e^- \to \pi^+\pi^-\pi^0$
5.79±0.42	1488	[19] KURDADZE	83B OLYA		$e^+e^- \to \pi^+\pi^-\pi^0$
5.89±0.54	433	[19] CORDIER	80 DM1		$e^+e^- \to \pi^+\pi^-\pi^0$
7.54±0.84	451	[19] BENAKSAS	72B OSPK		$e^+e^- \to \pi^+\pi^-\pi^0$

$\Gamma(e^+e^-) \times \Gamma(\pi^0\gamma)/\Gamma^2_{\mathrm{total}}$ $\Gamma_8\Gamma_2/\Gamma^2$

VALUE (units 10^{-6})	EVTS	DOCUMENT ID		TECN	COMMENT
$6.37^{+0.17}_{-0.15}$ OUR FIT					
6.44±0.18 OUR AVERAGE					
6.50±0.11±0.20	36500	[21] ACHASOV	03 SND		0.60–0.97 $e^+e^- \to \pi^0\gamma$
6.34±0.21±0.21	10625	[19] DOLINSKY	89 ND		$e^+e^- \to \pi^0\gamma$

$\Gamma(e^+e^-) \times \Gamma(\eta\gamma)/\Gamma^2_{\text{total}}$ $\Gamma_8\Gamma_5/\Gamma^2$

VALUE (units 10^{-8})	EVTS	DOCUMENT ID		TECN	COMMENT
3.53±0.35 OUR FIT					
3.3 ±0.4 OUR AVERAGE					
3.41±0.52±0.21	23k	[22,23] AKHMETSHIN	01B	CMD2	$e^+e^- \to \eta\gamma$
3.25±0.51±0.10	312	[24] ACHASOV	00D	SND	$e^+e^- \to \eta\gamma$

[18] Update of AKHMETSHIN 00C.
[19] Recalculated by us from the cross section in the peak.
[20] From the combined fit of ANTONELLI 92, ACHASOV 01E, ACHASOV 02E, and ACHASOV 03D data on the $\pi^+\pi^-\pi^0$ and ANTONELLI 92 on the $\omega\pi^+\pi^-$ final states. Supersedes ACHASOV 99E and ACHASOV 02E.
[21] Using $\sigma_{\phi\to\pi^0\gamma}$ from ACHASOV 00 and m_ω= 782.57 MeV in the model with the energy-independent phase of ρ-ω interference equal to $(-10.2 \pm 7.0)^\circ$.
[22] From the $\eta \to 3\pi^0$ decay and using B($\eta \to 3\pi^0$)= $(32.24 \pm 0.29) \times 10^{-2}$.
[23] The combined fit from 600 to 1380 MeV taking into account $\rho(770)$, $\omega(782)$, $\phi(1020)$, and $\rho(1450)$ (mass and width fixed at 1450 MeV and 310 MeV respectively).
[24] From the $\eta \to 3\pi^0$ decay and using B($\eta \to 3\pi^0$) = $(32.2 \pm 0.4) \times 10^{-2}$.

$\omega(782)$ BRANCHING RATIOS

$\Gamma(\text{neutrals})/\Gamma(\pi^+\pi^-\pi^0)$ $(\Gamma_2+\Gamma_4)/\Gamma_1$

VALUE	EVTS	DOCUMENT ID		TECN	COMMENT
0.102±0.008 OUR FIT					
0.103$^{+0.011}_{-0.010}$ OUR AVERAGE					
0.15 ±0.04	46	AGUILAR-...	72B	HBC	3.9,4.6 K^-p
0.10 ±0.03	19	BARASH	67B	HBC	0.0 $\overline{p}p$
0.134±0.026	850	DIGIUGNO	66B	CNTR	1.4 π^-p
0.097±0.016	348	FLATTE	66	HBC	1.4 – 1.7 $K^-p \to \Lambda$MM
0.06 $^{+0.05}_{-0.02}$		JAMES	66	HBC	2.1 π^+p
0.08 ±0.03	35	KRAEMER	64	DBC	1.2 π^+d
• • • We do not use the following data for averages, fits, limits, etc. • • •					
0.11 ±0.02	20	BUSCHBECK	63	HBC	1.5 K^-p

$\Gamma(\pi^+\pi^-)/\Gamma(\pi^+\pi^-\pi^0)$ Γ_3/Γ_1

See also $\Gamma(\pi^+\pi^-)/\Gamma_{\text{total}}$.

VALUE	DOCUMENT ID		TECN	COMMENT
0.0191±0.0030 OUR FIT Error includes scale factor of 1.4.				
0.026 ±0.005 OUR AVERAGE				
0.021 $^{+0.028}_{-0.009}$	[26] RATCLIFF	72	ASPK	15 $\pi^-p \to n2\pi$
0.028 ±0.006	BEHREND	71	ASPK	Photoproduction
0.022 $^{+0.009}_{-0.01}$	[27] ROOS	70	RVUE	

$\Gamma(\pi^0\gamma)/\Gamma(\pi^+\pi^-\pi^0)$ Γ_2/Γ_1

VALUE	EVTS	DOCUMENT ID		TECN	COMMENT
0.1001$^{+0.0031}_{-0.0026}$ OUR FIT Error includes scale factor of 1.1.					
0.097 ±0.005 OUR AVERAGE					
0.0994±0.0036±0.0038		[28] AULCHENKO	00A	SND	$e^+e^- \to \pi^+\pi^-\pi^0\pi^0$, $\pi^0\pi^0\gamma$
0.084 ±0.013		KEYNE	76	CNTR	$\pi^-p \to \omega n$
0.109 ±0.025		BENAKSAS	72C	OSPK	$e^+e^- \to \pi^0\gamma$
0.081 ±0.020		BALDIN	71	HLBC	2.9 π^+p
0.13 ±0.04		JACQUET	69B	HLBC	2.05 $\pi^+p \to \pi^+p\omega$
• • • We do not use the following data for averages, fits, limits, etc. • • •					
0.097 ±0.002 ±0.005	1.2M	[29,30] ACHASOV	03D	RVUE	0.44–2.00 $e^+e^- \to \pi^+\pi^-\pi^0$
0.099 ±0.007		[29] DOLINSKY	89	ND	$e^+e^- \to \pi^0\gamma$

$\Gamma(\pi^+\pi^-\gamma)/\Gamma(\pi^+\pi^-\pi^0)$ Γ_{10}/Γ_1

VALUE	CL%	DOCUMENT ID		TECN	COMMENT
• • • We do not use the following data for averages, fits, limits, etc. • • •					
<0.066	90	KALBFLEISCH	75	HBC	2.18 $K^-p \to \Lambda\pi^+\pi^-\gamma$
<0.05	90	FLATTE	66	HBC	1.2 – 1.7 $K^-p \to \Lambda\pi^+\pi^-\gamma$

$\Gamma(\pi^+\pi^-\gamma)/\Gamma_{\text{total}}$ Γ_{10}/Γ

VALUE	CL%	DOCUMENT ID		TECN	COMMENT
<0.0036	95	WEIDENAUER	90	ASTE	$p\overline{p} \to \pi^+\pi^-\pi^+\pi^-\gamma$
• • • We do not use the following data for averages, fits, limits, etc. • • •					
<0.004	95	BITYUKOV	88B	SPEC	32 $\pi^-p \to \pi^+\pi^-\gamma$X

$\Gamma(\pi^+\pi^-\pi^+\pi^-)/\Gamma_{\text{total}}$ Γ_{11}/Γ

VALUE	CL%	DOCUMENT ID		TECN	COMMENT
<1 × 10^{-3}	90	KURDADZE	88	OLYA	$e^+e^- \to \pi^+\pi^-\pi^+\pi^-$

$\Gamma(\pi^+\pi^-\pi^0\pi^0)/\Gamma_{\text{total}}$ Γ_9/Γ

VALUE (units 10^{-2})	CL%	DOCUMENT ID		TECN	COMMENT
<2	90	KURDADZE	86	OLYA	$e^+e^- \to \pi^+\pi^-\pi^0\pi^0$

$\Gamma(\mu^+\mu^-)/\Gamma(\pi^+\pi^-\pi^0)$ Γ_{14}/Γ_1

VALUE (units 10^{-3})	CL%	DOCUMENT ID		TECN	COMMENT
<0.2	90	WILSON	69	OSPK	12 π^-C → Fe
• • • We do not use the following data for averages, fits, limits, etc. • • •					
<1.7	74	FLATTE	66	HBC	1.2 – 1.7 $K^-p \to \Lambda\mu^+\mu^-$
<1.2		BARBARO-...	65	HBC	2.7 K^-p

$\Gamma(\pi^0\pi^0\gamma)/\Gamma_{\text{total}}$ Γ_{12}/Γ

VALUE (units 10^{-5})	EVTS	DOCUMENT ID		TECN	COMMENT
6.7±1.1 OUR FIT					
6.5±1.2 OUR AVERAGE					
6.4$^{+2.4}_{-2.0}$±0.8	190	[31] AKHMETSHIN	04B	CMD2	0.6–0.97 $e^+e^- \to \pi^0\pi^0\gamma$
6.6$^{+1.4}_{-1.3}$±0.6	295	ACHASOV	02F	SND	0.36–0.97 $e^+e^- \to \pi^0\pi^0\gamma$
• • • We do not use the following data for averages, fits, limits, etc. • • •					
11.8$^{+2.1}_{-1.9}$±1.4	190	[32] AKHMETSHIN	04B	CMD2	0.6–0.97 $e^+e^- \to \pi^0\pi^0\gamma$
7.8±2.7±2.0	63	[31,33] ACHASOV	00G	SND	$e^+e^- \to \pi^0\pi^0\gamma$
12.7±2.3±2.5	63	[32,33] ACHASOV	00G	SND	$e^+e^- \to \pi^0\pi^0\gamma$

$\Gamma(\pi^0\pi^0\gamma)/\Gamma(\pi^0\gamma)$ Γ_{12}/Γ_2

VALUE	CL%	EVTS	DOCUMENT ID		TECN	COMMENT
(7.6 ±1.3) × 10^{-4} OUR FIT						
0.00085±0.00029		40 ± 14	ALDE	94B	GAM2	38$\pi^-p \to \pi^0\pi^0\gamma n$
• • • We do not use the following data for averages, fits, limits, etc. • • •						
< 0.005	90		DOLINSKY	89	ND	$e^+e^- \to \pi^0\pi^0\gamma$
< 0.18	95		KEYNE	76	CNTR	$\pi^-p \to \omega n$
< 0.15	90		BENAKSAS	72C	OSPK	e^+e^-
< 0.14			BALDIN	71	HLBC	2.9 π^+p
< 0.1	90		BARMIN	64	HLBC	1.3–2.8 π^-p

$\Gamma(\eta\pi^0)/\Gamma_{\text{total}}$ Γ_{16}/Γ

Violates C conservation.

VALUE	CL%	DOCUMENT ID		TECN	COMMENT
<0.001	90	ALDE	94B	GAM2	38$\pi^-p \to \eta\pi^0 n$

$\Gamma(\eta\pi^0\gamma)/\Gamma_{\text{total}}$ Γ_{13}/Γ

VALUE (units 10^{-5})	CL%	DOCUMENT ID		TECN	COMMENT
<3.3	90	AKHMETSHIN	04B	CMD2	0.6–0.97 $e^+e^- \to \eta\pi^0\gamma$

$[\Gamma(\eta\gamma)+\Gamma(\eta\pi^0)]/\Gamma(\pi^+\pi^-\pi^0)$ $(\Gamma_5+\Gamma_{16})/\Gamma_1$

VALUE	CL%	DOCUMENT ID		TECN	COMMENT
<0.016	90	[34] FLATTE	66	HBC	1.2 – 1.7 $K^-p \to \Lambda\pi^+\pi^-$MM
• • • We do not use the following data for averages, fits, limits, etc. • • •					
<0.045	95	JACQUET	69B	HLBC	2.05 $\pi^+p \to \pi^+p\omega$

$\Gamma(\text{neutrals})/\Gamma(\text{charged particles})$ $(\Gamma_2+\Gamma_4)/(\Gamma_1+\Gamma_3)$

VALUE	DOCUMENT ID		TECN	COMMENT
0.100±0.008 OUR FIT				
0.124±0.021	FELDMAN	67C	OSPK	1.2 π^-p

$\Gamma(\pi^0\pi^0\gamma)/\Gamma(\pi^+\pi^-\pi^0)$ Γ_{12}/Γ_1

VALUE	CL%	DOCUMENT ID		TECN	COMMENT
<0.00045	90	DOLINSKY	89	ND	$e^+e^- \to \pi^0\pi^0\gamma$
• • • We do not use the following data for averages, fits, limits, etc. • • •					
<0.08	95	JACQUET	69B	HLBC	2.05 $\pi^+p \to \pi^+p\omega$

$\Gamma(\eta\gamma)/\Gamma(\pi^0\gamma)$ Γ_5/Γ_2

VALUE	DOCUMENT ID		TECN	COMMENT
• • • We do not use the following data for averages, fits, limits, etc. • • •				
0.0098±0.0024	[35] ALDE	93	GAM2	38$\pi^-p \to \omega n$
0.0082±0.0033	[36] DOLINSKY	89	ND	$e^+e^- \to \eta\gamma$
0.010 ±0.045	APEL	72B	OSPK	4–8 $\pi^-p \to n3\gamma$

$\Gamma(\pi^0\mu^+\mu^-)/\Gamma_{\text{total}}$ Γ_7/Γ

VALUE (units 10^{-4})	DOCUMENT ID		TECN	COMMENT
0.96±0.23 OUR FIT				
0.96±0.23	DZHELYADIN	81B	CNTR	25–33 $\pi^-p \to \omega n$

$\Gamma(\pi^0e^+e^-)/\Gamma_{\text{total}}$ Γ_6/Γ

VALUE (units 10^{-4})	EVTS	DOCUMENT ID		TECN	COMMENT
5.9±1.9 OUR FIT					
5.9±1.9	43	DOLINSKY	88	ND	$e^+e^- \to \pi^0e^+e^-$

Meson Particle Listings

$\omega(782)$

$\Gamma(e^+e^-)/\Gamma_{\text{total}}$ Γ_8/Γ

VALUE (units 10^{-4})	EVTS	DOCUMENT ID		TECN	COMMENT
0.714±0.013 OUR FIT		Error includes scale factor of 1.1.			
• • • We do not use the following data for averages, fits, limits, etc. • • •					
0.700±0.016	11200	[37,38] AKHMETSHIN	04	CMD2	$e^+e^- \to \pi^+\pi^-\pi^0$
0.752±0.004±0.024	1.2M	[37,39] ACHASOV	03D	RVUE	0.44–2.00 $e^+e^- \to \pi^+\pi^-\pi^0$
0.714±0.036		[37] DOLINSKY	89	ND	$e^+e^- \to \pi^+\pi^-\pi^0$
0.72 ±0.03		[37] BARKOV	87	CMD	$e^+e^- \to \pi^+\pi^-\pi^0$
0.64 ±0.04	1488	[37] KURDADZE	83B	OLYA	$e^+e^- \to \pi^+\pi^-\pi^0$
0.675±0.069	433	[37] CORDIER	80	DM1	$e^+e^- \to \pi^+\pi^-\pi^0$
0.83 ±0.10	451	[37] BENAKSAS	72B	OSPK	$e^+e^- \to \pi^+\pi^-\pi^0$
0.77 ±0.06		[40] AUGUSTIN	69D	OSPK	$e^+e^- \to \pi^+\pi^-\pi^0$
0.65 ±0.13	33	[41] ASTVACAT...	68	OSPK	Assume SU(3)+mixing

$\Gamma(\mu^+\mu^-)/\Gamma_{\text{total}}$ Γ_{14}/Γ

VALUE (units 10^{-5})	EVTS	DOCUMENT ID		TECN	COMMENT
9.0±3.1 OUR FIT					
9.0±2.9±1.1	18	HEISTER	02C	ALEP	$Z \to \mu^+\mu^- + X$

$\Gamma(\text{neutrals})/\Gamma_{\text{total}}$ $(\Gamma_2+\Gamma_4)/\Gamma$

VALUE	EVTS	DOCUMENT ID		TECN	COMMENT
0.091±0.006 OUR FIT					
0.081±0.011 OUR AVERAGE					
0.075±0.025		BIZZARRI	71	HBC	0.0 $p\overline{p}$
0.079±0.019		DEINET	69B	OSPK	1.5 $\pi^- p$
0.084±0.015		BOLLINI	68C	CNTR	2.1 $\pi^- p$
• • • We do not use the following data for averages, fits, limits, etc. • • •					
0.073±0.018	42	BASILE	72B	CNTR	1.67 $\pi^- p$

$\Gamma(\pi^+\pi^-)/\Gamma_{\text{total}}$ Γ_3/Γ

See also $\Gamma(\pi^+\pi^-)/\Gamma(\pi^+\pi^-\pi^0)$.

VALUE (units 10^{-2})	EVTS	DOCUMENT ID		TECN	COMMENT
1.70±0.27 OUR FIT		Error includes scale factor of 1.4.			
1.57±0.24 OUR AVERAGE		Error includes scale factor of 1.2.			
1.30±0.24±0.05	11200	[42] AKHMETSHIN	04	CMD2	$e^+e^- \to \pi^+\pi^-\pi^0$
$2.38^{+1.77}_{-0.90}\pm0.18$	5.4k	[43] ACHASOV	02E	SND	1.1–1.38 $e^+e^- \to \pi^+\pi^-\pi^0$
2.3 ±0.5		BARKOV	85	OLYA	$e^+e^- \to \pi^+\pi^-$
$1.6\ ^{+0.9}_{-0.7}$		QUENZER	78	DM1	$e^+e^- \to \pi^+\pi^-$
3.6 ±1.9		BENAKSAS	72	OSPK	$e^+e^- \to \pi^+\pi^-$
• • • We do not use the following data for averages, fits, limits, etc. • • •					
2.01±0.29		[44] BENAYOUN	03	RVUE	$e^+e^- \to \pi^+\pi^-$
1.9 ±0.3		[45] GARDNER	99	RVUE	$e^+e^- \to \pi^+\pi^-$
2.3 ±0.4		[46] BENAYOUN	98	RVUE	$e^+e^- \to \pi^+\pi^-$, $\mu^+\mu^-$
1.0 ±0.11		[47] WICKLUND	78	ASPK	3,4,6 $\pi^\pm N$
1.22±0.30		ALVENSLEB...	71C	CNTR	Photoproduction
$1.3\ ^{+1.2}_{-0.9}$		MOFFEIT	71	HBC	2.8,4.7 γp
$0.80^{+0.28}_{-0.20}$		[48] BIGGS	70B	CNTR	4.2γ C $\to \pi^+\pi^-$ C

$\Gamma(\pi^+\pi^-)/\Gamma(\pi^0\gamma)$ Γ_3/Γ_2

VALUE	EVTS	DOCUMENT ID		TECN	COMMENT
0.20±0.04	1.98M	[49] ALOISIO	03	KLOE	1.02 $e^+e^- \to \pi^+\pi^-\pi^0$

$\Gamma(\pi^0\pi^0\gamma)/\Gamma(\text{neutrals})$ $\Gamma_{12}/(\Gamma_2+\Gamma_4)$

VALUE	CL%	DOCUMENT ID		TECN	COMMENT
• • • We do not use the following data for averages, fits, limits, etc. • • •					
0.22±0.07		[25] DAKIN	72	OSPK	1.4 $\pi^- p \to n$MM
<0.19	90	DEINET	69B	OSPK	

[25] See $\Gamma(\pi^0\gamma)/\Gamma(\text{neutrals})$.

$\Gamma(\pi^0\gamma)/\Gamma(\text{neutrals})$ $\Gamma_2/(\Gamma_2+\Gamma_4)$

VALUE	CL%	DOCUMENT ID		TECN	COMMENT
• • • We do not use the following data for averages, fits, limits, etc. • • •					
0.78±0.07		[50] DAKIN	72	OSPK	1.4 $\pi^- p \to n$MM
>0.81	90	DEINET	69B	OSPK	

$\Gamma(\eta\gamma)/\Gamma_{\text{total}}$ Γ_5/Γ

VALUE (units 10^{-4})	EVTS	DOCUMENT ID		TECN	COMMENT
4.9 ±0.5 OUR FIT					
6.3 ±1.3 OUR AVERAGE		Error includes scale factor of 1.2.			
6.6 ±1.7		[51] ABELE	97E	CBAR	0.0 $p\overline{p} \to 5\gamma$
8.3 ±2.1		ALDE	93	GAM2	38$\pi^- p \to \omega n$
$3.0\ ^{+2.5}_{-1.8}$		[52] ANDREWS	77	CNTR	6.7–10 γ Cu
• • • We do not use the following data for averages, fits, limits, etc. • • •					
5.10±0.72±0.34	23k	[53] AKHMETSHIN	01B	CMD2	$e^+e^- \to \eta\gamma$
4.60±0.72±0.19	312	[54,55] ACHASOV	00D	SND	$e^+e^- \to \eta\gamma$
0.7 to 5.5		[56] CASE	00	CBAR	0.0 $p\overline{p} \to \eta\eta\gamma$
$6.56^{+2.41}_{-2.55}$	3525	[52,57] BENAYOUN	96	RVUE	$e^+e^- \to \eta\gamma$
7.3 ±2.9		[52,55] DOLINSKY	89	ND	$e^+e^- \to \eta\gamma$

$\Gamma(\pi^0\mu^+\mu^-)/\Gamma(\mu^+\mu^-)$ Γ_7/Γ_{14}

VALUE	EVTS	DOCUMENT ID		TECN	COMMENT
• • • We do not use the following data for averages, fits, limits, etc. • • •					
1.2±0.6	30	[58] DZHELYADIN	79	CNTR	25–33 $\pi^- p$

$\Gamma(\pi^+\pi^-\pi^0)/\Gamma_{\text{total}}$ Γ_1/Γ

VALUE	EVTS	DOCUMENT ID		TECN	COMMENT
• • • We do not use the following data for averages, fits, limits, etc. • • •					
0.8965±0.0016±0.0048	1.2M	[37,39] ACHASOV	03D	RVUE	0.44–2.00 $e^+e^- \to \pi^+\pi^-\pi^0$
0.880 ±0.020 ±0.032	11200	[37,59] AKHMETSHIN	00C	CMD2	$e^+e^- \to \pi^+\pi^-\pi^0$
0.8942±0.0062		[37] DOLINSKY	89	ND	$e^+e^- \to \pi^+\pi^-\pi^0$

$\Gamma(3\pi^0)/\Gamma_{\text{total}}$ Γ_{17}/Γ

Violates C conservation.

VALUE	CL%	DOCUMENT ID		TECN	COMMENT
<0.0003	90	PROKOSHKIN	95	GAM2	38 $\pi^- p \to 3\pi^0 n$

$\Gamma(3\pi^0)/\Gamma(\pi^+\pi^-\pi^0)$ Γ_{17}/Γ_1

Violates C conservation.

VALUE	CL%	DOCUMENT ID		TECN	COMMENT
• • • We do not use the following data for averages, fits, limits, etc. • • •					
<0.009	90	BARBERIS	01		450 $pp \to p_f 3\pi^0 p_s$

$\Gamma(3\gamma)/\Gamma_{\text{total}}$ Γ_{15}/Γ

VALUE (units 10^{-4})	CL%	DOCUMENT ID		TECN	COMMENT
<1.9	95	[60] ABELE	97E	CBAR	0.0 $\overline{p}p \to 5\gamma$
• • • We do not use the following data for averages, fits, limits, etc. • • •					
<2	90	[60] PROKOSHKIN	95	GAM2	38 $\pi^- p \to 3\gamma n$

$\Gamma(\pi^0\gamma)/\Gamma_{\text{total}}$ Γ_2/Γ

VALUE (units 10^{-2})	EVTS	DOCUMENT ID		TECN	COMMENT
• • • We do not use the following data for averages, fits, limits, etc. • • •					
9.34±0.15±0.31	36500	[29] ACHASOV	03	SND	0.60–0.97 $e^+e^- \to \pi^0\gamma$
8.65±0.16±0.42	1.2M	[37,39] ACHASOV	03D	RVUE	0.44–2.00 $e^+e^- \to \pi^+\pi^-\pi^0$
8.39±0.24	9975	[61] BENAYOUN	96	RVUE	$e^+e^- \to \pi^0\gamma$
8.88±0.62	10625	[29] DOLINSKY	89	ND	$e^+e^- \to \pi^0\gamma$

[26] Significant interference effect observed. NB of $\omega \to 3\pi$ comes from an extrapolation.
[27] ROOS 70 combines ABRAMOVICH 70 and BIZZARRI 70.
[28] From $\sigma_0^{\omega\pi^0 \to \pi^0\pi^0\gamma}(m_\phi)/\sigma_0^{\omega\pi^0 \to \pi^+\pi^-\pi^0}(m_\phi)$ with a phase-space correction factor of 1/1.023.
[29] Not independent of the corresponding $\Gamma(e^+e^-)\times\Gamma(\pi^0\gamma)/\Gamma^2_{\text{total}}$.
[30] Using ACHASOV 03.
[31] In the model assuming the $\rho \to \pi^0\pi^0\gamma$ decay via the $\omega\pi$ and $f_0(600)\gamma$ mechanisms.
[32] In the model assuming the $\rho \to \pi^0\pi^0\gamma$ decay via the $\omega\pi$ mechanism only.
[33] Superseded by ACHASOV 02F.
[34] Restated by us using B($\eta \to$ charged modes) = 29.2%.
[35] Model independent determination.
[36] Solution corresponding to constructive ω-ρ interference.
[37] Not independent of the corresponding $\Gamma(e^+e^-)\times\Gamma(\pi^+\pi^-\pi^0)/\Gamma^2_{\text{total}}$.
[38] Using B($\omega \to \pi^+\pi^-\pi^0$) = 0.891 ± 0.007. Update of AKHMETSHIN 00C.
[39] Using ACHASOV 03, ACHASOV 03D and B($\omega \to \pi^+\pi^-$) = (1.70 ± 0.28)%.
[40] Rescaled by us to correspond to ω width 8.4 MeV. Systematic errors underestimated.
[41] Not resolved from ρ decay. Error statistical only.
[42] Update of AKHMETSHIN 02.
[43] From the $m_{\pi^+\pi^-}$ spectrum taking into account the interference of the $\rho\pi$ and $\omega\pi$ amplitudes.
[44] Using the data of AKHMETSHIN 02 in the hidden local symmetry model.
[45] Using the data of BARKOV 85.
[46] Using the data of BARKOV 85 in the hidden local symmetry model.
[47] From a model-dependent analysis assuming complete coherence.
[48] Re-evaluated under $\Gamma(\pi^+\pi^-)/\Gamma(\pi^+\pi^-\pi^0)$ by BEHREND 71 using more accurate $\omega \to \rho$ photoproduction cross-section ratio.
[49] Using the data of ALOISIO 02D.
[50] Error statistical only. Authors obtain good fit also assuming $\pi^0\gamma$ as the only neutral decay.
[51] No flat $\eta\eta\gamma$ background assumed.
[52] Solution corresponding to constructive ω-ρ interference.
[53] Using B($\omega \to e^+e^-$)= (7.07 ± 0.19) × 10^{-5} and using B($\eta \to 3\pi^0$)= (32.24 ± 0.29) × 10^{-2}. Solution corresponding to constructive ω-ρ interference. The combined fit from 600 to 1380 MeV taking into account $\rho(770)$, $\omega(782)$, $\phi(1020)$, and $\rho(1450)$ (mass and width fixed at 1450 MeV and 310 MeV respectively). Not independent of the corresponding $\Gamma(e^+e^-)\times\Gamma(\eta\gamma)/\Gamma^2_{\text{total}}$.
[54] Using B($\omega \to e^+e^-$) = (7.07 ± 0.19) × 10^{-5} and B($\eta \to 3\pi^0$) = (32.2 ± 0.4) × 10^{-2}.
[55] Not independent of the corresponding $\Gamma(e^+e^-)\times\Gamma(\eta\gamma)/\Gamma^2_{\text{total}}$.
[56] Depending on the degree of coherence with the flat $\eta\eta\gamma$ background and using B($\omega \to \pi^0\gamma$)=(8.5 ± 0.5) × 10^{-2}.
[57] Reanalysis of DRUZHININ 84, DOLINSKY 89, DOLINSKY 91 taking into account the triangle anomaly contributions.
[58] Superseded by DZHELYADIN 81B result above.
[59] Using $\Gamma(e^+e^-)$=0.60 ± 0.02 keV.
[60] From direct 3γ decay search.
[61] Reanalysis of DRUZHININ 84, DOLINSKY 89, DOLINSKY 91 taking into account the triangle anomaly contributions.

$\omega(782)$ REFERENCES

AKHMETSHIN 04 PL B578 285 R.R. Akhmetshin *et al.* (Novosibirsk CMD-2 Collab.)
AKHMETSHIN 04B PL B580 119 R.R. Akhmetshin *et al.* (Novosibirsk CMD-2 Collab.)
ACHASOV 03 PL B559 171 M.N. Achasov *et al.* (Novosibirsk SND Collab.)
ACHASOV 03D PR D68 052006 M.N. Achasov *et al.* (Novosibirsk SND Collab.)
ALOISIO 03 PL B561 55 A. Aloisio *et al.* (KLOE Collab.)
BENAYOUN 03 EPJ C29 397 M. Benayoun *et al.*
ACHASOV 02E PR D66 032001 M.N. Achasov *et al.* (Novosibirsk SND Collab.)
ACHASOV 02F PL B537 201 M.N. Achasov *et al.* (Novosibirsk SND Collab.)
AKHMETSHIN 02 PL B527 161 R.R. Akhmetshin *et al.* (Novosibirsk CMD-2 Collab.)
ALOISIO 02D PL B537 21 A. Aloisio *et al.* (KLOE Collab.)
HEISTER 02C PL B528 19 A. Heister *et al.* (ALEPH Collab.)
ACHASOV 01E PR D63 072002 M.N. Achasov *et al.* (Novosibirsk SND Collab.)
AKHMETSHIN 01B PL B509 217 R.R. Akhmetshin *et al.* (Novosibirsk CMD-2 Collab.)
BARBERIS 01 PL B507 14 D. Barberis *et al.*
ACHASOV 00 EPJ C12 25 M.N. Achasov *et al.* (Novosibirsk SND Collab.)
ACHASOV 00D JETPL 72 282 M.N. Achasov *et al.* (Novosibirsk SND Collab.)
Translated from ZETFP 72 411.
ACHASOV 00G JETPL 71 355 M.N. Achasov *et al.* (Novosibirsk SND Collab.)
Translated from ZETFP 71 519.
AKHMETSHIN 00C PL B476 33 R.R. Akhmetshin *et al.* (Novosibirsk CMD-2 Collab.)
AULCHENKO 00A JETP 90 927 V.M. Aulchenko *et al.* (Novosibirsk SND Collab.)
Translated from ZETF 117 1067.
CASE 00 PR D61 032002 T. Case *et al.* (Crystal Barrel Collab.)
ACHASOV 99E PL B462 365 M.N. Achasov *et al.* (Novosibirsk SND Collab.)
GARDNER 99 PR D59 076002 S. Gardner, H.B. O'Connell
BENAYOUN 98 EPJ C2 269 M. Benayoun *et al.* (IPNP, NOVO, ADLD+)
ABELE 97E PL B411 361 A. Abele *et al.* (Crystal Barrel Collab.)
BENAYOUN 96 ZPHY C72 221 M. Benayoun *et al.* (IPNP, NOVO)
PROKOSHKIN 95 SPD 40 273 Y.D. Prokoshkin, V.D. Samoilenko (SERP)
Translated from DANS 342 610.
WURZINGER 95 PR C51 443 R. Wurzinger *et al.* (BONN, ORSAY, SACL+)
ALDE 94B PL B340 122 D.M. Alde *et al.* (SERP, BELG, LANL, LAPP+)
AMSLER 94C PL B327 425 C. Amsler *et al.* (Crystal Barrel Collab.)
ALDE 93 PAN 56 1229 D.M. Alde *et al.* (SERP, LAPP, LANL, BELG+)
Translated from YAF 56 137.
Also 94 ZPHY C61 35 D.M. Alde *et al.* (SERP, LAPP, LANL, BELG+)
AMSLER 93B PL B311 362 C. Amsler *et al.* (Crystal Barrel Collab.)
WEIDENAUER 93 ZPHY C59 387 P. Weidenauer *et al.* (ASTERIX Collab.)
ANTONELLI 92 ZPHY C56 15 A. Antonelli *et al.* (DM2 Collab.)
DOLINSKY 91 PRPL 202 99 S.I. Dolinsky *et al.* (NOVO)
WEIDENAUER 90 ZPHY C47 353 P. Weidenauer *et al.* (ASTERIX Collab.)
DOLINSKY 89 ZPHY C42 511 S.I. Dolinsky *et al.* (NOVO)
BITYUKOV 88B SJNP 47 800 S.I. Bityukov *et al.* (SERP)
Translated from YAF 47 1258.
DOLINSKY 88 SJNP 48 277 S.I. Dolinsky *et al.* (NOVO)
Translated from YAF 48 442.
KURDADZE 88 JETPL 47 512 L.M. Kurdadze *et al.* (NOVO)
Translated from ZETFP 47 432.
AULCHENKO 87 PL B186 432 V.M. Aulchenko *et al.* (NOVO)
BARKOV 87 JETPL 46 164 L.M. Barkov *et al.* (NOVO)
Translated from ZETFP 46 132.
KURDADZE 86 JETPL 43 643 L.M. Kurdadze *et al.* (NOVO)
Translated from ZETFP 43 497.
BARKOV 85 NP B256 365 L.M. Barkov *et al.* (NOVO)
DRUZHININ 84 PL 144B 136 V.P. Druzhinin *et al.* (NOVO)
KURDADZE 83B JETPL 36 274 A.M. Kurdadze *et al.* (NOVO)
Translated from ZETFP 36 221.
DZHELYADIN 81B PL 102B 296 R.I. Dzhelyadin *et al.* (SERP)
CORDIER 80 NP B172 13 A. Cordier *et al.* (LALO)
ROOS 80 LNC 27 321 M. Roos, A. Pellinen (HELS)
BENKHEIRI 79 NP B150 268 P. Benkheiri *et al.* (EPOL, CERN, CDEF+)
DZHELYADIN 79 PL 84B 143 R.I. Dzhelyadin *et al.* (SERP)
COOPER 78B NP B146 1 A.M. Cooper *et al.* (TATA, CERN, CDEF+)
QUENZER 78 PL 76B 512 A. Quenzer *et al.* (LALO)
VANAPEL... 78 NP B133 245 G.W. van Apeldoorn *et al.* (ZEEM)
WICKLUND 78 PR D17 1197 A.B. Wicklund *et al.* (ANL)
ANDREWS 77 PRL 38 198 D.E. Andrews *et al.* (ROCH)
GESSAROLI 77 NP B126 382 R. Gessaroli *et al.* (BGNA, FIRZ, GENO+)
KEYNE 76 PR D14 28 J. Keyne *et al.* (LOIC, SHMP)
Also 73B PR D8 2789 D.M. Binnie *et al.* (LOIC, SHMP)
KALBFLEISCH 75 PR D11 987 G.R. Kalbfleisch, R.C. Strand, J.W. Chapman (BNL+)
AGUILAR-... 72B PR D6 29 M. Aguilar-Benitez *et al.* (BNL)
APEL 72B PL 41B 234 W.D. Apel *et al.* (KARLK, KARLE, PISA)
BASILE 72B Phil. Conf. 153 M. Basile *et al.* (CERN)
BENAKSAS 72 PL 39B 289 D. Benaksas *et al.* (ORSAY)
BENAKSAS 72B PL 42B 507 D. Benaksas *et al.* (ORSAY)
BENAKSAS 72C PL 42B 511 D. Benaksas *et al.* (ORSAY)
BORENSTEIN 72 PR D5 1559 S.R. Borenstein *et al.* (BNL, MICH)
BROWN 72 PL 42B 117 R.M. Brown *et al.* (ILL, ILLC)
DAKIN 72 PR D6 2321 J.T. Dakin *et al.* (PRIN)
RATCLIFF 72 PL 38B 345 B.N. Ratcliff *et al.* (SLAC)
ALVENSLEB... 71C PRL 27 888 H. Alvensleben *et al.* (DESY)
BALDIN 71 SJNP 13 758 A.B. Baldin *et al.* (ITEP)
Translated from YAF 13 1318.
BEHREND 71 PRL 27 61 H.J. Behrend *et al.* (ROCH, CORN, FNAL)
BIZZARRI 71 NP B27 140 R. Bizzarri *et al.* (CERN, CDEF)
COYNE 71 NP B32 333 D.G. Coyne *et al.* (LRL)
MOFFEIT 71 NP B29 349 K.C. Moffeit *et al.* (LRL, UCB, SLAC+)
ABRAMOVI... 70 NP B20 209 M. Abramovich *et al.* (CERN)
BIGGS 70B PRL 24 1201 P.J. Biggs *et al.* (DARE)
BIZZARRI 70 PRL 25 1385 R. Bizzarri *et al.* (ROMA, SYRA)
ROOS 70 DNPL/R7 173 M. Roos (CERN)
Proc. Daresbury Study Weekend No. 1.
AUGUSTIN 69D PL 28B 513 J.E. Augustin *et al.* (ORSAY)
BIZZARRI 69 NP B14 169 R. Bizzarri *et al.* (CERN, CDEF)
DEINET 69B PL 30B 426 W. Deinet *et al.* (KARL, CERN)
JACQUET 69B NC 63A 743 F. Jacquet *et al.* (EPOL, BERG)
WILSON 69 Private Comm. R. Wilson (HARV)
Also 69 PR 178 2095 A.A. Wehmann *et al.* (HARV, CASE, SLAC+)
ASTVACAT... 68 PL 27B 45 R.G. Astvatsaturov *et al.* (JINR, MOSU)
BOLLINI 68C NC 56A 531 D. Bollini *et al.* (CERN, BGNA, STRB)
BARASH 67B PR 156 1399 N. Barash *et al.* (COLU)
FELDMAN 67C PR 159 1219 M. Feldman *et al.* (PENN)
DIGIUGNO 66B NC 44A 1272 G. Di Giugno *et al.* (NAPL, FRAS, TRST)
FLATTE 66 PR 145 1050 S.M. Flatte *et al.* (LRL)
JAMES 66 PR 142 896 F.E. James, H.L. Kraybill (YALE, BNL)
BARBARO-... 65 PRL 14 279 A. Barbaro-Galtieri, R.D. Tripp (LRL)
BARMIN 64 JETP 18 1289 V.V. Barmin *et al.* (ITEP)
Translated from ZETF 45 1879.
KRAEMER 64 PR 136B 496 R.W. Kraemer *et al.* (JHU, NWES, WOOD)
BUSCHBECK 63 Siena Conf. 1 166 B. Buschbeck *et al.* (VIEN, CERN, ANIK)

OTHER RELATED PAPERS

AZIMOV 03 EPJ A16 209 Ya.I. Azimov
BENAYOUN 01 EPJ C22 503 M. Benayoun, H.B. O'Connell
GOKALP 01B EPJ C22 327 A. Gokalp, Y. Sarac, O. Yilmaz
DELBOURGO 99B PR D59 113006 R. Delbourgo *et al.*
GARDNER 98 PR D57 2716 S. Gardner, H.B. O'Connell
Also 00A PR D62 019903 (errata) S. Gardner, H.B. O'Connell
ABELE 97F PL B411 354 A. Abele *et al.* (Crystal Barrel Collab.)
DOLINSKY 86 PL B174 453 S.I. Dolinsky *et al.* (NOVO)
KURDADZE 83 JETPL 37 733 L.M. Kurdadze *et al.* (NOVO)
Translated from ZETFP 37 613.
ALFF-... 62B PRL 9 325 C. Alff-Steinberger *et al.* (COLU, RUTG)
STEVENSON 62 PR 125 687 M.L. Stevenson *et al.* (LRL)
MAGLICH 61 PRL 7 178 B.C. Maglich *et al.* (LRL)
PEVSNER 61 PRL 7 421 A. Pevsner *et al.* (JHU)
XUONG 61 PRL 7 327 H. Nguyen Ngoc, G.R. Lynch (LRL)

$\eta'(958)$

$I^G(J^{PC}) = 0^+(0^{-+})$

$\eta'(958)$ MASS

VALUE (MeV)	EVTS	DOCUMENT ID		TECN	COMMENT
957.78±0.14 OUR AVERAGE					
957.9 ±0.2 ±0.6	4800	WURZINGER	96	SPEC	1.68 $pd \to {}^3\mathrm{He}\eta'$
959 ±1	630	BELADIDZE	92C	VES	36 $\pi^-\mathrm{Be} \to \pi^-\eta'\eta\mathrm{Be}$
958 ±1	340	ARMSTRONG	91B	OMEG	300 $pp \to pp\eta\pi^+\pi^-$
958.2 ±0.4	622	AUGUSTIN	90	DM2	$J/\psi \to \gamma\eta\pi^+\pi^-$
957.8 ±0.2	2420	AUGUSTIN	90	DM2	$J/\psi \to \gamma\gamma\pi^+\pi^-$
956.3 ±1.0	143	GIDAL	87	MRK2	$e^+e^- \to e^+e^-\eta\pi^+\pi^-$
957.46±0.33		DUANE	74	MMS	$\pi^- p \to n\mathrm{MM}$
958.2 ±0.5	1414	DANBURG	73	HBC	2.2 $K^- p \to \Lambda X^0$
958 ±1	400	JACOBS	73	HBC	2.9 $K^- p \to \Lambda X^0$
956.1 ±1.1	3415	BASILE	71	CNTR	1.6 $\pi^- p \to nX^0$
957.4 ±1.4	535	BASILE	71	CNTR	1.6 $\pi^- p \to nX^0$
957 ±1		RITTENBERG	69	HBC	1.7–2.7 $K^- p$

$\eta'(958)$ WIDTH

VALUE (MeV)	EVTS	DOCUMENT ID	TECN	CHG	COMMENT
0.202±0.016 OUR FIT Error includes scale factor of 1.3.					
0.30 ±0.09 OUR AVERAGE					
0.40 ±0.22	4800	WURZINGER 96	SPEC		1.68 $pd \to {}^3\mathrm{He}\eta'$
0.28 ±0.10	1000	BINNIE 79	MMS	0	$\pi^- p \to n\mathrm{MM}$

$\eta'(958)$ DECAY MODES

	Mode	Fraction (Γ_i/Γ)		Scale factor/ Confidence level
Γ_1	$\pi^+\pi^-\eta$	(44.3 ±1.5) %		S=1.2
Γ_2	$\rho^0\gamma$(including non-resonant $\pi^+\pi^-\gamma$)	(29.5 ±1.0) %		S=1.2
Γ_3	$\pi^0\pi^0\eta$	(20.9 ±1.2) %		S=1.2
Γ_4	$\omega\gamma$	(3.03±0.31) %		
Γ_5	$\gamma\gamma$	(2.12±0.14) %		S=1.3
Γ_6	$3\pi^0$	(1.56±0.26)	$\times 10^{-3}$	
Γ_7	$\mu^+\mu^-\gamma$	(1.04±0.26)	$\times 10^{-4}$	
Γ_8	$\pi^+\pi^-\pi^0$	< 5	%	CL=90%
Γ_9	$\pi^0\rho^0$	< 4	%	CL=90%
Γ_{10}	$\pi^+\pi^+\pi^-\pi^-$	< 1	%	CL=90%
Γ_{11}	$\pi^+\pi^+\pi^-\pi^-$ neutrals	< 1	%	CL=95%
Γ_{12}	$\pi^+\pi^+\pi^-\pi^-\pi^0$	< 1	%	CL=90%
Γ_{13}	6π	< 1	%	CL=90%
Γ_{14}	$\pi^+\pi^-e^+e^-$	< 6	$\times 10^{-3}$	CL=90%
Γ_{15}	γe^+e^-	< 9	$\times 10^{-4}$	CL=90%
Γ_{16}	$\pi^0\gamma\gamma$	< 8	$\times 10^{-4}$	CL=90%
Γ_{17}	$4\pi^0$	< 5	$\times 10^{-4}$	CL=90%
Γ_{18}	e^+e^-	< 2.1	$\times 10^{-7}$	CL=90%

Charge conjugation (C), Parity (P), Lepton family number (LF) violating modes

Γ_{19}	$\pi^+\pi^-$	P,CP	< 2	%		CL=90%
Γ_{20}	$\pi^0\pi^0$	P,CP	< 9	$\times 10^{-4}$		CL=90%
Γ_{21}	$\pi^0e^+e^-$	C	[a] < 1.4	$\times 10^{-3}$		CL=90%
Γ_{22}	ηe^+e^-	C	[a] < 2.4	$\times 10^{-3}$		CL=90%
Γ_{23}	3γ	C	< 1.0	$\times 10^{-4}$		CL=90%
Γ_{24}	$\mu^+\mu^-\pi^0$	C	[a] < 6.0	$\times 10^{-5}$		CL=90%
Γ_{25}	$\mu^+\mu^-\eta$	C	[a] < 1.5	$\times 10^{-5}$		CL=90%
Γ_{26}	$e\mu$	LF	< 4.7	$\times 10^{-4}$		CL=90%

[a] C parity forbids this to occur as a single-photon process.

CONSTRAINED FIT INFORMATION

An overall fit to the total width, a partial width, 2 combinations of partial widths obtained from integrated cross section, and 16 branching ratios uses 48 measurements and one constraint to determine 7 parameters. The overall fit has a $\chi^2 = 35.6$ for 42 degrees of freedom.

The following *off-diagonal* array elements are the correlation coefficients $\langle \delta p_i \delta p_j \rangle / (\delta p_i \cdot \delta p_j)$, in percent, from the fit to parameters p_i, including the branching fractions, $x_i \equiv \Gamma_i/\Gamma_{\rm total}$. The fit constrains the x_i whose labels appear in this array to sum to one.

	x_1	x_2	x_3	x_4	x_5	x_6
x_2	−39					
x_3	−74	−29				
x_4	−33	−24	32			
x_5	−25	−12	26	8		
x_6	−27	−11	35	11	9	
Γ	32	−3	−24	−5	−88	−8

	Mode	Rate (MeV)	Scale factor
Γ_1	$\pi^+\pi^-\eta$	0.090 ±0.008	1.2
Γ_2	$\rho^0\gamma$ (including non-resonant $\pi^+\pi^-\gamma$)	0.060 ±0.005	1.3
Γ_3	$\pi^0\pi^0\eta$	0.042 ±0.004	1.6
Γ_4	$\omega\gamma$	0.0061 ±0.0008	1.2
Γ_5	$\gamma\gamma$	0.00429±0.00015	1.1
Γ_6	$3\pi^0$	(3.1 ±0.6) × 10^{-4}	1.1

$\eta'(958)$ PARTIAL WIDTHS

$\Gamma(\gamma\gamma)$ Γ_5

VALUE (keV)	EVTS	DOCUMENT ID		TECN	COMMENT
4.29±0.15 OUR FIT Error includes scale factor of 1.1.					
4.28±0.19 OUR AVERAGE					
4.17±0.10±0.27	2000	[1] ACCIARRI	98B	L3	$e^+e^- \to e^+e^-\pi^+\pi^-\gamma$
4.53±0.29±0.51	266	KARCH	92	CBAL	$e^+e^- \to e^+e^-\eta\pi^0\pi^0$
3.61±0.13±0.48		[2] BEHREND	91	CELL	$e^+e^- \to e^+e^-\eta'(958)$
4.6 ±1.1 ±0.6	23	BARU	90	MD1	$e^+e^- \to e^+e^-\pi^+\pi^-\gamma$
4.57±0.25±0.44		BUTLER	90	MRK2	$e^+e^- \to e^+e^-\eta'(958)$
5.08±0.24±0.71	547	[3] ROE	90	ASP	$e^+e^- \to e^+e^-2\gamma$
3.8 ±0.7 ±0.6	34	AIHARA	88C	TPC	$e^+e^- \to e^+e^-\eta\pi^+\pi^-$
4.9 ±0.5 ±0.5	136	[4] WILLIAMS	88	CBAL	$e^+e^- \to e^+e^-2\gamma$
• • • We do not use the following data for averages, fits, limits, etc. • • •					
4.7 ±0.6 ±0.9	143	[5] GIDAL	87	MRK2	$e^+e^- \to e^+e^-\eta\pi^+\pi^-$
4.0 ±0.9		[6] BARTEL	85E	JADE	$e^+e^- \to e^+e^-2\gamma$

[1] No non-resonant $\pi^+\pi^-$ contribution found.
[2] Reevaluated by us using $B(\eta' \to \rho(770)\gamma) = (30.2 \pm 1.3)\%$.
[3] Reevaluated by us using $B(\eta' \to \gamma\gamma) = (2.11 \pm 0.13)\%$.
[4] Reevaluated by us using $B(\eta' \to \gamma\gamma) = (2.11 \pm 0.13)\%$.
[5] Superseded by BUTLER 90.
[6] Systematic error not evaluated.

$\eta'(958)$ $\Gamma(i)\Gamma(\gamma\gamma)/\Gamma(\text{total})$

This combination of a partial width with the partial width into $\gamma\gamma$ and with the total width is obtained from the integrated cross section into channel(i) in the $\gamma\gamma$ annihilation.

$\Gamma(\gamma\gamma) \times \Gamma(\rho^0\gamma(\text{including non-resonant } \pi^+\pi^-\gamma))/\Gamma_{\rm total}$ $\Gamma_5\Gamma_2/\Gamma$

VALUE (keV)	EVTS	DOCUMENT ID		TECN	COMMENT
1.27±0.05 OUR FIT Error includes scale factor of 1.2.					
1.26±0.07 OUR AVERAGE Error includes scale factor of 1.2.					
1.09±0.04±0.13		BEHREND	91	CELL	$e^+e^- \to e^+e^-\rho(770)^0\gamma$
1.35±0.09±0.21		AIHARA	87	TPC	$e^+e^- \to e^+e^-\rho\gamma$
1.13±0.04±0.13	867	ALBRECHT	87B	ARG	$e^+e^- \to e^+e^-\rho\gamma$
1.53±0.09±0.21		ALTHOFF	84E	TASS	$e^+e^- \to e^+e^-\rho\gamma$
1.14±0.08±0.11	243	BERGER	84B	PLUT	$e^+e^- \to e^+e^-\rho\gamma$
1.73±0.34±0.35	95	JENNI	83	MRK2	$e^+e^- \to e^+e^-\rho\gamma$
1.49±0.13±0.027	213	BARTEL	82B	JADE	$e^+e^- \to e^+e^-\rho\gamma$
• • • We do not use the following data for averages, fits, limits, etc. • • •					
1.85±0.31±0.24	43	BEHREND	83B	CELL	$e^+e^- \to e^+e^-\rho\gamma$

$\Gamma(\gamma\gamma) \times \Gamma(\pi^0\pi^0\eta)/\Gamma_{\rm total}$ $\Gamma_5\Gamma_3/\Gamma$

VALUE (keV)	DOCUMENT ID		TECN	COMMENT
0.90±0.06 OUR FIT Error includes scale factor of 1.2.				
0.92±0.06±0.11	[7] KARCH	92	CBAL	$e^+e^- \to e^+e^-\eta\pi^0\pi^0$
• • • We do not use the following data for averages, fits, limits, etc. • • •				
0.95±0.05±0.08	[8] KARCH	90	CBAL	$e^+e^- \to e^+e^-\eta\pi^0\pi^0$
1.00±0.08±0.10	[8,9] ANTREASYAN	87	CBAL	$e^+e^- \to e^+e^-\eta\pi^0\pi^0$

[7] Reevaluated by us using $B(\eta \to \gamma\gamma) = (39.21 \pm 0.34)\%$. Supersedes ANTREASYAN 87 and KARCH 90.
[8] Superseded by KARCH 92.
[9] Using $BR(\eta \to 2\gamma) = (38.9 \pm 0.5)\%$.

$\eta'(958)$ α PARAMETER

$|\text{MATRIX ELEMENT}|^2 = (1 + \alpha y)^2 + cx^2$

VALUE	DOCUMENT ID		TECN	COMMENT
−0.058±0.013	[10] ALDE	86	GAM2	38 $\pi^- p \to n\eta 2\pi^0$
• • • We do not use the following data for averages, fits, limits, etc. • • •				
−0.08 ±0.03	[10] KALBFLEISCH	74	RVUE	$\eta' \to \eta\pi^+\pi^-$

[10] May not necessarily be the same for $\eta' \to \eta\pi^+\pi^-$ and $\eta' \to \eta\pi^0\pi^0$.

$\eta'(958)$ β PARAMETER

See the "Note on η Decay Parameters" in our 1994 edition Physical Review **D50** 1173 (1994), p. 1454.

$|\text{MATRIX ELEMENT}|^2 = (1 + 2\beta Z)$

VALUE	DOCUMENT ID		TECN	COMMENT
−0.1 ±0.3	ALDE	87B	GAM2	38 $\pi^- p \to n3\pi^0$

$\eta'(958)$ BRANCHING RATIOS

$\Gamma(\pi^+\pi^-\eta(\text{neutral decay}))/\Gamma_{\rm total}$ $0.714\Gamma_1/\Gamma$

VALUE	EVTS	DOCUMENT ID		TECN	COMMENT
0.316±0.010 OUR FIT Error includes scale factor of 1.2.					
0.314±0.026	281	RITTENBERG	69	HBC	1.7–2.7 $K^- p$

$\Gamma(\pi^+\pi^-\text{neutrals})/\Gamma_{\rm total}$ $(0.714\Gamma_1+0.286\Gamma_3+0.89\Gamma_4)/\Gamma$

VALUE	EVTS	DOCUMENT ID		TECN	COMMENT
0.403±0.008 OUR FIT Error includes scale factor of 1.2.					
0.36 ±0.05 OUR AVERAGE					
0.4 ±0.1	39	LONDON	66	HBC	2.24 $K^- p \to \Lambda\pi^+\pi^-$ neutrals
0.35 ±0.06	33	BADIER	65B	HBC	3 $K^- p$

$\Gamma(\pi^+\pi^-\eta(\text{charged decay}))/\Gamma_{\rm total}$ $0.286\Gamma_1/\Gamma$

VALUE	EVTS	DOCUMENT ID		TECN	COMMENT
0.127±0.004 OUR FIT Error includes scale factor of 1.2.					
0.116±0.013 OUR AVERAGE					
0.123±0.014	107	RITTENBERG	69	HBC	1.7–2.7 $K^- p$
0.10 ±0.04	10	LONDON	66	HBC	2.24 $K^- p \to \Lambda\pi^+\pi^-\pi^+\pi^-\pi^0$
0.07 ±0.04	7	BADIER	65B	HBC	3 $K^- p$

$[\Gamma(\pi^0\pi^0\eta(\text{charged decay})) + \Gamma(\omega(\text{charged decay})\gamma)]/\Gamma_{\rm total}$ $(0.286\Gamma_3+0.89\Gamma_4)/\Gamma$

VALUE	EVTS	DOCUMENT ID		TECN	COMMENT
0.087±0.005 OUR FIT Error includes scale factor of 1.2.					
0.045±0.029	42	RITTENBERG	69	HBC	1.7–2.7 $K^- p$

$\Gamma(\text{neutrals})/\Gamma_{\rm total}$ $(0.714\Gamma_3+0.09\Gamma_4+\Gamma_5)/\Gamma$

VALUE	EVTS	DOCUMENT ID		TECN	COMMENT
0.173±0.009 OUR FIT Error includes scale factor of 1.2.					
0.187±0.017 OUR AVERAGE					
0.185±0.022	535	BASILE	71	CNTR	1.6 $\pi^- p \to nX^0$
0.189±0.026	123	RITTENBERG	69	HBC	1.7–2.7 $K^- p$

$\Gamma(\rho^0\gamma(\text{including non-resonant } \pi^+\pi^-\gamma))/\Gamma_{\rm total}$ Γ_2/Γ

VALUE	EVTS	DOCUMENT ID		TECN	COMMENT
0.295±0.010 OUR FIT Error includes scale factor of 1.2.					
0.319±0.030 OUR AVERAGE					
0.329±0.033	298	RITTENBERG	69	HBC	1.7–2.7 $K^- p$
0.2 ±0.1	20	LONDON	66	HBC	2.24 $K^- p \to \Lambda\pi^+\pi^-\gamma$
0.34 ±0.09	35	BADIER	65B	HBC	3 $K^- p$

$\Gamma(\rho^0\gamma(\text{including non-resonant } \pi^+\pi^-\gamma))/\Gamma(\pi\pi\eta)$ $\Gamma_2/(\Gamma_1+\Gamma_3)$

VALUE	DOCUMENT ID		TECN	COMMENT
0.453±0.022 OUR FIT Error includes scale factor of 1.2.				
0.426±0.028 OUR AVERAGE				
0.43 ±0.02 ±0.02	BARBERIS	98C	OMEG	450 $pp \to p_f \eta' p_s$
0.31 ±0.15	DAVIS	68	HBC	5.5 $K^- p$

$\Gamma(\gamma e^+e^-)/\Gamma_{total}$ Γ_{15}/Γ

VALUE	CL%	DOCUMENT ID		TECN	COMMENT
< 0.9	90	BRIERE	00	CLEO	10.6 e^+e^-

$\Gamma(\pi^0 e^+e^-)/\Gamma_{total}$ Γ_{21}/Γ

VALUE (units 10^{-3})	CL%	DOCUMENT ID		TECN	COMMENT
< 1.4	90	BRIERE	00	CLEO	10.6 e^+e^-
• • • We do not use the following data for averages, fits, limits, etc. • • •					
< 13	90	RITTENBERG	65	HBC	2.7 K^-p

$\Gamma(\eta e^+e^-)/\Gamma_{total}$ Γ_{22}/Γ

VALUE (units 10^{-3})	CL%	DOCUMENT ID		TECN	COMMENT
< 2.4	90	BRIERE	00	CLEO	10.6 e^+e^-
• • • We do not use the following data for averages, fits, limits, etc. • • •					
< 11	90	RITTENBERG	65	HBC	2.7 K^-p

$\Gamma(\pi^0\rho^0)/\Gamma_{total}$ Γ_9/Γ

VALUE	CL%	DOCUMENT ID		TECN	COMMENT
< 0.04	90	RITTENBERG	65	HBC	2.7 K^-p

$\Gamma(\pi^+\pi^-e^+e^-)/\Gamma_{total}$ Γ_{14}/Γ

VALUE	CL%	DOCUMENT ID		TECN	COMMENT
< 0.006	90	RITTENBERG	65	HBC	2.7 K^-p

$\Gamma(6\pi)/\Gamma_{total}$ Γ_{13}/Γ

VALUE	CL%	DOCUMENT ID		TECN	COMMENT
< 0.01	90	LONDON	66	HBC	Compilation

$\Gamma(\omega\gamma)/\Gamma(\pi^+\pi^-\eta)$ Γ_4/Γ_1

VALUE	EVTS	DOCUMENT ID		TECN	COMMENT
0.069 ± 0.008 OUR FIT	Error includes scale factor of 1.1.				
0.068 ± 0.013	68	ZANFINO	77	ASPK	8.4 π^-p

$\Gamma(\rho^0\gamma(\text{including non-resonant } \pi^+\pi^-\gamma))/[\Gamma(\pi^+\pi^-\eta)+\Gamma(\pi^0\pi^0\eta)+\Gamma(\omega\gamma)]$ $\Gamma_2/(\Gamma_1+\Gamma_3+\Gamma_4)$

VALUE	DOCUMENT ID		TECN	COMMENT
0.433 ± 0.021 OUR FIT	Error includes scale factor of 1.2.			
0.25 ± 0.14	DAUBER	64	HBC	1.95 K^-p

$\Gamma(\gamma\gamma)/\Gamma_{total}$ Γ_5/Γ

VALUE	EVTS	DOCUMENT ID		TECN	COMMENT
0.0212 ± 0.0014 OUR FIT	Error includes scale factor of 1.3.				
0.0196 ± 0.0015 OUR AVERAGE					
0.0200 ± 0.0018		[11] STANTON	80	SPEC	8.45 $\pi^-p \to n\pi^+\pi^-2\gamma$
0.025 ± 0.007		DUANE	74	MMS	$\pi^-p \to n$MM
0.0171 ± 0.0033	68	DALPIAZ	72	CNTR	1.6 $\pi^-p \to nX^0$
$0.020\ ^{+0.008}_{-0.006}$	31	HARVEY	71	OSPK	3.65 $\pi^-p \to nX^0$
• • • We do not use the following data for averages, fits, limits, etc. • • •					
0.018 ± 0.002	6000	[12] APEL	79	NICE	15–40 $\pi^-p \to n2\gamma$

[11] Includes APEL 79 result.
[12] Data is included in STANTON 80 evaluation.

$\Gamma(e^+e^-)/\Gamma_{total}$ Γ_{18}/Γ

VALUE (units 10^{-7})	CL%	DOCUMENT ID		TECN	COMMENT
< 2.1	90	VOROBYEV	88	ND	$e^+e^- \to \pi^+\pi^-\eta$

$\Gamma(\pi^+\pi^-)/\Gamma_{total}$ Γ_{19}/Γ

VALUE	CL%	DOCUMENT ID		TECN	COMMENT
< 0.02	90	RITTENBERG	69	HBC	1.7–2.7 K^-p
• • • We do not use the following data for averages, fits, limits, etc. • • •					
< 0.08	95	DANBURG	73	HBC	2.2 $K^-p \to \Lambda X^0$

$\Gamma(\pi^+\pi^-\pi^0)/\Gamma_{total}$ Γ_8/Γ

VALUE	CL%	DOCUMENT ID		TECN	COMMENT
< 0.05	90	RITTENBERG	69	HBC	1.7–2.7 K^-p
• • • We do not use the following data for averages, fits, limits, etc. • • •					
< 0.09	95	DANBURG	73	HBC	2.2 $K^-p \to \Lambda X^0$

$\Gamma(\pi^+\pi^+\pi^-\pi^-\text{neutrals})/\Gamma_{total}$ Γ_{11}/Γ

VALUE	CL%	DOCUMENT ID		TECN	COMMENT
< 0.01	95	DANBURG	73	HBC	2.2 $K^-p \to \Lambda X^0$
• • • We do not use the following data for averages, fits, limits, etc. • • •					
< 0.01	90	RITTENBERG	69	HBC	1.7–2.7 K^-p

$\Gamma(\pi^+\pi^+\pi^-\pi^-\pi^0)/\Gamma_{total}$ Γ_{12}/Γ

VALUE	CL%	DOCUMENT ID		TECN	COMMENT
< 0.01	90	RITTENBERG	69	HBC	1.7–2.7 K^-p

$\Gamma(\pi^+\pi^+\pi^-\pi^-)/\Gamma_{total}$ Γ_{10}/Γ

VALUE	CL%	DOCUMENT ID		TECN	COMMENT
< 0.01	90	RITTENBERG	69	HBC	1.7–2.7 K^-p

$\Gamma(\pi^0\pi^0\eta(3\pi^0\text{ decay}))/\Gamma_{total}$ $0.321\,\Gamma_3/\Gamma$

VALUE	EVTS	DOCUMENT ID		TECN	COMMENT
0.067 ± 0.004 OUR FIT	Error includes scale factor of 1.2.				
0.11 ± 0.06	4	BENSINGER	70	DBC	2.2 π^+d

$\Gamma(\rho^0\gamma(\text{including non-resonant } \pi^+\pi^-\gamma))/\Gamma(\pi^+\pi^-\eta(\text{neutral decay}))$ $\Gamma_2/0.714\,\Gamma_1$

VALUE	EVTS	DOCUMENT ID		TECN	COMMENT
0.93 ± 0.05 OUR FIT	Error includes scale factor of 1.2.				
1.01 ± 0.09 OUR AVERAGE					
1.07 ± 0.17		BELADIDZE	92C	VES	36 π^-Be $\to \pi^-\eta'\eta$Be
0.92 ± 0.14	473	DANBURG	73	HBC	2.2 $K^-p \to \Lambda X^0$
1.11 ± 0.18	192	JACOBS	73	HBC	2.9 $K^-p \to \Lambda X^0$

$\Gamma(\gamma\gamma)/\Gamma(\pi^0\pi^0\eta(\text{neutral decay}))$ $\Gamma_5/0.714\,\Gamma_3$

VALUE	EVTS	DOCUMENT ID		TECN	COMMENT
0.142 ± 0.010 OUR FIT	Error includes scale factor of 1.6.				
0.188 ± 0.058	16	APEL	72	OSPK	3.8 $\pi^-p \to nX^0$

$\Gamma(\mu^+\mu^-\gamma)/\Gamma(\gamma\gamma)$ Γ_7/Γ_5

VALUE (units 10^{-3})	EVTS	DOCUMENT ID		TECN	COMMENT
4.9 ± 1.2	33	VIKTOROV	80	CNTR	25,33 $\pi^-p \to 2\mu\gamma$

$\Gamma(\mu^+\mu^-\eta)/\Gamma_{total}$ Γ_{25}/Γ

VALUE (units 10^{-5})	CL%	DOCUMENT ID		TECN	COMMENT
< 1.5	90	DZHELYADIN	81	CNTR	30 $\pi^-p \to \eta' n$

$\Gamma(\mu^+\mu^-\pi^0)/\Gamma_{total}$ Γ_{24}/Γ

VALUE (units 10^{-5})	CL%	DOCUMENT ID		TECN	COMMENT
< 6.0	90	DZHELYADIN	81	CNTR	30 $\pi^-p \to \eta' n$

$\Gamma(3\pi^0)/\Gamma(\pi^0\pi^0\eta)$ Γ_6/Γ_3

VALUE (units 10^{-4})	DOCUMENT ID		TECN	COMMENT
74 ± 12 OUR FIT				
74 ± 12 OUR AVERAGE				
74 ± 15	ALDE	87B	GAM2	38 $\pi^-p \to n6\gamma$
75 ± 18	BINON	84	GAM2	30–40 $\pi^-p \to n6\gamma$

$\Gamma(\gamma\gamma)/\Gamma(\pi^0\pi^0\eta)$ Γ_5/Γ_3

VALUE	DOCUMENT ID		TECN	COMMENT
0.101 ± 0.007 OUR FIT	Error includes scale factor of 1.6.			
0.105 ± 0.010 OUR AVERAGE	Error includes scale factor of 1.9.			
0.091 ± 0.009	AMSLER	93	CBAR	0.0 $\bar{p}p$
0.112 ± 0.002 ± 0.006	ALDE	87B	GAM2	38 $\pi^-p \to n2\gamma$

$\Gamma(\omega\gamma)/\Gamma(\pi^0\pi^0\eta)$ Γ_4/Γ_3

VALUE	DOCUMENT ID		TECN	COMMENT
0.145 ± 0.014 OUR FIT				
0.147 ± 0.016	ALDE	87B	GAM2	38 $\pi^-p \to n4\gamma$

$\Gamma(3\gamma)/\Gamma(\pi^0\pi^0\eta)$ Γ_{23}/Γ_3

VALUE (units 10^{-4})	CL%	DOCUMENT ID		TECN	COMMENT
< 4.6	90	ALDE	87B	GAM2	38 $\pi^-p \to n3\gamma$

$\Gamma(\pi^0\gamma\gamma)/\Gamma(\pi^0\pi^0\eta)$ Γ_{16}/Γ_3

VALUE (units 10^{-4})	CL%	DOCUMENT ID		TECN	COMMENT
< 37	90	ALDE	87B	GAM2	38 $\pi^-p \to n4\gamma$

$\Gamma(\pi^0\pi^0)/\Gamma(\pi^0\pi^0\eta)$ Γ_{20}/Γ_3

VALUE (units 10^{-4})	CL%	DOCUMENT ID		TECN	COMMENT
< 45	90	ALDE	87B	GAM2	38 $\pi^-p \to n4\gamma$

$\Gamma(4\pi^0)/\Gamma(\pi^0\pi^0\eta)$ Γ_{17}/Γ_3

VALUE (units 10^{-4})	CL%	DOCUMENT ID		TECN	COMMENT
< 23	90	ALDE	87B	GAM2	38 $\pi^-p \to n8\gamma$

$\Gamma(e\mu)/\Gamma_{total}$ Γ_{26}/Γ

VALUE (units 10^{-4})	CL%	DOCUMENT ID		TECN	COMMENT
< 4.7	90	BRIERE	00	CLEO	10.6 e^+e^-

Meson Particle Listings

$\eta'(958)$, $f_0(980)$

$\eta'(958)$ C-NONCONSERVING DECAY PARAMETER

See the note on η decay parameters in the Stable Particle Particle Listings for definition of this parameter.

DECAY ASYMMETRY PARAMETER FOR $\pi^+\pi^-\gamma$

VALUE	EVTS	DOCUMENT ID		TECN	COMMENT
−0.01 ±0.04 OUR AVERAGE					
−0.019±0.056		AIHARA	87	TPC	$2\gamma \to \pi^+\pi^-\gamma$
−0.069±0.078	295	GRIGORIAN	75	STRC	2.1 π^-p
0.00 ±0.10	103	KALBFLEISCH	75	HBC	2.18 $K^-p \to \Lambda\pi^+\pi^-\gamma$
0.07 ±0.08	152	RITTENBERG	65	HBC	2.1–2.7 K^-p

$\eta'(958)$ REFERENCES

BRIERE	00	PRL 84 26	R. Briere *et al.*	(CLEO Collab.)
ACCIARRI	98B	PL B418 389	M. Acciarri *et al.*	(L3 Collab.)
BARBERIS	98C	PL B440 225	D. Barberis *et al.*	(WA 102 Collab.)
WURZINGER	96	PL B374 283	R. Wurzinger *et al.*	(BONN, ORSAY, SACL+)
PDG	94	PR D50 1173	L. Montanet *et al.*	(CERN, LBL, BOST+)
AMSLER	93	ZPHY C58 175	C. Amsler *et al.*	(Crystal Barrel Collab.)
BELADIDZE	92C	SJNP 55 1535 Translated from YAF 55 2748.	G.M. Beladidze, S.I. Bityukov, G.V. Borisov	(SERP+)
KARCH	92	ZPHY C54 33	K. Karch *et al.*	(Crystal Ball Collab.)
ARMSTRONG	91B	ZPHY C52 389	T.A. Armstrong *et al.*	(ATHU, BARI, BIRM+)
BEHREND	91	ZPHY C49 401	H.J. Behrend *et al.*	(CELLO Collab.)
AUGUSTIN	90	PR D42 10	J.E. Augustin *et al.*	(DM2 Collab.)
BARU	90	ZPHY C48 581	S.E. Baru *et al.*	(MD-1 Collab.)
BUTLER	90	PR D42 1368	F. Butler *et al.*	(Mark II Collab.)
KARCH	90	PL B249 353	K. Karch *et al.*	(Crystal Ball Collab.)
ROE	90	PR D41 17	N.A. Roe *et al.*	(ASP Collab.)
AIHARA	88C	PR D38 1	H. Aihara *et al.*	(TPC-2γ Collab.)
VOROBYEV	88	SJNP 48 273 Translated from YAF 48 436.	P.V. Vorobiev *et al.*	(NOVO)
WILLIAMS	88	PR D38 1365	D.A. Williams *et al.*	(Crystal Ball Collab.)
AIHARA	87	PR D35 2650	H. Aihara *et al.*	(TPC-2γ Collab.) JP
ALBRECHT	87B	PL B199 457	H. Albrecht *et al.*	(ARGUS Collab.)
ALDE	87B	ZPHY C36 603	D.M. Alde *et al.*	(LANL, BELG, SERP, LAPP)
ANTREASYAN	87	PR D36 2633	D. Antreasyan *et al.*	(Crystal Ball Collab.)
GIDAL	87	PRL 59 2012	G. Gidal *et al.*	(LBL, SLAC, HARV)
ALDE	86	PL B177 115	D.M. Alde *et al.*	(SERP, BELG, LANL, LAPP)
BARTEL	85E	PL 160B 421	W. Bartel *et al.*	(JADE Collab.)
ALTHOFF	84E	PL 147B 487	M. Althoff *et al.*	(TASSO Collab.)
BERGER	84B	PL 142B 125	C. Berger	(PLUTO Collab.)
BINON	84	PL 140B 264	F.G. Binon *et al.*	(SERP, BELG, LAPP+)
BEHREND	83B	PL 125B 518	H.J. Behrend *et al.*	(CELLO Collab.)
Also	82C	PL 114B 378	H.J. Behrend *et al.*	(CELLO Collab.)
JENNI	83	PR D27 1031	P. Jenni *et al.*	(SLAC, LBL)
BARTEL	82B	PL 113B 190	W. Bartel *et al.*	(JADE Collab.)
DZHELYADIN	81	PL 105B 239	R.I. Dzhelyadin *et al.*	(SERP)
STANTON	80	PL 92B 353	N.R. Stanton *et al.*	(OSU, CARL, MCGI+)
VIKTOROV	80	SJNP 32 520 Translated from YAF 32 1005.	V.A. Viktorov *et al.*	(SERP)
APEL	79	PL 83B 131	W.D. Apel, K.H. Augenstein, E. Bertolucci	(KARLK+)
BINNIE	79	PL 83B 141	D.M. Binnie *et al.*	(LOIC)
ZANFINO	77	PRL 38 930	C. Zanfino *et al.*	(CARL, MCGI, OHIO+)
GRIGORIAN	75	NP B91 232	A. Grigorian *et al.*	(+)
KALBFLEISCH	75	PR D11 987	G.R. Kalbfleisch, R.C. Strand, J.W. Chapman	(BNL+)
DUANE	74	PRL 32 425	A. Duane *et al.*	(LOIC, SHMP)
KALBFLEISCH	74	PR D10 916	G.R. Kalbfleisch	(BNL)
DANBURG	73	PR D8 3744	J.S. Danburg *et al.*	(BNL, MICH) JP
JACOBS	73	PR D8 18	S.M. Jacobs *et al.*	(BRAN, UMD, SYRA+) JP
APEL	72	PL 40B 680	W.D. Apel *et al.*	(KARLK, KARLE, PISA)
DALPIAZ	72	PL 42B 377	P.F. Dalpiaz *et al.*	(CERN)
BASILE	71	NC 3A 371	M. Basile *et al.*	(CERN, BGNA, STRB)
HARVEY	71	PRL 27 885	E.H. Harvey *et al.*	(MINN, MICH)
BENSINGER	70	PL 33B 505	J.R. Bensinger *et al.*	(WISC)
RITTENBERG	69	Thesis UCRL 18863	A. Rittenberg	(LRL) I
DAVIS	68	PL 27B 532	R. Davis *et al.*	(NWES, ANL)
LONDON	66	PR 143 1034	G.W. London *et al.*	(BNL, SYRA) JP
BADIER	65B	PL 17 337	J. Badier *et al.*	(EPOL, SACL, AMST)
RITTENBERG	65	PRL 15 556	A. Rittenberg, G.R. Kalbfleisch	(LRL, BNL)
DAUBER	64	PRL 13 449	P.M. Dauber *et al.*	(UCLA) JP

OTHER RELATED PAPERS

BENAYOUN	03B	EPJ C31 525	M. Benayoun *et al.*	
BENAYOUN	99B	PR D59 114027	M. Benayoun *et al.*	
PROKOSHKIN	99	PAN 62 356 Translated from YAF 62 396.	Yu.D. Prokoshkin	
GRONBERG	98	PR D57 33	J. Gronberg *et al.*	(CLEO Collab.)
ABELE	97B	PL B402 195	A. Abele *et al.*	(Crystal Barrel Collab.)
GENOVESE	94	ZPHY C61 425	M. Genovese, D.B. Lichtenberg, E. Predazzi	(TORI+)
BENAYOUN	93	ZPHY C58 31	M. Benayoun *et al.*	(CDEF, CERN, BARI)
KAMAL	92	PL B284 421	A.N. Kamal, Q.P. Xu	(ALBE)
BICKERSTAFF	82	ZPHY C16 171	R.P. Bickerstaff, B.H.J. McKellar	(MELB)
KIENZLE	65	PL 19 438	W. Kienzle *et al.*	(CERN)
TRILLING	65	PL 19 427	G.H. Trilling *et al.*	(LRL)
GOLDBERG	64	PRL 12 546	M. Goldberg *et al.*	(SYRA, BNL)
GOLDBERG	64B	PRL 13 249	M. Goldberg *et al.*	(SYRA, BNL)
KALBFLEISCH	64	PRL 12 527	G.R. Kalbfleisch *et al.*	(LRL) JP
KALBFLEISCH	64B	PRL 13 349	G.R. Kalbfleisch, O.I. Dahl, A. Rittenberg	(LRL) JP

$f_0(980)$

$I^G(J^{PC}) = 0^+(0^{++})$

See also the minireview on scalar mesons under $f_0(600)$. (See the index for the page number.)

$f_0(980)$ MASS

VALUE (MeV)	EVTS	DOCUMENT ID		TECN	COMMENT
980 ±10 OUR ESTIMATE					
• • • We do not use the following data for averages, fits, limits, etc. • • •					
1031 ± 8		[1] ANISOVICH	03	RVUE	
1037 ±31		TIKHOMIROV	03	SPEC	40.0 π^- C → $K^0_S K^0_S K^0_L$ X
973 ± 1	2438	[2] ALOISIO	02D	KLOE	$e^+e^- \to \pi^0\pi^0\gamma$
977 ± 3 ±2	848	[3] AITALA	01A	E791	$D^+_s \to \pi^-\pi^+\pi^+$
969.8± 4.5	419	[4] ACHASOV	00H	SND	$e^+e^- \to \pi^0\pi^0\gamma$
985 $^{+16}_{-12}$	419	[5,6] ACHASOV	00H	SND	$e^+e^- \to \pi^0\pi^0\gamma$
976 ± 5 ±6		[7] AKHMETSHIN	99B	CMD2	$e^+e^- \to \pi^+\pi^-\gamma$
977 ± 3 ±6	268	[7] AKHMETSHIN	99C	CMD2	$e^+e^- \to \pi^0\pi^0\gamma$
975 ± 4 ±6		[8] AKHMETSHIN	99C	CMD2	$e^+e^- \to \pi^0\pi^0\gamma$
975 ± 4 ±6		[9] AKHMETSHIN	99C	CMD2	$e^+e^- \to \pi^+\pi^-\gamma$, $\pi^0\pi^0\gamma$
985 ±10		BARBERIS	99	OMEG	450 $pp \to p_s p_f K^+K^-$
982 ± 3		BARBERIS	99B	OMEG	450 $pp \to p_s p_f \pi^+\pi^-$
982 ± 3		BARBERIS	99C	OMEG	450 $pp \to p_s p_f \pi^0\pi^0$
987 ± 6 ±6		[10] BARBERIS	99D	OMEG	450 $pp \to K^+K^-$, $\pi^+\pi^-$
989 ±15		BELLAZZINI	99	GAM4	450 $pp \to pp\pi^0\pi^0$
991 ± 3		[11] KAMINSKI	99	RVUE	$\pi\pi \to \pi\pi$, $K\overline{K}$, $\sigma\sigma$
~ 980		[11] OLLER	99	RVUE	$\pi\pi \to \pi\pi$, $K\overline{K}$
~ 993.5		OLLER	99B	RVUE	$\pi\pi \to \pi\pi$, $K\overline{K}$
~ 987		[11] OLLER	99C	RVUE	$\pi\pi \to \pi\pi$, $K\overline{K}$, $\eta\eta$
957 ± 6		[12] ACKERSTAFF	98Q	OPAL	$Z \to f_0$ X
960 ±10		ALDE	98	GAM4	
1015 ±15		[11] ANISOVICH	98B	RVUE	Compilation
1008		[13] LOCHER	98	RVUE	$\pi\pi \to \pi\pi$, $K\overline{K}$
955 ±10		[12] ALDE	97	GAM2	450 $pp \to pp\pi^0\pi^0$
994 ± 9		[14] BERTIN	97C	OBLX	0.0 $\overline{p}p \to \pi^+\pi^-\pi^0$
993.2± 6.5 ±6.9		[15] ISHIDA	96	RVUE	$\pi\pi \to \pi\pi$, $K\overline{K}$
1006		TORNQVIST	96	RVUE	$\pi\pi \to \pi\pi$, $K\overline{K}$, $K\pi$, $\eta\pi$
997 ± 5	3k	[16] ALDE	95B	GAM2	38 $\pi^-p \to \pi^0\pi^0n$
960 ±10	10k	[17] ALDE	95B	GAM2	38 $\pi^-p \to \pi^0\pi^0n$
994 ± 5		AMSLER	95B	CBAR	0.0 $\overline{p}p \to 3\pi^0$
~ 996		[18] AMSLER	95D	CBAR	0.0 $\overline{p}p \to \pi^0\pi^0\pi^0$, $\pi^0\eta\eta$, $\pi^0\pi^0\eta$
987 ± 6		[19] ANISOVICH	95	RVUE	
1015		JANSSEN	95	RVUE	$\pi\pi \to \pi\pi$, $K\overline{K}$
983		[20] BUGG	94	RVUE	$\overline{p}p \to \eta 2\pi^0$
973 ± 2		[21] KAMINSKI	94	RVUE	$\pi\pi \to \pi\pi$, $K\overline{K}$
988		[22] ZOU	94B	RVUE	
988 ±10		[23] MORGAN	93	RVUE	$\pi\pi(K\overline{K}) \to \pi\pi(K\overline{K})$, $J/\psi \to \phi\pi\pi(K\overline{K})$, $D_s \to \pi(\pi\pi)$
971.1± 4.0		[12] AGUILAR-...	91	EHS	400 pp
979 ± 4		[24] ARMSTRONG	91	OMEG	300 $pp \to pp\pi\pi$, $pp K\overline{K}$
956 ±12		BREAKSTONE	90	SFM	$pp \to pp\pi^+\pi^-$
959.4± 6.5		[12] AUGUSTIN	89	DM2	$J/\psi \to \omega\pi^+\pi^-$
978 ± 9		[12] ABACHI	86B	HRS	$e^+e^- \to \pi^+\pi^-$X
985.0 $^{+\ 9.0}_{-39.0}$		ETKIN	82B	MPS	23 $\pi^-p \to n2K^0_S$
974 ± 4		[24] GIDAL	81	MRK2	$J/\psi \to \pi^+\pi^-$X
975		[25] ACHASOV	80	RVUE	
986 ±10		[24] AGUILAR-...	78	HBC	0.7 $\overline{p}p \to K^0_S K^0_S$
969 ± 5		[24] LEEPER	77	ASPK	2–2.4 $\pi^-p \to \pi^+\pi^-n$, K^+K^-n
987 ± 7		[24] BINNIE	73	CNTR	$\pi^-p \to n$MM
1012 ± 6		[26] GRAYER	73	ASPK	17 $\pi^-p \to \pi^+\pi^-n$
1007 ±20		[26] HYAMS	73	ASPK	17 $\pi^-p \to \pi^+\pi^-n$
997 ± 6		[26] PROTOPOP...	73	HBC	7 $\pi^+p \to \pi^+p\pi^+\pi^-$

[1] K-matrix pole from combined analysis of $\pi^-p \to \pi^0\pi^0n$, $\pi^-p \to K\overline{K}n$, $\pi^+\pi^- \to \pi^+\pi^-$, $\overline{p}p \to \pi^0\pi^0\pi^0$, $\pi^0\eta\eta$, $\pi^0\pi^0\eta$, $\pi^+\pi^-\pi^0$, $K^+K^-\pi^0$, $K^0_SK^0_S\pi^0$, $K^+K^0_S\pi^-$ at rest, $\overline{p}n \to \pi^-\pi^-\pi^+$, $K^0_SK^-\pi^0$, $K^0_SK^0_S\pi^-$ at rest.

[2] From the negative interference with the $f_0(600)$ meson of AITALA 01B using the ACHASOV 89 parameterization for the $f_0(980)$, a Breit-Wigner for the $f_0(600)$, and ACHASOV 01F for the $\rho\pi$ contribution.

[3] Coupled-channel Breit-Wigner, couplings $g_\pi = 0.09 \pm 0.01 \pm 0.01$, $g_K = 0.02 \pm 0.04 \pm 0.03$.

[4] Supersedes ACHASOV 98I. Using the model of ACHASOV 89.

[5] Supersedes ACHASOV 98I.
[6] In the "narrow resonance" approximation.
[7] Assuming $\Gamma(f_0) = 40$ MeV.
[8] From a narrow pole fit taking into account $f_0(980)$ and $f_0(1200)$ intermediate mechanisms.
[9] From the combined fit of the photon spectra in the reactions $e^+e^- \to \pi^+\pi^-\gamma$, $\pi^0\pi^0\gamma$.
[10] Supersedes BARBERIS 99 and BARBERIS 99B
[11] T-matrix pole.
[12] From invariant mass fit.
[13] On sheet II in a 2 pole solution. The other pole is found on sheet III at (1039−93i) MeV.
[14] On sheet II in a 2 pole solution. The other pole is found on sheet III at (963-29i) MeV.
[15] Reanalysis of data from HYAMS 73, GRAYER 74, SRINIVASAN 75, and ROSSELET 77 using the interfering amplitude method.
[16] At high $|t|$.
[17] At low $|t|$.
[18] On sheet II in a 4-pole solution, the other poles are found on sheet III at (953−55i) MeV and on sheet IV at (938−35i) MeV.
[19] Combined fit of ALDE 95B, ANISOVICH 94, AMSLER 94D.
[20] On sheet II in a 2 pole solution. The other pole is found on sheet III at (996−103i) MeV.
[21] From sheet II pole position.
[22] On sheet II in a 2 pole solution. The other pole is found on sheet III at (797−185i) MeV and can be interpreted as a shadow pole.
[23] On sheet II in a 2 pole solution. The other pole is found on sheet III at (978−28i) MeV.
[24] From coupled channel analysis.
[25] Coupled channel analysis with finite width corrections.
[26] Included in AGUILAR-BENITEZ 78 fit.

$f_0(980)$ WIDTH

Width determination very model dependent. Peak width in $\pi\pi$ is about 50 MeV, but decay width can be much larger.

VALUE (MeV)	EVTS	DOCUMENT ID		TECN	COMMENT
40 to 100 OUR ESTIMATE					
• • • We do not use the following data for averages, fits, limits, etc. • • •					
64 ± 16		[27] ANISOVICH	03	RVUE	
121 ± 23		TIKHOMIROV	03	SPEC	40.0 π^- C → $K^0_S K^0_S K^0_L$ X
~ 70		[28] BRAMON	02	RVUE	1.02 e^+e^- → $\pi^0\pi^0\gamma$
44 ± 2 ± 2	848	[29] AITALA	01A	E791	$D^+_s \to \pi^-\pi^+\pi^+$
201 ± 28	419	[30] ACHASOV	00H	SND	$e^+e^- \to \pi^0\pi^0\gamma$
122 ± 13	419	[31,32] ACHASOV	00H	SND	$e^+e^- \to \pi^0\pi^0\gamma$
56 ± 20		[33] AKHMETSHIN	99C	CMD2	$e^+e^- \to \pi^0\pi^0\gamma$
65 ± 20		BARBERIS	99	OMEG	450 $pp \to p_s p_f K^+K^-$
80 ± 10		BARBERIS	99B	OMEG	450 $pp \to p_s p_f \pi^+\pi^-$
80 ± 10		BARBERIS	99C	OMEG	450 $pp \to p_s p_f \pi^0\pi^0$
48 ± 12 ± 8		[34] BARBERIS	99D	OMEG	450 $pp \to K^+K^-$, $\pi^+\pi^-$
65 ± 25		BELLAZZINI	99	GAM4	450 $pp \to pp\pi^0\pi^0$
71 ± 14		[35] KAMINSKI	99	RVUE	$\pi\pi \to \pi\pi$, $K\overline{K}$, $\sigma\sigma$
~ 28		[35] OLLER	99	RVUE	$\pi\pi \to \pi\pi$, $K\overline{K}$
~ 25		OLLER	99B	RVUE	$\pi\pi \to \pi\pi$, $K\overline{K}$
~ 14		[35] OLLER	99C	RVUE	$\pi\pi \to \pi\pi$, $K\overline{K}$, $\eta\eta$
70 ± 20		ALDE	98	GAM4	
86 ± 16		[35] ANISOVICH	98B	RVUE	Compilation
54		[36] LOCHER	98	RVUE	$\pi\pi \to \pi\pi$, $K\overline{K}$
69 ± 15		[37] ALDE	97	GAM2	450 $pp \to pp\pi^0\pi^0$
38 ± 20		[38] BERTIN	97C	OBLX	0.0 $\overline{p}p \to \pi^+\pi^-\pi^0$
~ 100		[39] ISHIDA	96	RVUE	$\pi\pi \to \pi\pi$, $K\overline{K}$
34		TORNQVIST	96	RVUE	$\pi\pi \to \pi\pi$, $K\overline{K}$, $K\pi$, $\eta\pi$
48 ± 10	3k	[40] ALDE	95B	GAM2	38 $\pi^-p \to \pi^0\pi^0 n$
95 ± 20	10k	[41] ALDE	95B	GAM2	38 $\pi^-p \to \pi^0\pi^0 n$
26 ± 10		AMSLER	95B	CBAR	0.0 $\overline{p}p \to 3\pi^0$
~ 112		[42] AMSLER	95D	CBAR	0.0 $\overline{p}p \to \pi^0\pi^0\pi^0$, $\pi^0\eta\eta$, $\pi^0\pi^0\eta$
80 ± 12		[43] ANISOVICH	95	RVUE	
30		JANSSEN	95	RVUE	$\pi\pi \to \pi\pi$, $K\overline{K}$
74		[44] BUGG	94	RVUE	$\overline{p}p \to \eta 2\pi^0$
29 ± 2		[45] KAMINSKI	94	RVUE	$\pi\pi \to \pi\pi$, $K\overline{K}$
46		[46] ZOU	94B	RVUE	
48 ± 12		[47] MORGAN	93	RVUE	$\pi\pi(K\overline{K}) \to \pi\pi(K\overline{K})$, $J/\psi \to \phi\pi\pi(K\overline{K})$, $D_s \to \pi(\pi\pi)$
37.4 ± 10.6		[37] AGUILAR-...	91	EHS	400 pp
72 ± 8		[48] ARMSTRONG	91	OMEG	300 $pp \to pp\pi\pi$, $pp\overline{K}K$
110 ± 30		BREAKSTONE	90	SFM	$pp \to pp\pi^+\pi^-$
29 ± 13		[37] ABACHI	86B	HRS	$e^+e^- \to \pi^+\pi^-$X
120 ±281 ±20		ETKIN	82B	MPS	23 $\pi^-p \to n2K^0_S$
28 ± 10		[48] GIDAL	81	MRK2	$J/\psi \to \pi^+\pi^-$X
70 to 300		[49] ACHASOV	80	RVUE	
100 ± 80		[50] AGUILAR-...	78	HBC	0.7 $\overline{p}p \to K^0_S K^0_S$
30 ± 8		[48] LEEPER	77	ASPK	2–2.4 $\pi^-p \to \pi^+\pi^-n$, K^+K^-n
48 ± 14		[48] BINNIE	73	CNTR	$\pi^-p \to n$MM
32 ± 10		[51] GRAYER	73	ASPK	17 $\pi^-p \to \pi^+\pi^-n$
30 ± 10		[51] HYAMS	73	ASPK	17 $\pi^-p \to \pi^+\pi^-n$
54 ± 16		[51] PROTOPOP...	73	HBC	7 $\pi^+p \to \pi^+p\pi^+\pi^-$

[27] K-matrix pole from combined analysis of $\pi^-p \to \pi^0\pi^0 n$, $\pi^-p \to K\overline{K}n$, $\pi^+\pi^- \to \pi^+\pi^-$, $\overline{p}p \to \pi^0\pi^0\pi^0$, $\pi^0\eta\eta$, $\pi^0\pi^0\eta$, $\pi^+\pi^-\pi^0$, $K^+K^-\pi^0$, $K^0_S K^0_S \pi^0$, $K^+K^0_S\pi^-$ at rest, $\overline{p}n \to \pi^-\pi^-\pi^+$, $K^0_S K^-\pi^0$, $K^0_S K^0_S \pi^-$ at rest.
[28] Using the data of AKHMETSHIN 99C, ACHASOV 00H, and ALOISIO 02D.
[29] Breit-Wigner width.
[30] Supersedes ACHASOV 98I. Using the model of ACHASOV 89.
[31] Supersedes ACHASOV 98I.
[32] In the "narrow resonance" approximation.
[33] From the combined fit of the photon spectra in the reactions $e^+e^- \to \pi^+\pi^-\gamma$, $\pi^0\pi^0\gamma$.
[34] Supersedes BARBERIS 99 and BARBERIS 99B
[35] T-matrix pole.
[36] On sheet II in a 2 pole solution. The other pole is found on sheet III at (1039−93i) MeV.
[37] From invariant mass fit.
[38] On sheet II in a 2 pole solution. The other pole is found on sheet III at (963-29i) MeV.
[39] Reanalysis of data from HYAMS 73, GRAYER 74, SRINIVASAN 75, and ROSSELET 77 using the interfering amplitude method.
[40] At high $|t|$.
[41] At low $|t|$.
[42] On sheet II in a 4-pole solution, the other poles are found on sheet III at (953−55i) MeV and on sheet IV at (938−35i) MeV.
[43] Combined fit of ALDE 95B, ANISOVICH 94,
[44] On sheet II in a 2 pole solution. The other pole is found on sheet III at (996−103i) MeV.
[45] From sheet II pole position.
[46] On sheet II in a 2 pole solution. The other pole is found on sheet III at (797−185i) MeV and can be interpreted as a shadow pole.
[47] On sheet II in a 2 pole solution. The other pole is found on sheet III at (978−28i) MeV.
[48] From coupled channel analysis.
[49] Coupled channel analysis with finite width corrections.
[50] From coupled channel fit to the HYAMS 73 and PROTOPOPESCU 73 data. With a simultaneous fit to the $\pi\pi$ phase-shifts, inelasticity and to the $K^0_S K^0_S$ invariant mass.
[51] Included in AGUILAR-BENITEZ 78 fit.

$f_0(980)$ DECAY MODES

	Mode	Fraction (Γ_j/Γ)
Γ_1	$\pi\pi$	dominant
Γ_2	$K\overline{K}$	seen
Γ_3	$\gamma\gamma$	seen
Γ_4	e^+e^-	

$f_0(980)$ PARTIAL WIDTHS

$\Gamma(\gamma\gamma)$ Γ_3

VALUE (keV)	EVTS	DOCUMENT ID		TECN	COMMENT
$0.39^{+0.10}_{-0.13}$ OUR AVERAGE Error includes scale factor of 1.5. See the ideogram below.					
$0.28^{+0.09}_{-0.13}$		[52] BOGLIONE	99	RVUE	$\gamma\gamma \to \pi^+\pi^-$, $\pi^0\pi^0$
0.63 ± 0.14		[53] MORGAN	90	RVUE	$\gamma\gamma \to \pi^+\pi^-$, $\pi^0\pi^0$
0.42 ± 0.06 ± 0.18	60	[54] OEST	90	JADE	$e^+e^- \to e^+e^-\pi^0\pi^0$
• • • We do not use the following data for averages, fits, limits, etc. • • •					
0.29 ± 0.07 ± 0.12		[55,56] BOYER	90	MRK2	$e^+e^- \to e^+e^-\pi^+\pi^-$
0.31 ± 0.14 ± 0.09		[55,56] MARSISKE	90	CBAL	$e^+e^- \to e^+e^-\pi^0\pi^0$

[52] Supersedes MORGAN 90.
[53] From amplitude analysis of BOYER 90 and MARSISKE 90, data corresponds to resonance parameters $m = 989$ MeV, $\Gamma = 61$ MeV.
[54] OEST 90 quote systematic errors $^{+0.08}_{-0.18}$. We use ±0.18.
[55] From analysis allowing arbitrary background unconstrained by unitarity.
[56] Data included in MORGAN 90, BOGLIONE 99 analyses.

Meson Particle Listings

$f_0(980)$, $a_0(980)$

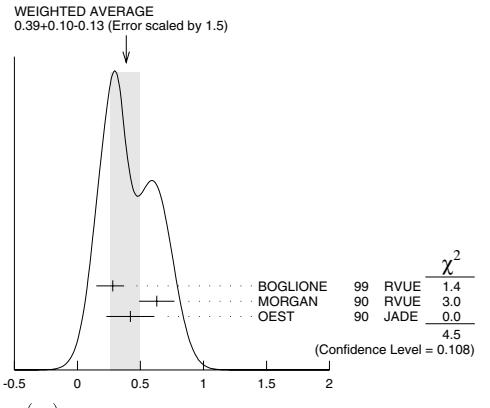

$\Gamma(e^+e^-)$ Γ_4

VALUE (eV)	CL%	DOCUMENT ID		TECN	COMMENT
<8.4	90	VOROBYEV	88	ND	$e^+e^- \to \pi^0\pi^0$

$f_0(980)$ BRANCHING RATIOS

$\Gamma(\pi\pi)/[\Gamma(\pi\pi)+\Gamma(K\overline{K})]$ $\Gamma_1/(\Gamma_1+\Gamma_2)$

VALUE	DOCUMENT ID		TECN	COMMENT
• • • We do not use the following data for averages, fits, limits, etc. • • •				
0.84 ± 0.02	[57] ANISOVICH	02D	SPEC	Combined fit
~ 0.68	OLLER	99B	RVUE	$\pi\pi \to \pi\pi,\ K\overline{K}$
0.67 ± 0.09	[58] LOVERRE	80	HBC	$4\ \pi^- p \to n 2K^0_S$
$0.81^{+0.09}_{-0.04}$	[58] CASON	78	STRC	$7\ \pi^- p \to n 2K^0_S$
0.78 ± 0.03	[58] WETZEL	76	OSPK	$8.9\ \pi^- p \to n 2K^0_S$

[57] From a combined K-matrix analysis of Crystal Barrel ($0.\ p\overline{p} \to \pi^0\pi^0\pi^0,\ \pi^0\eta\eta,\ \pi^0\pi^0\eta$), GAMS ($\pi p \to \pi^0\pi^0 n,\ \eta\eta n,\ \eta\eta' n$), and BNL ($\pi p \to K\overline{K} n$) data.

[58] Measure $\pi\pi$ elasticity assuming two resonances coupled to the $\pi\pi$ and $K\overline{K}$ channels only.

$f_0(980)$ REFERENCES

ANISOVICH	03	EPJ A16 229	V.V. Anisovich *et al.*	
TIKHOMIROV	03	PAN 66 828 Translated from YAF 66 860.	G.D. Tikhomirov *et al.*	
ALOISIO	02D	PL B537 21	A. Aloisio *et al.*	(KLOE Collab.)
ANISOVICH	02D	PAN 65 1545 Translated from YAF 65 1583.	V.V. Anisovich *et al.*	
BRAMON	02	EPJ C26 253	A. Bramon *et al.*	
ACHASOV	01F	PR D63 094007	N.N. Achasov *et al.*	(Novosibirsk SND Collab.)
AITALA	01A	PRL 86 765	E.M. Aitala *et al.*	(FNAL E791 Collab.)
AITALA	01B	PRL 86 770	E.M. Aitala *et al.*	(FNAL E791 Collab.)
ACHASOV	00H	PL B485 349	M.N. Achasov *et al.*	(Novosibirsk SND Collab.)
AKHMETSHIN	99B	PL B462 371	R.R. Akhmetshin *et al.*	(Novosibirsk CMD-2 Collab.)
AKHMETSHIN	99C	PL B462 380	R.R. Akhmetshin *et al.*	(Novosibirsk CMD-2 Collab.)
BARBERIS	99	PL B453 305	D. Barberis *et al.*	(Omega Expt.)
BARBERIS	99B	PL B453 316	D. Barberis *et al.*	(Omega Expt.)
BARBERIS	99C	PL B453 325	D. Barberis *et al.*	(Omega Expt.)
BARBERIS	99D	PL B462 462	D. Barberis *et al.*	(Omega Expt.)
BELLAZZINI	99	PL B467 296	R. Bellazzini *et al.*	
BOGLIONE	99	EPJ C9 11	M. Boglione, M.R. Pennington	
KAMINSKI	99	EPJ C9 141	R. Kaminski, L. Lesniak, B. Loiseau	(CRAC, PARIN)
OLLER	99	PR D60 099906 (erratum)	J.A. Oller *et al.*	
OLLER	99B	NP A652 407 (erratum)	J.A. Oller, E. Oset	
OLLER	99C	PR D60 074023	J.A. Oller, E. Oset	
ACHASOV	98I	PL B440 442	M.N. Achasov *et al.*	
ACKERSTAFF	98Q	EPJ C4 19	K. Ackerstaff *et al.*	(OPAL Collab.)
ALDE	98	EPJ A3 361	D. Alde *et al.*	(GAM4 Collab.)
Also	99	PAN 62 405 Translated from YAF 62 446.	D. Alde *et al.*	(GAMS Collab.)
ANISOVICH	98B	UFN 41 419	V.V. Anisovich *et al.*	
LOCHER	98	EPJ C4 317	M.P. Locher *et al.*	(PSI)
ALDE	97	PL B397 350	D.M. Alde *et al.*	(GAMS Collab.)
BERTIN	97C	PL B408 476	A. Bertin *et al.*	(OBELIX Collab.)
ISHIDA	96	PTP 95 745	S. Ishida *et al.*	(TOKY, MIYA, KEK)
TORNQVIST	96	PRL 76 1575	N.A. Tornqvist, M. Roos	(HELS)
ALDE	95B	ZPHY C66 375	D.M. Alde *et al.*	(GAMS Collab.)
AMSLER	95B	PL B342 433	C. Amsler *et al.*	(Crystal Barrel Collab.)
AMSLER	95D	PL B355 425	C. Amsler *et al.*	(Crystal Barrel Collab.)
ANISOVICH	95	PL B355 363	V.V. Anisovich *et al.*	(PNPI, SERP)
JANSSEN	95	PR D52 2690	G. Janssen *et al.*	(STON, ADLD, JULI)
AMSLER	94D	PL B333 277	C. Amsler *et al.*	(Crystal Barrel Collab.)
ANISOVICH	94	PL B323 233	V.V. Anisovich *et al.*	(Crystal Barrel Collab.)
BUGG	94	PR D50 4412	D.V. Bugg *et al.*	(LOQM)
KAMINSKI	94	PR D50 3145	R. Kaminski, L. Lesniak, J.P. Maillet	(CRAC+)
ZOU	94B	PR D50 591	B.S. Zou, D.V. Bugg	(LOQM)
MORGAN	93	PR D48 1185	D. Morgan, M.R. Pennington	(RAL, DURH)
AGUILAR-...	91	ZPHY C50 405	M. Aguilar-Benitez *et al.*	(LEBC-EHS Collab.)
ARMSTRONG	91	ZPHY C51 351	T.A. Armstrong *et al.*	(ATHU, BARI, BIRM+)
BOYER	90	PR D42 1350	J. Boyer *et al.*	(Mark II Collab.)
BREAKSTONE	90	ZPHY C48 569	A.M. Breakstone *et al.*	(ISU, BGNA, CERN+)
MARSISKE	90	PR D41 3324	H. Marsiske *et al.*	(Crystal Ball Collab.)
MORGAN	90	ZPHY C48 623	D. Morgan, M.R. Pennington	(RAL, DURH)
OEST	90	ZPHY C47 343	T. Oest *et al.*	(JADE Collab.)
ACHASOV	89	NP B315 465	N.N. Achasov, V.N. Ivanchenko	
AUGUSTIN	89	NP B320 1	J.E. Augustin, G. Cosme	(DM2 Collab.)
VOROBYEV	88	SJNP 48 273 Translated from YAF 48 436.	P.V. Vorobiev *et al.*	(NOVO)
ABACHI	86B	PRL 57 1990	S. Abachi *et al.*	(PURD, ANL, IND, MICH+)
ETKIN	82B	PR D25 1786	A. Etkin *et al.*	(BNL, CUNY, TUFTS, VAND)
GIDAL	81	PL 107B 153	G. Gidal *et al.*	(SLAC, LBL)
ACHASOV	80	SJNP 32 566 Translated from YAF 32 1098.	N.N. Achasov, S.A. Devyanin, G.N. Shestakov	(NOVM)
LOVERRE	80	ZPHY C6 187	P.F. Loverre *et al.*	(CERN, CDEF, MADR+) IJP
AGUILAR-...	78	NP B140 73	M. Aguilar-Benitez *et al.*	(MADR, BOMB+)
CASON	78	PRL 41 271	N.M. Cason *et al.*	(NDAM, ANL)
LEEPER	77	PR D16 2054	R.J. Leeper *et al.*	(ISU)
ROSSELET	77	PR D15 574	L. Rosselet *et al.*	(GEVA, SACL)
WETZEL	76	NP B115 208	W. Wetzel *et al.*	(ETH, CERN, LOIC)
SRINIVASAN	75	PR D12 681	V. Srinivasan *et al.*	(NDAM, ANL)
GRAYER	74	NP B75 189	G. Grayer *et al.*	(CERN, MPIM)
BINNIE	73	PRL 31 1534	D.M. Binnie *et al.*	(LOIC, SHMP)
GRAYER	73	Tallahassee	G. Grayer *et al.*	(CERN, MPIM)
HYAMS	73	NP B64 134	B.D. Hyams *et al.*	(CERN, MPIM)
PROTOPOP...	73	PR D7 1279	S.D. Protopopescu *et al.*	(LBL)

OTHER RELATED PAPERS

ACHASOV	03E	NP A728 425	N.N. Achasov
ANISOVICH	03B	PAN 66 741 Translated from YAF 66 772.	V.V. Anisovich, V.A. Nikonov, A.V. Sarantsev
ANISOVICH	03D	PAN 66 928 Translated from YAF 66 960.	V.V. Anisovich, A.V. Sarantsev
BEDAIGA	03	PR D68 036001	I. Bedaiga, M. Nielsen
BOGLIONE	03	EPJ C30 503	M. Boglione, M.R. Pennington
CHEN	03	PR D67 094011	C.-H. Chen
COLANGELO	03	PL B559 49	P. Colangelo, F. De Fazio
PALOMAR	03	NP A729 743	J.E. Palomar *et al.*
ACHASOV	02G	PL B534 83	N.N. Achasov, A.V. Kiselev
ANISOVICH	02C	PAN 65 497 Translated from YAF 65 523.	A.V. Anisovich *et al.*
BLACK	02	PRL 88 181603	D. Black, M. Harada, J. Schechter
CLOSE	02B	JPG 28 R249	F.E. Close, N. Tornqvist
KAMINSKI	02	EPJ Direct C4 1	R. Kaminski, L. Lesniak, K. Rybicki
KLEEFELD	02	PR D66 034007	F. Kleefeld, E. van Beveren, G. Rupp
RUPP	02	PR D65 078501	G. Rupp, E. van Beveren, M.D. Scadron
SHAKIN	02	PR D65 078502	C.M. Shakin, H. Wang
TESHIMA	02	JPG 28 1391	T. Teshima, I. Kitamura, N. Morisita
VOLKOV	02	PAN 65 1657 Translated from YAF 65 1701.	M.K. Volkov, V.L. Yudichev
ACHASOV	01F	PR D63 094007	N.N. Achasov *et al.* (Novosibirsk SND Collab.)
CLOSE	01	PL B515 13	F.E. Close, A. Kirk
GOKALP	01	PR D64 053017	A. Gokalp, O. Yilmaz
SUROVTSEV	01	PR D63 054024	Y.S. Surovtsev, D. Krupa, M. Nagy
MARKUSHIN	00	EPJ A8 389	V.E. Markushin
WANG	00A	PR D62 017503	Z. Wang
ABREU	99J	PL B449 364	P. Abreu *et al.* (DELPHI Collab.)
ANISOVICH	99D	PL B452 180	A.V. Anisovich *et al.*
Also	99F	NP A651 253	A.V. Anisovich *et al.*
ANISOVICH	99H	PL B467 289	A.V. Anisovich, V.V. Anisovich
BLACK	99	PR D59 074026	D. Black *et al.*
DELBOURGO	99	PL B446 332	R. Delbourgo, D. Liu, M. Scadron
MARCO	99	PL B470 20	E. Marco *et al.*
MINKOWSKI	99	EPJ C9 283	P. Minkowski, W. Ochs
ACHASOV	98G	JETPL 67 464	N.N. Achasov *et al.*
ACHASOV	98J	SPU 41 1149	N.N. Achasov
CHLIAPNIK...	98	PL B423 401	P.V. Chliapnikov, V.A. Uvarov
PROKOSHKIN	97	SPD 42 117 Translated from DANS 353 323.	Y.D. Prokoshkin *et al.* (SERP)
AU	87	PR D35 1633	K.L. Au, D. Morgan, M.R. Pennington (DURH, RAL)
AKESSON	86	NP B264 154	T. Akesson *et al.* (Axial Field Spec. Collab.)
BEVEREN	86	ZPHY C30 615	E. van Beveren *et al.* (NIJM, BIEL)
MENNESSIER	83	ZPHY C16 241	G. Mennessier (MONP)
BARBER	82	ZPHY C12 1	D.P. Barber *et al.* (DARE, LANC, SHEF)
ETKIN	82C	PR D25 2446	A. Etkin *et al.* (BNL, CUNY, TUFTS, VAND)
SRINIVASAN	75	PR D12 681	V. Srinivasan *et al.* (NDAM, ANL)
BIGI	62	CERN Conf. 247	A. Bigi *et al.* (CERN)
BINGHAM	62	CERN Conf. 240	H.H. Bingham *et al.* (EPOL, CERN)
ERWIN	62	PRL 9 34	A.R. Erwin *et al.* (WISC, BNL)
WANG	61	JETP 13 323 Translated from ZETF 40 464.	K.-C. Wang *et al.* (JINR)

$a_0(980)$

$I^G(J^{PC}) = 1^-(0^{++})$

See our minireview on scalar mesons under $f_0(600)$. (See the index for the page number.)

$a_0(980)$ MASS

VALUE (MeV)	DOCUMENT ID
984.7±1.2 OUR AVERAGE Includes data from the 2 datablocks that follow this one. Error includes scale factor of 1.5. See the ideogram below.	

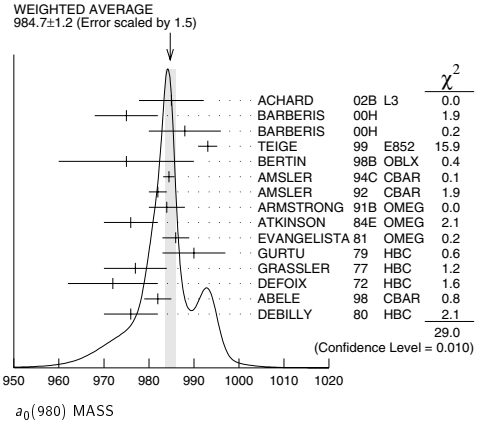

$\eta\pi$ FINAL STATE ONLY

VALUE (MeV)	EVTS	DOCUMENT ID		TECN	CHG	COMMENT
The data in this block is included in the average printed for a previous datablock.						
985.1 ± 1.3 OUR AVERAGE Error includes scale factor of 1.5. See the ideogram below.						
985 ± 4 ±6	318	ACHARD	02B	L3		183–209 $e^+e^- \to e^+e^-\eta\pi^+\pi^-$
975 ± 7		BARBERIS	00H			450 $pp \to p_f\eta\pi^0 p_s$
988 ± 8		BARBERIS	00H			450 $pp \to \Delta_f^{++}\eta\pi^- p_s$
993.1 ± 2.1		[1] TEIGE	99	E852		18.3 $\pi^- p \to \eta\pi^+\pi^- n$
975 ±15		BERTIN	98B	OBLX		0.0 $\overline{p}p \to K^\pm K_S\pi^\mp$
984.45 ± 1.23 ±0.34		AMSLER	94C	CBAR		0.0 $\overline{p}p \to \omega\eta\pi^0$
982 ± 2		[2] AMSLER	92	CBAR		0.0 $\overline{p}p \to \eta\eta\pi^0$
984 ± 4	1040	[2] ARMSTRONG	91B	OMEG	±	300 $pp \to pp\eta\pi^+\pi^-$
976 ± 6		ATKINSON	84E	OMEG	±	25–55 $\gamma p \to \eta\pi n$
986 ± 3	500	[3] EVANGELISTA	81	OMEG	±	12 $\pi^- p \to \eta\pi^+\pi^-\pi^- p$
990 ± 7	145	[3] GURTU	79	HBC	±	4.2 $K^- p \to \Lambda\eta 2\pi$
977 ± 7		GRASSLER	77	HBC	–	16 $\pi^\mp p \to p\eta 3\pi$
972 ±10	150	DEFOIX	72	HBC	±	0.7 $\overline{p}p \to 7\pi$
• • • We do not use the following data for averages, fits, limits, etc. • • •						
995 $^{+52}_{-10}$	36	[4] ACHASOV	00F	SND		$e^+e^- \to \eta\pi^0\gamma$
994 $^{+33}_{-8}$	36	[5] ACHASOV	00F	SND		$e^+e^- \to \eta\pi^0\gamma$
~ 1055		[6] OLLER	99	RVUE		$\eta\pi$, $K\overline{K}$
~ 1009.2		[6] OLLER	99B	RVUE		$\pi\pi \to \pi\pi$, $K\overline{K}$
988 ± 6		[6] ANISOVICH	98B	RVUE		Compilation
987		TORNQVIST	96	RVUE		$\pi\pi \to \pi\pi$, $K\overline{K}$, $K\pi$, $\eta\pi$
991		JANSSEN	95	RVUE		$\eta\pi \to \eta\pi$, $K\overline{K}$, $K\pi$, $\eta\pi$
980 ±11	47	CONFORTO	78	OSPK	–	4.5 $\pi^- p \to pX^-$
978 ±16	50	CORDEN	78	OMEG	±	12–15 $\pi^- p \to n\eta 2\pi$
989 ± 4	70	WELLS	75	HBC	–	3.1–6 $K^- p \to \Lambda\eta 2\pi$
970 ±15	20	BARNES	69C	HBC	–	4–5 $K^- p \to \Lambda\eta 2\pi$
980 ±10		CAMPBELL	69	DBC	±	2.7 $\pi^+ d$
980 ±10	15	MILLER	69B	HBC	–	4.5 $K^- N \to \eta\pi\Lambda$
980 ±10	30	AMMAR	68	HBC	±	5.5 $K^- p \to \Lambda\eta 2\pi$

[1] Breit-Wigner fit, average between $a_0^\pm$ and a_0^0. The fit favors a slightly heavier $a_0^\pm$.
[2] From a single Breit-Wigner fit.
[3] From $f_1(1285)$ decay.
[4] Supersedes ACHASOV 98B. Using the model of ACHASOV 89.
[5] Supersedes ACHASOV 98B. Using the model of JAFFE 77.
[6] T-matrix pole.

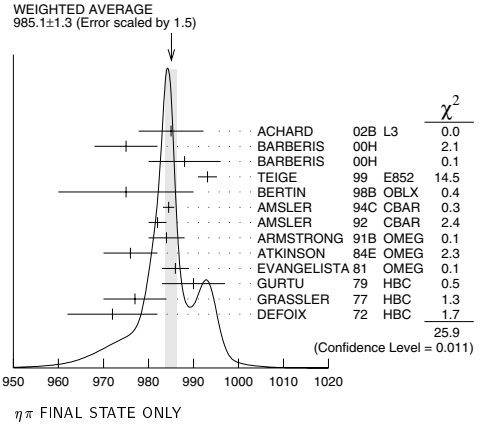

$\eta\pi$ FINAL STATE ONLY

$K\overline{K}$ ONLY

VALUE (MeV)	EVTS	DOCUMENT ID		TECN	CHG	COMMENT
The data in this block is included in the average printed for a previous datablock.						
980.8± 2.7 OUR AVERAGE						
982 ± 3		[7] ABELE	98	CBAR		0.0 $\overline{p}p \to K_L^0 K^\pm\pi^\mp$
976 ± 6	316	DEBILLY	80	HBC	±	1.2–2 $\overline{p}p \to f_1(1285)\omega$
• • • We do not use the following data for averages, fits, limits, etc. • • •						
~ 1053		[8] OLLER	99C	RVUE		$\pi\pi \to \pi\pi$, $K\overline{K}$
1016 ±10	100	[9] ASTIER	67	HBC	±	0.0 $\overline{p}p$
1003.3 ± 7.0	143	[10] ROSENFELD	65	RVUE	±	

[7] T-matrix pole on sheet II, the pole on sheet III is at 1006-i49 MeV.
[8] T-matrix pole.
[9] ASTIER 67 includes data of BARLOW 67, CONFORTO 67, ARMENTEROS 65.
[10] Plus systematic errors.

$a_0(980)$ WIDTH

VALUE (MeV)	EVTS	DOCUMENT ID		TECN	CHG	COMMENT
50 to 100 OUR ESTIMATE Width determination very model dependent. Peak width in $\eta\pi$ is about 60 MeV, but decay width can be much larger.						
• • • We do not use the following data for averages, fits, limits, etc. • • •						
50 ±13 ±4	318	ACHARD	02B	L3		183–209 $e^+e^- \to e^+e^-\eta\pi^+\pi^-$
72 ±16		BARBERIS	00H			450 $pp \to p_f\eta\pi^0 p_s$
61 ±19		BARBERIS	00H			450 $pp \to \Delta_f^{++}\eta\pi^- p_s$
~ 42		[11] OLLER	99	RVUE		$\eta\pi$, $K\overline{K}$
~ 112		[11] OLLER	99B	RVUE		$\pi\pi \to \eta\pi$, $K\overline{K}$
71 ± 7		TEIGE	99	E852		18.3 $\pi^- p \to \eta\pi^+\pi^- n$
92 ±20		[11] ANISOVICH	98B	RVUE		Compilation
65 ±10		BERTIN	98B	OBLX		0.0 $\overline{p}p \to K^\pm K_S\pi^\mp$
~ 100		TORNQVIST	96	RVUE		$\pi\pi \to \pi\pi$, $K\overline{K}$, $K\pi$, $\eta\pi$
202		JANSSEN	95	RVUE		$\eta\pi \to \eta\pi$, $K\overline{K}$, $K\pi$, $\eta\pi$
54.12 ± 0.34 ± 0.12		AMSLER	94C	CBAR		0.0 $\overline{p}p \to \omega\eta\pi^0$
54 ±10		[12] AMSLER	92	CBAR		0.0 $\overline{p}p \to \eta\eta\pi^0$
95 ±14	1040	[12] ARMSTRONG	91B	OMEG	±	300 $pp \to pp\eta\pi^+\pi^-$
62 ±15	500	[13] EVANGELISTA	81	OMEG	±	12 $\pi^- p \to \eta\pi^+\pi^-\pi^- p$
60 ±20	145	[13] GURTU	79	HBC	±	4.2 $K^- p \to \Lambda\eta 2\pi$
60 $^{+50}_{-30}$	47	CONFORTO	78	OSPK	–	4.5 $\pi^- p \to pX^-$
86.0 $^{+60.0}_{-50.0}$	50	CORDEN	78	OMEG	±	12–15 $\pi^- p \to n\eta 2\pi$
44 ±22		GRASSLER	77	HBC	–	16 $\pi^\mp p \to p\eta 3\pi$
80 to 300		[14] FLATTE	76	RVUE	–	4.2 $K^- p \to \Lambda\eta 2\pi$
16.0 $^{+25.0}_{-16.0}$	70	WELLS	75	HBC	–	3.1–6 $K^- p \to \Lambda\eta 2\pi$
30 ± 5	150	DEFOIX	72	HBC	±	0.7 $\overline{p}p \to 7\pi$
40 ±15		CAMPBELL	69	DBC	±	2.7 $\pi^+ d$
60 ±30	15	MILLER	69B	HBC	–	4.5 $K^- N \to \eta\pi\Lambda$
80 ±30	30	AMMAR	68	HBC	±	5.5 $K^- p \to \Lambda\eta 2\pi$

[11] T-matrix pole.
[12] From a single Breit-Wigner fit.
[13] From $f_1(1285)$ decay.
[14] Using a two-channel resonance parametrization of GAY 76B data.

$K\overline{K}$ ONLY

VALUE (MeV)	EVTS	DOCUMENT ID		TECN	CHG	COMMENT
92± 8		[15] ABELE	98	CBAR		0.0 $\overline{p}p \to K_L^0 K^\pm\pi^\mp$
• • • We do not use the following data for averages, fits, limits, etc. • • •						
~ 24		[16] OLLER	99C	RVUE		$\pi\pi \to \pi\pi$, $K\overline{K}$
~ 25	100	[17] ASTIER	67	HBC	±	
57 ±13	143	[18] ROSENFELD	65	RVUE	±	

[15] T-matrix pole on sheet II, the pole on sheet III is at 1006-i49 MeV.
[16] T-matrix pole.
[17] ASTIER 67 includes data of BARLOW 67, CONFORTO 67, ARMENTEROS 65.
[18] Plus systematic errors.

$a_0(980)$ DECAY MODES

	Mode	Fraction (Γ_i/Γ)
Γ_1	$\eta\pi$	dominant
Γ_2	$K\overline{K}$	seen
Γ_3	$\rho\pi$	
Γ_4	$\gamma\gamma$	seen
Γ_5	e^+e^-	

Meson Particle Listings

$a_0(980)$, $\phi(1020)$

$a_0(980)$ PARTIAL WIDTHS

$\Gamma(\gamma\gamma)$ Γ_4

VALUE (keV)	DOCUMENT ID		TECN	
• • • We do not use the following data for averages, fits, limits, etc. • • •				
0.30 ± 0.10	[19] AMSLER	98	RVUE	

[19] Using $\Gamma_{\gamma\gamma} B(a0(980) \to \eta\pi) = 0.24 \pm 0.08$ keV.

$a_0(980)$ $\Gamma(i)\Gamma(\gamma\gamma)/\Gamma(\text{total})$

$\Gamma(\eta\pi) \times \Gamma(\gamma\gamma)/\Gamma_{\text{total}}$ $\Gamma_1\Gamma_4/\Gamma$

VALUE (keV)	EVTS	DOCUMENT ID		TECN	COMMENT
$0.24^{+0.08}_{-0.07}$ OUR AVERAGE					
$0.28 \pm 0.04 \pm 0.10$	44	OEST	90	JADE	$e^+e^- \to e^+e^-\pi^0\eta$
$0.19 \pm 0.07^{+0.10}_{-0.07}$		ANTREASYAN	86	CBAL	$e^+e^- \to e^+e^-\pi^0\eta$

$\Gamma(\eta\pi) \times \Gamma(e^+e^-)/\Gamma_{\text{total}}$ $\Gamma_1\Gamma_5/\Gamma$

VALUE (eV)	CL%	DOCUMENT ID		TECN	COMMENT
<1.5	90	VOROBYEV	88	ND	$e^+e^- \to \pi^0\eta$

$a_0(980)$ BRANCHING RATIOS

$\Gamma(K\overline{K})/\Gamma(\eta\pi)$ Γ_2/Γ_1

VALUE	DOCUMENT ID		TECN	CHG	COMMENT
0.183 ± 0.024 OUR AVERAGE	Error includes scale factor of 1.2.				
0.57 ± 0.16	[20] BARGIOTTI	03	OBLX		$\overline{p}p$
0.23 ± 0.05	[21] ABELE	98	CBAR		0.0 $\overline{p}p \to K_L^0 K^\pm \pi^\mp$
$0.166 \pm 0.01 \pm 0.02$	[22] BARBERIS	98C	OMEG		450 $pp \to p_f f_1(1285) p_s$
• • • We do not use the following data for averages, fits, limits, etc. • • •					
~ 0.60	OLLER	99B	RVUE		$\pi\pi \to \eta\pi, K\overline{K}$
1.16 ± 0.18	[23] BUGG	94	RVUE		$\overline{p}p \to \eta\eta\pi^0$
0.7 ± 0.3	[22] CORDEN	78	OMEG		12–15 $\pi^- p \to n\eta 2\pi$
0.25 ± 0.08	[22] DEFOIX	72	HBC	$\pm$	0.7 $\overline{p} \to 7\pi$

$\Gamma(\rho\pi)/\Gamma(\eta\pi)$ Γ_3/Γ_1

$\rho\pi$ forbidden.

VALUE	CL%	DOCUMENT ID		TECN	CHG	COMMENT
• • • We do not use the following data for averages, fits, limits, etc. • • •						
< 0.25	70	AMMAR	70	HBC	$\pm$	4.1,5.5 $K^- p \to \Lambda\eta 2\pi$

[20] Coupled channel analysis of $\pi^+\pi^-\pi^0$, $K^+K^-\pi^0$, and $K^\pm K_S^0 \pi^\mp$.
[21] Using $\pi^0\pi^0\eta$ from AMSLER 94D.
[22] From the decay of $f_1(1285)$.
[23] BUGG 94 uses AMSLER 94C data. This is a ratio of couplings.

$a_0(980)$ REFERENCES

BARGIOTTI	03	EPJ C26 371	M. Bargiotti *et al.*	(OBELIX Collab.)
ACHARD	02B	PL B526 269	P. Achard *et al.*	(L3 Collab.)
ACHASOV	00F	PL B479 53	M.N. Achasov *et al.*	(Novosibirsk SND Collab.)
BARBERIS	00H	PL B488 225	D. Barberis *et al.*	(WA 102 Collab.)
OLLER	99	PR D60 099906 (erratum)	J.A. Oller *et al.*	
OLLER	99B	NP A652 407 (erratum)	J.A. Oller, E. Oset	
OLLER	99C	PR D60 074023	J.A. Oller, E. Oset	
TEIGE	99	PR D59 012001	S. Teige *et al.*	(BNL E852 Collab.)
ABELE	98	PR D57 3860	A. Abele *et al.*	(Crystal Barrel Collab.)
ACHASOV	98B	PL B438 441	M.N. Achasov *et al.*	(Novosibirsk SND Collab.)
AMSLER	98	RMP 70 1293	C. Amsler	
ANISOVICH	98B	UFN 41 419	V.V. Anisovich *et al.*	
BARBERIS	98C	PL B440 225	D. Barberis *et al.*	(WA 102 Collab.)
BERTIN	98B	PL B434 180	A. Bertin *et al.*	(OBELIX Collab.)
TORNQVIST	96	PRL 76 1575	N.A. Tornqvist, M. Roos	(HELS)
JANSSEN	95	PR D52 2690	G. Janssen *et al.*	(STON, ADLD, JUL)
AMSLER	94C	PL B327 425	C. Amsler *et al.*	(Crystal Barrel Collab.)
AMSLER	94D	PL B333 277	C. Amsler *et al.*	(Crystal Barrel Collab.)
BUGG	94	PR D50 4412	D.V. Bugg *et al.*	(LOQM)
AMSLER	92	PL B291 347	C. Amsler *et al.*	(Crystal Barrel Collab.)
ARMSTRONG	91B	ZPHY C52 389	T.A. Armstrong *et al.*	(ATHU, BARI, BIRM+)
OEST	90	ZPHY C47 343	T. Oest *et al.*	(JADE Collab.)
ACHASOV	89	NP B315 465	N.N. Achasov, V.N. Ivanchenko	
VOROBYEV	88	SJNP 48 273 Translated from YAF 48 436.	P.V. Vorobiev *et al.*	(NOVO)
ANTREASYAN	86	PR D33 1847	D. Antreasyan *et al.*	(Crystal Ball Collab.)
ATKINSON	84E	PL 138B 459	M. Atkinson *et al.*	(BONN, CERN, GLAS+)
EVANGELISTA	81	NP B178 197	C. Evangelista *et al.*	(BARI, BONN, CERN+)
DEBILLY	80	NP B176 1	L. de Billy *et al.*	(CURIN, LAUS, NEUC+)
GURTU	79	NP B151 181	A. Gurtu *et al.*	(CERN, ZEEM, NIJM, OXF)
CONFORTO	78	LNC 23 419	B. Conforto *et al.*	(RHEL, TNTO, CHIC+)
CORDEN	78	NP B144 253	M.J. Corden *et al.*	(BIRM, RHEL, TELA+)
GRASSLER	77	NP B121 189	H. Grassler *et al.*	(AACH3, BERL, BONN+)
JAFFE	77	PR D15 267,281	R. Jaffe	(MIT)
FLATTE	76	PL 63B 224	S.M. Flatte	(CERN)
GAY	76B	PL 63B 220	J.B. Gay *et al.*	(CERN, AMST, NIJM) JP
WELLS	75	NP B101 333	J. Wells *et al.*	(OXF)
DEFOIX	72	NP B44 125	C. Defoix *et al.*	(CDEF, CERN)
AMMAR	70	PR D2 430	R. Ammar *et al.*	(KANS, NWES, ANL, WISC)
BARNES	69C	PRL 23 610	V.E. Barnes *et al.*	(BNL, SYRA)
CAMPBELL	69	PRL 22 1204	J.H. Campbell *et al.*	(PURD)
MILLER	69B	PL 29B 255	D.H. Miller *et al.*	(PURD)
Also	69	PR 188 2011	W.L. Yen *et al.*	(PURD)
AMMAR	68	PRL 21 1832	R. Ammar *et al.*	(NWES, ANL)
ASTIER	67	PL 25B 294	A. Astier *et al.*	(CDEF, CERN, IRAD)

Includes data of BARLOW 67, CONFORTO 67, and ARMENTEROS 65.

BARLOW	67	NC 50A 701	J. Barlow *et al.*	(CERN, CDEF, IRAD, LIVP)
CONFORTO	67	NP B3 469	G. Conforto *et al.*	(CERN, CDEF, IPNP+)
ARMENTEROS	65	PL 17 344	R. Armenteros *et al.*	(CERN, CDEF)
ROSENFELD	65	Oxford Conf. 58	A.H. Rosenfeld	(LRL)

OTHER RELATED PAPERS

ACHASOV	03B	PR D68 014006	N.N. Achsaov, A.V. Kiselev	
ACHASOV	03E	NP A728 425	N.N. Achasov	
PALOMAR	03	NP A729 743	J.E. Palomar *et al.*	
ACHASOV	02G	PL B534 83	N.N Achasov, A.V. Kiselev	
BLACK	02	PRL 88 181603	D. Black, M. Harada, J. Schechter	
BOGLIONE	02	PR D65 114010	M. Boglione, M.R. Pennington	
CLOSE	02B	JPG 28 R249	F.E. Close, N. Tornqvist	
FURMAN	02	PL B538 266	A. Furman, L. Lesniak	
ACHASOV	01F	PR D63 094007	N.N. Achasov *et al.*	(Novosibirsk SND Collab.)
CLOSE	01	PL B515 13	F.E. Close, A. Kirk	
ANISOVICH	99D	PL B452 180	A.V. Anisovich *et al.*	
Also	99F	NP A651 253	A.V. Anisovich *et al.*	
MARCO	99	PL B470 20	E. Marco *et al.*	
ACHASOV	98J	SPU 41 1149	N.N. Achasov	
TORNQVIST	90	NPBPS 21 196	N.A. Tornqvist	(HELS)
WEINSTEIN	90	PR D41 2236	J. Weinstein, N. Isgur	(TNTO)
ACHASOV	88B	ZPHY C41 309	N.N. Achasov, G.N. Shestakov	(NOVM)
BEVEREN	86	ZPHY C30 615	E. van Beveren *et al.*	(NIJM, BIEL)
TORNQVIST	82	PRL 49 624	N.A. Tornqvist	(HELS)
BRAMON	80	PL 93B 65	A. Bramon, E. Masso	(BARC)
TURKOT	63	Siena Conf. 1 661	F. Turkot *et al.*	(BNL, PITT)

$\phi(1020)$

$I^G(J^{PC}) = 0^-(1^{--})$

$\phi(1020)$ MASS

We average mass and width values only when the systematic errors have been evaluated.

VALUE (MeV)	EVTS	DOCUMENT ID		TECN	COMMENT
1019.456 ± 0.020 OUR AVERAGE	Error includes scale factor of 1.1.				
1019.483 ± 0.011 ± 0.025	272k	[1] AKHMETSHIN	04	CMD2	$e^+e^- \to K_L^0 K_S^0$
1019.42 ± 0.05	1900k	[2] ACHASOV	01E	SND	$e^+e^- \to K^+K^-, K_S K_L, \pi^+\pi^-\pi^0$
1019.40 ± 0.04 ± 0.05	23k	AKHMETSHIN	01B	CMD2	$e^+e^- \to \eta\gamma$
1019.36 ± 0.12		[3] ACHASOV	00B	SND	$e^+e^- \to \eta\gamma$
1019.38 ± 0.07 ± 0.08	2200	[4] AKHMETSHIN	99F	CMD2	$e^+e^- \to \pi^+\pi^- \geq 2\gamma$
1019.51 ± 0.07 ± 0.10	11169	AKHMETSHIN	98	CMD2	$e^+e^- \to \pi^+\pi^-\pi^0$
1019.5 ± 0.4		BARBERIS	98	OMEG	450 $pp \to pp 2K^+ 2K^-$
1019.42 ± 0.06	55600	AKHMETSHIN	95	CMD2	$e^+e^- \to$ hadrons
1019.7 ± 0.3	2012	DAVENPORT	86	MPSF	400 $pA \to 4KX$
1019.7 ± 0.1 ± 0.1	5079	ALBRECHT	85D	ARG	10 $e^+e^- \to K^+K^-X$
1019.3 ± 0.1	1500	ARENTON	82	AEMS	11.8 polar. $pp \to KK$
1019.67 ± 0.17	25080	[5] PELLINEN	82	RVUE	
1019.52 ± 0.13	3681	BUKIN	78C	OLYA	$e^+e^- \to$ hadrons
• • • We do not use the following data for averages, fits, limits, etc. • • •					
1019.8 ± 0.7		ARMSTRONG	86	OMEG	85 $\pi^+/pp \to \pi^+/p4Kp$
1020.1 ± 0.11	5526	[6] ATKINSON	86	OMEG	20–70 γp
1019.7 ± 1.0		BEBEK	86	CLEO	$e^+e^- \to \Upsilon(4S)$
1019.411 ± 0.008	642k	[7] DIJKSTRA	86	SPEC	100–200 $\pi^\pm, \overline{p}, p, K^\pm$, on Be
1020.9 ± 0.2		[6] FRAME	86	OMEG	13 $K^+p \to \phi K^+ p$
1021.0 ± 0.2		[6] ARMSTRONG	83B	OMEG	18.5 $K^-p \to K^-K^+\Lambda$
1020.0 ± 0.5		[6] ARMSTRONG	83B	OMEG	18.5 $K^-p \to K^-K^+\Lambda$
1019.7 ± 0.3		[6] BARATE	83	GOLI	190 π^- Be $\to 2\mu X$
1019.8 ± 0.2 ± 0.5	766	IVANOV	81	OLYA	1–1.4 $e^+e^- \to K^+K^-$
1019.4 ± 0.5	337	COOPER	78B	HBC	0.7–0.8 $\overline{p}p \to K_S^0 K_L^0 \pi^+\pi^-$
1020 ± 1	383	[6] BALDI	77	CNTR	10 $\pi^-p \to \pi^-\phi p$
1018.9 ± 0.6	800	COHEN	77	ASPK	6 $\pi^\pm N \to K^+K^-N$
1019.7 ± 0.5	454	KALBFLEISCH	76	HBC	2.18 $K^-p \to \Lambda K\overline{K}$
1019.4 ± 0.8	984	BESCH	74	CNTR	2 $\gamma p \to pK^+K^-$
1020.3 ± 0.4	100	BALLAM	73	HBC	2.8–9.3 γp
1019.4 ± 0.7		BINNIE	73B	CNTR	$\pi^-p \to \phi n$
1019.6 ± 0.5	120	[8] AGUILAR-...	72B	HBC	3.9,4.6 $K^-p \to \Lambda K^+K^-$
1019.9 ± 0.5	100	[8] AGUILAR-...	72B	HBC	3.9,4.6 $K^-p \to K^-pK^+K^-$
1020.4 ± 0.5	131	COLLEY	72	HBC	10 $K^+p \to K^+p\phi$
1019.9 ± 0.3	410	STOTTLE...	71	HBC	2.9 $K^-p \to \Sigma/\Lambda K\overline{K}$

[1] Update of AKHMETSHIN 01D
[2] From the combined fit assuming that the total $\phi(1020)$ production cross section is saturated by those of K^+K^-, K_SK_L, $\pi^+\pi^-\pi^0$, and $\eta\gamma$ decays modes and using ACHASOV 00B for the $\eta\gamma$ decay mode.
[3] Using a total width of 4.43 ± 0.05 MeV. Systematic uncertainty included.
[4] Using a total width of 4.43 ± 0.05 MeV.
[5] PELLINEN 82 review includes AKERLOF 77, DAUM 81, BALDI 77, AYRES 74, DEGROOT 74.
[6] Systematic errors not evaluated.
[7] Weighted and scaled average of 12 measurements of DIJKSTRA 86.
[8] Mass errors enlarged by us to $\Gamma/\sqrt{N}$; see the note with the $K^*(892)$ mass.

$\phi(1020)$ WIDTH

We average mass and width values only when the systematic errors have been evaluated.

VALUE (MeV)		EVTS	DOCUMENT ID		TECN	COMMENT
4.26 ±0.05	**OUR AVERAGE**		Error includes scale factor of 1.7. See the ideogram below.			
4.280±0.033±0.025		272k	[9] AKHMETSHIN	04	CMD2	$e^+e^- \to K_L^0K_S^0$
4.21 ±0.04		1900k	[10] ACHASOV	01E	SND	$e^+e^- \to K^+K^-$, K_SK_L, $\pi^+\pi^-\pi^0$
4.44 ±0.09		55600	AKHMETSHIN	95	CMD2	$e^+e^- \to$ hadrons
4.5 ±0.7		1500	ARENTON	82	AEMS	11.8 polar. $pp \to KK$
4.2 ±0.6		766	[11] IVANOV	81	OLYA	1–1.4 $e^+e^- \to K^+K^-$
4.3 ±0.6			[11] CORDIER	80	DM1	$e^+e^- \to \pi^+\pi^-\pi^0$
4.36 ±0.29		3681	[11] BUKIN	78C	OLYA	$e^+e^- \to$ hadrons
4.4 ±0.6		984	[11] BESCH	74	CNTR	$2\gamma p \to pK^+K^-$
4.67 ±0.72		681	[11] BALAKIN	71	OSPK	$e^+e^- \to$ hadrons
4.09 ±0.29			BIZOT	70	OSPK	$e^+e^- \to$ hadrons
• • • We do not use the following data for averages, fits, limits, etc. • • •						
4.45 ±0.06		271k	DIJKSTRA	86	SPEC	100 π^- Be
3.6 ±0.8		337	[11] COOPER	78B	HBC	0.7–0.8 $\overline{p}p \to K_S^0K_L^0\pi^+\pi^-$
4.5 ±0.50		1300	[11,12] AKERLOF	77	SPEC	400 $pA \to K^+K^-X$
4.5 ±0.8		500	[11,12] AYRES	74	ASPK	3–6 $\pi^-p \to K^+K^-n$, $K^-p \to K^+K^-\Lambda/\Sigma^0$
3.81 ±0.37			COSME	74B	OSPK	$e^+e^- \to K_L^0K_S^0$
3.8 ±0.7		454	[11] BORENSTEIN	72	HBC	2.18 $K^-p \to KKn$

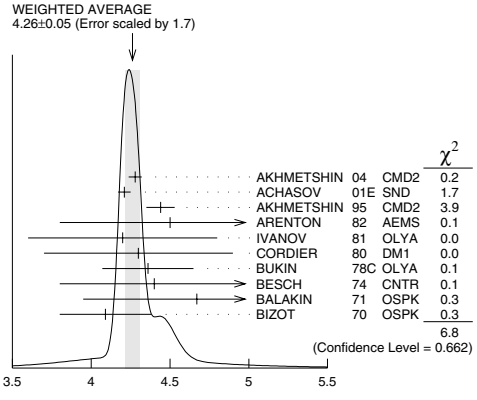

[9] Update of AKHMETSHIN 01D
[10] From the combined fit assuming that the total $\phi(1020)$ production cross section is saturated by those of K^+K^-, K_SK_L, $\pi^+\pi^-\pi^0$, and $\eta\gamma$ decays modes and using ACHASOV 00B for the $\eta\gamma$ decay mode.
[11] Width errors enlarged by us to $4\Gamma/\sqrt{N}$; see the note with the $K^*(892)$ mass.
[12] Systematic errors not evaluated.

$\phi(1020)$ DECAY MODES

	Mode	Fraction (Γ_i/Γ)	Scale factor/ Confidence level
Γ_1	K^+K^-	(49.1 ±0.6) %	S=1.2
Γ_2	$K_L^0K_S^0$	(34.0 ±0.5) %	S=1.1
Γ_3	$\rho\pi$ + $\pi^+\pi^-\pi^0$	(15.4 ±0.5) %	S=1.3
Γ_4	$\rho\pi$		
Γ_5	$\pi^+\pi^-\pi^0$		
Γ_6	$\eta\gamma$	(1.295±0.025) %	S=1.1
Γ_7	$\pi^0\gamma$	(1.23 ±0.10) $\times10^{-3}$	
Γ_8	e^+e^-	(2.98 ±0.04) $\times10^{-4}$	S=1.1
Γ_9	$\mu^+\mu^-$	(2.85 ±0.19) $\times10^{-4}$	
Γ_{10}	ηe^+e^-	(1.15 ±0.10) $\times10^{-4}$	
Γ_{11}	$\pi^+\pi^-$	(7.3 ±1.3) $\times10^{-5}$	
Γ_{12}	$\omega\pi^0$	(5.2 $^{+1.3}_{-1.1}$) $\times10^{-5}$	
Γ_{13}	$\omega\gamma$	< 5 %	CL=84%
Γ_{14}	$\rho\gamma$	< 1.2 $\times10^{-5}$	CL=90%
Γ_{15}	$\pi^+\pi^-\gamma$	(4.1 ±1.3) $\times10^{-5}$	
Γ_{16}	$f_0(980)\gamma$	(4.40 ±0.21) $\times10^{-4}$	
Γ_{17}	$\pi^0\pi^0\gamma$	(1.09 ±0.06) $\times10^{-4}$	
Γ_{18}	$\pi^+\pi^-\pi^+\pi^-$	(3.9 $^{+2.8}_{-2.2}$) $\times10^{-6}$	
Γ_{19}	$\pi^+\pi^+\pi^-\pi^-\pi^0$	< 4.6 $\times10^{-6}$	CL=90%
Γ_{20}	$\pi^0e^+e^-$	(1.12 ±0.28) $\times10^{-5}$	
Γ_{21}	$\pi^0\eta\gamma$	(8.3 ±0.5) $\times10^{-5}$	
Γ_{22}	$a_0(980)\gamma$	(7.6 ±0.6) $\times10^{-5}$	
Γ_{23}	$\eta'(958)\gamma$	(6.2 ±0.7) $\times10^{-5}$	S=1.1
Γ_{24}	$\eta\pi^0\pi^0\gamma$	< 2 $\times10^{-5}$	CL=90%
Γ_{25}	$\mu^+\mu^-\gamma$	(1.4 ±0.5) $\times10^{-5}$	
Γ_{26}	$\rho\gamma\gamma$	< 5 $\times10^{-4}$	CL=90%
Γ_{27}	$\eta\pi^+\pi^-$	< 1.8 $\times10^{-5}$	CL=90%
Γ_{28}	$\eta\mu^+\mu^-$	< 9.4 $\times10^{-6}$	CL=90%

CONSTRAINED FIT INFORMATION

An overall fit to 25 branching ratios uses 67 measurements and one constraint to determine 12 parameters. The overall fit has a $\chi^2 = 55.8$ for 56 degrees of freedom.

The following *off-diagonal* array elements are the correlation coefficients $\langle\delta x_i\delta x_j\rangle/(\delta x_i\cdot\delta x_j)$, in percent, from the fit to the branching fractions, $x_i \equiv \Gamma_i/\Gamma_{\rm total}$. The fit constrains the x_i whose labels appear in this array to sum to one.

x_2	−68									
x_3	−64	−13								
x_6	−25	24	3							
x_7	−10	9	1	8						
x_8	49	−53	−8	−47	−17					
x_9	−7	8	1	7	3	−15				
x_{11}	−4	4	1	3	1	−7	1			
x_{16}	0	0	0	0	0	0	0	0		
x_{18}	−1	1	0	1	0	−2	0	0	0	
x_{22}	0	0	0	0	0	0	0	0	0	0
x_{23}	−5	4	1	18	1	−8	1	1	0	0
	x_1	x_2	x_3	x_6	x_7	x_8	x_9	x_{11}	x_{16}	x_{18}

x_{23}	0
	x_{22}

$\phi(1020)$ PARTIAL WIDTHS

$\Gamma(\eta\gamma)$ Γ_6

VALUE (keV)	DOCUMENT ID		TECN	COMMENT
• • • We do not use the following data for averages, fits, limits, etc. • • •				
58.9±0.5±2.4	ACHASOV	00	SND	$e^+e^- \to \eta\gamma$

$\Gamma(\pi^0\gamma)$ Γ_7

VALUE (keV)	DOCUMENT ID		TECN	COMMENT
• • • We do not use the following data for averages, fits, limits, etc. • • •				
$5.40\pm0.16^{+0.43}_{-0.40}$	ACHASOV	00	SND	$e^+e^- \to \pi^0\gamma$

$\Gamma(e^+e^-)$ Γ_8

VALUE (keV)	EVTS	DOCUMENT ID		TECN	COMMENT
1.27±0.04 OUR EVALUATION					
• • • We do not use the following data for averages, fits, limits, etc. • • •					
1.27±0.03	272k	[13] AKHMETSHIN	04	CMD2	$e^+e^- \to K_L^0K_S^0$

[13] Using $B(\phi \to K_L^0K_S^0) = 0.337 \pm 0.005$ and $\Gamma_{\rm total} = 4.26 \pm 0.05$ MeV. Update of AKHMETSHIN 99D.

$\phi(1020)\ \Gamma(i)\Gamma(e^+e^-)/\Gamma^2(\text{total})$

$\Gamma(e^+e^-) \times \Gamma(K^+K^-)/\Gamma^2_{\rm total}$ $\Gamma_8\Gamma_1/\Gamma^2$

VALUE (units 10^{-5})	EVTS	DOCUMENT ID		TECN	COMMENT
14.60±0.33 OUR FIT	Error includes scale factor of 1.2.				
13.93±0.14±0.99	1000k	[14] ACHASOV	01E	SND	$e^+e^- \to K^+K^-$, K_SK_L, $\pi^+\pi^-\pi^0$

$\Gamma(e^+e^-) \times \Gamma(K_L^0 K_S^0)/\Gamma_{total}^2$ $\Gamma_8\Gamma_2/\Gamma^2$

VALUE (units 10^{-5})	EVTS	DOCUMENT ID		TECN	COMMENT
10.11±0.14 OUR FIT					
10.06±0.16 OUR AVERAGE					
10.01±0.04±0.17	272k	[15] AKHMETSHIN	04	CMD2	$e^+e^- \to K_L^0 K_S^0$
10.27±0.07±0.34	500k	[14] ACHASOV	01E	SND	$e^+e^- \to K^+K^-$, $K_S K_L$, $\pi^+\pi^-\pi^0$

$\Gamma(e^+e^-) \times [\Gamma(\rho\pi) + \Gamma(\pi^+\pi^-\pi^0)]/\Gamma_{total}^2$ $\Gamma_8\Gamma_3/\Gamma^2$

VALUE (units 10^{-5})	EVTS	DOCUMENT ID		TECN	COMMENT
4.60 ±0.14 OUR FIT	Error includes scale factor of 1.2.				
4.52 ±0.19 OUR AVERAGE					
4.665±0.042±0.261	400k	[14] ACHASOV	01E	SND	$e^+e^- \to K^+K^-$, $K_S K_L$, $\pi^+\pi^-\pi^0$
4.35 ±0.27 ±0.08	11169	[16] AKHMETSHIN	98	CMD2	$e^+e^- \to \pi^+\pi^-\pi^0$

$\Gamma(e^+e^-) \times \Gamma(\eta\gamma)/\Gamma_{total}^2$ $\Gamma_8\Gamma_6/\Gamma^2$

VALUE (units 10^{-6})	EVTS	DOCUMENT ID		TECN	COMMENT
3.85 ±0.07 OUR FIT	Error includes scale factor of 1.2.				
3.89 ±0.08 OUR AVERAGE	Error includes scale factor of 1.2.				
3.850±0.041±0.159	23k	[17,18] AKHMETSHIN	01B	CMD2	$e^+e^- \to \eta\gamma$
4.00 ±0.04 ±0.11		[19] ACHASOV	00	SND	$e^+e^- \to \eta\gamma$
3.765±0.092±0.143		[20] ACHASOV	00B	SND	$e^+e^- \to \eta\gamma$
4.017±0.035±0.124	23k	[21] ACHASOV	00D	SND	$e^+e^- \to \eta\gamma$
3.53 ±0.08 ±0.17	2200	[20,22] AKHMETSHIN	99F	CMD2	$e^+e^- \to \eta\gamma$
• • • We do not use the following data for averages, fits, limits, etc. • • •					
3.848±0.036±0.070		[23] ACHASOV	00B	SND	$e^+e^- \to \eta\gamma$

$\Gamma(e^+e^-) \times \Gamma(\pi^0\gamma)/\Gamma_{total}^2$ $\Gamma_8\Gamma_7/\Gamma^2$

VALUE (units 10^{-7})	DOCUMENT ID		TECN	COMMENT
3.67±0.28 OUR FIT				
$3.67\pm0.10^{+0.27}_{-0.25}$	[24] ACHASOV	00	SND	$e^+e^- \to \pi^0\gamma$

$\Gamma(e^+e^-) \times \Gamma(\mu^+\mu^-)/\Gamma_{total}^2$ $\Gamma_8\Gamma_9/\Gamma^2$

VALUE (units 10^{-8})	DOCUMENT ID		TECN	COMMENT
8.5 ±0.6 OUR FIT				
8.8 ±0.9 OUR AVERAGE	Error includes scale factor of 1.5. See the ideogram below.			
8.36±0.59±0.37	ACHASOV	01G	SND	$e^+e^- \to \mu^+\mu^-$
9.9 ±1.4 ±0.9	[22] ACHASOV	99C	SND	$e^+e^- \to \mu^+\mu^-$
14.4 ±3.0	[16] VASSERMAN	81	OLYA	$e^+e^- \to \mu^+\mu^-$
8.6 ±5.9	[16] AUGUSTIN	73	OSPK	$e^+e^- \to \mu^+\mu^-$

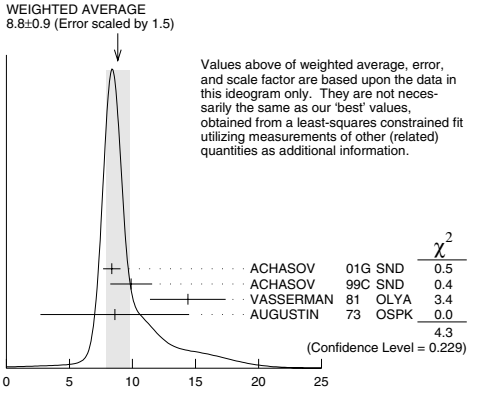

$\Gamma(e^+e^-) \times \Gamma(\mu^+\mu^-)/\Gamma_{total}^2$ $\Gamma_8\Gamma_9/\Gamma^2$

$\Gamma(e^+e^-) \times \Gamma(\pi^+\pi^-)/\Gamma_{total}^2$ $\Gamma_8\Gamma_{11}/\Gamma^2$

VALUE (units 10^{-8})	DOCUMENT ID		TECN	COMMENT
2.2 ±0.4 OUR FIT				
2.2 ±0.4 OUR AVERAGE				
2.1 ±0.3 ±0.3	[22] ACHASOV	00C	SND	$e^+e^- \to \pi^+\pi^-$
$1.95^{+1.15}_{-0.87}$	[16] GOLUBEV	86	ND	$e^+e^- \to \pi^+\pi^-$
$6.01^{+3.19}_{-2.51}$	[16] VASSERMAN	81	OLYA	$e^+e^- \to \pi^+\pi^-$

$\Gamma(e^+e^-) \times \Gamma(\pi^+\pi^-\pi^+\pi^-)/\Gamma_{total}^2$ $\Gamma_8\Gamma_{18}/\Gamma^2$

VALUE (units 10^{-9})	EVTS	DOCUMENT ID		TECN	COMMENT
$1.2\ ^{+0.8}_{-0.7}$ OUR FIT					
1.17±0.52±0.64	3285	[22] AKHMETSHIN	00E	CMD2	$e^+e^- \to \pi^+\pi^-\pi^+\pi^-$

[14] From the combined fit assuming that the total $\phi(1020)$ production cross section is saturated by those of K^+K^-, $K_S K_L$, $\pi^+\pi^-\pi^0$, and $\eta\gamma$ decays modes and using ACHASOV 00B for the $\eta\gamma$ decay mode.
[15] Update of AKHMETSHIN 01D
[16] Recalculated by us from the cross section in the peak.
[17] From the $\eta \to 3\pi^0$ decay and using $B(\eta \to 3\pi^0) = (32.24 \pm 0.29) \times 10^{-2}$.
[18] The combined fit from 600 to 1380 MeV taking into account $\rho(770)$, $\omega(782)$, $\phi(1020)$, and $\rho(1450)$ (mass and width fixed at 1450 MeV and 310 MeV respectively).
[19] From the $\eta \to 2\gamma$ decay and using $B(\eta \to 2\gamma) = (39.21 \pm 0.34) \times 10^{-2}$.
[20] From the $\eta \to \pi^+\pi^-\pi^0$ decay and using $B(\eta \to \pi^+\pi^-\pi^0) = (23.1 \pm 0.5) \times 10^{-2}$.
[21] From the $\eta \to 3\pi^0$ decay and using $B(\eta \to 3\pi^0) = (32.2 \pm 0.4) \times 10^{-2}$.
[22] Recalculated by the authors from the cross section in the peak.
[23] Using various decay modes of the η from ACHASOV 98F, ACHASOV 00, and ACHASOV 00B.
[24] From the $\pi^0 \to 2\gamma$ decay and using $B(\pi^0 \to 2\gamma) = (98.798 \pm 0.032) \times 10^{-2}$.

$\phi(1020)$ BRANCHING RATIOS

$\Gamma(K^+K^-)/\Gamma_{total}$ Γ_1/Γ

VALUE	EVTS	DOCUMENT ID		TECN	COMMENT
0.491±0.006 OUR FIT	Error includes scale factor of 1.2.				
0.493±0.010 OUR AVERAGE					
0.492±0.012	2913	AKHMETSHIN	95	CMD2	$e^+e^- \to K^+K^-$
0.44 ±0.05	321	KALBFLEISCH	76	HBC	2.18 $K^-p \to \Lambda K^+K^-$
0.49 ±0.06	270	DEGROOT	74	HBC	4.2 $K^-p \to \Lambda\phi$
0.540±0.034	565	BALAKIN	71	OSPK	$e^+e^- \to K^+K^-$
0.48 ±0.04	252	LINDSEY	66	HBC	2.1–2.7 $K^-p \to \Lambda K^+K^-$
• • • We do not use the following data for averages, fits, limits, etc. • • •					
0.476±0.017	1000k	[25] ACHASOV	01E	SND	$e^+e^- \to K^+K^-$, $K_S K_L$, $\pi^+\pi^-\pi^0$

$\Gamma(K_L^0 K_S^0)/\Gamma_{total}$ Γ_2/Γ

VALUE	EVTS	DOCUMENT ID		TECN	COMMENT
0.340±0.005 OUR FIT	Error includes scale factor of 1.1.				
0.331±0.009 OUR AVERAGE					
0.335±0.010	40644	AKHMETSHIN	95	CMD2	$e^+e^- \to K_L^0 K_S^0$
0.326±0.035		DOLINSKY	91	ND	$e^+e^- \to K_L^0 K_S^0$
0.310±0.024		DRUZHININ	84	ND	$e^+e^- \to K_L^0 K_S^0$
• • • We do not use the following data for averages, fits, limits, etc. • • •					
0.351±0.013	500k	[25] ACHASOV	01E	SND	$e^+e^- \to K^+K^-$, $K_S K_L$, $\pi^+\pi^-\pi^0$
0.27 ±0.03	133	KALBFLEISCH	76	HBC	2.18 $K^-p \to \Lambda K_L^0 K_S^0$
0.257±0.030	95	BALAKIN	71	OSPK	$e^+e^- \to K_L^0 K_S^0$
0.40 ±0.04	167	LINDSEY	66	HBC	2.1–2.7 $K^-p \to \Lambda K_L^0 K_S^0$

$[\Gamma(\rho\pi) + \Gamma(\pi^+\pi^-\pi^0)]/\Gamma_{total}$ Γ_3/Γ

VALUE	EVTS	DOCUMENT ID		TECN	COMMENT
0.154±0.005 OUR FIT	Error includes scale factor of 1.3.				
0.151±0.009 OUR AVERAGE	Error includes scale factor of 1.7.				
0.161±0.008	11761	AKHMETSHIN	95	CMD2	$e^+e^- \to \pi^+\pi^-\pi^0$
0.143±0.007		DOLINSKY	91	ND	$e^+e^- \to \pi^+\pi^-\pi^0$
• • • We do not use the following data for averages, fits, limits, etc. • • •					
0.159±0.008	400k	[25] ACHASOV	01E	SND	$e^+e^- \to K^+K^-$, $K_S K_L$, $\pi^+\pi^-\pi^0$
0.145±0.009±0.003	11169	[26] AKHMETSHIN	98	CMD2	$e^+e^- \to \pi^+\pi^-\pi^0$
0.139±0.007		[27] PARROUR	76B	OSPK	e^+e^-

$\Gamma(K_L^0 K_S^0)/\Gamma(K\overline{K})$ $\Gamma_2/(\Gamma_1+\Gamma_2)$

VALUE	EVTS	DOCUMENT ID		TECN	COMMENT
0.409±0.006 OUR FIT	Error includes scale factor of 1.1.				
0.45 ±0.04 OUR AVERAGE					
0.44 ±0.07		LONDON	66	HBC	2.24 $K^-p \to \Lambda K\overline{K}$
0.48 ±0.07	52	BADIER	65B	HBC	3 K^-p
0.40 ±0.10	34	SCHLEIN	63	HBC	1.95 $K^-p \to \Lambda K\overline{K}$

$[\Gamma(\rho\pi) + \Gamma(\pi^+\pi^-\pi^0)]/\Gamma(K\overline{K})$ $\Gamma_3/(\Gamma_1+\Gamma_2)$

VALUE	DOCUMENT ID		TECN	COMMENT
0.186±0.006 OUR FIT	Error includes scale factor of 1.2.			
0.24 ±0.04 OUR AVERAGE				
0.237±0.039	CERRADA	77B	HBC	4.2 $K^-p \to \Lambda 3\pi$
0.30 ±0.15	LONDON	66	HBC	2.24 $K^-p \to \Lambda\pi^+\pi^-\pi^0$

$[\Gamma(\rho\pi) + \Gamma(\pi^+\pi^-\pi^0)]/\Gamma(K_L^0 K_S^0)$ Γ_3/Γ_2

VALUE	EVTS	DOCUMENT ID		TECN	COMMENT
0.455±0.015 OUR FIT	Error includes scale factor of 1.2.				
0.51 ±0.05 OUR AVERAGE					
0.56 ±0.07	3681	BUKIN	78C	OLYA	$e^+e^- \to K_L^0 K_S^0$, $\pi^+\pi^-\pi^0$
0.47 ±0.06	516	COSME	74	OSPK	$e^+e^- \to \pi^+\pi^-\pi^0$

$\Gamma(\eta\gamma)/\Gamma(\pi^0\gamma)$ Γ_6/Γ_7

VALUE	DOCUMENT ID		TECN	COMMENT
• • • We do not use the following data for averages, fits, limits, etc. • • •				
$10.9\pm0.3^{+0.7}_{-0.8}$	ACHASOV	00	SND	$e^+e^-\to\eta\gamma,\pi^0\gamma$

$\Gamma(\mu^+\mu^-)/\Gamma_{\rm total}$ Γ_9/Γ

VALUE (units 10^{-4})	DOCUMENT ID		TECN	COMMENT
2.85 ± 0.19 OUR FIT				
2.5 ± 0.4 OUR AVERAGE				
2.69 ± 0.46	[28] HAYES	71	CNTR	8.3,9.8 γ C $\to\mu^+\mu^-$ X
2.17 ± 0.60	[28] EARLES	70	CNTR	6.0 γ C $\to\mu^+\mu^-$ X
• • • We do not use the following data for averages, fits, limits, etc. • • •				
$2.87\pm0.20\pm0.14$	[29] ACHASOV	01G	SND	$e^+e^-\to\mu^+\mu^-$
$3.30\pm0.45\pm0.32$	[26] ACHASOV	99C	SND	$e^+e^-\to\mu^+\mu^-$
4.83 ± 1.02	[30] VASSERMAN	81	OLYA	$e^+e^-\to\mu^+\mu^-$
2.87 ± 1.98	[30] AUGUSTIN	73	OSPK	$e^+e^-\to\mu^+\mu^-$

$\Gamma(\eta\gamma)/\Gamma_{\rm total}$ Γ_6/Γ

VALUE	EVTS	DOCUMENT ID		TECN	COMMENT
0.01295 ± 0.00025 OUR FIT Error includes scale factor of 1.1.					
0.0126 ± 0.0004 OUR AVERAGE					
$0.01246\pm0.00025\pm0.0005$	710k	[31] ACHASOV	98F	SND	$e^+e^-\to7\gamma$
0.0118 ± 0.0011	279	[32] AKHMETSHIN	95	CMD2	$e^+e^-\to\pi^+\pi^-3\gamma$
0.0130 ± 0.0006		[33] DRUZHININ	84	ND	$e^+e^-\to3\gamma$
0.014 ± 0.002		[34] DRUZHININ	84	ND	$e^+e^-\to6\gamma$
0.0088 ± 0.0020	290	KURDADZE	83C	OLYA	$e^+e^-\to3\gamma$
0.0135 ± 0.0029		ANDREWS	77	CNTR	6.7–10 γCu
0.015 ± 0.004	54	[33] COSME	76	OSPK	e^+e^-
• • • We do not use the following data for averages, fits, limits, etc. • • •					
$0.01287\pm0.00013\pm0.0006$	3	[35,36] AKHMETSHIN	01B	CMD2	$e^+e^-\to\eta\gamma$
$0.01338\pm0.00012\pm0.0005$	2	[37] ACHASOV	00	SND	$e^+e^-\to\eta\gamma$
$0.01287\pm0.00012\pm0.0004$	2	[38] ACHASOV	00B	SND	$e^+e^-\to\eta\gamma$
$0.01259\pm0.00030\pm0.0005$	9	[39] ACHASOV	00B	SND	$e^+e^-\to\eta\gamma$
$0.01343\pm0.00012\pm0.0005$	5.2k	[31] ACHASOV	00D	SND	$e^+e^-\to\eta\gamma$
$0.0118\pm0.0003\pm0.0006$	2200	[40] AKHMETSHIN	99F	CMD2	$e^+e^-\to\eta\gamma$
0.0121 ± 0.0007		[41] BENAYOUN	96	RVUE	0.54-1.04 $e^+e^-\to\eta\gamma$

$\Gamma(\pi^+\pi^-\gamma)/\Gamma_{\rm total}$ Γ_{15}/Γ

VALUE (units 10^{-4})	CL%	EVTS	DOCUMENT ID		TECN	COMMENT
$0.41\pm0.12\pm0.04$		30175	[42] AKHMETSHIN	99B	CMD2	$e^+e^-\to\pi^+\pi^-\gamma$
• • • We do not use the following data for averages, fits, limits, etc. • • •						
<0.3	90		[43] AKHMETSHIN	97C	CMD2	$e^+e^-\to\pi^+\pi^-\gamma$
<600	90		KALBFLEISCH	75	HBC	2.18 $K^-p\to\Lambda\pi^+\pi^-\gamma$
<70	90		COSME	74	OSPK	$e^+e^-\to\pi^+\pi^-\gamma$
<400	90		LINDSEY	65	HBC	2.1–2.7 $K^-p\to\Lambda\pi^+\pi^-$ neutrals

$\Gamma(\omega\gamma)/\Gamma_{\rm total}$ Γ_{13}/Γ

VALUE	CL%	DOCUMENT ID		TECN	COMMENT
<0.05	84	LINDSEY	66	HBC	2.1–2.7 $K^-p\to\Lambda\pi^+\pi^-$ neutrals

$\Gamma(\rho\gamma)/\Gamma_{\rm total}$ Γ_{14}/Γ

VALUE (units 10^{-4})	CL%	DOCUMENT ID		TECN	COMMENT
<0.12	90	[44] AKHMETSHIN	99B	CMD2	$e^+e^-\to\pi^+\pi^-\gamma$
• • • We do not use the following data for averages, fits, limits, etc. • • •					
<7	90	AKHMETSHIN	97C	CMD2	$e^+e^-\to\pi^+\pi^-\gamma$
<200	84	LINDSEY	66	HBC	2.1–2.7 $K^-p\to\Lambda\pi^+\pi^-$ neutrals

$\Gamma(e^+e^-)/\Gamma_{\rm total}$ Γ_8/Γ

VALUE (units 10^{-4})	EVTS	DOCUMENT ID		TECN	COMMENT
2.98 ± 0.04 OUR FIT Error includes scale factor of 1.1.					
2.98 ± 0.07 OUR AVERAGE Error includes scale factor of 1.1.					
2.93 ± 0.14	1900k	[45] ACHASOV	01E	SND	$e^+e^-\to K^+K^-,K_SK_L,\pi^+\pi^-\pi^0$
2.88 ± 0.09	55600	AKHMETSHIN	95	CMD2	$e^+e^-\to$ hadrons
3.00 ± 0.21	3681	BUKIN	78C	OLYA	$e^+e^-\to$ hadrons
3.10 ± 0.14		[46] PARROUR	76	OSPK	e^+e^-
3.3 ± 0.3		COSME	74	OSPK	$e^+e^-\to$ hadrons
2.81 ± 0.25	681	BALAKIN	71	OSPK	$e^+e^-\to$ hadrons
3.50 ± 0.27		CHATELUS	71	OSPK	e^+e^-

$\Gamma(\pi^0\gamma)/\Gamma_{\rm total}$ Γ_7/Γ

VALUE (units 10^{-3})	EVTS	DOCUMENT ID		TECN	COMMENT
1.31 ± 0.13 OUR AVERAGE					
1.30 ± 0.13		DRUZHININ	84	ND	$e^+e^-\to3\gamma$
1.4 ± 0.5	32	COSME	76	OSPK	e^+e^-
• • • We do not use the following data for averages, fits, limits, etc. • • •					
$1.226\pm0.036^{+0.096}_{-0.089}$		[47] ACHASOV	00	SND	$e^+e^-\to\pi^0\gamma$
1.26 ± 0.17		[41] BENAYOUN	96	RVUE	0.54-1.04 $e^+e^-\to\pi^0\gamma$

$\Gamma(\pi^+\pi^-)/\Gamma_{\rm total}$ Γ_{11}/Γ

VALUE (units 10^{-4})	CL%	DOCUMENT ID		TECN	COMMENT
• • • We do not use the following data for averages, fits, limits, etc. • • •					
$0.71\pm0.11\pm0.09$		[26] ACHASOV	00C	SND	$e^+e^-\to\pi^+\pi^-$
$0.65^{+0.38}_{-0.29}$		[26] GOLUBEV	86	ND	$e^+e^-\to\pi^+\pi^-$
$2.01^{+1.07}_{-0.84}$		[26] VASSERMAN	81	OLYA	$e^+e^-\to\pi^+\pi^-$
<6.6	95	BUKIN	78B	OLYA	$e^+e^-\to\pi^+\pi^-$
<2.7	95	ALVENSLEB...	72	CNTR	6.7 γ C $\to$ C$\pi^+\pi^-$

$\Gamma(\omega\pi^0)/\Gamma_{\rm total}$ Γ_{12}/Γ

VALUE (units 10^{-5})	DOCUMENT ID		TECN	COMMENT
$5.2^{+1.3}_{-1.1}$	[48,49] AULCHENKO	00A	SND	$e^+e^-\to\pi^+\pi^-\pi^0\pi^0$
• • • We do not use the following data for averages, fits, limits, etc. • • •				
~5.4	[50] ACHASOV	00E	SND	$e^+e^-\to\pi^0\pi^0\gamma$
$5.5^{+1.6}_{-1.4}\pm0.3$	[49,51] AULCHENKO	00A	SND	$e^+e^-\to\pi^+\pi^-\pi^0\pi^0$
$4.8^{+1.9}_{-1.7}\pm0.8$	[50] ACHASOV	99	SND	$e^+e^-\to\pi^+\pi^-\pi^0\pi^0$

$\Gamma(K^0_LK^0_S)/\Gamma(K^+K^-)$ Γ_2/Γ_1

VALUE	EVTS	DOCUMENT ID		TECN	COMMENT
0.692 ± 0.017 OUR FIT Error includes scale factor of 1.1.					
0.740 ± 0.031 OUR AVERAGE					
0.70 ± 0.06	2732	BUKIN	78C	OLYA	$e^+e^-\to K^0_LK^0_S$
0.82 ± 0.08		LOSTY	78	HBC	4.2 $K^-p\to\phi$hyperon
0.71 ± 0.05		LAVEN	77	HBC	10 $K^-p\to K^+K^-\Lambda$
0.71 ± 0.08		LYONS	77	HBC	3–4 $K^-p\to\Lambda\phi$
0.89 ± 0.10	144	AGUILAR-...	72B	HBC	3.9,4.6 K^-p
• • • We do not use the following data for averages, fits, limits, etc. • • •					
0.68 ± 0.03		[52] AKHMETSHIN	95	CMD2	$e^+e^-\to K^0_LK^0_S,K^+K^-$

$\left[\Gamma(\rho\pi)+\Gamma(\pi^+\pi^-\pi^0)\right]/\Gamma(K^+K^-)$ Γ_3/Γ_1

VALUE	EVTS	DOCUMENT ID		TECN	COMMENT
0.315 ± 0.012 OUR FIT Error includes scale factor of 1.2.					
0.28 ± 0.09	34	AGUILAR-...	72B	HBC	3.9,4.6 K^-p

$\Gamma(\eta e^+e^-)/\Gamma_{\rm total}$ Γ_{10}/Γ

VALUE (units 10^{-4})	EVTS	DOCUMENT ID		TECN	COMMENT
1.15 ± 0.10 OUR AVERAGE					
$1.19\pm0.19\pm0.12$	213	[53] ACHASOV	01B	SND	$e^+e^-\to\gamma\gamma e^+e^-$
$1.14\pm0.10\pm0.06$	355	[54] AKHMETSHIN	01	CMD2	$e^+e^-\to\eta e^+e^-$
$1.3^{+0.8}_{-0.6}$	7	GOLUBEV	85	ND	$e^+e^-\to\gamma\gamma e^+e^-$
• • • We do not use the following data for averages, fits, limits, etc. • • •					
$1.13\pm0.14\pm0.07$	183	[55] AKHMETSHIN	01	CMD2	$e^+e^-\to\eta e^+e^-$
$1.21\pm0.14\pm0.09$	130	[56] AKHMETSHIN	01	CMD2	$e^+e^-\to\eta e^+e^-$
$1.04\pm0.20\pm0.08$	42	[57] AKHMETSHIN	01	CMD2	$e^+e^-\to\eta e^+e^-$

$\Gamma(\eta'(958)\gamma)/\Gamma_{\rm total}$ Γ_{23}/Γ

VALUE (units 10^{-5})	CL%	EVTS	DOCUMENT ID		TECN	COMMENT
6.2 ± 0.7 OUR FIT Error includes scale factor of 1.1.						
$6.7^{+2.8}_{-2.4}\pm0.8$		12	[58] AULCHENKO	03B	SND	$e^+e^-\to\eta'\gamma$
• • • We do not use the following data for averages, fits, limits, etc. • • •						
$6.7^{+5.0}_{-4.2}\pm1.5$		7	AULCHENKO	03B	SND	$e^+e^-\to7\gamma$
$6.10\pm0.61\pm0.43$		120	[59] ALOISIO	02E	KLOE	1.02 $e^+e^-\to\pi^+\pi^-3\gamma$
$8.2^{+2.1}_{-1.9}\pm1.1$		21	[60] AKHMETSHIN	00B	CMD2	$e^+e^-\to\pi^+\pi^-3\gamma$
$4.9^{+2.2}_{-1.8}\pm0.6$		9	[61] AKHMETSHIN	00F	CMD2	$e^+e^-\to\pi^+\pi^-\pi^+\pi^-\geq2\gamma$
6.4 ± 1.6		30	[62] AKHMETSHIN	00F	CMD2	$e^+e^-\to\eta'(958)\gamma$
$6.7^{+3.4}_{-2.9}\pm1.0$		5	[63] AULCHENKO	99	SND	$e^+e^-\to\pi^+\pi^-3\gamma$
<11	90		AULCHENKO	98	SND	$e^+e^-\to7\gamma$
$12^{+7}_{-5}\pm2$		6	[60] AKHMETSHIN	97B	CMD2	$e^+e^-\to\pi^+\pi^-3\gamma$
<41	90		DRUZHININ	87	ND	$e^+e^-\to\gamma\eta\pi^+\pi^-$

Meson Particle Listings

$\phi(1020)$

$\Gamma(\eta\pi^0\pi^0\gamma)/\Gamma_{total}$ Γ_{24}/Γ

VALUE (units 10^{-5})	CL%	DOCUMENT ID		TECN	COMMENT
<2	90	AULCHENKO	98	SND	$e^+e^- \to 7\gamma$

$\Gamma(\pi^0\pi^0\gamma)/\Gamma_{total}$ Γ_{17}/Γ

VALUE (units 10^{-4})	CL%	EVTS	DOCUMENT ID		TECN	COMMENT
1.09 ±0.06 OUR AVERAGE						
1.09 ±0.03 ±0.05		2438	ALOISIO	02D	KLOE	$e^+e^- \to \pi^0\pi^0\gamma$
1.08 ±0.17 ±0.09		268	AKHMETSHIN	99C	CMD2	$e^+e^- \to \pi^0\pi^0\gamma$
• • • We do not use the following data for averages, fits, limits, etc. • • •						
1.158±0.093±0.052		419 [64,65]	ACHASOV	00H	SND	$e^+e^- \to \pi^0\pi^0\gamma$
<10	90		DRUZHININ	87	ND	$e^+e^- \to 5\gamma$

$\Gamma(\pi^0\pi^0\gamma)/\Gamma(\eta\gamma)$ Γ_{17}/Γ_6

VALUE (units 10^{-2})	EVTS	DOCUMENT ID		TECN	COMMENT
0.865±0.070±0.017	419	[65] ACHASOV	00H	SND	$e^+e^- \to \pi^0\pi^0\gamma$
• • • We do not use the following data for averages, fits, limits, etc. • • •					
0.90 ±0.08 ±0.07	164	ACHASOV	98I	SND	$e^+e^- \to 5\gamma$

$\Gamma(\pi^+\pi^+\pi^-\pi^-\pi^0)/\Gamma_{total}$ Γ_{19}/Γ

VALUE (units 10^{-6})	CL%	DOCUMENT ID		TECN	COMMENT
< 4.6	90	AKHMETSHIN	00E	CMD2	$e^+e^- \to \pi^+\pi^-\pi^+\pi^-\pi^0$
• • • We do not use the following data for averages, fits, limits, etc. • • •					
<150	95	BARKOV	88	CMD	$e^+e^- \to \pi^+\pi^-\pi^+\pi^-\pi^0$

$\Gamma(\pi^+\pi^-\pi^+\pi^-)/\Gamma_{total}$ Γ_{18}/Γ

VALUE (units 10^{-6})	CL%	EVTS	DOCUMENT ID		TECN	COMMENT
• • • We do not use the following data for averages, fits, limits, etc. • • •						
3.93±1.74±2.14		3285	AKHMETSHIN	00E	CMD2	$e^+e^- \to \pi^+\pi^-\pi^+\pi^-$
<870	90		CORDIER	79	WIRE	$e^+e^- \to \pi^+\pi^-\pi^+\pi^-$

$\Gamma(f_0(980)\gamma)/\Gamma_{total}$ Γ_{16}/Γ

VALUE (units 10^{-4})	CL%	EVTS	DOCUMENT ID		TECN	COMMENT
4.40±0.21 OUR FIT						
4.44±0.21 OUR AVERAGE						
4.47±0.21		2438	[66] ALOISIO	02D	KLOE	$e^+e^- \to \pi^0\pi^0\gamma$
2.90±0.21±1.54			[67] AKHMETSHIN	99C	CMD2	$e^+e^- \to \pi^+\pi^-\gamma$, $\pi^0\pi^0\gamma$
• • • We do not use the following data for averages, fits, limits, etc. • • •						
3.5 ±0.3 $^{+1.3}_{-0.5}$		419 [64,68]	ACHASOV	00H	SND	$e^+e^- \to \pi^0\pi^0\gamma$
1.93±0.46±0.50		27188	[69] AKHMETSHIN	99B	CMD2	$e^+e^- \to \pi^+\pi^-\gamma$
3.05±0.25±0.72		268	[70] AKHMETSHIN	99C	CMD2	$e^+e^- \to \pi^0\pi^0\gamma$
1.5 ±0.5		268	[71] AKHMETSHIN	99C	CMD2	$e^+e^- \to \pi^0\pi^0\gamma$
3.42±0.30±0.36		164	[68] ACHASOV	98I	SND	$e^+e^- \to 5\gamma$
< 1	90		[72] AKHMETSHIN	97C	CMD2	$e^+e^- \to \pi^+\pi^-\gamma$
< 7	90		[73] AKHMETSHIN	97C	CMD2	$e^+e^- \to \pi^+\pi^-\gamma$
<20	90		DRUZHININ	87	ND	$e^+e^- \to \pi^0\pi^0\gamma$

$\Gamma(f_0(980)\gamma)/\Gamma(\eta\gamma)$ Γ_{16}/Γ_6

VALUE (units 10^{-2})	EVTS	DOCUMENT ID		TECN	COMMENT
3.40±0.18 OUR FIT Error includes scale factor of 1.1.					
2.6 ±0.2 $^{+0.8}_{-0.3}$	419	[68] ACHASOV	00H	SND	$e^+e^- \to \pi^0\pi^0\gamma$

$\Gamma(\pi^0e^+e^-)/\Gamma_{total}$ Γ_{20}/Γ

VALUE (units 10^{-5})	CL%	EVTS	DOCUMENT ID		TECN	COMMENT
1.12±0.28 OUR AVERAGE						
1.01±0.28±0.29		52	[74] ACHASOV	02D	SND	$e^+e^- \to \pi^0e^+e^-$
1.22±0.34±0.21		46	[75] AKHMETSHIN	01C	CMD2	$e^+e^- \to \pi^0e^+e^-$
• • • We do not use the following data for averages, fits, limits, etc. • • •						
<12	90		DOLINSKY	88	ND	$e^+e^- \to \pi^0e^+e^-$

$\Gamma(\pi^0\eta\gamma)/\Gamma_{total}$ Γ_{21}/Γ

VALUE (units 10^{-5})	CL%	EVTS	DOCUMENT ID		TECN	COMMENT
8.3 ±0.5 OUR AVERAGE						
8.51±0.51±0.57		607	[76] ALOISIO	02C	KLOE	$e^+e^- \to \eta\pi^0\gamma$
7.96±0.60±0.40		197	[77] ALOISIO	02C	KLOE	$e^+e^- \to \eta\pi^0\gamma$
8.8 ±1.4 ±0.9		36	[78] ACHASOV	00F	SND	$e^+e^- \to \eta\pi^0\gamma$
9.0 ±2.4 ±1.0		80	AKHMETSHIN	99C	CMD2	$e^+e^- \to \eta\pi^0\gamma$
• • • We do not use the following data for averages, fits, limits, etc. • • •						
8.3 ±2.3 ±1.2		20	ACHASOV	98B	SND	$e^+e^- \to 5\gamma$
<250	90		DOLINSKY	91	ND	$e^+e^- \to \pi^0\eta\gamma$

$\Gamma(a_0(980)\gamma)/\Gamma_{total}$ Γ_{22}/Γ

VALUE (units 10^{-5})	CL%	EVTS	DOCUMENT ID		TECN	COMMENT
7.6±0.6 OUR FIT						
7.6±0.6 OUR AVERAGE						
7.4±0.7			[79] ALOISIO	02C	KLOE	$e^+e^- \to \eta\pi^0\gamma$
8.8±1.7		36	[80] ACHASOV	00F	SND	$e^+e^- \to \eta\pi^0\gamma$
• • • We do not use the following data for averages, fits, limits, etc. • • •						
11 ±2			[81] GOKALP	02	RVUE	$e^+e^- \to \eta\pi^0\gamma$
<500	90		DOLINSKY	91	ND	$e^+e^- \to \pi^0\eta\gamma$

$\Gamma(f_0(980)\gamma)/\Gamma(a_0(980)\gamma)$ Γ_{16}/Γ_{22}

VALUE (units 10^{-5})	DOCUMENT ID		TECN	COMMENT
6.1±0.6	[82] ALOISIO	02C	KLOE	$e^+e^- \to \eta\pi^0\gamma$

$\Gamma(\eta'(958)\gamma)/\Gamma(K_L^0K_S^0)$ Γ_{23}/Γ_2

VALUE (units 10^{-4})	EVTS	DOCUMENT ID		TECN	COMMENT
1.83±0.21 OUR FIT Error includes scale factor of 1.1.					
1.46 $^{+0.64}_{-0.54}$ ±0.18	9	[83] AKHMETSHIN	00F	CMD2	$e^+e^- \to \pi^+\pi^-\pi^+\pi^- \geq 2\gamma$

$\Gamma(\eta'(958)\gamma)/\Gamma(\eta\gamma)$ Γ_{23}/Γ_6

VALUE (units 10^{-3})	EVTS	DOCUMENT ID		TECN	COMMENT
4.8 ±0.5 OUR FIT Error includes scale factor of 1.1.					
4.9 ±0.5 OUR AVERAGE					
4.70±0.47±0.31	120	[84] ALOISIO	02E	KLOE	1.02 $e^+e^- \to \pi^+\pi^-3\gamma$
6.5 $^{+1.7}_{-1.5}$ ±0.8	21	AKHMETSHIN	00B	CMD2	$e^+e^- \to \pi^+\pi^-3\gamma$
• • • We do not use the following data for averages, fits, limits, etc. • • •					
9.5 $^{+5.2}_{-4.0}$ ±1.4	6	[85] AKHMETSHIN	97B	CMD2	$e^+e^- \to \pi^+\pi^-3\gamma$

$\Gamma(\mu^+\mu^-\gamma)/\Gamma_{total}$ Γ_{25}/Γ

VALUE (units 10^{-5})	EVTS	DOCUMENT ID		TECN	COMMENT
1.43±0.45±0.14	27188	[69] AKHMETSHIN	99B	CMD2	$e^+e^- \to \mu^+\mu^-\gamma$
• • • We do not use the following data for averages, fits, limits, etc. • • •					
2.3 ±1.0	824 ± 33	[86] AKHMETSHIN	97C	CMD2	$e^+e^- \to \mu^+\mu^-\gamma$

$\Gamma(\rho\gamma\gamma)/\Gamma_{total}$ Γ_{26}/Γ

VALUE (units 10^{-4})	CL%	DOCUMENT ID		TECN	COMMENT
<5	90	AKHMETSHIN	98	CMD2	$e^+e^- \to \pi^+\pi^-\gamma\gamma$

$\Gamma(\eta\pi^+\pi^-)/\Gamma_{total}$ Γ_{27}/Γ

VALUE (units 10^{-5})	CL%	DOCUMENT ID		TECN	COMMENT
< 1.8	90	AKHMETSHIN	00E	CMD2	$e^+e^- \to \pi^+\pi^-\pi^+\pi^-\pi^0$
• • • We do not use the following data for averages, fits, limits, etc. • • •					
<30	90	AKHMETSHIN	98	CMD2	$e^+e^- \to \pi^+\pi^-\gamma\gamma$

$\Gamma(\eta\mu^+\mu^-)/\Gamma_{total}$ Γ_{28}/Γ

VALUE (units 10^{-6})	CL%	DOCUMENT ID		TECN	COMMENT
<9.4	90	AKHMETSHIN	01	CMD2	$e^+e^- \to \eta e^+e^-$

$\Gamma(\pi^+\pi^-\pi^0)/\Gamma_{total}$ Γ_5/Γ

VALUE	CL%	EVTS	DOCUMENT ID		TECN	COMMENT
• • • We do not use the following data for averages, fits, limits, etc. • • •						
≃ 0.0087		1.98M [87,88]	ALOISIO	03	KLOE	1.02 $e^+e^- \to \pi^+\pi^-\pi^0$
<0.0006	90		[89] ACHASOV	02	SND	1.02 $e^+e^- \to \pi^+\pi^-\pi^0$
<0.23	90		[89] CORDIER	80	DM1	$e^+e^- \to \pi^+\pi^-\pi^0$
<0.20	90		[89] PARROUR	76B	OSPK	$e^+e^- \to \pi^+\pi^-\pi^0$

[25] Using $B(\phi \to e^+e^-) = (2.93 \pm 0.14) \times 10^{-4}$.
[26] Using $B(\phi \to e^+e^-) = (2.99 \pm 0.08) \times 10^{-4}$.
[27] Using $\Gamma(\phi) = 4.1$ Mev. If interference between the $\rho\pi$ and 3π modes is neglected, the fraction of the $\rho\pi$ is more than 80% at the 90% confidence level.
[28] Neglecting interference between resonance and continuum.
[29] Using $B(\phi \to e^+e^-) = (2.91 \pm 0.07) \times 10^{-4}$.
[30] Recalculated by us using $B(\phi \to e^+e^-) = (2.99 \pm 0.08) \times 10^{-4}$.
[31] Using $B(\phi \to e^+e^-) = (2.99 \pm 0.08) \times 10^{-4}$ and $B(\eta \to 3\pi^0) = (32.2 \pm 0.4) \times 10^{-2}$.
[32] From $\pi^+\pi^-\pi^0$ decay mode of η.
[33] From 2γ decay mode of η.
[34] From $3\pi^0$ decay mode of η.
[35] Using $B(\phi \to e^+e^-) = (2.99 \pm 0.08) \times 10^{-4}$ and $B(\eta \to 3\pi^0) = (32.24 \pm 0.29) \times 10^{-2}$.
[36] The combined fit from 600 to 1380 MeV taking into account $\rho(770)$, $\omega(782)$, $\phi(1020)$, and $\rho(1450)$ (mass and width fixed at 1450 MeV and 310 MeV respectively).
[37] From the $\eta \to 2\gamma$ decay and using $B(\phi \to e^+e^-) = (2.99 \pm 0.08) \times 10^{-4}$.
[38] Using various decay modes of the η from ACHASOV 98F, ACHASOV 00, and ACHASOV 00B and $B(\phi \to e^+e^-) = (2.99 \pm 0.08) \times 10^{-4}$.
[39] From the $\eta \to \pi^+\pi^-\pi^0$ decay and $B(\phi \to e^+e^-) = (2.99 \pm 0.08) \times 10^{-4}$.
[40] From $\pi^+\pi^-\pi^0$ decay mode of η and using $B(\phi \to e^+e^-) = (2.99 \pm 0.08) \times 10^{-4}$.
[41] Reanalysis of DRUZHININ 84, DOLINSKY 89, and DOLINSKY 91 taking into account a triangle anomaly contribution.
[42] For $E_\gamma > 20$ MeV and assuming that $B(\phi(1020) \to f_0(980)\gamma)$ is negligible. Supersedes AKHMETSHIN 97C.
[43] For $E_\gamma > 20$ MeV and assuming that $B(\phi(1020) \to f_0(980)\gamma)$ is negligible.
[44] Supersedes AKHMETSHIN 97C.
[45] From the combined fit assuming that the total $\phi(1020)$ production cross section is saturated by those of K^+K^-, K_SK_L, $\pi^+\pi^-\pi^0$, and $\eta\gamma$ decays modes and using ACHASOV 00B for the $\eta\gamma$ decay mode.
[46] Using total width 4.2 MeV. They detect 3π mode and observe significant interference with ω tail. This is accounted for in the result quoted above.
[47] From the $\pi^0 \to 2\gamma$ decay and using $B(\phi \to e^+e^-) = (2.99 \pm 0.08) \times 10^{-4}$.
[48] Using the 1996 and 1998 data.
[49] $(2.3 \pm 0.3)\%$ correction for other decay modes of the $\omega(782)$ applied.
[50] Using the 1996 data.
[51] Using the 1998 data.
[52] Theoretical analysis of BRAMON 00 taking into account phase-space difference, electromagnetic radiative corrections, as well as isospin breaking, predicts 0.62. FISCHBACH 02 calculates additional corrections caused by the close threshold and predicts 0.68.
[53] Using $B(\eta \to \gamma\gamma) = (39.25 \pm 0.32)\%$, $B(\phi \to \eta\gamma) = (1.26 \pm 0.06)\%$, and $B(\phi \to e^+e^-) = (3.00 \pm 0.06) \times 10^{-4}$.
[54] The average of the branching ratios separately obtained from the $\eta \to \gamma\gamma$, $3\pi^0$, $\pi^+\pi^-\pi^0$ decays.
[55] From $\eta \to \gamma\gamma$ decays and using $B(\eta \to \gamma\gamma) = (39.33 \pm 0.25) \times 10^{-2}$, $B(\eta \to \pi^+\pi^-\gamma) = (4.75 \pm 11) \times 10^{-2}$, and $B(\phi \to \eta\gamma) = (1.297 \pm 0.033) \times 10^{-2}$.
[56] From $\eta \to 3\pi^0$ decays and using $B(\pi^0 \to \gamma\gamma) = (98.798 \pm 0.033) \times 10^{-2}$, $B(\eta \to 3\pi^0) = (32.24 \pm 0.29) \times 10^{-2}$, $B(\eta \to \pi^+\pi^-\gamma) = (4.75 \pm 0.11) \times 10^{-2}$, and $B(\phi \to \eta\gamma) = (1.297 \pm 0.033) \times 10^{-2}$.
[57] From $\eta \to \pi^+\pi^-\pi^0$ decays and using $B(\pi^0 \to \gamma\gamma) = (98.798 \pm 0.033) \times 10^{-2}$, $B(\pi^0 \to e^+e^-\gamma) = (1.198 \pm 0.032) \times 10^{-2}$, $B(\eta \to \pi^+\pi^-\pi^0) = (23.0 \pm 0.4) \times 10^{-2}$, $B(\phi \to \pi^+\pi^-\pi^0) = (15.5 \pm 0.6) \times 10^{-2}$, and $B(\phi \to \eta\gamma) = (1.297 \pm 0.033) \times 10^{-2}$.
[58] Averaging AULCHENKO 03B with AULCHENKO 99.
[59] Using $B(\phi \to \eta\gamma) = (1.297 \pm 0.033)\%$.
[60] Using the value $B(\phi \to \eta\gamma) = (1.26 \pm 0.06) \times 10^{-2}$.
[61] Using $B(\phi \to K_L^0 K_S^0) = (33.8 \pm 0.6)\%$.
[62] Averaging AKHMETSHIN 00B with AKHMETSHIN 00F.
[63] Using the value $B(\eta' \to \eta\pi^+\pi^-) = (43.7 \pm 1.5) \times 10^{-2}$ and $B(\eta \to \gamma\gamma) = (39.25 \pm 0.31) \times 10^{-2}$.
[64] Using the value $B(\phi \to \eta\gamma) = (1.338 \pm 0.053) \times 10^{-2}$.
[65] Supersedes ACHASOV 98I. Excluding $\omega\pi^0$.
[66] From the negative interference with the $f_0(600)$ meson of AITALA 01B using the ACHASOV 89 parameterization for the $f_0(980)$, a Breit-Wigner for the $f_0(600)$, and ACHASOV 01F for the $\rho\pi$ contribution.
[67] From the combined fit of the photon spectra in the reactions $e^+e^- \to \pi^+\pi^-\gamma$, $\pi^0\pi^0\gamma$.
[68] Assuming that the $\pi^0\pi^0\gamma$ final state is completely determined by the $f_0\gamma$ mechanism, neglecting the decay $B(\phi \to K\overline{K}\gamma)$ and using $B(f_0 \to \pi^+\pi^-) = 2B(f_0 \to \pi^0\pi^0)$.
[69] For $E_\gamma > 20$ MeV. Supersedes AKHMETSHIN 97C.
[70] Neglecting other intermediate mechanisms ($\rho\pi$, $\sigma\gamma$).
[71] A narrow pole fit taking into account $f_0(980)$ and $f_0(1200)$ intermediate mechanisms.
[72] For destructive interference with the Bremsstrahlung process
[73] For constructive interference with the Bremsstrahlung process
[74] Using various branching ratios from the 2000 Edition of this Review (PDG 00).
[75] Using $B(\pi^0 \to \gamma\gamma) = 0.98798 \pm 0.00032$, $B(\phi \to \eta\gamma) = (1.297 \pm 0.033) \times 10^{-2}$, and $B(\eta \to \pi^+\pi^-\gamma) = (4.75 \pm 0.11) \times 10^{-2}$.
[76] From the decay mode $\eta \to \gamma\gamma$.
[77] From the decay mode $\eta \to \pi^+\pi^-\pi^0$.
[78] Supersedes ACHASOV 98B.
[79] Using $M_{a_0(980)} = 984.8$ MeV and assuming $a_0(980)\gamma$ dominance.
[80] Assuming $a_0(980)\gamma$ dominance in the $\eta\pi^0\gamma$ final state.
[81] Using data of ACHASOV 00F.
[82] Using results of ALOISIO 02D and assuming that $f_0(980)$ decays into $\pi\pi$ only and $a_0(980)$ into $\eta\pi$ only.
[83] Using various branching ratios of K_S^0, K_L^0, η, η' from the 2000 edition (The European Physical Journal **C15** 1 (2000)) of this Review.
[84] From the decay mode $\eta' \to \eta\pi^+\pi^-$, $\eta \to \gamma\gamma$.
[85] Superseded by AKHMETSHIN 00B.
[86] For $E_\gamma > 20$ MeV.
[87] From a fit without limitations on charged and neutral ρ masses and widths.
[88] Adding the direct and $\omega\pi$ contributions and considering the interference between the $\rho\pi$ and $\pi^+\pi^-\pi^0$.
[89] Neglecting the interference between the $\rho\pi$ and $\pi^+\pi^-\pi^0$.

$\pi^+\pi^-\pi^0$ / $\rho\pi$ AMPLITUDE RATIO a_1 IN DECAY OF $\phi \to \pi^+\pi^-\pi^0$

VALUE	CL%	EVTS	DOCUMENT ID		TECN	COMMENT
0.090 ± 0.011 ± 0.006		1.98M	[91,92] ALOISIO	03	KLOE	1.02 $e^+e^- \to \pi^+\pi^-\pi^0$
• • • We do not use the following data for averages, fits, limits, etc. • • •						
$-0.06 < a_1 < 0.06$		500k	[93] ACHASOV	02	SND	$e^+e^- \to \pi^+\pi^-\pi^0$
$-0.16 < a_1 < 0.11$	90		[90] AKHMETSHIN	98	CMD2	$e^+e^- \to \pi^+\pi^-\gamma\gamma$

[90] Dalitz plot analysis of 9735 events taking into account interference between the contact and $\rho\pi$ terms and assuming zero phase for the contact term.
[91] From a fit without limitations on charged and neutral ρ masses and widths.
[92] Recalculated by us to match the notations of AKHMETSHIN 98.
[93] Recalculated by the authors to match the notations of AKHMETSHIN 98.

$\phi(1020)$ REFERENCES

AKHMETSHIN 04 PL B578 285 R.R. Akhmetshin *et al.* (Novosibirsk CMD-2 Collab.)
ALOISIO 03 PL B561 55 A. Aloisio *et al.* (KLOE Collab.)
AULCHENKO 03B JETP 97 24 V.M. Aulchenko *et al.* (Novosibirsk SND Collab.)
Translated from ZETF 124 28.
ACHASOV 02 PR D65 032002 M.N. Achasov *et al.* (Novosibirsk SND Collab.)
ACHASOV 02D JETPL 75 449 M.N. Achasov *et al.* (Novosibirsk SND Collab.)
Translated from ZETFP 75 539.
ALOISIO 02C PL B536 209 A. Aloisio *et al.* (KLOE Collab.)
ALOISIO 02D PL B537 21 A. Aloisio *et al.* (KLOE Collab.)
ALOISIO 02E PL B541 45 A. Aloisio *et al.* (KLOE Collab.)
FISCHBACH 02 PL B526 355 E. Fischbach, A.W. Overhauser, B. Woodahl
GOKALP 02 JPG 28 2783 A. Gokalp *et al.*
ACHASOV 01B PL B504 275 M.N. Achasov *et al.* (Novosibirsk SND Collab.)
ACHASOV 01E PR D63 072002 M.N. Achasov *et al.* (Novosibirsk SND Collab.)
ACHASOV 01F PR D63 094007 N.N. Achasov *et al.* (Novosibirsk SND Collab.)
ACHASOV 01G PRL 86 1698 M.N. Achasov *et al.* (Novosibirsk SND Collab.)
AITALA 01B PRL 86 770 E.M. Aitala *et al.* (FNAL E791 Collab.)
AKHMETSHIN 01 PL B501 191 R.R. Akhmetshin *et al.* (Novosibirsk CMD-2 Collab.)
AKHMETSHIN 01B PL B509 217 R.R. Akhmetshin *et al.* (Novosibirsk CMD-2 Collab.)
AKHMETSHIN 01C PL B503 237 R.R. Akhmetshin *et al.* (Novosibirsk CMD-2 Collab.)
AKHMETSHIN 01D PL B508 217 (erratum) R.R. Akhmetshin *et al.* (Novosibirsk CMD-2 Collab.)
Also 99D PL B466 385 R.R. Akhmetshin *et al.*
ACHASOV 00 EPJ C12 25 M.N. Achasov *et al.* (Novosibirsk SND Collab.)
ACHASOV 00B JETP 90 17 M.N. Achasov *et al.* (Novosibirsk SND Collab.)
Translated from ZETF 117 22.
ACHASOV 00C PL B474 188 M.N. Achasov *et al.* (Novosibirsk SND Collab.)
ACHASOV 00D JETPL 72 282 M.N. Achasov *et al.* (Novosibirsk SND Collab.)
Translated from ZETFP 72 411.
ACHASOV 00E NP B569 158 M.N. Achasov *et al.* (Novosibirsk SND Collab.)
ACHASOV 00F PL B479 53 M.N. Achasov *et al.* (Novosibirsk SND Collab.)
ACHASOV 00H PL B485 349 M.N. Achasov *et al.* (Novosibirsk SND Collab.)
AKHMETSHIN 00B PL B473 337 R.R. Akhmetshin *et al.* (Novosibirsk CMD-2 Collab.)
AKHMETSHIN 00E PL B491 81 R.R. Akhmetshin *et al.* (Novosibirsk CMD-2 Collab.)
AKHMETSHIN 00F PL B494 26 R.R. Akhmetshin *et al.* (Novosibirsk CMD-2 Collab.)
AULCHENKO 00A JETP 90 927 V.M. Aulchenko *et al.* (Novosibirsk SND Collab.)
Translated from ZETF 117 1067.
BRAMON 00 PL B486 406 A. Bramon *et al.*
PDG 00 EPJ C15 1 D.E. Groom *et al.*
ACHASOV 99 PL B449 122 M.N. Achasov *et al.*
ACHASOV 99C PL B456 304 M.N. Achasov *et al.*
AKHMETSHIN 99B PL B462 371 R.R. Akhmetshin *et al.* (Novosibirsk CMD-2 Collab.)
AKHMETSHIN 99C PL B462 380 R.R. Akhmetshin *et al.* (Novosibirsk CMD-2 Collab.)
AKHMETSHIN 99D PL B466 385 R.R. Akhmetshin *et al.*
AKHMETSHIN 99F PL B460 242 R.R. Akhmetshin *et al.* (Novosibirsk CMD-2 Collab.)
AULCHENKO 99 JETPL 69 97 V.M. Aulchenko *et al.*
Translated from ZETFP 69 87.
ACHASOV 98B PL B438 441 M.N. Achasov *et al.* (Novosibirsk SND Collab.)
ACHASOV 98F JETPL 68 573 M.N. Achasov *et al.* (Novosibirsk SND Collab.)
ACHASOV 98I PL B440 442 M.N. Achasov *et al.*
AKHMETSHIN 98 PL B434 426 R.R. Akhmetshin *et al.*
AULCHENKO 98 PL B436 199 V.M. Aulchenko *et al.* (Novosibirsk SND Collab.)
BARBERIS 98 PL B432 436 D. Barberis *et al.* (Omega Expt.)
AKHMETSHIN 97B PL B415 445 R.R. Akhmetshin *et al.* (NOVO, BOST, PITT+)
AKHMETSHIN 97C PL B415 452 R.R. Akhmetshin *et al.* (Novosibirsk CMD-2 Collab.)
BENAYOUN 96 ZPHY C72 221 M. Benayoun *et al.* (IPNP, NOVO)
AKHMETSHIN 95 PL B364 199 R.R. Akhmetshin *et al.* (Novosibirsk CMD-2 Collab.)
DOLINSKY 91 PRPL 202 99 S.I. Dolinsky *et al.* (NOVO)
ACHASOV 89 NP B315 465 N.N. Achasov, V.N. Ivanchenko
DOLINSKY 89 ZPHY C42 511 S.I. Dolinsky *et al.* (NOVO)
BARKOV 88 SJNP 47 248 L.M. Barkov *et al.* (NOVO)
Translated from YAF 47 393.
DOLINSKY 88 SJNP 48 277 S.I. Dolinsky *et al.* (NOVO)
Translated from YAF 48 442.
DRUZHININ 87 ZPHY C37 1 V.P. Druzhinin *et al.* (NOVO)
ARMSTRONG 86 PL 166B 245 T.A. Armstrong *et al.* (ATHU, BARI, BIRM+)
ATKINSON 86 ZPHY C30 521 M. Atkinson *et al.* (BONN, CERN, GLAS+)
BEBEK 86 PRL 56 1893 C. Bebek *et al.* (CLEO Collab.)
DAVENPORT 86 PR 33 2519 T.F. Davenport (TUFTS, ARIZ, FNAL, FSU, NDAM+)
DIJKSTRA 86 ZPHY C31 375 H. Dijkstra *et al.* (ANIK, BRIS, CERN+)
FRAME 86 NP B276 667 D. Frame *et al.* (GLAS)
GOLUBEV 86 SJNP 44 409 V.B. Golubev *et al.* (NOVO)
Translated from YAF 44 633.
ALBRECHT 85D PL 153B 343 H. Albrecht *et al.* (ARGUS Collab.)
GOLUBEV 85 SJNP 41 756 V.B. Golubev *et al.* (NOVO)
Translated from YAF 41 1183.
DRUZHININ 84 PL 144B 136 V.P. Druzhinin *et al.* (NOVO)
ARMSTRONG 83B NP B224 193 T.A. Armstrong *et al.* (BARI, BIRM, CERN+)
BARATE 83 PL 121B 449 R. Barate *et al.* (SACL, LOIC, SHMP, IND)
KURDADZE 83C JETPL 38 366 L.M. Kurdadze *et al.* (NOVO)
Translated from ZETFP 38 306.
ARENTON 82 PR D25 2241 M.W. Arenton *et al.* (ANL, ILL)
PELLINEN 82 PS 25 599 A. Pellinen, M. Roos (HELS)
DAUM 81 PL 100B 439 C. Daum *et al.* (AMST, BRIS, CERN, CRAC+)
IVANOV 81 PL 107B 297 P.M. Ivanov *et al.* (NOVO)
Also 82 Private Comm. S.I. Eidelman (NOVO)
VASSERMAN 81 PL 99B 62 I.B. Vasserman *et al.* (NOVO)
Also 82 SJNP 35 240 L.M. Kurdadze *et al.*
Translated from YAF 35 352.
CORDIER 80 NP B172 13 A. Cordier *et al.* (LALO)
CORDIER 79 PL 81B 389 A. Cordier *et al.* (LALO)
BUKIN 78B SJNP 27 521 A.D. Bukin *et al.* (NOVO)
Translated from YAF 27 985.
BUKIN 78C SJNP 27 516 A.D. Bukin *et al.* (NOVO)
Translated from YAF 27 976.

COOPER	78B	NP B146 1	A.M. Cooper *et al.*	(TATA, CERN, CDEF+)
LOSTY	78	NP B133 38	M.J. Losty *et al.*	(CERN, AMST, NIJM+)
AKERLOF	77	PRL 39 861	C.W. Akerlof *et al.*	(FNAL, MICH, PURD)
ANDREWS	77	PRL 38 198	D.E. Andrews *et al.*	(ROCH)
BALDI	77	PL 68B 381	R. Baldi *et al.*	(GEVA)
CERRADA	77B	NP B126 241	M. Cerrada *et al.*	(AMST, CERN, NIJM+)
COHEN	77	PRL 38 269	D. Cohen *et al.*	(ANL)
LAVEN	77	NP B127 43	H. Laven *et al.*	(AACH3, BERL, CERN, LOIC+)
LYONS	77	NP B125 207	L. Lyons, A.M. Cooper, A.G. Clark	(OXF)
COSME	76	PL 63B 352	G. Cosme *et al.*	(ORSAY)
KALBFLEISCH	76	PR D13 22	G.R. Kalbfleisch, R.C. Strand, J.W. Chapman	(BNL+)
PARROUR	76	PL 63B 357	G. Parrour *et al.*	(ORSAY)
PARROUR	76B	PL 63B 362	G. Parrour *et al.*	(ORSAY)
KALBFLEISCH	75	PR D11 987	G.R. Kalbfleisch, R.C. Strand, J.W. Chapman	(BNL+)
AYRES	74	PRL 32 1463	D.S. Ayres *et al.*	(ANL)
BESCH	74	NP B70 257	H.J. Besch *et al.*	(BONN)
COSME	74	PL 48B 155	G. Cosme *et al.*	(ORSAY)
COSME	74B	PL 48B 159	G. Cosme *et al.*	(ORSAY)
DEGROOT	74	NP B74 77	A.J. de Groot *et al.*	(AMST, NIJM)
AUGUSTIN	73	PRL 30 462	J.E. Augustin *et al.*	(ORSAY)
BALLAM	73	PR D7 3150	J. Ballam *et al.*	(SLAC, LBL)
BINNIE	73B	PR D8 2789	D.M. Binnie *et al.*	(LOIC, SHMP)
AGUILAR-...	72B	PR D6 29	M. Aguilar-Benitez *et al.*	(BNL)
ALVENSLEB...	72	PRL 28 66	H. Alvensleben *et al.*	(MIT, DESY)
BORENSTEIN	72	PR D5 1559	S.R. Borenstein *et al.*	(BNL, MICH)
COLLEY	72	NP B50 1	D.C. Colley *et al.*	(BIRM, GLAS)
BALAKIN	71	PL 34B 328	V.E. Balakin *et al.*	(NOVO)
CHATELUS	71	Thesis LAL 1247	Y. Chatelus	(STRB)
Also	70	PL 32 416	J.C. Bizot *et al.*	(ORSAY)
HAYES	71	PR D4 899	S. Hayes *et al.*	(CORN)
STOTTLE...	71	Thesis ORO 2504 170	A.R. Stottlemyer	(UMD)
BIZOT	70	PL 32 416	J.C. Bizot *et al.*	(ORSAY)
Also	69	Liverpool Sym. 69	J.P. Perez-y-Jorba	
EARLES	70	PRL 25 1312	D.R. Earles *et al.*	(NEAS)
LINDSEY	66	PR 147 913	J.S. Lindsey, G. Smith	(LRL)
LONDON	66	PR 143 1034	G.W. London *et al.*	(BNL, SYRA) IGJPC
BADIER	65B	PL 17 337	J. Badier *et al.*	(EPOL, SACL, AMST)
LINDSEY	65	PRL 15 221	J.S. Lindsey, G.A. Smith	(LRL)
LINDSEY 65 data included in LINDSEY 66.				
SCHLEIN	63	PRL 10 368	P.E. Schlein *et al.*	(UCLA) IGJP

OTHER RELATED PAPERS

ACHASOV	03B	PR D68 014006	N.N. Achsaov, A.V. Kiselev	
BOGLIONE	03	EPJ C30 503	M. Boglione, M.R. Pennington	
ACHASOV	02L	PAN 65 1887 Translated from YAF 65 1939.	N.N. Achasov *et al.*	
ANISOVICH	02C	PAN 65 497 Translated from YAF 65 523.	A.V. Anisovich *et al.*	
BRAMON	02	EPJ C26 253	A. Bramon *et al.*	
ACHASOV	01F	PR D63 094007	N.N. Achasov *et al.*	(Novosibirsk SND Collab.)
BENAYOUN	01	EPJ C22 503	M. Benayoun, H.B. O'Connell	
CLOSE	01	PL B515 13	F.E. Close, A. Kirk	
GOKALP	01	PR D64 053017	A. Gokalp, O. Yilmaz	
MARKUSHIN	00	EPJ A8 389	V.E. Markushin	
ACHASOV	99B	PAN 62 442 Translated from YAF 62 484.	M.N. Achasov *et al.*	
MARCO	99	PL B470 20	E. Marco *et al.*	
OLLER	98B	PL B426 7	J.A. Oller	
ACHASOV	95	PLB 363 106	N.N. Achasov, V.V. Gubin	(NOVM)
KAMAL	92	PL B284 421	A.N. Kamal, Q.P. Xu	(ALBE)
GEORGIO...	85	PL 152B 428	C. Georgiopoulos *et al.*	(TUFTS, ARIZ, FNAL+)
GELFAND	63B	PRL 11 438	N. Gelfand *et al.*	(COLU, RUTG)
BERTANZA	62	PRL 9 180	L. Bertanza *et al.*	(BNL, SYRA)

$h_1(1170)$ $I^G(J^{PC}) = 0^-(1^{+-})$

$h_1(1170)$ MASS

VALUE (MeV)	*DOCUMENT ID*		*TECN*	*CHG*	*COMMENT*
1170±20 OUR ESTIMATE					
• • • We do not use the following data for averages, fits, limits, etc. • • •					
1168± 4	ANDO	92	SPEC		$8\ \pi^- p \rightarrow \pi^+\pi^-\pi^0 n$
1166± 5±3	[1] ANDO	92	SPEC		$8\ \pi^- p \rightarrow \pi^+\pi^-\pi^0 n$
1190±60	[2] DANKOWY...	81	SPEC	0	$8\ \pi p \rightarrow 3\pi n$

[1] Average and spread of values using 2 variants of the model of BOWLER 75.
[2] Uses the model of BOWLER 75.

$h_1(1170)$ WIDTH

VALUE (MeV)	*DOCUMENT ID*		*TECN*	*CHG*	*COMMENT*
360±40 OUR ESTIMATE					
• • • We do not use the following data for averages, fits, limits, etc. • • •					
345± 6	ANDO	92	SPEC		$8\ \pi^- p \rightarrow \pi^+\pi^-\pi^0 n$
375± 6±34	[3] ANDO	92	SPEC		$8\ \pi^- p \rightarrow \pi^+\pi^-\pi^0 n$
320±50	[4] DANKOWY...	81	SPEC	0	$8\ \pi p \rightarrow 3\pi n$

[3] Average and spread of values using 2 variants of the model of BOWLER 75.
[4] Uses the model of BOWLER 75.

$h_1(1170)$ DECAY MODES

	Mode	Fraction (Γ_i/Γ)
Γ_1	$\rho\pi$	seen

$h_1(1170)$ BRANCHING RATIOS

$\Gamma(\rho\pi)/\Gamma_{\text{total}}$ Γ_1/Γ

VALUE	*DOCUMENT ID*		*TECN*	*COMMENT*
• • • We do not use the following data for averages, fits, limits, etc. • • •				
seen	ANDO	92	SPEC	$8\ \pi^- p \rightarrow \pi^+\pi^-\pi^0 n$
seen	ATKINSON	84	OMEG	20–70 $\gamma p \rightarrow \pi^+\pi^-\pi^0 p$
seen	DANKOWY...	81	SPEC	$8\ \pi p \rightarrow 3\pi n$

$h_1(1170)$ REFERENCES

ANDO	92	PL B291 496	A. Ando *et al.*	(KEK, KYOT, NIRS, SAGA+)
ATKINSON	84	NP B231 15	M. Atkinson *et al.*	(BONN, CERN, GLAS+)
DANKOWY...	81	PRL 46 580	J.A. Dankowych *et al.*	(TNTO, BNL, CARL+)
BOWLER	75	NP B97 227	M.G. Bowler *et al.*	(OXFTP, DARE)

$b_1(1235)$ $I^G(J^{PC}) = 1^+(1^{+-})$

$b_1(1235)$ MASS

VALUE (MeV)	*EVTS*	*DOCUMENT ID*		*TECN*	*CHG*	*COMMENT*
1229.5± 3.2 OUR AVERAGE Error includes scale factor of 1.6. See the ideogram below.						
1225 ± 5		WEIDENAUER	93	ASTE		$\overline{p}p \rightarrow 2\pi^+2\pi^-\pi^0$
1235 ±15		ALDE	92C	GAM2		$38{,}100\ \pi^- p \rightarrow \omega\pi^0 n$
1236 ±16		FUKUI	91	SPEC		$8.95\ \pi^- p \rightarrow \omega\pi^0 n$
1222 ± 6		ATKINSON	84E	OMEG	±	25–$55\ \gamma p \rightarrow \omega\pi X$
1237 ± 7		ATKINSON	84E	OMEG	0	25–$55\ \gamma p \rightarrow \omega\pi X$
1239 ± 5		EVANGELISTA	81	OMEG	–	$12\ \pi^- p \rightarrow \omega\pi p$
1251 ± 8	450	GESSAROLI	77	HBC	–	$11\ \pi^- p \rightarrow \pi^-\omega p$
1245 ±11	890	FLATTE	76C	HBC	–	$4.2\ K^- p \rightarrow \pi^-\omega\Sigma^+$
1222 ± 4	1400	CHALOUPKA	74	HBC	–	$3.9\ \pi^- p$
1220 ± 7	600	KARSHON	74B	HBC	+	$4.9\ \pi^+ p$
• • • We do not use the following data for averages, fits, limits, etc. • • •						
1190 ±10		AUGUSTIN	89	DM2	±	$e^+e^- \rightarrow 5\pi$
1213 ± 5		ATKINSON	84C	OMEG	0	20–$70\ \gamma p$
1271 ±11		COLLICK	84	SPEC	+	$200\ \pi^+ Z \rightarrow Z\pi\omega$

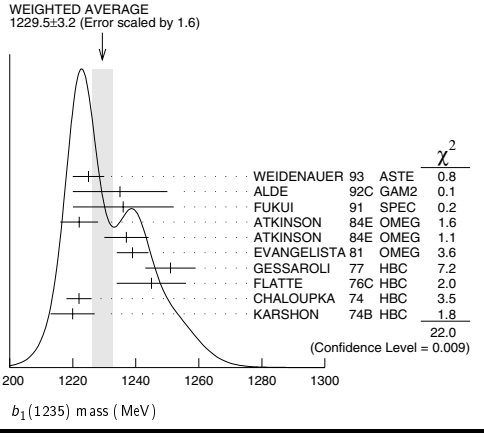

$b_1(1235)$ WIDTH

VALUE (MeV)	*EVTS*	*DOCUMENT ID*		*TECN*	*CHG*	*COMMENT*
142± 9 OUR AVERAGE Error includes scale factor of 1.2.						
113±12		WEIDENAUER	93	ASTE		$\overline{p}p \rightarrow 2\pi^+2\pi^-\pi^0$
160±30		ALDE	92C	GAM2		$38{,}100\ \pi^- p \rightarrow \omega\pi^0 n$
151±31		FUKUI	91	SPEC		$8.95\ \pi^- p \rightarrow \omega\pi^0 n$
170±15		EVANGELISTA	81	OMEG	–	$12\ \pi^- p \rightarrow \omega\pi p$
170±50	225	BALTAY	78B	HBC	+	$15\ \pi^+ p \rightarrow p4\pi$
155±32	450	GESSAROLI	77	HBC	–	$11\ \pi^- p \rightarrow \pi^-\omega p$
182±45	890	FLATTE	76C	HBC	–	$4.2\ K^- p \rightarrow \pi^-\omega\Sigma^+$
135±20	1400	CHALOUPKA	74	HBC	–	$3.9\ \pi^- p$
156±22	600	KARSHON	74B	HBC	+	$4.9\ \pi^+ p$

• • • We do not use the following data for averages, fits, limits, etc. • • •

210±19	AUGUSTIN	89	DM2	±	$e^+e^- \to 5\pi$
231±14	ATKINSON	84C	OMEG	0	20–70 γp
232±29	COLLICK	84	SPEC	+	200 π^+Z → Z$\pi\omega$

$b_1(1235)$ DECAY MODES

	Mode	Fraction (Γ_i/Γ)		Confidence level
Γ_1	$\omega\pi$ [D/S amplitude ratio = 0.277 ± 0.027]	dominant		
Γ_2	$\pi^\pm\gamma$	$(1.6\pm0.4)\times10^{-3}$		
Γ_3	$\eta\rho$	seen		
Γ_4	$\pi^+\pi^+\pi^-\pi^0$	< 50	%	84%
Γ_5	$(K\overline{K})^\pm\pi^0$	< 8	%	90%
Γ_6	$K^0_S K^0_L \pi^\pm$	< 6	%	90%
Γ_7	$K^0_S K^0_S \pi^\pm$	< 2	%	90%
Γ_8	$\phi\pi$	< 1.5	%	84%

$b_1(1235)$ PARTIAL WIDTHS

$\Gamma(\pi^\pm\gamma)$ Γ_2

VALUE (keV)	DOCUMENT ID		TECN	CHG	COMMENT
230±60	COLLICK	84	SPEC	+	200 π^+Z → Z$\pi\omega$

$b_1(1235)$ D-wave/S-wave AMPLITUDE RATIO IN DECAY OF $b_1(1235) \to \omega\pi$

VALUE	EVTS	DOCUMENT ID		TECN	CHG	COMMENT
0.277±0.027 OUR AVERAGE		Error includes scale factor of 2.4. See the ideogram below.				
0.269±0.009±0.010		NOZAR	02	MPS	–	18 $\pi^- p \to \omega\pi^- p$
0.23 ±0.03		AMSLER	94C	CBAR		0.0 $\overline{p}p \to \omega\eta\pi^0$
0.45 ±0.04		AMSLER	93B	CBAR		0.0 $\overline{p}p \to \omega\pi^0\pi^0$
0.235±0.047		ATKINSON	84C	OMEG		20–70 γp
0.4 $^{+0.1}_{-0.1}$		GESSAROLI	77	HBC	–	11 $\pi^- p \to \pi^-\omega p$
0.21 ±0.08		CHUNG	75B	HBC	+	7.1 $\pi^+ p$
0.3 ±0.1		CHALOUPKA	74	HBC	–	3.9–7.5 $\pi^- p$
0.35 ±0.25	600	KARSHON	74B	HBC	+	4.9 $\pi^+ p$

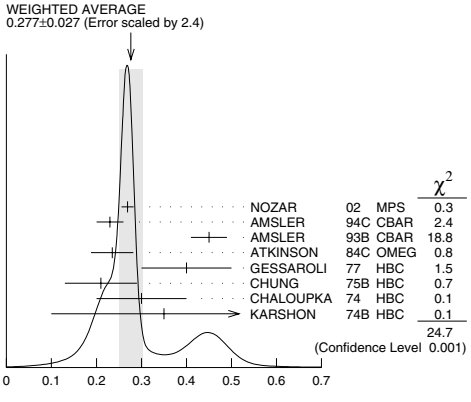

$b_1(1235)$ D-wave/S-wave amplitude ratio in decay of $b_1(1235) \to \omega\pi$

$b_1(1235)$ D-wave/S-wave AMPLITUDE PHASE DIFFERENCE IN DECAY OF $b_1(1235) \to \omega\pi$

VALUE (°)	DOCUMENT ID		TECN	CHG	COMMENT
10.5±2.4±3.9	NOZAR	02	MPS	–	18 $\pi^- p \to \omega\pi^- p$

$b_1(1235)$ BRANCHING RATIOS

$\Gamma(\eta\rho)/\Gamma(\omega\pi)$ Γ_3/Γ_1

VALUE	DOCUMENT ID		TECN	COMMENT
<0.10	ATKINSON	84D	OMEG	20–70 γp

$\Gamma(\pi^+\pi^+\pi^-\pi^0)/\Gamma(\omega\pi)$ Γ_4/Γ_1

VALUE	DOCUMENT ID		TECN	CHG	COMMENT
<0.5	ABOLINS	63	HBC	+	3.5 $\pi^+ p$

$\Gamma((K\overline{K})^\pm\pi^0)/\Gamma(\omega\pi)$ Γ_5/Γ_1

VALUE	CL%	DOCUMENT ID		TECN	CHG	COMMENT
<0.08	90	BALTAY	67	HBC	±	0.0 $\overline{p}p$

$\Gamma(K^0_S K^0_L\pi^\pm)/\Gamma(\omega\pi)$ Γ_6/Γ_1

VALUE	CL%	DOCUMENT ID		TECN	CHG	COMMENT
<0.06	90	BALTAY	67	HBC	±	0.0 $\overline{p}p$

$\Gamma(K^0_S K^0_S\pi^\pm)/\Gamma(\omega\pi)$ Γ_7/Γ_1

VALUE	CL%	DOCUMENT ID		TECN	CHG	COMMENT
<0.02	90	BALTAY	67	HBC	±	0.0 $\overline{p}p$

$\Gamma(\phi\pi)/\Gamma(\omega\pi)$ Γ_8/Γ_1

VALUE	CL%	DOCUMENT ID		TECN	CHG	COMMENT
<0.004	95	VIKTOROV	96	SPEC	0	32.5 $\pi^- p \to K^+K^-\pi^0 n$

• • • We do not use the following data for averages, fits, limits, etc. • • •

<0.04	95	BIZZARRI	69	HBC	±	0.0 $\overline{p}p$
<0.015		DAHL	67	HBC		1.6–4.2 $\pi^- p$

$b_1(1235)$ REFERENCES

NOZAR	02	PL B541 35	M. Nozar *et al.*
VIKTOROV	96	PAN 59 1184	V.A. Viktorov *et al.* (SERP)
		Translated from YAF 59 1239.	
AMSLER	94C	PL B327 425	C. Amsler *et al.* (Crystal Barrel Collab.)
AMSLER	93B	PL B311 362	C. Amsler *et al.* (Crystal Barrel Collab.)
WEIDENAUER	93	ZPHY C59 387	P. Weidenauer *et al.* (ASTERIX Collab.)
ALDE	92C	ZPHY C54 553	D.M. Alde *et al.* (BELG, SERP, KEK, LANL+)
FUKUI	91	PL B257 241	S. Fukui *et al.* (SUGI, NAGO, KEK, KYOT+)
AUGUSTIN	89	NP B320 1	J.E. Augustin, G. Cosme (DM2 Collab.)
ATKINSON	84C	NP B243 1	M. Atkinson *et al.* (BONN, CERN, GLAS+) JP
ATKINSON	84D	NP B242 269	M. Atkinson *et al.* (BONN, CERN, GLAS+)
ATKINSON	84E	PL 138B 459	M. Atkinson *et al.* (BONN, CERN, GLAS+)
COLLICK	84	PRL 53 2374	B. Collick *et al.* (MINN, ROCH, FNAL)
EVANGELISTA	81	NP B178 197	C. Evangelista *et al.* (BARI, BONN, CERN+)
BALTAY	78B	PR D17 62	C. Baltay *et al.* (COLU, BING)
GESSAROLI	77	NP B126 382	R. Gessaroli *et al.* (BGNA, FIRZ, GENO+) JP
FLATTE	76C	PL 64B 225	S.M. Flatte *et al.* (CERN, AMST, NUM+) JP
CHUNG	75B	PR D11 2426	S.U. Chung *et al.* (BNL, LBL, UCSC) JP
CHALOUPKA	74	PL 51B 407	V. Chaloupka *et al.* (CERN) JP
KARSHON	74B	PR D10 3608	U. Karshon *et al.* (REHO) JP
BIZZARRI	69	NP B14 169	R. Bizzarri *et al.* (CERN, CDEF)
BALTAY	67	PRL 18 93	C. Baltay *et al.* (COLU)
DAHL	67	PR 163 1377	O.I. Dahl *et al.* (LRL)
ABOLINS	63	PRL 11 381	M.A. Abolins *et al.* (UCSD)

OTHER RELATED PAPERS

GOLOVKIN	97	ZPHY A359 435	S.V. Golovkin *et al.* (SERP, ITEP)
BRAU	88	PR D37 2379	J.E. Brau *et al.* JP
ATKINSON	84C	NP B243 1	M. Atkinson *et al.* (BONN, CERN, GLAS+) JP
GOLDHABER	65	PRL 15 118	G. Goldhaber *et al.* (LRL)
CARMONY	64	PRL 12 254	D.D. Carmony *et al.* (UCB) JP
BONDAR	63B	PL 5 209	L. Bondar *et al.* (AACH, BIRM, HAMB, LOIC+)

$a_1(1260)$

$I^G(J^{PC}) = 1^-(1^{++})$

THE $a_1(1260)$ AND $a_1(1640)$

Updated December 2003 by S. Eidelman (Novosibirsk).

The main experimental data on the $a_1(1260)$ may be grouped into two classes:

(1) Hadronic Production: This comprises diffractive production with incident π^- (DAUM 80, 81B) and charge-exchange production with low-energy π^- (DANKOWYCH 81, ANDO 92). The 1980's experiments explain the $I^GLJ^P = 1^+S0^+$ data using a phenomenological amplitude consisting of a rescattered Deck amplitude plus a direct resonance-production term. They agree on an $a_1(1260)$ mass of about 1270 MeV and a width of 300–380 MeV. ANDO 92 finds rather lower values for the mass (1121 MeV) and width (239 MeV) in a partial-wave analysis based on the isobar model of the $\pi^+\pi^-\pi^0$ system. However, in this analysis, only Breit-Wigner terms were considered. Recently BARBERIS 98B studied central production of the $\pi^+\pi^-\pi^0$ system, and observed the $a_1(1260)$ meson with a mass of 1240 MeV and a width of about 400 MeV.

CONDO 93 found no evidence for charge-exchange photoproduction of the $a_1(1260)$ (but found a clear signal of $a_2(1320)$ photoproduction). Similarly, MOLCHANOV 01 found no evidence

for Coulomb production of $a_1(1260)$ studying coherent production of three pions (but observed a prominent signal of $a_2(1320)$). They show that it is consistent with either an extremely large $a_1(1260)$ hadronic width, or with a small radiative width to $\pi\gamma$, which could be accommodated if the a_1 mass is somewhat below 1260 MeV.

(2) τ Decay: Various experiments reported good data on $\tau \to a_1(1260)\nu_\tau \to \rho\pi\nu_\tau$ (RUCKSTUHL 86, SCHMIDKE 86, ALBRECHT 86B, BAND 87, ACKERSTAFF 97R, ABREU 98G, and ASNER 00). They are somewhat inconsistent concerning the $a_1(1260)$ mass, which can, however, be attributed to model-dependent systematic uncertainties (BOWLER 86, ALBRECHT 93C, ACKERSTAFF 97R). They all find a width greater than 400 MeV.

The discrepancies between the hadronic- and τ-decay results have stimulated several reanalyses. BASDEVANT 77, 78 used the early diffractive dissociation and τ decay data, and showed that they could be well reproduced with an a_1 resonance mass of 1180 ± 50 MeV and width of 400 ± 50 MeV. Later, BOWLER 86, TORNQVIST 87, ISGUR 89, and IVANOV 91 have studied the process $\tau \to 3\pi\nu_\tau$. Despite quite different approaches, they all found a good overall description of the τ-decay data with an $a_1(1260)$ mass near 1230 MeV, consistent with the hadronic data. However, their widths remain significantly larger (400–600 MeV) than those extracted from diffractive-hadronic data. This is also the case with the later OPAL experiment (ACKERSTAFF 97R). In the high statistics analysis of ACKERSTAFF 97R, the models of ISGUR 89 and KUHN 90 are used to fit distributions of the 3π invariant mass, as well as the 2π invariant mass projections of the Dalitz plot, and neither model is found to provide a completely satisfactory description of the data. Another recent high statistics analysis of ABREU 98G obtains a good description of the $\tau \to 3\pi$ data using the model of FEINDT 90, which includes the $a_1(1640)$ meson, most probably a radial excitation of the $a_1(1260)$ meson (BARNES 97), with a mass of 1700 MeV and a width of 300 MeV. A similar signal has been observed in various hadroproduction processes: by AMELIN 95B and CHUNG 02 in the D-wave of the $\rho\pi$ state, by GOUZ 92 in the $f_1(1285)\pi$ state, and by BAKER 99 in the $f_0(600)\pi$ state, as well as by BAKER 03 in the $\omega\pi^+\pi^-$ state. The existence of such a resonance is also suggested by the very big data sample of ASNER 00, which shows an excess of events at high 3π mass. Their data are better described by the a_1' contribution, though at a level below that reported by ABREU 98G. Since the statistical significance of the a_1' contribution is 2–3 standard deviations only, they conclude that more data is needed to establish the a_1' existence.

ASNER 00 has also performed the analysis of the substructures in the Dalitz plot and found significant contributions of the a_1 decay to $f_0(600)\pi$, $f_0(1370)\pi$, and $f_2(1270)\pi$. The contribution of the $a_1 \to f_0(600)\pi$ at a similar level has independently been observed in $e^+e^- \to 4\pi$ annihilation (AKHMETSHIN 99E), where the $2\pi^+2\pi^-$ final state was shown to be dominated by the $a_1(1260)\pi$ mechanism. Note that existence of the isoscalar contributions to the two-pion state, in addition to the isovector one ($\rho\pi$), will influence the ratio $B(a_1^- \to \pi^-\pi^+\pi^-)/B(a_1^- \to \pi^-\pi^0\pi^0)$, which should be equal to 1 for the pure $\rho\pi$ state. The fit of ASNER 00 improves when the $K\overline{K}^*(892)$ threshold is included. Recently DRUTSKOY 02 found direct evidence for the decay mode $a_1(1260) \to K\overline{K}^*(892)+$ c.c. in B-meson decays.

BOWLER 88 showed that good fits to both the hadronic and the τ-decay data could be obtained with a width of about 400 MeV. However, applying the same type of analysis to the ANDO 92 data, the low mass and narrow width they obtained with the Breit-Wigner PWA do not change appreciably.

$a_1(1260)$ MASS

VALUE (MeV)	EVTS	DOCUMENT ID		TECN	CHG	COMMENT
1230±40 OUR ESTIMATE						
• • • We do not use the following data for averages, fits, limits, etc. • • •						
1331 ±10± 3	37k	[1] ASNER	00	CLE2		10.6 $e^+e^- \to \tau^+\tau^-, \tau^- \to \pi^-\pi^0\pi^0\nu_\tau$
1255 ± 7± 6	5904	[2] ABREU	98G	DLPH		e^+e^-
1207 ± 5± 8	5904	[3] ABREU	98G	DLPH		e^+e^-
1196 ± 4± 5	5904	[4,5] ABREU	98G	DLPH		e^+e^-
1240 ±10		BARBERIS	98B			450 $pp \to p_f\pi^+\pi^-\pi^0 p_s$
1262 ± 9± 7		[2,6] ACKERSTAFF	97R	OPAL		$E^{ee}_{\rm cm}$= 88–94, $\tau \to 3\pi\nu$
1210 ± 7± 2		[3,6] ACKERSTAFF	97R	OPAL		$E^{ee}_{\rm cm}$= 88–94, $\tau \to 3\pi\nu$
1211 ± 7^{+50}_{-0}		[3] ALBRECHT	93C	ARG		$\tau^+ \to \pi^+\pi^+\pi^-\nu$
1121 ± 8		[7] ANDO	92	SPEC		8 $\pi^- p \to \pi^+\pi^-\pi^0 n$
1242 ±37		[8] IVANOV	91	RVUE		$\tau \to \pi^+\pi^+\pi^-\nu$
1260 ±14		[9] IVANOV	91	RVUE		$\tau \to \pi^+\pi^+\pi^-\nu$
1250 ± 9		[10] IVANOV	91	RVUE		$\tau \to \pi^+\pi^+\pi^-\nu$
1208 ±15		ARMSTRONG	90	OMEG	0	300.0$pp \to pp\pi^+\pi^-\pi^0$
1220 ±15		[11] ISGUR	89	RVUE		$\tau^+ \to \pi^+\pi^+\pi^-\nu$
1260 ±25		[12] BOWLER	88	RVUE		
1166 ±18±11		BAND	87	MAC		$\tau^+ \to \pi^+\pi^+\pi^-\nu$
1164 ±41±23		BAND	87	MAC		$\tau^+ \to \pi^+\pi^0\pi^0\nu$
1250 ±40		[11] TORNQVIST	87	RVUE		
1046 ±11		ALBRECHT	86B	ARG		$\tau^+ \to \pi^+\pi^+\pi^-\nu$
1056 ±20±15		RUCKSTUHL	86	DLCO		$\tau^+ \to \pi^+\pi^+\pi^-\nu$
1194 ±14±10		SCHMIDKE	86	MRK2		$\tau^+ \to \pi^+\pi^+\pi^-\nu$
1255 ±23		BELLINI	85	SPEC		40 $\pi^- A \to \pi^-\pi^+\pi^- A$
1240 ±80		[13] DANKOWYY...	81	SPEC	0	8.45 $\pi^- p \to n3\pi$
1280 ±30		[13] DAUM	81B	CNTR		63,94 $\pi^- p \to p3\pi$
1041 ±13		[14] GAVILLET	77	HBC	+	4.2 $K^- p \to \Sigma 3\pi$

[1] From a fit to the 3π mass spectrum including the $K\overline{K}^*(892)$ threshold.
[2] Uses the model of KUHN 90.
[3] Uses the model of ISGUR 89.
[4] Includes the effect of a possible a_1' state.
[5] Uses the model of FEINDT 90.
[6] Supersedes AKERS 95P.
[7] Average and spread of values using 2 variants of the model of BOWLER 75.
[8] Reanalysis of RUCKSTUHL 86.
[9] Reanalysis of SCHMIDKE 86.
[10] Reanalysis of ALBRECHT 86B.
[11] From a combined reanalysis of ALBRECHT 86B, SCHMIDKE 86, and RUCKSTUHL 86.
[12] From a combined reanalysis of ALBRECHT 86B and DAUM 81B.
[13] Uses the model of BOWLER 75.
[14] Produced in K^- backward scattering.

$a_1(1260)$ WIDTH

VALUE (MeV)	EVTS	DOCUMENT ID		TECN	CHG	COMMENT
250 to 600 OUR ESTIMATE						
• • • We do not use the following data for averages, fits, limits, etc. • • •						
460± 85	205	[15] DRUTSKOY	02	BELL		$B \to D^{(*)}K^-K^{*0}$
814± 36± 13	37k	[16] ASNER	00	CLE2		10.6 $e^+e^- \to \tau^+\tau^-, \tau^- \to \pi^-\pi^0\pi^0\nu_\tau$
450± 50	22k	[17] AKHMETSHIN	99E	CMD2		1.05–1.38 $e^+e^- \to \pi^+\pi^-\pi^0\pi^0$
570± 10		[18] BONDAR	99	RVUE		$e^+e^- \to 4\pi, \tau \to 3\pi\nu_\tau$
587± 27± 21	5904	[19] ABREU	98G	DLPH		e^+e^-
478± 3± 15	5904	[20] ABREU	98G	DLPH		e^+e^-
425± 14± 8	5904	[21,22] ABREU	98G	DLPH		e^+e^-

$400\pm$ 35		BARBERIS	98B	450 $pp \to p_f \pi^+\pi^-\pi^0 p_s$
$621\pm$ 32 $\pm$ 58	[19,23]	ACKERSTAFF	97R OPAL	$E_{\rm cm}^{ee}$= 88–94, $\tau \to {}^{3\pi}\nu$
$457\pm$ 15 $\pm$ 17	[20,23]	ACKERSTAFF	97R OPAL	$E_{\rm cm}^{ee}$= 88–94, $\tau \to {}^{3\pi}\nu$
$446\pm$ 21 $^{+140}_{-\ 0}$	[20]	ALBRECHT	93C ARG	$\tau^+ \to \pi^+\pi^+\pi^-\nu$
$239\pm$ 11		ANDO	92 SPEC	8 $\pi^- p \to \pi^+\pi^-\pi^0 n$
$266\pm$ 13 $\pm$ 4	[24]	ANDO	92 SPEC	8 $\pi^- p \to \pi^+\pi^-\pi^0 n$
465^{+228}_{-143}	[25]	IVANOV	91 RVUE	$\tau \to \pi^+\pi^+\pi^-\nu$
$298^{+\ 40}_{-\ 34}$	[26]	IVANOV	91 RVUE	$\tau \to \pi^+\pi^+\pi^-\nu$
$488\pm$ 32	[27]	IVANOV	91 RVUE	$\tau \to \pi^+\pi^+\pi^-\nu$
$430\pm$ 50		ARMSTRONG	90 OMEG 0	300.0 $pp \to pp\pi^+\pi^-\pi^0$
$420\pm$ 40	[28]	ISGUR	89 RVUE	$\tau^+ \to \pi^+\pi^+\pi^-\nu$
$396\pm$ 43	[29]	BOWLER	88 RVUE	
$405\pm$ 75 $\pm$ 25		BAND	87 MAC	$\tau^+ \to \pi^+\pi^+\pi^-\nu$
$419\pm108\pm$ 57		BAND	87 MAC	$\tau^+ \to \pi^+\pi^0\pi^0\nu$
$521\pm$ 27		ALBRECHT	86B ARG	$\tau^+ \to \pi^+\pi^+\pi^-\nu$
$476^{+132}_{-120}\pm$ 54		RUCKSTUHL	86 DLCO	$\tau^+ \to \pi^+\pi^+\pi^-\nu$
$462\pm$ 56 $\pm$ 30		SCHMIDKE	86 MRK2	$\tau^+ \to \pi^+\pi^+\pi^-\nu$
$292\pm$ 40		BELLINI	85 SPEC	40 $\pi^- A \to \pi^-\pi^+\pi^- A$
380 ± 100	[30]	DANKOWSY...	81 SPEC 0	8.45 $\pi^- p \to n3\pi$
$300\pm$ 50	[30]	DAUM	81B CNTR	63,94 $\pi^- p \to p3\pi$
$230\pm$ 50	[31]	GAVILLET	77 HBC +	4.2 $K^- p \to \Sigma 3\pi$

[15] From a fit of the $K^- K^{*0}$ distribution assuming m_{a_1} = 1230 MeV and purely resonant production of the $K^- K^{*0}$ system.
[16] From a fit to the 3π mass spectrum including the $K\overline{K}^*(892)$ threshold.
[17] Using the $a_1(1260)$ mass of 1230 MeV.
[18] From AKHMETSHIN 99E and ASNER 00 data using the $a_1(1260)$ mass of 1230 MeV.
[19] Uses the model of KUHN 90.
[20] Uses the model of ISGUR 89.
[21] Includes the effect of a possible a_1' state.
[22] Uses the model of FEINDT 90.
[23] Supersedes AKERS 95P.
[24] Average and spread of values using 2 variants of the model of BOWLER 75.
[25] Reanalysis of RUCKSTUHL 86.
[26] Reanalysis of SCHMIDKE 86.
[27] Reanalysis of ALBRECHT 86B.
[28] From a combined reanalysis of ALBRECHT 86B, SCHMIDKE 86, and RUCKSTUHL 86.
[29] From a combined reanalysis of ALBRECHT 86B and DAUM 81B.
[30] Uses the model of BOWLER 75.
[31] Produced in K^- backward scattering.

$a_1(1260)$ DECAY MODES

	Mode	Fraction (Γ_i/Γ)
Γ_1	$\pi^+\pi^-\pi^0$	
Γ_2	$\pi^0\pi^0\pi^0$	
Γ_3	$(\rho\pi)_{S-\rm wave}$	seen
Γ_4	$(\rho\pi)_{D-\rm wave}$	seen
Γ_5	$(\rho(1450)\pi)_{S-\rm wave}$	seen
Γ_6	$(\rho(1450)\pi)_{D-\rm wave}$	seen
Γ_7	$\sigma\pi$	seen
Γ_8	$f_0(980)\pi$	not seen
Γ_9	$f_0(1370)\pi$	seen
Γ_{10}	$f_2(1270)\pi$	seen
Γ_{11}	$K\overline{K}^*(892)+$ c.c.	seen
Γ_{12}	$\pi\gamma$	seen

$a_1(1260)$ PARTIAL WIDTHS

$\Gamma(\pi\gamma)$ Γ_{12}

VALUE (keV)	DOCUMENT ID	TECN	COMMENT
640 $\pm$ 246	ZIELINSKI	84C SPEC	200 $\pi^+ Z \to Z 3\pi$

D-wave/S-wave AMPLITUDE RATIO IN DECAY OF $a_1(1260) \to \rho\pi$

VALUE	DOCUMENT ID	TECN	COMMENT
-0.108 ± 0.016 OUR AVERAGE			
$-0.14\ \pm0.04\ \pm0.07$	[34] CHUNG	02 MPS	18.3 $\pi^- p \to \pi^+\pi^-\pi^- p$
$-0.10\ \pm0.02\ \pm0.02$	[32,33] ACKERSTAFF	97R OPAL	$E_{\rm cm}^{ee}$= 88–94, $\tau \to {}^{3\pi}\nu$
$-0.11\ \pm0.02$	[32] ALBRECHT	93C ARG	$\tau^+ \to \pi^+\pi^+\pi^-\nu$

[32] Uses the model of ISGUR 89.
[33] Supersedes AKERS 95P.
[34] Deck-type background not subtracted.

$a_1(1260)$ BRANCHING RATIOS

$\Gamma((\rho\pi)_{S-\rm wave})/\Gamma_{\rm total}$ Γ_3/Γ

VALUE (units 10^{-2})	EVTS	DOCUMENT ID	TECN	COMMENT
• • • We do not use the following data for averages, fits, limits, etc. • • •				
60.19	37k	[35] ASNER	00 CLE2	10.6 $e^+e^- \to \tau^+\tau^-$, $\tau^- \to \pi^-\pi^0\pi^0\nu_\tau$

$\Gamma((\rho\pi)_{D-\rm wave})/\Gamma_{\rm total}$ Γ_4/Γ

VALUE (units 10^{-2})	EVTS	DOCUMENT ID	TECN	COMMENT
• • • We do not use the following data for averages, fits, limits, etc. • • •				
$1.30\pm0.60\pm0.22$	37k	[35] ASNER	00 CLE2	10.6 $e^+e^- \to \tau^+\tau^-$, $\tau^- \to \pi^-\pi^0\pi^0\nu_\tau$

$\Gamma((\rho(1450)\pi)_{S-\rm wave})/\Gamma_{\rm total}$ Γ_5/Γ

VALUE (units 10^{-2})	EVTS	DOCUMENT ID	TECN	COMMENT
• • • We do not use the following data for averages, fits, limits, etc. • • •				
$0.56\pm0.84\pm0.32$	37k	[35,36] ASNER	00 CLE2	10.6 $e^+e^- \to \tau^+\tau^-$, $\tau^- \to \pi^-\pi^0\pi^0\nu_\tau$

$\Gamma((\rho(1450)\pi)_{D-\rm wave})/\Gamma_{\rm total}$ Γ_6/Γ

VALUE (units 10^{-2})	EVTS	DOCUMENT ID	TECN	COMMENT
• • • We do not use the following data for averages, fits, limits, etc. • • •				
$2.04\pm1.20\pm0.28$	37k	[35,36] ASNER	00 CLE2	10.6 $e^+e^- \to \tau^+\tau^-$, $\tau^- \to \pi^-\pi^0\pi^0\nu_\tau$

$\Gamma(\sigma\pi)/\Gamma_{\rm total}$ Γ_7/Γ

VALUE (units 10^{-2})	EVTS	DOCUMENT ID	TECN	COMMENT
• • • We do not use the following data for averages, fits, limits, etc. • • •				
seen		CHUNG	02 MPS	18.3 $\pi^- p \to \pi^+\pi^-\pi^- p$
$18.76\pm4.29\pm1.48$	37k	[35,37] ASNER	00 CLE2	10.6 $e^+e^- \to \tau^+\tau^-$, $\tau^- \to \pi^-\pi^0\pi^0\nu_\tau$

$\Gamma(f_0(980)\pi)/\Gamma_{\rm total}$ Γ_8/Γ

VALUE (units 10^{-2})	EVTS	DOCUMENT ID	TECN	COMMENT
• • • We do not use the following data for averages, fits, limits, etc. • • •				
not seen	37k	ASNER	00 CLE2	10.6 $e^+e^- \to \tau^+\tau^-$, $\tau^- \to \pi^-\pi^0\pi^0\nu_\tau$

$\Gamma(f_0(1370)\pi)/\Gamma_{\rm total}$ Γ_9/Γ

VALUE (units 10^{-2})	EVTS	DOCUMENT ID	TECN	COMMENT
• • • We do not use the following data for averages, fits, limits, etc. • • •				
$7.40\pm2.71\pm1.26$	37k	[35,38] ASNER	00 CLE2	10.6 $e^+e^- \to \tau^+\tau^-$, $\tau^- \to \pi^-\pi^0\pi^0\nu_\tau$

$\Gamma(f_2(1270)\pi)/\Gamma_{\rm total}$ Γ_{10}/Γ

VALUE (units 10^{-2})	EVTS	DOCUMENT ID	TECN	COMMENT
• • • We do not use the following data for averages, fits, limits, etc. • • •				
$1.19\pm0.49\pm0.17$	37k	[35,39] ASNER	00 CLE2	10.6 $e^+e^- \to \tau^+\tau^-$, $\tau^- \to \pi^-\pi^0\pi^0\nu_\tau$

$\Gamma(K\overline{K}^*(892)+\text{c.c.})/\Gamma_{\rm total}$ Γ_{11}/Γ

VALUE (units 10^{-2})	EVTS	DOCUMENT ID	TECN	COMMENT
• • • We do not use the following data for averages, fits, limits, etc. • • •				
8 to 15	205	[40] DRUTSKOY	02 BELL	$B \to D^{(*)} K^- K^{*0}$
$3.3\pm0.5\pm0.1$	37k	[41] ASNER	00 CLE2	10.6 $e^+e^- \to \tau^+\tau^-$, $\tau^- \to \pi^-\pi^0\pi^0\nu_\tau$

$\Gamma(\sigma\pi)/\Gamma((\rho\pi)_{S-\rm wave})$ Γ_7/Γ_3

VALUE	EVTS	DOCUMENT ID	TECN	COMMENT
• • • We do not use the following data for averages, fits, limits, etc. • • •				
~ 0.3	28k	AKHMETSHIN 99E	CMD2	1.05–1.38 $e^+e^- \to \pi^+\pi^-\pi^+\pi^-$
0.003 ± 0.003		[42] LONGACRE	82 RVUE	

$\Gamma(\pi^0\pi^0\pi^0)/\Gamma(\pi^+\pi^-\pi^0)$ Γ_2/Γ_1

VALUE	CL%	DOCUMENT ID	COMMENT
• • • We do not use the following data for averages, fits, limits, etc. • • •			
<0.008	90	[43] BARBERIS	01 450 $pp \to p_f 3\pi^0 p_s$

[35] From a fit to the Dalitz plot.
[36] Assuming for $\rho(1450)$ mass and width of 1370 and 386 MeV respectively.
[37] Assuming for σ mass and width of 860 and 880 MeV respectively.
[38] Assuming for $f_0(1370)$ mass and width of 1186 and 350 MeV respectively.
[39] Assuming for $f_2(1270)$ mass and width of 1275 and 185 MeV respectively.
[40] From a comparison to ALAM 94 assuming purely resonant production of the $K^- K^{*0}$ system.
[41] From a fit to the 3π mass spectrum including the $K\overline{K}^*(892)$ threshold.
[42] Uses multichannel Aitchison-Bowler model (BOWLER 75). Uses data from GAVILLET 77, DAUM 80, and DANKOWYCH 81.
[43] Inconsistent with observations of $\sigma\pi$, $f_0(1370)\pi$, and $f_2(1270)\pi$ decay modes.

Meson Particle Listings

$a_1(1260)$, $f_2(1270)$

$a_1(1260)$ REFERENCES

CHUNG	02	PR D65 072001	S.U. Chung *et al.*	
DRUTSKOY	02	PL B542 171	A. Drutskoy *et al.*	(BELLE Collab.)
BARBERIS	01	PL B507 14	D. Barberis *et al.*	
ASNER	00	PR D61 012002	D.M. Asner *et al.*	(CLEO Collab.)
AKHMETSHIN	99E	PL B466 392	R.R. Akhmetshin *et al.*	(Novosibirsk CMD-2 Collab.)
BONDAR	99	PL B466 403	A.E. Bondar *et al.*	(Novosibirsk CMD-2 Collab.)
ABREU	98G	PL B426 411	P. Abreu *et al.*	(DELPHI Collab.)
BARBERIS	98B	PL B422 399	D. Barberis *et al.*	(WA 102 Collab.)
ACKERSTAFF	97R	ZPHY C75 593	K. Ackerstaff *et al.*	(OPAL Collab.)
AKERS	95P	ZPHY C67 45	R. Akers *et al.*	(OPAL Collab.)
ALAM	94	PR D50 43	M.S. Alam *et al.*	(CLEO Collab.)
ALBRECHT	93C	ZPHY C58 61	H. Albrecht *et al.*	(ARGUS Collab.)
ANDO	92	PL B291 496	A. Ando *et al.*	(KEK, KYOT, NIRS, SAGA+)
IVANOV	91	ZPHY C49 563	Y.P. Ivanov, A.A. Osipov, M.K. Volkov	(JINR)
ARMSTRONG	90	ZPHY C48 213	T.A. Armstrong, M. Benayoun, W. Beusch	
FEINDT	90	ZPHY C48 681	M. Feindt	(HAMB)
KUHN	90	ZPHY C48 445	J.H. Kühn *et al.*	(MPIM)
ISGUR	89	PR D39 1357	N. Isgur, C. Morningstar, C. Reader	(TNTO)
BOWLER	88	PL B209 99	M.G. Bowler	(OXF)
BAND	87	PL B198 297	H.R. Band *et al.*	(MAC Collab.)
TORNQVIST	87	ZPHY C36 695	N.A. Törnqvist	(HELS)
ALBRECHT	86B	ZPHY C33 7	H. Albrecht *et al.*	(ARGUS Collab.)
RUCKSTUHL	86	PRL 56 2132	W. Ruckstuhl *et al.*	(DELCO Collab.)
SCHMIDKE	86	PRL 57 527	W.B. Schmidke *et al.*	(Mark II Collab.)
BELLINI	85	SJNP 41 781	D. Bellini *et al.*	
		Translated from YAF 41 1223.		
ZIELINSKI	84C	PRL 52 1195	M. Zielinski *et al.*	(ROCH, MINN, FNAL)
LONGACRE	82	PR D26 83	R.S. Longacre	(BNL)
DANKOWYC...	81	PRL 46 580	J.A. Dankowych *et al.*	(TNTO, BNL, CARL+)
DAUM	81B	NP B182 269	C. Daum *et al.*	(AMST, CERN, CRAC, MPIM+)
DAUM	80	PL 89B 281	C. Daum *et al.*	(AMST, CERN, CRAC, MPIM+) JP
GAVILLET	77	PL 69B 119	P. Gavillet *et al.*	(AMST, CERN, NIJM+) JP
BOWLER	75	NP B97 227	M.G. Bowler *et al.*	(OXFTP, DARE)

OTHER RELATED PAPERS

BAKER	03	PL B563 140	C.A. Baker *et al.*	
CHUNG	02	PR D65 072001	S.U. Chung *et al.*	
FEUILLAT	01	PL B501 37	M. Feuillat, J.L. Lucio, M.J. Pestieau	
MOLCHANOV	01	PL B521 171	V.V. Molchanov *et al.*	(FNAL SELEX Collab.)
BAKER	99	PL B449 114	C.A. Baker *et al.*	
ZAIMIDOROGA	99	PAN 30 1	O.A. Zaimidoroga	
		Translated from SJPN 30 5.		
BARNES	97	PR D55 4157	T. Barnes *et al.*	(ORNL, RAL, MCHS)
AMELIN	95B	PL B356 595	D.V. Amelin *et al.*	(SERP, TBIL)
BOLONKIN	95	PAN 58 1535	B.V. Bolonkin *et al.*	(ITEP)
		Translated from YAF 58 1628.		
WINGATE	95	PRL 74 4596	M. Wingate, T. de Grand	(COLO, FSU)
CONDO	93	PR D48 3045	G.T. Condo *et al.*	(SLAC Hybrid Collab.)
GOUZ	92	Dallas HEP 92, p. 572	Yu.P. Gouz *et al.*	(VES Collab.)
		Proceedings XXVI Int. Conf. on High Energy Physics		
IIZUKA	89	PR D39 3357	J. Iizuka, H. Koibuchi, F. Masuda	(NAGO, IBAR+)
BOWLER	86	PL B182 400	M.G. Bowler	(OXF)
BASDEVANT	78	PRL 40 994	J.L. Basdevant, E.L. Berger	(FNAL, ANL) JP
BASDEVANT	77	PR D16 657	J.L. Basdevant, E.L. Berger	(FNAL, ANL) JP
ADERHOLZ	64	PL 10 226	M. Aderholz *et al.*	(AACH3, BERL, BIRM+)
GOLDHABER	64	PRL 12 336	G. Goldhaber *et al.*	(LRL, UCB)
LANDER	64	PRL 13 346A	R.L. Lander *et al.*	(UCSD) JP
BELLINI	63	NC 29 896	G. Bellini *et al.*	(MILA)

$f_2(1270)$

$I^G(J^{PC}) = 0^+(2^{++})$

$f_2(1270)$ MASS

VALUE (MeV)	*EVTS*	*DOCUMENT ID*		*TECN*	*COMMENT*
1275.4± 1.2 OUR AVERAGE					
1283 ± 5		ALDE	98	GAM4	100 $\pi^- p \to \pi^0\pi^0 n$
1278 ± 5		[1] BERTIN	97C	OBLX	0.0 $\overline{p}p \to \pi^+\pi^-\pi^0$
1272 ± 8	200k	PROKOSHKIN	94	GAM2	38 $\pi^- p \to \pi^0\pi^0 n$
1269.7± 5.2	5730	AUGUSTIN	89	DM2	$e^+e^- \to 5\pi$
1283 ± 8	400	[2] ALDE	87	GAM4	100 $\pi^- p \to 4\pi^0 n$
1274 ± 5		[2] AUGUSTIN	87	DM2	$J/\psi \to \gamma\pi^+\pi^-$
1283 ± 6		[3] LONGACRE	86	MPS	22 $\pi^- p \to n2K^0_S$
1276 ± 7		COURAU	84	DLCO	$e^+e^- \to e^+e^-\pi^+\pi^-$
1273.3± 2.3		[4] CHABAUD	83	ASPK	17 $\pi^- p$ polarized
1280 ± 4		[5] CASON	82	STRC	8 $\pi^+ p \to \Delta^{++}\pi^0\pi^0$
1281 ± 7	11600	GIDAL	81	MRK2	J/ψ decay
1282 ± 5		[6] CORDEN	79	OMEG	12–15 $\pi^- p \to n2\pi$
1269 ± 4	10k	APEL	75	NICE	40 $\pi^- p \to n2\pi^0$
1272 ± 4	4600	ENGLER	74	DBC	6 $\pi^+ n \to \pi^+\pi^- p$
1277 ± 4	5300	FLATTE	71	HBC	7.0 $\pi^+ p$
1273 ± 8		[2] STUNTEBECK	70	HBC	8 $\pi^- p$, 5.4 $\pi^+ d$
1265 ± 8		BOESEBECK	68	HBC	8 $\pi^+ p$
• • • We do not use the following data for averages, fits, limits, etc. • • •					
1251 ±10		TIKHOMIROV	03	SPEC	40.0 $\overline{n}C \to K^0_S K^0_S K^0_L X$
1260 ±10		[7] ALDE	97	GAM2	450 $pp \to pp\pi^0\pi^0$
1278 ± 6		[7] GRYGOREV	96	SPEC	40 $\pi^- N \to K^0_S K^0_S X$
1262 ±11		AGUILAR-...	91	EHS	400 pp
1275 ±10		AKER	91	CBAR	0.0 $\overline{p}p \to 3\pi^0$
1220 ±10		BREAKSTONE	90	SFM	$pp \to pp\pi^+\pi^-$
1288 ±12		ABACHI	86B	HRS	$e^+e^- \to \pi^+\pi^- X$
1284 ±30	3k	BINON	83	GAM2	38 $\pi^- p \to n2\eta$
1280 ±20	3k	APEL	82	CNTR	25 $\pi^- p \to n2\pi^0$
1284 ±10	16000	DEUTSCH...	76	HBC	16 $\pi^+ p$
1258 ±10	600	TAKAHASHI	72	HBC	8 $\pi^- p \to n2\pi$
1275 ±13		ARMENISE	70	HBC	9 $\pi^+ n \to p\pi^+\pi^-$
1261 ± 5	1960	[2] ARMENISE	68	DBC	5.1 $\pi^+ n \to p\pi^+$MM$^-$
1270 ±10	360	[2] ARMENISE	68	DBC	5.1 $\pi^+ n \to p\pi^0$MM
1268 ± 6		[8] JOHNSON	68	HBC	3.7–4.2 $\pi^- p$

[1] T-matrix pole.
[2] Mass errors enlarged by us to $\Gamma/\sqrt{N}$; see the note with the $K^*(892)$ mass.
[3] From a partial-wave analysis of data using a K-matrix formalism with 5 poles.
[4] From an energy-independent partial-wave analysis.
[5] From an amplitude analysis of the reaction $\pi^+\pi^- \to 2\pi^0$.
[6] From an amplitude analysis of $\pi^+\pi^- \to \pi^+\pi^-$ scattering data.
[7] Systematic uncertainties not estimated.
[8] JOHNSON 68 includes BONDAR 63, LEE 64, DERADO 65, EISNER 67.

$f_2(1270)$ WIDTH

VALUE (MeV)	*EVTS*	*DOCUMENT ID*		*TECN*	*COMMENT*
185.1 $^{+\ 3.5}_{-\ 2.6}$ OUR FIT Error includes scale factor of 1.5.					
184.3 $^{+\ 4.0}_{-\ 2.6}$ OUR AVERAGE Error includes scale factor of 1.6. See the ideogram below.					
171 ±10		ALDE	98	GAM4	100 $\pi^- p \to \pi^0\pi^0 n$
204 ±20		[9] BERTIN	97C	OBLX	0.0 $\overline{p}p \to \pi^+\pi^-\pi^0$
192 ± 5	200k	PROKOSHKIN	94	GAM2	38 $\pi^- p \to \pi^0\pi^0 n$
180 ±24		AGUILAR-...	91	EHS	400 pp
169 ± 9	5730	[10] AUGUSTIN	89	DM2	$e^+e^- \to 5\pi$
150 ±30	400	[10] ALDE	87	GAM4	100 $\pi^- p \to 4\pi^0 n$
186 $^{+\ 9}_{-\ 2}$		[11] LONGACRE	86	MPS	22 $\pi^- p \to n2K^0_S$
179.2 $^{+\ 6.9}_{-\ 6.6}$		[12] CHABAUD	83	ASPK	17 $\pi^- p$ polarized
160 ±11		DENNEY	83	LASS	10 $\pi^+ N$
196 ±10	3k	APEL	82	CNTR	25 $\pi^- p \to n2\pi^0$
152 ± 9		[13] CASON	82	STRC	8 $\pi^+ p \to \Delta^{++}\pi^0\pi^0$
186 ±27	11600	GIDAL	81	MRK2	J/ψ decay
216 ±13		[14] CORDEN	79	OMEG	12–15 $\pi^- p \to n2\pi$
190 ±10	10k	APEL	75	NICE	40 $\pi^- p \to n2\pi^0$
192 ±16	4600	ENGLER	74	DBC	6 $\pi^+ n \to \pi^+\pi^- p$
183 ±15	5300	FLATTE	71	HBC	7 $\pi^+ p \to \Delta^{++} f_2$
196 ±30		[10] STUNTEBECK	70	HBC	8 $\pi^- p$, 5.4 $\pi^+ d$
216 ±20	1960	[10] ARMENISE	68	DBC	5.1 $\pi^+ n \to p\pi^+$MM$^-$
128 ±27		[10] BOESEBECK	68	HBC	8 $\pi^+ p$
176 ±21		[10,15] JOHNSON	68	HBC	3.7–4.2 $\pi^- p$
• • • We do not use the following data for averages, fits, limits, etc. • • •					
121 ±26		TIKHOMIROV	03	SPEC	40.0 $\overline{n}C \to K^0_S K^0_S K^0_L X$
187 ±20		[16] ALDE	97	GAM2	450 $pp \to pp\pi^0\pi^0$
184 ±10		[16] GRYGOREV	96	SPEC	40 $\pi^- N \to K^0_S K^0_S X$
200 ±10		AKER	91	CBAR	0.0 $\overline{p}p \to 3\pi^0$
240 ±40	3k	BINON	83	GAM2	38 $\pi^- p \to n2\eta$
187 ±30	650	[10] ANTIPOV	77	CIBS	25 $\pi^- p \to p3\pi$
225 ±38	16000	DEUTSCH...	76	HBC	16 $\pi^+ p$
166 ±28	600	[10] TAKAHASHI	72	HBC	8 $\pi^- p \to n2\pi$
173 ±53		[10] ARMENISE	70	HBC	9 $\pi^+ n \to p\pi^+\pi^-$

[9] T-matrix pole.
[10] Width errors enlarged by us to $4\Gamma/\sqrt{N}$; see the note with the $K^*(892)$ mass.
[11] From a partial-wave analysis of data using a K-matrix formalism with 5 poles.
[12] From an energy-independent partial-wave analysis.
[13] From an amplitude analysis of the reaction $\pi^+\pi^- \to 2\pi^0$.
[14] From an amplitude analysis of $\pi^+\pi^- \to \pi^+\pi^-$ scattering data.
[15] JOHNSON 68 includes BONDAR 63, LEE 64, DERADO 65, EISNER 67.
[16] Systematic uncertainties not estimated.

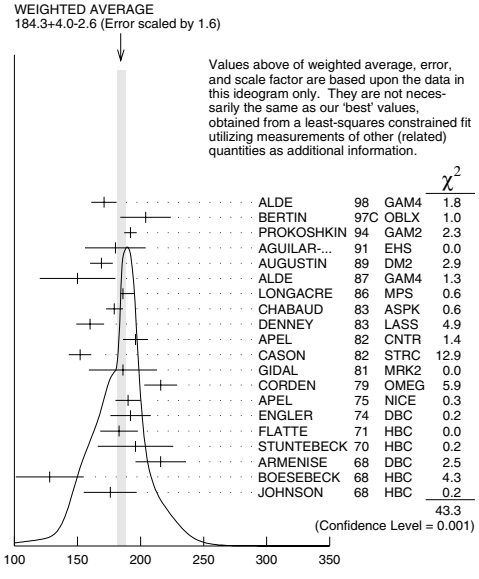

$f_2(1270)$ width (MeV)

$f_2(1270)$ DECAY MODES

	Mode	Fraction (Γ_i/Γ)	Scale factor/ Confidence level
Γ_1	$\pi\pi$	$(84.8\ ^{+2.5}_{-1.3})$ %	S=1.3
Γ_2	$\pi^+\pi^-2\pi^0$	$(7.1\ ^{+1.5}_{-2.7})$ %	S=1.3
Γ_3	$K\overline{K}$	(4.6 ± 0.4) %	S=2.7
Γ_4	$2\pi^+2\pi^-$	(2.8 ± 0.4) %	S=1.2
Γ_5	$\eta\eta$	$(4.5\pm1.0)\times10^{-3}$	S=2.4
Γ_6	$4\pi^0$	$(3.0\pm1.0)\times10^{-3}$	
Γ_7	$\gamma\gamma$	$(1.41\pm0.13)\times10^{-5}$	
Γ_8	$\eta\pi\pi$	$< 8\times10^{-3}$	CL=95%
Γ_9	$K^0K^-\pi^+$ + c.c.	$< 3.4\times10^{-3}$	CL=95%
Γ_{10}	e^+e^-	$< 6\times10^{-10}$	CL=90%

CONSTRAINED FIT INFORMATION

An overall fit to the total width, 4 partial widths, a combination of partial widths obtained from integrated cross sections, and 6 branching ratios uses 42 measurements and one constraint to determine 8 parameters. The overall fit has a $\chi^2 = 74.4$ for 35 degrees of freedom.

The following *off-diagonal* array elements are the correlation coefficients $\langle\delta p_i\delta p_j\rangle/(\delta p_i\cdot\delta p_j)$, in percent, from the fit to parameters p_i, including the branching fractions, $x_i \equiv \Gamma_i/\Gamma_{\rm total}$. The fit constrains the x_i whose labels appear in this array to sum to one.

	x_1	x_2	x_3	x_4	x_5	x_6	x_7
x_2	−92						
x_3	12	−38					
x_4	11	−37	1				
x_5	2	−9	0	0			
x_6	0	−7	0	0	0		
x_7	11	−8	−8	1	0	0	
Γ	−79	73	−12	−8	−3	0	−15

	Mode	Rate (MeV)	Scale factor
Γ_1	$\pi\pi$	$156.9\ ^{+4.0}_{-1.2}$	
Γ_2	$\pi^+\pi^-2\pi^0$	$13.1\ ^{+2.9}_{-5.1}$	1.3
Γ_3	$K\overline{K}$	8.5 ± 0.8	2.7
Γ_4	$2\pi^+2\pi^-$	5.2 ± 0.7	1.2
Γ_5	$\eta\eta$	0.83 ± 0.18	2.4
Γ_6	$4\pi^0$	0.55 ± 0.19	
Γ_7	$\gamma\gamma$	0.00260 ± 0.00024	

$f_2(1270)$ PARTIAL WIDTHS

$\Gamma(\pi\pi)$ Γ_1

VALUE (MeV)	DOCUMENT ID		TECN	COMMENT
$156.9\ ^{+4.0}_{-1.2}$ OUR FIT				
$157.0\ ^{+6.0}_{-1.0}$	[18] LONGACRE	86	MPS	$22\,\pi^-p\to n2K^0_S$

$\Gamma(K\overline{K})$ Γ_3

VALUE (MeV)	DOCUMENT ID		TECN	COMMENT
8.5 ±0.8 OUR FIT Error includes scale factor of 2.7.				
$9.0\ ^{+0.7}_{-0.3}$	[18] LONGACRE	86	MPS	$22\,\pi^-p\to n2K^0_S$

$\Gamma(\eta\eta)$ Γ_5

VALUE (MeV)	DOCUMENT ID		TECN	COMMENT
0.83±0.18 OUR FIT Error includes scale factor of 2.4.				
1.0 ±0.1	[18] LONGACRE	86	MPS	$22\,\pi^-p\to n2K^0_S$

$\Gamma(\gamma\gamma)$ Γ_7

The value of this width depends on the theoretical model used. Unitarised models with scalars give values clustering around $\simeq 2.6$ keV; without an S-wave contribution, values are systematically higher (typically around 3 keV).

VALUE (keV)	EVTS	DOCUMENT ID		TECN	COMMENT
2.60±0.24 OUR FIT					
$2.71\ ^{+0.26}_{-0.23}$ OUR AVERAGE					
2.84 ± 0.35		BOGLIONE	99	RVUE	$\gamma\gamma\to\pi^+\pi^-,\pi^0\pi^0$
$2.58\pm0.13\ ^{+0.36}_{-0.27}$		[19] BEHREND	92	CELL	$e^+e^-\to e^+e^-\pi^+\pi^-$
• • • We do not use the following data for averages, fits, limits, etc. • • •					
$2.93\pm0.23\pm0.32$		[17] YABUKI	95	VNS	
$3.10\pm0.35\pm0.35$		[20] BLINOV	92	MD1	$e^+e^-\to e^+e^-\pi^+\pi^-$
$2.27\pm0.47\pm0.11$		ADACHI	90D	TOPZ	$e^+e^-\to e^+e^-\pi^+\pi^-$
$3.15\pm0.04\pm0.39$		BOYER	90	MRK2	$e^+e^-\to e^+e^-\pi^+\pi^-$
$3.19\pm0.16\ ^{+0.29}_{-0.28}$		MARSISKE	90	CBAL	$e^+e^-\to e^+e^-\pi^0\pi^0$
2.35 ± 0.65		[21] MORGAN	90	RVUE	$\gamma\gamma\to\pi^+\pi^-,\pi^0\pi^0$
$3.19\pm0.09\ ^{+0.22}_{-0.38}$	2177	OEST	90	JADE	$e^+e^-\to e^+e^-\pi^0\pi^0$
$3.2\ \pm0.1\ \pm0.4$		[22] AIHARA	86B	TPC	$e^+e^-\to e^+e^-\pi^+\pi^-$
$2.5\ \pm0.1\ \pm0.5$		BEHREND	84B	CELL	$e^+e^-\to e^+e^-\pi^+\pi^-$
$2.85\pm0.25\pm0.5$		[23] BERGER	84	PLUT	$e^+e^-\to e^+e^-2\pi$
$2.70\pm0.05\pm0.20$		COURAU	84	DLCO	$e^+e^-\to e^+e^-\pi^+\pi^-$
$2.52\pm0.13\pm0.38$		[24] SMITH	84C	MRK2	$e^+e^-\to e^+e^-\pi^+\pi^-$
$2.7\ \pm0.2\ \pm0.6$		EDWARDS	82F	CBAL	$e^+e^-\to e^+e^-2\pi^0$
$2.9\ ^{+0.6}_{-0.4}\ \pm0.6$		[25] EDWARDS	82F	CBAL	$e^+e^-\to e^+e^-2\pi^0$
$3.2\ \pm0.2\ \pm0.6$		BRANDELIK	81B	TASS	$e^+e^-\to e^+e^-\pi^+\pi^-$
$3.6\ \pm0.3\ \pm0.5$		ROUSSARIE	81	MRK2	$e^+e^-\to e^+e^-\pi^+\pi^-$
$2.3\ \pm0.8$		[26] BERGER	80B	PLUT	e^+e^-

[17] With a narrow scalar state around 1220 MeV.

$\Gamma(e^+e^-)$ Γ_{10}

VALUE (eV)	CL%	DOCUMENT ID		TECN	COMMENT
<0.11	90	ACHASOV	00K	SND	$e^+e^-\to\pi^0\pi^0$
• • • We do not use the following data for averages, fits, limits, etc. • • •					
<1.7	90	VOROBYEV	88	ND	$e^+e^-\to\pi^0\pi^0$

[18] From a partial-wave analysis of data using a K-matrix formalism with 5 poles.
[19] Using a unitarized model with a 300 - 500 keV wide scalar at 1100 MeV.
[20] Using the unitarized model of LYTH 85.
[21] Error includes spread of different solutions. Data of MARK2 and CRYSTAL BALL used in the analysis. Authors report strong correlations with $\gamma\gamma$ width of $f_0(1370)$: $\Gamma(f_2) + 1/4\ \Gamma(f^0) = 3.6 \pm 0.3$ KeV.
[22] Radiative corrections modify the partial widths; for instance the COURAU 84 value becomes 2.66 ± 0.21 in the calculation of LANDRO 86.
[23] Using the MENNESSIER 83 model.
[24] Superseded by BOYER 90.
[25] If helicity = 2 assumption is not made.
[26] Using mass, width and $B(f_2(1270) \to 2\pi)$ from PDG 78.

$f_2(1270)$ Γ(i)Γ(γγ)/Γ(total)

$\Gamma(K\overline{K}) \times \Gamma(\gamma\gamma)/\Gamma_{total}$ — $\Gamma_3\Gamma_7/\Gamma$

VALUE (keV)	DOCUMENT ID		TECN	COMMENT
0.120±0.014 OUR FIT	Error includes scale factor of 1.3.			
0.091±0.007±0.027	[27] ALBRECHT	90G	ARG	$e^+e^- \to e^+e^-K^+K^-$
• • • We do not use the following data for averages, fits, limits, etc. • • •				
0.104±0.007±0.072	[28] ALBRECHT	90G	ARG	$e^+e^- \to e^+e^-K^+K^-$

[27] Using an incoherent background.
[28] Using a coherent background.

$f_2(1270)$ BRANCHING RATIOS

$\Gamma(\pi\pi)/\Gamma_{total}$ — Γ_1/Γ

VALUE	EVTS	DOCUMENT ID		TECN	COMMENT
$0.848^{+0.025}_{-0.013}$ OUR FIT	Error includes scale factor of 1.3.				
0.837±0.020 OUR AVERAGE					
0.849±0.025		CHABAUD	83	ASPK	17 π^-p polarized
0.85 ±0.05	250	BEAUPRE	71	HBC	8 $\pi^+p \to \Delta^{++}f_2$
0.8 ±0.04	600	OH	70	HBC	1.26 $\pi^-p \to \pi^+\pi^-n$

$\Gamma(\pi^+\pi^-2\pi^0)/\Gamma(\pi\pi)$ — Γ_2/Γ_1

Should be twice $\Gamma(2\pi^+2\pi^-)/\Gamma(\pi\pi)$ if decay is $\rho\rho$. (See ASCOLI 68D.)

VALUE	EVTS	DOCUMENT ID		TECN	COMMENT
$0.083^{+0.019}_{-0.034}$ OUR FIT	Error includes scale factor of 1.3.				
0.15 ±0.06	600	EISENBERG	74	HBC	4.9 $\pi^+p \to \Delta^{++}f_2$
• • • We do not use the following data for averages, fits, limits, etc. • • •					
0.07		EMMS	75D	DBC	4 $\pi^+n \to pf_2$

$\Gamma(K\overline{K})/\Gamma(\pi\pi)$ — Γ_3/Γ_1

We average only experiments which either take into account $f_2(1270)$-$a_2(1320)$ interference explicitly or demonstrate that $a_2(1320)$ production is negligible.

VALUE	EVTS	DOCUMENT ID		TECN	COMMENT
$0.054^{+0.005}_{-0.006}$ OUR FIT	Error includes scale factor of 2.7.				
$0.041^{+0.004}_{-0.005}$ OUR AVERAGE					
0.045±0.01		[29] BARGIOTTI	03	OBLX	$\overline{p}p$
$0.037^{+0.008}_{-0.021}$		ETKIN	82B	MPS	23 $\pi^-p \to n2K^0_S$
0.045±0.009		CHABAUD	81	ASPK	17 π^-p polarized
0.039±0.008		LOVERRE	80	HBC	4 $\pi^-p \to K\overline{K}N$
• • • We do not use the following data for averages, fits, limits, etc. • • •					
0.036±0.005		[30] COSTA...	80	OMEG	1–2.2 $\pi^-p \to K^+K^-n$
0.030±0.005		[31] MARTIN	79	RVUE	
0.027±0.009		[32] POLYCHRO...	79	STRC	7 $\pi^-p \to n2K^0_S$
0.025±0.015		EMMS	75D	DBC	4 $\pi^+n \to pf_2$
0.031±0.012	20	ADERHOLZ	69	HBC	8 $\pi^+p \to K^+K^-\pi^+p$

$\Gamma(2\pi^+2\pi^-)/\Gamma(\pi\pi)$ — Γ_4/Γ_1

VALUE	EVTS	DOCUMENT ID		TECN	COMMENT
0.033±0.005 OUR FIT	Error includes scale factor of 1.2.				
0.033±0.004 OUR AVERAGE	Error includes scale factor of 1.1.				
0.024±0.006	160	EMMS	75D	DBC	4 $\pi^+n \to pf_2$
0.051±0.025	70	EISENBERG	74	HBC	4.9 $\pi^+p \to \Delta^{++}f_2$
$0.043^{+0.007}_{-0.011}$	285	LOUIE	74	HBC	3.9 $\pi^-p \to nf_2$
0.037±0.007	154	ANDERSON	73	DBC	6 $\pi^+n \to pf_2$
0.047±0.013		OH	70	HBC	1.26 $\pi^-p \to \pi^+\pi^-n$

$\Gamma(\eta\eta)/\Gamma_{total}$ — Γ_5/Γ

VALUE (units 10^{-3})	DOCUMENT ID		TECN	COMMENT
4.5±1.0 OUR FIT	Error includes scale factor of 2.4.			
3.1±0.8 OUR AVERAGE	Error includes scale factor of 1.3.			
2.8±0.7	ALDE	86D	GAM4	100 $\pi^-p \to 2\eta n$
5.2±1.7	BINON	83	GAM2	38 $\pi^-p \to 2\eta n$

$\Gamma(\eta\eta)/\Gamma(\pi\pi)$ — Γ_5/Γ_1

VALUE	CL%	DOCUMENT ID		TECN	COMMENT
0.003 ±0.001		BARBERIS	00E		450 $pp \to p_f\eta\eta p_s$
• • • We do not use the following data for averages, fits, limits, etc. • • •					
<0.05	95	EDWARDS	82F	CBAL	$e^+e^- \to e^+e^-2\eta$
<0.016	95	EMMS	75D	DBC	4 $\pi^+n \to pf_2$
<0.09	95	EISENBERG	74	HBC	4.9 $\pi^+p \to \Delta^{++}f_2$

$\Gamma(4\pi^0)/\Gamma_{total}$ — Γ_6/Γ

VALUE	EVTS	DOCUMENT ID		TECN	COMMENT
0.0030±0.0010 OUR FIT					
0.003 ±0.001	400± 50	ALDE	87	GAM4	100 $\pi^-p \to 4\pi^0n$

$\Gamma(\eta\pi\pi)/\Gamma(\pi\pi)$ — Γ_8/Γ_1

VALUE	CL%	DOCUMENT ID		TECN	COMMENT
<0.010	95	EMMS	75D	DBC	4 $\pi^+n \to pf_2$

$\Gamma(K^0K^-\pi^+ + c.c.)/\Gamma(\pi\pi)$ — Γ_9/Γ_1

VALUE	CL%	DOCUMENT ID		TECN	COMMENT
<0.004	95	EMMS	75D	DBC	4 $\pi^+n \to pf_2$

$\Gamma(e^+e^-)/\Gamma_{total}$ — Γ_{10}/Γ

VALUE (units 10^{-10})	CL%	DOCUMENT ID		TECN	COMMENT
<6	90	ACHASOV	00K	SND	$e^+e^- \to \pi^0\pi^0$

[29] Coupled channel analysis of $\pi^+\pi^-\pi^0$, $K^+K^-\pi^0$, and $K^\pm K^0_S\pi^\mp$.
[30] Re-evaluated by CHABAUD 83.
[31] Includes PAWLICKI 77 data.
[32] Takes into account the $f_2(1270)$-$f'_2(1525)$ interference.

$f_2(1270)$ REFERENCES

BARGIOTTI	03	EPJ C26 371	M. Bargiotti *et al.*	(OBELIX Collab.)
TIKHOMIROV	03	PAN 66 828 Translated from YAF 66 860.	G.D. Tikhomirov *et al.*	
ACHASOV	00K	PL B492 8	M.N. Achasov *et al.*	(Novosibirsk SND Collab.)
BARBERIS	00E	PL B479 59	D. Barberis *et al.*	(WA 102 Collab.)
BOGLIONE	99	EPJ C9 11	M. Boglione, M.R. Pennington	
ALDE	98	EPJ A3 361	D. Alde *et al.*	(GAM4 Collab.)
Also	99	PAN 62 405 Translated from YAF 62 446.	D. Alde *et al.*	(GAMS Collab.)
ALDE	97	PL B397 350	D.M. Alde *et al.*	(GAMS Collab.)
BERTIN	97C	PL B408 476	A. Bertin *et al.*	(OBELIX Collab.)
GRYGOREV	96	PAN 59 2105 Translated from YAF 59 2187.	V.K. Grigoriev, O.N. Baloshin, B.P. Barkov	(ITEP)
YABUKI	95	JPSJ 64 435	F. Yabuki *et al.*	(VENUS Collab.)
PROKOSHKIN	94	SPD 39 420 Translated from DANS 336 613.	Y.D. Prokoshkin, A.A. Kondashov	(SERP)
BEHREND	92	ZPHY C56 381	H.J. Behrend	(CELLO Collab.)
BLINOV	92	ZPHY C53 33	A.E. Blinov *et al.*	(NOVO)
AGUILAR-...	91	ZPHY C50 405	M. Aguilar-Benitez *et al.*	(LEBC-EHS Collab.)
AKER	91	PL B260 249	E. Aker *et al.*	(Crystal Barrel Collab.)
ADACHI	90D	PL B234 185	I. Adachi *et al.*	(TOPAZ Collab.)
ALBRECHT	90G	ZPHY C48 183	H. Albrecht *et al.*	(ARGUS Collab.)
BOYER	90	PR D42 1350	J. Boyer *et al.*	(Mark II Collab.)
BREAKSTONE	90	ZPHY C48 569	A.M. Breakstone *et al.*	(ISU, BGNA, CERN+)
MARSISKE	90	PR D41 3324	H. Marsiske *et al.*	(Crystal Ball Collab.)
MORGAN	90	ZPHY C48 623	D. Morgan, M.R. Pennington	(RAL, DURH)
OEST	90	ZPHY C47 343	T. Oest *et al.*	(JADE Collab.)
AUGUSTIN	89	NP B320 1	J.E. Augustin, G. Cosme	(DM2 Collab.)
VOROBYEV	88	SJNP 48 273 Translated from YAF 48 436.	P.V. Vorobiev *et al.*	(NOVO)
ALDE	87	PL B198 286	D.M. Alde *et al.*	(LANL, BRUX, SERP, LAPP)
AUGUSTIN	87	ZPHY C36 369	J.E. Augustin *et al.*	(LALO, CLER, FRAS+)
ABACHI	86B	PRL 57 1990	S. Abachi *et al.*	(PURD, ANL, IND, MICH+)
AIHARA	86B	PRL 57 404	H. Aihara *et al.*	(TPC-2γ Collab.)
ALDE	86D	NP B269 485	D.M. Alde *et al.*	(BELG, LAPP, SERP, CERN+)
LANDRO	86	PL B172 445	M. Landro, K.J. Mork, H.A. Olsen	(UTRO)
LONGACRE	86	PL B177 223	R.S. Longacre *et al.*	(BNL, BRAN, CUNY+)
LYTH	85	JPG 11 459	D.H. Lyth	
BEHREND	84B	ZPHY C23 223	H.J. Behrend *et al.*	(CELLO Collab.)
BERGER	84	ZPHY C26 199	C. Berger *et al.*	(PLUTO Collab.)
COURAU	84	PL 147B 227	A. Courau *et al.*	(CIT, SLAC)
SMITH	84C	PR D30 851	J.R. Smith *et al.*	(SLAC, LBL, HARV)
BINON	83	NC 78A 313	F.G. Binon *et al.*	(BELG, LAPP, SERP+)
Also	83B	SJNP 38 561 Translated from YAF 38 934.	F.G. Binon *et al.*	(BELG, LAPP, SERP+)
CHABAUD	83	NP B223 1	V. Chabaud *et al.*	(CERN, CRAC, MPIM)
DENNEY	83	PR D28 2726	D.L. Denney *et al.*	(IOWA, MICH)
MENNESSIER	83	ZPHY C16 241	G. Mennessier	(MONP)
APEL	82	NP B201 197	W.D. Apel *et al.*	(KARLK, KARLE, PISA, SERP+)
CASON	82	PRL 48 1316	N.M. Cason *et al.*	(NDAM, ANL)
EDWARDS	82F	PL 110B 82	C. Edwards *et al.*	(CIT, HARV, PRIN+)
ETKIN	82B	PR D25 1786	A. Etkin *et al.*	(BNL, CUNY, TUFTS, VAND)
BRANDELIK	81B	ZPHY C10 117	R. Brandelik *et al.*	(TASSO Collab.)
CHABAUD	81	APP B12 575	V. Chabaud *et al.*	(CERN, CRAC, MPIM)
GIDAL	81	PL 107B 153	G. Gidal *et al.*	(SLAC, LBL)
ROUSSARIE	81	PL 105B 304	A. Roussarie *et al.*	(SLAC, LBL)
BERGER	80B	PL 94B 254	C. Berger *et al.*	(PLUTO Collab.)
COSTA...	80	NP B175 402	G. Costa de Beauregard *et al.*	(BARI, BONN+)
LOVERRE	80	ZPHY C6 187	P.F. Loverre *et al.*	(CERN, CDEF, MADR+)
CORDEN	79	NP B157 250	M.J. Corden *et al.*	(BIRM, RHEL, TELA+)
MARTIN	79	NP B158 520	A.D. Martin, E.N. Ozmutlu	(DURH)
POLYCHRO...	79	PR D19 1317	V.A. Polychronakos *et al.*	(NDAM, ANL)
PDG	78	PL 75B	C. Bricman *et al.*	
ANTIPOV	77	NP B119 45	Y.M. Antipov *et al.*	(SERP, GEVA)
PAWLICKI	77	PR D15 3196	A.J. Pawlicki *et al.*	(ANL)
DEUTSCH...	76	NP B103 426	M. Deutschmann *et al.*	(AACH3, BERL, BONN+)
APEL	75	PL 57B 398	W.D. Apel *et al.*	(KARLK, KARLE, PISA, SERP+)
EMMS	75D	NP B96 155	M.J. Emms *et al.*	(BIRM, DURH, RHEL)
EISENBERG	74	PL 52B 239	Y. Eisenberg *et al.*	(REHO)
ENGLER	74	PR D10 2070	A. Engler *et al.*	(CMU, CASE)
LOUIE	74	PL 48B 385	J. Louie *et al.*	(SACL, CERN)
ANDERSON	73	PRL 31 562	J.C. Anderson *et al.*	(CMU, CASE)
TAKAHASHI	72	PR D6 1266	K. Takahashi *et al.*	(TOHOK, PENN, NDAM+)
BEAUPRE	71	NP B28 77	J.V. Beaupre *et al.*	(AACH, BERL, CERN)
FLATTE	71	PL 34B 551	S.M. Flatte *et al.*	(LBL)
ARMENISE	70	LNC 4 199	N. Armenise *et al.*	(BARI, BGNA, FIRZ)
OH	70	PR D1 2494	B.Y. Oh *et al.*	(WISC, TNTO) JP
STUNTEBECK	70	PL 32B 391	P.H. Stuntebeck *et al.*	(NDAM)
ADERHOLZ	69	NP B11 259	M. Aderholz *et al.*	(AACH3, BERL, CERN+)
ARMENISE	68	NC 54A 999	N. Armenise *et al.*	(BARI, BGNA, FIRZ+)
ASCOLI	68D	PRL 21 1712	G. Ascoli *et al.*	(ILL)
BOESEBECK	68	NP B4 501	K. Boesebeck *et al.*	(AACH, BERL, CERN)
JOHNSON	68	PR 176 1651	P.B. Johnson *et al.*	(NDAM, PURD, SLAC)
EISNER	67	PR 164 1699	R.L. Eisner *et al.*	(PURD)
DERADO	65	PRL 14 872	I. Derado *et al.*	(NDAM)
LEE	64	PRL 12 342	Y.Y. Lee *et al.*	(MICH)
BONDAR	63	PL 5 153	L. Bondar *et al.*	(AACH, BIRM, BONN, DESY+)

OTHER RELATED PAPERS

LI	01	JPG 27 807	D.-M. Li, H. Yu, Q.-X. Shen

$f_1(1285)$

$I^G(J^{PC}) = 0^+(1^{++})$

$f_1(1285)$ MASS

VALUE (MeV)	CL%	EVTS	DOCUMENT ID		TECN	COMMENT
1281.8± 0.6 OUR AVERAGE			Error includes scale factor of 1.6. See the ideogram below.			
1274 ± 6		237	ABDALLAH	03H	DLPH	91.2 $e^+e^-\to K^0_S K^\pm\pi^\mp$ + X
1280 ± 4	95		ACCIARRI	01G	L3	
1288 ± 4 ± 5		20k	ADAMS	01B	E852	18 GeV $\pi^- p\to K^+K^-\pi^0 n$
1284 ± 6		1400	ALDE	97B	GAM4	100 $\pi^- p\to \eta\pi^0\pi^0 n$
1281 ± 1			BARBERIS	97B	OMEG	450 $pp\to pp2(\pi^+\pi^-)$
1281 ± 1			BARBERIS	97C	OMEG	450 $pp\to ppK^0_S K^\pm\pi^\mp$
1280 ± 2			[1] ANTINORI	95	OMEG	300,450 $pp\to pp2(\pi^+\pi^-)$
1282.2± 1.5			LEE	94	MPS2	18 $\pi^- p\to K^+\overline{K}^0 2\pi^- p$
1279 ± 5			FUKUI	91C	SPEC	8.95 $\pi^- p\to \eta\pi^+\pi^- n$
1278 ± 2		140	ARMSTRONG	89	OMEG	300 $pp\to K\overline{K}\pi pp$
1278 ± 2			ARMSTRONG	89G	OMEG	85 $\pi^+ p\to 4\pi\pi p$, $pp\to 4\pi pp$
1280.1± 2.1		60	RATH	89	MPS	21.4 $\pi^- p\to K^0_S K^0_S\pi^0 n$
1285 ± 1		4750	[2] BIRMAN	88	MPS	8 $\pi^- p\to K^+\overline{K}^0\pi^- n$
1280 ± 1		504	BITYUKOV	88	SPEC	32.5 $\pi^- p\to K^+K^-\pi^0 n$
1280 ± 4			ANDO	86	SPEC	8 $\pi^- p\to \eta\pi^+\pi^- n$
1277 ± 2		420	REEVES	86	SPEC	6.6 $p\overline{p}\to KK\pi X$
1285 ± 2			CHUNG	85	SPEC	8 $\pi^- p\to NK\overline{K}\pi$
1279 ± 2		604	ARMSTRONG	84	OMEG	85 $\pi^+ p\to K\overline{K}\pi\pi p$, $pp\to K\overline{K}\pi pp$
1286 ± 1			CHAUVAT	84	SPEC	ISR 31.5 pp
1278 ± 4			EVANGELISTA	81	OMEG	12 $\pi^- p\to \eta\pi^+\pi^-\overline{n}p$
1283 ± 3		103	DIONISI	80	HBC	4 $\pi^- p\to K\overline{K}\pi n$
1282 ± 2		320	NACASCH	78	HBC	0.7,0.76 $\overline{p}p\to K\overline{K}3\pi$
1279 ± 5		210	GRASSLER	77	HBC	16 $\pi^+ p$
1286 ± 3		180	DUBOC	72	HBC	1.2 $\overline{p}p\to 2K4\pi$
1283 ± 5			DAHL	67	HBC	1.6–4.2 $\pi^- p$
• • • We do not use the following data for averages, fits, limits, etc. • • •						
1281.9± 0.5			[3] SOSA	99	SPEC	$pp\to p_{\rm slow}(K^0_S K^+\pi^-) p_{\rm fast}$
1282.8± 0.6			[3] SOSA	99	SPEC	$pp\to p_{\rm slow}(K^0_S K^-\pi^+) p_{\rm fast}$
1270 ±10			AMELIN	95	VES	37 $\pi^- N\to \pi^-\pi^+\pi^-\gamma N$
1280 ± 2			ABATZIS	94	OMEG	450 $pp\to pp2(\pi^+\pi^-)$
1282 ± 4			ARMSTRONG	93C	E760	$\overline{p}p\to\pi^0\eta\eta\to 6\gamma$
1270 ± 6 ±10			ARMSTRONG	92C	OMEG	300 $pp\to pp\pi^+\pi^-\gamma$
1264 ± 8			AUGUSTIN	90	DM2	$J/\psi\to\gamma\eta\pi^+\pi^-$
1281 ± 1			ARMSTRONG	89E	OMEG	300 $pp\to pp2(\pi^+\pi^-)$
1279 ± 6 ±10		16	BECKER	87	MRK3	$e^+e^-\to\phi K\overline{K}\pi$
1286 ± 9			GIDAL	87	MRK2	$e^+e^-\to e^+e^-\eta\pi^+\pi^-$
1287 ± 5		353	BITYUKOV	84B	SPEC	32 $\pi^- p\to K^+K^-\pi^0 n$
~ 1279			[4] TORNQVIST	82B	RVUE	
1275 ± 6		31	BROMBERG	80	SPEC	100 $\pi^- p\to K\overline{K}\pi X$
1288 ± 9		200	GURTU	79	HBC	4.2 $K^- p\to n\eta 2\pi$
~ 1275.0		46	[5] STANTON	79	CNTR	8.5 $\pi^- p\to n2\gamma 2\pi$
1271 ±10		34	CORDEN	78	OMEG	12–15 $\pi^- p\to K^+K^-\pi n$
1295 ±12		85	CORDEN	78	OMEG	12–15 $\pi^- p\to n5\pi$
1292 ±10		150	DEFOIX	72	HBC	0.7 $\overline{p}p\to 7\pi$
1280 ± 3		500	[6] THUN	72	MMS	13.4 $\pi^- p$
1303 ± 8			BARDADIN-...	71	HBC	8 $\pi^+ p\to p6\pi$
1283 ± 6			BOESEBECK	71	HBC	16.0 $\pi p\to p5\pi$
1270 ±10			CAMPBELL	69	DBC	2.7 $\pi^+ d$
1285 ± 7			LORSTAD	69	HBC	0.7 $\overline{p}p$, 4,5-body
1290 ± 7			D'ANDLAU	68	HBC	1.2 $\overline{p}p$, 5–6 body

[1] Supersedes ABATZIS 94, ARMSTRONG 89E.
[2] From partial wave analysis of $K^+\overline{K}^0\pi^-$ system.
[3] No systematic error given.
[4] From a unitarized quark-model calculation.
[5] From phase shift analysis of $\eta\pi^+\pi^-$ system.
[6] Seen in the missing mass spectrum.

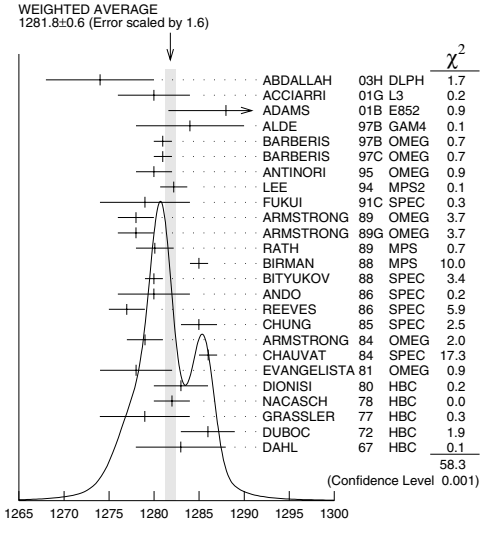

$f_1(1285)$ mass (MeV)

$f_1(1285)$ WIDTH

Only experiments giving width error less than 20 MeV are kept for averaging.

VALUE (MeV)	EVTS	DOCUMENT ID		TECN	COMMENT
24.1± 1.1 OUR AVERAGE		Error includes scale factor of 1.3. See the ideogram below.			
29 ±12	237	ABDALLAH	03H	DLPH	91.2 $e^+e^-\to K^0_S K^\pm\pi^\mp$ + X
45 ± 9 ± 7	20k	ADAMS	01B	E852	18 GeV $\pi^- p\to K^+K^-\pi^0 n$
55 ±18	1400	ALDE	97B	GAM4	100 $\pi^- p\to \eta\pi^0\pi^0 n$
24 ± 3		BARBERIS	97B	OMEG	450 $pp\to pp2(\pi^+\pi^-)$
20 ± 2		BARBERIS	97C	OMEG	450 $pp\to ppK^0_S K^\pm\pi^\mp$
36 ± 5		[7] ANTINORI	95	OMEG	300,450 $pp\to pp2(\pi^+\pi^-)$
29.0± 4.1		LEE	94	MPS2	18 $\pi^- p\to K^+\overline{K}^0 2\pi^- p$
25 ± 4	140	ARMSTRONG	89	OMEG	300 $pp\to K\overline{K}\pi pp$
22 ± 2	4750	[8] BIRMAN	88	MPS	8 $\pi^- p\to K^+\overline{K}^0\pi^- n$
25 ± 4	504	BITYUKOV	88	SPEC	32.5 $\pi^- p\to K^+K^-\pi^0 n$
19 ± 5		ANDO	86	SPEC	8 $\pi^- p\to \eta\pi^+\pi^- n$
32 ± 8	420	REEVES	86	SPEC	6.6 $p\overline{p}\to KK\pi X$
22 ± 2		CHUNG	85	SPEC	8 $\pi^- p\to NK\overline{K}\pi$
32 ± 3	604	ARMSTRONG	84	OMEG	85 $\pi^+ p\to K\overline{K}\pi\pi p$, $pp\to K\overline{K}\pi pp$
24 ± 3		CHAUVAT	84	SPEC	ISR 31.5 pp
29 ±10	103	DIONISI	80	HBC	4 $\pi^- p\to K\overline{K}\pi n$
28.3± 6.7	320	NACASCH	78	HBC	0.7,0.76 $\overline{p}p\to K\overline{K}3\pi$
• • • We do not use the following data for averages, fits, limits, etc. • • •					
18.2± 1.2		[9] SOSA	99	SPEC	$pp\to p_{\rm slow}(K^0_S K^+\pi^-) p_{\rm fast}$
19.4± 1.5		[9] SOSA	99	SPEC	$pp\to p_{\rm slow}(K^0_S K^-\pi^+) p_{\rm fast}$
40 ± 5		ABATZIS	94	OMEG	450 $pp\to pp2(\pi^+\pi^-)$
44 ±20		AUGUSTIN	90	DM2	$J/\psi\to\gamma\eta\pi^+\pi^-$
31 ± 5		ARMSTRONG	89E	OMEG	300 $pp\to pp2(\pi^+\pi^-)$
41 ±12		ARMSTRONG	89G	OMEG	85 $\pi^+ p\to 4\pi\pi p$, $pp\to 4\pi pp$

17.9 ± 10.9		60	RATH	89	MPS	21.4 $\pi^- p \rightarrow K^0_S K^0_S \pi^0 n$
14	$^{+20}_{-14}$ ±10	16	BECKER	87	MRK3	$e^+e^- \rightarrow \phi K \overline{K} \pi$
26	±12		EVANGELISTA	81	OMEG	12 $\pi^- p \rightarrow \eta \pi^+ \pi^- \pi^- p$
25	±15	200	GURTU	79	HBC	4.2 $K^- p \rightarrow n \eta 2\pi$
~ 10			[10] STANTON	79	CNTR	8.5 $\pi^- p \rightarrow n 2\gamma 2\pi$
24	±18	210	GRASSLER	77	HBC	16 $\pi^+ p$
28	± 5	150	[11] DEFOIX	72	HBC	0.7 $\overline{p}p \rightarrow 7\pi$
46	± 9	180	[11] DUBOC	72	HBC	1.2 $\overline{p}p \rightarrow 2K4\pi$
37	± 5	500	[12] THUN	72	MMS	13.4 $\pi^- p$
10	±10		BOESEBECK	71	HBC	16.0 $\pi p \rightarrow p5\pi$
30	±15		CAMPBELL	69	DBC	2.7 $\pi^+ d$
60	±15		[11] LORSTAD	69	HBC	0.7 $\overline{p}p$, 4,5-body
35	±10		[11] DAHL	67	HBC	1.6–4.2 $\pi^- p$

[7] Supersedes ABATZIS 94, ARMSTRONG 89E.
[8] From partial wave analysis of $K^+ \overline{K}{}^0 \pi^-$ system.
[9] No systematic error given.
[10] From phase shift analysis of $\eta\pi^+\pi^-$ system.
[11] Resolution is not unfolded.
[12] Seen in the missing mass spectrum.

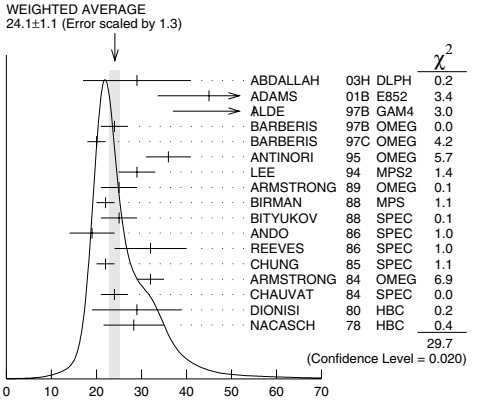

$f_1(1285)$ width (MeV)

$f_1(1285)$ DECAY MODES

	Mode	Fraction (Γ_j/Γ)	Scale factor/ Confidence level
Γ_1	4π	$(33.1^{+2.1}_{-1.8})$ %	S=1.3
Γ_2	$\pi^0\pi^0\pi^+\pi^-$	$(22.0^{+1.4}_{-1.2})$ %	S=1.3
Γ_3	$2\pi^+2\pi^-$	$(11.0^{+0.7}_{-0.6})$ %	S=1.3
Γ_4	$\rho^0\pi^+\pi^-$	$(11.0^{+0.7}_{-0.6})$ %	S=1.3
Γ_5	$\rho^0\rho^0$	seen	
Γ_6	$4\pi^0$	$< 7 \times 10^{-4}$	CL=90%
Γ_7	$\eta\pi\pi$	(52 ±16) %	
Γ_8	$a_0(980)\pi$ [ignoring $a_0(980) \rightarrow K\overline{K}$]	(36 ± 7) %	
Γ_9	$\eta\pi\pi$ [excluding $a_0(980)\pi$]	(16 ± 7) %	
Γ_{10}	$K\overline{K}\pi$	(9.0± 0.4) %	S=1.1
Γ_{11}	$K\overline{K}^*(892)$	not seen	
Γ_{12}	$\gamma\rho^0$	(5.5± 1.3) %	S=2.8
Γ_{13}	$\phi\gamma$	(7.4± 2.6) $\times 10^{-4}$	
Γ_{14}	$\gamma\gamma^*$		
Γ_{15}	$\gamma\gamma$		

CONSTRAINED FIT INFORMATION

An overall fit to 7 branching ratios uses 16 measurements and one constraint to determine 5 parameters. The overall fit has a $\chi^2 = 24.7$ for 12 degrees of freedom.

The following *off-diagonal* array elements are the correlation coefficients $\langle \delta x_i \delta x_j \rangle / (\delta x_i \cdot \delta x_j)$, in percent, from the fit to the branching fractions, $x_i \equiv \Gamma_i/\Gamma_{\text{total}}$. The fit constrains the x_i whose labels appear in this array to sum to one.

x_8	−17			
x_9	−8	−95		
x_{10}	46	−9	−4	
x_{12}	−36	−4	−2	−34
	x_1	x_8	x_9	x_{10}

$f_1(1285)$ Γ(i)$\Gamma(\gamma\gamma)/\Gamma$(total)

$\Gamma(\eta\pi\pi) \times \Gamma(\gamma\gamma)/\Gamma_{\text{total}}$ — **$\Gamma_7\Gamma_{15}/\Gamma = (\Gamma_8+\Gamma_9)\Gamma_{15}/\Gamma$**

VALUE (keV)	CL%	DOCUMENT ID		TECN	COMMENT
<0.62	95	GIDAL	87	MRK2	$e^+e^- \rightarrow e^+e^-\eta\pi^+\pi^-$

$\Gamma(\eta\pi\pi) \times \Gamma(\gamma\gamma^*)/\Gamma_{\text{total}}$ — **$\Gamma_7\Gamma_{14}/\Gamma = (\Gamma_8+\Gamma_9)\Gamma_{14}/\Gamma$**

VALUE (keV)	EVTS	DOCUMENT ID		TECN	COMMENT
1.4 ±0.4 OUR AVERAGE	Error includes scale factor of 1.4.				
1.18 ± 0.25 ± 0.20	26	[13,14] AIHARA	88B	TPC	$e^+e^- \rightarrow e^+e^-\eta\pi^+\pi^-$
2.30 ± 0.61 ± 0.42		[13,15] GIDAL	87	MRK2	$e^+e^- \rightarrow e^+e^-\eta\pi^+\pi^-$
• • • We do not use the following data for averages, fits, limits, etc. • • •					
1.8 ±0.3 ±0.3	420	[16] ACHARD	02B	L3	183–209 $e^+e^- \rightarrow e^+e^-\eta\pi^+\pi^-$

[13] Assuming a ρ-pole form factor.
[14] Published value multiplied by $\eta\pi\pi$ branching ratio 0.49.
[15] Published value divided by 2 and multiplied by the $\eta\pi\pi$ branching ratio 0.49.
[16] Published value multiplied by the $\eta\pi\pi$ branching ratio 0.52.

$f_1(1285)$ BRANCHING RATIOS

$\Gamma(K\overline{K}\pi)/\Gamma(4\pi)$ — **Γ_{10}/Γ_1**

VALUE	DOCUMENT ID		TECN	COMMENT
0.271 ± 0.016 OUR FIT	Error includes scale factor of 1.3.			
0.271 ± 0.016 OUR AVERAGE	Error includes scale factor of 1.2.			
0.265 ± 0.014	[17] BARBERIS	97C	OMEG	450 $pp \rightarrow ppK^0_S K^\pm\pi^\mp$
0.28 ±0.05	[18] ARMSTRONG	89E	OMEG	300 $pp \rightarrow pp f_1(1285)$
0.37 ±0.03 ±0.05	[19] ARMSTRONG	89G	OMEG	85 $\pi p \rightarrow 4\pi X$

[17] Using $2(\pi^+\pi^-)$ data from BARBERIS 97B.
[18] Assuming $\rho\pi\pi$ and $a_0(980)\pi$ intermediate states.
[19] 4π consistent with being entirely $\rho\pi\pi$.

$\Gamma(\pi^0\pi^0\pi^+\pi^-)/\Gamma_{\text{total}}$ — **$\Gamma_2/\Gamma = \frac{2}{3}\Gamma_1/\Gamma$**

VALUE	DOCUMENT ID
$0.220^{+0.014}_{-0.012}$ OUR FIT	Error includes scale factor of 1.3.

$\Gamma(2\pi^+2\pi^-)/\Gamma_{\text{total}}$ — **$\Gamma_3/\Gamma = \frac{1}{3}\Gamma_1/\Gamma$**

VALUE	DOCUMENT ID
$0.110^{+0.007}_{-0.006}$ OUR FIT	Error includes scale factor of 1.3.

$\Gamma(\rho^0\pi^+\pi^-)/\Gamma_{\text{total}}$ — **$\Gamma_4/\Gamma = \frac{1}{3}\Gamma_1/\Gamma$**

VALUE	DOCUMENT ID
$0.110^{+0.007}_{-0.006}$ OUR FIT	Error includes scale factor of 1.3.

$\Gamma(\rho^0\rho^0)/\Gamma_{\text{total}}$ — **Γ_5/Γ**

VALUE	DOCUMENT ID		TECN	COMMENT
• • • We do not use the following data for averages, fits, limits, etc. • • •				
seen	BARBERIS	00C		450 $pp \rightarrow p_f 4\pi p_s$

$\Gamma(K\overline{K}\pi)/\Gamma(\eta\pi\pi)$ — **$\Gamma_{10}/\Gamma_7 = \Gamma_{10}/(\Gamma_8+\Gamma_9)$**

VALUE	DOCUMENT ID		TECN	COMMENT
0.171 ± 0.013 OUR FIT	Error includes scale factor of 1.1.			
0.170 ± 0.012 OUR AVERAGE				
0.166 ± 0.01 ±0.008	BARBERIS	98C	OMEG	450 $pp \rightarrow p_f f_1(1285) p_s$
0.42 ±0.15	GURTU	79	HBC	4.2 $K^- p$
0.5 ±0.2	[20] CORDEN	78	OMEG	12–15 $\pi^- p$
0.20 ±0.08	[21] DEFOIX	72	HBC	0.7 $\overline{p}p \rightarrow 7\pi$
0.16 ±0.08	CAMPBELL	69	DBC	2.7 $\pi^+ d$

[20] CORDEN 78 assumes low-mass $\eta\pi\pi$ region is dominantly 1^{++}. See BARBERIS 98C and MANAK 00A for discussion.
[21] $K\overline{K}$ system characterized by the $I = 1$ threshold enhancement. (See under $a_0(980)$).

$\Gamma(a_0(980)\pi$ [ignoring $a_0(980) \to K\overline{K}]) / \Gamma(\eta\pi\pi)$ $\Gamma_8/\Gamma_7 = \Gamma_8/(\Gamma_8+\Gamma_9)$

VALUE	CL%	EVTS	DOCUMENT ID		TECN	COMMENT
0.69 ± 0.13 OUR FIT						
$0.69^{+0.13}_{-0.12}$ OUR AVERAGE						
0.72 ± 0.15			GURTU	79	HBC	4.2 $K^- p$
$0.6^{+0.3}_{-0.2}$			CORDEN	78	OMEG	12–15 $\pi^- p$
• • • We do not use the following data for averages, fits, limits, etc. • • •						
> 0.69	95	318	ACHARD	02B	L3	183–209 $e^+e^- \to e^+e^-\eta\pi^+\pi^-$
0.28 ± 0.07		1400	ALDE	97B	GAM4	100 $\pi^- p \to \eta\pi^0\pi^0 n$
1.0 ± 0.3			GRASSLER	77	HBC	16 $\pi^\mp p$

$\Gamma(4\pi)/\Gamma(\eta\pi\pi)$ $\Gamma_1/\Gamma_7 = \Gamma_1/(\Gamma_8+\Gamma_9)$

VALUE	DOCUMENT ID		TECN	COMMENT
0.63 ± 0.06 OUR FIT Error includes scale factor of 1.2.				
0.41 ± 0.14 OUR AVERAGE				
0.37 ± 0.11 ± 0.11	BOLTON	92	MRK3	$J/\psi \to \gamma f_1(1285)$
0.64 ± 0.40	GURTU	79	HBC	4.2 $K^- p$
• • • We do not use the following data for averages, fits, limits, etc. • • •				
0.93 ± 0.30	[22] GRASSLER	77	HBC	16 $\pi^\mp p$

[22] Assuming $\rho\pi\pi$ and $a_0(980)\pi$ intermediate states.

$\Gamma(K\overline{K}^*(892))/\Gamma_{\text{total}}$ Γ_{11}/Γ

VALUE	DOCUMENT ID		TECN	COMMENT
not seen	NACASCH	78	HBC	0.7,0.76 $\overline{p}p \to K\overline{K}3\pi$

$\Gamma(\rho^0\pi^+\pi^-)/\Gamma(2\pi^+2\pi^-)$ Γ_4/Γ_3

VALUE	DOCUMENT ID		TECN	COMMENT
• • • We do not use the following data for averages, fits, limits, etc. • • •				
1.0 ± 0.4	GRASSLER	77	HBC	16 GeV $\pi^\pm p$

$\Gamma(4\pi^0)/\Gamma_{\text{total}}$ Γ_6/Γ

VALUE (units 10^{-4})	CL%	DOCUMENT ID		TECN	COMMENT
< 7	90	ALDE	87	GAM4	100 $\pi^- p \to 4\pi^0 n$

$\Gamma(\phi\gamma)/\Gamma(K\overline{K}\pi)$ Γ_{13}/Γ_{10}

VALUE (units 10^{-2})	CL%	EVTS	DOCUMENT ID		TECN	COMMENT
0.82 ± 0.21 ± 0.20		19	BITYUKOV	88	SPEC	32.5 $\pi^- p \to K^+K^-\pi^0 n$
• • • We do not use the following data for averages, fits, limits, etc. • • •						
< 0.50	95		BARBERIS	98C	OMEG	450 $pp \to p_f f_1(1285) p_s$
< 0.93	95		AMELIN	95	VES	37 $\pi^- N \to \pi^-\pi^+\pi^-\gamma N$

$\Gamma(\gamma\rho^0)/\Gamma(K\overline{K}\pi)$ Γ_{12}/Γ_{10}

VALUE	CL%	DOCUMENT ID		TECN	COMMENT
• • • We do not use the following data for averages, fits, limits, etc. • • •					
> 0.035	90	[23] COFFMAN	90	MRK3	$J/\psi \to \gamma\gamma\pi^+\pi^-$

[23] Using $B(J/\psi \to \gamma f_1(1285) \to \gamma\gamma\rho^0) = 0.25 \times 10^{-4}$ and $B(J/\psi \to \gamma f_1(1285) \to \gamma K\overline{K}\pi) =< 0.72 \times 10^{-3}$.

$\Gamma(\gamma\rho^0)/\Gamma(2\pi^+2\pi^-)$ $\Gamma_{12}/\Gamma_3 = \Gamma_{12}/\frac{1}{3}\Gamma_1$

VALUE	DOCUMENT ID		TECN	COMMENT
0.50 ± 0.13 OUR FIT Error includes scale factor of 2.5.				
0.45 ± 0.18	[24] COFFMAN	90	MRK3	$J/\psi \to \gamma\gamma\pi^+\pi^-$

[24] Using $B(J/\psi \to \gamma f_1(1285) \to \gamma\gamma\rho^0) = 0.25 \times 10^{-4}$ and $B(J/\psi \to \gamma f_1(1285) \to \gamma 2\pi^+2\pi^-) = 0.55 \times 10^{-4}$ given by MIR 88.

$\Gamma(\gamma\rho^0)/\Gamma_{\text{total}}$ Γ_{12}/Γ

VALUE	CL%	DOCUMENT ID		TECN	COMMENT
0.055 ± 0.013 OUR FIT Error includes scale factor of 2.8.					
0.028 ± 0.007 ± 0.006		AMELIN	95	VES	37 $\pi^- N \to \pi^-\pi^+\pi^-\gamma N$
• • • We do not use the following data for averages, fits, limits, etc. • • •					
< 0.05	95	BITYUKOV	91B	SPEC	32 $\pi^- p \to \pi^+\pi^-\gamma n$

$\Gamma(\eta\pi\pi)/\Gamma(\gamma\rho^0)$ $\Gamma_7/\Gamma_{12} = (\Gamma_8+\Gamma_9)/\Gamma_{12}$

VALUE	DOCUMENT ID		TECN	COMMENT
9.5 ± 2.0 OUR FIT Error includes scale factor of 2.5.				
7.9 ± 0.9 OUR AVERAGE				
10.0 ± 1.0 ± 2.0	BARBERIS	98C	OMEG	450 $pp \to p_f f_1(1285) p_s$
7.5 ± 1.0	[25] ARMSTRONG	92C	OMEG	300 $pp \to pp\pi^+\pi^-\gamma$, $pp\eta\pi^+\pi^-$

[25] Published value multiplied by 1.5.

$f_1(1285)$ REFERENCES

ABDALLAH	03H	PL B569 129	J. Abdallah *et al.*	(DELPHI Collab.)
ACHARD	02B	PL B526 269	P. Achard *et al.*	(L3 Collab.)
ACCIARRI	01G	PL B501 1	M. Acciarri *et al.*	(L3 Collab.)
ADAMS	01B	PL B516 264	G.S. Adams *et al.*	(BNL E852 Collab.)
BARBERIS	00C	PL B471 440	D. Barberis *et al.*	(WA 102 Collab.)
MANAK	00A	PR D62 012003	J.J. Manak *et al.*	(BNL E852 Collab.)
SOSA	99	PRL 83 913	M. Sosa *et al.*	
BARBERIS	98C	PL B440 225	D. Barberis *et al.*	(WA 102 Collab.)
ALDE	97B	PAN 60 386 Translated from YAF 60 458.	D. Alde *et al.*	(GAMS Collab.)
BARBERIS	97B	PL B413 217	D. Barberis *et al.*	(WA 102 Collab.)
BARBERIS	97C	PL B413 225	D. Barberis *et al.*	(WA 102 Collab.)
AMELIN	95	ZPHY C66 71	D.V. Amelin *et al.*	(VES Collab.)
ANTINORI	95	PL B353 589	F. Antinori *et al.*	(ATHU, BARI, BIRM+)
ABATZIS	94	PL B324 509	S. Abatzis *et al.*	(ATHU, BARI, BIRM+)
LEE	94	PL B323 227	J.H. Lee *et al.*	(BNL, IND, KYUN, MASD+)
ARMSTRONG	93C	PL B307 394	T.A. Armstrong *et al.*	(FNAL, FERR, GENO+)
ARMSTRONG	92C	ZPHY C54 371	T.A. Armstrong *et al.*	(ATHU, BARI, BIRM+)
BOLTON	92	PL B278 495	T. Bolton *et al.*	(Mark III Collab.)
BITYUKOV	91B	SJNP 54 318 Translated from YAF 54 529.	S.I. Bityukov *et al.*	(SERP)
FUKUI	91C	PL B267 293	S. Fukui *et al.*	(SUGI, NAGO, KEK, KYOT+)
AUGUSTIN	90	PR D42 10	J.E. Augustin *et al.*	(DM2 Collab.)
COFFMAN	90	PR D41 1410	D.M. Coffman *et al.*	(Mark III Collab.)
ARMSTRONG	89	PL B221 216	T.A. Armstrong *et al.*	(CERN, CDEF, BIRM+) JPC
ARMSTRONG	89E	PL B228 536	T.A. Armstrong, M. Benayoun	(ATHU, BARI, BIRM+)
ARMSTRONG	89G	ZPHY C43 55	T.A. Armstrong *et al.*	(CERN, BIRM, BARI+)
RATH	89	PR D40 693	M.G. Rath *et al.*	(NDAM, BRAN, BNL, CUNY+)
AIHARA	88B	PL B209 107	H. Aihara *et al.*	(TPC-2γ Collab.)
BIRMAN	88	PRL 61 1557	A. Birman *et al.*	(BNL, FSU, IND, MASD) JP
BITYUKOV	88	PL B203 327	S.I. Bityukov *et al.*	(SERP)
MIR	88	Photon-Photon 88, 126 Conference	R. Mir	(Mark III Collab.)
ALDE	87	PL B198 286	D.M. Alde *et al.*	(LANL, BRUX, SERP, LAPP)
BECKER	87	PRL 59 186	J.J. Becker *et al.*	(Mark III Collab.)
GIDAL	87	PRL 59 2012	G. Gidal *et al.*	(LBL, SLAC, HARV)
ANDO	86	PRL 57 1296	A. Ando *et al.*	(KEK, KYOT, NIRS, SAGA+) IJP
REEVES	86	PR D34 1960	D.F. Reeves *et al.*	(FLOR, BNL, IND+) JP
CHUNG	85	PRL 55 779	S.U. Chung *et al.*	(BNL, FLOR, IND+) JP
ARMSTRONG	84	PL 146B 273	T.A. Armstrong *et al.*	(ATHU, BARI, BIRM+) JP
BITYUKOV	84B	PL 144B 133	S.I. Bityukov *et al.*	(SERP)
CHAUVAT	84	PL 148B 382	P. Chauvat *et al.*	(CERN, CLER, UCLA+)
TORNQVIST	82B	NP B203 268	N.A. Tornqvist	(HELS)
EVANGELISTA	81	NP B178 197	C. Evangelista *et al.*	(BARI, BONN, CERN+)
BROMBERG	80	PR D22 1513	C.M. Bromberg *et al.*	(CIT, FNAL, ILLC+)
DIONISI	80	NP B169 1	C. Dionisi *et al.*	(CERN, MADR, CDEF+)
GURTU	79	NP B151 181	A. Gurtu *et al.*	(CERN, ZEEM, NUM, OXF)
STANTON	79	PRL 42 346	N.R. Stanton *et al.*	(OSU, CARL, MCGI+) JP
CORDEN	78	NP B144 253	M.J. Corden *et al.*	(BIRM, RHEL, TELA+) JP
NACASCH	78	NP B135 203	R. Nacasch *et al.*	(PARIS, MADR, CERN)
GRASSLER	77	NP B121 189	H. Grassler *et al.*	(AACH3, BERL, BONN+)
DEFOIX	72	NP B44 125	C. Defoix *et al.*	(CDEF, CERN)
DUBOC	72	NP B46 429	J. Duboc *et al.*	(PARIS, LIVP)
THUN	72	PRL 28 1733	R. Thun *et al.*	(STON, NEAS)
BARDADIN-...	71	PR D4 2711	M. Bardadin-Otwinowska *et al.*	(WARS)
BOESEBECK	71	PL 34B 659	K. Boesebeck	(AACH, BERL, BONN, CERN, CRAC+)
CAMPBELL	69	PRL 22 1294	J.H. Campbell *et al.*	(PURD)
LORSTAD	69	NP B14 63	B. Lorstad *et al.*	(CDEF, CERN) JP
D'ANDLAU	68	NP B5 693	C. d'Andlau *et al.*	(CDEF, CERN, IRAD+) IJP
DAHL	67	PR 163 1377	O.I. Dahl *et al.*	(LRL) IJP

OTHER RELATED PAPERS

AIHARA	88C	PR D38 1	H. Aihara *et al.*	(TPC-2γ Collab.) JPC
ASTON	85	PR D32 2255	D. Aston *et al.*	(SLAC, CARL, CNRC)
ATKINSON	84E	PL 138B 459	M. Atkinson *et al.*	(BONN, CERN, GLAS+)
GAVILLET	82	ZPHY C16 119	P. Gavillet *et al.*	(CERN, CDEF, PADO+)
D'ANDLAU	65	PL 17 347	C. d'Andlau *et al.*	(CDEF, CERN, IRAD+)
MILLER	65	PRL 14 1074	D.H. Miller *et al.*	(LRL, UCB)

$\eta(1295)$ $I^G(J^{PC}) = 0^+(0^{-+})$

See also the mini-review under non-$q\overline{q}$ candidates. (See the index for the page number.)

$\eta(1295)$ MASS

VALUE (MeV)	EVTS	DOCUMENT ID		TECN	COMMENT
1294 ± 4 OUR AVERAGE Error includes scale factor of 1.6. See the ideogram below.					
1302 ± 9 ± 8	20k	ADAMS	01B	E852	18 GeV $\pi^- p \to K^+K^-\pi^0 n$
1282 ± 5	9082	MANAK	00A	MPS	18 $\pi^- p \to \eta\pi^+\pi^- n$
1299 ± 4	2100	ALDE	97B	GAM4	100 $\pi^- p \to \eta\pi^0\pi^0 n$
1295 ± 4		FUKUI	91C	SPEC	8.95 $\pi^- p \to \eta\pi^+\pi^- n$
• • • We do not use the following data for averages, fits, limits, etc. • • •					
~ 1275		STANTON	79	CNTR	8.4 $\pi^- p \to n\eta 2\pi$

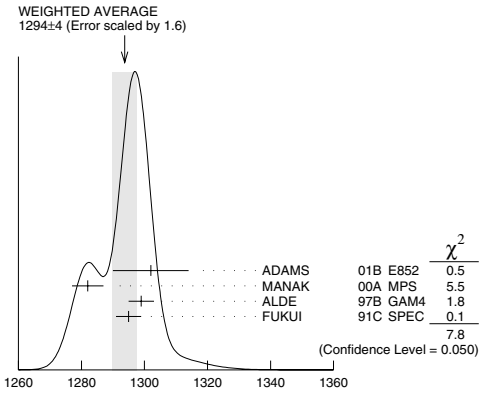

$\eta(1295)$ WIDTH

VALUE (MeV)	EVTS	DOCUMENT ID		TECN	COMMENT
55 ± 5 OUR AVERAGE					
57 ± 23 ± 21	20k	ADAMS	01B	E852	18 GeV $\pi^- p \rightarrow K^+ K^- \pi^0 n$
66 ± 13	9082	MANAK	00A	MPS	18 $\pi^- p \rightarrow \eta \pi^+ \pi^- n$
53 ± 6		FUKUI	91C	SPEC	8.95 $\pi^- p \rightarrow \eta \pi^+ \pi^- n$
• • • We do not use the following data for averages, fits, limits, etc. • • •					
< 40	2100	ALDE	97B	GAM4	100 $\pi^- p \rightarrow \eta \pi^0 \pi^0 n$
~ 70		STANTON	79	CNTR	8.4 $\pi^- p \rightarrow n \eta 2\pi$

$\eta(1295)$ DECAY MODES

	Mode	Fraction (Γ_i/Γ)
Γ_1	$\eta \pi^+ \pi^-$	seen
Γ_2	$a_0(980)\pi$	seen
Γ_3	$\gamma\gamma$	
Γ_4	$\eta \pi^0 \pi^0$	seen
Γ_5	$\eta(\pi\pi)$S-wave	seen
Γ_6	$\sigma\eta$	

$\eta(1295)$ $\Gamma(i)\Gamma(\gamma\gamma)/\Gamma(\text{total})$

$\Gamma(\eta\pi^+\pi^-) \times \Gamma(\gamma\gamma)/\Gamma_{\text{total}}$ $\Gamma_1\Gamma_3/\Gamma$

VALUE (keV)	CL%	DOCUMENT ID		TECN	COMMENT
< 0.066	95	ACCIARRI	01G	L3	183–202 $e^+e^- \rightarrow e^+e^-\eta\pi^+\pi^-$
• • • We do not use the following data for averages, fits, limits, etc. • • •					
< 0.6	90	AIHARA	88C	TPC	$e^+e^- \rightarrow e^+e^-\eta\pi^+\pi^-$
< 0.3		ANTREASYAN	87	CBAL	$e^+e^- \rightarrow e^+e^-\eta\pi\pi$

$\eta(1295)$ BRANCHING RATIOS

$\Gamma(a_0(980)\pi)/\Gamma_{\text{total}}$ Γ_2/Γ

VALUE	DOCUMENT ID		TECN	COMMENT
• • • We do not use the following data for averages, fits, limits, etc. • • •				
not seen	BERTIN	97	OBLX	0.0 $\overline{p}p \rightarrow K^\pm(K^0)\pi^\mp\pi^+\pi^-$
seen	BIRMAN	88	MPS	8 $\pi^- p \rightarrow K^+ \overline{K}{}^0 \pi^- n$
large	ANDO	86	SPEC	8 $\pi^- p \rightarrow \eta \pi^+ \pi^- n$
large	STANTON	79	CNTR	8.4 $\pi^- p \rightarrow n\eta 2\pi$

$\Gamma(a_0(980)\pi)/\Gamma(\eta\pi^0\pi^0)$ Γ_2/Γ_4

VALUE	DOCUMENT ID		TECN	COMMENT
0.65 ± 0.10	[1] ALDE	97B	GAM4	100 $\pi^- p \rightarrow \eta \pi^0 \pi^0 n$

[1] Assuming that $a_0(980)$ decays only to $\eta\pi$.

$\Gamma(\eta(\pi\pi)_{S\text{-wave}})/\Gamma(\eta\pi^0\pi^0)$ Γ_5/Γ_4

VALUE	DOCUMENT ID		TECN	COMMENT
0.35 ± 0.10	ALDE	97B	GAM4	100 $\pi^- p \rightarrow \eta \pi^0 \pi^0 n$

$\Gamma(a_0(980)\pi)/\Gamma(\sigma\eta)$ Γ_2/Γ_6

VALUE	EVTS	DOCUMENT ID		TECN	COMMENT
0.48 ± 0.22	9082	MANAK	00A	MPS	18 $\pi^- p \rightarrow \eta \pi^+ \pi^- n$

$\eta(1295)$ REFERENCES

ACCIARRI	01G	PL B501 1	M. Acciarri *et al.*	(L3 Collab.)
ADAMS	01B	PL B516 264	G.S. Adams *et al.*	(BNL E852 Collab.)
MANAK	00A	PR D62 012003	J.J. Manak *et al.*	(BNL E852 Collab.)
ALDE	97B	PAN 60 386	D. Alde *et al.*	(GAMS Collab.)
		Translated from YAF 60 458.		
BERTIN	97	PL B400 226	A. Bertin *et al.*	(OBELIX Collab.)
FUKUI	91C	PL B267 293	S. Fukui *et al.*	(SUGI, NAGO, KEK, KYOT+)
AIHARA	88C	PR D38 1	H. Aihara *et al.*	(TPC-2γ Collab.)
BIRMAN	88	PRL 61 1557	A. Birman *et al.*	(BNL, FSU, IND, MASD) JP
ANTREASYAN	87	PR D36 2633	D. Antreasyan *et al.*	(Crystal Ball Collab.)
ANDO	86	PRL 57 1296	A. Ando *et al.*	(KEK, KYOT, NIRS, SAGA+) IJP
STANTON	79	PRL 42 346	N.R. Stanton *et al.*	(OSU, CARL, MCGI+) JP

OTHER RELATED PAPERS

ANISOVICH	00F	EPJ A6 247	A.V. Anisovich *et al.*

$\pi(1300)$

$I^G(J^{PC}) = 1^-(0^{-+})$

$\pi(1300)$ MASS

VALUE (MeV)	DOCUMENT ID		TECN	COMMENT
1300 ± 100 OUR ESTIMATE				
• • • We do not use the following data for averages, fits, limits, etc. • • •				
1343 ± 15 ± 24	CHUNG	02	MPS	18.3 $\pi^- p \rightarrow \pi^+\pi^-\pi^- p$
1375 ± 40	ABELE	01	CBAR	0.0 $\overline{p}d \rightarrow \pi^- 4\pi^0 p$
1275 ± 15	BERTIN	97D	OBLX	0.05 $\overline{p}p \rightarrow 2\pi^+ 2\pi^-$
~ 1114	ABELE	96	CBAR	0.0 $\overline{p}p \rightarrow 5\pi^0$
1190 ± 30	ZIELINSKI	84	SPEC	200 $\pi^+ Z \rightarrow Z 3\pi$
1240 ± 30	BELLINI	82	SPEC	40 $\pi^- A \rightarrow A 3\pi$
1273 ± 50	[1] AARON	81	RVUE	
1342 ± 20	BONESINI	81	OMEG	12 $\pi^- p \rightarrow p 3\pi$
~ 1400	DAUM	81B	SPEC	63,94 $\pi^- p$

[1] Uses multichannel Aitchison-Bowler model (BOWLER 75). Uses data from DAUM 80 and DANKOWYCH 81.

$\pi(1300)$ WIDTH

VALUE (MeV)	DOCUMENT ID		TECN	COMMENT
200 to 600 OUR ESTIMATE				
• • • We do not use the following data for averages, fits, limits, etc. • • •				
449 ± 39 ± 47	CHUNG	02	MPS	18.3 $\pi^- p \rightarrow \pi^+\pi^-\pi^- p$
268 ± 50	ABELE	01	CBAR	0.0 $\overline{p}d \rightarrow \pi^- 4\pi^0 p$
218 ± 100	BERTIN	97D	OBLX	0.05 $\overline{p}p \rightarrow 2\pi^+ 2\pi^-$
~ 340	ABELE	96	CBAR	0.0 $\overline{p}p \rightarrow 5\pi^0$
440 ± 80	ZIELINSKI	84	SPEC	200 $\pi^+ Z \rightarrow Z 3\pi$
360 ± 120	BELLINI	82	SPEC	40 $\pi^- A \rightarrow A 3\pi$
580 ± 100	[2] AARON	81	RVUE	
220 ± 70	BONESINI	81	OMEG	12 $\pi^- p \rightarrow p 3\pi$
~ 600	DAUM	81B	SPEC	63,94 $\pi^- p$

[2] Uses multichannel Aitchison-Bowler model (BOWLER 75). Uses data from DAUM 80 and DANKOWYCH 81.

$\pi(1300)$ DECAY MODES

	Mode	Fraction (Γ_i/Γ)
Γ_1	$\rho\pi$	seen
Γ_2	$\pi(\pi\pi)_{S\text{-wave}}$	seen
Γ_3	$\gamma\gamma$	

$\pi(1300)$ $\Gamma(i)\Gamma(\gamma\gamma)/\Gamma(\text{total})$

$\Gamma(\rho\pi) \times \Gamma(\gamma\gamma)/\Gamma_{\text{total}}$ $\Gamma_1\Gamma_3/\Gamma$

VALUE (keV)	CL%	DOCUMENT ID		TECN	COMMENT
< 0.085	90	ACCIARRI	97T	L3	$e^+e^- \rightarrow e^+e^-\pi^+\pi^-\pi^0$
< 0.54	90	ALBRECHT	97B	ARG	$e^+e^- \rightarrow e^+e^-\pi^+\pi^-\pi^0$

$\pi(1300)$ BRANCHING RATIOS

$\Gamma(\pi(\pi\pi)_{S\text{-wave}})/\Gamma(\rho\pi)$ Γ_2/Γ_1

VALUE	CL%	DOCUMENT ID		TECN	COMMENT
• • • We do not use the following data for averages, fits, limits, etc. • • •					
seen		CHUNG	02	MPS	18.3 $\pi^- p \rightarrow \pi^+\pi^-\pi^- p$
< 0.15	90	ABELE	01	CBAR	0.0 $\overline{p}d \rightarrow \pi^- 4\pi^0 p$
2.12		[3] AARON	81	RVUE	

[3] Uses multichannel Aitchison-Bowler model (BOWLER 75). Uses data from DAUM 80 and DANKOWYCH 81.

$\pi(1300)$ REFERENCES

CHUNG	02	PR D65 072001	S.U. Chung *et al.*	
ABELE	01	EPJ C19 667	A. Abele *et al.*	(Crystal Barrel Collab.)
ACCIARRI	97T	PL B413 147	M. Acciarri *et al.*	(L3 Collab.)
ALBRECHT	97B	ZPHY C74 469	H. Albrecht *et al.*	(ARGUS Collab.)
BERTIN	97D	PL B414 220	A. Bertin *et al.*	(OBELIX Collab.)
ABELE	96	PL B380 453	A. Abele *et al.*	(Crystal Barrel Collab.)
ZIELINSKI	84	PR D30 1855	M. Zielinski *et al.*	(ROCH, MINN, FNAL)
BELLINI	82	PRL 48 1697	G. Bellini *et al.*	(MILA, BGNA, JINR)
AARON	81	PR D24 1207	R.A. Aaron, R.S. Longacre	(NEAS, BNL)
BONESINI	81	PL 103B 75	M. Bonesini *et al.*	(MILA, LIVP, DARE+)
DANKOWY...	81	PRL 46 580	J.A. Dankowych *et al.*	(TNTO, BNL, CARL+)
DAUM	81B	NP B182 269	C. Daum *et al.*	(AMST, CERN, CRAC, MPIM+)
DAUM	80	PL 89B 281	C. Daum *et al.*	(AMST, CERN, CRAC, MPIM+)
BOWLER	75	NP B97 227	M.G. Bowler *et al.*	(OXFTP, DARE)

OTHER RELATED PAPERS

ASNER	00	PR D61 012002	D.M. Asner *et al.*	(CLEO Collab.)
ZAIMIDOROGA	99	PAN 30 1 Translated from SJPN 30 5.	O.A. Zaimidoroga	
ACKERSTAFF	97R	ZPHY C75 593	K. Ackerstaff *et al.*	(OPAL Collab.)
ALBRECHT	95C	PL B349 576	H. Albrecht *et al.*	(ARGUS Collab.)

$a_2(1320)$

$I^G(J^{PC}) = 1^-(2^{++})$

$a_2(1320)$ MASS

VALUE (MeV)	DOCUMENT ID

1318.3±0.6 OUR AVERAGE Includes data from the 4 datablocks that follow this one. Error includes scale factor of 1.2.

3π MODE

VALUE (MeV)	EVTS	DOCUMENT ID	TECN	CHG	COMMENT

The data in this block is included in the average printed for a previous datablock.

1318.9± 1.4 OUR AVERAGE Error includes scale factor of 1.4. See the ideogram below.

1326	± 2	±2		CHUNG	02	MPS	18.3 $\pi^- p \to \pi^+\pi^-\pi^- p$
1317	± 3			BARBERIS	98B		450 $pp \to p_f \pi^+\pi^-\pi^0 p_s$
1323	± 4	±3		ACCIARRI	97T	L3	$e^+e^- \to e^+e^-\pi^+\pi^-\pi^0$
1320	± 7			ALBRECHT	97B	ARG	$e^+e^- \to e^+e^-\pi^+\pi^-\pi^0$
1311.3	± 1.6	±3.0	72400	AMELIN	96	VES	36 $\pi^- p \to \pi^+\pi^-\pi^0 n$
1310	± 5			ARMSTRONG	90	OMEG	0 300.0 $pp \to pp\pi^+\pi^-\pi^0$
1323.8	± 2.3		4022	AUGUSTIN	89	DM2	± $J/\psi \to \rho^\pm a_2^\mp$
1320.6	± 3.1		3562	AUGUSTIN	89	DM2	0 $J/\psi \to \rho^0 a_2^0$
1317	± 2		25000	[1] DAUM	80C	SPEC	– 63,94 $\pi^- p \to 3\pi p$
1320	±10		1097	[1] BALTAY	78B	HBC	+0 15 $\pi^+ p \to p4\pi$
1306	± 8			FERRERSORIA	78	OMEG	– 9 $\pi^- p \to p3\pi$
1318	± 7		1600	[1] EMMS	75	DBC	0 4 $\pi^+ n \to p(3\pi)^0$
1315	± 5			[1] ANTIPOV	73C	CNTR	– 25,40 $\pi^- p \to p\eta\pi^-$
1306	± 9		1580	CHALOUPKA	73	HBC	– 3.9 $\pi^- p$

• • • We do not use the following data for averages, fits, limits, etc. • • •

1305	±14			CONDO	93	SHF	$\gamma p \to \eta\pi^+\pi^+\pi^-$
1310	± 2			[1] EVANGELISTA	81	OMEG	– 12 $\pi^- p \to 3\pi p$
1343	±11		490	BALTAY	78B	HBC	0 15 $\pi^+ p \to \Delta 3\pi$
1309	± 5		5000	BINNIE	71	MMS	– $\pi^- p$ near a_2 threshold
1299	± 6		28000	BOWEN	71	MMS	– 5 $\pi^- p$
1300	± 6		24000	BOWEN	71	MMS	+ 5 $\pi^+ p$
1309	± 4		17000	BOWEN	71	MMS	– 7 $\pi^- p$
1306	± 4		941	ALSTON-...	70	HBC	+ 7.0 $\pi^+ p \to 3\pi p$

[1] From a fit to $J^P = 2^+$ $\rho\pi$ partial wave.

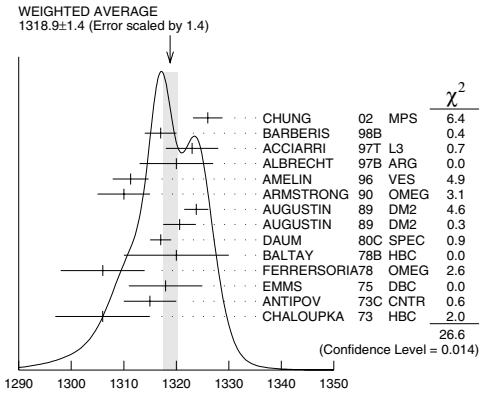

$a_2(1320)$ mass, 3π mode (MeV)

$K^\pm K^0_S$ MODE

VALUE (MeV)	EVTS	DOCUMENT ID	TECN	CHG	COMMENT

The data in this block is included in the average printed for a previous datablock.

1318.1± 0.7 OUR AVERAGE

1319	± 5	4700	[2,3] CLELAND	82B	SPEC	+	50 $\pi^+ p \to K^0_S K^+ p$
1324	± 6	5200	[2,3] CLELAND	82B	SPEC	–	50 $\pi^- p \to K^0_S K^- p$
1320	± 2	4000	CHABAUD	80	SPEC	–	17 π^- A $\to K^0_S K^-$ A
1312	± 4	11000	CHABAUD	78	SPEC	–	9.8 $\pi^- p \to K^- K^0_S p$
1316	± 2	4730	CHABAUD	78	SPEC	–	18.8 $\pi^- p \to K^- K^0_S p$
1318	± 1		[2,4] MARTIN	78D	SPEC	–	10 $\pi^- p \to K^0_S K^- p$
1320	± 2	2724	MARGULIE	76	SPEC	–	23 $\pi^- p \to K^- K^0_S p$
1313	± 4	730	FOLEY	72	CNTR	–	20.3 $\pi^- p \to K^- K^0_S p$
1319	± 3	1500	[4] GRAYER	71	ASPK	–	17.2 $\pi^- p \to K^- K^0_S p$

• • • We do not use the following data for averages, fits, limits, etc. • • •

1330	±11	1000	[2,3] CLELAND	82B	SPEC	+	30 $\pi^+ p \to K^0_S K^+ p$
1324	± 5	350	HYAMS	78	ASPK	+	12.7 $\pi^+ p \to K^+ K^0_S p$

[2] From a fit to $J^P = 2^+$ partial wave.
[3] Number of events evaluated by us.
[4] Systematic error in mass scale subtracted.

$\eta\pi$ MODE

VALUE (MeV)	EVTS	DOCUMENT ID	TECN	CHG	COMMENT

The data in this block is included in the average printed for a previous datablock.

1317.7±1.4 OUR AVERAGE

1308	±9		BARBERIS	00H			450 $pp \to p_f \eta\pi^0 p_s$
1316	±9		BARBERIS	00H			450 $pp \to \Delta_f^{++}\eta\pi^- p_s$
1317	±1	±2	THOMPSON	97	MPS		18 $\pi^- p \to \eta\pi^- p$
1315	±5	±2	[5] AMSLER	94D	CBAR		0.0 $\bar{p}p \to \pi^0\pi^0\eta$
1325.1	±5.1		AOYAGI	93	BKEI		$\pi^- p \to \eta\pi^- p$
1317.7	±1.4	±2.0	BELADIDZE	93	VES		37$\pi^- N \to \eta\pi^- N$
1323	±8	1000	[6] KEY	73	OSPK	–	6 $\pi^- p \to p\pi^-\eta$

• • • We do not use the following data for averages, fits, limits, etc. • • •

1324	±5		ARMSTRONG	93C	E760	0	$\bar{p}p \to \pi^0\eta\eta \to 6\gamma$
1336.2	±1.7	2561	DELFOSSE	81	SPEC	+	$\pi^\pm p \to p\pi^\pm\eta$
1330.7	±2.4	1653	DELFOSSE	81	SPEC	–	$\pi^\pm p \to p\pi^\pm\eta$
1324	±8	6200	[6,7] CONFORTO	73	OSPK	–	6 $\pi^- p \to p$MM$^-$

[5] The systematic error of 2 MeV corresponds to the spread of solutions.
[6] Error includes 5 MeV systematic mass-scale error.
[7] Missing mass with enriched MMS $= \eta\pi^-$, $\eta = 2\gamma$.

$\eta'\pi$ MODE

VALUE (MeV)	DOCUMENT ID	TECN	COMMENT

The data in this block is included in the average printed for a previous datablock.

1322 ± 7 OUR AVERAGE

1318 ± 8 $^{+3}_{-5}$	IVANOV	01	MPS		18 $\pi^- p \to \eta'\pi^- p$
1327.0 ±10.7	BELADIDZE	93	VES		37$\pi^- N \to \eta'\pi^- N$

$a_2(1320)$ WIDTH

3π MODE

VALUE (MeV)	EVTS	DOCUMENT ID		TECN	CHG	COMMENT
104.7± 1.9 OUR AVERAGE						
108 ± 3 ±15		CHUNG	02	MPS		18.3 $\pi^- p \to \pi^+\pi^-\pi^- p$
120 ±10		BARBERIS	98B			450 $pp \to p_f \pi^+\pi^-\pi^0 p_s$
105 ±10 ±11		ACCIARRI	97T	L3		$e^+e^- \to e^+e^-\pi^+\pi^-\pi^0$
120 ±10		ALBRECHT	97B	ARG		$e^+e^- \to e^+e^-\pi^+\pi^-\pi^0$
103.0± 6.0± 3.3	72400	AMELIN	96	VES		36 $\pi^- p \to \pi^+\pi^-\pi^0 n$
120 ±10		ARMSTRONG	90	OMEG	0	300.0$p p \to p p \pi^+\pi^-\pi^0$
107.0± 9.7	4022	AUGUSTIN	89	DM2	±	$J/\psi \to \rho^\pm a_2^\mp$
118.5±12.5	3562	AUGUSTIN	89	DM2	0	$J/\psi \to \rho^0 a_2^0$
97 ± 5		[8] EVANGELISTA	81	OMEG	–	12 $\pi^- p \to 3\pi p$
96 ± 9	25000	[8] DAUM	80C	SPEC	–	63,94 $\pi^- p \to 3\pi p$
110 ±15	1097	[8] BALTAY	78B	HBC	+0	15 $\pi^+ p \to p 4\pi$
112 ±18	1600	[8] EMMS	75	DBC	0	4 $\pi^+ n \to p(3\pi)^0$
122 ±14	1200	[8,9] WAGNER	75	HBC	0	7 $\pi^+ p \to \Delta^{++}(3\pi)^0$
115 ±15		[8] ANTIPOV	73C	CNTR	–	25,40 $\pi^- p \to p\eta\pi^-$
99 ±15	1580	CHALOUPKA	73	HBC	–	3.9 $\pi^- p$
105 ± 5	28000	BOWEN	71	MMS	–	5 $\pi^- p$
99 ± 5	24000	BOWEN	71	MMS	+	5 $\pi^+ p$
103 ± 5	17000	BOWEN	71	MMS	–	7 $\pi^- p$
• • • We do not use the following data for averages, fits, limits, etc. • • •						
120 ±40		CONDO	93	SHF		$\gamma p \to \eta\pi^+\pi^+\pi^-$
115 ±14	490	BALTAY	78B	HBC	0	15 $\pi^+ p \to \Delta 3\pi$
72 ±16	5000	BINNIE	71	MMS	–	$\pi^- p$ near a_2 threshold
79 ±12	941	ALSTON-...	70	HBC	+	7.0 $\pi^+ p \to 3\pi p$

[8] From a fit to $J^P = 2^+$ $\rho\pi$ partial wave.
[9] Width errors enlarged by us to $4\Gamma/\sqrt{N}$; see the note with the $K^*(892)$ mass.

$K^\pm K^0_S$ AND $\eta\pi$ MODES

VALUE (MeV)	DOCUMENT ID
107 ±5 OUR ESTIMATE	
110.4±1.7 OUR AVERAGE	Includes data from the 2 datablocks that follow this one.

$K^\pm K^0_S$ MODE

VALUE (MeV)	EVTS	DOCUMENT ID		TECN	CHG	COMMENT
The data in this block is included in the average printed for a previous datablock.						
109.8± 2.4 OUR AVERAGE						
112 ±20	4700	[10,11] CLELAND	82B	SPEC	+	50 $\pi^+ p \to K^0_S K^+ p$
120 ±25	5200	[10,11] CLELAND	82B	SPEC	–	50 $\pi^- p \to K^0_S K^- p$
106 ± 4	4000	CHABAUD	80	SPEC	–	17 $\pi^- A \to K^0_S K^- A$
126 ±11	11000	CHABAUD	78	SPEC	–	9.8 $\pi^- p \to K^- K^0_S p$
101 ± 8	4730	CHABAUD	78	SPEC	–	18.8 $\pi^- p \to K^- K^0_S p$
113 ± 4		[10,12] MARTIN	78D	SPEC	–	10 $\pi^- p \to K^0_S K^- p$
105 ± 8	2724	[12] MARGULIE	76	SPEC	–	23 $\pi^- p \to K^- K^0_S p$
113 ±19	730	FOLEY	72	CNTR	–	20.3 $\pi^- p \to K^- K^0_S p$
123 ±13	1500	[12] GRAYER	71	ASPK	–	17.2 $\pi^- p \to K^- K^0_S p$
• • • We do not use the following data for averages, fits, limits, etc. • • •						
121 ±51	1000	[10,11] CLELAND	82B	SPEC	+	30 $\pi^+ p \to K^0_S K^+ p$
110 ±18	350	HYAMS	78	ASPK	+	12.7 $\pi^+ p \to K^+ K^0_S p$

[10] From a fit to $J^P = 2^+$ partial wave.
[11] Number of events evaluated by us.
[12] Width errors enlarged by us to $4\Gamma/\sqrt{N}$; see the note with the $K^*(892)$ mass.

$\eta\pi$ MODE

VALUE (MeV)	EVTS	DOCUMENT ID		TECN	CHG	COMMENT
The data in this block is included in the average printed for a previous datablock.						
111.1± 2.4 OUR AVERAGE						
115 ±20		BARBERIS	00H			450 $pp \to p_f \eta\pi^0 p_s$
112 ±14		BARBERIS	00H			450 $pp \to \Delta_f^{++}\eta\pi^- p_s$
112 ± 3 ±2		[13] AMSLER	94D	CBAR		0.0 $\bar{p}p \to \pi^0\pi^0\eta$
103 ± 6 ±3		BELADIDZE	93	VES		37$\pi^- N \to \eta\pi^- N$
112.2± 5.7	2561	DELFOSSE	81	SPEC	+	$\pi^\pm p \to p\pi^\pm\eta$
116.6± 7.7	1653	DELFOSSE	81	SPEC	–	$\pi^\pm p \to p\pi^\pm\eta$
108 ± 9	1000	KEY	73	OSPK	–	6 $\pi^- p \to p\pi^-\eta$
• • • We do not use the following data for averages, fits, limits, etc. • • •						
127 ± 2 ±2		[14] THOMPSON	97	MPS		18 $\pi^- p \to \eta\pi^- p$
118 ±10		ARMSTRONG	93C	E760	0	$\bar{p}p \to \pi^0\eta\eta \to 6\gamma$
104 ± 9	6200	[15] CONFORTO	73	OSPK	–	6 $\pi^- p \to p$MM$^-$

[13] The systematic error of 2 MeV corresponds to the spread of solutions.
[14] Resolution is not unfolded.
[15] Missing mass with enriched MMS $= \eta\pi^-$, $\eta = 2\gamma$.

$\eta'\pi$ MODE

VALUE (MeV)	DOCUMENT ID		TECN	COMMENT
119±25 OUR AVERAGE				
140± 35 ± 20	IVANOV	01	MPS	18 $\pi^- p \to \eta'\pi^- p$
106± 32	BELADIDZE	93	VES	37$\pi^- N \to \eta'\pi^- N$

$a_2(1320)$ DECAY MODES

	Mode	Fraction (Γ_j/Γ)	Scale factor/ Confidence level
Γ_1	$\rho\pi$	(70.1 ±2.7) %	S=1.2
Γ_2	$\eta\pi$	(14.5 ±1.2) %	
Γ_3	$\omega\pi\pi$	(10.6 ±3.2) %	S=1.3
Γ_4	$K\overline{K}$	(4.9 ±0.8) %	
Γ_5	$\eta'(958)\pi$	(5.3 ±0.9) $\times 10^{-3}$	
Γ_6	$\pi^\pm\gamma$	(2.68±0.31) $\times 10^{-3}$	
Γ_7	$\gamma\gamma$	(9.4 ±0.7) $\times 10^{-6}$	
Γ_8	$\pi^+\pi^-\pi^-$	< 8 %	CL=90%
Γ_9	e^+e^-	< 6 $\times 10^{-9}$	CL=90%

CONSTRAINED FIT INFORMATION

An overall fit to 5 branching ratios uses 18 measurements and one constraint to determine 4 parameters. The overall fit has a $\chi^2 = 9.3$ for 15 degrees of freedom.

The following *off-diagonal* array elements are the correlation coefficients $\langle \delta x_i \delta x_j \rangle / (\delta x_i \cdot \delta x_j)$, in percent, from the fit to the branching fractions, $x_i \equiv \Gamma_i/\Gamma_{\text{total}}$. The fit constrains the x_i whose labels appear in this array to sum to one.

	x_1	x_2	x_3
x_2	10		
x_3	−89	−46	
x_4	−1	−2	−24

$a_2(1320)$ PARTIAL WIDTHS

$\Gamma(\pi^\pm\gamma)$ Γ_6

VALUE (keV)	EVTS	DOCUMENT ID		TECN	CHG	COMMENT
287± 30 OUR AVERAGE						
284± 25±25	7100	MOLCHANOV	01	SELX		600 $\pi^- A \to \pi^+\pi^-\pi^- A$
295± 60		CIHANGIR	82	SPEC	+	200 $\pi^+ A$
• • • We do not use the following data for averages, fits, limits, etc. • • •						
461±110		[18] MAY	77	SPEC	±	9.7 γA

$\Gamma(\gamma\gamma)$ Γ_7

VALUE (keV)	EVTS	DOCUMENT ID		TECN	CHG	COMMENT
1.00±0.06 OUR AVERAGE						
0.98±0.05±0.09		ACCIARRI	97T	L3		$e^+e^- \to e^+e^-\pi^+\pi^-\pi^0$
0.96±0.03±0.13		ALBRECHT	97B	ARG		$e^+e^- \to e^+e^-\pi^+\pi^-\pi^0$
1.26±0.26±0.18	36	BARU	90	MD1		$e^+e^- \to e^+e^-\pi^+\pi^-\pi^0$
1.00±0.07±0.15	415	BEHREND	90C	CELL	0	$e^+e^- \to e^+e^-\pi^+\pi^-\pi^0$
1.03±0.13±0.21		BUTLER	90	MRK2		$e^+e^- \to e^+e^-\pi^+\pi^-\pi^0$
1.01±0.14±0.22	85	OEST	90	JADE		$e^+e^- \to e^+e^-\pi^0\eta$
0.90±0.27±0.15	56	[16] ALTHOFF	86	TASS	0	$e^+e^- \to e^+e^- 3\pi$
1.14±0.20±0.26		[17] ANTREASYAN	86	CBAL	0	$e^+e^- \to e^+e^-\pi^0\eta$
1.06±0.18±0.19		BERGER	84C	PLUT	0	$e^+e^- \to e^+e^- 3\pi$
• • • We do not use the following data for averages, fits, limits, etc. • • •						
$0.81 \pm 0.19^{+0.42}_{-0.11}$	35	[16] BEHREND	83B	CELL	0	$e^+e^- \to e^+e^- 3\pi$
0.77±0.18±0.27	22	[17] EDWARDS	82F	CBAL	0	$e^+e^- \to e^+e^-\pi^0\eta$

[16] From $\rho\pi$ decay mode.
[17] From $\eta\pi^0$ decay mode.

$\Gamma(e^+e^-)$ Γ_9

VALUE (eV)	CL%	DOCUMENT ID		TECN	COMMENT
< 0.56	90	ACHASOV	00K	SND	$e^+e^- \to \pi^0\pi^0$
• • • We do not use the following data for averages, fits, limits, etc. • • •					
< 25	90	VOROBYEV	88	ND	$e^+e^- \to \pi^0\eta$

[18] Assuming one-pion exchange.

$a_2(1320)$ Γ(i)$\Gamma(\gamma\gamma)/\Gamma$(total)

$\Gamma(K\overline{K}) \times \Gamma(\gamma\gamma)/\Gamma_{\text{total}}$ $\Gamma_4\Gamma_7/\Gamma$

VALUE (keV)	DOCUMENT ID		TECN	COMMENT
0.126 ± 0.007 ± 0.028	[19] ALBRECHT	90G	ARG	$e^+e^- \to e^+e^-K^+K^-$
• • • We do not use the following data for averages, fits, limits, etc. • • •				
0.081 ± 0.006 ± 0.027	[20] ALBRECHT	90G	ARG	$e^+e^- \to e^+e^-K^+K^-$

[19] Using an incoherent background.
[20] Using a coherent background.

$a_2(1320)$ BRANCHING RATIOS

$\Gamma(K\overline{K})/\Gamma(\rho\pi)$ Γ_4/Γ_1

VALUE	EVTS	DOCUMENT ID		TECN	CHG	COMMENT
0.070 ± 0.012 OUR FIT						
0.078 ± 0.017		CHABAUD	78	RVUE		
• • • We do not use the following data for averages, fits, limits, etc. • • •						
0.011 ± 0.003		[21] BERTIN	98B	OBLX		$0.0\ \overline{p}p \to K^\pm K_S \pi^\mp$
0.056 ± 0.014	50	[22] CHALOUPKA	73	HBC	−	$3.9\ \pi^- p$
0.097 ± 0.018	113	[22] ALSTON-...	71	HBC	+	$7.0\ \pi^+ p$
0.06 ± 0.03		[22] ABRAMOVI...	70B	HBC	−	$3.93\ \pi^- p$
0.054 ± 0.022		[22] CHUNG	68	HBC	−	$3.2\ \pi^- p$

[21] Using 4π data from BERTIN 97D.
[22] Included in CHABAUD 78 review.

$\Gamma(\eta\pi)/[\Gamma(\rho\pi)+\Gamma(\eta\pi)+\Gamma(K\overline{K})]$ $\Gamma_2/(\Gamma_1+\Gamma_2+\Gamma_4)$

VALUE	EVTS	DOCUMENT ID		TECN	CHG	COMMENT
0.162 ± 0.012 OUR FIT						
0.140 ± 0.028 OUR AVERAGE						
0.13 ± 0.04		ESPIGAT	72	HBC	±	$0.0\ \overline{p}p$
0.15 ± 0.04	34	BARNHAM	71	HBC	+	$3.7\ \pi^+ p$

$\Gamma(\eta\pi)/\Gamma(\rho\pi)$ Γ_2/Γ_1

VALUE	EVTS	DOCUMENT ID		TECN	CHG	COMMENT
0.207 ± 0.018 OUR FIT						
0.213 ± 0.020 OUR AVERAGE						
0.18 ± 0.05		FORINO	76	HBC		$11\ \pi^- p$
0.22 ± 0.05	52	ANTIPOV	73	CNTR	−	$40\ \pi^- p$
0.211 ± 0.044	149	CHALOUPKA	73	HBC	−	$3.9\ \pi^- p$
0.246 ± 0.042	167	ALSTON-...	71	HBC	+	$7.0\ \pi^+ p$
0.25 ± 0.09	15	BOECKMANN	70	HBC	+	$5.0\ \pi^+ p$
0.23 ± 0.08	22	ASCOLI	68	HBC	−	$5\ \pi^- p$
0.12 ± 0.08		CHUNG	68	HBC	−	$3.2\ \pi^- p$
0.22 ± 0.09		CONTE	67	HBC	−	$11.0\ \pi^- p$

$\Gamma(\eta'(958)\pi)/\Gamma_{\text{total}}$ Γ_5/Γ

VALUE	CL%	DOCUMENT ID		TECN	CHG	COMMENT
• • • We do not use the following data for averages, fits, limits, etc. • • •						
< 0.006	95	ALDE	92B	GAM2		$38,100\ \pi^- p \to \eta'\pi^0 n$
< 0.02	97	BARNHAM	71	HBC	+	$3.7\ \pi^+ p$
0.004 ± 0.004		BOESEBECK	68	HBC	+	$8\ \pi^+ p$

$\Gamma(\eta'(958)\pi)/\Gamma(\rho\pi)$ Γ_5/Γ_1

VALUE	CL%	DOCUMENT ID		TECN	CHG	COMMENT
• • • We do not use the following data for averages, fits, limits, etc. • • •						
< 0.011	90	EISENSTEIN	73	HBC	−	$5\ \pi^- p$
< 0.04		ALSTON-...	71	HBC	+	$7.0\ \pi^+ p$
$0.04\ ^{+0.03}_{-0.04}$		BOECKMANN	70	HBC	0	$5.0\ \pi^+ p$

$\Gamma(K\overline{K})/[\Gamma(\rho\pi)+\Gamma(\eta\pi)+\Gamma(K\overline{K})]$ $\Gamma_4/(\Gamma_1+\Gamma_2+\Gamma_4)$

VALUE	EVTS	DOCUMENT ID		TECN	CHG	COMMENT
0.054 ± 0.009 OUR FIT						
0.048 ± 0.012 OUR AVERAGE						
0.05 ± 0.02		TOET	73	HBC	+	$5\ \pi^+ p$
0.09 ± 0.04		TOET	73	HBC	0	$5\ \pi^+ p$
0.03 ± 0.02	8	DAMERI	72	HBC	−	$11\ \pi^- p$
0.06 ± 0.03	17	BARNHAM	71	HBC	+	$3.7\ \pi^+ p$
• • • We do not use the following data for averages, fits, limits, etc. • • •						
0.020 ± 0.004		[23] ESPIGAT	72	HBC	±	$0.0\ \overline{p}p$

[23] Not averaged because of discrepancy between masses from $K\overline{K}$ and $\rho\pi$ modes.

$\Gamma(\pi^+\pi^-\pi^-)/\Gamma(\rho\pi)$ Γ_8/Γ_1

VALUE	CL%	DOCUMENT ID		TECN	CHG	COMMENT
< 0.12	90	ABRAMOVI...	70B	HBC	−	$3.93\ \pi^- p$

$\Gamma(\pi^\pm\gamma)/\Gamma_{\text{total}}$ Γ_6/Γ

VALUE	DOCUMENT ID		TECN	COMMENT
• • • We do not use the following data for averages, fits, limits, etc. • • •				
$0.005\ ^{+0.005}_{-0.003}$	[24] EISENBERG	72	HBC	4.3,5.25,7.5 γp

[24] Pion-exchange model used in this estimation.

$\Gamma(\omega\pi\pi)/\Gamma(\rho\pi)$ Γ_3/Γ_1

VALUE	EVTS	DOCUMENT ID		TECN	CHG	COMMENT
0.15 ± 0.05 OUR FIT Error includes scale factor of 1.3.						
0.15 ± 0.05 OUR AVERAGE Error includes scale factor of 1.3. See the ideogram below.						
0.28 ± 0.09	60	DIAZ	74	DBC	0	$6\ \pi^+ n$
0.18 ± 0.08		[25] KARSHON	74	HBC		Avg. of above two
0.10 ± 0.05	279	CHALOUPKA	73	HBC	−	$3.9\ \pi^- p$
• • • We do not use the following data for averages, fits, limits, etc. • • •						
0.29 ± 0.08	140	[25] KARSHON	74	HBC	0	$4.9\ \pi^+ p$
0.10 ± 0.04	60	[25] KARSHON	74	HBC	+	$4.9\ \pi^+ p$
0.19 ± 0.08		DEFOIX	73	HBC	0	$0.7\ \overline{p}p$

[25] KARSHON 74 suggest an additional $I = 0$ state strongly coupled to $\omega\pi\pi$ which could explain discrepancies in branching ratios and masses. We use a central value and a systematic spread.

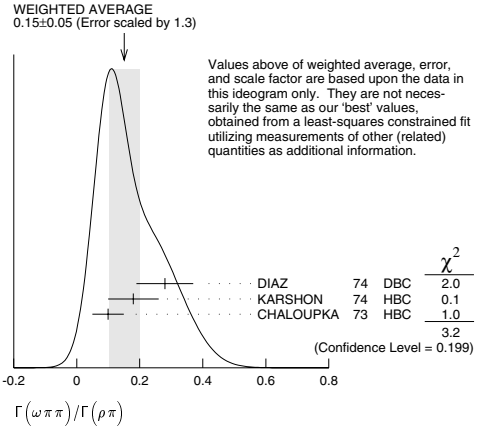

$\Gamma(\eta'(958)\pi)/\Gamma(\eta\pi)$ Γ_5/Γ_2

VALUE	DOCUMENT ID		TECN	COMMENT
0.037 ± 0.006 OUR AVERAGE				
0.032 ± 0.009	ABELE	97C	CBAR	$0.0\ \overline{p}p \to \pi^0\pi^0\eta'$
0.047 ± 0.010 ± 0.004	[26] BELADIDZE	93	VES	$37\pi^- N \to a_2^- N$
0.034 ± 0.008 ± 0.005	BELADIDZE	92	VES	$36\pi^- C \to a_2^- C$

[26] Using $B(\eta' \to \pi^+\pi^-\eta) = 0.441$, $B(\eta \to \gamma\gamma) = 0.389$ and $B(\eta \to \pi^+\pi^-\pi^0) = 0.236$.

$\Gamma(K\overline{K})/\Gamma(\eta\pi)$ Γ_4/Γ_2

VALUE	DOCUMENT ID		TECN	COMMENT
• • • We do not use the following data for averages, fits, limits, etc. • • •				
0.08 ± 0.02	[27] BERTIN	98B	OBLX	$0.0\ \overline{p}p \to K^\pm K_S \pi^\mp$

[27] Using $\eta\pi\pi$ data from AMSLER 94D.

$\Gamma(e^+e^-)/\Gamma_{\text{total}}$ Γ_9/Γ

VALUE (units 10^{-9})	CL%	DOCUMENT ID		TECN	COMMENT
< 6	90	ACHASOV	00K	SND	$e^+e^- \to \pi^0\pi^0$

$a_2(1320)$ REFERENCES

CHUNG	02	PR D65 072001	S.U. Chung *et al.*	
IVANOV	01	PRL 86 3977	E.I. Ivanov *et al.*	
MOLCHANOV	01	PL B521 171	V.V. Molchanov *et al.*	(FNAL SELEX Collab.)
ACHASOV	00K	PL B492 8	M.N. Achasov *et al.*	(Novosibirsk SND Collab.)
BARBERIS	00H	PL B488 225	D. Barberis *et al.*	(WA 102 Collab.)
BARBERIS	98B	PL B422 399	D. Barberis *et al.*	(WA 102 Collab.)
BERTIN	98B	PL B434 180	A. Bertin *et al.*	(OBELIX Collab.)
ABELE	97C	PL B404 179	A. Abele *et al.*	(Crystal Barrel Collab.)
ACCIARRI	97T	PL B413 147	M. Acciarri *et al.*	(L3 Collab.)
ALBRECHT	97B	ZPHY C74 469	H. Albrecht *et al.*	(ARGUS Collab.)
THOMPSON	97	PRL 79 1630	D.R. Thompson *et al.*	(E852 Collab.)
AMELIN	96	ZPHY C70 71	D.V. Amelin *et al.*	(SERP, TBIL)
AMSLER	94D	PL B333 277	C. Amsler *et al.*	(Crystal Barrel Collab.)
AOYAGI	93	PL B314 246	H. Aoyagi *et al.*	(BKEI Collab.)
ARMSTRONG	93C	PL B307 394	T.A. Armstrong *et al.*	(FNAL, FERR, GENO+)
BELADIDZE	93	PL B313 276	G.M. Beladidze *et al.*	(VES Collab.)
CONDO	93	PR D48 3045	G.T. Condo *et al.*	(SLAC Hybrid Collab.)
ALDE	92B	ZPHY C54 549	D.M. Alde *et al.*	(SERP, BELG, LANL, LAPP+)

Meson Particle Listings

$a_2(1320)$, $f_0(1370)$

BELADIDZE 92 ZPHY C54 235 G.M. Beladidze *et al.* (VES Collab.)
ALBRECHT 90G ZPHY C48 183 H. Albrecht *et al.* (ARGUS Collab.)
ARMSTRONG 90 ZPHY C48 213 T.A. Armstrong, M. Benayoun, W. Beusch
BARU 90 ZPHY C48 581 S.E. Baru *et al.* (MD-1 Collab.)
BEHREND 90C ZPHY C46 583 H.J. Behrend *et al.* (CELLO Collab.)
BUTLER 90 PR D42 1368 F. Butler *et al.* (Mark II Collab.)
OEST 90 ZPHY C47 343 T. Oest *et al.* (JADE Collab.)
AUGUSTIN 89 NP B320 1 J.E. Augustin, G. Cosme (DM2 Collab.)
VOROBYEV 88 SJNP 48 273 P.V. Vorobiev *et al.* (NOVO)
Translated from YAF 48 436.
ALTHOFF 86 ZPHY C31 537 M. Althoff *et al.* (TASSO Collab.)
ANTREASYAN 86 PR D33 1847 D. Antreasyan *et al.* (Crystal Ball Collab.)
BERGER 84C PL 149B 427 C. Berger *et al.* (PLUTO Collab.)
BEHREND 83B PL 125B 518 H.J. Behrend *et al.* (CELLO Collab.)
CIHANGIR 82 PL 117B 123 S. Cihangir *et al.* (FNAL, MINN, ROCH)
CLELAND 82B NP B208 228 W.E. Cleland *et al.* (DURH, GEVA, LAUS+)
EDWARDS 82F PL 110B 82 C. Edwards *et al.* (CIT, HARV, PRIN+)
DELFOSSE 81 NP B183 349 A. Delfosse *et al.* (GEVA, LAUS)
EVANGELISTA 81 NP B178 197 C. Evangelista *et al.* (BARI, BONN, CERN+)
CHABAUD 80 NP B175 189 V. Chabaud *et al.* (CERN, MPIM, AMST)
DAUM 80C PL 89B 276 C. Daum *et al.* (AMST, CERN, CRAC, MPIM+) JP
BALTAY 78B PR D17 62 C. Baltay *et al.* (COLU, BING)
CHABAUD 78 NP B145 349 V. Chabaud *et al.* (CERN, MPIM)
FERRERSORIA 78 PL 74B 287 A. Ferrer Soria *et al.* (ORSAY, CERN, CDEF+)
HYAMS 78 NP B146 303 B.D. Hyams *et al.* (CERN, MPIM, ATEN)
MARTIN 78D PL 74B 417 A.D. Martin *et al.* (DURH, GEVA) JP
MAY 77 PR D16 1983 E.N. May *et al.* (ROCH, CORN)
FORINO 76 NC 35A 465 A. Forino *et al.* (BGNA, FIRZ, GENO, MILA+)
MARGULIE 76 PR D14 667 M. Margulies *et al.* (BNL, CUNY)
EMMS 75 PL 58B 117 M.J. Emms *et al.* (BIRM, DURH, RHEL) JP
WAGNER 75 PL 58B 201 F. Wagner, M. Tabak, D.M. Chew (LBL) JP
DIAZ 74 PRL 32 260 J. Diaz *et al.* (CASE, CMU)
KARSHON 74 PRL 32 852 U. Karshon *et al.* (REHO)
ANTIPOV 73 NP B63 175 Y.M. Antipov *et al.* (CERN, SERP) JP
ANTIPOV 73C NP B63 153 Y.M. Antipov *et al.* (CERN, SERP) JP
CHALOUPKA 73 PL 44B 211 V. Chaloupka *et al.* (CERN)
CONFORTO 73 PL 45B 154 G. Conforto *et al.* (EFI, FNAL, TNTO+)
DEFOIX 73 PL 43B 141 C. Defoix *et al.* (CDEF)
EISENSTEIN 73 PR D7 278 L. Eisenstein *et al.* (ILL)
KEY 73 PRL 30 503 A.W. Key *et al.* (TNTO, EFI, FNAL, WISC)
TOET 73 NP B63 248 D.Z. Toet *et al.* (NIJM, BONN, DURH, TORI)
DAMERI 72 NC 9A 1 M. Dameri *et al.* (GENO, MILA, SACL)
EISENBERG 72 PR D5 15 Y. Eisenberg *et al.* (REHO, SLAC, TELA)
ESPIGAT 72 NP B36 93 P. Espigat *et al.* (CERN, CDEF)
FOLEY 72 PR D6 747 K.J. Foley *et al.* (BNL, CUNY)
ALSTON-... 71 PL 34B 156 M. Alston-Garnjost *et al.* (LRL)
BARNHAM 71 PRL 26 1494 K.W.J. Barnham *et al.* (LBL)
BINNIE 71 PL 36B 257 D.M. Binnie *et al.* (LOIC, SHMP)
BOWEN 71 PRL 26 1663 D.R. Bowen *et al.* (NEAS, STON)
GRAYER 71 PL 34B 333 G. Grayer *et al.* (CERN, MPIM)
ABRAMOVI... 70B NP B23 466 M. Abramovich *et al.* (CERN) JP
ALSTON-... 70 PL 33B 607 M. Alston-Garnjost *et al.* (LRL)
BOECKMANN 70 NP B16 221 K. Boeckmann *et al.* (BONN, DURH, NIJM+)
ASCOLI 68 PRL 20 1321 G. Ascoli *et al.* (ILL) JP
BOESEBECK 68 NP B4 501 K. Boesebeck *et al.* (AACH, BERL, CERN)
CHUNG 68 PR 165 1491 S.U. Chung *et al.* (LRL)
CONTE 67 NC 51A 175 F. Conte *et al.* (GENO, HAMB, MILA, SACL)

OTHER RELATED PAPERS

ALDE 99B PAN 62 421 D. Alde *et al.* (GAMS Collab.)
Translated from YAF 62 462.
JENNI 83 PR D27 1031 P. Jenni *et al.* (SLAC, LBL)
BEHREND 82C PL 114B 378 H.J. Behrend *et al.* (CELLO Collab.)
ADERHOLZ 65 PR 138B 897 M. Aderholz (AACH3, BERL, BIRM, BONN, HAMB+)
ALITTI 65 PL 15 69 J. Alitti *et al.* (SACL, BGNA) JP
CHUNG 65 PRL 15 325 S.U. Chung *et al.* (LRL)
FORINO 65B PL 19 68 A. Forino *et al.* (BGNA, BARI, FIRZ, ORSAY+)
LEFEBVRES 65 PL 19 434 F. Lefebvres *et al.*
SEIDLITZ 65 PRL 15 217 L. Seidlitz, O.I. Dahl, D.H. Miller (LRL)
ADERHOLZ 64 PL 10 226 M. Aderholz *et al.* (AACH3, BERL, BIRM+)
CHUNG 64 PRL 12 621 S.U. Chung *et al.* (LRL)
GOLDHABER 64 PRL 12 336 G. Goldhaber *et al.* (LRL, UCB)
LANDER 64 PRL 13 346A R.L. Lander *et al.* (UCSD)

$f_0(1370)$

$I^G(J^{PC}) = 0^+(0^{++})$

See also the mini-reviews on scalar mesons under $f_0(600)$ and on non-$q\overline{q}$ candidates. (See the index for the page number.)

$f_0(1370)$ T-MATRIX POLE POSITION

Note that $\Gamma \approx 2\ \mathrm{Im}(\sqrt{s_{\mathrm{pole}}})$.

VALUE (MeV)		DOCUMENT ID		TECN	COMMENT
(1200–1500) − *i*(150–250) OUR ESTIMATE					
• • • We do not use the following data for averages, fits, limits, etc. • • •					
$(1373 \pm 15) - i(137 \pm 10)$	[12]	BARGIOTTI	03	OBLX	$\overline{p}p$
$(1302 \pm 17) - i(166 \pm 18)$	[1]	BARBERIS	00C		450 $pp \rightarrow p_f 4\pi p_s$
$(1312 \pm 25 \pm 10) - i(109 \pm 22 \pm 15)$		BARBERIS	99D	OMEG	450 $pp \rightarrow K^+K^-$, $\pi^+\pi^-$
$(1406 \pm 19) - i(80 \pm 6)$	[2]	KAMINSKI	99	RVUE	$\pi\pi \rightarrow \pi\pi$, $K\overline{K}$, $\sigma\sigma$
$(1300 \pm 20) - i(120 \pm 20)$		ANISOVICH	98B	RVUE	Compilation
$(1290 \pm 15) - i(145 \pm 15)$		BARBERIS	97B	OMEG	450 $pp \rightarrow$ $pp2(\pi^+\pi^-)$
$(1548 \pm 40) - i(560 \pm 40)$		BERTIN	97C	OBLX	0.0 $\overline{p}p \rightarrow \pi^+\pi^-\pi^0$
$(1380 \pm 40) - i(180 \pm 25)$		ABELE	96B	CBAR	0.0 $\overline{p}p \rightarrow \pi^0 K_L^0 K_L^0$
$(1300 \pm 15) - i(115 \pm 8)$		BUGG	96	RVUE	
$(1330 \pm 50) - i(150 \pm 40)$	[3]	AMSLER	95B	CBAR	$\overline{p}p \rightarrow 3\pi^0$
$(1360 \pm 35) - i(150–300)$	[3]	AMSLER	95C	CBAR	$\overline{p}p \rightarrow \pi^0\eta\eta$
$(1390 \pm 30) - i(190 \pm 40)$	[4]	AMSLER	95D	CBAR	$\overline{p}p \rightarrow 3\pi^0, \pi^0\eta\eta$, $\pi^0\pi^0\eta$
$1346 - i249$	[5,6]	JANSSEN	95	RVUE	$\pi\pi \rightarrow \pi\pi$, $K\overline{K}$
$1214 - i168$	[6,7]	TORNQVIST	95	RVUE	$\pi\pi \rightarrow \pi\pi$, $K\overline{K}$, $K\pi$, $\eta\pi$
$1364 - i139$		AMSLER	94D	CBAR	$\overline{p}p \rightarrow \pi^0\pi^0\eta$
$(1365^{+20}_{-55}) - i(134 \pm 35)$		ANISOVICH	94	CBAR	$\overline{p}p \rightarrow 3\pi^0, \pi^0\eta\eta$
$(1340 \pm 40) - i(127^{+30}_{-20})$	[8]	BUGG	94	RVUE	$\overline{p}p \rightarrow 3\pi^0, \eta\eta\pi^0$, $\eta\pi^0\pi^0$
$(1430 \pm 5) - i(73 \pm 13)$	[9]	KAMINSKI	94	RVUE	$\pi\pi \rightarrow \pi\pi$, $K\overline{K}$
$1515 - i214$	[6,10]	ZOU	93	RVUE	$\pi\pi \rightarrow \pi\pi$, $K\overline{K}$
$1420 - i220$	[11]	AU	87	RVUE	$\pi\pi \rightarrow \pi\pi$, $K\overline{K}$

[1] Average between $\pi^+\pi^- 2\pi^0$ and $2(\pi^+\pi^-)$.
[2] T-matrix pole on sheet − − −.
[3] Supersedes ANISOVICH 94.
[4] Coupled-channel analysis of $\overline{p}p \rightarrow 3\pi^0$, $\pi^0\eta\eta$, and $\pi^0\pi^0\eta$ on sheet IV. Demonstrates explicitly that $f_0(600)$ and $f_0(1370)$ are two different poles.
[5] Analysis of data from FALVARD 88.
[6] The pole is on Sheet III. Demonstrates explicitly that $f_0(600)$ and $f_0(1370)$ are two different poles.
[7] Uses data from BEIER 72B, OCHS 73, HYAMS 73, GRAYER 74, ROSSELET 77, CASON 83, ASTON 88, and ARMSTRONG 91B. Coupled channel analysis with flavor symmetry and all light two-pseudoscalars systems.
[8] Reanalysis of ANISOVICH 94 data.
[9] T-matrix pole on sheet III.
[10] Analysis of data from OCHS 73, GRAYER 74, and ROSSELET 77.
[11] Analysis of data from OCHS 73,GRAYER 74, BECKER 79, and CASON 83.
[12] Coupled channel analysis of $\pi^+\pi^-\pi^0$, $K^+K^-\pi^0$, and $K^\pm K_S^0\pi^\mp$.

$f_0(1370)$ BREIT-WIGNER MASS OR K-MATRIX POLE PARAMETER

VALUE (MeV)	DOCUMENT ID
1200 to 1500 OUR ESTIMATE	

$\pi\pi$ MODE

VALUE (MeV)	EVTS	DOCUMENT ID		TECN	COMMENT
• • • We do not use the following data for averages, fits, limits, etc. • • •					
$1434 \pm 18 \pm 9$	848	AITALA	01A	E791	$D_s^+ \rightarrow \pi^-\pi^+\pi^+$
1308 ± 10		BARBERIS	99B	OMEG	450 $pp \rightarrow p_s p_f \pi^+\pi^-$
1315 ± 50		BELLAZZINI	99	GAM4	450 $pp \rightarrow pp\pi^0\pi^0$
1315 ± 30		ALDE	98	GAM4	100 $\pi^- p \rightarrow \pi^0\pi^0 n$
1280 ± 55		BERTIN	98	OBLX	0.05–0.405 $\overline{n}p \rightarrow$ $\pi^+\pi^+\pi^-$
1186	[13,14]	TORNQVIST	95	RVUE	$\pi\pi \rightarrow \pi\pi$, $K\overline{K}$, $K\pi$, $\eta\pi$
1472 ± 12		ARMSTRONG	91	OMEG	300 $pp \rightarrow pp\pi\pi$, $pp K\overline{K}$
1275 ± 20		BREAKSTONE	90	SFM	62 $pp \rightarrow pp\pi^+\pi^-$
1420 ± 20		AKESSON	86	SPEC	63 $pp \rightarrow pp\pi^+\pi^-$
1256		FROGGATT	77	RVUE	$\pi^+\pi^-$ channel

[13] Uses data from BEIER 72B, OCHS 73, HYAMS 73, GRAYER 74, ROSSELET 77, CASON 83, ASTON 88, and ARMSTRONG 91B. Coupled channel analysis with flavor symmetry and all light two-pseudoscalars systems.
[14] Also observed by ASNER 00 in $\tau^- \rightarrow \pi^-\pi^0\pi^0\nu_\tau$ decays

$K\overline{K}$ MODE

VALUE (MeV)	DOCUMENT ID		TECN	COMMENT
• • • We do not use the following data for averages, fits, limits, etc. • • •				
1391 ± 10	TIKHOMIROV	03	SPEC	40.0 π^- C $\rightarrow K_S^0 K_S^0 K_L^0$ X
1440 ± 50	BOLONKIN	88	SPEC	40 $\pi^- p \rightarrow K_S^0 K_S^0 n$
1463 ± 9	ETKIN	82B	MPS	23 $\pi^- p \rightarrow n 2K_S^0$
1425 ± 15	WICKLUND	80	SPEC	6 $\pi N \rightarrow K^+K^-N$
~ 1300	POLYCHRO...	79	STRC	7 $\pi^- p \rightarrow n 2K_S^0$

4π MODE $2(\pi\pi)_S{+}\rho\rho$

VALUE (MeV)	DOCUMENT ID		TECN	COMMENT
• • • We do not use the following data for averages, fits, limits, etc. • • •				
1395 ± 40	ABELE	01	CBAR	0.0 $\overline{p}d \rightarrow \pi^- 4\pi^0 p$
1374 ± 38	AMSLER	94	CBAR	0.0 $\overline{p}p \rightarrow \pi^+\pi^- 3\pi^0$
1345 ± 12	ADAMO	93	OBLX	$\overline{n}p \rightarrow 3\pi^+ 2\pi^-$
1386 ± 30	GASPERO	93	DBC	0.0 $\overline{p}n \rightarrow 2\pi^+ 3\pi^-$

$\eta\eta$ MODE

VALUE (MeV)	DOCUMENT ID		TECN	COMMENT
• • • We do not use the following data for averages, fits, limits, etc. • • •				
1430	AMSLER	92	CBAR	0.0 $\overline{p}p \rightarrow \pi^0\eta\eta$
1220 ± 40	ALDE	86D	GAM4	100 $\pi^- p \rightarrow n 2\eta$

COUPLED CHANNEL MODE

VALUE (MeV)	DOCUMENT ID		TECN
• • • We do not use the following data for averages, fits, limits, etc. • • •			
1306 ± 20	[15] ANISOVICH	03	RVUE

[15] K-matrix pole from combined analysis of $\pi^- p \rightarrow \pi^0\pi^0 n$, $\pi^- p \rightarrow K\overline{K} n$, $\pi^+\pi^- \rightarrow \pi^+\pi^-$, $\overline{p}p \rightarrow \pi^0\pi^0\pi^0$, $\pi^0\eta\eta$, $\pi^0\pi^0\eta$, $\pi^+\pi^-\pi^0$, $K^+K^-\pi^0$, $K_S^0 K_S^0\pi^0$, $K^+K_S^0\pi^-$ at rest, $\overline{p}n \rightarrow \pi^-\pi^-\pi^+$, $K_S^0 K^-\pi^0$, $K_S^0 K_S^0\pi^-$ at rest.

$f_0(1370)$ BREIT-WIGNER WIDTH

VALUE (MeV)	DOCUMENT ID
200 to 500 OUR ESTIMATE	

$\pi\pi$ MODE

VALUE (MeV)	EVTS	DOCUMENT ID		TECN	COMMENT
• • • We do not use the following data for averages, fits, limits, etc. • • •					
$173 \pm 32 \pm 6$	848	AITALA	01A	E791	$D_s^+ \to \pi^-\pi^+\pi^+$
222 ± 20		BARBERIS	99B	OMEG	450 $pp \to p_s p_f \pi^+\pi^-$
255 ± 60		BELLAZZINI	99	GAM4	450 $pp \to pp\pi^0\pi^0$
190 ± 50		ALDE	98	GAM4	100 $\pi^- p \to \pi^0\pi^0 n$
323 ± 13		BERTIN	98	OBLX	0.05–0.405 $\overline{n}p \to \pi^+\pi^+\pi^-$
350		[16,17] TORNQVIST	95	RVUE	$\pi\pi \to \pi\pi$, $K\overline{K}$, $K\pi$, $\eta\pi$
195 ± 33		ARMSTRONG	91	OMEG	300 $pp \to pp\pi\pi$, $pp K\overline{K}$
285 ± 60		BREAKSTONE	90	SFM	62 $pp \to pp\pi^+\pi^-$
460 ± 50		AKESSON	86	SPEC	63 $pp \to pp\pi^+\pi^-$
~ 400		[18] FROGGATT	77	RVUE	$\pi^+\pi^-$ channel

[16] Uses data from BEIER 72B, OCHS 73, HYAMS 73, GRAYER 74, ROSSELET 77, CASON 83, ASTON 88, and ARMSTRONG 91B. Coupled channel analysis with flavor symmetry and all light two-pseudoscalars systems.

[17] Also observed by ASNER 00 in $\tau^- \to \pi^-\pi^0\pi^0\nu_\tau$ decays

[18] Width defined as distance between 45 and 135° phase shift.

$K\overline{K}$ MODE

VALUE (MeV)	DOCUMENT ID		TECN	COMMENT
• • • We do not use the following data for averages, fits, limits, etc. • • •				
55 ± 26	TIKHOMIROV	03	SPEC	40.0 $\pi^- C \to K^0_S K^0_S K^0_L X$
250 ± 80	BOLONKIN	88	SPEC	40 $\pi^- p \to K^0_S K^0_S n$
118^{+138}_{-16}	ETKIN	82B	MPS	23 $\pi^- p \to n 2K^0_S$
160 ± 30	WICKLUND	80	SPEC	6 $\pi N \to K^+K^- N$
~ 150	POLYCHRO...	79	STRC	7 $\pi^- p \to n 2K^0_S$

4π MODE $2(\pi\pi)_S$+$\rho\rho$

VALUE (MeV)	DOCUMENT ID		TECN	COMMENT
• • • We do not use the following data for averages, fits, limits, etc. • • •				
275 ± 55	ABELE	01	CBAR	0.0 $\overline{p}d \to \pi^- 4\pi^0 p$
375 ± 61	AMSLER	94	CBAR	0.0 $\overline{p}p \to \pi^+\pi^- 3\pi^0$
398 ± 26	ADAMO	93	OBLX	$\overline{n}p \to 3\pi^+ 2\pi^-$
310 ± 50	GASPERO	93	DBC	0.0 $\overline{p}n \to 2\pi^+ 3\pi^-$

$\eta\eta$ MODE

VALUE (MeV)	DOCUMENT ID		TECN	COMMENT
• • • We do not use the following data for averages, fits, limits, etc. • • •				
250	AMSLER	92	CBAR	0.0 $\overline{p}p \to \pi^0\eta\eta$
320 ± 40	ALDE	86D	GAM4	100 $\pi^- p \to n 2\eta$

COUPLED CHANNEL MODE

VALUE (MeV)	DOCUMENT ID		TECN
• • • We do not use the following data for averages, fits, limits, etc. • • •			
147^{+30}_{-50}	[19] ANISOVICH	03	RVUE

[19] K-matrix pole from combined analysis of $\pi^- p \to \pi^0\pi^0 n$, $\pi^- p \to K\overline{K} n$, $\pi^+\pi^- \to \pi^+\pi^-$, $\overline{p}p \to \pi^0\pi^0\pi^0$, $\pi^0\eta\eta$, $\pi^0\pi^0\eta$, $\pi^+\pi^-\pi^0$, $K^+K^-\pi^0$, $K^0_S K^0_S \pi^0$, $K^+K^0_S\pi^-$ at rest, $\overline{p}n \to \pi^-\pi^-\pi^+$, $K^0_S K^-\pi^0$, $K^0_S K^0_S \pi^-$ at rest.

$f_0(1370)$ DECAY MODES

	Mode	Fraction (Γ_i/Γ)
Γ_1	$\pi\pi$	seen
Γ_2	4π	seen
Γ_3	$4\pi^0$	seen
Γ_4	$2\pi^+2\pi^-$	seen
Γ_5	$\pi^+\pi^-2\pi^0$	seen
Γ_6	$\rho\rho$	dominant
Γ_7	$2(\pi\pi)_S$-wave	seen
Γ_8	$\pi(1300)\pi$	seen
Γ_9	$a_1(1260)\pi$	seen
Γ_{10}	$\eta\eta$	seen
Γ_{11}	$K\overline{K}$	seen
Γ_{12}	$\gamma\gamma$	seen
Γ_{13}	e^+e^-	not seen

$f_0(1370)$ PARTIAL WIDTHS

$\Gamma(\gamma\gamma)$ Γ_{12}

See $\gamma\gamma$ widths under $f_0(600)$ and MORGAN 90.

$\Gamma(e^+e^-)$ Γ_{13}

VALUE (eV)	CL%	DOCUMENT ID		TECN	COMMENT
<20	90	VOROBYEV	88	ND	$e^+e^- \to \pi^0\pi^0$

$f_0(1370)$ BRANCHING RATIOS

$\Gamma(\pi\pi)/\Gamma_{total}$ Γ_1/Γ

VALUE	DOCUMENT ID		TECN	COMMENT
• • • We do not use the following data for averages, fits, limits, etc. • • •				
0.26 ± 0.09	BUGG	96	RVUE	
<0.15	[20] AMSLER	94	CBAR	$\overline{p}p \to \pi^+\pi^- 3\pi^0$
<0.20	GASPERO	93	DBC	0.0 $\overline{p}n \to$ hadrons

[20] Using AMSLER 95B ($3\pi^0$).

$\Gamma(4\pi)/\Gamma_{total}$ $\Gamma_2/\Gamma = (\Gamma_3+\Gamma_4+\Gamma_5)/\Gamma$

VALUE	DOCUMENT ID		TECN	COMMENT
• • • We do not use the following data for averages, fits, limits, etc. • • •				
0.80 ± 0.04	GASPERO	93	DBC	0.0 $\overline{p}n \to$ hadrons

$\Gamma(4\pi^0)/\Gamma_{total}$ Γ_3/Γ

VALUE	DOCUMENT ID		TECN	COMMENT
• • • We do not use the following data for averages, fits, limits, etc. • • •				
seen	ABELE	96	CBAR	0.0 $\overline{p}p \to 5\pi^0$

$\Gamma(2\pi^+2\pi^-)/\Gamma(4\pi)$ $\Gamma_4/\Gamma_2 = \Gamma_4/(\Gamma_3+\Gamma_4+\Gamma_5)$

VALUE	DOCUMENT ID		TECN	COMMENT
• • • We do not use the following data for averages, fits, limits, etc. • • •				
0.420 ± 0.014	[21] GASPERO	93	DBC	0.0 $\overline{p}n \to 2\pi^+ 3\pi^-$

[21] Model-dependent evaluation.

$\Gamma(\pi^+\pi^-2\pi^0)/\Gamma(4\pi)$ $\Gamma_5/\Gamma_2 = \Gamma_5/(\Gamma_3+\Gamma_4+\Gamma_5)$

VALUE	DOCUMENT ID		TECN	COMMENT
• • • We do not use the following data for averages, fits, limits, etc. • • •				
0.512 ± 0.019	[22] GASPERO	93	DBC	0.0 $\overline{p}n \to$ hadrons

[22] Model-dependent evaluation.

$\Gamma(\rho\rho)/\Gamma(2(\pi\pi)_S\text{-wave})$ Γ_6/Γ_7

VALUE	DOCUMENT ID		TECN	COMMENT
• • • We do not use the following data for averages, fits, limits, etc. • • •				
large	BARBERIS	00C		450 $pp \to p_f 4\pi p_s$
1.6 ± 0.2	AMSLER	94	CBAR	$\overline{p}p \to \pi^+\pi^- 3\pi^0$
0.58 ± 0.16	GASPERO	93	DBC	0.0 $\overline{p}n \to 2\pi^+ 3\pi^-$

$\Gamma(2(\pi\pi)_S\text{-wave})/\Gamma(4\pi)$ Γ_7/Γ_2

VALUE	DOCUMENT ID		TECN	COMMENT
• • • We do not use the following data for averages, fits, limits, etc. • • •				
5.6 ± 2.6	[23] ABELE	01	CBAR	0.0 $\overline{p}d \to \pi^- 4\pi^0 p$

$\Gamma(2(\pi\pi)_S\text{-wave})/\Gamma(4\pi)$ Γ_7/Γ_2

VALUE	DOCUMENT ID		TECN	COMMENT
• • • We do not use the following data for averages, fits, limits, etc. • • •				
0.51 ± 0.09	ABELE	01B	CBAR	0.0 $\overline{p}n \to 5\pi$

$\Gamma(\rho\rho)/\Gamma(4\pi)$ Γ_6/Γ_2

VALUE	DOCUMENT ID		TECN	COMMENT
• • • We do not use the following data for averages, fits, limits, etc. • • •				
0.26 ± 0.07	ABELE	01B	CBAR	0.0 $\overline{p}n \to 5\pi$

$\Gamma(\pi(1300)\pi)/\Gamma(4\pi)$ Γ_8/Γ_2

VALUE	DOCUMENT ID		TECN	COMMENT
• • • We do not use the following data for averages, fits, limits, etc. • • •				
0.17 ± 0.06	ABELE	01B	CBAR	0.0 $\overline{p}n \to 5\pi$

$\Gamma(a_1(1260)\pi)/\Gamma(4\pi)$ Γ_9/Γ_2

VALUE	DOCUMENT ID		TECN	COMMENT
• • • We do not use the following data for averages, fits, limits, etc. • • •				
0.06 ± 0.02	ABELE	01B	CBAR	0.0 $\overline{p}n \to 5\pi$

$\Gamma(K\overline{K})/\Gamma_{total}$ Γ_{11}/Γ

VALUE	DOCUMENT ID		TECN
• • • We do not use the following data for averages, fits, limits, etc. • • •			
0.35 ± 0.13	BUGG	96	RVUE

$\Gamma(K\overline{K})/\Gamma(\pi\pi)$ Γ_{11}/Γ_1

VALUE	DOCUMENT ID		TECN	COMMENT
• • • We do not use the following data for averages, fits, limits, etc. • • •				
0.91 ± 0.20	[24] BARGIOTTI	03	OBLX	$\overline{p}p$
0.12 ± 0.06	[25] ANISOVICH	02D	SPEC	Combined fit
$0.46 \pm 0.15 \pm 0.11$	BARBERIS	99D	OMEG	450 $pp \to K^+K^-$, $\pi^+\pi^-$

Meson Particle Listings

$f_0(1370)$, $h_1(1380)$, $\pi_1(1400)$

$\Gamma(\eta\eta)/\Gamma(4\pi)$ **$\Gamma_{10}/\Gamma_2 = \Gamma_{10}/(\Gamma_3+\Gamma_4+\Gamma_5)$**

VALUE	DOCUMENT ID		TECN	COMMENT
• • • We do not use the following data for averages, fits, limits, etc. • • •				
$(28 \pm 11) \times 10^{-3}$	[25] ANISOVICH	02D	SPEC	Combined fit
$(4.7 \pm 2.0) \times 10^{-3}$	BARBERIS	00E		450 $pp \to p_f \eta\eta p_s$

[23] From the combined data of ABELE 96 and ABELE 96C.
[24] Coupled channel analysis of $\pi^+\pi^-\pi^0$, $K^+K^-\pi^0$, and $K^\pm K^0_S\pi^\mp$.
[25] From a combined K-matrix analysis of Crystal Barrel (0. $p\overline{p} \to \pi^0\pi^0\pi^0$, $\pi^0\eta\eta$, $\pi^0\pi^0\eta$), GAMS ($\pi p \to \pi^0\pi^0 n$, $\eta\eta n$, $\eta\eta' n$), and BNL ($\pi p \to K\overline{K} n$) data.

$f_0(1370)$ REFERENCES

ANISOVICH	03	EPJ A16 229	V.V. Anisovich *et al.*	
BARGIOTTI	03	EPJ C26 371	M. Bargiotti *et al.*	(OBELIX Collab.)
TIKHOMIROV	03	PAN 66 828	G.D. Tikhomirov *et al.*	
		Translated from YAF 66 860.		
ANISOVICH	02D	PAN 65 1545	V.V. Anisovich *et al.*	
		Translated from YAF 65 1583.		
ABELE	01	EPJ C19 667	A. Abele *et al.*	(Crystal Barrel Collab.)
ABELE	01B	EPJ C21 261	A. Abele *et al.*	(Crystal Barrel Collab.)
AITALA	01A	PRL 86 765	E.M. Aitala *et al.*	(FNAL E791 Collab.)
ASNER	00	PR D61 012002	D.M. Asner *et al.*	(CLEO Collab.)
BARBERIS	00C	PL B471 440	D. Barberis *et al.*	(WA 102 Collab.)
BARBERIS	00E	PL B479 59	D. Barberis *et al.*	(WA 102 Collab.)
BARBERIS	99B	PL B453 316	D. Barberis *et al.*	(Omega Expt.)
BARBERIS	99D	PL B462 462	D. Barberis *et al.*	(Omega Expt.)
BELLAZZINI	99	PL B467 296	R. Bellazzini *et al.*	
KAMINSKI	99	EPJ C9 141	R. Kaminski, L. Lesniak, B. Loiseau	(CRAC, PARIN)
ALDE	98	EPJ A3 361	D. Alde *et al.*	(GAM4 Collab.)
Also	99	PAN 62 405	D. Alde *et al.*	(GAMS Collab.)
		Translated from YAF 62 446.		
ANISOVICH	98B	UFN 41 419	V.V. Anisovich *et al.*	
BERTIN	98	PR D57 55	A. Bertin *et al.*	(OBELIX Collab.)
BARBERIS	97B	PL B413 217	D. Barberis *et al.*	(WA 102 Collab.)
BERTIN	97C	PL B408 476	A. Bertin *et al.*	(OBELIX Collab.)
ABELE	96	PL B380 453	A. Abele *et al.*	(Crystal Barrel Collab.)
ABELE	96B	PL B385 425	A. Abele *et al.*	(Crystal Barrel Collab.)
ABELE	96C	NP A609 562	A. Abele *et al.*	(Crystal Barrel Collab.)
BUGG	96	NP B471 59	D.V. Bugg, A.V. Sarantsev, B.S. Zou	(LOQM, PNPI)
AMSLER	95B	PL B342 433	C. Amsler *et al.*	(Crystal Barrel Collab.)
AMSLER	95C	PL B353 571	C. Amsler *et al.*	(Crystal Barrel Collab.)
AMSLER	95D	PL B355 425	C. Amsler *et al.*	(Crystal Barrel Collab.)
JANSSEN	95	PR D52 2690	G. Janssen *et al.*	(STON, ADLD, JULI)
TORNQVIST	95	ZPHY C68 647	N.A. Tornqvist	(HELS)
AMSLER	94	PL B322 431	C. Amsler *et al.*	(Crystal Barrel Collab.) JPC
AMSLER	94D	PL B333 277	C. Amsler *et al.*	(Crystal Barrel Collab.)
ANISOVICH	94	PL B323 233	V.V. Anisovich *et al.*	(Crystal Barrel Collab.) JPC
BUGG	94	PR D50 4412	D.V. Bugg *et al.*	(LOQM)
KAMINSKI	94	PR D50 3145	R. Kaminski, L. Lesniak, J.P. Maillet	(CRAC+)
ADAMO	93	NP A558 13C	A. Adamo *et al.*	(OBELIX Collab.) JPC
GASPERO	93	NP A562 407	M. Gaspero	(ROMA1) JPC
ZOU	93	PR D48 3948	B.S. Zou, D.V. Bugg	(LOQM)
AMSLER	92	PL B291 347	C. Amsler *et al.*	(Crystal Barrel Collab.)
ARMSTRONG	91	ZPHY C51 351	T.A. Armstrong *et al.*	(ATHU, BARI, BIRM+)
ARMSTRONG	91B	ZPHY C52 389	T.A. Armstrong *et al.*	(ATHU, BARI, BIRM+)
BREAKSTONE	90	ZPHY C48 569	A.M. Breakstone *et al.*	(ISU, BGNA, CERN+)
MORGAN	90	ZPHY C48 623	D. Morgan, M.R. Pennington	(RAL, DURH)
ASTON	88	NP B296 493	D. Aston *et al.*	(SLAC, NAGO, CINC, INUS)
BOLONKIN	88	NP B309 426	B.V. Bolonkin *et al.*	(ITEP, SERP)
FALVARD	88	PR D38 2706	A. Falvard *et al.*	(CLER, FRAS, LALO+)
VOROBYEV	88	SJNP 48 273	P.V. Vorobiev *et al.*	(NOVO)
		Translated from YAF 48 436.		
AU	87	PR D35 1633	K.L. Au, D. Morgan, M.R. Pennington	(DURH, RAL)
AKESSON	86	NP B264 154	T. Akesson *et al.*	(Axial Field Spec. Collab.)
ALDE	86D	NP B269 485	D.M. Alde *et al.*	(BELG, LAPP, SERP, CERN+)
CASON	83	PR D28 1586	N.M. Cason *et al.*	(NDAM, ANL)
ETKIN	82B	PR D25 1786	A. Etkin *et al.*	(BNL, CUNY, TUFTS, VAND)
WICKLUND	80	PRL 45 1469	A.B. Wicklund *et al.*	(ANL)
BECKER	79	NP B151 46	H. Becker *et al.*	(MPIM, CERN, ZEEM, CRAC)
POLYCHRO...	79	PR D19 1317	V.A. Polychronakos *et al.*	(NDAM, ANL)
FROGGATT	77	NP B129 89	C.D. Froggatt, J.L. Petersen	(GLAS, NORD)
ROSSELET	77	PR D15 574	L. Rosselet *et al.*	(GEVA, SACL)
GRAYER	74	NP B75 189	G. Grayer *et al.*	(CERN, MPIM)
HYAMS	73	NP B64 134	B.D. Hyams *et al.*	(CERN, MPIM)
OCHS	73	Thesis	W. Ochs	(MPIM, MUNI)
BEIER	72B	PRL 29 511	E.W. Beier *et al.*	(PENN)

OTHER RELATED PAPERS

ANISOVICH	03B	PAN 66 741	V.V. Anisovich, V.A. Nikonov, A.V. Sarantsev	
		Translated from YAF 66 772.		
ANISOVICH	03D	PAN 66 928	V.V. Anisovich, A.V. Sarantsev	
		Translated from YAF 66 960.		
GARMASH	02	PR D65 092005	A. Garmash *et al.*	(BELLE Collab.)
JIN	02	PR D66 057505	H. Jin, X. Zhang	
KLEEFELD	02	PR D66 034007	F. Kleefeld, E. van Beveren, G. Rupp	
RUPP	02	PR D65 078501	G. Rupp, E. vanBeveren, M.D. Scadron	
SHAKIN	02	PR D65 078502	C.M. Shakin, H. Wang	
TESHIMA	02	JPG 28 1391	T. Teshima, I. Kitamura, N. Morisita	
VOLKOV	02	PAN 65 1657	M.K. Volkov, V.L. Yudichev	
		Translated from YAF 65 1701.		
KOPP	01	PR D63 092001	S. Kopp *et al.*	(CLEO Collab.)
LI	01B	EPJ C19 529	D.-M. Li, H. Yu, Q.-X. Shen	
SUROVTSEV	01	PR D63 054024	Y.S. Surovtsev, D. Krupa, M. Nagy	
AKHMETSHIN	00C	PL B476 33	R.R. Akhmetshin *et al.*	(Novosibirsk CMD-2 Collab.)
KAMINSKI	00	APP B31 895	R. Kaminski, L. Lesniak, K. Rybicki	
SADOVSKY	00	NP A655 131c	S.A. Sadovsky	
BEVEREN	99	EPJ C10 469	E. Van Beveren, G. Rupp	
ISHIDA	99	PTP 101 661	M. Ishida	
MINKOWSKI	99	EPJ C9 283	P. Minkowski, W. Ochs	
ACHASOV	98D	PAN 61 224	N.N. Achasov, V.V. Gubin	
ACHASOV	98E	PR D58 054011	N.N. Achasov, G.N. Shestakov	
AMSLER	98	RMP 70 1293	C. Amsler	
ANISOVICH	98	PL B437 209	V.V. Anisovich *et al.*	
BLACK	98	PR D58 054012	D. Black *et al.*	
LOCHER	98	EPJ C4 317	M.P. Locher *et al.*	(PSI)
NARISON	98	NP B509 312	S. Narison	
ANISOVICH	97	PL B395 123	A.V. Anisovich, A.V. Sarantsev	(PNPI)
KAMINSKI	97	ZPHY C74 79	R. Kaminski, L. Lesniak, K. Rybicki	(CRAC)
PROKOSHKIN	97	SPD 42 117	Y.D. Prokoshkin *et al.*	(SERP)
		Translated from DANS 353 323.		
TORNQVIST	96	PRL 76 1575	N.A. Tornqvist, M. Roos	(HELS)
GASPERO	95	NP A588 861	M. Gaspero	(ROMA)
KLEMPT	95	PL B361 160	E. Klempt *et al.*	
ZOU	94B	PR D50 591	B.S. Zou, D.V. Bugg	(LOQM)
CLOSE	93A	PL B319 291	F.E. Close *et al.*	
CLOSE	93B	NP B389 513	F.E. Close, N. Isgur, S. Kumano	
MORGAN	93	PR D48 1185	D. Morgan, M.R. Pennington	(RAL, DURH)
LI	91	PR D43 2161	Z.P. Li *et al.*	(TENN)
BARNES	85	PL B165 434	T. Barnes	
BIZZARRI	69	NP B14 169	R. Bizzarri *et al.*	(CERN, CDEF)
BETTINI	66	NC 42A 695	A. Bettini *et al.*	(PADO, PISA)

$h_1(1380)$ $I^G(J^{PC}) = ?^-(1^{+-})$

OMITTED FROM SUMMARY TABLE
Seen in partial-wave analysis of the $K\overline{K}\pi$ system. Needs confirmation.

$h_1(1380)$ MASS

VALUE (MeV)	DOCUMENT ID		TECN	COMMENT
1386±19 OUR AVERAGE				
1440±60	ABELE	97H	CBAR	$\overline{p}p \to K^0_L K^0_S \pi^0 \pi^0$
1380±20	ASTON	88C	LASS	11 $K^- p \to K^0_S K^\pm \pi^\mp \Lambda$

$h_1(1380)$ WIDTH

VALUE (MeV)	DOCUMENT ID		TECN	COMMENT
91±30 OUR AVERAGE Error includes scale factor of 1.1.				
170±80	ABELE	97H	CBAR	$\overline{p}p \to K^0_L K^0_S \pi^0 \pi^0$
80±30	ASTON	88C	LASS	11 $K^- p \to K^0_S K^\pm \pi^\mp \Lambda$

$h_1(1380)$ DECAY MODES

	Mode
Γ_1	$K\overline{K}^*(892)+$ c.c.

$h_1(1380)$ REFERENCES

ABELE	97H	PL B415 280	A. Abele *et al.*	(Crystal Barrel Collab.)
ASTON	88C	PL B201 573	D. Aston *et al.*	(SLAC, NAGO, CINC, INUS)

$\pi_1(1400)$ $I^G(J^{PC}) = 1^-(1^{-+})$

See also the mini-review under non-$q\overline{q}$ candidates. (See the index for the page number.)

$\pi_1(1400)$ MASS

VALUE (MeV)			DOCUMENT ID		TECN	CHG	COMMENT
1376 ±17 OUR AVERAGE							
1360	±25		ABELE	99	CBAR		0.0 $\overline{p}p \to \pi^0\pi^0\eta$
1400	±20	±20	ABELE	98B	CBAR		0.0 $\overline{p}n \to \pi^-\pi^0\eta$
1370	±16	$^{+50}_{-30}$	[1] THOMPSON	97	MPS		18 $\pi^- p \to \eta\pi^- p$
• • • We do not use the following data for averages, fits, limits, etc. • • •							
1323.1	± 4.6		[2] AOYAGI	93	BKEI		$\pi^- p \to \eta\pi^- p$
1406	±20		[3] ALDE	88B	GAM4	0	100 $\pi^- p \to \eta\pi^0 n$

[1] Natural parity exchange, questioned by DZIERBA 03.
[2] Unnatural parity exchange.
[3] Seen in the P_0-wave intensity of the $\eta\pi^0$ system, unnatural parity exchange.

$\pi_1(1400)$ WIDTH

VALUE (MeV)			DOCUMENT ID		TECN	CHG	COMMENT
300 ±40 OUR AVERAGE							
220	±90		ABELE	99	CBAR		0.0 $\overline{p}p \to \pi^0\pi^0\eta$
310	±50	$^{+50}_{-30}$	ABELE	98B	CBAR		0.0 $\overline{p}n \to \pi^-\pi^0\eta$
385	±40	$^{+65}_{-105}$	[4] THOMPSON	97	MPS		18 $\pi^- p \to \eta\pi^- p$
• • • We do not use the following data for averages, fits, limits, etc. • • •							
143.2	±12.5		[5] AOYAGI	93	BKEI		$\pi^- p \to \eta\pi^- p$
180	±20		[6] ALDE	88B	GAM4	0	100 $\pi^- p \to \eta\pi^0 n$

[4] Resolution is not unfolded, natural parity exchange, questioned by DZIERBA 03.
[5] Unnatural parity exchange.
[6] Seen in the P_0-wave intensity of the $\eta\pi^0$ system, unnatural parity exchange.

$\pi_1(1400)$ DECAY MODES

	Mode	Fraction (Γ_i/Γ)
Γ_1	$\eta\pi^0$	seen
Γ_2	$\eta\pi^-$	seen
Γ_3	$\eta'\pi$	

$\pi_1(1400)$ BRANCHING RATIOS

$\Gamma(\eta\pi^0)/\Gamma_{total}$ Γ_1/Γ

VALUE	DOCUMENT ID		TECN	CHG	COMMENT
• • • We do not use the following data for averages, fits, limits, etc. • • •					
not seen	PROKOSHKIN	95B	GAM4		$100\ \pi^- p \to \eta\pi^0 n$
not seen	[7] BUGG	94	RVUE		$\overline{p}p \to \eta 2\pi^0$
not seen	[8] APEL	81	NICE	0	$40\ \pi^- p \to \eta\pi^0 n$

[7] Using Crystal Barrel data.

[8] A general fit allowing S, D, and P waves (including m=0) is not done because of limited statistics.

$\Gamma(\eta\pi^-)/\Gamma_{total}$ Γ_2/Γ

VALUE	DOCUMENT ID		TECN	COMMENT
• • • We do not use the following data for averages, fits, limits, etc. • • •				
possibly seen	BELADIDZE	93	VES	$37\pi^- N \to \eta\pi^- N$

$\Gamma(\eta'\pi)/\Gamma(\eta\pi^0)$ Γ_3/Γ_1

VALUE	CL%	DOCUMENT ID		TECN	COMMENT
• • • We do not use the following data for averages, fits, limits, etc. • • •					
<0.80	95	BOUTEMEUR	90	GAM4	$100\ \pi^- p \to 4\gamma n$

$\pi_1(1400)$ REFERENCES

DZIERBA	03	PR D67 094015	A.R. Dzierba *et al.*	
ABELE	99	PL B446 349	A. Abele *et al.*	(Crystal Barrel Collab.)
ABELE	98B	PL B423 175	A. Abele *et al.*	(Crystal Barrel Collab.)
THOMPSON	97	PRL 79 1630	D.R. Thompson *et al.*	(E852 Collab.)
PROKOSHKIN	95B	PAN 58 606 Translated from YAF 58 662.	Y.D. Prokoshkin, S.A. Sadovsky	(SERP)
BUGG	94	PR D50 4412	D.V. Bugg *et al.*	(LOQM)
AOYAGI	93	PL B314 246	H. Aoyagi *et al.*	(BKEI Collab.)
BELADIDZE	93	PL B313 276	G.M. Beladidze *et al.*	(VES Collab.)
BOUTEMEUR	90	Hadron 89 Conf. p 119	M. Boutemeur, M. Poulet	(SERP, BELG, LANL+)
ALDE	88B	PL B205 397	D.M. Alde *et al.*	(SERP, BELG, LANL, LAPP) IGJPC
APEL	81	NP B193 269	W.D. Apel *et al.*	(SERP, CERN)

OTHER RELATED PAPERS

BERNARD	03	PR D68 074505	C. Bernard *et al.*	
JIN	03	PR D67 014025	H.Y. Jin, J.G. Korener, T.G. Steele	
SZCZEPANIAK	03B	PRL 91 092002	A.P. Szczepaniak *et al.*	
ZHANG	03	PR D67 074020	A. Zhang, T.G. Steele	
ACHASOV	02J	PAN 65 552 Translated from YAF 65 579.	N.N. Achasov, G.N. Shestakov	
CHUNG	02C	EPL A15 539	S.U. Chung, E. Klempt, J.G. Korener	
ZHANG	02	PR D65 096005	R. Zhang *et al.*	
IDDIR	01	PL B507 183	F. Iddir, A.S. Safir	
SADOVSKY	00	NP A655 131c	S.A. Sadovsky	
ALDE	99B	PAN 62 421 Translated from YAF 62 462.	D. Alde *et al.*	(GAMS Collab.)
CHUNG	99	PR D60 092001	S.U. Chung *et al.*	(BNL E852 Collab.)
DONNACHIE	98	PR D58 114012	A. Donnachie *et al.*	
LACOCK	97	PL B401 308	P. Lacock *et al.*	(EDIN, LIVP)
SVEC	97C	PR D56 4355	M. Svec	(MCGI)
PROKOSHKIN	95C	PAN 58 853 Translated from YAF 58 921.	Y.D. Prokoshkin, S.A. Sadovsky	(SERP)
KALASHNIK...	94	ZPHY C62 323	Y.S. Kalashnikova	(ITEP)
TUAN	88	PL B213 537	S.F. Tuan, T. Ferbel, R.H. Dalitz	(HAWA, ROCH+)
ZIELINSKI	87	ZPHY C34 255	M. Zielinski	(ROCH)

$\eta(1405)$
was $\eta(1440)$

$I^G(J^{PC}) = 0^+(0^{-+})$

THE $\eta(1405)$, $\eta(1475)$, $f_1(1420)$, AND $f_1(1510)$

Revised December 2003 by M. Aguilar-Benitez (CIEMAT), C. Amsler (Zürich), and A. Masoni (INFN Cagliari).

A pseudoscalar meson decaying into $K\overline{K}\pi$ was first observed in the 1400–1500 mass region in $p\overline{p}$ annihilation at rest into $(K\overline{K}\pi)\pi^+\pi^-$ (BAILLON 67). This state was reported to decay through $a_0(980)\pi$ and $K^*(892)\overline{K}$ with roughly equal contributions. It was then observed in radiative $J/\psi(1S)$ decay into $K\overline{K}\pi$ (SCHARRE 80, EDWARDS 82E, AUGUSTIN 90). This meson was previously called $\eta(1440)$. However, there is now evidence for the existence of two pseudoscalars in this mass region, and accordingly, we have split the $\eta(1440)$ into $\eta(1405)$ and $\eta(1475)$. The former decays mainly through $a_0(980)\pi$ (or direct $K\overline{K}\pi$), and the latter mainly to $K^*(892)\overline{K}$.

The simultaneous observation of two pseudoscalars is reported in three production mechanisms: $\pi^- p$ (RATH 89, ADAMS 01); radiative $J/\psi(1S)$ decay (BAI 90C, AUGUSTIN 92); and $\overline{p}p$ annihilation at rest (BERTIN 95,97, CICALO 99, NICHITIU 02). All of them give values for the masses, widths, and decay modes in reasonable agreement. However, AUGUSTIN 92 finds the state decaying into $K^*(892)\overline{K}$ at a lower mass than the state decaying into $a_0(980)\pi$.

In $J/\psi(1S)$ radiative decay, the $\eta(1405)$ decays into $K\overline{K}\pi$ through $a_0(980)\pi$, and hence, a signal is also expected in the $\eta\pi\pi$ mass spectrum. This was indeed observed by MARK III in $\eta\pi^+\pi^-$ (BOLTON 92B). This state is also observed in $\overline{p}p$ annihilation at rest into $\eta\pi^+\pi^-\pi^0\pi^0$, where it decays into $\eta\pi\pi$ (AMSLER 95F). The intermediate $a_0(980)\pi$ accounts for roughly half of the $\eta\pi\pi$ signal, in agreement with MARK III (BOLTON 92B) and DM2 (AUGUSTIN 90).

The $\eta(1475)$ could be the first radial excitation of the η', with the $\eta(1295)$ being the first radial excitation of the η. Ideal mixing, suggested by the $\eta(1295)$ and $\pi(1300)$ mass degeneracy, would then imply that the second isoscalar in the nonet is mainly $s\overline{s}$, and hence, couples to $K^*\overline{K}$, in agreement with observation. Its width also matches the expected width for the radially excited $s\overline{s}$ state (CLOSE 97, BARNES 97).

An investigation of the $K\overline{K}\pi$ and $\eta\pi\pi$ channels in $\gamma\gamma$ collisions was performed (ACCIARRI 01G). They observed the $\eta(1475)$ in $K\overline{K}\pi$, but not the $\eta(1405)$ in $\eta\pi\pi$. Since gluonium production is presumably suppressed in $\gamma\gamma$ collisions, the ACCIARRI 01G results suggest that this latter state has a large gluonic content (CLOSE 97B, LI 03C). The gluonium interpretation, however, is not favored by lattice gauge theories, which predict the 0^{-+} state above 2 GeV (BALI 93).

Let us now deal with 1^{++} isoscalars. The $f_1(1420)$, decaying to $K^*\overline{K}$, was first reported in $\pi^- p$ reactions at 4 GeV/c (DIONISI 80). However, later analyses found that the 1400–1500 MeV region was far more complex (CHUNG 85, REEVES 86, BIRMAN 88, ADAMS 01). A reanalysis of the MARK III data in

radiative $J/\psi(1S)$ decay to $K\overline{K}\pi$ (BAI 90C) shows the $f_1(1420)$ decaying into $K^*\overline{K}$. Also, a $C=+1$ state is observed in tagged $\gamma\gamma$ collisions (*e.g.*, BEHREND 89).

In $\pi^- p \to \eta\pi\pi n$ charge-exchange reactions at 8–9 GeV/c, the $\eta\pi\pi$ mass spectrum is dominated by the $\eta(1405/1475)$, and $\eta(1295)$ (ANDO 86, FUKUI 91C), and at 100 GeV/c ALDE 97B report $\eta(1295)$ and $\eta(1405/1475)$ decaying to $\eta\pi^0\pi^0$, with a weak $f_1(1285)$ signal and no evidence for the $f_1(1420)$.

Axial (1^{++}) mesons are not observed in $\overline{p}p$ annihilation at rest in liquid hydrogen, which proceeds dominantly through S-wave annihilation. However, in gaseous hydrogen, P-wave annihilation is enhanced, and indeed, BERTIN 97 report the $f_1(1420)$ decaying into $K^*\overline{K}$.

The $f_1(1420)$, decaying into $K\overline{K}\pi$, is also seen in pp central production, together with the $f_1(1285)$. The latter decays via $a_0(980)\pi$, and the former only via $K^*\overline{K}$, while no pseudoscalar is observed (ARMSTRONG 89, BARBERIS 97C). The $K_S K_S \pi^0$ decay mode of the $f_1(1420)$ establishes unambiguously C=+1. On the other hand, there is no evidence for any state decaying into $\eta\pi\pi$ around 1400 MeV, and hence, the $\eta\pi\pi$ mode of the $f_1(1420)$ must be suppressed (ARMSTRONG 91B).

We now turn to the experimental evidence for the $f_1(1510)$. Two states, the $f_1(1420)$ and $f_1(1510)$, decaying to $K^*\overline{K}$, compete for the $s\overline{s}$ assignment in the 1^{++} nonet. The $f_1(1510)$ was seen in $K^- p \to \Lambda K\overline{K}\pi$ at 4 GeV/c (GAVILLET 82) and at 11 GeV/c (ASTON 88C). Evidence is also reported in $\pi^- p$ at 8 GeV/c, based on the phase motion of the 1^{++} $K^*\overline{K}$ wave (BIRMAN 88). The absence of the $f_1(1420)$ in $K^- p$ (ASTON 88C) argues against being the $s\overline{s}$ member of the 1^{++} nonet. However, the $f_1(1420)$ was indeed reported in $K^- p$, but not in $\pi^- p$ (BITYUKOV 84).

Two experiments do not observe the $f_1(1510)$ in $K^- p$ (BITYUKOV 84, KING 91). It is also not seen in radiative $J/\psi(1S)$ decay (BAI 90C, AUGUSTIN 92), central collisions (BARBERIS 97C), or in $\gamma\gamma$ collisions (AIHARA 88C), although, surprisingly for an $s\overline{s}$ state, a signal is reported in 4π decays (BAUER 93B). These facts leads to the conclusion that the $f_1(1510)$ is not well established (CLOSE 97D).

Assigning the $f_1(1420)$ to the 1^{++} nonet, one finds a nonet mixing angle of $\sim 50°$ (CLOSE 97D). However, arguments favoring the $f_1(1420)$ being a hybrid $q\overline{q}g$ meson or a four-quark state were put forward by ISHIDA 89 and by CALDWELL 90, respectively, while LONGACRE 90 argued for a molecular state formed by the π orbiting in a P-wave around an S-wave $K\overline{K}$ state.

Summarizing, there is convincing evidence for the $f_1(1420)$ decaying into $K^*\overline{K}$, and for two pseudoscalars in the 1400-1500 MeV region, the $\eta(1405)$ and $\eta(1475)$, decaying to $a_0(980)\pi$ and $K^*\overline{K}$, respectively. The $f_1(1510)$ is not well established.

References may be found at the end of the $\eta(1405)$, $\eta(1475)$ $f_1(1420)$, and $f_1(1510)$ Listings.

$\eta(1405)$ MASS

VALUE (MeV)	DOCUMENT ID
1410.3±2.6 OUR AVERAGE	Includes data from the 2 datablocks that follow this one. Error includes scale factor of 2.2. See the ideogram below.

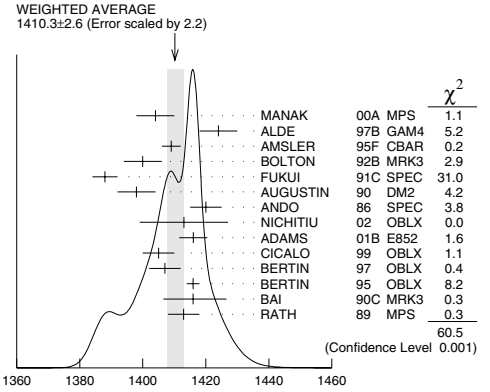

$\eta\pi\pi$ MODE

VALUE (MeV)	EVTS	DOCUMENT ID		TECN	COMMENT
The data in this block is included in the average printed for a previous datablock.					
1405±5 OUR AVERAGE		Error includes scale factor of 2.6. See the ideogram below.			
1404±6	9082	MANAK	00A	MPS	18 $\pi^- p \to \eta\pi^+\pi^- n$
1424±6	2200	ALDE	97B	GAM4	100 $\pi^- p \to \eta\pi^0\pi^0 n$
1409±3		AMSLER	95F	CBAR	0 $\overline{p}p \to \pi^+\pi^-\pi^0\pi^0\eta$
1400±6		[1] BOLTON	92B	MRK3	$J/\psi \to \gamma\eta\pi^+\pi^-$
1388±4		FUKUI	91C	SPEC	8.95 $\pi^- p \to \eta\pi^+\pi^- n$
1398±6	261	[2] AUGUSTIN	90	DM2	$J/\psi \to \gamma\eta\pi^+\pi^-$
1420±5		ANDO	86	SPEC	8 $\pi^- p \to \eta\pi^+\pi^- n$
• • • We do not use the following data for averages, fits, limits, etc. • • •					
1385±7		BAI	99	BES	$J/\psi \to \gamma\pi^+\pi^-$

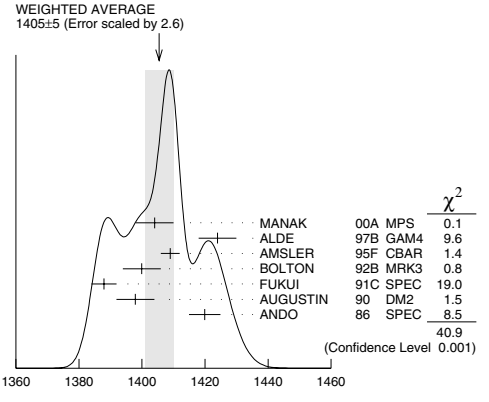

$K\overline{K}\pi$ MODE ($a_0(980)\pi$ or direct $K\overline{K}\pi$)

VALUE (MeV)	EVTS	DOCUMENT ID		TECN	COMMENT
The data in this block is included in the average printed for a previous datablock.					
1413.9± 1.7 OUR AVERAGE		Error includes scale factor of 1.1.			
1413 ±14	3651	[3] NICHITIU	02	OBLX	
1416 ± 4 ±2	20k	ADAMS	01B	E852	18 GeV $\pi^- p \to K^+K^-\pi^0 n$
1405 ± 5		[4] CICALO	99	OBLX	0 $\overline{p}p \to K^\pm K^0_S \pi^\mp \pi^+\pi^-$
1407 ± 5		[4] BERTIN	97	OBLX	0 $\overline{p}p \to K^\pm (K^0)\pi^\mp\pi^+\pi^-$
1416 ± 2		[4] BERTIN	95	OBLX	0 $\overline{p}p \to K\overline{K}\pi\pi\pi$
1416 ± 8 $^{+7}_{-5}$	700	[5] BAI	90C	MRK3	$J/\psi \to \gamma K^0_S K^\pm \pi^\mp$
1413 ± 5		[5] RATH	89	MPS	21.4 $\pi^- p \to n K^0_S K^0_S \pi^0$
• • • We do not use the following data for averages, fits, limits, etc. • • •					
1459 ± 5		[6] AUGUSTIN	92	DM2	$J/\psi \to \gamma K\overline{K}\pi$

$\pi\pi\gamma$ MODE

VALUE (MeV)		DOCUMENT ID		TECN	COMMENT
• • • We do not use the following data for averages, fits, limits, etc. • • •					
1401 ± 18		[7,8] AUGUSTIN	90	DM2	$J/\psi \to \pi^+\pi^-\gamma\gamma$
1432 ± 8		[8] COFFMAN	90	MRK3	$J/\psi \to \pi^+\pi^-2\gamma$

4π MODE

VALUE (MeV)	EVTS	DOCUMENT ID		TECN	COMMENT
• • • We do not use the following data for averages, fits, limits, etc. • • •					
1420 ± 20		BUGG	95	MRK3	$J/\psi \to \gamma\pi^+\pi^-\pi^+\pi^-$
1489 ± 12	3270	[9] BISELLO	89B	DM2	$J/\psi \to 4\pi\gamma$

$K\overline{K}\pi$ MODE (unresolved)

VALUE (MeV)	EVTS	DOCUMENT ID		TECN	COMMENT
• • • We do not use the following data for averages, fits, limits, etc. • • •					
1442 ± 10	410	[10] BAI	98C	BES	$J/\psi \to \gamma K^+K^-\pi^0$
1445 ± 8	693	[10] AUGUSTIN	90	DM2	$J/\psi \to \gamma K^0_S K^\pm\pi^\mp$
1433 ± 8	296	[10] AUGUSTIN	90	DM2	$J/\psi \to \gamma K^+K^-\pi^0$
1413 ± 8	500	[10] DUCH	89	ASTE	$\overline{p}p \to \pi^+\pi^-K^\pm\pi^\mp K^0$
1453 ± 7	170	[10] RATH	89	MPS	$21.4\ \pi^-p \to K^0_S K^0_S\pi^0 n$
1419 ± 1	8800	[10] BIRMAN	88	MPS	$8\ \pi^-p \to K^+\overline{K}{}^0\pi^- n$
1424 ± 3	620	[10] REEVES	86	SPEC	$6.6\ p\overline{p} \to K\overline{K}\pi X$
1421 ± 2		[10] CHUNG	85	SPEC	$8\ \pi^-p \to K\overline{K}\pi n$
1440^{+20}_{-15}	174	[10] EDWARDS	82E	CBAL	$J/\psi \to \gamma K^+K^-\pi^0$
1440^{+10}_{-15}		[10] SCHARRE	80	MRK2	$J/\psi \to \gamma K^0_S K^\pm\pi^\mp$
1425 ± 7	800	[10,11] BAILLON	67	HBC	$0\ \overline{p}p \to K\overline{K}\pi\pi\pi$

[1] From fit to the $a_0(980)\pi$ 0^{-+} partial wave.
[2] Best fit with a single Breit Wigner.
[3] Decaying dominantly directly to $K^+K^-\pi^0$.
[4] Decaying into $(K\overline{K})_S\pi$, $(K\pi)_S\overline{K}$, and $a_0(980)\pi$.
[5] From fit to the $a_0(980)\pi$ 0^{-+} partial wave. Cannot rule out a $a_0(980)\pi$ 1^{++} partial wave.
[6] Excluded from averaging because averaging would be meaningless.
[7] Best fit with a single Breit Wigner.
[8] This peak in the $\gamma\rho$ channel may not be related to the $\eta(1405)$.
[9] Estimated by us from various fits.
[10] These experiments identify only one pseudoscalar in the 1400–1500 range. Data could also refer to $\eta(1475)$.
[11] From best fit of 0^{-+} partial wave , 50% $K^*(892)K$, 50% $a_0(980)\pi$.

$\eta(1405)$ WIDTH

VALUE (MeV)	DOCUMENT ID
51 ± 4 OUR AVERAGE Includes data from the 2 datablocks that follow this one. Error includes scale factor of 2.2. See the ideogram below.	

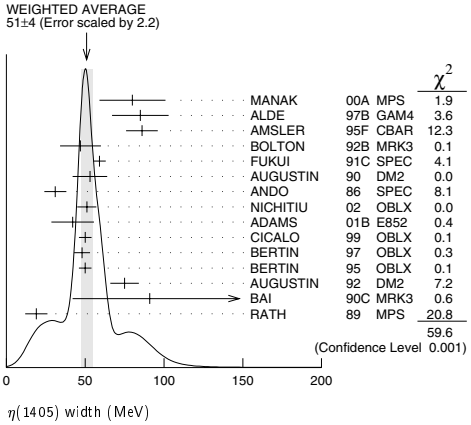

$\eta(1405)$ width (MeV)

$\eta\pi\pi$ MODE

VALUE (MeV)	EVTS	DOCUMENT ID		TECN	COMMENT
The data in this block is included in the average printed for a previous datablock.					
56 ± 6 OUR AVERAGE Error includes scale factor of 2.1. See the ideogram below.					
80 ± 21	9082	MANAK	00A	MPS	$18\ \pi^-p \to \eta\pi^+\pi^- n$
85 ± 18	2200	ALDE	97B	GAM4	$100\ \pi^-p \to \eta\pi^0\pi^0 n$
86 ± 10		AMSLER	95F	CBAR	$0\ \overline{p}p \to \pi^+\pi^-\pi^0\pi^0\eta$
47 ± 13		[12] BOLTON	92B	MRK3	$J/\psi \to \gamma\eta\pi^+\pi^-$
59 ± 4		FUKUI	91C	SPEC	$8.95\ \pi^-p \to \eta\pi^+\pi^- n$
53 ± 11		[13] AUGUSTIN	90	DM2	$J/\psi \to \gamma\eta\pi^+\pi^-$
31 ± 7		ANDO	86	SPEC	$8\ \pi^-p \to \eta\pi^+\pi^- n$

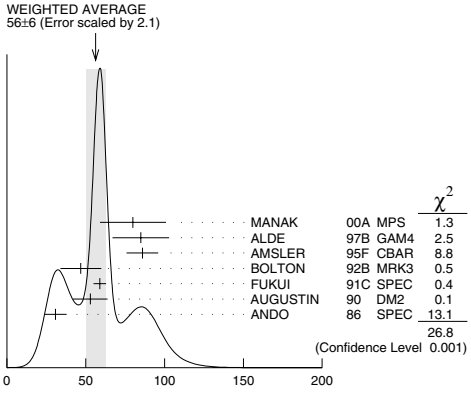

$\eta(1405)$ width $\eta\pi\pi$ mode (MeV)

$K\overline{K}\pi$ MODE ($a_0(980)\pi$ or direct $K\overline{K}\pi$)

VALUE (MeV)	EVTS	DOCUMENT ID		TECN	COMMENT
The data in this block is included in the average printed for a previous datablock.					
48 ± 4 OUR AVERAGE Error includes scale factor of 2.1. See the ideogram below.					
51 ± 6	3651	[14] NICHITIU	02	OBLX	
$42\pm10\pm9$	20k	ADAMS	01B	E852	$18\ \text{GeV}\ \pi^-p \to K^+K^-\pi^0 n$
50 ± 4		CICALO	99	OBLX	$0\ \overline{p}p \to K^\pm K^0_S\pi^\mp\pi^+\pi^-$
48 ± 5		[15] BERTIN	97	OBLX	$0.0\ \overline{p}p \to K^\pm(K^0)_S\pi^\mp\pi^+\pi^-$
50 ± 4		[15] BERTIN	95	OBLX	$0\ \overline{p}p \to K\overline{K}\pi\pi\pi$
75 ± 9		AUGUSTIN	92	DM2	$J/\psi \to \gamma K\overline{K}\pi$
91^{+67+15}_{-31-38}		[16] BAI	90C	MRK3	$J/\psi \to \gamma K^0_S K^\pm\pi^\mp$
19 ± 7		[16] RATH	89	MPS	$21.4\ \pi^-p \to nK^0_S K^0_S\pi^0$

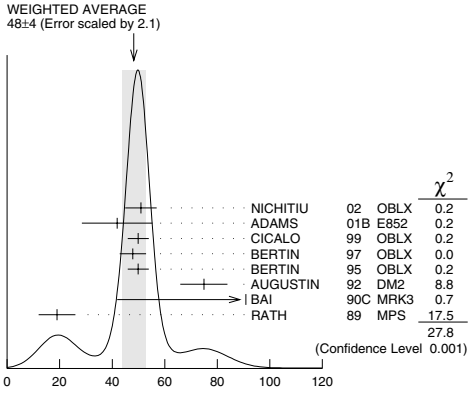

$\eta(1405)$ width $K\overline{K}\pi$ mode ($a_0(980)$ π dominant)

$\pi\pi\gamma$ MODE

VALUE (MeV)	DOCUMENT ID		TECN	COMMENT
• • • We do not use the following data for averages, fits, limits, etc. • • •				
174 ± 44	AUGUSTIN	90	DM2	$J/\psi \to \pi^+\pi^-\gamma\gamma$
90 ± 26	[17] COFFMAN	90	MRK3	$J/\psi \to \pi^+\pi^-2\gamma$

4π MODE

VALUE (MeV)	EVTS	DOCUMENT ID		TECN	COMMENT
• • • We do not use the following data for averages, fits, limits, etc. • • •					
160 ± 30		BUGG	95	MRK3	$J/\psi \to \gamma\pi^+\pi^-\pi^+\pi^-$
144 ± 13	3270	[18] BISELLO	89B	DM2	$J/\psi \to 4\pi\gamma$

$K\overline{K}\pi$ MODE (unresolved)

VALUE (MeV)	EVTS	DOCUMENT ID		TECN	COMMENT
• • • We do not use the following data for averages, fits, limits, etc. • • •					

93±14	296	[19] AUGUSTIN	90	DM2	$J/\psi \to \gamma K^+ K^- \pi^0$
105±10	693	[19] AUGUSTIN	90	DM2	$J/\psi \to \gamma K^0_S K^\pm \pi^\mp$
62±16	500	[19] DUCH	89	ASTE	$\overline{p}p \to K\overline{K}\pi\pi\pi$
100±11	170	[19] RATH	89	MPS	21.4 $\pi^- p \to K^0_S K^0_S \pi^0 n$
66± 2	8800	[19] BIRMAN	88	MPS	8 $\pi^- p \to K^+ \overline{K}^0 \pi^- n$
60±10	620	[19] REEVES	86	SPEC	6.6 $p\overline{p} \to K K \pi X$
60±10		[19] CHUNG	85	SPEC	8 $\pi^- p \to K\overline{K}\pi n$
55^{+20}_{-30}	174	[19] EDWARDS	82E	CBAL	$J/\psi \to \gamma K^+ K^- \pi^0$
50^{+30}_{-20}		[19] SCHARRE	80	MRK2	$J/\psi \to \gamma K^0_S K^\pm \pi^\mp$
80±10	800	[19,20] BAILLON	67	HBC	0.0 $\overline{p}p \to K\overline{K}\pi\pi\pi$

[12] From fit to the $a_0(980)\,\pi\ 0^{-+}$ partial wave.
[13] From $\eta\pi^+\pi^-$ mass distribution - mainly $a_0(980)\pi$ - no spin–parity determination available.
[14] Decaying dominantly directly to $K^+K^-\pi^0$.
[15] Decaying into $(K\overline{K})_S\pi$, $(K\pi)_S\overline{K}$, and $a_0(980)\pi$.
[16] From fit to the $a_0(980)\,\pi\ 0^{-+}$ partial wave, but $a_0(980)\,\pi\ 1^{++}$ cannot be excluded.
[17] This peak in the $\gamma\rho$ channel may not be related to the $\eta(1405)$.
[18] Estimated by us from various fits.
[19] These experiments identify only one pseudoscalar in the 1400–1500 range. Data could also refer to $\eta(1475)$.
[20] From best fit to 0^{-+} partial wave, 50% $K^*(892)K$, 50% $a_0(980)\pi$.

$\eta(1405)$ DECAY MODES

	Mode	Fraction (Γ_i/Γ)
Γ_1	$K\overline{K}\pi$	seen
Γ_2	$\eta\pi\pi$	seen
Γ_3	$a_0(980)\pi$	seen
Γ_4	$\eta(\pi\pi)_{S\text{-wave}}$	seen
Γ_5	$f_0(980)\eta$	seen
Γ_6	4π	seen
Γ_7	$\gamma\gamma$	
Γ_8	$\rho^0\gamma$	
Γ_9	$K^*(892)K$	seen

$\eta(1405)$ $\Gamma(i)\Gamma(\gamma\gamma)/\Gamma(\text{total})$

$\Gamma(\eta\pi\pi) \times \Gamma(\gamma\gamma)/\Gamma_{\text{total}}$ $\Gamma_2\Gamma_7/\Gamma$

VALUE (keV)	CL%	DOCUMENT ID	TECN	COMMENT
< 0.095	95	ACCIARRI	01G L3	183–202 $e^+e^- \to e^+e^-\eta\pi^+\pi^-$

$\Gamma(\rho^0\gamma) \times \Gamma(\gamma\gamma)/\Gamma_{\text{total}}$ $\Gamma_8\Gamma_7/\Gamma$

VALUE (keV)	CL%	DOCUMENT ID	TECN	COMMENT
• • • We do not use the following data for averages, fits, limits, etc. • • •				
< 1.5	95	ALTHOFF	84E TASS	$e^+e^- \to e^+e^-\pi^+\pi^-\gamma$

$\eta(1405)$ BRANCHING RATIOS

$\Gamma(\eta\pi\pi)/\Gamma(K\overline{K}\pi)$ Γ_2/Γ_1

VALUE	CL%	DOCUMENT ID	TECN	COMMENT
• • • We do not use the following data for averages, fits, limits, etc. • • •				
< 0.5	90	EDWARDS	83B CBAL	$J/\psi \to \eta\pi\pi\gamma$
< 1.1	90	SCHARRE	80 MRK2	$J/\psi \to \eta\pi\pi\gamma$
< 1.5	95	FOSTER	68B HBC	0.0 $\overline{p}p$

$\Gamma(a_0(980)\pi)/\Gamma(K\overline{K}\pi)$ Γ_3/Γ_1

VALUE	EVTS	DOCUMENT ID	TECN	COMMENT
• • • We do not use the following data for averages, fits, limits, etc. • • •				
~ 0.15		[21] BERTIN	95 OBLX	0 $\overline{p}p \to K\overline{K}\pi\pi\pi$
~ 0.8	500	[21] DUCH	89 ASTE	$\overline{p}p \to \pi^+\pi^- K^\pm\pi^\mp K^0$
~ 0.75		[21] REEVES	86 SPEC	6.6 $p\overline{p} \to K K \pi X$

$\Gamma(a_0(980)\pi)/\Gamma(\eta\pi\pi)$ Γ_3/Γ_2

VALUE	EVTS	DOCUMENT ID	TECN	COMMENT
• • • We do not use the following data for averages, fits, limits, etc. • • •				
0.29±0.10		ABELE	98E CBAR	0 $p\overline{p} \to \eta\pi^0\pi^0\pi^0$
0.19±0.04	2200	[22] ALDE	97B GAM4	100 $\pi^- p \to \eta\pi^0\pi^0 n$
0.56±0.04±0.03		[22] AMSLER	95F CBAR	0 $\overline{p}p \to \pi^+\pi^-\pi^0\pi^0\eta$

$\Gamma(a_0(980)\pi)/\Gamma(\eta(\pi\pi)_{S\text{-wave}})$ Γ_3/Γ_4

VALUE	EVTS	DOCUMENT ID	TECN	COMMENT
• • • We do not use the following data for averages, fits, limits, etc. • • •				
0.91±0.12		ANISOVICH	01 SPEC	0.0 $\overline{p}p \to \eta\pi^+\pi^-\pi^+\pi^-$
0.15±0.04	9082	MANAK	00A MPS	18 $\pi^- p \to \eta\pi^+\pi^- n$
0.70±0.12±0.20		[23] BAI	99 BES	$J/\psi \to \gamma\eta\pi^+\pi^-$

$\Gamma(\rho^0\gamma)/\Gamma(K\overline{K}\pi)$ Γ_8/Γ_1

VALUE	DOCUMENT ID	TECN	COMMENT
0.0152±0.0038	[24] COFFMAN	90 MRK3	$J/\psi \to \gamma\gamma\pi^+\pi^-$

$\Gamma(\eta(\pi\pi)_{S\text{-wave}})/\Gamma(\eta\pi\pi)$ Γ_4/Γ_2

VALUE	EVTS	DOCUMENT ID	TECN	COMMENT
• • • We do not use the following data for averages, fits, limits, etc. • • •				
0.81±0.04	2200	ALDE	97B GAM4	100 $\pi^- p \to \eta\pi^0\pi^0 n$

$\Gamma(a_0(980)\pi)/\Gamma(\eta(\pi\pi)_{S\text{-wave}})$ Γ_3/Γ_4

VALUE	DOCUMENT ID	TECN	COMMENT
• • • We do not use the following data for averages, fits, limits, etc. • • •			
0.32±0.07	[25] ANISOVICH	99I SPEC	0.9–1.2 $\overline{p}p \to \eta 3\pi^0$

$\Gamma(K^*(892)K)/\Gamma(a_0(980)\pi)$ Γ_9/Γ_3

VALUE	DOCUMENT ID	TECN	COMMENT
• • • We do not use the following data for averages, fits, limits, etc. • • •			
0.084±0.024	[26] ADAMS	01B E852	18 GeV $\pi^- p \to K^+K^-\pi^0 n$

[21] Assuming that the $a_0(980)$ decays only into $K\overline{K}$.
[22] Assuming that the $a_0(980)$ decays only into $\eta\pi$.
[23] Assuming that the $a_0(980)$ decays only into $\eta\pi$.
[24] Using $B(J/\psi \to \gamma\eta(1405) \to \gamma K\overline{K}\pi)=4.2\times10^{-3}$ and $B(J/\psi \to \gamma\eta(1405) \to \gamma\gamma\rho^0)=6.4\times10^{-5}$ and assuming that the $\gamma\rho^0$ signal does not come from the $f_1(1420)$.
[25] Using preliminary Crystal Barrel data.
[26] Statistical error only.

$\eta(1405)$ REFERENCES

NICHITIU	02	PL B545 261	F. Nichitiu *et al.* (OBELIX Collab.)
ACCIARRI	01G	PL B501 1	M. Acciarri *et al.* (L3 Collab.)
ADAMS	01B	PL B516 264	G.S. Adams *et al.* (BNL E852 Collab.)
ANISOVICH	01	NP A690 567	A.V. Anisovich *et al.*
MANAK	00A	PR D62 012003	J.J. Manak *et al.* (BNL E852 Collab.)
ANISOVICH	99I	PL B468 304	A.V. Anisovich *et al.*
BAI	99	PL B446 356	J.Z. Bai *et al.* (BES Collab.)
CICALO	99	PL B462 453	C. Cicalo *et al.* (OBELIX Collab.)
ABELE	98E	NP B514 45	A. Abele *et al.* (Crystal Barrel Collab.)
BAI	98C	PL B440 217	J.Z. Bai *et al.* (BES Collab.)
ALDE	97B	PAN 60 386 Translated from YAF 60 458.	D. Alde *et al.* (GAMS Collab.)
BERTIN	97	PL B400 226	A. Bertin *et al.* (OBELIX Collab.)
AMSLER	95F	PL B358 389	C. Amsler *et al.* (Crystal Barrel Collab.)
BERTIN	95	PL B361 187	A. Bertin *et al.* (OBELIX Collab.)
BUGG	95	PL B353 378	D.V. Bugg *et al.* (LOQM, PNPI, WASH)
AUGUSTIN	92	PR D46 1951	J.E. Augustin, G. Cosme (DM2 Collab.)
BOLTON	92B	PRL 69 1328	T. Bolton *et al.* (Mark III Collab.)
FUKUI	91C	PL B267 293	S. Fukui *et al.* (SUGI, NAGO, KEK, KYOT+)
AUGUSTIN	90	PR D42 10	J.E. Augustin *et al.* (DM2 Collab.)
BAI	90C	PRL 65 2507	Z. Bai *et al.* (Mark III Collab.)
COFFMAN	90	PR D41 1410	D.M. Coffman *et al.* (Mark III Collab.)
BISELLO	89B	PR D39 701	G. Busetto *et al.* (DM2 Collab.)
DUCH	89	ZPHY C45 223	K.D. Duch *et al.* (ASTERIX Collab.) JP
RATH	89	PR D40 693	M.G. Rath *et al.* (NDAM, BRAN, BNL, CUNY+)
BIRMAN	88	PRL 61 1557	A. Birman *et al.* (BNL, FSU, IND, MASD) JP
ANDO	86	PRL 57 1296	A. Ando *et al.* (KEK, KYOT, NIRS, SAGA+) IJP
REEVES	86	PR D34 1960	D.F. Reeves *et al.* (FLOR, BNL, IND+) JP
CHUNG	85	PRL 55 779	S.U. Chung *et al.* (BNL, FLOR, IND+) JP
ALTHOFF	84E	PL 147B 487	M. Althoff *et al.* (TASSO Collab.)
EDWARDS	83B	PRL 51 859	C. Edwards *et al.* (CIT, HARV, PRIN+)
EDWARDS	82E	PRL 49 259	C. Edwards *et al.* (CIT, HARV, PRIN+)
Also	83	PRL 50 219	C. Edwards *et al.* (CIT, HARV, PRIN+)
SCHARRE	80	PL 97B 329	D.L. Scharre *et al.* (SLAC, LBL)
FOSTER	68B	NP B8 174	M. Foster *et al.* (CERN, CDEF)
BAILLON	67	NC 50A 393	P.H. Baillon *et al.* (CERN, CDEF, IRAD)

OTHER RELATED PAPERS

LI	03C	EPJ C28 335	D.M. Li *et al.*
LI	03D	IJMP A18 3335	D.M. Li *et al.*
ANISOVICH	00F	EPJ A6 247	A.V. Anisovich *et al.*
CARVALHO	99	EPJ C7 95	W.S. Carvalho *et al.*
NEKRASOV	98	EPJ C5 507	M.L. Nekrasov
BERTIN	96	PL B385 493	A. Bertin *et al.* (Obelix Collab.)
FARRAR	96	PRL 76 4111	G.R. Farrar (RUTG)
AMELIN	95	ZPHY C66 71	D.V. Amelin *et al.* (VES Collab.)
GENOVESE	94	ZPHY C61 425	M. Genovese, D.B. Lichtenberg, E. Predazzi (TORI+)
BALI	93	PL B309 378	G.S. Bali *et al.* (LIVP)
AHMAD	89	NP B (PROC.)8 50	S. Ahmad *et al.* (ASTERIX Collab.)
ARMSTRONG	89	PL B221 216	T.A. Armstrong *et al.* (CERN, CDEF, BIRM+)
ARMSTRONG	87	ZPHY C34 23	T.A. Armstrong *et al.* (CERN, BIRM, BARI+)
ARMSTRONG	84	PL 146B 273	T.A. Armstrong *et al.* (ATHU, BARI, BIRM+)
DIONISI	80	NP B169 1	C. Dionisi *et al.* (CERN, MADR, CDEF+)
DEFOIX	72	NP B44 125	C. Defoix *et al.* (CDEF, CERN)
DUBOC	72	NP B46 429	J. Duboc *et al.* (PARIS, LIVP)
LORSTAD	69	NP B14 63	B. Lorstad *et al.* (CDEF, CERN)

$f_1(1420)$

$I^G(J^{PC}) = 0^+(1^{++})$

See the minireview under $\eta(1405)$.

$f_1(1420)$ MASS

VALUE (MeV)	EVTS	DOCUMENT ID		TECN	COMMENT
1426.3± 0.9 OUR AVERAGE		Error includes scale factor of 1.1.			
1426 ± 6	711	ABDALLAH	03H	DLPH	91.2 $e^+e^- \to K^0_S K^\pm \pi^\mp + X$
1420 ±14	3651	NICHITIU	02	OBLX	
1428 ± 4 ± 2	20k	ADAMS	01B	E852	18 GeV $\pi^- p \to K^+ K^- \pi^0 n$
1426 ± 1		BARBERIS	97C	OMEG	450 $pp \to pp K^0_S K^\pm \pi^\mp$
1425 ± 8		BERTIN	97	OBLX	0.0 $\overline{p}p \to K^\pm(K^0)\pi^\mp\pi^+\pi^-$
1435 ± 9		PROKOSHKIN	97B	GAM4	100 $\pi^- p \to \eta\pi^0\pi^0 n$
1430 ± 4		[1] ARMSTRONG	92E	OMEG	85,300 $\pi^+ p$, $pp \to \pi^+ p$, $pp(K\overline{K}\pi)$
1462 ±20		[2] AUGUSTIN	92	DM2	$J/\psi \to \gamma K\overline{K}\pi$
1443 $^{+7}_{-6}$ $^{+3}_{-2}$	1100	BAI	90C	MRK3	$J/\psi \to \gamma K^0_S K^\pm \pi^\mp$
1425 ±10	17	BEHREND	89	CELL	$\gamma\gamma \to K^0_S K^\pm \pi^\mp$
1442 ± 5 $^{+10}_{-17}$	111	BECKER	87	MRK3	e^+e^-, $\omega K\overline{K}\pi$
1423 ± 4		GIDAL	87B	MRK2	$e^+e^- \to e^+e^- K\overline{K}\pi$
1417 ±13	13	AIHARA	86C	TPC	$e^+e^- \to e^+e^- K\overline{K}\pi$
1422 ± 3		CHAUVAT	84	SPEC	ISR 31.5 pp
1440 ±10		[3] BROMBERG	80	SPEC	100 $\pi^- p \to K\overline{K}\pi X$
1426 ± 6	221	DIONISI	80	HBC	4 $\pi^- p \to K\overline{K}\pi n$
1420 ±20		DAHL	67	HBC	1.6–4.2 $\pi^- p$
• • • We do not use the following data for averages, fits, limits, etc. • • •					
1430.8± 0.9		[4] SOSA	99	SPEC	$pp \to p_{\rm slow}(K^0_S K^+\pi^-) p_{\rm fast}$
1433.4± 0.8		[4] SOSA	99	SPEC	$pp \to p_{\rm slow}(K^0_S K^-\pi^+) p_{\rm fast}$
1429 ± 3	389	ARMSTRONG	89	OMEG	300 $pp \to K\overline{K}\pi pp$
1425 ± 2	1520	ARMSTRONG	84	OMEG	85 $\pi^+ p$, $pp \to (\pi^+, p)(K\overline{K}\pi)p$
~ 1420		BITYUKOV	84	SPEC	32 $K^- p \to K^+ K^- \pi^0 Y$

[1] This result supersedes ARMSTRONG 84, ARMSTRONG 89.
[2] From fit to the $K^*(892)\,K\ 1^{++}$ partial wave.
[3] Mass error increased to account for $a_0(980)$ mass cut uncertainties.
[4] No systematic error given.

$f_1(1420)$ WIDTH

VALUE (MeV)	EVTS	DOCUMENT ID		TECN	COMMENT
54.9± 2.6 OUR AVERAGE					
51 ±14	711	ABDALLAH	03H	DLPH	91.2 $e^+e^- \to K^0_S K^\pm \pi^\mp + X$
61 ± 8	3651	NICHITIU	02	OBLX	
38 ± 9 ±6	20k	ADAMS	01B	E852	18 GeV $\pi^- p \to K^+ K^- \pi^0 n$
58 ± 4		BARBERIS	97C	OMEG	450 $pp \to pp K^0_S K^\pm \pi^\mp$
45 ±10		BERTIN	97	OBLX	0.0 $\overline{p}p \to K^\pm(K^0)\pi^\mp\pi^+\pi^-$
90 ±25		PROKOSHKIN	97B	GAM4	100 $\pi^- p \to \eta\pi^0\pi^0 n$
58 ±10		[5] ARMSTRONG	92E	OMEG	85,300 $\pi^+ p$, $pp \to \pi^+ p$, $pp(K\overline{K}\pi)$
129 ±41		[6] AUGUSTIN	92	DM2	$J/\psi \to \gamma K\overline{K}\pi$
68 $^{+29}_{-18}$ $^{+8}_{-9}$	1100	BAI	90C	MRK3	$J/\psi \to \gamma K^0_S K^\pm \pi^\mp$
42 ±22	17	BEHREND	89	CELL	$\gamma\gamma \to K^0_S K^\pm \pi^\mp$
40 $^{+17}_{-13}$ ±5	111	BECKER	87	MRK3	$e^+e^- \to \omega K\overline{K}\pi$
35 $^{+47}_{-20}$	13	AIHARA	86C	TPC	$e^+e^- \to e^+e^- K\overline{K}\pi$
47 ±10		CHAUVAT	84	SPEC	ISR 31.5 pp
62 ±14		BROMBERG	80	SPEC	100 $\pi^- p \to K\overline{K}\pi X$
40 ±15	221	DIONISI	80	HBC	4 $\pi^- p \to K\overline{K}\pi n$
60 ±20		DAHL	67	HBC	1.6–4.2 $\pi^- p$
• • • We do not use the following data for averages, fits, limits, etc. • • •					
68.7± 2.9		[7] SOSA	99	SPEC	$pp \to p_{\rm slow}(K^0_S K^+\pi^-) p_{\rm fast}$
58.8± 3.3		[7] SOSA	99	SPEC	$pp \to p_{\rm slow}(K^0_S K^-\pi^+) p_{\rm fast}$
58 ± 8	389	ARMSTRONG	89	OMEG	300 $pp \to K\overline{K}\pi pp$
62 ± 5	1520	ARMSTRONG	84	OMEG	85 $\pi^+ p$, $pp \to (\pi^+, p)(K\overline{K}\pi)p$
~ 50		BITYUKOV	84	SPEC	32 $K^- p \to K^+ K^- \pi^0 Y$

[5] This result supersedes ARMSTRONG 84, ARMSTRONG 89.
[6] From fit to the $K^*(892)\,K\ 1^{++}$ partial wave.
[7] No systematic error given.

$f_1(1420)$ DECAY MODES

	Mode	Fraction (Γ_i/Γ)
Γ_1	$K\overline{K}\pi$	dominant
Γ_2	$K\overline{K}^*(892)+$ c.c.	dominant
Γ_3	$\eta\pi\pi$	possibly seen
Γ_4	$a_0(980)\pi$	
Γ_5	$\pi\pi\rho$	
Γ_6	4π	
Γ_7	$\rho^0\gamma$	
Γ_8	$\phi\gamma$	seen

$f_1(1420)$ $\Gamma(i)\Gamma(\gamma\gamma)/\Gamma(\text{total})$

$\Gamma(K\overline{K}\pi) \times /\Gamma_{\rm total}$ $\Gamma_1\Gamma_0/\Gamma$

VALUE (keV)	CL%	DOCUMENT ID		TECN	COMMENT
1.7±0.4 OUR AVERAGE					
3.0±0.9±0.7		[8,9] BEHREND	89	CELL	$e^+e^- \to e^+e^- K^0_S K\pi$
$2.3^{+1.0}_{-0.9}$±0.8		HILL	89	JADE	$e^+e^- \to e^+e^- K^\pm K^0_S \pi^\mp$
1.3±0.5±0.3		AIHARA	88B	TPC	$e^+e^- \to e^+e^- K^\pm K^0_S \pi^\mp$
1.6±0.7±0.3		[8,10] GIDAL	87B	MRK2	$e^+e^- \to e^+e^- K\overline{K}\pi$
• • • We do not use the following data for averages, fits, limits, etc. • • •					
<8.0	95	JENNI	83	MRK2	$e^+e^- \to e^+e^- K\overline{K}\pi$

[8] Assume a ρ-pole form factor.
[9] A ϕ - pole form factor gives considerably smaller widths.
[10] Published value divided by 2.

$f_1(1420)$ BRANCHING RATIOS

$\Gamma(K\overline{K}^*(892)+\text{c.c.})/\Gamma(K\overline{K}\pi)$ Γ_2/Γ_1

VALUE	DOCUMENT ID		TECN	COMMENT
• • • We do not use the following data for averages, fits, limits, etc. • • •				
0.76±0.06	BROMBERG	80	SPEC	100 $\pi^- p \to K\overline{K}\pi X$
0.86±0.12	DIONISI	80	HBC	4 $\pi^- p \to K\overline{K}\pi n$

$\Gamma(\pi\pi\rho)/\Gamma(K\overline{K}\pi)$ Γ_5/Γ_1

VALUE	CL%	DOCUMENT ID		TECN	COMMENT
• • • We do not use the following data for averages, fits, limits, etc. • • •					
<0.3	95	CORDEN	78	OMEG	12–15 $\pi^- p$
<2.0		DAHL	67	HBC	1.6–4.2 $\pi^- p$

$\Gamma(\eta\pi\pi)/\Gamma(K\overline{K}\pi)$ Γ_3/Γ_1

VALUE	CL%	DOCUMENT ID		TECN	COMMENT
<0.1	95	ARMSTRONG	91B	OMEG	300 $pp \to pp\eta\pi^+\pi^-$
• • • We do not use the following data for averages, fits, limits, etc. • • •					
1.35±0.75		KOPKE	89	MRK3	$J/\psi \to \omega\eta\pi\pi(K\overline{K}\pi)$
<0.6	90	GIDAL	87	MRK2	$e^+e^- \to e^+e^-\eta\pi^+\pi^-$
<0.5	95	CORDEN	78	OMEG	12–15 $\pi^- p$
1.5 ±0.8		DEFOIX	72	HBC	0.7 $\overline{p}p$

$\Gamma(a_0(980)\pi)/\Gamma(\eta\pi\pi)$ Γ_4/Γ_3

VALUE	CL%	DOCUMENT ID		TECN	COMMENT
>0.1	90	PROKOSHKIN	97B	GAM4	100 $\pi^- p \to \eta\pi^0\pi^0 n$
• • • We do not use the following data for averages, fits, limits, etc. • • •					
not seen in either mode		ANDO	86	SPEC	8 $\pi^- p$
not seen in either mode		CORDEN	78	OMEG	12–15 $\pi^- p$
0.4±0.2		DEFOIX	72	HBC	0.7 $\overline{p}p \to 7\pi$

$\Gamma(4\pi)/\Gamma(K\overline{K}^*(892)+\text{c.c.})$ Γ_6/Γ_2

VALUE	CL%	DOCUMENT ID		TECN	COMMENT
• • • We do not use the following data for averages, fits, limits, etc. • • •					
<0.90	95	DIONISI	80	HBC	4 $\pi^- p$

$\Gamma(K\overline{K}\pi)/[\Gamma(K\overline{K}^*(892)+\text{c.c.})+\Gamma(a_0(980)\pi)]$ $\Gamma_1/(\Gamma_2+\Gamma_4)$

VALUE	DOCUMENT ID		TECN	COMMENT
• • • We do not use the following data for averages, fits, limits, etc. • • •				
0.65±0.27	[11] DIONISI	80	HBC	4 $\pi^- p$

[11] Calculated using $\Gamma(K\overline{K})/\Gamma(\eta\pi) = 0.24 \pm 0.07$ for $a_0(980)$ fractions.

$\Gamma(a_0(980)\pi)/\Gamma(K\overline{K}^*(892)+\text{c.c.})$ Γ_4/Γ_2

VALUE	CL%	DOCUMENT ID		TECN	COMMENT
0.04 ±0.01 ±0.01		BARBERIS	98C	OMEG	450 $pp \to p_f f_1(1420) p_s$
• • • We do not use the following data for averages, fits, limits, etc. • • •					
<0.04	68	ARMSTRONG	84	OMEG	85 $\pi^+ p$

$\Gamma(4\pi)/\Gamma(K\overline{K}\pi)$ Γ_6/Γ_1

VALUE	CL%	DOCUMENT ID		TECN	COMMENT
<0.62	95	ARMSTRONG	89G	OMEG	85 $\pi p \to 4\pi X$

$\Gamma(\rho^0\gamma)/\Gamma_{\text{total}}$ Γ_7/Γ

VALUE	CL%	DOCUMENT ID		TECN	COMMENT
<0.08	95	[12] ARMSTRONG	92C	SPEC	300 $pp \to pp\pi^+\pi^-\gamma$

[12] Using the data on the $\overline{K}K\pi$ mode from ARMSTRONG 89.

$\Gamma(\rho^0\gamma)/\Gamma(K\overline{K}\pi)$ Γ_7/Γ_1

VALUE	CL%	DOCUMENT ID		TECN	COMMENT
<0.02	95	BARBERIS	98C	OMEG	450 $pp \to p_f f_1(1420) p_s$

$\Gamma(\phi\gamma)/\Gamma(K\overline{K}\pi)$ Γ_8/Γ_1

VALUE	DOCUMENT ID		TECN	COMMENT
0.003 ±0.001 ±0.001	BARBERIS	98C	OMEG	450 $pp \to p_f f_1(1420) p_s$

$f_1(1420)$ REFERENCES

ABDALLAH	03H	PL B569 129	J. Abdallah *et al.*	(DELPHI Collab.)
NICHITIU	02	PL B545 261	F. Nichitiu *et al.*	(OBELIX Collab.)
ADAMS	01B	PL B516 264	G.S. Adams *et al.*	(BNL E852 Collab.)
SOSA	99	PRL 83 913	M. Sosa *et al.*	
BARBERIS	98C	PL B440 225	D. Barberis *et al.*	(WA 102 Collab.)
BARBERIS	97C	PL B413 225	D. Barberis *et al.*	(WA 102 Collab.)
BERTIN	97	PL B400 226	A. Bertin *et al.*	(OBELIX Collab.)
PROKOSHKIN	97B	SPD 42 298 Translated from DANS 354 751.	Yu.D. Prokoshkin, S.A. Sadovsky	
ARMSTRONG	92C	ZPHY C54 371	T.A. Armstrong *et al.*	(ATHU, BARI, BIRM+)
ARMSTRONG	92E	ZPHY C56 29	T.A. Armstrong *et al.*	(ATHU, BARI, BIRM+) JPC
AUGUSTIN	92	PR D46 1951	J.E. Augustin, G. Cosme	(DM2 Collab.)
ARMSTRONG	91B	ZPHY C52 389	T.A. Armstrong *et al.*	(ATHU, BARI, BIRM+)
BAI	90C	PRL 65 2507	Z. Bai *et al.*	(Mark III Collab.)
ARMSTRONG	89	PL B221 216	T.A. Armstrong *et al.*	(CERN, CDEF, BIRM+) JPC
ARMSTRONG	89G	ZPHY C43 55	T.A. Armstrong *et al.*	(CERN, BIRM, BARI+)
BEHREND	89	ZPHY C42 367	H.J. Behrend *et al.*	(CELLO Collab.)
HILL	89	ZPHY C42 355	P. Hill *et al.*	(JADE Collab.) JP
KOPKE	89	PRPL 174 67	L. Kopke *et al.*	(CERN)
AIHARA	88B	PL B209 107	H. Aihara *et al.*	(TPC-2γ Collab.)
BECKER	87	PRL 59 186	J.J. Becker *et al.*	(Mark III Collab.) JP
GIDAL	87	PRL 59 2012	G. Gidal *et al.*	(LBL, SLAC, HARV)
GIDAL	87B	PRL 59 2016	G. Gidal *et al.*	(LBL, SLAC, HARV)
AIHARA	86C	PRL 57 2500	H. Aihara *et al.*	(TPC-2γ Collab.) JP
ANDO	86	PRL 57 1296	A. Ando *et al.*	(KEK, KYOT, NIRS, SAGA+)
ARMSTRONG	84	PL 146B 273	T.A. Armstrong *et al.*	(ATHU, BARI, BIRM+) JP
BITYUKOV	84	SJNP 39 735 Translated from YAF 39 1165.	S. Bityukov *et al.*	(SERP)
CHAUVAT	84	PL 148B 382	P. Chauvat *et al.*	(CERN, CLER, UCLA+)
JENNI	83	PR D27 1031	P. Jenni *et al.*	(SLAC, LBL)
BROMBERG	80	PR D22 1513	C.M. Bromberg *et al.*	(CIT, FNAL, ILLC+)
DIONISI	80	NP B169 1	C. Dionisi *et al.*	(CERN, MADR, CDEF+) IJP
CORDEN	78	NP B144 253	M.J. Corden *et al.*	(BIRM, RHEL, TELA+)
DEFOIX	72	NP B44 125	C. Defoix *et al.*	(CDEF, CERN)
DAHL	67	PR 163 1377	O.I. Dahl *et al.*	(LRL) IJP
Also	65	PRL 14 1074	D.H. Miller *et al.*	(LRL, UCB)

OTHER RELATED PAPERS

PROKOSHKIN	99	PAN 62 356 Translated from YAF 62 396.	Yu.D. Prokoshkin	
IIZUKA	91	PTP 86 885	J. Iizuka, H. Koibuchi	(NAGO)
ISHIDA	89	PTP 82 119	S. Ishida *et al.*	(NIHO)
AIHARA	88C	PR D38 1	H. Aihara *et al.*	(TPC-2γ Collab.) JPC
BITYUKOV	88	PL B203 327	S.I. Bityukov *et al.*	(SERP)
PROTOPOP...	87B	Hadron 87 Conf.	S.D. Protopopescu, S.U. Chung	(BNL)

$\omega(1420)$

$I^G(J^{PC}) = 0^-(1^{--})$

$\omega(1420)$ MASS

VALUE (MeV)	EVTS	DOCUMENT ID		TECN	COMMENT
(1400–1450) OUR ESTIMATE					
• • • We do not use the following data for averages, fits, limits, etc. • • •					
1400 ± 50 ± 130	1.2M	[1] ACHASOV	03D	RVUE	0.44–2.00 $e^+e^- \to \pi^+\pi^-\pi^0$
1450 ± 10		[2] HENNER	02	RVUE	1.2–2.0 $e^+e^- \to \rho\pi, \omega\pi\pi$
1373 ± 70	177	[3] AKHMETSHIN	00D	CMD2	1.2–1.38 $e^+e^- \to \omega\pi^+\pi^-$
1370 ± 25	5095	ANISOVICH	00H	SPEC	0.0 $p\overline{p} \to \omega\pi^0\pi^0\pi^0$
1400^{+100}_{-200}		[4] ACHASOV	98H	RVUE	$e^+e^- \to \pi^+\pi^-\pi^0$
~ 1400		[5] ACHASOV	98H	RVUE	$e^+e^- \to \omega\pi^+\pi^-$
~ 1460		[6] ACHASOV	98H	RVUE	$e^+e^- \to K^+K^-$
1440 ± 70		[7] CLEGG	94	RVUE	
1419 ± 31	315	[8] ANTONELLI	92	DM2	1.34–2.4$e^+e^- \to \rho\pi$

[1] From the combined fit of ANTONELLI 92, ACHASOV 01E, ACHASOV 02E, and ACHASOV 03D data on the $\pi^+\pi^-\pi^0$ and ANTONELLI 92 on the $\omega\pi^+\pi^-$ final states. Supersedes ACHASOV 99E and ACHASOV 02E.

[2] Using results of CORDIER 81 and preliminary data of DOLINSKY 91 and ANTONELLI 92.

[3] Using the data of AKHMETSHIN 00D and ANTONELLI 92. The $\rho\pi$ dominance for the energy dependence of the $\omega(1420)$ and $\omega(1650)$ width assumed.

[4] Using data from BARKOV 87, DOLINSKY 91, and ANTONELLI 92.

[5] Using the data from ANTONELLI 92.

[6] Using the data from IVANOV 81 and BISELLO 88B.

[7] From a fit to two Breit-Wigner functions and using the data of DOLINSKY 91 and ANTONELLI 92.

[8] From a fit to two Breit-Wigner functions interfering between them and with the ω,ϕ tails with fixed $(+,-,+)$ phases.

$\omega(1420)$ WIDTH

VALUE (MeV)	EVTS	DOCUMENT ID		TECN	COMMENT
(180–250) OUR ESTIMATE					
• • • We do not use the following data for averages, fits, limits, etc. • • •					
$870^{+500}_{-300} \pm 450$	1.2M	[9] ACHASOV	03D	RVUE	0.44–2.00 $e^+e^- \to \pi^+\pi^-\pi^0$
199 ± 15		[10] HENNER	02	RVUE	1.2–2.0 $e^+e^- \to \rho\pi, \omega\pi\pi$
188 ± 45	177	[11] AKHMETSHIN	00D	CMD2	1.2–1.38 $e^+e^- \to \omega\pi^+\pi^-$
360^{+100}_{-60}	5095	ANISOVICH	00H	SPEC	0.0 $p\overline{p} \to \omega\pi^0\pi^0\pi^0$
240 ± 70		[12] CLEGG	94	RVUE	
174 ± 59	315	[13] ANTONELLI	92	DM2	1.34–2.4$e^+e^- \to \rho\pi$

[9] From the combined fit of ANTONELLI 92, ACHASOV 01E, ACHASOV 02E, and ACHASOV 03D data on the $\pi^+\pi^-\pi^0$ and ANTONELLI 92 on the $\omega\pi^+\pi^-$ final states. Supersedes ACHASOV 99E and ACHASOV 02E.

[10] Using results of CORDIER 81 and preliminary data of DOLINSKY 91 and ANTONELLI 92.

[11] Using the data of AKHMETSHIN 00D and ANTONELLI 92. The $\rho\pi$ dominance for the energy dependence of the $\omega(1420)$ and $\omega(1650)$ width assumed.

[12] From a fit to two Breit-Wigner functions and using the data of DOLINSKY 91 and ANTONELLI 92.

[13] From a fit to two Breit-Wigner functions interfering between them and with the ω,ϕ tails with fixed $(+,-,+)$ phases.

$\omega(1420)$ DECAY MODES

	Mode	Fraction (Γ_j/Γ)
Γ_1	$\rho\pi$	dominant
Γ_2	$\omega\pi\pi$	seen
Γ_3	$b_1(1235)\pi$	seen
Γ_4	e^+e^-	seen

$\omega(1420)$ $\Gamma(i)\Gamma(e^+e^-)/\Gamma^2(\text{total})$

$\Gamma(\rho\pi) \times \Gamma(e^+e^-)/\Gamma^2_{\text{total}}$ $\Gamma_1\Gamma_4/\Gamma^2$

VALUE (units 10^{-6})	EVTS	DOCUMENT ID		TECN	COMMENT
• • • We do not use the following data for averages, fits, limits, etc. • • •					
0.65 ±0.13 ±0.21	1.2M	[14,15] ACHASOV	03D	RVUE	0.44–2.00 $e^+e^- \to \pi^+\pi^-\pi^0$
0.625 ± 0.160		[16,17] CLEGG	94	RVUE	
0.466 ± 0.178		[18,20] ANTONELLI	92	DM2	1.34–2.4$e^+e^- \to \rho\pi$

[14] Calculated by us from the cross section at the peak.

[15] From the combined fit of ANTONELLI 92, ACHASOV 01E, ACHASOV 02E, and ACHASOV 03D data on the $\pi^+\pi^-\pi^0$ and ANTONELLI 92 on the $\omega\pi^+\pi^-$ final states. Supersedes ACHASOV 99E and ACHASOV 02E.

[16] From a fit to two Breit-Wigner functions and using the data of DOLINSKY 91 and ANTONELLI 92.

[17] From the partial and leptonic width given by the authors.

[18] From the product of the leptonic width and partial branching ratio given by the authors.

$\Gamma(\omega\pi\pi) \times \Gamma(e^+e^-)/\Gamma^2_{\text{total}}$ $\Gamma_2\Gamma_4/\Gamma^2$

VALUE (units 10^{-8})	EVTS	DOCUMENT ID		TECN	COMMENT
• • • We do not use the following data for averages, fits, limits, etc. • • •					
1.3 ± 1.3	612	[19] AKHMETSHIN	00D	CMD2	1.2–2.4 $e^+e^- \to \omega\pi^+\pi^-$

[19] Using the data of AKHMETSHIN 00D and ANTONELLI 92. The $\rho\pi$ dominance for the energy dependence of the $\omega(1420)$ and $\omega(1650)$ width assumed.

[20] From a fit to two Breit-Wigner functions interfering between them and with the ω,ϕ tails with fixed $(+,-,+)$ phases.

$\omega(1420)$ BRANCHING RATIOS

$\Gamma(\omega\pi\pi)/\Gamma_{\text{total}}$ Γ_2/Γ

VALUE	DOCUMENT ID		TECN	COMMENT
• • • We do not use the following data for averages, fits, limits, etc. • • •				
0.301 ± 0.029	[22] HENNER	02	RVUE	1.2–2.0 $e^+e^- \to \rho\pi, \omega\pi\pi$
possibly seen	AKHMETSHIN	00D	CMD2	$e^+e^- \to \omega\pi^+\pi^-$

$\Gamma(\omega\pi\pi)/\Gamma(b_1(1235)\pi)$ Γ_2/Γ_3

VALUE	EVTS	DOCUMENT ID		TECN	COMMENT
• • • We do not use the following data for averages, fits, limits, etc. • • •					
0.60 ± 0.16	5095	ANISOVICH	00H	SPEC	0.0 $p\overline{p} \to \omega\pi^0\pi^0\pi^0$

$\Gamma(\rho\pi)/\Gamma_{\text{total}}$ Γ_1/Γ

VALUE	DOCUMENT ID		TECN	COMMENT
• • • We do not use the following data for averages, fits, limits, etc. • • •				
0.699 ± 0.029	[22] HENNER	02	RVUE	1.2–2.0 $e^+e^- \to \rho\pi$, $\omega\pi\pi$

$\Gamma(e^+e^-)/\Gamma_{\text{total}}$ Γ_4/Γ

VALUE (units 10^{-7})	EVTS	DOCUMENT ID		TECN	COMMENT
• • • We do not use the following data for averages, fits, limits, etc. • • •					
$\sim$ 6.6	1.2M	[21,23] ACHASOV	03D	RVUE	0.44–2.00 $e^+e^- \to \pi^+\pi^-\pi^0$
23 $\pm$1		[22] HENNER	02	RVUE	1.2–2.0 $e^+e^- \to \rho\pi$, $\omega\pi\pi$

[21] Assuming that the $\omega(1420)$ decays into $\rho\pi$ only.
[22] Assuming that the $\omega(1420)$ decays into $\rho\pi$ and $\omega\pi\pi$ only.
[23] Calculated by us from the cross section at the peak.

$\omega(1420)$ REFERENCES

ACHASOV	03D	PR D68 052006	M.N. Achasov *et al.*	(Novosibirsk SND Collab.)
ACHASOV	02E	PR D66 032001	M.N. Achasov *et al.*	(Novosibirsk SND Collab.)
HENNER	02	EPJ C26 3	V.K. Henner *et al.*	
ACHASOV	01E	PR D63 072002	M.N. Achasov *et al.*	(Novosibirsk SND Collab.)
AKHMETSHIN	00D	PL B489 125	R.R. Akhmetshin *et al.*	(Novosibirsk CMD-2 Collab.)
ANISOVICH	00H	PL B485 341	A.V. Anisovich *et al.*	
ACHASOV	99E	PL B462 365	M.N. Achasov *et al.*	(Novosibirsk SND Collab.)
ACHASOV	98H	PR D57 4334	N.N. Achasov, A.A. Kozhevnikov	
CLEGG	94	ZPHY C62 455	A.B. Clegg, A. Donnachie	(LANC, MCHS)
ANTONELLI	92	ZPHY C56 15	A. Antonelli *et al.*	(DM2 Collab.)
DOLINSKY	91	PRPL 202 99	S.I. Dolinsky *et al.*	(NOVO)
BISELLO	88B	ZPHY C39 13	D. Bisello *et al.*	(PADO, CLER, FRAS+)
BARKOV	87	JETPL 46 164 Translated from ZETFP 46 132.	L.M. Barkov *et al.*	(NOVO)
CORDIER	81	PL 106B 155	A. Cordier *et al.*	(ORSAY)
IVANOV	81	PL 107B 297	P.M. Ivanov *et al.*	(NOVO)

OTHER RELATED PAPERS

ACHASOV	02B	PAN 65 153 Translated from YAF 65 158.	N.N. Achasov, A.A. Kozhevnikov	
CLOSE	02	PR D65 092003	F.E. Close, A. Donnachie, Yu.S. Kalashnikova	
ACHASOV	00J	PR D62 117503	N.N. Achasov, A.A. Kozhevnikov	
ABELE	99D	PL B468 178	A. Abele *et al.*	(Crystal Barrel Collab.)
BELOZEROVA	98	PPN 29 63 Translated from FECAY 29 148.	T.S. Belozerova, V.K. Henner	
ACHASOV	97F	PAN 60 2029 Translated from YAF 60 2212.	N.N. Achasov, A.A. Kozhevnikov	(NOVM)
ATKINSON	87	ZPHY C34 157	M. Atkinson *et al.*	(BONN, CERN, GLAS+)
ATKINSON	84	NP B231 15	M. Atkinson *et al.*	(BONN, CERN, GLAS+)
ATKINSON	83B	PL 127B 132	M. Atkinson *et al.*	(BONN, CERN, GLAS+)

$f_2(1430)$

$I^G(J^{PC}) = 0^+(2^{++})$

OMITTED FROM SUMMARY TABLE

This entry lists nearby peaks observed in the D wave of the $K\overline{K}$ and $\pi^+\pi^-$ systems. Needs confirmation.

$f_2(1430)$ MASS

VALUE (MeV)	DOCUMENT ID		TECN	COMMENT
$\approx$ 1430 OUR ESTIMATE				
• • • We do not use the following data for averages, fits, limits, etc. • • •				
1453 $\pm$ 4	[2] VLADIMIRSKY	01	SPEC	40 $\pi^-p \to K^0_S K^0_S n$
1421 $\pm$ 5	AUGUSTIN	87	DM2	$J/\psi \to \gamma\pi^+\pi^-$
1480 $\pm$50	AKESSON	86	SPEC	$pp \to pp\pi^+\pi^-$
1436^{+26}_{-16}	DAUM	84	CNTR	17–18 $\pi^-p \to K^+K^-n$
1412 $\pm$ 3	DAUM	84	CNTR	63 $\pi^-p \to K^0_S K^0_S n$, K^+K^-n
1439^{+5}_{-6}	[1] BEUSCH	67	OSPK	5,7,12 $\pi^-p \to K^0_S K^0_S n$

[1] Not seen by WETZEL 76.
[2] $J^{PC} = 0^{++}$ or 2^{++}.

$f_2(1430)$ WIDTH

VALUE (MeV)	DOCUMENT ID		TECN	COMMENT
• • • We do not use the following data for averages, fits, limits, etc. • • •				
13 $\pm$ 5	[4] VLADIMIRSKY	01	SPEC	40 $\pi^-p \to K^0_S K^0_S n$
30 $\pm$ 9	AUGUSTIN	87	DM2	$J/\psi \to \gamma\pi^+\pi^-$
150 $\pm$50	AKESSON	86	SPEC	$pp \to pp\pi^+\pi^-$
81^{+56}_{-29}	DAUM	84	CNTR	17–18 $\pi^-p \to K^+K^-n$
14 $\pm$ 6	DAUM	84	CNTR	63 $\pi^-p \to K^0_S K^0_S n$, K^+K^-n
43^{+17}_{-18}	[3] BEUSCH	67	OSPK	5,7,12 $\pi^-p \to K^0_S K^0_S n$

[3] Not seen by WETZEL 76.
[4] $J^{PC} = 0^{++}$ or 2^{++}.

$f_2(1430)$ DECAY MODES

	Mode
Γ_1	$K\overline{K}$
Γ_2	$\pi\pi$

$f_2(1430)$ REFERENCES

VLADIMIRSKY	01	PAN 64 1895 Translated from YAF 64 1979.	V.V. Vladimirsky *et al.*	
AUGUSTIN	87	ZPHY C36 369	J.E. Augustin *et al.*	(LALO, CLER, FRAS+)
AKESSON	86	NP B264 154	T. Akesson *et al.*	(Axial Field Spec. Collab.)
DAUM	84	ZPHY C23 339	C. Daum *et al.*	(AMST, CERN, CRAC, MPIM+) JP
WETZEL	76	NP B115 208	W. Wetzel *et al.*	(ETH, CERN, LOIC)
BEUSCH	67	PL 25B 357	W. Beusch *et al.*	(ETH, CERN)

$a_0(1450)$

$I^G(J^{PC}) = 1^-(0^{++})$

See minireview on scalar mesons under $f_0(1370)$.

$a_0(1450)$ MASS

VALUE (MeV)	EVTS	DOCUMENT ID		TECN	COMMENT
1474 $\pm$19 OUR AVERAGE					
1480 $\pm$30		ABELE	98	CBAR	0.0 $\overline{p}p \to K^0_L K^\pm\pi^\mp$
1470 $\pm$25		[1] AMSLER	95D	CBAR	0.0 $\overline{p}p \to \pi^0\pi^0\pi^0$, $\pi^0\eta\eta$, $\pi^0\pi^0\eta$
• • • We do not use the following data for averages, fits, limits, etc. • • •					
1441^{+40}_{-15}	35280	[4] BAKER	03	SPEC	$\overline{p}p \to \omega\pi^+\pi^-\pi^0$
1303 $\pm$16		[5] BARGIOTTI	03	OBLX	$\overline{p}p$
1296 $\pm$10		[2] AMSLER	02	CBAR	0.9 $\overline{p}p \to \pi^0\pi^0\eta$
1565 $\pm$30		[2] ANISOVICH	98B	RVUE	Compilation
1290 $\pm$10		BERTIN	98B	OBLX	0.0 $\overline{p}p \to K^\pm K_S\pi^\mp$
1450 $\pm$40		AMSLER	94D	CBAR	0.0 $\overline{p}p \to \pi^0\pi^0\eta$
1435 $\pm$40		BUGG	94	RVUE	$\overline{p}p \to \eta 2\pi^0$
1410 $\pm$25		ETKIN	82C	MPS	23 $\pi^-p \to n2K^0_S$
$\sim$ 1300		MARTIN	78	SPEC	10 $K^\pm p \to K^0_S\pi p$
1255 $\pm$ 5		[3] CASON	76		

[1] Coupled-channel analysis of AMSLER 95B, AMSLER 95C, and AMSLER 94D.
[2] T-matrix pole.
[3] Isospin 0 not excluded.
[4] From the pole position.
[5] Coupled channel analysis of $\pi^+\pi^-\pi^0$, $K^+K^-\pi^0$, and $K^\pm K^0_S\pi^\mp$.

$a_0(1450)$ WIDTH

VALUE (MeV)	EVTS	DOCUMENT ID		TECN	COMMENT
265 $\pm$13 OUR AVERAGE					
265 $\pm$15		ABELE	98	CBAR	0.0 $\overline{p}p \to K^0_L K^\pm\pi^\mp$
265 $\pm$30		[6] AMSLER	95D	CBAR	0.0 $\overline{p}p \to \pi^0\pi^0\pi^0$, $\pi^0\eta\eta$, $\pi^0\pi^0\eta$
• • • We do not use the following data for averages, fits, limits, etc. • • •					
110 $\pm$14	35280	[9] BAKER	03	SPEC	$\overline{p}p \to \omega\pi^+\pi^-\pi^0$
92 $\pm$16		[10] BARGIOTTI	03	OBLX	$\overline{p}p$
81 $\pm$21		[7] AMSLER	02	CBAR	0.9 $\overline{p}p \to \pi^0\pi^0\eta$
292 $\pm$40		[7] ANISOVICH	98B	RVUE	Compilation
80 $\pm$ 5		BERTIN	98B	OBLX	0.0 $\overline{p}p \to K^\pm K_S\pi^\mp$
270 $\pm$40		AMSLER	94D	CBAR	0.0 $\overline{p}p \to \pi^0\pi^0\eta$
270 $\pm$40		BUGG	94	RVUE	$\overline{p}p \to \eta 2\pi^0$
230 $\pm$30		ETKIN	82C	MPS	23 $\pi^-p \to n2K^0_S$
$\sim$ 250		MARTIN	78	SPEC	10 $K^\pm p \to K^0_S\pi p$
79 $\pm$10		[8] CASON	76		

[6] Coupled-channel analysis of AMSLER 95B, AMSLER 95C, and AMSLER 94D.
[7] T-matrix pole.
[8] Isospin 0 not excluded.
[9] From the pole position.
[10] Coupled channel analysis of $\pi^+\pi^-\pi^0$, $K^+K^-\pi^0$, and $K^\pm K^0_S\pi^\mp$.

Meson Particle Listings

$a_0(1450)$, $\rho(1450)$

$a_0(1450)$ DECAY MODES

	Mode	Fraction (Γ_i/Γ)
Γ_1	$\pi\eta$	seen
Γ_2	$\pi\eta'(958)$	seen
Γ_3	$K\overline{K}$	seen
Γ_4	$\omega\pi\pi$	seen

$\Gamma(\pi\eta'(958))/\Gamma(\pi\eta)$ Γ_2/Γ_1

VALUE	DOCUMENT ID		TECN	COMMENT
0.35 ± 0.16	[11] ABELE	98	CBAR	0.0 $\overline{p}p \to K^0_L K^\pm \pi^\mp$
• • • We do not use the following data for averages, fits, limits, etc. • • •				
0.43 ± 0.19	ABELE	97C	CBAR	0.0 $\overline{p}p \to \pi^0\pi^0\eta'$

[11] Using $\pi^0\eta$ from AMSLER 94D.

$\Gamma(K\overline{K})/\Gamma(\pi\eta)$ Γ_3/Γ_1

VALUE	DOCUMENT ID		TECN	COMMENT
0.88 ± 0.23	[11] ABELE	98	CBAR	0.0 $\overline{p}p \to K^0_L K^\pm \pi^\mp$

$\Gamma(\omega\pi\pi)/\Gamma(\pi\eta)$ Γ_4/Γ_1

VALUE	EVTS	DOCUMENT ID		TECN	COMMENT
• • • We do not use the following data for averages, fits, limits, etc. • • •					
10.7 ± 2.3	35 280	[12] BAKER	03	SPEC	$\overline{p}p \to \omega\pi^+\pi^-\pi^0$

[12] Using results on $\overline{p}p \to a_0(1450)^0\pi^0$, $a_0(1450) \to \eta\pi^0$ from ABELE 96C and assuming the $\omega\rho$ mechanism for the $\omega\pi\pi$ state.

$a_0(1450)$ REFERENCES

BAKER	03	PL B563 140	C.A. Baker *et al.*	
BARGIOTTI	03	EPJ C26 371	M. Bargiotti *et al.*	(OBELIX Collab.)
AMSLER	02	EPJ C23 29	C. Amsler *et al.*	
ABELE	98	PR D57 3860	A. Abele *et al.*	(Crystal Barrel Collab.)
ANISOVICH	98B	UFN 41 419	V.V. Anisovich *et al.*	
BERTIN	98B	PL B434 180	A. Bertin *et al.*	(OBELIX Collab.)
ABELE	97C	PL B404 179	A. Abele *et al.*	(Crystal Barrel Collab.)
ABELE	96C	NP A609 562	A. Abele *et al.*	(Crystal Barrel Collab.)
AMSLER	95B	PL B342 433	C. Amsler *et al.*	(Crystal Barrel Collab.)
AMSLER	95C	PL B353 571	C. Amsler *et al.*	(Crystal Barrel Collab.)
AMSLER	95D	PL B355 425	C. Amsler *et al.*	(Crystal Barrel Collab.)
AMSLER	94D	PL B333 277	C. Amsler *et al.*	(Crystal Barrel Collab.) IGJPC
BUGG	94	PR D50 4412	D.V. Bugg *et al.*	(LOQM)
ETKIN	82C	PR D25 2446	A. Etkin *et al.*	(BNL, CUNY, TUFTS, VAND)
MARTIN	78	NP B134 392	A.D. Martin *et al.*	(DURH, GEVA)
CASON	76	PRL 36 1485	N.M. Cason *et al.*	(NDAM, ANL)

OTHER RELATED PAPERS

FURMAN	02	PL B538 266	A. Furman, L. Lesniak	
BARBERIS	00H	PL B488 225	D. Barberis *et al.*	(WA 102 Collab.)
MASONI	99	EPJ C8 385	A. Masoni	
AMSLER	98	RMP 70 1293	C. Amsler	

$\rho(1450)$

$I^G(J^{PC}) = 1^+(1^{--})$

See the mini-review under the $\rho(1700)$.

$\rho(1450)$ MASS

VALUE (MeV)	DOCUMENT ID
1465 ± 25 OUR ESTIMATE This is only an educated guess; the error given is larger than the error on the average of the published values.	

$\eta\rho^0$ MODE

VALUE (MeV)	DOCUMENT ID		TECN	COMMENT
• • • We do not use the following data for averages, fits, limits, etc. • • •				
1497 ± 14	[1] AKHMETSHIN	01B	CMD2	$e^+e^- \to \eta\gamma$
1421 ± 15	[2] AKHMETSHIN	00D	CMD2	$e^+e^- \to \eta\pi^+\pi^-$
1470 ± 20	ANTONELLI	88	DM2	$e^+e^- \to \eta\pi^+\pi^-$
1446 ± 10	FUKUI	88	SPEC	8.95 $\pi^-p \to \eta\pi^+\pi^-n$

[1] Using the data of AKHMETSHIN 01B on $e^+e^- \to \eta\gamma$, AKHMETSHIN 00D and ANTONELLI 88 on $e^+e^- \to \eta\pi^+\pi^-$.

[2] Using the data of ANTONELLI 88, DOLINSKY 91, and AKHMETSHIN 00D. The energy-independent width of the $\rho(1450)$ and $\rho(1700)$ mesons assumed.

$\omega\pi$ MODE

VALUE (MeV)	EVTS	DOCUMENT ID		TECN	COMMENT
• • • We do not use the following data for averages, fits, limits, etc. • • •					
1582 ± 17 ± 25	2382	[3] AKHMETSHIN	03B	CMD2	$e^+e \to \pi^0\pi^0\gamma$
$1349 \pm 25 \,^{+10}_{-\ 5}$	341	[4] ALEXANDER	01B	CLE2	$B \to D^{(*)}\omega\pi^-$
1523 ± 10		[5] EDWARDS	00A	CLE2	$\tau^- \to \omega\pi^-\nu_\tau$
1463 ± 25		[6] CLEGG	94	RVUE	
1250		[7] ASTON	80C	OMEG	20–70 $\gamma p \to \omega\pi^0 p$
1290 ± 40		[7] BARBER	80C	SPEC	3–5 $\gamma p \to \omega\pi^0 p$

[3] Using the data of AKHMETSHIN 03B and BISELLO 91B assuming the $\omega\pi^0$ and $\pi^+\pi^-$ mass dependence of the total width. $\rho(1700)$ mass and width fixed at 1700 MeV and 240 MeV, respectively.

[4] Using Breit-Wigner parameterization of the $\rho(1450)$ and assuming the $\omega\pi^-$ mass dependence for the total width.

[5] Mass-independent width parameterization. $\rho(1700)$ mass and width fixed at 1700 MeV and 235 MeV respectively.

[6] Using data from BISELLO 91B, DOLINSKY 86 and ALBRECHT 87L.

[7] Not separated from $b_1(1235)$, not pure $J^P = 1^-$ effect.

4π MODE

VALUE (MeV)	DOCUMENT ID		TECN	COMMENT
• • • We do not use the following data for averages, fits, limits, etc. • • •				
1435 ± 40	ABELE	01B	CBAR	0.0 $\overline{p}n \to 2\pi^-2\pi^0\pi^+$
1350 ± 50	ACHASOV	97	RVUE	$e^+e^- \to 2(\pi^+\pi^-)$
1449 ± 4	[8] ARMSTRONG	89E	OMEG	300 $pp \to pp2(\pi^+\pi^-)$

[8] Not clear whether this observation has I=1 or 0.

$\pi\pi$ MODE

VALUE (MeV)	EVTS	DOCUMENT ID		TECN	COMMENT
• • • We do not use the following data for averages, fits, limits, etc. • • •					
1406 ± 15	87k	[9,10] ANDERSON	00A	CLE2	$\tau^- \to \pi^-\pi^0\nu_\tau$
~ 1368		[11] ABELE	99C	CBAR	0.0 $\overline{p}d \to \pi^+\pi^-\pi^-p$
1348 ± 33		BERTIN	98	OBLX	0.05–0.405 $\overline{n}p \to \pi^+\pi^+\pi^-$
1411 ± 14		[12] ABELE	97	CBAR	$\overline{p}n \to \pi^-\pi^0\pi^0$
$1370 \,^{+\ 90}_{-\ 70}$		ACHASOV	97	RVUE	$e^+e^- \to \pi^+\pi^-$
1380 ± 24		[13] BARATE	97M	ALEP	$\tau^- \to \pi^-\pi^0\nu_\tau$
1359 ± 40		[10] BERTIN	97C	OBLX	0.0 $\overline{p}p \to \pi^+\pi^-\pi^0$
1282 ± 37		BERTIN	97D	OBLX	0.05 $\overline{p}p \to 2\pi^+2\pi^-$
1424 ± 25		BISELLO	89	DM2	$e^+e^- \to \pi^+\pi^-$
1292 ± 17		[14] KURDADZE	83	OLYA	0.64–1.4 $e^+e^- \to \pi^+\pi^-$

[9] From the GOUNARIS 68 parametrization of the pion form factor.

[10] $\rho(1700)$ mass and width fixed at 1700 MeV and 235 MeV, respectively.

[11] $\rho(1700)$ mass and width fixed at 1780 MeV and 275 MeV respectively.

[12] T-matrix pole.

[13] Fixing $\rho(1450)$ width to 310 MeV and $\rho(1700)$ mass and width to 1700 MeV and 235 MeV respectively.

[14] Using for $\rho(1700)$ mass and width 1600 ± 20 and 300 ± 10 MeV respectively.

$\phi\pi$ MODE

VALUE (MeV)	DOCUMENT ID		TECN	CHG	COMMENT
• • • We do not use the following data for averages, fits, limits, etc. • • •					
1480 ± 40	[15,16] BITYUKOV	87	SPEC	0	32.5 $\pi^-p \to \phi\pi^0 n$

[15] DONNACHIE 91 suggests this is a different particle.

[16] Not seen by ABELE 97H.

$K\overline{K}$ MODE

VALUE (MeV)	EVTS	DOCUMENT ID		TECN	CHG	COMMENT
• • • We do not use the following data for averages, fits, limits, etc. • • •						
1422.8 ± 6.5	27k	[17] ABELE	99D	CBAR	±	0.0 $\overline{p}p \to K^+K^-\pi^0$

[17] K-matrix pole. Isospin not determined, could be $\omega(1420)$.

MIXED MODES

VALUE (MeV)	DOCUMENT ID		TECN	COMMENT
• • • We do not use the following data for averages, fits, limits, etc. • • •				
1265.5 ± 75.3	DUBNICKA	89	RVUE	$e^+e^- \to \pi^+\pi^-$

$\rho(1450)$ WIDTH

VALUE (MeV)	DOCUMENT ID
400 ± 60 OUR ESTIMATE This is only an educated guess; the error given is larger than the error on the average of the published values.	

$\eta\rho^0$ MODE

VALUE (MeV)	DOCUMENT ID		TECN	COMMENT
• • • We do not use the following data for averages, fits, limits, etc. • • •				
226 ± 44	[18] AKHMETSHIN	01B	CMD2	$e^+e^- \to \eta\gamma$
211 ± 31	[19] AKHMETSHIN	00D	CMD2	$e^+e^- \to \eta\pi^+\pi^-$
230 ± 30	ANTONELLI	88	DM2	$e^+e^- \to \eta\pi^+\pi^-$
60 ± 15	FUKUI	88	SPEC	8.95 $\pi^-p \to \eta\pi^+\pi^-n$

[18] Using the data of AKHMETSHIN 01B on $e^+e^- \to \eta\gamma$, AKHMETSHIN 00D and ANTONELLI 88 on $e^+e^- \to \eta\pi^+\pi^-$.

[19] Using the data of ANTONELLI 88, DOLINSKY 91, and AKHMETSHIN 00D. The energy-independent width of the $\rho(1450)$ and $\rho(1700)$ mesons assumed.

$\omega\pi$ MODE

VALUE (MeV)	EVTS	DOCUMENT ID		TECN	COMMENT
The data in this block is included in the average printed for a previous datablock.					
• • • We do not use the following data for averages, fits, limits, etc. • • •					
$429\pm\ 42\pm10$	2382	[20] AKHMETSHIN	03B	CMD2	$e^+e^- \to \pi^0\pi^0\gamma$
$547\pm\ 86^{+46}_{-45}$	341	[21] ALEXANDER	01B	CLE2	$B \to D^{(*)}\omega\pi^-$
$400\pm\ 35$		[22] EDWARDS	00A	CLE2	$\tau^- \to \omega\pi^-\nu_\tau$
$311\pm\ 62$		[23] CLEGG	94	RVUE	
300		[24] ASTON	80C	OMEG	20–70 $\gamma p \to \omega\pi^0 p$
320 ± 100		[24] BARBER	80C	SPEC	3–5 $\gamma p \to \omega\pi^0 p$

[20] Using the data of AKHMETSHIN 03B and BISELLO 91B assuming the $\omega\pi^0$ and $\pi^+\pi^-$ mass dependence of the total width. $\rho(1700)$ mass and width fixed at 1700 MeV and 240 MeV, respectively.
[21] Using Breit-Wigner parameterization of the $\rho(1450)$ and assuming the $\omega\pi^-$ mass dependence for the total width.
[22] Mass-independent width parameterization. $\rho(1700)$ mass and width fixed at 1700 MeV and 235 MeV respectively.
[23] Using data from BISELLO 91B, DOLINSKY 86 and ALBRECHT 87L.
[24] Not separated from $b_1(1235)$, not pure $J^P = 1^-$ effect.

4π MODE

VALUE (MeV)	DOCUMENT ID		TECN	COMMENT
• • • We do not use the following data for averages, fits, limits, etc. • • •				
325 ± 100	ABELE	01B	CBAR	$0.0\ \overline{p}n \to 2\pi^-2\pi^0\pi^+$

$\pi\pi$ MODE

VALUE (MeV)	EVTS	DOCUMENT ID		TECN	COMMENT
• • • We do not use the following data for averages, fits, limits, etc. • • •					
455 ± 41	87k	[25,26] ANDERSON	00A	CLE2	$\tau^- \to \pi^-\pi^0\nu_\tau$
~ 374		[27] ABELE	99C	CBAR	$0.0\ \overline{p}d \to \pi^+\pi^-\pi^-p$
275 ± 10		BERTIN	98	OBLX	0.05–0.405 $\overline{n}p \to \pi^+\pi^+\pi^-\pi^-$
343 ± 20		[28] ABELE	97	CBAR	$\overline{p}n \to \pi^-\pi^0\pi^0$
310 ± 40		[26] BERTIN	97C	OBLX	$0.0\ \overline{p}p \to \pi^+\pi^-\pi^0$
236 ± 36		BERTIN	97D	OBLX	$0.05\ \overline{p}p \to 2\pi^+2\pi^-$
269 ± 31		BISELLO	89	DM2	$e^+e^- \to \pi^+\pi^-$
218 ± 46		[29] KURDADZE	83	OLYA	0.64–1.4 $e^+e^- \to \pi^+\pi^-$

[25] From the GOUNARIS 68 parametrization of the pion form factor.
[26] $\rho(1700)$ mass and width fixed at 1700 MeV and 235 MeV, respectively.
[27] $\rho(1700)$ mass and width fixed at 1780 MeV and 275 MeV respectively.
[28] T-matrix pole.
[29] Using for $\rho(1700)$ mass and width 1600 ± 20 and 300 ± 10 MeV respectively.

$\phi\pi$ MODE

VALUE (MeV)	DOCUMENT ID		TECN	CHG	COMMENT
• • • We do not use the following data for averages, fits, limits, etc. • • •					
130 ± 60	[30,31] BITYUKOV	87	SPEC	0	32.5 $\pi^-p \to \phi\pi^0 n$

[30] DONNACHIE 91 suggests this is a different particle.
[31] Not seen by ABELE 97H.

$K\overline{K}$ MODE

VALUE (MeV)	EVTS	DOCUMENT ID		TECN	CHG	COMMENT
• • • We do not use the following data for averages, fits, limits, etc. • • •						
146.5 ± 10.5	27k	[32] ABELE	99D	CBAR	$\pm$	$0.0\ \overline{p}p \to K^+K^-\pi^0$

[32] K-matrix pole. Isospin not determined, could be $\omega(1420)$.

MIXED MODES

VALUE (MeV)	DOCUMENT ID		TECN	COMMENT
• • • We do not use the following data for averages, fits, limits, etc. • • •				
391 ± 70	DUBNICKA	89	RVUE	$e^+e^- \to \pi^+\pi^-$

$\rho(1450)$ DECAY MODES

	Mode	Fraction (Γ_i/Γ)	Confidence level
Γ_1	$\pi\pi$	seen	
Γ_2	4π	seen	
Γ_3	$\omega\pi$	<2.0 %	95%
Γ_4	$a_1(1260)\pi$		
Γ_5	$h_1(1170)\pi$		
Γ_6	$\pi(1300)\pi$		
Γ_7	$\rho\rho$		
Γ_8	$\rho(\pi\pi)_{S\text{-wave}}$		
Γ_9	e^+e^-	seen	
Γ_{10}	$\eta\rho$	<4 %	
Γ_{11}	$a_2(1320)\pi$	not seen	
Γ_{12}	$\phi\pi$	<1 %	
Γ_{13}	$K\overline{K}$	$<1.6\times10^{-3}$	95%
Γ_{14}	$\eta\gamma$	possibly seen	

$\rho(1450)$ Γ(i)$\Gamma(e^+e^-)/\Gamma$(total)

$\Gamma(\pi\pi) \times \Gamma(e^+e^-)/\Gamma_{\text{total}}$ $\Gamma_1\Gamma_9/\Gamma$

VALUE (keV)	DOCUMENT ID		TECN	COMMENT
• • • We do not use the following data for averages, fits, limits, etc. • • •				
0.12	[33] DIEKMAN	88	RVUE	$e^+e^- \to \pi^+\pi^-$
$0.027^{+0.015}_{-0.010}$	[34] KURDADZE	83	OLYA	0.64–1.4 $e^+e^- \to \pi^+\pi^-$

$\Gamma(\eta\rho) \times \Gamma(e^+e^-)/\Gamma_{\text{total}}$ $\Gamma_{10}\Gamma_9/\Gamma$

VALUE (eV)	DOCUMENT ID		TECN	COMMENT
• • • We do not use the following data for averages, fits, limits, etc. • • •				
74 ± 20	[35] AKHMETSHIN	00D	CMD2	$e^+e^- \to \eta\pi^+\pi^-$
91 ± 19	ANTONELLI	88	DM2	$e^+e^- \to \eta\pi^+\pi^-$

$\Gamma(\phi\pi) \times \Gamma(e^+e^-)/\Gamma_{\text{total}}$ $\Gamma_{12}\Gamma_9/\Gamma$

VALUE (eV)	CL%	DOCUMENT ID		TECN	COMMENT
<70	90	[36] AULCHENKO	87B	ND	$e^+e^- \to K^0_S K^0_L \pi^0$

$\Gamma(\eta\gamma) \times \Gamma(e^+e^-)/\Gamma_{\text{total}}$ $\Gamma_{14}\Gamma_9/\Gamma$

VALUE (units 10^{-9})	DOCUMENT ID		TECN	COMMENT
• • • We do not use the following data for averages, fits, limits, etc. • • •				
$10.0\pm2.2\pm1.5$	[37] AKHMETSHIN	01B	CMD2	$e^+e^- \to \eta\gamma$

[33] Using total width = 235 MeV.
[34] Using for $\rho(1700)$ mass and width 1600 ± 20 and 300 ± 10 MeV respectively.
[35] Using the data of ANTONELLI 88, DOLINSKY 91, and AKHMETSHIN 00D. The energy-independent width of the $\rho(1450)$ and $\rho(1700)$ mesons assumed.
[36] Using mass 1480 ± 40 MeV and total width 130 ± 60 MeV of BITYUKOV 87.
[37] Using the data of AKHMETSHIN 01B on $e^+e^- \to \eta\gamma$, AKHMETSHIN 00D and ANTONELLI 88 on $e^+e^- \to \eta\pi^+\pi^-$.

$\rho(1450)$ BRANCHING RATIOS

$\Gamma(\eta\rho)/\Gamma_{\text{total}}$ Γ_{10}/Γ

VALUE	DOCUMENT ID		TECN
<0.04	DONNACHIE	87B	RVUE

$\Gamma(a_2(1320)\pi)/\Gamma_{\text{total}}$ Γ_{11}/Γ

VALUE	DOCUMENT ID		TECN	COMMENT
• • • We do not use the following data for averages, fits, limits, etc. • • •				
not seen	AMELIN	00	VES	37 $\pi^-p \to \eta\pi^+\pi^-n$

$\Gamma(\phi\pi)/\Gamma(\omega\pi)$ Γ_{12}/Γ_3

VALUE	CL%	DOCUMENT ID		TECN	CHG	COMMENT
>0.5	95	BITYUKOV	87	SPEC	0	32.5 $\pi^-p \to \phi\pi^0 n$

$\Gamma(\omega\pi)/\Gamma(4\pi)$ Γ_3/Γ_2

VALUE	DOCUMENT ID		TECN
<0.14	CLEGG	88	RVUE

$\Gamma(a_1(1260)\pi)/\Gamma(4\pi)$ Γ_4/Γ_2

VALUE	DOCUMENT ID		TECN	COMMENT
• • • We do not use the following data for averages, fits, limits, etc. • • •				
0.27 ± 0.08	[38] ABELE	01B	CBAR	$0.0\ \overline{p}n \to 5\pi$

$\Gamma(h_1(1170)\pi)/\Gamma(4\pi)$ Γ_5/Γ_2

VALUE	DOCUMENT ID		TECN	COMMENT
• • • We do not use the following data for averages, fits, limits, etc. • • •				
0.08 ± 0.04	[38] ABELE	01B	CBAR	$0.0\ \overline{p}n \to 5\pi$

$\Gamma(\pi(1300)\pi)/\Gamma(4\pi)$ Γ_6/Γ_2

VALUE	DOCUMENT ID		TECN	COMMENT
• • • We do not use the following data for averages, fits, limits, etc. • • •				
0.37 ± 0.13	[38] ABELE	01B	CBAR	$0.0\ \overline{p}n \to 5\pi$

$\Gamma(\rho\rho)/\Gamma(4\pi)$ Γ_7/Γ_2

VALUE	DOCUMENT ID		TECN	COMMENT
• • • We do not use the following data for averages, fits, limits, etc. • • •				
0.11 ± 0.05	[38] ABELE	01B	CBAR	$0.0\ \overline{p}n \to 5\pi$

$\Gamma(\rho(\pi\pi)_{S\text{-wave}})/\Gamma(4\pi)$ Γ_8/Γ_2

VALUE	DOCUMENT ID		TECN	COMMENT
• • • We do not use the following data for averages, fits, limits, etc. • • •				
0.17 ± 0.09	[38] ABELE	01B	CBAR	$0.0\ \overline{p}n \to 5\pi$

$\Gamma(\pi\pi)/\Gamma(4\pi)$ Γ_1/Γ_2

VALUE	DOCUMENT ID		TECN	COMMENT
• • • We do not use the following data for averages, fits, limits, etc. • • •				
0.37 ± 0.10	[38,39] ABELE	01B	CBAR	$0.0\ \overline{p}n \to 5\pi$

Meson Particle Listings

$\rho(1450)$, $\eta(1475)$

$\Gamma(\eta\rho)/\Gamma(\omega\pi)$ Γ_{10}/Γ_3

VALUE	DOCUMENT ID		TECN	COMMENT
~ 0.24	[40] DONNACHIE	91	RVUE	
• • • We do not use the following data for averages, fits, limits, etc. • • •				
>2	FUKUI	91	SPEC	8.95 $\pi^- p \to \omega\pi^0 n$

$\Gamma(\omega\pi)/\Gamma_{total}$ Γ_3/Γ

VALUE	DOCUMENT ID		TECN
~ 0.21	CLEGG	94	RVUE

$\Gamma(\pi\pi)/\Gamma(\omega\pi)$ Γ_1/Γ_3

VALUE	DOCUMENT ID		TECN
~ 0.32	CLEGG	94	RVUE

$\Gamma(\phi\pi)/\Gamma_{total}$ Γ_{12}/Γ

VALUE	DOCUMENT ID		TECN	COMMENT
<0.01	[40] DONNACHIE	91	RVUE	
• • • We do not use the following data for averages, fits, limits, etc. • • •				
not seen	ABELE	97H	CBAR	$\bar{p}p \to K_L^0 K_S^0 \pi^0 \pi^0$

$\Gamma(K\overline{K})/\Gamma(\omega\pi)$ Γ_{13}/Γ_3

VALUE	DOCUMENT ID		TECN
<0.08	[40] DONNACHIE	91	RVUE

[38] $\omega\pi$ not included.
[39] Using ABELE 97.
[40] Using data from BISELLO 91B, DOLINSKY 86 and ALBRECHT 87L.

$\rho(1450)$ REFERENCES

AKHMETSHIN	03B	PL B562 173	R.R. Akhmetshin *et al.* (Novosibirsk CMD-2 Collab.)
ABELE	01B	EPJ C21 261	A. Abele *et al.* (Crystal Barrel Collab.)
AKHMETSHIN	01B	PL B509 217	R.R. Akhmetshin *et al.* (Novosibirsk CMD-2 Collab.)
ALEXANDER	01B	PR D64 092001	J.P. Alexander *et al.* (CLEO Collab.)
AKHMETSHIN	00D	PL B489 125	R.R. Akhmetshin *et al.* (Novosibirsk CMD-2 Collab.)
AMELIN	00	NP A668 83	D. Amelin *et al.* (VES Collab.)
ANDERSON	00A	PR D61 112002	S. Anderson *et al.* (CLEO Collab.)
EDWARDS	00A	PR D61 072003	K.W. Edwards *et al.* (CLEO Collab.)
ABELE	99C	PL B450 275	A. Abele *et al.* (Crystal Barrel Collab.)
ABELE	99D	PL B468 178	A. Abele *et al.* (Crystal Barrel Collab.)
BERTIN	98	PR D57 55	A. Bertin *et al.* (OBELIX Collab.)
ABELE	97	PL B391 191	A. Abele *et al.* (Crystal Barrel Collab.)
ABELE	97H	PL B415 280	A. Abele *et al.* (Crystal Barrel Collab.)
ACHASOV	97	PR D55 2663	N.N. Achasov *et al.* (NOVM)
BARATE	97M	ZPHY C76 15	R. Barate *et al.* (ALEPH Collab.)
BERTIN	97C	PL B408 476	A. Bertin *et al.* (OBELIX Collab.)
BERTIN	97D	PL B414 220	A. Bertin *et al.* (OBELIX Collab.)
CLEGG	94	ZPHY C62 455	A.B. Clegg, A. Donnachie (LANC, MCHS)
BISELLO	91B	NPBPS B21 111	D. Bisello (DM2 Collab.)
DOLINSKY	91	PRPL 202 99	S.I. Dolinsky *et al.* (NOVO)
DONNACHIE	91	ZPHY C51 689	A. Donnachie, A.B. Clegg (MCHS, LANC)
FUKUI	91	PL B257 241	S. Fukui *et al.* (SUGI, NAGO, KEK, KYOT+)
ARMSTRONG	89E	PL B228 536	T.A. Armstrong, M. Benayoun (ATHU, BARI, BIRM+)
BISELLO	89	PL B220 321	D. Bisello *et al.* (DM2 Collab.)
DUBNICKA	89	JPG 15 1349	S. Dubnicka *et al.* (JINR, SLOV)
ANTONELLI	88	PL B212 133	A. Antonelli *et al.* (DM2 Collab.)
CLEGG	88	ZPHY C40 313	A.B. Clegg, A. Donnachie (MCHS, LANC)
DIEKMAN	88	PRPL 159 101	B. Diekmann (BONN)
FUKUI	88	PL B202 441	S. Fukui *et al.* (SUGI, NAGO, KEK, KYOT+)
ALBRECHT	87L	PL B185 223	H. Albrecht *et al.* (ARGUS Collab.)
AULCHENKO	87B	JETPL 45 145 Translated from ZETFP 45 118.	V.M. Aulchenko *et al.* (NOVO)
BITYUKOV	87	PL B188 383	S.I. Bityukov *et al.* (SERP)
DONNACHIE	87B	ZPHY C34 257	A. Donnachie, A.B. Clegg (MCHS, LANC)
DOLINSKY	86	PL B174 453	S.I. Dolinsky *et al.* (NOVO)
KURDADZE	83	JETPL 37 733 Translated from ZETFP 37 613.	L.M. Kurdadze *et al.* (NOVO)
ASTON	80C	PL 92B 211	D. Aston (BONN, CERN, EPOL, GLAS, LANC+)
BARBER	80C	ZPHY C4 169	D.P. Barber *et al.* (DARE, LANC, SHEF)
GOUNARIS	68	PRL 21 244	G.J. Gounaris, J.J. Sakurai

OTHER RELATED PAPERS

ACHASOV	03C	JETP 96 789 Translated from ZETF 123 899.	M.N. Achasov *et al.* (Novosibirsk SND Collab.)
ACHASOV	02B	PAN 65 153 Translated from YAF 65 158.	N.N. Achasov, A.A. Kozhevnikov
CLOSE	02	PR D65 092003	F.E. Close, A. Donnachie, Yu.S. Kalashnikova
ADAMS	01B	PL B516 264	G.S. Adams *et al.* (BNL E852 Collab.)
ACHASOV	00I	PL B486 29	M.N. Achasov *et al.* (Novosibirsk SND Collab.)
ACHASOV	00J	PR D62 117503	N.N. Achasov, A.A. Kozhevnikov
AULCHENKO	00A	JETP 90 927 Translated from ZETF 117 1067.	V.M. Aulchenko *et al.* (Novosibirsk SND Collab.)
BELOZEROVA	98	PPN 29 63 Translated from FECAY 29 148.	T.S. Belozerova, V.K. Henner
ABELE	97H	PL B415 280	A. Abele *et al.* (Crystal Barrel Collab.)
BARNES	97	PR D55 4157	T. Barnes *et al.* (ORNL, RAL, MCHS)
CLOSE	97C	PR D56 1584	F.E. Close *et al.* (RAL, MCHS)
URHEIM	97	NPBPS 55C 359	J. Urheim (CLEO Collab.)
ACHASOV	96B	PAN 59 1262 Translated from YAF 59 1319.	N.N. Achasov, G.N. Shestakov (NOVM)
MURADOV	94	PAN 57 864	R.K. Muradov (BAKU)
LANDSBERG	92	SJNP 55 1051 Translated from YAF 55 1896.	L.G. Landsberg (SERP)
BRAU	88	PR D37 2379	J.E. Brau *et al.*
KURDADZE	86	JETPL 43 643 Translated from ZETFP 43 497.	L.M. Kurdadze *et al.* (NOVO)
BARKOV	85	NP B256 365	L.M. Barkov *et al.* (NOVO)
BISELLO	85	LAL 85-15	D. Bisello *et al.* (PADO, LALO, CLER+)
ABE	84B	PRL 53 751	K. Abe *et al.*
ATKINSON	84C	NP B243 1	M. Atkinson *et al.* (BONN, CERN, GLAS+)
CORDIER	82	PL 109B 129	A. Cordier *et al.* (LALO)
BISELLO	81	PL 107B 145	D. Bisello *et al.* (DM1 Collab.)
KILLIAN	80	PR D21 3005	T.J. Killian *et al.* (CORN)
COSME	76	PL 63B 352	G. Cosme *et al.* (ORSAY)
BINGHAM	72B	PL 41B 635	H.H. Bingham *et al.* (LBL, UCB, SLAC)
FRENKIEL	72	NP B47 61	P. Frenkiel *et al.* (CDEF, CERN)
LAYSSAC	71	NC 6A 134	J. Layssac, F.M. Renard (MONP)

$\eta(1475)$ was $\eta(1440)$

$I^G(J^{PC}) = 0^+(0^{-+})$

See also the $\eta(1405)$.

$\eta(1475)$ MASS

$K\overline{K}\pi$ MODE ($K^*(892)$ K dominant)

VALUE (MeV)	EVTS	DOCUMENT ID		TECN	COMMENT
1476± 4 OUR AVERAGE Error includes scale factor of 1.4. See the ideogram below.					
1460±19	3651	NICHITIU	02	OBLX	
1485± 8± 5	20k	ADAMS	01B	E852	18 GeV $\pi^- p \to K^+K^-\pi^0 n$
1500±10		CICALO	99	OBLX	0 $\bar{p}p \to K^\pm K_S^0 \pi^\mp \pi^+ \pi^-$
1464±10		BERTIN	97	OBLX	0 $\bar{p}p \to K^\pm (K^0) \pi^\mp \pi^+ \pi^-$
1460±10		BERTIN	95	OBLX	0 $\bar{p}p \to K\overline{K}\pi\pi\pi$
$1490^{+14+3}_{-\ 8-16}$	1100	BAI	90C	MRK3	$J/\psi \to \gamma K_S^0 K^\pm \pi^\mp$
1475± 4		RATH	89	MPS	21.4 $\pi^- p \to n K_S^0 K_S^0 \pi^0$
• • • We do not use the following data for averages, fits, limits, etc. • • •					
1421±14		AUGUSTIN	92	DM2	$J/\psi \to \gamma K\overline{K}\pi$

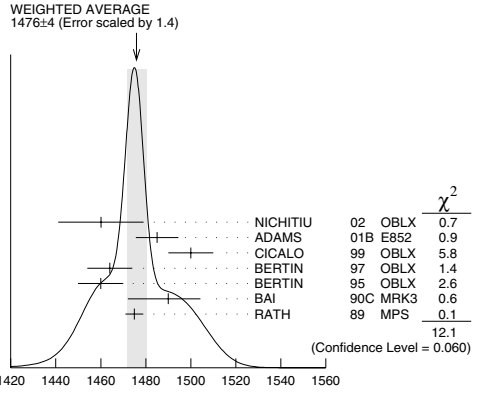

$\eta(1405)$ mass, $K\overline{K}\pi$ mode ($K^*(892)$ K dominant) (MeV)

$\eta(1475)$ WIDTH

$K\overline{K}\pi$ MODE ($K^*(892)$ K dominant)

VALUE (MeV)	EVTS	DOCUMENT ID		TECN	COMMENT
87± 9 OUR AVERAGE Error includes scale factor of 1.6. See the ideogram below.					
120±19	3651	NICHITIU	02	OBLX	
98±18± 3	20k	ADAMS	01B	E852	18 GeV $\pi^- p \to K^+K^-\pi^0 n$
100±20		CICALO	99	OBLX	0 $\bar{p}p \to K^\pm K_S^0 \pi^\mp \pi^+ \pi^-$
105±15		BERTIN	97	OBLX	0.0 $\bar{p}p \to K^\pm (K^0) \pi^\mp \pi^+ \pi^-$
105±15		BERTIN	95	OBLX	0 $\bar{p}p \to K\overline{K}\pi\pi\pi$
63±18		AUGUSTIN	92	DM2	$J/\psi \to \gamma K\overline{K}\pi$
54^{+37+13}_{-21-24}		BAI	90C	MRK3	$J/\psi \to \gamma K_S^0 K^\pm \pi^\mp$
51±13		RATH	89	MPS	21.4 $\pi^- p \to n K_S^0 K_S^0 \pi^0$

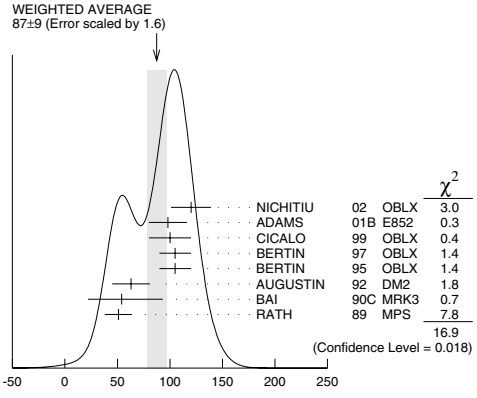

$\eta(1405)$ width $K\overline{K}\pi$ mode ($K^*(892)$ K dominant)

$\eta(1475)$ DECAY MODES

	Mode	Fraction (Γ_i/Γ)
Γ_1	$K\overline{K}\pi$	dominant
Γ_2	$K\overline{K}^*(892)+$ c.c.	seen
Γ_3	$a_0(980)\pi$	seen
Γ_4	$\gamma\gamma$	seen

$\eta(1475)$ Γ(i)$\Gamma(\gamma\gamma)/\Gamma$(total)

$\Gamma(K\overline{K}\pi) \times \Gamma(\gamma\gamma)/\Gamma_{\text{total}}$ $\Gamma_1\Gamma_4/\Gamma$

VALUE (keV)	DOCUMENT ID		TECN	COMMENT
0.212±0.050±0.023	[1] ACCIARRI	01G	L3	183–202 $e^+e^- \to e^+e^- K^0_S K^\pm\pi^\mp$

[1] Signal compatible with K^*K decay.

$\eta(1475)$ BRANCHING RATIOS

$\Gamma(K\overline{K}^*(892)+\text{c.c.})/\Gamma(K\overline{K}\pi)$ Γ_2/Γ_1

VALUE	DOCUMENT ID		TECN	COMMENT
• • • We do not use the following data for averages, fits, limits, etc. • • •				
0.50±0.10	[2] BAILLON	67	HBC	0.0 $\overline{p}p \to K\overline{K}\pi\pi\pi$

$\Gamma(K\overline{K}^*(892)+\text{c.c.})/[\Gamma(K\overline{K}^*(892)+\text{c.c.})+\Gamma(a_0(980)\pi)]$ $\Gamma_2/(\Gamma_2+\Gamma_3)$

VALUE	CL%	DOCUMENT ID		TECN	COMMENT
• • • We do not use the following data for averages, fits, limits, etc. • • •					
<0.25	90	EDWARDS	82E	CBAL	$J/\psi \to K^+K^-\pi^0\gamma$

[2] Data could also refer to $\eta(1405)$.

$\eta(1475)$ REFERENCES

NICHITIU	02	PL B545 261	F. Nichitiu *et al.*	(OBELIX Collab.)
ACCIARRI	01G	PL B501 1	M. Acciarri *et al.*	(L3 Collab.)
ADAMS	01B	PL B516 264	G.S. Adams *et al.*	(BNL E852 Collab.)
CICALO	99	PL B462 453	C. Cicalo *et al.*	(OBELIX Collab.)
BERTIN	97	PL B400 226	A. Bertin *et al.*	(OBELIX Collab.)
BERTIN	95	PL B361 187	A. Bertin *et al.*	(OBELIX Collab.)
AUGUSTIN	92	PR D46 1951	J.E. Augustin, G. Cosme	(DM2 Collab.)
BAI	90C	PRL 65 2507	Z. Bai *et al.*	(Mark III Collab.)
RATH	89	PR D40 693	M.G. Rath *et al.*	(NDAM, BRAN, BNL, CUNY+)
EDWARDS	82E	PRL 49 259	C. Edwards *et al.*	(CIT, HARV, PRIN+)
BAILLON	67	NC 50A 393	P.H. Baillon *et al.*	(CERN, CDEF, IRAD)

$f_0(1500)$ $I^G(J^{PC}) = 0^+(0^{++})$

See also the mini-reviews on scalar mesons under $f_0(600)$ and on non-$q\overline{q}$ candidates. (See the index for the page number.)

$f_0(1500)$ MASS

VALUE (MeV)	EVTS	DOCUMENT ID		TECN	COMMENT
1507± 5 OUR AVERAGE		Error includes scale factor of 1.2.			
1515±12		[1] BARBERIS	00A		450 $pp \to p_f\eta\eta p_s$
1511± 9		[1,2] BARBERIS	00C		450 $pp \to p_f 4\pi p_s$
1510± 8		[1] BARBERIS	00E		450 $pp \to p_f\eta\eta p_s$
1522±25		BERTIN	98	OBLX	0.05–0.405 $\overline{n}p \to \pi^+\pi^+\pi^-$
1449±20		[1] BERTIN	97C	OBLX	0.0 $\overline{p}p \to \pi^+\pi^-\pi^0$
1515±20		ABELE	96B	CBAR	0.0 $\overline{p}p \to \pi^0 K^0_L K^0_L$
1500±15		[3] AMSLER	95B	CBAR	0.0 $\overline{p}p \to 3\pi^0$
1505±15		[4] AMSLER	95C	CBAR	0.0 $\overline{p}p \to \eta\eta\pi^0$
• • • We do not use the following data for averages, fits, limits, etc. • • •					
$1489^{+\ 8}_{-\ 4}$		[13] ANISOVICH	03	RVUE	
1490±30		[5] ABELE	01	CBAR	0.0 $\overline{p}d \to \pi^- 4\pi^0 p$
1497±10		[5] BARBERIS	99	OMEG	450 $pp \to p_s p_f K^+K^-$
1502±10		[5] BARBERIS	99B	OMEG	450 $pp \to p_s p_f \pi^+\pi^-$
1502±12±10		[6] BARBERIS	99D	OMEG	450 $pp \to K^+K^-$, $\pi^+\pi^-$
1530±45		[5] BELLAZZINI	99	GAM4	450 $pp \to pp\pi^0\pi^0$
1505±18		[5] FRENCH	99		300 $pp \to p_f(K^+K^-)p_s$
1447±27		[7] KAMINSKI	99	RVUE	$\pi\pi \to \pi\pi$, $K\overline{K}$, $\sigma\sigma$
1580±80		[5] ALDE	98	GAM4	100 $\pi^- p \to \pi^0\pi^0 n$
1499± 8		[1] ANISOVICH	98B	RVUE	Compilation
~ 1520		REYES	98	SPEC	800 $pp \to p_s p_f K^0_S K^0_S$
1510±20		[1] BARBERIS	97B	OMEG	450 $pp \to pp2(\pi^+\pi^-)$
~ 1475		FRABETTI	97D	E687	$D^\pm_s \to \pi^\mp\pi^\pm\pi^\pm$
~ 1505		ABELE	96	CBAR	0.0 $\overline{p}p \to 5\pi^0$
1500± 8		[1] ABELE	96C	RVUE	Compilation
1460±20	120	[5] AMELIN	96B	VES	37 $\pi^- A \to \eta\eta\pi^- A$
1500± 8		BUGG	96	RVUE	
1500±10		[8] AMSLER	95D	CBAR	0.0 $\overline{p}p \to \pi^0\pi^0\pi^0$, $\pi^0\eta\eta$, $\pi^0\pi^0\eta$
1445± 5		[9] ANTINORI	95	OMEG	300,450 $pp \to pp2(\pi^+\pi^-)$
1497±30		[5] ANTINORI	95	OMEG	300,450 $pp \to pp\pi^+\pi^-$
~ 1505		BUGG	95	MRK3	$J/\psi \to \gamma\pi^+\pi^-\pi^+\pi^-$
1446± 5		[5] ABATZIS	94	OMEG	450 $pp \to pp2(\pi^+\pi^-)$
1545±25		[5] AMSLER	94E	CBAR	0.0 $\overline{p}p \to \pi^0\eta\eta'$
1520±25		[1,10] ANISOVICH	94	CBAR	0.0 $\overline{p}p \to 3\pi^0, \pi^0\eta\eta$
1505±20		[1,11] BUGG	94	RVUE	$\overline{p}p \to 3\pi^0, \eta\eta\pi^0$, $\eta\pi^0\pi^0$
1560±25		[5] AMSLER	92	CBAR	0.0 $\overline{p}p \to \pi^0\eta\eta$
1550±45±30		[5] BELADIDZE	92C	VES	36 π^- Be $\to \pi^-\eta'\eta$ Be
1449± 4		[5] ARMSTRONG	89E	OMEG	300 $pp \to pp2(\pi^+\pi^-)$
1610±20		[5] ALDE	88	GAM4	300 $\pi^- N \to \pi^- N 2\eta$
~ 1525		ASTON	88D	LASS	11 $K^- p \to K^0_S K^0_S \Lambda$
1570±20	600	[5] ALDE	87	GAM4	100 $\pi^- p \to 4\pi^0 n$
1575±45		[12] ALDE	86D	GAM4	100 $\pi^- p \to 2\eta n$
1568±33		[5] BINON	84C	GAM2	38 $\pi^- p \to \eta\eta' n$
1592±25		[5] BINON	83	GAM2	38 $\pi^- p \to 2\eta n$
1525± 5		[5] GRAY	83	DBC	0.0 $\overline{p}N \to 3\pi$

[1] T-matrix pole.
[2] Average between $\pi^+\pi^- 2\pi^0$ and $2(\pi^+\pi^-)$.
[3] T-matrix pole, supersedes ANISOVICH 94.
[4] T-matrix pole, supersedes ANISOVICH 94 and AMSLER 92.
[5] Breit-Wigner mass.
[6] Supersedes BARBERIS 99 and BARBERIS 99B.
[7] T-matrix pole on sheet $--+$.
[8] T-matrix pole. Coupled-channel analysis of AMSLER 95B, AMSLER 95C, and AMSLER 94D.
[9] Supersedes ABATZIS 94, ARMSTRONG 89E. Breit-Wigner mass.
[10] From a simultaneous analysis of the annihilations $\overline{p}p \to 3\pi^0, \pi^0\eta\eta$.
[11] Reanalysis of ANISOVICH 94 data.
[12] From central value and spread of two solutions. Breit-Wigner mass.
[13] K-matrix pole from combined analysis of $\pi^- p \to \pi^0\pi^0 n$, $\pi^- p \to K\overline{K} n$, $\pi^+\pi^- \to \pi^+\pi^-$, $\overline{p}p \to \pi^0\pi^0\pi^0, \pi^0\eta\eta, \pi^0\pi^0\eta, \pi^+\pi^-\pi^0, K^+K^-\pi^0, K^0_S K^0_S \pi^0$, $K^+K^0_S\pi^-$ at rest, $\overline{p}n \to \pi^-\pi^-\pi^+, K^0_S K^-\pi^0, K^0_S K^0_S \pi^-$ at rest.

$f_0(1500)$ WIDTH

VALUE (MeV)	EVTS	DOCUMENT ID		TECN	COMMENT
109± 7 OUR AVERAGE					
110± 24		[14] BARBERIS	00A		450 $pp \to p_f \eta\eta p_s$
102± 18		[14,15] BARBERIS	00C		450 $pp \to p_f 4\pi p_s$
110± 16		[14] BARBERIS	00E		450 $pp \to p_f \eta\eta p_s$
108± 33		BERTIN	98	OBLX	0.05–0.405 $\overline{n}p \to \pi^+\pi^+\pi^-$
114± 30		[14] BERTIN	97C	OBLX	0.0 $\overline{p}p \to \pi^+\pi^-\pi^0$
105± 15		ABELE	96B	CBAR	0.0 $\overline{p}p \to \pi^0 K^0_L K^0_L$
120± 25		[16] AMSLER	95B	CBAR	0.0 $\overline{p}p \to 3\pi^0$
120± 30		[17] AMSLER	95C	CBAR	0.0 $\overline{p}p \to \eta\eta\pi^0$
• • • We do not use the following data for averages, fits, limits, etc. • • •					
102± 10		[27] ANISOVICH	03	RVUE	
140± 40		[18] ABELE	01	CBAR	0.0 $\overline{p}d \to \pi^- 4\pi^0 p$
104± 25		[18] BARBERIS	99	OMEG	450 $pp \to p_s p_f K^+K^-$
131± 15		[18] BARBERIS	99B	OMEG	450 $pp \to p_s p_f \pi^+\pi^-$
98± 18±16		[19] BARBERIS	99D	OMEG	450 $pp \to K^+K^-, \pi^+\pi^-$
160± 50		[18] BELLAZZINI	99	GAM4	450 $pp \to pp\pi^0\pi^0$
100± 33		[18] FRENCH	99		300 $pp \to p_f(K^+K^-)p_s$
108± 46		[20] KAMINSKI	99	RVUE	$\pi\pi \to \pi\pi, K\overline{K}, \sigma\sigma$
280±100		[21] ALDE	98	GAM4	100 $\pi^- p \to \pi^0\pi^0 n$
130± 20		[14] ANISOVICH	98B	RVUE	Compilation
120± 35		[14] BARBERIS	97B	OMEG	450 $pp \to pp2(\pi^+\pi^-)$
~ 100		FRABETTI	97D	E687	$D_s^\pm \to \pi^\mp\pi^\pm\pi^\pm$
~ 169		ABELE	96	CBAR	0.0 $\overline{p}p \to 5\pi^0$
100± 30	120	[18] AMELIN	96B	VES	37 $\pi^- A \to \eta\eta\pi^- A$
132± 15		BUGG	96	RVUE	
154± 30		[22] AMSLER	95D	CBAR	0.0 $\overline{p}p \to \pi^0\pi^0\pi^0, \pi^0\eta\eta, \pi^0\pi^0\eta$
65± 10		[23] ANTINORI	95	OMEG	300,450 $pp \to pp2(\pi^+\pi^-)$
199± 30		[18] ANTINORI	95	OMEG	300,450 $pp \to pp\pi^+\pi^-$
56± 12		[18] ABATZIS	94	OMEG	450 $pp \to pp2(\pi^+\pi^-)$
100± 40		[18] AMSLER	94E	CBAR	0.0 $\overline{p}p \to \pi^0\eta\eta'$
$148^{+\ 20}_{-\ 25}$		[14,24] ANISOVICH	94	CBAR	0.0 $\overline{p}p \to 3\pi^0, \pi^0\eta\eta$
150± 20		[14,25] BUGG	94	RVUE	$\overline{p}p \to 3\pi^0, \eta\eta\pi^0, \eta\pi^0\pi^0$
245± 50		[18] AMSLER	92	CBAR	0.0 $\overline{p}p \to \pi^0\eta\eta$
153± 67±50		[18] BELADIDZE	92C	VES	36 π^-Be $\to \pi^-\eta'\eta$Be
78± 18		[18] ARMSTRONG	89E	OMEG	300 $pp \to pp2(\pi^+\pi^-)$
170± 40		[18] ALDE	88	GAM4	300 $\pi^- N \to \pi^- N 2\eta$
150± 20	600	[18] ALDE	87	GAM4	100 $\pi^- p \to 4\pi^0 n$
265± 65		[26] ALDE	86D	GAM4	100 $\pi^- p \to 2\eta n$
260± 60		[18] BINON	84C	GAM2	38 $\pi^- p \to \eta\eta' n$
210± 40		[18] BINON	83	GAM2	38 $\pi^- p \to 2\eta n$
101± 13		[18] GRAY	83	DBC	0.0 $\overline{p}N \to 3\pi$

[14] T-matrix pole.
[15] Average between $\pi^+\pi^-2\pi^0$ and $2(\pi^+\pi^-)$.
[16] T-matrix pole, supersedes ANISOVICH 94.
[17] T-matrix pole, supersedes ANISOVICH 94 and AMSLER 92.
[18] Breit-Wigner width.
[19] Supersedes BARBERIS 99 and BARBERIS 99B.
[20] T-matrix pole on sheet $--+$.
[21] Breit-Wigner width.
[22] T-matrix pole. Coupled-channel analysis of AMSLER 95B, AMSLER 95C, and AMSLER 94D.
[23] Supersedes ABATZIS 94, ARMSTRONG 89E. Breit-Wigner mass.
[24] From a simultaneous analysis of the annihilations $\overline{p}p \to 3\pi^0, \pi^0\eta\eta$.
[25] Reanalysis of ANISOVICH 94 data.
[26] From central value and spread of two solutions. Breit-Wigner mass.
[27] K-matrix pole from combined analysis of $\pi^- p \to \pi^0\pi^0 n$, $\pi^- p \to K\overline{K}n$, $\pi^+\pi^- \to \pi^+\pi^-$, $\overline{p}p \to \pi^0\pi^0\pi^0, \pi^0\eta\eta, \pi^0\pi^0\eta, \pi^+\pi^-\pi^0, K^+K^-\pi^0, K^0_S K^0_S\pi^0, K^+K^0_S\pi^-$ at rest, $\overline{p}n \to \pi^-\pi^-\pi^+, K^0_S K^-\pi^0, K^0_S K^0_S\pi^-$ at rest.

$f_0(1500)$ DECAY MODES

	Mode	Fraction (Γ_i/Γ)	Scale factor
Γ_1	$\eta\eta'(958)$	(1.9±0.8) %	1.7
Γ_2	$\eta\eta$	(5.1±0.9) %	1.4
Γ_3	4π	(49.5±3.3) %	1.2
Γ_4	$4\pi^0$	seen	
Γ_5	$2\pi^+2\pi^-$	seen	
Γ_6	$2(\pi\pi)_S$-wave		
Γ_7	$\rho\rho$		
Γ_8	$\pi(1300)\pi$		
Γ_9	$a_1(1260)\pi$		
Γ_{10}	$\pi\pi$	(34.9±2.3) %	1.2
Γ_{11}	$\pi^+\pi^-$	seen	
Γ_{12}	$2\pi^0$	seen	
Γ_{13}	$K\overline{K}$	(8.6±1.0) %	1.1
Γ_{14}	$\gamma\gamma$	not seen	

CONSTRAINED FIT INFORMATION

An overall fit to 6 branching ratios uses 10 measurements and one constraint to determine 5 parameters. The overall fit has a $\chi^2 = 11.4$ for 6 degrees of freedom.

The following *off-diagonal* array elements are the correlation coefficients $\langle \delta x_i \delta x_j \rangle / (\delta x_i \cdot \delta x_j)$, in percent, from the fit to the branching fractions, $x_i \equiv \Gamma_i/\Gamma_{\rm total}$. The fit constrains the x_i whose labels appear in this array to sum to one.

x_2	29			
x_3	−31	−52		
x_{10}	−5	11	−83	
x_{13}	6	33	−67	39
	x_1	x_2	x_3	x_{10}

$f_0(1500)$ $\Gamma(i)\Gamma(\gamma\gamma)/\Gamma(\text{total})$

$\Gamma(\pi\pi) \times \Gamma(\gamma\gamma)/\Gamma_{\rm total}$ $\Gamma_{10}\Gamma_{14}/\Gamma$

VALUE (keV)	CL%	DOCUMENT ID	TECN	COMMENT
• • • We do not use the following data for averages, fits, limits, etc. • • •				
not seen		ACCIARRI	01H L3	$\gamma\gamma \to K^0_S K^0_S$, $E^{ee}_{\rm cm}$ = 91, 183–209 GeV
<0.46	95	BARATE	00E ALEP	$\gamma\gamma \to \pi^+\pi^-$

$f_0(1500)$ BRANCHING RATIOS

$\Gamma(\eta\eta)/\Gamma(\pi\pi)$ Γ_2/Γ_{10}

VALUE	DOCUMENT ID		TECN	COMMENT
0.145±0.027 OUR FIT Error includes scale factor of 1.5.				
0.14 ±0.04 OUR AVERAGE Error includes scale factor of 1.7. See the ideogram below.				
0.080±0.033	AMSLER	02	CBAR	0.9 $\overline{p}p \to \pi^0\eta\eta, \pi^0\pi^0\pi^0$
0.18 ±0.03	BARBERIS	00E		450 $pp \to p_f \eta\eta p_s$
0.230±0.097	[28] AMSLER	95C	CBAR	0.0 $\overline{p}p \to \eta\eta\pi^0$
• • • We do not use the following data for averages, fits, limits, etc. • • •				
0.11 ±0.03	[29] ANISOVICH	02D	SPEC	Combined fit
0.078±0.013	[30] ABELE	96C	RVUE	Compilation
0.157±0.060	[31] AMSLER	95D	CBAR	0.0 $\overline{p}p \to \pi^0\pi^0\pi^0, \pi^0\eta\eta, \pi^0\pi^0\eta$

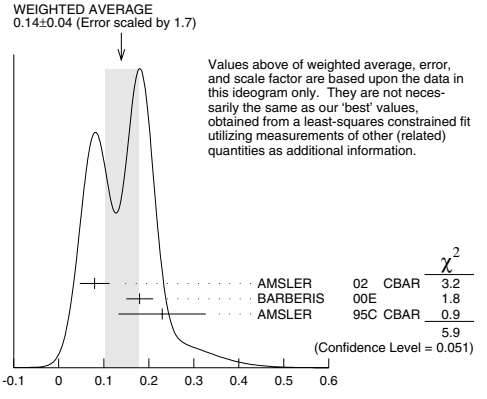

$\Gamma(\eta\eta)/\Gamma(\pi\pi)$ Γ_2/Γ_{10}

$\Gamma(K\overline{K})/\Gamma(\eta\eta)$ Γ_{13}/Γ_2

VALUE	CL%	DOCUMENT ID	TECN	COMMENT
1.69±0.33 OUR FIT Error includes scale factor of 1.4.				
1.85±0.41		BARBERIS	00E	450 $pp \to p_f \eta\eta p_s$
• • • We do not use the following data for averages, fits, limits, etc. • • •				
1.5 ±0.6		[29] ANISOVICH	02D SPEC	Combined fit
<0.4	90	[32] PROKOSHKIN	91 GAM4	300 $\pi^- p \to \pi^- p\eta\eta$
<0.6		[33] BINON	83 GAM2	38 $\pi^- p \to 2\eta n$

$\Gamma(K\overline{K})/\Gamma(\pi\pi)$ Γ_{13}/Γ_{10}

VALUE	DOCUMENT ID		TECN	COMMENT
0.246±0.026 OUR FIT				
0.241±0.028 OUR AVERAGE				
0.25 ±0.03	[34] BARGIOTTI	03	OBLX	$\overline{p}p$
0.19 ±0.07	[35] ABELE	98	CBAR	$0.0\,\overline{p}p \rightarrow K_L^0 K^\pm \pi^\mp$
• • • We do not use the following data for averages, fits, limits, etc. • • •				
0.16 ±0.05	[29] ANISOVICH	02D	SPEC	Combined fit
0.33 ±0.03 ±0.07	BARBERIS	99D	OMEG	$450\,pp \rightarrow K^+K^-, \pi^+\pi^-$
0.20 ±0.08	[36] ABELE	96B	CBAR	$0.0\,\overline{p}p \rightarrow \pi^0 K_L^0 K_L^0$

$\Gamma(\eta\eta'(958))/\Gamma(\pi\pi)$ Γ_1/Γ_{10}

VALUE	DOCUMENT ID		TECN	COMMENT
0.055±0.024 OUR FIT Error includes scale factor of 1.8.				
0.095±0.026	BARBERIS	00A		$450\,pp \rightarrow p_f \eta\eta p_s$
• • • We do not use the following data for averages, fits, limits, etc. • • •				
0.005±0.003	[29] ANISOVICH	02D	SPEC	Combined fit

$\Gamma(\eta\eta'(958))/\Gamma(\eta\eta)$ Γ_1/Γ_2

VALUE	DOCUMENT ID		TECN	COMMENT
0.38±0.16 OUR FIT Error includes scale factor of 1.9.				
0.29±0.10	[37] AMSLER	95C	CBAR	$0.0\,\overline{p}p \rightarrow \eta\eta\pi^0$
• • • We do not use the following data for averages, fits, limits, etc. • • •				
0.05±0.03	[29] ANISOVICH	02D	SPEC	Combined fit
0.84±0.23	ABELE	96C	RVUE	Compilation
2.7 ±0.8	BINON	84C	GAM2	$38\,\pi^- p \rightarrow \eta\eta' n$

$\Gamma(\pi\pi)/\Gamma_{\text{total}}$ Γ_{10}/Γ

VALUE	DOCUMENT ID		TECN
• • • We do not use the following data for averages, fits, limits, etc. • • •			
0.454±0.104	BUGG	96	RVUE

$\Gamma(\pi^+\pi^-)/\Gamma_{\text{total}}$ Γ_{11}/Γ

VALUE	DOCUMENT ID		TECN	COMMENT
• • • We do not use the following data for averages, fits, limits, etc. • • •				
seen	BERTIN	98	OBLX	0.05–$0.405\ \overline{n}p \rightarrow \pi^+\pi^+\pi^-$
possibly seen	FRABETTI	97D	E687	$D_s^\pm \rightarrow \pi^\mp\pi^\pm\pi^\pm$

$\Gamma(K\overline{K})/\Gamma_{\text{total}}$ Γ_{13}/Γ

VALUE	DOCUMENT ID		TECN
• • • We do not use the following data for averages, fits, limits, etc. • • •			
0.044±0.021	BUGG	96	RVUE

$\Gamma(\eta\eta)/\Gamma_{\text{total}}$ Γ_2/Γ

VALUE	DOCUMENT ID		TECN	COMMENT
• • • We do not use the following data for averages, fits, limits, etc. • • •				
large	ALDE	88	GAM4	$300\,\pi^- N \rightarrow \eta\eta\pi^- N$
large	BINON	83	GAM2	$38\,\pi^- p \rightarrow 2\eta n$

$\Gamma(4\pi)/\Gamma(\pi\pi)$ Γ_3/Γ_{10}

VALUE	DOCUMENT ID		TECN	COMMENT
1.42±0.18 OUR FIT Error includes scale factor of 1.2.				
1.42±0.18 OUR AVERAGE Error includes scale factor of 1.2.				
1.37±0.16	BARBERIS	00D		$450\,pp \rightarrow p_f 4\pi p_s$
2.1 ±0.6	[38] AMSLER	98	RVUE	
• • • We do not use the following data for averages, fits, limits, etc. • • •				
2.1 ±0.2	[29] ANISOVICH	02D	SPEC	Combined fit
3.4 ±0.8	[38] ABELE	96	CBAR	$0.0\,\overline{p}p \rightarrow 5\pi^0$

$\Gamma(4\pi^0)/\Gamma(\eta\eta)$ Γ_4/Γ_2

VALUE	DOCUMENT ID		TECN	COMMENT
• • • We do not use the following data for averages, fits, limits, etc. • • •				
0.8±0.3	ALDE	87	GAM4	$100\,\pi^- p \rightarrow 4\pi^0 n$

$\Gamma(\rho\rho)/\Gamma(2(\pi\pi)_{S\text{-wave}})$ Γ_7/Γ_6

VALUE	DOCUMENT ID		COMMENT
• • • We do not use the following data for averages, fits, limits, etc. • • •			
3.3±0.5	BARBERIS	00C	$450\,pp \rightarrow p_f \pi^+\pi^- 2\pi^0 p_s$
2.6±0.4	BARBERIS	00C	$450\,pp \rightarrow p_f 2(\pi^+\pi^-) p_s$

$\Gamma(2(\pi\pi)_{S\text{-wave}})/\Gamma(\pi\pi)$ Γ_6/Γ_{10}

VALUE	DOCUMENT ID		TECN	COMMENT
• • • We do not use the following data for averages, fits, limits, etc. • • •				
0.42±0.26	[39] ABELE	01	CBAR	$0.0\,\overline{p}d \rightarrow \pi^- 4\pi^0 p$

$\Gamma(2(\pi\pi)_{S\text{-wave}})/\Gamma(4\pi)$ Γ_6/Γ_3

VALUE	DOCUMENT ID		TECN	COMMENT
• • • We do not use the following data for averages, fits, limits, etc. • • •				
0.26±0.07	ABELE	01B	CBAR	$0.0\,\overline{p}n \rightarrow 5\pi$

$\Gamma(\rho\rho)/\Gamma(4\pi)$ Γ_7/Γ_3

VALUE	DOCUMENT ID		TECN	COMMENT
• • • We do not use the following data for averages, fits, limits, etc. • • •				
0.13±0.08	ABELE	01B	CBAR	$0.0\,\overline{p}n \rightarrow 5\pi$

$\Gamma(\pi(1300)\pi)/\Gamma(4\pi)$ Γ_8/Γ_3

VALUE	DOCUMENT ID		TECN	COMMENT
• • • We do not use the following data for averages, fits, limits, etc. • • •				
0.50±0.25	ABELE	01B	CBAR	$0.0\,\overline{p}n \rightarrow 5\pi$

$\Gamma(a_1(1260)\pi)/\Gamma(4\pi)$ Γ_9/Γ_3

VALUE	DOCUMENT ID		TECN	COMMENT
• • • We do not use the following data for averages, fits, limits, etc. • • •				
0.12±0.05	ABELE	01B	CBAR	$0.0\,\overline{p}n \rightarrow 5\pi$

[28] Using AMSLER 95B ($3\pi^0$).
[29] From a combined K-matrix analysis of Crystal Barrel (0. $p\overline{p} \rightarrow \pi^0\pi^0\pi^0$, $\pi^0\eta\eta$, $\pi^0\pi^0\eta$), GAMS ($\pi p \rightarrow \pi^0\pi^0 n$, $\eta\eta n$, $\eta\eta' n$), and BNL ($\pi p \rightarrow K\overline{K}n$) data.
[30] 2π width determined to be 60 ± 12 MeV.
[31] Coupled-channel analysis of AMSLER 95B, AMSLER 95C, and AMSLER 94D.
[32] Combining results of GAM4 with those of WA76 on $K\overline{K}$ central production.
[33] Using ETKIN 82B and COHEN 80.
[34] Coupled channel analysis of $\pi^+\pi^-\pi^0$, $K^+K^-\pi^0$, and $K^\pm K_S^0\pi^\mp$.
[35] Using $\pi^0\pi^0$ from AMSLER 95B.
[36] Using AMSLER 95B ($3\pi^0$), AMSLER 94C ($2\pi^0\eta$) and SU(3).
[37] Using AMSLER 94E ($\eta\eta'\pi^0$).
[38] Excluding $\rho\rho$ contribution to 4π.
[39] From the combined data of ABELE 96 and ABELE 96C.

$f_0(1500)$ REFERENCES

ANISOVICH	03	EPJ A16 229	V.V. Anisovich *et al.*	
BARGIOTTI	03	EPJ C26 371	M. Bargiotti *et al.*	(OBELIX Collab.)
AMSLER	02	EPJ C23 29	C. Amsler *et al.*	
ANISOVICH	02D	PAN 65 1545	V.V. Anisovich *et al.*	
		Translated from YAF 65 1583.		
ABELE	01	EPJ C19 667	A. Abele *et al.*	(Crystal Barrel Collab.)
ABELE	01B	EPJ C21 261	A. Abele *et al.*	(Crystal Barrel Collab.)
ACCIARRI	01H	PL B501 173	M. Acciarri *et al.*	(L3 Collab.)
BARATE	00E	PL B472 189	R. Barate *et al.*	(ALEPH Collab.)
BARBERIS	00A	PL B471 429	D. Barberis *et al.*	(WA 102 Collab.)
BARBERIS	00C	PL B471 440	D. Barberis *et al.*	(WA 102 Collab.)
BARBERIS	00D	PL B474 423	D. Barberis *et al.*	(WA 102 Collab.)
BARBERIS	00E	PL B479 59	D. Barberis *et al.*	(WA 102 Collab.)
BARBERIS	99	PL B453 305	D. Barberis *et al.*	(Omega Expt.)
BARBERIS	99B	PL B453 316	D. Barberis *et al.*	(Omega Expt.)
BARBERIS	99D	PL B462 462	D. Barberis *et al.*	(Omega Expt.)
BELLAZZINI	99	PL B467 296	R. Bellazzini *et al.*	
FRENCH	99	PL B460 213	B. French *et al.*	(WA76 Collab.)
KAMINSKI	99	EPJ C9 141	R. Kaminski, L. Lesniak, B. Loiseau	(CRAC, PARIN)
ABELE	98	PR D57 3860	A. Abele *et al.*	(Crystal Barrel Collab.)
ALDE	98	EPJ A3 361	D. Alde *et al.*	(GAM4 Collab.)
Also	99	PAN 62 405	D. Alde *et al.*	(GAMS Collab.)
		Translated from YAF 62 446.		
AMSLER	98	RMP 70 1293	C. Amsler	
ANISOVICH	98B	UFN 41 419	V.V. Anisovich *et al.*	
BERTIN	98	PR D57 55	A. Bertin *et al.*	(OBELIX Collab.)
REYES	98	PRL 81 4079	M.A. Reyes *et al.*	
BARBERIS	97B	PL B413 217	D. Barberis *et al.*	(WA 102 Collab.)
BERTIN	97C	PL B408 476	A. Bertin *et al.*	(OBELIX Collab.)
FRABETTI	97D	PL B407 79	P.L. Frabetti *et al.*	(FNAL E687 Collab.)
ABELE	96	PL B380 453	A. Abele *et al.*	(Crystal Barrel Collab.)
ABELE	96B	PL B385 425	A. Abele *et al.*	(Crystal Barrel Collab.)
ABELE	96C	NP A609 562	A. Abele *et al.*	(Crystal Barrel Collab.)
AMELIN	96B	PAN 59 976	D.V. Amelin *et al.*	(SERP, TBIL)
		Translated from YAF 59 1021.		
BUGG	96	NP B471 59	D.V. Bugg, A.V. Sarantsev, B.S. Zou	(LOQM, PNPI)
AMSLER	95B	PL B342 433	C. Amsler *et al.*	(Crystal Barrel Collab.)
AMSLER	95C	PL B353 571	C. Amsler *et al.*	(Crystal Barrel Collab.)
AMSLER	95D	PL B355 425	C. Amsler *et al.*	(Crystal Barrel Collab.)
ANTINORI	95	PL B353 589	F. Antinori *et al.*	(ATHU, BARI, BIRM+)
BUGG	95	PL B353 378	D.V. Bugg *et al.*	(LOQM, PNPI, WASH)
ABATZIS	94	PL B324 509	S. Abatzis *et al.*	(ATHU, BARI, BIRM+)
AMSLER	94C	PL B327 425	C. Amsler *et al.*	(Crystal Barrel Collab.)
AMSLER	94D	PL B333 277	C. Amsler *et al.*	(Crystal Barrel Collab.)
AMSLER	94E	PL B340 259	C. Amsler *et al.*	(Crystal Barrel Collab.)
ANISOVICH	94	PL B323 233	V.V. Anisovich *et al.*	(Crystal Barrel Collab.)
BUGG	94	PR D50 4412	D.V. Bugg *et al.*	(LOQM)
AMSLER	92	PL B291 347	C. Amsler *et al.*	(Crystal Barrel Collab.)
BELADIDZE	92C	SJNP 55 1535	G.M. Beladidze, S.I. Bityukov, G.V. Borisov	(SERP+)
		Translated from YAF 55 2748.		
PROKOSHKIN	91	SPD 36 155	Y.D. Prokoshkin	(GAM2, GAM4 Collab.)
		Translated from DANS 316 900.		
ARMSTRONG	89E	PL B228 536	T.A. Armstrong, M. Benayoun	(ATHU, BARI, BIRM+)
ALDE	88	PL B201 160	D.M. Alde *et al.*	(SERP, BELG, LANL, LAPP+)
ASTON	88D	NP B301 525	D. Aston *et al.*	(SLAC, NAGO, CINC, INUS)
ALDE	87	PL B198 286	D.M. Alde *et al.*	(LANL, BRUX, SERP, LAPP)
ALDE	86D	NP B269 485	D.M. Alde *et al.*	(BELG, LAPP, SERP, CERN+)
BINON	84C	NC 80A 363	F.G. Binon *et al.*	(BELG, LAPP, SERP+)
BINON	83	NC 78A 313	F.G. Binon *et al.*	(BELG, LAPP, SERP+)
Also	83B	SJNP 38 561	F.G. Binon *et al.*	(BELG, LAPP, SERP+)
		Translated from YAF 38 934.		
GRAY	83	PR D27 307	L. Gray *et al.*	(SYRA)
ETKIN	82B	PR D25 1786	A. Etkin *et al.*	(BNL, CUNY, TUFTS, VAND)
COHEN	80	PR D22 2595	D. Cohen *et al.*	(ANL)

OTHER RELATED PAPERS

ANISOVICH	03B	PAN 66 741	V.V. Anisovich, V.A. Nikonov, A.V. Sarantsev	
		Translated from YAF 66 772.		
DEWITT	03	PR D68 054026	M.A. DeWitt, H.M. Choi, C.R. Ji	
AMSLER	02B	PL B541 22	C. Amsler	
GARMASH	02	PR D65 092005	A. Garmash *et al.*	(BELLE Collab.)
JIN	02	PR D66 057505	H. Jin, X. Zhang	
KLEEFELD	02	PR D66 034007	F. Kleefeld, E. van Beveren, G. Rupp	
RUPP	02	PR D65 078501	G. Rupp, E. van Beveren, M.D. Scadron	
SHAKIN	02	PR D65 078502	C.M. Shakin, H. Wang	
TESHIMA	02	JPG 28 1391	T. Teshima, I. Kitamura, N. Morisita	
VOLKOV	02	PAN 65 1657	M.K. Volkov, V.L. Yudichev	
		Translated from YAF 65 1701.		

LI	01B	EPJ C19 529	D.-M. Li, H. Yu, Q.-X. Shen	
SUROVTSEV	01	PR D63 054024	Y.S. Surovtsev, D. Krupa, M. Nagy	
BAI	00A	PL B472 207	J.Z. Bai *et al.*	(BES Collab.)
ANISOVICH	99H	PL B467 289	A.V. Anisovich, V.V. Anisovich	
AMSLER	98	RMP 70 1293	C. Amsler	
STROHMEIER	98	PL B438 21	M. Strohmeier *et al.*	
ANISOVICH	97	PL B395 123	A.V. Anisovich, A.V. Sarantsev	(PNPI)
KAMINSKI	97B	PL B413 130	R. Kaminski, L. Lesniak, B. Loiseau	(CRAC, IPN)
PROKOSHKIN	97	SPD 42 117 Translated from DANS 353 323.	Y.D. Prokoshkin *et al.*	(SERP)
AMSLER	96	PR D53 295	C. Amsler, F.E. Close	(ZURI, RAL)
GASPERO	95	NP A588 861	M. Gaspero	(ROMA)
SLAUGHTER	88	MPL A3 1361	M.D. Slaughter	(LANL)
BRIDGES	86B	PRL 56 215	D.L. Bridges *et al.*	(SYRA, CASE)

$f_1(1510)$

$I^G(J^{PC}) = 0^+(1^{++})$

OMITTED FROM SUMMARY TABLE

See the minireview under $\eta(1405)$.

$f_1(1510)$ MASS

VALUE (MeV)	*EVTS*	*DOCUMENT ID*		*TECN*	*COMMENT*
1518± 5 OUR AVERAGE		Error includes scale factor of 1.7. See the ideogram below.			
1530±10		ASTON	88C	LASS	11 $K^- p \to K^0_S K^\pm \pi^\mp \Lambda$
1512± 4	600	[1] BIRMAN	88	MPS	8 $\pi^- p \to K^+ \overline{K}{}^0 \pi^- n$
1526± 6	271	GAVILLET	82	HBC	4.2 $K^- p \to \Lambda K K \pi$
• • • We do not use the following data for averages, fits, limits, etc. • • •					
~ 1525		[2] BAUER	93B		$\gamma\gamma^* \to \pi^+\pi^-\pi^0\pi^0$

[1] From partial wave analysis of $K^+ \overline{K}{}^0 \pi^-$ state.

[2] Not seen by AIHARA 88C in the $K^0_S K^\pm \pi^\mp$ final state.

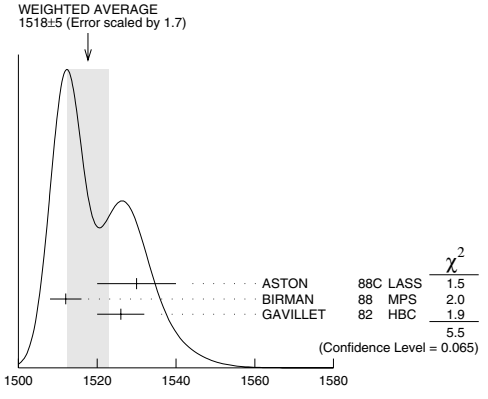

$f_1(1510)$ mass (MeV)

$f_1(1510)$ WIDTH

VALUE (MeV)	*EVTS*	*DOCUMENT ID*		*TECN*	*COMMENT*
73±25 OUR AVERAGE		Error includes scale factor of 2.5. See the ideogram below.			
100±40		ASTON	88C	LASS	11 $K^- p \to K^0_S K^\pm \pi^\mp \Lambda$
35±15	600	[3] BIRMAN	88	MPS	8 $\pi^- p \to K^+ \overline{K}{}^0 \pi^- n$
107±15	271	GAVILLET	82	HBC	4.2 $K^- p \to \Lambda K K \pi$

[3] From partial wave analysis of $K^+ \overline{K}{}^0 \pi^-$ state.

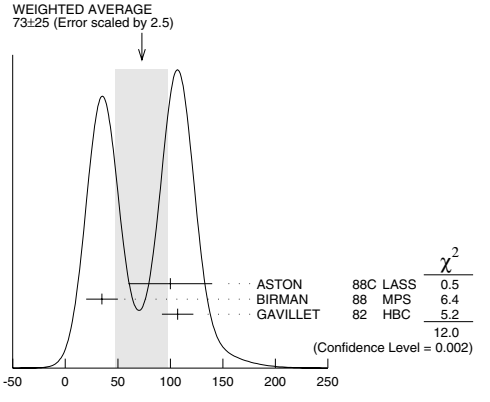

$f_1(1510)$ width (MeV)

$f_1(1510)$ DECAY MODES

	Mode	Fraction (Γ_j/Γ)
Γ_1	$K\overline{K}{}^*(892)+$ c.c.	seen

$f_1(1510)$ REFERENCES

BAUER	93B	PR D48 3976	D.A. Bauer *et al.*	(SLAC)
AIHARA	88C	PR D38 1	H. Aihara *et al.*	(TPC-2γ Collab.)
ASTON	88C	PL B201 573	D. Aston *et al.*	(SLAC, NAGO, CINC, INUS) JP
BIRMAN	88	PRL 61 1557	A. Birman *et al.*	(BNL, FSU, IND, MASD) JP
GAVILLET	82	ZPHY C16 119	P. Gavillet *et al.*	(CERN, CDEF, PADO+)

OTHER RELATED PAPERS

ABELE	97G	PL B415 289	A. Abele *et al.*	
CLOSE	97D	ZPHY C76 469	F.E. Close *et al.*	
KING	91	NPBPS B21 11	E. King *et al.*	(FSU, BNL+)
AIHARA	88C	PR D38 1	H. Aihara *et al.*	(TPC-2γ Collab.)
BITYUKOV	84	SJNP 39 735 Translated from YAF 39 1165.	S. Bityukov *et al.*	(SERP)

$f_2'(1525)$

$I^G(J^{PC}) = 0^+(2^{++})$

$f_2'(1525)$ MASS

VALUE (MeV)	*DOCUMENT ID*
1525±5 OUR ESTIMATE	This is only an educated guess; the error given is larger than the error on the average of the published values.

PRODUCED BY PION BEAM

VALUE (MeV)	*EVTS*	*DOCUMENT ID*		*TECN*	*COMMENT*
• • • We do not use the following data for averages, fits, limits, etc. • • •					
1521±13		TIKHOMIROV	03	SPEC	40.0 π^- C $\to K^0_S K^0_S K^0_L X$
1547^{+10}_{-2}		[2] LONGACRE	86	MPS	22 $\pi^- p \to K^0_S K^0_S n$
1496^{+9}_{-8}		[3] CHABAUD	81	ASPK	6 $\pi^- p \to K^+ K^- n$
1497^{+8}_{-9}		CHABAUD	81	ASPK	18.4 $\pi^- p \to K^+ K^- n$
1492±29		GORLICH	80	ASPK	17 π^- p polarized $\to K^+ K^- n$
1502±25		[4] CORDEN	79	OMEG	12–15 $\pi^- p \to \pi^+ \pi^- n$
1480	14	CRENNELL	66	HBC	6.0 $\pi^- p \to K^0_S K^0_S n$

PRODUCED BY $K^\pm$ BEAM

VALUE (MeV)	*EVTS*	*DOCUMENT ID*		*TECN*	*COMMENT*
1523.5± 1.3 OUR AVERAGE		Includes data from the datablock that follows this one. Error includes scale factor of 1.1.			
1526.8± 4.3		ASTON	88D	LASS	11 $K^- p \to K^0_S K^0_S \Lambda$
1504 ±12		BOLONKIN	86	SPEC	40 $K^- p \to K^0_S K^0_S Y$
1529 ± 3		ARMSTRONG	83B	OMEG	18.5 $K^- p \to K^- K^+ \Lambda$
1521 ± 6	650	AGUILAR-...	81B	HBC	4.2 $K^- p \to \Lambda K^+ K^-$
1521 ± 3	572	ALHARRAN	81	HBC	8.25 $K^- p \to \Lambda K \overline{K}$
1522 ± 6	123	BARREIRO	77	HBC	4.15 $K^- p \to \Lambda K^0_S K^0_S$
1528 ± 7	166	EVANGELISTA	77	OMEG	10 $K^- p \to K^+ K^- (\Lambda, \Sigma)$
1527 ± 3	120	BRANDENB...	76C	ASPK	13 $K^- p \to K^+ K^- (\Lambda, \Sigma)$
1519 ± 7	100	AGUILAR-...	72B	HBC	3.9,4.6 $K^- p \to K \overline{K} (\Lambda, \Sigma)$
• • • We do not use the following data for averages, fits, limits, etc. • • •					
1513 ±10		[5] BARKOV	99	SPEC	40 $K^- p \to K^0_S K^0_S y$

PRODUCED IN e^+e^- ANNIHILATION

VALUE (MeV)	EVTS	DOCUMENT ID		TECN	COMMENT
The data in this block is included in the average printed for a previous datablock.					
1520.6± 2.3 OUR AVERAGE Error includes scale factor of 1.1.					
1518 ± 1 ± 3		ABE	04	BELL	10.6 $e^+e^- \to e^+e^- K^+K^-$
1519 ± 2 $^{+15}_{-5}$		BAI	03G	BES	$J/\psi \to \gamma K\overline{K}$
1523 ± 6	331	[6] ACCIARRI	01H	L3	91, 183–209 $e^+e^- \to e^+e^- K^0_S K^0_S$
1535 ± 5 ± 4		ABREU	96C	DLPH	$Z^0 \to K^+K^- + X$
1516 ± 5 $^{+9}_{-15}$		BAI	96C	BES	$J/\psi \to \gamma K^+K^-$
1531.6 ±10.0		AUGUSTIN	88	DM2	$J/\psi \to \gamma K^+K^-$
1515 ± 5		[7] FALVARD	88	DM2	$J/\psi \to \phi K^+K^-$
1525 ±10 ±10		BALTRUSAIT...	87	MRK3	$J/\psi \to \gamma K^+K^-$
• • • We do not use the following data for averages, fits, limits, etc. • • •					
1529 ±10		ACCIARRI	95J	L3	Repl. by ACCIARRI 01H
1496 ± 2		[8] FALVARD	88	DM2	$J/\psi \to \phi K^+K^-$

PRODUCED IN $\overline{p}p$ ANNIHILATION

VALUE (MeV)	DOCUMENT ID		TECN	COMMENT
• • • We do not use the following data for averages, fits, limits, etc. • • •				
1508±9	[9] AMSLER	02	CBAR	0.9 $\overline{p}p \to \pi^0\eta\eta$, $\pi^0\pi^0\pi^0$

CENTRAL PRODUCTION

VALUE (MeV)	DOCUMENT ID		TECN	COMMENT
1515±15	BARBERIS	99	OMEG	450 $pp \to p_s p_f K^+K^-$

PRODUCED IN ep COLLISIONS

VALUE (MeV)	EVTS	DOCUMENT ID		TECN	COMMENT
• • • We do not use the following data for averages, fits, limits, etc. • • •					
1537 $^{+9}_{-8}$	84	[1] CHEKANOV	04	ZEUS	$ep \to K^0_S K^0_S X$

[1] Systematic errors not estimated.
[2] From a partial-wave analysis of data using a K-matrix formalism with 5 poles.
[3] CHABAUD 81 is a reanalysis of PAWLICKI 77 data.
[4] From an amplitude analysis where the $f_2'(1525)$ width and elasticity are in complete disagreement with the values obtained from $K\overline{K}$ channel, making the solution dubious.
[5] Systematic errors not estimated.
[6] Supersedes ACCIARRI 95J.
[7] From an analysis ignoring interference with $f_0(1710)$.
[8] From an analysis including interference with $f_0(1710)$.
[9] T-matrix pole.

$f_2'(1525)$ WIDTH

VALUE (MeV)	DOCUMENT ID		COMMENT
73 $^{+6}_{-5}$ OUR FIT			
76±10	PDG	90	For fitting

PRODUCED BY PION BEAM

VALUE (MeV)	DOCUMENT ID		TECN	COMMENT
• • • We do not use the following data for averages, fits, limits, etc. • • •				
102±42	TIKHOMIROV	03	SPEC	40.0 π^- C $\to K^0_S K^0_S K^0_L X$
108 $^{+5}_{-2}$	[11] LONGACRE	86	MPS	22 $\pi^- p \to K^0_S K^0_S n$
69 $^{+22}_{-16}$	[12] CHABAUD	81	ASPK	6 $\pi^- p \to K^+K^- n$
137 $^{+23}_{-21}$	CHABAUD	81	ASPK	18.4 $\pi^- p \to K^+K^- n$
150 $^{+83}_{-50}$	GORLICH	80	ASPK	17 $\pi^- p$ polarized $\to K^+K^- n$
165±42	[13] CORDEN	79	OMEG	12–15 $\pi^- p \to \pi^+\pi^- n$
92 $^{+39}_{-22}$	[14] POLYCHRO...	79	STRC	7 $\pi^- p \to n K^0_S K^0_S$

PRODUCED BY $K^\pm$ BEAM

VALUE (MeV)	EVTS	DOCUMENT ID		TECN	COMMENT
80.3± 2.7 OUR AVERAGE Includes data from the datablock that follows this one.					
90 ±12		ASTON	88D	LASS	11 $K^- p \to K^0_S K^0_S \Lambda$
73 ±18		BOLONKIN	86	SPEC	40 $K^- p \to K^0_S K^0_S Y$
83 ±15		ARMSTRONG	83B	OMEG	18.5 $K^- p \to K^- K^+ \Lambda$
85 ±16	650	AGUILAR-...	81B	HBC	4.2 $K^- p \to \Lambda K^+ K^-$
80 $^{+14}_{-11}$	572	ALHARRAN	81	HBC	8.25 $K^- p \to \Lambda K\overline{K}$
72 ±25	166	EVANGELISTA	77	OMEG	10 $K^- p \to K^+K^-(\Lambda,\Sigma)$
69 ±22	100	AGUILAR-...	72B	HBC	3.9,4.6 $K^- p \to K\overline{K}(\Lambda,\Sigma)$
• • • We do not use the following data for averages, fits, limits, etc. • • •					
75 ±20		[15] BARKOV	99	SPEC	40 $K^- p \to K^0_S K^0_S y$
62 $^{+19}_{-14}$	123	BARREIRO	77	HBC	4.15 $K^- p \to \Lambda K^0_S K^0_S$
61 ± 8	120	BRANDENB...	76C	ASPK	13 $K^- p \to K^+K^-(\Lambda,\Sigma)$

PRODUCED IN e^+e^- ANNIHILATION

VALUE (MeV)	EVTS	DOCUMENT ID		TECN	COMMENT
The data in this block is included in the average printed for a previous datablock.					
80± 4 OUR AVERAGE Error includes scale factor of 1.4. See the ideogram below.					
82± 2± 3		ABE	04	BELL	10.6 $e^+e^- \to e^+e^- K^+K^-$
75± 4 $^{+15}_{-5}$		BAI	03G	BES	$J/\psi \to \gamma K\overline{K}$
100±15	331	[16] ACCIARRI	01H	L3	91, 183–209 $e^+e^- \to e^+e^- K^0_S K^0_S$
60±20±19		ABREU	96C	DLPH	$Z^0 \to K^+K^- + X$
60± 23 $^{+13}_{-20}$		BAI	96C	BES	$J/\psi \to \gamma K^+K^-$
103±30		AUGUSTIN	88	DM2	$J/\psi \to \gamma K^+K^-$
62±10		[17] FALVARD	88	DM2	$J/\psi \to \phi K^+K^-$
85±35		BALTRUSAIT...	87	MRK3	$J/\psi \to \gamma K^+K^-$
• • • We do not use the following data for averages, fits, limits, etc. • • •					
76±40		ACCIARRI	95J	L3	Repl. by ACCIARRI 01H
100± 3		[18] FALVARD	88	DM2	$J/\psi \to \phi K^+K^-$

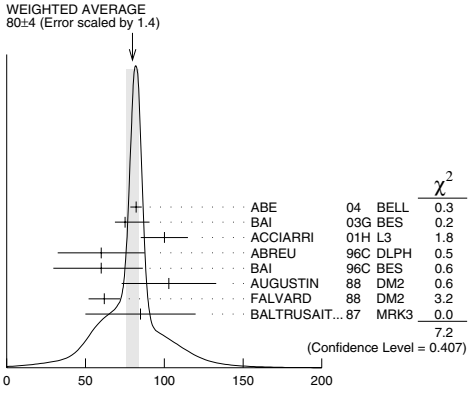

Produced in e^+e^- annihilation

PRODUCED IN $\overline{p}p$ ANNIHILATION

VALUE (MeV)	DOCUMENT ID		TECN	COMMENT
79±8	[19] AMSLER	02	CBAR	0.9 $\overline{p}p \to \pi^0\eta\eta$, $\pi^0\pi^0\pi^0$

CENTRAL PRODUCTION

VALUE (MeV)	DOCUMENT ID		TECN	COMMENT
70±25	BARBERIS	99	OMEG	450 $pp \to p_s p_f K^+K^-$

PRODUCED IN ep COLLISIONS

VALUE (MeV)	EVTS	DOCUMENT ID		TECN	COMMENT
• • • We do not use the following data for averages, fits, limits, etc. • • •					
50 $^{+34}_{-22}$	84	[10] CHEKANOV	04	ZEUS	$ep \to K^0_S K^0_S X$

[10] Systematic errors not estimated.
[11] From a partial-wave analysis of data using a K-matrix formalism with 5 poles.
[12] CHABAUD 81 is a reanalysis of PAWLICKI 77 data.
[13] From an amplitude analysis where the $f_2'(1525)$ width and elasticity are in complete disagreement with the values obtained from $K\overline{K}$ channel, making the solution dubious.
[14] From a fit to the D with $f_2(1270)$-$f_2'(1525)$ interference. Mass fixed at 1516 MeV.
[15] Systematic errors not estimated.
[16] Supersedes ACCIARRI 95J.
[17] From an analysis ignoring interference with $f_0(1710)$.
[18] From an analysis including interference with $f_0(1710)$.
[19] T-matrix pole.

$f_2'(1525)$ DECAY MODES

	Mode	Fraction (Γ_i/Γ)
Γ_1	$K\overline{K}$	(88.8 ±3.1) %
Γ_2	$\eta\eta$	(10.3 ±3.1) %
Γ_3	$\pi\pi$	(8.2 ±1.5) $\times 10^{-3}$
Γ_4	$K\overline{K}^*(892)+$ c.c.	
Γ_5	$\pi K\overline{K}$	
Γ_6	$\pi\pi\eta$	
Γ_7	$\pi^+\pi^+\pi^-\pi^-$	
Γ_8	$\gamma\gamma$	(1.11 ±0.14) $\times 10^{-6}$

Meson Particle Listings

$f_2'(1525)$

CONSTRAINED FIT INFORMATION

An overall fit to the total width, 2 partial widths, a combination of partial widths obtained from integrated cross sections, and 3 branching ratios uses 15 measurements and one constraint to determine 5 parameters. The overall fit has a $\chi^2 = 14.0$ for 11 degrees of freedom.

The following *off-diagonal* array elements are the correlation coefficients $\langle \delta p_i \delta p_j \rangle / (\delta p_i \cdot \delta p_j)$, in percent, from the fit to parameters p_i, including the branching fractions, $x_i \equiv \Gamma_i/\Gamma_{\rm total}$. The fit constrains the x_i whose labels appear in this array to sum to one.

x_2	−100			
x_3	−3	−1		
x_8	−8	8	1	
Γ	−32	32	−1	−53
	x_1	x_2	x_3	x_8

	Mode	Rate (MeV)
Γ_1	$K\overline{K}$	$65\ ^{+5}_{-4}$
Γ_2	$\eta\eta$	7.6 ± 2.5
Γ_3	$\pi\pi$	0.60 ± 0.12
Γ_8	$\gamma\gamma$	$(8.1 \pm 0.9) \times 10^{-5}$

$f_2'(1525)$ PARTIAL WIDTHS

$\Gamma(K\overline{K})$ Γ_1

VALUE (MeV)	DOCUMENT ID		TECN	COMMENT
$65\ ^{+5}_{-4}$ OUR FIT				
$63\ ^{+6}_{-5}$	[20] LONGACRE	86	MPS	$22\ \pi^- p \to K^0_S K^0_S n$

$\Gamma(\pi\pi)$ Γ_3

VALUE (MeV)	DOCUMENT ID		TECN	COMMENT
0.60 ± 0.12 OUR FIT				
$1.4\ ^{+1.0}_{-0.5}$	[20] LONGACRE	86	MPS	$22\ \pi^- p \to K^0_S K^0_S n$

$\Gamma(\eta\eta)$ Γ_2

VALUE (MeV)	DOCUMENT ID		TECN	COMMENT
7.6 ± 2.5 OUR FIT				
• • • We do not use the following data for averages, fits, limits, etc. • • •				
$24\ ^{+3}_{-1}$	[20] LONGACRE	86	MPS	$22\ \pi^- p \to K^0_S K^0_S n$

[20] From a partial-wave analysis of data using a K-matrix formalism with 5 poles.

$f_2'(1525)$ Γ(i)$\Gamma(\gamma\gamma)/\Gamma$(total)

$\Gamma(K\overline{K}) \times \Gamma(\gamma\gamma)/\Gamma_{\rm total}$ $\Gamma_1\Gamma_8/\Gamma$

VALUE (keV)	EVTS	DOCUMENT ID		TECN	COMMENT
0.072 ± 0.007 OUR FIT					
0.072 ± 0.007 OUR AVERAGE					
$0.0564 \pm 0.0048 \pm 0.0116$		ABE	04	BELL	$10.6\ e^+e^- \to e^+e^-K^+K^-$
$0.076 \pm 0.006 \pm 0.011$	331	[23] ACCIARRI	01H	L3	91, 183–209 $e^+e^- \to e^+e^-K^0_S K^0_S$
$0.067 \pm 0.008 \pm 0.015$		[21] ALBRECHT	90G	ARG	$e^+e^- \to e^+e^-K^+K^-$
$0.11\ ^{+0.03}_{-0.02} \pm 0.02$		BEHREND	89C	CELL	$e^+e^- \to e^+e^-K^0_S K^0_S$
$0.10\ ^{+0.04}_{-0.03}\ ^{+0.03}_{-0.02}$		BERGER	88	PLUT	$e^+e^- \to e^+e^-K^0_S K^0_S$
$0.12 \pm 0.07 \pm 0.04$		[21] AIHARA	86B	TPC	$e^+e^- \to e^+e^-K^+K^-$
$0.11 \pm 0.02 \pm 0.04$		[21] ALTHOFF	83	TASS	$e^+e^- \to e^+e^-K\overline{K}$
• • • We do not use the following data for averages, fits, limits, etc. • • •					
$0.093 \pm 0.018 \pm 0.022$		[21] ACCIARRI	95J	L3	Repl. by ACCIARRI 01H
$0.0314 \pm 0.0050 \pm 0.0077$		[22] ALBRECHT	90G	ARG	$e^+e^- \to e^+e^-K^+K^-$

[21] Using an incoherent background.
[22] Using a coherent background.
[23] Supersedes ACCIARRI 95J.

$f_2'(1525)$ BRANCHING RATIOS

$\Gamma(\eta\eta)/\Gamma(K\overline{K})$ Γ_2/Γ_1

VALUE	CL%	DOCUMENT ID		TECN	COMMENT
0.12 ± 0.04 OUR FIT					
0.11 ± 0.04		[24] PROKOSHKIN	91	GAM4	$300\ \pi^- p \to \pi^- p\eta\eta$
• • • We do not use the following data for averages, fits, limits, etc. • • •					
< 0.14	90	BARBERIS	00E		$450\ pp \to p_f \eta\eta p_s$
< 0.50		BARNES	67	HBC	$4.6,5.0\ K^- p$

[24] Combining results of GAM4 with those of WA76 on $K\overline{K}$ central production and results of CBAL, MRK3 and DM2 on $J/\psi \to \gamma\eta\eta$.

$\Gamma(\pi\pi)/\Gamma_{\rm total}$ Γ_3/Γ

VALUE	CL%	DOCUMENT ID		TECN	COMMENT
0.0082 ± 0.0016 OUR FIT					
0.0075 ± 0.0016 OUR AVERAGE					
0.007 ± 0.002		COSTA...	80	OMEG	$10\ \pi^- p \to K^+K^- n$
$0.027\ ^{+0.071}_{-0.013}$		[25] GORLICH	80	ASPK	$17,18\ \pi^- p$
0.0075 ± 0.0025		[25,26] MARTIN	79	RVUE	
• • • We do not use the following data for averages, fits, limits, etc. • • •					
< 0.06	95	AGUILAR-...	81B	HBC	$4.2\ K^- p \to \Lambda K^+K^-$
0.19 ± 0.03		CORDEN	79	OMEG	12–15 $\pi^- p \to \pi^+\pi^- n$
< 0.045	95	BARREIRO	77	HBC	$4.15\ K^- p \to \Lambda K^0_S K^0_S$
0.012 ± 0.004		[25] PAWLICKI	77	SPEC	$6\ \pi N \to K^+K^- N$
< 0.063	90	BRANDENB...	76C	ASPK	$13\ K^- p \to K^+K^-(\Lambda, \Sigma)$
< 0.0086		[25] BEUSCH	75B	OSPK	$8.9\ \pi^- p \to K^0\overline{K}^0 n$

[25] Assuming that the $f_2'(1525)$ is produced by an one-pion exchange production mechanism.
[26] MARTIN 79 uses the PAWLICKI 77 data with different input value of the $f_2'(1525) \to K\overline{K}$ branching ratio.

$\Gamma(\pi\pi)/\Gamma(K\overline{K})$ Γ_3/Γ_1

VALUE	DOCUMENT ID		TECN	COMMENT
0.0092 ± 0.0018 OUR FIT				
0.075 ± 0.035	AUGUSTIN	87	DM2	$J/\psi \to \gamma\pi^+\pi^-$

$\Gamma(\pi\pi\eta)/\Gamma(K\overline{K})$ Γ_6/Γ_1

VALUE	CL%	DOCUMENT ID		TECN	COMMENT
• • • We do not use the following data for averages, fits, limits, etc. • • •					
< 0.41	95	AGUILAR-...	72B	HBC	$3.9,4.6\ K^- p$
< 0.3	67	AMMAR	67	HBC	

$[\Gamma(K\overline{K}^*(892) + \text{c.c.}) + \Gamma(\pi K\overline{K})]/\Gamma(K\overline{K})$ $(\Gamma_4+\Gamma_5)/\Gamma_1$

VALUE	CL%	DOCUMENT ID		TECN	COMMENT
• • • We do not use the following data for averages, fits, limits, etc. • • •					
< 0.35	95	AGUILAR-...	72B	HBC	$3.9,4.6\ K^- p$
< 0.4	67	AMMAR	67	HBC	

$\Gamma(\pi^+\pi^+\pi^-\pi^-)/\Gamma(K\overline{K})$ Γ_7/Γ_1

VALUE	CL%	DOCUMENT ID		TECN	COMMENT
• • • We do not use the following data for averages, fits, limits, etc. • • •					
< 0.32	95	AGUILAR-...	72B	HBC	$3.9,4.6\ K^- p$

$\Gamma(\eta\eta)/\Gamma_{\rm total}$ Γ_2/Γ

VALUE	DOCUMENT ID		TECN	COMMENT
• • • We do not use the following data for averages, fits, limits, etc. • • •				
0.10 ± 0.03	[27] PROKOSHKIN	91	GAM4	$300\ \pi^- p \to \pi^- p\eta\eta$

[27] Combining results of GAM4 with those of WA76 on $K\overline{K}$ central production and results of CBAL, MRK3 and DM2 on $J/\psi \to \gamma\eta\eta$.

$f_2'(1525)$ REFERENCES

ABE	04	EPJ C32 323	K. Abe *et al.* (BELLE Collab.)
CHEKANOV	04	PL B578 33	S. Chekanov *et al.* (ZEUS Collab.)
BAI	03G	PR D68 052003	J.Z. Bai *et al.* (BES Collab.)
TIKHOMIROV	03	PAN 66 828 Translated from YAF 66 860.	G.D. Tikhomirov *et al.*
AMSLER	02	EPJ C23 29	C. Amsler *et al.*
ACCIARRI	01H	PL B501 173	M. Acciarri *et al.* (L3 Collab.)
BARBERIS	00E	PL B479 59	D. Barberis *et al.* (WA 102 Collab.)
BARBERIS	99	PL B453 305	D. Barberis *et al.* (Omega Expt.)
BARKOV	99	JETPL 70 248 Translated from ZETFP 70 242.	B.P. Barkov *et al.*
ABREU	96C	PL B379 309	P. Abreu *et al.* (DELPHI Collab.)
BAI	96C	PRL 77 3959	J.Z. Bai *et al.* (BES Collab.)
ACCIARRI	95J	PL B363 118	M. Acciarri *et al.* (L3 Collab.)
PROKOSHKIN	91	SPD 36 155 Translated from DANS 316 900.	Y.D. Prokoshkin (GAM2, GAM4 Collab.)
ALBRECHT	90G	ZPHY C48 183	H. Albrecht *et al.* (ARGUS Collab.)
PDG	90	PL B239	J.J. Hernandez *et al.* (IFIC, BOST, CIT+)
BEHREND	89C	ZPHY C43 91	H.J. Behrend *et al.* (CELLO Collab.)
ASTON	88D	NP B301 525	D. Aston *et al.* (SLAC, NAGO, CINC, INUS)
AUGUSTIN	88	PRL 60 2238	J.E. Augustin *et al.* (DM2 Collab.)
BERGER	88	ZPHY C37 329	C. Berger *et al.* (PLUTO Collab.)
FALVARD	88	PR D38 2706	A. Falvard *et al.* (CLER, FRAS, LALO+)
AUGUSTIN	87	ZPHY C36 369	J.E. Augustin *et al.* (LALO, CLER, FRAS+)
BALTRUSAIT...	87	PR D35 2077	R.M. Baltrusaitis *et al.* (Mark III Collab.)
AIHARA	86B	PRL 57 404	H. Aihara *et al.* (TPC-2γ Collab.)
BOLONKIN	86	SJNP 43 776 Translated from YAF 43 1211.	B.V. Bolonkin *et al.* (ITEP) JP

LONGACRE	86	PL B177 223	R.S. Longacre *et al.*	(BNL, BRAN, CUNY+)
ALTHOFF	83	PL 121B 216	M. Althoff *et al.*	(TASSO Collab.)
ARMSTRONG	83B	NP B224 193	T.A. Armstrong *et al.*	(BARI, BIRM, CERN+)
AGUILAR-...	81B	ZPHY C8 313	M. Aguilar-Benitez *et al.*	(CERN, CDEF+)
ALHARRAN	81	NP B191 26	S. Al-Harran *et al.*	(BIRM, CERN, GLAS+)
CHABAUD	81	APP B12 575	V. Chabaud *et al.*	(CERN, CRAC, MPIM)
COSTA...	80	NP B175 402	G. Costa de Beauregard *et al.*	(BARI, BONN+)
GORLICH	80	NP B174 16	L. Gorlich *et al.*	(CRAC, MPIM, CERN+)
CORDEN	79	NP B157 250	M.J. Corden *et al.*	(BIRM, RHEL, TELA+) JP
MARTIN	79	NP B158 520	A.D. Martin, E.N. Ozmutlu	(DURH)
POLYCHRO...	79	PR D19 1317	V.A. Polychronakos *et al.*	(NDAM, ANL)
BARREIRO	77	NP B121 237	F. Barreiro *et al.*	(CERN, AMST, NIJM+)
EVANGELISTA	77	NP B127 384	C. Evangelista *et al.*	(BARI, BONN, CERN+)
PAWLICKI	77	PR D15 3196	A.J. Pawlicki *et al.*	(ANL) IJP
BRANDENB...	76C	NP B104 413	G.W. Brandenburg *et al.*	(SLAC)
BEUSCH	75B	PL 60B 101	W. Beusch *et al.*	(CERN, ETH)
AGUILAR-...	72B	PR D6 29	M. Aguilar-Benitez *et al.*	(BNL)
AMMAR	67	PRL 19 1071	R. Ammar *et al.*	(NWES, ANL) JP
BARNES	67	PRL 19 964	V.E. Barnes *et al.*	(BNL, SYRA) IJPC
CRENNELL	66	PRL 16 1025	D.J. Crennell *et al.*	(BNL) I

OTHER RELATED PAPERS

LI	01	JPG 27 807	D.-M. Li, H. Yu, Q.-X. Shen	
ALBERICO	98	PL B438 430	A. Alberico *et al.*	(Obelix Collab.)
JENNI	83	PR D27 1031	P. Jenni *et al.*	(SLAC, LBL)
ARMSTRONG	82	PL 110B 77	T.A. Armstrong *et al.*	(BARI, BIRM, CERN+)
ETKIN	82B	PR D25 1786	A. Etkin *et al.*	(BNL, CUNY, TUFTS, VAND)
ABRAMS	67B	PRL 18 620	G.S. Abrams *et al.*	(UMD)
BARNES	65	PRL 15 322	V.E. Barnes *et al.*	(BNL, SYRA)

$f_2(1565)$

$I^G(J^{PC}) = 0^+(2^{++})$

OMITTED FROM SUMMARY TABLE

Seen in antinucleon-nucleon annihilation at rest. Needs confirmation.

$f_2(1565)$ MASS

VALUE (MeV)			*DOCUMENT ID*			*TECN*	*COMMENT*
1546	**±12**	**OUR AVERAGE**	Error includes scale factor of 1.6. See the ideogram below.				
1552	±13		[1] AMSLER	02	CBAR		0.9 $\overline{p}p \to \pi^0\eta\eta$, $\pi^0\pi^0\pi^0$
1550	±10	±20	AMELIN	00	VES		37 $\pi^- p \to \eta\pi^+\pi^- n$
1575	±18		BERTIN	98	OBLX		0.05–0.405 $\overline{n}p \to$ $\pi^+\pi^+\pi^-$
1507	±15		[1] BERTIN	97C	OBLX		0.0 $\overline{p}p \to \pi^+\pi^-\pi^0$
1565	±20		MAY	90	ASTE		0.0 $\overline{p}p \to \pi^+\pi^-\pi^0$
• • • We do not use the following data for averages, fits, limits, etc. • • •							
1544.7	± 3.0		VLADIMIRSKII	00	SPEC		40 $\pi^- p \to K^0_S K^0_S X$
1598	±11	± 9	BAKER	99B	SPEC		0 $\overline{p}p \to \omega\omega\pi^0$
1534	±20		[2] ABELE	96C	RVUE		Compilation
~ 1552			[3] AMSLER	95D	CBAR		0.0 $\overline{p}p \to \pi^0\pi^0\pi^0$, $\pi^0\eta\eta$, $\pi^0\pi^0\eta$
1598	±72		BALOSHIN	95	SPEC		40 π^- C $\to K^0_S K^0_S X$
1566	$^{+80}_{-50}$		[4] ANISOVICH	94	CBAR		0.0 $\overline{p}p \to 3\pi^0, \eta\eta\pi^0$
1502	± 9		ADAMO	93	OBLX		$\overline{n}p \to \pi^+\pi^+\pi^-$
1488	±10		[5] ARMSTRONG	93C	E760		$\overline{p}p \to \pi^0\eta\eta \to 6\gamma$
1508	±10		[5] ARMSTRONG	93D	E760		$\overline{p}p \to 3\pi^0 \to 6\gamma$
1525	±10		[5] ARMSTRONG	93D	E760		$\overline{p}p \to \eta\pi^0\pi^0 \to 6\gamma$
~ 1504			[6] WEIDENAUER	93	ASTE		0.0 $\overline{p}N \to 3\pi^-2\pi^+$
1540	±15		[5] ADAMO	92	OBLX		$\overline{n}p \to \pi^+\pi^+\pi^-$
1515	±10		[7] AKER	91	CBAR		0.0 $\overline{p}p \to 3\pi^0$
1477	± 5		BRIDGES	86C	DBC		0.0 $\overline{p}N \to 3\pi^-2\pi^+$

[1] T-matrix pole.
[2] T-matrix pole, large coupling to $\rho\rho$ and $\omega\omega$, could be $f_2(1640)$.
[3] Coupled-channel analysis of AMSLER 95B, AMSLER 95C, and AMSLER 94D.
[4] From a simultaneous analysis of the annihilations $\overline{p}p \to 3\pi^0, \pi^0\eta\eta$ including AKER 91 data.
[5] J^P not determined, could be partly $f_0(1500)$.
[6] J^P not determined.
[7] Superseded by AMSLER 95B.

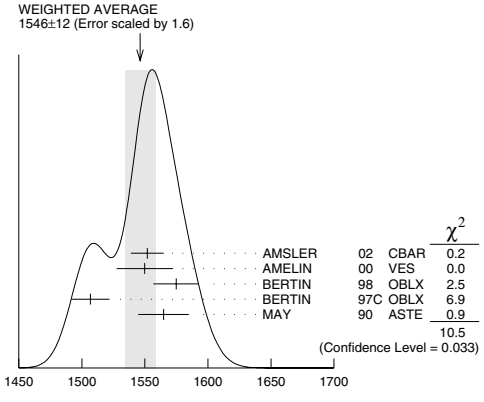

$f_2(1565)$ WIDTH

VALUE (MeV)			*DOCUMENT ID*			*TECN*	*COMMENT*
126	**± 12**	**OUR AVERAGE**					
113	± 23		[8] AMSLER	02	CBAR		0.9 $\overline{p}p \to \pi^0\eta\eta$, $\pi^0\pi^0\pi^0$
130	± 20	±40	AMELIN	00	VES		37 $\pi^- p \to \eta\pi^+\pi^- n$
119	± 24		BERTIN	98	OBLX		0.05–0.405 $\overline{n}p \to$ $\pi^+\pi^+\pi^-$
130	± 20		[8] BERTIN	97C	OBLX		0.0 $\overline{p}p \to \pi^+\pi^-\pi^0$
170	± 40		MAY	90	ASTE		0.0 $\overline{p}p \to \pi^+\pi^-\pi^0$
• • • We do not use the following data for averages, fits, limits, etc. • • •							
103.3	± 3.0		VLADIMIRSKII	00	SPEC		40 $\pi^- p \to K^0_S K^0_S X$
180	± 60		[9] ABELE	96C	RVUE		Compilation
~ 142			[10] AMSLER	95D	CBAR		0.0 $\overline{p}p \to \pi^0\pi^0\pi^0$, $\pi^0\eta\eta$, $\pi^0\pi^0\eta$
263	±101		BALOSHIN	95	SPEC		40 π^- C $\to K^0_S K^0_S X$
166	$^{+80}_{-20}$		[11] ANISOVICH	94	CBAR		0.0 $\overline{p}p \to 3\pi^0, \eta\eta\pi^0$
130	± 10		[12] ADAMO	93	OBLX		$\overline{n}p \to \pi^+\pi^+\pi^-$
148	± 27		[13] ARMSTRONG	93C	E760		$\overline{p}p \to \pi^0\eta\eta \to 6\gamma$
103	± 15		[13] ARMSTRONG	93D	E760		$\overline{p}p \to 3\pi^0 \to 6\gamma$
111	± 10		[13] ARMSTRONG	93D	E760		$\overline{p}p \to \eta\pi^0\pi^0 \to 6\gamma$
~ 206			[14] WEIDENAUER	93	ASTE		0.0 $\overline{p}N \to 3\pi^-2\pi^+$
132	± 37		[13] ADAMO	92	OBLX		$\overline{n}p \to \pi^+\pi^+\pi^-$
120	± 10		[15] AKER	91	CBAR		0.0 $\overline{p}p \to 3\pi^0$
116	± 9		BRIDGES	86C	DBC		0.0 $\overline{p}N \to 3\pi^-2\pi^+$

[8] T-matrix pole.
[9] T-matrix pole, large coupling to $\rho\rho$ and $\omega\omega$, could be $f_2(1640)$.
[10] Coupled-channel analysis of AMSLER 95B, AMSLER 95C, and AMSLER 94D.
[11] From a simultaneous analysis of the annihilations $\overline{p}p \to 3\pi^0, \pi^0\eta\eta$ including AKER 91 data.
[12] Supersedes ADAMO 92.
[13] J^P not determined, could be partly $f_0(1500)$.
[14] J^P not determined.
[15] Superseded by AMSLER 95B.

$f_2(1565)$ DECAY MODES

	Mode	Fraction (Γ_i/Γ)
Γ_1	$\pi\pi$	seen
Γ_2	$\pi^+\pi^-$	seen
Γ_3	$\pi^0\pi^0$	seen
Γ_4	$\rho^0\rho^0$	seen
Γ_5	$2\pi^+2\pi^-$	seen
Γ_6	$\eta\eta$	seen
Γ_7	$a_2(1320)\pi$	
Γ_8	$\omega\omega$	seen

$f_2(1565)$ BRANCHING RATIOS

$\Gamma(\pi\pi)/\Gamma_{\text{total}}$ Γ_1/Γ

VALUE	*DOCUMENT ID*		*TECN*	*COMMENT*
• • • We do not use the following data for averages, fits, limits, etc. • • •				
seen	BAKER	99B	SPEC	0 $\overline{p}p \to \omega\omega\pi^0$

$\Gamma(\pi^+\pi^-)/\Gamma_{\text{total}}$ Γ_2/Γ

VALUE	DOCUMENT ID		TECN	COMMENT
• • • We do not use the following data for averages, fits, limits, etc. • • •				
seen	BERTIN	98	OBLX	0.05–0.405 $\overline{n}p \to \pi^+\pi^+\pi^-$
not seen	[16] ANISOVICH	94B	RVUE	$\overline{p}p \to \pi^+\pi^-\pi^0$
seen	MAY	89	ASTE	$\overline{p}p \to \pi^+\pi^-\pi^0$

[16] ANISOVICH 94B is from a reanalysis of MAY 90.

$\Gamma(\pi^+\pi^-)/\Gamma(\rho^0\rho^0)$ Γ_2/Γ_4

VALUE	DOCUMENT ID	TECN	COMMENT
• • • We do not use the following data for averages, fits, limits, etc. • • •			
0.042 ± 0.013	BRIDGES	86B DBC	$\overline{p}N \to 3\pi^-2\pi^+$

$\Gamma(\pi^0\pi^0)/\Gamma_{\text{total}}$ Γ_3/Γ

VALUE	DOCUMENT ID	TECN	COMMENT
seen	AMSLER	95B CBAR	0.0 $\overline{p}p \to 3\pi^0$

$\Gamma(\eta\eta)/\Gamma(\pi^0\pi^0)$ Γ_6/Γ_3

VALUE	DOCUMENT ID	TECN	COMMENT
• • • We do not use the following data for averages, fits, limits, etc. • • •			
$0.024 \pm 0.005 \pm 0.012$	[17] ARMSTRONG	93C E760	$\overline{p}p \to \pi^0\eta\eta \to 6\gamma$

[17] J^P not determined, could be partly $f_0(1500)$.

$\Gamma(\omega\omega)/\Gamma_{\text{total}}$ Γ_8/Γ

VALUE	DOCUMENT ID	TECN	COMMENT
• • • We do not use the following data for averages, fits, limits, etc. • • •			
seen	BAKER	99B SPEC	0 $\overline{p}p \to \omega\omega\pi^0$

$f_2(1565)$ REFERENCES

AMSLER	02	EPJ C23 29	C. Amsler *et al.*
AMELIN	00	NP A668 83	D. Amelin *et al.* (VES Collab.)
VLADIMIRSKII	00	JETPL 26 486	V.V. Vladimirskii *et al.*
		Translated from ZETFP 72 698.	
BAKER	99B	PL B467 147	C.A. Baker *et al.*
BERTIN	98	PR D57 55	A. Bertin *et al.* (OBELIX Collab.)
BERTIN	97C	PL B408 476	A. Bertin *et al.* (OBELIX Collab.)
ABELE	96C	NP A609 562	A. Abele *et al.* (Crystal Barrel Collab.)
AMSLER	95B	PL B342 433	C. Amsler *et al.* (Crystal Barrel Collab.)
AMSLER	95C	PL B353 571	C. Amsler *et al.* (Crystal Barrel Collab.)
AMSLER	95D	PL B355 425	C. Amsler *et al.* (Crystal Barrel Collab.)
BALOSHIN	95	PAN 58 46	O.N. Baloshin *et al.* (ITEP)
		Translated from YAF 58 50.	
AMSLER	94D	PL B333 277	C. Amsler *et al.* (Crystal Barrel Collab.)
ANISOVICH	94	PL B323 233	V.V. Anisovich *et al.* (Crystal Barrel Collab.)
ANISOVICH	94B	PR D50 1972	V.V. Anisovich *et al.* (LOQM)
ADAMO	93	NP A558 13C	A. Adamo *et al.* (OBELIX Collab.)
ARMSTRONG	93C	PL B307 394	T.A. Armstrong *et al.* (FNAL, FERR, GENO+)
ARMSTRONG	93D	PL B307 399	T.A. Armstrong *et al.* (FNAL, FERR, GENO+)
WEIDENAUER	93	ZPHY C59 387	P. Weidenauer *et al.* (ASTERIX Collab.)
ADAMO	92	PL B287 368	A. Adamo *et al.* (OBELIX Collab.)
AKER	91	PL B260 249	E. Aker *et al.* (Crystal Barrel Collab.)
MAY	90	ZPHY C46 203	B. May *et al.* (ASTERIX Collab.)
MAY	89	PL B225 450	B. May *et al.* (ASTERIX Collab.) IJP
BRIDGES	86B	PRL 56 215	D.L. Bridges *et al.* (SYRA, CASE)
BRIDGES	86C	PRL 57 1534	D.L. Bridges *et al.* (SYRA)

$h_1(1595)$ $I^G(J^{PC}) = 0^-(1^{+-})$

OMITTED FROM SUMMARY TABLE

Seen in a partial-wave analysis of the $\omega\eta$ system produced in the reaction $\pi^- p \to \omega\eta n$ at 18 GeV/c.

$h_1(1595)$ MASS

VALUE (MeV)	DOCUMENT ID	TECN	COMMENT
$1594 \pm 15^{+10}_{-60}$	EUGENIO	01 SPEC	18 $\pi^- p \to \omega\eta n$

$h_1(1595)$ WIDTH

VALUE (MeV)	DOCUMENT ID	TECN	COMMENT
$384 \pm 60^{+70}_{-100}$	EUGENIO	01 SPEC	18 $\pi^- p \to \omega\eta n$

$h_1(1595)$ DECAY MODES

	Mode	Fraction (Γ_i/Γ)
Γ_1	$\omega\eta$	seen

$h_1(1595)$ REFERENCES

EUGENIO	01	PL B497 190	P. Eugenio *et al.*

$\pi_1(1600)$ $I^G(J^{PC}) = 1^-(1^{-+})$

$\pi_1(1600)$ MASS

VALUE (MeV)	DOCUMENT ID		TECN	COMMENT
1596^{+25}_{-14} OUR AVERAGE				
$1597 \pm 10^{+45}_{-10}$	IVANOV	01	MPS	18 $\pi^- p \to \eta'\pi^- p$
$1593 \pm 8^{+29}_{-47}$	[1] ADAMS	98B	MPS	18.3 $\pi^- p \to \pi^+\pi^-\pi^- p$

[1] Natural parity exchange.

$\pi_1(1600)$ WIDTH

VALUE (MeV)	DOCUMENT ID		TECN	COMMENT
312^{+64}_{-24} OUR AVERAGE Error includes scale factor of 1.1.				
$340 \pm 40 \pm 50$	IVANOV	01	MPS	18 $\pi^- p \to \eta'\pi^- p$
$168 \pm 20^{+150}_{-12}$	[2] ADAMS	98B	MPS	18.3 $\pi^- p \to \pi^+\pi^-\pi^- p$

[2] Natural parity exchange.

$\pi_1(1600)$ DECAY MODES

	Mode	Fraction (Γ_i/Γ)
Γ_1	$\pi\pi\pi$	seen
Γ_2	$\rho^0\pi^-$	seen
Γ_3	$f_2(1270)\pi^-$	not seen
Γ_4	$b_1(1235)\pi$	
Γ_5	$\eta'(958)\pi^-$	seen

$\pi_1(1600)$ BRANCHING RATIOS

$\Gamma(\rho^0\pi^-)/\Gamma_{\text{total}}$ Γ_2/Γ

VALUE	DOCUMENT ID		TECN	COMMENT
• • • We do not use the following data for averages, fits, limits, etc. • • •				
seen	[3] ADAMS	98B	MPS	18.3 $\pi^- p \to \pi^+\pi^-\pi^- p$

$\Gamma(\eta'(958)\pi^-)/\Gamma_{\text{total}}$ Γ_5/Γ

VALUE	DOCUMENT ID		TECN	COMMENT
• • • We do not use the following data for averages, fits, limits, etc. • • •				
seen	IVANOV	01	MPS	18 $\pi^- p \to \eta'\pi^- p$

$\Gamma(f_2(1270)\pi^-)/\Gamma_{\text{total}}$ Γ_3/Γ

VALUE	DOCUMENT ID		TECN	COMMENT
• • • We do not use the following data for averages, fits, limits, etc. • • •				
not seen	CHUNG	02	MPS	18.3 $\pi^- p \to \pi^+\pi^-\pi^- p$

$\Gamma(b_1(1235)\pi)/\Gamma_{\text{total}}$ Γ_4/Γ

VALUE	EVTS	DOCUMENT ID		TECN	COMMENT
• • • We do not use the following data for averages, fits, limits, etc. • • •					
seen	35280	[4] BAKER	03	SPEC	$\overline{p}p \to \omega\pi^+\pi^-\pi^0$

[3] Natural parity exchange.

[4] $B((b_1\pi)_{D-wave})/B((b_1\pi)_{S\text{-wave}}) = 0.3 \pm 0.1$.

$\pi_1(1600)$ REFERENCES

BAKER	03	PL B563 140	C.A. Baker *et al.*
CHUNG	02	PR D65 072001	S.U. Chung *et al.*
IVANOV	01	PRL 86 3977	E.I. Ivanov *et al.*
ADAMS	98B	PRL 81 5760	G.S. Adams *et al.* (MPS Collab.)

OTHER RELATED PAPERS

BERNARD	03	PR D68 074505	C. Bernard *et al.*
JIN	03	PR D67 014025	H.Y. Jin, J.G. Korener, T.G. Steele
SZCZEPANIAK	03B	PRL 91 092002	A.P. Szczepaniak *et al.*
ZHANG	03	PR D67 074020	A. Zhang, T.G. Steele
ACHASOV	02J	PAN 65 552	N.N. Achasov, G.N. Shestakov
		Translated from YAF 65 579.	
CHUNG	02C	EPL A15 539	S.U. Chung, E. Klempt, J.G. Korener
ZHANG	02	PR D65 096005	R. Zhang *et al.*
IDDIR	01	PL B507 183	F. Iddir, A.S. Safir

$a_1(1640)$

$I^G(J^{PC}) = 1^-(1^{++})$

OMITTED FROM SUMMARY TABLE

Seen in the amplitude analysis of the $3\pi^0$ system produced in $\overline{p}p \to 4\pi^0$. Possibly seen in the study of the hadronic structure in decay $\tau \to 3\pi\nu_\tau$ (ABREU 98G and ASNER 00). Needs confirmation. See the Note under $a_1(1260)$.

$a_1(1640)$ MASS

VALUE (MeV)	EVTS	DOCUMENT ID		TECN	COMMENT
1647±22 OUR AVERAGE		Error includes scale factor of 1.4. See the ideogram below.			
1630±20	35280	[1] BAKER	03	SPEC	$\overline{p}p \to \omega\pi^+\pi^-\pi^0$
1714± 9±36		CHUNG	02	MPS	18.3 $\pi^- p \to \pi^+\pi^-\pi^- p$
1640±12±30		BAKER	99	SPEC	1.94 $\overline{p}p \to 4\pi^0$
• • • We do not use the following data for averages, fits, limits, etc. • • •					
1670±90		BELLINI	85	SPEC	40 $\pi^- A \to \pi^-\pi^+\pi^- A$

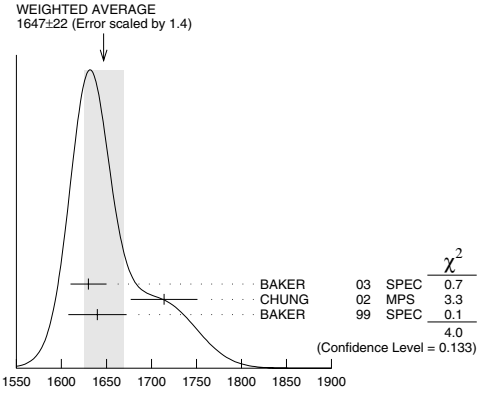

$a_1(1640)$ mass

[1] Using the $a_1(1260)$ mass and width results of BOWLER 88.

$a_1(1640)$ WIDTH

VALUE (MeV)	EVTS	DOCUMENT ID		TECN	COMMENT
254± 27 OUR AVERAGE		Error includes scale factor of 1.1.			
225± 30	35280	[2] BAKER	03	SPEC	$\overline{p}p \to \omega\pi^+\pi^-\pi^0$
308± 37±62		CHUNG	02	MPS	18.3 $\pi^- p \to \pi^+\pi^-\pi^- p$
300± 22±40		BAKER	99	SPEC	1.94 $\overline{p}p \to 4\pi^0$
• • • We do not use the following data for averages, fits, limits, etc. • • •					
300±100		BELLINI	85	SPEC	40 $\pi^- A \to \pi^-\pi^+\pi^- A$

[2] Using the $a_1(1260)$ mass and width results of BOWLER 88.

$a_1(1640)$ DECAY MODES

	Mode	Fraction (Γ_i/Γ)
Γ_1	$\pi\pi\pi$	seen
Γ_2	$f_2(1270)\pi$	seen
Γ_3	$\sigma\pi$	seen
Γ_4	$\rho\pi$ $_{S-wave}$	seen
Γ_5	$\rho\pi$ $_{D-wave}$	seen
Γ_6	$\omega\pi\pi$	seen
Γ_7	$f_1(1285)\pi$	seen

$a_1(1640)$ BRANCHING RATIOS

$\Gamma(f_2(1270)\pi)/\Gamma(\sigma\pi)$ Γ_2/Γ_3

VALUE	DOCUMENT ID		TECN	COMMENT
• • • We do not use the following data for averages, fits, limits, etc. • • •				
0.24±0.07	BAKER	99	SPEC	1.94 $\overline{p}p \to 4\pi^0$

$\Gamma(\rho\pi_{D-wave})/\Gamma_{total}$ Γ_5/Γ

VALUE	DOCUMENT ID		TECN	COMMENT
• • • We do not use the following data for averages, fits, limits, etc. • • •				
seen	CHUNG	02	MPS	18.3 $\pi^- p \to \pi^+\pi^-\pi^- p$
seen	AMELIN	95B	VES	36 $\pi^- A \to \pi^+\pi^-\pi^- A$

$\Gamma(\omega\pi\pi)/\Gamma_{total}$ Γ_6/Γ

VALUE	EVTS	DOCUMENT ID		TECN	COMMENT
• • • We do not use the following data for averages, fits, limits, etc. • • •					
seen	35280	[3] BAKER	03	SPEC	$\overline{p}p \to \omega\pi^+\pi^-\pi^0$

$\Gamma(f_1(1285)\pi)/\Gamma_{total}$ Γ_7/Γ

VALUE	DOCUMENT ID		TECN	COMMENT
• • • We do not use the following data for averages, fits, limits, etc. • • •				
seen	LEE	94	MPS2	18 $\pi^- p \to K^+\overline{K}^0\pi^-\pi^- p$

[3] Assuming the $\omega\rho$ mechanism for the $\omega\pi\pi$ state.

$a_1(1640)$ REFERENCES

BAKER	03	PL B563 140	C.A. Baker *et al.*	
CHUNG	02	PR D65 072001	S.U. Chung *et al.*	
ASNER	00	PR D61 012002	D.M. Asner *et al.*	(CLEO Collab.)
BAKER	99	PL B449 114	C.A. Baker *et al.*	
ABREU	98G	PL B426 411	P. Abreu *et al.*	(DELPHI Collab.)
AMELIN	95B	PL B356 595	D.V. Amelin *et al.*	(SERP, TBIL)
LEE	94	PL B323 227	J.H. Lee *et al.*	(BNL, IND, KYUN, MASD+)
BOWLER	88	PL B209 99	M.G. Bowler	(OXF)
BELLINI	85	SJNP 41 781	D. Bellini *et al.*	

Translated from YAF 41 1223.

OTHER RELATED PAPERS

BARNES	97	PR D55 4157	T. Barnes *et al.*	(ORNL, RAL, MCHS)
GOUZ	92	Dallas HEP 92, p. 572	Yu.P. Gouz *et al.*	(VES Collab.)

Proceedings XXVI Int. Conf. on High Energy Physics

$f_2(1640)$

$I^G(J^{PC}) = 0^+(2^{++})$

OMITTED FROM SUMMARY TABLE

$f_2(1640)$ MASS

VALUE (MeV)	DOCUMENT ID		TECN	COMMENT
1638± 6 OUR AVERAGE	Error includes scale factor of 1.2.			
1620±16	BUGG	95	MRK3	$J/\psi \to \gamma\pi^+\pi^-\pi^+\pi^-$
1647± 7	ADAMO	92	OBLX	$\overline{n}p \to 3\pi^+2\pi^-$
1590±30	BELADIDZE	92B	VES	36 $\pi^- p \to \omega\omega n$
1635± 7	ALDE	90	GAM2	38 $\pi^- p \to \omega\omega n$
• • • We do not use the following data for averages, fits, limits, etc. • • •				
1643± 7	[1] ALDE	89B	GAM2	38 $\pi^- p \to \omega\omega n$

[1] Superseded by ALDE 90.

$f_2(1640)$ WIDTH

VALUE (MeV)	CL%	DOCUMENT ID		TECN	COMMENT
99^{+28}_{-24} OUR AVERAGE		Error includes scale factor of 2.1. See the ideogram below.			
140^{+60}_{-20}		BUGG	95	MRK3	$J/\psi \to \gamma\pi^+\pi^-\pi^+\pi^-$
58±20		ADAMO	92	OBLX	$\overline{n}p \to 3\pi^+2\pi^-$
100±20		BELADIDZE	92B	VES	36 $\pi^- p \to \omega\omega n$
• • • We do not use the following data for averages, fits, limits, etc. • • •					
< 70	90	ALDE	90	GAM2	38 $\pi^- p \to \omega\omega n$

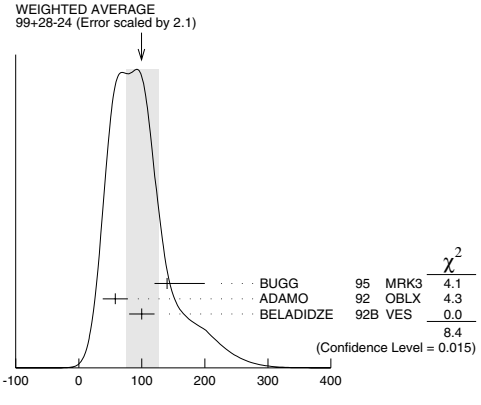

$f_2(1640)$ width (MeV)

$f_2(1640)$ DECAY MODES

	Mode	Fraction (Γ_i/Γ)
Γ_1	$\omega\omega$	seen
Γ_2	4π	seen

$f_2(1640)$ REFERENCES

BUGG	95	PL B353 378	D.V. Bugg *et al.*	(LOQM, PNPI, WASH) JP
ADAMO	92	PL B287 368	A. Adamo *et al.*	(OBELIX Collab.)
BELADIDZE	92B	ZPHY C54 367	G.M. Beladidze *et al.*	(VES Collab.)
ALDE	90	PL B241 600	D.M. Alde *et al.*	(SERP, BELG, LANL, LAPP+)
ALDE	89B	PL B216 451	D.M. Alde *et al.*	(SERP, BELG, LANL, LAPP+) IGJPC

OTHER RELATED PAPERS

PROKOSHKIN	99	PAN 62 356 Translated from YAF 62 396.	Yu.D. Prokoshkin

$\eta_2(1645)$ $I^G(J^{PC}) = 0^+(2^{-+})$

$\eta_2(1645)$ MASS

VALUE (MeV)	DOCUMENT ID		TECN	CHG	COMMENT
1617± 5 OUR AVERAGE					
1613± 8	BARBERIS	00B			450 $pp \to p_f \eta\pi^+\pi^- p_s$
1617± 8	BARBERIS	00C			450 $pp \to p_f 4\pi p_s$
1620±20	BARBERIS	97B	OMEG		450 $pp \to pp2(\pi^+\pi^-)$
1645±14±15	ADOMEIT	96	CBAR	0	1.94 $\overline{p}p \to \eta 3\pi^0$
• • • We do not use the following data for averages, fits, limits, etc. • • •					
1645± 6±20	ANISOVICH	00E	SPEC		1.94 $\overline{p}p \to \eta 3\pi^0$

$\eta_2(1645)$ WIDTH

VALUE (MeV)	DOCUMENT ID		TECN	CHG	COMMENT
181±11 OUR AVERAGE					
185±17	BARBERIS	00B			450 $pp \to p_f \eta\pi^+\pi^- p_s$
177±18	BARBERIS	00C			450 $pp \to p_f 4\pi p_s$
180±25	BARBERIS	97B	OMEG		450 $pp \to pp2(\pi^+\pi^-)$
$180^{+40}_{-21}\pm25$	ADOMEIT	96	CBAR	0	1.94 $\overline{p}p \to \eta 3\pi^0$
• • • We do not use the following data for averages, fits, limits, etc. • • •					
200±25	ANISOVICH	00E	SPEC		1.94 $\overline{p}p \to \eta 3\pi^0$

$\eta_2(1645)$ DECAY MODES

	Mode	Fraction (Γ_i/Γ)
Γ_1	$a_2(1320)\pi$	seen
Γ_2	$K\overline{K}\pi$	seen
Γ_3	$K^*\overline{K}$	seen
Γ_4	$\eta\pi^+\pi^-$	seen
Γ_5	$a_0(980)\pi$	seen
Γ_6	$f_2(1270)\eta$	not seen

$\eta_2(1645)$ BRANCHING RATIOS

$\Gamma(K\overline{K}\pi)/\Gamma(a_2(1320)\pi)$ Γ_2/Γ_1

VALUE	DOCUMENT ID		TECN	COMMENT
0.07 ±0.03	[1] BARBERIS	97C	OMEG	450 $pp \to pp K\overline{K}\pi$

[1] Using $2(\pi^+\pi^-)$ data from BARBERIS 97B.

$\Gamma(a_2(1320)\pi)/\Gamma(a_0(980)\pi)$ Γ_1/Γ_5

VALUE	DOCUMENT ID		COMMENT
13.0±2.7	BARBERIS	00B	450 $pp \to p_f \eta\pi^+\pi^- p_s$

$\Gamma(f_2(1270)\eta)/\Gamma_{total}$ Γ_6/Γ

VALUE	DOCUMENT ID		COMMENT
• • • We do not use the following data for averages, fits, limits, etc. • • •			
not seen	BARBERIS	00B	450 $pp \to p_f \eta\pi^+\pi^- p_s$

$\eta_2(1645)$ REFERENCES

ANISOVICH	00E	PL B477 19	A.V. Anisovich *et al.*	
BARBERIS	00B	PL B471 435	D. Barberis *et al.*	(WA 102 Collab.)
BARBERIS	00C	PL B471 440	D. Barberis *et al.*	(WA 102 Collab.)
BARBERIS	97B	PL B413 217	D. Barberis *et al.*	(WA 102 Collab.)
BARBERIS	97C	PL B413 225	D. Barberis *et al.*	(WA 102 Collab.)
ADOMEIT	96	ZPHY C71 227	J. Adomeit *et al.*	(Crystal Barrel Collab.)

$\omega(1650)$ was $\omega(1600)$ $I^G(J^{PC}) = 0^-(1^{--})$

$\omega(1650)$ MASS

VALUE (MeV)	EVTS	DOCUMENT ID		TECN	CHG	COMMENT
1670± 30 OUR ESTIMATE						
1700± 20		EUGENIO	01	SPEC		18 $\pi^- p \to \omega\eta n$
1705± 26	612	[1] AKHMETSHIN	00D	CMD2		$e^+e^- \to \omega\pi^+\pi^-$
1662± 13	750	[2] ANTONELLI	92	DM2		1.34–2.4 $e^+e^- \to \rho\pi, \omega\pi\pi$
• • • We do not use the following data for averages, fits, limits, etc. • • •						
1770± 50±60	1.2M	[3] ACHASOV	03D	RVUE		0.44–2.00 $e^+e^- \to \pi^+\pi^-\pi^0$
1619± 5		[4] HENNER	02	RVUE		1.2–2.0 $e^+e^- \to \rho\pi, \omega\pi\pi$
1820^{+190}_{-150}		[5] ACHASOV	98H	RVUE		$e^+e^- \to \pi^+\pi^-\pi^0$
1840^{+100}_{-70}		[6] ACHASOV	98H	RVUE		$e^+e^- \to \omega\pi^+\pi^-$
1780^{+170}_{-300}		[7] ACHASOV	98H	RVUE		$e^+e^- \to K^+K^-$
~ 2100		[8] ACHASOV	98H	RVUE		$e^+e^- \to K^0_S K^\pm\pi^\mp$
1606± 9		[9] CLEGG	94	RVUE		
1670± 20		ATKINSON	83B	OMEG		20–70 $\gamma p \to 3\pi X$
1657± 13		CORDIER	81	DM1		$e^+e^- \to \omega 2\pi$
1679± 34	21	ESPOSITO	80	FRAM		$e^+e^- \to 3\pi$
1652± 17		COSME	79	OSPK	0	$e^+e^- \to 3\pi$

[1] Using the data of AKHMETSHIN 00D and ANTONELLI 92. The $\rho\pi$ dominance for the energy dependence of the $\omega(1420)$ and $\omega(1650)$ width assumed.
[2] From the combined fit of the $\rho\pi$ and $\omega\pi\pi$ final states.
[3] From the combined fit of ANTONELLI 92, ACHASOV 01E, ACHASOV 02E, and ACHASOV 03D data on the $\pi^+\pi^-\pi^0$ and ANTONELLI 92 on the $\omega\pi^+\pi^-$ final states. Supersedes ACHASOV 99E and ACHASOV 02E.
[4] Using results of CORDIER 81 and preliminary data of DOLINSKY 91 and ANTONELLI 92.
[5] Using data from BARKOV 87, DOLINSKY 91, and ANTONELLI 92.
[6] Using the data from ANTONELLI 92.
[7] Using the data from IVANOV 81 and BISELLO 88B.
[8] Using the data from BISELLO 91C.
[9] From a fit to two Breit-Wigner functions and using the data of DOLINSKY 91 and ANTONELLI 92.

$\omega(1650)$ WIDTH

VALUE (MeV)	EVTS	DOCUMENT ID		TECN	CHG	COMMENT
315± 35 OUR ESTIMATE						
250± 50		EUGENIO	01	SPEC		18 $\pi^- p \to \omega\eta n$
370± 25	612	[10] AKHMETSHIN	00D	CMD2		$e^+e^- \to \omega\pi^+\pi^-$
280± 24	750	[11] ANTONELLI	92	DM2		1.34–2.4 $e^+e^- \to \rho\pi, \omega\pi\pi$
• • • We do not use the following data for averages, fits, limits, etc. • • •						
$490^{+200}_{-150}\pm130$	1.2M	[12] ACHASOV	03D	RVUE		0.44–2.00 $e^+e^- \to \pi^+\pi^-\pi^0$
250± 14		[13] HENNER	02	RVUE		1.2–2.0 $e^+e^- \to \rho\pi, \omega\pi\pi$
113± 20		[14] CLEGG	94	RVUE		
160± 20		ATKINSON	83B	OMEG		20–70 $\gamma p \to 3\pi X$
136± 46		CORDIER	81	DM1		$e^+e^- \to \omega 2\pi$
99± 49	21	ESPOSITO	80	FRAM		$e^+e^- \to 3\pi$
42± 17		COSME	79	OSPK	0	$e^+e^- \to 3\pi$

[10] Using the data of AKHMETSHIN 00D and ANTONELLI 92. The $\rho\pi$ dominance for the energy dependence of the $\omega(1420)$ and $\omega(1650)$ width assumed.
[11] From the combined fit of the $\rho\pi$ and $\omega\pi\pi$ final states.
[12] From the combined fit of ANTONELLI 92, ACHASOV 01E, ACHASOV 02E, and ACHASOV 03D data on the $\pi^+\pi^-\pi^0$ and ANTONELLI 92 on the $\omega\pi^+\pi^-$ final states. Supersedes ACHASOV 99E and ACHASOV 02E.
[13] Using results of CORDIER 81 and preliminary data of DOLINSKY 91 and ANTONELLI 92.
[14] From a fit to two Breit-Wigner functions and using the data of DOLINSKY 91 and ANTONELLI 92.

$\omega(1650)$ DECAY MODES

	Mode	Fraction (Γ_i/Γ)
Γ_1	$\rho\pi$	seen
Γ_2	$\omega\pi\pi$	seen
Γ_3	$\omega\eta$	seen
Γ_4	e^+e^-	seen

$\omega(1650)$ $\Gamma(i)\Gamma(e^+e^-)/\Gamma^2(\text{total})$

$\Gamma(\rho\pi) \times \Gamma(e^+e^-)/\Gamma^2_{\text{total}}$ $\Gamma_1\Gamma_4/\Gamma^2$

VALUE (units 10^{-6})	EVTS	DOCUMENT ID		TECN	COMMENT
• • • We do not use the following data for averages, fits, limits, etc. • • •					
$1.2\ {}^{+0.4}_{-0.1} \pm 0.8$	1.2M	15,16 ACHASOV	03D	RVUE	0.44–2.00 $e^+e^- \to \pi^+\pi^-\pi^0$
0.921 ± 0.230		17,18 CLEGG	94	RVUE	
0.479 ± 0.050	750	19,20 ANTONELLI	92	DM2	1.34–2.4 $e^+e^- \to \rho\pi$, $\omega\pi\pi$

$\Gamma(\omega\pi\pi) \times \Gamma(e^+e^-)/\Gamma^2_{\text{total}}$ $\Gamma_2\Gamma_4/\Gamma^2$

VALUE (units 10^{-6})	EVTS	DOCUMENT ID		TECN	COMMENT
• • • We do not use the following data for averages, fits, limits, etc. • • •					
$0.41 \pm 0.09 \pm 0.13$	1.2M	15,16 ACHASOV	03D	RVUE	0.44–2.00 $e^+e^- \to \pi^+\pi^-\pi^0$
0.540 ± 0.095		21 AKHMETSHIN	00D	CMD2	1.2–1.38 $e^+e^- \to \omega\pi^+\pi^-$
0.318 ± 0.080		17,18 CLEGG	94	RVUE	
0.607 ± 0.061	750	19,20 ANTONELLI	92	DM2	1.34–2.4 $e^+e^- \to \rho\pi$, $\omega\pi\pi$

$\Gamma(\omega\eta) \times \Gamma(e^+e^-)/\Gamma^2_{\text{total}}$ $\Gamma_3\Gamma_4/\Gamma^2$

VALUE (units 10^{-6})	CL%	DOCUMENT ID		TECN	COMMENT
• • • We do not use the following data for averages, fits, limits, etc. • • •					
< 6	90	22 AKHMETSHIN	03B	CMD2	$e^+e \to \eta\pi^0\gamma$

[15] Calculated by us from the cross section at the peak.
[16] From the combined fit of ANTONELLI 92, ACHASOV 01E, ACHASOV 02E, and ACHASOV 03D data on the $\pi^+\pi^-\pi^0$ and ANTONELLI 92 on the $\omega\pi^+\pi^-$ final states. Supersedes ACHASOV 99E and ACHASOV 02E.
[17] From a fit to two Breit-Wigner functions and using the data of DOLINSKY 91 and ANTONELLI 92.
[18] From the partial and leptonic width given by the authors.
[19] From the combined fit of the $\rho\pi$ and $\omega\pi\pi$ final states.
[20] From the product of the leptonic width and partial branching ratio given by the authors.
[21] Using the data of AKHMETSHIN 00D and ANTONELLI 92. The $\rho\pi$ dominance for the energy dependence of the $\omega(1420)$ and $\omega(1650)$ width assumed.
[22] $\omega(1650)$ mass and width fixed at 1700 MeV and 250 MeV, respectively.

$\omega(1650)$ BRANCHING RATIOS

$\Gamma(\omega\pi\pi)/\Gamma_{\text{total}}$ Γ_2/Γ

VALUE	EVTS	DOCUMENT ID		TECN	COMMENT
• • • We do not use the following data for averages, fits, limits, etc. • • •					
~ 0.35	1.2M	24 ACHASOV	03D	RVUE	0.44–2.00 $e^+e^- \to \pi^+\pi^-\pi^0$
0.620 ± 0.014		25 HENNER	02	RVUE	1.2–2.0 $e^+e^- \to \rho\pi$, $\omega\pi\pi$

$\Gamma(\rho\pi)/\Gamma_{\text{total}}$ Γ_1/Γ

VALUE	EVTS	DOCUMENT ID		TECN	COMMENT
• • • We do not use the following data for averages, fits, limits, etc. • • •					
~ 0.65	1.2M	24 ACHASOV	03D	RVUE	0.44–2.00 $e^+e^- \to \pi^+\pi^-\pi^0$
0.380 ± 0.014		25 HENNER	02	RVUE	1.2–2.0 $e^+e^- \to \rho\pi$, $\omega\pi\pi$

$\Gamma(e^+e^-)/\Gamma_{\text{total}}$ Γ_4/Γ

VALUE (units 10^{-7})	EVTS	DOCUMENT ID		TECN	COMMENT
• • • We do not use the following data for averages, fits, limits, etc. • • •					
~ 18	1.2M	23,25 ACHASOV	03D	RVUE	0.44–2.00 $e^+e^- \to \pi^+\pi^-\pi^0$
32 ± 1		25 HENNER	02	RVUE	1.2–2.0 $e^+e^- \to \rho\pi$, $\omega\pi\pi$

[23] Calculated by us from the cross section at the peak.
[24] From the combined fit of ANTONELLI 92, ACHASOV 01E, ACHASOV 02E, and ACHASOV 03D data on the $\pi^+\pi^-\pi^0$ and ANTONELLI 92 on the $\omega\pi^+\pi^-$ final states. Supersedes ACHASOV 99E and ACHASOV 02E.
[25] Assuming that the $\omega(1650)$ decays into $\rho\pi$ and $\omega\pi\pi$ only.

$\omega(1650)$ REFERENCES

ACHASOV	03D	PR D68 052006	M.N. Achasov *et al.*	(Novosibirsk SND Collab.)
AKHMETSHIN	03B	PL B562 173	R.R. Akhmetshin *et al.*	(Novosibirsk CMD-2 Collab.)
ACHASOV	02E	PR D66 032001	M.N. Achasov *et al.*	(Novosibirsk SND Collab.)
HENNER	02	EPJ C26 3	V.K. Henner *et al.*	
ACHASOV	01E	PR D63 072002	M.N. Achasov *et al.*	(Novosibirsk SND Collab.)
EUGENIO	01	PL B497 190	P. Eugenio *et al.*	
AKHMETSHIN	00D	PL B489 125	R.R. Akhmetshin *et al.*	(Novosibirsk CMD-2 Collab.)
ACHASOV	99E	PL B462 365	M.N. Achasov *et al.*	(Novosibirsk SND Collab.)
ACHASOV	98H	PR D57 4334	N.N. Achasov, A.A. Kozhevnikov	
CLEGG	94	ZPHY C62 455	A.B. Clegg, A. Donnachie	(LANC, MCHS)
ANTONELLI	92	ZPHY C56 15	A. Antonelli *et al.*	(DM2 Collab.)
BISELLO	91C	ZPHY C52 227	D. Bisello *et al.*	(DM2 Collab.)
DOLINSKY	91	PRPL 202 99	S.I. Dolinsky *et al.*	(NOVO)
BISELLO	88B	ZPHY C39 13	D. Bisello *et al.*	(PADO, CLER, FRAS+)
BARKOV	87	JETPL 46 164 Translated from ZETFP 46 132.	L.M. Barkov *et al.*	(NOVO)
ATKINSON	83B	PL 127B 132	M. Atkinson *et al.*	(BONN, CERN, GLAS+)
CORDIER	81	PL 106B 155	A. Cordier *et al.*	(ORSAY)
IVANOV	81	PL 107B 297	P.M. Ivanov *et al.*	(NOVO)
ESPOSITO	80	LNC 28 195	B. Esposito *et al.*	(FRAS, NAPL, PADO+)
COSME	79	NP B152 215	G. Cosme *et al.*	(IPN)

OTHER RELATED PAPERS

AKHMETSHIN	03	PL B551 27	R.R. Akhmetshin *et al.*	(Novosibirsk CMD-2 Collab.)
Also	02	PAN 65 1222 Translated from YAF 65 1255.	E.V. Anashkin, V.M. Aulchenko, R.R. Akhmetshin	
ACHASOV	02B	PAN 65 153 Translated from YAF 65 158.	N.N. Achasov, A.A. Kozhevnikov	
CLOSE	02	PR D65 092003	F.E. Close, A. Donnachie, Yu.S. Kalashnikova	
ACHASOV	00J	PR D62 117503	N.N. Achasov, A.A. Kozhevnikov	
ANISOVICH	00H	PL B485 341	A.V. Anisovich *et al.*	
ABELE	99D	PL B468 178	A. Abele *et al.*	(Crystal Barrel Collab.)
BELOZEROVA	98	PPN 29 63 Translated from FECAY 29 148.	T.S. Belozerova, V.K. Henner	
ACHASOV	97F	PAN 60 2029 Translated from YAF 60 2212.	N.N. Achasov, A.A. Kozhevnikov	(NOVM)
DOLINSKY	91	PRPL 202 99	S.I. Dolinsky *et al.*	(NOVO)
ATKINSON	87	ZPHY C34 157	M. Atkinson *et al.*	(BONN, CERN, GLAS+)
ATKINSON	84	NP B231 15	M. Atkinson *et al.*	(BONN, CERN, GLAS+)

$\omega_3(1670)$

$I^G(J^{PC}) = 0^-(3^{--})$

$\omega_3(1670)$ MASS

VALUE (MeV)	EVTS	DOCUMENT ID		TECN	COMMENT
1667 ± 4 OUR AVERAGE					
$1665.3 \pm 5.2 \pm 4.5$	23400	AMELIN	96	VES	36 $\pi^-p \to \pi^+\pi^-\pi^0 n$
1685 ± 20	60	BAUBILLIER	79	HBC	8.2 K^-p backward
1673 ± 12	430	1,2 BALTAY	78E	HBC	15 $\pi^+p \to \Delta 3\pi$
1650 ± 12		CORDEN	78B	OMEG	8–12 $\pi^-p \to N3\pi$
1669 ± 11	600	2 WAGNER	75	HBC	7 $\pi^+p \to \Delta^{++}3\pi$
1678 ± 14	500	DIAZ	74	DBC	6 $\pi^+n \to p3\pi^0$
1660 ± 13	200	DIAZ	74	DBC	6 $\pi^+n \to p\omega\pi^0\pi^0$
1679 ± 17	200	MATTHEWS	71D	DBC	7.0 $\pi^+n \to p3\pi^0$
1670 ± 20		KENYON	69	DBC	8 $\pi^+n \to p3\pi^0$
• • • We do not use the following data for averages, fits, limits, etc. • • •					
~ 1700	110	1 CERRADA	77B	HBC	4.2 $K^-p \to \Lambda 3\pi$
1695 ± 20		BARNES	69B	HBC	4.6 $K^-p \to \omega 2\pi X$
1636 ± 20		ARMENISE	68B	DBC	5.1 $\pi^+n \to p3\pi^0$

[1] Phase rotation seen for $J^P = 3^-$ $\rho\pi$ wave.
[2] From a fit to $I(J^P) = 0(3^-)$ $\rho\pi$ partial wave.

$\omega_3(1670)$ WIDTH

VALUE (MeV)	EVTS	DOCUMENT ID		TECN	COMMENT
168±10 OUR AVERAGE					
$149 \pm 19 \pm 7$	23400	AMELIN	96	VES	36 $\pi^-p \to \pi^+\pi^-\pi^0 n$
160 ± 80	60	3 BAUBILLIER	79	HBC	8.2 K^-p backward
173 ± 16	430	4,5 BALTAY	78E	HBC	15 $\pi^+p \to \Delta 3\pi$
253 ± 39		CORDEN	78B	OMEG	8–12 $\pi^-p \to N3\pi$
173 ± 28	600	3,5 WAGNER	75	HBC	7 $\pi^+p \to \Delta^{++}3\pi$
167 ± 40	500	DIAZ	74	DBC	6 $\pi^+n \to p3\pi^0$
122 ± 39	200	DIAZ	74	DBC	6 $\pi^+n \to p\omega\pi^0\pi^0$
155 ± 40	200	3 MATTHEWS	71D	DBC	7.0 $\pi^+n \to p3\pi^0$
• • • We do not use the following data for averages, fits, limits, etc. • • •					
90 ± 20		BARNES	69B	HBC	4.6 $K^-p \to \omega 2\pi$
100 ± 40		KENYON	69	DBC	8 $\pi^+n \to p3\pi^0$
112 ± 60		ARMENISE	68B	DBC	5.1 $\pi^+n \to p3\pi^0$

[3] Width errors enlarged by us to $4\Gamma/\sqrt{N}$; see the note with the $K^*(892)$ mass.
[4] Phase rotation seen for $J^P = 3^-$ $\rho\pi$ wave.
[5] From a fit to $I(J^P) = 0(3^-)$ $\rho\pi$ partial wave.

$\omega_3(1670)$ DECAY MODES

	Mode	Fraction (Γ_i/Γ)
Γ_1	$\rho\pi$	seen
Γ_2	$\omega\pi\pi$	seen
Γ_3	$b_1(1235)\pi$	possibly seen

$\omega_3(1670)$ BRANCHING RATIOS

$\Gamma(\omega\pi\pi)/\Gamma(\rho\pi)$ Γ_2/Γ_1

VALUE	EVTS	DOCUMENT ID		TECN	COMMENT
• • • We do not use the following data for averages, fits, limits, etc. • • •					
0.71 ± 0.27	100	DIAZ	74	DBC	6 $\pi^+n \to p5\pi^0$

$\Gamma(b_1(1235)\pi)/\Gamma(\rho\pi)$ Γ_3/Γ_1

VALUE	DOCUMENT ID		TECN	COMMENT
possibly seen	DIAZ	74	DBC	6 $\pi^+n \to p5\pi^0$

$\Gamma(b_1(1235)\pi)/\Gamma(\omega\pi\pi)$ Γ_3/Γ_2

VALUE	CL%	DOCUMENT ID		TECN	COMMENT
• • • We do not use the following data for averages, fits, limits, etc. • • •					
> 0.75	68	BAUBILLIER	79	HBC	8.2 K^-p backward

Meson Particle Listings

$\omega_3(1670)$, $\pi_2(1670)$

$\omega_3(1670)$ REFERENCES

AMELIN	96	ZPHY C70 71	D.V. Amelin *et al.*	(SERP, TBIL)
BAUBILLIER	79	PL 89B 131	M. Baubillier *et al.*	(BIRM, CERN, GLAS+)
BALTAY	78E	PRL 40 87	C. Baltay, C.V. Cautis, M. Kalelkar	(COLU) JP
CORDEN	78B	NP B138 235	M.J. Corden *et al.*	(BIRM, RHEL, TELA+)
CERRADA	77B	NP B126 241	M. Cerrada *et al.*	(AMST, CERN, NIJM+) JP
WAGNER	75	PL 58B 201	F. Wagner, M. Tabak, D.M. Chew	(LBL) JP
DIAZ	74	PRL 32 260	J. Díaz *et al.*	(CASE, CMU)
MATTHEWS	71D	PR D3 2561	J.A.J. Matthews *et al.*	(TNTO, WISC)
BARNES	69B	PRL 23 142	V.E. Barnes *et al.*	(BNL)
KENYON	69	PRL 23 146	I.R. Kenyon *et al.*	(BNL, UCND, ORNL)
ARMENISE	68B	PL 26B 336	N. Armenise *et al.*	(BARI, BGNA, FIRZ+)

OTHER RELATED PAPERS

MATTHEWS	71	LNC 1 361	J.A.J. Matthews *et al.*	(TNTO, WISC)
ARMENISE	70	LNC 4 199	N. Armenise *et al.*	(BARI, BGNA, FIRZ)

$\pi_2(1670)$

$I^G(J^{PC}) = 1^-(2^{-+})$

$\pi_2(1670)$ MASS

VALUE (MeV)	EVTS	DOCUMENT ID		TECN	CHG	COMMENT
1672.4± 3.2 OUR AVERAGE		Error includes scale factor of 1.4. See the ideogram below.				
1676 ± 3 ± 8		[1] CHUNG	02	MPS		18.3 $\pi^- p \to \pi^+\pi^-\pi^- p$
1685 ±10 ±30		[2] BARBERIS	01			450 $pp \to p_f 3\pi^0 p_s$
1687 ± 9 ±15		AMELIN	99	VES		37 $\pi^- A \to \omega\pi^-\pi^0 A^*$
1669 ± 4		BARBERIS	98B			450 $pp \to p_f \rho\pi p_s$
1670 ± 4		BARBERIS	98B			450 $pp \to p_f f_2(1270)\pi p_s$
1730 ±20		[3] AMELIN	95B	VES		36 $\pi^- A \to \pi^+\pi^-\pi^- A$
1690 ±14		[4] BERDNIKOV	94	VES		37 $\pi^- A \to K^+K^-\pi^- A$
1710 ±20	700	ANTIPOV	87	SIGM	–	50 π^- Cu $\to \mu^+\mu^-\pi^-$ Cu
1676 ± 6		[4] EVANGELISTA	81	OMEG	–	12 $\pi^- p \to 3\pi p$
1657 ±14		[4,5] DAUM	80D	SPEC	–	63–94 $\pi p \to 3\pi$ X
1662 ±10	2000	[4] BALTAY	77	HBC	+	15 $\pi^+ p \to p3\pi$
• • • We do not use the following data for averages, fits, limits, etc. • • •						
1742 ±31 ±49		ANTREASYAN	90	CBAL		$e^+e^- \to e^+e^-\pi^0\pi^0\pi^0$
1624 ±21		[1] BELLINI	85	SPEC		40 $\pi^- A \to \pi^-\pi^+\pi^- A$
1622 ±35		[6] BELLINI	85	SPEC		40 $\pi^- A \to \pi^-\pi^+\pi^- A$
1693 ±28		[7] BELLINI	85	SPEC		40 $\pi^- A \to \pi^-\pi^+\pi^- A$
1710 ±20		[8] DAUM	81B	SPEC	–	63,94 $\pi^- p$
1660 ±10		[4] ASCOLI	73	HBC	–	5–25 $\pi^- p \to p\pi_2$

[1] From $f_2(1270)\pi$ decay.
[2] From a fit to the invariant mass distribution.
[3] From a fit to $J^{PC} = 2^{-+}$ $f_2(1270)\pi$, $f_0(1370)\pi$ waves.
[4] From a fit to $J^P = 2^-$ S-wave $f_2(1270)\pi$ partial wave.
[5] Clear phase rotation seen in 2^-S, 2^-P, 2^-D waves. We quote central value and spread of single-resonance fits to three channels.
[6] From $\rho\pi$ decay.
[7] From $\sigma\pi$ decay.
[8] From a two-resonance fit to four 2^-0^+ waves. This should not be averaged with all the single resonance fits.

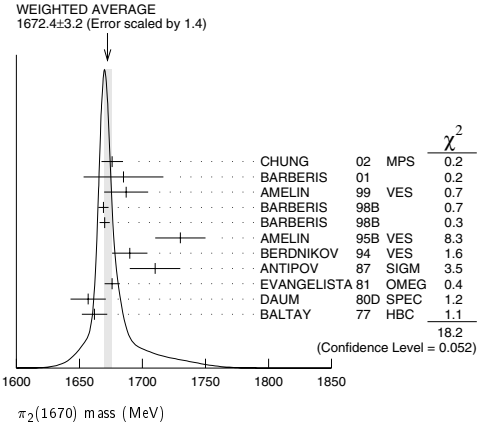

$\pi_2(1670)$ WIDTH

VALUE (MeV)	EVTS	DOCUMENT ID		TECN	CHG	COMMENT
259± 9 OUR AVERAGE		Error includes scale factor of 1.3. See the ideogram below.				
254 ± 3 ±31		[9] CHUNG	02	MPS		18.3 $\pi^- p \to \pi^+\pi^-\pi^- p$
265 ± 30 ±40		[10] BARBERIS	01			450 $pp \to p_f 3\pi^0 p_s$
168 ± 43 ±53		AMELIN	99	VES		37 $\pi^- A \to \omega\pi^-\pi^0 A^*$
268 ± 15		BARBERIS	98B			450 $pp \to p_f \rho\pi p_s$
256 ± 15		BARBERIS	98B			450 $pp \to p_f f_2(1270)\pi p_s$
310 ± 20		[11] AMELIN	95B	VES		36 $\pi^- A \to \pi^+\pi^-\pi^- A$
190 ± 50		[12] BERDNIKOV	94	VES		37 $\pi^- A \to K^+K^-\pi^- A$
170 ± 80	700	ANTIPOV	87	SIGM	–	50 π^- Cu $\to \mu^+\mu^-\pi^-$ Cu
260 ± 20		[12] EVANGELISTA	81	OMEG	–	12 $\pi^- p \to 3\pi p$
219 ± 20		[12,13] DAUM	80D	SPEC	–	63–94 $\pi p \to 3\pi$ X
285 ± 60	2000	[12] BALTAY	77	HBC	+	15 $\pi^+ p \to p3\pi$
• • • We do not use the following data for averages, fits, limits, etc. • • •						
236 ± 49 ±36		ANTREASYAN	90	CBAL		$e^+e^- \to e^+e^-\pi^0\pi^0\pi^0$
304 ± 22		[9] BELLINI	85	SPEC		40 $\pi^- A \to \pi^-\pi^+\pi^- A$
404 ±108		[14] BELLINI	85	SPEC		40 $\pi^- A \to \pi^-\pi^+\pi^- A$
330 ± 90		[15] BELLINI	85	SPEC		40 $\pi^- A \to \pi^-\pi^+\pi^- A$
312 ± 50		[16] DAUM	81B	SPEC	–	63,94 $\pi^- p$
270 ± 60		[12] ASCOLI	73	HBC	–	5–25 $\pi^- p \to p\pi_2$

[9] From $f_2(1270)\pi$ decay.
[10] From a fit to the invariant mass distribution.
[11] From a fit to $J^{PC} = 2^{-+}$ $f_2(1270)\pi$, $f_0(1370)\pi$ waves.
[12] From a fit to $J^P = 2^-$ $f_2(1270)\pi$ partial wave.
[13] Clear phase rotation seen in 2^-S, 2^-P, 2^-D waves. We quote central value and spread of single-resonance fits to three channels.
[14] From $\rho\pi$ decay.
[15] From $\sigma\pi$ decay.
[16] From a two-resonance fit to four 2^-0^+ waves. This should not be averaged with all the single resonance fits.

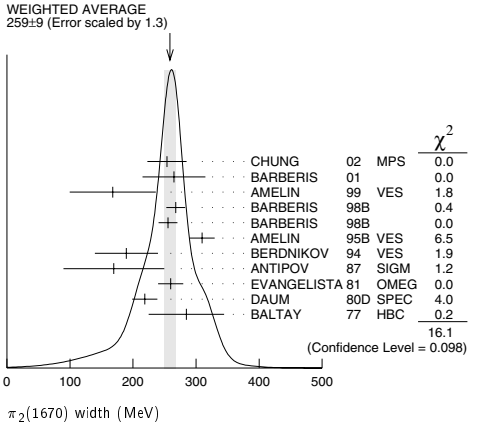

$\pi_2(1670)$ DECAY MODES

	Mode	Fraction (Γ_i/Γ)	Confidence level
Γ_1	3π	(95.8±1.4) %	
Γ_2	$\pi^+\pi^-\pi^0$		
Γ_3	$\pi^0\pi^0\pi^0$		
Γ_4	$f_2(1270)\pi$	(56.2±3.2) %	
Γ_5	$\rho\pi$	(31 ±4) %	
Γ_6	$\sigma\pi$	(10.9±3.4) %	
Γ_7	$(\pi\pi)_{S\text{-wave}}$	(8.7±3.4) %	
Γ_8	$K\overline{K}^*(892)+$ c.c.	(4.2±1.4) %	
Γ_9	$\omega\rho$	(2.7±1.1) %	
Γ_{10}	$\gamma\gamma$		
Γ_{11}	$\eta\pi$		
Γ_{12}	$\pi^\pm 2\pi^+ 2\pi^-$		
Γ_{13}	$\rho(1450)\pi$	< 3.6 $\times 10^{-3}$	97.7%
Γ_{14}	$b_1(1235)\pi$	< 1.9 $\times 10^{-3}$	97.7%

CONSTRAINED FIT INFORMATION

An overall fit to 4 branching ratios uses 6 measurements and one constraint to determine 4 parameters. The overall fit has a $\chi^2 = 1.9$ for 3 degrees of freedom.

The following *off-diagonal* array elements are the correlation coefficients $\langle \delta x_i \delta x_j \rangle / (\delta x_i \cdot \delta x_j)$, in percent, from the fit to the branching fractions, $x_i \equiv \Gamma_i/\Gamma_{total}$. The fit constrains the x_i whose labels appear in this array to sum to one.

x_5	−53			
x_7	−29	−59		
x_8	−8	−21	−9	
	x_4	x_5	x_7	

$\pi_2(1670)$ PARTIAL WIDTHS

$\Gamma(\gamma\gamma)$ **Γ_{10}**

VALUE (keV)	CL%	DOCUMENT ID		TECN	CHG	COMMENT
<0.072	90	[17] ACCIARRI	97T	L3		$e^+e^- \to e^+e^-\pi^+\pi^-\pi^0$
<0.19	90	[17] ALBRECHT	97B	ARG		$e^+e^- \to e^+e^-\pi^+\pi^-\pi^0$
• • • We do not use the following data for averages, fits, limits, etc. • • •						
$1.41 \pm 0.23 \pm 0.28$		ANTREASYAN	90	CBAL	0	$e^+e^- \to e^+e^-\pi^0\pi^0\pi^0$
$0.8 \pm 0.3 \pm 0.12$		[18] BEHREND	90C	CELL	0	$e^+e^- \to e^+e^-\pi^+\pi^-\pi^0$
$1.3 \pm 0.3 \pm 0.2$		[19] BEHREND	90C	CELL	0	$e^+e^- \to e^+e^-\pi^+\pi^-\pi^0$

[17] Decaying into $f_2(1270)\pi$ and $\rho\pi$.
[18] Constructive interference between $f_2(1270)\pi$, $\rho\pi$ and background.
[19] Incoherent Ansatz.

$\pi_2(1670)$ BRANCHING RATIOS

$\Gamma(3\pi)/\Gamma_{total}$ **$\Gamma_1/\Gamma = (\Gamma_4+\Gamma_5+\Gamma_7)/\Gamma$**

VALUE	DOCUMENT ID
0.958 ± 0.014 OUR FIT	

$\Gamma(\pi^0\pi^0\pi^0)/\Gamma(\pi^+\pi^-\pi^0)$ **Γ_3/Γ_2**

VALUE	DOCUMENT ID		COMMENT
0.29 ± 0.03 ± 0.05	[20] BARBERIS	01	$450\ pp \to p_f 3\pi^0 p_s$

$\Gamma(\rho\pi)/\Gamma(\pi^\pm\pi^+\pi^-)$ **$\frac{1}{2}\Gamma_5/(0.567\Gamma_4+\frac{1}{2}\Gamma_5+0.624\Gamma_7)$**

VALUE	DOCUMENT ID		TECN	CHG	COMMENT
0.29 ± 0.04 OUR FIT					
0.29 ± 0.05	[21] DAUM	81B	SPEC		63,94 π^-p
• • • We do not use the following data for averages, fits, limits, etc. • • •					
<0.3	BARTSCH	68	HBC	+	$8\ \pi^+p \to 3\pi p$

$\Gamma(f_2(1270)\pi)/\Gamma(\pi^\pm\pi^+\pi^-)$ **$0.567\Gamma_4/(0.567\Gamma_4+\frac{1}{2}\Gamma_5+0.624\Gamma_7)$**
(With $f_2(1270) \to \pi^+\pi^-$.)

VALUE	DOCUMENT ID		TECN	CHG	COMMENT
0.604 ± 0.035 OUR FIT					
0.60 ± 0.05 OUR AVERAGE	Error includes scale factor of 1.3. See the ideogram below.				
0.61 ± 0.04	[21] DAUM	81B	SPEC		63,94 π^-p
$0.76\ ^{+0.24}_{-0.34}$	ARMENISE	69	DBC	+	$5.1\ \pi^+d \to d3\pi$
0.35 ± 0.20	BALTAY	68	HBC	+	7–8.5 π^+p
• • • We do not use the following data for averages, fits, limits, etc. • • •					
0.59	BARTSCH	68	HBC	+	$8\ \pi^+p \to 3\pi p$

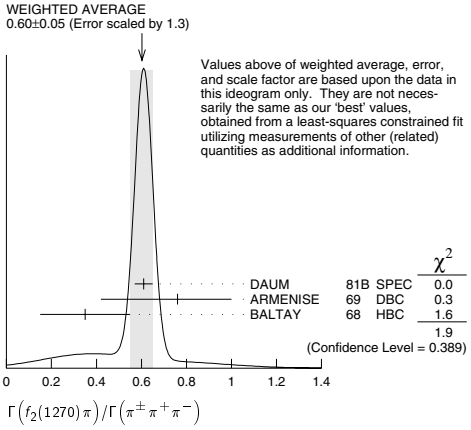

$\Gamma(\rho\pi)/\Gamma(f_2(1270)\pi)$ **$\Gamma_5/0.564\Gamma_4$**
(With $f_2(1270) \to \pi^+\pi^-$.)

VALUE	DOCUMENT ID		TECN	COMMENT
0.97 ± 0.09 OUR AVERAGE	Error includes scale factor of 1.9.			
$0.76 \pm 0.07 \pm 0.10$	CHUNG	02	MPS	$18.3\ \pi^-p \to \pi^+\pi^-\pi^-p$
1.01 ± 0.05	BARBERIS	98B		$450\ pp \to p_f\pi^+\pi^-\pi^0 p_s$

$\Gamma(\eta\pi)/\Gamma(\pi^\pm\pi^+\pi^-)$ **$\Gamma_{11}/(0.567\Gamma_4+\frac{1}{2}\Gamma_5+0.624\Gamma_7)$**
(All η decays.)

VALUE	DOCUMENT ID		TECN	CHG	COMMENT
<0.09	BALTAY	68	HBC	+	7–8.5 π^+p
• • • We do not use the following data for averages, fits, limits, etc. • • •					
<0.10	CRENNELL	70	HBC	−	$6\ \pi^-p \to f_2\pi^-N$

$\Gamma(\pi^\pm 2\pi^+ 2\pi^-)/\Gamma(\pi^\pm\pi^+\pi^-)$ **$\Gamma_{12}/(0.567\Gamma_4+\frac{1}{2}\Gamma_5+0.624\Gamma_7)$**

VALUE	DOCUMENT ID		TECN	CHG	COMMENT
<0.10	CRENNELL	70	HBC	−	$6\ \pi^-p \to f_2\pi^-N$
<0.1	BALTAY	68	HBC	+	7,8.5 π^+p

$\Gamma(\rho(1450)\pi)/\Gamma_{total}$ **Γ_{13}/Γ**

VALUE	CL%	DOCUMENT ID		TECN	COMMENT
<0.0036	97.7	AMELIN	99	VES	$37\ \pi^-A \to \omega\pi^-\pi^0 A^*$

$\Gamma(b_1(1235)\pi)/\Gamma_{total}$ **Γ_{14}/Γ**

VALUE	CL%	DOCUMENT ID		TECN	COMMENT
<0.0019	97.7	AMELIN	99	VES	$37\ \pi^-A \to \omega\pi^-\pi^0 A^*$

$\Gamma((\pi\pi)_{S\text{-wave}})/\Gamma(\pi^\pm\pi^+\pi^-)$ **$0.624\Gamma_7/(0.567\Gamma_4+\frac{1}{2}\Gamma_5+0.624\Gamma_7)$**
(With $(\pi\pi)_{S\text{-wave}} \to \pi^+\pi^-$.)

VALUE	DOCUMENT ID		TECN	COMMENT
0.10 ± 0.04 OUR FIT				
0.10 ± 0.05	[21] DAUM	81B	SPEC	63,94 π^-p

$\Gamma(K\overline{K}^*(892)+\text{c.c.})/\Gamma(f_2(1270)\pi)$ **Γ_8/Γ_4**

VALUE	DOCUMENT ID		TECN	CHG	COMMENT
0.075 ± 0.025 OUR FIT					
0.075 ± 0.025	[22] ARMSTRONG	82B	OMEG	−	$16\ \pi^-p \to K^+K^-\pi^-p$

$\Gamma(\omega\rho)/\Gamma_{total}$ **Γ_9/Γ**

VALUE	DOCUMENT ID		TECN	COMMENT
0.027 ± 0.004 ± 0.010	[23] AMELIN	99	VES	$37\ \pi^-A \to \omega\pi^-\pi^0 A^*$

$\Gamma(\sigma\pi)/\Gamma(f_2(1270)\pi)$ **Γ_6/Γ_4**

VALUE	DOCUMENT ID		TECN	COMMENT
0.19 ± 0.06 OUR AVERAGE				
$0.17 \pm 0.02 \pm 0.07$	CHUNG	02	MPS	$18.3\ \pi^-p \to \pi^+\pi^-\pi^-p$
0.24 ± 0.10	[24,25] BAKER	99	SPEC	$1.94\ \overline{p}p \to 4\pi^0$

***D*-wave/*S*-wave RATIO FOR $\pi_2(1670) \to f_2(1270)\pi$**

VALUE	DOCUMENT ID		TECN	COMMENT
−0.18 ± 0.06	[24] BAKER	99	SPEC	$1.94\ \overline{p}p \to 4\pi^0$
• • • We do not use the following data for averages, fits, limits, etc. • • •				
0.22 ± 0.10	[21] DAUM	81B	SPEC	63,94 π^-p

***F*-wave/*P*-wave RATIO FOR $\pi_2(1670) \to \rho\pi$**

VALUE	DOCUMENT ID		TECN	COMMENT
−0.72 ± 0.07 ± 0.14	CHUNG	02	MPS	$18.3\ \pi^-p \to \pi^+\pi^-\pi^-p$

[20] Using BARBERIS 98B.
[21] From a two-resonance fit to four 2^-0^+ waves.
[22] From a partial-wave analysis of $K^+K^-\pi^-$ system.
[23] Normalized to the $B(\pi_2(1670) \to f_2\pi)$.
[24] Using preliminary CBAR data.
[25] With the $\sigma\pi$ in L=2 and the $f_2(1270)\pi$ in L=0.

$\pi_2(1670)$ REFERENCES

CHUNG	02	PR D65 072001	S.U. Chung *et al.*
BARBERIS	01	PL B507 14	D. Barberis *et al.*
AMELIN	99	PAN 62 445 Translated from YAF 62 487.	D.V. Amelin *et al.* (VES Collab.)
BAKER	99	PL B449 114	C.A. Baker *et al.*
BARBERIS	98B	PL B422 399	D. Barberis *et al.* (WA 102 Collab.)
ACCIARRI	97T	PL B413 147	M. Acciarri *et al.* (L3 Collab.)
ALBRECHT	97B	ZPHY C74 469	H. Albrecht *et al.* (ARGUS Collab.)
AMELIN	95B	PL B356 595	D.V. Amelin *et al.* (SERP, TBIL)
BERDNIKOV	94	PL B337 219	E.B. Berdnikov *et al.* (SERP, TBIL)
ANTREASYAN	90	ZPHY C48 561	D. Antreasyan *et al.* (Crystal Ball Collab.)
BEHREND	90C	ZPHY C46 583	H.J. Behrend *et al.* (CELLO Collab.)
ANTIPOV	87	EPL 4 403	Y.M. Antipov *et al.* (SERP, JINR, INRM+)
BELLINI	85	SJNP 41 781 Translated from YAF 41 1223.	D. Bellini *et al.*

Meson Particle Listings

$\pi_2(1670)$, $\phi(1680)$

ARMSTRONG	82B	NP B202 1	T.A. Armstrong, B. Baccari	(AACH3, BARI, BONN+)
DAUM	81B	NP B182 269	C. Daum *et al.*	(AMST, CERN, CRAC, MPIM+)
EVANGELISTA	81	NP B178 197	C. Evangelista *et al.*	(BARI, BONN, CERN+)
Also	81B	NP B186 594	C. Evangelista	
DAUM	80D	PL 89B 285	C. Daum *et al.*	(AMST, CERN, CRAC, MPIM+) JP
BALTAY	77	PRL 39 591	C. Baltay, C.V. Cautis, M. Kalelkar	(COLU) JP
ASCOLI	73	PR D7 669	G. Ascoli	(ILL, TNTO, GENO, HAMB, MILA+) JP
CRENNELL	70	PRL 24 781	D.J. Crennell *et al.*	(BNL)
ARMENISE	69	LNC 2 501	N. Armenise *et al.*	(BARI, BGNA, FIRZ)
BALTAY	68	PRL 20 887	C. Baltay *et al.*	(COLU, ROCH, RUTG, YALE) I
BARTSCH	68	NP B7 345	J. Bartsch *et al.*	(AACH, BERL, CERN) JP

OTHER RELATED PAPERS

PAGE	03	PL B566 108	P. Page, S. Capstick	
ZAIMIDOROGA	99	PAN 30 1 Translated from SJPN 30 5.	O.A. Zaimidoroga	
CHEN	83B	PR D28 2304	T.Y. Chen *et al.*	(ARIZ, FNAL, FLOR, NDAM+)
LEEDOM	83	PR D27 1426	I.D. Leedom *et al.*	(PURD, TNTO)
BELLINI	82B	NP B199 1	G. Bellini *et al.*	(CERN, MILA, JINR+)
DAUM	81B	NP B182 269	C. Daum *et al.*	(AMST, CERN, CRAC, MPIM+)
PERNEGR	78	NP B134 436	J. Pernegr *et al.*	(ETH, CERN, LOIC+)
FOCACCI	66	PRL 17 890	M.N. Focacci *et al.*	(CERN)
LEVRAT	66	PL 22 714	B. Levrat *et al.*	
VETLITSKY	66	PL 21 579	I.A. Vetlitsky *et al.*	(ITEP)
FORINO	65B	PL 19 68	A. Forino *et al.*	(BGNA, BARI, FIRZ, ORSAY+)

$\phi(1680)$

$I^G(J^{PC}) = 0^-(1^{--})$

$\phi(1680)$ MASS

e^+e^- PRODUCTION

VALUE (MeV)	EVTS	DOCUMENT ID		TECN	COMMENT
1680±20 OUR ESTIMATE					
• • • We do not use the following data for averages, fits, limits, etc. • • •					
1623±20	948	[1] AKHMETSHIN	03	CMD2	1.05–1.38 $e^+e^- \to K_L^0 K_S^0$
~ 1500		[2] ACHASOV	98H	RVUE	$e^+e^- \to \pi^+\pi^-\pi^0$, $\omega\pi^+\pi^-$, K^+K^-
~ 1900		[3] ACHASOV	98H	RVUE	$e^+e^- \to K_S^0 K^\pm\pi^\mp$
1700±20		[4] CLEGG	94	RVUE	$e^+e^- \to K^+K^-$, $K_S^0 K\pi$
1657±27	367	BISELLO	91C	DM2	$e^+e^- \to K_S^0 K^\pm\pi^\mp$
1655±17		[5] BISELLO	88B	DM2	$e^+e^- \to K^+K^-$
1680±10		[6] BUON	82	DM1	$e^+e^- \to$ hadrons
1677±12		[7] MANE	82	DM1	$e^+e^- \to K_S^0 K\pi$

PHOTOPRODUCTION

VALUE (MeV)	DOCUMENT ID		TECN	COMMENT
• • • We do not use the following data for averages, fits, limits, etc. • • •				
1753± 3	[8] LINK	02K	FOCS	20–160 $\gamma p \to K^+K^-p$
1726±22	[8] BUSENITZ	89	TPS	$\gamma p \to K^+K^-X$
1760±20	[8] ATKINSON	85C	OMEG	20–70 $\gamma p \to K\overline{K}X$
1690±10	[8] ASTON	81F	OMEG	25–70 $\gamma p \to K^+K^-X$

[1] From the combined fit of AKHMETSHIN 03 and MANE 81 also including ρ, ω, and ϕ. Neither isospin nor flavor structure known.
[2] Using data from IVANOV 81, BARKOV 87, BISELLO 88B, DOLINSKY 91, and ANTONELLI 92.
[3] Using the data from BISELLO 91C.
[4] Using BISELLO 88B and MANE 82 data.
[5] From global fit including ρ, ω, ϕ and $\rho(1700)$ assume mass 1570 MeV and width 510 MeV for ρ radial excitation.
[6] From global fit of ρ, ω, ϕ and their radial excitations to channels $\omega\pi^+\pi^-$, K^+K^-, $K_S^0K_L^0$, $K_S^0K^\pm\pi^\mp$. Assume mass 1570 MeV and width 510 MeV for ρ radial excitations, mass 1570 and width 500 MeV for ω radial excitation.
[7] Fit to one channel only, neglecting interference with ω, $\rho(1700)$.
[8] We list here a state decaying into K^+K^- possibly different from $\phi(1680)$.

$\phi(1680)$ WIDTH

e^+e^- PRODUCTION

VALUE (MeV)	EVTS	DOCUMENT ID		TECN	COMMENT
150±50 OUR ESTIMATE This is only an educated guess; the error given is larger than the error on the average of the published values.					
• • • We do not use the following data for averages, fits, limits, etc. • • •					
139±60	948	[9] AKHMETSHIN	03	CMD2	1.05–1.38 $e^+e^- \to K_L^0 K_S^0$
300±60		[10] CLEGG	94	RVUE	$e^+e^- \to K^+K^-$, $K_S^0 K\pi$
146±55	367	BISELLO	91C	DM2	$e^+e^- \to K_S^0 K^\pm\pi^\mp$
207±45		[11] BISELLO	88B	DM2	$e^+e^- \to K^+K^-$
185±22		[12] BUON	82	DM1	$e^+e^- \to$ hadrons
102±36		[13] MANE	82	DM1	$e^+e^- \to K_S^0 K\pi$

PHOTOPRODUCTION

VALUE (MeV)	DOCUMENT ID		TECN	COMMENT
• • • We do not use the following data for averages, fits, limits, etc. • • •				
122±63	[14] LINK	02K	FOCS	20–160 $\gamma p \to K^+K^-p$
121±47	[14] BUSENITZ	89	TPS	$\gamma p \to K^+K^-X$
80±40	[14] ATKINSON	85C	OMEG	20–70 $\gamma p \to K\overline{K}X$
100±40	[14] ASTON	81F	OMEG	25–70 $\gamma p \to K^+K^-X$

[9] From the combined fit of AKHMETSHIN 03 and MANE 81 also including ρ, ω, and ϕ. Neither isospin nor flavor structure known.
[10] Using BISELLO 88B and MANE 82 data.
[11] From global fit including ρ, ω, ϕ and $\rho(1700)$
[12] From global fit of ρ, ω, ϕ and their radial excitations to channels $\omega\pi^+\pi^-$, K^+K^-, $K_S^0K_L^0$, $K_S^0K^\pm\pi^\mp$. Assume mass 1570 MeV and width 510 MeV for ρ radial excitations, mass 1570 and width 500 MeV for ω radial excitation.
[13] Fit to one channel only, neglecting interference with ω, $\rho(1700)$.
[14] We list here a state decaying into K^+K^- possibly different from $\phi(1680)$.

$\phi(1680)$ DECAY MODES

	Mode	Fraction (Γ_i/Γ)
Γ_1	$K\overline{K}^*(892)+$ c.c.	dominant
Γ_2	$K_S^0K\pi$	seen
Γ_3	$K\overline{K}$	seen
Γ_4	$K_L^0K_S^0$	
Γ_5	e^+e^-	seen
Γ_6	$\omega\pi\pi$	not seen
Γ_7	$K^+K^-\pi^0$	

$\phi(1680)$ $\Gamma(i)\Gamma(e^+e^-)/\Gamma^2(\text{total})$

This combination of a branching ratio into channel (i) and branching ratio into e^+e^- is directly measured and obtained from the cross section at the peak. We list only data that have not been used to determine the branching ratio into (i) or e^+e^-.

$\Gamma(K_L^0K_S^0) \times \Gamma(e^+e^-)/\Gamma^2_{\text{total}}$ $\Gamma_4\Gamma_5/\Gamma^2$

VALUE (units 10^{-6})	EVTS	DOCUMENT ID		TECN	COMMENT
• • • We do not use the following data for averages, fits, limits, etc. • • •					
0.131±0.059	948	[15] AKHMETSHIN	03	CMD2	1.05–1.38 $e^+e^- \to K_L^0K_S^0$

$\Gamma(K\overline{K}^*(892)+\text{c.c.}) \times \Gamma(e^+e^-)/\Gamma^2_{\text{total}}$ $\Gamma_1\Gamma_5/\Gamma^2$

VALUE (units 10^{-6})	EVTS	DOCUMENT ID		TECN	COMMENT
• • • We do not use the following data for averages, fits, limits, etc. • • •					
3.29±1.57	367	[16] BISELLO	91C	DM2	1.35–2.40 $e^+e^- \to K_S^0K^\pm\pi^\mp$

[15] From the combined fit of AKHMETSHIN 03 and MANE 81 also including ρ, ω, and ϕ. Neither isospin nor flavor structure known. Recalculated by us.
[16] Recalculated by us with the published value of $B(K\overline{K}^*(892) +$ c.c.$) \times \Gamma(e^+e^-)$.

$\phi(1680)$ BRANCHING RATIOS

$\Gamma(K\overline{K}^*(892)+\text{c.c.})/\Gamma(K_S^0K\pi)$ Γ_1/Γ_2

VALUE	DOCUMENT ID		TECN	COMMENT
dominant	MANE	82	DM1	$e^+e^- \to K_S^0K^\pm\pi^\mp$

$\Gamma(K\overline{K})/\Gamma(K\overline{K}^*(892)+\text{c.c.})$ Γ_3/Γ_1

VALUE	DOCUMENT ID		TECN	COMMENT
• • • We do not use the following data for averages, fits, limits, etc. • • •				
0.07±0.01	BUON	82	DM1	e^+e^-

$\Gamma(\omega\pi\pi)/\Gamma(K\overline{K}^*(892)+\text{c.c.})$ Γ_6/Γ_1

VALUE	DOCUMENT ID		TECN	COMMENT
<0.10	BUON	82	DM1	e^+e^-

$\phi(1680)$ REFERENCES

AKHMETSHIN	03	PL B551 27	R.R. Akhmetshin *et al.*	(Novosibirsk CMD-2 Collab.)
Also	02	PAN 65 1222 Translated from YAF 65 1255.	E.V. Anashkin, V.M. Aulchenko, R.R. Akhmetshin	
LINK	02K	PL B545 50	J.M. Link *et al.*	(FNAL FOCUS Collab.)
ACHASOV	98H	PR D57 4334	N.N. Achasov, A.A. Kozhevnikov	
CLEGG	94	ZPHY C62 455	A.B. Clegg, A. Donnachie	(LANC, MCHS)
ANTONELLI	92	ZPHY C56 15	A. Antonelli *et al.*	(DM2 Collab.)
BISELLO	91C	ZPHY C52 227	D. Bisello *et al.*	(DM2 Collab.)
DOLINSKY	91	PRPL 202 99	S.I. Dolinsky *et al.*	(NOVO)
BUSENITZ	89	PR D40 1	J.K. Busenitz *et al.*	(ILL, FNAL)
BISELLO	88B	ZPHY C39 13	D. Bisello *et al.*	(PADO, CLER, FRAS+)
BARKOV	87	JETPL 46 164 Translated from ZETFP 46 132.	L.M. Barkov *et al.*	(NOVO)
ATKINSON	85C	ZPHY C27 233	M. Atkinson *et al.*	(BONN, CERN, GLAS+)
BUON	82	PL 118B 221	J. Buon *et al.*	(LALO, MONP)
MANE	82	PL 112B 178	F. Mane *et al.*	(LALO)
ASTON	81F	PL 104B 231	D. Aston	(BONN, CERN, EPOL, GLAS, LANC+)
IVANOV	81	PL 107B 297	P.M. Ivanov *et al.*	(NOVO)
MANE	81	PL 99B 261	F. Mane *et al.*	(ORSAY)

OTHER RELATED PAPERS

CLOSE	02	PR D65 092003	F.E. Close, A. Donnachie, Yu.S. Kalashnikova	
LINK	02K	PL B545 50	J.M. Link *et al.*	(FNAL FOCUS Collab.)
ABELE	99D	PL B468 178	A. Abele *et al.*	(Crystal Barrel Collab.)
ACHASOV	97F	PAN 60 2029	N.N. Achasov, A.A. Kozhevnikov	(NOVM)
		Translated from YAF 60 2212.		
ATKINSON	86C	ZPHY C30 541	M. Atkinson *et al.*	(BONN, CERN, GLAS+)
ATKINSON	84	NP B231 15	M. Atkinson *et al.*	(BONN, CERN, GLAS+)
ATKINSON	84B	NP B231 1	M. Atkinson *et al.*	(BONN, CERN, GLAS+)
ATKINSON	83C	NP B229 269	M. Atkinson *et al.*	(BONN, CERN, GLAS+)
CORDIER	81	PL 106B 155	A. Cordier *et al.*	(ORSAY)
MANE	81	PL 99B 261	F. Mane *et al.*	(ORSAY)
ASTON	80F	NP B174 269	D. Aston	(BONN, CERN, EPOL, GLAS, LANC+)

$\rho_3(1690)$

$I^G(J^{PC}) = 1^+(3^{--})$

$\rho_3(1690)$ MASS

VALUE (MeV)	DOCUMENT ID
1688.8±2.1 OUR AVERAGE	Includes data from the 5 datablocks that follow this one.

2π MODE

VALUE (MeV)	EVTS	DOCUMENT ID		TECN	CHG	COMMENT
The data in this block is included in the average printed for a previous datablock.						
1686± 4 OUR AVERAGE						
1677±14		EVANGELISTA	81	OMEG	−	12 $\pi^- p \to 2\pi p$
1679±11	476	BALTAY	78B	HBC	0	15 $\pi^+ p \to \pi^+\pi^- n$
1678±12	175	[1] ANTIPOV	77	CIBS	0	25 $\pi^- p \to p3\pi$
1690± 7	600	[1] ENGLER	74	DBC	0	6 $\pi^+ n \to \pi^+\pi^- p$
1693± 8		[2] GRAYER	74	ASPK	0	17 $\pi^- p \to \pi^+\pi^- n$
1678±12		MATTHEWS	71C	DBC	0	7 $\pi^+ N$
• • • We do not use the following data for averages, fits, limits, etc. • • •						
1734±10		[3] CORDEN	79	OMEG		12–15 $\pi^- p \to n2\pi$
1692±12		[2,4] ESTABROOKS	75	RVUE		17 $\pi^- p \to \pi^+\pi^- n$
1737±23		ARMENISE	70	DBC	0	9 $\pi^+ N$
1650±35	122	BARTSCH	70B	HBC	+	8 $\pi^+ p \to N2\pi$
1687±21		STUNTEBECK	70	HDBC	0	8 $\pi^- p$, 5.4 $\pi^+ d$
1683±13		ARMENISE	68	DBC	0	5.1 $\pi^+ d$
1670±30		GOLDBERG	65	HBC	0	6 $\pi^+ d$, 8 $\pi^- p$

[1] Mass errors enlarged by us to $\Gamma/\sqrt{N}$; see the note with the $K^*(892)$ mass.
[2] Uses same data as HYAMS 75.
[3] From a phase shift solution containing a $f_2'(1525)$ width two times larger than the $K\overline{K}$ result.
[4] From phase-shift analysis. Error takes account of spread of different phase-shift solutions.

$K\overline{K}$ AND $K\overline{K}\pi$ MODES

VALUE (MeV)	EVTS	DOCUMENT ID		TECN	CHG	COMMENT
The data in this block is included in the average printed for a previous datablock.						
1696± 4 OUR AVERAGE						
1699± 5		ALPER	80	CNTR	0	62 $\pi^- p \to K^+ K^- n$
1698±12	6k	[5,6] MARTIN	78D	SPEC		10 $\pi p \to K^0_S K^- p$
1692± 6		BLUM	75	ASPK	0	18.4 $\pi^- p \to n K^+ K^-$
1690±16		ADERHOLZ	69	HBC	+	8 $\pi^+ p \to K\overline{K}\pi$
• • • We do not use the following data for averages, fits, limits, etc. • • •						
1694± 8		[7] COSTA...	80	OMEG		10 $\pi^- p \to K^+ K^- n$

[5] From a fit to $J^P = 3^-$ partial wave.
[6] Systematic error on mass scale subtracted.
[7] They cannot distinguish between $\rho_3(1690)$ and $\omega_3(1670)$.

$(4\pi)^\pm$ MODE

VALUE (MeV)	EVTS	DOCUMENT ID		TECN	CHG	COMMENT
The data in this block is included in the average printed for a previous datablock.						
1686± 5 OUR AVERAGE Error includes scale factor of 1.1.						
1694± 6		[8] EVANGELISTA	81	OMEG	−	12 $\pi^- p \to p4\pi$
1665±15	177	BALTAY	78B	HBC	+	15 $\pi^+ p \to p4\pi$
1670±10		THOMPSON	74	HBC	+	13 $\pi^+ p$
1687±20		CASON	73	HBC	−	8,18.5 $\pi^- p$
1685±14		[9] CASON	73	HBC	−	8,18.5 $\pi^- p$
1680±40	144	BARTSCH	70B	HBC	+	8 $\pi^+ p \to N4\pi$
1689±20	102	[9] BARTSCH	70B	HBC	+	8 $\pi^+ p \to N2\rho$
1705±21		CASO	70	HBC	−	11.2 $\pi^- p \to n\rho 2\pi$
• • • We do not use the following data for averages, fits, limits, etc. • • •						
1718±10		[10] EVANGELISTA	81	OMEG	−	12 $\pi^- p \to p4\pi$
1673± 9		[11] EVANGELISTA	81	OMEG	−	12 $\pi^- p \to p4\pi$
1733± 9	66	[9] KLIGER	74	HBC	−	4.5 $\pi^- p \to p4\pi$
1630±15		HOLMES	72	HBC	+	10–12 $K^+ p$
1720±15		BALTAY	68	HBC	+	7, 8.5 $\pi^+ p$

[8] From $\rho^-\rho^0$ mode, not independent of the other two EVANGELISTA 81 entries.
[9] From $\rho^\pm\rho^0$ mode.
[10] From $a_2(1320)^-\pi^0$ mode, not independent of the other two EVANGELISTA 81 entries.
[11] From $a_2(1320)^0\pi^-$ mode, not independent of the other two EVANGELISTA 81 entries.

$\omega\pi$ MODE

VALUE (MeV)	DOCUMENT ID		TECN	CHG	COMMENT
The data in this block is included in the average printed for a previous datablock.					
1681± 7 OUR AVERAGE					
1670±25	[12] ALDE	95	GAM2		38 $\pi^- p \to \omega\pi^0 n$
1690±15	EVANGELISTA	81	OMEG	−	12 $\pi^- p \to \omega\pi p$
1666±14	GESSAROLI	77	HBC		11 $\pi^- p \to \omega\pi p$
1686± 9	THOMPSON	74	HBC	+	13 $\pi^+ p$
• • • We do not use the following data for averages, fits, limits, etc. • • •					
1654±24	BARNHAM	70	HBC	+	10 $K^+ p \to \omega\pi X$

[12] Supersedes ALDE 92C.

$\eta\pi^+\pi^-$ MODE

(For difficulties with MMS experiments, see the $a_2(1320)$ mini-review in the 1973 edition.)

VALUE (MeV)	DOCUMENT ID		TECN	CHG	COMMENT
The data in this block is included in the average printed for a previous datablock.					
1682±12 OUR AVERAGE					
1685±10±20	AMELIN	00	VES		37 $\pi^- p \to \eta\pi^+\pi^- n$
1680±15	FUKUI	88	SPEC	0	8.95 $\pi^- p \to \eta\pi^+\pi^- n$
• • • We do not use the following data for averages, fits, limits, etc. • • •					
1700±47	[13] ANDERSON	69	MMS	−	16 $\pi^- p$ backward
1632±15	[13,14] FOCACCI	66	MMS	−	7–12 $\pi^- p \to p$MM
1700±15	[13,14] FOCACCI	66	MMS	−	7–12 $\pi^- p \to p$MM
1748±15	[13,14] FOCACCI	66	MMS	−	7–12 $\pi^- p \to p$MM

[13] Seen in 2.5–3 GeV/c $\overline{p}p$. $2\pi^+2\pi^-$, with 0, 1, 2 $\pi^+\pi^-$ pairs in ρ band not seen by OREN 74 (2.3 GeV/c $\overline{p}p$) with more statistics. (Jan. 1976)
[14] Not seen by BOWEN 72.

$\rho_3(1690)$ WIDTH

2π, $K\overline{K}$, AND $K\overline{K}\pi$ MODES

VALUE (MeV)	DOCUMENT ID
161±10 OUR AVERAGE	Includes data from the 5 datablocks that follow this one. Error includes scale factor of 1.5. See the ideogram below.

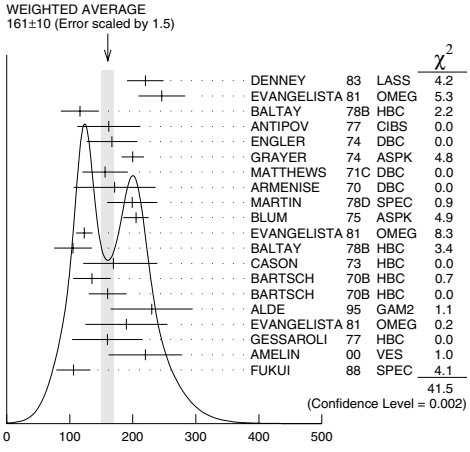

$\rho_3(1690)$ width, 2π, $K\overline{K}$, and $K\overline{K}\pi$ modes (MeV)

2π MODE

VALUE (MeV)	EVTS	DOCUMENT ID		TECN	CHG	COMMENT
The data in this block is included in the average printed for a previous datablock.						
186±14 OUR AVERAGE Error includes scale factor of 1.3. See the ideogram below.						
220±29		DENNEY	83	LASS		10 $\pi^+ N$
246±37		EVANGELISTA	81	OMEG	−	12 $\pi^- p \to 2\pi p$
116±30	476	BALTAY	78B	HBC	0	15 $\pi^+ p \to \pi^+\pi^- n$
162±50	175	[15] ANTIPOV	77	CIBS	0	25 $\pi^- p \to p3\pi$

Meson Particle Listings

$\rho_3(1690)$

167 ± 40	600	ENGLER	74	DBC	0	6 $\pi^+ n \to \pi^+\pi^- p$
200 ± 18	[16]	GRAYER	74	ASPK	0	17 $\pi^- p \to \pi^+\pi^- n$
156 ± 36		MATTHEWS	71C	DBC	0	7 $\pi^+ N$
171 ± 65		ARMENISE	70	DBC	0	9 $\pi^+ d$
• • • We do not use the following data for averages, fits, limits, etc. • • •						
322 ± 35	[17]	CORDEN	79	OMEG		12–15 $\pi^- p \to n 2\pi$
240 ± 30	[16,18]	ESTABROOKS	75	RVUE		17 $\pi^- p \to \pi^+\pi^- n$
180 ± 30	122	BARTSCH	70B	HBC	+	8 $\pi^+ p \to N 2\pi$
267^{+72}_{-46}		STUNTEBECK	70	HDBC	0	8 $\pi^- p$, 5.4 $\pi^+ d$
188 ± 49		ARMENISE	68	DBC	0	5.1 $\pi^+ d$
180 ± 40		GOLDBERG	65	HBC	0	6 $\pi^+ d$, 8 $\pi^- p$

[15] Width errors enlarged by us to $4\Gamma/\sqrt{N}$; see the note with the $K^*(892)$ mass.
[16] Uses same data as HYAMS 75 and BECKER 79.
[17] From a phase shift solution containing a $f_2'(1525)$ width two times larger than the $K\overline{K}$ result.
[18] From phase-shift analysis. Error takes account of spread of different phase-shift solutions.

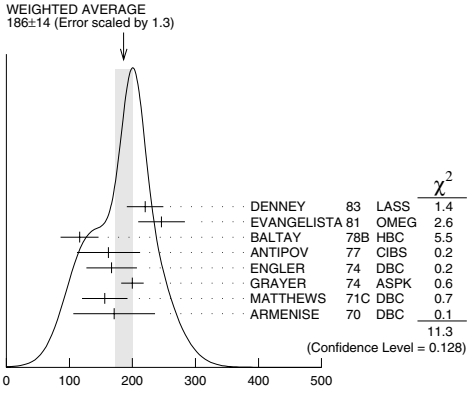

$\rho_3(1690)$ width, 2π mode (MeV)

$K\overline{K}$ AND $K\overline{K}\pi$ MODES

VALUE (MeV)	EVTS	DOCUMENT ID		TECN	CHG	COMMENT
The data in this block is included in the average printed for a previous datablock.						
204±18 OUR AVERAGE						
199 ± 40	6000	[19] MARTIN	78D	SPEC		10 $\pi p \to K^0_S K^- p$
205 ± 20		BLUM	75	ASPK	0	18.4 $\pi^- p \to n K^+ K^-$
• • • We do not use the following data for averages, fits, limits, etc. • • •						
219 ± 4		ALPER	80	CNTR	0	62 $\pi^- p \to K^+ K^- n$
186 ± 11		[20] COSTA...	80	OMEG		10 $\pi^- p \to K^+ K^- n$
112 ± 60		ADERHOLZ	69	HBC	+	8 $\pi^+ p \to K\overline{K}\pi$

[19] From a fit to $J^P = 3^-$ partial wave.
[20] They cannot distinguish between $\rho_3(1690)$ and $\omega_3(1670)$.

$(4\pi)^\pm$ MODE

VALUE (MeV)	EVTS	DOCUMENT ID		TECN	CHG	COMMENT
The data in this block is included in the average printed for a previous datablock.						
129±10 OUR AVERAGE						
123 ± 13		[21] EVANGELISTA	81	OMEG	–	12 $\pi^- p \to p 4\pi$
105 ± 30	177	BALTAY	78B	HBC	+	15 $\pi^+ p \to p 4\pi$
169^{+70}_{-48}		CASON	73	HBC	–	8,18.5 $\pi^- p$
135 ± 30	144	BARTSCH	70B	HBC	+	8 $\pi^+ p \to N 4\pi$
160 ± 30	102	BARTSCH	70B	HBC	+	8 $\pi^+ p \to N 2\rho$
• • • We do not use the following data for averages, fits, limits, etc. • • •						
230 ± 28		[22] EVANGELISTA	81	OMEG	–	12 $\pi^- p \to p 4\pi$
184 ± 33		[23] EVANGELISTA	81	OMEG	–	12 $\pi^- p \to p 4\pi$
150	66	[24] KLIGER	74	HBC	–	4.5 $\pi^- p \to p 4\pi$
106 ± 25		THOMPSON	74	HBC	+	13 $\pi^+ p$
125^{+83}_{-35}		[24] CASON	73	HBC	–	8,18.5 $\pi^- p$
130 ± 30		HOLMES	72	HBC	+	10–12 $K^+ p$
180 ± 30	90	[24] BARTSCH	70B	HBC	+	8 $\pi^+ p \to N a_2\pi$
100 ± 35		BALTAY	68	HBC	+	7, 8.5 $\pi^+ p$

[21] From $\rho^-\rho^0$ mode, not independent of the other two EVANGELISTA 81 entries.
[22] From $a_2(1320)^-\pi^0$ mode, not independent of the other two EVANGELISTA 81 entries.
[23] From $a_2(1320)^0\pi^-$ mode, not independent of the other two EVANGELISTA 81 entries.
[24] From $\rho^\pm\rho^0$ mode.

$\omega\pi$ MODE

VALUE (MeV)	DOCUMENT ID		TECN	CHG	COMMENT
The data in this block is included in the average printed for a previous datablock.					
190±40 OUR AVERAGE					
230 ± 65	[25] ALDE	95	GAM2		38 $\pi^- p \to \omega\pi^0 n$
190 ± 65	EVANGELISTA	81	OMEG	–	12 $\pi^- p \to \omega\pi p$
160 ± 56	GESSAROLI	77	HBC		11 $\pi^- p \to \omega\pi p$
• • • We do not use the following data for averages, fits, limits, etc. • • •					
89 ± 25	THOMPSON	74	HBC	+	13 $\pi^+ p$
130^{+73}_{-43}	BARNHAM	70	HBC	+	10 $K^+ p \to \omega\pi X$

[25] Supersedes ALDE 92C.

$\eta\pi^+\pi^-$ MODE

(For difficulties with MMS experiments, see the $a_2(1320)$ mini-review in the 1973 edition.)

VALUE (MeV)	DOCUMENT ID		TECN	CHG	COMMENT
The data in this block is included in the average printed for a previous datablock.					
126±40 OUR AVERAGE Error includes scale factor of 1.8.					
$220\pm30\pm50$	AMELIN	00	VES		37 $\pi^- p \to \eta\pi^+\pi^- n$
106 ± 27	FUKUI	88	SPEC	0	8.95 $\pi^- p \to \eta\pi^+\pi^- n$
• • • We do not use the following data for averages, fits, limits, etc. • • •					
195	[26] ANDERSON	69	MMS	–	16 $\pi^- p$ backward
< 21	[26,27] FOCACCI	66	MMS	–	7–12 $\pi^- p \to p$MM
< 30	[26,27] FOCACCI	66	MMS	–	7–12 $\pi^- p \to p$MM
< 38	[26,27] FOCACCI	66	MMS	–	7–12 $\pi^- p \to p$MM

[26] Seen in 2.5–3 GeV/c $\overline{p}p$. $2\pi^+ 2\pi^-$, with 0, 1, 2 $\pi^+\pi^-$ pairs in ρ^0 band not seen by OREN 74 (2.3 GeV/c $\overline{p}p$) with more statistics. (Jan. 1979)
[27] Not seen by BOWEN 72.

$\rho_3(1690)$ DECAY MODES

	Mode	Fraction (Γ_i/Γ)	Scale factor
Γ_1	4π	(71.1 ± 1.9) %	
Γ_2	$\pi^\pm\pi^+\pi^-\pi^0$	(67 ±22) %	
Γ_3	$\omega\pi$	(16 ± 6) %	
Γ_4	$\pi\pi$	(23.6 ± 1.3) %	
Γ_5	$K\overline{K}\pi$	(3.8 ± 1.2) %	
Γ_6	$K\overline{K}$	(1.58± 0.26) %	1.2
Γ_7	$\eta\pi^+\pi^-$	seen	
Γ_8	$\rho(770)\eta$	seen	
Γ_9	$\pi\pi\rho$ Excluding 2ρ and $a_2(1320)\pi$.	seen	
Γ_{10}	$a_2(1320)\pi$	seen	
Γ_{11}	$\rho\rho$	seen	
Γ_{12}	$\phi\pi$		
Γ_{13}	$\eta\pi$		
Γ_{14}	$\pi^\pm 2\pi^+ 2\pi^-\pi^0$		

CONSTRAINED FIT INFORMATION

An overall fit to 5 branching ratios uses 10 measurements and one constraint to determine 4 parameters. The overall fit has a $\chi^2 = 14.7$ for 7 degrees of freedom.

The following *off-diagonal* array elements are the correlation coefficients $\langle \delta x_i \delta x_j \rangle / (\delta x_i \cdot \delta x_j)$, in percent, from the fit to the branching fractions, $x_i \equiv \Gamma_i/\Gamma_{\text{total}}$. The fit constrains the x_i whose labels appear in this array to sum to one.

x_4	−77		
x_5	−74	17	
x_6	−15	2	0
	x_1	x_4	x_5

$\rho_3(1690)$ BRANCHING RATIOS

$\Gamma(\pi\pi)/\Gamma_{\text{total}}$ Γ_4/Γ

VALUE	DOCUMENT ID		TECN	CHG	COMMENT
0.236±0.013 OUR FIT					
0.243±0.013 OUR AVERAGE					
$0.259^{+0.018}_{-0.019}$	BECKER	79	ASPK	0	17 $\pi^- p$ polarized
0.23 ±0.02	CORDEN	79	OMEG		12–15 $\pi^- p \to n 2\pi$
0.22 ±0.04	[28] MATTHEWS	71C	HDBC	0	7 $\pi^+ n \to \pi^- p$
• • • We do not use the following data for averages, fits, limits, etc. • • •					
0.245 ± 0.006	[29] ESTABROOKS	75	RVUE		17 $\pi^- p \to \pi^+\pi^- n$

[28] One-pion-exchange model used in this estimation.
[29] From phase-shift analysis of HYAMS 75 data.

$\Gamma(\pi\pi)/\Gamma(\pi^\pm\pi^+\pi^-\pi^0)$ Γ_4/Γ_2

VALUE	DOCUMENT ID		TECN	CHG	COMMENT
0.35 ± 0.11	CASON	73	HBC	−	8,18.5 π^-p
• • • We do not use the following data for averages, fits, limits, etc. • • •					
< 0.2	HOLMES	72	HBC	+	10–12 K^+p
< 0.12	BALLAM	71B	HBC	−	16 π^-p

$\Gamma(\pi\pi)/\Gamma(4\pi)$ Γ_4/Γ_1

VALUE	DOCUMENT ID		TECN	CHG	COMMENT
0.332 ± 0.026 OUR FIT Error includes scale factor of 1.1.					
0.30 ± 0.10	BALTAY	78B	HBC	0	15 $\pi^+p \to p4\pi$

$\Gamma(K\overline{K})/\Gamma(\pi\pi)$ Γ_6/Γ_4

VALUE	DOCUMENT ID		TECN	CHG	COMMENT
0.067 ± 0.011 OUR FIT Error includes scale factor of 1.2.					
$0.118^{+0.039}_{-0.032}$ OUR AVERAGE Error includes scale factor of 1.7. See the ideogram below.					
$0.191^{+0.040}_{-0.037}$	GORLICH	80	ASPK	0	17,18 π^-p polarized
0.08 ± 0.03	BARTSCH	70B	HBC	+	8 π^+p
$0.08^{+0.08}_{-0.03}$	CRENNELL	68B	HBC		6.0 π^-p

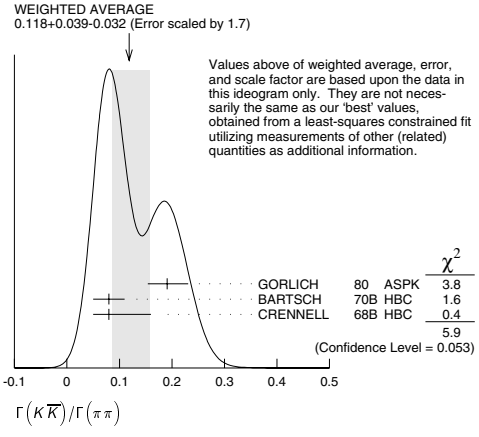

$\Gamma(K\overline{K}\pi)/\Gamma(\pi\pi)$ Γ_5/Γ_4

VALUE	DOCUMENT ID		TECN	CHG	COMMENT
0.16 ± 0.05 OUR FIT					
0.16 ± 0.05	[30] BARTSCH	70B	HBC	+	8 π^+p

[30] Increased by us to correspond to $B(\rho_3(1690) \to \pi\pi)$=0.24.

$[\Gamma(\pi\pi\rho)+\Gamma(a_2(1320)\pi)+\Gamma(\rho\rho)]/\Gamma(\pi^\pm\pi^+\pi^-\pi^0)$ $(\Gamma_9+\Gamma_{10}+\Gamma_{11})/\Gamma_2$

VALUE	DOCUMENT ID		TECN	CHG	COMMENT
0.94 ± 0.09 OUR AVERAGE					
0.96 ± 0.21	BALTAY	78B	HBC	+	15 $\pi^+p \to p4\pi$
0.88 ± 0.15	BALLAM	71B	HBC	−	16 π^-p
1 ± 0.15	BARTSCH	70B	HBC	+	8 π^+p
consistent with 1	CASO	68	HBC	−	11 π^-p

$\Gamma(\rho\rho)/\Gamma(\pi^\pm\pi^+\pi^-\pi^0)$ Γ_{11}/Γ_2

VALUE	EVTS	DOCUMENT ID		TECN	CHG	COMMENT
• • • We do not use the following data for averages, fits, limits, etc. • • •						
0.12 ± 0.11		BALTAY	78B	HBC	+	15 $\pi^+p \to p4\pi$
0.56	66	KLIGER	74	HBC	−	4.5 $\pi^-p \to p4\pi$
0.13 ± 0.09		[31] THOMPSON	74	HBC	+	13 π^+p
0.7 ± 0.15		BARTSCH	70B	HBC	+	8 π^+p

[31] $\rho\rho$ and $a_2(1320)\pi$ modes are indistinguishable.

$\Gamma(\rho\rho)/[\Gamma(\pi\pi\rho)+\Gamma(a_2(1320)\pi)+\Gamma(\rho\rho)]$ $\Gamma_{11}/(\Gamma_9+\Gamma_{10}+\Gamma_{11})$

VALUE	DOCUMENT ID		TECN	CHG	COMMENT
• • • We do not use the following data for averages, fits, limits, etc. • • •					
0.48 ± 0.16	CASO	68	HBC	−	11 π^-p

$\Gamma(a_2(1320)\pi)/\Gamma(\pi^\pm\pi^+\pi^-\pi^0)$ Γ_{10}/Γ_2

VALUE	DOCUMENT ID		TECN	CHG	COMMENT
• • • We do not use the following data for averages, fits, limits, etc. • • •					
0.66 ± 0.08	BALTAY	78B	HBC	+	15 $\pi^+p \to p4\pi$
0.36 ± 0.14	[32] THOMPSON	74	HBC	+	13 π^+p
not seen	CASON	73	HBC	−	8,18.5 π^-p
0.6 ± 0.15	BARTSCH	70B	HBC	+	8 π^+p
0.6	BALTAY	68	HBC	+	7,8.5 π^+p

[32] $\rho\rho$ and $a_2(1320)\pi$ modes are indistinguishable.

$\Gamma(\omega\pi)/\Gamma(\pi^\pm\pi^+\pi^-\pi^0)$ Γ_3/Γ_2

VALUE	CL%	DOCUMENT ID		TECN	CHG	COMMENT
0.23 ± 0.05 OUR AVERAGE Error includes scale factor of 1.2.						
0.33 ± 0.07		THOMPSON	74	HBC	+	13 π^+p
0.12 ± 0.07		BALLAM	71B	HBC	−	16 π^-p
0.25 ± 0.10		BALTAY	68	HBC	+	7,8.5 π^+p
0.25 ± 0.10		JOHNSTON	68	HBC	−	7.0 π^-p
• • • We do not use the following data for averages, fits, limits, etc. • • •						
< 0.11	95	BALTAY	78B	HBC	+	15 $\pi^+p \to p4\pi$
< 0.09		KLIGER	74	HBC	−	4.5 $\pi^-p \to p4\pi$

$\Gamma(\phi\pi)/\Gamma(\pi^\pm\pi^+\pi^-\pi^0)$ Γ_{12}/Γ_2

VALUE	DOCUMENT ID		TECN	CHG	COMMENT
• • • We do not use the following data for averages, fits, limits, etc. • • •					
< 0.11	BALTAY	68	HBC	+	7,8.5 π^+p

$\Gamma(\pi^\pm 2\pi^+ 2\pi^-\pi^0)/\Gamma(\pi^\pm\pi^+\pi^-\pi^0)$ Γ_{14}/Γ_2

VALUE	DOCUMENT ID		TECN	CHG	COMMENT
• • • We do not use the following data for averages, fits, limits, etc. • • •					
< 0.15	BALTAY	68	HBC	+	7,8.5 π^+p

$\Gamma(\eta\pi)/\Gamma(\pi^\pm\pi^+\pi^-\pi^0)$ Γ_{13}/Γ_2

VALUE	DOCUMENT ID		TECN	CHG	COMMENT
• • • We do not use the following data for averages, fits, limits, etc. • • •					
< 0.02	THOMPSON	74	HBC	+	13 π^+p

$\Gamma(K\overline{K})/\Gamma_{total}$ Γ_6/Γ

VALUE	DOCUMENT ID		TECN	CHG	COMMENT
0.0158 ± 0.0026 OUR FIT Error includes scale factor of 1.2.					
0.0130 ± 0.0024 OUR AVERAGE					
0.013 ± 0.003	COSTA...	80	OMEG	0	10 $\pi^-p \to K^+K^-n$
0.013 ± 0.004	[33] MARTIN	78B	SPEC	−	10 $\pi p \to K^0_S K^-p$

[33] From $(\Gamma_4\Gamma_6)^{1/2} = 0.056 \pm 0.034$ assuming $B(\rho_3(1690) \to \pi\pi) = 0.24$.

$\Gamma(\omega\pi)/[\Gamma(\omega\pi)+\Gamma(\rho\rho)]$ $\Gamma_3/(\Gamma_3+\Gamma_{11})$

VALUE	DOCUMENT ID		TECN	CHG	COMMENT
• • • We do not use the following data for averages, fits, limits, etc. • • •					
0.22 ± 0.08	CASON	73	HBC	−	8,18.5 π^-p

$\Gamma(\eta\pi^+\pi^-)/\Gamma_{total}$ Γ_7/Γ

VALUE	DOCUMENT ID		TECN	COMMENT
seen	FUKUI	88	SPEC	8.95 $\pi^-p \to \eta\pi^+\pi^-n$

$\Gamma(a_2(1320)\pi)/\Gamma(\rho(770)\eta)$ Γ_{10}/Γ_8

VALUE	DOCUMENT ID		TECN	COMMENT
5.5 ± 2.0	AMELIN	00	VES	37 $\pi^-p \to \eta\pi^+\pi^-n$

$\rho_3(1690)$ REFERENCES

AMELIN	00	NP A668 83	D. Amelin *et al.* (VES Collab.)
ALDE	95	ZPHY C66 379	D.M. Alde *et al.* (GAMS Collab.) JP
ALDE	92C	ZPHY C54 553	D.M. Alde *et al.* (BELG, SERP, KEK, LANL+)
FUKUI	88	PL B202 441	S. Fukui *et al.* (SUGI, NAGO, KEK, KYOT+)
DENNEY	83	PR D28 2726	D.L. Denney *et al.* (IOWA, MICH)
EVANGELISTA	81	NP B178 197	C. Evangelista *et al.* (BARI, BONN, CERN+)
ALPER	80	PL 94B 422	B. Alper *et al.* (AMST, CERN, CRAC, MPIM+)
COSTA...	80	NP B175 402	G. Costa de Beauregard *et al.* (BARI, BONN+)
GORLICH	80	NP B174 16	L. Gorlich *et al.* (CRAC, MPIM, CERN+)
BECKER	79	NP B151 46	H. Becker *et al.* (MPIM, CERN, ZEEM, CRAC)
CORDEN	79	NP B157 250	M.J. Corden *et al.* (BIRM, RHEL, TELA+) JP
BALTAY	78B	PR D17 62	C. Baltay *et al.* (COLU, BING)
MARTIN	78B	NP B140 158	A.D. Martin *et al.* (DURH, GEVA)
MARTIN	78D	PL 74B 417	A.D. Martin *et al.* (DURH, GEVA)
ANTIPOV	77	NP B119 45	Y.M. Antipov *et al.* (SERP, GEVA)
GESSAROLI	77	NP B126 382	R. Gessaroli *et al.* (BGNA, FIRZ, GENO+)
BLUM	75	PL 57B 403	W. Blum *et al.* (CERN, MPIM) JP
ESTABROOKS	75	NP B95 322	P.G. Estabrooks, A.D. Martin (DURH)
HYAMS	75	NP B100 205	B.D. Hyams *et al.* (CERN, MPIM)
ENGLER	74	PR D10 2070	A. Engler *et al.* (CMU, CASE)
GRAYER	74	NP B75 189	G. Grayer *et al.* (CERN, MPIM)
KLIGER	74	SJNP 19 428	G.K. Kliger *et al.* (ITEP)

Translated from YAF 19 839.

OREN	74	NP B71 189	Y. Oren *et al.*	(ANL, OXF)
THOMPSON	74	NP B69 220	G. Thompson *et al.*	(PURD)
CASON	73	PR D7 1971	N.M. Cason *et al.*	(NDAM)
BOWEN	72	PRL 29 890	D.R. Bowen *et al.*	(NEAS, STON)
HOLMES	72	PR D6 3336	R. Holmes *et al.*	(ROCH)
BALLAM	71B	PR D3 2606	J. Ballam *et al.*	(SLAC)
MATTHEWS	71C	NP B33 1	J.A.J. Matthews *et al.*	(TNTO, WISC) JP
ARMENISE	70	LNC 4 199	N. Armenise *et al.*	(BARI, BGNA, FIRZ)
BARNHAM	70	PRL 24 1083	K.W.J. Barnham *et al.*	(BIRM)
BARTSCH	70B	NP B22 109	J. Bartsch *et al.*	(AACH, BERL, CERN)
CASO	70	LNC 3 707	C. Caso *et al.*	(GENO, HAMB, MILA, SACL)
STUNTEBECK	70	PL 32B 391	P.H. Stuntebeck *et al.*	(NDAM)
ADERHOLZ	69	NP B11 259	M. Aderholz *et al.*	(AACH3, BERL, CERN+)
ANDERSON	69	PRL 22 1390	E.W. Anderson *et al.*	(BNL, CMU)
ARMENISE	68	NC 54A 999	N. Armenise *et al.*	(BARI, BGNA, FIRZ+) I
BALTAY	68	PRL 20 887	C. Baltay *et al.*	(COLU, ROCH, RUTG, YALE) I
CASO	68	NC 54A 983	C. Caso *et al.*	(GENO, HAMB, MILA, SACL)
CRENNELL	68B	PL 28B 136	D.J. Crennell *et al.*	(BNL)
JOHNSTON	68	PRL 20 1414	T.F. Johnston *et al.*	(TNTO, WISC) IJP
FOCACCI	66	PRL 17 890	M.N. Focacci *et al.*	(CERN)
GOLDBERG	65	PL 17 354	M. Goldberg *et al.*	(CERN, EPOL, ORSAY+)

OTHER RELATED PAPERS

BARNETT	83B	PL 120B 455	B. Barnett *et al.*	(JHU)
EHRLICH	66	PR 152 1194	R. Ehrlich, W. Selove, H. Yuta	(PENN)
LEVRAT	66	PL 22 714	B. Levrat *et al.*	
SEGUINOT	66	PL 19 712	J. Seguinot *et al.*	
BELLINI	65	NC 40A 948	G. Bellini *et al.*	(MILA)
DEUTSCH...	65	PL 18 351	M. Deutschmann *et al.*	(AACH3, BERL, CERN)
FORINO	65	PL 19 65	A. Forino *et al.*	(BGNA, ORSAY, SACL)

$\rho(1700)$

$I^G(J^{PC}) = 1^+(1^{--})$

THE $\rho(1450)$ AND THE $\rho(1700)$

Updated December 2003 by S. Eidelman (Novosibirsk) and J. Hernandez (Valencia).

In our 1988 edition, we replaced the $\rho(1600)$ entry with two new ones, the $\rho(1450)$ and the $\rho(1700)$, because there was emerging evidence that the 1600-MeV region actually contains two ρ-like resonances. ERKAL 86 had pointed out this possibility with a theoretical analysis on the consistency of 2π and 4π electromagnetic form factors and the $\pi\pi$ scattering length. DONNACHIE 87, with a full analysis of data on the 2π and 4π final states in e^+e^- annihilation and photoproduction reactions, had also argued that in order to obtain a consistent picture, two resonances were necessary. The existence of $\rho(1450)$ was supported by the analysis of $\eta\rho^0$ mass spectra obtained in photoproduction and e^+e^- annihilation (DONNACHIE 87B), as well as that of $e^+e^- \to \omega\pi$ (DONNACHIE 91).

The analysis of DONNACHIE 87 was further extended by CLEGG 88, 94 to include new data on 4π systems produced in e^+e^- annihilation, and in τ decays (τ decays to 4π and e^+e^- annihilation to 4π can be related by the Conserved Vector Current assumption). These systems were successfully analyzed using interfering contributions from two ρ-like states, and from the tail of the $\rho(770)$ decaying into two-body states. While specific conclusions on $\rho(1450) \to 4\pi$ were obtained, little could be said about the $\rho(1700)$.

Independent evidence for two 1^- states is provided by KILLIAN 80 in 4π electroproduction at $\langle Q^2 \rangle = 1$ (GeV/c)^2, and by FUKUI 88 in a high-statistics sample of the $\eta\pi\pi$ system in $\pi^- p$ charge exchange.

This scenario with two overlapping resonances is supported by other data. BISELLO 89 measured the pion form factor in the interval 1.35–2.4 GeV, and observed a deep minimum around 1.6 GeV. The best fit was obtained with the hypothesis of ρ-like resonances at 1420 and 1770 MeV, with widths of about 250 MeV. ANTONELLI 88 found that the $e^+e^- \to \eta\pi^+\pi^-$ cross section is better fitted with two fully interfering Breit-Wigners, with parameters in fair agreement with those of DONNACHIE 87 and BISELLO 89. These results can be considered as a confirmation of the $\rho(1450)$.

Decisive evidence for the $\pi\pi$ decay mode of both $\rho(1450)$ and $\rho(1700)$ came from recent results in $\overline{p}p$ annihilation at rest (ABELE 97). It was shown that these resonances also possess a $K\overline{K}$ decay mode (ABELE 98, BERTIN 98B, ABELE 99D). High statistics studies of the decays $\tau \to \pi\pi\nu_\tau$ (BARATE 97M, URHEIM 97), and $\tau \to 4\pi\nu_\tau$ (EDWARDS 00), also require the $\rho(1450)$, but are not sensitive to the $\rho(1700)$, because it is too close to the τ mass.

The structure of these ρ states is not yet completely clear. BARNES 97 and CLOSE 97C claim that $\rho(1450)$ has a mass consistent with radial $2S$, but its decays show characteristics of hybrids, and suggest that this state may be a $2S$-hybrid mixture. DONNACHIE 99 argues that hybrid states could have a 4π decay mode dominated by the $a_1\pi$. Such behavior has recently been observed by AKHMETSHIN 99E in $e^+e^- \to 4\pi$ in the energy range 1.05–1.38 GeV, and by EDWARDS 00 in $\tau \to 4\pi$ decays. ALEXANDER 01B observed the $\rho(1450) \to \omega\pi$ decay mode in B-meson decays, however, didn't find $\rho(1700) \to \omega\pi^0$. A similar conclusion is made by AKHMETSHIN 03B who studied the process $e^+e^- \to \omega\pi^0$. Various decay modes of the $\rho(1450)$ and $\rho(1700)$ were observed in $\overline{p}n$ and $\overline{p}p$ annihilation (ABELE 01B, BARGIOTTI 03B), but no definite conclusions could be drawn. More data should be collected to clarify the nature of the ρ states, particularly in the energy range above 1.6 GeV.

We also list under the $\rho(1450)$ the $\phi\pi$ state with $J^{PC} = 1^{--}$ or $C(1480)$ observed by BITYUKOV 87. While ACHASOV 96B shows that it may be a threshold effect, CLEGG 88 and LANDSBERG 92 suggest two independent vector states with this decay mode. Note, however, that $C(1480)$ in its $\phi\pi$ decay mode was not confirmed by e^+e^- (DOLINSKY 91, BISELLO 91C) and $\overline{p}p$ (ABELE 97H) experiments.

Several observations on the $\omega\pi$ system in the 1200-MeV region (FRENKIEL 72, COSME 76, BARBER 80C, ASTON 80C, ATKINSON 84C, BRAU 88, AMSLER 93B) may be interpreted in terms of either $J^P = 1^-$ $\rho(770) \to \omega\pi$ production (LAYSSAC 71), or $J^P = 1^+$ $b_1(1235)$ production (BRAU 88, AMSLER 93B). We argue that no special entry for a $\rho(1250)$ is needed. The LASS amplitude analysis (ASTON 91B) showing evidence for $\rho(1270)$ is preliminary and needs confirmation. For completeness, the relevant observations are listed under the $\rho(1450)$.

Evidence for ρ-like mesons decaying into 6π states was first noted by CLEGG 90 in the analysis of 6π mass spectra from e^+e^- annihilation (BISELLO 81, CASTRO 88) and diffractive photoproduction (ATKINSON 85). CLEGG 90 argued that two states at about 2.1 and 1.8 GeV exist: while the former is a candidate for a new resonance ($\rho(2150)$), the latter could be a manifestation of the $\rho(1700)$ distorted by threshold effects. Recently, the E687 Collaboration at Fermilab reported an observation of a narrow dip structure at 1.9 GeV/c^2 in the $3\pi^+3\pi^-$ diffractive photoproduction (FRABETTI 01). A similar effect of the dip in the cross section of $e^+e^- \to 6\pi$ around 1.9 GeV has been earlier reported by DM2 (CASTRO 88), where 6π

included both $3\pi^+3\pi^-$ and $2\pi^+2\pi^-2\pi^0$. Later the dip in the R value (the total cross section of $e^+e^- \to$ hadrons divided by the cross section of $e^+e^- \to \mu^+\mu^-$) was observed by ANTONELLI 96, again around 1.9 GeV. This energy is close to the $N\overline{N}$ threshold, which hints to the possible relation between the dip and $N\overline{N}$, *e.g.*, the frequently discussed narrow $N\overline{N}$ resonance or just a threshold effect. Such behaviour is also characteristic of exotic objects like vector $q\overline{q}$ hybrids. Note that AGNELLO 02 failed to find this state in the reaction $\overline{n}p \to 3\pi^+2\pi^-\pi^0$. Recent reanalysis of the E687 data by FRABETTI 04 shows that a dip may arise due to interference of a narrow object with a broad $\rho(1700)$ independently of the nature of the former. We list these observations under a separate particle $\rho(1900)$, which needs confirmation.

$\rho(1700)$ MASS

$\eta\rho^0$ AND $\pi^+\pi^-$ MODES

VALUE (MeV)	DOCUMENT ID
1720±20 OUR ESTIMATE	

$\eta\rho^0$ MODE

VALUE (MeV)	DOCUMENT ID		TECN	COMMENT
The data in this block is included in the average printed for a previous datablock.				
• • • We do not use the following data for averages, fits, limits, etc. • • •				
1740±20	ANTONELLI	88	DM2	$e^+e^- \to \eta\pi^+\pi^-$
1701±15	[2] FUKUI	88	SPEC	8.95 $\pi^- p \to \eta\pi^+\pi^- n$

$\pi\pi$ MODE

VALUE (MeV)	DOCUMENT ID		TECN	COMMENT
The data in this block is included in the average printed for a previous datablock.				
• • • We do not use the following data for averages, fits, limits, etc. • • •				
1780 $^{+37}_{-29}$	[3] ABELE	97	CBAR	$\overline{p}n \to \pi^-\pi^0\pi^0$
1719 ±15	[3] BERTIN	97C	OBLX	0.0 $\overline{p}p \to \pi^+\pi^-\pi^0$
1730 ±30	CLEGG	94	RVUE	$e^+e^- \to \pi^+\pi^-$
1768 ±21	BISELLO	89	DM2	$e^+e^- \to \pi^+\pi^-$
1745.7±91.9	DUBNICKA	89	RVUE	$e^+e^- \to \pi^+\pi^-$
1546 ±26	GESHKEN...	89	RVUE	
1650	[4] ERKAL	85	RVUE	20–70 $\gamma p \to \gamma\pi$
1550 ±70	ABE	84B	HYBR	20 $\gamma p \to \pi^+\pi^- p$
1590 ±20	[5] ASTON	80	OMEG	20–70 $\gamma p \to p2\pi$
1600 ±10	[6] ATIYA	79B	SPEC	50 γC $\to$ C2π
1598 $^{+24}_{-22}$	BECKER	79	ASPK	17 $\pi^- p$ polarized
1659 ±25	[4] LANG	79	RVUE	
1575	[4] MARTIN	78C	RVUE	17 $\pi^- p \to \pi^+\pi^- n$
1610 ±30	[4] FROGGATT	77	RVUE	17 $\pi^- p \to \pi^+\pi^- n$
1590 ±20	[7] HYAMS	73	ASPK	17 $\pi^- p \to \pi^+\pi^- n$

$\pi\omega$ MODE

VALUE (MeV)	DOCUMENT ID		TECN	COMMENT
• • • We do not use the following data for averages, fits, limits, etc. • • •				
1550 to 1620	[8] ACHASOV	00I	SND	$e^+e^- \to \pi^0\pi^0\gamma$
1580 to 1710	[9] ACHASOV	00I	SND	$e^+e^- \to \pi^0\pi^0\gamma$
1710±90	ACHASOV	97	RVUE	$e^+e^- \to \omega\pi^0$

$K\overline{K}$ MODE

VALUE (MeV)	EVTS	DOCUMENT ID		TECN	CHG	COMMENT
• • • We do not use the following data for averages, fits, limits, etc. • • •						
1740.8±22.2	27k	[1] ABELE	99D	CBAR	±	0.0 $\overline{p}p \to K^+K^-\pi^0$
1582 ±36	1600	CLELAND	82B	SPEC	±	50 $\pi p \to K^0_S K^\pm p$

[1] K-matrix pole. Isospin not determined, could be $\omega(1650)$ or $\phi(1680)$.

$2(\pi^+\pi^-)$ MODE

VALUE (MeV)	EVTS	DOCUMENT ID		TECN	COMMENT
• • • We do not use the following data for averages, fits, limits, etc. • • •					
1851 $^{+27}_{-24}$		ACHASOV	97	RVUE	$e^+e^- \to 2(\pi^+\pi^-)$
1570± 20		[10] CORDIER	82	DM1	$e^+e^- \to 2(\pi^+\pi^-)$
1520± 30		[5] ASTON	81E	OMEG	20–70 $\gamma p \to p4\pi$
1654± 25		[11] DIBIANCA	81	DBC	$\pi^+ d \to pp2(\pi^+\pi^-)$
1666± 39		[10] BACCI	80	FRAG	$e^+e^- \to 2(\pi^+\pi^-)$
1780	34	KILLIAN	80	SPEC	11 $e^- p \to 2(\pi^+\pi^-)$
1500		[12] ATIYA	79B	SPEC	50 γC $\to$ C4$\pi^\pm$
1570± 60	65	[13] ALEXANDER	75	HBC	7.5 $\gamma p \to p4\pi$
1550± 60		[5] CONVERSI	74	OSPK	$e^+e^- \to 2(\pi^+\pi^-)$
1550± 50	160	SCHACHT	74	STRC	5.5–9 $\gamma p \to p4\pi$
1450±100	340	SCHACHT	74	STRC	9–18 $\gamma p \to p4\pi$
1430± 50	400	BINGHAM	72B	HBC	9.3 $\gamma p \to p4\pi$

$\pi^+\pi^-\pi^0\pi^0$ MODE

VALUE (MeV)	DOCUMENT ID		TECN	COMMENT
• • • We do not use the following data for averages, fits, limits, etc. • • •				
1660±30	ATKINSON	85B	OMEG	20–70 γp

$3(\pi^+\pi^-)$ AND $2(\pi^+\pi^-\pi^0)$ MODES

VALUE (MeV)	DOCUMENT ID		TECN	COMMENT
• • • We do not use the following data for averages, fits, limits, etc. • • •				
1730±34	[14] FRABETTI	04	E687	$\gamma p \to 3\pi^+ 3\pi^- p$
1783±15	CLEGG	90	RVUE	$e^+e^- \to 3(\pi^+\pi^-)2(\pi^+\pi^-\pi^0)$

[2] Assuming $\rho^+ f_0(1370)$ decay mode interferes with $a_1(1260)^+\pi$ background. From a two Breit-Wigner fit.
[3] T-matrix pole.
[4] From phase shift analysis of HYAMS 73 data.
[5] Simple relativistic Breit-Wigner fit with constant width.
[6] An additional 40 MeV uncertainty in both the mass and width is present due to the choice of the background shape.
[7] Included in BECKER 79 analysis.
[8] Taking into account both $\rho(1450)$ and $\rho(1700)$ contributions. Using the data of ACHASOV 00I on $e^+e^- \to \omega\pi^0$ and of EDWARDS 00A on $\tau^- \to \omega\pi^-\nu_\tau$. $\rho(1450)$ mass and width fixed at 1400 MeV and 500 MeV respectively.
[9] Taking into account the $\rho(1700)$ contribution only. Using the data of ACHASOV 00I on $e^+e^- \to \omega\pi^0$ and of EDWARDS 00A on $\tau^- \to \omega\pi^-\nu_\tau$.
[10] Simple relativistic Breit-Wigner fit with model dependent width.
[11] One peak fit result.
[12] Parameters roughly estimated, not from a fit.
[13] Skew mass distribution compensated by Ross-Stodolsky factor.
[14] From a fit with two resonances with the JACOB 72 continuum.

$\rho(1700)$ WIDTH

$\eta\rho^0$ AND $\pi^+\pi^-$ MODES

VALUE (MeV)	DOCUMENT ID
250±100 OUR ESTIMATE	

$\eta\rho^0$ MODE

VALUE (MeV)	DOCUMENT ID		TECN	COMMENT
The data in this block is included in the average printed for a previous datablock.				
• • • We do not use the following data for averages, fits, limits, etc. • • •				
150±30	ANTONELLI	88	DM2	$e^+e^- \to \eta\pi^+\pi^-$
282±44	[16] FUKUI	88	SPEC	8.95 $\pi^- p \to \eta\pi^+\pi^- n$

$\pi\pi$ MODE

VALUE (MeV)	DOCUMENT ID		TECN	COMMENT
The data in this block is included in the average printed for a previous datablock.				
• • • We do not use the following data for averages, fits, limits, etc. • • •				
275 ± 45	[17] ABELE	97	CBAR	$\overline{p}n \to \pi^-\pi^0\pi^0$
310 ± 40	[17] BERTIN	97C	OBLX	0.0 $\overline{p}p \to \pi^+\pi^-\pi^0$
400 ±100	CLEGG	94	RVUE	$e^+e^- \to \pi^+\pi^-$
224 ± 22	BISELLO	89	DM2	$e^+e^- \to \pi^+\pi^-$
242.5±163.0	DUBNICKA	89	RVUE	$e^+e^- \to \pi^+\pi^-$
620 ± 60	GESHKEN...	89	RVUE	
<315	[18] ERKAL	85	RVUE	20–70 $\gamma p \to \gamma\pi$
280 $^{+30}_{-80}$	ABE	84B	HYBR	20 $\gamma p \to \pi^+\pi^- p$
230 ± 80	[19] ASTON	80	OMEG	20–70 $\gamma p \to p2\pi$
283 ± 14	[20] ATIYA	79B	SPEC	50 γC $\to$ C2π
175 $^{+98}_{-53}$	BECKER	79	ASPK	17 $\pi^- p$ polarized
232 ± 34	[18] LANG	79	RVUE	
340	[18] MARTIN	78C	RVUE	17 $\pi^- p \to \pi^+\pi^- n$
300 ±100	[18] FROGGATT	77	RVUE	17 $\pi^- p \to \pi^+\pi^- n$
180 ± 50	[21] HYAMS	73	ASPK	17 $\pi^- p \to \pi^+\pi^- n$

$K\overline{K}$ MODE

VALUE (MeV)	EVTS	DOCUMENT ID		TECN	CHG	COMMENT
• • • We do not use the following data for averages, fits, limits, etc. • • •						
187.2± 26.7	27k	[15] ABELE	99D	CBAR	±	0.0 $\overline{p}p \to K^+K^-\pi^0$
265 ±120	1600	CLELAND	82B	SPEC	±	50 $\pi p \to K^0_S K^\pm p$

[15] K-matrix pole. Isospin not determined, could be $\omega(1650)$ or $\phi(1680)$.

Meson Particle Listings

$\rho(1700)$

$2(\pi^+\pi^-)$ MODE

VALUE (MeV)	EVTS	DOCUMENT ID		TECN	COMMENT
• • • We do not use the following data for averages, fits, limits, etc. • • •					
510± 40		[22] CORDIER	82	DM1	$e^+e^- \to 2(\pi^+\pi^-)$
400± 50		[19] ASTON	81E	OMEG	20–70 $\gamma p \to p4\pi$
400±146		[23] DIBIANCA	81	DBC	$\pi^+ d \to pp2(\pi^+\pi^-)$
700±160		[22] BACCI	80	FRAG	$e^+e^- \to 2(\pi^+\pi^-)$
100	34	KILLIAN	80	SPEC	11 $e^- p \to 2(\pi^+\pi^-)$
600		[24] ATIYA	79B	SPEC	50 γC $\to$ C4$\pi^\pm$
340±160	65	[25] ALEXANDER	75	HBC	7.5 $\gamma p \to p4\pi$
360±100		[19] CONVERSI	74	OSPK	$e^+e^- \to 2(\pi^+\pi^-)$
400±120	160	[26] SCHACHT	74	STRC	5.5–9 $\gamma p \to p4\pi$
850±200	340	[26] SCHACHT	74	STRC	9–18 $\gamma p \to p4\pi$
650±100	400	BINGHAM	72B	HBC	9.3 $\gamma p \to p4\pi$

$\pi^+\pi^-\pi^0\pi^0$ MODE

VALUE (MeV)	DOCUMENT ID		TECN	COMMENT
• • • We do not use the following data for averages, fits, limits, etc. • • •				
300±50	ATKINSON	85B	OMEG	20–70 γp

$\omega\pi^0$ MODE

VALUE (MeV)	DOCUMENT ID		TECN	COMMENT
• • • We do not use the following data for averages, fits, limits, etc. • • •				
350 to 580	[27] ACHASOV	00I	SND	$e^+e^- \to \pi^0\pi^0\gamma$
490 to 1040	[28] ACHASOV	00I	SND	$e^+e^- \to \pi^0\pi^0\gamma$

$3(\pi^+\pi^-)$ AND $2(\pi^+\pi^-\pi^0)$ MODES

VALUE (MeV)	DOCUMENT ID		TECN	COMMENT
• • • We do not use the following data for averages, fits, limits, etc. • • •				
315±100	[29] FRABETTI	04	E687	$\gamma p \to 3\pi^+3\pi^- p$
285± 20	CLEGG	90	RVUE	$e^+e^- \to 3(\pi^+\pi^-)2(\pi^+\pi^-\pi^0)$

[16] Assuming $\rho^+ f_0(1370)$ decay mode interferes with $a_1(1260)^+\pi$ background. From a two Breit-Wigner fit.
[17] T-matrix pole.
[18] From phase shift analysis of HYAMS 73 data.
[19] Simple relativistic Breit-Wigner fit with constant width.
[20] An additional 40 MeV uncertainty in both the mass and width is present due to the choice of the background shape.
[21] Included in BECKER 79 analysis.
[22] Simple relativistic Breit-Wigner fit with model-dependent width.
[23] One peak fit result.
[24] Parameters roughly estimated, not from a fit.
[25] Skew mass distribution compensated by Ross-Stodolsky factor.
[26] Width errors enlarged by us to $4\Gamma/\sqrt{N}$; see the note with the $K^*(892)$ mass.
[27] Taking into account both $\rho(1450)$ and $\rho(1700)$ contributions. Using the data of ACHASOV 00I on $e^+e^- \to \omega\pi^0$ and of EDWARDS 00A on $\tau^- \to \omega\pi^-\nu_\tau$. $\rho(1450)$ mass and width fixed at 1400 MeV and 500 MeV respectively.
[28] Taking into account the $\rho(1700)$ contribution only. Using the data of ACHASOV 00I on $e^+e^- \to \omega\pi^0$ and of EDWARDS 00A on $\tau^- \to \omega\pi^-\nu_\tau$.
[29] From a fit with two resonances with the JACOB 72 continuum.

$\rho(1700)$ DECAY MODES

	Mode	Fraction (Γ_i/Γ)
Γ_1	4π	
Γ_2	$2(\pi^+\pi^-)$	large
Γ_3	$\rho\pi\pi$	dominant
Γ_4	$\rho^0\pi^+\pi^-$	large
Γ_5	$\rho^0\pi^0\pi^0$	
Γ_6	$\rho^\pm\pi^\mp\pi^0$	large
Γ_7	$a_1(1260)\pi$	seen
Γ_8	$h_1(1170)\pi$	seen
Γ_9	$\pi(1300)\pi$	seen
Γ_{10}	$\rho\rho$	seen
Γ_{11}	$\pi^+\pi^-$	seen
Γ_{12}	$\pi\pi$	seen
Γ_{13}	$K\overline{K}^*(892)+$ c.c.	seen
Γ_{14}	$\eta\rho$	seen
Γ_{15}	$a_2(1320)\pi$	not seen
Γ_{16}	$K\overline{K}$	seen
Γ_{17}	e^+e^-	seen
Γ_{18}	$\pi^0\omega$	seen

$\rho(1700)$ $\Gamma(i)\Gamma(e^+e^-)/\Gamma(\text{total})$

This combination of a partial width with the partial width into e^+e^- and with the total width is obtained from the cross-section into channel i in e^+e^- annihilation.

$\Gamma(2(\pi^+\pi^-)) \times \Gamma(e^+e^-)/\Gamma_{\text{total}}$ $\quad \Gamma_2\Gamma_{17}/\Gamma$

VALUE (keV)	DOCUMENT ID		TECN	COMMENT
• • • We do not use the following data for averages, fits, limits, etc. • • •				
2.6 ±0.2	DELCOURT	81B	DM1	$e^+e^- \to 2(\pi^+\pi^-)$
2.83±0.42	BACCI	80	FRAG	$e^+e^- \to 2(\pi^+\pi^-)$

$\Gamma(\pi^+\pi^-) \times \Gamma(e^+e^-)/\Gamma_{\text{total}}$ $\quad \Gamma_{11}\Gamma_{17}/\Gamma$

VALUE (keV)	DOCUMENT ID		TECN	COMMENT
• • • We do not use the following data for averages, fits, limits, etc. • • •				
0.13	[30] DIEKMAN	88	RVUE	$e^+e^- \to \pi^+\pi^-$
$0.029^{+0.016}_{-0.012}$	KURDADZE	83	OLYA	0.64–1.4 $e^+e^- \to \pi^+\pi^-$

[30] Using total width = 220 MeV.

$\Gamma(K\overline{K}^*(892)+\text{c.c.}) \times \Gamma(e^+e^-)/\Gamma_{\text{total}}$ $\quad \Gamma_{13}\Gamma_{17}/\Gamma$

VALUE (keV)	DOCUMENT ID		TECN	COMMENT
• • • We do not use the following data for averages, fits, limits, etc. • • •				
0.305 ± 0.071	[31] BIZOT	80	DM1	e^+e^-

$\Gamma(\eta\rho) \times \Gamma(e^+e^-)/\Gamma_{\text{total}}$ $\quad \Gamma_{14}\Gamma_{17}/\Gamma$

VALUE (eV)	DOCUMENT ID		TECN	COMMENT
• • • We do not use the following data for averages, fits, limits, etc. • • •				
7 ± 3	ANTONELLI	88	DM2	$e^+e^- \to \eta\pi^+\pi^-$

$\Gamma(K\overline{K}) \times \Gamma(e^+e^-)/\Gamma_{\text{total}}$ $\quad \Gamma_{16}\Gamma_{17}/\Gamma$

VALUE (keV)	DOCUMENT ID		TECN	COMMENT
• • • We do not use the following data for averages, fits, limits, etc. • • •				
0.035 ± 0.029	[31] BIZOT	80	DM1	e^+e^-

$\Gamma(\rho\pi\pi) \times \Gamma(e^+e^-)/\Gamma_{\text{total}}$ $\quad \Gamma_3\Gamma_{17}/\Gamma$

VALUE (keV)	DOCUMENT ID		TECN	COMMENT
• • • We do not use the following data for averages, fits, limits, etc. • • •				
3.510 ± 0.090	[31] BIZOT	80	DM1	e^+e^-

[31] Model dependent.

$\rho(1700)$ BRANCHING RATIOS

$\Gamma(\pi^+\pi^-)/\Gamma_{\text{total}}$ $\quad \Gamma_{11}/\Gamma$

VALUE	DOCUMENT ID		TECN	COMMENT
• • • We do not use the following data for averages, fits, limits, etc. • • •				
$0.287^{+0.043}_{-0.042}$	BECKER	79	ASPK	17 $\pi^- p$ polarized
0.15 to 0.30	[32] MARTIN	78C	RVUE	17 $\pi^- p \to \pi^+\pi^- n$
<0.20	[33] COSTA...	77B	RVUE	$e^+e^- \to 2\pi$, 4π
0.30 ±0.05	[32] FROGGATT	77	RVUE	17 $\pi^- p \to \pi^+\pi^- n$
<0.15	[34] EISENBERG	73	HBC	5 $\pi^+ p \to \Delta^{++}2\pi$
0.25 ±0.05	[35] HYAMS	73	ASPK	17 $\pi^- p \to \pi^+\pi^- n$

[32] From phase shift analysis of HYAMS 73 data.
[33] Estimate using unitarity, time reversal invariance, Breit-Wigner.
[34] Estimated using one-pion-exchange model.
[35] Included in BECKER 79 analysis.

$\Gamma(\pi^+\pi^-)/\Gamma(2(\pi^+\pi^-))$ $\quad \Gamma_{11}/\Gamma_2$

VALUE	DOCUMENT ID		TECN	COMMENT
• • • We do not use the following data for averages, fits, limits, etc. • • •				
0.13±0.05	ASTON	80	OMEG	20–70 $\gamma p \to p2\pi$
<0.14	[36] DAVIER	73	STRC	6–18 $\gamma p \to p4\pi$
<0.2	[37] BINGHAM	72B	HBC	9.3 $\gamma p \to p2\pi$

[36] Upper limit is estimate.
[37] 2σ upper limit.

$\Gamma(\pi\pi)/\Gamma(4\pi)$ $\quad \Gamma_{12}/\Gamma_1$

VALUE	DOCUMENT ID		TECN	COMMENT
• • • We do not use the following data for averages, fits, limits, etc. • • •				
0.16±0.04	[42,43] ABELE	01B	CBAR	0.0 $\overline{p}n \to 5\pi$

$\Gamma(K\overline{K}^*(892)+\text{c.c.})/\Gamma(2(\pi^+\pi^-))$ $\quad \Gamma_{13}/\Gamma_2$

VALUE	DOCUMENT ID		TECN	COMMENT
• • • We do not use the following data for averages, fits, limits, etc. • • •				
0.15±0.03	[38] DELCOURT	81B	DM1	$e^+e^- \to \overline{K}K\pi$

[38] Assuming $\rho(1700)$ and ω radial excitations to be degenerate in mass.

$\Gamma(\eta\rho)/\Gamma_{\text{total}}$ $\quad \Gamma_{14}/\Gamma$

VALUE	CL%	DOCUMENT ID		TECN	COMMENT
• • • We do not use the following data for averages, fits, limits, etc. • • •					
possibly seen		AKHMETSHIN	00D	CMD2	$e^+e^- \to \eta\pi^+\pi^-$
<0.04		DONNACHIE	87B	RVUE	
<0.02	58	ATKINSON	86B	OMEG	20–70 γp

$\Gamma(a_2(1320)\pi)/\Gamma_{\text{total}}$ $\quad \Gamma_{15}/\Gamma$

VALUE	DOCUMENT ID		TECN	COMMENT
• • • We do not use the following data for averages, fits, limits, etc. • • •				
not seen	AMELIN	00	VES	37 $\pi^- p \to \eta\pi^+\pi^- n$

$\Gamma(\eta\rho)/\Gamma(2(\pi^+\pi^-))$ Γ_{14}/Γ_2

VALUE	DOCUMENT ID		TECN	COMMENT
• • • We do not use the following data for averages, fits, limits, etc. • • •				
0.123 ± 0.027	DELCOURT	82	DM1	$e^+e^- \to \pi^+\pi^-$ MM
~ 0.1	ASTON	80	OMEG	20–70 γp

$\Gamma(\pi^+\pi^-\text{neutrals})/\Gamma(2(\pi^+\pi^-))$ $(\Gamma_5+\Gamma_6+0.714\Gamma_{14})/\Gamma_2$

VALUE	DOCUMENT ID		TECN	COMMENT
• • • We do not use the following data for averages, fits, limits, etc. • • •				
2.6 ± 0.4	[39] BALLAM	74	HBC	9.3 γp

[39] Upper limit. Background not subtracted.

$\Gamma(\pi^0\omega)/\Gamma_{\text{total}}$ Γ_{18}/Γ

VALUE	EVTS	DOCUMENT ID		TECN	COMMENT
• • • We do not use the following data for averages, fits, limits, etc. • • •					
not seen	2382	AKHMETSHIN	03B	CMD2	$e^+e \to \pi^0\pi^0\gamma$
seen		ACHASOV	97	RVUE	$e^+e^- \to \omega\pi^0$

$\Gamma(a_1(1260)\pi)/\Gamma(4\pi)$ Γ_7/Γ_1

VALUE	DOCUMENT ID		TECN	COMMENT
• • • We do not use the following data for averages, fits, limits, etc. • • •				
0.16 ± 0.05	[42] ABELE	01B	CBAR	0.0 $\overline{p}n \to 5\pi$

$\Gamma(h_1(1170)\pi)/\Gamma(4\pi)$ Γ_8/Γ_1

VALUE	DOCUMENT ID		TECN	COMMENT
• • • We do not use the following data for averages, fits, limits, etc. • • •				
0.17 ± 0.06	[42] ABELE	01B	CBAR	0.0 $\overline{p}n \to 5\pi$

$\Gamma(\pi(1300)\pi)/\Gamma(4\pi)$ Γ_9/Γ_1

VALUE	DOCUMENT ID		TECN	COMMENT
• • • We do not use the following data for averages, fits, limits, etc. • • •				
0.30 ± 0.10	[42] ABELE	01B	CBAR	0.0 $\overline{p}n \to 5\pi$

$\Gamma(\rho\rho)/\Gamma(4\pi)$ Γ_{10}/Γ_1

VALUE	DOCUMENT ID		TECN	COMMENT
• • • We do not use the following data for averages, fits, limits, etc. • • •				
0.09 ± 0.03	[42] ABELE	01B	CBAR	0.0 $\overline{p}n \to 5\pi$

$\Gamma(\rho\pi\pi)/\Gamma(4\pi)$ Γ_3/Γ_1

VALUE	DOCUMENT ID		TECN	COMMENT
• • • We do not use the following data for averages, fits, limits, etc. • • •				
0.28 ± 0.06	[42] ABELE	01B	CBAR	0.0 $\overline{p}n \to 5\pi$

$\Gamma(K\overline{K})/\Gamma(2(\pi^+\pi^-))$ Γ_{16}/Γ_2

VALUE	CL%	DOCUMENT ID		TECN	CHG	COMMENT
• • • We do not use the following data for averages, fits, limits, etc. • • •						
0.015 ± 0.010		[40] DELCOURT	81B	DM1		$e^+e^- \to K\overline{K}$
< 0.04	95	BINGHAM	72B	HBC	0	9.3 γp

[40] Assuming $\rho(1700)$ and ω radial excitations to be degenerate in mass.

$\Gamma(K\overline{K})/\Gamma(K\overline{K}^*(892)+\text{c.c.})$ Γ_{16}/Γ_{13}

VALUE	DOCUMENT ID		TECN	COMMENT
• • • We do not use the following data for averages, fits, limits, etc. • • •				
0.052 ± 0.026	BUON	82	DM1	e^+e^- → hadrons

$\Gamma(\rho^0\pi^+\pi^-)/\Gamma(2(\pi^+\pi^-))$ Γ_4/Γ_2

VALUE	EVTS	DOCUMENT ID		TECN	COMMENT
• • • We do not use the following data for averages, fits, limits, etc. • • •					
~ 1.0		DELCOURT	81B	DM1	$e^+e^- \to 2(\pi^+\pi^-)$
0.7 ± 0.1	500	SCHACHT	74	STRC	5.5–18 $\gamma p \to p4\pi$
0.80		[41] BINGHAM	72B	HBC	9.3 $\gamma p \to p4\pi$

[41] The $\pi\pi$ system is in S-wave.

$\Gamma(\rho^0\pi^0\pi^0)/\Gamma(\rho^\pm\pi^\mp\pi^0)$ Γ_5/Γ_6

VALUE	DOCUMENT ID		TECN	CHG	COMMENT
• • • We do not use the following data for averages, fits, limits, etc. • • •					
< 0.10	ATKINSON	85B	OMEG		20–70 γp
< 0.15	ATKINSON	82	OMEG	0	20–70 $\gamma p \to p4\pi$

[42] $\omega\pi$ not included.
[43] Using ABELE 97.

$\rho(1700)$ REFERENCES

FRABETTI	04	PL B578 290	P.L. Frabetti *et al.* (FNAL E687 Collab.)
AKHMETSHIN	03B	PL B562 173	R.R. Akhmetshin *et al.* (Novosibirsk CMD-2 Collab.)
ABELE	01B	EPJ C21 261	A. Abele *et al.* (Crystal Barrel Collab.)
ACHASOV	00I	PL B486 29	M.N. Achasov *et al.* (Novosibirsk SND Collab.)
AKHMETSHIN	00D	PL B489 125	R.R. Akhmetshin *et al.* (Novosibirsk CMD-2 Collab.)
AMELIN	00	NP A668 83	D. Amelin *et al.* (VES Collab.)
EDWARDS	00A	PR D61 072003	K.W. Edwards *et al.* (CLEO Collab.)
ABELE	99D	PL B468 178	A. Abele *et al.* (Crystal Barrel Collab.)
ABELE	97	PL B391 191	A. Abele *et al.* (Crystal Barrel Collab.)
ACHASOV	97	PR D55 2663	N.N. Achasov *et al.* (NOVM)
BERTIN	97C	PL B408 476	A. Bertin *et al.* (OBELIX Collab.)
CLEGG	94	ZPHY C62 455	A.B. Clegg, A. Donnachie (LANC, MCHS)
CLEGG	90	ZPHY C45 677	A.B. Clegg, A. Donnachie (LANC, MCHS)
BISELLO	89	PL B220 321	D. Bisello *et al.* (DM2 Collab.)
DUBNICKA	89	JPG 15 1349	S. Dubnicka *et al.* (JINR, SLOV)
GESHKEN...	89	ZPHY C45 351	B.V. Geshkenbein (ITEP)
ANTONELLI	88	PL B212 133	A. Antonelli *et al.* (DM2 Collab.)
DIEKMAN	88	PRPL 159 101	B. Diekmann (BONN)
FUKUI	88	PL B202 441	S. Fukui *et al.* (SUGI, NAGO, KEK, KYOT+)
DONNACHIE	87B	ZPHY C34 257	A. Donnachie, A.B. Clegg (MCHS, LANC)
ATKINSON	86B	ZPHY C30 531	M. Atkinson *et al.* (BONN, CERN, GLAS+)
ATKINSON	85B	ZPHY C26 499	M. Atkinson *et al.* (BONN, CERN, GLAS+)
ERKAL	85	ZPHY C29 485	C. Erkal, M.G. Olsson (WISC)
ABE	84B	PRL 53 751	K. Abe *et al.*
KURDADZE	83	JETPL 37 733	L.M. Kurdadze *et al.* (NOVO)
		Translated from ZETFP 37 613.	
ATKINSON	82	PL 108B 55	M. Atkinson *et al.* (BONN, CERN, GLAS+)
BUON	82	PL 118B 221	J. Buon *et al.* (LALO, MONP)
CLELAND	82B	NP B208 228	W.E. Cleland *et al.* (DURH, GEVA, LAUS+)
CORDIER	82	PL 109B 129	A. Cordier *et al.* (LALO)
DELCOURT	82	PL 113B 93	B. Delcourt *et al.* (LALO)
ASTON	81E	NP B189 15	D. Aston (BONN, CERN, EPOL, GLAS, LANC+)
DELCOURT	81B	Bonn Conf. 205	B. Delcourt (ORSAY)
Also	82	PL 109B 129	A. Cordier *et al.* (LALO)
DIBIANCA	81	PR D23 595	F.A. di Bianca *et al.* (CASE, CMU)
ASTON	80	PL 92B 215	D. Aston (BONN, CERN, EPOL, GLAS, LANC+)
BACCI	80	PL 95B 139	C. Bacci *et al.* (ROMA, FRAS)
BIZOT	80	Madison Conf. 546	J.C. Bizot *et al.* (LALO, MONP)
KILLIAN	80	PR D21 3005	T.J. Killian *et al.* (CORN)
ATIYA	79B	PRL 43 1691	M.S. Atiya *et al.* (COLU, ILL, FNAL)
BECKER	79	NP B151 46	H. Becker *et al.* (MPIM, CERN, ZEEM, CRAC)
LANG	79	PR D19 956	C.B. Lang, A. Mas-Parareda (GRAZ)
MARTIN	78C	ANP 114 1	A.D. Martin, M.R. Pennington (CERN)
COSTA...	77B	PL 71B 345	B. Costa de Beauregard, B. Pire, T.N. Truong (EPOL)
FROGGATT	77	NP B129 89	C.D. Froggatt, J.L. Petersen (GLAS, NORD)
ALEXANDER	75	PL 57B 487	G. Alexander *et al.* (TELA)
BALLAM	74	NP B76 375	J. Ballam *et al.* (SLAC, LBL, MPIM)
CONVERSI	74	PL 52B 493	M. Conversi *et al.* (ROMA, FRAS)
SCHACHT	74	NP B81 205	P. Schacht *et al.* (MPIM)
DAVIER	73	NP B58 31	M. Davier *et al.* (SLAC)
EISENBERG	73	PL 43B 149	Y. Eisenberg *et al.* (REHO)
HYAMS	73	NP B64 134	B.D. Hyams *et al.* (CERN, MPIM)
BINGHAM	72B	PL 41B 635	H.H. Bingham *et al.* (LBL, UCB, SLAC) IGJP
JACOB	72	PR D5 1847	M. Jacob, R. Slansky

OTHER RELATED PAPERS

ACHASOV	03C	JETP 96 789	M.N. Achasov *et al.* (Novosibirsk SND Collab.)
		Translated from ZETF 123 899.	
AKHMETSHIN	03	PL B551 27	R.R. Akhmetshin *et al.* (Novosibirsk CMD-2 Collab.)
Also	02	PAN 65 1222	E.V. Anashkin, V.M. Aulchenko, R.R. Akhmetshin
		Translated from YAF 65 1255.	
BARGIOTTI	03B	PL B561 233	M. Bargiotti *et al.*
ACHASOV	02B	PAN 65 153	N.N. Achasov, A.A. Kozhevnikov
		Translated from YAF 65 158.	
AGNELLO	02	PL B527 39	M. Agnello *et al.* (OBELIX Collab.)
CLOSE	02	PR D65 092003	F.E. Close, A. Donnachie, Yu.S. Kalashnikova
FRABETTI	01	PL B514 240	P.L. Frabetti *et al.* (FNAL E687 Collab.)
ACHASOV	00J	PR D62 117503	N.N. Achasov, A.A. Kozhevnikov
ANDERSON	00A	PR D61 112002	S. Anderson *et al.* (CLEO Collab.)
EDWARDS	00A	PR D61 072003	K.W. Edwards *et al.* (CLEO Collab.)
ABELE	99C	PL B450 275	A. Abele *et al.* (Crystal Barrel Collab.)
DONNACHIE	99	PR D60 114011	A. Donnachie, Yu.S. Kalashnikova
KULZINGER	99	EPJ C7 73	G. Kulzinger *et al.*
ANTONELLI	98	NP B517 3	A. Antonelli *et al.* (FENICE Collab.)
BELOZEROVA	98	PPN 29 63	T.S. Belozerova, V.K. Henner
		Translated from FECAY 29 148.	
BARNES	97	PR D55 4157	T. Barnes *et al.* (ORNL, RAL, MCHS)
CLOSE	97C	PR D56 1584	F.E. Close *et al.* (RAL, MCHS)
URHEIM	97	NPBPS 55C 359	J. Urheim (CLEO Collab.)
ACHASOV	96B	PAN 59 1262	N.N. Achasov, G.N. Shestakov (NOVM)
		Translated from YAF 59 1311.	
ANTONELLI	96	PL B365 427	A. Antonelli *et al.* (FENICE Collab.)
AMSLER	93B	PL B311 362	C. Amsler *et al.* (Crystal Barrel Collab.)
LANDSBERG	92	SJNP 55 1051	L.G. Landsberg (SERP)
		Translated from YAF 55 1896.	
ASTON	91B	NPBPS 21 105	D. Aston *et al.* (LASS Collab.)
DONNACHIE	91	ZPHY C51 689	A. Donnachie, A.B. Clegg (MCHS, LANC)
ACHASOV	88C	PL B209 373	N.N. Achasov, A.A. Kozhevnikov (NOVM)
BRAU	88	PR D37 2379	J.E. Brau *et al.* JP
CASTRO	88	Preprint LAL-88-58	A. Castro *et al.* (DM2 Collab.)
ERKAL	86	ZPHY C31 615	C. Erkal, M.G. Olsson (WISC)
ATKINSON	85	ZPHY C29 333	M. Atkinson *et al.* (BONN, CERN, GLAS+)
BARKOV	85	NP B256 365	L.M. Barkov *et al.* (NOVO)
ATKINSON	84C	NP B243 1	M. Atkinson *et al.* (BONN, CERN, GLAS+) JP
ATKINSON	83B	PL 127B 132	M. Atkinson *et al.* (BONN, CERN, GLAS+)
ATKINSON	83C	NP B229 269	M. Atkinson *et al.* (BONN, CERN, GLAS+)
AUGUSTIN	83	LAL 83-21	J.E. Augustin *et al.* (LALO, PADO, FRAS)
SHAMBROOM	82	PR D26 1	W.D. Shambroom *et al.* (HARV, EFI, ILL+)
BISELLO	81	PL 107B 145	D. Bisello *et al.* (DM1 Collab.)
ASTON	80C	PL 92B 211	D. Aston (BONN, CERN, EPOL, GLAS, LANC+)
BARBER	80C	ZPHY C4 169	D.P. Barber *et al.* (DARE, LANC, SHEF)
KILLIAN	80	PR D21 3005	T.J. Killian *et al.* (CORN)
COSME	76	PL 63B 352	G. Cosme *et al.* (ORSAY)
FRENKIEL	72	NP B47 61	P. Frenkiel *et al.* (CDEF, CERN)
ALVENSLEB...	71	PRL 26 273	H. Alvensleben *et al.* (DESY, MIT) G
BRAUN	71	NP B30 213	H.M. Braun *et al.* (STRB) G
BULOS	71	PRL 26 149	F. Bulos *et al.* (SLAC, UMD, IBM, LBL) G
LAYSSAC	71	NC 6A 134	J. Layssac, F.M. Renard (MONP)

Meson Particle Listings

$\rho(1700)$, $a_2(1700)$, $f_0(1710)$

$a_2(1700)$

$I^G(J^{PC}) = 1^-(2^{++})$

OMITTED FROM SUMMARY TABLE

$a_2(1700)$ MASS

VALUE (MeV)	DOCUMENT ID		TECN	COMMENT
1732±16 OUR AVERAGE	Error includes scale factor of 1.9. See the ideogram below.			
1737± 5±7	ABE	04	BELL	10.6 $e^+e^- \to e^+e^-K^+K^-$
1698±44	[1] AMSLER	02	CBAR	0.9 $\overline{p}p \to \pi^0\eta\eta$
1660±40	ABELE	99B	CBAR	1.94 $\overline{p}p \to \pi^0\eta\eta$
• • • We do not use the following data for averages, fits, limits, etc. • • •				
~ 1775	[2] GRYGOREV	99	SPEC	40 $\pi^-p \to K^0_S K^0_S n$
1752±21±4	ACCIARRI	97T	L3	$\gamma\gamma \to \pi^+\pi^-\pi^0$

[1] T-matrix pole.
[2] Possibly two $J^P = 2^+$ resonances with isospins 0 and 1.

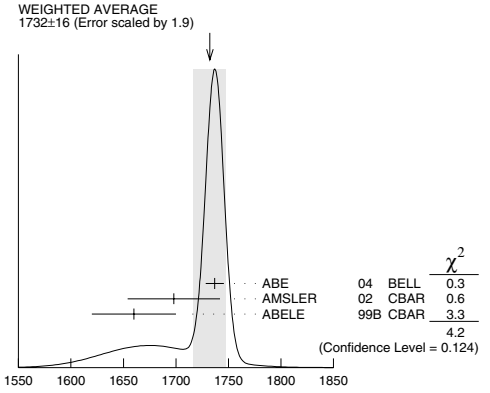

$a_2(1700)$ mass (MeV)

$a_2(1700)$ WIDTH

VALUE (MeV)	DOCUMENT ID		TECN	COMMENT
194± 40 OUR AVERAGE	Error includes scale factor of 1.6. See the ideogram below.			
151± 22±24	ABE	04	BELL	10.6 $e^+e^- \to e^+e^-K^+K^-$
265± 55	[3] AMSLER	02	CBAR	0.9 $\overline{p}p \to \pi^0\eta\eta$
280± 70	ABELE	99B	CBAR	1.94 $\overline{p}p \to \pi^0\eta\eta$
• • • We do not use the following data for averages, fits, limits, etc. • • •				
150±110±34	ACCIARRI	97T	L3	$\gamma\gamma \to \pi^+\pi^-\pi^0$

[3] T-matrix pole.

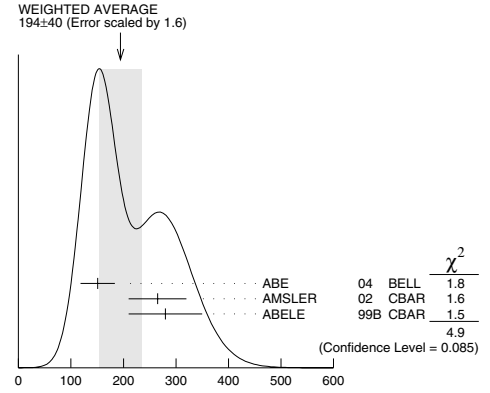

$a_2(1700)$ width

$a_2(1700)$ DECAY MODES

	Mode	Fraction (Γ_i/Γ)
Γ_1	$\eta\pi$	seen
Γ_2	$\gamma\gamma$	
Γ_3	$\rho\pi$	
Γ_4	$f_2(1270)\pi$	
Γ_5	$K\overline{K}$	seen

$a_2(1700)$ $\Gamma(i)\Gamma(\gamma\gamma)/\Gamma(\text{total})$

$[\Gamma(\rho\pi) + \Gamma(f_2(1270)\pi)] \times \Gamma(\gamma\gamma)/\Gamma_{\text{total}}$ $\quad (\Gamma_3+\Gamma_4)\Gamma_2/\Gamma$

VALUE (keV)	DOCUMENT ID	TECN	COMMENT
0.29±0.04±0.02	ACCIARRI	97T L3	$\gamma\gamma \to \pi^+\pi^-\pi^0$

$\Gamma(K\overline{K}) \times \Gamma(\gamma\gamma)/\Gamma_{\text{total}}$ $\quad \Gamma_5\Gamma_2/\Gamma$

VALUE (eV)	DOCUMENT ID		TECN	COMMENT
• • • We do not use the following data for averages, fits, limits, etc. • • •				
20.6±4.2±4.6	[4] ABE	04	BELL	10.6 $e^+e^- \to e^+e^-K^+K^-$

[4] Assuming spin 2.

$a_2(1700)$ REFERENCES

ABE	04	EPJ C32 323	K. Abe *et al.*	(BELLE Collab.)
AMSLER	02	EPJ C23 29	C. Amsler *et al.*	
ABELE	99B	EPJ C8 67	A. Abele *et al.*	(Crystal Barrel Collab.)
GRYGOREV	99	PAN 62 470	V.K. Grygorev *et al.*	
		Translated from YAF 62 513.		
ACCIARRI	97T	PL B413 147	M. Acciarri *et al.*	(L3 Collab.)

OTHER RELATED PAPERS

BAKER	03	PL B563 140	C.A. Baker *et al.*	
BARBERIS	00H	PL B488 225	D. Barberis *et al.*	(WA 102 Collab.)

$f_0(1710)$

$I^G(J^{PC}) = 0^+(0^{++})$

THE $f_0(1710)$

Updated April 2002 by M. Doser (CERN).

The $f_0(1710)$ is seen in the radiative decay $J/\psi(1S) \to \gamma f_0(1710)$; therefore $C = +1$. It decays into 2η and $K^0_S K^0_S$, which implies $I^G J^{PC} = 0^+(even)^{++}$. The spin of the $f_0(1710)$ has been controversial, but evidence for spin 0 has accumulated recently in all production modes.

An analysis of radiative $J/\psi(1S)$ decays at BES into $\pi^+\pi^-\pi^+\pi^-$ (BAI 00) clearly favors spin 0. Combined amplitude analyses of the K^+K^-, K_SK_S, and $\pi^+\pi^-$ systems produced in $J/\psi(1S)$ radiative decay by MARK III (CHEN 91 and more recently DUNWOODIE 97) find a large spin-0 component, as well as reproducing known parameters of the $f_2(1270)$ and $f_2'(1525)$. In addition, a recent reanalysis (BUGG 95) of the 4π channel from MARK III, allowing both $\rho\rho$ and two $\pi\pi$ S waves, also finds a 0^{++} assignment for the $f_0(1710)$. Earlier analyses of this final state (BISELLO 89B, BALTRUSAITIS 86B) found only pseudoscalar activity in the $f_0(1710)$ region, but considered only the process $J/\psi(1S) \to \gamma\rho\rho$. Similarly, earlier analyses of the K^+K^- system based on less statistics (BALTRUSAITIS 87, BAI 96) found a spin of 2 for the $f_0(1710)$.

A similar situation is present in central production, with earlier analyses favoring spin 2 over spin 0 (ARMSTRONG 89D). More recent analyses with greater statistics [BARBERIS 99 (K^+K^-,K_SK_S), BARBERIS 99B ($\pi^+\pi^-$), and FRENCH 99 (K^+K^-)], however, clearly indicate spin 0, and exclude spin 2. Generally, analyses preferring spin 2 concentrate on angular distributions in the $f_J(1710)$ region, and do not include possible interferences or distortion due to the nearby $f_2'(1525)$.

The $f_0(1710)$ is also observed in $K\overline{K}$ (FALVARD 88) in $J/\psi(1S) \to \omega K\overline{K}$ and $J/\psi(1S) \to \phi K\overline{K}$, but with no spin-parity analysis, as well as in $\eta\eta$ in radiative $J/\psi(1S)$ decays (EDWARDS 82). It is also clearly seen in 300-GeV/c pp central production in both K^+K^- and $K^0_SK^0_S$ (ARMSTRONG 89D). Mass and width are determined via a fit to non-interfering Breit-Wigners over a polynomial background, which leads to large systematic errors for the width. ARMSTRONG 93C also sees a broad peak in $\eta\eta$ at 1747 MeV, which may be the $f_0(1710)$.

This resonance is not observed in the hypercharge-exchange reactions $K^-p \to K^0_SK^0_S\Lambda$ (ASTON 88D) and $K^-p \to K^0_SK^0_SY^*$ (BOLONKIN 86); these non-observations are explained by a spin of 0 (LINDENBAUM 92). It is not observed in $\overline{p}p$ interactions, neither via its $\pi\pi$ nor its $\eta\eta$ decay (AMSLER 02). A possible observation in $\gamma\gamma$ collisions leading to K_SK_S (BRACCINI 99, but no spin determination), and a non-observation in $\gamma\gamma \to \pi^+\pi^-$ (BARATE 00E), are consistent with a large $\overline{s}s$ component.

References

References may be found at the end of the $f_0(1710)$ Listing.

$f_0(1710)$ MASS

VALUE (MeV)	EVTS	DOCUMENT ID		TECN	COMMENT
1714 ± 5 OUR AVERAGE					
1740 ± 4 $^{+10}_{-25}$		[1] BAI	03G	BES	$J/\psi \to \gamma K\overline{K}$
1740 $^{+30}_{-25}$		[1] BAI	00A	BES	$J/\psi \to \gamma(\pi^+\pi^-\pi^+\pi^-)$
1698 ± 18		[2] BARBERIS	00E		450 $pp \to p_f\eta\eta p_s$
1710 ± 12 ± 11		[3] BARBERIS	99D	OMEG	450 $pp \to K^+K^-, \pi^+\pi^-$
1710 ± 25		[4] FRENCH	99		300 $pp \to p_f(K^+K^-)p_s$
1707 ± 10		[5] AUGUSTIN	88	DM2	$J/\psi \to \gamma K^+K^-, K^0_SK^0_S$
1698 ± 15		[5] AUGUSTIN	87	DM2	$J/\psi \to \gamma\pi^+\pi^-$
1720 ± 10 ± 10		[6] BALTRUSAIT...87		MRK3	$J/\psi \to \gamma K^+K^-$
1742 ± 15		[5] WILLIAMS	84	MPSF	200 $\pi^-N \to 2K^0_S$X
1670 ± 50		BLOOM	83	CBAL	$J/\psi \to \gamma 2\eta$
• • • We do not use the following data for averages, fits, limits, etc. • • •					
1726 ± 7	74	[7] CHEKANOV	04	ZEUS	$ep \to K^0_SK^0_SX$
1732 +15		[8] ANISOVICH	03	RVUE	
1682 ± 16		TIKHOMIROV	03	SPEC	40.0 π^-C $\to K^0_SK^0_SK^0_L$X
1670 ± 26	3651	[1,9] NICHITIU	02	OBLX	
1767 ± 14	221	[10] ACCIARRI	01H	L3	$\gamma\gamma \to K^0_SK^0_S$, E^{ee}_{cm}= 91, 183–209 GeV
1770 ± 12		[11,12] ANISOVICH	99B	SPEC	0.6–1.2 $p\overline{p} \to \eta\eta\pi^0$
1730 ± 15		[1] BARBERIS	99	OMEG	450 $pp \to p_sp_fK^+K^-$
1750 ± 20		[1] BARBERIS	99B	OMEG	450 $pp \to p_sp_f\pi^+\pi^-$
1750 ± 30		[13] ANISOVICH	98B	RVUE	Compilation
1720 ± 39		BAI	98H	BES	$J/\psi \to \gamma\pi^0\pi^0$
1775 ± 1.5	57	[14] BARKOV	98		$\pi^-p \to K^0_SK^0_Sn$
1690 ± 11		[15] ABREU	96C	DLPH	$Z^0 \to K^+K^-$ + X
1696 ± 5 $^{+9}_{-34}$		[6] BAI	96C	BES	$J/\psi \to \gamma K^+K^-$
1781 ± 8 $^{+10}_{-31}$		[1] BAI	96C	BES	$J/\psi \to \gamma K^+K^-$
1768 ± 14		BALOSHIN	95	SPEC	40 π^-C $\to K^0_SK^0_S$X
1750 ± 15		[16] BUGG	95	MRK3	$J/\psi \to \gamma\pi^+\pi^-\pi^+\pi^-$
1620 ± 16		[6] BUGG	95	MRK3	$J/\psi \to \gamma\pi^+\pi^-\pi^+\pi^-$
1748 ± 10		[5] ARMSTRONG	93C	E760	$\overline{p}p \to \pi^0\eta\eta \to 6\gamma$
~ 1750		BREAKSTONE	93	SFM	$pp \to pp\pi^+\pi^-\pi^+\pi^-$
1744 ± 15		[17] ALDE	92D	GAM2	38 $\pi^-p \to \eta\eta n$
1713 ± 10		[18] ARMSTRONG	89D	OMEG	300 $pp \to ppK^+K^-$
1706 ± 10		[18] ARMSTRONG	89D	OMEG	300 $pp \to ppK^0_SK^0_S$
1700 ± 15		[6] BOLONKIN	88	SPEC	40 $\pi^-p \to K^0_SK^0_Sn$
1720 ± 60		[1] BOLONKIN	88	SPEC	40 $\pi^-p \to K^0_SK^0_Sn$
1638 ± 10		[19] FALVARD	88	DM2	$J/\psi \to \phi K^+K^-, K^0_SK^0_S$
1690 ± 4		[20] FALVARD	88	DM2	$J/\psi \to \phi K^+K^-, K^0_SK^0_S$
1755 ± 8		[21] ALDE	86C	GAM2	38 $\pi^-p \to n2\eta$
1730 $^{+2}_{-10}$		[22] LONGACRE	86	RVUE	22 $\pi^-p \to n2K^0_S$
1650 ± 50		BURKE	82	MRK2	$J/\psi \to \gamma\rho$
1640 ± 50		[23,24] EDWARDS	82D	CBAL	$J/\psi \to \gamma 2\eta$
1730 ± 10 ± 20		[25] ETKIN	82C	MPS	23 $\pi^-p \to n2K^0_S$

[1] $J^P = 0^+$.
[2] T-matrix pole.
[3] Supersedes BARBERIS 99 and BARBERIS 99B.
[4] $J^P = 0^+$, supersedes by ARMSTRONG 89D.
[5] No J^{PC} determination.
[6] $J^P = 2^+$.
[7] Systematic errors not estimated.
[8] K-matrix pole, assuming $J^P = 0^+$, from combined analysis of $\pi^-p \to \pi^0\pi^0n$, $\pi^-p \to K\overline{K}n$, $\pi^+\pi^- \to \pi^+\pi^-$, $\overline{p}p \to \pi^0\pi^0\pi^0$, $\pi^0\eta\eta$, $\pi^0\pi^0\eta$, $\pi^+\pi^-\pi^0$, $K^+K^-\pi^0$, $K^0_SK^0_S\pi^0$, $K^+K^0_S\pi^-$ at rest, $\overline{p}n \to \pi^-\pi^-\pi^+$, $K^0_SK^-\pi^0$, $K^0_SK^0_S\pi^-$ at rest.
[9] Decaying to $f_0(1370)\pi\pi$.
[10] Spin 2 dominant, isospin not determined, could also be I=1.
[11] $J^P = 0^+$.
[12] Not seen by AMSLER 02.
[13] T-matrix pole, assuming $J^P = 0^+$
[14] No J^{PC} determination.
[15] No J^{PC} determination, width not determined.
[16] From a fit to the 0^+ partial wave.
[17] ALDE 92D combines all the GAMS-2000 data.
[18] $J^P = 2^+$, superseded by FRENCH 99.
[19] From an analysis ignoring interference with $f'_2(1525)$.
[20] From an analysis including interference with $f'_2(1525)$.
[21] Superseded by ALDE 92D.
[22] Uses MRK3 data. From a partial-wave analysis of data using a K-matrix formalism with 5 poles, but assuming spin 2. Fit with constrained inelasticity.
[23] $J^P = 2^+$ preferred.
[24] From fit neglecting nearby $f'_2(1525)$. Replaced by BLOOM 83.
[25] Superseded by LONGACRE 86.

$f_0(1710)$ WIDTH

VALUE (MeV)	CL%	EVTS	DOCUMENT ID		TECN	COMMENT
140 ± 10 OUR AVERAGE			Error includes scale factor of 1.2.			
166 $^{+5}_{-8}$ $^{+15}_{-10}$			[26] BAI	03G	BES	$J/\psi \to \gamma K\overline{K}$
120 $^{+50}_{-40}$			[26] BAI	00A	BES	$J/\psi \to \gamma(\pi^+\pi^-\pi^+\pi^-)$
120 ± 26			[27] BARBERIS	00E		450 $pp \to p_f\eta\eta p_s$
126 ± 16 ± 18			[28] BARBERIS	99D	OMEG	450 $pp \to K^+K^-, \pi^+\pi^-$
105 ± 34			[29] FRENCH	99		300 $pp \to p_f(K^+K^-)p_s$
166.4 ± 33.2			[30] AUGUSTIN	88	DM2	$J/\psi \to \gamma K^+K^-, K^0_SK^0_S$
136 ± 28			[30] AUGUSTIN	87	DM2	$J/\psi \to \gamma\pi^+\pi^-$
130 ± 20			[31] BALTRUSAIT...87		MRK3	$J/\psi \to \gamma K^+K^-$
57 ± 38			[5] WILLIAMS	84	MPSF	200 $\pi^-N \to 2K^0_S$X
160 ± 80			BLOOM	83	CBAL	$J/\psi \to \gamma 2\eta$
• • • We do not use the following data for averages, fits, limits, etc. • • •						
38 $^{+20}_{-14}$		74	[32] CHEKANOV	04	ZEUS	$ep \to K^0_SK^0_SX$
144 ± 30			[33,34] ANISOVICH	03	RVUE	
320 $^{+50}_{-20}$			[34,35] ANISOVICH	03	RVUE	
102 ± 26			TIKHOMIROV	03	SPEC	40.0 π^-C $\to K^0_SK^0_SK^0_L$X
267 ± 44		3651	[26,36] NICHITIU	02	OBLX	
187 ± 60		221	[37] ACCIARRI	01H	L3	$\gamma\gamma \to K^0_SK^0_S$, E^{ee}_{cm}= 91, 183–209 GeV
220 ± 40			[38,39] ANISOVICH	99B	SPEC	0.6–1.2 $p\overline{p} \to \eta\eta\pi^0$
100 ± 25			[26] BARBERIS	99	OMEG	450 $pp \to p_sp_fK^+K^-$
160 ± 30			[26] BARBERIS	99B	OMEG	450 $pp \to p_sp_f\pi^+\pi^-$
250 ± 140			[40] ANISOVICH	98B	RVUE	Compilation
30 ± 7		57	[41] BARKOV	98		$\pi^-p \to K^0_SK^0_Sn$
103 ± 18 $^{+30}_{-11}$			[31] BAI	96C	BES	$J/\psi \to \gamma K^+K^-$
85 ± 24 $^{+22}_{-19}$			[26] BAI	96C	BES	$J/\psi \to \gamma K^+K^-$
56 ± 19			BALOSHIN	95	SPEC	40 π^-C $\to K^0_SK^0_S$X
160 ± 40			[42] BUGG	95	MRK3	$J/\psi \to \gamma\pi^+\pi^-\pi^+\pi^-$
160 $^{+60}_{-20}$			[31] BUGG	95	MRK3	$J/\psi \to \gamma\pi^+\pi^-\pi^+\pi^-$

264	± 25		[30] ARMSTRONG	93C	E760	$\overline{p}p \to \pi^0\eta\eta \to 6\gamma$
200	to 300		BREAKSTONE	93	SFM	$pp \to pp\pi^+\pi^-\pi^+\pi^-$
< 80		90	[43] ALDE	92D	GAM2	$38\ \pi^- p \to \eta\eta N^*$
181	± 30		[44] ARMSTRONG	89D	OMEG	$300\ pp \to pp K^+K^-$
104	± 30		[44] ARMSTRONG	89D	OMEG	$300\ pp \to pp K^0_S K^0_S$
30	± 20		[31] BOLONKIN	88	SPEC	$40\ \pi^- p \to K^0_S K^0_S n$
350	±150		[26] BOLONKIN	88	SPEC	$40\ \pi^- p \to K^0_S K^0_S n$
148	± 17		[45] FALVARD	88	DM2	$J/\psi \to \phi K^+K^-$, $K^0_S K^0_S$
184	± 6		[46] FALVARD	88	DM2	$J/\psi \to \phi K^+K^-$, $K^0_S K^0_S$
122	$^{+\ 74}_{-\ 15}$		[47] LONGACRE	86	RVUE	$22\ \pi^- p \to n2K^0_S$
200	±100		BURKE	82	MRK2	$J/\psi \to \gamma 2\rho$
220	$^{+100}_{-\ 70}$		[48,49] EDWARDS	82D	CBAL	$J/\psi \to \gamma 2\eta$
200.0	$^{+156.0}_{-\ 9.0}$		[50] ETKIN	82B	MPS	$23\ \pi^- p \to n2K^0_S$

[26] $J^P = 0^+$.
[27] T-matrix pole.
[28] Supersedes BARBERIS 99 and BARBERIS 99B.
[29] $J^P = 0^+$, supersedes by ARMSTRONG 89D.
[30] No J^{PC} determination.
[31] $J^P = 2^+$.
[32] Systematic errors not estimated.
[33] (Solution I)
[34] K-matrix pole, assuming $J^P = 0^+$, from combined analysis of $\pi^- p \to \pi^0\pi^0 n$, $\pi^- p \to K\overline{K}n$, $\pi^+\pi^- \to \pi^+\pi^-$, $\overline{p}p \to \pi^0\pi^0\pi^0$, $\pi^0\eta\eta$, $\pi^0\pi^0\eta$, $\pi^+\pi^-\pi^0$, $K^+K^-\pi^0$, $K^0_S K^0_S\pi^0$, $K^+K^0_S\pi^-$ at rest, $\overline{p}n \to \pi^-\pi^-\pi^+$, $K^0_S K^-\pi^0$, $K^0_S K^0_S\pi^-$ at rest.
[35] (Solution I)
[36] Decaying to $f_0(1370)\pi\pi$.
[37] Spin 2 dominant, isospin not determined, could also be I=1.
[38] $J^P = 0^+$.
[39] Not seen by AMSLER 02.
[40] T-matrix pole, assuming $J^P = 0^+$
[41] No J^{PC} determination.
[42] From a fit to the 0^+ partial wave.
[43] ALDE 92D combines all the GAMS-2000 data.
[44] $J^P = 2^+$, (0^+ excluded).
[45] From an analysis ignoring interference with $f'_2(1525)$.
[46] From an analysis including interference with $f'_2(1525)$.
[47] Uses MRK3 data. From a partial-wave analysis of data using a K-matrix formalism with 5 poles, but assuming spin 2. Fit with constrained inelasticity.
[48] $J^P = 2^+$ preferred.
[49] From fit neglecting nearby $f'_2(1525)$. Replaced by BLOOM 83.
[50] From an amplitude analysis of the $K^0_S K^0_S$ system, superseded by LONGACRE 86.

$f_0(1710)$ DECAY MODES

	Mode	Fraction (Γ_i/Γ)
Γ_1	$K\overline{K}$	seen
Γ_2	$\eta\eta$	seen
Γ_3	$\pi\pi$	seen
Γ_4	$\gamma\gamma$	

$f_0(1710)$ Γ(i)$\Gamma(\gamma\gamma)/\Gamma$(total)

$\Gamma(K\overline{K}) \times \Gamma(\gamma\gamma)/\Gamma_{\text{total}}$ $\quad \Gamma_1\Gamma_4/\Gamma$

VALUE (eV)	CL%	DOCUMENT ID		TECN	COMMENT
<110	95	[52] BEHREND	89C	CELL	$\gamma\gamma \to K^0_S K^0_S$
• • • We do not use the following data for averages, fits, limits, etc. • • •					
49 ± 11 ± 13		[53] ACCIARRI	01H	L3	$\gamma\gamma \to K^0_S K^0_S$, E^{ee}_{cm}= 91, 183–209 GeV
<480	95	ALBRECHT	90G	ARG	$\gamma\gamma \to K^+K^-$
<280	95	[52] ALTHOFF	85B	TASS	$\gamma\gamma \to K\overline{K}\pi$

$\Gamma(\pi\pi) \times \Gamma(\gamma\gamma)/\Gamma_{\text{total}}$ $\quad \Gamma_3\Gamma_4/\Gamma$

VALUE (keV)	CL%	DOCUMENT ID		TECN	COMMENT
<0.82	95	[51] BARATE	00E	ALEP	$\gamma\gamma \to \pi^+\pi^-$

[51] Assuming spin 0.
[52] Assuming helicity 2.
[53] Spin 2 dominant, isospin not determined, could also be I=1.

$f_0(1710)$ BRANCHING RATIOS

$\Gamma(K\overline{K})/\Gamma_{\text{total}}$ $\quad \Gamma_1/\Gamma$

VALUE	DOCUMENT ID		TECN	COMMENT
• • • We do not use the following data for averages, fits, limits, etc. • • •				
$0.38^{+0.09}_{-0.19}$	[54,55] LONGACRE	86	MPS	$22\ \pi^- p \to n2K^0_S$

$\Gamma(\eta\eta)/\Gamma_{\text{total}}$ $\quad \Gamma_2/\Gamma$

VALUE	DOCUMENT ID		TECN
• • • We do not use the following data for averages, fits, limits, etc. • • •			
$0.18^{+0.03}_{-0.13}$	[54,55] LONGACRE	86	RVUE

$\Gamma(\pi\pi)/\Gamma_{\text{total}}$ $\quad \Gamma_3/\Gamma$

VALUE	DOCUMENT ID		TECN	COMMENT
• • • We do not use the following data for averages, fits, limits, etc. • • •				
not seen	AMSLER	02	CBAR	$0.9\ \overline{p}p \to \pi^0\eta\eta$, $\pi^0\pi^0\pi^0$
$0.039^{+0.002}_{-0.024}$	[54,55] LONGACRE	86	RVUE	

$\Gamma(\pi\pi)/\Gamma(K\overline{K})$ $\quad \Gamma_3/\Gamma_1$

VALUE	DOCUMENT ID		TECN	COMMENT
0.2 ±0.024±0.036	BARBERIS	99D	OMEG	$450\ pp \to K^+K^-$, $\pi^+\pi^-$
• • • We do not use the following data for averages, fits, limits, etc. • • •				
$5.8\ ^{+9.1}_{-5.5}$	[56] ANISOVICH	02D	SPEC	Combined fit
0.39 ± 0.14	ARMSTRONG	91	OMEG	$300\ pp \to pp\pi\pi$, $pp K\overline{K}$

$\Gamma(\eta\eta)/\Gamma(K\overline{K})$ $\quad \Gamma_2/\Gamma_1$

VALUE	CL%	DOCUMENT ID		TECN	COMMENT
0.48 ± 0.15		BARBERIS	00E		$450\ pp \to p_f\eta\eta p_s$
• • • We do not use the following data for averages, fits, limits, etc. • • •					
$0.46^{+0.70}_{-0.38}$		[56] ANISOVICH	02D	SPEC	Combined fit
<0.02	90	[57] PROKOSHKIN	91	GA24	$300\ \pi^- p \to \pi^- p\eta\eta$

[54] From a partial-wave analysis of data using a K-matrix formalism with 5 poles, but assuming spin 2.
[55] Fit with constrained inelasticity.
[56] From a combined K-matrix analysis of Crystal Barrel (0. $p\overline{p} \to \pi^0\pi^0\pi^0$, $\pi^0\eta\eta$, $\pi^0\pi^0\eta$), GAMS ($\pi p \to \pi^0\pi^0 n$, $\eta\eta n$, $\eta\eta' n$), and BNL ($\pi p \to K\overline{K}n$) data.
[57] Combining results of GAM4 with those of ARMSTRONG 89D.

$f_0(1710)$ REFERENCES

CHEKANOV	04	PL B578 33	S. Chekanov *et al.*	(ZEUS Collab.)
ANISOVICH	03	EPJ A16 229	V.V. Anisovich *et al.*	
BAI	03G	PR D68 052003	J.Z. Bai *et al.*	(BES Collab.)
TIKHOMIROV	03	PAN 66 828 Translated from YAF 66 860.	G.D. Tikhomirov *et al.*	
AMSLER	02	EPJ C23 29	C. Amsler *et al.*	
ANISOVICH	02D	PAN 65 1545 Translated from YAF 65 1583.	V.V. Anisovich *et al.*	
NICHITIU	02	PL B545 261	F. Nichitiu *et al.*	(OBELIX Collab.)
ACCIARRI	01H	PL B501 173	M. Acciarri *et al.*	(L3 Collab.)
BAI	00A	PL B472 207	J.Z. Bai *et al.*	(BES Collab.)
BARATE	00E	PL B472 189	R. Barate *et al.*	(ALEPH Collab.)
BARBERIS	00E	PL B479 59	D. Barberis *et al.*	(WA 102 Collab.)
ANISOVICH	99B	PL B449 154	A.V. Anisovich *et al.*	
BARBERIS	99	PL B453 305	D. Barberis *et al.*	(Omega Expt.)
BARBERIS	99B	PL B453 316	D. Barberis *et al.*	(Omega Expt.)
BARBERIS	99D	PL B462 462	D. Barberis *et al.*	(Omega Expt.)
FRENCH	99	PL B460 213	B. French *et al.*	(WA76 Collab.)
ANISOVICH	98B	UFN 41 419	V.V. Anisovich *et al.*	
BAI	98H	PRL 81 1179	J.Z. Bai *et al.*	(BES Collab.)
BARKOV	98	JEPTL 68 764	B.P. Barkov *et al.*	
ABREU	96C	PL B379 309	P. Abreu *et al.*	(DELPHI Collab.)
BAI	96C	PRL 77 3959	J.Z. Bai *et al.*	(BES Collab.)
BALOSHIN	95	PAN 58 46 Translated from YAF 58 50.	O.N. Baloshin *et al.*	(ITEP)
BUGG	95	PL B353 378	D.V. Bugg *et al.*	(LOQM, PNPI, WASH)
ARMSTRONG	93C	PL B307 394	T.A. Armstrong *et al.*	(FNAL, FERR, GENO+)
BREAKSTONE	93	ZPHY C58 251	A.M. Breakstone *et al.*	(IOWA, CERN, DORT+)
ALDE	92D	PL B284 457	D.M. Alde *et al.*	(GAM2 Collab.)
Also	91	SJNP 54 451 Translated from YAF 54 745.	D.M. Alde *et al.*	(GAM2 Collab.)
ARMSTRONG	91	ZPHY C51 351	T.A. Armstrong *et al.*	(ATHU, BARI, BIRM+)
PROKOSHKIN	91	SPD 36 155 Translated from DANS 316 900.	Y.D. Prokoshkin	(GAM2, GAM4 Collab.)
ALBRECHT	90G	ZPHY C48 183	H. Albrecht *et al.*	(ARGUS Collab.)
ARMSTRONG	89D	PL B227 186	T.A. Armstrong, M. Benayoun	(ATHU, BARI, BIRM+)
BEHREND	89C	ZPHY C43 91	H.J. Behrend *et al.*	(CELLO Collab.)
AUGUSTIN	88	PRL 60 2238	J.E. Augustin *et al.*	(DM2 Collab.)
BOLONKIN	88	NP B309 426	B.V. Bolonkin *et al.*	(ITEP, SERP)
FALVARD	88	PR D38 2706	A. Falvard *et al.*	(CLER, FRAS, LALO+)
AUGUSTIN	87	ZPHY C36 369	J.E. Augustin *et al.*	(LALO, CLER, FRAS+)
BALTRUSAIT...	87	PR D35 2077	R.M. Baltrusaitis *et al.*	(Mark III Collab.)
ALDE	86C	PL B182 105	D.M. Alde *et al.*	(SERP, BELG, LANL, LAPP)
LONGACRE	86	PL B177 223	R.S. Longacre *et al.*	(BNL, BRAN, CUNY+)
ALTHOFF	85B	ZPHY C29 189	M. Althoff *et al.*	(TASSO Collab.)
WILLIAMS	84	PR D30 877	E.G.H. Williams *et al.*	(VAND, NDAM, TUFTS+)
BLOOM	83	ARNS 33 143	E.D. Bloom, C. Peck	(SLAC, CIT)
BURKE	82	PRL 49 632	D.L. Burke *et al.*	(LBL, SLAC)
EDWARDS	82D	PRL 48 458	C. Edwards *et al.*	(CIT, HARV, PRIN+)
ETKIN	82B	PR D25 1786	A. Etkin *et al.*	(BNL, CUNY, TUFTS, VAND)
ETKIN	82C	PR D25 2446	A. Etkin *et al.*	(BNL, CUNY, TUFTS, VAND)

OTHER RELATED PAPERS

ANISOVICH	03B	PAN 66 741 Translated from YAF 66 772.	V.V. Anisovich, V.A. Nikonov, A.V. Sarantsev	
AMSLER	02B	PL B541 22	C. Amsler	
JIN	02	PR D66 057505	H. Jin, X. Zhang	
KLEEFELD	02	PR D66 034007	F. Kleefeld, E. van Beveren, G. Rupp	
RUPP	02	PR D65 078501	G. Rupp, E. vanBeveren, M.D. Scadron	
SHAKIN	02	PR D65 078502	C.M. Shakin, H. Wang	
TESHIMA	02	JPG 28 1391	T. Teshima, I. Kitamura, N. Morisita	
VOLKOV	02	PAN 65 1657 Translated from YAF 65 1701.	M.K. Volkov, V.L. Yudichev	

LI	01B	EPJ C19 529	D.-M. Li, H. Yu, Q.-X. Shen	
VOLKOV	01	PAN 64 2006	M.K. Volkov, V.L. Yudichev	
		Translated from YAF 64 2091.		
ANISOVICH	99H	PL B467 289	A.V. Anisovich, V.V. Anisovich	
GRYGOREV	99	PAN 62 470	V.K. Grygorev *et al.*	
		Translated from YAF 62 513.		
PROKOSHKIN	99	PAN 62 356	Yu.D. Prokoshkin	
		Translated from YAF 62 396.		
ANISOVICH	97	PL B395 123	A.V. Anisovich, A.V. Sarantsev	(PNPI)
LINDENBAUM	92	PL B274 492	S.J. Lindenbaum, R.S. Longacre	(BNL)
BISELLO	89B	PR D39 701	G. Busetto *et al.*	(DM2 Collab.)
ASTON	88D	NP B301 525	D. Aston *et al.*	(SLAC, NAGO, CINC, INUS)
AKESSON	86	NP B264 154	T. Akesson *et al.*	(Axial Field Spec. Collab.)
ARMSTRONG	86B	PL 167B 133	T.A. Armstrong *et al.*	(ATHU, BARI, BIRM+)
BALTRUSAIT...	86B	PR D33 1222	R.M. Baltrusaitis *et al.*	(Mark III Collab.)
ALTHOFF	83	PL 121B 216	M. Althoff *et al.*	(TASSO Collab.)
BARNETT	83B	PL 120B 455	B. Barnett *et al.*	(JHU)
BARNES	82B	NP B198 380	T. Barnes, F.E. Close, S. Monaghan	(RHEL, OXFTP)
TANIMOTO	82	PL 116B 198	M. Tanimoto	(BIEL)

$\eta(1760)$

$I^G(J^{PC}) = 0^+(0^{-+})$

OMITTED FROM SUMMARY TABLE

Seen by DM2 in the $\rho\rho$ system (BISELLO 89B). Structure in this region has been reported before in the same system (BALTRUSAITIS 86B) and in the $\omega\omega$ system (BALTRUSAITIS 85C, BISELLO 87). Needs confirmation.

$\eta(1760)$ MASS

VALUE (MeV)	*EVTS*	*DOCUMENT ID*		*TECN*	*COMMENT*
1760±11	320	[1] BISELLO	89B	DM2	$J/\psi \to 4\pi\gamma$

[1] Estimated by us from various fits.

$\eta(1760)$ WIDTH

VALUE (MeV)	*EVTS*	*DOCUMENT ID*		*TECN*	*COMMENT*
60±16	320	[2] BISELLO	89B	DM2	$J/\psi \to 4\pi\gamma$

[2] Estimated by us from various fits.

$\eta(1760)$ REFERENCES

BISELLO	89B	PR D39 701	G. Busetto *et al.*	(DM2 Collab.)
BISELLO	87	PL B192 239	D. Bisello *et al.*	(PADO, CLER, FRAS+)
BALTRUSAIT...	86B	PR D33 1222	R.M. Baltrusaitis *et al.*	(Mark III Collab.)
BALTRUSAIT...	85C	PRL 55 1723	R.M. Baltrusaitis *et al.*	(CIT, UCSC+)

OTHER RELATED PAPERS

BAI	99	PL B446 356	J.Z. Bai *et al.*	(BES Collab.)

$\pi(1800)$

$I^G(J^{PC}) = 1^-(0^{-+})$

See also minireview under non-$q\overline{q}$ candidates. (See the index for the page number.)

$\pi(1800)$ MASS

VALUE (MeV)	*EVTS*	*DOCUMENT ID*		*TECN*	*CHG*	*COMMENT*
1812±14 OUR AVERAGE Error includes scale factor of 2.3. See the ideogram below.						
1774±18±20		[1] CHUNG	02	MPS		18.3 $\pi^- p \to \pi^+\pi^-\pi^- p$
1863± 9±10		[2] CHUNG	02	MPS		18.3 $\pi^- p \to \pi^+\pi^-\pi^- p$
1840±10±10	1200	AMELIN	96B	VES	–	37 $\pi^- A \to \eta\eta\pi^- A$
1775± 7±10		[3] AMELIN	95B	VES	–	36 $\pi^- A \to \pi^+\pi^-\pi^- A$
1790±14		[4] BERDNIKOV	94	VES	–	37 $\pi^- A \to K^+K^-\pi^- A$
1873±33±20		BELADIDZE	92C	VES	–	36 π^-Be $\to \pi^-\eta'\eta$Be
1814±10±23	426± 57	BITYUKOV	91	VES	–	36 π^-C $\to \pi^-\eta\eta$C
1770±30	1100	BELLINI	82	SPEC	–	40 π^-A $\to 3\pi$A
• • • We do not use the following data for averages, fits, limits, etc. • • •						
1737± 5±15		AMELIN	99	VES		37 $\pi^- A \to \omega\pi^-\pi^0 A^*$

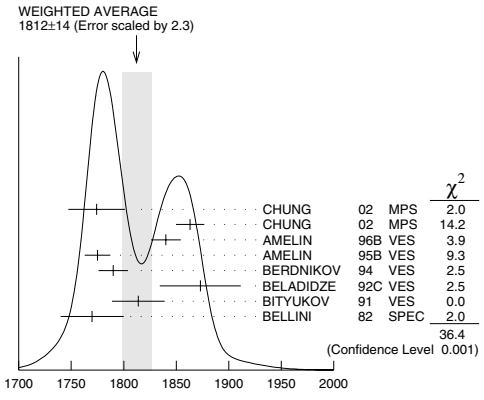

[1] In the $f_0(980)\pi$ wave.
[2] In the $f_0(600)\pi$ wave.
[3] From a fit to $J^{PC} = 0^{-+}$ $f_0(980)\pi$, $f_0(1370)\pi$ waves.
[4] From a fit to $J^{PC} = 0^{-+}$ $K_0^*(1430)K^-$ and $f_0(980)\pi^-$ waves.

$\pi(1800)$ WIDTH

VALUE (MeV)	*EVTS*	*DOCUMENT ID*		*TECN*	*CHG*	*COMMENT*
207±13 OUR AVERAGE						
223±48±50		[7] CHUNG	02	MPS		18.3 $\pi^- p \to \pi^+\pi^-\pi^- p$
191±21±20		[8] CHUNG	02	MPS		18.3 $\pi^- p \to \pi^+\pi^-\pi^- p$
210±30±30	1200	AMELIN	96B	VES	–	37 $\pi^- A \to \eta\eta\pi^- A$
190±15±15		[5] AMELIN	95B	VES	–	36 $\pi^- A \to \pi^+\pi^-\pi^- A$
210±70		[6] BERDNIKOV	94	VES	–	37 $\pi^- A \to K^+K^-\pi^- A$
225±35±20		BELADIDZE	92C	VES	–	36 π^-Be $\to \pi^-\eta'\eta$Be
205±18±32	426± 57	BITYUKOV	91	VES	–	36 π^-C $\to \pi^-\eta\eta$C
310±50	1100	BELLINI	82	SPEC	–	40 π^-A $\to 3\pi$A
• • • We do not use the following data for averages, fits, limits, etc. • • •						
259±19± 6		AMELIN	99	VES		37 $\pi^- A \to \omega\pi^-\pi^0 A^*$

[5] From a fit to $J^{PC} = 0^{-+}$ $f_0(980)\pi$, $f_0(1370)\pi$ waves.
[6] From a fit to $J^{PC} = 0^{-+}$ $K_0^*(1430)K^-$ and $f_0(980)\pi^-$ waves.
[7] In the $f_0(980)\pi$ wave.
[8] In the $f_0(600)\pi$ wave.

$\pi(1800)$ DECAY MODES

	Mode	Fraction (Γ_i/Γ)
Γ_1	$\pi^+\pi^-\pi^-$	seen
Γ_2	$f_0(600)\pi^-$	seen
Γ_3	$f_0(980)\pi^-$	seen
Γ_4	$f_0(1370)\pi^-$	seen
Γ_5	$f_0(1500)\pi^-$	not seen
Γ_6	$\rho\pi^-$	not seen
Γ_7	$\eta\eta\pi^-$	seen
Γ_8	$a_0(980)\eta$	seen
Γ_9	$f_0(1500)\pi^-$	seen
Γ_{10}	$\eta\eta'(958)\pi^-$	seen
Γ_{11}	$K_0^*(1430)K^-$	seen
Γ_{12}	$K^*(892)K^-$	not seen

$\pi(1800)$ BRANCHING RATIOS

$\Gamma(f_0(980)\pi^-)/\Gamma(f_0(600)\pi^-)$ Γ_3/Γ_2

VALUE	*DOCUMENT ID*		*TECN*	*COMMENT*
0.44±0.08±0.38	[10] CHUNG	02	MPS	18.3 $\pi^- p \to \pi^+\pi^-\pi^- p$

$\Gamma(f_0(980)\pi^-)/\Gamma(f_0(1370)\pi^-)$ Γ_3/Γ_4

VALUE	*DOCUMENT ID*		*TECN*	*CHG*	*COMMENT*
1.7±1.3	AMELIN	95B	VES	–	36 $\pi^- A \to \pi^+\pi^-\pi^- A$

Meson Particle Listings

$\pi(1800)$, $f_2(1810)$

$\Gamma(f_0(1370)\pi^-)/\Gamma_{total}$ Γ_4/Γ

VALUE	DOCUMENT ID		TECN	CHG	COMMENT
seen	BELLINI	82	SPEC	–	$40\ \pi^- A \rightarrow 3\pi A$

$\Gamma(f_0(1500)\pi^-)/\Gamma_{total}$ Γ_5/Γ

VALUE	DOCUMENT ID		TECN	COMMENT
• • • We do not use the following data for averages, fits, limits, etc. • • •				
not seen	CHUNG	02	MPS	$18.3\ \pi^- p \rightarrow \pi^+\pi^-\pi^- p$

$\Gamma(\eta\eta\pi^-)/\Gamma(\pi^+\pi^-\pi^-)$ Γ_7/Γ_1

VALUE	EVTS	DOCUMENT ID		TECN	CHG	COMMENT
0.5 ±0.1	1200	AMELIN	96B	VES	–	$37\ \pi^- A \rightarrow \eta\eta\pi^- A$

$\Gamma(f_0(1500)\pi^-)/\Gamma(a_0(980)\eta)$ Γ_9/Γ_8

VALUE	EVTS	DOCUMENT ID		TECN	CHG	COMMENT
0.08 ±0.03	1200	[9] AMELIN	96B	VES	–	$37\ \pi^- A \rightarrow \eta\eta\pi^- A$

[9] Assuming that $f_0(1500)$ decays only to $\eta\eta$ and $a_0(980)$ decays only to $\eta\pi$.

$\Gamma(\eta\eta'(958)\pi^-)/\Gamma(\eta\eta\pi^-)$ Γ_{10}/Γ_7

VALUE	EVTS	DOCUMENT ID		TECN	CHG	COMMENT
0.29±0.06 OUR AVERAGE						
0.29±0.07		BELADIDZE	92C	VES	–	$36\ \pi^-$Be $\rightarrow \pi^-\eta'\eta$Be
0.3 ±0.1	426± 57	BITYUKOV	91	VES	–	$36\ \pi^- C \rightarrow \pi^-\eta\eta C$

$\Gamma(K_0^*(1430)K^-)/\Gamma_{total}$ Γ_{11}/Γ

VALUE	DOCUMENT ID		TECN	CHG	COMMENT
seen	BERDNIKOV	94	VES	–	$37\ \pi^- A \rightarrow K^+K^-\pi^- A$

$\Gamma(K^*(892)K^-)/\Gamma_{total}$ Γ_{12}/Γ

VALUE	DOCUMENT ID		TECN	CHG	COMMENT
• • • We do not use the following data for averages, fits, limits, etc. • • •					
not seen	BERDNIKOV	94	VES	–	$37\ \pi^- A \rightarrow K^+K^-\pi^- A$

$\Gamma(\rho\pi^-)/\Gamma(f_0(980)\pi^-)$ Γ_6/Γ_3

VALUE	CL%	DOCUMENT ID		TECN	CHG	COMMENT
• • • We do not use the following data for averages, fits, limits, etc. • • •						
<0.25		CHUNG	02	MPS		$18.3\ \pi^- p \rightarrow \pi^+\pi^-\pi^- p$
<0.14	90	AMELIN	95B	VES	–	$36\ \pi^- A \rightarrow \pi^+\pi^-\pi^- A$

$\Gamma(\rho\pi^-)/\Gamma_{total}$ Γ_6/Γ

VALUE	DOCUMENT ID		TECN	CHG	COMMENT
not seen	BELLINI	82	SPEC	–	$40\ \pi^- A \rightarrow 3\pi A$

[10] Assuming that $f_0(980)$ decays only to $\pi\pi$.

$\pi(1800)$ REFERENCES

CHUNG	02	PR D65 072001	S.U. Chung *et al.*	
AMELIN	99	PAN 62 445 Translated from YAF 62 487.	D.V. Amelin *et al.*	(VES Collab.)
AMELIN	96B	PAN 59 976 Translated from YAF 59 1021.	D.V. Amelin *et al.*	(SERP, TBIL) IGJPC
AMELIN	95B	PL B356 595	D.V. Amelin *et al.*	(SERP, TBIL)
BERDNIKOV	94	PL B337 219	E.B. Berdnikov *et al.*	(SERP, TBIL)
BELADIDZE	92C	SJNP 55 1535 Translated from YAF 55 2748.	G.M. Beladidze, S.I. Bityukov, G.V. Borisov	(SERP+)
BITYUKOV	91	PL B268 137	S.I. Bityukov *et al.*	(SERP, TBIL)
BELLINI	82	PRL 48 1697	G. Bellini *et al.*	(MILA, BGNA, JINR)

OTHER RELATED PAPERS

ZAIMIDOROGA	99	PAN 30 1 Translated from SJPN 30 5.	O.A. Zaimidoroga	
BORISOV	92	SJNP 55 1441 Translated from YAF 55 2583.	G.V. Borisov, S.S. Gershtein, A.M. Zaitsev	(SERP)

$f_2(1810)$ $I^G(J^{PC}) = 0^+(2^{++})$

OMITTED FROM SUMMARY TABLE

Needs confirmation.

$f_2(1810)$ MASS

VALUE (MeV)	EVTS	DOCUMENT ID		TECN	COMMENT
1815±12 OUR AVERAGE Error includes scale factor of 1.4. See the ideogram below.					
1800 ± 30	40	ALDE	88D	GAM4	$300\ \pi^- p \rightarrow \pi^- p 4\pi^0$
1806 ± 10	1600	ALDE	87	GAM4	$100\ \pi^- p \rightarrow 4\pi^0 n$
1870 ± 40		[1] ALDE	86D	GAM4	$100\ \pi^- p \rightarrow \eta\eta n$
1857^{+35}_{-24}		[2] COSTA...	80	OMEG	$10\ \pi^- p \rightarrow K^+K^- n$
• • • We do not use the following data for averages, fits, limits, etc. • • •					
1858^{+18}_{-71}		[3] LONGACRE	86	RVUE	Compilation
1799 ± 15		[4] CASON	82	STRC	$8\ \pi^+ p \rightarrow \Delta^{++}\pi^0\pi^0$

[1] Seen in only one solution.

[2] Error increased by spread of two solutions. Included in LONGACRE 86 global analysis.

[3] From a partial-wave analysis of data using a K-matrix formalism with 5 poles. Includes compilation of several other experiments.

[4] From an amplitude analysis of the reaction $\pi^+\pi^- \rightarrow 2\pi^0$. The resonance in the $2\pi^0$ final state is not confirmed by PROKOSHKIN 97.

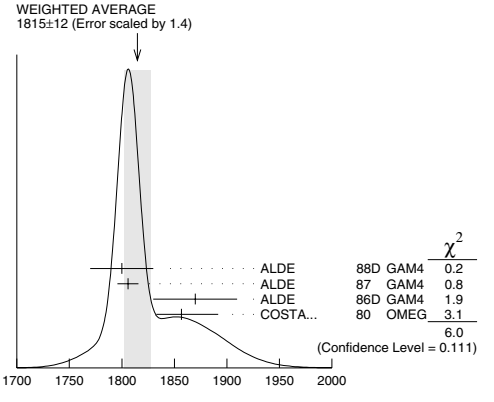

$f_2(1810)$ WIDTH

VALUE (MeV)	EVTS	DOCUMENT ID		TECN	COMMENT
197± 22 OUR AVERAGE Error includes scale factor of 1.5. See the ideogram below.					
160 ± 30	40	ALDE	88D	GAM4	$300\ \pi^- p \rightarrow \pi^- p 4\pi^0$
190 ± 20	1600	ALDE	87	GAM4	$100\ \pi^- p \rightarrow 4\pi^0 n$
250 ± 30		[5] ALDE	86D	GAM4	$100\ \pi^- p \rightarrow \eta\eta n$
185^{+102}_{-139}		[6] COSTA...	80	OMEG	$10\ \pi^- p \rightarrow K^+K^- n$
• • • We do not use the following data for averages, fits, limits, etc. • • •					
388^{+15}_{-21}		[7] LONGACRE	86	RVUE	Compilation
280^{+42}_{-35}		[8] CASON	82	STRC	$8\ \pi^+ p \rightarrow \Delta^{++}\pi^0\pi^0$

[5] Seen in only one solution.

[6] Error increased by spread of two solutions. Included in LONGACRE 86 global analysis.

[7] From a partial-wave analysis of data using a K-matrix formalism with 5 poles. Includes compilation of several other experiments.

[8] From an amplitude analysis of the reaction $\pi^+\pi^- \rightarrow 2\pi^0$. The resonance in the $2\pi^0$ final state is not confirmed by PROKOSHKIN 97.

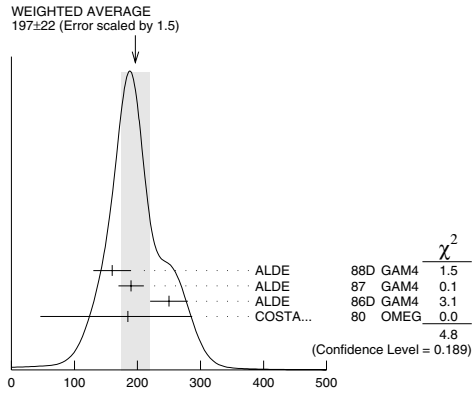

$f_2(1810)$ width (MeV)

$f_2(1810)$ DECAY MODES

	Mode	Fraction (Γ_i/Γ)
Γ_1	$\pi\pi$	
Γ_2	$\eta\eta$	
Γ_3	$4\pi^0$	seen
Γ_4	K^+K^-	

$f_2(1810)$ BRANCHING RATIOS

$\Gamma(\pi\pi)/\Gamma_{total}$ Γ_1/Γ

VALUE	DOCUMENT ID		TECN	COMMENT
• • • We do not use the following data for averages, fits, limits, etc. • • •				
not seen	AMSLER	02	CBAR	0.9 $\overline{p}p \to \pi^0\eta\eta$, $\pi^0\pi^0\pi^0$
not seen	PROKOSHKIN	97	GAM2	38 $\pi^-p \to \pi^0\pi^0n$
$0.21^{+0.02}_{-0.03}$	[9] LONGACRE	86	RVUE	Compilation
0.44 ± 0.03	[10] CASON	82	STRC	8 $\pi^+p \to \Delta^{++}\pi^0\pi^0$

[9] From a partial-wave analysis of data using a K-matrix formalism with 5 poles. Includes compilation of several other experiments.
[10] Included in LONGACRE 86 global analysis.

$\Gamma(\eta\eta)/\Gamma_{total}$ Γ_2/Γ

VALUE	DOCUMENT ID		TECN	COMMENT
• • • We do not use the following data for averages, fits, limits, etc. • • •				
$0.008^{+0.028}_{-0.003}$	[9] LONGACRE	86	RVUE	Compilation

$\Gamma(\pi\pi)/\Gamma(4\pi^0)$ Γ_1/Γ_3

VALUE	DOCUMENT ID		TECN	COMMENT
• • • We do not use the following data for averages, fits, limits, etc. • • •				
<0.75	ALDE	87	GAM4	100 $\pi^-p \to 4\pi^0n$

$\Gamma(4\pi^0)/\Gamma(\eta\eta)$ Γ_3/Γ_2

VALUE	DOCUMENT ID		TECN	COMMENT
• • • We do not use the following data for averages, fits, limits, etc. • • •				
0.8 ± 0.3	ALDE	87	GAM4	100 $\pi^-p \to 4\pi^0n$

$\Gamma(K^+K^-)/\Gamma_{total}$ Γ_4/Γ

VALUE	DOCUMENT ID		TECN	COMMENT
• • • We do not use the following data for averages, fits, limits, etc. • • •				
$0.003^{+0.019}_{-0.002}$	[9] LONGACRE	86	RVUE	Compilation
seen	COSTA...	80	OMEG	10 $\pi^-p \to K^+K^-n$

$f_2(1810)$ REFERENCES

AMSLER	02	EPJ C23 29	C. Amsler *et al.*
PROKOSHKIN	97	SPD 42 117 Translated from DANS 353 323.	Y.D. Prokoshkin *et al.* (SERP)
ALDE	88D	SJNP 47 810 Translated from YAF 47 1273.	D.M. Alde *et al.* (SERP, BELG, LANL, LAPP+)
ALDE	87	PL B198 286	D.M. Alde *et al.* (LANL, BRUX, SERP, LAPP)
ALDE	86D	NP B269 485	D.M. Alde *et al.* (BELG, LAPP, SERP, CERN+)
LONGACRE	86	PL B177 223	R.S. Longacre *et al.* (BNL, BRAN, CUNY+)
CASON	82	PRL 48 1316	N.M. Cason *et al.* (NDAM, ANL)
COSTA...	80	NP B175 402	G. Costa de Beauregard *et al.* (BARI, BONN+)

OTHER RELATED PAPERS

AKER	91	PL B260 249	E. Aker *et al.* (Crystal Barrel Collab.)
CASON	83	PR D28 1586	N.M. Cason *et al.* (NDAM, ANL)
ETKIN	82B	PR D25 1786	A. Etkin *et al.* (BNL, CUNY, TUFTS, VAND)

$\phi_3(1850)$

$I^G(J^{PC}) = 0^-(3^{--})$

$\phi_3(1850)$ MASS

VALUE (MeV)	EVTS	DOCUMENT ID		TECN	COMMENT
1854 ± 7 OUR AVERAGE					
1855 ± 10		ASTON	88E	LASS	11 $K^-p \to K^-K^+\Lambda$, $K^0_S K^\pm\pi^\mp\Lambda$
1870^{+30}_{-20}	430	ARMSTRONG	82	OMEG	18.5 $K^-p \to K^-K^+\Lambda$
1850 ± 10	123	ALHARRAN	81B	HBC	8.25 $K^-p \to K\overline{K}\Lambda$

$\phi_3(1850)$ WIDTH

VALUE (MeV)	EVTS	DOCUMENT ID		TECN	COMMENT
87^{+28}_{-23} OUR AVERAGE Error includes scale factor of 1.2.					
64 ± 31		ASTON	88E	LASS	11 $K^-p \to K^-K^+\Lambda$, $K^0_S K^\pm\pi^\mp\Lambda$
160^{+90}_{-50}	430	ARMSTRONG	82	OMEG	18.5 $K^-p \to K^-K^+\Lambda$
80^{+40}_{-30}	123	ALHARRAN	81B	HBC	8.25 $K^-p \to K\overline{K}\Lambda$

$\phi_3(1850)$ DECAY MODES

	Mode	Fraction (Γ_i/Γ)
Γ_1	$K\overline{K}$	seen
Γ_2	$K\overline{K}^*(892)+$ c.c.	seen

$\phi_3(1850)$ BRANCHING RATIOS

$\Gamma(K\overline{K}^*(892)+\text{c.c.})/\Gamma(K\overline{K})$ Γ_2/Γ_1

VALUE	DOCUMENT ID		TECN	COMMENT
$0.55^{+0.85}_{-0.45}$	ASTON	88E	LASS	11 $K^-p \to K^-K^+\Lambda$, $K^0_S K^\pm\pi^\mp\Lambda$
• • • We do not use the following data for averages, fits, limits, etc. • • •				
0.8 ± 0.4	ALHARRAN	81B	HBC	8.25 $K^-p \to K\overline{K}\pi\Lambda$

$\phi_3(1850)$ REFERENCES

ASTON	88E	PL B208 324	D. Aston *et al.* (SLAC, NAGO, CINC, INUS) IGJPC
ARMSTRONG	82	PL 110B 77	T.A. Armstrong *et al.* (BARI, BIRM, CERN+) JP
ALHARRAN	81B	PL 101B 357	S. Al-Harran *et al.* (BIRM, CERN, GLAS+)

OTHER RELATED PAPERS

CORDIER	82B	PL 110B 335	A. Cordier *et al.* (LALO)
ASTON	80B	PL 92B 219	D. Aston (BONN, CERN, EPOL, GLAS, LANC+)

$\eta_2(1870)$

$I^G(J^{PC}) = 0^+(2^{-+})$

OMITTED FROM SUMMARY TABLE
Needs confirmation.

$\eta_2(1870)$ MASS

VALUE (MeV)	EVTS	DOCUMENT ID		TECN	CHG	COMMENT
1842 ± 8 OUR AVERAGE						
1835 ± 12		BARBERIS	00B			450 $pp \to p_f\eta\pi^+\pi^-p_s$
1844 ± 13		BARBERIS	00C			450 $pp \to p_f 4\pi p_s$
1840 ± 25		BARBERIS	97B	OMEG		450 $pp \to pp2(\pi^+\pi^-)$
$1875\pm20\pm35$		ADOMEIT	96	CBAR	0	1.94 $\overline{p}p \to \eta3\pi^0$
$1881\pm32\pm40$	26	KARCH	92	CBAL		$e^+e^- \to e^+e^-\eta\pi^0\pi^0$
• • • We do not use the following data for averages, fits, limits, etc. • • •						
$1860\pm5\pm15$		ANISOVICH	00E	SPEC		1.94 $\overline{p}p \to \eta3\pi^0$
1840 ± 15		BAI	99	BES		$J/\psi \to \gamma\eta\pi^+\pi^-$

$\eta_2(1870)$ WIDTH

VALUE (MeV)	EVTS	DOCUMENT ID		TECN	CHG	COMMENT
225 ± 14 OUR AVERAGE						
235 ± 22		BARBERIS	00B			450 $pp \to p_f \eta\pi^+\pi^- p_s$
228 ± 23		BARBERIS	00C			450 $pp \to p_f 4\pi p_s$
200 ± 40		BARBERIS	97B	OMEG		450 $pp \to pp2(\pi^+\pi^-)$
200 ± 25 ± 45		ADOMEIT	96	CBAR	0	1.94 $\overline{p}p \to \eta 3\pi^0$
221 ± 92 ± 44	26	KARCH	92	CBAL		$e^+e^- \to e^+e^-\eta\pi^0\pi^0$
• • • We do not use the following data for averages, fits, limits, etc. • • •						
$250 \pm 25^{+50}_{-35}$		ANISOVICH	00E	SPEC		1.94 $\overline{p}p \to \eta 3\pi^0$
170 ± 40		BAI	99	BES		$J/\psi \to \gamma\eta\pi^+\pi^-$

$\eta_2(1870)$ DECAY MODES

	Mode
Γ_1	$\eta\pi\pi$
Γ_2	$a_2(1320)\pi$
Γ_3	$f_2(1270)\eta$
Γ_4	$a_0(980)\pi$

$\eta_2(1870)$ BRANCHING RATIOS

$\Gamma(a_2(1320)\pi)/\Gamma(f_2(1270)\eta)$ Γ_2/Γ_3

VALUE	DOCUMENT ID		TECN	CHG	COMMENT
6 ± 5 OUR AVERAGE Error includes scale factor of 2.3.					
20.4 ± 6.6	BARBERIS	00B			450 $pp \to p_f \eta\pi^+\pi^- p_s$
4.1 ± 2.3	ADOMEIT	96	CBAR	0	1.94 $\overline{p}p \to \eta 3\pi^0$

$\Gamma(a_2(1320)\pi)/\Gamma(a_0(980)\pi)$ Γ_2/Γ_4

VALUE	DOCUMENT ID		COMMENT
32.6 ± 12.6	BARBERIS	00B	450 $pp \to p_f \eta\pi^+\pi^- p_s$

$\eta_2(1870)$ REFERENCES

ANISOVICH	00E	PL B477 19	A.V. Anisovich *et al.*	
BARBERIS	00B	PL B471 435	D. Barberis *et al.*	(WA 102 Collab.)
BARBERIS	00C	PL B471 440	D. Barberis *et al.*	(WA 102 Collab.)
BAI	99	PL B446 356	J.Z. Bai *et al.*	(BES Collab.)
BARBERIS	97B	PL B413 217	D. Barberis *et al.*	(WA 102 Collab.)
ADOMEIT	96	ZPHY C71 227	J. Adomeit *et al.*	(Crystal Barrel Collab.)
KARCH	92	ZPHY C54 33	K. Karch *et al.*	(Crystal Ball Collab.)

OTHER RELATED PAPERS

KARCH	90	PL B249 353	K. Karch *et al.*	(Crystal Ball Collab.)

$\rho(1900)$ $I^G(J^{PC}) = 1^+(1^{--})$

OMITTED FROM SUMMARY TABLE

See the mini-review under the $\rho(1700)$.

$\rho(1900)$ MASS

VALUE (MeV)	DOCUMENT ID		TECN	COMMENT
• • • We do not use the following data for averages, fits, limits, etc. • • •				
1910 ± 10	[1,2] FRABETTI	04	E687	$\gamma p \to 3\pi^+ 3\pi^- p$
1870 ± 10	ANTONELLI	96	SPEC	$e^+e^- \to$ hadrons

[1] From a fit with two resonances with the JACOB 72 continuum.
[2] Supersedes FRABETTI 01.

$\rho(1900)$ WIDTH

VALUE (MeV)	DOCUMENT ID		TECN	COMMENT
• • • We do not use the following data for averages, fits, limits, etc. • • •				
37 ± 13	[3,4] FRABETTI	04	E687	$\gamma p \to 3\pi^+ 3\pi^- p$
10 ± 5	ANTONELLI	96	SPEC	$e^+e^- \to$ hadrons

[3] From a fit with two resonances with the JACOB 72 continuum.
[4] Supersedes FRABETTI 01.

$\rho(1900)$ DECAY MODES

	Mode	Fraction (Γ_i/Γ)
Γ_1	6π	seen
Γ_2	$3\pi^+ 3\pi^-$	seen
Γ_3	hadrons	seen
Γ_4	e^+e^-	seen
Γ_5	$\overline{N}N$	not seen

$\rho(1900)$ BRANCHING RATIOS

$\Gamma(6\pi)/\Gamma_{total}$ Γ_1/Γ

VALUE	DOCUMENT ID		TECN	COMMENT
not seen	AGNELLO	02	OBLX	$\overline{n}p \to 3\pi^+ 2\pi^- \pi^0$
seen	FRABETTI	01	E687	$\gamma p \to 3\pi^+ 3\pi^- p$
seen	ANTONELLI	96	SPEC	$e^+e^- \to$ hadrons

$\rho(1900)$ REFERENCES

FRABETTI	04	PL B578 290	P.L. Frabetti *et al.*	(FNAL E687 Collab.)
AGNELLO	02	PL B527 39	M. Agnello *et al.*	(OBELIX Collab.)
FRABETTI	01	PL B514 240	P.L. Frabetti *et al.*	(FNAL E687 Collab.)
ANTONELLI	96	PL B365 427	A. Antonelli *et al.*	(FENICE Collab.)
JACOB	72	PR D5 1847	M. Jacob, R. Slansky	

OTHER RELATED PAPERS

DATTA	03B	PL B567 273	A. Datta, P.J. O'Donnel	
PAGE	99	PR D59 034016	P.R. Page, E.S. Swanson, A.P. Szczepaniak	
CLEGG	90	ZPHY C45 677	A.B. Clegg, A. Donnachie	(LANC, MCHS)
CASTRO	88	Preprint LAL-88-58	A. Castro *et al.*	(DM2 Collab.)

$f_2(1910)$ $I^G(J^{PC}) = 0^+(2^{++})$

OMITTED FROM SUMMARY TABLE

We list here two different peaks with close masses and widths seen in the mass distributions of $\omega\omega$ and $\eta\eta'$ final states. ALDE 91B argues that they are of different nature.

$f_2(1910)$ MASS

$f_2(1910)$ $\omega\omega$ MODE

VALUE (MeV)	DOCUMENT ID		TECN	COMMENT
1915 ± 7 OUR AVERAGE Error includes scale factor of 1.2.				
1934 ± 20	ANISOVICH	00J	SPEC	
1897 ± 11	BARBERIS	00F		450 $pp \to p_f \omega\omega p_s$
1920 ± 10	BELADIDZE	92B	VES	36 $\pi^- p \to \omega\omega n$
1924 ± 14	ALDE	90	GAM2	38 $\pi^- p \to \omega\omega n$

$f_2(1910)$ $\eta\eta'$ MODE

VALUE (MeV)	DOCUMENT ID		TECN	COMMENT
1934 ± 16	[1] BARBERIS	00A		450 $pp \to p_f \eta\eta' p_s$
• • • We do not use the following data for averages, fits, limits, etc. • • •				
1911 ± 10	ALDE	91B	GAM2	38 $\pi^- p \to \eta\eta' n$

[1] Also compatible with $J^{PC}=1^{-+}$.

$f_2(1910)$ WIDTH

$f_2(1910)$ $\omega\omega$ MODE

VALUE (MeV)	DOCUMENT ID		TECN	COMMENT
163 ± 50 OUR AVERAGE Error includes scale factor of 3.4. See the ideogram below.				
271 ± 25	ANISOVICH	00J	SPEC	
202 ± 32	BARBERIS	00F		450 $pp \to p_f \omega\omega p_s$
90 ± 20	BELADIDZE	92B	VES	36 $\pi^- p \to \omega\omega n$
91 ± 50	ALDE	90	GAM2	38 $\pi^- p \to \omega\omega n$

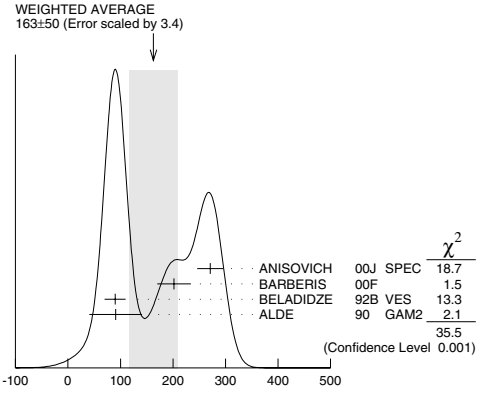

$f_2(1910)$ $\omega\omega$ MODE WIDTH(MeV)

$f_2(1910)$ $\eta\eta'$ MODE

VALUE (MeV)	DOCUMENT ID		TECN	COMMENT
141±41	[2] BARBERIS	00A		450 $pp \rightarrow p_f \eta\eta' p_s$
• • • We do not use the following data for averages, fits, limits, etc. • • •				
90±35	ALDE	91B	GAM2	38 $\pi^- p \rightarrow \eta\eta' n$

[2] Also compatible with $J^{PC}=1^{-+}$.

$f_2(1910)$ DECAY MODES

	Mode	Fraction (Γ_i/Γ)
Γ_1	$\pi^0\pi^0$	
Γ_2	$K^0_S K^0_S$	
Γ_3	$\eta\eta$	seen
Γ_4	$\omega\omega$	seen
Γ_5	$\eta\eta'$	seen
Γ_6	$\eta'\eta'$	
Γ_7	$\rho\rho$	seen

$f_2(1910)$ BRANCHING RATIOS

$\Gamma(\pi^0\pi^0)/\Gamma(\eta\eta')$ Γ_1/Γ_5

VALUE	DOCUMENT ID		TECN	COMMENT
• • • We do not use the following data for averages, fits, limits, etc. • • •				
<0.1	ALDE	89	GAM2	38$\pi^- p \rightarrow \eta\eta' n$

$\Gamma(\eta\eta)/\Gamma(\eta\eta')$ Γ_3/Γ_5

VALUE	CL%	DOCUMENT ID		TECN	COMMENT
• • • We do not use the following data for averages, fits, limits, etc. • • •					
<0.05	90	ALDE	91B	GAM2	38 $\pi^- p \rightarrow \eta\eta' n$

$\Gamma(K^0_S K^0_S)/\Gamma(\eta\eta')$ Γ_2/Γ_5

VALUE	CL%	DOCUMENT ID		TECN	COMMENT
• • • We do not use the following data for averages, fits, limits, etc. • • •					
<0.066	90	BALOSHIN	86	SPEC	40$\pi p \rightarrow K^0_S K^0_S n$

$\Gamma(\eta'\eta')/\Gamma_{\text{total}}$ Γ_6/Γ

VALUE	DOCUMENT ID		TECN	COMMENT
• • • We do not use the following data for averages, fits, limits, etc. • • •				
probably not seen	BARBERIS	00A		450 $pp \rightarrow p_f \eta'\eta' p_s$
possibly seen	BELADIDZE	92D	VES	37 $\pi^- p \rightarrow \eta'\eta' n$

$\Gamma(\rho\rho)/\Gamma(\omega\omega)$ Γ_7/Γ_4

VALUE	DOCUMENT ID		COMMENT
• • • We do not use the following data for averages, fits, limits, etc. • • •			
2.6±0.4	BARBERIS	00F	450 $pp \rightarrow p_f \omega\omega p_s$

$\Gamma(\omega\omega)/\Gamma(\eta\eta')$ Γ_4/Γ_5

VALUE	DOCUMENT ID		COMMENT
• • • We do not use the following data for averages, fits, limits, etc. • • •			
2.6±0.6	BARBERIS	00F	450 $pp \rightarrow p_f \omega\omega p_s$

$f_2(1910)$ REFERENCES

ANISOVICH	00J	PL B491 47	A.V. Anisovich *et al.*	
BARBERIS	00A	PL B471 429	D. Barberis *et al.*	(WA 102 Collab.)
BARBERIS	00F	PL B484 198	D. Barberis *et al.*	(WA 102 Collab.)
BELADIDZE	92B	ZPHY C54 367	G.M. Beladidze *et al.*	(VES Collab.)
BELADIDZE	92D	ZPHY C57 13	G.M. Beladidze *et al.*	(VES Collab.)
ALDE	91B	SJNP 54 455 Translated from YAF 54 751.	D.M. Alde *et al.*	(SERP, BELG, LANL, LAPP+)
Also	92	PL B276 375	D.M. Alde *et al.*	(BELG, SERP, KEK, LANL+)
ALDE	90	PL B241 600	D.M. Alde *et al.*	(SERP, BELG, LANL, LAPP+)
ALDE	89	PL B216 447	D.M. Alde *et al.*	(SERP, BELG, LANL, LAPP)
Also	88E	SJNP 48 1035 Translated from YAF 48 1724.	D.M. Alde *et al.*	(BELG, SERP, LANL, LAPP)
BALOSHIN	86	SJNP 43 959 Translated from YAF 43 1487.	O.N. Baloshin *et al.*	(ITEP)

OTHER RELATED PAPERS

LEE	94	PL B323 227	J.H. Lee *et al.*	(BNL, IND, KYUN, MASD+)

$f_2(1950)$

$I^G(J^{PC}) = 0^+(2^{++})$

$f_2(1950)$ MASS

VALUE (MeV)	DOCUMENT ID		TECN	CHG	COMMENT
1945±13 OUR AVERAGE Error includes scale factor of 1.6. See the ideogram below.					
2010±25	ANISOVICH	00J	SPEC		
1940±50	BAI	00A	BES		$J/\psi \rightarrow \gamma(\pi^+\pi^-\pi^+\pi^-)$
1980±22	[1] BARBERIS	00C			450 $pp \rightarrow pp4\pi$
1940±22	[2] BARBERIS	00C			450 $pp \rightarrow pp2\pi 2\pi^0$
1980±50	ANISOVICH	99B	SPEC		1.35–1.94 $p\overline{p} \rightarrow \eta\eta\pi^0$
1960±30	BARBERIS	97B	OMEG		450 $pp \rightarrow pp2(\pi^+\pi^-)$
1918±12	ANTINORI	95	OMEG		300,450 $pp \rightarrow pp2(\pi^+\pi^-)$
• • • We do not use the following data for averages, fits, limits, etc. • • •					
1980± 2±14	ABE	04	BELL		10.6 $e^+e^- \rightarrow e^+e^- K^+K^-$
1867±46	[3] AMSLER	02	CBAR		0.9 $\overline{p}p \rightarrow \pi^0\eta\eta,\ \pi^0\pi^0\pi^0$
~ 1996	HASAN	94	RVUE		$\overline{p}p \rightarrow \pi\pi$
~ 1990	[4] OAKDEN	94	RVUE		0.36–1.55 $\overline{p}p \rightarrow \pi\pi$
1950±15	[5] ASTON	91	LASS	0	11 $K^- p \rightarrow \Lambda K\overline{K}\pi\pi$

[1] Decaying into $\pi^+\pi^- 2\pi^0$.
[2] Decaying into $2(\pi^+\pi^-)$.
[3] T-matrix pole.
[4] From solution B of amplitude analysis of data on $\overline{p}p \rightarrow \pi\pi$. See however KLOET 96 who fit $\pi^+\pi^-$ only and find waves only up to $J=3$ to be important but not significantly resonant.
[5] Cannot determine spin to be 2.

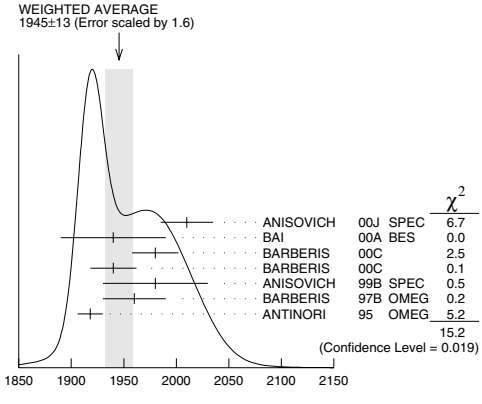

$f_2(1950)$ mass (MeV)

$f_2(1950)$ WIDTH

VALUE (MeV)	DOCUMENT ID		TECN	CHG	COMMENT
475± 19 OUR AVERAGE					
495± 35	ANISOVICH	00J	SPEC		
380^{+120}_{-90}	BAI	00A	BES		$J/\psi \rightarrow \gamma(\pi^+\pi^-\pi^+\pi^-)$
520± 50	[6] BARBERIS	00C			450 $pp \rightarrow pp4\pi$
485± 55	[7] BARBERIS	00C			450 $pp \rightarrow pp4\pi$
500±100	ANISOVICH	99B	SPEC		1.35–1.94 $p\overline{p} \rightarrow \eta\eta\pi^0$
460± 40	BARBERIS	97B	OMEG		450 $pp \rightarrow pp2(\pi^+\pi^-)$
390± 60	ANTINORI	95	OMEG		300,450 $pp \rightarrow pp2(\pi^+\pi^-)$

• • • We do not use the following data for averages, fits, limits, etc. • • •

297 ± 12 ± 6	ABE	04	BELL		10.6 $e^+e^- \to e^+e^-K^+K^-$
385 ± 58	[8] AMSLER	02	CBAR		0.9 $\overline{p}p \to \pi^0\eta\eta$, $\pi^0\pi^0\pi^0$
~ 134	HASAN	94	RVUE		$\overline{p}p \to \pi\pi$
~ 100	[9] OAKDEN	94	RVUE		0.36–1.55 $\overline{p}p \to \pi\pi$
250 ± 50	[10] ASTON	91	LASS	0	11 $K^-p \to \Lambda K\overline{K}\pi\pi$

[6] Decaying into $\pi^+\pi^-2\pi^0$.
[7] Decaying into $2(\pi^+\pi^-)$.
[8] T-matrix pole.
[9] From solution B of amplitude analysis of data on $\overline{p}p \to \pi\pi$. See however KLOET 96 who fit $\pi^+\pi^-$ only and find waves only up to $J = 3$ to be important but not significantly resonant.
[10] Cannot determine spin to be 2.

$f_2(1950)$ DECAY MODES

	Mode	Fraction (Γ_i/Γ)
Γ_1	$K^*(892)\overline{K}^*(892)$	seen
Γ_2	$\pi^+\pi^-$	seen
Γ_3	4π	seen
Γ_4	$\pi^+\pi^-\pi^+\pi^-$	
Γ_5	$a_2(1320)\pi$	
Γ_6	$f_2(1270)\pi\pi$	
Γ_7	$\eta\eta$	seen
Γ_8	$K\overline{K}$	seen
Γ_9	$\gamma\gamma$	seen

$f_2(1950)$ Γ(i)$\Gamma(\gamma\gamma)/\Gamma$(total)

$\Gamma(K\overline{K}) \times \Gamma(\gamma\gamma)/\Gamma_{total}$ $\Gamma_8\Gamma_9/\Gamma$

VALUE (eV)	DOCUMENT ID		TECN	COMMENT
• • • We do not use the following data for averages, fits, limits, etc. • • •				
122 ± 4 ± 26	[11] ABE	04	BELL	10.6 $e^+e^- \to e^+e^-K^+K^-$

[11] Assuming spin 2.

$f_2(1950)$ BRANCHING RATIOS

$\Gamma(K^*(892)\overline{K}^*(892))/\Gamma_{total}$ Γ_1/Γ

VALUE	DOCUMENT ID		TECN	CHG	COMMENT
seen	ASTON	91	LASS	0	11 $K^-p \to \Lambda K\overline{K}\pi\pi$

$\Gamma(a_2(1320)\pi)/\Gamma_{total}$ Γ_5/Γ

VALUE	DOCUMENT ID		TECN	COMMENT
• • • We do not use the following data for averages, fits, limits, etc. • • •				
not seen	BARBERIS	00B		450 $pp \to p_f\eta\pi^+\pi^-p_s$
not seen	BARBERIS	00C		450 $pp \to p_f4\pi p_s$
possibly seen	BARBERIS	97B	OMEG	450 $pp \to pp2(\pi^+\pi^-)$

$\Gamma(\eta\eta)/\Gamma(4\pi)$ Γ_7/Γ_3

VALUE	CL%	DOCUMENT ID		COMMENT
• • • We do not use the following data for averages, fits, limits, etc. • • •				
$< 5.0 \times 10^{-3}$	90	BARBERIS	00E	450 $pp \to p_f\eta\eta p_s$

$\Gamma(\eta\eta)/\Gamma(\pi^+\pi^-)$ Γ_7/Γ_2

VALUE	DOCUMENT ID		TECN	COMMENT
0.14 ± 0.05	AMSLER	02	CBAR	0.9 $\overline{p}p \to \pi^0\eta\eta$, $\pi^0\pi^0\pi^0$

$f_2(1950)$ REFERENCES

ABE	04	EPJ C32 323	K. Abe *et al.*	(BELLE Collab.)
AMSLER	02	EPJ C23 29	C. Amsler *et al.*	
ANISOVICH	00J	PL B491 47	A.V. Anisovich *et al.*	
BAI	00A	PL B472 207	J.Z. Bai *et al.*	(BES Collab.)
BARBERIS	00B	PL B471 435	D. Barberis *et al.*	(WA 102 Collab.)
BARBERIS	00C	PL B471 440	D. Barberis *et al.*	(WA 102 Collab.)
BARBERIS	00E	PL B479 59	D. Barberis *et al.*	(WA 102 Collab.)
ANISOVICH	99B	PL B449 154	A.V. Anisovich *et al.*	
BARBERIS	97B	PL B413 217	D. Barberis *et al.*	(WA 102 Collab.)
KLOET	96	PR D53 6120	W.M. Kloet, F. Myhrer	(RUTG, NORD)
ANTINORI	95	PL B353 589	F. Antinori *et al.*	(ATHU, BARI, BIRM+) JP
HASAN	94	PL B334 215	A. Hasan, D.V. Bugg	(LOQM)
OAKDEN	94	NP A574 731	M.N. Oakden, M.R. Pennington	(DURH)
ASTON	91	NPBPS B21 5	D. Aston *et al.*	(LASS Collab.)

OTHER RELATED PAPERS

ALBRECHT	88N	PL B212 528	H. Albrecht *et al.*	(ARGUS Collab.)
ALBRECHT	87Q	PL B198 255	H. Albrecht *et al.*	(ARGUS Collab.)
ARMSTRONG	87C	ZPHY C34 33	T.A. Armstrong *et al.*	(CERN, BIRM, BARI+)

$\rho_3(1990)$ $I^G(J^{PC}) = 1^+(3^{--})$

OMITTED FROM SUMMARY TABLE

$\rho_3(1990)$ MASS

VALUE (MeV)	DOCUMENT ID		TECN	COMMENT
• • • We do not use the following data for averages, fits, limits, etc. • • •				
1982 ± 14	[1] ANISOVICH	02	SPEC	0.6–1.9 $p\overline{p} \to \omega\pi^0$, $\omega\eta\pi^0$, $\pi^+\pi^-$
~ 2007	HASAN	94		

[1] From the combined analysis of ANISOVICH 00J, ANISOVICH 01D, ANISOVICH 01E, and ANISOVICH 02.

$\rho_3(1990)$ WIDTH

VALUE (MeV)	DOCUMENT ID		TECN	COMMENT
• • • We do not use the following data for averages, fits, limits, etc. • • •				
188 ± 24	[2] ANISOVICH	02	SPEC	0.6–1.9 $p\overline{p} \to \omega\pi^0$, $\omega\eta\pi^0$, $\pi^+\pi^-$
~ 267	HASAN	94		

[2] From the combined analysis of ANISOVICH 00J, ANISOVICH 01D, ANISOVICH 01E, and ANISOVICH 02.

$\rho_3(1990)$ REFERENCES

ANISOVICH	02	PL B542 8	A.V. Anisovich *et al.*
ANISOVICH	01D	PL B508 6	A.V. Anisovich *et al.*
ANISOVICH	01E	PL B513 281	A.V. Anisovich *et al.*
ANISOVICH	00J	PL B491 47	A.V. Anisovich *et al.*
HASAN	94	PL B334 215	A. Hasan, D.V. Bugg (LOQM)

$f_2(2010)$ $I^G(J^{PC}) = 0^+(2^{++})$

See also the mini-review under non-$q\overline{q}$ candidates. (See the index for the page number.)

$f_2(2010)$ MASS

VALUE (MeV)	DOCUMENT ID		TECN	COMMENT
2011^{+62}_{-76}	[1] ETKIN	88	MPS	22 $\pi^-p \to \phi\phi n$
• • • We do not use the following data for averages, fits, limits, etc. • • •				
1980 ± 20	[2] BOLONKIN	88	SPEC	40 $\pi^-p \to K^0_SK^0_Sn$
2050^{+90}_{-50}	ETKIN	85	MPS	22 $\pi^-p \to 2\phi n$
2120^{+20}_{-120}	LINDENBAUM	84	RVUE	
2160 ± 50	ETKIN	82	MPS	22 $\pi^-p \to 2\phi n$

[1] Includes data of ETKIN 85. The percentage of the resonance going into $\phi\phi$ 2^{++} S_2, D_2, and D_0 is 98^{+1}_{-3}, 0^{+1}_{-0}, and 2^{+2}_{-1}, respectively.
[2] Statistically very weak, only 1.4 s.d.

$f_2(2010)$ WIDTH

VALUE (MeV)	DOCUMENT ID		TECN	COMMENT
202^{+67}_{-62}	[3] ETKIN	88	MPS	22 $\pi^-p \to \phi\phi n$
• • • We do not use the following data for averages, fits, limits, etc. • • •				
145 ± 50	[4] BOLONKIN	88	SPEC	40 $\pi^-p \to K^0_SK^0_Sn$
200^{+160}_{-50}	ETKIN	85	MPS	22 $\pi^-p \to 2\phi n$
300^{+150}_{-50}	LINDENBAUM	84	RVUE	
310 ± 70	ETKIN	82	MPS	22 $\pi^-p \to 2\phi n$

[3] Includes data of ETKIN 85.
[4] Statistically very weak, only 1.4 s.d.

$f_2(2010)$ DECAY MODES

	Mode	Fraction (Γ_i/Γ)
Γ_1	$\phi\phi$	seen

$f_2(2010)$ REFERENCES

BOLONKIN	88	NP B309 426	B.V. Bolonkin *et al.*	(ITEP, SERP)
ETKIN	88	PL B201 568	A. Etkin *et al.*	(BNL, CUNY)
ETKIN	85	PL 165B 217	A. Etkin *et al.*	(BNL, CUNY)
LINDENBAUM	84	CNPP 13 285	S.J. Lindenbaum	(CUNY)
ETKIN	82	PRL 49 1620	A. Etkin *et al.*	(BNL, CUNY)
Also	83	Brighton Conf. 351	S.J. Lindenbaum	(BNL, CUNY)

OTHER RELATED PAPERS

ANISOVICH	99D	PL B452 180	A.V. Anisovich *et al.*	
Also	99F	NP A651 253	A.V. Anisovich *et al.*	
ANISOVICH	99F	NP A651 253	A.V. Anisovich *et al.*	
LANDBERG	96	PR D53 2839	C. Landberg *et al.*	(BNL, CUNY, RPI)
GREEN	86	PRL 56 1639	D.R. Green *et al.*	(FNAL, ARIZ, FSU+)
BOOTH	84	NP B242 51	P.S.L. Booth *et al.*	(LIVP, GLAS, CERN)
EISENHAND...	75	NP B96 109	E. Eisenhandler *et al.*	(LOQM, LIVP, DARE+)

$f_0(2020)$

$I^G(J^{PC}) = 0^+(0^{++})$

OMITTED FROM SUMMARY TABLE

Needs confirmation.

$f_0(2020)$ MASS

VALUE (MeV)	DOCUMENT ID		TECN	COMMENT
1992±16	[1,2] BARBERIS	00C		450 $pp \to p_f 4\pi p_s$
• • • We do not use the following data for averages, fits, limits, etc. • • •				
2040±38	ANISOVICH	00J	SPEC	
2010±60	ALDE	98	GAM4	100 $\pi^- p \to \pi^0\pi^0 n$
2020±35	BARBERIS	97B	OMEG	450 $pp \to pp2(\pi^+\pi^-)$

[1] Average between $\pi^+\pi^-2\pi^0$ and $2(\pi^+\pi^-)$.
[2] T-matrix pole.

$f_0(2020)$ WIDTH

VALUE (MeV)	DOCUMENT ID		TECN	COMMENT
442± 60	[3,4] BARBERIS	00C		450 $pp \to p_f 4\pi p_s$
• • • We do not use the following data for averages, fits, limits, etc. • • •				
405± 40	ANISOVICH	00J	SPEC	
240±100	ALDE	98	GAM4	100 $\pi^- p \to \pi^0\pi^0 n$
410± 50	BARBERIS	97B	OMEG	450 $pp \to pp2(\pi^+\pi^-)$

[3] Average between $\pi^+\pi^-2\pi^0$ and $2(\pi^+\pi^-)$.
[4] T-matrix pole.

$f_0(2020)$ DECAY MODES

	Mode	Fraction (Γ_i/Γ)
Γ_1	$\rho\pi\pi$	seen
Γ_2	$\pi^0\pi^0$	seen
Γ_3	$\rho\rho$	seen
Γ_4	$\omega\omega$	seen

$f_0(2020)$ BRANCHING RATIOS

$\Gamma(\rho\rho)/\Gamma(\omega\omega)$ **Γ_3/Γ_4**

VALUE	DOCUMENT ID		COMMENT
• • • We do not use the following data for averages, fits, limits, etc. • • •			
~ 3	BARBERIS	00F	450 $pp \to p_f \omega\omega p_s$

$f_0(2020)$ REFERENCES

ANISOVICH	00J	PL B491 47	A.V. Anisovich *et al.*	
BARBERIS	00C	PL B471 440	D. Barberis *et al.*	(WA 102 Collab.)
BARBERIS	00F	PL B484 198	D. Barberis *et al.*	(WA 102 Collab.)
ALDE	98	EPJ A3 361	D. Alde *et al.*	(GAM4 Collab.)
Also	99	PAN 62 405 Translated from YAF 62 446.	D. Alde *et al.*	(GAMS Collab.)
BARBERIS	97B	PL B413 217	D. Barberis *et al.*	(WA 102 Collab.)

$a_4(2040)$

$I^G(J^{PC}) = 1^-(4^{++})$

$a_4(2040)$ MASS

VALUE (MeV)	DOCUMENT ID		TECN	CHG	COMMENT
2010±12 OUR AVERAGE					
1996±25±43	CHUNG	02	MPS		18.3 $\pi^- p \to 3\pi p$
$2000 \pm 40^{+60}_{-20}$	IVANOV	01	MPS		18 $\pi^- p \to \eta'\pi^- p$
1944± 8±50	[1] AMELIN	99	VES		37 $\pi^- A \to \omega\pi^-\pi^0 A^*$
2005±25	ANISOVICH	99E	SPEC		
2010±20	[2] DONSKOV	96	GAM2	0	38 $\pi^- p \to \eta\pi^0 n$
2040±30	[3] CLELAND	82B	SPEC	±	50 $\pi p \to K^0_S K^\pm p$
2030±50	[4] CORDEN	78C	OMEG	0	15 $\pi^- p \to 3\pi n$
• • • We do not use the following data for averages, fits, limits, etc. • • •					
2005^{+25}_{-45}	ANISOVICH	01F	SPEC		2.0 $\bar{p}p \to 3\pi^0$, $\pi^0\eta$, $\pi^0\eta'$
1903±10	[5] BALDI	78	SPEC	–	10 $\pi^- p \to pK^0_S K^-$

[1] May be a different state.
[2] From a simultaneous fit to the G_+ and G_0 wave intensities.
[3] From an amplitude analysis.
[4] $J^P = 4^+$ is favored, though $J^P = 2^+$ cannot be excluded.
[5] From a fit to the Y^0_8 moment. Limited by phase space.

$a_4(2040)$ WIDTH

VALUE (MeV)	DOCUMENT ID		TECN	CHG	COMMENT
353± 40 OUR AVERAGE					
298± 81±85	CHUNG	02	MPS		18.3 $\pi^- p \to 3\pi p$
$350 \pm 100^{+70}_{-50}$	IVANOV	01	MPS		18 $\pi^- p \to \eta'\pi^- p$
324± 26±75	[6] AMELIN	99	VES		37 $\pi^- A \to \omega\pi^-\pi^0 A^*$
360± 80	ANISOVICH	99E	SPEC		
370± 80	[7] DONSKOV	96	GAM2	0	38 $\pi^- p \to \eta\pi^0 n$
380±150	[8] CLELAND	82B	SPEC	±	50 $\pi p \to K^0_S K^\pm p$
510±200	[9] CORDEN	78C	OMEG	0	15 $\pi^- p \to 3\pi n$
• • • We do not use the following data for averages, fits, limits, etc. • • •					
180± 30	ANISOVICH	01F	SPEC		2.0 $\bar{p}p \to 3\pi^0$, $\pi^0\eta$, $\pi^0\eta'$
166± 43	[10] BALDI	78	SPEC	–	10 $\pi^- p \to pK^0_S K^-$

[6] May be a different state.
[7] From a simultaneous fit to the G_+ and G_0 wave intensities.
[8] From an amplitude analysis.
[9] $J^P = 4^+$ is favored, though $J^P = 2^+$ cannot be excluded.
[10] From a fit to the Y^0_8 moment. Limited by phase space.

$a_4(2040)$ DECAY MODES

	Mode	Fraction (Γ_i/Γ)
Γ_1	$K\overline{K}$	seen
Γ_2	$\pi^+\pi^-\pi^0$	seen
Γ_3	$\rho\pi$	seen
Γ_4	$f_2(1270)\pi$	seen
Γ_5	$\eta\pi^0$	seen
Γ_6	$\eta'(958)\pi$	seen

$a_4(2040)$ BRANCHING RATIOS

$\Gamma(K\overline{K})/\Gamma_{\text{total}}$ **Γ_1/Γ**

VALUE	DOCUMENT ID		TECN	CHG	COMMENT
seen	BALDI	78	SPEC	±	10 $\pi^- p \to K^0_S K^- p$

$\Gamma(\pi^+\pi^-\pi^0)/\Gamma_{\text{total}}$ **Γ_2/Γ**

VALUE	DOCUMENT ID		TECN	CHG	COMMENT
seen	CORDEN	78C	OMEG	0	15 $\pi^- p \to 3\pi n$

$\Gamma(\rho\pi)/\Gamma(f_2(1270)\pi)$ **Γ_3/Γ_4**

VALUE	DOCUMENT ID		TECN	COMMENT
1.1 ±0.2 ±0.2	CHUNG	02	MPS	18.3 $\pi^- p \to 3\pi p$

$\Gamma(\eta\pi^0)/\Gamma_{\text{total}}$ **Γ_5/Γ**

VALUE	DOCUMENT ID		TECN	CHG	COMMENT
seen	DONSKOV	96	GAM2	0	38 $\pi^- p \to \eta\pi^0 n$

$a_4(2040)$ REFERENCES

CHUNG	02	PR D65 072001	S.U. Chung *et al.*	
ANISOVICH	01F	PL B517 261	A.V. Anisovich *et al.*	
IVANOV	01	PRL 86 3977	E.I. Ivanov *et al.*	
AMELIN	99	PAN 62 445 Translated from YAF 62 487.	D.V. Amelin *et al.*	(VES Collab.)
ANISOVICH	99E	PL B452 187	A.V. Anisovich *et al.*	
DONSKOV	96	PAN 59 982 Translated from YAF 59 1027.	S.V. Donskov *et al.*	(GAMS Collab.) IGJPC
CLELAND	82B	NP B208 228	W.E. Cleland *et al.*	(DURH, GEVA, LAUS+)
BALDI	78	PL 74B 413	R. Baldi *et al.*	(GEVA) JP
CORDEN	78C	NP B136 77	M.J. Corden *et al.*	(BIRM, RHEL, TELA+) JP

OTHER RELATED PAPERS

DELFOSSE	81	NP B183 349	A. Delfosse *et al.*	(GEVA, LAUS)

$f_4(2050)$ $I^G(J^{PC}) = 0^+(4^{++})$

$f_4(2050)$ MASS

VALUE (MeV)	EVTS	DOCUMENT ID		TECN	COMMENT
2034±11 OUR AVERAGE		Error includes scale factor of 1.6. See the ideogram below.			
1998±15		ALDE	98	GAM4	100 $\pi^- p \to \pi^0\pi^0 n$
1970±30		BELADIDZE	92B	VES	36 $\pi^- p \to \omega\omega n$
2060±20		ALDE	90	GAM2	38 $\pi^- p \to \omega\omega n$
2038±30		AUGUSTIN	87	DM2	$J/\psi \to \gamma\pi^+\pi^-$
2086±15		BALTRUSAIT...	87	MRK3	$J/\psi \to \gamma\pi^+\pi^-$
2000±60		ALDE	86D	GAM4	100 $\pi^- p \to n2\eta$
2020±20	40k	[1] BINON	84B	GAM2	38 $\pi^- p \to n2\pi^0$
2015±28		[2] CASON	82	STRC	8 $\pi^+ p \to \Delta^{++}\pi^0\pi^0$
2031^{+25}_{-36}		ETKIN	82B	MPS	23 $\pi^- p \to n2K^0_S$
2020±30	700	APEL	75	NICE	40 $\pi^- p \to n2\pi^0$
2050±25		BLUM	75	ASPK	18.4 $\pi^- p \to nK^+K^-$
• • • We do not use the following data for averages, fits, limits, etc. • • •					
2018± 6		ANISOVICH	00J	SPEC	2.0 $\overline{p}p \to \eta\pi^0\pi^0$, $\pi^0\pi^0$, $\eta\eta$, $\eta\eta'$, $\pi\pi$
~ 2000		[3] MARTIN	98	RVUE	$N\overline{N} \to \pi\pi$
~ 2010		[4] MARTIN	97	RVUE	$N\overline{N} \to \pi\pi$
~ 2040		[5] OAKDEN	94	RVUE	0.36–1.55 $\overline{p}p \to \pi\pi$
~ 1990		[6] OAKDEN	94	RVUE	0.36–1.55 $\overline{p}p \to \pi\pi$
1978± 5		[7] ALPER	80	CNTR	62 $\pi^- p \to K^+K^- n$
2040±10		[7] ROZANSKA	80	SPRK	18 $\pi^- p \to p\overline{p}n$
1935±13		[7] CORDEN	79	OMEG	12–15 $\pi^- p \to n2\pi$
1988± 7		EVANGELISTA	79B	OMEG	10 $\pi^- p \to K^+K^- n$
1922±14		[8] ANTIPOV	77	CIBS	25 $\pi^- p \to p3\pi$

[1] From a partial-wave analysis of the data.
[2] From an amplitude analysis of the reaction $\pi^+\pi^- \to 2\pi^0$.
[3] Energy-dependent analysis.
[4] Single energy analysis.
[5] From solution A of amplitude analysis of data on $\overline{p}p \to \pi\pi$. See however KLOET 96 who fit $\pi^+\pi^-$ only and find waves only up to $J = 3$ to be important but not significantly resonant.
[6] From solution B of amplitude analysis of data on $\overline{p}p \to \pi\pi$. See however KLOET 96 who fit $\pi^+\pi^-$ only and find waves only up to $J = 3$ to be important but not significantly resonant.
[7] $I(J^P) = 0(4^+)$ from amplitude analysis assuming one-pion exchange.
[8] Width errors enlarged by us to $4\Gamma/\sqrt{N}$; see the note with the $K^*(892)$ mass.

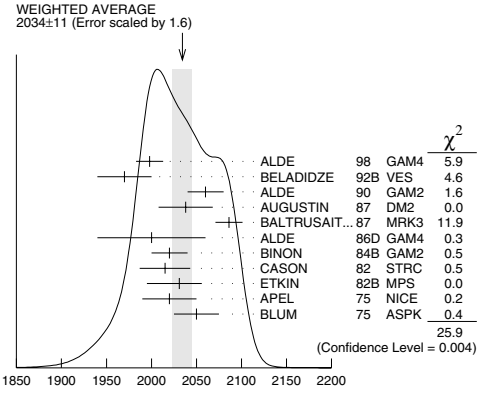

$f_4(2050)$ mass (MeV)

$f_4(2050)$ WIDTH

VALUE (MeV)	EVTS	DOCUMENT ID		TECN	COMMENT
222± 19 OUR AVERAGE		Error includes scale factor of 1.8. See the ideogram below.			
395± 40		ALDE	98	GAM4	100 $\pi^- p \to \pi^0\pi^0 n$
300± 50		BELADIDZE	92B	VES	36 $\pi^- p \to \omega\omega n$
170± 60		ALDE	90	GAM2	38 $\pi^- p \to \omega\omega n$
304± 60		AUGUSTIN	87	DM2	$J/\psi \to \gamma\pi^+\pi^-$
210± 63		BALTRUSAIT...	87	MRK3	$J/\psi \to \gamma\pi^+\pi^-$
400±100		ALDE	86D	GAM4	100 $\pi^- p \to n2\eta$
240± 40	40k	[9] BINON	84B	GAM2	38 $\pi^- p \to n2\pi^0$
190± 14		DENNEY	83	LASS	10 $\pi^+ n/\pi^+ p$
186^{+103}_{-58}		[10] CASON	82	STRC	8 $\pi^+ p \to \Delta^{++}\pi^0\pi^0$
305^{+36}_{-119}		ETKIN	82B	MPS	23 $\pi^- p \to n2K^0_S$
180± 60	700	APEL	75	NICE	40 $\pi^- p \to n2\pi^0$
225^{+120}_{-70}		BLUM	75	ASPK	18.4 $\pi^- p \to nK^+K^-$
• • • We do not use the following data for averages, fits, limits, etc. • • •					
182± 7		ANISOVICH	00J	SPEC	2.0 $\overline{p}p \to \eta\pi^0\pi^0$, $\pi^0\pi^0$, $\eta\eta$, $\eta\eta'$, $\pi\pi$
~ 170		[11] MARTIN	98	RVUE	$N\overline{N} \to \pi\pi$
~ 200		[12] MARTIN	97	RVUE	$N\overline{N} \to \pi\pi$
~ 60		[13] OAKDEN	94	RVUE	0.36–1.55 $\overline{p}p \to \pi\pi$
~ 80		[14] OAKDEN	94	RVUE	0.36–1.55 $\overline{p}p \to \pi\pi$
243± 16		[15] ALPER	80	CNTR	62 $\pi^- p \to K^+K^- n$
140± 15		[15] ROZANSKA	80	SPRK	18 $\pi^- p \to p\overline{p}n$
263± 57		[15] CORDEN	79	OMEG	12–15 $\pi^- p \to n2\pi$
100± 28		EVANGELISTA	79B	OMEG	10 $\pi^- p \to K^+K^- n$
107± 56		[16] ANTIPOV	77	CIBS	25 $\pi^- p \to p3\pi$

[9] From a partial-wave analysis of the data.
[10] From an amplitude analysis of the reaction $\pi^+\pi^- \to 2\pi^0$.
[11] Energy-dependent analysis.
[12] Single energy analysis.
[13] From solution A of amplitude analysis of data on $\overline{p}p \to \pi\pi$. See however KLOET 96 who fit $\pi^+\pi^-$ only and find waves only up to $J = 3$ to be important but not significantly resonant.
[14] From solution B of amplitude analysis of data on $\overline{p}p \to \pi\pi$. See however KLOET 96 who fit $\pi^+\pi^-$ only and find waves only up to $J = 3$ to be important but not significantly resonant.
[15] $I(J^P) = 0(4^+)$ from amplitude analysis assuming one-pion exchange.
[16] Width errors enlarged by us to $4\Gamma/\sqrt{N}$; see the note with the $K^*(892)$ mass.

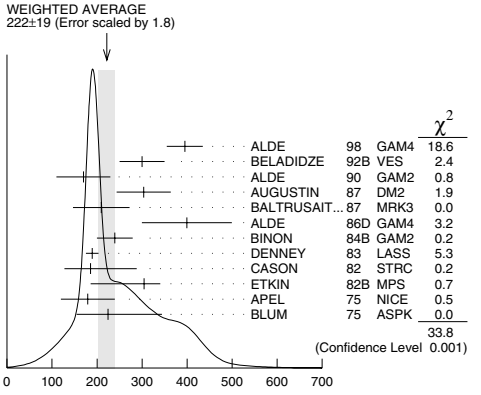

$f_4(2050)$ WIDTH

$f_4(2050)$ DECAY MODES

	Mode	Fraction (Γ_i/Γ)
Γ_1	$\omega\omega$	not seen
Γ_2	$\pi\pi$	(17.0±1.5) %
Γ_3	$K\overline{K}$	$(6.8^{+3.4}_{-1.8}) \times 10^{-3}$
Γ_4	$\eta\eta$	$(2.1\pm0.8) \times 10^{-3}$
Γ_5	$4\pi^0$	< 1.2 %
Γ_6	$\gamma\gamma$	
Γ_7	$a_2(1320)\pi$	seen

$f_4(2050)$ $\Gamma(i)\Gamma(\gamma\gamma)/\Gamma(\text{total})$

$\Gamma(K\overline{K}) \times \Gamma(\gamma\gamma)/\Gamma_{\text{total}}$ $\Gamma_3\Gamma_6/\Gamma$

VALUE (keV)	CL%	DOCUMENT ID		TECN	COMMENT
• • • We do not use the following data for averages, fits, limits, etc. • • •					
<0.29	95	ALTHOFF	85B	TASS	$\gamma\gamma \to K\overline{K}\pi$

$\Gamma(\pi\pi) \times \Gamma(\gamma\gamma)/\Gamma_{total}$ $\Gamma_2\Gamma_6/\Gamma$

VALUE (keV)	CL%	EVTS	DOCUMENT ID		TECN	COMMENT
<1.1	95	13 ± 4	OEST	90	JADE	$e^+e^- \to e^+e^-\pi^0\pi^0$

$f_4(2050)$ BRANCHING RATIOS

$\Gamma(\omega\omega)/\Gamma_{total}$ Γ_1/Γ

VALUE	DOCUMENT ID		TECN	COMMENT
• • • We do not use the following data for averages, fits, limits, etc. • • •				
not seen	BARBERIS	00F		450 $pp \to p_f \omega\omega p_s$

$\Gamma(\omega\omega)/\Gamma(\pi\pi)$ Γ_1/Γ_2

VALUE	DOCUMENT ID		TECN	COMMENT
1.5 ±0.3	ALDE	90	GAM2	38 $\pi^- p \to \omega\omega n$

$\Gamma(\pi\pi)/\Gamma_{total}$ Γ_2/Γ

VALUE	DOCUMENT ID		TECN	COMMENT
0.170±0.015 OUR AVERAGE				
0.18 ±0.03	[17] BINON	83C	GAM2	38 $\pi^- p \to n4\gamma$
0.16 ±0.03	[17] CASON	82	STRC	8 $\pi^+ p \to \Delta^{++}\pi^0\pi^0$
0.17 ±0.02	[17] CORDEN	79	OMEG	12–15 $\pi^- p \to n2\pi$

[17] Assuming one pion exchange.

$\Gamma(K\overline{K})/\Gamma(\pi\pi)$ Γ_3/Γ_2

VALUE	DOCUMENT ID		TECN	COMMENT
$0.04\ ^{+0.02}_{-0.01}$	ETKIN	82B	MPS	23 $\pi^- p \to n2K^0_S$

$\Gamma(\eta\eta)/\Gamma_{total}$ Γ_4/Γ

VALUE (units 10^{-3})	DOCUMENT ID		TECN	COMMENT
2.1±0.8	ALDE	86D	GAM4	100 $\pi^- p \to n4\gamma$

$\Gamma(4\pi^0)/\Gamma_{total}$ Γ_5/Γ

VALUE	DOCUMENT ID		TECN	COMMENT
<0.012	ALDE	87	GAM4	100 $\pi^- p \to 4\pi^0 n$

$\Gamma(a_2(1320)\pi)/\Gamma_{total}$ Γ_7/Γ

VALUE	DOCUMENT ID		TECN	COMMENT
• • • We do not use the following data for averages, fits, limits, etc. • • •				
seen	AMELIN	00	VES	37 $\pi^- p \to \eta\pi^+\pi^- n$

$f_4(2050)$ REFERENCES

AMELIN	00	NP A668 83	D. Amelin *et al.*	(VES Collab.)
ANISOVICH	00J	PL B491 47	A.V. Anisovich *et al.*	
BARBERIS	00F	PL B484 198	D. Barberis *et al.*	(WA 102 Collab.)
ALDE	98	EPJ A3 361	D. Alde *et al.*	(GAM4 Collab.)
Also	99	PAN 62 405	D. Alde *et al.*	(GAMS Collab.)
		Translated from YAF 62 446.		
MARTIN	98	PR C57 3492	B.R. Martin *et al.*	
MARTIN	97	PR C56 1114	B.R. Martin, G.C. Oades	(LOUC, AARH)
KLOET	96	PR D53 6120	W.M. Kloet, F. Myhrer	(RUTG, NORD)
OAKDEN	94	NP A574 731	M.N. Oakden, M.R. Pennington	(DURH)
BELADIDZE	92B	ZPHY C54 367	G.M. Beladidze *et al.*	(VES Collab.)
ALDE	90	PL B241 600	D.M. Alde *et al.*	(SERP, BELG, LANL, LAPP+)
OEST	90	ZPHY C47 343	T. Oest *et al.*	(JADE Collab.)
ALDE	87	PL B198 286	D.M. Alde *et al.*	(LANL, BRUX, SERP, LAPP)
AUGUSTIN	87	ZPHY C36 369	J.E. Augustin *et al.*	(LALO, CLER, FRAS+)
BALTRUSAIT...	87	PR D35 2077	R.M. Baltrusaitis *et al.*	(Mark III Collab.)
ALDE	86D	NP B269 485	D.M. Alde *et al.*	(BELG, LAPP, SERP, CERN+)
ALTHOFF	85B	ZPHY C29 189	M. Althoff *et al.*	(TASSO Collab.)
BINON	84B	LNC 39 41	F.G. Binon *et al.*	(SERP, BELG, LAPP)
BINON	83C	SJNP 38 723	F.G. Binon *et al.*	(SERP, BRUX+)
		Translated from YAF 38 1199.		
DENNEY	83	PR D28 2726	D.L. Denney *et al.*	(IOWA, MICH)
CASON	82	PRL 48 1316	N.M. Cason *et al.*	(NDAM, ANL)
ETKIN	82B	PR D25 1786	A. Etkin *et al.*	(BNL, CUNY, TUFTS, VAND)
ALPER	80	PL 94B 422	B. Alper *et al.*	(AMST, CERN, CRAC, MPIM+)
ROZANSKA	80	NP B162 505	M. Rozanska *et al.*	(MPIM, CERN)
CORDEN	79	NP B157 250	M.J. Corden *et al.*	(BIRM, RHEL, TELA+) JP
EVANGELISTA	79B	NP B154 381	C. Evangelista *et al.*	(BARI, BONN, CERN+)
ANTIPOV	77	NP B119 45	Y.M. Antipov *et al.*	(SERP, GEVA)
APEL	75	PL 57B 398	W.D. Apel *et al.*	(KARLK, KARLE, PISA, SERP+) JP
BLUM	75	PL 57B 403	W. Blum *et al.*	(CERN, MPIM) JP

OTHER RELATED PAPERS

ANISOVICH	99D	PL B452 180	A.V. Anisovich *et al.*	
Also	99F	NP A651 253	A.V. Anisovich *et al.*	
ANISOVICH	99F	NP A651 253	A.V. Anisovich *et al.*	
PROKOSHKIN	97	SPD 42 117	Y.D. Prokoshkin *et al.*	(SERP)
		Translated from DANS 353 323.		
CASON	83	PR D28 1586	N.M. Cason *et al.*	(NDAM, ANL)
GOTTESMAN	80	PR D22 1503	S.R. Gottesman *et al.*	(SYRA, BRAN, BNL+)
EISENHAND...	75	NP B96 109	E. Eisenhandler *et al.*	(LOQM, LIVP, DARE+)
WAGNER	74	London Conf. 2 27	F. Wagner	(MPIM)

$\pi_2(2100)$ $I^G(J^{PC}) = 1^-(2^{-+})$

OMITTED FROM SUMMARY TABLE

Needs confirmation.

$\pi_2(2100)$ MASS

VALUE (MeV)	DOCUMENT ID		TECN	COMMENT
2090± 29 OUR AVERAGE				
2090± 30	[1] AMELIN	95B	VES	36 $\pi^- A \to \pi^+\pi^-\pi^- A$
2100±150	[2] DAUM	81B	CNTR	63,94 $\pi^- p \to 3\pi X$

[1] From a fit to $J^{PC} = 2^{-+}$ $f_2(1270)\pi$, $(\pi\pi)_S\pi$ waves.

[2] From a two-resonance fit to four 2^-0^+ waves.

$\pi_2(2100)$ WIDTH

VALUE (MeV)	DOCUMENT ID		TECN	COMMENT
625± 50 OUR AVERAGE Error includes scale factor of 1.2.				
520±100	[3] AMELIN	95B	VES	36 $\pi^- A \to \pi^+\pi^-\pi^- A$
651± 50	[4] DAUM	81B	CNTR	63,94 $\pi^- p \to 3\pi X$

[3] From a fit to $J^{PC} = 2^{-+}$ $f_2(1270)\pi$, $(\pi\pi)_S\pi$ waves.

[4] From a two-resonance fit to four 2^-0^+ waves.

$\pi_2(2100)$ DECAY MODES

	Mode	Fraction (Γ_i/Γ)
Γ_1	3π	seen
Γ_2	$\rho\pi$	seen
Γ_3	$f_2(1270)\pi$	seen
Γ_4	$(\pi\pi)_S\pi$	seen

$\pi_2(2100)$ BRANCHING RATIOS

$\Gamma(\rho\pi)/\Gamma(3\pi)$ Γ_2/Γ_1

VALUE	DOCUMENT ID		TECN	COMMENT
0.19±0.05	[5] DAUM	81B	CNTR	63,94 $\pi^- p$

$\Gamma(f_2(1270)\pi)/\Gamma(3\pi)$ Γ_3/Γ_1

VALUE	DOCUMENT ID		TECN	COMMENT
0.36±0.09	[5] DAUM	81B	CNTR	63,94 $\pi^- p$

$\Gamma((\pi\pi)_S\pi)/\Gamma(3\pi)$ Γ_4/Γ_1

VALUE	DOCUMENT ID		TECN	COMMENT
0.45±0.07	[5] DAUM	81B	CNTR	63,94 $\pi^- p$

***D*-wave/*S*-wave RATIO FOR $\pi_2(2100) \to f_2(1270)\pi$**

VALUE	DOCUMENT ID		TECN	COMMENT
0.39±0.23	[5] DAUM	81B	CNTR	63,94 $\pi^- p$

[5] From a two-resonance fit to four 2^-0^+ waves.

$\pi_2(2100)$ REFERENCES

AMELIN	95B	PL B356 595	D.V. Amelin *et al.*	(SERP, TBIL)
DAUM	81B	NP B182 269	C. Daum *et al.*	(AMST, CERN, CRAC, MPIM+)

$f_0(2100)$ $I^G(J^{PC}) = 0^+(0^{++})$

OMITTED FROM SUMMARY TABLE

Needs confirmation.

$f_0(2100)$ MASS

VALUE (MeV)	DOCUMENT ID		TECN	COMMENT
2103± 7 OUR AVERAGE				
2105±15	ANISOVICH	00B	SPEC	
2102±13	ANISOVICH	00J	SPEC	2.0 $\overline{p}p \to \eta\pi^0\pi^0$, $\pi^0\pi^0$, $\eta\eta$, $\eta\eta'$, $\pi^+\pi^-$
2090±30	BAI	00A	BES	$J/\psi \to \gamma(\pi^+\pi^-\pi^+\pi^-)$
2105±10	ANISOVICH	99K	SPEC	0.6–1.94 $\overline{p}p \to \eta\eta$, $\eta\eta'$
• • • We do not use the following data for averages, fits, limits, etc. • • •				
~2104	BUGG	95		

$f_0(2100)$ WIDTH

VALUE (MeV)	DOCUMENT ID		TECN	COMMENT
206 ± 15 OUR AVERAGE				
200 ± 25	ANISOVICH	00B	SPEC	
211 ± 29	ANISOVICH	00J	SPEC	2.0 $\overline{p}p \to \eta\pi^0\pi^0$, $\pi^0\pi^0$, $\eta\eta$, $\eta\eta'$, $\pi^+\pi^-$
330 ± 100	BAI	00A	BES	$J/\psi \to \gamma(\pi^+\pi^-\pi^+\pi^-)$
200 ± 25	ANISOVICH	99K	SPEC	0.6–1.94 $\overline{p}p \to \eta\eta$, $\eta\eta'$
• • • We do not use the following data for averages, fits, limits, etc. • • •				
~ 203	BUGG		95	

$f_0(2100)$ REFERENCES

ANISOVICH	00B	NP A662 319	A.V. Anisovich *et al.*	
ANISOVICH	00J	PL B491 47	A.V. Anisovich *et al.*	
BAI	00A	PL B472 207	J.Z. Bai *et al.*	(BES Collab.)
ANISOVICH	99K	PL B468 309	A.V. Anisovich *et al.*	
BUGG	95	PL B353 378	D.V. Bugg *et al.*	(LOQM, PNPI, WASH)

$f_2(2150)$

$I^G(J^{PC}) = 0^+(2^{++})$

OMITTED FROM SUMMARY TABLE
This entry was previously called T_0.

$f_2(2150)$ MASS

$f_2(2150)$ MASS, COMBINED MODES (MeV)

VALUE (MeV)	DOCUMENT ID
2156±11 OUR AVERAGE Includes data from the 2 datablocks that follow this one.	

$\eta\eta$ MODE

VALUE (MeV)	DOCUMENT ID		TECN	COMMENT
The data in this block is included in the average printed for a previous datablock.				
2157±12 OUR AVERAGE				
2151 ± 16	BARBERIS	00E		450 $pp \to p_f\eta\eta p_s$
2175 ± 20	PROKOSHKIN	95D	GAM4	300 $\pi^- N \to \pi^- N 2\eta$, 450 $pp \to pp2\eta$
2130 ± 35	SINGOVSKI	94	GAM4	450 $pp \to pp2\eta$
• • • We do not use the following data for averages, fits, limits, etc. • • •				
2140 ± 30	[1] ABELE	99B	CBAR	
seen	[2] ANISOVICH	99B	SPEC	1.35–1.94 $\overline{p}p \to \eta\eta\pi^0$
2105 ± 10	[2] ANISOVICH	99K	RVUE	0.6–1.94 $\overline{p}p \to \eta\eta$, $\eta\eta'$
2104 ± 20	[3] ARMSTRONG	93C	E760	$\overline{p}p \to \pi^0\eta\eta \to 6\gamma$

[1] Spin not determined.
[2] $J^{PC} = 0^{++}$.
[3] No J^{PC} determination.

$\eta\pi\pi$ MODE

VALUE (MeV)	DOCUMENT ID		TECN	CHG	COMMENT
The data in this block is included in the average printed for a previous datablock.					
2135 ± 20 ± 45	ADOMEIT	96	CBAR	0	1.94 $\overline{p}p \to \eta 3\pi^0$

$\overline{p}p \to \pi\pi$

VALUE (MeV)	DOCUMENT ID		TECN	COMMENT
• • • We do not use the following data for averages, fits, limits, etc. • • •				
~ 2226	HASAN	94	RVUE	$\overline{p}p \to \pi\pi$
~ 2090	[4] OAKDEN	94	RVUE	0.36–1.55 $\overline{p}p \to \pi\pi$
~ 2120	[5] OAKDEN	94	RVUE	0.36–1.55 $\overline{p}p \to \pi\pi$
~ 2170	[6] MARTIN	80B	RVUE	
~ 2150	[6] MARTIN	80C	RVUE	
~ 2150	[7] DULUDE	78B	OSPK	1–2 $\overline{p}p \to \pi^0\pi^0$

[4] OAKDEN 94 makes an amplitude analysis of LEAR data on $\overline{p}p \to \pi\pi$ using a method based on Barrelet zeros. This is solution A. The amplitude analysis of HASAN 94 includes earlier data as well, and assume that the data can be parametrized in terms of towers of nearly degenerate resonances on the leading Regge trajectory. See also KLOET 96 and MARTIN 97 who make related analyses.
[5] From solution B of amplitude analysis of data on $\overline{p}p \to \pi\pi$.
[6] $I(J^P) = 0(2^+)$ from simultaneous analysis of $p\overline{p} \to \pi^-\pi^+$ and $\pi^0\pi^0$.
[7] $I^G(J^P) = 0^+(2^+)$ from partial-wave amplitude analysis.

S-CHANNEL $\overline{p}p$, $\overline{N}N$ or $\overline{K}K$

VALUE (MeV)	DOCUMENT ID		TECN	CHG	COMMENT
• • • We do not use the following data for averages, fits, limits, etc. • • •					
$2139^{+\ 8}_{-\ 9}$	[8] EVANGELISTA	97	SPEC		0.6-2.4 $\overline{p}p \to K^0_S K^0_S$
~ 2190	[8] CUTTS	78B	CNTR		0.97–3 $\overline{p}p \to \overline{N}N$
2155 ± 15	[8,9] COUPLAND	77	CNTR	0	0.7–2.4 $\overline{p}p \to \overline{p}p$
2193 ± 2	[8,10] ALSPECTOR	73	CNTR		$\overline{p}p$ S channel

[8] Isospins 0 and 1 not separated.
[9] From a fit to the total elastic cross section.
[10] Referred to as T or T region by ALSPECTOR 73.

$K\overline{K}$ MODE

VALUE (MeV)	DOCUMENT ID		TECN	COMMENT
2130 ± 35	BARBERIS	99	OMEG	450 $pp \to p_s p_f K^+K^-$

$f_2(2150)$ WIDTH

$f_2(2150)$ WIDTH, COMBINED MODES (MeV)

VALUE (MeV)	DOCUMENT ID
167±30 OUR AVERAGE Includes data from the 2 datablocks that follow this one. Error includes scale factor of 1.5. See the ideogram below.	

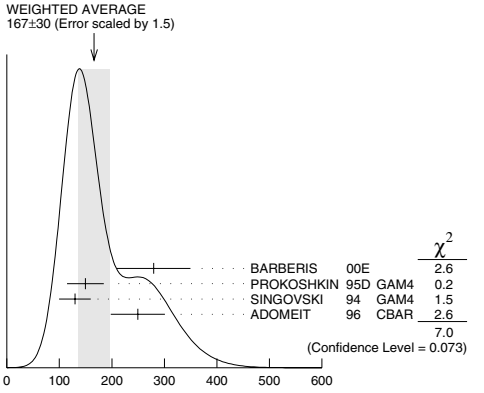

$f_2(2150)$ WIDTH, COMBINED MODES (MeV)

$\eta\eta$ MODE

VALUE (MeV)	DOCUMENT ID		TECN	COMMENT
The data in this block is included in the average printed for a previous datablock.				
152±30 OUR AVERAGE Error includes scale factor of 1.4. See the ideogram below.				
280 ± 70	BARBERIS	00E		450 $pp \to p_f\eta\eta p_s$
150 ± 35	PROKOSHKIN	95D	GAM4	300 $\pi^- N \to \pi^- N 2\eta$, 450 $pp \to pp2\eta$
130 ± 30	SINGOVSKI	94	GAM4	450 $pp \to pp2\eta$
• • • We do not use the following data for averages, fits, limits, etc. • • •				
310 ± 50	[11] ABELE	99B	CBAR	
seen	[12] ANISOVICH	99B	SPEC	1.35–1.94 $\overline{p}p \to \eta\eta\pi^0$
200 ± 25	[13] ANISOVICH	99K	RVUE	0.6–1.94 $\overline{p}p \to \eta\eta$, $\eta\eta'$
203 ± 10	[14] ARMSTRONG	93C	E760	$\overline{p}p \to \pi^0\eta\eta \to 6\gamma$

[11] Spin not determined.
[12] $J^{PC} = 0^{++}$
[13] PWA gives $J^{PC} = 0^{++}$.
[14] No J^{PC} determination.

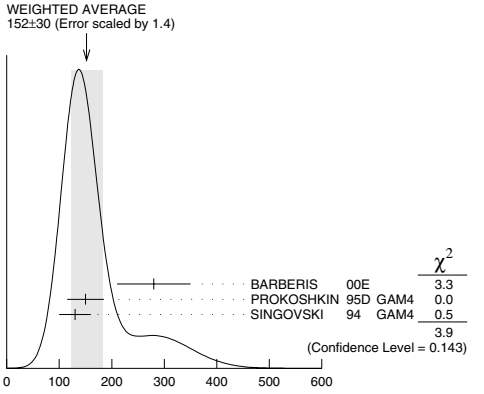

$f_2(2150)$ WIDTH, $\eta\eta$ MODE (MeV)

$\eta\pi\pi$ MODE

VALUE (MeV)	DOCUMENT ID		TECN	CHG	COMMENT
The data in this block is included in the average printed for a previous datablock.					
250 ± 25 ± 45	ADOMEIT	96	CBAR	0	1.94 $\overline{p}p \to \eta 3\pi^0$

$\overline{p}p \rightarrow \pi\pi$

VALUE (MeV)	DOCUMENT ID		TECN	COMMENT
250 OUR ESTIMATE				
• • • We do not use the following data for averages, fits, limits, etc. • • •				
~ 226	HASAN	94	RVUE	$\overline{p}p \rightarrow \pi\pi$
~ 70	[15] OAKDEN	94	RVUE	0.36–1.55 $\overline{p}p \rightarrow \pi\pi$
~ 250	[16] MARTIN	80B	RVUE	
~ 250	[16] MARTIN	80C	RVUE	
~ 250	[17] DULUDE	78B	OSPK	1–2 $\overline{p}p \rightarrow \pi^0\pi^0$

[15] See however KLOET 96 who fit $\pi^+\pi^-$ only and find waves only up to $J = 3$ to be important but not significantly resonant.
[16] $I(J^P) = 0(2^+)$ from simultaneous analysis of $p\overline{p} \rightarrow \pi^-\pi^+$ and $\pi^0\pi^0$.
[17] $I^G(J^P) = 0^+(2^+)$ from partial-wave amplitude analysis.

S-CHANNEL $\overline{p}p$, $\overline{N}N$ or $\overline{K}K$

VALUE (MeV)	DOCUMENT ID		TECN	CHG	COMMENT
• • • We do not use the following data for averages, fits, limits, etc. • • •					
56^{+31}_{-16}	[18] EVANGELISTA	97	SPEC		0.6-2.4 $\overline{p}p \rightarrow K^0_S K^0_S$
135 ± 75	[19,20] COUPLAND	77	CNTR	0	0.7–2.4 $\overline{p}p \rightarrow \overline{p}p$
98 ± 8	[20] ALSPECTOR	73	CNTR		$\overline{p}p$ S channel

[18] Isospin 0 and 2 not separated.
[19] From a fit to the total elastic cross section.
[20] Isospins 0 and 1 not separated.

$K\overline{K}$ MODE

VALUE (MeV)	DOCUMENT ID		TECN	COMMENT
270±50	BARBERIS	99	OMEG	450 $pp \rightarrow p_s p_f K^+ K^-$

$f_2(2150)$ DECAY MODES

	Mode	Fraction (Γ_i/Γ)
Γ_1	$\pi\pi$	
Γ_2	$\eta\eta$	seen
Γ_3	$K\overline{K}$	seen
Γ_4	$f_2(1270)\eta$	seen
Γ_5	$a_2(1320)\pi$	seen

$f_2(2150)$ BRANCHING RATIOS

$\Gamma(K\overline{K})/\Gamma(\eta\eta)$ Γ_3/Γ_2

VALUE	CL%	DOCUMENT ID		TECN	COMMENT
1.28±0.23		BARBERIS	00E		450 $pp \rightarrow p_f \eta\eta p_s$
• • • We do not use the following data for averages, fits, limits, etc. • • •					
< 0.1	95	[21] PROKOSHKIN	95D	GAM4	300 $\pi^- N \rightarrow \pi^- N 2\eta$, 450 $pp \rightarrow pp2\eta$

[21] Using data from ARMSTRONG 89D.

$\Gamma(\pi\pi)/\Gamma(\eta\eta)$ Γ_1/Γ_2

VALUE	CL%	DOCUMENT ID		TECN	COMMENT
• • • We do not use the following data for averages, fits, limits, etc. • • •					
< 0.33	95	[22] PROKOSHKIN	95D	GAM4	300 $\pi^- N \rightarrow \pi^- N 2\eta$, 450 $pp \rightarrow pp2\eta$

[22] Derived from a $\pi^0\pi^0/\eta\eta$ limit.

$\Gamma(f_2(1270)\eta)/\Gamma(a_2(1320)\pi)$ Γ_4/Γ_5

VALUE	DOCUMENT ID		TECN	COMMENT
0.79±0.11	[23] ADOMEIT	96	CBAR	1.94 $\overline{p}p \rightarrow \eta 3\pi^0$

[23] Using B($a_2(1320) \rightarrow \eta\pi$) = 0.145

$f_2(2150)$ REFERENCES

BARBERIS	00E	PL B479 59	D. Barberis *et al.* (WA 102 Collab.)
ABELE	99B	EPJ C8 67	A. Abele *et al.* (Crystal Barrel Collab.)
ANISOVICH	99B	PL B449 154	A.V. Anisovich *et al.*
ANISOVICH	99K	PL B468 309	A.V. Anisovich *et al.*
BARBERIS	99	PL B453 305	D. Barberis *et al.* (Omega Expt.)
EVANGELISTA	97	PR D56 3803	C. Evangelista *et al.* (LEAR Collab.)
MARTIN	97	PR C56 1114	B.R. Martin, G.C. Oades (LOUC, AARH)
ADOMEIT	96	ZPHY C71 227	J. Adomeit *et al.* (Crystal Barrel Collab.)
KLOET	96	PR D53 6120	W.M. Kloet, F. Myhrer (RUTG, NORD)
PROKOSHKIN	95D	SPD 40 495	Y.D. Prokoshkin (SERP) IGJPC
		Translated from DANS 344 469.	
HASAN	94	PL B334 215	A. Hasan, D.V. Bugg (LOQM)
OAKDEN	94	NP A574 731	M.N. Oakden, M.R. Pennington (DURH)
SINGOVSKI	94	NC 107A 1911	A.V. Singovsky (SERP)
ARMSTRONG	93C	PL B307 394	T.A. Armstrong *et al.* (FNAL, FERR, GENO+)
ARMSTRONG	89D	PL B227 186	T.A. Armstrong, M. Benayoun (ATHU, BARI, BIRM+)
MARTIN	80B	NP B176 355	B.R. Martin, D. Morgan (LOUC, RHEL) JP
MARTIN	80C	NP B169 216	A.D. Martin, M.R. Pennington (DURH) JP
CUTTS	78B	PR D17 16	D. Cutts *et al.* (STON, WISC)
DULUDE	78B	PL 79B 335	R.S. Dulude *et al.* (BROW, MIT, BARI) JP
COUPLAND	77	PL 71B 460	M. Coupland *et al.* (LOQM, RHEL)
ALSPECTOR	73	PRL 30 511	J. Alspector *et al.* (RUTG, UPNJ)

OTHER RELATED PAPERS

EISENHAND...	75	NP B96 109	E. Eisenhandler *et al.* (LOQM, LIVP, DARE+)
FIELDS	71	PRL 27 1749	T. Fields *et al.* (ANL, OXF)
YOH	71	PRL 26 922	J.K. Yoh *et al.* (CIT, BNL, ROCH)

$\rho(2150)$

$I^G(J^{PC}) = 1^+(1^{--})$

OMITTED FROM SUMMARY TABLE

This entry was previously called $T_1(2190)$.

$\rho(2150)$ MASS

$e^+e^- \rightarrow \pi^+\pi^-, K^+K^-, 6\pi$

VALUE (MeV)	DOCUMENT ID		TECN	CHG	COMMENT
2149±17 OUR AVERAGE Includes data from the datablock that follows this one.					
2153±37	BIAGINI	91	RVUE		$e^+e^- \rightarrow \pi^+\pi^-, K^+K^-$
2110±50	[2] CLEGG	90	RVUE	0	$e^+e^- \rightarrow 3(\pi^+\pi^-), 2(\pi^+\pi^-\pi^0)$

$\overline{p}p \rightarrow \pi\pi$

VALUE (MeV)	DOCUMENT ID		TECN	COMMENT
• • • We do not use the following data for averages, fits, limits, etc. • • •				
~ 2191	HASAN	94	RVUE	$\overline{p}p \rightarrow \pi\pi$
~ 1988	HASAN	94	RVUE	$\overline{p}p \rightarrow \pi\pi$
~ 2070	[1] OAKDEN	94	RVUE	0.36–1.55 $\overline{p}p \rightarrow \pi\pi$
~ 2170	[3] MARTIN	80B	RVUE	
~ 2100	[3] MARTIN	80C	RVUE	

[1] See however KLOET 96 who fit $\pi^+\pi^-$ only and find waves only up to $J = 3$ to be important but not significantly resonant.

S-CHANNEL $\overline{N}N$

VALUE (MeV)	DOCUMENT ID		TECN	CHG	COMMENT
• • • We do not use the following data for averages, fits, limits, etc. • • •					
2110±35	[4] ANISOVICH	02	SPEC		0.6–1.9 $p\overline{p} \rightarrow \omega\pi^0, \omega\eta\pi^0, \pi^+\pi^-$
~ 2190	[5] CUTTS	78B	CNTR		0.97–3 $\overline{p}p \rightarrow \overline{N}N$
2155±15	[5,6] COUPLAND	77	CNTR	0	0.7–2.4 $\overline{p}p \rightarrow \overline{p}p$
2193± 2	[5,7] ALSPECTOR	73	CNTR		$\overline{p}p$ S channel
2190±10	[8] ABRAMS	70	CNTR		S channel $\overline{p}N$

$\pi^- p \rightarrow \omega\pi^0 n$

VALUE (MeV)	DOCUMENT ID		TECN	COMMENT
The data in this block is included in the average printed for a previous datablock.				
2155±21 OUR AVERAGE				
2140±30	ALDE	95	GAM2	38 $\pi^- p \rightarrow \omega\pi^0 n$
2170±30	ALDE	92C	GAM4	100 $\pi^- p \rightarrow \omega\pi^0 n$

[2] Includes ATKINSON 85.
[3] $I(J^P) = 1(1^-)$ from simultaneous analysis of $p\overline{p} \rightarrow \pi^-\pi^+$ and $\pi^0\pi^0$.
[4] From the combined analysis of ANISOVICH 00J, ANISOVICH 01D, ANISOVICH 01E, and ANISOVICH 02.
[5] Isospins 0 and 1 not separated.
[6] From a fit to the total elastic cross section.
[7] Referred to as T or T region by ALSPECTOR 73.
[8] Seen as bump in $I = 1$ state. See also COOPER 68. PEASLEE 75 confirm $\overline{p}p$ results of ABRAMS 70, no narrow structure.

$\rho(2150)$ WIDTH

$e^+e^- \rightarrow \pi^+\pi^-, K^+K^-, 6\pi$

VALUE (MeV)	DOCUMENT ID		TECN	CHG	COMMENT
363± 50 OUR AVERAGE Includes data from the datablock that follows this one.					
389± 79	BIAGINI	91	RVUE		$e^+e^- \rightarrow \pi^+\pi^-, K^+K^-$
410±100	[10] CLEGG	90	RVUE	0	$e^+e^- \rightarrow 3(\pi^+\pi^-), 2(\pi^+\pi^-\pi^0)$

$\overline{p}p \rightarrow \pi\pi$

VALUE (MeV)	DOCUMENT ID		TECN	COMMENT
• • • We do not use the following data for averages, fits, limits, etc. • • •				
~ 296	HASAN	94	RVUE	$\overline{p}p \rightarrow \pi\pi$
~ 244	HASAN	94	RVUE	$\overline{p}p \rightarrow \pi\pi$
~ 40	[9] OAKDEN	94	RVUE	0.36–1.55 $\overline{p}p \rightarrow \pi\pi$
~ 250	[11] MARTIN	80B	RVUE	
~ 200	[11] MARTIN	80C	RVUE	

[9] See however KLOET 96 who fit $\pi^+\pi^-$ only and find waves only up to $J = 3$ to be important but not significantly resonant.

S-CHANNEL $\overline{N}N$

VALUE (MeV)	DOCUMENT ID		TECN	CHG	COMMENT
• • • We do not use the following data for averages, fits, limits, etc. • • •					
230±50	[12] ANISOVICH	02	SPEC		0.6–1.9 $p\overline{p} \rightarrow \omega\pi^0, \omega\eta\pi^0, \pi^+\pi^-$
135 ± 75	[13,14] COUPLAND	77	CNTR	0	0.7–2.4 $\overline{p}p \rightarrow \overline{p}p$
98 ± 8	[14] ALSPECTOR	73	CNTR		$\overline{p}p$ S channel
~ 85	[15] ABRAMS	70	CNTR		S channel $\overline{p}N$

$\pi^- p \to \omega\pi^0 n$

VALUE (MeV)	DOCUMENT ID		TECN	COMMENT
The data in this block is included in the average printed for a previous datablock.				
320±70	ALDE	95	GAM2	38 $\pi^- p \to \omega\pi^0 n$
• • • We do not use the following data for averages, fits, limits, etc. • • •				
~ 300	ALDE	92C	GAM4	100 $\pi^- p \to \omega\pi^0 n$

[10] Includes ATKINSON 85.
[11] $I(J^P) = 1(1^-)$ from simultaneous analysis of $p\overline{p} \to \pi^-\pi^+$ and $\pi^0\pi^0$.
[12] From the combined analysis of ANISOVICH 00J, ANISOVICH 01D, ANISOVICH 01E, and ANISOVICH 02.
[13] From a fit to the total elastic cross section.
[14] Isospins 0 and 1 not separated.
[15] Seen as bump in $I = 1$ state. See also COOPER 68. PEASLEE 75 confirm $\overline{p}p$ results of ABRAMS 70, no narrow structure.

$\rho(2150)$ REFERENCES

ANISOVICH	02	PL B542 8	A.V. Anisovich *et al.*	
ANISOVICH	01D	PL B508 6	A.V. Anisovich *et al.*	
ANISOVICH	01E	PL B513 281	A.V. Anisovich *et al.*	
ANISOVICH	00J	PL B491 47	A.V. Anisovich *et al.*	
KLOET	96	PR D53 6120	W.M. Kloet, F. Myhrer	(RUTG, NORD)
ALDE	95	ZPHY C66 379	D.M. Alde *et al.*	(GAMS Collab.) JP
HASAN	94	PL B334 215	A. Hasan, D.V. Bugg	(LOQM)
OAKDEN	94	NP A574 731	M.N. Oakden, M.R. Pennington	(DURH)
ALDE	92C	ZPHY C54 553	D.M. Alde *et al.*	(BELG, SERP, KEK, LANL+)
BIAGINI	91	NC 104A 363	M.E. Biagini *et al.*	(FRAS, PRAG)
CLEGG	90	ZPHY C45 677	A.B. Clegg, A. Donnachie	(LANC, MCHS)
ATKINSON	85	ZPHY C29 333	M. Atkinson *et al.*	(BONN, CERN, GLAS+)
MARTIN	80B	NP B176 355	B.R. Martin, D. Morgan	(LOUC, RHEL) JP
MARTIN	80C	NP B169 216	A.D. Martin, M.R. Pennington	(DURH) JP
CUTTS	78B	PR D17 16	D. Cutts *et al.*	(STON, WISC)
COUPLAND	77	PL 71B 460	M. Coupland *et al.*	(LOQM, RHEL)
PEASLEE	75	PL 57B 189	D.C. Peaslee *et al.*	(CANB, BARI, BROW+)
ALSPECTOR	73	PRL 30 511	J. Alspector *et al.*	(RUTG, UPNJ)
ABRAMS	70	PR D1 1917	R.J. Abrams *et al.*	(BNL)
COOPER	68	PRL 20 1059	W.A. Cooper *et al.*	(ANL)

OTHER RELATED PAPERS

AMELIN	00	NP A668 83	D. Amelin *et al.*	(VES Collab.)
EISENHAND...	75	NP B96 109	E. Eisenhandler *et al.*	(LOQM, LIVP, DARE+)
BRICMAN	69	PL 29B 451	C. Bricman *et al.*	(CERN, CAEN, SACL)
ABRAMS	67C	PRL 18 1209	R.J. Abrams *et al.*	(BNL)

$f_0(2200)$

$I^G(J^{PC}) = 0^+(0^{++})$

OMITTED FROM SUMMARY TABLE
Seen at DCI in the $K^0_S K^0_S$ system. Not seen in Υ radiative decays (BARU 89). Needs confirmation.

$f_0(2200)$ MASS

VALUE (MeV)	DOCUMENT ID		TECN	CHG	COMMENT
2197±17	[1] AUGUSTIN	88	DM2	0	$J/\psi \to \gamma K^0_S K^0_S$
• • • We do not use the following data for averages, fits, limits, etc. • • •					
~ 2122	HASAN	94	RVUE		$\overline{p}p \to \pi\pi$
~ 2321	HASAN	94	RVUE		$\overline{p}p \to \pi\pi$

[1] Cannot determine spin to be 0.

$f_0(2200)$ WIDTH

VALUE (MeV)	DOCUMENT ID		TECN	CHG	COMMENT
201±51	[2] AUGUSTIN	88	DM2	0	$J/\psi \to \gamma K^0_S K^0_S$
• • • We do not use the following data for averages, fits, limits, etc. • • •					
~ 273	HASAN	94	RVUE		$\overline{p}p \to \pi\pi$
~ 223	HASAN	94	RVUE		$\overline{p}p \to \pi\pi$

[2] Cannot determine spin to be 0.

$f_0(2200)$ REFERENCES

HASAN	94	PL B334 215	A. Hasan, D.V. Bugg	(LOQM)
BARU	89	ZPHY C42 505	S.E. Baru *et al.*	(NOVO)
AUGUSTIN	88	PRL 60 2238	J.E. Augustin *et al.*	(DM2 Collab.)

OTHER RELATED PAPERS

EISENHAND...	75	NP B96 109	E. Eisenhandler *et al.*	(LOQM, LIVP, DARE+)

$f_J(2220)$

$I^G(J^{PC}) = 0^+(2^{++} \text{ or } 4^{++})$

OMITTED FROM SUMMARY TABLE
Needs confirmation.

THE $f_J(2220)$

Updated April 2002 by M. Doser (CERN).

This state has been seen in $J/\psi(1S)$ radiative decay into $K\overline{K}$ (K^+K^- and $K^0_S K^0_S$ modes seen (BALTRUSAITIS 86D, BAI 96B)). An upper limit from DM2 for these modes (AUGUSTIN 88) is at the level at which observation is claimed. There are also indications for further decay modes ($\pi^+\pi^-$ and $\overline{p}p$ (BAI 96B) and $\pi^0\pi^0$ (BAI 98H)) in the same production process, although again at the level at which previous upper limits had been obtained (BALTRUSAITIS 86D). This is also seen in $\eta\eta$ (ALDE 86B), $K^0_S K^0_S$ (ASTON 88D), and in K^+K^- (ALDE 88F), albeit with very low statistics. Its J^{PC} is determined from the angular distributions of these observations. It is not seen in Υ radiative decays (BARU 89, MASEK 02), B inclusive decays (BEHRENDS 84), or in $\gamma\gamma$ (GODANG 97, ALAM 98C, ACCIARRI 01H), which would not be surprising if it were a glueball, since its two-photon width would then be expected to be small. It is also not seen in formation in $\overline{p}p \to K^+K^-$ (BARDIN 87, SCULLI 87), in $\overline{p}p \to K_S K_S$ (BARNES 93, EVANGELISTA 97), $\overline{p}p \to \phi\phi$ (EVANGELISTA 98), in $\overline{p}p \to \eta\eta$ (AMSLER 01), or in $\overline{p}p \to \pi\pi$ (HASAN 96, AMSLER 01). The upper limit in $\overline{p}p$ formation can be related to the claimed decay into $\overline{p}p$ to give a lower limit for the process $J/\psi(1S) \to \gamma\xi$ of $\sim 2.3 \times 10^{-3}$ (GODFREY 99). Such a signal should be visible in the inclusive photon spectrum (BLOOM 85). The limit also leads to the conclusion that the reported two-body final states constitute only a small fraction of all decay modes of the ξ. A recent speculation that a handfull of events may have been seen in charmless B decays (CHUA 02) underlines that observation of further decay modes and confirmation of the $p\overline{p}$ decay would be very desireable.

References

References may be found at the end of the $f_J(2220)$ Listing.

$f_J(2220)$ MASS

VALUE (MeV)	EVTS	DOCUMENT ID		TECN	COMMENT
2231.1± 3.5 OUR AVERAGE					
2235 ± 4 ± 6	74	BAI	96B	BES	$e^+e^- \to J/\psi \to \gamma\pi^+\pi^-$
2230 $^{+6}_{-7}$ ±16	46	BAI	96B	BES	$e^+e^- \to J/\psi \to \gamma K^+K^-$
2232 $^{+8}_{-7}$ ±15	23	BAI	96B	BES	$e^+e^- \to J/\psi \to \gamma K^0_S K^0_S$
2235 ± 4 ± 5	32	BAI	96B	BES	$e^+e^- \to J/\psi \to \gamma p\overline{p}$
2209 $^{+17}_{-15}$ ±10		ASTON	88F	LASS	11 $K^- p \to K^+K^-\Lambda$
2230 ±20		BOLONKIN	88	SPEC	40 $\pi^- p \to K^0_S K^0_S n$
2220 ±10	41	[1] ALDE	86B	GA24	38–100 $\pi p \to n\eta\eta'$
2230 ± 6 ±14	93	BALTRUSAIT...	86D	MRK3	$e^+e^- \to \gamma K^+K^-$
2232 ± 7 ± 7	23	BALTRUSAIT...	86D	MRK3	$e^+e^- \to \gamma K^0_S K^0_S$
• • • We do not use the following data for averages, fits, limits, etc. • • •					
2246 ±36		BAI	98H	BES	$J/\psi \to \gamma\pi^0\pi^0$

[1] ALDE 86B uses data from both the GAMS-2000 and GAMS-4000 detectors.

$f_J(2220)$ WIDTH

VALUE (MeV)	CL%	EVTS	DOCUMENT ID		TECN	COMMENT
$23^{+\ 8}_{-\ 7}$ OUR AVERAGE						
$19^{+\ 13}_{-\ 11} \pm 12$		74	BAI	96B	BES	$e^+e^- \to J/\psi \to \gamma\pi^+\pi^-$
$20^{+\ 20}_{-\ 15} \pm 17$		46	BAI	96B	BES	$e^+e^- \to J/\psi \to \gamma K^+K^-$
$20^{+\ 25}_{-\ 16} \pm 14$		23	BAI	96B	BES	$e^+e^- \to J/\psi \to \gamma K^0_S K^0_S$
$15^{+\ 12}_{-\ 9} \pm 9$		32	BAI	96B	BES	$e^+e^- \to J/\psi \to \gamma p\overline{p}$
$60^{+107}_{-\ 57}$			ASTON	88F	LASS	$11\ K^-p \to K^+K^-\Lambda$
80 ± 30			BOLONKIN	88	SPEC	$40\ \pi^-p \to K^0_S K^0_S n$
$26^{+\ 20}_{-\ 16} \pm 17$		93	BALTRUSAIT...	86D	MRK3	$e^+e^- \to \gamma K^+K^-$
$18^{+\ 23}_{-\ 15} \pm 10$		23	BALTRUSAIT...	86D	MRK3	$e^+e^- \to \gamma K^0_S K^0_S$
• • • We do not use the following data for averages, fits, limits, etc. • • •						
<80	90		ALDE	87C	GAM2	$38\ \pi^-p \to \eta'\eta n$

$f_J(2220)$ DECAY MODES

	Mode	Fraction (Γ_i/Γ)
Γ_1	$\pi\pi$	seen
Γ_2	$\pi^+\pi^-$	seen
Γ_3	$K\overline{K}$	seen
Γ_4	$p\overline{p}$	
Γ_5	$\gamma\gamma$	not seen
Γ_6	$\eta\eta'(958)$	seen
Γ_7	$\phi\phi$	not seen
Γ_8	$\eta\eta$	not seen

$f_J(2220)$ Γ(i)$\Gamma(\gamma\gamma)/\Gamma$(total)

$\Gamma(K\overline{K}) \times \Gamma(\gamma\gamma)/\Gamma_{\text{total}}$ — **$\Gamma_3\Gamma_5/\Gamma$**

VALUE (eV)	CL%	DOCUMENT ID		TECN	COMMENT
$<\ 1.4$	95	[2] ACCIARRI	01H	L3	$\gamma\gamma \to K^0_S K^0_S$, E^{ee}_{cm}= 91, 183–209 GeV
• • • We do not use the following data for averages, fits, limits, etc. • • •					
$<\ 5.6$	95	[2] GODANG	97	CLE2	$\gamma\gamma \to K^0_S K^0_S$
$<\ 86$	95	[2] ALBRECHT	90G	ARG	$\gamma\gamma \to K^+K^-$
<1000	95	[3] ALTHOFF	85B	TASS	$\gamma\gamma$, $K\overline{K}\pi$

$\Gamma(\pi\pi) \times \Gamma(\gamma\gamma)/\Gamma_{\text{total}}$ — **$\Gamma_1\Gamma_5/\Gamma$**

VALUE (eV)	CL%	DOCUMENT ID		TECN	COMMENT
<2.5	95	ALAM	98C	CLE2	$\gamma\gamma \to \pi^+\pi^-$

[2] Assuming $J^P = 2^+$.
[3] True for $J^P = 0^+$ and $J^P = 2^+$.

$f_J(2220)$ Γ(i)$\Gamma(p\overline{p})/\Gamma^2$(total)

$\Gamma(p\overline{p}) \times \Gamma(\pi\pi)/\Gamma^2_{\text{total}}$ — **$\Gamma_4\Gamma_1/\Gamma^2$**

VALUE (units 10^{-5})	CL%	DOCUMENT ID		TECN	COMMENT
<18	95	[4] AMSLER	01	CBAR	1.4–$1.5\ p\overline{p} \to \pi^0\pi^0$
• • • We do not use the following data for averages, fits, limits, etc. • • •					
<(11–42)	99	[5] HASAN	96	SPEC	1.35–$1.55\ p\overline{p} \to \pi^+\pi^-$

$\Gamma(p\overline{p}) \times \Gamma(\phi\phi)/\Gamma^2_{\text{total}}$ — **$\Gamma_4\Gamma_7/\Gamma^2$**

VALUE (units 10^{-5})	CL%	DOCUMENT ID		TECN	COMMENT
<6	95	[6] EVANGELISTA	98	SPEC	1.1-$2.0\ p\overline{p} \to \phi\phi$

$\Gamma(p\overline{p}) \times \Gamma(\eta\eta)/\Gamma^2_{\text{total}}$ — **$\Gamma_4\Gamma_8/\Gamma^2$**

VALUE (units 10^{-5})	CL%	DOCUMENT ID		TECN	COMMENT
<4	95	[4] AMSLER	01	CBAR	1.4–$1.5\ p\overline{p} \to \eta\eta$

[4] For $J^P = 2^+$ in the mass range 2222–2240 MeV and the total width between 10 and 20 MeV.
[5] For $J^P = 2^+$ and $J^P = 4^+$ in the mass range 2220–2245 MeV and the total width of 15 MeV.
[6] For $J^P = 2^+$, the mass of 2235 MeV and the total width of 15 MeV.

$f_J(2220)$ BRANCHING RATIOS

$\Gamma(p\overline{p})/\Gamma_{\text{total}}$ — **Γ_4/Γ**

VALUE (units 10^{-4})	CL%	DOCUMENT ID		TECN	COMMENT
• • • We do not use the following data for averages, fits, limits, etc. • • •					
<3.0	95	[8] EVANGELISTA	97	SPEC	1.96-$2.40\ \overline{p}p \to K^0_S K^0_S$
<1.1	99.7	[7] BARNES	93	SPEC	1.3-$1.5\ \overline{p}p \to K^0_S K^0_S$
<2.6	99.7	[7] BARDIN	87	CNTR	1.3-$1.5\ \overline{p}p \to K^+K^-$
<3.6	99.7	[7] SCULLI	87	CNTR	1.29-$1.55\ \overline{p}p \to K^+K^-$

[7] Assuming Γ = 30-35 MeV, $J^P = 2^+$ and B($f_J(2220) \to K\overline{K}$) = 100%.

$\Gamma(\pi\pi)/\Gamma(K\overline{K})$ — **Γ_1/Γ_3**

VALUE	DOCUMENT ID		TECN	COMMENT
1.0±0.5	BAI	96B	BES	$e^+e^- \to J/\psi \to \gamma 2\pi, K\overline{K}$

$\Gamma(p\overline{p})/\Gamma(K\overline{K})$ — **Γ_4/Γ_3**

VALUE	DOCUMENT ID		TECN	COMMENT
0.17±0.09	BAI	96B	BES	$e^+e^- \to J/\psi \to \gamma p\overline{p}, K\overline{K}$

[8] Assuming $\Gamma \sim 20$ MeV, $J^P = 2^+$ and B($f_J(2220) \to K\overline{K}$) = 100%.

$f_J(2220)$ REFERENCES

ACCIARRI	01H	PL B501 173	M. Acciarri *et al.* (L3 Collab.)
AMSLER	01	PL B520 175	C. Amsler *et al.* (Crystal Barrel Collab.)
ALAM	98C	PRL 81 3328	M.S. Alam *et al.* (CLEO Collab.)
BAI	98H	PRL 81 1179	J.Z. Bai *et al.* (BES Collab.)
EVANGELISTA	98	PR D57 5370	C. Evangelista *et al.* (JETSET Collab.)
EVANGELISTA	97	PR D56 3803	C. Evangelista *et al.* (LEAR Collab.)
GODANG	97	PRL 79 3829	R. Godang *et al.* (CLEO Collab.)
BAI	96B	PRL 76 3502	J.Z. Bai *et al.* (BES Collab.)
HASAN	96	PL B388 376	A. Hasan, D.V. Bugg (BRUN, LOQM)
BARNES	93	PL B309 469	P.D. Barnes, P. Birien, W.H. Breunlich
ALBRECHT	90G	ZPHY C48 183	H. Albrecht *et al.* (ARGUS Collab.)
ASTON	88F	PL B215 199	D. Aston *et al.* (SLAC, NAGO, CINC, INUS) JP
BOLONKIN	88	NP B309 426	B.V. Bolonkin *et al.* (ITEP, SERP)
ALDE	87C	SJNP 45 255	D. Alde *et al.* Translated from YAF 45 405.
BARDIN	87	PL B195 292	G. Bardin *et al.* (SACL, FERR, CERN, PADO+)
SCULLI	87	PRL 58 1715	J. Sculli *et al.* (NYU, BNL)
ALDE	86B	PL B177 120	D.M. Alde *et al.* (SERP, BELG, LANL, LAPP)
BALTRUSAIT...	86D	PRL 56 107	R.M. Baltrusaitis (CIT, UCSC, ILL, SLAC+)
ALTHOFF	85B	ZPHY C29 189	M. Althoff *et al.* (TASSO Collab.)

OTHER RELATED PAPERS

CHUA	02	PL B544 139	C.-K. Chua, W.-S. Hou, S.U. Tsai
MASEK	02	PR D65 072002	G. Masek *et al.* (CLEO Collab.)
LIU	00A	JPG 26 L59	L.C. Liu, W.H. Ma
WANG	00A	PR D62 017503	Z. Wang
ANISOVICH	99D	PL B452 180	A.V. Anisovich *et al.*
Also	99F	NP A651 253	A.V. Anisovich *et al.*
ANISOVICH	99F	NP A651 253	A.V. Anisovich *et al.*
PROKOSHKIN	99	PAN 62 356	Yu.D. Prokoshkin Translated from YAF 62 396.
HUANG	96	PL B380 189	T. Huang *et al.* (BHEP, BEIJ)
BARDIN	87	PL B195 292	G. Bardin *et al.* (SACL, FERR, CERN, PADO+)
YAOUANC	85	ZPHY C28 309	A. Le Yaouanc *et al.* (ORSAY, TOKY)
GODFREY	84	PL 141B 439	S. Godfrey, R. Kokoski, N. Isgur (TNTO)
SHATZ	84	PL 138B 209	M.P. Shatz (CIT)
WILLEY	84	PRL 52 585	R.S. Willey (PITT)
EISENHAND...	75	NP B96 109	E. Eisenhandler *et al.* (LOQM, LIVP, DARE+)

$\eta(2225)$

$I^G(J^{PC}) = 0^+(0^{-+})$

OMITTED FROM SUMMARY TABLE
Seen in $J/\psi \to \gamma\phi\phi$. Needs confirmation.

$\eta(2225)$ MASS

VALUE (MeV)	DOCUMENT ID		TECN	COMMENT
2220±18 OUR AVERAGE				
$2230 \pm 25 \pm 15$	BAI	90B	MRK3	$J/\psi \to \gamma K^+K^-K^+K^-$
$2214 \pm 20 \pm 13$	BAI	90B	MRK3	$J/\psi \to \gamma K^+K^-K^0_S K^0_L$
• • • We do not use the following data for averages, fits, limits, etc. • • •				
~ 2220	BISELLO	86B	DM2	$J/\psi \to \gamma K^+K^-K^+K^-$

$\eta(2225)$ WIDTH

VALUE (MeV)	DOCUMENT ID		TECN	COMMENT
$150^{+\ 300}_{-\ 60} \pm 60$	BAI	90B	MRK3	$J/\psi \to \gamma K^+K^-K^+K^-$
• • • We do not use the following data for averages, fits, limits, etc. • • •				
$\sim\ 80$	BISELLO	86B	DM2	$J/\psi \to \gamma K^+K^-K^+K^-$

$\eta(2225)$ REFERENCES

BAI	90B	PRL 65 1309	Z. Bai *et al.* (Mark III Collab.)
BISELLO	86B	PL B179 294	D. Bisello *et al.* (DM2 Collab.)

Meson Particle Listings

$\rho_3(2250)$, $f_2(2300)$

$\rho_3(2250)$

$I^G(J^{PC}) = 1^+(3^{--})$

OMITTED FROM SUMMARY TABLE

Contains results mostly from formation experiments. For further production experiments see the Further States entry. See also $\rho(2150)$, $f_2(2150)$, $f_4(2300)$, $\rho_5(2350)$.

$\rho_3(2250)$ MASS

$\overline{p}p \to \pi\pi$ or $K\overline{K}$

VALUE (MeV)	DOCUMENT ID		TECN	CHG	COMMENT
• • • We do not use the following data for averages, fits, limits, etc. • • •					
~ 2232	HASAN	94	RVUE		$\overline{p}p \to \pi\pi$
~ 2007	HASAN	94	RVUE		$\overline{p}p \to \pi\pi$
~ 2090	[1] OAKDEN	94	RVUE		0.36–1.55 $\overline{p}p \to \pi\pi$
~ 2250	[2] MARTIN	80B	RVUE		
~ 2300	[2] MARTIN	80C	RVUE		
~ 2140	[3] CARTER	78B	CNTR	0	0.7–2.4 $\overline{p}p \to K^-K^+$
~ 2150	[4] CARTER	77	CNTR	0	0.7–2.4 $\overline{p}p \to \pi\pi$

[1] See however KLOET 96 who fit $\pi^+\pi^-$ only and find waves only up to $J = 3$ to be important but not significantly resonant.
[2] $I(J^P) = 1(3^-)$ from simultaneous analysis of $p\overline{p} \to \pi^-\pi^+$ and $\pi^0\pi^0$.
[3] $I = 0, 1$. $J^P = 3^-$ from Barrelet-zero analysis.
[4] $I(J^P) = 1(3^-)$ from amplitude analysis.

S-CHANNEL $\overline{N}N$

VALUE (MeV)	DOCUMENT ID		TECN	CHG	COMMENT
• • • We do not use the following data for averages, fits, limits, etc. • • •					
2260 ± 20	[5] ANISOVICH	02	SPEC		0.6–1.9 $p\overline{p} \to \omega\pi^0, \omega\eta\pi^0, \pi^+\pi^-$
~ 2190	[6] CUTTS	78B	CNTR		0.97–3 $\overline{p}p \to \overline{N}N$
2155 ± 15	[6,7] COUPLAND	77	CNTR	0	0.7–2.4 $\overline{p}p \to \overline{p}p$
2193 ± 2	[6,8] ALSPECTOR	73	CNTR		$\overline{p}p$ S channel
2190 ± 10	[9] ABRAMS	70	CNTR		S channel $\overline{p}N$

[5] From the combined analysis of ANISOVICH 00J, ANISOVICH 01D, ANISOVICH 01E, and ANISOVICH 02.
[6] Isospins 0 and 1 not separated.
[7] From a fit to the total elastic cross section.
[8] Referred to as T or T region by ALSPECTOR 73.
[9] Seen as bump in $I = 1$ state. See also COOPER 68. PEASLEE 75 confirm $\overline{p}p$ results of ABRAMS 70, no narrow structure.

$\pi^-p \to \eta\pi\pi$

VALUE (MeV)	DOCUMENT ID		TECN	COMMENT
• • • We do not use the following data for averages, fits, limits, etc. • • •				
2290 ± 20 ± 30	AMELIN	00	VES	37 $\pi^-p \to \eta\pi^+\pi^-n$

$\rho_3(2250)$ WIDTH

$\overline{p}p \to \pi\pi$ or $K\overline{K}$

VALUE (MeV)	DOCUMENT ID		TECN	CHG	COMMENT
• • • We do not use the following data for averages, fits, limits, etc. • • •					
~ 220	HASAN	94	RVUE		$\overline{p}p \to \pi\pi$
~ 287	HASAN	94	RVUE		$\overline{p}p \to \pi\pi$
~ 60	[10] OAKDEN	94	RVUE		0.36–1.55 $\overline{p}p \to \pi\pi$
~ 250	[11] MARTIN	80B	RVUE		
~ 200	[11] MARTIN	80C	RVUE		
~ 150	[12] CARTER	78B	CNTR	0	0.7–2.4 $\overline{p}p \to K^-K^+$
~ 200	[13] CARTER	77	CNTR	0	0.7–2.4 $\overline{p}p \to \pi\pi$

[10] See however KLOET 96 who fit $\pi^+\pi^-$ only and find waves only up to $J = 3$ to be important but not significantly resonant.
[11] $I(J^P) = 1(3^-)$ from simultaneous analysis of $p\overline{p} \to \pi^-\pi^+$ and $\pi^0\pi^0$.
[12] $I = 0, 1$. $J^P = 3^-$ from Barrelet-zero analysis.
[13] $I(J^P) = 1(3^-)$ from amplitude analysis.

S-CHANNEL $\overline{N}N$

VALUE (MeV)	DOCUMENT ID		TECN	CHG	COMMENT
• • • We do not use the following data for averages, fits, limits, etc. • • •					
160 ± 25	[14] ANISOVICH	02	SPEC		0.6–1.9 $p\overline{p} \to \omega\pi^0, \omega\eta\pi^0, \pi^+\pi^-$
135 ± 75	[15,16] COUPLAND	77	CNTR	0	0.7–2.4 $\overline{p}p \to \overline{p}p$
98 ± 8	[16] ALSPECTOR	73	CNTR		$\overline{p}p$ S channel
~ 85	[17] ABRAMS	70	CNTR		S channel $\overline{p}N$

[14] From the combined analysis of ANISOVICH 00J, ANISOVICH 01D, ANISOVICH 01E, and ANISOVICH 02.
[15] From a fit to the total elastic cross section.
[16] Isospins 0 and 1 not separated.
[17] Seen as bump in $I = 1$ state. See also COOPER 68. PEASLEE 75 confirm $\overline{p}p$ results of ABRAMS 70, no narrow structure.

$\pi^-p \to \eta\pi\pi$

VALUE (MeV)	DOCUMENT ID		TECN	COMMENT
• • • We do not use the following data for averages, fits, limits, etc. • • •				
230 ± 50 ± 80	AMELIN	00	VES	37 $\pi^-p \to \eta\pi^+\pi^-n$

$\rho_3(2250)$ REFERENCES

ANISOVICH	02	PL B542 8	A.V. Anisovich *et al.*
ANISOVICH	01D	PL B508 6	A.V. Anisovich *et al.*
ANISOVICH	01E	PL B513 281	A.V. Anisovich *et al.*
AMELIN	00	NP A668 83	D. Amelin *et al.* (VES Collab.)
ANISOVICH	00J	PL B491 47	A.V. Anisovich *et al.*
KLOET	96	PR D53 6120	W.M. Kloet, F. Myhrer (RUTG, NORD)
HASAN	94	PL B334 215	A. Hasan, D.V. Bugg (LOQM)
OAKDEN	94	NP A574 731	M.N. Oakden, M.R. Pennington (DURH)
MARTIN	80B	NP B176 355	B.R. Martin, D. Morgan (LOUC, RHEL) JP
MARTIN	80C	NP B169 216	A.D. Martin, M.R. Pennington (DURH) JP
CARTER	78B	NP B141 467	A.A. Carter (LOQM)
CUTTS	78B	PR D17 16	D. Cutts *et al.* (STON, WISC)
CARTER	77	PL 67B 117	A.A. Carter *et al.* (LOQM, RHEL) JP
COUPLAND	77	PL 71B 460	M. Coupland *et al.* (LOQM, RHEL)
PEASLEE	75	PL 57B 189	D.C. Peaslee *et al.* (CANB, BARI, BROW+)
ALSPECTOR	73	PRL 30 511	J. Alspector *et al.* (RUTG, UPNJ)
ABRAMS	70	PR D1 1917	R.J. Abrams *et al.* (BNL)
COOPER	68	PRL 20 1059	W.A. Cooper *et al.* (ANL)

OTHER RELATED PAPERS

MARTIN	79B	PL 86B 93	A.D. Martin, M.R. Pennington (DURH)
CARTER	78	NP B132 176	A.A Carter (LOQM) JP
CARTER	77B	PL 67B 122	A.A. Carter (LOQM) JP
CARTER	77C	NP B127 202	A.A. Carter *et al.* (LOQM, DARE, RHEL)
ZEMANY	76	NP B103 537	P.D. Zemany *et al.* (MSU)
EISENHAND...	75	NP B96 109	E. Eisenhandler *et al.* (LOQM, LIVP, DARE+)
BERTANZA	74	NC 23A 209	L. Bertanza *et al.* (PISA, PADO, TORI)
BETTINI	73	NC 15A 563	A. Bettini *et al.* (PADO, LBL, PISA+)
DONNACHIE	73	LNC 7 285	A. Donnachie, P.R. Thomas (MCHS)
NICHOLSON	73	PR D7 2572	H. Nicholson *et al.* (CIT, ROCH, BNL)
FIELDS	71	PRL 27 1749	T. Fields *et al.* (ANL, OXF)
YOH	71	PRL 26 922	J.K. Yoh *et al.* (CIT, BNL, ROCH)
ABRAMS	67C	PRL 18 1209	R.J. Abrams *et al.* (BNL)

$f_2(2300)$

$I^G(J^{PC}) = 0^+(2^{++})$

See also the mini-review under non-$q\overline{q}$ candidates. (See the index for the page number.)

$f_2(2300)$ MASS

VALUE (MeV)	DOCUMENT ID		TECN	COMMENT
2297±28	[1] ETKIN	88	MPS	22 $\pi^-p \to \phi\phi n$
• • • We do not use the following data for averages, fits, limits, etc. • • •				
2327 ± 9 ± 6	ABE	04	BELL	10.6 $e^+e^- \to e^+e^-K^+K^-$
2240 ± 15	ANISOVICH	00J	SPEC	$p\overline{p} \to \pi^0\pi^0\eta$
2231 ± 10	BOOTH	86	OMEG	85 π^-Be $\to 2\phi$Be
2220^{+90}_{-20}	LINDENBAUM	84	RVUE	
2320 ± 40	ETKIN	82	MPS	22 $\pi^-p \to 2\phi n$

[1] Includes data of ETKIN 85. The percentage of the resonance going into $\phi\phi$ 2^{++} S_2, D_2, and D_0 is 6^{+15}_{-5}, 25^{+18}_{-14}, and 69^{+16}_{-27}, respectively.

$f_2(2300)$ WIDTH

VALUE (MeV)	DOCUMENT ID		TECN	COMMENT
149±41	[2] ETKIN	88	MPS	22 $\pi^-p \to \phi\phi n$
• • • We do not use the following data for averages, fits, limits, etc. • • •				
275 ± 36 ± 20	ABE	04	BELL	10.6 $e^+e^- \to e^+e^-K^+K^-$
241 ± 30	ANISOVICH	00J	SPEC	$p\overline{p} \to \pi^0\pi^0\eta$
133 ± 50	BOOTH	86	OMEG	85 π^-Be $\to 2\phi$Be
200 ± 50	LINDENBAUM	84	RVUE	
220 ± 70	ETKIN	82	MPS	22 $\pi^-p \to 2\phi n$

[2] Includes data of ETKIN 85.

$f_2(2300)$ DECAY MODES

	Mode	Fraction (Γ_i/Γ)
Γ_1	$\phi\phi$	seen
Γ_2	$K\overline{K}$	seen
Γ_3	$\gamma\gamma$	seen

$f_2(2300)$ Γ(i)$\Gamma(\gamma\gamma)/\Gamma$(total)

$\Gamma(K\overline{K}) \times \Gamma(\gamma\gamma)/\Gamma_{\text{total}}$ $\qquad$ $\Gamma_2\Gamma_3/\Gamma$

VALUE (eV)	DOCUMENT ID		TECN	COMMENT
• • • We do not use the following data for averages, fits, limits, etc. • • •				
44 ± 6 ± 12	[3] ABE	04	BELL	10.6 $e^+e^- \to e^+e^-K^+K^-$

[3] Assuming spin 2.

$f_2(2300)$ REFERENCES

ABE	04	EPJ C32 323	K. Abe *et al.*	(BELLE Collab.)
ANISOVICH	00J	PL B491 47	A.V. Anisovich *et al.*	
ETKIN	88	PL B201 568	A. Etkin *et al.*	(BNL, CUNY)
BOOTH	86	NP B273 677	P.S.L. Booth *et al.*	(LIVP, GLAS, CERN)
ETKIN	85	PL 165B 217	A. Etkin *et al.*	(BNL, CUNY)
LINDENBAUM	84	CNPP 13 285	S.J. Lindenbaum	(CUNY)
ETKIN	82	PRL 49 1620	A. Etkin *et al.*	(BNL, CUNY)

OTHER RELATED PAPERS

AMELIN	00	NP A668 83	D. Amelin *et al.*	(VES Collab.)
BOLONKIN	00	JETPL 72 166 Translated from ZETFP 72 240.	B.V. Bolonkin *et al.*	
BARBERIS	98	PL B432 436	D. Barberis *et al.*	(Omega Expt.)
LANDBERG	96	PR D53 2839	C. Landberg *et al.*	(BNL, CUNY, RPI)
GREEN	86	PRL 56 1639	D.R. Green *et al.*	(FNAL, ARIZ, FSU+)
BOOTH	84	NP B242 51	P.S.L. Booth *et al.*	(LIVP, GLAS, CERN)
EISENHAND...	75	NP B96 109	E. Eisenhandler *et al.*	(LOQM, LIVP, DARE+)

$f_4(2300)$

$I^G(J^{PC}) = 0^+(4^{++})$

OMITTED FROM SUMMARY TABLE

This entry was previously called $U_0(2350)$. Contains results mostly from formation experiments. For further production experiments see the Further States entry. See also $\rho(2150)$, $f_2(2150)$, $\rho_3(2250)$, $\rho_5(2350)$.

$f_4(2300)$ MASS

$\overline{p}p \to \pi\pi$ or $\overline{K}K$

VALUE (MeV)		DOCUMENT ID		TECN	COMMENT
• • • We do not use the following data for averages, fits, limits, etc. • • •					
~ 2314		HASAN	94	RVUE	$\overline{p}p \to \pi\pi$
~ 2300	[1]	MARTIN	80B	RVUE	
~ 2300	[1]	MARTIN	80C	RVUE	
~ 2340	[2]	CARTER	78B	CNTR	0.7–2.4 $\overline{p}p \to K^-K^+$
~ 2330		DULUDE	78B	OSPK	1–2 $\overline{p}p \to \pi^0\pi^0$
~ 2310	[3]	CARTER	77	CNTR	0.7–2.4 $\overline{p}p \to \pi\pi$

[1] $I(J^P) = 0(4^+)$ from simultaneous analysis of $p\overline{p} \to \pi^-\pi^+$ and $\pi^0\pi^0$.
[2] $I(J^P) = 0(4^+)$ from Barrelet-zero analysis.
[3] $I(J^P) = 0(4^+)$ from amplitude analysis.

S-CHANNEL $\overline{p}p$ or $\overline{N}N$

VALUE (MeV)		DOCUMENT ID		TECN	COMMENT
• • • We do not use the following data for averages, fits, limits, etc. • • •					
2283 ± 17		ANISOVICH	00J	SPEC	
~ 2380	[4]	CUTTS	78B	CNTR	0.97–3 $\overline{p}p \to \overline{N}N$
2345 ± 15	[4,5]	COUPLAND	77	CNTR	0.7–2.4 $\overline{p}p \to \overline{p}p$
2359 ± 2	[4,6]	ALSPECTOR	73	CNTR	$\overline{p}p$ S channel
2375 ± 10		ABRAMS	70	CNTR	S channel $\overline{N}N$

[4] Isospins 0 and 1 not separated.
[5] From a fit to the total elastic cross section.
[6] Referred to as U or U region by ALSPECTOR 73.

$\pi^- p \to \eta\pi\pi n$

VALUE (MeV)	DOCUMENT ID		TECN	COMMENT
• • • We do not use the following data for averages, fits, limits, etc. • • •				
2330 ± 20 ± 40	AMELIN	00	VES	37 $\pi^- p \to \eta\pi^+\pi^- n$

pp CENTRAL PRODUCTION

VALUE (MeV)	DOCUMENT ID		COMMENT
2332 ± 15	BARBERIS	00F	450 $pp \to p_f\omega\omega p_s$

$f_4(2300)$ WIDTH

$\overline{p}p \to \pi\pi$ or $\overline{K}K$

VALUE (MeV)		DOCUMENT ID		TECN	COMMENT
• • • We do not use the following data for averages, fits, limits, etc. • • •					
~ 278		HASAN	94	RVUE	$\overline{p}p \to \pi\pi$
~ 200	[7]	MARTIN	80C	RVUE	
~ 150	[8]	CARTER	78B	CNTR	0.7–2.4 $\overline{p}p \to K^-K^+$
~ 210	[9]	CARTER	77	CNTR	0.7–2.4 $\overline{p}p \to \pi\pi$

[7] $I(J^P) = 0(4^+)$ from simultaneous analysis of $p\overline{p} \to \pi^-\pi^+$ and $\pi^0\pi^0$.
[8] $I(J^P) = 0(4^+)$ from Barrelet-zero analysis.
[9] $I(J^P) = 0(4^+)$ from amplitude analysis.

S-CHANNEL $\overline{p}p$ or $\overline{N}N$

VALUE (MeV)		DOCUMENT ID		TECN	COMMENT
• • • We do not use the following data for averages, fits, limits, etc. • • •					
310 ± 25		ANISOVICH	00J	SPEC	
135^{+150}_{-65}	[10,11]	COUPLAND	77	CNTR	0.7–2.4 $\overline{p}p \to \overline{p}p$
165^{+18}_{-8}	[11]	ALSPECTOR	73	CNTR	$\overline{p}p$ S channel
~ 190		ABRAMS	70	CNTR	S channel $\overline{N}N$

[10] From a fit to the total elastic cross section.
[11] Isospins 0 and 1 not separated.

$\pi^- p \to \eta\pi\pi n$

VALUE (MeV)	DOCUMENT ID		TECN	COMMENT
• • • We do not use the following data for averages, fits, limits, etc. • • •				
235 ± 50 ± 40	AMELIN	00	VES	37 $\pi^- p \to \eta\pi^+\pi^- n$

pp CENTRAL PRODUCTION

VALUE (MeV)	DOCUMENT ID		COMMENT
260±57	BARBERIS	00F	450 $pp \to p_f\omega\omega p_s$

$f_4(2300)$ DECAY MODES

	Mode	Fraction (Γ_i/Γ)
Γ_1	$\rho\rho$	seen
Γ_2	$\omega\omega$	seen
Γ_3	$\eta\pi\pi$	seen
Γ_4	$\pi\pi$	seen
Γ_5	$K\overline{K}$	seen
Γ_6	$N\overline{N}$	seen

$f_4(2300)$ BRANCHING RATIOS

$\Gamma(\rho\rho)/\Gamma(\omega\omega)$ Γ_1/Γ_2

VALUE	DOCUMENT ID		COMMENT
• • • We do not use the following data for averages, fits, limits, etc. • • •			
2.8 ± 0.5	BARBERIS	00F	450 $pp \to p_f\omega\omega p_s$

$f_4(2300)$ REFERENCES

AMELIN	00	NP A668 83	D. Amelin *et al.*	(VES Collab.)
ANISOVICH	00J	PL B491 47	A.V. Anisovich *et al.*	
BARBERIS	00F	PL B484 198	D. Barberis *et al.*	(WA 102 Collab.)
HASAN	94	PL B334 215	A. Hasan, D.V. Bugg	(LOQM)
MARTIN	80B	NP B176 355	B.R. Martin, D. Morgan	(LOUC, RHEL) JP
MARTIN	80C	NP B169 216	A.D. Martin, M.R. Pennington	(DURH) JP
CARTER	78B	NP B141 467	A.A. Carter	(LOQM)
CUTTS	78B	PR D17 16	D. Cutts *et al.*	(STON, WISC)
DULUDE	78B	PL 79B 335	R.S. Dulude *et al.*	(BROW, MIT, BARI) JP
CARTER	77	PL 67B 117	A.A. Carter *et al.*	(LOQM, RHEL) JP
COUPLAND	77	PL 71B 460	M. Coupland *et al.*	(LOQM, RHEL)
ALSPECTOR	73	PRL 30 511	J. Alspector *et al.*	(RUTG, UPNJ)
ABRAMS	70	PR D1 1917	R.J. Abrams *et al.*	(BNL)

OTHER RELATED PAPERS

ANISOVICH	99D	PL B452 180	A.V. Anisovich *et al.*	
Also	99F	NP A651 253	A.V. Anisovich *et al.*	
ANISOVICH	99F	NP A651 253	A.V. Anisovich *et al.*	
EISENHAND...	75	NP B96 109	E. Eisenhandler *et al.*	(LOQM, LIVP, DARE+)
FIELDS	71	PRL 27 1749	T. Fields *et al.*	(ANL, OXF)
YOH	71	PRL 26 922	J.K. Yoh *et al.*	(CIT, BNL, ROCH)
BRICMAN	69	PL 29B 451	C. Bricman *et al.*	(CERN, CAEN, SACL)

$f_2(2340)$

$I^G(J^{PC}) = 0^+(2^{++})$

See also the mini-review under non-$q\overline{q}$ candidates. (See the index for the page number.)

$f_2(2340)$ MASS

VALUE (MeV)		DOCUMENT ID		TECN	COMMENT
2339±55	[1]	ETKIN	88	MPS	22 $\pi^- p \to \phi\phi n$
• • • We do not use the following data for averages, fits, limits, etc. • • •					
2392 ± 10		BOOTH	86	OMEG	85 π^-Be $\to 2\phi$Be
2360 ± 20		LINDENBAUM	84	RVUE	

[1] Includes data of ETKIN 85. The percentage of the resonance going into $\phi\phi$ 2^{++} S_2, D_2, and D_0 is 37 ± 19, 4^{+12}_{-4}, and 59^{+21}_{-19}, respectively.

$f_2(2340)$ WIDTH

VALUE (MeV)		DOCUMENT ID		TECN	COMMENT
$\mathbf{319^{+81}_{-69}}$	[2]	ETKIN	88	MPS	22 $\pi^- p \to \phi\phi n$
• • • We do not use the following data for averages, fits, limits, etc. • • •					
198 ± 50		BOOTH	86	OMEG	85 π^-Be $\to 2\phi$Be
150^{+150}_{-50}		LINDENBAUM	84	RVUE	

[2] Includes data of ETKIN 85.

$f_2(2340)$ DECAY MODES

	Mode	Fraction (Γ_i/Γ)
Γ_1	$\phi\phi$	seen

Meson Particle Listings

$f_2(2340)$, $\rho_5(2350)$, $a_6(2450)$

$f_2(2340)$ REFERENCES

ETKIN	88	PL B201 568	A. Etkin *et al.*	(BNL, CUNY)
BOOTH	86	NP B273 677	P.S.L. Booth *et al.*	(LIVP, GLAS, CERN)
ETKIN	85	PL 165B 217	A. Etkin *et al.*	(BNL, CUNY)
LINDENBAUM	84	CNPP 13 285	S.J. Lindenbaum	(CUNY)

OTHER RELATED PAPERS

BOLONKIN	00	JETPL 72 166 Translated from ZETFP 72 240.	B.V. Bolonkin *et al.*	
ANISOVICH	99D	PL B452 180	A.V. Anisovich *et al.*	
Also	99F	NP A651 253	A.V. Anisovich *et al.*	
ANISOVICH	99F	NP A651 253	A.V. Anisovich *et al.*	
LANDBERG	96	PR D53 2839	C. Landberg *et al.*	(BNL, CUNY, RPI)
GREEN	86	PRL 56 1639	D.R. Green *et al.*	(FNAL, ARIZ, FSU+)
BOOTH	84	NP B242 51	P.S.L. Booth *et al.*	(LIVP, GLAS, CERN)
EISENHAND...	75	NP B96 109	E. Eisenhandler *et al.*	(LOQM, LIVP, DARE+)

$\rho_5(2350)$

$I^G(J^{PC}) = 1^+(5^{--})$

OMITTED FROM SUMMARY TABLE

This entry was previously called $U_1(2400)$. See also the Further States entry. See also $\rho(2150)$, $f_2(2150)$, $\rho_3(2250)$, $f_4(2300)$.

$\rho_5(2350)$ MASS

$\pi^- p \to \omega\pi^0 n$

VALUE (MeV)	DOCUMENT ID		TECN	COMMENT
2330±35	ALDE	95	GAM2	38 $\pi^- p \to \omega\pi^0 n$

VALUE (MeV)	DOCUMENT ID		TECN	CHG	COMMENT
• • • We do not use the following data for averages, fits, limits, etc. • • •					
~ 2303	HASAN	94	RVUE		$\overline{p}p \to \pi\pi$
~ 2300	[1] MARTIN	80B	RVUE		
~ 2250	[1] MARTIN	80C	RVUE		
~ 2500	[2] CARTER	78B	CNTR	0	0.7–2.4 $\overline{p}p \to K^-K^+$
~ 2480	[3] CARTER	77	CNTR	0	0.7–2.4 $\overline{p}p \to \pi\pi$

S-CHANNEL $\overline{N}N$

VALUE (MeV)	DOCUMENT ID		TECN	CHG	COMMENT
• • • We do not use the following data for averages, fits, limits, etc. • • •					
2300±45	[4] ANISOVICH	02	SPEC		0.6–1.9 $p\overline{p} \to \omega\pi^0, \omega\eta\pi^0, \pi^+\pi^-$
2295±30	ANISOVICH	00J	SPEC		
~ 2380	[5] CUTTS	78B	CNTR		0.97–3 $\overline{p}p \to \overline{N}N$
2345±15	[5,6] COUPLAND	77	CNTR	0	0.7–2.4 $\overline{p}p \to \overline{p}p$
2359± 2	[5,7] ALSPECTOR	73	CNTR		$\overline{p}p$ S channel
2350±10	[8] ABRAMS	70	CNTR		S channel $\overline{N}N$
2360±25	[9] OH	70B	HDBC	−0	$\overline{p}(pn)$, $K^*K2\pi$

$\pi^- p \to K^+K^- n$

VALUE (MeV)	DOCUMENT ID		TECN	CHG	COMMENT
• • • We do not use the following data for averages, fits, limits, etc. • • •					
2307±6	ALPER	80	CNTR	0	62 $\pi^- p \to K^+K^- n$

[1] $I(J^P) = 1(5^-)$ from simultaneous analysis of $p\overline{p} \to \pi^-\pi^+$ and $\pi^0\pi^0$.
[2] $I = 0(1)$; $J^P = 5^-$ from Barrelet-zero analysis.
[3] $I(J^P) = 1(5^-)$ from amplitude analysis.
[4] From the combined analysis of ANISOVICH 00J, ANISOVICH 01D, ANISOVICH 01E, and ANISOVICH 02.
[5] Isospins 0 and 1 not separated.
[6] From a fit to the total elastic cross section.
[7] Referred to as U or U region by ALSPECTOR 73.
[8] For $I = 1$ $\overline{N}N$.
[9] No evidence for this bump seen in the $\overline{p}p$ data of CHAPMAN 71B. Narrow state not confirmed by OH 73 with more data.

$\rho_5(2350)$ WIDTH

$\pi^- p \to \omega\pi^0 n$

VALUE (MeV)	DOCUMENT ID		TECN	COMMENT
400±100	ALDE	95	GAM2	38 $\pi^- p \to \omega\pi^0 n$

$\overline{p}p \to \pi\pi$ or $\overline{K}K$

VALUE (MeV)	DOCUMENT ID		TECN	CHG	COMMENT
• • • We do not use the following data for averages, fits, limits, etc. • • •					
~ 169	HASAN	94	RVUE		$\overline{p}p \to \pi\pi$
~ 250	[10] MARTIN	80B	RVUE		
~ 300	[10] MARTIN	80C	RVUE		
~ 150	[11] CARTER	78B	CNTR	0	0.7–2.4 $\overline{p}p \to K^-K^+$
~ 210	[12] CARTER	77	CNTR	0	0.7–2.4 $\overline{p}p \to \pi\pi$

S-CHANNEL $\overline{N}N$

VALUE (MeV)	DOCUMENT ID		TECN	CHG	COMMENT
• • • We do not use the following data for averages, fits, limits, etc. • • •					
260± 75	[13] ANISOVICH	02	SPEC		0.6–1.9 $p\overline{p} \to \omega\pi^0, \omega\eta\pi^0, \pi^+\pi^-$
235^{+65}_{-40}	ANISOVICH	00J	SPEC		
135^{+150}_{-65}	[14,15] COUPLAND	77	CNTR	0	0.7–2.4 $\overline{p}p \to \overline{p}p$
165^{+18}_{-8}	[15] ALSPECTOR	73	CNTR		$\overline{p}p$ S channel
< 60	[16] OH	70B	HDBC	−0	$\overline{p}(pn)$, $K^*K2\pi$
~ 140	ABRAMS	67C	CNTR		S channel $\overline{p}N$

$\pi^- p \to K^+K^- n$

VALUE (MeV)	DOCUMENT ID		TECN	CHG	COMMENT
• • • We do not use the following data for averages, fits, limits, etc. • • •					
245±20	ALPER	80	CNTR	0	62 $\pi^- p \to K^+K^- n$

[10] $I(J^P) = 1(5^-)$ from simultaneous analysis of $p\overline{p} \to \pi^-\pi^+$ and $\pi^0\pi^0$.
[11] $I = 0(1)$; $J^P = 5^-$ from Barrelet-zero analysis.
[12] $I(J^P) = 1(5^-)$ from amplitude analysis.
[13] From the combined analysis of ANISOVICH 00J, ANISOVICH 01D, ANISOVICH 01E, and ANISOVICH 02.
[14] From a fit to the total elastic cross section.
[15] Isospins 0 and 1 not separated.
[16] No evidence for this bump seen in the $\overline{p}p$ data of CHAPMAN 71B. Narrow state not confirmed by OH 73 with more data.

$\rho_5(2350)$ REFERENCES

ANISOVICH	02	PL B542 8	A.V. Anisovich *et al.*	
ANISOVICH	01D	PL B508 6	A.V. Anisovich *et al.*	
ANISOVICH	01E	PL B513 281	A.V. Anisovich *et al.*	
ANISOVICH	00J	PL B491 47	A.V. Anisovich *et al.*	
ALDE	95	ZPHY C66 379	D.M. Alde *et al.*	(GAMS Collab.) JP
HASAN	94	PL B334 215	A. Hasan, D.V. Bugg	(LOQM)
ALPER	80	PL 94B 422	B. Alper *et al.*	(AMST, CERN, CRAC, MPIM+)
MARTIN	80B	NP B176 355	B.R. Martin, D. Morgan	(LOUC, RHEL) JP
MARTIN	80C	NP B169 216	A.D. Martin, M.R. Pennington	(DURH) JP
CARTER	78B	NP B141 467	A.A. Carter	(LOQM)
CUTTS	78B	PR D17 16	D. Cutts *et al.*	(STON, WISC)
CARTER	77	PL 67B 117	A.A. Carter *et al.*	(LOQM, RHEL) JP
COUPLAND	77	PL 71B 460	M. Coupland *et al.*	(LOQM, RHEL)
ALSPECTOR	73	PRL 30 511	J. Alspector *et al.*	(RUTG, UPNJ)
OH	73	NP B51 57	B.Y. Oh *et al.*	(MSU)
CHAPMAN	71B	PR D4 1275	J.W. Chapman *et al.*	(MICH)
ABRAMS	70	PR D1 1917	R.J. Abrams *et al.*	(BNL)
OH	70B	PRL 24 1257	B.Y. Oh *et al.*	(MSU)
ABRAMS	67C	PRL 18 1209	R.J. Abrams *et al.*	(BNL)

OTHER RELATED PAPERS

EISENHAND...	75	NP B96 109	E. Eisenhandler *et al.*	(LOQM, LIVP, DARE+)
CASO	70	LNC 3 707	C. Caso *et al.*	(GENO, HAMB, MILA, SACL)
BRICMAN	69	PL 29B 451	C. Bricman *et al.*	(CERN, CAEN, SACL)

$a_6(2450)$

$I^G(J^{PC}) = 1^-(6^{++})$

OMITTED FROM SUMMARY TABLE

Needs confirmation.

$a_6(2450)$ MASS

VALUE (MeV)	DOCUMENT ID		TECN	CHG	COMMENT
2450±130	[1] CLELAND	82B	SPEC	±	50 $\pi p \to K^0_S K^\pm p$

[1] From an amplitude analysis.

$a_6(2450)$ WIDTH

VALUE (MeV)	DOCUMENT ID		TECN	CHG	COMMENT
400±250	[2] CLELAND	82B	SPEC	±	50 $\pi p \to K^0_S K^\pm p$

[2] From an amplitude analysis.

$a_6(2450)$ DECAY MODES

	Mode
Γ_1	$K\overline{K}$

$a_6(2450)$ REFERENCES

CLELAND	82B	NP B208 228	W.E. Cleland *et al.*	(DURH, GEVA, LAUS+)

$f_6(2510)$

$I^G(J^{PC}) = 0^+(6^{++})$

OMITTED FROM SUMMARY TABLE

Needs confirmation.

$f_6(2510)$ MASS

VALUE (MeV)	DOCUMENT ID		TECN	COMMENT
2465±50 OUR AVERAGE	Error includes scale factor of 2.1.			
2420±30	ALDE	98	GAM4	100 $\pi^- p \rightarrow \pi^0\pi^0 n$
2510±30	BINON	84B	GAM2	38 $\pi^- p \rightarrow n2\pi^0$

$f_6(2510)$ WIDTH

VALUE (MeV)	DOCUMENT ID		TECN	COMMENT
255±40 OUR AVERAGE				
270±60	ALDE	98	GAM4	100 $\pi^- p \rightarrow \pi^0\pi^0 n$
240±60	BINON	84B	GAM2	38 $\pi^- p \rightarrow n2\pi^0$

$f_6(2510)$ DECAY MODES

	Mode	Fraction (Γ_i/Γ)
Γ_1	$\pi\pi$	(6.0±1.0) %

$f_6(2510)$ BRANCHING RATIOS

$\Gamma(\pi\pi)/\Gamma_{\text{total}}$ Γ_1/Γ

VALUE	DOCUMENT ID		TECN	COMMENT
0.06 ±0.01	[1] BINON	83C	GAM2	38 $\pi^- p \rightarrow n4\gamma$

[1] Assuming one pion exchange and using data of BOLOTOV 74.

$f_6(2510)$ REFERENCES

ALDE	98	EPJ A3 361	D. Alde *et al.*	(GAM4 Collab.)
Also	99	PAN 62 405 Translated from YAF 62 446.	D. Alde *et al.*	(GAMS Collab.)
BINON	84B	LNC 39 41	F.G. Binon *et al.*	(SERP, BELG, LAPP) JP
BINON	83C	SJNP 38 723 Translated from YAF 38 1199.	F.G. Binon *et al.*	(SERP, BRUX+)
BOLOTOV	74	PL 52B 489	V.N. Bolotov *et al.*	(SERP)

OTHER RELATED PAPERS

BOLONKIN	00	JETPL 72 166 Translated from ZETFP 72 240.	B.V. Bolonkin *et al.*	
PROKOSHKIN	99	PAN 62 356 Translated from YAF 62 396.	Yu.D. Prokoshkin	
EISENHAND...	75	NP B96 109	E. Eisenhandler *et al.*	(LOQM, LIVP, DARE+)

OTHER LIGHT MESONS

Further States

OMITTED FROM SUMMARY TABLE

This section contains states observed by a single group OR STATES POORLY ESTABLISHED that thus need confirmation. Publications that exclude earlier claims in this section are listed under 'Other Related Papers.'

QUANTUM NUMBERS, MASSES, WIDTHS, AND BRANCHING RATIOS

$X(1110)$ $I^G(J^{PC}) = 0^+(\text{even}^{++})$

MASS (MeV)	WIDTH (MeV)	DOCUMENT ID		TECN	COMMENT
1107±4	111 ± 8 ± 15	DAFTARI	87	DBC	0. $\overline{p}n \to \rho^-\pi^+\pi^-$

$f_0(1200\text{–}1600)$ $I^G(J^{PC}) = 0^+(0^{++})$

MASS (MeV)	WIDTH (MeV)	DOCUMENT ID		TECN
1480^{+100}_{-150}	1030^{+80}_{-170}	[1] ANISOVICH	03	SPEC
1530^{+90}_{-250}	560 ± 40	[2] ANISOVICH	03	SPEC

$X(1420)$ $I^G(J^{PC}) = 2^+(0^{++})$

MASS (MeV)	WIDTH (MeV)	DOCUMENT ID		TECN	COMMENT
1420±20	160 ± 10	FILIPPI	00	OBLX	0 $\overline{n}p \to \pi^+\pi^+\pi^-$

$X(1600)$ $I^G(J^{PC}) = 2^+(2^{++})$

MASS (MeV)	WIDTH (MeV)	DOCUMENT ID		TECN	COMMENT
1600±100	400 ± 200	[3] ALBRECHT	91F	ARG	10.2 $e^+e^- \to e^+e^-2(\pi^+\pi^-)$

$X(1650)$ $I^G(J^{PC}) = 0^-(?^{?-})$

MASS (MeV)	WIDTH (MeV)	EVTS	DOCUMENT ID		TECN	COMMENT
1652±7	<50	100	PROKOSHKIN	96	GAM2	32,38 $\pi p \to \omega\eta n$

$X(1750)$ $I^G(J^{PC}) = ?^?(1^{--})$

MASS (MeV)	WIDTH (MeV)	DOCUMENT ID		TECN	COMMENT
1753.5 ±1.5±2.3	122.2 ± 6.2 ± 8.0	LINK		02K FOCS	20–160 $\gamma p \to K^+K^-p$

$B(X(1750) \to \overline{K}^*(892)^0K^0 \to K^\pm\pi^\mp K^0_S)/B(X(1750) \to K^+K^-)$

VALUE	CL%	DOCUMENT ID		TECN
<0.065	90	LINK		02K FOCS

$B(X(1750) \to \overline{K}^*(892)^\pm K^\mp \to K^\pm\pi^\mp K^0_S)/B(X(1750) \to K^+K^-)$

VALUE	CL%	DOCUMENT ID		TECN
<0.183	90	LINK		02K FOCS

$X(1775)$ $I^G(J^{PC}) = 1^-(?^{-+})$

MASS (MeV)	WIDTH (MeV)	DOCUMENT ID		TECN	COMMENT
1763±20	192 ± 60	CONDO	91	SHF	$\gamma p \to (p\pi^+)(\pi^+\pi^-\pi^-)$
1787±18	118 ± 60	CONDO	91	SHF	$\gamma p \to n\pi^+\pi^+\pi^-$

$X(1855)$ $I^G(J^{PC}) = ?^?(?^{??})$

MASS (MeV)	WIDTH (MeV)	DOCUMENT ID		TECN	COMMENT
1856.6±5	20 ± 5	BRIDGES	86D	SPEC	0. $\overline{p}d \to \pi\pi N$

$X(1860)$ $I^G(J^{PC}) = ?^?(?^{??})$

MASS (MeV)	WIDTH (MeV)	DOCUMENT ID		TECN	COMMENT
1859^{+6}_{-27}	<30	BAI	03F	BES2	$J/\psi \to \gamma p\overline{p}$

$X(1870)$ $I^G(J^{PC}) = ?^?(?^{??})$

MASS (MeV)	WIDTH (MeV)	DOCUMENT ID		TECN	COMMENT
~ 1870	~ 10	DALKAROV	97	RVUE	0.0 $\overline{p}d \to p3\pi^-2\pi^+$

$X(1870)$ $I^G(J^{PC}) = ?^?(2^{??})$

MASS (MeV)	WIDTH (MeV)	DOCUMENT ID		TECN	COMMENT
1870±40	250 ± 30	ALDE	86D	GAM4	100 $\pi^-p \to 2\eta X$

$a_3(1875)$ $I^G(J^{PC}) = 0^+(1^{--})$

MASS (MeV)	WIDTH (MeV)	DOCUMENT ID		TECN	COMMENT
1874±43±96	385 ± 121 ± 114	CHUNG	02	MPS	18.3 $\pi^-p \to \pi^+\pi^-\pi^-p$

$B(a_3(1875) \to f_2(1270)\pi)/B(a_3(1875) \to \rho\pi)$

VALUE	DOCUMENT ID		TECN	COMMENT
0.8±0.2	[4] CHUNG	02	MPS	18.3 $\pi^-p \to \pi^+\pi^-\pi^-p$

$B(a_3(1875) \to \rho_3(1690)\pi)/B(a_3(1875) \to \rho\pi)$

VALUE	DOCUMENT ID		TECN	COMMENT
0.9±0.3	[4] CHUNG	02	MPS	18.3 $\pi^-p \to \pi^+\pi^-\pi^-p$

$\pi_2(1880)$ $I^G(J^{PC}) = 1^-(2^{-+})$

MASS (MeV)	WIDTH (MeV)	DOCUMENT ID		COMMENT
1880±20	255 ± 45	ANISOVICH	01B	$\overline{p}p \to (a_2(1320)\eta)\pi^0$

$a_1(1930)$ $I^G(J^{PC}) = 0^-(1^{++})$

MASS (MeV)	WIDTH (MeV)	DOCUMENT ID		TECN	COMMENT
1930^{+30}_{-70}	155 ± 45	ANISOVICH	01F	SPEC	2.0 $\overline{p}p \to 3\pi^0$, $\pi^0\eta$, $\pi^0\eta'$

$X(1935)$ $I^G(J^{PC}) = 1^+(1^{-?})$

MASS (MeV)	WIDTH (MeV)	DOCUMENT ID		TECN	COMMENT
1935±20	215 ± 30	EVANGELISTA	79	OMEG	10,16 $\pi^-p \to \overline{p}pn$

$\rho_2(1940)$ $I^G(J^{PC}) = 1^+(2^{--})$

MASS (MeV)	WIDTH (MeV)	DOCUMENT ID		TECN	COMMENT
1940±40	155 ± 40	[5] ANISOVICH	02	SPEC	0.6–1.9 $p\overline{p} \to \omega\pi^0$, $\omega\eta\pi^0$, $\pi^+\pi^-$

$\omega_3(1945)$ $I^G(J^{PC}) = 0^-(3^{--})$

MASS (MeV)	WIDTH (MeV)	DOCUMENT ID		TECN	COMMENT
1945±20	115 ± 22	[6] ANISOVICH	02B	SPEC	0.6–1.9 $p\overline{p} \to \omega\eta$, $\omega\pi^0\pi^0$

$\omega(1960)$ $I^G(J^{PC}) = 0^-(1^{--})$

MASS (MeV)	WIDTH (MeV)	DOCUMENT ID		TECN	COMMENT
1960±25	195 ± 60	[6] ANISOVICH	02B	SPEC	0.6–1.9 $p\overline{p} \to \omega\eta$, $\omega\pi^0\pi^0$

$b_1(1960)$ $I^G(J^{PC}) = 1^+(1^{+-})$

MASS (MeV)	WIDTH (MeV)	DOCUMENT ID		TECN	COMMENT
1960±35	230 ± 50	[5] ANISOVICH	02	SPEC	0.6–1.9 $p\overline{p} \to \omega\pi^0$, $\omega\eta\pi^0$, $\pi^+\pi^-$

$\rho(1965)$ $I^G(J^{PC}) = 1^+(1^{--})$

MASS (MeV)	WIDTH (MeV)	DOCUMENT ID		TECN	COMMENT
1970±30	260 ± 45	[5] ANISOVICH	02	SPEC	0.6–1.9 $p\overline{p} \to \omega\pi^0$, $\omega\eta\pi^0$, $\pi^+\pi^-$
2000±30	295 ± 85	ANISOVICH	00J	SPEC	

$h_1(1965)$ $I^G(J^{PC}) = 0^-(1^{+-})$

MASS (MeV)	WIDTH (MeV)	DOCUMENT ID		TECN	COMMENT
1965±45	345 ± 75	[6] ANISOVICH	02B	SPEC	0.6–1.9 $p\overline{p} \to \omega\eta$, $\omega\pi^0\pi^0$

$f_1(1970)$ $I^G(J^{PC}) = 0^+(1^{++})$

MASS (MeV)	WIDTH (MeV)	DOCUMENT ID		TECN
1971±15	240 ± 45	ANISOVICH	00J	SPEC

X(1970) $I^G(J^{PC}) = ?^?(?^{??})$

MASS (MeV)	WIDTH (MeV)	DOCUMENT ID		TECN	COMMENT
1970±10	40 ± 20	CHLIAPNIK...	80	HBC	32 $K^+p \to 2K^0_S 2\pi X$

X(1975) $I^G(J^{PC}) = ?^?(?^{??})$

MASS (MeV)	WIDTH (MeV)	EVTS	DOCUMENT ID		TECN	COMMENT
1973±15	80	30	CASO	70	HBC	11.2 $\pi^- p \to \rho 2\pi$

ω_2(1975) $I^G(J^{PC}) = 0^-(2^{--})$

MASS (MeV)	WIDTH (MeV)	DOCUMENT ID		TECN	COMMENT
1975±20	175 ± 25	[6] ANISOVICH	02B	SPEC	0.6–1.9 $p\overline{p} \to \omega\eta, \omega\pi^0\pi^0$

a_2(1990) $I^G(J^{PC}) = 1^-(2^{++})$

MASS (MeV)	WIDTH (MeV)	DOCUMENT ID		TECN
1990^{+15}_{-30}	190 ± 50	ANISOVICH	99C	SPEC

ρ(2000) $I^G(J^{PC}) = 1^+(1^{--})$

MASS (MeV)	WIDTH (MeV)	DOCUMENT ID		TECN
2000±30	295 ± 85	ANISOVICH	00J	SPEC

f_2(2000) $I^G(J^{PC}) = 0^+(2^{++})$

MASS (MeV)	WIDTH (MeV)	DOCUMENT ID		TECN
2001±10	312 ± 32	ANISOVICH	00J	SPEC

X(2000) $I^G(J^{PC}) = 1^-(?^{?+})$

MASS (MeV)	WIDTH (MeV)	DOCUMENT ID		TECN	CHG	COMMENT
1964±35	225 ± 50	[7] ARMSTRONG	93D	E760		$\overline{p}p \to 3\pi^0 \to 6\gamma$
~ 2100	~ 500	[7] ANTIPOV	77	CIBS	–	25 $\pi^- p \to p\pi^-\rho_3$
2214±15	355 ± 21	[8] BALTAY	77	HBC	0	15 $\pi^- p \to \Delta^{++}3\pi$
2080±40	340 ± 80	KALELKAR	75	HBC	+	15 $\pi^+ p \to p\pi^+\rho_3$

X(2000) $I^G(J^{PC}) = ?^?(4^{++})$

MASS (MeV)	WIDTH (MeV)	DOCUMENT ID		TECN	COMMENT
1998±3±5	<15	VLADIMIRSKY	03	SPEC	$\pi^- p \to K^0_S K^0_S M M$

π_2(2005) $I^G(J^{PC}) = 1^-(2^{-+})$

MASS (MeV)	WIDTH (MeV)	DOCUMENT ID		TECN	COMMENT
2005±15	200 ± 40	ANISOVICH	01F	SPEC	2.0 $\overline{p}p \to 3\pi^0, \pi^0\eta, \pi^0\eta'$

η(2010) $I^G(J^{PC}) = 0^+(0^{-+})$

MASS (MeV)	WIDTH (MeV)	DOCUMENT ID		TECN
2010^{+35}_{-60}	270 ± 60	ANISOVICH	00J	SPEC

a_0(2020) $I^G(J^{PC}) = 1^-(0^{++})$

MASS (MeV)	WIDTH (MeV)	DOCUMENT ID		TECN
2025±30	330 ± 75	ANISOVICH	99C	SPEC

X(2020) $I^G(J^{PC}) = ?^?(?^{??})$

MASS (MeV)	WIDTH (MeV)	DOCUMENT ID		TECN	COMMENT
2015±3	10 ± 4	FERRER	99	RVUE	$\pi p \to p p \overline{p} \pi(\pi)$

h_3(2025) $I^G(J^{PC}) = 0^-(3^{--})$

MASS (MeV)	WIDTH (MeV)	DOCUMENT ID		TECN	COMMENT
2025±20	145 ± 30	[6] ANISOVICH	02B	SPEC	0.6–1.9 $p\overline{p} \to \omega\eta, \omega\pi^0\pi^0$

b_3(2025) $I^G(J^{PC}) = 1^+(3^{+-})$

MASS (MeV)	WIDTH (MeV)	DOCUMENT ID		TECN	COMMENT
2032±12	117 ± 11	[5] ANISOVICH	02	SPEC	0.6–1.9 $p\overline{p} \to \omega\pi^0, \omega\eta\pi^0, \pi^+\pi^-$

η_2(2030) $I^G(J^{PC}) = 0^+(2^{-+})$

MASS (MeV)	WIDTH (MeV)	DOCUMENT ID		TECN
2030±5±15	205 ± 10 ± 15	ANISOVICH	00E	SPEC

$B(a_2\pi)_{L=0}/B(a_2\pi)_{L=2}$

VALUE	DOCUMENT ID		TECN
0.74±0.17	[9] ANISOVICH	00E	SPEC

$B(a_0\pi)/B(a_2\pi)_{L=2}$

VALUE	DOCUMENT ID		TECN
0.072±0.016	[9] ANISOVICH	00E	SPEC

$B(f_2\eta)/B(a_2\pi)_{L=2}$

VALUE	DOCUMENT ID		TECN
0.074±0.026	[9] ANISOVICH	00E	SPEC

f_3(2050) $I^G(J^{PC}) = 0^+(3^{++})$

MASS (MeV)	WIDTH (MeV)	DOCUMENT ID		TECN
2048±8	213 ± 34	ANISOVICH	00J	SPEC

f_0(2060) $I^G(J^{PC}) = 0^+(0^{++})$

MASS (MeV)	WIDTH (MeV)	DOCUMENT ID		TECN	COMMENT
~ 2050	~ 120	[10] OAKDEN	94	RVUE	0.36–1.55 $\overline{p}p \to \pi\pi$
~ 2060	~ 50	[10] OAKDEN	94	RVUE	0.36–1.55 $\overline{p}p \to \pi\pi$

π(2070) $I^G(J^{PC}) = 0^-(0^{-+})$

MASS (MeV)	WIDTH (MeV)	DOCUMENT ID		TECN	COMMENT
2070±35	310^{+100}_{-50}	ANISOVICH	01F	SPEC	2.0 $\overline{p}p \to 3\pi^0, \pi^0\eta, \pi^0\eta'$

a_3(2070) $I^G(J^{PC}) = 1^-(3^{++})$

MASS (MeV)	WIDTH (MeV)	DOCUMENT ID		TECN
2070±20	170 ± 40	ANISOVICH	99C	SPEC

a_2(2080) $I^G(J^{PC}) = 1^-(2^{++})$

MASS (MeV)	WIDTH (MeV)	DOCUMENT ID		TECN
2060±20	195 ± 30	ANISOVICH	99C	SPEC
2100^{+10}_{-30}	360^{+40}_{-100}	ANISOVICH	99E	SPEC

X(2080) $I^G(J^{PC}) = ?^?(?^{??})$

MASS (MeV)	WIDTH (MeV)	DOCUMENT ID		TECN	COMMENT
2080±10	110 ± 20	KREYMER	80	STRC	13 $\pi^- d \to p\overline{p}n(n_s)$

X(2080) $I^G(J^{PC}) = ?^?(3^{-?})$

MASS (MeV)	WIDTH (MeV)	DOCUMENT ID		TECN	COMMENT
2080±10	190 ± 15	ROZANSKA	80	SPRK	18 $\pi^- p \to p\overline{p}n$

η(2100) $I^G(J^{PC}) = 0^+(0^{-+})$

MASS (MeV)	WIDTH (MeV)	EVTS	DOCUMENT ID		TECN	COMMENT
2103±50	187 ± 75	586	[11] BISELLO	89B	DM2	$J/\psi \to 4\pi\gamma$

X(2100) $I^G(J^{PC}) = ?^?(0^{??})$

MASS (MeV)	WIDTH (MeV)	DOCUMENT ID		TECN	COMMENT
2100±40	250 ± 40	ALDE	86D	GAM4	100 $\pi^- p \to 2\eta X$

X(2110) $I^G(J^{PC}) = 1^+(3^{-?})$

MASS (MeV)	WIDTH (MeV)	DOCUMENT ID		TECN	COMMENT
2110±10	330 ± 20	EVANGELISTA	79	OMEG	10,16 $\pi^- p \to \overline{p}pn$

f_2(2140) $I^G(J^{PC}) = 0^+(2^{++})$

MASS (MeV)	WIDTH (MeV)	EVTS	DOCUMENT ID		TECN	COMMENT
2141±12	49 ± 28	389	GREEN	86	MPSF	400 $pA \to 4KX$

ω(2145) $I^G(J^{PC}) = 0^-(1^{--})$

MASS (MeV)	WIDTH (MeV)	DOCUMENT ID		TECN	COMMENT
2150±20	235 ± 30	ANISOVICH	01C	SPEC	0.6–1.9 $\overline{p}p \to \omega\eta$
2145±20	200 ± 25	ANISOVICH	00D	SPEC	

$X(2150)$ $I^G(J^{PC}) = ?^?(2^{+?})$

MASS (MeV)	WIDTH (MeV)	DOCUMENT ID		TECN	COMMENT
2150 ± 10	260 ± 10	ROZANSKA	80	SPRK	18 $\pi^- p \to p\overline{p}n$

$a_2(2175)$ $I^G(J^{PC}) = 0^-(2^{++})$

MASS (MeV)	WIDTH (MeV)	DOCUMENT ID		TECN	COMMENT
2175 ± 40	310^{+90}_{-45}	ANISOVICH	01F	SPEC	2.0 $\overline{p}p \to 3\pi^0$, $\pi^0\eta$, $\pi^0\eta'$

$\eta(2190)$ $I^G(J^{PC}) = 0^+(0^{-+})$

MASS (MeV)	WIDTH (MeV)	DOCUMENT ID		TECN
2190 ± 50	850 ± 100	BUGG	99	BES

$\omega_2(2195)$ $I^G(J^{PC}) = 0^-(2^{--})$

MASS (MeV)	WIDTH (MeV)	DOCUMENT ID		TECN	COMMENT
2195 ± 30	225 ± 40	[6] ANISOVICH	02B	SPEC	0.6–1.9 $p\overline{p} \to \omega\eta$, $\omega\pi^0\pi^0$

$\omega(2205)$ $I^G(J^{PC}) = 0^-(1^{--})$

MASS (MeV)	WIDTH (MeV)	DOCUMENT ID		TECN	COMMENT
2205 ± 30	350 ± 90	[6] ANISOVICH	02B	SPEC	0.6–1.9 $p\overline{p} \to \omega\eta$, $\omega\pi^0\pi^0$

$X(2210)$ $I^G(J^{PC}) = ?^?(?^{??})$

MASS (MeV)	WIDTH (MeV)	DOCUMENT ID		TECN	COMMENT
2210^{+79}_{-21}	203^{+437}_{-87}	EVANGELISTA	79B	OMEG	10 $\pi^- p \to K^+K^- n$

$X(2210)$ $I^G(J^{PC}) = ?^?(?^{??})$

MASS (MeV)	WIDTH (MeV)	DOCUMENT ID		TECN	COMMENT
2207 ± 22	130	CASO	70	HBC	11.2 $\pi^- p$

$h_1(2215)$ $I^G(J^{PC}) = 0^-(1^{+-})$

MASS (MeV)	WIDTH (MeV)	DOCUMENT ID		TECN	COMMENT
2215 ± 40	325 ± 55	[6] ANISOVICH	02B	SPEC	0.6–1.9 $p\overline{p} \to \omega\eta$, $\omega\pi^0\pi^0$

$b_1(2240)$ $I^G(J^{PC}) = 1^+(1^{+-})$

MASS (MeV)	WIDTH (MeV)	DOCUMENT ID		TECN	COMMENT
2240 ± 35	320 ± 85	[5] ANISOVICH	02	SPEC	0.6–1.9 $p\overline{p} \to \omega\pi^0$, $\omega\eta\pi^0$, $\pi^+\pi^-$

$\rho_2(2240)$ $I^G(J^{PC}) = 1^+(2^{--})$

MASS (MeV)	WIDTH (MeV)	DOCUMENT ID		TECN	COMMENT
2225 ± 35	335^{+100}_{-50}	[5] ANISOVICH	02	SPEC	0.6–1.9 $p\overline{p} \to \omega\pi^0$, $\omega\eta\pi^0$, $\pi^+\pi^-$

$\rho_4(2240)$ $I^G(J^{PC}) = 1^+(4^{--})$

MASS (MeV)	WIDTH (MeV)	DOCUMENT ID		TECN	COMMENT
2230 ± 25	210 ± 30	[5] ANISOVICH	02	SPEC	0.6–1.9 $p\overline{p} \to \omega\pi^0$, $\omega\eta\pi^0$, $\pi^+\pi^-$

$\pi_2(2245)$ $I^G(J^{PC}) = 0^-(2^{-+})$

MASS (MeV)	WIDTH (MeV)	DOCUMENT ID		TECN	COMMENT
2245 ± 60	320^{+100}_{-40}	ANISOVICH	01F	SPEC	2.0 $\overline{p}p \to 3\pi^0$, $\pi^0\eta$, $\pi^0\eta'$

$\eta_2(2250)$ $I^G(J^{PC}) = 0^+(2^{-+})$

MASS (MeV)	WIDTH (MeV)	DOCUMENT ID		TECN
2248 ± 20	280 ± 20	ANISOVICH	00I	SPEC
2267 ± 14	290 ± 50	ANISOVICH	00J	SPEC

$\pi_4(2250)$ $I^G(J^{PC}) = 1^-(4^{-+})$

MASS (MeV)	WIDTH (MeV)	DOCUMENT ID		TECN	COMMENT
2250 ± 15	215 ± 25	ANISOVICH	01F	SPEC	2.0 $\overline{p}p \to 3\pi^0$, $\pi^0\eta$, $\pi^0\eta'$

$\omega_4(2250)$ $I^G(J^{PC}) = 0^-(4^{--})$

MASS (MeV)	WIDTH (MeV)	DOCUMENT ID		TECN	COMMENT
2250 ± 30	150 ± 50	[6] ANISOVICH	02B	SPEC	0.6–1.9 $p\overline{p} \to \omega\eta$, $\omega\pi^0\pi^0$

$\omega_3(2255)$ $I^G(J^{PC}) = 0^-(3^{--})$

MASS (MeV)	WIDTH (MeV)	DOCUMENT ID		TECN	COMMENT
2255 ± 15	175 ± 30	[6] ANISOVICH	02B	SPEC	0.6–1.9 $p\overline{p} \to \omega\eta$, $\omega\pi^0\pi^0$

$X(2260)$ $I^G(J^{PC}) = 0^+(4^{+?})$

MASS (MeV)	WIDTH (MeV)	DOCUMENT ID		TECN	COMMENT
2260 ± 20	400 ± 100	EVANGELISTA	79	OMEG	10,16 $\pi^- p \to \overline{p}pn$

$\rho(2265)$ $I^G(J^{PC}) = 1^+(1^{--})$

MASS (MeV)	WIDTH (MeV)	DOCUMENT ID		TECN	COMMENT
2265 ± 40	325 ± 80	[5] ANISOVICH	02	SPEC	0.6–1.9 $p\overline{p} \to \omega\pi^0$, $\omega\eta\pi^0$, $\pi^+\pi^-$

$a_1(2270)$ $I^G(J^{PC}) = 1^-(1^{++})$

MASS (MeV)	WIDTH (MeV)	DOCUMENT ID		TECN	COMMENT
2270^{+55}_{-40}	305^{+70}_{-40}	ANISOVICH	01F	SPEC	2.0 $\overline{p}p \to 3\pi^0$, $\pi^0\eta$, $\pi^0\eta'$

$a_2(2270)$ $I^G(J^{PC}) = 1^-(2^{++})$

MASS (MeV)	WIDTH (MeV)	DOCUMENT ID		TECN
2265 ± 20	235^{+60}_{-35}	ANISOVICH	99C	SPEC
2280 ± 30	280 ± 50	ANISOVICH	99E	SPEC

$h_3(2275)$ $I^G(J^{PC}) = 0^-(3^{+-})$

MASS (MeV)	WIDTH (MeV)	DOCUMENT ID		TECN	COMMENT
2275 ± 25	190 ± 45	[6] ANISOVICH	02B	SPEC	0.6–1.9 $p\overline{p} \to \omega\eta$, $\omega\pi^0\pi^0$

$a_4(2280)$ $I^G(J^{PC}) = 1^-(4^{++})$

MASS (MeV)	WIDTH (MeV)	DOCUMENT ID		TECN
2300 ± 20	230 ± 40	ANISOVICH	99C	SPEC
2260 ± 15	180 ± 20	ANISOVICH	99E	SPEC

$\eta(2280)$ $I^G(J^{PC}) = 0^+(0^{-+})$

MASS (MeV)	WIDTH (MeV)	DOCUMENT ID		TECN
2285 ± 20	325 ± 30	ANISOVICH	00J	SPEC
2320 ± 15	230 ± 35	[12] ANISOVICH	00M	SPEC

$\rho(2280)$ $I^G(J^{PC}) = 1^+(1^{--})$

MASS (MeV)	WIDTH (MeV)	DOCUMENT ID		TECN	COMMENT
2280 ± 50	440 ± 110	ATKINSON	85	OMEG	20–70 $\gamma p \to p\omega\pi^+\pi^-\pi^0$

$\omega_3(2285)$ $I^G(J^{PC}) = 0^-(3^{--})$

MASS (MeV)	WIDTH (MeV)	DOCUMENT ID		TECN	COMMENT
2285 ± 60	230 ± 40	[6] ANISOVICH	02B	SPEC	0.6–1.9 $p\overline{p} \to \omega\eta$, $\omega\pi^0\pi^0$

$f_3(2300)$ $I^G(J^{PC}) = 0^+(3^{++})$

MASS (MeV)	WIDTH (MeV)	DOCUMENT ID		TECN
2303 ± 15	214 ± 29	ANISOVICH	00J	SPEC

$\rho_3(2300)$ $I^G(J^{PC}) = 1^+(3^{--})$

MASS (MeV)	WIDTH (MeV)	DOCUMENT ID		TECN
2300^{+50}_{-80}	340 ± 50	ANISOVICH	00J	SPEC

$a_3(2310)$ $I^G(J^{PC}) = 1^-(3^{++})$

MASS (MeV)	WIDTH (MeV)	DOCUMENT ID		TECN
2310 ± 40	180^{+120}_{-60}	ANISOVICH	99C	SPEC

$f_1(2310)$ $I^G(J^{PC}) = 0^+(1^{++})$

MASS (MeV)	WIDTH (MeV)	DOCUMENT ID		TECN
2310±60	255 ± 70	ANISOVICH	00J	SPEC

$\eta_4(2320)$ $I^G(J^{PC}) = 0^+(4^{-+})$

MASS (MeV)	WIDTH (MeV)	DOCUMENT ID		TECN
2328±38	240 ± 90	ANISOVICH	00J	SPEC

$f_0(2330)$ $I^G(J^{PC}) = 0^+(0^{++})$

MASS (MeV)	WIDTH (MeV)	DOCUMENT ID		TECN
• • • We do not use the following data for averages, fits, limits, etc. • • •				
2337±14	217 ± 33	ANISOVICH	00J	SPEC
~ 2321	~ 223	HASAN	94	

$\omega(2330)$ $I^G(J^{PC}) = 0^-(1^{--})$

MASS (MeV)	WIDTH (MeV)	DOCUMENT ID		TECN	COMMENT
2330±30	435 ± 75	ATKINSON	88	OMEG	25–50 $\gamma p \rightarrow \rho^{\pm}\rho^0\pi^{\mp}$

$a_1(2340)$ $I^G(J^{PC}) = 1^-(1^{++})$

MASS (MeV)	WIDTH (MeV)	DOCUMENT ID		TECN
2340±40	230 ± 70	ANISOVICH	99E	SPEC

$X(2340)$ $I^G(J^{PC}) = ?^?(?^{??})$

MASS (MeV)	WIDTH (MeV)	EVTS	DOCUMENT ID		TECN	COMMENT
2340±20	180 ± 60	126	[13] BALTAY	75	HBC	15 $\pi^+p \rightarrow p5\pi$

$\pi(2360)$ $I^G(J^{PC}) = 0^-(0^{-+})$

MASS (MeV)	WIDTH (MeV)	DOCUMENT ID		TECN	COMMENT
2360±25	300^{+100}_{-50}	ANISOVICH	01F	SPEC	2.0 $\overline{p}p \rightarrow 3\pi^0$, $\pi^0\eta$, $\pi^0\eta'$

$X(2360)$ $I^G(J^{PC}) = ?^?(4^{+?})$

MASS (MeV)	WIDTH (MeV)	DOCUMENT ID		TECN	COMMENT
2360±10	430 ± 30	ROZANSKA	80	SPRK	18 $\pi^-p \rightarrow p\overline{p}n$

$X(2440)$ $I^G(J^{PC}) = ?^?(5^{-?})$

MASS (MeV)	WIDTH (MeV)	DOCUMENT ID		TECN	COMMENT
2440±10	310 ± 20	ROZANSKA	80	SPRK	18 $\pi^-p \rightarrow p\overline{p}n$

$X(2680)$ $I^G(J^{PC}) = ?^?(?^{??})$

MASS (MeV)	WIDTH (MeV)	DOCUMENT ID		TECN	COMMENT
2676±27	150	CASO	70	HBC	11.2 $\pi^-p \rightarrow \rho^-\pi^+\pi^-p$

$X(2710)$ $I^G(J^{PC}) = ?^?(6^{+?})$

MASS (MeV)	WIDTH (MeV)	DOCUMENT ID		TECN	COMMENT
2710±20	170 ± 40	ROZANSKA	80	SPRK	18 $\pi^-p \rightarrow p\overline{p}n$

$X(2750)$ $I^G(J^{PC}) = ?^?(7^{-?})$

MASS (MeV)	WIDTH (MeV)	DOCUMENT ID		TECN	COMMENT
2747±32	195 ± 75	DENNEY	83	LASS	10 $\pi^+p \rightarrow K^+K^-\pi^+p$

$X(3250)$ $I^G(J^{PC}) = ?^?(?^{??})$ 3-Body Decays

MASS (MeV)	WIDTH (MeV)	DOCUMENT ID		TECN	COMMENT
3250±8±20	45 ± 18	ALEEV	93	BIS2	$X(3250) \rightarrow \Lambda\overline{p}K^+$
3265±7±20	40 ± 18	ALEEV	93	BIS2	$X(3250) \rightarrow \overline{\Lambda}pK^-$

$X(3250)$ $I^G(J^{PC}) = ?^?(?^{??})$ 4-Body Decays

MASS (MeV)	WIDTH (MeV)	DOCUMENT ID		TECN	COMMENT
3245±8±20	25 ± 11	ALEEV	93	BIS2	$X(3250) \rightarrow \Lambda\overline{p}K^+\pi^{\pm}$
3250±9±20	50 ± 20	ALEEV	93	BIS2	$X(3250) \rightarrow \overline{\Lambda}pK^-\pi^{\mp}$
3270±8±20	25 ± 11	ALEEV	93	BIS2	$X(3250) \rightarrow K^0_S p\overline{p}K^{\pm}$

FOOTNOTES for Further States

[1] K-matrix pole from combined analysis of $\pi^-p \rightarrow \pi^0\pi^0n$, $\pi^-p \rightarrow K\overline{K}n$, $\pi^+\pi^- \rightarrow \pi^+\pi^-$, $\overline{p}p \rightarrow \pi^0\pi^0\pi^0$, $\pi^0\eta\eta$, $\pi^0\pi^0\eta$, $\pi^+\pi^-\pi^0$, $K^+K^-\pi^0$, $K^0_SK^0_S\pi^0$, $K^+K^0_S\pi^-$ at rest, $\overline{p}n \rightarrow \pi^-\pi^-\pi^+$, $K^0_SK^-\pi^0$, $K^0_SK^0_S\pi^-$ at rest.

[2] K-matrix pole from combined analysis of $\pi^-p \rightarrow \pi^0\pi^0n$, $\pi^-p \rightarrow K\overline{K}n$, $\overline{p}p \rightarrow \pi^0\pi^0\pi^0$, $\pi^0\eta\eta$, $\pi^0\pi^0\eta$ at rest.

[3] Our estimate.

[4] Using the observable fractions of 50.0% $\rho\pi$, 56.5% $f_2\pi$, and 11.8% $\rho_3\pi$.

[5] From the combined analysis of ANISOVICH 00J, ANISOVICH 01D, ANISOVICH 01E, and ANISOVICH 02.

[6] From the combined analysis of ANISOVICH 00D, ANISOVICH 01C, and ANISOVICH 02B.

[7] Cannot determine spin to be 3.

[8] BALTAY 77 favors $J^P = ,3^+$.

[9] Corrected for all decay modes.

[10] See SEMENOV 99 and KLOET 96.

[11] ASTON 81B sees no peak, has 850 events in Ajinenko+Barth bins. ARESTOV 80 sees no peak.

[12] Combined fit along with data of ANISOVICH 00J.

[13] Dominant decay into $\rho^0\rho^0\pi^+$. BALTAY 78 finds confirmation in $2\pi^+\pi^-2\pi^0$ events which contain $\rho^+\rho^0\pi^0$ and $2\rho^+\pi^-$.

REFERENCES for Further States

ANISOVICH	03	EPJ A16 229	V.V. Anisovich *et al.*
BAI	03F	PRL 91 022001	J.Z. Bai *et al.* (BES Collab.)
VLADIMIRSKY	03	PAN 66 700	V.V. Vladimirsky *et al.*
		Translated from YAF 66 729.	
ANISOVICH	02	PL B542 8	A.V. Anisovich *et al.*
ANISOVICH	02B	PL B542 19	A.V. Anisovich *et al.*
CHUNG	02	PR D65 072001	S.U. Chung *et al.*
LINK	02K	PL B545 50	J.M. Link *et al.* (FNAL FOCUS Collab.)
ANISOVICH	01B	PL B500 222	A.V. Anisovich *et al.*
ANISOVICH	01C	PL B507 23	A.V. Anisovich *et al.*
ANISOVICH	01D	PL B508 6	A.V. Anisovich *et al.*
ANISOVICH	01E	PL B513 281	A.V. Anisovich *et al.*
ANISOVICH	01F	PL B517 261	A.V. Anisovich *et al.*
ANISOVICH	00D	PL B476 15	A.V. Anisovich *et al.*
ANISOVICH	00E	PL B477 19	A.V. Anisovich *et al.*
ANISOVICH	00I	PL B491 40	A.V. Anisovich *et al.*
ANISOVICH	00J	PL B491 47	A.V. Anisovich *et al.*
ANISOVICH	00M	PL B496 145	A.V. Anisovich *et al.*
FILIPPI	00	PL B495 284	A. Filippi *et al.* (OBELIX Experiment)
ANISOVICH	99C	PL B452 173	A.V. Anisovich *et al.*
ANISOVICH	99E	PL B452 187	A.V. Anisovich *et al.*
BUGG	99	PL B458 511	D.V. Bugg *et al.*
FERRER	99	EPJ C10 249	A. Ferrer *et al.*
SEMENOV	99	SPU 42 847	S.V. Semenov
		Translated from UFN 42 937.	
DALKAROV	97	PL B392 229	O.D. Dalkarov *et al.* (LEBD)
KLOET	96	PR D53 6120	W.M. Kloet, F. Myhrer (RUTG, NORD)
PROKOSHKIN	96	SPD 41 247	Y.D. Prokoshkin, V.D. Samoilenko (SERP)
		Translated from DANS 348 481.	
HASAN	94	PL B334 215	A. Hasan, D.V. Bugg (LOQM)
OAKDEN	94	NP A574 731	M.N. Oakden, M.R. Pennington (DURH)
ALEEV	93	PAN 56 1358	A.N. Aleev *et al.* (BIS-2 Collab.)
		Translated from YAF 56 100.	
ARMSTRONG	93D	PL B307 399	T.A. Armstrong *et al.* (FNAL, FERR, GENO+)
ALBRECHT	91F	ZPHY C50 1	H. Albrecht *et al.* (ARGUS Collab.)
CONDO	91	PR D43 2787	G.T. Condo *et al.* (SLAC Hybrid Collab.)
BISELLO	89B	PR D39 701	G. Busetto *et al.* (DM2 Collab.)
ATKINSON	88	ZPHY C38 535	M. Atkinson *et al.* (BONN, CERN, GLAS+)
DAFTARI	87	PRL 58 859	I.K. Daftari *et al.* (SYRA)
ALDE	86D	NP B269 485	D.M. Alde *et al.* (BELG, LAPP, SERP, CERN+)
BRIDGES	86D	PL B180 313	D.L. Bridges *et al.* (SYRA, BNL, CASE+)
GREEN	86	PRL 56 1639	D.R. Green *et al.* (FNAL, ARIZ, FSU+)
ATKINSON	85	ZPHY C29 333	M. Atkinson *et al.* (BONN, CERN, GLAS+)
DENNEY	83	PR D28 2726	D.L. Denney *et al.* (IOWA, MICH)
ASTON	81B	NP B189 205	D. Aston *et al.* (BONN, CERN, EPOL, GLAS+)
ARESTOV	80	IHEP 80-165	Y.I. Arestov *et al.* (SERP)
CHLIAPNIK...	80	ZPHY C3 285	P.V. Chliapnikov *et al.* (SERP, BRUX, MONS)
KREYMER	80	PR D22 36	A.E. Kreymer *et al.* (IND., PURD, SLAC+)
ROZANSKA	80	NP B162 505	M. Rozanska *et al.* (MPIM, CERN)
EVANGELISTA	79	NP B153 253	C. Evangelista *et al.* (BARI, BONN, CERN+)
EVANGELISTA	79B	NP B154 381	C. Evangelista *et al.* (BARI, BONN, CERN+)
BALTAY	78	PR D17 52	C. Baltay *et al.* (COLU, BING)
ANTIPOV	77	NP B119 45	Y.M. Antipov *et al.* (SERP, GEVA)
BALTAY	77	PRL 39 591	C. Baltay, C.V. Cautis, M. Kalelkar (COLU)
BALTAY	75	PRL 35 891	C. Baltay *et al.* (COLU, BING)
KALELKAR	75	Thesis Nevis 207	M.S. Kalelkar (COLU)
CASO	70	LNC 3 707	C. Caso *et al.* (GENO, HAMB, MILA, SACL)

OTHER RELATED PAPERS

ROSNER	03B	PR D68 014004	J.L. Rosner
ABE	02K	PRL 88 181803	K. Abe *et al.* (BELLE Collab.)
ABE	02W	PRL 89 151802	K. Abe *et al.* (BELLE Collab.)
ANISOVICH	01E	PL B513 281	A.V. Anisovich *et al.*
ABELE	00B	EPJ C17 583	A. Abele *et al.*
BARNES	00	PR C62 055203	P.D. Barnes *et al.*
BOLONKIN	00	JETPL 72 166	B.V. Bolonkin *et al.*
		Translated from ZETFP 72 240.	
ANISOVICH	99F	NP A651 253	A.V. Anisovich *et al.*
CHIBA	99	PR C60 035204	M. Chiba *et al.*
BUZZO	97	ZPHY C76 475	A. Buzzo *et al.* (JETSET Collab.)
CHIBA	97	PR D55 40	M. Chiba *et al.* (FUKI, INUS, KEK, SANG+)
BARNES	94	PL B331 203	P.D. Barnes *et al.* (PS185 Collab.)
CARBONELL	93	PL B306 407	J. Carbonell, K.V. Protasov, O.D. Dalkarov (ISNG+)
FERRER	93	NP A558 191c	A. Ferrer, A.A. Grigorian (WA56 Collab.)
CHIBA	91	PR D44 1933	M. Chiba *et al.* (FUKI, KEK, SANG, OSAK+)
GRAF	91	PR D44 1945	N.A. Graf *et al.* (UCI, PENN, NMSU, KARLK+)
TANIMORI	90	PR D41 744	T. Tanimori *et al.* (KEK, INUS, KYOT+)
ALBRECHT	89M	PL B217 205	H. Albrecht *et al.* (ARGUS Collab.)
BEHREND	89D	PL B218 493	H.J. Behrend *et al.* (CELLO Collab.)
BUSENITZ	89	PR D40 1	J.K. Busenitz *et al.* (ILL, FNAL)
CHIBA	88	PL B202 447	M. Chiba, K. Doi (FUKI, INUS, KEK, SANG, OSAK+)
CHIBA	87	PR D36 3321	M. Chiba *et al.* (FUKI, INUS, KEK, SANG+)
FRANKLIN	87	PL B184 111	J. Franklin
LIU	87	PRL 58 2288	K.F. Liu, B.A. Li (STON)
ADIELS	86	PL B182 405	L. Adiels *et al.* (STOH, BASL, LASL, THES+)
ANGELOPO...	86	PL B178 441	A. Angelopoulos *et al.* (ATHU, UCI, KARLK+)
ARMSTRONG	86C	PL B175 383	T.A. Armstrong *et al.* (BNL, HOUS, PENN+)
BRIDGES	86	PRL 56 211	D.L. Bridges *et al.* (BLSU, BNL, CASE+)
BRIDGES	86B	PRL 56 215	D.L. Bridges *et al.* (SYRA, CASE)
BRIDGES	86C	PRL 57 1534	D.L. Bridges *et al.* (SYRA)

Meson Particle Listings

Further States

BRIDGES	86D	PL B180 313	D.L. Bridges *et al.*	(SYRA, BNL, CASE+)
DOVER	86	PRL 57 1207	C.B. Dover *et al.*	(BNL)
ANGELOPO...	85	PL 159B 210	A. Angelopoulos *et al.*	(ATHU, UCI, UNM+)
BODENKAMP	85	NP B255 717	J. Bodenkamp *et al.*	(KARLK, KARLE, DESY)
ADIELS	84	PL 138B 235	L. Adiels *et al.*	(BASL, KARLK, KARLE, STOH+)
ATKINSON	84F	NP B239 1	M. Atkinson *et al.*	(BONN, CERN, GLAS+)
AZOOZ	84	NP B244 277	F. Azooz, I. Butterworth	(LOIC, RHEL, SACL+)
CLOUGH	84	PL 146B 299	A.S. Clough *et al.*	(SURR, LOQM, ANIK+)
AZOOZ	83	PL 122B 471	F. Azooz, I. Butterworth	(LOIC, RHEL, SACL+)
BARNETT	83	PR D27 493	B. Barnett *et al.*	(JHU)
BODENKAMP	83	PL 133B 275	J. Bodenkamp *et al.*	(KARLK, KARLE, DESY)
RICHTER	83	PL 126B 284	B. Richter, L. Adiels	(BASL, KARLK, KARLE, STOH+)
AJALTOUNI	82	NP B209 301	Z. Ajaltouni *et al.*	(CERN, NEUC+)
ASTON	81B	NP B189 205	D. Aston *et al.*	(BONN, CERN, EPOL, GLAS+)
BANKS	81	PL 100B 191	A.D. Banks *et al.*	(LIVP, CERN)
CHUNG	81	PRL 46 395	S.U. Chung *et al.*	(BNL, BRAN, CINC+)
HARRIS	81	ZPHY C9 275	R.M. Harris *et al.*	(SEAT, UCB)
ARESTOV	80	IHEP 80-165	Y.I. Arestov *et al.*	(SERP)
ASTON	80D	PL 93B 517	D. Aston	(BONN, CERN, EPOL, GLAS, LANC+)
BIONTA	80	PRL 44 909	R.M. Bionta *et al.*	(BNL, CMU, FNAL+)
CARROLL	80	PRL 44 1572	A.S. Carroll *et al.*	(BNL, PRIN)
DAUM	80E	PL 90B 475	C. Daum *et al.*	(AMST, CERN, CRAC, MPIM+)
DEFOIX	80	NP B162 12	C. Defoix *et al.*	(CDEF, PISA)
HAMILTON	80	PRL 44 1179	R.P. Hamilton *et al.*	(LBL, BNL, MTHO)
HAMILTON	80B	PRL 44 1182	R.P. Hamilton *et al.*	(LBL, BNL, MTHO)
KREYMER	80	PR D22 36	A.E. Kreymer *et al.*	(IND, PURD, SLAC+)
ALBERI	79	PL 83B 247	G. Alberi *et al.*	(TRST, CERN, IFRJ)
ARMSTRONG	79	PL B85 304	T.A. Armstrong *et al.*	(DESY, GLAS)
BARTALUCCI	79	NC 49A 207	S. Bartalucci *et al.*	(DESY, FRAS)
DELCOURT	79	PL 86B 395	B. Delcourt *et al.*	(LALO)
GIBBARD	79	PRL 42 1593	B.G. Gibbard *et al.*	(CORN)
SAKAMOTO	79	NP B158 410	S. Sakamoto *et al.*	(INUS)
CARTER	78B	NP B141 467	A.A. Carter	(LOQM)
ESPOSITO	78	LNC 22 305	B. Esposito, F. Felicetti	(FRAS, NAPL, PADO+)
PAVLOPO...	78	PL 72B 415	P. Pavlopoulos *et al.*	(KARLK, KARLE, BASL+)
PETERSON	78	PR D18 3955	D. Peterson *et al.*	(CORN, HARV)
BENKHEIRI	77	PL 68B 483	P. Benkheiri *et al.*	(CERN, CDEF, EPOL+)
BRUCKNER	77	PL 67B 222	W. Bruckner *et al.*	(MPIH, HEIDP, CERN)
ABASHIAN	76	PR D13 5	A. Abashian *et al.*	(ILL, ANL, CHIC+)
BRAUN	76	PL 60B 481	H.M. Braun *et al.*	(STRB)
CHALOUPKA	76	PL 61B 487	V. Chaloupka *et al.*	(CERN, LIVP, MONS+)
ALSTON-...	75	PRL 35 1685	M. Alston-Garnjost *et al.*	(LBL, MTHO)
D'ANDLAU	75	PL 58B 223	C. d'Andlau *et al.*	(CDEF, PISA)
KALOGERO...	75	PRL 34 1047	T. Kalogeropoulos, G.S. Tzanakos	(SYRA)
CARROLL	74	PRL 32 247	A.S. Carroll *et al.*	(BNL)
THOMPSON	74	NP B69 220	G. Thompson *et al.*	(PURD)
DONALD	73	NP B61 333	R.A. Donald *et al.*	(LIVP, PARIS)
ALEXANDER	72	NP B45 29	G. Alexander *et al.*	(TELA)
ANTIPOV	72	PL 40 147	Y.M. Antipov *et al.*	(SERP)
TAKAHASHI	72	PR D6 1266	K. Takahashi *et al.*	(TOHOK, PENN, NDAM+)
BENVENUTI	71	PRL 27 283	A.C. Benvenuti *et al.*	(WISC)
SABAU	71	LNC 1 514	M. Sabeu, J.L. Uretsky	(BUCH, ANL)
BAUD	70	PL 31B 549	R. Baud *et al.*	(CERN Boson Spectrometer Collab.)
ANDERSON	69	PRL 22 1390	E.W. Anderson *et al.*	(BNL, CMU)
BOESEBECK	68	NP B4 501	K. Boesebeck *et al.*	(AACH, BERL, CERN)
HUSON	68	PL 28B 208	R. Huson *et al.*	(ORSAY, MILA, UCLA)
ALLES-...	67B	NC 50A 776	V. Alles-Borelli *et al.*	(CERN, BONN)
DANYSZ	67B	NC 51A 801	J.A. Danysz, B.R. French, V. Simak	(CERN)
CHIKOVANI	66	PL 22 233	G.E. Chikovani *et al.*	(SERP)
FOCACCI	66	PRL 17 890	M.N. Focacci *et al.*	(CERN)

STRANGE MESONS
($S = \pm 1$, $C = B = 0$)

$K^+ = u\overline{s}$, $K^0 = d\overline{s}$, $\overline{K}^0 = \overline{d}s$, $K^- = \overline{u}s$, similarly for K^*'s

$K^{\pm}$ $I(J^P) = \frac{1}{2}(0^-)$

THE CHARGED KAON MASS

Revised 1994 by T.G. Trippe (LBNL).

The average of the six charged kaon mass measurements which we use in the Particle Listings is

$$m_{K^{\pm}} = 493.677 \pm 0.013 \text{ MeV (S = 2.4)} , \quad (1)$$

where the error has been increased by the scale factor S. The large scale factor indicates a serious disagreement between different input data. The average before scaling the error is

$$m_{K^{\pm}} = 493.677 \pm 0.005 \text{ MeV} ,$$
$$\chi^2 = 22.9 \text{ for 5 D.F., Prob. } = 0.04\% , \quad (2)$$

where the high χ^2 and correspondingly low χ^2 probability further quantify the disagreement.

The main disagreement is between the two most recent and precise results,

$$m_{K^{\pm}} = 493.696 \pm 0.007 \text{ MeV} \quad \text{DENISOV 91}$$
$$m_{K^{\pm}} = 493.636 \pm 0.011 \text{ MeV (S = 1.5)} \quad \text{GALL 88}$$
$$\text{Average} = 493.679 \pm 0.006 \text{ MeV}$$
$$\chi^2 = 21.2 \text{ for 1 D.F., Prob. } = 0.0004\% , \quad (3)$$

both of which are measurements of x-ray energies from kaonic atoms. Comparing the average in Eq. (3) with the overall average in Eq. (2), it is clear that DENISOV 91 and GALL 88 dominate the overall average, and that their disagreement is responsible for most of the high χ^2.

The GALL 88 measurement was made using four different kaonic atom transitions, K^- Pb ($9 \to 8$), K^- Pb ($11 \to 10$), K^- W ($9 \to 8$), and K^- W ($11 \to 10$). The $m_{K^{\pm}}$ values they obtain from each of these transitions is shown in the Particle Listings and in Fig. 1. Their K^- Pb ($9 \to 8$) $m_{K^{\pm}}$is below and somewhat inconsistent with their other three transitions. The average of their four measurements is

$$m_{K^{\pm}} = 493.636 \pm 0.007 ,$$
$$\chi^2 = 7.0 \text{ for 3 D.F., Prob. } = 7.2\% . \quad (4)$$

This is a low but acceptable χ^2 probability so, to be conservative, GALL 88 scaled up the error on their average by S=1.5 to obtain their published error ± 0.011 shown in Eq. (3) above and used in the Particle Listings average.

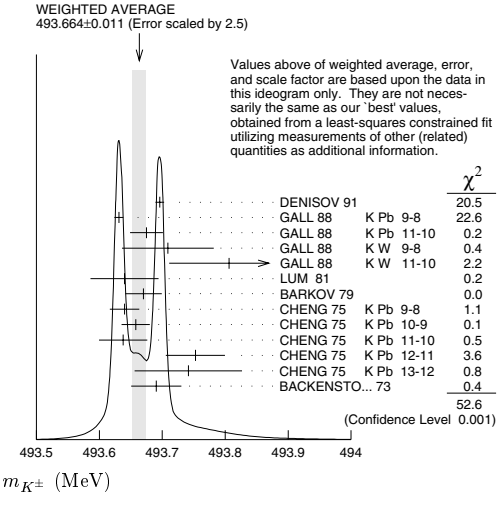

Figure 1: Ideogram of $m_{K^{\pm}}$ mass measurements. GALL 88 and CHENG 75 measurements are shown separately for each transition they measured.

The ideogram in Fig. 1 shows that the DENISOV 91 measurement and the GALL 88 K^- Pb ($9 \to 8$) measurement yield two well-separated peaks. One might suspect the GALL 88 K^- Pb ($9 \to 8$) measurement since it is responsible both for the internal inconsistency in the GALL 88 measurements and the disagreement with DENISOV 91.

To see if the disagreement could result from a systematic problem with the K^- Pb ($9 \to 8$) transition, we have separated the CHENG 75 data, which also used K^- Pb, into its separate transitions. Figure 1 shows that the CHENG 75 and GALL 88 K^- Pb ($9 \to 8$) values are consistent, suggesting the possibility of a common effect such as contaminant nuclear γ rays near the K^- Pb ($9 \to 8$) transition energy, although the CHENG 75 errors are too large to make a strong conclusion. The average of all 13 measurements has a χ^2 of 52.6 as shown in Fig. 1 and the first line of Table 1, yielding an unacceptable χ^2 probability of 0.00005%. The second line of Table 1 excludes both the GALL 88 and CHENG 75 measurements of the K^- Pb ($9 \to 8$) transition and yields a χ^2 probability of 43%. The third [fourth] line of Table 1 excludes only the GALL 88 K^- Pb ($9 \to 8$) [DENISOV 91] measurement and yields a χ^2 probability of 20% [8.6%]. Table 1 shows that removing both measurements of the K^- Pb ($9 \to 8$) transition produces the most consistent set of data, but that excluding only the GALL 88 K^- Pb ($9 \to 8$) transition or DENISOV 91 also produces acceptable probabilities.

Table 1: $m_{K^{\pm}}$ averages for some combinations of Fig. 1 data.

$m_{K^{\pm}}$ (MeV)	χ^2	D.F.	Prob. (%)	Measurements used
493.664 ± 0.004	52.6	12	0.00005	all 13 measurements
493.690 ± 0.006	10.1	10	43	no K^- Pb(9→8)
493.687 ± 0.006	14.6	11	20	no GALL 88 K^- Pb(9→8)
493.642 ± 0.006	17.8	11	8.6	no DENISOV 91

Yu.M. Ivanov, representing DENISOV 91, has estimated corrections needed for the older experiments because of improved ^{192}Ir and ^{198}Au calibration γ-ray energies. He estimates that CHENG 75 and BACKENSTOSS 73 $m_{K^{\pm}}$ values could be raised by about 15 keV and 22 keV, respectively. With these estimated corrections, Table 1 becomes Table 2. The last line of Table 2 shows that if such corrections are assumed, then GALL 88 K^- Pb (9 → 8) is inconsistent with the rest of the data even when DENISOV 91 is excluded. Yu.M. Ivanov warns that these are rough estimates. Accordingly, we do not use Table 2 to reject the GALL 88 K^- Pb (9 → 8) transition, but we note that a future reanalysis of the CHENG 75 data could be useful because it might provide supporting evidence for such a rejection.

Table 2: $m_{K^{\pm}}$ averages for some combinations of Fig. 1 data after raising CHENG 75 and BACKENSTOSS 73 values by 0.015 and 0.022 MeV respectively.

$m_{K^{\pm}}$ (MeV)	χ^2	D.F.	Prob. (%)	Measurements used
493.666 ± 0.004	53.9	12	0.00003	all 13 measurements
493.693 ± 0.006	9.0	10	53	no K^- Pb(9→8)
493.690 ± 0.006	11.5	11	40	no GALL 88 K^- Pb(9→8)
493.645 ± 0.006	23.0	11	1.8	no DENISOV 91

The GALL 88 measurement uses a Ge semiconductor spectrometer which has a resolution of about 1 keV, so they run the risk of some contaminant nuclear γ rays. Studies of γ rays following stopped π^- and Σ^- absorption in nucleii (unpublished) do not show any evidence for contaminants according to GALL 88 spokesperson, B.L. Roberts. The DENISOV 91 measurement uses a crystal diffraction spectrometer with a resolution of 6.3 eV for radiation at 22.1 keV to measure the 4f-3d transition in K^- ^{12}C. The high resolution and the light nucleus reduce the probability for overlap by contaminant γ rays, compared with the measurement of GALL 88. The DENISOV 91 measurement is supported by their high-precision measurement of the 4d-2p transition energy in π^- ^{12}C, which is good agreement with the calculated energy.

While we suspect that the GALL 88 K^- Pb (9 → 8) measurements could be the problem, we are unable to find clear grounds for rejecting it. Therefore, we retain their measurement in the average and accept the large scale factor until further information can be obtained from new measurements and/or from reanalysis of GALL 88 and CHENG 75 data.

We thank B.L. Roberts (Boston Univ.) and Yu.M. Ivanov (Petersburg Nuclear Physics Inst.) for their extensive help in understanding this problem.

$K^{\pm}$ MASS

VALUE (MeV)	DOCUMENT ID		TECN	CHG	COMMENT
493.677±0.016 OUR FIT Error includes scale factor of 2.8.					
493.677±0.013 OUR AVERAGE Error includes scale factor of 2.4. See the ideogram below.					
493.696±0.007	[1] DENISOV	91	CNTR	–	Kaonic atoms
493.636±0.011	[2] GALL	88	CNTR	–	Kaonic atoms
493.640±0.054	LUM	81	CNTR	–	Kaonic atoms
493.670±0.029	BARKOV	79	EMUL	±	$e^+e^- \to K^+K^-$
493.657±0.020	[2] CHENG	75	CNTR	–	Kaonic atoms
493.691±0.040	BACKENSTO...73		CNTR	–	Kaonic atoms
• • • We do not use the following data for averages, fits, limits, etc. • • •					
493.631±0.007	GALL	88	CNTR	–	K^- Pb (9→ 8)
493.675±0.026	GALL	88	CNTR	–	K^- Pb (11→ 10)
493.709±0.073	GALL	88	CNTR	–	K^- W (9→ 8)
493.806±0.095	GALL	88	CNTR	–	K^- W (11→ 10)
493.640±0.022±0.008	[3] CHENG	75	CNTR	–	K^- Pb (9→ 8)
493.658±0.019±0.012	[3] CHENG	75	CNTR	–	K^- Pb (10→ 9)
493.638±0.035±0.016	[3] CHENG	75	CNTR	–	K^- Pb (11→ 10)
493.753±0.042±0.021	[3] CHENG	75	CNTR	–	K^- Pb (12→ 11)
493.742±0.081±0.027	[3] CHENG	75	CNTR	–	K^- Pb (13→ 12)

[1] Error increased from 0.0059 based on the error analysis in IVANOV 92.
[2] This value is the authors' combination of all of the separate transitions listed for this paper.
[3] The CHENG 75 values for separate transitions were calculated from their Table 7 transition energies. The first error includes a 20% systematic error in the noncircular contaminant shift. The second error is due to a ±5 eV uncertainty in the theoretical transition energies.

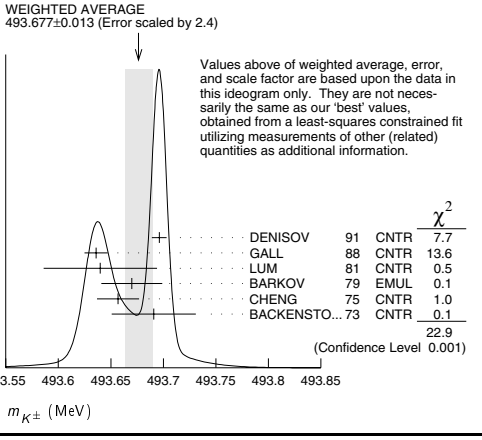

$m_{K^+} - m_{K^-}$

Test of *CPT*.

VALUE (MeV)	EVTS	DOCUMENT ID		TECN	CHG
−0.032±0.090	1.5M	[4] FORD	72	ASPK	±

[4] FORD 72 uses $m_{\pi^+} - m_{\pi^-} = +28 \pm 70$ keV.

$K^{\pm}$ MEAN LIFE

VALUE (10^{-8} s)	EVTS	DOCUMENT ID		TECN	CHG	COMMENT
1.2384±0.0024 OUR FIT Error includes scale factor of 2.0.						
1.2385±0.0025 OUR AVERAGE Error includes scale factor of 2.1. See the ideogram below.						
1.2451±0.0030	250k	KOPTEV	95	CNTR		K at rest, U target
1.2368±0.0041	150k	KOPTEV	95	CNTR		K at rest, Cu target
1.2380±0.0016	3M	OTT	71	CNTR	+	K at rest
1.2272±0.0036		LOBKOWICZ	69	CNTR	+	K in flight
1.2443±0.0038		FITCH	65B	CNTR	+	K at rest
• • • We do not use the following data for averages, fits, limits, etc. • • •						
1.2415±0.0024	400k	[5] KOPTEV	95	CNTR		K at rest
1.221 ±0.011		FORD	67	CNTR	±	
1.231 ±0.011		BOYARSKI	62	CNTR	+	

[5] KOPTEV 95 report this weighted average of their U-target and Cu-target results, where they have weighted by $1/\sigma$ rather than $1/\sigma^2$.

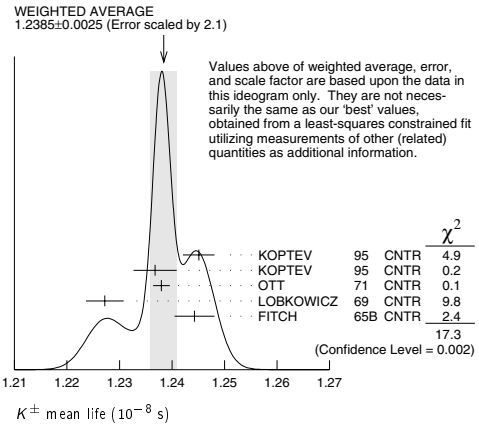

$(\tau_{K^+} - \tau_{K^-}) / \tau_{average}$

This quantity is a measure of CPT invariance in weak interactions.

VALUE (%)		DOCUMENT ID		TECN
0.11 ±0.09 OUR AVERAGE	Error includes scale factor of 1.2.			
0.090±0.078		LOBKOWICZ	69	CNTR
0.47 ±0.30		FORD	67	CNTR

RARE KAON DECAYS

(Revised November 2003 by L. Littenberg, BNL and G. Valencia, Iowa State University)

A. Introduction: There are several useful reviews on rare kaon decays and related topics [1–14]. The current activity in rare kaon decays can be divided roughly into four categories:

1. Searches for explicit violations of the Standard Model
2. Measurements of Standard Model parameters
3. Searches for CP violation
4. Studies of strong interactions at low energy.

The paradigm of Category 1 is the lepton flavor violating decay $K_L \to \mu e$. Category 2 includes processes such as $K^+ \to \pi^+ \nu\overline{\nu}$, which is sensitive to $|V_{td}|$. Much of the interest in Category 3 is focused on the decays $K_L \to \pi^0 \ell\overline{\ell}$, where $\ell \equiv e, \mu, \nu$. Category 4 includes reactions like $K^+ \to \pi^+ \ell^+ \ell^-$ which constitute a testing ground for the ideas of chiral perturbation theory. Other reactions of this type are $K_L \to \pi^0 \gamma\gamma$ and $K_L \to \ell^+ \ell^- \gamma$. The former is important in understanding a CP-conserving contribution to $K_L \to \pi^0 \ell^+ \ell^-$, whereas the latter could shed light on long distance contributions to $K_L \to \mu^+ \mu^-$.

The interplay between Categories 2-4 can be illustrated in Fig. 1. The modes $K \to \pi\nu\overline{\nu}$ are the cleanest ones theoretically. They can provide accurate determinations of certain CKM parameters (shown in the figure). In combination with alternate determinations of these parameters they also constrain new interactions. The modes $K_L \to \pi^0 e^+ e^-$ and $K_L \to \mu^+ \mu^-$ are also sensitive to CKM parameters. However, they suffer from a series of hadronic uncertainties that can be addressed, at least in part, through a systematic study of the additional modes indicated in the figure.

B. Explicit violations of the Standard Model: Most of the activity here is in searches for lepton flavor violation (LFV).

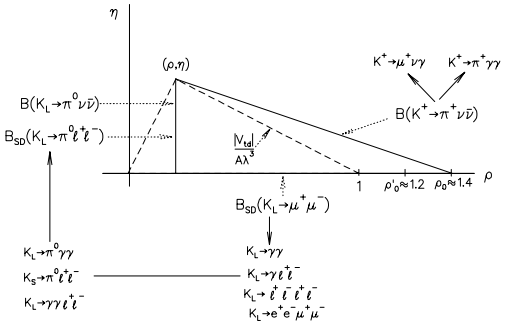

Figure 1: Role of rare kaon decays in determining the unitarity triangle. The solid arrows point to auxiliary modes needed to interpret the main results.

This is motivated by the fact that many extensions of the minimal Standard Model violate lepton flavor and by the potential to access very high energy scales. For example, the tree-level exchange of a LFV vector boson of mass M_X that couples to left-handed fermions with electroweak strength and without mixing angles yields $B(K_L \to \mu e) = 4.7 \times 10^{-12} (148 \text{ TeV}/M_X)^4$ [5]. This simple dimensional analysis may be used to read from Table 1 that the reaction $K_L \to \mu e$ is already probing scales of over 100 TeV. Table 1 summarizes the present experimental situation vis a vis LFV. The decays $K_L \to \mu^{\pm} e^{\mp}$ and $K^+ \to \pi^+ e^{\mp} \mu^{\pm}$ (or $K_L \to \pi^0 e^{\mp} \mu^{\pm}$) provide complementary information on potential family number violating interactions since the former is sensitive to parity-odd couplings and the latter is sensitive to parity-even couplings. Limits on certain lepton-number violating kaon decays [15,16] also exist. Related searches in μ and τ processes are discussed in our section "Tests of Conservation Laws".

Table 1: Searches for lepton flavor violation in K decay

Mode	90% CL upper limit	Exp't	Yr./Ref.
$K^+ \to \pi^+ e^- \mu^+$	1.2×10^{-11}	BNL-865 (prelim.)	2003/Ref. 17
$K^+ \to \pi^+ e^+ \mu^-$	5.2×10^{-10}	BNL-865	2001/Ref. 15
$K_L \to \mu e$	4.7×10^{-12}	BNL-871	1998/Ref. 18
$K_L \to \pi^0 e\mu$	3.4×10^{-10}	KTeV (prelim.)	2003/Ref. 19

Physics beyond the SM is also pursued through the search for $K^+ \to \pi^+ X^0$, where X^0 is a very light, noninteracting particle (*e.g.* hyperphoton, axion, familon, *etc.*). The 90% CL upper limit on this process is 5.9×10^{-11} [20].

C. Measurements of Standard Model parameters: Until 1997, searches for $K^+ \to \pi^+ \nu\overline{\nu}$ were motivated by the possibility of observing non-SM physics because the sensitivity attained was far short of the SM prediction for this decay [21] and long-distance contributions are known to be quite small [2,22]. Since then, BNL-787 has observed two candidate events [20,23], yielding a branching ratio of $(1.57^{+1.75}_{-0.82}) \times 10^{-10}$ [20]. At this level,

this reaction becomes interesting from the point of view of constraining SM parameters. An upgrade to the experiment to collect roughly an order of magnitude more sensitivity is in progress [24]. A new experiment with a sensitivity goal of $\sim 10^{-12}$/event was given scientific approval at FNAL [25] in 2001, but as of the end of 2003 its outlook is less certain. In the future this mode may provide grounds for precision tests of the flavor structure of the Standard Model [26]. The branching ratio can be written in terms of the very well-measured K_{e3} rate as [2]:

$$\mathrm{B}(K^+ \to \pi^+ \nu\overline{\nu}) = \frac{\alpha^2 \mathrm{B}(K^+ \to \pi^o e^+ \nu)}{V_{us}^2 2\pi^2 \sin^4\theta_W} \times \sum_{l=e,\mu,\tau} |V_{cs}^* V_{cd} X_{NL}^{\ell} + V_{ts}^* V_{td} X(m_t)|^2 \quad (1)$$

to eliminate the *a priori* unknown hadronic matrix element. Isospin breaking corrections to the ratio of matrix elements reduce this rate by 10% [27]. In Eq. (1) the Inami-Lim function $X(m_t)$ is of order 1 [28], and X_{NL}^{ℓ} is several hundred times smaller. This form exhibits the strong dependence of this branching ratio on $|V_{td}|$. QCD corrections, which mainly affect X_{NL}^{ℓ}, are known at next-to-leading order [12,29] and lead to a residual error of $< 10\%$ for the decay amplitude. Evaluating the constants in Eq. (1), one can cast this result in terms of the CKM parameters A, ρ and η (see our Section on "The Cabibbo-Kobayashi-Maskawa mixing matrix") [12]

$$\mathrm{B}(K^+ \to \pi^+ \nu\overline{\nu}) \approx 1.0 \times 10^{-10} A^4 [\eta^2 + (\rho_o - \rho)^2] \quad (2)$$

where $\rho_o \equiv 1 + (\frac{2}{3}X_{NL}^e + \frac{1}{3}X_{NL}^\tau)/(A^2 V_{us}^4 X(m_t)) \approx 1.4$. Thus, $\mathrm{B}(K^+ \to \pi^+ \nu\overline{\nu})$ determines a circle in the ρ, η plane with center $(\rho_o, 0)$ and radius $\approx \frac{1}{A^2}\sqrt{\frac{\mathrm{B}(K^+ \to \pi^+ \nu\overline{\nu})}{1.0\times 10^{-10}}}$. Current constraints on the CKM parameters lead to a predicted branching ratio $(7.2 \pm 2.1) \times 10^{-11}$ [30], near the lower end of the BNL-787 measurement.

The decay $K_L \to \mu^+\mu^-$ also has a short distance contribution sensitive to the CKM parameter ρ, given by [12]:

$$\mathrm{B}_{\mathrm{SD}}(K_L \to \mu^+\mu^-) \approx 1.6 \times 10^{-9} A^4 (\rho_o' - \rho)^2 \quad (3)$$

where ρ_o' depends on the charm quark mass and is approximately 1.2. This decay, however, is dominated by a long-distance contribution from a two-photon intermediate state. The absorptive (imaginary) part of the long-distance component is determined by the measured rate for $K_L \to \gamma\gamma$ to be $\mathrm{B}_{\mathrm{abs}}(K_L \to \mu^+\mu^-) = (7.07 \pm 0.18) \times 10^{-9}$; and it almost completely saturates the observed rate $\mathrm{B}(K_L \to \mu^+\mu^-) = (7.18 \pm 0.17) \times 10^{-9}$ [31]. The difference between the observed rate and the absorptive component can be attributed to the (coherent) sum of the short-distance amplitude and the real part of the long-distance amplitude. In order to use this mode to constrain ρ it is, therefore, necessary to know the real part of the long-distance contribution. Unlike the absorptive part, the real part of the long-distance contribution cannot be derived from the measured rate for $K_L \to \gamma\gamma$. At present it is not possible to compute this long-distance component reliably, and therefore it is not possible to constrain ρ from this mode in a model independent way [32]. Several hadronic models exist to estimate this long-distance component [33,34] and are commonly used to place rough bounds on new physics contributions to the $K_L \to \mu^+\mu^-$ rate [35,36]. The decay $K_L \to e^+e^-$ is completely dominated by long distance physics and is easier to estimate. The result, $B(K_L \to e^+e^-) \sim 9 \times 10^{-12}$ [32,34], is in good agreement with the BNL-871 measurement, $(8.7^{+5.7}_{-4.1}) \times 10^{-12}$ [37].

D. Searches for direct CP violation: The mode $K_L \to \pi^0\nu\overline{\nu}$ is dominantly CP-violating and free of hadronic uncertainties [2,38,39]. In the Standard Model this mode is dominated by an intermediate top-quark state and does not suffer from the small uncertainty associated with the charm-quark intermediate state that affects the mode $K^+ \to \pi^+\nu\overline{\nu}$. The branching ratio is given approximately by Ref. 12:

$$\mathrm{B}(K_L \to \pi^0\nu\overline{\nu}) \approx 4.1 \times 10^{-10} A^4 \eta^2 \, . \quad (4)$$

With current constraints on the CKM parameters this leads to a predicted branching ratio $(2.8 \pm 1.0) \times 10^{-11}$ [30]. The current experimental upper bound is $\mathrm{B}(K_L \to \pi^0\nu\overline{\nu}) \leq 5.9 \times 10^{-7}$ [40]. The 90% CL bound on $K^+ \to \pi^+\nu\bar{\nu}$ provides a nearly model independent bound $B(K_L \to \pi^0\nu\bar{\nu}) < 1.7 \times 10^{-9}$ [41]. A KEK experiment to reach the 3×10^{-10}/event level [42] is scheduled to begin data-taking in early 2004. The KOPIO [43] experiment aims to reach the 6×10^{-13}/event level for $K_L \to \pi^0\nu\overline{\nu}$ at the BNL AGS. A Letter of Intent for an experiment of similar sensitivity has been submitted to the J-PARC PAC [44].

There has been much theoretical work on possible contributions to ϵ'/ϵ and rare K decays in supersymmetric extensions of the SM. While in the simplest case of the MSSM with no new sources of flavor or CP violation the main effect is a suppression of the rare K decays [45], substantial enhancements are possible in more general SUSY models [35,46]. Other recent predictions of the possible effects of new physics on rare kaon decays include those of large extra dimensions [47] and of effective theories with minimal flavor violation [36].

The decay $K_L \to \pi^0 e^+ e^-$ also has sensitivity to the CKM parameter η through its CP-violating component. There are both direct and indirect CP-violating amplitudes which can interfere. The direct CP-violating amplitude is short distance dominated and has been calculated in detail within the SM [9]. The indirect CP-violating amplitude can be inferred from a measurement of $K_S \to \pi^0 e^+ e^-$. The complete CP-violating contribution to the rate can be written as [50]:

$$\mathrm{B}_{\mathrm{CPV}} \approx \left(15.3 a_s^2 \pm 35 A^2 \eta |a_s| + 74.4 A^4 \eta^2\right) \times 10^{-12}. \quad (5)$$

The parameter a_s has recently been extracted by NA48 from a measurement of the decay $K_S \to \pi^0 e^+ e^-$ with the result $|a_s| = 1.06^{+0.26}_{-0.21} \pm 0.07$ [51]. With current constraints on the CKM parameters this implies that

$$\mathrm{B}_{\mathrm{CPV}} \approx (17.2 \pm 9.4 + 4.7) \times 10^{-12}. \quad (6)$$

The indirect CP violation is larger than the direct CP violation. While the sign of the interference is *a priori* unknown, arguments in favor of a positive sign have been put forward in Ref. 52.

This mode also has a CP-conserving component dominated by a two-photon intermediate state that cannot be computed reliably at present. This component has an absorptive part that can be, in principle, determined from a detailed analysis of $K_L \to \pi^0\gamma\gamma$. To understand the rate and the shape of the distribution $d\Gamma/dm_{\gamma\gamma}$ in $K_L \to \pi^0\gamma\gamma$ within chiral perturbation theory it is necessary to go beyond leading order, and this introduces three (a priori) unknown parameters [53]. Both KTeV and NA48 analyze their $K_L \to \pi^0\gamma\gamma$ data assuming vector meson dominance and extract from this analysis a bound on the CP-conserving rate in $K_L \to \pi^0 e^+e^-$ using the model of Ref. [54]. The two experiments report conflicting results. The more recent NA48 data finds a negligible rate in the low $m_{\gamma\gamma}$ region suggesting a very small CP-conserving component in $K_L \to \pi^0 e^+e^-$, $B_{\rm CP}(K_L \to \pi^0 e^+e^-) = (0.47^{+0.22}_{-0.18}) \times 10^{-12}$ [55]. On the other hand KTeV reported a larger fraction of $K_L \to \pi^0\gamma\gamma$ in the low $m_{\gamma\gamma}$ region, favoring a larger CP-conserving rate $B_{\rm CP}(K_L \to \pi^0 e^+e^-)$ between $1 - 2 \times 10^{-12}$ [56]. In addition to this difference between the two experiments, there remain two other sources of uncertainty in the prediction for the CP-conserving rate in $K_L \to \pi^0 e^+e^-$. The first one arises from the way the $K_L \to \pi^0\gamma\gamma$ amplitude is parameterized [57] assuming vector meson dominance, and the second one reflects the model dependence of the form factor connecting the two modes [52]. For the $K_L \to \pi^0\gamma\gamma$ rates, KTeV finds $B(K_L \to \pi^0\gamma\gamma) = (1.68 \pm 0.07_{\rm stat} \pm 0.08_{\rm sys}) \times 10^{-6}$ [56], whereas NA48 finds $B(K_L \to \pi^0\gamma\gamma) = (1.36 \pm 0.03_{\rm stat} \pm 0.03_{\rm sys} \pm 0.03_{\rm norm}) \times 10^{-6}$ [55].

The related process, $K_L \to \pi^0\gamma e^+e^-$, is potentially an additional background in some region of phase space [58]. This process has been observed with a branching ratio of $(2.34 \pm 0.35_{\rm stat} \pm 0.13_{\rm sys}) \times 10^{-8}$ [59].

The decay $K_L \to \gamma\gamma e^+e^-$ constitutes the dominant background to $K_L \to \pi^0 e^+e^-$. It was first observed by BNL-845 [60] and subsequently confirmed with a much larger sample by FNAL-799 [61]. It has been estimated that this background will enter at the level of 3×10^{-10} [62,63], comparable to or larger than the signal level. Because of this, the observation of $K_L \to \pi^0 e^+e^-$ will depend on background subtraction with good statistics. Possible alternative strategies are discussed in Ref. 52 and references cited therein.

The published 90% CL upper bound for the process $K_L \to \pi^0 e^+e^-$ is 5.1×10^{-10} [63]. There is now a preliminary 90% CL upper bound of 2.8×10^{-10} [64]. For the closely related muonic process, the published upper bound is $\mathrm{B}(K_L \to \pi^0\mu^+\mu^-) \leq 3.8 \times 10^{-10}$ [65]. KTeV has additional data corresponding to about a factor 1.3 in sensitivity for the latter reaction that is still to be analyzed.

A recent study of $K_L \to \pi^0\mu^+\mu^-$ has indicated that it might be possible to extract the direct CP-violating contribution by a joint study of the Dalitz plot variables and the components of the μ^+ polarization [66]. The latter tends to be quite substantial so that large statistics may not be necessary.

E. Other long distance dominated modes:

The decays $K^+ \to \pi^+\ell^+\ell^-$ ($\ell = e$ or μ) have received considerable attention. The rate and spectrum have been measured for both the electron and muon modes [67,68]. Ref. 50 has proposed a parameterization inspired by chiral perturbation theory, which provides a successful description of data but indicates the presence of large corrections beyond leading order. More work is needed to fully understand the origin of these large corrections.

Much information has been recorded by KTeV and NA48 on the rates and spectrum for the Dalitz pair conversion modes $K_L \to \ell^+\ell^-\gamma$ [69], and $K_L \to \ell^+\ell^-\ell'^+\ell'^-$ for $\ell, \ell' = e$ or μ [16,70–72]. All these results are used to test hadronic models and could further our understanding of the long distance component in $K_L \to \mu^+\mu^-$.

References

1. D. Bryman, Int. J. Mod. Phys. **A4**, 79 (1989).
2. J. Hagelin and L. Littenberg, Prog. in Part. Nucl. Phys. **23**, 1 (1989).
3. R. Battiston *et al.*, Phys. Reports **214**, 293 (1992).
4. L.Littenberg and G. Valencia, Ann. Rev. Nucl. and Part. Sci. **43**, 729 (1993).
5. J. Ritchie and S. Wojcicki, Rev. Mod. Phys. **65**, 1149 (1993).
6. B. Winstein and L. Wolfenstein, Rev. Mod. Phys. **65**, 1113 (1993).
7. G. D'Ambrosio, G. Ecker, G. Isidori and H. Neufeld, *Radiative Non-Leptonic Kaon Decays*, in The DAΦNE Physics Handbook (second edition), eds. L. Maiani, G. Pancheri, and N. Paver (Frascati), Vol. I, 265 (1995).
8. A. Pich, Rept. on Prog. in Phys. **58**, 563 (1995).
9. G. Buchalla, A.J. Buras, and M.E. Lautenbacher, Rev. Mod. Phys. **68**, 1125 (1996).
10. G. D'Ambrosio and G. Isidori, Int. J. Mod. Phys. **A13**, 1 (1996).
11. P. Buchholz and B. Renk Prog. in Part. Nucl. Phys. **39**, 253 (1997).
12. A.J. Buras and R. Fleischer, TUM-HEP-275-97, `hep-ph/9704376`, *Heavy Flavours II*, World Scientific, eds. A.J. Buras and M. Lindner (1997), 65–238.
13. A.J. Buras, TUM-HEP-349-99, Lectures given at Lake Louise Winter Institute: Electroweak Physics, Lake Louise, Alberta, Canada, 14–20 Feb. 1999.
14. A.R. Barker and S.H. Kettell, Ann. Rev. Nucl. and Part. Sci. **50**, 249 (2000).
15. R. Appel *et al.*, Phys. Rev. Lett. **85**, 2877 (2000).
16. A. Alavi-Harati *et al.*, Phys. Rev. Lett. **90**, 141801 (2003).
17. A. Sher "Lepton Flavor Violating Decay $K^+ \to \pi^+\mu^+e^-$", Universität Zürich Thesis, Oct 2003; R. Appel *et al.*, Phys. Rev. Lett. **85**, 2450 (2000).
18. D. Ambrose *et al.*, Phys. Rev. Lett. **81**, 5734 (1998).
19. A. Bellavance "Search for the lepton-flavor-number violating decay $K_L \to \pi^0\mu^\pm e^\mp$ in the full E799II KTeV dataset" Rice University Thesis, Jan 2003.

20. S. Adler *et al.*, Phys. Rev. Lett. **88**, 041803 (2002).
21. I. Bigi and F. Gabbiani, Nucl. Phys. **B367**, 3 (1991).
22. M. Lu and M.B. Wise, Phys. Lett. **B324**, 461 (1994); A.F. Falk, A. Lewandowski, and A.A. Petrov, Phys. Lett. **B505**, 107 (2001).
23. S. Adler *et al.*, Phys. Rev. Lett. **84**, 3768 (2000).
24. M. Aoki *et al.*, AGS Proposal 949, October 1998.
25. P.S. Cooper, Nucl. Phys. (Proc. Supp.) **B99N3**, 121 (2001).
26. G. D'Ambrosio and G. Isidori, Phys. Lett. **B530**, 108 (2002).
27. W. Marciano and Z. Parsa, Phys. Rev. **D53**, 1 (1996).
28. T. Inami and C.S. Lim, Prog. Theor. Phys. **65**, 297 (1981); erratum Prog. Theor. Phys. **65**, 172 (1981).
29. G. Buchalla and A.J. Buras Nucl. Phys. **B548**, 309 (1999); M. Misiak and J. Urban, Phys. Lett. **B451**, 161 (1999).
30. M. Battaglia *et al.*, "The CKM matrix and the unitarity triangle", hep-ph/0304132.
31. D. Ambrose *et al.*, Phys. Rev. Lett. **84**, 1389 (2000).
32. G. Valencia, Nucl. Phys. **B517**, 339 (1998).
33. G. D'Ambrosio, G. Isidori, and J. Portoles, Phys. Lett. **B423**, 385 (1998).
34. D. Gomez-Dumm and A. Pich, Phys. Rev. Lett. **80**, 4633 (1998).
35. A.J. Buras and L. Silvestrini Nucl. Phys. **B546**, 299 (1999).
36. G. D'Ambrosio *et al.*, Nucl. Phys. **B645**, 155 (2002).
37. D. Ambrose *et al.*, Phys. Rev. Lett. **81**, 4309 (1998).
38. L. Littenberg, Phys. Rev. **D39**, 3322 (1989).
39. G. Buchalla and G. Isidori Phys. Lett. **B440**, 170 (1998).
40. A. Alavi-Harati *et al.*, Phys. Rev. **D61**, 072006 (2000).
41. Y. Grossman and Y. Nir, Phys. Lett. **B398**, 163 (1997).
42. T.Inagaki *et al.*, KEK Internal 96-13, November 1996.
43. I-H. Chiang *et al.*, "KOPIO—a search for $K_L \to \pi^0\nu\bar{\nu}$", in RSVP proposal to the National Science Foundation (October 1999).
44. Y.B. Hsiung *et al.*, "Measurement of the $K_L \to \pi^0\nu\bar{\nu}$ Branching Ratio", submitted to the J-PARC Committee for Nuclear and Particle Physics Experimental Facility.
45. A.J. Buras *et al.*, Nucl. Phys. **B592**, 55 (2001).
46. F. Gabbiani *et al.*, Nucl. Phys. **B477**, 321 (1996); Y. Nir and M.P. Worah, Phys. Lett. **B423**, 319 (1998); A.J. Buras, A. Romanino, and L. Silvestrini, Nucl. Phys. **B520**, 3 (1998); G. Colangelo and G. Isidori, JHEP **9809**, 009 (1998); A.J. Buras *et al.*, Nucl. Phys. **B566**, 3 (2000).
47. A.J. Buras, M. Spranger, and A. Weiler, Nucl. Phys. **B660**, 225 (2003).
48. G. Ecker, A. Pich, and E. de Rafael, Nucl. Phys. **B303**, 665 (1988).
49. A. Lai *et al.*, Phys. Lett. **B514**, 253 (2001).
50. G. D'Ambrosio *et al.*, JHEP **9808**, 004 (1998); C.O. Dib, I. Dunietz, and F.J. Gilman, Phys. Rev. **D39**, 2639 (1989).
51. J.R. Batley *et al.*, hep-ex/0309075.
52. G. Buchalla, G. D'Ambrosio, and G. Isidori, "Extracting short-distance physics from $K_{(L,S)} \to \pi^0 e^+ e^-$ decays", hep-ph/0308000.
53. G. Ecker, A. Pich, and E. de Rafael, Phys. Lett. **237B**, 481 (1990); L. Cappiello, G. D'Ambrosio, and M. Miragliuolo, Phys. Lett. **B298**, 423 (1993); A. Cohen, G. Ecker, and A. Pich, Phys. Lett. **B304**, 347 (1993).
54. J.F. Donoghue and F. Gabbiani, Phys. Rev. **D51**, 2187 (1995).
55. A. Lai *et al.*, Phys. Lett. **B536**, 229 (2002).
56. A. Alavi-Harati *et al.*, Phys. Rev. Lett. **83**, 917 (1999).
57. F. Gabbiani and G. Valencia, Phys. Rev. **D64**, 094008 (2001); F. Gabbiani and G. Valencia, Phys. Rev. **D66**, 074006 (2002).
58. J. Donoghue and F. Gabbiani, Phys. Rev. **D56**, 1605 (1997).
59. A. Alavi-Harati *et al.*, Phys. Rev. Lett. **87**, 021801 (2001).
60. W.M. Morse *et al.*, Phys. Rev. **D45**, 36 (1992).
61. A. Alavi-Harati *et al.*, Phys. Rev. **D64**, 012003 (2001).
62. H.B. Greenlee, Phys. Rev. **D42**, 3724 (1990).
63. A. Alavi-Harati *et al.*, Phys. Rev. Lett. **86**, 397 (2001).
64. A. Alavi-Harati *et al.*, hep-ex/0309072 .
65. A. Alavi-Harati *et al.*, Phys. Rev. Lett. **84**, 5279 (2000).
66. M.V. Diwan, H. Ma and T.L. Trueman, Phys. Rev. **D65**, 054020 (2002).
67. R. Appel *et al.*, Phys. Rev. Lett. **83**, 4482 (1999).
68. S.C. Adler *et al.*, Phys. Rev. Lett. **79**, 4756 (1997); R. Appel *et al.*, Phys. Rev. Lett. **84**, 2580 (2000); H.K. Park *et al.*, Phys. Rev. Lett. **88**, 111801 (2002).
69. A. Alavi-Harati *et al.*, Phys. Rev. Lett. **87**, 071801 (2001).
70. A. Alavi-Harati *et al.*, Phys. Rev. Lett. **86**, 5425 (2001).
71. Jason R. LaDue "Understanding Dalitz Decays of the K_L in particular the decays of $K_L \to e^+e^-\gamma$ and $K_L \to e^+e^-e^+e^-$" University of Colorado Thesis, May 2003.
72. V. Fanti *et al.*, Phys. Lett. **B458**, 458 (1999).

K^+ DECAY MODES

K^- modes are charge conjugates of the modes below.

	Mode	Fraction (Γ_i/Γ)	Scale factor/ Confidence level
	Leptonic and semileptonic modes		
Γ_1	$e^+\nu_e$	$(1.55 \pm 0.07) \times 10^{-5}$	
Γ_2	$\mu^+\nu_\mu$	(63.43 ± 0.17) %	S=1.2
Γ_3	$\pi^0 e^+\nu_e$ Called K^+_{e3}.	(4.87 ± 0.06) %	S=1.2
Γ_4	$\pi^0\mu^+\nu_\mu$ Called $K^+_{\mu3}$.	(3.27 ± 0.06) %	S=1.2
Γ_5	$\pi^0\pi^0 e^+\nu_e$	$(2.1 \pm 0.4) \times 10^{-5}$	
Γ_6	$\pi^+\pi^- e^+\nu_e$	$(4.08 \pm 0.09) \times 10^{-5}$	
Γ_7	$\pi^+\pi^-\mu^+\nu_\mu$	$(1.4 \pm 0.9) \times 10^{-5}$	
Γ_8	$\pi^0\pi^0\pi^0 e^+\nu_e$	$< 3.5 \times 10^{-6}$	CL=90%
	Hadronic modes		
Γ_9	$\pi^+\pi^0$	(21.13 ± 0.14) %	S=1.1
Γ_{10}	$\pi^+\pi^0\pi^0$	(1.73 ± 0.04) %	S=1.2
Γ_{11}	$\pi^+\pi^+\pi^-$	(5.576 ± 0.031) %	S=1.1
	Leptonic and semileptonic modes with photons		
Γ_{12}	$\mu^+\nu_\mu\gamma$	[a,b] $(5.50 \pm 0.28) \times 10^{-3}$	
Γ_{13}	$\pi^0 e^+\nu_e\gamma$	[a,b] $(2.65 \pm 0.20) \times 10^{-4}$	
Γ_{14}	$\pi^0 e^+\nu_e\gamma$ (SD)	[c] $< 5.3 \times 10^{-5}$	CL=90%
Γ_{15}	$\pi^0\mu^+\nu_\mu\gamma$	[a,b] $< 6.1 \times 10^{-5}$	CL=90%
Γ_{16}	$\pi^0\pi^0 e^+\nu_e\gamma$	$< 5 \times 10^{-6}$	CL=90%

Hadronic modes with photons

Γ_{17}	$\pi^+\pi^0\gamma$	[a,b]	$(\ 2.75 \pm 0.15\ )\times10^{-4}$		
Γ_{18}	$\pi^+\pi^0\gamma$ (DE)	[b,d]	$(\ 4.4 \pm 0.8\ )\times10^{-6}$		
Γ_{19}	$\pi^+\pi^0\pi^0\gamma$	[a,b]	$(\ 7.4\ ^{+5.5}_{-2.9}\ )\times10^{-6}$		
Γ_{20}	$\pi^+\pi^+\pi^-\gamma$	[a,b]	$(\ 1.04 \pm 0.31\ )\times10^{-4}$		
Γ_{21}	$\pi^+\gamma\gamma$	[b]	$(\ 1.10 \pm 0.32\ )\times10^{-6}$		
Γ_{22}	$\pi^+3\gamma$	[b]	$<\ 1.0$	$\times10^{-4}$	CL=90%

Leptonic modes with $\ell\overline{\ell}$ pairs

Γ_{23}	$e^+\nu_e\nu\overline{\nu}$		$<\ 6$	$\times10^{-5}$	CL=90%
Γ_{24}	$\mu^+\nu_\mu\nu\overline{\nu}$		$<\ 6.0$	$\times10^{-6}$	CL=90%
Γ_{25}	$e^+\nu_e e^+e^-$		$(\ 2.48 \pm 0.20\ )\times10^{-8}$		
Γ_{26}	$\mu^+\nu_\mu e^+e^-$		$(\ 7.06 \pm 0.31\ )\times10^{-8}$		
Γ_{27}	$e^+\nu_e\mu^+\mu^-$		$<\ 5$	$\times10^{-7}$	CL=90%
Γ_{28}	$\mu^+\nu_\mu\mu^+\mu^-$		$<\ 4.1$	$\times10^{-7}$	CL=90%

Lepton Family number (LF), Lepton number (L), $\Delta S = \Delta Q$ (SQ) violating modes, or $\Delta S = 1$ weak neutral current ($S1$) modes

Γ_{29}	$\pi^+\pi^+e^-\overline{\nu}_e$	SQ	$<\ 1.2$	$\times10^{-8}$	CL=90%
Γ_{30}	$\pi^+\pi^+\mu^-\overline{\nu}_\mu$	SQ	$<\ 3.0$	$\times10^{-6}$	CL=95%
Γ_{31}	$\pi^+e^+e^-$	$S1$	$(\ 2.88 \pm 0.13\ )\times10^{-7}$		
Γ_{32}	$\pi^+\mu^+\mu^-$	$S1$	$(\ 8.1 \pm 1.4\ )\times10^{-8}$		S=2.7
Γ_{33}	$\pi^+\nu\overline{\nu}$	$S1$	$(\ 1.6\ ^{+1.8}_{-0.8}\ )\times10^{-10}$		
Γ_{34}	$\pi^+\pi^0\nu\overline{\nu}$	$S1$	$<\ 4.3$	$\times10^{-5}$	CL=90%
Γ_{35}	$\mu^-\nu e^+e^+$	LF	$<\ 2.0$	$\times10^{-8}$	CL=90%
Γ_{36}	$\mu^+\nu_e$	LF	[e] $<\ 4$	$\times10^{-3}$	CL=90%
Γ_{37}	$\pi^+\mu^+e^-$	LF	$<\ 2.8$	$\times10^{-11}$	CL=90%
Γ_{38}	$\pi^+\mu^-e^+$	LF	$<\ 5.2$	$\times10^{-10}$	CL=90%
Γ_{39}	$\pi^-\mu^+e^+$	L	$<\ 5.0$	$\times10^{-10}$	CL=90%
Γ_{40}	$\pi^-e^+e^+$	L	$<\ 6.4$	$\times10^{-10}$	CL=90%
Γ_{41}	$\pi^-\mu^+\mu^+$	L	[e] $<\ 3.0$	$\times10^{-9}$	CL=90%
Γ_{42}	$\mu^+\overline{\nu}_e$	L	[e] $<\ 3.3$	$\times10^{-3}$	CL=90%
Γ_{43}	$\pi^0e^+\overline{\nu}_e$	L	$<\ 3$	$\times10^{-3}$	CL=90%
Γ_{44}	$\pi^+\gamma$		[f] $<\ 3.6$	$\times10^{-7}$	CL=90%

[a] Most of this radiative mode, the low-momentum γ part, is also included in the parent mode listed without γ's.

[b] See the Particle Listings below for the energy limits used in this measurement.

[c] Structure-dependent part.

[d] Direct-emission branching fraction.

[e] Derived from an analysis of neutrino-oscillation experiments.

[f] Violates angular-momentum conservation.

CONSTRAINED FIT INFORMATION

An overall fit to the mean life, 2 decay rate, and 19 branching ratios uses 48 measurements and one constraint to determine 8 parameters. The overall fit has a $\chi^2 = 49.8$ for 41 degrees of freedom.

The following *off-diagonal* array elements are the correlation coefficients $\langle \delta p_i \delta p_j \rangle / (\delta p_i \cdot \delta p_j)$, in percent, from the fit to parameters p_i, including the branching fractions, $x_i \equiv \Gamma_i/\Gamma_{\rm total}$. The fit constrains the x_i whose labels appear in this array to sum to one.

x_3	−51						
x_4	−50	77					
x_5	−3	6	4				
x_9	−67	−17	−16	−1			
x_{10}	−23	−1	−1	0	−2		
x_{11}	−23	10	7	1	−6	14	
Γ	7	−3	−2	0	2	−5	−33
	x_2	x_3	x_4	x_5	x_9	x_{10}	x_{11}

	Mode	Rate (10^8 s^{-1})	Scale factor
Γ_2	$\mu^+\nu_\mu$	0.5122 ± 0.0017	1.4
Γ_3	$\pi^0e^+\nu_e$ Called K^+_{e3}.	0.0393 ± 0.0005	1.2
Γ_4	$\pi^0\mu^+\nu_\mu$ Called $K^+_{\mu3}$.	0.0264 ± 0.0005	1.2
Γ_5	$\pi^0\pi^0e^+\nu_e$	$(1.71\ ^{+0.34}_{-0.30}) \times10^{-5}$	
Γ_9	$\pi^+\pi^0$	0.1706 ± 0.0011	1.1
Γ_{10}	$\pi^+\pi^0\pi^0$	0.01395 ± 0.00031	1.2
Γ_{11}	$\pi^+\pi^+\pi^-$	0.04503 ± 0.00023	1.1

$K^{\pm}$ DECAY RATES

$\Gamma(\mu^+\nu_\mu)$ Γ_2

VALUE (10^6 s^{-1})	DOCUMENT ID		TECN	CHG
51.22 ± 0.17 OUR FIT Error includes scale factor of 1.4.				
51.2 ± 0.8	FORD	67	CNTR	±

$\Gamma(\pi^+\pi^+\pi^-)$ Γ_{11}

VALUE (10^6 s^{-1})	EVTS	DOCUMENT ID		TECN	CHG
4.503 ± 0.023 OUR FIT Error includes scale factor of 1.1.					
4.511 ± 0.024		[6] FORD	70	ASPK	
• • • We do not use the following data for averages, fits, limits, etc. • • •					
4.529 ± 0.032	3.2M	[6] FORD	70	ASPK	
4.496 ± 0.030		[6] FORD	67	CNTR	±

[6] First FORD 70 value is second FORD 70 combined with FORD 67.

$(\Gamma(K^+) - \Gamma(K^-)) / \Gamma(K)$

$K^{\pm} \to \mu^{\pm}\nu_\mu$ RATE DIFFERENCE/AVERAGE

Test of CPT conservation.

VALUE (%)	DOCUMENT ID		TECN
−0.54 ± 0.41	FORD	67	CNTR

$K^{\pm} \to \pi^{\pm}\pi^+\pi^-$ RATE DIFFERENCE/AVERAGE

Test of CP conservation.

VALUE (%)	EVTS	DOCUMENT ID		TECN	CHG
0.07 ± 0.12 OUR AVERAGE					
0.08 ± 0.12		[7] FORD	70	ASPK	
−0.50 ± 0.90		FLETCHER	67	OSPK	
• • • We do not use the following data for averages, fits, limits, etc. • • •					
−0.02 ± 0.16		[8] SMITH	73	ASPK	±
0.10 ± 0.14	3.2M	[7] FORD	70	ASPK	
−0.04 ± 0.21		[7] FORD	67	CNTR	

[7] First FORD 70 value is second FORD 70 combined with FORD 67.
[8] SMITH 73 value of $K^{\pm} \to \pi^{\pm}\pi^+\pi^-$ rate difference is derived from SMITH 73 value of $K^{\pm} \to \pi^{\pm}2\pi^0$ rate difference.

$K^{\pm} \to \pi^{\pm}\pi^0\pi^0$ RATE DIFFERENCE/AVERAGE

Test of CP conservation.

VALUE (%)	EVTS	DOCUMENT ID		TECN	CHG
0.0 ± 0.6 OUR AVERAGE					
0.08 ± 0.58		SMITH	73	ASPK	±
−1.1 ± 1.8	1802	HERZO	69	OSPK	

$K^{\pm} \to \pi^{\pm}\pi^0$ RATE DIFFERENCE/AVERAGE

Test of CPT conservation.

VALUE (%)	DOCUMENT ID		TECN
0.8 ± 1.2	HERZO	69	OSPK

$K^{\pm} \to \pi^{\pm}\pi^0\gamma$ RATE DIFFERENCE/AVERAGE

Test of CP conservation.

VALUE (%)	EVTS	DOCUMENT ID		TECN	CHG	COMMENT
0.9 ± 3.3 OUR AVERAGE						
0.8 ± 5.8	2461	SMITH	76	WIRE	±	E_π 55–90 MeV
1.0 ± 4.0	4000	ABRAMS	73B	ASPK	±	E_π 51–100 MeV

K^+ BRANCHING RATIOS

Leptonic and semileptonic modes

$\Gamma(e^+\nu_e)/\Gamma(\mu^+\nu_\mu)$ Γ_1/Γ_2

VALUE (units 10^{-5})	EVTS	DOCUMENT ID		TECN	CHG
2.45 ± 0.11 OUR AVERAGE					
2.51 ± 0.15	404	HEINTZE	76	SPEC	+
2.37 ± 0.17	534	HEARD	75B	SPEC	+
2.42 ± 0.42	112	CLARK	72	OSPK	+

$\Gamma(\mu^+\nu_\mu)/\Gamma_{\rm total}$ Γ_2/Γ

VALUE (units 10^{-2})	EVTS	DOCUMENT ID		TECN	CHG	COMMENT
63.43 ± 0.17 OUR FIT Error includes scale factor of 1.2.						
63.24 ± 0.44	62k	CHIANG	72	OSPK	+	1.84 GeV/c K^+

$\Gamma(\pi^0e^+\nu_e)/\Gamma_{\rm total}$ Γ_3/Γ

VALUE (units 10^{-2})	EVTS	DOCUMENT ID		TECN	CHG	COMMENT
4.87 ± 0.06 OUR FIT Error includes scale factor of 1.2.						
4.84 ± 0.09 OUR AVERAGE						
4.86 ± 0.10	3516	CHIANG	72	OSPK	+	1.84 GeV/c K^+
4.7 ± 0.3	429	SHAKLEE	64	HLBC	+	
• • • We do not use the following data for averages, fits, limits, etc. • • •						
5.0 ± 0.5		ROE	61	HLBC	+	

$\Gamma(\pi^0 e^+ \nu_e)/\Gamma(\mu^+ \nu_\mu)$ Γ_3/Γ_2

VALUE	EVTS	DOCUMENT ID		TECN	CHG
0.0767±0.0011 OUR FIT Error includes scale factor of 1.3.					
0.0752±0.0024 OUR AVERAGE					
0.069 ±0.006	350	ZELLER	69	ASPK	+
0.0775±0.0033	960	BOTTERILL	68C	ASPK	+
0.069 ±0.006	561	GARLAND	68	OSPK	+
0.0791±0.0054	295	[9] AUERBACH	67	OSPK	+

[9] AUERBACH 67 changed from 0.0797 ± 0.0054. See comment with ratio $\Gamma(\pi^0\mu^+\nu_\mu)/\Gamma(\mu^+\nu_\mu)$. The value 0.0785 ± 0.0025 given in AUERBACH 67 is an average of AUERBACH 67 $\Gamma(\pi^0 e^+\nu_e)/\Gamma(\mu^+\nu_\mu)$ and CESTER 66 $\Gamma(\pi^0 e^+\nu_e)/\left[\Gamma(\mu^+\nu_\mu) + \Gamma(\pi^+\pi^0)\right]$.

$\Gamma(\pi^0 e^+ \nu_e)/[\Gamma(\mu^+\nu_\mu) + \Gamma(\pi^+\pi^0)]$ $\Gamma_3/(\Gamma_2+\Gamma_9)$

VALUE (units 10^{-2})	EVTS	DOCUMENT ID		TECN	CHG
5.76±0.08 OUR FIT Error includes scale factor of 1.2.					
6.02±0.15 OUR AVERAGE					
6.16±0.22	5110	ESCHSTRUTH	68	OSPK	+
5.89±0.21	1679	CESTER	66	OSPK	+
• • • We do not use the following data for averages, fits, limits, etc. • • •					
5.92±0.65		[10] WEISSENBE...	76	SPEC	+

[10] Value calculated from WEISSENBERG 76 ($\pi^0 e\nu$), ($\mu\nu$), and ($\pi\pi^0$) values to eliminate dependence on our 1974 ($\pi 2\pi^0$) and ($\pi\pi^+\pi^-$) fractions.

$\Gamma(\pi^0 e^+ \nu_e)/\Gamma(\pi^+\pi^0)$ Γ_3/Γ_9

VALUE	EVTS	DOCUMENT ID		TECN	CHG	COMMENT
0.230±0.004 OUR FIT Error includes scale factor of 1.2.						
0.221±0.012	786	[11] LUCAS	73B	HBC	–	Dalitz pairs only

[11] LUCAS 73B gives $N(K_{e3}) = 786 \pm 3.1\%$, $N(2\pi) = 3564 \pm 3.1\%$. We divide.

$\Gamma(\pi^0 e^+ \nu_e)/\Gamma(\pi^+\pi^+\pi^-)$ Γ_3/Γ_{11}

VALUE	EVTS	DOCUMENT ID		TECN	CHG
0.873±0.012 OUR FIT Error includes scale factor of 1.2.					
0.868±0.021 OUR AVERAGE					
0.867±0.027	2768	BARMIN	87	XEBC	+
0.856±0.040	2827	BRAUN	75	HLBC	+
0.90 ±0.06	230	BORREANI	64	HBC	+
• • • We do not use the following data for averages, fits, limits, etc. • • •					
0.850±0.019	4385	[12] HAIDT	71	HLBC	+
0.846±0.021	4385	[12] EICHTEN	68	HLBC	+
0.94 ±0.09	854	BELLOTTI	67B	HLBC	

[12] HAIDT 71 is a reanalysis of EICHTEN 68. Not included in average because of large discrepancy in $\Gamma(\pi^0\mu^+\nu)/\Gamma(\pi^0 e^+\nu)$ with more precise results.

$\Gamma(\pi^0\mu^+\nu_\mu)/\Gamma_{\text{total}}$ Γ_4/Γ

VALUE (units 10^{-2})	EVTS	DOCUMENT ID		TECN	CHG	COMMENT
3.27±0.06 OUR FIT Error includes scale factor of 1.2.						
3.33±0.16	2345	CHIANG	72	OSPK	+	1.84 GeV/c K^+
• • • We do not use the following data for averages, fits, limits, etc. • • •						
2.8 ±0.4		[13] TAYLOR	59	EMUL	+	

[13] Earlier experiments not averaged.

$\Gamma(\pi^0\mu^+\nu_\mu)/\Gamma(\mu^+\nu_\mu)$ Γ_4/Γ_2

VALUE	EVTS	DOCUMENT ID		TECN	CHG
0.0515 $^{+0.0010}_{-0.0009}$ OUR FIT Error includes scale factor of 1.2.					
0.0483±0.0027 OUR AVERAGE					
0.0480±0.0037	424	[14] GARLAND	68	OSPK	+
0.0486±0.0040	307	[15] AUERBACH	67	OSPK	+
• • • We do not use the following data for averages, fits, limits, etc. • • •					
0.054 ±0.009	240	ZELLER	69	ASPK	+

[14] GARLAND 68 changed from 0.055 ± 0.004 in agreement with μ-spectrum calculation of GAILLARD 70 appendix B. L.G.Pondrom, (private communication 73).

[15] AUERBACH 67 changed from 0.0602 ± 0.0046 by erratum which brings the μ-spectrum calculation into agreement with GAILLARD 70 appendix B.

$\Gamma(\pi^0\mu^+\nu_\mu)/\Gamma(\pi^0 e^+\nu_e)$ Γ_4/Γ_3

VALUE	EVTS	DOCUMENT ID		TECN	CHG	COMMENT
0.672±0.007 OUR FIT						
0.672±0.007 OUR AVERAGE						
0.671±0.007±0.008	24k	HORIE	01	SPEC		
0.670±0.014		[16] HEINTZE	77	SPEC	+	
0.698±0.025	3480	[17] CHIANG	72	OSPK	+	1.84 GeV/c K^+
0.667±0.017	5601	BOTTERILL	68B	ASPK	+	
• • • We do not use the following data for averages, fits, limits, etc. • • •						
0.608±0.014	1585	[18] BRAUN	75	HLBC	+	
0.705±0.063	554	[19] LUCAS	73B	HBC	–	Dalitz pairs only
0.596±0.025		[20] HAIDT	71	HLBC	+	
0.604±0.022	1398	[20] EICHTEN	68	HLBC		
0.703±0.056	1509	CALLAHAN	66B	HLBC		

[16] HEINTZE 77 value from fit to λ_0. Assumes μ-e universality.

[17] CHIANG 72 $\Gamma(\pi^0\mu^+\nu_\mu)/\Gamma(\pi^0 e^+\nu_e)$ is statistically independent of CHIANG 72 $\Gamma(\pi^0\mu^+\nu_\mu)/\Gamma_{\text{total}}$ and $\Gamma(\pi^0 e^+\nu_e)/\Gamma_{\text{total}}$.

[18] BRAUN 75 value is from form factor fit. Assumes μ-e universality.

[19] LUCAS 73B gives $N(K_{\mu 3}) = 554 \pm 7.6\%$, $N(K_{e3}) = 786 \pm 3.1\%$. We divide.

[20] HAIDT 71 is a reanalysis of EICHTEN 68. Not included in average because of large discrepancy with more precise results.

$[\Gamma(\pi^0\mu^+\nu_\mu) + \Gamma(\pi^+\pi^0)]/\Gamma_{\text{total}}$ $(\Gamma_4+\Gamma_9)/\Gamma$

We combine these two modes for experiments measuring them in xenon bubble chamber because of difficulties of separating them there.

VALUE (units 10^{-2})	EVTS	DOCUMENT ID		TECN	CHG
24.40±0.14 OUR FIT Error includes scale factor of 1.1.					
• • • We do not use the following data for averages, fits, limits, etc. • • •					
25.4 ±0.9	886	SHAKLEE	64	HLBC	+
23.4 ±1.1		ROE	61	HLBC	+

$\Gamma(\pi^0\mu^+\nu_\mu)/\Gamma(\pi^+\pi^+\pi^-)$ Γ_4/Γ_{11}

VALUE	EVTS	DOCUMENT ID		TECN	CHG	COMMENT
0.586±0.010 OUR FIT Error includes scale factor of 1.2.						
0.63 ±0.07	2845	[21] BISI	65B	BC	+	HBC+HLBC
• • • We do not use the following data for averages, fits, limits, etc. • • •						
0.503±0.019	1505	[22] HAIDT	71	HLBC	+	
0.510±0.017	1505	[22] EICHTEN	68	HLBC	+	

[21] Error enlarged for background problems. See GAILLARD 70.

[22] HAIDT 71 is a reanalysis of EICHTEN 68. Not included in average because of large discrepancy in $\Gamma(\pi^0\mu^+\nu)/\Gamma(\pi^0 e^+\nu)$ with more precise results.

$\Gamma(\pi^0\pi^0 e^+\nu_e)/\Gamma_{\text{total}}$ Γ_5/Γ

VALUE (units 10^{-5})	EVTS	DOCUMENT ID		TECN	CHG
2.1 ±0.4 OUR FIT					
2.54±0.89	10	BARMIN	88B	HLBC	+

$\Gamma(\pi^0\pi^0 e^+\nu_e)/\Gamma(\pi^0 e^+\nu_e)$ Γ_5/Γ_3

VALUE (units 10^{-4})	EVTS	DOCUMENT ID		TECN	CHG
4.3 $^{+0.9}_{-0.7}$ OUR FIT					
4.1 $^{+1.0}_{-0.7}$ OUR AVERAGE					
4.2 $^{+1.0}_{-0.9}$	25	BOLOTOV	86B	CALO	–
3.8 $^{+5.0}_{-1.2}$	2	LJUNG	73	HLBC	+

$\Gamma(\pi^+\pi^- e^+\nu_e)/\Gamma(\pi^+\pi^+\pi^-)$ Γ_6/Γ_{11}

VALUE (units 10^{-4})	EVTS	DOCUMENT ID		TECN	CHG
7.31±0.16 OUR AVERAGE					
7.35±0.01±0.19	388k	[23] PISLAK	01	B865	
7.21±0.32	30k	ROSSELET	77	SPEC	+
• • • We do not use the following data for averages, fits, limits, etc. • • •					
7.36±0.68	500	BOURQUIN	71	ASPK	
7.0 ±0.9	106	SCHWEINB...	71	HLBC	+
5.83±0.63	269	ELY	69	HLBC	+

[23] PISLAK 01 reports $\Gamma(\pi^+\pi^- e^+\nu_e)/\Gamma_{\text{total}} = (4.109 \pm 0.008 \pm 0.110) \times 10^{-5}$ using the PDG 00 value $\Gamma(\pi^+\pi^+\pi^-)/\Gamma_{\text{total}} = (5.59 \pm 0.05) \times 10^{-2}$. We divide by the PDG value and unfold its error from the systematic error. PISLAK 03 gives additional details on the branching ratio measurement and gives improved errors on the S-wave π-π scattering length: $a_0^0 = 0.216 \pm 0.013(\text{stat.}) \pm 0.002(\text{syst.}) \pm 0.002(\text{theor.})$.

$\Gamma(\pi^+\pi^-\mu^+\nu_\mu)/\Gamma_{\text{total}}$ Γ_7/Γ

VALUE (units 10^{-5})	EVTS	DOCUMENT ID		TECN	CHG
• • • We do not use the following data for averages, fits, limits, etc. • • •					
0.77 $^{+0.54}_{-0.50}$	1	CLINE	65	FBC	+

$\Gamma(\pi^+\pi^-\mu^+\nu_\mu)/\Gamma(\pi^+\pi^+\pi^-)$ Γ_7/Γ_{11}

VALUE (units 10^{-4})	EVTS	DOCUMENT ID		TECN	CHG
2.57±1.55	7	BISI	67	DBC	+
• • • We do not use the following data for averages, fits, limits, etc. • • •					
~ 2.5	1	GREINER	64	EMUL	+

$\Gamma(\pi^0\pi^0\pi^0 e^+\nu_e)/\Gamma_{\text{total}}$ Γ_8/Γ

VALUE (units 10^{-6})	CL%	EVTS	DOCUMENT ID		TECN	CHG
<3.5	90	0	BOLOTOV	88	SPEC	–
• • • We do not use the following data for averages, fits, limits, etc. • • •						
<9	90	0	BARMIN	92	XEBC	+

Hadronic modes

$\Gamma(\pi^+\pi^0)/\Gamma_{\text{total}}$ Γ_9/Γ

VALUE (units 10^{-2})	EVTS	DOCUMENT ID		TECN	CHG	COMMENT
21.13±0.14 OUR FIT Error includes scale factor of 1.1.						
21.18±0.28	16k	CHIANG	72	OSPK	+	1.84 GeV/c K^+
• • • We do not use the following data for averages, fits, limits, etc. • • •						
21.0 ±0.6		CALLAHAN	65	HLBC		See $\Gamma(\pi^+\pi^0)/\Gamma(\pi^+\pi^+\pi^-)$

$\Gamma(\pi^+\pi^0)/\Gamma(\pi^+\pi^+\pi^-)$ Γ_9/Γ_{11}

VALUE	EVTS	DOCUMENT ID		TECN	CHG
3.789±0.033 OUR FIT	Error includes scale factor of 1.1.				
3.96 ±0.15	1045	CALLAHAN	66	FBC	+

$\Gamma(\pi^+\pi^0)/\Gamma(\mu^+\nu_\mu)$ Γ_9/Γ_2

VALUE	EVTS	DOCUMENT ID		TECN	CHG	COMMENT
0.3331±0.0028 OUR FIT	Error includes scale factor of 1.1.					
0.3316±0.0032 OUR AVERAGE						
0.3329±0.0047±0.0010	45k	USHER	92	SPEC	+	$p\overline{p}$ at rest
0.3355 ±0.0057		[24] WEISSENBE...	76	SPEC	+	
0.305 ±0.018	1600	ZELLER	69	ASPK	+	
0.3277±0.0065	4517	[25] AUERBACH	67	OSPK	+	
• • • We do not use the following data for averages, fits, limits, etc. • • •						
0.328 ±0.005	25k	[24] WEISSENBE...	74	STRC	+	

[24] WEISSENBERG 76 revises WEISSENBERG 74.
[25] AUERBACH 67 changed from 0.3253 ± 0.0065. See comment with ratio $\Gamma(\pi^0\mu^+\nu_\mu)/\Gamma(\mu^+\nu_\mu)$.

$\Gamma(\pi^+\pi^0\pi^0)/\Gamma_{total}$ Γ_{10}/Γ

VALUE (units 10^{-2})	EVTS	DOCUMENT ID		TECN	CHG	COMMENT
1.73±0.04 OUR FIT	Error includes scale factor of 1.2.					
1.77±0.07 OUR AVERAGE	Error includes scale factor of 1.4. See the ideogram below.					
1.84±0.06	1307	CHIANG	72	OSPK	+	1.84 GeV/c K^+
1.53±0.11	198	[26] PANDOULAS	70	EMUL	+	
1.8 ±0.2	108	SHAKLEE	64	HLBC	+	
1.7 ±0.2		ROE	61	HLBC	+	
• • • We do not use the following data for averages, fits, limits, etc. • • •						
1.5 ±0.2		[27] TAYLOR	59	EMUL	+	

[26] Includes events of TAYLOR 59.
[27] Earlier experiments not averaged.

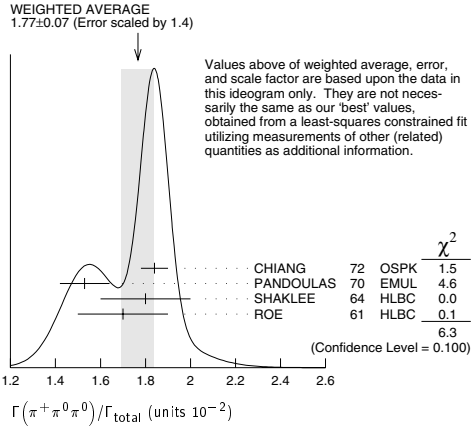

$\Gamma(\pi^+\pi^0\pi^0)/\Gamma(\pi^+\pi^0)$ Γ_{10}/Γ_9

VALUE	EVTS	DOCUMENT ID		TECN	CHG	COMMENT
0.0818±0.0019 OUR FIT	Error includes scale factor of 1.2.					
0.081 ±0.005	574	[28] LUCAS	73B	HBC	–	Dalitz pairs only

[28] LUCAS 73B gives $N(\pi 2\pi^0) = 574 \pm 5.9\%$, $N(2\pi) = 3564 \pm 3.1\%$. We quote $0.5\,N(\pi 2\pi^0)/N(2\pi)$ where 0.5 is because only Dalitz pair π^0's were used.

$\Gamma(\pi^+\pi^0\pi^0)/\Gamma(\pi^+\pi^+\pi^-)$ Γ_{10}/Γ_{11}

VALUE	EVTS	DOCUMENT ID		TECN	CHG	COMMENT
0.310±0.007 OUR FIT	Error includes scale factor of 1.1.					
0.303±0.009	2027	BISI	65	BC	+	HBC+HLBC
• • • We do not use the following data for averages, fits, limits, etc. • • •						
0.393±0.099	17	YOUNG	65	EMUL	+	

$\Gamma(\pi^+\pi^+\pi^-)/\Gamma_{total}$ Γ_{11}/Γ

VALUE (units 10^{-2})	EVTS	DOCUMENT ID		TECN	CHG	COMMENT
5.576±0.031 OUR FIT	Error includes scale factor of 1.1.					
5.50 ±0.10 OUR AVERAGE	Error includes scale factor of 1.3. See the ideogram below.					
5.34 ±0.21	693	[29] PANDOULAS	70	EMUL	+	
5.71 ±0.15		DEMARCO	65	HBC		
5.54 ±0.12	2332	CALLAHAN	64	HLBC	+	
5.1 ±0.2	540	SHAKLEE	64	HLBC	+	
5.7 ±0.3		ROE	61	HLBC	+	
• • • We do not use the following data for averages, fits, limits, etc. • • •						
5.56 ±0.20	2330	[30] CHIANG	72	OSPK	+	1.84 GeV/c K^+
6.0 ±0.4	44	YOUNG	65	EMUL	+	

[29] Includes events of TAYLOR 59.
[30] Value is not independent of CHIANG 72 $\Gamma(\mu^+\nu_\mu)/\Gamma_{total}$, $\Gamma(\pi^+\pi^0)/\Gamma_{total}$, $\Gamma(\pi^+\pi^0\pi^0)/\Gamma_{total}$, $\Gamma(\pi^0\mu^+\nu_\mu)/\Gamma_{total}$, and $\Gamma(\pi^0 e^+\nu_e)/\Gamma_{total}$.

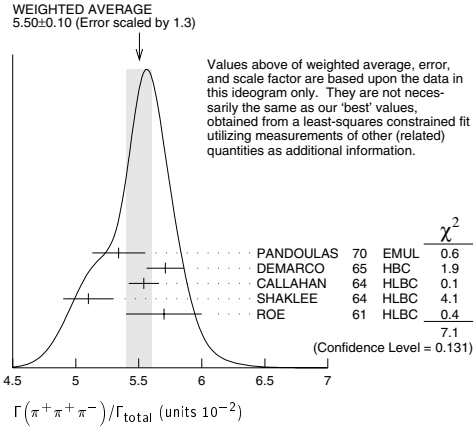

Leptonic and semileptonic modes with photons

$\Gamma(\mu^+\nu_\mu\gamma)/\Gamma_{total}$ Γ_{12}/Γ

VALUE (units 10^{-3})	EVTS	DOCUMENT ID		TECN	CHG	COMMENT
5.50±0.28 OUR AVERAGE						
6.6 ±1.5		[31,32] DEMIDOV	90	XEBC		$P(\mu)$ <231.5 MeV/c
6.0 ±0.9		BARMIN	88	HLBC	+	$P(\mu)$ <231.5 MeV/c
5.4 ±0.3		[33] AKIBA	85	SPEC		$P(\mu)$ <231.5 MeV/c
• • • We do not use the following data for averages, fits, limits, etc. • • •						
3.5 ±0.8		[32,34] DEMIDOV	90	XEBC		$E(\gamma) > 20$ MeV
3.2 ±0.5	57	[35] BARMIN	88	HLBC	+	$E(\gamma) > 20$ MeV

[31] $P(\mu)$ cut given in DEMIDOV 90 paper, 235.1 MeV/c, is a misprint according to authors (private communication).
[32] DEMIDOV 90 quotes only inner bremsstrahlung (IB) part.
[33] Assumes μ-e universality and uses constraints from $K \to e\nu\gamma$.
[34] Not independent of above DEMIDOV 90 value. Cuts differ.
[35] Not independent of above BARMIN 88 value. Cuts differ.

$\Gamma(\pi^0 e^+\nu_e\gamma)/\Gamma(\pi^0 e^+\nu_e)$ Γ_{13}/Γ_3

VALUE (units 10^{-2})	EVTS	DOCUMENT ID		TECN	CHG	COMMENT
0.54±0.04 OUR AVERAGE	Error includes scale factor of 1.1.					
0.46±0.08	82	[36] BARMIN	91	XEBC		$E(\gamma) > 10$ MeV, $0.6 < \cos\theta_{e\gamma} < 0.9$
0.56±0.04	192	[37] BOLOTOV	86B	CALO	–	$E(\gamma) > 10$ MeV
0.76±0.28	13	[38] ROMANO	71	HLBC		$E(\gamma) > 10$ MeV
• • • We do not use the following data for averages, fits, limits, etc. • • •						
1.51±0.25	82	[36] BARMIN	91	XEBC		$E(\gamma) > 10$ MeV, $\cos\theta_{e\gamma} < 0.98$
0.48±0.20	16	[39] LJUNG	73	HLBC	+	$E(\gamma) > 30$ MeV
$0.22^{+0.15}_{-0.10}$		[39] LJUNG	73	HLBC	+	$E(\gamma) > 30$ MeV
0.53±0.22		[38] ROMANO	71	HLBC	+	$E(\gamma) > 30$ MeV

[36] BARMIN 91 quotes branching ratio $\Gamma(K \to e\pi^0\nu\gamma)/\Gamma_{all}$. The measured normalization is $[\Gamma(K \to e\pi^0\nu) + \Gamma(K \to \pi^+\pi^+\pi^-)]$. For comparison with other experiments we used $\Gamma(K \to e\pi^0\nu)/\Gamma_{all} = 0.0482$ to calculate the values quoted here.
[37] $\cos\theta(e\gamma)$ between 0.6 and 0.9.
[38] Both ROMANO 71 values are for $\cos\theta(e\gamma)$ between 0.6 and 0.9. Second value is for comparison with second LJUNG 73 value. We use lowest $E(\gamma)$ cut for Summary Table value. See ROMANO 71 for E_γ dependence.
[39] First LJUNG 73 value is for $\cos\theta(e\gamma) < 0.9$, second value is for $\cos\theta(e\gamma)$ between 0.6 and 0.9 for comparison with ROMANO 71.

$\Gamma(\pi^0 e^+\nu_e\gamma(SD))/\Gamma_{total}$ Γ_{14}/Γ

Structure-dependent part.

VALUE (units 10^{-5})	CL%	DOCUMENT ID		TECN	CHG
<5.3	90	BOLOTOV	86B	CALO	–

$\Gamma(\pi^0\mu^+\nu_\mu\gamma)/\Gamma_{total}$ Γ_{15}/Γ

VALUE (units 10^{-5})	CL%	EVTS	DOCUMENT ID		TECN	CHG	COMMENT
<6.1	90	0	LJUNG	73	HLBC	+	$E(\gamma) > 30$ MeV

Meson Particle Listings

$K^{\pm}$

$\Gamma(\pi^0\pi^0 e^+\nu_e\gamma)/\Gamma_{total}$ Γ_{16}/Γ

VALUE (units 10^{-6})	CL%	EVTS	DOCUMENT ID		TECN	CHG	COMMENT
<5	90	0	BARMIN	92	XEBC	+	$E_\gamma > 10$ MeV

Hadronic modes with photons

$\Gamma(\pi^+\pi^0\gamma)/\Gamma_{total}$ Γ_{17}/Γ

VALUE (units 10^{-4})	CL%	EVTS	DOCUMENT ID		TECN	CHG	COMMENT
2.75±0.15 OUR AVERAGE							
2.71±0.45		140	BOLOTOV	87	WIRE	−	$T\pi^-$ 55–90 MeV
2.87±0.32		2461	SMITH	76	WIRE	±	$T\pi^\pm$ 55–90 MeV
2.71±0.19		2100	ABRAMS	72	ASPK	±	$T\pi^+$ 55–90 MeV
• • • We do not use the following data for averages, fits, limits, etc. • • •							
$1.5\ ^{+1.1}_{-0.6}$			[40] LJUNG	73	HLBC	+	$T\pi^+$ 55–80 MeV
$2.6\ ^{+1.5}_{-1.1}$			[40] LJUNG	73	HLBC	+	$T\pi^+$ 55–90 MeV
$6.8\ ^{+3.7}_{-2.1}$		17	[40] LJUNG	73	HLBC	+	$T\pi^+$ 55–102 MeV
2.4 ±0.8		24	EDWARDS	72	OSPK		$T\pi^+$ 58–90 MeV
<1.0		0	[41] MALTSEV	70	HLBC	+	$T\pi^+$ <55 MeV
<1.9	90	0	EMMERSON	69	OSPK		$T\pi^+$ 55–80 MeV
2.2 ±0.7		18	CLINE	64	FBC	+	$T\pi^+$ 55–80 MeV

[40] The LJUNG 73 values are not independent.
[41] MALTSEV 70 selects low π^+ energy to enhance direct emission contribution.

$\Gamma(\pi^+\pi^0\gamma(DE))/\Gamma_{total}$ Γ_{18}/Γ

Direct emission (DE) part of $\Gamma(\pi^+\pi^0\gamma)/\Gamma_{total}$, assuming that interference (INT) component is zero.

VALUE (units 10^{-6})	EVTS	DOCUMENT ID		TECN	CHG	COMMENT
4.4±0.8 OUR AVERAGE						
3.2±1.3±1.0	4k	[42] ALIEV	03	K470	+	$T\pi^+$ 55–90 MeV
4.7±0.8±0.3	20k	[43] ADLER	00C	B787	+	$T\pi^+$ 55–90 MeV
• • • We do not use the following data for averages, fits, limits, etc. • • •						
6.1±2.5±1.9	4k	[42] ALIEV	03	K470	+	$T\pi^+$ full range
$20.5\pm4.6\ ^{+3.9}_{-2.3}$		BOLOTOV	87	WIRE	−	$T\pi^-$ 55–90 MeV
15.6±3.5±5.0		ABRAMS	72	ASPK	±	$T\pi^\pm$ 55–90 MeV

[42] ALIEV 03 "$T\pi^+$ full range" result is extrapolated from their $T\pi > 35$ MeV measurement. They calculate the "$T\pi^+$ 55–90 MeV" result for comparison with other experiments. They measure the INT component to be $(-0.58\ ^{+0.91}_{-0.83})$% of the inner bremsstrahlung (IB) component. The DE component is measured assuming INT=0.
[43] ADLER 00C measures the INT component to be (-0.4 ± 1.6)% of the inner bremsstrahlung (IB) component. The DE component is measured assuming INT=0.

$\Gamma(\pi^+\pi^0\pi^0\gamma)/\Gamma(\pi^+\pi^0\pi^0)$ Γ_{19}/Γ_{10}

VALUE (units 10^{-4})	DOCUMENT ID		TECN	CHG	COMMENT
$\mathbf{4.3\ ^{+3.2}_{-1.7}}$	BOLOTOV	85	SPEC	−	$E(\gamma) > 10$ MeV

$\Gamma(\pi^+\pi^+\pi^-\gamma)/\Gamma_{total}$ Γ_{20}/Γ

VALUE (units 10^{-4})	EVTS	DOCUMENT ID		TECN	CHG	COMMENT
1.04±0.31 OUR AVERAGE						
1.10±0.48	7	BARMIN	89	XEBC		$E(\gamma) > 5$ MeV
1.0 ±0.4		STAMER	65	EMUL	+	$E(\gamma) > 11$ MeV

$\Gamma(\pi^+\gamma\gamma)/\Gamma_{total}$ Γ_{21}/Γ

All values given here assume a phase space pion energy spectrum.

VALUE (units 10^{-7})	CL%	EVTS	DOCUMENT ID		TECN	CHG	COMMENT
11 ± 3 ±1		31	[44] KITCHING	97	B787		
• • • We do not use the following data for averages, fits, limits, etc. • • •							
< 10	90	0	ATIYA	90B	B787		$T\pi$ 117–127 MeV
< 84	90	0	ASANO	82	CNTR	+	$T\pi$ 117–127 MeV
−420 ±520		0	ABRAMS	77	SPEC	+	$T\pi$ <92 MeV
< 350	90	0	LJUNG	73	HLBC	+	6–102, 114–127 MeV
< 500	90	0	KLEMS	71	OSPK	+	$T\pi$ <117 MeV
−100 ±600			CHEN	68	OSPK	+	$T\pi$ 60–90 MeV

[44] KITCHING 97 is extrapolated from their model-independent branching fraction $(6.0\pm1.5\pm0.7)\times10^{-7}$ for 100 MeV/c<P_{π^+}< 180 MeV/c using Chiral Perturbation Theory.

$\Gamma(\pi^+3\gamma)/\Gamma_{total}$ Γ_{22}/Γ

Values given here assume a phase space pion energy spectrum.

VALUE (units 10^{-4})	CL%	DOCUMENT ID		TECN	CHG	COMMENT
<1.0	90	ASANO	82	CNTR	+	$T(\pi)$ 117–127 MeV
• • • We do not use the following data for averages, fits, limits, etc. • • •						
<3.0	90	KLEMS	71	OSPK	+	$T(\pi)$ >117 MeV

Leptonic modes with $\ell\bar{\ell}$ pairs

$\Gamma(e^+\nu_e\nu\overline{\nu})/\Gamma(e^+\nu_e)$ Γ_{23}/Γ_1

VALUE	CL%	EVTS	DOCUMENT ID		TECN	CHG
<3.8	90	0	HEINTZE	79	SPEC	+

$\Gamma(\mu^+\nu_\mu\nu\overline{\nu})/\Gamma_{total}$ Γ_{24}/Γ

VALUE (units 10^{-6})	CL%	EVTS	DOCUMENT ID		TECN	CHG
<6.0	90	0	[45] PANG	73	CNTR	+

[45] PANG 73 assumes μ spectrum from ν-ν interaction of BARDIN 70.

$\Gamma(e^+\nu_e e^+e^-)/\Gamma_{total}$ Γ_{25}/Γ

VALUE (units 10^{-8})	EVTS	DOCUMENT ID		TECN	CHG	COMMENT
2.48± 0.14±0.14	410	POBLAGUEV	02	B865	+	m_{ee} >150 MeV
• • • We do not use the following data for averages, fits, limits, etc. • • •						
20 ±20	4	DIAMANT-...	76	SPEC	+	$m_{e^+e^-}$ >140 MeV

$\Gamma(\mu^+\nu_\mu e^+e^-)/\Gamma_{total}$ Γ_{26}/Γ

VALUE (units 10^{-8})	EVTS	DOCUMENT ID		TECN	CHG	COMMENT
7.06± 0.16±0.26	2.7k	POBLAGUEV	02	B865	+	m_{ee} >145 MeV
• • • We do not use the following data for averages, fits, limits, etc. • • •						
100 ±30	14	DIAMANT-...	76	SPEC	+	$m_{e^+e^-}$ >140 MeV

$\Gamma(e^+\nu_e\mu^+\mu^-)/\Gamma_{total}$ Γ_{27}/Γ

VALUE	CL%	DOCUMENT ID		TECN
$\mathbf{<5\times10^{-7}}$	90	ADLER	98	B787

$\Gamma(\mu^+\nu_\mu\mu^+\mu^-)/\Gamma_{total}$ Γ_{28}/Γ

VALUE (units 10^{-7})	CL%	DOCUMENT ID		TECN	CHG
<4.1	90	ATIYA	89	B787	+

Lepton Family number (LF), Lepton number (L), $\Delta S = \Delta Q$ (SQ) violating modes, or $\Delta S = 1$ weak neutral current ($S1$) modes

$\Gamma(\pi^+\pi^+e^-\overline{\nu}_e)/\Gamma_{total}$ Γ_{29}/Γ

Test of $\Delta S = \Delta Q$ rule.

VALUE (units 10^{-7})	CL%	EVTS	DOCUMENT ID		TECN	CHG
• • • We do not use the following data for averages, fits, limits, etc. • • •						
< 9.0	95	0	SCHWEINB...	71	HLBC	+
< 6.9	95	0	ELY	69	HLBC	+
<20.	95		BIRGE	65	FBC	+

$\Gamma(\pi^+\pi^+e^-\overline{\nu}_e)/\Gamma(\pi^+\pi^-e^+\nu_e)$ Γ_{29}/Γ_6

Test of $\Delta S = \Delta Q$ rule.

VALUE (units 10^{-4})	CL%	EVTS	DOCUMENT ID		TECN
< 3	90	3	[46] BLOCH	76	SPEC
• • • We do not use the following data for averages, fits, limits, etc. • • •					
<130.	95	0	BOURQUIN	71	ASPK

[46] BLOCH 76 quotes 3.6×10^{-4} at CL = 95%, we convert.

$\Gamma(\pi^+\pi^+\mu^-\overline{\nu}_\mu)/\Gamma_{total}$ Γ_{30}/Γ

Test of $\Delta S = \Delta Q$ rule.

VALUE (units 10^{-6})	CL%	EVTS	DOCUMENT ID		TECN	CHG
<3.0	95	0	BIRGE	65	FBC	+

$\Gamma(\pi^+e^+e^-)/\Gamma_{total}$ Γ_{31}/Γ

Test for $\Delta S = 1$ weak neutral current. Allowed by combined first-order weak and electromagnetic interactions.

VALUE (units 10^{-7})	EVTS	DOCUMENT ID		TECN	CHG
2.88±0.13 OUR AVERAGE					
2.94±0.05±0.14	10300	[47] APPEL	99	SPEC	+
2.75±0.23±0.13	500	[48] ALLIEGRO	92	SPEC	+
2.7 ±0.5	41	[49] BLOCH	75	SPEC	+

[47] APPEL 99 establishes vector nature of this decay and determines form factor $f(Z)=f_0(1+\delta Z)$, $Z=M^2_{ee}/m^2_K$, $\delta=2.14\pm0.13\pm0.15$.
[48] ALLIEGRO 92 assumes a vector interaction with a form factor given by $\lambda = 0.105\pm0.035\pm0.015$ and a correlation coefficient of −0.82.
[49] BLOCH 75 assumes a vector interaction.

$\Gamma(\pi^+\mu^+\mu^-)/\Gamma_{total}$ Γ_{32}/Γ

Test for $\Delta S = 1$ weak neutral current. Allowed by higher-order electroweak interactions.

VALUE (units 10^{-8})	CL%	EVTS	DOCUMENT ID		TECN	CHG
8.1 ±1.4 OUR AVERAGE Error includes scale factor of 2.7. See the ideogram below.						
9.8 ±1.0 ±0.5		110	[50] PARK	02	HYCP	±
9.22±0.60±0.49		402	[51] MA	00	B865	+
5.0 ±0.4 ±0.9		207	[52] ADLER	97C	B787	+
• • • We do not use the following data for averages, fits, limits, etc. • • •						
9.7 ±1.2 ±0.4		65	PARK	02	HYCP	+
10.0 ±1.9 ±0.7		35	PARK	02	HYCP	−
<23	90		ATIYA	89	B787	+

[50] PARK 02 "±" result comes from combining $K^+\to\pi^+\mu^+\mu^-$ and $K^-\to\pi^-\mu^+\mu^-$, assuming CP is conserved.
[51] MA 00 establishes vector nature of this decay and determines form factor $f(Z)=f_0(1+\delta Z)$, $Z=M^2_{\mu\mu}/m^2_K$, $\delta=2.45\ ^{+1.30}_{-0.95}$.
[52] ADLER 97C gives systematic error 0.7×10^{-8} and theoretical uncertainty 0.6×10^{-8}, which we combine in quadrature to obtain our second error.

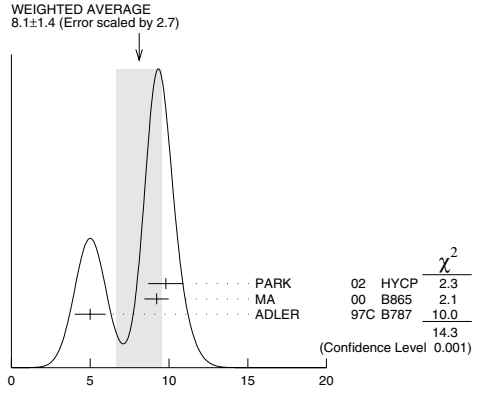

$\Gamma\left(\pi^+\mu^+\mu^-\right)/\Gamma_{\text{total}}$ Γ_{32}/Γ

$\Gamma\left(\pi^+\nu\overline{\nu}\right)/\Gamma_{\text{total}}$ Γ_{33}/Γ

Test for $\Delta S = 1$ weak neutral current. Allowed by higher-order electroweak interactions. Branching ratio values are extrapolated from the momentum or energy regions shown in the comments assuming Standard Model phase space except for those labeled "Scalar" or "Tensor" to indicate the assumed non-Standard-Model interaction.

VALUE (units 10^{-9})	CL%	EVTS	DOCUMENT ID		TECN	CHG	COMMENT
$\mathbf{0.157^{+0.175}_{-0.082}}$		2	ADLER	02	B787		$P_\pi > 211$ MeV/c
• • • We do not use the following data for averages, fits, limits, etc. • • •							
< 4.2	90	1	ADLER	02C	B787		$140 < P_\pi < 195$ MeV/c
< 4.7	90		ADLER	02C	B787		Scalar
< 2.5	90		ADLER	02C	B787		Tensor
$0.15^{+0.34}_{-0.12}$		1	ADLER	00	B787		In ADLER 02
$0.42^{+0.97}_{-0.35}$		1	ADLER	97	B787		
< 2.4	90		ADLER	96	B787		
< 7.5	90		ATIYA	93	B787	+	$T(\pi)$ 115–127 MeV
< 5.2	90		[53] ATIYA	93	B787	+	
< 17	90	0	ATIYA	93B	B787	+	$T(\pi)$ 60–100 MeV
< 34	90		ATIYA	90	B787	+	
< 140	90		ASANO	81B	CNTR	+	$T(\pi)$ 116–127 MeV

[53] Combining ATIYA 93 and ATIYA 93B results. Superseded by ADLER 96.

$\Gamma\left(\pi^+\pi^0\nu\overline{\nu}\right)/\Gamma_{\text{total}}$ Γ_{34}/Γ

Test for $\Delta S = 1$ weak neutral current. Allowed by higher-order electroweak interactions.

VALUE (units 10^{-5})	CL%	DOCUMENT ID		TECN
< 4.3	90	[54] ADLER	01	SPEC

[54] Search region defined by 90 MeV/c < P_{π^+} < 188 MeV/c and 135 MeV < E_{π^0} < 180 MeV.

$\Gamma\left(\mu^-\nu e^+e^+\right)/\Gamma\left(\pi^+\pi^-e^+\nu_e\right)$ Γ_{35}/Γ_6

Test of lepton family number conservation.

VALUE (units 10^{-3})	CL%	EVTS	DOCUMENT ID		TECN	CHG
< 0.5	90	0	[55] DIAMANT-...	76	SPEC	+

[55] DIAMANT-BERGER 76 quotes this result times our 1975 $\pi^+\pi^-e\nu$ BR ratio.

$\Gamma\left(\mu^+\nu_e\right)/\Gamma_{\text{total}}$ Γ_{36}/Γ

Forbidden by lepton family number conservation.

VALUE	CL%	EVTS	DOCUMENT ID		TECN	CHG	COMMENT
< 0.004	90	0	[56] LYONS	81	HLBC	0	200 GeV K^+ narrow band ν beam
• • • We do not use the following data for averages, fits, limits, etc. • • •							
< 0.012	90		[56] COOPER	82	HLBC		Wideband ν beam

[56] COOPER 82 and LYONS 81 limits on ν_e observation are here interpreted as limits on lepton family number violation in the absence of mixing.

$\Gamma\left(\pi^+\mu^+e^-\right)/\Gamma_{\text{total}}$ Γ_{37}/Γ

Test of lepton family number conservation.

VALUE (units 10^{-10})	CL%	EVTS	DOCUMENT ID		TECN	CHG
< 0.28	90		[57] APPEL	00	RVUE	+
• • • We do not use the following data for averages, fits, limits, etc. • • •						
< 0.39	90		APPEL	00	B865	+
< 2.1	90	0	LEE	90	SPEC	+

[57] This result combines APPEL 00 BNL-E865 1996 data, BNL-E865 1995 data from BERGMAN 97 and PISLAK 97 theses, and LEE 90 BNL-E777 data.

$\Gamma\left(\pi^+\mu^-e^+\right)/\Gamma_{\text{total}}$ Γ_{38}/Γ

Test of lepton family number conservation.

VALUE (units 10^{-10})	CL%	EVTS	DOCUMENT ID		TECN	CHG
< 5.2	90	0	APPEL	00B	B865	+
• • • We do not use the following data for averages, fits, limits, etc. • • •						
< 70	90	0	[58] DIAMANT-...	76	SPEC	+

[58] Measurement actually applies to the sum of the $\pi^+\mu^-e^+$ and $\pi^-\mu^+e^+$ modes.

$\Gamma\left(\pi^-\mu^+e^+\right)/\Gamma_{\text{total}}$ Γ_{39}/Γ

Test of total lepton number conservation.

VALUE (units 10^{-10})	CL%	EVTS	DOCUMENT ID		TECN	CHG
< 5.0	90	0	APPEL	00B	B865	+
• • • We do not use the following data for averages, fits, limits, etc. • • •						
< 70	90	0	[59] DIAMANT-...	76	SPEC	+

[59] Measurement actually applies to the sum of the $\pi^+\mu^-e^+$ and $\pi^-\mu^+e^+$ modes.

$\Gamma\left(\pi^-e^+e^+\right)/\Gamma_{\text{total}}$ Γ_{40}/Γ

Test of total lepton number conservation.

VALUE	CL%	EVTS	DOCUMENT ID		TECN	CHG
< 6.4 × 10^{-10}	90	0	APPEL	00B	B865	+
• • • We do not use the following data for averages, fits, limits, etc. • • •						
< 9.2 × 10^{-9}	90	0	DIAMANT-...	76	SPEC	+
< 1.5 × 10^{-5}			CHANG	68	HBC	–

$\Gamma\left(\pi^-\mu^+\mu^+\right)/\Gamma_{\text{total}}$ Γ_{41}/Γ

Forbidden by total lepton number conservation.

VALUE	CL%	EVTS	DOCUMENT ID		TECN	CHG
< 3.0 × 10^{-9}	90	0	APPEL	00B	B865	+
• • • We do not use the following data for averages, fits, limits, etc. • • •						
< 1.5 × 10^{-4}	90		[60] LITTENBERG	92	HBC	

[60] LITTENBERG 92 is from retroactive data analysis of CHANG 68 bubble chamber data.

$\Gamma\left(\mu^+\overline{\nu}_e\right)/\Gamma_{\text{total}}$ Γ_{42}/Γ

Forbidden by total lepton number conservation.

VALUE (units 10^{-3})	CL%	DOCUMENT ID		TECN	COMMENT
< 3.3	90	[61] COOPER	82	HLBC	Wideband ν beam

[61] COOPER 82 limit on $\overline{\nu}_e$ observation is here interpreted as a limit on lepton number violation in the absence of mixing.

$\Gamma\left(\pi^0e^+\overline{\nu}_e\right)/\Gamma_{\text{total}}$ Γ_{43}/Γ

Forbidden by total lepton number conservation.

VALUE	CL%	DOCUMENT ID		TECN	COMMENT
< 0.003	90	[62] COOPER	82	HLBC	Wideband ν beam

[62] COOPER 82 limit on $\overline{\nu}_e$ observation is here interpreted as a limit on lepton number violation in the absence of mixing.

$\Gamma\left(\pi^+\gamma\right)/\Gamma_{\text{total}}$ Γ_{44}/Γ

Violates angular momentum conservation. Current interest in this decay is as a search for exotic physics such as a vacuum expectation value of a new vector field, non-local Superstring effects, or departures from Lorentz invariance, as discussed in ADLER 02B.

VALUE (units 10^{-7})	CL%	DOCUMENT ID		TECN	CHG
< 3.6	90	ADLER	02B	B787	+
• • • We do not use the following data for averages, fits, limits, etc. • • •					
< 14	90	ASANO	82	CNTR	+
< 40	90	[63] KLEMS	71	OSPK	+

[63] Test of model of Selleri, Nuovo Cimento **60A** 291 (1969).

K^+ LONGITUDINAL POLARIZATION OF EMITTED μ^+

VALUE	CL%	DOCUMENT ID		TECN	CHG	COMMENT
< −0.990	90	[64] AOKI	94	SPEC	+	
• • • We do not use the following data for averages, fits, limits, etc. • • •						
< −0.990	90	IMAZATO	92	SPEC	+	Repl. by AOKI 94
−0.970 ± 0.047		[65] YAMANAKA	86	SPEC	+	
−1.0 ± 0.1		[65] CUTTS	69	SPRK	+	
−0.96 ± 0.12		[65] COOMBES	57	CNTR	+	

[64] AOKI 94 measures $\xi P_\mu = -0.9996 \pm 0.0030 \pm 0.0048$. The above limit is obtained by summing the statistical and systematic errors in quadrature, normalizing to the physically significant region ($|\xi P_\mu| < 1$) and assuming that $\xi = 1$, its maximum value.

[65] Assumes $\xi = 1$.

DALITZ PLOT PARAMETERS FOR $K \to 3\pi$ DECAYS

Revised 1999 by T.G. Trippe (LBNL).

The Dalitz plot distribution for $K^{\pm} \to \pi^{\pm}\pi^{\pm}\pi^{\mp}$, $K^{\pm} \to \pi^0\pi^0\pi^{\pm}$, and $K_L^0 \to \pi^+\pi^-\pi^0$ can be parameterized by a series expansion such as that introduced by Weinberg [1]. We use the form

$$|M|^2 \propto 1 + g\frac{(s_3 - s_0)}{m_{\pi^+}^2} + h\left[\frac{s_3 - s_0}{m_{\pi^+}^2}\right]^2 + j\ \frac{(s_2 - s_1)}{m_{\pi^+}^2} + k\left[\frac{s_2 - s_1}{m_{\pi^+}^2}\right]^2 + f\ \frac{(s_2 - s_1)}{m_{\pi^+}^2}\frac{(s_3 - s_0)}{m_{\pi^+}^2} + \cdots , \quad (1)$$

where $m_{\pi^+}^2$ has been introduced to make the coefficients g, h, j, and k dimensionless, and

$$s_i = (P_K - P_i)^2 = (m_K - m_i)^2 - 2m_K T_i\ ,\ i = 1, 2, 3,$$
$$s_0 = \frac{1}{3}\sum_i s_i = \frac{1}{3}(m_K^2 + m_1^2 + m_2^2 + m_3^2)\quad .$$

Here the P_i are four-vectors, m_i and T_i are the mass and kinetic energy of the i^{th} pion, and the index 3 is used for the odd pion.

The coefficient g is a measure of the slope in the variable s_3 (or T_3) of the Dalitz plot, while h and k measure the quadratic dependence on s_3 and $(s_2 - s_1)$, respectively. The coefficient j is related to the asymmetry of the plot and must be zero if CP invariance holds. Note also that if CP is good, g, h, and k must be the same for $K^+ \to \pi^+\pi^+\pi^-$ as for $K^- \to \pi^-\pi^-\pi^+$.

Since different experiments use different forms for $|M|^2$, in order to compare the experiments we have converted to g, h, j, and k whatever coefficients have been measured. Where such conversions have been done, the measured coefficient a_y, a_t, a_u, or a_v is given in the comment at the right. For definitions of these coefficients, details of this conversion, and discussion of the data, see the April 1982 version of this note [2].

References

1. S. Weinberg, Phys. Rev. Lett. **4**, 87 (1960).
2. Particle Data Group, Phys. Lett. **111B**, 69 (1982).

ENERGY DEPENDENCE OF $K^{\pm}$ DALITZ PLOT

$|\text{matrix element}|^2 = 1 + gu + hu^2 + kv^2$
where $u = (s_3 - s_0)\ /\ m_{\pi}^2$ and $v = (s_2 - s_1)\ /\ m_{\pi}^2$

LINEAR COEFFICIENT $g_{\tau+}$ FOR $K^+ \to \pi^+\pi^+\pi^-$

Some experiments use Dalitz variables x and y. In the comments we give a_y = coefficient of y term. See note above on "Dalitz Plot Parameters for $K \to 3\pi$ Decays." For discussion of the conversion of a_y to g, see the earlier version of the same note in the *Review* published in Physics Letters **111B** 70 (1982).

VALUE	EVTS	DOCUMENT ID		TECN	CHG	COMMENT
−0.2154±0.0035 OUR AVERAGE		Error includes scale factor of 1.4. See the ideogram below.				
−0.2221±0.0065	225k	DEVAUX	77	SPEC	+	a_y=.2814 ± .0082
−0.2157±0.0028	750k	FORD	72	ASPK	+	a_y=.2734 ± .0035
−0.200 ±0.009	39819	[66] HOFFMASTER	72	HLBC	+	
• • • We do not use the following data for averages, fits, limits, etc. • • •						
−0.196 ±0.012	17898	[67] GRAUMAN	70	HLBC	+	a_y=0.228 ± 0.030
−0.218 ±0.016	9994	[68] BUTLER	68	HBC	+	a_y=0.277 ± 0.020
−0.22 ±0.024	5428	[68,69] ZINCHENKO	67	HBC	+	a_y=0.28 ± 0.03

[66] HOFFMASTER 72 includes GRAUMAN 70 data.
[67] Emulsion data added — all events included by HOFFMASTER 72.
[68] Experiments with large errors not included in average.
[69] Also includes DBC events.

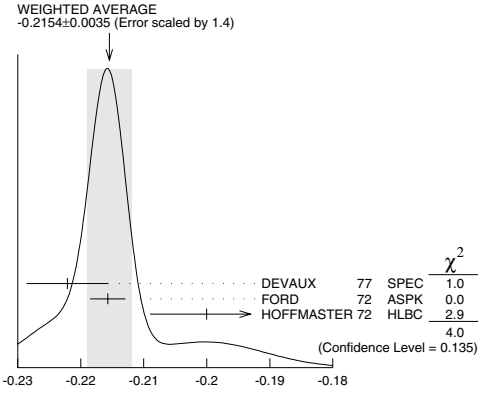

Linear energy dependence for $K^+ \to \pi^+\pi^+\pi^-$

QUADRATIC COEFFICIENT h FOR $K^+ \to \pi^+\pi^+\pi^-$

VALUE	EVTS	DOCUMENT ID		TECN	CHG
0.012 ±0.008 OUR AVERAGE		Error includes scale factor of 1.4. See the ideogram below.			
−0.0006±0.0143	225k	DEVAUX	77	SPEC	+
0.0187±0.0062	750k	FORD	72	ASPK	+
−0.009 ±0.014	39819	HOFFMASTER	72	HLBC	+

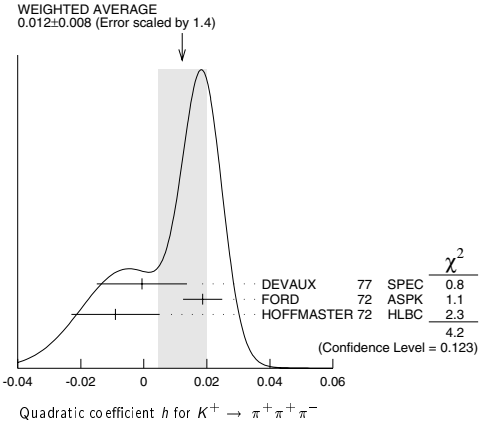

Quadratic coefficient h for $K^+ \to \pi^+\pi^+\pi^-$

QUADRATIC COEFFICIENT k FOR $K^+ \to \pi^+\pi^+\pi^-$

VALUE	EVTS	DOCUMENT ID		TECN	CHG
−0.0101±0.0034 OUR AVERAGE		Error includes scale factor of 2.1. See the ideogram below.			
−0.0205±0.0039	225k	DEVAUX	77	SPEC	+
−0.0075±0.0019	750k	FORD	72	ASPK	+
−0.0105±0.0045	39819	HOFFMASTER	72	HLBC	+

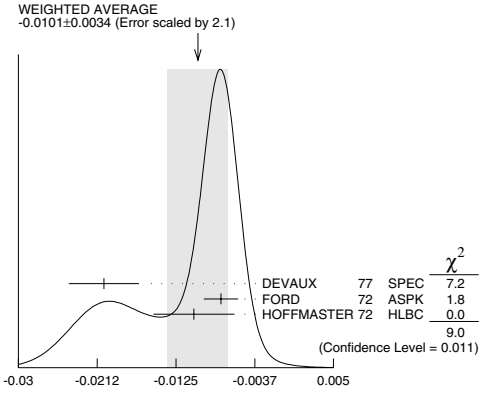

Quadratic coefficient k for $K^+ \to \pi^+\pi^+\pi^-$

LINEAR COEFFICIENT $g_{\tau-}$ FOR $K^- \to \pi^-\pi^-\pi^+$

Some experiments use Dalitz variables x and y. In the comments we give a_y = coefficient of y term. See note above on "Dalitz Plot Parameters for $K \to 3\pi$ Decays." For discussion of the conversion of a_y to g, see the earlier version of the same note in the *Review* published in Physics Letters **111B** 70 (1982).

VALUE	EVTS	DOCUMENT ID		TECN	CHG	COMMENT
−0.217 ±0.007 OUR AVERAGE		Error includes scale factor of 2.5.				
−0.2186±0.0028	750k	FORD	72	ASPK	−	a_y=.2770 ± .0035
−0.193 ±0.010	50919	MAST	69	HBC	−	a_y=0.244 ± 0.013
• • • We do not use the following data for averages, fits, limits, etc. • • •						
−0.199 ±0.008	81k	[70] LUCAS	73	HBC	−	a_y=0.252 ± 0.011
−0.190 ±0.023	5778	[71,72] MOSCOSO	68	HBC	−	a_y=0.242 ± 0.029
−0.220 ±0.035	1347	[73] FERRO-LUZZI	61	HBC	−	a_y=0.28 ± 0.045

[70] Quadratic dependence is required by K^0_L experiments. For comparison we average only those $K^{\pm}$ experiments which quote quadratic fit values.
[71] Experiments with large errors not included in average.
[72] Also includes DBC events.
[73] No radiative corrections included.

QUADRATIC COEFFICIENT h FOR $K^- \to \pi^-\pi^-\pi^+$

VALUE	EVTS	DOCUMENT ID		TECN	CHG
0.010 ±0.006 OUR AVERAGE					
0.0125±0.0062	750k	FORD	72	ASPK	−
−0.001 ±0.012	50919	MAST	69	HBC	−

QUADRATIC COEFFICIENT k FOR $K^- \to \pi^-\pi^-\pi^+$

VALUE	EVTS	DOCUMENT ID		TECN	CHG
−0.0084±0.0019 OUR AVERAGE					
−0.0083±0.0019	750k	FORD	72	ASPK	−
−0.014 ±0.012	50919	MAST	69	HBC	−

$(g_{\tau+} - g_{\tau-}) / (g_{\tau+} + g_{\tau-})$ FOR $K^{\pm} \to \pi^{\pm}\pi^+\pi^-$

A nonzero value for this quantity indicates CP violation.

VALUE (%)	EVTS	DOCUMENT ID		TECN
−0.70±0.53	3.2M	FORD	70	ASPK

LINEAR COEFFICIENT g FOR $K^{\pm} \to \pi^{\pm}\pi^0\pi^0$

Unless otherwise stated, all experiments include terms quadratic in $(s_3 - s_0) / m^2_{\pi^+}$. See note above on "Dalitz Plot Parameters for $K \to 3\pi$ Decays."

See BATUSOV 98 for a discussion of the discrepancy between their result and others, especially BOLOTOV 86. At this time we have no way to resolve the discrepancy so we depend on the large scale factor as a warning.

VALUE	EVTS	DOCUMENT ID		TECN	CHG	COMMENT
0.638±0.020 OUR AVERAGE		Error includes scale factor of 2.5. See the ideogram below.				
0.627±0.004±0.010	252k	[74,75] AJINENKO	03B	ISTR	−	
0.736±0.014±0.012	33k	BATUSOV	98	SPEC	+	
0.582±0.021	43k	BOLOTOV	86	CALO	−	
0.670±0.054	3263	BRAUN	76B	HLBC	+	
0.630±0.038	5635	SHEAFF	75	HLBC	+	
0.510±0.060	27k	SMITH	75	WIRE	+	
0.67 ±0.06	1365	AUBERT	72	HLBC	+	
0.544±0.048	4048	DAVISON	69	HLBC	+	Also emulsion
• • • We do not use the following data for averages, fits, limits, etc. • • •						
0.518±0.039	815	[76] SHIN	00	SPEC	+	
0.806±0.220	4639	[77] BERTRAND	76	EMUL	+	
0.484±0.084	574	[76] LUCAS	73B	HBC	−	Dalitz pairs only
0.527±0.102	198	[77] PANDOULAS	70	EMUL	+	
0.586±0.098	1874	[76] BISI	65	HLBC	+	Also HBC
0.48 ±0.04	1792	[76] KALMUS	64	HLBC	+	

[74] Measured using in-flight decays of the 25 GeV negative secondary beam.
[75] They form new world averages $g_- = (0.617 \pm 0.018)$ and $g_+ = (0.684 \pm 0.033)$ which give $\Delta g_{\tau'} = 0.051 \pm 0.028$.
[76] Authors give linear fit only.
[77] Experiments with large errors not included in average.

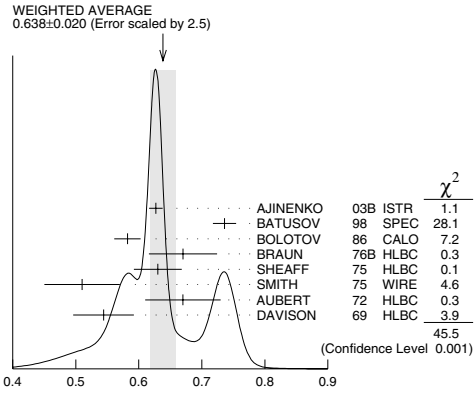

Linear energy dependence for $K^{\pm} \to \pi^{\pm}\pi^0\pi^0$

QUADRATIC COEFFICIENT h FOR $K^{\pm} \to \pi^{\pm}\pi^0\pi^0$

VALUE	EVTS	DOCUMENT ID		TECN	CHG	COMMENT
0.051±0.013 OUR AVERAGE		Error includes scale factor of 1.4. See the ideogram below.				
0.046±0.004±0.012	252k	[78] AJINENKO	03B	ISTR	−	
0.128±0.015±0.024	33k	BATUSOV	98	SPEC	+	
0.037±0.024	43k	BOLOTOV	86	CALO	−	
0.152±0.082	3263	BRAUN	76B	HLBC	+	
0.041±0.030	5635	SHEAFF	75	HLBC	+	
0.009±0.040	27k	SMITH	75	WIRE	+	
−0.01 ±0.08	1365	AUBERT	72	HLBC	+	
0.026±0.050	4048	DAVISON	69	HLBC	+	Also emulsion
• • • We do not use the following data for averages, fits, limits, etc. • • •						
0.164±0.121	4639	[79] BERTRAND	76	EMUL	+	
0.018±0.124	198	[79] PANDOULAS	70	EMUL	+	

[78] Measured using in-flight decays of the 25 GeV negative secondary beam.
[79] Experiments with large errors not included in average.

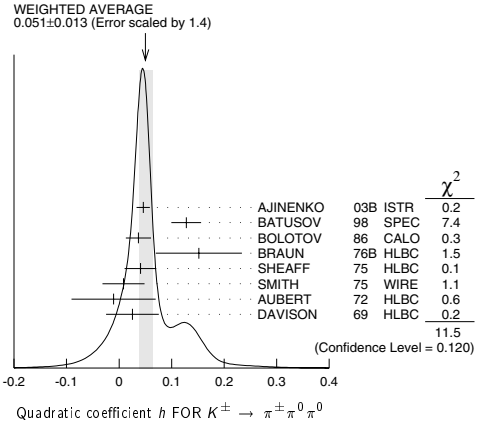

Quadratic coefficient h FOR $K^{\pm} \to \pi^{\pm}\pi^0\pi^0$

QUADRATIC COEFFICIENT k FOR $K^{\pm} \to \pi^{\pm}\pi^0\pi^0$

VALUE	EVTS	DOCUMENT ID		TECN	CHG
0.004 ±0.007 OUR AVERAGE		Error includes scale factor of 3.2.			
0.001 ±0.001 ±0.002	252k	[80] AJINENKO	03B	ISTR	−
0.0197±0.0045±0.0029	33k	BATUSOV	98	SPEC	+
• • • We do not use the following data for averages, fits, limits, etc. • • •					
0.043 ±0.020	815	SHIN	00	SPEC	+

[80] Measured using in-flight decays of the 25 GeV negative secondary beam.

$K^{\pm}_{\ell 3}$ AND $K^{0}_{\ell 3}$ FORM FACTORS

Revised January 2004 by T.G. Trippe (LBNL).

Assuming that only the vector current contributes to $K \to \pi\ell\nu$ decays, we write the matrix element as

$$M \propto f_+(t)\left[(P_K + P_\pi)_\mu \overline{\ell}\gamma_\mu(1+\gamma_5)\nu\right] + f_-(t)\left[m_\ell\overline{\ell}(1+\gamma_5)\nu\right] \ , \quad (1)$$

where P_K and P_π are the four-momenta of the K and π mesons, m_ℓ is the lepton mass, and f_+ and f_- are dimensionless form factors which can depend only on $t = (P_K - P_\pi)^2$, the square of the four-momentum transfer to the leptons. If time-reversal invariance holds, f_+ and f_- are relatively real. $K_{\mu 3}$ experiments, discussed immediately below, measure f_+ and f_-, while K_{e3} experiments, discussed further below, are sensitive only to f_+ because the small electron mass makes the f_- term negligible.

For this edition, fits to the form factor data have been made with and without the assumption of μ-e universality, as described near the end of the note.

$K_{\mu 3}$ Experiments. Analyses of $K_{\mu 3}$ data frequently assume a linear dependence of f_+ and f_- on t, *i.e.*,

$$f_\pm(t) = f_\pm(0)\left[1 + \lambda_\pm(t/m_\pi^2)\right] \quad (2)$$

Most $K_{\mu 3}$ data are adequately described by Eq. (2) for f_+ and a constant f_- (*i.e.*, $\lambda_- = 0$). There are two equivalent parametrizations commonly used in these analyses:

(1) $\lambda_+, \xi(0)$ parametrization. Analyses of $K_{\mu 3}$ data often introduce the ratio of the two form factors

$$\xi(t) = f_-(t)/f_+(t) \ . \quad (3)$$

The $K_{\mu 3}$ decay distribution is then described by the two parameters λ_+ and $\xi(0)$ (assuming time reversal invariance and $\lambda_- = 0$). These parameters can be determined by three different methods:

Method A. By studying the Dalitz plot or the pion spectrum of $K_{\mu 3}$ decay. The Dalitz plot density is (see, *e.g.*, Chounet *et al.* [1]):

$$\rho(E_\pi, E_\mu) \propto f_+^2(t)\left[A + B\xi(t) + C\xi(t)^2\right] \ ,$$

where

$$A = m_K\left(2E_\mu E_\nu - m_K E'_\pi\right) + m_\mu^2\left(\frac{1}{4}E'_\pi - E_\nu\right) \ ,$$

$$B = m_\mu^2\left(E_\nu - \frac{1}{2}E'_\pi\right) \ ,$$

$$C = \frac{1}{4}m_\mu^2 E'_\pi \ ,$$

$$E'_\pi = E_\pi^{\max} - E_\pi = \left(m_K^2 + m_\pi^2 - m_\mu^2\right)/2m_K - E_\pi \ . \quad (4)$$

Here E_π, E_μ, and E_ν are, respectively, the pion, muon, and neutrino energies in the kaon center of mass. The density ρ is fit to the data to determine the values of $\lambda_+, \xi(0)$, and their correlation.

Method B. By measuring the $K_{\mu 3}/K_{e3}$ branching ratio and comparing it with the theoretical ratio (see, *e.g.*, Fearing *et al.* [2]) as given in terms of λ_+ and $\xi(0)$, assuming μ-e universality:

$$\Gamma(K^\pm_{\mu 3})/\Gamma(K^\pm_{e3}) = 0.6457 + 1.4115\lambda_+ + 0.1264\xi(0) + 0.0192\xi(0)^2 + 0.0080\lambda_+\xi(0) \ ,$$

$$\Gamma(K^0_{\mu 3})/\Gamma(K^0_{e3}) = 0.6452 + 1.3162\lambda_+ + 0.1264\xi(0) + 0.0186\xi(0)^2 + 0.0064\lambda_+\xi(0) \ . \quad (5)$$

This cannot determine λ_+ and $\xi(0)$ simultaneously but simply fixes a relationship between them.

Method C. By measuring the muon polarization in $K_{\mu 3}$ decay. In the rest frame of the K, the μ is expected to be polarized in the direction $\mathbf{A}$ with $\mathbf{P} = \mathbf{A}/\left|\mathbf{A}\right|$, where $\mathbf{A}$ is given (Cabibbo and Maksymowicz [3]) by

$$\mathbf{A} = a_1(\xi)\mathbf{p}_\mu - a_2(\xi)\left[\frac{\mathbf{p}_\mu}{m_\mu}\left(m_K - E_\pi + \frac{\mathbf{p}_\pi\cdot\mathbf{p}_\mu}{\left|\mathbf{p}_\mu\right|^2}(E_\mu - m_\mu)\right) + \mathbf{p}_\pi\right] + m_K \mathrm{Im}\xi(t)(\mathbf{p}_\pi \times \mathbf{p}_\mu) \ . \quad (6)$$

If time-reversal invariance holds, ξ is real, and thus there is no polarization perpendicular to the K-decay plane. Polarization experiments measure the weighted average of $\xi(t)$ over the t range of the experiment, where the weighting accounts for the variation with t of the sensitivity to $\xi(t)$.

(2) λ_+, λ_0 parametrization. Most of the more recent $K_{\mu 3}$ analyses have parameterized in terms of the form factors f_+ and f_0 which are associated with vector and scalar exchange, respectively, to the lepton pair. f_0 is related to f_+ and f_- by

$$f_0(t) = f_+(t) + \left[t/(m_K^2 - m_\pi^2)\right] f_-(t) \ . \quad (7)$$

Here $f_0(0)$ must equal $f_+(0)$ unless $f_-(t)$ diverges at $t = 0$. The earlier assumption that f_+ is linear in t and f_- is constant leads to f_0 linear in t:

$$f_0(t) = f_0(0)\left[1 + \lambda_0(t/m_\pi^2)\right] \ . \quad (8)$$

With the assumption that $f_0(0) = f_+(0)$, the two parametrizations, $(\lambda_+, \xi(0))$ and (λ_+, λ_0) are equivalent as long as correlation information is retained. (λ_+, λ_0) correlations tend to be less strong than $(\lambda_+, \xi(0))$ correlations.

The experimental results for $\xi(0)$ and its correlation with λ_+ are listed in the $K^\pm$ and K^0_L sections of the Particle Listings in section $\xi_{\rm A}$, $\xi_{\rm B}$, or $\xi_{\rm C}$ depending on whether method A, B, or C discussed above was used. The corresponding values of λ_+ are also listed.

Because recent experiments tend to use the (λ_+, λ_0) parametrization, we include a subsection for λ_0 results. Wherever possible we have converted $\xi(0)$ results into λ_0 results and vice versa.

See the 1982 version of this note [4] for additional discussion of the $K^0_{\mu 3}$ parameters, correlations, and conversion between parametrizations.

K_{e3} Experiments. Analysis of K_{e3} data is simpler than that of $K_{\mu 3}$ because the second term of the matrix element assuming a pure vector current [Eq. (1) above] can be neglected. Here f_+ is usually assumed to be linear in t, and the linear coefficient λ_+ of Eq. (2) is determined.

If we remove the assumption of a pure vector current, then the matrix element for the decay, in addition to the terms in Eq. (1), would contain

$$+2m_K f_S \overline{\ell}(1+\gamma_5)\nu$$
$$+(2f_T/m_K)(P_K)_\lambda (P_\pi)_\mu \overline{\ell}\,\sigma_{\lambda\mu}(1+\gamma_5)\nu\ , \qquad (9)$$

where f_S is the scalar form factor, and f_T is the tensor form factor. In the case of the K_{e3} decays where the f_- term can be neglected, experiments have yielded limits on $|f_S/f_+|$ and $|f_T/f_+|$.

Fits for $K_{\ell 3}$ Form Factors. Fits are made for the two parameters λ_+ and λ_0 and their correlation, or equivalently for λ_+ and $\xi(0)$ and their correlation. The fits are done both with and without assuming μ-e universality. This assumption sets $\lambda_+(K_{\mu 3}) = \lambda_+(K_{e3})$ so that the more precise λ_+ values from K_{e3} can be included with the $K_{\mu 3}$ data in the fit. In addition it allows the $K_{\mu 3}/K_{e3}$ branching ratio to be used in the determination of $\xi(0)$ or λ_0 as a function of λ_+. Without this assumption, $\lambda_+(K_{e3})$ values are averaged separately and excluded from the fit to $K_{\mu 3}$ data, and branching ratio data are not used. The Kaon Particle Listings show the results with and without assuming μ-e universality.

References

1. L.M. Chounet, J.M. Gaillard, and M.K. Gaillard, Phys. Reports **4C**, 199 (1972).
2. H.W. Fearing, E. Fischbach, and J. Smith, Phys. Rev. **D2**, 542 (1970).
3. N. Cabibbo and A. Maksymowicz, Phys. Lett. **9**, 352 (1964).
4. Particle Data Group, Phys. Lett. **111B**, 73 (1982).

$K^{\pm}_{\ell 3}$ FORM FACTORS

In the form factor comments, the following symbols are used.

f_+ and f_- are form factors for the vector matrix element.

f_S and f_T refer to the scalar and tensor term.

$f_0 = f_+ + f_- t/(m_K^2 - m_\pi^2)$.

λ_+, λ_-, and λ_0 are the linear expansion coefficients of f_+, f_-, and f_0.

λ_+ refers to the $K^{\pm}_{\mu 3}$ value except in the $K^{\pm}_{e3}$ sections.

$d\xi(0)/d\lambda_+$ is the correlation between $\xi(0)$ and λ_+ in $K^{\pm}_{\mu 3}$.

$d\lambda_0/d\lambda_+$ is the correlation between λ_0 and λ_+ in $K^{\pm}_{\mu 3}$.

t = momentum transfer to the π in units of m_π^2.

DP = Dalitz plot analysis.

PI = π spectrum analysis.

MU = μ spectrum analysis.

POL = μ polarization analysis.

BR = $K^{\pm}_{\mu 3}/K^{\pm}_{e3}$ branching ratio analysis.

E = positron or electron spectrum analysis.

RC = radiative corrections.

λ_+ (LINEAR ENERGY DEPENDENCE OF f_+ IN $K^{\pm}_{e3}$ DECAY)

For radiative correction of $K^{\pm}_{e3}$ Dalitz plot, see GINSBERG 67 and BECHERRAWY 70.

Results labeled OUR FIT are discussed in the review "$K^{\pm}_{\ell 3}$ and $K^0_{\ell 3}$ Form Factors" above.

VALUE (units 10^{-2})		EVTS	DOCUMENT ID		TECN	CHG	COMMENT
2.78 ±0.07	**OUR FIT**		Error includes scale factor of 1.5. Assumes μ-e universality.				
2.77 ±0.05	**OUR AVERAGE**						
2.774 ±0.047	±0.032	919k	[81] YUSHCHENKO	04B	ISTR	–	
2.78 ±0.26	±0.30	41k	SHIMIZU	00	SPEC	+	DP, uses RC
1.8 ±0.7		3000	ARTEMOV	97B	SPEC	–	DP
2.84 ±0.27	±0.20	32k	[82] AKIMENKO	91	SPEC		PI, no RC
2.9 ±0.4		62k	[83] BOLOTOV	88	SPEC		PI, no RC
2.7 ±0.8			[84] BRAUN	73B	HLBC	+	DP, no RC
2.9 ±1.1		4017	CHIANG	72	OSPK	+	DP, RC negligible
2.7 ±1.0		2707	STEINER	71	HLBC	+	DP, uses RC
4.5 ±1.5		1458	BOTTERILL	70	OSPK		PI, uses RC
4.5 $^{+1.7}_{-1.8}$		854	BELLOTTI	67B	FBC	+	DP, uses RC
1.6 ±1.6		1393	IMLAY	67	OSPK	+	DP, no RC
2.8 $^{+1.3}_{-1.4}$		515	KALMUS	67	FBC	+	e^+, PI, no RC
• • • We do not use the following data for averages, fits, limits, etc. • • •							
2.93 ±0.15	±0.2	130k	[85] AJINENKO	02	SPEC		DP, uses RC
2.5 ±0.7			[86] BRAUN	74	HLBC	+	$K_{\mu 3}/K_{e3}$ vs. t

[81] This should be considered a mean slope. A significant quadratic non-linearity is observed, with linear and quadratic form factor parameters $\lambda_+ = 0.02324 \pm 0.00152 \pm 0.00032$ and $\lambda'_+ = 0.00084 \pm 0.00027 \pm 0.00031$.

[82] AKIMENKO 91 state that radiative corrections would raise λ_+ by 0.0013.

[83] BOLOTOV 88 state radiative corrections of GINSBERG 67 would raise λ_+ by 0.002.

[84] BRAUN 73B states that radiative corrections of GINSBERG 67 would lower λ^e_+ by 0.002 but that radiative corrections of BECHERRAWY 70 disagrees and would raise λ^e_+ by 0.005.

[85] Superseded by YUSHCHENKO 04B.

[86] BRAUN 74 is a combined $K_{\mu 3}$-K_{e3} result. It is not independent of BRAUN 73C ($K_{\mu 3}$) and BRAUN 73B (K_{e3}) form factor results.

$\xi_A = f_-/f_+$ (determined from $K^{\pm}_{\mu 3}$ spectra)

Results labeled OUR FIT are discussed in the review "$K^{\pm}_{\ell 3}$ and $K^0_{\ell 3}$ Form Factors" above. ξ_A is $\xi(0)$ determined by Method A of that review. The parameter $\xi(0)$ is redundant with λ_0 below and is not put into the Meson Summary Table.

VALUE	$d\xi(0)/d\lambda_+$	EVTS	DOCUMENT ID		TECN	CHG	COMMENT
−0.125 ±0.023	**OUR FIT**		Error includes scale factor of 1.5. Correlation is $d\xi(0)/d\lambda_+ = -16.3$. Assumes μ-e universality.				
−0.14 ±0.05	**OUR FIT**		Error includes scale factor of 1.8. Correlation is $d\xi(0)/d\lambda_+ = -16.6$.				
−0.116 ±0.030	−17	540k	[87] YUSHCHENKO	04	ISTR	–	DP
+0.54 ±0.39	−12	3000	[87] ARTEMOV	97B	SPEC	–	DP
−0.27 ±0.25	−17	3973	WHITMAN	80	SPEC	+	DP
−0.8 ±0.8	−20	490	[88] ARNOLD	74	HLBC	+	DP
−0.57 ±0.24	−9	6527	[89] MERLAN	74	ASPK	+	DP
−0.36 ±0.40	−19	1897	[90] BRAUN	73C	HLBC	+	DP
−0.62 ±0.28	−12	4025	[91] ANKENBRA...	72	ASPK	+	PI
+0.45 ±0.28	−15	3480	[92] CHIANG	72	OSPK	+	DP
−0.5 ±0.8	−26	2041	[93] KIJEWSKI	69	OSPK	+	PI
+0.72 ±0.93	−17	444	CALLAHAN	66B	FBC	+	PI
• • • We do not use the following data for averages, fits, limits, etc. • • •							
−0.14 ±0.10	−18	112k	[87,94] AJINENKO	03	ISTR	–	DP
−1.1 ±0.56	−29	3240	[95] HAIDT	71	HLBC	+	DP
−0.5 ±0.9	none	78	EISLER	68	HLBC	+	PI, λ_+=0
0.0 $^{+1.1}_{-0.9}$		2648	[96] CALLAHAN	66B	FBC	+	μ, λ_+=0
+0.7 ±0.5		87	GIACOMELLI	64	EMUL	+	MU+BR, λ_+=0
−0.08 ±0.7			[97] JENSEN	64	XEBC	+	DP+BR
+1.8 ±0.6		76	BROWN	62B	XEBC	+	DP+BR, λ_+=0

[87] Calculated from λ_+, λ_0, and $d\lambda_0/d\lambda_+$.

[88] ARNOLD 74 figure 4 was used to obtain ξ_A and $d\xi(0)/d\lambda_+$.

[89] MERLAN 74 figure 5 was used to obtain $d\xi(0)/d\lambda_+$.

[90] BRAUN 73C gives $\xi(t) = -0.34 \pm 0.20$, $d\xi(t)/d\lambda_+ = -14$ for $\lambda_+ = 0.027$, $t = 6.6$. We calculate above $\xi(0)$ and $d\xi(0)/d\lambda_+$ for their $\lambda_+ = 0.025 \pm 0.017$.

[91] ANKENBRANDT 72 figure 3 was used to obtain $d\xi(0)/d\lambda_+$.

[92] CHIANG 72 figure 10 was used to obtain $d\xi(0)/d\lambda_+$. Fit had $\lambda_- = \lambda_+$ but would not change for $\lambda_- = 0$. L.Pondrom, (private communication 74).

[93] KIJEWSKI 69 figure 17 was used to obtain $d\xi(0)/d\lambda_+$ and errors.

[94] Superseded by YUSHCHENKO 04.

[95] HAIDT 71 table 8 (Dalitz plot analysis) gives $d\xi(0)/d\lambda_+ = (-1.1+0.5)/(0.050-0.029) = -29$, error raised from 0.50 to agree with $d\xi(0) = 0.20$ for fixed λ_+. Not included in fit because of large disagreement with more precise $K_{\mu 3}/K_{e3}$ branching ratio measurement.

[96] CALLAHAN 66 table 1 (π analysis) gives $d\xi(0)/d\lambda_+ = (0.72-0.05)/(0-0.04) = -17$, error raised from 0.80 to agree with $d\xi(0) = 0.37$ for fixed λ_+. t unknown.

[97] JENSEN 64 gives $\lambda_+^{\mu} = \lambda_+^{e} = -0.020 \pm 0.027$. $d\xi(0)/d\lambda_+$ unknown. Includes SHAKLEE 64 $\xi_B(K_{\mu 3}/K_{e3})$.

$\xi_B = f_-/f_+$ (determined from $K^{\pm}_{\mu 3}/K^{\pm}_{e3}$)

The $K^{\pm}_{\mu 3}/K^{\pm}_{e3}$ branching ratio fixes a relationship between $\xi(0)$ and λ_+ if μ-e universality is assumed. We quote the author's $\xi(0)$ and associated λ_+ but do not average because the λ_+ values differ. The result labeled OUR FIT below does not use these ξ_B values. Instead it uses the authors $K^{+}_{\mu 3}/K^{+}_{e3}$ branching ratios to obtain the fitted $K^{\pm}_{\mu 3}/K^{\pm}_{e3}$ ratio which is then converted to KL3FIT value below, as discussed in the review "$K^{\pm}_{\ell 3}$ and $K^{0}_{\ell 3}$ Form Factors" above. ξ_B is $\xi(0)$ determined by Method B of that review. The parameter $\xi(0)$ is redundant with λ_0 below and is not put into the Meson Summary Table.

VALUE	EVTS	DOCUMENT ID		TECN	CHG	COMMENT
-0.125 ± 0.023 OUR FIT		Error includes scale factor of 1.5. Correlation is $d\xi(0)/d\lambda_+ = -16.3$. Assumes μ-e universality.				
-0.13 ± 0.06		[98] KL3FIT	04	RVUE		$\lambda_+ = 0.030$
• • • We do not use the following data for averages, fits, limits, etc. • • •						
-0.12 ± 0.12	55k	[99] HEINTZE	77	CNTR	+	$\lambda_+ = 0.029$
0.0 ± 0.15	5825	CHIANG	72	OSPK	+	$\lambda_+ = 0.03$, fig.10
-0.81 ± 0.27	1505	[100] HAIDT	71	HLBC	+	$\lambda_+ = 0.028$, fig.8
-0.35 ± 0.22		[101] BOTTERILL	70	OSPK	+	$\lambda_+ = 0.045 \pm 0.015$
$+0.91 \pm 0.82$		ZELLER	69	ASPK	+	$\lambda_+ = 0.023$
-0.08 ± 0.15	5601	[101] BOTTERILL	68B	ASPK	+	$\lambda_+ = 0.023 \pm 0.008$
-0.60 ± 0.20	1398	[100] EICHTEN	68	HLBC	+	See note
$+1.0 \pm 0.6$	986	GARLAND	68	OSPK	+	$\lambda_+ = 0$
$+0.75 \pm 0.50$	306	AUERBACH	67	OSPK	+	$\lambda_+ = 0$
$+0.4 \pm 0.4$	636	CALLAHAN	66B	FBC	+	$\lambda_+ = 0$
$+0.6 \pm 0.5$		BISI	65B	HBC	+	$\lambda_+ = 0$
$+0.8 \pm 0.6$	500	CUTTS	65	OSPK	+	$\lambda_+ = 0$
$-0.17 \, {}^{+0.75}_{-0.99}$		SHAKLEE	64	XEBC	+	$\lambda_+ = 0$

[98] KL3FIT value is from fitted $K^{\pm}_{\mu 3}/K^{\pm}_{e3}$ branching ratio. $d\xi(0)/d\lambda_+ = -11.6$.

[99] Calculated by us from λ_0 and λ_+ given below.

[100] EICHTEN 68 has $\lambda_+ = 0.023 \pm 0.008$, $t = 4$, independent of λ_-. Replaced by HAIDT 71.

[101] BOTTERILL 70 is re-evaluation of BOTTERILL 68B with different λ_+.

$\xi_C = f_-/f_+$ (determined from μ polarization in $K^{\pm}_{\mu 3}$)

The μ polarization is a measure of $\xi(t)$. No assumptions on λ_{+-} are necessary, but t (weighted by sensitivity to $\xi(t)$) should be specified. In λ_+, $\xi(0)$ parametrization this is $\xi(0)$ for $\lambda_+ = 0$. $d\xi/d\lambda = \xi t$. For radiative correction to muon polarization in $K^{\pm}_{\mu 3}$, see GINSBERG 71. Results labeled OUR FIT are discussed in the review "$K^{\pm}_{\ell 3}$ and $K^{0}_{\ell 3}$ Form Factors" above. ξ_C is $\xi(0)$ determined by Method C of that review. The parameter $\xi(0)$ is redundant with λ_0 below and is not put into the Meson Summary Table.

VALUE	EVTS	DOCUMENT ID		TECN	CHG	COMMENT
-0.125 ± 0.023 OUR FIT		Error includes scale factor of 1.5. Correlation is $d\xi(0)/d\lambda_+ = -16.3$. Assumes μ-e universality.				
-0.14 ± 0.05 OUR FIT		Error includes scale factor of 1.8. Correlation is $d\xi(0)/d\lambda_+ = -16.6$.				
-0.95 ± 0.3	3133	[102] CUTTS	69	OSPK	+	Total pol. t=4.0
-1.0 ± 0.3	6000	[103] BETTELS	68	HLBC	+	Total pol. t=4.9
• • • We do not use the following data for averages, fits, limits, etc. • • •						
-0.25 ± 1.20	1585	[104] BRAUN	75	HLBC	+	POL, t=4.2
-0.64 ± 0.27	40k	[105] MERLAN	74	ASPK	+	POL, $d\xi(0)/d\lambda_+ = +1.7$

[102] CUTTS 69 $t = 4.0$ was calculated from figure 8. $d\xi(0)/d\lambda_+ = \xi t = -0.95 \times 4 = -3.8$.

[103] BETTELS 68 $d\xi(0)/d\lambda_+ = \xi t = -1.0 \times 4.9 = -4.9$.

[104] BRAUN 75 $d\xi(0)/d\lambda_+ = \xi t = -0.25 \times 4.2 = -1.0$.

[105] MERLAN 74 polarization result (figure 5) not possible. See discussion of polarization experiments in note on "$K_{\ell 3}$ Form Factors" in the 1982 edition of this *Review* [Physics Letters **111B** (1982)].

λ_+ (LINEAR ENERGY DEPENDENCE OF f_+ IN $K^{\pm}_{\mu 3}$ DECAY)

See also the corresponding entries and footnotes in sections ξ_A, ξ_C, and λ_0. For radiative correction of $K^{\pm}_{\mu 3}$ Dalitz plot, see GINSBERG 70 and BECHERRAWY 70. Results labeled OUR FIT are discussed in the review "$K^{\pm}_{\ell 3}$ and $K^{0}_{\ell 3}$ Form Factors" above.

VALUE (units 10^{-2})	EVTS	DOCUMENT ID		TECN	CHG	COMMENT
2.78 ± 0.07 OUR FIT		Error includes scale factor of 1.5. Assumes μ-e universality.				
2.84 ± 0.27 OUR FIT		Error includes scale factor of 1.8.				
$2.77 \pm 0.13 \pm 0.09$	540k	YUSHCHENKO	04	ISTR	−	DP
1.4 ± 2.4	3000	ARTEMOV	97B	SPEC	−	DP
5.0 ± 1.3	3973	WHITMAN	80	SPEC	+	DP
2.5 ± 3.0	490	ARNOLD	74	HLBC	+	DP
2.7 ± 1.9	6527	MERLAN	74	ASPK	+	DP
2.5 ± 1.7	1897	BRAUN	73C	HLBC	+	DP
2.4 ± 1.9	4025	[106] ANKENBRA...	72	ASPK	+	PI
-0.6 ± 1.5	3480	CHIANG	72	OSPK	+	DP
0.9 ± 2.6	2041	KIJEWSKI	69	OSPK	+	PI
0.0 ± 5.0	444	CALLAHAN	66B	FBC	+	PI
• • • We do not use the following data for averages, fits, limits, etc. • • •						
3.21 ± 0.45	112k	[107] AJINENKO	03	ISTR	−	DP
2.9 ± 2.4	3000	[108] ARTEMOV	97	SPEC	−	DP
5.0 ± 1.8	3240	[109] HAIDT	71	HLBC	+	DP

[106] ANKENBRANDT 72 λ_+ from figure 3 to match $d\xi(0)/d\lambda_+$. Text gives 0.024 ± 0.022.

[107] Superseded by YUSHCHENKO 04.

[108] Superseded by ARTEMOV 97B.

[109] Not included in fit because of large discrepancy in $K_{\mu 3}/K_{e3}$ branching ratio with more precise experiments.

λ_0 (LINEAR ENERGY DEPENDENCE OF f_0 IN $K^{\pm}_{\mu 3}$ DECAY)

Wherever possible, we have converted the above values of $\xi(0)$ into values of λ_0 using the associated λ_+^{μ} and $d\xi/d\lambda$. Results labeled OUR FIT are discussed in the review "$K^{\pm}_{\ell 3}$ and $K^{0}_{\ell 3}$ Form Factors" above.

VALUE (units 10^{-2})	$d\lambda_0/d\lambda_+$	EVTS	DOCUMENT ID		TECN	CHG	COMMENT
1.74 ± 0.22 OUR FIT			Error includes scale factor of 1.8. Correlation is $d\lambda_0/d\lambda_+ = -0.34$.				
1.77 ± 0.16 OUR FIT			Error includes scale factor of 1.5. Correlation is $d\lambda_0/d\lambda_+ = -0.32$. Assumes μ-e universality.				
$+2.0 \pm 0.5$	$+0.06$		[110] KL3FIT	04	RVUE		$\lambda_+ = 0.030$
$+1.83 \pm 0.11 \pm 0.06$	-0.348	540k	YUSHCHENKO	04	ISTR	−	DP
$+5.8 \pm 2.0$	$+0.0$	3000	[111] ARTEMOV	97B	SPEC	−	DP
$+2.9 \pm 1.1$	-0.37	3973	WHITMAN	80	SPEC	+	DP
-4.0 ± 4.0	-0.62	490	ARNOLD	74	HLBC	+	DP
-1.9 ± 1.5	$+0.27$	6527	[112] MERLAN	74	ASPK	+	DP
-0.8 ± 2.0	-0.53	1897	[113] BRAUN	73C	HLBC	+	DP
-2.6 ± 1.3	$+0.03$	4025	[114] ANKENBRA...	72	ASPK	+	PI
$+3.0 \pm 1.4$	-0.21	3480	[114] CHIANG	72	OSPK	+	DP
-5.6 ± 2.4	$+0.69$	3133	[115] CUTTS	69	OSPK	+	POL
-3.1 ± 4.5	-1.10	2041	[114] KIJEWSKI	69	OSPK	+	PI
-6.3 ± 2.4	$+0.60$	6000	[115] BETTELS	68	HLBC	+	POL
$+5.8 \pm 3.6$	-0.37	444	[114] CALLAHAN	66B	FBC	+	PI
• • • We do not use the following data for averages, fits, limits, etc. • • •							
$+2.09 \pm 0.45$	-0.46	112k	[116] AJINENKO	03	ISTR	−	DP
$+1.9 \pm 0.64$		24k	[117] HORIE	01	SPEC	+	BR
$+6.2 \pm 2.4$	$+0.0$	3000	[118] ARTEMOV	97	SPEC	−	DP
$+1.9 \pm 1.0$	$+0.03$	55k	[119] HEINTZE	77	SPEC	+	BR
$+0.8 \pm 9.7$	$+0.92$	1585	[115] BRAUN	75	HLBC	+	POL
-1.7 ± 1.1			[120] BRAUN	74	HLBC	+	$K_{\mu 3}/K_{e3}$ vs. t
-3.9 ± 2.9	-1.34	3240	[114] HAIDT	71	HLBC	+	DP

[110] KL3FIT 04 value is from our fitted value of the $K^{\pm}_{\mu 3}/K^{\pm}_{e3}$ branching ratio. Assumes $\mu - e$ universality.

[111] ARTEMOV 97B does not give $d\lambda_0/d\lambda_+$ so we take it to be zero.

[112] MERLAN 74 λ_0 and $d\lambda_0/d\lambda_+$ were calculated by us from ξ_A, λ_+^{μ}, and $d\xi(0)/d\lambda_+$. Their figure 6 gives $\lambda_0 = -0.025 \pm 0.012$ and no $d\lambda_0/d\lambda_+$.

[113] This value and error are taken from BRAUN 75 but correspond to the BRAUN 73C λ_+^{μ} result. $d\lambda_0/d\lambda_+$ is from BRAUN 73C $d\xi(0)/d\lambda_+$ in ξ_A above.

[114] λ_0 calculated by us from $\xi(0)$, λ_+^{μ}, and $d\xi(0)/d\lambda_+$.

[115] λ_0 value is for $\lambda_+ = 0.03$ calculated by us from $\xi(0)$ and $d\xi(0)/d\lambda_+$.

[116] Superseded by YUSHCHENKO 04.

[117] HORIE 01 assumes μ-e universality in $K^{+}_{\ell 3}$ decay and uses SHIMIZU 00 value $\lambda = 0.0278 \pm 0.0040$ from $K^{\pm}_{e3}$ decay. Enters fit via $K_{\mu 3}/K_{e3}$ branching ratio.

[118] ARTEMOV 97 does not give $d\lambda_0/d\lambda_+$ so we take it to be zero. Superseded by ARTEMOV 97B.

[119] HEINTZE 77 uses $\lambda_+ = 0.029 \pm 0.003$. $d\lambda_0/d\lambda_+$ estimated by us. Enters fit via $K_{\mu 3}/K_{e3}$ branching ratio.

[120] BRAUN 74 is a combined $K_{\mu 3}$-K_{e3} result. It is not independent of BRAUN 73C ($K_{\mu 3}$) and BRAUN 73B (K_{e3}) form factor results.

$|f_S/f_+|$ FOR $K^\pm_{e3}$ DECAY

Ratio of scalar to f_+ couplings.

VALUE (units 10^{-2})	CL%	EVTS	DOCUMENT ID		TECN	CHG	COMMENT
$-0.3^{+0.8}_{-0.7}$ OUR AVERAGE							
$-0.37^{+0.66}_{-0.56}\pm0.41$		919k	YUSHCHENKO	04B	ISTR	−	
$0.2\pm2.6\pm1.4$		41k	SHIMIZU	00	SPEC	+	λ_+, f_S, f_T fit
• • • We do not use the following data for averages, fits, limits, etc. • • •							
$-1.9^{+2.5}_{-1.6}$		130k	[121] AJINENKO	02	SPEC		λ_+, f_S fit
$7.0\pm1.6\pm1.6$		32k	AKIMENKO	91	SPEC		λ_+, f_S, f_T, ϕ fit
0 ± 10		2827	[122] BRAUN	75	HLBC	+	
<13	90	4017	CHIANG	72	OSPK	+	
14^{+3}_{-4}		2707	[122] STEINER	71	HLBC	+	λ_+, f_S, f_T, ϕ fit
<23	90		BOTTERILL	68C	ASPK		
<18	90		BELLOTTI	67B	HLBC		
<30	95		KALMUS	67	HLBC	+	

[121] Superseded by YUSHCHENKO 04B.
[122] Statistical errors only.

$|f_T/f_+|$ FOR $K^\pm_{e3}$ DECAY

Ratio of tensor to f_+ couplings.

VALUE (units 10^{-2})	CL%	EVTS	DOCUMENT ID		TECN	CHG	COMMENT
-1.2 ± 2.3 OUR AVERAGE							
$1.2\pm2.1\pm1.1$		919k	YUSHCHENKO	04B	ISTR	−	
$1\pm14\pm9$		41k	SHIMIZU	00	SPEC	+	λ_+, f_S, f_T fit
• • • We do not use the following data for averages, fits, limits, etc. • • •							
$-4.5^{+6.0}_{-5.7}$		130k	[123] AJINENKO	02	SPEC		λ_+, f_T fit
$53^{+9}_{-10}\pm10$		32k	AKIMENKO	91	SPEC		λ_+, f_S, f_T, ϕ fit
7 ± 37		2827	[124] BRAUN	75	HLBC	+	
$<75.$	90	4017	CHIANG	72	OSPK	+	
24^{+16}_{-14}		2707	[124] STEINER	71	HLBC	+	λ_+, f_S, f_T, ϕ fit
$<58.$	90		BOTTERILL	68C	ASPK		
$<58.$	90		BELLOTTI	67B	HLBC		
$<110.$	95		KALMUS	67	HLBC	+	

[123] Superseded by YUSHCHENKO 04B.
[124] Statistical errors only.

f_S/f_+ FOR $K^\pm_{\mu3}$ DECAY

Ratio of scalar to f_+ couplings.

VALUE (units 10^{-2})	EVTS	DOCUMENT ID		TECN	CHG	COMMENT
$0.17\pm0.14\pm0.54$	540k	[125] YUSHCHENKO	04	ISTR	−	DP
• • • We do not use the following data for averages, fits, limits, etc. • • •						
$0.4\pm0.5\pm0.5$	112k	[126] AJINENKO	03	ISTR	−	DP

[125] The second error is the theoretical error from the uncertainty in the chiral perturbation theory prediction for λ_0, ±0.0053, combined in quadrature with the systematic error ±0.0009.
[126] The second error is the theoretical error from the uncertainty in the chiral perturbation theory prediction for λ_0. Superseded by YUSHCHENKO 04.

f_T/f_+ FOR $K^\pm_{\mu3}$ DECAY

Ratio of tensor to f_+ couplings.

VALUE (units 10^{-2})	EVTS	DOCUMENT ID		TECN	CHG	COMMENT
-0.1 ± 0.7 OUR AVERAGE						
$-0.07\pm0.71\pm0.20$	540k	YUSHCHENKO	04	ISTR	−	DP
2 ± 12	1585	BRAUN	75	HLBC		
• • • We do not use the following data for averages, fits, limits, etc. • • •						
$-2.1\pm2.8\pm1.4$	112k	[127] AJINENKO	03	ISTR	−	DP

[127] The second error is the theoretical error from the uncertainty in the chiral perturbation theory prediction for λ_0. Superseded by YUSHCHENKO 04.

DECAY FORM FACTORS FOR $K^\pm \to \pi^+\pi^- e^\pm \nu_e$

Given in PISLAK 01, ROSSELET 77, BEIER 73, and BASILE 71C.

DECAY FORM FACTOR FOR $K^\pm \to \pi^0\pi^0 e^\pm \nu$

Given in BOLOTOV 86B and BARMIN 88B.

$K^\pm \to \ell^\pm\nu\gamma$ FORM FACTORS

For definitions of the axial-vector F_A and vector F_V form factor, see the "Note on $\pi^\pm \to \ell^\pm\nu\gamma$ and $K^\pm \to \ell^\pm\nu\gamma$ Form Factors" in the $\pi^\pm$ section. In the kaon literature, often different definitions $a_K = F_A/m_K$ and $v_K = F_V/m_K$ are used.

$F_A + F_V$, SUM OF AXIAL-VECTOR AND VECTOR FORM FACTOR FOR $K \to e\nu_e\gamma$

VALUE	EVTS	DOCUMENT ID		TECN
0.148 ± 0.010 OUR AVERAGE				
0.147 ± 0.011	51	[128] HEINTZE	79	SPEC
$0.150^{+0.018}_{-0.023}$	56	[129] HEARD	75	SPEC

[128] HEINTZE 79 quotes absolute value of $|F_A + F_V|\sin\theta_c$. We use $\sin\theta_c = V_{us} = 0.2205$.
[129] HEARD 75 quotes absolute value of $|F_A + F_V|\sin\theta_c$. We use $\sin\theta_c = V_{us} = 0.2205$.

$F_A + F_V$, SUM OF AXIAL-VECTOR AND VECTOR FORM FACTOR FOR $K \to \mu\nu_\mu\gamma$

VALUE	CL%	EVTS	DOCUMENT ID		TECN	CHG
$0.165\pm0.007\pm0.011$		2588	[130] ADLER	00B	B787	+
• • • We do not use the following data for averages, fits, limits, etc. • • •						
-1.2 to 1.1	90		DEMIDOV	90	XEBC	
<0.23	90		[130] AKIBA	85	SPEC	

[130] Quotes absolute value. Sign not determined.

$F_A - F_V$, DIFFERENCE OF AXIAL-VECTOR AND VECTOR FORM FACTOR FOR $K \to e\nu_e\gamma$

VALUE	EVTS	DOCUMENT ID		TECN
<0.49	90	[131] HEINTZE	79	SPEC

[131] HEINTZE 79 quotes $|F_A - F_V| < \sqrt{11}\,|F_A + F_V|$.

$F_A - F_V$, DIFFERENCE OF AXIAL-VECTOR AND VECTOR FORM FACTOR FOR $K \to \mu\nu_\mu\gamma$

VALUE	CL%	EVTS	DOCUMENT ID		TECN	CHG
-0.24 to 0.04	90	2588	ADLER	00B	B787	+
• • • We do not use the following data for averages, fits, limits, etc. • • •						
-2.2 to 0.6	90		DEMIDOV	90	XEBC	
-2.5 to 0.3	90		AKIBA	85	SPEC	

$K^\pm$ CHARGE RADIUS

VALUE (fm)	DOCUMENT ID		COMMENT
0.560 ± 0.031 OUR AVERAGE			
0.580 ± 0.040	AMENDOLIA	86B	$Ke \to Ke$
0.530 ± 0.050	DALLY	80	$Ke \to Ke$
• • • We do not use the following data for averages, fits, limits, etc. • • •			
0.620 ± 0.037	BLATNIK	79	VMD + dispersion relations

CP VIOLATION TESTS IN K^+ AND K^- DECAYS

$$\Delta(K^\pm_{\pi\mu\mu}) = \frac{\Gamma(K^+_{\pi\mu\mu}) - \Gamma(K^-_{\pi\mu\mu})}{\Gamma(K^+_{\pi\mu\mu}) + \Gamma(K^-_{\pi\mu\mu})}$$

VALUE	DOCUMENT ID		TECN
$-0.02\pm0.11\pm0.04$	PARK	02	HYCP

T VIOLATION TESTS IN K^+ AND K^- DECAYS

P_T in $K^+ \to \pi^0\mu^+\nu_\mu$

T-violating muon polarization. Sensitive to new sources of CP violation beyond the Standard Model.

VALUE (units 10^{-3})	EVTS	DOCUMENT ID		TECN	CHG
$-4.2\pm4.9\pm0.9$	3.9M	ABE	99S	K246	+

P_T in $K^+ \to \mu^+\nu_\mu\gamma$

T-violating muon polarization. Sensitive to new sources of CP violation beyond the Standard Model.

VALUE (units 10^{-2})	EVTS	DOCUMENT ID		TECN	CHG
$-0.64\pm1.85\pm0.10$	114k	[132] ANISIMOVSKY	03	K246	+

[132] Muons stopped and polarization measured from decay to positrons.

Im(ξ) in $K^+ \to \pi^0\mu^+\nu_\mu$ DECAY (from transverse μ pol.)

Test of T reversal invariance.

VALUE	EVTS	DOCUMENT ID		TECN	CHG	COMMENT
-0.014 ± 0.014 OUR AVERAGE						
$-0.013\pm0.016\pm0.003$	3.9M	ABE	99S	CNTR	+	p_T K^+ at rest
-0.016 ± 0.025	20M	CAMPBELL	81	CNTR	+	Pol.

$K^\pm$ REFERENCES

KL3FIT	04	RPP 2004 edition	T.G. Trippe	(PDG Collab.)
$K^\pm_{\mu3}$ and $K^0_{\mu3}$ Form Factors review in K^+ Listings.				
YUSHCHENKO	04	PL B581 31	O.P. Yushchenko *et al.*	(IHEP, INRM)
YUSHCHENKO	04B	hep-ex/0404030 PL B (to be publ.)	O.P. Yushchenko *et al.*	(IHEP, INRM)
AJINENKO	03	PAN 66 105 Translated from YAF 66 107.	I.V. Ajinenko *et al.*	(IHEP, INRM)
AJINENKO	03B	PL B567 159	I.V. Ajinenko *et al.*	(IHEP, INRM)
ALIEV	03	PL B554 7	M.A. Aliev *et al.*	(KEK E470 Collab.)
ANISIMOVSKY	03	PL B562 166	V.V. Anisimovsky *et al.*	
PISLAK	03	PR D67 072004	S. Pislak *et al.*	(BNL E865 Collab.)
ADLER	02	PRL 88 041803	S. Adler *et al.*	(BNL E787 Collab.)
ADLER	02B	PR D65 052009	S. Adler *et al.*	(BNL E787 Collab.)
ADLER	02C	PL B537 211	S. Adler *et al.*	(BNL E787 Collab.)
AJINENKO	02	PAN 65 2064 Translated from YAF 65 2125.	I.V. Ajinenko *et al.*	(IHEP, INRM)

Meson Particle Listings

$K^{\pm}$

PARK 02 PRL 88 111801 H.K. Park *et al.* (HyperCP Collab.)
POBLAGUEV 02 PRL 89 061803 A.A. Poblaguev *et al.* (BNL 865 Collab.)
ADLER 01 PR D63 032004 S. Adler *et al.* (BNL E787 Collab.)
HORIE 01 PL B513 311 K. Horie *et al.* (KEK E426 Collab.)
PISLAK 01 PRL 87 221801 S. Pislak *et al.* (BNL E865 Collab.)
Also 03 PR D67 072004 S. Pislak *et al.* (BNL E865 Collab.)
ADLER 00 PRL 84 3768 S. Adler *et al.* (BNL E787 Collab.)
ADLER 00B PRL 85 2256 S. Adler *et al.* (BNL E787 Collab.)
ADLER 00C PRL 85 4856 S. Adler *et al.* (BNL E787 Collab.)
APPEL 00 PRL 85 2450 R. Appel *et al.* (BNL 865 Collab.)
Also 97 Thesis, Yale Univ. D.R. Bergman
Also 97 Thesis, Univ. Zurich S. Pislak
APPEL 00B PRL 85 2877 R. Appel *et al.* (BNL 865 Collab.)
MA 00 PRL 84 2580 H. Ma *et al.* (BNL 865 Collab.)
PDG 00 EPJ C15 1 D.E. Groom *et al.*
SHIMIZU 00 PL B495 33 S. Shimizu *et al.* (KEK E246 Collab.)
SHIN 00 EPJ C12 627 Y.-H. Shin *et al.* (KEK E246 Collab.)
ABE 99S PRL 83 4253 M. Abe *et al.* (KEK E246 Collab.)
APPEL 99 PRL 83 4482 R. Appel *et al.* (BNL 865 Collab.)
ADLER 98 PR D58 012003 S. Adler *et al.* (BNL E787 Collab.)
BATUSOV 98 NP B516 3 V.Y. Batusov *et al.*
ADLER 97 PRL 79 2204 S. Adler *et al.* (BNL E787 Collab.)
ADLER 97C PRL 79 4756 S. Adler *et al.* (BNL E787 Collab.)
ARTEMOV 97 PAN 60 218 V.M. Artemov *et al.* (JINR)
Translated from YAF 60 277.
ARTEMOV 97B PAN 60 2023 V.M. Artemov *et al.*
Translated from YAF 60 2205.
BERGMAN 97 Thesis, Yale Univ. D.R. Bergman
KITCHING 97 PRL 79 4079 P. Kitching *et al.* (BNL E787 Collab.)
PISLAK 97 Thesis, Univ. Zurich S. Pislak
ADLER 96 PRL 76 1421 S. Adler *et al.* (BNL E787 Collab.)
KOPTEV 95 JETPL 61 877 V.P. Koptev *et al.* (PNPI)
Translated from ZETFP 61 865.
AOKI 94 PR D50 69 M. Aoki *et al.* (INUS, KEK, TOKMS)
ATIYA 93 PRL 70 2521 M.S. Atiya *et al.* (BNL E787 Collab.)
Also 93C PRL 71 305 (erratum) M.S. Atiya *et al.* (BNL E787 Collab.)
ATIYA 93B PR D48 R1 M.S. Atiya *et al.* (BNL E787 Collab.)
ALLIEGRO 92 PRL 68 278 C. Alliegro *et al.* (BNL, FNAL, PSI+)
BARMIN 92 SJNP 55 547 V.V. Barmin *et al.* (ITEP)
Translated from YAF 55 976.
IMAZATO 92 PRL 69 877 J. Imazato *et al.* (KEK, INUS, TOKY+)
IVANOV 92 THESIS Yu.M. Ivanov (PNPI)
LITTENBERG 92 PRL 68 443 L.S. Littenberg, R.E. Shrock (BNL, STON)
USHER 92 PR D45 3961 T. Usher *et al.* (UCI)
AKIMENKO 91 PL B259 225 S.A. Akimenko *et al.* (SERP, JINR, TBIL+)
BARMIN 91 SJNP 53 606 V.V. Barmin *et al.* (ITEP)
Translated from YAF 53 981.
DENISOV 91 JETPL 54 558 A.S. Denisov *et al.* (PNPI)
Translated from ZETFP 54 567.
Also 92 THESIS Yu.M. Ivanov (PNPI)
ATIYA 90 PRL 64 21 M.S. Atiya *et al.* (BNL E787 Collab.)
ATIYA 90B PRL 65 1188 M.S. Atiya *et al.* (BNL E787 Collab.)
DEMIDOV 90 SJNP 52 1006 V.S. Demidov *et al.* (ITEP)
Translated from YAF 52 1595.
LEE 90 PRL 64 165 A.M. Lee *et al.* (BNL, FNAL, VILL, WASH+)
ATIYA 89 PRL 63 2177 M.S. Atiya *et al.* (BNL E787 Collab.)
BARMIN 89 SJNP 50 421 V.V. Barmin *et al.* (ITEP)
Translated from YAF 50 679.
BARMIN 88 SJNP 47 643 V.V. Barmin *et al.* (ITEP)
Translated from YAF 47 1011.
BARMIN 88B SJNP 48 1032 V.V. Barmin *et al.* (ITEP)
Translated from YAF 48 1719.
BOLOTOV 88 JETPL 47 7 V.N. Bolotov *et al.* (ASCI)
Translated from ZETFP 47 8.
GALL 88 PRL 60 186 K.P. Gall *et al.* (BOST, MIT, WILL, CIT+)
BARMIN 87 SJNP 45 62 V.V. Barmin *et al.* (ITEP)
Translated from YAF 45 97.
BOLOTOV 87 SJNP 45 1023 V.N. Bolotov *et al.* (INRM)
Translated from YAF 45 1652.
AMENDOLIA 86B PL B178 435 S.R. Amendolia *et al.* (CERN NA7 Collab.)
BOLOTOV 86 SJNP 44 73 V.N. Bolotov *et al.* (INRM)
Translated from YAF 44 117.
BOLOTOV 86B SJNP 44 68 V.N. Bolotov *et al.* (INRM)
Translated from YAF 44 108.
YAMANAKA 86 PR D34 85 T. Yamanaka *et al.* (KEK, TOKY)
Also 84 PRL 52 329 R.S. Hayano *et al.* (TOKY, KEK)
AKIBA 85 PR D32 2911 Y. Akiba *et al.* (TOKY, TINT, TSUK, KEK)
BOLOTOV 85 JETPL 42 481 V.N. Bolotov *et al.* (INRM)
Translated from ZETFP 42 390.
ASANO 82 PL 113B 195 Y. Asano *et al.* (KEK, TOKY, INUS, OSAK)
COOPER 82 PL 112B 97 A.M. Cooper *et al.* (RL)
PDG 82 PL 111B M. Roos *et al.* (HELS, CIT, CERN)
PDG 82B PL 111B 70 M. Roos *et al.* (HELS, CIT, CERN)
ASANO 81B PL 107 159 Y. Asano *et al.* (KEK, TOKY, INUS, OSAK)
CAMPBELL 81 PRL 47 1032 M.K. Campbell *et al.* (YALE, BNL)
Also 83 PR D27 1056 S.R. Blatt *et al.* (YALE, BNL)
LUM 81 PR D23 2522 G.K. Lum *et al.* (LBL, NBS+)
LYONS 81 ZPHY C10 215 L. Lyons, C. Albajar, G. Myatt (OXF)
DALLY 80 PRL 45 232 E.B. Dally *et al.* (UCLA+)
WHITMAN 80 PR D21 652 R. Whitman *et al.* (ILLC, BNL, ILL)
BARKOV 79 NP B148 53 L.M. Barkov *et al.* (NOVO, KIAE)
BLATNIK 79 LNC 24 39 S. Blatnik, J. Stahov, C.B. Lang (TUZL, GRAZ)
HEINTZE 79 NP B149 365 J. Heintze *et al.* (HEIDP, CERN)
ABRAMS 77 PR D15 22 R.J. Abrams *et al.* (BNL)
DEVAUX 77 NP B126 11 B. Devaux *et al.* (SACL, GEVA)
HEINTZE 77 PL 70B 482 J. Heintze *et al.* (HEIDP, CERN)
ROSSELET 77 PR D15 574 L. Rosselet *et al.* (GEVA, SACL)
BERTRAND 76 NP B114 387 D. Bertrand *et al.* (BRUX, KIDR, DUUC+)
BLOCH 76 PL 60B 393 P. Bloch *et al.* (GEVA, SACL)
BRAUN 76B LNC 17 521 H.M. Braun *et al.* (AACH3, BARI, BELG+)
DIAMANT-... 76 PL 62B 485 A.M. Diamant-Berger *et al.* (SACL, GEVA)
HEINTZE 76 PL 60B 302 J. Heintze *et al.* (HEIDP)
SMITH 76 NP B109 173 K.M. Smith *et al.* (GLAS, LIVP, OXF+)
WEISSENBE... 76 NP B115 55 A.O. Weissenberg *et al.* (ITEP, LEBD)
BLOCH 75 PL 56B 201 P. Bloch *et al.* (SACL, GEVA)
BRAUN 75 NP B89 210 H.M. Braun *et al.* (AACH3, BARI, BRUX+)
CHENG 75 NP A254 381 S.C. Cheng *et al.* (COLU, YALE)
HEARD 75 PL 55B 324 K.S. Heard *et al.* (CERN, HEIDH)
HEARD 75B PL 55B 327 K.S. Heard *et al.* (CERN, HEIDH)
SHEAFF 75 PR D12 2570 M. Sheaff (WISC)
SMITH 75 NP B91 45 K.M. Smith *et al.* (GLAS, LIVP, OXF+)
ARNOLD 74 PR D9 1221 C.L. Arnold, B.P. Roe, D. Sinclair (MICH)
BRAUN 74 PL 51B 393 H.M. Braun *et al.* (AACH3, BARI, BRUX+)
MERLAN 74 PR D9 107 S. Merlan *et al.* (YALE, BNL, LASL)
WEISSENBE... 74 PL 48B 474 A.O. Weissenberg *et al.* (ITEP, LEBD)
ABRAMS 73B PRL 30 500 R.J. Abrams *et al.* (BNL)
BACKENSTO... 73 PL 43B 431 G. Backenstoss *et al.* (CERN, KARLK, KARLE+)
BEIER 73 PRL 30 399 E.W. Beier *et al.* (PENN)
BRAUN 73B PL 47B 185 H.M. Braun, M. Cornelssen (AACH3, BARI, BRUX+)
Also 75 NP B89 210 H.M. Braun *et al.* (AACH3, BARI, BRUX+)
BRAUN 73C PL 47B 182 H.M. Braun, M. Cornelssen (AACH3, BARI, BRUX+)
Also 75 NP B89 210 H.M. Braun *et al.* (AACH3, BARI, BRUX+)
LJUNG 73 PR D8 1307 D. Ljung, D. Cline (WISC)
Also 72 PRL 28 523 D. Ljung (WISC)
Also 72 PRL 28 1287 D. Cline, D. Ljung (WISC)
Also 69 PRL 23 326 U. Camerini *et al.* (WISC)
LUCAS 73 PR D8 719 P.W. Lucas, H.D. Taft, W.J. Willis (YALE)
LUCAS 73B PR D8 727 P.W. Lucas, H.D. Taft, W.J. Willis (YALE)
PANG 73 PR D8 1989 C.Y. Pang *et al.* (EFI, ARIZ, LBL)
Also 72 PL 40B 699 G.D. Cable *et al.* (EFI, LBL)
SMITH 73 NP B60 411 K.M. Smith *et al.* (GLAS, LIVP, OXF+)
ABRAMS 72 PRL 29 1118 R.J. Abrams *et al.* (BNL)
ANKENBRA... 72 PRL 28 1472 C.M. Ankenbrandt *et al.* (BNL, LASL, FNAL+)
AUBERT 72 NC 12A 509 B. Aubert *et al.* (ORSAY, BRUX, EPOL)
CHIANG 72 PR D6 1254 I.H. Chiang *et al.* (ROCH, WISC)
CLARK 72 PRL 29 1274 A.R. Clark *et al.* (LBL)
EDWARDS 72 PR D5 2720 R.T. Edwards *et al.* (ILL)
FORD 72 PL 38B 335 W.T. Ford *et al.* (PRIN)
HOFFMASTER 72 NP B36 1 S. Hoffmaster *et al.* (STEV, SETO, LEHI)
BASILE 71C PL 36B 619 P. Basile *et al.* (SACL, GEVA)
BOURQUIN 71 PL 36B 615 M.H. Bourquin *et al.* (GEVA, SACL)
GINSBERG 71 PR D4 2893 E.S. Ginsberg (MIT)
HAIDT 71 PR D3 10 D. Haidt (AACH, BARI, CERN, EPOL, NIJM+)
Also 69 PL 29B 691 D. Haidt *et al.* (AACH, BARI, CERN, EPOL+)
KLEMS 71 PR D4 66 J.H. Klems, R.H. Hildebrand, R. Stiening (CHIC+)
Also 70 PRL 24 1086 J.H. Klems, R.H. Hildebrand, R. Stiening (LRL+)
Also 70B PR 25 473 J.H. Klems, R.H. Hildebrand, R. Stiening (LRL+)
OTT 71 PR D3 52 R.J. Ott, T.W. Pritchard (LOQM)
ROMANO 71 PL 36B 525 F. Romano *et al.* (BARI, CERN, ORSAY)
SCHWEINB... 71 PL 36B 246 W. Schweinberger (AACH, BELG, CERN, NIJM+)
STEINER 71 PL 36B 521 H.J. Steiner (AACH, BARI, CERN, EPOL, ORSAY+)
BARDIN 70 PL 32B 121 D.Y. Bardin, S.N. Bilenky, B.M. Pontecorvo (JINR)
BECHERRAWY 70 PR D1 1452 T. Becherrawy (ROCH)
BOTTERILL 70 PL 31B 325 D.R. Botterill *et al.* (OXF)
FORD 70 PRL 25 1370 W.T. Ford *et al.* (PRIN)
GAILLARD 70 CERN 70-14 J.M. Gaillard, L.M. Chounet (CERN, ORSAY)
GINSBERG 70 PR D1 229 E.S. Ginsberg (HAIF)
GRAUMAN 70 PR D1 1277 J. Grauman *et al.* (STEV, SETO, LEHI)
Also 69 PRL 23 737 J.U. Grauman *et al.* (STEV, SETO, LEHI)
MALTSEV 70 SJNP 10 678 E.I. Maltsev *et al.* (JINR)
Translated from YAF 10 1195.
PANDOULAS 70 PR D2 1205 D. Pandoulas *et al.* (STEV, SETO)
CUTTS 69 PR 184 1380 D. Cutts *et al.* (LRL, MIT)
Also 68 PRL 20 955 D. Cutts *et al.* (LRL, MIT)
DAVISON 69 PR 180 1333 D.C. Davison *et al.* (UCR)
ELY 69 PR 180 1319 R.P. Ely *et al.* (LOUC, WISC, LRL)
EMMERSON 69 PRL 23 393 J.M.L. Emmerson, T.W. Quirk (OXF)
HERZO 69 PR 186 1403 D. Herzo *et al.* (ILL)
KIJEWSKI 69 Thesis UCRL 18433 P.K. Kijewski (LBL)
LOBKOWICZ 69 PR 185 1676 F. Lobkowicz *et al.* (ROCH, BNL)
Also 66 PRL 17 548 F. Lobkowicz *et al.* (ROCH, BNL)
MAST 69 PR 183 1200 T.S. Mast *et al.* (LRL)
SELLERI 69 NC 60A 291 F. Selleri
ZELLER 69 PR 182 1420 M.E. Zeller *et al.* (UCLA, LRL)
BETTELS 68 NC 56A 1106 J. Bettels (AACH, BARI, BERG, CERN, EPOL+)
Also 71 PR D3 10 D. Haidt (AACH, BARI, CERN, EPOL, NIJM+)
BOTTERILL 68B PRL 21 766 D.R. Botterill *et al.* (OXF)
BOTTERILL 68C PR 174 1661 D.R. Botterill *et al.* (OXF)
BUTLER 68 UCRL 18420 W.D. Butler *et al.* (LRL)
CHANG 68 PRL 20 510 C.Y. Chang *et al.* (UMD, RUTG)
CHEN 68 PRL 20 73 M. Chen *et al.* (LRL, MIT)
EICHTEN 68 PL 27B 586 T. Eichten (AACH, BARI, CERN, EPOL, ORSAY+)
EISLER 68 PR 169 1090 F.R. Eisler *et al.* (RUTG)
ESCHSTRUTH 68 PR 165 1487 P.T. Eschstruth *et al.* (PRIN, PENN)
GARLAND 68 PR 167 1225 R. Garland *et al.* (COLU, RUTG, WISC)
MOSCOSO 68 Thesis L. Moscoso (ORSAY)
AUERBACH 67 PR 155 1505 L.B. Auerbach *et al.* (PENN, PRIN)
Also 74 PR D9 3216 L.B. Auerbach
Erratum.
BELLOTTI 67B NC 52A 1287 E. Bellotti, E. Fiorini, A. Pullia (MILA)
Also 66B PL 20 690 E. Bellotti *et al.* (MILA)
BISI 67 PL 25B 572 V. Bisi *et al.* (TORI)
FLETCHER 67 PRL 19 98 C.R. Fletcher *et al.* (ILL)
FORD 67 PRL 18 1214 W.T. Ford *et al.* (PRIN)
GINSBERG 67 PR 162 1570 E.S. Ginsberg (MASB)
IMLAY 67 PR 160 1203 R.L. Imlay *et al.* (PRIN)
KALMUS 67 PR 159 1187 G.E. Kalmus, A. Kernan (LRL)
ZINCHENKO 67 Thesis Rutgers A.I. Zinchenko (RUTG)
CALLAHAN 66 NC 44A 90 A.C. Callahan (WISC)
CALLAHAN 66B PR 150 1153 A.C. Callahan *et al.* (WISC, LRL, UCR+)
CESTER 66 PL 21 343 R. Cester *et al.* (PPA)
See footnote 1 in AUERBACH 67.
Also 67 PR 155 1505 L.B. Auerbach *et al.* (PENN, PRIN)
BIRGE 65 PR 139B 1600 R.W. Birge *et al.* (LRL, WISC)
BISI 65 NC 35 768 V. Bisi *et al.* (TORI)
BISI 65B PR 139B 1068 V. Bisi *et al.* (TORI)
CALLAHAN 65 PRL 15 129 A. Callahan, D. Cline (WISC)
CLINE 65 PL 15 293 D. Cline, W.F. Fry (WISC)
CUTTS 65 PR 138B 969 D. Cutts, T. Elioff, R. Stiening (LRL)
DEMARCO 65 PR 140B 1430 A. de Marco, C. Grosso, G. Rinaudo (TORI, CERN)
FITCH 65B PR 140B 1088 V.L. Fitch, C.A. Quarles, H.C. Wilkins (PRIN+)
STAMER 65 PR 138B 440 P. Stamer *et al.* (STEV)
YOUNG 65 Thesis UCRL 16362 P.S. Young (LRL)
Also 67 PR 156 1464 P.S. Young, W.Z. Osborne, W.H. Barkas (LRL)
BORREANI 64 PL 12 123 G. Borreani, G. Rinaudo, A.E. Werbrouck (TORI)
CALLAHAN 64 PR 136B 1463 A. Callahan, R. March, R. Stark (WISC)
CLINE 64 PRL 13 101 D. Cline, W.F. Fry (WISC)
GIACOMELLI 64 NC 34 1134 G. Giacomelli *et al.* (BGNA, MUNI)
GREINER 64 PRL 13 284 D.E. Greiner, W.Z. Osborne, W.H. Barkas (LRL)
JENSEN 64 PR 136B 1431 G.L. Jensen *et al.* (MICH)
KALMUS 64 PRL 13 99 G.E. Kalmus *et al.* (LRL, WISC)
SHAKLEE 64 PR 136B 1423 F.S. Shaklee *et al.* (MICH)
BOYARSKI 62 PR 128 2398 A.M. Boyarski *et al.* (MIT)
BROWN 62B PRL 8 450 J.L. Brown *et al.* (LRL, MICH)
FERRO-LUZZI 61 NC 22 1087 M. Ferro-Luzzi *et al.* (LRL)
ROE 61 PRL 7 346 B.P. Roe *et al.* (MICH, LRL)
TAYLOR 59 PR 114 359 S. Taylor *et al.* (COLU)
COOMBES 57 PR 108 1348 C.A. Coombes *et al.* (LBL)

OTHER RELATED PAPERS

LITTENBERG 93 ARNPS 43 729 L.S. Littenberg, G. Valencia (BNL, FNAL)
Rare and Radiative Kaon Decays
RITCHIE 93 RMP 65 1149 J.L. Ritchie, S.G. Wojcicki
"Rare K Decays"
BATTISTON 92 PRPL 214 293 R. Battiston *et al.* (PGIA, CERN, TRSTT)
Status and Perspectives of K Decay Physics
BRYMAN 89 UMP A4 79 D.A. Bryman (TRIU)
"Rare Kaon Decays"
CHOUNET 72 PRPL 4C 199 L.M. Chounet, J.M. Gaillard, M.K. Gaillard (ORSAY+)
FEARING 70 PR D2 542 H.W. Fearing, E. Fischbach, J. Smith (STON, BOHR)
HAIDT 69B PL 29B 696 D. Haidt *et al.* (AACH, BARI, CERN, EPOL+)
CRONIN 68B Vienna Conf. 241 J.W. Cronin (PRIN)
Rapporteur talk.

WILLIS	67	Heidelberg Conf. 273	W.J. Willis	(YALE)
Rapporteur talk.				
CABIBBO	66	Berkeley Conf. 33	N. Cabibbo	(CERN)
ADAIR	64	PL 12 67	R.K. Adair, L.B. Leipuner	(YALE, BNL)
CABIBBO	64	PL 9 352	N. Cabibbo, A. Maksymowicz	(CERN)
Also	64B	PL 11 360	N. Cabibbo, A. Maksymowicz	(CERN)
Also	65	PL 14 72	N. Cabibbo, A. Maksymowicz	(CERN)
BIRGE	63	PRL 11 35	R.W. Birge *et al.*	(LRL, WISC, BARI)
BLOCK	62B	CERN Conf. 371	M.M. Block, L. Lendinara, L. Monari	(NWES, BGNA)
BRENE	61	NP 22 553	N. Brene, L. Egardt, B. Qvist	(NORD)

K^0

$I(J^P) = \frac{1}{2}(0^-)$

K^0 MASS

VALUE (MeV)	EVTS	DOCUMENT ID		TECN	COMMENT
497.648 ± 0.022 OUR FIT					
497.648 ± 0.022 OUR AVERAGE					
497.625 ± 0.001 ± 0.031	655k	LAI	02	NA48	K^0_L beam
497.661 ± 0.033	3713	BARKOV	87B	CMD	$e^+e^- \to K^0_L K^0_S$
497.742 ± 0.085	780	BARKOV	85B	CMD	$e^+e^- \to K^0_L K^0_S$
• • • We do not use the following data for averages, fits, limits, etc. • • •					
497.44 ± 0.50		FITCH	67	OSPK	
498.9 ± 0.5	4500	BALTAY	66	HBC	K^0 from $\overline{p}p$
497.44 ± 0.33	2223	KIM	65B	HBC	K^0 from $\overline{p}p$
498.1 ± 0.4		CHRISTENS...	64	OSPK	

$m_{K^0} - m_{K^\pm}$

VALUE (MeV)	EVTS	DOCUMENT ID		TECN	CHG	COMMENT
3.972 ± 0.027 OUR FIT	Error includes scale factor of 1.2.					
• • • We do not use the following data for averages, fits, limits, etc. • • •						
3.95 ± 0.21	417	HILL	68B	DBC	+	$K^+d \to K^0pp$
3.90 ± 0.25	9	BURNSTEIN	65	HBC	−	
3.71 ± 0.35	7	KIM	65B	HBC	−	$K^-p \to n\overline{K}^0$
5.4 ± 1.1		CRAWFORD	59	HBC	+	
3.9 ± 0.6		ROSENFELD	59	HBC	−	

K^0 MEAN SQUARE CHARGE RADIUS

VALUE (fm^2)	DOCUMENT ID		TECN	COMMENT
−0.076 ± 0.018 OUR AVERAGE	Error includes scale factor of 1.1.			
−0.090 ± 0.021	LAI	03C	NA48	$K^0_L \to \pi^+\pi^- e^+e^-$
−0.054 ± 0.026	MOLZON	78		K_S regen. by electrons
• • • We do not use the following data for averages, fits, limits, etc. • • •				
−0.087 ± 0.046	BLATNIK	79		VMD + dispersion relations
−0.050 ± 0.130	FOETH	69B		K_S regen. by electrons

T-VIOLATION PARAMETER IN K^0-$\overline{K}^0$ MIXING

The asymmetry $A_T = \frac{\Gamma(\overline{K}^0 \to K^0) - \Gamma(K^0 \to \overline{K}^0)}{\Gamma(\overline{K}^0 \to K^0) + \Gamma(K^0 \to \overline{K}^0)}$ must vanish if T invariance holds.

ASYMMETRY A_T IN K^0-$\overline{K}^0$ MIXING

VALUE (units 10^{-3})	EVTS	DOCUMENT ID		TECN
6.6 ± 1.3 ± 1.0	640k	[1] ANGELOPO...	98E	CPLR

[1] ANGELOPOULOS 98E measures the asymmetry $A_T = [\Gamma(\overline{K}^0_{t=0} \to e^+\pi^-\nu_{t=\tau}) - \Gamma(K^0_{t=0} \to e^-\pi^+\overline{\nu}_{t=\tau})]/[\Gamma(\overline{K}^0_{t=0} \to e^+\pi^-\nu_{t=\tau}) + \Gamma(K^0_{t=0} \to e^-\pi^+\overline{\nu}_{t=\tau})]$ as a function of the neutral-kaon eigentime τ. The initial strangeness of the neutral kaon is tagged by the charge of the accompanying charged kaon in the reactions $p\overline{p} \to K^-\pi^+K^0$ and $p\overline{p} \to K^+\pi^-\overline{K}^0$. The strangeness at the time of the decay is tagged by the lepton charge. The reported result is the average value of A_T over the interval $1\tau_S < \tau < 20\tau_S$. From this value of A_T ANGELOPOULOS 01B, assuming CPT invariance in the $e\pi\nu$ decay amplitude, determine the T-violating as $\Delta S{=}\Delta S$ conserving parameter (for its definition, see Review below) $4\mathrm{Re}(\epsilon) = (6.2 \pm 1.4 \pm 1.0) \times 10^{-3}$.

CPT INVARIANCE TESTS IN NEUTRAL KAON DECAY

Revised 2003 by P. Bloch (CERN).

The time evolution of a neutral kaon state state is described by

$$\frac{d}{dt}\Psi = -i\Lambda\Psi \ , \qquad \Lambda \equiv M - \frac{i}{2}\Gamma \tag{1}$$

where M and Γ are Hermitian 2×2 matrices known as the mass and decay matrices. The corresponding eigenvalues are $\lambda_{L,S} = m_{L,S} - \frac{i}{2}\gamma_{L,S}$. CPT invariance requires the diagonal elements of Λ to be equal. The CPT-violation complex parameter δ is defined as

$$\delta = \frac{\Lambda_{\overline{K}^0\overline{K}^0} - \Lambda_{K^0K^0}}{2(\lambda_L - \lambda_S)} = \delta_\parallel \exp\left(i\phi_{SW}\right) + \delta_\perp \exp\left(i(\phi_{SW} + \frac{\pi}{2})\right) \tag{2}$$

where we have introduced the projections $\delta_\parallel$ and $\delta_\perp$ respectively parallel and perpendicular to the superweak direction $\phi_{SW} = \tan^{-1}(2\Delta m/\Delta\gamma)$, where $\Delta m = m_L - m_S$ and $\Delta\gamma = \gamma_S - \gamma_L$, the positive mass and width differences between K_L and K_S. These projections are linked to the mass and width difference between K^0 and $\overline{K}^0$:

$$\delta_\parallel = \frac{1}{4}\frac{\gamma_{K^0} - \gamma_{\overline{K}^0}}{\sqrt{\Delta m^2 + \left(\frac{\Delta\gamma}{2}\right)^2}} \ , \ \delta_\perp = \frac{1}{2}\frac{m_{K^0} - m_{\overline{K}^0}}{\sqrt{\Delta m^2 + \left(\frac{\Delta\gamma}{2}\right)^2}} \ . \tag{3}$$

$\mathrm{Re}(\delta)$ can be directly measured by studying the time evolution of the strangeness content of initially pure K^0 and $\overline{K}^0$ states, for example through the asymmetry

$$A_{CPT} = \frac{P[\overline{K}^0 \to \overline{K}^0(t)] - P[K^0 \to K^0(t)]}{P[\overline{K}^0 \to \overline{K}^0(t)] + P[K^0 \to K^0(t)]} = 4\mathrm{Re}(\delta) \tag{4}$$

where $P[a \to b(t)]$ is the probability that the pure initial state a is seen as state b at proper time t. This method has been used by tagging the initial strangeness with strong interactions and the final strangeness with the semileptonic decay (a more appropriate combination of semileptonic rates allows to be independent of any direct CPT violation in the decay itself) and yields today's best value of $\mathrm{Re}(\delta)$, compatible with zero with an error of $\sim 3\times 10^{-4}$.

As an alternative it has been proposed to compare the semileptonic charge asymmetries for K_L and K_S

$$\delta_{L,S} = \frac{R(K_{L,S} \to \pi^-\ell^+\nu) - R(K_{L,S} \to \pi^+\ell^-\overline{\nu})}{R(K_{L,S} \to \pi^-\ell^+\nu) + R(K_{L,S} \to \pi^+\ell^-\overline{\nu})} \ ,$$
$$\delta_S - \delta_L = 4\mathrm{Re}(\delta) \ . \tag{5}$$

δ_L has been accurately measured and δ_S should be measured in the near future with tagged K_S at ϕ factories. Note however that Eq. (5) assumes CPT invariance in the $\Delta S = -\Delta Q$ semileptonic decay amplitude.

$\delta_\perp$ can be obtained from the measurement of the $\pi\pi$ decays CP-violation parameters η_{+-} and η_{00}. Figure 1 shows the various contributions to $\eta_{\pi\pi}$ [1]. The T-violation parameter ϵ_T

$$\epsilon_T = i\frac{|\Lambda_{K^0\overline{K}^0}|^2 - |\Lambda_{\overline{K}^0K^0}|^2}{\Delta\gamma(\lambda_L - \lambda_S)} \tag{6}$$

has been defined in such a way that it is exactly aligned along the superweak direction [‡]. A_I (resp. B_I) is the CPT-conserving (resp. violating) decay amplitude for the $\pi\pi$ Isospin I state, ε' is the direct CP/CPT-violation parameter $[\varepsilon' = 1/3(\eta_{+-} - \eta_{00})]$ and $\delta\phi = \frac{1}{2}\left[\varphi_\Gamma - \arg(A_0^*\overline{A}_0)\right]$ is the phase difference between

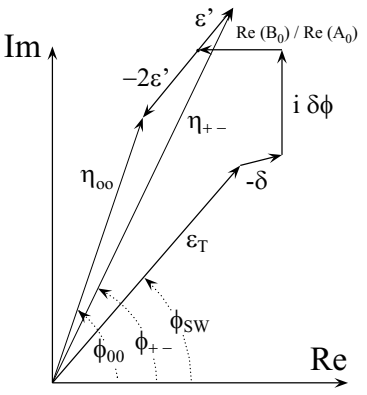

Figure 1: *CP*- and *CPT*-violation parameters in 2π decay.

the $I = 0$ component of the decay amplitude and the matrix element $\Gamma_{K^0\overline{K}^0}$. From Fig. 1 one obtains

$$\delta_\perp = |\eta_{+-}|(\phi_{SW} - \frac{2}{3}\phi_{+-} - \frac{1}{3}\phi_{00}) - \frac{\mathrm{Re}(B_0)}{\mathrm{Re}(A_0)}\sin(\phi_{SW}) + \delta\phi \quad \cos(\phi_{SW}) \ . \qquad (7)$$

The present accuracy on the term $|\eta_{+-}|(\phi_{SW} - \frac{2}{3}\phi_{+-} - \frac{1}{3}\phi_{00})$ is 2.6×10^{-5}. $\delta\phi$ gets contributions from *CP* violation in semileptonic and 3π decays [2,3] and can only be neglected at the present time if one assumes that η_{000} is not significantly larger than η_{+-0}. Furthermore, B_0 is not directly measured, so additional assumptions (for example, *CPT* conservation in the decay which implies $B_0 = 0$) or a combination with other measurements are necessary to obtain $\delta_\perp$.

If one assumes unitarity, one can measure $\mathrm{Im}(\delta)$ using the Bell-Steinberger relation which relates K_S and K_L decay amplitudes into all final states f:

$$\mathrm{Re}(\epsilon_T) - i\mathrm{Im}(\delta) = \frac{1}{2(i\Delta m + \frac{1}{2}(\gamma_L + \gamma_S))} \times \sum A_{f_L} A^*_{f_S} \ . \qquad (8)$$

Since the $\pi\pi$ amplitudes dominate, the result relies also strongly on the $\phi_{\pi\pi}$ phase measurements. The advantage is that B_0 does not enter. Using all available data, one obtains a value of $\mathrm{Im}(\delta)$ compatible with zero with a precision of 5×10^{-5}. The precision here is also limited by the poor measurement of η_{000}.

The results on $\mathrm{Re}(\delta)$ and $\mathrm{Im}(\delta)$ can be combined to obtain $\delta_\parallel$ and $\delta_\perp$ and therefore the K^0–$\overline{K}^0$ mass and width difference shown in Fig. 2. The current accuracy is a few 10^{-18} GeV for both.

If one assumes that *CPT* is conserved in the decays ($\gamma_{K^0} = \gamma_{\overline{K}^0}$, $\delta_\parallel = 0$, $B_I = 0$), the phase of δ is known, and the $\delta_\perp$ and Bell-Steinberger methods are identical. Assuming in addition

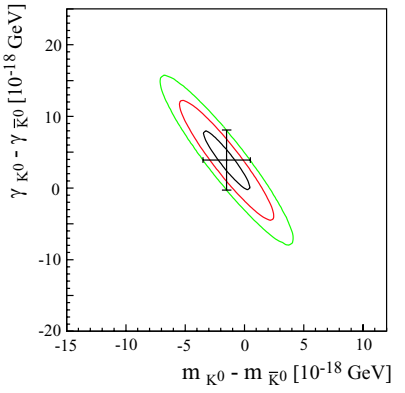

Figure 2: K^0–$\overline{K}^0$ mass vs width difference.

$\eta_{+-0} = \eta_{000}$, one in this case obtains a limit for $|m_{K^0} - m_{\overline{K}^0}|$ of 4.4×10^{-19} GeV (90%CL).

Footnotes and References

[‡] Many authors have a different definition of the T-violation parameter, $\epsilon = (\Lambda_{\overline{K}^0 K^0} - \Lambda_{K^0\overline{K}^0})/(2(\lambda_L - \lambda_S))$. ϵ is not exactly aligned with the superweak direction. The two definitions can be related through $\epsilon = \epsilon_T + i\delta\phi$.

1. See for instance, C.D. Buchanan *et al.*, Phys. Rev. **D45**, 4088 (1992). See also the Second Daphne Handbook, Ed. L.Maiani *et al.*, INFN Frascati (1995).
2. V.V. Barmin *et al.*, Nucl. Phys. **B247**, 293 (1984).
3. L. Lavoura, Mod. Phys. Lett. **A7**, 1367 (1992).

CPT-VIOLATION PARAMETERS

In K^0-$\overline{K}^0$ mixing, if *CP*-violating interactions include a *T* conserving part then

$$|K_S\rangle = [|K_1\rangle + (\epsilon + \delta)|K_2\rangle]/\sqrt{1 + |\epsilon + \delta|^2}$$
$$|K_L\rangle = [|K_2\rangle + (\epsilon - \delta)|K_1\rangle]/\sqrt{1 + |\epsilon - \delta|^2}$$

where

$$|K_1\rangle = [|K^0\rangle + |\overline{K}^0\rangle]/\sqrt{2}$$
$$|K_2\rangle = [|K^0\rangle - |\overline{K}^0\rangle]/\sqrt{2}$$

and

$$|\overline{K}^0\rangle = CP|K^0\rangle.$$

The parameter δ specifies the *CPT*-violating part.

Estimates of δ are given below assuming the validity of the $\Delta S = \Delta Q$ rule. See also THOMSON 95 for a test of *CPT*-symmetry conservation in K^0 decays using the Bell-Steinberger relation.

REAL PART OF δ

A nonzero value violates *CPT* invariance.

VALUE (units 10^{-4})	EVTS	DOCUMENT ID		TECN	COMMENT
2.9 ± 2.6 ± 0.6	1.3M	[2] ANGELOPO...	98F	CPLR	
• • • We do not use the following data for averages, fits, limits, etc. • • •					
2.4 ± 2.8		[3] APOSTOLA...	99B	RVUE	
180 ± 200	6481	[4] DEMIDOV	95		$K_{\ell 3}$ reanalysis

[2] If $\Delta S = \Delta Q$ is not assumed, ANGELOPOULOS 98F finds $\mathrm{Re}\delta = (3.0 \pm 3.3 \pm 0.6) \times 10^{-4}$.
[3] APOSTOLAKIS 99B assumes only unitarity and combines CPLEAR and other results.
[4] DEMIDOV 95 reanalyzes data from HART 73 and NIEBERGALL 74.

IMAGINARY PART OF δ

A nonzero value violates *CPT* invariance.

VALUE (units 10^{-3})	EVTS	DOCUMENT ID		TECN	COMMENT
0.024 ± 0.050		[5] APOSTOLA...	99B	RVUE	
• • • We do not use the following data for averages, fits, limits, etc. • • •					
− 0.9 ± 2.9 ± 1.0	1.3M	[6] ANGELOPO...	98F	CPLR	
21 ± 37	6481	[7] DEMIDOV	95		$K_{\ell 3}$ reanalysis

[5] APOSTOLAKIS 99B assumes only unitarity and combines CPLEAR and other results.
[6] If $\Delta S = \Delta Q$ is not assumed, ANGELOPOULOS 98F finds $\mathrm{Im}\delta = (-15 \pm 23 \pm 3) \times 10^{-3}$.
[7] DEMIDOV 95 reanalyzes data from HART 73 and NIEBERGALL 74.

$|m_{K^0} - m_{\overline{K}^0}| / m_{\text{average}}$

A test of CPT invariance. "Our Evaluation" is described in the "Tests of Conservation Laws" section. It assumes CPT invariance in the decay and neglects some contributions from decay channels other than $\pi\pi$.

VALUE	CL%	DOCUMENT ID	TECN
$< 10^{-18}$ (CL = 90%) OUR EVALUATION			
• • • We do not use the following data for averages, fits, limits, etc. • • •			
$(-3 \pm 4) \times 10^{-18}$		[8] ANGELOPO... 99B	RVUE

[8] ANGELOPOULOS 99B assumes only unitarity and combines CPLEAR and other results.

$(\Gamma_{K^0} - \Gamma_{\overline{K}^0})/m_{\text{average}}$

A test of CPT invariance.

VALUE	DOCUMENT ID	TECN
$(7.8 \pm 8.4) \times 10^{-18}$	[9] ANGELOPO... 99B	RVUE

[9] ANGELOPOULOS 99B assumes only unitarity and combines CPLEAR with other results. Correlated with $(m_{K^0} - m_{\overline{K}^0}) / m_{\text{average}}$ with a correlation coefficient of -0.95.

K^0 REFERENCES

LAI	03C	EPJ C30 33	A. Lai *et al.*	(CERN NA48 Collab.)
LAI	02	PL B533 196	A. Lai *et al.*	(CERN NA48 Collab.)
ANGELOPO...	01B	EPJ C22 55	A. Angelopoulos *et al.*	(CPLEAR Collab.)
ANGELOPO...	99B	PL B471 332	A. Angelopoulos *et al.*	(CPLEAR Collab.)
APOSTOLA...	99B	PL B456 297	A. Apostolakis *et al.*	(CPLEAR Collab.)
ANGELOPO...	98E	PL B444 43	A. Angelopoulos *et al.*	(CPLEAR Collab.)
ANGELOPO...	98F	PL B444 52	A. Angelopoulos *et al.*	(CPLEAR Collab.)
Also	01B	EPJ C22 55	A. Angelopoulos *et al.*	(CPLEAR Collab.)
DEMIDOV	95	PAN 58 968 From YAF 58 1041.	V. Demidov, K. Gusev, E. Shabalin	(ITEP)
THOMSON	95	PR D51 1412	G.B. Thomson, Y. Zou	(RUTG)
BARKOV	87B	SJNP 46 630 Translated from YAF 46 1088.	L.M. Barkov *et al.*	(NOVO)
BARKOV	85B	JETPL 42 138 Translated from ZETFP 42 113.	L.M. Barkov *et al.*	(NOVO)
BLATNIK	79	LNC 24 39	S. Blatnik, J. Stahov, C.B. Lang	(TUZL, GRAZ)
MOLZON	78	PRL 41 1213	W.R. Molzon *et al.*	(EFI+)
NIEBERGALL	74	PL 49B 103	F. Niebergall *et al.*	(CERN, ORSAY, VIEN)
HART	73	NP B66 317	J.C. Hart *et al.*	(CAVE, RHEL)
FOETH	69B	PL 30B 276	H. Foeth *et al.*	(AACH, CERN, TORI)
HILL	68B	PR 168 1534	D.G. Hill *et al.*	(BNL, CMU)
FITCH	67	PR 164 1711	V.L. Fitch *et al.*	(PRIN)
BALTAY	66	PR 142 932	C. Baltay *et al.*	(YALE, BNL)
BURNSTEIN	65	PR 138B 895	R.A. Burnstein, H.A. Rubin	(UMD)
KIM	65B	PR 140B 1334	J.K. Kim, L. Kirsch, D. Miller	(COLU)
CHRISTENS...	64	PRL 13 138	J.H. Christenson *et al.*	(PRIN)
CRAWFORD	59	PRL 2 112	F.S. Crawford *et al.*	(LRL)
ROSENFELD	59	PRL 2 110	A.H. Rosenfeld, F.T. Solmitz, R.D. Tripp	(LRL)

K^0_S

$I(J^P) = \frac{1}{2}(0^-)$

K^0_S MEAN LIFE

For earlier measurements, beginning with BOLDT 58B, see our 1986 edition, Physics Letters **170B** 130 (1986).

OUR FIT is described in the note on "CP violation in K_L decays" in the K^0_L Particle Listings. The result labeled "OUR FIT Assuming CPT" ["OUR FIT Not assuming CPT"] includes all measurements except those with the comment "Not assuming CPT" ["Assuming CPT"]. Measurements with neither comment do not assume CPT and enter both fits.

VALUE (10^{-10} s)	EVTS	DOCUMENT ID	TECN	COMMENT
0.8953 ±0.0006	**OUR FIT**	Error includes scale factor of 1.4. Assuming CPT		
0.8958 ±0.0006	**OUR FIT**	Error includes scale factor of 1.2. Not assuming CPT		
0.8965 ±0.0007		[1,2] ALAVI-HARATI 03	KTEV	Assuming CPT
0.8958 ±0.0013		[2,3] ALAVI-HARATI 03	KTEV	Not assuming CPT
0.89598 ±0.00048 ±0.00051	16M	LAI 02C	NA48	
0.8971 ±0.0021		BERTANZA 97	NA31	
0.8941 ±0.0014 ±0.0009		SCHWINGEN... 95	E773	Assuming CPT
0.8929 ±0.0016		GIBBONS 93	E731	Assuming CPT
• • • We do not use the following data for averages, fits, limits, etc. • • •				
0.8920 ±0.0044	214k	GROSSMAN 87	SPEC	
0.905 ±0.007		[4] ARONSON 82B	SPEC	
0.881 ±0.009	26k	ARONSON 76	SPEC	
0.8926 ±0.0032 ±0.0002		[5] CARITHERS 75	SPEC	
0.8937 ±0.0048	6M	GEWENIGER 74B	ASPK	
0.8958 ±0.0045	50k	[6] SKJEGGEST... 72	HBC	
0.856 ±0.008	19994	[7] DONALD 68B	HBC	
0.872 ±0.009	20000	[7,8] HILL 68	DBC	

[1] This ALAVI-HARATI 03 fit has Δm and τ_S free but constrains ϕ_{+-} to the Superweak value, i.e. assumes CPT. This τ_S value is correlated with their $\Delta m = m_{K^0_L} - m_{K^0_S}$ measurement in the K^0_L listings. The correlation coefficient $\rho(\tau_S, \Delta m) = -0.396$.
[2] The two ALAVI-HARATI 03 values use the same data. The first enters the "assuming CPT" fit and the second enters the "not assuming CPT" fit.
[3] This ALAVI-HARATI 03 fit has Δm, ϕ_{+-}, and τ_{K_S} free. See ϕ_{+-} in the "K_L CP violation" section for correlation information.
[4] ARONSON 82 find that K^0_S mean life may depend on the kaon energy.
[5] CARITHERS 75 measures the Δm dependence of the total decay rate (inverse mean life) to be $\Gamma(K^0_S) = [(1.122 \pm 0.004) + 0.16(\Delta m - 0.5348)/\Delta m]\, 10^{10}$/s, or, in terms of mean life, CARITHERS 75 measures $\tau_S = (0.8913 \pm 0.0032) - 0.238\,[\Delta m - 0.5348]$ (10^{-10} s). We have adjusted the measurement to use our best values of ($\Delta m = 0.5292 \pm 0.0010$) ($10^{10}$ $\hbar$ s^{-1}). Our first error is their experiment's error and our second error is the systematic error from using our best values.
[6] HILL 68 has been changed by the authors from the published value (0.865 ± 0.009) because of a correction in the shift due to η_{+-}. SKJEGGESTAD 72 and HILL 68 give detailed discussions of systematics encountered in this type of experiment.
[7] Pre-1971 experiments are excluded from the average because of disagreement with later more precise experiments.
[8] HILL 68 has been changed by the authors from the published value (0.865 ± 0.009) because of a correction in the shift due to η_{+-}. SKJEGGESTAD 72 and HILL 68 give detailed discussions of systematics encountered in this type of experiment.

K^0_S DECAY MODES

	Mode	Fraction (Γ_i/Γ)	Scale factor/ Confidence level
	Hadronic modes		
Γ_1	$\pi^0\pi^0$	(31.05 ± 0.14) %	S=1.1
Γ_2	$\pi^+\pi^-$	(68.95 ± 0.14) %	S=1.1
Γ_3	$\pi^+\pi^-\pi^0$	$(3.2\ ^{+1.2}_{-1.0}) \times 10^{-7}$	
	Modes with photons or $\ell\overline{\ell}$ pairs		
Γ_4	$\pi^+\pi^-\gamma$	[a,b] $(1.79 \pm 0.05) \times 10^{-3}$	
Γ_5	$\pi^+\pi^- e^+ e^-$	$(4.69 \pm 0.30) \times 10^{-5}$	
Γ_6	$\pi^0\gamma\gamma$	[b] $(4.9 \pm 1.8) \times 10^{-8}$	
Γ_7	$\gamma\gamma$	$(2.80 \pm 0.07) \times 10^{-6}$	
	Semileptonic modes		
Γ_8	$\pi^\pm e^\mp \nu_e$	[c] $(6.9 \pm 0.4) \times 10^{-4}$	
Γ_9	$\pi^\pm \mu^\mp \nu_\mu$	[c]	
	***CP* violating (*CP*) and $\Delta S = 1$ weak neutral current (*S1*) modes**		
Γ_{10}	$3\pi^0$	*CP* $< 1.4 \times 10^{-5}$	CL=90%
Γ_{11}	$\mu^+\mu^-$	*S1* $< 3.2 \times 10^{-7}$	CL=90%
Γ_{12}	e^+e^-	*S1* $< 1.4 \times 10^{-7}$	CL=90%
Γ_{13}	$\pi^0 e^+ e^-$	*S1* [b] $(3.0\ ^{+1.5}_{-1.2}) \times 10^{-9}$	

[a] Most of this radiative mode, the low-momentum γ part, is also included in the parent mode listed without γ's.
[b] See the Particle Listings below for the energy limits used in this measurement.
[c] The value is for the sum of the charge states or particle/antiparticle states indicated.

CONSTRAINED FIT INFORMATION

An overall fit to 3 branching ratios uses 14 measurements and one constraint to determine 2 parameters. The overall fit has a $\chi^2 = 18.8$ for 13 degrees of freedom.

The following *off-diagonal* array elements are the correlation coefficients $\langle \delta x_i \delta x_j \rangle / (\delta x_i \cdot \delta x_j)$, in percent, from the fit to the branching fractions, $x_i \equiv \Gamma_i/\Gamma_{\text{total}}$. The fit constrains the x_i whose labels appear in this array to sum to one.

x_2	-100
	x_1

K^0_S DECAY RATES

$\Gamma(\pi^\pm e^\mp \nu_e)$ Γ_8

VALUE (10^6 s^{-1})	EVTS	DOCUMENT ID	TECN	COMMENT
• • • We do not use the following data for averages, fits, limits, etc. • • •				
8.1 ±1.6	75	[9] AKHMETSHIN 99	CMD2	Tagged K^0_S using $\phi \to K^0_L K^0_S$
7.50 ±0.08		[10] PDG 98		
seen		BURGUN 72	HBC	$K^+ p \to K^0 p \pi^+$
9.3 ±2.5		AUBERT 65	HLBC	$\Delta S = \Delta Q$, CP cons. not assumed

[9] AKHMETSHIN 99 is from a measured branching ratio $B(K^0_S \to \pi e \nu_e) = (7.2 \pm 1.4) \times 10^{-4}$ and $\tau_{K^0_S} = (0.8934 \pm 0.0008) \times 10^{-10}$ s. Not independent of measured branching ratio.

[10] PDG 98 from K^0_L measurements, assuming that $\Delta S = \Delta Q$ in K^0 decay so that $\Gamma(K^0_S \to \pi^\pm e^\mp \nu_e) = \Gamma(K^0_L \to \pi^\pm e^\mp \nu_e)$.

$\Gamma(\pi^\pm \mu^\mp \nu_\mu)$ Γ_9

VALUE (10^6 s^{-1})	DOCUMENT ID	
• • • We do not use the following data for averages, fits, limits, etc. • • •		
5.25 ± 0.07	[11] PDG	98

[11] PDG 98 from K^0_L measurements, assuming that $\Delta S = \Delta Q$ in K^0 decay so that $\Gamma(K^0_S \to \pi^\pm \mu^\mp \nu_\mu) = \Gamma(K^0_L \to \pi^\pm \mu^\mp \nu_\mu)$.

K^0_S BRANCHING RATIOS

Hadronic modes

$\Gamma(\pi^0\pi^0)/\Gamma_{total}$ Γ_1/Γ

VALUE	EVTS	DOCUMENT ID		TECN
0.3105 ± 0.0014 OUR FIT Error includes scale factor of 1.1.				
0.318 ± 0.015 OUR AVERAGE Error includes scale factor of 1.4. See the ideogram below.				
0.335 ± 0.014	1066	BROWN	63	HLBC
0.288 ± 0.021	198	CHRETIEN	63	HLBC
0.30 ± 0.035		BROWN	61	HLBC

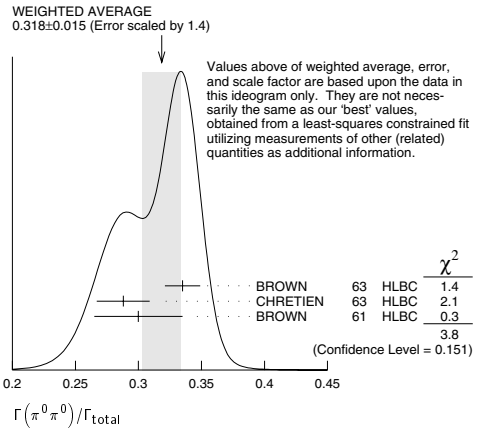

$\Gamma(\pi^+\pi^-)/\Gamma_{total}$ Γ_2/Γ

VALUE	EVTS	DOCUMENT ID		TECN	COMMENT
0.6895 ± 0.0014 OUR FIT Error includes scale factor of 1.1.					
0.670 ± 0.010	3447	DOYLE	69	HBC	$\pi^- p \to \Lambda K^0$

$\Gamma(\pi^+\pi^-)/\Gamma(\pi^0\pi^0)$ Γ_2/Γ_1

VALUE	EVTS	DOCUMENT ID		TECN	COMMENT
2.221 ± 0.014 OUR FIT Error includes scale factor of 1.1.					
2.225 ± 0.014 OUR AVERAGE Error includes scale factor of 1.1.					
2.236 ± 0.003 ± 0.015	766k	ALOISIO	02B	KLOE	Incl. Rad. Decays $(\pi^+\pi^-\gamma)$
2.11 ± 0.09	1315	EVERHART	76	WIRE	$\pi^- p \to \Lambda K^0$
2.169 ± 0.094	16k	COWELL	74	OSPK	$\pi^- p \to \Lambda K^0$
2.16 ± 0.08	4799	HILL	73	DBC	$K^+ d \to K^0 pp$
2.22 ± 0.10	3068	[12] ALITTI	72	HBC	$K^+ p \to \pi^+ p K^0$
2.22 ± 0.08	6380	MORSE	72B	DBC	$K^+ n \to K^0 p$
2.10 ± 0.11	701	[13] NAGY	72	HLBC	$K^+ n \to K^0 p$
2.22 ± 0.095	6150	[14] BALTAY	71	HBC	$K p \to K^0$ neutrals
2.282 ± 0.043	7944	[15] MOFFETT	70	OSPK	$K^+ n \to K^0 p$
2.10 ± 0.06	3700	MORFIN	69	HLBC	$K^+ n \to K^0 p$
• • • We do not use the following data for averages, fits, limits, etc. • • •					
2.12 ± 0.17	267	[13] BOZOKI	69	HLBC	
2.285 ± 0.055	3016	[15] GOBBI	69	OSPK	$K^+ n \to K^0 p$

[12] The directly measured quantity is $K^0_S \to \pi^+\pi^-/\text{all } K^0 = 0.345 \pm 0.005$.

[13] NAGY 72 is a final result which includes BOZOKI 69.

[14] The directly measured quantity is $K^0_S \to \pi^+\pi^-/\text{all } \overline{K^0} = 0.345 \pm 0.005$.

[15] MOFFETT 70 is a final result which includes GOBBI 69.

$\Gamma(\pi^+\pi^-\pi^0)/\Gamma_{total}$ Γ_3/Γ

VALUE (units 10^{-7})	EVTS	DOCUMENT ID		TECN	COMMENT
$3.2^{+1.2}_{-1.0}$ OUR AVERAGE					
$2.5^{+1.3}_{-1.0}\pm 0.5 \pm 0.6$	500k	[16] ADLER	97B	CPLR	
$4.8^{+2.2}_{-1.6}\pm 1.1$		[17] ZOU	96	E621	
• • • We do not use the following data for averages, fits, limits, etc. • • •					
$4.1^{+2.5}_{-1.9}+0.5-0.6$		[18] ADLER	96E	CPLR	Sup. by ADLER 97B
$3.9^{+5.4}_{-1.8}+0.9-0.7$		[19] THOMSON	94	E621	Sup. by ZOU 96

[16] ADLER 97B find the *CP*-conserving parameters $\text{Re}(\lambda) = (28 \pm 7 \pm 3) \times 10^{-3}$, $\text{Im}(\lambda) = (-10 \pm 8 \pm 2) \times 10^{-3}$. They estimate $B(K^0_S \to \pi^+\pi^-\pi^0)$ from $\text{Re}(\lambda)$ and the K^0_L decay parameters. See also ANGELOPOULOS 98C.

[17] ZOU 96 is from the measured quantities $|\rho_{+-0}| = 0.039^{+0.009}_{-0.006} \pm 0.005$ and $\phi_\rho = (-9 \pm 18)^\circ$.

[18] ADLER 96E is from the measured quantities $\text{Re}(\lambda) = 0.036 \pm 0.010^{+0.002}_{-0.003}$ and $\text{Im}(\lambda)$ consistent with zero. Note that the quantity λ is the same as ρ_{+-0} used in other footnotes.

[19] THOMSON 94 calculates this branching ratio from their measurements $|\rho_{+-0}| = 0.035^{+0.019}_{-0.011} \pm 0.004$ and $\phi_\rho = (-59 \pm 48)^\circ$ where $|\rho_{+-0}| e^{i\phi_\rho} = A(K^0_S \to \pi^+\pi^-\pi^0, I = 2)/A(K^0_L \to \pi^+\pi^-\pi^0)$.

Modes with photons or $\ell\bar{\ell}$ pairs

$\Gamma(\pi^+\pi^-\gamma)/\Gamma(\pi^+\pi^-)$ Γ_4/Γ_2

VALUE (units 10^{-3})	EVTS	DOCUMENT ID		TECN	COMMENT
2.60 ± 0.08 OUR AVERAGE					
2.56 ± 0.09	1286	RAMBERG	93	E731	p_γ >50 MeV/c
2.68 ± 0.15		[20] TAUREG	76	SPEC	p_γ >50 MeV/c
2.8 ± 0.6		[21] BURGUN	73	HBC	p_γ >50 MeV/c
• • • We do not use the following data for averages, fits, limits, etc. • • •					
7.10 ± 0.22	3723	RAMBERG	93	E731	p_γ >20 MeV/c
3.0 ± 0.6	29	[22] BOBISUT	74	HLBC	p_γ >40 MeV/c

[20] TAUREG 76 find direct emission contribution < 0.06, CL = 90%.

[21] BURGUN 73 estimates that direct emission contribution is 0.3 ± 0.6.

[22] BOBISUT 74 not included in average because p_γ cut differs. Estimates direct emission contribution to be 0.5 or less, CL = 95%.

$\Gamma(\pi^+\pi^- e^+ e^-)/\Gamma_{total}$ Γ_5/Γ

VALUE (units 10^{-5})	EVTS	DOCUMENT ID		TECN	COMMENT
4.69 ± 0.30	676	[23] LAI	03C	NA48	1998+1999 data
• • • We do not use the following data for averages, fits, limits, etc. • • •					
4.71 ± 0.23 ± 0.22	620	[23,24] LAI	03C	NA48	1999 data
4.5 ± 0.7 ± 0.4	56	LAI	00B	NA48	1998 data

[23] Uses normalization $BR(K_L \to \pi^+\pi^-\pi^0) * BR(\pi^0 \to e^+ e^-) = (1.505 \pm 0.047) \times 10^{-3}$ from our 2000 Edition.

[24] Second error is 0.16(syst) ± 0.15(norm) combined in quadrature.

$\Gamma(\pi^0\gamma\gamma)/\Gamma_{total}$ Γ_6/Γ

VALUE (units 10^{-8})	CL%	EVTS	DOCUMENT ID		TECN	COMMENT
4.9 ± 1.6 ± 0.9		17	[25] LAI	04	NA48	$m^2_{\gamma\gamma}/m^2_K > 0.2$
• • • We do not use the following data for averages, fits, limits, etc. • • •						
<33	90		LAI	03B	NA48	$m^2_{\gamma\gamma}/m^2_K > 0.2$

[25] Spectrum also measured and found consistent with the one generated by a constant matrix element.

$\Gamma(\gamma\gamma)/\Gamma_{total}$ Γ_7/Γ

VALUE (units 10^{-6})	CL%	EVTS	DOCUMENT ID		TECN
2.80 ± 0.07 OUR AVERAGE					
2.81 ± 0.07 ± 0.01		7.5k	[26] LAI	03	NA48
2.58 ± 0.36 ± 0.22		149	LAI	00	NA48
2.4 ± 0.9		35	[27] BARR	95B	NA31
• • • We do not use the following data for averages, fits, limits, etc. • • •					
2.2 ± 1.1		16	[28] BARR	95B	NA31
< 13	90		BALATS	89	SPEC
2.4 ± 1.2		19	BURKHARDT	87	NA31
<133	90		BARMIN	86B	XEBC

[26] LAI 03 reports 2.78 ± 0.06 ± 0.04 for $B(K^0_S \to \pi^0\pi^0) = (31.39 \pm 0.28) \times 10^{-2}$. We rescale to our best value $B(K^0_S \to \pi^0\pi^0) = (31.05 \pm 0.14) \times 10^{-2}$. Our first error is their experiment's error and our second error is the systematic error from using our best value.

[27] BARR 95B quotes this as the combined BARR 95B + BURKHARDT 87 result after rescaling BURKHARDT 87 to use same branching ratios and lifetimes as BARR 95B.

[28] BARR 95B result is calculated using $B(K_L \to \gamma\gamma) = (5.86 \pm 0.17) \times 10^{-4}$.

Semileptonic modes

$\Gamma(\pi^\pm e^\mp \nu_e)/\Gamma_{total}$ Γ_8/Γ

VALUE (units 10^{-4})	EVTS	DOCUMENT ID		TECN	COMMENT
6.9 ±0.4 OUR AVERAGE					
6.91±0.34±0.15	624	[29] ALOISIO	02	KLOE	Tagged K^0_S using $\phi \to K^0_L K^0_S$
7.2 ±1.4	75	AKHMETSHIN	99	CMD2	Tagged K^0_S using $\phi \to K^0_L K^0_S$

[29] Uses the PDG 00 value for $B(K^0_S \to \pi^+\pi^-)$.

CP violating (CP) and $\Delta S = 1$ weak neutral current ($S1$) modes

$\Gamma(3\pi^0)/\Gamma_{total}$ Γ_{10}/Γ

Violates CP conservation.

VALUE (units 10^{-5})	CL%	EVTS	DOCUMENT ID		TECN
<1.4	90	7M	ACHASOV	99D	SND
• • • We do not use the following data for averages, fits, limits, etc. • • •					
<1.9	90	17300	[30] ANGELOPO...	98B	CPLR
<3.7	90		BARMIN	83	HLBC

[30] ANGELOPOULOS 98B is from $\mathrm{Im}(\eta_{000}) = -0.05 \pm 0.12 \pm 0.05$, assuming $\mathrm{Re}(\eta_{000}) = \mathrm{Re}(\epsilon) = 1.635 \times 10^{-3}$ and using the value $B(K^0_L \to \pi^0\pi^0\pi^0) = 0.2112 \pm 0.0027$.

$\Gamma(\mu^+\mu^-)/\Gamma_{total}$ Γ_{11}/Γ

Test for $\Delta S = 1$ weak neutral current. Allowed by first-order weak interaction combined with electromagnetic interaction.

VALUE (units 10^{-5})	CL%	DOCUMENT ID		TECN
<0.032	90	GJESDAL	73	ASPK
• • • We do not use the following data for averages, fits, limits, etc. • • •				
<0.7	90	HYAMS	69B	OSPK

$\Gamma(e^+e^-)/\Gamma_{total}$ Γ_{12}/Γ

Test for $\Delta S = 1$ weak neutral current. Allowed by first-order weak interaction combined with electromagnetic interaction.

VALUE (units 10^{-7})	CL%	EVTS	DOCUMENT ID		TECN	COMMENT
< 1.4	90		ANGELOPO...	97	CPLR	
• • • We do not use the following data for averages, fits, limits, etc. • • •						
< 28	90	0	BLICK	94	CNTR	Hyperon facility
<100	90		BARMIN	86	XEBC	

$\Gamma(\pi^0 e^+ e^-)/\Gamma_{total}$ Γ_{13}/Γ

Test for $\Delta S = 1$ weak neutral current. Allowed by first-order weak interaction combined with electromagnetic interaction.

VALUE (units 10^{-9})	CL%	EVTS	DOCUMENT ID		TECN	COMMENT
$3.0^{+1.5}_{-1.2} \pm 0.2$		7	[31] BATLEY	03	NA48	$m_{ee} > 0.165$ GeV
• • • We do not use the following data for averages, fits, limits, etc. • • •						
< 140	90		LAI	01	NA48	
< 1100	90	0	BARR	93B	NA31	
<45000	90		GIBBONS	88	E731	

[31] BATLEY 03 extrapolate also to the full kinematical region using a constant form factor and a vector matrix element. The resulting branching ratio is $(5.8^{+2.9}_{-2.4}) \times 10^{-9}$.

CP VIOLATION IN $K_S \to 3\pi$

Written 1996 by T. Nakada (Paul Scherrer Institute) and L. Wolfenstein (Carnegie-Mellon University).

The possible final states for the decay $K^0 \to \pi^+\pi^-\pi^0$ have isospin $I = 0$, 1, 2, and 3. The $I = 0$ and $I = 2$ states have $CP = +1$ and K_S can decay into them without violating CP symmetry, but they are expected to be strongly suppressed by centrifugal barrier effects. The $I = 1$ and $I = 3$ states, which have no centrifugal barrier, have $CP = -1$ so that the K_S decay to these requires CP violation.

In order to see CP violation in $K_S \to \pi^+\pi^-\pi^0$, it is necessary to observe the interference between K_S and K_L decay, which determines the amplitude ratio

$$\eta_{+-0} = \frac{A(K_S \to \pi^+\pi^-\pi^0)}{A(K_L \to \pi^+\pi^-\pi^0)} \ . \qquad (1)$$

If η_{+-0} is obtained from an integration over the whole Dalitz plot, there is no contribution from the $I = 0$ and $I = 2$ final states and a nonzero value of η_{+-0} is entirely due to CP violation.

Only $I = 1$ and $I = 3$ states, which are $CP = -1$, are allowed for $K^0 \to \pi^0\pi^0\pi^0$ decays and the decay of K_S into $3\pi^0$ is an unambiguous sign of CP violation. Similarly to η_{+-0}, η_{000} is defined as

$$\eta_{000} = \frac{A(K_S \to \pi^0\pi^0\pi^0)}{A(K_L \to \pi^0\pi^0\pi^0)} \ . \qquad (2)$$

If one assumes that CPT invariance holds and that there are no transitions to $I = 3$ (or to nonsymmetric $I = 1$ states), it can be shown that

$$\eta_{+-0} = \eta_{000} = \epsilon + i\frac{\mathrm{Im}\ a_1}{\mathrm{Re}\ a_1} \ . \qquad (3)$$

With the Wu-Yang phase convention, a_1 is the weak decay amplitude for K^0 into $I = 1$ final states; ϵ is determined from CP violation in $K_L \to 2\pi$ decays. The real parts of η_{+-0} and η_{000} are equal to $\mathrm{Re}(\epsilon)$. Since currently-known upper limits on $|\eta_{+-0}|$ and $|\eta_{000}|$ are much larger than $|\epsilon|$, they can be interpreted as upper limits on $\mathrm{Im}(\eta_{+-0})$ and $\mathrm{Im}(\eta_{000})$ and so as limits on the CP-violating phase of the decay amplitude a_1.

CP-VIOLATION PARAMETERS IN K^0_S DECAY

$\mathrm{Im}(\eta_{+-0})^2 = \Gamma(K^0_S \to \pi^+\pi^-\pi^0, CP\text{-violating}) / \Gamma(K^0_L \to \pi^+\pi^-\pi^0)$

CPT assumed valid (i.e. $\mathrm{Re}(\eta_{+-0}) \simeq 0$).

VALUE	CL%	EVTS	DOCUMENT ID		TECN
• • • We do not use the following data for averages, fits, limits, etc. • • •					
<0.23	90	601	[32] BARMIN	85	HLBC
<0.12	90	384	METCALF	72	ASPK

[32] BARMIN 85 find $\mathrm{Re}(\eta_{+-0}) = (0.05 \pm 0.17)$ and $\mathrm{Im}(\eta_{+-0}) = (0.15 \pm 0.33)$. Includes events of BALDO-CEOLIN 75.

$\mathrm{Im}(\eta_{+-0}) = \mathrm{Im}(A(K^0_S \to \pi^+\pi^-\pi^0, CP\text{-violating}) / A(K^0_L \to \pi^+\pi^-\pi^0))$

VALUE	EVTS	DOCUMENT ID		TECN	COMMENT
$-0.002 \pm 0.009^{+0.002}_{-0.001}$	500k	[33] ADLER	97B	CPLR	
• • • We do not use the following data for averages, fits, limits, etc. • • •					
$-0.002 \pm 0.018 \pm 0.003$	137k	[34] ADLER	96D	CPLR	Sup. by ADLER 97B
$-0.015 \pm 0.017 \pm 0.025$	272k	[35] ZOU	94	SPEC	

[33] ADLER 97B also find $\mathrm{Re}(\eta_{+-0}) = -0.002 \pm 0.007^{+0.004}_{-0.001}$. See also ANGELOPOULOS 98C.

[34] The ADLER 96D fit also yields $\mathrm{Re}(\eta_{+-0}) = 0.006 \pm 0.013 \pm 0.001$ with a correlation $+0.66$ between real and imaginary parts. Their results correspond to $|\eta_{+-0}| < 0.037$ with 90% CL.

[35] ZOU 94 use theoretical constraint $\mathrm{Re}(\eta_{+-0}) = \mathrm{Re}(\epsilon) = 0.0016$. Without this constraint they find $\mathrm{Im}(\eta_{+-0}) = 0.019 \pm 0.061$ and $\mathrm{Re}(\eta_{+-0}) = 0.019 \pm 0.027$.

$\mathrm{Im}(\eta_{000})^2 = \Gamma(K^0_S \to 3\pi^0) / \Gamma(K^0_L \to 3\pi^0)$

CPT assumed valid (i.e. $\mathrm{Re}(\eta_{000}) \simeq 0$). This limit determines branching ratio $\Gamma(3\pi^0)/\Gamma_{total}$ above.

VALUE	CL%	EVTS	DOCUMENT ID		TECN	COMMENT
• • • We do not use the following data for averages, fits, limits, etc. • • •						
<0.1	90	632	[36] BARMIN	83	HLBC	
<0.28	90		[37] GJESDAL	74B	SPEC	Indirect meas.

[36] BARMIN 83 find $\mathrm{Re}(\eta_{000}) = (-0.08 \pm 0.18)$ and $\mathrm{Im}(\eta_{000}) = (-0.05 \pm 0.27)$. Assuming CPT invariance they obtain the limit quoted above.

[37] GJESDAL 74B uses $K2\pi$, $K_{\mu 3}$, and K_{e3} decay results, unitarity, and CPT. Calculates $|(\eta_{000})| = 0.26 \pm 0.20$. We convert to upper limit.

$\mathrm{Im}(\eta_{000}) = \mathrm{Im}(A(K^0_S \to \pi^0\pi^0\pi^0)/A(K^0_L \to \pi^0\pi^0\pi^0))$

$K^0_S \to \pi^0\pi^0\pi^0$ violates CP conservation, in contrast to $K^0_S \to \pi^+\pi^-\pi^0$ which has a CP-conserving part.

VALUE	EVTS	DOCUMENT ID		TECN
$-0.05 \pm 0.12 \pm 0.05$	17300	[38] ANGELOPO...	98B	CPLR

[38] ANGELOPOULOS 98B assumes $\mathrm{Re}(\eta_{000}) = \mathrm{Re}(\epsilon) = 1.635 \times 10^{-3}$. Without assuming CPT invariance, they obtain $\mathrm{Re}(\eta_{000}) = 0.18 \pm 0.14 \pm 0.06$ and $\mathrm{Im}(\eta_{000}) = 0.15 \pm 0.20 \pm 0.03$.

Meson Particle Listings

K^0_S, K^0_L

DECAY-PLANE ASYMMETRY IN $\pi^+\pi^-e^+e^-$ DECAYS

This is the *CP*-violating asymmetry

$$A = \frac{N_{\sin\phi\cos\phi>0.0} - N_{\sin\phi\cos\phi<0.0}}{N_{\sin\phi\cos\phi>0.0} + N_{\sin\phi\cos\phi<0.0}}$$

where ϕ is the angle between the e^+e^- and $\pi^+\pi^-$ planes in the K^0_S rest frame.

CP asymmetry A in $K^0_S \to \pi^+\pi^-e^+e^-$

VALUE (%)	DOCUMENT ID		TECN	COMMENT
−1.1 ± 4.1	LAI	03C	NA48	1998+1999 data
• • • We do not use the following data for averages, fits, limits, etc. • • •				
0.5 ± 4.0 ± 1.6	LAI	03C	NA48	1999 data

K^0_S REFERENCES

LAI	04	PL B578 276	A. Lai *et al.*	(CERN NA48 Collab.)
ALAVI-HARATI	03	PR D67 012005	A. Alavi-Harati *et al.*	(FNAL KTeV Collab.)
Also	04	Erratum (to be publ.)	A. Alavi-Harati *et al.*	(FNAL KTeV Collab.)
BATLEY	03	PL B576 43	J.R. Batley *et al.*	(CERN NA48 Collab.)
LAI	03	PL B551 7	A. Lai *et al.*	(CERN NA48 Collab.)
LAI	03B	PL B556 105	A. Lai *et al.*	(CERN NA48 Collab.)
LAI	03C	EPJ C30 33	A. Lai *et al.*	(CERN NA48 Collab.)
ALOISIO	02	PL B535 37	A. Aloisio *et al.*	(KLOE Collab.)
ALOISIO	02B	PL B538 21	A. Aloisio *et al.*	(KLOE Collab.)
LAI	02C	PL B537 28	A. Lai *et al.*	(CERN NA48 Collab.)
LAI	01	PL B514 253	A. Lai *et al.*	(CERN NA48 Collab.)
LAI	00	PL B493 29	A. Lai *et al.*	(CERN NA48 Collab.)
LAI	00B	PL B496 137	A. Lai *et al.*	(CERN NA48 Collab.)
PDG	00	EPJ C15 1	D.E. Groom *et al.*	
ACHASOV	99D	PL B459 674	M.N. Achasov *et al.*	
AKHMETSHIN	99	PL B456 90	R.R. Akhmetshin *et al.*	(Novosibirsk CMD-2 Collab.)
ANGELOPO...	98B	PL B425 391	A. Angelopoulos *et al.*	(CPLEAR Collab.)
ANGELOPO...	98C	EPJ C5 389	A. Angelopoulos *et al.*	(CPLEAR Collab.)
PDG	98	EPJ C3 1	C. Caso *et al.*	
ADLER	97B	PL B407 193	R. Adler *et al.*	(CPLEAR Collab.)
ANGELOPO...	97	PL B413 232	A. Angelopoulos *et al.*	(CPLEAR Collab.)
BERTANZA	97	ZPHY C73 629	L. Bertanza	(PISA, CERN, EDIN, MANZ, ORSAY+)
ADLER	96D	PL B370 167	R. Adler *et al.*	(CPLEAR Collab.)
ADLER	96E	PL B374 313	R. Adler *et al.*	(CPLEAR Collab.)
ZOU	96	PL B369 362	Y. Zou *et al.*	(RUTG, MINN, MICH)
BARR	95B	PL B351 579	G.D. Barr *et al.*	(CERN, EDIN, MANZ, LALO+)
SCHWINGEN...	95	PRL 74 4376	B. Schwingenheuer *et al.*	(EFI, CHIC+)
BLICK	94	PL B334 234	A.M. Blick *et al.*	(SERP, JINR)
THOMSON	94	PL B337 411	G.B. Thomson *et al.*	(RUTG, MINN, MICH)
ZOU	94	PL B329 519	Y. Zou *et al.*	(RUTG, MINN, MICH)
BARR	93B	PL B304 381	G.D. Barr *et al.*	(CERN, EDIN, MANZ, LALO+)
GIBBONS	93	PRL 70 1199	L.K. Gibbons *et al.*	(FNAL E731 Collab.)
Also	97	PR D55 6625	L.K. Gibbons *et al.*	(FNAL E731 Collab.)
RAMBERG	93	PRL 70 2525	E. Ramberg *et al.*	(FNAL E731 Collab.)
BALATS	89	SJNP 49 828 Translated from YAF 49 1332.	M.Y. Balats *et al.*	(ITEP)
GIBBONS	88	PRL 61 2661	L.K. Gibbons *et al.*	(FNAL E731 Collab.)
BURKHARDT	87	PL B199 139	H. Burkhardt *et al.*	(CERN, EDIN, MANZ+)
GROSSMAN	87	PRL 59 18	N. Grossman *et al.*	(MINN, MICH, RUTG)
BARMIN	86	SJNP 44 622 Translated from YAF 44 965.	V.V. Barmin *et al.*	(ITEP)
BARMIN	86B	NC 96A 159	V.V. Barmin *et al.*	(ITEP, PADO)
PDG	86B	PL 170B 130	M. Aguilar-Benitez *et al.*	(CERN, CIT+)
BARMIN	85	NC 85A 67	V.V. Barmin *et al.*	(ITEP, PADO)
Also	85B	SJNP 41 759 Translated from YAF 41 1187.	V.V. Barmin *et al.*	(ITEP)
BARMIN	83	PL 128B 129	V.V. Barmin *et al.*	(ITEP, PADO)
Also	84	SJNP 39 269 Translated from YAF 39 428.	V.V. Barmin *et al.*	(ITEP, PADO)
ARONSON	82	PRL 48 1078	S.H. Aronson *et al.*	(BNL, CHIC, STAN+)
ARONSON	82B	PRL 48 1306	S.H. Aronson *et al.*	(BNL, CHIC, PURD)
Also	82B	PL 116B 73	E. Fischbach *et al.*	(PURD, BNL, CHIC)
Also	83	PR D28 476	S.H. Aronson *et al.*	(BNL, CHIC, PURD)
Also	83B	PR D28 495	S.H. Aronson *et al.*	(BNL, CHIC, PURD)
ARONSON	76	NC 32A 236	S.H. Aronson *et al.*	(WISC, EFI, UCSD+)
EVERHART	76	PR D14 661	G.C. Everhart *et al.*	(PENN)
TAUREG	76	PL 65B 92	H. Taureg *et al.*	(HEIDH, CERN, DORT)
BALDO-...	75	NC 25A 688	M. Baldo-Ceolin *et al.*	(PADO, WISC)
CARITHERS	75	PRL 34 1244	W.C.J. Carithers *et al.*	(COLU, NYU)
BOBISUT	74	LNC 11 646	F. Bobisut *et al.*	(PADO)
COWELL	74	PR D10 2083	P.L. Cowell *et al.*	(STON, COLU)
GEWENIGER	74B	PL 48B 487	C. Geweniger *et al.*	(CERN, HEIDH)
GJESDAL	74B	PL 52B 119	S. Gjesdal *et al.*	(CERN, HEIDH)
BURGUN	73	PL 46B 481	G. Burgun *et al.*	(SACL, CERN)
GJESDAL	73	PL 44B 217	S. Gjesdal *et al.*	(CERN, HEIDH)
HILL	73	PR D8 1290	D.G. Hill *et al.*	(BNL, CMU)
ALITTI	72	PL 39B 568	J. Alitti, E. Lesquoy, A. Muller	(SACL)
BURGUN	72	NP B50 194	G. Burgun *et al.*	(SACL, CERN, OSLO)
METCALF	72	PL 40B 703	M. Metcalf *et al.*	(CERN, IPN, WIEN)
MORSE	72B	PRL 28 388	R. Morse *et al.*	(COLO, PRIN, UMD)
NAGY	72	NP B47 94	E. Nagy, F. Telbisz, G. Vesztergombi	(BUDA)
Also	69	PL 30B 498	G. Bozoki *et al.*	(BUDA)
SKJEGGEST...	72	NP B48 343	O. Skjeggestad *et al.*	(OSLO, CERN, SACL)
BALTAY	71	PRL 27 1678	C. Baltay *et al.*	(COLU)
Also	71	Thesis Nevis 187	W.A. Cooper	(COLU)
MOFFETT	70	BAPS 15 512	R. Moffett *et al.*	(ROCH)
BOZOKI	69	PL 30B 498	G. Bozoki *et al.*	(BUDA)
DOYLE	69	Thesis UCRL 18139	J.C. Doyle	(LRL)
GOBBI	69	PRL 22 682	B. Gobbi *et al.*	(ROCH)
HYAMS	69B	PL 29B 521	B.D. Hyams *et al.*	(CERN, MPIM)
MORFIN	69	PRL 23 660	J.G. Morfin, D. Sinclair	(MICH)
DONALD	68B	PL 27B 58	R.A. Donald *et al.*	(LIVP, CERN, IPNP+)
HILL	68	PR 171 1418	D.G. Hill *et al.*	(BNL, CMU)
AUBERT	65	PL 17 59	B. Aubert *et al.*	(EPOL, ORSAY)
BROWN	63	PR 130 769	J.L. Brown *et al.*	(LRL, MICH)
CHRETIEN	63	PR 131 2208	M. Chretien *et al.*	(BRAN, BROW, HARV+)
BROWN	61	NC 19 1155	J.L. Brown *et al.*	(MICH)
BOLDT	58B	PRL 1 150	E. Boldt, D.O. Caldwell, Y. Pal	(MIT)

OTHER RELATED PAPERS

LITTENBERG	93	ARNPS 43 729 Rare and Radiative Kaon Decays	L.S. Littenberg, G. Valencia	(BNL, FNAL)
BATTISTON	92	PRPL 214 293 Status and Perspectives of K Decay Physics	R. Battiston *et al.*	(PGIA, CERN, TRSTT)
TRILLING	65B	UCRL 16473 Updated from 1965 Argonne Conference, page 115.	G.N. Trilling	(LRL)
CRAWFORD	62	CERN Conf. 827	F.S. Crawford	(LRL)
FITCH	61	NC 22 1160	V.L. Fitch, P.A. Piroue, R.B. Perkins	(PRIN+)
GOOD	61	PR 124 1223	R.H. Good *et al.*	(LRL)
BIRGE	60	Rochester Conf. 601	R.W. Birge *et al.*	(LRL, WISC)
MULLER	60	PRL 4 418	F. Muller *et al.*	(LRL, BNL)

K^0_L $I(J^P) = \frac{1}{2}(0^-)$

$m_{K^0_L} - m_{K^0_S}$

For earlier measurements, beginning with GOOD 61 and FITCH 61, see our 1986 edition, Physics Letters **170B** 132 (1986).

OUR FIT is described in the note on "*CP* violation in K_L decays" in the K^0_L Particle Listings. The result labeled "OUR FIT Assuming *CPT*" ["OUR FIT Not assuming *CPT*"] includes all measurements except those with the comment "Not assuming *CPT*" ["Assuming *CPT*"]. Measurements with neither comment do not assume *CPT* and enter both fits.

VALUE (10^{10} $\hbar$ s^{-1})		DOCUMENT ID		TECN	COMMENT
0.5292 ± 0.0010	**OUR FIT**	Error includes scale factor of 1.2. Assuming *CPT*			
0.5290 ± 0.0016	**OUR FIT**	Error includes scale factor of 1.2. Not assuming *CPT*			
0.5261 ± 0.0015		[1,2] ALAVI-HARATI	03	KTEV	Assuming *CPT*
0.5288 ± 0.0043		[2,3] ALAVI-HARATI	03	KTEV	Not assuming *CPT*
0.5240 ± 0.0044 ± 0.0033		APOSTOLA...	99C	CPLR	K^0-$\overline{K}^0$ to $\pi^+\pi^-$
0.5297 ± 0.0030 ± 0.0022		[4] SCHWINGEN...	95	E773	20–160 GeV K beams
0.5286 ± 0.0028		[5] GIBBONS	93	E731	Assuming *CPT*
0.5257 ± 0.0049 ± 0.0021		[4] GIBBONS	93C	E731	Not assuming *CPT*
0.5340 ± 0.00255 ± 0.0015		[6] GEWENIGER	74C	SPEC	Gap method
0.5334 ± 0.0040 ± 0.0015		[6] GJESDAL	74	SPEC	Charge asymmetry in $K^0_{\ell 3}$
• • • We do not use the following data for averages, fits, limits, etc. • • •					
0.5343 ± 0.0063 ± 0.0025		[7] ANGELOPO...	01	CPLR	
0.5295 ± 0.0020 ± 0.0003		[8] ANGELOPO...	98D	CPLR	Assuming *CPT*
0.5307 ± 0.0013		[9] ADLER	96C	RVUE	
0.5274 ± 0.0029 ± 0.0005		[8] ADLER	95	CPLR	Sup. by ANGELOPOULOS 98D
0.482 ± 0.014		[10] ARONSON	82B	SPEC	E=30–110 GeV
0.534 ± 0.007		[11] CARNEGIE	71	ASPK	Gap method
0.542 ± 0.006		[11] ARONSON	70	ASPK	Gap method
0.542 ± 0.006		CULLEN	70	CNTR	

[1] ALAVI-HARATI 03 fit Δm and $\tau_{K^0_S}$ simultaneously. ϕ_{+-} is constrained to the Superweak value, i.e. *CPT* is assumed. See "K^0_S Mean Life" section for correlation information.

[2] The two ALAVI-HARATI 03 values use the same data. The first enters the "Assuming *CPT*" fit and the second enters the "Not assuming *CPT*" fit. They use 40–160 GeV K beams.

[3] ALAVI-HARATI 03 fit Δm, ϕ_{+-}, and τ_{K_S} simultaneously. See ϕ_{+-} in the "K_L *CP* violation" section for correlation information.

[4] Fits Δm and ϕ_{+-} simultaneously. GIBBONS 93C systematic error is from B. Winstein via private communication. 20–160 GeV K beams.

[5] GIBBONS 93 value assume $\phi_{+-} = \phi_{00} = \phi_{SW} = (43.7 \pm 0.2)^\circ$, i.e. assumes *CPT*. 20–160 GeV K beams.

[6] These two experiments have a common systematic error due to the uncertainty in the momentum scale, as pointed out in WAHL 89.

[7] ANGELOPOULOS 01 uses strong interactions strangeness tagging at two different times.

[8] Uses $\overline{K}^0_{e3}$ and K^0_{e3} strangeness tagging at production and decay. Assumes *CPT* conservation on $\Delta S = -\Delta Q$ transitions.

[9] ADLER 96C is the result of a fit which includes nearly the same data as entered into the "OUR FIT" value above.

[10] ARONSON 82 find that Δm may depend on the kaon energy.

[11] ARONSON 70 and CARNEGIE 71 use K^0_S mean life $= (0.862 \pm 0.006) \times 10^{-10}$ s. We have not attempted to adjust these values for the subsequent change in the K^0_S mean life or in η_{+-}.

K^0_L MEAN LIFE

VALUE (10^{-8} s)	EVTS	DOCUMENT ID		TECN
5.18 ± 0.04	**OUR FIT**	Error includes scale factor of 1.1.		
5.15 ± 0.04	**OUR AVERAGE**			
5.154 ± 0.044	0.4M	VOSBURGH	72	CNTR
5.15 ± 0.14		DEVLIN	67	CNTR
• • • We do not use the following data for averages, fits, limits, etc. • • •				
5.0 ± 0.5		[12] LOWYS	67	HLBC
6.1 $^{+1.5}_{-1.2}$	1700	ASTBURY	65C	CNTR
5.3 ± 0.6		FUJII	64	OSPK
5.1 $^{+2.4}_{-1.3}$	15	DARMON	62	FBC
8.1 $^{+3.2}_{-2.4}$	34	BARDON	58	CNTR

[12] Sum of partial decay rates.

K_L^0 DECAY MODES

	Mode		Fraction (Γ_i/Γ)	Scale factor/ Confidence level
	Semileptonic modes			
Γ_1	$\pi^\pm e^\mp \nu_e$ Called K^0_{e3}.	[a]	(38.81 ±0.27) %	S=1.1
Γ_2	$\pi^- e^+ \nu_e$			
Γ_3	$\pi^+ e^- \overline{\nu}_e$			
Γ_4	$\pi^\pm \mu^\mp \nu_\mu$ Called $K^0_{\mu3}$.	[a]	(27.19 ±0.25) %	S=1.1
Γ_5	$\pi^- \mu^+ \nu_\mu$			
Γ_6	$\pi^+ \mu^- \overline{\nu}_\mu$			
Γ_7	$(\pi\mu\text{atom})\nu$		(1.06 ±0.11) $\times 10^{-7}$	
Γ_8	$\pi^0 \pi^\pm e^\mp \nu$	[a]	(5.18 ±0.29) $\times 10^{-5}$	
	Hadronic modes, including Charge conjugation × Parity Violating (*CPV*) modes			
Γ_9	$3\pi^0$		(21.05 ±0.23) %	S=1.1
Γ_{10}	$\pi^+ \pi^- \pi^0$		(12.59 ±0.19) %	S=1.6
Γ_{11}	$\pi^+ \pi^-$	*CPV*	(2.090±0.025) $\times 10^{-3}$	S=1.1
Γ_{12}	$\pi^0 \pi^0$	*CPV*	(9.32 ±0.12) $\times 10^{-4}$	S=1.1
	Semileptonic modes with photons			
Γ_{13}	$\pi^\pm e^\mp \nu_e \gamma$	[a,b,c]	(3.53 ±0.06) $\times 10^{-3}$	
Γ_{14}	$\pi^\pm \mu^\mp \nu_\mu \gamma$		(5.7 $^{+0.6}_{-0.7}$) $\times 10^{-4}$	
	Hadronic modes with photons or $\ell\overline{\ell}$ pairs			
Γ_{15}	$\pi^0 \pi^0 \gamma$		< 5.6 $\times 10^{-6}$	
Γ_{16}	$\pi^+ \pi^- \gamma$	[b,c]	(4.39 ±0.12) $\times 10^{-5}$	S=1.8
Γ_{17}	$\pi^0 2\gamma$	[c]	(1.41 ±0.12) $\times 10^{-6}$	S=2.8
Γ_{18}	$\pi^0 \gamma e^+ e^-$		(2.3 ±0.4) $\times 10^{-8}$	
	Other modes with photons or $\ell\overline{\ell}$ pairs			
Γ_{19}	2γ		(5.90 ±0.07) $\times 10^{-4}$	S=1.1
Γ_{20}	3γ		< 2.4 $\times 10^{-7}$	CL=90%
Γ_{21}	$e^+ e^- \gamma$		(10.0 ±0.5) $\times 10^{-6}$	S=1.5
Γ_{22}	$\mu^+ \mu^- \gamma$		(3.59 ±0.11) $\times 10^{-7}$	S=1.3
Γ_{23}	$e^+ e^- \gamma\gamma$	[c]	(5.95 ±0.33) $\times 10^{-7}$	
Γ_{24}	$\mu^+ \mu^- \gamma\gamma$	[c]	(1.0 $^{+0.8}_{-0.6}$) $\times 10^{-8}$	
	Charge conjugation × Parity (*CP*) or Lepton Family number (*LF*) violating modes, or $\Delta S = 1$ weak neutral current (*S1*) modes			
Γ_{25}	$\mu^+ \mu^-$	*S1*	(7.27 ±0.14) $\times 10^{-9}$	
Γ_{26}	$e^+ e^-$	*S1*	(9 $^{+6}_{-4}$) $\times 10^{-12}$	
Γ_{27}	$\pi^+ \pi^- e^+ e^-$	*S1* [c]	(3.11 ±0.19) $\times 10^{-7}$	
Γ_{28}	$\pi^0 \pi^0 e^+ e^-$	*S1*	< 6.6 $\times 10^{-9}$	CL=90%
Γ_{29}	$\mu^+ \mu^- e^+ e^-$	*S1*	(2.69 ±0.27) $\times 10^{-9}$	
Γ_{30}	$e^+ e^- e^+ e^-$	*S1*	(3.75 ±0.27) $\times 10^{-8}$	
Γ_{31}	$\pi^0 \mu^+ \mu^-$	*CP,S1* [d]	< 3.8 $\times 10^{-10}$	CL=90%
Γ_{32}	$\pi^0 e^+ e^-$	*CP,S1* [d]	< 5.1 $\times 10^{-10}$	CL=90%
Γ_{33}	$\pi^0 \nu\overline{\nu}$	*CP,S1* [e]	< 5.9 $\times 10^{-7}$	CL=90%
Γ_{34}	$e^\pm \mu^\mp$	*LF* [a]	< 4.7 $\times 10^{-12}$	CL=90%
Γ_{35}	$e^\pm e^\pm \mu^\mp \mu^\mp$	*LF* [a]	< 4.12 $\times 10^{-11}$	CL=90%
Γ_{36}	$\pi^0 \mu^\pm e^\mp$	*LF* [a]	< 6.2 $\times 10^{-9}$	CL=90%

[a] The value is for the sum of the charge states or particle/antiparticle states indicated.

[b] Most of this radiative mode, the low-momentum γ part, is also included in the parent mode listed without γ's.

[c] See the Particle Listings below for the energy limits used in this measurement.

[d] Allowed by higher-order electroweak interactions.

[e] Violates *CP* in leading order. Test of direct *CP* violation since the indirect *CP*-violating and *CP*-conserving contributions are expected to be suppressed.

CONSTRAINED FIT INFORMATION

An overall fit to the mean life, 3 decay rate, and 15 branching ratios uses 50 measurements and one constraint to determine 9 parameters. The overall fit has a $\chi^2 = 43.7$ for 42 degrees of freedom.

The following *off-diagonal* array elements are the correlation coefficients $\langle \delta p_i \delta p_j \rangle / (\delta p_i \cdot \delta p_j)$, in percent, from the fit to parameters p_i, including the branching fractions, $x_i \equiv \Gamma_i/\Gamma_{\text{total}}$. The fit constrains the x_i whose labels appear in this array to sum to one.

	x_1	x_4	x_9	x_{10}	x_{11}	x_{12}	x_{16}	x_{19}
x_4	−38							
x_9	−48	−37						
x_{10}	−34	−33	−5					
x_{11}	−25	−21	34	20				
x_{12}	−27	−22	42	16	86			
x_{16}	−9	−8	13	8	37	32		
x_{19}	−42	−33	86	−1	42	50	16	
Γ	0	0	0	0	0	0	0	0

	Mode		Rate (10^8 s^{-1})	Scale factor
Γ_1	$\pi^\pm e^\mp \nu_e$ Called K^0_{e3}.	[a]	0.0750±0.0008	1.1
Γ_4	$\pi^\pm \mu^\mp \nu_\mu$ Called $K^0_{\mu3}$.	[a]	0.0525±0.0007	1.1
Γ_9	$3\pi^0$		0.0407±0.0006	1.1
Γ_{10}	$\pi^+ \pi^- \pi^0$		0.0243±0.0004	1.5
Γ_{11}	$\pi^+ \pi^-$		(4.04 ±0.06) $\times 10^{-4}$	1.1
Γ_{12}	$\pi^0 \pi^0$		(1.800 ±0.027) $\times 10^{-4}$	1.1
Γ_{16}	$\pi^+ \pi^- \gamma$	[b,c]	(8.48 ±0.25) $\times 10^{-6}$	1.7
Γ_{19}	2γ		(1.140 ±0.016) $\times 10^{-4}$	1.1

K_L^0 DECAY RATES

$\Gamma(\pi^+\pi^-\pi^0)$ Γ_{10}

VALUE (10^6 s^{-1})	*EVTS*	*DOCUMENT ID*		*TECN*	*COMMENT*
2.43±0.04 OUR FIT Error includes scale factor of 1.5.					
2.38±0.09 OUR AVERAGE					
2.32 $^{+0.13}_{-0.15}$	192	BALDO-...	75	HLBC	Assumes *CP*
2.35 ±0.20	180	[13] JAMES	72	HBC	Assumes *CP*
2.71 ±0.28	99	CHO	71	DBC	Assumes *CP*
2.12 ±0.33	50	MEISNER	71	HBC	Assumes *CP*
2.20 ±0.35	53	WEBBER	70	HBC	Assumes *CP*
2.62 $^{+0.28}_{-0.27}$	136	BEHR	66	HLBC	Assumes *CP*
• • • We do not use the following data for averages, fits, limits, etc. • • •					
2.5 ±0.3	98	[13] JAMES	71	HBC	Assumes *CP*
3.26±0.77	18	ANDERSON	65	HBC	
1.4 ±0.4	14	FRANZINI	65	HBC	

[13] JAMES 72 is a final measurement and includes JAMES 71.

$\Gamma(\pi^\pm e^\mp \nu_e)$ Γ_1

VALUE (10^6 s^{-1})	*EVTS*	*DOCUMENT ID*		*TECN*	*COMMENT*
7.50±0.08 OUR FIT Error includes scale factor of 1.1.					
7.7 ±0.5 OUR AVERAGE					
7.81±0.56	620	CHAN	71	HBC	
7.52 $^{+0.85}_{-0.72}$		AUBERT	65	HLBC	$\Delta S = \Delta Q$, *CP* assumed

$\Gamma(\pi^\pm e^\mp \nu_e) + \Gamma(\pi^\pm \mu^\mp \nu_\mu)$ $(\Gamma_1+\Gamma_4)$

VALUE (10^6 s^{-1})	*EVTS*	*DOCUMENT ID*		*TECN*	*COMMENT*
12.75±0.12 OUR FIT Error includes scale factor of 1.1.					
11.9 ±0.6 OUR AVERAGE Error includes scale factor of 1.2.					
12.4 ±0.7	410	[14] BURGUN	72	HBC	$K^+ p \to K^0 p \pi^+$
13.1 ±1.3	252	[14] WEBBER	71	HBC	$K^- p \to n\overline{K}^0$
11.6 ±0.9	393	[14,15] CHO	70	DBC	$K^+ n \to K^0 p$
9.85 $^{+1.15}_{-1.05}$	109	[14] FRANZINI	65	HBC	
• • • We do not use the following data for averages, fits, limits, etc. • • •					
8.47±1.69	126	[14] MANN	72	HBC	$K^- p \to n\overline{K}^0$
10.3 ±0.8	335	[15] HILL	67	DBC	$K^+ n \to K^0 p$

[14] Assumes $\Delta S = \Delta Q$ rule.

[15] CHO 70 includes events of HILL 67.

K_L^0 BRANCHING RATIOS

Semileptonic modes

$\Gamma(\pi^\pm e^\mp \nu_e) + \Gamma(\pi^\pm \mu^\mp \nu_\mu)/\Gamma_{total}$ $(\Gamma_1+\Gamma_4)/\Gamma$

VALUE	DOCUMENT ID
0.6599±0.0029 OUR FIT	Error includes scale factor of 1.3.

$\Gamma(\pi^\pm \mu^\mp \nu_\mu)/\Gamma(\pi^\pm e^\mp \nu_e)$ Γ_4/Γ_1

VALUE	EVTS	DOCUMENT ID		TECN
0.701±0.009 OUR FIT				
$0.697^{+0.010}_{-0.009}$ OUR AVERAGE				
0.702±0.011	33k	CHO	80	HBC
0.662±0.037	10k	WILLIAMS	74	ASPK
0.741±0.044	6700	BRANDENB...	73	HBC
0.662±0.030	1309	EVANS	73	HLBC
0.71 ±0.05	770	BUDAGOV	68	HLBC
• • • We do not use the following data for averages, fits, limits, etc. • • •				
0.68 ±0.08	3548	BASILE	70	OSPK

$\Gamma((\pi\mu\,\text{atom})\nu)/\Gamma(\pi^\pm \mu^\mp \nu_\mu)$ Γ_7/Γ_4

VALUE (units 10^{-7})	EVTS	DOCUMENT ID		TECN
3.90±0.39	155	[16] ARONSON	86	SPEC
• • • We do not use the following data for averages, fits, limits, etc. • • •				
seen	18	COOMBES	76	WIRE

[16] ARONSON 86 quote theoretical value of $(4.31 \pm 0.08) \times 10^{-7}$.

$\Gamma(\pi^0 \pi^\pm e^\mp \nu)/\Gamma_{total}$ Γ_8/Γ

VALUE (units 10^{-5})	CL%	EVTS	DOCUMENT ID		TECN
5.18±0.29 OUR AVERAGE					
5.16±0.20±0.22		729	MAKOFF	93	E731
6.2 ±2.0		16	CARROLL	80C	SPEC
• • • We do not use the following data for averages, fits, limits, etc. • • •					
< 220	90		[17] DONALDSON	74	SPEC

[17] DONALDSON 74 uses $K_L^0 \to \pi^+\pi^-\pi^0/(\text{all } K_L^0)$ decays = 0.126.

Hadronic modes, including Charge conjugation × Parity Violating (*CPV*) modes

$\Gamma(3\pi^0)/\Gamma_{total}$ Γ_9/Γ

VALUE	EVTS	DOCUMENT ID		TECN
0.2105±0.0023 OUR FIT	Error includes scale factor of 1.1.			
0.2105±0.0028	38k	[18] KREUTZ	95	NA31

[18] KREUTZ 95 measure $3\pi^0$, $\pi^+\pi^-\pi^0$, and $\pi e \nu_e$ modes. They assume PDG 1992 values for $\pi\mu\nu_\mu$, 2π, and 2γ modes.

$\Gamma(3\pi^0)/\Gamma(\pi^\pm e^\mp \nu_e)$ Γ_9/Γ_1

VALUE	EVTS	DOCUMENT ID		TECN
0.542±0.008 OUR FIT	Error includes scale factor of 1.1.			
0.545±0.004±0.009	38k	[19] KREUTZ	95	NA31

[19] KREUTZ 95 measurement excluded from fit because it is not independent of their $\Gamma(3\pi^0)/\Gamma_{total}$ measurement, which is in the fit.

$\Gamma(3\pi^0)/[\Gamma(\pi^\pm e^\mp \nu_e) + \Gamma(\pi^\pm \mu^\mp \nu_\mu) + \Gamma(\pi^+\pi^-\pi^0)]$ $\Gamma_9/(\Gamma_1+\Gamma_4+\Gamma_{10})$

VALUE	EVTS	DOCUMENT ID		TECN	COMMENT
0.268±0.004 OUR FIT	Error includes scale factor of 1.1.				
0.260±0.011 OUR AVERAGE					
0.251±0.014	549	BUDAGOV	68	HLBC	ORSAY measur.
0.277±0.021	444	BUDAGOV	68	HLBC	Ecole polytec.meas
$0.31^{+0.07}_{-0.06}$	29	KULYUKINA	68	CC	
0.24 ±0.08	24	ANIKINA	64	CC	

$\Gamma(3\pi^0)/\Gamma(\pi^+\pi^-\pi^0)$ Γ_9/Γ_{10}

VALUE	EVTS	DOCUMENT ID		TECN	COMMENT
1.673±0.032 OUR FIT	Error includes scale factor of 1.3.				
1.63 ±0.05 OUR AVERAGE	Error includes scale factor of 1.4.				
1.611±0.014±0.034	38k	[20] KREUTZ	95	NA31	
1.80 ±0.13	1010	BUDAGOV	68	HLBC	
2.0 ±0.6	188	ALEKSANYAN	64B	FBC	
• • • We do not use the following data for averages, fits, limits, etc. • • •					
1.65 ±0.07	883	BARMIN	72B	HLBC	Error statistical only

[20] KREUTZ 95 excluded from fit because it is not independent of their $\Gamma(3\pi^0)/\Gamma_{total}$ measurement, which is in the fit.

$\Gamma(\pi^+\pi^-\pi^0)/\Gamma_{total}$ Γ_{10}/Γ

VALUE	DOCUMENT ID
0.1259±0.0019 OUR FIT	Error includes scale factor of 1.6.

$\Gamma(\pi^+\pi^-\pi^0)/\Gamma(\pi^\pm e^\mp \nu_e)$ Γ_{10}/Γ_1

VALUE	EVTS	DOCUMENT ID		TECN
0.324±0.006 OUR FIT	Error includes scale factor of 1.6.			
0.336±0.003±0.007	28k	KREUTZ	95	NA31

$\Gamma(\pi^+\pi^-\pi^0)/[\Gamma(\pi^\pm e^\mp \nu_e) + \Gamma(\pi^\pm \mu^\mp \nu_\mu) + \Gamma(\pi^+\pi^-\pi^0)]$ $\Gamma_{10}/(\Gamma_1+\Gamma_4+\Gamma_{10})$

VALUE	EVTS	DOCUMENT ID		TECN	COMMENT
0.1602±0.0024 OUR FIT	Error includes scale factor of 1.7.				
0.1588±0.0024 OUR AVERAGE	Error includes scale factor of 1.4. See the ideogram below.				
0.163 ±0.003	6499	CHO	77	HBC	
0.1605±0.0038	1590	ALEXANDER	73B	HBC	
0.146 ±0.004	3200	BRANDENB...	73	HBC	
0.159 ±0.010	558	EVANS	73	HLBC	
0.167 ±0.016	1402	KULYUKINA	68	CC	
0.161 ±0.005		HOPKINS	67	HBC	
0.162 ±0.015	126	HAWKINS	66	HBC	
0.159 ±0.015	326	ASTBURY	65B	CC	
0.178 ±0.017	566	GUIDONI	65	HBC	
• • • We do not use the following data for averages, fits, limits, etc. • • •					
0.144 ±0.004	1729	HOPKINS	65	HBC	See HOPKINS 67

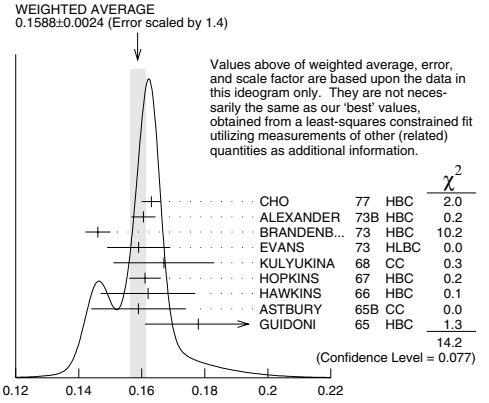

$\Gamma(\pi^+\pi^-\pi^0)/[\Gamma(\pi^\pm e^\mp \nu_e) + \Gamma(\pi^\pm \mu^\mp \nu_\mu) + \Gamma(\pi^+\pi^-\pi^0)]$

$\Gamma(\pi^+\pi^-)/\Gamma_{total}$ Γ_{11}/Γ

Violates *CP* conservation.

VALUE (units 10^{-3})	DOCUMENT ID	
2.090±0.025 OUR FIT	Error includes scale factor of 1.1.	
2.081±0.048	ETAFIT	04

$\Gamma(\pi^+\pi^-)/[\Gamma(\pi^\pm e^\mp \nu_e) + \Gamma(\pi^\pm \mu^\mp \nu_\mu)]$ $\Gamma_{11}/(\Gamma_1+\Gamma_4)$

Violates *CP* conservation.

VALUE (units 10^{-3})	EVTS	DOCUMENT ID		TECN	COMMENT
3.17±0.05 OUR FIT	Error includes scale factor of 1.1.				
3.08±0.10 OUR AVERAGE					
3.13±0.14	1687	COUPAL	85	SPEC	η_{+-}=2.28 ± 0.06
3.04±0.14	2703	DEVOE	77	SPEC	η_{+-}=2.25 ± 0.05
• • • We do not use the following data for averages, fits, limits, etc. • • •					
2.51±0.23	309	[21] DEBOUARD	67	OSPK	η_{+-}=2.00 ± 0.09
2.35±0.19	525	[21] FITCH	67	OSPK	η_{+-}=1.94 ± 0.08

[21] Old experiments excluded from fit. See subsection on η_{+-} in section on "PARAMETERS FOR $K_L^0 \to 2\pi$ DECAY" below for average η_{+-} of these experiments and for note on discrepancy.

$\Gamma(\pi^+\pi^-)/[\Gamma(\pi^\pm e^\mp \nu_e) + \Gamma(\pi^\pm \mu^\mp \nu_\mu) + \Gamma(\pi^+\pi^-\pi^0)]$ $\Gamma_{11}/(\Gamma_1+\Gamma_4+\Gamma_{10})$

Violates *CP* conservation.

VALUE (units 10^{-3})	EVTS	DOCUMENT ID		TECN	COMMENT
2.659±0.035 OUR FIT	Error includes scale factor of 1.1.				
• • • We do not use the following data for averages, fits, limits, etc. • • •					
2.60 ±0.07	4200	[22] MESSNER	73	ASPK	η_{+-} = 2.23 ± 0.05

[22] From same data as $\Gamma(\pi^+\pi^-)/\Gamma(\pi^+\pi^-\pi^0)$ MESSNER 73, but with different normalization.

$\Gamma(\pi^+\pi^-)/\Gamma(\pi^+\pi^-\pi^0)$ Γ_{11}/Γ_{10}

Violates *CP* conservation.

VALUE (units 10^{-2})	EVTS	DOCUMENT ID		TECN	COMMENT
1.660±0.028 OUR FIT	Error includes scale factor of 1.2.				
1.64 ±0.04	4200	MESSNER	73	ASPK	η_{+-} = 2.23

$\Gamma(\pi^0\pi^0)/\Gamma_{total}$ Γ_{12}/Γ

Violates *CP* conservation.

VALUE (units 10^{-3})	DOCUMENT ID
0.932±0.012 OUR FIT	Error includes scale factor of 1.1.

$\Gamma(\pi^0\pi^0)/\Gamma(\pi^+\pi^-)$ Γ_{12}/Γ_{11}

Violates CP conservation.

VALUE	DOCUMENT ID	
0.4458±0.0029 OUR FIT		
0.4458±0.0030	ETAFIT	04

$\Gamma(\pi^0\pi^0)/\Gamma(3\pi^0)$ Γ_{12}/Γ_9

Violates CP conservation.

VALUE (units 10^{-2})	EVTS	DOCUMENT ID		TECN	COMMENT
0.443±0.006 OUR FIT					
0.39 ±0.06 OUR AVERAGE					
0.37 ±0.08	29	BARMIN	70	HLBC	η_{00}=2.02 ± 0.23
0.32 ±0.15	30	BUDAGOV	70	HLBC	η_{00}=1.9 ± 0.5
0.46 ±0.11	57	BANNER	69	OSPK	η_{00}=2.2 ± 0.3

Semileptonic modes with photons

$\Gamma(\pi^\pm e^\mp \nu_e \gamma)/\Gamma(\pi^\pm e^\mp \nu_e)$ Γ_{13}/Γ_1

VALUE (units 10^{-2})	EVTS	DOCUMENT ID		TECN	COMMENT
0.910±0.014 OUR AVERAGE					
$0.908\pm0.008^{+0.013}_{-0.012}$	15k	ALAVI-HARATI	01J	KTEV	$E^*_\gamma \geq 30$ MeV, $\theta^*_{e\gamma} \geq 20^\circ$
$0.934\pm0.036^{+0.055}_{-0.039}$	1384	LEBER	96	NA31	$E^*_\gamma \geq 30$ MeV, $\theta^*_{e\gamma} \geq 20^\circ$

$\Gamma(\pi^\pm \mu^\mp \nu_\mu \gamma)/\Gamma(\pi^\pm \mu^\mp \nu_\mu)$ Γ_{14}/Γ_4

VALUE (units 10^{-3})	EVTS	DOCUMENT ID		TECN	COMMENT
$\mathbf{2.08\pm0.17^{+0.16}_{-0.21}}$	252	BENDER	98	NA48	$E^*_\gamma \geq 30$ MeV

Hadronic modes with photons or $\ell\bar{\ell}$ pairs

$\Gamma(\pi^0\pi^0\gamma)/\Gamma_{\text{total}}$ Γ_{15}/Γ

VALUE (units 10^{-6})	CL%	EVTS	DOCUMENT ID		TECN
< 5.6			BARR	94	NA31
• • • We do not use the following data for averages, fits, limits, etc. • • •					
<230	90	0	ROBERTS	94	E799

$\Gamma(\pi^+\pi^-\gamma)/\Gamma_{\text{total}}$ Γ_{16}/Γ

For earlier limits see our 1992 edition Physical Review **D45,** 1 June, Part II (1992).

VALUE (units 10^{-5})	EVTS	DOCUMENT ID		TECN	COMMENT
4.39±0.12 OUR FIT Error includes scale factor of 1.8.					
4.61±0.14 OUR AVERAGE					
4.66±0.15	3136	[23] RAMBERG	93	E731	E_γ >20 MeV
4.41±0.32	1062	[24] CARROLL	80B	SPEC	E_γ >20 MeV
• • • We do not use the following data for averages, fits, limits, etc. • • •					
1.52±0.16	516	[25] CARROLL	80B	SPEC	E_γ >20 MeV
2.89±0.28	546	[26] CARROLL	80B	SPEC	

[23] RAMBERG 93 finds that fraction of Direct Emission (DE) decays with E_γ >20 MeV is 0.685 ± 0.041.

[24] Both components. Uses $K^0_L \to \pi^+\pi^-\pi^0/(\text{all } K^0_L)$ decays = 0.1239.

[25] Internal Bremsstrahlung component only.

[26] Direct γ emission component only.

$\Gamma(\pi^+\pi^-\gamma)/\Gamma(\pi^+\pi^-)$ Γ_{16}/Γ_{11}

VALUE (units 10^{-2})	EVTS	DOCUMENT ID		TECN	COMMENT
2.10 ±0.05 OUR FIT Error includes scale factor of 2.1.					
2.08 ±0.02 ±0.02	8669	[27] ALAVI-HARATI	01B	KTEV	E^*_γ >20 MeV

[27] ALAVI-HARATI 01B includes both Direct Emission (DE) and Inner Bremsstrahlung (IB) processes. They also report DE/(DE+IB)= 0.683 ± 0.011. The paper reports results for ρ propagator, linear, and quadratic form factors.

$\Gamma(\pi^0 2\gamma)/\Gamma_{\text{total}}$ Γ_{17}/Γ

VALUE (units 10^{-6})	CL%	EVTS	DOCUMENT ID		TECN	COMMENT
1.41±0.12 OUR AVERAGE Error includes scale factor of 2.8. See the ideogram below.						
1.35±0.04±0.02		2.5k	[28] LAI	02B	NA48	
1.68±0.07±0.08		884	[29] ALAVI-HARATI	99B	KTEV	
1.7 ±0.2 ±0.2		63	[30] BARR	92	NA31	
• • • We do not use the following data for averages, fits, limits, etc. • • •						
1.86±0.60±0.60		60	PAPADIMITR...91		E731	$m_{\gamma\gamma}$ > 280 MeV
<5.1	90		PAPADIMITR...91		E731	$m_{\gamma\gamma}$ < 264 MeV
2.1 ±0.6		14	[31] BARR	90C	NA31	$m_{\gamma\gamma}$ > 280 MeV

[28] LAI 02B reports 1.36 ± 0.03 ± 0.03 for $B(K^0_L \to \pi^0\pi^0) = 9.27\times10^{-4}$. We rescale to our best value $B(K^0_L \to \pi^0\pi^0) = (9.32 \pm 0.12)\times10^{-4}$. Our first error is their experiment's error and our second error is the systematic error from using our best value. They also find that $B(\pi^0 2\gamma,\ m_{\gamma\gamma}$ <110 MeV) < 0.6×10^{-8}(90% CL).

[29] ALAVI-HARATI 99B finds that $\Gamma(\pi^0 2\gamma,\ m_{\gamma\gamma}$ <240 MeV)) / $\Gamma(\pi^0 2\gamma) = (17.3 \pm 1.3 \pm 1.5)\%$.

[30] BARR 92 find that $\Gamma(\pi^0 2\gamma,\ m_{\gamma\gamma}$ <240 MeV)/$\Gamma(\pi^0 2\gamma)$< 0.09 (90% CL).

[31] BARR 90C superseded by BARR 92.

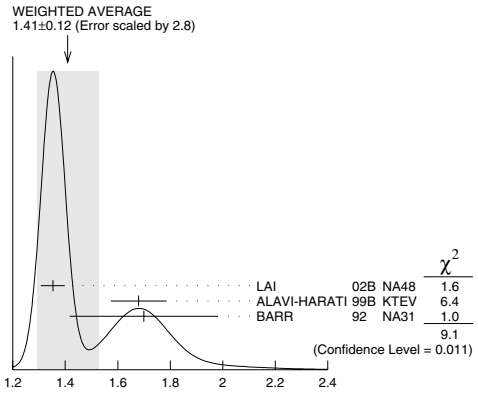

$\Gamma(\pi^0 2\gamma)/\Gamma_{\text{total}}$ Γ_{17}/Γ

$\Gamma(\pi^0\gamma e^+e^-)/\Gamma_{\text{total}}$ Γ_{18}/Γ

VALUE (units 10^{-8})	CL%	EVTS	DOCUMENT ID		TECN
2.34±0.35±0.13		44	ALAVI-HARATI	01E	KTEV
• • • We do not use the following data for averages, fits, limits, etc. • • •					
<71	90	0	MURAKAMI	99	SPEC

Other modes with photons or $\ell\bar{\ell}$ pairs

$\Gamma(2\gamma)/\Gamma_{\text{total}}$ Γ_{19}/Γ

VALUE (units 10^{-4})	EVTS	DOCUMENT ID		TECN	COMMENT
5.90±0.07 OUR FIT Error includes scale factor of 1.1.					
• • • We do not use the following data for averages, fits, limits, etc. • • •					
4.54±0.84		[32] BANNER	72B	OSPK	
4.5 ±1.0	23	ENSTROM	71	OSPK	K^0_L 1.5–9 GeV/c
5.0 ±1.0		[33] REPELLIN	71	OSPK	
5.5 ±1.1	90	KUNZ	68	OSPK	Norm.to 3 π(C+N)

[32] This value uses $(\eta_{00}/\eta_{+-})^2 = 1.05 \pm 0.14$. In general, $\Gamma(2\gamma)/\Gamma_{\text{total}} = [(4.32\pm0.55)\times10^{-4}]\,[(\eta_{00}/\eta_{+-})^2]$.

[33] Assumes regeneration amplitude in copper at 2 GeV is 22 mb. To evaluate for a given regeneration amplitude and error, multiply by (regeneration amplitude/22mb)^2.

$\Gamma(2\gamma)/\Gamma(3\pi^0)$ Γ_{19}/Γ_9

VALUE (units 10^{-3})	EVTS	DOCUMENT ID		TECN	COMMENT
2.801±0.017 OUR FIT					
2.802±0.018 OUR AVERAGE					
2.79 ±0.02 ±0.02	27k	ADINOLFI	03	KLOE	
2.81 ±0.01 ±0.02		LAI	03	NA48	
• • • We do not use the following data for averages, fits, limits, etc. • • •					
2.13 ±0.43	28	BARMIN	71	HLBC	
2.24 ±0.28	115	BANNER	69	OSPK	
2.5 ±0.7	16	ARNOLD	68B	HLBC	Vacuum decay

$\Gamma(2\gamma)/\Gamma(\pi^0\pi^0)$ Γ_{19}/Γ_{12}

VALUE	EVTS	DOCUMENT ID		TECN
0.633±0.008 OUR FIT				
0.632±0.004±0.008	110k	BURKHARDT	87	NA31

$\Gamma(3\gamma)/\Gamma_{\text{total}}$ Γ_{20}/Γ

VALUE	CL%	DOCUMENT ID		TECN
$\mathbf{<2.4\times10^{-7}}$	90	[34] BARR	95C	NA31

[34] Assumes a phase-space decay distribution.

$\Gamma(e^+e^-\gamma)/\Gamma_{\text{total}}$ Γ_{21}/Γ

VALUE (units 10^{-6})	EVTS	DOCUMENT ID		TECN
10.0±0.5 OUR AVERAGE Error includes scale factor of 1.5. See the ideogram below.				
10.6±0.2±0.4	6864	[35] FANTI	99B	NA48
9.2±0.5±0.5	1053	BARR	90B	NA31
$9.1\pm0.4^{+0.6}_{-0.5}$	919	OHL	90B	B845

[35] For FANTI 99B, the ±0.4 systematic error includes for uncertainties in the calculation, primarily uncertainties in the $\pi^0 \to e^+e^-\gamma$ and $K^0_L \to \pi^0\pi^0$ branching ratios, evaluated using our 1999 Web edition values.

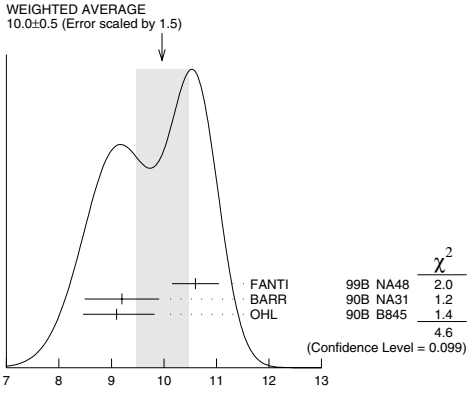

$\Gamma(\mu^+\mu^-\gamma)/\Gamma_{\rm total}$ Γ_{22}/Γ

VALUE (units 10^{-7})	EVTS	DOCUMENT ID		TECN
3.59±0.11 OUR AVERAGE		Error includes scale factor of 1.3.		
3.62±0.04±0.08	9100	ALAVI-HARATI	01G	KTEV
3.4 ±0.6 ±0.4	45	FANTI	97	NA48
3.23±0.23±0.19	197	SPENCER	95	E799

$\Gamma(e^+e^-\gamma\gamma)/\Gamma_{\rm total}$ Γ_{23}/Γ

VALUE (units 10^{-7})	EVTS	DOCUMENT ID		TECN	COMMENT
5.95±0.33 OUR AVERAGE					
5.84±0.15±0.32	1543	ALAVI-HARATI	01F	KTEV	$E_\gamma^*>5$ MeV
8.0 ±1.5 $^{+1.4}_{-1.2}$	40	SETZU	98	NA31	$E_\gamma>5$ MeV
6.5 ±1.2 ±0.6	58	NAKAYA	94	E799	$E_\gamma>5$ MeV
6.6 ±3.2		MORSE	92	B845	$E_\gamma>5$ MeV

$\Gamma(\mu^+\mu^-\gamma\gamma)/\Gamma_{\rm total}$ Γ_{24}/Γ

VALUE (units 10^{-9})	EVTS	DOCUMENT ID		TECN	COMMENT
10.4$^{+7.5}_{-5.9}$±0.7	4	ALAVI-HARATI	00E	KTEV	$m_{\gamma\gamma}\geq 1$ MeV/c^2

Charge conjugation × Parity (*CP*) or Lepton Family number (*LF*) violating modes, or $\Delta S=1$ weak neutral current (*S1*) modes

$\Gamma(\mu^+\mu^-)/\Gamma(\pi^+\pi^-)$ Γ_{25}/Γ_{11}

Test for $\Delta S=1$ weak neutral current. Allowed by higher-order electroweak interaction.

VALUE (units 10^{-6})	EVTS	DOCUMENT ID		TECN	COMMENT
3.48 ±0.05 OUR AVERAGE					
3.474±0.057	6210	AMBROSE	00	B871	
3.87 ±0.30	179	[36] AKAGI	95	SPEC	
3.38 ±0.17	707	HEINSON	95	B791	
• • • We do not use the following data for averages, fits, limits, etc. • • •					
3.9 ±0.3 ±0.1	178	[37] AKAGI	91B	SPEC	In AKAGI 95
3.45 ±0.18 ±0.13	368	[38] HEINSON	91	SPEC	In HEINSON 95
4.1 ±0.5	54	INAGAKI	89	SPEC	In AKAGI 91B
2.8 ±0.3 ±0.2	87	MATHIAZHA...	89B	SPEC	In HEINSON 91

[36] AKAGI 95 gives this number multiplied by the PDG 1992 average for $\Gamma(K_L^0\to\pi^+\pi^-)/\Gamma(\text{total})$.

[37] AKAGI 91B give this number multiplied by the 1990 PDG average for $\Gamma(K_L^0\to\pi^+\pi^-)/\Gamma(\text{total})$.

[38] HEINSON 91 give $\Gamma(K_L^0\to\mu\mu)/\Gamma_{\rm total}$. We divide out the $\Gamma(K_L^0\to\pi^+\pi^-)/\Gamma_{\rm total}$ PDG average which they used.

$\Gamma(e^+e^-)/\Gamma_{\rm total}$ Γ_{26}/Γ

Test for $\Delta S=1$ weak neutral current. Allowed by higher-order electroweak interaction.

VALUE (units 10^{-10})	CL%	EVTS	DOCUMENT ID		TECN
0.087$^{+0.057}_{-0.041}$		4	AMBROSE	98	B871
• • • We do not use the following data for averages, fits, limits, etc. • • •					
<1.6	90	1	AKAGI	95	SPEC
<0.41	90	0	[39] ARISAKA	93B	B791

[39] ARISAKA 93B includes all events with <6 MeV radiated energy.

$\Gamma(\pi^+\pi^-e^+e^-)/\Gamma_{\rm total}$ Γ_{27}/Γ

Test for $\Delta S=1$ weak neutral current. Allowed by higher-order electroweak interaction.

VALUE (units 10^{-7})	CL%	EVTS	DOCUMENT ID		TECN	COMMENT
3.11±0.19 OUR AVERAGE						
3.08±0.09±0.18		1125	[40] LAI	03C	NA48	
3.2 ±0.6 ±0.4		37	ADAMS	98	KTEV	
4.4 ±1.3 ±0.5		13	TAKEUCHI	98	SPEC	
• • • We do not use the following data for averages, fits, limits, etc. • • •						
<4.6	90		NOMURA	97	SPEC	$m_{ee}>4$ MeV

[40] LAI 03C second error is 0.15(syst)±0.10(norm) combined in quadrature. The normalization uses BR($K_L\to\pi^+\pi^-\pi^0$) * BR($\pi^0\to e^+e^-$) = (1.505 ± 0.047) × 10^{-3} from our 2000 Edition.

$\Gamma(\pi^0\pi^0e^+e^-)/\Gamma_{\rm total}$ Γ_{28}/Γ

Test for $\Delta S=1$ weak neutral current. Allowed by higher-order electroweak interaction.

VALUE (units 10^{-9})	CL%	EVTS	DOCUMENT ID		TECN
<6.6	90	1	ALAVI-HARATI	02C	E799

$\Gamma(\mu^+\mu^-e^+e^-)/\Gamma_{\rm total}$ Γ_{29}/Γ

Test for $\Delta S=1$ weak neutral current. Allowed by higher-order electroweak interaction.

VALUE (units 10^{-9})	CL%	EVTS	DOCUMENT ID		TECN	COMMENT
2.69±0.27 OUR AVERAGE						
2.69±0.24±0.12		131	[41] ALAVI-HARATI	03B	KTEV	
2.9 $^{+6.7}_{-2.4}$		1	GU	96	E799	
• • • We do not use the following data for averages, fits, limits, etc. • • •						
2.62±0.40±0.17		43	ALAVI-HARATI	01H	KTEV	Sup. by ALAVI-HARATI 03B
<4900	90		BALATS	83	SPEC	

[41] ALAVI-HARATI 03B also measures the linear slope $\alpha=-1.59\pm0.37$.

$\Gamma(e^+e^-e^+e^-)/\Gamma_{\rm total}$ Γ_{30}/Γ

Test for $\Delta S=1$ weak neutral current. Allowed by higher-order electroweak interaction.

VALUE (units 10^{-8})	EVTS	DOCUMENT ID		TECN	COMMENT
3.75±0.27 OUR AVERAGE					
3.72±0.18±0.23	441	ALAVI-HARATI	01D	KTEV	
6 ±2 ±1	18	[42] AKAGI	95	SPEC	$m_{ee}>470$ MeV
3.96±0.78±0.32	27	GU	94	E799	
3.07±1.25±0.26	6	VAGINS	93	B845	
• • • We do not use the following data for averages, fits, limits, etc. • • •					
7 ±3 ±2	6	[42] AKAGI	95	SPEC	$m_{ee}>470$ MeV
10.4 ±3.7 ±1.1	8	[43] BARR	95	NA31	
6 ±2 ±1	18	AKAGI	93	CNTR	Sup. by AKAGI 95
4 ±3	2	BARR	91	NA31	Sup. by BARR 95

[42] Values are for the total branching fraction, acceptance-corrected for the m_{ee} cuts shown.

[43] Distribution of angles between two e^+e^- pair planes favors $CP=-1$ for K_L^0.

$\Gamma(\pi^0\mu^+\mu^-)/\Gamma_{\rm total}$ Γ_{31}/Γ

Violates *CP* in leading order. Test for $\Delta S=1$ weak neutral current. Allowed by higher-order electroweak interaction.

VALUE (units 10^{-9})	CL%	EVTS	DOCUMENT ID		TECN
<0.38	90		ALAVI-HARATI	00D	KTEV
• • • We do not use the following data for averages, fits, limits, etc. • • •					
<5.1	90	0	HARRIS	93	E799

$\Gamma(\pi^0e^+e^-)/\Gamma_{\rm total}$ Γ_{32}/Γ

Violates *CP* in leading order. Direct and indirect *CP*-violating contributions are expected to be comparable and to dominate the *CP*-conserving part. LAI 02B result suggests that *CP*-violation effects dominate. Test for $\Delta S=1$ weak neutral current. Allowed by higher-order electroweak interaction.

VALUE (units 10^{-10})	CL%	EVTS	DOCUMENT ID		TECN	COMMENT
< 5.1	90	2	ALAVI-HARATI	01	KTEV	
• • • We do not use the following data for averages, fits, limits, etc. • • •						
0.0047$^{+0.0022}_{-0.0018}$			[44] LAI	02B	NA48	*CP*-conserving part
0.01 to 0.02			ALAVI-HARATI	99B	KTEV	*CP*-conserving part
< 43	90	0	HARRIS	93B	E799	
< 75	90	0	BARKER	90	E731	
< 55	90	0	OHL	90	B845	
< 400	90		BARR	88	NA31	
<3200	90		JASTRZEM...	88	SPEC	

[44] LAI 02B uses the absence of a signal in $K_L^0\to\pi^0\gamma\gamma$ with $m(\gamma\gamma)<m(\pi^0)$ and their a_V value to predict this value.

$\Gamma(\pi^0\nu\overline{\nu})/\Gamma_{\rm total}$ Γ_{33}/Γ

Violates *CP* in leading order. Test of direct *CP* violation since the indirect *CP*-violating and *CP*-conserving contributions are expected to be suppressed. Test of $\Delta S=1$ weak neutral current.

VALUE (units 10^{-5})	CL%	EVTS	DOCUMENT ID		TECN
< 0.059	90	0	ALAVI-HARATI	00	KTEV
• • • We do not use the following data for averages, fits, limits, etc. • • •					
< 0.16	90	0	ADAMS	99	KTEV
< 5.8	90	0	WEAVER	94	E799
<22	90	0	GRAHAM	92	CNTR

$\Gamma(e^\pm\mu^\mp)/\Gamma_{\rm total}$ Γ_{34}/Γ

Test of lepton family number conservation.

VALUE (units 10^{-11})	CL%	EVTS	DOCUMENT ID		TECN
<0.47	90		AMBROSE	98B	B871
• • • We do not use the following data for averages, fits, limits, etc. • • •					
<9.4	90	0	AKAGI	95	SPEC
<3.9	90	0	ARISAKA	93	B791
<3.3	90	0	[45] ARISAKA	93	B791

[45] This is the combined result of ARISAKA 93 and MATHIAZHAGAN 89.

$\Gamma(e^\pm e^\pm \mu^\mp \mu^\mp)/\Gamma_{total}$ Γ_{35}/Γ

Test of lepton family number conservation.

VALUE (units 10^{-11})	CL%	EVTS	DOCUMENT ID		TECN	COMMENT
< 4.12	90	0	ALAVI-HARATI 03B		KTEV	
• • • We do not use the following data for averages, fits, limits, etc. • • •						
< 12.3	90	0	[46] ALAVI-HARATI 01H		KTEV	Sup. by ALAVI-HARATI 03B
<610	90	0	[46] GU	96	E799	

[46] Assuming uniform phase space distribution.

$\Gamma(\pi^0 \mu^\pm e^\mp)/\Gamma_{total}$ Γ_{36}/Γ

Test of lepton family number conservation.

VALUE	CL%	DOCUMENT ID		TECN
$<6.2\times10^{-9}$	90	ARISAKA	98	E799

ENERGY DEPENDENCE OF K^0_L DALITZ PLOT

For discussion, see note on Dalitz plot parameters in the $K^\pm$ section of the Particle Listings above. For definitions of a_y, a_t, a_u, and a_y, see the earlier version of the same note in the 1982 edition of this *Review* published in Physics Letters **111B** 70 (1982).

$|\text{matrix element}|^2 = 1 + gu + hu^2 + jv + kv^2 + fuv$

where $u = (s_3 - s_0)\ /\ m^2_\pi$ and $v = (s_2 - s_1)\ /\ m^2_\pi$

LINEAR COEFFICIENT g FOR $K^0_L \to \pi^+\pi^-\pi^0$

VALUE	EVTS	DOCUMENT ID		TECN	COMMENT
0.678 ±0.008 OUR AVERAGE		Error includes scale factor of 1.5. See the ideogram below.			
0.6823±0.0044±0.0044	500k	ANGELOPO...	98C	CPLR	
0.681 ±0.024	6499	CHO	77	HBC	
0.620 ±0.023	4709	PEACH	77	HBC	
0.677 ±0.010	509k	MESSNER	74	ASPK	$a_y = -0.917 \pm 0.013$
• • • We do not use the following data for averages, fits, limits, etc. • • •					
0.69 ±0.07	192	[47] BALDO-...	75	HLBC	
0.590 ±0.022	56k	[47] BUCHANAN	75	SPEC	$a_u = -0.277 \pm 0.010$
0.619 ±0.027	20k	[47,48] BISI	74	ASPK	$a_t = -0.282 \pm 0.011$
0.612 ±0.032		[47] ALEXANDER	73B	HBC	
0.73 ±0.04	3200	[47] BRANDENB...	73	HBC	
0.608 ±0.043	1486	[47] KRENZ	72	HLBC	$a_t = -0.277 \pm 0.018$
0.650 ±0.012	29k	[47] ALBROW	70	ASPK	$a_y = -0.858 \pm 0.015$
0.593 ±0.022	36k	[47,49] BUCHANAN	70	SPEC	$a_u = -0.278 \pm 0.010$
0.664 ±0.056	4400	[47] SMITH	70	OSPK	$a_t = -0.306 \pm 0.024$
0.400 ±0.045	2446	[47] BASILE	68B	OSPK	$a_t = -0.188 \pm 0.020$
0.649 ±0.044	1350	[47] HOPKINS	67	HBC	$a_t = -0.294 \pm 0.018$
0.428 ±0.055	1198	[47] NEFKENS	67	OSPK	$a_u = -0.204 \pm 0.025$

[47] Quadratic dependence required by some experiments. (See sections on "QUADRATIC COEFFICIENT h" and "QUADRATIC COEFFICIENT k" below.) Correlations prevent us from averaging results of fits not including g, h, and k terms.

[48] BISI 74 value comes from quadratic fit with quad. term consistent with zero. g error is thus larger than if linear fit were used.

[49] BUCHANAN 70 result revised by BUCHANAN 75 to include radiative correlations and to use more reliable K^0_L momentum spectrum of second experiment (had same beam).

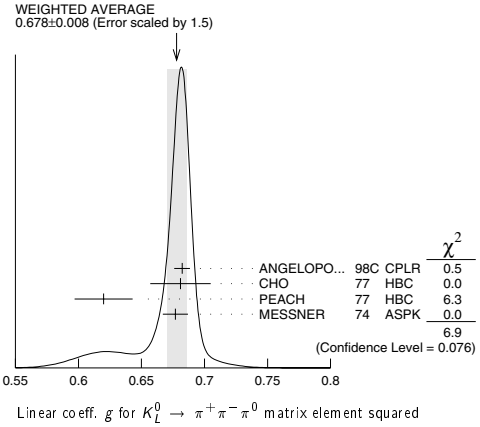

Linear coeff. g for $K^0_L \to \pi^+\pi^-\pi^0$ matrix element squared

QUADRATIC COEFFICIENT h FOR $K^0_L \to \pi^+\pi^-\pi^0$

VALUE	EVTS	DOCUMENT ID		TECN
0.076±0.006 OUR AVERAGE				
0.061±0.004±0.015	500k	ANGELOPO...	98C	CPLR
0.095±0.032	6499	CHO	77	HBC
0.048±0.036	4709	PEACH	77	HBC
0.079±0.007	509k	MESSNER	74	ASPK
• • • We do not use the following data for averages, fits, limits, etc. • • •				
−0.011±0.018	29k	[50] ALBROW	70	ASPK
0.043±0.052	4400	[50] SMITH	70	OSPK

See notes in section "LINEAR COEFFICIENT g FOR $K^0_L \to \pi^+\pi^-\pi^0$ |MATRIX ELEMENT|^2" above.

[50] Quadratic coefficients h and k required by some experiments. (See section on "QUADRATIC COEFFICIENT K" below.) Correlations prevent us from averaging results of fits not including g, h, and k terms.

QUADRATIC COEFFICIENT k FOR $K^0_L \to \pi^+\pi^-\pi^0$

VALUE	EVTS	DOCUMENT ID		TECN
0.0099±0.0015 OUR AVERAGE				
0.0104±0.0017±0.0024	500k	ANGELOPO...	98C	CPLR
0.024 ±0.010	6499	CHO	77	HBC
−0.008 ±0.012	4709	PEACH	77	HBC
0.0097±0.0018	509k	MESSNER	74	ASPK

LINEAR COEFFICIENT j FOR $K^0_L \to \pi^+\pi^-\pi^0$ (CP-VIOLATING TERM)

Listed in CP-violation section below.

QUADRATIC COEFFICIENT f FOR $K^0_L \to \pi^+\pi^-\pi^0$ (CP-VIOLATING TERM)

Listed in CP-violation section below.

QUADRATIC COEFFICIENT h FOR $K^0_L \to \pi^0\pi^0\pi^0$

VALUE (units 10^{-3})	EVTS	DOCUMENT ID		TECN
−5.0±1.4 OUR AVERAGE		Error includes scale factor of 1.7.		
−6.1±0.9±0.5	14.7M	LAI	01B	NA48
−3.3±1.1±0.7	5M	[51] SOMALWAR	92	E731

[51] SOMALWAR 92 chose m_{π^+} as normalization to make it compatible with the Particle Data Group $K^0_L \to \pi^+\pi^-\pi^0$ definitions.

K^0_L FORM FACTORS

For discussion, see note on form factors in the $K^\pm$ section of the Particle Listings above.

In the form factor comments, the following symbols are used.

f_+ and f_- are form factors for the vector matrix element.
f_S and f_T refer to the scalar and tensor term.
$f_0 = f_+ + f_- t/(m^2_K - m^2_\pi)$.
λ_+, λ_-, and λ_0 are the linear expansion coefficients of f_+, f_-, and f_0.
λ_+ refers to the $K^0_{\mu3}$ value except in the K^0_{e3} sections.
$d\xi(0)/d\lambda_+$ is the correlation between $\xi(0)$ and λ_+ in $K^0_{\mu3}$.
$d\lambda_0/d\lambda_+$ is the correlation between λ_0 and λ_+ in $K^0_{\mu3}$.
t = momentum transfer to the π in units of m^2_π.
DP = Dalitz plot analysis.
PI = π spectrum analysis.
MU = μ spectrum analysis.
POL= μ polarization analysis.
BR = $K^0_{\mu3}/K^0_{e3}$ branching ratio analysis.
E = positron or electron spectrum analysis.
RC = radiative corrections.

λ_+ (LINEAR ENERGY DEPENDENCE OF f_+ IN $K^0_{\ell3}$ DECAY)

For radiative correction of K^0_{e3} DP, see GINSBERG 67 and BECHERRAWY 70. Results labeled OUR FIT are discussed in the review "$K^\pm_{\ell3}$ and $K^0_{\ell3}$ Form Factors" in the $K^\pm$ Listings.

VALUE	EVTS	DOCUMENT ID		TECN	COMMENT
0.0300±0.0020 OUR FIT		Error includes scale factor of 2.0. Assumes μ-e universality.			
0.0291±0.0018 OUR AVERAGE		Error includes scale factor of 1.5. See the ideogram below.			
0.0245±0.0012±0.0022	366k	APOSTOLA...	00	CPLR	DP
0.0306±0.0034	74k	BIRULEV	81	SPEC	DP
0.025 ±0.005	12k	[52] ENGLER	78B	HBC	DP
0.0348±0.0044	18k	HILL	78	STRC	DP
0.0312±0.0025	500k	GJESDAL	76	SPEC	DP
0.0270±0.0028	25k	BLUMENTHAL	75	SPEC	DP
0.044 ±0.006	24k	BUCHANAN	75	SPEC	DP
0.023 ±0.005	42k	BISI	71	ASPK	DP
0.05 ±0.01	16k	CHIEN	71	ASPK	DP, no RC

• • • We do not use the following data for averages, fits, limits, etc. • • •

0.029 ±0.005	19k	[52] CHO	80	HBC	DP
0.040 ±0.012	2171	WANG	74	OSPK	DP
0.045 ±0.014	5600	ALBROW	73	ASPK	DP
0.019 ±0.013	1871	BRANDENB...	73	HBC	PI transv.
0.022 ±0.014	1910	NEUHOFER	72	ASPK	PI
0.02 ±0.013	1000	ARONSON	68	OSPK	PI
+0.023 ±0.012	4800	BASILE	68	OSPK	DP, no RC

[52] ENGLER 78B uses an unique K_{e3} subset of CHO 80 events and is less subject to systematic effects.

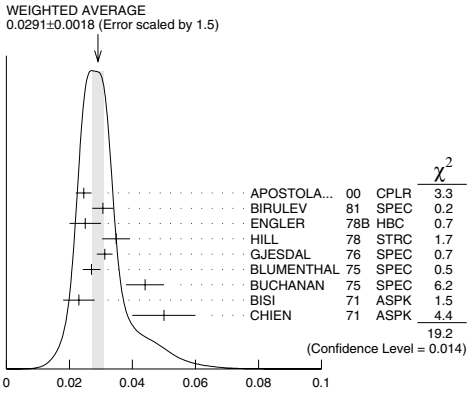

λ_+ (Linear energy dependence of f_+, K_{e3} decay)

$\xi_A = f_-/f_+$ (determined from $K^0_{\mu 3}$ spectra)

Results labeled OUR FIT are discussed in the review "$K^{\pm}_{\ell 3}$ and $K^0_{\ell 3}$ Form Factors" in the $K^{\pm}$ Listings. ξ_A is $\xi(0)$ determined by Method *A* of that review. The parameter $\xi(0)$ is redundant with λ_0 below and is not put into the Meson Summary Table.

VALUE	$d\xi(0)/d\lambda_+$	EVTS	DOCUMENT ID		TECN	COMMENT
−0.01±0.06 OUR FIT Error includes scale factor of 2.0. Correlation is $d\xi(0)/d\lambda_+ = -13.2$. Assumes μ-e universality.						
−0.08±0.09 OUR FIT Error includes scale factor of 2.3. Correlation is $d\xi(0)/d\lambda_+ = -13.7$.						
−0.10±0.09	−12	150k	[53] BIRULEV	81	SPEC	DP
+0.26±0.16	−13	14k	[54] CHO	80	HBC	DP
+0.13±0.23	−20	16k	[54] HILL	79	STRC	DP
−0.25±0.22	−5.9	32k	[55] BUCHANAN	75	SPEC	DP
−0.11±0.07	−17	1.6M	[56] DONALDSON	74B	SPEC	DP
• • • We do not use the following data for averages, fits, limits, etc. • • •						
−1.00±0.45	−20	1385	[57] PEACH	73	HLBC	DP
−1.5 ±0.7	−28	9086	[58] ALBROW	72	ASPK	DP
+0.50±0.61	unknown	16k	[59] DALLY	72	ASPK	DP
−3.9 ±0.4		3140	[60] BASILE	70	OSPK	DP, indep of λ_+
$-0.68^{+0.12}_{-0.20}$	−26	16k	[59] CHIEN	70	ASPK	DP
+1.2 ±0.8	−18	1341	[61] CARPENTER	66	OSPK	DP

[53] BIRULEV 81 error, $d\xi(0)/d\lambda_+$ calculated by us from λ_0, λ_+. $d\lambda_0/d\lambda_+ = 0$ used.

[54] HILL 79 and CHO 80 calculated by us from λ_0, λ_+, and $d\lambda_0/d\lambda_+$.

[55] BUCHANAN 75 is calculated by us from λ_0, λ_+ and $d\lambda_0/d\lambda_+$ because their appendix A value -0.20 ± 22 assumes $\xi(t)$ constant, i.e. $\lambda_- = \lambda_+$.

[56] DONALDSON 74B gives $\xi = -0.11 \pm 0.02$ not including systematics. Above error and $d\xi(0)/d\lambda_+$ were calculated by us from λ_0 and λ_+ errors (which include systematics) and $d\lambda_0/d\lambda_+$.

[57] PEACH 73 gives $\xi(0) = -0.95 \pm 0.45$ for $\lambda_+ = \lambda_- = 0.025$. The above value is for $\lambda_- = 0$. K.Peach, private communication (1974).

[58] ALBROW 72 fit has λ_- free, gets $\lambda_- = -0.030 \pm 0.060$ or $\Lambda = +0.15^{+0.17}_{-0.11}$.

[59] CHIEN 70 errors are statistical only. $d\xi(0)/d\lambda_+$ from figure 4. DALLY 72 is a reanalysis of CHIEN 70. The DALLY 72 result is not compatible with assumption $\lambda_- = 0$ so not included in our fit. The nonzero λ_- value and the relatively large λ_+ value found by DALLY 72 come mainly from a single low t bin (figures 1,2). The (f_+,ξ) correlation was ignored. We estimate from figure 2 that fixing $\lambda_- = 0$ would give $\xi(0) = -1.4 \pm 0.3$ and would add 10 to χ^2. $d\xi(0)/d\lambda_+$ is not given.

[60] BASILE 70 is incompatible with all other results. Authors suggest that efficiency estimates might be responsible.

[61] CARPENTER 66 $\xi(0)$ is for $\lambda_+ = 0$. $d\xi(0)/d\lambda_+$ is from figure 9.

$\xi_B = f_-/f_+$ (determined from $K^0_{\mu 3}/K^0_{e3}$)

The $K^0_{\mu 3}/K^0_{e3}$ branching ratio fixes a relationship between $\xi(0)$ and λ_+ if μ-e universality is assumed. We quote the author's $\xi(0)$ and associated λ_+ but do not average because the λ_+ values differ. The result labeled OUR FIT below does not use these ξ_b values. Instead it uses the authors $K^0_{\mu 3}/K^0_{e3}$ branching ratios to obtain the fitted $K^0_{\mu 3}/K^0_{e3}$ ratio which is then converted to the KL3FIT value below, as discussed in the review "$K^{\pm}_{\ell 3}$ and $K^0_{\ell 3}$ Form Factors" in the $K^{\pm}$ Listings. ξ_B is $\xi(0)$ determined by Method *B* of that review. The parameter $\xi(0)$ is redundant with λ_0 below and is not put into the Meson Summary Table.

VALUE	EVTS	DOCUMENT ID		TECN	COMMENT
−0.01±0.06 OUR FIT Error includes scale factor of 2.0. Correlation is $d\xi/d\lambda_+ = -13.2$. Assumes μ-e universality.					
0.13±0.07		[62] KL3FIT	04	RVUE	$\lambda_+ = 0.030$
• • • We do not use the following data for averages, fits, limits, etc. • • •					
0.5 ±0.4	6700	BRANDENB...	73	HBC	BR, $\lambda_+ = 0.019 \pm 0.013$
−0.08±0.25	1309	[63] EVANS	73	HLBC	BR, $\lambda_+ = 0.02$
−0.5 ±0.5	3548	BASILE	70	OSPK	BR, $\lambda_+ = 0.02$
+0.45±0.28	569	BEILLIERE	69	HLBC	BR, $\lambda_+ = 0$
−0.22±0.30	1309	[63] EVANS	69	HLBC	
$+0.2\ ^{+0.8}_{-1.2}$		KULYUKINA	68	CC	BR, $\lambda_+ = 0$
+1.1 ±1.1	389	ADAIR	64	HBC	BR, $\lambda_+ = 0$
$+0.66^{+0.9}_{-1.3}$		LUERS	64	HBC	BR, $\lambda_+ = 0$

[62] KL3FIT value is from fitted $K^0_{\mu 3}/K^0_{e3}$ branching ratio. $d\xi(0)/d\lambda_+ = -10.2$.

[63] EVANS 73 replaces EVANS 69.

$\xi_C = f_-/f_+$ (determined from μ polarization in $K^0_{\mu 3}$)

The μ polarization is a measure of $\xi(t)$. No assumptions on λ_{+-} are necessary, but t (weighted by sensitivity to $\xi(t)$) should be specified. In λ_+, $\xi(0)$ parametrization this is $\xi(0)$ for $\lambda_+ = 0$. $d\xi/d\lambda = \xi t$. For radiative correction to μ polarization in $K^0_{\mu 3}$, see GINSBERG 73. Results labeled OUR FIT are discussed in the review "$K^{\pm}_{\ell 3}$ and $K^0_{\ell 3}$ Form Factors" in the $K^{\pm}$ Listings. ξ_C is $\xi(0)$ determined by Method *C* of that review. The parameter $\xi(0)$ is redundant with λ_0 below and is not put into the Meson Summary Table.

VALUE	EVTS	DOCUMENT ID		TECN	COMMENT
−0.01 ±0.06 OUR FIT Error includes scale factor of 2.0. Correlation is $d\xi(0)/d\lambda_+ = -13.2$. Assumes μ-e universality.					
−0.08 ±0.09 OUR FIT Error includes scale factor of 2.3. Correlation is $d\xi(0)/d\lambda_+ = -13.7$.					
+0.178±0.105	207k	[64] CLARK	77	SPEC	POL, $d\xi(0)/d\lambda_+ = +0.68$
−0.385±0.105	2.2M	[65] SANDWEISS	73	CNTR	POL, $d\xi(0)/d\lambda_+ = -6$
• • • We do not use the following data for averages, fits, limits, etc. • • •					
$-1.81\ ^{+0.50}_{-0.26}$		[66] LONGO	69	CNTR	POL, $t = 3.3$
−1.6 ±0.5	638	[67] ABRAMS	68B	OSPK	Polarization
−1.2 ±0.5	2608	[67] AUERBACH	66B	OSPK	Polarization

[64] CLARK 77 $t = +3.80$, $d\xi(0)/d\lambda_+ = \xi(t)t = 0.178 \times 3.80 = +0.68$.

[65] SANDWEISS 73 is for $\lambda_+ = 0$ and $t = 0$.

[66] LONGO 69 $t = 3.3$ calculated from $d\xi(0)/d\lambda_+ = -6.0$ (table 1) divided by $\xi = -1.81$.

[67] t value not given.

λ_+ (LINEAR ENERGY DEPENDENCE OF f_+ IN $K^0_{\mu 3}$ DECAY)

See also the corresponding entries and notes in section "$\xi_A = f_-/f_+$" above and section "λ_0 (LINEAR ENERGY DEPENDENCE OF f_0 IN $K^0_{\mu 3}$ DECAY)" below. For radiative correction of $K^0_{\mu 3}$ Dalitz plot see GINSBERG 70 and BECHERRAWY 70. Results labeled OUR FIT are discussed in the review "$K^{\pm}_{\ell 3}$ and $K^0_{\ell 3}$ Form Factors" in the $K^{\pm}$ Listings.

VALUE	EVTS	DOCUMENT ID		TECN	COMMENT
0.0300±0.0020 OUR FIT Error includes scale factor of 2.0. Assumes μ-e universality.					
0.033 ±0.005 OUR FIT Error includes scale factor of 2.3.					
0.0427±0.0044	150k	BIRULEV	81	SPEC	DP
0.028 ±0.010	14k	CHO	80	HBC	DP
0.028 ±0.011	16k	HILL	79	STRC	DP
0.046 ±0.030	32k	BUCHANAN	75	SPEC	DP
0.030 ±0.003	1.6M	DONALDSON	74B	SPEC	DP
• • • We do not use the following data for averages, fits, limits, etc. • • •					
0.0337±0.0033	129k	DZHORD...	77	SPEC	Repl. by BIRULEV 81
0.046 ±0.008	82k	ALBRECHT	74	WIRE	Repl. by BIRULEV 81
0.085 ±0.015	9086	ALBROW	72	ASPK	DP
0.11 ±0.04	16k	DALLY	72	ASPK	DP
0.07 ±0.02	16k	CHIEN	70	ASPK	Repl. by DALLY 72

λ_0 (LINEAR ENERGY DEPENDENCE OF f_0 IN $K^0_{\mu 3}$ DECAY)

Wherever possible, we have converted the above values of $\xi(0)$ into values of λ_0 using the associated λ^{μ}_{+} and $d\xi(0)/d\lambda_+$. Results labeled OUR FIT are discussed in the review "$K^{\pm}_{\ell 3}$ and $K^0_{\ell 3}$ Form Factors" in the $K^{\pm}$ Listings.

VALUE	$d\lambda_0/d\lambda_+$	EVTS	DOCUMENT ID		TECN	COMMENT
0.030 ±0.005 OUR FIT	Error includes scale factor of 2.0. Correlation is $d\lambda_0/d\lambda_+ = -0.12$. Assumes μ-e universality.					
0.027 ±0.006 OUR FIT	Error includes scale factor of 2.3. Correlation is $d\lambda_0/d\lambda_+ = -0.17$.					
0.041 ±0.006	0.13		[68] KL3FIT	04	RVUE	$\lambda_+ = 0.030$
0.0341±0.0067	unknown	150k	[69] BIRULEV	81	SPEC	DP
+0.050 ±0.008	−0.11	14k	CHO	80	HBC	DP
+0.039 ±0.010	−0.67	16k	HILL	79	STRC	DP
+0.047 ±0.009	1.06	207k	[70] CLARK	77	SPEC	POL
+0.025 ±0.019	+0.5	32k	[71] BUCHANAN	75	SPEC	DP
+0.019 ±0.004	−0.47	1.6M	[72] DONALDSON	74B	SPEC	DP
−0.018 ±0.009	+0.49	2.2M	[70] SANDWEISS	73	CNTR	POL
• • • We do not use the following data for averages, fits, limits, etc. • • •						
0.041 ±0.008		14k	[73] CHO	80	HBC	BR, $\lambda_+ = 0.028$
+0.0485±0.0076		47k	DZHORD...	77	SPEC	In BIRULEV 81
+0.024 ±0.011		82k	ALBRECHT	74	WIRE	In BIRULEV 81
+0.06 ±0.03		6700	[74] BRANDENB...	73	HBC	BR, $\lambda_+ = 0.019 \pm 0.013$
−0.060 ±0.038	−0.71	1385	[75] PEACH	73	HLBC	DP
−0.043 ±0.052	−1.39	9086	[76] ALBROW	72	ASPK	DP
−0.067 ±0.227	unknown	16k	[77] DALLY	72	ASPK	DP
−0.333 ±0.034	+1.	3140	[78] BASILE	70	OSPK	DP
$-0.140\ ^{+0.043}_{-0.022}$	+0.49		[70] LONGO	69	CNTR	POL
+0.08 ±0.07	−0.54	1371	[70] CARPENTER	66	OSPK	DP

[68] KL3FIT 04 value is from our fitted value of the $K^{\pm}_{\mu 3}/K^{\pm}_{e3}$ branching ratio. Assumes $\mu - e$ universality.

[69] BIRULEV 81 gives $d\lambda_0/d\lambda_+ = -1.5$, giving an unreasonably narrow error ellipse which dominates all other results. We use $d\lambda_0/d\lambda_+ = 0$.

[70] λ_0 value is for $\lambda_+ = 0.03$ calculated by us from $\xi(0)$ and $d\xi(0)/d\lambda_+$.

[71] BUCHANAN 75 value is from their appendix A and uses only $K_{\mu 3}$ data. $d\lambda_0/d\lambda_+$ was obtained by private communication, C.Buchanan, 1976.

[72] DONALDSON 74B $d\lambda_0/d\lambda_+$ obtained from figure 18.

[73] CHO 80 BR result not independent of their Dalitz plot result.

[74] Fit for λ_0 does not include this value but instead includes the $K_{\mu 3}/K_{e3}$ result from this experiment.

[75] PEACH 73 assumes $\lambda_+ = 0.025$. Calculated by us from $\xi(0)$ and $d\xi(0)/d\lambda_+$.

[76] ALBROW 72 λ_0 is calculated by us from ξ_A, λ_+ and $d\xi(0)/d\lambda_+$. They give $\lambda_0 = -0.043 \pm 0.039$ for $\lambda_- = 0$. We use our larger calculated error.

[77] DALLY 72 gives $f_0 = 1.20 \pm 0.35$, $\lambda_0 = -0.080 \pm 0.272$, $\lambda_0{}' = -0.006 \pm 0.045$, but with a different definition of λ_0. Our quoted λ_0 is his λ_0/f_0. We cannot calculate true λ_0 error without his (λ_0, f_0) correlations. See also note on DALLY 72 in section ξ_A.

[78] BASILE 70 λ_0 is for $\lambda_+ = 0$. Calculated by us from ξ_A with $d\xi(0)/d\lambda_+ = 0$. BASILE 70 is incompatible with all other results. Authors suggest that efficiency estimates might be responsible.

$|f_S/f_+|$ FOR K^0_{e3} DECAY

Ratio of scalar to f_+ couplings.

VALUE	CL%	EVTS	DOCUMENT ID		TECN	COMMENT
<0.04	68	25k	BLUMENTHAL	75	SPEC	
• • • We do not use the following data for averages, fits, limits, etc. • • •						
<0.095	95	18k	HILL	78	STRC	
<0.07	68	48k	BIRULEV	76	SPEC	See also BIRULEV 81
<0.19	95	5600	ALBROW	73	ASPK	
<0.15	68		KULYUKINA	67	CC	

$|f_T/f_+|$ FOR K^0_{e3} DECAY

Ratio of tensor to f_+ couplings.

VALUE	CL%	EVTS	DOCUMENT ID		TECN	COMMENT
<0.23	68	25k	BLUMENTHAL	75	SPEC	
• • • We do not use the following data for averages, fits, limits, etc. • • •						
<0.40	95	18k	HILL	78	STRC	
<0.34	68	48k	BIRULEV	76	SPEC	See also BIRULEV 81
<1.0	95	5600	ALBROW	73	ASPK	
<1.0	68		KULYUKINA	67	CC	

$|f_T/f_+|$ FOR $K^0_{\mu 3}$ DECAY

Ratio of tensor to f_+ couplings.

VALUE	DOCUMENT ID		TECN
0.12±0.12	BIRULEV	81	SPEC

α_{K^*} DECAY FORM FACTOR FOR $K_L \to e^+e^-\gamma$

α_{K^*} is the constant in the model of BERGSTROM 83 which measures the relative strength of the vector-vector transition $K_L \to K^*\gamma$ with $K^* \to \rho, \omega, \phi \to \gamma^*$ and the pseudoscalar-pseudoscalar transition $K_L \to \pi, \eta, \eta' \to \gamma\gamma^*$.

VALUE	EVTS	DOCUMENT ID		TECN
−0.33 ±0.05 OUR AVERAGE				
−0.36 ±0.06 ±0.02	6864	FANTI	99B	NA48
−0.28 ±0.13		BARR	90B	NA31
$-0.280\ ^{+0.099}_{-0.090}$		OHL	90B	B845

α_{K^*} DECAY FORM FACTOR FOR $K_L \to \mu^+\mu^-\gamma$

α_{K^*} is the constant in the model of BERGSTROM 83 described in the previous section.

VALUE	EVTS	DOCUMENT ID		TECN
−0.158±0.027 OUR AVERAGE				
$-0.160\ ^{+0.026}_{-0.028}$	9100	ALAVI-HARATI	01G	KTEV
$-0.04\ ^{+0.24}_{-0.21}$		FANTI	97	NA48

$\alpha^{\rm eff}_{K^*}$ DECAY FORM FACTOR FOR $K_L \to e^+e^-e^+e^-$

$\alpha^{\rm eff}_{K^*}$ is the parameter describing the relative strength of an intermediate pseudoscalar decay amplitude and a vector meson decay amplitude in the model of BERGSTROM 83. It takes into account both the radiative effects and the form factor. Since there are two e^+e^- pairs here compared with one in $e^+e^-\gamma$ decays, a factorized expression is used for the $e^+e^-e^+e^-$ decay form factor.

VALUE	EVTS	DOCUMENT ID		TECN
−0.14±0.16±0.15	441	ALAVI-HARATI	01D	KTEV

a_1/a_2 FORM FACTOR FOR M1 DIRECT EMISSION AMPLITUDE

Form factor $= \tilde{g}_{M1}\left[1 + \frac{a_1/a_2}{(M_\rho^2 - M_K^2) + 2M_K E^*_\gamma}\right]$ as described in ALAVI-HARATI 00B.

VALUE (GeV^2)	EVTS	DOCUMENT ID		TECN	COMMENT
−0.734±0.022 OUR AVERAGE					
$-0.81\ ^{+0.07}_{-0.13}$ ±0.02		[79] LAI	03C	NA48	$\pi^+\pi^-e^+e^-$
−0.737±0.026±0.022		[80] ALAVI-HARATI	01B		$\pi^+\pi^-\gamma$
−0.720±0.028±0.009	1766	[81] ALAVI-HARATI	00B	KTEV	$\pi^+\pi^-e^+e^-$

[79] LAI 03C also measured $\tilde{g}_{M1} = 0.99\ ^{+0.28}_{-0.27} \pm 0.07$.

[80] ALAVI-HARATI 01B fit gives $\chi^2/\text{DOF} = 38.8/27$. Linear and quadratic fits give $\chi^2/\text{DOF} = 43.2/27$ and $37.6/26$ respectively.

[81] ALAVI-HARATI 00B also measured $\tilde{g}_{M1} = 1.35\ ^{+0.20}_{-0.17} \pm 0.04$.

DECAY FORM FACTORS FOR $K^0_L \to \pi^{\pm}\pi^0 e^{\mp}\nu_e$

Given in MAKOFF 93.

a_V, VECTOR MESON EXCHANGE CONTRIBUTION

VALUE	DOCUMENT ID		TECN	COMMENT
−0.54±0.12 OUR AVERAGE	Error includes scale factor of 2.8. See the ideogram below.			
−0.46±0.03±0.04	LAI	02B	NA48	$K^0_L \to \pi^0 2\gamma$
−0.67±0.21±0.12	ALAVI-HARATI	01E	KTEV	$K^0_L \to \pi^0 e^+ e^- \gamma$
−0.72±0.05±0.06	ALAVI-HARATI	99B	KTEV	$K^0_L \to \pi^0 2\gamma$

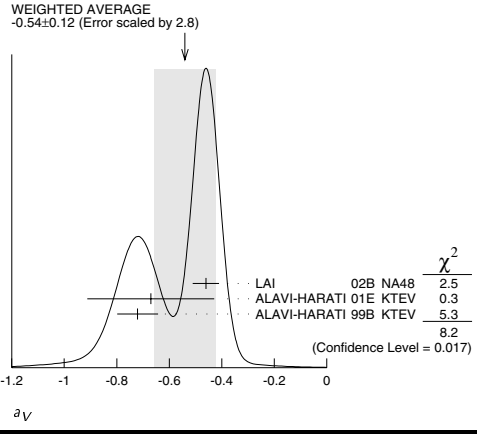

CP VIOLATION IN K_L DECAYS

Revised March 2004 by L. Wolfenstein (Carnegie-Mellon University) and T.G. Trippe (LBNL).

The symmetries C (particle-antiparticle interchange) and P (space inversion) hold for strong and electromagnetic interactions. After the discovery of large C and P violation in the weak interactions, it appeared that the product CP was a good symmetry. In 1964 CP violation was observed in K^0 decays at a level given by the parameter $\epsilon \approx 2.3 \times 10^{-3}$.

A unified treatment of CP violation in K, D, B, and B_s mesons is given in "CP Violation in Meson Decays" by D. Kirkby and Y. Nir in this *Review*. A recent book by

K. Kleinknecht [1] gives a more detailed review including a thorough discussion of the experimental techniques used to determine CP violation parameters. Here we give a concise summary of the formalism needed to define the parameters of CP violation in K_L decays and a description of our fits for the best values of these parameters.

1. Formalism for CP violation in Kaon decay:

CP violation has been observed in the semi-leptonic decays $K_L^0 \to \pi^\mp \ell^\pm \nu$ and in the nonleptonic decay $K_L^0 \to 2\pi$. The experimental numbers that have been measured are

$$\delta_L = \frac{\Gamma(K_L^0 \to \pi^- \ell^+ \nu) - \Gamma(K_L^0 \to \pi^+ \ell^- \nu)}{\Gamma(K_L^0 \to \pi^- \ell^+ \nu) + \Gamma(K_L^0 \to \pi^+ \ell^- \nu)} \quad (1a)$$

$$\eta_{+-} = A(K_L^0 \to \pi^+\pi^-)/A(K_S^0 \to \pi^+\pi^-) = |\eta_{+-}|\, e^{i\phi_{+-}} \quad (1b)$$

$$\eta_{00} = A(K_L^0 \to \pi^0\pi^0)/A(K_S^0 \to \pi^0\pi^0) = |\eta_{00}|\, e^{i\phi_{00}} \ . \quad (1c)$$

CP violation can occur either in the K^0–$\overline{K}^0$ mixing or in the decay amplitudes. Assuming CPT invariance, the mass eigenstates of the K^0–$\overline{K}^0$ system can be written

$$|K_S\rangle = p|K^0\rangle + q|\overline{K}^0\rangle \ , \qquad |K_L\rangle = p|K^0\rangle - q|\overline{K}^0\rangle \ . \quad (2)$$

If CP invariance held, we would have $q = p$ so that K_S would be CP even and K_L CP odd. (We define $|\overline{K}^0\rangle$ as CP $|K^0\rangle$). CP violation in K^0–$\overline{K}^0$ mixing is then given by the parameter $\widetilde{\epsilon}$ where

$$\frac{p}{q} = \frac{(1+\widetilde{\epsilon})}{(1-\widetilde{\epsilon})} \ . \quad (3)$$

CP violation can also occur in the decay amplitudes

$$A(K^0 \to \pi\pi(I)) = A_I e^{i\delta_I} \ , \qquad A(\overline{K}^0 \to \pi\pi(I)) = A_I^* e^{i\delta_I} \ , \quad (4)$$

where I is the isospin of $\pi\pi$, δ_I is the final-state phase shift, and A_I would be real if CP invariance held. The CP-violating observables are usually expressed in terms of ϵ and ϵ' defined by

$$\eta_{+-} = \epsilon + \epsilon' \ , \qquad \eta_{00} = \epsilon - 2\epsilon' \ , \quad (5a)$$

One can then show [2]

$$\epsilon = \widetilde{\epsilon} + i\ (\mathrm{Im}\ A_0/\mathrm{Re}\ A_0) \ , \quad (5b)$$

$$\sqrt{2}\epsilon' = ie^{i(\delta_2-\delta_0)}(\mathrm{Re}\, A_2/\mathrm{Re}\, A_0)\ (\mathrm{Im}\, A_2/\mathrm{Re}\, A_2 - \mathrm{Im}\, A_0/\mathrm{Re}\, A_0) \ , \quad (5c)$$

$$\delta_L = 2\mathrm{Re}\,\epsilon/(1+|\epsilon|^2) \approx 2\mathrm{Re}\,\epsilon \ . \quad (5d)$$

In Eqs. (5a) small corrections of order $\epsilon' \times \mathrm{Re}\ (A_2/A_0)$ are neglected and Eq. (5d) assumes the $\Delta S = \Delta Q$ rule.

The quantities Im A_0, Im A_2, and Im $\widetilde{\epsilon}$ depend on the choice of phase convention since one can change the phases of K^0 and $\overline{K}^0$ by a transformation of the strange quark state $|s\rangle \to |s\rangle\, e^{i\alpha}$; of course, observables are unchanged. It is possible by a choice of phase convention to set Im A_0 or Im A_2 or Im $\widetilde{\epsilon}$ to zero, but none of these is zero with the usual phase conventions in the Standard Model. The choice Im $A_0 = 0$ is called the Wu-Yang phase convention [3] in which case $\epsilon = \widetilde{\epsilon}$. The value of ϵ' is independent of phase convention and a nonzero value demonstrates CP violation in the decay amplitudes, referred to as direct CP violation. The possibility that direct CP violation is essentially zero and that CP violation occurs only in the mixing matrix was referred to as the superweak theory [4].

By applying CPT invariance and unitarity the phase of ϵ is given approximately by

$$\phi_\epsilon \approx \tan^{-1}\frac{2(m_{K_L} - m_{K_S})}{\Gamma_{K_S} - \Gamma_{K_L}} \approx 43.51 \pm 0.05^\circ \quad (6a)$$

while Eq. (5c) gives the phase of ϵ' to be

$$\phi_{\epsilon'} = \delta_2 - \delta_0 + \frac{\pi}{2} \approx 48 \pm 4^\circ \ , \quad (6b)$$

where the numerical value is based on an analysis of π–π scattering [5]. The approximation in Eq. (6a) depends on the assumption that direct CP violation is very small in all K^0 decays. This is expected to be good to a few tenths of a degree as indicated by the small value of ϵ' and of η_{+-0}, the CP-violation parameter in the decay $K_S \to \pi^+\pi^-\pi^0$ [6], although limits on η_{000} are still poor. The relation in Eq. (6a) is exact in the superweak theory so this is sometimes called the superweak phase ϕ_{SW}. An important point for the analysis is that $\cos(\phi_{\epsilon'} - \phi_\epsilon) \simeq 1$. The consequence is that only two real quantities need be measured, the magnitude of ϵ and the value of (ϵ'/ϵ) including its sign. The measured quantity $|\eta_{00}/\eta_{+-}|^2$, which is very close to unity so that we can write

$$|\eta_{00}/\eta_{+-}|^2 \approx 1 - 6\mathrm{Re}\,(\epsilon'/\epsilon) \approx 1 - 6\epsilon'/\epsilon \ . \quad (7a)$$

$$\mathrm{Re}(\epsilon'/\epsilon) \approx \tfrac{1}{3}(1 - |\eta_{00}/\eta_{+-}|) \ . \quad (7b)$$

From the experimental measurements in this Edition of the *Review of Particle Physics* and the fits discussed in the next section, one finds

$$|\epsilon| = (2.284 \pm 0.014) \times 10^{-3} \ , \quad (8a)$$

$$\phi_\epsilon = (43.5 \pm 0.7)^\circ \ , \quad (8b)$$

$$\mathrm{Re}(\epsilon'/\epsilon) \approx \epsilon'/\epsilon = (1.67 \pm 0.26) \times 10^{-3} \ , \quad (8c)$$

$$\phi_{+-} = (43.4 \pm 0.7)^\circ \ , \quad (8d)$$

$$\phi_{00} - \phi_{+-} = (0.2 \pm 0.4)^\circ \ , \quad (8e)$$

$$\delta_L = (3.27 \pm 0.12) \times 10^{-3} \ . \quad (8f)$$

Direct CP violation, as indicated by ϵ'/ϵ, is expected in the Standard Model. However the numerical value cannot be reliably predicted because of theoretical uncertainties [7]. The value of δ_L agrees with Eq. (5d). The values of ϕ_{+-} and $\phi_{00} - \phi_{+-}$ are used to set limits on CPT violation. [See Tests of Conservation Laws.]

2. Fits for K_L^0 CP-violation parameters:

In recent years, K_L^0 CP-violation experiments have improved our knowledge of CP-violation parameters and their consistency with the expectations of CPT invariance and unitarity. To determine the best values of the CP-violation parameters in $K_L^0 \to \pi^+\pi^-$ and $\pi^0\pi^0$ decay, we make two types of

fits, one for the phases ϕ_{+-} and ϕ_{00} jointly with Δm and τ_S, and the other for the amplitudes $|\eta_{+-}|$ and $|\eta_{00}|$ jointly with the $K_L^0 \to \pi\pi$ branching fractions.

Fits to ϕ_{+-}, ϕ_{00}, $\Delta\phi$, Δm, and τ_S data: These are joint fits to the data on ϕ_{+-}, ϕ_{00}, the phase difference $\Delta\phi = \phi_{00} - \phi_{+-}$, the K_L^0–K_S^0 mass difference Δm, and the K_S^0 mean life τ_S, including the effects of correlations.

Measurements of ϕ_{+-} and ϕ_{00} are highly correlated with Δm and τ_S. Some measurements of τ_S are correlated with Δm. The correlations are given in the footnotes of the ϕ_{+-} and ϕ_{00} sections of the K_L^0 Particle Listings and the τ_S section of the K_S^0 Particle listings.

In most cases, the correlations are quoted as 100%, *i.e.*with the value and error of ϕ_{+-} or ϕ_{00} given at a fixed value of Δm and τ_S with additional terms specifying the dependence of the value on Δm and τ_S. These cases lead to diagonal bands in Figs. [1] and [2]. The KTeV experiment [8] quotes its results as values of ϕ_{+-}, Δm, and τ_S with correlations, leading to the ellipses labeled "b".

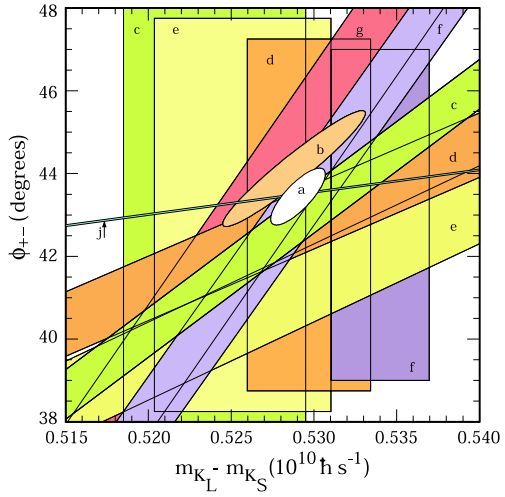

Figure 1: ϕ_{+-} vs Δm for experiments which do not assume CPT invariance. Δm measurements appear as vertical bands spanning $\Delta m \pm 1\sigma$, cut near the top and bottom to aid the eye. Most ϕ_{+-} measurements appear as diagonal bands spanning $\phi_{+-} \pm \sigma_\phi$. Data are labeled by letters: "b"–FNAL KTeV, "c"–CERN CPLEAR, "d"–FNAL E773, "e"–FNAL E731, "f"–CERN, "g"–CERN NA31, and are cited in Table 1. The narrow band "j" shows ϕ_{SW}. The ellipse "a" shows the $\chi^2 = 1$ contour of the fit result. See full-color version on color pages at end of book.

The data on τ_S, Δm, and ϕ_{+-} shown in Figs. [1] and [2]. are combined with data on ϕ_{00} and $\phi_{00} - \phi_{+-}$ in two fits, one without assuming CPT and the other with this assumption. The results without assuming CPT are shown as ellipses labeled "a". These ellipses are seen to be in good agreement with the superweak phase

$$\phi_{SW} = \tan^{-1}\left(\frac{2\Delta m}{\Delta\Gamma}\right) = \tan^{-1}\left(\frac{2\Delta m \tau_S \tau_L}{\hbar(\tau_L - \tau_S)}\right) . \qquad (9)$$

In Figs. [1] and [2], ϕ_{SW} is shown as narrow bands labeled "j".

Table 1: References, Document ID's, and sources corresponding to the letter labels in the figures. The data are given in the ϕ_{+-} and Δm sections of the K_L Particle Listings, and the τ_S section of the K_S Particle Listings.

Label	Source	PDG Document ID	Ref.
a	this review	OUR FIT	
b	FNAL KTeV	ALAVI-HARATI 03	[8]
c	CERN CPLEAR	APOSTOLAKIS 99C	[9]
d	FNAL E773	SCHWINGENHEUER 95	[10]
e	FNAL E731	GIBBONS 93,93C	[11,12]
f	CERN	GEWENIGER 74B,74C	[13,14]
g	CERN NA31	CAROSI 90	[15]
h	CERN NA48	LAI 02C	[16]
i	CERN NA31	BERTANZA 97	[17]
j	this review	SUPERWEAK 04	

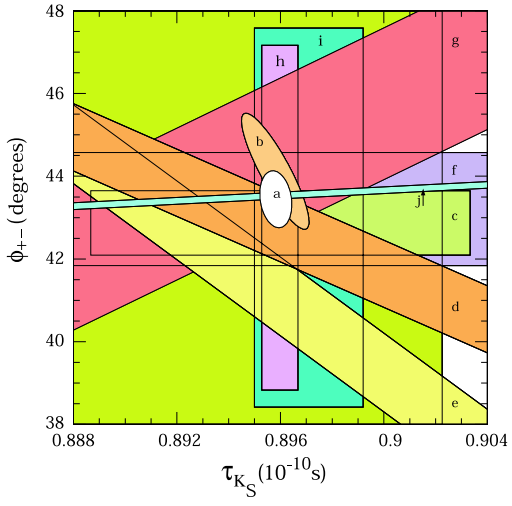

Figure 2: ϕ_{+-} vs τ_S. τ_S measurements appear as vertical bands spanning $\tau_S \pm 1\sigma$, some of which are cut near the top and bottom to aid the eye. Most ϕ_{+-} measurements appear as diagonal or horizontal bands spanning $\phi_{+-} \pm \sigma_\phi$. Data are labeled by letters: "b"–FNAL KTeV, "c"–CERN CPLEAR, "d"–FNAL E773, "e"–FNAL E731, "f"–CERN, "g"–CERN NA31, "h"–CERN NA48, "i"–CERN NA31, and are cited in Table 1. The narrow band "j" shows ϕ_{SW}. The ellipse "a" shows the fit result's $\chi^2 = 1$ contour. Color version at end of book.

Table 2 column 2, "Fit w/o CPT," gives the resulting fitted parameters, while Table 3 gives the correlation matrix for this fit. The white ellipses labeled "a" in Fig. 1 and Fig. 2 are the $\chi^2 = 1$ contours for this fit.

For experiments which have dependencies on unseen fit parameters, that is, parameters other than those shown on the x or y axis of the figure, their band positions are evaluated using the fit results and their band widths include the fitted uncertainty in the unseen parameters. This is also true for the $\phi_{\rm SW}$ bands.

If CPT invariance and unitarity are assumed, then by Eq. (6a), the phase of ϵ is constrained to be approximately equal to

$$\phi_{\rm SW} = (43.507 \pm 0.0004)^\circ + 54(\Delta m = 0.5290)^\circ + 32(\tau_S - 0.8958) \quad (10)$$

where we have linearized the Δm and τ_S dependence of Eq. (9). The error ± 0.0004 is due to the uncertainty in τ_L. Here Δm has units $10^{10}\,\hbar\,{\rm s}^{-1}$ and τ_S has units 10^{-10} s.

If in addition we use the observation that $Re(\epsilon'/\epsilon) \ll 1$ and $cos(\phi_{\epsilon'} - \phi_\epsilon) \simeq 1$, as well as the numerical value of $\phi_{\epsilon'} - \phi_\epsilon$ given in Eq. (6b), then Eqs. (5a), which are sketched in Fig. 3, lead to the constraint

$$\begin{aligned} \phi_{00} - \phi_{+-} &\approx -3\ {\rm Im}\left(\frac{\epsilon'}{\epsilon}\right) \\ &\approx -3\ {\rm Re}\left(\frac{\epsilon'}{\epsilon}\right) \tan(\phi_{\epsilon'} - \phi_\epsilon) \\ &\approx -0.023^\circ \pm 0.020^\circ \end{aligned} \quad (11)$$

so that $\phi_{+-} \approx \phi_{00} \approx \phi_\epsilon \approx \phi_{\rm SW}$.

In the fit assuming CPT we constrain $\phi_\epsilon = \phi_{\rm SW}$ using the linear expression in Eq. (10) and constrain $\phi_{00} - \phi_{+-}$ using Eq. (11). These constraints are inserted into the Data Listings with the Document ID of SUPERWEAK 04. Some additional data for which the authors assumed CPT are added to this fit or substitute for other less precise data for which the authors did not make this assumption. See the data listings for details.

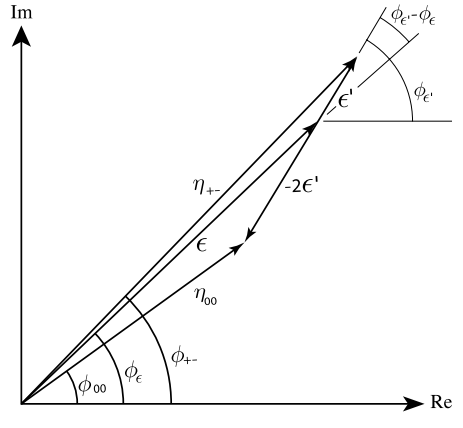

Figure 3: Sketch of Eqs. (5a). Not to scale.

The results of this fit are shown in Table 2, column 3, "Fit w/CPT," and the correlation matrix is shown in Table 4. The Δm precision is improved by the CPT assumption.

Table 2: Fit results for ϕ_{+-}, Δm, τ_S, ϕ_{00}, $\Delta\phi = \phi_{00} - \phi_{+-}$, and ϕ_ϵ without and with the CPT assumption.

Quantity(units)	Fit w/o CPT	Fit w/ CPT
$\phi_{+-}(^\circ)$	43.4 ± 0.7 (S=1.3)	43.52 ± 0.06 (S=1.3)
$\Delta m(10^{10}\hbar\ {\rm s}^{-1})$	0.5290 ± 0.0016 (S=1.2)	0.5292 ± 0.0010 (S=1.2)
$\tau_S(10^{-10}{\rm s})$	0.8958 ± 0.0006 (S=1.2)	0.8953 ± 0.0006 (S=1.4)
$\phi_{00}(^\circ)$	43.7 ± 0.8 (S=1.2)	43.50 ± 0.06 (S=1.3)
$\Delta\phi(^\circ)$	0.2 ± 0.4	-0.022 ± 0.041 (S=2.1)
$\phi_\epsilon(^\circ)$	43.5 ± 0.7 (S=1.3)	43.51 ± 0.05 (S=1.2)
χ^2	17.3	21.8
No. Deg. Freedom	13	17

Table 3: Correlation matrix for the results of the fit without the CPT assumption

	ϕ_{+-}	Δm	τ_S	ϕ_{00}	$\Delta\phi$	ϕ_ϵ
ϕ_{+-}	1.00	0.79	−0.19	0.85	0.00	0.98
Δm	0.79	1.00	−0.16	0.69	0.03	0.78
τ_S	−0.19	−0.16	1.00	−0.15	0.01	−0.18
ϕ_{00}	0.85	0.69	−0.15	1.00	0.53	0.94
$\Delta\phi$	0.00	0.03	0.01	0.53	1.00	0.21
ϕ_ϵ	0.98	0.78	−0.18	0.94	0.21	1.00

Table 4: Correlation matrix for the results of the fit with the CPT assumption

	ϕ_{+-}	Δm	τ_S	ϕ_{00}	$\Delta\phi$	ϕ_ϵ
ϕ_{+-}	1.00	0.92	0.32	0.76	−0.26	0.97
Δm	0.92	1.00	0.00	0.84	−0.02	0.94
τ_S	0.32	0.00	1.00	0.30	0.01	0.33
ϕ_{00}	0.76	0.84	0.30	1.00	0.44	0.89
$\Delta\phi$	−0.26	−0.02	0.01	0.44	1.00	−0.02
ϕ_ϵ	0.97	0.94	0.33	0.89	−0.02	1.00

Fits for ϵ'/ϵ, $|\eta_{+-}|$, $|\eta_{00}|$, and B($K_L \to \pi\pi$)

We list measurements of $|\eta_{+-}|$, $|\eta_{00}|$, $|\eta_{00}/\eta_{+-}|$ and ϵ'/ϵ. Independent information on $|\eta_{+-}|$ and $|\eta_{00}|$ can be obtained from measurements of the K^0_L and K^0_S lifetimes (τ_L, τ_S) and branching ratios (B) to $\pi\pi$, using the relations

$$|\eta_{+-}| = \left[\frac{{\rm B}(K^0_L \to \pi^+\pi^-)}{\tau_L}\ \frac{\tau_S}{{\rm B}(K^0_S \to \pi^+\pi^-)}\right]^{1/2}, \quad (12a)$$

$$|\eta_{00}| = \left[\frac{{\rm B}(K^0_L \to \pi^0\pi^0)}{\tau_L}\ \frac{\tau_S}{{\rm B}(K^0_S \to \pi^0\pi^0)}\right]^{1/2}. \quad (12b)$$

For historical reasons the branching ratio fits and the CP-violation fits are done separately, but we want to include the influence of $|\eta_{+-}|$, $|\eta_{00}|$, $|\eta_{00}/\eta_{+-}|$, and ϵ'/ϵ measurements on $B(K^0_L \to \pi^+\pi^-)$ and $B(K^0_L \to \pi^0\pi^0)$ and vice versa. We approximate a global fit to all of these measurements by first performing two independent fits: 1) BRFIT, a fit to the K^0_L branching ratios, rates, and mean life, and 2) ETAFIT, a fit to the $|\eta_{+-}|$, $|\eta_{00}|$, $|\eta_{+-}/\eta_{00}|$, and ϵ'/ϵ measurements. The results from fit 1, along with the K^0_S values from this edition are used to compute values of $|\eta_{+-}|$ and $|\eta_{00}|$ which are included as measurements in the $|\eta_{00}|$ and $|\eta_{+-}|$ sections with a document ID of BRFIT 04. Thus the fit values of $|\eta_{+-}|$ and $|\eta_{00}|$ given in this edition include both the direct measurements and the results from the branching ratio fit.

The process is reversed in order to include the direct $|\eta|$ measurements in the branching ratio fit. The results from fit 2 above (before including BRFIT 04 values) are used along with the K^0_L and K^0_S mean lives and the $K^0_S \to \pi\pi$ branching fractions to compute the K^0_L branching ratios $\Gamma(K^0_L \to \pi^+\pi^-)/\Gamma(\text{total})$ and $\Gamma(K^0_L \to \pi^0\pi^0)/\Gamma(K^0_L \to \pi^+\pi^-)$. These branching ratio values are included as measurements in the branching ratio section with a document ID of ETAFIT 04. Thus the K^0_L branching ratio fit values in this edition include the results of direct measurements of $|\eta_{+-}|$, $|\eta_{00}|$, $|\eta_{00}/\eta_{+-}|$, and ϵ'/ϵ. A more detailed discussion of these fits is given in the 1990 edition of this *Review* [18].

References

1. K. Kleinknecht, "Uncovering CP violation: experimental clarification in the neutral K meson and B meson systems", Springer Tracts in Modern Physics, vol. 195 (Springer Verlag 2003).
2. B. Winstein and L. Wolfenstein, Rev. Mod. Phys. **65**, 1113 (1993).
3. T.T. Wu and C.N. Yang, Phys. Rev. Lett. **13**, 380 (1964).
4. L. Wolfenstein, Phys. Rev. Lett. **13**, 562 (1964); L. Wolfenstein, Comm. Nucl. Part. Phys. **21**, 275 (1994).
5. E. Chell and M.G. Olsson, Phys. Rev. **D48**, 4076 (1993).
6. R. Adler *et al.*, (CPLEAR Collaboration), Phys. Lett. **B407**, 193 (1997); P. Bloch, *Proceedings of Workshop on K Physics* (Orsay 1996), ed. L. Iconomidou-Fayard, Edition Frontieres, Gif-sur-Yvette, France (1997) p. 307.
7. G. Buchalla, A.J. Buras, and M.E. Lautenbacher, Rev. Mod. Phys. **68**, 1125 (1996); S. Bosch *et al.*, Nucl. Phys. **B565**, 3 (2000); S. Bertolini, M. Fabrichesi, and J.O. Egg, Rev. Mod. Phys. **72**, 65 (2000).
8. A. Alavi-Harati *et al.*, Phys. Rev. **D67**, 012005 (2003); See also *erratum*, Alavi-Harati *et al.*, Phys. Rev. **D**, to be published, for corrections to correlation coefficients.
9. A. Apostolakis *et al.*, Phys. Lett. **B458**, 545 (1999).
10. B. Schwingenheuer *et al.*, Phys. Rev. Lett. **74**, 4376 (1995).
11. L.K. Gibbons *et al.*, Phys. Rev. Lett. **70**, 1199 (1993) and footnote in Ref. [10].
12. L.K. Gibbons, Thesis, RX-1487, Univ. of Chicago, 1993.
13. C. Geweniger *et al.*, Phys. Lett. **48B**, 487 (1974).
14. C. Geweniger *et al.*, Phys. Lett. **52B**, 108 (1974).
15. R. Carosi *et al.*, Phys. Lett. **B237**, 303 (1990).
16. A. Lai *et al.*, Phys. Lett. **B537**, 28 (2002).
17. L. Bertanza *et al.*, Z. Phys. **C73**, 629 (1997).
18. J.J. Hernandez *et al.*, Phys. Lett. **B239**, 1 (1990).

CP-VIOLATION PARAMETERS IN K^0_L DECAYS

CHARGE ASYMMETRY IN $K^0_{\ell 3}$ DECAYS

Such asymmetry violates CP. It is related to $\mathrm{Re}(\epsilon)$.

δ_L = weighted average of $\delta_L(\mu)$ and $\delta_L(e)$

VALUE (%)	EVTS	DOCUMENT ID		TECN	COMMENT
0.327 ± 0.012 OUR AVERAGE		Includes data from the 2 datablocks that follow this one.			
0.333 ± 0.050	33M	WILLIAMS	73	ASPK	$K_{\mu 3} + K_{e3}$

$\delta_L(\mu) = [\Gamma(\pi^-\mu^+\nu_\mu) - \Gamma(\pi^+\mu^-\overline{\nu}_\mu)]/\mathrm{SUM}$

Only the combined value below is put into the Meson Summary Table.

VALUE (%)	EVTS	DOCUMENT ID		TECN
The data in this block is included in the average printed for a previous datablock.				
0.304 ± 0.025 OUR AVERAGE				
0.313 ± 0.029	15M	GEWENIGER	74	ASPK
0.278 ± 0.051	7.7M	PICCIONI	72	ASPK
• • • We do not use the following data for averages, fits, limits, etc. • • •				
0.60 ± 0.14	4.1M	MCCARTHY	73	CNTR
0.57 ± 0.17	1M	[82] PACIOTTI	69	OSPK
0.403 ± 0.134	1M	[82] DORFAN	67	OSPK

[82] PACIOTTI 69 is a reanalysis of DORFAN 67 and is corrected for $\mu^+\mu^-$ range difference in MCCARTHY 72.

$\delta_L(e) = [\Gamma(\pi^- e^+\nu_e) - \Gamma(\pi^+ e^-\overline{\nu}_e)]/\mathrm{SUM}$

Only the combined value below is put into the Meson Summary Table.

VALUE (%)	EVTS	DOCUMENT ID		TECN
The data in this block is included in the average printed for a previous datablock.				
0.333 ± 0.014 OUR AVERAGE				
0.341 ± 0.018	34M	GEWENIGER	74	ASPK
0.318 ± 0.038	40M	FITCH	73	ASPK
0.346 ± 0.033	10M	MARX	70	CNTR
0.246 ± 0.059	10M	[83] SAAL	69	CNTR
• • • We do not use the following data for averages, fits, limits, etc. • • •				
0.36 ± 0.18	600k	ASHFORD	72	ASPK
0.224 ± 0.036	10M	[83] BENNETT	67	CNTR

[83] SAAL 69 is a reanalysis of BENNETT 67.

PARAMETERS FOR $K^0_L \to 2\pi$ DECAY

$\eta_{+-} = A(K^0_L \to \pi^+\pi^-) / A(K^0_S \to \pi^+\pi^-)$

$\eta_{00} = A(K^0_L \to \pi^0\pi^0) / A(K^0_S \to \pi^0\pi^0)$

The fitted values of $|\eta_{+-}|$ and $|\eta_{00}|$ given below are the results of a fit to $|\eta_{+-}|$, $|\eta_{00}|$, $|\eta_{00}/\eta_{+-}|$, and $\mathrm{Re}(\epsilon'/\epsilon)$. Independent information on $|\eta_{+-}|$ and $|\eta_{00}|$ can be obtained from the fitted values of the $K^0_L \to \pi\pi$ and $K^0_S \to \pi\pi$ branching ratios and the K^0_L and K^0_S lifetimes. This information is included as data in the $|\eta_{+-}|$ and $|\eta_{00}|$ sections with a Document ID "BRFIT." See the note "CP violation in K_L decays" above for details.

$|\eta_{00}| = |A(K^0_L \to 2\pi^0) / A(K^0_S \to 2\pi^0)|$

VALUE (units 10^{-3})	DOCUMENT ID		TECN	COMMENT
2.276 ± 0.014 OUR FIT				
2.280 ± 0.025 OUR AVERAGE				
2.278 ± 0.025	BRFIT	04		
2.47 ± 0.31 ± 0.24	ANGELOPO...	98	CPLR	
2.33 ± 0.18	CHRISTENS...	79	ASPK	
• • • We do not use the following data for averages, fits, limits, etc. • • •				
2.49 ± 0.40	[84] ADLER	96B	CPLR	Sup. by ANGELOPOULOS 98
2.71 ± 0.37	[85] WOLFF	71	OSPK	Cu reg., 4γ's
2.95 ± 0.63	[85] CHOLLET	70	OSPK	Cu reg., 4γ's

[84] Error is statistical only.

[85] CHOLLET 70 gives $|\eta_{00}| = (1.23 \pm 0.24)\times$(regeneration amplitude, 2 GeV/c Cu)/10000mb. WOLFF 71 gives $|\eta_{00}| = (1.13 \pm 0.12)\times$(regeneration amplitude, 2 GeV/c Cu)/10000mb. We compute both $|\eta_{00}|$ values for (regeneration amplitude, 2 GeV/c Cu) = 24 ± 2mb. This regeneration amplitude results from averaging over FAISSNER 69, extrapolated using optical-model calculations of Bohm et al., Physics Letters **27B** 594 (1968) and the data of BALATS 71. (From H. Faissner, private communication).

$|\eta_{+-}| = |A(K^0_L \to \pi^+\pi^-) / A(K^0_S \to \pi^+\pi^-)|$

VALUE (units 10^{-3})	EVTS	DOCUMENT ID		TECN	COMMENT
2.288±0.014 OUR FIT					
2.286±0.017 OUR AVERAGE					
2.289±0.024		BRFIT	04		
2.264±0.023±0.027	70M	[86] APOSTOLA...	99C	CPLR	K^0-$\overline{K}^0$ asymmetry
2.30 ±0.035		GEWENIGER	74B	ASPK	
• • • We do not use the following data for averages, fits, limits, etc. • • •					
2.310±0.043±0.031		[87] ADLER	95B	CPLR	K^0-$\overline{K}^0$ asymmetry
2.32 ±0.14 ±0.03	10^5	ADLER	92B	CPLR	K^0-$\overline{K}^0$ asymmetry

[86] APOSTOLAKIS 99C report $(2.264 \pm 0.023 \pm 0.026 + 9.1[\tau_S - 0.8934]) \times 10^{-3}$. We evaluate for our 1998 best value $\tau_S = (0.8934 \pm 0.0008) \times 10^{-10}$ s.

[87] ADLER 95B report $(2.312 \pm 0.043 \pm 0.030 - 1[\Delta m - 0.5274] + 9.1[\tau_S - 0.8926]) \times 10^{-3}$. We evaluate for our 1996 best values $\Delta m = (0.5304 \pm 0.0014) \times 10^{-10}$ $\hbar s^{-1}$ and $\tau_S = (0.8927 \pm 0.0009) \times 10^{-10}$ s. Superseded by APOSTOLAKIS 99C.

$|\epsilon| = (2|\eta_{+-}| + |\eta_{00}|)/3$

This expression is a very good approximation, good to about one part in 10^{-4} because of the small measured value of $\phi_{00} - \phi_{+-}$ and small theoretical ambiguities.

VALUE (units 10^{-3})	DOCUMENT ID
2.284±0.014 OUR FIT	

$|\eta_{00}/\eta_{+-}|$

VALUE	EVTS	DOCUMENT ID		TECN
0.9950±0.0008 OUR FIT Error includes scale factor of 1.6.				
0.9930±0.0020 OUR AVERAGE				
0.9931±0.0020		[88,89] BARR	93D	NA31
0.9904±0.0084±0.0036		[90] WOODS	88	E731
• • • We do not use the following data for averages, fits, limits, etc. • • •				
0.9939±0.0013±0.0015	1M	[88] BARR	93D	NA31
0.9899±0.0020±0.0025		[88] BURKHARDT	88	NA31

[88] This is the square root of the ratio R given by BURKHARDT 88 and BARR 93D.

[89] This is the combined results from BARR 93D and BURKHARDT 88, taking into account a common systematic uncertainty of 0.0014.

[90] We calculate $|\eta_{00}/\eta_{+-}| = 1 - 3(\epsilon'/\epsilon)$ from WOODS 88 (ϵ'/ϵ) value.

$\mathrm{Re}(\epsilon'/\epsilon) = (1 - |\eta_{00}/\eta_{+-}|)/3$

VALUE (units 10^{-3})	DOCUMENT ID		TECN	COMMENT
1.67±0.26 OUR FIT Error includes scale factor of 1.6.				
1.67±0.23 OUR AVERAGE Error includes scale factor of 1.4. See the ideogram below.				
2.07±0.28	ALAVI-HARATI	03	KTEV	
1.47±0.22	BATLEY	02	NA48	
2.3 ±0.65	[91,92] BARR	93D	NA31	
0.74±0.52±0.29	GIBBONS	93B	E731	
• • • We do not use the following data for averages, fits, limits, etc. • • •				
1.53±0.26	LAI	01C	NA48	Incl. in BATLEY 02
2.80±0.30±0.28	ALAVI-HARATI	99D	KTEV	In ALAVI-HARATI 03
1.85±0.45±0.58	FANTI	99C	NA48	In LAI 01C
2.0 ±0.7	[93] BARR	93D	NA31	
−0.4 ±1.4 ±0.6	PATTERSON	90	E731	in GIBBONS 93B
3.3 ±1.1	[93] BURKHARDT	88	NA31	
3.2 ±2.8 ±1.2	[91] WOODS	88	E731	

[91] These values are derived from $|\eta_{00}/\eta_{+-}|$ measurements. They enter the average in this section but enter the fit via the $|\eta_{00}/\eta_{+-}|$ only.

[92] This is the combined results from BARR 93D and BURKHARDT 88, taking into account their common systematic uncertainty.

[93] These values are derived from $|\eta_{00}/\eta_{+-}|$ measurements.

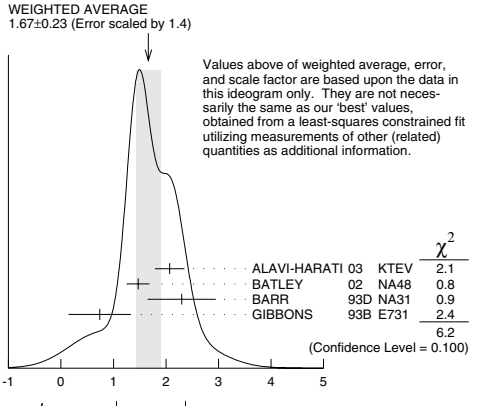

$\mathrm{Re}(\epsilon'/\epsilon) = (1 - |\eta_{00}/\eta_{+-}|)/3$

ϕ_{+-}, PHASE of η_{+-}

The dependence of the phase on Δm and τ_S is given for each experiment in the comments below, where Δm is the $K^0_L - K^0_S$ mass difference in units 10^{10} $\hbar s^{-1}$ and τ_S is the K_S mean life in units 10^{-10} s. We also give the regeneration phase ϕ_f in the comments below.

OUR FIT is described in the note on "CP violation in K_L decays" in the K^0_L Particle Listings. Most experiments in this section are included in both the "Not Assuming CPT" and "Assuming CPT" fits. In the latter fit, they have little direct influence on ϕ_{+-} because their errors are large compared to that assuming CPT, but they influence Δm and τ_S through their dependencies on these parameters, which are given in the footnotes. Only ALAVI-HARATI 03 is excluded from the "Assuming CPT" fit because we explicitly include their Δm and τ_S measurements which assume CPT.

VALUE (°)	EVTS	DOCUMENT ID		TECN	COMMENT
43.52±0.06 OUR FIT		Error includes scale factor of 1.3. Assuming CPT			
43.4 ±0.7 OUR FIT		Error includes scale factor of 1.3. Not assuming CPT			
44.12±0.72±1.20		[94] ALAVI-HARATI	03	KTEV	Not assuming CPT
42.9 ±0.6 ±0.3	70M	[95] APOSTOLA...	99C	CPLR	K^0-$\overline{K}^0$ asymmetry
43.0 ±0.8 ±0.2		[96,97] SCHWINGEN...	95	E773	$CH_{1.1}$ regenerator
41.4 ±0.9 ±0.3		[97,98] GIBBONS	93	E731	B_4C regenerator
44.4 ±1.6 ±0.6		[99] CAROSI	90	NA31	Vacuum regen.
43.3 ±1.0 ±0.5		[100] GEWENIGER	74B	ASPK	Vacuum regen.
• • • We do not use the following data for averages, fits, limits, etc. • • •					
42.5 ±0.4 ±0.4		[101,102] ADLER	96C	RVUE	
43.4 ±1.1 ±0.3		[103] ADLER	95B	CPLR	K^0-$\overline{K}^0$ asymmetry
42.3 ±4.4 ±1.4	10^5	[104] ADLER	92B	CPLR	K^0-$\overline{K}^0$ asymmetry
47.7 ±2.0 ±0.9		[97,105] KARLSSON	90	E731	
44.3 ±2.8 ±0.2		[106] CARITHERS	75	SPEC	C regenerator

[94] ALAVI-HARATI 03 ϕ_{+-} is correlated with their $\Delta m = m_{K^0_L} - m_{K^0_S}$ and τ_{K_S} measurements in the K^0_L and K^0_S sections respectively. The correlation coefficients are $\rho(\phi_{+-}, \Delta m) = +0.955$, $\rho(\phi_{+-}, \tau_S) = -0.871$, and $\rho(\tau_S, \Delta m) = -0.840$. CPT is not assumed. Uses scintillator Pb regenerator.

[95] APOSTOLAKIS 99C measures $\phi_{+-} = (43.19 \pm 0.53 \pm 0.28) + 300\,[\Delta m - 0.5301]$ (°). We have adjusted the measurement to use our best values of $(\Delta m = 0.5292 \pm 0.0010)$ $(10^{10}\ \hbar\ s^{-1})$. Our first error is their experiment's error and our second error is the systematic error from using our best values.

[96] SCHWINGENHEUER 95 measures $\phi_{+-} = (43.53 \pm 0.76) + 173\,[\Delta m - 0.5282] - 275\,[\tau_S - 0.8926]$ (°). We have adjusted the measurement to use our best values of $(\Delta m = 0.5292 \pm 0.0010)$ $(10^{10}\ \hbar\ s^{-1})$, $(\tau_S = 0.8953 \pm 0.0006)$ $(10^{-10}$ s). Our first error is their experiment's error and our second error is the systematic error from using our best values.

[97] These experiments measure $\phi_{+-} - \phi_f$ and calculate the regeneration phase from the power law momentum dependence of the regeneration amplitude using analyticity and dispersion relations. SCHWINGENHEUER 95 [GIBBONS 93] includes a systematic error of 0.35° [0.5°] for uncertainties in their modeling of the regeneration amplitude. See the discussion of these systematic errors, including criticism that they could be underestimated, in the note on "C violation in K^0_L decay."

[98] GIBBONS 93 measures $\phi_{+-} = (42.21 \pm 0.9) + 189\,[\Delta m - 0.5257] - 460\,[\tau_S - 0.8922]$ (°). We have adjusted the measurement to use our best values of $(\Delta m = 0.5292 \pm 0.0010)$ $(10^{10}\ \hbar\ s^{-1})$, $(\tau_S = 0.8953 \pm 0.0006)$ $(10^{-10}$ s). Our first error is their experiment's error and our second error is the systematic error from using our best values. This is actually reported in SCHWINGENHEUER 95, footnote 8. GIBBONS 93 reports $\phi_{+-} = (42.2 \pm 1.4)°$. They measure $\phi_{+-} - \phi_f$ and calculate the regeneration phase ϕ_f from the power law momentum dependence of the regeneration amplitude using analyticity. An error of 0.6° is included for possible uncertainties in the regeneration phase.

[99] CAROSI 90 measures $\phi_{+-} = (46.9 \pm 1.4 \pm 0.7) + 579\,[\Delta m - 0.5351] + 303\,[\tau_S - 0.8922]$ (°). We have adjusted the measurement to use our best values of $(\Delta m = 0.5292 \pm 0.0010)$ $(10^{10}\ \hbar\ s^{-1})$, $(\tau_S = 0.8953 \pm 0.0006)$ $(10^{-10}$ s). Our first error is their experiment's error and our second error is the systematic error from using our best values.

[100] GEWENIGER 74B measures $\phi_{+-} = (49.4 \pm 1.0) + 565\,[\Delta m - 0.540]$ (°). We have adjusted the measurement to use our best values of $(\Delta m = 0.5292 \pm 0.0010)$ $(10^{10}\ \hbar\ s^{-1})$. Our first error is their experiment's error and our second error is the systematic error from using our best values.

[101] ADLER 96C measures $\phi_{+-} = (43.82 \pm 0.41) + 339\,[\Delta m - 0.5307] - 252\,[\tau_S - 0.8922]$ (°). We have adjusted the measurement to use our best values of $(\Delta m = 0.5292 \pm 0.0010)$ $(10^{10}\ \hbar\ s^{-1})$, $(\tau_S = 0.8953 \pm 0.0006)$ $(10^{-10}$ s). Our first error is their experiment's error and our second error is the systematic error from using our best values.

[102] ADLER 96C is the result of a fit which includes nearly the same data as entered into the "OUR FIT" value in the 1996 edition of this Review (Physical Review **D54** 1 (1996)).

[103] ADLER 95B measures $\phi_{+-} = (42.7 \pm 0.9 \pm 0.6) + 316\,[\Delta m - 0.5274] + 30\,[\tau_S - 0.8926]$ (°). We have adjusted the measurement to use our best values of $(\Delta m = 0.5292 \pm 0.0010)$ $(10^{10}\ \hbar\ s^{-1})$, $(\tau_S = 0.8953 \pm 0.0006)$ $(10^{-10}$ s). Our first error is their experiment's error and our second error is the systematic error from using our best values.

[104] ADLER 92B quote separately two systematic errors: ±0.4 from their experiment and ±1.0 degrees due to the uncertainty in the value of Δm.

[105] KARLSSON 90 systematic error does not include regeneration phase uncertainty.

[106] CARITHERS 75 measures $\phi_{+-} = (45.5 \pm 2.8) + 224\,[\Delta m - 0.5348]$ (°). We have adjusted the measurement to use our best values of $(\Delta m = 0.5292 \pm 0.0010)$ $(10^{10}\ \hbar\ s^{-1})$. Our first error is their experiment's error and our second error is the systematic error from using our best values. $\phi_f = -40.9 \pm 2.6°$.

ϕ_{00}, PHASE OF η_{00}

See comment in ϕ_{+-} header above for treatment of Δm and τ_S dependence, as well as for the inclusion of data in both the "Assuming *CPT*" and "Not Assuming *CPT*" fits.

OUR FIT is described in the note on "*CP* violation in K_L decays" in the K^0_L Particle Listings.

VALUE (°)	DOCUMENT ID		TECN	COMMENT
43.50±0.06 OUR FIT	Error includes scale factor of 1.3.			Assuming *CPT*
43.7 ±0.8 OUR FIT	Error includes scale factor of 1.2.			Not assuming *CPT*
44.5 ±2.3 ±0.6	[107] CAROSI	90	NA31	
• • • We do not use the following data for averages, fits, limits, etc. • • •				
41.6 ±5.9 ±0.2	[108] ANGELOPO...	98	CPLR	
50.8 ±7.1 ±1.7	[109] ADLER	96B	CPLR	Sup. by ANGELOPOULOS 98
47.4 ±1.4 ±0.9	[110] KARLSSON	90	E731	

[107] CAROSI 90 measures $\phi_{00} = (47.1 \pm 2.1 \pm 1.0) + 579\,[\Delta m - 0.5351] + 252\,[\tau_S - 0.8922]$ (°). We have adjusted the measurement to use our best values of ($\Delta m = 0.5292 \pm 0.0010$) ($10^{10}\ \hbar\ s^{-1}$), ($\tau_S = 0.8953 \pm 0.0006$) ($10^{-10}$ s). Our first error is their experiment's error and our second error is the systematic error from using our best values.

[108] ANGELOPOULOS 98 measures $\phi_{00} = (42.0 \pm 5.6 \pm 1.9) + 240\,[\Delta m - 0.5307]$ (°). We have adjusted the measurement to use our best values of ($\Delta m = 0.5292 \pm 0.0010$) ($10^{10}\ \hbar\ s^{-1}$). Our first error is their experiment's error and our second error is the systematic error from using our best values. The τ_S dependence is negligible.

[109] ADLER 96B identified initial neutral kaon individually as being a K^0 or a $\overline{K}{}^0$. The systematic uncertainty is $\pm 1.5°$ combined in quadrature with $\pm 0.8°$ due to Δm.

[110] KARLSSON 90 systematic error does not include regeneration phase uncertainty.

$\phi_\epsilon = (2\phi_{+-} + \phi_{00})/3$

This expression is a very good approximation, good to about 10^{-3} degrees because of the small measured values of $\phi_{00} - \phi_{+-}$ and Re ϵ'/ϵ, and small theoretical ambiguities.

VALUE (°)	DOCUMENT ID		COMMENT
43.51 ±0.05 OUR FIT	Error includes scale factor of 1.2. Assuming *CPT*		
43.5 ±0.7 OUR FIT	Error includes scale factor of 1.3. Not assuming *CPT*		
43.5105±0.0004±0.0548	[111] SUPERWEAK	04	Assuming *CPT*

[111] SUPERWEAK 04 is a fake measurement used to impose the *CPT* or Superweak constraint $\phi_{+-} = \phi_{SW} = 2\,\frac{\Delta m}{\hbar}\,(\frac{\tau_S \tau_L}{\tau_L - \tau_S})$. This "measurement" is linearized using values near the RPP 2004 edition values of Δm, τ_S and τ_L, and then adjusted to our current values as described in the following "measurement". SUPERWEAK 04 measures $\phi_\epsilon = (43.5131 \pm 0.0004) + 54\,[\Delta m - 0.5290] + 32\,[\tau_S - 0.8958]$ (°). We have adjusted the measurement to use our best values of ($\Delta m = 0.5292 \pm 0.0010$) ($10^{10}\ \hbar\ s^{-1}$), ($\tau_S = 0.8953 \pm 0.0006$) ($10^{-10}$ s). Our first error is their experiment's error and our second error is the systematic error from using our best values.

DECAY-PLANE ASYMMETRY IN $\pi^+\pi^-e^+e^-$ DECAYS

This is the *CP*-violating asymmetry

$$A = \frac{N_{\sin\phi\cos\phi>0.0} - N_{\sin\phi\cos\phi<0.0}}{N_{\sin\phi\cos\phi>0.0} + N_{\sin\phi\cos\phi<0.0}}$$

where ϕ is the angle between the e^+e^- and $\pi^+\pi^-$ planes in the K^0_L rest frame.

CP ASYMMETRY *A* in $K^0_L \to \pi^+\pi^-e^+e^-$

VALUE (%)	DOCUMENT ID		TECN
13.8±2.2 OUR AVERAGE			
14.2±3.0±1.9	LAI	03C	NA48
13.6±2.5±1.2	ALAVI-HARATI	00B	KTEV

PARAMETERS FOR $e^+e^-e^+e^-$ DECAYS

These are the *CP*-violating parameters in the ϕ distribution, where ϕ is the angle between the planes of the two e^+e^- paris in the kaon rest frame:

$$d\Gamma/d\phi \propto 1 + \beta_{CP}\cos(2\phi) + \gamma_{CP}\sin(2\phi)$$

β_{CP} from $K^0_L \to e^+e^-e^+e^-$

VALUE	EVTS	DOCUMENT ID		TECN	COMMENT
−0.23±0.09±0.02	441	ALAVI-HARATI	01D	KTEV	$M_{ee} > 8$ MeV/c^2

γ_{CP} from $K^0_L \to e^+e^-e^+e^-$

VALUE	EVTS	DOCUMENT ID		TECN	COMMENT
−0.09±0.09±0.02	441	ALAVI-HARATI	01D	KTEV	$M_{ee} > 8$ MeV/c^2

CHARGE ASYMMETRY IN $\pi^+\pi^-\pi^0$ DECAYS

These are *CP*-violating charge-asymmetry parameters, defined at beginning of section "LINEAR COEFFICIENT *g* FOR $K^0_L \to \pi^+\pi^-\pi^0$ above.

See also note on Dalitz plot parameters in $K^\pm$ section and note on "*CP* violation in K_L decays" above.

LINEAR COEFFICIENT *j* FOR $K^0_L \to \pi^+\pi^-\pi^0$

VALUE	EVTS	DOCUMENT ID		TECN
0.0012±0.0008 OUR AVERAGE				
0.0010±0.0024±0.0030	500k	ANGELOPO...	98C	CPLR
−0.001 ±0.011	6499	CHO	77	
0.001 ±0.003	4709	PEACH	77	
0.0013±0.0009	3M	SCRIBANO	70	
0.0 ±0.017	4400	SMITH	70	OSPK
0.001 ±0.004	238k	BLANPIED	68	

QUADRATIC COEFFICIENT *f* FOR $K^0_L \to \pi^+\pi^-\pi^0$

VALUE	EVTS	DOCUMENT ID		TECN
0.0045±0.0024±0.0059	500k	ANGELOPO...	98C	CPLR

PARAMETERS for $K^0_L \to \pi^+\pi^-\gamma$ DECAY

$|\eta_{+-\gamma}| = |A(K^0_L \to \pi^+\pi^-\gamma,\ CP \text{ violating})/A(K^0_S \to \pi^+\pi^-\gamma)|$

VALUE (units 10^{-3})	EVTS	DOCUMENT ID		TECN
2.35 ±0.07 OUR AVERAGE				
2.359±0.062±0.040	9045	MATTHEWS	95	E773
2.15 ±0.26 ±0.20	3671	RAMBERG	93B	E731

$\phi_{+-\gamma}$ = phase of $\eta_{+-\gamma}$

VALUE (°)	EVTS	DOCUMENT ID		TECN
44 ± 4 OUR AVERAGE				
43.8± 3.5± 1.9	9045	MATTHEWS	95	E773
72 ±23 ±17	3671	RAMBERG	93B	E731

$|\epsilon'_{+-\gamma}|/\epsilon$ for $K^0_L \to \pi^+\pi^-\gamma$

VALUE	CL%	EVTS	DOCUMENT ID		TECN
<0.3	90	3671	[112] RAMBERG	93B	E731

[112] RAMBERG 93B limit on $|\epsilon'_{+-\gamma}|/\epsilon$ assumes than any difference between η_{+-} and $\eta_{+-\gamma}$ is due to direct *CP* violation.

T VIOLATION TESTS IN K^0_L DECAYS

Im(ξ) in $K^0_{\mu 3}$ DECAY (from transverse μ pol.)

Test of *T* reversal invariance.

VALUE	EVTS	DOCUMENT ID		TECN	COMMENT
−0.007±0.026 OUR AVERAGE					
0.009±0.030	12M	MORSE	80	CNTR	Polarization
0.35 ±0.30	207k	[113] CLARK	77	SPEC	POL, t=0
−0.085±0.064	2.2M	[114] SANDWEISS	73	CNTR	POL, t=0
−0.02 ±0.08		LONGO	69	CNTR	POL, t=3.3
−0.2 ±0.6		ABRAMS	68B	OSPK	Polarization
• • • We do not use the following data for averages, fits, limits, etc. • • •					
0.012±0.026		SCHMIDT	79	CNTR	Repl. by MORSE 80

[113] CLARK 77 value has additional $\xi(0)$ dependence $+0.21\,\mathrm{Re}\,[\xi(0)]$.

[114] SANDWEISS 73 value corrected from value quoted in their paper due to new value of Re(ξ). See footnote 4 of SCHMIDT 79.

CPT-INVARIANCE TESTS IN K^0_L DECAYS

PHASE DIFFERENCE $\phi_{00} - \phi_{+-}$

Test of *CPT*.

OUR FIT is described in the note on "*CP* violation in K_L decays" in the K^0_L Particle Listings.

VALUE (°)	DOCUMENT ID		TECN	COMMENT
−0.02 ±0.04 OUR FIT	Error includes scale factor of 2.1. Assuming *CPT*			
0.2 ±0.4 OUR FIT	Not assuming *CPT*			
−0.023±0.020	[115] SUPERWEAK	04		Assuming *CPT*
0.39 ±0.22 ±0.45	[116] ALAVI-HARATI	03	KTEV	
−0.30 ±0.88	[117] SCHWINGEN...	95		Combined E731, E773
• • • We do not use the following data for averages, fits, limits, etc. • • •				
0.62 ±0.71 ±0.75	SCHWINGEN...	95	E773	
−1.6 ±1.2	[118] GIBBONS	93	E731	
0.2 ±2.6 ±1.2	[119] CAROSI	90	NA31	
−0.3 ±2.4 ±1.2	KARLSSON	90	E731	

[115] SUPERWEAK 04 is a fake experiment to constrain ϕ_{00}-ϕ_{+-} to a small value as described in the note "*CP* violation in K_L decays."

[116] ALAVI-HARATI 03 fit Re(ϵ'/ϵ), Im(ϵ'/ϵ), Δm, τ_S, and ϕ_{+-} simultaneously, not assuming *CPT*. Phase difference is obtained from $\phi_{00} - \phi_{+-} \approx -3\,\mathrm{Im}(\epsilon'/\epsilon)$ for small $|\epsilon'/\epsilon|$.

[117] This SCHWINGENHEUER 95 values is the combined result of SCHWINGENHEUER 95 and GIBBONS 93, accounting for correlated systematic errors.

[118] GIBBONS 93 give detailed dependence of systematic error on lifetime (see the section on the K^0_S mean life) and mass difference (see the section on $m_{K^0_L} - m_{K^0_S}$).

[119] CAROSI 90 is excluded from the fit because it it is not independent of ϕ_{+-} and ϕ_{00} values.

PHASE DIFFERENCE $\phi_{+-} - \phi_{SW}$

Test of *CPT*. The Superweak phase $\phi_{SW} \equiv \tan^{-1}(2\Delta m/\Delta\Gamma)$ where $\Delta m = m_{K^0_L} - m_{K^0_S}$ and $\Delta\Gamma = \hbar(\tau_L - \tau_S)/(\tau_L \tau_S)$.

VALUE (°)	DOCUMENT ID		TECN
0.61±0.62±1.01	[120] ALAVI-HARATI	03	KTEV

[120] ALAVI-HARATI 03 fit is the same as their ϕ_{+-}, τ_{K_S}, Δm fit, except that the parameter $\phi_{+-} - \phi_{SW}$ is used in place of ϕ.

$\mathrm{Re}(\frac{2}{3}\eta_{+-} + \frac{1}{3}\eta_{00}) - \frac{\delta_L}{2}$
Test of CPT

VALUE (units 10^{-6})	DOCUMENT ID		TECN	COMMENT
-3 ± 35	[121] ALAVI-HARATI 02		E799	Uses δ_L from K_{e3} decays

[121] ALAVI-HARATI 02 uses PDG 00 values of η_{+-} and η_{00}.

$\Delta S = \Delta Q$ IN K^0 DECAYS

The relative amount of $\Delta S \neq \Delta Q$ component present is measured by the parameter x, defined as

$$x = A(\overline{K}^0 \to \pi^- \ell^+ \nu)/A(K^0 \to \pi^- \ell^+ \nu) \ .$$

We list $\mathrm{Re}\{x\}$ and $\mathrm{Im}\{x\}$ for K_{e3} and $K_{\mu 3}$ combined.

$x = A(\overline{K}^0 \to \pi^- \ell^+ \nu)/A(K^0 \to \pi^- \ell^+ \nu) = A(\Delta S = -\Delta Q)/A(\Delta S = \Delta Q)$

REAL PART OF x

VALUE	EVTS	DOCUMENT ID		TECN	COMMENT
$-0.0018 \pm 0.0041 \pm 0.0045$		ANGELOPO...	98D	CPLR	K_{e3} from K^0
• • • We do not use the following data for averages, fits, limits, etc. • • •					
$0.10 \ ^{+0.18}_{-0.19}$	79	SMITH	75B	WIRE	$\pi^- p \to K^0 \Lambda$
0.04 ± 0.03	4724	NIEBERGALL	74	ASPK	$K^+ p \to K^0 p \pi^+$
-0.008 ± 0.044	1757	FACKLER	73	OSPK	K_{e3} from K^0
-0.03 ± 0.07	1367	HART	73	OSPK	K_{e3} from $K^0 \Lambda$
-0.070 ± 0.036	1079	MALLARY	73	OSPK	K_{e3} from $K^0 \Lambda X$
0.03 ± 0.06	410	[122] BURGUN	72	HBC	$K^+ p \to K^0 p \pi^+$
$0.04 \ ^{+0.10}_{-0.13}$	100	[123] GRAHAM	72	OSPK	$K_{\mu 3}$ from $K^0 \Lambda$
-0.05 ± 0.09	442	[123] GRAHAM	72	OSPK	$\pi^- p \to K^0 \Lambda$
$0.26 \ ^{+0.10}_{-0.14}$	126	MANN	72	HBC	$K^- p \to n \overline{K}^0$
-0.13 ± 0.11	342	[123] MANTSCH	72	OSPK	K_{e3} from $K^0 \Lambda$
$0.04 \ ^{+0.07}_{-0.08}$	222	[122] BURGUN	71	HBC	$K^+ p \to K^0 p \pi^+$
$0.25 \ ^{+0.07}_{-0.09}$	252	WEBBER	71	HBC	$K^- p \to n \overline{K}^0$
0.12 ± 0.09	215	[124] CHO	70	DBC	$K^+ d \to K^0 pp$
-0.020 ± 0.025		[125] BENNETT	69	CNTR	Charge asym+ Cu regen.
$0.09 \ ^{+0.14}_{-0.16}$	686	LITTENBERG	69	OSPK	$K^+ n \to K^0 p$
0.03 ± 0.03		[125] BENNETT	68	CNTR	
$0.09 \ ^{+0.07}_{-0.09}$	121	JAMES	68	HBC	$\overline{p} p$
$0.17 \ ^{+0.16}_{-0.35}$	116	FELDMAN	67B	OSPK	$\pi^- p \to K^0 \Lambda$
0.17 ± 0.10	335	[124] HILL	67	DBC	$K^+ d \to K^0 pp$
$0.035 \ ^{+0.11}_{-0.13}$	196	AUBERT	65	HLBC	K^+ charge exchange
$0.06 \ ^{+0.18}_{-0.44}$	152	[126] BALDO-...	65	HLBC	K^+ charge exchange
$-0.08 \ ^{+0.16}_{-0.28}$	109	[127] FRANZINI	65	HBC	$\overline{p} p$

[122] BURGUN 72 is a final result which includes BURGUN 71.
[123] First GRAHAM 72 value is second GRAHAM 72 value combined with MANTSCH 72.
[124] CHO 70 is analysis of unambiguous events in new data and HILL 67.
[125] BENNETT 69 is a reanalysis of BENNETT 68.
[126] BALDO-CEOLIN 65 gives x and θ converted by us to $\mathrm{Re}(x)$ and $\mathrm{Im}(x)$.
[127] FRANZINI 65 gives x and θ for $\mathrm{Re}(x)$ and $\mathrm{Im}(x)$. See SCHMIDT 67.

IMAGINARY PART OF x

Assumes $m_{K_L^0} - m_{K_S^0}$ positive. See Listings above.

VALUE	EVTS	DOCUMENT ID		TECN	COMMENT
$0.0012 \pm 0.0019 \pm 0.0009$	640k	ANGELOPO...	01B	CPLR	K_{e3} from K^0
• • • We do not use the following data for averages, fits, limits, etc. • • •					
0.0012 ± 0.0019	640k	[128] ANGELOPO...	98E	CPLR	K_{e3} from K^0
$-0.10 \ ^{+0.16}_{-0.19}$	79	SMITH	75B	WIRE	$\pi^- p \to K^0 \Lambda$
-0.06 ± 0.05	4724	NIEBERGALL	74	ASPK	$K^+ p \to K^0 p \pi^+$
-0.017 ± 0.060	1757	FACKLER	73	OSPK	K_{e3} from K^0
0.09 ± 0.07	1367	HART	73	OSPK	K_{e3} from $K^0 \Lambda$
$0.107 \ ^{+0.092}_{-0.074}$	1079	MALLARY	73	OSPK	K_{e3} from $K^0 \Lambda X$
$0.07 \ ^{+0.06}_{-0.07}$	410	[129] BURGUN	72	HBC	$K^+ p \to K^0 p \pi^+$
$0.12 \ ^{+0.17}_{-0.16}$	100	[130] GRAHAM	72	OSPK	$K_{\mu 3}$ from $K^0 \Lambda$
0.05 ± 0.13	442	[130] GRAHAM	72	OSPK	$\pi^- p \to K^0 \Lambda$
$0.21 \ ^{+0.15}_{-0.12}$	126	MANN	72	HBC	$K^- p \to n \overline{K}^0$
-0.04 ± 0.16	342	[130] MANTSCH	72	OSPK	K_{e3} from $K^0 \Lambda$
$0.12 \ ^{+0.08}_{-0.09}$	222	[129] BURGUN	71	HBC	$K^+ p \to K^0 p \pi^+$
0.0 ± 0.08	252	WEBBER	71	HBC	$K^- p \to n \overline{K}^0$
-0.08 ± 0.07	215	[131] CHO	70	DBC	$K^+ d \to K^0 pp$
$-0.11 \ ^{+0.10}_{-0.11}$	686	LITTENBERG	69	OSPK	$K^+ n \to K^0 p$
$+0.22 \ ^{+0.37}_{-0.29}$	121	JAMES	68	HBC	$\overline{p} p$
0.0 ± 0.25	116	FELDMAN	67B	OSPK	$\pi^- p \to K^0 \Lambda$
-0.20 ± 0.10	335	[131] HILL	67	DBC	$K^+ d \to K^0 pp$
$-0.21 \ ^{+0.11}_{-0.15}$	196	AUBERT	65	HLBC	K^+ charge exchange
$-0.44 \ ^{+0.32}_{-0.19}$	152	[132] BALDO-...	65	HLBC	K^+ charge exchange
$+0.24 \ ^{+0.40}_{-0.30}$	109	[133] FRANZINI	65	HBC	$\overline{p} p$

[128] Superseded by ANGELOPOULOS 01B.
[129] BURGUN 72 is a final result which includes BURGUN 71.
[130] First GRAHAM 72 value is second GRAHAM 72 value combined with MANTSCH 72.
[131] Footnote 10 of HILL 67 should read $+0.58$, not -0.58 (private communication) CHO 70 is analysis of unambiguous events in new data and HILL 67.
[132] BALDO-CEOLIN 65 gives x and θ converted by us to $\mathrm{Re}(x)$ and $\mathrm{Im}(x)$.
[133] FRANZINI 65 gives x and θ for $\mathrm{Re}(x)$ and $\mathrm{Im}(x)$. See SCHMIDT 67.

K_L^0 REFERENCES

BRFIT	04	RPP 2004 edition	T.G. Trippe	(PDG Collab.)
CP violation in K_L decays				
ETAFIT	04	RPP 2004 edition	T.G. Trippe	(PDG Collab.)
CP violation in K_L decays				
KL3FIT	04	RPP 2004 edition	T.G. Trippe	(PDG Collab.)
$K_{\mu 3}^{\pm}$ and $K_{\mu 3}^0$ Form Factors review in K^+ Listings.				
SUPERWEAK	04	RPP 2004 edition	T.G. Trippe	(PDG Collab.)
CP violation in K_L decays				
ADINOLFI	03	PL B566 61	M. Adinolfi *et al.*	(KLOE Collab.)
ALAVI-HARATI	03	PR D67 012005	A. Alavi-Harati *et al.*	(FNAL KTeV Collab.)
Also	04	Erratum (to be publ.)	A. Alavi-Harati *et al.*	(FNAL KTeV Collab.)
ALAVI-HARATI	03B	PRL 90 141801	A. ALavi-Harati *et al.*	(FNAL KTeV Collab.)
LAI	03	PL B551 7	A. Lai *et al.*	(CERN NA48 Collab.)
LAI	03C	EPJ C30 33	A. Lai *et al.*	(CERN NA48 Collab.)
ALAVI-HARATI	02	PRL 88 181601	A. Alavi-Harati *et al.*	(FNAL KTeV Collab.)
ALAVI-HARATI	02C	PRL 89 211801	A. Alavi-Harati *et al.*	(FNAL KTeV Collab.)
BATLEY	02	PL B544 97	J.R. Batley *et al.*	(CERN NA48 Collab.)
LAI	02B	PL B536 229	A. Lai *et al.*	(CERN NA48 Collab.)
ALAVI-HARATI	01	PRL 86 397	A. Alavi-Harati *et al.*	(FNAL KTeV Collab.)
ALAVI-HARATI	01B	PRL 86 761	A. Alavi-Harati *et al.*	(FNAL KTeV Collab.)
ALAVI-HARATI	01D	PRL 86 5425	A. Alavi-Harati *et al.*	(FNAL KTeV Collab.)
ALAVI-HARATI	01E	PRL 87 021801	A. Alavi-Harati *et al.*	(FNAL KTeV Collab.)
ALAVI-HARATI	01F	PR D64 012003	A. Alavi-Harati *et al.*	(FNAL KTeV Collab.)
ALAVI-HARATI	01G	PRL 87 071801	A. Alavi-Harati *et al.*	(FNAL KTeV Collab.)
ALAVI-HARATI	01H	PRL 87 111802	A. Alavi-Harati *et al.*	(FNAL KTeV Collab.)
ALAVI-HARATI	01J	PR D64 112004	A. Alavi-Harati *et al.*	(FNAL KTeV Collab.)
ANGELOPO...	01	PL B503 49	A. Angelopoulos *et al.*	(CPLEAR Collab.)
ANGELOPO...	01B	EPJ C22 55	A. Angelopoulos *et al.*	(CPLEAR Collab.)
LAI	01B	PL B515 261	A. Lai *et al.*	(CERN NA48 Collab.)
LAI	01C	EPJ C22 231	A. Lai *et al.*	(CERN NA48 Collab.)
ALAVI-HARATI	00	PR D61 072006	A. Alavi-Harati *et al.*	(FNAL KTeV Collab.)
ALAVI-HARATI	00B	PRL 84 408	A. Alavi-Harati *et al.*	(FNAL KTeV Collab.)
ALAVI-HARATI	00D	PRL 84 5279	A. Alavi-Harati *et al.*	(FNAL KTeV Collab.)
ALAVI-HARATI	00E	PR D62 112001	A. Alavi-Harati *et al.*	(FNAL KTeV Collab.)
AMBROSE	00	PRL 84 1389	D. Ambrose *et al.*	(BNL E871 Collab.)
APOSTOLA...	00	PL B473 186	A. Apostolakis *et al.*	(CPLEAR Collab.)
PDG	00	EPJ C15 1	D.E. Groom *et al.*	
ADAMS	99	PL B447 240	J. Adams *et al.*	(FNAL KTeV Collab.)
ALAVI-HARATI	99B	PRL 83 917	A. Alavi-Harati *et al.*	(FNAL KTeV Collab.)
ALAVI-HARATI	99D	PRL 83 22	A. Alavi-Harati *et al.*	(FNAL KTeV Collab.)
APOSTOLA...	99C	PL B458 545	A. Apostolakis *et al.*	(CPLEAR Collab.)
Also	00B	EPJ C18 41	A. Apostolakis *et al.*	(CPLEAR Collab.)
FANTI	99B	PL B458 553	V. Fanti *et al.*	(CERN NA48 Collab.)
FANTI	99C	PL B465 335	V. Fanti *et al.*	(CERN NA48 Collab.)
MURAKAMI	99	PL B463 333	K. Murakami *et al.*	(KEK E162 Collab.)
ADAMS	98	PRL 81 4123	J. Adams *et al.*	(FNAL KTeV Collab.)
AMBROSE	98	PRL 81 4309	D. Ambrose *et al.*	(BNL E871 Collab.)
AMBROSE	98B	PRL 81 5734	D. Ambrose *et al.*	(BNL E871 Collab.)
ANGELOPO...	98	PL B420 191	A. Angelopoulos *et al.*	(CPLEAR Collab.)
ANGELOPO...	98C	EPJ C5 389	A. Angelopoulos *et al.*	(CPLEAR Collab.)
ANGELOPO...	98D	PL B444 38	A. Angelopoulos *et al.*	(CPLEAR Collab.)
Also	01B	EPJ C22 55	A. Angelopoulos *et al.*	(CPLEAR Collab.)
ANGELOPO...	98E	PL B444 43	A. Angelopoulos *et al.*	(CPLEAR Collab.)
ARISAKA	98	PL B432 230	K. Arisaka *et al.*	(FNAL E799 Collab.)
BENDER	98	PL B418 411	M. Bender *et al.*	(CERN NA48 Collab.)
SETZU	98	PL B420 205	M.G. Setzu *et al.*	
TAKEUCHI	98	PL B443 409	Y. Takeuchi *et al.*	(KYOT, KEK, HIRO)
FANTI	97	ZPHY C76 653	V. Fanti *et al.*	(CERN NA48 Collab.)
NOMURA	97	PL B408 445	T. Nomura *et al.*	(KYOT, KEK, HIRO)
ADLER	96B	ZPHY C70 211	R. Adler *et al.*	(CPLEAR Collab.)
ADLER	96C	PL B369 367	R. Adler *et al.*	(CPLEAR Collab.)
GU	96	PRL 76 4312	P. Gu *et al.*	(RUTG, UCLA, EFI, COLO+)
LEBER	96	PL B369 69	F. Leber *et al.*	(MANZ, CERN, EDIN, ORSAY+)
PDG	96	PR D54 1	R. M. Barnett *et al.*	
ADLER	95	PL B363 237	R. Adler *et al.*	(CPLEAR Collab.)
ADLER	95B	PL B363 243	R. Adler *et al.*	(CPLEAR Collab.)
AKAGI	95	PR D51 2061	T. Akagi *et al.*	(TOHOK, TOKY, KYOT, KEK)
BARR	95	ZPHY C65 361	G.D. Barr *et al.*	(CERN, EDIN, MANZ, LALO+)
BARR	95C	PL B358 399	G.D. Barr *et al.*	(CERN, EDIN, MANZ, LALO+)
HEINSON	95	PR D51 985	A.P. Heinson *et al.*	(BNL E791 Collab.)
KREUTZ	95	ZPHY C65 67	A. Kreutz *et al.*	(SIEG, EDIN, MANZ, ORSAY+)
MATTHEWS	95	PRL 75 2803	J.N. Matthews *et al.*	(RUTG, EFI, ELMT+)
SCHWINGEN...	95	PRL 74 4376	B. Schwingenheuer *et al.*	(EFI, CHIC+)
SPENCER	95	PRL 74 3323	M.B. Spencer *et al.*	(UCLA, EFI, COLO+)
BARR	94	PL B328 528	G.D. Barr *et al.*	(CERN, EDIN, MANZ, LALO+)
GU	94	PRL 72 3000	P. Gu *et al.*	(RUTG, UCLA, EFI, COLO+)
NAKAYA	94	PRL 73 2169	T. Nakaya *et al.*	(OSAK, UCLA, EFI, COLU+)
ROBERTS	94	PR D50 1874	D. Roberts *et al.*	(UCLA, EFI, COLU+)
WEAVER	94	PRL 72 3758	M. Weaver *et al.*	(UCLA, EFI, COLU, ELMT+)
AKAGI	93	PR D47 R2644	T. Akagi *et al.*	(TOHOK, TOKY, KYOT, KEK)
ARISAKA	93	PRL 70 1049	K. Arisaka *et al.*	(BNL E791 Collab.)
ARISAKA	93B	PRL 71 3910	K. Arisaka *et al.*	(BNL E791 Collab.)
BARR	93D	PL B317 233	G.D. Barr *et al.*	(CERN, EDIN, MANZ, LALO+)

See key on page 323

Meson Particle Listings

K_L^0

GIBBONS 93 PRL 70 1199 L.K. Gibbons *et al.* (FNAL E731 Collab.)
Also 97 PR D55 6625 L.K. Gibbons *et al.* (FNAL E731 Collab.)
GIBBONS 93B PRL 70 1203 L.K. Gibbons *et al.* (FNAL E731 Collab.)
GIBBONS 93C Thesis RX-1487 L.K. Gibbons (CHIC)
Also 97 PR D55 6625 L.K. Gibbons *et al.* (FNAL E731 Collab.)
HARRIS 93 PRL 71 3914 D.A. Harris *et al.* (EFI, UCLA, COLO+)
HARRIS 93B PRL 71 3918 D.A. Harris *et al.* (EFI, UCLA, COLO+)
MAKOFF 93 PRL 70 1591 G. Makoff *et al.* (FNAL E731 Collab.)
Also 95 PRL 75 2069 (erratum) G. Makoff *et al.*
RAMBERG 93 PRL 70 2525 E. Ramberg *et al.* (FNAL E731 Collab.)
RAMBERG 93B PRL 70 2529 E.J. Ramberg *et al.* (FNAL E731 Collab.)
VAGINS 93 PRL 71 35 M.R. Vagins *et al.* (BNL E845 Collab.)
ADLER 92B PL B286 180 R. Adler *et al.* (CPLEAR Collab.)
Also 92 SJNP 55 840 R. Adler *et al.* (CPLEAR Collab.)
BARR 92 PL B284 440 G.D. Barr *et al.* (CERN, EDIN, MANZ, LALO+)
GRAHAM 92 PL B295 169 G.E. Graham *et al.* (FNAL E731 Collab.)
MORSE 92 PR D45 36 W.M. Morse *et al.* (BNL, YALE, VASS)
PDG 92 PR D45, 1 June, Part II K. Hikasa *et al.* (KEK, LBL, BOST+)
SOMALWAR 92 PRL 68 2580 S.V. Somalwar *et al.* (FNAL E731 Collab.)
AKAGI 91B PRL 67 2618 T. Akagi *et al.* (TOHOK, TOKY, KYOT, KEK)
BARR 91 PL B259 389 G.D. Barr *et al.* (CERN, EDIN, MANZ, LALO+)
HEINSON 91 PR D44 R1 A.P. Heinson *et al.* (UCI, UCLA, LANL+)
PAPADIMITR... 91 PR D44 R573 V. Papadimitriou *et al.* (FNAL E731 Collab.)
BARKER 90 PR D41 3546 A.R. Barker *et al.* (FNAL E731 Collab.)
Also 88 PRL 61 2661 L.K. Gibbons *et al.* (FNAL E731 Collab.)
BARR 90B PL B240 283 G.D. Barr *et al.* (CERN, EDIN, MANZ, LALO+)
BARR 90C PL B242 523 G.D. Barr *et al.* (CERN, EDIN, MANZ, LALO+)
CAROSI 90 PL B237 303 R. Carosi *et al.* (CERN, EDIN, MANZ, LALO+)
KARLSSON 90 PRL 64 2976 M. Karlsson *et al.* (FNAL E731 Collab.)
OHL 90 PRL 64 2755 K.E. Ohl *et al.* (BNL E845 Collab.)
OHL 90B PRL 65 1407 K.E. Ohl *et al.* (BNL E845 Collab.)
PATTERSON 90 PRL 64 1491 J.R. Patterson *et al.* (FNAL E731 Collab.)
INAGAKI 89 PR D40 1712 T. Inagaki *et al.* (KEK, TOKY, KYOT)
MATHIAZHA... 89 PRL 63 2181 C. Mathiazhagan *et al.* (UCI, UCLA, LANL+)
MATHIAZHA... 89B PRL 63 2185 C. Mathiazhagan *et al.* (UCI, UCLA, LANL+)
WAHL 89 CERN-EP/89-86 H. Wahl (CERN)
BARR 88 PL B214 303 G.D. Barr *et al.* (CERN, EDIN, MANZ, LALO+)
BURKHARDT 88 PL B206 169 H. Burkhardt *et al.* (CERN, EDIN, MANZ+)
JASTRZEM... 88 PRL 61 2300 E. Jastrzembski *et al.* (BNL, YALE)
WOODS 88 PRL 60 1695 M. Woods *et al.* (FNAL E731 Collab.)
BURKHARDT 87 PL B199 139 H. Burkhardt *et al.* (CERN, EDIN, MANZ+)
ARONSON 86 PR D33 3180 S.H. Aronson *et al.* (BNL, CHIC, STAN+)
Also 82 PRL 48 1078 S.H. Aronson *et al.* (BNL, CHIC, STAN+)
PDG 86C PL 170B 132 M. Aguilar-Benitez *et al.* (CERN, CIT+)
COUPAL 85 PRL 55 566 D.P. Coupal *et al.* (CHIC, SACL)
BALATS 83 SJNP 38 556 M.Y. Balats *et al.* (ITEP)
Translated from YAF 38 927.
BERGSTROM 83 PL 131B 229 L. Bergstrom, E. Masso, P. Singer (CERN)
ARONSON 82 PRL 48 1078 S.H. Aronson *et al.* (BNL, CHIC, STAN+)
ARONSON 82B PRL 48 1306 S.H. Aronson *et al.* (BNL, CHIC, PURD)
Also 82B PL 116B 73 E. Fischbach *et al.* (PURD, BNL, CHIC)
Also 83 PR D28 476 S.H. Aronson *et al.* (BNL, CHIC, PURD)
Also 83B PR D28 495 S.H. Aronson *et al.* (BNL, CHIC, PURD)
PDG 82B PL 111B 70 M. Roos *et al.* (HELS, CIT, CERN)
BIRULEV 81 NP B182 1 V.K. Birulev *et al.* (JINR)
Also 80 SJNP 31 622 V.K. Birulev *et al.* (JINR)
Translated from YAF 31 1204.
CARROLL 80B PRL 44 529 A.S. Carroll *et al.* (BNL, ROCH)
CARROLL 80C PL 96B 407 A.S. Carroll *et al.* (BNL, ROCH)
CHO 80 PR D22 2688 Y. Cho *et al.* (ANL, CMU)
MORSE 80 PR D21 1750 W.M. Morse *et al.* (BNL, YALE)
CHRISTENS... 79 PRL 43 1209 J.H. Christenson *et al.* (NYU)
HILL 79 NP B153 39 D.G. Hill *et al.* (BNL, SLAC, SBER)
SCHMIDT 79 PRL 43 556 M.P. Schmidt *et al.* (YALE, BNL)
ENGLER 78B PR D18 623 A. Engler *et al.* (CMU, ANL)
HILL 78 PL 73B 403 D.G. Hill *et al.* (BNL, SLAC, SBER)
CHO 77 PR D15 587 Y. Cho *et al.* (ANL, CMU)
CLARK 77 PR D15 553 A.R. Clark *et al.* (LBL)
Also 75 Thesis LBL-4275 G. Shen (LBL)
DEVOE 77 PR D16 565 R. Devoe *et al.* (EFI, ANL)
DZHORD... 77 SJNP 26 478 V.P. Dzhordzhadze *et al.* (JINR)
Translated from YAF 26 910.
PEACH 77 NP B127 399 K.J. Peach *et al.* (BGNA, EDIN, GLAS+)
BIRULEV 76 SJNP 24 178 V.K. Birulev *et al.* (JINR)
Translated from YAF 24 340.
COOMBES 76 PRL 37 249 R.W. Coombes *et al.* (STAN, NYU)
GJESDAL 76 NP B109 118 G. Gjesdal *et al.* (CERN, HEIDH)
BALDO-... 75 NC 25A 688 M. Baldo-Ceolin *et al.* (PADO, WISC)
BLUMENTHAL 75 PRL 34 164 R.B. Blumenthal *et al.* (PENN, CHIC, TEMP)
BUCHANAN 75 PR D11 457 C.D. Buchanan *et al.* (UCLA, SLAC, JHU)
CARITHERS 75 PRL 34 1244 W.C.J. Carithers *et al.* (COLU, NYU)
SMITH 75B Thesis UCSD unpub. J.G. Smith (UCSD)
ALBRECHT 74 PL 48B 393 K.F. Albrecht (JINR, BERL, BUDA, PRAG, SERP+)
BISI 74 PL 50B 504 V. Bisi, M.I. Ferrero (TORI)
DONALDSON 74 Thesis SLAC-0184 G. Donaldson (SLAC)
Also 76 PR D14 2839 G. Donaldson *et al.* (SLAC)
DONALDSON 74B PR D9 2960 G. Donaldson *et al.* (SLAC, UCSC)
Also 73B PRL 31 337 G. Donaldson *et al.* (SLAC, UCSC)
GEWENIGER 74 PL 48B 483 C. Geweniger *et al.* (CERN, HEIDH)
Also 74 Thesis CERN Int. 74-4 V. Luth (CERN)
GEWENIGER 74B PL 48B 487 C. Geweniger *et al.* (CERN, HEIDH)
Also 74B PL 52B 119 S. Gjesdal *et al.* (CERN, HEIDH)
GEWENIGER 74C PL 52B 108 C. Geweniger *et al.* (CERN, HEIDH)
GJESDAL 74 PL 52B 113 S. Gjesdal *et al.* (CERN, HEIDH)
MESSNER 74 PRL 33 1458 R. Messner *et al.* (COLO, SLAC, UCSC)
NIEBERGALL 74 PL 49B 103 F. Niebergall *et al.* (CERN, ORSAY, VIEN)
WANG 74 PR D9 540 L. Wang *et al.* (UMD, BNL)
WILLIAMS 74 PRL 33 240 H.H. Williams *et al.* (BNL, YALE)
ALBROW 73 NP B58 22 M.G. Albrow *et al.* (MCHS, DARE)
ALEXANDER 73B NP B65 301 G. Alexander *et al.* (TELA, HEID)
BRANDENB... 73 PR D8 1978 G.W. Brandenburg *et al.* (SLAC)
EVANS 73 PR D7 36 G.R. Evans *et al.* (EDIN, CERN)
Also 69 PRL 23 427 G.R. Evans *et al.* (EDIN, CERN)
FACKLER 73 PRL 31 847 O. Fackler *et al.* (MIT)
FITCH 73 PRL 31 1524 V.L. Fitch *et al.* (PRIN)
Also 72 Thesis COO-3072-13 R.C. Webb (PRIN)
GINSBERG 73 PR D8 3887 E.S. Ginsberg, J. Smith (MIT, STON)
HART 73 NP B66 317 J.C. Hart *et al.* (CAVE, RHEL)
MALLARY 73 PR D7 1953 M.L. Mallary *et al.* (CIT)
Also 70 PRL 25 1214 F.J. Sciulli *et al.* (CIT)
MCCARTHY 73 PR D7 687 R.L. McCarthy *et al.* (LBL)
Also 72 PL 42B 291 R.L. McCarthy *et al.* (LBL)
Also 71 Thesis LBL-550 R.L. McCarthy (LBL)
MESSNER 73 PRL 30 876 R. Messner *et al.* (COLO, SLAC, UCSC)
PEACH 73 PL 43B 441 K.J. Peach *et al.* (EDIN, CERN, AACH)
SANDWEISS 73 PRL 30 1002 J. Sandweiss *et al.* (YALE, ANL)
WILLIAMS 73 PRL 31 1521 H.H. Williams *et al.* (BNL, YALE)
ALBROW 72 NP B44 1 M.G. Albrow *et al.* (MCHS, DARE)
ASHFORD 72 PL 38B 47 V.A. Ashford *et al.* (UCSD)
BANNER 72B PRL 29 237 M. Banner *et al.* (PRIN)
BARMIN 72B SJNP 15 638 V.V. Barmin *et al.* (ITEP)
Translated from YAF 15 1152.
BURGUN 72 NP B50 194 G. Burgun *et al.* (SACL, CERN, OSLO)
DALLY 72 PL 41B 647 E.B. Dally *et al.* (SLAC, JHU, UCLA)
Also 70 PL 33B 627 C.Y. Chien *et al.* (JHU, SLAC, UCLA)
Also 71 PL 35B 261 C.Y. Chien *et al.* (JHU, SLAC, UCLA)
GRAHAM 72 NC 9A 166 M.F. Graham *et al.* (ILL, NEAS)
JAMES 72 NP B49 1 F. James *et al.* (CERN, SACL, OSLO)
KRENZ 72 LNC 4 213 W. Krenz *et al.* (AACH, CERN, EDIN)
MANN 72 PR D6 137 W.A. Mann *et al.* (MASA, BNL, YALE)
MANTSCH 72 NC 9A 160 P.M. Mantsch *et al.* (ILL, NEAS)
MCCARTHY 72 PL 42B 291 R.L. McCarthy *et al.* (LBL)
NEUHOFER 72 PL 41B 642 G. Neuhofer *et al.* (CERN, ORSAY, VIEN)
PICCIONI 72 PRL 29 1412 R. Piccioni *et al.* (SLAC)
Also 74 PR D9 2939 R. Piccioni *et al.* (SLAC, UCSC, COLO)
VOSBURGH 72 PR D6 1834 K.G. Vosburgh *et al.* (RUTG, MASA)
Also 71 PRL 26 866 K.G. Vosburgh *et al.* (RUTG, MASA)
BALATS 71 SJNP 13 53 M.Y. Balats *et al.* (ITEP)
Translated from YAF 13 93.
BARMIN 71 PL 35B 604 V.V. Barmin *et al.* (ITEP)
BISI 71 PL 36B 533 V. Bisi *et al.* (AACH, CERN, TORI)
BURGUN 71 LNC 2 1169 G. Burgun *et al.* (SACL, CERN, OSLO)
CARNEGIE 71 PR D4 1 R.K. Carnegie *et al.* (PRIN)
CHAN 71 Thesis LBL-350 J.H.S. Chan (LBL)
CHIEN 71 PL 35B 361 C.Y. Chien *et al.* (JHU, SLAC, UCLA)
Also 72 PL 41B 647 E.B. Dally *et al.* (SLAC, JHU, UCLA)
CHO 71 PR D3 1557 Y. Cho *et al.* (CMU, BNL, CASE)
ENSTROM 71 PR D4 2629 J. Enstrom *et al.* (SLAC, STAN)
Also 70 Thesis SLAC-0125 J.E. Enstrom (STAN)
JAMES 71 PL 35B 265 F. James *et al.* (CERN, SACL, OSLO)
MEISNER 71 PR D3 59 G.W. Meisner *et al.* (MASA, BNL, YALE)
REPELLIN 71 PL 36B 603 J.P. Repellin *et al.* (ORSAY, CERN)
WEBBER 71 PR D3 64 B.R. Webber *et al.* (LRL)
Also 68 PRL 21 498 B.R. Webber *et al.* (LRL)
Also 69 Thesis UCRL 19226 B.R. Webber (LRL)
WOLFF 71 PL 36B 517 B. Wolff *et al.* (ORSAY, CERN)
ALBROW 70 PL 33B 516 M.G. Albrow *et al.* (MCHS, DARE)
ARONSON 70 PRL 25 1057 S.H. Aronson *et al.* (EFI, ILLC, SLAC)
BARMIN 70 PL 33B 377 V.V. Barmin *et al.* (ITEP, JINR)
BASILE 70 PR D2 78 P. Basile *et al.* (SACL)
BECHERRAWY 70 PR D1 1452 T. Becherrawy (ROCH)
BUCHANAN 70 PL 33B 623 C.D. Buchanan *et al.* (SLAC, JHU, UCLA)
Also 71 Private Comm. A.J. Cox
BUDAGOV 70 PR D2 815 I.A. Budagov *et al.* (CERN, ORSAY, EPOL)
Also 68B PL 28B 215 I.A. Budagov *et al.* (CERN, ORSAY, EPOL)
CHIEN 70 PL 33B 627 C.Y. Chien *et al.* (JHU, SLAC, UCLA)
Also 71 Private Comm. A.J. Cox
CHO 70 PR D1 3031 Y. Cho *et al.* (CMU, BNL, CASE)
Also 67 PRL 19 668 D.G. Hill *et al.* (BNL, CMU)
CHOLLET 70 PL 31B 658 J.C. Chollet *et al.* (CERN)
CULLEN 70 PL 32B 523 M. Cullen *et al.* (AACH, CERN, TORI)
GINSBERG 70 PR D1 229 E.S. Ginsberg (HAIF)
MARX 70 PL 32B 219 J. Marx *et al.* (COLU, HARV, CERN)
Also 70B Thesis Nevis 179 J. Marx (COLU)
SCRIBANO 70 PL 32B 224 A. Scribano *et al.* (PISA, COLU, HARV)
SMITH 70 PL 32B 133 R.C. Smith *et al.* (UMD, BNL)
WEBBER 70 PR D1 1967 B.R. Webber *et al.* (LRL)
Also 69 Thesis UCRL 19226 B.R. Webber (LRL)
BANNER 69 PR 188 2033 M. Banner *et al.* (PRIN)
Also 68 PRL 21 1103 M. Banner *et al.* (PRIN)
Also 68 PRL 21 1107 J.W. Cronin, J.K. Liu, J.E. Pilcher (PRIN)
BEILLIERE 69 PL 30B 202 P. Beilliere, G. Boutang, J. Limon (EPOL)
BENNETT 69 PL 29B 317 S. Bennett *et al.* (COLU, BNL)
EVANS 69 PRL 23 427 G.R. Evans *et al.* (EDIN, CERN)
FAISSNER 69 PL 30B 204 H. Faissner *et al.* (AACH3, CERN, TORI)
LITTENBERG 69 PRL 22 654 L.S. Littenberg *et al.* (UCSD)
LONGO 69 PR 181 1808 M.J. Longo, K.K. Young, J.A. Helland (MICH, UCLA)
PACIOTTI 69 Thesis UCRL 19446 M.A. Paciotti (LRL)
SAAL 69 Thesis H.J. Saal (COLU)
ABRAMS 68B PR 176 1603 R.J. Abrams *et al.* (ILL)
ARNOLD 68B PL 28B 56 R.G. Arnold *et al.* (CERN, ORSAY)
ARONSON 68 PRL 20 287 S.H. Aronson, K.W. Chen (PRIN)
Also 69 PR 175 1708 S.H. Aronson, K.W. Chen (PRIN)
BASILE 68 PL 26B 542 P. Basile *et al.* (SACL)
BASILE 68B PL 28B 58 P. Basile *et al.* (SACL)
BENNETT 68 PL 27B 244 S. Bennett *et al.* (COLU, CERN)
BLANPIED 68 PRL 21 1650 W.A. Blanpied *et al.* (CASE, HARV, MCGI)
BOHM 68B PL 27B 594 A. Bohm *et al.*
BUDAGOV 68 NC 57A 182 I.A. Budagov *et al.* (CERN, ORSAY, IPNP)
Also 68B PL 28B 215 I.A. Budagov *et al.* (CERN, ORSAY, EPOL)
JAMES 68 NP B8 365 F. James, H. Briand (IPNP, CERN)
Also 68 PRL 21 257 J.A. Helland, M.J. Longo, K.K. Young (UCLA, CERN)
KULYUKINA 68 JETP 26 20 L.A. Kulyukina *et al.* (JINR)
Translated from ZETF 53 29.
KUNZ 68 Thesis PU-68-46 P.F. Kunz (PRIN)
BENNETT 67 PRL 19 993 S. Bennett *et al.* (COLU)
DEBOUARD 67 NC 52A 662 X. de Bouard *et al.* (CERN)
Also 65 PL 15 58 X. de Bouard *et al.* (CERN, ORSAY, MPIM)
DEVLIN 67 PRL 18 54 T.J. Devlin *et al.* (PRIN, UMD)
Also 68 PR 169 1045 G.A. Sayer *et al.* (UMD, PPA, PRIN)
DORFAN 67 PRL 19 987 D.E. Dorfan *et al.* (SLAC, LRL)
FELDMAN 67B PR 155 1611 L. Feldman *et al.* (PENN)
FITCH 67 PR 164 1711 V.L. Fitch *et al.* (PRIN)
GINSBERG 67 PR 162 1570 E.S. Ginsberg (MASB)
HILL 67 PRL 19 668 D.G. Hill *et al.* (BNL, CMU)
HOPKINS 67 PRL 19 185 H.W.K. Hopkins, T.C. Bacon, F.R. Eisler (BNL)
KULYUKINA 67 Preprint L.A. Kulyukina *et al.* (JINR)
LOWYS 67 PL 24B 75 J.P. Lowys *et al.* (EPOL, ORSAY)
NEFKENS 67 PR 157 1233 B.M.K. Nefkens *et al.* (ILL)
SCHMIDT 67 Thesis Nevis 160 P. Schmidt (COLU)
AUERBACH 66B PRL 17 980 L.B. Auerbach *et al.* (PENN)
BEHR 66 PL 22 540 L. Behr *et al.* (EPOL, MILA, PADO, ORSAY)
CARPENTER 66 PR 142 871 D.W. Carpenter *et al.* (ILL)
HAWKINS 66 PL 21 238 C.J.B. Hawkins (YALE)
Also 67 PR 156 1444 C.J.B. Hawkins (YALE)
ANDERSON 65 PRL 14 475 J.A. Anderson *et al.* (LRL, WISC)
ASTBURY 65B PL 18 175 P. Astbury *et al.* (CERN, ZURI)
ASTBURY 65C PL 18 178 P. Astbury *et al.* (CERN, ZURI)
AUBERT 65 PL 17 59 B. Aubert *et al.* (EPOL, ORSAY)
Also 67 PL 24B 75 J.P. Lowys *et al.* (EPOL, ORSAY)
BALDO-... 65 NC 38 684 M. Baldo-Ceolin *et al.* (PADO)
FRANZINI 65 PR 140B 127 P. Franzini *et al.* (COLU, RUTG)
GUIDONI 65 Argonne Conf. 49 P. Guidoni *et al.* (BNL, YALE)
HOPKINS 65 Argonne Conf. 67 H.W.K. Hopkins, T.C. Bacon, F. Eisler (VAND+)
ADAIR 64 PL 12 67 R.K. Adair, L.B. Leipuner (YALE, BNL)
ALEKSANYAN 64B Dubna Conf. 2 102 A.S. Aleksanyan *et al.* (YERE)
Also 64 JETP 19 1019 A.S. Aleksanyan *et al.* (LEBD, MPEI, YERE)
Translated from ZETF 46 1504.
ANIKINA 64 JETP 19 42 M.K. Anikina *et al.* (GEOR, JINR)
Translated from ZETF 46 59.

Meson Particle Listings

K^0_L, $K^*_0(800)$, $K^*(892)$

FUJII 64 Dubna Conf. 2 146 T. Fujii *et al.* (BNL, UMD, MIT)
LUERS 64 PR 133B 1276 D. Luers *et al.* (BNL)
DARMON 62 PL 3 57 J. Darmon, A. Rousset, J. Six (EPOL)
FITCH 61 NC 22 1160 V.L. Fitch, P.A. Piroue, R.B. Perkins (PRIN+)
GOOD 61 PR 124 1223 R.H. Good *et al.* (LRL)
BARDON 58 ANP 5 156 M. Bardon, K. Lande, L.M. Lederman (COLU, BNL)

OTHER RELATED PAPERS

HAYAKAWA 93 PR D48 1150 M. Hayakawa, A.I. Sanda (NAGO)
"Searching for *T*, *CP*, *CPT*, $\Delta S = \Delta Q$ Rule Violations in the Neutral *K* Meson System: A Guide"
LITTENBERG 93 ARNPS 43 729 L.S. Littenberg, G. Valencia (BNL, FNAL)
Rare and Radiative Kaon Decays
RITCHIE 93 RMP 65 1149 J.L. Ritchie, S.G. Wojcicki
"Rare *K* Decays"
WINSTEIN 93 RMP 65 1113 B. Winstein, L. Wolfenstein
"The Search for Direct *CP* Violation"
BATTISTON 92 PRPL 214 293 R. Battiston *et al.* (PGIA, CERN, TRSTT)
Status and Perspectives of *K* Decay Physics
DIB 92 PR D46 2265 C.O. Dib, R.D. Peccei (UCLA)
Tests of *CPT* conservation in the neutral kaon system.
KLEINKNECHT 92 CNPP 20 281 K. Kleinknecht (MANZ)
New Results on *CP* Violation in Decays of Neutral *K* Mesons.
KLEINKNECHT 90 ZPHY C46 S57 K. Kleinknecht (MANZ)
PEACH 90 JPG 16 131 K.J. Peach (EDIN)
BRYMAN 89 IJMP A4 79 D.A. Bryman (TRIU)
"Rare Kaon Decays"
KLEINKNECHT 76 ARNS 26 1 K. Kleinknecht (DORT)
GINSBERG 73 PR D8 3887 E.S. Ginsberg, J. Smith (MIT, STON)
GINSBERG 70 PR D1 229 E.S. Ginsberg (HAIF)
HEUSSE 70 LNC 3 449 P. Heusse *et al.* (ORSAY)
CRONIN 68C Vienna Conf. 281 J.W. Cronin (PRIN)
RUBBIA 67 PL 24B 531 C. Rubbia, J. Steinberger (CERN, COLU)
Also 66C PL 23 167 C. Rubbia, J. Steinberger (CERN, COLU)
Also 66C PL 20 207 C. Alff-Steinberger *et al.* (CERN)
Also 66B PL 21 595 C. Alff-Steinberger *et al.* (CERN)
AUERBACH 66 PR 149 1052 L.B. Auerbach *et al.* (PENN)
Also 65 PRL 14 192 L.B. Auerbach *et al.* (PENN)
FIRESTONE 66B PRL 17 116 A. Firestone *et al.* (YALE, BNL)
BEHR 65 Argonne Conf. 59 L. Behr *et al.* (EPOL, MILA, PADO)
MESTVIRISHH... 65 JINR P 2449 A.N. Mestvirishvili *et al.* (JINR)
TRILLING 65B UCRL 16473 G.N. Trilling (LRL)
Updated from 1965 Argonne Conference, page 115.
JOVANOV... 63 BNL Conf. 42 J.V. Jovanovich *et al.* (BNL, UMD)

$K^*_0(800)$ or κ

$I(J^P) = \frac{1}{2}(0^+)$

OMITTED FROM SUMMARY TABLE

The existence of this state is controversial.

$K^*_0(800)$ MASS

VALUE (MeV)	*EVTS*	*DOCUMENT ID*		*TECN*	*COMMENT*
• • • We do not use the following data for averages, fits, limits, etc. • • •					
722±60		[1] BUGG	03	RVUE	11 $K^- p \to K^- \pi^+ n$
797±19±43	15090	[2] AITALA	02	E791	$D^+ \to K^- \pi^+ \pi^+$
905^{+65}_{-30}		[3] ISHIDA	97B	RVUE	11 $K^- p \to K^- \pi^+ n$

[1] T-matrix pole. Reanalysis of ASTON 88 data.
[2] Not seen by KOPP 01 using 7070 events of $D^0 \to K^- \pi^+ \pi^0$. Possibly seen by LINK 02E in $D^+ \to K^- \pi^+ \mu^+ \nu_\mu$.
[3] Reanalysis of ASTON 88 using interfering Breit-Wigner amplitudes.

$K^*_0(800)$ WIDTH

VALUE (MeV)	*EVTS*	*DOCUMENT ID*		*TECN*	*COMMENT*
• • • We do not use the following data for averages, fits, limits, etc. • • •					
772±100		[4] BUGG	03	RVUE	11 $K^- p \to K^- \pi^+ n$
410± 43±87	15090	[5] AITALA	02	E791	$D^+ \to K^- \pi^+ \pi^+$
545^{+235}_{-110}		[6] ISHIDA	97B	RVUE	11 $K^- p \to K^- \pi^+ n$

[4] T-matrix pole. Reanalysis of ASTON 88 data.
[5] Not seen by KOPP 01 using 7070 events of $D^0 \to K^- \pi^+ \pi^0$. Possibly seen by LINK 02E in $D^+ \to K^- \pi^+ \mu^+ \nu_\mu$.
[6] Reanalysis of ASTON 88 using interfering Breit-Wigner amplitudes.

$K^*_0(800)$ REFERENCES

BUGG 03 PL B572 1 D.V. Bugg
AITALA 02 PRL 89 121801 E.M. Aitala *et al.* (FNAL E791 Collab.)
LINK 02E PL B535 43 J.M. Link *et al.* (FNAL FOCUS Collab.)
KOPP 01 PR D63 092001 S. Kopp *et al.* (CLEO Collab.)
ISHIDA 97B PTP 98 621 S. Ishida *et al.*
ASTON 88 NP B296 493 D. Aston *et al.* (SLAC, NAGO, CINC, INUS)

OTHER RELATED PAPERS

SEMENOV 03 PAN 66 526 S.V. Semenov
Translated from YAF 66 553.
BEVEREN 01B EPJ C22 493 E. van Beveren

$K^*(892)$

$I(J^P) = \frac{1}{2}(1^-)$

$K^*(892)$ MASS

CHARGED ONLY

VALUE (MeV)	*EVTS*	*DOCUMENT ID*		*TECN*	*CHG*	*COMMENT*
891.66±0.26 OUR AVERAGE						
892.6 ±0.5	5840	BAUBILLIER	84B	HBC	–	8.25 $K^- p \to \overline{K}^0 \pi^- p$
888 ±3		NAPIER	84	SPEC	+	200 $\pi^- p \to 2K^0_S X$
891 ±1		NAPIER	84	SPEC	–	200 $\pi^- p \to 2K^0_S X$
891.7 ±2.1	3700	BARTH	83	HBC	+	70 $K^+ p \to K^0 \pi^+ X$
891 ±1	4100	TOAFF	81	HBC	–	6.5 $K^- p \to \overline{K}^0 \pi^- p$
892.8 ±1.6		AJINENKO	80	HBC	+	32 $K^+ p \to K^0 \pi^+ X$
890.7 ±0.9	1800	AGUILAR-...	78B	HBC	±	0.76 $\overline{p} p \to K^\mp K^0_S \pi^\pm$
886.6 ±2.4	1225	BALAND	78	HBC	±	12 $\overline{p} p \to (K\pi)^\pm X$
891.7 ±0.6	6706	COOPER	78	HBC	±	0.76 $\overline{p} p \to (K\pi)^\pm X$
891.9 ±0.7	9000	[2] PALER	75	HBC	–	14.3 $K^- p \to (K\pi)^- X$
892.2 ±1.5	4404	AGUILAR-...	71B	HBC	–	3.9,4.6 $K^- p \to (K\pi)^- p$
891 ±2	1000	CRENNELL	69D	DBC	–	3.9 $K^- N \to K^0 \pi^- X$
890 ±3.0	720	BARLOW	67	HBC	±	1.2 $\overline{p} p \to (K^0\pi)^\pm K^\mp$
889 ±3.0	600	BARLOW	67	HBC	±	1.2 $\overline{p} p \to (K^0\pi)^\pm K\pi$
891 ±2.3	620	[3] DEBAERE	67B	HBC	+	3.5 $K^+ p \to K^0 \pi^+ p$
891.0 ±1.2	1700	[4] WOJCICKI	64	HBC	–	1.7 $K^- p \to \overline{K}^0 \pi^- p$
• • • We do not use the following data for averages, fits, limits, etc. • • •						
893.5 ±1.1	27k	[1] ABELE	99D	CBAR	±	0.0 $\overline{p} p \to K^+ K^- \pi^0$
890.4 ±0.2 ±0.5	79709± 801	[5] BIRD	89	LASS	–	11 $K^- p \to \overline{K}^0 \pi^- p$
890.0 ±2.3	800	[3,4] CLELAND	82	SPEC	+	30 $K^+ p \to K^0_S \pi^+ p$
896.0 ±1.1	3200	[3,4] CLELAND	82	SPEC	+	50 $K^+ p \to K^0_S \pi^+ p$
893 ±1	3600	[3,4] CLELAND	82	SPEC	–	50 $K^+ p \to K^0_S \pi^- p$
896.0 ±1.9	380	DELFOSSE	81	SPEC	+	50 $K^\pm p \to K^\pm \pi^0 p$
886.0 ±2.3	187	DELFOSSE	81	SPEC	–	50 $K^\pm p \to K^\pm \pi^0 p$
894.2 ±2.0	765	[3] CLARK	73	HBC	–	3.13 $K^- p \to \overline{K}^0 \pi^- p$
894.3 ±1.5	1150	[3,4] CLARK	73	HBC	–	3.3 $K^- p \to \overline{K}^0 \pi^- p$
892.0 ±2.6	341	[3] SCHWEING...	68	HBC	–	5.5 $K^- p \to \overline{K}^0 \pi^- p$

[1] K-matrix pole.

NEUTRAL ONLY

VALUE (MeV)	*EVTS*	*DOCUMENT ID*		*TECN*	*CHG*	*COMMENT*
896.10±0.27 OUR AVERAGE		Error includes scale factor of 1.4. See the ideogram below.				
896 ±2		BARBERIS	98E	OMEG		450 $pp \to p_f p_s K^* \overline{K}^*$
895.9 ±0.5 ±0.2		ASTON	88	LASS	0	11 $K^- p \to K^- \pi^+ n$
894.52±0.63	25k	[2] ATKINSON	86	OMEG		20–70 γp
894.63±0.76	20k	[2] ATKINSON	86	OMEG		20–70 γp
897 ±1	28k	EVANGELISTA	80	OMEG	0	10 $\pi^- p \to K^+ \pi^- (\Lambda, \Sigma)$
898.4 ±1.4	1180	AGUILAR-...	78B	HBC	0	0.76 $\overline{p} p \to K^\mp K^0_S \pi^\pm$
894.9 ±1.6		WICKLUND	78	ASPK	0	3,4,6 $K^\pm N \to (K\pi)^0 N$
897.6 ±0.9		BOWLER	77	DBC	0	5.4 $K^+ d \to K^+ \pi^- p p$
895.5 ±1.0	3600	MCCUBBIN	75	HBC	0	3.6 $K^- p \to K^- \pi^+ n$
897.1 ±0.7	22k	[2] PALER	75	HBC	0	14.3 $K^- p \to (K\pi)^0 X$
896.0 ±0.6	10k	FOX	74	RVUE	0	2 $K^- p \to K^- \pi^+ n$
896.0 ±0.6		FOX	74	RVUE	0	2 $K^+ n \to K^+ \pi^- p$
896 ±2		[6] MATISON	74	HBC	0	12 $K^+ p \to K^+ \pi^- \Delta$
896 ±1	3186	LEWIS	73	HBC	0	2.1–2.7 $K^+ p \to K \pi \pi p$
894.0 ±1.3		[6] LINGLIN	73	HBC	0	2–13 $K^+ p \to K^+ \pi^- \pi^+ p$
898.4 ±1.3	1700	[3] BUCHNER	72	DBC	0	4.6 $K^+ n \to K^+ \pi^- p$
897.9 ±1.1	2934	[3] AGUILAR-...	71B	HBC	0	3.9,4.6 $K^- p \to K^- \pi^+ n$
898.0 ±0.7	5362	[3] AGUILAR-...	71B	HBC	0	3.9,4.6 $K^- p \to K^- \pi^+ \pi^- p$
895 ±1	4300	[4] HABER	70	DBC	0	3 $K^- N \to K^- \pi^+ X$
893.7 ±2.0	10k	DAVIS	69	HBC	0	12 $K^+ p \to K^+ \pi^- \pi^+ p$
894.7 ±1.4	1040	[3] DAUBER	67B	HBC	0	2.0 $K^- p \to K^- \pi^+ \pi^- p$
• • • We do not use the following data for averages, fits, limits, etc. • • •						
900.7 ±1.1	5900	BARTH	83	HBC	0	70 $K^+ p \to K^+ \pi^- X$

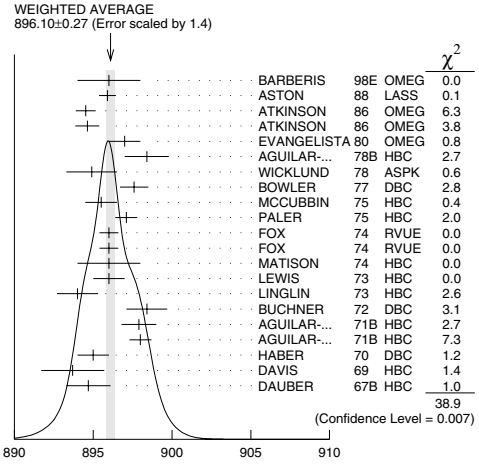

[2] Inclusive reaction. Complicated background and phase-space effects.
[3] Mass errors enlarged by us to $\Gamma/\sqrt{N}$. See note.
[4] Number of events in peak reevaluated by us.
[5] From a partial wave amplitude analysis.
[6] From pole extrapolation.

$K^*(892)$ MASSES AND MASS DIFFERENCES

Unrealistically small errors have been reported by some experiments. We use simple "realistic" tests for the minimum errors on the determination of a mass and width from a sample of N events:

$$\delta_{\min}(m) = \frac{\Gamma}{\sqrt{N}}, \quad \delta_{\min}(\Gamma) = 4\frac{\Gamma}{\sqrt{N}}\ . \tag{1}$$

We consistently increase unrealistic errors before averaging. For a detailed discussion, see the 1971 edition of this Note.

$m_{K^*(892)^0} - m_{K^*(892)^\pm}$

VALUE (MeV)	EVTS	DOCUMENT ID		TECN	CHG	COMMENT
6.7±1.2 OUR AVERAGE						
7.7±1.7	2980	AGUILAR-...	78B	HBC	±0	0.76 $\overline{p}p \to K^\mp K^0_S \pi^\pm$
5.7±1.7	7338	AGUILAR-...	71B	HBC	−0	3.9,4.6 $K^- p$
6.3±4.1	283	[7] BARASH	67B	HBC		0.0 $\overline{p}p$

[7] Number of events in peak reevaluated by us.

$K^*(892)$ RANGE PARAMETER

All from partial wave amplitude analyses.

VALUE (GeV^{-1})	DOCUMENT ID		TECN	CHG	COMMENT
3.4±0.7	ASTON	88	LASS	0	11 $K^- p \to K^- \pi^+ n$
• • • We do not use the following data for averages, fits, limits, etc. • • •					
12.1±3.2±3.0	BIRD	89	LASS	−	11 $K^- p \to \overline{K}^0 \pi^- p$

$K^*(892)$ WIDTH

VALUE (MeV)	EVTS	DOCUMENT ID		TECN	CHG	COMMENT
CHARGED ONLY						
50.8±0.9 OUR FIT						
50.8±0.9 OUR AVERAGE						
49 ±2	5840	BAUBILLIER	84B	HBC	−	8.25 $K^- p \to \overline{K}^0 \pi^- p$
56 ±4		NAPIER	84	SPEC	−	200 $\pi^- p \to 2K^0_S X$
51 ±2	4100	TOAFF	81	HBC	−	6.5 $K^- p \to \overline{K}^0 \pi^- p$
50.5±5.6		AJINENKO	80	HBC	+	32 $K^+ p \to K^0 \pi^+ X$
45.8±3.6	1800	AGUILAR-...	78B	HBC	±	0.76 $\overline{p}p \to K^\mp K^0_S \pi^\pm$
52.0±2.5	6706	[9] COOPER	78	HBC	±	0.76 $\overline{p}p \to (K\pi)^\pm X$
52.1±2.2	9000	[10] PALER	75	HBC	−	14.3 $K^- p \to (K\pi)^- X$
46.3±6.7	765	[9] CLARK	73	HBC	−	3.13 $K^- p \to \overline{K}^0 \pi^- p$
48.2±5.7	1150	[9,11] CLARK	73	HBC	−	3.3 $K^- p \to \overline{K}^0 \pi^- p$
54.3±3.3	4404	[9] AGUILAR-...	71B	HBC	−	3.9,4.6 $K^- p \to (K\pi)^- p$
46 ±5	1700	[9,11] WOJCICKI	64	HBC	−	1.7 $K^- p \to \overline{K}^0 \pi^- p$
• • • We do not use the following data for averages, fits, limits, etc. • • •						
54.8±1.7	27k	[8] ABELE	99D	CBAR	±	0.0 $\overline{p}p \to K^+ K^- \pi^0$
45.2±1 ±2	79709±801	[12] BIRD	89	LASS	−	11 $K^- p \to \overline{K}^0 \pi^- p$
42.8±7.1	3700	BARTH	83	HBC	+	70 $K^+ p \to K^0 \pi^+ X$
64.0±9.2	800	[9,11] CLELAND	82	SPEC	+	30 $K^+ p \to K^0_S \pi^+ p$
62.0±4.4	3200	[9,11] CLELAND	82	SPEC	+	50 $K^+ p \to K^0_S \pi^+ p$
55 ±4	3600	[9,11] CLELAND	82	SPEC	−	50 $K^+ p \to K^0_S \pi^- p$
62.6±3.8	380	DELFOSSE	81	SPEC	+	50 $K^\pm p \to K^\pm \pi^0 p$
50.5±3.9	187	DELFOSSE	81	SPEC	−	50 $K^\pm p \to K^\pm \pi^0 p$

[8] K-matrix pole.

NEUTRAL ONLY

VALUE (MeV)	EVTS	DOCUMENT ID		TECN	CHG	COMMENT
50.7±0.6 OUR FIT Error includes scale factor of 1.1.						
50.7±0.6 OUR AVERAGE Error includes scale factor of 1.1.						
54 ±3		BARBERIS	98E	OMEG		450 $pp \to p_f p_s K^* \overline{K}^*$
50.8±0.8±0.9		ASTON	88	LASS	0	11 $K^- p \to K^- \pi^+ n$
46.5±4.3	5900	BARTH	83	HBC	0	70 $K^+ p \to K^+ \pi^- X$
54 ±2	28k	EVANGELISTA	80	OMEG	0	10 $\pi^- p \to K^+ \pi^- (\Lambda, \Sigma)$
45.9±4.8	1180	AGUILAR-...	78B	HBC	0	0.76 $\overline{p}p \to K^\mp K^0_S \pi^\pm$
51.2±1.7		WICKLUND	78	ASPK	0	3,4,6 $K^\pm N \to (K\pi)^0 N$
48.9±2.5		BOWLER	77	DBC	0	5.4 $K^+ d \to K^+ \pi^- p p$
48 $^{+3}_{-2}$	3600	MCCUBBIN	75	HBC	0	3.6 $K^- p \to K^- \pi^+ n$
50.6±2.5	22k	[10] PALER	75	HBC	0	14.3 $K^- p \to (K\pi)^0 X$
47 ±2	10k	FOX	74	RVUE	0	2 $K^- p \to K^- \pi^+ n$
51 ±2		FOX	74	RVUE	0	2 $K^+ n \to K^+ \pi^- p$
46.0±3.3	3186	[9] LEWIS	73	HBC	0	2.1–2.7 $K^+ p \to K \pi \pi p$
51.4±5.0	1700	[9] BUCHNER	72	DBC	0	4.6 $K^+ n \to K^+ \pi^- p$
55.8 $^{+4.2}_{-3.4}$	2934	[9] AGUILAR-...	71B	HBC	0	3.9,4.6 $K^- p \to K^- \pi^+ n$
48.5±2.7	5362	AGUILAR-...	71B	HBC	0	3.9,4.6 $K^- p \to K^- \pi^+ \pi^- p$
54.0±3.3	4300	[9,11] HABER	70	DBC	0	3 $K^- N \to K^- \pi^+ X$
53.2±2.1	10k	[9] DAVIS	69	HBC	0	12 $K^+ p \to K^+ \pi^- \pi^+ p$
44 ±5.5	1040	[9] DAUBER	67B	HBC	0	2.0 $K^- p \to K^- \pi^+ \pi^- p$

[9] Width errors enlarged by us to $4 \times \Gamma/\sqrt{N}$; see note.
[10] Inclusive reaction. Complicated background and phase-space effects.
[11] Number of events in peak reevaluated by us.
[12] From a partial wave amplitude analysis.

$K^*(892)$ DECAY MODES

	Mode	Fraction (Γ_j/Γ)	Confidence level
Γ_1	$K\pi$	~ 100 %	
Γ_2	$(K\pi)^\pm$	(99.901±0.009) %	
Γ_3	$(K\pi)^0$	(99.770±0.020) %	
Γ_4	$K^0\gamma$	(2.30 ±0.20) × 10^{-3}	
Γ_5	$K^\pm\gamma$	(9.9 ±0.9) × 10^{-4}	
Γ_6	$K\pi\pi$	< 7 × 10^{-4}	95%

CONSTRAINED FIT INFORMATION

An overall fit to the total width and a partial width uses 13 measurements and one constraint to determine 3 parameters. The overall fit has a $\chi^2 = 7.8$ for 11 degrees of freedom.

The following *off-diagonal* array elements are the correlation coefficients $\langle \delta p_i \delta p_j \rangle / (\delta p_i \cdot \delta p_j)$, in percent, from the fit to parameters p_i, including the branching fractions, $x_i \equiv \Gamma_i / \Gamma_{total}$. The fit constrains the x_i whose labels appear in this array to sum to one.

x_5	−100	
Γ	19	−19
	x_2	x_5

	Mode	Rate (MeV)
Γ_2	$(K\pi)^\pm$	50.7 ±0.9
Γ_5	$K^\pm\gamma$	0.050±0.005

CONSTRAINED FIT INFORMATION

An overall fit to the total width and a partial width uses 19 measurements and one constraint to determine 3 parameters. The overall fit has a $\chi^2 = 19.7$ for 17 degrees of freedom.

The following *off-diagonal* array elements are the correlation coefficients $\langle \delta p_i \delta p_j \rangle / (\delta p_i \cdot \delta p_j)$, in percent, from the fit to parameters p_i, including the branching fractions, $x_i \equiv \Gamma_i / \Gamma_{total}$. The fit constrains the x_i whose labels appear in this array to sum to one.

x_4	−100	
Γ	14	−14
	x_3	x_4

	Mode	Rate (MeV)	Scale factor
Γ_3	$(K\pi)^0$	50.6 ±0.6	1.1
Γ_4	$K^0\gamma$	0.117±0.010	

$K^*(892)$ PARTIAL WIDTHS

$\Gamma(K^0\gamma)$ **Γ_4**

VALUE (keV)	EVTS	DOCUMENT ID		TECN	CHG	COMMENT
116 ±10 OUR FIT						
116.5± 9.9	584	CARLSMITH	86	SPEC	0	$K^0_L A \to K^0_S \pi^0 A$

$\Gamma(K^\pm\gamma)$ **Γ_5**

VALUE (keV)	DOCUMENT ID		TECN	CHG	COMMENT
50± 5 OUR FIT					
50± 5 OUR AVERAGE					
48±11	BERG	83	SPEC	−	156 $K^- A \to \overline{K}\pi A$
51± 5	CHANDLEE	83	SPEC	+	200 $K^+ A \to K\pi A$

$K^*(892)$ BRANCHING RATIOS

$\Gamma(K^0\gamma)/\Gamma_{total}$ **Γ_4/Γ**

VALUE (units 10^{-3})	DOCUMENT ID		TECN	CHG	COMMENT
2.30±0.20 OUR FIT					
• • • We do not use the following data for averages, fits, limits, etc. • • •					
1.5 ±0.7	CARITHERS	75B	CNTR	0	8–16 $\overline{K}^0 A$

$\Gamma(K^\pm\gamma)/\Gamma_{total}$ **Γ_5/Γ**

VALUE (units 10^{-3})	CL%	DOCUMENT ID		TECN	CHG	COMMENT
0.99±0.09 OUR FIT						
• • • We do not use the following data for averages, fits, limits, etc. • • •						
<1.6	95	BEMPORAD	73	CNTR	+	10–16 $K^+ A$

$\Gamma(K\pi\pi)/\Gamma((K\pi)^\pm)$ **Γ_6/Γ_2**

VALUE	CL%	DOCUMENT ID		TECN	CHG	COMMENT
<0.0007	95	JONGEJANS	78	HBC		4 $K^- p \to p\overline{K}^0 2\pi$
• • • We do not use the following data for averages, fits, limits, etc. • • •						
<0.002		WOJCICKI	64	HBC	−	1.7 $K^- p \to \overline{K}^0 \pi^- p$

$K^*(892)$ REFERENCES

ABELE	99D	PL B468 178	A. Abele *et al.*	(Crystal Barrel Collab.)
BARBERIS	98E	PL B436 204	D. Barberis *et al.*	(Omega Expt.)
BIRD	89	SLAC-332	P.F. Bird	(SLAC)
ASTON	88	NP B296 493	D. Aston *et al.*	(SLAC, NAGO, CINC, INUS)
ATKINSON	86	ZPHY C30 521	M. Atkinson *et al.*	(BONN, CERN, GLAS+)
CARLSMITH	86	PRL 56 18	D. Carlsmith *et al.*	(EFI, SACL)
BAUBILLIER	84B	ZPHY C26 37	M. Baubillier *et al.*	(BIRM, CERN, GLAS+)
NAPIER	84	PL 149B 514	A. Napier *et al.*	(TUFTS, ARIZ, FNAL, FLOR+)
BARTH	83	NP B223 296	M. Barth *et al.*	(BRUX, CERN, GENO, MONS+)
BERG	83	Thesis UMI 83-21652	D.M. Berg	(ROCH)
CHANDLEE	83	PRL 51 168	C. Chandlee *et al.*	(ROCH, FNAL, MINN)
CLELAND	82	NP B208 189	W.E. Cleland *et al.*	(DURH, GEVA, LAUS+)
DELFOSSE	81	NP B183 349	A. Delfosse *et al.*	(GEVA, LAUS)
TOAFF	81	PR D23 1500	S. Toaff *et al.*	(ANL, KANS)
AJINENKO	80	ZPHY C5 177	I.V. Ajinenko *et al.*	(SERP, BRUX, MONS+)
EVANGELISTA	80	NP B165 383	C. Evangelista *et al.*	(BARI, BONN, CERN+)
AGUILAR-...	78B	NP B141 101	M. Aguilar-Benitez *et al.*	(MADR, TATA+)
BALAND	78	NP B140 220	J.F. Baland *et al.*	(MONS, BELG, CERN+)
COOPER	78	NP B136 365	A.M. Cooper *et al.*	(TATA, CERN, CDEF+)
JONGEJANS	78	NP B139 383	B. Jongejans *et al.*	(ZEEM, CERN, NIJM+)
WICKLUND	78	PR D17 1197	A.B. Wicklund *et al.*	(ANL)
BOWLER	77	NP B126 31	M.G. Bowler *et al.*	(OXF)
CARITHERS	75B	PRL 35 349	W.C.J. Carithers *et al.*	(ROCH, MCGI)
MCCUBBIN	75	NP B86 13	N.A. McCubbin, L. Lyons	(OXF)
PALER	75	NP B96 1	K. Paler *et al.*	(RHEL, SACL, EPOL)
FOX	74	NP B80 403	G.C. Fox, M.L. Grãs	(CIT)
MATISON	74	PR D9 1872	M.J. Matison *et al.*	(LBL)
BEMPORAD	73	NP B51 1	C. Bemporad *et al.*	(CERN, ETH, LOIC)
CLARK	73	NP B54 432	A.G. Clark, L. Lyons, D. Radojicic	(OXF)
LEWIS	73	NP B60 283	P.H. Lewis *et al.*	(LOWC, LOIC, CDEF)
LINGLIN	73	NP B55 408	D. Linglin	(CERN)
BUCHNER	72	NP B45 333	K. Buchner *et al.*	(MPIM, CERN, BRUX)
AGUILAR-...	71B	PR D4 2583	M. Aguilar-Benitez, R.L. Eisner, J.B. Kinson	(BNL)
HABER	70	NP B17 289	B. Haber *et al.*	(REHO, SACL, BGNA, EPOL)
CRENNELL	69D	PRL 22 487	D.J. Crennell *et al.*	(BNL)
DAVIS	69	PRL 23 1071	P.J. Davis *et al.*	(LRL)
SCHWEING...	68	PR 166 1317	F. Schweingruber *et al.*	(ANL, NWES)
BARASH	67B	PR 156 1399	N. Barash *et al.*	(COLU)
BARLOW	67	NC 50A 701	J. Barlow *et al.*	(CERN, CDEF, IRAD, LIVP)
DAUBER	67B	PR 153 1403	P.M. Dauber *et al.*	(UCLA)
DEBAERE	67B	NC 51A 401	W. de Baere *et al.*	(BRUX, CERN)
WOJCICKI	64	PR 135B 484	S.G. Wojcicki	(LRL)

OTHER RELATED PAPERS

BENAYOUN	99B	PR D59 114027	M. Benayoun *et al.*	
KAMAL	92	PL B284 421	A.N. Kamal, Q.P. Xu	(ALBE)
NAPIER	84	PL 149B 514	A. Napier *et al.*	(TUFTS, ARIZ, FNAL, FLOR+)
CLELAND	82	NP B208 189	W.E. Cleland *et al.*	(DURH, GEVA, LAUS+)
ALEXANDER	62	PRL 8 447	G. Alexander *et al.*	(LRL)
ALSTON	61	PRL 6 300	M.H. Alston *et al.*	(LRL)

$K_1(1270)$ $I(J^P) = \frac{1}{2}(1^+)$

$K_1(1270)$ MASS

VALUE (MeV)	DOCUMENT ID
1273±7 OUR AVERAGE	Includes data from the 2 datablocks that follow this one.

PRODUCED BY K^-, BACKWARD SCATTERING, HYPERON EXCHANGE

VALUE (MeV)	EVTS	DOCUMENT ID		TECN	CHG	COMMENT
The data in this block is included in the average printed for a previous datablock.						
1275±10	700	GAVILLET	78	HBC	+	4.2 $K^- p \to \Xi^- (K\pi\pi)^+$

PRODUCED BY K BEAMS

VALUE (MeV)	DOCUMENT ID		TECN	CHG	COMMENT
The data in this block is included in the average printed for a previous datablock.					
1270±10	DAUM	81C	CNTR	−	63 $K^- p \to K^- 2\pi p$
• • • We do not use the following data for averages, fits, limits, etc. • • •					
~ 1276	[1] TORNQVIST	82B	RVUE		
~ 1300	VERGEEST	79	HBC	−	4.2 $K^- p \to (\overline{K}\pi\pi)^- p$
1289±25	[2] CARNEGIE	77	ASPK	±	13 $K^\pm p \to (K\pi\pi)^\pm p$
~ 1300	BRANDENB...	76	ASPK	±	13 $K^\pm p \to (K\pi\pi)^\pm p$
~ 1270	OTTER	76	HBC	−	10,14,16 $K^- p \to (\overline{K}\pi\pi)^- p$
1260	DAVIS	72	HBC	+	12 $K^+ p$
1234±12	FIRESTONE	72B	DBC	+	12 $K^+ d$

[1] From a unitarized quark-model calculation.
[2] From a model-dependent fit with Gaussian background to BRANDENBURG 76 data.

PRODUCED BY BEAMS OTHER THAN K MESONS

VALUE (MeV)	EVTS	DOCUMENT ID		TECN	CHG	COMMENT
• • • We do not use the following data for averages, fits, limits, etc. • • •						
1294±10	310	RODEBACK	81	HBC		4 $\pi^- p \to \Lambda K 2\pi$
1300	40	CRENNELL	72	HBC	0	4.5 $\pi^- p \to \Lambda K 2\pi$
1242^{+9}_{-10}		[3] ASTIER	69	HBC	0	$\overline{p}p$
1300	45	CRENNELL	67	HBC	0	6 $\pi^- p \to \Lambda K 2\pi$

[3] This was called the C meson.

$K_1(1270)$ WIDTH

VALUE (MeV)	DOCUMENT ID
90±20 OUR ESTIMATE	This is only an educated guess; the error given is larger than the error on the average of the published values.
87± 7 OUR AVERAGE	Includes data from the 2 datablocks that follow this one.

PRODUCED BY K^-, BACKWARD SCATTERING, HYPERON EXCHANGE

VALUE (MeV)	EVTS	DOCUMENT ID		TECN	CHG	COMMENT
The data in this block is included in the average printed for a previous datablock.						
75±15	700	GAVILLET	78	HBC	+	4.2 $K^- p \rightarrow \Xi^- K\pi\pi$

PRODUCED BY K BEAMS

VALUE (MeV)	DOCUMENT ID		TECN	CHG	COMMENT
The data in this block is included in the average printed for a previous datablock.					
90± 8	DAUM	81C	CNTR	–	63 $K^- p \rightarrow K^- 2\pi p$
• • • We do not use the following data for averages, fits, limits, etc. • • •					
~ 150	VERGEEST	79	HBC	–	4.2 $K^- p \rightarrow (\overline{K}\pi\pi)^- p$
150±71	[4] CARNEGIE	77	ASPK	±	13 $K^\pm p \rightarrow (K\pi\pi)^\pm p$
~ 200	BRANDENB...	76	ASPK	±	13 $K^\pm p \rightarrow (K\pi\pi)^\pm p$
120	DAVIS	72	HBC	+	12 $K^+ p$
188±21	FIRESTONE	72B	DBC	+	12 $K^+ d$

[4] From a model-dependent fit with Gaussian background to BRANDENBURG 76 data.

PRODUCED BY BEAMS OTHER THAN K MESONS

VALUE (MeV)	EVTS	DOCUMENT ID		TECN	CHG	COMMENT
• • • We do not use the following data for averages, fits, limits, etc. • • •						
66±15	310	RODEBACK	81	HBC		4 $\pi^- p \rightarrow \Lambda K 2\pi$
60	40	CRENNELL	72	HBC	0	4.5 $\pi^- p \rightarrow \Lambda K 2\pi$
127^{+7}_{-25}		ASTIER	69	HBC	0	$\overline{p}p$
60	45	CRENNELL	67	HBC	0	6 $\pi^- p \rightarrow \Lambda K 2\pi$

$K_1(1270)$ DECAY MODES

	Mode	Fraction (Γ_i/Γ)
Γ_1	$K\rho$	(42 ±6) %
Γ_2	$K_0^*(1430)\pi$	(28 ±4) %
Γ_3	$K^*(892)\pi$	(16 ±5) %
Γ_4	$K\omega$	(11.0±2.0) %
Γ_5	$K f_0(1370)$	(3.0±2.0) %
Γ_6	γK^0	seen

$K_1(1270)$ PARTIAL WIDTHS

$\Gamma(K\rho)$ Γ_1

VALUE (MeV)	DOCUMENT ID		TECN	CHG	COMMENT
• • • We do not use the following data for averages, fits, limits, etc. • • •					
57±5	MAZZUCATO	79	HBC	+	4.2 $K^- p \rightarrow \Xi^- (K\pi\pi)^+$
75±6	CARNEGIE	77B	ASPK	±	13 $K^\pm p \rightarrow (K\pi\pi)^\pm p$

$\Gamma(K_0^*(1430)\pi)$ Γ_2

VALUE (MeV)	DOCUMENT ID		TECN	CHG	COMMENT
• • • We do not use the following data for averages, fits, limits, etc. • • •					
26±6	CARNEGIE	77B	ASPK	±	13 $K^\pm p \rightarrow (K\pi\pi)^\pm p$

$\Gamma(K^*(892)\pi)$ Γ_3

VALUE (MeV)	DOCUMENT ID		TECN	CHG	COMMENT
• • • We do not use the following data for averages, fits, limits, etc. • • •					
14±11	MAZZUCATO	79	HBC	+	4.2 $K^- p \rightarrow \Xi^- (K\pi\pi)^+$
2± 2	CARNEGIE	77B	ASPK	±	13 $K^\pm p \rightarrow (K\pi\pi)^\pm p$

$\Gamma(K\omega)$ Γ_4

VALUE (MeV)	DOCUMENT ID		TECN	CHG	COMMENT
• • • We do not use the following data for averages, fits, limits, etc. • • •					
4±4	MAZZUCATO	79	HBC	+	4.2 $K^- p \rightarrow \Xi^- (K\pi\pi)^+$
24±3	CARNEGIE	77B	ASPK	±	13 $K^\pm p \rightarrow (K\pi\pi)^\pm p$

$\Gamma(K f_0(1370))$ Γ_5

VALUE (MeV)	DOCUMENT ID		TECN	CHG	COMMENT
• • • We do not use the following data for averages, fits, limits, etc. • • •					
22±5	CARNEGIE	77B	ASPK	±	13 $K^\pm p \rightarrow (K\pi\pi)^\pm p$

$\Gamma(\gamma K^0)$ Γ_6

VALUE (keV)	DOCUMENT ID		TECN	COMMENT
73.2± 6.1±28.3	ALAVI-HARATI	02B	KTEV	$K + A \rightarrow K^* + A$

$K_1(1270)$ BRANCHING RATIOS

$\Gamma(K\rho)/\Gamma_{total}$ Γ_1/Γ

VALUE	DOCUMENT ID		TECN	COMMENT
0.42±0.06	[5] DAUM	81C	CNTR	63 $K^- p \rightarrow K^- 2\pi p$
• • • We do not use the following data for averages, fits, limits, etc. • • •				
dominant	RODEBACK	81	HBC	4 $\pi^- p \rightarrow \Lambda K 2\pi$

$\Gamma(K_0^*(1430)\pi)/\Gamma_{total}$ Γ_2/Γ

VALUE	DOCUMENT ID		TECN	COMMENT
0.28±0.04	[5] DAUM	81C	CNTR	63 $K^- p \rightarrow K^- 2\pi p$

$\Gamma(K^*(892)\pi)/\Gamma_{total}$ Γ_3/Γ

VALUE	DOCUMENT ID		TECN	COMMENT
0.16±0.05	[5] DAUM	81C	CNTR	63 $K^- p \rightarrow K^- 2\pi p$

$\Gamma(K\omega)/\Gamma_{total}$ Γ_4/Γ

VALUE	DOCUMENT ID		TECN	COMMENT
0.11 ±0.02	[5] DAUM	81C	CNTR	63 $K^- p \rightarrow K^- 2\pi p$

$\Gamma(K\omega)/\Gamma(K\rho)$ Γ_4/Γ_1

VALUE	CL%	DOCUMENT ID	TECN	COMMENT
• • • We do not use the following data for averages, fits, limits, etc. • • •				
<0.30	95	RODEBACK	81 HBC	4 $\pi^- p \rightarrow \Lambda K 2\pi$

$\Gamma(K f_0(1370))/\Gamma_{total}$ Γ_5/Γ

VALUE	DOCUMENT ID		TECN	COMMENT
0.03 ±0.02	[5] DAUM	81C	CNTR	63 $K^- p \rightarrow K^- 2\pi p$

D-wave/S-wave RATIO FOR $K_1(1270) \rightarrow K^*(892)\pi$

VALUE	DOCUMENT ID		TECN	COMMENT
1.0±0.7	[5] DAUM	81C	CNTR	63 $K^- p \rightarrow K^- 2\pi p$

[5] Average from low and high t data.

$K_1(1270)$ REFERENCES

ALAVI-HARATI	02B	PRL 89 072001	A. Alavi-Harati *et al.* (FNAL KTeV Collab.)
TORNQVIST	82B	NP B203 268	N.A. Tornqvist (HELS)
DAUM	81C	NP B187 1	C. Daum *et al.* (AMST, CERN, CRAC, MPIM+)
RODEBACK	81	ZPHY C9 9	S. Rodeback *et al.* (CERN, CDEF, MADR+)
MAZZUCATO	79	NP B156 532	M. Mazzucato *et al.* (CERN, ZEEM, NIJM+)
VERGEEST	79	NP B158 265	J.S.M. Vergeest *et al.* (NIJM, AMST, CERN+)
GAVILLET	78	PL 76B 517	P. Gavillet *et al.* (AMST, CERN, NIJM+) JP
CARNEGIE	77	NP B127 509	R.K. Carnegie *et al.* (SLAC)
CARNEGIE	77B	PL 68B 287	R.K. Carnegie *et al.* (SLAC)
BRANDENB...	76	PRL 26 703	G.W. Brandenburg *et al.* (SLAC) JP
OTTER	76	NP B106 77	G. Otter *et al.* (AACH3, BERL, CERN, LOIC+) JP
CRENNELL	72	PR D6 1220	D.J. Crennell *et al.* (BNL)
DAVIS	72	PR D5 2688	P.J. Davis *et al.* (LBL)
FIRESTONE	72B	PR D5 505	A. Firestone *et al.* (LBL)
ASTIER	69	NP B10 65	A. Astier *et al.* (CDEF, CERN, IPNP, LIVP) IJP
CRENNELL	67	PRL 19 44	D.J. Crennell *et al.* (BNL) I

OTHER RELATED PAPERS

SUZUKI	93	PR D47 1252	M. Suzuki (LBL)
BAUBILLIER	82B	NP B202 21	M. Baubillier *et al.* (BIRM, CERN, GLAS+)
FERNANDEZ	82	ZPHY C16 95	C. Fernandez *et al.* (MADR, CERN, CDEF+) JP
GAVILLET	82	ZPHY C16 119	P. Gavillet *et al.* (CERN, CDEF, PADO+)
SHEN	66	PRL 17 726	B.C. Shen *et al.* (LRL)
Also	66	Private Comm.	G. Goldhaber (LRL)
ALMEIDA	65	PL 16 184	S.P. Almeida *et al.* (CAVE)
ARMENTEROS	64	PL 9 207	R. Armenteros *et al.* (CERN, CDEF)
Also	66	PR 145 1095	N. Barash *et al.* (COLU)

$K_1(1400)$ $I(J^P) = \frac{1}{2}(1^+)$

$K_1(1400)$ MASS

VALUE (MeV)	DOCUMENT ID		TECN	CHG	COMMENT
1402± 7 OUR AVERAGE					
1373±14±18	[1] ASTON	87	LASS	0	11 $K^- p \rightarrow \overline{K}^0 \pi^+ \pi^- n$
1392±18	BAUBILLIER	82B	HBC	0	8.25 $K^- p \rightarrow K^0_S \pi^+ \pi^- n$
1410±25	DAUM	81C	CNTR	–	63 $K^- p \rightarrow K^- 2\pi p$
1415±15	ETKIN	80	MPS	0	6 $K^- p \rightarrow \overline{K}^0 \pi^+ \pi^- n$
1404±10	[2] CARNEGIE	77	ASPK	±	13 $K^\pm p \rightarrow (K\pi\pi)^\pm p$
• • • We do not use the following data for averages, fits, limits, etc. • • •					
~ 1350	[3] TORNQVIST	82B	RVUE		
~ 1400	VERGEEST	79	HBC	–	4.2 $K^- p \rightarrow (\overline{K}\pi\pi)^- p$
~ 1400	BRANDENB...	76	ASPK	±	13 $K^\pm p \rightarrow (K\pi\pi)^\pm p$
1420	DAVIS	72	HBC	+	12 $K^+ p$
1368±18	FIRESTONE	72B	DBC	+	12 $K^+ d$

[1] From partial-wave analysis of $K^0 \pi^+ \pi^-$ system.
[2] From a model-dependent fit with Gaussian background to BRANDENBURG 76 data.
[3] From a unitarized quark-model calculation.

$K_1(1400)$ WIDTH

VALUE (MeV)	DOCUMENT ID		TECN	CHG	COMMENT
174±13 OUR AVERAGE	Error includes scale factor of 1.6. See the ideogram below.				
188±54±60	[4] ASTON	87	LASS	0	11 $K^-p \to \overline{K}^0\pi^+\pi^-n$
276±65	BAUBILLIER	82B	HBC	0	8.25 $K^-p \to K^0_S\pi^+\pi^-n$
195±25	DAUM	81C	CNTR	–	63 $K^-p \to K^-2\pi p$
180±10	ETKIN	80	MPS	0	6 $K^-p \to \overline{K}^0\pi^+\pi^-n$
142±16	[5] CARNEGIE	77	ASPK	±	13 $K^\pm p \to (K\pi\pi)^\pm p$
• • • We do not use the following data for averages, fits, limits, etc. • • •					
~ 200	VERGEEST	79	HBC	–	4.2 $K^-p \to (\overline{K}\pi\pi)^-p$
~ 160	BRANDENB...	76	ASPK	±	13 $K^\pm p \to (K\pi\pi)^\pm p$
80	DAVIS	72	HBC	+	12 K^+p
241±30	FIRESTONE	72B	DBC	+	12 K^+d

[4] From partial-wave analysis of $K^0\pi^+\pi^-$ system.
[5] From a model-dependent fit with Gaussian background to BRANDENBURG 76 data.

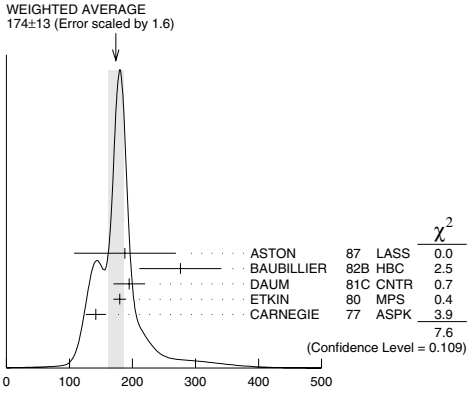

$K_1(1400)$ DECAY MODES

	Mode	Fraction (Γ_i/Γ)
Γ_1	$K^*(892)\pi$	(94 ±6) %
Γ_2	$K\rho$	(3.0±3.0) %
Γ_3	$Kf_0(1370)$	(2.0±2.0) %
Γ_4	$K\omega$	(1.0±1.0) %
Γ_5	$K_0^*(1430)\pi$	not seen
Γ_6	γK^0	seen

$K_1(1400)$ PARTIAL WIDTHS

$\Gamma(K^*(892)\pi)$ Γ_1

VALUE (MeV)	DOCUMENT ID		TECN	CHG	COMMENT
117±10	CARNEGIE	77	ASPK	±	13 $K^\pm p \to (K\pi\pi)^\pm p$

$\Gamma(K\rho)$ Γ_2

VALUE (MeV)	DOCUMENT ID		TECN	CHG	COMMENT
2 ±1	CARNEGIE	77	ASPK	±	13 $K^\pm p \to (K\pi\pi)^\pm p$

$\Gamma(K\omega)$ Γ_4

VALUE (MeV)	DOCUMENT ID		TECN	CHG	COMMENT
23±12	CARNEGIE	77	ASPK	±	13 $K^\pm p \to (K\pi\pi)^\pm p$

$\Gamma(\gamma K^0)$ Γ_6

VALUE (keV)	DOCUMENT ID		TECN	COMMENT
280.8±23.2±40.4	ALAVI-HARATI	02B	KTEV	$K + A \to K^* + A$

$K_1(1400)$ BRANCHING RATIOS

$\Gamma(K^*(892)\pi)/\Gamma_{total}$ Γ_1/Γ

VALUE	DOCUMENT ID		TECN	COMMENT
0.94±0.06	[6] DAUM	81C	CNTR	63 $K^-p \to K^-2\pi p$

$\Gamma(K\rho)/\Gamma_{total}$ Γ_2/Γ

VALUE	DOCUMENT ID		TECN	COMMENT
0.03 ±0.03	[6] DAUM	81C	CNTR	63 $K^-p \to K^-2\pi p$

$\Gamma(Kf_0(1370))/\Gamma_{total}$ Γ_3/Γ

VALUE	DOCUMENT ID		TECN	COMMENT
0.02 ±0.02	[6] DAUM	81C	CNTR	63 $K^-p \to K^-2\pi p$

$\Gamma(K\omega)/\Gamma_{total}$ Γ_4/Γ

VALUE	DOCUMENT ID		TECN	COMMENT
0.01 ±0.01	[6] DAUM	81C	CNTR	63 $K^-p \to K^-2\pi p$

$\Gamma(K_0^*(1430)\pi)/\Gamma_{total}$ Γ_5/Γ

VALUE	DOCUMENT ID		TECN	COMMENT
not seen	[6] DAUM	81C	CNTR	63 $K^-p \to K^-2\pi p$

D-wave/S-wave RATIO FOR $K_1(1400) \to K^*(892)\pi$

VALUE	DOCUMENT ID		TECN	COMMENT
0.04 ±0.01	[6] DAUM	81C	CNTR	63 $K^-p \to K^-2\pi p$

[6] Average from low and high t data.

$K_1(1400)$ REFERENCES

ALAVI-HARATI	02B	PRL 89 072001	A. Alavi-Harati *et al.* (FNAL KTeV Collab.)
ASTON	87	NP B292 693	D. Aston *et al.* (SLAC, NAGO, CINC, INUS)
BAUBILLIER	82B	NP B202 21	M. Baubillier *et al.* (BIRM, CERN, GLAS+)
TORNQVIST	82B	NP B203 268	N.A. Tornqvist (HELS)
DAUM	81C	NP B187 1	C. Daum *et al.* (AMST, CERN, CRAC, MPIM+)
ETKIN	80	PR D22 42	A. Etkin *et al.* (BNL, CUNY) JP
VERGEEST	79	NP B158 265	J.S.M. Vergeest *et al.* (NIJM, AMST, CERN+)
CARNEGIE	77	NP B127 509	R.K. Carnegie *et al.* (SLAC)
BRANDENB...	76	PRL 26 703	G.W. Brandenburg *et al.* (SLAC) JP
DAVIS	72	PR D5 2688	P.J. Davis *et al.* (LBL)
FIRESTONE	72B	PR D5 505	A. Firestone *et al.* (LBL)

OTHER RELATED PAPERS

SUZUKI	93	PR D47 1252	M. Suzuki (LBL)
FERNANDEZ	82	ZPHY C16 95	C. Fernandez *et al.* (MADR, CERN, CDEF+)
SHEN	66	PRL 17 726	B.C. Shen *et al.* (LRL)
Also	66	Private Comm.	G. Goldhaber (LRL)
ALMEIDA	65	PL 16 184	S.P. Almeida *et al.* (CAVE)
ARMENTEROS	64	PL 9 207	R. Armenteros *et al.* (CERN, CDEF)
Also	66	PR 145 1095	N. Barash *et al.* (COLU)

$K^*(1410)$ $I(J^P) = \frac{1}{2}(1^-)$

$K^*(1410)$ MASS

VALUE (MeV)	DOCUMENT ID		TECN	CHG	COMMENT
1414±15 OUR AVERAGE	Error includes scale factor of 1.3.				
1380±21±19	ASTON	88	LASS	0	11 $K^-p \to K^-\pi^+n$
1420± 7±10	ASTON	87	LASS	0	11 $K^-p \to \overline{K}^0\pi^+\pi^-n$
• • • We do not use the following data for averages, fits, limits, etc. • • •					
1367±54	BIRD	89	LASS	–	11 $K^-p \to \overline{K}^0\pi^-p$
1474±25	BAUBILLIER	82B	HBC	0	8.25 $K^-p \to \overline{K}^0 2\pi n$
1500±30	ETKIN	80	MPS	0	6 $K^-p \to \overline{K}^0\pi^+\pi^-n$

$K^*(1410)$ WIDTH

VALUE (MeV)	DOCUMENT ID		TECN	CHG	COMMENT
232± 21 OUR AVERAGE	Error includes scale factor of 1.1.				
176± 52±22	ASTON	88	LASS	0	11 $K^-p \to K^-\pi^+n$
240± 18±12	ASTON	87	LASS	0	11 $K^-p \to \overline{K}^0\pi^+\pi^-n$
• • • We do not use the following data for averages, fits, limits, etc. • • •					
114±101	BIRD	89	LASS	–	11 $K^-p \to \overline{K}^0\pi^-p$
275± 65	BAUBILLIER	82B	HBC	0	8.25 $K^-p \to \overline{K}^0 2\pi n$
500±100	ETKIN	80	MPS	0	6 $K^-p \to \overline{K}^0\pi^+\pi^-n$

$K^*(1410)$ DECAY MODES

	Mode	Fraction (Γ_i/Γ)	Confidence level
Γ_1	$K^*(892)\pi$	> 40 %	95%
Γ_2	$K\pi$	(6.6±1.3) %	
Γ_3	$K\rho$	< 7 %	95%
Γ_4	γK^0	seen	

$K^*(1410)$ PARTIAL WIDTHS

$\Gamma(\gamma K^0)$ Γ_4

VALUE (keV)	CL%	DOCUMENT ID		TECN	COMMENT
<52.9	90	ALAVI-HARATI	02B	KTEV	$K + A \to K^* + A$

$K^*(1410)$ BRANCHING RATIOS

$\Gamma(K\rho)/\Gamma(K^*(892)\pi)$ Γ_3/Γ_1

VALUE	CL%	DOCUMENT ID		TECN	CHG	COMMENT
<0.17	95	ASTON	84	LASS	0	11 $K^-p \to \overline{K}^0 2\pi n$

$\Gamma(K\pi)/\Gamma(K^*(892)\pi)$ Γ_2/Γ_1

VALUE	CL%	DOCUMENT ID		TECN	CHG	COMMENT
<0.16	95	ASTON	84	LASS	0	11 $K^-p \to \overline{K}^0 2\pi n$

$\Gamma(K\pi)/\Gamma_{\text{total}}$ Γ_2/Γ

VALUE	DOCUMENT ID		TECN	CHG	COMMENT
0.066±0.010±0.008	ASTON	88	LASS	0	11 $K^-p \to K^-\pi^+n$

$K^*(1410)$ REFERENCES

ALAVI-HARATI	02B	PRL 89 072001	A. Alavi-Harati *et al.*	(FNAL KTeV Collab.)
BIRD	89	SLAC-332	P.F. Bird	(SLAC)
ASTON	88	NP B296 493	D. Aston *et al.*	(SLAC, NAGO, CINC, INUS)
ASTON	87	NP B292 693	D. Aston *et al.*	(SLAC, NAGO, CINC, INUS)
ASTON	84	PL 149B 258	D. Aston *et al.*	(SLAC, CARL, OTTA) JP
BAUBILLIER	82B	NP B202 21	M. Baubillier *et al.*	(BIRM, CERN, GLAS+)
ETKIN	80	PR D22 42	A. Etkin *et al.*	(BNL, CUNY) JP

$K_0^*(1430)$

$I(J^P) = \frac{1}{2}(0^+)$

See our minireview in the 1994 edition and in this edition under the $f_0(600)$.

$K_0^*(1430)$ MASS

VALUE (MeV)	EVTS	DOCUMENT ID		TECN	CHG	COMMENT
1412 ± 6		[1] ASTON	88	LASS	0	11 $K^-p \to K^-\pi^+n$
• • • We do not use the following data for averages, fits, limits, etc. • • •						
~ 1419		[2] BUGG	03	RVUE		11 $K^-p \to K^-\pi^+n$
~ 1440		[3] LI	03	RVUE		11 $K^-p \to K^-\pi^+n$
1459 ± 9	15090	[4] AITALA	02	E791		$D^+ \to K^-\pi^+\pi^+$
~ 1440		[5] JAMIN	00	RVUE		$Kp \to Kp$
1436 ± 8		[6] BARBERIS	98E	OMEG		450 $pp \to p_f p_s K^+K^-\pi^+\pi^-$
1415 ±25		[2] ANISOVICH	97C	RVUE		11 $K^-p \to K^-\pi^+n$
~ 1450		[7] TORNQVIST	96	RVUE		$\pi\pi \to \pi\pi$, $K\overline{K}$, $K\pi$
~ 1430		BAUBILLIER	84B	HBC	–	8.25 $K^-p \to \overline{K}^0\pi^-p$
~ 1425		[8,9] ESTABROOKS	78	ASPK		13 $K^\pm p \to K^\pm\pi^\pm(n,\Delta)$
~ 1450.0		MARTIN	78	SPEC		10 $K^\pm p \to K^0_S\pi p$

[1] Uses a model for the background, without this background they get a mass 1340 MeV, where the phase shift passes 90°.
[2] T-matrix pole. Reanalysis of ASTON 88 data.
[3] Breit-Wigner fit. Using ASTON 88.
[4] Assuming a low-mass scalar $K\pi$ resonance, $\kappa(800)$.
[5] T-matrix pole. Using data from ESTABROOKS 78 and ASTON 88.
[6] J^P not determined, could be $K_2^*(1430)$.
[7] T-matrix pole.
[8] Mass defined by pole position.
[9] From elastic $K\pi$ partial-wave analysis.

$K_0^*(1430)$ WIDTH

VALUE (MeV)	EVTS	DOCUMENT ID		TECN	CHG	COMMENT
294±23		ASTON	88	LASS	0	11 $K^-p \to K^-\pi^+n$
• • • We do not use the following data for averages, fits, limits, etc. • • •						
~ 316		[10] BUGG	03	RVUE		11 $K^-p \to K^-\pi^+n$
~ 350		[11] LI	03	RVUE		11 $K^-p \to K^-\pi^+n$
175±17	15090	[12] AITALA	02	E791		$D^+ \to K^-\pi^+\pi^+$
~ 300		[13] JAMIN	00	RVUE		$Kp \to Kp$
196±45		[14] BARBERIS	98E	OMEG		450 $pp \to p_f p_s K^+K^-\pi^+\pi^-$
330±50		[10] ANISOVICH	97C	RVUE		11 $K^-p \to K^-\pi^+n$
~ 320		[15] TORNQVIST	96	RVUE		$\pi\pi \to \pi\pi$, $K\overline{K}$, $K\pi$
~ 200		BAUBILLIER	84B	HBC	–	8.25 $K^-p \to \overline{K}^0\pi^-p$
200 to 300		[16] ESTABROOKS	78	ASPK		13 $K^\pm p \to K^\pm\pi^\pm(n,\Delta)$

[10] T-matrix pole. Reanalysis of ASTON 88 data.
[11] Breit-Wigner fit. Using ASTON 88.
[12] Assuming a low-mass scalar $K\pi$ resonance, $\kappa(800)$.
[13] T-matrix pole. Using data from ESTABROOKS 78 and ASTON 88.
[14] J^P not determined, could be $K_2^*(1430)$.
[15] T-matrix pole.
[16] From elastic $K\pi$ partial-wave analysis.

$K_0^*(1430)$ DECAY MODES

	Mode	Fraction (Γ_i/Γ)
Γ_1	$K\pi$	(93±10) %

$K_0^*(1430)$ BRANCHING RATIOS

$\Gamma(K\pi)/\Gamma_{\text{total}}$ Γ_1/Γ

VALUE	DOCUMENT ID		TECN	CHG	COMMENT
0.93±0.04±0.09	ASTON	88	LASS	0	11 $K^-p \to K^-\pi^+n$

$K_0^*(1430)$ REFERENCES

BUGG	03	PL B572 1	D.V. Bugg	
LI	03	PR D67 034025	L. Li, B. Zou, G. Li	
AITALA	02	PRL 89 121801	E.M. Aitala *et al.*	(FNAL E791 Collab.)
JAMIN	00	NP B587 331	M. Jamin *et al.*	
BARBERIS	98E	PL B436 204	D. Barberis *et al.*	(Omega Expt.)
ANISOVICH	97C	PL B413 137	A.V. Anisovich, A.V. Sarantsev	
TORNQVIST	96	PRL 76 1575	N.A. Tornqvist, M. Roos	(HELS)
ASTON	88	NP B296 493	D. Aston *et al.*	(SLAC, NAGO, CINC, INUS)
BAUBILLIER	84B	ZPHY C26 37	M. Baubillier *et al.*	(BIRM, CERN, GLAS+)
ESTABROOKS	78	NP B133 490	P.G. Estabrooks *et al.*	(MCGI, CARL, DURH+)
MARTIN	78	NP B134 392	A.D. Martin *et al.*	(DURH, GEVA)

OTHER RELATED PAPERS

SHAKIN	00	PR D62 114014	C.M. Shakin, H. Wang	
BEVEREN	99	EPJ C10 469	E. Van Beveren, G. Rupp	
OLLER	99	PR D60 099906 (erratum)	J.A. Oller *et al.*	
OLLER	99C	PR D60 074023	J.A. Oller, E. Oset	
TORNQVIST	82	PRL 49 624	N.A. Tornqvist	(HELS)
GOLDBERG	69	PL 30B 434	J. Goldberg *et al.*	(SABRE Collab.)
TRIPPE	68	PL 28B 203	T.G. Trippe *et al.*	(UCLA)

$K_2^*(1430)$

$I(J^P) = \frac{1}{2}(2^+)$

We consider that phase-shift analyses provide more reliable determinations of the mass and width.

$K_2^*(1430)$ MASS

CHARGED ONLY, WITH FINAL STATE $K\pi$

VALUE (MeV)	EVTS	DOCUMENT ID		TECN	CHG	COMMENT
1425.6± 1.5 OUR AVERAGE		Error includes scale factor of 1.1.				
1420 ± 4	1587	BAUBILLIER	84B	HBC	–	8.25 $K^-p \to \overline{K}^0\pi^-p$
1436 ± 5.5	400	[1,2] CLELAND	82	SPEC	+	30 $K^+p \to K^0_S\pi^+p$
1430 ± 3.2	1500	[1,2] CLELAND	82	SPEC	+	50 $K^+p \to K^0_S\pi^+p$
1430 ± 3.2	1200	[1,2] CLELAND	82	SPEC	–	50 $K^+p \to K^0_S\pi^-p$
1423 ± 5	935	TOAFF	81	HBC	–	6.5 $K^-p \to \overline{K}^0\pi^-p$
1428.0± 4.6		[3] MARTIN	78	SPEC	+	10 $K^\pm p \to K^0_S\pi p$
1423.8± 4.6		[3] MARTIN	78	SPEC	–	10 $K^\pm p \to K^0_S\pi p$
1420.0± 3.1	1400	AGUILAR-...	71B	HBC	–	3.9,4.6 K^-p
1425 ± 8.0	225	[1,2] BARNHAM	71C	HBC	+	$K^+p \to K^0\pi^+p$
1416 ±10	220	CRENNELL	69D	DBC	–	3.9 $K^-N \to \overline{K}^0\pi^-N$
1414 ±13.0	60	[1] LIND	69	HBC	+	9 $K^+p \to K^0\pi^+p$
1427 ±12	63	[1] SCHWEING...	68	HBC	–	5.5 $K^-p \to \overline{K}\pi N$
1423 ±11.0	39	[1] BASSANO	67	HBC	–	4.6–5.0 $K^-p \to \overline{K}^0\pi^-p$
• • • We do not use the following data for averages, fits, limits, etc. • • •						
1423.4± 2 ±3	24809± 820	[4] BIRD	89	LASS	–	11 $K^-p \to \overline{K}^0\pi^-p$

NEUTRAL ONLY

VALUE (MeV)	EVTS	DOCUMENT ID		TECN	CHG	COMMENT
1432.4± 1.3 OUR AVERAGE						
1431.2± 1.8± 0.7		[5] ASTON	88	LASS	0	11 $K^-p \to K^-\pi^+n$
1434 ± 4 ± 6		[5] ASTON	87	LASS	0	11 $K^-p \to \overline{K}^0\pi^+\pi^-n$
1433 ± 6 ±10		[5] ASTON	84B	LASS	0	11 $K^-p \to \overline{K}^0 2\pi n$
1471 ±12		[5] BAUBILLIER	82B	HBC	0	8.25 $K^-p \to N K^0_S\pi\pi$
1428 ± 3		[5] ASTON	81C	LASS	0	11 $K^-p \to K^-\pi^+n$
1434 ± 2		[5] ESTABROOKS	78	ASPK	0	13 $K^\pm p \to pK\pi$
1440 ±10		[5] BOWLER	77	DBC	0	5.5 $K^+d \to K\pi pp$
• • • We do not use the following data for averages, fits, limits, etc. • • •						
1420 ± 7	300	HENDRICK	76	DBC		8.25 $K^+N \to K^+\pi N$
1421.6± 4.2	800	MCCUBBIN	75	HBC	0	3.6 $K^-p \to K^-\pi^+n$
1420.1± 4.3		[6] LINGLIN	73	HBC	0	2–13 $K^+p \to K^+\pi^-X$
1419.1± 3.7	1800	AGUILAR-...	71B	HBC	0	3.9,4.6 K^-p
1416 ± 6	600	CORDS	71	DBC	0	9 $K^+n \to K^+\pi^-p$
1421.1± 2.6	2200	DAVIS	69	HBC	0	12 $K^+p \to K^+\pi^-X$

[1] Errors enlarged by us to $\Gamma/\sqrt{N}$; see the note with the $K^*(892)$ mass.
[2] Number of events in peak re-evaluated by us.
[3] Systematic error added by us.
[4] From a partial wave amplitude analysis.
[5] From phase shift or partial-wave analysis.
[6] From pole extrapolation, using world K^+p data summary tape.

$K_2^*(1430)$ WIDTH

CHARGED ONLY, WITH FINAL STATE $K\pi$

VALUE (MeV)	EVTS	DOCUMENT ID		TECN	CHG	COMMENT
98.5± 2.7 OUR FIT	Error includes scale factor of 1.1.					
98.5± 2.9 OUR AVERAGE	Error includes scale factor of 1.1.					
109 ±22	400	[7,8] CLELAND	82	SPEC	+	30 $K^+p \to K^0_S\pi^+p$
124 ±12.8	1500	[7,8] CLELAND	82	SPEC	+	50 $K^+p \to K^0_S\pi^+p$
113 ±12.8	1200	[7,8] CLELAND	82	SPEC	−	50 $K^+p \to K^0_S\pi^-p$
85 ±16	935	TOAFF	81	HBC	−	6.5 $K^-p \to \overline{K}^0\pi^-p$
96.5± 3.8		MARTIN	78	SPEC	+	10 $K^\pm p \to K^0_S\pi p$
97.7± 4.0		MARTIN	78	SPEC	−	10 $K^\pm p \to K^0_S\pi p$
$94.7^{+15.1}_{-12.5}$	1400	AGUILAR-...	71B	HBC	−	3.9,4.6 K^-p
• • • We do not use the following data for averages, fits, limits, etc. • • •						
98 ± 4 ±4	24809± 820	[9] BIRD	89	LASS	−	11 $K^-p \to \overline{K}^0\pi^-p$

NEUTRAL ONLY

VALUE (MeV)	EVTS	DOCUMENT ID		TECN	CHG	COMMENT
109 ± 5 OUR AVERAGE	Error includes scale factor of 1.9. See the ideogram below.					
116.5± 3.6± 1.7		[10] ASTON	88	LASS	0	11 $K^-p \to K^-\pi^+n$
129 ±15 ±15		[10] ASTON	87	LASS	0	11 $K^-p \to \overline{K}^0\pi^+\pi^-n$
131 ±24 ±20		[10] ASTON	84B	LASS	0	11 $K^-p \to \overline{K}^0 2\pi n$
143 ±34		[10] BAUBILLIER	82B	HBC	0	8.25 $K^-p \to NK^0_S\pi\pi$
98 ± 8		[10] ASTON	81C	LASS	0	11 $K^-p \to K^-\pi^+n$
140 ±30		[10] ETKIN	80	SPEC	0	6 $K^-p \to \overline{K}^0\pi^+\pi^-n$
98 ± 5		[10] ESTABROOKS	78	ASPK	0	13 $K^\pm p \to pK\pi$
• • • We do not use the following data for averages, fits, limits, etc. • • •						
125 ±29	300	[7] HENDRICK	76	DBC		8.25 $K^+N \to K^+\pi N$
116 ±18	800	MCCUBBIN	75	HBC	0	3.6 $K^-p \to K^-\pi^+n$
61 ±14		[11] LINGLIN	73	HBC	0	2–13 $K^+p \to K^+\pi^-X$
$116.6^{+10.3}_{-15.5}$	1800	AGUILAR-...	71B	HBC	0	3.9,4.6 K^-p
144 ±24.0	600	[7] CORDS	71	DBC	0	9 $K^+n \to K^+\pi^-p$
101 ±10	2200	DAVIS	69	HBC	0	12 $K^+p \to K^+\pi^-\pi^+p$

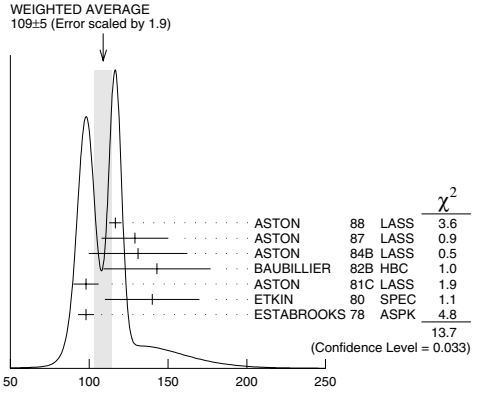

[7] Errors enlarged by us to $4\Gamma/\sqrt{N}$; see the note with the $K^*(892)$ mass.
[8] Number of events in peak re-evaluated by us.
[9] From a partial wave amplitude analysis.
[10] From phase shift or partial-wave analysis.
[11] From pole extrapolation, using world K^+p data summary tape.

$K_2^*(1430)$ DECAY MODES

	Mode	Fraction (Γ_i/Γ)	Scale factor/ Confidence level
Γ_1	$K\pi$	(49.9±1.2) %	
Γ_2	$K^*(892)\pi$	(24.7±1.5) %	
Γ_3	$K^*(892)\pi\pi$	(13.4±2.2) %	
Γ_4	$K\rho$	(8.7±0.8) %	S=1.2
Γ_5	$K\omega$	(2.9±0.8) %	
Γ_6	$K^+\gamma$	$(2.4\pm0.5)\times10^{-3}$	S=1.1
Γ_7	$K\eta$	$(1.5^{+3.4}_{-1.0})\times10^{-3}$	S=1.3
Γ_8	$K\omega\pi$	$< 7.2 \times10^{-4}$	CL=95%
Γ_9	$K^0\gamma$	$< 9 \times10^{-4}$	CL=90%

CONSTRAINED FIT INFORMATION

An overall fit to the total width, a partial width, and 10 branching ratios uses 31 measurements and one constraint to determine 8 parameters. The overall fit has a $\chi^2 = 20.2$ for 24 degrees of freedom.

The following *off-diagonal* array elements are the correlation coefficients $\langle\delta p_i \delta p_j\rangle/(\delta p_i \cdot \delta p_j)$, in percent, from the fit to parameters p_i, including the branching fractions, $x_i \equiv \Gamma_i/\Gamma_{\text{total}}$. The fit constrains the x_i whose labels appear in this array to sum to one.

	x_1	x_2	x_3	x_4	x_5	x_6	x_7
x_2	−9						
x_3	−40	−73					
x_4	−8	36	−52				
x_5	−11	−3	−26	−7			
x_6	−1	−1	−1	−1	0		
x_7	−4	−7	−5	−5	−2	0	
Γ	0	0	0	0	0	−13	0

	Mode	Rate (MeV)	Scale factor
Γ_1	$K\pi$	49.1 ±1.8	
Γ_2	$K^*(892)\pi$	24.3 ±1.6	
Γ_3	$K^*(892)\pi\pi$	13.2 ±2.2	
Γ_4	$K\rho$	8.5 ±0.8	1.2
Γ_5	$K\omega$	2.9 ±0.8	
Γ_6	$K^+\gamma$	0.24±0.05	1.1
Γ_7	$K\eta$	$0.15^{+0.33}_{-0.10}$	1.3

$K_2^*(1430)$ PARTIAL WIDTHS

$\Gamma(K^+\gamma)$ Γ_6

VALUE (keV)	DOCUMENT ID		TECN	CHG	COMMENT
241±50 OUR FIT	Error includes scale factor of 1.1.				
240±45	CIHANGIR	82	SPEC	+	200 $K^+Z \to ZK^+\pi^0$, $ZK^0_S\pi^+$

$\Gamma(K^0\gamma)$ Γ_9

VALUE (keV)	CL%	DOCUMENT ID		TECN	CHG	COMMENT
< 5.4	90	ALAVI-HARATI	02B	KTEV		$K + A \to K^* + A$
• • • We do not use the following data for averages, fits, limits, etc. • • •						
<84	90	CARLSMITH	87	SPEC	0	60–200 $K^0_L A \to K^0_S\pi^0 A$

$K_2^*(1430)$ BRANCHING RATIOS

$\Gamma(K\pi)/\Gamma_{\text{total}}$ Γ_1/Γ

VALUE	DOCUMENT ID		TECN	CHG	COMMENT
0.499±0.012 OUR FIT					
0.488±0.014 OUR AVERAGE					
0.485±0.006±0.020	[12] ASTON	88	LASS	0	11 $K^-p \to K^-\pi^+n$
0.49 ±0.02	[12] ESTABROOKS	78	ASPK	±	13 $K^\pm p \to pK\pi$

$\Gamma(K^*(892)\pi)/\Gamma(K\pi)$ Γ_2/Γ_1

VALUE	DOCUMENT ID		TECN	CHG	COMMENT
0.496±0.034 OUR FIT					
0.47 ±0.04 OUR AVERAGE					
0.44 ±0.09	ASTON	84B	LASS	0	11 $K^-p \to \overline{K}^0 2\pi n$
0.62 ±0.19	LAUSCHER	75	HBC	0	10,16 $K^-p \to K^-\pi^+n$
0.54 ±0.16	DEHM	74	DBC	0	4.6 K^+N
0.47 ±0.08	AGUILAR-...	71B	HBC		3.9,4.6 K^-p
0.47 ±0.10	BASSANO	67	HBC	−0	4.6,5.0 K^-p
0.45 ±0.13	BADIER	65C	HBC	−	3 K^-p

$\Gamma(K\omega)/\Gamma(K\pi)$ Γ_5/Γ_1

VALUE	DOCUMENT ID		TECN	CHG	COMMENT
0.059±0.017 OUR FIT					
0.070±0.035 OUR AVERAGE					
0.05 ±0.04	AGUILAR-...	71B	HBC		3.9,4.6 K^-p
0.13 ±0.07	BASSOMPIE...	69	HBC	0	5 K^+p

$\Gamma(K\rho)/\Gamma(K\pi)$ Γ_4/Γ_1

VALUE	DOCUMENT ID		TECN	CHG	COMMENT
0.174±0.017 OUR FIT	Error includes scale factor of 1.2.				
$0.150^{+0.029}_{-0.017}$ OUR AVERAGE					
0.18 ±0.05	ASTON	84B	LASS	0	11 $K^-p \to \overline{K}^0 2\pi n$
$0.02^{+0.10}_{-0.02}$	DEHM	74	DBC	0	4.6 K^+N
0.16 ±0.05	AGUILAR-...	71B	HBC		3.9,4.6 K^-p
0.14 ±0.10	BASSANO	67	HBC	−0	4.6,5.0 K^-p
0.14 ±0.07	BADIER	65C	HBC	−	3 K^-p

$\Gamma(K\rho)/\Gamma(K^*(892)\pi)$ Γ_4/Γ_2

VALUE	DOCUMENT ID	TECN	CHG	COMMENT
0.350±0.031 OUR FIT	Error includes scale factor of 1.4.			
0.354±0.033 OUR AVERAGE	Error includes scale factor of 1.4. See the ideogram below.			
0.293±0.032±0.020	ASTON	87 LASS	0	11 $K^-p \to \overline{K}^0\pi^+\pi^-n$
0.38 ±0.09	BAUBILLIER	82B HBC	0	8.25 $K^-p \to NK^0_S\pi\pi$
0.39 ±0.03	DAUM	81C CNTR		63 $K^-p \to K^-2\pi p$

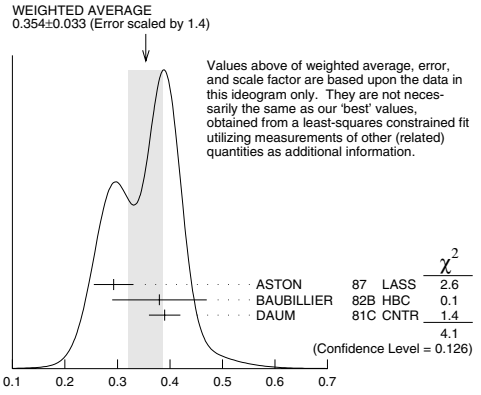

$\Gamma(K\rho)/\Gamma(K^*(892)\pi)$

$\Gamma(K\omega)/\Gamma(K^*(892)\pi)$ Γ_5/Γ_2

VALUE	DOCUMENT ID	TECN	CHG	COMMENT
0.118±0.034 OUR FIT				
0.10 ±0.04	FIELD	67 HBC	–	3.8 K^-p

$\Gamma(K\eta)/\Gamma(K^*(892)\pi)$ Γ_7/Γ_2

VALUE	DOCUMENT ID	TECN	CHG	COMMENT
$0.006^{+0.014}_{-0.004}$ OUR FIT	Error includes scale factor of 1.2.			
0.07 ±0.04	FIELD	67 HBC	–	3.8 K^-p

$\Gamma(K\eta)/\Gamma(K\pi)$ Γ_7/Γ_1

VALUE	CL%	DOCUMENT ID	TECN	CHG	COMMENT
$0.0030^{+0.0068}_{-0.0020}$ OUR FIT		Error includes scale factor of 1.3.			
0 ±0.0056		[13] ASTON	88B LASS	–	11 $K^-p \to K^-\eta p$
• • • We do not use the following data for averages, fits, limits, etc. • • •					
<0.04	95	AGUILAR-...	71B HBC		3.9,4.6 K^-p
<0.065		[14] BASSOMPIE...	69 HBC		5.0 K^+p
<0.02		BISHOP	69 HBC		3.5 K^+p

$\Gamma(K^*(892)\pi\pi)/\Gamma_{total}$ Γ_3/Γ

VALUE	DOCUMENT ID	TECN	CHG	COMMENT
0.134±0.022 OUR FIT				
0.12 ±0.04	[15] GOLDBERG	76 HBC	–	3 $K^-p \to p\overline{K}^0\pi\pi\pi$

$\Gamma(K^*(892)\pi\pi)/\Gamma(K\pi)$ Γ_3/Γ_1

VALUE	DOCUMENT ID	TECN	CHG	COMMENT
0.27±0.05 OUR FIT				
0.21±0.08	[14,15] JONGEJANS	78 HBC	–	4 $K^-p \to p\overline{K}^0\pi\pi\pi$

$\Gamma(K\omega\pi)/\Gamma_{total}$ Γ_8/Γ

VALUE (units 10^{-3})	CL%	EVTS	DOCUMENT ID	TECN	COMMENT
<0.72	95	0	JONGEJANS 78	HBC	4 $K^-p \to p\overline{K}^0 4\pi$

[12] From phase shift analysis.
[13] ASTON 88B quote < 0.0092 at CL=95%. We convert this to a central value and 1 sigma error in order to be able to use it in our constrained fit.
[14] Restated by us.
[15] Assuming $\pi\pi$ system has isospin 1, which is supported by the data.

$K_2^*(1430)$ REFERENCES

ALAVI-HARATI	02B	PRL 89 072001	A. Alavi-Harati *et al.*	(FNAL KTeV Collab.)
BIRD	89	SLAC-332	P.F. Bird	(SLAC)
ASTON	88	NP B296 493	D. Aston *et al.*	(SLAC, NAGO, CINC, INUS)
ASTON	88B	PL B201 169	D. Aston *et al.*	(SLAC, NAGO, CINC, INUS)
ASTON	87	NP B292 693	D. Aston *et al.*	(SLAC, NAGO, CINC, INUS)
CARLSMITH	87	PR D36 3502	D. Carlsmith *et al.*	(EFI, SACL)
ASTON	84B	NP B247 261	D. Aston *et al.*	(SLAC, CARL, OTTA)
BAUBILLIER	84B	ZPHY C26 37	M. Baubillier *et al.*	(BIRM, CERN, GLAS+)
BAUBILLIER	82B	NP B202 21	M. Baubillier *et al.*	(BIRM, CERN, GLAS+)
CIHANGIR	82	PL 117B 123	S. Cihangir *et al.*	(FNAL, MINN, ROCH)
CLELAND	82	NP B208 189	W.E. Cleland *et al.*	(DURH, GEVA, LAUS+)
ASTON	81C	PL 106B 235	D. Aston *et al.*	(SLAC, CARL, OTTA) JP
DAUM	81C	NP B187 1	C. Daum *et al.*	(AMST, CERN, CRAC, MPIM+)
TOAFF	81	PR D23 1500	S. Toaff *et al.*	(ANL, KANS)
ETKIN	80	PR D22 42	A. Etkin *et al.*	(BNL, CUNY) JP
ESTABROOKS	78	NP B133 490	P.G. Estabrooks *et al.*	(MCGI, CARL, DURH+)
Also	78B	PR D17 658	P.G. Estabrooks *et al.*	(MCGI, CARL, DURH+)
JONGEJANS	78	NP B139 383	B. Jongejans *et al.*	(ZEEM, CERN, NIJM+)
MARTIN	78	NP B134 392	A.D. Martin *et al.*	(DURH, GEVA)
BOWLER	77	NP B126 31	M.G. Bowler *et al.*	(OXF)
GOLDBERG	76	LNC 17 253	J. Goldberg	(HAIF)
HENDRICK	76	NP B112 189	K. Hendrickx *et al.*	(MONS, SACL, PARIS+)
LAUSCHER	75	NP B86 189	P. Lauscher *et al.*	(ABCLV Collab.) JP
MCCUBBIN	75	NP B86 13	N.A. McCubbin, L. Lyons	(OXF)
DEHM	74	NP B75 47	G. Dehm *et al.*	(MPIM, BRUX, MONS, CERN)
LINGLIN	73	NP B55 408	D. Linglin	(CERN)
AGUILAR-...	71B	PR D4 2583	M. Aguilar-Benitez, R.L. Eisner, J.B. Kinson	(BNL)
BARNHAM	71C	NP B28 171	K.W.J. Barnham *et al.*	(BIRM, GLAS)
CORDS	71	PR D4 1974	D. Cords *et al.*	(PURD, UCD, IUPU)
BASSOMPIE...	69	NP B13 189	G. Bassompierre *et al.*	(CERN, BRUX) JP
BISHOP	69	NP B9 403	J.M. Bishop *et al.*	(WISC)
CRENNELL	69D	PRL 22 487	D.J. Crennell *et al.*	(BNL)
DAVIS	69	PRL 23 1071	P.J. Davis *et al.*	(LRL)
LIND	69	NP B14 1	V.G. Lind *et al.*	(LRL) JP
SCHWEING...	68	PR 166 1317	F. Schweingruber *et al.*	(ANL, NWES)
Also	67	Thesis	F.L. Schweingruber	(NWES, NWES)
BASSANO	67	PRL 19 968	D. Bassano *et al.*	(BNL, SYRA)
FIELD	67	PL 24B 638	J.H. Field *et al.*	(UCSD)
BADIER	65C	PL 19 612	J. Badier *et al.*	(EPOL, SACL, AMST)

OTHER RELATED PAPERS

BEVEREN	01B	EPJ C22 493	E. van Beveren	
BARBERIS	98E	PL B436 204	D. Barberis *et al.*	(Omega Expt.)
ATKINSON	86	ZPHY C30 521	M. Atkinson *et al.*	(BONN, CERN, GLAS+)
BAUBILLIER	82B	NP B202 21	M. Baubillier *et al.*	(BIRM, CERN, GLAS+)
CHUNG	65	PRL 15 325	S.U. Chung *et al.*	(LRL)
FOCARDI	65	PL 16 351	S. Focardi *et al.*	(BGNA, SACL)
HAQUE	65	PL 14 338	N. Haque *et al.*	
HARDY	65	PRL 14 401	L.M. Hardy *et al.*	(LRL)

$K(1460)$ $I(J^P) = \frac{1}{2}(0^-)$

OMITTED FROM SUMMARY TABLE

Observed in $K\pi\pi$ partial-wave analysis.

$K(1460)$ MASS

VALUE (MeV)	DOCUMENT ID	TECN	CHG	COMMENT
• • • We do not use the following data for averages, fits, limits, etc. • • •				
~ 1460	DAUM	81C CNTR	–	63 $K^-p \to K^-2\pi p$
~ 1400	[1] BRANDENB...	76B ASPK	±	13 $K^\pm p \to K^+2\pi p$

[1] Coupled mainly to $Kf_0(1370)$. Decay into $K^*(892)\pi$ seen.

$K(1460)$ WIDTH

VALUE (MeV)	DOCUMENT ID	TECN	CHG	COMMENT
• • • We do not use the following data for averages, fits, limits, etc. • • •				
~ 260	DAUM	81C CNTR	–	63 $K^-p \to K^-2\pi p$
~ 250	[2] BRANDENB...	76B ASPK	±	13 $K^\pm p \to K^+2\pi p$

[2] Coupled mainly to $Kf_0(1370)$. Decay into $K^*(892)\pi$ seen.

$K(1460)$ DECAY MODES

	Mode	Fraction (Γ_i/Γ)
Γ_1	$K^*(892)\pi$	seen
Γ_2	$K\rho$	seen
Γ_3	$K_0^*(1430)\pi$	seen

$K(1460)$ PARTIAL WIDTHS

$\Gamma(K^*(892)\pi)$ Γ_1

VALUE (MeV)	DOCUMENT ID	TECN	COMMENT
• • • We do not use the following data for averages, fits, limits, etc. • • •			
~ 109	DAUM	81C CNTR	63 $K^-p \to K^-2\pi p$

$\Gamma(K\rho)$ Γ_2

VALUE (MeV)	DOCUMENT ID	TECN	COMMENT
• • • We do not use the following data for averages, fits, limits, etc. • • •			
~ 34	DAUM	81C CNTR	63 $K^-p \to K^-2\pi p$

$\Gamma(K_0^*(1430)\pi)$ Γ_3

VALUE (MeV)	DOCUMENT ID	TECN	COMMENT
• • • We do not use the following data for averages, fits, limits, etc. • • •			
~ 117	DAUM	81C CNTR	63 $K^-p \to K^-2\pi p$

$K(1460)$ REFERENCES

DAUM	81C	NP B187 1	C. Daum *et al.*	(AMST, CERN, CRAC, MPIM+)
BRANDENB...	76B	PRL 36 1239	G.W. Brandenburg *et al.*	(SLAC) JP

OTHER RELATED PAPERS

TANIMOTO	82	PL 116B 198	M. Tanimoto	(BIEL)
VERGEEST	79	NP B158 265	J.S.M. Vergeest *et al.*	(NIJM, AMST, CERN+)

$K_2(1580)$

$I(J^P) = \frac{1}{2}(2^-)$

OMITTED FROM SUMMARY TABLE

Seen in partial-wave analysis of the $K^-\pi^+\pi^-$ system. Needs confirmation.

$K_2(1580)$ MASS

VALUE (MeV)	DOCUMENT ID		CHG	COMMENT
• • • We do not use the following data for averages, fits, limits, etc. • • •				
~ 1580	OTTER	79	–	10,14,16 K^-p

$K_2(1580)$ WIDTH

VALUE (MeV)	DOCUMENT ID		CHG	COMMENT
• • • We do not use the following data for averages, fits, limits, etc. • • •				
~ 110	OTTER	79	–	10,14,16 K^-p

$K_2(1580)$ DECAY MODES

	Mode	Fraction (Γ_i/Γ)
Γ_1	$K^*(892)\pi$	seen
Γ_2	$K_2^*(1430)\pi$	possibly seen

$K_2(1580)$ BRANCHING RATIOS

$\Gamma(K^*(892)\pi)/\Gamma_{total}$ **Γ_1/Γ**

VALUE	DOCUMENT ID		TECN	CHG	COMMENT
seen	OTTER	79	HBC	–	10,14,16 K^-p

$\Gamma(K_2^*(1430)\pi)/\Gamma_{total}$ **Γ_2/Γ**

VALUE	DOCUMENT ID		TECN	CHG	COMMENT
possibly seen	OTTER	79	HBC	–	10,14,16 K^-p

$K_2(1580)$ REFERENCES

OTTER 79 NP B147 1 G. Otter *et al.* (AACH3, BERL, CERN, LOIC+) JP

$K(1630)$

$I(J^P) = \frac{1}{2}(?^?)$

OMITTED FROM SUMMARY TABLE

Seen as a narrow peak, compatible with the experimental resolution, in the invariant mass of the $K_S^0\pi^+\pi^-$ system produced in π^-p interactions at high momentum transfers.

$K(1630)$ MASS

VALUE (MeV)	EVTS	DOCUMENT ID	TECN	COMMENT
1629±7	~ 75	KARNAUKHOV98	BC	16.0 $\pi^-p \to (K_S^0\pi^+\pi^-)X^+\pi^-X^0$

$K(1630)$ WIDTH

VALUE (MeV)	EVTS	DOCUMENT ID	TECN	COMMENT
16^{+19}_{-16}	~ 75	[1] KARNAUKHOV98	BC	16.0 $\pi^-p \to (K_S^0\pi^+\pi^-)X^+\pi^-X^0$

[1] Compatible with an experimental resolution of 14 ± 1 MeV.

$K(1630)$ DECAY MODES

	Mode
Γ_1	$K_S^0\pi^+\pi^-$

$K(1630)$ REFERENCES

KARNAUKHOV 98 PAN 61 203 V.M. Karnaukhov, C. Coca, V.I. Moroz
Translated from YAF 61 252.

OTHER RELATED PAPERS

KARNAUKHOV 00 PAN 63 588 V.M. Karnaukhov, C. Coca, V.I. Moroz
Translated from YAF 63 652.

$K_1(1650)$

$I(J^P) = \frac{1}{2}(1^+)$

OMITTED FROM SUMMARY TABLE

This entry contains various peaks in strange meson systems ($K^+\phi$, $K\pi\pi$) reported in partial-wave analysis in the 1600–1900 mass region.

$K_1(1650)$ MASS

VALUE (MeV)	DOCUMENT ID		TECN	CHG	COMMENT
1650±50	FRAME	86	OMEG	+	13 $K^+p \to \phi K^+p$
• • • We do not use the following data for averages, fits, limits, etc. • • •					
~ 1840	ARMSTRONG	83	OMEG	–	18.5 $K^-p \to 3Kp$
~ 1800	DAUM	81C	CNTR	–	63 $K^-p \to K^-2\pi p$

$K_1(1650)$ WIDTH

VALUE (MeV)	DOCUMENT ID		TECN	CHG	COMMENT
150±50	FRAME	86	OMEG	+	13 $K^+p \to \phi K^+p$
• • • We do not use the following data for averages, fits, limits, etc. • • •					
~ 250	DAUM	81C	CNTR	–	63 $K^-p \to K^-2\pi p$

$K_1(1650)$ DECAY MODES

	Mode
Γ_1	$K\pi\pi$
Γ_2	$K\phi$

$K_1(1650)$ REFERENCES

FRAME 86 NP B276 667 D. Frame *et al.* (GLAS)
ARMSTRONG 83 NP B221 1 T.A. Armstrong *et al.* (BARI, BIRM, CERN+)
DAUM 81C NP B187 1 C. Daum *et al.* (AMST, CERN, CRAC, MPIM+)

$K^*(1680)$

$I(J^P) = \frac{1}{2}(1^-)$

$K^*(1680)$ MASS

VALUE (MeV)	DOCUMENT ID		TECN	CHG	COMMENT
1717±27 OUR AVERAGE Error includes scale factor of 1.4.					
1677±10±32	ASTON	88	LASS	0	11 $K^-p \to K^-\pi^+n$
1735±10±20	ASTON	87	LASS	0	11 $K^-p \to \overline{K}^0\pi^+\pi^-n$
• • • We do not use the following data for averages, fits, limits, etc. • • •					
1678±64	BIRD	89	LASS	–	11 $K^-p \to \overline{K}^0\pi^-p$
1800±70	ETKIN	80	MPS	0	6 $K^-p \to \overline{K}^0\pi^+\pi^-n$
~ 1650	ESTABROOKS	78	ASPK	0	13 $K^\pm p \to K^\pm\pi^\pm n$

$K^*(1680)$ WIDTH

VALUE (MeV)	DOCUMENT ID		TECN	CHG	COMMENT
322±110 OUR AVERAGE Error includes scale factor of 4.2.					
205± 16±34	ASTON	88	LASS	0	11 $K^-p \to K^-\pi^+n$
423± 18±30	ASTON	87	LASS	0	11 $K^-p \to \overline{K}^0\pi^+\pi^-n$
• • • We do not use the following data for averages, fits, limits, etc. • • •					
454±270	BIRD	89	LASS	–	11 $K^-p \to \overline{K}^0\pi^-p$
170± 30	ETKIN	80	MPS	0	6 $K^-p \to \overline{K}^0\pi^+\pi^-n$
250 to 300	ESTABROOKS	78	ASPK	0	13 $K^\pm p \to K^\pm\pi^\pm n$

$K^*(1680)$ DECAY MODES

	Mode	Fraction (Γ_i/Γ)
Γ_1	$K\pi$	(38.7±2.5) %
Γ_2	$K\rho$	($31.4^{+4.7}_{-2.1}$) %
Γ_3	$K^*(892)\pi$	($29.9^{+2.2}_{-4.7}$) %

CONSTRAINED FIT INFORMATION

An overall fit to 4 branching ratios uses 4 measurements and one constraint to determine 3 parameters. The overall fit has a $\chi^2 = 2.9$ for 2 degrees of freedom.

The following *off-diagonal* array elements are the correlation coefficients $\langle \delta x_i \delta x_j \rangle / (\delta x_i \cdot \delta x_j)$, in percent, from the fit to the branching fractions, $x_i \equiv \Gamma_i / \Gamma_{total}$. The fit constrains the x_i whose labels appear in this array to sum to one.

x_2	−36		
x_3	−39	−72	
	x_1	x_2	

$K^*(1680)$ BRANCHING RATIOS

$\Gamma(K\pi)/\Gamma_{total}$ — **Γ_1/Γ**

VALUE	DOCUMENT ID		TECN	CHG	COMMENT
0.387±0.026 OUR FIT					
0.388±0.014±0.022	ASTON	88	LASS	0	11 $K^-p \to K^-\pi^+n$

$\Gamma(K\pi)/\Gamma(K^*(892)\pi)$ — **Γ_1/Γ_3**

VALUE	DOCUMENT ID		TECN	CHG	COMMENT
$1.30^{+0.23}_{-0.14}$ OUR FIT					
2.8 ±1.1	ASTON	84	LASS	0	11 $K^-p \to \overline{K}^0 2\pi n$

$\Gamma(K\rho)/\Gamma(K\pi)$ — **Γ_2/Γ_1**

VALUE	DOCUMENT ID		TECN	CHG	COMMENT
$0.81^{+0.14}_{-0.09}$ OUR FIT					
1.2 ±0.4	ASTON	84	LASS	0	11 $K^-p \to \overline{K}^0 2\pi n$

$\Gamma(K\rho)/\Gamma(K^*(892)\pi)$ — **Γ_2/Γ_3**

VALUE	DOCUMENT ID		TECN	CHG	COMMENT
$1.05^{+0.27}_{-0.11}$ OUR FIT					
$0.97\pm0.09^{+0.30}_{-0.10}$	ASTON	87	LASS	0	11 $K^-p \to \overline{K}^0\pi^+\pi^-n$

$K^*(1680)$ REFERENCES

BIRD	89	SLAC-332	P.F. Bird	(SLAC)
ASTON	88	NP B296 493	D. Aston *et al.*	(SLAC, NAGO, CINC, INUS)
ASTON	87	NP B292 693	D. Aston *et al.*	(SLAC, NAGO, CINC, INUS)
ASTON	84	PL 149B 258	D. Aston *et al.*	(SLAC, CARL, OTTA) JP
ETKIN	80	PR D22 42	A. Etkin *et al.*	(BNL, CUNY) JP
ESTABROOKS	78	NP B133 490	P.G. Estabrooks *et al.*	(MCGI, CARL, DURH+) JP

$K_2(1770)$

$I(J^P) = \frac{1}{2}(2^-)$

THE $K_2(1770)$ AND THE $K_2(1820)$

A partial-wave analysis of the $K^-\omega$ system based on about 100,000 $K^-p \to K^-\omega p$ events (ASTON 93) gives evidence for two $q\bar{q}$ D-wave states near 1.8 GeV. A previous analysis based on about 200,000 diffractively produced $K^-p \to K^-\pi^+\pi^-p$ events (DAUM 81) gave evidence for two $J^P = 2^-$ states in this region, with masses $\sim$ 1780 MeV and $\sim$ 1840 MeV and widths $\sim$ 200 MeV, in good agreement with the results of ASTON 93. In contrast, the masses obtained using a single resonance do not agree well: ASTON 93 obtains 1728 ± 7 MeV, while DAUM 81 estimates $\sim$ 1820 MeV. We conclude that there are indeed two K_2 resonances here.

We list under the $K_2(1770)$ other measurements that do not resolve the two-resonance structure of the enhancement.

References

References may be found at the end of the $K_2(1770)$ Listing.

$K_2(1770)$ MASS

VALUE (MeV)	EVTS	DOCUMENT ID		TECN	CHG	COMMENT
1773± 8		[1] ASTON	93	LASS		11 $K^-p \to K^-\omega p$
• • • We do not use the following data for averages, fits, limits, etc. • • •						
1743±15		TIKHOMIROV	03	SPEC		40.0 π^- C → $K^0_S K^0_S K^0_L$ X
1810±20		FRAME	86	OMEG	+	13 $K^+p \to \phi K^+p$
~ 1730		ARMSTRONG	83	OMEG	−	18.5 $K^-p \to 3Kp$
~ 1780		[2] DAUM	81C	CNTR	−	63 $K^-p \to K^-2\pi p$
1710±15	60	CHUNG	74	HBC	−	7.3 $K^-p \to K^-\omega p$
1767± 6		BLIEDEN	72	MMS	−	11–16 K^-p
1730±20	306	[3] FIRESTONE	72B	DBC	+	12 K^+d
1765±40		[4] COLLEY	71	HBC	+	10 $K^+p \to K2\pi N$
1740		DENEGRI	71	DBC	−	12.6 $K^-d \to \overline{K}2\pi d$
1745±20		AGUILAR-...	70C	HBC	−	4.6 K^-p
1780±15		BARTSCH	70C	HBC	−	10.1 K^-p
1760±15		LUDLAM	70	HBC	−	12.6 K^-p

[1] From a partial wave analysis of the $K^-\omega$ system.
[2] From a partial wave analysis of the $K^-2\pi$ system.
[3] Produced in conjunction with excited deuteron.
[4] Systematic errors added correspond to spread of different fits.

$K_2(1770)$ WIDTH

VALUE (MeV)	EVTS	DOCUMENT ID		TECN	CHG	COMMENT
186±14		[5] ASTON	93	LASS		11 $K^-p \to K^-\omega p$
• • • We do not use the following data for averages, fits, limits, etc. • • •						
147±70		TIKHOMIROV	03	SPEC		40.0 π^- C → $K^0_S K^0_S K^0_L$ X
140±40		FRAME	86	OMEG	+	13 $K^+p \to \phi K^+p$
~ 220		ARMSTRONG	83	OMEG	−	18.5 $K^-p \to 3Kp$
~ 210		[6] DAUM	81C	CNTR	−	63 $K^-p \to K^-2\pi p$
110±50	60	CHUNG	74	HBC	−	7.3 $K^-p \to K^-\omega p$
100±26		BLIEDEN	72	MMS	−	11–16 K^-p
210±30	306	[7] FIRESTONE	72B	DBC	+	12 K^+d
90±70		[8] COLLEY	71	HBC	+	10 $K^+p \to K2\pi N$
130		DENEGRI	71	DBC	−	12.6 $K^-d \to \overline{K}2\pi d$
100±50		AGUILAR-...	70C	HBC	−	4.6 K^-p
138±40		BARTSCH	70C	HBC	−	10.1 K^-p
50^{+40}_{-20}		LUDLAM	70	HBC	−	12.6 K^-p

[5] From a partial wave analysis of the $K^-\omega$ system.
[6] From a partial wave analysis of the $K^-2\pi$ system.
[7] Produced in conjunction with excited deuteron.
[8] Systematic errors added correspond to spread of different fits.

$K_2(1770)$ DECAY MODES

	Mode	Fraction (Γ_i/Γ)
Γ_1	$K\pi\pi$	
Γ_2	$K_2^*(1430)\pi$	dominant
Γ_3	$K^*(892)\pi$	seen
Γ_4	$K f_2(1270)$	seen
Γ_5	$K f_0(980)$	
Γ_6	$K\phi$	seen
Γ_7	$K\omega$	seen

$K_2(1770)$ BRANCHING RATIOS

$\Gamma(K_2^*(1430)\pi)/\Gamma(K\pi\pi)$ — **Γ_2/Γ_1**
($K_2^*(1430) \to K\pi$)

VALUE	DOCUMENT ID		TECN	CHG	COMMENT
• • • We do not use the following data for averages, fits, limits, etc. • • •					
~ 0.03	DAUM	81C	CNTR		63 $K^-p \to K^-2\pi p$
~ 1.0	[9] FIRESTONE	72B	DBC	+	12 K^+d
<1.0	COLLEY	71	HBC		10 K^+p
0.2 ±0.2	AGUILAR-...	70C	HBC	−	4.6 K^-p
<1.0	BARTSCH	70C	HBC	−	10.1 K^-p
1.0	BARBARO-...	69	HBC	+	12.0 K^+p

[9] Produced in conjunction with excited deuteron.

$\Gamma(K^*(892)\pi)/\Gamma(K\pi\pi)$ — **Γ_3/Γ_1**

VALUE	DOCUMENT ID		TECN	COMMENT
• • • We do not use the following data for averages, fits, limits, etc. • • •				
~ 0.23	DAUM	81C	CNTR	63 $K^-p \to K^-2\pi p$

$\Gamma(K f_2(1270))/\Gamma(K\pi\pi)$ — **Γ_4/Γ_1**
($f_2(1270) \to \pi\pi$)

VALUE	DOCUMENT ID		TECN	COMMENT
• • • We do not use the following data for averages, fits, limits, etc. • • •				
~ 0.74	DAUM	81C	CNTR	63 $K^-p \to K^-2\pi p$

$\Gamma(K f_0(980))/\Gamma_{total}$ Γ_5/Γ

VALUE	DOCUMENT ID	TECN	COMMENT
• • • We do not use the following data for averages, fits, limits, etc. • • •			
possibly seen	TIKHOMIROV 03	SPEC	40.0 $\pi^- C \to K_S^0 K_S^0 K_L^0 X$

$\Gamma(K\phi)/\Gamma_{total}$ Γ_6/Γ

VALUE	DOCUMENT ID	TECN	CHG	COMMENT
seen	ARMSTRONG 83	OMEG	–	18.5 $K^- p \to K^- \phi N$

$\Gamma(K\omega)/\Gamma_{total}$ Γ_7/Γ

VALUE	DOCUMENT ID	TECN	CHG	COMMENT
seen	OTTER 81	HBC	±	8.25,10,16 $K^\pm p$
seen	CHUNG 74	HBC	–	7.3 $K^- p \to K^- \omega p$

$K_2(1770)$ REFERENCES

TIKHOMIROV 03	PAN 66 828 Translated from YAF 66 860.	G.D. Tikhomirov *et al.*	
ASTON 93	PL B308 186	D. Aston *et al.*	(SLAC, NAGO, CINC, INUS)
FRAME 86	NP B276 667	D. Frame *et al.*	(GLAS)
ARMSTRONG 83	NP B221 1	T.A. Armstrong *et al.*	(BARI, BIRM, CERN+)
DAUM 81C	NP B187 1	C. Daum *et al.*	(AMST, CERN, CRAC, MPIM+)
OTTER 81	NP B181 1	G. Otter	(AACH3, BERL, LOIC, VIEN, BIRM+)
CHUNG 74	PL 51B 413	S.U. Chung *et al.*	(BNL)
BLIEDEN 72	PL 39B 668	H.R. Blieden *et al.*	(STON, NEAS)
FIRESTONE 72B	PR D5 505	A. Firestone *et al.*	(LBL)
COLLEY 71	NP B26 71	D.C. Colley *et al.*	(BIRM, GLAS)
DENEGRI 71	NP B28 13	D. Denegri *et al.*	(JHU) JP
AGUILAR-... 70C	PRL 25 54	M. Aguilar-Benitez *et al.*	(BNL)
BARTSCH 70C	PL 33B 186	J. Bartsch *et al.*	(AACH, BERL, CERN+)
LUDLAM 70	PR D2 1234	T. Ludlam, J. Sandweiss, A.J. Slaughter	(YALE)
BARBARO-... 69	PRL 22 1207	A. Barbaro-Galtieri *et al.*	(LRL)

OTHER RELATED PAPERS

BERLINGHIERI 67	PRL 18 1087	J.C. Berlinghieri *et al.*	(ROCH) I
CARMONY 67	PRL 18 615	D.D. Carmony, T. Hendricks, R.L. Lander	(UCSD)
JOBES 67	PL 26B 49	M. Jobes *et al.*	(BIRM, CERN, BRUX)
BARTSCH 66	PL 22 357	J. Bartsch *et al.*	(AACH, BERL, CERN+)

$K_3^*(1780)$

$I(J^P) = \frac{1}{2}(3^-)$

$K_3^*(1780)$ MASS

VALUE (MeV)	EVTS	DOCUMENT ID	TECN	CHG	COMMENT
1776± 7 OUR AVERAGE		Error includes scale factor of 1.1.			
1781± 8± 4		[1] ASTON	88 LASS	0	11 $K^- p \to K^- \pi^+ n$
1740±14±15		[1] ASTON	87 LASS	0	11 $K^- p \to \overline{K}^0 \pi^+ \pi^- n$
1779±11		[2] BALDI	76 SPEC	+	10 $K^+ p \to K^0 \pi^+ p$
1776±26		[3] BRANDENB...	76D ASPK	0	13 $K^\pm p \to K^\pm \pi^\mp N$
• • • We do not use the following data for averages, fits, limits, etc. • • •					
1720±10±15	6111	[4] BIRD	89 LASS	–	11 $K^- p \to \overline{K}^0 \pi^- p$
1749±10		ASTON	88B LASS	–	11 $K^- p \to K^- \eta p$
1780± 9	300	BAUBILLIER	84B HBC	–	8.25 $K^- p \to \overline{K}^0 \pi^- p$
1790±15		BAUBILLIER	82B HBC	0	8.25 $K^- p \to K_S^0 2\pi N$
1784± 9	2060	CLELAND	82 SPEC	±	50 $K^+ p \to K_S^0 \pi^\pm p$
1786±15		[5] ASTON	81D LASS	0	11 $K^- p \to K^- \pi^+ n$
1762± 9	190	TOAFF	81 HBC	–	6.5 $K^- p \to \overline{K}^0 \pi^- p$
1850±50		ETKIN	80 MPS	0	6 $K^- p \to \overline{K}^0 \pi^+ \pi^-$
1812±28		BEUSCH	78 OMEG		10 $K^- p \to \overline{K}^0 \pi^+ \pi^- n$
1786± 8		CHUNG	78 MPS	0	6 $K^- p \to K^- \pi^+ n$

[1] From energy-independent partial-wave analysis.
[2] From a fit to Y_6^2 moment. $J^P = 3^-$ found.
[3] Confirmed by phase shift analysis of ESTABROOKS 78, yields $J^P = 3^-$.
[4] From a partial wave amplitude analysis.
[5] From a fit to the Y_6^0 moment.

$K_3^*(1780)$ WIDTH

VALUE (MeV)	EVTS	DOCUMENT ID	TECN	CHG	COMMENT
159±21 OUR AVERAGE		Error includes scale factor of 1.3. See the ideogram below.			
203±30± 8		[6] ASTON	88 LASS	0	11 $K^- p \to K^- \pi^+ n$
171±42±20		[6] ASTON	87 LASS	0	11 $K^- p \to \overline{K}^0 \pi^+ \pi^- n$
135±22		[7] BALDI	76 SPEC	+	10 $K^+ p \to K^0 \pi^+ p$
• • • We do not use the following data for averages, fits, limits, etc. • • •					
187^{+31}_{-20}	6111	[8] BIRD	89 LASS	–	11 $K^- p \to \overline{K}^0 \pi^- p$
193^{+51}_{-37}		ASTON	88B LASS	–	11 $K^- p \to K^- \eta p$
99±30	300	BAUBILLIER	84B HBC	–	8.25 $K^- p \to \overline{K}^0 \pi^- p$
~ 130		BAUBILLIER	82B HBC	0	8.25 $K^- p \to K_S^0 2\pi N$
191±24	2060	CLELAND	82 SPEC	±	50 $K^+ p \to K_S^0 \pi^\pm p$
225±60		[9] ASTON	81D LASS	0	11 $K^- p \to K^- \pi^+ n$
~ 80	190	TOAFF	81 HBC	–	6.5 $K^- p \to \overline{K}^0 \pi^- p$
240±50		ETKIN	80 MPS	0	6 $K^- p \to \overline{K}^0 \pi^+ \pi^-$
181±44		[10] BEUSCH	78 OMEG		10 $K^- p \to \overline{K}^0 \pi^+ \pi^- n$
96±31		CHUNG	78 MPS	0	6 $K^- p \to K^- \pi^+ n$
270±70		[11] BRANDENB...	76D ASPK	0	13 $K^\pm p \to K^\pm \pi^\mp N$

[6] From energy-independent partial-wave analysis.
[7] From a fit to Y_6^2 moment. $J^P = 3^-$ found.
[8] From a partial wave amplitude analysis.
[9] From a fit to Y_6^0 moment.
[10] Errors enlarged by us to $4\Gamma/\sqrt{N}$; see the note with the $K^*(892)$ mass.
[11] ESTABROOKS 78 find that BRANDENBURG 76D data are consistent with 175 MeV width. Not averaged.

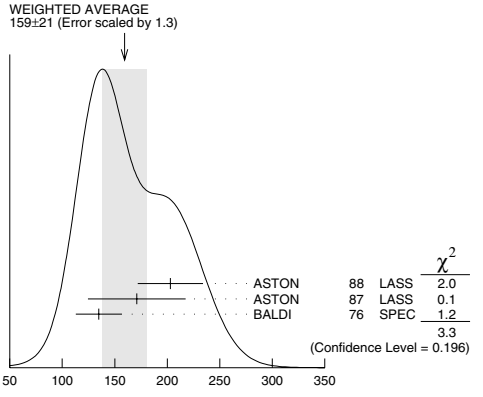

$K_3^*(1780)$ DECAY MODES

	Mode	Fraction (Γ_i/Γ)	Confidence level
Γ_1	$K\rho$	(31 ± 9) %	
Γ_2	$K^*(892)\pi$	(20 ± 5) %	
Γ_3	$K\pi$	(18.8± 1.0) %	
Γ_4	$K\eta$	(30 ±13) %	
Γ_5	$K_2^*(1430)\pi$	< 16 %	95%

CONSTRAINED FIT INFORMATION

An overall fit to 3 branching ratios uses 4 measurements and one constraint to determine 4 parameters. The overall fit has a $\chi^2 = 0.0$ for 1 degrees of freedom.

The following *off-diagonal* array elements are the correlation coefficients $\langle \delta x_i \delta x_j \rangle / (\delta x_i \cdot \delta x_j)$, in percent, from the fit to the branching fractions, $x_i \equiv \Gamma_i/\Gamma_{total}$. The fit constrains the x_i whose labels appear in this array to sum to one.

x_2	85		
x_3	18	21	
x_4	−98	−94	−27
	x_1	x_2	x_3

$K_3^*(1780)$ BRANCHING RATIOS

$\Gamma(K\rho)/\Gamma(K^*(892)\pi)$ Γ_1/Γ_2

VALUE	DOCUMENT ID	TECN	CHG	COMMENT
1.52±0.23 OUR FIT				
1.52±0.21±0.10	ASTON 87	LASS	0	11 $K^- p \to \overline{K}^0 \pi^+ \pi^- n$

$\Gamma(K^*(892)\pi)/\Gamma(K\pi)$ Γ_2/Γ_3

VALUE	DOCUMENT ID	TECN	CHG	COMMENT
1.09±0.26 OUR FIT				
1.09±0.26	ASTON 84B	LASS	0	11 $K^-p \to \overline{K}^0 2\pi n$

$\Gamma(K\pi)/\Gamma_{total}$ Γ_3/Γ

VALUE	DOCUMENT ID	TECN	CHG	COMMENT
0.188±0.010 OUR FIT				
0.188±0.010 OUR AVERAGE				
0.187±0.008±0.008	ASTON 88	LASS	0	11 $K^-p \to K^-\pi^+ n$
0.19 ±0.02	ESTABROOKS 78	ASPK	0	13 $K^\pm p \to K\pi N$

$\Gamma(K\eta)/\Gamma(K\pi)$ Γ_4/Γ_3

VALUE	DOCUMENT ID	TECN	CHG	COMMENT
1.6 ±0.7 OUR FIT				
• • • We do not use the following data for averages, fits, limits, etc. • • •				
0.41±0.050	[12] BIRD 89	LASS	–	11 $K^-p \to \overline{K}^0\pi^- p$
0.50±0.18	ASTON 88B	LASS	–	11 $K^-p \to K^-\eta p$

[12] This result supersedes ASTON 88B.

$\Gamma(K_2^*(1430)\pi)/\Gamma(K^*(892)\pi)$ Γ_5/Γ_2

VALUE	CL%	DOCUMENT ID	TECN	CHG	COMMENT
<0.78	95	ASTON 87	LASS	0	11 $K^-p \to \overline{K}^0\pi^+\pi^- n$

$K_3^*(1780)$ REFERENCES

BIRD	89	SLAC-332	P.F. Bird	(SLAC)
ASTON	88	NP B296 493	D. Aston *et al.*	(SLAC, NAGO, CINC, INUS)
ASTON	88B	PL B201 169	D. Aston *et al.*	(SLAC, NAGO, CINC, INUS) JP
ASTON	87	NP B292 693	D. Aston *et al.*	(SLAC, NAGO, CINC, INUS)
ASTON	84B	NP B247 261	D. Aston *et al.*	(SLAC, CARL, OTTA)
BAUBILLIER	84B	ZPHY C26 37	M. Baubillier *et al.*	(BIRM, CERN, GLAS+)
BAUBILLIER	82B	NP B202 21	M. Baubillier *et al.*	(BIRM, CERN, GLAS+)
CLELAND	82	NP B208 189	W.E. Cleland *et al.*	(DURH, GEVA, LAUS+)
ASTON	81D	PL 99B 502	D. Aston *et al.*	(SLAC, CARL, OTTA) JP
TOAFF	81	PR D23 1500	S. Toaff *et al.*	(ANL, KANS)
ETKIN	80	PR D22 42	A. Etkin *et al.*	(BNL, CUNY) JP
BEUSCH	78	PL 74B 282	W. Beusch *et al.*	(CERN, AACH3, ETH) JP
CHUNG	78	PRL 40 355	S.U. Chung *et al.*	(BNL, BRAN, CUNY+) JP
ESTABROOKS	78	NP B133 490	P.G. Estabrooks *et al.*	(MCGI, CARL, DURH+) JP
Also	78B	PR D17 658	P.G. Estabrooks *et al.*	(MCGI, CARL, DURH+)
BALDI	76	PL 63B 344	R. Baldi *et al.*	(GEVA) JP
BRANDENB...	76D	PL 60B 478	G.W. Brandenburg *et al.*	(SLAC) JP

OTHER RELATED PAPERS

AGUILAR-...	73	PRL 30 672	M. Aguilar-Benitez *et al.*	(BNL)
WALUCH	73	PR D8 2837	V. Waluch, S.M. Flatte, J.H. Friedman	(LBL)
CARMONY	71	PRL 27 1160	D.D. Carmony *et al.*	(PURD, UCD, IUPU)
FIRESTONE	71	PL 36B 513	A. Firestone *et al.*	(LBL)

$K_2(1820)$ $I(J^P) = \frac{1}{2}(2^-)$

Observed by ASTON 93 from a partial wave analysis of the $K^-\omega$ system. See mini-review under $K_2(1770)$.

$K_2(1820)$ MASS

VALUE (MeV)	DOCUMENT ID	TECN	COMMENT
1816±13	[1] ASTON 93	LASS	11 $K^-p \to K^-\omega p$
• • • We do not use the following data for averages, fits, limits, etc. • • •			
~ 1840	[2] DAUM 81C	CNTR	63 $K^-p \to K^-2\pi p$

[1] From a partial wave analysis of the $K^-\omega$ system.
[2] From a partial wave analysis of the $K^-2\pi$ system.

$K_2(1820)$ WIDTH

VALUE (MeV)	DOCUMENT ID	TECN	COMMENT
276±35	[3] ASTON 93	LASS	11 $K^-p \to K^-\omega p$
• • • We do not use the following data for averages, fits, limits, etc. • • •			
~ 230	[4] DAUM 81C	CNTR	63 $K^-p \to K^-2\pi p$

[3] From a partial wave analysis of the $K^-\omega$ system.
[4] From a partial wave analysis of the $K^-2\pi$ system.

$K_2(1820)$ DECAY MODES

	Mode	Fraction (Γ_i/Γ)
Γ_1	$K\pi\pi$	
Γ_2	$K_2^*(1430)\pi$	seen
Γ_3	$K^*(892)\pi$	seen
Γ_4	$Kf_2(1270)$	seen
Γ_5	$K\omega$	seen

$K_2(1820)$ BRANCHING RATIOS

$\Gamma(K_2^*(1430)\pi)/\Gamma(K\pi\pi)$ Γ_2/Γ_1

VALUE	DOCUMENT ID	TECN	COMMENT
• • • We do not use the following data for averages, fits, limits, etc. • • •			
~ 0.77	DAUM 81C	CNTR	63 $K^-p \to \overline{K}2\pi p$

$\Gamma(K^*(892)\pi)/\Gamma(K\pi\pi)$ Γ_3/Γ_1

VALUE	DOCUMENT ID	TECN	COMMENT
• • • We do not use the following data for averages, fits, limits, etc. • • •			
~ 0.05	DAUM 81C	CNTR	63 $K^-p \to \overline{K}2\pi p$

$\Gamma(Kf_2(1270))/\Gamma(K\pi\pi)$ Γ_4/Γ_1

VALUE	DOCUMENT ID	TECN	COMMENT
• • • We do not use the following data for averages, fits, limits, etc. • • •			
~ 0.18	DAUM 81C	CNTR	63 $K^-p \to \overline{K}2\pi p$

$K_2(1820)$ REFERENCES

ASTON	93	PL B308 186	D. Aston *et al.*	(SLAC, NAGO, CINC, INUS)
DAUM	81C	NP B187 1	C. Daum *et al.*	(AMST, CERN, CRAC, MPIM+)

$K(1830)$ $I(J^P) = \frac{1}{2}(0^-)$

OMITTED FROM SUMMARY TABLE

Seen in partial-wave analysis of $K^-\phi$ system. Needs confirmation.

$K(1830)$ MASS

VALUE (MeV)	DOCUMENT ID	TECN	CHG	COMMENT
• • • We do not use the following data for averages, fits, limits, etc. • • •				
~ 1830	ARMSTRONG 83	OMEG	–	18.5 $K^-p \to 3Kp$

$K(1830)$ WIDTH

VALUE (MeV)	DOCUMENT ID	TECN	CHG	COMMENT
• • • We do not use the following data for averages, fits, limits, etc. • • •				
~ 250	ARMSTRONG 83	OMEG	–	18.5 $K^-p \to 3Kp$

$K(1830)$ DECAY MODES

	Mode
Γ_1	$K\phi$

$K(1830)$ REFERENCES

ARMSTRONG	83	NP B221 1	T.A. Armstrong *et al.*	(BARI, BIRM, CERN+) JP

$K_0^*(1950)$ $I(J^P) = \frac{1}{2}(0^+)$

OMITTED FROM SUMMARY TABLE

Seen in partial-wave analysis of the $K^-\pi^+$ system. Needs confirmation.

$K_0^*(1950)$ MASS

VALUE (MeV)	DOCUMENT ID	TECN	CHG	COMMENT
1945±10±20	[1] ASTON 88	LASS	0	11 $K^-p \to K^-\pi^+ n$
• • • We do not use the following data for averages, fits, limits, etc. • • •				
1820±40	[2] ANISOVICH 97C	RVUE		11 $K^-p \to K^-\pi^+ n$

[1] We take the central value of the two solutions and the larger error given.
[2] T-matrix pole. Reanalysis of ASTON 88 data.

$K_0^*(1950)$ WIDTH

VALUE (MeV)	DOCUMENT ID	TECN	CHG	COMMENT
201± 34±79	[3] ASTON 88	LASS	0	11 $K^-p \to K^-\pi^+ n$
• • • We do not use the following data for averages, fits, limits, etc. • • •				
250±100	[4] ANISOVICH 97C	RVUE		11 $K^-p \to K^-\pi^+ n$

[3] We take the central value of the two solutions and the larger error given.
[4] T-matrix pole. Reanalysis of ASTON 88 data.

$K_0^*(1950)$ DECAY MODES

	Mode	Fraction (Γ_i/Γ)
Γ_1	$K\pi$	(52±14) %

$K_0^*(1950)$ BRANCHING RATIOS

$\Gamma(K\pi)/\Gamma_{total}$ — **Γ_1/Γ**

VALUE	DOCUMENT ID		TECN	CHG	COMMENT
0.52±0.08±0.12	[5] ASTON	88	LASS	0	11 $K^-p \to K^-\pi^+n$

[5] We take the central value of the two solutions and the larger error given.

$K_0^*(1950)$ REFERENCES

ANISOVICH	97C	PL B413 137	A.V. Anisovich, A.V. Sarantsev
ASTON	88	NP B296 493	D. Aston *et al.* (SLAC, NAGO, CINC, INUS)

OTHER RELATED PAPERS

JAMIN	00	NP B587 331	M. Jamin *et al.*
SHAKIN	00	PR D62 114014	C.M. Shakin, H. Wang

$K_2^*(1980)$ $I(J^P) = \frac{1}{2}(2^+)$

OMITTED FROM SUMMARY TABLE
Needs confirmation.

$K_2^*(1980)$ MASS

VALUE (MeV)	EVTS	DOCUMENT ID		TECN	CHG	COMMENT
1973± 8±25		ASTON	87	LASS	0	11 $K^-p \to \overline{K}^0\pi^+\pi^-n$
• • • We do not use the following data for averages, fits, limits, etc. • • •						
2020±20		TIKHOMIROV	03	SPEC		40.0 $\bar{p}$ C → $K_S^0K_S^0K_L^0$X
1978±40	241± 47	BIRD	89	LASS	–	11 $K^-p \to \overline{K}^0\pi^-p$

$K_2^*(1980)$ WIDTH

VALUE (MeV)	EVTS	DOCUMENT ID		TECN	CHG	COMMENT
373±33±60		ASTON	87	LASS	0	11 $K^-p \to \overline{K}^0\pi^+\pi^-n$
• • • We do not use the following data for averages, fits, limits, etc. • • •						
180±70		TIKHOMIROV	03	SPEC		40.0 $\bar{p}$ C → $K_S^0K_S^0K_L^0$X
398±47	241± 47	BIRD	89	LASS	–	11 $K^-p \to \overline{K}^0\pi^-p$

$K_2^*(1980)$ DECAY MODES

	Mode
Γ_1	$K^*(892)\pi$
Γ_2	$K\rho$
Γ_3	$Kf_2(1270)$

$K_2^*(1980)$ BRANCHING RATIOS

$\Gamma(K\rho)/\Gamma(K^*(892)\pi)$ — **Γ_2/Γ_1**

VALUE	DOCUMENT ID		TECN	CHG	COMMENT
1.49±0.24±0.09	ASTON	87	LASS	0	11 $K^-p \to \overline{K}^0\pi^+\pi^-n$

$\Gamma(Kf_2(1270))/\Gamma_{total}$ — **Γ_3/Γ**

VALUE	DOCUMENT ID		TECN	COMMENT
• • • We do not use the following data for averages, fits, limits, etc. • • •				
possibly seen	TIKHOMIROV	03	SPEC	40.0 $\bar{p}$ C → $K_S^0K_S^0K_L^0$X

$K_2^*(1980)$ REFERENCES

TIKHOMIROV	03	PAN 66 828 Translated from YAF 66 860.	G.D. Tikhomirov *et al.*
BIRD	89	SLAC-332	P.F. Bird (SLAC)
ASTON	87	NP B292 693	D. Aston *et al.* (SLAC, NAGO, CINC, INUS)

$K_4^*(2045)$ $I(J^P) = \frac{1}{2}(4^+)$

$K_4^*(2045)$ MASS

VALUE (MeV)	EVTS	DOCUMENT ID		TECN	CHG	COMMENT
2045± 9 OUR AVERAGE		Error includes scale factor of 1.1.				
2062± 14±13		[1] ASTON	86	LASS	0	11 $K^-p \to K^-\pi^+n$
2039± 10	400	[2,3] CLELAND	82	SPEC	±	50 $K^+p \to K_S^0\pi^\pm p$
2070^{+100}_{-40}		[4] ASTON	81C	LASS	0	11 $K^-p \to K^-\pi^+n$
• • • We do not use the following data for averages, fits, limits, etc. • • •						
2079± 7	431	TORRES	86	MPSF		400 $pA \to 4KX$
2088± 20	650	BAUBILLIER	82	HBC	–	8.25 $K^-p \to K_S^0\pi^-p$
2115± 46	488	CARMONY	77	HBC	0	9 $K^+d \to K^+\pi$'s X

[1] From a fit to all moments.
[2] From a fit to 8 moments.
[3] Number of events evaluated by us.
[4] From energy-independent partial-wave analysis.

$K_4^*(2045)$ WIDTH

VALUE (MeV)	EVTS	DOCUMENT ID		TECN	CHG	COMMENT
198± 30 OUR AVERAGE						
221± 48±27		[5] ASTON	86	LASS	0	11 $K^-p \to K^-\pi^+n$
189± 35	400	[6,7] CLELAND	82	SPEC	±	50 $K^+p \to K_S^0\pi^\pm p$
• • • We do not use the following data for averages, fits, limits, etc. • • •						
61± 58	431	TORRES	86	MPSF		400 $pA \to 4KX$
170^{+100}_{-50}	650	BAUBILLIER	82	HBC	–	8.25 $K^-p \to K_S^0\pi^-p$
240^{+500}_{-100}		[8] ASTON	81C	LASS	0	11 $K^-p \to K^-\pi^+n$
300±200		CARMONY	77	HBC	0	9 $K^+d \to K^+\pi$'s X

[5] From a fit to all moments.
[6] From a fit to 8 moments.
[7] Number of events evaluated by us.
[8] From energy-independent partial-wave analysis.

$K_4^*(2045)$ DECAY MODES

	Mode	Fraction (Γ_j/Γ)
Γ_1	$K\pi$	(9.9±1.2) %
Γ_2	$K^*(892)\pi\pi$	(9 ±5) %
Γ_3	$K^*(892)\pi\pi\pi$	(7 ±5) %
Γ_4	$\rho K\pi$	(5.7±3.2) %
Γ_5	$\omega K\pi$	(5.0±3.0) %
Γ_6	$\phi K\pi$	(2.8±1.4) %
Γ_7	$\phi K^*(892)$	(1.4±0.7) %

$K_4^*(2045)$ BRANCHING RATIOS

$\Gamma(K\pi)/\Gamma_{total}$ — **Γ_1/Γ**

VALUE	DOCUMENT ID		TECN	CHG	COMMENT
0.099±0.012	ASTON	88	LASS	0	11 $K^-p \to K^-\pi^+n$

$\Gamma(K^*(892)\pi\pi)/\Gamma(K\pi)$ — **Γ_2/Γ_1**

VALUE	DOCUMENT ID		TECN	CHG	COMMENT
0.89±0.53	BAUBILLIER	82	HBC	–	8.25 $K^-p \to pK_S^0 3\pi$

$\Gamma(K^*(892)\pi\pi\pi)/\Gamma(K\pi)$ — **Γ_3/Γ_1**

VALUE	DOCUMENT ID		TECN	CHG	COMMENT
0.75±0.49	BAUBILLIER	82	HBC	–	8.25 $K^-p \to pK_S^0 3\pi$

$\Gamma(\rho K\pi)/\Gamma(K\pi)$ — **Γ_4/Γ_1**

VALUE	DOCUMENT ID		TECN	CHG	COMMENT
0.58±0.32	BAUBILLIER	82	HBC	–	8.25 $K^-p \to pK_S^0 3\pi$

$\Gamma(\omega K\pi)/\Gamma(K\pi)$ — **Γ_5/Γ_1**

VALUE	DOCUMENT ID		TECN	CHG	COMMENT
0.50±0.30	BAUBILLIER	82	HBC	–	8.25 $K^-p \to pK_S^0 3\pi$

$\Gamma(\phi K\pi)/\Gamma_{total}$ — **Γ_6/Γ**

VALUE	DOCUMENT ID		TECN	COMMENT
0.028±0.014	[9] TORRES	86	MPSF	400 $pA \to 4KX$

$\Gamma(\phi K^*(892))/\Gamma_{total}$ — **Γ_7/Γ**

VALUE	DOCUMENT ID		TECN	COMMENT
0.014±0.007	[9] TORRES	86	MPSF	400 $pA \to 4KX$

[9] Error determination is model dependent.

$K_4^*(2045)$ REFERENCES

ASTON	88	NP B296 493	D. Aston *et al.*	(SLAC, NAGO, CINC, INUS)
ASTON	86	PL B180 308	D. Aston *et al.*	(SLAC, NAGO, CINC, INUS)
TORRES	86	PR 34 707	S. Torres *et al.*	(VPI, ARIZ, FNAL, FSU+)
BAUBILLIER	82	PL 118B 447	M. Baubillier *et al.*	(BIRM, CERN, GLAS+)
CLELAND	82	NP B208 189	W.E. Cleland *et al.*	(DURH, GEVA, LAUS+)
ASTON	81C	PL 106B 235	D. Aston *et al.*	(SLAC, CARL, OTTA) JP
CARMONY	77	PR D16 1251	D.D. Carmony *et al.*	(PURD, UCD, IUPU)

OTHER RELATED PAPERS

BROMBERG	80	PR D22 1513	C.M. Bromberg *et al.*	(CIT, FNAL, ILLC+)
CARMONY	71	PRL 27 1160	D.D. Carmony *et al.*	(PURD, UCD, IUPU)

$K_2(2250)$ $I(J^P) = \frac{1}{2}(2^-)$

OMITTED FROM SUMMARY TABLE

This entry contains various peaks in strange meson systems reported in the 2150–2260 MeV region, as well as enhancements seen in the antihyperon-nucleon system, either in the mass spectra or in the $J^P = 2^-$ wave.

$K_2(2250)$ MASS

VALUE (MeV)	*EVTS*	*DOCUMENT ID*		*TECN*	*CHG*	*COMMENT*
2247±17 OUR AVERAGE						
2200±40		[1] ARMSTRONG	83C	OMEG	–	18 $K^-p \to \Lambda\overline{p}X$
2235±50		[1] BAUBILLIER	81	HBC	–	8 $K^-p \to \Lambda\overline{p}X$
2260±20		[1] CLELAND	81	SPEC	±	50 $K^+p \to \Lambda\overline{p}X$
• • • We do not use the following data for averages, fits, limits, etc. • • •						
2280±20		TIKHOMIROV	03	SPEC		40.0 π^- C $\to K_S^0 K_S^0 K_L^0 X$
2147± 4	37	CHLIAPNIK...	79	HBC	+	32 $K^+p \to \overline{\Lambda}pX$
2240±20	20	LISSAUER	70	HBC		9 K^+p

[1] $J^P = 2^-$ from moments analysis.

$K_2(2250)$ WIDTH

VALUE (MeV)	*EVTS*	*DOCUMENT ID*		*TECN*	*CHG*	*COMMENT*
180±30 OUR AVERAGE		Error includes scale factor of 1.4.				
150±30		[2] ARMSTRONG	83C	OMEG	–	18 $K^-p \to \Lambda\overline{p}X$
210±30		[2] CLELAND	81	SPEC	±	50 $K^+p \to \Lambda\overline{p}X$
• • • We do not use the following data for averages, fits, limits, etc. • • •						
180±60		TIKHOMIROV	03	SPEC		40.0 π^- C $\to K_S^0 K_S^0 K_L^0 X$
~ 200		[2] BAUBILLIER	81	HBC	–	8 $K^-p \to \Lambda\overline{p}X$
~ 40	37	CHLIAPNIK...	79	HBC	+	32 $K^+p \to \overline{\Lambda}pX$
80±20	20	LISSAUER	70	HBC		9 K^+p

[2] $J^P = 2^-$ from moments analysis.

$K_2(2250)$ DECAY MODES

	Mode
Γ_1	$K\pi\pi$
Γ_2	$Kf_2(1270)$
Γ_3	$K^*(892)f_0(980)$
Γ_4	$p\overline{\Lambda}$

$K_2(2250)$ REFERENCES

TIKHOMIROV	03	PAN 66 828 Translated from YAF 66 860.	G.D. Tikhomirov *et al.*	
ARMSTRONG	83C	NP B227 365	T.A. Armstrong *et al.*	(BARI, BIRM, CERN+)
BAUBILLIER	81	NP B183 1	M. Baubillier *et al.*	(BIRM, CERN, GLAS+) JP
CLELAND	81	NP B184 1	W.E. Cleland *et al.*	(PITT, GEVA, LAUS+) JP
CHLIAPNIK...	79	NP B158 253	P.V. Chliapnikov *et al.*	(CERN, BELG, MONS)
LISSAUER	70	NP B18 491	D. Lissauer *et al.*	(LBL)

OTHER RELATED PAPERS

ALEXANDER	68B	PRL 20 755	G. Alexander *et al.*	(LRL)

$K_3(2320)$ $I(J^P) = \frac{1}{2}(3^+)$

OMITTED FROM SUMMARY TABLE

Seen in the $J^P = 3^+$ wave of the antihyperon-nucleon system. Needs confirmation.

$K_3(2320)$ MASS

VALUE (MeV)	*DOCUMENT ID*		*TECN*	*CHG*	*COMMENT*
2324±24 OUR AVERAGE					
2330±40	[1] ARMSTRONG	83C	OMEG	–	18 $K^-p \to \Lambda\overline{p}X$
2320±30	[1] CLELAND	81	SPEC	±	50 $K^+p \to \Lambda\overline{p}X$

[1] $J^P = 3^+$ from moments analysis.

$K_3(2320)$ WIDTH

VALUE (MeV)	*DOCUMENT ID*		*TECN*	*CHG*	*COMMENT*
150±30	[2] ARMSTRONG	83C	OMEG	–	18 $K^-p \to \Lambda\overline{p}X$
• • • We do not use the following data for averages, fits, limits, etc. • • •					
~ 250	[2] CLELAND	81	SPEC	±	50 $K^+p \to \Lambda\overline{p}X$

[2] $J^P = 3^+$ from moments analysis.

$K_3(2320)$ DECAY MODES

	Mode
Γ_1	$p\overline{\Lambda}$

$K_3(2320)$ REFERENCES

ARMSTRONG	83C	NP B227 365	T.A. Armstrong *et al.*	(BARI, BIRM, CERN+)
CLELAND	81	NP B184 1	W.E. Cleland *et al.*	(PITT, GEVA, LAUS+)

$K_5^*(2380)$ $I(J^P) = \frac{1}{2}(5^-)$

OMITTED FROM SUMMARY TABLE

Needs confirmation.

$K_5^*(2380)$ MASS

VALUE (MeV)	*DOCUMENT ID*		*TECN*	*CHG*	*COMMENT*
2382±14±19	[1] ASTON	86	LASS	0	11 $K^-p \to K^-\pi^+n$

[1] From a fit to all the moments.

$K_5^*(2380)$ WIDTH

VALUE (MeV)	*DOCUMENT ID*		*TECN*	*CHG*	*COMMENT*
178±37±32	[2] ASTON	86	LASS	0	11 $K^-p \to K^-\pi^+n$

[2] From a fit to all the moments.

$K_5^*(2380)$ DECAY MODES

	Mode	Fraction (Γ_i/Γ)
Γ_1	$K\pi$	(6.1±1.2) %

$K_5^*(2380)$ BRANCHING RATIOS

$\Gamma(K\pi)/\Gamma_{total}$ Γ_1/Γ

VALUE	*DOCUMENT ID*		*TECN*	*CHG*	*COMMENT*
0.061±0.012	ASTON	88	LASS	0	11 $K^-p \to K^-\pi^+n$

$K_5^*(2380)$ REFERENCES

ASTON	88	NP B296 493	D. Aston *et al.*	(SLAC, NAGO, CINC, INUS)
ASTON	86	PL B180 308	D. Aston *et al.*	(SLAC, NAGO, CINC, INUS)

Meson Particle Listings

$K_5^*(2380)$, $K_4(2500)$, $K(3100)$

$K_4(2500)$

$I(J^P) = \frac{1}{2}(4^-)$

OMITTED FROM SUMMARY TABLE

Needs confirmation.

$K_4(2500)$ MASS

VALUE (MeV)	DOCUMENT ID		TECN	CHG	COMMENT
2490±20	[1] CLELAND	81	SPEC	±	50 $K^+p \to \Lambda\overline{p}$

[1] $J^P = 4^-$ from moments analysis.

$K_4(2500)$ WIDTH

VALUE (MeV)	DOCUMENT ID		TECN	CHG	COMMENT
• • • We do not use the following data for averages, fits, limits, etc. • • •					
~ 250	[2] CLELAND	81	SPEC	±	50 $K^+p \to \Lambda\overline{p}$

[2] $J^P = 4^-$ from moments analysis.

$K_4(2500)$ DECAY MODES

	Mode
Γ_1	$p\overline{\Lambda}$

$K_4(2500)$ REFERENCES

CLELAND 81 NP B184 1 W.E. Cleland *et al.* (PITT, GEVA, LAUS+)

$K(3100)$

$I^G(J^{PC}) = ?^?(?^{??})$

OMITTED FROM SUMMARY TABLE

Narrow peak observed in several ($\Lambda\overline{p}$ + pions) and ($\overline{\Lambda}p$ + pions) states in Σ^- Be reactions by BOURQUIN 86 and in np and nA reactions by ALEEV 93. Not seen by BOEHNLEIN 91. If due to strong decays, this state has exotic quantum numbers (B=0,Q=+1,S=−1 for $\Lambda\overline{p}\pi^+\pi^+$ and $I \geq 3/2$ for $\Lambda\overline{p}\pi^-$). Needs confirmation.

$K(3100)$ MASS

VALUE (MeV)	DOCUMENT ID
≈ 3100 OUR ESTIMATE	

3-BODY DECAYS

VALUE (MeV)	DOCUMENT ID		TECN	COMMENT
3054±11 OUR AVERAGE				
3060± 7±20	[1] ALEEV	93	BIS2	$K(3100) \to \Lambda\overline{p}\pi^+$
3056± 7±20	[1] ALEEV	93	BIS2	$K(3100) \to \overline{\Lambda}p\pi^-$
3055± 8±20	[1] ALEEV	93	BIS2	$K(3100) \to \Lambda\overline{p}\pi^-$
3045± 8±20	[1] ALEEV	93	BIS2	$K(3100) \to \overline{\Lambda}p\pi^+$

4-BODY DECAYS

VALUE (MeV)	DOCUMENT ID		TECN	COMMENT
3059±11 OUR AVERAGE				
3067± 6±20	[1] ALEEV	93	BIS2	$K(3100) \to \Lambda\overline{p}\pi^+\pi^+$
3060± 8±20	[1] ALEEV	93	BIS2	$K(3100) \to \Lambda\overline{p}\pi^+\pi^-$
3055± 7±20	[1] ALEEV	93	BIS2	$K(3100) \to \overline{\Lambda}p\pi^-\pi^-$
3052± 8±20	[1] ALEEV	93	BIS2	$K(3100) \to \overline{\Lambda}p\pi^-\pi^+$
• • • We do not use the following data for averages, fits, limits, etc. • • •				
3105±30	BOURQUIN	86	SPEC	$K(3100) \to \Lambda\overline{p}\pi^+\pi^+$
3115±30	BOURQUIN	86	SPEC	$K(3100) \to \Lambda\overline{p}\pi^+\pi^-$

5-BODY DECAYS

VALUE (MeV)	DOCUMENT ID		TECN	COMMENT
• • • We do not use the following data for averages, fits, limits, etc. • • •				
3095±30	BOURQUIN	86	SPEC	$K(3100) \to \Lambda\overline{p}\pi^+\pi^+\pi^-$

[1] Supersedes ALEEV 90.

$K(3100)$ WIDTH

3-BODY DECAYS

VALUE (MeV)	DOCUMENT ID		TECN	COMMENT
• • • We do not use the following data for averages, fits, limits, etc. • • •				
42±16	[2] ALEEV	93	BIS2	$K(3100) \to \Lambda\overline{p}\pi^+$
36±15	[2] ALEEV	93	BIS2	$K(3100) \to \overline{\Lambda}p\pi^-$
50±18	[2] ALEEV	93	BIS2	$K(3100) \to \Lambda\overline{p}\pi^-$
30±15	[2] ALEEV	93	BIS2	$K(3100) \to \overline{\Lambda}p\pi^+$

4-BODY DECAYS

VALUE (MeV)	CL%	DOCUMENT ID		TECN	COMMENT
• • • We do not use the following data for averages, fits, limits, etc. • • •					
22± 8		[2] ALEEV	93	BIS2	$K(3100) \to \Lambda\overline{p}\pi^+\pi^+$
28±12		[2] ALEEV	93	BIS2	$K(3100) \to \Lambda\overline{p}\pi^+\pi^-$
32±15		[2] ALEEV	93	BIS2	$K(3100) \to \overline{\Lambda}p\pi^-\pi^-$
30±15		[2] ALEEV	93	BIS2	$K(3100) \to \overline{\Lambda}p\pi^-\pi^+$
<30	90	BOURQUIN	86	SPEC	$K(3100) \to \Lambda\overline{p}\pi^+\pi^+$
<80	90	BOURQUIN	86	SPEC	$K(3100) \to \Lambda\overline{p}\pi^+\pi^-$

5-BODY DECAYS

VALUE (MeV)	CL%	DOCUMENT ID	TECN	COMMENT
• • • We do not use the following data for averages, fits, limits, etc. • • •				
<30	90	BOURQUIN	86 SPEC	$K(3100) \to \Lambda\overline{p}\pi^+\pi^+\pi^-$

[2] Supersedes ALEEV 90.

$K(3100)$ DECAY MODES

	Mode
Γ_1	$K(3100)^0 \to \Lambda\overline{p}\pi^+$
Γ_2	$K(3100)^{--} \to \Lambda\overline{p}\pi^-$
Γ_3	$K(3100)^- \to \Lambda\overline{p}\pi^+\pi^-$
Γ_4	$K(3100)^+ \to \Lambda\overline{p}\pi^+\pi^+$
Γ_5	$K(3100)^0 \to \Lambda\overline{p}\pi^+\pi^+\pi^-$
Γ_6	$K(3100)^0 \to \Sigma(1385)^+\overline{p}$

$\Gamma(\Sigma(1385)^+\overline{p})/\Gamma(\Lambda\overline{p}\pi^+)$ **Γ_6/Γ_1**

VALUE	CL%	DOCUMENT ID		TECN	COMMENT
<0.04	90	ALEEV	93	BIS2	$K(3100)^0 \to \Sigma(1385)^+\overline{p}$

$K(3100)$ REFERENCES

ALEEV 93 PAN 56 1358 A.N. Aleev *et al.* (BIS-2 Collab.)
Translated from YAF 56 100.
BOEHNLEIN 91 NPBPS B21 174 A. Boehnlein *et al.* (FLOR, BNL, IND+)
ALEEV 90 ZPHY C47 533 A.N. Aleev *et al.* (BIS-2 Collab.)
BOURQUIN 86 PL B172 113 M.H. Bourquin *et al.* (GEVA, RAL, HEIDP+)

CHARMED MESONS ($C = \pm 1$)

$D^+ = c\overline{d}$, $D^0 = c\overline{u}$, $\overline{D}^0 = \overline{c}u$, $D^- = \overline{c}d$, similarly for D^*'s

$D^{\pm}$

$I(J^P) = \frac{1}{2}(0^-)$

$D^{\pm}$ MASS

The fit includes $D^{\pm}$, D^0, $D_s^{\pm}$, $D^{*\pm}$, D^{*0}, and $D_s^{*\pm}$ mass and mass difference measurements.

VALUE (MeV)	EVTS	DOCUMENT ID		TECN	COMMENT
1869.4 ± 0.5 OUR FIT	Error includes scale factor of 1.1.				
1869.4 ± 0.5 OUR AVERAGE					
1870.0 ± 0.5 ± 1.0	317	BARLAG	90C	ACCM	π^- Cu 230 GeV
1863 ± 4		DERRICK	84	HRS	e^+e^- 29 GeV
1869.4 ± 0.6	[1]	TRILLING	81	RVUE	e^+e^- 3.77 GeV
• • • We do not use the following data for averages, fits, limits, etc. • • •					
1875 ± 10	9	ADAMOVICH	87	EMUL	Photoproduction
1860 ± 16	6	ADAMOVICH	84	EMUL	Photoproduction
1868.4 ± 0.5	[1]	SCHINDLER	81	MRK2	e^+e^- 3.77 GeV
1874 ± 5		GOLDHABER	77	MRK1	D^0, D^+ recoil spectra
1868.3 ± 0.9	[1]	PERUZZI	77	MRK1	e^+e^- 3.77 GeV
1874 ± 11		PICCOLO	77	MRK1	e^+e^- 4.03, 4.41 GeV
1876 ± 15	50	PERUZZI	76	MRK1	$K^{\mp}\pi^{\pm}\pi^{\pm}$

[1] PERUZZI 77 and SCHINDLER 81 errors do not include the 0.13% uncertainty in the absolute SPEAR energy calibration. TRILLING 81 uses the high precision $J/\psi(1S)$ and $\psi(2S)$ measurements of ZHOLENTZ 80 to determine this uncertainty and combines the PERUZZI 77 and SCHINDLER 81 results to obtain the value quoted.

$D^{\pm}$ MEAN LIFE

Measurements with an error $> 100 \times 10^{-15}$ s have been omitted from the Listings.

VALUE (10^{-15} s)	EVTS	DOCUMENT ID		TECN	COMMENT
1040 ± 7 OUR AVERAGE					
1039.4 ± 4.3 ± 7.0	110k	LINK	02F	FOCS	γ nucleus, ≈ 180 GeV
1033.6 ± 22.1 $^{+\ 9.9}_{-12.7}$	3777	BONVICINI	99	CLE2	$e^+e^- \approx \Upsilon(4S)$
1048 ± 15 ± 11	9k	FRABETTI	94D	E687	$D^+ \to K^-\pi^+\pi^+$
• • • We do not use the following data for averages, fits, limits, etc. • • •					
1075 ± 40 ± 18	2455	FRABETTI	91	E687	γ Be, $D^+ \to K^-\pi^+\pi^+$
1030 ± 80 ± 60	200	ALVAREZ	90	NA14	γ, $D^+ \to K^-\pi^+\pi^+$
1050 $^{+\ 77}_{-\ 72}$	317	[2] BARLAG	90C	ACCM	π^- Cu 230 GeV
1050 ± 80 ± 70	363	ALBRECHT	88I	ARG	e^+e^- 10 GeV
1090 ± 30 ± 25	2992	RAAB	88	E691	Photoproduction

[2] BARLAG 90C estimates the systematic error to be negligible.

D^+ DECAY MODES

D^- modes are charge conjugates of the modes below.

	Mode	Fraction (Γ_i/Γ)		Scale factor/ Confidence level
	Inclusive modes			
Γ_1	e^+ anything	(17.2 ± 1.9)	%	
Γ_2	K^- anything	(27.5 ± 2.4)	%	
Γ_3	$\overline{K}^0$ anything + K^0 anything	(61 ± 8)	%	
Γ_4	K^+ anything	(5.5 ± 1.6)	%	
Γ_5	η anything	[a] < 13	%	CL=90%
Γ_6	ϕ anything	< 1.8	%	CL=90%
Γ_7	ϕe^+ anything	< 1.6	%	CL=90%
Γ_8	μ^+ anything			
	Leptonic and semileptonic modes			
Γ_9	$\mu^+\nu_\mu$	(8 $^{+17}_{-\ 5}$) $\times 10^{-4}$		
Γ_{10}	$\overline{K}^0\ell^+\nu_\ell$	[b] (6.8 ± 0.8)	%	
Γ_{11}	$\overline{K}^0 e^+\nu_e$	(6.7 ± 0.9)	%	
Γ_{12}	$\overline{K}^0\mu^+\nu_\mu$	(7.0 $^{+\ 3.0}_{-\ 2.0}$)	%	
Γ_{13}	$K^-\pi^+e^+\nu_e$	(4.5 $^{+\ 1.0}_{-\ 0.8}$)	%	S=1.1
Γ_{14}	$\overline{K}^*(892)^0 e^+\nu_e$ $\times$ B($\overline{K}^*(892)^0 \to K^-\pi^+$)	(3.7 ± 0.5)	%	
Γ_{15}	$K^-\pi^+e^+\nu_e$ nonresonant	< 7	$\times 10^{-3}$	CL=90%
Γ_{16}	$K^-\pi^+\mu^+\nu_\mu$	(4.00 ± 0.32)	%	
	In the fit as $\frac{2}{3}\Gamma_{28} + \Gamma_{18}$, where $\frac{2}{3}\Gamma_{28} = \Gamma_{17}$.			
Γ_{17}	$\overline{K}^*(892)^0\mu^+\nu_\mu$ $\times$ B($\overline{K}^*(892)^0 \to K^-\pi^+$)	(3.7 ± 0.3)	%	
Γ_{18}	$K^-\pi^+\mu^+\nu_\mu$ nonresonant	(3.3 ± 1.3)	$\times 10^{-3}$	
Γ_{19}	$\overline{K}^0\pi^+\pi^-e^+\nu_e$			
Γ_{20}	$K^-\pi^+\pi^0e^+\nu_e$			
Γ_{21}	$(\overline{K}^*(892)\pi)^0 e^+\nu_e$	< 1.2	%	CL=90%
Γ_{22}	$(\overline{K}\pi\pi)^0 e^+\nu_e$ non-$\overline{K}^*(892)$	< 9	$\times 10^{-3}$	CL=90%
Γ_{23}	$K^-\pi^+\pi^0\mu^+\nu_\mu$	< 1.7	$\times 10^{-3}$	CL=90%
Γ_{24}	$\pi^0\ell^+\nu_\ell$	[c] (3.1 ± 1.5)	$\times 10^{-3}$	
Γ_{25}	$\pi^+\pi^-e^+\nu_e$			
	Fractions of some of the following modes with resonances have already appeared above as submodes of particular charged-particle modes.			
Γ_{26}	$\overline{K}^*(892)^0\ell^+\nu_\ell$	[b] (5.73 ± 0.35)	%	
Γ_{27}	$\overline{K}^*(892)^0 e^+\nu_e$	(5.5 ± 0.7)	%	S=1.4
Γ_{28}	$\overline{K}^*(892)^0\mu^+\nu_\mu$	(5.5 ± 0.4)	%	
Γ_{29}	$\overline{K}_1(1270)^0\mu^+\nu_\mu$	< 4	%	CL=95%
Γ_{30}	$\overline{K}^*(1410)^0\mu^+\nu_\mu$			
Γ_{31}	$\overline{K}^*_2(1430)^0\mu^+\nu_\mu$	< 1.0	%	CL=95%
Γ_{32}	$\rho^0 e^+\nu_e$	(2.5 ± 1.0)	$\times 10^{-3}$	
Γ_{33}	$\rho^0\mu^+\nu_\mu$	(3.4 ± 0.8)	$\times 10^{-3}$	
Γ_{34}	$\phi e^+\nu_e$	< 2.09	%	CL=90%
Γ_{35}	$\phi\mu^+\nu_\mu$	< 3.72	%	CL=90%
Γ_{36}	$\eta\ell^+\nu_\ell$	< 5	$\times 10^{-3}$	CL=90%
Γ_{37}	$\eta'(958)\mu^+\nu_\mu$	< 1.1	%	CL=90%
	Hadronic modes with a $\overline{K}$ or $\overline{K}K\overline{K}$			
Γ_{38}	$\overline{K}^0\pi^+$	(2.82 ± 0.19)	%	
Γ_{39}	$K^-\pi^+\pi^+$	[d] (9.2 ± 0.6)	%	
Γ_{40}	$K_0^*(800)^0\pi^+$			
Γ_{41}	$\overline{K}^*(892)^0\pi^+$ $\times$ B($\overline{K}^*(892)^0 \to K^-\pi^+$)	(1.30 ± 0.13)	%	
Γ_{42}	$\overline{K}_0^*(1430)^0\pi^+$ $\times$ B($\overline{K}_0^*(1430)^0 \to K^-\pi^+$)	(2.3 ± 0.3)	%	
Γ_{43}	$\overline{K}^*_2(1430)^0\pi^+$ $\times$ B($\overline{K}^*_2(1430)^0 \to K^-\pi^+$)			
Γ_{44}	$\overline{K}^*(1680)^0\pi^+$ $\times$ B($\overline{K}^*(1680)^0 \to K^-\pi^+$)	(3.8 ± 0.8)	$\times 10^{-3}$	
Γ_{45}	$K^-\pi^+\pi^+$ nonresonant	(8.8 ± 0.9)	%	
Γ_{46}	$\overline{K}^0\pi^+\pi^0$	[d] (9.7 ± 3.0)	%	S=1.1
Γ_{47}	$\overline{K}^0\rho^+$	(6.6 ± 2.5)	%	
Γ_{48}	$\overline{K}^*(892)^0\pi^+$ $\times$ B($\overline{K}^*(892)^0 \to \overline{K}^0\pi^0$)	(6.5 ± 0.6)	$\times 10^{-3}$	
Γ_{49}	$\overline{K}^0\pi^+\pi^0$ nonresonant	(1.3 ± 1.1)	%	
Γ_{50}	$K^-\pi^+\pi^+\pi^0$	[d] (6.5 ± 1.1)	%	
Γ_{51}	$\overline{K}^*(892)^0\rho^+$ total $\times$ B($\overline{K}^*(892)^0 \to K^-\pi^+$)	(1.4 ± 0.9)	%	
Γ_{52}	$\overline{K}_1(1400)^0\pi^+$ $\times$ B($\overline{K}_1(1400)^0 \to K^-\pi^+\pi^0$)	(2.2 ± 0.6)	%	
Γ_{53}	$K^-\rho^+\pi^+$ total	(3.1 ± 1.1)	%	
Γ_{54}	$K^-\rho^+\pi^+$ 3-body	(1.1 ± 0.4)	%	
Γ_{55}	$\overline{K}^*(892)^0\pi^+\pi^0$ total $\times$ B($\overline{K}^*(892)^0 \to K^-\pi^+$)	(4.5 ± 0.9)	%	
Γ_{56}	$\overline{K}^*(892)^0\pi^+\pi^0$ 3-body $\times$ B($\overline{K}^*(892)^0 \to K^-\pi^+$)	(2.9 ± 0.9)	%	
Γ_{57}	$K^*(892)^-\pi^+\pi^+$ 3-body $\times$ B($K^*(892)^- \to K^-\pi^0$)	(7 ± 3)	$\times 10^{-3}$	
Γ_{58}	$K^-\pi^+\pi^+\pi^0$ nonresonant	[e] (1.2 ± 0.6)	%	
Γ_{59}	$\overline{K}^0\pi^+\pi^+\pi^-$	[d] (7.1 ± 1.0)	%	
Γ_{60}	$\overline{K}^0 a_1(1260)^+$ $\times$ B($a_1(1260)^+ \to \pi^+\pi^+\pi^-$)	(4.0 ± 0.9)	%	
Γ_{61}	$\overline{K}_1(1400)^0\pi^+$ $\times$ B($\overline{K}_1(1400)^0 \to \overline{K}^0\pi^+\pi^-$)	(2.2 ± 0.6)	%	
Γ_{62}	$K^*(892)^-\pi^+\pi^+$ 3-body $\times$ B($K^*(892)^- \to \overline{K}^0\pi^-$)	(1.4 ± 0.6)	%	
Γ_{63}	$\overline{K}^0\rho^0\pi^+$ total	(4.3 ± 0.9)	%	
Γ_{64}	$\overline{K}^0\rho^0\pi^+$ 3-body	(5 ± 5)	$\times 10^{-3}$	
Γ_{65}	$\overline{K}^0\pi^+\pi^+\pi^-$ nonresonant	(9 ± 4)	$\times 10^{-3}$	
Γ_{66}	$K^-3\pi^+\pi^-$	[d] (6.2 ± 0.8)	$\times 10^{-3}$	S=1.3
Γ_{67}	$\overline{K}^*(892)^0\pi^+\pi^+\pi^-$ $\times$ B($\overline{K}^*(892)^0 \to K^-\pi^+$)	(2.1 ± 0.8)	$\times 10^{-3}$	

Meson Particle Listings

$D^{\pm}$

Γ_{68}	$\overline{K}^*(892)^0\rho^0\pi^+$ × B($\overline{K}^*(892)^0 \to K^-\pi^+$)	(2.0 ± 0.5) × 10^{-3}		
Γ_{69}	$\overline{K}^*(892)^0\pi^+\pi^+\pi^-$ no-ρ × B($\overline{K}^*(892)^0 \to K^-\pi^+$)	(2.9 ± 1.1) × 10^{-3}		
Γ_{70}	$K^-\rho^0\pi^+\pi^+$	(1.94 ± 0.35) × 10^{-3}		S=1.1
Γ_{71}	$K^-3\pi^+\pi^-$ nonresonant	(4.3 ± 3.2) × 10^{-4}		
Γ_{72}	$K^-2\pi^+2\pi^0$			
Γ_{73}	$\overline{K}^0 2\pi^+\pi^-\pi^0$			
Γ_{74}	$\overline{K}^0 3\pi^+2\pi^-$			
Γ_{75}	$K^-3\pi^+\pi^-\pi^0$			
Γ_{76}	$\overline{K}^0\overline{K}^0K^+$	(1.8 ± 0.8) %		
Γ_{77}	$K^+K^-\overline{K}^0\pi^+$	(5.5 ± 1.4) × 10^{-4}		

Fractions of some of the following modes with resonances have already appeared above as submodes of particular charged-particle modes.

Γ_{78}	$\overline{K}^0\rho^+$	(6.6 ± 2.5) %		
Γ_{79}	$\overline{K}^0 a_1(1260)^+$	(8.2 ± 1.7) %		
Γ_{80}	$\overline{K}^0 a_2(1320)^+$	< 3 × 10^{-3}		CL=90%
Γ_{81}	$K_0^*(800)^0\pi^+$			
Γ_{82}	$\overline{K}^*(892)^0\pi^+$	(1.95 ± 0.19) %		
Γ_{83}	$\overline{K}^*(892)^0\rho^+$ total	(2.1 ± 1.4) %	[e]	
Γ_{84}	$\overline{K}^*(892)^0\rho^+$ S-wave	(1.7 ± 1.6) %	[e]	
Γ_{85}	$\overline{K}^*(892)^0\rho^+$ P-wave	< 1 × 10^{-3}		CL=90%
Γ_{86}	$\overline{K}^*(892)^0\rho^+$ D-wave	(10 ± 7) × 10^{-3}		
Γ_{87}	$\overline{K}^*(892)^0\rho^+$ D-wave longitudinal	< 7 × 10^{-3}		CL=90%
Γ_{88}	$\overline{K}_1(1270)^0\pi^+$	< 7 × 10^{-3}		CL=90%
Γ_{89}	$\overline{K}_1(1400)^0\pi^+$	(5.0 ± 1.3) %		
Γ_{90}	$\overline{K}^*(1410)^0\pi^+$			
Γ_{91}	$\overline{K}_0^*(1430)^0\pi^+$	(3.8 ± 0.4) %		
Γ_{92}	$\overline{K}_2^*(1430)^0\pi^+$			
Γ_{93}	$\overline{K}^*(1680)^0\pi^+$	(1.47 ± 0.31) %		
Γ_{94}	$\overline{K}^*(892)^0\pi^+\pi^0$ total	(6.8 ± 1.4) %		
Γ_{95}	$\overline{K}^*(892)^0\pi^+\pi^0$ 3-body	(4.3 ± 1.4) %	[e]	
Γ_{96}	$K^*(892)^-\pi^+\pi^+$ total	—		
Γ_{97}	$K^*(892)^-\pi^+\pi^+$ 3-body	(2.1 ± 0.9) %		
Γ_{98}	$K^-\rho^+\pi^+$ total	(3.1 ± 1.1) %		
Γ_{99}	$K^-\rho^+\pi^+$ 3-body	(1.1 ± 0.4) %		
Γ_{100}	$\overline{K}^0\rho^0\pi^+$ total	(4.3 ± 0.9) %		CL=90%
Γ_{101}	$\overline{K}^0\rho^0\pi^+$ 3-body	(5 ± 5) × 10^{-3}		
Γ_{102}	$\overline{K}^0 f_0(980)\pi^+$			
Γ_{103}	$\overline{K}^*(892)^0\pi^+\pi^+\pi^-$	(3.2 ± 1.2) × 10^{-3}		S=2.0
Γ_{104}	$\overline{K}^*(892)^0\rho^0\pi^+$	(3.0 ± 0.7) × 10^{-3}		S=1.3
Γ_{105}	$\overline{K}^*(892)^0\pi^+\pi^+\pi^-$ no-ρ	(4.4 ± 1.7) × 10^{-3}		
Γ_{106}	$K^-\rho^0\pi^+\pi^+$	(1.94 ± 0.35) × 10^{-3}		
Γ_{107}	$\overline{K}^*(892)^0 a_1(1260)^+$	(9.1 ± 1.9) × 10^{-3}		

Pionic modes

Γ_{108}	$\pi^+\pi^0$	(2.6 ± 0.7) × 10^{-3}		
Γ_{109}	$\pi^+\pi^+\pi^-$	(3.1 ± 0.4) × 10^{-3}		
Γ_{110}	$\sigma\pi^+$	(2.2 ± 0.5) × 10^{-3}		
Γ_{111}	$\rho^0\pi^+$	(1.05 ± 0.18) × 10^{-3}		
Γ_{112}	$f_0(980)\pi^+$ × B($f_0 \to \pi^+\pi^-$)	(1.9 ± 0.5) × 10^{-4}	[f]	
Γ_{113}	$f_2(1270)\pi^+$ × B($f_2 \to \pi^+\pi^-$)	(6.1 ± 1.1) × 10^{-4}		
Γ_{114}	$f_0(1370)\pi^+$ × B($f_0(1370) \to \pi^+\pi^-$)			
Γ_{115}	$\rho(1450)^0\pi^+$ × B($\rho(1450)^0 \to \pi^+\pi^-$)			
Γ_{116}	$\pi^+\pi^+\pi^-$ nonresonant	(2.4 ± 2.1) × 10^{-4}		
Γ_{117}	$\pi^+\pi^+\pi^-\pi^0$	—		
Γ_{118}	$\eta\pi^+$ × B($\eta \to \pi^+\pi^-\pi^0$)	(6.8 ± 1.4) × 10^{-4}		
Γ_{119}	$\omega\pi^+$ × B($\omega \to \pi^+\pi^-\pi^0$)	< 6 × 10^{-3}		CL=90%
Γ_{120}	$3\pi^+2\pi^-$	(1.82 ± 0.25) × 10^{-3}		S=1.2
Γ_{121}	$3\pi^+2\pi^-\pi^0$			

Fractions of some of the following modes with resonances have already appeared above as submodes of particular charged-particle modes.

Γ_{122}	$\eta\pi^+$	(3.0 ± 0.6) × 10^{-3}		
Γ_{123}	$\rho^0\pi^+$	(1.05 ± 0.18) × 10^{-3}		
Γ_{124}	$\omega\pi^+$	< 7 × 10^{-3}		CL=90%
Γ_{125}	$\eta\rho^+$	< 7 × 10^{-3}		CL=90%
Γ_{126}	$\eta'(958)\pi^+$	(5.1 ± 1.0) × 10^{-3}		
Γ_{127}	$\eta'(958)\rho^+$	< 5 × 10^{-3}		CL=90%
Γ_{128}	$f_2(1270)\pi^+$	(1.08 ± 0.20) × 10^{-3}		

Hadronic modes with a $K\overline{K}$ pair

Γ_{129}	$K^+\overline{K}^0$	(5.9 ± 0.6) × 10^{-3}		S=1.2
Γ_{130}	$K^+K^-\pi^+$	(8.9 ± 0.8) × 10^{-3}	[d]	
Γ_{131}	$\phi\pi^+$ × B($\phi \to K^+K^-$)	(3.1 ± 0.3) × 10^{-3}		
Γ_{132}	$K^+\overline{K}^*(892)^0$ × B($\overline{K}^{*0} \to K^-\pi^+$)	(2.9 ± 0.4) × 10^{-3}		
Γ_{133}	$K^+K^-\pi^+$ nonresonant	(4.6 ± 0.9) × 10^{-3}		
Γ_{134}	$K^0\overline{K}^0\pi^+$	—		
Γ_{135}	$K^*(892)^+\overline{K}^0$ × B($K^{*+} \to K^0\pi^+$)	(2.1 ± 0.9) %		
Γ_{136}	$K^+K^-\pi^+\pi^0$	—		
Γ_{137}	$\phi\pi^+\pi^0$ × B($\phi \to K^+K^-$)	(1.1 ± 0.5) %		
Γ_{138}	$\phi\rho^+$ × B($\phi \to K^+K^-$)	< 7 × 10^{-3}		CL=90%
Γ_{139}	$K^+K^-\pi^+\pi^0$ non-ϕ	(1.5 $^{+\ 0.7}_{-\ 0.6}$) %		
Γ_{140}	$K^+\overline{K}^0\pi^+\pi^-$	(4.0 ± 0.7) × 10^{-3}		
Γ_{141}	$K^0K^-\pi^+\pi^+$	(5.5 ± 0.8) × 10^{-3}		
Γ_{142}	$K^*(892)^+\overline{K}^*(892)^0$ × B^2($K^*(892)^+ \to K^0\pi^+$)	(1.2 ± 0.5) %		
Γ_{143}	$K^0K^-\pi^+\pi^+$ (non-$K^{*+}\overline{K}^{*0}$)	< 7.9 × 10^{-3}		CL=90%
Γ_{144}	$K^+K^-\pi^+\pi^+\pi^-$	(2.5 ± 1.3) × 10^{-4}		
Γ_{145}	$K^+K^-\pi^+\pi^+\pi^-$ nonresonant			

Fractions of the following modes with resonances have already appeared above as submodes of particular charged-particle modes.

Γ_{146}	$\phi\pi^+$	(6.2 ± 0.6) × 10^{-3}		
Γ_{147}	$\phi\pi^+\pi^0$	(2.3 ± 1.0) %		
Γ_{148}	$\phi\rho^+$	< 1.5 %		CL=90%
Γ_{149}	$\phi\pi^+\pi^+\pi^-$			
Γ_{150}	$K^+\overline{K}^*(892)^0$	(4.3 ± 0.6) × 10^{-3}		
Γ_{151}	$K^*(892)^+\overline{K}^0$	(3.1 ± 1.4) %		
Γ_{152}	$K^*(892)^+\overline{K}^*(892)^0$	(2.6 ± 1.1) %		

Doubly Cabibbo suppressed (DC) modes, $\Delta C = 1$ weak neutral current ($C1$) modes, or Lepton Family number (LF) or Lepton number (L) violating modes

Γ_{153}	$K^+\pi^+\pi^-$	DC	(7.0 ± 1.5) × 10^{-4}		
Γ_{154}	$K^+\rho^0$	DC	(2.6 ± 1.2) × 10^{-4}		
Γ_{155}	$K^*(892)^0\pi^+$	DC	(3.7 ± 1.7) × 10^{-4}	[g]	
Γ_{156}	$K^+\pi^+\pi^-$ nonresonant	DC	(2.5 ± 1.2) × 10^{-4}		
Γ_{157}	$K^+K^+K^-$	DC	(8.7 ± 2.1) × 10^{-5}		
Γ_{158}	ϕK^+	DC	< 1.3 × 10^{-4}	[g]	CL=90%
Γ_{159}	$\pi^+e^+e^-$	$C1$	< 5.2 × 10^{-5}		CL=90%
Γ_{160}	$\pi^+\mu^+\mu^-$	$C1$	< 8.8 × 10^{-6}		CL=90%
Γ_{161}	$\rho^+\mu^+\mu^-$	$C1$	< 5.6 × 10^{-4}		CL=90%
Γ_{162}	$K^+e^+e^-$		< 2.0 × 10^{-4}	[h]	CL=90%
Γ_{163}	$K^+\mu^+\mu^-$		< 9.2 × 10^{-6}	[h]	CL=90%
Γ_{164}	$\pi^+e^\pm\mu^\mp$	LF	< 3.4 × 10^{-5}		CL=90%
Γ_{165}	$\pi^+e^+\mu^-$				
Γ_{166}	$\pi^+e^-\mu^+$				
Γ_{167}	$K^+e^\pm\mu^\mp$	LF	< 6.8 × 10^{-5}	[i]	CL=90%
Γ_{168}	$K^+e^+\mu^-$				
Γ_{169}	$K^+e^-\mu^+$				
Γ_{170}	$\pi^-e^+e^+$	L	< 9.6 × 10^{-5}		CL=90%
Γ_{171}	$\pi^-\mu^+\mu^+$	L	< 4.8 × 10^{-6}		CL=90%
Γ_{172}	$\pi^-e^+\mu^+$	L	< 5.0 × 10^{-5}		CL=90%
Γ_{173}	$\rho^-\mu^+\mu^+$	L	< 5.6 × 10^{-4}		CL=90%
Γ_{174}	$K^-e^+e^+$	L	< 1.2 × 10^{-4}		CL=90%
Γ_{175}	$K^-\mu^+\mu^+$	L	< 1.3 × 10^{-5}		CL=90%
Γ_{176}	$K^-e^+\mu^+$	L	< 1.3 × 10^{-4}		CL=90%
Γ_{177}	$K^*(892)^-\mu^+\mu^+$	L	< 8.5 × 10^{-4}		CL=90%

Γ_{178} A dummy mode used by the fit. (31 ± 5) %

[a] This is a weighted average of $D^{\pm}$ (44%) and D^0 (56%) branching fractions. See "D^+ and $D^0 \to$ (η anything) / (total D^+ and D^0)" under "D^+ Branching Ratios" in these Particle Listings.

[b] This value averages the e^+ and μ^+ branching fractions, after making a small phase-space adjustment to the μ^+ fraction to be able to use it as an e^+ fraction; hence our ℓ^+ here is really an e^+.

[c] An ℓ indicates an e or a μ mode, not a sum over these modes.

[d] The branching fraction for this mode may differ from the sum of the submodes that contribute to it, due to interference effects. See the relevant papers.

[e] The two experiments measuring this fraction are in serious disagreement. See the Particle Listings.

[f] This value includes only $\pi^+\pi^-$ decays of the intermediate resonance, because branching fractions of this resonance are not known.

[g] Unseen decay modes of the resonance are included.

[h] This mode is not a useful test for a $\Delta C=1$ weak neutral current because both quarks must change flavor in this decay.

[i] The value is for the sum of the charge states or particle/antiparticle states indicated.

CONSTRAINED FIT INFORMATION

An overall fit to 33 branching ratios uses 58 measurements and one constraint to determine 20 parameters. The overall fit has a $\chi^2 = 47.9$ for 39 degrees of freedom.

The following *off-diagonal* array elements are the correlation coefficients $\langle \delta x_i \delta x_j \rangle / (\delta x_i \cdot \delta x_j)$, in percent, from the fit to the branching fractions, $x_i \equiv \Gamma_i/\Gamma_{\rm total}$. The fit constrains the x_i whose labels appear in this array to sum to one.

x_{13}	6									
x_{18}	6	2								
x_{27}	17	33	7							
x_{28}	33	13	19	39						
x_{38}	38	14	16	42	85					
x_{39}	38	15	17	44	88	96				
x_{46}	0	0	0	0	0	0	0			
x_{50}	9	3	4	10	20	22	23	0		
x_{59}	11	4	5	13	27	29	30	0	18	
x_{66}	19	8	9	22	45	49	51	0	12	15
x_{70}	13	5	6	15	31	34	35	0	8	11
x_{82}	25	10	11	29	58	63	66	0	15	20
x_{89}	6	2	3	7	14	15	16	0	31	37
x_{97}	3	1	1	4	8	8	9	0	29	13
x_{103}	7	3	3	8	16	18	19	0	4	6
x_{104}	9	4	4	11	22	24	25	0	6	8
x_{120}	18	7	8	21	42	46	48	0	11	14
x_{129}	23	9	10	27	54	60	62	0	14	19
x_{178}	−37	−30	−12	−42	−53	−56	−58	−57	−46	−46
	x_{11}	x_{13}	x_{18}	x_{27}	x_{28}	x_{38}	x_{39}	x_{46}	x_{50}	x_{59}

x_{70}	68								
x_{82}	34	23							
x_{89}	8	5	10						
x_{97}	4	3	6	12					
x_{103}	28	19	12	3	2				
x_{104}	34	23	16	4	2	56			
x_{120}	88	60	31	7	4	25	30		
x_{129}	31	21	40	10	5	11	15	29	
x_{178}	−32	−22	−40	−46	−32	−14	−17	−30	−36
	x_{66}	x_{70}	x_{82}	x_{89}	x_{97}	x_{103}	x_{104}	x_{120}	x_{129}

D^+ BRANCHING RATIOS

See the "Note on D Mesons" above. Some now-obsolete measurements have been omitted from these Listings.

c-quark decays

$\Gamma(c \to e^+ \text{anything})/\Gamma(c \to \text{anything})$

We only put the average of e^+ and μ^+ measurements from $Z^0 \to c\overline{c}$ decays in the Summary Table; see the second data block below.

VALUE	EVTS	DOCUMENT ID		TECN	COMMENT
$0.103 \pm 0.009^{+0.009}_{-0.008}$	378	[3] ABBIENDI	99K	OPAL	$Z^0 \to c\overline{c}$

[3] ABBIENDI 99K uses the excess of right-sign over wrong-sign leptons opposite reconstructed $D^*(2010)^+ \to D^0\pi^+$ decays in $Z^0 \to c\overline{c}$.

$\Gamma(c \to \mu^+ \text{anything})/\Gamma(c \to \text{anything})$

We only put the average of e^+ and μ^+ measurements from $Z^0 \to c\overline{c}$ decays in the Summary Table; see the next data block.

VALUE	EVTS	DOCUMENT ID		TECN	COMMENT
0.088 ± 0.005 OUR AVERAGE					
$0.093 \pm 0.009 \pm 0.009$	88	KAYIS-TOPAK.	02	CHRS	ν_μ emulsion
$0.095 \pm 0.007^{+0.014}_{-0.013}$	2829	ASTIER	00D	NOMD	ν_μ Fe $\to \mu^-\mu^+$X
$0.090 \pm 0.007^{+0.007}_{-0.006}$	476	[4] ABBIENDI	99K	OPAL	$Z^0 \to c\overline{c}$
$0.086 \pm 0.017^{+0.008}_{-0.007}$	69	[5] ALBRECHT	92F	ARG	$e^+e^- \approx 10$ GeV
$0.078 \pm 0.009 \pm 0.012$		ONG	88	MRK2	e^+e^- 29 GeV
$0.078 \pm 0.015 \pm 0.02$		BARTEL	87	JADE	e^+e^- 34.6 GeV
$0.082 \pm 0.012^{+0.02}_{-0.01}$		ALTHOFF	84G	TASS	e^+e^- 34.5 GeV
• • • We do not use the following data for averages, fits, limits, etc. • • •					
$0.089 \pm 0.018 \pm 0.025$		BARTEL	85J	JADE	See BARTEL 87

[4] ABBIENDI 99K uses the excess of right-sign over wrong-sign leptons opposite reconstructed $D^*(2010)^+ \to D^0\pi^+$ decays in $Z^0 \to c\overline{c}$.

[5] ALBRECHT 92F uses the excess of right-sign over wrong-sign leptons in a sample of events tagged by fully reconstructed $D^*(2010)^+ \to D^0\pi^+$ decays.

$\Gamma(c \to \ell^+ \text{anything})/\Gamma(c \to \text{anything})$

This is an average (not a sum) of e^+ and μ^+ measurements.

VALUE	EVTS	DOCUMENT ID		TECN	COMMENT
0.096 ± 0.004 OUR AVERAGE					
$0.0958 \pm 0.0042 \pm 0.0028$	1828	[6] ABREU	00O	DLPH	$Z^0 \to c\overline{c}$
$0.095 \pm 0.006^{+0.007}_{-0.006}$	854	[7] ABBIENDI	99K	OPAL	$Z^0 \to c\overline{c}$

[6] ABREU 00O uses leptons opposite fully reconstructed $D^*(2010)^+$, D^+, or D^0 mesons.

[7] ABBIENDI 99K uses the excess of right-sign over wrong-sign leptons opposite reconstructed $D^*(2010)^+ \to D^0\pi^+$ decays in $Z^0 \to c\overline{c}$.

$\Gamma(c \to D^*(2010)^+ \text{anything})/\Gamma(c \to \text{anything})$

VALUE	EVTS	DOCUMENT ID		TECN	COMMENT
$0.255 \pm 0.015 \pm 0.008$	2371	[8] ABREU	00O	DLPH	$Z^0 \to c\overline{c}$

[8] ABREU 00O uses slow pions opposite fully reconstructed $D^*(2010)^+$, D^+, or D^0 mesons as a signal of $D^*(2010)^-$ production.

Inclusive modes

$\Gamma(e^+ \text{anything})/\Gamma_{\rm total}$ Γ_1/Γ

VALUE	EVTS	DOCUMENT ID		TECN	COMMENT
0.172 ± 0.019 OUR AVERAGE					
$0.20\ ^{+0.09}_{-0.07}$		AGUILAR-...	87E	HYBR	πp, pp 360, 400 GeV
$0.170 \pm 0.019 \pm 0.007$	158	BALTRUSAIT...	85B	MRK3	e^+e^- 3.77 GeV
0.168 ± 0.064	23	SCHINDLER	81	MRK2	e^+e^- 3.771 GeV
• • • We do not use the following data for averages, fits, limits, etc. • • •					
$0.220^{+0.044}_{-0.022}$		BACINO	80	DLCO	e^+e^- 3.77 GeV

D^+ and $D^0 \to (e^+ \text{anything})$ / (total D^+ and D^0)

If measured at the $\psi(3770)$, this quantity is a weighted average of D^+ (44%) and D^0 (56%) branching fractions. Only experiments at $E_{\rm cm} = 3.77$ GeV are included in the average here. We don't put this result in the Summary Table.

VALUE	EVTS	DOCUMENT ID		TECN	COMMENT
0.110 ± 0.011 OUR AVERAGE		Error includes scale factor of 1.1.			
0.117 ± 0.011	295	BALTRUSAIT...	85B	MRK3	e^+e^- 3.77 GeV
0.10 ± 0.032		[9] SCHINDLER	81	MRK2	e^+e^- 3.771 GeV
0.072 ± 0.028		FELLER	78	MRK1	e^+e^- 3.772 GeV
• • • We do not use the following data for averages, fits, limits, etc. • • •					
$0.096 \pm 0.004 \pm 0.011$	2207	[10] ALBRECHT	96C	ARG	$e^+e^- \approx 10$ GeV
$0.134 \pm 0.015 \pm 0.010$		[11] ABE	93E	VNS	e^+e^- 58 GeV
$0.098 \pm 0.009^{+0.006}_{-0.005}$	240	[12] ALBRECHT	92F	ARG	$e^+e^- \approx 10$ GeV
$0.096 \pm 0.007 \pm 0.015$		[13] ONG	88	MRK2	e^+e^- 29 GeV
$0.116^{+0.011}_{-0.009}$		[13] PAL	86	DLCO	e^+e^- 29 GeV
$0.091 \pm 0.009 \pm 0.013$		[13] AIHARA	85	TPC	e^+e^- 29 GeV
$0.092 \pm 0.022 \pm 0.040$		[13] ALTHOFF	84J	TASS	e^+e^- 34.6 GeV
0.091 ± 0.013		[13] KOOP	84	DLCO	See PAL 86
0.08 ± 0.015		[14] BACINO	79	DLCO	e^+e^- 3.772 GeV

[9] Isolates D^+ and $D^0 \to e^+$X and weights for relative production (44%–56%).

[10] ALBRECHT 96C uses e^- in the hemisphere opposite to $D^{*+} \to D^0\pi^+$ events.

[11] ABE 93E also measures forward-backward asymmetries and fragmentation functions for c and b quarks.

[12] ALBRECHT 92F uses the excess of right-sign over wrong-sign leptons in a sample of events tagged by fully reconstructed $D^*(2010)^+ \to D^0\pi^+$ decays.

[13] Average BR for charm $\to e^+$X. Unlike at $E_{\rm cm} = 3.77$ GeV, the admixture of charmed mesons is unknown.

[14] Not independent of BACINO 80 measurements of $\Gamma(e^+ \text{anything})/\Gamma_{\rm total}$ for the D^+ and D^0 separately.

$\Gamma(K^-\text{ anything})/\Gamma_{\text{total}}$ Γ_2/Γ

VALUE	EVTS	DOCUMENT ID		TECN	COMMENT
0.275±0.024 OUR AVERAGE					
$0.278^{+0.036}_{-0.031}$		[15] BARLAG	92C	ACCM	π^- Cu 230 GeV
0.271±0.023±0.024		COFFMAN	91	MRK3	e^+e^- 3.77 GeV
• • • We do not use the following data for averages, fits, limits, etc. • • •					
0.17 ±0.07		AGUILAR-...	87E	HYBR	πp, pp 360, 400 GeV
$0.16\ ^{+0.08}_{-0.07}$		AGUILAR-...	86B	HYBR	See AGUILAR-BENITEZ 87E
0.19 ±0.05	26	SCHINDLER	81	MRK2	e^+e^- 3.771 GeV
0.10 ±0.07	3	VUILLEMIN	78	MRK1	e^+e^- 3.772 GeV

[15] BARLAG 92C computes the branching fraction using topological normalization.

$[\Gamma(\overline{K}^0\text{ anything})+\Gamma(K^0\text{ anything})]/\Gamma_{\text{total}}$ Γ_3/Γ

VALUE	EVTS	DOCUMENT ID		TECN	COMMENT
0.612±0.065±0.043		COFFMAN	91	MRK3	e^+e^- 3.77 GeV
• • • We do not use the following data for averages, fits, limits, etc. • • •					
0.52 ±0.18	15	SCHINDLER	81	MRK2	e^+e^- 3.771 GeV
0.39 ±0.29	3	VUILLEMIN	78	MRK1	e^+e^- 3.772 GeV

$\Gamma(K^+\text{ anything})/\Gamma_{\text{total}}$ Γ_4/Γ

VALUE	EVTS	DOCUMENT ID		TECN	COMMENT
0.055±0.013±0.009		COFFMAN	91	MRK3	e^+e^- 3.77 GeV
• • • We do not use the following data for averages, fits, limits, etc. • • •					
$0.08\ ^{+0.06}_{-0.05}$		AGUILAR-...	87E	HYBR	πp, pp 360, 400 GeV
0.06 ±0.04	12	SCHINDLER	81	MRK2	e^+e^- 3.771 GeV
0.06 ±0.06	2	VUILLEMIN	78	MRK1	e^+e^- 3.772 GeV

D^+ and $D^0 \to$ (η anything) / (total D^+ and D^0)

If measured at the $\psi(3770)$, this quantity is a weighted average of D^+ (44%) and D^0 (56%) branching fractions. Only the experiment at $E_{\text{cm}} = 3.77$ GeV is used.

VALUE	DOCUMENT ID		TECN	COMMENT
<0.13	PARTRIDGE	81	CBAL	e^+e^- 3.77 GeV
• • • We do not use the following data for averages, fits, limits, etc. • • •				
<0.02	[16] BRANDELIK	79	DASP	e^+e^- 4.03 GeV

[16] The BRANDELIK 79 result is based on the absence of an η signal at $E_{\text{cm}} = 4.03$ GeV. PARTRIDGE 81 observes a substantially higher η cross section at 4.03 GeV.

$\Gamma(\phi\text{ anything})/\Gamma_{\text{total}}$ Γ_6/Γ

VALUE	CL%	DOCUMENT ID		TECN	COMMENT
<0.018	90	[17] BAI	00C	BES	$e^+e^- \to D\overline{D}^*, D^*\overline{D}^*$

[17] BAI 00C finds the average (ϕ anything) branching fraction for the 4.03-GeV mix of D^+ and D^0 mesons to be (1.34 ± 0.52 ± 0.12)%.

$\Gamma(\phi e^+\text{ anything})/\Gamma_{\text{total}}$ Γ_7/Γ

VALUE	CL%	DOCUMENT ID		TECN	COMMENT
<0.016	90	BAI	00C	BES	$e^+e^- \to D\overline{D}^*, D^*\overline{D}^*$

Leptonic and semileptonic modes

$\Gamma(\mu^+\nu_\mu)/\Gamma_{\text{total}}$ Γ_9/Γ

See the "Note on Pseudoscalar-Meson Decay Constants" in the Listings for the $\pi^{\pm}$.

VALUE	CL%	EVTS	DOCUMENT ID		TECN	COMMENT
0.0008 $^{+0.0016+0.0005}_{-0.0005-0.0002}$		1	[18] BAI	98B	BES	$e^+e^- \to D^{*+}D^-$
• • • We do not use the following data for averages, fits, limits, etc. • • •						
< 0.00072	90		ADLER	88B	MRK3	e^+e^- 3.77 GeV
< 0.02	90	0	[19] AUBERT	83	SPEC	μ^+ Fe, 250 GeV

[18] BAI 98B obtains $f_D = (300^{+180+80}_{-150-40})$ MeV from this measurement.

[19] AUBERT 83 obtains an upper limit 0.014 assuming the final state contains equal amounts of (D^+,D^-), $(D^+,\overline{D}^0)$, (D^-,D^0), and $(D^0,\overline{D}^0)$. We quote the limit they get under more general assumptions.

$\Gamma(\overline{K}^0\ell^+\nu_\ell)/\Gamma_{\text{total}}$ Γ_{10}/Γ

We average our $\overline{K}^0 e^+\nu_e$ and $\overline{K}^0\mu^+\nu_\mu$ branching fractions, after multiplying the latter by a phase-space factor of 1.03 to be able to use it with the $\overline{K}^0 e^+\nu_e$ fraction. Hence our ℓ^+ here is really an e^+.

VALUE	DOCUMENT ID		COMMENT
0.068±0.008 OUR AVERAGE			
0.067±0.009	PDG	04	Our $\Gamma(\overline{K}^0 e^+\nu_e)/\Gamma_{\text{total}}$
$0.072^{+0.031}_{-0.021}$	PDG	04	1.03 × our $\Gamma(\overline{K}^0\mu^+\nu_\mu)/\Gamma_{\text{total}}$

$\Gamma(\overline{K}^0 e^+\nu_e)/\Gamma_{\text{total}}$ Γ_{11}/Γ

VALUE	EVTS	DOCUMENT ID		TECN	COMMENT
0.067±0.009 OUR FIT					
$0.06\ ^{+0.022}_{-0.013}$**±0.007**	13	BAI	91	MRK3	$e^+e^- \approx$ 3.77 GeV

$\Gamma(\overline{K}^0 e^+\nu_e)/\Gamma(\overline{K}^0\pi^+)$ Γ_{11}/Γ_{38}

VALUE	EVTS	DOCUMENT ID		TECN	COMMENT
2.37±0.31 OUR FIT					
2.60±0.35±0.26	186	[20] BEAN	93C	CLE2	$e^+e^- \approx \Upsilon(4S)$

[20] BEAN 93C uses $\overline{K}^0\mu^+\nu_\mu$ as well as $\overline{K}^0 e^+\nu_e$ events and makes a small phase-space adjustment to the number of the μ^+ events to use them as e^+ events.

$\Gamma(\overline{K}^0 e^+\nu_e)/\Gamma(K^-\pi^+\pi^+)$ Γ_{11}/Γ_{39}

VALUE	DOCUMENT ID		TECN	COMMENT
0.72±0.09 OUR FIT				
0.66±0.09±0.14	ANJOS	91C	E691	γ Be 80–240 GeV

$\Gamma(\overline{K}^0\mu^+\nu_\mu)/\Gamma_{\text{total}}$ Γ_{12}/Γ

VALUE	EVTS	DOCUMENT ID		TECN	COMMENT
0.07 $^{+0.028}_{-0.016}$**±0.012**	14	BAI	91	MRK3	$e^+e^- \approx$ 3.77 GeV

$\Gamma(\overline{K}^0\mu^+\nu_\mu)/\Gamma(\mu^+\text{anything})$ Γ_{12}/Γ_8

VALUE	EVTS	DOCUMENT ID		COMMENT
• • • We do not use the following data for averages, fits, limits, etc. • • •				
0.76±0.06	84	[21] AOKI	88	π^- emulsion

[21] From topological branching ratios in emulsion with an identified muon.

$\Gamma(K^-\pi^+e^+\nu_e)/\Gamma_{\text{total}}$ Γ_{13}/Γ

VALUE	CL%	EVTS	DOCUMENT ID		TECN	COMMENT
0.045 $^{+0.010}_{-0.008}$ **OUR FIT** Error includes scale factor of 1.1.						
0.035 $^{+0.012}_{-0.007}$**±0.004**		14	[22] BAI	91	MRK3	$e^+e^- \approx$ 3.77 GeV
• • • We do not use the following data for averages, fits, limits, etc. • • •						
<0.057	90		[23] AGUILAR-...	87F	HYBR	πp, pp 360, 400 GeV

[22] BAI 91 finds that a fraction $0.79^{+0.15+0.09}_{-0.17-0.03}$ of combined D^+ and D^0 decays to $\overline{K}\pi e^+\nu_e$ (24 events) are $\overline{K}^*(892)e^+\nu_e$.

[23] AGUILAR-BENITEZ 87F computes the branching fraction using topological normalization.

$\Gamma(\overline{K}^*(892)^0\ell^+\nu_\ell)/\Gamma_{\text{total}}$ Γ_{26}/Γ

We average our $\overline{K}^{*0}e^+\nu_e$ and $\overline{K}^{*0}\mu^+\nu_\mu$ branching fractions, after multiplying the latter by a phase-space factor of 1.05 to be able to use it with the $\overline{K}^{*0}e^+\nu_e$ fraction. Hence our ℓ^+ here is really an e^+.

VALUE	DOCUMENT ID		COMMENT
0.0573±0.0035 OUR AVERAGE			
0.055 ±0.007	PDG	04	Our $\Gamma(\overline{K}^{*0}e^+\nu_e)/\Gamma_{\text{total}}$
0.058 ±0.004	PDG	04	1.05 × our $\Gamma(\overline{K}^{*0}\mu^+\nu_\mu)/\Gamma_{\text{total}}$

$\Gamma(\overline{K}^*(892)^0 e^+\nu_e)/\Gamma(K^-\pi^+e^+\nu_e)$ Γ_{27}/Γ_{13}

Unseen decay modes of the $\overline{K}^*(892)^0$ are included. See the end of the D^+ Listings for measurements of $D^+ \to \overline{K}^*(892)^0\ell^+\nu_\ell$ form-factor ratios.

VALUE	EVTS	DOCUMENT ID		TECN	COMMENT
1.23 $^{+0.23}_{-0.26}$ **OUR FIT** Error includes scale factor of 1.1.					
1.0 ±0.3	35	ADAMOVICH	91	OMEG	π^- 340 GeV

$\Gamma(\overline{K}^*(892)^0 e^+\nu_e)/\Gamma(K^-\pi^+\pi^+)$ Γ_{27}/Γ_{39}

Unseen decay modes of the $\overline{K}^*(892)^0$ are included. See the end of the D^+ Listings for measurements of $D^+ \to \overline{K}^*(892)^0\ell^+\nu_\ell$ form-factor ratios.

VALUE	EVTS	DOCUMENT ID		TECN	COMMENT
0.60±0.07 OUR FIT Error includes scale factor of 1.8.					
0.61±0.07 OUR AVERAGE Error includes scale factor of 1.6. See the ideogram below.					
0.74±0.04±0.05		BRANDENB...	02	CLE2	$e^+e^- \approx \Upsilon(4S)$
0.62±0.15±0.09	35	ADAMOVICH	91	OMEG	π^- 340 GeV
0.55±0.08±0.10	880	ALBRECHT	91	ARG	$e^+e^- \approx$ 10.4 GeV
0.49±0.04±0.05		ANJOS	89B	E691	Photoproduction
• • • We do not use the following data for averages, fits, limits, etc. • • •					
0.67±0.09±0.07	710	[24] BEAN	93C	CLE2	See BRANDENBURG 02

[24] BEAN 93C uses $\overline{K}^{*0}\mu^+\nu_\mu$ as well as $\overline{K}^{*0}e^+\nu_e$ events and makes a small phase-space adjustment to the number of the μ^+ events to use them as e^+ events.

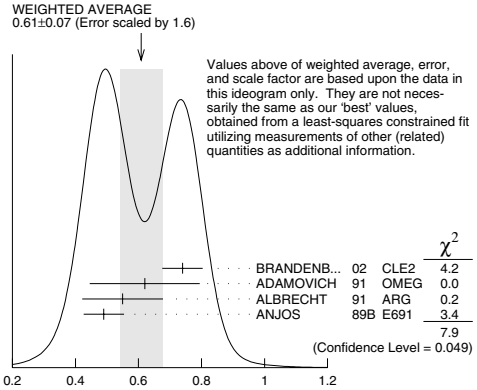

$\Gamma(K^-\pi^+e^+\nu_e$ nonresonant$)/\Gamma_{total}$ Γ_{15}/Γ

VALUE	CL%	DOCUMENT ID		TECN	COMMENT
<0.007	90	[25] ANJOS	89B	E691	Photoproduction

[25] ANJOS 89B assumes a $\Gamma(D^+ \to K^-\pi^+\pi^+)/\Gamma_{total} = 9.1 \pm 1.3 \pm 0.4\%$.

$\Gamma(K^-\pi^+\mu^+\nu_\mu)/\Gamma_{total}$ $\Gamma_{16}/\Gamma = (\Gamma_{18}+\frac{2}{3}\Gamma_{28})/\Gamma$

The value here is calculated from $\frac{2}{3}B(\overline{K}^*(892)^0\mu^+\nu_\mu) + B(K^-\pi^+\mu^+\nu_\mu$ nonresonant).

VALUE	DOCUMENT ID
0.0400±0.0032 OUR FIT	

$\Gamma(\overline{K}^*(892)^0\mu^+\nu_\mu)/\Gamma_{total}$ Γ_{28}/Γ

Unseen decay modes of the $\overline{K}^*(892)^0$ are included. See the end of the D^+ Listings for measurements of $D^+ \to \overline{K}^*(892)^0\ell^+\nu_\ell$ form-factor ratios.

VALUE	EVTS	DOCUMENT ID		TECN	COMMENT
• • • We do not use the following data for averages, fits, limits, etc. • • •					
0.0325±0.0071±0.0075	224	[26] KODAMA	92C	E653	π^- emulsion 600 GeV

[26] KODAMA 92C measures $\Gamma(D^+ \to \overline{K}^{*0}\mu^+\nu_\mu)/\Gamma(D^0 \to K^-\mu^+\nu_\mu) = 0.43 \pm 0.09 \pm 0.09$ and then uses $\Gamma(D^0 \to K^-\mu^+\nu_\mu) = (7.0 \pm 0.7) \times 10^{10}\,s^{-1}$ to get the quoted branching fraction. See also the footnote to KODAMA 92C in the next data block.

$\Gamma(\overline{K}^*(892)^0\mu^+\nu_\mu)/\Gamma(K^-\pi^+\pi^+)$ Γ_{28}/Γ_{39}

Unseen decay modes of the $\overline{K}^*(892)^0$ are included. See the end of the D^+ Listings for measurements of $D^+ \to \overline{K}^*(892)^0\ell^+\nu_\ell$ form-factor ratios.

VALUE	EVTS	DOCUMENT ID		TECN	COMMENT
0.597±0.021 OUR FIT					
0.597±0.022 OUR AVERAGE					
0.72 ±0.10 ±0.05		BRANDENB...	02	CLE2	$e^+e^- \approx \Upsilon(4S)$
0.602±0.010±0.021	12k	[27] LINK	02J	FOCS	γ nucleus, ≈ 180 GeV
0.56 ±0.04 ±0.06	875	FRABETTI	93E	E687	γBe $\overline{E}_\gamma \approx$ 200 GeV
0.46 ±0.07 ±0.08	224	[28] KODAMA	92C	E653	π^- emulsion 600 GeV

[27] This LINK 02J result includes the effects of an interference of a small S-wave $K^-\pi^+$ amplitude with the dominant $\overline{K}^{*0}$ amplitude. (The interference effect is reported in LINK 02E.)

[28] KODAMA 92C also uses the same $\overline{K}^{*0}\mu^+\nu_\mu$ events normalizing instead with $D^0 \to K^-\mu^+\nu_\mu$ events, as reported in the preceding data block.

$\Gamma(K^-\pi^+\mu^+\nu_\mu$ nonresonant$)/\Gamma(K^-\pi^+\mu^+\nu_\mu)$ $\Gamma_{18}/\Gamma_{16} = \Gamma_{18}/(\Gamma_{18}+\frac{2}{3}\Gamma_{28})$

VALUE	DOCUMENT ID		TECN	COMMENT
0.083±0.029 OUR FIT				
0.083±0.029	FRABETTI	93E	E687	< 0.12 (90% CL)

$\Gamma(\overline{K}^0\pi^+\pi^-e^+\nu_e)/\Gamma_{total}$ Γ_{19}/Γ

VALUE	EVTS	DOCUMENT ID		TECN	COMMENT
• • • We do not use the following data for averages, fits, limits, etc. • • •					
$0.022^{+0.047}_{-0.006}\pm0.004$	1	[29] AGUILAR-...	87F	HYBR	πp, pp 360, 400 GeV

[29] AGUILAR-BENITEZ 87F computes the branching fraction using topological normalization.

$\Gamma(K^-\pi^+\pi^0e^+\nu_e)/\Gamma_{total}$ Γ_{20}/Γ

VALUE	EVTS	DOCUMENT ID		TECN	COMMENT
• • • We do not use the following data for averages, fits, limits, etc. • • •					
$0.044^{+0.052}_{-0.013}\pm0.007$	2	[30] AGUILAR-...	87F	HYBR	πp, pp 360, 400 GeV

[30] AGUILAR-BENITEZ 87F computes the branching fraction using topological normalization.

$\Gamma((\overline{K}^*(892)\pi)^0e^+\nu_e)/\Gamma_{total}$ Γ_{21}/Γ

Unseen decay modes of the $\overline{K}^*(892)$ are included.

VALUE	CL%	DOCUMENT ID		TECN	COMMENT
<0.012	90	ANJOS	92	E691	Photoproduction

$\Gamma((\overline{K}\pi\pi)^0e^+\nu_e$ non-$\overline{K}^*(892))/\Gamma_{total}$ Γ_{22}/Γ

VALUE	CL%	DOCUMENT ID		TECN	COMMENT
<0.009	90	ANJOS	92	E691	Photoproduction

$\Gamma(K^-\pi^+\pi^0\mu^+\nu_\mu)/\Gamma(K^-\pi^+\mu^+\nu_\mu)$ $\Gamma_{23}/\Gamma_{16} = \Gamma_{23}/(\Gamma_{18}+\frac{2}{3}\Gamma_{28})$

VALUE	CL%	DOCUMENT ID		TECN	COMMENT
<0.042	90	FRABETTI	93E	E687	γBe $\overline{E}_\gamma \approx$ 200 GeV

$\Gamma(\overline{K}_1(1270)^0\mu^+\nu_\mu)/\Gamma(\overline{K}^*(892)^0\mu^+\nu_\mu)$ Γ_{29}/Γ_{28}

VALUE	CL%	DOCUMENT ID		TECN	COMMENT
<0.78	95	ABE	99P	CDF	$\overline{p}p$ 1.8 TeV

$\Gamma(\overline{K}^*(1410)^0\mu^+\nu_\mu)/\Gamma(\overline{K}^*(892)^0\mu^+\nu_\mu)$ Γ_{30}/Γ_{28}

VALUE	CL%	DOCUMENT ID		TECN	COMMENT
• • • We do not use the following data for averages, fits, limits, etc. • • •					
<0.60	95	ABE	99P	CDF	$\overline{p}p$ 1.8 TeV

$\Gamma(\overline{K}_2^*(1430)^0\mu^+\nu_\mu)/\Gamma(\overline{K}^*(892)^0\mu^+\nu_\mu)$ Γ_{31}/Γ_{28}

VALUE	CL%	DOCUMENT ID		TECN	COMMENT
<0.19	95	ABE	99P	CDF	$\overline{p}p$ 1.8 TeV

$\Gamma(\pi^0\ell^+\nu_\ell)/\Gamma(\overline{K}^0\ell^+\nu_\ell)$ Γ_{24}/Γ_{10}

VALUE	EVTS	DOCUMENT ID		TECN	COMMENT
0.046±0.014±0.017	100	[31] BARTELT	97	CLE2	$e^+e^- \approx \Upsilon(4S)$
• • • We do not use the following data for averages, fits, limits, etc. • • •					
0.085±0.027±0.014	53	[32] ALAM	93	CLE2	See BARTELT 97

[31] BARTELT 97 thus directly measures the product of ratios squared of CKM matrix elements and form factors at q^2=0: $|V_{cd}/V_{cs}|^2 \cdot |f_+^\pi(0)/f_+^K(0)|^2 = 0.046 \pm 0.014 \pm 0.017$.

[32] ALAM 93 thus directly measures the product of ratios squared of CKM matrix elements and form factors at q^2=0: $|V_{cd}/V_{cs}|^2 \cdot |f_+^\pi(0)/f_+^K(0)|^2 = 0.085 \pm 0.027 \pm 0.014$.

$\Gamma(\pi^+\pi^-e^+\nu_e)/\Gamma_{total}$ Γ_{25}/Γ

VALUE	CL%	DOCUMENT ID		TECN	COMMENT
• • • We do not use the following data for averages, fits, limits, etc. • • •					
<0.057	90	[33] AGUILAR-...	87F	HYBR	πp, pp 360, 400 GeV

[33] AGUILAR-BENITEZ 87F computes the branching fraction using topological normalization.

$\Gamma(\rho^0e^+\nu_e)/\Gamma_{total}$ Γ_{32}/Γ

VALUE	CL%	DOCUMENT ID		TECN	COMMENT
• • • We do not use the following data for averages, fits, limits, etc. • • •					
<0.0037	90	BAI	91	MRK3	$e^+e^- \approx$ 3.77 GeV

$\Gamma(\rho^0e^+\nu_e)/\Gamma(\overline{K}^*(892)^0e^+\nu_e)$ Γ_{32}/Γ_{27}

VALUE	EVTS	DOCUMENT ID		TECN	COMMENT
0.045±0.014±0.009	49	[34] AITALA	97	E791	π^- nucleus, 500 GeV

[34] AITALA 97 explicitly subtracts $D^+ \to \eta' e^+\nu_e$ and other backgrounds to get this result.

$\Gamma(\rho^0\mu^+\nu_\mu)/\Gamma(\overline{K}^*(892)^0\mu^+\nu_\mu)$ Γ_{33}/Γ_{28}

VALUE	EVTS	DOCUMENT ID		TECN	COMMENT
0.061±0.014 OUR AVERAGE					
0.051±0.015±0.009	54	[35] AITALA	97	E791	π^- nucleus, 500 GeV
0.079±0.019±0.013	39	[36] FRABETTI	97	E687	γ Be, $\overline{E}_\gamma \approx$ 220 GeV
• • • We do not use the following data for averages, fits, limits, etc. • • •					
$0.044^{+0.031}_{-0.025}\pm0.014$	4	[37] KODAMA	93C	E653	π^- emulsion 600 GeV

[35] AITALA 97 explicitly subtracts $D^+ \to \eta'\mu^+\nu_\mu$ and other backgrounds to get this result.

[36] Because the reconstruction efficiency for photons is low, this FRABETTI 97 result also includes any $D^+ \to \eta'\mu^+\nu_\mu \to \gamma\rho^0\mu^+\nu_\mu$ events in the numerator.

[37] This KODAMA 93C result is based on a final signal of $4.0^{+2.8}_{-2.3}\pm1.3$ events; the estimates of backgrounds that affect this number are somewhat model dependent.

$\Gamma(\phi e^+\nu_e)/\Gamma_{total}$ Γ_{34}/Γ

Decay modes of the ϕ not included in the search are corrected for.

VALUE	CL%	DOCUMENT ID		TECN	COMMENT
<0.0209	90	BAI	91	MRK3	$e^+e^- \approx$ 3.77 GeV

$\Gamma(\phi\mu^+\nu_\mu)/\Gamma_{total}$ Γ_{35}/Γ

Decay modes of the ϕ not included in the search are corrected for.

VALUE	CL%	DOCUMENT ID		TECN	COMMENT
<0.0372	90	BAI	91	MRK3	$e^+e^- \approx$ 3.77 GeV

$\Gamma(\eta\ell^+\nu_\ell)/\Gamma(\pi^0\ell^+\nu_\ell)$ Γ_{36}/Γ_{24}

VALUE	CL%	DOCUMENT ID		TECN	COMMENT
<1.5	90	BARTELT	97	CLE2	$e^+e^- \approx \Upsilon(4S)$

$\Gamma(\eta'(958)\mu^+\nu_\mu)/\Gamma(\overline{K}^*(892)^0\mu^+\nu_\mu)$ Γ_{37}/Γ_{28}

Decay modes of the $\eta'(958)$ not included in the search are corrected for.

VALUE	CL%	DOCUMENT ID		TECN	COMMENT
<0.20	90	KODAMA	93B	E653	π^- emulsion 600 GeV

Hadronic modes with a $\overline{K}$ or $\overline{K}K\overline{K}$

$\Gamma(\overline{K}^0\pi^+)/\Gamma_{\text{total}}$ Γ_{38}/Γ

VALUE	EVTS	DOCUMENT ID		TECN	COMMENT
0.0282±0.0019 OUR FIT					
0.032 ±0.004 OUR AVERAGE					
0.032 ±0.005 ±0.002	161	ADLER	88C	MRK3	e^+e^- 3.77 GeV
0.033 ±0.009	36	[38] SCHINDLER	81	MRK2	e^+e^- 3.771 GeV
0.033 ±0.013	17	[39] PERUZZI	77	MRK1	e^+e^- 3.77 GeV

[38] SCHINDLER 81 (MARK-2) measures $\sigma(e^+e^- \to \psi(3770)) \times$ branching fraction to be 0.14 ± 0.03 nb. We use the MARK-3 (ADLER 88C) value of $\sigma = 4.2 \pm 0.6 \pm 0.3$ nb.

[39] PERUZZI 77 (MARK-1) measures $\sigma(e^+e^- \to \psi(3770)) \times$ branching fraction to be 0.14 ± 0.05 nb. We use the MARK-3 (ADLER 88C) value of $\sigma = 4.2 \pm 0.6 \pm 0.3$ nb.

$\Gamma(\overline{K}^0\pi^+)/\Gamma(K^-\pi^+\pi^+)$ Γ_{38}/Γ_{39}

It is generally assumed for modes such as $D^+ \to \overline{K}^0\pi^+$ that
$\Gamma(D^+ \to \overline{K}^0\pi^+) = 2\Gamma(D^+ \to K^0_S\pi^+)$;
it is the latter Γ that is actually measured. BIGI 95 points out that interference between Cabibbo-allowed and doubly Cabibbo-suppressed amplitudes, where both occur, could invalidate this assumption by a few percent.

VALUE	EVTS	DOCUMENT ID		TECN	COMMENT
0.306 ±0.006 OUR FIT					
0.307 ±0.005 OUR AVERAGE					
0.3060±0.0046±0.0032	10.6k	LINK	02B	FOCS	γ nucleus, $\overline{E}_\gamma \approx 180$ GeV
0.348 ±0.024 ±0.022	473	[40] BISHAI	97	CLE2	$e^+e^- \approx \Upsilon(4S)$
0.274 ±0.030 ±0.031	264	ANJOS	90C	E691	Photoproduction

[40] See BISHAI 97 for an isospin analysis of $D^+ \to \overline{K}\pi$ amplitudes.

$\Gamma(K^-\pi^+\pi^+)/\Gamma_{\text{total}}$ Γ_{39}/Γ

VALUE	EVTS	DOCUMENT ID		TECN	COMMENT
0.092±0.006 OUR FIT					
0.091±0.007 OUR AVERAGE					
0.093±0.006±0.008	1502	[41] BALEST	94	CLE2	$e^+e^- \approx \Upsilon(4S)$
0.091±0.013±0.004	1164	ADLER	88C	MRK3	e^+e^- 3.77 GeV
0.091±0.019	239	[42] SCHINDLER	81	MRK2	e^+e^- 3.771 GeV
0.086±0.020	85	[43] PERUZZI	77	MRK1	e^+e^- 3.77 GeV
• • • We do not use the following data for averages, fits, limits, etc. • • •					
$0.064^{+0.015}_{-0.014}$		[44] BARLAG	92C	ACCM	π^- Cu 230 GeV
$0.063^{+0.028}_{-0.014}\pm0.011$	8	[44] AGUILAR-...	87F	HYBR	πp, pp 360, 400 GeV

[41] BALEST 94 measures the ratio of $D^+ \to K^-\pi^+\pi^+$ and $D^0 \to K^-\pi^+$ branching fractions to be 2.35 ± 0.16 ± 0.16 and uses their absolute measurement of the $D^0 \to K^-\pi^+$ fraction (AKERIB 93).

[42] SCHINDLER 81 (MARK-2) measures $\sigma(e^+e^- \to \psi(3770)) \times$ branching fraction to be 0.38 ± 0.05 nb. We use the MARK-3 (ADLER 88C) value of $\sigma = 4.2 \pm 0.6 \pm 0.3$ nb.

[43] PERUZZI 77 (MARK-1) measures $\sigma(e^+e^- \to \psi(3770)) \times$ branching fraction to be 0.36 ± 0.06 nb. We use the MARK-3 (ADLER 88C) value of $\sigma = 4.2 \pm 0.6 \pm 0.3$ nb.

[44] AGUILAR-BENITEZ 87F and BARLAG 92C compute the branching fraction by topological normalization.

REVIEW OF CHARM DALITZ-PLOT ANALYSES

Written November 2003 by D. Asner (University of Pittsburgh)

Weak nonleptonic decays of charm mesons are expected to proceed dominantly through resonant two-body decays in several theoretical models [1]. The Dalitz-plot analysis technique [2,3] has been applied to the decays $D \to rc$, $r \to ab$ where the decay products a, b, and c are K or π and the intermediate state r is a scalar, vector, or tensor meson. Table 1 lists published analyses of $D \to \overline{K}\pi\pi$, $\to \pi\pi\pi$, $\to \overline{K}K\pi$, and $\to \overline{K}K\overline{K}$ decays. The analyses include studies of doubly Cabibbo-suppressed decays [4,5], searches for CP violation [5–8], properties of established light mesons [9–11], and properties of $\pi\pi$ [4,11,12] and $K\pi$ [13] S-wave states. Future studies could improve sensitivity to D^0–$\overline{D}^0$ mixing [14].

The amplitude of the process, $D \to rc, r \to ab$, is given by the product of three factors: the angular distributions [15,16] of final-state particles, the barrier form factors [17,18] for the production of rc and ab, respectively, and the dynamical function describing the resonance r. Usually r is modeled with a Breit-Wigner, and the nonresonant contribution is parameterized as an S-wave with no variation in magnitude or phase across the Dalitz plot. Some more recent analyses have used the K-matrix formalism [19] with the P-vector approximation [20] to describe the $\pi\pi$ S-wave.

In the following, we discuss a number of subjects of current interest.

Table 1: Reported Dalitz Plot Analyses.

Decay	Experiment(s)
$D^0 \to K^0_S\pi^+\pi^-$	Mark II [21], Mark III [22], E691 [24], E687 [23,26], ARGUS [25], CLEO [4]
$D^0 \to K^-\pi^+\pi^0$	Mark III [22], E687 [26], E691 [24], CLEO [6]
$D^0 \to \overline{K}^0K^+\pi^-$	BABAR [27]
$D^0 \to K^0K^-\pi^+$	BABAR [27]
$D^0 \to \pi^+\pi^-\pi^0$	CLEO [8]
$D^0 \to K^0_SK^+K^-$	BABAR [27]
$D^+ \to K^-\pi^+\pi^+$	Mark III [22], E687 [26], E691 [24], E791 [13]
$D^+ \to \overline{K}^0\pi^+\pi^0$	Mark III [22]
$D^+ \to \pi^+\pi^+\pi^-$	E687 [9], E791 [12], FOCUS [11]
$D^+ \to K^+K^-\pi^+$	FOCUS [29]
$D^+_s \to K^+K^-\pi^+$	E687 [30], FOCUS [29]
$D^+_s \to \pi^+\pi^+\pi^-$	E687 [9], E791 [10], FOCUS [11]

$D^0 \to K^0_S\pi^+\pi^-$ — Several experiments have analyzed the decay $D^0 \to K^0_S\pi^+\pi^-$. The earliest analyses, by Mark II [21], Mark III [22], and E687 [23], assumed only two intermediate resonances, $K^0_S\rho^0$, $K^*(892)^-\pi^+$, and a significant nonresonant component. Additional resonances were considered by E691 [24] but were not found to be statistically significant. ARGUS [25] and E687 [26], with more events, fit the Dalitz plot with six intermediate resonances: $K^*(892)^-\pi^+$, $K^*_0(1430)^-\pi^+$, $K^0_S\rho^0$, $K^0_Sf_0(975)$, $K^0_Sf_2(1270)$, and $K^0_Sf_0(1400)$. The nonresonant contribution was negligible. The early and later E687 results [23, 26] were consistent under similar assumptions. The most precise results are from CLEO [4], which includes three additional resonances: $K^0_S\omega, K^*(1680)^-\pi^+$ and the doubly Cabibbo-suppressed $K^*(892)^+\pi^-$. They find a much smaller nonresonant contribution than did the earliest experiments.

It is not straightforward to compare or combine results using different descriptions of the angular distributions, barrier factors, resonant parametrizations, and different sets of resonances. Some of the earlier results [22–24], did not include barrier factors [17, 18]. Most of the earlier results [22–24, 26] used the Zemach formalism [15] to describe the angular shape of the decay pattern, while the more recent results [25, 4] use the helicity formalism [16].

The significance of the nonresonant component in the smaller data samples has been attributed to the presence of the broad scalar resonances $K_0^*(1430)^-$ and $f_0(1370)$ that were later observed in the larger data samples. The observation of a small but significant nonresonant component in the largest data samples suggests the presence of additional broad scalar resonances, the $\kappa(800)$ and $\sigma(500)$. The CLEO analysis could accomodate the $\sigma(500)$ in lieu of the nonresonant component, but found no evidence for the $\kappa(800)$.

$D^0 \to \pi^+\pi^-\pi^0$ and $D^0 \to \overline{K}^0 K^+ K^-$ — The only significant contribution to the resonant substructure of $D^0 \to \pi^+\pi^-\pi^0$ is in the $\rho\pi$ channels. A small nonresonant component is observed but all other $\pi\pi$ resonances, including the $\sigma(500)$, yielded fit fractions consistent with zero. The CLEO [8] results for $D^0 \to \pi^+\pi^-\pi^0$ are given in Table 2.

Table 2: Dalitz fit results of $D^0 \to \pi^+\pi^-\pi^0$.

Resonance	Amplitude	Phase(°)	Fit fraction(%)
ρ^+	1. (fixed)	0. (fixed)	$76.5 \pm 1.8 \pm 4.8$
ρ^0	$0.56 \pm 0.02 \pm 0.07$	$10 \pm 3 \pm 3$	$23.9 \pm 1.8 \pm 4.6$
ρ^-	$0.65 \pm 0.03 \pm 0.04$	$-4 \pm 3 \pm 4$	$32.3 \pm 2.1 \pm 2.2$
nonresonant	$1.03 \pm 0.17 \pm 0.31$	$77 \pm 8 \pm 11$	$2.7 \pm 0.9 \pm 1.7$

The BABAR [27] results for $D^0 \to \overline{K}^0 K^+ K^-$ are given in Table 3. The non-ϕ resonant substructure in K^+K^- is significant. Resonant contributions from $a_0(980)^0$, $a_0(980)^+$, and $f_0(980)$ are observed. The nonresonant and the doubly Cabibbo-suppressed contributions are consistent with zero.

Table 3: Dalitz fit results of $D^0 \to \overline{K}^0 K^+ K^-$.

Resonance	Phase(°)	Fit fraction(%)
$\overline{K}^0\phi$	0. (fixed)	$45.4 \pm 1.6 \pm 1.0$
$\overline{K}^0 a_0(980)$	109 ± 5	$60.9 \pm 7.5 \pm 13.3$
$\overline{K}^0 f_0(980)$	-161 ± 14	$12.2 \pm 3.1 \pm 8.6$
$a_0(980)^+ K^-$	-53 ± 4	$34.3 \pm 3.2 \pm 6.8$
$a_0(980)^- K^+$	-13 ± 15	$3.2 \pm 1.9 \pm 0.5$
nonresonant	40 ± 44	$0.4 \pm 0.3 \pm 0.8$

Charm Dalitz-plot analyses might be useful for calibrating tools used in B decays: specifically, to extract α from $B^0 \to \pi^+\pi^-\pi^0$, β from $B^0 \to \overline{K}^0 K^+ K^-$, and γ from $B^\pm \to DK^\pm$ followed by $D \to \overline{K}^0 K^+ K^-$ or $D \to \overline{K}^0 \pi^+\pi^-$ [28].

$D^+ \to \pi^+\pi^+\pi^-$: a $\sigma(500)$ or $f_0(600)$ — The decay $D^+ \to \pi^+\pi^+\pi^-$ has been studied by the E687 [9], E791 [12] and FOCUS [11] experiments. The E687 experiment considered the $\rho(770)^0\pi^+$, $f_0(980)\pi^+$, $f_2(1270)\pi^+$, and a nonresonant component. The E791 experiment included in addition $f_0(1370)\pi^+$ and $\rho(1450)^0\pi^+$. Both analyses found a very large fraction ($\sim 50\%$) for the nonresonant contribution, perhaps indicating a broad scalar contribution. E791 found the nonresonant amplitude to be consistent with zero if a broad scalar resonance was included in the fit. FOCUS analyzed its data sample using both the Breit-Wigner formalism and the K-matrix formalism. The Breit-Wigner analysis included $\rho(770), f_0(980), f_2(1270), f_0(1500), \sigma(500)$, and a nonresonant contribution. Applying the K-matrix formalism to the S wave and parameterizing the $\rho(770)$ and $f_2(1270)$ with the Breit-Wigner functions also described the FOCUS data well.

None of these analyses has modeled the dynamics of the $\pi^+\pi^+$ interaction. Consideration of the $I = 2$ S-wave and D-wave phase shifts, also measured in $\pi^+ p \to \pi^+\pi^+ n$ [31], could affect the $\pi^+\pi^-$ S-wave result.

E791 finds additional evidence that the low mass $\pi\pi$ feature is resonant by examining the phase of the $\pi\pi$ amplitude in the vicinity of the reported $\sigma(500)$ mass. A phase variation with invariant $\pi\pi$ mass is consistent with a resonant contribution [32].

Table 4 gives the parameters of the $\sigma(500)$ determined in charm Dalitz plot analyses. A consistent relative phase between the $\sigma(500)$ and $\rho(770)$ resonances is observed.

Table 4: Parameters of the $\sigma(500)$ resonance. The amplitude and phase are relative to the $\rho(770)$.

Experiment	E791 [12]	CLEO [4]	FOCUS [11]
Decay Mode	$D^+ \to \pi^+\pi^+\pi^-$	$D^0 \to K^0_S\pi^+\pi^-$	$D^+ \to \pi^+\pi^+\pi^-$
Amplitude	$1.17 \pm 0.13 \pm 0.06$	0.57 ± 0.13	—
Phase(°)	$205.7 \pm 8.0 \pm 5.2$	214 ± 11	200 ± 31
m(MeV/c^2)	$478^{+24}_{-23} \pm 17$	513 ± 32	443 ± 27
Γ(MeV/c^2)	$324^{+42}_{-40} \pm 21$	335 ± 67	443 ± 80

$D^+ \to K^-\pi^+\pi^+$: a $\kappa(800)$? — Indication of a broad $K\pi$ scalar intermediate resonance has been reported by E791 in the decay $D^+ \to K^-\pi^+\pi^+$ [13]. Fitting the Dalitz plot with $\overline{K}^*(892)^0\pi^+$, $\overline{K}^*_0(1430)^0\pi^+$, $\overline{K}^*_2(1430)^0\pi^+$, and $\overline{K}^*(1680)^0\pi^+$, plus a constant nonresonant component, E791 finds results consistent with earlier results from E691 and E687 with a nonresonant fit fraction of over 90%. Having reconstructed more events than the other experiments, E791 was led to include an extra low-mass S-wave $\overline{K}\pi$ resonance to account for the poor fit already seen by earlier experiments: A $\kappa(800)$ with $m = 797 \pm 19 \pm 43$ MeV/c^2 and $\Gamma = 410 \pm 43 \pm 87$ MeV/c^2 much improved the fits. The $\kappa(800)$ is now the dominant resonance and the nonresonant fit fraction is reduced from $90.9 \pm 2.6\%$ to $13.0 \pm 5.8 \pm 4.4\%$. As discussed with the $\sigma(500)$, the $K^-\pi^+$ S-wave result could be affected by modeling the dynamics of the $I = 2$ $\pi^+\pi^+$ interaction.

E791 also modeled the $K\pi$ S-wave phase variation as a function of $K\pi$ mass with the $K_0^*(1430)$ resonance only and a nonresonant component following the parameterization of LASS [33]. It was necessary to relax the unitarity constraint to describe the E791 data [34]. The $K\pi$ S-wave phase behavior in this model is consistent with the model that includes the κ resonance.

CLEO allowed scalar $K\pi$ resonances in the fit to $D^0 \to K^-\pi^+\pi^0$ [6] and $D^0 \to K^0_S\pi^+\pi^-$ [4] and observed a significant contribution for only $K^*_0(1430)$ [35]. BABAR has analyzed the decay $D^0 \to K^0K^-\pi^+$ and $D^0 \to \overline{K}^0K^+\pi^-$ [27]. They fit the former Dalitz plot with both positively charged and neutral $\overline{K}^*(892)$, $\overline{K}^*_0(1430)$, $\overline{K}^*_2(1430)$, $\overline{K}^*(1680)$ and $a_0(980)^-$, $a_0(1450)^-$, $a_2(1310)^-$ resonances, and a nonresonant component. The second Dalitz plot is fit with the identical resonances except for the $a_2(1310)^-$. A good fit is obtained in both cases without including the κ.

$f_0(980)$, $f_0(1370)$ and $f_0(1500)$ — The proximity of the $K\overline{K}$ threshold requires a coupled-channel or Flatte parametrization [36] of the $f_0(980)$ in charm Dalitz-plot analyses. The width of the $f_0(980)$ is poorly known. E791 used a coupled-channel Breit-Wigner function, following the parametrization of Ref. [37], to describe the $f_0(980)$ in $D^+_s \to \pi^+\pi^+\pi^-$ [10], and measured $m_r = 977 \pm 3 \pm 2$ MeV/c^2, $g_{\pi\pi} = 0.09 \pm 0.01 \pm 0.01$, and $g_{KK} = 0.02 \pm 0.04 \pm 0.03$. Results similar to these are desirable for input to the analysis of the $D^+_s \to K^+K^-\pi^+$ [29], which includes the $f_0(980)$ and $a_0(980)$.

The quark content of the $f_0(1370)$ and $f_0(1500)$ can perhaps be inferred from how they populate various Dalitz plots. The E791 analysis of $D^+ \to \pi^+\pi^+\pi^-$ [12] finds a contribution from the $f_0(1370)$ but not the $f_0(1500)$. The FOCUS analysis [11] of this decay does not find a significant contribution from the $f_0(1370)$. For the $D^+_s \to \pi^+\pi^+\pi^-$, E687 [9] and FOCUS [11] do not see the $f_0(1370)$ but do see a resonance with parameters similar to the $f_0(1500)$, while E791 [10] observes a $\pi\pi$ resonance ($m = 1434 \pm 18 \pm 9$ MeV/c^2 and $\Gamma = 172 \pm 32 \pm 6$ MeV/c^2) that is not consistent with either meson. BABAR has found no evidence for either the $f_0(1370)$ or the $f_0(1500)$ in $D^0 \to \overline{K}^0K^+K^-$ [27], while CLEO has observed the $f_0(1370)$ in $D^0 \to K^0_S\pi^+\pi^-$ [4]. Future analyses will present a clearer picture only if the same resonances and model of decay amplitudes are applied to all Dalitz-plot fits.

Doubly Cabibbo-Suppressed Decays — There are two classes of multibody doubly Cabibbo-suppressed (DCS) decays of charm mesons. The first consists of those in which the DCS and corresponding Cabbibo-favored (CF) decays populate distinct Dalitz plots: the pairs $D^0 \to K^+\pi^-\pi^0$ and $D^0 \to K^-\pi^+\pi^0$, or $D^+ \to K^+\pi^+\pi^-$ and $D^+ \to K^-\pi^+\pi^+$, are examples. CLEO [5] has reported $\dfrac{\mathcal{B}(D^0 \to K^+\pi^-\pi^0)}{\mathcal{B}(D^0 \to K^-\pi^+\pi^0)} = (0.43^{+0.11}_{-0.10} \pm 0.07)\%$.

The second class consists of decays where the DCS and CF modes populate the same Dalitz plot: for example, $D^0 \to K^{*-}\pi^+$ and $D^0 \to K^{*+}\pi^-$ both contribute to $D^0 \to K^0_S\pi^+\pi^-$. In this case, the potential for interference of DCS and CF amplitudes increases the sensitivity to the DCS amplitude. CLEO [4] has reported the relative amplitudes and phases to be $(7.1 \pm 1.3^{+2.6\,+2.6}_{-0.6\,-0.6})\%$ and $(189 \pm 10 \pm 3^{+15}_{-5})^\circ$, respectively, corresponding to $\dfrac{\mathcal{B}(D^0 \to K^*(892)^+\pi^-)}{\mathcal{B}(D^0 \to K^*(892)^-\pi^+)} = (0.5 \pm 0.2^{+0.5\,+0.4}_{-0.1\,-0.1})\%$.

CP Violation — In the limit of CP conservation, charge conjugate decays will have the same Dalitz-plot distribution. The $D^{*\pm}$ tag enables the discrimination between D^0 and $\overline{D}^0$. The integrated CP violation across the Dalitz plot is determined from

$$\mathcal{A}_{CP} = \int \frac{|\mathcal{M}|^2 - |\overline{\mathcal{M}}|^2}{|\mathcal{M}|^2 + |\overline{\mathcal{M}}|^2}\, dm^2_{ab}\, dm^2_{bc} \Big/ \int dm^2_{ab}\, dm^2_{bc}\,,$$

where $\mathcal{M}$ and $\overline{\mathcal{M}}$ are the D^0 and $\overline{D}^0$ Dalitz-plot amplitudes. This expression is less sensitive to CP violation than the individual resonant submodes reported in Ref. [7]. Table 5 reports the results for CP violation. No evidence of CP violation has been observed.

Table 5: Dalitz-plot-integrated CP violation.

Experiment	Decay mode	$\mathcal{A}_{CP}(\%)$
CLEO [6]	$D^0 \to K^-\pi^+\pi^0$	-3.1 ± 8.6
CLEO [5]	$D^0 \to K^+\pi^-\pi^0$	$+9^{+22}_{-25}$
CLEO [7]	$D^0 \to K^0_S\pi^+\pi^-$	$-3.9 \pm 3.4^{+1.4}_{-2.2} \pm 2.7$
CLEO [8]	$D^0 \to \pi^+\pi^-\pi^0$	$+1^{+9}_{-7} \pm 9$

The possibility of interference between CP–conserving and CP–violating amplitudes provides a more sensitive probe of CP violation. The constraints on the square of the CP–violating amplitude obtained in the resonant submodes of $D^0 \to K^0_S\pi^+\pi^-$ range form 4.5–to–29 $\times 10^{-4}$ at 95% confidence level [7].

References

1. M Bauer, B. Stech and M. Wirbel, Z. Phys. **C34**, 103 (1987);
P. Bedaque, A. Das and V.S. Mathur, Phys. Rev. **D49**, 269 (1994);
L.-L. Chau and H.-Y. Cheng, Phys. Rev. **D36**, 137 (1987);
K. Terasaki, Int. J. Mod. Phys. **A10**, 3207 (1995);
F. Buccella, M. Lusignoli and A. Pugliese, Phys. Lett. **B379**, 249 (1996).
2. R. H. Dalitz, *Phil. Mag.* **44**, 1068 (1953).
3. See the note on Kinematics in this *Review*.
4. H. Muramatsu *et al.* (CLEO Collab.), Phys. Rev. Lett. **89**, 251802 (2002); erratum, Phys. Rev. Lett. **90**, 059901 (2003).
5. G. Brandenburg *et al.* (CLEO Collab.), Phys. Rev. Lett. **87**, 071802 (2001).
6. S. Kopp *et al.* (CLEO Collab.), Phys. Rev. **D63**, 092001 (2001).
7. D. M. Asner *et al.* (CLEO Collab.), `hep-ex/0311033` .
8. V. V. Frolov *et al.* (CLEO Collab.), `hep-ex/0306048`, contributed to the International Europhysics Conference on High Energy Physics (EPS 2003).
9. P. L. Frabetti *et al.* (E687 Collab.), Phys. Lett. **B407**, 79 (1997).
10. E. M. Aitala *et al.* (E791 Collab.), Phys. Rev. Lett. **86**, 765 (2001).
11. S. Malvezzi, `hep-ex/0307055`, contributed to the High Energy Physics Workshop on Scalar Mesons, 2003;
J.M. Link *et al.* (FOCUS Collab.), Phys. Lett. **B** (submitted), `hep-ex/0312040`.

12. E. M. Aitala *et al.* (E791 Collab.), Phys. Rev. Lett. **86**, 770 (2001).
13. E. M. Aitala *et al.* (E791 Collab.), Phys. Rev. Lett. **89**, 121801 (2002).
14. See the note on "D^0–$\overline{D}^0$ Mixing" in this *Review*; Dalitz analysis of the wrong sign rate $D^0 \to K^+\pi^-\pi^0$ [5] and the time dependence of Dalitz analysis of $D^0 \to K^0_S\pi^+\pi^-$ [4] are two candidate processes.
15. C. Zemach, Phys. Rev. **B133**, 1201 (1964); C. Zemach, Phys. Rev. **B140**, 97 (1965).
16. S. U. Chung, Phys. Rev. **D48**, 1225, (1993); J. D. Richman, CALT-68-1148.
17. J. Blatt and V. Weisskopf, *Theoretical Nuclear Physics*, New York: John Wiley & Sons (1952).
18. F. von Hippel and C. Quigg, Phys. Rev. **D5**, 624, (1972).
19. S.U. Chung *et al.*, Ann. Phys. **4**, 404 (1995).
20. I.J.R. Aitchison, Nucl. Phys. **A189**, 417 (1972).
21. R. H. Schindler *et al.* (Mark II Collab.), Phys. Rev. **D28**, 78 (1981).
22. J. Adler *et al.* (Mark III Collab.), Phys. Lett. **B196**, 107 (1987).
23. P.L. Frabetti *et al.* (E687 Collab.), Phys. Lett. **B286**, 195 (1992).
24. J.C. Anjos *et al.* (E691 Collab.), Phys. Rev. **D48**, 56 (1993).
25. H. Albecht *et al.* (ARGUS Collab.), Phys. Lett. **B308**, 435 (1993).
26. P.L. Frabetti *et al.* (E687 Collab.), Phys. Lett. **B331**, 217 (1994).
27. B. Aubert *et al.* (BABAR Collab.), hep-ex/0207089; contributed to the 31st International Conference on High Energy Physics (ICHEP 2002).
28. A. Giri *et al.*, Phys. Rev. **D68**, 054018 (2003).
29. S. Malvezzi, AIP Conf. Proc. **549**, 569 (2002).
30. P. L. Frabetti *et al.* (E687 Collab.), Phys. Lett. **B351**, 591 (1995).
31. W. Hoogland *et al.*, Nucl. Phys. **B69**, 266 (1974).
32. I. Bediaga (E791 Collab.), hep-ex/0307008; contributed to the High Energy Physics Workshop on Scalar Mesons, 2003.
33. D. Aston *et al.* (LASS Collab.), Nucl. Phys. **B296**, 493 (1988).
34. C. Gobel (E791 Collab.), hep-ex/0307003.
35. See the note on Scalar Mesons in this *Review*.
36. S. M. Flatte, Phys. Lett. **B63**, 224 (1976).
37. T. A. Armstrong *et al.* (WA76 Collab.), Z. Phys. **C51**, 351 (1991).

$\Gamma(K_0^*(800)^0\pi^+)/\Gamma(K^-\pi^+\pi^+)$ Γ_{81}/Γ_{39}

The $K_0^*(800)$ is a broad scalar resonance that may not exist and is not included in the Summary Tables. AITALA 02 finds that including such a resonance in the fit to the $D^+ \to K^-\pi^+\pi^+$ Dalitz plot greatly improves the fit. However, the results of AITALA 02 for the $D^+ \to K^-\pi^+\pi^+$ Dalitz plot analysis so disagree with earlier analyses that averaging the results makes no sense. For now, we exclude AITALA 02 from the average.

VALUE	DOCUMENT ID	TECN	COMMENT
• • • We do not use the following data for averages, fits, limits, etc. • • •			
$0.478 \pm 0.121 \pm 0.053$	AITALA	02 E791	π^- nucleus, 500 GeV

$\Gamma(\overline{K}^*(892)^0\pi^+)/\Gamma(K^-\pi^+\pi^+)$ Γ_{82}/Γ_{39}

Unseen decay modes of the $\overline{K}^*(892)^0$ are included.

VALUE	DOCUMENT ID	TECN	COMMENT
0.212 ± 0.016 OUR FIT			
0.210 ± 0.015 OUR AVERAGE			
$0.206 \pm 0.009 \pm 0.014$	FRABETTI	94G E687	γBe, $\overline{E}_\gamma \approx 220$ GeV
$0.255 \pm 0.014 \pm 0.050$	ANJOS	93 E691	γBe 90–260 GeV
$0.21 \pm 0.06 \pm 0.06$	ALVAREZ	91B NA14	Photoproduction
$0.20 \pm 0.02 \pm 0.11$	ADLER	87 MRK3	e^+e^- 3.77 GeV
• • • We do not use the following data for averages, fits, limits, etc. • • •			
$0.185 \pm 0.015 \pm 0.014$	[45] AITALA	02 E791	π^- nucleus, 500 GeV

[45] AITALA 02 includes a broad scalar $K_0^*(800)$ in the fit to the $D^+ \to K^-\pi^+\pi^+$ Dalitz plot. This (a) greatly improves the fit, and (b) gives results in other channels that greatly disagree with previous analyses. The disagreement is so large that it makes no sense to average the results with those of earlier experiments. For now, we exclude AITALA 02 from the average.

$\Gamma(\overline{K}_0^*(1430)^0\pi^+)/\Gamma(K^-\pi^+\pi^+)$ Γ_{91}/Γ_{39}

Unseen decay modes of the $\overline{K}_0^*(1430)^0$ are included.

VALUE	DOCUMENT ID	TECN	COMMENT
0.41 ± 0.04 OUR AVERAGE			
$0.458 \pm 0.035 \pm 0.094$	FRABETTI	94G E687	γBe, $\overline{E}_\gamma \approx 220$ GeV
$0.400 \pm 0.031 \pm 0.027$	ANJOS	93 E691	γBe 90–260 GeV
• • • We do not use the following data for averages, fits, limits, etc. • • •			
$0.202 \pm 0.023 \pm 0.008$	[46] AITALA	02 E791	π^- nucleus, 500 GeV

[46] AITALA 02 includes a broad scalar $K_0^*(800)$ in the fit to the $D^+ \to K^-\pi^+\pi^+$ Dalitz plot. This (a) greatly improves the fit, and (b) gives results in other channels that greatly disagree with previous analyses. The disagreement is so large that it makes no sense to average the results with those of earlier experiments. For now, we exclude AITALA 02 from the average.

$\Gamma(\overline{K}_2^*(1430)^0\pi^+)/\Gamma(K^-\pi^+\pi^+)$ Γ_{92}/Γ_{39}

Unseen decay modes of the $\overline{K}_2^*(1430)^0$ are included.

VALUE	DOCUMENT ID	TECN	COMMENT
• • • We do not use the following data for averages, fits, limits, etc. • • •			
$0.015 \pm 0.003 \pm 0.006$	[47] AITALA	02 E791	π^- nucleus, 500 GeV

[47] AITALA 02 includes a broad scalar $K_0^*(800)$ in the fit to the $D^+ \to K^-\pi^+\pi^+$ Dalitz plot. This (a) greatly improves the fit, and (b) gives results in other channels that greatly disagree with previous analyses. The disagreement is so large that it makes no sense to average the results with those of earlier experiments. For now, we exclude AITALA 02 from the average.

$\Gamma(\overline{K}^*(1680)^0\pi^+)/\Gamma(K^-\pi^+\pi^+)$ Γ_{93}/Γ_{39}

Unseen decay modes of the $\overline{K}^*(1680)^0$ are included.

VALUE	DOCUMENT ID	TECN	COMMENT
0.160 ± 0.032 OUR AVERAGE Error includes scale factor of 1.1.			
$0.182 \pm 0.023 \pm 0.028$	FRABETTI	94G E687	γBe, $\overline{E}_\gamma \approx 220$ GeV
$0.113 \pm 0.015 \pm 0.050$	ANJOS	93 E691	γBe 90–260 GeV
• • • We do not use the following data for averages, fits, limits, etc. • • •			
$0.097 \pm 0.027 \pm 0.012$	[48] AITALA	02 E791	π^- nucleus, 500 GeV

[48] AITALA 02 includes a broad scalar $K_0^*(800)$ in the fit to the $D^+ \to K^-\pi^+\pi^+$ Dalitz plot. This (a) greatly improves the fit, and (b) gives results in other channels that greatly disagree with previous analyses. The disagreement is so large that it makes no sense to average the results with those of earlier experiments. For now, we exclude AITALA 02 from the average.

$\Gamma(K^-\pi^+\pi^+ \text{nonresonant})/\Gamma(K^-\pi^+\pi^+)$ Γ_{45}/Γ_{39}

VALUE	DOCUMENT ID	TECN	COMMENT
0.95 ± 0.07 OUR AVERAGE			
$0.998 \pm 0.037 \pm 0.072$	FRABETTI	94G E687	γBe, $\overline{E}_\gamma \approx 220$ GeV
$0.838 \pm 0.088 \pm 0.275$	ANJOS	93 E691	γBe 90–260 GeV
$0.79 \pm 0.07 \pm 0.15$	ADLER	87 MRK3	e^+e^- 3.77 GeV
• • • We do not use the following data for averages, fits, limits, etc. • • •			
$0.130 \pm 0.058 \pm 0.044$	[49] AITALA	02 E791	π^- nucleus, 500 GeV

[49] AITALA 02 includes a broad scalar $K_0^*(800)$ in the fit to the $D^+ \to K^-\pi^+\pi^+$ Dalitz plot. This (a) greatly improves the fit, and (b) gives results in other channels that greatly disagree with previous analyses. The disagreement is so large that it makes no sense to average the results with those of earlier experiments. For now, we exclude AITALA 02 from the average.

$\Gamma(\overline{K}^0\pi^+\pi^0)/\Gamma_{\text{total}}$ Γ_{46}/Γ

VALUE	EVTS	DOCUMENT ID	TECN	COMMENT
0.097 ± 0.030 OUR FIT Error includes scale factor of 1.1.				
0.107 ± 0.029 OUR AVERAGE				
$0.102 \pm 0.025 \pm 0.016$	159	ADLER	88C MRK3	e^+e^- 3.77 GeV
0.19 ± 0.12	10	[50] SCHINDLER	81 MRK2	e^+e^- 3.771 GeV

[50] SCHINDLER 81 (MARK-2) measures $\sigma(e^+e^- \to \psi(3770)) \times$ branching fraction to be 0.78 ± 0.48 nb. We use the MARK-3 (ADLER 88C) value of $\sigma = 4.2 \pm 0.6 \pm 0.3$ nb.

$\Gamma(\overline{K}^0\rho^+)/\Gamma(\overline{K}^0\pi^+\pi^0)$ Γ_{47}/Γ_{46}

VALUE	DOCUMENT ID	TECN	COMMENT
0.68 ± 0.08 ± 0.12	ADLER	87 MRK3	e^+e^- 3.77 GeV

$\Gamma(\overline{K}^*(892)^0\pi^+)/\Gamma(\overline{K}^0\pi^+\pi^0)$ Γ_{82}/Γ_{46}

Unseen decay modes of the $\overline{K}^*(892)^0$ are included.

VALUE	DOCUMENT ID		TECN	COMMENT
0.20±0.06 OUR FIT				
0.57±0.18±0.18	ADLER	87	MRK3	e^+e^- 3.77 GeV

$\Gamma(\overline{K}^0\pi^+\pi^0$ nonresonant$)/\Gamma(\overline{K}^0\pi^+\pi^0)$ Γ_{49}/Γ_{46}

VALUE	DOCUMENT ID		TECN	COMMENT
0.13±0.07±0.08	ADLER	87	MRK3	e^+e^- 3.77 GeV

$\Gamma(K^-\pi^+\pi^+\pi^0)/\Gamma_{\text{total}}$ Γ_{50}/Γ

VALUE	EVTS	DOCUMENT ID		TECN	COMMENT
0.065±0.011 OUR FIT					
0.058±0.012±0.012	142	COFFMAN	92B	MRK3	e^+e^- 3.77 GeV
• • • We do not use the following data for averages, fits, limits, etc. • • •					
$0.034^{+0.056}_{-0.070}$		[51] BARLAG	92C	ACCM	π^- Cu 230 GeV
$0.022^{+0.047}_{-0.006}\pm0.004$	1	[51] AGUILAR-...	87F	HYBR	πp, pp 360, 400 GeV
$0.063^{+0.014}_{-0.013}\pm0.012$	175	BALTRUSAIT...	86E	MRK3	See COFFMAN 92B

[51] AGUILAR-BENITEZ 87F and BARLAG 92C compute the branching fraction by topological normalization.

$\Gamma(K^-\pi^+\pi^+\pi^0)/\Gamma(K^-\pi^+\pi^+)$ Γ_{50}/Γ_{39}

VALUE	EVTS	DOCUMENT ID		TECN	COMMENT
0.70±0.12 OUR FIT					
0.76±0.11±0.12	91	ANJOS	92C	E691	γBe 90–260 GeV
• • • We do not use the following data for averages, fits, limits, etc. • • •					
0.69±0.10±0.16		ANJOS	89E	E691	See ANJOS 92C
$0.57^{+0.65}_{-0.17}$	1	AGUILAR-...	83B	HYBR	π^-p, 360 GeV

$\Gamma(\overline{K}^*(892)^0\rho^+$total$)/\Gamma(K^-\pi^+\pi^+\pi^0)$ Γ_{83}/Γ_{50}

Unseen decay modes of the $\overline{K}^*(892)^0$ are included.

VALUE	DOCUMENT ID		TECN	COMMENT
0.33±0.165±0.12	[52] ANJOS	92C	E691	γBe 90–260 GeV

[52] See, however, the next entry, where the two experiments disagree completely.

$\Gamma(\overline{K}^*(892)^0\rho^+$ S-wave$)/\Gamma(K^-\pi^+\pi^+\pi^0)$ Γ_{84}/Γ_{50}

Unseen decay modes of the $\overline{K}^*(892)^0$ are included. The two experiments here disagree completely.

VALUE	DOCUMENT ID		TECN	COMMENT
0.26 ±0.25 OUR AVERAGE	Error includes scale factor of 3.1.			
0.15 ±0.075±0.045	ANJOS	92C	E691	γBe 90–260 GeV
0.833±0.116±0.165	COFFMAN	92B	MRK3	e^+e^- 3.77 GeV

$\Gamma(\overline{K}^*(892)^0\rho^+$ P-wave$)/\Gamma_{\text{total}}$ Γ_{85}/Γ

Unseen decay modes of the $\overline{K}^*(892)^0$ are included.

VALUE	CL%	DOCUMENT ID		TECN	COMMENT
<0.001	90	ANJOS	92C	E691	γBe 90–260 GeV
• • • We do not use the following data for averages, fits, limits, etc. • • •					
<0.005	90	COFFMAN	92B	MRK3	e^+e^- 3.77 GeV

$\Gamma(\overline{K}^*(892)^0\rho^+$ D-wave$)/\Gamma(K^-\pi^+\pi^+\pi^0)$ Γ_{86}/Γ_{50}

Unseen decay modes of the $\overline{K}^*(892)^0$ are included.

VALUE	DOCUMENT ID		TECN	COMMENT
0.15±0.09±0.045	ANJOS	92C	E691	γBe 90–260 GeV

$\Gamma(\overline{K}^*(892)^0\rho^+$ D-wave longitudinal$)/\Gamma_{\text{total}}$ Γ_{87}/Γ

Unseen decay modes of the $\overline{K}^*(892)^0$ are included.

VALUE	CL%	DOCUMENT ID		TECN	COMMENT
<0.007	90	COFFMAN	92B	MRK3	e^+e^- 3.77 GeV

$\Gamma(\overline{K}_1(1400)^0\pi^+)/\Gamma(K^-\pi^+\pi^+\pi^0)$ Γ_{89}/Γ_{50}

Unseen decay modes of the $\overline{K}_1(1400)^0$ are included.

VALUE	DOCUMENT ID		TECN	COMMENT
0.77 ±0.20 OUR FIT				
0.907±0.218±0.180	COFFMAN	92B	MRK3	e^+e^- 3.77 GeV

$\Gamma(K^-\rho^+\pi^+$total$)/\Gamma(K^-\pi^+\pi^+\pi^0)$ Γ_{98}/Γ_{50}

This includes $\overline{K}^*(892)^0\rho^+$, *etc.* The next entry gives the specifically 3-body fraction.

VALUE	DOCUMENT ID		TECN	COMMENT
0.48±0.13±0.09	ANJOS	92C	E691	γBe 90–260 GeV

$\Gamma(K^-\rho^+\pi^+$ 3-body$)/\Gamma(K^-\pi^+\pi^+\pi^0)$ Γ_{99}/Γ_{50}

VALUE	DOCUMENT ID		TECN	COMMENT
0.17 ±0.06 OUR AVERAGE				
0.18 ±0.08 ±0.04	ANJOS	92C	E691	γBe 90–260 GeV
0.159±0.065±0.060	COFFMAN	92B	MRK3	e^+e^- 3.77 GeV

$\Gamma(\overline{K}^*(892)^0\pi^+\pi^0$total$)/\Gamma(K^-\pi^+\pi^+\pi^0)$ Γ_{94}/Γ_{50}

This includes $\overline{K}^*(892)^0\rho^+$, *etc.* The next two entries give the specifically 3-body fraction. Unseen decay modes of the $\overline{K}^*(892)^0$ are included.

VALUE	DOCUMENT ID		TECN	COMMENT
1.05±0.11±0.08	ANJOS	92C	E691	γBe 90–260 GeV

$\Gamma(\overline{K}^*(892)^0\pi^+\pi^0$ 3-body$)/\Gamma_{\text{total}}$ Γ_{95}/Γ

Unseen decay modes of the $\overline{K}^*(892)^0$ are included.

VALUE	CL%	DOCUMENT ID		TECN	COMMENT
• • • We do not use the following data for averages, fits, limits, etc. • • •					
<0.008	90	[53] COFFMAN	92B	MRK3	e^+e^- 3.77 GeV

[53] See, however, the next entry: ANJOS 92C sees a large signal in this channel.

$\Gamma(\overline{K}^*(892)^0\pi^+\pi^0$ 3-body$)/\Gamma(K^-\pi^+\pi^+\pi^0)$ Γ_{95}/Γ_{50}

Unseen decay modes of the $\overline{K}^*(892)^0$ are included.

VALUE	DOCUMENT ID		TECN	COMMENT
0.66±0.09±0.17	ANJOS	92C	E691	γBe 90–260 GeV

$\Gamma(K^*(892)^-\pi^+\pi^+$ 3-body$)/\Gamma(K^-\pi^+\pi^+\pi^0)$ Γ_{97}/Γ_{50}

Unseen decay modes of the $K^*(892)^-$ are included.

VALUE	DOCUMENT ID		TECN	COMMENT
0.32±0.14 OUR FIT	Error includes scale factor of 1.1.			
0.24±0.12±0.09	ANJOS	92C	E691	γBe 90–260 GeV

$\Gamma(K^-\pi^+\pi^+\pi^0$ nonresonant$)/\Gamma_{\text{total}}$ Γ_{58}/Γ

VALUE	CL%	DOCUMENT ID		TECN	COMMENT
• • • We do not use the following data for averages, fits, limits, etc. • • •					
<0.002	90	[54] ANJOS	92C	E691	γBe 90–260 GeV

[54] Whereas ANJOS 92C finds no signal here, COFFMAN 92B finds a fairly large one; see the next entry.

$\Gamma(K^-\pi^+\pi^+\pi^0$ nonresonant$)/\Gamma(K^-\pi^+\pi^+\pi^0)$ Γ_{58}/Γ_{50}

VALUE	DOCUMENT ID		TECN	COMMENT
0.184±0.070±0.050	COFFMAN	92B	MRK3	e^+e^- 3.77 GeV

$\Gamma(\overline{K}^0\pi^+\pi^+\pi^-)/\Gamma_{\text{total}}$ Γ_{59}/Γ

VALUE	EVTS	DOCUMENT ID		TECN	COMMENT
$0.071^{+0.010}_{-0.009}$ OUR FIT					
0.071±0.016 OUR AVERAGE					
0.066±0.015±0.005	168	ADLER	88C	MRK3	e^+e^- 3.77 GeV
0.12 ±0.05	21	[55] SCHINDLER	81	MRK2	e^+e^- 3.771 GeV
• • • We do not use the following data for averages, fits, limits, etc. • • •					
$0.042^{+0.019}_{-0.017}$		[56] BARLAG	92C	ACCM	π^- Cu 230 GeV
$0.243^{+0.064}_{-0.041}\pm0.041$	11	[56] AGUILAR-...	87F	HYBR	πp, pp 360, 400 GeV

[55] SCHINDLER 81 (MARK-2) measures $\sigma(e^+e^- \to \psi(3770)) \times$ branching fraction to be 0.51 ± 0.08 nb. We use the MARK-3 (ADLER 88C) value of $\sigma = 4.2 \pm 0.6 \pm 0.3$ nb.

[56] AGUILAR-BENITEZ 87F and BARLAG 92C compute the branching fraction by topological normalization.

$\Gamma(\overline{K}^0\pi^+\pi^+\pi^-)/\Gamma(K^-\pi^+\pi^+)$ Γ_{59}/Γ_{39}

VALUE	EVTS	DOCUMENT ID		TECN	COMMENT
0.77±0.10 OUR FIT					
0.77±0.07±0.11	229	ANJOS	92C	E691	γBe 90–260 GeV

$\Gamma(\overline{K}^0 a_1(1260)^+)/\Gamma(\overline{K}^0\pi^+\pi^+\pi^-)$ Γ_{79}/Γ_{59}

Unseen decay modes of the $a_1(1260)^+$ are included, assuming that the $a_1(1260)^+$ decays entirely to $\rho\pi$ [or at least to $(\pi\pi)_{I=1}\ \pi$].

VALUE	DOCUMENT ID		TECN	COMMENT
1.15 ±0.19 OUR AVERAGE	Error includes scale factor of 1.1.			
1.66 ±0.28 ±0.40	ANJOS	92C	E691	γBe 90–260 GeV
1.078±0.114±0.140	COFFMAN	92B	MRK3	e^+e^- 3.77 GeV

$\Gamma(\overline{K}^0 a_2(1320)^+)/\Gamma_{\text{total}}$ Γ_{80}/Γ

Unseen decay modes of the $a_2(1320)^+$ are included.

VALUE	CL%	DOCUMENT ID		TECN	COMMENT
<0.003	90	ANJOS	92C	E691	γBe 90–260 GeV
• • • We do not use the following data for averages, fits, limits, etc. • • •					
<0.008	90	COFFMAN	92B	MRK3	e^+e^- 3.77 GeV

$\Gamma(\overline{K}_1(1270)^0\pi^+)/\Gamma_{\text{total}}$ Γ_{88}/Γ

Unseen decay modes of the $\overline{K}_1(1270)^0$ are included.

VALUE	CL%	DOCUMENT ID		TECN	COMMENT
<0.007	90	ANJOS	92C	E691	γBe 90–260 GeV
• • • We do not use the following data for averages, fits, limits, etc. • • •					
<0.011	90	COFFMAN	92B	MRK3	e^+e^- 3.77 GeV

$\Gamma(\overline{K}_1(1400)^0\pi^+)/\Gamma_{\text{total}}$ Γ_{89}/Γ

Unseen decay modes of the $\overline{K}_1(1400)^0$ are included.

VALUE	CL%	DOCUMENT ID		TECN	COMMENT
• • • We do not use the following data for averages, fits, limits, etc. • • •					
<0.009	90	[57] ANJOS	92C	E691	γBe 90–260 GeV

[57] ANJOS 92C sees no evidence for $\overline{K}_1(1400)^0\pi^+$ in either the $\overline{K}^0\pi^+\pi^+\pi^-$ or $K^-\pi^+\pi^+\pi^0$ channels, whereas COFFMAN 92B finds the $\overline{K}_1(1400)^0\pi^+$ branching fraction to be large; see the next entry.

$\Gamma(\overline{K}_1(1400)^0\pi^+)/\Gamma(\overline{K}^0\pi^+\pi^+\pi^-)$ Γ_{89}/Γ_{59}

Unseen decay modes of the $\overline{K}_1(1400)^0$ are included.

VALUE	DOCUMENT ID	TECN	COMMENT
0.70 ±0.17 OUR FIT			
0.623±0.106±0.180	COFFMAN	92B MRK3	e^+e^- 3.77 GeV

$\Gamma(\overline{K}^*(1410)^0\pi^+)/\Gamma_{\text{total}}$ Γ_{90}/Γ

VALUE	CL%	DOCUMENT ID	TECN	COMMENT
• • • We do not use the following data for averages, fits, limits, etc. • • •				
<0.007	90	COFFMAN	92B MRK3	e^+e^- 3.77 GeV

$\Gamma(K^*(892)^-\pi^+\pi^+\text{total})/\Gamma(\overline{K}^0\pi^+\pi^+\pi^-)$ Γ_{96}/Γ_{59}

Unseen decay modes of the $K^*(892)^-$ are included.

VALUE	EVTS	DOCUMENT ID	TECN	COMMENT
• • • We do not use the following data for averages, fits, limits, etc. • • •				
0.41±0.14	14	ALEEV	94 BIS2	nN 20–70 GeV

$\Gamma(K^*(892)^-\pi^+\pi^+\text{3-body})/\Gamma_{\text{total}}$ Γ_{97}/Γ

Unseen decay modes of the $\overline{K}^*(892)^0$ are included.

VALUE	CL%	DOCUMENT ID	TECN	COMMENT
0.021±0.009 OUR FIT				
• • • We do not use the following data for averages, fits, limits, etc. • • •				
<0.013	90	COFFMAN	92B MRK3	e^+e^- 3.77 GeV

$\Gamma(K^*(892)^-\pi^+\pi^+\text{3-body})/\Gamma(\overline{K}^0\pi^+\pi^+\pi^-)$ Γ_{97}/Γ_{59}

Unseen decay modes of the $K^*(892)^-$ are included.

VALUE	DOCUMENT ID	TECN	COMMENT
0.29±0.13 OUR FIT Error includes scale factor of 1.1.			
0.50±0.09±0.21	ANJOS	92C E691	γBe 90–260 GeV

$\Gamma(\overline{K}^0\rho^0\pi^+\text{total})/\Gamma(\overline{K}^0\pi^+\pi^+\pi^-)$ Γ_{100}/Γ_{59}

This includes $\overline{K}^0 a_1(1260)^+$. The next two entries give the specifically 3-body reaction.

VALUE	CL%	DOCUMENT ID	TECN	COMMENT
0.60±0.10±0.17	90	ANJOS	92C E691	γBe 90–260 GeV

$\Gamma(\overline{K}^0\rho^0\pi^+\text{3-body})/\Gamma_{\text{total}}$ Γ_{101}/Γ

VALUE	CL%	DOCUMENT ID	TECN	COMMENT
• • • We do not use the following data for averages, fits, limits, etc. • • •				
<0.004	90	COFFMAN	92B MRK3	e^+e^- 3.77 GeV

$\Gamma(\overline{K}^0\rho^0\pi^+\text{3-body})/\Gamma(\overline{K}^0\pi^+\pi^+\pi^-)$ Γ_{101}/Γ_{59}

VALUE	DOCUMENT ID	TECN	COMMENT
0.07±0.04±0.06	ANJOS	92C E691	γBe 90–260 GeV

$\Gamma(\overline{K}^0 f_0(980)\pi^+)/\Gamma_{\text{total}}$ Γ_{102}/Γ

VALUE	CL%	DOCUMENT ID	TECN	COMMENT
• • • We do not use the following data for averages, fits, limits, etc. • • •				
<0.005	90	ANJOS	92C E691	γBe 90–260 GeV

$\Gamma(\overline{K}^0\pi^+\pi^+\pi^-\text{ nonresonant})/\Gamma(\overline{K}^0\pi^+\pi^+\pi^-)$ Γ_{65}/Γ_{59}

VALUE	DOCUMENT ID	TECN	COMMENT
0.12±0.06 OUR AVERAGE			
0.10±0.04 ±0.06	ANJOS	92C E691	γBe 90–260 GeV
0.17±0.056±0.100	COFFMAN	92B MRK3	e^+e^- 3.77 GeV

$\Gamma(K^-3\pi^+\pi^-)/\Gamma(K^-\pi^+\pi^+)$ Γ_{66}/Γ_{39}

VALUE	EVTS	DOCUMENT ID	TECN	COMMENT
0.067±0.007 OUR FIT Error includes scale factor of 1.5.				
0.066±0.008 OUR AVERAGE Error includes scale factor of 1.6. See the ideogram below.				
0.058±0.002±0.006	2923	LINK	03D FOCS	γ nucleus, $\overline{E}_\gamma \approx 180$ GeV
0.077±0.008±0.010	239	FRABETTI	97C E687	γBe, $\overline{E}_\gamma \approx 200$ GeV
0.09 ±0.01 ±0.01	113	ANJOS	90D E691	Photoproduction

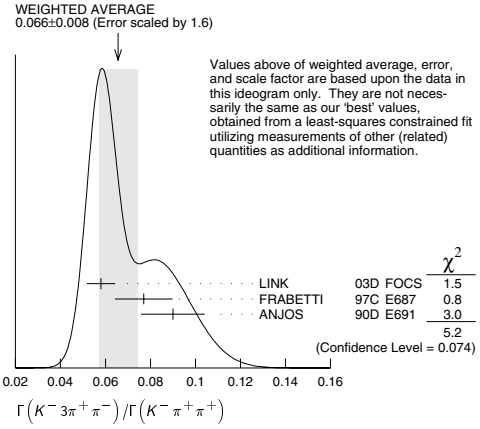

$\Gamma(\overline{K}^*(892)^0\pi^+\pi^+\pi^-)/\Gamma(K^-3\pi^+\pi^-)$ Γ_{103}/Γ_{66}

Unseen decay modes of the $\overline{K}^*(892)^0$ are included.

VALUE	DOCUMENT ID	TECN	COMMENT
0.51±0.19 OUR FIT Error includes scale factor of 2.2.			
0.46±0.33 OUR AVERAGE Error includes scale factor of 3.3.			
0.32±0.06±0.09	LINK	03D FOCS	γ nucleus, $\overline{E}_\gamma \approx 180$ GeV
1.25±0.12±0.23	ANJOS	90D E691	Photoproduction

$\Gamma(\overline{K}^*(892)^0\rho^0\pi^+)/\Gamma(K^-\pi^+\pi^+)$ Γ_{104}/Γ_{39}

Unseen decay modes of the $\overline{K}^*(892)^0$ are included.

VALUE	DOCUMENT ID	TECN	COMMENT
0.033±0.008 OUR FIT Error includes scale factor of 1.4.			
0.023±0.010±0.006	FRABETTI	97C E687	γBe, $\overline{E}_\gamma \approx 200$ GeV

$\Gamma(\overline{K}^*(892)^0\rho^0\pi^+)/\Gamma(K^-3\pi^+\pi^-)$ Γ_{104}/Γ_{66}

Unseen decay modes of the $\overline{K}^*(892)^0$ are included.

VALUE	DOCUMENT ID	TECN	COMMENT
0.49±0.11 OUR FIT Error includes scale factor of 1.5.			
0.60±0.05±0.09	LINK	03D FOCS	γ nucleus, $\overline{E}_\gamma \approx 180$ GeV

$\Gamma(\overline{K}^*(892)^0\rho^0\pi^+)/\Gamma(\overline{K}^*(892)^0\pi^+\pi^+\pi^-)$ $\Gamma_{104}/\Gamma_{103}$

VALUE	DOCUMENT ID	TECN	COMMENT
0.95±0.24 OUR FIT Error includes scale factor of 1.4.			
0.75±0.17±0.19	ANJOS	90D E691	Photoproduction

$\Gamma(\overline{K}^*(892)^0\pi^+\pi^+\pi^-\text{ no-}\rho)/\Gamma(K^-\pi^+\pi^+)$ Γ_{105}/Γ_{39}

Unseen decay modes of the $\overline{K}^*(892)^0$ are included.

VALUE	DOCUMENT ID	TECN	COMMENT
0.048±0.015±0.011	FRABETTI	97C E687	γBe, $\overline{E}_\gamma \approx 200$ GeV

$\Gamma(K^-\rho^0\pi^+\pi^+)/\Gamma(K^-\pi^+\pi^+)$ Γ_{70}/Γ_{39}

VALUE	DOCUMENT ID	TECN	COMMENT
0.021±0.004 OUR FIT Error includes scale factor of 1.2.			
0.034±0.009±0.005	FRABETTI	97C E687	γBe, $\overline{E}_\gamma \approx 200$ GeV

$\Gamma(K^-\rho^0\pi^+\pi^+)/\Gamma(K^-3\pi^+\pi^-)$ Γ_{70}/Γ_{66}

VALUE	DOCUMENT ID	TECN	COMMENT
0.31±0.04 OUR FIT			
0.30±0.04±0.01	LINK	03D FOCS	γ nucleus, $\overline{E}_\gamma \approx 180$ GeV

$\Gamma(\overline{K}^*(892)^0 a_1(1260)^+)/\Gamma(K^-\pi^+\pi^+)$ Γ_{107}/Γ_{39}

Unseen decay modes of the $\overline{K}^*(892)^0$ and $a_1(1260)^+$ are included.

VALUE	DOCUMENT ID	TECN	COMMENT
0.099±0.008±0.018	LINK	03D FOCS	γ nucleus, $\overline{E}_\gamma \approx 180$ GeV

$\Gamma(K^-3\pi^+\pi^-\text{ nonresonant})/\Gamma(K^-3\pi^+\pi^-)$ Γ_{71}/Γ_{66}

VALUE	CL%	DOCUMENT ID	TECN	COMMENT
0.07 ±0.05±0.01		LINK	03D FOCS	γ nucleus, $\overline{E}_\gamma \approx 180$ GeV
• • • We do not use the following data for averages, fits, limits, etc. • • •				
<0.026	90	FRABETTI	97C E687	γBe, $\overline{E}_\gamma \approx 200$ GeV

$\Gamma(K^-2\pi^+2\pi^0)/\Gamma_{\text{total}}$ Γ_{72}/Γ

VALUE	EVTS	DOCUMENT ID	TECN	COMMENT
• • • We do not use the following data for averages, fits, limits, etc. • • •				
<0.015		[58] BARLAG	92C ACCM	π^- Cu 230 GeV
$0.022^{+0.047}_{-0.008}\pm0.004$	1	[58] AGUILAR-...	87F HYBR	πp, pp 360, 400 GeV

[58] AGUILAR-BENITEZ 87F and BARLAG 92C compute the branching fraction by topological normalization.

$\Gamma(\overline{K}^0 2\pi^+\pi^-\pi^0)/\Gamma_{\text{total}}$ Γ_{73}/Γ

VALUE	EVTS	DOCUMENT ID	TECN	COMMENT
• • • We do not use the following data for averages, fits, limits, etc. • • •				
$0.099^{+0.036}_{-0.070}$		[59] BARLAG	92C ACCM	π^- Cu 230 GeV
$0.044^{+0.052}_{-0.013}\pm0.007$	2	[59] AGUILAR-...	87F HYBR	πp, pp 360, 400 GeV

[59] AGUILAR-BENITEZ 87F and BARLAG 92C compute the branching fraction by topological normalization.

$\Gamma(\overline{K}^0 3\pi^+2\pi^-)/\Gamma_{\text{total}}$ Γ_{74}/Γ

VALUE	DOCUMENT ID	TECN	COMMENT
• • • We do not use the following data for averages, fits, limits, etc. • • •			
0.0008±0.0007	[60] BARLAG	92C ACCM	π^- Cu 230 GeV

[60] BARLAG 92C computes the branching fraction using topological normalization.

$\Gamma(K^-3\pi^+\pi^-\pi^0)/\Gamma_{\text{total}}$ Γ_{75}/Γ

VALUE	DOCUMENT ID	TECN	COMMENT
• • • We do not use the following data for averages, fits, limits, etc. • • •			
0.0020±0.0018	[61] BARLAG	92C ACCM	π^- Cu 230 GeV

[61] BARLAG 92C computes the branching fraction using topological normalization.

$\Gamma(\overline{K}^0 K^0 K^+)/\Gamma(K^-\pi^+\pi^+)$ Γ_{76}/Γ_{39}

VALUE	EVTS	DOCUMENT ID		TECN	COMMENT
0.20 ± 0.09 OUR AVERAGE		Error includes scale factor of 2.4.			
0.14 ± 0.04 ± 0.02	39	ALBRECHT	94I	ARG	$e^+e^-\approx 10$ GeV
0.34 ± 0.07	70	AMMAR	91	CLEO	$e^+e^-\approx 10.5$ GeV

$\Gamma(K^+K^-\overline{K}^0\pi^+)/\Gamma(\overline{K}^0\pi^+\pi^+\pi^-)$ Γ_{77}/Γ_{59}

VALUE	EVTS	DOCUMENT ID		TECN	COMMENT
0.0077 ± 0.0015 ± 0.0009	35	LINK	01C	FOCS	γ nucleus, $\overline{E}_\gamma \approx 180$ GeV

Pionic modes

$\Gamma(\pi^+\pi^0)/\Gamma(K^-\pi^+\pi^+)$ Γ_{108}/Γ_{39}

VALUE	EVTS	DOCUMENT ID		TECN	COMMENT
0.028 ± 0.006 ± 0.005	34	SELEN	93	CLE2	$e^+e^-\approx \Upsilon(4S)$

$\Gamma(\pi^+\pi^+\pi^-)/\Gamma(K^-\pi^+\pi^+)$ Γ_{109}/Γ_{39}

VALUE	EVTS	DOCUMENT ID		TECN	COMMENT
0.0341 $^{+0.0035}_{-0.0042}$ OUR AVERAGE		Error includes scale factor of 1.7. See the ideogram below.			
0.0311 ± 0.0018 $^{+0.0016}_{-0.0026}$	1172	AITALA	01B	E791	π^- nucleus, 500 GeV
0.043 ± 0.003 ± 0.003	236	FRABETTI	97D	E687	γ Be $\approx$ 200 GeV
0.035 ± 0.007 ± 0.003	83	ANJOS	89	E691	Photoproduction
• • • We do not use the following data for averages, fits, limits, etc. • • •					
0.032 ± 0.011 ± 0.003	20	ADAMOVICH	93	WA82	π^- 340 GeV
0.042 ± 0.016 ± 0.010	57	BALTRUSAIT...85E		MRK3	e^+e^- 3.77 GeV

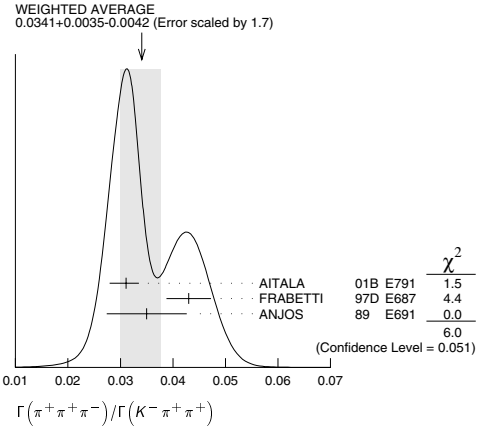

$\Gamma(\sigma\pi^+)/\Gamma(\pi^+\pi^+\pi^-)$ $\Gamma_{110}/\Gamma_{109}$

Unseen decay modes of the σ are included.

VALUE	DOCUMENT ID			TECN	COMMENT
0.695 ± 0.135 ± 0.032	[62] AITALA		01B	E791	π^- nucleus, 500 GeV

[62] See AITALA 01B for the magnitude and phase of this amplitude relative to the $\rho^0\pi^+$ amplitude. The branching ratio given here is 3/2 the paper's value, to allow for $\pi^0\pi^0$ decays.

$\Gamma(\rho^0\pi^+)/\Gamma(\pi^+\pi^+\pi^-)$ $\Gamma_{111}/\Gamma_{109}$

VALUE	DOCUMENT ID			TECN	COMMENT
0.336 ± 0.032 ± 0.022	AITALA		01B	E791	π^- nucleus, 500 GeV
• • • We do not use the following data for averages, fits, limits, etc. • • •					
0.289 ± 0.055 ± 0.058	[63] FRABETTI		97D	E687	γ Be $\approx$ 200 GeV

[63] FRABETTI 97D also includes $f_2(1270)\pi^+$ and $f_0(980)\pi^+$ modes in the fit, but the resulting decay fractions are not statistically significant.

$\Gamma(\rho^0\pi^+)/\Gamma(K^-\pi^+\pi^+)$ Γ_{111}/Γ_{39}

VALUE	CL%	DOCUMENT ID		TECN	COMMENT
• • • We do not use the following data for averages, fits, limits, etc. • • •					
< 0.015	90	ANJOS	89	E691	Photoproduction

$\Gamma(f_0(980)\pi^+ \times B(f_0 \to \pi^+\pi^-))/\Gamma(\pi^+\pi^+\pi^-)$ $\Gamma_{112}/\Gamma_{109}$

This includes only the $\pi^+\pi^-$ decays of the $f_0(980)$, because branching fractions of this resonance are not known.

VALUE	DOCUMENT ID			TECN	COMMENT
0.062 ± 0.013 ± 0.004	[64] AITALA		01B	E791	π^- nucleus, 500 GeV

[64] See AITALA 01B for the magnitude and phase of this amplitude relative to the $\rho^0\pi^+$ amplitude.

$\Gamma(f_2(1270)\pi^+)/\Gamma(\pi^+\pi^+\pi^-)$ $\Gamma_{128}/\Gamma_{109}$

Unseen decay modes of the $f_2(1270)$ are included.

VALUE	DOCUMENT ID			TECN	COMMENT
0.343 ± 0.044 ± 0.007	[65] AITALA		01B	E791	π^- nucleus, 500 GeV

[65] See AITALA 01B for the magnitude and phase of this amplitude relative to the $\rho^0\pi^+$ amplitude.

$\Gamma(f_0(1370)\pi^+ \times B(f_0(1370) \to \pi^+\pi^-))/\Gamma(\pi^+\pi^+\pi^-)$ $\Gamma_{114}/\Gamma_{109}$

This includes only the $\pi^+\pi^-$ decays of the $f_0(1370)$, because branching fractions of this resonance are not known.

VALUE	DOCUMENT ID			TECN	COMMENT
• • • We do not use the following data for averages, fits, limits, etc. • • •					
0.023 ± 0.015 ± 0.008	[66] AITALA		01B	E791	π^- nucleus, 500 GeV

[66] This AITALA 01B result does not have enough statistical significance to advance it to the Summary Tables.

$\Gamma(\rho(1450)^0\pi^+ \times B(\rho(1450)^0 \to \pi^+\pi^-))/\Gamma(\pi^+\pi^+\pi^-)$ $\Gamma_{115}/\Gamma_{109}$

This includes only the $\pi^+\pi^-$ decays of the $\rho(1450)$, because branching fractions of this resonance are not known.

VALUE	DOCUMENT ID			TECN	COMMENT
• • • We do not use the following data for averages, fits, limits, etc. • • •					
0.007 ± 0.007 ± 0.003	[67] AITALA		01B	E791	π^- nucleus, 500 GeV

[67] This AITALA 01B result does not have enough statistical significance to advance it to the Summary Tables.

$\Gamma(\pi^+\pi^+\pi^-$ nonresonant$)/\Gamma(\pi^+\pi^+\pi^-)$ $\Gamma_{116}/\Gamma_{109}$

The big difference between the results here of AITALA 01B and FRABETTI 97D is the addition of the $\sigma\pi^+$ channel to the AITALA 01B fit.

VALUE	DOCUMENT ID			TECN	COMMENT
0.078 ± 0.060 ± 0.027	[68] AITALA		01B	E791	π^- nucleus, 500 GeV
• • • We do not use the following data for averages, fits, limits, etc. • • •					
0.589 ± 0.105 ± 0.081	[69] FRABETTI		97D	E687	γ Be $\approx$ 200 GeV

[68] See AITALA 01B for the magnitude and phase of this amplitude relative to the $\rho^0\pi^+$ amplitude.

[69] FRABETTI 97D also includes $f_2(1270)\pi^+$ and $f_0(980)\pi^+$ modes in the fit, but the resulting decay fractions are not statistically significant.

$\Gamma(\pi^+\pi^+\pi^-$ nonresonant$)/\Gamma(K^-\pi^+\pi^+)$ Γ_{116}/Γ_{39}

VALUE	DOCUMENT ID			TECN	COMMENT
• • • We do not use the following data for averages, fits, limits, etc. • • •					
0.027 ± 0.007 ± 0.002	ANJOS		89	E691	Photoproduction

$\Gamma(\pi^+\pi^+\pi^-\pi^0)/\Gamma_{\text{total}}$ Γ_{117}/Γ

VALUE	DOCUMENT ID			TECN	COMMENT
• • • We do not use the following data for averages, fits, limits, etc. • • •					
0.019 $^{+0.015}_{-0.012}$	[70] BARLAG		92C	ACCM	π^- Cu 230 GeV

[70] BARLAG 92C computes the branching fraction using topological normalization.

$\Gamma(\pi^+\pi^+\pi^-\pi^0)/\Gamma(K^-\pi^+\pi^+)$ Γ_{117}/Γ_{39}

VALUE	CL%	DOCUMENT ID		TECN	COMMENT
• • • We do not use the following data for averages, fits, limits, etc. • • •					
< 0.4	90	ANJOS	89E	E691	Photoproduction

$\Gamma(\eta\pi^+)/\Gamma(\phi\pi^+)$ $\Gamma_{122}/\Gamma_{146}$

Unseen decay modes of the η are included.

VALUE	EVTS	DOCUMENT ID		TECN	COMMENT
0.49 ± 0.08	275	JESSOP	98	CLE2	$e^+e^-\approx \Upsilon(4S)$

$\Gamma(\eta\pi^+)/\Gamma(K^-\pi^+\pi^+)$ Γ_{122}/Γ_{39}

Unseen decay modes of the η are included.

VALUE	CL%	EVTS	DOCUMENT ID		TECN	COMMENT
• • • We do not use the following data for averages, fits, limits, etc. • • •						
0.083 ± 0.023 ± 0.014		99	DAOUDI	92	CLE2	See JESSOP 98
< 0.12	90		ANJOS	89E	E691	Photoproduction

$\Gamma(\omega\pi^+)/\Gamma(K^-\pi^+\pi^+)$ Γ_{124}/Γ_{39}

Unseen decay modes of the ω are included.

VALUE	CL%	DOCUMENT ID		TECN	COMMENT
< 0.08	90	ANJOS	89E	E691	Photoproduction

$\Gamma(3\pi^+2\pi^-)/\Gamma(K^-\pi^+\pi^+)$ Γ_{120}/Γ_{39}

VALUE	EVTS	DOCUMENT ID		TECN	COMMENT
0.0198 ± 0.0024 OUR FIT		Error includes scale factor of 1.3.			
0.023 ± 0.004 ± 0.002	58	FRABETTI	97C	E687	γ Be, $\overline{E}_\gamma \approx 200$ GeV

$\Gamma(3\pi^+2\pi^-)/\Gamma(K^-3\pi^+\pi^-)$ Γ_{120}/Γ_{66}

VALUE	EVTS	DOCUMENT ID		TECN	COMMENT
0.294 ± 0.020 OUR FIT					
0.290 ± 0.017 ± 0.011	835	LINK	03D	FOCS	γ nucleus, $\overline{E}_\gamma \approx 180$ GeV

$\Gamma(\eta\rho^+)/\Gamma(\phi\pi^+)$ $\Gamma_{125}/\Gamma_{146}$

Unseen decay modes of the η are included.

VALUE	CL%	DOCUMENT ID		TECN	COMMENT
< 1.11	90	JESSOP	98	CLE2	$e^+e^-\approx \Upsilon(4S)$

$\Gamma(\eta\rho^+)/\Gamma(K^-\pi^+\pi^+)$ Γ_{125}/Γ_{39}

Unseen decay modes of the η are included.

VALUE	CL%	DOCUMENT ID	TECN	COMMENT
• • • We do not use the following data for averages, fits, limits, etc. • • •				
<0.13	90	DAOUDI	92 CLE2	See JESSOP 98

$\Gamma(3\pi^+2\pi^-\pi^0)/\Gamma_{\text{total}}$ Γ_{121}/Γ

VALUE	DOCUMENT ID	TECN	COMMENT
• • • We do not use the following data for averages, fits, limits, etc. • • •			
$0.0029^{+0.0029}_{-0.0020}$	[71] BARLAG	92C ACCM	π^- Cu 230 GeV

[71] BARLAG 92C computes the branching fraction using topological normalization.

$\Gamma(\eta'(958)\pi^+)/\Gamma(\phi\pi^+)$ $\Gamma_{126}/\Gamma_{146}$

Unseen decay modes of the $\eta'(958)$ are included.

VALUE	EVTS	DOCUMENT ID	TECN	COMMENT
0.82 ± 0.14	126	JESSOP	98 CLE2	$e^+e^-\approx\Upsilon(4S)$

$\Gamma(\eta'(958)\pi^+)/\Gamma(K^-\pi^+\pi^+)$ Γ_{126}/Γ_{39}

Unseen decay modes of the $\eta'(958)$ are included.

VALUE	CL%	DOCUMENT ID	TECN	COMMENT
• • • We do not use the following data for averages, fits, limits, etc. • • •				
<0.1	90	DAOUDI	92 CLE2	See JESSOP 98
<0.1	90	ALVAREZ	91 NA14	Photoproduction
<0.13	90	ANJOS	91B E691	γBe, $\overline{E}_\gamma\approx 145$ GeV

$\Gamma(\eta'(958)\rho^+)/\Gamma(\phi\pi^+)$ $\Gamma_{127}/\Gamma_{146}$

Unseen decay modes of the $\eta'(958)$ are included.

VALUE	CL%	DOCUMENT ID	TECN	COMMENT
< 0.86	90	JESSOP	98 CLE2	$e^+e^-\approx\Upsilon(4S)$

$\Gamma(\eta'(958)\rho^+)/\Gamma(K^-\pi^+\pi^+)$ Γ_{127}/Γ_{39}

Unseen decay modes of the $\eta'(958)$ are included.

VALUE	CL%	DOCUMENT ID	TECN	COMMENT
• • • We do not use the following data for averages, fits, limits, etc. • • •				
<0.17	90	DAOUDI	92 CLE2	See JESSOP 98

Hadronic modes with a $K\overline{K}$ pair

$\Gamma(K^+\overline{K}^0)/\Gamma(\overline{K}^0\pi^+)$ Γ_{129}/Γ_{38}

It is generally assumed for modes such as $D^+\to\overline{K}^0\pi^+$ that $\Gamma(D^+\to\overline{K}^0\pi^+)=2\Gamma(D^+\to K^0_S\pi^+)$; it is the latter Γ that is actually measured. BIGI 95 points out that interference between Cabibbo-allowed and doubly Cabibbo-suppressed amplitudes, where both occur, could invalidate this assumption by a few percent.

VALUE	EVTS	DOCUMENT ID	TECN	COMMENT
0.211 ± 0.018 OUR FIT Error includes scale factor of 1.3.				
0.263 ± 0.035 OUR AVERAGE				
$0.25\pm0.04\pm0.02$	129	FRABETTI	95 E687	γBe $\overline{E}_\gamma\approx 200$ GeV
$0.271\pm0.065\pm0.039$	69	ANJOS	90C E691	γBe
$0.317\pm0.086\pm0.048$	31	BALTRUSAIT...85E	MRK3	e^+e^- 3.77 GeV
0.25 ± 0.15	6	SCHINDLER	81 MRK2	e^+e^- 3.771 GeV
• • • We do not use the following data for averages, fits, limits, etc. • • •				
$0.1996\pm0.0119\pm0.0096$	949	[72] LINK	02B FOCS	γ nucleus, $\overline{E}_\gamma\approx 180$ GeV
$0.222\pm0.041\pm0.029$	70	[73] BISHAI	97 CLE2	$e^+e^-\approx\Upsilon(4S)$

[72] This LINK 02B result is redundant with a result in the next datablock.
[73] This BISHAI 97 result is redundant with results elsewhere in the Listings.

$\Gamma(K^+\overline{K}^0)/\Gamma(K^-\pi^+\pi^+)$ Γ_{129}/Γ_{39}

VALUE	EVTS	DOCUMENT ID	TECN	COMMENT
0.064 ± 0.005 OUR FIT Error includes scale factor of 1.3.				
0.062 ± 0.004 OUR AVERAGE				
$0.0604\pm0.0035\pm0.0030$	949	LINK	02B FOCS	γ nucleus, $\overline{E}_\gamma\approx 180$ GeV
$0.077\pm0.014\pm0.007$	70	[74] BISHAI	97 CLE2	$e^+e^-\approx\Upsilon(4S)$

[74] See BISHAI 97 for an isospin analysis of $D^+\to K\overline{K}$ amplitudes.

$\Gamma(K^+K^-\pi^+)/\Gamma(K^-\pi^+\pi^+)$ Γ_{130}/Γ_{39}

VALUE	DOCUMENT ID	TECN	COMMENT
0.097 ± 0.006 OUR AVERAGE			
$0.093\pm0.010^{+0.008}_{-0.006}$	JUN	00 SELX	Σ^- nucleus, 600 GeV
$0.0976\pm0.0042\pm0.0046$	FRABETTI	95B E687	Dalitz plot analysis

$\Gamma(\phi\pi^+)/\Gamma(K^-\pi^+\pi^+)$ Γ_{146}/Γ_{39}

Unseen decay modes of the ϕ are included.

VALUE	EVTS	DOCUMENT ID	TECN	COMMENT
0.068 ± 0.005 OUR AVERAGE				
$0.058\pm0.006\pm0.006$		FRABETTI	95B E687	Dalitz plot analysis
$0.062\pm0.017\pm0.006$	19	ADAMOVICH	93 WA82	π^- 340 GeV
$0.077\pm0.011\pm0.005$	128	DAOUDI	92 CLE2	$e^+e^-\approx 10.5$ GeV
$0.098\pm0.032\pm0.014$	12	ALVAREZ	90C NA14	Photoproduction
$0.071\pm0.008\pm0.007$	84	ANJOS	88 E691	Photoproduction
$0.084\pm0.021\pm0.011$	21	BALTRUSAIT...85E	MRK3	e^+e^- 3.77 GeV

$\Gamma(K^+\overline{K}^*(892)^0)/\Gamma(K^-\pi^+\pi^+)$ Γ_{150}/Γ_{39}

Unseen decay modes of the $\overline{K}^*(892)^0$ are included.

VALUE	EVTS	DOCUMENT ID	TECN	COMMENT
0.047 ± 0.005 OUR AVERAGE		Error includes scale factor of 1.2.		
$0.044\pm0.003\pm0.004$		[75] FRABETTI	95B E687	Dalitz plot analysis
$0.058\pm0.009\pm0.006$	73	ANJOS	88 E691	Photoproduction
$0.048\pm0.021\pm0.011$	14	BALTRUSAIT...85E	MRK3	e^+e^- 3.77 GeV

[75] See FRABETTI 95B for evidence also of $\overline{K}^*_0(1430)^0K^+$ in the $D^+\to K^+K^-\pi^+$ Dalitz plot.

$\Gamma(K^+K^-\pi^+\text{ nonresonant})/\Gamma(K^-\pi^+\pi^+)$ Γ_{133}/Γ_{39}

VALUE	EVTS	DOCUMENT ID	TECN	COMMENT
0.050 ± 0.009 OUR AVERAGE				
$0.049\pm0.008\pm0.006$	95	ANJOS	88 E691	Photoproduction
$0.059\pm0.026\pm0.009$	37	BALTRUSAIT...85E	MRK3	e^+e^- 3.77 GeV

$\Gamma(K^*(892)^+\overline{K}^0)/\Gamma(\overline{K}^0\pi^+)$ Γ_{151}/Γ_{38}

Unseen decay modes of the $K^*(892)^+$ are included.

VALUE	EVTS	DOCUMENT ID	TECN	COMMENT
1.1 ± 0.3 ± 0.4	67	FRABETTI	95 E687	γBe $\overline{E}_\gamma\approx 200$ GeV

$\Gamma(\phi\pi^+\pi^0)/\Gamma_{\text{total}}$ Γ_{147}/Γ

Unseen decay modes of the ϕ are included.

VALUE	DOCUMENT ID	TECN	COMMENT
0.023 ± 0.010	[76] BARLAG	92C ACCM	π^- Cu 230 GeV

[76] BARLAG 92C computes the branching fraction using topological normalization.

$\Gamma(\phi\pi^+\pi^0)/\Gamma(K^-\pi^+\pi^+)$ Γ_{147}/Γ_{39}

Unseen decay modes of the ϕ are included.

VALUE	CL%	DOCUMENT ID	TECN	COMMENT
• • • We do not use the following data for averages, fits, limits, etc. • • •				
<0.58	90	ALVAREZ	90C NA14	Photoproduction
<0.28	90	ANJOS	89E E691	Photoproduction

$\Gamma(\phi\rho^+)/\Gamma(K^-\pi^+\pi^+)$ Γ_{148}/Γ_{39}

Unseen decay modes of the ϕ are included.

VALUE	CL%	DOCUMENT ID	TECN	COMMENT
< 0.16	90	DAOUDI	92 CLE2	$e^+e^-\approx 10.5$ GeV

$\Gamma(K^+K^-\pi^+\pi^0\text{ non-}\phi)/\Gamma_{\text{total}}$ Γ_{139}/Γ

VALUE	DOCUMENT ID	TECN	COMMENT
$\mathbf{0.015^{+0.007}_{-0.006}}$	[77] BARLAG	92C ACCM	π^- Cu 230 GeV

[77] BARLAG 92C computes the branching fraction using topological normalization.

$\Gamma(K^+K^-\pi^+\pi^0\text{ non-}\phi)/\Gamma(K^-\pi^+\pi^+)$ Γ_{139}/Γ_{39}

VALUE	CL%	DOCUMENT ID	TECN	COMMENT
• • • We do not use the following data for averages, fits, limits, etc. • • •				
<0.25	90	ANJOS	89E E691	Photoproduction

$\Gamma(K^+\overline{K}^0\pi^+\pi^-)/\Gamma(\overline{K}^0\pi^+\pi^+\pi^-)$ Γ_{140}/Γ_{59}

VALUE	EVTS	DOCUMENT ID	TECN	COMMENT
0.0562 ± 0.0039 ± 0.0040	469	LINK	01C FOCS	γ nucleus, $\overline{E}_\gamma\approx 180$ GeV

$\Gamma(K^+\overline{K}^0\pi^+\pi^-)/\Gamma_{\text{total}}$ Γ_{140}/Γ

VALUE	CL%	DOCUMENT ID	TECN	COMMENT
• • • We do not use the following data for averages, fits, limits, etc. • • •				
<0.02	90	ALBRECHT	92B ARG	$e^+e^-\simeq 10.4$ GeV

$\Gamma(K^0K^-\pi^+\pi^+)/\Gamma(\overline{K}^0\pi^+\pi^+\pi^-)$ Γ_{141}/Γ_{59}

VALUE	EVTS	DOCUMENT ID	TECN	COMMENT
0.0768 ± 0.0041 ± 0.0032	670	LINK	01C FOCS	γ nucleus, $\overline{E}_\gamma\approx 180$ GeV

$\Gamma(K^0K^-\pi^+\pi^+)/\Gamma_{\text{total}}$ Γ_{141}/Γ

VALUE	CL%	DOCUMENT ID	TECN	COMMENT
• • • We do not use the following data for averages, fits, limits, etc. • • •				
$0.01\pm0.005\pm0.003$		ALBRECHT	92B ARG	$e^+e^-\simeq 10.4$ GeV
<0.003		[78] BARLAG	92C ACCM	π^- Cu 230 GeV

[78] BARLAG 92C computes the branching fraction using topological normalization.

$\Gamma(K^*(892)^+\overline{K}^*(892)^0)/\Gamma_{\text{total}}$ Γ_{152}/Γ

Unseen decay modes of the $K^*(892)$'s are included.

VALUE	DOCUMENT ID	TECN	COMMENT
0.026 ± 0.008 ± 0.007	ALBRECHT	92B ARG	$e^+e^-\simeq 10.4$ GeV

$\Gamma(K^0K^-\pi^+\pi^+(\text{non-}K^{*+}\overline{K}^{*0}))/\Gamma_{\text{total}}$ Γ_{143}/Γ

VALUE	CL%	DOCUMENT ID	TECN	COMMENT
< 0.0079	90	ALBRECHT	92B ARG	$e^+e^-\simeq 10.4$ GeV

$\Gamma(K^+K^-\pi^+\pi^+\pi^-)/\Gamma(K^-3\pi^+\pi^-)$ Γ_{144}/Γ_{66}

VALUE	EVTS	DOCUMENT ID	TECN	COMMENT
0.040 ± 0.009 ± 0.019	38	LINK	03D FOCS	γ nucleus, $\overline{E}_\gamma\approx 180$ GeV

$\Gamma(\phi\pi^+\pi^+\pi^-)/\Gamma_{\text{total}}$ Γ_{149}/Γ

Unseen decay modes of the ϕ are included.

VALUE	CL%	EVTS	DOCUMENT ID	TECN	COMMENT
• • • We do not use the following data for averages, fits, limits, etc. • • •					
<0.002	90	0	ANJOS	88 E691	Photoproduction

$\Gamma(\phi\pi^+\pi^+\pi^-)/\Gamma(K^-\pi^+\pi^+)$ Γ_{149}/Γ_{39}

Unseen decay modes of the ϕ are included.

VALUE	CL%	DOCUMENT ID	TECN	COMMENT
• • • We do not use the following data for averages, fits, limits, etc. • • •				
<0.031	90	ALVAREZ	90C NA14	Photoproduction

$\Gamma(\phi\pi^+\pi^+\pi^-)/\Gamma(\phi\pi^+)$ $\Gamma_{149}/\Gamma_{146}$

VALUE	CL%	DOCUMENT ID	TECN	COMMENT
• • • We do not use the following data for averages, fits, limits, etc. • • •				
<0.6	90	FRABETTI	92 E687	γ Be

$\Gamma(K^+K^-\pi^+\pi^+\pi^-\text{ nonresonant})/\Gamma_{\text{total}}$ Γ_{145}/Γ

VALUE	CL%	EVTS	DOCUMENT ID	TECN	COMMENT
• • • We do not use the following data for averages, fits, limits, etc. • • •					
<0.03	90	12	ANJOS	88 E691	Photoproduction

Rare or forbidden modes

$\Gamma(K^+\pi^+\pi^-)/\Gamma(K^-\pi^+\pi^+)$ Γ_{153}/Γ_{39}

VALUE	EVTS	DOCUMENT ID	TECN	COMMENT
0.0075 ± 0.0016 OUR AVERAGE				
$0.0077\pm0.0017\pm0.0008$	59	AITALA	97C E791	π^- nucleus, 500 GeV
$0.0072\pm0.0023\pm0.0017$	21	FRABETTI	95E E687	γ Be, $\overline{E}_\gamma = 220$ GeV

$\Gamma(K^+\rho^0)/\Gamma(K^+\pi^+\pi^-)$ $\Gamma_{154}/\Gamma_{153}$

VALUE	DOCUMENT ID	TECN	COMMENT
$0.37\pm0.14\pm0.07$	AITALA	97C E791	π^- nucleus, 500 GeV

$\Gamma(K^+\rho^0)/\Gamma(K^-\pi^+\pi^+)$ Γ_{154}/Γ_{39}

VALUE	CL%	DOCUMENT ID	TECN	COMMENT
• • • We do not use the following data for averages, fits, limits, etc. • • •				
<0.0067	90	FRABETTI	95E E687	γ Be, $\overline{E}_\gamma = 220$ GeV

$\Gamma(K^*(892)^0\pi^+)/\Gamma(K^+\pi^+\pi^-)$ $\Gamma_{155}/\Gamma_{153}$

Unseen decay modes of the $K^*(892)^0$ are included.

VALUE	DOCUMENT ID	TECN	COMMENT
$0.53\pm0.21\pm0.02$	AITALA	97C E791	π^- nucleus, 500 GeV

$\Gamma(K^*(892)^0\pi^+)/\Gamma(K^-\pi^+\pi^+)$ Γ_{155}/Γ_{39}

Unseen decay modes of the $K^*(892)^0$ are included.

VALUE	CL%	DOCUMENT ID	TECN	COMMENT
• • • We do not use the following data for averages, fits, limits, etc. • • •				
<0.0021	90	FRABETTI	95E E687	γ Be, $\overline{E}_\gamma = 220$ GeV

$\Gamma(K^+\pi^+\pi^-\text{ nonresonant})/\Gamma(K^+\pi^+\pi^-)$ $\Gamma_{156}/\Gamma_{153}$

VALUE	DOCUMENT ID	TECN	COMMENT
$0.36\pm0.14\pm0.07$	AITALA	97C E791	π^- nucleus, 500 GeV

$\Gamma(K^+K^+K^-)/\Gamma(K^-\pi^+\pi^+)$ Γ_{157}/Γ_{39}

A doubly Cabibbo-suppressed decay with no simple spectator process possible.

VALUE (units 10^{-4})	CL%	EVTS	DOCUMENT ID	TECN	COMMENT
$9.49\pm\ 2.17\pm\ 0.22$		65	[79] LINK	02I FOCS	γ nucleus, ≈ 180 GeV
• • • We do not use the following data for averages, fits, limits, etc. • • •					
<16	90		[80] FRABETTI	95F E687	γ Be, $\overline{E}_\gamma \approx 220$ GeV
$570\ \pm200\ \pm70$		13	ADAMOVICH	93 WA82	π^- 340 GeV

[79] LINK 02I finds little evidence for ϕK^+ or $f_0(980)K^+$ submodes.

[80] Using the $\phi\pi^+$ mode to normalize, FRABETTI 95F gets $\Gamma(K^+K^+K^-)/\Gamma(\phi\pi^+) < 0.025$.

$\Gamma(\phi K^+)/\Gamma(\phi\pi^+)$ $\Gamma_{158}/\Gamma_{146}$

A doubly Cabibbo-suppressed decay with no simple spectator process possible.

VALUE	CL%	EVTS	DOCUMENT ID	TECN	COMMENT
<0.021	90		FRABETTI	95F E687	γ Be, $\overline{E}_\gamma \approx 220$ GeV
• • • We do not use the following data for averages, fits, limits, etc. • • •					
$0.058\ ^{+0.032}_{-0.026}\pm0.007$		4	[81] ANJOS	92D E691	γ Be, $\overline{E}_\gamma = 145$ GeV

[81] The evidence of ANJOS 92D is a small excess of events $(4.5\ ^{+2.4}_{-2.0})$.

$\Gamma(\pi^+e^+e^-)/\Gamma_{\text{total}}$ Γ_{159}/Γ

A test for the $\Delta C = 1$ weak neutral current. Allowed by higher-order electroweak interactions.

VALUE	CL%	EVTS	DOCUMENT ID	TECN	COMMENT
$<5.2\times10^{-5}$	90		AITALA	99G E791	π^- N 500 GeV
• • • We do not use the following data for averages, fits, limits, etc. • • •					
$<1.1\times10^{-4}$	90		FRABETTI	97B E687	γ Be, $\overline{E}_\gamma \approx 220$ GeV
$<6.6\times10^{-5}$	90		AITALA	96 E791	π^- N 500 GeV
$<2.5\times10^{-3}$	90		WEIR	90B MRK2	e^+e^- 29 GeV
$<2.6\times10^{-3}$	90	39	HAAS	88 CLEO	e^+e^- 10 GeV

$\Gamma(\pi^+\mu^+\mu^-)/\Gamma_{\text{total}}$ Γ_{160}/Γ

A test for the $\Delta C = 1$ weak neutral current. Allowed by higher-order electroweak interactions.

VALUE	CL%	EVTS	DOCUMENT ID	TECN	COMMENT
$<8.8\times10^{-6}$	90		LINK	03F FOCS	γ nucleus, $\overline{E}_\gamma \approx 180$ GeV
• • • We do not use the following data for averages, fits, limits, etc. • • •					
$<1.5\times10^{-5}$	90		AITALA	99G E791	π^- N 500 GeV
$<8.9\times10^{-5}$	90		FRABETTI	97B E687	γ Be, $\overline{E}_\gamma \approx 220$ GeV
$<1.8\times10^{-5}$	90		AITALA	96 E791	π^- N 500 GeV
$<2.2\times10^{-4}$	90	0	KODAMA	95 E653	π^- emulsion 600 GeV
$<5.9\times10^{-3}$	90		WEIR	90B MRK2	e^+e^- 29 GeV
$<2.9\times10^{-3}$	90	36	HAAS	88 CLEO	e^+e^- 10 GeV

$\Gamma(\rho^+\mu^+\mu^-)/\Gamma_{\text{total}}$ Γ_{161}/Γ

A test for the $\Delta C = 1$ weak neutral current. Allowed by higher-order electroweak interactions.

VALUE	CL%	EVTS	DOCUMENT ID	TECN	COMMENT
$<5.6\times10^{-4}$	90	0	KODAMA	95 E653	π^- emulsion 600 GeV

$\Gamma(K^+e^+e^-)/\Gamma_{\text{total}}$ Γ_{162}/Γ

VALUE	CL%	DOCUMENT ID	TECN	COMMENT
$<2.0\times10^{-4}$	90	AITALA	99G E791	π^- N 500 GeV
$<2.0\times10^{-4}$	90	FRABETTI	97B E687	γ Be, $\overline{E}_\gamma \approx 220$ GeV
• • • We do not use the following data for averages, fits, limits, etc. • • •				
$<4.8\times10^{-3}$	90	WEIR	90B MRK2	e^+e^- 29 GeV

$\Gamma(K^+\mu^+\mu^-)/\Gamma_{\text{total}}$ Γ_{163}/Γ

VALUE	CL%	EVTS	DOCUMENT ID	TECN	COMMENT
$<9.2\times10^{-6}$	90		LINK	03F FOCS	γ nucleus, $\overline{E}_\gamma \approx 180$ GeV
• • • We do not use the following data for averages, fits, limits, etc. • • •					
$<4.4\times10^{-5}$	90		AITALA	99G E791	π^- N 500 GeV
$<9.7\times10^{-5}$	90		FRABETTI	97B E687	γ Be, $\overline{E}_\gamma \approx 220$ GeV
$<3.2\times10^{-4}$	90	0	KODAMA	95 E653	π^- emulsion 600 GeV
$<9.2\times10^{-3}$	90		WEIR	90B MRK2	e^+e^- 29 GeV

$\Gamma(\pi^+e^\pm\mu^\mp)/\Gamma_{\text{total}}$ Γ_{164}/Γ

A test of lepton-family-number conservation.

VALUE	CL%	DOCUMENT ID	TECN	COMMENT
$<3.4\times10^{-5}$	90	AITALA	99G E791	π^- N 500 GeV

$\Gamma(\pi^+e^+\mu^-)/\Gamma_{\text{total}}$ Γ_{165}/Γ

A test of lepton-family-number conservation.

VALUE	CL%	DOCUMENT ID	TECN	COMMENT
• • • We do not use the following data for averages, fits, limits, etc. • • •				
$<1.1\times10^{-4}$	90	FRABETTI	97B E687	γ Be, $\overline{E}_\gamma \approx 220$ GeV
$<3.3\times10^{-3}$	90	WEIR	90B MRK2	e^+e^- 29 GeV

$\Gamma(\pi^+e^-\mu^+)/\Gamma_{\text{total}}$ Γ_{166}/Γ

A test of lepton-family-number conservation.

VALUE	CL%	DOCUMENT ID	TECN	COMMENT
• • • We do not use the following data for averages, fits, limits, etc. • • •				
$<1.3\times10^{-4}$	90	FRABETTI	97B E687	γ Be, $\overline{E}_\gamma \approx 220$ GeV
$<3.3\times10^{-3}$	90	WEIR	90B MRK2	e^+e^- 29 GeV

$\Gamma(K^+e^\pm\mu^\mp)/\Gamma_{\text{total}}$ Γ_{167}/Γ

A test of lepton-family-number conservation.

VALUE	CL%	DOCUMENT ID	TECN	COMMENT
$<6.8\times10^{-5}$	90	AITALA	99G E791	π^- N 500 GeV

$\Gamma(K^+e^+\mu^-)/\Gamma_{\text{total}}$ Γ_{168}/Γ

A test of lepton-family-number conservation.

VALUE	CL%	DOCUMENT ID	TECN	COMMENT
• • • We do not use the following data for averages, fits, limits, etc. • • •				
$<1.3\times10^{-4}$	90	FRABETTI	97B E687	γ Be, $\overline{E}_\gamma \approx 220$ GeV
$<3.4\times10^{-3}$	90	WEIR	90B MRK2	e^+e^- 29 GeV

$\Gamma(K^+e^-\mu^+)/\Gamma_{\text{total}}$ Γ_{169}/Γ

A test of lepton-family-number conservation.

VALUE	CL%	DOCUMENT ID	TECN	COMMENT
• • • We do not use the following data for averages, fits, limits, etc. • • •				
$<1.2\times10^{-4}$	90	FRABETTI	97B E687	γ Be, $\overline{E}_\gamma \approx 220$ GeV
$<3.4\times10^{-3}$	90	WEIR	90B MRK2	e^+e^- 29 GeV

$\Gamma(\pi^- e^+ e^+)/\Gamma_{total}$ Γ_{170}/Γ

A test of lepton-number conservation.

VALUE	CL%	DOCUMENT ID		TECN	COMMENT
$< 9.6 \times 10^{-5}$	90	AITALA	99G	E791	π^- N 500 GeV
• • • We do not use the following data for averages, fits, limits, etc. • • •					
$< 1.1 \times 10^{-4}$	90	FRABETTI	97B	E687	γ Be, $\overline{E}_\gamma \approx$ 220 GeV
$< 4.8 \times 10^{-3}$	90	WEIR	90B	MRK2	e^+e^- 29 GeV

$\Gamma(\pi^- \mu^+ \mu^+)/\Gamma_{total}$ Γ_{171}/Γ

A test of lepton-number conservation.

VALUE	CL%	EVTS	DOCUMENT ID		TECN	COMMENT
$< 4.8 \times 10^{-6}$	90		LINK	03F	FOCS	γ nucleus, $\overline{E}_\gamma \approx$ 180 GeV
• • • We do not use the following data for averages, fits, limits, etc. • • •						
$< 1.7 \times 10^{-5}$	90		AITALA	99G	E791	π^- N 500 GeV
$< 8.7 \times 10^{-5}$	90		FRABETTI	97B	E687	γ Be, $\overline{E}_\gamma \approx$ 220 GeV
$< 2.2 \times 10^{-4}$	90	0	KODAMA	95	E653	π^- emulsion 600 GeV
$< 6.8 \times 10^{-3}$	90		WEIR	90B	MRK2	e^+e^- 29 GeV

$\Gamma(\pi^- e^+ \mu^+)/\Gamma_{total}$ Γ_{172}/Γ

A test of lepton-number conservation.

VALUE	CL%	DOCUMENT ID		TECN	COMMENT
$< 5.0 \times 10^{-5}$	90	AITALA	99G	E791	π^- N 500 GeV
• • • We do not use the following data for averages, fits, limits, etc. • • •					
$< 1.1 \times 10^{-4}$	90	FRABETTI	97B	E687	γ Be, $\overline{E}_\gamma \approx$ 220 GeV
$< 3.7 \times 10^{-3}$	90	WEIR	90B	MRK2	e^+e^- 29 GeV

$\Gamma(\rho^- \mu^+ \mu^+)/\Gamma_{total}$ Γ_{173}/Γ

A test of lepton-number conservation.

VALUE	CL%	EVTS	DOCUMENT ID		TECN	COMMENT
$< 5.6 \times 10^{-4}$	90	0	KODAMA	95	E653	π^- emulsion 600 GeV

$\Gamma(K^- e^+ e^+)/\Gamma_{total}$ Γ_{174}/Γ

A test of lepton-number conservation.

VALUE	CL%	DOCUMENT ID		TECN	COMMENT
$< 1.2 \times 10^{-4}$	90	FRABETTI	97B	E687	γ Be, $\overline{E}_\gamma \approx$ 220 GeV
• • • We do not use the following data for averages, fits, limits, etc. • • •					
$< 9.1 \times 10^{-3}$	90	WEIR	90B	MRK2	e^+e^- 29 GeV

$\Gamma(K^- \mu^+ \mu^+)/\Gamma_{total}$ Γ_{175}/Γ

A test of lepton-number conservation.

VALUE	CL%	EVTS	DOCUMENT ID		TECN	COMMENT
$< 1.3 \times 10^{-5}$	90		LINK	03F	FOCS	γ nucleus, $\overline{E}_\gamma \approx$ 180 GeV
• • • We do not use the following data for averages, fits, limits, etc. • • •						
$< 1.2 \times 10^{-4}$	90		FRABETTI	97B	E687	γ Be, $\overline{E}_\gamma \approx$ 220 GeV
$< 3.2 \times 10^{-4}$	90	0	KODAMA	95	E653	π^- emulsion 600 GeV
$< 4.3 \times 10^{-3}$	90		WEIR	90B	MRK2	e^+e^- 29 GeV

$\Gamma(K^- e^+ \mu^+)/\Gamma_{total}$ Γ_{176}/Γ

A test of lepton-number conservation.

VALUE	CL%	DOCUMENT ID		TECN	COMMENT
$< 1.3 \times 10^{-4}$	90	FRABETTI	97B	E687	γ Be, $\overline{E}_\gamma \approx$ 220 GeV
• • • We do not use the following data for averages, fits, limits, etc. • • •					
$< 4.0 \times 10^{-3}$	90	WEIR	90B	MRK2	e^+e^- 29 GeV

$\Gamma(K^*(892)^- \mu^+ \mu^+)/\Gamma_{total}$ Γ_{177}/Γ

A test of lepton-number conservation.

VALUE	CL%	EVTS	DOCUMENT ID		TECN	COMMENT
$< 8.5 \times 10^{-4}$	90	0	KODAMA	95	E653	π^- emulsion 600 GeV

$D^{\pm}$ *CP*-VIOLATING DECAY-RATE ASYMMETRIES

$A_{CP}(K^0_S \pi^{\pm})$ in $D^{\pm} \to K^0_S \pi^{\pm}$

This is the difference between D^+ and D^- partial widths for these modes divided by the sum of the widths.

VALUE	EVTS	DOCUMENT ID		TECN	COMMENT
$-0.016 \pm 0.015 \pm 0.009$	10.6k	[82] LINK	02B	FOCS	γ nucleus, $\overline{E}_\gamma \approx$ 180 GeV

[82] LINK 02B measures $N(D^+ \to K^0_S \pi^+)/N(D^+ \to K^- \pi^+ \pi^+)$, the ratio of numbers of events observed, and similarly for the D^-.

$A_{CP}(K^0_S K^{\pm})$ in $D^{\pm} \to K^0_S K^{\pm}$

This is the difference between D^+ and D^- partial widths for these modes divided by the sum of the widths.

VALUE	EVTS	DOCUMENT ID		TECN	COMMENT
$+0.071 \pm 0.061 \pm 0.012$	949	[83] LINK	02B	FOCS	γ nucleus, $\overline{E}_\gamma \approx$ 180 GeV
• • • We do not use the following data for averages, fits, limits, etc. • • •					
$+0.069 \pm 0.060 \pm 0.015$	949	[84] LINK	02B	FOCS	γ nucleus, $\overline{E}_\gamma \approx$ 180 GeV

[83] LINK 02B measures $N(D^+ \to K^0_S K^+)/N(D^+ \to K^0_S \pi^+)$, the ratio of numbers of events observed, and similarly for the D^-.

[84] LINK 02B measures $N(D^+ \to K^0_S K^+)/N(D^+ \to K^- \pi^+ \pi^+)$, the ratio of numbers of events observed, and similarly for the D^-.

$A_{CP}(K^+ K^- \pi^{\pm})$ in $D^{\pm} \to K^+ K^- \pi^{\pm}$

This is the difference between D^+ and D^- partial widths for these modes divided by the sum of the widths.

VALUE	EVTS	DOCUMENT ID		TECN	COMMENT
0.002 ± 0.011 OUR AVERAGE					
$+0.006 \pm 0.011 \pm 0.005$	14k	[85] LINK	00B	FOCS	
-0.014 ± 0.029		[85] AITALA	97B	E791	$-0.062 < A_{CP} < +0.034$ (90% CL)
-0.031 ± 0.068		[85] FRABETTI	94I	E687	$-0.14 < A_{CP} < +0.081$ (90% CL)

[85] FRABETTI 94I, AITALA 98C, and LINK 00B measure $N(D^+ \to K^- K^+ \pi^+)/N(D^+ \to K^- \pi^+ \pi^+)$, the ratio of numbers of events observed, and similarly for the D^-.

$A_{CP}(K^{\pm} K^{*0})$ in $D^+ \to K^+ \overline{K}^{*0}$, $D^- \to K^- K^{*0}$

This is the difference between D^+ and D^- partial widths for these modes divided by the sum of the widths.

VALUE	DOCUMENT ID		TECN	COMMENT
-0.02 ± 0.05 OUR AVERAGE				
-0.010 ± 0.050	[86] AITALA	97B	E791	$-0.092 < A_{CP} < +0.072$ (90% CL)
-0.12 ± 0.13	[86] FRABETTI	94I	E687	$-0.33 < A_{CP} < +0.094$ (90% CL)

[86] FRABETTI 94I and AITALA 97B measure $N(D^+ \to K^+ \overline{K}^*(892)^0)/N(D^+ \to K^- \pi^+ \pi^+)$, the ratio of numbers of events observed, and similarly for the D^-.

$A_{CP}(\phi \pi^{\pm})$ in $D^{\pm} \to \phi \pi^{\pm}$

This is the difference between D^+ and D^- partial widths for these modes divided by the sum of the widths.

VALUE	DOCUMENT ID		TECN	COMMENT
-0.014 ± 0.033 OUR AVERAGE				
-0.028 ± 0.036	[87] AITALA	97B	E791	$-0.087 < A_{CP} < +0.031$ (90% CL)
$+0.066 \pm 0.086$	[87] FRABETTI	94I	E687	$-0.075 < A_{CP} < +0.21$ (90% CL)

[87] FRABETTI 94I and AITALA 97B measure $N(D^+ \to \phi \pi^+)/N(D^+ \to K^- \pi^+ \pi^+)$, the ratio of numbers of events observed, and similarly for the D^-.

$A_{CP}(\pi^+ \pi^- \pi^{\pm})$ in $D^{\pm} \to \pi^+ \pi^- \pi^{\pm}$

This is the difference between D^+ and D^- partial widths for these modes divided by the sum of the widths.

VALUE	DOCUMENT ID		TECN	COMMENT
-0.017 ± 0.042	[88] AITALA	97B	E791	$-0.086 < A_{CP} < +0.052$ (90% CL)

[88] AITALA 97B measure $N(D^+ \to \pi^+ \pi^- \pi^+)/N(D^+ \to K^- \pi^+ \pi^+)$, the ratio of numbers of events observed, and similarly for the D^-.

$D^{\pm}$ PRODUCTION CROSS SECTION AT $\psi(3770)$

A compilation of the cross sections for the direct production of $D^{\pm}$ mesons at or near the $\psi(3770)$ peak in e^+e^- production.

VALUE (nanobarns)	DOCUMENT ID		TECN	COMMENT
• • • We do not use the following data for averages, fits, limits, etc. • • •				
$4.2 \pm 0.6 \pm 0.3$	[89] ADLER	88C	MRK3	e^+e^- 3.768 GeV
5.5 ± 1.0	[90] PARTRIDGE	84	CBAL	e^+e^- 3.771 GeV
$6.00 \pm 0.72 \pm 1.02$	[91] SCHINDLER	80	MRK2	e^+e^- 3.771 GeV
9.1 ± 2.0	[92] PERUZZI	77	MRK1	e^+e^- 3.774 GeV

[89] This measurement compares events with one detected D to those with two detected D mesons, to determine the the absolute cross section. ADLER 88C measure the ratio of cross sections (neutral to charged) to be $1.36 \pm 0.23 \pm 0.14$. This measurement does not include the decays of the $\psi(3770)$ not associated with charmed particle production.

[90] This measurement comes from a scan of the $\psi(3770)$ resonance and a fit to the cross section. PARTRIDGE 84 measures 6.4 ± 1.15 nb for the cross section. We take the phase space division of neutral and charged D mesons in $\psi(3770)$ decay to be 1.33, and we assume that the $\psi(3770)$ is an isosinglet to evaluate the cross sections. The noncharm decays (e.g. radiative) of the $\psi(3770)$ are included in this measurement and may amount to a few percent correction.

[91] This measurement comes from a scan of the $\psi(3770)$ resonance and a fit to the cross section. SCHINDLER 80 assume the phase space division of neutral and charged D mesons in $\psi(3770)$ decay to be 1.33, and that the $\psi(3770)$ is an isosinglet. The noncharm decays (e.g. radiative) of the $\psi(3770)$ are included in this measurement and may amount to a few percent correction.

[92] This measurement comes from a scan of the $\psi(3770)$ resonance and a fit to the cross section. The phase space division of neutral and charged D mesons in $\psi(3770)$ decay is taken to be 1.33, and $\psi(3770)$ is assumed to be an isosinglet. The noncharm decays (e.g. radiative) of the $\psi(3770)$ are included in this measurement and may amount to a few percent correction. We exclude this measurement from the average because of uncertainties in the contamination from τ lepton pairs. Also see RAPIDIS 77.

$D^+ \to \overline{K}^*(892)^0 \ell^+ \nu_\ell$ FORM FACTORS

$r_V \equiv V(0)/A_1(0)$ in $D^+ \to \overline{K}^*(892)^0 \ell^+ \nu_\ell$

VALUE	EVTS	DOCUMENT ID		TECN	COMMENT
1.62 ± 0.08 OUR AVERAGE		Error includes scale factor of 1.5. See the ideogram below.			
$1.504 \pm 0.057 \pm 0.039$	15k	[93] LINK	02L	FOCS	$\overline{K}^*(892)^0 \mu^+ \nu_\mu$
$1.45 \pm 0.23 \pm 0.07$	763	ADAMOVICH	99	BEAT	$\overline{K}^*(892)^0 \mu^+ \nu_\mu$
$1.90 \pm 0.11 \pm 0.09$	3000	[94] AITALA	98B	E791	$\overline{K}^*(892)^0 e^+ \nu_e$
$1.84 \pm 0.11 \pm 0.09$	3034	AITALA	98F	E791	$\overline{K}^*(892)^0 \mu^+ \nu_\mu$
$1.74 \pm 0.27 \pm 0.28$	874	FRABETTI	93E	E687	$\overline{K}^*(892)^0 \mu^+ \nu_\mu$
$2.00 \pm 0.34 \pm 0.16$	305	KODAMA	92	E653	$\overline{K}^*(892)^0 \mu^+ \nu_\mu$
• • • We do not use the following data for averages, fits, limits, etc. • • •					
$2.0 \pm 0.6 \pm 0.3$	183	ANJOS	90E	E691	$\overline{K}^*(892)^0 e^+ \nu_e$

[93] LINK 02L includes the effects of interference with an S-wave background. This much improves the goodness of fit, but does not much shift the values of the form factors.

[94] This is slightly different from the AITALA 98B value: see ref. [5] in AITALA 98F.

Meson Particle Listings

$D^{\pm}$

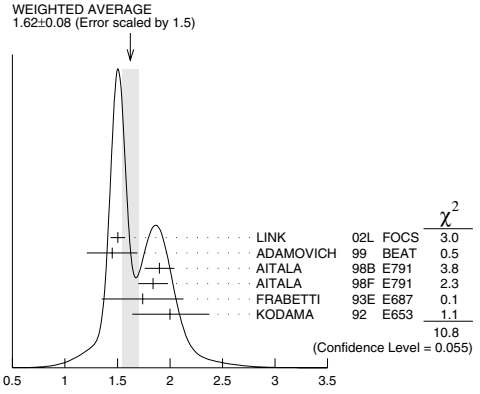

$r_V \equiv V(0)/A_1(0)$ in $D^+ \to \overline{K}^*(892)^0 \ell^+ \nu_\ell$

$r_2 \equiv A_2(0)/A_1(0)$ in $D^+ \to \overline{K}^*(892)^0 \ell^+ \nu_\ell$

VALUE	EVTS	DOCUMENT ID		TECN	COMMENT
0.83 ±0.05 OUR AVERAGE					
0.875±0.049±0.064	15k	[95] LINK	02L	FOCS	$\overline{K}^*(892)^0 \mu^+ \nu_\mu$
1.00 ±0.15 ±0.03	763	ADAMOVICH	99	BEAT	$\overline{K}^*(892)^0 \mu^+ \nu_\mu$
0.71 ±0.08 ±0.09	3000	AITALA	98B	E791	$\overline{K}^*(892)^0 e^+ \nu_e$
0.75 ±0.08 ±0.09	3034	AITALA	98F	E791	$\overline{K}^*(892)^0 \mu^+ \nu_\mu$
0.78 ±0.18 ±0.10	874	FRABETTI	93E	E687	$\overline{K}^*(892)^0 \mu^+ \nu_\mu$
0.82 $^{+0.22}_{-0.23}$ ±0.11	305	KODAMA	92	E653	$\overline{K}^*(892)^0 \mu^+ \nu_\mu$
• • • We do not use the following data for averages, fits, limits, etc. • • •					
0.0 ±0.5 ±0.2	183	ANJOS	90E	E691	$\overline{K}^*(892)^0 e^+ \nu_e$

[95] LINK 02L includes the effects of interference with an S-wave background. This much improves the goodness of fit, but does not much shift the values of the form factors.

$r_3 \equiv A_3(0)/A_1(0)$ in $D^+ \to \overline{K}^*(892)^0 \ell^+ \nu_\ell$

VALUE	EVTS	DOCUMENT ID	TECN	COMMENT
0.04±0.33±0.29	3034	AITALA	98F E791	$\overline{K}^*(892)^0 \mu^+ \nu_\mu$

Γ_L/Γ_T in $D^+ \to \overline{K}^*(892)^0 \ell^+ \nu_\ell$

VALUE	EVTS	DOCUMENT ID		TECN	COMMENT
1.13±0.08 OUR AVERAGE					
1.09±0.10±0.02	763	ADAMOVICH	99	BEAT	$\overline{K}^*(892)^0 \mu^+ \nu_\mu$
1.20±0.13±0.13	874	FRABETTI	93E	E687	$\overline{K}^*(892)^0 \mu^+ \nu_\mu$
1.18±0.18±0.08	305	KODAMA	92	E653	$\overline{K}^*(892)^0 \mu^+ \nu_\mu$
• • • We do not use the following data for averages, fits, limits, etc. • • •					
1.8 $^{+0.6}_{-0.4}$ ±0.3	183	ANJOS	90E	E691	$\overline{K}^*(892)^0 e^+ \nu_e$

Γ_+/Γ_- in $D^+ \to \overline{K}^*(892)^0 \ell^+ \nu_\ell$

VALUE	EVTS	DOCUMENT ID		TECN	COMMENT
0.22±0.06 OUR AVERAGE Error includes scale factor of 1.6.					
0.28±0.05±0.02	763	ADAMOVICH	99	BEAT	$\overline{K}^*(892)^0 \mu^+ \nu_\mu$
0.16±0.05±0.02	305	KODAMA	92	E653	$\overline{K}^*(892)^0 \mu^+ \nu_\mu$
• • • We do not use the following data for averages, fits, limits, etc. • • •					
0.15 $^{+0.07}_{-0.05}$ ±0.03	183	ANJOS	90E	E691	$\overline{K}^*(892)^0 e^+ \nu_e$

$D^{\pm}$ REFERENCES

PDG	04		S. Eidelman *et al.*	
LINK	03D	PL B561 225	J.M. Link *et al.*	(FNAL FOCUS Collab.)
LINK	03F	PL B572 21	J.M. Link *et al.*	(FNAL FOCUS Collab.)
AITALA	02	PRL 89 121801	E.M. Aitala *et al.*	(FNAL E791 Collab.)
BRANDENB...	02	PRL 89 222001	G. Brandenburg *et al.*	(CLEO Collab.)
KAYIS-TOPAK...	02	PL B549 48	A. Kayis-Topaksu *et al.*	(CERN CHORUS Collab.)
LINK	02B	PRL 88 041602	J.M. Link *et al.*	(FNAL FOCUS Collab.)
Also	02D	PRL 88 159903 (erratum)	J.M. Link *et al.*	(FNAL FOCUS Collab.)
LINK	02E	PL B535 43	J.M. Link *et al.*	(FNAL FOCUS Collab.)
LINK	02F	PL B537 192	J.M. Link *et al.*	(FNAL FOCUS Collab.)
LINK	02I	PL B541 227	J.M. Link *et al.*	(FNAL FOCUS Collab.)
LINK	02J	PL B541 243	J.M. Link *et al.*	(FNAL FOCUS Collab.)
LINK	02L	PL B544 89	J.M. Link *et al.*	(FNAL FOCUS Collab.)
AITALA	01B	PRL 86 770	E.M. Aitala *et al.*	(FNAL E791 Collab.)
LINK	01C	PRL 87 162001	J.M. Link *et al.*	(FNAL FOCUS Collab.)
ABREU	00O	EPJ C12 209	P. Abreu *et al.*	(DELPHI Collab.)
ASTIER	00D	PL B486 35	P. Astier *et al.*	(CERN NOMAD Collab.)
BAI	00C	PR D62 052001	J.Z. Bai *et al.*	(BEPC BES Collab.)
JUN	00	PRL 84 1857	S.Y. Jun *et al.*	(FNAL SELEX Collab.)
LINK	00B	PL B491 232	J.M. Link *et al.*	(FNAL FOCUS Collab.)
Also	00D	PL B495 443 (errata)	J.M. Link *et al.*	(FNAL FOCUS Collab.)
ABBIENDI	99K	EPJ C8 573	G. Abbiendi *et al.*	(OPAL Collab.)
ABE	99P	PR D60 092005	F. Abe *et al.*	(CDF Collab.)
ADAMOVICH	99	EPJ C6 35	M. Adamovich *et al.*	(CERN BEATRICE Collab.)
AITALA	99G	PL B462 401	E.M. Aitala *et al.*	(FNAL E791 Collab.)
BONVICINI	99	PRL 82 4586	G. Bonvicini *et al.*	(CLEO Collab.)
AITALA	98B	PRL 80 1393	E.M. Aitala *et al.*	(FNAL E791 Collab.)
AITALA	98C	PL B421 405	E.M. Aitala *et al.*	(FNAL E791 Collab.)
AITALA	98F	PL B440 435	E.M. Aitala *et al.*	(FNAL E791 Collab.)
BAI	98B	PL B429 188	J.Z. Bai *et al.*	(BEPC BES Collab.)
JESSOP	98	PR D58 052002	C.P. Jessop *et al.*	(CLEO Collab.)
AITALA	97	PL B397 325	E.M. Aitala *et al.*	(FNAL E791 Collab.)
AITALA	97B	PL B403 377	E.M. Aitala *et al.*	(FNAL E791 Collab.)
AITALA	97C	PL B404 187	E.M. Aitala *et al.*	(FNAL E791 Collab.)
BARTELT	97	PL B405 373	J. Bartelt *et al.*	(CLEO Collab.)
BISHAI	97	PRL 78 3261	M. Bishai *et al.*	(CLEO Collab.)
FRABETTI	97	PL B391 235	P.L. Frabetti *et al.*	(FNAL E687 Collab.)
FRABETTI	97B	PL B398 239	P.L. Frabetti *et al.*	(FNAL E687 Collab.)
FRABETTI	97C	PL B401 131	P.L. Frabetti *et al.*	(FNAL E687 Collab.)
FRABETTI	97D	PL B407 79	P.L. Frabetti *et al.*	(FNAL E687 Collab.)
AITALA	96	PRL 76 364	E.M. Aitala *et al.*	(FNAL E791 Collab.)
ALBRECHT	96C	PL B374 249	H. Albrecht *et al.*	(ARGUS Collab.)
BIGI	95	PL B349 363	I.I. Bigi, H. Yamamoto	(NDAM, HARV)
FRABETTI	95	PL B346 199	P.L. Frabetti *et al.*	(FNAL E687 Collab.)
FRABETTI	95B	PL B351 591	P.L. Frabetti *et al.*	(FNAL E687 Collab.)
FRABETTI	95E	PL B359 403	P.L. Frabetti *et al.*	(FNAL E687 Collab.)
FRABETTI	95F	PL B363 259	P.L. Frabetti *et al.*	(FNAL E687 Collab.)
KODAMA	95	PL B345 85	K. Kodama *et al.*	(FNAL E653 Collab.)
ALBRECHT	94I	ZPHY C64 375	H. Albrecht *et al.*	(ARGUS Collab.)
ALEEV	94	PAN 57 1370 Translated from YF 57 1443	A.N. Aleev *et al.*	(Serpukhov BIS-2 Collab.)
BALEST	94	PRL 72 2328	R. Balest *et al.*	(CLEO Collab.)
FRABETTI	94D	PL B323 459	P.L. Frabetti *et al.*	(FNAL E687 Collab.)
FRABETTI	94G	PL B331 217	P.L. Frabetti *et al.*	(FNAL E687 Collab.)
FRABETTI	94I	PR D50 R2953	P.L. Frabetti *et al.*	(FNAL E687 Collab.)
ABE	93E	PL B313 288	K. Abe *et al.*	(VENUS Collab.)
ADAMOVICH	93	PL B305 177	M.I. Adamovich *et al.*	(CERN WA82 Collab.)
AKERIB	93	PRL 71 3070	D.S. Akerib *et al.*	(CLEO Collab.)
ALAM	93	PRL 71 1311	M.S. Alam *et al.*	(CLEO Collab.)
ANJOS	93	PR D48 56	J.C. Anjos *et al.*	(FNAL E691 Collab.)
BEAN	93C	PL B317 647	A. Bean *et al.*	(CLEO Collab.)
FRABETTI	93E	PL B307 262	P.L. Frabetti *et al.*	(FNAL E687 Collab.)
KODAMA	93B	PL B313 260	K. Kodama *et al.*	(FNAL E653 Collab.)
KODAMA	93C	PL B316 455	K. Kodama *et al.*	(FNAL E653 Collab.)
SELEN	93	PRL 71 1973	M.A. Selen *et al.*	(CLEO Collab.)
ALBRECHT	92B	ZPHY C53 361	H. Albrecht *et al.*	(ARGUS Collab.)
ALBRECHT	92F	PL B278 202	H. Albrecht *et al.*	(ARGUS Collab.)
ANJOS	92	PR D45 R2177	J.C. Anjos *et al.*	(FNAL E691 Collab.)
ANJOS	92C	PR D46 1941	J.C. Anjos *et al.*	(FNAL E691 Collab.)
ANJOS	92D	PRL 69 2892	J.C. Anjos *et al.*	(FNAL E691 Collab.)
BARLAG	92C	ZPHY C55 383	S. Barlag *et al.*	(ACCMOR Collab.)
Also	90D	ZPHY C48 29	S. Barlag *et al.*	(ACCMOR Collab.)
COFFMAN	92B	PR D45 2196	D.M. Coffman *et al.*	(Mark III Collab.)
DAOUDI	92	PR D45 3965	M. Daoudi *et al.*	(CLEO Collab.)
FRABETTI	92	PL B281 167	P.L. Frabetti *et al.*	(FNAL E687 Collab.)
KODAMA	92	PL B274 246	K. Kodama *et al.*	(FNAL E653 Collab.)
KODAMA	92C	PL B286 187	K. Kodama *et al.*	(FNAL E653 Collab.)
ADAMOVICH	91	PL B268 142	M.I. Adamovich *et al.*	(WA82 Collab.)
ALBRECHT	91	PL B255 634	H. Albrecht *et al.*	(ARGUS Collab.)
ALVAREZ	91	PL B255 639	M.P. Alvarez *et al.*	(CERN NA14/2 Collab.)
ALVAREZ	91B	ZPHY C50 11	M.P. Alvarez *et al.*	(CERN NA14/2 Collab.)
AMMAR	91	PR D44 3383	R. Ammar *et al.*	(CLEO Collab.)
ANJOS	91B	PR D43 R2063	J.C. Anjos *et al.*	(FNAL E691 Collab.)
ANJOS	91C	PRL 67 1507	J.C. Anjos *et al.*	(FNAL TPS Collab.)
BAI	91	PRL 66 1011	Z. Bai *et al.*	(Mark III Collab.)
COFFMAN	91	PL B263 135	D.M. Coffman *et al.*	(Mark III Collab.)
FRABETTI	91	PL B263 584	P.L. Frabetti *et al.*	(FNAL E687 Collab.)
ALVAREZ	90	ZPHY C47 539	M.P. Alvarez *et al.*	(CERN NA14/2 Collab.)
ALVAREZ	90C	PL B246 261	M.P. Alvarez *et al.*	(CERN NA14/2 Collab.)
ANJOS	90C	PR D41 2705	J.C. Anjos *et al.*	(FNAL E691 Collab.)
ANJOS	90D	PR D42 2414	J.C. Anjos *et al.*	(FNAL E691 Collab.)
ANJOS	90E	PRL 65 2630	J.C. Anjos *et al.*	(FNAL E691 Collab.)
BARLAG	90C	ZPHY C46 563	S. Barlag *et al.*	(ACCMOR Collab.)
WEIR	90B	PR D41 1384	A.J. Weir *et al.*	(Mark II Collab.)
ANJOS	89	PRL 62 125	J.C. Anjos *et al.*	(FNAL E691 Collab.)
ANJOS	89B	PRL 62 722	J.C. Anjos *et al.*	(FNAL E691 Collab.)
ANJOS	89E	PL B223 267	J.C. Anjos *et al.*	(FNAL E691 Collab.)
ADLER	88B	PRL 60 1375	J. Adler *et al.*	(Mark III Collab.)
ADLER	88C	PRL 60 89	J. Adler *et al.*	(Mark III Collab.)
ALBRECHT	88I	PL B210 267	H. Albrecht *et al.*	(ARGUS Collab.)
ANJOS	88	PRL 60 897	J.C. Anjos *et al.*	(FNAL E691 Collab.)
AOKI	88	PL B209 113	S. Aoki *et al.*	(WA75 Collab.)
HAAS	88	PRL 60 1614	P. Haas *et al.*	(CLEO Collab.)
ONG	88	PRL 60 2587	R.A. Ong *et al.*	(Mark II Collab.)
RAAB	88	PR D37 2391	J.R. Raab *et al.*	(FNAL E691 Collab.)
ADAMOVICH	87	EPL 4 887	M.I. Adamovich *et al.*	(Photon Emulsion Collab.)
ADLER	87	PL B196 107	J. Adler *et al.*	(Mark III Collab.)
AGUILAR-...	87E	ZPHY C36 551	M. Aguilar-Benitez *et al.*	(LEBC-EHS Collab.)
Also	88B	ZPHY C40 321	M. Aguilar-Benitez *et al.*	(LEBC-EHS Collab.)
AGUILAR-...	87F	ZPHY C36 559	M. Aguilar-Benitez *et al.*	(LEBC-EHS Collab.)
Also	88	ZPHY C38 520 erratum	M. Aguilar-Benitez *et al.*	(LEBC-EHS Collab.)
BARTEL	87	ZPHY C33 339	W. Bartel *et al.*	(JADE Collab.)
AGUILAR-...	86B	ZPHY C31 491	M. Aguilar-Benitez *et al.*	(LEBC-EHS Collab.)
BALTRUSAIT...	86E	PRL 56 2140	R.M. Baltrusaitis *et al.*	(Mark III Collab.)
PAL	86	PR D33 2708	T. Pal *et al.*	(DELCO Collab.)
AIHARA	85	ZPHY C27 39	H. Aihara *et al.*	(TPC Collab.)
BALTRUSAIT...	85B	PRL 54 1976	R.M. Baltrusaitis *et al.*	(Mark III Collab.)
BALTRUSAIT...	85E	PRL 55 150	R.M. Baltrusaitis *et al.*	(Mark III Collab.)
BARTEL	85J	PL 163B 277	W. Bartel *et al.*	(JADE Collab.)
ADAMOVICH	84	PL 140B 119	M.I. Adamovich *et al.*	(CERN WA58 Collab.)
ALTHOFF	84G	ZPHY C22 219	M. Althoff *et al.*	(TASSO Collab.)
ALTHOFF	84J	PL 146B 443	M. Althoff *et al.*	(TASSO Collab.)
DERRICK	84	PRL 53 1971	M. Derrick *et al.*	(HRS Collab.)
KOOP	84	PRL 52 970	D.E. Koop *et al.*	(DELCO Collab.)
PARTRIDGE	84	Thesis CALT-68-1150	R.A. Partridge	(Crystal Ball Collab.)
AGUILAR-...	83B	PL 123B 98	M. Aguilar-Benitez *et al.*	(LEBC-EHS Collab.)
AUBERT	83	NP B213 31	J.J. Aubert *et al.*	(EMC Collab.)
PARTRIDGE	81	PRL 47 760	R. Partridge *et al.*	(Crystal Ball Collab.)
SCHINDLER	81	PR D24 78	R.H. Schindler *et al.*	(Mark II Collab.)
TRILLING	81	PRPL 75 57	G.H. Trilling	(LBL, UCB) J
BACINO	80	PRL 45 329	W.J. Bacino *et al.*	(DELCO Collab.)
SCHINDLER	80	PR D21 2716	R.H. Schindler *et al.*	(Mark II Collab.)
ZHOLENTZ	80	PL 96B 214	A.A. Zholentz *et al.*	(NOVO)
Also	81	SJNP 34 814 Translated from YAF 34 1471.	A.A. Zholents *et al.*	(NOVO)
BACINO	79	PRL 43 1073	W.J. Bacino *et al.*	(DELCO Collab.)
BRANDELIK	79	PL 80B 412	R. Brandelik *et al.*	(DASP Collab.)
FELLER	78	PRL 40 274	J.M. Feller *et al.*	(Mark I Collab.)
VUILLEMIN	78	PRL 41 1149	V. Vuillemin *et al.*	(Mark I Collab.)
GOLDHABER	77	PL 69B 503	G. Goldhaber *et al.*	(Mark I Collab.)
PERUZZI	77	PRL 39 1301	I. Peruzzi *et al.*	(Mark I Collab.)
PICCOLO	77	PL 70B 260	M. Piccolo *et al.*	(Mark I Collab.)
RAPIDIS	77	PRL 39 526	P.A. Rapidis *et al.*	(Mark I Collab.)
PERUZZI	76	PRL 37 569	I. Peruzzi *et al.*	(Mark I Collab.)

OTHER RELATED PAPERS

RICHMAN	95	RMP 67 893	J.D. Richman, P.R. Burchat	(UCSB, STAN)
ROSNER	95	CNPP 21 369	J. Rosner	(CHIC)

D^0

$I(J^P) = \frac{1}{2}(0^-)$

D^0 MASS

The fit includes $D^\pm$, D^0, $D_s^\pm$, $D^{*\pm}$, D^{*0}, and $D_s^{*\pm}$ mass and mass difference measurements.

VALUE (MeV)	EVTS	DOCUMENT ID		TECN	COMMENT
1864.6± 0.5 OUR FIT Error includes scale factor of 1.1.					
1864.1± 1.0 OUR AVERAGE					
1864.6± 0.3±1.0	641	BARLAG	90C	ACCM	π^- Cu 230 GeV
1852 ± 7	16	ADAMOVICH	87	EMUL	Photoproduction
1861 ± 4		DERRICK	84	HRS	e^+e^- 29 GeV
• • • We do not use the following data for averages, fits, limits, etc. • • •					
1856 ±36	22	ADAMOVICH	84B	EMUL	Photoproduction
1847 ± 7	1	FIORINO	81	EMUL	$\gamma N \to \overline{D}^0 +$
1863.8± 0.5		[1] SCHINDLER	81	MRK2	e^+e^- 3.77 GeV
1864.7± 0.6		[1] TRILLING	81	RVUE	e^+e^- 3.77 GeV
1863.0± 2.5	238	ASTON	80E	OMEG	$\gamma p \to \overline{D}^0$
1860 ± 2	143	[2] AVERY	80	SPEC	$\gamma N \to D^{*+}$
1869 ± 4	35	[2] AVERY	80	SPEC	$\gamma N \to D^{*+}$
1854 ± 6	94	[2] ATIYA	79	SPEC	$\gamma N \to D^0\overline{D}^0$
1850 ±15	64	BALTAY	78C	HBC	$\nu N \to K^0\pi\pi$
1863 ± 3		GOLDHABER	77	MRK1	D^0, D^+ recoil spectra
1863.3± 0.9		[1] PERUZZI	77	MRK1	e^+e^- 3.77 GeV
1868 ±11		PICCOLO	77	MRK1	e^+e^- 4.03, 4.41 GeV
1865 ±15	234	GOLDHABER	76	MRK1	$K\pi$ and $K3\pi$

[1] PERUZZI 77 and SCHINDLER 81 errors do not include the 0.13% uncertainty in the absolute SPEAR energy calibration. TRILLING 81 uses the high precision $J/\psi(1S)$ and $\psi(2S)$ measurements of ZHOLENTZ 80 to determine this uncertainty and combines the PERUZZI 77 and SCHINDLER 81 results to obtain the value quoted. TRILLING 81 enters the fit in the $D^\pm$ mass, and PERUZZI 77 and SCHINDLER 81 enter in the $m_{D^\pm} - m_{D^0}$, below.

[2] Error does not include possible systematic mass scale shift, estimated to be less than 5 MeV.

$m_{D^\pm} - m_{D^0}$

The fit includes $D^\pm$, D^0, $D_s^\pm$, $D^{*\pm}$, D^{*0}, and $D_s^{*\pm}$ mass and mass difference measurements.

VALUE (MeV)	DOCUMENT ID		TECN	COMMENT
4.78±0.10 OUR FIT Error includes scale factor of 1.1.				
4.74±0.28 OUR AVERAGE				
4.7 ±0.3	[3] SCHINDLER	81	MRK2	e^+e^- 3.77 GeV
5.0 ±0.8	[3] PERUZZI	77	MRK1	e^+e^- 3.77 GeV

[3] See the footnote on TRILLING 81 in the D^0 and $D^\pm$ sections on the mass.

D^0 MEAN LIFE

Measurements with an error $> 20 \times 10^{-15}$ s have been omitted from the average.

VALUE (10^{-15} s)	EVTS	DOCUMENT ID		TECN	COMMENT
410.3± 1.5 OUR AVERAGE					
409.6± 1.1± 1.5	210k	LINK	02F	FOCS	γ nucleus, ≈ 180 GeV
407.9± 6.0± 4.3	10k	KUSHNIR...	01	SELX	$D^0 \to K^-\pi^+$, $K^-\pi^+\pi^+\pi^-$
413 ± 3 ± 4	35k	AITALA	99E	E791	$K^-\pi^+$
408.5± 4.1$^{+\ 3.5}_{-\ 3.4}$	25k	BONVICINI	99	CLE2	$e^+e^- \approx \Upsilon(4S)$
413 ± 4 ± 3	16k	FRABETTI	94D	E687	$K^-\pi^+$, $K^-\pi^+\pi^+\pi^-$
424 ±11 ± 7	5118	FRABETTI	91	E687	$K^-\pi^+$, $K^-\pi^+\pi^+\pi^-$
• • • We do not use the following data for averages, fits, limits, etc. • • •					
417 ±18 ±15	890	ALVAREZ	90	NA14	$K^-\pi^+$, $K^-\pi^+\pi^+\pi^-$
388 $^{+23}_{-21}$	641	[4] BARLAG	90C	ACCM	π^- Cu 230 GeV
480 ±40 ±30	776	ALBRECHT	88I	ARG	e^+e^- 10 GeV
422 ± 8 ±10	4212	RAAB	88	E691	Photoproduction
420 ±50	90	BARLAG	87B	ACCM	K^- and π^- 200 GeV

[4] BARLAG 90C estimate systematic error to be negligible.

D^0–$\overline{D}^0$ MIXING

Revised November 2003 by D. Asner (University of Pittsburgh)

Standard Model contributions to D^0–$\overline{D}^0$ mixing are strongly suppressed by CKM and GIM factors. Thus the observation of D^0–$\overline{D}^0$ mixing might be evidence for physics beyond the Standard Model. See Burdman and Shipsey [1] for a review of D^0–$\overline{D}^0$ mixing, Nelson [2] for a compilation of mixing predictions, and Ref. [3] for subsequent predictions.

Formalism: The time evolution of the D^0–$\overline{D}^0$ system is described by the Schrödinger equation

$$i\frac{\partial}{\partial t}\begin{pmatrix} D^0(t) \\ \overline{D}^0(t) \end{pmatrix} = \left(\mathbf{M} - \tfrac{i}{2}\mathbf{\Gamma}\right)\begin{pmatrix} D^0(t) \\ \overline{D}^0(t) \end{pmatrix}, \quad (1)$$

where the $\mathbf{M}$ and $\mathbf{\Gamma}$ matrices are Hermitian, and CPT invariance requires $M_{11} = M_{22} \equiv M$ and $\Gamma_{11} = \Gamma_{22} \equiv \Gamma$. The off-diagonal elements of these matrices describe the dispersive and absorptive parts of D^0–$\overline{D}^0$ mixing.

The two eigenstates D_1 and D_2 of the effective Hamiltonian matrix $(\mathbf{M} - \frac{i}{2}\mathbf{\Gamma})$ are given by

$$|D_{1,2}\rangle = p|D^0\rangle \pm q|\overline{D}^0\rangle\,. \quad (2)$$

The corresponding eigenvalues are

$$\lambda_{1,2} \equiv m_{1,2} - \tfrac{i}{2}\Gamma_{1,2} = \left(M - \tfrac{i}{2}\Gamma\right) \pm \frac{q}{p}\left(M_{12} - \tfrac{i}{2}\Gamma_{12}\right), \quad (3)$$

where m_1 and Γ_1 are the mass and width of the D_1, etc., and

$$\left|\frac{q}{p}\right|^2 = \frac{M_{12}^* - \frac{i}{2}\Gamma_{12}^*}{M_{12} - \frac{i}{2}\Gamma_{12}}\,. \quad (4)$$

We extend the formalism of this Review's note on "B^0–$\overline{B}^0$ Mixing" [4]. In addition to the "right-sign" instantaneous decay amplitudes $\overline{A}_f \equiv \langle f|H|\overline{D}^0\rangle$ and $A_{\overline{f}} \equiv \langle \overline{f}|H|D^0\rangle$ for CP conjugate final states f and $\overline{f}$, we include the "wrong-sign" amplitudes $\overline{A}_{\overline{f}} \equiv \langle \overline{f}|H|\overline{D}^0\rangle$ and $A_f \equiv \langle f|H|D^0\rangle$.

It is usual to normalize the wrong-sign decay distributions to the integrated rate of right-sign decays and to express time in units of the precisely measured D^0 mean lifetime, $\overline{\tau}_{D^0} = 1/\Gamma = 2/(\Gamma_1 + \Gamma_2)$. Starting from a pure $|D^0\rangle$ or $|\overline{D}^0\rangle$ state at $t = 0$, the time-dependent rates of production of the wrong-sign final states relative to the integrated right-sign states are then

$$r(t) = \frac{\left|\langle f|H|D^0(t)\rangle\right|^2}{\left|\overline{A}_f\right|^2} = \left|\frac{q}{p}\right|^2 \left|g_+(t)\,\chi_f^{-1} + g_-(t)\right|^2 \quad (5)$$

and

$$\overline{r}(t) = \frac{\left|\langle \overline{f}|H|\overline{D}^0(t)\rangle\right|^2}{\left|A_{\overline{f}}\right|^2} = \left|\frac{p}{q}\right|^2 \left|g_+(t)\,\chi_{\overline{f}} + g_-(t)\right|^2, \quad (6)$$

where

$$\chi_f = \frac{q\overline{A}_f}{pA_f} \quad (7)$$

and

$$g_\pm(t) = \frac{1}{2}\left(e^{-iz_1 t} \pm e^{-iz_2 t}\right), \quad z_{1,2} = \frac{\lambda_{1,2}}{\Gamma}\,. \quad (8)$$

Note that a change in the convention for the relative phase of D^0 and $\overline{D}^0$ would cancel between q/p and $\overline{A}_f/A_f$ and leave χ_f invariant.

Since D^0–$\overline{D}^0$ mixing is a small effect, the identification tag of the initial particle as a D^0 or a $\overline{D}^0$ must be extremely accurate. The usual tag is the charge of the distinctive slow

pion in the decay sequence $D^{*+} \to D^0\pi^+$ or $D^{*-} \to \overline{D}^0\pi^-$. In current experiments, the mis-tag probability is about one per thousand. Another tag of comparable accuracy is identification of one of the D's from $\psi(3770) \to D^0\overline{D}^0$.

We expand $r(t)$ and $\overline{r}(t)$ to second order in time for modes where the ratio of decay amplitudes $R_D = |A_f/\overline{A}_f|^2$ is very small. We define reduced mixing amplitudes x and y by

$$x \equiv \frac{2M_{12}}{\Gamma} = \frac{m_1 - m_2}{\Gamma} = \frac{\Delta m}{\Gamma} \tag{9}$$

and

$$y \equiv \frac{\Gamma_{12}}{\Gamma} = \frac{\Gamma_1 - \Gamma_2}{2\Gamma} = \frac{\Delta\Gamma}{2\Gamma}. \tag{10}$$

In these equations, the middle relation holds in the limit of CP conservation, in which case the subscripts 1 and 2 indicate the CP-even and CP-odd eigenstates, respectively.

Semileptonic decays: In semileptonic decays, $A_f = \overline{A}_{\overline{f}} = 0$ in the Standard Model. Then in the limit of weak mixing, where $|ix + y| \ll 1$, $r(t)$ is given by

$$r(t) = |g_-(t)|^2 \left|\frac{q}{p}\right|^2 \approx \frac{e^{-t}}{4}(x^2 + y^2)\, t^2 \left|\frac{q}{p}\right|^2 . \tag{11}$$

For $\overline{r}(t)$ one replaces q/p here by p/q; and in the limit of CP conservation, $r(t) = \overline{r}(t)$, and the time-integrated mixing rate relative to the time-integrated right-sign decay rate is

$$R_M = \int_0^\infty r(t)dt \approx \frac{1}{2}(x^2 + y^2)\,. \tag{12}$$

The results from semileptonic decays are summarized in Table 1. The most sensitive mixing limit is from the FOCUS experiment [5]. Searching for the decay $D^0 \to K^+\mu^-\overline{\nu}_\mu$, it found $R_M < 1.31 \times 10^{-3}$ at the 95% C.L., assuming CP conservation. Semileptonic decays are less sensitive to mixing than are hadronic decays and thus have received less attention recently.

Table 1: Results for R_M in D^0 semileptonic decays.

Year	Exper.	Final State(s)	R_M
2002	FOCUS [5]	$K^+\mu^-\overline{\nu}_\mu$	$< 1.31 \times 10^{-3}$ (95% C.L.)
2002	CLEO [6]	$K^{*+}e^-\overline{\nu}_e$	$< 8.6 \times 10^{-3}$ (95% C.L.)
1996	E791 [7]	$K^+\ell^-\overline{\nu}_\ell$	$< 5.0 \times 10^{-3}$ (90% C.L.)

Wrong-sign decays to hadronic non-CP eigenstates: Consider the final state $f = K^+\pi^-$, where A_f is doubly Cabibbo-suppressed, and the ratio of decay amplitudes is

$$\frac{A_f}{\overline{A}_f} = -\sqrt{R_D}\, e^{-i\delta}, \qquad \left|\frac{A_f}{\overline{A}_f}\right| \sim O(\tan^2\theta_c)\,, \tag{13}$$

where R_D is the doubly Cabibbo-suppressed decay rate relative to the Cabibbo-favored rate, and δ is a strong phase difference between doubly Cabibbo-suppressed and Cabibbo-favored processes. The minus sign originates from the sign of V_{us} relative to V_{cd}.

We characterize the violation of CP in the mixing amplitude, the decay amplitude, and the interference between mixing and decay, by real-valued parameters A_M, A_D, and ϕ. We adopt a parameterization similar to that of Nir [8] and CLEO [9] and express these quantities in a way that is convenient to describe the three types of CP violation:

$$\left|\frac{q}{p}\right| = 1 + A_M\,, \tag{14}$$

$$\chi_f^{-1} \equiv \frac{pA_f}{q\overline{A}_f} = \frac{-\sqrt{R_D}(1 + A_D)}{(1 + A_M)}\, e^{-i(\delta+\phi)}\,, \tag{15}$$

$$\chi_{\overline{f}} \equiv \frac{q\overline{A}_{\overline{f}}}{pA_{\overline{f}}} = -\frac{-\sqrt{R_D}(1 + A_M)}{(1 + A_D)}\, e^{-i(\delta-\phi)}\,. \tag{16}$$

In general, $\chi_{\overline{f}}$ and χ_f^{-1} are independent complex numbers. To leading order,

$$r(t) = e^{-t} \times \Big[R_D(1 + A_D)^2 + \sqrt{R_D}(1 + A_M)(1 + A_D)y'_-\, t + \frac{(1 + A_M)^2 R_M}{2}\, t^2\Big] \tag{17}$$

and

$$\overline{r}(t) = e^{-t} \times \left[\frac{R_D}{(1+A_D)^2} + \frac{\sqrt{R_D}}{(1+A_D)(1+A_M)} y'_+ t + \frac{R_M}{2(1+A_M)^2}\, t^2\right], \tag{18}$$

where

$$y'_\pm \equiv y'\cos\phi \pm x'\sin\phi = y\cos(\delta \mp \phi) - x\sin(\delta \mp \phi) \tag{19}$$

$$y' \equiv y\cos\delta - x\sin\delta, \quad x' \equiv x\cos\delta + y\sin\delta\,, \tag{20}$$

and R_M is the mixing rate relative to the time-integrated right-sign rate.

The differences between the three terms in Eq. (17) and Eq. (18) probe the three fundamental types of CP violation. In the limit of CP conservation, A_M, A_D, and ϕ are all zero, and then $r(t) = \overline{r}(t)$:

$$r(t) = \overline{r}(t) = e^{-t}\left(R_D + \sqrt{R_D}\, y' t + \frac{1}{2} R_M\, t^2\right), \tag{21}$$

and the time-integrated wrong-sign rate relative to the integrated right-sign rate is

$$R = \int_0^\infty r(t)\, dt = R_D + \sqrt{R_D}\, y' + R_M\,. \tag{22}$$

The ratio R of time-integrated wrong- and right-sign rates is the most readily accessible experimental quantity. The observations of non-zero R in $D^0 \to K^+\pi^-$ decay are summarized in Table 2. There has been improvement in precision since 1999, and the average, $R = (0.365 \pm 0.021)\,\%$, from recent experiments is about two standard deviations from the average of $R = (0.81 \pm 0.23)\,\%$ of the pre-1999 results. We restrict the subsequent discussion to the post-1999 experiments.

Table 2: Results for R in $D^0 \to K^+\pi^-$.

Year	Exper.	Technique	$R_D(\times 10^{-3})$	$A_D(\%)$
2003	BABAR [10]	$e^+e^- \to \Upsilon(4S)$	$3.57 \pm 0.22 \pm 0.27$	$9.5 \pm 6.1 \pm 8.3$
2002	Belle [11]	$e^+e^- \to \Upsilon(4S)$	$3.72 \pm 0.25^{+0.09}_{-0.14}$	-
2001	FOCUS [12]	γ BeO	$4.04 \pm 0.85 \pm 0.25$	-
2000	CLEO [9]	$e^+e^- \to \Upsilon(4S)$	$3.32^{+0.63}_{-0.65} \pm 0.40$	$2^{+19}_{-20} \pm 1$
1998	E791 [13]	π^-Pt	$6.8^{+3.4}_{-3.3} \pm 0.7$	-
1998	Aleph [14]	$e^+e^- \to Z^0$	$18.4 \pm 5.9 \pm 3.4$	-
1994	CLEO [15]	$e^+e^- \to \Upsilon(4S)$	$7.7 \pm 2.5 \pm 2.5$	-

The contributions to R can be extracted by fitting the $D^0 \to K^+\pi^-$ decay rates. Comparison of results is complicated because some experiments include CP violating terms, some do not. CLEO [9] and BABAR [10] allowed for CP violation in all three terms (i.e. measure $r(t)$ and $\overline{r}(t)$), and then quote limits on the mixing amplitudes after averaging D^0 and $\overline{D}^0$. A preliminary FOCUS result [12] assumes CP conservation. The results for y' and $x'^2/2$ are summarized in Table 3. Figure 1 shows the two-dimensional allowed regions.

Table 3: Results from studies of the time dependence $r(t)$.

Year	Exper.	y' (95% C.L.)	$x'^2/2$ (95% C.L.)
2003	BABAR [10]	$-5.6 < y' < 3.9$ %	< 0.11 %
2001	FOCUS [12]	$-12.4 < y' < -0.5$ %	< 0.076 %
2000	CLEO [9]	$-5.8 < y' < 1.0$ %	< 0.041 %

Extraction of the amplitudes x and y from the results in Table 3 requires knowledge of the relative strong phase δ, a subject of theoretical discussion [16, 17]. In most cases, it appears difficult for theory to accommodate $\delta > 25°$, although the judicious placement of a $K\pi$ resonance could allow δ to be as large as 50°.

A quantum interference effect that provides useful sensitivity to δ arises in the decay chain $\psi(3770) \to D^0\overline{D}^0 \to (f_{cp})(K^+\pi^-)$, where f_{cp} denotes a CP eigenstate from D^0 decay, such as K^+K^-[1, 18]. Here, the amplitude triangle relation

$$\sqrt{2}\,A(D_\pm \to K^-\pi^+) = A(D^0 \to K^-\pi^+) \pm A(\overline{D}^0 \to K^-\pi^+), \tag{23}$$

where $D_\pm$ denotes a CP eigenstate, implies that

$$1 \pm 2\sqrt{R_D}\cos\delta = 2\,\frac{B(D_\pm \to K^-\pi^+)}{B(D^0 \to K^-\pi^+)}, \tag{24}$$

or

$$\cos\delta = \frac{B(D_+ \to K^-\pi^+) - B(D_- \to K^-\pi^+)}{2\sqrt{R_D}\,B(D^0 \to K^-\pi^+)}, \tag{25}$$

neglecting CP violation and exploiting $R_D \ll \sqrt{R_D}$. Projections for 3 fb^{-1} of data at the $\psi(3770)$ indicate that δ could be measured to 20° if $|\cos\delta| \sim 1$, and to a few degrees if $\cos\delta \sim 0$ [19].

The strong phase δ might also be determined by constructing amplitude quadrangles from a complete set of branching fraction measurements of the other doubly Cabibbo-suppressed D decays to two pseudoscalars [20]. This analysis would have to assume that the amplitudes from both $\Delta I = 1$ and $\Delta I = 0$ that populate the total $I = 1/2$ $K\pi$ state have the same strong phase relative to the amplitude that populates the total $I = 3/2$ $K\pi$ state.

The Dalitz-plot analyses of doubly Cabibbo-suppressed D decays to a pseudoscalar and a vector allow the measurement of the relative strong phase between some amplitudes, providing additional contraints to the amplitude quadrangle [21] and thus the determination of the strong phase difference between the relevant doubly Cabibbo-suppressed and Cabibbo-favored amplitudes. In $D^0 \to K_S\pi\pi$, the doubly Cabibbo-suppressed and Cabibbo-favored decay amplitudes occupy the same Dalitz plot, which allows direct measurement of the relative strong phase. CLEO has measured the relative phase between $D^0 \to K^*(892)^+\pi^-$ and $D^0 \to K^*(892)^-\pi^+$ to be $(189 \pm 10 \pm 3^{+15}_{-5})°$ [22], consistent with the 180° expected from Cabibbo factors and a small strong phase.

There are several results for R measured in multibody final states with nonzero strangeness. Here R, defined in Eq. (22), becomes an average over the Dalitz space, weighted by experimental efficiencies and acceptance. The results are summarized in Table 4.

Table 4: Results for R in $D^0 \to K^{(*)+}\pi^-(n\pi)$.

Year	Exper.	D^0 Final State	$R(\%)$
2002	CLEO [22]	$K^*(892)^+\pi^-$	$0.5 \pm 0.2^{+0.6}_{-0.1}$
2001	CLEO [23]	$K^+\pi^-\pi^+\pi^-$	$0.41^{+0.12}_{-0.11} \pm 0.04$
2001	CLEO [24]	$K^+\pi^-\pi^0$	$0.43^{+0.11}_{-0.10} \pm 0.07$
1998	E791 [13]	$K^+\pi^-\pi^+\pi^-$	$0.68^{+0.34}_{-0.33} \pm 0.07$

For multibody final states, Eqs. (13)–(22) apply to one point in the Dalitz space. Although x and y do not vary across the Dalitz space, knowledge of the resonant substructure is needed to extrapolate the strong phase difference δ from point to point. Both the sign and magnitude of x and y are experimentally accessible by studying the time-dependent resonant substructure in decay modes such as $D^0 \to K_S\pi^+\pi^-$ [25].

Decays to CP Eigenstates: When the final state f is a CP eigenstate, there is no distinction between f and $\overline{f}$, and then $A_f = A_{\overline{f}}$ and $\overline{A}_{\overline{f}} = \overline{A}_f$. We denote final states with CP eigenvalues ± 1 by $f_\pm$. In analogy with Eqs. (5)–(6), the decay rates to CP eigenstates are then

$$\begin{aligned} r_\pm(t) &= \frac{\left|\langle f_\pm|H|D^0(t)\rangle\right|^2}{\left|\overline{A}_\pm\right|^2} \\ &= \frac{1}{4}\left|h_\pm(t)\left(\frac{A_\pm}{\overline{A}_\pm} \pm \frac{q}{p}\right) + h_\mp(t)\left(\frac{A_\pm}{\overline{A}_\pm} \mp \frac{q}{p}\right)\right|^2, \\ &\propto \frac{1}{|p|^2}\left|h_\pm(t) + \eta_\pm h_\mp(t)\right|^2, \end{aligned} \tag{26}$$

and

$$\overline{r}_\pm(t) = \frac{\left|\langle f_\pm|H|\overline{D}^0(t)\rangle\right|^2}{|A_\pm|^2} \propto \frac{1}{|q|^2}\left|h_\pm(t) - \eta_\pm h_\mp(t)\right|^2, \quad (27)$$

where

$$h_\pm(t) = g_+(t) \pm g_-(t) = e^{-iz_\pm t}, \quad (28)$$

and

$$\eta_\pm \equiv \frac{pA_\pm \mp q\overline{A}_\pm}{pA_\pm \pm q\overline{A}_\pm} = \frac{1 \mp \chi_\pm}{1 \pm \chi_\pm}, \quad (29)$$

and the variable $\eta_\pm$ describes CP violation; $\eta_\pm$ can receive contributions from each of the three fundamental types of CP violation.

The quantity y may be measured by comparing the rate for decays to non-CP eigenstates such as $D^0 \to K^-\pi^+$ with decays to CP eigenstates such as $D^0 \to K^+K^-$ [17]. A positive y would make K^+K^- decays appear to have a higher decay rate than $K^-\pi^+$ decays. The decay rate for a D^0 into a CP eigenstate is not described by a single exponential in the presence of CP violation.

In the limit of weak mixing, where $|ix+y| \ll 1$, and small CP violation, where $|A_M|$, $|A_D|$, and $|\sin\phi| \ll 1$, the time dependence of decays to CP eigenstates is proportional to a single exponential:

$$r_\pm(t) \propto e^{-[1\pm\left|\frac{p}{q}\right|(y\cos\phi - x\sin\phi)]t}, \quad (30)$$

$$\overline{r}_\pm(t) \propto e^{-[1\pm\left|\frac{q}{p}\right|(y\cos\phi + x\sin\phi)]t}, \quad (31)$$

$$r_\pm(t) + \overline{r}_\pm(t) \propto e^{-(1\pm y_{CP})t}. \quad (32)$$

Here

$$y_{CP} = y\cos\phi\left[\frac{1}{2}\left(\left|\frac{p}{q}\right| + \left|\frac{q}{p}\right|\right) + \frac{A_{\rm prod}}{2}\left(\left|\frac{p}{q}\right| - \left|\frac{q}{p}\right|\right)\right] - x\sin\phi\left[\frac{1}{2}\left(\left|\frac{p}{q}\right| - \left|\frac{q}{p}\right|\right) + \frac{A_{\rm prod}}{2}\left(\left|\frac{p}{q}\right| + \left|\frac{q}{p}\right|\right)\right], \quad (33)$$

and

$$A_{\rm prod} \equiv \frac{N(D^0) - N(\overline{D}^0)}{N(D^0) + N(\overline{D}^0)} \quad (34)$$

is defined as the production asymmetry of the D^0 and $\overline{D}^0$. Note that deviations from the decay rate measured in non-CP eigenstates does not require $y \neq 0$ but can be due to $x\sin\phi \neq 0$. This possibility is distinguished by a relative sign difference in the exponents of Eqs. (30) and (31) describing the D^0 and $\overline{D}^0$ samples, respectively.

In the limit of CP conservation, $A_\pm = \pm\overline{A}_\pm$, $\eta_\pm = 0$, $y = y_{CP}$, and

$$r_\pm(t)\left|\overline{A}_\pm\right|^2 = \overline{r}_\pm(t)\left|A_\pm\right|^2 = e^{-(1\pm y_{CP})t}. \quad (35)$$

The possibility of CP violation has not been considered in general in any of the analyses of y, although specific cases have been considered. Belle [26] and BABAR [27] have allowed CP violation in interference and mixing. Neither result considered CP violation in direct decay. All measurements are relative to the $D^0 \to K^-\pi^+$ decay rate. The current status of measurements of y is summarized in Table 5 and in Fig. 1.

Table 5: Results for y from $D^0 \to K^+K^-$ and $\pi^+\pi^-$.

Year	Exper.	D^0 Final State(s)	$y(\%)$
2003	Belle [26]	K^+K^-	$y_{CP} = 1.15 \pm 0.69 \pm 0.38$
2003	BABAR [27]	$K^+K^-, \pi^+\pi^-$	$y\cos\phi = 0.8 \pm 0.4^{+0.5}_{-0.4}$
2001	CLEO [28]	$K^+K^-, \pi^+\pi^-$	$y_{CP} = -1.1 \pm 2.5 \pm 1.4$
2001	Belle [29]	K^+K^-	$y_{CP} = -0.5 \pm 1.0^{+0.7}_{-0.8}$
2000	FOCUS [30]	K^+K^-	$y_{CP} = 3.4 \pm 1.4 \pm 0.7$
1999	E791 [31]	K^+K^-	$y_{CP} = 0.8 \pm 2.9 \pm 1.0$

Substantial work on the integrated CP asymmetries in decays to CP eigenstates indicates that A_{CP} is consistent with zero at the few percent level [32]. The expression for the integrated CP asymmetry that includes the possibility of CP violation in mixing is

$$A_{CP} = \frac{\Gamma(D^0 \to f_\pm) - \Gamma(\overline{D}^0 \to f_\pm)}{\Gamma(D^0 \to f_\pm) + \Gamma(\overline{D}^0 \to f_\pm)} \quad (36)$$

$$= \frac{|q|^2 - |p|^2}{|q|^2 + |p|^2} + 2\mathrm{Re}(\eta_\pm). \quad (37)$$

References

1. G. Burdman and I. Shipsey, Ann. Rev. Nucl. and Part. Sci. **53**, 431 (2003).
2. H.N. Nelson, in *Proceedings of the 19th Intl. Symp. on Lepton and Photon Interactions at High Energy LP99*, ed. J.A. Jaros and M.E. Peskin, SLAC (1999).
3. A.A. Petrov, `hep-ph/0311371`, contributed to Flavor Physics and CP Violation (FPCP2003), Paris, June 2003; I.I. Bigi and N.G. Uraltsev, Nucl. Phys. **B592**, 92 (2001); Z. Ligeti, AIP Conf. Proc. **618**, 298 (2002), `hep-ph/0205316`; A.F. Falk *et al.*, Phys. Rev. **D65**, 054034 (2002); C.K. Chua and W.S. Hou, `hep-ph/0110106`.
4. See the review on B^0–$\overline{B}^0$ mixing in this *Review*.
5. K. Stenson, presented at the April Meeting of the American Physical Society (APS 03), Philadelphia, Pennsylvania, April 5-8, 2003; M. Hosack, (FOCUS Collab.), Fermilab-Thesis-2002-25.
6. S. McGee in *Fundamental Interactions, Proceedings of the 17th Lake Louise Winter Institute*, edited by A. Astbury *et al.*, World Scientific Publishing Co. Pte. Ltd. (2002).
7. E.M. Aitala *et al.*, (E791 Collab.), Phys. Rev. Lett. **77**, 2384 (1996).
8. Y. Nir, Lectures given at 27th SLAC Summer Institute on Particle Physics: CP Violation in and Beyond the Standard Model (SSI 99), Stanford, California, 7-16 Jul 1999. Published in Trieste 1999, *Particle Physics* pp. 165-243.
9. R. Godang *et al.*, (CLEO Collab.), Phys. Rev. Lett. **84**, 5038 (2000).
10. B. Aubert *et al.*, (BABAR Collab.), Phys. Rev. Lett. **91**, 171801 (2003).
11. K. Abe *et al.*, (Belle Collab.), `hep-ex/0208051` contributed to the *31st International*

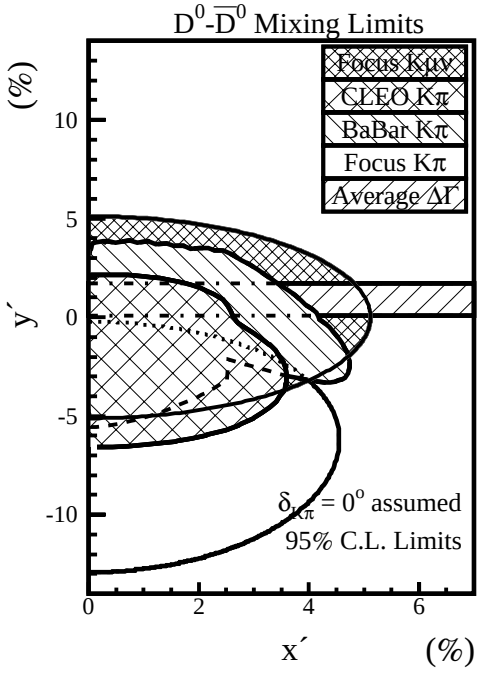

Figure 1: Current allowed regions in the plane of y' versus x'. The regions for CLEO and BaBar allow CP violation in the decay amplitude, in the mixing amplitude, and in the interference between these two processes. The FOCUS result does not allow CP violation. The allowed region for $\Delta\Gamma$ is the average of the y_{CP} [26, 28–31] results and the BABAR measurement of $y\cos\phi$ [27] and does not include $y = 0$. We assume $\delta = 0$ to place the $\Delta\Gamma$ results. A non-zero value for δ would rotate this confidence region clockwise about the origin by an angle δ. See full-color version on color pages at end of book.

Conference on High-Energy Physics (ICHEP 2002), Amsterdam, The Netherlands, (24-31 July 2002).

12. J.M. Link, (FOCUS Collab.), Phys. Rev. Lett. **86**, 2955 (2001);
J.M. Link, (FOCUS Collab.), hep-ex/0106093, presented at the *36th Rencontres de Moriond on Electroweak Interactions and Unified Theories*, Les Arcs, France, (March 10-17, 2001).
13. E.M. Aitala *et al.*, (E791 Collab.), Phys. Rev. **D57**, 13 (1998).
14. R. Barate *et al.*, (ALEPH Collab.), Phys. Lett. **B436**, 211 (1998).
15. D. Cinabro *et al.*, (CLEO Collab.), Phys. Rev. Lett. **72**, 1406 (1994).
16. L. Chau and H. Cheng, Phys. Lett. **B333**, 514 (1994);
T.E. Browder and S. Pakvasa, Phys. Lett. **B383**, 475 (1995);
A.F. Falk, Y. Nir, and A.A. Petrov, JHEP **9912**, 19 (1999);
M. Gronau and J.L. Rosner, Phys. Lett. **B500**, 247 (2001);
G. Blaylock, A. Seiden, and Y. Nir, Phys. Lett. **B355**, 555 (1995).
17. S. Bergmann *et al.*, Phys. Lett. **B486**, 418 (2000).
18. M. Gronau, Y. Grossman, and J.L. Rosner, Phys. Lett. **B508**, 37 (2001).
19. R.A. Briere *et al.*, (CLEO Collab.), CLNS 01-1742, July 2001.
20. E. Golowich and S. Pakvasa, Phys. Lett. **B505**, 94 (2001).
21. C.W. Chiang and J.L. Rosner, Phys. Rev. **D65**, 054007 (2002).
22. H. Muramatsu *et al.*, (CLEO Collab.), Phys. Rev. Lett. **89**, 251802 (2002) [Erratum-ibid. **90**, 059901 (2003)].
23. S.A. Dytman *et al.*, (CLEO Collab.), Phys. Rev. **D64**, 111101 (2001).
24. G. Brandenburg *et al.*, (CLEO Collab.), Phys. Rev. Lett. **87**, 071802 (2001).
25. D.M. Asner, UCRL-JC-147296.
26. K. Abe *et al.*, (Belle Collab.), hep-ex/0308034, contributed to the 21st International Symposium on Lepton and Photon Interactions at High Energies, (LP 03), Batavia, Illinois, 11-16 Aug 2003.
27. B. Aubert *et al.*, (BABAR Collab.), Phys. Rev. Lett. **91**, 121801 (2003).
28. S.E. Csorna *et al.*, (CLEO Collab.), Phys. Rev. **D65**, 092001 (2002).
29. K. Abe *et al.*, (Belle Collab.), Phys. Rev. Lett. **88**, 162001 (2002).
30. J.M. Link *et al.*, (FOCUS Collab.), Phys. Lett. **B485**, 62 (2000).
31. E.M. Aitala *et al.*, (E791 Collab.), Phys. Rev. **83**, 32 (1999).
32. See the tabulation of A_{CP} results in the decays of D^0 and D^+ in this *Review*.

$|m_{D_1^0} - m_{D_2^0}|$

The D_1^0 and D_2^0 are the mass eigenstates of the D^0 meson, as described in the note on "D^0-$\overline{D}^0$ Mixing," above.

VALUE (10^{10} $\hbar$ s^{-1})	CL%	DOCUMENT ID		TECN	COMMENT
< 7	95	[5] GODANG	00	CLE2	e^+e^-
• • • We do not use the following data for averages, fits, limits, etc. • • •					
< 11	95	[6] AUBERT	03Z	BABR	e^+e^-, 10.6 GeV
< 32	90	[7,8] AITALA	98	E791	π^- nucleus, 500 GeV
< 24	90	[9] AITALA	96C	E791	π^- nucleus, 500 GeV
< 21	90	[8,10] ANJOS	88C	E691	Photoproduction

[5] This GODANG 00 limit is inferred from the D^0-$\overline{D}^0$ mixing ratio $\Gamma(K^+\pi^-$ (via $\overline{D}^0$))/$\Gamma(K^-\pi^+)$ given near the end of this D^0 Listings. Decay-time information is used to distinguish DCS decays from D^0-$\overline{D}^0$ mixing. The limit allows interference between the DCS and mixing ratios, and also allows CP violation. The strong phase between $D^0 \to K^+\pi^-$ and $\overline{D}^0 \to K^+\pi^-$ is assumed to be small. If an arbitrary relative strong phase is allowed, the limit degrades by a factor of two.

[6] This AUBERT 03Z limit is inferred from the D^0-$\overline{D}^0$ mixing ratio $\Gamma(K^+\pi^-$ (via $\overline{D}^0$))/$\Gamma(K^-\pi^+)$ given near the end of this D^0 Listings. Decay-time information is used to distinguish DCS decays from D^0-$\overline{D}^0$ mixing. The limit allows interference between the DCS and mixing ratios, and also allows CP violation. The strong phase between $D^0 \to K^+\pi^-$ and $\overline{D}^0 \to K^+\pi^-$ is assumed to be small. If an arbitrary relative strong phase is allowed, the limit degrades by 20%.

[7] AITALA 98 allows interference between the doubly Cabibbo-suppressed and mixing amplitudes, and also allows CP violation in this term, but assumes that A_D=A_R=0. See the note on "D^0-$\overline{D}^0$ Mixing," above.

[8] This limit is inferred from R_M for $f = K^+\pi^-$ and $f = K^+\pi^-\pi^+\pi^-$. See the note on "D^0-$\overline{D}^0$ Mixing," above. Decay-time information is used to distinguish doubly Cabibbo-suppressed decays from D^0-$\overline{D}^0$ mixing.

[9] This limit is inferred from R_M for $f = K^+\ell^-\overline{\nu}_\ell$. See the note on "$D^0$-$\overline{D}^0$ Mixing," above.

[10] ANJOS 88C assumes that $y = 0$. See the note on "D^0-$\overline{D}^0$ Mixing," above. Without this assumption, the limit degrades by about a factor of two.

$(\Gamma_{D_1^0} - \Gamma_{D_2^0})/\Gamma = 2y$

The D_1^0 and D_2^0 are the mass eigenstates of the D^0 meson, as described in the note on "D^0-$\overline{D}^0$ Mixing," above.

VALUE	CL%	EVTS	DOCUMENT ID		TECN	COMMENT
0.016 ±0.010 OUR AVERAGE						
$0.016 \pm 0.008 \,^{+0.010}_{-0.008}$		450k	[11] AUBERT	03P	BABR	$e^+e^- \approx \Upsilon(4S)$
$-0.010 \pm 0.020 \,^{+0.014}_{-0.016}$		18k	[12] ABE	02I	BELL	$e^+e^- \approx \Upsilon(4S)$
$-0.024 \pm 0.050 \pm 0.028$		3393	[13] CSORNA	02	CLE2	$e^+e^- \approx \Upsilon(4S)$
$0.0684 \pm 0.0278 \pm 0.0148$		10k	[12] LINK	00	FOCS	γ nucleus
$+0.016 \pm 0.058 \pm 0.021$			[12] AITALA	99E	E791	$K^-\pi^+$, K^+K^-
• • • We do not use the following data for averages, fits, limits, etc. • • •						
$0.016 \,^{+0.062}_{-0.128}$			[14,15] AUBERT	03Z	BABR	e^+e^-, 10.6 GeV
$-0.050 \,^{+0.028}_{-0.032} \pm 0.006$			[15] GODANG	00	CLE2	e^+e^-
$\lvert\Delta\Gamma\rvert/\Gamma < 0.26$	90		[16,17] AITALA	98	E791	π^- nucleus, 500 GeV
$\lvert\Delta\Gamma\rvert/\Gamma < 0.20$	90		[18] AITALA	96C	E791	π^- nucleus, 500 GeV
$\lvert\Delta\Gamma\rvert/\Gamma < 0.17$	90		[17,19] ANJOS	88C	E691	Photoproduction

[11] AUBERT 03P measures $\Upsilon \equiv 2\tau^0/(\tau^+ + \tau^-) - 1$, where τ^0 is the $D^0 \to K^-\pi^+$ (and $\overline{D}^0 \to K^+\pi^-$) lifetime, and τ^+ and τ^- are the D^0 and $\overline{D}^0$ lifetimes to CP-even states (here K^-K^+ and $\pi^-\pi^+$). In the limit of CP conservation, $\Upsilon = y \equiv \Delta\Gamma/2\Gamma$ (we list $2y = \Delta\Gamma/\Gamma$). AUBERT 03P also uses $\tau^+ - \tau^-$ to get $\Delta Y = -0.008 \pm 0.006 \pm 0.002$.

[12] LINK 00, AITALA 99E, and ABE 02I measure the lifetime difference between $D^0 \to K^-K^+$ (CP even) decays and $D^0 \to K^-\pi^+$ (CP mixed) decays, or $y_{CP} = [\Gamma(CP+) - \Gamma(CP-)]/[\Gamma(CP+) + \Gamma(CP-)]$. We list $2y_{CP} = \Delta\Gamma/\Gamma$.

[13] CSORNA 02 measures the lifetime difference between $D^0 \to K^-K^+$ and $\pi^-\pi^+$ (CP even) decays and $D^0 \to K^-\pi^+$ (CP mixed) decays, or $y_{CP} = [\Gamma(CP+) - \Gamma(CP-)]/[\Gamma(CP+) + \Gamma(CP-)]$. We list $2y_{CP} = \Delta\Gamma/\Gamma$.

[14] The range of this AUBERT 03Z measurement is for 95% confidence level.

[15] The GODANG 00 and AUBERT 03Z limits are inferred from the D^0-$\overline{D}^0$ mixing ratio $\Gamma(K^+\pi^-$ (via $\overline{D}^0))/\Gamma(K^-\pi^+)$ given near the end of this D^0 Listings. Decay-time information is used to distinguish DCS decays from D^0-$\overline{D}^0$ mixing. The limit allows interference between the DCS and mixing ratios, and also allows CP violation. The phase between $D^0 \to K^+\pi^-$ and $\overline{D}^0 \to K^+\pi^-$ is assumed to be small. This is a measurement of y' and is not the same as the y_{CP} of our note above on "D^0-$\overline{D}^0$ Mixing."

[16] AITALA 98 allows interference between the doubly Cabibbo-suppressed and mixing amplitudes, and also allows CP violation in this term, but assumes that $A_D = A_R = 0$. See the note on "D^0-$\overline{D}^0$ Mixing," above.

[17] This limit is inferred from R_M for $f = K^+\pi^-$ and $f = K^+\pi^-\pi^+\pi^-$. See the note on "D^0-$\overline{D}^0$ Mixing," above. Decay-time information is used to distinguish doubly Cabibbo-suppressed decays from D^0-$\overline{D}^0$ mixing.

[18] This limit is inferred from R_M for $f = K^+\ell^-\overline{\nu}_\ell$. See the note on "$D^0$-$\overline{D}^0$ Mixing," above.

[19] ANJOS 88C assumes that $y = 0$. See the note on "D^0-$\overline{D}^0$ Mixing," above. Without this assumption, the limit degrades by about a factor of two.

D^0 DECAY MODES

$\overline{D}^0$ modes are charge conjugates of the modes below.

	Mode		Fraction (Γ_i/Γ)	Scale factor/ Confidence level
	Inclusive modes			
Γ_1	e^+ anything	[a]	(6.87 ± 0.28) %	
Γ_2	μ^+ anything		(6.5 ± 0.8) %	
Γ_3	K^- anything		(53 ± 4) %	S=1.3
Γ_4	$\overline{K}^0$ anything + K^0 anything		(42 ± 5) %	
Γ_5	K^+ anything		$(3.4 \,^{+0.6}_{-0.4})$ %	
Γ_6	η anything	[b]	< 13 %	CL=90%
Γ_7	ϕ anything		(1.7 ± 0.8) %	
	Semileptonic modes			
Γ_8	$K^-\ell^+\nu_\ell$	[c]	(3.43 ± 0.14) %	S=1.2
Γ_9	$K^-e^+\nu_e$		(3.58 ± 0.18) %	S=1.1
Γ_{10}	$K^-\mu^+\nu_\mu$		(3.19 ± 0.17) %	
Γ_{11}	$K^-\pi^0e^+\nu_e$		$(1.1 \,^{+0.8}_{-0.6})$ %	S=1.6
Γ_{12}	$\overline{K}^0\pi^-e^+\nu_e$		(1.8 ± 0.8) %	S=1.6
Γ_{13}	$\overline{K}^*(892)^-e^+\nu_e$ × B($K^*(892)^- \to \overline{K}^0\pi^-$)		(1.43 ± 0.23) %	
Γ_{14}	$K^*(892)^-\ell^+\nu_\ell$			
Γ_{15}	$\overline{K}^*(892)^0\pi^-e^+\nu_e$			
Γ_{16}	$K^-\pi^+\pi^-\mu^+\nu_\mu$		< 1.2 × 10^{-3}	CL=90%
Γ_{17}	$(\overline{K}^*(892)\pi)^-\mu^+\nu_\mu$		< 1.4 × 10^{-3}	CL=90%
Γ_{18}	$\pi^-e^+\nu_e$		(3.6 ± 0.6) × 10^{-3}	

A fraction of the following resonance mode has already appeared above as a submode of a charged-particle mode.

Γ_{19}	$K^*(892)^-e^+\nu_e$		(2.15 ± 0.35) %	
	Hadronic modes with a $\overline{K}$ or $\overline{K}K\overline{K}$			
Γ_{20}	$K^-\pi^+$		(3.80 ± 0.09) %	
Γ_{21}	$\overline{K}^0\pi^0$		(2.30 ± 0.22) %	
Γ_{22}	$\overline{K}^0\pi^+\pi^-$	[d]	(5.97 ± 0.35) %	S=1.1
Γ_{23}	$\overline{K}^0\rho^0$		$(1.55 \,^{+0.12}_{-0.16})$ %	
Γ_{24}	$\overline{K}^0\omega$ × B($\omega \to \pi^+\pi^-$)		(3.9 ± 0.9) × 10^{-4}	
Γ_{25}	$\overline{K}^0 f_0(980)$ × B($f_0(980) \to \pi^+\pi^-$)		$(2.8 \,^{+0.6}_{-0.4})$ × 10^{-3}	
Γ_{26}	$\overline{K}^0 f_2(1270)$ × B($f_2(1270) \to \pi^+\pi^-$)		$(2.6 \,^{+2.3}_{-1.4})$ × 10^{-4}	
Γ_{27}	$\overline{K}^0 f_0(1370)$ × B($f_0(1370) \to \pi^+\pi^-$)		$(5.1 \,^{+1.2}_{-1.3})$ × 10^{-3}	
Γ_{28}	$K^*(892)^-\pi^+$ × B($K^*(892)^- \to \overline{K}^0\pi^-$)		(3.9 ± 0.3) %	
Γ_{29}	$K_0^*(1430)^-\pi^+$ × B($K_0^*(1430)^- \to \overline{K}^0\pi^-$)		$(6.1 \,^{+1.2}_{-0.8})$ × 10^{-3}	
Γ_{30}	$K_2^*(1430)^-\pi^+$ × B($K_2^*(1430)^- \to \overline{K}^0\pi^-$)		$(1.0 \,^{+0.7}_{-0.4})$ × 10^{-3}	
Γ_{31}	$K^*(1680)^-\pi^+$ × B($K^*(1680)^- \to \overline{K}^0\pi^-$)		$(2.1 \,^{+1.0}_{-0.9})$ × 10^{-3}	
Γ_{32}	$K^*(892)^+\pi^-$ × B($K^*(892)^+ \to K^0\pi^+$)		$(2.0 \,^{+2.6}_{-0.9})$ × 10^{-4}	
Γ_{33}	$\overline{K}^0\pi^+\pi^-$ nonresonant		$(5.4 \,^{+12.0}_{-3.4})$ × 10^{-4}	
Γ_{34}	$K^-\pi^+\pi^0$	[d]	(13.0 ± 0.8) %	S=1.3
Γ_{35}	$K^-\rho^+$		(10.1 ± 0.8) %	
Γ_{36}	$K^-\rho(1700)^+$ × B($\rho(1700)^+ \to \pi^+\pi^0$)		(7.4 ± 1.6) × 10^{-3}	
Γ_{37}	$K^*(892)^-\pi^+$ × B($K^*(892)^- \to K^-\pi^0$)		(1.97 ± 0.13) %	
Γ_{38}	$\overline{K}^*(892)^0\pi^0$ × B($\overline{K}^*(892)^0 \to K^-\pi^+$)		(1.87 ± 0.27) %	
Γ_{39}	$K_0^*(1430)^-\pi^+$ × B($K_0^*(1430)^- \to K^-\pi^0$)		$(3.0 \,^{+0.6}_{-0.4})$ × 10^{-3}	
Γ_{40}	$\overline{K}_0^*(1430)^0\pi^0$ × B($\overline{K}_0^*(1430)^0 \to K^-\pi^+$)		$(5.3 \,^{+4.2}_{-1.4})$ × 10^{-3}	
Γ_{41}	$K^*(1680)^-\pi^+$ × B($K^*(1680)^- \to K^-\pi^0$)		(1.1 ± 0.5) × 10^{-3}	
Γ_{42}	$K^-\pi^+\pi^0$ nonresonant		$(1.04 \,^{+0.50}_{-0.19})$ %	
Γ_{43}	$\overline{K}^0\pi^0\pi^0$		—	
Γ_{44}	$\overline{K}^*(892)^0\pi^0$ × B($\overline{K}^*(892)^0 \to \overline{K}^0\pi^0$)		(9.3 ± 1.3) × 10^{-3}	
Γ_{45}	$\overline{K}^0\pi^0\pi^0$ nonresonant		(8.5 ± 2.2) × 10^{-3}	
Γ_{46}	$K^-\pi^+\pi^+\pi^-$	[d]	(7.46 ± 0.31) %	
Γ_{47}	$K^-\pi^+\rho^0$ total		(6.2 ± 0.4) %	
Γ_{48}	$K^-\pi^+\rho^0$ 3-body		(4.7 ± 2.1) × 10^{-3}	
Γ_{49}	$\overline{K}^*(892)^0\rho^0$ × B($\overline{K}^*(892)^0 \to K^-\pi^+$)		(9.7 ± 2.1) × 10^{-3}	
Γ_{50}	$K^-a_1(1260)^+$ × B($a_1(1260)^+ \to \pi^+\pi^+\pi^-$)		(3.6 ± 0.6) %	
Γ_{51}	$\overline{K}^*(892)^0\pi^+\pi^-$ total × B($\overline{K}^*(892)^0 \to K^-\pi^+$)		(1.5 ± 0.4) %	
Γ_{52}	$\overline{K}^*(892)^0\pi^+\pi^-$ 3-body × B($\overline{K}^*(892)^0 \to K^-\pi^+$)		(9.5 ± 2.1) × 10^{-3}	
Γ_{53}	$K_1(1270)^-\pi^+$ × B($K_1(1270)^- \to K^-\pi^+\pi^-$)	[e]	(2.9 ± 0.3) × 10^{-3}	
Γ_{54}	$K^-\pi^+\pi^+\pi^-$ nonresonant		(1.74 ± 0.25) %	
Γ_{55}	$\overline{K}^0\pi^+\pi^-\pi^0$	[d]	(10.9 ± 1.3) %	
Γ_{56}	$\overline{K}^0\eta \times$ B($\eta \to \pi^+\pi^-\pi^0$)		(1.74 ± 0.25) × 10^{-3}	
Γ_{57}	$\overline{K}^0\omega \times$ B($\omega \to \pi^+\pi^-\pi^0$)		(2.1 ± 0.4) %	
Γ_{58}	$K^*(892)^-\rho^+$ × B($K^*(892)^- \to \overline{K}^0\pi^-$)		(4.4 ± 1.7) %	
Γ_{59}	$\overline{K}^*(892)^0\rho^0$ × B($\overline{K}^*(892)^0 \to \overline{K}^0\pi^0$)		(4.8 ± 1.1) × 10^{-3}	
Γ_{60}	$K_1(1270)^-\pi^+$ × B($K_1(1270)^- \to \overline{K}^0\pi^-\pi^0$)	[e]	(4.5 ± 1.2) × 10^{-3}	

See key on page 323

Γ_{61}	$\overline{K}^*(892)^0\pi^+\pi^-$ 3-body × B($\overline{K}^*(892)^0 \to \overline{K}^0\pi^0$)	(4.7 ± 1.0) × 10^{-3}	
Γ_{62}	$\overline{K}^0\pi^+\pi^-\pi^0$ nonresonant	(2.3 ± 2.3) %	
Γ_{63}	$K^-\pi^+\pi^0\pi^0$		
Γ_{64}	$K^-\pi^+\pi^+\pi^-\pi^0$	(4.0 ± 0.4) %	
Γ_{65}	$\overline{K}^*(892)^0\pi^+\pi^-\pi^0$ × B($\overline{K}^*(892)^0 \to K^-\pi^+$)	(1.2 ± 0.6) %	
Γ_{66}	$\overline{K}^*(892)^0\eta$ × B($\overline{K}^*(892)^0 \to K^-\pi^+$) × B($\eta \to \pi^+\pi^-\pi^0$)	(2.7 ± 0.6) × 10^{-3}	
Γ_{67}	$K^-\pi^+\omega$ × B($\omega \to \pi^+\pi^-\pi^0$)	(2.7 ± 0.5) %	
Γ_{68}	$\overline{K}^*(892)^0\omega$ × B($\overline{K}^*(892)^0 \to K^-\pi^+$) × B($\omega \to \pi^+\pi^-\pi^0$)	(6.5 ± 2.4) × 10^{-3}	
Γ_{69}	$\overline{K}^0\pi^+\pi^+\pi^-\pi^-$	(6.4 ± 1.8) × 10^{-3}	
Γ_{70}	$\overline{K}^0\pi^+\pi^-\pi^0\pi^0(\pi^0)$		
Γ_{71}	$\overline{K}^0K^+K^-$	(1.03 ± 0.10) %	
	In the fit as $\frac{1}{2}\Gamma_{86} + \Gamma_{73}$, where $\frac{1}{2}\Gamma_{86} = \Gamma_{72}$.		
Γ_{72}	$\overline{K}^0\phi$ × B($\phi \to K^+K^-$)	(4.7 ± 0.6) × 10^{-3}	
Γ_{73}	$\overline{K}^0K^+K^-$ non-ϕ	(5.6 ± 0.9) × 10^{-3}	
Γ_{74}	$K^0_SK^0_SK^0_S$	(9.2 ± 1.6) × 10^{-4}	
Γ_{75}	$K^+K^-K^-\pi^+$	(2.04 ± 0.30) × 10^{-4}	
Γ_{76}	$K^+K^-\overline{K}^*(892)^0$ × B($\overline{K}^*(892)^0 \to K^-\pi^+$)	(4.1 ± 1.7) × 10^{-5}	
Γ_{77}	$K^-\pi^+\phi$ × B($\phi \to K^+K^-$)	(3.8 ± 1.6) × 10^{-5}	
Γ_{78}	$\phi\overline{K}^*(892)^0$ × B($\phi \to K^+K^-$) × B($\overline{K}^*(892)^0 \to K^-\pi^+$)	(1.0 ± 0.2) × 10^{-4}	
Γ_{79}	$K^+K^-K^-\pi^+$ nonresonant	(3.1 ± 1.4) × 10^{-5}	
Γ_{80}	$K^+K^-\overline{K}^0\pi^0$		

Fractions of many of the following modes with resonances have already appeared above as submodes of particular charged-particle modes. (Modes for which there are only upper limits and $\overline{K}^*(892)\rho$ submodes only appear below.)

Γ_{81}	$\overline{K}^0\eta$	(7.7 ± 1.1) × 10^{-3}		
Γ_{82}	$\overline{K}^0\rho^0$	(1.55 $^{+0.12}_{-0.16}$) %		
Γ_{83}	$K^-\rho^+$	(10.1 ± 0.8) %		S=1.2
Γ_{84}	$\overline{K}^0\omega$	(2.3 ± 0.4) %		
Γ_{85}	$\overline{K}^0\eta'(958)$	(1.88 ± 0.28) %		
Γ_{86}	$\overline{K}^0\phi$	(9.4 ± 1.1) × 10^{-3}		
Γ_{87}	$K^-a_1(1260)^+$	(7.2 ± 1.1) %		
Γ_{88}	$\overline{K}^0a_1(1260)^0$	< 1.9	%	CL=90%
Γ_{89}	$\overline{K}^0f_2(1270)$	(4.7 $^{+4.1}_{-2.4}$) × 10^{-4}		
Γ_{90}	$K^-a_2(1320)^+$	< 2	× 10^{-3}	CL=90%
Γ_{91}	$K^*(892)^-\pi^+$	(5.9 ± 0.4) %		S=1.1
Γ_{92}	$\overline{K}^*(892)^0\pi^0$	(2.8 ± 0.4) %		S=1.1
Γ_{93}	$\overline{K}^*(892)^0\pi^+\pi^-$ total	(2.2 ± 0.5) %		
Γ_{94}	$\overline{K}^*(892)^0\pi^+\pi^-$ 3-body	(1.42 ± 0.31) %		
Γ_{95}	$K^-\pi^+\rho^0$ total	(6.2 ± 0.4) %		
Γ_{96}	$K^-\pi^+\rho^0$ 3-body	(4.7 ± 2.1) × 10^{-3}		
Γ_{97}	$\overline{K}^*(892)^0\rho^0$	(1.45 ± 0.32) %		
Γ_{98}	$\overline{K}^*(892)^0\rho^0$ transverse	(1.5 ± 0.5) %		
Γ_{99}	$\overline{K}^*(892)^0\rho^0$ S-wave	(2.8 ± 0.6) %		
Γ_{100}	$\overline{K}^*(892)^0\rho^0$ S-wave long.	< 3	× 10^{-3}	CL=90%
Γ_{101}	$\overline{K}^*(892)^0\rho^0$ P-wave	< 3	× 10^{-3}	CL=90%
Γ_{102}	$\overline{K}^*(892)^0\rho^0$ D-wave	(1.9 ± 0.6) %		
Γ_{103}	$K^*(892)^-\rho^+$	(6.6 ± 2.6) %		
Γ_{104}	$K^*(892)^-\rho^+$ longitudinal	(3.2 ± 1.3) %		
Γ_{105}	$K^*(892)^-\rho^+$ transverse	(3.4 ± 2.0) %		
Γ_{106}	$K^*(892)^-\rho^+$ P-wave	< 1.5	%	CL=90%
Γ_{107}	$K^-\pi^+f_0(980)$			
Γ_{108}	$\overline{K}^*(892)^0f_0(980)$			
Γ_{109}	$K_1(1270)^-\pi^+$ [e]	(1.14 ± 0.31) %		
Γ_{110}	$K_1(1400)^-\pi^+$	< 1.2	%	CL=90%
Γ_{111}	$\overline{K}_1(1400)^0\pi^0$	< 3.7	%	CL=90%
Γ_{112}	$K^*(1410)^-\pi^+$			
Γ_{113}	$K^*_0(1430)^-\pi^+$	(9.8 $^{+2.0}_{-1.3}$) × 10^{-3}		
Γ_{114}	$\overline{K}^*_0(1430)^0\pi^0$	(8.6 $^{+6.8}_{-2.3}$) × 10^{-3}		
Γ_{115}	$K^*_2(1430)^-\pi^+$	(2.0 $^{+1.3}_{-0.7}$) × 10^{-3}		
Γ_{116}	$\overline{K}^*_2(1430)^0\pi^0$	< 3.3	× 10^{-3}	CL=90%
Γ_{117}	$K^*(1680)^-\pi^+$	(8.2 $^{+3.9}_{-3.5}$) × 10^{-3}		S=1.2
Γ_{118}	$\overline{K}^*(892)^0\pi^+\pi^-\pi^0$	(1.8 ± 0.9) %		
Γ_{119}	$\overline{K}^*(892)^0\eta$	(1.8 ± 0.4) %		
Γ_{120}	$K^-\pi^+\omega$	(3.0 ± 0.6) %		
Γ_{121}	$\overline{K}^*(892)^0\omega$	(1.1 ± 0.4) %		
Γ_{122}	$K^-\pi^+\eta'(958)$	(6.9 ± 1.8) × 10^{-3}		
Γ_{123}	$\overline{K}^*(892)^0\eta'(958)$	< 1.0	× 10^{-3}	CL=90%
Γ_{124}	$K^-\pi^+\phi$	(7.6 ± 3.1) × 10^{-5}		
Γ_{125}	$K^+K^-\overline{K}^*(892)^0$	(6.1 ± 2.5) × 10^{-5}		
Γ_{126}	$\phi\overline{K}^*(892)^0$	(3.0 ± 0.6) × 10^{-4}		

Pionic modes

Γ_{127}	$\pi^+\pi^-$	(1.38 ± 0.05) × 10^{-3}		
Γ_{128}	$\pi^0\pi^0$	(8.4 ± 2.2) × 10^{-4}		
Γ_{129}	$\pi^+\pi^-\pi^0$	(1.1 ± 0.4) %		
Γ_{130}	$\pi^+\pi^+\pi^-\pi^-$	(7.3 ± 0.5) × 10^{-3}		
Γ_{131}	$\pi^+\pi^+\pi^-\pi^-\pi^0$			
Γ_{132}	$\pi^+\pi^+\pi^+\pi^-\pi^-\pi^-$			

Hadronic modes with a $K\overline{K}$ pair

Γ_{133}	K^+K^-	(3.89 $^{+0.12}_{-0.15}$) × 10^{-3}		S=1.2
Γ_{134}	$K^0\overline{K}^0$	(7.1 ± 1.9) × 10^{-4}		S=1.2
Γ_{135}	$K^0K^-\pi^+$	(6.9 ± 1.0) × 10^{-3}		
Γ_{136}	$\overline{K}^*(892)^0K^0$ × B($\overline{K}^{*0} \to K^-\pi^+$)	< 1.1	× 10^{-3}	CL=90%
Γ_{137}	$K^*(892)^+K^-$ × B($K^{*+} \to K^0\pi^+$)	(2.5 ± 0.5) × 10^{-3}		
Γ_{138}	$K^0K^-\pi^+$ nonresonant	(2.3 ± 2.3) × 10^{-3}		
Γ_{139}	$\overline{K}^0K^+\pi^-$	(5.3 ± 1.0) × 10^{-3}		
Γ_{140}	$K^*(892)^0\overline{K}^0$ × B($K^{*0} \to K^+\pi^-$)	< 6	× 10^{-4}	CL=90%
Γ_{141}	$K^*(892)^-K^+$ × B($K^{*-} \to \overline{K}^0\pi^-$)	(1.3 ± 0.7) × 10^{-3}		
Γ_{142}	$\overline{K}^0K^+\pi^-$ nonresonant	(3.8 $^{+2.3}_{-1.9}$) × 10^{-3}		
Γ_{143}	$K^+K^-\pi^0$	(1.24 ± 0.35) × 10^{-3}		
Γ_{144}	$K^0_SK^0_S\pi^0$	< 5.9	× 10^{-4}	
Γ_{145}	$K^+K^-\pi^+\pi^-$ [f]	(2.49 ± 0.23) × 10^{-3}		
Γ_{146}	$\phi\pi^+\pi^-$ × B($\phi \to K^+K^-$)	(5.3 ± 1.4) × 10^{-4}		
Γ_{147}	$\phi\rho^0$ × B($\phi \to K^+K^-$)	(2.9 ± 1.5) × 10^{-4}		
Γ_{148}	$K^+K^-\rho^0$ 3-body	(9.0 ± 2.3) × 10^{-4}		
Γ_{149}	$K^*(892)^0K^-\pi^+$ + c.c. [g] × B($K^{*0} \to K^+\pi^-$)	< 5	× 10^{-4}	
Γ_{150}	$K^*(892)^0\overline{K}^*(892)^0$ × B^2($K^{*0} \to K^+\pi^-$)	(6 ± 2) × 10^{-4}		
Γ_{151}	$K^+K^-\pi^+\pi^-$ non-ϕ			
Γ_{152}	$K^+K^-\pi^+\pi^-$ nonresonant	< 8	× 10^{-4}	CL=90%
Γ_{153}	$K^0\overline{K}^0\pi^+\pi^-$	(7.5 ± 2.9) × 10^{-3}		
Γ_{154}	$K^+K^-\pi^+\pi^-\pi^0$	(3.1 ± 2.0) × 10^{-3}		

Fractions of most of the following modes with resonances have already appeared above as submodes of particular charged-particle modes.

Γ_{155}	$\overline{K}^*(892)^0K^0$	< 1.7	× 10^{-3}	CL=90%
Γ_{156}	$K^*(892)^+K^-$	(3.8 ± 0.8) × 10^{-3}		
Γ_{157}	$K^*(892)^0\overline{K}^0$	< 9	× 10^{-4}	CL=90%
Γ_{158}	$K^*(892)^-K^+$	(2.0 ± 1.1) × 10^{-3}		
Γ_{159}	$\phi\pi^0$	(7.5 ± 0.5) × 10^{-4}		
Γ_{160}	$\phi\eta$	(1.4 ± 0.5) × 10^{-4}		
Γ_{161}	$\phi\omega$	< 2.1	× 10^{-3}	CL=90%
Γ_{162}	$\phi\pi^+\pi^-$	(1.06 ± 0.28) × 10^{-3}		
Γ_{163}	$\phi\rho^0$	(5.7 ± 3.0) × 10^{-4}		
Γ_{164}	$\phi\pi^+\pi^-$ 3-body	(7 ± 5) × 10^{-4}		
Γ_{165}	$K^*(892)^0K^-\pi^+$ + c.c. [g]	< 7	× 10^{-4}	CL=90%
Γ_{166}	$K^*(892)^0K^-\pi^+$			
Γ_{167}	$\overline{K}^*(892)^0K^+\pi^-$			
Γ_{168}	$K^*(892)^0\overline{K}^*(892)^0$	(1.4 ± 0.5) × 10^{-3}		

Radiative modes

Γ_{169}	$\rho^0\gamma$	< 2.4	× 10^{-4}	CL=90%
Γ_{170}	$\omega\gamma$	< 2.4	× 10^{-4}	CL=90%
Γ_{171}	$\phi\gamma$	(2.5 $^{+0.7}_{-0.6}$) × 10^{-5}		
Γ_{172}	$\overline{K}^*(892)^0\gamma$	< 7.6	× 10^{-4}	CL=90%

Doubly Cabibbo suppressed (*DC*) modes, $\Delta C = 2$ forbidden via mixing (*C2M*) modes, $\Delta C = 1$ weak neutral current (*C1*) modes, Lepton Family number (*LF*) violating modes, or Lepton number (*L*) violating modes

Γ_{173}	$K^+\ell^-\overline{\nu}_\ell$(via $\overline{D}^0$)	*C2M*	<	1.7	$\times 10^{-4}$	CL=90%
Γ_{174}	$K^+\pi^-$	*DC*		(1.38 ± 0.11)	$\times 10^{-4}$	
Γ_{175}	$K^+\pi^-$ (via $\overline{D}^0$)	*C2M*	<	1.6	$\times 10^{-5}$	CL=95%
Γ_{176}	$K^*(892)^+\pi^-$			($3.0\ ^{+\ 3.8}_{-\ 1.3}$)	$\times 10^{-4}$	
Γ_{177}	$K^+\pi^-\pi^0$			(5.6 ± 1.7)	$\times 10^{-4}$	
Γ_{178}	$K^+\pi^-\pi^+\pi^-$	*DC*		(3.1 ± 1.0)	$\times 10^{-4}$	
Γ_{179}	$K^+\pi^-\pi^+\pi^-$ (via $\overline{D}^0$)	*C2M*	<	4	$\times 10^{-4}$	CL=90%
Γ_{180}	$K^+\pi^-$ or $K^+\pi^-\pi^+\pi^-$(via $\overline{D}^0$)		<	1.0	$\times 10^{-3}$	CL=90%
Γ_{181}	μ^- anything (via $\overline{D}^0$)	*C2M*	<	4	$\times 10^{-4}$	CL=90%
Γ_{182}	$\gamma\gamma$	*C1*	<	2.8	$\times 10^{-5}$	CL=90%
Γ_{183}	e^+e^-	*C1*	<	6.2	$\times 10^{-6}$	CL=90%
Γ_{184}	$\mu^+\mu^-$	*C1*	<	4.1	$\times 10^{-6}$	CL=90%
Γ_{185}	$\pi^0 e^+e^-$	*C1*	<	4.5	$\times 10^{-5}$	CL=90%
Γ_{186}	$\pi^0\mu^+\mu^-$	*C1*	<	1.8	$\times 10^{-4}$	CL=90%
Γ_{187}	ηe^+e^-	*C1*	<	1.1	$\times 10^{-4}$	CL=90%
Γ_{188}	$\eta\mu^+\mu^-$	*C1*	<	5.3	$\times 10^{-4}$	CL=90%
Γ_{189}	$\pi^+\pi^-e^+e^-$	*C1*	<	3.73	$\times 10^{-4}$	CL=90%
Γ_{190}	$\rho^0 e^+e^-$	*C1*	<	1.0	$\times 10^{-4}$	CL=90%
Γ_{191}	$\pi^+\pi^-\mu^+\mu^-$	*C1*	<	3.0	$\times 10^{-5}$	CL=90%
Γ_{192}	$\rho^0\mu^+\mu^-$	*C1*	<	2.2	$\times 10^{-5}$	CL=90%
Γ_{193}	ωe^+e^-	*C1*	<	1.8	$\times 10^{-4}$	CL=90%
Γ_{194}	$\omega\mu^+\mu^-$	*C1*	<	8.3	$\times 10^{-4}$	CL=90%
Γ_{195}	$K^-K^+e^+e^-$	*C1*	<	3.15	$\times 10^{-4}$	CL=90%
Γ_{196}	ϕe^+e^-	*C1*	<	5.2	$\times 10^{-5}$	CL=90%
Γ_{197}	$K^-K^+\mu^+\mu^-$	*C1*	<	3.3	$\times 10^{-5}$	CL=90%
Γ_{198}	$\phi\mu^+\mu^-$	*C1*	<	3.1	$\times 10^{-5}$	CL=90%
Γ_{199}	$\overline{K}^0 e^+e^-$		[*h*] <	1.1	$\times 10^{-4}$	CL=90%
Γ_{200}	$\overline{K}^0\mu^+\mu^-$		[*h*] <	2.6	$\times 10^{-4}$	CL=90%
Γ_{201}	$K^-\pi^+e^+e^-$	*C1*	<	3.85	$\times 10^{-4}$	CL=90%
Γ_{202}	$\overline{K}^*(892)^0 e^+e^-$		[*h*] <	4.7	$\times 10^{-5}$	CL=90%
Γ_{203}	$K^-\pi^+\mu^+\mu^-$	*C1*	<	3.59	$\times 10^{-4}$	CL=90%
Γ_{204}	$\overline{K}^*(892)^0\mu^+\mu^-$		[*h*] <	2.4	$\times 10^{-5}$	CL=90%
Γ_{205}	$\pi^+\pi^-\pi^0\mu^+\mu^-$	*C1*	<	8.1	$\times 10^{-4}$	CL=90%
Γ_{206}	$\mu^\pm e^\mp$	*LF*	[*i*] <	8.1	$\times 10^{-6}$	CL=90%
Γ_{207}	$\pi^0 e^\pm\mu^\mp$	*LF*	[*i*] <	8.6	$\times 10^{-5}$	CL=90%
Γ_{208}	$\eta e^\pm\mu^\mp$	*LF*	[*i*] <	1.0	$\times 10^{-4}$	CL=90%
Γ_{209}	$\pi^+\pi^-e^\pm\mu^\mp$	*LF*	[*i*] <	1.5	$\times 10^{-5}$	CL=90%
Γ_{210}	$\rho^0 e^\pm\mu^\mp$	*LF*	[*i*] <	4.9	$\times 10^{-5}$	CL=90%
Γ_{211}	$\omega e^\pm\mu^\mp$	*LF*	[*i*] <	1.2	$\times 10^{-4}$	CL=90%
Γ_{212}	$K^-K^+e^\pm\mu^\mp$	*LF*	[*i*] <	1.8	$\times 10^{-4}$	CL=90%
Γ_{213}	$\phi e^\pm\mu^\mp$	*LF*	[*i*] <	3.4	$\times 10^{-5}$	CL=90%
Γ_{214}	$\overline{K}^0 e^\pm\mu^\mp$	*LF*	[*i*] <	1.0	$\times 10^{-4}$	CL=90%
Γ_{215}	$K^-\pi^+e^\pm\mu^\mp$	*LF*	[*i*] <	5.53	$\times 10^{-4}$	CL=90%
Γ_{216}	$\overline{K}^*(892)^0 e^\pm\mu^\mp$	*LF*	[*i*] <	8.3	$\times 10^{-5}$	CL=90%
Γ_{217}	$\pi^-\pi^-e^+e^+$ + c.c.	*L*	<	1.12	$\times 10^{-4}$	CL=90%
Γ_{218}	$\pi^-\pi^-\mu^+\mu^+$ + c.c.	*L*	<	2.9	$\times 10^{-5}$	CL=90%
Γ_{219}	$K^-\pi^-e^+e^+$ + c.c.	*L*	<	2.06	$\times 10^{-4}$	CL=90%
Γ_{220}	$K^-\pi^-\mu^+\mu^+$ + c.c.	*L*	<	3.9	$\times 10^{-4}$	CL=90%
Γ_{221}	$K^-K^-e^+e^+$ + c.c.	*L*	<	1.52	$\times 10^{-4}$	CL=90%
Γ_{222}	$K^-K^-\mu^+\mu^+$ + c.c.	*L*	<	9.4	$\times 10^{-5}$	CL=90%
Γ_{223}	$\pi^-\pi^-e^+\mu^+$ + c.c.	*L*	<	7.9	$\times 10^{-5}$	CL=90%
Γ_{224}	$K^-\pi^-e^+\mu^+$ + c.c.	*L*	<	2.18	$\times 10^{-4}$	CL=90%
Γ_{225}	$K^-K^-e^+\mu^+$ + c.c.	*L*	<	5.7	$\times 10^{-5}$	CL=90%
Γ_{226}	A dummy mode used by the fit.			(10.8 ± 3.4) %		S=1.1

[*a*] The exclusive e^+ modes $K^-e^+\nu_e$, $K^-\pi^0e^+\nu_e$, $\overline{K}^0\pi^-e^+\nu_e$ and $\pi^-e^+\nu_e$ are constrained to equal this (well-measured) inclusive fraction.

[*b*] This is a weighted average of $D^\pm$ (44%) and D^0 (56%) branching fractions. See "D^+ and $D^0 \to$ (η anything) / (total D^+ and D^0)" under "D^+ Branching Ratios" in these Particle Listings.

[*c*] This value averages the e^+ and μ^+ branching fractions, after making a small phase-space adjustment to the μ^+ fraction to be able to use it as an e^+ fraction; hence our ℓ^+ here is really an e^+.

[*d*] The branching fraction for this mode may differ from the sum of the submodes that contribute to it, due to interference effects. See the relevant papers.

[*e*] The two experiments measuring this fraction are in serious disagreement. See the Particle Listings.

[*f*] The experiments on the division of this charge mode amongst its submodes disagree, and the submode branching fractions here add up to considerably more than the charged-mode fraction.

[*g*] However, these upper limits are in serious disagreement with values obtained in another experiment.

[*h*] This mode is not a useful test for a ΔC=1 weak neutral current because both quarks must change flavor in this decay.

[*i*] The value is for the sum of the charge states or particle/antiparticle states indicated.

CONSTRAINED FIT INFORMATION

An overall fit to 58 branching ratios uses 125 measurements and one constraint to determine 32 parameters. The overall fit has a $\chi^2 = 67.2$ for 94 degrees of freedom.

The following *off-diagonal* array elements are the correlation coefficients $\langle \delta x_i \delta x_j \rangle / (\delta x_i \cdot \delta x_j)$, in percent, from the fit to the branching fractions, $x_i \equiv \Gamma_i/\Gamma_{\rm total}$. The fit constrains the x_i whose labels appear in this array to sum to one.

x_9	6									
x_{10}	31	19								
x_{11}	0	−8	−1							
x_{12}	−1	−15	−3	−91						
x_{18}	1	24	5	−4	−8					
x_{19}	1	10	3	−1	−1	2				
x_{20}	13	46	42	−3	−7	11	8			
x_{21}	1	6	5	0	−1	1	16	11		
x_{22}	2	10	8	−1	−1	2	28	18	58	
x_{34}	3	11	9	−1	−2	3	10	22	22	33
x_{46}	5	18	17	−1	−3	4	3	40	5	8
x_{55}	1	4	3	0	−1	1	12	8	24	42
x_{64}	3	9	8	−1	−1	2	2	19	2	4
x_{73}	1	4	3	0	−1	1	11	7	22	38
x_{81}	1	4	3	0	−1	1	11	7	54	40
x_{84}	1	3	3	0	−1	1	9	6	19	34
x_{86}	1	5	4	0	−1	1	14	9	29	51
x_{91}	2	9	7	−1	−1	2	25	17	51	88
x_{92}	1	5	4	0	−1	1	6	10	18	19
x_{94}	1	3	3	0	0	1	1	7	1	1
x_{98}	1	2	2	0	0	0	1	4	2	4
x_{109}	0	2	2	0	0	0	4	4	9	16
x_{113}	1	3	2	0	0	1	8	5	16	28
x_{117}	0	1	1	0	0	0	3	2	6	9
x_{119}	1	3	3	0	0	1	2	6	5	8
x_{133}	9	32	30	−2	−5	8	6	71	8	13
x_{134}	0	2	2	0	0	0	6	4	12	20
x_{135}	1	4	4	0	−1	1	9	9	19	33
x_{139}	1	4	3	0	−1	1	7	7	13	23
x_{156}	1	3	2	0	0	1	7	5	15	25
x_{226}	−28	−17	−24	0	1	−4	−30	−33	−47	−70
	x_2	x_9	x_{10}	x_{11}	x_{12}	x_{18}	x_{19}	x_{20}	x_{21}	x_{22}

x_{46}	9									
x_{55}	14	5								
x_{64}	4	28	2							
x_{73}	12	3	16	1						
x_{81}	14	3	17	1	15					
x_{84}	11	3	38	1	13	13				
x_{86}	17	4	21	2	−4	20	17			
x_{91}	36	7	37	3	33	35	30	45		
x_{92}	43	4	8	2	7	11	6	10	20	
x_{94}	2	18	1	5	1	1	1	1	1	1
x_{98}	2	10	8	3	1	2	3	2	3	1
x_{109}	5	4	37	1	6	6	14	8	14	3
x_{113}	9	2	12	1	10	11	9	14	25	5
x_{117}	7	1	4	0	3	4	3	5	9	4
x_{119}	23	2	3	1	3	3	3	4	8	10
x_{133}	16	29	6	14	5	5	4	6	12	7
x_{134}	7	2	9	1	8	8	7	10	18	4
x_{135}	11	4	14	2	12	13	11	17	29	6
x_{139}	8	3	10	1	9	9	8	12	20	5
x_{156}	8	2	11	1	9	10	8	13	22	5
x_{226}	−56	−27	−66	−20	−28	−33	−43	−37	−67	−36
	x_{34}	x_{46}	x_{55}	x_{64}	x_{73}	x_{81}	x_{84}	x_{86}	x_{91}	x_{92}

x_{98}	2									
x_{109}	1	3								
x_{113}	0	1	4							
x_{117}	0	0	1	3						
x_{119}	0	0	1	2	2					
x_{133}	5	3	3	4	2	4				
x_{134}	0	1	3	6	2	2	3			
x_{135}	1	1	5	9	3	3	6	7		
x_{139}	1	1	4	6	2	2	5	5	8	
x_{156}	0	1	4	7	2	2	4	5	8	6
x_{226}	−14	−22	−33	−25	−19	−25	−24	−15	−26	−20
	x_{94}	x_{98}	x_{109}	x_{113}	x_{117}	x_{119}	x_{133}	x_{134}	x_{135}	x_{139}

x_{226}	−20
	x_{156}

D^0 BRANCHING RATIOS

Some older now obsolete results have been omitted from these Listings.

Inclusive modes

$\Gamma(e^+ \text{anything})/\Gamma_{\text{total}}$ $\Gamma_1/\Gamma = (\Gamma_9+\Gamma_{11}+\Gamma_{12}+\Gamma_{18})/\Gamma$

VALUE	EVTS	DOCUMENT ID		TECN	COMMENT
0.0687±0.0028 OUR FIT					
0.0675±0.0029 OUR AVERAGE					
0.069 ±0.003 ±0.005	1670	ALBRECHT	96C	ARG	$e^+e^- \approx$ 10 GeV
0.0664±0.0018±0.0029	4609	[20] KUBOTA	96B	CLE2	$e^+e^- \approx \Upsilon(4S)$
0.075 ±0.011 ±0.004	137	BALTRUSAIT...	85B	MRK3	e^+e^- 3.77 GeV
• • • We do not use the following data for averages, fits, limits, etc. • • •					
0.15 ±0.05		AGUILAR-...	87E	HYBR	πp, pp 360, 400 GeV
0.055 ±0.037	12	SCHINDLER	81	MRK2	e^+e^- 3.771 GeV

[20] KUBOTA 96B uses $D^{*+} \to D^0\pi^+$ (and charge conjugate) events in which the D^0 subsequently decays to $X e^+ \nu_e$.

$\Gamma(\mu^+ \text{anything})/\Gamma_{\text{total}}$ Γ_2/Γ

VALUE	EVTS	DOCUMENT ID		TECN	COMMENT
0.065±0.008 OUR FIT					
0.060±0.007±0.012	310	ALBRECHT	96C	ARG	$e^+e^- \approx$ 10 GeV

$\Gamma(K^- \text{anything})/\Gamma_{\text{total}}$ Γ_3/Γ

VALUE	EVTS	DOCUMENT ID		TECN	COMMENT
0.53 ±0.04 OUR AVERAGE		Error includes scale factor of 1.3. See the ideogram below.			
$0.546^{+0.039}_{-0.038}$		[21] BARLAG	92C	ACCM	π^- Cu 230 GeV
0.609±0.032±0.052		COFFMAN	91	MRK3	e^+e^- 3.77 GeV
0.42 ±0.08		AGUILAR-...	87E	HYBR	πp, pp 360, 400 GeV
0.55 ±0.11	121	SCHINDLER	81	MRK2	e^+e^- 3.771 GeV
0.35 ±0.10	19	VUILLEMIN	78	MRK1	e^+e^- 3.772 GeV

[21] BARLAG 92C computes the branching fraction using topological normalization.

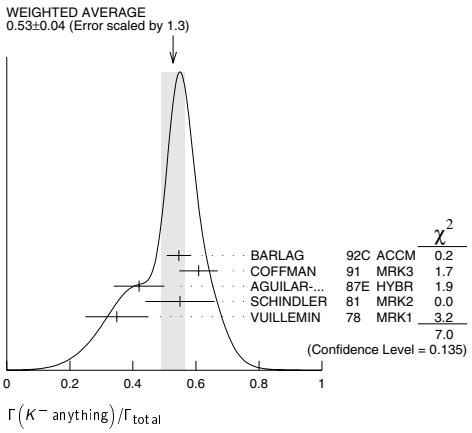

$[\Gamma(\overline{K}^0 \text{anything}) + \Gamma(K^0 \text{anything})]/\Gamma_{\text{total}}$ Γ_4/Γ

VALUE	EVTS	DOCUMENT ID		TECN	COMMENT
0.42 ±0.05 OUR AVERAGE					
0.455±0.050±0.032		COFFMAN	91	MRK3	e^+e^- 3.77 GeV
0.29 ±0.11	13	SCHINDLER	81	MRK2	e^+e^- 3.771 GeV
0.57 ±0.26	6	VUILLEMIN	78	MRK1	e^+e^- 3.772 GeV

$\Gamma(K^+ \text{anything})/\Gamma_{\text{total}}$ Γ_5/Γ

VALUE	EVTS	DOCUMENT ID		TECN	COMMENT
$0.034^{+0.006}_{-0.004}$ OUR AVERAGE					
$0.034^{+0.007}_{-0.005}$		[22] BARLAG	92C	ACCM	π^- Cu 230 GeV
0.028±0.009±0.004		COFFMAN	91	MRK3	e^+e^- 3.77 GeV
$0.03^{+0.05}_{-0.02}$		AGUILAR-...	87E	HYBR	πp, pp 360, 400 GeV
0.08 ±0.03	25	SCHINDLER	81	MRK2	e^+e^- 3.771 GeV

[22] BARLAG 92C computes the branching fraction using topological normalization.

$\Gamma(\phi \text{anything})/\Gamma_{\text{total}}$ Γ_7/Γ

VALUE	EVTS	DOCUMENT ID		TECN	COMMENT
$0.0171^{+0.0076}_{-0.0071}\pm0.0017$	9	[23] BAI	00C	BES	$e^+e^- \to D\overline{D}^*$, $D^*\overline{D}^*$

[23] BAI 00C finds the average (ϕ anything) branching fraction for the 4.03-GeV mix of D^+ and D^0 mesons to be (1.34 ± 0.52 ± 0.12)%.

Semileptonic modes

$\Gamma(K^-\ell^+\nu_\ell)/\Gamma_{\text{total}}$ Γ_8/Γ

We average our $K^- e^+ \nu_e$ and $K^- \mu^+ \nu_\mu$ branching fractions, after multiplying the latter by a phase-space factor of 1.03 to be able to use it with the $K^- e^+ \nu_e$ fraction. Hence our ℓ^+ here is really an e^+.

VALUE	DOCUMENT ID		COMMENT
0.0343±0.0014 OUR AVERAGE	Error includes scale factor of 1.2.		
0.0358±0.0018	PDG	04	Our $\Gamma(K^- e^+ \nu_e)/\Gamma_{\text{total}}$
0.0329±0.0017	PDG	04	1.03 × our $\Gamma(K^- \mu^+ \nu_\mu)/\Gamma_{\text{total}}$

$\Gamma(K^- e^+ \nu_e)/\Gamma_{\text{total}}$ Γ_9/Γ

VALUE	EVTS	DOCUMENT ID		TECN	COMMENT
0.0358±0.0018 OUR FIT		Error includes scale factor of 1.1.			
0.034 ±0.005 ±0.004	55	ADLER	89	MRK3	e^+e^- 3.77 GeV

$\Gamma(K^- e^+ \nu_e)/\Gamma(K^-\pi^+)$ Γ_9/Γ_{20}

VALUE	EVTS	DOCUMENT ID		TECN	COMMENT
0.94 ±0.04 OUR FIT					
0.95 ±0.04 OUR AVERAGE					
0.978±0.027±0.044	2510	[24] BEAN	93C	CLE2	$e^+e^- \approx \Upsilon(4S)$
0.90 ±0.06 ±0.06	584	[25] CRAWFORD	91B	CLEO	$e^+e^- \approx$ 10.5 GeV
0.91 ±0.07 ±0.11	250	[26] ANJOS	89F	E691	Photoproduction

[24] BEAN 93C uses $K^-\mu^+\nu_\mu$ as well as $K^- e^+ \nu_e$ events and makes a small phase-space adjustment to the number of the μ^+ events to use them as e^+ events. A pole mass of 2.00 ± 0.12 ± 0.18 GeV/c^2 is obtained from the q^2 dependence of the decay rate.

[25] CRAWFORD 91B uses $K^- e^+ \nu_e$ and $K^-\mu^+\nu_\mu$ candidates to measure a pole mass of $2.1^{+0.4}_{-0.2}{}^{+0.3}_{-0.2}$ GeV/c^2 from the q^2 dependence of the decay rate.

[26] ANJOS 89F measures a pole mass of $2.1^{+0.4}_{-0.2}$ ± 0.2 GeV/c^2 from the q^2 dependence of the decay rate.

$\Gamma(K^-\mu^+\nu_\mu)/\Gamma(K^-\pi^+)$ Γ_{10}/Γ_{20}

VALUE	EVTS	DOCUMENT ID		TECN	COMMENT
0.84 ±0.04 OUR FIT					
0.84 ±0.04 OUR AVERAGE					
0.852±0.034±0.028	1897	[27] FRABETTI	95G	E687	γBe $\overline{E}_\gamma$= 220 GeV
0.82 ±0.13 ±0.13	338	[28] FRABETTI	93I	E687	γBe $\overline{E}_\gamma$= 221 GeV
0.79 ±0.08 ±0.09	231	[29] CRAWFORD	91B	CLEO	e^+e^- ≈ 10.5 GeV

[27] FRABETTI 95G extracts the ratio of form factors $f_-(0)/f_+(0) = -1.3^{+3.6}_{-3.4} \pm 0.6$, and measures a pole mass of $1.87^{+0.11+0.07}_{-0.08-0.06}$ GeV/c^2 from the q^2 dependence of the decay rate.

[28] FRABETTI 93I measures a pole mass of $2.1^{+0.7+0.7}_{-0.3-0.3}$ GeV/c^2 from the q^2 dependence of the decay rate.

[29] CRAWFORD 91B measures a pole mass of 2.00 ± 0.12 ± 0.18 GeV/c^2 from the q^2 dependence of the decay rate.

$\Gamma(K^-\mu^+\nu_\mu)/\Gamma(\mu^+\text{anything})$ Γ_{10}/Γ_{2}

VALUE	EVTS	DOCUMENT ID		TECN	COMMENT
0.49 ±0.06 OUR FIT					
0.472±0.051±0.040	232	KODAMA	94	E653	π^- emulsion 600 GeV
• • • We do not use the following data for averages, fits, limits, etc. • • •					
0.32 ±0.05 ±0.05	124	KODAMA	91	EMUL	pA 800 GeV

$\Gamma(K^-\pi^0e^+\nu_e)/\Gamma_{\text{total}}$ Γ_{11}/Γ

VALUE	EVTS	DOCUMENT ID		TECN	COMMENT
$\mathbf{0.011^{+0.008}_{-0.006}}$ **OUR FIT** Error includes scale factor of 1.6.					
$\mathbf{0.016^{+0.013}_{-0.005}\pm0.002}$	4	[30] BAI	91	MRK3	e^+e^- ≈ 3.77 GeV

[30] BAI 91 finds that a fraction $0.79^{+0.15+0.09}_{-0.17-0.03}$ of combined D^+ and D^0 decays to $\overline{K}\pi e^+\nu_e$ (24 events) are $\overline{K}^*(892)e^+\nu_e$. BAI 91 uses 56 $K^-e^+\nu_e$ events to measure a pole mass of 1.8 ± 0.3 ± 0.2 GeV/c^2 from the q^2 dependence of the decay rate.

$\Gamma(\overline{K}^0\pi^-e^+\nu_e)/\Gamma_{\text{total}}$ Γ_{12}/Γ

VALUE	EVTS	DOCUMENT ID		TECN	COMMENT
0.018±0.008 OUR FIT Error includes scale factor of 1.6.					
$\mathbf{0.028^{+0.017}_{-0.008}\pm0.003}$	6	[31] BAI	91	MRK3	e^+e^- ≈ 3.77 GeV

[31] BAI 91 finds that a fraction $0.79^{+0.15+0.09}_{-0.17-0.03}$ of combined D^+ and D^0 decays to $\overline{K}\pi e^+\nu_e$ (24 events) are $\overline{K}^*(892)e^+\nu_e$.

$\Gamma(K^*(892)^-e^+\nu_e)/\Gamma(K^-e^+\nu_e)$ Γ_{19}/Γ_{9}

Unseen decay modes of the $K^*(892)^-$ are included.

VALUE	DOCUMENT ID		TECN	COMMENT
0.60±0.10 OUR FIT				
0.51±0.18±0.06	CRAWFORD	91B	CLEO	e^+e^- ≈ 10.5 GeV

$\Gamma(K^*(892)^-e^+\nu_e)/\Gamma(\overline{K}^0\pi^+\pi^-)$ Γ_{19}/Γ_{22}

Unseen decay modes of the $\overline{K}^*(892)^-$ are included.

VALUE	EVTS	DOCUMENT ID		TECN	COMMENT
0.36±0.06 OUR FIT					
0.38±0.06±0.03	152	[32] BEAN	93C	CLE2	e^+e^- ≈ $\Upsilon(4S)$

[32] BEAN 93C uses $K^{*-}\mu^+\nu_\mu$ as well as $K^{*-}e^+\nu_e$ events and makes a small phase-space adjustment to the number of the μ^+ events to use them as e^+ events.

$\Gamma(K^*(892)^-\ell^+\nu_\ell)/\Gamma(\overline{K}^0\pi^+\pi^-)$ Γ_{14}/Γ_{22}

This an average of the $K^*(892)^-e^+\nu_e$ and $K^*(892)^-\mu^+\nu_\mu$ ratios. Unseen decay modes of the $K^*(892)^-$ are included.

VALUE	EVTS	DOCUMENT ID		TECN	COMMENT
• • • We do not use the following data for averages, fits, limits, etc. • • •					
0.24±0.07±0.06	137	[33] ALEXANDER	90B	CLEO	e^+e^- 10.5–11 GeV

[33] ALEXANDER 90B cannot exclude extra π^0's in the final state. See nearby data blocks for more detailed results.

$\Gamma(\overline{K}^*(892)^0\pi^-e^+\nu_e)/\Gamma(K^*(892)^-e^+\nu_e)$ Γ_{15}/Γ_{19}

Unseen decay modes of the $\overline{K}^*(892)^0$ are included.

VALUE	CL%	DOCUMENT ID		TECN	COMMENT
• • • We do not use the following data for averages, fits, limits, etc. • • •					
<0.64	90	[34] CRAWFORD	91B	CLEO	e^+e^- ≈ 10.5 GeV

[34] The limit on $(\overline{K}^*(892)\pi)^-\mu^+\nu_\mu$ below is much stronger.

$\Gamma(K^-\pi^+\pi^-\mu^+\nu_\mu)/\Gamma(K^-\mu^+\nu_\mu)$ Γ_{16}/Γ_{10}

VALUE	CL%	DOCUMENT ID		TECN	COMMENT
<0.037	90	KODAMA	93B	E653	π^- emulsion 600 GeV

$\Gamma((\overline{K}^*(892)\pi)^-\mu^+\nu_\mu)/\Gamma(K^-\mu^+\nu_\mu)$ Γ_{17}/Γ_{10}

VALUE	CL%	DOCUMENT ID		TECN	COMMENT
<0.043	90	[35] KODAMA	93B	E653	π^- emulsion 600 GeV

[35] KODAMA 93B searched in $K^-\pi^+\pi^-\mu^+\nu_\mu$, but the limit includes other $(\overline{K}^*(892)\pi)^-$ charge states.

$\Gamma(\pi^-e^+\nu_e)/\Gamma_{\text{total}}$ Γ_{18}/Γ

VALUE	EVTS	DOCUMENT ID		TECN	COMMENT
0.0036±0.0006 OUR FIT					
$\mathbf{0.0039^{+0.0023}_{-0.0011}\pm0.0004}$	7	[36] ADLER	89	MRK3	e^+e^- 3.77 GeV

[36] This result of ADLER 89 gives $|\frac{V_{cd}}{V_{cs}}\cdot\frac{f_+^\pi(0)}{f_+^K(0)}|^2 = 0.057^{+0.038}_{-0.015} \pm 0.005$.

$\Gamma(\pi^-e^+\nu_e)/\Gamma(K^-e^+\nu_e)$ Γ_{18}/Γ_{9}

VALUE	EVTS	DOCUMENT ID		TECN	COMMENT
0.101±0.017 OUR FIT					
0.101±0.018 OUR AVERAGE					
0.101±0.020±0.003	91	[37] FRABETTI	96B	E687	γ Be, $\overline{E}_\gamma$ ≈ 200 GeV
0.103±0.039±0.013	87	[38] BUTLER	95	CLE2	< 0.156 (90% CL)

[37] FRABETTI 96B uses both e and μ events, and makes a small correction to the μ events to make them effectively e events. This result gives $|\frac{V_{cd}}{V_{cs}}\cdot\frac{f_+^\pi(0)}{f_+^K(0)}|^2 = 0.050\pm0.011\pm0.002$.

[38] BUTLER 95 has 87 ± 33 $\pi^-e^+\nu_e$ events. The result gives $|\frac{V_{cd}}{V_{cs}}\cdot\frac{f_+^\pi(0)}{f_+^K(0)}|^2 = 0.052 \pm 0.020 \pm 0.007$.

Hadronic modes with a $\overline{K}$ or $\overline{K}K\overline{K}$

$\Gamma(K^-\pi^+)/\Gamma_{\text{total}}$ Γ_{20}/Γ

We list measurements *before* radiative corrections are made.

VALUE	EVTS	DOCUMENT ID		TECN	COMMENT
0.0380±0.0009 OUR FIT					
0.0385±0.0009 OUR AVERAGE					
0.0382±0.0007±0.0012		[39] ARTUSO	98	CLE2	CLEO average
0.0390±0.0009±0.0012	5392	[40] BARATE	97C	ALEP	From Z decays
0.045 ±0.006 ±0.004		[41] ALBRECHT	94	ARG	e^+e^- ≈ $\Upsilon(4S)$
0.0341±0.0012±0.0028	1173	[40] ALBRECHT	94F	ARG	e^+e^- ≈ $\Upsilon(4S)$
0.0362±0.0034±0.0044		[40] DECAMP	91J	ALEP	From Z decays
0.045 ±0.008 ±0.005	56	[40] ABACHI	88	HRS	e^+e^- 29 GeV
0.042 ±0.004 ±0.004	930	ADLER	88C	MRK3	e^+e^- 3.77 GeV
0.041 ±0.006	263	[42] SCHINDLER	81	MRK2	e^+e^- 3.771 GeV
0.043 ±0.010	130	[43] PERUZZI	77	MRK1	e^+e^- 3.77 GeV
• • • We do not use the following data for averages, fits, limits, etc. • • •					
0.0381±0.0015±0.0016	1165	[44] ARTUSO	98	CLE2	e^+e^- at $\Upsilon(4S)$
0.0369±0.0011±0.0016		[45] COAN	98	CLE2	See ARTUSO 98
0.0391±0.0008±0.0017	4208	[40,46] AKERIB	93	CLE2	See ARTUSO 98

[39] This combines the CLEO results of ARTUSO 98, COAN 98, and AKERIB 93.

[40] ABACHI 88, DECAMP 91J, AKERIB 93, ALBRECHT 94F, and BARATE 97C use $D^*(2010)^+ \to D^0\pi^+$ decays. The π^+ is both slow and of low p_T with respect to the event thrust axis or nearest jet (≈ D^{*+} direction). The excess number of such π^+'s over background gives the number of $D^*(2010)^+ \to D^0\pi^+$ events, and the fraction with $D^0 \to K^-\pi^+$ gives the $D^0 \to K^-\pi^+$ branching fraction.

[41] ALBRECHT 94 uses D^0 mesons from $\overline{B}^0 \to D^{*+}\ell^-\overline{\nu}_\ell$ decays. This is a different set of events than used by ALBRECHT 94F.

[42] SCHINDLER 81 (MARK-2) measures $\sigma(e^+e^- \to \psi(3770)) \times$ branching fraction to be 0.24 ± 0.02 nb. We use the MARK-3 (ADLER 88C) value of σ = 5.8 ± 0.5 ± 0.6 nb.

[43] PERUZZI 77 (MARK-1) measures $\sigma(e^+e^- \to \psi(3770)) \times$ branching fraction to be 0.25 ± 0.05 nb. We use the MARK-3 (ADLER 88C) value of σ = 5.8 ± 0.5 ± 0.6 nb.

[44] ARTUSO 98, following ALBRECHT 94, uses D^0 mesons from $\overline{B}^0 \to D^*(2010)^+X\ell^-\overline{\nu}_\ell$ decays. Our average uses the CLEO average of this value with the values of COAN 98 and AKERIB 93.

[45] COAN 98 assumes that $\Gamma(B \to \overline{D}X\ell^+\nu)/\Gamma(B \to X\ell^+\nu) = 1.0 - 3|V_{ub}/V_{cb}|^2 - 0.010 \pm 0.005$, the last term accounting for $\overline{B} \to D_s^+KX\ell^-\overline{\nu}$. COAN 98 is included in the CLEO average in ARTUSO 98.

[46] This AKERIB 93 value does not include radiative corrections; with them, the value is 0.0395 ± 0.0008 ± 0.0017. AKERIB 93 is included in the CLEO average in ARTUSO 98.

$\Gamma(\overline{K}^0\pi^0)/\Gamma(K^-\pi^+)$ Γ_{21}/Γ_{20}

VALUE	EVTS	DOCUMENT ID		TECN	COMMENT
0.60±0.06 OUR FIT					
1.36±0.23±0.22	119	ANJOS	92B	E691	γBe 80–240 GeV

$\Gamma(\overline{K}^0\pi^0)/\Gamma(\overline{K}^0\pi^+\pi^-)$ Γ_{21}/Γ_{22}

VALUE	EVTS	DOCUMENT ID		TECN	COMMENT
0.385±0.031 OUR FIT					
0.378±0.033 OUR AVERAGE					
0.44 ±0.02 ±0.05	1942	PROCARIO	93B	CLE2	e^+e^- 10.36–10.7 GeV
0.34 ±0.04 ±0.02	92	[47] ALBRECHT	92P	ARG	e^+e^- ≈ 10 GeV
0.36 ±0.04 ±0.08	104	KINOSHITA	91	CLEO	e^+e^- ~ 10.7 GeV

[47] This value is calculated from numbers in Table 1 of ALBRECHT 92P.

$\Gamma(\overline{K}^0\pi^+\pi^-)/\Gamma_{\text{total}}$ Γ_{22}/Γ

VALUE	EVTS	DOCUMENT ID		TECN	COMMENT
0.0597±0.0035 OUR FIT Error includes scale factor of 1.1.					
0.055 ±0.005 OUR AVERAGE					
0.0503±0.0039±0.0049	284	[48] ALBRECHT	94F	ARG	e^+e^- ≈ $\Upsilon(4S)$
0.064 ±0.005 ±0.010		ADLER	87	MRK3	e^+e^- 3.77 GeV
0.052 ±0.016	32	[49] SCHINDLER	81	MRK2	e^+e^- 3.771 GeV
0.079 ±0.023	28	[50] PERUZZI	77	MRK1	e^+e^- 3.77 GeV

[48] See the footnote on the ALBRECHT 94F measurement of $\Gamma(K^-\pi^+)/\Gamma_{\text{total}}$ for the method used.

[49] SCHINDLER 81 (MARK-2) measures $\sigma(e^+e^- \to \psi(3770)) \times$ branching fraction to be 0.30 ± 0.08 nb. We use the MARK-3 (ADLER 88C) value of $\sigma = 5.8 \pm 0.5 \pm 0.6$ nb.

[50] PERUZZI 77 (MARK-1) measures $\sigma(e^+e^- \to \psi(3770)) \times$ branching fraction to be 0.46 ± 0.12 nb. We use the MARK-3 (ADLER 88C) value of $\sigma = 5.8 \pm 0.5 \pm 0.6$ nb.

$\Gamma(\overline{K}^0\pi^+\pi^-)/\Gamma(K^-\pi^+)$ Γ_{22}/Γ_{20}

VALUE	EVTS	DOCUMENT ID		TECN	COMMENT
1.57 ± 0.09 OUR FIT Error includes scale factor of 1.1.					
1.65 ± 0.17 OUR AVERAGE					
1.61 ± 0.10 ± 0.15	856	FRABETTI	94J	E687	γBe $\overline{E}_\gamma$=220 GeV
1.7 ± 0.8	35	AVERY	80	SPEC	$\gamma N \to D^{*+}$
2.8 ± 1.0	116	PICCOLO	77	MRK1	e^+e^- 4.03, 4.41 GeV

$\Gamma(\overline{K}^0\rho^0)/\Gamma(\overline{K}^0\pi^+\pi^-)$ Γ_{23}/Γ_{22}

VALUE	DOCUMENT ID		TECN	COMMENT
$0.259^{+0.014}_{-0.023}$ OUR AVERAGE Error includes scale factor of 1.1.				
$0.264 \pm 0.009^{+0.010}_{-0.026}$	MURAMATSU	02	CLE2	$e^+e^- \approx$ 10 GeV
$0.350 \pm 0.028 \pm 0.067$	FRABETTI	94G	E687	γBe, $\overline{E}_\gamma \approx$ 220 GeV
$0.227 \pm 0.032 \pm 0.009$	ALBRECHT	93D	ARG	$e^+e^- \approx$ 10 GeV
• • • We do not use the following data for averages, fits, limits, etc. • • •				
$0.215 \pm 0.051 \pm 0.037$	ANJOS	93	E691	γBe 90–260 GeV
$0.20 \pm 0.06 \pm 0.03$	FRABETTI	92B	E687	γBe $\overline{E}_\gamma$= 221 GeV
$0.12 \pm 0.01 \pm 0.07$	ADLER	87	MRK3	e^+e^- 3.77 GeV

$\Gamma(\overline{K}^0 f_0(980) \times B(f_0 \to \pi^+\pi^-))/\Gamma(\overline{K}^0\pi^+\pi^-)$ Γ_{25}/Γ_{22}

This includes only $\pi^+\pi^-$ decays of the $f_0(980)$, because branching fractions of this resonance are not known.

VALUE	DOCUMENT ID		TECN	COMMENT
$0.047^{+0.010}_{-0.007}$ OUR AVERAGE				
$0.043 \pm 0.005^{+0.012}_{-0.006}$	MURAMATSU	02	CLE2	$e^+e^- \approx$ 10 GeV
$0.068 \pm 0.016 \pm 0.018$	FRABETTI	94G	E687	γBe, $\overline{E}_\gamma \approx$ 220 GeV
$0.046 \pm 0.018 \pm 0.006$	ALBRECHT	93D	ARG	$e^+e^- \approx$ 10 GeV

$\Gamma(\overline{K}^0 f_2(1270))/\Gamma(\overline{K}^0\pi^+\pi^-)$ Γ_{89}/Γ_{22}

Unseen decay modes of the $f_2(1270)$ are included. Note the large difference between MURAMATSU 02 and earlier measurements.

VALUE	DOCUMENT ID		TECN	COMMENT
$0.008^{+0.007}_{-0.004}$ OUR AVERAGE				
$0.0048 \pm 0.0027^{+0.0065}_{-0.0029}$	MURAMATSU	02	CLE2	$e^+e^- \approx$ 10 GeV
$0.065 \pm 0.025 \pm 0.030$	FRABETTI	94G	E687	γBe, $\overline{E}_\gamma \approx$ 220 GeV
$0.088 \pm 0.037 \pm 0.014$	ALBRECHT	93D	ARG	$e^+e^- \approx$ 10 GeV

$\Gamma(\overline{K}^0 f_0(1370) \times B(f_0 \to \pi^+\pi^-))/\Gamma(\overline{K}^0\pi^+\pi^-)$ Γ_{27}/Γ_{22}

This includes only $\pi^+\pi^-$ decays of the $f_0(1370)$, because branching fractions of this resonance are not known.

VALUE	DOCUMENT ID		TECN	COMMENT
$0.085^{+0.019}_{-0.021}$ OUR AVERAGE				
$0.099 \pm 0.011^{+0.028}_{-0.044}$	MURAMATSU	02	CLE2	$e^+e^- \approx$ 10 GeV
$0.077 \pm 0.022 \pm 0.031$	FRABETTI	94G	E687	γBe, $\overline{E}_\gamma \approx$ 220 GeV
$0.082 \pm 0.028 \pm 0.013$	ALBRECHT	93D	ARG	$e^+e^- \approx$ 10 GeV

$\Gamma(K^*(892)^-\pi^+)/\Gamma(\overline{K}^0\pi^+\pi^-)$ Γ_{91}/Γ_{22}

Unseen decay modes of the $K^*(892)^-$ are included.

VALUE	EVTS	DOCUMENT ID		TECN	COMMENT
$0.997^{+0.030}_{-0.034}$ OUR FIT					
$0.991^{+0.028}_{-0.040}$ OUR AVERAGE					
$0.986 \pm 0.020^{+0.027}_{-0.063}$		MURAMATSU	02	CLE2	$e^+e^- \approx$ 10 GeV
$0.938 \pm 0.054 \pm 0.038$		FRABETTI	94G	E687	γBe, $\overline{E}_\gamma \approx$ 220 GeV
$1.08 \pm 0.063 \pm 0.045$		ALBRECHT	93D	ARG	$e^+e^- \approx$ 10 GeV
• • • We do not use the following data for averages, fits, limits, etc. • • •					
$0.720 \pm 0.145 \pm 0.185$		ANJOS	93	E691	γBe 90–260 GeV
$0.96 \pm 0.12 \pm 0.075$		FRABETTI	92B	E687	γBe $\overline{E}_\gamma$= 221 GeV
$0.84 \pm 0.06 \pm 0.08$		ADLER	87	MRK3	e^+e^- 3.77 GeV
$1.05^{+0.23}_{-0.26}{}^{+0.07}_{-0.09}$	25	SCHINDLER	81	MRK2	e^+e^- 3.771 GeV

$\Gamma(K_0^*(1430)^-\pi^+)/\Gamma(\overline{K}^0\pi^+\pi^-)$ Γ_{113}/Γ_{22}

Unseen decay modes of the $K_0^*(1430)^-$ are included.

VALUE	DOCUMENT ID		TECN	COMMENT
$0.165^{+0.033}_{-0.021}$ OUR FIT				
$0.154^{+0.034}_{-0.019}$ OUR AVERAGE				
$0.118 \pm 0.011^{+0.050}_{-0.018}$	MURAMATSU	02	CLE2	$e^+e^- \approx$ 10 GeV
$0.176 \pm 0.044 \pm 0.047$	FRABETTI	94G	E687	γBe, $\overline{E}_\gamma \approx$ 220 GeV
$0.208 \pm 0.055 \pm 0.034$	ALBRECHT	93D	ARG	$e^+e^- \approx$ 10 GeV

$\Gamma(K_2^*(1430)^-\pi^+)/\Gamma(\overline{K}^0\pi^+\pi^-)$ Γ_{115}/Γ_{22}

Unseen decay modes of the $K_2^*(1430)^-$ are included.

VALUE	CL%	DOCUMENT ID		TECN	COMMENT
$0.033 \pm 0.006^{+0.020}_{-0.010}$		MURAMATSU	02	CLE2	$e^+e^- \approx$ 10 GeV
• • • We do not use the following data for averages, fits, limits, etc. • • •					
<0.15	90	ALBRECHT	93D	ARG	$e^+e^- \approx$ 10 GeV

$\Gamma(K^*(1680)^-\pi^+)/\Gamma(\overline{K}^0\pi^+\pi^-)$ Γ_{117}/Γ_{22}

Unseen decay modes of the $K^*(1680)^-$ are included.

VALUE	DOCUMENT ID		TECN	COMMENT
$0.14^{+0.07}_{-0.06}$ OUR FIT Error includes scale factor of 1.2.				
$0.085 \pm 0.016^{+0.069}_{-0.059}$	MURAMATSU	02	CLE2	$e^+e^- \approx$ 10 GeV

$\Gamma(\overline{K}^0\pi^+\pi^-$ nonresonant$)/\Gamma(\overline{K}^0\pi^+\pi^-)$ Γ_{33}/Γ_{22}

Neither FRABETTI 94G nor ALBRECHT 93D sees evidence for a nonresonant component.

VALUE	DOCUMENT ID		TECN	COMMENT
$0.009 \pm 0.004^{+0.020}_{-0.004}$	MURAMATSU	02	CLE2	$e^+e^- \approx$ 10 GeV
• • • We do not use the following data for averages, fits, limits, etc. • • •				
$0.263 \pm 0.024 \pm 0.041$	ANJOS	93	E691	γBe 90–260 GeV
$0.26 \pm 0.08 \pm 0.05$	FRABETTI	92B	E687	γBe $\overline{E}_\gamma$= 221 GeV
$0.33 \pm 0.05 \pm 0.10$	ADLER	87	MRK3	e^+e^- 3.77 GeV

$\Gamma(K^-\pi^+\pi^0)/\Gamma_{\text{total}}$ Γ_{34}/Γ

VALUE	EVTS	DOCUMENT ID		TECN	COMMENT
0.130 ± 0.008 OUR FIT Error includes scale factor of 1.3.					
0.131 ± 0.016 OUR AVERAGE					
$0.133 \pm 0.012 \pm 0.013$	931	ADLER	88C	MRK3	e^+e^- 3.77 GeV
0.117 ± 0.043	37	[51] SCHINDLER	81	MRK2	e^+e^- 3.771 GeV

[51] SCHINDLER 81 (MARK-2) measures $\sigma(e^+e^- \to \psi(3770)) \times$ branching fraction to be 0.68 ± 0.23 nb. We use the MARK-3 (ADLER 88C) value of $\sigma = 5.8 \pm 0.5 \pm 0.6$ nb.

$\Gamma(K^-\pi^+\pi^0)/\Gamma(K^-\pi^+)$ Γ_{34}/Γ_{20}

VALUE	EVTS	DOCUMENT ID		TECN	COMMENT
3.42 ± 0.22 OUR FIT Error includes scale factor of 1.3.					
3.47 ± 0.30 OUR AVERAGE Error includes scale factor of 1.5. See the ideogram below.					
$3.81 \pm 0.07 \pm 0.26$	10k	BARISH	96	CLE2	$e^+e^- \approx \Upsilon(4S)$
$3.04 \pm 0.16 \pm 0.34$	931	[52] ALBRECHT	92P	ARG	$e^+e^- \approx$ 10 GeV
4.0 ± 0.9 ± 1.0	69	ALVAREZ	91B	NA14	Photoproduction
2.8 ± 0.14 ± 0.52	1050	KINOSHITA	91	CLEO	$e^+e^- \sim$ 10.7 GeV
4.2 ± 1.4	41	SUMMERS	84	E691	Photoproduction

[52] This value is calculated from numbers in Table 1 of ALBRECHT 92P.

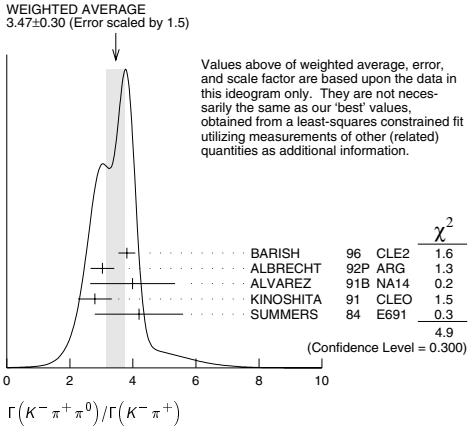

$\Gamma(K^-\rho^+)/\Gamma(K^-\pi^+\pi^0)$ Γ_{35}/Γ_{34}

VALUE	EVTS	DOCUMENT ID		TECN	COMMENT
0.78 ± 0.04 OUR AVERAGE					
$0.788 \pm 0.019 \pm 0.048$		KOPP	01	CLE2	$e^+e^- \approx$ 10.6 GeV
$0.765 \pm 0.041 \pm 0.054$		FRABETTI	94G	E687	γBe, $\overline{E}_\gamma \approx$ 220 GeV
• • • We do not use the following data for averages, fits, limits, etc. • • •					
$0.647 \pm 0.039 \pm 0.150$		ANJOS	93	E691	γBe 90–260 GeV
0.81 ± 0.03 ± 0.06		ADLER	87	MRK3	e^+e^- 3.77 GeV
$0.31^{+0.20}_{-0.14}$	13	SUMMERS	84	E691	Photoproduction
$0.85^{+0.11}_{-0.15}{}^{+0.09}_{-0.10}$	31	SCHINDLER	81	MRK2	e^+e^- 3.771 GeV

$\Gamma(K^-\rho(1700)^+ \times B(\rho(1700)^+ \to \pi^+\pi^0))/\Gamma(K^-\pi^+\pi^0)$ Γ_{36}/Γ_{34}

This only includes $\pi^+\pi^0$ decays of the $\rho(1700)^+$, because branching fractions of this resonance are not known.

VALUE	DOCUMENT ID		TECN	COMMENT
0.057 ± 0.008 ± 0.009	KOPP	01	CLE2	$e^+e^- \approx 10.6$ GeV

$\Gamma(K^*(892)^-\pi^+)/\Gamma(K^-\pi^+\pi^0)$ Γ_{91}/Γ_{34}

Unseen decay modes of the $K^*(892)^-$ are included.

VALUE	DOCUMENT ID		TECN	COMMENT
0.457 ± 0.034 OUR FIT Error includes scale factor of 1.2.				
0.48 $^{+0.08}_{-0.04}$ OUR AVERAGE				
$0.483 \pm 0.021 ^{+0.081}_{-0.032}$	KOPP	01	CLE2	$e^+e^- \approx 10.6$ GeV
$0.444 \pm 0.084 \pm 0.147$	FRABETTI	94G	E687	γBe, $\overline{E}_\gamma \approx 220$ GeV
• • • We do not use the following data for averages, fits, limits, etc. • • •				
$0.252 \pm 0.033 \pm 0.035$	ANJOS	93	E691	γBe 90–260 GeV
$0.36 \pm 0.06 \pm 0.09$	ADLER	87	MRK3	e^+e^- 3.77 GeV

$\Gamma(\overline{K}^*(892)^0\pi^0)/\Gamma(K^-\pi^+\pi^0)$ Γ_{92}/Γ_{34}

Unseen decay modes of the $\overline{K}^*(892)^0$ are included.

VALUE	DOCUMENT ID		TECN	COMMENT
0.214 ± 0.027 OUR FIT Error includes scale factor of 1.1.				
0.204 ± 0.025 OUR AVERAGE				
$0.191 \pm 0.014 \pm 0.024$	KOPP	01	CLE2	$e^+e^- \approx 10.6$ GeV
$0.248 \pm 0.047 \pm 0.023$	FRABETTI	94G	E687	γBe, $\overline{E}_\gamma \approx 220$ GeV
• • • We do not use the following data for averages, fits, limits, etc. • • •				
$0.213 \pm 0.027 \pm 0.035$	ANJOS	93	E691	γBe 90–260 GeV
$0.20 \pm 0.03 \pm 0.05$	ADLER	87	MRK3	e^+e^- 3.77 GeV

$\Gamma(K_0^*(1430)^-\pi^+)/\Gamma(K^-\pi^+\pi^0)$ Γ_{113}/Γ_{34}

Unseen decay modes of the $K_0^*(1430)^-$ are included.

VALUE	DOCUMENT ID		TECN	COMMENT
0.075 $^{+0.016}_{-0.010}$ OUR FIT				
0.107 ± 0.019 ± 0.045	KOPP	01	CLE2	$e^+e^- \approx 10.6$ GeV

$\Gamma(\overline{K}_0^*(1430)^0\pi^0)/\Gamma(K^-\pi^+\pi^0)$ Γ_{114}/Γ_{34}

Unseen decay modes of the $\overline{K}_0^*(1430)^0$ are included.

VALUE	DOCUMENT ID		TECN	COMMENT
0.066 ± 0.010 $^{+0.051}_{-0.014}$	KOPP	01	CLE2	$e^+e^- \approx 10.6$ GeV

$\Gamma(K^*(1680)^-\pi^+)/\Gamma(K^-\pi^+\pi^0)$ Γ_{117}/Γ_{34}

Unseen decay modes of the $K^*(1680)^-$ are included.

VALUE	DOCUMENT ID		TECN	COMMENT
0.063 $^{+0.031}_{-0.027}$ OUR FIT Error includes scale factor of 1.2.				
0.101 ± 0.023 ± 0.033	KOPP	01	CLE2	$e^+e^- \approx 10.6$ GeV

$\Gamma(K^-\pi^+\pi^0 \text{ nonresonant})/\Gamma(K^-\pi^+\pi^0)$ Γ_{42}/Γ_{34}

VALUE	EVTS	DOCUMENT ID		TECN	COMMENT
0.080 $^{+0.038}_{-0.014}$ OUR AVERAGE					
$0.075 \pm 0.009 ^{+0.056}_{-0.011}$		KOPP	01	CLE2	$e^+e^- \approx 10.6$ GeV
$0.101 \pm 0.033 \pm 0.040$		FRABETTI	94G	E687	γBe, $\overline{E}_\gamma \approx 220$ GeV
• • • We do not use the following data for averages, fits, limits, etc. • • •					
$0.036 \pm 0.004 \pm 0.018$		ANJOS	93	E691	γBe 90–260 GeV
$0.09 \pm 0.02 \pm 0.04$		ADLER	87	MRK3	e^+e^- 3.77 GeV
0.51 ± 0.22	21	SUMMERS	84	E691	Photoproduction

$\Gamma(\overline{K}^*(892)^0\pi^0)/\Gamma(\overline{K}^0\pi^0)$ Γ_{92}/Γ_{21}

Unseen decay modes of the $\overline{K}^*(892)^0$ are included.

VALUE	EVTS	DOCUMENT ID		TECN	COMMENT
1.22 ± 0.20 OUR FIT Error includes scale factor of 1.2.					
1.65 $^{+0.39}_{-0.31}$ ± 0.20	122	PROCARIO	93B	CLE2	$\overline{K}^0\pi^0\pi^0$ Dalitz plot

$\Gamma(\overline{K}_2^*(1430)^0\pi^0)/\Gamma(\overline{K}^*(892)^0\pi^0)$ Γ_{116}/Γ_{92}

Unseen decay modes of the $\overline{K}_2^*(1430)^0$ and $\overline{K}^*(892)^0$ are included.

VALUE	CL%	DOCUMENT ID		TECN	COMMENT
< 0.12	90	PROCARIO	93B	CLE2	$\overline{K}^0\pi^0\pi^0$ Dalitz plot

$\Gamma(\overline{K}^0\pi^0\pi^0 \text{ nonresonant})/\Gamma(\overline{K}^0\pi^0)$ Γ_{45}/Γ_{21}

VALUE	EVTS	DOCUMENT ID		TECN	COMMENT
0.37 ± 0.08 ± 0.04	76	PROCARIO	93B	CLE2	$\overline{K}^0\pi^0\pi^0$ Dalitz plot

$\Gamma(K^-\pi^+\pi^+\pi^-)/\Gamma_{\text{total}}$ Γ_{46}/Γ

VALUE	EVTS	DOCUMENT ID		TECN	COMMENT
0.0746 ± 0.0031 OUR FIT					
0.075 ± 0.006 OUR AVERAGE Error includes scale factor of 1.3. See the ideogram below.					
$0.079 \pm 0.015 \pm 0.009$		[53] ALBRECHT	94	ARG	$e^+e^- \approx \Upsilon(4S)$
$0.0680 \pm 0.0027 \pm 0.0057$	1430	[54] ALBRECHT	94F	ARG	$e^+e^- \approx \Upsilon(4S)$
$0.091 \pm 0.008 \pm 0.008$	992	ADLER	88C	MRK3	e^+e^- 3.77 GeV
0.117 ± 0.025	185	[55] SCHINDLER	81	MRK2	e^+e^- 3.771 GeV
0.062 ± 0.019	44	[56] PERUZZI	77	MRK1	e^+e^- 3.77 GeV

[53] ALBRECHT 94 uses D^0 mesons from $\overline{B}^0 \to D^{*+}\ell^-\overline{\nu}_\ell$ decays. This is a different set of events than used by ALBRECHT 94F.

[54] See the footnote on the ALBRECHT 94F measurement of $\Gamma(K^-\pi^+)/\Gamma_{\text{total}}$ for the method used.

[55] SCHINDLER 81 (MARK-2) measures $\sigma(e^+e^- \to \psi(3770)) \times$ branching fraction to be 0.68 ± 0.11 nb. We use the MARK-3 (ADLER 88C) value of $\sigma = 5.8 \pm 0.5 \pm 0.6$ nb.

[56] PERUZZI 77 (MARK-1) measures $\sigma(e^+e^- \to \psi(3770)) \times$ branching fraction to be 0.36 ± 0.10 nb. We use the MARK-3 (ADLER 88C) value of $\sigma = 5.8 \pm 0.5 \pm 0.6$ nb.

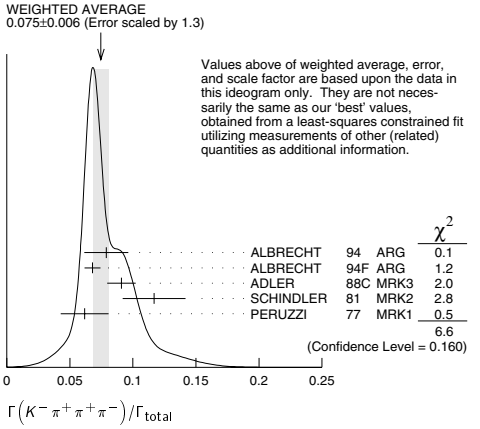

$\Gamma(K^-\pi^+\pi^+\pi^-)/\Gamma(K^-\pi^+)$ Γ_{46}/Γ_{20}

VALUE	EVTS	DOCUMENT ID		TECN	COMMENT
1.96 ± 0.08 OUR FIT					
1.97 ± 0.09 OUR AVERAGE					
$1.94 \pm 0.07 ^{+0.09}_{-0.11}$		JUN	00	SELX	Σ^- nucleus, 600 GeV
$1.7 \pm 0.2 \pm 0.2$	1745	ANJOS	92C	E691	γBe 90–260 GeV
$1.90 \pm 0.25 \pm 0.20$	337	ALVAREZ	91B	NA14	Photoproduction
$2.12 \pm 0.16 \pm 0.09$		BORTOLETTO	88	CLEO	e^+e^- 10.55 GeV
2.0 ± 0.9	48	BAILEY	86	ACCM	π^-Be fixed target
$2.17 \pm 0.28 \pm 0.23$		ALBRECHT	85F	ARG	e^+e^- 10 GeV
2.0 ± 1.0	10	BAILEY	83B	SPEC	π^-Be $\to D^0$
2.2 ± 0.8	214	PICCOLO	77	MRK1	e^+e^- 4.03, 4.41 GeV

$\Gamma(K^-\pi^+\rho^0\text{total})/\Gamma(K^-\pi^+\pi^+\pi^-)$ Γ_{47}/Γ_{46}

This includes $K^-a_1(1260)^+$, $\overline{K}^*(892)^0\rho^0$, etc. The next entry gives the specifically 3-body fraction. We rely on the MARK III and E691 full amplitude analyses of the $K^-\pi^+\pi^+\pi^-$ channel for values of the resonant substructure.

VALUE	DOCUMENT ID		TECN	COMMENT
0.835 ± 0.035 OUR AVERAGE				
$0.80 \pm 0.03 \pm 0.05$	ANJOS	92C	E691	γBe 90–260 GeV
$0.855 \pm 0.032 \pm 0.030$	COFFMAN	92B	MRK3	e^+e^- 3.77 GeV
• • • We do not use the following data for averages, fits, limits, etc. • • •				
$0.98 \pm 0.12 \pm 0.10$	ALVAREZ	91B	NA14	Photoproduction

$\Gamma(K^-\pi^+\rho^0\text{3-body})/\Gamma(K^-\pi^+\pi^+\pi^-)$ Γ_{48}/Γ_{46}

We rely on the MARK III and E691 full amplitude analyses of the $K^-\pi^+\pi^+\pi^-$ channel for values of the resonant substructure.

VALUE	EVTS	DOCUMENT ID		TECN	COMMENT
0.063 ± 0.028 OUR AVERAGE					
$0.05 \pm 0.03 \pm 0.02$		ANJOS	92C	E691	γBe 90–260 GeV
$0.084 \pm 0.022 \pm 0.04$		COFFMAN	92B	MRK3	e^+e^- 3.77 GeV
• • • We do not use the following data for averages, fits, limits, etc. • • •					
$0.77 \pm 0.06 \pm 0.06$		[57] ALVAREZ	91B	NA14	Photoproduction
$0.85 ^{+0.11}_{-0.22}$	180	PICCOLO	77	MRK1	e^+e^- 4.03, 4.41 GeV

[57] This value is for ρ^0 $(K^-\pi^+)$-nonresonant. ALVAREZ 91B cannot determine what fraction of this is $K^-a_1(1260)^+$.

$\Gamma(\overline{K}^*(892)^0\rho^0)/\Gamma(K^-\pi^+\pi^+\pi^-)$ Γ_{97}/Γ_{46}

Unseen decay modes of the $\overline{K}^*(892)^0$ are included. We rely on the MARK III and E691 full amplitude analyses of the $K^-\pi^+\pi^+\pi^-$ channel for values of the resonant substructure.

VALUE	EVTS	DOCUMENT ID		TECN	COMMENT
0.195 ± 0.03 ± 0.03		ANJOS	92C	E691	γBe 90–260 GeV
• • • We do not use the following data for averages, fits, limits, etc. • • •					
0.34 ± 0.09 ± 0.09		ALVAREZ	91B	NA14	Photoproduction
0.75 ± 0.3	5	BAILEY	83B	SPEC	π Be → D^0
$0.15\ ^{+0.16}_{-0.15}$	20	PICCOLO	77	MRK1	e^+e^- 4.03, 4.41 GeV

$\Gamma(\overline{K}^*(892)^0\rho^0\text{transverse})/\Gamma(K^-\pi^+\pi^+\pi^-)$ Γ_{98}/Γ_{46}

Unseen decay modes of the $\overline{K}^*(892)^0$ are included.

VALUE	DOCUMENT ID		TECN	COMMENT
0.21 ± 0.07 OUR FIT				
0.213 ± 0.024 ± 0.075	COFFMAN	92B	MRK3	e^+e^- 3.77 GeV

$\Gamma(\overline{K}^*(892)^0\rho^0\,S\text{-wave})/\Gamma(K^-\pi^+\pi^+\pi^-)$ Γ_{99}/Γ_{46}

Unseen decay modes of the $\overline{K}^*(892)^0$ are included.

VALUE	DOCUMENT ID		TECN	COMMENT
0.375 ± 0.045 ± 0.06	ANJOS	92C	E691	γBe 90–260 GeV

$\Gamma(\overline{K}^*(892)^0\rho^0\,S\text{-wave long.})/\Gamma_{\text{total}}$ Γ_{100}/Γ

Unseen decay modes of the $\overline{K}^*(892)^0$ are included.

VALUE	CL%	DOCUMENT ID		TECN	COMMENT
< 0.003	90	COFFMAN	92B	MRK3	e^+e^- 3.77 GeV

$\Gamma(\overline{K}^*(892)^0\rho^0\,P\text{-wave})/\Gamma_{\text{total}}$ Γ_{101}/Γ

Unseen decay modes of the $\overline{K}^*(892)^0$ are included.

VALUE	CL%	DOCUMENT ID		TECN	COMMENT
< 0.003	90	COFFMAN	92B	MRK3	e^+e^- 3.77 GeV
• • • We do not use the following data for averages, fits, limits, etc. • • •					
< 0.009	90	ANJOS	92C	E691	γBe 90–260 GeV

$\Gamma(\overline{K}^*(892)^0\rho^0\,D\text{-wave})/\Gamma(K^-\pi^+\pi^+\pi^-)$ Γ_{102}/Γ_{46}

Unseen decay modes of the $\overline{K}^*(892)^0$ are included.

VALUE	DOCUMENT ID		TECN	COMMENT
0.255 ± 0.045 ± 0.06	ANJOS	92C	E691	γBe 90–260 GeV

$\Gamma(K^-\pi^+ f_0(980))/\Gamma_{\text{total}}$ Γ_{107}/Γ

VALUE	CL%	DOCUMENT ID		TECN	COMMENT
• • • We do not use the following data for averages, fits, limits, etc. • • •					
< 0.011	90	ANJOS	92C	E691	γBe 90–260 GeV

$\Gamma(\overline{K}^*(892)^0 f_0(980))/\Gamma_{\text{total}}$ Γ_{108}/Γ

VALUE	CL%	DOCUMENT ID		TECN	COMMENT
• • • We do not use the following data for averages, fits, limits, etc. • • •					
< 0.007	90	ANJOS	92C	E691	γBe 90–260 GeV

$\Gamma(K^-a_1(1260)^+)/\Gamma(K^-\pi^+\pi^+\pi^-)$ Γ_{87}/Γ_{46}

Unseen decay modes of the $a_1(1260)^+$ are included, assuming that the $a_1(1260)^+$ decays entirely to $\rho\pi$ [or at least to $(\pi\pi)_{I=1}\ \pi$].

VALUE	DOCUMENT ID		TECN	COMMENT
0.97 ± 0.14 OUR AVERAGE				
0.94 ± 0.13 ± 0.20	ANJOS	92C	E691	γBe 90–260 GeV
0.984 ± 0.048 ± 0.16	COFFMAN	92B	MRK3	e^+e^- 3.77 GeV

$\Gamma(K^-a_2(1320)^+)/\Gamma_{\text{total}}$ Γ_{90}/Γ

Unseen decay modes of the $a_2(1320)^+$ are included.

VALUE	CL%	DOCUMENT ID		TECN	COMMENT
< 0.002	90	ANJOS	92C	E691	γBe 90–260 GeV
• • • We do not use the following data for averages, fits, limits, etc. • • •					
< 0.006	90	COFFMAN	92B	MRK3	e^+e^- 3.77 GeV

$\Gamma(K_1(1270)^-\pi^+)/\Gamma(K^-\pi^+\pi^+\pi^-)$ Γ_{109}/Γ_{46}

Unseen decay modes of the $K_1(1270)^-$ are included. The MARK3 and E691 experiments disagree considerably here.

VALUE	CL%	DOCUMENT ID		TECN	COMMENT
0.15 ± 0.04 OUR FIT					
0.194 ± 0.056 ± 0.088	COFFMAN	92B	MRK3	e^+e^- 3.77 GeV	
• • • We do not use the following data for averages, fits, limits, etc. • • •					
< 0.013	90	ANJOS	92C	E691	γBe 90–260 GeV

$\Gamma(K_1(1400)^-\pi^+)/\Gamma_{\text{total}}$ Γ_{110}/Γ

VALUE	CL%	DOCUMENT ID		TECN	COMMENT
< 0.012	90	COFFMAN	92B	MRK3	e^+e^- 3.77 GeV

$\Gamma(K^*(1410)^-\pi^+)/\Gamma_{\text{total}}$ Γ_{112}/Γ

VALUE	CL%	DOCUMENT ID		TECN	COMMENT
• • • We do not use the following data for averages, fits, limits, etc. • • •					
< 0.012	90	COFFMAN	92B	MRK3	e^+e^- 3.77 GeV

$\Gamma(\overline{K}^*(892)^0\pi^+\pi^-\text{total})/\Gamma(K^-\pi^+\pi^+\pi^-)$ Γ_{93}/Γ_{46}

This includes $\overline{K}^*(892)^0\rho^0$, *etc.* The next entry gives the specifically 3-body fraction. Unseen decay modes of the $\overline{K}^*(892)^0$ are included.

VALUE	DOCUMENT ID		TECN	COMMENT
0.30 ± 0.06 ± 0.03	ANJOS	92C	E691	γBe 90–260 GeV

$\Gamma(\overline{K}^*(892)^0\pi^+\pi^-\text{3-body})/\Gamma(K^-\pi^+\pi^+\pi^-)$ Γ_{94}/Γ_{46}

Unseen decay modes of the $\overline{K}^*(892)^0$ are included.

VALUE	DOCUMENT ID		TECN	COMMENT
0.19 ± 0.04 OUR FIT				
0.18 ± 0.04 OUR AVERAGE				
0.165 ± 0.03 ± 0.045	ANJOS	92C	E691	γBe 90–260 GeV
0.210 ± 0.027 ± 0.06	COFFMAN	92B	MRK3	e^+e^- 3.77 GeV

$\Gamma(K^-\pi^+\pi^+\pi^-\text{nonresonant})/\Gamma(K^-\pi^+\pi^+\pi^-)$ Γ_{54}/Γ_{46}

VALUE	DOCUMENT ID		TECN	COMMENT
0.233 ± 0.032 OUR AVERAGE				
0.23 ± 0.02 ± 0.03	ANJOS	92C	E691	γBe 90–260 GeV
0.242 ± 0.025 ± 0.06	COFFMAN	92B	MRK3	e^+e^- 3.77 GeV

$\Gamma(\overline{K}^0\pi^+\pi^-\pi^0)/\Gamma_{\text{total}}$ Γ_{55}/Γ

VALUE	EVTS	DOCUMENT ID		TECN	COMMENT
0.109 ± 0.013 OUR FIT					
0.103 ± 0.022 ± 0.025	140	COFFMAN	92B	MRK3	e^+e^- 3.77 GeV
• • • We do not use the following data for averages, fits, limits, etc. • • •					
$0.134\ ^{+0.032}_{-0.033}$	[58]	BARLAG	92C	ACCM	π^- Cu 230 GeV

[58] BARLAG 92C computes the branching fraction using topological normalization.

$\Gamma(\overline{K}^0\pi^+\pi^-\pi^0)/\Gamma(\overline{K}^0\pi^+\pi^-)$ Γ_{55}/Γ_{22}

VALUE	EVTS	DOCUMENT ID		TECN	COMMENT
1.82 ± 0.20 OUR FIT					
1.86 ± 0.23 OUR AVERAGE					
1.80 ± 0.20 ± 0.21	190	[59] ALBRECHT	92P	ARG	$e^+e^-\approx 10$ GeV
2.8 ± 0.8 ± 0.8	46	ANJOS	92C	E691	γBe 90–260 GeV
1.85 ± 0.26 ± 0.30	158	KINOSHITA	91	CLEO	$e^+e^-\sim 10.7$ GeV

[59] This value is calculated from numbers in Table 1 of ALBRECHT 92P.

$\Gamma(\overline{K}^0\eta)/\Gamma(K^-\pi^+)$ Γ_{81}/Γ_{20}

Unseen decay modes of the η are included.

VALUE	CL%	DOCUMENT ID		TECN	COMMENT
• • • We do not use the following data for averages, fits, limits, etc. • • •					
< 0.64	90	ALBRECHT	89D	ARG	e^+e^- 10 GeV

$\Gamma(\overline{K}^0\eta)/\Gamma(\overline{K}^0\pi^0)$ Γ_{81}/Γ_{21}

Unseen decay modes of the η are included.

VALUE	EVTS	DOCUMENT ID		TECN	COMMENT
0.33 ± 0.04 OUR FIT					
0.32 ± 0.04 ± 0.03	225	PROCARIO	93B	CLE2	$\eta\to\gamma\gamma$

$\Gamma(\overline{K}^0\eta)/\Gamma(\overline{K}^0\pi^+\pi^-)$ Γ_{81}/Γ_{22}

Unseen decay modes of the η are included.

VALUE	EVTS	DOCUMENT ID		TECN	COMMENT
0.128 ± 0.017 OUR FIT					
0.14 ± 0.02 ± 0.02	80	PROCARIO	93B	CLE2	$\eta\to\pi^+\pi^-\pi^0$

$\Gamma(\overline{K}^0\omega)/\Gamma(K^-\pi^+)$ Γ_{84}/Γ_{20}

Unseen decay modes of the ω are included.

VALUE	DOCUMENT ID		TECN	COMMENT
0.60 ± 0.09 OUR FIT				
1.00 ± 0.36 ± 0.20	ALBRECHT	89D	ARG	e^+e^- 10 GeV

$\Gamma(\overline{K}^0\omega)/\Gamma(\overline{K}^0\pi^+\pi^-)$ Γ_{84}/Γ_{22}

Unseen decay modes of the ω are included.

VALUE	EVTS	DOCUMENT ID		TECN	COMMENT
0.39 ± 0.06 OUR FIT					
0.36 ± 0.07 OUR AVERAGE					
$0.42 \pm 0.13\ ^{+0.06}_{-0.05}$		MURAMATSU	02	CLE2	$e^+e^-\approx 10$ GeV
0.29 ± 0.08 ± 0.05	16	[60] ALBRECHT	92P	ARG	$e^+e^-\approx 10$ GeV
0.54 ± 0.14 ± 0.16	40	KINOSHITA	91	CLEO	$e^+e^-\sim 10.7$ GeV

[60] This value is calculated from numbers in Table 1 of ALBRECHT 92P.

$\Gamma(\overline{K}^0\omega)/\Gamma(\overline{K}^0\pi^+\pi^-\pi^0)$ Γ_{84}/Γ_{55}

Unseen decay modes of the ω are included.

VALUE	DOCUMENT ID		TECN	COMMENT
0.212 ± 0.034 OUR FIT				
0.220 ± 0.048 ± 0.0116	COFFMAN	92B	MRK3	e^+e^- 3.77 GeV

$\Gamma(\overline{K}^0\eta'(958))/\Gamma(\overline{K}^0\pi^+\pi^-)$ Γ_{85}/Γ_{22}

Unseen decay modes of the $\eta'(958)$ are included.

VALUE	EVTS	DOCUMENT ID		TECN	COMMENT
0.32 ± 0.04 OUR AVERAGE					
0.31 ± 0.02 ± 0.04	594	PROCARIO	93B	CLE2	$\eta'\to\eta\pi^+\pi^-$, $\rho^0\gamma$
0.37 ± 0.13 ± 0.06	18	[61] ALBRECHT	92P	ARG	$e^+e^-\approx 10$ GeV

[61] This value is calculated from numbers in Table 1 of ALBRECHT 92P.

$\Gamma(K^*(892)^-\rho^+)/\Gamma(\overline{K}^0\pi^+\pi^-\pi^0)$ Γ_{103}/Γ_{55}

Unseen decay modes of the $K^*(892)^-$ are included.

VALUE	DOCUMENT ID		TECN	COMMENT
0.606 ± 0.188 ± 0.126	COFFMAN	92B	MRK3	e^+e^- 3.77 GeV

$\Gamma(K^*(892)^-\rho^+\text{longitudinal})/\Gamma(\overline{K}^0\pi^+\pi^-\pi^0)$ Γ_{104}/Γ_{55}

Unseen decay modes of the $K^*(892)^-$ are included.

VALUE	DOCUMENT ID		TECN	COMMENT
0.290 ± 0.111	COFFMAN	92B	MRK3	e^+e^- 3.77 GeV

$\Gamma(K^*(892)^-\rho^+\text{transverse})/\Gamma(\overline{K}^0\pi^+\pi^-\pi^0)$ Γ_{105}/Γ_{55}

Unseen decay modes of the $K^*(892)^-$ are included.

VALUE	DOCUMENT ID		TECN	COMMENT
0.317 ± 0.180	COFFMAN	92B	MRK3	e^+e^- 3.77 GeV

$\Gamma(K^*(892)^-\rho^+ P\text{-wave})/\Gamma_{\text{total}}$ Γ_{106}/Γ

Unseen decay modes of the $K^*(892)^-$ are included.

VALUE	CL%	DOCUMENT ID		TECN	COMMENT
< 0.015	90	[62] COFFMAN	92B	MRK3	e^+e^- 3.77 GeV

[62] Obtained using other $\overline{K}^*(892)\rho$ P-wave limits and isospin relations.

$\Gamma(\overline{K}^*(892)^0\rho^0\text{transverse})/\Gamma(\overline{K}^0\pi^+\pi^-\pi^0)$ Γ_{98}/Γ_{55}

Unseen decay modes of the $\overline{K}^*(892)^0$ are included.

VALUE	DOCUMENT ID		TECN	COMMENT
0.14 ± 0.05 OUR FIT				
0.126 ± 0.111	COFFMAN	92B	MRK3	e^+e^- 3.77 GeV

$\Gamma(\overline{K}^0 a_1(1260)^0)/\Gamma_{\text{total}}$ Γ_{88}/Γ

Unseen decay modes of the $a_1(1260)^+$ are included, assuming that the $a_1(1260)^+$ decays entirely to $\rho\pi$ [or at least to $(\pi\pi)_{I=1}\ \pi$].

VALUE	CL%	DOCUMENT ID		TECN	COMMENT
< 0.019	90	COFFMAN	92B	MRK3	e^+e^- 3.77 GeV

$\Gamma(K_1(1270)^-\pi^+)/\Gamma(\overline{K}^0\pi^+\pi^-\pi^0)$ Γ_{109}/Γ_{55}

Unseen decay modes of the $K_1(1270)^-$ are included.

VALUE	DOCUMENT ID		TECN	COMMENT
0.105 ± 0.028 OUR FIT				
0.10 ± 0.03	COFFMAN	92B	MRK3	e^+e^- 3.77 GeV

$\Gamma(\overline{K}_1(1400)^0\pi^0)/\Gamma_{\text{total}}$ Γ_{111}/Γ

VALUE	CL%	DOCUMENT ID		TECN	COMMENT
< 0.037	90	COFFMAN	92B	MRK3	e^+e^- 3.77 GeV

$\Gamma(\overline{K}^*(892)^0\pi^+\pi^-\text{3-body})/\Gamma(\overline{K}^0\pi^+\pi^-\pi^0)$ Γ_{94}/Γ_{55}

Unseen decay modes of the $\overline{K}^*(892)^0$ are included.

VALUE	DOCUMENT ID		TECN	COMMENT
0.130 ± 0.034 OUR FIT Error includes scale factor of 1.1.				
0.191 ± 0.105	COFFMAN	92B	MRK3	e^+e^- 3.77 GeV

$\Gamma(\overline{K}^0\pi^+\pi^-\pi^0\text{nonresonant})/\Gamma(\overline{K}^0\pi^+\pi^-\pi^0)$ Γ_{62}/Γ_{55}

VALUE	DOCUMENT ID		TECN	COMMENT
0.210 ± 0.147 ± 0.150	COFFMAN	92B	MRK3	e^+e^- 3.77 GeV

$\Gamma(K^-\pi^+\pi^0\pi^0)/\Gamma_{\text{total}}$ Γ_{63}/Γ

VALUE	EVTS	DOCUMENT ID		TECN	COMMENT
• • • We do not use the following data for averages, fits, limits, etc. • • •					
0.177 ± 0.029		[63] BARLAG	92C	ACCM	π^- Cu 230 GeV
0.149 ± 0.037 ± 0.030	24	[64] ADLER	88C	MRK3	e^+e^- 3.77 GeV
$0.209^{+0.074}_{-0.043} \pm 0.012$	9	[63] AGUILAR-...	87F	HYBR	πp, pp 360, 400 GeV

[63] AGUILAR-BENITEZ 87F and BARLAG 92C compute the branching fraction using topological normalization. They do not distinguish the presence of a third π^0, and thus are not included in the average.

[64] ADLER 88C uses an absolute normalization method finding this decay channel opposite a detected $\overline{D}^0 \to K^+\pi^-$ in pure $D\overline{D}$ events.

$\Gamma(K^-\pi^+\pi^+\pi^-\pi^0)/\Gamma(K^-\pi^+)$ Γ_{64}/Γ_{20}

VALUE	EVTS	DOCUMENT ID		TECN	COMMENT
1.06 ± 0.10 OUR FIT					
0.98 ± 0.11 ± 0.11	225	[65] ALBRECHT	92P	ARG	e^+e^- ≈ 10 GeV

[65] This value is calculated from numbers in Table 1 of ALBRECHT 92P.

$\Gamma(K^-\pi^+\pi^+\pi^-\pi^0)/\Gamma(K^-\pi^+\pi^+\pi^-)$ Γ_{64}/Γ_{46}

VALUE	EVTS	DOCUMENT ID		TECN	COMMENT
0.54 ± 0.05 OUR FIT					
0.56 ± 0.07 OUR AVERAGE					
$0.55 \pm 0.07^{+0.12}_{-0.09}$	167	KINOSHITA	91	CLEO	e^+e^- ~10.7 GeV
0.57 ± 0.06 ± 0.05	180	ANJOS	90D	E691	Photoproduction

$\Gamma(\overline{K}^*(892)^0\pi^+\pi^-\pi^0)/\Gamma(K^-\pi^+\pi^+\pi^-\pi^0)$ Γ_{118}/Γ_{64}

Unseen decay modes of the $\overline{K}^*(892)^0$ are included.

VALUE	DOCUMENT ID		TECN	COMMENT
0.45 ± 0.15 ± 0.15	ANJOS	90D	E691	Photoproduction

$\Gamma(\overline{K}^*(892)^0\eta)/\Gamma(K^-\pi^+)$ Γ_{119}/Γ_{20}

Unseen decay modes of the $\overline{K}^*(892)^0$ and η are included.

VALUE	EVTS	DOCUMENT ID		TECN	COMMENT
0.46 ± 0.12 OUR FIT					
$\mathbf{0.58 \pm 0.19^{+0.24}_{-0.28}}$	46	KINOSHITA	91	CLEO	e^+e^- ~10.7 GeV

$\Gamma(\overline{K}^*(892)^0\eta)/\Gamma(K^-\pi^+\pi^0)$ Γ_{119}/Γ_{34}

Unseen decay modes of the $\overline{K}^*(892)^0$ and η are included.

VALUE	EVTS	DOCUMENT ID		TECN	COMMENT
0.135 ± 0.034 OUR FIT					
0.13 ± 0.02 ± 0.03	214	PROCARIO	93B	CLE2	$\overline{K}^{*0}\eta \to K^-\pi^+/\gamma\gamma$

$\Gamma(K^-\pi^+\omega)/\Gamma(K^-\pi^+)$ Γ_{120}/Γ_{20}

Unseen decay modes of the ω are included.

VALUE	EVTS	DOCUMENT ID		TECN	COMMENT
0.78 ± 0.12 ± 0.10	99	[66] ALBRECHT	92P	ARG	e^+e^- ≈ 10 GeV

[66] This value is calculated from numbers in Table 1 of ALBRECHT 92P.

$\Gamma(\overline{K}^*(892)^0\omega)/\Gamma(K^-\pi^+)$ Γ_{121}/Γ_{20}

Unseen decay modes of the $\overline{K}^*(892)^0$ and ω are included.

VALUE	EVTS	DOCUMENT ID		TECN	COMMENT
0.28 ± 0.11 ± 0.04	17	[67] ALBRECHT	92P	ARG	e^+e^- ≈ 10 GeV

[67] This value is calculated from numbers in Table 1 of ALBRECHT 92P.

$\Gamma(\overline{K}^*(892)^0\omega)/\Gamma(K^-\pi^+\pi^+\pi^-\pi^0)$ Γ_{121}/Γ_{64}

Unseen decay modes of the $\overline{K}^*(892)^0$ and ω are included.

VALUE	CL%	DOCUMENT ID		TECN	COMMENT
• • • We do not use the following data for averages, fits, limits, etc. • • •					
< 0.44	90	[68] ANJOS	90D	E691	Photoproduction

[68] Recovered from the published limit, $\Gamma(\overline{K}^*(892)^0\omega)/\Gamma_{\text{total}}$, in order to make our normalization consistent.

$\Gamma(K^-\pi^+\eta'(958))/\Gamma(K^-\pi^+\pi^+\pi^-)$ Γ_{122}/Γ_{46}

Unseen decay modes of the $\eta'(958)$ are included.

VALUE	EVTS	DOCUMENT ID		TECN	COMMENT
0.093 ± 0.014 ± 0.019	286	PROCARIO	93B	CLE2	$\eta' \to \eta\pi^+\pi^-$, $\rho^0\gamma$

$\Gamma(\overline{K}^*(892)^0\eta'(958))/\Gamma(K^-\pi^+\eta'(958))$ $\Gamma_{123}/\Gamma_{122}$

Unseen decay modes of the $\overline{K}^*(892)^0$ are included.

VALUE	CL%	DOCUMENT ID		TECN
< 0.15	90	PROCARIO	93B	CLE2

$\Gamma(\overline{K}^0\pi^+\pi^+\pi^-\pi^-)/\Gamma(\overline{K}^0\pi^+\pi^-)$ Γ_{69}/Γ_{22}

VALUE	EVTS	DOCUMENT ID		TECN	COMMENT
0.107 ± 0.029 OUR AVERAGE	Error includes scale factor of 1.8. See the ideogram below.				
0.07 ± 0.02 ± 0.01	11	[69] ALBRECHT	92P	ARG	e^+e^- ≈ 10 GeV
0.149 ± 0.026	56	AMMAR	91	CLEO	e^+e^- ≈ 10.5 GeV
0.18 ± 0.07 ± 0.04	6	ANJOS	90D	E691	Photoproduction

[69] This value is calculated from numbers in Table 1 of ALBRECHT 92P.

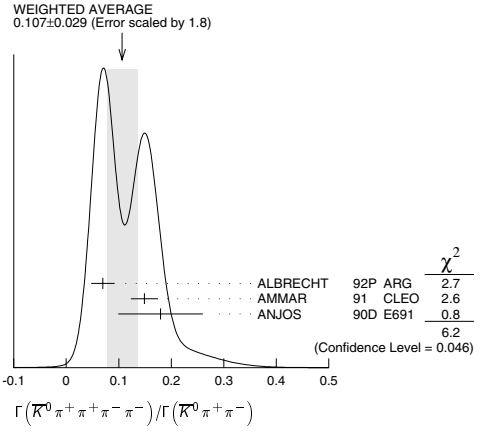

$\Gamma(\overline{K}^0\pi^+\pi^-\pi^0\pi^0(\pi^0))/\Gamma_{\text{total}}$ Γ_{70}/Γ

VALUE	EVTS	DOCUMENT ID		TECN	COMMENT
• • • We do not use the following data for averages, fits, limits, etc. • • •					
$0.106^{+0.073}_{-0.029} \pm 0.006$	4	[70] AGUILAR-...	87F	HYBR	πp, pp 360, 400 GeV

[70] AGUILAR-BENITEZ 87F computes the branching fraction using topological normalization, and does not distinguish the presence of a third π^0.

$\Gamma(\overline{K}^0 K^+ K^-)/\Gamma(\overline{K}^0\pi^+\pi^-)$ $\Gamma_{71}/\Gamma_{22} = (\Gamma_{73}+\frac{1}{2}\Gamma_{86})/\Gamma_{22}$

VALUE	EVTS	DOCUMENT ID		TECN	COMMENT
0.172±0.014 OUR FIT					
0.178±0.019 OUR AVERAGE					
0.20 ±0.05 ±0.04	47	FRABETTI	92B	E687	γBe $\overline{E}_\gamma$= 221 GeV
0.170±0.022	136	AMMAR	91	CLEO	$e^+e^-\approx$ 10.5 GeV
0.24 ±0.08		BEBEK	86	CLEO	e^+e^- near $\Upsilon(4S)$
0.185±0.055	52	ALBRECHT	85B	ARG	e^+e^- 10 GeV

$\Gamma(\overline{K}^0\phi)/\Gamma(\overline{K}^0\pi^+\pi^-)$ Γ_{86}/Γ_{22}

Unseen decay modes of the ϕ are included.

VALUE	EVTS	DOCUMENT ID		TECN	COMMENT
0.158±0.016 OUR FIT					
0.156±0.017 OUR AVERAGE					
0.13 ±0.06 ±0.02	13	FRABETTI	92B	E687	γBe $\overline{E}_\gamma$= 221 GeV
0.163±0.023	63	AMMAR	91	CLEO	$e^+e^-\approx$ 10.5 GeV
0.155±0.033	56	ALBRECHT	87E	ARG	e^+e^- 10 GeV
0.14 ±0.05	29	BEBEK	86	CLEO	e^+e^- near $\Upsilon(4S)$
• • • We do not use the following data for averages, fits, limits, etc. • • •					
0.186±0.052	26	ALBRECHT	85B	ARG	See ALBRECHT 87E

$\Gamma(\overline{K}^0 K^+ K^-\text{non-}\phi)/\Gamma(\overline{K}^0\pi^+\pi^-)$ Γ_{73}/Γ_{22}

VALUE	EVTS	DOCUMENT ID		TECN	COMMENT
0.093±0.014 OUR FIT					
0.088±0.019 OUR AVERAGE					
0.11 ±0.04 ±0.03	20	FRABETTI	92B	E687	γBe $\overline{E}_\gamma$= 221 GeV
0.084±0.020		ALBRECHT	87E	ARG	e^+e^- 10 GeV

$\Gamma(K^0_S K^0_S K^0_S)/\Gamma(\overline{K}^0\pi^+\pi^-)$ Γ_{74}/Γ_{22}

VALUE	EVTS	DOCUMENT ID		TECN	COMMENT
0.0154±0.0025 OUR AVERAGE					
0.0139±0.0019±0.0024	61	ASNER	96B	CLE2	$e^+e^-\approx\Upsilon(4S)$
0.035 ±0.012 ±0.006	10	FRABETTI	94J	E687	γBe $\overline{E}_\gamma$=220 GeV
0.016 ±0.005	22	AMMAR	91	CLEO	$e^+e^-\approx$ 10.5 GeV
0.017 ±0.007 ±0.005	5	ALBRECHT	90C	ARG	$e^+e^-\approx$ 10 GeV

$\Gamma(K^+K^-K^-\pi^+)/\Gamma(K^-\pi^+\pi^+\pi^-)$ Γ_{75}/Γ_{46}

VALUE	EVTS	DOCUMENT ID		TECN	COMMENT
0.0027 ±0.0004 OUR AVERAGE		Error includes scale factor of 1.1.			
0.00257±0.00034±0.00024	143	LINK	03G	FOCS	γ nucleus, $\overline{E}_\gamma\approx$ 180 GeV
0.0054 ±0.0016 ±0.0008	18	AITALA	01D	E791	π^- nucleus, 500 GeV
0.0028 ±0.0007 ±0.0001	20	FRABETTI	95C	E687	γBe, $\overline{E}_\gamma\approx$ 200 GeV

$\Gamma(\phi\overline{K}^*(892)^0)/\Gamma(K^+K^-K^-\pi^+)$ Γ_{126}/Γ_{75}

Unseen decay modes of the ϕ and $\overline{K}^*(892)^0$ are included.

VALUE	DOCUMENT ID		TECN	COMMENT
1.46±0.18±0.03	LINK	03G	FOCS	γ nucleus, $\overline{E}_\gamma\approx$ 180 GeV

$\Gamma(K^-\pi^+\phi)/\Gamma(K^+K^-K^-\pi^+)$ Γ_{124}/Γ_{75}

Unseen decay modes of the ϕ are included.

VALUE	EVTS	DOCUMENT ID		TECN	COMMENT
0.37±0.12±0.08		LINK	03G	FOCS	γ nucleus, $\overline{E}_\gamma\approx$ 180 GeV
• • • We do not use the following data for averages, fits, limits, etc. • • •					
1.4 ±0.6	13	[71] AITALA	01D	E791	π^- nucleus, 500 GeV

[71] This AITALA 01D result is from a projection fit, not a full amplitude analysis.

$\Gamma(K^+K^-\overline{K}^*(892)^0)/\Gamma(K^+K^-K^-\pi^+)$ Γ_{125}/Γ_{75}

Unseen decay modes of the $\overline{K}^*(892)^0$ are included.

VALUE	DOCUMENT ID		TECN	COMMENT
0.30±0.11±0.03	LINK	03G	FOCS	γ nucleus, $\overline{E}_\gamma\approx$ 180 GeV

$\Gamma(K^+K^-K^-\pi^+\text{nonresonant})/\Gamma(K^+K^-K^-\pi^+)$ Γ_{79}/Γ_{75}

VALUE	DOCUMENT ID		TECN	COMMENT
0.15±0.06±0.02	LINK	03G	FOCS	γ nucleus, $\overline{E}_\gamma\approx$ 180 GeV

$\Gamma(K^+K^-\overline{K}^0\pi^0)/\Gamma_{\text{total}}$ Γ_{80}/Γ

VALUE	DOCUMENT ID		TECN	COMMENT
• • • We do not use the following data for averages, fits, limits, etc. • • •				
$0.0072^{+0.0048}_{-0.0035}$	[72] BARLAG	92C	ACCM	π^- Cu 230 GeV

[72] BARLAG 92C computes the branching fraction using topological normalization.

Pionic modes

$\Gamma(\pi^+\pi^-)/\Gamma(K^-\pi^+)$ Γ_{127}/Γ_{20}

VALUE	EVTS	DOCUMENT ID		TECN	COMMENT
0.0362±0.0010 OUR AVERAGE					
0.0353±0.0012±0.0006	3453	LINK	03	FOCS	γ nucleus, $\overline{E}_\gamma\approx$ 180 GeV
0.0351±0.0016±0.0017	710	CSORNA	02	CLE2	$e^+e^-\approx\Upsilon(4S)$
0.040 ±0.002 ±0.003	2043	AITALA	98C	E791	π^- nucleus, 500 GeV
0.043 ±0.007 ±0.003	177	FRABETTI	94C	E687	γBe $\overline{E}_\gamma$= 220 GeV
0.0348±0.0030±0.0023	227	SELEN	93	CLE2	$e^+e^-\approx\Upsilon(4S)$
0.055 ±0.008 ±0.005	120	ANJOS	91D	E691	Photoproduction
0.050 ±0.007 ±0.005	110	ALEXANDER	90	CLEO	e^+e^- 10.5–11 GeV
• • • We do not use the following data for averages, fits, limits, etc. • • •					
0.048 ±0.013 ±0.008	51	ADAMOVICH	92	OMEG	π^- 340 GeV
0.040 ±0.007 ±0.006	57	ALBRECHT	90C	ARG	$e^+e^-\approx$ 10 GeV
0.033 ±0.010 ±0.006	39	BALTRUSAIT...	85E	MRK3	e^+e^- 3.77 GeV
0.033 ±0.015		ABRAMS	79D	MRK2	e^+e^- 3.77 GeV

$\Gamma(\pi^0\pi^0)/\Gamma(K^-\pi^+)$ Γ_{128}/Γ_{20}

VALUE	EVTS	DOCUMENT ID		TECN	COMMENT
0.022±0.004±0.004	40	SELEN	93	CLE2	$e^+e^-\approx\Upsilon(4S)$

$\Gamma(\pi^+\pi^-\pi^0)/\Gamma_{\text{total}}$ Γ_{129}/Γ

VALUE	EVTS	DOCUMENT ID		TECN	COMMENT
0.011 ±0.004 ±0.002	10	[73] BALTRUSAIT...	85E	MRK3	e^+e^- 3.77 GeV
• • • We do not use the following data for averages, fits, limits, etc. • • •					
$0.0390^{+0.0100}_{-0.0095}$		[74] BARLAG	92C	ACCM	π^- Cu 230 GeV

[73] All the BALTRUSAITIS 85E events are consistent with $\rho^0\pi^0$.

[74] BARLAG 92C computes the branching fraction using topological normalization. Possible contamination by extra π^0's may partly explain the unexpectedly large value.

$\Gamma(\pi^+\pi^+\pi^-\pi^-)/\Gamma(K^-\pi^+\pi^+\pi^-)$ Γ_{130}/Γ_{46}

VALUE	EVTS	DOCUMENT ID		TECN	COMMENT
0.098±0.006 OUR AVERAGE					
0.095±0.007±0.002	814	FRABETTI	95C	E687	γBe, $\overline{E}_\gamma\approx$ 200 GeV
0.115±0.023±0.016	64	ADAMOVICH	92	OMEG	π^- 340 GeV
0.108±0.024±0.008	79	FRABETTI	92	E687	γBe
0.102±0.013	345	[75] AMMAR	91	CLEO	$e^+e^-\approx$ 10.5 GeV
0.096±0.018±0.007	66	ANJOS	91	E691	γBe 80–240 GeV

[75] AMMAR 91 finds 1.25 ± 0.25 ± 0.25 ρ^0's per $\pi^+\pi^+\pi^-\pi^-$ decay, but can't untangle the resonant substructure ($\rho^0\rho^0$, $a_1^\pm\pi^\mp$, $\rho^0\pi^+\pi^-$).

$\Gamma(\pi^+\pi^+\pi^-\pi^-\pi^0)/\Gamma_{\text{total}}$ Γ_{131}/Γ

VALUE	DOCUMENT ID		TECN	COMMENT
• • • We do not use the following data for averages, fits, limits, etc. • • •				
$0.0192^{+0.0041}_{-0.0038}$	[76] BARLAG	92C	ACCM	π^- Cu 230 GeV

[76] BARLAG 92C computes the branching fraction using topological normalization.

$\Gamma(\pi^+\pi^+\pi^+\pi^-\pi^-\pi^-)/\Gamma_{\text{total}}$ Γ_{132}/Γ

VALUE	DOCUMENT ID		TECN	COMMENT
• • • We do not use the following data for averages, fits, limits, etc. • • •				
0.0004±0.0003	[77] BARLAG	92C	ACCM	π^- Cu 230 GeV

[77] BARLAG 92C computes the branching fraction using topological normalization.

Hadronic modes with a $K\overline{K}$ pair

$\Gamma(K^+K^-)/\Gamma(K^-\pi^+)$ Γ_{133}/Γ_{20}

VALUE	EVTS	DOCUMENT ID		TECN	COMMENT
$0.1023^{+0.0022}_{-0.0027}$ OUR FIT		Error includes scale factor of 1.4.			
0.1023±0.0021 OUR AVERAGE		Error includes scale factor of 1.3. See the ideogram below.			
0.0993±0.0014±0.0014	11k	LINK	03	FOCS	γ nucleus, $\overline{E}_\gamma\approx$ 180 GeV
0.1040±0.0033±0.0027	1900	CSORNA	02	CLE2	$e^+e^-\approx\Upsilon(4S)$
0.109 ±0.003 ±0.003	3317	AITALA	98C	E791	π^- nucleus, 500 GeV
0.116 ±0.007 ±0.007	1102	ASNER	96B	CLE2	$e^+e^-\approx\Upsilon(4S)$
0.109 ±0.007 ±0.009	581	FRABETTI	94C	E687	γBe $\overline{E}_\gamma$= 220 GeV
0.107 ±0.010 ±0.009	193	ANJOS	91D	E691	Photoproduction
0.117 ±0.010 ±0.007	249	ALEXANDER	90	CLEO	e^+e^- 10.5–11 GeV
• • • We do not use the following data for averages, fits, limits, etc. • • •					
0.107 ±0.029 ±0.015	103	ADAMOVICH	92	OMEG	π^- 340 GeV
0.138 ±0.027 ±0.010	155	FRABETTI	92	E687	γBe
0.16 ±0.05	34	ALVAREZ	91B	NA14	Photoproduction
0.10 ±0.02 ±0.01	131	ALBRECHT	90C	ARG	$e^+e^-\approx$ 10 GeV
0.122 ±0.018 ±0.012	118	BALTRUSAIT...	85E	MRK3	e^+e^- 3.77 GeV
0.113 ±0.030		ABRAMS	79D	MRK2	e^+e^- 3.77 GeV

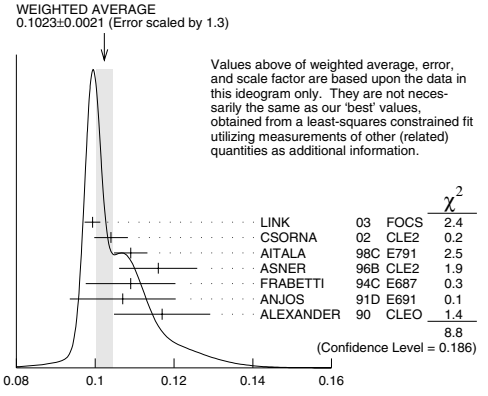

$\Gamma(K^+K^-)/\Gamma(K^-\pi^+)$

$\Gamma(K^+K^-)/\Gamma(\pi^+\pi^-)$ $\Gamma_{133}/\Gamma_{127}$

The unused results here are redundant with $\Gamma(K^+K^-)/\Gamma(K^-\pi^+)$ and $\Gamma(\pi^+\pi^-)/\Gamma(K^-\pi^+)$ measurements by the same experiments.

VALUE	EVTS	DOCUMENT ID	TECN	COMMENT
• • • We do not use the following data for averages, fits, limits, etc. • • •				
2.81±0.10±0.06		LINK 03	FOCS	γ nucleus, $\overline{E}_\gamma \approx$ 180 GeV
2.96±0.16±0.15	710	CSORNA 02	CLE2	$e^+e^- \approx \Upsilon(4S)$
2.75±0.15±0.16		AITALA 98C	E791	π^- nucleus, 500 GeV
2.53±0.46±0.19		FRABETTI 94C	E687	γBe $\overline{E}_\gamma$= 220 GeV
2.23±0.81±0.46		ADAMOVICH 92	OMEG	π^- 340 GeV
1.95±0.34±0.22		ANJOS 91D	E691	Photoproduction
2.5 ±0.7		ALBRECHT 90C	ARG	$e^+e^- \approx$ 10 GeV
2.35±0.37±0.28		ALEXANDER 90	CLEO	e^+e^- 10.5–11 GeV

$\Gamma(K^0\overline{K}^0)/\Gamma(\overline{K}^0\pi^+\pi^-)$ Γ_{134}/Γ_{22}

VALUE	EVTS	DOCUMENT ID	TECN	COMMENT
0.0119±0.0033 OUR FIT Error includes scale factor of 1.3.				
0.0117±0.0033 OUR AVERAGE Error includes scale factor of 1.3. See the ideogram below.				
0.0101±0.0022±0.0016	26	ASNER 96B	CLE2	$e^+e^- \approx \Upsilon(4S)$
0.039 ±0.013 ±0.013	20	FRABETTI 94J	E687	γBe $\overline{E}_\gamma$=220 GeV
0.021 $^{+0.011}_{-0.008}$ ±0.002	5	ALEXANDER 90	CLEO	e^+e^- 10.5–11 GeV

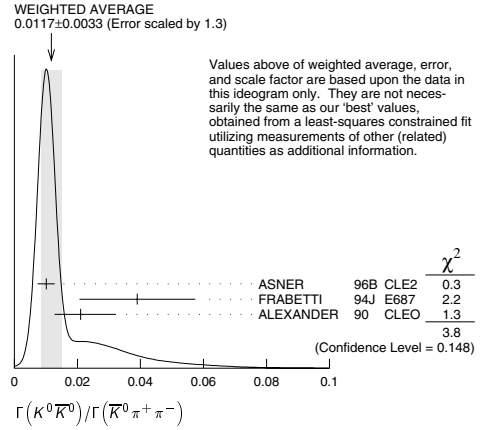

$\Gamma(K^0\overline{K}^0)/\Gamma(\overline{K}^0\pi^+\pi^-)$

$\Gamma(K^0\overline{K}^0)/\Gamma(K^+K^-)$ $\Gamma_{134}/\Gamma_{133}$

VALUE	EVTS	DOCUMENT ID	TECN	COMMENT
0.18±0.05 OUR FIT Error includes scale factor of 1.3.				
0.24±0.16	4	[78] CUMALAT 88	SPEC	nN 0–800 GeV

[78] Includes a correction communicated to us by the authors of CUMALAT 88.

$\Gamma(K^0K^-\pi^+)/\Gamma(K^-\pi^+)$ Γ_{135}/Γ_{20}

VALUE	DOCUMENT ID	TECN	COMMENT
0.183±0.027 OUR FIT			
0.16 ±0.06	[79] ANJOS 91	E691	γBe 80–240 GeV

[79] The factor 100 at the top of column 2 of Table I of ANJOS 91 should be omitted.

$\Gamma(K^0K^-\pi^+)/\Gamma(\overline{K}^0\pi^+\pi^-)$ Γ_{135}/Γ_{22}

VALUE	EVTS	DOCUMENT ID	TECN	COMMENT
0.116±0.017 OUR FIT Error includes scale factor of 1.1.				
0.119±0.021 OUR AVERAGE Error includes scale factor of 1.3.				
0.108±0.019	61	AMMAR 91	CLEO	$e^+e^- \approx$ 10.5 GeV
0.16 ±0.03 ±0.02	39	ALBRECHT 90C	ARG	$e^+e^- \approx$ 10 GeV

$\Gamma(\overline{K}^*(892)^0K^0)/\Gamma(\overline{K}^0\pi^+\pi^-)$ Γ_{155}/Γ_{22}

Unseen decay modes of the $\overline{K}^*(892)^0$ are included.

VALUE	CL%	DOCUMENT ID	TECN	COMMENT
<0.029	90	AMMAR 91	CLEO	$e^+e^- \approx$ 10.5 GeV
• • • We do not use the following data for averages, fits, limits, etc. • • •				
<0.03	90	ALBRECHT 90C	ARG	$e^+e^- \approx$ 10 GeV

$\Gamma(K^*(892)^+K^-)/\Gamma(K^-\pi^+)$ Γ_{156}/Γ_{20}

Unseen decay modes of the $K^*(892)^+$ are included.

VALUE	DOCUMENT ID	TECN	COMMENT
0.100±0.021 OUR FIT			
0.16 $^{+0.08}_{-0.06}$	[80] ANJOS 91	E691	γBe 80–240 GeV

[80] The factor 100 at the top of column 2 of Table I of ANJOS 91 should be omitted.

$\Gamma(K^*(892)^+K^-)/\Gamma(\overline{K}^0\pi^+\pi^-)$ Γ_{156}/Γ_{22}

Unseen decay modes of the $K^*(892)^+$ are included.

VALUE	EVTS	DOCUMENT ID	TECN	COMMENT
0.064±0.013 OUR FIT				
0.058±0.014 OUR AVERAGE				
0.064±0.018	23	AMMAR 91	CLEO	$e^+e^- \approx$ 10.5 GeV
0.05 ±0.02 ±0.01	15	ALBRECHT 90C	ARG	$e^+e^- \approx$ 10 GeV

$\Gamma(K^0K^-\pi^+\text{nonresonant})/\Gamma(K^-\pi^+)$ Γ_{138}/Γ_{20}

VALUE	DOCUMENT ID	TECN	COMMENT
0.06±0.06	[81] ANJOS 91	E691	γBe 80–240 GeV

[81] The factor 100 at the top of column 2 of Table I of ANJOS 91 should be omitted.

$\Gamma(\overline{K}^0K^+\pi^-)/\Gamma(K^-\pi^+)$ Γ_{139}/Γ_{20}

VALUE	DOCUMENT ID	TECN	COMMENT
0.139±0.027 OUR FIT			
0.10 ±0.05	[82] ANJOS 91	E691	γBe 80–240 GeV

[82] The factor 100 at the top of column 2 of Table I of ANJOS 91 should be omitted.

$\Gamma(\overline{K}^0K^+\pi^-)/\Gamma(\overline{K}^0\pi^+\pi^-)$ Γ_{139}/Γ_{22}

VALUE	EVTS	DOCUMENT ID	TECN	COMMENT
0.088±0.017 OUR FIT				
0.098±0.020	55	AMMAR 91	CLEO	$e^+e^- \approx$ 10.5 GeV

$\Gamma(K^*(892)^0\overline{K}^0)/\Gamma(\overline{K}^0\pi^+\pi^-)$ Γ_{157}/Γ_{22}

Unseen decay modes of the $K^*(892)^0$ are included.

VALUE	CL%	DOCUMENT ID	TECN	COMMENT
<0.015	90	AMMAR 91	CLEO	$e^+e^- \approx$ 10.5 GeV

$\Gamma(K^*(892)^-K^+)/\Gamma(\overline{K}^0\pi^+\pi^-)$ Γ_{158}/Γ_{22}

Unseen decay modes of the $K^*(892)^-$ are included.

VALUE	EVTS	DOCUMENT ID	TECN	COMMENT
0.034±0.019	12	AMMAR 91	CLEO	$e^+e^- \approx$ 10.5 GeV

$\Gamma(\overline{K}^0K^+\pi^-\text{nonresonant})/\Gamma(K^-\pi^+)$ Γ_{142}/Γ_{20}

VALUE	DOCUMENT ID	TECN	COMMENT
0.10 $^{+0.06}_{-0.05}$	[83] ANJOS 91	E691	γBe 80–240 GeV

[83] The factor 100 at the top of column 2 of Table I of ANJOS 91 should be omitted.

$\Gamma(K^+K^-\pi^0)/\Gamma(K^-\pi^+\pi^0)$ Γ_{143}/Γ_{34}

VALUE	EVTS	DOCUMENT ID	TECN	COMMENT
0.0095±0.0026	151	ASNER 96B	CLE2	$e^+e^- \approx \Upsilon(4S)$

$\Gamma(K^0_SK^0_S\pi^0)/\Gamma_{\text{total}}$ Γ_{144}/Γ

VALUE	DOCUMENT ID	TECN	COMMENT
<0.00059	ASNER 96B	CLE2	$e^+e^- \approx \Upsilon(4S)$

$\Gamma(\phi\pi^0)/\Gamma_{\text{total}}$ Γ_{159}/Γ

VALUE	CL%	DOCUMENT ID	TECN	COMMENT
• • • We do not use the following data for averages, fits, limits, etc. • • •				
<0.0014	90	ALBRECHT 94I	ARG	$e^+e^-\approx$ 10 GeV

$\Gamma(\phi\pi^0)/\Gamma(K^+K^-)$ $\Gamma_{159}/\Gamma_{133}$

VALUE	EVTS	DOCUMENT ID	TECN	COMMENT
0.194±0.006±0.009	1254	TAJIMA 04	BELL	e^+e^- at $\Upsilon(4S)$

$\Gamma(\phi\eta)/\Gamma_{\text{total}}$ Γ_{160}/Γ

VALUE	CL%	DOCUMENT ID	TECN	COMMENT
• • • We do not use the following data for averages, fits, limits, etc. • • •				
<0.0028	90	ALBRECHT 94I	ARG	$e^+e^-\approx$ 10 GeV

$\Gamma(\phi\eta)/\Gamma(K^+K^-)$ $\Gamma_{160}/\Gamma_{133}$

VALUE (units 10^{-2})	EVTS	DOCUMENT ID		TECN	COMMENT
3.59 ± 1.14 ± 0.18	31	TAJIMA	04	BELL	e^+e^- at $\Upsilon(4S)$

$\Gamma(\phi\omega)/\Gamma_{\text{total}}$ Γ_{161}/Γ

VALUE	CL%	DOCUMENT ID		TECN	COMMENT
< 0.0021	90	ALBRECHT	94I	ARG	$e^+e^-\approx 10$ GeV

$\Gamma(K^+K^-\pi^+\pi^-)/\Gamma(K^-\pi^+\pi^+\pi^-)$ Γ_{145}/Γ_{46}

VALUE	EVTS	DOCUMENT ID		TECN	COMMENT
0.0334 ± 0.0028 OUR AVERAGE					
0.0313 ± 0.0037 ± 0.0036	136	AITALA	98D	E791	π^- nucleus, 500 GeV
0.035 ± 0.004 ± 0.002	244	FRABETTI	95C	E687	γ Be, $\overline{E}_\gamma \approx 200$ GeV
0.041 ± 0.007 ± 0.005	114	ALBRECHT	94I	ARG	$e^+e^-\approx 10$ GeV
0.0314 ± 0.010	89	AMMAR	91	CLEO	$e^+e^-\approx 10.5$ GeV
$0.028\ ^{+0.008}_{-0.007}$		ANJOS	91	E691	γ Be 80–240 GeV

$\Gamma(\phi\pi^+\pi^-)/\Gamma(K^-\pi^+\pi^+\pi^-)$ Γ_{162}/Γ_{46}

Unseen decay modes of the ϕ are included.

VALUE	EVTS	DOCUMENT ID		TECN	COMMENT
0.014 ± 0.004 OUR AVERAGE		Error includes scale factor of 1.5. See the ideogram below.			
0.011 ± 0.003		FRABETTI	95C	E687	γ Be, $\overline{E}_\gamma \approx 200$ GeV
0.020 ± 0.006 ± 0.005	28	ALBRECHT	94I	ARG	$e^+e^-\approx 10$ GeV
0.024 ± 0.006	34	[84] AMMAR	91	CLEO	$e^+e^-\approx 10.5$ GeV
• • • We do not use the following data for averages, fits, limits, etc. • • •					
$0.0076\ ^{+0.0066}_{-0.0049}$	3	ANJOS	91	E691	γ Be 80–240 GeV

[84] AMMAR 91 measures $\phi\rho^0$, but notes that $\phi\rho^0$ dominates $\phi\pi^+\pi^-$. We put the measurement here to keep from having more $\phi\rho^0$ than $\phi\pi^+\pi^-$.

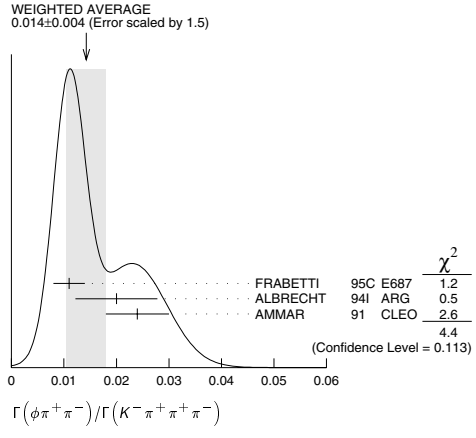

$\Gamma(\phi\rho^0)/\Gamma(K^-\pi^+\pi^+\pi^-)$ Γ_{163}/Γ_{46}

Unseen decay modes of the ϕ are included.

VALUE	EVTS	DOCUMENT ID		TECN	COMMENT
0.008 ± 0.004 OUR AVERAGE		Error includes scale factor of 1.5. See the ideogram below.			
0.02 ± 0.009 ± 0.008		AITALA	98D	E791	π^- nucleus, 500 GeV
0.005 ± 0.003		FRABETTI	95C	E687	γ Be, $\overline{E}_\gamma \approx 200$ GeV
0.020 ± 0.006 ± 0.005	28	ALBRECHT	94I	ARG	$e^+e^-\approx 10$ GeV

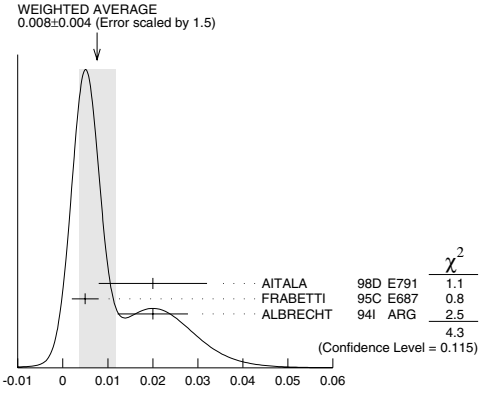

$\Gamma(\phi\pi^+\pi^-\text{3-body})/\Gamma(K^-\pi^+\pi^+\pi^-)$ Γ_{164}/Γ_{46}

Unseen decay modes of the ϕ are included.

VALUE	CL%	DOCUMENT ID		TECN	COMMENT
0.009 ± 0.004 ± 0.005		AITALA	98D	E791	π^- nucleus, 500 GeV
• • • We do not use the following data for averages, fits, limits, etc. • • •					
< 0.006	90	FRABETTI	95C	E687	γ Be, $\overline{E}_\gamma \approx 200$ GeV

$\Gamma(K^+K^-\rho^0\text{3-body})/\Gamma(K^-\pi^+\pi^+\pi^-)$ Γ_{148}/Γ_{46}

VALUE	DOCUMENT ID		TECN	COMMENT
0.012 ± 0.003	FRABETTI	95C	E687	γ Be, $\overline{E}_\gamma \approx 200$ GeV

$\Gamma(K^*(892)^0K^-\pi^+ + \text{c.c.})/\Gamma(K^-\pi^+\pi^+\pi^-)$ Γ_{165}/Γ_{46}

Unseen decay modes of the $K^*(892)^0$ are included.

VALUE	CL%	DOCUMENT ID		TECN	COMMENT
< 0.01	90	[85] AITALA	98D	E791	π^- nucleus, 500 GeV
• • • We do not use the following data for averages, fits, limits, etc. • • •					
< 0.017	90	[85] FRABETTI	95C	E687	γ Be, $\overline{E}_\gamma \approx 200$ GeV
$0.010\ ^{+0.016}_{-0.010}$		ANJOS	91	E691	γ Be 80–240 GeV

[85] These upper limits are in conflict with values in the next two data blocks.

$\Gamma(K^*(892)^0K^-\pi^+)/\Gamma(K^-\pi^+\pi^+\pi^-)$ Γ_{166}/Γ_{46}

The $K^{*0}K^-\pi^+$ and $\overline{K}^{*0}K^+\pi^-$ modes are distinguished by the charge of the pion in $D^*(2010)^\pm \to D^0\pi^\pm$ decays. Unseen decay modes of the $K^*(892)^0$ are included.

VALUE	EVTS	DOCUMENT ID		TECN	COMMENT
• • • We do not use the following data for averages, fits, limits, etc. • • •					
0.043 ± 0.014 ± 0.009	55	[86] ALBRECHT	94I	ARG	$e^+e^-\approx 10$ GeV

[86] This ALBRECHT 94I value is in conflict with upper limits given above.

$\Gamma(\overline{K}^*(892)^0K^+\pi^-)/\Gamma(K^-\pi^+\pi^+\pi^-)$ Γ_{167}/Γ_{46}

The $K^{*0}K^-\pi^+$ and $\overline{K}^{*0}K^+\pi^-$ modes are distinguished by the charge of the pion in $D^*(2010)^\pm \to D^0\pi^\pm$ decays. Unseen decay modes of the $\overline{K}^*(892)^0$ are included.

VALUE	EVTS	DOCUMENT ID		TECN	COMMENT
• • • We do not use the following data for averages, fits, limits, etc. • • •					
0.023 ± 0.013 ± 0.009	30	[87] ALBRECHT	94I	ARG	$e^+e^-\approx 10$ GeV

[87] This ALBRECHT 94I value is in conflict with upper limits given above.

$\Gamma(K^*(892)^0\overline{K}^*(892)^0)/\Gamma(K^-\pi^+\pi^+\pi^-)$ Γ_{168}/Γ_{46}

Unseen decay modes of the $K^*(892)^0$ and $\overline{K}^*(892)^0$ are included.

VALUE	CL%	EVTS	DOCUMENT ID		TECN	COMMENT
0.018 ± 0.007 OUR AVERAGE			Error includes scale factor of 1.2.			
0.016 ± 0.006			FRABETTI	95C	E687	γ Be, $\overline{E}_\gamma \approx 200$ GeV
$0.036\ ^{+0.020}_{-0.016}$		11	ANJOS	91	E691	γ Be 80–240 GeV
• • • We do not use the following data for averages, fits, limits, etc. • • •						
< 0.02	90		AITALA	98D	E791	π^- nucleus, 500 GeV
< 0.033	90		[88] AMMAR	91	CLEO	$e^+e^-\approx 10.5$ GeV

[88] A corrected value (G. Moneti, private communication).

$\Gamma(K^+K^-\pi^+\pi^-\text{non-}\phi)/\Gamma_{\text{total}}$ Γ_{151}/Γ

VALUE	DOCUMENT ID		TECN	COMMENT
• • • We do not use the following data for averages, fits, limits, etc. • • •				
0.0017 ± 0.0005	[89] BARLAG	92C	ACCM	π^- Cu 230 GeV

[89] BARLAG 92C computes the branching fraction using topological normalization.

$\Gamma(K^+K^-\pi^+\pi^-\text{ nonresonant})/\Gamma(K^-\pi^+\pi^+\pi^-)$ Γ_{152}/Γ_{46}

VALUE	CL%	DOCUMENT ID		TECN	COMMENT
< 0.011	90	FRABETTI	95C	E687	γBe, $\overline{E}_\gamma \approx 200$ GeV
• • • We do not use the following data for averages, fits, limits, etc. • • •					
$0.001^{+0.011}_{-0.001}$		ANJOS	91	E691	γBe 80–240 GeV

$\Gamma(K^0\overline{K}^0\pi^+\pi^-)/\Gamma(\overline{K}^0\pi^+\pi^-)$ Γ_{153}/Γ_{22}

VALUE	EVTS	DOCUMENT ID		TECN	COMMENT
0.126 ± 0.038 ± 0.030	25	ALBRECHT	94I	ARG	$e^+e^- \approx 10$ GeV

$\Gamma(K^+K^-\pi^+\pi^-\pi^0)/\Gamma_{\text{total}}$ Γ_{154}/Γ

VALUE	DOCUMENT ID		TECN	COMMENT
0.0031 ± 0.0020	[90] BARLAG	92C	ACCM	π^- Cu 230 GeV

[90] BARLAG 92C computes the branching fraction using topological normalization.

Radiative modes

$\Gamma(\rho^0\gamma)/\Gamma_{\text{total}}$ Γ_{169}/Γ

VALUE	CL%	DOCUMENT ID		TECN
< 2.4 × 10⁻⁴	90	ASNER	98	CLE2

$\Gamma(\omega\gamma)/\Gamma_{\text{total}}$ Γ_{170}/Γ

VALUE	CL%	DOCUMENT ID		TECN
< 2.4 × 10⁻⁴	90	ASNER	98	CLE2

$\Gamma(\phi\gamma)/\Gamma_{\text{total}}$ Γ_{171}/Γ

VALUE	CL%	DOCUMENT ID		TECN
• • • We do not use the following data for averages, fits, limits, etc. • • •				
< 1.9 × 10⁻⁴	90	ASNER	98	CLE2

$\Gamma(\phi\gamma)/\Gamma(K^+K^-)$ $\Gamma_{171}/\Gamma_{133}$

VALUE (units 10^{-3})	EVTS	DOCUMENT ID		TECN	COMMENT
$\mathbf{6.31^{+1.70}_{-1.48}{}^{+0.30}_{-0.36}}$	28	TAJIMA	04	BELL	e^+e^- at $\Upsilon(4S)$

$\Gamma(\overline{K}^*(892)^0\gamma)/\Gamma_{\text{total}}$ Γ_{172}/Γ

VALUE	CL%	DOCUMENT ID		TECN
< 7.6 × 10⁻⁴	90	ASNER	98	CLE2

Rare or forbidden modes

$\Gamma(K^+\ell^-\overline{\nu}_\ell(\text{via }\overline{D}^0))/\Gamma(K^-\ell^+\nu_\ell)$ Γ_{173}/Γ_8

This is a limit on R_M without the complications of possible doubly-Cabibbo-suppressed decays that occur when using hadronic modes. For the limits on $|m_1 - m_2|$ and $(\Gamma_1 - \Gamma_2)/\Gamma$ that come from the best mixing limit, see near the beginning of these D^0 Listings.

VALUE	CL%	DOCUMENT ID		TECN	COMMENT
< 0.005	90	[91] AITALA	96C	E791	π^- nucleus, 500 GeV

[91] AITALA 96C uses $D^{*+} \to D^0\pi^+$ (and charge conjugate) decays to identify the charm at production and $D^0 \to K^-\ell^+\nu_\ell$ (and charge conjugate) decays to identify the charm at decay.

$\Gamma(K^+\pi^-)/\Gamma(K^-\pi^+)$ Γ_{174}/Γ_{20}

This is R_D in the note on "D^0-$\overline{D}^0$ Mixing." near the start of the D^0 Listings. The experiments here use the charge of the pion in $D^*(2010)^\pm \to (D^0 \text{ or } \overline{D}^0)\,\pi^\pm$ decay to tell whether a D^0 or a $\overline{D}^0$ was born. The $D^0 \to K^+\pi^-$ decay can occur directly by doubly Cabibbo-suppressed (DCS) decay, or indirectly by $D^0 \to \overline{D}^0$ mixing followed by $\overline{D}^0 \to K^+\pi^-$ decay. Some of the experiments can use the decay-time information to disentangle the two mechanisms. Here, we list the experimental branching ratio, which if there is no mixing is the DCS ratio. See the next data block for limits on the mixing ratio R_M, see the section on CP-violating asymmetries near the end of this D^0 Listing for values of A_D, and see the note on "D^0-$\overline{D}^0$ Mixing" for limits on x' and y'.

Some early limits have been omitted from this Listing; see our 1998 edition (EPJ **C3** 1).

VALUE	CL%	EVTS	DOCUMENT ID		TECN	COMMENT
0.00362 ± 0.00029 OUR AVERAGE						
0.00359 ± 0.00020 ± 0.00027			[92] AUBERT	03Z	BABR	e^+e^-, 10.6 GeV
0.00404 ± 0.00085 ± 0.00025		149	[93] LINK	01	FOCS	γ nucleus
$0.00332^{+0.00063}_{-0.00065} \pm 0.00040$		45	[94] GODANG	00	CLE2	e^+e^-
$0.0068\ ^{+0.0034}_{-0.0033} \pm 0.0007$		34	[95] AITALA	98	E791	π^- nucleus, 500 GeV
• • • We do not use the following data for averages, fits, limits, etc. • • •						
0.0184 ± 0.0059 ± 0.0034		19	[96] BARATE	98W	ALEP	e^+e^- at Z^0
0.0077 ± 0.0025 ± 0.0025		19	[97] CINABRO	94	CLE2	$e^+e^- \approx \Upsilon(4S)$
< 0.011	90		[97] AMMAR	91	CLEO	$e^+e^- \approx 10.5$ GeV
< 0.015	90	1 ± 6	[98] ANJOS	88C	E691	Photoproduction
< 0.014	90		[97] ALBRECHT	87K	ARG	e^+e^- 10 GeV

[92] This AUBERT 03Z result is for no mixing or CP violation. If CP violation but no mixing is allowed, R_D=0.00357 ± 0.00022 ± 0.00027. If only mixing is allowed, the 95% confidence-level interval is $(2.4 < R_D < 4.9)\times10^{-3}$. If both mixing and CP violation are allowed, this interval becomes $(2.3 < R_D < 5.2)\times10^{-3}$.

[93] This LINK 01 result assumes no mixing or CP violation; see Fig. 4 of the paper for the DCS value as a function of the (unknown) mixing parameters x' and y'. See also the note on "D^0-$\overline{D}^0$ Mixing" near the start of the D^0 Listings for results on x' and y' from FOCUS and other experiments.

[94] This GODANG 00 result assumes no D^0-$\overline{D}^0$ mixing (R_M=0 in the note on "D^0-$\overline{D}^0$ Mixing" near the start of the D^0 Listings) but allows CP violation. The DCS ratio becomes 0.0048 ± 0.0012 ± 0.0004 when mixing is allowed.

[95] This AITALA 98 result assumes no CP violation or mixing (R_M=0 in the note on "D^0-$\overline{D}^0$ Mixing" near the start of the D^0 Listings). The DCS ratio becomes $0.0090^{+0.0120}_{-0.0109} \pm 0.0044$ when mixing is allowed.

[96] BARATE 98W gets $0.0177^{+0.0060}_{-0.0056} \pm 0.0031$ for the DCS ratio when mixing is allowed, assuming no interference between the DCS and mixing amplitudes ($y' = 0$ in the note on "D^0-$\overline{D}^0$ Mixing" near the start of the D^0 Listings).

[97] CINABRO 94, AMMAR 91, and ALBRECHT 87K cannot distinguish between doubly Cabibbo-suppressed decay and D^0-$\overline{D}^0$ mixing.

[98] ANJOS 88C allows mixing but assumes no interference between the DCS and mixing amplitudes ($y' = 0$ in the note on "D^0-$\overline{D}^0$ Mixing" near the start of the D^0 Listings). When interference is allowed, the limit degrades to 0.049.

$\Gamma(K^+\pi^-(\text{via }\overline{D}^0))/\Gamma(K^-\pi^+)$ Γ_{175}/Γ_{20}

This is R_M in the note on "D^0-$\overline{D}^0$ Mixing" near the start of the D^0 Listings. The experiments here (1) use the charge of the pion in $D^*(2010)^\pm \to (D^0 \text{ or } \overline{D}^0)\,\pi^\pm$ decay to tell whether a D^0 or a $\overline{D}^0$ was born; and (2) use the decay-time distribution to disentangle doubly Cabibbo-suppressed decay and mixing. For the limits on $|m_1 - m_2|$ and $(\Gamma_1 - \Gamma_2)/\Gamma$ that come from the best mixing limit, see near the beginning of these D^0 Listings.

VALUE	CL%	EVTS	DOCUMENT ID		TECN	COMMENT
< 0.00041	95		[99] GODANG	00	CLE2	e^+e^-
• • • We do not use the following data for averages, fits, limits, etc. • • •						
< 0.0013	95		[100] AUBERT	03Z	BABR	e^+e^-, 10.6 GeV
< 0.0092	95		[101] BARATE	98W	ALEP	e^+e^- at Z^0
< 0.005	90	1 ± 4	[102] ANJOS	88C	E691	Photoproduction

[99] This GODANG 00 result allows CP violation and assumes that the strong phase between $D^0 \to K^+\pi^-$ and $\overline{D}^0 \to K^+\pi^-$ is small, and limits only $D^0 \to \overline{D}^0$ transitions via off-shell intermediate states. The limit on transitions via on-shell intermediate states is 0.0017.

[100] This AUBERT 03Z result allows CP violation and assumes that the strong phase between $D^0 \to K^+\pi^-$ and $\overline{D}^0 \to K^+\pi^-$ is small, and limits only $D^0 \to \overline{D}^0$ transitions via off-shell intermediate states. The limit on transitions via on-shell intermediate states is 0.0016.

[101] This BARATE 98W result assumes no interference between the DCS and mixing amplitudes ($y' = 0$ in the note on "D^0-$\overline{D}^0$ Mixing" near the start of the D^0 Listings). When interference is allowed, the limit degrades to 0.036 (95%CL).

[102] This ANJOS 88C result assumes no interference between the DCS and mixing amplitudes ($y' = 0$ in the note on "D^0-$\overline{D}^0$ Mixing" near the start of the D^0 Listings). When interference is allowed, the limit degrades to 0.019.

$\Gamma(K^*(892)^+\pi^-)/\Gamma(K^*(892)^-\pi^+)$ Γ_{176}/Γ_{91}

Unseen decay modes of the $K^*(892)^+$ are included.

VALUE	DOCUMENT ID		TECN	COMMENT
$\mathbf{0.005 \pm 0.002\ ^{+0.006}_{-0.001}}$	MURAMATSU	02	CLE2	$e^+e^- \approx 10$ GeV

$\Gamma(K^+\pi^-\pi^0)/\Gamma(K^-\pi^+\pi^0)$ Γ_{177}/Γ_{34}

The experiments here use the charge of the pion in $D^*(2010)^\pm \to (D^0 \text{ or } \overline{D}^0)\,\pi^\pm$ decay to tell whether a D^0 or a $\overline{D}^0$ was born. The $D^0 \to K^+\pi^-\pi^0$ decay can occur directly by doubly Cabibbo-suppressed (DCS) decay, or indirectly by $D^0 \to \overline{D}^0$ mixing followed by $\overline{D}^0 \to K^+\pi^-\pi^0$ decay.

VALUE	EVTS	DOCUMENT ID		TECN	COMMENT
$\mathbf{0.0043^{+0.0011}_{-0.0010} \pm 0.0007}$	38	[103] BRANDENB...	01	CLE2	$e^+e^- \approx \Upsilon(4S)$

[103] BRANDENBURG 01 does not distinguish between doubly Cabbibbo-suppressed decay and D^0-$\overline{D}^0$ mixing.

$\Gamma(K^+\pi^-\pi^+\pi^-)/\Gamma(K^-\pi^+\pi^+\pi^-)$ Γ_{178}/Γ_{46}

The experiments here use the charge of the pion in $D^*(2010)^\pm \to (D^0 \text{ or } \overline{D}^0)\,\pi^\pm$ decay to tell whether a D^0 or a $\overline{D}^0$ was born. The $D^0 \to K^+\pi^-\pi^+\pi^-$ decay can occur directly by doubly Cabibbo-suppressed (DCS) decay, or indirectly by $D^0 \to \overline{D}^0$ mixing followed by $\overline{D}^0 \to K^+\pi^-\pi^+\pi^-$ decay. Some of the experiments can use the decay-time information to disentangle the two mechanisms. Here, we list the experimental branching ratio, which if there is no mixing is the DCS ratio; in the next data block we give the limits on the mixing ratio.

Some early limits have been omitted from this Listing; see our 1998 edition (EPJ **C3** 1).

VALUE	CL%	EVTS	DOCUMENT ID		TECN	COMMENT
0.0042 ± 0.0013 OUR AVERAGE						
$0.0044^{+0.0013}_{-0.0012} \pm 0.0006$		54	[104] DYTMAN	01	CLE2	$e^+e^- \approx \Upsilon(4S)$
$0.0025^{+0.0036}_{-0.0034} \pm 0.0003$			[105] AITALA	98	E791	π^- nucleus, 500 GeV

• • • We do not use the following data for averages, fits, limits, etc. • • •

< 0.018	90		[104] AMMAR	91	CLEO	$e^+e^- \approx$ 10.5 GeV
< 0.018	90	5 ± 12	[106] ANJOS	88C	E691	Photoproduction

[104] AMMAR 91 cannot and DYTMAN 01 does not distinguish between doubly Cabibbo-suppressed decay and D^0-$\overline{D}^0$ mixing.

[105] This AITALA 98 result assumes no D^0-$\overline{D}^0$ mixing (R_M in the note on "D^0-$\overline{D}^0$ Mixing"). It becomes $-0.0020^{+0.0117}_{-0.0106} \pm 0.0035$ when mixing is allowed and decay-time information is used to distinguish doubly Cabibbo-suppressed decays from mixing.

[106] ANJOS 88C uses decay-time information to distinguish doubly Cabibbo-suppressed (DCS) decays from D^0-$\overline{D}^0$ mixing. However, the result assumes no interference between the DCS and mixing amplitudes ($y' = 0$ in the note on "D^0-$\overline{D}^0$ Mixing" near the start of the D^0 Listings). When interference is allowed, the limit degrades to 0.033.

$\Gamma(K^+\pi^-\pi^+\pi^-$ (via $\overline{D}^0))/\Gamma(K^-\pi^+\pi^+\pi^-)$ Γ_{179}/Γ_{46}

This is a D^0-$\overline{D}^0$ mixing limit. The experiments here (1) use the charge of the pion in $D^*(2010)^\pm \to (D^0$ or $\overline{D}^0)\,\pi^\pm$ decay to tell whether a D^0 or a $\overline{D}^0$ was born; and (2) use the decay-time distribution to disentangle doubly Cabibbo-suppressed decay and mixing. For the limits on $\left|m_{D_1^0} - m_{D_2^0}\right|$ and $(\Gamma_{D_1^0} - \Gamma_{D_2^0})/\Gamma_{D^0}$ that come from the best mixing limit, see near the beginning of these D^0 Listings.

VALUE	CL%	EVTS	DOCUMENT ID		TECN	COMMENT
< 0.005	90	0 ± 4	[107] ANJOS	88C	E691	Photoproduction

[107] ANJOS 88C uses decay-time information to distinguish doubly Cabibbo-suppressed (DCS) decays from D^0-$\overline{D}^0$ mixing. However, the result assumes no interference between the DCS and mixing amplitudes ($y' = 0$ in the note on "D^0-$\overline{D}^0$ Mixing" near the start of the D^0 Listings). When interference is allowed, the limit degrades to 0.007.

$\Gamma(K^+\pi^-$ or $K^+\pi^-\pi^+\pi^-$ (via $\overline{D}^0))/\Gamma(K^-\pi^+$ or $K^-\pi^+\pi^+\pi^-)$ Γ_{180}/Γ_0

This is a D^0-$\overline{D}^0$ mixing limit. For the limits on $\left|m_{D_1^0} - m_{D_2^0}\right|$ and $(\Gamma_{D_1^0} - \Gamma_{D_2^0})/\Gamma_{D^0}$ that come from the best mixing limit, see near the beginning of these D^0 Listings.

VALUE	CL%	DOCUMENT ID		TECN	COMMENT
< 0.0085	90	[108] AITALA	98	E791	π^- nucleus, 500 GeV
• • • We do not use the following data for averages, fits, limits, etc. • • •					
< 0.0037	90	[109] ANJOS	88C	E691	Photoproduction

[108] AITALA 98 uses decay-time information to distinguish doubly Cabibbo-suppressed decays from D^0-$\overline{D}^0$ mixing. The fit allows interference between the two amplitudes, and also allows CP violation in this term. The central value obtained is $0.0039^{+0.0036}_{-0.0032} \pm 0.0016$. When interference is disallowed, the result becomes $0.0021 \pm 0.0009 \pm 0.0002$.

[109] This combines results of ANJOS 88C on $K^+\pi^-$ and $K^+\pi^-\pi^+\pi^-$ (via $\overline{D}^0$) reported in the data block above (see footnotes there). It assumes no interference.

$\Gamma(\mu^-$ anything (via $\overline{D}^0))/\Gamma(\mu^+$ anything) Γ_{181}/Γ_2

This is a D^0-$\overline{D}^0$ mixing limit. See the somewhat better limits above.

VALUE	CL%	DOCUMENT ID		TECN	COMMENT
< 0.0056	90	LOUIS	86	SPEC	π^- W 225 GeV
• • • We do not use the following data for averages, fits, limits, etc. • • •					
< 0.012	90	BENVENUTI	85	CNTR	μ C, 200 GeV
< 0.044	90	BODEK	82	SPEC	π^-, pFe $\to D^0$

$\Gamma(\gamma\gamma)/\Gamma(\pi^0\pi^0)$ $\Gamma_{182}/\Gamma_{128}$

$D^0 \to \gamma\gamma$ is a flavor-changing neutral-current decay, forbidden in the Standard Model at the tree level.

VALUE	CL%	DOCUMENT ID		TECN	COMMENT
< 0.033	90	COAN	03	CLE2	$e^+e^- \approx \Upsilon(4S)$

$\Gamma(e^+e^-)/\Gamma_{\text{total}}$ Γ_{183}/Γ

A test for the $\Delta C = 1$ weak neutral current. Allowed by first-order weak interaction combined with electromagnetic interaction.

VALUE	CL%	EVTS	DOCUMENT ID		TECN	COMMENT
< 6.2 × 10⁻⁶	90		AITALA	99G	E791	π^- N 500 GeV
• • • We do not use the following data for averages, fits, limits, etc. • • •						
$< 8.19 \times 10^{-6}$	90		PRIPSTEIN	00	E789	p nucleus, 800 GeV
$< 1.3 \times 10^{-5}$	90	0	FREYBERGER	96	CLE2	$e^+e^- \approx \Upsilon(4S)$
$< 1.3 \times 10^{-4}$	90		ADLER	88	MRK3	e^+e^- 3.77 GeV
$< 1.7 \times 10^{-4}$	90	7	ALBRECHT	88G	ARG	e^+e^- 10 GeV
$< 2.2 \times 10^{-4}$	90	8	HAAS	88	CLEO	e^+e^- 10 GeV

$\Gamma(\mu^+\mu^-)/\Gamma_{\text{total}}$ Γ_{184}/Γ

A test for the $\Delta C = 1$ weak neutral current. Allowed by first-order weak interaction combined with electromagnetic interaction.

VALUE	CL%	EVTS	DOCUMENT ID		TECN	COMMENT
< 4.1 × 10⁻⁶	90		ADAMOVICH	97	BEAT	π^- Cu, W 350 GeV
• • • We do not use the following data for averages, fits, limits, etc. • • •						
$< 1.56 \times 10^{-5}$	90		PRIPSTEIN	00	E789	p nucleus, 800 GeV
$< 5.2 \times 10^{-6}$	90		AITALA	99G	E791	π^- N 500 GeV
$< 4.2 \times 10^{-6}$	90		ALEXOPOU...	96	E771	p Si, 800 GeV
$< 3.4 \times 10^{-5}$	90	1	FREYBERGER	96	CLE2	$e^+e^- \approx \Upsilon(4S)$
$< 7.6 \times 10^{-6}$	90	0	ADAMOVICH	95	BEAT	See ADAMOVICH 97
$< 4.4 \times 10^{-5}$	90	0	KODAMA	95	E653	π^- emulsion 600 GeV
$< 3.1 \times 10^{-5}$	90		[110] MISHRA	94	E789	-4.1 ± 4.8 events
$< 7.0 \times 10^{-5}$	90	3	ALBRECHT	88G	ARG	e^+e^- 10 GeV
$< 1.1 \times 10^{-5}$	90		LOUIS	86	SPEC	π^- W 225 GeV
$< 3.4 \times 10^{-4}$	90		AUBERT	85	EMC	Deep inelast. μ N

[110] Here MISHRA 94 uses "the statistical approach advocated by the PDG." For an alternate approach, giving a limit of 9×10^{-6} at 90% confidence level, see the paper.

$\Gamma(\pi^0e^+e^-)/\Gamma_{\text{total}}$ Γ_{185}/Γ

A test for the $\Delta C = 1$ weak neutral current. Allowed by higher-order electroweak interactions.

VALUE	CL%	EVTS	DOCUMENT ID	TECN	COMMENT
< 4.5 × 10⁻⁵	90	0	FREYBERGER 96	CLE2	$e^+e^- \approx \Upsilon(4S)$

$\Gamma(\pi^0\mu^+\mu^-)/\Gamma_{\text{total}}$ Γ_{186}/Γ

A test for the ΔC=1 weak neutral current. Allowed by higher-order electroweak interactions.

VALUE	CL%	EVTS	DOCUMENT ID		TECN	COMMENT
< 1.8 × 10⁻⁴	90	2	KODAMA	95	E653	π^- emulsion 600 GeV
• • • We do not use the following data for averages, fits, limits, etc. • • •						
$< 5.4 \times 10^{-4}$	90	3	FREYBERGER	96	CLE2	$e^+e^- \approx \Upsilon(4S)$

$\Gamma(\eta e^+e^-)/\Gamma_{\text{total}}$ Γ_{187}/Γ

A test for the $\Delta C = 1$ weak neutral current. Allowed by higher-order electroweak interactions.

VALUE	CL%	EVTS	DOCUMENT ID	TECN	COMMENT
< 1.1 × 10⁻⁴	90	0	FREYBERGER 96	CLE2	$e^+e^- \approx \Upsilon(4S)$

$\Gamma(\eta\mu^+\mu^-)/\Gamma_{\text{total}}$ Γ_{188}/Γ

A test for the $\Delta C = 1$ weak neutral current. Allowed by higher-order electroweak interactions.

VALUE	CL%	EVTS	DOCUMENT ID	TECN	COMMENT
< 5.3 × 10⁻⁴	90	0	FREYBERGER 96	CLE2	$e^+e^- \approx \Upsilon(4S)$

$\Gamma(\pi^+\pi^-e^+e^-)/\Gamma_{\text{total}}$ Γ_{189}/Γ

A test for the $\Delta C = 1$ weak neutral current. Allowed by higher-order electroweak interactions.

VALUE	CL%	EVTS	DOCUMENT ID	TECN	COMMENT
< 3.73 × 10⁻⁴	90	9	AITALA	01C E791	π^- nucleus, 500 GeV

$\Gamma(\rho^0e^+e^-)/\Gamma_{\text{total}}$ Γ_{190}/Γ

A test for the $\Delta C = 1$ weak neutral current. Allowed by higher-order electroweak interactions.

VALUE	CL%	EVTS	DOCUMENT ID		TECN	COMMENT
< 1.0 × 10⁻⁴	90	2	[111] FREYBERGER	96	CLE2	$e^+e^- \approx \Upsilon(4S)$
• • • We do not use the following data for averages, fits, limits, etc. • • •						
$< 1.24 \times 10^{-4}$	90	1	AITALA	01C	E791	π^- nucleus, 500 GeV
$< 4.5 \times 10^{-4}$	90	2	HAAS	88	CLEO	e^+e^- 10 GeV

[111] This FREYBERGER 96 limit is obtained using a phase-space model. The limit changes to $< 1.8 \times 10^{-4}$ using a photon pole amplitude model.

$\Gamma(\pi^+\pi^-\mu^+\mu^-)/\Gamma_{\text{total}}$ Γ_{191}/Γ

A test for the $\Delta C = 1$ weak neutral current. Allowed by higher-order electroweak interactions.

VALUE	CL%	EVTS	DOCUMENT ID	TECN	COMMENT
< 3.0 × 10⁻⁵	90	2	AITALA	01C E791	π^- nucleus, 500 GeV

$\Gamma(\rho^0\mu^+\mu^-)/\Gamma_{\text{total}}$ Γ_{192}/Γ

A test for the $\Delta C = 1$ weak neutral current. Allowed by higher-order electroweak interactions.

VALUE	CL%	EVTS	DOCUMENT ID		TECN	COMMENT
< 2.2 × 10⁻⁵	90	0	AITALA	01C	E791	π^- nucleus, 500 GeV
• • • We do not use the following data for averages, fits, limits, etc. • • •						
$< 4.9 \times 10^{-4}$	90	1	[112] FREYBERGER	96	CLE2	$e^+e^- \approx \Upsilon(4S)$
$< 2.3 \times 10^{-4}$	90	0	KODAMA	95	E653	π^- emulsion 600 GeV
$< 8.1 \times 10^{-4}$	90	5	HAAS	88	CLEO	e^+e^- 10 GeV

[112] This FREYBERGER 96 limit is obtained using a phase-space model. The limit changes to $< 4.5 \times 10^{-4}$ using a photon pole amplitude model.

$\Gamma(\omega e^+e^-)/\Gamma_{\text{total}}$ Γ_{193}/Γ

A test for the $\Delta C = 1$ weak neutral current. Allowed by higher-order electroweak interactions.

VALUE	CL%	EVTS	DOCUMENT ID		TECN	COMMENT
< 1.8 × 10⁻⁴	90	1	[113] FREYBERGER	96	CLE2	$e^+e^- \approx \Upsilon(4S)$

[113] This FREYBERGER 96 limit is obtained using a phase-space model. The limit changes to $< 2.7 \times 10^{-4}$ using a photon pole amplitude model.

$\Gamma(\omega\mu^+\mu^-)/\Gamma_{\text{total}}$ Γ_{194}/Γ

A test for the $\Delta C = 1$ weak neutral current. Allowed by higher-order electroweak interactions.

VALUE	CL%	EVTS	DOCUMENT ID		TECN	COMMENT
< 8.3 × 10⁻⁴	90	0	[114] FREYBERGER	96	CLE2	$e^+e^- \approx \Upsilon(4S)$

[114] This FREYBERGER 96 limit is obtained using a phase-space model. The limit changes to $< 6.5 \times 10^{-4}$ using a photon pole amplitude model.

$\Gamma(K^-K^+e^+e^-)/\Gamma_{\text{total}}$ Γ_{195}/Γ

A test for the $\Delta C = 1$ weak neutral current. Allowed by higher-order electroweak interactions.

VALUE	CL%	EVTS	DOCUMENT ID	TECN	COMMENT
< 3.15 × 10⁻⁴	90	9	AITALA	01C E791	π^- nucleus, 500 GeV

$\Gamma(\phi e^+ e^-)/\Gamma_{total}$ Γ_{196}/Γ

A test for the $\Delta C = 1$ weak neutral current. Allowed by higher-order electroweak interactions.

VALUE	CL%	EVTS	DOCUMENT ID		TECN	COMMENT
$< 5.2 \times 10^{-5}$	90	2	[115] FREYBERGER	96	CLE2	$e^+e^- \approx \Upsilon(4S)$
• • • We do not use the following data for averages, fits, limits, etc. • • •						
$< 5.9 \times 10^{-5}$	90	0	AITALA	01C	E791	π^- nucleus, 500 GeV

[115] This FREYBERGER 96 limit is obtained using a phase-space model. The limit changes to $< 7.6 \times 10^{-5}$ using a photon pole amplitude model.

$\Gamma(K^- K^+ \mu^+ \mu^-)/\Gamma_{total}$ Γ_{197}/Γ

A test for the $\Delta C = 1$ weak neutral current. Allowed by higher-order electroweak interactions.

VALUE	CL%	EVTS	DOCUMENT ID	TECN	COMMENT
$< 3.3 \times 10^{-5}$	90	0	AITALA	01C E791	π^- nucleus, 500 GeV

$\Gamma(\phi \mu^+ \mu^-)/\Gamma_{total}$ Γ_{198}/Γ

A test for the $\Delta C = 1$ weak neutral current. Allowed by higher-order electroweak interactions.

VALUE	CL%	EVTS	DOCUMENT ID		TECN	COMMENT
$< 3.1 \times 10^{-5}$	90	0	AITALA	01C	E791	π^- nucleus, 500 GeV
• • • We do not use the following data for averages, fits, limits, etc. • • •						
$< 4.1 \times 10^{-4}$	90	0	[116] FREYBERGER	96	CLE2	$e^+e^- \approx \Upsilon(4S)$

[116] This FREYBERGER 96 limit is obtained using a phase-space model. The limit changes to $< 2.4 \times 10^{-4}$ using a photon pole amplitude model.

$\Gamma(\overline{K}^0 e^+ e^-)/\Gamma_{total}$ Γ_{199}/Γ

Not a useful test for $\Delta C = 1$ weak neutral current because both quarks must change flavor.

VALUE	CL%	EVTS	DOCUMENT ID		TECN	COMMENT
$< 1.1 \times 10^{-4}$	90	0	FREYBERGER	96	CLE2	$e^+e^- \approx \Upsilon(4S)$
• • • We do not use the following data for averages, fits, limits, etc. • • •						
$< 1.7 \times 10^{-3}$	90		ADLER	89C	MRK3	e^+e^- 3.77 GeV

$\Gamma(\overline{K}^0 \mu^+ \mu^-)/\Gamma_{total}$ Γ_{200}/Γ

Not a useful test for $\Delta C = 1$ weak neutral current because both quarks must change flavor.

VALUE	CL%	EVTS	DOCUMENT ID		TECN	COMMENT
$< 2.6 \times 10^{-4}$	90	2	KODAMA	95	E653	π^- emulsion 600 GeV
• • • We do not use the following data for averages, fits, limits, etc. • • •						
$< 6.7 \times 10^{-4}$	90	1	FREYBERGER	96	CLE2	$e^+e^- \approx \Upsilon(4S)$

$\Gamma(K^- \pi^+ e^+ e^-)/\Gamma_{total}$ Γ_{201}/Γ

A test for the $\Delta C = 1$ weak neutral current. Allowed by higher-order electroweak interactions.

VALUE	CL%	EVTS	DOCUMENT ID	TECN	COMMENT
$< 3.85 \times 10^{-4}$	90	6	AITALA	01C E791	π^- nucleus, 500 GeV

$\Gamma(\overline{K}^*(892)^0 e^+ e^-)/\Gamma_{total}$ Γ_{202}/Γ

Not a useful test for $\Delta C = 1$ weak neutral current because both quarks must change flavor.

VALUE	CL%	EVTS	DOCUMENT ID		TECN	COMMENT
$< 4.7 \times 10^{-5}$	90	2	AITALA	01C	E791	π^- nucleus, 500 GeV
• • • We do not use the following data for averages, fits, limits, etc. • • •						
$< 1.4 \times 10^{-4}$	90	1	[117] FREYBERGER	96	CLE2	$e^+e^- \approx \Upsilon(4S)$

[117] This FREYBERGER 96 limit is obtained using a phase-space model. The limit changes to $< 2.0 \times 10^{-4}$ using a photon pole amplitude model.

$\Gamma(K^- \pi^+ \mu^+ \mu^-)/\Gamma_{total}$ Γ_{203}/Γ

A test for the $\Delta C = 1$ weak neutral current. Allowed by higher-order electroweak interactions.

VALUE	CL%	EVTS	DOCUMENT ID	TECN	COMMENT
$< 3.59 \times 10^{-4}$	90	12	AITALA	01C E791	π^- nucleus, 500 GeV

$\Gamma(\overline{K}^*(892)^0 \mu^+ \mu^-)/\Gamma_{total}$ Γ_{204}/Γ

Not a useful test for $\Delta C = 1$ weak neutral current because both quarks must change flavor.

VALUE	CL%	EVTS	DOCUMENT ID		TECN	COMMENT
$< 2.4 \times 10^{-5}$	90	3	AITALA	01C	E791	π^- nucleus, 500 GeV
• • • We do not use the following data for averages, fits, limits, etc. • • •						
$< 1.18 \times 10^{-3}$	90	1	[118] FREYBERGER	96	CLE2	$e^+e^- \approx \Upsilon(4S)$

[118] This FREYBERGER 96 limit is obtained using a phase-space model. The limit changes to $< 1.0 \times 10^{-3}$ using a photon pole amplitude model.

$\Gamma(\pi^+ \pi^- \pi^0 \mu^+ \mu^-)/\Gamma_{total}$ Γ_{205}/Γ

A test for the $\Delta C = 1$ weak neutral current. Allowed by higher-order electroweak interactions.

VALUE	CL%	EVTS	DOCUMENT ID	TECN	COMMENT
$< 8.1 \times 10^{-4}$	90	1	KODAMA	95 E653	π^- emulsion 600 GeV

$\Gamma(\mu^\pm e^\mp)/\Gamma_{total}$ Γ_{206}/Γ

A test of lepton family number conservation.

VALUE	CL%	EVTS	DOCUMENT ID		TECN	COMMENT
$< 8.1 \times 10^{-6}$	90		AITALA	99G	E791	π^- N 500 GeV
• • • We do not use the following data for averages, fits, limits, etc. • • •						
$< 1.72 \times 10^{-5}$	90		PRIPSTEIN	00	E789	p nucleus, 800 GeV
$< 1.9 \times 10^{-5}$	90	2	[119] FREYBERGER	96	CLE2	$e^+e^- \approx \Upsilon(4S)$
$< 1.0 \times 10^{-4}$	90	4	ALBRECHT	88G	ARG	e^+e^- 10 GeV
$< 2.7 \times 10^{-4}$	90	9	HAAS	88	CLEO	e^+e^- 10 GeV
$< 1.2 \times 10^{-4}$	90		BECKER	87C	MRK3	e^+e^- 3.77 GeV
$< 9 \times 10^{-4}$	90		PALKA	87	SILI	200 GeV πp
$< 21 \times 10^{-4}$	90	0	[120] RILES	87	MRK2	e^+e^- 29 GeV

[119] This is the corrected result given in the erratum to FREYBERGER 96.
[120] RILES 87 assumes $B(D \to K\pi) = 3.0\%$ and has production model dependency.

$\Gamma(\pi^0 e^\pm \mu^\mp)/\Gamma_{total}$ Γ_{207}/Γ

A test of lepton family number conservation. The value is for the sum of the two charge states.

VALUE	CL%	EVTS	DOCUMENT ID	TECN	COMMENT
$< 8.6 \times 10^{-5}$	90	2	FREYBERGER 96	CLE2	$e^+e^- \approx \Upsilon(4S)$

$\Gamma(\eta e^\pm \mu^\mp)/\Gamma_{total}$ Γ_{208}/Γ

A test of lepton family number conservation. The value is for the sum of the two charge states.

VALUE	CL%	EVTS	DOCUMENT ID	TECN	COMMENT
$< 1.0 \times 10^{-4}$	90	0	FREYBERGER 96	CLE2	$e^+e^- \approx \Upsilon(4S)$

$\Gamma(\pi^+ \pi^- e^\pm \mu^\mp)/\Gamma_{total}$ Γ_{209}/Γ

A test of lepton family-number conservation. The value is for the sum of the two charge states.

VALUE	CL%	EVTS	DOCUMENT ID	TECN	COMMENT
$< 1.5 \times 10^{-5}$	90	1	AITALA	01C E791	π^- nucleus, 500 GeV

$\Gamma(\rho^0 e^\pm \mu^\mp)/\Gamma_{total}$ Γ_{210}/Γ

A test of lepton family number conservation. The value is for the sum of the two charge states.

VALUE	CL%	EVTS	DOCUMENT ID		TECN	COMMENT
$< 4.9 \times 10^{-5}$	90	0	[121] FREYBERGER	96	CLE2	$e^+e^- \approx \Upsilon(4S)$
• • • We do not use the following data for averages, fits, limits, etc. • • •						
$< 6.6 \times 10^{-5}$	90	1	AITALA	01C	E791	π^- nucleus, 500 GeV

[121] This FREYBERGER 96 limit is obtained using a phase-space model. The limit changes to $< 5.0 \times 10^{-5}$ using a photon pole amplitude model.

$\Gamma(\omega e^\pm \mu^\mp)/\Gamma_{total}$ Γ_{211}/Γ

A test of lepton family number conservation. The value is for the sum of the two charge states.

VALUE	CL%	EVTS	DOCUMENT ID		TECN	COMMENT
$< 1.2 \times 10^{-4}$	90	0	[122] FREYBERGER	96	CLE2	$e^+e^- \approx \Upsilon(4S)$

[122] This FREYBERGER 96 limit is obtained using a phase-space model. The same limit is obtained using a photon pole amplitude model.

$\Gamma(K^- K^+ e^\pm \mu^\mp)/\Gamma_{total}$ Γ_{212}/Γ

A test of lepton family-number conservation. The value is for the sum of the two charge states.

VALUE	CL%	EVTS	DOCUMENT ID	TECN	COMMENT
$< 1.8 \times 10^{-4}$	90	5	AITALA	01C E791	π^- nucleus, 500 GeV

$\Gamma(\phi e^\pm \mu^\mp)/\Gamma_{total}$ Γ_{213}/Γ

A test of lepton family number conservation. The value is for the sum of the two charge states.

VALUE	CL%	EVTS	DOCUMENT ID		TECN	COMMENT
$< 3.4 \times 10^{-5}$	90	0	[123] FREYBERGER	96	CLE2	$e^+e^- \approx \Upsilon(4S)$
• • • We do not use the following data for averages, fits, limits, etc. • • •						
$< 4.7 \times 10^{-5}$	90	0	AITALA	01C	E791	π^- nucleus, 500 GeV

[123] This FREYBERGER 96 limit is obtained using a phase-space model. The limit changes to $< 3.3 \times 10^{-5}$ using a photon pole amplitude model.

$\Gamma(\overline{K}^0 e^\pm \mu^\mp)/\Gamma_{total}$ Γ_{214}/Γ

A test of lepton family number conservation. The value is for the sum of the two charge states.

VALUE	CL%	EVTS	DOCUMENT ID	TECN	COMMENT
$< 1.0 \times 10^{-4}$	90	0	FREYBERGER 96	CLE2	$e^+e^- \approx \Upsilon(4S)$

$\Gamma(K^- \pi^+ e^\pm \mu^\mp)/\Gamma_{total}$ Γ_{215}/Γ

A test of lepton family-number conservation. The value is for the sum of the two charge states.

VALUE	CL%	EVTS	DOCUMENT ID	TECN	COMMENT
$< 5.53 \times 10^{-4}$	90	15	AITALA	01C E791	π^- nucleus, 500 GeV

$\Gamma(\overline{K}^*(892)^0 e^\pm \mu^\mp)/\Gamma_{total}$ Γ_{216}/Γ

A test of lepton family number conservation. The value is for the sum of the two charge states.

VALUE	CL%	EVTS	DOCUMENT ID	TECN	COMMENT
$< 8.3 \times 10^{-5}$	90	9	AITALA	01C E791	π^- nucleus, 500 GeV
• • • We do not use the following data for averages, fits, limits, etc. • • •					
$< 1.0 \times 10^{-4}$	90	0	[124] FREYBERGER 96	CLE2	$e^+e^- \approx \Upsilon(4S)$

[124] This FREYBERGER 96 limit is obtained using a phase-space model. The same limit is obtained using a photon pole amplitude model.

$\Gamma(\pi^-\pi^-e^+e^+ + \text{c.c.})/\Gamma_{\text{total}}$ Γ_{217}/Γ

A test of lepton-number conservation. The value is for the sum of the two charge states.

VALUE	CL%	EVTS	DOCUMENT ID		TECN	COMMENT
$<1.12\times10^{-4}$	90	1	AITALA	01C	E791	π^- nucleus, 500 GeV

$\Gamma(\pi^-\pi^-\mu^+\mu^+ + \text{c.c.})/\Gamma_{\text{total}}$ Γ_{218}/Γ

A test of lepton-number conservation. The value is for the sum of the two charge states.

VALUE	CL%	EVTS	DOCUMENT ID		TECN	COMMENT
$<2.9\times10^{-5}$	90	1	AITALA	01C	E791	π^- nucleus, 500 GeV

$\Gamma(K^-\pi^-e^+e^+ + \text{c.c.})/\Gamma_{\text{total}}$ Γ_{219}/Γ

A test of lepton-number conservation. The value is for the sum of the two charge states.

VALUE	CL%	EVTS	DOCUMENT ID		TECN	COMMENT
$<2.06\times10^{-4}$	90	2	AITALA	01C	E791	π^- nucleus, 500 GeV

$\Gamma(K^-\pi^-\mu^+\mu^+ + \text{c.c.})/\Gamma_{\text{total}}$ Γ_{220}/Γ

A test of lepton-number conservation. The value is for the sum of the two charge states.

VALUE	CL%	EVTS	DOCUMENT ID		TECN	COMMENT
$<3.9\times10^{-4}$	90	14	AITALA	01C	E791	π^- nucleus, 500 GeV

$\Gamma(K^-K^-e^+e^+ + \text{c.c.})/\Gamma_{\text{total}}$ Γ_{221}/Γ

A test of lepton-number conservation. The value is for the sum of the two charge states.

VALUE	CL%	EVTS	DOCUMENT ID		TECN	COMMENT
$<1.52\times10^{-4}$	90	2	AITALA	01C	E791	π^- nucleus, 500 GeV

$\Gamma(K^-K^-\mu^+\mu^+ + \text{c.c.})/\Gamma_{\text{total}}$ Γ_{222}/Γ

A test of lepton-number conservation. The value is for the sum of the two charge states.

VALUE	CL%	EVTS	DOCUMENT ID		TECN	COMMENT
$<9.4\times10^{-5}$	90	1	AITALA	01C	E791	π^- nucleus, 500 GeV

$\Gamma(\pi^-\pi^-e^+\mu^+ + \text{c.c.})/\Gamma_{\text{total}}$ Γ_{223}/Γ

A test of lepton-number conservation. The value is for the sum of the two charge states.

VALUE	CL%	EVTS	DOCUMENT ID		TECN	COMMENT
$<7.9\times10^{-5}$	90	4	AITALA	01C	E791	π^- nucleus, 500 GeV

$\Gamma(K^-\pi^-e^+\mu^+ + \text{c.c.})/\Gamma_{\text{total}}$ Γ_{224}/Γ

A test of lepton-number conservation. The value is for the sum of the two charge states.

VALUE	CL%	EVTS	DOCUMENT ID		TECN	COMMENT
$<2.18\times10^{-4}$	90	7	AITALA	01C	E791	π^- nucleus, 500 GeV

$\Gamma(K^-K^-e^+\mu^+ + \text{c.c.})/\Gamma_{\text{total}}$ Γ_{225}/Γ

A test of lepton-number conservation. The value is for the sum of the two charge states.

VALUE	CL%	EVTS	DOCUMENT ID		TECN	COMMENT
$<5.7\times10^{-5}$	90	0	AITALA	01C	E791	π^- nucleus, 500 GeV

D^0 *CP*-VIOLATING DECAY-RATE ASYMMETRIES

$A_{CP}(K^+K^-)$ in $D^0, \overline{D}^0 \to K^+K^-$

This is the difference between D^0 and $\overline{D}^0$ partial widths for these modes divided by the sum of the widths. The D^0 and $\overline{D}^0$ are distinguished by the charge of the parent D^*: $D^{*+} \to D^0\pi^+$ and $D^{*-} \to \overline{D}^0\pi^-$.

VALUE	EVTS	DOCUMENT ID		TECN	COMMENT
0.005 ± 0.016 OUR AVERAGE					
$0.000\pm0.022\pm0.008$	3023	[125] CSORNA	02	CLE2	$e^+e^- \approx \Upsilon(4S)$
$-0.001\pm0.022\pm0.015$	3330	[125] LINK	00B	FOCS	
$-0.010\pm0.049\pm0.012$	609	[125] AITALA	98C	E791	$-0.093 < A_{CP} < +0.073$ (90% CL)
$+0.080\pm0.061$		BARTELT	95	CLE2	$-0.022 < A_{CP} < +0.18$ (90%CL)
$+0.024\pm0.084$		[125] FRABETTI	94I	E687	$-0.11 < A_{CP} < +0.16$ (90% CL)

[125] FRABETTI 94I, AITALA 98C, LINK 00B, and CSORNA 02 measure $N(D^0 \to K^+K^-)/N(D^0 \to K^-\pi^+)$, the ratio of numbers of events observed, and similarly for the $\overline{D}^0$.

$A_{CP}(K^0_S K^0_S)$ in $D^0, \overline{D}^0 \to K^0_S K^0_S$

This is the difference between D^0 and $\overline{D}^0$ partial widths for these modes divided by the sum of the widths. The D^0 and $\overline{D}^0$ are distinguished by the charge of the parent D^*: $D^{*+} \to D^0\pi^+$ and $D^{*-} \to \overline{D}^0\pi^-$.

VALUE	EVTS	DOCUMENT ID		TECN	COMMENT
-0.23 ± 0.19	65	BONVICINI	01	CLE2	$e^+e^- \approx 10.6$ GeV

$A_{CP}(\pi^+\pi^-)$ in $D^0, \overline{D}^0 \to \pi^+\pi^-$

This is the difference between D^0 and $\overline{D}^0$ partial widths for these modes divided by the sum of the widths. The D^0 and $\overline{D}^0$ are distinguished by the charge of the parent D^*: $D^{*+} \to D^0\pi^+$ and $D^{*-} \to \overline{D}^0\pi^-$.

VALUE	EVTS	DOCUMENT ID		TECN	COMMENT
0.021 ± 0.026 OUR AVERAGE					
$0.019\pm0.032\pm0.008$	1136	[126] CSORNA	02	CLE2	$e^+e^- \approx \Upsilon(4S)$
$+0.048\pm0.039\pm0.025$	1177	[126] LINK	00B	FOCS	
$-0.049\pm0.078\pm0.030$	343	[126] AITALA	98C	E791	$-0.186 < A_{CP} < +0.088$ (90% CL)

[126] AITALA 98C, LINK 00B, and CSORNA 02 measure $N(D^0 \to \pi^+\pi^-)/N(D^0 \to K^-\pi^+)$, the ratio of numbers of events observed, and similarly for the $\overline{D}^0$.

$A_{CP}(\pi^0\pi^0)$ in $D^0, \overline{D}^0 \to \pi^0\pi^0$

This is the difference between D^0 and $\overline{D}^0$ partial widths for these modes divided by the sum of the widths. The D^0 and $\overline{D}^0$ are distinguished by the charge of the parent D^*: $D^{*+} \to D^0\pi^+$ and $D^{*-} \to \overline{D}^0\pi^-$.

VALUE	EVTS	DOCUMENT ID		TECN	COMMENT
$+0.001\pm0.048$	810	BONVICINI	01	CLE2	$e^+e^- \approx 10.6$ GeV

$A_{CP}(K^0_S\phi)$ in $D^0, \overline{D}^0 \to K^0_S\phi$

This is the difference between D^0 and $\overline{D}^0$ partial widths for these modes divided by the sum of the widths. The D^0 and $\overline{D}^0$ are distinguished by the charge of the parent D^*: $D^{*+} \to D^0\pi^+$ and $D^{*-} \to \overline{D}^0\pi^-$.

VALUE	DOCUMENT ID		TECN	COMMENT
-0.028 ± 0.094	BARTELT	95	CLE2	$-0.182 < A_{CP} < +0.126$ (90%CL)

$A_{CP}(K^0_S\pi^0)$ in $D^0, \overline{D}^0 \to K^0_S\pi^0$

This is the difference between D^0 and $\overline{D}^0$ partial widths for these modes divided by the sum of the widths. The D^0 and $\overline{D}^0$ are distinguished by the charge of the parent D^*: $D^{*+} \to D^0\pi^+$ and $D^{*-} \to \overline{D}^0\pi^-$.

VALUE	EVTS	DOCUMENT ID		TECN	COMMENT
$+0.001\pm0.013$	9099	BONVICINI	01	CLE2	$e^+e^- \approx 10.6$ GeV
• • • We do not use the following data for averages, fits, limits, etc. • • •					
-0.018 ± 0.030		BARTELT	95	CLE2	See BONVICINI 01

$A_{CP}(K^\pm\pi^\mp)$ in $D^0 \to K^+\pi^-, \overline{D}^0 \to K^-\pi^+$

This is the difference between D^0 and $\overline{D}^0$ partial widths for these modes divided by the sum of the widths. The D^0 and $\overline{D}^0$ are distinguished by the charge of the parent D^*: $D^{*+} \to D^0\pi^+$ and $D^{*-} \to \overline{D}^0\pi^-$.

VALUE	EVTS	DOCUMENT ID		TECN	COMMENT
0.08 ± 0.09 OUR AVERAGE					
$+0.095\pm0.061\pm0.083$		[127] AUBERT	03Z	BABR	e^+e^-, 10.6 GeV
$+0.02\ ^{+0.19}_{-0.20}\ \pm0.01$	45	[128] GODANG	00	CLE2	$-0.43 < A_{CP} < +0.34$ (95%CL)

[127] This AUBERT 03Z limit assumes no mixing. If mixing is allowed, the 95% confidence-level interval is $(-2.8 < A_D < 4.9)\times10^{-3}$.

[128] This GODANG 00 result assumes no D^0-$\overline{D}^0$ mixing; it becomes $-0.01\ ^{+0.16}_{-0.17} \pm 0.01$ when mixing is allowed.

$A_{CP}(K^\mp\pi^\pm\pi^0)$ in $D^0 \to K^-\pi^+\pi^0, \overline{D}^0 \to K^+\pi^-\pi^0$

This is the difference between D^0 and $\overline{D}^0$ partial widths for these modes divided by the sum of the widths. The D^0 and $\overline{D}^0$ are distinguished by the charge of the parent D^*: $D^{*+} \to D^0\pi^+$ and $D^{*-} \to \overline{D}^0\pi^-$.

VALUE	DOCUMENT ID		TECN	COMMENT
-0.031 ± 0.086	[129] KOPP	01	CLE2	$e^+e^- \approx 10.6$ GeV

[129] KOPP 01 fits separately the D^0 and $\overline{D}^0$ Dalitz plots and then calculates the integrated difference of normalized densities divided by the integrated sum.

$A_{CP}(K^\pm\pi^\mp\pi^0)$ in $D^0 \to K^+\pi^-\pi^0, \overline{D}^0 \to K^-\pi^+\pi^0$

This is the difference between D^0 and $\overline{D}^0$ partial widths for these modes divided by the sum of the widths. The D^0 and $\overline{D}^0$ are distinguished by the charge of the parent D^*: $D^{*+} \to D^0\pi^+$ and $D^{*-} \to \overline{D}^0\pi^-$.

VALUE	EVTS	DOCUMENT ID		TECN	COMMENT
$+0.09\ ^{+0.25}_{-0.22}$	38	BRANDENB...	01	CLE2	$e^+e^- \approx \Upsilon(4S)$

D^0 *CPT*-VIOLATING DECAY-RATE ASYMMETRIES

$A_{CPT}(K^\mp\pi^\pm)$ in $D^0 \to K^-\pi^+, \overline{D}^0 \to K^+\pi^-$

$A_{CPT}(t)$ is defined in terms of the time-dependent decay probabilities $P(D^0 \to K^-\pi^+)$ and $\overline{P}(\overline{D}^0 \to K^+\pi^-)$ by $A_{CPT}(t) = (\overline{P}-P)/(\overline{P}+P)$. For small mixing parameters $x \equiv \Delta m/\Gamma$ and $y \equiv \Delta\Gamma/2\Gamma$ (as is the case), and times t, $A_{CPT}(t)$ reduces to $[\, y\ Re\,\xi - x\ Im\,\xi\,]\ \Gamma t$, where ξ is the *CPT*-violating parameter.

The following is actually $y\ Re\,\xi - x\ Im\,\xi$.

VALUE	DOCUMENT ID		TECN	COMMENT
$0.0083\pm0.0065\pm0.0041$	LINK	03B	FOCS	γ nucleus, $\overline{E}_\gamma \approx 180$ GeV

D^0 PRODUCTION CROSS SECTION AT $\psi(3770)$

A compilation of the cross sections for the direct production of D^0 mesons at or near the $\psi(3770)$ peak in e^+e^- production.

VALUE (nanobarns)	DOCUMENT ID		TECN	COMMENT
• • • We do not use the following data for averages, fits, limits, etc. • • •				
$5.8\ \pm0.5\ \pm0.6$	[130] ADLER	88C	MRK3	e^+e^- 3.768 GeV
$7.3\ \pm1.3$	[131] PARTRIDGE	84	CBAL	e^+e^- 3.771 GeV
$8.00\pm0.95\pm1.21$	[132] SCHINDLER	80	MRK2	e^+e^- 3.771 GeV
$11.5\ \pm2.5$	[133] PERUZZI	77	MRK1	e^+e^- 3.774 GeV

Meson Particle Listings

D^0, $D^*(2007)^0$

130 This measurement compares events with one detected D to those with two detected D mesons, to determine the the absolute cross section. ADLER 88C find the ratio of cross sections (neutral to charged) to be $1.36 \pm 0.23 \pm 0.14$.

131 This measurement comes from a scan of the $\psi(3770)$ resonance and a fit to the cross section. PARTRIDGE 84 measures 6.4 ± 1.15 nb for the cross section. We take the phase space division of neutral and charged D mesons in $\psi(3770)$ decay to be 1.33, and we assume that the $\psi(3770)$ is an isosinglet to evaluate the cross sections. The noncharm decays (e.g. radiative) of the $\psi(3770)$ are included in this measurement and may amount to a few percent correction.

132 This measurement comes from a scan of the $\psi(3770)$ resonance and a fit to the cross section. SCHINDLER 80 assume the phase space division of neutral and charged D mesons in $\psi(3770)$ decay to be 1.33, and that the $\psi(3770)$ is an isosinglet. The noncharm decays (e.g. radiative) of the $\psi(3770)$ are included in this measurement and may amount to a few percent correction.

133 This measurement comes from a scan of the $\psi(3770)$ resonance and a fit to the cross section. The phase space division of neutral and charged D mesons in $\psi(3770)$ decay is taken to be 1.33, and $\psi(3770)$ is assumed to be an isosinglet. The noncharm decays (e.g. radiative) of the $\psi(3770)$ are included in this measurement and may amount to a few percent correction. We exclude this measurement from the average because of uncertainties in the contamination from τ lepton pairs. Also see RAPIDIS 77.

D^0 REFERENCES

PDG	04		S. Eidelman *et al.*	
TAJIMA	04	PRL 92 101803	O. Tajima *et al.*	(BELLE Collab.)
AUBERT	03P	PRL 91 121801	B. Aubert *et al.*	(BaBar Collab.)
AUBERT	03Z	PRL 91 171801	B. Aubert *et al.*	(BaBar Collab.)
COAN	03	PRL 90 101801	T.E. Coan *et al.*	(CLEO Collab.)
LINK	03	PL B555 167	J.M. Link *et al.*	(FNAL FOCUS Collab.)
LINK	03B	PL B556 7	J.M. Link *et al.*	(FNAL FOCUS Collab.)
LINK	03G	PL B575 190	J.M. Link *et al.*	(FNAL FOCUS Collab.)
ABE	02I	PRL 88 162001	K. Abe *et al.*	(KEK BELLE Collab.)
CSORNA	02	PR D65 092001	S.E. Csorna *et al.*	(CLEO Collab.)
LINK	02F	PL B537 192	J.M. Link *et al.*	(FNAL FOCUS Collab.)
MURAMATSU	02	PRL 89 251802	H. Muramatsu *et al.*	(CLEO Collab.)
Also	03	PRL 90 059901 (erratum)	H. Muramatsu *et al.*	(CLEO Collab.)
AITALA	01C	PRL 86 3969	E.M. Aitala *et al.*	(FNAL E791 Collab.)
AITALA	01D	PR D64 112003	E.M. Aitala *et al.*	(FNAL E791 Collab.)
BONVICINI	01	PR D63 071101R	G. Bonvicini *et al.*	(CLEO Collab.)
BRANDENB...	01	PRL 87 071802	G. Brandenburg *et al.*	(CLEO Collab.)
DYTMAN	01	PR D64 111101 (R)	S.A. Dytman *et al.*	(CLEO Collab.)
KOPP	01	PR D63 092001	S. Kopp *et al.*	(CLEO Collab.)
KUSHNIR...	01	PRL 86 5243	A. Kushnirenko *et al.*	(FNAL SELEX Collab.)
LINK	01	PRL 86 2955	J.M. Link *et al.*	(FNAL FOCUS Collab.)
BAI	00C	PR D62 052001	J.Z. Bai *et al.*	(BEPC BES Collab.)
GODANG	00	PRL 84 5038	R. Godang *et al.*	(CLEO Collab.)
JUN	00	PRL 84 1857	S.Y. Jun *et al.*	(FNAL SELEX Collab.)
LINK	00	PL B485 62	J.M. Link *et al.*	(FNAL FOCUS Collab.)
LINK	00B	PL B491 232	J.M. Link *et al.*	(FNAL FOCUS Collab.)
Also	00D	PL B495 443 (errata)	J.M. Link *et al.*	(FNAL FOCUS Collab.)
PRIPSTEIN	00	PR D61 032005	D. Pripstein *et al.*	(FNAL E789 Collab.)
AITALA	99E	PRL 83 32	E.M. Aitala *et al.*	(FNAL E791 Collab.)
AITALA	99G	PL B462 401	E.M. Aitala *et al.*	(FNAL E791 Collab.)
BONVICINI	99	PRL 82 4586	G. Bonvicini *et al.*	(CLEO Collab.)
AITALA	98	PR D57 13	E.M. Aitala *et al.*	(FNAL E791 Collab.)
AITALA	98C	PL B421 405	E.M. Aitala *et al.*	(FNAL E791 Collab.)
AITALA	98D	PL B423 185	E.M. Aitala *et al.*	(FNAL E791 Collab.)
ARTUSO	98	PRL 80 3193	M. Artuso *et al.*	(CLEO Collab.)
ASNER	98	PR D58 092001	D.M. Asner *et al.*	(CLEO Collab.)
BARATE	98W	PL B436 211	R. Barate *et al.*	(ALEPH Collab.)
COAN	98	PRL 80 1150	T.E. Coan *et al.*	(CLEO Collab.)
ADAMOVICH	97	PL B408 469	M.I. Adamovich *et al.*	(CERN BEATRICE Collab.)
BARATE	97C	PL B403 367	R. Barate *et al.*	(ALEPH Collab.)
AITALA	96C	PRL 77 2384	E.M. Aitala *et al.*	(FNAL E791 Collab.)
ALBRECHT	96C	PL B374 249	H. Albrecht *et al.*	(ARGUS Collab.)
ALEXOPOU...	96	PRL 77 2380	T. Alexopoulos *et al.*	(FNAL E771 Collab.)
ASNER	96B	PR D54 4211	D.M. Asner *et al.*	(CLEO Collab.)
BARISH	96	PL B373 334	B.C. Barish *et al.*	(CLEO Collab.)
FRABETTI	96B	PL B382 312	P.L. Frabetti *et al.*	(FNAL E687 Collab.)
FREYBERGER	96	PRL 76 3065	A. Freyberger *et al.*	(CLEO Collab.)
Also	96B	PRL 77 2147 (errata)	A. Freyberger *et al.*	(CLEO Collab.)
KUBOTA	96B	PR D54 2994	Y. Kubota *et al.*	(CLEO Collab.)
ADAMOVICH	95	PL B353 563	M.I. Adamovich *et al.*	(CERN BEATRICE Collab.)
BARTELT	95	PR D52 4860	J.E. Bartelt *et al.*	(CLEO Collab.)
BUTLER	95	PR D52 2656	F. Butler *et al.*	(CLEO Collab.)
FRABETTI	95C	PL B354 486	P.L. Frabetti *et al.*	(FNAL E687 Collab.)
FRABETTI	95G	PL B364 127	P.L. Frabetti *et al.*	(FNAL E687 Collab.)
KODAMA	95	PL B345 85	K. Kodama *et al.*	(FNAL E653 Collab.)
ALBRECHT	94	PL B324 249	H. Albrecht *et al.*	(ARGUS Collab.)
ALBRECHT	94F	PL B340 125	H. Albrecht *et al.*	(ARGUS Collab.)
ALBRECHT	94I	ZPHY C64 375	H. Albrecht *et al.*	(ARGUS Collab.)
CINABRO	94	PRL 72 1406	D. Cinabro *et al.*	(CLEO Collab.)
FRABETTI	94C	PL B321 295	P.L. Frabetti *et al.*	(FNAL E687 Collab.)
FRABETTI	94D	PL B323 459	P.L. Frabetti *et al.*	(FNAL E687 Collab.)
FRABETTI	94G	PL B331 217	P.L. Frabetti *et al.*	(FNAL E687 Collab.)
FRABETTI	94I	PR D50 R2953	P.L. Frabetti *et al.*	(FNAL E687 Collab.)
FRABETTI	94J	PL B340 254	P.L. Frabetti *et al.*	(FNAL E687 Collab.)
KODAMA	94	PL B336 605	K. Kodama *et al.*	(FNAL E653 Collab.)
MISHRA	94	PR D50 R9	C.S. Mishra *et al.*	(FNAL E789 Collab.)
AKERIB	93	PRL 71 3070	D.S. Akerib *et al.*	(CLEO Collab.)
ALBRECHT	93D	PL B308 435	H. Albrecht *et al.*	(ARGUS Collab.)
ANJOS	93	PR D48 56	J.C. Anjos *et al.*	(FNAL E691 Collab.)
BEAN	93C	PL B317 647	A. Bean *et al.*	(CLEO Collab.)
FRABETTI	93I	PL B315 203	P.L. Frabetti *et al.*	(FNAL E687 Collab.)
KODAMA	93B	PL B313 260	K. Kodama *et al.*	(FNAL E653 Collab.)
PROCARIO	93B	PR D48 4007	M. Procario *et al.*	(CLEO Collab.)
SELEN	93	PRL 71 1973	M.A. Selen *et al.*	(CLEO Collab.)
ADAMOVICH	92	PL B280 163	M.I. Adamovich *et al.*	(CERN WA82 Collab.)
ALBRECHT	92P	ZPHY C56 7	H. Albrecht *et al.*	(ARGUS Collab.)
ANJOS	92B	PR D46 R1	J.C. Anjos *et al.*	(FNAL E691 Collab.)
ANJOS	92C	PR D46 1941	J.C. Anjos *et al.*	(FNAL E691 Collab.)
BARLAG	92C	ZPHY C55 383	S. Barlag *et al.*	(ACCMOR Collab.)
Also	90D	ZPHY C48 29	S. Barlag *et al.*	(ACCMOR Collab.)
COFFMAN	92B	PR D45 2196	D.M. Coffman *et al.*	(Mark III Collab.)
Also	90	PRL 64 2615	J. Adler *et al.*	(Mark III Collab.)
FRABETTI	92	PL B281 167	P.L. Frabetti *et al.*	(FNAL E687 Collab.)
FRABETTI	92B	PL B286 195	P.L. Frabetti *et al.*	(FNAL E687 Collab.)
ALVAREZ	91B	ZPHY C50 11	M.P. Alvarez *et al.*	(CERN NA14/2 Collab.)
AMMAR	91	PR D44 3383	R. Ammar *et al.*	(CLEO Collab.)
ANJOS	91	PR D43 R635	J.C. Anjos *et al.*	(FNAL-TPS Collab.)
ANJOS	91D	PR D44 R3371	J.C. Anjos *et al.*	(FNAL-TPS Collab.)
BAI	91	PRL 66 1011	Z. Bai *et al.*	(Mark III Collab.)
COFFMAN	91	PL B263 135	D.M. Coffman *et al.*	(Mark III Collab.)
CRAWFORD	91B	PR D44 3394	G. Crawford *et al.*	(CLEO Collab.)
DECAMP	91J	PL B266 218	D. Decamp *et al.*	(ALEPH Collab.)
FRABETTI	91	PL B263 584	P.L. Frabetti *et al.*	(FNAL E687 Collab.)
KINOSHITA	91	PR D43 2836	K. Kinoshita *et al.*	(CLEO Collab.)
KODAMA	91	PRL 66 1819	K. Kodama *et al.*	(FNAL E653 Collab.)
ALBRECHT	90C	ZPHY C46 9	H. Albrecht *et al.*	(ARGUS Collab.)
ALEXANDER	90	PRL 65 1184	J. Alexander *et al.*	(CLEO Collab.)
ALEXANDER	90B	PRL 65 1531	J. Alexander *et al.*	(CLEO Collab.)
ALVAREZ	90	ZPHY C47 539	M.P. Alvarez *et al.*	(CERN NA14/2 Collab.)
ANJOS	90D	PR D42 2414	J.C. Anjos *et al.*	(FNAL E691 Collab.)
BARLAG	90C	ZPHY C46 563	S. Barlag *et al.*	(ACCMOR Collab.)
ADLER	89	PRL 62 1821	J. Adler *et al.*	(Mark III Collab.)
ADLER	89C	PR D40 906	J. Adler *et al.*	(Mark III Collab.)
ALBRECHT	89D	ZPHY C43 181	H. Albrecht *et al.*	(ARGUS Collab.)
ANJOS	89F	PRL 62 1587	J.C. Anjos *et al.*	(FNAL E691 Collab.)
ABACHI	88	PL B205 411	S. Abachi *et al.*	(HRS Collab.)
ADLER	88	PR D37 2023	J. Adler *et al.*	(Mark III Collab.)
ADLER	88C	PRL 60 89	J. Adler *et al.*	(Mark III Collab.)
ALBRECHT	88G	PL B209 380	H. Albrecht *et al.*	(ARGUS Collab.)
ALBRECHT	88I	PL B210 267	H. Albrecht *et al.*	(ARGUS Collab.)
ANJOS	88C	PRL 60 1239	J.C. Anjos *et al.*	(FNAL E691 Collab.)
BORTOLETTO	88	PR D37 1719	D. Bortoletto *et al.*	(CLEO Collab.)
Also	89D	PR D39 1471 erratum	D. Bortoletto *et al.*	(CLEO Collab.)
CUMALAT	88	PL B210 253	J.P. Cumalat *et al.*	(E-400 Collab.)
HAAS	88	PRL 60 1614	P. Haas *et al.*	(CLEO Collab.)
RAAB	88	PR D37 2391	J.R. Raab *et al.*	(FNAL E691 Collab.)
ADAMOVICH	87	EPL 4 887	M.I. Adamovich *et al.*	(Photon Emulsion Collab.)
ADLER	87	PL B196 107	J. Adler *et al.*	(Mark III Collab.)
AGUILAR-...	87E	ZPHY C36 551	M. Aguilar-Benitez *et al.*	(LEBC-EHS Collab.)
Also	88B	ZPHY C40 321	M. Aguilar-Benitez *et al.*	(LEBC-EHS Collab.)
AGUILAR-...	87F	ZPHY C36 559	M. Aguilar-Benitez *et al.*	(LEBC-EHS Collab.)
Also	88	ZPHY C38 520 erratum	M. Aguilar-Benitez *et al.*	(LEBC-EHS Collab.)
ALBRECHT	87E	ZPHY C33 359	H. Albrecht *et al.*	(ARGUS Collab.)
ALBRECHT	87K	PL B199 447	H. Albrecht *et al.*	(ARGUS Collab.)
BARLAG	87B	ZPHY C37 17	S. Barlag *et al.*	(ACCMOR Collab.)
BECKER	87C	PL B193 147	J.J. Becker *et al.*	(Mark III Collab.)
Also	87D	PL B198 590 erratum	J.J. Becker *et al.*	(Mark III Collab.)
PALKA	87	PL B189 238	H. Palka *et al.*	(ACCMOR Collab.)
RILES	87	PR D35 2914	K. Riles *et al.*	(Mark II Collab.)
BAILEY	86	ZPHY C30 51	R. Bailey *et al.*	(ACCMOR Collab.)
BEBEK	86	PRL 56 1893	C. Bebek *et al.*	(CLEO Collab.)
LOUIS	86	PRL 56 1027	W.C. Louis *et al.*	(PRIN, CHIC, ISU)
ALBRECHT	85B	PL 150B 525	H. Albrecht *et al.*	(ARGUS Collab.)
ALBRECHT	85F	PL 150B 235	H. Albrecht *et al.*	(ARGUS Collab.)
AUBERT	85	PL 155B 461	J.J. Aubert *et al.*	(EMC Collab.)
BALTRUSAIT...	85B	PRL 54 1976	R.M. Baltrusaitis *et al.*	(Mark III Collab.)
BALTRUSAIT...	85E	PRL 55 150	R.M. Baltrusaitis *et al.*	(Mark III Collab.)
BENVENUTI	85	PL 158B 531	A.C. Benvenuti *et al.*	(BCDMS Collab.)
ADAMOVICH	84B	PL 140B 123	M.I. Adamovich *et al.*	(CERN WA58 Collab.)
DERRICK	84	PRL 53 1971	M. Derrick *et al.*	(HRS Collab.)
PARTRIDGE	84	Thesis CALT-68-1150	R.A. Partridge	(Crystal Ball Collab.)
SUMMERS	84	PRL 52 410	D.J. Summers *et al.*	(UCSB, CARL, COLO+)
BAILEY	83B	PL 132B 237	R. Bailey *et al.*	(ACCMOR Collab.)
BODEK	82	PL 113B 82	A. Bodek *et al.*	(ROCH, CIT, CHIC, FNAL+)
FIORINO	81	LNC 30 166	A. Fiorino *et al.*	
SCHINDLER	81	PR D24 78	R.H. Schindler *et al.*	(Mark II Collab.)
TRILLING	81	PRPL 75 57	G.H. Trilling	(LBL, UCB) J
ASTON	80E	PL 94B 113	D. Aston *et al.*	(BONN, CERN, EPOL, GLAS+)
AVERY	80	PRL 44 1309	P. Avery *et al.*	(ILL, FNAL, COLU)
SCHINDLER	80	PR D21 2716	R.H. Schindler *et al.*	(Mark II Collab.)
ZHOLENTZ	80	PL 96B 214	A.A. Zholents *et al.*	(NOVO)
Also	81	SJNP 34 814 Translated from YAF 34 1471.	A.A. Zholents *et al.*	(NOVO)
ABRAMS	79D	PRL 43 481	G.S. Abrams *et al.*	(Mark II Collab.)
ATIYA	79	PRL 43 414	M.S. Atiya *et al.*	(COLU, ILL, FNAL)
BALTAY	78C	PRL 41 73	C. Baltay *et al.*	(COLU, BNL)
VUILLEMIN	78	PRL 41 1149	V. Vuillemin *et al.*	(Mark I Collab.)
GOLDHABER	77	PL 69B 503	G. Goldhaber *et al.*	(Mark I Collab.)
PERUZZI	77	PRL 39 1301	I. Peruzzi *et al.*	(Mark I Collab.)
PICCOLO	77	PL 70B 260	M. Piccolo *et al.*	(Mark I Collab.)
RAPIDIS	77	PRL 39 526	P.A. Rapidis *et al.*	(Mark I Collab.)
GOLDHABER	76	PRL 37 255	G. Goldhaber *et al.*	(Mark I Collab.)

OTHER RELATED PAPERS

RICHMAN	95	RMP 67 893	J.D. Richman, P.R. Burchat	(UCSB, STAN)
ROSNER	95	CNPP 21 369	J. Rosner	(CHIC)

$D^*(2007)^0$

$I(J^P) = \frac{1}{2}(1^-)$
I, J, P need confirmation.

J consistent with 1, value 0 ruled out (NGUYEN 77).

$D^*(2007)^0$ MASS

The fit includes $D^\pm$, D^0, $D_s^\pm$, $D^{*\pm}$, D^{*0}, and $D_s^{*\pm}$ mass and mass difference measurements.

VALUE (MeV)	DOCUMENT ID	TECN	COMMENT
2006.7±0.5 OUR FIT Error includes scale factor of 1.1.			
• • • We do not use the following data for averages, fits, limits, etc. • • •			
2006 ±1.5	[1] GOLDHABER 77	MRK1	e^+e^-

[1] From simultaneous fit to $D^*(2010)^+$, $D^*(2007)^0$, D^+, and D^0.

$m_{D^*(2007)^0} - m_{D^0}$

The fit includes $D^\pm$, D^0, $D_s^\pm$, $D^{*\pm}$, D^{*0}, and $D_s^{*\pm}$ mass and mass difference measurements.

VALUE (MeV)	EVTS	DOCUMENT ID	TECN	COMMENT
142.12±0.07 OUR FIT				
142.12±0.07 OUR AVERAGE				
142.2 ±0.3 ±0.2	145	ALBRECHT 95F	ARG	$e^+e^- \to$ hadrons
142.12±0.05±0.05	1176	BORTOLETTO 92B	CLE2	$e^+e^- \to$ hadrons
• • • We do not use the following data for averages, fits, limits, etc. • • •				
142.2 ±2.0		SADROZINSKI 80	CBAL	$D^{*0} \to D^0\pi^0$
142.7 ±1.7		[2] GOLDHABER 77	MRK1	e^+e^-

[2] From simultaneous fit to $D^*(2010)^+$, $D^*(2007)^0$, D^+, and D^0.

$D^*(2007)^0$ WIDTH

VALUE (MeV)	CL%	DOCUMENT ID		TECN	COMMENT
<2.1	90	[3] ABACHI	88B	HRS	$D^{*0} \to D^+\pi^-$

[3] Assuming $m_{D^{*0}} = 2007.2 \pm 2.1$ MeV/c^2.

$D^*(2007)^0$ DECAY MODES

$\overline{D}{}^*(2007)^0$ modes are charge conjugates of modes below.

	Mode	Fraction (Γ_j/Γ)
Γ_1	$D^0\pi^0$	(61.9 ± 2.9) %
Γ_2	$D^0\gamma$	(38.1 ± 2.9) %

CONSTRAINED FIT INFORMATION

An overall fit to a branching ratio uses 3 measurements and one constraint to determine 2 parameters. The overall fit has a $\chi^2 = 0.5$ for 2 degrees of freedom.

The following *off-diagonal* array elements are the correlation coefficients $\langle \delta x_i \delta x_j \rangle / (\delta x_i \cdot \delta x_j)$, in percent, from the fit to the branching fractions, $x_i \equiv \Gamma_i/\Gamma_{\rm total}$. The fit constrains the x_i whose labels appear in this array to sum to one.

x_2	−100
	x_1

$D^*(2007)^0$ BRANCHING RATIOS

$\Gamma(D^0\pi^0)/\Gamma_{\rm total}$ Γ_1/Γ

VALUE	EVTS	DOCUMENT ID		TECN	COMMENT
0.619 ± 0.029 OUR FIT					
• • • We do not use the following data for averages, fits, limits, etc. • • •					
0.596 ± 0.035 ± 0.028	858	[4] ALBRECHT	95F	ARG	$e^+e^- \to$ hadrons
0.636 ± 0.023 ± 0.033	1097	[4] BUTLER	92	CLE2	$e^+e^- \to$ hadrons

$\Gamma(D^0\gamma)/\Gamma_{\rm total}$ Γ_2/Γ

VALUE	EVTS	DOCUMENT ID		TECN	COMMENT
0.381 ± 0.029 OUR FIT					
0.381 ± 0.029 OUR AVERAGE					
0.404 ± 0.035 ± 0.028	456	[4] ALBRECHT	95F	ARG	$e^+e^- \to$ hadrons
0.364 ± 0.023 ± 0.033	621	[4] BUTLER	92	CLE2	$e^+e^- \to$ hadrons
0.37 ± 0.08 ± 0.08		ADLER	88D	MRK3	e^+e^-
• • • We do not use the following data for averages, fits, limits, etc. • • •					
0.47 ± 0.23		LOW	87	HRS	29 GeV e^+e^-
0.53 ± 0.13		BARTEL	85G	JADE	e^+e^-, hadrons
0.47 ± 0.12		COLES	82	MRK2	e^+e^-
0.45 ± 0.15		GOLDHABER	77	MRK1	e^+e^-

[4] The BUTLER 92 and ALBRECHT 95F branching ratios are not independent, they have been constrained by the authors to sum to 100%.

$D^*(2007)^0$ REFERENCES

ALBRECHT	95F	ZPHY C66 63	H. Albrecht *et al.*	(ARGUS Collab.)
BORTOLETTO	92B	PRL 69 2046	D. Bortoletto *et al.*	(CLEO Collab.)
BUTLER	92	PRL 69 2041	F. Butler *et al.*	(CLEO Collab.)
ABACHI	88B	PL B212 533	S. Abachi *et al.*	(ANL, IND, MICH, PURD+)
ADLER	88D	PL B208 152	J. Adler *et al.*	(Mark III Collab.)
LOW	87	PL B183 232	E.H. Low *et al.*	(HRS Collab.)
BARTEL	85G	PL 161B 197	W. Bartel *et al.*	(JADE Collab.)
COLES	82	PR D26 2190	M.W. Coles *et al.*	(LBL, SLAC)
SADROZINSKI	80	Madison Conf. 681	H.F.W. Sadrozinski *et al.*	(PRIN, CIT+)
GOLDHABER	77	PL 69B 503	G. Goldhaber *et al.*	(Mark I Collab.)
NGUYEN	77	PRL 39 262	H.K. Nguyen *et al.*	(LBL, SLAC) J

OTHER RELATED PAPERS

EDWARDS	02	PR D65 012002	K.W. Edwards *et al.*	(CLEO Collab.)
SEMENOV	99	SPU 42 847 Translated from UFN 42 937.	S.V. Semenov	
KAMAL	92	PL B284 421	A.N. Kamal, Q.P. Xu	(ALBE)
TRILLING	81	PRPL 75 57	G.H. Trilling	(LBL, UCB)
GOLDHABER	76	PRL 37 255	G. Goldhaber *et al.*	(Mark I Collab.)

$D^*(2010)^\pm$

$I(J^P) = \frac{1}{2}(1^-)$
I, J, P need confirmation.

$D^*(2010)^\pm$ MASS

The fit includes $D^\pm$, D^0, $D_s^\pm$, $D^{*\pm}$, D^{*0}, and $D_s^{*\pm}$ mass and mass difference measurements.

VALUE (MeV)	DOCUMENT ID		TECN	CHG	COMMENT
2010.0 ± 0.5 OUR FIT Error includes scale factor of 1.1.					
• • • We do not use the following data for averages, fits, limits, etc. • • •					
2008 ± 3	[1] GOLDHABER	77	MRK1	±	e^+e^-
2008.6 ± 1.0	[2] PERUZZI	77	MRK1	±	e^+e^-

[1] From simultaneous fit to $D^*(2010)^+$, $D^*(2007)^0$, D^+, and D^0; not independent of FELDMAN 77B mass difference below.
[2] PERUZZI 77 mass not independent of FELDMAN 77B mass difference below and PERUZZI 77 D^0 mass value.

$m_{D^*(2010)^+} - m_{D^+}$

The fit includes $D^\pm$, D^0, $D_s^\pm$, $D^{*\pm}$, D^{*0}, and $D_s^{*\pm}$ mass and mass difference measurements.

VALUE (MeV)	EVTS	DOCUMENT ID	TECN	COMMENT
140.64 ± 0.10 OUR FIT Error includes scale factor of 1.1.				
140.64 ± 0.08 ± 0.06	620	BORTOLETTO 92B	CLE2	$e^+e^- \to$ hadrons

$m_{D^*(2010)^+} - m_{D^0}$

The fit includes $D^\pm$, D^0, $D_s^\pm$, $D^{*\pm}$, D^{*0}, and $D_s^{*\pm}$ mass and mass difference measurements.

VALUE (MeV)	EVTS	DOCUMENT ID		TECN	COMMENT
145.421 ± 0.010 OUR FIT Error includes scale factor of 1.1.					
145.421 ± 0.010 OUR AVERAGE					
145.412 ± 0.002 ± 0.012		ANASTASSOV	02	CLE2	$D^{*\pm} \to D^0\pi^\pm \to (K\pi)\pi^\pm$
145.54 ± 0.08	611	[3] ADINOLFI	99	BEAT	$D^{*\pm} \to D^0\pi^\pm$
145.45 ± 0.02		[3] BREITWEG	99	ZEUS	$D^{*\pm} \to D^0\pi^\pm \to (K\pi)\pi^\pm$
145.42 ± 0.05		[3] BREITWEG	99	ZEUS	$D^{*\pm} \to D^0\pi^\pm \to (K^-3\pi)\pi^\pm$
145.5 ± 0.15	103	[4] ADLOFF	97B	H1	$D^{*\pm} \to D^0\pi^\pm$
145.44 ± 0.08	152	[4] BREITWEG	97	ZEUS	$D^{*\pm} \to D^0\pi^\pm$, $D^0 \to K^-3\pi$
145.42 ± 0.11	199	[4] BREITWEG	97	ZEUS	$D^{*\pm} \to D^0\pi^\pm$, $D^0 \to K^-\pi^+$
145.4 ± 0.2	48	[4] DERRICK	95	ZEUS	$D^{*\pm} \to D^0\pi^\pm$
145.39 ± 0.06 ± 0.03		BARLAG	92B	ACCM	π^- 230 GeV
145.5 ± 0.2	115	[4] ALEXANDER	91B	OPAL	$D^{*\pm} \to D^0\pi^\pm$
145.30 ± 0.06		[4] DECAMP	91J	ALEP	$D^{*\pm} \to D^0\pi^\pm$
145.40 ± 0.05 ± 0.10		ABACHI	88B	HRS	$D^{*\pm} \to D^0\pi^\pm$
145.46 ± 0.07 ± 0.03		ALBRECHT	85F	ARG	$D^{*\pm} \to D^0\pi^\pm$
145.5 ± 0.3	28	BAILEY	83	SPEC	$D^{*\pm} \to D^0\pi^\pm$
145.5 ± 0.3	60	FITCH	81	SPEC	π^- A
145.3 ± 0.5	30	FELDMAN	77B	MRK1	$D^{*+} \to D^0\pi^+$
• • • We do not use the following data for averages, fits, limits, etc. • • •					
145.44 ± 0.09	122	[4] BREITWEG	97B	ZEUS	$D^{*\pm} \to D^0\pi^\pm$, $D^0 \to K^-\pi^+$
145.8 ± 1.5	16	AHLEN	83	HRS	$D^{*+} \to D^0\pi^+$
145.1 ± 1.8	12	BAILEY	83	SPEC	$D^{*\pm} \to D^0\pi^\pm$
145.1 ± 0.5	14	BAILEY	83	SPEC	$D^{*\pm} \to D^0\pi^\pm$
145.5 ± 0.5	14	YELTON	82	MRK2	29 $e^+e^- \to K^-\pi^+$
~ 145.5		AVERY	80	SPEC	γ A
145.2 ± 0.6	2	BLIETSCHAU	79	BEBC	νp

[3] Statistical errors only.
[4] Systematic error not evaluated.

$m_{D^*(2010)^+} - m_{D^*(2007)^0}$

VALUE (MeV)	DOCUMENT ID		TECN	COMMENT
• • • We do not use the following data for averages, fits, limits, etc. • • •				
2.6 ± 1.8	[5] PERUZZI	77	MRK1	e^+e^-

[5] Not independent of FELDMAN 77B mass difference above, PERUZZI 77 D^0 mass, and GOLDHABER 77 $D^*(2007)^0$ mass.

$D^*(2010)^\pm$ WIDTH

VALUE (keV)	CL%	EVTS	DOCUMENT ID	TECN	COMMENT
96 ± 4 ± 22			ANASTASSOV 02	CLE2	$D^{*\pm} \to D^0\pi^\pm \to (K\pi)\pi^\pm$
• • • We do not use the following data for averages, fits, limits, etc. • • •					
<131	90	110	BARLAG	92B ACCM	π^- 230 GeV

Meson Particle Listings

$D^*(2010)^\pm$, $D_1(2420)^0$

$D^*(2010)^\pm$ DECAY MODES

$D^*(2010)^-$ modes are charge conjugates of the modes below.

	Mode	Fraction (Γ_i/Γ)
Γ_1	$D^0\pi^+$	(67.7 ± 0.5) %
Γ_2	$D^+\pi^0$	(30.7 ± 0.5) %
Γ_3	$D^+\gamma$	(1.6 ± 0.4) %

CONSTRAINED FIT INFORMATION

An overall fit to 3 branching ratios uses 6 measurements and one constraint to determine 3 parameters. The overall fit has a $\chi^2 = 0.3$ for 4 degrees of freedom.

The following *off-diagonal* array elements are the correlation coefficients $\langle \delta x_i \delta x_j \rangle / (\delta x_i \cdot \delta x_j)$, in percent, from the fit to the branching fractions, $x_i \equiv \Gamma_i/\Gamma_{total}$. The fit constrains the x_i whose labels appear in this array to sum to one.

x_2	−62	
x_3	−43	−44
	x_1	x_2

$D^*(2010)^+$ BRANCHING RATIOS

$\Gamma(D^0\pi^+)/\Gamma_{total}$ — Γ_1/Γ

VALUE	DOCUMENT ID		TECN	COMMENT
0.677 ± 0.005 OUR FIT				
0.677 ± 0.006 OUR AVERAGE				
0.6759 ± 0.0029 ± 0.0064	[6,7,8] BARTELT	98	CLE2	e^+e^-
0.688 ± 0.024 ± 0.013	ALBRECHT	95F	ARG	$e^+e^- \to$ hadrons
0.681 ± 0.010 ± 0.013	[6] BUTLER	92	CLE2	$e^+e^- \to$ hadrons
• • • We do not use the following data for averages, fits, limits, etc. • • •				
0.57 ± 0.04 ± 0.04	ADLER	88D	MRK3	e^+e^-
0.44 ± 0.10	COLES	82	MRK2	e^+e^-
0.6 ± 0.15	[8] GOLDHABER	77	MRK1	e^+e^-

$\Gamma(D^+\pi^0)/\Gamma_{total}$ — Γ_2/Γ

VALUE	EVTS	DOCUMENT ID		TECN	COMMENT
0.307 ± 0.005 OUR FIT					
0.3073 ± 0.0013 ± 0.0062		[6,7,8] BARTELT	98	CLE2	e^+e^-
• • • We do not use the following data for averages, fits, limits, etc. • • •					
0.312 ± 0.011 ± 0.008	1404	ALBRECHT	95F	ARG	$e^+e^- \to$ hadrons
0.308 ± 0.004 ± 0.008	410	[6] BUTLER	92	CLE2	$e^+e^- \to$ hadrons
0.26 ± 0.02 ± 0.02		ADLER	88D	MRK3	e^+e^-
0.34 ± 0.07		COLES	82	MRK2	e^+e^-

$\Gamma(D^+\gamma)/\Gamma_{total}$ — Γ_3/Γ

VALUE	CL%	EVTS	DOCUMENT ID		TECN	COMMENT
0.016 ± 0.004 OUR FIT						
0.016 ± 0.005 OUR AVERAGE						
0.0168 ± 0.0042 ± 0.0029			[6,7] BARTELT	98	CLE2	e^+e^-
0.011 ± 0.014 ± 0.016		12	[6] BUTLER	92	CLE2	$e^+e^- \to$ hadrons
• • • We do not use the following data for averages, fits, limits, etc. • • •						
< 0.052	90		ALBRECHT	95F	ARG	$e^+e^- \to$ hadrons
0.17 ± 0.05 ± 0.05			ADLER	88D	MRK3	e^+e^-
0.22 ± 0.12			[9] COLES	82	MRK2	e^+e^-

[6] The branching ratios are not independent, they have been constrained by the authors to sum to 100%.
[7] Systematic error includes theoretical error on the prediction of the ratio of hadronic modes.
[8] Assuming that isospin is conserved in the decay.
[9] Not independent of $\Gamma(D^0\pi^+)/\Gamma_{total}$ and $\Gamma(D^+\pi^0)/\Gamma_{total}$ measurement.

$D^*(2010)^\pm$ REFERENCES

ANASTASSOV	02	PR D65 032003	A. Anastassov *et al.*	(CLEO Collab.)
ADINOLFI	99	NP B547 3	M. Adinolfi *et al.*	(Beatrice Collab.)
BREITWEG	99	EPJ C6 67	J. Breitweg *et al.*	(ZEUS Collab.)
BARTELT	98	PRL 80 3919	J. Bartelt *et al.*	(CLEO II Collab.)
ADLOFF	97B	ZPHY C72 593	C. Adloff *et al.*	(H1 Collab.)
BREITWEG	97	PL B401 192	J. Breitweg *et al.*	(ZEUS Collab.)
BREITWEG	97B	PL B407 402	J. Breitweg *et al.*	(ZEUS Collab.)
ALBRECHT	95F	ZPHY C66 63	H. Albrecht *et al.*	(ARGUS Collab.)
DERRICK	95	PL B349 225	M. Derrick *et al.*	(ZEUS Collab.)
BARLAG	92B	PL B278 480	S. Barlag *et al.*	(ACCMOR Collab.)
BORTOLETTO	92B	PRL 69 2046	D. Bortoletto *et al.*	(CLEO Collab.)
BUTLER	92	PRL 69 2041	F. Butler *et al.*	(CLEO Collab.)
ALEXANDER	91B	PL B262 341	G. Alexander *et al.*	(OPAL Collab.)
DECAMP	91J	PL B266 218	D. Decamp *et al.*	(ALEPH Collab.)
ABACHI	88B	PL B212 533	S. Abachi *et al.*	(ANL, IND, MICH, PURD+)
ADLER	88D	PL B208 152	J. Adler *et al.*	(Mark III Collab.)
ALBRECHT	85F	PL 150B 235	H. Albrecht *et al.*	(ARGUS Collab.)
AHLEN	83	PRL 51 1147	S.P. Ahlen *et al.*	(ANL, IND, LBL+)
BAILEY	83	PL 132B 230	R. Bailey *et al.*	(AMST, BRIS, CERN, CRAC+)
COLES	82	PR D26 2190	M.W. Coles *et al.*	(LBL, SLAC)
YELTON	82	PRL 49 430	J.M. Yelton *et al.*	(SLAC, LBL, UCB+)
FITCH	81	PRL 46 761	V.L. Fitch *et al.*	(PRIN, SACL, TORI+)
AVERY	80	PRL 44 1309	P. Avery *et al.*	(ILL, FNAL, COLU)
BLIETSCHAU	79	PL 86B 108	J. Blietschau *et al.*	(AACH3, BONN, CERN+)
FELDMAN	77B	PRL 38 1313	G.J. Feldman *et al.*	(Mark I Collab.)
GOLDHABER	77	PL 69B 503	G. Goldhaber *et al.*	(Mark I Collab.)
PERUZZI	77	PRL 39 1301	I. Peruzzi *et al.*	(Mark I Collab.)

OTHER RELATED PAPERS

AHMED	01	PRL 87 251801	S. Ahmed *et al.*	(CLEO Collab.)
SEMENOV	99	SPU 42 847 Translated from UFN 42 937.	S.V. Semenov	
NUSSINOV	98	PL B418 383	S. Nussinov	
KAMAL	92	PL B284 421	A.N. Kamal, Q.P. Xu	(ALBE)
ALTHOFF	83C	PL 126B 493	M. Althoff *et al.*	(TASSO Collab.)
BEBEK	82	PRL 49 610	C. Bebek *et al.*	(HARV, OSU, ROCH, RUTG+)
TRILLING	81	PRPL 75 57	G.H. Trilling	(LBL, UCB)
PERUZZI	76	PRL 37 569	I. Peruzzi *et al.*	(Mark I Collab.)

$D_1(2420)^0$

$I(J^P) = \frac{1}{2}(1^+)$
I, J, P need confirmation.

Seen in $D^*(2010)^+\pi^-$. $J^P = 1^+$ according to ALBRECHT 89H.

$D_1(2420)^0$ MASS

VALUE (MeV)	EVTS	DOCUMENT ID		TECN	COMMENT
2422.2 ± 1.8 OUR AVERAGE Error includes scale factor of 1.2.					
2421 $^{+1}_{-2}$ ± 2	286	AVERY	94C	CLE2	$e^+e^- \to D^{*+}\pi^-X$
2422 ± 2 ± 2	51	FRABETTI	94B	E687	$\gamma Be \to D^{*+}\pi^-X$
2428 ± 3 ± 2	279	AVERY	90	CLEO	$e^+e^- \to D^{*+}\pi^-X$
2414 ± 2 ± 5	171	ALBRECHT	89H	ARG	$e^+e^- \to D^{*+}\pi^-X$
2428 ± 8 ± 5	171	ANJOS	89C	TPS	$\gamma N \to D^{*+}\pi^-X$
• • • We do not use the following data for averages, fits, limits, etc. • • •					
2425 ± 3	235	[1] ABREU	98M	DLPH	e^+e^-

[1] No systematic error given.

$D_1(2420)^0$ WIDTH

VALUE (MeV)	EVTS	DOCUMENT ID		TECN	COMMENT
18.9 $^{+4.6}_{-3.5}$ OUR AVERAGE					
20 $^{+6}_{-5}$ ± 3	286	AVERY	94C	CLE2	$e^+e^- \to D^{*+}\pi^-X$
15 ± 8 ± 4	51	FRABETTI	94B	E687	$\gamma Be \to D^{*+}\pi^-X$
23 $^{+8}_{-6}$ $^{+10}_{-3}$	279	AVERY	90	CLEO	$e^+e^- \to D^{*+}\pi^-X$
13 ± 6 $^{+10}_{-5}$	171	ALBRECHT	89H	ARG	$e^+e^- \to D^{*+}\pi^-X$
• • • We do not use the following data for averages, fits, limits, etc. • • •					
58 ±14 ±10	171	ANJOS	89C	TPS	$\gamma N \to D^{*+}\pi^-X$

$D_1(2420)^0$ DECAY MODES

$\overline{D}_1(2420)^0$ modes are charge conjugates of modes below.

	Mode	Fraction (Γ_i/Γ)
Γ_1	$D^*(2010)^+\pi^-$	seen
Γ_2	$D^+\pi^-$	not seen

$D_1(2420)^0$ BRANCHING RATIOS

$\Gamma(D^*(2010)^+\pi^-)/\Gamma_{total}$ — Γ_1/Γ

VALUE	DOCUMENT ID	TECN	COMMENT
seen	ACKERSTAFF	97W OPAL	$e^+e^- \to D^{*+}\pi^-X$
seen	AVERY	90 CLEO	$e^+e^- \to D^{*+}\pi^-X$
seen	ALBRECHT	89H ARG	$e^+e^- \to D^*\pi^-X$
seen	ANJOS	89C TPS	$\gamma N \to D^{*+}\pi^-X$

$\Gamma(D^+\pi^-)/\Gamma(D^*(2010)^+\pi^-)$ — Γ_2/Γ_1

VALUE	CL%	DOCUMENT ID	TECN	COMMENT
< 0.24	90	AVERY	90 CLEO	$e^+e^- \to D^+\pi^-X$

$D_1(2420)^0$ REFERENCES

ABREU	98M	PL B426 231	P. Abreu *et al.*	(DELPHI Collab.)
ACKERSTAFF	97W	ZPHY C76 425	K. Ackerstaff *et al.*	(OPAL Collab.)
AVERY	94C	PL B331 236	P. Avery *et al.*	(CLEO Collab.)
FRABETTI	94B	PRL 72 324	P.L. Frabetti *et al.*	(FNAL E687 Collab.)
AVERY	90	PR D41 774	P. Avery, D. Besson	(CLEO Collab.)
ALBRECHT	89H	PL B232 398	H. Albrecht *et al.*	(ARGUS Collab.) JP
ANJOS	89C	PRL 62 1717	J.C. Anjos *et al.*	(FNAL E691 Collab.)

OTHER RELATED PAPERS

SEMENOV	99	SPU 42 847 Translated from UFN 42 937.	S.V. Semenov	

$D_1(2420)^{\pm}$

$I(J^P) = \frac{1}{2}(?^?)$
I needs confirmation.

OMITTED FROM SUMMARY TABLE
Seen in $D^*(2007)^0\pi^+$. $J^P = 0^+$ ruled out.

$D_1(2420)^{\pm}$ MASS

VALUE (MeV)	EVTS	DOCUMENT ID		TECN	COMMENT
2427±5 OUR AVERAGE	Error includes scale factor of 2.0.				
2425±2±2	146	BERGFELD	94B	CLE2	$e^+e^- \to D^{*0}\pi^+X$
2443±7±5	190	ANJOS	89C	TPS	$\gamma N \to D^0\pi^+X^0$

$m_{D_1^0(2420)^{\pm}} - m_{D_1^0(2420)^0}$

VALUE (MeV)	DOCUMENT ID		TECN	COMMENT
$4^{+2}_{-3}\pm3$	BERGFELD	94B	CLE2	$e^+e^- \to$ hadrons

$D_1(2420)^{\pm}$ WIDTH

VALUE (MeV)	EVTS	DOCUMENT ID		TECN	COMMENT
28± 8 OUR AVERAGE					
$26^{+}_{-}\,^{8}_{7}\pm4$	146	BERGFELD	94B	CLE2	$e^+e^- \to D^{*0}\pi^+X$
41±19±8	190	ANJOS	89C	TPS	$\gamma N \to D^0\pi^+X^0$

$D_1(2420)^{\pm}$ DECAY MODES

$D_1^*(2420)^-$ modes are charge conjugates of modes below.

	Mode	Fraction (Γ_i/Γ)
Γ_1	$D^*(2007)^0\pi^+$	seen
Γ_2	$D^0\pi^+$	not seen

$D_1(2420)^{\pm}$ BRANCHING RATIOS

$\Gamma(D^*(2007)^0\pi^+)/\Gamma_{\text{total}}$ Γ_1/Γ

VALUE	DOCUMENT ID		TECN	COMMENT
seen	ANJOS	89C	TPS	$\gamma N \to D^0\pi^+X^0$

$\Gamma(D^0\pi^+)/\Gamma(D^*(2007)^0\pi^+)$ Γ_2/Γ_1

VALUE	CL%	DOCUMENT ID		TECN	COMMENT
• • • We do not use the following data for averages, fits, limits, etc. • • •					
<0.18	90	BERGFELD	94B	CLE2	$e^+e^- \to$ hadrons

$D_1(2420)^{\pm}$ REFERENCES

BERGFELD	94B	PL B340 194	T. Bergfeld *et al.*	(CLEO Collab.)
ANJOS	89C	PRL 62 1717	J.C. Anjos *et al.*	(FNAL E691 Collab.)

OTHER RELATED PAPERS

SEMENOV	99	SPU 42 847 Translated from UFN 42 937.	S.V. Semenov

$D_2^*(2460)^0$

$I(J^P) = \frac{1}{2}(2^+)$
$J^P = 2^+$ assignment strongly favored(ALBRECHT 89B).

$D_2^*(2460)0$ MASS

VALUE (MeV)	EVTS	DOCUMENT ID		TECN	COMMENT
2458.9±2.0 OUR AVERAGE	Error includes scale factor of 1.2.				
2465 ±3 ±3	486	AVERY	94C	CLE2	$e^+e^- \to D^+\pi^-X$
2453 ±3 ±2	128	FRABETTI	94B	E687	γBe $\to D^+\pi^-X$
2461 ±3 ±1	440	AVERY	90	CLEO	$e^+e^- \to D^{*+}\pi^-X$
2455 ±3 ±5	337	ALBRECHT	89B	ARG	$e^+e^- \to D^+\pi^-X$
2459 ±3 ±2	153	ANJOS	89C	TPS	$\gamma N \to D^+\pi^-X$
• • • We do not use the following data for averages, fits, limits, etc. • • •					
2461 ±6	126	[1] ABREU	98M	DLPH	e^+e^-
2466 ±7	1	ASRATYAN	95	BEBC	53,40 $\nu(\overline{\nu}) \to p + X$, $d + X$

[1] No systematic error given.

$D_2^*(2460)^0$ WIDTH

VALUE (MeV)	EVTS	DOCUMENT ID		TECN	COMMENT
23± 5 OUR AVERAGE					
$28^{+}_{-}\,^{8}_{7}\pm6$	486	AVERY	94C	CLE2	$e^+e^- \to D^+\pi^-X$
25±10± 5	128	FRABETTI	94B	E687	γBe $\to D^+\pi^-X$
$20^{+}_{-}\,^{9}_{12}\,^{9}_{10}$	440	AVERY	90	CLEO	$e^+e^- \to D^{*+}\pi^-X$
$15^{+13}_{-10}\,^{+5}_{-10}$	337	ALBRECHT	89B	ARG	$e^+e^- \to D^+\pi^-X$
20±10± 5	153	ANJOS	89C	TPS	$\gamma N \to D^+\pi^-X$

$D_2^*(2460)^0$ DECAY MODES

$\overline{D}_2^*(2460)^0$ modes are charge conjugates of modes below.

	Mode	Fraction (Γ_i/Γ)
Γ_1	$D^+\pi^-$	seen
Γ_2	$D^*(2010)^+\pi^-$	seen

$D_2^*(2460)^0$ BRANCHING RATIOS

$\Gamma(D^+\pi^-)/\Gamma_{\text{total}}$ Γ_1/Γ

VALUE	DOCUMENT ID		TECN	COMMENT
seen	ALBRECHT	89B	ARG	$e^+e^- \to D^+\pi^-X$
seen	ANJOS	89C	TPS	$\gamma N \to D^+\pi^-X$

$\Gamma(D^*(2010)^+\pi^-)/\Gamma_{\text{total}}$ Γ_2/Γ

VALUE	DOCUMENT ID		TECN	COMMENT
seen	ACKERSTAFF	97W	OPAL	$e^+e^- \to D^{*+}\pi^-X$
seen	AVERY	90	CLEO	$e^+e^- \to D^{*+}\pi^-X$
seen	ALBRECHT	89H	ARG	$e^+e^- \to D^*\pi^-X$

$\Gamma(D^+\pi^-)/\Gamma(D^*(2010)^+\pi^-)$ Γ_1/Γ_2

VALUE	DOCUMENT ID		TECN	COMMENT
2.3±0.6 OUR AVERAGE				
2.2± 0.7± 0.6	AVERY	94C	CLE2	$e^+e^- \to D^{*+}\pi^-X$
2.3± 0.8	AVERY	90	CLEO	e^+e^-
3.0± 1.1± 1.5	ALBRECHT	89H	ARG	$e^+e^- \to D^*\pi^-X$

$D_2^*(2460)^0$ REFERENCES

ABREU	98M	PL B426 231	P. Abreu *et al.*	(DELPHI Collab.)
ACKERSTAFF	97W	ZPHY C76 425	K. Ackerstaff *et al.*	(OPAL Collab.)
ASRATYAN	95	ZPHY C68 43	A.E. Asratyan *et al.*	(BIRM, BELG, CERN+)
AVERY	94C	PL B331 236	P. Avery *et al.*	(CLEO Collab.)
FRABETTI	94B	PRL 72 324	P.L. Frabetti *et al.*	(FNAL E687 Collab.)
AVERY	90	PR D41 774	P. Avery, D. Besson	(CLEO Collab.)
ALBRECHT	89B	PL B221 422	H. Albrecht *et al.*	(ARGUS Collab.) JP
ALBRECHT	89H	PL B232 398	H. Albrecht *et al.*	(ARGUS Collab.) JP
ANJOS	89C	PRL 62 1717	J.C. Anjos *et al.*	(FNAL E691 Collab.)

OTHER RELATED PAPERS

SEMENOV	99	SPU 42 847 Translated from UFN 42 937.	S.V. Semenov

$D_2^*(2460)^{\pm}$

$I(J^P) = \frac{1}{2}(2^+)$
$J^P = 2^+$ assignment strongly favored(ALBRECHT 89B).

$D_2^*(2460)^{\pm}$ MASS

VALUE (MeV)	EVTS	DOCUMENT ID		TECN	COMMENT
2459±4 OUR AVERAGE	Error includes scale factor of 1.7. See the ideogram below.				
2463±3±3	310	BERGFELD	94B	CLE2	$e^+e^- \to D^0\pi^+X$
2453±3±2	185	FRABETTI	94B	E687	γBe $\to D^0\pi^+X$
2469±4±6		ALBRECHT	89F	ARG	$e^+e^- \to D^0\pi^+X$

Meson Particle Listings

$D_2^*(2460)^\pm$, $D^*(2640)^\pm$

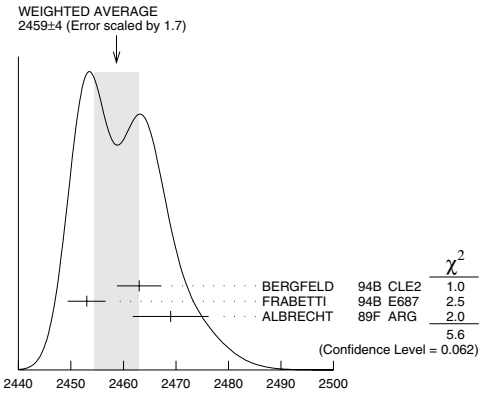

$m_{D_2^*(2460)^\pm} - m_{D_2^*(2460)^0}$

VALUE (MeV)			DOCUMENT ID		TECN	COMMENT
0.9±3.3 OUR AVERAGE			Error includes scale factor of 1.1.			
− 2	±4	±4	BERGFELD	94B	CLE2	$e^+e^- \to$ hadrons
0	±4		FRABETTI	94B	E687	γBe $\to D\pi X$
14	±5	±8	ALBRECHT	89F	ARG	$e^+e^- \to D^0\pi^+X$

$D_2^*(2460)^\pm$ WIDTH

VALUE (MeV)	EVTS	DOCUMENT ID		TECN	COMMENT
$25 \pm \frac{8}{7}$ OUR AVERAGE					
$27 \pm \frac{11}{8} \pm 5$	310	BERGFELD	94B	CLE2	$e^+e^- \to D^0\pi^+X$
23± 9±5	185	FRABETTI	94B	E687	γBe $\to D^0\pi^+X$

$D_2^*(2460)^\pm$ DECAY MODES

$D_2^*(2460)^-$ modes are charge conjugates of modes below.

	Mode	Fraction (Γ_i/Γ)
Γ_1	$D^0\pi^+$	seen
Γ_2	$D^{*0}\pi^+$	seen

$D_2^*(2460)^\pm$ BRANCHING RATIOS

$\Gamma(D^0\pi^+)/\Gamma_{total}$ **Γ_1/Γ**

VALUE	DOCUMENT ID		TECN	COMMENT
seen	ALBRECHT	89F	ARG	$e^+e^- \to D^0\pi^+X$

$\Gamma(D^0\pi^+)/\Gamma(D^{*0}\pi^+)$ **Γ_1/Γ_2**

VALUE	DOCUMENT ID		TECN	COMMENT
1.9±1.1±0.3	BERGFELD	94B	CLE2	$e^+e^- \to$ hadrons

$D_2^*(2460)^\pm$ REFERENCES

BERGFELD	94B	PL B340 194	T. Bergfeld *et al.*	(CLEO Collab.)
FRABETTI	94B	PRL 72 324	P.L. Frabetti *et al.*	(FNAL E687 Collab.)
ALBRECHT	89B	PL B221 422	H. Albrecht *et al.*	(ARGUS Collab.)
ALBRECHT	89F	PL B231 208	H. Albrecht *et al.*	(ARGUS Collab.)

$D^*(2640)^\pm$ $I(J^P) = \frac{1}{2}(?^?)$

OMITTED FROM SUMMARY TABLE

Seen in Z decays by ABREU 98M. Not seen by ABBIENDI 01N. Needs confirmation.

$D^*(2640)^\pm$ MASS

VALUE (MeV)	EVTS	DOCUMENT ID		TECN	COMMENT
2637±2±6	66 ± 14	ABREU	98M	DLPH	$e^+e^- \to D^{*+}\pi^+\pi^-X$

$D^*(2640)^\pm$ WIDTH

VALUE (MeV)	CL%	DOCUMENT ID		TECN	COMMENT
<15	95	ABREU	98M	DLPH	$e^+e^- \to D^{*+}\pi^+\pi^-X$

$D^*(2640)^+$ DECAY MODES

$D^*(2640)^-$ modes are charge conjugates of modes below.

	Mode	Fraction (Γ_i/Γ)
Γ_1	$D^*(2010)^+\pi^+\pi^-$	seen

$D^*(2640)^\pm$ REFERENCES

ABBIENDI	01N	EPJ C20 445	G. Abbiendi *et al.*	(OPAL Collab.)
ABREU	98M	PL B426 231	P. Abreu *et al.*	(DELPHI Collab.)

CHARMED, STRANGE MESONS ($C = S = \pm 1$)

$D_s^+ = c\bar{s}$, $D_s^- = \bar{c}s$, similarly for D_s^*'s

$D_s^\pm$ was $F^\pm$

$I(J^P) = 0(0^-)$

The angular distributions of the decays of the ϕ and $\overline{K}^*(892)^0$ in the $\phi\pi^+$ and $K^+\overline{K}^*(892)^0$ modes strongly indicate that the spin is zero. The parity given is that expected of a $c\bar{s}$ ground state.

$D_s^\pm$ MASS

The fit includes $D^\pm$, D^0, $D_s^\pm$, $D^{*\pm}$, D^{*0}, and $D_s^{*\pm}$ mass and mass difference measurements. Measurements of the $D_s^\pm$ mass with an error greater than 10 MeV are omitted from the fit and average. A number of early measurements have been omitted altogether.

VALUE (MeV)	EVTS	DOCUMENT ID		TECN	COMMENT
1968.3 ± 0.5 OUR FIT Error includes scale factor of 1.2.					
1969.0 ± 1.4 OUR AVERAGE Error includes scale factor of 1.5. See the ideogram below.					
1967.0 ± 1.0 ± 1.0	54	BARLAG	90C	ACCM	π^- Cu 230 GeV
1969.3 ± 1.4 ± 1.4		ALBRECHT	88	ARG	e^+e^- 9.4–10.6 GeV
1972.7 ± 1.5 ± 1.0	21	BECKER	87B	SILI	200 GeV π,K,p
1972.4 ± 3.7 ± 3.7	27	BLAYLOCK	87	MRK3	e^+e^- 4.14 GeV
1963 ± 3 ± 3	30	DERRICK	85B	HRS	e^+e^- 29 GeV
1970 ± 5 ± 5	104	CHEN	83C	CLEO	e^+e^- 10.5 GeV
• • • We do not use the following data for averages, fits, limits, etc. • • •					
1968.3 ± 0.7 ± 0.7	290	[1] ANJOS	88	E691	Photoproduction
1980 ± 15	6	USHIDA	86	EMUL	ν wideband
1973.6 ± 2.6 ± 3.0	163	ALBRECHT	85D	ARG	e^+e^- 10 GeV
1948 ± 28 ± 10	65	AIHARA	84D	TPC	e^+e^- 29 GeV
1975 ± 9 ± 10	49	ALTHOFF	84	TASS	e^+e^- 14–25 GeV
1975 ± 4	3	BAILEY	84	ACCM	hadron$^+$ Be $\rightarrow$ $\phi\pi^+$X

[1] ANJOS 88 enters the fit via $m_{D_s^\pm} - m_{D^\pm}$ (see below).

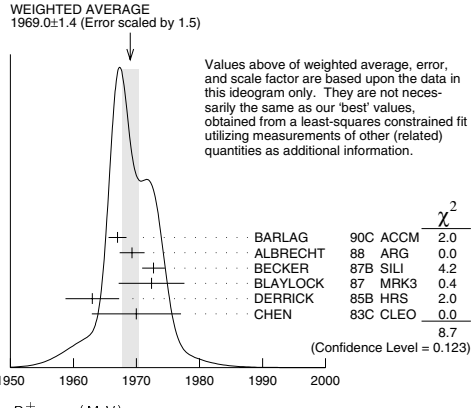

$m_{D_s^\pm} - m_{D^\pm}$

The fit includes $D^\pm$, D^0, $D_s^\pm$, $D^{*\pm}$, D^{*0}, and $D_s^{*\pm}$ mass and mass difference measurements.

VALUE (MeV)	EVTS	DOCUMENT ID		TECN	COMMENT
98.87 ± 0.31 OUR FIT Error includes scale factor of 1.4.					
98.85 ± 0.25 OUR AVERAGE Error includes scale factor of 1.1.					
99.41 ± 0.38 ± 0.21		ACOSTA	03D	CDF2	$\bar{p}p$, $\sqrt{s}$ = 1.96 TeV
98.4 ± 0.1 ± 0.3	48k	AUBERT	02G	BABR	$e^+e^- \approx \Upsilon(4S)$
99.5 ± 0.6 ± 0.3		BROWN	94	CLE2	$e^+e^- \approx \Upsilon(4S)$
98.5 ± 1.5	555	CHEN	89	CLEO	e^+e^- 10.5 GeV
99.0 ± 0.8	290	ANJOS	88	E691	Photoproduction

$D_s^\pm$ MEAN LIFE

Measurements with an error greater than 100×10^{-15} s or with fewer than 100 events have been omitted from the Listings.

VALUE (10^{-15} s)	EVTS	DOCUMENT ID		TECN	COMMENT
490 ± 9 OUR AVERAGE Error includes scale factor of 1.1.					
472.5 ± 17.2 ± 6.6	760	IORI	01	SELX	600 GeV Σ^-, π^-, p
518 ± 14 ± 7	1662	AITALA	99	E791	π^- nucleus, 500 GeV
486.3 ± 15.0 $^{+4.9}_{-5.1}$	2167	[2] BONVICINI	99	CLE2	$e^+e^- \approx \Upsilon(4S)$
475 ± 20 ± 7	900	FRABETTI	93F	E687	γBe, $\phi\pi^+$
500 ± 60 ± 30	104	FRABETTI	90	E687	γBe, $\phi\pi^+$
470 ± 40 ± 20	228	RAAB	88	E691	Photoproduction

[2] BONVICINI 99 obtains 1.19 ± 0.04 for the ratio of D_s^+ to D^0 lifetimes.

D_s^+ DECAY MODES

Unless otherwise noted, the branching fractions for modes with a resonance in the final state include all the decay modes of the resonance. D_s^- modes are charge conjugates of the modes below.

	Mode		Fraction (Γ_j/Γ)	Scale factor/ Confidence level
	Inclusive modes			
Γ_1	K^- anything		(13 $^{+14}_{-12}$) %	
Γ_2	$\overline{K}^0$ anything + K^0 anything		(39 ± 28) %	
Γ_3	K^+ anything		(20 $^{+18}_{-14}$) %	
Γ_4	(non-$K\overline{K}$) anything		(64 ± 17) %	
Γ_5	e^+ anything		(8 $^{+6}_{-5}$) %	
Γ_6	ϕ anything		(18 $^{+15}_{-10}$) %	
	Leptonic and semileptonic modes			
Γ_7	$\mu^+\nu_\mu$		(5.0 ± 1.9) $\times 10^{-3}$	S=1.3
Γ_8	$\tau^+\nu_\tau$		(6.4 ± 1.5) %	
Γ_9	$\phi\ell^+\nu_\ell$	[a]	(2.0 ± 0.5) %	
Γ_{10}	$\eta\ell^+\nu_\ell$ + $\eta'(958)\ell^+\nu_\ell$	[a]	(3.4 ± 1.0) %	
Γ_{11}	$\eta\ell^+\nu_\ell$	[a]	(2.5 ± 0.7) %	
Γ_{12}	$\eta'(958)\ell^+\nu_\ell$	[a]	(8.9 ± 3.3) $\times 10^{-3}$	
	Hadronic modes with a $K\overline{K}$ pair (including from a ϕ)			
Γ_{13}	$K^+\overline{K}^0$		(3.6 ± 1.1) %	
Γ_{14}	$K^+K^-\pi^+$	[b]	(4.4 ± 1.2) %	
Γ_{15}	$\phi\pi^+$	[c]	(3.6 ± 0.9) %	
Γ_{16}	$K^+\overline{K}^*(892)^0$	[c]	(3.3 ± 0.9) %	
Γ_{17}	$f_0(980)\pi^+$ $\times$ B($f_0 \rightarrow K^+K^-$)	[d]	(4.9 ± 2.3) $\times 10^{-3}$	
Γ_{18}	$K^+\overline{K}_0^*(1430)^0$	[c]	(7 ± 4) $\times 10^{-3}$	
Γ_{19}	$f_0(1710)\pi^+$ $\times$ B($f_0 \rightarrow K^+K^-$)			
Γ_{20}	$K^+K^-\pi^+$ nonresonant		(9 ± 4) $\times 10^{-3}$	
Γ_{21}	$K^0\overline{K}^0\pi^+$		—	
Γ_{22}	$K^*(892)^+\overline{K}^0$	[c]	(4.3 ± 1.4) %	
Γ_{23}	$K^+K^-\pi^+\pi^0$		—	
Γ_{24}	$\phi\pi^+\pi^0$	[c]	(9 ± 5) %	
Γ_{25}	$\phi\rho^+$	[c]	(6.7 ± 2.3) %	
Γ_{26}	$\phi\pi^+\pi^0$ 3-body	[c]	< 2.6 %	CL=90%
Γ_{27}	$K^+K^-\pi^+\pi^0$ non-ϕ		< 9 %	CL=90%
Γ_{28}	$K^+\overline{K}^0\pi^+\pi^-$		(2.5 ± 0.9) %	
Γ_{29}	$K^0K^-\pi^+\pi^+$		(4.3 ± 1.5) %	
Γ_{30}	$K^*(892)^+\overline{K}^*(892)^0$	[c]	(5.8 ± 2.5) %	
Γ_{31}	$K^0K^-\pi^+\pi^+$(non-$K^{*+}\overline{K}^{*0}$)		< 2.9 %	CL=90%
Γ_{32}	$K^+K^-\pi^+\pi^+\pi^-$		(7.1 ± 2.2) $\times 10^{-3}$	
Γ_{33}	$\phi\pi^+\pi^+\pi^-$	[c]	(9.7 ± 2.6) $\times 10^{-3}$	
Γ_{34}	$K^+K^-\rho^0\pi^+$ non-ϕ		< 2.1 $\times 10^{-4}$	CL=90%
Γ_{35}	$\phi\rho^0\pi^+$	[c]	(1.06 ± 0.35) %	
Γ_{36}	$\phi a_1(1260)^+$	[c]	(2.5 ± 0.8) %	
Γ_{37}	$K^+K^-\pi^+\pi^+\pi^-$ nonresonant		(7 ± 6) $\times 10^{-4}$	
	Hadronic modes without K's			
Γ_{38}	$\pi^+\pi^+\pi^-$		(1.01 ± 0.28) %	S=1.1
Γ_{39}	$\rho^0\pi^+$		< 7 $\times 10^{-4}$	CL=90%
Γ_{40}	$f_0(980)\pi^+ \times$ B($f_0 \rightarrow \pi^+\pi^-$)	[e]	(5.7 ± 1.7) $\times 10^{-3}$	
Γ_{41}	$f_2(1270)\pi^+$	[c]	(3.5 ± 1.2) $\times 10^{-3}$	
Γ_{42}	$f_0(1370)\pi^+$ $\times$ B($f_0 \rightarrow \pi^+\pi^-$)	[e]	(3.3 ± 1.2) $\times 10^{-3}$	

Γ_{43}	$\rho(1450)^0\pi^+$ × B($\rho^0 \to \pi^+\pi^-$)	[e]	(4.4 ± 2.5) × 10^{-4}		
Γ_{44}	$f_0(1500)\pi^+$ × B($f_0 \to \pi^+\pi^-$)				
Γ_{45}	$\pi^+\pi^+\pi^-$ nonresonant		(5 $^{+22}_{-5}$) × 10^{-5}		
Γ_{46}	$\pi^+\pi^+\pi^-\pi^0$		< 12	%	CL=90%
Γ_{47}	$\eta\pi^+$	[c]	(1.7 ± 0.5) %		
Γ_{48}	$\omega\pi^+$	[c]	(2.8 ± 1.1) × 10^{-3}		
Γ_{49}	$3\pi^+2\pi^-$		(6.5 ± 1.8) × 10^{-3}		
Γ_{50}	$\pi^+\pi^+\pi^-\pi^0\pi^0$		—		
Γ_{51}	$\eta\rho^+$	[c]	(10.8 ± 3.1) %		
Γ_{52}	$\eta\pi^+\pi^0$ 3-body	[c]	< 4	%	CL=90%
Γ_{53}	$3\pi^+2\pi^-\pi^0$		(4.9 ± 3.2) %		
Γ_{54}	$\eta'(958)\pi^+$	[c]	(3.9 ± 1.0) %		
Γ_{55}	$3\pi^+2\pi^-2\pi^0$		—		
Γ_{56}	$\eta'(958)\rho^+$	[c]	(10.1 ± 2.8) %		
Γ_{57}	$\eta'(958)\pi^+\pi^0$ 3-body	[c]	< 1.4	%	CL=90%

Modes with one or three K's

Γ_{58}	$K^0\pi^+$		< 8	× 10^{-3}	CL=90%
Γ_{59}	$K^+\pi^+\pi^-$		(1.0 ± 0.4) %		
Γ_{60}	$K^+\rho^0$		< 2.9	× 10^{-3}	CL=90%
Γ_{61}	$K^*(892)^0\pi^+$	[c]	(6.5 ± 2.8) × 10^{-3}		
Γ_{62}	$K^+K^+K^-$		(4.0 ± 1.7) × 10^{-4}		
Γ_{63}	ϕK^+	[c]	< 5	× 10^{-4}	CL=90%

$\Delta C = 1$ weak neutral current ($C1$) modes, Lepton family number (LF), or Lepton number (L) violating modes

Γ_{64}	$\pi^+e^+e^-$		[f] < 2.7	× 10^{-4}	CL=90%
Γ_{65}	$\pi^+\mu^+\mu^-$		[f] < 2.6	× 10^{-5}	CL=90%
Γ_{66}	$K^+e^+e^-$	$C1$	< 1.6	× 10^{-3}	CL=90%
Γ_{67}	$K^+\mu^+\mu^-$	$C1$	< 3.6	× 10^{-5}	CL=90%
Γ_{68}	$K^*(892)^+\mu^+\mu^-$	$C1$	< 1.4	× 10^{-3}	CL=90%
Γ_{69}	$\pi^+e^\pm\mu^\mp$	LF	[g] < 6.1	× 10^{-4}	CL=90%
Γ_{70}	$K^+e^\pm\mu^\mp$	LF	[g] < 6.3	× 10^{-4}	CL=90%
Γ_{71}	$\pi^-e^+e^+$	L	< 6.9	× 10^{-4}	CL=90%
Γ_{72}	$\pi^-\mu^+\mu^+$	L	< 2.9	× 10^{-5}	CL=90%
Γ_{73}	$\pi^-e^+\mu^+$	L	< 7.3	× 10^{-4}	CL=90%
Γ_{74}	$K^-e^+e^+$	L	< 6.3	× 10^{-4}	CL=90%
Γ_{75}	$K^-\mu^+\mu^+$	L	< 1.3	× 10^{-5}	CL=90%
Γ_{76}	$K^-e^+\mu^+$	L	< 6.8	× 10^{-4}	CL=90%
Γ_{77}	$K^*(892)^-\mu^+\mu^+$	L	< 1.4	× 10^{-3}	CL=90%
Γ_{78}	A dummy mode used by the fit.		(82 ± 5) %		

[a] For now, we average together measurements of the $Xe^+\nu_e$ and $X\mu^+\nu_\mu$ branching fractions. This is the *average*, not the *sum*.

[b] The branching fraction for this mode may differ from the sum of the submodes that contribute to it, due to interference effects. See the relevant papers.

[c] This branching fraction includes all the decay modes of the final-state resonance.

[d] This value includes only K^+K^- decays of the intermediate resonance, because branching fractions of this resonance are not known.

[e] This value includes only $\pi^+\pi^-$ decays of the intermediate resonance, because branching fractions of this resonance are not known.

[f] This mode is not a useful test for a ΔC=1 weak neutral current because both quarks must change flavor in this decay.

[g] The value is for the sum of the charge states or particle/antiparticle states indicated.

CONSTRAINED FIT INFORMATION

An overall fit to 12 branching ratios uses 24 measurements and one constraint to determine 9 parameters. The overall fit has a $\chi^2 = 13.0$ for 16 degrees of freedom.

The following *off-diagonal* array elements are the correlation coefficients $\langle \delta x_i \delta x_j \rangle / (\delta x_i \cdot \delta x_j)$, in percent, from the fit to the branching fractions, $x_i \equiv \Gamma_i/\Gamma_{\rm total}$. The fit constrains the x_i whose labels appear in this array to sum to one.

x_9	70							
x_{11}	60	85						
x_{12}	45	64	54					
x_{14}	66	88	75	56				
x_{15}	72	96	81	61	92			
x_{16}	67	89	76	57	93	93		
x_{38}	63	84	72	54	86	88	84	
x_{78}	−73	−96	−86	−66	−96	−98	−96	−89
	x_7	x_9	x_{11}	x_{12}	x_{14}	x_{15}	x_{16}	x_{38}

D_s^+ BRANCHING RATIOS

A few older, now obsolete results have been omitted. They may be found in earlier editions.

Inclusive modes

$\Gamma(K^-\text{ anything})/\Gamma_{\rm total}$ Γ_1/Γ

VALUE	DOCUMENT ID		TECN	COMMENT
$0.13^{+0.14}_{-0.12}\pm0.02$	COFFMAN	91	MRK3	e^+e^- 4.14 GeV

$[\Gamma(\overline{K}^0\text{ anything}) + \Gamma(K^0\text{ anything})]/\Gamma_{\rm total}$ Γ_2/Γ

VALUE	DOCUMENT ID		TECN	COMMENT
$0.39^{+0.28}_{-0.27}\pm0.04$	COFFMAN	91	MRK3	e^+e^- 4.14 GeV

$\Gamma(K^+\text{ anything})/\Gamma_{\rm total}$ Γ_3/Γ

VALUE	DOCUMENT ID		TECN	COMMENT
$0.20^{+0.18}_{-0.13}\pm0.04$	COFFMAN	91	MRK3	e^+e^- 4.14 GeV

$\Gamma((\text{non-}K\overline{K})\text{ anything})/\Gamma_{\rm total}$ Γ_4/Γ

VALUE	DOCUMENT ID		TECN	COMMENT
$0.64\pm0.17\pm0.03$	[3] COFFMAN	91	MRK3	e^+e^- 4.14 GeV

[3] COFFMAN 91 uses the direct measurements of the kaon content to determine this non-$K\overline{K}$ fraction. This number implies that a large fraction of D_s^+ decays involve η, η', and/or non-spectator decays.

$\Gamma(e^+\text{ anything})/\Gamma_{\rm total}$ Γ_5/Γ

VALUE	CL%	DOCUMENT ID		TECN	COMMENT
$0.077^{+0.057+0.024}_{-0.043-0.021}$		BAI	97	BES	$e^+e^- \to D_s^+D_s^-$
• • • We do not use the following data for averages, fits, limits, etc. • • •					
<0.20	90	[4] BAI	90	MRK3	e^+e^- 4.14 GeV

[4] Expressed as a value, the BAI 90 result is $\Gamma(e^+\text{anything})/\Gamma_{\rm total} = 0.05 \pm 0.05 \pm 0.02$.

$\Gamma(\phi\text{ anything})/\Gamma_{\rm total}$ Γ_6/Γ

VALUE	EVTS	DOCUMENT ID		TECN	COMMENT
$0.178^{+0.151+0.006}_{-0.072-0.063}$	3	BAI	98	BES	$e^+e^- \to D_s^+D_s^-$

Leptonic and semileptonic modes

D_s^+ DECAY CONSTANT

Written October 2003 by A. Edwards and P. Burchat (Stanford University)

In the Standard Model, the D_s^+ leptonic branching fractions are related to the D_s^+ decay constant f_{D_s} by the equation [1]

$$\mathrm{B}(D_s^+ \to \ell^+\nu_\ell) = \frac{G_F^2}{8\pi}|V_{cs}|^2 f_{D_s}^2 \frac{\tau_{D_s}}{\hbar} m_{D_s} m_\ell^2 \left(1 - \frac{m_\ell^2}{m_{D_s}^2}\right)^2 . \quad (1)$$

Hence, measurements of $\mathrm{B}(D_s^+ \to \ell^+\nu_\ell)$ can be used to extract f_{D_s}. Eight experiments have published measurements of the branching fraction for D_s^+ decaying to $\mu^+\nu_\mu$ or $\tau^+\nu_\tau$: WA75

(AOKI 93), BES (BAI 95), E653 (KODAMA 96), L3 (ACCIARRI 97F), CLEO (CHADHA 98), BEATRICE (ALEXANDROV 00), OPAL (ABBIENDI 01L), and ALEPH (HEISTER 02I). All these experiments except BES either explicitly or implicitly measure the leptonic branching fraction relative to the branching fraction for $D_s^+ \to \phi\pi^+$, or for semileptonic D_s^+ or D^0 decays. The semileptonic D_s^+ branching fraction is in turn measured relative to $B(D_s^+ \to \phi\pi^+)$. The fractional experimental uncertainty on $B(D_s^+ \to \phi\pi^+)$ is currently 25%. The LEP experiments (L3, OPAL, ALEPH) share a 23% correlated uncertainty in the normalization of the leptonic branching fraction. They use the partial decay rate for $Z \to c\bar{c}$ and the D_s^+ production rate in $Z \to c\bar{c}$ events, which in turn depends on the assumed value of $B(D_s^+ \to \phi\pi^+)$. BES uses the relative number of events in which one or two D_s decays are fully reconstructed to determine the absolute $D_s^+ \to \mu^+\nu_\mu$ branching fraction; however, only three events are observed in which one D_s^+ decays to a hadronic final state and the other decays to $\mu^+\nu_\mu$ or $\tau^+\nu_\tau$.

We determine the world average value of f_{D_s} from the experimental measurements of the D_s^+ leptonic branching fractions, assuming lepton universality, taking into account correlated uncertainties, and using a consistent and up-to-date set of input parameters [2] for the μ, τ, and D_s^+ masses, the D_s^+ lifetime, V_{cs}, $B(D_s^+ \to \phi\pi^+)$, and the relative D_s^+ branching fractions. Although the uncertainty on $B(D_s^+ \to \phi\pi^+)$ is by far the largest correlated uncertainty, we also take into account correlated uncertainties in the input parameters. Weighting each measurement by its uncorrelated uncertainty, we determine the average leptonic branching fraction for all experiments except BES to be $B(D_s^+ \to \mu^+\nu_\mu) = 0.00547 \pm 0.00067 \pm 0.00132$, where the second uncertainty in the average is the correlated uncertainty due to $B(D_s^+ \to \phi\pi^+)$. Since the above average is less (by 1.5σ) than the BES result of $B(D_s^+ \to \mu^+\nu_\mu) = 0.015^{+0.013+0.003}_{-0.006-0.002}$, the negative uncertainties on the BES measurement are used to calculate the weighted average for all experiments:

$$B(D_s^+ \to \mu^+\nu_\mu) = 0.00596 \pm 0.00144 \ . \qquad (2)$$

Using this value of the branching fraction and including the relatively minor uncertainties on the other parameters in Eq. (1), we extract the world average D_s^+ decay constant:

$$f_{D_s} = (267 \pm 33) \ \text{MeV} \ . \qquad (3)$$

References

1. See the note on "Pseudoscalar-Meson Decay Constants" at the beginning of the Meson Particle Listings.
2. Review of Particle Properties 2004.

$\Gamma(\mu^+\nu_\mu)/\Gamma_{\text{total}}$ Γ_7/Γ

See the "Note on Pseudoscalar-Meson Decay Constants" in the Listings for the $\pi^\pm$.

VALUE	EVTS	DOCUMENT ID		TECN	COMMENT
• • • We do not use the following data for averages, fits, limits, etc. • • •					
$0.0068 \pm 0.0011 \pm 0.0018$	553	[5] HEISTER	02I	ALEP	Z decays
$0.015\ ^{+0.013}_{-0.006}\ ^{+0.003}_{-0.002}$	3	[6] BAI	95	BES	$e^+e^- \to D_s^+ D_s^-$
$0.004\ ^{+0.0018}_{-0.0014}\ ^{+0.0020}_{-0.0019}$	8	[7] AOKI	93	WA75	π^- emulsion 350 GeV
< 0.03	0	[8] AUBERT	83	SPEC	μ^+Fe, 250 GeV

[5] This HEISTER 02I result is not actually an independent measurement of the absolute $\mu^+\nu_\mu$ branching fraction, but is in fact based on our $\phi\pi^+$ branching fraction of $3.6 \pm 0.9\%$, so it cannot be included in our overall fit. HEISTER 02I combines its $D_s^+ \to \tau^+\nu_\tau$ and $\mu^+\nu_\mu$ branching fractions to get $f_{D_s} = (285 \pm 19 \pm 40)$ MeV.

[6] BAI 95 uses one actual $D_s^+ \to \mu^+\nu_\mu$ event together with two $D_s^+ \to \tau^+\nu_\tau$ events and assumes μ-τ universality. This value of $\Gamma(\mu^+\nu_\mu)/\Gamma_{\text{total}}$ gives a pseudoscalar decay constant of $(430^{+150}_{-130} \pm 40)$ MeV.

[7] AOKI 93 assumes the ratio of production cross sections of the D_s^+ and D^0 is 0.27. The value of $\Gamma(\mu^+\nu_\mu)/\Gamma_{\text{total}}$ gives a pseudoscalar decay constant $f_{D_s} = (232 \pm 45 \pm 52)$ MeV.

[8] AUBERT 83 assume that the $D_s^\pm$ production rate is 20% of total charm production rate.

$\Gamma(\mu^+\nu_\mu)/\Gamma(\phi\pi^+)$ Γ_7/Γ_{15}

See the "Note on Pseudoscalar-Meson Decay Constants" in the Listings for the $\pi^\pm$.

VALUE	EVTS	DOCUMENT ID		TECN	COMMENT
0.14 ±0.04 OUR FIT Error includes scale factor of 1.4.					
0.19 ±0.04 OUR AVERAGE					
$0.23 \pm 0.06 \pm 0.04$	18	[9] ALEXANDROV	00	BEAT	π^- nucleus, 350 GeV
$0.173 \pm 0.023 \pm 0.035$	182	[10] CHADHA	98	CLE2	$e^+e^- \approx \Upsilon(4S)$
• • • We do not use the following data for averages, fits, limits, etc. • • •					
$0.245 \pm 0.052 \pm 0.074$	39	[11] ACOSTA	94	CLE2	See CHADHA 98

[9] ALEXANDROV 00 uses $f_D^2/f_{D_s}^2 = 0.82 \pm 0.09$ from a lattice-gauge-theory calculation to get the relative numbers of $D^+ \to \mu^+\nu_\mu$ and $D_s^+ \to \mu^+\nu_\mu$ events. The present result leads to $f_{D_s} = (323 \pm 44 \pm 36)$ MeV.

[10] CHADHA 98 obtains $f_{D_s} = (280 \pm 19 \pm 28 \pm 34)$ MeV from this measurement, using $\Gamma(D_s^+ \to \phi\pi^+)/\Gamma(\text{total}) = 0.036 \pm 0.009$.

[11] ACOSTA 94 obtains $f_{D_s} = (344 \pm 37 \pm 52 \pm 42)$ MeV from this measurement, using $\Gamma(D_s^+ \to \phi\pi^+)/\Gamma(\text{total}) = 0.037 \pm 0.009$.

$\Gamma(\mu^+\nu_\mu)/\Gamma(\phi\ell^+\nu_\ell)$ Γ_7/Γ_9

See the "Note on Pseudoscalar-Meson Decay Constants" in the Listings for the $\pi^\pm$.

VALUE	EVTS	DOCUMENT ID		TECN	COMMENT
0.25±0.07 OUR FIT Error includes scale factor of 1.5.					
0.16±0.06±0.03	23	[12] KODAMA	96	E653	π^- emulsion, 600 GeV

[12] KODAMA 96 obtains $f_{D_s} = (194 \pm 35 \pm 20 \pm 14)$ MeV from this measurement, using $\Gamma(D_s^+ \to \phi\ell^+\nu)/\Gamma_{\text{total}} = 0.0188 \pm 0.0029$. The third error is from the uncertainty on $\phi\ell^+\nu_\ell$ branching fraction.

$\Gamma(\tau^+\nu_\tau)/\Gamma_{\text{total}}$ Γ_8/Γ

See the "Note on Pseudoscalar-Meson Decay Constants" in the Listings for the $\pi^\pm$.

VALUE	EVTS	DOCUMENT ID		TECN	COMMENT
0.064 ±0.015 OUR AVERAGE					
$0.0579 \pm 0.0077 \pm 0.0184$	881	[13] HEISTER	02I	ALEP	Z decays
$0.070 \pm 0.021 \pm 0.020$	22	[14] ABBIENDI	01L	OPAL	$D_s^{*+} \to \gamma D_s^+$ from Z's
$0.074 \pm 0.028 \pm 0.024$	16	[15] ACCIARRI	97F	L3	$D_s^{*+} \to \gamma D_s^+$ from Z's

[13] HEISTER 02I combines its $D_s^+ \to \tau^+\nu_\tau$ and $\mu^+\nu_\mu$ branching fractions to get $f_{D_s} = (285 \pm 19 \pm 40)$ MeV.

[14] This ABBIENDI 01L value gives a decay constant f_{D_s} of $(286 \pm 44 \pm 41)$ MeV.

[15] The second ACCIARRI 97F error here combines in quadrature systematic (0.016) and normalization (0.018) errors. The branching fraction gives $f_{D_s} = (309 \pm 58 \pm 33 \pm 38)$ MeV.

$\Gamma(\phi\ell^+\nu_\ell)/\Gamma(\phi\pi^+)$ Γ_9/Γ_{15}

For now, we average together measurements of the $\Gamma(\phi e^+\nu_e)/\Gamma(\phi\pi^+)$ and $\Gamma(\phi\mu^+\nu_\mu)/\Gamma(\phi\pi^+)$ ratios. See the end of the D_s^+ Listings for measurements of $D_s^+ \to \phi\ell^+\nu_\ell$ form-factor ratios.

VALUE	EVTS	DOCUMENT ID		TECN	COMMENT
0.55 ±0.04 OUR FIT					
0.54 ±0.04 OUR AVERAGE					
$0.540 \pm 0.033 \pm 0.048$	793	[16] LINK	02J	FOCS	γ nucleus, ≈ 180 GeV
$0.54 \pm 0.05 \pm 0.04$	367	[17] BUTLER	94	CLE2	$e^+e^- \approx \Upsilon(4S)$
$0.58 \pm 0.17 \pm 0.07$	97	[18] FRABETTI	93G	E687	γBe $\bar{E}_\gamma = 220$ GeV
$0.57 \pm 0.15 \pm 0.15$	104	[19] ALBRECHT	91	ARG	$e^+e^- \approx 10.4$ GeV
$0.49 \pm 0.10\ ^{+0.10}_{-0.14}$	54	[20] ALEXANDER	90B	CLEO	e^+e^- 10.5–11 GeV

[16] LINK 02J measures the $\Gamma(\phi\mu^+\nu_\mu)/\Gamma(\phi\pi^+)$ ratio.

[17] BUTLER 94 uses both $\phi e^+\nu_e$ and $\phi\mu^+\nu_\mu$ events, and makes a phase-space adjustment to the latter to use them as $\phi e^+\nu_e$ events.

[18] FRABETTI 93G measures the $\Gamma(\phi\mu^+\nu_\mu)/\Gamma(\phi\pi^+)$ ratio.

[19] ALBRECHT 91 measures the $\Gamma(\phi e^+\nu_e)/\Gamma(\phi\pi^+)$ ratio.

[20] ALEXANDER 90B measures an average of the $\Gamma(\phi e^+\nu_e)/\Gamma(\phi\pi^+)$ and $\Gamma(\phi\mu^+\nu_\mu)/\Gamma(\phi\pi^+)$ ratios.

Meson Particle Listings

$D_s^\pm$

$\Gamma(\eta\ell^+\nu_\ell)/\Gamma(\phi\ell^+\nu_\ell)$ Γ_{11}/Γ_9

Unseen decay modes of the η and the ϕ are included.

VALUE	EVTS	DOCUMENT ID		TECN	COMMENT
1.27 ± 0.19 OUR FIT					
1.24 ± 0.12 ± 0.15	440	[21] BRANDENB...	95	CLE2	$e^+e^-\approx\Upsilon(4S)$

[21] BRANDENBURG 95 uses both e^+ and μ^+ events and makes a phase-space adjustment to use the μ^+ events as e^+ events.

$\Gamma(\eta'(958)\ell^+\nu_\ell)/\Gamma(\phi\ell^+\nu_\ell)$ Γ_{12}/Γ_9

Unseen decay modes of the resonances are included.

VALUE	CL%	EVTS	DOCUMENT ID		TECN	COMMENT
0.44 ± 0.13 OUR FIT						
0.43 ± 0.11 ± 0.07		29	[22] BRANDENB...	95	CLE2	$e^+e^-\approx\Upsilon(4S)$
• • • We do not use the following data for averages, fits, limits, etc. • • •						
< 1.6	90		[23] KODAMA	93B	E653	π^- emulsion 600 GeV

[22] BRANDENBURG 95 uses both e^+ and μ^+ events and makes a phase-space adjustment to use the μ^+ events as e^+ events.
[23] KODAMA 93B uses μ^+ events.

$[\Gamma(\eta\ell^+\nu_\ell)+\Gamma(\eta'(958)\ell^+\nu_\ell)]/\Gamma(\phi\ell^+\nu_\ell)$ $\Gamma_{10}/\Gamma_9=(\Gamma_{11}+\Gamma_{12})/\Gamma_9$

Unseen decay modes of the resonances are included.

VALUE	EVTS	DOCUMENT ID		TECN	COMMENT
1.72 ± 0.23 OUR FIT					
3.9 ± 1.6	13	[24] KODAMA	93	E653	π^- emulsion 600 GeV
• • • We do not use the following data for averages, fits, limits, etc. • • •					
1.67 ± 0.17 ± 0.17		[25] BRANDENB...	95	CLE2	$e^+e^-\approx\Upsilon(4S)$

[24] KODAMA 93 uses μ^+ events.
[25] This BRANDENBURG 95 data is redundant with data in previous blocks.

Hadronic modes with a $K\overline{K}$ pair.

$\Gamma(K^+\overline{K}{}^0)/\Gamma(\phi\pi^+)$ Γ_{13}/Γ_{15}

VALUE	EVTS	DOCUMENT ID		TECN	COMMENT
1.01 ± 0.16 OUR AVERAGE					
1.15 ± 0.31 ± 0.19	68	ANJOS	90C	E691	γ Be
0.92 ± 0.32 ± 0.20		ADLER	89B	MRK3	e^+e^- 4.14 GeV
0.99 ± 0.17 ± 0.10		CHEN	89	CLEO	e^+e^- 10 GeV

$\Gamma(\phi\pi^+)/\Gamma_{\text{total}}$ Γ_{15}/Γ

We now have model-independent measurements of this branching fraction, and so we no longer use the earlier, model-dependent results.

VALUE	CL%	EVTS	DOCUMENT ID		TECN	COMMENT
0.036 ± 0.009 OUR FIT						
0.036 ± 0.009 OUR AVERAGE						
0.0359 ± 0.0077 ± 0.0048			[26] ARTUSO	96	CLE2	e^+e^- at $\Upsilon(4S)$
$0.039\ ^{+0.051}_{-0.019}\ ^{+0.018}_{-0.011}$			[27] BAI	95C	BES	e^+e^- 4.03 GeV
• • • We do not use the following data for averages, fits, limits, etc. • • •						
0.051 ± 0.004 ± 0.008			[28] BUTLER	94	CLE2	$e^+e^-\approx\Upsilon(4S)$
< 0.048	90		MUHEIM	94		
0.046 ± 0.015			[29] MUHEIM	94		
0.031 ± 0.009			[29] MUHEIM	94		
0.031 ± 0.009 ± 0.006			[28] FRABETTI	93G	E687	γBe $\overline{E}_\gamma$= 220 GeV
0.024 ± 0.010			[28] ALBRECHT	91	ARG	$e^+e^-\approx$ 10.4 GeV
< 0.041	90	0	[27] ADLER	90B	MRK3	e^+e^- 4.14 GeV
$0.031 \pm 0.006\ ^{+0.011}_{-0.009}$			[28] ALEXANDER	90B	CLEO	e^+e^- 10.5–11 GeV
0.048 ± 0.017 ± 0.019			[30] ALVAREZ	90C	NA14	Photoproduction
> 0.034	90		[28] ANJOS	90B	E691	γBe, $\overline{E}_\gamma\approx$ 145 GeV
0.02 ± 0.01		405	[31] CHEN	89	CLEO	e^+e^- 10 GeV
0.033 ± 0.016 ± 0.010		9	[31] BRAUNSCH...	87	TASS	e^+e^- 35–44 GeV
0.033 ± 0.011		30	[31] DERRICK	85B	HRS	e^+e^- 29 GeV

[26] ARTUSO 96 uses partially reconstructed $\overline{B}{}^0\to D^{*+}D_s^{*-}$ decays to get a model-independent value for $\Gamma(D_s^-\to\phi\pi^-)/\Gamma(D^0\to K^-\pi^+)$ of 0.92 ± 0.20 ± 0.11.
[27] BAI 95C uses $e^+e^-\to D_s^+D_s^-$ events in which one or both of the $D_s^\pm$ are observed to obtain the first model-independent measurement of the $D_s^+\to\phi\pi^+$ branching fraction, without assumptions about $\sigma(D_s^\pm)$. However, with only two "doubly-tagged" events, the statistical error is very large. ADLER 90B used the same method to set a limit.
[28] BUTLER 94, FRABETTI 93G, ALBRECHT 91, ALEXANDER 90B, and ANJOS 90B measure the ratio $\Gamma(D_s^+\to\phi\ell^+\nu_\ell)/\Gamma(D_s^+\to\phi\pi^+)$, where $\ell=e$ and/or μ, and then use a theoretical calculation of the ratio of widths $\Gamma(D_s^+\to\phi\ell^+\nu_\ell)/\Gamma(D^+\to\overline{K}{}^{*0}\ell^+\nu)$. Not everyone uses the same value for this ratio.
[29] The two MUHEIM 94 values here are model-dependent calculations based on distinct data sets. The first uses measurements of the $D_2^*(2460)^0$ and $D_{s1}(2536)^+$, the second uses B-decay factorization and $\Gamma(D_s^+\to\mu^+\nu_\mu)/\Gamma(D_s^+\to\phi\ell^+\nu_\ell)$. A third calculation using the semileptonic width of $D_s^+\to\phi\ell^+\nu_\ell$ is not independent of other results listed here. Note also the upper limit, based on the sum of established D_s^+ branching ratios.
[30] ALVAREZ 90C relies on the Lund model to estimate the ratio of D_s^+ to D^+ cross sections.
[31] Values based on crude estimates of the $D_s^\pm$ production level. DERRICK 85B errors are statistical only.

$\Gamma(\phi\pi^+)/\Gamma(K^+K^-\pi^+)$ Γ_{15}/Γ_{14}

Unseen decay modes of the ϕ are included.

VALUE	DOCUMENT ID		TECN	COMMENT
0.81 ± 0.08 OUR FIT				
0.807 ± 0.067 ± 0.096	FRABETTI	95B	E687	Dalitz plot analysis

$\Gamma(K^+\overline{K}{}^*(892)^0)/\Gamma(K^+K^-\pi^+)$ Γ_{16}/Γ_{14}

Unseen decay modes of the $\overline{K}{}^*(892)^0$ are included.

VALUE	DOCUMENT ID		TECN	COMMENT
0.75 ± 0.07 OUR FIT				
0.717 ± 0.069 ± 0.060	FRABETTI	95B	E687	Dalitz plot analysis

$\Gamma(K^+\overline{K}{}^*(892)^0)/\Gamma(\phi\pi^+)$ Γ_{16}/Γ_{15}

Unseen decay modes of the resonances are included.

VALUE	EVTS	DOCUMENT ID		TECN	COMMENT
0.92 ± 0.09 OUR FIT					
0.95 ± 0.10 OUR AVERAGE					
0.85 ± 0.34 ± 0.20	9	ALVAREZ	90C	NA14	Photoproduction
0.84 ± 0.30 ± 0.22		ADLER	89B	MRK3	e^+e^- 4.14 GeV
1.05 ± 0.17 ± 0.12		CHEN	89	CLEO	e^+e^- 10 GeV
0.87 ± 0.13 ± 0.05	117	ANJOS	88	E691	Photoproduction
1.44 ± 0.37	87	ALBRECHT	87F	ARG	e^+e^- 10 GeV

$\Gamma(f_0(980)\pi^+\times B(f_0\to K^+K^-))/\Gamma(K^+K^-\pi^+)$ Γ_{17}/Γ_{14}

This includes only the K^+K^- decays of the $f_0(980)$, because branching fractions of this resonance are not known.

VALUE	DOCUMENT ID		TECN	COMMENT
0.11 ± 0.035 ± 0.026	FRABETTI	95B	E687	Dalitz plot analysis

$\Gamma(f_0(1710)\pi^+\times B(f_0\to K^+K^-))/\Gamma(K^+K^-\pi^+)$ Γ_{19}/Γ_{14}

This includes only K^+K^- decays of the $f_0(1710)$, because branching fractions of this resonance are not known.

VALUE	DOCUMENT ID		TECN	COMMENT
• • • We do not use the following data for averages, fits, limits, etc. • • •				
0.034 ± 0.023 ± 0.035	[32] FRABETTI	95B	E687	Dalitz plot analysis

[32] In other words, FRABETTI 95B doesn't see this resonance.

$\Gamma(K^+\overline{K}{}_0^*(1430)^0)/\Gamma(K^+K^-\pi^+)$ Γ_{18}/Γ_{14}

Unseen decay modes of the $\overline{K}{}_0^*(1430)^0$ are included.

VALUE	DOCUMENT ID		TECN	COMMENT
0.150 ± 0.052 ± 0.052	FRABETTI	95B	E687	Dalitz plot analysis

$\Gamma(K^+K^-\pi^+\text{nonresonant})/\Gamma(\phi\pi^+)$ Γ_{20}/Γ_{15}

VALUE	EVTS	DOCUMENT ID		TECN	COMMENT
0.25 ± 0.07 ± 0.05	48	ANJOS	88	E691	Photoproduction

$\Gamma(K^*(892)^+\overline{K}{}^0)/\Gamma(\phi\pi^+)$ Γ_{22}/Γ_{15}

Unseen decay modes of the resonances are included.

VALUE	DOCUMENT ID		TECN	COMMENT
1.20 ± 0.21 ± 0.13	CHEN	89	CLEO	e^+e^- 10 GeV

$\Gamma(K^*(892)^+\overline{K}{}^0)/\Gamma(K^+\overline{K}{}^0)$ Γ_{22}/Γ_{13}

Unseen decay modes of the $K^*(892)^+$ are included.

VALUE	CL%	DOCUMENT ID		TECN	COMMENT
• • • We do not use the following data for averages, fits, limits, etc. • • •					
< 0.9	90	FRABETTI	95	E687	γBe $\overline{E}_\gamma\approx$ 200 GeV

$\Gamma(\phi\pi^+\pi^0)/\Gamma(\phi\pi^+)$ Γ_{24}/Γ_{15}

VALUE	CL%	EVTS	DOCUMENT ID		TECN	COMMENT
2.4 ± 1.0 ± 0.5		11	ANJOS	89E	E691	Photoproduction
• • • We do not use the following data for averages, fits, limits, etc. • • •						
< 2.6	90		ALVAREZ	90C	NA14	Photoproduction

$\Gamma(\phi\rho^+)/\Gamma(\phi\pi^+)$ Γ_{25}/Γ_{15}

VALUE	EVTS	DOCUMENT ID		TECN	COMMENT
$\mathbf{1.86\pm0.26\ ^{+0.29}_{-0.40}}$	253	AVERY	92	CLE2	$e^+e^-\simeq$ 10.5 GeV

$\Gamma(\phi\pi^+\pi^0\text{ 3-body})/\Gamma(\phi\pi^+)$ Γ_{26}/Γ_{15}

VALUE	CL%	DOCUMENT ID		TECN	COMMENT
< 0.71	90	DAOUDI	92	CLE2	$e^+e^-\approx$ 10.5 GeV

$\Gamma(K^+K^-\pi^+\pi^0\text{ non-}\phi)/\Gamma(\phi\pi^+)$ Γ_{27}/Γ_{15}

VALUE	CL%	DOCUMENT ID		TECN	COMMENT
< 2.4	90	ANJOS	89E	E691	Photoproduction

$\Gamma(K^+\overline{K}{}^0\pi^+\pi^-)/\Gamma(\phi\pi^+)$ Γ_{28}/Γ_{15}

VALUE	CL%	DOCUMENT ID		TECN	COMMENT
• • • We do not use the following data for averages, fits, limits, etc. • • •					
< 0.77	90	ALBRECHT	92B	ARG	$e^+e^-\simeq$ 10.4 GeV

$\Gamma(K^+\overline{K}{}^0\pi^+\pi^-)/\Gamma(K^0K^-\pi^+\pi^+)$ Γ_{28}/Γ_{29}

VALUE	EVTS	DOCUMENT ID		TECN	COMMENT
0.586 ± 0.052 ± 0.043	476	LINK	01C	FOCS	γ nucleus, $\overline{E}_\gamma\approx$ 180 GeV

$\Gamma(K^0 K^- \pi^+ \pi^+)/\Gamma(\phi\pi^+)$ Γ_{29}/Γ_{15}

VALUE	DOCUMENT ID	TECN	COMMENT
1.2 ±0.2 ±0.2	ALBRECHT 92B	ARG	e^+e^- ≃ 10.4 GeV

$\Gamma(K^*(892)^+ \overline{K}^*(892)^0)/\Gamma(\phi\pi^+)$ Γ_{30}/Γ_{15}

Unseen decay modes of the resonances are included.

VALUE	DOCUMENT ID	TECN	COMMENT
1.6 ± 0.4 ± 0.4	ALBRECHT 92B	ARG	e^+e^- ≃ 10.4 GeV

$\Gamma(K^0 K^- \pi^+ \pi^+ (\text{non-}K^{*+}\overline{K}^{*0}))/\Gamma(\phi\pi^+)$ Γ_{31}/Γ_{15}

VALUE	CL%	DOCUMENT ID	TECN	COMMENT
<0.80	90	ALBRECHT 92B	ARG	e^+e^- ≃ 10.4 GeV

$\Gamma(K^+ K^- \pi^+ \pi^+ \pi^-)/\Gamma(K^+ K^- \pi^+)$ Γ_{32}/Γ_{14}

VALUE	EVTS	DOCUMENT ID	TECN	COMMENT
0.160 ± 0.027 OUR AVERAGE				
0.150 ± 0.019 ± 0.025	240	LINK 03D	FOCS	γ nucleus, $\overline{E}_\gamma$ ≈ 180 GeV
0.188 ± 0.036 ± 0.040	75	FRABETTI 97C	E687	γ Be, $\overline{E}_\gamma$ ≈ 200 GeV

$\Gamma(\phi\pi^+\pi^+\pi^-)/\Gamma(\phi\pi^+)$ Γ_{33}/Γ_{15}

VALUE	CL%	EVTS	DOCUMENT ID	TECN	COMMENT
0.269 ± 0.027 OUR AVERAGE					
0.249 ± 0.024 ± 0.021		136	LINK 03D	FOCS	γ nucleus, $\overline{E}_\gamma$ ≈ 180 GeV
0.28 ±0.06 ±0.01		40	FRABETTI 97C	E687	γ Be, $\overline{E}_\gamma$ ≈ 200 GeV
0.58 ±0.21 ±0.10		21	FRABETTI 92	E687	γ Be
0.42 ±0.13 ±0.07		19	ANJOS 88	E691	Photoproduction
1.11 ±0.37 ±0.28		62	ALBRECHT 85D	ARG	e^+e^- 10 GeV
• • • We do not use the following data for averages, fits, limits, etc. • • •					
<0.24	90		ALVAREZ 90C	NA14	Photoproduction

$\Gamma(\phi\pi^+\pi^+\pi^-)/\Gamma(K^+K^-\pi^+\pi^+\pi^-)$ Γ_{33}/Γ_{32}

Unseen decay modes of the ϕ are included.

VALUE	EVTS	DOCUMENT ID	TECN	COMMENT
• • • We do not use the following data for averages, fits, limits, etc. • • •				
0.42 ± 0.10 ± 0.12	136	[33] LINK 03D	FOCS	γ nucleus, $\overline{E}_\gamma$ ≈ 180 GeV

[33] This LINK 03D result is redundant with its $\Gamma(\phi\pi^+\pi^+\pi^-)/\Gamma(\phi\pi^+)$ result above.

$\Gamma(K^+K^-\rho^0\pi^+\text{non-}\phi)/\Gamma(K^+K^-\pi^+\pi^+\pi^-)$ Γ_{34}/Γ_{32}

VALUE	CL%	DOCUMENT ID	TECN	COMMENT
<0.03	90	LINK 03D	FOCS	γ nucleus, $\overline{E}_\gamma$ ≈ 180 GeV

$\Gamma(\phi\rho^0\pi^+)/\Gamma(K^+K^-\pi^+\pi^+\pi^-)$ Γ_{35}/Γ_{32}

Unseen decay modes of the ϕ are included.

VALUE	DOCUMENT ID	TECN	COMMENT
1.50 ± 0.12 ± 0.08	LINK 03D	FOCS	γ nucleus, $\overline{E}_\gamma$ ≈ 180 GeV

$\Gamma(\phi a_1(1260)^+)/\Gamma(K^+K^-\pi^+)$ Γ_{36}/Γ_{14}

Unseen decay modes of the ϕ and $a_1(1260)^+$ are included.

VALUE	DOCUMENT ID	TECN	COMMENT
0.559 ± 0.078 ± 0.044	LINK 03D	FOCS	γ nucleus, $\overline{E}_\gamma$ ≈ 180 GeV

$\Gamma(K^+K^-\pi^+\pi^+\pi^-\text{nonresonant})/\Gamma(K^+K^-\pi^+\pi^+\pi^-)$ Γ_{37}/Γ_{32}

VALUE	DOCUMENT ID	TECN	COMMENT
0.10 ± 0.06 ± 0.05	LINK 03D	FOCS	γ nucleus, $\overline{E}_\gamma$ ≈ 180 GeV

Pionic modes

$\Gamma(\pi^+\pi^+\pi^-)/\Gamma(K^+K^-\pi^+)$ Γ_{38}/Γ_{14}

VALUE	EVTS	DOCUMENT ID	TECN	COMMENT
0.227 ± 0.033 OUR FIT	Error includes scale factor of 1.1.			
0.265 ± 0.041 ± 0.031	98	FRABETTI 97D	E687	γ Be ≈ 200 GeV

$\Gamma(\pi^+\pi^+\pi^-)/\Gamma(\phi\pi^+)$ Γ_{38}/Γ_{15}

VALUE	EVTS	DOCUMENT ID	TECN	COMMENT
0.28 ±0.04 OUR FIT	Error includes scale factor of 1.3.			
0.27 ±0.04 OUR AVERAGE	Error includes scale factor of 1.3. See the ideogram below.			
$0.245 \pm 0.028^{+0.019}_{-0.012}$	848	AITALA 01A	E791	π^- nucleus, 500 GeV
0.33 ±0.10 ±0.04	29	ADAMOVICH 93	WA82	π^- 340 GeV
0.44 ±0.10 ±0.04	68	ANJOS 89	E691	Photoproduction

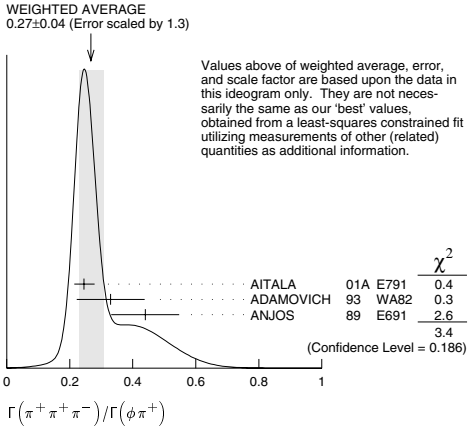

$\Gamma(\rho^0\pi^+)/\Gamma(\pi^+\pi^+\pi^-)$ Γ_{39}/Γ_{38}

VALUE	CL%	DOCUMENT ID	TECN	COMMENT
<0.073	90	FRABETTI 97D	E687	γ Be ≈ 200 GeV
• • • We do not use the following data for averages, fits, limits, etc. • • •				
0.058 ± 0.023 ± 0.037		[34] AITALA 01A	E791	π^- nucleus, 500 GeV

[34] This AITALA 01A result does not have enough statistical significance to prefer it to the FRABETTI 97D limit.

$\Gamma(\rho^0\pi^+)/\Gamma(\phi\pi^+)$ Γ_{39}/Γ_{15}

VALUE	CL%	DOCUMENT ID	TECN	COMMENT
• • • We do not use the following data for averages, fits, limits, etc. • • •				
<0.08	90	ANJOS 89	E691	Photoproduction
<0.22	90	ALBRECHT 87G	ARG	e^+e^- 10 GeV

$\Gamma(f_0(980)\pi^+ \times B(f_0 \to \pi^+\pi^-))/\Gamma(\pi^+\pi^+\pi^-)$ Γ_{40}/Γ_{38}

This includes only the $\pi^+\pi^-$ decays of the $f_0(980)$, because branching fractions of this resonance are not known. In general, we favor the results of AITALA 01A over those of FRABETTI 97D (848 ± 44 events versus 98 ± 12). It makes no sense to average them.

VALUE	DOCUMENT ID	TECN	COMMENT
0.565 ± 0.043 ± 0.047	AITALA 01A	E791	π^- nucleus, 500 GeV
• • • We do not use the following data for averages, fits, limits, etc. • • •			
1.074 ± 0.140 ± 0.043	FRABETTI 97D	E687	γ Be ≈ 200 GeV

$\Gamma(f_0(980)\pi^+ \times B(f_0 \to \pi^+\pi^-))/\Gamma(\phi\pi^+)$ Γ_{40}/Γ_{15}

This includes only the $\pi^+\pi^-$ decays of the $f_0(980)$, because branching fractions of this resonance are not known.

VALUE	DOCUMENT ID	TECN	COMMENT
• • • We do not use the following data for averages, fits, limits, etc. • • •			
0.28 ± 0.10 ± 0.03	ANJOS 89	E691	Photoproduction

$\Gamma(f_2(1270)\pi^+)/\Gamma(\pi^+\pi^+\pi^-)$ Γ_{41}/Γ_{38}

Unseen decay modes of the $f_2(1270)$ are included. In general, we favor the results of AITALA 01A over those of FRABETTI 97D (848 ± 44 events versus 98 ± 12). It makes no sense to average them.

VALUE	DOCUMENT ID	TECN	COMMENT
0.349 ± 0.059 ± 0.011	[35] AITALA 01A	E791	π^- nucleus, 500 GeV
• • • We do not use the following data for averages, fits, limits, etc. • • •			
0.22 ±0.10 ±0.03	FRABETTI 97D	E687	γ Be ≈ 200 GeV

[35] See AITALA 01A for the magnitude and phase of this amplitude relative to the $f_0(980)\pi^+$ amplitude.

$\Gamma(f_0(1370)\pi^+ \times B(f_0 \to \pi^+\pi^-))/\Gamma(\pi^+\pi^+\pi^-)$ Γ_{42}/Γ_{38}

This includes only the $\pi^+\pi^-$ decays of the $f_0(1370)$, because branching fractions of this resonance are not known.

VALUE	DOCUMENT ID	TECN	COMMENT
0.324 ± 0.077 ± 0.017	[36] AITALA 01A	E791	π^- nucleus, 500 GeV

[36] See AITALA 01A for the magnitude and phase of this amplitude relative to the $f_0(980)\pi^+$ amplitude.

$\Gamma(\rho(1450)^0\pi^+ \times B(\rho^0 \to \pi^+\pi^-))/\Gamma(\pi^+\pi^+\pi^-)$ Γ_{43}/Γ_{38}

This includes only the $\pi^+\pi^-$ decays of the $\rho(1450)^0$, because branching fractions of this resonance are not known.

VALUE	DOCUMENT ID	TECN	COMMENT
0.044 ± 0.021 ± 0.002	[37] AITALA 01A	E791	π^- nucleus, 500 GeV

[37] See AITALA 01A for the magnitude and phase of this amplitude relative to the $f_0(980)\pi^+$ amplitude.

$\Gamma(f_0(1500)\pi^+ \times B(f_0 \to \pi^+\pi^-))/\Gamma(\pi^+\pi^+\pi^-)$ Γ_{44}/Γ_{38}

This includes only $\pi^+\pi^-$ decays of the $f_0(1500)$, because branching fractions of this resonance are not known. In general, we favor the results of AITALA 01A over those of FRABETTI 97D (848 ± 44 events versus 98 ± 12).

VALUE	DOCUMENT ID	TECN	COMMENT
• • • We do not use the following data for averages, fits, limits, etc. • • •			
0.274 ± 0.114 ± 0.019	[38] FRABETTI	97D E687	γ Be ≈ 200 GeV

[38] FRABETTI 97D calls this mode $S(1475)\pi^+$, but finds the mass and width of this $S(1475)$ to be in excellent agreement with those of the $f_0(1500)$.

$\Gamma(\pi^+\pi^+\pi^-$ nonresonant$)/\Gamma(\pi^+\pi^+\pi^-)$ Γ_{45}/Γ_{38}

In general, we favor the results of AITALA 01A over those of FRABETTI 97D (848 ± 44 events versus 98 ± 12).

VALUE	CL%	DOCUMENT ID	TECN	COMMENT
0.005 ± 0.014 ± 0.017		AITALA	01A E791	π^- nucleus, 500 GeV
• • • We do not use the following data for averages, fits, limits, etc. • • •				
< 0.269	90	[39] FRABETTI	97D E687	γ Be ≈ 200 GeV

[39] See FRABETTI 97D on the difficulty of disentangling the $f_0(1500)\pi^+$ and nonresonant modes.

$\Gamma(\pi^+\pi^+\pi^-$ nonresonant$)/\Gamma(\phi\pi^+)$ Γ_{45}/Γ_{15}

VALUE	DOCUMENT ID	TECN	COMMENT
• • • We do not use the following data for averages, fits, limits, etc. • • •			
0.29 ± 0.09 ± 0.03	ANJOS	89 E691	Photoproduction

$\Gamma(\pi^+\pi^+\pi^-\pi^0)/\Gamma(\phi\pi^+)$ Γ_{46}/Γ_{15}

VALUE	CL%	DOCUMENT ID	TECN	COMMENT
< 3.3	90	ANJOS	89E E691	Photoproduction

$\Gamma(\eta\pi^+)/\Gamma(\phi\pi^+)$ Γ_{47}/Γ_{15}

Unseen decay modes of the resonances are included.

VALUE	CL%	EVTS	DOCUMENT ID	TECN	COMMENT
0.48 ± 0.03 ± 0.04		920	JESSOP	98 CLE2	$e^+e^- \approx \Upsilon(4S)$
• • • We do not use the following data for averages, fits, limits, etc. • • •					
0.54 ± 0.09 ± 0.06		165	ALEXANDER	92 CLE2	See JESSOP 98
< 1.5	90		ANJOS	89E E691	Photoproduction

$\Gamma(\omega\pi^+)/\Gamma(\phi\pi^+)$ Γ_{48}/Γ_{15}

Unseen decay modes of the resonances are included.

VALUE	CL%	DOCUMENT ID	TECN	COMMENT
• • • We do not use the following data for averages, fits, limits, etc. • • •				
< 0.5	90	ANJOS	89E E691	Photoproduction

$\Gamma(\omega\pi^+)/\Gamma(\eta\pi^+)$ Γ_{48}/Γ_{47}

VALUE	DOCUMENT ID	TECN	COMMENT
0.16 ± 0.04 ± 0.03	BALEST	97 CLE2	$e^+e^- \approx \Upsilon(4S)$

$\Gamma(3\pi^+2\pi^-)/\Gamma(K^+K^-\pi^+)$ Γ_{49}/Γ_{14}

VALUE	EVTS	DOCUMENT ID	TECN	COMMENT
0.146 ± 0.014 OUR AVERAGE				
0.145 ± 0.011 ± 0.010	671	LINK	03D FOCS	γ nucleus, $\overline{E}_\gamma \approx$ 180 GeV
0.158 ± 0.042 ± 0.031	37	FRABETTI	97C E687	γ Be, $\overline{E}_\gamma \approx$ 200 GeV

$\Gamma(3\pi^+2\pi^-)/\Gamma(\phi\pi^+)$ Γ_{49}/Γ_{15}

VALUE	CL%	DOCUMENT ID	TECN	COMMENT
• • • We do not use the following data for averages, fits, limits, etc. • • •				
< 0.29	90	ANJOS	89 E691	Photoproduction

$\Gamma(\eta\rho^+)/\Gamma(\phi\pi^+)$ Γ_{51}/Γ_{15}

Unseen decay modes of the resonances are included.

VALUE	EVTS	DOCUMENT ID	TECN	COMMENT
2.98 ± 0.20 ± 0.39	447	JESSOP	98 CLE2	$e^+e^- \approx \Upsilon(4S)$
• • • We do not use the following data for averages, fits, limits, etc. • • •				
$2.86 \pm 0.38^{+0.36}_{-0.38}$	217	AVERY	92 CLE2	See JESSOP 98

$\Gamma(\eta\pi^+\pi^0$ 3-body$)/\Gamma(\phi\pi^+)$ Γ_{52}/Γ_{15}

Unseen decay modes of the resonances are included.

VALUE	CL%	DOCUMENT ID	TECN	COMMENT
< 1.1	90	JESSOP	98 CLE2	$e^+e^- \approx \Upsilon(4S)$
• • • We do not use the following data for averages, fits, limits, etc. • • •				
< 0.82	90	[40] DAOUDI	92 CLE2	See JESSOP 98

[40] We use the JESSOP 98 limit, even though the DAOUDI 92 limit, from the same experiment but with a much smaller data sample, is more restrictive.

$\Gamma(3\pi^+2\pi^-\pi^0)/\Gamma_{\text{total}}$ Γ_{53}/Γ

VALUE	DOCUMENT ID	TECN	COMMENT
$\mathbf{0.049^{+0.033}_{-0.030}}$	BARLAG	92C ACCM	π^- 230 GeV

$\Gamma(\eta'(958)\pi^+)/\Gamma(\phi\pi^+)$ Γ_{54}/Γ_{15}

Unseen decay modes of the resonances are included.

VALUE	CL%	EVTS	DOCUMENT ID	TECN	COMMENT
1.08 ± 0.09 OUR AVERAGE					
1.03 ± 0.06 ± 0.07		537	JESSOP	98 CLE2	$e^+e^- \approx \Upsilon(4S)$
2.5 ± 1.0 $^{+1.5}_{-0.4}$		22	ALVAREZ	91 NA14	Photoproduction
2.5 ± 0.5 ± 0.3		215	ALBRECHT	90D ARG	$e^+e^- \approx$ 10.4 GeV
• • • We do not use the following data for averages, fits, limits, etc. • • •					
1.20 ± 0.15 ± 0.11		281	ALEXANDER	92 CLE2	See JESSOP 98
< 1.3	90		ANJOS	91B E691	γ Be, $\overline{E}_\gamma \approx$ 145 GeV

$\Gamma(\eta'(958)\rho^+)/\Gamma(\phi\pi^+)$ Γ_{56}/Γ_{15}

Unseen decay modes of the resonances are included.

VALUE	EVTS	DOCUMENT ID	TECN	COMMENT
2.78 ± 0.28 ± 0.30	137	JESSOP	98 CLE2	$e^+e^- \approx \Upsilon(4S)$
• • • We do not use the following data for averages, fits, limits, etc. • • •				
$3.44 \pm 0.62^{+0.44}_{-0.46}$	68	AVERY	92 CLE2	See JESSOP 98

$\Gamma(\eta'(958)\pi^+\pi^0$ 3-body$)/\Gamma(\phi\pi^+)$ Γ_{57}/Γ_{15}

Unseen decay modes of the resonances are included.

VALUE	CL%	DOCUMENT ID	TECN	COMMENT
< 0.4	90	JESSOP	98 CLE2	$e^+e^- \approx \Upsilon(4S)$
• • • We do not use the following data for averages, fits, limits, etc. • • •				
< 0.85	90	DAOUDI	92 CLE2	See JESSOP 98

Modes with one or three K's

$\Gamma(K^0\pi^+)/\Gamma(\phi\pi^+)$ Γ_{58}/Γ_{15}

VALUE	CL%	DOCUMENT ID	TECN	COMMENT
< 0.21	90	ADLER	89B MRK3	e^+e^- 4.14 GeV

$\Gamma(K^0\pi^+)/\Gamma(K^+\overline{K}^0)$ Γ_{58}/Γ_{13}

VALUE	CL%	DOCUMENT ID	TECN	COMMENT
• • • We do not use the following data for averages, fits, limits, etc. • • •				
< 0.53	90	FRABETTI	95 E687	γBe $\overline{E}_\gamma \approx$ 200 GeV

$\Gamma(K^+\pi^+\pi^-)/\Gamma(\phi\pi^+)$ Γ_{59}/Γ_{15}

VALUE	EVTS	DOCUMENT ID	TECN	COMMENT
0.28 ± 0.06 ± 0.05	85	FRABETTI	95E E687	γBe, $\overline{E}_\gamma$ = 220 GeV

$\Gamma(K^+\rho^0)/\Gamma(\phi\pi^+)$ Γ_{60}/Γ_{15}

VALUE	CL%	DOCUMENT ID	TECN	COMMENT
< 0.08	90	FRABETTI	95E E687	γBe, $\overline{E}_\gamma$ = 220 GeV

$\Gamma(K^*(892)^0\pi^+)/\Gamma(\phi\pi^+)$ Γ_{61}/Γ_{15}

Unseen decay modes of the resonances are included.

VALUE	EVTS	DOCUMENT ID	TECN	COMMENT
0.18 ± 0.05 ± 0.04	25	FRABETTI	95E E687	γBe, $\overline{E}_\gamma$ = 220 GeV

$\Gamma(K^+K^+K^-)/\Gamma(K^+K^-\pi^+)$ Γ_{62}/Γ_{14}

VALUE	EVTS	DOCUMENT ID	TECN	COMMENT
$\mathbf{0.00895 \pm 0.00212^{+0.00224}_{-0.00231}}$	31	LINK	02I FOCS	γ nucleus, ≈ 180 GeV

$\Gamma(K^+K^+K^-)/\Gamma(\phi\pi^+)$ Γ_{62}/Γ_{15}

VALUE	CL%	DOCUMENT ID	TECN	COMMENT
• • • We do not use the following data for averages, fits, limits, etc. • • •				
< 0.016	90	FRABETTI	95F E687	γBe, $\overline{E}_\gamma \approx$ 220 GeV

$\Gamma(\phi K^+)/\Gamma(\phi\pi^+)$ Γ_{63}/Γ_{15}

VALUE	CL%	DOCUMENT ID	TECN	COMMENT
< 0.013	90	FRABETTI	95F E687	γBe, $\overline{E}_\gamma \approx$ 220 GeV
• • • We do not use the following data for averages, fits, limits, etc. • • •				
< 0.071	90	ANJOS	92D E691	γBe, $\overline{E}_\gamma$ = 145 GeV

Rare or forbidden modes

$\Gamma(\pi^+e^+e^-)/\Gamma_{\text{total}}$ Γ_{64}/Γ

This mode is not a useful test for a ΔC=1 weak neutral current because both quarks must change flavor in this decay.

VALUE	CL%	DOCUMENT ID	TECN	COMMENT
$\mathbf{< 2.7 \times 10^{-4}}$	90	AITALA	99G E791	π^- N 500 GeV

$\Gamma(\pi^+\mu^+\mu^-)/\Gamma_{\text{total}}$ Γ_{65}/Γ

This mode is not a useful test for a ΔC=1 weak neutral current because both quarks must change flavor in this decay.

VALUE	CL%	EVTS	DOCUMENT ID	TECN	COMMENT
$\mathbf{< 2.6 \times 10^{-5}}$	90		LINK	03F FOCS	γ nucleus, $\overline{E}_\gamma \approx$ 180 GeV
• • • We do not use the following data for averages, fits, limits, etc. • • •					
$< 1.4 \times 10^{-4}$	90		AITALA	99G E791	π^- N 500 GeV
$< 4.3 \times 10^{-4}$	90	0	KODAMA	95 E653	π^- emulsion 600 GeV

$\Gamma(K^+e^+e^-)/\Gamma_{total}$ Γ_{66}/Γ

A test for the ΔC=1 weak neutral current. Allowed by higher-order electroweak interactions.

VALUE	CL%	DOCUMENT ID		TECN	COMMENT
$<1.6\times10^{-3}$	90	AITALA	99G	E791	π^- N 500 GeV

$\Gamma(K^+\mu^+\mu^-)/\Gamma_{total}$ Γ_{67}/Γ

A test for the ΔC=1 weak neutral current. Allowed by higher-order electroweak interactions.

VALUE	CL%	EVTS	DOCUMENT ID		TECN	COMMENT
$<3.6\times10^{-5}$	90		LINK	03F	FOCS	γ nucleus, $\overline{E}_\gamma\approx$ 180 GeV
• • • We do not use the following data for averages, fits, limits, etc. • • •						
$<1.4\times10^{-4}$	90		AITALA	99G	E791	π^- N 500 GeV
$<5.9\times10^{-4}$	90	0	KODAMA	95	E653	π^- emulsion 600 GeV

$\Gamma(K^*(892)^+\mu^+\mu^-)/\Gamma_{total}$ Γ_{68}/Γ

A test for the ΔC=1 weak neutral current. Allowed by higher-order electroweak interactions.

VALUE	CL%	EVTS	DOCUMENT ID		TECN	COMMENT
$<1.4\times10^{-3}$	90	0	KODAMA	95	E653	π^- emulsion 600 GeV

$\Gamma(\pi^+e^\pm\mu^\mp)/\Gamma_{total}$ Γ_{69}/Γ

A test of lepton-family-number conservation.

VALUE	CL%	DOCUMENT ID		TECN	COMMENT
$<6.1\times10^{-4}$	90	AITALA	99G	E791	π^- N 500 GeV

$\Gamma(K^+e^\pm\mu^\mp)/\Gamma_{total}$ Γ_{70}/Γ

A test of lepton-family-number conservation.

VALUE	CL%	DOCUMENT ID		TECN	COMMENT
$<6.3\times10^{-4}$	90	AITALA	99G	E791	π^- N 500 GeV

$\Gamma(\pi^-e^+e^+)/\Gamma_{total}$ Γ_{71}/Γ

A test of lepton-number conservation.

VALUE	CL%	DOCUMENT ID		TECN	COMMENT
$<6.9\times10^{-4}$	90	AITALA	99G	E791	π^- N 500 GeV

$\Gamma(\pi^-\mu^+\mu^+)/\Gamma_{total}$ Γ_{72}/Γ

A test of lepton-number conservation.

VALUE	CL%	EVTS	DOCUMENT ID		TECN	COMMENT
$<2.9\times10^{-5}$	90		LINK	03F	FOCS	γ nucleus, $\overline{E}_\gamma\approx$ 180 GeV
• • • We do not use the following data for averages, fits, limits, etc. • • •						
$<8.2\times10^{-5}$	90		AITALA	99G	E791	π^- N 500 GeV
$<4.3\times10^{-4}$	90	0	KODAMA	95	E653	π^- emulsion 600 GeV

$\Gamma(\pi^-e^+\mu^+)/\Gamma_{total}$ Γ_{73}/Γ

A test of lepton-number conservation.

VALUE	CL%	DOCUMENT ID		TECN	COMMENT
$<7.3\times10^{-4}$	90	AITALA	99G	E791	π^- N 500 GeV

$\Gamma(K^-e^+e^+)/\Gamma_{total}$ Γ_{74}/Γ

A test of lepton-number conservation.

VALUE	CL%	DOCUMENT ID		TECN	COMMENT
$<6.3\times10^{-4}$	90	AITALA	99G	E791	π^- N 500 GeV

$\Gamma(K^-\mu^+\mu^+)/\Gamma_{total}$ Γ_{75}/Γ

A test of lepton-number conservation.

VALUE	CL%	EVTS	DOCUMENT ID		TECN	COMMENT
$<1.3\times10^{-5}$	90		LINK	03F	FOCS	γ nucleus, $\overline{E}_\gamma\approx$ 180 GeV
• • • We do not use the following data for averages, fits, limits, etc. • • •						
$<1.8\times10^{-4}$	90		AITALA	99G	E791	π^- N 500 GeV
$<5.9\times10^{-4}$	90	0	KODAMA	95	E653	π^- emulsion 600 GeV

$\Gamma(K^-e^+\mu^+)/\Gamma_{total}$ Γ_{76}/Γ

A test of lepton-number conservation.

VALUE	CL%	DOCUMENT ID		TECN	COMMENT
$<6.8\times10^{-4}$	90	AITALA	99G	E791	π^- N 500 GeV

$\Gamma(K^*(892)^-\mu^+\mu^+)/\Gamma_{total}$ Γ_{77}/Γ

A test of lepton-number conservation.

VALUE	CL%	EVTS	DOCUMENT ID		TECN	COMMENT
$<1.4\times10^{-3}$	90	0	KODAMA	95	E653	π^- emulsion 600 GeV

$D_s^+ \to \phi\ell^+\nu_\ell$ FORM FACTORS

$r_2 \equiv A_2(0)/A_1(0)$ in $D_s^+ \to \phi\ell^+\nu_\ell$

VALUE	EVTS	DOCUMENT ID		TECN	COMMENT
1.60 ± 0.24 OUR AVERAGE					
$1.57\pm0.25\pm0.19$	271	AITALA	99D	E791	$\phi e^+\nu_e$, $\phi\mu^+\nu_\mu$
$1.4\ \pm0.5\ \pm0.3$	308	AVERY	94B	CLE2	$\phi e^+\nu_e$
$1.1\ \pm0.8\ \pm0.1$	90	FRABETTI	94F	E687	$\phi\mu^+\nu_\mu$
$2.1\ ^{+0.6}_{-0.5}\ \pm0.2$	19	KODAMA	93	E653	$\phi\mu^+\nu_\mu$

$r_v \equiv V(0)/A_1(0)$ in $D_s^+ \to \phi\ell^+\nu_\ell$

VALUE	EVTS	DOCUMENT ID		TECN	COMMENT
1.92 ± 0.32 OUR AVERAGE					
$2.27\pm0.35\pm0.22$	271	AITALA	99D	E791	$\phi e^+\nu_e$, $\phi\mu^+\nu_\mu$
$0.9\ \pm0.6\ \pm0.3$	308	AVERY	94B	CLE2	$\phi e^+\nu_e$
$1.8\ \pm0.9\ \pm0.2$	90	FRABETTI	94F	E687	$\phi\mu^+\nu_\mu$
$2.3\ ^{+1.1}_{-0.9}\ \pm0.4$	19	KODAMA	93	E653	$\phi\mu^+\nu_\mu$

Γ_L/Γ_T in $D_s^+ \to \phi\ell^+\nu_\ell$

VALUE	EVTS	DOCUMENT ID		TECN	COMMENT
0.72 ± 0.18 OUR AVERAGE					
$1.0\ \pm0.3\ \pm0.2$	308	AVERY	94B	CLE2	$\phi e^+\nu_e$
$1.0\ \pm0.5\ \pm0.1$	90	[41] FRABETTI	94F	E687	$\phi\mu^+\nu_\mu$
$0.54\pm0.21\pm0.10$	19	[41] KODAMA	93	E653	$\phi\mu^+\nu_\mu$

[41] FRABETTI 94F and KODAMA 93 evaluate Γ_L/Γ_T for a lepton mass of zero.

$D_s^\pm$ REFERENCES

ACOSTA	03D	PR D68 072004	D. Acosta *et al.*	(FNAL CDF-II Collab.)
LINK	03D	PL B561 225	J.M. Link *et al.*	(FNAL FOCUS Collab.)
LINK	03F	PL B572 21	J.M. Link *et al.*	(FNAL FOCUS Collab.)
AUBERT	02G	PR D65 091104R	B. Aubert *et al.*	(BaBar Collab.)
HEISTER	02I	PL B528 1	A. Heister *et al.*	(ALEPH Collab.)
LINK	02I	PL B541 227	J.M. Link *et al.*	(FNAL FOCUS Collab.)
LINK	02J	PL B541 243	J.M. Link *et al.*	(FNAL FOCUS Collab.)
ABBIENDI	01L	PL B516 236	G. Abbiendi *et al.*	(OPAL Collab.)
AITALA	01A	PRL 86 765	E.M. Aitala *et al.*	(FNAL E791 Collab.)
IORI	01	PL B523 22	M. Iori *et al.*	(FNAL SELEX Collab.)
LINK	01C	PRL 87 162001	J.M. Link *et al.*	(FNAL FOCUS Collab.)
ALEXANDROV	00	PL B478 31	Y. Alexandrov *et al.*	(CERN BEATRICE Collab.)
AITALA	99	PL B445 449	E.M. Aitala *et al.*	(FNAL E791 Collab.)
AITALA	99D	PL B450 294	E.M. Aitala *et al.*	(FNAL E791 Collab.)
AITALA	99G	PL B462 401	E.M. Aitala *et al.*	(FNAL E791 Collab.)
BONVICINI	99	PRL 82 4586	G. Bonvicini *et al.*	(CLEO Collab.)
BAI	98	PR D57 28	J.Z. Bai *et al.*	(BEPC BES Collab.)
CHADHA	98	PR D58 032002	M. Chada *et al.*	(CLEO Collab.)
JESSOP	98	PR D58 052002	C.P. Jessop *et al.*	(CLEO Collab.)
ACCIARRI	97F	PL B396 327	M. Acciarri *et al.*	(L3 Collab.)
BAI	97	PR D56 3779	J.Z. Bai *et al.*	(BES Collab.)
BALEST	97	PRL 79 1436	R. Balest *et al.*	(CLEO Collab.)
FRABETTI	97C	PL B401 131	P.L. Frabetti *et al.*	(FNAL E687 Collab.)
FRABETTI	97D	PL B407 79	P.L. Frabetti *et al.*	(FNAL E687 Collab.)
ARTUSO	96	PL B378 364	M. Artuso *et al.*	(CLEO Collab.)
KODAMA	96	PL B382 299	K. Kodama *et al.*	(FNAL E653 Collab.)
BAI	95	PRL 74 4599	J.Z. Bai *et al.*	(BES Collab.)
BAI	95C	PR D52 3781	J.Z. Bai *et al.*	(BES Collab.)
BRANDENB...	95	PRL 75 3804	G.W. Brandenburg *et al.*	(CLEO Collab.)
FRABETTI	95	PL B346 199	P.L. Frabetti *et al.*	(FNAL E687 Collab.)
FRABETTI	95B	PL B351 591	P.L. Frabetti *et al.*	(FNAL E687 Collab.)
FRABETTI	95E	PL B359 403	P.L. Frabetti *et al.*	(FNAL E687 Collab.)
FRABETTI	95F	PL B363 259	P.L. Frabetti *et al.*	(FNAL E687 Collab.)
KODAMA	95	PL B345 85	K. Kodama *et al.*	(FNAL E653 Collab.)
ACOSTA	94	PR D49 5690	D. Acosta *et al.*	(CLEO Collab.)
AVERY	94B	PL B337 405	P. Avery *et al.*	(CLEO Collab.)
BROWN	94	PR D50 1884	D. Brown *et al.*	(CLEO Collab.)
BUTLER	94	PL B324 255	F. Butler *et al.*	(CLEO Collab.)
FRABETTI	94F	PL B328 187	P.L. Frabetti *et al.*	(FNAL E687 Collab.)
MUHEIM	94	PR D49 3767	F. Muheim, S. Stone	(SYRA)
ADAMOVICH	93	PL B305 177	M.I. Adamovich *et al.*	(CERN WA82 Collab.)
AOKI	93	PTP 89 131	S. Aoki *et al.*	(CERN WA75 Collab.)
FRABETTI	93F	PRL 71 827	P.L. Frabetti *et al.*	(FNAL E687 Collab.)
FRABETTI	93G	PL B313 253	P.L. Frabetti *et al.*	(FNAL E687 Collab.)
KODAMA	93	PL B309 483	K. Kodama *et al.*	(FNAL E653 Collab.)
KODAMA	93B	PL B313 260	K. Kodama *et al.*	(FNAL E653 Collab.)
ALBRECHT	92B	ZPHY C53 361	H. Albrecht *et al.*	(ARGUS Collab.)
ALEXANDER	92	PRL 68 1275	J. Alexander *et al.*	(CLEO Collab.)
ANJOS	92D	PRL 69 2892	J.C. Anjos *et al.*	(FNAL E691 Collab.)
AVERY	92	PRL 68 1279	P. Avery *et al.*	(CLEO Collab.)
BARLAG	92C	ZPHY C55 383	S. Barlag *et al.*	(ACCMOR Collab.)
Also	90D	ZPHY C48 29	S. Barlag *et al.*	(ACCMOR Collab.)
DAOUDI	92	PR D45 3965	M. Daoudi *et al.*	(CLEO Collab.)
FRABETTI	92	PL B281 167	P.L. Frabetti *et al.*	(FNAL E687 Collab.)
ALBRECHT	91	PL B255 634	H. Albrecht *et al.*	(ARGUS Collab.)
ALVAREZ	91	PL B255 639	M.P. Alvarez *et al.*	(CERN NA14/2 Collab.)
ANJOS	91B	PR D43 R2063	J.C. Anjos *et al.*	(FNAL E691 Collab.)
COFFMAN	91	PL B263 135	D.M. Coffman *et al.*	(Mark III Collab.)
ADLER	90B	PRL 64 169	J.C. Adler *et al.*	(Mark III Collab.)
ALBRECHT	90D	PL B245 315	H. Albrecht *et al.*	(ARGUS Collab.)
ALEXANDER	90B	PRL 65 1531	J. Alexander *et al.*	(CLEO Collab.)
ALVAREZ	90C	PL B246 261	M.P. Alvarez *et al.*	(CERN NA14/2 Collab.)
ANJOS	90B	PRL 64 2885	J.C. Anjos *et al.*	(FNAL E691 Collab.)
ANJOS	90C	PR D41 2705	J.C. Anjos *et al.*	(FNAL E691 Collab.)
BAI	90	PRL 65 686	Z. Bai *et al.*	(Mark III Collab.)
BARLAG	90C	ZPHY C46 563	S. Barlag *et al.*	(ACCMOR Collab.)
FRABETTI	90	PL B251 639	P.L. Frabetti *et al.*	(FNAL E687 Collab.)
ADLER	89B	PRL 63 1211	J. Adler *et al.*	(Mark III Collab.)
Also	89D	PRL 63 2858 erratum	J. Adler *et al.*	(Mark III Collab.)
ANJOS	89	PRL 62 125	J.C. Anjos *et al.*	(FNAL E691 Collab.)
ANJOS	89E	PL B223 267	J.C. Anjos *et al.*	(FNAL E691 Collab.)
CHEN	89	PL B226 192	W.Y. Chen *et al.*	(CLEO Collab.)
ALBRECHT	88	PL B207 349	H. Albrecht *et al.*	(ARGUS Collab.)
ANJOS	88	PRL 60 897	J.C. Anjos *et al.*	(FNAL E691 Collab.)
RAAB	88	PR D37 2391	J.R. Raab *et al.*	(FNAL E691 Collab.)
ALBRECHT	87F	PL B179 398	H. Albrecht *et al.*	(ARGUS Collab.)
ALBRECHT	87G	PL B195 102	H. Albrecht *et al.*	(ARGUS Collab.)
BECKER	87B	PL B184 277	H. Becker *et al.*	(NA11 and NA32 Collab.)
BLAYLOCK	87	PRL 58 2171	G.T. Blaylock *et al.*	(Mark III Collab.)
BRAUNSCH...	87	ZPHY C35 317	W. Braunschweig *et al.*	(TASSO Collab.)
USHIDA	86	PRL 56 1767	N. Ushida *et al.*	(FNAL E531 Collab.)
ALBRECHT	85D	PL 153B 343	H. Albrecht *et al.*	(ARGUS Collab.)
DERRICK	85B	PRL 54 2568	M. Derrick *et al.*	(HRS Collab.)
AIHARA	84D	PRL 53 2465	H. Aihara *et al.*	(TPC Collab.)
ALTHOFF	84	PL 136B 130	M. Althoff *et al.*	(TASSO Collab.)
BAILEY	84	PL 139B 320	R. Bailey *et al.*	(ACCMOR Collab.)
AUBERT	83	NP B213 31	J.J. Aubert *et al.*	(EMC Collab.)
CHEN	83C	PRL 51 634	A. Chen *et al.*	(CLEO Collab.)

OTHER RELATED PAPERS

RICHMAN	95	RMP 67 893	J.D. Richman, P.R. Burchat	(UCSB, STAN)

Meson Particle Listings

$D_s^{*\pm}$, $D_{sJ}^*(2317)^\pm$

$D_s^{*\pm}$

$I(J^P) = 0(?^?)$

J^P is natural, width and decay modes consistent with 1^-.

$D_s^{*\pm}$ MASS

The fit includes $D^\pm$, D^0, $D_s^\pm$, $D^{*\pm}$, D^{*0}, and $D_s^{*\pm}$ mass and mass difference measurements.

VALUE (MeV)	DOCUMENT ID		TECN	COMMENT
2112.1±0.7 OUR FIT Error includes scale factor of 1.1.				
2106.6±2.1±2.7	[1] BLAYLOCK	87	MRK3	$e^+e^- \to D_s^\pm\gamma X$

[1] Assuming $D_s^\pm$ mass = 1968.7 ± 0.9 MeV.

$m_{D_s^{*\pm}} - m_{D_s^\pm}$

The fit includes $D^\pm$, D^0, $D_s^\pm$, $D^{*\pm}$, D^{*0}, and $D_s^{*\pm}$ mass and mass difference measurements.

VALUE (MeV)	EVTS	DOCUMENT ID		TECN	COMMENT
143.8 ± 0.4 OUR FIT					
143.9 ± 0.4 OUR AVERAGE					
143.76± 0.39±0.40		GRONBERG	95	CLE2	e^+e^-
144.22± 0.47±0.37		BROWN	94	CLE2	e^+e^-
142.5 ± 0.8 ±1.5		[2] ALBRECHT	88	ARG	$e^+e^- \to D_s^\pm\gamma X$
139.5 ± 8.3 ±9.7	60	AIHARA	84D	TPC	$e^+e^- \to$ hadrons
• • • We do not use the following data for averages, fits, limits, etc. • • •					
143.0 ±18.0	8	ASRATYAN	85	HLBC	FNAL 15-ft, ν-^{2}H
110 ±46		BRANDELIK	79	DASP	$e^+e^- \to D_s^\pm\gamma X$

[2] Result includes data of ALBRECHT 84B.

$D_s^{*\pm}$ WIDTH

VALUE (MeV)	CL%	DOCUMENT ID		TECN	COMMENT
< 1.9	90	GRONBERG	95	CLE2	e^+e^-
< 4.5	90	ALBRECHT	88	ARG	$E_{cm}^{ee} = 10.2$ GeV
• • • We do not use the following data for averages, fits, limits, etc. • • •					
< 4.9	90	BROWN	94	CLE2	e^+e^-
<22	90	BLAYLOCK	87	MRK3	$e^+e^- \to D_s^\pm\gamma X$

D_s^{*+} DECAY MODES

D_s^{*-} modes are charge conjugates of the modes below.

	Mode	Fraction (Γ_i/Γ)
Γ_1	$D_s^+\gamma$	(94.2±2.5) %
Γ_2	$D_s^+\pi^0$	(5.8±2.5) %

CONSTRAINED FIT INFORMATION

An overall fit to a branching ratio uses 1 measurements and one constraint to determine 2 parameters. The overall fit has a $\chi^2 = 0.0$ for 0 degrees of freedom.

The following *off-diagonal* array elements are the correlation coefficients $\langle \delta x_i \delta x_j \rangle / (\delta x_i \cdot \delta x_j)$, in percent, from the fit to the branching fractions, $x_i \equiv \Gamma_i/\Gamma_{total}$. The fit constrains the x_i whose labels appear in this array to sum to one.

x_2 | −100
x_1

D_s^{*+} BRANCHING RATIOS

$\Gamma(D_s^+\gamma)/\Gamma_{total}$ **Γ_1/Γ**

VALUE	DOCUMENT ID		TECN	COMMENT
0.942±0.026 OUR FIT				
• • • We do not use the following data for averages, fits, limits, etc. • • •				
seen	ASRATYAN	91	HLBC	$\overline{\nu}_\mu$ Ne
seen	ALBRECHT	88	ARG	$e^+e^- \to D_s^\pm\gamma X$
seen	AIHARA	84D		
seen	ALBRECHT	84B		
seen	BRANDELIK	79		

$\Gamma(D_s^+\pi^0)/\Gamma(D_s^+\gamma)$ **Γ_2/Γ_1**

VALUE	DOCUMENT ID		TECN	COMMENT
0.062±0.029 OUR FIT				
$0.062^{+0.020}_{-0.018}\pm0.022$	GRONBERG	95	CLE2	e^+e^-

$D_s^{*\pm}$ REFERENCES

GRONBERG	95	PRL 75 3232	J. Gronberg *et al.* (CLEO Collab.)
BROWN	94	PR D50 1884	D. Brown *et al.* (CLEO Collab.)
ASRATYAN	91	PL B257 525	A.E. Asratyan *et al.* (ITEP, BELG, SACL+)
ALBRECHT	88	PL B207 349	H. Albrecht *et al.* (ARGUS Collab.)
BLAYLOCK	87	PRL 58 2171	G.T. Blaylock *et al.* (Mark III Collab.)
ASRATYAN	85	PL 156B 441	A.E. Asratyan *et al.* (ITEP, SERP)
AIHARA	84D	PRL 53 2465	H. Aihara *et al.* (TPC Collab.)
ALBRECHT	84B	PL 146B 111	H. Albrecht *et al.* (ARGUS Collab.)
BRANDELIK	79	PL 80B 412	R. Brandelik *et al.* (DASP Collab.)

OTHER RELATED PAPERS

KAMAL	92	PL B284 421	A.N. Kamal, Q.P. Xu (ALBE)
BRANDELIK	78C	PL 76B 361	R. Brandelik *et al.* (DASP Collab.)
BRANDELIK	77B	PL 70B 132	R. Brandelik *et al.* (DASP Collab.)

$D_{sJ}^*(2317)^\pm$

$I(J^P) = 0(0^+)$
J, P need confirmation.

J^P is natural, low mass and decay angular distribution consistent with 0^+.

$D_{sJ}^*(2317)^\pm$ MASS

VALUE (MeV)	EVTS	DOCUMENT ID		TECN	COMMENT
2317.4±0.9 OUR FIT Error includes scale factor of 1.1.					
• • • We do not use the following data for averages, fits, limits, etc. • • •					
2317.2±0.5±0.9	761	[1] MIKAMI	04	BELL	10.6 e^+e^-
2316.8±0.4±3.0	1267± 53	[1,2] AUBERT	03G	BABR	10.6 e^+e^-
2317.6±1.3	273± 33	[1,3] AUBERT	03G	BABR	10.6 e^+e^-
2319.8±2.1±2.0	24	[1] KROKOVNY	03B	BELL	10.6 e^+e^-

[1] Not independent of the corresponding $m_{D_{sJ}^*(2317)} - m_{D_s}$.
[2] From $D_s^+ \to K^+K^-\pi^+$ decay.
[3] From $D_s^+ \to K^+K^-\pi^+\pi^0$ decay.

$m_{D_{sJ}^*(2317)^\pm} - m_{D_s^\pm}$

VALUE (MeV)	EVTS	DOCUMENT ID		TECN	COMMENT
349.2±0.7 OUR FIT					
349.2±0.7 OUR AVERAGE					
348.7±0.5±0.7	761	MIKAMI	04	BELL	10.6 e^+e^-
349.6±0.4±3.0	1267	[4,5] AUBERT	03G	BABR	10.6 e^+e^-
350.0±1.2±1.0	135	BESSON	03	CLE2	10.6 e^+e^-
351.3±2.1±1.9	24	[6] KROKOVNY	03B	BELL	10.6 e^+e^-
• • • We do not use the following data for averages, fits, limits, etc. • • •					
350.2±1.3	273	[7,8] AUBERT	03G	BABR	10.6 e^+e^-

[4] From $D_s^+ \to K^+K^-\pi^+$ decay.
[5] Recalculated by us using $m_{D_s^+} = 1967.20 \pm 0.03$ MeV.
[6] Recalculated by us using $m_{D_s^+} = 1968.5 \pm 0.6$ MeV.
[7] From $D_s^+ \to K^+K^-\pi^+\pi^0$ decay.
[8] Recalculated by us using $m_{D_s^+} = 1967.4 \pm 0.2$ MeV. Systematic errors not estimated.

$D_{sJ}^*(2317)^\pm$ WIDTH

VALUE (MeV)	CL%	EVTS	DOCUMENT ID		TECN	COMMENT
< 4.6	90	761	MIKAMI	04	BELL	10.6 e^+e^-
• • • We do not use the following data for averages, fits, limits, etc. • • •						
<10			AUBERT	03G	BABR	10.6 e^+e^-
< 7	90	135	BESSON	03	CLE2	10.6 e^+e^-

$D_{sJ}^*(2317)^\pm$ DECAY MODES

$D_{sJ}^*(2317)^-$ modes are charge conjugates of modes below.

	Mode
Γ_1	$D_s^+\pi^0$
Γ_2	$D_s^+\gamma$
Γ_3	$D_s^*(2112)^+\gamma$
Γ_4	$D_s^+\gamma\gamma$
Γ_5	$D_s^*(2112)^+\pi^0$
Γ_6	$D_s^+\pi^+\pi^-$

$D^*_{sJ}(2317)^\pm$ BRANCHING RATIOS

$\Gamma(D_s^+\pi^0)/\Gamma_{total}$ Γ_1/Γ

VALUE	EVTS	DOCUMENT ID		TECN	COMMENT
• • • We do not use the following data for averages, fits, limits, etc. • • •					
seen	1540 ± 62	AUBERT	03G	BABR	10.6 e^+e^-

$\Gamma(D_s^+\gamma)/\Gamma(D_s^+\pi^0)$ Γ_2/Γ_1

VALUE	CL%	DOCUMENT ID		TECN	COMMENT
< 0.05	90	MIKAMI	04	BELL	10.6 e^+e^-
• • • We do not use the following data for averages, fits, limits, etc. • • •					
< 0.052	90	BESSON	03	CLE2	10.6 e^+e^-

$\Gamma(D_s^*(2112)^+\gamma)/\Gamma(D_s^+\pi^0)$ Γ_3/Γ_1

VALUE	CL%	DOCUMENT ID		TECN	COMMENT
< 0.059	90	BESSON	03	CLE2	10.6 e^+e^-
• • • We do not use the following data for averages, fits, limits, etc. • • •					
< 0.18	90	MIKAMI	04	BELL	10.6 e^+e^-

$\Gamma(D_s^+\gamma\gamma)/\Gamma(D_s^+\pi^0)$ Γ_4/Γ_1

VALUE	DOCUMENT ID		TECN	COMMENT
• • • We do not use the following data for averages, fits, limits, etc. • • •				
not seen	AUBERT	03G	BABR	10.6 e^+e^-

$\Gamma(D_s^*(2112)^+\pi^0)/\Gamma(D_s^+\pi^0)$ Γ_5/Γ_1

VALUE	CL%	DOCUMENT ID		TECN	COMMENT
< 0.11	90	BESSON	03	CLE2	10.6 e^+e^-

$\Gamma(D_s^+\pi^+\pi^-)/\Gamma(D_s^+\pi^0)$ Γ_6/Γ_1

VALUE	CL%	DOCUMENT ID		TECN	COMMENT
< 0.004	90	MIKAMI	04	BELL	10.6 e^+e^-
• • • We do not use the following data for averages, fits, limits, etc. • • •					
< 0.019	90	BESSON	03	CLE2	10.6 e^+e^-

$D^*_{sJ}(2317)^\pm$ REFERENCES

MIKAMI	04	PRL 92 012002	Y. Mikami *et al.*	(BELLE Collab.)
AUBERT	03G	PRL 90 242001	B. Aubert *et al.*	(BaBar Collab.)
BESSON	03	PR D68 032002	D. Besson *et al.*	(CLEO Collab.)
KROKOVNY	03B	PRL 91 262002	P. Krokovny *et al.*	(BELLE Collab.)

OTHER RELATED PAPERS

BROWDER	04	PL B578 365	T.E. Browder, S. Pakvasa, A.A. Petrov
SADZIKOWSKI	04	PL B579 39	M. Sadzikowski
BALI	03	PR D68 071501	G.S. Bali
BARDEEN	03	PR D68 054024	W.A. Bardeen *et al.*
BARNES	03	PR D68 054006	T. Barnes *et al.*
CAHN	03	PR D68 037502	R.N. Cahn, J.D. Jackson
CHENG	03C	PL B566 193	H.-Y. Cheng, W.-S. Hou
COLANGELO	03B	PL B570 180	P. Colangelo, F. De Fazio
DATTA	03C	PL B572 164	A. Datta, P.J. O'Donnell
SZCZEPANIAK	03	PL B567 23	A.P. Szczepaniak
TERASAKI	03	PR D68 011501	K. Terasaki
VANBEVEREN	03	PRL 91 012003	E. van Beveren, G. Rupp

$D_{sJ}(2460)^\pm$

$I(J^P) = 0(1^+)$

Zero spin excluded by the observation of the decay to $D_s^+\gamma$, the decay angular distribution consistent with spin 1.

$D_{sJ}(2460)^\pm$ MASS

VALUE (MeV)	EVTS	DOCUMENT ID		TECN	COMMENT
2459.3 ± 1.3 OUR FIT Error includes scale factor of 1.3.					
• • • We do not use the following data for averages, fits, limits, etc. • • •					
2456.5 ± 1.3 ± 1.3	126	[1,2] MIKAMI	04	BELL	10.6 e^+e^-
2459.5 ± 1.3 ± 2.0	152	[3,4] MIKAMI	04	BELL	10.6 e^+e^-
2459.9 ± 0.9 ± 1.6	60	[3,4] MIKAMI	04	BELL	10.6 e^+e^-
2459.2 ± 1.6 ± 2.0	57	KROKOVNY	03B	BELL	10.6 e^+e^-

[1] Not independent of the corresponding $m_{D_{sJ}(2460)^\pm} - m_{D_s^{*\pm}}$.

[2] Using $m_{D_s^{*+}} = 2112.4 \pm 0.7$ MeV.

[3] Not independent of the corresponding $m_{D_{sJ}(2460)^\pm} - m_{D_s^\pm}$.

[4] Using $m_{D_s^+} = 1968.5 \pm 0.6$ MeV.

$m_{D_{sJ}(2460)^\pm} - m_{D_s^{*\pm}}$

VALUE (MeV)	EVTS	DOCUMENT ID		TECN	COMMENT
347.2 ± 1.2 OUR FIT Error includes scale factor of 1.3.					
347.1 ± 2.2 OUR AVERAGE Error includes scale factor of 1.9. See the ideogram below.					
344.1 ± 1.3 ± 1.1	126	MIKAMI	04	BELL	10.6 e^+e^-
351.2 ± 1.7 ± 1.0	41	BESSON	03	CLE2	10.6 e^+e^-
346.8 ± 1.6 ± 1.9	57	[5] KROKOVNY	03B	BELL	10.6 e^+e^-

[5] Recalculated by us using $m_{D_s^{*+}} = 2112.4 \pm 0.7$ MeV.

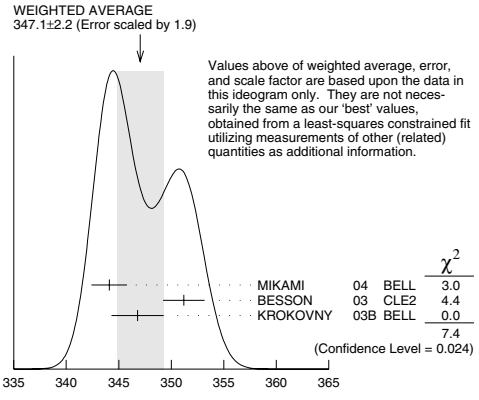

$m_{D_{sJ}(2460)^\pm} - m_{D_s^\pm}$

VALUE (MeV)	EVTS	DOCUMENT ID		TECN	COMMENT
491.0 ± 1.2 OUR FIT Error includes scale factor of 1.3.					
491.3 ± 1.4 OUR AVERAGE					
491.0 ± 1.3 ± 1.9	152	[6] MIKAMI	04	BELL	10.6 e^+e^-
491.4 ± 0.9 ± 1.5	60	[7] MIKAMI	04	BELL	10.6 e^+e^-

[6] From the decay to $D_s^\pm\gamma$.

[7] From the decay to $D_s^\pm\pi^+\pi^-$.

$D_{sJ}(2460)^\pm$ WIDTH

VALUE (MeV)	CL%	EVTS	DOCUMENT ID		TECN	COMMENT
< 5.5	90	126	MIKAMI	04	BELL	10.6 e^+e^-
• • • We do not use the following data for averages, fits, limits, etc. • • •						
< 7	90	41	BESSON	03	CLE2	10.6 e^+e^-

$D_{sJ}(2460)^+$ DECAY MODES

$D_{sJ}(2460)^-$ modes are charge conjugates of the modes below.

	Mode
Γ_1	$D_s^{*+}\pi^0$
Γ_2	$D_s^+\gamma$
Γ_3	$D_s^+\pi^+\pi^-$
Γ_4	$D_s^{*+}\gamma$
Γ_5	$D^*_{sJ}(2317)^+\gamma$

$D_{sJ}(2460)^\pm$ BRANCHING RATIOS

$\Gamma(D_s^{*+}\pi^0)/\Gamma_{total}$ Γ_1/Γ

VALUE	EVTS	DOCUMENT ID		TECN	COMMENT
• • • We do not use the following data for averages, fits, limits, etc. • • •					
seen	41	BESSON	03	CLE2	10.6 e^+e^-

$\Gamma(D_s^+\gamma)/\Gamma(D_s^{*+}\pi^0)$ Γ_2/Γ_1

VALUE	CL%	EVTS	DOCUMENT ID		TECN	COMMENT
0.44 ± 0.09 OUR AVERAGE						
0.55 ± 0.13 ± 0.08		152	MIKAMI	04	BELL	10.6 e^+e^-
0.38 ± 0.11 ± 0.04		38	KROKOVNY	03B	BELL	10.6 e^+e^-
• • • We do not use the following data for averages, fits, limits, etc. • • •						
< 0.49	90		BESSON	03	CLE2	10.6 e^+e^-

Meson Particle Listings

$D_{sJ}(2460)^{\pm}$, $D_{s1}(2536)^{\pm}$

$\Gamma(D_s^+\pi^+\pi^-)/\Gamma(D_s^{*+}\pi^0)$ Γ_3/Γ_1

VALUE	CL%	EVTS	DOCUMENT ID		TECN	COMMENT
0.14 ± 0.04 ± 0.02		60	MIKAMI	04	BELL	10.6 e^+e^-
• • • We do not use the following data for averages, fits, limits, etc. • • •						
< 0.08	90		BESSON	03	CLE2	10.6 e^+e^-

$\Gamma(D_s^{*+}\gamma)/\Gamma(D_s^{*+}\pi^0)$ Γ_4/Γ_1

VALUE	CL%	DOCUMENT ID		TECN	COMMENT
< 0.16	90	BESSON	03	CLE2	10.6 e^+e^-
• • • We do not use the following data for averages, fits, limits, etc. • • •					
< 0.31	90	MIKAMI	04	BELL	10.6 e^+e^-

$\Gamma(D_{sJ}^*(2317)^+\gamma)/\Gamma(D_s^{*+}\pi^0)$ Γ_5/Γ_1

VALUE	CL%	DOCUMENT ID		TECN	COMMENT
• • • We do not use the following data for averages, fits, limits, etc. • • •					
< 0.58	90	BESSON	03	CLE2	10.6 e^+e^-

$D_s(2460)^{\pm}$ REFERENCES

MIKAMI	04	PRL 92 012002	Y. Mikami *et al.*	(BELLE Collab.)
BESSON	03	PR D68 032002	D. Besson *et al.*	(CLEO Collab.)
KROKOVNY	03B	PRL 91 262002	P. Krokovny *et al.*	(BELLE Collab.)

OTHER RELATED PAPERS

BROWDER	04	PL B578 365	T.E. Browder, S. Pakvasa, A.A. Petrov
SADZIKOWSKI	04	PL B579 39	M. Sadzikowski
AUBERT	03G	PRL 90 242001	B. Aubert *et al.* (BaBar Collab.)
BARDEEN	03	PR D68 054024	W.A. Bardeen *et al.*
BARNES	03	PR D68 054006	T. Barnes *et al.*
CAHN	03	PR D68 037502	R.N. Cahn, J.D. Jackson
COLANGELO	03B	PL B570 180	P. Colangelo, F. De Fazio
DATTA	03C	PL B572 164	A. Datta, P.J. O'Donnell

$D_{s1}(2536)^{\pm}$

$I(J^P) = 0(1^+)$
J, P need confirmation.

Seen in $D^*(2010)^+K^0$. Not seen in D^+K^0 or D^0K^+. $J^P = 1^+$ assignment strongly favored.

$D_{s1}(2536)^{\pm}$ MASS

VALUE (MeV)	EVTS	DOCUMENT ID		TECN	COMMENT
2535.35 ± 0.34 ± 0.5 OUR EVALUATION					
2535.34 ± 0.31 OUR AVERAGE					
2535.3 ± 0.7	92	[1] HEISTER	02B	ALEP	$e^+e^- \to D^{*+}K^0X$, $D^{*0}K^+X$
2534.2 ± 1.2	9	ASRATYAN	94	BEBC	$\nu N \to D^*K^0X, D^{*0}K^{\pm}X$
2535 ± 0.6 ± 1	75	FRABETTI	94B	E687	γBe $\to D^{*+}K^0X$, $D^{*0}K^+X$
2535.3 ± 0.2 ± 0.5	134	ALEXANDER	93	CLE2	$e^+e^- \to D^{*0}K^+X$
2534.8 ± 0.6 ± 0.6	44	ALEXANDER	93	CLE2	$e^+e^- \to D^{*+}K^0X$
2535.2 ± 0.5 ± 1.5	28	ALBRECHT	92R	ARG	10.4 $e^+e^- \to D^{*0}K^+X$
2536.6 ± 0.7 ± 0.4		AVERY	90	CLEO	$e^+e^- \to D^{*+}K^0X$
2535.9 ± 0.6 ± 2.0		ALBRECHT	89E	ARG	$D_{s1}^* \to D^*(2010)K^0$
• • • We do not use the following data for averages, fits, limits, etc. • • •					
2535 ± 28		[2] ASRATYAN	88	HLBC	$\nu N \to D_S\gamma\gamma X$

[1] Calculated using $m_{D^*(2010)^{\pm}} = 2010.0 \pm 0.5$ MeV, $m_{D^*(2007)^0} = 2006.7 \pm 0.5$ MeV, and the mass difference below.
[2] Not seen in D^*K.

$m_{D_{s1}(2536)^{\pm}} - m_{D_s^*(2111)}$

VALUE (MeV)	DOCUMENT ID		TECN	COMMENT
424 ± 28	ASRATYAN	88	HLBC	$D_s^{*\pm}\gamma$

$m_{D_{s1}(2536)^{\pm}} - m_{D^*(2010)^{\pm}}$

VALUE (MeV)	EVTS	DOCUMENT ID		TECN	COMMENT
525.3 ± 0.6 ± 0.1	41	HEISTER	02B	ALEP	$e^+e^- \to D^{*+}K^0X$

$m_{D_{s1}(2536)^{\pm}} - m_{D^*(2007)^0}$

VALUE (MeV)	EVTS	DOCUMENT ID		TECN	COMMENT
528.1 ± 1.5 OUR AVERAGE					
528.7 ± 1.9 ± 0.5	51	HEISTER	02B	ALEP	$e^+e^- \to D^{*0}K^+X$
527.3 ± 2.2	29	ACKERSTAFF	97W	OPAL	$e^+e^- \to D^{*0}K^+X$

$D_{s1}(2536)^{\pm}$ WIDTH

VALUE (MeV)	CL%	EVTS	DOCUMENT ID		TECN	COMMENT
< 2.3	90		ALEXANDER	93	CLEO	$e^+e^- \to D^{*0}K^+X$
• • • We do not use the following data for averages, fits, limits, etc. • • •						
< 3.2	90	75	FRABETTI	94B	E687	γBe $\to D^{*+}K^0X$, $D^{*0}K^+X$
< 3.9	90		ALBRECHT	92R	ARG	10.4 $e^+e^- \to D^{*0}K^+X$
< 5.44	90		AVERY	90	CLEO	$e^+e^- \to D^{*+}K^0X$
< 4.6	90		ALBRECHT	89E	ARG	$D_{s1}^* \to D^*(2010)K^0$

$D_{s1}(2536)^+$ DECAY MODES

$D_{s1}(2536)^-$ modes are charge conjugates of the modes below.

	Mode	Fraction (Γ_j/Γ)
Γ_1	$D^*(2010)^+K^0$	seen
Γ_2	$D^*(2007)^0K^+$	seen
Γ_3	D^+K^0	not seen
Γ_4	D^0K^+	not seen
Γ_5	$D_s^{*+}\gamma$	possibly seen

$D_{s1}(2536)^+$ BRANCHING RATIOS

$\Gamma(D^+K^0)/\Gamma(D^*(2010)^+K^0)$ Γ_3/Γ_1

VALUE	CL%	DOCUMENT ID		TECN	COMMENT
< 0.40	90	ALEXANDER	93	CLEO	$e^+e^- \to D^{*+}K^0X$
< 0.43	90	ALBRECHT	89E	ARG	$D_{s1}^* \to D^*(2010)K^0$

$\Gamma(D_s^{*+}\gamma)/\Gamma_{\text{total}}$ Γ_5/Γ

VALUE	DOCUMENT ID		TECN	COMMENT
possibly seen	ASRATYAN	88	HLBC	$\nu N \to D_S\gamma\gamma X$

$\Gamma(D^0K^+)/\Gamma(D^*(2007)^0K^+)$ Γ_4/Γ_2

VALUE	CL%	DOCUMENT ID		TECN	COMMENT
< 0.12	90	ALEXANDER	93	CLEO	$e^+e^- \to D^{*0}K^+X$

$\Gamma(D_s^{*+}\gamma)/\Gamma(D^*(2007)^0K^+)$ Γ_5/Γ_2

VALUE	CL%	DOCUMENT ID		TECN	COMMENT
< 0.42	90	ALEXANDER	93	CLEO	$e^+e^- \to D^{*0}K^+X$

$\Gamma(D^*(2007)^0K^+)/\Gamma(D^*(2010)^+K^0)$ Γ_2/Γ_1

VALUE	EVTS	DOCUMENT ID		TECN	COMMENT
1.27 ± 0.21 OUR AVERAGE					
1.32 ± 0.47 ± 0.23	92	[3] HEISTER	02B	ALEP	$e^+e^- \to D^{*+}K^0X$, $D^{*0}K^+X$
1.9 $^{+1.1}_{-0.9}$ ± 0.4	35	[3] ACKERSTAFF	97W	OPAL	$e^+e^- \to D^{*0}K^+X$, $D^{*+}K^0X$
1.1 ± 0.3		ALEXANDER	93	CLEO	$e^+e^- \to D^{*0}K^+X, D^{*+}K^0X$
1.4 ± 0.3 ± 0.2		[4] ALBRECHT	92R	ARG	10.4 $e^+e^- \to D^{*0}K^+X, D^{*+}K^0X$

[3] Ratio of the production rates measured in Z^0 decays.
[4] Evaluated by us from published inclusive cross-sections.

$D_{s1}(2536)^{\pm}$ REFERENCES

HEISTER	02B	PL B526 34	A. Heister *et al.*	(ALEPH Collab.)
ACKERSTAFF	97W	ZPHY C76 425	K. Ackerstaff *et al.*	(OPAL Collab.)
ASRATYAN	94	ZPHY C 61 563	A.E. Asratyan *et al.*	(BIRM, BELG, CERN+)
FRABETTI	94B	PRL 72 324	P.L. Frabetti *et al.*	(FNAL E687 Collab.)
ALEXANDER	93	PL B303 377	J. Alexander *et al.*	(CLEO Collab.)
ALBRECHT	92R	PL B297 425	H. Albrecht *et al.*	(ARGUS Collab.)
AVERY	90	PR D41 774	P. Avery, D. Besson	(CLEO Collab.)
ALBRECHT	89E	PL B230 162	H. Albrecht *et al.*	(ARGUS Collab.)
ASRATYAN	88	ZPHY C40 483	A.E. Asratyan *et al.*	(ITEP, SERP)

OTHER RELATED PAPERS

SEMENOV	99	SPU 42 847 Translated from UFN 42 937.	S.V. Semenov

See key on page 323

$D_{s2}(2573)^{\pm}$

$I(J^P) = 0(?^?)$

J^P is natural, width and decay modes consistent with 2^+.

$D_{s2}(2573)^{\pm}$ MASS

VALUE (MeV)	EVTS	DOCUMENT ID		TECN	CHG	COMMENT
2572.4 ± 1.5 OUR AVERAGE						
2568.6 ± 3.2	64	[1] HEISTER	02B	ALEP		$e^+e^- \to D^0K^+X$
2574.5 ± 3.3 ± 1.6		ALBRECHT	96	ARG		$e^+e^- \to D^0K^+X$
$2573.2^{+1.7}_{-1.6} \pm 0.9$	217	KUBOTA	94	CLE2	+	$e^+e^- \sim$ 10.5 GeV

[1] Calculated using $m_{D^0} = 1864.5 \pm 0.5$ and the mass difference below.

$m_{D_{s2}(2573)^{\pm}} - m_{D^0}$

VALUE (MeV)	EVTS	DOCUMENT ID		TECN	COMMENT
704 ± 3 ± 1	64	HEISTER	02B	ALEP	$e^+e^- \to D^0K^+X$

$D_{s2}(2573)^{\pm}$ WIDTH

VALUE (MeV)	EVTS	DOCUMENT ID		TECN	CHG	COMMENT
15^{+5}_{-4} OUR AVERAGE						
$10.4 \pm 8.3 \pm 3.0$		ALBRECHT	96	ARG		$e^+e^- \to D^0K^+X$
$16^{+5}_{-4} \pm 3$	217	KUBOTA	94	CLE2	+	$e^+e^- \sim$ 10.5 GeV

$D_{s2}(2573)^+$ DECAY MODES

$D_{s2}(2573)^-$ modes are charge conjugates of the modes below.

	Mode	Fraction (Γ_i/Γ)
Γ_1	D^0K^+	seen
Γ_2	$D^*(2007)^0K^+$	not seen

$D_{s2}(2573)^+$ BRANCHING RATIOS

$\Gamma(D^0K^+)/\Gamma_{total}$ Γ_1/Γ

VALUE	EVTS	DOCUMENT ID		TECN	CHG	COMMENT
seen	217	KUBOTA	94	CLE2	±	$e^+e^- \sim$ 10.5 GeV

$\Gamma(D^*(2007)^0K^+)/\Gamma(D^0K^+)$ Γ_2/Γ_1

VALUE	CL%	DOCUMENT ID		TECN	CHG	COMMENT
< 0.33	90	KUBOTA	94	CLE2	+	$e^+e^- \sim$ 10.5 GeV

$D_{s2}(2573)^{\pm}$ REFERENCES

HEISTER	02B	PL B526 34	A. Heister *et al.*	(ALEPH Collab.)
ALBRECHT	96	ZPHY C69 405	H. Albrecht *et al.*	(ARGUS Collab.)
KUBOTA	94	PRL 72 1972	Y. Kubota *et al.*	(CLEO Collab.)

OTHER RELATED PAPERS

SEMENOV	99	SPU 42 847 Translated from UFN 42 937.	S.V. Semenov

BOTTOM MESONS
($B = \pm 1$)

$B^+ = u\overline{b}$, $B^0 = d\overline{b}$, $\overline{B}^0 = \overline{d}b$, $B^- = \overline{u}b$, similarly for B^*'s

B-particle organization

Many measurements of B decays involve admixtures of B hadrons. Previously we arbitrarily included such admixtures in the $B^\pm$ section, but because of their importance we have created two new sections: "$B^\pm/B^0$ Admixture" for $\Upsilon(4S)$ results and "$B^\pm/B^0/B_s^0$/b-baryon Admixture" for results at higher energies. Most inclusive decay branching fractions and χ_b at high energy are found in the Admixture sections. B^0-$\overline{B}^0$ mixing data are found in the B^0 section, while B_s^0-$\overline{B}_s^0$ mixing data and B-$\overline{B}$ mixing data for a B^0/B_s^0 admixture are found in the B_s^0 section. CP-violation data are found in the $B^\pm$, B^0, and $B^\pm$ B^0 Admixture sections. b-baryons are found near the end of the Baryon section. Recently, we also created a new section: "V_{cb} and V_{ub} CKM Matrix Elements."

The organization of the B sections is now as follows, where bullets indicate particle sections and brackets indicate reviews.

[Production and Decay of b-flavored Hadrons]
[A Short Note on HFAG Activities]
- $B^\pm$
  - mass, mean life
  - branching fractions
  - CP violation
- B^0
  - mass, mean life
  - branching fractions
  - polarization in B^0 decay
  - [B-$\overline{B}$ Mixing]
  - B^0-$\overline{B}^0$ mixing
  - CP violation
- $B^\pm$ B^0 Admixture
  - branching fractions, CP violation
  - CP violation
- $B^\pm/B^0/B_s^0$/b-baryon Admixture
  - mean life
  - production fractions
  - branching fractions
  - χ_b at high energy
- V_{cb} and V_{ub} CKM Matrix Elements
  - [Determination of V_{cb}]
  - [Determination of V_{ub}]

- B^*
  - mass
- $B_J^*(5732)$
  - mass, width
- B_s^0
  - mass, mean life
  - branching fractions
  - polarizaton in B_s^0 decay
  - B_s^0-$\overline{B}_s^0$ mixing
- B_s^*
  - mass
- $B_{sJ}^*(5850)$
  - mass, width
- $B_c^\pm$
  - mass, mean life
  - branching fractions

At end of Baryon Listings:
- Λ_b
  - mass, mean life
  - branching fractions
- Ξ_b^0, Ξ_b^-
  - mean life
- b-baryon Admixture
  - mean life
  - branching fractions

PRODUCTION AND DECAY OF *b*-FLAVORED HADRONS

Updated December 2003 by Y. Kwon (Yonsei University, Seoul, Korea).

In the summer of 2001—almost four decades after CP violation was first discovered in the decay of neutral kaons—the BABAR and Belle collaborations reported the first observation of CP violation in the B meson system [1,2]. The measurement of the CP-violation parameter $\sin 2\beta (= \sin 2\phi_1)$ [3] marks the culmination of a very significant experimental and theoretical program that started in 1973 when Kobayashi and Maskawa proposed their model of the quark mixing matrix. Other recent developments in the physics of B mesons include new results on penguin decays, improved measurements of rare hadronic B decays, as well as new determinations of the CKM matrix elements V_{cb} and V_{ub} [4,5].

The structure of this mini-review is organized as follows. First, we briefly update the results on b quark production and discuss the spectroscopy and the lifetimes of b-flavored hadrons. Then after a brief description of basic properties of B meson decays, we give a short description of the experimental results on CP violation in B meson decays. More details about formalism and implications of CP violations are described in a separate mini-review [6] in this *Review* . This review closes with a description and update on hadronic and rare decays of B mesons.

Production and spectroscopy: Elementary particles are characterized by their masses, lifetimes, and internal quantum numbers. The bound states with a $\overline{b}$ antiquark and a u or d quark are referred to as the B_d (B^0) and the B_u (B^+) mesons, respectively. The first excitation is called the B^* meson. B^{**} is the generic name for the four orbitally excited ($L = 1$) B-meson states that correspond to the P-wave mesons in the charm system, D^{**}. Mesons containing an s or a c quark are denoted B_s^0 and B_c^+, respectively.

Although the b quark was discovered in a fixed-target experiment at Fermilab in 1977, most of the experimental information on b-flavored hadrons has come from colliding-beam machines. Currently, experimental studies of b decay are performed at the $\Upsilon(4S)$ resonance near production threshold, as well as at higher energies in proton-antiproton collisions and Z decays. High-energy $p\overline{p}$ collisions at the Tevatron produce b-flavored hadrons with very large cross-section ($\sigma_{b\overline{b}} \sim 50\mu b$), but it is only possible to trigger on a very small fraction of the decays because of limited acceptance and large background.

The $b\bar{b}$ production cross-section at the Z and $\Upsilon(4S)$ resonances are about 6.6 nb and 1.1 nb, respectively.

By far the largest samples of B mesons have been collected by the e^+e^- collider detectors running at $\Upsilon(4S)$ ("B-Factories"). As of this writing, both Belle and BABAR have accumulated approximately 150 fb^{-1}. The $\Upsilon(4S)$ resonance decays only to $B^0\overline{B}^0$ and B^+B^- pairs, while at high-energy collider experiments, heavier states such as B_s^0 or B_c^+ mesons and b-flavored baryons are produced as well. The current experimental limit for non-$B\overline{B}$ decays of the $\Upsilon(4S)$ is less than 4% at the 95% confidence level (CL) [7]. The $\bar{b}$ (or b) quarks produced at high-energy collider experiments hadronize as B^0, B^+, B_s^0, and B_c^+ mesons (or their antiparticles), or as baryons containing $\bar{b}$ (or b) quarks.

For quantitative studies of B decays, the initial composition of the data sample must be known. In particular, the ratio f_+/f_0 of charged to neutral $\Upsilon(4S)$ decays is crucial to calculate the decay branching fractions for B-factory experiments. CLEO and BABAR have measured the ratio $(f_+/f_0)(\tau_+/\tau_0)$ with exclusive $B \to \psi K^{(*)}$ [8,9] and $B \to D^*\ell\nu$ [10] decays, where τ_+/τ_0 is the B^+/B^0 lifetime ratio (*see next section*). By using the world-average value of τ_+ and τ_0 Belle also extracted the value of f_+/f_0 [11]. Using the current average of τ_+/τ_0, the average becomes $f_+/f_0 = 1.044 \pm 0.050$ [12]. This is consistent with equal production of B^+B^- and $B^0\overline{B}^0$ pairs, and unless explicitly stated otherwise, we will assume $f_+/f_0 = 1$. This assumption is further supported by the near equality of the B^+ and B^0 masses. Again using exclusive $B \to J/\psi K^{(*)}$ decays, CLEO determined these masses to $m(B^0) = 5.2791 \pm 0.0007 \pm 0.0003$ GeV/c^2 and $m(B^+) = 5.2791 \pm 0.0004 \pm 0.0004$ GeV/c^2, respectively [13].

More diverse species of b-flavored hadrons are produced in the experiments at the Z resonance and in the high-energy $p\overline{p}$ collisions. Table 1 shows the fractions f_d, f_u, f_s, and $f_{\rm baryon}$ of B^0, B^+, B_s^0, and b baryons in an unbiased sample of weakly decaying b hadrons produced at the Z resonance and in $p\overline{p}$ collisions [12]. A detailed account can be found elsewhere in this *Review* [14]. The values assume identical hadronization in $p\overline{p}$ collisions and in Z decay, even though these could, in principle, differ because of the different momentum distributions of the b–quark in these processes.

Table 1: Fractions of weakly decaying b-hadron species in $Z \to b\bar{b}$ decay and in $p\overline{p}$ collisions at $\sqrt{s} = 1.8$ TeV.

b hadron	Fraction [%]
B^+, B^0	39.7 ± 1.0
B_s^0	10.7 ± 1.1
b baryons	9.9 ± 1.7

To date, the existence of several b-flavored mesons (B^+, B^0, B_s^0, B_c^+, and various excitations), as well as the Λ_b baryon has been established. Using exclusive hadronic decays such as $B_s^0 \to J/\psi\phi$ and $\Lambda_b \to J/\psi\Lambda$, the masses of these states are now known with the precision of a few MeV. The current world averages of the B_s^0 and the Λ_b mass are 5.3696 ± 0.0024 GeV/c^2 and 5.624 ± 0.009 GeV/c^2, respectively. Clear evidence for the B_c^+, the last weakly decaying bottom meson, has been published by CDF [15]. They reconstruct the semileptonic decay $B_c^+ \to J/\psi\ell X$, and extract a B_c^+ mass of $6.40 \pm 0.39 \pm 0.13$ GeV/c^2. First indications of Ξ_b production have been presented by the LEP Collaborations [16,17].

Excited B-meson states have been observed by CLEO, LEP, CUSB, and CDF. The current world average of the B^*–B mass difference is 45.78 ± 0.35 MeV/c^2. Evidence for B^{**} production has been presented by the LEP and CDF experiments [18]. Inclusively reconstructing a bottom hadron candidate combined with a charged pion from the primary vertex, they see the B^{**} as a broad resonance around 5.697 ± 0.009 GeV/c^2 in the $M(B\pi) - M(B)$ mass distribution [19]. Due to the inclusive approach, the mass resolution is limited to about 40 MeV, which makes it very difficult to identify the narrow states, B_1^* and B_2^*, separately. The LEP experiments have also provided evidence for excited B_s^{**} states.

Lifetimes: Precise lifetimes are key in extracting the weak parameters that are important for understanding the role of the CKM matrix in CP violation, such as the determination of V_{cb} and $B_s^0\overline{B}_s^0$ mixing measurements. In the naive spectator model, the heavy quark can decay only via the external spectator mechanism, and thus, the lifetimes of all mesons and baryons containing b quarks would be equal. Nonspectator effects, such as the interference between contributing amplitudes, modify this simple picture and give rise to a lifetime hierarchy for b-flavored hadrons similar to the one in the charm sector. However, since the lifetime differences are expected to scale as $1/m_Q^2$, where m_Q is the mass of the heavy quark, the variation in the b system should be significantly smaller, of order 10% or less [20]. For the b system we expect

$$\tau(B^+) \geq \tau(B^0) \approx \tau(B_s^0) > \tau(\Lambda_b^0) \gg \tau(B_c^+) . \quad (1)$$

In the B_c^+, both quarks can decay weakly, resulting in its much shorter lifetime. Measurements of lifetimes for the various b-flavored hadrons thus provide a means to determine the importance of non-spectator mechanisms in the b sector.

Over the past years, advanced algorithms based on impact parameter or decay length measurements exploiting the potential of silicon vertex detectors resulted in improvement of lifetime measurements. However, in order to reach the precision necessary to test theoretical predictions, the results from different experiments need to be averaged. This is a challenging task that requires detailed knowledge of common systematic uncertainties, and correlations between the results from different experiments. The average lifetimes for b-flavored hadrons

given in this edition have been determined by the Heavy Flavor Averaging Group (HFAG) [12]. A detailed description of the procedures and the treatment of correlated and uncorrelated errors can be found in [21]. The asymmetric B factories are now making significant contributions to the B^+ and B^0 lifetime measurements. Their use of fully–reconstructed B decays yield measurements with much reduced statistical and systematic uncertainties. The measurements are free, for example, from systematics associated with modelling of fragmentation. The new world average b-hadron lifetimes are summarized in Table 2.

Table 2: Summary of inclusive and exclusive b-hadron lifetime measurements.

Particle	Lifetime [ps]
B^0	1.536 ± 0.014
B^+	1.671 ± 0.018
B_s^0	1.461 ± 0.057
B_c^+	$0.46^{+0.18}_{-0.16} \pm 0.03$
b baryon	1.208 ± 0.051
Λ_b	1.229 ± 0.080
Ξ_b	$1.39^{+0.34}_{-0.28}$
b hadron	1.564 ± 0.014

For comparison with theory, lifetime ratios are preferred. Experimentally we find

$$\frac{\tau_{B^+}}{\tau_{B^0}} = 1.086 \pm 0.017\,, \quad \frac{\tau_{B_s^0}}{\tau_{B^0}} = 0.951 \pm 0.038\,,$$

$$\frac{\tau_{\Lambda_b}}{\tau_{B^0}} = 0.800 \pm 0.053\,,$$

while theory makes the following predictions [22]

$$\frac{\tau_{B^+}}{\tau_{B^0}} = 1 + 0.05 \left(\frac{f_B}{200\ \text{MeV}}\right)^2\,, \quad \frac{\tau_{B_s^0}}{\tau_{B^0}} = 1 \pm 0.01\,, \quad \frac{\tau_{\Lambda_b}}{\tau_{B^0}} = 0.9\ .$$

In conclusion, the pattern of measured B-meson lifetimes follows the theoretical expectations, and non-spectator effects are observed to be small. The short B_c^+ lifetime has been predicted correctly. However, the Λ_b-baryon lifetime may be somewhat smaller than expected. As has been noted by several authors, the observed value of the Λ_b lifetime is difficult to accommodate theoretically [23–29].

Similar to the kaon system, neutral B mesons contain short- and long-lived components. The Standard Model predicts that the lifetime difference is significantly smaller. The most stringent limit on the lifetime difference of neutral B_d mesons is recently obtained by BABAR: $-0.156 < \Delta\Gamma_d/\Gamma_d < 0.042$ at 90% CL [30] where $\Delta\Gamma_d \equiv \Gamma_H - \Gamma_L$ with $\Gamma_H(\Gamma_L)$ being the decay width of the heavier (lighter) B_d meson. They measure the time-dependence of $\Upsilon(4S)$ decays where one neutral B is fully reconstructed and the other B is identified as being either B^0 or $\overline{B}^0$. In this analysis, possible violations in CP, T, and CPT are fully considered. The limit on the lifetime difference for B_s^0 is $|\Delta\Gamma_s|/\Gamma_s < 0.54$ at 95% CL. This result is based on a combination [12] of the various B_s^0 proper time measurements. A more restrictive limit for the B_s^0 system ($|\Delta\Gamma_s|/\Gamma_s < 0.29$) can be obtained if one assumes $\Gamma_s = \Gamma_d$.

***B* meson decay properties:** B^+ and B^0 mesons are the lightest elements of the b-flavored hadrons, hence they decay via weak interactions. Since the mass of a b-quark is much larger than its partner quark (d or u), B meson decays are mostly described by the decay of the b quark ("spectator model"). The dominant decay mode of a b-quark is $b \to cW^*$ where the virtual W^* eventually materializes either into a pair of leptons, $\ell\nu$ ("semileptonic decay") or into a pair of quarks which then hadronizes. The decays in which the spectator quark combines with one of the quarks from W^* are suppressed because the colors of the quarks from different sources must match ("color-suppression").

Couplings of quarks to the W boson are described by the Cabibbo-Kobayashi-Maskawa (CKM) matrix. The regular pattern of the three lepton and quark families is one of the most intriguing puzzles in particle physics. The existence of families gives rise to many of the free parameters in the Standard Model, in particular the fermion masses, and the elements of the CKM matrix. In the Standard Model (SM) of three generations, the CKM matrix is parameterized by three real parameters and one complex phase. This complex phase can become a source of CP violations in B meson decays. A more detailed discussion of the CKM matrix and CP violation can be found elsewhere in this *Review* [6,31].

Semileptonic B decays $B \to X_c\ell\nu$ and $B \to X_u\ell\nu$ provide an excellent laboratory to measure CKM elements $|V_{cb}|$ and $|V_{ub}|$ respectively, because the strong interaction effects are much simplified due to the two leptons in the final state. Both exclusive decays and inclusive decays can be used and the nature of uncertainties are quite complimentary. For exclusive decay analysis a knowledge about the form factors for the exclusive hadronic system $X_{c(u)}$ is required. For inclusive analysis, it is usually required to restrict the available phase-space of the decay products to suppress backgrounds; subsequently uncertainties are introduced in the extrapolation to the full phase-space. Moreover, restriction to a small corner of the phase-space may result in break-down of the operator product expansion scheme, thus making theoretical calculations unreliable. A more detailed discussion of the B semileptonic decays and extraction of $|V_{cb}|$ and $|V_{ub}|$ are described elsewhere in the *Review* [4,5].

On the other hand, hadronic decays of B are complicated because of strong interaction effects caused by the surrounding cloud of light quarks and gluons. While this complicates the extraction of CKM matrix elements, it also provides a great opportunity to study perturbative and non-perturbative QCD, hadronization, and Final State Interaction (FSI) effects, etc.

Other (non-spectator) decay processes include W-exchange and annihilation decays both of which occur at tree level processes. Higher-order loop-induced flavor-changing neutral current (FCNC) decay processes ("Penguin decays") are also available. In the Standard Model, these decays are much suppressed

in comparison to the spectator decays. Penguin decays are experimentally established by observations of $B \to K^*\gamma$ and recently $B \to K^{(*)}\ell^+\ell^-$. Some observed decay modes such as $B^0 \to D_s^- K^+$ may be interpreted as a W-exchange process. There has not been any experimental evidence for annihilation decays of B.

Experimental results on CP violation in B decays: The determination of all the parameters of the CKM matrix is required to fully define the Standard Model, and is central to the experimental program in heavy-flavor physics. In the framework of the Standard Model, the CKM matrix must be unitary, *i.e.* $VV^\dagger = 1$. This gives rise to relationships between the matrix elements that can be visualized as triangles in the complex plane, for example

$$V_{ub}^* V_{ud} + V_{cb}^* V_{cd} + V_{tb}^* V_{td} = 0\,.$$

The interior angles of the triangle can be expressed in terms of the CKM elements

$$\alpha = \phi_2 = arg(-\frac{V_{ud}V_{ub}^*}{V_{td}V_{tb}^*})\,,$$

$$\beta = \phi_1 = arg(-\frac{V_{cd}V_{cb}^*}{V_{td}V_{tb}^*})\,,$$

$$\gamma = \phi_3 = arg(-\frac{V_{cd}V_{cb}^*}{V_{ud}V_{ub}^*})\,.$$

The most precise measurements of the angle β have come from the two energy-asymmetric B-factories running at $\Upsilon(4S)$, KEKB and PEP-II, by analyzing time-dependent CP asymmetries in $b \to c\bar{c}s$ decay modes including $B \to J/\psi K_S$. Given the tiny boost the B mesons receive in the $\Upsilon(4S)$ rest frame, asymmetric beam energies are required to improve the precision of time-dependence measurement. At KEKB, for example, the boost is $\beta\gamma = 0.43$, and the typical B meson decay length is dilated from $\approx 20\ \mu m$ to $\approx 200\ \mu m$. PEP-II uses a slightly larger boost, $\beta\gamma = 0.55$.

In the decay chain $\Upsilon(4S) \to B^0\overline{B}^0 \to f_{CP} f_{\rm tag}$, in which one of the B mesons decays at time t_{CP} to f_{CP} and the other decays at time $t_{\rm tag}$ to a final state $f_{\rm tag}$ that distinguishes between B^0 and $\overline{B}^0$, the decay rate has a time dependence given by [6]

$$\mathcal{P}^q_{f_{CP}}(\Delta t) = \frac{e^{-|\Delta t|/\tau}}{4\tau}\left[1 + q\cdot\{S\sin(\Delta m_d \Delta t) - C\cos(\Delta m_d \Delta t)\}\right],$$

where τ is the B^0 lifetime, Δm_d is the mass difference between the two B^0 mass eigenstates, and $\Delta t = t_{CP} - t_{\rm tag}$. The parameter q is determined by identifying the b-quark flavor of the accompanying B meson ("flavor tagging") using inclusive features of the charged particles in $f_{\rm tag}$. For instance, $q = +1(-1)$ when the tagging B meson is a B^0 ($\overline{B}^0$). The CP-violating parameters S and C are expressed as

$$C = \frac{1-|\lambda|^2}{1+|\lambda|^2}, \qquad S = \frac{2Im\lambda}{1+|\lambda|^2},$$

where λ is a complex parameter that depends on both B^0-$\overline{B}^0$ mixing and on the amplitudes for B^0 and $\overline{B}^0$ decay to f_{CP}. In the SM, to a good approximation, $|\lambda|$ is equal to the absolute value of the ratio of the $\overline{B}^0$ to B^0 decay amplitudes. In the absence of direct CP violation, $|\lambda| = 1$. For $b \to c\bar{c}s$ transition, the SM predicts $S = -\xi \sin 2\beta$, where $\xi = +1(-1)$ for CP-even (-odd) final states, and $C = 0$.

In the summer of 2001, both BABAR [1] and Belle [2] reported first significant measurements of $\sin 2\beta$, thereby establishing CP violation in the B^0 meson decays. Both experiments have updated their results recently. Using a data sample of 88 million $B\overline{B}$ pairs, BABAR [32] obtained $\sin 2\beta = 0.741 \pm 0.067 \pm 0.034$, while with 152 million $B\overline{B}$ pairs, Belle [33] reported $\sin 2\beta = 0.733 \pm 0.057 \pm 0.028$. Averaging the latest results from the two experiments we find

$$\sin 2\beta = \sin 2\phi_1 = 0.736 \pm 0.049.$$

This value is consistent with CKM expectations.

Charmless B decays mediated by the $b \to s$ penguin transition are potentially sensitive to new CP-violating phases from physics beyond the SM [34]. In the SM, measurement of S in the $b \to s\bar{s}s$ transition should yield approximately the same value ($-\xi \sin 2\beta$) as in the $b \to c\bar{c}s$ modes. Both BABAR and Belle measured S for $B \to \eta' K_S$ and ϕK_S. Both final states are CP-odd ($\xi = -1$). Belle also measured S for $B \to K^+K^-K_S$ (non-resonant). From an angular analysis, Belle concludes that $K^+K^-K_S$ is primarily CP-even [35]. The average value of effective $\sin 2\beta (\equiv \sin 2\beta_{\rm eff})$ for $b \to s$ penguin transitions calculated by HFAG is 0.24 ± 0.15 where the error is dominantly statistical. The largest deviation from $b \to c\bar{c}s$ result ($\sin 2\beta = 0.736$) comes from Belle's $B \to \phi K_S$ mode where they measure $\sin 2\beta_{\rm eff} = -0.96 \pm 0.50^{+0.09}_{-0.11}$. For the same mode, BABAR measures $\sin 2\beta_{\rm eff} = +0.45 \pm 0.43 \pm 0.07$. There is a 2.1 σ discrepancy between Belle and BABAR.

Experimental work on the determination of the other two angles of the unitarity triangle is also underway. Much larger data samples will be needed to obtain precision results and to challenge the Standard Model. Information on $\sin 2\alpha$ can be extracted from $B \to \pi^+\pi^-$ decays following a procedure similar to the one outlined above. Unfortunately, these decays suffer from fairly small branching fractions ($\mathcal{O}(10^{-6})$) and sizeable contributions from penguin diagrams that complicate the extraction of the CP phases. Because of this, the time-dependent asymmetry in $B \to \pi^+\pi^-$ will not be proportional to $\sin\alpha$, but to $\sin 2\alpha_{\rm eff}$, with an unknown correction to α. Despite these difficulties, attempts to measure CP asymmetries in the $\pi^+\pi^-$ mode have been reported. Using 113 fb^{-1}, BABAR [36] extracts $S(= \sqrt{1-C^2} \times \sin 2\alpha_{\rm eff}) = -0.40 \pm 0.22 \pm 0.03$ and Belle [37] finds $S = -1.23 \pm 0.41^{+0.08}_{-0.07}$ with 78 fb^{-1}. The contribution from direct CP violation in the $B \to \pi^+\pi^-$ decay shows up as a nonzero amplitude C. Both experiments have determined C simultaneously with S. BABAR finds $C = -0.19 \pm 0.19 \pm 0.05$, while Belle measures $C = -0.77 \pm 0.27 \pm 0.08$. BABAR also measured CP-violation parameters in the related mode $B^0 \to \rho^\pm\pi^\mp$ and obtained $S_{\rho\pi} = -0.13 \pm 0.18 \pm 0.04$ and $C_{\rho\pi} = 0.35 \pm 0.13 \pm 0.05$ [38].

The time- and flavor-integrated charge asymmetry $A_{CP}^{\rho\pi}$ is also measured as $-0.114 \pm 0.062 \pm 0.027$. The decay $B^0 \to \rho^+\rho^-$ is another promising mode for measuring α and has the advantage of a larger expected decay rate and smaller uncertainty in penguin contaminations. Based on the recent limit on $B^0 \to \rho^0\rho^0$ and the measurements of $B^+ \to \rho^+\rho^0$ branching fraction [79], BABAR sets an upper limit on the penguin pollution to $B^0 \to \rho^+\rho^-$ [81].

Several methods have been suggested to measure the third angle, $\gamma \approx \arg(V_{ub})$ [39]. However, they require very large data samples (such as for $B \to DK$), measurements of B_s^0 decays or suffer from large theoretical uncertainties, rendering γ particularly difficult to measure.

Gronau and Wyler [40] first suggested that decays of the type $B \to DK$ can be used to extract the angle γ. An example of such Cabibbo–suppressed modes, $B^- \to D^0K^-$ was first observed by CLEO [41] and later confirmed by Belle [42] and BABAR [43]. By selecting CP eigenstates for the D^0 meson decay mode, both Belle and BABAR have limited direct CP violation in these decays [43,44].

The decay amplitudes for $B^+ \to D^0K^+$ and $B^+ \to \overline{D}^0K^+$ can interfere if the D^0 and $\overline{D}^0$ decay to a common final state, such as $K_S\pi^+\pi^-$. Since the Cabibbo-suppressed $B^+ \to D^0K^+$ amplitude involves V_{ub}, the phase difference measures the angle γ. Belle made a preliminary attempt of a $D^0 \to K_S\pi^+\pi^-$ Dalitz plot analysis for this channel to simultaneously determine γ and an unknown strong phase [45].

The Cabibbo-favoured $B^0 \to D^{(*)-}\pi^+$ amplitude can have interference with the doubly Cabibbo-suppressed amplitude of $\overline{B}^0 \to D^{(*)-}\pi^+$. The relative weak phase between these two amplitudes is γ and, when combined with the $B^0\overline{B}^0$ mixing phase, the total phase difference is $-(2\beta+\gamma)$. Therefore $B^0 \to D^{(*)\pm}\pi^\mp$ decays can provide sensitivity to γ. The interpretation of the observables in terms of unitarity angles requires external input on the ratio of magnitude of the two amplitudes. Due to the disparate strength of the two interfering amplitudes, CP asymmetry is expected to be small, hence the possible occurrence of CP violation on the tag side may become an important obstacle. Preliminary results on measuring the CP-violating amplitudes in the partially and fully reconstructed $B^0 \to D^{(*)\pm}\pi^\mp$ decays have been made by BABAR [46,47] and Belle [48].

Hadronic B decays: The experimental results on hadronic B decays have steadily improved over the past years and the measurements have reached a sufficient precision to challenge our understanding of the dynamics of these decays. It has been suggested that in analogy to semileptonic decays, two-body hadronic decays of B mesons can be expressed as the product of two independent hadronic currents, one describing the formation of a charm meson, and the other the hadronization of the remaining $\overline{u}d$ (or $\overline{c}s$) system from the virtual W^-. Qualitatively, for a B decay with a large energy release, the $\overline{u}d$ pair, which is produced as a color singlet, travels fast enough to leave the interaction region without influencing the second hadron formed from the c quark and the spectator antiquark. The assumption that the amplitude can be expressed as the product of two hadronic currents is called "factorization" in this paper. Recent theoretical work has provided a more solid foundation for this hypothesis [49,50].

With a good neutral particle detection and hadron identification capabilities of B-factory detectors, a substantial fraction of hadronic B decay events can be fully reconstructed. Because of the kinematic constraint of $\Upsilon(4S)$, the energy sum of the final-state particles of a B meson decay is always equal to one half of the total energy in the center of mass frame. As a result, the two variables, ΔE (energy difference) and M_B (B candidate mass with a beam-energy constraint) are very effective to suppress combinatorial background both from $\Upsilon(4S)$ and $e^+e^- \to q\bar{q}$ continuum events. In particular, the energy-constraint in M_B improves the signal resolution by almost an order of magnitude.

Such a kinematically clean environment of B meson decays provides a very nice laboratory to search for new states. For instance, quark-level $b \to c\bar{c}s$ decays have been used to search for new charmonium and charm-strange mesons and study their properties in detail. Recently, BABAR discovered a new narrow charm-strange state $D_{sJ}(2317)$ [51] and CLEO observed a similar state $D_{sJ}(2460)$ [52]. But the properties of these new states were largely unknown. Belle later observed $B \to DD_{sJ}(2317)$ and $B \to DD_{sJ}(2460)$, which helped identify some quantum numbers of $D_{sJ}(2460)$ [53].

In the $B \to$ charmonium mode, several new modes have been added. In particular, Belle studied $B \to \{J/\psi\pi^+\pi^-\}K^+$ decays and looked for new states that decay to $J/\psi\pi^+\pi^-$. A new very narrow state was discovered at 3.872 GeV which approximately coincides with the sum of D^0 and D^{*0} masses [54]. This state was also confirmed by CDF [55]. The detailed properties of this new state are not known yet.

Most branching fractions for exclusive $B \to J/\psi K^{(*)}$ transitions are updated. Being a vector-vector final state, the CP eigenvalue of $J/\psi K^*$ depends on its polarization state. Therefore, the polarization needs to be measured in order to extract CP violation parameters from this decay. Updated measurements of the polarization in $B \to J/\psi K^*$ have been made by Belle, BABAR, CDF and CLEO and an outstanding discrepancy between theory and experiment [56] is resolved. The decay amplitudes for $B \to \phi K^*$ are also measured and the fraction of longitudinal polarization is $0.41 \pm 0.10 \pm 0.04$ [57].

$B^0 \to D^{(*)+}D^{(*)-}$ decays are also sensitive to the CKM unitarity angle β. However, the theoretically uncertain penguin contribution with different weak phases may shift the observed asymmetry by an amount that depends on the penguin/tree ratio. This shift is expected to be small in models based on factorization and heavy-quark symmetry. $B^0 \to D^{*+}D^{*-}$ decays have been observed by CLEO [58] and BABAR [59] with an average branching fraction of $(8.7 \pm 1.8) \times 10^{-4}$. By studying the polarization of this mode, BABAR determines the CP-odd

fraction as $0.063 \pm 0.055 \pm 0.09$ as well as the CP-violating parameter $Im(\lambda) = 0.05 \pm 0.29 \pm 0.10$ [60] which the SM predicts to be $-\sin 2\beta$ in the absence of penguin contamination. $B^0 \to D^{*-}D^+$ decay is first observed by Belle [61] and confirmed by BABAR [62]. The average branching fraction for this mode is $(9.3 \pm 1.5) \times 10^{-4}$. BABAR also set bounds on the CP-violating parameters for this mode.

Angular distributions have been studied for other B decays to two vector mesons, in $B \to D^*\rho$ [63] and $B \to D^*D_s^*$ [64,65]. These results can be used to test the factorization hypothesis as suggested by Körner and Goldstein [66] by comparing exclusive hadronic B decays to the corresponding semileptonic modes. For certain $b \to c$ decays with large energy release it is expected that factorization works well. An example is given by the longitudinal polarization of ρ mesons in $B \to D^*\rho$ decays. CLEO's result of $\Gamma_L/\Gamma = 0.885 \pm 0.016 \pm 0.012$ [63] agrees well with the factorization expectation, 0.85 – 0.88 [67–70]. Within the experimental precision (10 – 30%) and over the limited q^2 range ($\sim M_\rho^2$) probed so far, the measurements agree with factorization predictions. The average fraction of longitudinal polarization for $B \to D^*D_s^*$ is determined as 0.52 ± 0.05 which is again consistent with predictions based on factorization.

The $B^0 \to \overline{D}^{(*)0}h^0$ decay modes, where h^0 is a light neutral meson, are expected to proceed via an internal spectator diagram and to be color-suppressed relative to external spectator decays such as $B^0 \to \overline{D}^{(*)-}\pi^+$. The contribution of the W-exchange diagram is usually assumed to be negligible [71]. In the charm meson decays, the effect of color suppression is obscured by effects of final state interactions, or reduced by non-factorizable contributions. Color suppression is, however, believed to be operative in the B meson system. Until recently, the $B \to$ charmonium transitions were the only identified color-suppressed B decays. Belle, CLEO and BABAR have now reported the observations of $B^0 \to \overline{D}^0\pi^0$ and $D^{*0}\pi^0$ [73–74]. Belle and BABAR also observed many other color-suppressed modes including $B^0 \to D^0\rho^0$ [75], $B^0 \to D^0\eta$, $D^0\omega$ [74,75] and $B^0 \to D^{*0}\eta$, $D^{*0}\omega$ [74]. The measured branching fractions are consistently higher than recent theoretical predictions based on naive factorization hypothesis [71]. Combining these results with previous measurements of other $B \to D^{(*)}\pi$ final states, it is possible to extract the strong interaction phase δ_I between the isospin 1/2 and 3/2 amplitudes in the $D\pi$ and $D^*\pi$ final states. The results from all three experiments are consistent with δ_I being approximately 30°. These results suggest the possibility of significant nonfactorizable effects such as final-state re-scattering.

The decay $B^0 \to D_s^- K^+$ is expected to occur either via a W exchange diagram or via final-state rescattering process. Because of uncertainties in final-state interaction effects, predictions for its branching fraction vary over a wide range. Therefore measurement of this decay can provide a useful probe of B decay dynamics. Belle [82] observed this decay and BABAR [83] also found an evidence for it. The average branching fraction is $\mathrm{B}(B^0 \to D_s^- K^+) = (3.8 \pm 1.3) \times 10^{-5}$.

Rare B decays: All B-meson decays that do not occur through the usual $b \to c$ transition are known as rare B decays. These include both semileptonic and hadronic $b \to u$ decays that are suppressed at leading order by the small CKM matrix element V_{ub}, as well as higher order processes such as electromagnetic and gluonic penguin decays.

Charmless B meson decays into two-body hadronic final states such as $B \to \pi\pi$ and $K\pi$ are experimentally clean and provide good opportunities to probe new physics and search for indirect and direct CP violations. The final state particles in these decays tend to have larger momenta than average B decay products, therefore the event environment is cleaner than $b \to c$ decays. Over the past years, many such modes have been observed by BABAR, Belle and CLEO. Branching fractions are typically around 10^{-5}, for exclusive channels. Because of high-momenta for final state particles, the dominant source of background is from $e^+e^- \to q\bar{q}$ continuum events and sophisticated background suppression techniques exploiting the event shape variables are essential for these analyses. The results are in general consistent between the three experiments and confirm the larger than expected rate for gluonic penguin decays such as $B \to K\pi$.

Several rare decay modes such as $B^0 \to K^+\pi^-$ have contributions from both $b \to u$ tree diagram and $b \to sg$ penguin diagram processes. If the size of each contribution is comparable to each other, the interference between them may cause direct CP violation which may show up as a charge asymmetry in time-independent decay rate measurement. The average charge asymmetry in the $K^+\pi^-$ mode is -0.095 ± 0.028 [12]. No clear evidence for direct CP violation have been found in other modes.

The fact that $B^0 \to \pi^+\pi^-$ also can have interference between tree and penguin processes makes it difficult to extract a unitarity angle α from time-dependent CP asymmetry measurements. In order to extract α unambiguously, an isospin analysis has been suggested [76]. A crucial element for the isospin analysis is a flavor-specific measurement of $B^0 \to \pi^0\pi^0$ and $\overline{B}^0 \to \pi^0\pi^0$. Recently BABAR observed the $B^0 \to \pi^0\pi^0$ decays and measured the flavor-averaged branching fraction $\mathrm{B}(B^0 \to \pi^0\pi^0) = (2.1 \pm 0.6 \pm 0.3) \times 10^{-6}$ [77]. Belle also reported evidence for the same mode and measured the flavor-averaged branching fraction $(1.7 \pm 0.6 \pm 0.2) \times 10^{-6}$ [78]. The decays $B \to \rho\rho$ are also expected to provide important information on CP violation. Both BABAR [79] and Belle [80] have observed $B^+ \to \rho^+\rho^0$ and measured its polarization. BABAR have observed $B^0 \to \rho^+\rho^-$ and measured its polarization as well [81].

The decay $B^0 \to D_s^+\pi^-$ proceeds via $b \to u$ tree diagram where D_s is produced from the vertex of virtual W hadronization. Therefore, it is sensitive to $|V_{ub}|$, although actual extraction of $|V_{ub}|$ becomes obscured by unknown non-factorizable strong-interaction effects. Both Belle [82] and BABAR [83] found evidences for this mode, and the average branching fraction is $\mathrm{B}(B^0 \to D_s^+\pi^-) = (2.7 \pm 1.0) \times 10^{-5}$.

Electroweak penguin decays:

The observation of the decay $B \to K^*(892)\gamma$, reported in 1993 by the CLEO experiment, provided first evidence for the one-loop FCNC penguin diagram [84]. Using larger data samples, CLEO, Belle and BABAR have updated this analysis and have added several new decay modes such as $B \to K_2^*(1430)\gamma$. So far no evidence for the decays $B \to \rho\gamma$ and $B \to \omega\gamma$ has been found. BABAR obtained the most stringent upper limit for the ratio $\mathrm{B}(B \to (\rho/\omega)\gamma)/\mathrm{B}(B \to K^*\gamma) < 0.047$ at 90% CL [85]. The limit on the ratio of branching fractions implies that $|V_{td}/V_{ts}| < 0.34$ at 90% CL.

The observed branching fractions were used to constrain a large class of Standard Model extensions [86]. However, due to the uncertainties in the hadronization, only the inclusive $b \to s\gamma$ rate can be reliably compared with theoretical calculations. This rate can be measured from the endpoint of the inclusive photon spectrum in B decay. The current PDG average of the CLEO [87] and the Belle [88] measurements for the B meson is $\mathrm{B}(B \to X_s\gamma) = (3.3 \pm 0.4) \times 10^{-4}$. Consistent results have been reported by ALEPH for inclusive b–hadrons produced at the Z. The measured branching fraction can be compared to recent theoretical calculations by Chetyrkin, Misiak, Munz and by Kagan and Neubert which predict $\mathrm{B}(b \to s\gamma) = (3.29 \pm 0.33) \times 10^{-4}$ [89–91].

According to the SM, the CP asymmetry in $b \to s\gamma$ is smaller than 1 %, but some non-SM models allow significanly larger CP asymmetry (~ 10 %) without altering the inclusive branching fraction [92–94]. CLEO has searched for CP violation in this mode, and set a range on $A_{CP}(b \to s\gamma)$ at 90 % CL as $-0.27 < A_{CP} < 0.10$ [95]. Belle also set a preliminary range as $-0.107 < A_{CP} < 0.099$ at 90 % CL [96]. CP asymmetry in the exclusive $B \to K^*\gamma$ mode is also searched for by CLEO [97] and BABAR [98]. The PDG average of the asymmetry is $A_{CP}(B \to K^*\gamma) = -0.01 \pm 0.07$.

In addition, CLEO has measured the inclusive photon energy spectrum for $b \to s\gamma$ [99]. Analyzing the shape of the spectrum they obtained the first and second moment for photon energies above 2 GeV:

$$< E_\gamma >= 2.346 \pm 0.032 \pm 0.011 \text{ GeV} \qquad (2)$$

and

$$< E_\gamma^2 > - < E_\gamma >^2 = 0.0226 \pm 0.0066 \pm 0.0020 \text{ GeV}^2 . \qquad (3)$$

These results can be used to extract non-perturbative HQET parameters that are needed for the determination of the CKM matrix element V_{ub}.

Additional information on FCNC processes can be obtained from $B \to X_s\ell^+\ell^-$ decays which are mediated by electroweak penguin and W-box diagrams. Exclusive $B \to K\ell^+\ell^-$ decay was first observed by Belle [100]. Recently, both BABAR [101] and Belle [102] updated the measurments and the PDG average of the branching fraction is

$$\mathrm{B}(B \to K\ell^+\ell^-) = (0.54 \pm 0.08) \times 10^{-6}.$$

The branching fraction for $B \to K^*(892)\ell^+\ell^-$ is also measured by both experiments and the average value is

$$\mathrm{B}(B \to K^*\ell^+\ell^-) = (1.05 \pm 0.20) \times 10^{-6}.$$

The branching fraction of inclusive $B \to X_s\ell^+\ell^-$ decays is measured by Belle [103]:

$$\mathrm{B}(B \to X_s\ell^+\ell^-) = (6.1 \pm 1.4^{+1.4}_{-1.1}) \times 10^{-6}.$$

These results are consistent with SM expectations.

Summary and Outlook: The study of B mesons continues to be one of the most productive fields in particle physics. CP violation has been observed for the first time outside the kaon system. Many hadronic $b \to u$ transitions and gluonic penguin decays have been observed, and the emerging pattern is still full of surprises. The coming years look equally promising. Each of the asymmetric B-factory experiments, Belle and BABAR, has accumulated data samples well over 100 fb^{-1}. Run II at Fermilab has begun and new results from CDF and D0 can be expected soon. These experiments promise a rich spectrum of rare and precision measurements that have the potential to affect fundamentally our understanding of the Standard Model and CP-violating phenomena.

References

1. BABAR Collab., B. Aubert *et al.*, Phys. Rev. Lett. **87**, 091801 (2001).
2. Belle Collab., K. Abe *et al.*, Phys. Rev. Lett. **87**, 091802 (2001).
3. Currently two different notations (ϕ_1, ϕ_2, ϕ_3) and (α, β, γ) are used in the literature for CKM unitarity angles. In this mini-review, we use the latter notation following the other mini-reviews in this *Review* . The two notations are related by $\phi_1 = \beta$, $\phi_2 = \alpha$ and $\phi_3 = \gamma$.
4. See the "Status of $|V_{ub}|$ Measurements" by L. Gibbons and M. Battaglia in this *Review* .
5. See the "Status of $|V_{cb}|$ Measurements" by M. Artuso and E. Barberio in this *Review* .
6. See the "CP Violation in Meson Decays" by D. Kirby and Y. Nir in this *Review* .
7. CLEO Collab., B. Barish *et al.*, Phys. Rev. Lett. **76**, 1570 (1996).
8. CLEO Collab., J.P. Alexander *et al.*, Phys. Rev. Lett. **86**, 2737 (2001).
9. BABAR Collab., B. Aubert *et al.*, Phys. Rev. **D65**, 032001 (2002).
10. CLEO Collab., S.B. Athar *et al.*, Phys. Rev. **D66**, 052003 (2002).
11. Belle Collab., N.C. Hastings *et al.*, Phys. Rev. **D67**, 052004 (2003).
12. Heavy Flavor Averaging Group, `http://www.slac.stanford.edu/xorg/hfag/`.
13. CLEO Collab., S.E. Csorna *et al.*, Phys. Rev. **D61**, 111101 (2000).
14. See the "Review on B–$\overline{B}$ Mixing" by O. Schneider in this *Review* .
15. CDF Collab., F. Abe *et al.*, Phys. Rev. Lett. **81**, 2432 (1998);

CDF Collab., F. Abe *et al.*, Phys. Rev. **D58**, 112004 (1998).
16. ALEPH Collab., D. Buskulic *et al.*, Phys. Lett. **B384**, 449 (1996).
17. DELPHI Collab., P. Abreu *et al.*, Z. Phys. **C68**, 541 (1995).
18. F. Ukegawa, "Spectroscopy and lifetime of bottom and charm hadrons", hep-ex/0002031, *Proceedings of 3rd International Conference on B Physics and CP Violation*, (BCONF99), Taipei, Taiwan, (1999).
19. V. Ciulli, "Spectroscopy of excited b and c states", hep-ex/9911044, *Proceedings of the 8th International Conference on Heavy Flavours*, Southampton (1999).
20. I.I. Bigi, UND-HEP-99-BIG07, hep-ph/0001003, *Proceedings of the 3rd International Conference on B Physics and CP Violation*, Taipei (1999).
21. D. Abbaneo *et al.*, "Combined results on b-hadron production rates and decay properties" CERN EP-2001/050 (2001).
22. I.I. Bigi *et al.*, in "B Decays," 2nd edition, S. Stone (ed.), World Scientific, Singapore, 1994.
23. N. Uraltsev, Phys. Lett. **B376**, 303 (1996).
24. M. Neubert and C.T. Sachrajda, Nucl. Phys. **B483**, 339 (1997).
25. J.L. Rosner, Phys. Lett. **B379**, 267 (1996).
26. M. Voloshin, Phys. Reports **320**, 275 (1999).
27. B. Guberina, B. Melic, and H. Stefancic, Phys. Lett. **B469**, 253 (1999).
28. P. Colangelo and F. De Fazio, Phys. Lett. **B387**, 371 (1996);
P. Colangelo, *Proceedings of the 28th International Conference on High Energy Physics*, Warsaw (1996).
29. G. Altarelli *et al.*, Phys. Lett. **B382**, 409 (1996).
30. BABAR Collab., B. Aubert *et al.*, hep-ex/0311037, submitted to Phys. Rev. Lett.
31. See the "CKM Quark Mixing Matrix" by F.J. Gilman, K. Kleinknecht, and B. Renk in this *Review* .
32. BABAR Collab., B. Aubert *et al.*, Phys. Rev. Lett. **89**, 201802 (2002).
33. Belle Collab., K. Abe *et al.*, Belle-CONF-0353 (2003).
34. Y. Grossman and M.P. Worah, Phys. Lett. **B395**, 241 (1997).
35. Belle Collab., K. Abe *et al.*, Belle-CONF-0344 (2003).
36. BABAR Collab., Preliminary result presented at Lepton-Photon 2003 (2003).
37. Belle Collab., K. Abe *et al.*, Phys. Rev. **D68**, 012001 (2003).
38. The results originally published in Phys. Rev. Lett. **91**, 201802 (2003) are updated at Lepton-Photon 2003 (2003).
39. See, for example, "The BABAR Physics Book", SLAC-R-504, P.F. Harrison and H.R. Quinn, Ed., and references therein.
40. M. Gronau and D. Wyler, Phys. Lett. **B265**, 172 (1991).
41. CLEO Collab., M. Athanas *et al.*, Phys. Rev. Lett. **80**, 5493 (1998).
42. Belle Collab., K. Abe *et al.*, Phys. Rev. Lett. **87**, 111801 (2001).
43. BABAR Collab., B. Aubert *et al.*, hep-ex/0207087.
44. Belle Collab., S. Swain *et al.*, Phys. Rev. **D68**, 051101 (2003).
45. Belle Collab., K. Abe *et al.*, Belle-CONF-0343 (2003).
46. BABAR Collab., B. Aubert *et al.*, hep-ex/0310037, submitted to Phys. Rev. Lett.
47. BABAR Collab., B. Aubert *et al.*, BABAR-CONF-03/022 (2003).
48. Belle Collab., K. Abe *et al.*, Belle-CONF-0341 (2003).
49. M. Neubert, "Aspects of QCD Factorization", hep-ph/0110093 *Proceedings of HF9*, Pasadena (2001) and references therein.
50. Z. Ligeti, M. Luke, and M. Wise, Phys. Lett. **B507**, 142 (2001).
51. BABAR Collab., B. Aubert *et al.*, Phys. Rev. Lett. **90**, 242001 (2003).
52. CLEO Collab., D. Besson *et al.*, Phys. Rev. **D68**, 032002 (2003).
53. Belle Collab., P. Krokovny *et al.*, hep-ex/0308019, to be published in Phys. Rev. Lett.
54. Belle Collab., S.-K. Choi *et al.*, hep-ex/0309032, to be published in Phys. Rev. Lett.
55. CDF II Collab., D. Acosta *et al.*, hep-ex/0312021, submitted to Phys. Rev. Lett.
56. K. Honscheid, *Proceedings of the International b20 Symposium*, Chicago (1997).
57. Belle Collab., K.-F. Chen *et al.*, Phys. Rev. Lett. **91**, 201801 (2003).
58. CLEO Collab., E. Lipeles *et al.*, Phys. Rev. **D62**, 032005 (2003).
59. BABAR Collab., B. Aubert *et al.*, Phys. Rev. Lett. **89**, 061801 (2002).
60. BABAR Collab., B. Aubert *et al.*, Phys. Rev. Lett. **91**, 131801 (2003).
61. Belle Collab., K. Abe *et al.*, Phys. Rev. Lett. **89**, 122001 (2003).
62. BABAR Collab., B. Aubert *et al.*, Phys. Rev. Lett. **90**, 221801 (2003).
63. S.E. Csorna *et al.*, CLEO Collab., Phys. Rev. **D67**, 112002 (2003).
64. BABAR Collab., B. Aubert *et al.*, Phys. Rev. **D67**, 092003 (2003).
65. CLEO Collab., S. Ahmed *et al.*, Phys. Rev. **D62**, 112003 (2003).
66. J. Körner and G. Goldstein Phys. Lett. **B89**, 105 (1979).
67. J.L. Rosner, Phys. Rev. **D42**, 3732 (1990).
68. M. Neubert, Phys. Lett. **B264**, 455 (1991).
69. G. Kramer, T. Mannel, and W.F. Palmer, Z. Phys. **C55**, 497 (1992).
70. A. Dighe, I. Dunietz, and R.Fleischer, Eur. Phys. J. **C6**, 647 (1999).
71. M. Neubert and B. Stech, in *Heavy Flavors II*, ed. by A.J. Buras and M. Lindner (World Scientific, Singapore, 1998).
72. CLEO Collab., T. Coan *et al.*, Phys. Rev. Lett. **88**, 062001, (2002).
73. Belle Collab., K. Abe *et al.*, Phys. Rev. Lett. **88**, 052002 (2002).
74. BABAR Collab., B. Aubert *et al.*, hep-ex/0310028, submitted to Phys. Rev. **D**.

75. Belle Collab., A. Satpathy *et al.*, Phys. Lett. **B553**, 159 (2003).
76. M. Gronau and D. London, Phys. Rev. Lett. **65**, 3381 (1990).
77. BABAR Collab., B. Aubert *et al.*, hep-ex/0308012, to be published in Phys. Rev. Lett.
78. Belle Collab., S.H. Lee *et al.*, hep-ex/0308040, to be published in Phys. Rev. Lett.
79. BABAR Collab., B. Aubert *et al.*, Phys. Rev. Lett. **91**, 171802 (2003).
80. Belle Collab., J. Zhang *et al.*, Phys. Rev. Lett. **91**, 221801 (2003).
81. BABAR Collab., B. Aubert *et al.*, hep-ex/0311017, to be published in Phys. Rev. **D**.
82. Belle Collab., P. Krokovny *et al.*, Phys. Rev. Lett. **89**, 231804 (2002).
83. BABAR Collab., B. Aubert *et al.*, Phys. Rev. Lett. **90**, 181803 (2003).
84. CLEO Collab., R. Ammar *et al.*, Phys. Rev. Lett. **71**, 674 (1993).
85. BABAR Collab., B. Aubert *et al.*, hep-ex/0306038, to be published in Phys. Rev. Lett.
86. J.L. Hewett, Phys. Rev. Lett. **70**, 1045 (1993).
87. CLEO Collab., S. Chen *et al.*, Phys. Rev. Lett. **87**, 251807 (2001).
88. Belle Collab., K. Abe *et al.*, Phys. Lett. **B511**, 151 (2001).
89. K. Chetyrkin, M. Misiak, and M. Münz, Phys. Lett. **B400**, 206 (1997); Erratum-ibid, Phys. Lett. **B425**, 414 (1998).
90. A.J. Buras, A. Kwiatkowski, and N. Pott, Phys. Lett. **B414**, 157 (1997); Erratum-ibid, Phys. Lett. **B434**, 459 (1998).
91. A.L. Kagan and Matthias Neubert, Eur. Phys. J. **C7**, 5 (1999).
92. K. Kiers, A. Soni and G. Wu, Phys. Rev. **D62**, 116004 (2000).
93. A.L. Kagan and M. Neubert, Phys. Rev. **D58**, 094012 (1998).
94. S. Baek and P. Ko, Phys. Rev. Lett. **83**, 488 (1998).
95. CLEO Collab., T.E. Coan *et al.*, Phys. Rev. Lett. **86**, 5661 (2001).
96. Belle Collab., K. Abe *et al.*, Belle-CONF-0348 (2003).
97. CLEO Collab., T.E. Coan *et al.*, Phys. Rev. Lett. **84**, 5283 (2000).
98. BABAR Collab., B. Aubert *et al.*, Phys. Rev. Lett. **88**, 101805 (2002).
99. CLEO Collab., S. Chen *et al.*, Phys. Rev. Lett. **87**, 251807 (2001).
100. Belle Collab., K. Abe *et al.*, Phys. Rev. Lett. **88**, 021801 (2001).
101. BABAR Collab., B. Aubert *et al.*, Phys. Rev. Lett. **91**, 221802 (2003).
102. Belle Collab., A. Ishikawa *et al.*, Phys. Rev. Lett. **91**, 261601 (2003).
103. Belle Collab., J. Kaneko *et al.*, Phys. Rev. Lett. **90**, 021801 (2003).

A NOTE ON HFAG ACTIVITIES

Written December 2003 D. Kirkby (UC, Irvine) and Y. Sakai (KEK).

The Heavy Flavor Averaging Group (HFAG) has been formed, continuing the activities of LEP Heavy Flavor Steering group, to provide the averages for measurements dedicated to the b-flavor related quantities. The HFAG consists of representatives and contacts from the experimental groups: BaBar, Belle, CDF, CLEO, DØ , LEP, and SLD.

In the averaging, the input parameters used in the various analyses are adjusted (rescaled) to common values, and all known correlations are taking into account. The HFAG provides averages for b-hadron lifetimes, B-oscillation parameters, semileptonic parameters, rare decay branching fractions, and CP-violation measurements. The averages provided by the HFAG are listed as "OUR EVALUATION" with a note mentioning about it.

The complete listing of averages and more detailed information on the averaging are available at;

http://www.slac.stanford.edu/xorg/hfag and also at http://belle.kek.jp/mirror/hfag (KEK mirror site).

$B^{\pm}$

$I(J^P) = \frac{1}{2}(0^-)$

Quantum numbers not measured. Values shown are quark-model predictions.

See also the $B^{\pm}/B^0$ ADMIXTURE and $B^{\pm}/B^0/B_s^0/b$-baryon ADMIXTURE sections.

$B^{\pm}$ MASS

The fit uses m_{B^+}, $(m_{B^0} - m_{B^+})$, and m_{B^0} to determine m_{B^+}, m_{B^0}, and the mass difference.

VALUE (MeV)	EVTS	DOCUMENT ID		TECN	COMMENT
5279.0 ± 0.5 OUR FIT					
5279.1 ± 0.5 OUR AVERAGE					
5279.1 ± 0.4 ± 0.4	526	[1] CSORNA	00	CLE2	$e^+e^- \to \Upsilon(4S)$
5279.1 ± 1.7 ± 1.4	147	ABE	96B	CDF	$p\overline{p}$ at 1.8 TeV
• • • We do not use the following data for averages, fits, limits, etc. • • •					
5278.8 ± 0.54 ± 2.0	362	ALAM	94	CLE2	$e^+e^- \to \Upsilon(4S)$
5278.3 ± 0.4 ± 2.0		BORTOLETTO	92	CLEO	$e^+e^- \to \Upsilon(4S)$
5280.5 ± 1.0 ± 2.0		[2] ALBRECHT	90J	ARG	$e^+e^- \to \Upsilon(4S)$
5275.8 ± 1.3 ± 3.0	32	ALBRECHT	87C	ARG	$e^+e^- \to \Upsilon(4S)$
5278.2 ± 1.8 ± 3.0	12	[3] ALBRECHT	87D	ARG	$e^+e^- \to \Upsilon(4S)$
5278.6 ± 0.8 ± 2.0		BEBEK	87	CLEO	$e^+e^- \to \Upsilon(4S)$

[1] CSORNA 00 uses fully reconstructed 526 $B^+ \to J/\psi^{(\prime)}K^+$ events and invariant masses without beam constraint.
[2] ALBRECHT 90J assumes 10580 for $\Upsilon(4S)$ mass. Supersedes ALBRECHT 87C and ALBRECHT 87D.
[3] Found using fully reconstructed decays with $J/\psi(1S)$. ALBRECHT 87D assume $m_{\Upsilon(4S)}$ = 10577 MeV.

$B^{\pm}$ MEAN LIFE

See $B^{\pm}/B^0/B_s^0/b$-baryon ADMIXTURE section for data on B-hadron mean life averaged over species of bottom particles.

"OUR EVALUATION" is an average using rescaled values of the data listed below. The average and rescaling were performed by the Heavy Flavor Averaging Group (HFAG) and are described at http://www.slac.stanford.edu/xorg/hfag/. The averaging/rescaling procedure takes into account corrections between the measurements and asymmetric lifetime errors.

VALUE (10^{-12} s)	EVTS	DOCUMENT ID		TECN	COMMENT
1.671 ± 0.018 OUR EVALUATION					
1.695 ± 0.026 ± 0.015		[4] ABE	02H	BELL	$e^+e^- \to \Upsilon(4S)$

$1.636 \pm 0.058 \pm 0.025$		[5] ACOSTA	02C	CDF	$p\overline{p}$ at 1.8 TeV
$1.673 \pm 0.032 \pm 0.023$		[4] AUBERT	01F	BABR	$e^+e^- \rightarrow \Upsilon(4S)$
$1.648 \pm 0.049 \pm 0.035$		[6] BARATE	00R	ALEP	$e^+e^- \rightarrow Z$
$1.643 \pm 0.037 \pm 0.025$		[7] ABBIENDI	99J	OPAL	$e^+e^- \rightarrow Z$
$1.637 \pm 0.058 ^{+0.045}_{-0.043}$		[6] ABE	98Q	CDF	$p\overline{p}$ at 1.8 TeV
$1.66 \pm 0.06 \pm 0.03$		[7] ACCIARRI	98S	L3	$e^+e^- \rightarrow Z$
$1.66 \pm 0.06 \pm 0.05$		[7] ABE	97J	SLD	$e^+e^- \rightarrow Z$
$1.58 ^{+0.21}_{-0.18} ^{+0.04}_{-0.03}$	94	[5] BUSKULIC	96J	ALEP	$e^+e^- \rightarrow Z$
$1.61 \pm 0.16 \pm 0.12$		[6,8] ABREU	95Q	DLPH	$e^+e^- \rightarrow Z$
$1.72 \pm 0.08 \pm 0.06$		[9] ADAM	95	DLPH	$e^+e^- \rightarrow Z$
$1.52 \pm 0.14 \pm 0.09$		[6] AKERS	95T	OPAL	$e^+e^- \rightarrow Z$
• • • We do not use the following data for averages, fits, limits, etc. • • •					
$1.68 \pm 0.07 \pm 0.02$		[5] ABE	98B	CDF	Repl. by ACOSTA 02C
$1.56 \pm 0.13 \pm 0.06$		[6] ABE	96C	CDF	Repl. by ABE 98Q
$1.58 \pm 0.09 \pm 0.03$		[10] BUSKULIC	96J	ALEP	$e^+e^- \rightarrow Z$
$1.58 \pm 0.09 \pm 0.04$		[6] BUSKULIC	96J	ALEP	Repl. by BARATE 00R
1.70 ± 0.09		[11] ADAM	95	DLPH	$e^+e^- \rightarrow Z$
$1.61 \pm 0.16 \pm 0.05$	148	[5] ABE	94D	CDF	Repl. by ABE 98B
$1.30 ^{+0.33}_{-0.29} \pm 0.16$	92	[6] ABREU	93D	DLPH	Sup. by ABREU 95Q
$1.56 \pm 0.19 \pm 0.13$	134	[9] ABREU	93G	DLPH	Sup. by ADAM 95
$1.51 ^{+0.30}_{-0.28} ^{+0.12}_{-0.14}$	59	[6] ACTON	93C	OPAL	Sup. by AKERS 95T
$1.47 ^{+0.22}_{-0.19} ^{+0.15}_{-0.14}$	77	[6] BUSKULIC	93D	ALEP	Sup. by BUSKULIC 96J

[4] Events are selected in which one B meson is fully reconstructed while the second B meson is reconstructed inclusively.
[5] Measured mean life using fully reconstructed decays.
[6] Data analyzed using $D/D^*\ell$X event vertices.
[7] Data analyzed using charge of secondary vertex.
[8] ABREU 95Q assumes $B(B^0 \rightarrow D^{**-}\ell^+\nu_\ell) = 3.2 \pm 1.7\%$.
[9] Data analyzed using vertex-charge technique to tag B charge.
[10] Combined result of $D/D^*\ell$X analysis and fully reconstructed B analysis.
[11] Combined ABREU 95Q and ADAM 95 result.

B^+ DECAY MODES

B^- modes are charge conjugates of the modes below. Modes which do not identify the charge state of the B are listed in the $B^{\pm}/B^0$ ADMIXTURE section.

The branching fractions listed below assume 50% $B^0\overline{B}^0$ and 50% B^+B^- production at the $\Upsilon(4S)$. We have attempted to bring older measurements up to date by rescaling their assumed $\Upsilon(4S)$ production ratio to 50:50 and their assumed D, D_s, D^*, and ψ branching ratios to current values whenever this would affect our averages and best limits significantly.

Indentation is used to indicate a subchannel of a previous reaction. All resonant subchannels have been corrected for resonance branching fractions to the final state so the sum of the subchannel branching fractions can exceed that of the final state.

For inclusive branching fractions, *e.g.*, $B \rightarrow D^{\pm}$ anything, the values usually are multiplicities, not branching fractions. They can be greater than one.

	Mode	Fraction (Γ_i/Γ)	Scale factor/ Confidence level
	Semileptonic and leptonic modes		
Γ_1	$\ell^+\nu_\ell$ anything	[a] $(10.2 \pm 0.9)\%$	
Γ_2	$\overline{D}^0\ell^+\nu_\ell$	[a] $(2.15 \pm 0.22)\%$	
Γ_3	$\overline{D}^*(2007)^0\ell^+\nu_\ell$	[a] $(6.5 \pm 0.5)\%$	
Γ_4	$\overline{D}_1(2420)^0\ell^+\nu_\ell$	$(5.6 \pm 1.6) \times 10^{-3}$	
Γ_5	$\overline{D}_2^*(2460)^0\ell^+\nu_\ell$	$< 8 \times 10^{-3}$	CL=90%
Γ_6	$\pi^0 e^+\nu_e$	$(9.0 \pm 2.8) \times 10^{-5}$	
Γ_7	$\eta\ell^+\nu_\ell$	$(8 \pm 4) \times 10^{-5}$	
Γ_8	$\omega\ell^+\nu_\ell$	[a] $< 2.1 \times 10^{-4}$	CL=90%
Γ_9	$\omega\mu^+\nu_\mu$		
Γ_{10}	$\rho^0\ell^+\nu_\ell$	[a] $(1.34 ^{+0.32}_{-0.35}) \times 10^{-4}$	
Γ_{11}	$p\overline{p}e^+\nu_e$	$< 5.2 \times 10^{-3}$	CL=90%
Γ_{12}	$e^+\nu_e$	$< 1.5 \times 10^{-5}$	CL=90%
Γ_{13}	$\mu^+\nu_\mu$	$< 2.1 \times 10^{-5}$	CL=90%
Γ_{14}	$\tau^+\nu_\tau$	$< 5.7 \times 10^{-4}$	CL=90%
Γ_{15}	$e^+\nu_e\gamma$	$< 2.0 \times 10^{-4}$	CL=90%
Γ_{16}	$\mu^+\nu_\mu\gamma$	$< 5.2 \times 10^{-5}$	CL=90%
	D, D^*, or D_s modes		
Γ_{17}	$\overline{D}^0\pi^+$	$(4.98 \pm 0.29) \times 10^{-3}$	
Γ_{18}	$D_{CP(+1)}\pi^+$	[b]	
Γ_{19}	$D_{CP(-1)}\pi^+$	[b]	
Γ_{20}	$\overline{D}^0\rho^+$	$(1.34 \pm 0.18)\%$	
Γ_{21}	$\overline{D}^0K^+$	$(3.7 \pm 0.6) \times 10^{-4}$	S=1.1
Γ_{22}	$D_{CP(+1)}K^+$	[b]	
Γ_{23}	$D_{CP(-1)}K^+$	[b]	
Γ_{24}	$\overline{D}^0K^*(892)^+$	$(6.1 \pm 2.3) \times 10^{-4}$	
Γ_{25}	$\overline{D}^0K^+\overline{K}^0$	$(5.5 \pm 1.6) \times 10^{-4}$	
Γ_{26}	$\overline{D}^0K^+\overline{K}^*(892)^0$	$(7.5 \pm 1.7) \times 10^{-4}$	
Γ_{27}	$\overline{D}^0\pi^+\pi^+\pi^-$	$(1.1 \pm 0.4)\%$	
Γ_{28}	$\overline{D}^0\pi^+\pi^+\pi^-$ nonresonant	$(5 \pm 4) \times 10^{-3}$	
Γ_{29}	$\overline{D}^0\pi^+\rho^0$	$(4.2 \pm 3.0) \times 10^{-3}$	
Γ_{30}	$\overline{D}^0a_1(1260)^+$	$(5 \pm 4) \times 10^{-3}$	
Γ_{31}	$\overline{D}^0\omega\pi^+$	$(4.1 \pm 0.9) \times 10^{-3}$	
Γ_{32}	$D^*(2010)^-\pi^+\pi^+$	$(2.1 \pm 0.6) \times 10^{-3}$	
Γ_{33}	$D^-\pi^+\pi^+$	$< 1.4 \times 10^{-3}$	CL=90%
Γ_{34}	$\overline{D}^*(2007)^0\pi^+$	$(4.6 \pm 0.4) \times 10^{-3}$	
Γ_{35}	$\overline{D}^*(2007)^0\omega\pi^+$	$(4.5 \pm 1.2) \times 10^{-3}$	
Γ_{36}	$\overline{D}^*(2007)^0\rho^+$	$(9.8 \pm 1.7) \times 10^{-3}$	
Γ_{37}	$\overline{D}^*(2007)^0K^+$	$(3.6 \pm 1.0) \times 10^{-4}$	
Γ_{38}	$\overline{D}^*(2007)^0K^*(892)^+$	$(7.2 \pm 3.4) \times 10^{-4}$	
Γ_{39}	$\overline{D}^*(2007)^0K^+\overline{K}^0$	$< 1.06 \times 10^{-3}$	CL=90%
Γ_{40}	$\overline{D}^*(2007)^0K^+K^*(892)^0$	$(1.5 \pm 0.4) \times 10^{-3}$	
Γ_{41}	$\overline{D}^*(2007)^0\pi^+\pi^+\pi^-$	$(9.4 \pm 2.6) \times 10^{-3}$	
Γ_{42}	$\overline{D}^*(2007)^0a_1(1260)^+$	$(1.9 \pm 0.5)\%$	
Γ_{43}	$\overline{D}^*(2007)^0\pi^-\pi^+\pi^+\pi^0$	$(1.8 \pm 0.4)\%$	
Γ_{44}	$D^*(2010)^+\pi^0$	$< 1.7 \times 10^{-4}$	CL=90%
Γ_{45}	$\overline{D}^*(2010)^+K^0$	$< 9.5 \times 10^{-5}$	CL=90%
Γ_{46}	$D^*(2010)^-\pi^+\pi^+\pi^0$	$(1.5 \pm 0.7)\%$	
Γ_{47}	$D^*(2010)^-\pi^+\pi^+\pi^+\pi^-$	$< 1\%$	CL=90%
Γ_{48}	$\overline{D}_1^*(2420)^0\pi^+$	$(1.5 \pm 0.6) \times 10^{-3}$	S=1.3
Γ_{49}	$\overline{D}_1^*(2420)^0\rho^+$	$< 1.4 \times 10^{-3}$	CL=90%
Γ_{50}	$\overline{D}_2^*(2460)^0\pi^+$	$< 1.3 \times 10^{-3}$	CL=90%
Γ_{51}	$\overline{D}_2^*(2460)^0\rho^+$	$< 4.7 \times 10^{-3}$	CL=90%
Γ_{52}	$\overline{D}^0D_s^+$	$(1.3 \pm 0.4)\%$	
Γ_{53}	$\overline{D}^0D_{sJ}(2317)^+$	seen	
Γ_{54}	$\overline{D}^0D_{sJ}(2457)^+$	seen	
Γ_{55}	$\overline{D}^0D_{sJ}(2536)^+$	not seen	
Γ_{56}	$\overline{D}^*(2007)^0D_{sJ}(2536)^+$	not seen	
Γ_{57}	$\overline{D}^0D_{sJ}(2573)^+$	not seen	
Γ_{58}	$\overline{D}^*(2007)^0D_{sJ}(2573)^+$	not seen	
Γ_{59}	$\overline{D}^0D_s^{*+}$	$(9 \pm 4) \times 10^{-3}$	
Γ_{60}	$\overline{D}^*(2007)^0D_s^+$	$(1.2 \pm 0.5)\%$	
Γ_{61}	$\overline{D}^*(2007)^0D_s^{*+}$	$(2.7 \pm 1.0)\%$	
Γ_{62}	$D_s^{(*)+}\overline{D}^{**0}$	$(2.7 \pm 1.2)\%$	
Γ_{63}	$\overline{D}^*(2007)^0D^*(2010)^+$	$< 1.1\%$	CL=90%
Γ_{64}	$\overline{D}^0D^*(2010)^+ + \overline{D}^*(2007)^0D^+$	$< 1.3\%$	CL=90%
Γ_{65}	$\overline{D}^0D^+$	$< 6.7 \times 10^{-3}$	CL=90%
Γ_{66}	$\overline{D}^0D^+K^0$	$< 2.8 \times 10^{-3}$	CL=90%
Γ_{67}	$\overline{D}^*(2007)^0D^+K^0$	$< 6.1 \times 10^{-3}$	CL=90%
Γ_{68}	$\overline{D}^0\overline{D}^*(2010)^+K^0$	$(5.2 \pm 1.2) \times 10^{-3}$	
Γ_{69}	$\overline{D}^*(2007)^0D^*(2010)^+K^0$	$(7.8 \pm 2.6) \times 10^{-3}$	
Γ_{70}	$\overline{D}^0D^0K^+$	$(1.9 \pm 0.4) \times 10^{-3}$	
Γ_{71}	$\overline{D}^*(2010)^0D^0K^+$	$< 3.8 \times 10^{-3}$	CL=90%
Γ_{72}	$\overline{D}^0D^*(2007)^0K^+$	$(4.7 \pm 1.0) \times 10^{-3}$	
Γ_{73}	$\overline{D}^*(2007)^0D^*(2007)^0K^+$	$(5.3 \pm 1.6) \times 10^{-3}$	
Γ_{74}	$D^-D^+K^+$	$< 4 \times 10^{-4}$	CL=90%
Γ_{75}	$D^-D^*(2010)^+K^+$	$< 7 \times 10^{-4}$	CL=90%
Γ_{76}	$D^*(2010)^-D^+K^+$	$(1.5 \pm 0.4) \times 10^{-3}$	
Γ_{77}	$D^*(2010)^-D^*(2010)^+K^+$	$< 1.8 \times 10^{-3}$	CL=90%
Γ_{78}	$(\overline{D}+\overline{D}^*)(D+D^*)K$	$(3.5 \pm 0.6)\%$	
Γ_{79}	$D_s^+\pi^0$	$< 2.0 \times 10^{-4}$	CL=90%
Γ_{80}	$D_s^{*+}\pi^0$	$< 3.3 \times 10^{-4}$	CL=90%
Γ_{81}	$D_s^+\eta$	$< 5 \times 10^{-4}$	CL=90%
Γ_{82}	$D_s^{*+}\eta$	$< 8 \times 10^{-4}$	CL=90%
Γ_{83}	$D_s^+\rho^0$	$< 4 \times 10^{-4}$	CL=90%
Γ_{84}	$D_s^{*+}\rho^0$	$< 5 \times 10^{-4}$	CL=90%
Γ_{85}	$D_s^+\omega$	$< 5 \times 10^{-4}$	CL=90%
Γ_{86}	$D_s^{*+}\omega$	$< 7 \times 10^{-4}$	CL=90%
Γ_{87}	$D_s^+a_1(1260)^0$	$< 2.2 \times 10^{-3}$	CL=90%

Γ_{88}	$D_s^{*+} a_1(1260)^0$	<	1.6	$\times 10^{-3}$	CL=90%
Γ_{89}	$D_s^{+} \phi$	<	3.2	$\times 10^{-4}$	CL=90%
Γ_{90}	$D_s^{*+} \phi$	<	4	$\times 10^{-4}$	CL=90%
Γ_{91}	$D_s^{+} \overline{K}^0$	<	1.1	$\times 10^{-3}$	CL=90%
Γ_{92}	$D_s^{*+} \overline{K}^0$	<	1.1	$\times 10^{-3}$	CL=90%
Γ_{93}	$D_s^{+} \overline{K}^*(892)^0$	<	5	$\times 10^{-4}$	CL=90%
Γ_{94}	$D_s^{*+} \overline{K}^*(892)^0$	<	4	$\times 10^{-4}$	CL=90%
Γ_{95}	$D_s^{-} \pi^+ K^+$	<	8	$\times 10^{-4}$	CL=90%
Γ_{96}	$D_s^{*-} \pi^+ K^+$	<	1.2	$\times 10^{-3}$	CL=90%
Γ_{97}	$D_s^{-} \pi^+ K^*(892)^+$	<	6	$\times 10^{-3}$	CL=90%
Γ_{98}	$D_s^{*-} \pi^+ K^*(892)^+$	<	8	$\times 10^{-3}$	CL=90%

Charmonium modes

Γ_{99}	$\eta_c K^+$	(	9.0 $\pm$2.7)	$\times 10^{-4}$	
Γ_{100}	$J/\psi(1S) K^+$	(	1.00$\pm$0.04)	$\times 10^{-3}$	
Γ_{101}	$J/\psi(1S) K^+ \pi^+ \pi^-$	(	7.7 $\pm$2.0)	$\times 10^{-4}$	
Γ_{102}	$X(3872) K^+$	seen			
Γ_{103}	$J/\psi(1S) K^*(892)^+$	(	1.35$\pm$0.10)	$\times 10^{-3}$	
Γ_{104}	$J/\psi(1S) K(1270)^+$	(	1.8 $\pm$0.5)	$\times 10^{-3}$	
Γ_{105}	$J/\psi(1S) K(1400)^+$	<	5	$\times 10^{-4}$	CL=90%
Γ_{106}	$J/\psi(1S) \phi K^+$	(	5.2 $\pm$1.7)	$\times 10^{-5}$	S=1.2
Γ_{107}	$J/\psi(1S) \pi^+$	(	4.0 $\pm$0.5)	$\times 10^{-5}$	
Γ_{108}	$J/\psi(1S) \rho^+$	<	7.7	$\times 10^{-4}$	CL=90%
Γ_{109}	$J/\psi(1S) a_1(1260)^+$	<	1.2	$\times 10^{-3}$	CL=90%
Γ_{110}	$J/\psi(1S) p \overline{\Lambda}$	(	1.2 $^{+0.9}_{-0.6}$)	$\times 10^{-5}$	
Γ_{111}	$\psi(2S) K^+$	(	6.8 $\pm$0.4)	$\times 10^{-4}$	
Γ_{112}	$\psi(2S) K^*(892)^+$	(	9.2 $\pm$2.2)	$\times 10^{-4}$	
Γ_{113}	$\psi(2S) K^+ \pi^+ \pi^-$	(	1.9 $\pm$1.2)	$\times 10^{-3}$	
Γ_{114}	$\chi_{c0}(1P) K^+$	(	6.0 $^{+2.4}_{-2.1}$)	$\times 10^{-4}$	
Γ_{115}	$\chi_{c1}(1P) K^+$	(	6.8 $\pm$1.2)	$\times 10^{-4}$	
Γ_{116}	$\chi_{c1}(1P) K^*(892)^+$	<	2.1	$\times 10^{-3}$	CL=90%

K* or *K* **modes**

Γ_{117}	$K^0 \pi^+$	(	1.88$\pm$0.21)	$\times 10^{-5}$	
Γ_{118}	$K^+ \pi^0$	(	1.29$\pm$0.12)	$\times 10^{-5}$	
Γ_{119}	$\eta' K^+$	(	7.8 $\pm$0.5)	$\times 10^{-5}$	
Γ_{120}	$\eta' K^*(892)^+$	<	3.5	$\times 10^{-5}$	CL=90%
Γ_{121}	ηK^+	<	6.9	$\times 10^{-6}$	CL=90%
Γ_{122}	$\eta K^*(892)^+$	(	2.6 $^{+1.0}_{-0.9}$)	$\times 10^{-5}$	
Γ_{123}	ωK^+	(	9.2 $^{+2.8}_{-2.5}$)	$\times 10^{-6}$	
Γ_{124}	$\omega K^*(892)^+$	<	8.7	$\times 10^{-5}$	CL=90%
Γ_{125}	$K^*(892)^0 \pi^+$	(	1.9 $^{+0.6}_{-0.8}$)	$\times 10^{-5}$	
Γ_{126}	$K^*(892)^+ \pi^0$	<	3.1	$\times 10^{-5}$	CL=90%
Γ_{127}	$K^+ \pi^- \pi^+$	(	5.7 $\pm$0.4)	$\times 10^{-5}$	
Γ_{128}	$K^+ \pi^- \pi^+$ nonresonant	<	2.8	$\times 10^{-5}$	CL=90%
Γ_{129}	$K^+ f_0(980)$				
Γ_{130}	$K^+ \rho^0$	<	1.2	$\times 10^{-5}$	CL=90%
Γ_{131}	$K_2^*(1430)^0 \pi^+$	<	6.8	$\times 10^{-4}$	CL=90%
Γ_{132}	$K^- \pi^+ \pi^+$	<	1.8	$\times 10^{-6}$	CL=90%
Γ_{133}	$K^- \pi^+ \pi^+$ nonresonant	<	5.6	$\times 10^{-5}$	CL=90%
Γ_{134}	$K_1(1400)^0 \pi^+$	<	2.6	$\times 10^{-3}$	CL=90%
Γ_{135}	$K^0 \pi^+ \pi^0$	<	6.6	$\times 10^{-5}$	CL=90%
Γ_{136}	$K^0 \rho^+$	<	4.8	$\times 10^{-5}$	CL=90%
Γ_{137}	$K^*(892)^+ \pi^+ \pi^-$	<	1.1	$\times 10^{-3}$	CL=90%
Γ_{138}	$K^*(892)^+ \rho^0$	(	1.1 $\pm$0.4)	$\times 10^{-5}$	
Γ_{139}	$K^*(892)^+ K^*(892)^0$	<	7.1	$\times 10^{-5}$	CL=90%
Γ_{140}	$K_1(1400)^+ \rho^0$	<	7.8	$\times 10^{-4}$	CL=90%
Γ_{141}	$K_2^*(1430)^+ \rho^0$	<	1.5	$\times 10^{-3}$	CL=90%
Γ_{142}	$K^+ \overline{K}^0$	<	2.0	$\times 10^{-6}$	CL=90%
Γ_{143}	$\overline{K}^0 K^+ \pi^0$	<	2.4	$\times 10^{-5}$	CL=90%
Γ_{144}	$K^+ K_S^0 K_S^0$	(	1.34$\pm$0.24)	$\times 10^{-5}$	
Γ_{145}	$K_S^0 K_S^0 \pi^+$	<	3.2	$\times 10^{-6}$	CL=90%
Γ_{146}	$K^+ K^- \pi^+$	<	6.3	$\times 10^{-6}$	CL=90%
Γ_{147}	$K^+ K^- \pi^+$ nonresonant	<	7.5	$\times 10^{-5}$	CL=90%
Γ_{148}	$K^+ K^+ \pi^-$	<	1.3	$\times 10^{-6}$	CL=90%
Γ_{149}	$K^+ K^+ \pi^-$ nonresonant	<	8.79	$\times 10^{-5}$	CL=90%
Γ_{150}	$K^+ K^*(892)^0$	<	5.3	$\times 10^{-6}$	CL=90%
Γ_{151}	$K^+ f_J(2220)$				
Γ_{152}	$K^+ K^- K^+$	(	3.08$\pm$0.21)	$\times 10^{-5}$	
Γ_{153}	$K^+ \phi$	(	9.3 $\pm$1.0)	$\times 10^{-6}$	S=1.3
Γ_{154}	$K^+ K^- K^+$ nonresonant	<	3.8	$\times 10^{-5}$	CL=90%
Γ_{155}	$K^*(892)^+ K^+ K^-$	<	1.6	$\times 10^{-3}$	CL=90%
Γ_{156}	$K^*(892)^+ \phi$	(	9.6 $\pm$3.0)	$\times 10^{-6}$	S=1.9
Γ_{157}	$K_1(1400)^+ \phi$	<	1.1	$\times 10^{-3}$	CL=90%
Γ_{158}	$K_2^*(1430)^+ \phi$	<	3.4	$\times 10^{-3}$	CL=90%
Γ_{159}	$K^+ \phi \phi$	(	2.6 $^{+1.1}_{-0.9}$)	$\times 10^{-6}$	
Γ_{160}	$K^*(892)^+ \gamma$	(	3.8 $\pm$0.5)	$\times 10^{-5}$	
Γ_{161}	$K_1(1270)^+ \gamma$	<	9.9	$\times 10^{-5}$	CL=90%
Γ_{162}	$\phi K^+ \gamma$	(	3.4 $\pm$1.0)	$\times 10^{-6}$	
Γ_{163}	$K^+ \pi^- \pi^+ \gamma$	(	2.4 $^{+0.6}_{-0.5}$)	$\times 10^{-5}$	
Γ_{164}	$K^*(892)^0 \pi^+ \gamma$	(	2.0 $^{+0.7}_{-0.6}$)	$\times 10^{-5}$	
Γ_{165}	$K^+ \rho^0 \gamma$	<	2.0	$\times 10^{-5}$	CL=90%
Γ_{166}	$K^+ \pi^- \pi^+ \gamma$ nonresonant	<	9.2	$\times 10^{-6}$	CL=90%
Γ_{167}	$K_1(1400)^+ \gamma$	<	5.0	$\times 10^{-5}$	CL=90%
Γ_{168}	$K_2^*(1430)^+ \gamma$	<	1.4	$\times 10^{-3}$	CL=90%
Γ_{169}	$K^*(1680)^+ \gamma$	<	1.9	$\times 10^{-3}$	CL=90%
Γ_{170}	$K_3^*(1780)^+ \gamma$	<	5.5	$\times 10^{-3}$	CL=90%
Γ_{171}	$K_4^*(2045)^+ \gamma$	<	9.9	$\times 10^{-3}$	CL=90%

Light unflavored meson modes

Γ_{172}	$\rho^+ \gamma$	<	2.1	$\times 10^{-6}$	CL=90%
Γ_{173}	$\pi^+ \pi^0$	(	5.6 $^{+0.9}_{-1.1}$)	$\times 10^{-6}$	
Γ_{174}	$\pi^+ \pi^+ \pi^-$	(	1.1 $\pm$0.4)	$\times 10^{-5}$	
Γ_{175}	$\rho^0 \pi^+$	(	8.6 $\pm$2.0)	$\times 10^{-6}$	
Γ_{176}	$\pi^+ f_0(980)$	<	1.4	$\times 10^{-4}$	CL=90%
Γ_{177}	$\pi^+ f_2(1270)$	<	2.4	$\times 10^{-4}$	CL=90%
Γ_{178}	$\pi^+ \pi^- \pi^+$ nonresonant	<	4.1	$\times 10^{-5}$	CL=90%
Γ_{179}	$\pi^+ \pi^0 \pi^0$	<	8.9	$\times 10^{-4}$	CL=90%
Γ_{180}	$\rho^+ \pi^0$	<	4.3	$\times 10^{-5}$	CL=90%
Γ_{181}	$\pi^+ \pi^- \pi^+ \pi^0$	<	4.0	$\times 10^{-3}$	CL=90%
Γ_{182}	$\rho^+ \rho^0$	(	2.6 $\pm$0.6)	$\times 10^{-5}$	
Γ_{183}	$a_1(1260)^+ \pi^0$	<	1.7	$\times 10^{-3}$	CL=90%
Γ_{184}	$a_1(1260)^0 \pi^+$	<	9.0	$\times 10^{-4}$	CL=90%
Γ_{185}	$\omega \pi^+$	(	6.4 $^{+1.8}_{-1.6}$)	$\times 10^{-6}$	S=1.3
Γ_{186}	$\omega \rho^+$	<	6.1	$\times 10^{-5}$	CL=90%
Γ_{187}	$\eta \pi^+$	<	5.7	$\times 10^{-6}$	CL=90%
Γ_{188}	$\eta' \pi^+$	<	7.0	$\times 10^{-6}$	CL=90%
Γ_{189}	$\eta' \rho^+$	<	3.3	$\times 10^{-5}$	CL=90%
Γ_{190}	$\eta \rho^+$	<	1.5	$\times 10^{-5}$	CL=90%
Γ_{191}	$\phi \pi^+$	<	4.1	$\times 10^{-7}$	CL=90%
Γ_{192}	$\phi \rho^+$	<	1.6	$\times 10^{-5}$	
Γ_{193}	$\pi^+ \pi^+ \pi^+ \pi^- \pi^-$	<	8.6	$\times 10^{-4}$	CL=90%
Γ_{194}	$\rho^0 a_1(1260)^+$	<	6.2	$\times 10^{-4}$	CL=90%
Γ_{195}	$\rho^0 a_2(1320)^+$	<	7.2	$\times 10^{-4}$	CL=90%
Γ_{196}	$\pi^+ \pi^+ \pi^+ \pi^- \pi^- \pi^0$	<	6.3	$\times 10^{-3}$	CL=90%
Γ_{197}	$a_1(1260)^+ a_1(1260)^0$	<	1.3	%	CL=90%

Charged particle ($h^{\pm}$) modes

$h^{\pm} = K^{\pm}$ or $\pi^{\pm}$

Γ_{198}	$h^+ \pi^0$	(	1.6 $^{+0.7}_{-0.6}$)	$\times 10^{-5}$	
Γ_{199}	ωh^+	(	1.38$^{+0.27}_{-0.24}$)	$\times 10^{-5}$	
Γ_{200}	$h^+ X^0$(Familon)	<	4.9	$\times 10^{-5}$	CL=90%

Baryon modes

Γ_{201}	$p \overline{p} \pi^+$	<	3.7	$\times 10^{-6}$	CL=90%
Γ_{202}	$p \overline{p} \pi^+$ nonresonant	<	5.3	$\times 10^{-5}$	CL=90%
Γ_{203}	$p \overline{p} \pi^+ \pi^+ \pi^-$	<	5.2	$\times 10^{-4}$	CL=90%
Γ_{204}	$p \overline{p} K^+$	(	4.3 $^{+1.2}_{-1.0}$)	$\times 10^{-6}$	
Γ_{205}	$p \overline{p} K^+$ nonresonant	<	8.9	$\times 10^{-5}$	CL=90%
Γ_{206}	$p \overline{\Lambda}$	<	1.5	$\times 10^{-6}$	CL=90%
Γ_{207}	$p \overline{\Lambda} \gamma$				
Γ_{208}	$p \overline{\Sigma}^- \gamma$				
Γ_{209}	$p \overline{\Lambda} \pi^+ \pi^-$	<	2.0	$\times 10^{-4}$	CL=90%
Γ_{210}	$\overline{\Delta}^0 p$	<	3.8	$\times 10^{-4}$	CL=90%
Γ_{211}	$\Delta^{++} \overline{p}$	<	1.5	$\times 10^{-4}$	CL=90%
Γ_{212}	$D^+ p \overline{p}$	<	1.5	$\times 10^{-5}$	CL=90%
Γ_{213}	$D^*(2010)^+ p \overline{p}$	<	1.5	$\times 10^{-5}$	CL=90%
Γ_{214}	$\overline{\Lambda}_c^- p \pi^+$	(	2.1 $\pm$0.7)	$\times 10^{-4}$	
Γ_{215}	$\overline{\Lambda}_c^- p \pi^+ \pi^0$	(	1.8 $\pm$0.6)	$\times 10^{-3}$	
Γ_{216}	$\overline{\Lambda}_c^- p \pi^+ \pi^+ \pi^-$	(	2.3 $\pm$0.7)	$\times 10^{-3}$	
Γ_{217}	$\overline{\Lambda}_c^- p \pi^+ \pi^+ \pi^- \pi^0$	<	1.34	%	CL=90%

Γ_{218}	$\overline{\Sigma}_c(2455)^0\, p$		< 8	$\times 10^{-5}$	CL=90%
Γ_{219}	$\overline{\Sigma}_c(2520)^0\, p$		< 4.6	$\times 10^{-5}$	CL=90%
Γ_{220}	$\overline{\Sigma}_c(2455)^0\, p\pi^0$		(4.4 $\pm$1.8)	$\times 10^{-4}$	
Γ_{221}	$\overline{\Sigma}_c(2455)^0\, p\pi^-\pi^+$		(4.4 $\pm$1.7)	$\times 10^{-4}$	
Γ_{222}	$\overline{\Sigma}_c(2455)^{--}\, p\pi^+\pi^+$		(2.8 $\pm$1.2)	$\times 10^{-4}$	
Γ_{223}	$\overline{\Lambda}_c(2593)^-\,/\,\overline{\Lambda}_c(2625)^-\, p\pi^+$		< 1.9	$\times 10^{-4}$	CL=90%

Lepton Family number (LF) or Lepton number (L) violating modes, or $\Delta B = 1$ weak neutral current ($B1$) modes

Γ_{224}	$\pi^+ e^+ e^-$	$B1$	< 3.9	$\times 10^{-3}$	CL=90%
Γ_{225}	$\pi^+ \mu^+ \mu^-$	$B1$	< 9.1	$\times 10^{-3}$	CL=90%
Γ_{226}	$K^+ e^+ e^-$	$B1$	($6.3\ ^{+1.9}_{-1.7}$)	$\times 10^{-7}$	
Γ_{227}	$K^+ \mu^+ \mu^-$	$B1$	($4.5\ ^{+1.4}_{-1.2}$)	$\times 10^{-7}$	
Γ_{228}	$K^+ \ell^+ \ell^-$	$B1$ [a]	(5.3 $\pm$1.1)	$\times 10^{-7}$	
Γ_{229}	$K^+ \overline{\nu}\nu$	$B1$	< 2.4	$\times 10^{-4}$	CL=90%
Γ_{230}	$K^*(892)^+ e^+ e^-$	$B1$	< 4.6	$\times 10^{-6}$	CL=90%
Γ_{231}	$K^*(892)^+ \mu^+ \mu^-$	$B1$	< 2.2	$\times 10^{-6}$	CL=90%
Γ_{232}	$K^*(892)^+ \ell^+ \ell$	$B1$ [a]	< 2.2	$\times 10^{-6}$	CL=90%
Γ_{233}	$\pi^+ e^+ \mu^-$	LF	< 6.4	$\times 10^{-3}$	CL=90%
Γ_{234}	$\pi^+ e^- \mu^+$	LF	< 6.4	$\times 10^{-3}$	CL=90%
Γ_{235}	$K^+ e^+ \mu^-$	LF	< 8	$\times 10^{-7}$	CL=90%
Γ_{236}	$K^+ e^- \mu^+$	LF	< 6.4	$\times 10^{-3}$	CL=90%
Γ_{237}	$K^*(892)^+ e^\pm \mu^\mp$	LF	< 7.9	$\times 10^{-6}$	CL=90%
Γ_{238}	$\pi^- e^+ e^+$	L	< 1.6	$\times 10^{-6}$	CL=90%
Γ_{239}	$\pi^- \mu^+ \mu^+$	L	< 1.4	$\times 10^{-6}$	CL=90%
Γ_{240}	$\pi^- e^+ \mu^+$	L	< 1.3	$\times 10^{-6}$	CL=90%
Γ_{241}	$\rho^- e^+ e^+$	L	< 2.6	$\times 10^{-6}$	CL=90%
Γ_{242}	$\rho^- \mu^+ \mu^+$	L	< 5.0	$\times 10^{-6}$	CL=90%
Γ_{243}	$\rho^- e^+ \mu^+$	LF	< 3.3	$\times 10^{-6}$	CL=90%
Γ_{244}	$K^- e^+ e^+$	L	< 1.0	$\times 10^{-6}$	CL=90%
Γ_{245}	$K^- \mu^+ \mu^+$	L	< 1.8	$\times 10^{-6}$	CL=90%
Γ_{246}	$K^- e^+ \mu^+$	L	< 2.0	$\times 10^{-6}$	CL=90%
Γ_{247}	$K^*(892)^- e^+ e^+$	L	< 2.8	$\times 10^{-6}$	CL=90%
Γ_{248}	$K^*(892)^- \mu^+ \mu^+$	L	< 8.3	$\times 10^{-6}$	CL=90%
Γ_{249}	$K^*(892)^- e^+ \mu^+$	LF	< 4.4	$\times 10^{-6}$	CL=90%

[a] An ℓ indicates an e or a μ mode, not a sum over these modes.

[b] An $CP(\pm 1)$ indicates the CP=+1 and CP=−1 eigenstates of the D^0-$\overline{D}^0$ system.

CONSTRAINED FIT INFORMATION

An overall fit to 3 branching ratios uses 9 measurements and one constraint to determine 3 parameters. The overall fit has a χ^2 = 1.1 for 7 degrees of freedom.

The following *off-diagonal* array elements are the correlation coefficients $\langle \delta x_i \delta x_j \rangle / (\delta x_i \cdot \delta x_j)$, in percent, from the fit to the branching fractions, $x_i \equiv \Gamma_i/\Gamma_{\rm total}$. The fit constrains the x_i whose labels appear in this array to sum to one.

x_{107}	16
x_{100}	

B^+ BRANCHING RATIOS

$\Gamma(\ell^+ \nu_\ell \text{anything})/\Gamma_{\rm total}$ Γ_1/Γ

VALUE	DOCUMENT ID		TECN	COMMENT
0.1025 ± 0.0057 ± 0.0065	[12] ARTUSO	97	CLE2	$e^+e^- \to \Upsilon(4S)$
• • • We do not use the following data for averages, fits, limits, etc. • • •				
0.101 ± 0.018 ± 0.015	ATHANAS	94	CLE2	Sup. by ARTUSO 97

[12] ARTUSO 97 uses partial reconstruction of $B \to D^* \ell \nu_\ell$ and inclusive semileptonic branching ratio from BARISH 96B (0.1049 ± 0.0017 ± 0.0043).

$\Gamma(\overline{D}^0 \ell^+ \nu_\ell)/\Gamma_{\rm total}$ Γ_2/Γ

ℓ = e or μ, not sum over e and μ modes.

VALUE	DOCUMENT ID		TECN	COMMENT
0.0215 ± 0.0022 OUR AVERAGE				
0.0221 ± 0.0013 ± 0.0019	[13] BARTELT	99	CLE2	$e^+e^- \to \Upsilon(4S)$
0.016 ± 0.006 ± 0.003	[14] FULTON	91	CLEO	$e^+e^- \to \Upsilon(4S)$
• • • We do not use the following data for averages, fits, limits, etc. • • •				
0.0194 ± 0.0015 ± 0.0034	[15] ATHANAS	97	CLE2	Repl. by BARTELT 99

[13] Assumes equal production of B^+ and B^0 at the $\Upsilon(4S)$.

[14] FULTON 91 assumes equal production of $B^0\overline{B}^0$ and B^+B^- at the $\Upsilon(4S)$.

[15] ATHANAS 97 uses missing energy and missing momentum to reconstruct neutrino.

$\Gamma(\overline{D}^*(2007)^0 \ell^+ \nu_\ell)/\Gamma_{\rm total}$ Γ_3/Γ

ℓ = e or μ, not sum over e and μ modes.

VALUE	EVTS	DOCUMENT ID		TECN	COMMENT
0.065 ± 0.005 OUR AVERAGE					
0.0650 ± 0.0020 ± 0.0043		[16] ADAM	03	CLE2	$e^+e^- \to \Upsilon(4S)$
0.066 ± 0.016 ± 0.015		[17] ALBRECHT	92C	ARG	$e^+e^- \to \Upsilon(4S)$
• • • We do not use the following data for averages, fits, limits, etc. • • •					
0.0650 ± 0.0020 ± 0.0043		[18] BRIERE	02	CLE2	$e^+e^- \to \Upsilon(4S)$
0.0513 ± 0.0054 ± 0.0064	302	[19] BARISH	95	CLE2	Repl. by ADAM 03
seen	398	[20] SANGHERA	93	CLE2	$e^+e^- \to \Upsilon(4S)$
0.041 $\pm$0.008 $^{+0.008}_{-0.009}$		[21] FULTON	91	CLEO	$e^+e^- \to \Upsilon(4S)$
0.070 ± 0.018 ± 0.014		[22] ANTREASYAN	90B	CBAL	$e^+e^- \to \Upsilon(4S)$

[16] Simultaneous measurements of both $B^0 \to D^*(2010)^- \ell \nu$ and $B^+ \to \overline{D}(2007)^0 \ell \nu$.

[17] ALBRECHT 92C reports 0.058 ± 0.014 ± 0.013. We rescale using the method described in STONE 94 but with the updated PDG 94 B($D^0 \to K^-\pi^+$). Assumes equal production of $B^0\overline{B}^0$ and B^+B^- at the $\Upsilon(4S)$.

[18] The results are based on the same analysis and data sample reported in ADAM 03.

[19] BARISH 95 use B($D^0 \to K^-\pi^+$) = (3.91 ± 0.08 ± 0.17)% and B($D^{*0} \to D^0\pi^0$) = (63.6 ± 2.3 ± 3.3)%.

[20] Combining $\overline{D}^{*0}\ell^+\nu_\ell$ and $\overline{D}^{*-}\ell^+\nu_\ell$ SANGHERA 93 test $V-A$ structure and fit the decay angular distributions to obtain $A_{FB} = 3/4*(\Gamma^- - \Gamma^+)/\Gamma = 0.14 \pm 0.06 \pm 0.03$. Assuming a value of V_{cb}, they measure V, A_1, and A_2, the three form factors for the $D^*\ell\nu_\ell$ decay, where results are slightly dependent on model assumptions.

[21] Assumes equal production of $B^0\overline{B}^0$ and B^+B^- at the $\Upsilon(4S)$. Uncorrected for D and D^* branching ratio assumptions.

[22] ANTREASYAN 90B is average over B and $\overline{D}^*(2010)$ charge states.

$\Gamma(\overline{D}_1(2420)^0 \ell^+ \nu_\ell)/\Gamma_{\rm total}$ Γ_4/Γ

VALUE	DOCUMENT ID		TECN	COMMENT
0.0056 ± 0.0013 ± 0.0009	[23] ANASTASSOV	98	CLE2	$e^+e^- \to \Upsilon(4S)$

[23] ANASTASSOV 98 result is derived from the measurement of B($B^+ \to \overline{D}_1^0 \ell^+ \nu_\ell$)×B($\overline{D}_1^0 \to D^{*+}\pi^-$) = (0.373 ± 0.085 ± 0.052 ± 0.024)% by assuming B($\overline{D}_1^0 \to D^{*+}\pi^-$) = 67%, where the third error includes theoretical uncertainties.

$\Gamma(\overline{D}_2^*(2460)^0 \ell^+ \nu_\ell)/\Gamma_{\rm total}$ Γ_5/Γ

VALUE	CL%	DOCUMENT ID		TECN	COMMENT
< 8 × 10^-3	90	[24] ANASTASSOV	98	CLE2	$e^+e^- \to \Upsilon(4S)$

[24] ANASTASSOV 98 result is derived from the measurement of B($B^+ \to \overline{D}_2^{*0} \ell^+ \nu_\ell$)×B($\overline{D}_2^{*0} \to D^{*+}\pi^-$) < 0.16% at 90% CL by assuming B($\overline{D}_2^{*0} \to D^{*+}\pi^-$) = 20%.

$\Gamma(\pi^0 e^+ \nu_e)/\Gamma_{\rm total}$ Γ_6/Γ

VALUE (units 10^{-4})	CL%	DOCUMENT ID		TECN	COMMENT
0.9 ± 0.2 ± 0.2		[25] ALEXANDER	96T	CLE2	$e^+e^- \to \Upsilon(4S)$
• • • We do not use the following data for averages, fits, limits, etc. • • •					
<22	90	ANTREASYAN	90B	CBAL	$e^+e^- \to \Upsilon(4S)$

[25] Derived based in the reported B^0 result by assuming isospin symmetry: $\Gamma(B^0 \to \pi^-\ell^+\nu) = 2\Gamma(B^+ \to \pi^0\ell^+\nu)$.

$\Gamma(\eta \ell^+ \nu_\ell)/\Gamma_{\rm total}$ Γ_7/Γ

VALUE (units 10^{-4})	DOCUMENT ID		TECN	COMMENT
0.84 ± 0.31 ± 0.18	[26] ATHAR	03	CLE2	$e^+e^- \to \Upsilon(4S)$

[26] ATHAR 03 reports systematic errors 0.16 ± 0.09, which are experimental systematic and systematic due to model dependence. We combine these in quadrature.

$\Gamma(\omega \ell^+ \nu_\ell)/\Gamma_{\rm total}$ Γ_8/Γ

ℓ = e or μ, not sum over e and μ modes.

VALUE	CL%	DOCUMENT ID		TECN	COMMENT
< 2.1 × 10^-4	90	[27] BEAN	93B	CLE2	$e^+e^- \to \Upsilon(4S)$

[27] BEAN 93B limit set using ISGW Model. Using isospin and the quark model to combine $\Gamma(\rho^0\ell^+\nu_\ell)$ and $\Gamma(\rho^-\ell^+\nu_\ell)$ with this result, they obtain a limit <(1.6–2.7) × 10^{-4} at 90% CL for $B^+ \to \omega\ell^+\nu_\ell$. The range corresponds to the ISGW, WSB, and KS models. An upper limit on $|V_{ub}/V_{cb}|$ < 0.8–0.13 at 90% CL is derived as well.

$\Gamma(\omega \mu^+ \nu_\mu)/\Gamma_{\rm total}$ Γ_9/Γ

VALUE	DOCUMENT ID		TECN
• • • We do not use the following data for averages, fits, limits, etc. • • •			
seen	[28] ALBRECHT	91C	ARG

[28] In ALBRECHT 91C, one event is fully reconstructed providing evidence for the $b \to u$ transition.

$\Gamma(\rho^0 \ell^+ \nu_\ell)/\Gamma_{\rm total}$ Γ_{10}/Γ

ℓ = e or μ, not sum over e and μ modes.

VALUE (units 10^{-4})	CL%	DOCUMENT ID		TECN	COMMENT
1.34 ± 0.15 $^{+0.28}_{-0.32}$		[29] BEHRENS	00	CLE2	$e^+e^- \to \Upsilon(4S)$
• • • We do not use the following data for averages, fits, limits, etc. • • •					
1.40 ± 0.21 $^{+0.32}_{-0.33}$		[29] BEHRENS	00	CLE2	$e^+e^- \to \Upsilon(4S)$
1.2 $\pm$0.2 $^{+0.3}_{-0.4}$		[29] ALEXANDER	96T	CLE2	$e^+e^- \to \Upsilon(4S)$
<2.1	90	[30] BEAN	93B	CLE2	$e^+e^- \to \Upsilon(4S)$

[29] Derived based in the reported B^0 result by assuming isospin symmetry: $\Gamma(B^0 \to \rho^- \ell^+ \nu) = 2\Gamma(B^+ \to \rho^0 \ell^+ \nu) \approx 2\Gamma(B^+ \to \omega \ell^+ \nu)$.

[30] BEAN 93B limit set using ISGW Model. Using isospin and the quark model to combine $\Gamma(\omega^0 \ell^+ \nu_\ell)$ and $\Gamma(\rho^- \ell^+ \nu_\ell)$ with this result, they obtain a limit $< (1.6\text{–}2.7) \times 10^{-4}$ at 90% CL for $B^+ \to \rho^0 \ell^+ \nu_\ell$. The range corresponds to the ISGW, WSB, and KS models. An upper limit on $|V_{ub}/V_{cb}| < 0.8\text{–}0.13$ at 90% CL is derived as well.

$\Gamma(p\overline{p}e^+\nu_e)/\Gamma_{total}$ Γ_{11}/Γ

VALUE	CL%	DOCUMENT ID		TECN	COMMENT
$< 5.2 \times 10^{-3}$	90	[31] ADAM	03B	CLE2	$e^+e^- \to \Upsilon(4S)$

[31] Based on phase-space model; if V–A model is used, the 90% CL upper limit becomes $< 1.2 \times 10^{-3}$.

$\Gamma(e^+\nu_e)/\Gamma_{total}$ Γ_{12}/Γ

VALUE	CL%	DOCUMENT ID		TECN	COMMENT
$< 1.5 \times 10^{-5}$	90	ARTUSO	95	CLE2	$e^+e^- \to \Upsilon(4S)$

$\Gamma(\mu^+\nu_\mu)/\Gamma_{total}$ Γ_{13}/Γ

VALUE	CL%	DOCUMENT ID		TECN	COMMENT
$< 2.1 \times 10^{-5}$	90	ARTUSO	95	CLE2	$e^+e^- \to \Upsilon(4S)$

$\Gamma(\tau^+\nu_\tau)/\Gamma_{total}$ Γ_{14}/Γ

VALUE	CL%	DOCUMENT ID		TECN	COMMENT
$< 5.7 \times 10^{-4}$	90	[32] ACCIARRI	97F	L3	$e^+e^- \to Z$
• • • We do not use the following data for averages, fits, limits, etc. • • •					
$< 8.3 \times 10^{-4}$	90	[33] BARATE	01E	ALEP	$e^+e^- \to Z$
$< 8.4 \times 10^{-4}$	90	[34] BROWDER	01	CLE2	$e^+e^- \to \Upsilon(4S)$
$< 1.04 \times 10^{-2}$	90	[35] ALBRECHT	95D	ARG	$e^+e^- \to \Upsilon(4S)$
$< 2.2 \times 10^{-3}$	90	ARTUSO	95	CLE2	$e^+e^- \to \Upsilon(4S)$
$< 1.8 \times 10^{-3}$	90	[36] BUSKULIC	95	ALEP	$e^+e^- \to Z$

[32] ACCIARRI 97F uses missing-energy technique and $f(b \to B^-) = (38.2 \pm 2.5)\%$.

[33] The energy-flow and b-tagging algorithms were used.

[34] Assumes equal production of B^+ and B^0 at the $\Upsilon(4S)$.

[35] ALBRECHT 95D use full reconstruction of one B decay as tag.

[36] BUSKULIC 95 uses same missing-energy technique as in $\overline{b} \to \tau^+\nu_\tau$ X, but analysis is restricted to endpoint region of missing-energy distribution.

$\Gamma(e^+\nu_e\gamma)/\Gamma_{total}$ Γ_{15}/Γ

VALUE	CL%	DOCUMENT ID		TECN	COMMENT
$< 2.0 \times 10^{-4}$	90	[37] BROWDER	97	CLE2	$e^+e^- \to \Upsilon(4S)$

[37] BROWDER 97 uses the hermiticity of the CLEO II detector to reconstruct the neutrino energy and momentum.

$\Gamma(\mu^+\nu_\mu\gamma)/\Gamma_{total}$ Γ_{16}/Γ

VALUE	CL%	DOCUMENT ID		TECN	COMMENT
$< 5.2 \times 10^{-5}$	90	[38] BROWDER	97	CLE2	$e^+e^- \to \Upsilon(4S)$

[38] BROWDER 97 uses the hermiticity of the CLEO II detector to reconstruct the neutrino energy and momentum.

$\Gamma(\overline{D}^0\pi^+)/\Gamma_{total}$ Γ_{17}/Γ

VALUE	EVTS	DOCUMENT ID		TECN	COMMENT
0.00498 ± 0.00029 OUR AVERAGE					
$0.00497 \pm 0.00012 \pm 0.00029$		[39,40] AHMED	02B	CLE2	$e^+e^- \to \Upsilon(4S)$
$0.0050 \pm 0.0007 \pm 0.0006$	54	[41] BORTOLETTO	92	CLEO	$e^+e^- \to \Upsilon(4S)$
$0.0054 \,^{+0.0018}_{-0.0015} \,^{+0.0012}_{-0.0009}$	14	[42] BEBEK	87	CLEO	$e^+e^- \to \Upsilon(4S)$
• • • We do not use the following data for averages, fits, limits, etc. • • •					
$0.0055 \pm 0.0004 \pm 0.0005$	304	[43] ALAM	94	CLE2	Repl. by AHMED 02B
$0.0020 \pm 0.0008 \pm 0.0006$	12	[41] ALBRECHT	90J	ARG	$e^+e^- \to \Upsilon(4S)$
$0.0019 \pm 0.0010 \pm 0.0006$	7	[44] ALBRECHT	88K	ARG	$e^+e^- \to \Upsilon(4S)$

[39] Assumes equal production of B^+ and B^0 at the $\Upsilon(4S)$.

[40] AHMED 02B reports an additional uncertainty on the branching ratios to account for 4.5% uncertainty on relative production of B^0 and B^+, which is not included here.

[41] Assumes equal production of B^+ and B^0 at the $\Upsilon(4S)$ and uses the Mark III branching fractions for the D.

[42] BEBEK 87 value has been updated in BERKELMAN 91 to use same assumptions as noted for BORTOLETTO 92.

[43] ALAM 94 assume equal production of B^+ and B^0 at the $\Upsilon(4S)$ and use the CLEO II absolute $B(D^0 \to K^-\pi^+)$ and the PDG 1992 $B(D^0 \to K^-\pi^+\pi^0)/B(D^0 \to K^-\pi^+)$ and $B(D^0 \to K^-\pi^+\pi^+\pi^-)/B(D^0 \to K^-\pi^+)$.

[44] ALBRECHT 88K assumes $B^0\overline{B}^0 : B^+B^-$ ratio is 45:55. Superseded by ALBRECHT 90J.

$\Gamma(\overline{D}^0\rho^+)/\Gamma_{total}$ Γ_{20}/Γ

VALUE	EVTS	DOCUMENT ID		TECN	COMMENT
0.0134 ± 0.0018 OUR AVERAGE					
$0.0135 \pm 0.0012 \pm 0.0015$	212	[45] ALAM	94	CLE2	$e^+e^- \to \Upsilon(4S)$
$0.013 \pm 0.004 \pm 0.004$	19	[46] ALBRECHT	90J	ARG	$e^+e^- \to \Upsilon(4S)$
• • • We do not use the following data for averages, fits, limits, etc. • • •					
$0.021 \pm 0.008 \pm 0.009$	10	[47] ALBRECHT	88K	ARG	$e^+e^- \to \Upsilon(4S)$

[45] ALAM 94 assume equal production of B^+ and B^0 at the $\Upsilon(4S)$ and use the CLEO II absolute $B(D^0 \to K^-\pi^+)$ and the PDG 1992 $B(D^0 \to K^-\pi^+\pi^0)/B(D^0 \to K^-\pi^+)$ and $B(D^0 \to K^-\pi^+\pi^+\pi^-)/B(D^0 \to K^-\pi^+)$.

[46] Assumes equal production of B^+ and B^0 at the $\Upsilon(4S)$ and uses the Mark III branching fractions for the D.

[47] ALBRECHT 88K assumes $B^0\overline{B}^0 : B^+B^-$ ratio is 45:55.

$\Gamma(\overline{D}^0K^+)/\Gamma_{total}$ Γ_{21}/Γ

VALUE (units 10^{-4})	DOCUMENT ID		TECN	COMMENT
3.7 ±0.6 OUR AVERAGE	Error includes scale factor of 1.1.			
$4.19 \pm 0.57 \pm 0.40$	[48] ABE	01I	BELL	$e^+e^- \to \Upsilon(4S)$
$2.92 \pm 0.80 \pm 0.28$	[49] ATHANAS	98	CLE2	$e^+e^- \to \Upsilon(4S)$

[48] ABE 01I reports $B(B^+ \to \overline{D}^0K^+)/B(B^+ \to \overline{D}^0\pi^+) = 0.079 \pm 0.009 \pm 0.006$. We multiply by our best value $B(B^+ \to \overline{D}^0\pi^+) = (5.3 \pm 0.5) \times 10^{-3}$. Our first error is their experiment's error and the second error is systematic error from using our best value.

[49] ATHANAS 98 reports $[B(B^+ \to \overline{D}^0K^+)]/[B(B^+ \to \overline{D}^0\pi^+)] = 0.055 \pm 0.014 \pm 0.005$. We multiply by our best value $B(B^+ \to \overline{D}^0\pi^+) = (5.3 \pm 0.5) \times 10^{-3}$. Our first error is their experiment's error and our second error is the systematic error from using our best value.

$\Gamma(\overline{D}^0K^+)/\Gamma(\overline{D}^0\pi^+)$ Γ_{21}/Γ_{17}

VALUE	DOCUMENT ID		TECN	COMMENT
0.083 ± 0.010 OUR AVERAGE	Error includes scale factor of 1.4.			
$0.099 \,^{+0.014}_{-0.012} \pm 0.007 \pm 0.006$	[50] BORNHEIM	03	CLE2	$e^+e^- \to \Upsilon(4S)$
$0.077 \pm 0.005 \pm 0.006$	[51] SWAIN	03	BELL	$e^+e^- \to \Upsilon(4S)$
• • • We do not use the following data for averages, fits, limits, etc. • • •				
$0.094 \pm 0.009 \pm 0.007$	[51] ABE	03D	BELL	Repl. by SWAIN 03

[50] Assumes equal production of B^+ and B^0 at the $\Upsilon(4S)$.

[51] Flavor specific D^0 meson is reconstructed via $D^0 \to K^-\pi^+$.

$\Gamma(D_{CP(+1)}K^+)/\Gamma(D_{CP(+1)}\pi^+)$ Γ_{22}/Γ_{18}

VALUE	DOCUMENT ID		TECN	COMMENT
0.093 ± 0.018 ± 0.008	[52] SWAIN	03	BELL	$e^+e^- \to \Upsilon(4S)$
• • • We do not use the following data for averages, fits, limits, etc. • • •				
$0.125 \pm 0.036 \pm 0.010$	[52] ABE	03D	BELL	Repl. by SWAIN 03

[52] $CP = +1$ eigenstate of $D^0\overline{D}^0$ system is reconstructed via K^+K^- and $\pi^+\pi^-$.

$\Gamma(D_{CP(-1)}K^+)/\Gamma(D_{CP(-1)}\pi^+)$ Γ_{23}/Γ_{19}

VALUE	DOCUMENT ID		TECN	COMMENT
0.108 ± 0.019 ± 0.007	[53] SWAIN	03	BELL	$e^+e^- \to \Upsilon(4S)$
• • • We do not use the following data for averages, fits, limits, etc. • • •				
$0.119 \pm 0.028 \pm 0.006$	[53] ABE	03D	BELL	Repl. by SWAIN 03

[53] $CP = -1$ eigenstate of $D^0\overline{D}^0$ system is reconstructed via $K^0_S\pi^0$, $K^0_S\omega$, $K^0_S\phi$, $K^0_S\eta$, and $K^0_S\eta'$.

$\Gamma(\overline{D}^0K^*(892)^+)/\Gamma_{total}$ Γ_{24}/Γ

VALUE	DOCUMENT ID		TECN	COMMENT
$(6.1 \pm 1.6 \pm 1.7) \times 10^{-4}$	[54] MAHAPATRA	02	CLE2	$e^+e^- \to \Upsilon(4S)$

[54] Assumes equal production of B^+ and B^0 at the $\Upsilon(4S)$.

$\Gamma(\overline{D}^0K^+\overline{K}^0)/\Gamma_{total}$ Γ_{25}/Γ

VALUE (units 10^{-4})	DOCUMENT ID		TECN	COMMENT
5.5 ± 1.4 ± 0.8	[55] DRUTSKOY	02	BELL	$e^+e^- \to \Upsilon(4S)$

[55] Assumes equal production of B^+ and B^0 at the $\Upsilon(4S)$.

$\Gamma(\overline{D}^0K^+\overline{K}^*(892)^0)/\Gamma_{total}$ Γ_{26}/Γ

VALUE (units 10^{-4})	DOCUMENT ID		TECN	COMMENT
7.5 ± 1.3 ± 1.1	[56] DRUTSKOY	02	BELL	$e^+e^- \to \Upsilon(4S)$

[56] Assumes equal production of B^+ and B^0 at the $\Upsilon(4S)$.

$\Gamma(\overline{D}^0\pi^+\pi^+\pi^-)/\Gamma_{total}$ Γ_{27}/Γ

VALUE	DOCUMENT ID		TECN	COMMENT
0.0115 ± 0.0029 ± 0.0021	[57] BORTOLETTO	92	CLEO	$e^+e^- \to \Upsilon(4S)$

[57] BORTOLETTO 92 assumes equal production of B^+ and B^0 at the $\Upsilon(4S)$ and uses Mark III branching fractions for the D.

$\Gamma(\overline{D}^0\pi^+\pi^+\pi^-\text{ nonresonant})/\Gamma_{total}$ Γ_{28}/Γ

VALUE	DOCUMENT ID		TECN	COMMENT
0.0051 ± 0.0034 ± 0.0023	[58] BORTOLETTO	92	CLEO	$e^+e^- \to \Upsilon(4S)$

[58] BORTOLETTO 92 assumes equal production of B^+ and B^0 at the $\Upsilon(4S)$ and uses Mark III branching fractions for the D.

$\Gamma(\overline{D}^0\pi^+\rho^0)/\Gamma_{total}$ Γ_{29}/Γ

VALUE	DOCUMENT ID		TECN	COMMENT
0.0042 ± 0.0023 ± 0.0020	[59] BORTOLETTO	92	CLEO	$e^+e^- \to \Upsilon(4S)$

[59] BORTOLETTO 92 assumes equal production of B^+ and B^0 at the $\Upsilon(4S)$ and uses Mark III branching fractions for the D.

$\Gamma(\overline{D}^0a_1(1260)^+)/\Gamma_{total}$ Γ_{30}/Γ

VALUE	DOCUMENT ID		TECN	COMMENT
0.0045 ± 0.0019 ± 0.0031	[60] BORTOLETTO	92	CLEO	$e^+e^- \to \Upsilon(4S)$

[60] BORTOLETTO 92 assumes equal production of B^+ and B^0 at the $\Upsilon(4S)$ and uses Mark III branching fractions for the D.

$\Gamma(\overline{D}^0\omega\pi^+)/\Gamma_{total}$ Γ_{31}/Γ

VALUE	DOCUMENT ID		TECN	COMMENT
0.0041 ± 0.0007 ± 0.0006	[61] ALEXANDER	01B	CLE2	$e^+e^- \to \Upsilon(4S)$

[61] Assumes equal production of B^+ and B^0 at the $\Upsilon(4S)$. The signal is consistent with all observed $\omega\pi^+$ having proceeded through the ρ'^+ resonance at mass $1349 \pm 25^{+10}_{-5}$ MeV and width $547 \pm 86^{+46}_{-45}$ MeV.

$\Gamma(D^*(2010)^-\pi^+\pi^+)/\Gamma_{total}$ Γ_{32}/Γ

VALUE	CL%	EVTS	DOCUMENT ID		TECN	COMMENT
0.0021 ± 0.0006 OUR AVERAGE						
$0.0019 \pm 0.0007 \pm 0.0003$		14	[62] ALAM	94	CLE2	$e^+e^- \to \Upsilon(4S)$
$0.0026 \pm 0.0014 \pm 0.0007$		11	[63] ALBRECHT	90J	ARG	$e^+e^- \to \Upsilon(4S)$
$0.0024^{+0.0017}_{-0.0016} {}^{+0.0010}_{-0.0006}$		3	[64] BEBEK	87	CLEO	$e^+e^- \to \Upsilon(4S)$
• • • We do not use the following data for averages, fits, limits, etc. • • •						
< 0.004	90		[65] BORTOLETTO	92	CLEO	$e^+e^- \to \Upsilon(4S)$
$0.005 \pm 0.002 \pm 0.003$		7	[66] ALBRECHT	87C	ARG	$e^+e^- \to \Upsilon(4S)$

[62] ALAM 94 assume equal production of B^+ and B^0 at the $\Upsilon(4S)$ and use the CLEO II $B(D^*(2010)^+ \to D^0\pi^+)$ and absolute $B(D^0 \to K^-\pi^+)$ and the PDG 1992 $B(D^0 \to K^-\pi^+\pi^0)/B(D^0 \to K^-\pi^+)$ and $B(D^0 \to K^-\pi^+\pi^+\pi^-)/B(D^0 \to K^-\pi^+)$.

[63] Assumes equal production of B^+ and B^0 at the $\Upsilon(4S)$ and uses the Mark III branching fractions for the D.

[64] BEBEK 87 value has been updated in BERKELMAN 91 to use same assumptions as noted for BORTOLETTO 92.

[65] BORTOLETTO 92 assumes equal production of B^+ and B^0 at the $\Upsilon(4S)$ and uses Mark III branching fractions for the D and $D^*(2010)$. The authors also find the product branching fraction into $D^{**}\pi$ followed by $D^{**} \to D^*(2010)\pi$ to be $0.0014^{+0.0008}_{-0.0006} \pm 0.0003$ where D^{**} represents all orbitally excited D mesons.

[66] ALBRECHT 87C use PDG 86 branching ratios for D and $D^*(2010)$ and assume $B(\Upsilon(4S) \to B^+B^-) = 55\%$ and $B(\Upsilon(4S) \to B^0\overline{B}^0) = 45\%$. Superseded by ALBRECHT 90J.

$\Gamma(D^-\pi^+\pi^+)/\Gamma_{total}$ Γ_{33}/Γ

VALUE	CL%	EVTS	DOCUMENT ID		TECN	COMMENT
< 0.0014	90		[67] ALAM	94	CLE2	$e^+e^- \to \Upsilon(4S)$
• • • We do not use the following data for averages, fits, limits, etc. • • •						
< 0.007	90		[68] BORTOLETTO	92	CLEO	$e^+e^- \to \Upsilon(4S)$
$0.0025^{+0.0041}_{-0.0023} {}^{+0.0024}_{-0.0008}$		1	[69] BEBEK	87	CLEO	$e^+e^- \to \Upsilon(4S)$

[67] ALAM 94 assume equal production of B^+ and B^0 at the $\Upsilon(4S)$ and use the Mark III $B(D^+ \to K^-\pi^+\pi^+)$.

[68] BORTOLETTO 92 assumes equal production of B^+ and B^0 at the $\Upsilon(4S)$ and uses Mark III branching fractions for the D. The product branching fraction into $D_0^*(2340)\pi$ followed by $D_0^*(2340) \to D\pi$ is < 0.005 at 90%CL and into $D_2^*(2460)$ followed by $D_2^*(2460) \to D\pi$ is < 0.004 at 90%CL.

[69] BEBEK 87 assume the $\Upsilon(4S)$ decays 43% to $B^0\overline{B}^0$. $B(D^- \to K^+\pi^-\pi^-) = (9.1 \pm 1.3 \pm 0.4)\%$ is assumed.

$\Gamma(\overline{D}^*(2007)^0\pi^+)/\Gamma_{total}$ Γ_{34}/Γ

VALUE	EVTS	DOCUMENT ID		TECN	COMMENT
0.0046 ± 0.0004 OUR AVERAGE					
$0.00434 \pm 0.00047 \pm 0.00018$		[70] BRANDENB...	98	CLE2	$e^+e^- \to \Upsilon(4S)$
$0.0052 \pm 0.0007 \pm 0.0007$	71	[71] ALAM	94	CLE2	$e^+e^- \to \Upsilon(4S)$
$0.0072 \pm 0.0018 \pm 0.0016$		[72] BORTOLETTO	92	CLEO	$e^+e^- \to \Upsilon(4S)$
$0.0040 \pm 0.0014 \pm 0.0012$	9	[72] ALBRECHT	90J	ARG	$e^+e^- \to \Upsilon(4S)$
• • • We do not use the following data for averages, fits, limits, etc. • • •					
0.0027 ± 0.0044		[73] BEBEK	87	CLEO	$e^+e^- \to \Upsilon(4S)$

[70] BRANDENBURG 98 assume equal production of B^+ and B^0 at $\Upsilon(4S)$ and use the D^* reconstruction technique. The first error is their experiment's error and the second error is the systematic error from the PDG 96 value of $B(D^* \to D\pi)$.

[71] ALAM 94 assume equal production of B^+ and B^0 at the $\Upsilon(4S)$ and use the CLEO II $B(D^*(2007)^0 \to D^0\pi^0)$ and absolute $B(D^0 \to K^-\pi^+)$ and the PDG 1992 $B(D^0 \to K^-\pi^+\pi^0)/B(D^0 \to K^-\pi^+)$ and $B(D^0 \to K^-\pi^+\pi^+\pi^-)/B(D^0 \to K^-\pi^+)$.

[72] Assumes equal production of B^+ and B^0 at the $\Upsilon(4S)$ and uses Mark III branching fractions for the D and $D^*(2010)$.

[73] This is a derived branching ratio, using the inclusive pion spectrum and other two-body B decays. BEBEK 87 assume the $\Upsilon(4S)$ decays 43% to $B^0\overline{B}^0$.

$\Gamma(\overline{D}^*(2007)^0\omega\pi^+)/\Gamma_{total}$ Γ_{35}/Γ

VALUE	DOCUMENT ID		TECN	COMMENT
0.0045 ± 0.0010 ± 0.0007	[74] ALEXANDER	01B	CLE2	$e^+e^- \to \Upsilon(4S)$

[74] Assumes equal production of B^+ and B^0 at the $\Upsilon(4S)$. The signal is consistent with all observed $\omega\pi^+$ having proceeded through the ρ'^+ resonance at mass $1349 \pm 25^{+10}_{-5}$ MeV and width $547 \pm 86^{+46}_{-45}$ MeV.

$\Gamma(\overline{D}^*(2007)^0\rho^+)/\Gamma_{total}$ Γ_{36}/Γ

VALUE	EVTS	DOCUMENT ID		TECN	COMMENT
0.0098 ± 0.0017 OUR AVERAGE					
$0.0098 \pm 0.0006 \pm 0.0017$		[75] CSORNA	03	CLE2	$e^+e^- \to \Upsilon(4S)$
$0.010 \pm 0.006 \pm 0.004$	7	[76] ALBRECHT	90J	ARG	$e^+e^- \to \Upsilon(4S)$
• • • We do not use the following data for averages, fits, limits, etc. • • •					
$0.0168 \pm 0.0021 \pm 0.0028$	86	[77] ALAM	94	CLE2	$e^+e^- \to \Upsilon(4S)$

[75] Assumes equal production of B^0 and B^+ at the $\Upsilon(4S)$ resonance. The second error combines the systematic and theoretical uncertainties in quadrature. CSORNA 03 includes data used in ALAM 94. A full angular fit to three complex helicity amplitudes is performed.

[76] Assumes equal production of B^+ and B^0 at the $\Upsilon(4S)$ and uses Mark III branching fractions for the D and $D^*(2010)$.

[77] ALAM 94 assume equal production of B^+ and B^0 at the $\Upsilon(4S)$ and use the CLEO II $B(D^*(2007)^0 \to D^0\pi^0)$ and absolute $B(D^0 \to K^-\pi^+)$ and the PDG 1992 $B(D^0 \to K^-\pi^+\pi^0)/B(D^0 \to K^-\pi^+)$ and $B(D^0 \to K^-\pi^+\pi^+\pi^-)/B(D^0 \to K^-\pi^+)$. The nonresonant $\pi^+\pi^0$ contribution under the ρ^+ is negligible.

$\Gamma(\overline{D}^*(2007)^0K^+)/\Gamma_{total}$ Γ_{37}/Γ

VALUE	DOCUMENT ID		TECN	COMMENT
$(3.59 \pm 0.97 \pm 0.31) \times 10^{-4}$	[78] ABE	01I	BELL	$e^+e^- \to \Upsilon(4S)$

[78] ABE 01I reports $B(B^+ \to \overline{D}^*(2007)^0K^+)/B(B^+ \to \overline{D}^*(2007)^0\pi^+) = 0.078 \pm 0.019 \pm 0.009$. We multiply by our best value $B(B^+ \to \overline{D}^*(2007)^0\pi^+) = (4.6 \pm 0.4) \times 10^{-3}$. Our first error is their experiment's error and the second error is systematic error from using our best value.

$\Gamma(\overline{D}^*(2007)^0K^*(892)^+)/\Gamma_{total}$ Γ_{38}/Γ

VALUE	DOCUMENT ID		TECN	COMMENT
$(7.2 \pm 2.2 \pm 2.6) \times 10^{-4}$	[79] MAHAPATRA	02	CLE2	$e^+e^- \to \Upsilon(4S)$

[79] Assumes equal production of B^+ and B^0 at the $\Upsilon(4S)$ and an unpolarized final state.

$\Gamma(\overline{D}^*(2007)^0K^+\overline{K}^0)/\Gamma_{total}$ Γ_{39}/Γ

VALUE (units 10^{-4})	CL%	DOCUMENT ID		TECN	COMMENT
< 10.6	90	[80] DRUTSKOY	02	BELL	$e^+e^- \to \Upsilon(4S)$

[80] Assumes equal production of B^+ and B^0 at the $\Upsilon(4S)$.

$\Gamma(\overline{D}^*(2007)^0K^+K^*(892)^0)/\Gamma_{total}$ Γ_{40}/Γ

VALUE (units 10^{-4})	DOCUMENT ID		TECN	COMMENT
15.3 ± 3.1 ± 2.9	[81] DRUTSKOY	02	BELL	$e^+e^- \to \Upsilon(4S)$

[81] Assumes equal production of B^+ and B^0 at the $\Upsilon(4S)$.

$\Gamma(\overline{D}^*(2007)^0\pi^+\pi^+\pi^-)/\Gamma_{total}$ Γ_{41}/Γ

VALUE	EVTS	DOCUMENT ID		TECN	COMMENT
0.0094 ± 0.0020 ± 0.0017	48	[82,83] ALAM	94	CLE2	$e^+e^- \to \Upsilon(4S)$

[82] ALAM 94 assume equal production of B^+ and B^0 at the $\Upsilon(4S)$ and use the CLEO II $B(D^*(2007)^0 \to D^0\pi^0)$ and absolute $B(D^0 \to K^-\pi^+)$ and the PDG 1992 $B(D^0 \to K^-\pi^+\pi^0)/B(D^0 \to K^-\pi^+)$ and $B(D^0 \to K^-\pi^+\pi^+\pi^-)/B(D^0 \to K^-\pi^+)$.

[83] The three pion mass is required to be between 1.0 and 1.6 GeV consistent with an a_1 meson. (If this channel is dominated by a_1^+, the branching ratio for $\overline{D}^{*0}a_1^+$ is twice that for $\overline{D}^{*0}\pi^+\pi^+\pi^-$.)

$\Gamma(\overline{D}^*(2007)^0a_1(1260)^+)/\Gamma_{total}$ Γ_{42}/Γ

VALUE	DOCUMENT ID		TECN	COMMENT
0.0188 ± 0.0040 ± 0.0034	[84,85] ALAM	94	CLE2	$e^+e^- \to \Upsilon(4S)$

[84] ALAM 94 value is twice their $\Gamma(\overline{D}^*(2007)^0\pi^+\pi^+\pi^-)/\Gamma_{total}$ value based on their observation that the three pions are dominantly in the $a_1(1260)$ mass range 1.0 to 1.6 GeV.

[85] ALAM 94 assume equal production of B^+ and B^0 at the $\Upsilon(4S)$ and use the CLEO II $B(D^*(2007)^0 \to D^0\pi^0)$ and absolute $B(D^0 \to K^-\pi^+)$ and the PDG 1992 $B(D^0 \to K^-\pi^+\pi^0)/B(D^0 \to K^-\pi^+)$ and $B(D^0 \to K^-\pi^+\pi^+\pi^-)/B(D^0 \to K^-\pi^+)$.

$\Gamma(\overline{D}^*(2007)^0\pi^-\pi^+\pi^+\pi^0)/\Gamma_{total}$ Γ_{43}/Γ

VALUE	DOCUMENT ID		TECN	COMMENT
0.0180 ± 0.0024 ± 0.0027	[86] ALEXANDER	01B	CLE2	$e^+e^- \to \Upsilon(4S)$

[86] Assumes equal production of B^+ and B^0 at the $\Upsilon(4S)$. The signal is consistent with all observed $\omega\pi^+$ having proceeded through the ρ'^+ resonance at mass $1349 \pm 25^{+10}_{-5}$ MeV and width $547 \pm 86^{+46}_{-45}$ MeV.

$\Gamma(D^*(2010)^+\pi^0)/\Gamma_{total}$ Γ_{44}/Γ

VALUE	CL%	DOCUMENT ID		TECN	COMMENT
< 0.00017	90	[87] BRANDENB...	98	CLE2	$e^+e^- \to \Upsilon(4S)$

[87] BRANDENBURG 98 assume equal production of B^+ and B^0 at $\Upsilon(4S)$ and use the D^* partial reconstruction technique. The first error is their experiment's error and the second error is the systematic error from the PDG 96 value of $B(D^* \to D\pi)$.

$\Gamma(\overline{D}^*(2010)^+K^0)/\Gamma_{total}$ Γ_{45}/Γ

VALUE	CL%	DOCUMENT ID		TECN	COMMENT
< 9.5 × 10⁻⁵	90	[88] GRITSAN	01	CLE2	$e^+e^- \to \Upsilon(4S)$

[88] Assumes equal production of B^+ and B^0 at the $\Upsilon(4S)$.

$\Gamma(D^*(2010)^-\pi^+\pi^+\pi^0)/\Gamma_{total}$ Γ_{46}/Γ

VALUE	EVTS	DOCUMENT ID		TECN	COMMENT
0.0152±0.0071±0.0001	26	[89] ALBRECHT	90J	ARG	$e^+e^- \to \Upsilon(4S)$
• • • We do not use the following data for averages, fits, limits, etc. • • •					
0.043 ±0.013 ±0.026	24	[90] ALBRECHT	87C	ARG	$e^+e^- \to \Upsilon(4S)$

[89] ALBRECHT 90J reports $0.018 \pm 0.007 \pm 0.005$ for $B(D^*(2010)^+ \to D^0\pi^+) = 0.57 \pm 0.06$. We rescale to our best value $B(D^*(2010)^+ \to D^0\pi^+) = (67.7 \pm 0.5) \times 10^{-2}$. Our first error is their experiment's error and our second error is the systematic error from using our best value. Assumes equal production of B^+ and B^0 at the $\Upsilon(4S)$ and uses Mark III branching fractions for the D.

[90] ALBRECHT 87C use PDG 86 branching ratios for D and $D^*(2010)$ and assume $B(\Upsilon(4S) \to B^+B^-) = 55\%$ and $B(\Upsilon(4S) \to B^0\overline{B}^0) = 45\%$. Superseded by ALBRECHT 90J.

$\Gamma(D^*(2010)^-\pi^+\pi^+\pi^+\pi^-)/\Gamma_{total}$ Γ_{47}/Γ

VALUE	CL%	DOCUMENT ID		TECN	COMMENT
<0.01	90	[91] ALBRECHT	90J	ARG	$e^+e^- \to \Upsilon(4S)$

[91] Assumes equal production of B^+ and B^0 at the $\Upsilon(4S)$ and uses Mark III branching fractions for the D and $D^*(2010)$.

$\Gamma(\overline{D}_1^*(2420)^0\pi^+)/\Gamma_{total}$ Γ_{48}/Γ

VALUE	EVTS	DOCUMENT ID		TECN	COMMENT
0.0015±0.0006 OUR AVERAGE		Error includes scale factor of 1.3.			
0.0011±0.0005±0.0002	8	[92] ALAM	94	CLE2	$e^+e^- \to \Upsilon(4S)$
0.0025±0.0007±0.0006		[93] ALBRECHT	94D	ARG	$e^+e^- \to \Upsilon(4S)$

[92] ALAM 94 assume equal production of B^+ and B^0 at the $\Upsilon(4S)$ and use the CLEO II $B(D^*(2010)^+ \to D^0\pi^+)$ and absolute $B(D^0 \to K^-\pi^+)$ and the PDG 1992 $B(D^0 \to K^-\pi^+\pi^0)/B(D^0 \to K^-\pi^+)$ and assuming $B(D_1(2420)^0 \to D^*(2010)^+\pi^-) = 67\%$.

[93] ALBRECHT 94D assume equal production of B^+ and B^0 at the $\Upsilon(4S)$ and use the CLEO II $B(D^*(2010)^+ \to D^0\pi^+)$ assuming $B(D_1(2420)^0 \to D^*(2010)^+\pi^-) = 67\%$.

$\Gamma(\overline{D}_1^*(2420)^0\rho^+)/\Gamma_{total}$ Γ_{49}/Γ

VALUE	CL%	DOCUMENT ID		TECN	COMMENT
<0.0014	90	[94] ALAM	94	CLE2	$e^+e^- \to \Upsilon(4S)$

[94] ALAM 94 assume equal production of B^+ and B^0 at the $\Upsilon(4S)$ and use the CLEO II $B(D^*(2010)^+ \to D^0\pi^+)$ assuming $B(D_1(2420)^0 \to D^*(2010)^+\pi^-) = 67\%$.

$\Gamma(\overline{D}_2^*(2460)^0\pi^+)/\Gamma_{total}$ Γ_{50}/Γ

VALUE	CL%	DOCUMENT ID		TECN	COMMENT
<0.0013	90	[95] ALAM	94	CLE2	$e^+e^- \to \Upsilon(4S)$
• • • We do not use the following data for averages, fits, limits, etc. • • •					
<0.0028	90	[96] ALAM	94	CLE2	$e^+e^- \to \Upsilon(4S)$
<0.0023	90	[97] ALBRECHT	94D	ARG	$e^+e^- \to \Upsilon(4S)$

[95] ALAM 94 assume equal production of B^+ and B^0 at the $\Upsilon(4S)$ and use the Mark III $B(D^+ \to K^-\pi^+\pi^+)$ and $B(D_2^*(2460)^0 \to D^+\pi^-) = 30\%$.

[96] ALAM 94 assume equal production of B^+ and B^0 at the $\Upsilon(4S)$ and use the Mark III $B(D^+ \to K^-\pi^+\pi^+)$, the CLEO II $B(D^*(2010)^+ \to D^0\pi^+)$ and $B(D_2^*(2460)^0 \to D^*(2010)^+\pi^-) = 20\%$.

[97] ALBRECHT 94D assume equal production of B^+ and B^0 at the $\Upsilon(4S)$ and use the CLEO II $B(D^*(2010)^+ \to D^0\pi^+)$ and $B(D_2^*(2460)^0 \to D^*(2010)^+\pi^-) = 30\%$.

$\Gamma(\overline{D}_2^*(2460)^0\rho^+)/\Gamma_{total}$ Γ_{51}/Γ

VALUE	CL%	DOCUMENT ID		TECN	COMMENT
<0.0047	90	[98] ALAM	94	CLE2	$e^+e^- \to \Upsilon(4S)$
<0.005	90	[99] ALAM	94	CLE2	$e^+e^- \to \Upsilon(4S)$

[98] ALAM 94 assume equal production of B^+ and B^0 at the $\Upsilon(4S)$ and use the Mark III $B(D^+ \to K^-\pi^+\pi^+)$ and $B(D_2^*(2460)^0 \to D^+\pi^-) = 30\%$.

[99] ALAM 94 assume equal production of B^+ and B^0 at the $\Upsilon(4S)$ and use the Mark III $B(D^+ \to K^-\pi^+\pi^+)$, the CLEO II $B(D^*(2010)^+ \to D^0\pi^+)$ and $B(D_2^*(2460)^0 \to D^*(2010)^+\pi^-) = 20\%$.

$\Gamma(\overline{D}^0 D_s^+)/\Gamma_{total}$ Γ_{52}/Γ

VALUE	EVTS	DOCUMENT ID		TECN	COMMENT
0.013 ±0.004 OUR AVERAGE					
$0.0122 \pm 0.0032^{+0.0029}_{-0.0030}$		[100] GIBAUT	96	CLE2	$e^+e^- \to \Upsilon(4S)$
0.018 ±0.009 ±0.004		[101] ALBRECHT	92G	ARG	$e^+e^- \to \Upsilon(4S)$
0.016 ±0.007 ±0.004	5	[102] BORTOLETTO	90	CLEO	$e^+e^- \to \Upsilon(4S)$

[100] GIBAUT 96 reports $0.0126 \pm 0.0022 \pm 0.0025$ for $B(D_s^+ \to \phi\pi^+) = 0.035$. We rescale to our best value $B(D_s^+ \to \phi\pi^+) = (3.6 \pm 0.9) \times 10^{-2}$. Our first error is their experiment's error and our second error is the systematic error from using our best value.

[101] ALBRECHT 92G reports $0.024 \pm 0.012 \pm 0.004$ for $B(D_s^+ \to \phi\pi^+) = 0.027$. We rescale to our best value $B(D_s^+ \to \phi\pi^+) = (3.6 \pm 0.9) \times 10^{-2}$. Our first error is their experiment's error and our second error is the systematic error from using our best value. Assumes PDG 1990 D^0 branching ratios, e.g., $B(D^0 \to K^-\pi^+) = 3.71 \pm 0.25\%$.

[102] BORTOLETTO 90 reports 0.029 ± 0.013 for $B(D_s^+ \to \phi\pi^+) = 0.02$. We rescale to our best value $B(D_s^+ \to \phi\pi^+) = (3.6 \pm 0.9) \times 10^{-2}$. Our first error is their experiment's error and our second error is the systematic error from using our best value.

$\Gamma(\overline{D}^0 D_{sJ}(2317)^+)/\Gamma_{total}$ Γ_{53}/Γ

VALUE	DOCUMENT ID		TECN	COMMENT
seen	[103] KROKOVNY	03B	BELL	$e^+e^- \to \Upsilon(4S)$

[103] The product branching ratio for $B(B^+ \to \overline{D}^0 D_{sJ}(2317)^+) \times B(D_{sJ}(2317)^+ \to D_s\pi^0)$ is measured to be $(8.1^{+3.0}_{-2.7} \pm 2.4) \times 10^{-4}$.

$\Gamma(\overline{D}^0 D_{sJ}(2457)^+)/\Gamma_{total}$ Γ_{54}/Γ

VALUE	DOCUMENT ID		TECN	COMMENT
seen	[104] KROKOVNY	03B	BELL	$e^+e^- \to \Upsilon(4S)$

[104] The product branching ratio for $B(B^+ \to \overline{D}^0 D_{sJ}(2457)^+) \times B(D_{sJ}(2457)^+ \to D_s^{*+}\pi^0, D_s^+\gamma)$ are measured to be $(11.9^{+6.1}_{-4.9} \pm 3.6) \times 10^{-4}$ and $(5.6^{+1.6}_{-1.5} \pm 1.7) \times 10^{-4}$, respectively.

$\Gamma(\overline{D}^0 D_{sJ}(2536)^+)/\Gamma_{total}$ Γ_{55}/Γ

VALUE	DOCUMENT ID		TECN	COMMENT
not seen	[105] AUBERT	03X	BABR	$e^+e^- \to \Upsilon(4S)$

[105] No evidence is found for such decay and set a limit on $B(B \to \overline{D}^0 D_{sJ}(2536)^+) \times B(D_{sJ}(2536)^+ \to D^*(2007)^0 K^+) < 2 \times 10^{-4}$ at 90%CL.

$\Gamma(\overline{D}^*(2007)^0 D_{sJ}(2536)^+)/\Gamma_{total}$ Γ_{56}/Γ

VALUE	DOCUMENT ID		TECN	COMMENT
not seen	[106] AUBERT	03X	BABR	$e^+e^- \to \Upsilon(4S)$

[106] No evidence is found for such decay and set a limit on $B(B \to \overline{D}^*(2007)^0 D_{sJ}(2536)^+) \times B(D_{sJ}(2536)^+ \to D^*(2007)^0 K^+) < 7 \times 10^{-4}$ at 90%CL.

$\Gamma(\overline{D}^0 D_{sJ}(2573)^+)/\Gamma_{total}$ Γ_{57}/Γ

VALUE	DOCUMENT ID		TECN	COMMENT
not seen	[107] AUBERT	03X	BABR	$e^+e^- \to \Upsilon(4S)$

[107] No evidence is found for such decay and set a limit on $B(B \to \overline{D}^0 D_{sJ}(2573)^+) \times B(D_{sJ}(2573)^+ \to D^0 K^+) < 2 \times 10^{-4}$ at 90%CL.

$\Gamma(\overline{D}^*(2007)^0 D_{sJ}(2573)^+)/\Gamma_{total}$ Γ_{58}/Γ

VALUE	DOCUMENT ID		TECN	COMMENT
not seen	[108] AUBERT	03X	BABR	$e^+e^- \to \Upsilon(4S)$

[108] No evidence is found for such decay and set a limit on $B(B \to \overline{D}^*(2007)^0 D_{sJ}(2536)^+) \times B(D_{sJ}(2536)^+ \to D^0 K^+) < 5 \times 10^{-4}$ at 90%CL.

$\Gamma(\overline{D}^0 D_s^{*+})/\Gamma_{total}$ Γ_{59}/Γ

VALUE	DOCUMENT ID		TECN	COMMENT
0.009 ±0.004 OUR AVERAGE				
$0.0084 \pm 0.0031^{+0.0020}_{-0.0021}$	[109] GIBAUT	96	CLE2	$e^+e^- \to \Upsilon(4S)$
0.012 ±0.009 ±0.003	[110] ALBRECHT	92G	ARG	$e^+e^- \to \Upsilon(4S)$

[109] GIBAUT 96 reports $0.0087 \pm 0.0027 \pm 0.0017$ for $B(D_s^+ \to \phi\pi^+) = 0.035$. We rescale to our best value $B(D_s^+ \to \phi\pi^+) = (3.6 \pm 0.9) \times 10^{-2}$. Our first error is their experiment's error and our second error is the systematic error from using our best value.

[110] ALBRECHT 92G reports $0.016 \pm 0.012 \pm 0.003$ for $B(D_s^+ \to \phi\pi^+) = 0.027$. We rescale to our best value $B(D_s^+ \to \phi\pi^+) = (3.6 \pm 0.9) \times 10^{-2}$. Our first error is their experiment's error and our second error is the systematic error from using our best value. Assumes PDG 1990 D^0 branching ratios, e.g., $B(D^0 \to K^-\pi^+) = 3.71 \pm 0.25\%$.

$\Gamma(\overline{D}^*(2007)^0 D_s^+)/\Gamma_{total}$ Γ_{60}/Γ

VALUE	DOCUMENT ID		TECN	COMMENT
0.012±0.005 OUR AVERAGE				
0.014±0.005±0.003	[111] GIBAUT	96	CLE2	$e^+e^- \to \Upsilon(4S)$
0.010±0.007±0.002	[112] ALBRECHT	92G	ARG	$e^+e^- \to \Upsilon(4S)$

[111] GIBAUT 96 reports $0.0140 \pm 0.0043 \pm 0.0035$ for $B(D_s^+ \to \phi\pi^+) = 0.035$. We rescale to our best value $B(D_s^+ \to \phi\pi^+) = (3.6 \pm 0.9) \times 10^{-2}$. Our first error is their experiment's error and our second error is the systematic error from using our best value.

[112] ALBRECHT 92G reports $0.013 \pm 0.009 \pm 0.002$ for $B(D_s^+ \to \phi\pi^+) = 0.027$. We rescale to our best value $B(D_s^+ \to \phi\pi^+) = (3.6 \pm 0.9) \times 10^{-2}$. Our first error is their experiment's error and our second error is the systematic error from using our best value. Assumes PDG 1990 D^0 and $D^*(2007)^0$ branching ratios, e.g., $B(D^0 \to K^-\pi^+) = 3.71 \pm 0.25\%$ and $B(D^*(2007)^0 \to D^0\pi^0) = 55 \pm 6\%$.

$\Gamma(\overline{D}^*(2007)^0 D_s^{*+})/\Gamma_{total}$ Γ_{61}/Γ

VALUE	DOCUMENT ID		TECN	COMMENT
0.027±0.010 OUR AVERAGE				
0.030±0.011±0.007	[113] GIBAUT	96	CLE2	$e^+e^- \to \Upsilon(4S)$
0.023±0.013±0.006	[114] ALBRECHT	92G	ARG	$e^+e^- \to \Upsilon(4S)$

[113] GIBAUT 96 reports $0.0310 \pm 0.0088 \pm 0.0065$ for $B(D_s^+ \to \phi\pi^+) = 0.035$. We rescale to our best value $B(D_s^+ \to \phi\pi^+) = (3.6 \pm 0.9) \times 10^{-2}$. Our first error is their experiment's error and our second error is the systematic error from using our best value.

[114] ALBRECHT 92G reports $0.031 \pm 0.016 \pm 0.005$ for $B(D_s^+ \to \phi\pi^+) = 0.027$. We rescale to our best value $B(D_s^+ \to \phi\pi^+) = (3.6 \pm 0.9) \times 10^{-2}$. Our first error is their experiment's error and our second error is the systematic error from using our best value. Assumes PDG 1990 D^0 and $D^*(2007)^0$ branching ratios, e.g., $B(D^0 \to K^-\pi^+) = 3.71 \pm 0.25\%$ and $B(D^*(2007)^0 \to D^0\pi^0) = 55 \pm 6\%$.

$\Gamma(D_s^{(*)+}\overline{D}^{**0})/\Gamma_{total}$ Γ_{62}/Γ

VALUE	DOCUMENT ID		TECN	COMMENT
$(2.73\ \pm0.93\ \pm0.68)\times10^{-2}$	[115] AHMED	00B	CLE2	$e^+e^-\to\ \Upsilon(4S)$

[115] AHMED 00B reports their experiment's uncertainties ($\pm0.78\ \pm\ 0.48\ \pm\ 0.68$)%, where the first error is statistical, the second is systematic, and the third is the uncertainty in the $D_s\to\ \phi\pi$ branching fraction. We combine the first two in quadrature.

$\Gamma(\overline{D}^*(2007)^0\,D^*(2010)^+)/\Gamma_{total}$ Γ_{63}/Γ

VALUE	CL%	DOCUMENT ID		TECN	COMMENT
<0.011	90	BARATE	98Q	ALEP	$e^+e^-\to\ Z$

$[\Gamma(\overline{D}^0\,D^*(2010)^+)+\Gamma(\overline{D}^*(2007)^0\,D^+)]/\Gamma_{total}$ Γ_{64}/Γ

VALUE	CL%	DOCUMENT ID		TECN	COMMENT
<0.013	90	BARATE	98Q	ALEP	$e^+e^-\to\ Z$

$\Gamma(\overline{D}^0\,D^+)/\Gamma_{total}$ Γ_{65}/Γ

VALUE	CL%	DOCUMENT ID		TECN	COMMENT
<0.0067	90	BARATE	98Q	ALEP	$e^+e^-\to\ Z$

$\Gamma(\overline{D}^0\,D^+K^0)/\Gamma_{total}$ Γ_{66}/Γ

VALUE (units 10^{-3})	CL%	DOCUMENT ID		TECN	COMMENT
<2.8	90	[116] AUBERT	03X	BABR	$e^+e^-\to\ \Upsilon(4S)$

[116] Assumes equal production of B^+ and B^0 at the $\Upsilon(4S)$.

$\Gamma(\overline{D}^*(2007)^0\,D^+K^0)/\Gamma_{total}$ Γ_{67}/Γ

VALUE (units 10^{-3})	CL%	DOCUMENT ID		TECN	COMMENT
<6.1	90	[117] AUBERT	03X	BABR	$e^+e^-\to\ \Upsilon(4S)$

[117] Assumes equal production of B^+ and B^0 at the $\Upsilon(4S)$.

$\Gamma(\overline{D}^0\overline{D}^*(2010)^+K^0)/\Gamma_{total}$ Γ_{68}/Γ

VALUE (units 10^{-3})	DOCUMENT ID		TECN	COMMENT
$5.2^{+1.0}_{-0.9}\pm0.7$	[118] AUBERT	03X	BABR	$e^+e^-\to\ \Upsilon(4S)$

[118] Assumes equal production of B^+ and B^0 at the $\Upsilon(4S)$.

$\Gamma(\overline{D}^*(2007)^0\,D^*(2010)^+K^0)/\Gamma_{total}$ Γ_{69}/Γ

VALUE (units 10^{-3})	DOCUMENT ID		TECN	COMMENT
$7.8^{+2.3}_{-2.1}\pm1.4$	[119] AUBERT	03X	BABR	$e^+e^-\to\ \Upsilon(4S)$

[119] Assumes equal production of B^+ and B^0 at the $\Upsilon(4S)$.

$\Gamma(\overline{D}^0\,D^0\,K^+)/\Gamma_{total}$ Γ_{70}/Γ

VALUE (units 10^{-3})	DOCUMENT ID		TECN	COMMENT
$1.9\pm0.3\pm0.3$	[120] AUBERT	03X	BABR	$e^+e^-\to\ \Upsilon(4S)$

[120] Assumes equal production of B^+ and B^0 at the $\Upsilon(4S)$.

$\Gamma(\overline{D}^*(2010)^0\,D^0\,K^+)/\Gamma_{total}$ Γ_{71}/Γ

VALUE (units 10^{-3})	CL%	DOCUMENT ID		TECN	COMMENT
<3.8	90	[121] AUBERT	03X	BABR	$e^+e^-\to\ \Upsilon(4S)$

[121] Assumes equal production of B^+ and B^0 at the $\Upsilon(4S)$.

$\Gamma(\overline{D}^0\,D^*(2007)^0\,K^+)/\Gamma_{total}$ Γ_{72}/Γ

VALUE (units 10^{-3})	DOCUMENT ID		TECN	COMMENT
$4.7\pm0.7\pm0.7$	[122] AUBERT	03X	BABR	$e^+e^-\to\ \Upsilon(4S)$

[122] Assumes equal production of B^+ and B^0 at the $\Upsilon(4S)$.

$\Gamma(\overline{D}^*(2007)^0\,D^*(2007)^0\,K^+)/\Gamma_{total}$ Γ_{73}/Γ

VALUE (units 10^{-3})	DOCUMENT ID		TECN	COMMENT
$5.3^{+1.1}_{-1.0}\pm1.2$	[123] AUBERT	03X	BABR	$e^+e^-\to\ \Upsilon(4S)$

[123] Assumes equal production of B^+ and B^0 at the $\Upsilon(4S)$.

$\Gamma(D^-\,D^+\,K^+)/\Gamma_{total}$ Γ_{74}/Γ

VALUE (units 10^{-3})	CL%	DOCUMENT ID		TECN	COMMENT
<0.4	90	[124] AUBERT	03X	BABR	$e^+e^-\to\ \Upsilon(4S)$

[124] Assumes equal production of B^+ and B^0 at the $\Upsilon(4S)$.

$\Gamma(D^-\,D^*(2010)^+\,K^+)/\Gamma_{total}$ Γ_{75}/Γ

VALUE (units 10^{-3})	CL%	DOCUMENT ID		TECN	COMMENT
<0.7	90	[125] AUBERT	03X	BABR	$e^+e^-\to\ \Upsilon(4S)$

[125] Assumes equal production of B^+ and B^0 at the $\Upsilon(4S)$.

$\Gamma(D^*(2010)^-\,D^+\,K^+)/\Gamma_{total}$ Γ_{76}/Γ

VALUE (units 10^{-3})	DOCUMENT ID		TECN	COMMENT
$1.5\pm0.3\pm0.2$	[126] AUBERT	03X	BABR	$e^+e^-\to\ \Upsilon(4S)$

[126] Assumes equal production of B^+ and B^0 at the $\Upsilon(4S)$.

$\Gamma(D^*(2010)^-\,D^*(2010)^+\,K^+)/\Gamma_{total}$ Γ_{77}/Γ

VALUE (units 10^{-3})	CL%	DOCUMENT ID		TECN	COMMENT
<1.8	90	[127] AUBERT	03X	BABR	$e^+e^-\to\ \Upsilon(4S)$

[127] Assumes equal production of B^+ and B^0 at the $\Upsilon(4S)$.

$\Gamma((\overline{D}+\overline{D}^*)(D+D^*)\,K)/\Gamma_{total}$ Γ_{78}/Γ

VALUE (units 10^{-2})	DOCUMENT ID		TECN	COMMENT
$3.5\pm0.3\pm0.5$	[128] AUBERT	03X	BABR	$e^+e^-\to\ \Upsilon(4S)$

[128] Assumes equal production of B^+ and B^0 at the $\Upsilon(4S)$.

$\Gamma(D_s^+\pi^0)/\Gamma_{total}$ Γ_{79}/Γ

VALUE	CL%	DOCUMENT ID		TECN	COMMENT
<0.00020	90	[129] ALEXANDER	93B	CLE2	$e^+e^-\to\ \Upsilon(4S)$

[129] ALEXANDER 93B reports $<2.0\times10^{-4}$ for $B(D_s^+\to\ \phi\pi^+)=0.037$. We rescale to our best value $B(D_s^+\to\ \phi\pi^+)=0.036$.

$[\Gamma(D_s^+\pi^0)+\Gamma(D_s^{*+}\pi^0)]/\Gamma_{total}$ $(\Gamma_{79}+\Gamma_{80})/\Gamma$

VALUE	CL%	DOCUMENT ID		TECN	COMMENT
<0.0007	90	[130] ALBRECHT	93E	ARG	$e^+e^-\to\ \Upsilon(4S)$

[130] ALBRECHT 93E reports $<0.9\times10^{-3}$ for $B(D_s^+\to\ \phi\pi^+)=0.027$. We rescale to our best value $B(D_s^+\to\ \phi\pi^+)=0.036$.

$\Gamma(D_s^{*+}\pi^0)/\Gamma_{total}$ Γ_{80}/Γ

VALUE	CL%	DOCUMENT ID		TECN	COMMENT
<0.00033	90	[131] ALEXANDER	93B	CLE2	$e^+e^-\to\ \Upsilon(4S)$

[131] ALEXANDER 93B reports $<3.2\times10^{-4}$ for $B(D_s^+\to\ \phi\pi^+)=0.037$. We rescale to our best value $B(D_s^+\to\ \phi\pi^+)=0.036$.

$\Gamma(D_s^+\eta)/\Gamma_{total}$ Γ_{81}/Γ

VALUE	CL%	DOCUMENT ID		TECN	COMMENT
<0.0005	90	[132] ALEXANDER	93B	CLE2	$e^+e^-\to\ \Upsilon(4S)$

[132] ALEXANDER 93B reports $<4.6\times10^{-4}$ for $B(D_s^+\to\ \phi\pi^+)=0.037$. We rescale to our best value $B(D_s^+\to\ \phi\pi^+)=0.036$.

$\Gamma(D_s^{*+}\eta)/\Gamma_{total}$ Γ_{82}/Γ

VALUE	CL%	DOCUMENT ID		TECN	COMMENT
<0.0008	90	[133] ALEXANDER	93B	CLE2	$e^+e^-\to\ \Upsilon(4S)$

[133] ALEXANDER 93B reports $<7.5\times10^{-4}$ for $B(D_s^+\to\ \phi\pi^+)=0.037$. We rescale to our best value $B(D_s^+\to\ \phi\pi^+)=0.036$.

$\Gamma(D_s^+\rho^0)/\Gamma_{total}$ Γ_{83}/Γ

VALUE	CL%	DOCUMENT ID		TECN	COMMENT
<0.0004	90	[134] ALEXANDER	93B	CLE2	$e^+e^-\to\ \Upsilon(4S)$

[134] ALEXANDER 93B reports $<3.7\times10^{-4}$ for $B(D_s^+\to\ \phi\pi^+)=0.037$. We rescale to our best value $B(D_s^+\to\ \phi\pi^+)=0.036$.

$[\Gamma(D_s^+\rho^0)+\Gamma(D_s^+\overline{K}^*(892)^0)]/\Gamma_{total}$ $(\Gamma_{83}+\Gamma_{93})/\Gamma$

VALUE	CL%	DOCUMENT ID		TECN	COMMENT
<0.0025	90	[135] ALBRECHT	93E	ARG	$e^+e^-\to\ \Upsilon(4S)$

[135] ALBRECHT 93E reports $<3.4\times10^{-3}$ for $B(D_s^+\to\ \phi\pi^+)=0.027$. We rescale to our best value $B(D_s^+\to\ \phi\pi^+)=0.036$.

$\Gamma(D_s^{*+}\rho^0)/\Gamma_{total}$ Γ_{84}/Γ

VALUE	CL%	DOCUMENT ID		TECN	COMMENT
<0.0005	90	[136] ALEXANDER	93B	CLE2	$e^+e^-\to\ \Upsilon(4S)$

[136] ALEXANDER 93B reports $<4.8\times10^{-4}$ for $B(D_s^+\to\ \phi\pi^+)=0.037$. We rescale to our best value $B(D_s^+\to\ \phi\pi^+)=0.036$.

$[\Gamma(D_s^{*+}\rho^0)+\Gamma(D_s^{*+}\overline{K}^*(892)^0)]/\Gamma_{total}$ $(\Gamma_{84}+\Gamma_{94})/\Gamma$

VALUE	CL%	DOCUMENT ID		TECN	COMMENT
<0.0015	90	[137] ALBRECHT	93E	ARG	$e^+e^-\to\ \Upsilon(4S)$

[137] ALBRECHT 93E reports $<2.0\times10^{-3}$ for $B(D_s^+\to\ \phi\pi^+)=0.027$. We rescale to our best value $B(D_s^+\to\ \phi\pi^+)=0.036$.

$\Gamma(D_s^+\omega)/\Gamma_{total}$ Γ_{85}/Γ

VALUE	CL%	DOCUMENT ID		TECN	COMMENT
<0.0005	90	[138] ALEXANDER	93B	CLE2	$e^+e^-\to\ \Upsilon(4S)$
• • • We do not use the following data for averages, fits, limits, etc. • • •					
<0.0025	90	[139] ALBRECHT	93E	ARG	$e^+e^-\to\ \Upsilon(4S)$

[138] ALEXANDER 93B reports $<4.8\times10^{-4}$ for $B(D_s^+\to\ \phi\pi^+)=0.037$. We rescale to our best value $B(D_s^+\to\ \phi\pi^+)=0.036$.

[139] ALBRECHT 93E reports $<3.4\times10^{-3}$ for $B(D_s^+\to\ \phi\pi^+)=0.027$. We rescale to our best value $B(D_s^+\to\ \phi\pi^+)=0.036$.

$\Gamma(D_s^{*+}\omega)/\Gamma_{total}$ Γ_{86}/Γ

VALUE	CL%	DOCUMENT ID		TECN	COMMENT
<0.0007	90	[140] ALEXANDER	93B	CLE2	$e^+e^- \to \Upsilon(4S)$

• • • We do not use the following data for averages, fits, limits, etc. • • •

<0.0014	90	[141] ALBRECHT	93E	ARG	$e^+e^- \to \Upsilon(4S)$

[140] ALEXANDER 93B reports $< 6.8 \times 10^{-4}$ for $B(D_s^+ \to \phi\pi^+) = 0.037$. We rescale to our best value $B(D_s^+ \to \phi\pi^+) = 0.036$.

[141] ALBRECHT 93E reports $< 1.9 \times 10^{-3}$ for $B(D_s^+ \to \phi\pi^+) = 0.027$. We rescale to our best value $B(D_s^+ \to \phi\pi^+) = 0.036$.

$\Gamma(D_s^+ a_1(1260)^0)/\Gamma_{total}$ Γ_{87}/Γ

VALUE	CL%	DOCUMENT ID		TECN	COMMENT
<0.0022	90	[142] ALBRECHT	93E	ARG	$e^+e^- \to \Upsilon(4S)$

[142] ALBRECHT 93E reports $< 3.0 \times 10^{-3}$ for $B(D_s^+ \to \phi\pi^+) = 0.027$. We rescale to our best value $B(D_s^+ \to \phi\pi^+) = 0.036$.

$\Gamma(D_s^{*+} a_1(1260)^0)/\Gamma_{total}$ Γ_{88}/Γ

VALUE	CL%	DOCUMENT ID		TECN	COMMENT
<0.0016	90	[143] ALBRECHT	93E	ARG	$e^+e^- \to \Upsilon(4S)$

[143] ALBRECHT 93E reports $< 2.2 \times 10^{-3}$ for $B(D_s^+ \to \phi\pi^+) = 0.027$. We rescale to our best value $B(D_s^+ \to \phi\pi^+) = 0.036$.

$\Gamma(D_s^+\phi)/\Gamma_{total}$ Γ_{89}/Γ

VALUE	CL%	DOCUMENT ID		TECN	COMMENT
<0.00032	90	[144] ALEXANDER	93B	CLE2	$e^+e^- \to \Upsilon(4S)$

• • • We do not use the following data for averages, fits, limits, etc. • • •

<0.0013	90	[145] ALBRECHT	93E	ARG	$e^+e^- \to \Upsilon(4S)$

[144] ALEXANDER 93B reports $< 3.1 \times 10^{-4}$ for $B(D_s^+ \to \phi\pi^+) = 0.037$. We rescale to our best value $B(D_s^+ \to \phi\pi^+) = 0.036$.

[145] ALBRECHT 93E reports $< 1.7 \times 10^{-3}$ for $B(D_s^+ \to \phi\pi^+) = 0.027$. We rescale to our best value $B(D_s^+ \to \phi\pi^+) = 0.036$.

$\Gamma(D_s^{*+}\phi)/\Gamma_{total}$ Γ_{90}/Γ

VALUE	CL%	DOCUMENT ID		TECN	COMMENT
<0.0004	90	[146] ALEXANDER	93B	CLE2	$e^+e^- \to \Upsilon(4S)$

• • • We do not use the following data for averages, fits, limits, etc. • • •

<0.0016	90	[147] ALBRECHT	93E	ARG	$e^+e^- \to \Upsilon(4S)$

[146] ALEXANDER 93B reports $< 4.2 \times 10^{-4}$ for $B(D_s^+ \to \phi\pi^+) = 0.037$. We rescale to our best value $B(D_s^+ \to \phi\pi^+) = 0.036$.

[147] ALBRECHT 93E reports $< 2.1 \times 10^{-3}$ for $B(D_s^+ \to \phi\pi^+) = 0.027$. We rescale to our best value $B(D_s^+ \to \phi\pi^+) = 0.036$.

$\Gamma(D_s^+\overline{K}^0)/\Gamma_{total}$ Γ_{91}/Γ

VALUE	CL%	DOCUMENT ID		TECN	COMMENT
<0.0011	90	[148] ALEXANDER	93B	CLE2	$e^+e^- \to \Upsilon(4S)$

• • • We do not use the following data for averages, fits, limits, etc. • • •

<0.0019	90	[149] ALBRECHT	93E	ARG	$e^+e^- \to \Upsilon(4S)$

[148] ALEXANDER 93B reports $< 10.3 \times 10^{-4}$ for $B(D_s^+ \to \phi\pi^+) = 0.037$. We rescale to our best value $B(D_s^+ \to \phi\pi^+) = 0.036$.

[149] ALBRECHT 93E reports $< 2.5 \times 10^{-3}$ for $B(D_s^+ \to \phi\pi^+) = 0.027$. We rescale to our best value $B(D_s^+ \to \phi\pi^+) = 0.036$.

$\Gamma(D_s^{*+}\overline{K}^0)/\Gamma_{total}$ Γ_{92}/Γ

VALUE	CL%	DOCUMENT ID		TECN	COMMENT
<0.0011	90	[150] ALEXANDER	93B	CLE2	$e^+e^- \to \Upsilon(4S)$

• • • We do not use the following data for averages, fits, limits, etc. • • •

<0.0023	90	[151] ALBRECHT	93E	ARG	$e^+e^- \to \Upsilon(4S)$

[150] ALEXANDER 93B reports $< 10.9 \times 10^{-4}$ for $B(D_s^+ \to \phi\pi^+) = 0.037$. We rescale to our best value $B(D_s^+ \to \phi\pi^+) = 0.036$.

[151] ALBRECHT 93E reports $< 3.1 \times 10^{-3}$ for $B(D_s^+ \to \phi\pi^+) = 0.027$. We rescale to our best value $B(D_s^+ \to \phi\pi^+) = 0.036$.

$\Gamma(D_s^+\overline{K}^*(892)^0)/\Gamma_{total}$ Γ_{93}/Γ

VALUE	CL%	DOCUMENT ID		TECN	COMMENT
<0.0005	90	[152] ALEXANDER	93B	CLE2	$e^+e^- \to \Upsilon(4S)$

[152] ALEXANDER 93B reports $< 4.4 \times 10^{-4}$ for $B(D_s^+ \to \phi\pi^+) = 0.037$. We rescale to our best value $B(D_s^+ \to \phi\pi^+) = 0.036$.

$\Gamma(D_s^{*+}\overline{K}^*(892)^0)/\Gamma_{total}$ Γ_{94}/Γ

VALUE	CL%	DOCUMENT ID		TECN	COMMENT
<0.0004	90	[153] ALEXANDER	93B	CLE2	$e^+e^- \to \Upsilon(4S)$

[153] ALEXANDER 93B reports $< 4.3 \times 10^{-4}$ for $B(D_s^+ \to \phi\pi^+) = 0.037$. We rescale to our best value $B(D_s^+ \to \phi\pi^+) = 0.036$.

$\Gamma(D_s^-\pi^+K^+)/\Gamma_{total}$ Γ_{95}/Γ

VALUE	CL%	DOCUMENT ID		TECN	COMMENT
<0.0008	90	[154] ALBRECHT	93E	ARG	$e^+e^- \to \Upsilon(4S)$

[154] ALBRECHT 93E reports $< 1.1 \times 10^{-3}$ for $B(D_s^+ \to \phi\pi^+) = 0.027$. We rescale to our best value $B(D_s^+ \to \phi\pi^+) = 0.036$.

$\Gamma(D_s^{*-}\pi^+K^+)/\Gamma_{total}$ Γ_{96}/Γ

VALUE	CL%	DOCUMENT ID		TECN	COMMENT
<0.0012	90	[155] ALBRECHT	93E	ARG	$e^+e^- \to \Upsilon(4S)$

[155] ALBRECHT 93E reports $< 1.6 \times 10^{-3}$ for $B(D_s^+ \to \phi\pi^+) = 0.027$. We rescale to our best value $B(D_s^+ \to \phi\pi^+) = 0.036$.

$\Gamma(D_s^-\pi^+K^*(892)^+)/\Gamma_{total}$ Γ_{97}/Γ

VALUE	CL%	DOCUMENT ID		TECN	COMMENT
<0.006	90	[156] ALBRECHT	93E	ARG	$e^+e^- \to \Upsilon(4S)$

[156] ALBRECHT 93E reports $< 8.6 \times 10^{-3}$ for $B(D_s^+ \to \phi\pi^+) = 0.027$. We rescale to our best value $B(D_s^+ \to \phi\pi^+) = 0.036$.

$\Gamma(D_s^{*-}\pi^+K^*(892)^+)/\Gamma_{total}$ Γ_{98}/Γ

VALUE	CL%	DOCUMENT ID		TECN	COMMENT
<0.008	90	[157] ALBRECHT	93E	ARG	$e^+e^- \to \Upsilon(4S)$

[157] ALBRECHT 93E reports $< 1.1 \times 10^{-2}$ for $B(D_s^+ \to \phi\pi^+) = 0.027$. We rescale to our best value $B(D_s^+ \to \phi\pi^+) = 0.036$.

$\Gamma(\eta_c K^+)/\Gamma_{total}$ Γ_{99}/Γ

VALUE (units 10^{-3})	DOCUMENT ID		TECN	COMMENT
0.90±0.27 OUR AVERAGE				
$1.25 \pm 0.14^{+0.39}_{-0.40}$	[158] FANG	03	BELL	$e^+e^- \to \Upsilon(4S)$
$0.69^{+0.26}_{-0.21} \pm 0.22$	[159] EDWARDS	01	CLE2	$e^+e^- \to \Upsilon(4S)$

[158] Assumes equal production of B^+ and B^0 at the $\Upsilon(4S)$.

[159] EDWARDS 01 assumes equal production of B^0 and B^+ at the $\Upsilon(4S)$. The correlated uncertainties (28.3)% from $B(J/\psi(1S) \to \gamma\eta_c)$ in those modes have been accounted for.

$\Gamma(J/\psi(1S)K^+)/\Gamma_{total}$ Γ_{100}/Γ

VALUE (units 10^{-4})	EVTS	DOCUMENT ID		TECN	COMMENT
10.0± 0.4 OUR FIT					
10.1± 0.4 OUR AVERAGE					
10.1± 0.2±0.7		[160] ABE	03B	BELL	$e^+e^- \to \Upsilon(4S)$
10.1± 0.3±0.5		[160] AUBERT	02	BABR	$e^+e^- \to \Upsilon(4S)$
10.2± 0.8±0.7		[160] JESSOP	97	CLE2	$e^+e^- \to \Upsilon(4S)$
9.3± 3.1±0.2		[161] BORTOLETTO	92	CLEO	$e^+e^- \to \Upsilon(4S)$
8.1± 3.5±0.1	6	[162] ALBRECHT	90J	ARG	$e^+e^- \to \Upsilon(4S)$

• • • We do not use the following data for averages, fits, limits, etc. • • •

11.0± 1.5±0.9	59	[160] ALAM	94	CLE2	Repl. by JESSOP 97
22 ±10 ±2		BUSKULIC	92G	ALEP	$e^+e^- \to Z$
7 ± 4	3	[163] ALBRECHT	87D	ARG	$e^+e^- \to \Upsilon(4S)$
10 ± 7 ±2	3	[164] BEBEK	87	CLEO	$e^+e^- \to \Upsilon(4S)$
9 ± 5	3	[165] ALAM	86	CLEO	$e^+e^- \to \Upsilon(4S)$

[160] Assumes equal production of B^+ and B^0 at the $\Upsilon(4S)$.

[161] BORTOLETTO 92 reports $8 \pm 2 \pm 2$ for $B(J/\psi(1S) \to e^+e^-) = 0.069 \pm 0.009$. We rescale to our best value $B(J/\psi(1S) \to e^+e^-) = (5.93 \pm 0.10) \times 10^{-2}$. Our first error is their experiment's error and our second error is the systematic error from using our best value. Assumes equal production of B^+ and B^0 at the $\Upsilon(4S)$.

[162] ALBRECHT 90J reports $7 \pm 3 \pm 1$ for $B(J/\psi(1S) \to e^+e^-) = 0.069 \pm 0.009$. We rescale to our best value $B(J/\psi(1S) \to e^+e^-) = (5.93 \pm 0.10) \times 10^{-2}$. Our first error is their experiment's error and our second error is the systematic error from using our best value. Assumes equal production of B^+ and B^0 at the $\Upsilon(4S)$.

[163] ALBRECHT 87D assume $B^+B^-/B^0\overline{B}^0$ ratio is 55/45. Superseded by ALBRECHT 90J.

[164] BEBEK 87 value has been updated in BERKELMAN 91 to use same assumptions as noted for BORTOLETTO 92.

[165] ALAM 86 assumes $B^{\pm}/B^0$ ratio is 60/40.

$\Gamma(J/\psi(1S)K^+\pi^+\pi^-)/\Gamma_{total}$ Γ_{101}/Γ

VALUE (units 10^{-3})	CL%	EVTS	DOCUMENT ID		TECN	COMMENT
0.77±0.20 OUR AVERAGE						
$0.69 \pm 0.18 \pm 0.12$			[166] ACOSTA	02F	CDF	$p\overline{p}$ 1.8 TeV
$1.40 \pm 0.82 \pm 0.02$			[167] BORTOLETTO	92	CLEO	$e^+e^- \to \Upsilon(4S)$
$1.40 \pm 0.91 \pm 0.02$		6	[168] ALBRECHT	87D	ARG	$e^+e^- \to \Upsilon(4S)$

• • • We do not use the following data for averages, fits, limits, etc. • • •

<1.9	90		[169] ALBRECHT	90J	ARG	$e^+e^- \to \Upsilon(4S)$

[166] ACOSTA 02F uses as reference of $B(B \to J/\psi(1S)K^+) = (10.1 \pm 0.6) \times 10^{-4}$. The second error includes the systematic error and the uncertainties of the branching ratio.

[167] BORTOLETTO 92 reports $1.2 \pm 0.6 \pm 0.4$ for $B(J/\psi(1S) \to e^+e^-) = 0.069 \pm 0.009$. We rescale to our best value $B(J/\psi(1S) \to e^+e^-) = (5.93 \pm 0.10) \times 10^{-2}$. Our first error is their experiment's error and our second error is the systematic error from using our best value. Assumes equal production of B^+ and B^0 at the $\Upsilon(4S)$.

[168] ALBRECHT 87D reports 1.2 ± 0.8 for $B(J/\psi(1S) \to e^+e^-) = 0.069 \pm 0.009$. We rescale to our best value $B(J/\psi(1S) \to e^+e^-) = (5.93 \pm 0.10) \times 10^{-2}$. Our first error is their experiment's error and our second error is the systematic error from using our best value. They actually report 0.0011 ± 0.0007 assuming $B^+B^-/B^0\overline{B}^0$ ratio is 55/45. We rescale to 50/50. Analysis explicitly removes $B^+ \to \psi(2S)K^+$.

[169] ALBRECHT 90J reports < 1.6 for $B(J/\psi(1S) \to e^+e^-) = 0.069$. We rescale to our best value $B(J/\psi(1S) \to e^+e^-) = 0.0593$. Assumes equal production of B^+ and B^0 at the $\Upsilon(4S)$.

$\Gamma(X(3872)K^+)/\Gamma_{total}$ Γ_{102}/Γ

VALUE	DOCUMENT ID		TECN	COMMENT
seen	[170] CHOI	03	BELL	$e^+e^- \to \Upsilon(4S)$

[170] CHOI 03 reports $B(B^+ \to X(3872)K^+) \times B(X(3872) \to \pi^+\pi^- J/\psi(1S))/B(B^+ \to \psi(2S)K^+) \times B(\psi(2S) \to \pi^+\pi^0 J/\psi(1S)) = 0.063 \pm 0.012(\text{stat}) \pm 0.007(\text{syst})$ where the $X(3872)$ is a new meson state with a mass $3872.0 \pm 0.6 \pm 0.5$ MeV and a full width < 2.3 MeV at 90%CL.

$\Gamma(J/\psi(1S)K^*(892)^+)/\Gamma_{total}$ Γ_{103}/Γ

For polarization information see the Listings at the end of the "B^0 Branching Ratios" section.

VALUE (units 10^{-3})	EVTS	DOCUMENT ID		TECN	COMMENT
1.35 ± 0.10 OUR AVERAGE					
$1.28 \pm 0.07 \pm 0.14$		[171] ABE	02N	BELL	$e^+e^- \to \Upsilon(4S)$
$1.37 \pm 0.09 \pm 0.11$		[171] AUBERT	02	BABR	$e^+e^- \to \Upsilon(4S)$
$1.41 \pm 0.23 \pm 0.24$		[171] JESSOP	97	CLE2	$e^+e^- \to \Upsilon(4S)$
$1.58 \pm 0.47 \pm 0.27$		[172] ABE	96H	CDF	$p\overline{p}$ at 1.8 TeV
$1.51 \pm 1.09 \pm 0.02$		[173] BORTOLETTO	92	CLEO	$e^+e^- \to \Upsilon(4S)$
$1.86 \pm 1.30 \pm 0.03$	2	[174] ALBRECHT	90J	ARG	$e^+e^- \to \Upsilon(4S)$
• • • We do not use the following data for averages, fits, limits, etc. • • •					
$1.78 \pm 0.51 \pm 0.23$	13	[171] ALAM	94	CLE2	Sup. by JESSOP 97

[171] Assumes equal production of B^+ and B^0 at the $\Upsilon(4S)$.

[172] ABE 96H assumes that $B(B^+ \to J/\psi K^+) = (1.02 \pm 0.14) \times 10^{-3}$.

[173] BORTOLETTO 92 reports $1.3 \pm 0.9 \pm 0.3$ for $B(J/\psi(1S) \to e^+e^-) = 0.069 \pm 0.009$. We rescale to our best value $B(J/\psi(1S) \to e^+e^-) = (5.93 \pm 0.10) \times 10^{-2}$. Our first error is their experiment's error and our second error is the systematic error from using our best value. Assumes equal production of B^+ and B^0 at the $\Upsilon(4S)$.

[174] ALBRECHT 90J reports $1.6 \pm 1.1 \pm 0.3$ for $B(J/\psi(1S) \to e^+e^-) = 0.069 \pm 0.009$. We rescale to our best value $B(J/\psi(1S) \to e^+e^-) = (5.93 \pm 0.10) \times 10^{-2}$. Our first error is their experiment's error and our second error is the systematic error from using our best value. Assumes equal production of B^+ and B^0 at the $\Upsilon(4S)$.

$\Gamma(J/\psi(1S)K^*(892)^+)/\Gamma(J/\psi(1S)K^+)$ $\Gamma_{103}/\Gamma_{100}$

VALUE	DOCUMENT ID		TECN	COMMENT
1.40 ± 0.11 OUR AVERAGE				
$1.37 \pm 0.10 \pm 0.08$	[175] AUBERT	02	BABR	$e^+e^- \to \Upsilon(4S)$
$1.45 \pm 0.20 \pm 0.17$	[176] JESSOP	97	CLE2	$e^+e^- \to \Upsilon(4S)$
$1.92 \pm 0.60 \pm 0.17$	ABE	96Q	CDF	$p\overline{p}$

[175] Assumes equal production of B^+ and B^0 at the $\Upsilon(4S)$.

[176] JESSOP 97 assumes equal production of B^+ and B^0 at the $\Upsilon(4S)$. The measurement is actually measured as an average over kaon charged and neutral states.

$\Gamma(J/\psi(1S)K(1270)^+)/\Gamma_{total}$ Γ_{104}/Γ

VALUE (units 10^{-3})	DOCUMENT ID		TECN	COMMENT
1.80 ± 0.34 ± 0.39	[177] ABE	01L	BELL	$e^+e^- \to \Upsilon(4S)$

[177] Uses the PDG value of $B(B^+ \to J/\psi(1S)K^+) = (1.00 \pm 0.10) \times 10^{-3}$.

$\Gamma(J/\psi(1S)K(1400)^+)/\Gamma(J/\psi(1S)K(1270)^+)$ $\Gamma_{105}/\Gamma_{104}$

VALUE	CL%	DOCUMENT ID		TECN	COMMENT
< 0.30	90	ABE	01L	BELL	$e^+e^- \to \Upsilon(4S)$

$\Gamma(J/\psi(1S)\phi K^+)/\Gamma_{total}$ Γ_{106}/Γ

VALUE	DOCUMENT ID		TECN	COMMENT
(5.2 ± 1.7) × 10^{-5} OUR AVERAGE Error includes scale factor of 1.2.				
$(4.4 \pm 1.4 \pm 0.5) \times 10^{-5}$	[178] AUBERT	03O	BABR	$e^+e^- \to \Upsilon(4S)$
$(8.8^{+3.5}_{-3.0} \pm 1.3) \times 10^{-5}$	[179] ANASTASSOV	00	CLE2	$e^+e^- \to \Upsilon(4S)$

[178] Assumes equal production of B^+ and B^0 at the $\Upsilon(4S)$.

[179] ANASTASSOV 00 finds 10 events on a background of 0.5 ± 0.2. Assumes equal production of B^0 and B^+ at the $\Upsilon(4S)$, a uniform Dalitz plot distribution, isotropic $J/\psi(1S)$ and ϕ decays, and $B(B^+ \to J/\psi(1S)\phi K^+) = B(B^0 \to J/\psi(1S)\phi K^0)$.

$\Gamma(J/\psi(1S)\pi^+)/\Gamma_{total}$ Γ_{107}/Γ

VALUE	DOCUMENT ID		TECN	COMMENT
(4.0 ± 0.5) × 10^{-5} OUR FIT				
$(3.8 \pm 0.6 \pm 0.3) \times 10^{-5}$	[180] ABE	03B	BELL	$e^+e^- \to \Upsilon(4S)$

[180] Assumes equal production of B^+ and B^0 at the $\Upsilon(4S)$.

$\Gamma(J/\psi(1S)\pi^+)/\Gamma(J/\psi(1S)K^+)$ $\Gamma_{107}/\Gamma_{100}$

VALUE	EVTS	DOCUMENT ID		TECN	COMMENT
0.040 ± 0.005 OUR FIT					
0.042 ± 0.007 OUR AVERAGE					
$0.0391 \pm 0.0078 \pm 0.0019$		AUBERT	02F	BABR	$e^+e^- \to \Upsilon(4S)$
$0.05 \quad {}^{+0.019}_{-0.017} \pm 0.001$		ABE	96R	CDF	$p\overline{p}$ 1.8 TeV
0.052 ± 0.024		BISHAI	96	CLE2	$e^+e^- \to \Upsilon(4S)$
• • • We do not use the following data for averages, fits, limits, etc. • • •					
0.043 ± 0.023	5	[181] ALEXANDER	95	CLE2	Sup. by BISHAI 96

[181] Assumes equal production of B^+B^- and $B^0\overline{B}^0$ on $\Upsilon(4S)$.

$\Gamma(J/\psi(1S)\rho^+)/\Gamma_{total}$ Γ_{108}/Γ

VALUE	CL%	DOCUMENT ID		TECN	COMMENT
$< 7.7 \times 10^{-4}$	90	BISHAI	96	CLE2	$e^+e^- \to \Upsilon(4S)$

$\Gamma(J/\psi(1S)a_1(1260)^+)/\Gamma_{total}$ Γ_{109}/Γ

VALUE	CL%	DOCUMENT ID		TECN	COMMENT
$< 1.2 \times 10^{-3}$	90	BISHAI	96	CLE2	$e^+e^- \to \Upsilon(4S)$

$\Gamma(J/\psi(1S)p\overline{p})/\Gamma_{total}$ Γ_{110}/Γ

VALUE	CL%	DOCUMENT ID		TECN	COMMENT
$(12 \ {}^{+9}_{-6}) \times 10^{-6}$		[182] AUBERT	03K	BABR	$e^+e^- \to \Upsilon(4S)$
• • • We do not use the following data for averages, fits, limits, etc. • • •					
$< 4.1 \times 10^{-5}$	90	ZANG	04	BELL	$e^+e^- \to \Upsilon(4S)$

[182] Assumes equal production of B^+ and B^0 at the $\Upsilon(4S)$.

$\Gamma(\psi(2S)K^+)/\Gamma_{total}$ Γ_{111}/Γ

VALUE (units 10^{-4})	CL%	EVTS	DOCUMENT ID		TECN	COMMENT
6.8 ± 0.4 OUR AVERAGE						
6.9 ± 0.6			[183] ABE	03B	BELL	$e^+e^- \to \Upsilon(4S)$
$6.4 \pm 0.5 \pm 0.8$			[183] AUBERT	02	BABR	$e^+e^- \to \Upsilon(4S)$
$7.8 \pm 0.7 \pm 0.9$			[183] RICHICHI	01	CLE2	$e^+e^- \to \Upsilon(4S)$
$5.5 \pm 1.0 \pm 0.6$			[184] ABE	98O	CDF	$p\overline{p}$ 1.8 TeV
$18 \pm 8 \pm 4$		5	[183] ALBRECHT	90J	ARG	$e^+e^- \to \Upsilon(4S)$
• • • We do not use the following data for averages, fits, limits, etc. • • •						
$6.1 \pm 2.3 \pm 0.9$		7	[183] ALAM	94	CLE2	Repl. by RICHICHI 01
< 5	90		[183] BORTOLETTO	92	CLEO	$e^+e^- \to \Upsilon(4S)$
22 ± 17		3	[185] ALBRECHT	87D	ARG	$e^+e^- \to \Upsilon(4S)$

[183] Assumes equal production of B^+ and B^0 at the $\Upsilon(4S)$.

[184] ABE 98O reports $[B(B^+ \to \psi(2S)K^+)]/[B(B^+ \to J/\psi(1S)K^+)] = 0.558 \pm 0.082 \pm 0.056$. We multiply by our best value $B(B^+ \to J/\psi(1S)K^+) = (9.9 \pm 1.0) \times 10^{-4}$. Our first error is their experiment's error and our second error is the systematic error from using our best value.

[185] ALBRECHT 87D assume $B^+B^-/B^0\overline{B}^0$ ratio is 55/45. Superseded by ALBRECHT 90J.

$\Gamma(\psi(2S)K^+)/\Gamma(J/\psi(1S)K^+)$ $\Gamma_{111}/\Gamma_{100}$

VALUE	DOCUMENT ID		TECN	COMMENT
0.64 ± 0.06 ± 0.07	[186] AUBERT	02	BABR	$e^+e^- \to \Upsilon(4S)$

[186] Assumes equal production of B^+ and B^0 at the $\Upsilon(4S)$.

$\Gamma(\psi(2S)K^*(892)^+)/\Gamma_{total}$ Γ_{112}/Γ

VALUE (units 10^{-4})	CL%	DOCUMENT ID		TECN	COMMENT
9.2 ± 1.9 ± 1.2		[187] RICHICHI	01	CLE2	$e^+e^- \to \Upsilon(4S)$
• • • We do not use the following data for averages, fits, limits, etc. • • •					
< 30	90	[187] ALAM	94	CLE2	Repl. by RICHICHI 01
< 35	90	[187] BORTOLETTO	92	CLEO	$e^+e^- \to \Upsilon(4S)$
< 49	90	[187] ALBRECHT	90J	ARG	$e^+e^- \to \Upsilon(4S)$

[187] Assumes equal production of B^+ and B^0 at the $\Upsilon(4S)$.

$\Gamma(\psi(2S)K^+\pi^+\pi^-)/\Gamma_{total}$ Γ_{113}/Γ

VALUE	EVTS	DOCUMENT ID		TECN	COMMENT
0.0019 ± 0.0011 ± 0.0004	3	[188] ALBRECHT	90J	ARG	$e^+e^- \to \Upsilon(4S)$

[188] Assumes equal production of B^+ and B^0 at the $\Upsilon(4S)$.

$\Gamma(\chi_{c0}(1P)K^+)/\Gamma_{total}$ Γ_{114}/Γ

VALUE (units 10^{-4})	CL%	DOCUMENT ID		TECN	COMMENT
$6.0^{+2.1}_{-1.8} \pm 1.1$		[189] ABE	02B	BELL	$e^+e^- \to \Upsilon(4S)$
• • • We do not use the following data for averages, fits, limits, etc. • • •					
< 4.8	90	[190] EDWARDS	01	CLE2	$e^+e^- \to \Upsilon(4S)$

[189] ABE 02B measures the ratio of $B(B^+ \to \chi_c^0 K^+)/B(B^+ \to J/\psi(1S)K^+) = 0.60 + 0.21 - 0.18 \pm 0.05 \pm 0.08$, where the third error is due to the uncertainty in the $B(\chi_c^0 \to \pi^+\pi^-)$, and uses $B(B^+ \to J/\psi(1S)K^+) = (10.0 \pm 1.0) \times 10^{-4}$ to obtain the result.

[190] EDWARDS 01 assumes equal production of B^0 and B^+ at the $\Upsilon(4S)$. The correlated uncertainties (28.3)% from $B(J/\psi(1S) \to \gamma\eta_c)$ in those modes have been accounted for.

$\Gamma(\chi_{c1}(1P)K^+)/\Gamma_{total}$ Γ_{115}/Γ

VALUE (units 10^{-4})	EVTS	DOCUMENT ID		TECN	COMMENT
6.8± 1.2 OUR AVERAGE					
15.5± 5.4± 2.0		[191] ACOSTA	02F	CDF	$p\overline{p}$ 1.8 TeV
6.5± 1.0± 0.7		[192] AUBERT	02	BABR	$e^+e^- \to \Upsilon(4S)$
• • • We do not use the following data for averages, fits, limits, etc. • • •					
9.7± 4.0± 0.9	6	[193] ALAM	94	CLE2	$e^+e^- \to \Upsilon(4S)$
19 ±13 ±6		[194] ALBRECHT	92E	ARG	$e^+e^- \to \Upsilon(4S)$

[191] ACOSTA 02F uses as reference of $B(B \to J/\psi(1S)K^+) = (10.1 \pm 0.6) \times 10^{-4}$. The second error includes the systematic error and the uncertainties of the branching ratio.

[192] AUBERT 02 reports $7.5 \pm 0.9 \pm 0.8$ for $B(\chi_{c1}(1P) \to \gamma J/\psi(1S)) = 0.273 \pm 0.016$. We rescale to our best value $B(\chi_{c1}(1P) \to \gamma J/\psi(1S)) = (31.6 \pm 3.3) \times 10^{-2}$. Our first error is their experiment's error and our second error is the systematic error from using our best value. Assumes equal production of B^+ and B^0 at the $\Upsilon(4S)$.

[193] Assumes equal production of B^+ and B^0 at the $\Upsilon(4S)$.

[194] ALBRECHT 92E assumes no $\chi_{c2}(1P)$ production and $B(\Upsilon(4S) \to B^+B^-) = 50\%$.

$\Gamma(\chi_{c1}(1P)K^+)/\Gamma(J/\psi(1S)K^+)$ $\Gamma_{115}/\Gamma_{100}$

VALUE	DOCUMENT ID		TECN	COMMENT
0.65±0.07±0.07	[195] AUBERT	02	BABR	$e^+e^- \to \Upsilon(4S)$

[195] AUBERT 02 reports $0.75 \pm 0.08 \pm 0.05$ for $B(\chi_{c1}(1P) \to \gamma J/\psi(1S)) = 0.273 \pm 0.016$. We rescale to our best value $B(\chi_{c1}(1P) \to \gamma J/\psi(1S)) = (31.6 \pm 3.3) \times 10^{-2}$. Our first error is their experiment's error and our second error is the systematic error from using our best value. Assumes equal production of B^+ and B^0 at the $\Upsilon(4S)$.

$\Gamma(\chi_{c1}(1P)K^*(892)^+)/\Gamma_{total}$ Γ_{116}/Γ

VALUE	CL%	DOCUMENT ID		TECN	COMMENT
<0.0021	90	[196] ALAM	94	CLE2	$e^+e^- \to \Upsilon(4S)$

[196] Assumes equal production of B^+ and B^0 at the $\Upsilon(4S)$.

$\Gamma(K^0\pi^+)/\Gamma_{total}$ Γ_{117}/Γ

VALUE (units 10^{-5})	CL%	DOCUMENT ID		TECN	COMMENT
1.88±0.21 OUR AVERAGE					
$1.88^{+0.37}_{-0.33}{}^{+0.21}_{-0.18}$		[197] BORNHEIM	03	CLE2	$e^+e^- \to \Upsilon(4S)$
$1.94^{+0.31}_{-0.30} \pm 0.16$		[197] CASEY	02	BELL	$e^+e^- \to \Upsilon(4S)$
$1.82^{+0.33}_{-0.30} \pm 0.20$		[197] AUBERT	01E	BABR	$e^+e^- \to \Upsilon(4S)$
• • • We do not use the following data for averages, fits, limits, etc. • • •					
$1.37^{+0.57}_{-0.48}{}^{+0.19}_{-0.18}$		[197] ABE	01H	BELL	Repl. by CASEY 02
$1.82^{+0.46}_{-0.40} \pm 0.16$		[197] CRONIN-HEN..	00	CLE2	Repl. by BORNHEIM 03
$2.3^{+1.1}_{-1.0} \pm 0.36$		GODANG	98	CLE2	Repl. by CRONIN-HENNESSY 00
< 4.8	90	ASNER	96	CLE2	Repl. by GODANG 98
<19	90	ALBRECHT	91B	ARG	$e^+e^- \to \Upsilon(4S)$
<10	90	[198] AVERY	89B	CLEO	$e^+e^- \to \Upsilon(4S)$
<68	90	AVERY	87	CLEO	$e^+e^- \to \Upsilon(4S)$

[197] Assumes equal production of B^+ and B^0 at the $\Upsilon(4S)$.

[198] AVERY 89B reports $< 9 \times 10^{-5}$ assuming the $\Upsilon(4S)$ decays 43% to $B^0\overline{B}{}^0$. We rescale to 50%.

$\Gamma(K^+\pi^0)/\Gamma_{total}$ Γ_{118}/Γ

VALUE (units 10^{-5})	CL%	DOCUMENT ID		TECN	COMMENT
1.29±0.12 OUR AVERAGE					
$1.28^{+0.12}_{-0.11} \pm 0.10$		[199] AUBERT	03L	BABR	$e^+e^- \to \Upsilon(4S)$
$1.29^{+0.24}_{-0.22}{}^{+0.12}_{-0.11}$		[199] BORNHEIM	03	CLE2	$e^+e^- \to \Upsilon(4S)$
$1.3^{+0.25}_{-0.24} \pm 0.13$		[199] CASEY	02	BELL	$e^+e^- \to \Upsilon(4S)$
• • • We do not use the following data for averages, fits, limits, etc. • • •					
$1.63^{+0.35}_{-0.33}{}^{+0.16}_{-0.18}$		[199] ABE	01H	BELL	Repl. by CASEY 02
$1.08^{+0.21}_{-0.19} \pm 0.10$		[199] AUBERT	01E	BABR	Repl. by AUBERT 03L
$1.16^{+0.30}_{-0.27}{}^{+0.14}_{-0.13}$		[199] CRONIN-HEN..	00	CLE2	Repl. by BORNHEIM 03
<1.6	90	GODANG	98	CLE2	Repl. by CRONIN-HENNESSY 00
<1.4	90	ASNER	96	CLE2	Repl. by GODANG 98

[199] Assumes equal production of B^+ and B^0 at the $\Upsilon(4S)$.

$\Gamma(K^+\pi^0)/\Gamma(K^0\pi^+)$ $\Gamma_{118}/\Gamma_{117}$

VALUE	DOCUMENT ID		TECN	COMMENT
$\mathbf{2.38^{+0.98}_{-1.10}{}^{+0.39}_{-0.26}}$	[200] ABE	01H	BELL	$e^+e^- \to \Upsilon(4S)$

[200] Assumes equal production of B^+ and B^0 at the $\Upsilon(4S)$.

$\Gamma(\eta' K^+)/\Gamma_{total}$ Γ_{119}/Γ

VALUE (units 10^{-5})	DOCUMENT ID		TECN	COMMENT
7.8 ±0.5 OUR AVERAGE				
7.69±0.35±0.44	[201] AUBERT	03W	BABR	$e^+e^- \to \Upsilon(4S)$
$7.9^{+1.2}_{-1.1} \pm 0.9$	[201] ABE	01M	BELL	$e^+e^- \to \Upsilon(4S)$
$8.0^{+1.0}_{-0.9} \pm 0.7$	[201] RICHICHI	00	CLE2	$e^+e^- \to \Upsilon(4S)$
• • • We do not use the following data for averages, fits, limits, etc. • • •				
7.0 ±0.8 ±0.5	[201] AUBERT	01G	BABR	Repl. by AUBERT 03W
$6.5^{+1.5}_{-1.4} \pm 0.9$	BEHRENS	98	CLE2	Repl. by RICHICHI 00

[201] Assumes equal production of B^+ and B^0 at the $\Upsilon(4S)$.

$\Gamma(\eta' K^*(892)^+)/\Gamma_{total}$ Γ_{120}/Γ

VALUE	CL%	DOCUMENT ID		TECN	COMMENT
$\mathbf{<3.5 \times 10^{-5}}$	90	[202] RICHICHI	00	CLE2	$e^+e^- \to \Upsilon(4S)$
• • • We do not use the following data for averages, fits, limits, etc. • • •					
$<1.3 \times 10^{-4}$	90	BEHRENS	98	CLE2	Repl. by RICHICHI 00

[202] Assumes equal production of B^+ and B^0 at the $\Upsilon(4S)$.

$\Gamma(\eta K^+)/\Gamma_{total}$ Γ_{121}/Γ

VALUE	CL%	DOCUMENT ID		TECN	COMMENT
$\mathbf{<6.9 \times 10^{-6}}$	90	[203] RICHICHI	00	CLE2	$e^+e^- \to \Upsilon(4S)$
• • • We do not use the following data for averages, fits, limits, etc. • • •					
$<1.4 \times 10^{-5}$	90	BEHRENS	98	CLE2	Repl. by RICHICHI 00

[203] Assumes equal production of B^+ and B^0 at the $\Upsilon(4S)$.

$\Gamma(\eta K^*(892)^+)/\Gamma_{total}$ Γ_{122}/Γ

VALUE (units 10^{-5})	CL%	DOCUMENT ID		TECN	COMMENT
$\mathbf{2.64^{+0.96}_{-0.82} \pm 0.33}$		[204] RICHICHI	00	CLE2	$e^+e^- \to \Upsilon(4S)$
• • • We do not use the following data for averages, fits, limits, etc. • • •					
<3.0	90	BEHRENS	98	CLE2	Repl. by RICHICHI 00

[204] Assumes equal production of B^+ and B^0 at the $\Upsilon(4S)$.

$\Gamma(\omega K^+)/\Gamma_{total}$ Γ_{123}/Γ

VALUE (units 10^{-5})	CL%	DOCUMENT ID		TECN	COMMENT
$\mathbf{0.92^{+0.26}_{-0.23} \pm 0.10}$		[205] LU	02	BELL	$e^+e^- \to \Upsilon(4S)$
• • • We do not use the following data for averages, fits, limits, etc. • • •					
<0.4	90	[205] AUBERT	01G	BABR	$e^+e^- \to \Upsilon(4S)$
<0.79	90	[205] JESSOP	00	CLE2	$e^+e^- \to \Upsilon(4S)$
$1.5^{+0.7}_{-0.6} \pm 0.2$		[205] BERGFELD	98	CLE2	Repl. by JESSOP 00

[205] Assumes equal production of B^+ and B^0 at the $\Upsilon(4S)$.

$\Gamma(\omega K^*(892)^+)/\Gamma_{total}$ Γ_{124}/Γ

VALUE	CL%	DOCUMENT ID		TECN
$\mathbf{<8.7 \times 10^{-5}}$	90	[206] BERGFELD	98	CLE2

[206] Assumes equal production of B^+ and B^0 at the $\Upsilon(4S)$.

$\Gamma(K^*(892)^0\pi^+)/\Gamma_{total}$ Γ_{125}/Γ

VALUE (units 10^{-5})	CL%	DOCUMENT ID		TECN	COMMENT
$\mathbf{1.94^{+0.42}_{-0.39}{}^{+0.41}_{-0.71}}$		[207] GARMASH	02	BELL	$e^+e^- \to \Upsilon(4S)$
• • • We do not use the following data for averages, fits, limits, etc. • • •					
<11.9	90	[208] ABE	00C	SLD	$e^+e^- \to Z$
< 1.6	90	[209] JESSOP	00	CLE2	$e^+e^- \to \Upsilon(4S)$
<39	90	[210] ADAM	96D	DLPH	$e^+e^- \to Z$
< 4.1	90	ASNER	96	CLE2	Repl. by JESSOP 00
<48	90	[211] ABREU	95N	DLPH	Sup. by ADAM 96D
<17	90	ALBRECHT	91B	ARG	$e^+e^- \to \Upsilon(4S)$
<15	90	[212] AVERY	89B	CLEO	$e^+e^- \to \Upsilon(4S)$
<26	90	AVERY	87	CLEO	$e^+e^- \to \Upsilon(4S)$

[207] Uses a reference decay mode $B^+ \to \overline{D}{}^0\pi^+$ and $\overline{D}{}^0 \to K^+\pi^-$ with $B(B^+ \to \overline{D}{}^0\pi^+) \cdot B(\overline{D}{}^0 \to K^+\pi^-) = (20.3 \pm 2.0) \times 10^{-5}$.

[208] ABE 00C assumes $B(Z \to b\overline{b}) = (21.7 \pm 0.1)\%$ and the B fractions $f_{B^0} = f_{B^+} = (39.7^{+1.8}_{-2.2})\%$ and $f_{B_s} = (10.5^{+1.8}_{-2.2})\%$.

[209] Assumes equal production of B^+ and B^0 at the $\Upsilon(4S)$.

[210] ADAM 96D assumes $f_{B^0} = f_{B^-} = 0.39$ and $f_{B_s} = 0.12$.

[211] Assumes a B^0, B^- production fraction of 0.39 and a B_s production fraction of 0.12.

[212] AVERY 89B reports $< 1.3 \times 10^{-4}$ assuming the $\Upsilon(4S)$ decays 43% to $B^0\overline{B}{}^0$. We rescale to 50%.

$\Gamma(K^*(892)^+\pi^0)/\Gamma_{total}$ Γ_{126}/Γ

VALUE	CL%	DOCUMENT ID		TECN	COMMENT
$\mathbf{<3.1 \times 10^{-5}}$	90	[213] JESSOP	00	CLE2	$e^+e^- \to \Upsilon(4S)$
• • • We do not use the following data for averages, fits, limits, etc. • • •					
$<9.9 \times 10^{-5}$	90	ASNER	96	CLE2	Repl. by JESSOP 00

[213] Assumes equal production of B^+ and B^0 at the $\Upsilon(4S)$.

$\Gamma(K^+\pi^-\pi^+)/\Gamma_{total}$ Γ_{127}/Γ

VALUE	DOCUMENT ID	TECN	COMMENT
(5.7 ±0.4) × 10⁻⁵ OUR AVERAGE			
(5.36 ± 0.31 ± 0.51) × 10⁻⁵	[214] GARMASH 04	BELL	$e^+e^- \to \Upsilon(4S)$
(5.91 ± 0.38 ± 0.32) × 10⁻⁵	[215] AUBERT 03M	BABR	$e^+e^- \to \Upsilon(4S)$
• • • We do not use the following data for averages, fits, limits, etc. • • •			
(5.56 ± 0.58 ± 0.77) × 10⁻⁵	[216] GARMASH 02	BELL	Repl. by GARMASH 04

[214] Assumes equal production of B^+ and B^0 at the $\Upsilon(4S)$.

[215] Assumes equal production of B^0 and B^+ at the $\Upsilon(4S)$; charm and charmonium contributions are subtracted, otherwise no assumptions about intermediate resonances.

[216] Uses a reference decay mode $B^+ \to \overline{D}{}^0\pi^+$ and $\overline{D}{}^0 \to K^+\pi^-$ with $B(B^+ \to \overline{D}{}^0\pi^+)\cdot B(\overline{D}{}^0 \to K^+\pi^-) = (20.3 \pm 2.0) \times 10^{-5}$.

$\Gamma(K^+\pi^-\pi^+ \text{nonresonant})/\Gamma_{total}$ Γ_{128}/Γ

VALUE (units 10⁻⁵)	CL%	DOCUMENT ID	TECN	COMMENT
< 2.8	90	BERGFELD 96B	CLE2	$e^+e^- \to \Upsilon(4S)$
• • • We do not use the following data for averages, fits, limits, etc. • • •				
< 33	90	[217] ADAM 96D	DLPH	$e^+e^- \to Z$
< 40	90	[218] ABREU 95N	DLPH	Sup. by ADAM 96D
< 33	90	ALBRECHT 91E	ARG	$e^+e^- \to \Upsilon(4S)$
< 19	90	[219] AVERY 89B	CLEO	$e^+e^- \to \Upsilon(4S)$

[217] ADAM 96D assumes $f_{B^0} = f_{B^-} = 0.39$ and $f_{B_s} = 0.12$.

[218] Assumes a B^0, B^- production fraction of 0.39 and a B_s production fraction of 0.12.

[219] AVERY 89B reports < 1.7 × 10⁻⁴ assuming the $\Upsilon(4S)$ decays 43% to $B^0\overline{B}{}^0$. We rescale to 50%.

$\Gamma(K^+ f_0(980))/\Gamma_{total}$ Γ_{129}/Γ

VALUE (units 10⁻⁶)	CL%	DOCUMENT ID	TECN	COMMENT
seen		[220] GARMASH 02	BELL	$e^+e^- \to \Upsilon(4S)$
• • • We do not use the following data for averages, fits, limits, etc. • • •				
< 80	90	[221] AVERY 89B	CLEO	$e^+e^- \to \Upsilon(4S)$

[220] Uses a reference decay mode $B^+ \to \overline{D}{}^0\pi^+$ and $\overline{D}{}^0 \to K^+\pi^-$ with $B(B^+ \to \overline{D}{}^0\pi^+)\cdot B(\overline{D}{}^0 \to K^+\pi^-) = (20.3 \pm 2.0) \times 10^{-5}$ and reports $B(B^+ \to K^+ f_0(980)) \cdot B(f_0(980) \to \pi\pi) = (9.6^{+2.5}_{-2.3}{}^{+3.7}_{-1.7}) \times 10^{-6}$. Only charged pions from the $f_0(980)$ are used.

[221] AVERY 89B reports < 7 × 10⁻⁵ assuming the $\Upsilon(4S)$ decays 43% to $B^0\overline{B}{}^0$. We rescale to 50%.

$\Gamma(K^+\rho^0)/\Gamma_{total}$ Γ_{130}/Γ

VALUE	CL%	DOCUMENT ID	TECN	COMMENT
< 1.2 × 10⁻⁵	90	[222] GARMASH 02	BELL	$e^+e^- \to \Upsilon(4S)$
• • • We do not use the following data for averages, fits, limits, etc. • • •				
< 8.6 × 10⁻⁵	90	[223] ABE 00C	SLD	$e^+e^- \to Z$
< 1.7 × 10⁻⁵	90	[224] JESSOP 00	CLE2	$e^+e^- \to \Upsilon(4S)$
< 1.2 × 10⁻⁴	90	[225] ADAM 96D	DLPH	$e^+e^- \to Z$
< 1.9 × 10⁻⁵	90	ASNER 96	CLE2	Repl. by JESSOP 00
< 1.9 × 10⁻⁴	90	[226] ABREU 95N	DLPH	Sup. by ADAM 96D
< 1.8 × 10⁻⁴	90	ALBRECHT 91B	ARG	$e^+e^- \to \Upsilon(4S)$
< 8 × 10⁻⁵	90	[227] AVERY 89B	CLEO	$e^+e^- \to \Upsilon(4S)$
< 2.6 × 10⁻⁴	90	AVERY 87	CLEO	$e^+e^- \to \Upsilon(4S)$

[222] Uses a reference decay mode $B^+ \to \overline{D}{}^0\pi^+$ and $\overline{D}{}^0 \to K^+\pi^-$ with $B(B^+ \to \overline{D}{}^0\pi^+)\cdot B(\overline{D}{}^0 \to K^+\pi^-) = (20.3 \pm 2.0) \times 10^{-5}$.

[223] ABE 00C assumes $B(Z \to b\overline{b}) = (21.7 \pm 0.1)\%$ and the B fractions $f_{B^0} = f_{B^+} = (39.7^{+1.8}_{-2.2})\%$ and $f_{B_s} = (10.5^{+1.8}_{-2.2})\%$.

[224] Assumes equal production of B^+ and B^0 at the $\Upsilon(4S)$.

[225] ADAM 96D assumes $f_{B^0} = f_{B^-} = 0.39$ and $f_{B_s} = 0.12$.

[226] Assumes a B^0, B^- production fraction of 0.39 and a B_s production fraction of 0.12.

[227] AVERY 89B reports < 7 × 10⁻⁵ assuming the $\Upsilon(4S)$ decays 43% to $B^0\overline{B}{}^0$. We rescale to 50%.

$\Gamma(K_2^*(1430)^0\pi^+)/\Gamma_{total}$ Γ_{131}/Γ

VALUE	CL%	DOCUMENT ID	TECN	COMMENT
< 6.8 × 10⁻⁴	90	ALBRECHT 91B	ARG	$e^+e^- \to \Upsilon(4S)$

$\Gamma(K^-\pi^+\pi^+)/\Gamma_{total}$ Γ_{132}/Γ

VALUE	CL%	DOCUMENT ID	TECN	COMMENT
< 1.8 × 10⁻⁶	90	[228] AUBERT 03M	BABR	$e^+e^- \to \Upsilon(4S)$
• • • We do not use the following data for averages, fits, limits, etc. • • •				
< 4.5 × 10⁻⁶	90	[229] GARMASH 04	BELL	$e^+e^- \to \Upsilon(4S)$
< 7.0 × 10⁻⁶	90	[230] GARMASH 02	BELL	$e^+e^- \to \Upsilon(4S)$

[228] Assumes equal production of B^0 and B^+ at the $\Upsilon(4S)$; charm and charmonium contributions are subtracted, otherwise no assumptions about intermediate resonances.

[229] Assumes equal production of B^+ and B^0 at the $\Upsilon(4S)$.

[230] Uses a reference decay mode $B^+ \to \overline{D}{}^0\pi^+$ and $\overline{D}{}^0 \to K^+\pi^-$ with $B(B^+ \to \overline{D}{}^0\pi^+)\cdot B(\overline{D}{}^0 \to K^+\pi^-) = (20.3 \pm 2.0) \times 10^{-5}$.

$\Gamma(K^-\pi^+\pi^+ \text{nonresonant})/\Gamma_{total}$ Γ_{133}/Γ

VALUE	CL%	DOCUMENT ID	TECN	COMMENT
< 5.6 × 10⁻⁵	90	BERGFELD 96B	CLE2	$e^+e^- \to \Upsilon(4S)$

$\Gamma(K_1(1400)^0\pi^+)/\Gamma_{total}$ Γ_{134}/Γ

VALUE	CL%	DOCUMENT ID	TECN	COMMENT
< 2.6 × 10⁻³	90	ALBRECHT 91B	ARG	$e^+e^- \to \Upsilon(4S)$

$\Gamma(K^0\pi^+\pi^0)/\Gamma_{total}$ Γ_{135}/Γ

VALUE	CL%	DOCUMENT ID	TECN	COMMENT
< 66 × 10⁻⁶	90	[231] ECKHART 02	CLE2	$e^+e^- \to \Upsilon(4S)$

[231] Assumes equal production of B^+ and B^0 at the $\Upsilon(4S)$.

$\Gamma(K^0\rho^+)/\Gamma_{total}$ Γ_{136}/Γ

VALUE	CL%	DOCUMENT ID	TECN	COMMENT
< 4.8 × 10⁻⁵	90	ASNER 96	CLE2	$e^+e^- \to \Upsilon(4S)$

$\Gamma(K^*(892)^+\pi^+\pi^-)/\Gamma_{total}$ Γ_{137}/Γ

VALUE	CL%	DOCUMENT ID	TECN	COMMENT
< 1.1 × 10⁻³	90	ALBRECHT 91E	ARG	$e^+e^- \to \Upsilon(4S)$

$\Gamma(K^*(892)^+\rho^0)/\Gamma_{total}$ Γ_{138}/Γ

VALUE (units 10⁻⁶)	CL%	DOCUMENT ID	TECN	COMMENT
$10.6^{+3.0}_{-2.6} \pm 2.4$		[232] AUBERT 03V	BABR	$e^+e^- \to \Upsilon(4S)$
• • • We do not use the following data for averages, fits, limits, etc. • • •				
< 74	90	[233] GODANG 02	CLE2	$e^+e^- \to \Upsilon(4S)$
< 900	90	ALBRECHT 91B	ARG	$e^+e^- \to \Upsilon(4S)$

[232] Assumes equal production of B^+ and B^0 at the $\Upsilon(4S)$.

[233] Assumes a helicity 00 configuration. For a helicity 11 configuration, the limit decreases to 4.9 × 10⁻⁵.

$\Gamma(K^*(892)^+K^*(892)^0)/\Gamma_{total}$ Γ_{139}/Γ

VALUE	CL%	DOCUMENT ID	TECN	COMMENT
< 7.1 × 10⁻⁵	90	[234] GODANG 02	CLE2	$e^+e^- \to \Upsilon(4S)$

[234] Assumes a helicity 00 configuration. For a helicity 11 configuration, the limit decreases to 4.8 × 10⁻⁵.

$\Gamma(K_1(1400)^+\rho^0)/\Gamma_{total}$ Γ_{140}/Γ

VALUE	CL%	DOCUMENT ID	TECN	COMMENT
< 7.8 × 10⁻⁴	90	ALBRECHT 91B	ARG	$e^+e^- \to \Upsilon(4S)$

$\Gamma(K_2^*(1430)^+\rho^0)/\Gamma_{total}$ Γ_{141}/Γ

VALUE	CL%	DOCUMENT ID	TECN	COMMENT
< 1.5 × 10⁻³	90	ALBRECHT 91B	ARG	$e^+e^- \to \Upsilon(4S)$

$\Gamma(K^+\overline{K}{}^0)/\Gamma_{total}$ Γ_{142}/Γ

VALUE	CL%	DOCUMENT ID	TECN	COMMENT
< 2.0 × 10⁻⁶	90	[235] CASEY 02	BELL	$e^+e^- \to \Upsilon(4S)$
• • • We do not use the following data for averages, fits, limits, etc. • • •				
< 3.3 × 10⁻⁶	90	[235] BORNHEIM 03	CLE2	$e^+e^- \to \Upsilon(4S)$
< 5.0 × 10⁻⁶	90	[235] ABE 01H	BELL	$e^+e^- \to \Upsilon(4S)$
< 2.4 × 10⁻⁶	90	[235] AUBERT 01E	BABR	$e^+e^- \to \Upsilon(4S)$
< 5.1 × 10⁻⁶	90	[235] CRONIN-HEN..00	CLE2	$e^+e^- \to \Upsilon(4S)$
< 2.1 × 10⁻⁵	90	GODANG 98	CLE2	Repl. by CRONIN-HENNESSY 00

[235] Assumes equal production of B^+ and B^0 at the $\Upsilon(4S)$.

$\Gamma(\overline{K}{}^0K^+\pi^0)/\Gamma_{total}$ Γ_{143}/Γ

VALUE	CL%	DOCUMENT ID	TECN	COMMENT
< 24 × 10⁻⁶	90	[236] ECKHART 02	CLE2	$e^+e^- \to \Upsilon(4S)$

[236] Assumes equal production of B^+ and B^0 at the $\Upsilon(4S)$.

$\Gamma(K^+K_S^0K_S^0)/\Gamma_{total}$ Γ_{144}/Γ

VALUE (units 10⁻⁶)	DOCUMENT ID	TECN	COMMENT
13.4 ± 1.9 ± 1.5	[237] GARMASH 04	BELL	$e^+e^- \to \Upsilon(4S)$

[237] Assumes equal production of B^+ and B^0 at the $\Upsilon(4S)$.

$\Gamma(K_S^0K_S^0\pi^+)/\Gamma_{total}$ Γ_{145}/Γ

VALUE (units 10⁻⁶)	CL%	DOCUMENT ID	TECN	COMMENT
< 3.2	90	[238] GARMASH 04	BELL	$e^+e^- \to \Upsilon(4S)$

[238] Assumes equal production of B^+ and B^0 at the $\Upsilon(4S)$.

$\Gamma(K^+K^-\pi^+)/\Gamma_{total}$ Γ_{146}/Γ

VALUE	CL%	DOCUMENT ID	TECN	COMMENT
< 6.3 × 10⁻⁶	90	[239] AUBERT 03M	BABR	$e^+e^- \to \Upsilon(4S)$
• • • We do not use the following data for averages, fits, limits, etc. • • •				
< 13 × 10⁻⁶	90	[240] GARMASH 04	BELL	$e^+e^- \to \Upsilon(4S)$
< 1.2 × 10⁻⁵	90	[241] GARMASH 02	BELL	$e^+e^- \to \Upsilon(4S)$

[239] Assumes equal production of B^0 and B^+ at the $\Upsilon(4S)$; charm and charmonium contributions are subtracted, otherwise no assumptions about intermediate resonances.

[240] Assumes equal production of B^+ and B^0 at the $\Upsilon(4S)$.

[241] Uses a reference decay mode $B^+ \to \overline{D}{}^0\pi^+$ and $\overline{D}{}^0 \to K^+\pi^-$ with $B(B^+ \to \overline{D}{}^0\pi^+)\cdot B(\overline{D}{}^0 \to K^+\pi^-) = (20.3 \pm 2.0) \times 10^{-5}$.

$\Gamma(K^+K^-\pi^+\text{nonresonant})/\Gamma_{\text{total}}$ Γ_{147}/Γ

VALUE	CL%	DOCUMENT ID		TECN	COMMENT
$<7.5\times10^{-5}$	90	BERGFELD	96B	CLE2	$e^+e^-\to\Upsilon(4S)$

$\Gamma(K^+K^+\pi^-)/\Gamma_{\text{total}}$ Γ_{148}/Γ

VALUE	CL%	DOCUMENT ID		TECN	COMMENT
$<1.3\times10^{-6}$	90	[242] AUBERT	03M	BABR	$e^+e^-\to\Upsilon(4S)$
• • • We do not use the following data for averages, fits, limits, etc. • • •					
$<2.4\times10^{-6}$	90	[243] GARMASH	04	BELL	$e^+e^-\to\Upsilon(4S)$
$<3.2\times10^{-6}$	90	[244] GARMASH	02	BELL	$e^+e^-\to\Upsilon(4S)$

[242] Assumes equal production of B^0 and B^+ at the $\Upsilon(4S)$; charm and charmonium contributions are subtracted, otherwise no assumptions about intermediate resonances.
[243] Assumes equal production of B^+ and B^0 at the $\Upsilon(4S)$.
[244] Uses a reference decay mode $B^+\to\overline{D}^0\pi^+$ and $\overline{D}^0\to K^+\pi^-$ with $B(B^+\to\overline{D}^0\pi^+)\cdot B(\overline{D}^0\to K^+\pi^-)=(20.3\pm2.0)\times10^{-5}$.

$\Gamma(K^+K^+\pi^-\text{nonresonant})/\Gamma_{\text{total}}$ Γ_{149}/Γ

VALUE	CL%	DOCUMENT ID		TECN	COMMENT
$<8.79\times10^{-5}$	90	ABBIENDI	00B	OPAL	$e^+e^-\to Z$

$\Gamma(K^+K^*(892)^0)/\Gamma_{\text{total}}$ Γ_{150}/Γ

VALUE	CL%	DOCUMENT ID		TECN	COMMENT
$<5.3\times10^{-6}$	90	[245] JESSOP	00	CLE2	$e^+e^-\to\Upsilon(4S)$
• • • We do not use the following data for averages, fits, limits, etc. • • •					
$<1.29\times10^{-4}$	90	ABBIENDI	00B	OPAL	$e^+e^-\to Z$
$<1.38\times10^{-4}$	90	[246] ABE	00C	SLD	$e^+e^-\to Z$

[245] Assumes equal production of B^+ and B^0 at the $\Upsilon(4S)$.
[246] ABE 00C assumes $B(Z\to b\overline{b})=(21.7\pm0.1)\%$ and the B fractions $f_{B^0}=f_{B^+}=(39.7^{+1.8}_{-2.2})\%$ and $f_{B_s}=(10.5^{+1.8}_{-2.2})\%$.

$\Gamma(K^+f_J(2220))/\Gamma_{\text{total}}$ Γ_{151}/Γ

VALUE (units 10^{-6})		DOCUMENT ID		TECN	COMMENT
not seen		[247] HUANG	03	BELL	$e^+e^-\to\Upsilon(4S)$

[247] No evidence is found for such decay and set a limit on $B(B^+\to f_J(2220))\times B(f_J(2220)\to\phi\phi)<1.2\times10^{-6}$ at 90%CL where the $f_J(2220)$ is a possible glueball state.

$\Gamma(K^+K^-K^+)/\Gamma_{\text{total}}$ Γ_{152}/Γ

VALUE (units 10^{-5})	CL%	DOCUMENT ID		TECN	COMMENT
3.08 ± 0.21 OUR AVERAGE					
$3.28\pm0.18\pm0.28$		[248] GARMASH	04	BELL	$e^+e^-\to\Upsilon(4S)$
$2.96\pm0.21\pm0.16$		[249] AUBERT	03M	BABR	$e^+e^-\to\Upsilon(4S)$
• • • We do not use the following data for averages, fits, limits, etc. • • •					
$3.53\pm0.37\pm0.45$		[250] GARMASH	02	BELL	Repl. by GARMASH 04
<20	90	[251] ADAM	96D	DLPH	$e^+e^-\to Z$
<32	90	[252] ABREU	95N	DLPH	Sup. by ADAM 96D
<35	90	ALBRECHT	91E	ARG	$e^+e^-\to\Upsilon(4S)$

[248] Assumes equal production of B^+ and B^0 at the $\Upsilon(4S)$.
[249] Assumes equal production of B^0 and B^+ at the $\Upsilon(4S)$; charm and charmonium contributions are subtracted, otherwise no assumptions about intermediate resonances.
[250] Uses a reference decay mode $B^+\to\overline{D}^0\pi^+$ and $\overline{D}^0\to K^+\pi^-$ with $B(B^+\to\overline{D}^0\pi^+)\cdot B(\overline{D}^0\to K^+\pi^-)=(20.3\pm2.0)\times10^{-5}$.
[251] ADAM 96D assumes $f_{B^0}=f_{B^-}=0.39$ and $f_{B_s}=0.12$.
[252] Assumes a B^0, B^- production fraction of 0.39 and a B_s production fraction of 0.12.

$\Gamma(K^+\phi)/\Gamma_{\text{total}}$ Γ_{153}/Γ

VALUE (units 10^{-6})	CL%	DOCUMENT ID		TECN	COMMENT
9.3 ± 1.0 OUR AVERAGE		Error includes scale factor of 1.3. See the ideogram below.			
$10.0^{+0.9}_{-0.8}\pm0.5$		[253] AUBERT	04A	BABR	$e^+e^-\to\Upsilon(4S)$
$9.4\pm1.1\pm0.7$		[254] CHEN	03B	BELL	$e^+e^-\to\Upsilon(4S)$
$5.5^{+2.1}_{-1.8}\pm0.6$		[254] BRIERE	01	CLE2	$e^+e^-\to\Upsilon(4S)$
• • • We do not use the following data for averages, fits, limits, etc. • • •					
$14.6^{+3.0}_{-2.8}\pm2.0$		[255] GARMASH	02	BELL	Repl. by CHEN 03B
$7.7^{+1.6}_{-1.4}\pm0.8$		[254] AUBERT	01D	BABR	$e^+e^-\to\Upsilon(4S)$
<144	90	[256] ABE	00C	SLD	$e^+e^-\to Z$
<5	90	[254] BERGFELD	98	CLE2	
<280	90	[257] ADAM	96D	DLPH	$e^+e^-\to Z$
<12	90	ASNER	96	CLE2	$e^+e^-\to\Upsilon(4S)$
<440	90	[258] ABREU	95N	DLPH	Sup. by ADAM 96D
<180	90	ALBRECHT	91B	ARG	$e^+e^-\to\Upsilon(4S)$
<90	90	[259] AVERY	89B	CLEO	$e^+e^-\to\Upsilon(4S)$
<210	90	AVERY	87	CLEO	$e^+e^-\to\Upsilon(4S)$

[253] Assumes equal production of B^+ and B^0 at $\Upsilon(4S)$.
[254] Assumes equal production of B^+ and B^0 at the $\Upsilon(4S)$.
[255] Uses a reference decay mode $B^+\to\overline{D}^0\pi^+$ and $\overline{D}^0\to K^+\pi^-$ with $B(B^+\to\overline{D}^0\pi^+)\cdot B(\overline{D}^0\to K^+\pi^-)=(20.3\pm2.0)\times10^{-5}$.
[256] ABE 00C assumes $B(Z\to b\overline{b})=(21.7\pm0.1)\%$ and the B fractions $f_{B^0}=f_{B^+}=(39.7^{+1.8}_{-2.2})\%$ and $f_{B_s}=(10.5^{+1.8}_{-2.2})\%$.
[257] ADAM 96D assumes $f_{B^0}=f_{B^-}=0.39$ and $f_{B_s}=0.12$.
[258] Assumes a B^0, B^- production fraction of 0.39 and a B_s production fraction of 0.12.
[259] AVERY 89B reports $<8\times10^{-5}$ assuming the $\Upsilon(4S)$ decays 43% to $B^0\overline{B}^0$. We rescale to 50%.

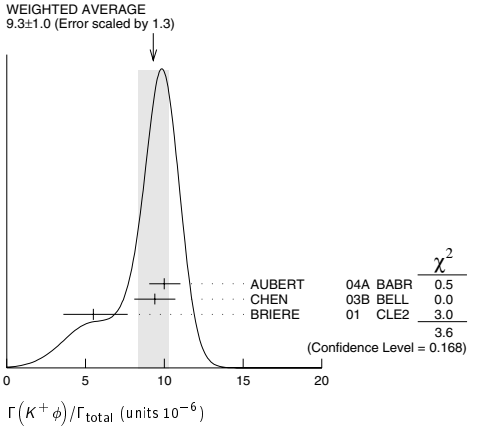

$\Gamma(K^+K^-K^+\text{nonresonant})/\Gamma_{\text{total}}$ Γ_{154}/Γ

VALUE (units 10^{-5})	CL%	DOCUMENT ID		TECN	COMMENT
<3.8	90	BERGFELD	96B	CLE2	$e^+e^-\to\Upsilon(4S)$

$\Gamma(K^*(892)^+K^+K^-)/\Gamma_{\text{total}}$ Γ_{155}/Γ

VALUE	CL%	DOCUMENT ID		TECN	COMMENT
$<1.6\times10^{-3}$	90	ALBRECHT	91E	ARG	$e^+e^-\to\Upsilon(4S)$

$\Gamma(K^*(892)^+\phi)/\Gamma_{\text{total}}$ Γ_{156}/Γ

VALUE (units 10^{-6})	CL%	DOCUMENT ID		TECN	COMMENT
9.6 ± 3.0 OUR AVERAGE		Error includes scale factor of 1.9.			
$12.7^{+2.2}_{-2.0}\pm1.1$		[260] AUBERT	03V	BABR	$e^+e^-\to\Upsilon(4S)$
$6.7^{+2.1}_{-1.9}{}^{+0.7}_{-1.0}$		[260] CHEN	03B	BELL	$e^+e^-\to\Upsilon(4S)$
• • • We do not use the following data for averages, fits, limits, etc. • • •					
$9.7^{+4.2}_{-3.4}\pm1.7$		[260] AUBERT	01D	BABR	Repl. by AUBERT 03V
<22.5	90	[260] BRIERE	01	CLE2	$e^+e^-\to\Upsilon(4S)$
<41	90	[260] BERGFELD	98	CLE2	
<70	90	ASNER	96	CLE2	$e^+e^-\to\Upsilon(4S)$
<1300	90	ALBRECHT	91B	ARG	$e^+e^-\to\Upsilon(4S)$

[260] Assumes equal production of B^+ and B^0 at the $\Upsilon(4S)$.

$\Gamma(K_1(1400)^+\phi)/\Gamma_{\text{total}}$ Γ_{157}/Γ

VALUE	CL%	DOCUMENT ID	TECN	COMMENT
$<1.1\times10^{-3}$	90	ALBRECHT	91B ARG	$e^+e^-\to\Upsilon(4S)$

$\Gamma(K_2^*(1430)^+\phi)/\Gamma_{\text{total}}$ Γ_{158}/Γ

VALUE	CL%	DOCUMENT ID	TECN	COMMENT
$<3.4\times10^{-3}$	90	ALBRECHT	91B ARG	$e^+e^-\to\Upsilon(4S)$

$\Gamma(K^+\phi\phi)/\Gamma_{\text{total}}$ Γ_{159}/Γ

VALUE (units 10^{-6})	DOCUMENT ID		TECN	COMMENT
$2.6^{+1.1}_{-0.9}\pm0.3$	[261] HUANG	03	BELL	$e^+e^-\to\Upsilon(4S)$

[261] Assumes equal production of B^0 and B^+ at the $\Upsilon(4S)$ and for a $\phi\phi$ invariant mass below 2.85 GeV/c^2.

$\Gamma(K^*(892)^+\gamma)/\Gamma_{\text{total}}$ Γ_{160}/Γ

VALUE (units 10^{-5})	CL%	EVTS	DOCUMENT ID		TECN	COMMENT
3.8 ± 0.5 OUR AVERAGE						
$3.83\pm0.62\pm0.22$			[262] AUBERT	02C	BABR	$e^+e^-\to\Upsilon(4S)$
$3.76^{+0.89}_{-0.83}\pm0.28$			[262] COAN	00	CLE2	$e^+e^-\to\Upsilon(4S)$

• • • We do not use the following data for averages, fits, limits, etc. • • •

$5.7 \pm 3.1 \pm 1.1$		5	[263] AMMAR	93	CLE2	Repl. by COAN 00
< 55	90		[264] ALBRECHT	89G	ARG	$e^+e^- \to \Upsilon(4S)$
< 55	90		[265] AVERY	89B	CLEO	$e^+e^- \to \Upsilon(4S)$
< 180	90		AVERY	87	CLEO	$e^+e^- \to \Upsilon(4S)$

[262] Assumes equal production of B^+ and B^0 at the $\Upsilon(4S)$.
[263] AMMAR 93 observed 4.1 ± 2.3 events above background.
[264] Assumes the $\Upsilon(4S)$ decays 45% to $B^0\overline{B}^0$.
[265] Assumes the $\Upsilon(4S)$ decays 43% to $B^0\overline{B}^0$.

$\Gamma(K_1(1270)^+\gamma)/\Gamma_{\text{total}}$ Γ_{161}/Γ

VALUE	CL%	DOCUMENT ID		TECN	COMMENT
$< 9.9 \times 10^{-5}$	90	[266] NISHIDA	02	BELL	$e^+e^- \to \Upsilon(4S)$
• • • We do not use the following data for averages, fits, limits, etc. • • •					
< 0.0073	90	[267] ALBRECHT	89G	ARG	$e^+e^- \to \Upsilon(4S)$

[266] Assumes equal production of B^+ and B^0 at the $\Upsilon(4S)$.
[267] ALBRECHT 89G reports < 0.0066 assuming the $\Upsilon(4S)$ decays 45% to $B^0\overline{B}^0$. We rescale to 50%.

$\Gamma(\phi K^+)/\Gamma_{\text{total}}$ Γ_{162}/Γ

VALUE (units 10^{-6})	DOCUMENT ID		TECN	COMMENT
$3.4 \pm 0.9 \pm 0.4$	[268] DRUTSKOY	04	BELL	$e^+e^- \to \Upsilon(4S)$

[268] Assumes equal production of B^+ and B^0 at $\Upsilon(4S)$.

$\Gamma(K^+\pi^-\pi^+\gamma)/\Gamma_{\text{total}}$ Γ_{163}/Γ

VALUE	DOCUMENT ID		TECN	COMMENT
$(2.4 \pm 0.5^{+0.4}_{-0.2}) \times 10^{-5}$	[269,270] NISHIDA	02	BELL	$e^+e^- \to \Upsilon(4S)$

[269] Assumes equal production of B^+ and B^0 at the $\Upsilon(4S)$.
[270] $M_{K\pi\pi} < 2.4$ GeV/c^2.

$\Gamma(K^*(892)^0\pi^+\gamma)/\Gamma_{\text{total}}$ Γ_{164}/Γ

VALUE	DOCUMENT ID		TECN	COMMENT
$(2.0^{+0.7}_{-0.6} \pm 0.2) \times 10^{-5}$	[271,272] NISHIDA	02	BELL	$e^+e^- \to \Upsilon(4S)$

[271] Assumes equal production of B^+ and B^0 at the $\Upsilon(4S)$.
[272] $M_{K\pi\pi} < 2.4$ GeV/c^2.

$\Gamma(K^+\rho^0\gamma)/\Gamma_{\text{total}}$ Γ_{165}/Γ

VALUE	CL%	DOCUMENT ID		TECN	COMMENT
$< 2.0 \times 10^{-5}$	90 [273,274]	NISHIDA	02	BELL	$e^+e^- \to \Upsilon(4S)$

[273] Assumes equal production of B^+ and B^0 at the $\Upsilon(4S)$.
[274] $M_{K\pi\pi} < 2.4$ GeV/c^2.

$\Gamma(K^+\pi^-\pi^+\gamma \text{ nonresonant})/\Gamma_{\text{total}}$ Γ_{166}/Γ

VALUE	CL%	DOCUMENT ID		TECN	COMMENT
$< 9.2 \times 10^{-6}$	90 [275,276]	NISHIDA	02	BELL	$e^+e^- \to \Upsilon(4S)$

[275] Assumes equal production of B^+ and B^0 at the $\Upsilon(4S)$.
[276] $M_{K\pi\pi} < 2.4$ GeV/c^2.

$\Gamma(K_1(1400)^+\gamma)/\Gamma_{\text{total}}$ Γ_{167}/Γ

VALUE	CL%	DOCUMENT ID		TECN	COMMENT
$< 5.0 \times 10^{-5}$	90	[277] NISHIDA	02	BELL	$e^+e^- \to \Upsilon(4S)$
• • • We do not use the following data for averages, fits, limits, etc. • • •					
< 0.0022	90	[278] ALBRECHT	89G	ARG	$e^+e^- \to \Upsilon(4S)$

[277] Assumes equal production of B^+ and B^0 at the $\Upsilon(4S)$.
[278] ALBRECHT 89G reports < 0.0020 assuming the $\Upsilon(4S)$ decays 45% to $B^0\overline{B}^0$. We rescale to 50%.

$\Gamma(K_2^*(1430)^+\gamma)/\Gamma_{\text{total}}$ Γ_{168}/Γ

VALUE	CL%	DOCUMENT ID		TECN	COMMENT
< 0.0014	90	[279] ALBRECHT	89G	ARG	$e^+e^- \to \Upsilon(4S)$

[279] ALBRECHT 89G reports < 0.0013 assuming the $\Upsilon(4S)$ decays 45% to $B^0\overline{B}^0$. We rescale to 50%.

$\Gamma(K^*(1680)^+\gamma)/\Gamma_{\text{total}}$ Γ_{169}/Γ

VALUE	CL%	DOCUMENT ID		TECN	COMMENT
< 0.0019	90	[280] ALBRECHT	89G	ARG	$e^+e^- \to \Upsilon(4S)$

[280] ALBRECHT 89G reports < 0.0017 assuming the $\Upsilon(4S)$ decays 45% to $B^0\overline{B}^0$. We rescale to 50%.

$\Gamma(K_3^*(1780)^+\gamma)/\Gamma_{\text{total}}$ Γ_{170}/Γ

VALUE	CL%	DOCUMENT ID		TECN	COMMENT
< 0.0055	90	[281] ALBRECHT	89G	ARG	$e^+e^- \to \Upsilon(4S)$

[281] ALBRECHT 89G reports < 0.005 assuming the $\Upsilon(4S)$ decays 45% to $B^0\overline{B}^0$. We rescale to 50%.

$\Gamma(K_4^*(2045)^+\gamma)/\Gamma_{\text{total}}$ Γ_{171}/Γ

VALUE	CL%	DOCUMENT ID		TECN	COMMENT
< 0.0099	90	[282] ALBRECHT	89G	ARG	$e^+e^- \to \Upsilon(4S)$

[282] ALBRECHT 89G reports < 0.0090 assuming the $\Upsilon(4S)$ decays 45% to $B^0\overline{B}^0$. We rescale to 50%.

$\Gamma(\rho^+\gamma)/\Gamma_{\text{total}}$ Γ_{172}/Γ

VALUE	CL%	DOCUMENT ID		TECN	COMMENT
$< 2.1 \times 10^{-6}$	90	[283] AUBERT	04C	BABR	$e^+e^- \to \Upsilon(4S)$
• • • We do not use the following data for averages, fits, limits, etc. • • •					
$< 1.3 \times 10^{-5}$	90	[284] COAN	00	CLE2	$e^+e^- \to \Upsilon(4S)$

[283] Assumes equal production of B^+ and B^0 at $\Upsilon(4S)$.
[284] Assumes equal production of B^+ and B^0 at the $\Upsilon(4S)$. No evidence for a nonresonant $K\pi\gamma$ contamination was seen; the central value assumes no contamination.

$\Gamma(\pi^+\pi^0)/\Gamma_{\text{total}}$ Γ_{173}/Γ

VALUE (units 10^{-5})	CL%	DOCUMENT ID		TECN	COMMENT
$0.56^{+0.09}_{-0.11}$ OUR AVERAGE					
$0.55^{+0.10}_{-0.19} \pm 0.06$		[285] AUBERT	03L	BABR	$e^+e^- \to \Upsilon(4S)$
$0.46^{+0.18}_{-0.16} \pm 0.06$		[285] BORNHEIM	03	CLE2	$e^+e^- \to \Upsilon(4S)$
$0.74^{+0.23}_{-0.22} \pm 0.09$		[285] CASEY	02	BELL	$e^+e^- \to \Upsilon(4S)$
• • • We do not use the following data for averages, fits, limits, etc. • • •					
< 1.34	90	[285] ABE	01H	BELL	$e^+e^- \to \Upsilon(4S)$
< 0.96	90	[285] AUBERT	01E	BABR	$e^+e^- \to \Upsilon(4S)$
< 1.27	90	[285] CRONIN-HEN...00		CLE2	$e^+e^- \to \Upsilon(4S)$
< 2.0	90	GODANG	98	CLE2	Repl. by CRONIN-HENNESSY 00
< 1.7	90	ASNER	96	CLE2	Repl. by GODANG 98
< 24	90	[286] ALBRECHT	90B	ARG	$e^+e^- \to \Upsilon(4S)$
< 230	90	[287] BEBEK	87	CLEO	$e^+e^- \to \Upsilon(4S)$

[285] Assumes equal production of B^+ and B^0 at the $\Upsilon(4S)$.
[286] ALBRECHT 90B limit assumes equal production of $B^0\overline{B}^0$ and B^+B^- at $\Upsilon(4S)$.
[287] BEBEK 87 assume the $\Upsilon(4S)$ decays 43% to $B^0\overline{B}^0$.

$\Gamma(\pi^+\pi^+\pi^-)/\Gamma_{\text{total}}$ Γ_{174}/Γ

VALUE (units 10^{-6})	CL%	DOCUMENT ID		TECN	COMMENT
$10.9 \pm 3.3 \pm 1.6$		[288] AUBERT	03M	BABR	$e^+e^- \to \Upsilon(4S)$
• • • We do not use the following data for averages, fits, limits, etc. • • •					
< 130	90	[289] ADAM	96D	DLPH	$e^+e^- \to Z$
< 220	90	[290] ABREU	95N	DLPH	Sup. by ADAM 96D
< 450	90	[291] ALBRECHT	90B	ARG	$e^+e^- \to \Upsilon(4S)$
< 190	90	[292] BORTOLETTO	89	CLEO	$e^+e^- \to \Upsilon(4S)$

[288] Assumes equal production of B^0 and B^+ at the $\Upsilon(4S)$; charm and charmonium contributions are subtracted, otherwise no assumptions about intermediate resonances.
[289] ADAM 96D assumes $f_{B^0} = f_{B^-} = 0.39$ and $f_{B_s} = 0.12$.
[290] Assumes a B^0, B^- production fraction of 0.39 and a B_s production fraction of 0.12.
[291] ALBRECHT 90B limit assumes equal production of $B^0\overline{B}^0$ and B^+B^- at $\Upsilon(4S)$.
[292] BORTOLETTO 89 reports $< 1.7 \times 10^{-4}$ assuming the $\Upsilon(4S)$ decays 43% to $B^0\overline{B}^0$. We rescale to 50%.

$\Gamma(\rho^0\pi^+)/\Gamma_{\text{total}}$ Γ_{175}/Γ

VALUE (units 10^{-5})	CL%	EVTS	DOCUMENT ID		TECN	COMMENT
0.86 ± 0.20 OUR AVERAGE						
$0.80^{+0.23}_{-0.20} \pm 0.07$			[293] GORDON	02	BELL	$e^+e^- \to \Upsilon(\text{rS})$
$1.04^{+0.33}_{-0.34} \pm 0.21$			[293] JESSOP	00	CLE2	$e^+e^- \to \Upsilon(4S)$
• • • We do not use the following data for averages, fits, limits, etc. • • •						
< 8.3	90		[294] ABE	00C	SLD	$e^+e^- \to Z$
< 16	90		[295] ADAM	96D	DLPH	$e^+e^- \to Z$
< 4.3	90		ASNER	96	CLE2	Repl. by JESSOP 00
< 26	90		[296] ABREU	95N	DLPH	Sup. by ADAM 96D
< 15	90		[297] ALBRECHT	90B	ARG	$e^+e^- \to \Upsilon(4S)$
< 17	90		[298] BORTOLETTO	89	CLEO	$e^+e^- \to \Upsilon(4S)$
< 23	90		[298] BEBEK	87	CLEO	$e^+e^- \to \Upsilon(4S)$
< 60	90	0	GILES	84	CLEO	Repl. by BEBEK 87

[293] Assumes equal production of B^+ and B^0 at the $\Upsilon(4S)$.
[294] ABE 00C assumes $B(Z \to b\overline{b}) = (21.7 \pm 0.1)\%$ and the B fractions $f_{B^0} = f_{B^+} = (39.7^{+1.8}_{-2.2})\%$ and $f_{B_s} = (10.5^{+1.8}_{-2.2})\%$.
[295] ADAM 96D assumes $f_{B^0} = f_{B^-} = 0.39$ and $f_{B_s} = 0.12$.
[296] Assumes a B^0, B^- production fraction of 0.39 and a B_s production fraction of 0.12.
[297] ALBRECHT 90B limit assumes equal production of $B^0\overline{B}^0$ and B^+B^- at $\Upsilon(4S)$.
[298] Papers assume the $\Upsilon(4S)$ decays 43% to $B^0\overline{B}^0$. We rescale to 50%.

$[\Gamma(K^*(892)^0\pi^+) + \Gamma(\rho^0\pi^+)]/\Gamma_{\text{total}}$ $(\Gamma_{125}+\Gamma_{175})/\Gamma$

VALUE	DOCUMENT ID		TECN	COMMENT
$(17^{+12}_{-8} \pm 2) \times 10^{-5}$	[299] ADAM	96D	DLPH	$e^+e^- \to Z$

[299] ADAM 96D assumes $f_{B^0} = f_{B^-} = 0.39$ and $f_{B_s} = 0.12$.

$\Gamma(\pi^+ f_0(980))/\Gamma_{total}$ Γ_{176}/Γ

VALUE	CL%	DOCUMENT ID		TECN	COMMENT
$<1.4\times10^{-4}$	90	[300] BORTOLETTO 89		CLEO	$e^+e^-\to\Upsilon(4S)$

[300] BORTOLETTO 89 reports $<1.2\times10^{-4}$ assuming the $\Upsilon(4S)$ decays 43% to $B^0\overline{B}^0$. We rescale to 50%.

$\Gamma(\pi^+ f_2(1270))/\Gamma_{total}$ Γ_{177}/Γ

VALUE	CL%	DOCUMENT ID		TECN	COMMENT
$<2.4\times10^{-4}$	90	[301] BORTOLETTO 89		CLEO	$e^+e^-\to\Upsilon(4S)$

[301] BORTOLETTO 89 reports $<2.1\times10^{-4}$ assuming the $\Upsilon(4S)$ decays 43% to $B^0\overline{B}^0$. We rescale to 50%.

$\Gamma(\pi^+\pi^-\pi^+ \text{nonresonant})/\Gamma_{total}$ Γ_{178}/Γ

VALUE	CL%	DOCUMENT ID		TECN	COMMENT
$<4.1\times10^{-5}$	90	BERGFELD	96B	CLE2	$e^+e^-\to\Upsilon(4S)$

$\Gamma(\pi^+\pi^0\pi^0)/\Gamma_{total}$ Γ_{179}/Γ

VALUE	CL%	DOCUMENT ID		TECN	COMMENT
$<8.9\times10^{-4}$	90	[302] ALBRECHT	90B	ARG	$e^+e^-\to\Upsilon(4S)$

[302] ALBRECHT 90B limit assumes equal production of $B^0\overline{B}^0$ and B^+B^- at $\Upsilon(4S)$.

$\Gamma(\rho^+\pi^0)/\Gamma_{total}$ Γ_{180}/Γ

VALUE	CL%	DOCUMENT ID		TECN	COMMENT
$<4.3\times10^{-5}$	90	[303] JESSOP	00	CLE2	$e^+e^-\to\Upsilon(4S)$
• • • We do not use the following data for averages, fits, limits, etc. • • •					
$<7.7\times10^{-5}$	90	ASNER	96	CLE2	Repl. by JESSOP 00
$<5.5\times10^{-4}$	90	[304] ALBRECHT	90B	ARG	$e^+e^-\to\Upsilon(4S)$

[303] Assumes equal production of B^+ and B^0 at the $\Upsilon(4S)$. Assumes no nonresonant contributions of $B^+\to\pi^+\pi^0\pi^0$.
[304] ALBRECHT 90B limit assumes equal production of $B^0\overline{B}^0$ and B^+B^- at $\Upsilon(4S)$.

$\Gamma(\pi^+\pi^-\pi^+\pi^0)/\Gamma_{total}$ Γ_{181}/Γ

VALUE	CL%	DOCUMENT ID		TECN	COMMENT
$<4.0\times10^{-3}$	90	[305] ALBRECHT	90B	ARG	$e^+e^-\to\Upsilon(4S)$

[305] ALBRECHT 90B limit assumes equal production of $B^0\overline{B}^0$ and B^+B^- at $\Upsilon(4S)$.

$\Gamma(\rho^+\rho^0)/\Gamma_{total}$ Γ_{182}/Γ

VALUE (units 10^{-5})	CL%	DOCUMENT ID		TECN	COMMENT
2.6 ±0.6 OUR AVERAGE					
$2.25^{+0.57}_{-0.54}\pm0.58$		[306] AUBERT	03V	BABR	$e^+e^-\to\Upsilon(4S)$
$3.17\pm0.71^{+0.38}_{-0.67}$		[307] ZHANG	03B	BELL	$e^+e^-\to\Upsilon(4S)$
• • • We do not use the following data for averages, fits, limits, etc. • • •					
<100	90	[308] ALBRECHT	90B	ARG	$e^+e^-\to\Upsilon(4S)$

[306] Assumes equal production of B^+ and B^0 at the $\Upsilon(4S)$.
[307] Assumes equal production of B^0 and B^+ at the $\Upsilon(4S)$ and the systematic error includes the error associated with the helicity-mix uncertainty.
[308] ALBRECHT 90B limit assumes equal production of $B^0\overline{B}^0$ and B^+B^- at $\Upsilon(4S)$.

$\Gamma(a_1(1260)^+\pi^0)/\Gamma_{total}$ Γ_{183}/Γ

VALUE	CL%	DOCUMENT ID		TECN	COMMENT
$<1.7\times10^{-3}$	90	[309] ALBRECHT	90B	ARG	$e^+e^-\to\Upsilon(4S)$

[309] ALBRECHT 90B limit assumes equal production of $B^0\overline{B}^0$ and B^+B^- at $\Upsilon(4S)$.

$\Gamma(a_1(1260)^0\pi^+)/\Gamma_{total}$ Γ_{184}/Γ

VALUE	CL%	DOCUMENT ID		TECN	COMMENT
$<9.0\times10^{-4}$	90	[310] ALBRECHT	90B	ARG	$e^+e^-\to\Upsilon(4S)$

[310] ALBRECHT 90B limit assumes equal production of $B^0\overline{B}^0$ and B^+B^- at $\Upsilon(4S)$.

$\Gamma(\omega\pi^+)/\Gamma_{total}$ Γ_{185}/Γ

VALUE (units 10^{-5})	CL%	DOCUMENT ID		TECN	COMMENT
$0.64^{+0.18}_{-0.16}$ **OUR AVERAGE** Error includes scale factor of 1.3. See the ideogram below.					
$0.42^{+0.20}_{-0.18}\pm0.05$		[311] LU	02	BELL	$e^+e^-\to\Upsilon(4S)$
$0.66^{+0.21}_{-0.18}\pm0.07$		[311] AUBERT	01G	BABR	$e^+e^-\to\Upsilon(4S)$
$1.13^{+0.33}_{-0.29}\pm0.14$		[311] JESSOP	00	CLE2	$e^+e^-\to\Upsilon(4S)$
• • • We do not use the following data for averages, fits, limits, etc. • • •					
<2.3	90	[311] BERGFELD	98	CLE2	Repl. by JESSOP 00
<40	90	[312] ALBRECHT	90B	ARG	$e^+e^-\to\Upsilon(4S)$

[311] Assumes equal production of B^+ and B^0 at the $\Upsilon(4S)$.
[312] ALBRECHT 90B limit assumes equal production of $B^0\overline{B}^0$ and B^+B^- at $\Upsilon(4S)$.

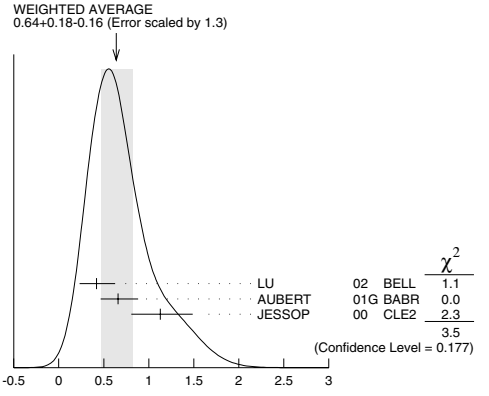

$\Gamma(\omega\pi^+)/\Gamma_{total}$ Γ_{185}/Γ

$\Gamma(\omega\rho^+)/\Gamma_{total}$ Γ_{186}/Γ

VALUE	CL%	DOCUMENT ID		TECN
$<6.1\times10^{-5}$	90	[313] BERGFELD	98	CLE2

[313] Assumes equal production of B^+ and B^0 at the $\Upsilon(4S)$.

$\Gamma(\eta\pi^+)/\Gamma_{total}$ Γ_{187}/Γ

VALUE	CL%	DOCUMENT ID		TECN	COMMENT
$<5.7\times10^{-6}$	90	[314] RICHICHI	00	CLE2	$e^+e^-\to\Upsilon(4S)$
• • • We do not use the following data for averages, fits, limits, etc. • • •					
$<1.5\times10^{-5}$	90	BEHRENS	98	CLE2	Repl. by RICHICHI 00
$<7.0\times10^{-4}$	90	[315] ALBRECHT	90B	ARG	$e^+e^-\to\Upsilon(4S)$

[314] Assumes equal production of B^+ and B^0 at the $\Upsilon(4S)$.
[315] ALBRECHT 90B limit assumes equal production of $B^0\overline{B}^0$ and B^+B^- at $\Upsilon(4S)$.

$\Gamma(\eta'\pi^+)/\Gamma_{total}$ Γ_{188}/Γ

VALUE	CL%	DOCUMENT ID		TECN	COMMENT
$<7.0\times10^{-6}$	90	[316] ABE	01M	BELL	$e^+e^-\to\Upsilon(4S)$
• • • We do not use the following data for averages, fits, limits, etc. • • •					
$<1.2\times10^{-5}$	90	[316] AUBERT	01G	BABR	$e^+e^-\to\Upsilon(4S)$
$<1.2\times10^{-5}$	90	[316] RICHICHI	00	CLE2	$e^+e^-\to\Upsilon(4S)$
$<3.1\times10^{-5}$	90	BEHRENS	98	CLE2	Repl. by RICHICHI 00

[316] Assumes equal production of B^+ and B^0 at the $\Upsilon(4S)$.

$\Gamma(\eta'\rho^+)/\Gamma_{total}$ Γ_{189}/Γ

VALUE	CL%	DOCUMENT ID		TECN	COMMENT
$<3.3\times10^{-5}$	90	[317] RICHICHI	00	CLE2	$e^+e^-\to\Upsilon(4S)$
• • • We do not use the following data for averages, fits, limits, etc. • • •					
$<4.7\times10^{-5}$	90	BEHRENS	98	CLE2	Repl. by RICHICHI 00

[317] Assumes equal production of B^+ and B^0 at the $\Upsilon(4S)$.

$\Gamma(\eta\rho^+)/\Gamma_{total}$ Γ_{190}/Γ

VALUE	CL%	DOCUMENT ID		TECN	COMMENT
$<1.5\times10^{-5}$	90	[318] RICHICHI	00	CLE2	$e^+e^-\to\Upsilon(4S)$
• • • We do not use the following data for averages, fits, limits, etc. • • •					
$<3.2\times10^{-5}$	90	BEHRENS	98	CLE2	Repl. by RICHICHI 00

[318] Assumes equal production of B^+ and B^0 at the $\Upsilon(4S)$.

$\Gamma(\phi\pi^+)/\Gamma_{total}$ Γ_{191}/Γ

VALUE	CL%	DOCUMENT ID		TECN	COMMENT
$<4.1\times10^{-7}$	90	[319] AUBERT	04A	BABR	$e^+e^-\to\Upsilon(4S)$
• • • We do not use the following data for averages, fits, limits, etc. • • •					
$<1.4\times10^{-6}$	90	[320] AUBERT	01D	BABR	$e^+e^-\to\Upsilon(4S)$
$<1.53\times10^{-4}$	90	[321] ABE	00C	SLD	$e^+e^-\to Z$
$<0.5\times10^{-5}$	90	[320] BERGFELD	98	CLE2	

[319] Assumes equal production of B^+ and B^0 at the $\Upsilon(4S)$.
[320] Assumes equal production of B^+ and B^0 at the $\Upsilon(4S)$.
[321] ABE 00C assumes $B(Z\to b\overline{b})=(21.7\pm0.1)\%$ and the B fractions $f_{B^0}=f_{B^+}=(39.7^{+1.8}_{-2.2})\%$ and $f_{B_s}=(10.5^{+1.8}_{-2.2})\%$.

$\Gamma(\phi\rho^+)/\Gamma_{total}$ Γ_{192}/Γ

VALUE	DOCUMENT ID		TECN
$<1.6\times10^{-5}$	[322] BERGFELD	98	CLE2

[322] Assumes equal production of B^+ and B^0 at the $\Upsilon(4S)$.

$\Gamma(\pi^+\pi^+\pi^+\pi^-\pi^-)/\Gamma_{total}$ Γ_{193}/Γ

VALUE	CL%	DOCUMENT ID		TECN	COMMENT
$<8.6\times10^{-4}$	90	[323] ALBRECHT	90B	ARG	$e^+e^-\to\Upsilon(4S)$

[323] ALBRECHT 90B limit assumes equal production of $B^0\overline{B}^0$ and B^+B^- at $\Upsilon(4S)$.

$\Gamma(\rho^0 a_1(1260)^+)/\Gamma_{total}$ Γ_{194}/Γ

VALUE	CL%	DOCUMENT ID		TECN	COMMENT
$< 6.2 \times 10^{-4}$	90	[324] BORTOLETTO	89	CLEO	$e^+e^- \to \Upsilon(4S)$
• • • We do not use the following data for averages, fits, limits, etc. • • •					
$< 6.0 \times 10^{-4}$	90	[325] ALBRECHT	90B	ARG	$e^+e^- \to \Upsilon(4S)$
$< 3.2 \times 10^{-3}$	90	[324] BEBEK	87	CLEO	$e^+e^- \to \Upsilon(4S)$

[324] BORTOLETTO 89 reports $< 5.4 \times 10^{-4}$ assuming the $\Upsilon(4S)$ decays 43% to $B^0\overline{B}^0$. We rescale to 50%.

[325] ALBRECHT 90B limit assumes equal production of $B^0\overline{B}^0$ and B^+B^- at $\Upsilon(4S)$.

$\Gamma(\rho^0 a_2(1320)^+)/\Gamma_{total}$ Γ_{195}/Γ

VALUE	CL%	DOCUMENT ID		TECN	COMMENT
$< 7.2 \times 10^{-4}$	90	[326] BORTOLETTO	89	CLEO	$e^+e^- \to \Upsilon(4S)$
• • • We do not use the following data for averages, fits, limits, etc. • • •					
$< 2.6 \times 10^{-3}$	90	[327] BEBEK	87	CLEO	$e^+e^- \to \Upsilon(4S)$

[326] BORTOLETTO 89 reports $< 6.3 \times 10^{-4}$ assuming the $\Upsilon(4S)$ decays 43% to $B^0\overline{B}^0$. We rescale to 50%.

[327] BEBEK 87reports $< 2.3 \times 10^{-3}$ assuming the $\Upsilon(4S)$ decays 43% to $B^0\overline{B}^0$. We rescale to 50%.

$\Gamma(\pi^+\pi^+\pi^+\pi^-\pi^-\pi^0)/\Gamma_{total}$ Γ_{196}/Γ

VALUE	CL%	DOCUMENT ID		TECN	COMMENT
$< 6.3 \times 10^{-3}$	90	[328] ALBRECHT	90B	ARG	$e^+e^- \to \Upsilon(4S)$

[328] ALBRECHT 90B limit assumes equal production of $B^0\overline{B}^0$ and B^+B^- at $\Upsilon(4S)$.

$\Gamma(a_1(1260)^+ a_1(1260)^0)/\Gamma_{total}$ Γ_{197}/Γ

VALUE	CL%	DOCUMENT ID		TECN	COMMENT
$< 1.3 \times 10^{-2}$	90	[329] ALBRECHT	90B	ARG	$e^+e^- \to \Upsilon(4S)$

[329] ALBRECHT 90B limit assumes equal production of $B^0\overline{B}^0$ and B^+B^- at $\Upsilon(4S)$.

$\Gamma(h^+\pi^0)/\Gamma_{total}$ Γ_{198}/Γ

$h^+ = K^+$ or π^+

VALUE	DOCUMENT ID		TECN	COMMENT
$(1.6^{+0.6}_{-0.5} \pm 0.36) \times 10^{-5}$	GODANG	98	CLE2	$e^+e^- \to \Upsilon(4S)$

$\Gamma(\omega h^+)/\Gamma_{total}$ Γ_{199}/Γ

$h^+ = K^+$ or π^+

VALUE (units 10^{-5})	DOCUMENT ID		TECN	COMMENT
$1.38^{+0.27}_{-0.24}$ OUR AVERAGE				
$1.34^{+0.33}_{-0.29} \pm 0.11$	[330] LU	02	BELL	$e^+e^- \to \Upsilon(4S)$
$1.43^{+0.36}_{-0.32} \pm 0.20$	[330] JESSOP	00	CLE2	$e^+e^- \to \Upsilon(4S)$
• • • We do not use the following data for averages, fits, limits, etc. • • •				
$2.5\ ^{+0.8}_{-0.7}\ \pm 0.3$	[330] BERGFELD	98	CLE2	Repl. by JESSOP 00

[330] Assumes equal production of B^+ and B^0 at the $\Upsilon(4S)$.

$\Gamma(h^+ X^0(\text{Familon}))/\Gamma_{total}$ Γ_{200}/Γ

VALUE	CL%	DOCUMENT ID		TECN	COMMENT
$< 4.9 \times 10^{-5}$	90	[331] AMMAR	01B	CLE2	$e^+e^- \to \Upsilon(4S)$

[331] AMMAR 01B searched for the two-body decay of the B meson to a massless neutral feebly-interacting particle X^0 such as the familon, the Nambu-Goldstone boson associated with a spontaneously broken global family symmetry.

$\Gamma(p\overline{p}\pi^+)/\Gamma_{total}$ Γ_{201}/Γ

VALUE	CL%	DOCUMENT ID		TECN	COMMENT
$< 3.7 \times 10^{-6}$	90	[332,333] ABE	02K	BELL	$e^+e^- \to \Upsilon(4S)$
• • • We do not use the following data for averages, fits, limits, etc. • • •					
$< 5.0 \times 10^{-4}$	90	[334] ABREU	95N	DLPH	Sup. by ADAM 96D
$< 1.6 \times 10^{-4}$	90	[335] BEBEK	89	CLEO	$e^+e^- \to \Upsilon(4S)$
$(5.7 \pm 1.5 \pm 2.1) \times 10^{-4}$		[336] ALBRECHT	88F	ARG	$e^+e^- \to \Upsilon(4S)$

[332] Assumes equal production of B^+ and B^0 at the $\Upsilon(4S)$.

[333] Explicitly vetoes resonant production of $p\overline{p}$ from Charmonium states.

[334] Assumes a B^0, B^- production fraction of 0.39 and a B_s production fraction of 0.12.

[335] BEBEK 89 reports $< 1.4 \times 10^{-4}$ assuming the $\Upsilon(4S)$ decays 43% to $B^0\overline{B}^0$. We rescale to 50%.

[336] ALBRECHT 88F reports $(5.2 \pm 1.4 \pm 1.9) \times 10^{-4}$ assuming the $\Upsilon(4S)$ decays 45% to $B^0\overline{B}^0$. We rescale to 50%.

$\Gamma(p\overline{p}\pi^+ \text{nonresonant})/\Gamma_{total}$ Γ_{202}/Γ

VALUE	CL%	DOCUMENT ID		TECN	COMMENT
$< 5.3 \times 10^{-5}$	90	BERGFELD	96B	CLE2	$e^+e^- \to \Upsilon(4S)$

$\Gamma(p\overline{p}\pi^+\pi^+\pi^-)/\Gamma_{total}$ Γ_{203}/Γ

VALUE	CL%	DOCUMENT ID		TECN	COMMENT
$< 5.2 \times 10^{-4}$	90	[337] ALBRECHT	88F	ARG	$e^+e^- \to \Upsilon(4S)$

[337] ALBRECHT 88F reports $< 4.7 \times 10^{-4}$ assuming the $\Upsilon(4S)$ decays 45% to $B^0\overline{B}^0$. We rescale to 50%.

$\Gamma(p\overline{p}K^+)/\Gamma_{total}$ Γ_{204}/Γ

VALUE	DOCUMENT ID		TECN	COMMENT
$(4.3^{+1.1}_{-0.9} \pm 0.5) \times 10^{-6}$	[338,339] ABE	02K	BELL	$e^+e^- \to \Upsilon(4S)$

[338] Assumes equal production of B^+ and B^0 at the $\Upsilon(4S)$.

[339] Explicitly vetoes resonant production of $p\overline{p}$ from Charmonium states.

$\Gamma(p\overline{p}K^+ \text{nonresonant})/\Gamma_{total}$ Γ_{205}/Γ

VALUE	CL%	DOCUMENT ID		TECN	COMMENT
$< 8.9 \times 10^{-5}$	90	BERGFELD	96B	CLE2	$e^+e^- \to \Upsilon(4S)$

$\Gamma(p\overline{\Lambda})/\Gamma_{total}$ Γ_{206}/Γ

VALUE	CL%	DOCUMENT ID		TECN	COMMENT
$< 1.5 \times 10^{-6}$	90	[340] BORNHEIM	03	CLE2	$e^+e^- \to \Upsilon(4S)$
• • • We do not use the following data for averages, fits, limits, etc. • • •					
$< 2.2 \times 10^{-6}$	90	[340] ABE	02O	BELL	$e^+e^- \to \Upsilon(4S)$
$< 2.6 \times 10^{-6}$	90	[341] COAN	99	CLE2	$e^+e^- \to \Upsilon(4S)$
$< 6 \times 10^{-5}$	90	[342] AVERY	89B	CLEO	$e^+e^- \to \Upsilon(4S)$
$< 9.3 \times 10^{-5}$	90	[343] ALBRECHT	88F	ARG	$e^+e^- \to \Upsilon(4S)$

[340] Assumes equal production of B^+ and B^0 at the $\Upsilon(4S)$.

[341] Assumes equal production of B^+ and B^0 at the $\Upsilon(4S)$.

[342] AVERY 89B reports $< 5 \times 10^{-5}$ assuming the $\Upsilon(4S)$ decays 43% to $B^0\overline{B}^0$. We rescale to 50%.

[343] ALBRECHT 88F reports $< 8.5 \times 10^{-5}$ assuming the $\Upsilon(4S)$ decays 45% to $B^0\overline{B}^0$. We rescale to 50%.

$[\Gamma(p\overline{\Lambda}\gamma) + \Gamma(p\overline{\Sigma}\gamma)]/\Gamma_{total}$ $(\Gamma_{207}+0.3\Gamma_{208})/\Gamma$

VALUE	CL%	DOCUMENT ID		TECN	COMMENT
$< 3.9 \times 10^{-6}$	90	[344] EDWARDS	03	CLE2	$e^+e^- \to \Upsilon(4S)$

[344] Corresponds to $E_\gamma > 1.5$ GeV. The limit changes to 3.3×10^{-6} for $E_\gamma > 2.0$ GeV.

$[\Gamma(p\overline{\Lambda}\gamma) + \Gamma(p\overline{\Sigma}\gamma)]/\Gamma_{total}$ $(0.4\Gamma_{207}+\Gamma_{208})/\Gamma$

VALUE	CL%	DOCUMENT ID		TECN	COMMENT
$< 7.9 \times 10^{-6}$	90	[345] EDWARDS	03	CLE2	$e^+e^- \to \Upsilon(4S)$

[345] Corresponds to $E_\gamma > 1.5$ GeV. The limit changes to 6.4×10^{-6} for $E_\gamma > 2.0$ GeV.

$\Gamma(p\overline{\Lambda}\pi^+\pi^-)/\Gamma_{total}$ Γ_{209}/Γ

VALUE	CL%	DOCUMENT ID		TECN	COMMENT
$< 2.0 \times 10^{-4}$	90	[346] ALBRECHT	88F	ARG	$e^+e^- \to \Upsilon(4S)$

[346] ALBRECHT 88F reports $< 1.8 \times 10^{-4}$ assuming the $\Upsilon(4S)$ decays 45% to $B^0\overline{B}^0$. We rescale to 50%.

$\Gamma(\overline{\Delta}^0 p)/\Gamma_{total}$ Γ_{210}/Γ

VALUE	CL%	DOCUMENT ID		TECN	COMMENT
$< 3.8 \times 10^{-4}$	90	[347] BORTOLETTO	89	CLEO	$e^+e^- \to \Upsilon(4S)$

[347] BORTOLETTO 89 reports $< 3.3 \times 10^{-4}$ assuming the $\Upsilon(4S)$ decays 43% to $B^0\overline{B}^0$. We rescale to 50%.

$\Gamma(\Delta^{++}\overline{p})/\Gamma_{total}$ Γ_{211}/Γ

VALUE	CL%	DOCUMENT ID		TECN	COMMENT
$< 1.5 \times 10^{-4}$	90	[348] BORTOLETTO	89	CLEO	$e^+e^- \to \Upsilon(4S)$

[348] BORTOLETTO 89 reports $< 1.3 \times 10^{-4}$ assuming the $\Upsilon(4S)$ decays 43% to $B^0\overline{B}^0$. We rescale to 50%.

$\Gamma(D^+ p\overline{p})/\Gamma_{total}$ Γ_{212}/Γ

VALUE	CL%	DOCUMENT ID		TECN	COMMENT
$< 1.5 \times 10^{-5}$	90	[349] ABE	02W	BELL	$e^+e^- \to \Upsilon(4S)$

[349] Assumes equal production of B^+ and B^0 at the $\Upsilon(4S)$.

$\Gamma(D^*(2010)^+ p\overline{p})/\Gamma_{total}$ Γ_{213}/Γ

VALUE	CL%	DOCUMENT ID		TECN	COMMENT
$< 1.5 \times 10^{-5}$	90	[350] ABE	02W	BELL	$e^+e^- \to \Upsilon(4S)$

[350] Assumes equal production of B^+ and B^0 at the $\Upsilon(4S)$.

$\Gamma(\overline{\Lambda}_c^- p\pi^+)/\Gamma_{total}$ Γ_{214}/Γ

VALUE (units 10^{-4})	DOCUMENT ID		TECN	COMMENT
2.1 ± 0.7 OUR AVERAGE				
$2.4 \pm 0.6 \pm 0.6$	[351] DYTMAN	02	CLE2	$e^+e^- \to \Upsilon(4S)$
$1.9 \pm 0.5 \pm 0.5$	[352] GABYSHEV	02	BELL	$e^+e^- \to \Upsilon(4S)$
• • • We do not use the following data for averages, fits, limits, etc. • • •				
$6.2^{+2.3}_{-2.0} \pm 1.6$	[353] FU	97	CLE2	Repl. by DYTMAN 02

[351] DYTMAN 02 reports $2.4^{+0.63}_{-0.62}$ for $B(\Lambda_c^+ \to pK^-\pi^+) = 0.05$. We rescale to our best value $B(\Lambda_c^+ \to pK^-\pi^+) = (5.0 \pm 1.3) \times 10^{-2}$. Our first error is their experiment's error and our second error is the systematic error from using our best value.

[352] GABYSHEV 02 reports $1.87^{+0.51}_{-0.49}$ for $B(\Lambda_c^+ \to pK^-\pi^+) = 0.05$. We rescale to our best value $B(\Lambda_c^+ \to pK^-\pi^+) = (5.0 \pm 1.3) \times 10^{-2}$. Our first error is their experiment's error and our second error is the systematic error from using our best value.

[353] FU 97 uses PDG 96 values of Λ_c branching fraction.

$\Gamma(\overline{\Lambda}_c^- p\pi^+\pi^0)/\Gamma_{total}$ Γ_{215}/Γ

VALUE (units 10^{-3})	CL%	DOCUMENT ID		TECN	COMMENT
$1.81\pm0.29^{+0.52}_{-0.50}$		[354,355] DYTMAN	02	CLE2	$e^+e^-\to\Upsilon(4S)$
• • • We do not use the following data for averages, fits, limits, etc. • • •					
<3.12	90	[356] FU	97	CLE2	$e^+e^-\to\Upsilon(4S)$

[354] Assumes equal production of B^+ and B^0 at the $\Upsilon(4S)$.
[355] DYTMAN 02 measurement uses $B(\Lambda_c^-\to\overline{p}K^+\pi^-)=5.0\pm1.3\%$. The second error includes the systematic and the uncertainty of the branching ratio.
[356] FU 97 uses PDG 96 values of Λ_c branching ratio.

$\Gamma(\overline{\Lambda}_c^- p\pi^+\pi^+\pi^-)/\Gamma_{total}$ Γ_{216}/Γ

VALUE (units 10^{-3})	CL%	DOCUMENT ID		TECN	COMMENT
$2.25\pm0.25^{+0.63}_{-0.61}$		[357,358] DYTMAN	02	CLE2	$e^+e^-\to\Upsilon(4S)$
• • • We do not use the following data for averages, fits, limits, etc. • • •					
<1.46	90	[359] FU	97	CLE2	$e^+e^-\to\Upsilon(4S)$

[357] Assumes equal production of B^+ and B^0 at the $\Upsilon(4S)$.
[358] DYTMAN 02 measurement uses $B(\Lambda_c^-\to\overline{p}K^+\pi^-)=5.0\pm1.3\%$. The second error includes the systematic and the uncertainty of the branching ratio.
[359] FU 97 uses PDG 96 values of Λ_c branching ratio.

$\Gamma(\overline{\Lambda}_c^- p\pi^+\pi^+\pi^-\pi^0)/\Gamma_{total}$ Γ_{217}/Γ

VALUE	CL%	DOCUMENT ID		TECN	COMMENT
$<1.34\times10^{-2}$	90	[360] FU	97	CLE2	$e^+e^-\to\Upsilon(4S)$

[360] FU 97 uses PDG 96 values of Λ_c branching ratio.

$\Gamma(\Sigma_c(2455)^0 p)/\Gamma_{total}$ Γ_{218}/Γ

VALUE	CL%	DOCUMENT ID		TECN	COMMENT
$<0.8\times10^{-4}$	90 [361,362]	DYTMAN	02	CLE2	$e^+e^-\to\Upsilon(4S)$
• • • We do not use the following data for averages, fits, limits, etc. • • •					
$<9.3\times10^{-5}$	90 [361,363]	GABYSHEV	02	BELL	$e^+e^-\to\Upsilon(4S)$

[361] Assumes equal production of B^+ and B^0 at the $\Upsilon(4S)$.
[362] DYTMAN 02 measurement uses $B(\Lambda_c^-\to\overline{p}K^+\pi^-)=5.0\pm1.3\%$. The second error includes the systematic and the uncertainty of the branching ratio.
[363] Uses the value for $\Lambda_c\to pK^-\pi^+$ branching ratio $(5.0\pm1.3)\%$.

$\Gamma(\Sigma_c(2520)^0 p)/\Gamma_{total}$ Γ_{219}/Γ

VALUE	CL%	DOCUMENT ID		TECN	COMMENT
$<4.6\times10^{-5}$	90 [364,365]	GABYSHEV	02	BELL	$e^+e^-\to\Upsilon(4S)$

[364] Assumes equal production of B^+ and B^0 at the $\Upsilon(4S)$.
[365] Uses the value for $\Lambda_c\to pK^-\pi^+$ branching ratio $(5.0\pm1.3)\%$.

$\Gamma(\Sigma_c(2455)^0 p\pi^0)/\Gamma_{total}$ Γ_{220}/Γ

VALUE (units 10^{-4})	DOCUMENT ID		TECN	COMMENT
$4.4\pm1.4\pm1.1$	[366,367] DYTMAN	02	CLE2	$e^+e^-\to\Upsilon(4S)$

[366] DYTMAN 02 reports 4.4 ± 1.4 for $B(\Lambda_c^+\to pK^-\pi^+)=0.05$. We rescale to our best value $B(\Lambda_c^+\to pK^-\pi^+)=(5.0\pm1.3)\times10^{-2}$. Our first error is their experiment's error and our second error is the systematic error from using our best value.
[367] Assumes equal production of B^+ and B^0 at the $\Upsilon(4S)$.

$\Gamma(\Sigma_c(2455)^0 p\pi^-\pi^+)/\Gamma_{total}$ Γ_{221}/Γ

VALUE (units 10^{-4})	DOCUMENT ID		TECN	COMMENT
$4.4\pm1.3\pm1.1$	[368,369] DYTMAN	02	CLE2	$e^+e^-\to\Upsilon(4S)$

[368] DYTMAN 02 reports 4.4 ± 1.3 for $B(\Lambda_c^+\to pK^-\pi^+)=0.05$. We rescale to our best value $B(\Lambda_c^+\to pK^-\pi^+)=(5.0\pm1.3)\times10^{-2}$. Our first error is their experiment's error and our second error is the systematic error from using our best value.
[369] Assumes equal production of B^+ and B^0 at the $\Upsilon(4S)$.

$\Gamma(\Sigma_c(2455)^{--} p\pi^+\pi^+)/\Gamma_{total}$ Γ_{222}/Γ

VALUE (units 10^{-4})	DOCUMENT ID		TECN	COMMENT
$2.8\pm1.0\pm0.7$	[370,371] DYTMAN	02	CLE2	$e^+e^-\to\Upsilon(4S)$

[370] DYTMAN 02 reports 2.8 ± 1.0 for $B(\Lambda_c^+\to pK^-\pi^+)=0.05$. We rescale to our best value $B(\Lambda_c^+\to pK^-\pi^+)=(5.0\pm1.3)\times10^{-2}$. Our first error is their experiment's error and our second error is the systematic error from using our best value.
[371] Assumes equal production of B^+ and B^0 at the $\Upsilon(4S)$.

$\Gamma(\overline{\Lambda}_c(2593)^- / \overline{\Lambda}_c(2625)^- p\pi^+)/\Gamma_{total}$ Γ_{223}/Γ

VALUE	CL%	DOCUMENT ID		TECN	COMMENT
$<1.9\times10^{-4}$	90 [372,373]	DYTMAN	02	CLE2	$e^+e^-\to\Upsilon(4S)$

[372] Assumes equal production of B^+ and B^0 at the $\Upsilon(4S)$.
[373] DYTMAN 02 measurement uses $B(\Lambda_c^-\to\overline{p}K^+\pi^-)=5.0\pm1.3\%$. The second error includes the systematic and the uncertainty of the branching ratio.

$\Gamma(\pi^+e^+e^-)/\Gamma_{total}$ Γ_{224}/Γ

Test for $\Delta B=1$ weak neutral current. Allowed by higher-order electroweak interactions.

VALUE	CL%	DOCUMENT ID		TECN	COMMENT
<0.0039	90	[374] WEIR	90B	MRK2	e^+e^- 29 GeV

[374] WEIR 90B assumes B^+ production cross section from LUND.

$\Gamma(\pi^+\mu^+\mu^-)/\Gamma_{total}$ Γ_{225}/Γ

Test for $\Delta B=1$ weak neutral current. Allowed by higher-order electroweak interactions.

VALUE	CL%	DOCUMENT ID		TECN	COMMENT
<0.0091	90	[375] WEIR	90B	MRK2	e^+e^- 29 GeV

[375] WEIR 90B assumes B^+ production cross section from LUND.

$\Gamma(K^+e^+e^-)/\Gamma_{total}$ Γ_{226}/Γ

Test for $\Delta B=1$ weak neutral current. Allowed by higher-order electroweak interactions.

VALUE (units 10^{-7})	CL%	DOCUMENT ID		TECN	COMMENT
$6.3^{+1.9}_{-1.7}\pm0.3$		[376] ISHIKAWA	03	BELL	$e^+e^-\to\Upsilon(4S)$
• • • We do not use the following data for averages, fits, limits, etc. • • •					
<14	90	[377] ABE	02	BELL	$e^+e^-\to\Upsilon(4S)$
<9	90	[377] AUBERT	02L	BABR	$e^+e^-\to\Upsilon(4S)$
<24	90	[378] ANDERSON	01B	CLE2	$e^+e^-\to\Upsilon(4S)$
<990	90	[379] ALBRECHT	91E	ARG	$e^+e^-\to\Upsilon(4S)$
<68000	90	[380] WEIR	90B	MRK2	e^+e^- 29 GeV
<600	90	[381] AVERY	89B	CLEO	$e^+e^-\to\Upsilon(4S)$
<2500	90	[382] AVERY	87	CLEO	$e^+e^-\to\Upsilon(4S)$

[376] Assumes equal production of B^0 and B^+ at $\Upsilon(4S)$. The second error is a total of systematic uncertainties including model dependence.
[377] Assumes equal production of B^+ and B^0 at the $\Upsilon(4S)$.
[378] The result is for di-lepton masses above 0.5 GeV.
[379] ALBRECHT 91E reports $<9.0\times10^{-5}$ assuming the $\Upsilon(4S)$ decays 45% to $B^0\overline{B}^0$. We rescale to 50%.
[380] WEIR 90B assumes B^+ production cross section from LUND.
[381] AVERY 89B reports $<5\times10^{-5}$ assuming the $\Upsilon(4S)$ decays 43% to $B^0\overline{B}^0$. We rescale to 50%.
[382] AVERY 87 reports $<2.1\times10^{-4}$ assuming the $\Upsilon(4S)$ decays 40% to $B^0\overline{B}^0$. We rescale to 50%.

$\Gamma(K^+\mu^+\mu^-)/\Gamma_{total}$ Γ_{227}/Γ

Test for $\Delta B=1$ weak neutral current. Allowed by higher-order electroweak interactions.

VALUE (units 10^{-6})	CL%	DOCUMENT ID		TECN	COMMENT
$0.45^{+0.14}_{-0.12}\pm0.03$		[383] ISHIKAWA	03	BELL	$e^+e^-\to\Upsilon(4S)$
• • • We do not use the following data for averages, fits, limits, etc. • • •					
$0.98^{+0.46}_{-0.36}\pm0.16$		[384] ABE	02	BELL	Repl. by ISHIKAWA 03
<1.2	90	[384] AUBERT	02L	BABR	$e^+e^-\to\Upsilon(4S)$
<3.68	90	[385] ANDERSON	01B	CLE2	$e^+e^-\to\Upsilon(4S)$
<5.2	90	[386] AFFOLDER	99B	CDF	$p\overline{p}$ at 1.8 TeV
<10	90	[387] ABE	96L	CDF	Repl. by AFFOLDER 99B
<240	90	[388] ALBRECHT	91E	ARG	$e^+e^-\to\Upsilon(4S)$
<6400	90	[389] WEIR	90B	MRK2	e^+e^- 29 GeV
<170	90	[390] AVERY	89B	CLEO	$e^+e^-\to\Upsilon(4S)$
<380	90	[391] AVERY	87	CLEO	$e^+e^-\to\Upsilon(4S)$

[383] Assumes equal production of B^0 and B^+ at $\Upsilon(4S)$. The second error is a total of systematic uncertainties including model dependence.
[384] Assumes equal production of B^+ and B^0 at the $\Upsilon(4S)$.
[385] The result is for di-lepton masses above 0.5 GeV.
[386] AFFOLDER 99B measured relative to $B^+\to J/\psi(1S)K^+$.
[387] ABE 96L measured relative to $B^+\to J/\psi(1S)K^+$ using PDG 94 branching ratios.
[388] ALBRECHT 91E reports $<2.2\times10^{-4}$ assuming the $\Upsilon(4S)$ decays 45% to $B^0\overline{B}^0$. We rescale to 50%.
[389] WEIR 90B assumes B^+ production cross section from LUND.
[390] AVERY 89B reports $<1.5\times10^{-4}$ assuming the $\Upsilon(4S)$ decays 43% to $B^0\overline{B}^0$. We rescale to 50%.
[391] AVERY 87 reports $<3.2\times10^{-4}$ assuming the $\Upsilon(4S)$ decays 40% to $B^0\overline{B}^0$. We rescale to 50%.

$\Gamma(K^+\ell^+\ell^-)/\Gamma_{total}$ Γ_{228}/Γ

VALUE (units 10^{-7})	DOCUMENT ID		TECN	COMMENT
$5.3^{+1.1}_{-1.0}\pm0.3$	[392] ISHIKAWA	03	BELL	$e^+e^-\to\Upsilon(4S)$

[392] Assumes equal production of B^0 and B^+ at $\Upsilon(4S)$.

$\Gamma(K^+\overline{\nu}\nu)/\Gamma_{total}$ Γ_{229}/Γ

Test for $\Delta B=1$ weak neutral current. Allowed by higher-order electroweak interactions.

VALUE	CL%	DOCUMENT ID		TECN	COMMENT
$<2.4\times10^{-4}$	90	[393] BROWDER	01	CLE2	$e^+e^-\to\Upsilon(4S)$

[393] Assumes equal production of B^+ and B^0 at the $\Upsilon(4S)$.

$\Gamma(K^*(892)^+e^+e^-)/\Gamma_{total}$ Γ_{230}/Γ

Test for $\Delta B=1$ weak neutral current. Allowed by higher-order electroweak interactions.

VALUE	CL%	DOCUMENT ID		TECN	COMMENT
$<4.6\times10^{-6}$	90	[394] ISHIKAWA	03	BELL	$e^+e^-\to\Upsilon(4S)$
• • • We do not use the following data for averages, fits, limits, etc. • • •					
$<8.9\times10^{-6}$	90	[395] ABE	02	BELL	Repl. by ISHIKAWA 03
$<9.5\times10^{-6}$	90	[395] AUBERT	02L	BABR	$e^+e^-\to\Upsilon(4S)$
$<6.9\times10^{-4}$	90	[396] ALBRECHT	91E	ARG	$e^+e^-\to\Upsilon(4S)$

[394] Assumes equal production of B^0 and B^+ at $\Upsilon(4S)$. The second error is a total of systematic uncertainties including model dependence.
[395] Assumes equal production of B^+ and B^0 at the $\Upsilon(4S)$.
[396] ALBRECHT 91E reports $<6.3\times10^{-4}$ assuming the $\Upsilon(4S)$ decays 45% to $B^0\overline{B}^0$. We rescale to 50%.

$\Gamma(K^*(892)^+\mu^+\mu^-)/\Gamma_{total}$ Γ_{231}/Γ

Test for $\Delta B = 1$ weak neutral current. Allowed by higher-order electroweak interactions.

VALUE	CL%	DOCUMENT ID		TECN	COMMENT
$< 2.2 \times 10^{-6}$	90	[397] ISHIKAWA	03	BELL	$e^+e^- \to \Upsilon(4S)$
• • • We do not use the following data for averages, fits, limits, etc. • • •					
$< 3.9 \times 10^{-6}$	90	[398] ABE	02	BELL	Repl. by ISHIKAWA 03
$< 17.0 \times 10^{-6}$	90	[398] AUBERT	02L	BABR	$e^+e^- \to \Upsilon(4S)$
$< 1.2 \times 10^{-3}$	90	[399] ALBRECHT	91E	ARG	$e^+e^- \to \Upsilon(4S)$

[397] Assumes equal production of B^0 and B^+ at $\Upsilon(4S)$. The second error is a total of systematic uncertainties including model dependence.
[398] Assumes equal production of B^+ and B^0 at the $\Upsilon(4S)$.
[399] ALBRECHT 91E reports $< 1.1 \times 10^{-3}$ assuming the $\Upsilon(4S)$ decays 45% to $B^0\overline{B}^0$. We rescale to 50%.

$\Gamma(K^*(892)^+\ell^+\ell)/\Gamma_{total}$ Γ_{232}/Γ

VALUE (units 10^{-7})	CL%	DOCUMENT ID		TECN	COMMENT
< 22	90	[400] ISHIKAWA	03	BELL	$e^+e^- \to \Upsilon(4S)$

[400] Assumes equal production of B^0 and B^+ at $\Upsilon(4S)$.

$\Gamma(\pi^+e^+\mu^-)/\Gamma_{total}$ Γ_{233}/Γ

Test of lepton family number conservation.

VALUE	CL%	DOCUMENT ID		TECN	COMMENT
< 0.0064	90	[401] WEIR	90B	MRK2	e^+e^- 29 GeV

[401] WEIR 90B assumes B^+ production cross section from LUND.

$\Gamma(\pi^+e^-\mu^+)/\Gamma_{total}$ Γ_{234}/Γ

Test of lepton family number conservation.

VALUE	CL%	DOCUMENT ID		TECN	COMMENT
< 0.0064	90	[402] WEIR	90B	MRK2	e^+e^- 29 GeV

[402] WEIR 90B assumes B^+ production cross section from LUND.

$\Gamma(K^+e^+\mu^-)/\Gamma_{total}$ Γ_{235}/Γ

Test of lepton family number conservation.

VALUE	CL%	DOCUMENT ID		TECN	COMMENT
< 0.8 $\times 10^{-6}$	90	[403] AUBERT	02L	BABR	$e^+e^- \to \Upsilon(4S)$
• • • We do not use the following data for averages, fits, limits, etc. • • •					
< 0.0064	90	[404] WEIR	90B	MRK2	e^+e^- 29 GeV

[403] Assumes equal production of B^+ and B^0 at the $\Upsilon(4S)$.
[404] WEIR 90B assumes B^+ production cross section from LUND.

$\Gamma(K^+e^-\mu^+)/\Gamma_{total}$ Γ_{236}/Γ

Test of lepton family number conservation.

VALUE	CL%	DOCUMENT ID		TECN	COMMENT
< 0.0064	90	[405] WEIR	90B	MRK2	e^+e^- 29 GeV

[405] WEIR 90B assumes B^+ production cross section from LUND.

$\Gamma(K^*(892)^+e^\pm\mu^\mp)/\Gamma_{total}$ Γ_{237}/Γ

Test of lepton family number conservation.

VALUE	CL%	DOCUMENT ID		TECN	COMMENT
< 7.9 × 10⁻⁶	90	[406] AUBERT	02L	BABR	$e^+e^- \to \Upsilon(4S)$

[406] Assumes equal production of B^+ and B^0 at the $\Upsilon(4S)$.

$\Gamma(\pi^-e^+e^+)/\Gamma_{total}$ Γ_{238}/Γ

Test of total lepton number conservation.

VALUE	CL%	DOCUMENT ID		TECN	COMMENT
< 1.6 $\times 10^{-6}$	90	[407] EDWARDS	02B	CLE2	$e^+e^- \to \Upsilon(4S)$
• • • We do not use the following data for averages, fits, limits, etc. • • •					
< 0.0039	90	[408] WEIR	90B	MRK2	e^+e^- 29 GeV

[407] Assumes equal production of B^+ and B^0 at the $\Upsilon(4S)$.
[408] WEIR 90B assumes B^+ production cross section from LUND.

$\Gamma(\pi^-\mu^+\mu^+)/\Gamma_{total}$ Γ_{239}/Γ

Test of total lepton number conservation.

VALUE	CL%	DOCUMENT ID		TECN	COMMENT
< 1.4 $\times 10^{-6}$	90	[409] EDWARDS	02B	CLE2	$e^+e^- \to \Upsilon(4S)$
• • • We do not use the following data for averages, fits, limits, etc. • • •					
< 0.0091	90	[410] WEIR	90B	MRK2	e^+e^- 29 GeV

[409] Assumes equal production of B^+ and B^0 at the $\Upsilon(4S)$.
[410] WEIR 90B assumes B^+ production cross section from LUND.

$\Gamma(\pi^-e^+\mu^+)/\Gamma_{total}$ Γ_{240}/Γ

Test of total lepton number conservation.

VALUE	CL%	DOCUMENT ID		TECN	COMMENT
< 1.3 $\times 10^{-6}$	90	[411] EDWARDS	02B	CLE2	$e^+e^- \to \Upsilon(4S)$
• • • We do not use the following data for averages, fits, limits, etc. • • •					
< 0.0064	90	[412] WEIR	90B	MRK2	e^+e^- 29 GeV

[411] Assumes equal production of B^+ and B^0 at the $\Upsilon(4S)$.
[412] WEIR 90B assumes B^+ production cross section from LUND.

$\Gamma(\rho^-e^+e^+)/\Gamma_{total}$ Γ_{241}/Γ

Test of total lepton number conservation.

VALUE (units 10^{-6})	CL%	DOCUMENT ID		TECN	COMMENT
< 2.6	90	[413] EDWARDS	02B	CLE2	$e^+e^- \to \Upsilon(4S)$

[413] Assumes equal production of B^+ and B^0 at the $\Upsilon(4S)$.

$\Gamma(\rho^-\mu^+\mu^+)/\Gamma_{total}$ Γ_{242}/Γ

Test of total lepton number conservation.

VALUE (units 10^{-6})	CL%	DOCUMENT ID		TECN	COMMENT
< 5.0	90	[414] EDWARDS	02B	CLE2	$e^+e^- \to \Upsilon(4S)$

[414] Assumes equal production of B^+ and B^0 at the $\Upsilon(4S)$.

$\Gamma(\rho^-e^+\mu^+)/\Gamma_{total}$ Γ_{243}/Γ

Test of lepton family number conservation.

VALUE (units 10^{-6})	CL%	DOCUMENT ID		TECN	COMMENT
< 3.3	90	[415] EDWARDS	02B	CLE2	$e^+e^- \to \Upsilon(4S)$

[415] Assumes equal production of B^+ and B^0 at the $\Upsilon(4S)$.

$\Gamma(K^-e^+e^+)/\Gamma_{total}$ Γ_{244}/Γ

Test of total lepton number conservation.

VALUE	CL%	DOCUMENT ID		TECN	COMMENT
< 1.0 $\times 10^{-6}$	90	[416] EDWARDS	02B	CLE2	$e^+e^- \to \Upsilon(4S)$
• • • We do not use the following data for averages, fits, limits, etc. • • •					
< 0.0039	90	[417] WEIR	90B	MRK2	e^+e^- 29 GeV

[416] Assumes equal production of B^+ and B^0 at the $\Upsilon(4S)$.
[417] WEIR 90B assumes B^+ production cross section from LUND.

$\Gamma(K^-\mu^+\mu^+)/\Gamma_{total}$ Γ_{245}/Γ

Test of total lepton number conservation.

VALUE	CL%	DOCUMENT ID		TECN	COMMENT
< 1.8 $\times 10^{-6}$	90	[418] EDWARDS	02B	CLE2	$e^+e^- \to \Upsilon(4S)$
• • • We do not use the following data for averages, fits, limits, etc. • • •					
< 0.0091	90	[419] WEIR	90B	MRK2	e^+e^- 29 GeV

[418] Assumes equal production of B^+ and B^0 at the $\Upsilon(4S)$.
[419] WEIR 90B assumes B^+ production cross section from LUND.

$\Gamma(K^-e^+\mu^+)/\Gamma_{total}$ Γ_{246}/Γ

Test of total lepton number conservation.

VALUE	CL%	DOCUMENT ID		TECN	COMMENT
< 2.0 $\times 10^{-6}$	90	[420] EDWARDS	02B	CLE2	$e^+e^- \to \Upsilon(4S)$
• • • We do not use the following data for averages, fits, limits, etc. • • •					
< 0.0064	90	[421] WEIR	90B	MRK2	e^+e^- 29 GeV

[420] Assumes equal production of B^+ and B^0 at the $\Upsilon(4S)$.
[421] WEIR 90B assumes B^+ production cross section from LUND.

$\Gamma(K^*(892)^-e^+e^+)/\Gamma_{total}$ Γ_{247}/Γ

Test of total lepton number conservation.

VALUE (units 10^{-6})	CL%	DOCUMENT ID		TECN	COMMENT
< 2.8	90	[422] EDWARDS	02B	CLE2	$e^+e^- \to \Upsilon(4S)$

[422] Assumes equal production of B^+ and B^0 at the $\Upsilon(4S)$.

$\Gamma(K^*(892)^-\mu^+\mu^+)/\Gamma_{total}$ Γ_{248}/Γ

Test of total lepton number conservation.

VALUE (units 10^{-6})	CL%	DOCUMENT ID		TECN	COMMENT
< 8.3	90	[423] EDWARDS	02B	CLE2	$e^+e^- \to \Upsilon(4S)$

[423] Assumes equal production of B^+ and B^0 at the $\Upsilon(4S)$.

$\Gamma(K^*(892)^-e^+\mu^+)/\Gamma_{total}$ Γ_{249}/Γ

Test of lepton family number conservation.

VALUE (units 10^{-6})	CL%	DOCUMENT ID		TECN	COMMENT
< 4.4	90	[424] EDWARDS	02B	CLE2	$e^+e^- \to \Upsilon(4S)$

[424] Assumes equal production of B^+ and B^0 at the $\Upsilon(4S)$.

POLARIZATION IN B^+ DECAY

Γ_L / Γ in $B^+ \to \overline{D}{}^{*0}\rho^+$

VALUE	DOCUMENT ID		TECN	COMMENT
0.892 ± 0.018 ± 0.016	CSORNA	03	CLE2	$e^+e^- \to \Upsilon(4S)$

Γ_L / Γ in $B^+ \to \phi K^*(892)^+$

VALUE	DOCUMENT ID		TECN	COMMENT
0.46 ± 0.12 ± 0.03	AUBERT	03V	BABR	$e^+e^- \to \Upsilon(4S)$

Γ_L / Γ in $B^+ \to \rho^0 K^*(892)^+$

VALUE	DOCUMENT ID		TECN	COMMENT
$0.96^{+0.04}_{-0.15} \pm 0.04$	AUBERT	03V	BABR	$e^+e^- \to \Upsilon(4S)$

Meson Particle Listings

$B^{\pm}$

Γ_L / Γ in $B^+ \to \rho^+\rho^0$

VALUE	DOCUMENT ID	TECN	COMMENT
0.96 $^{+0.05}_{-0.06}$ OUR AVERAGE			
$0.97\ ^{+0.03}_{-0.07} \pm 0.04$	AUBERT	03V BABR	$e^+e^- \to \Upsilon(4S)$
$0.948 \pm 0.106 \pm 0.021$	ZHANG	03B BELL	$e^+e^- \to \Upsilon(4S)$

CP VIOLATION

A_{CP} is defined as

$$\frac{B(B^- \to \overline{f}) - B(B^+ \to f)}{B(B^- \to \overline{f}) + B(B^+ \to f)},$$

the *CP*-violation charge asymmetry of exclusive B^- and B^+ decay.

$A_{CP}(B^+ \to J/\psi(1S)K^+)$

VALUE	DOCUMENT ID	TECN	COMMENT
-0.007 ± 0.019 OUR AVERAGE			
$-0.026 \pm 0.022 \pm 0.017$	ABE	03B BELL	$e^+e^- \to \Upsilon(4S)$
$0.003 \pm 0.030 \pm 0.004$	AUBERT	02F BABR	$e^+e^- \to \Upsilon(4S)$
$0.018 \pm 0.043 \pm 0.004$	[425] BONVICINI	00 CLE2	$e^+e^- \to \Upsilon(4S)$

[425] A $+0.3\%$ correction is applied due to a slightly higher reconstruction efficiency for the positive kaons.

$A_{CP}(B^+ \to J/\psi(1S)\pi^+)$

VALUE	DOCUMENT ID	TECN	COMMENT
-0.01 ± 0.13 OUR AVERAGE			
$-0.023 \pm 0.164 \pm 0.015$	ABE	03B BELL	$e^+e^- \to \Upsilon(4S)$
$0.01 \pm 0.22 \pm 0.01$	AUBERT	02F BABR	$e^+e^- \to \Upsilon(4S)$

$A_{CP}(B^+ \to \psi(2S)K^+)$

VALUE	DOCUMENT ID	TECN	COMMENT
-0.037 ± 0.025 OUR AVERAGE			
$-0.042 \pm 0.020 \pm 0.017$	ABE	03B BELL	$e^+e^- \to \Upsilon(4S)$
$0.02 \pm 0.091 \pm 0.01$	[426] BONVICINI	00 CLE2	$e^+e^- \to \Upsilon(4S)$

[426] A $+0.3\%$ correction is applied due to a slightly higher reconstruction efficiency for the positive kaons.

$A_{CP}(B^+ \to \overline{D}^0 K^+)$

VALUE	DOCUMENT ID	TECN	COMMENT
$0.04 \pm 0.06 \pm 0.03$	[427] SWAIN	03 BELL	$e^+e^- \to \Upsilon(4S)$
• • • We do not use the following data for averages, fits, limits, etc. • • •			
$0.003 \pm 0.080 \pm 0.037$	[428] ABE	03D BELL	Repl. by SWAIN 03

[427] Corresponds to 90% confidence range $-0.07 < A_{CP} < 0.15$.
[428] Corresponds to 90% confidence range $-0.15 < A_{CP} < 0.16$.

$A_{CP}(B^+ \to D_{CP(+1)}K^+)$

VALUE	DOCUMENT ID	TECN	COMMENT
$0.06 \pm 0.19 \pm 0.04$	[429] SWAIN	03 BELL	$e^+e^- \to \Upsilon(4S)$
• • • We do not use the following data for averages, fits, limits, etc. • • •			
$0.29 \pm 0.26 \pm 0.05$	[430] ABE	03D BELL	Repl. by SWAIN 03

[429] Corresponds to 90% confidence range $-0.26 < A_{CP} < 0.38$.
[430] Corresponds to 90% confidence range $-0.14 < A_{CP} < 0.73$.

$A_{CP}(B^+ \to D_{CP(-1)}K^+)$

VALUE	DOCUMENT ID	TECN	COMMENT
$-0.19 \pm 0.17 \pm 0.05$	[431] SWAIN	03 BELL	$e^+e^- \to \Upsilon(4S)$
• • • We do not use the following data for averages, fits, limits, etc. • • •			
$-0.22 \pm 0.24 \pm 0.04$	[432] ABE	03D BELL	Repl. by SWAIN 03

[431] Corresponds to 90% confidence range $-0.47 < A_{CP} < 0.11$.
[432] Corresponds to 90% confidence range $-0.62 < A_{CP} < 0.18$.

$A_{CP}(B^+ \to \pi^+\pi^0)$

VALUE	DOCUMENT ID	TECN	COMMENT
0.05 ± 0.15 OUR AVERAGE			
$-0.03\ ^{+0.18}_{-0.17} \pm 0.02$	[433] AUBERT	03L BABR	$e^+e^- \to \Upsilon(4S)$
$0.30 \pm 0.30\ ^{+0.06}_{-0.04}$	[434] CASEY	02 BELL	$e^+e^- \to \Upsilon(4S)$

[433] Corresponds to 90% confidence range $-0.32 < A_{CP} < 0.27$.
[434] Corresponds to 90% confidence range $-0.23 < A_{CP} < +0.86$.

$A_{CP}(B^+ \to K^+\pi^0)$

VALUE	DOCUMENT ID	TECN	COMMENT
-0.10 ± 0.08 OUR AVERAGE			
$-0.09 \pm 0.09 \pm 0.01$	[435] AUBERT	03L BABR	$e^+e^- \to \Upsilon(4S)$
$-0.02 \pm 0.19 \pm 0.02$	[436] CASEY	02 BELL	$e^+e^- \to \Upsilon(4S)$
-0.29 ± 0.23	[437] CHEN	00 CLE2	$e^+e^- \to \Upsilon(4S)$
• • • We do not use the following data for averages, fits, limits, etc. • • •			
$-0.059\ ^{+0.222}_{-0.196} \pm 0.055 \pm 0.017$	[438] ABE	01K BELL	Repl. by CASEY 02
$0.00 \pm 0.18 \pm 0.04$	[439] AUBERT	01E BABR	Repl. by AUBERT 03L

[435] Corresponds to 90% confidence range $-0.24 < A_{CP} < 0.06$.
[436] Corresponds to 90% confidence range $-0.35 < A_{CP} < +0.30$.
[437] Corresponds to 90% confidence range $-0.67 < A_{CP} < 0.09$.
[438] Corresponds to 90% confidence range $-0.40 < A_{CP} < 0.36$.
[439] Corresponds to 90% confidence range $-0.30 < A_{CP} < +0.30$.

$A_{CP}(B^+ \to K^0_S\pi^+)$

VALUE	DOCUMENT ID	TECN	COMMENT
0.03 ± 0.08 OUR AVERAGE Error includes scale factor of 1.1.			
$0.07\ ^{+0.09}_{-0.08}\ ^{+0.01}_{-0.03}$	[440] UNNO	03 BELL	$e^+e^- \to \Upsilon(4S)$
$-0.21 \pm 0.18 \pm 0.03$	[441] AUBERT	01E BABR	$e^+e^- \to \Upsilon(4S)$
0.18 ± 0.24	[442] CHEN	00 CLE2	$e^+e^- \to \Upsilon(4S)$
• • • We do not use the following data for averages, fits, limits, etc. • • •			
$0.46 \pm 0.15 \pm 0.02$	[443] CASEY	02 BELL	Repl. by UNNO 03
$0.098\ ^{+0.430}_{-0.343}\ ^{+0.020}_{-0.063}$	[444] ABE	01K BELL	Repl. by CASEY 02

[440] Corresponds to 90% confidence range $-0.10 < A_{CP} < +0.22$.
[441] Corresponds to 90% confidence range $-0.51 < A_{CP} < 0.09$.
[442] Corresponds to 90% confidence range $-0.22 < A_{CP} < 0.56$.
[443] Corresponds to 90% confidence range $+0.19 < A_{CP} < +0.72$.
[444] Corresponds to 90% confidence range $-0.53 < A_{CP} < 0.82$.

$A_{CP}(B^+ \to \pi^+\pi^-\pi^+)$

VALUE	DOCUMENT ID	TECN	COMMENT
$-0.39 \pm 0.33 \pm 0.12$	AUBERT	03M BABR	$e^+e^- \to \Upsilon(4S)$

$A_{CP}(B^+ \to \rho^+\rho^0)$

VALUE	DOCUMENT ID	TECN	COMMENT
-0.09 ± 0.16 OUR AVERAGE			
$-0.19 \pm 0.23 \pm 0.03$	AUBERT	03V BABR	$e^+e^- \to \Upsilon(4S)$
$0.00 \pm 0.22 \pm 0.03$	ZHANG	03B BELL	$e^+e^- \to \Upsilon(4S)$

$A_{CP}(B^+ \to K^+\pi^-\pi^+)$

VALUE	DOCUMENT ID	TECN	COMMENT
$0.01 \pm 0.07 \pm 0.03$	AUBERT	03M BABR	$e^+e^- \to \Upsilon(4S)$

$A_{CP}(B^+ \to K^+K^-K^+)$

VALUE	DOCUMENT ID	TECN	COMMENT
$0.02 \pm 0.07 \pm 0.03$	AUBERT	03M BABR	$e^+e^- \to \Upsilon(4S)$

$A_{CP}(B^+ \to K^+\eta')$

VALUE	DOCUMENT ID	TECN	COMMENT
0.009 ± 0.035 OUR AVERAGE			
$0.037 \pm 0.045 \pm 0.011$	[445] AUBERT	03W BABR	$e^+e^- \to \Upsilon(4S)$
$-0.11 \pm 0.11 \pm 0.02$	[446] AUBERT	02E BABR	$e^+e^- \to \Upsilon(4S)$
$-0.015 \pm 0.070 \pm 0.009$	[447] CHEN	02B BELL	$e^+e^- \to \Upsilon(4S)$
0.03 ± 0.12	[448] CHEN	00 CLE2	$e^+e^- \to \Upsilon(4S)$
• • • We do not use the following data for averages, fits, limits, etc. • • •			
$0.06 \pm 0.15 \pm 0.01$	[449] ABE	01M BELL	Repl. by CHEN 02B

[445] Corresponds to 90% confidence range $-0.04 < A_{CP} < 0.11$.
[446] Corresponds to 90% confidence range $-0.28 < A_{CP} < 0.07$.
[447] Corresponds to 90% confidence range $-0.13 < A_{CP} < 0.10$.
[448] Corresponds to 90% confidence range $-0.17 < A_{CP} < 0.23$.
[449] Corresponds to 90% confidence range $-0.20 < A_{CP} < 0.32$.

$A_{CP}(B^+ \to \omega\pi^+)$

VALUE	DOCUMENT ID	TECN	COMMENT
-0.21 ± 0.19 OUR AVERAGE			
$-0.01\ ^{+0.29}_{-0.31} \pm 0.03$	[450] AUBERT	02E BABR	$e^+e^- \to \Upsilon(4S)$
-0.34 ± 0.25	[451] CHEN	00 CLE2	$e^+e^- \to \Upsilon(4S)$

[450] Corresponds to 90% confidence range $-0.50 < A_{CP} < 0.46$.
[451] Corresponds to 90% confidence range $-0.75 < A_{CP} < 0.07$.

$A_{CP}(B^+ \to \omega K^+)$

VALUE	DOCUMENT ID	TECN	COMMENT
$-0.21 \pm 0.28 \pm 0.03$	[452] LU	02 BELL	$e^+e^- \to \Upsilon(4S)$

[452] Corresponds to 90% confidence range $-0.70 < A_{CP} < +0.38$.

$A_{CP}(B^+ \to \phi K^+)$

VALUE	DOCUMENT ID	TECN	COMMENT
0.03 ± 0.07 OUR AVERAGE			
$0.04 \pm 0.09 \pm 0.01$	[453] AUBERT	04A BABR	$e^+e^- \to \Upsilon(4S)$
$0.01 \pm 0.12 \pm 0.05$	[454] CHEN	03B BELL	$e^+e^- \to \Upsilon(4S)$
• • • We do not use the following data for averages, fits, limits, etc. • • •			
$-0.05 \pm 0.20 \pm 0.03$	[455] AUBERT	02E BABR	$e^+e^- \to \Upsilon(4S)$

[453] Corresponds to 90% confidence range $-0.10 < A_{CP} < 0.18$.
[454] Corresponds to 90% confidence range $-0.20 < A_{CP} < 0.22$.
[455] Corresponds to 90% confidence range $-0.37 < A_{CP} < 0.28$.

$A_{CP}(B^+ \to \phi K^*(892)^+)$

VALUE	DOCUMENT ID	TECN	COMMENT
0.09 ± 0.15 OUR AVERAGE			
$0.16 \pm 0.17 \pm 0.03$	AUBERT	03V BABR	$e^+e^- \to \Upsilon(4S)$
$-0.13 \pm 0.29\ ^{+0.08}_{-0.11}$	[456] CHEN	03B BELL	$e^+e^- \to \Upsilon(4S)$
• • • We do not use the following data for averages, fits, limits, etc. • • •			
$-0.43\ ^{+0.36}_{-0.30} \pm 0.06$	[457] AUBERT	02E BABR	Repl. by AUBERT 03V

[456] Corresponds to 90% confidence range $-0.64 < A_{CP} < 0.36$.
[457] Corresponds to 90% confidence range $-0.88 < A_{CP} < 0.18$.

$A_{CP}(B^+ \to \rho^0 K^*(892)^+)$

VALUE	DOCUMENT ID	TECN	COMMENT
$0.20^{+0.32}_{-0.29} \pm 0.04$	AUBERT	03V BABR	$e^+e^- \to \Upsilon(4S)$

$B^{\pm}$ REFERENCES

AUBERT	04A	PR D69 011102	B. Aubert *et al.*	(BABAR Collab.)
AUBERT	04C	PRL 92 111801	B. Aubert *et al.*	(BaBar Collab.)
DRUTSKOY	04	PRL 92 051801	A. Drutskoy *et al.*	(BELLE Collab.)
GARMASH	04	PR D69 012001	A. Garmash *et al.*	(BELLE Collab.)
ZANG	04	PR D69 017101	S.L. Zang *et al.*	(BELLE Collab.)
ABE	03B	PR D67 032003	K. Abe *et al.*	(BELLE Collab.)
ABE	03D	PRL 90 131803	K. Abe *et al.*	(BELLE Collab.)
ADAM	03	PR D67 032001	N.E. Adam *et al.*	(CLEO Collab.)
ADAM	03B	PR D68 012004	N.E. Adam *et al.*	(CLEO Collab.)
ATHAR	03	PR D68 072003	S.B. Athar *et al.*	(CLEO Collab.)
AUBERT	03K	PRL 90 231801	B. Aubert *et al.*	(BaBar Collab.)
AUBERT	03L	PRL 91 021801	B. Aubert *et al.*	(BaBar Collab.)
AUBERT	03M	PRL 91 051801	B. Aubert *et al.*	(BaBar Collab.)
AUBERT	03O	PRL 91 071801	B. Aubert *et al.*	(BaBar Collab.)
AUBERT	03V	PRL 91 171802	B. Aubert *et al.*	(BaBar Collab.)
AUBERT	03W	PRL 91 161801	B. Aubert *et al.*	(BaBar Collab.)
AUBERT	03X	PR D68 092001	B. Aubert *et al.*	(BaBar Collab.)
BORNHEIM	03	PR D68 052002	A. Bornheim *et al.*	(CLEO Collab.)
CHEN	03B	PRL 91 201801	K.-F. Chen *et al.*	(BELLE Collab.)
CHOI	03	PRL 91 262001	S.-K. Choi *et al.*	(BELLE Collab.)
CSORNA	03	PR D67 112002	S.E. Csorna *et al.*	(CLEO Collab.)
EDWARDS	03	PR D68 011102R	K.W. Edwards *et al.*	(CLEO Collab.)
FANG	03	PRL 90 071801	F. Fang *et al.*	(BELLE Collab.)
HUANG	03	PRL 91 241802	H.-C. Huang *et al.*	(BELLE Collab.)
ISHIKAWA	03	PRL 91 261601	A. Ishikawa *et al.*	(BELLE Collab.)
KROKOVNY	03B	PRL 91 262002	P. Krokovny *et al.*	(BELLE Collab.)
SWAIN	03	PR D68 051101R	S.K. Swain *et al.*	(BELLE Collab.)
UNNO	03	PR D68 011103R	Y. Unno *et al.*	(BELLE Collab.)
ZHANG	03B	PRL 91 221801	J. Zhang *et al.*	(BELLE Collab.)
ABE	02	PRL 88 021801	K. Abe *et al.*	(BELLE Collab.)
ABE	02B	PRL 88 031802	K. Abe *et al.*	(BELLE Collab.)
ABE	02H	PRL 88 171801	K. Abe *et al.*	(BELLE Collab.)
ABE	02K	PRL 88 181803	K. Abe *et al.*	(BELLE Collab.)
ABE	02N	PL B538 11	K. Abe *et al.*	(BELLE Collab.)
ABE	02O	PR D65 091103R	K. Abe *et al.*	(BELLE Collab.)
ABE	02W	PRL 89 151802	K. Abe *et al.*	(BELLE Collab.)
ACOSTA	02C	PR D65 092009	D. Acosta *et al.*	(CDF Collab.)
ACOSTA	02F	PR D66 052005	D. Acosta *et al.*	(CDF Collab.)
AHMED	02B	PR D66 031101R	S. Ahmed *et al.*	(CLEO Collab.)
AUBERT	02	PR D65 032001	B. Aubert *et al.*	(BaBar Collab.)
AUBERT	02C	PRL 88 101805	B. Aubert *et al.*	(BaBar Collab.)
AUBERT	02E	PR D65 051101R	B. Aubert *et al.*	(BaBar Collab.)
AUBERT	02F	PR D65 091101R	B. Aubert *et al.*	(BaBar Collab.)
AUBERT	02L	PRL 88 221801	B. Aubert *et al.*	(BaBar Collab.)
BRIERE	02	PRL 89 081803	R. Briere *et al.*	(CLEO Collab.)
CASEY	02	PR D66 092002	B.C.K. Casey *et al.*	(BELLE Collab.)
CHEN	02B	PL B546 196	K.-F. Chen *et al.*	(BELLE Collab.)
DRUTSKOY	02	PL B542 171	A. Drutskoy *et al.*	(BELLE Collab.)
DYTMAN	02	PR D66 091101R	S.A. Dytman *et al.*	(CLEO Collab.)
ECKHART	02	PRL 89 251801	E. Eckhart *et al.*	(CLEO Collab.)
EDWARDS	02B	PR D65 111102R	K.W. Edwards *et al.*	(CLEO Collab.)
GABYSHEV	02	PR D66 091102R	N. Gabyshev *et al.*	(BELLE Collab.)
GARMASH	02	PR D65 092005	A. Garmash *et al.*	(BELLE Collab.)
GODANG	02	PRL 88 021802	R. Godang *et al.*	(CLEO Collab.)
GORDON	02	PL B542 183	A. Gordon *et al.*	(BELLE Collab.)
LU	02	PRL 89 191801	R.-S. Lu *et al.*	(BELLE Collab.)
MAHAPATRA	02	PRL 88 101803	R. Mahapatra *et al.*	(CLEO Collab.)
NISHIDA	02	PRL 89 231801	S. Nishida *et al.*	(BELLE Collab.)
ABE	01H	PRL 87 101801	K. Abe *et al.*	(BELLE Collab.)
ABE	01I	PRL 87 111801	K. Abe *et al.*	(BELLE Collab.)
ABE	01K	PR D64 071101	K. Abe *et al.*	(BELLE Collab.)
ABE	01L	PRL 87 161601	K. Abe *et al.*	(BELLE Collab.)
ABE	01M	PL B517 309	K. Abe *et al.*	(BELLE Collab.)
ALEXANDER	01B	PR D64 092001	J.P. Alexander *et al.*	(CLEO Collab.)
AMMAR	01B	PRL 87 271801	R. Ammar *et al.*	(CLEO Collab.)
ANDERSON	01B	PRL 87 181803	S. Anderson *et al.*	(CLEO Collab.)
AUBERT	01D	PRL 87 151801	B. Aubert *et al.*	(BaBar Collab.)
AUBERT	01E	PRL 87 151802	B. Aubert *et al.*	(BaBar Collab.)
AUBERT	01F	PRL 87 201803	B. Aubert *et al.*	(BaBar Collab.)
AUBERT	01G	PRL 87 221802	B. Aubert *et al.*	(BaBar Collab.)
BARATE	01E	EPJ C19 213	R. Barate *et al.*	(ALEPH Collab.)
BRIERE	01	PRL 86 3718	R.A. Biere *et al.*	(CLEO Collab.)
BROWDER	01	PRL 86 2950	T.E. Browder *et al.*	(CLEO Collab.)
EDWARDS	01	PRL 86 30	K.W. Edwards *et al.*	(CLEO Collab.)
GRITSAN	01	PR D64 077501	A. Gritsan *et al.*	(CLEO Collab.)
RICHICHI	01	PR D63 031103R	S.J. Richichi *et al.*	(CLEO Collab.)
ABBIENDI	00B	PL B476 233	G. Abbiendi *et al.*	(OPAL Collab.)
ABE	00C	PR D62 071101R	K. Abe *et al.*	(SLD Collab.)
AHMED	00B	PR D62 112003	S. Ahmed *et al.*	(CLEO Collab.)
ANASTASSOV	00	PRL 84 1393	A. Anastassov *et al.*	(CLEO Collab.)
BARATE	00R	PL B492 275	R. Barate *et al.*	(ALEPH Collab.)
BEHRENS	00	PR D61 052001	B.H. Behrens *et al.*	(CLEO Collab.)
BONVICINI	00	PRL 84 5940	G. Bonvicini *et al.*	(CLEO Collab.)
CHEN	00	PRL 85 525	S. Chen *et al.*	(CLEO Collab.)
COAN	00	PRL 84 5283	T.E. Coan *et al.*	(CLEO Collab.)
CRONIN-HEN...	00	PRL 85 515	D. Cronin-Hennessy *et al.*	(CLEO Collab.)
CSORNA	00	PR D61 111101	S.E. Csorna *et al.*	(CLEO Collab.)
JESSOP	00	PRL 85 2881	C.P. Jessop *et al.*	(CLEO Collab.)
RICHICHI	00	PRL 85 520	S.J. Richichi *et al.*	(CLEO Collab.)
ABBIENDI	99J	EPJ C12 609	G. Abbiendi *et al.*	(OPAL Collab.)
AFFOLDER	99B	PRL 83 3378	T. Affolder *et al.*	(CDF Collab.)
BARTELT	99	PRL 82 3746	J. Bartelt *et al.*	(CLEO Collab.)
COAN	99	PR D59 111101	T.E. Coan *et al.*	(CLEO Collab.)
ABE	98B	PR D57 5382	F. Abe *et al.*	(CDF Collab.)
ABE	98O	PR D58 072001	F. Abe *et al.*	(CDF Collab.)
ABE	98Q	PR D58 092002	F. Abe *et al.*	(CDF Collab.)
ACCIARRI	98S	PL B438 417	M. Acciarri *et al.*	(L3 Collab.)
ANASTASSOV	98	PRL 80 4127	A. Anastassov *et al.*	(CLEO Collab.)
ATHANAS	98	PRL 80 5493	M. Athanas *et al.*	(CLEO Collab.)
BARATE	98Q	EPJ C4 387	R. Barate *et al.*	(ALEPH Collab.)
BEHRENS	98	PRL 80 3710	B.H. Behrens *et al.*	(CLEO Collab.)
BERGFELD	98	PRL 81 272	T. Bergfeld *et al.*	(CLEO Collab.)
BRANDENB...	98	PRL 80 2762	G. Brandenburg *et al.*	(CLEO Collab.)
GODANG	98	PRL 80 3456	R. Godang *et al.*	(CLEO Collab.)
ABE	97J	PRL 79 590	K. Abe *et al.*	(SLD Collab.)
ACCIARRI	97F	PL B396 327	M. Acciarri *et al.*	(L3 Collab.)
ARTUSO	97	PL B399 321	M. Artuso *et al.*	(CLEO Collab.)
ATHANAS	97	PRL 79 2208	M. Athanas *et al.*	(CLEO Collab.)
BROWDER	97	PR D56 11	T. Browder *et al.*	(CLEO Collab.)
FU	97	PRL 79 3125	X. Fu *et al.*	(CLEO Collab.)
JESSOP	97	PRL 79 4533	C.P. Jessop *et al.*	(CLEO Collab.)
ABE	96B	PR D53 3496	F. Abe *et al.*	(CDF Collab.)
ABE	96C	PRL 76 4462	F. Abe *et al.*	(CDF Collab.)
ABE	96H	PRL 76 2015	F. Abe *et al.*	(CDF Collab.)
ABE	96L	PRL 76 4675	F. Abe *et al.*	(CDF Collab.)
ABE	96Q	PR D54 6596	F. Abe *et al.*	(CDF Collab.)
ABE	96R	PRL 77 5176	F. Abe *et al.*	(CDF Collab.)
ADAM	96D	ZPHY C72 207	W. Adam *et al.*	(DELPHI Collab.)
ALEXANDER	96T	PRL 77 5000	J.P. Alexander *et al.*	(CLEO Collab.)
ASNER	96	PR D53 1039	D.M. Asner *et al.*	(CLEO Collab.)
BARISH	96B	PRL 76 1570	B.C. Barish *et al.*	(CLEO Collab.)
BERGFELD	96B	PRL 77 4503	T. Bergfeld *et al.*	(CLEO Collab.)
BISHAI	96	PL B369 186	M. Bishai *et al.*	(CLEO Collab.)
BUSKULIC	96J	ZPHY C71 31	D. Buskulic *et al.*	(ALEPH Collab.)
GIBAUT	96	PR D53 4734	D. Gibaut *et al.*	(CLEO Collab.)
PDG	96	PR D54 1	R. M. Barnett *et al.*	
ABREU	95N	PL B357 255	P. Abreu *et al.*	(DELPHI Collab.)
ABREU	95Q	ZPHY C68 13	P. Abreu *et al.*	(DELPHI Collab.)
ADAM	95	ZPHY C68 363	W. Adam *et al.*	(DELPHI Collab.)
AKERS	95T	ZPHY C67 379	R. Akers *et al.*	(OPAL Collab.)
ALBRECHT	95D	PL B353 554	H. Albrecht *et al.*	(ARGUS Collab.)
ALEXANDER	95	PL B341 435	J. Alexander *et al.*	(CLEO Collab.)
Also	95C	PL B347 469 (erratum)	J. Alexander *et al.*	(CLEO Collab.)
ARTUSO	95	PRL 75 785	M. Artuso *et al.*	(CLEO Collab.)
BARISH	95	PR D51 1014	B.C. Barish *et al.*	(CLEO Collab.)
BUSKULIC	95	PL B343 444	D. Buskulic *et al.*	(ALEPH Collab.)
ABE	94D	PRL 72 3456	F. Abe *et al.*	(CDF Collab.)
ALAM	94	PR D50 43	M.S. Alam *et al.*	(CLEO Collab.)
ALBRECHT	94D	PL B335 526	H. Albrecht *et al.*	(ARGUS Collab.)
ATHANAS	94	PRL 73 3503	M. Athanas *et al.*	(CLEO Collab.)
Also	95	PRL 74 3090 (erratum)	M. Athanas *et al.*	(CLEO Collab.)
PDG	94	PR D50 1173	L. Montanet *et al.*	(CERN, LBL, BOST+)
STONE	94	HEPSY 93-11	S. Stone	
Published in B Decays, 2nd Edition, World Scientific, Singapore				
ABREU	93D	ZPHY C57 181	P. Abreu *et al.*	(DELPHI Collab.)
ABREU	93G	PL B312 253	P. Abreu *et al.*	(DELPHI Collab.)
ACTON	93C	PL B307 247	P.D. Acton *et al.*	(OPAL Collab.)
ALBRECHT	93E	ZPHY C60 11	H. Albrecht *et al.*	(ARGUS Collab.)
ALEXANDER	93B	PL B319 365	J. Alexander *et al.*	(CLEO Collab.)
AMMAR	93	PRL 71 674	R. Ammar *et al.*	(CLEO Collab.)
BEAN	93B	PRL 70 2681	A. Bean *et al.*	(CLEO Collab.)
BUSKULIC	93D	PL B307 194	D. Buskulic *et al.*	(ALEPH Collab.)
Also	94H	PL B325 537 (errata)	D. Buskulic *et al.*	(ALEPH Collab.)
SANGHERA	93	PR D47 791	S. Sanghera *et al.*	(CLEO Collab.)
ALBRECHT	92C	PL B275 195	H. Albrecht *et al.*	(ARGUS Collab.)
ALBRECHT	92E	PL B277 209	H. Albrecht *et al.*	(ARGUS Collab.)
ALBRECHT	92G	ZPHY C54 1	H. Albrecht *et al.*	(ARGUS Collab.)
BORTOLETTO	92	PR D45 21	D. Bortoletto *et al.*	(CLEO Collab.)
BUSKULIC	92G	PL B295 396	D. Buskulic *et al.*	(ALEPH Collab.)
ALBRECHT	91B	PL B254 288	H. Albrecht *et al.*	(ARGUS Collab.)
ALBRECHT	91C	PL B255 297	H. Albrecht *et al.*	(ARGUS Collab.)
ALBRECHT	91E	PL B262 148	H. Albrecht *et al.*	(ARGUS Collab.)
BERKELMAN	91	ARNPS 41 1	K. Berkelman, S. Stone	(CORN, SYRA)
"Decays of B Mesons"				
FULTON	91	PR D43 651	R. Fulton *et al.*	(CLEO Collab.)
ALBRECHT	90B	PL B241 278	H. Albrecht *et al.*	(ARGUS Collab.)
ALBRECHT	90J	ZPHY C48 543	H. Albrecht *et al.*	(ARGUS Collab.)
ANTREASYAN	90B	ZPHY C48 553	D. Antreasyan *et al.*	(Crystal Ball Collab.)
BORTOLETTO	90	PRL 64 2117	D. Bortoletto *et al.*	(CLEO Collab.)
Also	92	PR D45 21	D. Bortoletto *et al.*	(CLEO Collab.)
WEIR	90B	PR D41 1384	A.J. Weir *et al.*	(Mark II Collab.)
ALBRECHT	89G	PL B229 304	H. Albrecht *et al.*	(ARGUS Collab.)
AVERY	89B	PL B223 470	P. Avery *et al.*	(CLEO Collab.)
BEBEK	89	PRL 62 8	C. Bebek *et al.*	(CLEO Collab.)
BORTOLETTO	89	PRL 62 2436	D. Bortoletto *et al.*	(CLEO Collab.)
ALBRECHT	88F	PL B209 119	H. Albrecht *et al.*	(ARGUS Collab.)
ALBRECHT	88K	PL B215 424	H. Albrecht *et al.*	(ARGUS Collab.)
ALBRECHT	87C	PL B185 218	H. Albrecht *et al.*	(ARGUS Collab.)
ALBRECHT	87D	PL B199 451	H. Albrecht *et al.*	(ARGUS Collab.)
AVERY	87	PL B183 429	P. Avery *et al.*	(CLEO Collab.)
BEBEK	87	PR D36 1289	C. Bebek *et al.*	(CLEO Collab.)
ALAM	86	PR D34 3279	M.S. Alam *et al.*	(CLEO Collab.)
PDG	86	PL 170B	M. Aguilar-Benitez *et al.*	(CERN, CIT+)
GILES	84	PR D30 2279	R. Giles *et al.*	(CLEO Collab.)

B^0

$I(J^P) = \frac{1}{2}(0^-)$

Quantum numbers not measured. Values shown are quark-model predictions.

See also the $B^{\pm}/B^0$ ADMIXTURE and $B^{\pm}/B^0/B_s^0$/b-baryon ADMIXTURE sections.

See the Note "Production and Decay of b-flavored Hadrons" at the beginning of the $B^{\pm}$ Particle Listings and the Note on "B^0-$\overline{B}^0$ Mixing" near the end of the B^0 Particle Listings.

B^0 MASS

The fit uses $m_{B^{+}}$, $(m_{B^0} - m_{B^+})$, and m_{B^0} to determine m_{B^+}, m_{B^0}, and the mass difference.

VALUE (MeV)	EVTS	DOCUMENT ID		TECN	COMMENT
5279.4 ± 0.5 OUR FIT					
5279.3 ± 0.7 OUR AVERAGE					
5279.1 ± 0.7 ± 0.3	135	[1] CSORNA	00	CLE2	$e^+e^- \to \Upsilon(4S)$
5281.3 ± 2.2 ± 1.4	51	ABE	96B	CDF	$p\overline{p}$ at 1.8 TeV
• • • We do not use the following data for averages, fits, limits, etc. • • •					
5279.2 ± 0.54 ± 2.0	340	ALAM	94	CLE2	$e^+e^- \to \Upsilon(4S)$
5278.0 ± 0.4 ± 2.0		BORTOLETTO	92	CLEO	$e^+e^- \to \Upsilon(4S)$
5279.6 ± 0.7 ± 2.0	40	[2] ALBRECHT	90J	ARG	$e^+e^- \to \Upsilon(4S)$
5278.2 ± 1.0 ± 3.0	40	ALBRECHT	87C	ARG	$e^+e^- \to \Upsilon(4S)$
5279.5 ± 1.6 ± 3.0	7	[3] ALBRECHT	87D	ARG	$e^+e^- \to \Upsilon(4S)$
5280.6 ± 0.8 ± 2.0		BEBEK	87	CLEO	$e^+e^- \to \Upsilon(4S)$

Meson Particle Listings

B^0

[1] CSORNA 00 uses fully reconstructed 135 $B^0 \to J/\psi^{(\prime)} K^0_S$ events and invariant masses without beam constraint.
[2] ALBRECHT 90J assumes 10580 for $\Upsilon(4S)$ mass. Supersedes ALBRECHT 87C and ALBRECHT 87D.
[3] Found using fully reconstructed decays with J/ψ. ALBRECHT 87D assume $m_{\Upsilon(4S)} =$ 10577 MeV.

$m_{B^0} - m_{B^+}$

VALUE (MeV)		DOCUMENT ID		TECN	COMMENT
0.33 ± 0.28 OUR FIT	Error includes scale factor of 1.1.				
0.34 ± 0.32 OUR AVERAGE	Error includes scale factor of 1.2.				
0.41 ± 0.25 ± 0.19		ALAM	94	CLE2	$e^+e^- \to \Upsilon(4S)$
−0.4 ± 0.6 ± 0.5		BORTOLETTO	92	CLEO	$e^+e^- \to \Upsilon(4S)$
−0.9 ± 1.2 ± 0.5		ALBRECHT	90J	ARG	$e^+e^- \to \Upsilon(4S)$
2.0 ± 1.1 ± 0.3	[4]	BEBEK	87	CLEO	$e^+e^- \to \Upsilon(4S)$

[4] BEBEK 87 actually measure the difference between half of $E_{\rm cm}$ and the $B^\pm$ or B^0 mass, so the $m_{B^0} - m_{B^\pm}$ is more accurate. Assume $m_{\Upsilon(4S)} =$ 10580 MeV.

$m_{B^0_H} - m_{B^0_L}$

See the B^0-$\overline{B}^0$ MIXING PARAMETERS section near the end of these B^0 Listings.

B^0 MEAN LIFE

See $B^\pm/B^0/B^0_s/b$-baryon ADMIXTURE section for data on B-hadron mean life averaged over species of bottom particles.

"OUR EVALUATION" is an average using rescaled values of the data listed below. The average and rescaling were performed by the Heavy Flavor Averaging Group (HFAG) and are described at http://www.slac.stanford.edu/xorg/hfag/. The averaging/rescaling procedure takes into account corrections between the measurements and asymmetric lifetime errors.

VALUE (10^{-12} s)	EVTS	DOCUMENT ID		TECN	COMMENT
1.536 ± 0.014 OUR EVALUATION					
$1.523^{+0.024}_{-0.023} \pm 0.022$		[5] AUBERT	03C	BABR	$e^+e^- \to \Upsilon(4S)$
1.533 ± 0.034 ± 0.038		[6] AUBERT	03H	BABR	$e^+e^- \to \Upsilon(4S)$
1.554 ± 0.030 ± 0.019		[7] ABE	02H	BELL	$e^+e^- \to \Upsilon(4S)$
1.497 ± 0.073 ± 0.032		[8] ACOSTA	02C	CDF	$p\overline{p}$ at 1.8 TeV
1.529 ± 0.012 ± 0.029		[9] AUBERT	02H	BABR	$e^+e^- \to \Upsilon(4S)$
1.546 ± 0.032 ± 0.022		[7] AUBERT	01F	BABR	$e^+e^- \to \Upsilon(4S)$
1.541 ± 0.028 ± 0.023		[9] ABBIENDI,G	00B	OPAL	$e^+e^- \to Z$
1.518 ± 0.053 ± 0.034		[10] BARATE	00R	ALEP	$e^+e^- \to Z$
1.523 ± 0.057 ± 0.053		[11] ABBIENDI	99J	OPAL	$e^+e^- \to Z$
$1.474 \pm 0.039^{+0.052}_{-0.051}$		[10] ABE	98Q	CDF	$p\overline{p}$ at 1.8 TeV
1.52 ± 0.06 ± 0.04		[11] ACCIARRI	98S	L3	$e^+e^- \to Z$
1.64 ± 0.08 ± 0.08		[11] ABE	97J	SLD	$e^+e^- \to Z$
1.532 ± 0.041 ± 0.040		[12] ABREU	97F	DLPH	$e^+e^- \to Z$
$1.25^{+0.15}_{-0.13} \pm 0.05$	121	[8] BUSKULIC	96J	ALEP	$e^+e^- \to Z$
$1.49^{+0.17}_{-0.15} {}^{+0.08}_{-0.06}$		[13] BUSKULIC	96J	ALEP	$e^+e^- \to Z$
$1.61^{+0.14}_{-0.13} \pm 0.08$		[10,14] ABREU	95Q	DLPH	$e^+e^- \to Z$
1.63 ± 0.14 ± 0.13		[15] ADAM	95	DLPH	$e^+e^- \to Z$
1.53 ± 0.12 ± 0.08		[10,16] AKERS	95T	OPAL	$e^+e^- \to Z$
• • • We do not use the following data for averages, fits, limits, etc. • • •					
1.58 ± 0.09 ± 0.02		[8] ABE	98B	CDF	Repl. by ACOSTA 02C
1.54 ± 0.08 ± 0.06		[10] ABE	96C	CDF	Repl. by ABE 98Q
1.55 ± 0.06 ± 0.03		[17] BUSKULIC	96J	ALEP	$e^+e^- \to Z$
1.61 ± 0.07 ± 0.04		[10] BUSKULIC	96J	ALEP	Repl. by BARATE 00R
1.62 ± 0.12		[18] ADAM	95	DLPH	$e^+e^- \to Z$
1.57 ± 0.18 ± 0.08	121	[8] ABE	94D	CDF	Repl. by ABE 98B
$1.17^{+0.29}_{-0.23} \pm 0.16$	96	[10] ABREU	93D	DLPH	Sup. by ABREU 95Q
1.55 ± 0.25 ± 0.18	76	[15] ABREU	93G	DLPH	Sup. by ADAM 95
$1.51^{+0.24}_{-0.23} {}^{+0.12}_{-0.14}$	78	[10] ACTON	93C	OPAL	Sup. by AKERS 95T
$1.52^{+0.20}_{-0.18} {}^{+0.07}_{-0.13}$	77	[10] BUSKULIC	93D	ALEP	Sup. by BUSKULIC 96J
$1.20^{+0.52}_{-0.36} {}^{+0.16}_{-0.14}$	15	[19] WAGNER	90	MRK2	$E^{ee}_{\rm cm} = 29$ GeV
$0.82^{+0.57}_{-0.37} \pm 0.27$		[20] AVERILL	89	HRS	$E^{ee}_{\rm cm} = 29$ GeV

[5] AUBERT 03C uses a sample of approximately 14,000 exclusively reconstructed $B^0 \to D^*(2010)^- \ell\nu$ and simultaneously measures the lifetime and oscillation frequency.
[6] Measurement performed with decays $B^0 \to D^{*-}\pi^+$ and $B^0 \to D^{*-}\rho^+$ using a partial reconstruction technique.
[7] Events are selected in which one B meson is fully reconstructed while the second B meson is reconstructed inclusively.
[8] Measured mean life using fully reconstructed decays.
[9] Data analyzed using partially reconstructed $\overline{B}^0 \to D^{*+}\ell^-\overline{\nu}$ decays.
[10] Data analyzed using $D/D^*\ell$X event vertices.
[11] Data analyzed using charge of secondary vertex.
[12] Data analyzed using inclusive $D/D^*\ell X$.
[13] Measured mean life using partially reconstructed $D^{*-}\pi^+$X vertices.
[14] ABREU 95Q assumes B($B^0 \to D^{**-}\ell^+\nu_\ell$) = 3.2 ± 1.7%.
[15] Data analyzed using vertex-charge technique to tag B charge.
[16] AKERS 95T assumes B($B^0 \to D_s^{(*)}D^{0(*)}$) = 5.0 ± 0.9% to find B^+/B^0 yield.
[17] Combined result of $D/D^*\ell$x analysis, fully reconstructed B analysis, and partially reconstructed $D^{*-}\pi^+$X analysis.
[18] Combined ABREU 95Q and ADAM 95 result.
[19] WAGNER 90 tagged B^0 mesons by their decays into $D^{*-}e^+\nu$ and $D^{*-}\mu^+\nu$ where the D^{*-} is tagged by its decay into $\pi^-\overline{D}^0$.
[20] AVERILL 89 is an estimate of the B^0 mean lifetime assuming that $B^0 \to D^{*+}$ + X always.

MEAN LIFE RATIO τ_{B^+}/τ_{B^0}

τ_{B^+}/τ_{B^0} (direct measurements)

"OUR EVALUATION" is an average using rescaled values of the data listed below. The average and rescaling were performed by the Heavy Flavor Averaging Group (HFAG) and are described at http://www.slac.stanford.edu/xorg/hfag/. The averaging/rescaling procedure takes into account corrections between the measurements and asymmetric lifetime errors.

VALUE	EVTS	DOCUMENT ID		TECN	COMMENT
The data in this block is included in the average printed for a previous datablock.					
1.086 ± 0.017 OUR EVALUATION					
1.091 ± 0.023 ± 0.014		[21] ABE	02H	BELL	$e^+e^- \to \Upsilon(4S)$
1.093 ± 0.066 ± 0.028		[22] ACOSTA	02C	CDF	$p\overline{p}$ at 1.8 TeV
1.082 ± 0.026 ± 0.012		[21] AUBERT	01F	BABR	$e^+e^- \to \Upsilon(4S)$
1.085 ± 0.059 ± 0.018		[23] BARATE	00R	ALEP	$e^+e^- \to Z$
1.079 ± 0.064 ± 0.041		[24] ABBIENDI	99J	OPAL	$e^+e^- \to Z$
$1.110 \pm 0.056^{+0.033}_{-0.030}$		[23] ABE	98Q	CDF	$p\overline{p}$ at 1.8 TeV
1.09 ± 0.07 ± 0.03		[24] ACCIARRI	98S	L3	$e^+e^- \to Z$
1.01 ± 0.07 ± 0.06		[24] ABE	97J	SLD	$e^+e^- \to Z$
$1.27^{+0.23}_{-0.19} {}^{+0.03}_{-0.02}$		[22] BUSKULIC	96J	ALEP	$e^+e^- \to Z$
$1.00^{+0.17}_{-0.15} \pm 0.10$		[23,25] ABREU	95Q	DLPH	$e^+e^- \to Z$
$1.06^{+0.13}_{-0.10} \pm 0.10$		[26] ADAM	95	DLPH	$e^+e^- \to Z$
0.99 ± 0.14 $^{+0.05}_{-0.04}$		[23,27] AKERS	95T	OPAL	$e^+e^- \to Z$
• • • We do not use the following data for averages, fits, limits, etc. • • •					
1.06 ± 0.07 ± 0.02		[22] ABE	98B	CDF	Repl. by ACOSTA 02C
1.01 ± 0.11 ± 0.02		[23] ABE	96C	CDF	Repl. by ABE 98Q
1.03 ± 0.08 ± 0.02		[28] BUSKULIC	96J	ALEP	$e^+e^- \to Z$
0.98 ± 0.08 ± 0.03		[23] BUSKULIC	96J	ALEP	Repl. by BARATE 00R
1.02 ± 0.16 ± 0.05	269	[22] ABE	94D	CDF	Repl. by ABE 98B
$1.11^{+0.51}_{-0.39}$ ± 0.11	188	[23] ABREU	93D	DLPH	Sup. by ABREU 95Q
$1.01^{+0.29}_{-0.22} \pm 0.12$	253	[26] ABREU	93G	DLPH	Sup. by ADAM 95
$1.0^{+0.33}_{-0.25} \pm 0.08$	130	ACTON	93C	OPAL	Sup. by AKERS 95T
0.96 $^{+0.19}_{-0.15}$ $^{+0.18}_{-0.12}$	154	[23] BUSKULIC	93D	ALEP	Sup. by BUSKULIC 96J

[21] Events are selected in which one B meson is fully reconstructed while the second B meson is reconstructed inclusively.
[22] Measured using fully reconstructed decays.
[23] Data analyzed using $D/D^*\ell$X vertices.
[24] Data analyzed using charge of secondary vertex.
[25] ABREU 95Q assumes B($B^0 \to D^{**-}\ell^+\nu_\ell$) = 3.2 ± 1.7%.
[26] Data analyzed using vertex-charge technique to tag B charge.
[27] AKERS 95T assumes B($B^0 \to D_s^{(*)}D^{0(*)}$) = 5.0 ± 0.9% to find B^+/B^0 yield.
[28] Combined result of $D/D^*\ell$X analysis and fully reconstructed B analysis.

τ_{B^+}/τ_{B^0} (inferred from branching fractions)

These measurements are inferred from the branching fractions for semileptonic decay or other spectator-dominated decays by assuming that the rates for such decays are equal for B^0 and B^+. We do not use measurements which assume equal production of B^0 and B^+ because of the large uncertainty in the production ratio.

VALUE	CL%	EVTS	DOCUMENT ID		TECN	COMMENT
The data in this block is included in the average printed for a previous datablock.						
• • • We do not use the following data for averages, fits, limits, etc. • • •						
$0.95^{+0.117}_{-0.080} \pm 0.091$			[29] ARTUSO	97	CLE2	$e^+e^- \to \Upsilon(4S)$
1.15 ± 0.17 ± 0.06			[30] JESSOP	97	CLE2	$e^+e^- \to \Upsilon(4S)$
0.93 ± 0.18 ± 0.12			[31] ATHANAS	94	CLE2	Sup. by ARTUSO 97
0.91 ± 0.27 ± 0.21			[32] ALBRECHT	92C	ARG	$e^+e^- \to \Upsilon(4S)$
1.0 ± 0.4		29	[32,33] ALBRECHT	92G	ARG	$e^+e^- \to \Upsilon(4S)$
0.89 ± 0.19 ± 0.13			[32] FULTON	91	CLEO	$e^+e^- \to \Upsilon(4S)$
1.00 ± 0.23 ± 0.14			[32] ALBRECHT	90L	ARG	$e^+e^- \to \Upsilon(4S)$
0.49 to 2.3	90		[34] BEAN	87B	CLEO	$e^+e^- \to \Upsilon(4S)$

[29] ARTUSO 97 uses partial reconstruction of $B \to D^* \ell \nu_\ell$ and independent of B^0 and B^+ production fraction.
[30] Assumes equal production of B^+ and B^0 at the $\Upsilon(4S)$.
[31] ATHANAS 94 uses events tagged by fully reconstructed B^- decays and partially or fully reconstructed B^0 decays.
[32] Assumes equal production of B^0 and B^+.
[33] ALBRECHT 92G data analyzed using $B \to D_s \overline{D}$, $D_s \overline{D}^*$, $D_s^* \overline{D}$, $D_s^* \overline{D}^*$ events.
[34] BEAN 87B assume the fraction of $B^0 \overline{B}^0$ events at the $\Upsilon(4S)$ is 0.41.

$|\Delta\Gamma_{B^0_d}|/\Gamma_{B^0_d}$

$\Gamma_{B^0_d}$ and $|\Delta\Gamma_{B^0_d}|$ are the decay rate average and difference between two B^0_d CP eigenstates.

VALUE	CL%	DOCUMENT ID		TECN	COMMENT
< 0.18	95	[35] ABDALLAH	03B	DLPH	$e^+e^- \to Z$
• • • We do not use the following data for averages, fits, limits, etc. • • •					
< 0.80	95	[36,37] BEHRENS	00B	CLE2	$e^+e^- \to \Upsilon(4S)$

[35] Using the measured $\tau_{B^0} = 1.55 \pm 0.03$ ps.
[36] BEHRENS 00B uses high-momentum lepton tags and partially reconstructed $\overline{B}^0 \to D^{*+}\pi^-$, ρ^- decays to determine the flavor of the B meson.
[37] Assumes $\Delta_{md} = 0.478 \pm 0.018\ \text{ps}^{-1}$ and $\tau_{B^0} = 1.548 \pm 0.032$ ps.

B^0 DECAY MODES

$\overline{B}^0$ modes are charge conjugates of the modes below. Reactions indicate the weak decay vertex and do not include mixing. Modes which do not identify the charge state of the B are listed in the $B^\pm/B^0$ ADMIXTURE section.

The branching fractions listed below assume 50% $B^0\overline{B}^0$ and 50% B^+B^- production at the $\Upsilon(4S)$. We have attempted to bring older measurements up to date by rescaling their assumed $\Upsilon(4S)$ production ratio to 50:50 and their assumed D, D_S, D^*, and ψ branching ratios to current values whenever this would affect our averages and best limits significantly.

Indentation is used to indicate a subchannel of a previous reaction. All resonant subchannels have been corrected for resonance branching fractions to the final state so the sum of the subchannel branching fractions can exceed that of the final state.

For inclusive branching fractions, *e.g.*, $B \to D^\pm$ anything, the values usually are multiplicities, not branching fractions. They can be greater than one.

	Mode	Fraction (Γ_i/Γ)	Scale factor/ Confidence level
Γ_1	$\ell^+ \nu_\ell$ anything	[a] (10.5 ±0.8) %	
Γ_2	$D^- \ell^+ \nu_\ell$	[a] (2.14±0.20) %	
Γ_3	$D^*(2010)^- \ell^+ \nu_\ell$	[a] (5.44±0.23) %	
Γ_4	$\rho^- \ell^+ \nu_\ell$	[a] (2.6 ±0.7) × 10^{-4}	
Γ_5	$\pi^- \ell^+ \nu_\ell$	[a] (1.33±0.22) × 10^{-4}	
	Inclusive modes		
Γ_6	$\pi^- \mu^+ \nu_\mu$		
Γ_7	K^+ anything	(78 ±8) %	
	***D*, *D**, or D_s modes**		
Γ_8	$D^- \pi^+$	(2.76±0.25) × 10^{-3}	
Γ_9	$D^- \rho^+$	(7.7 ±1.3) × 10^{-3}	
Γ_{10}	$D^- K^*(892)^+$	(3.7 ±1.8) × 10^{-4}	
Γ_{11}	$D^- \omega \pi^+$	(2.8 ±0.6) × 10^{-3}	
Γ_{12}	$D^- K^+$	(2.0 ±0.6) × 10^{-4}	
Γ_{13}	$D^- K^+ \overline{K}^0$	< 3.1 × 10^{-4}	CL=90%
Γ_{14}	$D^- K^+ \overline{K}^*(892)^0$	(8.8 ±1.9) × 10^{-4}	
Γ_{15}	$\overline{D}^0 \pi^0$	(2.7 ±0.8) × 10^{-4}	
Γ_{16}	$\overline{D}^0 \pi^+ \pi^-$	(8.0 ±1.6) × 10^{-4}	
Γ_{17}	$D^*(2010)^- \pi^+$	(2.76±0.21) × 10^{-3}	
Γ_{18}	$D^- \pi^+ \pi^+ \pi^-$	(8.0 ±2.5) × 10^{-3}	
Γ_{19}	($D^- \pi^+ \pi^+ \pi^-$) nonresonant	(3.9 ±1.9) × 10^{-3}	
Γ_{20}	$D^- \pi^+ \rho^0$	(1.1 ±1.0) × 10^{-3}	
Γ_{21}	$D^- a_1(1260)^+$	(6.0 ±3.3) × 10^{-3}	
Γ_{22}	$D^*(2010)^- \pi^+ \pi^0$	(1.5 ±0.5) %	
Γ_{23}	$D^*(2010)^- \rho^+$	(6.8 ±0.9) × 10^{-3}	
Γ_{24}	$D^*(2010)^- K^+$	(2.0 ±0.5) × 10^{-4}	
Γ_{25}	$D^*(2010)^- K^*(892)^+$	(3.8 ±1.5) × 10^{-4}	
Γ_{26}	$D^*(2010)^- K^+ \overline{K}^0$	< 4.7 × 10^{-4}	CL=90%
Γ_{27}	$D^*(2010)^- K^+ \overline{K}^*(892)^0$	(1.29±0.33) × 10^{-3}	
Γ_{28}	$D^*(2010)^- \pi^+ \pi^+ \pi^-$	(7.6 ±1.8) × 10^{-3}	S=1.4
Γ_{29}	($D^*(2010)^- \pi^+ \pi^+ \pi^-$) non-resonant	(0.0 ±2.5) × 10^{-3}	
Γ_{30}	$D^*(2010)^- \pi^+ \rho^0$	(5.7 ±3.2) × 10^{-3}	
Γ_{31}	$D^*(2010)^- a_1(1260)^+$	(1.30±0.27) %	
Γ_{32}	$D^*(2010)^- \pi^+ \pi^+ \pi^- \pi^0$	(1.76±0.27) %	
Γ_{33}	$D^*(2010)^+ \pi^+ \pi^- \pi^- \pi^0$	(1.8 ±0.7) %	
Γ_{34}	$D^*(2010)^- p\overline{p}\pi^+$	(6.5 ±1.6) × 10^{-4}	
Γ_{35}	$D^*(2010)^- p\overline{n}$	(1.5 ±0.4) × 10^{-3}	
Γ_{36}	$\overline{D}^*(2010)^- \omega \pi^+$	(2.9 ±0.5) × 10^{-3}	
Γ_{37}	$\overline{D}_2^*(2460)^- \pi^+$	< 2.2 × 10^{-3}	CL=90%
Γ_{38}	$\overline{D}_2^*(2460)^- \rho^+$	< 4.9 × 10^{-3}	CL=90%
Γ_{39}	$D^- D^+$	< 9.4 × 10^{-4}	CL=90%
Γ_{40}	$D^- D_s^+$	(8.0 ±3.0) × 10^{-3}	
Γ_{41}	$D^*(2010)^- D_s^+$	(1.07±0.29) %	
Γ_{42}	$D^- D_s^{*+}$	(1.0 ±0.5) %	
Γ_{43}	$D^*(2010)^- D_s^{*+}$	(1.9 ±0.5) %	
Γ_{44}	$D^- D_{sJ}(2317)^+$	seen	
Γ_{45}	$D^- D_{sJ}(2457)^+$	seen	
Γ_{46}	$D^- D_{sJ}(2536)^+$	not seen	
Γ_{47}	$D^*(2010)^- D_{sJ}(2536)^+$	not seen	
Γ_{48}	$D^- D_{sJ}(2573)^+$	not seen	
Γ_{49}	$D^*(2010)^- D_{sJ}(2573)^+$	not seen	
Γ_{50}	$D_s^+ \pi^-$	(2.7 ±1.0) × 10^{-5}	
Γ_{51}	$D_s^{*+} \pi^-$	< 4.1 × 10^{-5}	CL=90%
Γ_{52}	$D_s^+ \rho^-$	< 7 × 10^{-4}	CL=90%
Γ_{53}	$D_s^{*+} \rho^-$	< 8 × 10^{-4}	CL=90%
Γ_{54}	$D_s^+ a_1(1260)^-$	< 2.6 × 10^{-3}	CL=90%
Γ_{55}	$D_s^{*+} a_1(1260)^-$	< 2.2 × 10^{-3}	CL=90%
Γ_{56}	$D_s^- K^+$	(3.8 ±1.3) × 10^{-5}	
Γ_{57}	$D_s^{*-} K^+$	< 2.5 × 10^{-5}	CL=90%
Γ_{58}	$D_s^- K^*(892)^+$	< 9.9 × 10^{-4}	CL=90%
Γ_{59}	$D_s^{*-} K^*(892)^+$	< 1.1 × 10^{-3}	CL=90%
Γ_{60}	$D_s^- \pi^+ K^0$	< 5 × 10^{-3}	CL=90%
Γ_{61}	$D_s^{*-} \pi^+ K^0$	< 3.1 × 10^{-3}	CL=90%
Γ_{62}	$D_s^- \pi^+ K^*(892)^0$	< 4 × 10^{-3}	CL=90%
Γ_{63}	$D_s^{*-} \pi^+ K^*(892)^0$	< 2.0 × 10^{-3}	CL=90%
Γ_{64}	$\overline{D}^0 K^0$	(5.0 ±1.4) × 10^{-5}	
Γ_{65}	$\overline{D}^0 K^*(892)^0$	(4.8 ±1.2) × 10^{-5}	
Γ_{66}	$\overline{D}^0 \pi^0$	(2.91±0.28) × 10^{-4}	
Γ_{67}	$\overline{D}^0 \rho^0$	(2.9 ±1.1) × 10^{-4}	
Γ_{68}	$\overline{D}^0 \eta$	(2.2 ±0.5) × 10^{-4}	S=1.6
Γ_{69}	$\overline{D}^0 \eta'$	(1.7 ±0.4) × 10^{-4}	
Γ_{70}	$\overline{D}^0 \omega$	(2.5 ±0.6) × 10^{-4}	S=1.5
Γ_{71}	$D^0 K^*(892)^0$	< 1.8 × 10^{-5}	CL=90%
Γ_{72}	$\overline{D}^{*0} \gamma$	< 5.0 × 10^{-5}	CL=90%
Γ_{73}	$\overline{D}^*(2007)^0 \pi^0$	(2.7 ±0.5) × 10^{-4}	
Γ_{74}	$\overline{D}^*(2007)^0 \rho^0$	< 5.1 × 10^{-4}	CL=90%
Γ_{75}	$\overline{D}^*(2007)^0 \eta$	(2.6 ±0.6) × 10^{-4}	
Γ_{76}	$\overline{D}^*(2007)^0 \eta'$	< 2.6 × 10^{-4}	CL=90%
Γ_{77}	$\overline{D}^*(2007)^0 \pi^+ \pi^-$	(6.2 ±2.2) × 10^{-4}	
Γ_{78}	$\overline{D}^*(2007)^0 K^0$	< 6.6 × 10^{-5}	CL=90%
Γ_{79}	$\overline{D}^*(2007)^0 K^*(892)^0$	< 6.9 × 10^{-5}	CL=90%
Γ_{80}	$D^*(2007)^0 K^*(892)^0$	< 4.0 × 10^{-5}	CL=90%
Γ_{81}	$D^*(2007)^0 \pi^+ \pi^+ \pi^- \pi^-$	(3.0 ±0.9) × 10^{-3}	
Γ_{82}	$D^*(2010)^+ D^*(2010)^-$	(8.7 ±1.8) × 10^{-4}	
Γ_{83}	$\overline{D}^*(2007)^0 \omega$	(4.2 ±1.1) × 10^{-4}	
Γ_{84}	$D^*(2010)^+ D^-$	< 6.3 × 10^{-4}	CL=90%
Γ_{85}	$D^*(2010)^- D^+ + D^*(2010)^+ D^-$	(9.3 ±1.5) × 10^{-4}	
Γ_{86}	$D^*(2007)^0 \overline{D}^*(2007)^0$	< 2.7 %	CL=90%
Γ_{87}	$D^- D^0 K^+$	(1.7 ±0.4) × 10^{-3}	
Γ_{88}	$D^- D^*(2007)^0 K^+$	(4.6 ±1.0) × 10^{-3}	
Γ_{89}	$D^*(2010)^- D^0 K^+$	(3.1 $^{+0.6}_{-0.5}$) × 10^{-3}	
Γ_{90}	$D^*(2010)^- D^*(2007)^0 K^+$	(1.18±0.20) %	
Γ_{91}	$D^- D^+ K^0$	< 1.7 × 10^{-3}	CL=90%
Γ_{92}	$D^*(2010)^- D^+ K^0 + D^- D^*(2010)^+ K^0$	(6.5 ±1.6) × 10^{-3}	
Γ_{93}	$D^*(2010)^- D^*(2010)^+ K^0$	(8.8 ±1.9) × 10^{-3}	
Γ_{94}	$\overline{D}^0 D^0 K^0$	< 1.4 × 10^{-3}	CL=90%
Γ_{95}	$\overline{D}^0 D^*(2007)^0 K^0 + \overline{D}^*(2007)^0 D^0 K^0$	< 3.7 × 10^{-3}	CL=90%
Γ_{96}	$\overline{D}^*(2007)^0 D^*(2007)^0 K^0$	< 6.6 × 10^{-3}	CL=90%
Γ_{97}	$(\overline{D}+\overline{D}^*)(D+D^*)K$	(4.3 ±0.7) %	

Meson Particle Listings

B^0

Charmonium modes

Γ_{98}	$\eta_c K^0$		$(1.2 \pm 0.4) \times 10^{-3}$		
Γ_{99}	$\eta_c K^*(892)^0$		$(1.6 \pm 0.7) \times 10^{-3}$		
Γ_{100}	$J/\psi(1S) K^0$		$(8.5 \pm 0.5) \times 10^{-4}$		
Γ_{101}	$J/\psi(1S) K^+ \pi^-$		$(1.2 \pm 0.6) \times 10^{-3}$		
Γ_{102}	$J/\psi(1S) K^*(892)^0$		$(1.31 \pm 0.07) \times 10^{-3}$		
Γ_{103}	$J/\psi(1S) \phi K^0$		$(9.4 \pm 2.6) \times 10^{-5}$		
Γ_{104}	$J/\psi(1S) K(1270)^0$		$(1.3 \pm 0.5) \times 10^{-3}$		
Γ_{105}	$J/\psi(1S) \pi^0$		$(2.2 \pm 0.4) \times 10^{-5}$		
Γ_{106}	$J/\psi(1S) \eta$	$<$	2.7×10^{-5}		CL=90%
Γ_{107}	$J/\psi(1S) \pi^+ \pi^-$		$(4.6 \pm 0.9) \times 10^{-5}$		
Γ_{108}	$J/\psi(1S) \rho^0$		$(1.6 \pm 0.7) \times 10^{-5}$		
Γ_{109}	$J/\psi(1S) \omega$	$<$	2.7×10^{-4}		CL=90%
Γ_{110}	$J/\psi(1S) \phi$	$<$	9.2×10^{-6}		CL=90%
Γ_{111}	$J/\psi(1S) \eta'(958)$	$<$	6.3×10^{-5}		CL=90%
Γ_{112}	$J/\psi(1S) K^0 \pi^+ \pi^-$		$(1.0 \pm 0.4) \times 10^{-3}$		
Γ_{113}	$J/\psi(1S) K^0 \rho^0$		$(5.4 \pm 3.0) \times 10^{-4}$		
Γ_{114}	$J/\psi(1S) K^*(892)^+ \pi^-$		$(8 \pm 4) \times 10^{-4}$		
Γ_{115}	$J/\psi(1S) K^*(892)^0 \pi^+ \pi^-$		$(6.6 \pm 2.2) \times 10^{-4}$		
Γ_{116}	$J/\psi(1S) p\overline{p}$	$<$	1.9×10^{-6}		CL=90%
Γ_{117}	$\psi(2S) K^0$		$(6.2 \pm 0.7) \times 10^{-4}$		
Γ_{118}	$\psi(2S) K^+ \pi^-$	$<$	1×10^{-3}		CL=90%
Γ_{119}	$\psi(2S) K^*(892)^0$		$(8.0 \pm 1.3) \times 10^{-4}$		
Γ_{120}	$\chi_{c0}(1P) K^0$	$<$	5.0×10^{-4}		CL=90%
Γ_{121}	$\chi_{c1}(1P) K^0$		$(4.0 \, ^{+1.2}_{-1.0}) \times 10^{-4}$		
Γ_{122}	$\chi_{c1}(1P) K^*(892)^0$		$(4.1 \pm 1.5) \times 10^{-4}$		

K or K^* modes

Γ_{123}	$K^+ \pi^-$		$(1.85 \pm 0.11) \times 10^{-5}$		S=1.2
Γ_{124}	$K^0 \pi^0$		$(9.5 \, ^{+2.1}_{-1.9}) \times 10^{-6}$		
Γ_{125}	$\eta' K^0$		$(6.3 \pm 0.7) \times 10^{-5}$		S=1.1
Γ_{126}	$\eta' K^*(892)^0$	$<$	2.4×10^{-5}		CL=90%
Γ_{127}	$\eta K^*(892)^0$		$(1.4 \, ^{+0.6}_{-0.5}) \times 10^{-5}$		
Γ_{128}	ηK^0	$<$	9.3×10^{-6}		CL=90%
Γ_{129}	ωK^0	$<$	1.3×10^{-5}		CL=90%
Γ_{130}	$K^0_S X^0$ (Familon)	$<$	5.3×10^{-5}		CL=90%
Γ_{131}	$\omega K^*(892)^0$	$<$	2.3×10^{-5}		CL=90%
Γ_{132}	$K^+ K^-$				
Γ_{133}	$K^0 \overline{K}^0$	$<$	3.3×10^{-6}		CL=90%
Γ_{134}	$K^0_S K^0_S K^0_S$		$(4.2 \, ^{+1.8}_{-1.5}) \times 10^{-6}$		
Γ_{135}	$K^+ \pi^- \pi^0$	$<$	4.0×10^{-5}		CL=90%
Γ_{136}	$K^+ \rho^-$		$(7.3 \pm 1.8) \times 10^{-6}$		
Γ_{137}	$K^0 \pi^+ \pi^-$		$(4.7 \pm 0.7) \times 10^{-5}$		
Γ_{138}	$K^0 \rho^0$	$<$	3.9×10^{-5}		CL=90%
Γ_{139}	$K^0 f_0(980)$	$<$	3.6×10^{-4}		CL=90%
Γ_{140}	$K^*(892)^+ \pi^-$		$(1.6 \, ^{+0.6}_{-0.5}) \times 10^{-5}$		
Γ_{141}	$K^*(892)^0 \pi^0$	$<$	3.6×10^{-6}		CL=90%
Γ_{142}	$K^*_2(1430)^+ \pi^-$	$<$	1.8×10^{-5}		CL=90%
Γ_{143}	$K^0 K^- \pi^+$	$<$	2.1×10^{-5}		CL=90%
Γ_{144}	$K^+ K^- \pi^0$	$<$	1.9×10^{-5}		CL=90%
Γ_{145}	$K^0 K^+ K^-$		$(2.8 \pm 0.5) \times 10^{-5}$		
Γ_{146}	$K^0 \phi$		$(8.6 \, ^{+1.3}_{-1.1}) \times 10^{-6}$		
Γ_{147}	$K^- \pi^+ \pi^+ \pi^-$	[b] $<$	2.3×10^{-4}		CL=90%
Γ_{148}	$K^*(892)^0 \pi^+ \pi^-$	$<$	1.4×10^{-3}		CL=90%
Γ_{149}	$K^*(892)^0 \rho^0$	$<$	3.4×10^{-5}		CL=90%
Γ_{150}	$K^*(892)^0 f_0(980)$	$<$	1.7×10^{-4}		CL=90%
Γ_{151}	$K_1(1400)^+ \pi^-$	$<$	1.1×10^{-3}		CL=90%
Γ_{152}	$K^- a_1(1260)^+$	[b] $<$	2.3×10^{-4}		CL=90%
Γ_{153}	$K^*(892)^0 K^+ K^-$	$<$	6.1×10^{-4}		CL=90%
Γ_{154}	$K^*(892)^0 \phi$		$(1.07 \pm 0.11) \times 10^{-5}$		
Γ_{155}	$\overline{K}^*(892)^0 K^*(892)^0$	$<$	2.2×10^{-5}		CL=90%
Γ_{156}	$K^*(892)^0 K^*(892)^0$	$<$	3.7×10^{-5}		CL=90%
Γ_{157}	$K^*(892)^+ K^*(892)^-$	$<$	1.41×10^{-4}		CL=90%
Γ_{158}	$K_1(1400)^0 \rho^0$	$<$	3.0×10^{-3}		CL=90%
Γ_{159}	$K_1(1400)^0 \phi$	$<$	5.0×10^{-3}		CL=90%
Γ_{160}	$K^*_2(1430)^0 \rho^0$	$<$	1.1×10^{-3}		CL=90%
Γ_{161}	$K^*_2(1430)^0 \phi$	$<$	1.4×10^{-3}		CL=90%
Γ_{162}	$K^*(892)^0 \gamma$		$(4.3 \pm 0.4) \times 10^{-5}$		
Γ_{163}	$K^0 \phi \gamma$	$<$	8.3×10^{-6}		CL=90%
Γ_{164}	$K^+ \pi^- \gamma$		$(4.6 \pm 1.4) \times 10^{-6}$		
Γ_{165}	$K^*(1410) \gamma$	$<$	1.3×10^{-4}		CL=90%
Γ_{166}	$K^+ \pi^- \gamma$ nonresonant	$<$	2.6×10^{-6}		CL=90%
Γ_{167}	$K_1(1270)^0 \gamma$	$<$	7.0×10^{-3}		CL=90%
Γ_{168}	$K_1(1400)^0 \gamma$	$<$	4.3×10^{-3}		CL=90%
Γ_{169}	$K^*_2(1430)^0 \gamma$		$(1.3 \pm 0.5) \times 10^{-5}$		
Γ_{170}	$K^*(1680)^0 \gamma$	$<$	2.0×10^{-3}		CL=90%
Γ_{171}	$K^*_3(1780)^0 \gamma$	$<$	1.0 %		CL=90%
Γ_{172}	$K^*_4(2045)^0 \gamma$	$<$	4.3×10^{-3}		CL=90%

Light unflavored meson modes

Γ_{173}	$\rho^0 \gamma$	$<$	1.2×10^{-6}		CL=90%
Γ_{174}	$\omega \gamma$	$<$	1.0×10^{-6}		CL=90%
Γ_{175}	$\phi \gamma$	$<$	3.3×10^{-6}		CL=90%
Γ_{176}	$\pi^+ \pi^-$		$(4.8 \pm 0.5) \times 10^{-6}$		
Γ_{177}	$\pi^0 \pi^0$		$(1.9 \pm 0.5) \times 10^{-6}$		
Γ_{178}	$\eta \pi^0$	$<$	2.9×10^{-6}		CL=90%
Γ_{179}	$\eta \eta$	$<$	1.8×10^{-5}		CL=90%
Γ_{180}	$\eta' \pi^0$	$<$	5.7×10^{-6}		CL=90%
Γ_{181}	$\eta' \eta'$	$<$	4.7×10^{-5}		CL=90%
Γ_{182}	$\eta' \eta$	$<$	2.7×10^{-5}		CL=90%
Γ_{183}	$\eta' \rho^0$	$<$	1.2×10^{-5}		CL=90%
Γ_{184}	$\eta \rho^0$	$<$	1.0×10^{-5}		CL=90%
Γ_{185}	$\omega \eta$	$<$	1.2×10^{-5}		CL=90%
Γ_{186}	$\omega \eta'$	$<$	6.0×10^{-5}		CL=90%
Γ_{187}	$\omega \rho^0$	$<$	1.1×10^{-5}		CL=90%
Γ_{188}	$\omega \omega$	$<$	1.9×10^{-5}		CL=90%
Γ_{189}	$\phi \pi^0$	$<$	5×10^{-6}		CL=90%
Γ_{190}	$\phi \eta$	$<$	9×10^{-6}		CL=90%
Γ_{191}	$\phi \eta'$	$<$	3.1×10^{-5}		CL=90%
Γ_{192}	$\phi \rho^0$	$<$	1.3×10^{-5}		CL=90%
Γ_{193}	$\phi \omega$	$<$	2.1×10^{-5}		CL=90%
Γ_{194}	$\phi \phi$	$<$	1.2×10^{-5}		CL=90%
Γ_{195}	$\pi^+ \pi^- \pi^0$	$<$	7.2×10^{-4}		CL=90%
Γ_{196}	$\rho^0 \pi^0$	$<$	5.3×10^{-6}		CL=90%
Γ_{197}	$\rho^\mp \pi^\pm$	[c]	$(2.28 \pm 0.25) \times 10^{-5}$		
Γ_{198}	$\pi^+ \pi^- \pi^+ \pi^-$	$<$	2.3×10^{-4}		CL=90%
Γ_{199}	$\rho^0 \rho^0$	$<$	2.1×10^{-6}		CL=90%
Γ_{200}	$a_1(1260)^\mp \pi^\pm$	[c] $<$	4.9×10^{-4}		CL=90%
Γ_{201}	$a_2(1320)^\mp \pi^\pm$	[c] $<$	3.0×10^{-4}		CL=90%
Γ_{202}	$\pi^+ \pi^- \pi^0 \pi^0$	$<$	3.1×10^{-3}		CL=90%
Γ_{203}	$\rho^+ \rho^-$	$<$	2.2×10^{-3}		CL=90%
Γ_{204}	$a_1(1260)^0 \pi^0$	$<$	1.1×10^{-3}		CL=90%
Γ_{205}	$\omega \pi^0$	$<$	3×10^{-6}		CL=90%
Γ_{206}	$\pi^+ \pi^+ \pi^- \pi^- \pi^0$	$<$	9.0×10^{-3}		CL=90%
Γ_{207}	$a_1(1260)^+ \rho^-$	$<$	3.4×10^{-3}		CL=90%
Γ_{208}	$a_1(1260)^0 \rho^0$	$<$	2.4×10^{-3}		CL=90%
Γ_{209}	$\pi^+ \pi^+ \pi^+ \pi^- \pi^- \pi^-$	$<$	3.0×10^{-3}		CL=90%
Γ_{210}	$a_1(1260)^+ a_1(1260)^-$	$<$	2.8×10^{-3}		CL=90%
Γ_{211}	$\pi^+ \pi^+ \pi^+ \pi^- \pi^- \pi^- \pi^0$	$<$	1.1 %		CL=90%

Baryon modes

Γ_{212}	$p\overline{p}$	$<$	1.2×10^{-6}		CL=90%
Γ_{213}	$p\overline{p} \pi^+ \pi^-$	$<$	2.5×10^{-4}		CL=90%
Γ_{214}	$p\overline{p} K^0$	$<$	7.2×10^{-6}		CL=90%
Γ_{215}	$p\overline{\Lambda} \pi^-$		$(4.0 \, ^{+1.1}_{-1.0}) \times 10^{-6}$		
Γ_{216}	$p\overline{\Lambda} K^-$	$<$	8.2×10^{-7}		CL=90%
Γ_{217}	$p\overline{\Sigma}^0 \pi^-$	$<$	3.8×10^{-6}		CL=90%
Γ_{218}	$\overline{\Lambda} \Lambda$	$<$	1.0×10^{-6}		CL=90%
Γ_{219}	$\Delta^0 \overline{\Delta}^0$	$<$	1.5×10^{-3}		CL=90%
Γ_{220}	$\Delta^{++} \overline{\Delta}^{--}$	$<$	1.1×10^{-4}		CL=90%
Γ_{221}	$\overline{D}^0 p\overline{p}$		$(1.18 \pm 0.22) \times 10^{-4}$		
Γ_{222}	$\overline{D}^*(2007)^0 p\overline{p}$		$(1.2 \pm 0.4) \times 10^{-4}$		
Γ_{223}	$\overline{\Sigma}_c^{--} \Delta^{++}$	$<$	1.0×10^{-3}		CL=90%
Γ_{224}	$\overline{\Lambda}_c^- p \pi^+ \pi^-$		$(1.3 \pm 0.4) \times 10^{-3}$		
Γ_{225}	$\overline{\Lambda}_c^- p$		$(2.2 \pm 0.8) \times 10^{-5}$		
Γ_{226}	$\overline{\Lambda}_c^- p \pi^0$	$<$	5.9×10^{-4}		CL=90%
Γ_{227}	$\overline{\Lambda}_c^- p \pi^+ \pi^- \pi^0$	$<$	5.07×10^{-3}		CL=90%
Γ_{228}	$\overline{\Lambda}_c^- p \pi^+ \pi^- \pi^+ \pi^-$	$<$	2.74×10^{-3}		CL=90%
Γ_{229}	$\overline{\Sigma}_c(2520)^{--} p \pi^+$		$(1.6 \pm 0.7) \times 10^{-4}$		
Γ_{230}	$\overline{\Sigma}_c(2520)^0 p \pi^-$	$<$	1.21×10^{-4}		CL=90%
Γ_{231}	$\overline{\Sigma}_c(2455)^0 p \pi^-$		$(10 \pm 8) \times 10^{-5}$		S=1.7
Γ_{232}	$\overline{\Sigma}_c(2455)^{--} p \pi^+$		$(2.8 \pm 0.9) \times 10^{-4}$		
Γ_{233}	$\overline{\Lambda}_c(2593)^-$ / $\overline{\Lambda}_c(2625)^- p$	$<$	1.1×10^{-4}		CL=90%

Lepton Family number (LF) violating modes, or $\Delta B = 1$ weak neutral current ($B1$) modes

Γ_{234}	$\gamma\gamma$	$B1$	<	1.7	$\times 10^{-6}$	CL=90%
Γ_{235}	e^+e^-	$B1$	<	1.9	$\times 10^{-7}$	CL=90%
Γ_{236}	$\mu^+\mu^-$	$B1$	<	1.6	$\times 10^{-7}$	CL=90%
Γ_{237}	$K^0e^+e^-$	$B1$	<	5.4	$\times 10^{-7}$	CL=90%
Γ_{238}	$K^0\mu^+\mu^-$	$B1$		$(5.6\ ^{+2.9}_{-2.4})$	$\times 10^{-7}$	
Γ_{239}	$K^0\ell^+\ell^-$	$B1$	[a] <	6.8	$\times 10^{-7}$	CL=90%
Γ_{240}	$K^*(892)^0e^+e^-$	$B1$	<	2.4	$\times 10^{-6}$	CL=90%
Γ_{241}	$K^*(892)^0\mu^+\mu^-$	$B1$		(1.3 ± 0.4)	$\times 10^{-6}$	
Γ_{242}	$K^*(892)^0\nu\overline{\nu}$	$B1$	<	1.0	$\times 10^{-3}$	CL=90%
Γ_{243}	$K^*(892)^0\ell^+\ell^-$	$B1$	[a]	(1.17 ± 0.30)	$\times 10^{-6}$	
Γ_{244}	$e^\pm\mu^\mp$	LF	[c] <	1.7	$\times 10^{-7}$	CL=90%
Γ_{245}	$K^0e^\pm\mu^\mp$	LF	<	4.0	$\times 10^{-6}$	CL=90%
Γ_{246}	$K^*(892)^0e^\pm\mu^\mp$	LF	<	3.4	$\times 10^{-6}$	CL=90%
Γ_{247}	$e^\pm\tau^\mp$	LF	[c] <	5.3	$\times 10^{-4}$	CL=90%
Γ_{248}	$\mu^\pm\tau^\mp$	LF	[c] <	8.3	$\times 10^{-4}$	CL=90%

[a] An ℓ indicates an e or a μ mode, not a sum over these modes.

[b] B^0 and B^0_s contributions not separated. Limit is on weighted average of the two decay rates.

[c] The value is for the sum of the charge states or particle/antiparticle states indicated.

B^0 BRANCHING RATIOS

For branching ratios in which the charge of the decaying B is not determined, see the $B^\pm$ section.

$\Gamma(\ell^+\nu_\ell \text{anything})/\Gamma_{\text{total}}$ Γ_1/Γ

VALUE	DOCUMENT ID		TECN	COMMENT
0.105 ±0.008 OUR AVERAGE				
$0.1078\pm0.0060\pm0.0069$	[38] ARTUSO	97	CLE2	$e^+e^- \to \Upsilon(4S)$
$0.093\ \pm0.011\ \pm0.015$	ALBRECHT	94	ARG	$e^+e^- \to \Upsilon(4S)$
$0.099\ \pm0.030\ \pm0.009$	HENDERSON	92	CLEO	$e^+e^- \to \Upsilon(4S)$
• • • We do not use the following data for averages, fits, limits, etc. • • •				
$0.109\ \pm0.007\ \pm0.011$	ATHANAS	94	CLE2	Sup. by ARTUSO 97

[38] ARTUSO 97 uses partial reconstruction of $B \to D^*\ell\nu_\ell$ and inclusive semileptonic branching ratio from BARISH 96B ($0.1049 \pm 0.0017 \pm 0.0043$).

$\Gamma(D^-\ell^+\nu_\ell)/\Gamma_{\text{total}}$ Γ_2/Γ

ℓ denotes e or μ, not the sum.

"OUR EVALUATION" is an average using rescaled values of the data listed below. The average and rescaling were performed by the Heavy Flavor Averaging Group (HFAG) and are described at http://www.slac.stanford.edu/xorg/hfag/. The averaging/rescaling procedure takes into account corrections between the measurements.

VALUE	DOCUMENT ID		TECN	COMMENT
0.0214±0.0020 OUR EVALUATION				
0.0213±0.0018 OUR AVERAGE				
$0.0213\pm0.0012\pm0.0039$	ABE	02E	BELL	$e^+e^- \to \Upsilon(4S)$
$0.0209\pm0.0013\pm0.0018$	[39] BARTELT	99	CLE2	$e^+e^- \to \Upsilon(4S)$
$0.0235\pm0.0020\pm0.0044$	[40] BUSKULIC	97	ALEP	$e^+e^- \to Z$
• • • We do not use the following data for averages, fits, limits, etc. • • •				
$0.0187\pm0.0015\pm0.0032$	[41] ATHANAS	97	CLE2	Repl. by BARTELT 99
$0.018\ \pm0.006\ \pm0.003$	[42] FULTON	91	CLEO	$e^+e^- \to \Upsilon(4S)$
$0.020\ \pm0.007\ \pm0.006$	[43] ALBRECHT	89J	ARG	$e^+e^- \to \Upsilon(4S)$

[39] Assumes equal production of B^+ and B^0 at the $\Upsilon(4S)$.

[40] BUSKULIC 97 assumes fraction (B^+) = fraction (B^0) = (37.8 ± 2.2)% and PDG 96 values for B lifetime and branching ratio of D^* and D decays.

[41] ATHANAS 97 uses missing energy and missing momentum to reconstruct neutrino.

[42] FULTON 91 assumes assuming equal production of B^0 and B^+ at the $\Upsilon(4S)$ and uses Mark III D and D^* branching ratios.

[43] ALBRECHT 89J reports $0.018 \pm 0.006 \pm 0.005$. We rescale using the method described in STONE 94 but with the updated PDG 94 B($D^0 \to K^-\pi^+$).

$\Gamma(D^*(2010)^-\ell^+\nu_\ell)/\Gamma_{\text{total}}$ Γ_3/Γ

"OUR EVALUATION" is an average using rescaled values of the data listed below. The average and rescaling were performed by the Heavy Flavor Averaging Group (HFAG) and are described at http://www.slac.stanford.edu/xorg/hfag/. The averaging/rescaling procedure takes into account corrections between the measurements.

VALUE	EVTS	DOCUMENT ID		TECN	COMMENT
0.0544±0.0023 OUR EVALUATION					
0.0519±0.0032 OUR AVERAGE Error includes scale factor of 1.3. See the ideogram below.					
$0.0609\pm0.0019\pm0.0040$		[44] ADAM	03	CLE2	$e^+e^- \to \Upsilon(4S)$
$0.0459\pm0.0023\pm0.0040$		[45] ABE	02F	BELL	$e^+e^- \to \Upsilon(4S)$
$0.0470\pm0.0013\ ^{+0.0036}_{-0.0031}$		[46] ABREU	01H	DLPH	$e^+e^- \to Z$
$0.0526\pm0.0020\pm0.0046$		[47] ABBIENDI	00Q	OPAL	$e^+e^- \to Z$
$0.0553\pm0.0026\pm0.0052$		[48] BUSKULIC	97	ALEP	$e^+e^- \to Z$
• • • We do not use the following data for averages, fits, limits, etc. • • •					
$0.0609\pm0.0019\pm0.0040$		[49] BRIERE	02	CLE2	$e^+e^- \to \Upsilon(4S)$
$0.0508\pm0.0021\pm0.0066$		[50] ACKERSTAFF	97G	OPAL	Repl. by ABBIENDI 00Q
$0.0552\pm0.0017\pm0.0068$		[51] ABREU	96P	DLPH	Repl. by ABREU 01H
$0.0449\pm0.0032\pm0.0039$	376	[52] BARISH	95	CLE2	Repl. by ADAM 03
$0.0518\pm0.0030\pm0.0062$	410	[53] BUSKULIC	95N	ALEP	Sup. by BUSKULIC 97
$0.045\ \pm0.003\ \pm0.004$		[54] ALBRECHT	94	ARG	$e^+e^- \to \Upsilon(4S)$
$0.047\ \pm0.005\ \pm0.005$	235	[55] ALBRECHT	93	ARG	$e^+e^- \to \Upsilon(4S)$
seen	398	[56] SANGHERA	93	CLE2	$e^+e^- \to \Upsilon(4S)$
$0.070\ \pm0.018\ \pm0.014$		[57] ANTREASYAN	90B	CBAL	$e^+e^- \to \Upsilon(4S)$
		[58] ALBRECHT	89C	ARG	$e^+e^- \to \Upsilon(4S)$
$0.060\ \pm0.010\ \pm0.014$		[59] ALBRECHT	89J	ARG	$e^+e^- \to \Upsilon(4S)$
$0.040\ \pm0.004\ \pm0.006$		[60] BORTOLETTO	89B	CLEO	$e^+e^- \to \Upsilon(4S)$
$0.070\ \pm0.012\ \pm0.019$	47	[61] ALBRECHT	87J	ARG	$e^+e^- \to \Upsilon(4S)$

[44] Uses the combined fit of both $B^0 \to D^*(2010)^-\ell\nu$ and $B^+ \to \overline{D}(2007)^0\ell\nu$ samples.

[45] Assumes equal production of B^+ and B^0 at the $\Upsilon(4S)$.

[46] ABREU 01H measured using about 5000 partial reconstructed D^* sample.

[47] ABBIENDI 00Q assumes the fraction B($b \to B^0$)= $(39.7^{+1.8}_{-2.2})$%. This result is an average of two methods using exclusive and partial D^* reconstruction.

[48] BUSKULIC 97 assumes fraction (B^+) = fraction (B^0) = (37.8 ± 2.2)% and PDG 96 values for B lifetime and D^* and D branching fractions.

[49] The results are based on the same analysis and data sample reported in ADAM 03.

[50] ACKERSTAFF 97G assumes fraction (B^+) = fraction (B^0) = (37.8 ± 2.2)% and PDG 96 values for B lifetime and branching ratio of D^* and D decays.

[51] ABREU 96P result is the average of two methods using exclusive and partial D^* reconstruction.

[52] BARISH 95 use B($D^0 \to K^-\pi^+$) = $(3.91 \pm 0.08 \pm 0.17)$% and B($D^{*+} \to D^0\pi^+$) = $(68.1 \pm 1.0 \pm 1.3)$%.

[53] BUSKULIC 95N assumes fraction (B^+) = fraction (B^0) = $38.2 \pm 1.3 \pm 2.2$% and τ_{B^0} = 1.58 ± 0.06 ps. $\Gamma(D^{*-}\ell^+\nu_\ell)$/total = [5.18 − 0.13(fraction(B^0)− 38.2)− 1.5(τ_{B^0} − 1.58)]%.

[54] ALBRECHT 94 assumes B($D^{*+} \to D^0\pi^+$) = $68.1 \pm 1.0 \pm 1.3$%. Uses partial reconstruction of D^{*+} and is independent of D^0 branching ratios.

[55] ALBRECHT 93 reports $0.052 \pm 0.005 \pm 0.006$. We rescale using the method described in STONE 94 but with the updated PDG 94 B($D^0 \to K^-\pi^+$). We have taken their average e and μ value. They also obtain α= $2*\Gamma^0/(\Gamma^- + \Gamma^+) - 1 = 1.1 \pm 0.4 \pm 0.2$, $A_{AF} = 3/4*(\Gamma^- - \Gamma^+)/\Gamma = 0.2 \pm 0.08 \pm 0.06$ and a value of $|V_{cb}| = 0.036$–0.045 depending on model assumptions.

[56] Combining $\overline{D}^{*0}\ell^+\nu_\ell$ and $\overline{D}^{*-}\ell^+\nu_\ell$ SANGHERA 93 test $V-A$ structure and fit the decay angular distributions to obtain $A_{FB} = 3/4*(\Gamma^- - \Gamma^+)/\Gamma = 0.14 \pm 0.06 \pm 0.03$. Assuming a value of V_{cb}, they measure V, A_1, and A_2, the three form factors for the $D^*\ell\nu_\ell$ decay, where results are slightly dependent on model assumptions.

[57] ANTREASYAN 90B is average over B and $\overline{D}^*(2010)$ charge states.

[58] The measurement of ALBRECHT 89C suggests a D^* polarization γ_L/γ_T of 0.85 ± 0.45. or $\alpha = 0.7 \pm 0.9$.

[59] ALBRECHT 89J is ALBRECHT 87J value rescaled using B($D^*(2010)^- \to D^0\pi^-$) = $0.57 \pm 0.04 \pm 0.04$. Superseded by ALBRECHT 93.

[60] We have taken average of the BORTOLETTO 89B values for electrons and muons, $0.046 \pm 0.005 \pm 0.007$. We rescale using the method described in STONE 94 but with the updated PDG 94 B($D^0 \to K^-\pi^+$). The measurement suggests a D^* polarization parameter value $\alpha = 0.65 \pm 0.66 \pm 0.25$.

[61] ALBRECHT 87J assume μ-e universality, the B($\Upsilon(4S) \to B^0\overline{B}^0$) = 0.45, the B($D^0 \to K^-\pi^+$) = $(0.042 \pm 0.004 \pm 0.004)$, and the B($D^*(2010)^- \to D^0\pi^-$) = 0.49 ± 0.08. Superseded by ALBRECHT 89J.

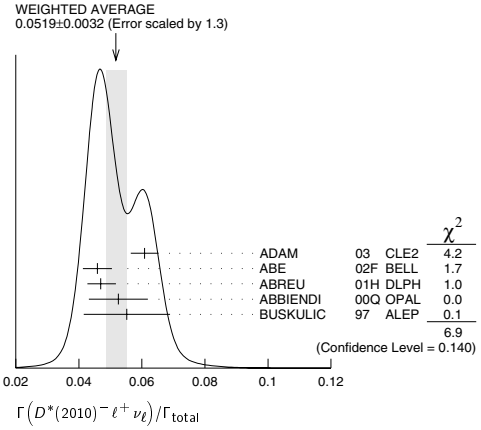

$\Gamma(\rho^- \ell^+ \nu_\ell)/\Gamma_{total}$ Γ_4/Γ

$\ell = e$ or μ, not sum over e and μ modes.

VALUE (units 10^{-4})	CL%	DOCUMENT ID		TECN	COMMENT
2.6 ±0.7 OUR AVERAGE					
$2.17 \pm 0.34 \,^{+0.62}_{-0.68}$		[62] ATHAR	03	CLE2	$e^+e^- \to \Upsilon(4S)$
$3.29 \pm 0.42 \pm 0.72$		[63] AUBERT	03E	BABR	$e^+e^- \to \Upsilon(4S)$
$2.57 \pm 0.29 \,^{+0.53}_{-0.62}$		[64] BEHRENS	00	CLE2	$e^+e^- \to \Upsilon(4S)$
• • • We do not use the following data for averages, fits, limits, etc. • • •					
$2.69 \pm 0.41 \,^{+0.61}_{-0.64}$		[65] BEHRENS	00	CLE2	$e^+e^- \to \Upsilon(4S)$
$2.5 \pm 0.4 \,^{+0.7}_{-0.9}$		[66] ALEXANDER	96T	CLE2	Repl. by BEHRENS 00
<4.1	90	[67] BEAN	93B	CLE2	$e^+e^- \to \Upsilon(4S)$

[62] ATHAR 03 reports systematic errors $^{+0.47}_{-0.5} \pm 0.41 \pm 0.01$, which are experimental systematic, systematic due to residual form-factor uncertainties in the signal, and systematic due to residual form-factor uncertainties in the cross-feed modes, respectively. We combine these in quadrature.

[63] Uses isospin constraints and extrapolation to all electron energies according to five different form-factor calculations. The second error combines the systematic and theoretical uncertainties in quadrature.

[64] Averaging with ALEXANDER 96T results including experimental and theoretical correlations considered, BEHRENS 00 reports systematic errors $^{+0.33}_{-0.46} \pm 0.41$, where the second error is theoretical model dependence. We combine these in quadrature.

[65] BEHRENS 00 reports $^{+0.35}_{-0.40} \pm 0.50$, where the second error is the theoretical model dependence. We combine these in quadrature. B^+ and B^0 decays combined using isospin symmetry: $\Gamma(B^0 \to \rho^- \ell^+ \nu) = 2\Gamma(B^+ \to \rho^0 \ell^+ \nu) \approx 2\Gamma(B^+ \to \omega \ell^+ \nu)$. No evidence for $\omega \ell \nu$ is reported.

[66] ALEXANDER 96T reports $^{+0.5}_{-0.7} \pm 0.5$ where the second error is the theoretical model dependence. We combine these in quadrature. B^+ and B^0 decays combined using isospin symmetry: $\Gamma(B^0 \to \rho^- \ell^+ \nu) = 2\Gamma(B^+ \to \rho^0 \ell^+ \nu) \approx 2\Gamma(B^+ \to \omega \ell^+ \nu)$. No evidence for $\omega \ell \nu$ is reported.

[67] BEAN 93B limit set using ISGW Model. Using isospin and the quark model to combine $\Gamma(\rho^0 \ell^+ \nu_\ell)$ and $\Gamma(\omega \ell^+ \nu_\ell)$ with this result, they obtain a limit $< (1.6\text{–}2.7) \times 10^{-4}$ at 90% CL for $B^+ \to (\omega \text{ or } \rho^0) \ell^+ \nu_\ell$. The range corresponds to the ISGW, WSB, and KS models. An upper limit on $|V_{ub}/V_{cb}| < 0.08\text{–}0.13$ at 90% CL is derived as well.

$\Gamma(\pi^- \ell^+ \nu_\ell)/\Gamma_{total}$ Γ_5/Γ

VALUE (units 10^{-4})	DOCUMENT ID		TECN	COMMENT
1.33 ± 0.18 ± 0.13	[68] ATHAR	03	CLE2	$e^+e^- \to \Upsilon(4S)$
• • • We do not use the following data for averages, fits, limits, etc. • • •				
1.8 ±0.4 ±0.4	[69] ALEXANDER	96T	CLE2	Repl. by ATHAR 03

[68] ATHAR 03 reports systematic errors $0.11 \pm 0.01 \pm 0.07$, which are experimental systematic, systematic due to residual form-factor uncertainties in the signal, and systematic due to residual form-factor uncertainties in the cross-feed modes, respectively. We combine these in quadrature.

[69] ALEXANDER 96T gives systematic errors $\pm 0.3 \pm 0.2$ where the second error reflects the estimated model dependence. We combine these in quadrature. Assumes isospin symmetry: $\Gamma(B^0 \to \pi^- \ell^+ \nu) = 2 \times \Gamma(B^+ \to \pi^0 \ell^+ \nu)$.

$\Gamma(\pi^- \mu^+ \nu_\mu)/\Gamma_{total}$ Γ_6/Γ

VALUE	DOCUMENT ID		TECN
• • • We do not use the following data for averages, fits, limits, etc. • • •			
seen	[70] ALBRECHT	91C	ARG

[70] In ALBRECHT 91C, one event is fully reconstructed providing evidence for the $b \to u$ transition.

$\Gamma(K^+ \text{anything})/\Gamma_{total}$ Γ_7/Γ

VALUE	DOCUMENT ID		TECN	COMMENT
0.78 ± 0.08	[71] ALBRECHT	96D	ARG	$e^+e^- \to \Upsilon(4S)$

[71] Average multiplicity.

$\Gamma(D^- \pi^+)/\Gamma_{total}$ Γ_8/Γ

VALUE	EVTS	DOCUMENT ID		TECN	COMMENT
0.00276 ± 0.00025 OUR AVERAGE					
$0.00268 \pm 0.00012 \pm 0.00024$		[72,73] AHMED	02B	CLE2	$e^+e^- \to \Upsilon(4S)$
0.0027 ±0.0006 ±0.0005		[74] BORTOLETTO	92	CLEO	$e^+e^- \to \Upsilon(4S)$
0.0048 ±0.0011 ±0.0011	22	[75] ALBRECHT	90J	ARG	$e^+e^- \to \Upsilon(4S)$
$0.0051 \,^{+0.0028}_{-0.0025} \,^{+0.0013}_{-0.0012}$	4	[76] BEBEK	87	CLEO	$e^+e^- \to \Upsilon(4S)$
• • • We do not use the following data for averages, fits, limits, etc. • • •					
0.0029 ±0.0004 ±0.0002	81	[77] ALAM	94	CLE2	Repl. by AHMED 02B
0.0031 ±0.0013 ±0.0010	7	[75] ALBRECHT	88K	ARG	$e^+e^- \to \Upsilon(4S)$

[72] Assumes equal production of B^+ and B^0 at the $\Upsilon(4S)$.

[73] AHMED 02B reports an additional uncertainty on the branching ratios to account for 4.5% uncertainty on relative production of B^0 and B^+, which is not included here.

[74] BORTOLETTO 92 assumes equal production of B^+ and B^0 at the $\Upsilon(4S)$ and uses Mark III branching fractions for the D.

[75] ALBRECHT 88K assumes $B^0\overline{B}^0 : B^+B^-$ production ratio is 45:55. Superseded by ALBRECHT 90J which assumes 50:50.

[76] BEBEK 87 value has been updated in BERKELMAN 91 to use same assumptions as noted for BORTOLETTO 92.

[77] ALAM 94 reports $[\mathrm{B}(B^0 \to D^- \pi^+) \times \mathrm{B}(D^+ \to K^- \pi^+ \pi^+)] = 0.000265 \pm 0.000032 \pm 0.000023$. We divide by our best value $\mathrm{B}(D^+ \to K^- \pi^+ \pi^+) = (9.2 \pm 0.6) \times 10^{-2}$. Our first error is their experiment's error and our second error is the systematic error from using our best value. Assumes equal production of B^+ and B^0 at the $\Upsilon(4S)$.

$\Gamma(D^- \rho^+)/\Gamma_{total}$ Γ_9/Γ

VALUE	EVTS	DOCUMENT ID		TECN	COMMENT
0.0077 ± 0.0013 OUR AVERAGE					
$0.0076 \pm 0.0013 \pm 0.0005$	79	[78] ALAM	94	CLE2	$e^+e^- \to \Upsilon(4S)$
0.009 ±0.005 ±0.003	9	[79] ALBRECHT	90J	ARG	$e^+e^- \to \Upsilon(4S)$
• • • We do not use the following data for averages, fits, limits, etc. • • •					
0.022 ±0.012 ±0.009	6	[79] ALBRECHT	88K	ARG	$e^+e^- \to \Upsilon(4S)$

[78] ALAM 94 reports $[\mathrm{B}(B^0 \to D^- \rho^+) \times \mathrm{B}(D^+ \to K^- \pi^+ \pi^+)] = 0.000704 \pm 0.000096 \pm 0.000070$. We divide by our best value $\mathrm{B}(D^+ \to K^- \pi^+ \pi^+) = (9.2 \pm 0.6) \times 10^{-2}$. Our first error is their experiment's error and our second error is the systematic error from using our best value. Assumes equal production of B^+ and B^0 at the $\Upsilon(4S)$.

[79] ALBRECHT 88K assumes $B^0\overline{B}^0 : B^+B^-$ production ratio is 45:55. Superseded by ALBRECHT 90J which assumes 50:50.

$\Gamma(D^- K^*(892)^+)/\Gamma_{total}$ Γ_{10}/Γ

VALUE	DOCUMENT ID		TECN	COMMENT
$(3.7 \pm 1.5 \pm 1.0) \times 10^{-4}$	[80] MAHAPATRA	02	CLE2	$e^+e^- \to \Upsilon(4S)$

[80] Assumes equal production of B^+ and B^0 at the $\Upsilon(4S)$.

$\Gamma(D^- \omega \pi^+)/\Gamma_{total}$ Γ_{11}/Γ

VALUE	DOCUMENT ID		TECN	COMMENT
0.0028 ± 0.0005 ± 0.0004	[81] ALEXANDER	01B	CLE2	$e^+e^- \to \Upsilon(4S)$

[81] Assumes equal production of B^+ and B^0 at the $\Upsilon(4S)$. The signal is consistent with all observed $\omega\pi^+$ having proceeded through the ρ'^+ resonance at mass $1349 \pm 25 \,^{+10}_{-5}$ MeV and width $547 \pm 86 \,^{+46}_{-45}$ MeV.

$\Gamma(D^- K^+)/\Gamma_{total}$ Γ_{12}/Γ

VALUE	DOCUMENT ID		TECN	COMMENT
$(2.04 \pm 0.50 \pm 0.27) \times 10^{-4}$	[82] ABE	01I	BELL	$e^+e^- \to \Upsilon(4S)$

[82] ABE 01I reports $\mathrm{B}(B^0 \to D^- K^+)/\mathrm{B}(B^0 \to D^- \pi^+) = 0.068 \pm 0.015 \pm 0.007$. We multiply by our best value $\mathrm{B}(B^0 \to D^- \pi^+) = (3.0 \pm 0.4) \times 10^{-3}$. Our first error is their experiment's error and the second error is systematic error from using our best value.

$\Gamma(D^- K^+ \overline{K}^0)/\Gamma_{total}$ Γ_{13}/Γ

VALUE (units 10^{-4})	CL%	DOCUMENT ID		TECN	COMMENT
<3.1	90	[83] DRUTSKOY	02	BELL	$e^+e^- \to \Upsilon(4S)$

[83] Assumes equal production of B^+ and B^0 at the $\Upsilon(4S)$.

$\Gamma(D^- K^+ \overline{K}^*(892)^0)/\Gamma_{total}$ Γ_{14}/Γ

VALUE (units 10^{-4})	DOCUMENT ID		TECN	COMMENT
8.8 ± 1.1 ± 1.5	[84] DRUTSKOY	02	BELL	$e^+e^- \to \Upsilon(4S)$

[84] Assumes equal production of B^+ and B^0 at the $\Upsilon(4S)$.

$\Gamma(\overline{D}^0 \pi^+ \pi^-)/\Gamma_{total}$ Γ_{16}/Γ

"OUR EVALUATION" is an average using rescaled values of the data listed below. The average and rescaling were performed by the Heavy Flavor Averaging Group (HFAG) and are described at http://www.slac.stanford.edu/xorg/hfag/. The averaging/rescaling procedure takes into account corrections between the measurements.

VALUE (units 10^{-4})	CL%	EVTS	DOCUMENT ID		TECN	COMMENT
8.0± 0.6±1.5			[85,86] SATPATHY	03	BELL	$e^+e^- \to \Upsilon(4S)$
• • • We do not use the following data for averages, fits, limits, etc. • • •						
< 16	90		[85] ALAM	94	CLE2	$e^+e^- \to \Upsilon(4S)$
< 70	90		[87] BORTOLETTO	92	CLEO	$e^+e^- \to \Upsilon(4S)$
<340	90		[88] BEBEK	87	CLEO	$e^+e^- \to \Upsilon(4S)$
700 ±500		5	[89] BEHRENDS	83	CLEO	$e^+e^- \to \Upsilon(4S)$

[85] Assumes equal production of B^+ and B^0 at the $\Upsilon(4S)$.

[86] No assumption about the intermediate mechanism is made in the analysis.

[87] BORTOLETTO 92 assumes equal production of B^+ and B^0 at the $\Upsilon(4S)$ and uses Mark III branching fractions for the D. The product branching fraction into $D_0^*(2340)\pi$ followed by $D_0^*(2340) \to D^0\pi$ is < 0.0001 at 90% CL and into $D_2^*(2460)$ followed by $D_2^*(2460) \to D^0\pi$ is < 0.0004 at 90% CL.

[88] BEBEK 87 assume the $\Upsilon(4S)$ decays 43% to $B^0\overline{B}^0$. We rescale to 50%. $\mathrm{B}(D^0 \to K^-\pi^+) = (4.2 \pm 0.4 \pm 0.4)\%$ and $\mathrm{B}(D^0 \to K^-\pi^+\pi^+\pi^-) = (9.1 \pm 0.8 \pm 0.8)\%$ were used.

[89] Corrected by us using assumptions: $\mathrm{B}(D^0 \to K^-\pi^+) = (0.042 \pm 0.006)$ and $\mathrm{B}(\Upsilon(4S) \to B^0\overline{B}^0) = 50\%$. The product branching ratio is $\mathrm{B}(B^0 \to \overline{D}^0\pi^+\pi^-)\mathrm{B}(\overline{D}^0 \to K^+\pi^-) = (0.39 \pm 0.26) \times 10^{-2}$.

$\Gamma(D^*(2010)^- \pi^+)/\Gamma_{total}$ Γ_{17}/Γ

VALUE	EVTS	DOCUMENT ID		TECN	COMMENT
0.00276 ± 0.00021 OUR AVERAGE					
$0.00281 \pm 0.00024 \pm 0.00005$		[90] BRANDENB...	98	CLE2	$e^+e^- \to \Upsilon(4S)$
0.0026 ±0.0003 ±0.0004	82	[91] ALAM	94	CLE2	$e^+e^- \to \Upsilon(4S)$
$0.00337 \pm 0.00096 \pm 0.00002$		[92] BORTOLETTO	92	CLEO	$e^+e^- \to \Upsilon(4S)$
$0.00236 \pm 0.00088 \pm 0.00002$	12	[93] ALBRECHT	90J	ARG	$e^+e^- \to \Upsilon(4S)$
$0.00236 \,^{+0.00150}_{-0.00110} \pm 0.00002$	5	[94] BEBEK	87	CLEO	$e^+e^- \to \Upsilon(4S)$

• • • We do not use the following data for averages, fits, limits, etc. • • •

0.010	±0.004	±0.001	8	[95] AKERS	94J OPAL	$e^+e^- \to Z$
0.0027	±0.0014	±0.0010	5	[96] ALBRECHT	87C ARG	$e^+e^- \to \Upsilon(4S)$
0.0035	±0.002	±0.002		[97] ALBRECHT	86F ARG	$e^+e^- \to \Upsilon(4S)$
0.017	±0.005	±0.005	41	[98] GILES	84 CLEO	$e^+e^- \to \Upsilon(4S)$

[90] BRANDENBURG 98 assume equal production of B^+ and B^0 at $\Upsilon(4S)$ and use the D^* reconstruction technique. The first error is their experiment's error and the second error is the systematic error from the PDG 96 value of $B(D^* \to D\pi)$.

[91] ALAM 94 assume equal production of B^+ and B^0 at the $\Upsilon(4S)$ and use the CLEO II $B(D^*(2010)^+ \to D^0\pi^+)$ and absolute $B(D^0 \to K^-\pi^+)$ and the PDG 1992 $B(D^0 \to K^-\pi^+\pi^0)/B(D^0 \to K^-\pi^+)$ and $B(D^0 \to K^-\pi^+\pi^+\pi^-)/B(D^0 \to K^-\pi^+)$.

[92] BORTOLETTO 92 reports $0.0040 \pm 0.0010 \pm 0.0007$ for $B(D^*(2010)^+ \to D^0\pi^+) = 0.57 \pm 0.06$. We rescale to our best value $B(D^*(2010)^+ \to D^0\pi^+) = (67.7 \pm 0.5) \times 10^{-2}$. Our first error is their experiment's error and our second error is the systematic error from using our best value. Assumes equal production of B^+ and B^0 at the $\Upsilon(4S)$ and uses Mark III branching fractions for the D.

[93] ALBRECHT 90J reports $0.0028 \pm 0.0009 \pm 0.0006$ for $B(D^*(2010)^+ \to D^0\pi^+) = 0.57 \pm 0.06$. We rescale to our best value $B(D^*(2010)^+ \to D^0\pi^+) = (67.7 \pm 0.5) \times 10^{-2}$. Our first error is their experiment's error and our second error is the systematic error from using our best value. Assumes equal production of B^+ and B^0 at the $\Upsilon(4S)$ and uses Mark III branching fractions for the D.

[94] BEBEK 87 reports $0.0028^{+0.0015}_{-0.0012}{}^{+0.0010}_{-0.0006}$ for $B(D^*(2010)^+ \to D^0\pi^+) = 0.57 \pm 0.06$. We rescale to our best value $B(D^*(2010)^+ \to D^0\pi^+) = (67.7 \pm 0.5) \times 10^{-2}$. Our first error is their experiment's error and our second error is the systematic error from using our best value. Updated in BERKELMAN 91 to use same assumptions as noted for BORTOLETTO 92 and ALBRECHT 90J.

[95] Assumes $B(Z \to b\overline{b}) = 0.217$ and 38% B_d production fraction.

[96] ALBRECHT 87C use PDG 86 branching ratios for D and $D^*(2010)$ and assume $B(\Upsilon(4S) \to B^+B^-) = 55\%$ and $B(\Upsilon(4S) \to B^0\overline{B}^0) = 45\%$. Superseded by ALBRECHT 90J.

[97] ALBRECHT 86F uses pseudomass that is independent of D^0 and D^+ branching ratios.

[98] Assumes $B(D^*(2010)^+ \to D^0\pi^+) = 0.60^{+0.08}_{-0.15}$. Assumes $B(\Upsilon(4S) \to B^0\overline{B}^0) = 0.40 \pm 0.02$ Does not depend on D branching ratios.

$\Gamma(D^-\pi^+\pi^+\pi^-)/\Gamma_{total}$ Γ_{18}/Γ

VALUE	DOCUMENT ID	TECN	COMMENT
0.0080 ± 0.0021 ± 0.0014	[99] BORTOLETTO92	CLEO	$e^+e^- \to \Upsilon(4S)$

[99] BORTOLETTO 92 assumes equal production of B^+ and B^0 at the $\Upsilon(4S)$ and uses Mark III branching fractions for the D.

$\Gamma((D^-\pi^+\pi^+\pi^-)\,\text{nonresonant})/\Gamma_{total}$ Γ_{19}/Γ

VALUE	DOCUMENT ID	TECN	COMMENT
0.0039 ± 0.0014 ± 0.0013	[100] BORTOLETTO92	CLEO	$e^+e^- \to \Upsilon(4S)$

[100] BORTOLETTO 92 assumes equal production of B^+ and B^0 at the $\Upsilon(4S)$ and uses Mark III branching fractions for the D.

$\Gamma(D^-\pi^+\rho^0)/\Gamma_{total}$ Γ_{20}/Γ

VALUE	DOCUMENT ID	TECN	COMMENT
0.0011 ± 0.0009 ± 0.0004	[101] BORTOLETTO92	CLEO	$e^+e^- \to \Upsilon(4S)$

[101] BORTOLETTO 92 assumes equal production of B^+ and B^0 at the $\Upsilon(4S)$ and uses Mark III branching fractions for the D.

$\Gamma(D^-a_1(1260)^+)/\Gamma_{total}$ Γ_{21}/Γ

VALUE	DOCUMENT ID	TECN	COMMENT
0.0060 ± 0.0022 ± 0.0024	[102] BORTOLETTO92	CLEO	$e^+e^- \to \Upsilon(4S)$

[102] BORTOLETTO 92 assumes equal production of B^+ and B^0 at the $\Upsilon(4S)$ and uses Mark III branching fractions for the D.

$\Gamma(D^*(2010)^-\pi^+\pi^0)/\Gamma_{total}$ Γ_{22}/Γ

VALUE	EVTS	DOCUMENT ID	TECN	COMMENT
0.0152 ± 0.0052 ± 0.0001	51	[103] ALBRECHT 90J	ARG	$e^+e^- \to \Upsilon(4S)$

• • • We do not use the following data for averages, fits, limits, etc. • • •

0.015 ±0.008 ±0.008	8	[104] ALBRECHT	87C ARG	$e^+e^- \to \Upsilon(4S)$

[103] ALBRECHT 90J reports $0.018 \pm 0.004 \pm 0.005$ for $B(D^*(2010)^+ \to D^0\pi^+) = 0.57 \pm 0.06$. We rescale to our best value $B(D^*(2010)^+ \to D^0\pi^+) = (67.7 \pm 0.5) \times 10^{-2}$. Our first error is their experiment's error and our second error is the systematic error from using our best value. Assumes equal production of B^+ and B^0 at the $\Upsilon(4S)$ and uses Mark III branching fractions for the D.

[104] ALBRECHT 87C use PDG 86 branching ratios for D and $D^*(2010)$ and assume $B(\Upsilon(4S) \to B^+B^-) = 55\%$ and $B(\Upsilon(4S) \to B^0\overline{B}^0) = 45\%$. Superseded by ALBRECHT 90J.

$\Gamma(D^*(2010)^-\rho^+)/\Gamma_{total}$ Γ_{23}/Γ

VALUE	EVTS	DOCUMENT ID	TECN	COMMENT
0.0068 ± 0.0009 OUR AVERAGE				
0.0068 ±0.0003 ±0.0009		[105] CSORNA 03	CLE2	$e^+e^- \to \Upsilon(4S)$
0.0160 ±0.0113 ±0.0001		[106] BORTOLETTO92	CLEO	$e^+e^- \to \Upsilon(4S)$
0.00589 ± 0.00352 ± 0.00004	19	[107] ALBRECHT 90J	ARG	$e^+e^- \to \Upsilon(4S)$

• • • We do not use the following data for averages, fits, limits, etc. • • •

0.0074 ±0.0010 ±0.0014	71	[108,109] ALAM 94	CLE2	$e^+e^- \to \Upsilon(4S)$
0.081 ±0.029 $^{+0.059}_{-0.024}$	19	[110] CHEN 85	CLEO	$e^+e^- \to \Upsilon(4S)$

[105] Assumes equal production of B^0 and B^+ at the $\Upsilon(4S)$ resonance. The second error combines the systematic and theoretical uncertainties in quadrature. CSORNA 03 includes data used in ALAM 94. A full angular fit to three complex helicity amplitudes is performed.

[106] BORTOLETTO 92 reports $0.019 \pm 0.008 \pm 0.011$ for $B(D^*(2010)^+ \to D^0\pi^+) = 0.57 \pm 0.06$. We rescale to our best value $B(D^*(2010)^+ \to D^0\pi^+) = (67.7 \pm 0.5) \times 10^{-2}$. Our first error is their experiment's error and our second error is the systematic error from using our best value. Assumes equal production of B^+ and B^0 at the $\Upsilon(4S)$ and uses Mark III branching fractions for the D.

[107] ALBRECHT 90J reports $0.007 \pm 0.003 \pm 0.003$ for $B(D^*(2010)^+ \to D^0\pi^+) = 0.57 \pm 0.06$. We rescale to our best value $B(D^*(2010)^+ \to D^0\pi^+) = (67.7 \pm 0.5) \times 10^{-2}$. Our first error is their experiment's error and our second error is the systematic error from using our best value. Assumes equal production of B^+ and B^0 at the $\Upsilon(4S)$ and uses Mark III branching fractions for the D.

[108] ALAM 94 assume equal production of B^+ and B^0 at the $\Upsilon(4S)$ and use the CLEO II $B(D^*(2010)^+ \to D^0\pi^+)$ and absolute $B(D^0 \to K^-\pi^+)$ and the PDG 1992 $B(D^0 \to K^-\pi^+\pi^0)/B(D^0 \to K^-\pi^+)$ and $B(D^0 \to K^-\pi^+\pi^+\pi^-)/B(D^0 \to K^-\pi^+)$.

[109] This decay is nearly completely longitudinally polarized, $\Gamma_L/\Gamma = (93 \pm 5 \pm 5)\%$, as expected from the factorization hypothesis (ROSNER 90). The nonresonant $\pi^+\pi^0$ contribution under the ρ^+ is less than 9% at 90% CL.

[110] Uses $B(D^* \to D^0\pi^+) = 0.6 \pm 0.15$ and $B(\Upsilon(4S) \to B^0\overline{B}^0) = 0.4$. Does not depend on D branching ratios.

$\Gamma(D^*(2010)^-K^+)/\Gamma_{total}$ Γ_{24}/Γ

VALUE	DOCUMENT ID	TECN	COMMENT
(2.04 ± 0.44 ± 0.16) × 10⁻⁴	[111] ABE 01I	BELL	$e^+e^- \to \Upsilon(4S)$

[111] ABE 01I reports $B(B^0 \to D^*(2010)^-K^+)/B(B^0 \to D^*(2010)^-\pi^+) = 0.074 \pm 0.015 \pm 0.006$. We multiply by our best value $B(B^0 \to D^*(2010)^-\pi^+) = (2.76 \pm 0.21) \times 10^{-3}$. Our first error is their experiment's error and the second error is systematic error from using our best value.

$\Gamma(D^*(2010)^-K^*(892)^+)/\Gamma_{total}$ Γ_{25}/Γ

VALUE	DOCUMENT ID	TECN	COMMENT
(3.8 ± 1.3 ± 0.8) × 10⁻⁴	[112] MAHAPATRA 02	CLE2	$e^+e^- \to \Upsilon(4S)$

[112] Assumes equal production of B^+ and B^0 at the $\Upsilon(4S)$ and an unpolarized final state.

$\Gamma(D^*(2010)^-K^+\overline{K}^0)/\Gamma_{total}$ Γ_{26}/Γ

VALUE (units 10^{-4})	CL%	DOCUMENT ID	TECN	COMMENT
< 4.7	90	[113] DRUTSKOY 02	BELL	$e^+e^- \to \Upsilon(4S)$

[113] Assumes equal production of B^+ and B^0 at the $\Upsilon(4S)$.

$\Gamma(D^*(2010)^-K^+\overline{K}^*(892)^0)/\Gamma_{total}$ Γ_{27}/Γ

VALUE (units 10^{-4})	DOCUMENT ID	TECN	COMMENT
12.9 ± 2.2 ± 2.5	[114] DRUTSKOY 02	BELL	$e^+e^- \to \Upsilon(4S)$

[114] Assumes equal production of B^+ and B^0 at the $\Upsilon(4S)$.

$\Gamma(D^*(2010)^-\pi^+\pi^+\pi^-)/\Gamma_{total}$ Γ_{28}/Γ

VALUE	CL%	EVTS	DOCUMENT ID	TECN	COMMENT
0.0076 ± 0.0018 OUR AVERAGE Error includes scale factor of 1.4. See the ideogram below.					
0.0063 ± 0.0010 ± 0.0011		49	[115,116] ALAM 94	CLE2	$e^+e^- \to \Upsilon(4S)$
0.0134 ± 0.0036 ± 0.0001			[117] BORTOLETTO92	CLEO	$e^+e^- \to \Upsilon(4S)$
0.0101 ± 0.0041 ± 0.0001		26	[118] ALBRECHT 90J	ARG	$e^+e^- \to \Upsilon(4S)$

• • • We do not use the following data for averages, fits, limits, etc. • • •

0.033 ±0.009 ±0.016		27	[119] ALBRECHT	87C ARG	$e^+e^- \to \Upsilon(4S)$
< 0.042	90		[120] BEBEK 87	CLEO	$e^+e^- \to \Upsilon(4S)$

[115] ALAM 94 assume equal production of B^+ and B^0 at the $\Upsilon(4S)$ and use the CLEO II $B(D^*(2010)^+ \to D^0\pi^+)$ and absolute $B(D^0 \to K^-\pi^+)$ and the PDG 1992 $B(D^0 \to K^-\pi^+\pi^0)/B(D^0 \to K^-\pi^+)$ and $B(D^0 \to K^-\pi^+\pi^+\pi^-)/B(D^0 \to K^-\pi^+)$.

[116] The three pion mass is required to be between 1.0 and 1.6 GeV consistent with an a_1 meson. (If this channel is dominated by a_1^+, the branching ratio for $\overline{D}^{*-}\pi^+\pi^+\pi^-$ is twice that for $\overline{D}^{*-}a_1^+$.)

[117] BORTOLETTO 92 reports $0.0159 \pm 0.0028 \pm 0.0037$ for $B(D^*(2010)^+ \to D^0\pi^+) = 0.57 \pm 0.06$. We rescale to our best value $B(D^*(2010)^+ \to D^0\pi^+) = (67.7 \pm 0.5) \times 10^{-2}$. Our first error is their experiment's error and our second error is the systematic error from using our best value. Assumes equal production of B^+ and B^0 at the $\Upsilon(4S)$ and uses Mark III branching fractions for the D.

[118] ALBRECHT 90J reports $0.012 \pm 0.003 \pm 0.004$ for $B(D^*(2010)^+ \to D^0\pi^+) = 0.57 \pm 0.06$. We rescale to our best value $B(D^*(2010)^+ \to D^0\pi^+) = (67.7 \pm 0.5) \times 10^{-2}$. Our first error is their experiment's error and our second error is the systematic error from using our best value. Assumes equal production of B^+ and B^0 at the $\Upsilon(4S)$ and uses Mark III branching fractions for the D.

[119] ALBRECHT 87C use PDG 86 branching ratios for D and $D^*(2010)$ and assume $B(\Upsilon(4S) \to B^+B^-) = 55\%$ and $B(\Upsilon(4S) \to B^0\overline{B}^0) = 45\%$. Superseded by ALBRECHT 90J.

[120] BEBEK 87 value has been updated in BERKELMAN 91 to use same assumptions as noted for BORTOLETTO 92.

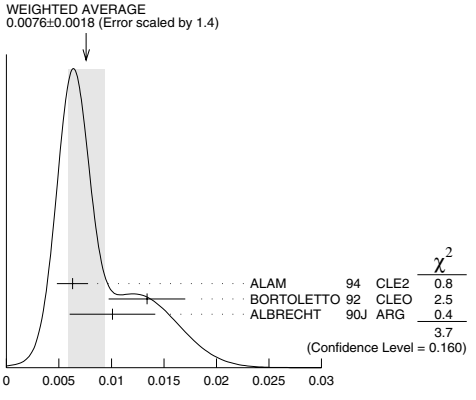

$\Gamma\left(D^*(2010)^-\pi^+\pi^+\pi^-\right)/\Gamma_{\rm total}$

$\Gamma\left((D^*(2010)^-\pi^+\pi^+\pi^-)\ \text{nonresonant}\right)/\Gamma_{\rm total}$ Γ_{29}/Γ

VALUE	DOCUMENT ID	TECN	COMMENT
0.0000±0.0019±0.0016	[121] BORTOLETTO 92	CLEO	$e^+e^- \to \Upsilon(4S)$

[121] BORTOLETTO 92 assumes equal production of B^+ and B^0 at the $\Upsilon(4S)$ and uses Mark III branching fractions for the D and $D^*(2010)$.

$\Gamma\left(D^*(2010)^-\pi^+\rho^0\right)/\Gamma_{\rm total}$ Γ_{30}/Γ

VALUE	DOCUMENT ID	TECN	COMMENT
0.00573±0.00317±0.00004	[122] BORTOLETTO 92	CLEO	$e^+e^- \to \Upsilon(4S)$

[122] BORTOLETTO 92 reports $0.0068 \pm 0.0032 \pm 0.0021$ for $B(D^*(2010)^+ \to D^0\pi^+) = 0.57 \pm 0.06$. We rescale to our best value $B(D^*(2010)^+ \to D^0\pi^+) = (67.7 \pm 0.5) \times 10^{-2}$. Our first error is their experiment's error and our second error is the systematic error from using our best value. Assumes equal production of B^+ and B^0 at the $\Upsilon(4S)$ and uses Mark III branching fractions for the D.

$\Gamma\left(D^*(2010)^-a_1(1260)^+\right)/\Gamma_{\rm total}$ Γ_{31}/Γ

VALUE	DOCUMENT ID	TECN	COMMENT
0.0130±0.0027 OUR AVERAGE			
$0.0126 \pm 0.0020 \pm 0.0022$	[123,124] ALAM 94	CLE2	$e^+e^- \to \Upsilon(4S)$
$0.0152 \pm 0.0070 \pm 0.0001$	[125] BORTOLETTO 92	CLEO	$e^+e^- \to \Upsilon(4S)$

[123] ALAM 94 value is twice their $\Gamma(D^*(2010)^-\pi^+\pi^+\pi^-)/\Gamma_{\rm total}$ value based on their observation that the three pions are dominantly in the $a_1(1260)$ mass range 1.0 to 1.6 GeV.

[124] ALAM 94 assume equal production of B^+ and B^0 at the $\Upsilon(4S)$ and use the CLEO II $B(D^*(2010)^+ \to D^0\pi^+)$ and absolute $B(D^0 \to K^-\pi^+)$ and the PDG 1992 $B(D^0 \to K^-\pi^+\pi^0)/B(D^0 \to K^-\pi^+)$ and $B(D^0 \to K^-\pi^+\pi^+\pi^-)/B(D^0 \to K^-\pi^+)$.

[125] BORTOLETTO 92 reports $0.018 \pm 0.006 \pm 0.006$ for $B(D^*(2010)^+ \to D^0\pi^+) = 0.57 \pm 0.06$. We rescale to our best value $B(D^*(2010)^+ \to D^0\pi^+) = (67.7 \pm 0.5) \times 10^{-2}$. Our first error is their experiment's error and our second error is the systematic error from using our best value. Assumes equal production of B^+ and B^0 at the $\Upsilon(4S)$ and uses Mark III branching fractions for the D.

$\Gamma\left(D^*(2010)^-\pi^+\pi^+\pi^-\pi^0\right)/\Gamma_{\rm total}$ Γ_{32}/Γ

VALUE	EVTS	DOCUMENT ID	TECN	COMMENT
0.0176±0.0027 OUR AVERAGE				
$0.0172 \pm 0.0014 \pm 0.0024$		[126] ALEXANDER 01B	CLE2	$e^+e^- \to \Upsilon(4S)$
$0.0345 \pm 0.0181 \pm 0.0003$	28	[127] ALBRECHT 90J	ARG	$e^+e^- \to \Upsilon(4S)$

[126] Assumes equal production of B^+ and B^0 at the $\Upsilon(4S)$. The signal is consistent with all observed $\omega\pi^+$ having proceeded through the ρ'^+ resonance at mass $1349 \pm 25^{+10}_{-\ 5}$ MeV and width $547 \pm 86^{+46}_{-45}$ MeV.

[127] ALBRECHT 90J reports $0.041 \pm 0.015 \pm 0.016$ for $B(D^*(2010)^+ \to D^0\pi^+) = 0.57 \pm 0.06$. We rescale to our best value $B(D^*(2010)^+ \to D^0\pi^+) = (67.7 \pm 0.5) \times 10^{-2}$. Our first error is their experiment's error and our second error is the systematic error from using our best value. Assumes equal production of B^+ and B^0 at the $\Upsilon(4S)$ and uses Mark III branching fractions for the D.

$\Gamma\left(D^*(2010)^-p\overline{p}\pi^+\right)/\Gamma_{\rm total}$ Γ_{34}/Γ

VALUE (units 10^{-4})	DOCUMENT ID	TECN	COMMENT
$\mathbf{6.5^{+1.3}_{-1.2}\pm1.0}$	[128] ANDERSON 01	CLE2	$e^+e^- \to \Upsilon(4S)$

[128] Assumes equal production of B^+ and B^0 at the $\Upsilon(4S)$.

$\Gamma\left(D^*(2010)^-p\overline{n}\right)/\Gamma_{\rm total}$ Γ_{35}/Γ

VALUE (units 10^{-4})	DOCUMENT ID	TECN	COMMENT
$\mathbf{14.5^{+3.4}_{-3.0}\pm2.7}$	[129] ANDERSON 01	CLE2	$e^+e^- \to \Upsilon(4S)$

[129] Assumes equal production of B^+ and B^0 at the $\Upsilon(4S)$.

$\Gamma\left(\overline{D}^*(2010)^-\omega\pi^+\right)/\Gamma_{\rm total}$ Γ_{36}/Γ

VALUE	DOCUMENT ID	TECN	COMMENT
0.0029±0.0003±0.0004	[130] ALEXANDER 01B	CLE2	$e^+e^- \to \Upsilon(4S)$

[130] Assumes equal production of B^+ and B^0 at the $\Upsilon(4S)$. The signal is consistent with all observed $\omega\pi^+$ having proceeded through the ρ'^+ resonance at mass $1349 \pm 25^{+10}_{-\ 5}$ MeV and width $547 \pm 86^{+46}_{-45}$ MeV.

$\Gamma\left(\overline{D}_2^*(2460)^-\pi^+\right)/\Gamma_{\rm total}$ Γ_{37}/Γ

VALUE	CL%	DOCUMENT ID	TECN	COMMENT
<0.0022	90	[131] ALAM 94	CLE2	$e^+e^- \to \Upsilon(4S)$

[131] ALAM 94 assumes equal production of B^+ and B^0 at the $\Upsilon(4S)$ and use the CLEO II absolute $B(D^0 \to K^-\pi^+)$ and $B(D_2^*(2460)^+ \to D^0\pi^+) = 30\%$.

$\Gamma\left(\overline{D}_2^*(2460)^-\rho^+\right)/\Gamma_{\rm total}$ Γ_{38}/Γ

VALUE	CL%	DOCUMENT ID	TECN	COMMENT
<0.0049	90	[132] ALAM 94	CLE2	$e^+e^- \to \Upsilon(4S)$

[132] ALAM 94 assumes equal production of B^+ and B^0 at the $\Upsilon(4S)$ and use the CLEO II absolute $B(D^0 \to K^-\pi^+)$ and $B(D_2^*(2460)^+ \to D^0\pi^+) = 30\%$.

$\Gamma\left(D^-D^+\right)/\Gamma_{\rm total}$ Γ_{39}/Γ

VALUE	CL%	DOCUMENT ID	TECN	COMMENT
<9.4 × 10⁻⁴	90	[133] LIPELES 00	CLE2	$e^+e^- \to \Upsilon(4S)$
• • • We do not use the following data for averages, fits, limits, etc. • • •				
$<5.9 \times 10^{-3}$	90	BARATE 98Q	ALEP	$e^+e^- \to Z$
$<1.2 \times 10^{-3}$	90	ASNER 97	CLE2	$e^+e^- \to \Upsilon(4S)$

[133] Assumes equal production of B^+ and B^0 at the $\Upsilon(4S)$.

$\Gamma\left(D^-D_s^+\right)/\Gamma_{\rm total}$ Γ_{40}/Γ

VALUE	EVTS	DOCUMENT ID	TECN	COMMENT
0.0080±0.0030 OUR AVERAGE				
$0.0084 \pm 0.0030^{+0.0020}_{-0.0021}$		[134] GIBAUT 96	CLE2	$e^+e^- \to \Upsilon(4S)$
$0.013 \pm 0.011 \pm 0.003$		[135] ALBRECHT 92G	ARG	$e^+e^- \to \Upsilon(4S)$
$0.007 \pm 0.004 \pm 0.002$		[136] BORTOLETTO 92	CLEO	$e^+e^- \to \Upsilon(4S)$
• • • We do not use the following data for averages, fits, limits, etc. • • •				
0.012 ± 0.007	3	[137] BORTOLETTO 90	CLEO	$e^+e^- \to \Upsilon(4S)$

[134] GIBAUT 96 reports $0.0087 \pm 0.0024 \pm 0.0020$ for $B(D_s^+ \to \phi\pi^+) = 0.035$. We rescale to our best value $B(D_s^+ \to \phi\pi^+) = (3.6 \pm 0.9) \times 10^{-2}$. Our first error is their experiment's error and our second error is the systematic error from using our best value.

[135] ALBRECHT 92G reports $0.017 \pm 0.013 \pm 0.006$ for $B(D_s^+ \to \phi\pi^+) = 0.027$. We rescale to our best value $B(D_s^+ \to \phi\pi^+) = (3.6 \pm 0.9) \times 10^{-2}$. Our first error is their experiment's error and our second error is the systematic error from using our best value. Assumes PDG 1990 D^+ branching ratios, e.g., $B(D^+ \to K^-\pi^+\pi^+) = 7.7 \pm 1.0\%$.

[136] BORTOLETTO 92 reports $0.0080 \pm 0.0045 \pm 0.0030$ for $B(D_s^+ \to \phi\pi^+) = 0.030 \pm 0.011$. We rescale to our best value $B(D_s^+ \to \phi\pi^+) = (3.6 \pm 0.9) \times 10^{-2}$. Our first error is their experiment's error and our second error is the systematic error from using our best value. Assumes equal production of B^+ and B^0 at the $\Upsilon(4S)$ and uses Mark III branching fractions for the D.

[137] BORTOLETTO 90 assume $B(D_s \to \phi\pi^+) = 2\%$. Superseded by BORTOLETTO 92.

$\Gamma\left(D^*(2010)^-D_s^+\right)/\Gamma_{\rm total}$ Γ_{41}/Γ

VALUE	EVTS	DOCUMENT ID	TECN	COMMENT
0.0107±0.0029 OUR AVERAGE				
$0.0103 \pm 0.0019 \pm 0.0025$		[138] AUBERT 03I	BABR	$e^+e^- \to \Upsilon(4S)$
$0.0110 \pm 0.0021^{+0.0026}_{-0.0027}$		[139] AHMED 00B	CLE2	$e^+e^- \to \Upsilon(4S)$
$0.010 \pm 0.008 \pm 0.003$		[140] ALBRECHT 92G	ARG	$e^+e^- \to \Upsilon(4S)$
$0.013 \pm 0.008 \pm 0.003$		[141] BORTOLETTO 92	CLEO	$e^+e^- \to \Upsilon(4S)$
• • • We do not use the following data for averages, fits, limits, etc. • • •				
$0.0090 \pm 0.0027 \pm 0.0022$		[142] GIBAUT 96	CLE2	Repl. by AHMED 00B
0.024 ± 0.014	3	[143] BORTOLETTO 90	CLEO	$e^+e^- \to \Upsilon(4S)$

[138] AUBERT 03I reports $0.0103 \pm 0.0014 \pm 0.0013$ for $B(D_s^+ \to \phi\pi^+) = 0.036$. We rescale to our best value $B(D_s^+ \to \phi\pi^+) = (3.6 \pm 0.9) \times 10^{-2}$. Our first error is their experiment's error and our second error is the systematic error from using our best value.

[139] AHMED 00B reports $0.0110 \pm 0.0018 \pm 0.0011$ for $B(D_s^+ \to \phi\pi^+) = 0.036$. We rescale to our best value $B(D_s^+ \to \phi\pi^+) = (3.6 \pm 0.9) \times 10^{-2}$. Our first error is their experiment's error and our second error is the systematic error from using our best value.

[140] ALBRECHT 92G reports $0.014 \pm 0.010 \pm 0.003$ for $B(D_s^+ \to \phi\pi^+) = 0.027$. We rescale to our best value $B(D_s^+ \to \phi\pi^+) = (3.6 \pm 0.9) \times 10^{-2}$. Our first error is their experiment's error and our second error is the systematic error from using our best value. Assumes PDG 1990 D^+ and $D^*(2010)^+$ branching ratios, e.g., $B(D^0 \to K^-\pi^+) = 3.71 \pm 0.25\%$, $B(D^+ \to K^-\pi^+\pi^+) = 7.1 \pm 1.0\%$, and $B(D^*(2010)^+ \to D^0\pi^+) = 55 \pm 4\%$.

[141] BORTOLETTO 92 reports $0.016 \pm 0.009 \pm 0.006$ for $B(D_s^+ \to \phi\pi^+) = 0.030 \pm 0.011$. We rescale to our best value $B(D_s^+ \to \phi\pi^+) = (3.6 \pm 0.9) \times 10^{-2}$. Our first error is their experiment's error and our second error is the systematic error from using our best value. Assumes equal production of B^+ and B^0 at the $\Upsilon(4S)$ and uses Mark III branching fractions for the D and $D^*(2010)$.

[142] GIBAUT 96 reports $0.0093 \pm 0.0023 \pm 0.0016$ for $B(D_s^+ \to \phi\pi^+) = 0.035$. We rescale to our best value $B(D_s^+ \to \phi\pi^+) = (3.6 \pm 0.9) \times 10^{-2}$. Our first error is their experiment's error and our second error is the systematic error from using our best value.

[143] BORTOLETTO 90 assume $B(D_s \to \phi\pi^+) = 2\%$. Superseded by BORTOLETTO 92.

$\Gamma(D^- D_s^{*+})/\Gamma_{total}$ Γ_{42}/Γ

VALUE	DOCUMENT ID		TECN	COMMENT
0.010±0.005 OUR AVERAGE				
0.010±0.004±0.002	[144] GIBAUT	96	CLE2	$e^+e^- \to \Upsilon(4S)$
0.020±0.014±0.005	[145] ALBRECHT	92G	ARG	$e^+e^- \to \Upsilon(4S)$

[144] GIBAUT 96 reports $0.0100 \pm 0.0035 \pm 0.0022$ for $B(D_s^+ \to \phi\pi^+) = 0.035$. We rescale to our best value $B(D_s^+ \to \phi\pi^+) = (3.6 \pm 0.9) \times 10^{-2}$. Our first error is their experiment's error and our second error is the systematic error from using our best value.

[145] ALBRECHT 92G reports $0.027 \pm 0.017 \pm 0.009$ for $B(D_s^+ \to \phi\pi^+) = 0.027$. We rescale to our best value $B(D_s^+ \to \phi\pi^+) = (3.6 \pm 0.9) \times 10^{-2}$. Our first error is their experiment's error and our second error is the systematic error from using our best value. Assumes PDG 1990 D^+ branching ratios, e.g., $B(D^+ \to K^-\pi^+\pi^+) = 7.7 \pm 1.0\%$.

$[\Gamma(D^*(2010)^- D_s^+) + \Gamma(D^*(2010)^- D_s^{*+})]/\Gamma_{total}$ $(\Gamma_{41}+\Gamma_{43})/\Gamma$

VALUE (units 10^{-2})	EVTS	DOCUMENT ID		TECN	COMMENT
0.030±0.008 OUR AVERAGE					
0.030±0.004±0.007		[146] AUBERT	03I	BABR	$e^+e^- \to \Upsilon(4S)$
4.1 ±1.1 ±1.0	22	[147] BORTOLETTO	90	CLEO	$e^+e^- \to \Upsilon(4S)$

[146] AUBERT 03I reports $0.0300 \pm 0.0019 \pm 0.0039$ for $B(D_s^+ \to \phi\pi^+) = 0.036$. We rescale to our best value $B(D_s^+ \to \phi\pi^+) = (3.6 \pm 0.9) \times 10^{-2}$. Our first error is their experiment's error and our second error is the systematic error from using our best value.

[147] BORTOLETTO 90 reports 7.5 ± 2.0 for $B(D_s^+ \to \phi\pi^+) = 0.02$. We rescale to our best value $B(D_s^+ \to \phi\pi^+) = (3.6 \pm 0.9) \times 10^{-2}$. Our first error is their experiment's error and our second error is the systematic error from using our best value.

$\Gamma(D^*(2010)^- D_s^{*+})/\Gamma_{total}$ Γ_{43}/Γ

VALUE	DOCUMENT ID		TECN	COMMENT
0.019±0.005 OUR AVERAGE				
0.020±0.003±0.005	[148] AUBERT	03I	BABR	$e^+e^- \to \Upsilon(4S)$
0.018±0.004±0.004	[149] AHMED	00B	CLE2	$e^+e^- \to \Upsilon(4S)$
0.019±0.011±0.005	[150] ALBRECHT	92G	ARG	$e^+e^- \to \Upsilon(4S)$
• • • We do not use the following data for averages, fits, limits, etc. • • •				
0.020±0.006±0.005	[151] GIBAUT	96	CLE2	Repl. by AHMED 00B

[148] AUBERT 03I reports $0.0197 \pm 0.0015 \pm 0.0030$ for $B(D_s^+ \to \phi\pi^+) = 0.036$. We rescale to our best value $B(D_s^+ \to \phi\pi^+) = (3.6 \pm 0.9) \times 10^{-2}$. Our first error is their experiment's error and our second error is the systematic error from using our best value.

[149] AHMED 00B reports $0.0182 \pm 0.0037 \pm 0.0025$ for $B(D_s^+ \to \phi\pi^+) = 0.036$. We rescale to our best value $B(D_s^+ \to \phi\pi^+) = (3.6 \pm 0.9) \times 10^{-2}$. Our first error is their experiment's error and our second error is the systematic error from using our best value.

[150] ALBRECHT 92G reports $0.026 \pm 0.014 \pm 0.006$ for $B(D_s^+ \to \phi\pi^+) = 0.027$. We rescale to our best value $B(D_s^+ \to \phi\pi^+) = (3.6 \pm 0.9) \times 10^{-2}$. Our first error is their experiment's error and our second error is the systematic error from using our best value. Assumes PDG 1990 D^+ and $D^*(2010)^+$ branching ratios, e.g., $B(D^0 \to K^-\pi^+) = 3.71 \pm 0.25\%$, $B(D^+ \to K^-\pi^+\pi^+) = 7.1 \pm 1.0\%$, and $B(D^*(2010)^+ \to D^0\pi^+) = 55 \pm 4\%$.

[151] GIBAUT 96 reports $0.0203 \pm 0.0050 \pm 0.0036$ for $B(D_s^+ \to \phi\pi^+) = 0.035$. We rescale to our best value $B(D_s^+ \to \phi\pi^+) = (3.6 \pm 0.9) \times 10^{-2}$. Our first error is their experiment's error and our second error is the systematic error from using our best value.

$\Gamma(D^- D_{sJ}(2317)^+)/\Gamma_{total}$ Γ_{44}/Γ

VALUE	DOCUMENT ID		TECN	COMMENT
seen	[152] KROKOVNY	03B	BELL	$e^+e^- \to \Upsilon(4S)$

[152] The product branching ratio for $B(B^0 \to D^- D_{sJ}(2317)^+) \times B(D_{sJ}(2317)^+ \to D_s\pi^0)$ is measured to be $(8.6^{+3.3}_{-2.6} \pm 2.6) \times 10^{-4}$.

$\Gamma(D^- D_{sJ}(2457)^+)/\Gamma_{total}$ Γ_{45}/Γ

VALUE	DOCUMENT ID		TECN	COMMENT
seen	[153] KROKOVNY	03B	BELL	$e^+e^- \to \Upsilon(4S)$

[153] The product branching ratio for $B(B^0 \to D^- D_{sJ}(2457)^+) \times B(D_{sJ}(2457)^+ \to D_s^{*+}\pi^0, D_s^+\gamma)$ are measured to be $(22.7^{+7.3}_{-6.2} \pm 6.8) \times 10^{-4}$ and $(8.2^{+2.2}_{-1.9} \pm 2.5) \times 10^{-4}$, respectively.

$\Gamma(D^- D_{sJ}(2536)^+)/\Gamma_{total}$ Γ_{46}/Γ

VALUE	DOCUMENT ID		TECN	COMMENT
not seen	[154] AUBERT	03X	BABR	$e^+e^- \to \Upsilon(4S)$

[154] No evidence is found for such decay and set a limit on $B(B^0 \to D^- D_{sJ}(2536)^+) \times B(D_{sJ}(2536)^+ \to D^*(2007)^0 K^+) < 5 \times 10^{-4}$ at 90%CL.

$\Gamma(D^*(2010)^- D_{sJ}(2536)^+)/\Gamma_{total}$ Γ_{47}/Γ

VALUE	DOCUMENT ID		TECN	COMMENT
not seen	[155] AUBERT	03X	BABR	$e^+e^- \to \Upsilon(4S)$

[155] No evidence is found for such decay and set a limit on $B(B^0 \to D^*(2010)^- D_{sJ}(2536)^+) \times B(D_{sJ}(2536)^+ \to D^*(2007)^0 K^+) < 7 \times 10^{-4}$ at 90%CL.

$\Gamma(D^- D_{sJ}(2573)^+)/\Gamma_{total}$ Γ_{48}/Γ

VALUE	DOCUMENT ID		TECN	COMMENT
not seen	[156] AUBERT	03X	BABR	$e^+e^- \to \Upsilon(4S)$

[156] No evidence is found for such decay and set a limit on $B(B^0 \to D^- D_{sJ}(2573)^+) \times B(D_{sJ}(2573)^+ \to D^0 K^+)$ such $< 1 \times 10^{-4}$ at 90%CL.

$\Gamma(D^*(2010)^- D_{sJ}(2573)^+)/\Gamma_{total}$ Γ_{49}/Γ

VALUE	DOCUMENT ID		TECN	COMMENT
not seen	[157] AUBERT	03X	BABR	$e^+e^- \to \Upsilon(4S)$

[157] No evidence is found for such decay and set a limit on $B(B^0 \to D^*(2010)^- D_{sJ}(2573)^+) \times B(D_{sJ}(2573)^+ \to D^0 K^+) < 2 \times 10^{-4}$ at 90%CL.

$\Gamma(D_s^+\pi^-)/\Gamma_{total}$ Γ_{50}/Γ

VALUE (units 10^{-6})	CL%	DOCUMENT ID		TECN	COMMENT
27±10 OUR AVERAGE					
$31. \pm 11. ^{+7.}_{-8.}$		[158] AUBERT	03D	BABR	$e^+e^- \to \Upsilon(4S)$
$24. ^{+11.}_{-9.} \pm 6.$		[159] KROKOVNY	02	BELL	$e^+e^- \to \Upsilon(4S)$
• • • We do not use the following data for averages, fits, limits, etc. • • •					
< 280	90	[160] ALEXANDER	93B	CLE2	$e^+e^- \to \Upsilon(4S)$
<1300	90	[161] BORTOLETTO	90	CLEO	$e^+e^- \to \Upsilon(4S)$

[158] AUBERT 03D reports $[B(B^0 \to D_s^+\pi^-) \times B(D_s^+ \to \phi\pi^+)] = 1.13 \pm 0.33 \pm 0.21$. We divide by our best value $B(D_s^+ \to \phi\pi^+) = (3.6 \pm 0.9) \times 10^{-2}$. Our first error is their experiment's error and our second error is the systematic error from using our best value.

[159] KROKOVNY 02 reports $[B(B^0 \to D_s^+\pi^-) \times B(D_s^+ \to \phi\pi^+)] = 0.86^{+0.37}_{-0.30} \pm 0.11$. We divide by our best value $B(D_s^+ \to \phi\pi^+) = (3.6 \pm 0.9) \times 10^{-2}$. Our first error is their experiment's error and our second error is the systematic error from using our best value.

[160] ALEXANDER 93B reports < 270 for $B(D_s^+ \to \phi\pi^+) = 0.037$. We rescale to our best value $B(D_s^+ \to \phi\pi^+) = 0.036$.

[161] BORTOLETTO 90 assume $B(D_s \to \phi\pi^+) = 2\%$.

$[\Gamma(D_s^+\pi^-) + \Gamma(D_s^- K^+)]/\Gamma_{total}$ $(\Gamma_{50}+\Gamma_{56})/\Gamma$

VALUE	CL%	DOCUMENT ID		TECN	COMMENT
<0.0013	90	[162] ALBRECHT	93E	ARG	$e^+e^- \to \Upsilon(4S)$

[162] ALBRECHT 93E reports $< 1.7 \times 10^{-3}$ for $B(D_s^+ \to \phi\pi^+) = 0.027$. We rescale to our best value $B(D_s^+ \to \phi\pi^+) = 0.036$.

$\Gamma(D_s^{*+}\pi^-)/\Gamma_{total}$ Γ_{51}/Γ

VALUE (units 10^{-5})	CL%	DOCUMENT ID		TECN	COMMENT
< 4.1	90	AUBERT	03D	BABR	$e^+e^- \to \Upsilon(4S)$
• • • We do not use the following data for averages, fits, limits, etc. • • •					
<50	90	[163] ALEXANDER	93B	CLE2	$e^+e^- \to \Upsilon(4S)$

[163] ALEXANDER 93B reports < 44 for $B(D_s^+ \to \phi\pi^+) = 0.037$. We rescale to our best value $B(D_s^+ \to \phi\pi^+) = 0.036$.

$[\Gamma(D_s^{*+}\pi^-) + \Gamma(D_s^{*-} K^+)]/\Gamma_{total}$ $(\Gamma_{51}+\Gamma_{57})/\Gamma$

VALUE	CL%	DOCUMENT ID		TECN	COMMENT
<0.0009	90	[164] ALBRECHT	93E	ARG	$e^+e^- \to \Upsilon(4S)$

[164] ALBRECHT 93E reports $< 1.2 \times 10^{-3}$ for $B(D_s^+ \to \phi\pi^+) = 0.027$. We rescale to our best value $B(D_s^+ \to \phi\pi^+) = 0.036$.

$\Gamma(D_s^+\rho^-)/\Gamma_{total}$ Γ_{52}/Γ

VALUE	CL%	DOCUMENT ID		TECN	COMMENT
<0.0007	90	[165] ALEXANDER	93B	CLE2	$e^+e^- \to \Upsilon(4S)$
• • • We do not use the following data for averages, fits, limits, etc. • • •					
<0.0016	90	[166] ALBRECHT	93E	ARG	$e^+e^- \to \Upsilon(4S)$

[165] ALEXANDER 93B reports $< 6.6 \times 10^{-4}$ for $B(D_s^+ \to \phi\pi^+) = 0.037$. We rescale to our best value $B(D_s^+ \to \phi\pi^+) = 0.036$.

[166] ALBRECHT 93E reports $< 2.2 \times 10^{-3}$ for $B(D_s^+ \to \phi\pi^+) = 0.027$. We rescale to our best value $B(D_s^+ \to \phi\pi^+) = 0.036$.

$\Gamma(D_s^{*+}\rho^-)/\Gamma_{total}$ Γ_{53}/Γ

VALUE	CL%	DOCUMENT ID		TECN	COMMENT
<0.0008	90	[167] ALEXANDER	93B	CLE2	$e^+e^- \to \Upsilon(4S)$
• • • We do not use the following data for averages, fits, limits, etc. • • •					
<0.0019	90	[168] ALBRECHT	93E	ARG	$e^+e^- \to \Upsilon(4S)$

[167] ALEXANDER 93B reports $< 7.4 \times 10^{-4}$ for $B(D_s^+ \to \phi\pi^+) = 0.037$. We rescale to our best value $B(D_s^+ \to \phi\pi^+) = 0.036$.

[168] ALBRECHT 93E reports $< 2.5 \times 10^{-3}$ for $B(D_s^+ \to \phi\pi^+) = 0.027$. We rescale to our best value $B(D_s^+ \to \phi\pi^+) = 0.036$.

$\Gamma(D_s^+ a_1(1260)^-)/\Gamma_{total}$ Γ_{54}/Γ

VALUE	CL%	DOCUMENT ID		TECN	COMMENT
< 0.0026	90	[169] ALBRECHT	93E	ARG	$e^+e^- \to \Upsilon(4S)$

[169] ALBRECHT 93E reports $< 3.5 \times 10^{-3}$ for $B(D_s^+ \to \phi\pi^+) = 0.027$. We rescale to our best value $B(D_s^+ \to \phi\pi^+) = 0.036$.

$\Gamma(D_s^{*+} a_1(1260)^-)/\Gamma_{total}$ Γ_{55}/Γ

VALUE	CL%	DOCUMENT ID		TECN	COMMENT
< 0.0022	90	[170] ALBRECHT	93E	ARG	$e^+e^- \to \Upsilon(4S)$

[170] ALBRECHT 93E reports $< 2.9 \times 10^{-3}$ for $B(D_s^+ \to \phi\pi^+) = 0.027$. We rescale to our best value $B(D_s^+ \to \phi\pi^+) = 0.036$.

$\Gamma(D_s^- K^+)/\Gamma_{total}$ Γ_{56}/Γ

VALUE (units 10^{-6})	CL%	DOCUMENT ID		TECN	COMMENT
38 ± 13 OUR AVERAGE					
$32. \pm 12. \pm 8.$		[171] AUBERT	03D	BABR	$e^+e^- \to \Upsilon(4S)$
$45.^{+14.}_{-12.} \pm 11.$		[172] KROKOVNY	02	BELL	$e^+e^- \to \Upsilon(4S)$
• • • We do not use the following data for averages, fits, limits, etc. • • •					
< 240	90	[173] ALEXANDER	93B	CLE2	$e^+e^- \to \Upsilon(4S)$
< 1300	90	[174] BORTOLETTO	90	CLEO	$e^+e^- \to \Upsilon(4S)$

[171] AUBERT 03D reports $[B(B^0 \to D_s^- K^+) \times B(D_s^+ \to \phi\pi^+)] = 1.16 \pm 0.36 \pm 0.24$. We divide by our best value $B(D_s^+ \to \phi\pi^+) = (3.6 \pm 0.9) \times 10^{-2}$. Our first error is their experiment's error and our second error is the systematic error from using our best value.

[172] KROKOVNY 02 reports $[B(B^0 \to D_s^- K^+) \times B(D_s^+ \to \phi\pi^+)] = 1.61^{+0.45}_{-0.38} \pm 0.21$. We divide by our best value $B(D_s^+ \to \phi\pi^+) = (3.6 \pm 0.9) \times 10^{-2}$. Our first error is their experiment's error and our second error is the systematic error from using our best value.

[173] ALEXANDER 93B reports < 230 for $B(D_s^+ \to \phi\pi^+) = 0.037$. We rescale to our best value $B(D_s^+ \to \phi\pi^+) = 0.036$.

[174] BORTOLETTO 90 assume $B(D_s \to \phi\pi^+) = 2\%$.

$\Gamma(D_s^{*-} K^+)/\Gamma_{total}$ Γ_{57}/Γ

VALUE (units 10^{-5})	CL%	DOCUMENT ID		TECN	COMMENT
< 2.5	90	AUBERT	03D	BABR	$e^+e^- \to \Upsilon(4S)$
• • • We do not use the following data for averages, fits, limits, etc. • • •					
< 17	90	[175] ALEXANDER	93B	CLE2	$e^+e^- \to \Upsilon(4S)$

[175] ALEXANDER 93B reports < 17 for $B(D_s^+ \to \phi\pi^+) = 0.037$. We rescale to our best value $B(D_s^+ \to \phi\pi^+) = 0.036$.

$\Gamma(D_s^- K^*(892)^+)/\Gamma_{total}$ Γ_{58}/Γ

VALUE	CL%	DOCUMENT ID		TECN	COMMENT
< 0.0010	90	[176] ALEXANDER	93B	CLE2	$e^+e^- \to \Upsilon(4S)$
• • • We do not use the following data for averages, fits, limits, etc. • • •					
< 0.0034	90	[177] ALBRECHT	93E	ARG	$e^+e^- \to \Upsilon(4S)$

[176] ALEXANDER 93B reports $< 9.7 \times 10^{-4}$ for $B(D_s^+ \to \phi\pi^+) = 0.037$. We rescale to our best value $B(D_s^+ \to \phi\pi^+) = 0.036$.

[177] ALBRECHT 93E reports $< 4.6 \times 10^{-3}$ for $B(D_s^+ \to \phi\pi^+) = 0.027$. We rescale to our best value $B(D_s^+ \to \phi\pi^+) = 0.036$.

$\Gamma(D_s^{*-} K^*(892)^+)/\Gamma_{total}$ Γ_{59}/Γ

VALUE	CL%	DOCUMENT ID		TECN	COMMENT
< 0.0011	90	[178] ALEXANDER	93B	CLE2	$e^+e^- \to \Upsilon(4S)$
• • • We do not use the following data for averages, fits, limits, etc. • • •					
< 0.004	90	[179] ALBRECHT	93E	ARG	$e^+e^- \to \Upsilon(4S)$

[178] ALEXANDER 93B reports $< 11.0 \times 10^{-4}$ for $B(D_s^+ \to \phi\pi^+) = 0.037$. We rescale to our best value $B(D_s^+ \to \phi\pi^+) = 0.036$.

[179] ALBRECHT 93E reports $< 5.8 \times 10^{-3}$ for $B(D_s^+ \to \phi\pi^+) = 0.027$. We rescale to our best value $B(D_s^+ \to \phi\pi^+) = 0.036$.

$\Gamma(D_s^- \pi^+ K^0)/\Gamma_{total}$ Γ_{60}/Γ

VALUE	CL%	DOCUMENT ID		TECN	COMMENT
< 0.005	90	[180] ALBRECHT	93E	ARG	$e^+e^- \to \Upsilon(4S)$

[180] ALBRECHT 93E reports $< 7.3 \times 10^{-3}$ for $B(D_s^+ \to \phi\pi^+) = 0.027$. We rescale to our best value $B(D_s^+ \to \phi\pi^+) = 0.036$.

$\Gamma(D_s^{*-} \pi^+ K^0)/\Gamma_{total}$ Γ_{61}/Γ

VALUE	CL%	DOCUMENT ID		TECN	COMMENT
< 0.0031	90	[181] ALBRECHT	93E	ARG	$e^+e^- \to \Upsilon(4S)$

[181] ALBRECHT 93E reports $< 4.2 \times 10^{-3}$ for $B(D_s^+ \to \phi\pi^+) = 0.027$. We rescale to our best value $B(D_s^+ \to \phi\pi^+) = 0.036$.

$\Gamma(D_s^- \pi^+ K^*(892)^0)/\Gamma_{total}$ Γ_{62}/Γ

VALUE	CL%	DOCUMENT ID		TECN	COMMENT
< 0.004	90	[182] ALBRECHT	93E	ARG	$e^+e^- \to \Upsilon(4S)$

[182] ALBRECHT 93E reports $< 5.0 \times 10^{-3}$ for $B(D_s^+ \to \phi\pi^+) = 0.027$. We rescale to our best value $B(D_s^+ \to \phi\pi^+) = 0.036$.

$\Gamma(D_s^{*-} \pi^+ K^*(892)^0)/\Gamma_{total}$ Γ_{63}/Γ

VALUE	CL%	DOCUMENT ID		TECN	COMMENT
< 0.0020	90	[183] ALBRECHT	93E	ARG	$e^+e^- \to \Upsilon(4S)$

[183] ALBRECHT 93E reports $< 2.7 \times 10^{-3}$ for $B(D_s^+ \to \phi\pi^+) = 0.027$. We rescale to our best value $B(D_s^+ \to \phi\pi^+) = 0.036$.

$\Gamma(\overline{D}^0 K^0)/\Gamma_{total}$ Γ_{64}/Γ

VALUE	DOCUMENT ID		TECN	COMMENT
$(5.0^{+1.3}_{-1.2} \pm 0.6) \times 10^{-5}$	[184] KROKOVNY	03	BELL	$e^+e^- \to \Upsilon(4S)$

[184] Assumes equal production of B^+ and B^0 at the $\Upsilon(4S)$.

$\Gamma(\overline{D}^0 K^*(892)^0)/\Gamma_{total}$ Γ_{65}/Γ

VALUE	DOCUMENT ID		TECN	COMMENT
$(4.8^{+1.1}_{-1.0} \pm 0.5) \times 10^{-5}$	[185] KROKOVNY	03	BELL	$e^+e^- \to \Upsilon(4S)$

[185] Assumes equal production of B^+ and B^0 at the $\Upsilon(4S)$.

$\Gamma(\overline{D}^0 \pi^0)/\Gamma_{total}$ Γ_{66}/Γ

VALUE (units 10^{-4})	CL%	DOCUMENT ID		TECN	COMMENT
2.91 ± 0.28 OUR AVERAGE					
$2.9 \pm 0.2 \pm 0.3$		[186] AUBERT	04B	BABR	$e^+e^- \to \Upsilon(4S)$
$3.1 \pm 0.4 \pm 0.5$		[186] ABE	02J	BELL	$e^+e^- \to \Upsilon(4S)$
$2.74^{+0.36}_{-0.32} \pm 0.55$		[186] COAN	02	CLE2	$e^+e^- \to \Upsilon(4S)$
• • • We do not use the following data for averages, fits, limits, etc. • • •					
< 1.2	90	[187] NEMATI	98	CLE2	Repl. by COAN 02
< 4.8	90	[188] ALAM	94	CLE2	Repl. by NEMATI 98

[186] Assumes equal production of B^+ and B^0 at the $\Upsilon(4S)$.

[187] NEMATI 98 assumes equal production of B^+ and B^0 at the $\Upsilon(4S)$ and use the PDG 96 values for D^0, D^{*0}, η, η', and ω branching fractions.

[188] ALAM 94 assume equal production of B^+ and B^0 at the $\Upsilon(4S)$ and use the CLEO II absolute $B(D^0 \to K^-\pi^+)$ and the PDG 1992 $B(D^0 \to K^-\pi^+\pi^0)/B(D^0 \to K^-\pi^+)$ and $B(D^0 \to K^-\pi^+\pi^+\pi^-)/B(D^0 \to K^-\pi^+)$.

$\Gamma(\overline{D}^0 \rho^0)/\Gamma_{total}$ Γ_{67}/Γ

VALUE (units 10^{-4})	CL%	EVTS	DOCUMENT ID		TECN	COMMENT
2.9 ± 1.0 ± 0.4			[189] SATPATHY	03	BELL	$e^+e^- \to \Upsilon(4S)$
• • • We do not use the following data for averages, fits, limits, etc. • • •						
< 3.9	90		[190] NEMATI	98	CLE2	$e^+e^- \to \Upsilon(4S)$
< 5.5	90		[191] ALAM	94	CLE2	Repl. by NEMATI 98
< 6.0	90		[192] BORTOLETTO	92	CLEO	$e^+e^- \to \Upsilon(4S)$
< 27.0	90	4	[193] ALBRECHT	88K	ARG	$e^+e^- \to \Upsilon(4S)$

[189] Assumes equal production of B^+ and B^0 at the $\Upsilon(4S)$.

[190] NEMATI 98 assumes equal production of B^+ and B^0 at the $\Upsilon(4S)$ and use the PDG 96 values for D^0, D^{*0}, η, η', and ω branching fractions.

[191] ALAM 94 assume equal production of B^+ and B^0 at the $\Upsilon(4S)$ and use the CLEO II absolute $B(D^0 \to K^-\pi^+)$ and the PDG 1992 $B(D^0 \to K^-\pi^+\pi^0)/B(D^0 \to K^-\pi^+)$ and $B(D^0 \to K^-\pi^+\pi^+\pi^-)/B(D^0 \to K^-\pi^+)$.

[192] BORTOLETTO 92 assumes equal production of B^+ and B^0 at the $\Upsilon(4S)$ and uses Mark III branching fractions for the D.

[193] ALBRECHT 88K reports < 0.003 assuming $B^0\overline{B}^0$:B^+B^- production ratio is 45:55. We rescale to 50%.

$\Gamma(\overline{D}^0 \eta)/\Gamma_{total}$ Γ_{68}/Γ

VALUE (units 10^{-4})	CL%	DOCUMENT ID		TECN	COMMENT
2.2 ± 0.5 OUR AVERAGE Error includes scale factor of 1.6.					
$2.5 \pm 0.2 \pm 0.3$		[194] AUBERT	04B	BABR	$e^+e^- \to \Upsilon(4S)$
$1.4^{+0.5}_{-0.4} \pm 0.3$		[194] ABE	02J	BELL	$e^+e^- \to \Upsilon(4S)$
• • • We do not use the following data for averages, fits, limits, etc. • • •					
< 1.3	90	[195] NEMATI	98	CLE2	$e^+e^- \to \Upsilon(4S)$
< 6.8	90	[196] ALAM	94	CLE2	Repl. by NEMATI 98

[194] Assumes equal production of B^+ and B^0 at the $\Upsilon(4S)$.

[195] NEMATI 98 assumes equal production of B^+ and B^0 at the $\Upsilon(4S)$ and use the PDG 96 values for D^0, D^{*0}, η, η', and ω branching fractions.

[196] ALAM 94 assume equal production of B^+ and B^0 at the $\Upsilon(4S)$ and use the CLEO II absolute $B(D^0 \to K^-\pi^+)$ and the PDG 1992 $B(D^0 \to K^-\pi^+\pi^0)/B(D^0 \to K^-\pi^+)$ and $B(D^0 \to K^-\pi^+\pi^+\pi^-)/B(D^0 \to K^-\pi^+)$.

$\Gamma(\overline{D}^0\eta')/\Gamma_{\text{total}}$ Γ_{69}/Γ

VALUE (units 10^{-4})	CL%	DOCUMENT ID		TECN	COMMENT
$1.7\pm0.4\pm0.2$		[197] AUBERT	04B	BABR	$e^+e^- \to \Upsilon(4S)$
• • • We do not use the following data for averages, fits, limits, etc. • • •					
9.4	90	[198] NEMATI	98	CLE2	$e^+e^- \to \Upsilon(4S)$
8.6	90	[199] ALAM	94	CLE2	Repl. by NEMATI 98

[197] Assumes equal production of B^+ and B^0 at the $\Upsilon(4S)$.

[198] NEMATI 98 assumes equal production of B^+ and B^0 at the $\Upsilon(4S)$ and use the PDG 96 values for D^0, D^{*0}, η, η', and ω branching fractions.

[199] ALAM 94 assume equal production of B^+ and B^0 at the $\Upsilon(4S)$ and use the CLEO II absolute $B(D^0 \to K^-\pi^+)$ and the PDG 1992 $B(D^0 \to K^-\pi^+\pi^0)/B(D^0 \to K^-\pi^+)$ and $B(D^0 \to K^-\pi^+\pi^+\pi^-)/B(D^0 \to K^-\pi^+)$.

$\Gamma(\overline{D}^0\eta')/\Gamma(\overline{D}^0\eta)$ Γ_{69}/Γ_{68}

VALUE	DOCUMENT ID		TECN	COMMENT
$0.7\ \pm0.2\ \pm0.1$	AUBERT	04B	BABR	$e^+e^- \to \Upsilon(4S)$

$\Gamma(\overline{D}^0\omega)/\Gamma_{\text{total}}$ Γ_{70}/Γ

VALUE (units 10^{-4})	CL%	DOCUMENT ID		TECN	COMMENT
2.5 ± 0.6 OUR AVERAGE		Error includes scale factor of 1.5.			
$3.0\pm0.3\pm0.4$		[200] AUBERT	04B	BABR	$e^+e^- \to \Upsilon(4S)$
$1.8\pm0.5^{+0.4}_{-0.3}$		[200] ABE	02J	BELL	$e^+e^- \to \Upsilon(4S)$
• • • We do not use the following data for averages, fits, limits, etc. • • •					
<5.1	90	[201] NEMATI	98	CLE2	$e^+e^- \to \Upsilon(4S)$
<6.3	90	[202] ALAM	94	CLE2	Repl. by NEMATI 98

[200] Assumes equal production of B^+ and B^0 at the $\Upsilon(4S)$.

[201] NEMATI 98 assumes equal production of B^+ and B^0 at the $\Upsilon(4S)$ and use the PDG 96 values for D^0, D^{*0}, η, η', and ω branching fractions.

[202] ALAM 94 assume equal production of B^+ and B^0 at the $\Upsilon(4S)$ and use the CLEO II absolute $B(D^0 \to K^-\pi^+)$ and the PDG 1992 $B(D^0 \to K^-\pi^+\pi^0)/B(D^0 \to K^-\pi^+)$ and $B(D^0 \to K^-\pi^+\pi^+\pi^-)/B(D^0 \to K^-\pi^+)$.

$\Gamma(D^0K^*(892)^0)/\Gamma_{\text{total}}$ Γ_{71}/Γ

VALUE	CL%	DOCUMENT ID		TECN	COMMENT
$<1.8\times10^{-5}$	90	[203] KROKOVNY	03	BELL	$e^+e^- \to \Upsilon(4S)$

[203] Assumes equal production of B^+ and B^0 at the $\Upsilon(4S)$.

$\Gamma(\overline{D}^{*0}\gamma)/\Gamma_{\text{total}}$ Γ_{72}/Γ

VALUE	CL%	DOCUMENT ID		TECN	COMMENT
$<5.0\times10^{-5}$	90	[204] ARTUSO	00	CLE2	$e^+e^- \to \Upsilon(4S)$

[204] Assumes equal production of B^+ and B^0 at the $\Upsilon(4S)$.

$\Gamma(\overline{D}^*(2007)^0\pi^0)/\Gamma_{\text{total}}$ Γ_{73}/Γ

VALUE (units 10^{-4})	CL%	DOCUMENT ID		TECN	COMMENT
$2.7\ \pm0.5$ OUR AVERAGE					
$2.9\ \pm0.4\ \pm0.5$		[205] AUBERT	04B	BABR	$e^+e^- \to \Upsilon(4S)$
$2.7\ ^{+0.8}_{-0.7}\ ^{+0.5}_{-0.6}$		[205] ABE	02J	BELL	$e^+e^- \to \Upsilon(4S)$
$2.20^{+0.59}_{-0.52}\pm0.79$		[205] COAN	02	CLE2	$e^+e^- \to \Upsilon(4S)$
• • • We do not use the following data for averages, fits, limits, etc. • • •					
<4.4	90	[206] NEMATI	98	CLE2	Repl. by COAN 02
<9.7	90	[207] ALAM	94	CLE2	Repl. by NEMATI 98

[205] Assumes equal production of B^+ and B^0 at the $\Upsilon(4S)$.

[206] NEMATI 98 assumes equal production of B^+ and B^0 at the $\Upsilon(4S)$ and use the PDG 96 values for D^0, D^{*0}, η, η', and ω branching fractions.

[207] ALAM 94 assume equal production of B^+ and B^0 at the $\Upsilon(4S)$ and use the CLEO II $B(D^*(2007)^0 \to D^0\pi^0)$ and absolute $B(D^0 \to K^-\pi^+)$ and the PDG 1992 $B(D^0 \to K^-\pi^+\pi^0)/B(D^0 \to K^-\pi^+)$ and $B(D^0 \to K^-\pi^+\pi^+\pi^-)/B(D^0 \to K^-\pi^+)$.

$\Gamma(\overline{D}^0\pi^0)/\Gamma(\overline{D}^*(2007)^0\pi^0)$ Γ_{15}/Γ_{73}

VALUE	DOCUMENT ID		TECN	COMMENT
$1.0\ \pm0.1\ \pm0.2$	AUBERT	04B	BABR	$e^+e^- \to \Upsilon(4S)$

$\Gamma(\overline{D}^*(2007)^0\rho^0)/\Gamma_{\text{total}}$ Γ_{74}/Γ

VALUE	CL%	DOCUMENT ID		TECN	COMMENT
$<5.1\ \times10^{-4}$	90	[208] SATPATHY	03	BELL	$e^+e^- \to \Upsilon(4S)$
• • • We do not use the following data for averages, fits, limits, etc. • • •					
<0.00056	90	[209] NEMATI	98	CLE2	$e^+e^- \to \Upsilon(4S)$
<0.00117	90	[210] ALAM	94	CLE2	Repl. by NEMATI 98

[208] Assumes equal production of B^+ and B^0 at the $\Upsilon(4S)$.

[209] NEMATI 98 assumes equal production of B^+ and B^0 at the $\Upsilon(4S)$ and use the PDG 96 values for D^0, D^{*0}, η, η', and ω branching fractions.

[210] ALAM 94 assume equal production of B^+ and B^0 at the $\Upsilon(4S)$ and use the CLEO II $B(D^*(2007)^0 \to D^0\pi^0)$ and absolute $B(D^0 \to K^-\pi^+)$ and the PDG 1992 $B(D^0 \to K^-\pi^+\pi^0)/B(D^0 \to K^-\pi^+)$ and $B(D^0 \to K^-\pi^+\pi^+\pi^-)/B(D^0 \to K^-\pi^+)$.

$\Gamma(\overline{D}^*(2007)^0\eta)/\Gamma_{\text{total}}$ Γ_{75}/Γ

VALUE (units 10^{-4})	CL%	DOCUMENT ID		TECN	COMMENT
$2.6\pm0.4\pm0.4$		[211] AUBERT	04B	BABR	$e^+e^- \to \Upsilon(4S)$
• • • We do not use the following data for averages, fits, limits, etc. • • •					
<4.6	90	[211] ABE	02J	BELL	$e^+e^- \to \Upsilon(4S)$
<2.6	90	[212] NEMATI	98	CLE2	$e^+e^- \to \Upsilon(4S)$
<6.9	90	[213] ALAM	94	CLE2	Repl. by NEMATI 98

[211] Assumes equal production of B^+ and B^0 at the $\Upsilon(4S)$.

[212] NEMATI 98 assumes equal production of B^+ and B^0 at the $\Upsilon(4S)$ and use the PDG 96 values for D^0, D^{*0}, η, η', and ω branching fractions.

[213] ALAM 94 assume equal production of B^+ and B^0 at the $\Upsilon(4S)$ and use the CLEO II $B(D^*(2007)^0 \to D^0\pi^0)$ and absolute $B(D^0 \to K^-\pi^+)$ and the PDG 1992 $B(D^0 \to K^-\pi^+\pi^0)/B(D^0 \to K^-\pi^+)$ and $B(D^0 \to K^-\pi^+\pi^+\pi^-)/B(D^0 \to K^-\pi^+)$.

$\Gamma(\overline{D}^0\eta)/\Gamma(\overline{D}^*(2007)^0\eta)$ Γ_{68}/Γ_{75}

VALUE	DOCUMENT ID		TECN	COMMENT
$0.9\ \pm0.2\ \pm0.1$	AUBERT	04B	BABR	$e^+e^- \to \Upsilon(4S)$

$\Gamma(\overline{D}^*(2007)^0\eta')/\Gamma(\overline{D}^*(2007)^0\eta)$ Γ_{76}/Γ_{75}

VALUE	DOCUMENT ID		TECN	COMMENT
$0.5\ \pm0.3\ \pm0.1$	AUBERT	04B	BABR	$e^+e^- \to \Upsilon(4S)$

$\Gamma(\overline{D}^*(2007)^0\eta')/\Gamma_{\text{total}}$ Γ_{76}/Γ

VALUE	CL%	DOCUMENT ID		TECN	COMMENT
<0.00026	90	[214] AUBERT	04B	BABR	$e^+e^- \to \Upsilon(4S)$
• • • We do not use the following data for averages, fits, limits, etc. • • •					
<0.0014	90	BRANDENB...	98	CLE2	$e^+e^- \to \Upsilon(4S)$
<0.0019	90	[215] NEMATI	98	CLE2	$e^+e^- \to \Upsilon(4S)$
<0.0027	90	[216] ALAM	94	CLE2	Repl. by NEMATI 98

[214] Assumes equal production of B^+ and B^0 at the $\Upsilon(4S)$.

[215] NEMATI 98 assumes equal production of B^+ and B^0 at the $\Upsilon(4S)$ and use the PDG 96 values for D^0, D^{*0}, η, η', and ω branching fractions.

[216] ALAM 94 assume equal production of B^+ and B^0 at the $\Upsilon(4S)$ and use the CLEO II $B(D^*(2007)^0 \to D^0\pi^0)$ and absolute $B(D^0 \to K^-\pi^+)$ and the PDG 1992 $B(D^0 \to K^-\pi^+\pi^0)/B(D^0 \to K^-\pi^+)$ and $B(D^0 \to K^-\pi^+\pi^+\pi^-)/B(D^0 \to K^-\pi^+)$.

$\Gamma(\overline{D}^0\eta')/\Gamma(\overline{D}^*(2007)^0\eta')$ Γ_{69}/Γ_{76}

VALUE	DOCUMENT ID		TECN	COMMENT
$1.3\pm0.8\pm0.2$	AUBERT	04B	BABR	$e^+e^- \to \Upsilon(4S)$

$\Gamma(\overline{D}^*(2007)^0\omega)/\Gamma_{\text{total}}$ Γ_{83}/Γ

VALUE (units 10^{-4})	CL%	DOCUMENT ID		TECN	COMMENT
$4.2\pm0.7\pm0.9$	90	[217] AUBERT	04B	BABR	$e^+e^- \to \Upsilon(4S)$
• • • We do not use the following data for averages, fits, limits, etc. • • •					
<7.9	90	[217] ABE	02J	BELL	$e^+e^- \to \Upsilon(4S)$
<7.4	90	[218] NEMATI	98	CLE2	$e^+e^- \to \Upsilon(4S)$
<21	90	[219] ALAM	94	CLE2	Repl. by NEMATI 98

[217] Assumes equal production of B^+ and B^0 at the $\Upsilon(4S)$.

[218] NEMATI 98 assumes equal production of B^+ and B^0 at the $\Upsilon(4S)$ and use the PDG 96 values for D^0, D^{*0}, η, η', and ω branching fractions.

[219] ALAM 94 assume equal production of B^+ and B^0 at the $\Upsilon(4S)$ and use the CLEO II $B(D^*(2007)^0 \to D^0\pi^0)$ and absolute $B(D^0 \to K^-\pi^+)$ and the PDG 1992 $B(D^0 \to K^-\pi^+\pi^0)/B(D^0 \to K^-\pi^+)$ and $B(D^0 \to K^-\pi^+\pi^+\pi^-)/B(D^0 \to K^-\pi^+)$.

$\Gamma(\overline{D}^0\omega)/\Gamma(\overline{D}^*(2007)^0\omega)$ Γ_{70}/Γ_{83}

VALUE	DOCUMENT ID		TECN	COMMENT
$0.7\ \pm0.1\ \pm0.1$	AUBERT	04B	BABR	$e^+e^- \to \Upsilon(4S)$

$\Gamma(\overline{D}^*(2007)^0\pi^+\pi^-)/\Gamma_{\text{total}}$ Γ_{77}/Γ

VALUE		DOCUMENT ID		TECN	COMMENT
$(6.2\pm1.2\pm1.8)\times10^{-4}$	[220,221]	SATPATHY	03	BELL	$e^+e^- \to \Upsilon(4S)$

[220] Assumes equal production of B^+ and B^0 at the $\Upsilon(4S)$.

[221] No assumption about the intermediate mechanism is made in the analysis.

$\Gamma(\overline{D}^*(2007)^0K^0)/\Gamma_{\text{total}}$ Γ_{78}/Γ

VALUE	CL%	DOCUMENT ID		TECN	COMMENT
$<6.6\times10^{-5}$	90	[222] KROKOVNY	03	BELL	$e^+e^- \to \Upsilon(4S)$

[222] Assumes equal production of B^+ and B^0 at the $\Upsilon(4S)$.

$\Gamma(\overline{D}^*(2007)^0K^*(892)^0)/\Gamma_{\text{total}}$ Γ_{79}/Γ

VALUE	CL%	DOCUMENT ID		TECN	COMMENT
$<6.9\times10^{-5}$	90	[223] KROKOVNY	03	BELL	$e^+e^- \to \Upsilon(4S)$

[223] Assumes equal production of B^+ and B^0 at the $\Upsilon(4S)$.

$\Gamma(D^*(2007)^0K^*(892)^0)/\Gamma_{\text{total}}$ Γ_{80}/Γ

VALUE	CL%	DOCUMENT ID		TECN	COMMENT
$<4.0\times10^{-5}$	90	[224] KROKOVNY	03	BELL	$e^+e^- \to \Upsilon(4S)$

[224] Assumes equal production of B^+ and B^0 at the $\Upsilon(4S)$.

$\Gamma(D^*(2007)^0\pi^+\pi^+\pi^-\pi^-)/\Gamma_{total}$ Γ_{81}/Γ

VALUE	DOCUMENT ID		TECN	COMMENT
3.0 ± 0.7 ± 0.6	[225] EDWARDS	02	CLE2	$e^+e^- \to \Upsilon(4S)$

[225] Assumes equal production of B^+ and B^0 at the $\Upsilon(4S)$.

$\Gamma(D^*(2007)^0\pi^+\pi^+\pi^-\pi^-)/\Gamma(D^*(2010)^+\pi^+\pi^-\pi^-\pi^0)$ Γ_{81}/Γ_{33}

VALUE	DOCUMENT ID		TECN	COMMENT
0.17 ± 0.04 ± 0.02	[226] EDWARDS	02	CLE2	$e^+e^- \to \Upsilon(4S)$

[226] Assumes equal production of B^+ and B^0 at the $\Upsilon(4S)$.

$\Gamma(D^*(2010)^+ D^*(2010)^-)/\Gamma_{total}$ Γ_{82}/Γ

VALUE	CL%	DOCUMENT ID		TECN	COMMENT
(8.7 ± 1.8) × 10⁻⁴ OUR AVERAGE					
$(8.3 \pm 1.6 \pm 1.2) \times 10^{-4}$		[227,228] AUBERT	02M	BABR	$e^+e^- \to \Upsilon(4S)$
$(9.9^{+4.2}_{-3.3} \pm 1.2) \times 10^{-4}$		[227] LIPELES	00	CLE2	$e^+e^- \to \Upsilon(4S)$
• • • We do not use the following data for averages, fits, limits, etc. • • •					
$(6.2^{+4.0}_{-2.9} \pm 1.0) \times 10^{-4}$		[229] ARTUSO	99	CLE2	Repl. by LIPELES 00
$< 6.1 \times 10^{-3}$	90	[230] BARATE	98Q	ALEP	$e^+e^- \to Z$
$< 2.2 \times 10^{-3}$	90	[231] ASNER	97	CLE2	Repl. by ARTUSO 99

[227] Assumes equal production of B^+ and B^0 at the $\Upsilon(4S)$.
[228] AUBERT 02M also assumes the measured CP-odd fraction of the final states is $0.22 \pm 0.18 \pm 0.03$.
[229] ARTUSO 99 uses $B(\Upsilon(4S) \to B^0\overline{B}^0) = (48 \pm 4)\%$.
[230] BARATE 98Q (ALEPH) observes 2 events with an expected background of 0.10 ± 0.03 which corresponds to a branching ratio of $(2.3^{+1.9}_{-1.2} \pm 0.4) \times 10^{-3}$.
[231] ASNER 97 at CLEO observes 1 event with an expected background of 0.022 ± 0.011. This corresponds to a branching ratio of $(5.3^{+7.1}_{-3.7} \pm 1.0) \times 10^{-4}$.

$\Gamma(D^*(2010)^+ D^-)/\Gamma_{total}$ Γ_{84}/Γ

VALUE	CL%	DOCUMENT ID		TECN	COMMENT
< 6.3 × 10⁻⁴	90	[232] LIPELES	00	CLE2	$e^+e^- \to \Upsilon(4S)$
• • • We do not use the following data for averages, fits, limits, etc. • • •					
$< 5.6 \times 10^{-3}$	90	BARATE	98Q	ALEP	$e^+e^- \to Z$
$< 1.8 \times 10^{-3}$	90	ASNER	97	CLE2	$e^+e^- \to \Upsilon(4S)$

[232] Assumes equal production of B^+ and B^0 at the $\Upsilon(4S)$.

$[\Gamma(D^*(2010)^- D^+) + \Gamma(D^*(2010)^+ D^-)]/\Gamma_{total}$ Γ_{85}/Γ

VALUE (units 10⁻³)		DOCUMENT ID		TECN	COMMENT
0.93 ± 0.15 OUR AVERAGE					
$0.88 \pm 0.10 \pm 0.13$		[233] AUBERT	03J	BABR	$e^+e^- \to \Upsilon(4S)$
$1.17 \pm 0.26^{+0.22}_{-0.25}$		[233,234] ABE	02Q	BELL	$e^+e^- \to \Upsilon(4S)$
• • • We do not use the following data for averages, fits, limits, etc. • • •					
$1.48 \pm 0.38^{+0.28}_{-0.31}$		[233,235] ABE	02Q	BELL	$e^+e^- \to \Upsilon(4S)$

[233] Assumes equal production of B^+ and B^0 at the $\Upsilon(4S)$.
[234] The measurement is performed using fully reconstructed D^* and D^+ decays.
[235] The measurement is performed using a partial reconstruction technique for the D^* and fully reconstructed D^+ decays as a cross check.

$\Gamma(D^*(2007)^0\overline{D}^*(2007)^0)/\Gamma_{total}$ Γ_{86}/Γ

VALUE	CL%	DOCUMENT ID		TECN	COMMENT
< 0.027	90	BARATE	98Q	ALEP	$e^+e^- \to Z$

$\Gamma(D^- D^0 K^+)/\Gamma_{total}$ Γ_{87}/Γ

VALUE (units 10⁻³)	DOCUMENT ID		TECN	COMMENT
1.7 ± 0.3 ± 0.3	[236] AUBERT	03X	BABR	$e^+e^- \to \Upsilon(4S)$

[236] Assumes equal production of B^+ and B^0 at the $\Upsilon(4S)$.

$\Gamma(D^- D^*(2007)^0 K^+)/\Gamma_{total}$ Γ_{88}/Γ

VALUE (units 10⁻³)	DOCUMENT ID		TECN	COMMENT
4.6 ± 0.7 ± 0.7	[237] AUBERT	03X	BABR	$e^+e^- \to \Upsilon(4S)$

[237] Assumes equal production of B^+ and B^0 at the $\Upsilon(4S)$.

$\Gamma(D^*(2010)^- D^0 K^+)/\Gamma_{total}$ Γ_{89}/Γ

VALUE (units 10⁻³)	DOCUMENT ID		TECN	COMMENT
3.1 $^{+0.4}_{-0.3}$ ± 0.4	[238] AUBERT	03X	BABR	$e^+e^- \to \Upsilon(4S)$

[238] Assumes equal production of B^+ and B^0 at the $\Upsilon(4S)$.

$\Gamma(D^*(2010)^- D^*(2007)^0 K^+)/\Gamma_{total}$ Γ_{90}/Γ

VALUE (units 10⁻³)	DOCUMENT ID		TECN	COMMENT
11.8 ± 1.0 ± 1.7	[239] AUBERT	03X	BABR	$e^+e^- \to \Upsilon(4S)$

[239] Assumes equal production of B^+ and B^0 at the $\Upsilon(4S)$.

$\Gamma(D^- D^+ K^0)/\Gamma_{total}$ Γ_{91}/Γ

VALUE (units 10⁻³)	CL%	DOCUMENT ID		TECN	COMMENT
< 1.7	90	[240] AUBERT	03X	BABR	$e^+e^- \to \Upsilon(4S)$

[240] Assumes equal production of B^+ and B^0 at the $\Upsilon(4S)$.

$[\Gamma(D^*(2010)^- D^+ K^0) + \Gamma(D^- D^*(2010)^+ K^0)]/\Gamma_{total}$ Γ_{92}/Γ

VALUE (units 10⁻³)	DOCUMENT ID		TECN	COMMENT
6.5 ± 1.2 ± 1.0	[241] AUBERT	03X	BABR	$e^+e^- \to \Upsilon(4S)$

[241] Assumes equal production of B^+ and B^0 at the $\Upsilon(4S)$.

$\Gamma(D^*(2010)^- D^*(2010)^+ K^0)/\Gamma_{total}$ Γ_{93}/Γ

VALUE (units 10⁻³)	DOCUMENT ID		TECN	COMMENT
8.8 $^{+1.5}_{-1.4}$ ± 1.3	[242] AUBERT	03X	BABR	$e^+e^- \to \Upsilon(4S)$

[242] Assumes equal production of B^+ and B^0 at the $\Upsilon(4S)$.

$\Gamma(\overline{D}^0 D^0 K^0)/\Gamma_{total}$ Γ_{94}/Γ

VALUE (units 10⁻³)	CL%	DOCUMENT ID		TECN	COMMENT
< 1.4	90	[243] AUBERT	03X	BABR	$e^+e^- \to \Upsilon(4S)$

[243] Assumes equal production of B^+ and B^0 at the $\Upsilon(4S)$.

$[\Gamma(\overline{D}^0 D^*(2007)^0 K^0) + \Gamma(\overline{D}^*(2007)^0 D^0 K^0)]/\Gamma_{total}$ Γ_{95}/Γ

VALUE (units 10⁻³)	CL%	DOCUMENT ID		TECN	COMMENT
< 3.7	90	[244] AUBERT	03X	BABR	$e^+e^- \to \Upsilon(4S)$

[244] Assumes equal production of B^+ and B^0 at the $\Upsilon(4S)$.

$\Gamma(\overline{D}^*(2007)^0 D^*(2007)^0 K^0)/\Gamma_{total}$ Γ_{96}/Γ

VALUE (units 10⁻³)	CL%	DOCUMENT ID		TECN	COMMENT
< 6.6	90	[245] AUBERT	03X	BABR	$e^+e^- \to \Upsilon(4S)$

[245] Assumes equal production of B^+ and B^0 at the $\Upsilon(4S)$.

$\Gamma((\overline{D}+\overline{D}^*)(D+D^*)K)/\Gamma_{total}$ Γ_{97}/Γ

VALUE (units 10⁻²)	DOCUMENT ID		TECN	COMMENT
4.3 ± 0.3 ± 0.6	[246] AUBERT	03X	BABR	$e^+e^- \to \Upsilon(4S)$

[246] Assumes equal production of B^+ and B^0 at the $\Upsilon(4S)$.

$\Gamma(\eta_c K^0)/\Gamma_{total}$ Γ_{98}/Γ

VALUE (units 10⁻³)	DOCUMENT ID		TECN	COMMENT
1.2 ± 0.4 OUR AVERAGE				
$1.23 \pm 0.23^{+0.40}_{-0.41}$	[247] FANG	03	BELL	$e^+e^- \to \Upsilon(4S)$
$1.09^{+0.55}_{-0.42} \pm 0.33$	[248] EDWARDS	01	CLE2	$e^+e^- \to \Upsilon(4S)$

[247] Assumes equal production of B^+ and B^0 at the $\Upsilon(4S)$.
[248] EDWARDS 01 assumes equal production of B^0 and B^+ at the $\Upsilon(4S)$. The correlated uncertainties (28.3)% from $B(J/\psi(1S) \to \gamma\eta_c)$ in those modes have been accounted for.

$\Gamma(\eta_c K^*(892)^0)/\Gamma_{total}$ Γ_{99}/Γ

VALUE (units 10⁻³)	DOCUMENT ID		TECN	COMMENT
1.62 ± 0.32 $^{+0.55}_{-0.60}$	[249] FANG	03	BELL	$e^+e^- \to \Upsilon(4S)$

[249] Assumes equal production of B^+ and B^0 at the $\Upsilon(4S)$.

$\Gamma(\eta_c K^*(892)^0)/\Gamma(\eta_c K^0)$ Γ_{99}/Γ_{98}

VALUE	DOCUMENT ID		TECN	COMMENT
1.33 ± 0.36 $^{+0.24}_{-0.33}$	FANG	03	BELL	$e^+e^- \to \Upsilon(4S)$

$\Gamma(J/\psi(1S) K^0)/\Gamma_{total}$ Γ_{100}/Γ

VALUE (units 10⁻⁴)	CL%	EVTS	DOCUMENT ID		TECN	COMMENT
8.5 ± 0.5 OUR AVERAGE						
$7.9 \pm 0.4 \pm 0.9$			[250] ABE	03B	BELL	$e^+e^- \to \Upsilon(4S)$
$8.3 \pm 0.4 \pm 0.5$			[250] AUBERT	02	BABR	$e^+e^- \to \Upsilon(4S)$
$9.5 \pm 0.8 \pm 0.6$			[250] AVERY	00	CLE2	$e^+e^- \to \Upsilon(4S)$
$11.5 \pm 2.3 \pm 1.7$			[251] ABE	96H	CDF	$p\overline{p}$ at 1.8 TeV
$7.0 \pm 4.1 \pm 0.1$			[252] BORTOLETTO	92	CLEO	$e^+e^- \to \Upsilon(4S)$
$9.3 \pm 7.3 \pm 0.2$		2	[253] ALBRECHT	90J	ARG	$e^+e^- \to \Upsilon(4S)$
• • • We do not use the following data for averages, fits, limits, etc. • • •						
$8.5^{+1.4}_{-1.2} \pm 0.6$			[250] JESSOP	97	CLE2	Repl. by AVERY 00
$7.5 \pm 2.4 \pm 0.8$		10	[252] ALAM	94	CLE2	Sup. by JESSOP 97
< 50	90		ALAM	86	CLEO	$e^+e^- \to \Upsilon(4S)$

[250] Assumes equal production of B^+ and B^0 at the $\Upsilon(4S)$.
[251] ABE 96H assumes that $B(B^+ \to J/\psi K^+) = (1.02 \pm 0.14) \times 10^{-3}$.
[252] BORTOLETTO 92 reports $6 \pm 3 \pm 2$ for $B(J/\psi(1S) \to e^+e^-) = 0.069 \pm 0.009$. We rescale to our best value $B(J/\psi(1S) \to e^+e^-) = (5.93 \pm 0.10) \times 10^{-2}$. Our first error is their experiment's error and our second error is the systematic error from using our best value. Assumes equal production of B^+ and B^0 at the $\Upsilon(4S)$.
[253] ALBRECHT 90J reports $8 \pm 6 \pm 2$ for $B(J/\psi(1S) \to e^+e^-) = 0.069 \pm 0.009$. We rescale to our best value $B(J/\psi(1S) \to e^+e^-) = (5.93 \pm 0.10) \times 10^{-2}$. Our first error is their experiment's error and our second error is the systematic error from using our best value. Assumes equal production of B^+ and B^0 at the $\Upsilon(4S)$.

$\Gamma(J/\psi(1S)K^+\pi^-)/\Gamma_{total}$ Γ_{101}/Γ

VALUE (units 10^{-3})	CL%	EVTS	DOCUMENT ID		TECN	COMMENT
1.16±0.56±0.02			[254] BORTOLETTO 92		CLEO	$e^+e^- \to \Upsilon(4S)$
• • • We do not use the following data for averages, fits, limits, etc. • • •						
<1.3	90		[255] ALBRECHT	87D	ARG	$e^+e^- \to \Upsilon(4S)$
<6.3	90	2	GILES	84	CLEO	$e^+e^- \to \Upsilon(4S)$

[254] BORTOLETTO 92 reports $1.0 \pm 0.4 \pm 0.3$ for $B(J/\psi(1S) \to e^+e^-) = 0.069 \pm 0.009$. We rescale to our best value $B(J/\psi(1S) \to e^+e^-) = (5.93 \pm 0.10) \times 10^{-2}$. Our first error is their experiment's error and our second error is the systematic error from using our best value. Assumes equal production of B^+ and B^0 at the $\Upsilon(4S)$.

[255] ALBRECHT 87D assume $B^+B^-/B^0\overline{B}^0$ ratio is 55/45. $K\pi$ system is specifically selected as nonresonant.

$\Gamma(J/\psi(1S)K^*(892)^0)/\Gamma_{total}$ Γ_{102}/Γ

VALUE (units 10^{-3})	EVTS	DOCUMENT ID		TECN	COMMENT
1.31±0.07 OUR AVERAGE					
1.29±0.05±0.13		[256] ABE	02N	BELL	$e^+e^- \to \Upsilon(4S)$
1.24±0.05±0.09		[256] AUBERT	02	BABR	$e^+e^- \to \Upsilon(4S)$
1.74±0.20±0.18		[257] ABE	98O	CDF	$p\overline{p}$ 1.8 TeV
1.32±0.17±0.17		[258] JESSOP	97	CLE2	$e^+e^- \to \Upsilon(4S)$
1.28±0.66±0.02		[259] BORTOLETTO	92	CLEO	$e^+e^- \to \Upsilon(4S)$
1.28±0.60±0.02	6	[260] ALBRECHT	90J	ARG	$e^+e^- \to \Upsilon(4S)$
4.1 ±1.8 ±0.1	5	[261] BEBEK	87	CLEO	$e^+e^- \to \Upsilon(4S)$
• • • We do not use the following data for averages, fits, limits, etc. • • •					
1.36±0.27±0.22		[262] ABE	96H	CDF	Sup. by ABE 98O
1.69±0.31±0.18	29	[263] ALAM	94	CLE2	Sup. by JESSOP 97
		[264] ALBRECHT	94G	ARG	$e^+e^- \to \Upsilon(4S)$
4.0 ±0.30		[265] ALBAJAR	91E	UA1	$E_{cm}^{p\overline{p}} = 630$ GeV
3.3 ±0.18	5	[266] ALBRECHT	87D	ARG	$e^+e^- \to \Upsilon(4S)$
4.1 ±0.18	5	[267] ALAM	86	CLEO	Repl. by BEBEK 87

[256] Assumes equal production of B^+ and B^0 at the $\Upsilon(4S)$.

[257] ABE 98O reports $[B(B^0 \to J/\psi(1S)K^*(892)^0)]/[B(B^+ \to J/\psi(1S)K^+)] = 1.76 \pm 0.14 \pm 0.15$. We multiply by our best value $B(B^+ \to J/\psi(1S)K^+) = (9.9 \pm 1.0) \times 10^{-4}$. Our first error is their experiment's error and our second error is the systematic error from using our best value.

[258] Assumes equal production of B^+ and B^0 at the $\Upsilon(4S)$.

[259] BORTOLETTO 92 reports $1.1 \pm 0.5 \pm 0.3$ for $B(J/\psi(1S) \to e^+e^-) = 0.069 \pm 0.009$. We rescale to our best value $B(J/\psi(1S) \to e^+e^-) = (5.93 \pm 0.10) \times 10^{-2}$. Our first error is their experiment's error and our second error is the systematic error from using our best value. Assumes equal production of B^+ and B^0 at the $\Upsilon(4S)$.

[260] ALBRECHT 90J reports $1.1 \pm 0.5 \pm 0.2$ for $B(J/\psi(1S) \to e^+e^-) = 0.069 \pm 0.009$. We rescale to our best value $B(J/\psi(1S) \to e^+e^-) = (5.93 \pm 0.10) \times 10^{-2}$. Our first error is their experiment's error and our second error is the systematic error from using our best value. Assumes equal production of B^+ and B^0 at the $\Upsilon(4S)$.

[261] BEBEK 87 reports $3.5 \pm 1.6 \pm 0.3$ for $B(J/\psi(1S) \to e^+e^-) = 0.069 \pm 0.009$. We rescale to our best value $B(J/\psi(1S) \to e^+e^-) = (5.93 \pm 0.10) \times 10^{-2}$. Our first error is their experiment's error and our second error is the systematic error from using our best value. Updated in BORTOLETTO 92 to use the same assumptions.

[262] ABE 96H assumes that $B(B^+ \to J/\psi K^+) = (1.02 \pm 0.14) \times 10^{-3}$.

[263] The neutral and charged B events together are predominantly longitudinally polarized, $\Gamma_L/\Gamma = 0.080 \pm 0.08 \pm 0.05$. This can be compared with a prediction using HQET, 0.73 (KRAMER 92). This polarization indicates that the $B \to \psi K^*$ decay is dominated by the $CP = -1$ CP eigenstate. Assumes equal production of B^+ and B^0 at the $\Upsilon(4S)$.

[264] ALBRECHT 94G measures the polarization in the vector-vector decay to be predominantly longitudinal, $\Gamma_T/\Gamma = 0.03 \pm 0.16 \pm 0.15$ making the neutral decay a CP eigenstate when the K^{*0} decays through $K_S^0\pi^0$.

[265] ALBAJAR 91E assumes B_d^0 production fraction of 36%.

[266] ALBRECHT 87D assume $B^+B^-/B^0\overline{B}^0$ ratio is 55/45. Superseded by ALBRECHT 90J.

[267] ALAM 86 assumes $B^\pm/B^0$ ratio is 60/40. The observation of the decay $B^+ \to J/\psi K^*(892)^+$ (HAAS 85) has been retracted in this paper.

$\Gamma(J/\psi(1S)K^*(892)^0)/\Gamma(J/\psi(1S)K^0)$ $\Gamma_{102}/\Gamma_{100}$

VALUE	DOCUMENT ID		TECN	COMMENT
1.48±0.12 OUR AVERAGE				
1.49±0.10±0.08	[268] AUBERT	02	BABR	$e^+e^- \to \Upsilon(4S)$
1.39±0.36±0.10	ABE	96Q	CDF	$p\overline{p}$

[268] Assumes equal production of B^+ and B^0 at the $\Upsilon(4S)$.

$\Gamma(J/\psi(1S)\phi K^0)/\Gamma_{total}$ Γ_{103}/Γ

VALUE	DOCUMENT ID		TECN	COMMENT
(9.4±2.6) × 10^{-5} OUR AVERAGE				
$(10.2 \pm 3.8 \pm 1.0) \times 10^{-5}$	[269] AUBERT	03O	BABR	$e^+e^- \to \Upsilon(4S)$
$(\ 8.8^{+3.5}_{-3.0} \pm 1.3) \times 10^{-5}$	[270] ANASTASSOV	00	CLE2	$e^+e^- \to \Upsilon(4S)$

[269] Assumes equal production of B^+ and B^0 at the $\Upsilon(4S)$.

[270] ANASTASSOV 00 finds 10 events on a background of 0.5 ± 0.2. Assumes equal production of B^0 and B^+ at the $\Upsilon(4S)$, a uniform Dalitz plot distribution, isotropic $J/\psi(1S)$ and ϕ decays, and $B(B^+ \to J/\psi(1S)\phi K^+) = B(B^0 \to J/\psi(1S)\phi K^0)$.

$\Gamma(J/\psi(1S)K(1270)^0)/\Gamma_{total}$ Γ_{104}/Γ

VALUE (units 10^{-3})	DOCUMENT ID		TECN	COMMENT
1.30±0.34±0.32	[271] ABE	01L	BELL	$e^+e^- \to \Upsilon(4S)$

[271] Assumes equal production of B^+ and B^0 at the $\Upsilon(4S)$ and uses the PDG value of $B(B^+ \to J/\psi(1S)K^+) = (1.00 \pm 0.10) \times 10^{-3}$.

$\Gamma(J/\psi(1S)\pi^0)/\Gamma_{total}$ Γ_{105}/Γ

VALUE (units 10^{-5})	CL%	EVTS	DOCUMENT ID		TECN	COMMENT
2.2±0.4 OUR AVERAGE						
2.3±0.5±0.2			[272] ABE	03B	BELL	$e^+e^- \to \Upsilon(4S)$
2.0±0.6±0.2			[272] AUBERT	02	BABR	$e^+e^- \to \Upsilon(4S)$
$2.5^{+1.1}_{-0.9} \pm 0.2$			[272] AVERY	00	CLE2	$e^+e^- \to \Upsilon(4S)$
• • • We do not use the following data for averages, fits, limits, etc. • • •						
< 32	90		[273] ACCIARRI	97C	L3	
< 5.8	90		BISHAI	96	CLE2	$e^+e^- \to \Upsilon(4S)$
<690	90	1	[274] ALEXANDER	95	CLE2	Sup. by BISHAI 96

[272] Assumes equal production of B^+ and B^0 at the $\Upsilon(4S)$.

[273] ACCIARRI 97C assumes B^0 production fraction (39.5 ± 4.0%) and B_s (12.0 ± 3.0%).

[274] Assumes equal production of B^+B^- and $B^0\overline{B}^0$ on $\Upsilon(4S)$.

$\Gamma(J/\psi(1S)\eta)/\Gamma_{total}$ Γ_{106}/Γ

VALUE	CL%	DOCUMENT ID		TECN	COMMENT
<2.7 × 10^{-5}	90	[275] AUBERT	03O	BABR	$e^+e^- \to \Upsilon(4S)$
• • • We do not use the following data for averages, fits, limits, etc. • • •					
$<1.2 \times 10^{-3}$	90	[276] ACCIARRI	97C	L3	

[275] Assumes equal production of B^+ and B^0 at the $\Upsilon(4S)$.

[276] ACCIARRI 97C assumes B^0 production fraction (39.5 ± 4.0%) and B_s (12.0 ± 3.0%).

$\Gamma(J/\psi(1S)\pi^+\pi^-)/\Gamma_{total}$ Γ_{107}/Γ

VALUE	DOCUMENT ID		TECN	COMMENT
(4.6±0.7±0.6) × 10^{-5}	[277] AUBERT	03B	BABR	$e^+e^- \to \Upsilon(4S)$

[277] Assumes equal production of B^+ and B^0 at the $\Upsilon(4S)$.

$\Gamma(J/\psi(1S)\rho^0)/\Gamma_{total}$ Γ_{108}/Γ

VALUE (units 10^{-5})	CL%	DOCUMENT ID		TECN	COMMENT
1.6±0.6±0.4		[278] AUBERT	03B	BABR	$e^+e^- \to \Upsilon(4S)$
• • • We do not use the following data for averages, fits, limits, etc. • • •					
<25	90	BISHAI	96	CLE2	$e^+e^- \to \Upsilon(4S)$

[278] Assumes equal production of B^+ and B^0 at the $\Upsilon(4S)$.

$\Gamma(J/\psi(1S)\omega)/\Gamma_{total}$ Γ_{109}/Γ

VALUE	CL%	DOCUMENT ID		TECN	COMMENT
<2.7 × 10^{-4}	90	BISHAI	96	CLE2	$e^+e^- \to \Upsilon(4S)$

$\Gamma(J/\psi(1S)\phi)/\Gamma_{total}$ Γ_{110}/Γ

VALUE (units 10^{-6})	CL%	DOCUMENT ID		TECN	COMMENT
<9.2	90	[279] AUBERT	03O	BABR	$e^+e^- \to \Upsilon(4S)$

[279] Assumes equal production of B^+ and B^0 at the $\Upsilon(4S)$.

$\Gamma(J/\psi(1S)\eta'(958))/\Gamma_{total}$ Γ_{111}/Γ

VALUE (units 10^{-5})	CL%	DOCUMENT ID		TECN	COMMENT
<6.3	90	[280] AUBERT	03O	BABR	$e^+e^- \to \Upsilon(4S)$

[280] Assumes equal production of B^+ and B^0 at the $\Upsilon(4S)$.

$\Gamma(J/\psi(1S)K^0\pi^+\pi^-)/\Gamma_{total}$ Γ_{112}/Γ

VALUE (units 10^{-4})	DOCUMENT ID		TECN	COMMENT
10.3±3.3±1.5	[281] AFFOLDER	02B	CDF	$p\overline{p}$ 1.8 TeV

[281] Uses $B^0 \to J/\psi(1S)K_S^0$ decay as a reference and $B(B^0 \to J/\psi(1S)K^0) = 8.3 \times 10^{-4}$.

$\Gamma(J/\psi(1S)K^0\rho^0)/\Gamma_{total}$ Γ_{113}/Γ

VALUE (units 10^{-4})	DOCUMENT ID		TECN	COMMENT
5.4±2.9±0.9	[282] AFFOLDER	02B	CDF	$p\overline{p}$ 1.8 TeV

[282] Uses $B^0 \to J/\psi(1S)K_S^0$ decay as a reference and $B(B^0 \to J/\psi(1S)K^0) = 8.3 \times 10^{-4}$.

$\Gamma(J/\psi(1S)K^*(892)^+\pi^-)/\Gamma_{total}$ Γ_{114}/Γ

VALUE (units 10^{-4})	DOCUMENT ID		TECN	COMMENT
7.7±4.1±1.3	[283] AFFOLDER	02B	CDF	$p\overline{p}$ 1.8 TeV

[283] Uses $B^0 \to J/\psi(1S)K_S^0$ decay as a reference and $B(B^0 \to J/\psi(1S)K^0) = 8.3 \times 10^{-4}$.

$\Gamma(J/\psi(1S)K^*(892)^0\pi^+\pi^-)/\Gamma_{total}$ Γ_{115}/Γ

VALUE (units 10^{-4})	DOCUMENT ID		TECN	COMMENT
6.6±1.9±1.1	[284] AFFOLDER	02B	CDF	$p\overline{p}$ 1.8 TeV

[284] Uses $B^0 \to J/\psi(1S)K^*(892)^0$ decay as a reference and $B(B^0 \to J/\psi(1S)K^0) = 12.4 \times 10^{-4}$.

Meson Particle Listings

B^0

$\Gamma(J/\psi(1S)p\overline{p})/\Gamma_{total}$ Γ_{116}/Γ

VALUE	CL%	DOCUMENT ID		TECN	COMMENT
$<1.9\times10^{-6}$	90	[285] AUBERT	03K	BABR	$e^+e^-\to\Upsilon(4S)$

[285] Assumes equal production of B^+ and B^0 at the $\Upsilon(4S)$.

$\Gamma(\psi(2S)K^0)/\Gamma_{total}$ Γ_{117}/Γ

VALUE (units 10^{-4})	CL%	DOCUMENT ID		TECN	COMMENT
6.2±0.7 OUR AVERAGE					
6.7±1.1		[286] ABE	03B	BELL	$e^+e^-\to\Upsilon(4S)$
6.9±1.1±1.1		[286] AUBERT	02	BABR	$e^+e^-\to\Upsilon(4S)$
5.0±1.1±0.6		[286] RICHICHI	01	CLE2	$e^+e^-\to\Upsilon(4S)$
• • • We do not use the following data for averages, fits, limits, etc. • • •					
< 8	90	[286] ALAM	94	CLE2	$e^+e^-\to\Upsilon(4S)$
<15	90	[286] BORTOLETTO	92	CLEO	$e^+e^-\to\Upsilon(4S)$
<28	90	[286] ALBRECHT	90J	ARG	$e^+e^-\to\Upsilon(4S)$

[286] Assumes equal production of B^+ and B^0 at the $\Upsilon(4S)$.

$\Gamma(\psi(2S)K^0)/\Gamma(J/\psi(1S)K^0)$ $\Gamma_{117}/\Gamma_{100}$

VALUE	DOCUMENT ID		TECN	COMMENT
0.82±0.13±0.12	[287] AUBERT	02	BABR	$e^+e^-\to\Upsilon(4S)$

[287] Assumes equal production of B^+ and B^0 at the $\Upsilon(4S)$.

$\Gamma(\psi(2S)K^+\pi^-)/\Gamma_{total}$ Γ_{118}/Γ

VALUE	CL%	DOCUMENT ID		TECN	COMMENT
<0.001	90	[288] ALBRECHT	90J	ARG	$e^+e^-\to\Upsilon(4S)$

[288] Assumes equal production of B^+ and B^0 at the $\Upsilon(4S)$.

$\Gamma(\psi(2S)K^*(892)^0)/\Gamma_{total}$ Γ_{119}/Γ

VALUE (units 10^{-4})	CL%	DOCUMENT ID		TECN	COMMENT
8.0±1.3 OUR AVERAGE					
7.6±1.1±1.0		[289] RICHICHI	01	CLE2	$e^+e^-\to\Upsilon(4S)$
9.0±2.2±0.9		[290] ABE	98O	CDF	$p\overline{p}$ 1.8 TeV
• • • We do not use the following data for averages, fits, limits, etc. • • •					
<19	90	[291] ALAM	94	CLE2	Repl. by RICHICHI 01
14 ±8 ±4		[291] BORTOLETTO	92	CLEO	$e^+e^-\to\Upsilon(4S)$
<23	90	[291] ALBRECHT	90J	ARG	$e^+e^-\to\Upsilon(4S)$

[289] Assumes equal production of B^+ and B^0 at the $\Upsilon(4S)$.

[290] ABE 98O reports $[B(B^0\to\psi(2S)K^*(892)^0)]/[B(B^+\to J/\psi(1S)K^+)]=0.908\pm0.194\pm0.10$. We multiply by our best value $B(B^+\to J/\psi(1S)K^+)=(9.9\pm1.0)\times10^{-4}$. Our first error is their experiment's error and our second error is the systematic error from using our best value.

[291] Assumes equal production of B^+ and B^0 at the $\Upsilon(4S)$.

$\Gamma(\chi_{c0}(1P)K^0)/\Gamma_{total}$ Γ_{120}/Γ

VALUE	CL%	DOCUMENT ID		TECN	COMMENT
$<5.0\times10^{-4}$	90	[292] EDWARDS	01	CLE2	$e^+e^-\to\Upsilon(4S)$

[292] EDWARDS 01 assumes equal production of B^0 and B^+ at the $\Upsilon(4S)$. The correlated uncertainties (28.3)% from $B(J/\psi(1S)\to\gamma\eta_c)$ in those modes have been accounted for.

$\Gamma(\chi_{c1}(1P)K^0)/\Gamma_{total}$ Γ_{121}/Γ

VALUE (units 10^{-4})	CL%	DOCUMENT ID		TECN	COMMENT
$4.0^{+1.2}_{-1.0}$ OUR AVERAGE					
$4.7\pm1.5\pm0.5$		[293] AUBERT	02	BABR	$e^+e^-\to\Upsilon(4S)$
$3.4^{+1.7}_{-1.2}\pm0.4$		[294] AVERY	00	CLE2	$e^+e^-\to\Upsilon(4S)$
• • • We do not use the following data for averages, fits, limits, etc. • • •					
<27	90	[295] ALAM	94	CLE2	$e^+e^-\to\Upsilon(4S)$

[293] AUBERT 02 reports $5.4\pm1.4\pm1.1$ for $B(\chi_{c1}(1P)\to\gamma J/\psi(1S))=0.273\pm0.016$. We rescale to our best value $B(\chi_{c1}(1P)\to\gamma J/\psi(1S))=(31.6\pm3.3)\times10^{-2}$. Our first error is their experiment's error and our second error is the systematic error from using our best value. Assumes equal production of B^+ and B^0 at the $\Upsilon(4S)$.

[294] AVERY 00 reports $3.9^{+1.9}_{-1.3}\pm0.4$ for $B(\chi_{c1}(1P)\to\gamma J/\psi(1S))=0.273\pm0.016$. We rescale to our best value $B(\chi_{c1}(1P)\to\gamma J/\psi(1S))=(31.6\pm3.3)\times10^{-2}$. Our first error is their experiment's error and our second error is the systematic error from using our best value. Assumes equal production of B^+ and B^0 at the $\Upsilon(4S)$.

[295] Assumes equal production of B^+ and B^0 at the $\Upsilon(4S)$.

$\Gamma(\chi_{c1}(1P)K^*(892)^0)/\Gamma_{total}$ Γ_{122}/Γ

VALUE (units 10^{-4})	CL%	DOCUMENT ID		TECN	COMMENT
4.1±1.4±0.4		[296] AUBERT	02	BABR	$e^+e^-\to\Upsilon(4S)$
• • • We do not use the following data for averages, fits, limits, etc. • • •					
<21	90	[297] ALAM	94	CLE2	$e^+e^-\to\Upsilon(4S)$

[296] AUBERT 02 reports $4.8\pm1.4\pm0.9$ for $B(\chi_{c1}(1P)\to\gamma J/\psi(1S))=0.273\pm0.016$. We rescale to our best value $B(\chi_{c1}(1P)\to\gamma J/\psi(1S))=(31.6\pm3.3)\times10^{-2}$. Our first error is their experiment's error and our second error is the systematic error from using our best value. Assumes equal production of B^+ and B^0 at the $\Upsilon(4S)$.

[297] BORTOLETTO 92 assumes equal production of B^+ and B^0 at the $\Upsilon(4S)$.

$\Gamma(\chi_{c1}(1P)K^0)/\Gamma(J/\psi(1S)K^0)$ $\Gamma_{121}/\Gamma_{100}$

VALUE	DOCUMENT ID		TECN	COMMENT
0.57±0.17±0.06	[298] AUBERT	02	BABR	$e^+e^-\to\Upsilon(4S)$

[298] AUBERT 02 reports $0.66\pm0.11\pm0.17$ for $B(\chi_{c1}(1P)\to\gamma J/\psi(1S))=0.273\pm0.016$. We rescale to our best value $B(\chi_{c1}(1P)\to\gamma J/\psi(1S))=(31.6\pm3.3)\times10^{-2}$. Our first error is their experiment's error and our second error is the systematic error from using our best value. Assumes equal production of B^+ and B^0 at the $\Upsilon(4S)$.

$\Gamma(\chi_{c1}(1P)K^*(892)^0)/\Gamma(\chi_{c1}(1P)K^0)$ $\Gamma_{122}/\Gamma_{121}$

VALUE	DOCUMENT ID		TECN	COMMENT
0.89±0.34±0.17	[299] AUBERT	02	BABR	$e^+e^-\to\Upsilon(4S)$

[299] Assumes equal production of B^+ and B^0 at the $\Upsilon(4S)$.

$\Gamma(K^+\pi^-)/\Gamma_{total}$ Γ_{123}/Γ

VALUE (units 10^{-5})	CL%	DOCUMENT ID		TECN	COMMENT
1.85±0.11 OUR AVERAGE		Error includes scale factor of 1.2.			
$1.80^{+0.23}_{-0.21}{}^{+0.12}_{-0.09}$		[300] BORNHEIM	03	CLE2	$e^+e^-\to\Upsilon(4S)$
$1.79\pm0.09\pm0.07$		[300] AUBERT	02Q	BABR	$e^+e^-\to\Upsilon(4S)$
$2.25\pm0.19\pm0.18$		[300] CASEY	02	BELL	$e^+e^-\to\Upsilon(4S)$
• • • We do not use the following data for averages, fits, limits, etc. • • •					
$1.93^{+0.34}_{-0.32}{}^{+0.15}_{-0.06}$		[300] ABE	01H	BELL	Repl. by CASEY 02
$1.67\pm0.16\pm0.13$		[300] AUBERT	01E	BABR	Repl. by AUBERT 02Q
< 6.6	90	[301] ABE	00C	SLD	$e^+e^-\to Z$
$1.72^{+0.25}_{-0.24}\pm0.12$		[300] CRONIN-HEN..	00	CLE2	Repl. by BORNHEIM 03
$1.5\ ^{+0.5}_{-0.4}\ \pm0.14$		GODANG	98	CLE2	Repl. by CRONIN-HENNESSY 00
$2.4\ ^{+1.7}_{-1.1}\ \pm0.2$		[302] ADAM	96D	DLPH	$e^+e^-\to Z$
< 1.7	90	ASNER	96	CLE2	Sup. by ADAM 96D
< 3.0	90	[303] BUSKULIC	96V	ALEP	$e^+e^-\to Z$
< 9	90	[304] ABREU	95N	DLPH	Sup. by ADAM 96D
< 8.1	90	[305] AKERS	94L	OPAL	$e^+e^-\to Z$
< 2.6	90	[306] BATTLE	93	CLE2	$e^+e^-\to\Upsilon(4S)$
<18	90	ALBRECHT	91B	ARG	$e^+e^-\to\Upsilon(4S)$
< 9	90	[307] AVERY	89B	CLEO	$e^+e^-\to\Upsilon(4S)$
<32	90	AVERY	87	CLEO	$e^+e^-\to\Upsilon(4S)$

[300] Assumes equal production of B^+ and B^0 at the $\Upsilon(4S)$.

[301] ABE 00C assumes $B(Z\to b\overline{b})=(21.7\pm0.1)\%$ and the B fractions $f_{B^0}=f_{B^+}=(39.7^{+1.8}_{-2.2})\%$ and $f_{B_s}=(10.5^{+1.8}_{-2.2})\%$.

[302] ADAM 96D assumes $f_{B^0}=f_{B^-}=0.39$ and $f_{B_s}=0.12$. Contributions from B^0 and B_s decays cannot be separated. Limits are given for the weighted average of the decay rates for the two neutral B mesons.

[303] BUSKULIC 96V assumes PDG 96 production fractions for B^0, B^+, B_s, b baryons.

[304] Assumes a B^0, B^- production fraction of 0.39 and a B_s production fraction of 0.12. Contributions from B^0 and B_s^0 decays cannot be separated. Limits are given for the weighted average of the decay rates for the two neutral B mesons.

[305] Assumes $B(Z\to b\overline{b})=0.217$ and B_d^0 (B_s^0) fraction 39.5% (12%).

[306] BATTLE 93 assumes equal production of $B^0\overline{B}{}^0$ and B^+B^- at $\Upsilon(4S)$.

[307] Assumes the $\Upsilon(4S)$ decays 43% to $B^0\overline{B}{}^0$.

$\Gamma(K^+\pi^-)/\Gamma(K^0\pi^0)$ $\Gamma_{123}/\Gamma_{124}$

VALUE	DOCUMENT ID		TECN	COMMENT
$1.20^{+0.50}_{-0.58}{}^{+0.22}_{-0.32}$	[308] ABE	01H	BELL	$e^+e^-\to\Upsilon(4S)$

[308] Assumes equal production of B^+ and B^0 at the $\Upsilon(4S)$.

$[\Gamma(K^+\pi^-)+\Gamma(\pi^+\pi^-)]/\Gamma_{total}$ $(\Gamma_{123}+\Gamma_{176})/\Gamma$

VALUE (units 10^{-5})	EVTS	DOCUMENT ID		TECN	COMMENT
1.9±0.6 OUR AVERAGE					
$2.8^{+1.5}_{-1.0}\pm2.0$		[309] ADAM	96D	DLPH	$e^+e^-\to Z$
$1.8^{+0.6}_{-0.5}{}^{+0.3}_{-0.4}$	17.2	ASNER	96	CLE2	$e^+e^-\to\Upsilon(4S)$
• • • We do not use the following data for averages, fits, limits, etc. • • •					
$2.4^{+0.8}_{-0.7}\pm0.2$		[310] BATTLE	93	CLE2	$e^+e^-\to\Upsilon(4S)$

[309] ADAM 96D assumes $f_{B^0}=f_{B^-}=0.39$ and $f_{B_s}=0.12$. Contributions from B^0 and B_s decays cannot be separated. Limits are given for the weighted average of the decay rates for the two neutral B mesons.

[310] BATTLE 93 assumes equal production of $B^0\overline{B}{}^0$ and B^+B^- at $\Upsilon(4S)$.

$\Gamma(K^0\pi^0)/\Gamma_{total}$ Γ_{124}/Γ

VALUE (units 10^{-5})	CL%	DOCUMENT ID		TECN	COMMENT
$0.95^{+0.21}_{-0.19}$ OUR AVERAGE					
$1.28^{+0.40}_{-0.33}{}^{+0.17}_{-0.14}$		[311] BORNHEIM	03	CLE2	$e^+e^-\to\Upsilon(4S)$
$0.80^{+0.33}_{-0.31}\pm0.16$		[311] CASEY	02	BELL	$e^+e^-\to\Upsilon(4S)$
$0.82^{+0.31}_{-0.27}\pm0.12$		[311] AUBERT	01E	BABR	$e^+e^-\to\Upsilon(4S)$

• • • We do not use the following data for averages, fits, limits, etc. • • •

$1.60^{+0.72}_{-0.59}{}^{+0.25}_{-0.27}$		[311] ABE	01H	BELL	Repl. by CASEY 02
$1.46^{+0.59}_{-0.51}{}^{+0.24}_{-0.33}$		[311] CRONIN-HEN..	00	CLE2	Repl. by BORNHEIM 03
<4.1	90	GODANG	98	CLE2	Repl. by CRONIN-HENNESSY 00
<4.0	90	ASNER	96	CLE2	Rep. by GODANG 98

[311] Assumes equal production of B^+ and B^0 at the $\Upsilon(4S)$.

$\Gamma(\eta' K^0)/\Gamma_{total}$ Γ_{125}/Γ

VALUE (units 10^{-5})		DOCUMENT ID		TECN	COMMENT
6.3 ±0.7 OUR AVERAGE	Error includes scale factor of 1.1.				
$6.06 \pm 0.56 \pm 0.46$		[312] AUBERT	03W	BABR	$e^+e^- \to \Upsilon(4S)$
$5.5\ ^{+1.9}_{-1.6} \pm 0.8$		[312] ABE	01M	BELL	$e^+e^- \to \Upsilon(4S)$
$8.9\ ^{+1.8}_{-1.6} \pm 0.9$		[312] RICHICHI	00	CLE2	$e^+e^- \to \Upsilon(4S)$
• • • We do not use the following data for averages, fits, limits, etc. • • •					
$4.2\ ^{+1.3}_{-1.1} \pm 0.4$		[312] AUBERT	01G	BABR	Repl. by AUBERT 03W
$4.7\ ^{+2.7}_{-2.0} \pm 0.9$		BEHRENS	98	CLE2	Repl. by RICHICHI 00

[312] Assumes equal production of B^+ and B^0 at the $\Upsilon(4S)$.

$\Gamma(\eta' K^*(892)^0)/\Gamma_{total}$ Γ_{126}/Γ

VALUE (units 10^{-5})	CL%	DOCUMENT ID		TECN	COMMENT
<2.4	90	[313] RICHICHI	00	CLE2	$e^+e^- \to \Upsilon(4S)$
• • • We do not use the following data for averages, fits, limits, etc. • • •					
<3.9	90	BEHRENS	98	CLE2	Repl. by RICHICHI 00

[313] Assumes equal production of B^+ and B^0 at the $\Upsilon(4S)$.

$\Gamma(\eta K^*(892)^0)/\Gamma_{total}$ Γ_{127}/Γ

VALUE (units 10^{-5})	CL%	DOCUMENT ID		TECN	COMMENT
$\mathbf{1.38^{+0.55}_{-0.46} \pm 0.16}$		[314] RICHICHI	00	CLE2	$e^+e^- \to \Upsilon(4S)$
• • • We do not use the following data for averages, fits, limits, etc. • • •					
<3.0	90	BEHRENS	98	CLE2	Repl. by RICHICHI 00

[314] Assumes equal production of B^+ and B^0 at the $\Upsilon(4S)$.

$\Gamma(\eta K^0)/\Gamma_{total}$ Γ_{128}/Γ

VALUE (units 10^{-6})	CL%	DOCUMENT ID		TECN	COMMENT
< 9.3	90	[315] RICHICHI	00	CLE2	$e^+e^- \to \Upsilon(4S)$
• • • We do not use the following data for averages, fits, limits, etc. • • •					
<33	90	BEHRENS	98	CLE2	Repl. by RICHICHI 00

[315] Assumes equal production of B^+ and B^0 at the $\Upsilon(4S)$.

$\Gamma(\omega K^0)/\Gamma_{total}$ Γ_{129}/Γ

VALUE (units 10^{-5})	CL%	DOCUMENT ID		TECN	COMMENT
<1.3	90	[316] AUBERT	01G	BABR	$e^+e^- \to \Upsilon(4S)$
• • • We do not use the following data for averages, fits, limits, etc. • • •					
<2.1	90	[316] JESSOP	00	CLE2	$e^+e^- \to \Upsilon(4S)$
<5.7	90	[316] BERGFELD	98	CLE2	Repl. by JESSOP 00

[316] Assumes equal production of B^+ and B^0 at the $\Upsilon(4S)$.

$\Gamma(K^0_S X^0(\text{Familon}))/\Gamma_{total}$ Γ_{130}/Γ

VALUE (units 10^{-5})	CL%	DOCUMENT ID		TECN	COMMENT
<5.3	90	[317] AMMAR	01B	CLE2	$e^+e^- \to \Upsilon(4S)$

[317] AMMAR 01B searched for the two-body decay of the B meson to a massless neutral feebly-interacting particle X^0 such as the familon, the Nambu-Goldstone boson associated with a spontaneously broken global family symmetry.

$\Gamma(\omega K^*(892)^0)/\Gamma_{total}$ Γ_{131}/Γ

VALUE	CL%	DOCUMENT ID		TECN
$\mathbf{<2.3 \times 10^{-5}}$	90	[318] BERGFELD	98	CLE2

[318] Assumes equal production of B^+ and B^0 at the $\Upsilon(4S)$.

$\Gamma(K^+K^-)/\Gamma_{total}$ Γ_{132}/Γ

VALUE (units 10^{-6})	CL%	DOCUMENT ID		TECN	COMMENT
< 0.6	90	[319] AUBERT	02Q	BABR	$e^+e^- \to \Upsilon(4S)$
• • • We do not use the following data for averages, fits, limits, etc. • • •					
< 0.8	90	[319] BORNHEIM	03	CLE2	$e^+e^- \to \Upsilon(4S)$
< 0.9	90	[319] CASEY	02	BELL	$e^+e^- \to \Upsilon(4S)$
< 2.7	90	[319] ABE	01H	BELL	$e^+e^- \to \Upsilon(4S)$
< 2.5	90	[319] AUBERT	01E	BABR	$e^+e^- \to \Upsilon(4S)$
< 66	90	[320] ABE	00C	SLD	$e^+e^- \to Z$
< 1.9	90	[319] CRONIN-HEN..	00	CLE2	$e^+e^- \to \Upsilon(4S)$
< 4.3	90	GODANG	98	CLE2	Repl. by CRONIN-HENNESSY 00
< 46		[321] ADAM	96D	DLPH	$e^+e^- \to Z$
< 4	90	ASNER	96	CLE2	Repl. by GODANG 98
< 18	90	[322] BUSKULIC	96V	ALEP	$e^+e^- \to Z$
<120	90	[323] ABREU	95N	DLPH	Sup. by ADAM 96D
< 7	90	[324] BATTLE	93	CLE2	$e^+e^- \to \Upsilon(4S)$

[319] Assumes equal production of B^+ and B^0 at the $\Upsilon(4S)$.

[320] ABE 00C assumes $B(Z \to b\overline{b}) = (21.7 \pm 0.1)\%$ and the B fractions $f_{B^0} = f_{B^+} = (39.7^{+1.8}_{-2.2})\%$ and $f_{B_s} = (10.5^{+1.8}_{-2.2})\%$.

[321] ADAM 96D assumes $f_{B^0} = f_{B^-} = 0.39$ and $f_{B_s} = 0.12$. Contributions from B^0 and B_s decays cannot be separated. Limits are given for the weighted average of the decay rates for the two neutral B mesons.

[322] BUSKULIC 96V assumes PDG 96 production fractions for B^0, B^+, B_s, b baryons.

[323] Assumes a B^0, B^- production fraction of 0.39 and a B_s production fraction of 0.12. Contributions from B^0 and B^0_s decays cannot be separated. Limits are given for the weighted average of the decay rates for the two neutral B mesons.

[324] BATTLE 93 assumes equal production of $B^0\overline{B}{}^0$ and B^+B^- at $\Upsilon(4S)$.

$\Gamma(K^0\overline{K}{}^0)/\Gamma_{total}$ Γ_{133}/Γ

VALUE	CL%	DOCUMENT ID		TECN	COMMENT
$\mathbf{<3.3 \times 10^{-6}}$	90	[325] BORNHEIM	03	CLE2	$e^+e^- \to \Upsilon(4S)$
• • • We do not use the following data for averages, fits, limits, etc. • • •					
$<4.1 \times 10^{-6}$	90	[325] CASEY	02	BELL	$e^+e^- \to \Upsilon(4S)$
$<1.7 \times 10^{-5}$	90	GODANG	98	CLE2	$e^+e^- \to \Upsilon(4S)$

[325] Assumes equal production of B^+ and B^0 at the $\Upsilon(4S)$.

$\Gamma(K^0_S K^0_S K^0_S)/\Gamma_{total}$ Γ_{134}/Γ

VALUE (units 10^{-6})	DOCUMENT ID		TECN	COMMENT
$\mathbf{4.2^{+1.6}_{-1.3} \pm 0.8}$	[326] GARMASH	04	BELL	$e^+e^- \to \Upsilon(4S)$

[326] Assumes equal production of B^+ and B^0 at the $\Upsilon(4S)$.

$\Gamma(K^+\pi^-\pi^0)/\Gamma_{total}$ Γ_{135}/Γ

VALUE	CL%	DOCUMENT ID		TECN	COMMENT
$\mathbf{<40 \times 10^{-6}}$	90	[327] ECKHART	02	CLE2	$e^+e^- \to \Upsilon(4S)$

[327] Assumes equal production of B^+ and B^0 at the $\Upsilon(4S)$.

$\Gamma(K^+\rho^-)/\Gamma_{total}$ Γ_{136}/Γ

VALUE (units 10^{-6})	CL%	DOCUMENT ID		TECN	COMMENT
$\mathbf{7.3^{+1.3}_{-1.2} \pm 1.3}$		[328] AUBERT	03T	BABR	$e^+e^- \to \Upsilon(4S)$
• • • We do not use the following data for averages, fits, limits, etc. • • •					
<32	90	[328] JESSOP	00	CLE2	$e^+e^- \to \Upsilon(4S)$
<35	90	ASNER	96	CLE2	Repl. by JESSOP 00

[328] Assumes equal production of B^+ and B^0 at the $\Upsilon(4S)$.

$\Gamma(K^0\pi^+\pi^-)/\Gamma_{total}$ Γ_{137}/Γ

VALUE (units 10^{-6})	CL%	DOCUMENT ID		TECN	COMMENT
47 ± 7 OUR AVERAGE					
$45.4 \pm 5.2 \pm 5.9$		[329] GARMASH	04	BELL	$e^+e^- \to \Upsilon(4S)$
$50\ ^{+10}_{-9} \pm 7$		[329] ECKHART	02	CLE2	$e^+e^- \to \Upsilon(4S)$
• • • We do not use the following data for averages, fits, limits, etc. • • •					
<440	90	ALBRECHT	91E	ARG	$e^+e^- \to \Upsilon(4S)$

[329] Assumes equal production of B^+ and B^0 at the $\Upsilon(4S)$.

$\Gamma(K^0\rho^0)/\Gamma_{total}$ Γ_{138}/Γ

VALUE	CL%	DOCUMENT ID		TECN	COMMENT
$\mathbf{<3.9 \times 10^{-5}}$	90	ASNER	96	CLE2	$e^+e^- \to \Upsilon(4S)$
• • • We do not use the following data for averages, fits, limits, etc. • • •					
$<3.2 \times 10^{-4}$	90	ALBRECHT	91B	ARG	$e^+e^- \to \Upsilon(4S)$
$<5.0 \times 10^{-4}$	90	[330] AVERY	89B	CLEO	$e^+e^- \to \Upsilon(4S)$
<0.064	90	[331] AVERY	87	CLEO	$e^+e^- \to \Upsilon(4S)$

[330] AVERY 89B reports $< 5.8 \times 10^{-4}$ assuming the $\Upsilon(4S)$ decays 43% to $B^0\overline{B}{}^0$. We rescale to 50%.

[331] AVERY 87 reports < 0.08 assuming the $\Upsilon(4S)$ decays 40% to $B^0\overline{B}{}^0$. We rescale to 50%.

$\Gamma(K^0 f_0(980))/\Gamma_{total}$ Γ_{139}/Γ

VALUE	CL%	DOCUMENT ID		TECN	COMMENT
$\mathbf{<3.6 \times 10^{-4}}$	90	[332] AVERY	89B	CLEO	$e^+e^- \to \Upsilon(4S)$

[332] AVERY 89B reports $< 4.2 \times 10^{-4}$ assuming the $\Upsilon(4S)$ decays 43% to $B^0\overline{B}{}^0$. We rescale to 50%.

$\Gamma(K^*(892)^+\pi^-)/\Gamma_{total}$ Γ_{140}/Γ

VALUE (units 10^{-6})	CL%	DOCUMENT ID		TECN	COMMENT
$\mathbf{16^{+6}_{-5} \pm 2}$		[333] ECKHART	02	CLE2	$e^+e^- \to \Upsilon(4S)$
• • • We do not use the following data for averages, fits, limits, etc. • • •					
< 72	90	ASNER	96	CLE2	$e^+e^- \to \Upsilon(4S)$
<620	90	ALBRECHT	91B	ARG	$e^+e^- \to \Upsilon(4S)$
<380	90	[334] AVERY	89B	CLEO	$e^+e^- \to \Upsilon(4S)$
<560	90	[335] AVERY	87	CLEO	$e^+e^- \to \Upsilon(4S)$

[333] Assumes equal production of B^+ and B^0 at the $\Upsilon(4S)$.

[334] AVERY 89B reports $< 4.4 \times 10^{-4}$ assuming the $\Upsilon(4S)$ decays 43% to $B^0\overline{B}{}^0$. We rescale to 50%.

[335] AVERY 87 reports $< 7 \times 10^{-4}$ assuming the $\Upsilon(4S)$ decays 40% to $B^0\overline{B}{}^0$. We rescale to 50%.

$\Gamma(K^*(892)^0\pi^0)/\Gamma_{total}$ Γ_{141}/Γ

VALUE	CL%	DOCUMENT ID		TECN	COMMENT
$<3.6\times10^{-6}$	90	232 JESSOP	00	CLE2	$e^+e^-\to\Upsilon(4S)$
• • • We do not use the following data for averages, fits, limits, etc. • • •					
$<2.8\times10^{-5}$	90	ASNER	96	CLE2	Repl. by JESSOP 00

$\Gamma(K_2^*(1430)^+\pi^-)/\Gamma_{total}$ Γ_{142}/Γ

VALUE	CL%	DOCUMENT ID		TECN	COMMENT
$<1.8\times10^{-5}$	90	336 GARMASH	04	BELL	$e^+e^-\to\Upsilon(4S)$
• • • We do not use the following data for averages, fits, limits, etc. • • •					
$<2.6\times10^{-3}$	90	ALBRECHT	91B	ARG	$e^+e^-\to\Upsilon(4S)$

336 Assumes equal production of B^+ and B^0 at the $\Upsilon(4S)$.

$\Gamma(K^0K^-\pi^+)/\Gamma_{total}$ Γ_{143}/Γ

VALUE	CL%	DOCUMENT ID		TECN	COMMENT
$<21\times10^{-6}$	90	337 ECKHART	02	CLE2	$e^+e^-\to\Upsilon(4S)$

337 Assumes equal production of B^+ and B^0 at the $\Upsilon(4S)$.

$\Gamma(K^+K^-\pi^0)/\Gamma_{total}$ Γ_{144}/Γ

VALUE	CL%	DOCUMENT ID		TECN	COMMENT
$<19\times10^{-6}$	90	338 ECKHART	02	CLE2	$e^+e^-\to\Upsilon(4S)$

338 Assumes equal production of B^+ and B^0 at the $\Upsilon(4S)$.

$\Gamma(K^0K^+K^-)/\Gamma_{total}$ Γ_{145}/Γ

VALUE (units 10^{-6})	CL%	DOCUMENT ID		TECN	COMMENT
$28.3\pm3.3\pm4.0$		339 GARMASH	04	BELL	$e^+e^-\to\Upsilon(4S)$
• • • We do not use the following data for averages, fits, limits, etc. • • •					
<1300	90	ALBRECHT	91E	ARG	$e^+e^-\to\Upsilon(4S)$

339 Assumes equal production of B^+ and B^0 at the $\Upsilon(4S)$.

$\Gamma(K^0\phi)/\Gamma_{total}$ Γ_{146}/Γ

VALUE (units 10^{-6})	CL%	DOCUMENT ID		TECN	COMMENT
$8.6^{+1.3}_{-1.1}$ OUR AVERAGE					
$8.4^{+1.5}_{-1.3}\pm0.5$		340 AUBERT	04A	BABR	$e^+e^-\to\Upsilon(4S)$
$9.0^{+2.2}_{-1.8}\pm0.7$		341 CHEN	03B	BELL	$e^+e^-\to\Upsilon(4S)$
• • • We do not use the following data for averages, fits, limits, etc. • • •					
$8.1^{+3.1}_{-2.5}\pm0.8$		341 AUBERT	01D	BABR	$e^+e^-\to\Upsilon(4S)$
<12.3	90	341 BRIERE	01	CLE2	$e^+e^-\to\Upsilon(4S)$
<31	90	341 BERGFELD	98	CLE2	
<88	90	ASNER	96	CLE2	$e^+e^-\to\Upsilon(4S)$
<720	90	ALBRECHT	91B	ARG	$e^+e^-\to\Upsilon(4S)$
<420	90	342 AVERY	89B	CLEO	$e^+e^-\to\Upsilon(4S)$
<1000	90	343 AVERY	87	CLEO	$e^+e^-\to\Upsilon(4S)$

340 Assumes equal production of B^+ and B^0 at $\Upsilon(4S)$.
341 Assumes equal production of B^+ and B^0 at the $\Upsilon(4S)$.
342 AVERY 89B reports $<4.9\times10^{-4}$ assuming the $\Upsilon(4S)$ decays 43% to $B^0\overline{B}^0$. We rescale to 50%.
343 AVERY 87 reports $<1.3\times10^{-3}$ assuming the $\Upsilon(4S)$ decays 40% to $B^0\overline{B}^0$. We rescale to 50%.

$\Gamma(K^-\pi^+\pi^+\pi^-)/\Gamma_{total}$ Γ_{147}/Γ

VALUE	CL%	DOCUMENT ID		TECN	COMMENT
$<2.3\times10^{-4}$	90	344 ADAM	96D	DLPH	$e^+e^-\to Z$
• • • We do not use the following data for averages, fits, limits, etc. • • •					
$<2.1\times10^{-4}$	90	345 ABREU	95N	DLPH	Sup. by ADAM 96D

344 ADAM 96D assumes $f_{B^0}=f_{B^-}=0.39$ and $f_{B_s}=0.12$. Contributions from B^0 and B_s decays cannot be separated. Limits are given for the weighted average of the decay rates for the two neutral B mesons.
345 Assumes a B^0, B^- production fraction of 0.39 and a B_s production fraction of 0.12. Contributions from B^0 and B_s^0 decays cannot be separated. Limits are given for the weighted average of the decay rates for the two neutral B mesons.

$\Gamma(K^*(892)^0\pi^+\pi^-)/\Gamma_{total}$ Γ_{148}/Γ

VALUE	CL%	DOCUMENT ID		TECN	COMMENT
$<1.4\times10^{-3}$	90	ALBRECHT	91E	ARG	$e^+e^-\to\Upsilon(4S)$

$\Gamma(K^*(892)^0\rho^0)/\Gamma_{total}$ Γ_{149}/Γ

VALUE	CL%	DOCUMENT ID		TECN	COMMENT
$<3.4\times10^{-5}$	90	346 GODANG	02	CLE2	$e^+e^-\to\Upsilon(4S)$
• • • We do not use the following data for averages, fits, limits, etc. • • •					
$<2.86\times10^{-4}$	90	347 ABE	00C	SLD	$e^+e^-\to Z$
$<4.6\times10^{-4}$	90	ALBRECHT	91B	ARG	$e^+e^-\to\Upsilon(4S)$
$<5.8\times10^{-4}$	90	348 AVERY	89B	CLEO	$e^+e^-\to\Upsilon(4S)$
$<9.6\times10^{-4}$	90	349 AVERY	87	CLEO	$e^+e^-\to\Upsilon(4S)$

346 Assumes a helicity 00 configuration. For a helicity 11 configuration, the limit decreases to 2.4×10^{-5}.
347 ABE 00C assumes $B(Z\to b\overline{b})=(21.7\pm0.1)\%$ and the B fractions $f_{B^0}=f_{B^+}=(39.7^{+1.8}_{-2.2})\%$ and $f_{B_s}=(10.5^{+1.8}_{-2.2})\%$.
348 AVERY 89B reports $<6.7\times10^{-4}$ assuming the $\Upsilon(4S)$ decays 43% to $B^0\overline{B}^0$. We rescale to 50%.
349 AVERY 87 reports $<1.2\times10^{-3}$ assuming the $\Upsilon(4S)$ decays 40% to $B^0\overline{B}^0$. We rescale to 50%.

$\Gamma(K^*(892)^0f_0(980))/\Gamma_{total}$ Γ_{150}/Γ

VALUE	CL%	DOCUMENT ID		TECN	COMMENT
$<1.7\times10^{-4}$	90	350 AVERY	89B	CLEO	$e^+e^-\to\Upsilon(4S)$

350 AVERY 89B reports $<2.0\times10^{-4}$ assuming the $\Upsilon(4S)$ decays 43% to $B^0\overline{B}^0$. We rescale to 50%.

$\Gamma(K_1(1400)^+\pi^-)/\Gamma_{total}$ Γ_{151}/Γ

VALUE	CL%	DOCUMENT ID		TECN	COMMENT
$<1.1\times10^{-3}$	90	ALBRECHT	91B	ARG	$e^+e^-\to\Upsilon(4S)$

$\Gamma(K^-a_1(1260)^+)/\Gamma_{total}$ Γ_{152}/Γ

VALUE	CL%	DOCUMENT ID		TECN	COMMENT
$<2.3\times10^{-4}$	90	351 ADAM	96D	DLPH	$e^+e^-\to Z$
• • • We do not use the following data for averages, fits, limits, etc. • • •					
$<3.9\times10^{-4}$	90	352 ABREU	95N	DLPH	Sup. by ADAM 96D

351 ADAM 96D assumes $f_{B^0}=f_{B^-}=0.39$ and $f_{B_s}=0.12$. Contributions from B^0 and B_s decays cannot be separated. Limits are given for the weighted average of the decay rates for the two neutral B mesons.
352 Assumes a B^0, B^- production fraction of 0.39 and a B_s production fraction of 0.12. Contributions from B^0 and B_s^0 decays cannot be separated. Limits are given for the weighted average of the decay rates for the two neutral B mesons.

$\Gamma(K^*(892)^0K^+K^-)/\Gamma_{total}$ Γ_{153}/Γ

VALUE	CL%	DOCUMENT ID		TECN	COMMENT
$<6.1\times10^{-4}$	90	ALBRECHT	91E	ARG	$e^+e^-\to\Upsilon(4S)$

$\Gamma(K^*(892)^0\phi)/\Gamma_{total}$ Γ_{154}/Γ

VALUE (units 10^{-6})	CL%	DOCUMENT ID		TECN	COMMENT
10.7 ± 1.1 OUR AVERAGE					
$11.2\pm1.3\pm0.8$		353 AUBERT	03V	BABR	$e^+e^-\to\Upsilon(4S)$
$10.0^{+1.6}_{-1.5}{}^{+0.7}_{-0.8}$		353 CHEN	03B	BELL	$e^+e^-\to\Upsilon(4S)$
$11.5^{+4.5}_{-3.7}{}^{+1.8}_{-1.7}$		353 BRIERE	01	CLE2	$e^+e^-\to\Upsilon(4S)$
• • • We do not use the following data for averages, fits, limits, etc. • • •					
$8.7^{+2.5}_{-2.1}\pm1.1$		353 AUBERT	01D	BABR	Repl. by AUBERT 03V
<384	90	354 ABE	00C	SLD	$e^+e^-\to Z$
<21	90	353 BERGFELD	98	CLE2	
<43	90	ASNER	96	CLE2	$e^+e^-\to\Upsilon(4S)$
<320	90	ALBRECHT	91B	ARG	$e^+e^-\to\Upsilon(4S)$
<380	90	355 AVERY	89B	CLEO	$e^+e^-\to\Upsilon(4S)$
<380	90	356 AVERY	87	CLEO	$e^+e^-\to\Upsilon(4S)$

353 Assumes equal production of B^+ and B^0 at the $\Upsilon(4S)$.
354 ABE 00C assumes $B(Z\to b\overline{b})=(21.7\pm0.1)\%$ and the B fractions $f_{B^0}=f_{B^+}=(39.7^{+1.8}_{-2.2})\%$ and $f_{B_s}=(10.5^{+1.8}_{-2.2})\%$.
355 AVERY 89B reports $<4.4\times10^{-4}$ assuming the $\Upsilon(4S)$ decays 43% to $B^0\overline{B}^0$. We rescale to 50%.
356 AVERY 87 reports $<4.7\times10^{-4}$ assuming the $\Upsilon(4S)$ decays 40% to $B^0\overline{B}^0$. We rescale to 50%.

$\Gamma(\overline{K}^*(892)^0K^*(892)^0)/\Gamma_{total}$ Γ_{155}/Γ

VALUE	CL%	DOCUMENT ID		TECN	COMMENT
$<2.2\times10^{-5}$	90	357 GODANG	02	CLE2	$e^+e^-\to\Upsilon(4S)$
• • • We do not use the following data for averages, fits, limits, etc. • • •					
$<4.69\times10^{-4}$	90	358 ABE	00C	SLD	$e^+e^-\to Z$

357 Assumes a helicity 00 configuration. For a helicity 11 configuration, the limit decreases to 1.9×10^{-5}.
358 ABE 00C assumes $B(Z\to b\overline{b})=(21.7\pm0.1)\%$ and the B fractions $f_{B^0}=f_{B^+}=(39.7^{+1.8}_{-2.2})\%$ and $f_{B_s}=(10.5^{+1.8}_{-2.2})\%$.

$\Gamma(K^*(892)^0K^*(892)^0)/\Gamma_{total}$ Γ_{156}/Γ

VALUE	CL%	DOCUMENT ID		TECN	COMMENT
$<3.7\times10^{-5}$	90	359 GODANG	02	CLE2	$e^+e^-\to\Upsilon(4S)$

359 Assumes a helicity 00 configuration. For a helicity 11 configuration, the limit decreases to 2.9×10^{-5}.

$\Gamma(K^*(892)^+K^*(892)^-)/\Gamma_{total}$ Γ_{157}/Γ

VALUE	CL%	DOCUMENT ID		TECN	COMMENT
$<1.41\times10^{-4}$	90	360 GODANG	02	CLE2	$e^+e^-\to\Upsilon(4S)$

360 Assumes a helicity 00 configuration. For a helicity 11 configuration, the limit decreases to 8.9×10^{-5}.

$\Gamma(K_1(1400)^0\rho^0)/\Gamma_{total}$ Γ_{158}/Γ

VALUE	CL%	DOCUMENT ID		TECN	COMMENT
$<3.0\times10^{-3}$	90	ALBRECHT	91B	ARG	$e^+e^-\to\Upsilon(4S)$

$\Gamma(K_1(1400)^0\phi)/\Gamma_{total}$ Γ_{159}/Γ

VALUE	CL%	DOCUMENT ID		TECN	COMMENT
$<5.0\times10^{-3}$	90	ALBRECHT	91B	ARG	$e^+e^-\to\Upsilon(4S)$

$\Gamma(K_2^*(1430)^0\rho^0)/\Gamma_{total}$ Γ_{160}/Γ

VALUE	CL%	DOCUMENT ID		TECN	COMMENT
$<1.1\times10^{-3}$	90	ALBRECHT	91B	ARG	$e^+e^-\to\Upsilon(4S)$

$\Gamma(K_2^*(1430)^0\phi)/\Gamma_{total}$ Γ_{161}/Γ

VALUE	CL%	DOCUMENT ID		TECN	COMMENT
$<1.4\times10^{-3}$	90	ALBRECHT	91B	ARG	$e^+e^-\to\Upsilon(4S)$

$\Gamma(K^*(892)^0\gamma)/\Gamma_{total}$ Γ_{162}/Γ

VALUE (units 10^{-5})	CL%	EVTS	DOCUMENT ID		TECN	COMMENT
4.3 ± 0.4 OUR AVERAGE						
$4.23\pm0.40\pm0.22$			[361] AUBERT	02C	BABR	$e^+e^-\to\Upsilon(4S)$
$4.55^{+0.72}_{-0.68}\pm0.34$			[362] COAN	00	CLE2	$e^+e^-\to\Upsilon(4S)$
• • • We do not use the following data for averages, fits, limits, etc. • • •						
<11	90		ACOSTA	02G	CDF	$p\overline{p}$ at 1.8 TeV
<21	90		[363] ADAM	96D	DLPH	$e^+e^-\to Z$
$4.0\pm1.7\pm0.8$		8	[364] AMMAR	93	CLE2	Repl. by COAN 00
<42	90		ALBRECHT	89G	ARG	$e^+e^-\to\Upsilon(4S)$
<24	90		[365] AVERY	89B	CLEO	$e^+e^-\to\Upsilon(4S)$
<210	90		AVERY	87	CLEO	$e^+e^-\to\Upsilon(4S)$

[361] Assumes equal production of B^+ and B^0 at the $\Upsilon(4S)$.
[362] Assumes equal production of B^+ and B^0 at the $\Upsilon(4S)$. No evidence for a nonresonant $K\pi\gamma$ contamination was seen; the central value assumes no contamination.
[363] ADAM 96D assumes $f_{B^0}=f_{B^-}=0.39$ and $f_{B_s}=0.12$.
[364] AMMAR 93 observed 6.6 ± 2.8 events above background.
[365] AVERY 89B reports $<2.8\times10^{-4}$ assuming the $\Upsilon(4S)$ decays 43% to $B^0\overline{B}^0$. We rescale to 50%.

$\Gamma(K^0\phi\gamma)/\Gamma_{total}$ Γ_{163}/Γ

VALUE (units 10^{-6})	CL%	DOCUMENT ID		TECN	COMMENT
<8.3	90	[366] DRUTSKOY	04	BELL	$e^+e^-\to\Upsilon(4S)$

[366] Assumes equal production of B^+ and B^0 at $\Upsilon(4S)$.

$\Gamma(K^+\pi^-\gamma)/\Gamma_{total}$ Γ_{164}/Γ

VALUE	DOCUMENT ID		TECN	COMMENT
$(4.6^{+1.3+0.5}_{-1.2-0.7})\times10^{-6}$	[367,368] NISHIDA	02	BELL	$e^+e^-\to\Upsilon(4S)$

[367] Assumes equal production of B^+ and B^0 at the $\Upsilon(4S)$.
[368] $1.25\ \mathrm{GeV}/c^2<M_{K\pi}<1.6\ \mathrm{GeV}/c^2$

$\Gamma(K^*(1410)\gamma)/\Gamma_{total}$ Γ_{165}/Γ

VALUE	CL%	DOCUMENT ID		TECN	COMMENT
$<1.3\times10^{-4}$	90	[369] NISHIDA	02	BELL	$e^+e^-\to\Upsilon(4S)$

[369] Assumes equal production of B^+ and B^0 at the $\Upsilon(4S)$.

$\Gamma(K^+\pi^-\gamma\ \text{nonresonant})/\Gamma_{total}$ Γ_{166}/Γ

VALUE	CL%	DOCUMENT ID		TECN	COMMENT
$<2.6\times10^{-6}$	90 [370,371]	NISHIDA	02	BELL	$e^+e^-\to\Upsilon(4S)$

[370] Assumes equal production of B^+ and B^0 at the $\Upsilon(4S)$.
[371] $1.25\ \mathrm{GeV}/c^2<M_{K\pi}<1.6\ \mathrm{GeV}/c^2$

$\Gamma(K_1(1270)^0\gamma)/\Gamma_{total}$ Γ_{167}/Γ

VALUE	CL%	DOCUMENT ID		TECN	COMMENT
<0.0070	90	[372] ALBRECHT	89G	ARG	$e^+e^-\to\Upsilon(4S)$

[372] ALBRECHT 89G reports <0.0078 assuming the $\Upsilon(4S)$ decays 45% to $B^0\overline{B}^0$. We rescale to 50%.

$\Gamma(K_1(1400)^0\gamma)/\Gamma_{total}$ Γ_{168}/Γ

VALUE	CL%	DOCUMENT ID		TECN	COMMENT
<0.0043	90	[373] ALBRECHT	89G	ARG	$e^+e^-\to\Upsilon(4S)$

[373] ALBRECHT 89G reports <0.0048 assuming the $\Upsilon(4S)$ decays 45% to $B^0\overline{B}^0$. We rescale to 50%.

$\Gamma(K_2^*(1430)^0\gamma)/\Gamma_{total}$ Γ_{169}/Γ

VALUE (units 10^{-5})	CL%	DOCUMENT ID		TECN	COMMENT
$1.3\pm0.5\pm0.1$		[374] NISHIDA	02	BELL	$e^+e^-\to\Upsilon(4S)$
• • • We do not use the following data for averages, fits, limits, etc. • • •					
<40	90	[375] ALBRECHT	89G	ARG	$e^+e^-\to\Upsilon(4S)$

[374] Assumes equal production of B^+ and B^0 at the $\Upsilon(4S)$.
[375] ALBRECHT 89G reports $<4.4\times10^{-4}$ assuming the $\Upsilon(4S)$ decays 45% to $B^0\overline{B}^0$. We rescale to 50%.

$\Gamma(K^*(1680)^0\gamma)/\Gamma_{total}$ Γ_{170}/Γ

VALUE	CL%	DOCUMENT ID		TECN	COMMENT
<0.0020	90	[376] ALBRECHT	89G	ARG	$e^+e^-\to\Upsilon(4S)$

[376] ALBRECHT 89G reports <0.0022 assuming the $\Upsilon(4S)$ decays 45% to $B^0\overline{B}^0$. We rescale to 50%.

$\Gamma(K_3^*(1780)^0\gamma)/\Gamma_{total}$ Γ_{171}/Γ

VALUE	CL%	DOCUMENT ID		TECN	COMMENT
<0.010	90	[377] ALBRECHT	89G	ARG	$e^+e^-\to\Upsilon(4S)$

[377] ALBRECHT 89G reports <0.011 assuming the $\Upsilon(4S)$ decays 45% to $B^0\overline{B}^0$. We rescale to 50%.

$\Gamma(K_4^*(2045)^0\gamma)/\Gamma_{total}$ Γ_{172}/Γ

VALUE	CL%	DOCUMENT ID		TECN	COMMENT
<0.0043	90	[378] ALBRECHT	89G	ARG	$e^+e^-\to\Upsilon(4S)$

[378] ALBRECHT 89G reports <0.0048 assuming the $\Upsilon(4S)$ decays 45% to $B^0\overline{B}^0$. We rescale to 50%.

$\Gamma(\rho^0\gamma)/\Gamma_{total}$ Γ_{173}/Γ

VALUE	CL%	DOCUMENT ID		TECN	COMMENT
$<1.2\times10^{-6}$	90	[379] AUBERT	04C	BABR	$e^+e^-\to\Upsilon(4S)$
• • • We do not use the following data for averages, fits, limits, etc. • • •					
$<1.7\times10^{-5}$	90	[380] COAN	00	CLE2	$e^+e^-\to\Upsilon(4S)$

[379] Assumes equal production of B^+ and B^0 at $\Upsilon(4S)$.
[380] Assumes equal production of B^+ and B^0 at the $\Upsilon(4S)$.

$\Gamma(\omega\gamma)/\Gamma_{total}$ Γ_{174}/Γ

VALUE	CL%	DOCUMENT ID		TECN	COMMENT
$<1.0\times10^{-6}$	90	[381] AUBERT	04C	BABR	$e^+e^-\to\Upsilon(4S)$
• • • We do not use the following data for averages, fits, limits, etc. • • •					
$<0.92\times10^{-5}$	90	[382] COAN	00	CLE2	$e^+e^-\to\Upsilon(4S)$

[381] Assumes equal production of B^+ and B^0 at $\Upsilon(4S)$.
[382] Assumes equal production of B^+ and B^0 at the $\Upsilon(4S)$.

$\Gamma(\phi\gamma)/\Gamma_{total}$ Γ_{175}/Γ

VALUE	CL%	DOCUMENT ID		TECN	COMMENT
$<0.33\times10^{-5}$	90	[383] COAN	00	CLE2	$e^+e^-\to\Upsilon(4S)$

[383] Assumes equal production of B^+ and B^0 at the $\Upsilon(4S)$.

$\Gamma(\pi^+\pi^-)/\Gamma_{total}$ Γ_{176}/Γ

VALUE (units 10^{-6})	CL%	EVTS	DOCUMENT ID		TECN	COMMENT
4.8 ± 0.5 OUR AVERAGE						
$4.5^{+1.4}_{-1.2}\pm0.5$			[384] BORNHEIM	03	CLE2	$e^+e^-\to\Upsilon(4S)$
$4.7\pm0.6\pm0.2$			[384] AUBERT	02Q	BABR	$e^+e^-\to\Upsilon(4S)$
$5.4\pm1.2\pm0.5$			[384] CASEY	02	BELL	$e^+e^-\to\Upsilon(4S)$
• • • We do not use the following data for averages, fits, limits, etc. • • •						
$5.6^{+2.3}_{-2.0}\pm0.4$			[384] ABE	01H	BELL	Repl. by CASEY 02
$4.1\pm1.0\pm0.7$			[384] AUBERT	01E	BABR	Repl. by AUBERT 02Q
<67	90		[385] ABE	00C	SLD	$e^+e^-\to Z$
$4.3^{+1.6}_{-1.4}\pm0.5$			[384] CRONIN-HEN..00		CLE2	Repl. by BORNHEIM 03
<15	90		GODANG	98	CLE2	Repl. by CRONIN-HENNESSY 00
<45	90		[386] ADAM	96D	DLPH	$e^+e^-\to Z$
<20	90		ASNER	96	CLE2	Repl. by GODANG 98
<41	90		[387] BUSKULIC	96V	ALEP	$e^+e^-\to Z$
<55	90		[388] ABREU	95N	DLPH	Sup. by ADAM 96D
<47	90		[389] AKERS	94L	OPAL	$e^+e^-\to Z$
<29	90		[390] BATTLE	93	CLE2	$e^+e^-\to\Upsilon(4S)$
<130	90		[390] ALBRECHT	90B	ARG	$e^+e^-\to\Upsilon(4S)$
<77	90		[391] BORTOLETTO	89	CLEO	$e^+e^-\to\Upsilon(4S)$
<260	90		[391] BEBEK	87	CLEO	$e^+e^-\to\Upsilon(4S)$
<500	90	4	GILES	84	CLEO	$e^+e^-\to\Upsilon(4S)$

[384] Assumes equal production of B^+ and B^0 at the $\Upsilon(4S)$.
[385] ABE 00C assumes $B(Z\to b\overline{b})=(21.7\pm0.1)\%$ and the B fractions $f_{B^0}=f_{B^+}=(39.7^{+1.8}_{-2.2})\%$ and $f_{B_s}=(10.5^{+1.8}_{-2.2})\%$.
[386] ADAM 96D assumes $f_{B^0}=f_{B^-}=0.39$ and $f_{B_s}=0.12$.
[387] BUSKULIC 96V assumes PDG 96 production fractions for B^0, B^+, B_s, b baryons.
[388] Assumes a B^0, B^- production fraction of 0.39 and a B_s production fraction of 0.12.
[389] Assumes $B(Z\to b\overline{b})=0.217$ and B_d^0 (B_s^0) fraction 39.5% (12%).
[390] Assumes equal production of $B^0\overline{B}^0$ and B^+B^- at $\Upsilon(4S)$.
[391] Paper assumes the $\Upsilon(4S)$ decays 43% to $B^0\overline{B}^0$. We rescale to 50%.

$\Gamma(\pi^+\pi^-)/\Gamma(K^+\pi^-)$ $\Gamma_{176}/\Gamma_{123}$

VALUE	DOCUMENT ID		TECN	COMMENT
$0.29^{+0.13+0.01}_{-0.12-0.02}$	[392] ABE	01H	BELL	$e^+e^-\to\Upsilon(4S)$

[392] Assumes equal production of B^+ and B^0 at the $\Upsilon(4S)$.

Meson Particle Listings

B^0

$\Gamma(\pi^0\pi^0)/\Gamma_{total}$ Γ_{177}/Γ

VALUE (units 10^{-6})	CL%	DOCUMENT ID		TECN	COMMENT
1.9±0.5 OUR AVERAGE					
2.1±0.6±0.3		[393] AUBERT	03S	BABR	$e^+e^- \to \Upsilon(4S)$
1.7±0.6±0.2		[393] LEE	03	BELL	$e^+e^- \to \Upsilon(4S)$
• • • We do not use the following data for averages, fits, limits, etc. • • •					
< 3.6	90	[393] AUBERT	03L	BABR	$e^+e^- \to \Upsilon(4S)$
< 4.4	90	[393] BORNHEIM	03	CLE2	$e^+e^- \to \Upsilon(4S)$
< 5.7	90	[393] ASNER	02	CLE2	$e^+e^- \to \Upsilon(4S)$
< 6.4	90	[393] CASEY	02	BELL	$e^+e^- \to \Upsilon(4S)$
< 9.3	90	GODANG	98	CLE2	Repl. by ASNER 02
< 9.1	90	ASNER	96	CLE2	Repl. by GODANG 98
<60	90	[394] ACCIARRI	95H	L3	$e^+e^- \to Z$

[393] Assumes equal production of B^+ and B^0 at the $\Upsilon(4S)$.
[394] ACCIARRI 95H assumes $f_{B^0} = 39.5 \pm 4.0$ and $f_{B_s} = 12.0 \pm 3.0\%$.

$\Gamma(\eta\pi^0)/\Gamma_{total}$ Γ_{178}/Γ

VALUE	CL%	DOCUMENT ID		TECN	COMMENT
<2.9 × 10⁻⁶	90	[395] RICHICHI	00	CLE2	$e^+e^- \to \Upsilon(4S)$
• • • We do not use the following data for averages, fits, limits, etc. • • •					
<8 × 10⁻⁶	90	BEHRENS	98	CLE2	Repl. by RICHICHI 00
<2.5 × 10⁻⁴	90	[396] ACCIARRI	95H	L3	$e^+e^- \to Z$
<1.8 × 10⁻³	90	[397] ALBRECHT	90B	ARG	$e^+e^- \to \Upsilon(4S)$

[395] Assumes equal production of B^+ and B^0 at the $\Upsilon(4S)$.
[396] ACCIARRI 95H assumes $f_{B^0} = 39.5 \pm 4.0$ and $f_{B_s} = 12.0 \pm 3.0\%$.
[397] ALBRECHT 90B limit assumes equal production of $B^0\overline{B}^0$ and B^+B^- at $\Upsilon(4S)$.

$\Gamma(\eta\eta)/\Gamma_{total}$ Γ_{179}/Γ

VALUE	CL%	DOCUMENT ID		TECN	COMMENT
<1.8 × 10⁻⁵	90	BEHRENS	98	CLE2	$e^+e^- \to \Upsilon(4S)$
• • • We do not use the following data for averages, fits, limits, etc. • • •					
<4.1 × 10⁻⁴	90	[398] ACCIARRI	95H	L3	$e^+e^- \to Z$

[398] ACCIARRI 95H assumes $f_{B^0} = 39.5 \pm 4.0$ and $f_{B_s} = 12.0 \pm 3.0\%$.

$\Gamma(\eta'\pi^0)/\Gamma_{total}$ Γ_{180}/Γ

VALUE	CL%	DOCUMENT ID		TECN	COMMENT
<5.7 × 10⁻⁶	90	[399] RICHICHI	00	CLE2	$e^+e^- \to \Upsilon(4S)$
• • • We do not use the following data for averages, fits, limits, etc. • • •					
<1.1 × 10⁻⁵	90	BEHRENS	98	CLE2	Repl. by RICHICHI 00

[399] Assumes equal production of B^+ and B^0 at the $\Upsilon(4S)$.

$\Gamma(\eta'\eta')/\Gamma_{total}$ Γ_{181}/Γ

VALUE	CL%	DOCUMENT ID		TECN	COMMENT
<4.7 × 10⁻⁵	90	BEHRENS	98	CLE2	$e^+e^- \to \Upsilon(4S)$

$\Gamma(\eta'\eta)/\Gamma_{total}$ Γ_{182}/Γ

VALUE	CL%	DOCUMENT ID		TECN	COMMENT
<2.7 × 10⁻⁵	90	BEHRENS	98	CLE2	$e^+e^- \to \Upsilon(4S)$

$\Gamma(\eta'\rho^0)/\Gamma_{total}$ Γ_{183}/Γ

VALUE	CL%	DOCUMENT ID		TECN	COMMENT
<1.2 × 10⁻⁵	90	[400] RICHICHI	00	CLE2	$e^+e^- \to \Upsilon(4S)$
• • • We do not use the following data for averages, fits, limits, etc. • • •					
<2.3 × 10⁻⁵	90	BEHRENS	98	CLE2	Repl. by RICHICHI 00

[400] Assumes equal production of B^+ and B^0 at the $\Upsilon(4S)$.

$\Gamma(\eta\rho^0)/\Gamma_{total}$ Γ_{184}/Γ

VALUE	CL%	DOCUMENT ID		TECN	COMMENT
<1.0 × 10⁻⁵	90	[401] RICHICHI	00	CLE2	$e^+e^- \to \Upsilon(4S)$
• • • We do not use the following data for averages, fits, limits, etc. • • •					
<1.3 × 10⁻⁵	90	BEHRENS	98	CLE2	Repl. by RICHICHI 00

[401] Assumes equal production of B^+ and B^0 at the $\Upsilon(4S)$.

$\Gamma(\omega\eta)/\Gamma_{total}$ Γ_{185}/Γ

VALUE	CL%	DOCUMENT ID		TECN
<1.2 × 10⁻⁵	90	[402] BERGFELD	98	CLE2

[402] Assumes equal production of B^+ and B^0 at the $\Upsilon(4S)$.

$\Gamma(\omega\eta')/\Gamma_{total}$ Γ_{186}/Γ

VALUE	CL%	DOCUMENT ID		TECN
<6.0 × 10⁻⁵	90	[403] BERGFELD	98	CLE2

[403] Assumes equal production of B^+ and B^0 at the $\Upsilon(4S)$.

$\Gamma(\omega\rho^0)/\Gamma_{total}$ Γ_{187}/Γ

VALUE	CL%	DOCUMENT ID		TECN
<1.1 × 10⁻⁵	90	[404] BERGFELD	98	CLE2

[404] Assumes equal production of B^+ and B^0 at the $\Upsilon(4S)$.

$\Gamma(\omega\omega)/\Gamma_{total}$ Γ_{188}/Γ

VALUE	CL%	DOCUMENT ID		TECN
<1.9 × 10⁻⁵	90	[405] BERGFELD	98	CLE2

[405] Assumes equal production of B^+ and B^0 at the $\Upsilon(4S)$.

$\Gamma(\phi\pi^0)/\Gamma_{total}$ Γ_{189}/Γ

VALUE	CL%	DOCUMENT ID		TECN
<0.5 × 10⁻⁵	90	[406] BERGFELD	98	CLE2

[406] Assumes equal production of B^+ and B^0 at the $\Upsilon(4S)$.

$\Gamma(\phi\eta)/\Gamma_{total}$ Γ_{190}/Γ

VALUE	CL%	DOCUMENT ID		TECN
<0.9 × 10⁻⁵	90	[407] BERGFELD	98	CLE2

[407] Assumes equal production of B^+ and B^0 at the $\Upsilon(4S)$.

$\Gamma(\phi\eta')/\Gamma_{total}$ Γ_{191}/Γ

VALUE	CL%	DOCUMENT ID		TECN
<3.1 × 10⁻⁵	90	[408] BERGFELD	98	CLE2

[408] Assumes equal production of B^+ and B^0 at the $\Upsilon(4S)$.

$\Gamma(\phi\rho^0)/\Gamma_{total}$ Γ_{192}/Γ

VALUE	CL%	DOCUMENT ID		TECN	COMMENT
<1.3 × 10⁻⁵	90	[409] BERGFELD	98	CLE2	
• • • We do not use the following data for averages, fits, limits, etc. • • •					
<1.56 × 10⁻⁴	90	[410] ABE	00C	SLD	$e^+e^- \to Z$

[409] Assumes equal production of B^+ and B^0 at the $\Upsilon(4S)$.
[410] ABE 00C assumes $B(Z \to b\overline{b})$=(21.7 ± 0.1)% and the B fractions $f_{B^0}=f_{B^+}=(39.7^{+1.8}_{-2.2})\%$ and $f_{B_s}=(10.5^{+1.8}_{-2.2})\%$.

$\Gamma(\phi\omega)/\Gamma_{total}$ Γ_{193}/Γ

VALUE	CL%	DOCUMENT ID		TECN
<2.1 × 10⁻⁵	90	[411] BERGFELD	98	CLE2

[411] Assumes equal production of B^+ and B^0 at the $\Upsilon(4S)$.

$\Gamma(\phi\phi)/\Gamma_{total}$ Γ_{194}/Γ

VALUE	CL%	DOCUMENT ID		TECN	COMMENT
<1.2 × 10⁻⁵	90	[412] BERGFELD	98	CLE2	
• • • We do not use the following data for averages, fits, limits, etc. • • •					
<3.21 × 10⁻⁴	90	[413] ABE	00C	SLD	$e^+e^- \to Z$
<3.9 × 10⁻⁵	90	ASNER	96	CLE2	$e^+e^- \to \Upsilon(4S)$

[412] Assumes equal production of B^+ and B^0 at the $\Upsilon(4S)$.
[413] ABE 00C assumes $B(Z \to b\overline{b})$=(21.7 ± 0.1)% and the B fractions $f_{B^0}=f_{B^+}=(39.7^{+1.8}_{-2.2})\%$ and $f_{B_s}=(10.5^{+1.8}_{-2.2})\%$.

$\Gamma(\pi^+\pi^-\pi^0)/\Gamma_{total}$ Γ_{195}/Γ

VALUE	CL%	DOCUMENT ID		TECN	COMMENT
<7.2 × 10⁻⁴	90	[414] ALBRECHT	90B	ARG	$e^+e^- \to \Upsilon(4S)$

[414] ALBRECHT 90B limit assumes equal production of $B^0\overline{B}^0$ and B^+B^- at $\Upsilon(4S)$.

$\Gamma(\rho^0\pi^0)/\Gamma_{total}$ Γ_{196}/Γ

VALUE	CL%	DOCUMENT ID		TECN	COMMENT
<5.3 × 10⁻⁶	90	[415] GORDON	02	BELL	$e^+e^- \to \Upsilon(rS)$
• • • We do not use the following data for averages, fits, limits, etc. • • •					
<5.5 × 10⁻⁶	90	[227] JESSOP	00	CLE2	$e^+e^- \to \Upsilon(4S)$
<2.4 × 10⁻⁵	90	ASNER	96	CLE2	Repl. by JESSOP 00
<4.0 × 10⁻⁴	90	[416] ALBRECHT	90B	ARG	$e^+e^- \to \Upsilon(4S)$

[415] Assumes equal production of B^+ and B^0 at the $\Upsilon(4S)$.
[416] ALBRECHT 90B limit assumes equal production of $B^0\overline{B}^0$ and B^+B^- at $\Upsilon(4S)$.

$\Gamma(\rho^\mp\pi^\pm)/\Gamma_{total}$ Γ_{197}/Γ

VALUE (units 10^{-5})	CL%	DOCUMENT ID		TECN	COMMENT
2.28±0.25 OUR AVERAGE					
$2.26 \pm 0.18 \pm 0.22$		[417] AUBERT	03T	BABR	$e^+e^- \to \Upsilon(4S)$
$2.08^{+0.60}_{-0.63}{}^{+0.28}_{-0.31}$		[417] GORDON	02	BELL	$e^+e^- \to \Upsilon(rS)$
$2.76^{+0.84}_{-0.74} \pm 0.42$		[417] JESSOP	00	CLE2	$e^+e^- \to \Upsilon(4S)$
• • • We do not use the following data for averages, fits, limits, etc. • • •					
< 8.8	90	ASNER	96	CLE2	Repl. by JESSOP 00
< 52	90	[418] ALBRECHT	90B	ARG	$e^+e^- \to \Upsilon(4S)$
<520	90	[419] BEBEK	87	CLEO	$e^+e^- \to \Upsilon(4S)$

[417] Assumes equal production of B^+ and B^0 at the $\Upsilon(4S)$.
[418] ALBRECHT 90B limit assumes equal production of $B^0\overline{B}^0$ and B^+B^- at $\Upsilon(4S)$.
[419] BEBEK 87 reports $< 6.1 \times 10^{-3}$ assuming the $\Upsilon(4S)$ decays 43% to $B^0\overline{B}^0$. We rescale to 50%.

$\Gamma(\pi^+\pi^-\pi^+\pi^-)/\Gamma_{total}$ Γ_{198}/Γ

VALUE	CL%	DOCUMENT ID		TECN	COMMENT
$<2.3\times10^{-4}$	90	[420] ADAM	96D	DLPH	$e^+e^-\to Z$
• • • We do not use the following data for averages, fits, limits, etc. • • •					
$<2.8\times10^{-4}$	90	[421] ABREU	95N	DLPH	Sup. by ADAM 96D
$<6.7\times10^{-4}$	90	[422] ALBRECHT	90B	ARG	$e^+e^-\to\Upsilon(4S)$

[420] ADAM 96D assumes $f_{B^0}=f_{B^-}=0.39$ and $f_{B_s}=0.12$.

[421] Assumes a B^0, B^- production fraction of 0.39 and a B_s production fraction of 0.12.

[422] ALBRECHT 90B limit assumes equal production of $B^0\overline{B}{}^0$ and B^+B^- at $\Upsilon(4S)$.

$\Gamma(\rho^0\rho^0)/\Gamma_{total}$ Γ_{199}/Γ

VALUE	CL%	DOCUMENT ID		TECN	COMMENT
$<2.1\ \times10^{-6}$	90	[423] AUBERT	03V	BABR	$e^+e^-\to\Upsilon(4S)$
• • • We do not use the following data for averages, fits, limits, etc. • • •					
$<1.8\ \times10^{-5}$	90	[424] GODANG	02	CLE2	$e^+e^-\to\Upsilon(4S)$
$<1.36\times10^{-4}$	90	[425] ABE	00C	SLD	$e^+e^-\to Z$
$<2.8\ \times10^{-4}$	90	[426] ALBRECHT	90B	ARG	$e^+e^-\to\Upsilon(4S)$
$<2.9\ \times10^{-4}$	90	[427] BORTOLETTO	89	CLEO	$e^+e^-\to\Upsilon(4S)$
$<4.3\ \times10^{-4}$	90	[427] BEBEK	87	CLEO	$e^+e^-\to\Upsilon(4S)$

[423] Assumes equal production of B^+ and B^0 at the $\Upsilon(4S)$.

[424] Assumes a helicity 00 configuration. For a helicity 11 configuration, the limit decreases to 1.4×10^{-5}.

[425] ABE 00C assumes $B(Z\to b\overline{b})=(21.7\pm0.1)\%$ and the B fractions $f_{B^0}=f_{B^+}=(39.7^{+1.8}_{-2.2})\%$ and $f_{B_s}=(10.5^{+1.8}_{-2.2})\%$.

[426] ALBRECHT 90B limit assumes equal production of $B^0\overline{B}{}^0$ and B^+B^- at $\Upsilon(4S)$.

[427] Paper assumes the $\Upsilon(4S)$ decays 43% to $B^0\overline{B}{}^0$. We rescale to 50%.

$\Gamma(a_1(1260)^\mp\pi^\pm)/\Gamma_{total}$ Γ_{200}/Γ

VALUE	CL%	DOCUMENT ID		TECN	COMMENT
$<4.9\times10^{-4}$	90	[428] BORTOLETTO	89	CLEO	$e^+e^-\to\Upsilon(4S)$
• • • We do not use the following data for averages, fits, limits, etc. • • •					
$<6.3\times10^{-4}$	90	[429] ALBRECHT	90B	ARG	$e^+e^-\to\Upsilon(4S)$
$<1.0\times10^{-3}$	90	[428] BEBEK	87	CLEO	$e^+e^-\to\Upsilon(4S)$

[428] Paper assumes the $\Upsilon(4S)$ decays 43% to $B^0\overline{B}{}^0$. We rescale to 50%.

[429] ALBRECHT 90B limit assumes equal production of $B^0\overline{B}{}^0$ and B^+B^- at $\Upsilon(4S)$.

$\Gamma(a_2(1320)^\mp\pi^\pm)/\Gamma_{total}$ Γ_{201}/Γ

VALUE	CL%	DOCUMENT ID		TECN	COMMENT
$<3.0\times10^{-4}$	90	[430] BORTOLETTO	89	CLEO	$e^+e^-\to\Upsilon(4S)$
• • • We do not use the following data for averages, fits, limits, etc. • • •					
$<1.4\times10^{-3}$	90	[430] BEBEK	87	CLEO	$e^+e^-\to\Upsilon(4S)$

[430] Paper assumes the $\Upsilon(4S)$ decays 43% to $B^0\overline{B}{}^0$. We rescale to 50%.

$\Gamma(\pi^+\pi^-\pi^0\pi^0)/\Gamma_{total}$ Γ_{202}/Γ

VALUE	CL%	DOCUMENT ID		TECN	COMMENT
$<3.1\times10^{-3}$	90	[431] ALBRECHT	90B	ARG	$e^+e^-\to\Upsilon(4S)$

[431] ALBRECHT 90B limit assumes equal production of $B^0\overline{B}{}^0$ and B^+B^- at $\Upsilon(4S)$.

$\Gamma(\rho^+\rho^-)/\Gamma_{total}$ Γ_{203}/Γ

VALUE	CL%	DOCUMENT ID		TECN	COMMENT
$<2.2\times10^{-3}$	90	[432] ALBRECHT	90B	ARG	$e^+e^-\to\Upsilon(4S)$

[432] ALBRECHT 90B limit assumes equal production of $B^0\overline{B}{}^0$ and B^+B^- at $\Upsilon(4S)$.

$\Gamma(a_1(1260)^0\pi^0)/\Gamma_{total}$ Γ_{204}/Γ

VALUE	CL%	DOCUMENT ID		TECN	COMMENT
$<1.1\times10^{-3}$	90	[433] ALBRECHT	90B	ARG	$e^+e^-\to\Upsilon(4S)$

[433] ALBRECHT 90B limit assumes equal production of $B^0\overline{B}{}^0$ and B^+B^- at $\Upsilon(4S)$.

$\Gamma(\omega\pi^0)/\Gamma_{total}$ Γ_{205}/Γ

VALUE	CL%	DOCUMENT ID		TECN	COMMENT
$<3\ \times10^{-6}$	90	[434] AUBERT	01G	BABR	$e^+e^-\to\Upsilon(4S)$
• • • We do not use the following data for averages, fits, limits, etc. • • •					
$<5.5\times10^{-6}$	90	[434] JESSOP	00	CLE2	$e^+e^-\to\Upsilon(4S)$
$<1.4\times10^{-5}$	90	[434] BERGFELD	98	CLE2	Repl. by JESSOP 00
$<4.6\times10^{-4}$	90	[435] ALBRECHT	90B	ARG	$e^+e^-\to\Upsilon(4S)$

[434] Assumes equal production of B^+ and B^0 at the $\Upsilon(4S)$.

[435] ALBRECHT 90B limit assumes equal production of $B^0\overline{B}{}^0$ and B^+B^- at $\Upsilon(4S)$.

$\Gamma(\pi^+\pi^+\pi^-\pi^-\pi^0)/\Gamma_{total}$ Γ_{206}/Γ

VALUE	CL%	DOCUMENT ID		TECN	COMMENT
$<9.0\times10^{-3}$	90	[436] ALBRECHT	90B	ARG	$e^+e^-\to\Upsilon(4S)$

[436] ALBRECHT 90B limit assumes equal production of $B^0\overline{B}{}^0$ and B^+B^- at $\Upsilon(4S)$.

$\Gamma(a_1(1260)^+\rho^-)/\Gamma_{total}$ Γ_{207}/Γ

VALUE	CL%	DOCUMENT ID		TECN	COMMENT
$<3.4\times10^{-3}$	90	[437] ALBRECHT	90B	ARG	$e^+e^-\to\Upsilon(4S)$

[437] ALBRECHT 90B limit assumes equal production of $B^0\overline{B}{}^0$ and B^+B^- at $\Upsilon(4S)$.

$\Gamma(a_1(1260)^0\rho^0)/\Gamma_{total}$ Γ_{208}/Γ

VALUE	CL%	DOCUMENT ID		TECN	COMMENT
$<2.4\times10^{-3}$	90	[438] ALBRECHT	90B	ARG	$e^+e^-\to\Upsilon(4S)$

[438] ALBRECHT 90B limit assumes equal production of $B^0\overline{B}{}^0$ and B^+B^- at $\Upsilon(4S)$.

$\Gamma(\pi^+\pi^+\pi^+\pi^-\pi^-\pi^-)/\Gamma_{total}$ Γ_{209}/Γ

VALUE	CL%	DOCUMENT ID		TECN	COMMENT
$<3.0\times10^{-3}$	90	[439] ALBRECHT	90B	ARG	$e^+e^-\to\Upsilon(4S)$

[439] ALBRECHT 90B limit assumes equal production of $B^0\overline{B}{}^0$ and B^+B^- at $\Upsilon(4S)$.

$\Gamma(a_1(1260)^+a_1(1260)^-)/\Gamma_{total}$ Γ_{210}/Γ

VALUE	CL%	DOCUMENT ID		TECN	COMMENT
$<2.8\times10^{-3}$	90	[440] BORTOLETTO	89	CLEO	$e^+e^-\to\Upsilon(4S)$
• • • We do not use the following data for averages, fits, limits, etc. • • •					
$<6.0\times10^{-3}$	90	[441] ALBRECHT	90B	ARG	$e^+e^-\to\Upsilon(4S)$

[440] BORTOLETTO 89 reports $<3.2\times10^{-3}$ assuming the $\Upsilon(4S)$ decays 43% to $B^0\overline{B}{}^0$. We rescale to 50%.

[441] ALBRECHT 90B limit assumes equal production of $B^0\overline{B}{}^0$ and B^+B^- at $\Upsilon(4S)$.

$\Gamma(\pi^+\pi^+\pi^+\pi^-\pi^-\pi^-\pi^0)/\Gamma_{total}$ Γ_{211}/Γ

VALUE	CL%	DOCUMENT ID		TECN	COMMENT
$<1.1\times10^{-2}$	90	[442] ALBRECHT	90B	ARG	$e^+e^-\to\Upsilon(4S)$

[442] ALBRECHT 90B limit assumes equal production of $B^0\overline{B}{}^0$ and B^+B^- at $\Upsilon(4S)$.

$\Gamma(p\overline{p})/\Gamma_{total}$ Γ_{212}/Γ

VALUE	CL%	DOCUMENT ID		TECN	COMMENT
$<1.2\times10^{-6}$	90	[443] ABE	02O	BELL	$e^+e^-\to\Upsilon(4S)$
• • • We do not use the following data for averages, fits, limits, etc. • • •					
$<1.4\times10^{-6}$	90	[443] BORNHEIM	03	CLE2	$e^+e^-\to\Upsilon(4S)$
$<7.0\times10^{-6}$	90	[444] COAN	99	CLE2	$e^+e^-\to\Upsilon(4S)$
$<1.8\times10^{-5}$	90	[445] BUSKULIC	96V	ALEP	$e^+e^-\to Z$
$<3.5\times10^{-4}$	90	[446] ABREU	95N	DLPH	Sup. by ADAM 96D
$<3.4\times10^{-5}$	90	[447] BORTOLETTO	89	CLEO	$e^+e^-\to\Upsilon(4S)$
$<1.2\times10^{-4}$	90	[448] ALBRECHT	88F	ARG	$e^+e^-\to\Upsilon(4S)$
$<1.7\times10^{-4}$	90	[447] BEBEK	87	CLEO	$e^+e^-\to\Upsilon(4S)$

[443] Assumes equal production of B^+ and B^0 at the $\Upsilon(4S)$.

[444] Assumes equal production of B^+ and B^0 at the $\Upsilon(4S)$.

[445] BUSKULIC 96V assumes PDG 96 production fractions for B^0, B^+, B_s, b baryons.

[446] Assumes a B^0, B^- production fraction of 0.39 and a B_s production fraction of 0.12.

[447] Paper assumes the $\Upsilon(4S)$ decays 43% to $B^0\overline{B}{}^0$. We rescale to 50%.

[448] ALBRECHT 88F reports $<1.3\times10^{-4}$ assuming the $\Upsilon(4S)$ decays 45% to $B^0\overline{B}{}^0$. We rescale to 50%.

$\Gamma(p\overline{p}\pi^+\pi^-)/\Gamma_{total}$ Γ_{213}/Γ

VALUE (units 10^{-4})	CL%	DOCUMENT ID		TECN	COMMENT
<2.5	90	[449] BEBEK	89	CLEO	$e^+e^-\to\Upsilon(4S)$
• • • We do not use the following data for averages, fits, limits, etc. • • •					
<9.5	90	[450] ABREU	95N	DLPH	Sup. by ADAM 96D
$5.4\pm1.8\pm2.0$		[451] ALBRECHT	88F	ARG	$e^+e^-\to\Upsilon(4S)$

[449] BEBEK 89 reports $<2.9\times10^{-4}$ assuming the $\Upsilon(4S)$ decays 43% to $B^0\overline{B}{}^0$. We rescale to 50%.

[450] Assumes a B^0, B^- production fraction of 0.39 and a B_s production fraction of 0.12.

[451] ALBRECHT 88F reports $6.0\pm2.0\pm2.2$ assuming the $\Upsilon(4S)$ decays 45% to $B^0\overline{B}{}^0$. We rescale to 50%.

$\Gamma(p\overline{p}K^0)/\Gamma_{total}$ Γ_{214}/Γ

VALUE	CL%	DOCUMENT ID		TECN	COMMENT
$<7.2\times10^{-6}$	90 [452,453]	ABE	02K	BELL	$e^+e^-\to\Upsilon(4S)$

[452] Assumes equal production of B^+ and B^0 at the $\Upsilon(4S)$.

[453] Explicitly vetoes resonant production of $p\overline{p}$ from Charmonium states.

$\Gamma(p\overline{\Lambda}\pi^-)/\Gamma_{total}$ Γ_{215}/Γ

VALUE (units 10^{-6})	CL%	DOCUMENT ID		TECN	COMMENT
$3.97^{+1.00}_{-0.80}\pm0.56$		[454] WANG	03	BELL	$e^+e^-\to\Upsilon(4S)$
• • • We do not use the following data for averages, fits, limits, etc. • • •					
<13	90	[454] COAN	99	CLE2	$e^+e^-\to\Upsilon(4S)$
<180	90	[455] ALBRECHT	88F	ARG	$e^+e^-\to\Upsilon(4S)$

[454] Assumes equal production of B^+ and B^0 at the $\Upsilon(4S)$.

[455] ALBRECHT 88F reports $<2.0\times10^{-4}$ assuming the $\Upsilon(4S)$ decays 45% to $B^0\overline{B}{}^0$. We rescale to 50%.

$\Gamma(p\overline{\Lambda}K^-)/\Gamma_{total}$ Γ_{216}/Γ

VALUE	CL%	DOCUMENT ID		TECN	COMMENT
$<8.2\times10^{-7}$	90	[456] WANG	03	BELL	$e^+e^-\to\Upsilon(4S)$

[456] Assumes equal production of B^+ and B^0 at the $\Upsilon(4S)$.

$\Gamma(p\overline{\Sigma}^0\pi^-)/\Gamma_{total}$ Γ_{217}/Γ

VALUE	CL%	DOCUMENT ID		TECN	COMMENT
$<3.8\times10^{-6}$	90	[457] WANG	03	BELL	$e^+e^-\to\Upsilon(4S)$

[457] Assumes equal production of B^+ and B^0 at the $\Upsilon(4S)$.

$\Gamma(\overline{\Lambda}\Lambda)/\Gamma_{total}$ Γ_{218}/Γ

VALUE	CL%	DOCUMENT ID		TECN	COMMENT
$<1.0\times10^{-6}$	90	[458] ABE	02O	BELL	$e^+e^-\to\Upsilon(4S)$
• • • We do not use the following data for averages, fits, limits, etc. • • •					
$<1.2\times10^{-6}$	90	[458] BORNHEIM	03	CLE2	$e^+e^-\to\Upsilon(4S)$
$<3.9\times10^{-6}$	90	[459] COAN	99	CLE2	$e^+e^-\to\Upsilon(4S)$

[458] Assumes equal production of B^+ and B^0 at the $\Upsilon(4S)$.
[459] Assumes equal production of B^+ and B^0 at the $\Upsilon(4S)$.

$\Gamma(\Delta^0\overline{\Delta}^0)/\Gamma_{total}$ Γ_{219}/Γ

VALUE	CL%	DOCUMENT ID		TECN	COMMENT
<0.0015	90	[460] BORTOLETTO89		CLEO	$e^+e^-\to\Upsilon(4S)$

[460] BORTOLETTO 89 reports <0.0018 assuming $\Upsilon(4S)$ decays 43% to $B^0\overline{B}^0$. We rescale to 50%.

$\Gamma(\Delta^{++}\overline{\Delta}^{--})/\Gamma_{total}$ Γ_{220}/Γ

VALUE	CL%	DOCUMENT ID		TECN	COMMENT
$<1.1\times10^{-4}$	90	[461] BORTOLETTO89		CLEO	$e^+e^-\to\Upsilon(4S)$

[461] BORTOLETTO 89 reports $<1.3\times10^{-4}$ assuming $\Upsilon(4S)$ decays 43% to $B^0\overline{B}^0$. We rescale to 50%.

$\Gamma(\overline{D}^0p\overline{p})/\Gamma_{total}$ Γ_{221}/Γ

VALUE	DOCUMENT ID		TECN	COMMENT
$(1.18\pm0.15\pm0.16)\times10^{-4}$	[462] ABE	02W	BELL	$e^+e^-\to\Upsilon(4S)$

[462] Assumes equal production of B^+ and B^0 at the $\Upsilon(4S)$.

$\Gamma(\overline{D}^*(2007)^0p\overline{p})/\Gamma_{total}$ Γ_{222}/Γ

VALUE	DOCUMENT ID		TECN	COMMENT
$(1.20^{+0.33}_{-0.29}\pm0.21)\times10^{-4}$	[463] ABE	02W	BELL	$e^+e^-\to\Upsilon(4S)$

[463] Assumes equal production of B^+ and B^0 at the $\Upsilon(4S)$.

$\Gamma(\overline{\Sigma}_c^{--}\Delta^{++})/\Gamma_{total}$ Γ_{223}/Γ

VALUE	CL%	DOCUMENT ID		TECN	COMMENT
<0.0010	90	[464] PROCARIO	94	CLE2	$e^+e^-\to\Upsilon(4S)$

[464] PROCARIO 94 reports <0.0012 for $B(\Lambda_c^+\to pK^-\pi^+)=0.043$. We rescale to our best value $B(\Lambda_c^+\to pK^-\pi^+)=0.050$.

$\Gamma(\overline{\Lambda}_c^-p\pi^+\pi^-)/\Gamma_{total}$ Γ_{224}/Γ

VALUE (units 10^{-3})		DOCUMENT ID		TECN	COMMENT
1.3 ±0.4 OUR AVERAGE					
1.7 ±0.3 ±0.4		[465] DYTMAN	02	CLE2	$e^+e^-\to\Upsilon(4S)$
1.10±0.20±0.29		[466] GABYSHEV	02	BELL	$e^+e^-\to\Upsilon(4S)$
• • • We do not use the following data for averages, fits, limits, etc. • • •					
$1.33^{+0.46}_{-0.42}\pm0.37$		[467] FU	97	CLE2	Repl. by DYTMAN 02

[465] DYTMAN 02 reports $1.67^{+0.27}_{-0.25}$ for $B(\Lambda_c^+\to pK^-\pi^+)=0.05$. We rescale to our best value $B(\Lambda_c^+\to pK^-\pi^+)=(5.0\pm1.3)\times10^{-2}$. Our first error is their experiment's error and our second error is the systematic error from using our best value.
[466] GABYSHEV 02 reports 1.1 ± 0.2 for $B(\Lambda_c^+\to pK^-\pi^+)=0.05$. We rescale to our best value $B(\Lambda_c^+\to pK^-\pi^+)=(5.0\pm1.3)\times10^{-2}$. Our first error is their experiment's error and our second error is the systematic error from using our best value.
[467] FU 97 uses PDG 96 values of Λ_c branching fraction.

$\Gamma(\overline{\Lambda}_c^-p)/\Gamma_{total}$ Γ_{225}/Γ

VALUE (units 10^{-5})	CL%	DOCUMENT ID		TECN	COMMENT
$2.19^{+0.56}_{-0.49}\pm0.65$		[468,469] GABYSHEV	03	BELL	$e^+e^-\to\Upsilon(4S)$
• • • We do not use the following data for averages, fits, limits, etc. • • •					
< 9	90	[468,470] DYTMAN	02	CLE2	$e^+e^-\to\Upsilon(4S)$
< 3.1	90	[468,471] GABYSHEV	02	BELL	$e^+e^-\to\Upsilon(4S)$
<21	90	[472] FU	97	CLE2	$e^+e^-\to\Upsilon(4S)$

[468] Assumes equal production of B^+ and B^0 at the $\Upsilon(4S)$.
[469] The second error for GABYSHEV 03 includes the systematic and the error of $\Lambda_c\to\overline{p}K^+\pi^-$ decay branching fraction.
[470] DYTMAN 02 measurement uses $B(\Lambda_c^-\to\overline{p}K^+\pi^-)=5.0\pm1.3\%$. The second error includes the systematic and the uncertainty of the branching ratio.
[471] Uses the value for $\Lambda_c\to pK^-\pi^+$ branching ratio $(5.0\pm1.3)\%$.
[472] FU 97 uses PDG 96 values of Λ_c branching ratio.

$\Gamma(\overline{\Lambda}_c^-p\pi^0)/\Gamma_{total}$ Γ_{226}/Γ

VALUE	CL%	DOCUMENT ID		TECN	COMMENT
$<5.9\times10^{-4}$	90	[473] FU	97	CLE2	$e^+e^-\to\Upsilon(4S)$

[473] FU 97 uses PDG 96 values of Λ_c branching ratio.

$\Gamma(\overline{\Lambda}_c^-p\pi^+\pi^-\pi^0)/\Gamma_{total}$ Γ_{227}/Γ

VALUE	CL%	DOCUMENT ID		TECN	COMMENT
$<5.07\times10^{-3}$	90	[474] FU	97	CLE2	$e^+e^-\to\Upsilon(4S)$

[474] FU 97 uses PDG 96 values of Λ_c branching ratio.

$\Gamma(\overline{\Lambda}_c^-p\pi^+\pi^-\pi^+\pi^-)/\Gamma_{total}$ Γ_{228}/Γ

VALUE	CL%	DOCUMENT ID		TECN	COMMENT
$<2.74\times10^{-3}$	90	[475] FU	97	CLE2	$e^+e^-\to\Upsilon(4S)$

[475] FU 97 uses PDG 96 values of Λ_c branching ratio.

$\Gamma(\overline{\Sigma}_c(2520)^{--}p\pi^+)/\Gamma_{total}$ Γ_{229}/Γ

VALUE (units 10^{-4})	DOCUMENT ID		TECN	COMMENT
$1.6\pm0.6\pm0.4$	[476] GABYSHEV	02	BELL	$e^+e^-\to\Upsilon(4S)$

[476] GABYSHEV 02 reports $1.63^{+0.64}_{-0.58}$ for $B(\Lambda_c^+\to pK^-\pi^+)=0.05$. We rescale to our best value $B(\Lambda_c^+\to pK^-\pi^+)=(5.0\pm1.3)\times10^{-2}$. Our first error is their experiment's error and our second error is the systematic error from using our best value.

$\Gamma(\overline{\Sigma}_c(2520)^0p\pi^-)/\Gamma_{total}$ Γ_{230}/Γ

VALUE	CL%	DOCUMENT ID		TECN	COMMENT
$<1.21\times10^{-4}$	90 [477,478]	GABYSHEV	02	BELL	$e^+e^-\to\Upsilon(4S)$

[477] Assumes equal production of B^+ and B^0 at the $\Upsilon(4S)$.
[478] Uses the value for $\Lambda_c\to pK^-\pi^+$ branching ratio $(5.0\pm1.3)\%$.

$\Gamma(\overline{\Sigma}_c(2455)^0p\pi^-)/\Gamma_{total}$ Γ_{231}/Γ

VALUE (units 10^{-4})	CL%	DOCUMENT ID		TECN	COMMENT
1.0±0.8 OUR AVERAGE		Error includes scale factor of 1.7.			
2.2±0.7±0.6		[479] DYTMAN	02	CLE2	$e^+e^-\to\Upsilon(4S)$
$0.5^{+0.5}_{-0.4}\pm0.1$	90	[480] GABYSHEV	02	BELL	$e^+e^-\to\Upsilon(4S)$

[479] DYTMAN 02 reports 2.2 ± 0.7 for $B(\Lambda_c^+\to pK^-\pi^+)=0.05$. We rescale to our best value $B(\Lambda_c^+\to pK^-\pi^+)=(5.0\pm1.3)\times10^{-2}$. Our first error is their experiment's error and our second error is the systematic error from using our best value.
[480] GABYSHEV 02 reports $0.48^{+0.46}_{-0.41}$ for $B(\Lambda_c^+\to pK^-\pi^+)=0.05$. We rescale to our best value $B(\Lambda_c^+\to pK^-\pi^+)=(5.0\pm1.3)\times10^{-2}$. Our first error is their experiment's error and our second error is the systematic error from using our best value.

$\Gamma(\overline{\Sigma}_c(2455)^{--}p\pi^+)/\Gamma_{total}$ Γ_{232}/Γ

VALUE (units 10^{-4})	DOCUMENT ID		TECN	COMMENT
2.8±0.9 OUR AVERAGE				
3.7±1.1±1.0	[481] DYTMAN	02	CLE2	$e^+e^-\to\Upsilon(4S)$
2.4±0.7±0.6	[482] GABYSHEV	02	BELL	$e^+e^-\to\Upsilon(4S)$

[481] DYTMAN 02 reports 3.7 ± 1.1 for $B(\Lambda_c^+\to pK^-\pi^+)=0.05$. We rescale to our best value $B(\Lambda_c^+\to pK^-\pi^+)=(5.0\pm1.3)\times10^{-2}$. Our first error is their experiment's error and our second error is the systematic error from using our best value.
[482] GABYSHEV 02 reports $2.38^{+0.75}_{-0.69}$ for $B(\Lambda_c^+\to pK^-\pi^+)=0.05$. We rescale to our best value $B(\Lambda_c^+\to pK^-\pi^+)=(5.0\pm1.3)\times10^{-2}$. Our first error is their experiment's error and our second error is the systematic error from using our best value.

$\Gamma(\overline{\Lambda}_c(2593)^-\ /\ \overline{\Lambda}_c(2625)^-p)/\Gamma_{total}$ Γ_{233}/Γ

VALUE	CL%	DOCUMENT ID		TECN	COMMENT
$<1.1\times10^{-4}$	90 [483,484]	DYTMAN	02	CLE2	$e^+e^-\to\Upsilon(4S)$

[483] Assumes equal production of B^+ and B^0 at the $\Upsilon(4S)$.
[484] DYTMAN 02 measurement uses $B(\Lambda_c^-\to\overline{p}K^+\pi^-)=5.0\pm1.3\%$. The second error includes the systematic and the uncertainty of the branching ratio.

$\Gamma(\gamma\gamma)/\Gamma_{total}$ Γ_{234}/Γ

Test for $\Delta B=1$ weak neutral current. Allowed by higher-order electroweak interactions.

VALUE	CL%	DOCUMENT ID		TECN	COMMENT
$<1.7\times10^{-6}$	90	[485] AUBERT	01I	BABR	$e^+e^-\to\Upsilon(4S)$
• • • We do not use the following data for averages, fits, limits, etc. • • •					
$<3.9\times10^{-5}$	90	[486] ACCIARRI	95I	L3	$e^+e^-\to Z$

[485] Assumes equal production of B^+ and B^0 at the $\Upsilon(4S)$.
[486] ACCIARRI 95I assumes $f_{B^0}=39.5\pm4.0$ and $f_{B_s}=12.0\pm3.0\%$.

$\Gamma(e^+e^-)/\Gamma_{total}$ Γ_{235}/Γ

Test for $\Delta B=1$ weak neutral current. Allowed by higher-order electroweak interactions.

VALUE	CL%	DOCUMENT ID		TECN	COMMENT
$<1.9\times10^{-7}$	90	[487] CHANG	03	BELL	$e^+e^-\to\Upsilon(4S)$
• • • We do not use the following data for averages, fits, limits, etc. • • •					
$<8.3\times10^{-7}$	90	[487] BERGFELD	00B	CLE2	$e^+e^-\to\Upsilon(4S)$
$<1.4\times10^{-5}$	90	[488] ACCIARRI	97B	L3	$e^+e^-\to Z$
$<5.9\times10^{-6}$	90	AMMAR	94	CLE2	Repl. by BERGFELD 00B
$<2.6\times10^{-5}$	90	[489] AVERY	89B	CLEO	$e^+e^-\to\Upsilon(4S)$
$<7.6\times10^{-5}$	90	[490] ALBRECHT	87D	ARG	$e^+e^-\to\Upsilon(4S)$
$<6.4\times10^{-5}$	90	[491] AVERY	87	CLEO	$e^+e^-\to\Upsilon(4S)$
$<3\ \times10^{-4}$	90	GILES	84	CLEO	Repl. by AVERY 87

[487] Assumes equal production of B^+ and B^0 at the $\Upsilon(4S)$.
[488] ACCIARRI 97B assume PDG 96 production fractions for B^+, B^0, B_s, and Λ_b.
[489] AVERY 89B reports $<3\times10^{-5}$ assuming the $\Upsilon(4S)$ decays 43% to $B^0\overline{B}^0$. We rescale to 50%.
[490] ALBRECHT 87D reports $<8.5\times10^{-5}$ assuming the $\Upsilon(4S)$ decays 45% to $B^0\overline{B}^0$. We rescale to 50%.
[491] AVERY 87 reports $<8\times10^{-5}$ assuming the $\Upsilon(4S)$ decays 40% to $B^0\overline{B}^0$. We rescale to 50%.

$\Gamma(\mu^+\mu^-)/\Gamma_{total}$ Γ_{236}/Γ

Test for $\Delta B = 1$ weak neutral current. Allowed by higher-order electroweak interactions.

VALUE	CL%	DOCUMENT ID		TECN	COMMENT
$< 1.6 \times 10^{-7}$	90	[492] CHANG	03	BELL	$e^+e^- \to \Upsilon(4S)$
• • • We do not use the following data for averages, fits, limits, etc. • • •					
$< 6.1 \times 10^{-7}$	90	[492] BERGFELD	00B	CLE2	$e^+e^- \to \Upsilon(4S)$
$< 4.0 \times 10^{-5}$	90	ABBOTT	98B	D0	$p\overline{p}$ 1.8 TeV
$< 6.8 \times 10^{-7}$	90	[493] ABE	98	CDF	$p\overline{p}$ at 1.8 TeV
$< 1.0 \times 10^{-5}$	90	[494] ACCIARRI	97B	L3	$e^+e^- \to Z$
$< 1.6 \times 10^{-6}$	90	[495] ABE	96L	CDF	Repl. by ABE 98
$< 5.9 \times 10^{-6}$	90	AMMAR	94	CLE2	$e^+e^- \to \Upsilon(4S)$
$< 8.3 \times 10^{-6}$	90	[496] ALBAJAR	91C	UA1	$E_{cm}^{p\overline{p}} = 630$ GeV
$< 1.2 \times 10^{-5}$	90	[497] ALBAJAR	91C	UA1	$E_{cm}^{p\overline{p}} = 630$ GeV
$< 4.3 \times 10^{-5}$	90	[498] AVERY	89B	CLEO	$e^+e^- \to \Upsilon(4S)$
$< 4.5 \times 10^{-5}$	90	[499] ALBRECHT	87D	ARG	$e^+e^- \to \Upsilon(4S)$
$< 7.7 \times 10^{-5}$	90	[500] AVERY	87	CLEO	$e^+e^- \to \Upsilon(4S)$
$< 2 \times 10^{-4}$	90	GILES	84	CLEO	Repl. by AVERY 87

[492] Assumes equal production of B^+ and B^0 at the $\Upsilon(4S)$.
[493] ABE 98 assumes production of $\sigma(B^0) = \sigma(B^+)$ and $\sigma(B_s)/\sigma(B^0) = 1/3$. They normalize to their measured $\sigma(B^0, p_T(B) > 6, |y| < 1.0) = 2.39 \pm 0.32 \pm 0.44\ \mu$b.
[494] ACCIARRI 97B assume PDG 96 production fractions for B^+, B^0, B_s, and Λ_b.
[495] ABE 96L assumes equal B^0 and B^+ production. They normalize to their measured $\sigma(B^+, p_T(B) > 6$ GeV/c, $|y| < 1) = 2.39 \pm 0.54\ \mu$b.
[496] B^0 and B_s^0 are not separated.
[497] Obtained from unseparated B^0 and B_s^0 measurement by assuming a $B^0{:}B_s^0$ ratio 2:1.
[498] AVERY 89B reports $< 5 \times 10^{-3}$ assuming the $\Upsilon(4S)$ decays 43% to $B^0\overline{B}^0$. We rescale to 50%.
[499] ALBRECHT 87D reports $< 5 \times 10^{-5}$ assuming the $\Upsilon(4S)$ decays 45% to $B^0\overline{B}^0$. We rescale to 50%.
[500] AVERY 87 reports $< 9 \times 10^{-5}$ assuming the $\Upsilon(4S)$ decays 40% to $B^0\overline{B}^0$. We rescale to 50%.

$\Gamma(K^0 e^+ e^-)/\Gamma_{total}$ Γ_{237}/Γ

Test for $\Delta B = 1$ weak neutral current. Allowed by higher-order electroweak interactions.

VALUE	CL%	DOCUMENT ID		TECN	COMMENT
$< 5.4 \times 10^{-7}$	90	[501] ISHIKAWA	03	BELL	$e^+e^- \to \Upsilon(4S)$
• • • We do not use the following data for averages, fits, limits, etc. • • •					
$< 2.7 \times 10^{-6}$	90	[502] ABE	02	BELL	Repl. by ISHIKAWA 03
$< 3.8 \times 10^{-6}$	90	[502] AUBERT	02L	BABR	$e^+e^- \to \Upsilon(4S)$
$< 8.45 \times 10^{-6}$	90	[503] ANDERSON	01B	CLE2	$e^+e^- \to \Upsilon(4S)$
$< 3.0 \times 10^{-4}$	90	ALBRECHT	91E	ARG	$e^+e^- \to \Upsilon(4S)$
$< 5.2 \times 10^{-4}$	90	[504] AVERY	87	CLEO	$e^+e^- \to \Upsilon(4S)$

[501] Assumes equal production of B^0 and B^+ at $\Upsilon(4S)$. The second error is a total of systematic uncertainties including model dependence.
[502] Assumes equal production of B^+ and B^0 at the $\Upsilon(4S)$.
[503] The result is for di-lepton masses above 0.5 GeV.
[504] AVERY 87 reports $< 6.5 \times 10^{-4}$ assuming the $\Upsilon(4S)$ decays 40% to $B^0\overline{B}^0$. We rescale to 50%.

$\Gamma(K^0\mu^+\mu^-)/\Gamma_{total}$ Γ_{238}/Γ

Test for $\Delta B = 1$ weak neutral current. Allowed by higher-order electroweak interactions.

VALUE (units 10^{-7})	CL%	DOCUMENT ID		TECN	COMMENT
$5.6^{+2.9}_{-2.3} \pm 0.5$		[505] ISHIKAWA	03	BELL	$e^+e^- \to \Upsilon(4S)$
• • • We do not use the following data for averages, fits, limits, etc. • • •					
< 33	90	[506] ABE	02	BELL	Repl. by ISHIKAWA 03
< 36	90	AUBERT	02L	BABR	$e^+e^- \to \Upsilon(4S)$
< 66.4	90	[507] ANDERSON	01B	CLE2	$e^+e^- \to \Upsilon(4S)$
< 5200	90	ALBRECHT	91E	ARG	$e^+e^- \to \Upsilon(4S)$
< 3600	90	[508] AVERY	87	CLEO	$e^+e^- \to \Upsilon(4S)$

[505] Assumes equal production of B^0 and B^+ at $\Upsilon(4S)$. The second error is a total of systematic uncertainties including model dependence.
[506] Assumes equal production of B^+ and B^0 at the $\Upsilon(4S)$.
[507] The result is for di-lepton masses above 0.5 GeV.
[508] AVERY 87 reports $< 4.5 \times 10^{-4}$ assuming the $\Upsilon(4S)$ decays 40% to $B^0\overline{B}^0$. We rescale to 50%.

$\Gamma(K^0\ell^+\ell^-)/\Gamma_{total}$ Γ_{239}/Γ

VALUE (units 10^{-7})	CL%	DOCUMENT ID		TECN	COMMENT
< 6.8	90	[509] ISHIKAWA	03	BELL	$e^+e^- \to \Upsilon(4S)$

[509] Assumes equal production of B^0 and B^+ at $\Upsilon(4S)$.

$\Gamma(K^*(892)^0 e^+ e^-)/\Gamma_{total}$ Γ_{240}/Γ

Test for $\Delta B = 1$ weak neutral current. Allowed by higher-order electroweak interactions.

VALUE	CL%	DOCUMENT ID		TECN	COMMENT
$< 2.4 \times 10^{-6}$	90	[510] ISHIKAWA	03	BELL	$e^+e^- \to \Upsilon(4S)$
• • • We do not use the following data for averages, fits, limits, etc. • • •					
$< 6.4 \times 10^{-6}$	90	[511] ABE	02	BELL	Repl. by ISHIKAWA 03
$< 6.7 \times 10^{-6}$	90	[511] AUBERT	02L	BABR	$e^+e^- \to \Upsilon(4S)$
$< 2.9 \times 10^{-4}$	90	ALBRECHT	91E	ARG	$e^+e^- \to \Upsilon(4S)$

[510] Assumes equal production of B^0 and B^+ at $\Upsilon(4S)$. The second error is a total of systematic uncertainties including model dependence.
[511] Assumes equal production of B^+ and B^0 at the $\Upsilon(4S)$.

$\Gamma(K^*(892)^0\mu^+\mu^-)/\Gamma_{total}$ Γ_{241}/Γ

Test for $\Delta B = 1$ weak neutral current. Allowed by higher-order electroweak interactions.

VALUE (units 10^{-6})	CL%	DOCUMENT ID		TECN	COMMENT
$1.33^{+0.42}_{-0.37} \pm 0.11$		[512] ISHIKAWA	03	BELL	$e^+e^- \to \Upsilon(4S)$
• • • We do not use the following data for averages, fits, limits, etc. • • •					
< 4.2	90	[513] ABE	02	BELL	$e^+e^- \to \Upsilon(4S)$
< 3.3	90	AUBERT	02L	BABR	$e^+e^- \to \Upsilon(4S)$
< 4.0	90	[514] AFFOLDER	99B	CDF	$p\overline{p}$ at 1.8 TeV
< 25	90	[515] ABE	96L	CDF	Repl. by AFFOLDER 99B
< 23	90	[516] ALBAJAR	91C	UA1	$E_{cm}^{p\overline{p}} = 630$ GeV
< 340	90	ALBRECHT	91E	ARG	$e^+e^- \to \Upsilon(4S)$

[512] Assumes equal production of B^0 and B^+ at $\Upsilon(4S)$. The second error is a total of systematic uncertainties including model dependence.
[513] Assumes equal production of B^+ and B^0 at the $\Upsilon(4S)$.
[514] AFFOLDER 99B measured relative to $B^0 \to J/\psi(1S)K^*(892)^0$.
[515] ABE 96L measured relative to $B^0 \to J/\psi(1S)K^*(892)^0$ using PDG 94 branching ratios.
[516] ALBAJAR 91C assumes 36% of $\overline{b}$ quarks give B^0 mesons.

$\Gamma(K^*(892)^0\ell^+\ell^-)/\Gamma_{total}$ Γ_{243}/Γ

VALUE (units 10^{-7})	DOCUMENT ID		TECN	COMMENT
$11.7^{+3.0}_{-2.7} \pm 0.9$	[517] ISHIKAWA	03	BELL	$e^+e^- \to \Upsilon(4S)$

[517] Assumes equal production of B^0 and B^+ at $\Upsilon(4S)$.

$\Gamma(K^*(892)^0\nu\overline{\nu})/\Gamma_{total}$ Γ_{242}/Γ

Test for $\Delta B = 1$ weak neutral current. Allowed by higher-order electroweak interactions.

VALUE	CL%	DOCUMENT ID		TECN	COMMENT
$< 1.0 \times 10^{-3}$	90	[518] ADAM	96D	DLPH	$e^+e^- \to Z$

[518] ADAM 96D assumes $f_{B^0} = f_{B^-} = 0.39$ and $f_{B_s} = 0.12$.

$\Gamma(e^\pm\mu^\mp)/\Gamma_{total}$ Γ_{244}/Γ

Test of lepton family number conservation. Allowed by higher-order electroweak interactions.

VALUE	CL%	DOCUMENT ID		TECN	COMMENT
$< 1.7 \times 10^{-7}$	90	[519] CHANG	03	BELL	$e^+e^- \to \Upsilon(4S)$
• • • We do not use the following data for averages, fits, limits, etc. • • •					
$< 15 \times 10^{-7}$	90	[519] BERGFELD	00B	CLE2	$e^+e^- \to \Upsilon(4S)$
$< 3.5 \times 10^{-6}$	90	ABE	98V	CDF	$p\overline{p}$ at 1.8 TeV
$< 1.6 \times 10^{-5}$	90	[520] ACCIARRI	97B	L3	$e^+e^- \to Z$
$< 5.9 \times 10^{-6}$	90	AMMAR	94	CLE2	$e^+e^- \to \Upsilon(4S)$
$< 3.4 \times 10^{-5}$	90	[521] AVERY	89B	CLEO	$e^+e^- \to \Upsilon(4S)$
$< 4.5 \times 10^{-5}$	90	[522] ALBRECHT	87D	ARG	$e^+e^- \to \Upsilon(4S)$
$< 7.7 \times 10^{-5}$	90	[523] AVERY	87	CLEO	$e^+e^- \to \Upsilon(4S)$
$< 3 \times 10^{-4}$	90	GILES	84	CLEO	Repl. by AVERY 87

[519] Assumes equal production of B^+ and B^0 at the $\Upsilon(4S)$.
[520] ACCIARRI 97B assume PDG 96 production fractions for B^+, B^0, B_s, and Λ_b.
[521] Paper assumes the $\Upsilon(4S)$ decays 43% to $B^0\overline{B}^0$. We rescale to 50%.
[522] ALBRECHT 87D reports $< 5 \times 10^{-5}$ assuming the $\Upsilon(4S)$ decays 45% to $B^0\overline{B}^0$. We rescale to 50%.
[523] AVERY 87 reports $< 9 \times 10^{-5}$ assuming the $\Upsilon(4S)$ decays 40% to $B^0\overline{B}^0$. We rescale to 50%.

$\Gamma(K^0 e^\pm\mu^\mp)/\Gamma_{total}$ Γ_{245}/Γ

Test of lepton family number conservation.

VALUE	CL%	DOCUMENT ID		TECN	COMMENT
$< 4.0 \times 10^{-6}$	90	[524] AUBERT	02L	BABR	$e^+e^- \to \Upsilon(4S)$

[524] Assumes equal production of B^+ and B^0 at the $\Upsilon(4S)$.

$\Gamma(K^*(892)^0 e^\pm\mu^\mp)/\Gamma_{total}$ Γ_{246}/Γ

Test of lepton family number conservation.

VALUE	CL%	DOCUMENT ID		TECN	COMMENT
$< 3.4 \times 10^{-6}$	90	[525] AUBERT	02L	BABR	$e^+e^- \to \Upsilon(4S)$

[525] Assumes equal production of B^+ and B^0 at the $\Upsilon(4S)$.

$\Gamma(e^\pm\tau^\mp)/\Gamma_{total}$ Γ_{247}/Γ

Test of lepton family number conservation. Allowed by higher-order electroweak interactions.

VALUE	CL%	DOCUMENT ID		TECN	COMMENT
$< 5.3 \times 10^{-4}$	90	AMMAR	94	CLE2	$e^+e^- \to \Upsilon(4S)$

$\Gamma(\mu^\pm\tau^\mp)/\Gamma_{total}$ Γ_{248}/Γ

Test of lepton family number conservation. Allowed by higher-order electroweak interactions.

VALUE	CL%	DOCUMENT ID		TECN	COMMENT
$< 8.3 \times 10^{-4}$	90	AMMAR	94	CLE2	$e^+e^- \to \Upsilon(4S)$

POLARIZATION IN B^0 DECAY

Γ_L/Γ in $B^0 \to J/\psi(1S)K^*(892)^0$

$\Gamma_L/\Gamma = 1$ would indicate that $B^0 \to J/\psi(1S)K^*(892)^0$ followed by $K^*(892)^0 \to K^0_S\pi^0$ is a pure CP eigenstate with $CP = -1$.

VALUE	EVTS	DOCUMENT ID		TECN	COMMENT
0.605 ± 0.022 OUR AVERAGE					
0.62 ± 0.02 ± 0.03		[526] ABE	02N	BELL	$e^+e^- \to \Upsilon(4S)$
0.597 ± 0.028 ± 0.024		[527] AUBERT	01H	BABR	$e^+e^- \to \Upsilon(4S)$
0.59 ± 0.06 ± 0.01		[528] AFFOLDER	00N	CDF	$p\overline{p}$ at 1.8 TeV
0.52 ± 0.07 ± 0.04		[529] JESSOP	97	CLE2	$e^+e^- \to \Upsilon(4S)$
0.65 ± 0.10 ± 0.04	65	ABE	95Z	CDF	$p\overline{p}$ at 1.8 TeV
0.97 ± 0.16 ± 0.15	13	[530] ALBRECHT	94G	ARG	$e^+e^- \to \Upsilon(4S)$
• • • We do not use the following data for averages, fits, limits, etc. • • •					
0.80 ± 0.08 ± 0.05	42	[530] ALAM	94	CLE2	Sup. by JESSOP 97

[526] Averaged over an admixture of B^0 and B^+ decays and the P wave fraction is $(19 \pm 2 \pm 3)\%$.
[527] Averaged over an admixture of B^0 and B^- decays and the P wave fraction is $(16.0 \pm 3.2 \pm 1.4) \times 10^{-2}$.
[528] AFFOLDER 00N measurements are based on 190 B^0 candidates obtained from a data sample of 89 pb^{-1}. The P-wave fraction is found to be $0.13^{+0.12}_{-0.09} \pm 0.06$.
[529] JESSOP 97 is the average over a mixture of B^0 and B^+ decays. The P-wave fraction is found to be $0.16 \pm 0.08 \pm 0.04$.
[530] Averaged over an admixture of B^0 and B^+ decays.

Γ_L/Γ in $B^0 \to \psi(2S)K^*(892)^0$

VALUE	DOCUMENT ID		TECN	COMMENT
0.45 ± 0.11 ± 0.04	[531] RICHICHI	01	CLE2	$e^+e^- \to \Upsilon(4S)$

[531] Averages between charged and neutral B mesons.

Γ_L/Γ in $B^0 \to D_s^{*+}D^{*-}$

VALUE	DOCUMENT ID		TECN	COMMENT
0.52 ± 0.05 OUR AVERAGE				
0.519 ± 0.050 ± 0.028	[532] AUBERT	03I	BABR	$e^+e^- \to \Upsilon(4S)$
0.506 ± 0.139 ± 0.036	AHMED	00B	CLE2	$e^+e^- \to \Upsilon(4S)$

[532] Measurement performed using partial reconstruction of D^{*-} decay.

Γ_L/Γ in $B^0 \to D^{*-}\rho^+$

VALUE	EVTS	DOCUMENT ID		TECN	COMMENT
0.885 ± 0.016 ± 0.012		CSORNA	03	CLE2	$e^+e^- \to \Upsilon(4S)$
• • • We do not use the following data for averages, fits, limits, etc. • • •					
0.93 ± 0.05 ± 0.05	76	ALAM	94	CLE2	$e^+e^- \to \Upsilon(4S)$

Γ_L/Γ in $B^0 \to D^{*+}D^{*-}$

VALUE	DOCUMENT ID		TECN	COMMENT
0.063 ± 0.055 ± 0.009	AUBERT	03Q	BABR	$e^+e^- \to \Upsilon(4S)$

Γ_L/Γ in $B^0 \to \phi K^*(892)^0$

VALUE	DOCUMENT ID		TECN	COMMENT
0.57 ± 0.11 OUR AVERAGE Error includes scale factor of 1.8.				
0.65 ± 0.07 ± 0.02	AUBERT	03V	BABR	$e^+e^- \to \Upsilon(4S)$
0.41 ± 0.10 ± 0.04	CHEN	03B	BELL	$e^+e^- \to \Upsilon(4S)$

B^0–$\overline{B}^0$ MIXING

Updated December 2003 by O. Schneider (Federal Institute of Technology, Lausanne).

There are two neutral B^0–$\overline{B}^0$ meson systems, B^0_d–$\overline{B}^0_d$ and B^0_s–$\overline{B}^0_s$ (generically denoted B^0_q–$\overline{B}^0_q$, $q = s, d$), which exhibit particle-antiparticle mixing [1]. This mixing phenomenon is described in Ref. 2. In the following, we adopt the notation introduced in Ref. 2, and assume CPT conservation throughout. In each system, the light (L) and heavy (H) mass eigenstates,

$$|B_{\rm L,H}\rangle = p|B^0_q\rangle \pm q|\overline{B}^0_q\rangle\,, \qquad (1)$$

have a mass difference $\Delta m_q = m_{\rm H} - m_{\rm L} > 0$, and a total decay width difference $\Delta\Gamma_q = \Gamma_{\rm H} - \Gamma_{\rm L}$. In the absence of CP violation in the mixing, $|q/p| = 1$, these differences are given by $\Delta m_q = 2|M_{12}|$ and $|\Delta\Gamma_q| = 2|\Gamma_{12}|$, where M_{12} and Γ_{12} are the off-diagonal elements of the mass and decay matrices [2]. The evolution of a pure $|B^0_q\rangle$ or $|\overline{B}^0_q\rangle$ state at $t = 0$ is given by

$$|B^0_q(t)\rangle = g_+(t)\,|B^0_q\rangle + \frac{q}{p}\,g_-(t)\,|\overline{B}^0_q\rangle\,, \qquad (2)$$

$$|\overline{B}^0_q(t)\rangle = g_+(t)\,|\overline{B}^0_q\rangle + \frac{p}{q}\,g_-(t)\,|B^0_q\rangle\,, \qquad (3)$$

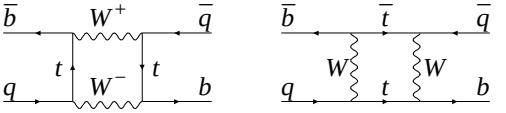

Figure 1: Dominant box diagrams for the $B^0_q \to \overline{B}^0_q$ transitions ($q = d$ or s). Similar diagrams exist where one or both t quarks are replaced with c or u quarks.

which means that the flavor states remain unchanged (+) or oscillate into each other (−) with time-dependent probabilities proportional to

$$|g_\pm(t)|^2 = \frac{e^{-\Gamma_q t}}{2}\left[\cosh\left(\frac{\Delta\Gamma_q}{2}t\right) \pm \cos(\Delta m_q\, t)\right]\,, \qquad (4)$$

where $\Gamma_q = (\Gamma_{\rm H} + \Gamma_{\rm L})/2$. In the absence of CP violation, the time-integrated mixing probability $\int |g_-(t)|^2\,dt/(\int |g_-(t)|^2\,dt + \int |g_+(t)|^2\,dt)$ is given by

$$\chi_q = \frac{x_q^2 + y_q^2}{2(x_q^2+1)}\,, \quad \text{where} \quad x_q = \frac{\Delta m_q}{\Gamma_q}\,, \quad y_q = \frac{\Delta\Gamma_q}{2\Gamma_q}\,. \qquad (5)$$

Standard Model predictions and phenomenology

In the Standard Model, the transitions $B^0_q \to \overline{B}^0_q$ and $\overline{B}^0_q \to B^0_q$ are due to the weak interaction. They are described, at the lowest order, by box diagrams involving two W bosons and two up-type quarks (see Fig. 1), as is the case for K^0–$\overline{K}^0$ mixing. However, the long range interactions arising from intermediate virtual states are negligible for the neutral B meson systems, because the large B mass is off the region of hadronic resonances. The calculation of the dispersive and absorptive parts of the box diagrams yields the following predictions for the off-diagonal element of the mass and decay matrices [3],

$$M_{12} = -\frac{G_F^2 m_W^2 \eta_B m_{B_q} B_{B_q} f_{B_q}^2}{12\pi^2}\, S_0(m_t^2/m_W^2)\,(V_{tq}^* V_{tb})^2\,, \qquad (6)$$

$$\Gamma_{12} = \frac{G_F^2 m_b^2 \eta'_B m_{B_q} B_{B_q} f_{B_q}^2}{8\pi} \times \left[(V_{tq}^* V_{tb})^2 + V_{tq}^* V_{tb} V_{cq}^* V_{cb}\; \mathcal{O}\left(\frac{m_c^2}{m_b^2}\right) + (V_{cq}^* V_{cb})^2\; \mathcal{O}\left(\frac{m_c^4}{m_b^4}\right)\right]\,, \qquad (7)$$

where G_F is the Fermi constant, m_W the W boson mass, and m_i the mass of quark i; m_{B_q}, f_{B_q} and B_{B_q} are the B^0_q mass, weak decay constant and bag parameter, respectively. The known function $S_0(x_t)$ can be approximated very well by $0.784\, x_t^{0.76}$ [4], and V_{ij} are the elements of the CKM matrix [5]. The QCD corrections η_B and η'_B are of order unity. The only non-negligible contributions to M_{12} are from box diagrams involving two top quarks. The phases of M_{12} and Γ_{12} satisfy

$$\phi_M - \phi_\Gamma = \pi + \mathcal{O}\left(\frac{m_c^2}{m_b^2}\right)\,, \qquad (8)$$

implying that the mass eigenstates have mass and width differences of opposite signs. This means that, like in the K^0–$\overline{K}^0$

system, the heavy state has a smaller decay width than that of the light state. Hence, $\Delta\Gamma$ is expected to be negative in the Standard Model.

Furthermore, the quantity

$$\left|\frac{\Gamma_{12}}{M_{12}}\right| \simeq \frac{3\pi}{2}\frac{m_b^2}{m_W^2}\frac{1}{S_0(m_t^2/m_W^2)} \sim \mathcal{O}\left(\frac{m_b^2}{m_t^2}\right) \qquad (9)$$

is small, and a power expansion of $|q/p|^2$ yields

$$\left|\frac{q}{p}\right|^2 = 1 + \left|\frac{\Gamma_{12}}{M_{12}}\right|\sin(\phi_M - \phi_\Gamma) + \mathcal{O}\left(\left|\frac{\Gamma_{12}}{M_{12}}\right|^2\right). \qquad (10)$$

Therefore, considering both Eqs. (8) and (9), the CP-violating parameter

$$1 - \left|\frac{q}{p}\right|^2 \simeq \mathrm{Im}\left(\frac{\Gamma_{12}}{M_{12}}\right) \qquad (11)$$

is expected to be very small: $\sim \mathcal{O}(10^{-3})$ for the B_d^0–$\overline{B}_d^0$ system and $\lesssim \mathcal{O}(10^{-4})$ for the B_s^0–$\overline{B}_s^0$ system [6].

In the approximation of negligible CP violation in mixing, the ratio $\Delta\Gamma_q/\Delta m_q$ is equal to the small quantity $|\Gamma_{12}/M_{12}|$ of Eq. (9); it is hence independent of CKM matrix elements, *i.e.*, the same for the B_d^0–$\overline{B}_d^0$ and B_s^0–$\overline{B}_s^0$ systems. It can be calculated with lattice QCD techniques; typical results are $\sim 5 \times 10^{-3}$ with quoted uncertainties of $\sim 30\%$. Given the current experimental knowledge (discussed below) on the mixing parameter x_q,

$$\begin{cases} x_d = 0.771 \pm 0.012 & (B_d^0\text{–}\overline{B}_d^0 \text{ system}) \\ x_s > 20.6 \text{ at } 95\% \text{ CL} & (B_s^0\text{–}\overline{B}_s^0 \text{ system}) \end{cases}, \qquad (12)$$

the Standard Model thus predicts that $\Delta\Gamma_d/\Gamma_d$ is very small (below 1%), but $\Delta\Gamma_s/\Gamma_s$ considerably larger ($\sim 10\%$). These width differences are caused by the existence of final states to which both the B_q^0 and $\overline{B}_q^0$ mesons can decay. Such decays involve $b \to c\overline{c}q$ quark-level transitions, which are Cabibbo-suppressed if $q = d$ and Cabibbo-allowed if $q = s$.

Experimental issues and methods for oscillation analyses

Time-integrated measurements of B^0–$\overline{B}^0$ mixing were published for the first time in 1987 by UA1 [7] and ARGUS [8], and since then by many other experiments. These measurements are typically based on counting same-sign and opposite-sign lepton pairs from the semileptonic decay of the produced $b\overline{b}$ pairs. Such analyses cannot easily separate the contributions from the different b-hadron species, therefore, the clean environment of $\Upsilon(4S)$ machines (where only B_d^0 and charged B_u mesons are produced) is in principle best suited to measure χ_d.

However, better sensitivity is obtained from time-dependent analyses aimed at the direct measurement of the oscillation frequencies Δm_d and Δm_s, from the proper time distributions of B_d^0 or B_s^0 candidates identified through their decay in (mostly) flavor-specific modes, and suitably tagged as mixed or unmixed. (This is particularly true for the B_s^0–$\overline{B}_s^0$ system, where the large value of x_s implies maximal mixing, *i.e.*, $\chi_s \simeq 1/2$.) In such analyses, the B_d^0 or B_s^0 mesons are either fully reconstructed, partially reconstructed from a charm meson, selected from a lepton with the characteristics of a $b \to \ell^-$ decay, or selected from a reconstructed displaced vertex. At high-energy colliders (LEP, SLC, Tevatron), the proper time $t = \frac{m_B}{p}L$ is measured from the distance L between the production vertex and the B decay vertex, and from an estimate of the B momentum p. At asymmetric B factories (KEKB, PEP-II), producing $e^+e^- \to \Upsilon(4S) \to B_d^0\overline{B}_d^0$ events with a boost $\beta\gamma$ (= 0.425, 0.55), the proper time difference between the two B candidates is estimated as $\Delta t \simeq \frac{\Delta z}{\beta\gamma c}$, where Δz is the spatial separation between the two B decay vertices along the boost direction. In all cases, the good resolution needed on the vertex positions is obtained with silicon detectors.

The average statistical significance $\mathcal{S}$ of a B_d^0 or B_s^0 oscillation signal can be approximated as [9]

$$\mathcal{S} \approx \sqrt{N/2}\, f_{\rm sig}\,(1-2\eta)\, e^{-(\Delta m\,\sigma_t)^2/2}, \qquad (13)$$

where N and $f_{\rm sig}$ are the number of candidates and the fraction of signal in the selected sample, η is the total mistag probability, and σ_t is the resolution on proper time (or proper time difference). The quantity $\mathcal{S}$ decreases very quickly as Δm increases; this dependence is controlled by σ_t, which is therefore a critical parameter for Δm_s analyses. At high-energy colliders, the proper time resolution $\sigma_t \sim \frac{m_B}{\langle p\rangle}\sigma_L \oplus t\frac{\sigma_p}{p}$ includes a constant contribution due to the decay length resolution σ_L (typically 0.05–0.3 ps), and a term due to the relative momentum resolution σ_p/p (typically 10–20% for partially reconstructed decays), which increases with proper time. At B factories, the boost of the B mesons is estimated from the known beam energies, and the term due to the spatial resolution dominates (typically 1–1.5 ps because of the much smaller B boost).

In order to tag a B candidate as mixed or unmixed, it is necessary to determine its flavor both in the initial state and in the final state. The initial and final state mistag probabilities, η_i and η_f, degrade $\mathcal{S}$ by a total factor $(1-2\eta) = (1-2\eta_i)(1-2\eta_f)$. In lepton-based analyses, the final state is tagged by the charge of the lepton from $b \to \ell^-$ decays; the biggest contribution to η_f is then due to $\overline{b} \to \overline{c} \to \ell^-$ decays. Alternatively, the charge of a reconstructed charm meson (D^{*-} from B_d^0 or D_s^- from B_s^0), or that of a kaon thought to come from a $b \to c \to s$ decay [10], can be used. For fully inclusive analyses based on topological vertexing, final state tagging techniques include jet charge [11] and charge dipole [12,13] methods.

At high-energy colliders, the methods to tag the initial state (*i.e.*, the state at production), can be divided in two groups: the ones that tag the initial charge of the $\overline{b}$ quark contained in the B candidate itself (same-side tag), and the ones that tag the initial charge of the other b quark produced in the event (opposite-side tag). On the same side, the charge of a track from the primary vertex is correlated with the production state of the B if that track is a decay product of a B^{**} state or the first particle in the fragmentation chain [14,15]. Jet- and vertex-charge techniques work on both sides and on the opposite side, respectively. Finally, the charge of a lepton from $b \to \ell^-$

or of a kaon from $b \to c \to s$ can be used as opposite side tags, keeping in mind that their performance is degraded due to integrated mixing. At SLC, the beam polarization produced a sizeable forward-backward asymmetry in the $Z \to b\overline{b}$ decays, and provided another very interesting and effective initial state tag based on the polar angle of the B candidate [12]. Initial state tags have also been combined to reach $\eta_i \sim 26\%$ at LEP [15,16], or even 22% at SLD [12] with full efficiency. In the case $\eta_f = 0$, this corresponds to an effective tagging efficiency (defined as $Q = \epsilon(1-2\eta)^2$, where ϵ is the tagging efficiency) in the range $23-31\%$. The equivalent figure at CDF is $\sim 3.5\%$ for Tevatron Run I [17] (expected to reach $\sim 5\%$ for Run II [18]), reflecting the fact that tagging is very challenging at hadron colliders.

At B factories, the flavor of a B^0_d meson at production cannot be determined, since the two neutral B mesons produced in a $\Upsilon(4S)$ decay evolve in a coherent P-wave state where they keep opposite flavors at any time. However, as soon as one of them decays, the other follows a time-evolution given by Eqs. (2) or (3), where t is replaced with Δt (which will take negative values half of the time). Hence, the "initial state" tag of a B can be taken as the final state tag of the other B. Effective tagging efficiencies $Q = 28-29\%$ are achieved by BABAR and Belle [19], using different techniques including $b \to \ell^-$ and $b \to c \to s$ tags. It is interesting to note that, in this case, mixing of this other B (*i.e.*, the coherent mixing occurring before the first B decay) does not contribute to the mistag probability.

In the absence of experimental evidence for a decay-width difference, oscillation analyses typically neglect $\Delta\Gamma$ in Eq. (4), and describe the data with the physics functions $\Gamma e^{-\Gamma t}(1 \pm \cos(\Delta m t))/2$ (high-energy colliders) or $\Gamma e^{-\Gamma|\Delta t|}(1 \pm \cos(\Delta m \Delta t))/4$ (asymmetric $\Upsilon(4S)$ machines). As can be seen from Eq. (4), a non-zero value of $\Delta\Gamma$ would effectively reduce the oscillation amplitude with a small time-dependent factor that would be very difficult to distinguish from time resolution effects. Measurements of Δm_d are usually extracted from the data using a maximum likelihood fit. No significant B^0_s–$\overline{B}^0_s$ oscillations have been seen so far. To extract information useful to set lower limits on Δm_s, B^0_s analyses follow a method [9] in which a B^0_s oscillation amplitude $\mathcal{A}$ is measured as a function of a fixed test value of Δm_s, using a maximum likelihood fit based on the functions $\Gamma_s e^{-\Gamma_s t}(1 \pm \mathcal{A}\cos(\Delta m_s t))/2$. To a very good approximation, the statistical uncertainty on $\mathcal{A}$ is Gaussian and equal to $1/\mathcal{S}$ from Eq. (13). If $\Delta m_s = \Delta m_s^{\rm true}$, one expects $\mathcal{A} = 1$ within the total uncertainty $\sigma_{\mathcal{A}}$; however, if Δm_s is (far) below its true value, a measurement consistent with $\mathcal{A} = 0$ is expected. A value of Δm_s can be excluded at 95% CL if $\mathcal{A} + 1.645\,\sigma_{\mathcal{A}} \leq 1$. If $\Delta m_s^{\rm true}$ is very large, one expects $\mathcal{A} = 0$, and all values of Δm_s such that $1.645\,\sigma_{\mathcal{A}}(\Delta m_s) < 1$ are expected to be excluded at 95% CL. Because of the proper time resolution, the quantity $\sigma_{\mathcal{A}}(\Delta m_s)$ is an increasing function of Δm_s, and one therefore expects to be able to exclude individual Δm_s values up to $\Delta m_s^{\rm sens}$, where $\Delta m_s^{\rm sens}$, called here the sensitivity of the analysis, is defined by $1.645\,\sigma_{\mathcal{A}}(\Delta m_s^{\rm sens}) = 1$.

B^0_d mixing studies

Many B^0_d–$\overline{B}^0_d$ oscillations analyses have been published by the ALEPH [20], BABAR [21], Belle [22], CDF [14], DELPHI [13,23], L3 [24], and OPAL [25] collaborations. Although a variety of different techniques have been used, the individual Δm_d results obtained at high-energy colliders have remarkably similar precision. Their average is compatible with the recent and more precise measurements from asymmetric B factories. The systematic uncertainties are not negligible; they are often dominated by sample composition, mistag probability, or b-hadron lifetime contributions. Before being combined, the measurements are adjusted on the basis of a common set of input values, including the b-hadron lifetimes and fractions published in this *Review*. Some measurements are statistically correlated. Systematic correlations arise both from common physics sources (fragmentation fractions, lifetimes, branching ratios of b hadrons), and from purely experimental or algorithmic effects (efficiency, resolution, tagging, background description). Combining all published measurements [13,14,20–25] and accounting for all identified correlations as described in Ref. 26, yields $\Delta m_d = 0.502 \pm 0.004(\text{stat}) \pm 0.005(\text{syst})$ ps^{-1}.

On the other hand, ARGUS and CLEO have published time-integrated measurements [27–29], which average to $\chi_d = 0.182 \pm 0.015$. Following Ref. 29, the width difference $\Delta\Gamma_d$ could in principle be extracted from the measured value of Γ_d and the above averages for Δm_d and χ_d (see Eq. (5)), provided that $\Delta\Gamma_d$ has a negligible impact on the Δm_d measurements. However, direct time-dependent studies yield stronger constraints: DELPHI published the result $|\Delta\Gamma_d|/\Gamma_d < 18\%$ at 95% CL [13], while BABAR recently obtained $-8.4\% < \text{sign}(\text{Re}\lambda_{\rm CP})\Delta\Gamma_{\rm d}/\Gamma_{\rm d} < 6.8\%$ at 90% CL [30].

Assuming $\Delta\Gamma_d = 0$ and no CP violation in mixing, and using the measured B^0_d lifetime, the Δm_d and χ_d results are combined to yield the world average

$$\Delta m_d = 0.502 \pm 0.007 \text{ ps}^{-1} \tag{14}$$

or, equivalently,

$$\chi_d = 0.186 \pm 0.004\,. \tag{15}$$

Evidence for CP violation in B^0_d mixing has been searched for, both with flavor-specific and inclusive B^0_d decays, in samples where the initial flavor state is tagged. In the case of semileptonic (or other flavor-specific) decays, where the final state tag is also available, the following asymmetry [2]

$$\mathcal{A}_{\rm SL} = \frac{N(\overline{B}^0_d(t) \to \ell^+\nu_\ell X) - N(B^0_d(t) \to \ell^-\overline{\nu}_\ell X)}{N(\overline{B}^0_d(t) \to \ell^+\nu_\ell X) + N(B^0_d(t) \to \ell^-\overline{\nu}_\ell X)} \simeq 1 - |q/p|^2_d \tag{16}$$

has been measured, either in time-integrated analyses at CLEO [28,29,31] and CDF [32], or in time-dependent analyses at LEP [33–35] and BABAR [30,36]. In the inclusive case,

also investigated at LEP [34,35,37], no final state tag is used, and the asymmetry [38]

$$\frac{N(B^0_d(t) \to \text{all}) - N(\overline{B}^0_d(t) \to \text{all})}{N(B^0_d(t) \to \text{all}) + N(\overline{B}^0_d(t) \to \text{all})} \simeq \mathcal{A}_{\rm SL}\left[\frac{x_d}{2}\sin(\Delta m_d\, t) - \sin^2\left(\frac{\Delta m_d\, t}{2}\right)\right] \quad (17)$$

must be measured as a function of the proper time to extract information on CP violation. In all cases, asymmetries compatible with zero have been found, with a precision limited by the available statistics. A simple average of all published results for the B^0_d meson [29,31,33,35–37] yields $\mathcal{A}_{\rm SL} = +0.002 \pm 0.013$, or $|q/p|_d = 0.999 \pm 0.006$, a result which does not yet constrain the Standard Model.

The Δm_d result of Eq. (14) provides an estimate of $2|M_{12}|$, and can be used, together with Eq. (6), to extract the magnitude of the CKM matrix element V_{td} within the Standard Model [39]. The main experimental uncertainties on the resulting estimate of $|V_{td}|$ come from m_t and Δm_d; however, the extraction is at present completely dominated by the uncertainty on the hadronic matrix element $f_{B_d}\sqrt{B_{B_d}} = 221 \pm 28^{+0}_{-22}$ MeV obtained from lattice QCD calculations [40].

B^0_s mixing studies

B^0_s–$\overline{B}^0_s$ oscillations have been the subject of many studies from ALEPH [15,41], CDF [42], DELPHI [13,16,43,44], OPAL [45], and SLD [12,46,47]. No oscillation signal has been found so far. The most sensitive analyses appear to be the ones based on inclusive lepton samples at LEP. Because of their better proper time resolution, the small data samples analyzed inclusively at SLD, as well as the few fully reconstructed B_s decays at LEP, turn out to be also very useful to explore the high Δm_s region.

All results are limited by the available statistics. They can easily be combined, since all experiments provide measurements of the B^0_s oscillation amplitude. All published results [12,13,16,41,42,43,45,46] are averaged using the procedure of Ref. 26 to yield the combined amplitudes $\mathcal{A}$ shown in Fig. 2 as a function of Δm_s. The individual results have been adjusted to common physics inputs, and all known correlations have been accounted for; the sensitivities of the inclusive analyses, which depend directly through Eq. (13) on the assumed fraction f_s of B^0_s mesons in an unbiased sample of weakly-decaying b hadrons, have also been rescaled to a common average of $f_s = 0.107 \pm 0.011$. The combined sensitivity for 95% CL exclusion of Δm_s values is found to be 17.8 ps^{-1}. All values of Δm_s below 14.4 ps^{-1} are excluded at 95% CL, which we express as

$$\Delta m_s > 14.4 \text{ ps}^{-1} \quad \text{at 95\% CL}. \quad (18)$$

The values between 14.4 and 21.8 ps^{-1} cannot be excluded, because the data is compatible with a signal in this region.

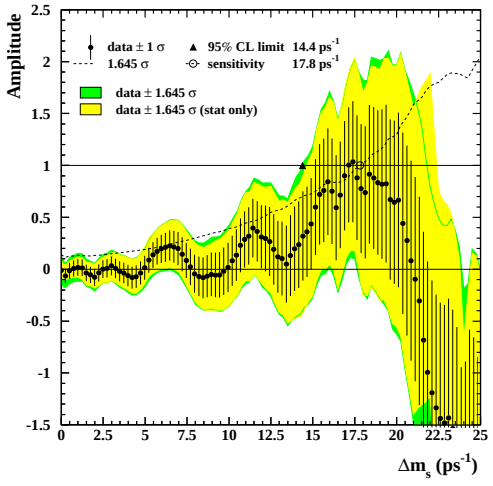

Figure 2: Combined measurements of the B^0_s oscillation amplitude as a function of Δm_s, including all results published by November 2003. The measurements are dominated by statistical uncertainties. Neighboring points are statistically correlated. See full-color version on color pages at end of book.

However, no deviation from $\mathcal{A} = 0$ is seen in Fig. 2 that would indicate the observation of a signal.

Some Δm_s analyses are still unpublished [44,47]. Including these in the above combination would yield $\Delta m_s > 14.6$ ps^{-1} at 95% CL with a sensitivity of 19.3 ps^{-1}.

The information on $|V_{ts}|$ obtained, in the framework of the Standard Model, from the combined amplitude spectrum, is hampered by the hadronic uncertainty, as in the B^0_d case. However, several uncertainties cancel in the frequency ratio

$$\frac{\Delta m_s}{\Delta m_d} = \frac{m_{B_s}}{m_{B_d}}\,\xi^2\left|\frac{V_{ts}}{V_{td}}\right|^2, \quad (19)$$

where $\xi = (f_{B_s}\sqrt{B_{B_s}})/(f_{B_d}\sqrt{B_{B_d}}) = 1.15 \pm 0.05^{+0.12}_{-0.00}$ is an SU(3) flavor-symmetry breaking factor obtained from lattice QCD calculations [40]. The CKM matrix can be constrained using the experimental results on Δm_d, Δm_s, $|V_{ub}/V_{cb}|$, ϵ_K, and $\sin(2\beta)$ together with theoretical inputs and unitarity conditions [39,48]. Given all measurements other than Δm_d and Δm_s, the constraint from our knowledge on the ratio $\Delta m_s/\Delta m_d$ is presently more effective in limiting the position of the apex of the CKM unitarity triangle than the one obtained from the Δm_d measurements alone, due to the reduced hadronic uncertainty in Eq. (19). We note also that it would be difficult for the Standard Model to accommodate values of Δm_s above ~ 25 ps^{-1} [48].

Information on $\Delta\Gamma_s$ can be obtained by studying the proper time distribution of untagged data samples enriched in B^0_s mesons [49]. In the case of an inclusive B^0_s selection [50], or a semileptonic B^0_s decay selection [16,51], both the short- and long-lived components are present, and the proper time distribution is a superposition of two exponentials with decay constants $\Gamma_s \pm \Delta\Gamma_s/2$. In principle, this provides sensitivity to

both Γ_s and $(\Delta\Gamma_s/\Gamma_s)^2$. Ignoring $\Delta\Gamma_s$ and fitting for a single exponential leads to an estimate of Γ_s with a relative bias proportional to $(\Delta\Gamma_s/\Gamma_s)^2$. An alternative approach, which is directly sensitive to first order in $\Delta\Gamma_s/\Gamma_s$, is to determine the lifetime of B_s^0 candidates decaying to CP eigenstates; measurements exist for $B_s^0 \to J/\psi\phi$ [52] and $B_s^0 \to D_s^{(*)+}D_s^{(*)-}$ [53], which are mostly CP-even states [54]. An estimate of $\Delta\Gamma_s/\Gamma_s$ has also been obtained directly from a measurement of the $B_s^0 \to D_s^{(*)+}D_s^{(*)-}$ branching ratio [53], under the assumption that these decays account for all the CP-even final states (however, no systematic uncertainty due to this assumption is given, so the average quoted below will not include this estimate).

Present data is not precise enough to efficiently constrain both Γ_s and $\Delta\Gamma_s/\Gamma_s$; since the B_s^0 and B_d^0 lifetimes are predicted to be equal within less than a percent [55], an expectation compatible with the current experimental data [56], the constraint $\Gamma_s = \Gamma_d$ can also be used to improve the extraction of $\Delta\Gamma_s/\Gamma_s$. Applying the combination procedure of Ref. 26 on the published results [16,51–53,57], yields

$$|\Delta\Gamma_s|/\Gamma_s < 0.54 \quad \text{at 95\% CL} \tag{20}$$

without external constraint, or

$$|\Delta\Gamma_s|/\Gamma_s < 0.29 \quad \text{at 95\% CL} \tag{21}$$

when constraining $1/\Gamma_s$ to the measured B_d^0 lifetime. These results are not yet precise enough to test Standard Model predictions.

Average b-hadron mixing and b-hadron production fractions at high energy

Let f_u, f_d, f_s and $f_{\rm baryon}$ be the fractions of B_u, B_d^0, B_s^0 and b-baryon composing an unbiased sample of weakly decaying b hadrons produced in high-energy colliders. LEP experiments have measured $f_s \times {\rm BR}(B_s^0 \to D_s^- \ell^+ \nu_\ell X)$ [58], ${\rm BR}(b \to \Lambda_b^0) \times {\rm BR}(\Lambda_b^0 \to \Lambda_c^+ \ell^- \overline{\nu}_\ell X)$ [59], and ${\rm BR}(b \to \Xi_b^-) \times {\rm BR}(\Xi_b^- \to \Xi^- \ell^- \overline{\nu}_\ell X)$ [60] from partially reconstructed final states, including a lepton, $f_{\rm baryon}$ from protons identified in b events [61], and the production rate of charged b hadrons [62]. The various b-hadron fractions have also been measured at CDF from electron-charm final states [63]. All these published results have been combined following the procedure and assumptions described in Ref. 26, to yield $f_u = f_d = (40.3 \pm 1.1)\%$, $f_s = (8.8 \pm 2.1)\%$, and $f_{\rm baryon} = (10.7 \pm 1.8)\%$ under the constraints

$$f_u = f_d \qquad \text{and} \qquad f_u + f_d + f_s + f_{\rm baryon} = 1\,. \tag{22}$$

Time-integrated mixing analyses performed with lepton pairs from $b\bar{b}$ events produced at high-energy colliders measure the quantity

$$\overline{\chi} = f'_d\,\chi_d + f'_s\,\chi_s\,, \tag{23}$$

where f'_d and f'_s are the fractions of B_d^0 and B_s^0 hadrons in a sample of semileptonic b-hadron decays. Assuming that all b hadrons have the same semileptonic decay width implies $f'_q = f_q/(\Gamma_q \tau_b)$ $(q = s, d)$, where τ_b is the average b-hadron lifetime. Hence $\overline{\chi}$ measurements can be used to improve our knowledge on the fractions f_u, f_d, f_s and $f_{\rm baryon}$.

Combining the above estimates of these fractions with the average $\overline{\chi} = 0.1257 \pm 0.0042$ (published in this *Review*), χ_d from Eq. (15), and $\chi_s = 1/2$ yields, under the constraints of Eq. (22),

$$f_u = f_d = (39.7 \pm 1.0)\%\,, \tag{24}$$

$$f_s = (10.7 \pm 1.1)\%\,, \tag{25}$$

$$f_{\rm baryon} = (9.9 \pm 1.7)\%\,, \tag{26}$$

showing that mixing information substantially reduces the uncertainty on f_s. These results and the averages quoted in Eqs. (14) and (15) for χ_d and Δm_d have been obtained in a consistent way by the B oscillations working group [26], taking into account the fact that many individual measurements of Δm_d depend on the assumed values for the b-hadron fractions.

Summary and prospects

B^0–$\overline{B}^0$ mixing has been and still is a field of intense study. The mass difference in the B_d^0–$\overline{B}_d^0$ system is very well measured (with an accuracy of 1.3%) but, despite an impressive theoretical effort, the hadronic uncertainty still limits the precision of the extracted estimate of $|V_{td}|$. The mass difference in the B_s^0–$\overline{B}_s^0$ system is much larger and still unmeasured. However, the current experimental lower limit on Δm_s already provides, together with Δm_d, a significant constraint on the CKM matrix within the Standard Model. No strong experimental evidence exists yet for the rather large decay width difference expected in the B_s^0–$\overline{B}_s^0$ system. It is interesting to recall that the ratio $\Delta\Gamma_s/\Delta m_s$ does not depend on CKM matrix elements in the Standard Model (see Eq. (9)), and that a measurement of either Δm_s or $\Delta\Gamma_s$ could be turned into a Standard Model prediction of the other one.

In the near future, the most promising prospects for B_s^0 mixing are from Run II at the Tevatron, where both Δm_s and $\Delta\Gamma_s$ are expected to be measured with fully reconstructed B_s^0 decays. The CDF and D0 collaborations expect to be able to observe B_s^0 oscillations with $2-3$ fb^{-1} of data, if Δm_s is consistent with the current Standard Model prediction [18]. Should this not be the case, then the discovery of B_s^0 oscillations will most likely be made at CERN's Large Hadron Collider scheduled to come into operation in 2007, where the LHC collaboration claims to have the potential to cover a Δm_s range up to ~ 68 ps^{-1} after 2 fb^{-1} of data (10^7 s) have been analyzed [64]. The BTeV experiment at Fermilab should have a comparable sensitivity to Δm_s and is expected to turn on in 2009 [65].

CP violation in B mixing, which has not been seen yet, as well as the phases involved in B mixing, will be further investigated with the large statistics that will become available at the B factories, the Tevatron, and the LHC.

B mixing may not have delivered all its secrets yet, because it is one of the phenomena where new physics might very well reveal itself (for example, new particles involved in the box

diagrams). Theoretical calculations in lattice QCD are becoming more reliable, and further progress in reducing hadronic uncertainties is expected. In the long term, a stringent check of the consistency, within the Standard Model, of the B^0_d and B^0_s mixing measurements, with all other measured observables in B physics (including CP asymmetries in B decays), will be possible, allowing to place limits on new physics or, better, discover new physics.

References

1. T.D. Lee and C.S. Wu, Ann. Rev. Nucl. Sci. **16**, 511 (1966); I.I. Bigi and A.I. Sanda, "CP violation," Cambridge Univ. Press, 2000; G.C. Branco, L. Lavoura, and J.P. Silva, "CP violation," Clarendon Press Oxford, 1999.
2. See the review on CP violation by D. Kirkby and Y. Nir in this publication.
3. A.J. Buras, W. Slominski, and H. Steger, Nucl. Phys. **B245**, 369 (1984).
4. T. Inami and C.S. Lim, Prog. Theor. Phys. **65**, 297 (1981); for the power-like approximation, see A.J. Buras and R. Fleischer, page 91 in "Heavy Flavours II," eds. A.J. Buras and M. Lindner, Singapore World Scientific (1998).
5. M. Kobayashi and K. Maskawa, Prog. Theor. Phys. **49**, 652 (1973).
6. I.I. Bigi *et al.*, in "CP violation," ed. C. Jarlskog, Singapore World Scientific, 1989.
7. C. Albajar *et al.* (**UA1**), Phys. Lett. **B186**, 247 (1987).
8. H. Albrecht *et al.* (**ARGUS**), Phys. Lett. **B192**, 245 (1987).
9. H.-G. Moser and A. Roussarie, Nucl. Instrum. Methods **384**, 491 (1997).
10. **SLD** collab., SLAC-PUB-7228, SLAC-PUB-7229 and SLAC-PUB-7230, contrib. to 28th Int. Conf. on High Energy Physics, Warsaw, 1996; J. Wittlin, PhD thesis, SLAC-R-582, 2001.
11. **ALEPH** collab., contrib. 596 to Int. Europhysics Conf. on High Energy Physics, Jerusalem, 1997.
12. K. Abe *et al.* (**SLD**), Phys. Rev. **D67**, 012006 (2003).
13. J. Abdallah *et al.* (**DELPHI**), Eur. Phys. J. **C28**, 155 (2003).
14. F. Abe *et al.* (**CDF**), Phys. Rev. Lett. **80**, 2057 (1998) and Phys. Rev. **D59**, 032001 (1999); Phys. Rev. **D60**, 051101 (1999); Phys. Rev. **D60**, 072003 (1999); T. Affolder *et al.* (**CDF**), Phys. Rev. **D60**, 112004 (1999).
15. R. Barate *et al.* (**ALEPH**), Eur. Phys. J. **C4**, 367 (1998); Eur. Phys. J. **C7**, 553 (1999).
16. P. Abreu *et al.* (**DELPHI**), Eur. Phys. J. **C16**, 555 (2000); Eur. Phys. J. **C18**, 229 (2000).
17. See tagging summary on page 160 of K. Anikeev *et al.*, "B physics at the Tevatron: Run II and beyond," FERMILAB-PUB-01/97, `hep-ph/0201071`, and references therein.
18. K.T. Pitts, "Mixings, lifetimes, spectroscopy and production of heavy flavour at the Tevatron," to appear in the procs. of the XXI Int. Symp. on Lepton and Photon Interactions at High Energies, Fermilab, August 2003.
19. B. Aubert *et al.* (**BABAR**), Phys. Rev. Lett. **89**, 201802 (2002); K. Abe *et al.* (**Belle**), Phys. Rev. **D66**, 071102(R) (2002).
20. D. Buskulic *et al.* (**ALEPH**), Z. Phys. **C75**, 397 (1997).
21. B. Aubert *et al.* (**BABAR**), Phys. Rev. Lett. **88**, 221802 (2002) and Phys. Rev. **D66**, 032003 (2002); Phys. Rev. Lett. **88**, 221803 (2002); Phys. Rev. **D67**, 072002 (2003).
22. K. Abe *et al.* (**Belle**), Phys. Rev. Lett. **86**, 3228 (2001); K. Hara *et al.* (**Belle**), Phys. Rev. Lett. **89**, 251803 (2002); T. Tomura *et al.* (**Belle**), Phys. Lett. **B542**, 207 (2002); N.C. Hastings *et al.* (**Belle**), Phys. Rev. **D67**, 052004 (2003); Y. Zheng *et al.* (**Belle**), Phys. Rev. **D67**, 092004 (2003).
23. P. Abreu *et al.* (**DELPHI**), Z. Phys. **C76**, 579 (1997).
24. M. Acciarri *et al.* (**L3**), Eur. Phys. J. **C5**, 195 (1998).
25. G. Alexander *et al.* (**OPAL**), Z. Phys. **C72**, 377 (1996); K. Ackerstaff *et al.* (**OPAL**), Z. Phys. **C76**, 401 (1997); Z. Phys. **C76**, 417 (1997); G. Abbiendi *et al.* (**OPAL**), Phys. Lett. **B493**, 266 (2000).
26. **ALEPH**, **CDF**, **DELPHI**, **L3**, **OPAL**, and **SLD** collab., "Combined results on b-hadron production rates and decay properties," CERN-EP/2001-050; the combined results on B mixing and b-hadron fractions published in this *Review* have been obtained by the B oscillations working group of the Heavy Flavour Averaging Group (HFAG); for more information, see `http://www.slac.stanford.edu/xorg/hfag/osc/`.
27. H. Albrecht *et al.* (**ARGUS**), Z. Phys. **C55**, 357 (1992); Phys. Lett. **B324**, 249 (1994).
28. J. Bartelt *et al.* (**CLEO**), Phys. Rev. Lett. **71**, 1680 (1993).
29. B.H. Behrens *et al.* (**CLEO**), Phys. Lett. **B490**, 36 (2000).
30. B. Aubert *et al.* (**BABAR**), `hep-ex/0311037`, SLAC-PUB-10247, submitted to Phys. Rev. Lett.
31. D.E. Jaffe *et al.* (**CLEO**), Phys. Rev. Lett. **86**, 5000 (2001).
32. F. Abe *et al.* (**CDF**), Phys. Rev. **D55**, 2546 (1997).
33. K. Ackerstaff *et al.* (**OPAL**), Z. Phys. **C76**, 401 (1997).
34. **DELPHI** collab., contrib. 449 to Int. Europhysics Conf. on High Energy Physics, Jerusalem, 1997.
35. R. Barate *et al.* (**ALEPH**), Eur. Phys. J. **C20**, 431 (2001).
36. B. Aubert *et al.* (**BABAR**), Phys. Rev. Lett. **88**, 231801 (2002).
37. G. Abbiendi *et al.* (**OPAL**), Eur. Phys. J. **C12**, 609 (2000).
38. M. Beneke, G. Buchalla, and I. Dunietz, Phys. Lett. **B393**, 132 (1997); I. Dunietz, Eur. Phys. J. **C7**, 197 (1999).
39. See the review on the CKM quark-mixing matrix by F.J. Gilman, K. Kleinknecht and B. Renk in this publication.
40. We quote here the global estimates from H. Wittig, `hep-ph/0310329`, talk at Int. Europhysics Conf. on High Energy Physics, Aachen, 2003; the second asymmetric error is due to the chiral extrapolation; for a recent review on lattice QCD calculations for heavy quarks see also A.S. Kronfeld, `hep-lat/0310063`, talk at XXI International Symposium on Lattice Field Theory, Tsukuba, 2003.
41. A. Heister *et al.* (**ALEPH**), Eur. Phys. J. **C29**, 143 (2003).
42. F. Abe *et al.* (**CDF**), Phys. Rev. Lett. **82**, 3576 (1999).
43. W. Adam *et al.* (**DELPHI**), Phys. Lett. **B414**, 382 (1997).
44. **DELPHI** collab., note 2002-073-CONF-607, contrib. 587 to Int. Conf. on High Energy Physics, Amsterdam, 2002.
45. G. Abbiendi *et al.* (**OPAL**), Eur. Phys. J. **C11**, 587 (1999); Eur. Phys. J. **C19**, 241 (2001).
46. K. Abe *et al.* (**SLD**), Phys. Rev. **D66**, 032009 (2002).

47. **SLD** collab., SLAC-PUB-8568, contrib. to 30th Int. Conf. on High Energy Physics, Osaka, 2000.
48. Workshop on the CKM matrix and the unitarity triangle, procs. eds. M. Battaglia *et al.*, hep-ph/0304132 and CERN-2003-002, 2003; the latest update on the CKM unitarity triangle fit can be found in M. Ciuchini *et al.*, hep-ph/0307195.
49. K. Hartkorn and H.-G. Moser, Eur. Phys. J. **C8**, 381 (1999).
50. M. Acciarri *et al.* (**L3**), Phys. Lett. **B438**, 417 (1998).
51. F. Abe *et al.* (**CDF**), Phys. Rev. **D59**, 032004 (1999).
52. F. Abe *et al.* (**CDF**), Phys. Rev. **D57**, 5382 (1998).
53. R. Barate *et al.* (**ALEPH**), Phys. Lett. **B486**, 286 (2000).
54. R. Aleksan *et al.*, Phys. Lett. **B316**, 567 (1993).
55. See for example M. Beneke, G. Buchalla, and I. Dunietz, Phys. Rev. **D54**, 4419 (1996).
56. See the review on production and decay of b-hadrons by Y. Kwon in this publication.
57. D. Buskulic *et al.* (**ALEPH**), Phys. Lett. **B377**, 205 (1996);
K. Ackerstaff *et al.* (**OPAL**), Phys. Lett. **B426**, 161 (1998).
58. P. Abreu *et al.* (**DELPHI**), Phys. Lett. **B289**, 199 (1992);
P.D. Acton *et al.* (**OPAL**), Phys. Lett. **B295**, 357 (1992);
D. Buskulic *et al.* (**ALEPH**), Phys. Lett. **B361**, 221 (1995).
59. P. Abreu *et al.* (**DELPHI**), Z. Phys. **C68**, 375 (1995);
R. Barate *et al.* (**ALEPH**), Eur. Phys. J. **C2**, 197 (1998).
60. P. Abreu *et al.* (**DELPHI**), Z. Phys. **C68**, 541 (1995);
D. Buskulic *et al.* (**ALEPH**), Phys. Lett. **B384**, 449 (1996).
61. R. Barate *et al.* (**ALEPH**), Eur. Phys. J. **C5**, 205 (1998).
62. J. Abdallah *et al.* (**DELPHI**), Phys. Lett. **B576**, 29 (2003).
63. F. Abe *et al.* (**CDF**), Phys. Rev. **D60**, 092005 (1999);
T. Affolder *et al.* (**CDF**), Phys. Rev. Lett. **84**, 1663 (2000).
64. R. Antunes Nobrega *et al.* (**LHCb**), "LHCb reoptimized detector and performance," Technical Design Report, CERN/LHCC 2003-030, September 2003.
65. See http://www-btev.fnal.gov/public/hep/ for more information on BTeV.

B^0-$\overline{B}^0$ MIXING PARAMETERS

For a discussion of B^0-$\overline{B}^0$ mixing see the note on "B^0-$\overline{B}^0$ Mixing" in the B^0 Particle Listings above.

χ_d is a measure of the time-integrated B^0-$\overline{B}^0$ mixing probability that a produced B^0 ($\overline{B}^0$) decays as a $\overline{B}^0$ (B^0). Mixing violates $\Delta B \neq 2$ rule.

$$\chi_d = \frac{x_d^2}{2(1+x_d^2)}$$

$$x_d = \frac{\Delta m_{B^0}}{\Gamma_{B^0}} = (m_{B^0_H} - m_{B^0_L})\,\tau_{B^0},$$

where H, L stand for heavy and light states of two B^0 CP eigenstates and $\tau_{B^0} = \frac{1}{0.5(\Gamma_{B^0_H}+\Gamma_{B^0_L})}$.

χ_d

This B^0-$\overline{B}^0$ mixing parameter is the probability (integrated over time) that a produced B^0 (or $\overline{B}^0$) decays as a $\overline{B}^0$ (or B^0), e.g. for inclusive lepton decays

$$\chi_d = \Gamma(B^0 \to \ell^- X \text{ (via } \overline{B}^0)) / \Gamma(B^0 \to \ell^{\pm} X)$$
$$= \Gamma(\overline{B}^0 \to \ell^+ X \text{ (via } B^0)) / \Gamma(\overline{B}^0 \to \ell^{\pm} X)$$

Where experiments have measured the parameter $r = \chi/(1-\chi)$, we have converted to χ. Mixing violates the $\Delta B \neq 2$ rule.

Note that the measurement of χ at energies higher than the $\Upsilon(4S)$ have not separated χ_d from χ_s where the subscripts indicate $B^0(\overline{b}d)$ or $B^0_s(\overline{b}s)$. They are listed in the $B^{\pm}/B^0/B^0_s/b$-baryon ADMIXTURE section.

The experiments at $\Upsilon(4S)$ make an assumption about the $B^0\overline{B}^0$ fraction and about the ratio of the $B^{\pm}$ and B^0 semileptonic branching ratios (usually that it equals one).

"OUR EVALUATION" is an average using rescaled values of the data listed below. The average and rescaling were performed by the Heavy Flavor Averaging Group (HFAG) and are described at http://www.slac.stanford.edu/xorg/hfag/. The averaging/rescaling procedure takes into account corrections between the measurements, includes χ_d calculated from Δm_{B^0} and τ_{B^0}.

VALUE	CL%	DOCUMENT ID		TECN	COMMENT
0.186±0.004 OUR EVALUATION					
0.182±0.015 OUR AVERAGE					
0.198±0.013±0.014		[533] BEHRENS	00B	CLE2	$e^+e^- \to \Upsilon(4S)$
0.16 ±0.04 ±0.04		[534] ALBRECHT	94	ARG	$e^+e^- \to \Upsilon(4S)$
0.149±0.023±0.022		[535] BARTELT	93	CLE2	$e^+e^- \to \Upsilon(4S)$
0.171±0.048		[536] ALBRECHT	92L	ARG	$e^+e^- \to \Upsilon(4S)$
• • • We do not use the following data for averages, fits, limits, etc. • • •					
0.20 ±0.13 ±0.12		[537] ALBRECHT	96D	ARG	$e^+e^- \to \Upsilon(4S)$
0.19 ±0.07 ±0.09		[538] ALBRECHT	96D	ARG	$e^+e^- \to \Upsilon(4S)$
0.24 ±0.12		[539] ELSEN	90	JADE	e^+e^- 35–44 GeV
$0.158^{+0.052}_{-0.059}$		ARTUSO	89	CLEO	$e^+e^- \to \Upsilon(4S)$
0.17 ±0.05		[540] ALBRECHT	87I	ARG	$e^+e^- \to \Upsilon(4S)$
<0.19	90	[541] BEAN	87B	CLEO	$e^+e^- \to \Upsilon(4S)$
<0.27	90	[542] AVERY	84	CLEO	$e^+e^- \to \Upsilon(4S)$

[533] BEHRENS 00B uses high-momentum lepton tags and partially reconstructed $\overline{B}^0 \to D^{*+}\pi^-, \rho^-$ decays to determine the flavor of the B meson.
[534] ALBRECHT 94 reports r=0.194 ± 0.062 ± 0.054. We convert to χ for comparison. Uses tagged events (lepton + pion from D^*).
[535] BARTELT 93 analysis performed using tagged events (lepton+pion from D^*). Using dilepton events they obtain $0.157 \pm 0.016^{+0.033}_{-0.028}$.
[536] ALBRECHT 92L is a combined measurement employing several lepton-based techniques. It uses all previous ARGUS data in addition to new data and therefore supersedes ALBRECHT 87I. A value of $r = 20.6 \pm 7.0\%$ is directly measured. The value can be used to measure $x = \Delta M/\Gamma = 0.72 \pm 0.15$ for the B_d meson. Assumes $f_{+-}/f_0 = 1.0 \pm 0.05$ and uses $\tau_{B^{\pm}}/\tau_{B^0} = (0.95 \pm 0.14)$ (f_{+-}/f_0).
[537] Uses $D^{*+}K^{\pm}$ correlations.
[538] Uses $(D^{*+}\ell^-)\,K^{\pm}$ correlations.
[539] These experiments see a combination of B_s and B_d mesons.
[540] ALBRECHT 87I is inclusive measurement with like-sign dileptons, with tagged B decays plus leptons, and one fully reconstructed event. Measures r=0.21 ± 0.08. We convert to χ for comparison. Superseded by ALBRECHT 92L.
[541] BEAN 87B measured $r < 0.24$; we converted to χ.
[542] Same-sign dilepton events. Limit assumes semileptonic BR for B^+ and B^0 equal. If $B^0/B^{\pm}$ ratio <0.58, no limit exists. The limit was corrected in BEAN 87B from $r < 0.30$ to $r < 0.37$. We converted this limit to χ.

$\Delta m_{B^0} = m_{B^0_H} - m_{B^0_L}$

$\Delta m_{B^0_s}$ is a measure of 2π times the B^0-$\overline{B}^0$ oscillation frequency in time-dependent mixing experiments.

The second "OUR EVALUATION" is an average using rescaled values of the data listed below. The average and rescaling were performed by the Heavy Flavor Averaging Group (HFAG) and are described at http://www.slac.stanford.edu/xorg/hfag/. The averaging/rescaling procedure takes into account corrections between the measurements.

The first "OUR EVALUATION" (0.502 ± 0.007), also provided by the HFAG, includes Δm_d calculated from χ_d measured at $\Upsilon(4S)$.

VALUE (10^{12} $\hbar$ s^{-1})	EVTS	DOCUMENT ID		TECN	COMMENT
0.502±0.007 OUR EVALUATION	First				
0.502±0.007 OUR EVALUATION	Second				
0.531±0.025±0.007		[543] ABDALLAH	03B	DLPH	$e^+e^- \to Z$
0.492±0.018±0.013		[544] AUBERT	03C	BABR	$e^+e^- \to \Upsilon(4S)$
0.503±0.008±0.010		[545] HASTINGS	03	BELL	$e^+e^- \to \Upsilon(4S)$
0.509±0.017±0.020		[546] ZHENG	03	BELL	$e^+e^- \to \Upsilon(4S)$
0.516±0.016±0.010		[547] AUBERT	02I	BABR	$e^+e^- \to \Upsilon(4S)$
0.493±0.012±0.009		[548] AUBERT	02J	BABR	$e^+e^- \to \Upsilon(4S)$
0.494±0.012±0.015		[549] HARA	02	BELL	$e^+e^- \to \Upsilon(4S)$

$0.528 \pm 0.017 \pm 0.011$	[550] TOMURA	02	BELL	$e^+e^- \to \Upsilon(4S)$	
$0.497 \pm 0.024 \pm 0.025$	[551] ABBIENDI,G	00B	OPAL	$e^+e^- \to Z$	
$0.503 \pm 0.064 \pm 0.071$	[552] ABE	99K	CDF	$p\overline{p}$ at 1.8 TeV	
$0.500 \pm 0.052 \pm 0.043$	[553] ABE	99Q	CDF	$p\overline{p}$ at 1.8 TeV	
$0.516 \pm 0.099 ^{+0.029}_{-0.035}$	[554] AFFOLDER	99C	CDF	$p\overline{p}$ at 1.8 TeV	
$0.471 ^{+0.078}_{-0.068} ^{+0.033}_{-0.034}$	[555] ABE	98C	CDF	$p\overline{p}$ at 1.8 TeV	
$0.458 \pm 0.046 \pm 0.032$	[556] ACCIARRI	98D	L3	$e^+e^- \to Z$	
$0.437 \pm 0.043 \pm 0.044$	[557] ACCIARRI	98D	L3	$e^+e^- \to Z$	
$0.472 \pm 0.049 \pm 0.053$	[558] ACCIARRI	98D	L3	$e^+e^- \to Z$	
$0.523 \pm 0.072 \pm 0.043$	[559] ABREU	97N	DLPH	$e^+e^- \to Z$	
$0.493 \pm 0.042 \pm 0.027$	[557] ABREU	97N	DLPH	$e^+e^- \to Z$	
$0.499 \pm 0.053 \pm 0.015$	[560] ABREU	97N	DLPH	$e^+e^- \to Z$	
$0.480 \pm 0.040 \pm 0.051$	[556] ABREU	97N	DLPH	$e^+e^- \to Z$	
$0.444 \pm 0.029 ^{+0.020}_{-0.017}$	[557] ACKERSTAFF	97U	OPAL	$e^+e^- \to Z$	
$0.430 \pm 0.043 ^{+0.028}_{-0.030}$	[556] ACKERSTAFF	97V	OPAL	$e^+e^- \to Z$	
$0.482 \pm 0.044 \pm 0.024$	[561] BUSKULIC	97D	ALEP	$e^+e^- \to Z$	
$0.404 \pm 0.045 \pm 0.027$	[557] BUSKULIC	97D	ALEP	$e^+e^- \to Z$	
$0.452 \pm 0.039 \pm 0.044$	[556] BUSKULIC	97D	ALEP	$e^+e^- \to Z$	
$0.539 \pm 0.060 \pm 0.024$	[562] ALEXANDER	96V	OPAL	$e^+e^- \to Z$	
$0.567 \pm 0.089 ^{+0.029}_{-0.023}$	[563] ALEXANDER	96V	OPAL	$e^+e^- \to Z$	
• • • We do not use the following data for averages, fits, limits, etc. • • •					
$0.516 \pm 0.016 \pm 0.010$	[564] AUBERT	02N	BABR	$e^+e^- \to \Upsilon(4S)$	
$0.463 \pm 0.008 \pm 0.016$	[548] ABE	01D	BELL	Repl. by HASTINGS 03	
$0.444 \pm 0.028 \pm 0.028$	[565] ACCIARRI	98D	L3	$e^+e^- \to Z$	
0.497 ± 0.035	[566] ABREU	97N	DLPH	$e^+e^- \to Z$	
$0.467 \pm 0.022 ^{+0.017}_{-0.015}$	[567] ACKERSTAFF	97V	OPAL	$e^+e^- \to Z$	
0.446 ± 0.032	[568] BUSKULIC	97D	ALEP	$e^+e^- \to Z$	
$0.531 ^{+0.050}_{-0.046} \pm 0.078$	[569] ABREU	96Q	DLPH	Sup. by ABREU 97N	
$0.496 ^{+0.055}_{-0.051} \pm 0.043$	[556] ACCIARRI	96E	L3	Repl. by ACCIARRI 98D	
$0.548 \pm 0.050 ^{+0.023}_{-0.019}$	[570] ALEXANDER	96V	OPAL	$e^+e^- \to Z$	
0.496 ± 0.046	[571] AKERS	95J	OPAL	Repl. by ACKERSTAFF 97V	
$0.462 ^{+0.040}_{-0.053} ^{+0.052}_{-0.035}$	[556] AKERS	95J	OPAL	Repl. by ACKERSTAFF 97V	
$0.50 \pm 0.12 \pm 0.06$	[559] ABREU	94M	DLPH	Sup. by ABREU 97N	
$0.508 \pm 0.075 \pm 0.025$	[562] AKERS	94C	OPAL	Repl. by ALEXANDER 96V	
$0.57 \pm 0.11 \pm 0.02$ 153	[563] AKERS	94H	OPAL	Repl. by ALEXANDER 96V	
$0.50 ^{+0.07}_{-0.06} ^{+0.11}_{-0.10}$	[556] BUSKULIC	94B	ALEP	Sup. by BUSKULIC 97D	
$0.52 ^{+0.10}_{-0.11} ^{+0.04}_{-0.03}$	[563] BUSKULIC	93K	ALEP	Sup. by BUSKULIC 97D	

[543] Events with a high transverse momentum lepton were removed and an inclusively reconstructed vertex was required.

[544] AUBERT 03C uses a sample of approximately 14,000 exclusively reconstructed $B^0 \to D^*(2010)^- \ell\nu$ and simultaneously measures the lifetime and oscillation frequency.

[545] HASTINGS 03 measurement based on the time evolution of dilepton events. It also reports $f_+/f_0 = 1.01 \pm 0.03 \pm 0.09$ and CPT violation parameters in B^0-$\overline{B}^0$ mixing.

[546] ZHENG 03 data analyzed using partially reconstructed $\overline{B}^0 \to D^{*-}\pi^+$ decay and a flavor tag based on the charge of the lepton from the accompanying B decay.

[547] Uses a tagged sample of fully-reconstructed neutral B decays at $\Upsilon(4S)$.

[548] Measured based on the time evolution of dilepton events in $\Upsilon(4S)$ decays.

[549] Uses a tagged sample of B^0 decays reconstructed in the mode $B^0 \to D^*\ell\nu$.

[550] Uses a tagged sample of fully-reconstructed hadronic B^0 decays at $\Upsilon(4S)$.

[551] Data analyzed using partially reconstructed $\overline{B}^0 \to D^{*+}\ell^-\overline{\nu}$ decay and a combination of flavor tags from the rest of the event.

[552] Uses di-muon events.

[553] Uses jet-charge and lepton-flavor tagging.

[554] Uses $\ell^- D^{*+} - \ell$ events.

[555] Uses π-B in the same side.

[556] Uses ℓ-ℓ.

[557] Uses ℓ-$Q_{\rm hem}$.

[558] Uses ℓ-ℓ with impact parameters.

[559] Uses $D^{*\pm}$-$Q_{\rm hem}$.

[560] Uses $\pi_s^\pm$ ℓ-$Q_{\rm hem}$.

[561] Uses $D^{*\pm}$-ℓ/$Q_{\rm hem}$.

[562] Uses $D^{*\pm}$ ℓ-$Q_{\rm hem}$.

[563] Uses $D^{*\pm}$-ℓ.

[564] AUBERT 02N result based on the same analysis and data sample reported in AUBERT 02I.

[565] ACCIARRI 98D combines results from ℓ-ℓ, ℓ-$Q_{\rm hem}$, and ℓ-ℓ with impact parameters.

[566] ABREU 97N combines results from $D^{*\pm}$-$Q_{\rm hem}$, ℓ-$Q_{\rm hem}$, $\pi_s^\pm$ ℓ-$Q_{\rm hem}$, and ℓ-ℓ.

[567] ACKERSTAFF 97V combines results from ℓ-ℓ, ℓ-$Q_{\rm hem}$, D^*-ℓ, and $D^{*\pm}$-$Q_{\rm hem}$.

[568] BUSKULIC 97D combines results from $D^{*\pm}$-ℓ/$Q_{\rm hem}$, ℓ-$Q_{\rm hem}$, and ℓ-ℓ.

[569] ABREU 96Q analysis performed using lepton, kaon, and jet-charge tags.

[570] ALEXANDER 96V combines results from $D^{*\pm}$-ℓ and $D^{*\pm}$ ℓ-$Q_{\rm hem}$.

[571] AKERS 95J combines results from charge measurement, $D^{*\pm}$ ℓ-$Q_{\rm hem}$ and ℓ-ℓ.

$x_d = \Delta m_{B^0}/\Gamma_{B^0}$

The second "OUR EVALUATION" is an average using rescaled values of the data listed below. The average and rescaling were performed by the Heavy Flavor Averaging Group (HFAG) and are described at http://www.slac.stanford.edu/xorg/hfag/. The averaging/rescaling procedure takes into account corrections between the measurements.

The first "OUR EVALUATION" (0.771 ± 0.012), also provided by the HFAG, includes χ_d measured at $\Upsilon(4S)$.

VALUE	DOCUMENT ID
0.771 ± 0.012 OUR EVALUATION	First
0.771 ± 0.012 OUR EVALUATION	Second

CP VIOLATION PARAMETERS

$\mathrm{Re}(\epsilon_{B^0})/(1+|\epsilon_{B^0}|^2)$

CP impurity in B^0_d system. It is obtained from either $a_{\ell\ell}$, the charge asymmetry in like-sign dilepton events or a_{cp}, the time-dependent asymmetry of inclusive B^0 and $\overline{B}^0$ decays.

VALUE (units 10^{-3})	DOCUMENT ID		TECN	COMMENT
0.5 ± 3.1 OUR AVERAGE				
$1.2 \pm 2.9 \pm 3.6$	[572] AUBERT	02K	BABR	$e^+e^- \to \Upsilon(4S)$
-3.2 ± 6.5	[573] BARATE	01D	ALEP	$e^+e^- \to Z$
$3.5 \pm 10.3 \pm 1.5$	[574] JAFFE	01	CLE2	$e^+e^- \to \Upsilon(4S)$
$1.2 \pm 13.8 \pm 3.2$	[575] ABBIENDI	99J	OPAL	$e^+e^- \to Z$
$2 \pm 7 \pm 3$	[576] ACKERSTAFF	97U	OPAL	$e^+e^- \to Z$
• • • We do not use the following data for averages, fits, limits, etc. • • •				
$4 \pm 18 \pm 3$	[577] BEHRENS	00B	CLE2	Repl. by JAFFE 01
< 45	[578] BARTELT	93	CLE2	$e^+e^- \to \Upsilon(4S)$

[572] AUBERT 02K uses the charge asymmetry in like-sign dilepton events.

[573] BARATE 01D measured by investigating time-dependent asymmetries in semileptonic and fully inclusive B^0_d decays.

[574] JAFFE 01 finds $a_{\ell\ell} = 0.013 \pm 0.050 \pm 0.005$ and combines with the previous BEHRENS 00B independent measurement.

[575] Data analyzed using the time-dependent asymmetry of inclusive B^0 decay. The production flavor of B^0 mesons is determined using both the jet charge and the charge of secondary vertex in the opposite hemisphere.

[576] ACKERSTAFF 97U assumes CPT and is based on measuring the charge asymmetry in a sample of B^0 decays defined by lepton and $Q_{\rm hem}$ tags. If CPT is not invoked, $\mathrm{Re}(\epsilon_B) = -0.006 \pm 0.010 \pm 0.006$ is found. The indirect CPT violation parameter is determined to $\mathrm{Im}(\delta B) = -0.020 \pm 0.016 \pm 0.006$.

[577] BEHRENS 00B uses high-momentum lepton tags and partially reconstructed $\overline{B}^0 \to D^{*+}\pi^-$, ρ^- decays to determine the flavor of the B meson.

[578] BARTELT 93 finds $a_{\ell\ell} = 0.031 \pm 0.096 \pm 0.032$ which corresponds to $|a_{\ell\ell}| < 0.18$, which yields the above $|\mathrm{Re}(\epsilon_{B^0})/(1+|\epsilon_{B^0}|^2|$.

$A_{T/CP}$

$A_{T/CP}$ is defined as

$$\frac{P(\overline{B}^0 \to B^0) - P(B^0 \to \overline{B}^0)}{P(\overline{B}^0 \to B^0) + P(B^0 \to \overline{B}^0)},$$

the CPT invariant asymmetry between the oscillation probabilities $P(\overline{B}^0 \to B^0)$ and $P(B^0 \to \overline{B}^0)$.

VALUE	DOCUMENT ID		TECN	COMMENT
0.005 ± 0.012 ± 0.014	[579] AUBERT	02K	BABR	$e^+e^- \to \Upsilon(4S)$

[579] AUBERT 02K uses the charge asymmetry in like-sign dilepton events.

A_{CP} ($B^0 \to K^+\pi^-$)

A_{CP} is defined as

$$\frac{B(\overline{B}^0 \to \overline{f}) - B(B^0 \to f)}{B(\overline{B}^0 \to \overline{f}) + B(B^0 \to f)},$$

the CP-violation charge asymmetry of exclusive B^0 and $\overline{B}^0$ decay.

VALUE	DOCUMENT ID		TECN	COMMENT
−0.09 ± 0.04 OUR AVERAGE				
$-0.102 \pm 0.050 \pm 0.016$	[580] AUBERT	02Q	BABR	$e^+e^- \to \Upsilon(4S)$
$-0.06 \pm 0.09 ^{+0.01}_{-0.02}$	[581] CASEY	02	BELL	$e^+e^- \to \Upsilon(4S)$
-0.04 ± 0.16	[582] CHEN	00	CLE2	$e^+e^- \to \Upsilon(4S)$
• • • We do not use the following data for averages, fits, limits, etc. • • •				
$-0.07 \pm 0.08 \pm 0.02$	[583] AUBERT	02D	BABR	Repl. by AUBERT 02Q
$0.044 ^{+0.186}_{-0.167} ^{+0.018}_{-0.021}$	[584] ABE	01K	BELL	Repl. by CASEY 02
$-0.19 \pm 0.10 \pm 0.03$	[585] AUBERT	01E	BABR	Repl. by AUBERT 02Q

[580] Corresponds to 90% confidence range $-0.188 < A_{CP} < -0.016$.

[581] Corresponds to 90% confidence range $-0.21 < A_{CP} < +0.09$.

[582] Corresponds to 90% confidence range $-0.30 < A_{CP} < 0.22$.

[583] Corresponds to 90% confidence range $-0.21 < A_{CP} < 0.07$.

[584] Corresponds to 90% confidence range $-0.25 < A_{CP} < 0.37$.

[585] Corresponds to 90% confidence range $-0.35 < A_{CP} < -0.03$.

$A_{CP}(B^0 \to \rho^+\pi^-)$

VALUE	DOCUMENT ID		TECN	COMMENT
$-0.18 \pm 0.08 \pm 0.03$	AUBERT	03T	BABR	$e^+e^- \to \Upsilon(4S)$

$A_{CP}(B^0 \to \rho^+K^-)$

VALUE	DOCUMENT ID		TECN	COMMENT
$0.28 \pm 0.17 \pm 0.08$	AUBERT	03T	BABR	$e^+e^- \to \Upsilon(4S)$

$A_{CP}(B^0 \to K^*(892)^+\pi^-)$

VALUE	DOCUMENT ID		TECN	COMMENT
$0.26^{+0.33}_{-0.34}{}^{+0.10}_{-0.08}$	[586] EISENSTEIN	03	CLE2	$e^+e^- \to \Upsilon(4S)$

[586] Corresponds to 90% confidence range $-0.31 < A_{CP} < 0.78$.

$A_{CP}(B^0 \to K^*(892)^0\phi)$

VALUE	DOCUMENT ID		TECN	COMMENT
0.05 ± 0.10 OUR AVERAGE				
$0.04 \pm 0.12 \pm 0.02$	AUBERT	03V	BABR	$e^+e^- \to \Upsilon(4S)$
$0.07 \pm 0.15^{+0.05}_{-0.03}$	[587] CHEN	03B	BELL	$e^+e^- \to \Upsilon(4S)$
• • • We do not use the following data for averages, fits, limits, etc. • • •				
$0.00 \pm 0.27 \pm 0.03$	[588] AUBERT	02E	BABR	Repl. by AUBERT 03V

[587] Corresponds to 90% confidence range $-0.18 < A_{CP} < 0.33$.
[588] Corresponds to 90% confidence range $-0.44 < A_{CP} < 0.44$.

$A_{CP}(B^0 \to D^*(2010)^+D^-)$

VALUE	DOCUMENT ID		TECN	COMMENT
$-0.03 \pm 0.11 \pm 0.05$	AUBERT	03J	BABR	$e^+e^- \to \Upsilon(4S)$

$C_{\pi\pi}$ $(B^0 \to \pi^+\pi^-)$

$C_{\pi\pi}$ is defined as $(1-|\lambda|^2)/(1+|\lambda|^2)$, where the quantity $\lambda = q/p\,\overline{A}_f/A_f$ is a phase convention independent observable quantity for the final state f. For details, see the note on "CP Violation in B Decay Standard Model Predictions" in the B^0 Particle Listings above.

VALUE	DOCUMENT ID		TECN	COMMENT
-0.51 ± 0.23 OUR AVERAGE	Error includes scale factor of 1.2.			
$-0.77 \pm 0.27 \pm 0.08$	[589] ABE	03G	BELL	$e^+e^- \to \Upsilon(4S)$
$-0.30 \pm 0.25 \pm 0.04$	[590] AUBERT	02Q	BABR	$e^+e^- \to \Upsilon(4S)$
• • • We do not use the following data for averages, fits, limits, etc. • • •				
$-0.94^{+0.31}_{-0.25} \pm 0.09$	[589] ABE	02M	BELL	Repl. by ABE 03G
$-0.25^{+0.45}_{-0.47} \pm 0.14$	[591] AUBERT	02D	BABR	Repl. by AUBERT 02Q

[589] Papers report $A_{\pi\pi}$ which has opposite sign to the convention used in this quantity ($C_{\pi\pi}$). We have done the conversion here.
[590] Corresponds to 90% confidence range $-0.72 < C_{\pi\pi} < 0.12$.
[591] Corresponds to 90% confidence range $-1.0 < C_{\pi\pi} < 0.47$.

$S_{\pi\pi}$ $(B^0 \to \pi^+\pi^-)$

$S_{\pi\pi} = 2\mathrm{Im}\lambda/(1+|\lambda|^2)$, see the note in the $C_{\pi\pi}$ datablock above.

VALUE	DOCUMENT ID		TECN	COMMENT
-0.5 ± 0.6 OUR AVERAGE	Error includes scale factor of 2.3.			
$-1.23 \pm 0.41^{+0.08}_{-0.07}$	ABE	03G	BELL	$e^+e^- \to \Upsilon(4S)$
$0.02 \pm 0.34 \pm 0.05$	[592] AUBERT	02Q	BABR	$e^+e^- \to \Upsilon(4S)$
• • • We do not use the following data for averages, fits, limits, etc. • • •				
$-1.21^{+0.38}_{-0.27}{}^{+0.16}_{-0.13}$	ABE	02M	BELL	Repl. by ABE 03G
$0.03^{+0.52}_{-0.56} \pm 0.11$	[593] AUBERT	02D	BABR	Repl. by AUBERT 02Q

[592] Corresponds to 90% confidence range $-0.54 < S_{\pi\pi} < 0.58$.
[593] Corresponds to 90% confidence range $-0.89 < S_{\pi\pi} < 0.85$.

$C_{\rho\pi}$ $(B^0 \to \rho^+\pi^-)$

VALUE	DOCUMENT ID		TECN	COMMENT
$0.36 \pm 0.18 \pm 0.04$	AUBERT	03T	BABR	$e^+e^- \to \Upsilon(4S)$

$S_{\rho\pi}$ $(B^0 \to \rho^+\pi^-)$

VALUE	DOCUMENT ID		TECN	COMMENT
$0.19 \pm 0.24 \pm 0.03$	AUBERT	03T	BABR	$e^+e^- \to \Upsilon(4S)$

$C_{\eta'(958)K}$ $(B^0 \to \eta'(958)K^0_S)$

VALUE	DOCUMENT ID		TECN	COMMENT
0.04 ± 0.13 OUR AVERAGE				
$0.01 \pm 0.16 \pm 0.04$	[594] ABE	03H	BELL	$e^+e^- \to \Upsilon(4S)$
$0.10 \pm 0.22 \pm 0.04$	AUBERT	03W	BABR	$e^+e^- \to \Upsilon(4S)$
• • • We do not use the following data for averages, fits, limits, etc. • • •				
$-0.26 \pm 0.22 \pm 0.03$	[594] ABE	03C	BELL	Repl. by ABE 03H
$-0.13 \pm 0.32^{+0.06}_{-0.09}$	[594] CHEN	02B	BELL	Repl. by ABE 03C

[594] BELLE Collab. quotes $A_{\eta'(958)K^0_S}$ which is equal to $-C_{\eta'(958)K^0_S}$.

$S_{\eta'(958)K}$ $(B^0 \to \eta'(958)K^0_S)$

VALUE	DOCUMENT ID		TECN	COMMENT
0.27 ± 0.21 OUR AVERAGE				
$0.43 \pm 0.27 \pm 0.05$	ABE	03H	BELL	$e^+e^- \to \Upsilon(4S)$
$0.02 \pm 0.34 \pm 0.03$	AUBERT	03W	BABR	$e^+e^- \to \Upsilon(4S)$
• • • We do not use the following data for averages, fits, limits, etc. • • •				
$0.71 \pm 0.37^{+0.05}_{-0.06}$	ABE	03C	BELL	Repl. by ABE 03H
$0.28 \pm 0.55^{+0.07}_{-0.08}$	CHEN	02B	BELL	Repl. by ABE 03C

$C_{\phi K^0_S}$ $(B^0 \to \phi K^0_S)$

VALUE	DOCUMENT ID		TECN	COMMENT
$0.15 \pm 0.29 \pm 0.07$	[595] ABE	03H	BELL	$e^+e^- \to \Upsilon(4S)$
• • • We do not use the following data for averages, fits, limits, etc. • • •				
$0.56 \pm 0.41 \pm 0.16$	[595] ABE	03C	BELL	Repl. by ABE 03H

[595] BELLE Collab. quotes $A_{\phi K^0_S}$ which is equal to $-C_{\phi K^0_S}$.

$S_{\phi K^0_S}$ $(B^0 \to \phi K^0_S)$

VALUE	DOCUMENT ID		TECN	COMMENT
$-0.96 \pm 0.50^{+0.09}_{-0.11}$	ABE	03H	BELL	$e^+e^- \to \Upsilon(4S)$
• • • We do not use the following data for averages, fits, limits, etc. • • •				
$-0.73 \pm 0.64 \pm 0.22$	ABE	03C	BELL	Repl. by ABE 03H

$C_{K^+K^-K^0_S}$ $(B^0 \to K^+K^-K^0_S)$

VALUE	DOCUMENT ID		TECN	COMMENT
$0.17 \pm 0.16 \pm 0.04$	[596] ABE	03H	BELL	$e^+e^- \to \Upsilon(4S)$
• • • We do not use the following data for averages, fits, limits, etc. • • •				
$0.40 \pm 0.33^{+0.28}_{-0.10}$	[596] ABE	03C	BELL	Repl. by ABE 03H

[596] BELLE Collab. quotes $A_{K^+K^-K^0_S}$ which is equal to $-C_{K^+K^-K^0_S}$.

$S_{K^+K^-K^0_S}$ $(B^0 \to K^+K^-K^0_S)$

VALUE	DOCUMENT ID		TECN	COMMENT
$-0.51 \pm 0.26 \pm 0.05$	ABE	03H	BELL	$e^+e^- \to \Upsilon(4S)$
• • • We do not use the following data for averages, fits, limits, etc. • • •				
$-0.49 \pm 0.43 \pm 0.11$	ABE	03C	BELL	Repl. by ABE 03H

$C_{D^*(2010)^-D^+}$ $(B^0 \to D^*(2010)^-D^+)$

VALUE	DOCUMENT ID		TECN	COMMENT
$-0.22 \pm 0.37 \pm 0.10$	AUBERT	03J	BABR	$e^+e^- \to \Upsilon(4S)$

$S_{D^*(2010)^-D^+}$ $(B^0 \to D^*(2010)^-D^+)$

VALUE	DOCUMENT ID		TECN	COMMENT
$-0.24 \pm 0.69 \pm 0.12$	AUBERT	03J	BABR	$e^+e^- \to \Upsilon(4S)$

$C_{D^*(2010)^+D^-}$ $(B^0 \to D^*(2010)^+D^-)$

VALUE	DOCUMENT ID		TECN	COMMENT
$-0.47 \pm 0.40 \pm 0.12$	AUBERT	03J	BABR	$e^+e^- \to \Upsilon(4S)$

$S_{D^*(2010)^+D^-}$ $(B^0 \to D^*(2010)^+D^-)$

VALUE	DOCUMENT ID		TECN	COMMENT
$-0.82 \pm 0.75 \pm 0.14$	AUBERT	03J	BABR	$e^+e^- \to \Upsilon(4S)$

$C_{J/\psi(1S)\pi^0}$ $(B^0 \to J/\psi(1S)\pi^0)$

VALUE	DOCUMENT ID		TECN	COMMENT
$0.38 \pm 0.41 \pm 0.09$	AUBERT	03N	BABR	$e^+e^- \to \Upsilon(4S)$

$S_{J/\psi(1S)\pi^0}$ $(B^0 \to J/\psi(1S)\pi^0)$

VALUE	DOCUMENT ID		TECN	COMMENT
$0.05 \pm 0.49 \pm 0.16$	AUBERT	03N	BABR	$e^+e^- \to \Upsilon(4S)$

$\Delta C_{\rho\pi}$ $(B^0 \to \rho^+\pi^-)$

$\Delta C_{\rho\pi}$ describes the asymmetry between the rates $\Gamma(B^0 \to \rho^+\pi^-) + \Gamma(\overline{B}{}^0 \rho^-\pi^+)$ and $\Gamma(B^0 \to \rho^-\pi^+) + \Gamma(\overline{B}{}^0 \to \rho^+\pi^-)$.

VALUE	DOCUMENT ID		TECN	COMMENT
$0.28^{+0.18}_{-0.19} \pm 0.04$	AUBERT	03T	BABR	$e^+e^- \to \Upsilon(4S)$

$\Delta S_{\rho\pi}$ $(B^0 \to \rho^+\pi^-)$

$\Delta S_{\rho\pi}$ is related to the strong phase difference between the amplitudes contributing to $B^0 \to \rho^+\pi^-$.

VALUE	DOCUMENT ID		TECN	COMMENT
$0.15 \pm 0.25 \pm 0.03$	AUBERT	03T	BABR	$e^+e^- \to \Upsilon(4S)$

$|\lambda|$ ($B^0 \to c\overline{c}K^0$)

The same λ quantity, defined in the $C_{\pi\pi}$ datablock above.

"OUR EVALUATION" is an average using rescaled values of the data listed below. The average and rescaling were performed by the Heavy Flavor Averaging Group (HFAG) and are described at http://www.slac.stanford.edu/xorg/hfag/. The averaging/rescaling procedure takes into account corrections between the measurements.

VALUE	DOCUMENT ID		TECN	COMMENT
0.949±0.045 OUR EVALUATION				
0.95 ±0.04 OUR AVERAGE				
0.950±0.049±0.025	[597] ABE	02Z	BELL	$e^+e^- \to \Upsilon(4S)$
0.948±0.051±0.030	[598] AUBERT	02P	BABR	$e^+e^- \to \Upsilon(4S)$

[597] Measured with both $\eta_f = \pm 1$ samples.

[598] Measured with the high purity of $\eta_f = -1$ samples.

$|\lambda|$ ($B^0 \to D^{*+}D^{*-}$)

The same λ quantity, defined in the $C_{\pi\pi}$ datablock above, but in C-even final state.

VALUE	DOCUMENT ID		TECN	COMMENT
0.75±0.19±0.02	AUBERT	03Q	BABR	$e^+e^- \to \Upsilon(4S)$

Im(λ) ($B^0 \to D^{*+}D^{*-}$)

The same λ quantity, defined in the $C_{\pi\pi}$ datablock above, but in C-even final state.

VALUE	DOCUMENT ID		TECN	COMMENT
0.05±0.29±0.10	AUBERT	03Q	BABR	$e^+e^- \to \Upsilon(4S)$

sin(2β)

For a discussion of CP violation, see the note on "CP Violation in B Decay Standard Model Predictions" in the B^0 Particle Listings above. sin(2β) is a measure of the CP-violating amplitude in the $B^0_d \to J/\psi(1S)K^0_S$.

"OUR EVALUATION" is an average using rescaled values of the data listed below. The average and rescaling were performed by the Heavy Flavor Averaging Group (HFAG) and are described at http://www.slac.stanford.edu/xorg/hfag/. The averaging/rescaling procedure takes into account corrections between the measurements.

VALUE	DOCUMENT ID		TECN	COMMENT
0.731±0.056 OUR EVALUATION				
0.73 ±0.05 OUR AVERAGE				
0.719±0.074±0.035	[599] ABE	02Z	BELL	$e^+e^- \to \Upsilon(4S)$
0.741±0.067±0.034	[600] AUBERT	02P	BABR	$e^+e^- \to \Upsilon(4S)$
$0.79\ ^{+0.41}_{-0.44}$	[601] AFFOLDER	00C	CDF	$p\overline{p}$ at 1.8 TeV
$0.84\ ^{+0.82}_{-1.04}$ ±0.16	[602] BARATE	00Q	ALEP	$e^+e^- \to Z$
$3.2\ ^{+1.8}_{-2.0}$ ±0.5	[603] ACKERSTAFF	98Z	OPAL	$e^+e^- \to Z$
• • • We do not use the following data for averages, fits, limits, etc. • • •				
0.99 ±0.14 ±0.06	[604] ABE	02U	BELL	$e^+e^- \to \Upsilon(4S)$
0.59 ±0.14 ±0.05	[605] AUBERT	02N	BABR	$e^+e^- \to \Upsilon(4S)$
$0.58\ ^{+0.32}_{-0.34}\ ^{+0.09}_{-0.10}$	ABASHIAN	01	BELL	Repl. by ABE 01G
0.99 ±0.14 ±0.06	[606] ABE	01G	BELL	Repl by ABE 02Z
0.34 ±0.20 ±0.05	AUBERT	01	BABR	Repl. by AUBERT 01B
0.59 ±0.14 ±0.05	[606] AUBERT	01B	BABR	Repl. by AUBERT 02P
1.8 ±1.1 ±0.3	[607] ABE	98U	CDF	Repl. by AFFOLDER 00C

[599] ABE 02Z result is based on 85×10^6 $B\overline{B}$ pairs.

[600] AUBERT 02P result is based on 88×10^6 $B\overline{B}$ pairs.

[601] AFFOLDER 00C uses about 400 $B^0 \to J/\psi(1S)K^0_S$ events. The production flavor of B^0 was determined using three tagging algorithms: a same-side tag, a jet-charge tag, and a soft-lepton tag.

[602] BARATE 00Q uses 23 candidates for $B^0 \to J/\psi(1S)K^0_S$ decays. A combination of jet-charge, vertex-charge, and same-side tagging techniques were used to determine the B^0 production flavor.

[603] ACKERSTAFF 98Z uses 24 candidates for $B^0_d \to J/\psi(1S)K^0_S$ decay. A combination of jet-charge and vertex-charge techniques were used to tag the B^0_d production flavor.

[604] ABE 02U result is based on the same analysis and data sample reported in ABE 01G.

[605] AUBERT 02N result based on the same analysis and data sample reported in AUBERT 01B.

[606] First observation of CP violation in B^0 meson system.

[607] ABE 98U uses 198 ± 17 $B^0_d \to J/\psi(1S)K^0$ events. The production flavor of B^0 was determined using the same side tagging technique.

$B^0 \to D^{*-}\ell^+\nu_\ell$ FORM FACTORS

R_1 (form factor ratio $\sim V/A_1$)

VALUE	DOCUMENT ID		TECN	COMMENT
1.18±0.30±0.12	DUBOSCQ	96	CLE2	$e^+e^- \to \Upsilon(4S)$

R_2 (form factor ratio $\sim A_2/A_1$)

VALUE	DOCUMENT ID		TECN	COMMENT
0.71±0.22±0.07	DUBOSCQ	96	CLE2	$e^+e^- \to \Upsilon(4S)$

$\rho^2_{A_1}$ (form factor slope)

VALUE	DOCUMENT ID		TECN	COMMENT
0.91±0.15±0.06	DUBOSCQ	96	CLE2	$e^+e^- \to \Upsilon(4S)$

B^0 REFERENCES

AUBERT	04A	PR D69 011102	B. Aubert *et al.* (BABAR Collab.)
AUBERT	04B	PR D69 032004	B. Aubert *et al.* (BABAR Collab.)
AUBERT	04C	PRL 92 111801	B. Aubert *et al.* (BaBar Collab.)
DRUTSKOY	04	PRL 92 051801	A. Drutskoy *et al.* (BELLE Collab.)
GARMASH	04	PR D69 012001	A. Garmash *et al.* (BELLE Collab.)
ABDALLAH	03B	EPJ C28 155	J. Abdallah *et al.* (DELPHI Collab.)
ABE	03B	PR D67 032003	K. Abe *et al.* (BELLE Collab.)
ABE	03C	PR D67 031102R	K. Abe *et al.* (BELLE Collab.)
ABE	03G	PR D68 012001	K. Abe *et al.* (BELLE Collab.)
ABE	03H	PRL 91 261602	K. Abe *et al.* (BELLE Collab.)
ADAM	03	PR D67 032001	N.E. Adam *et al.* (CLEO Collab.)
ATHAR	03	PR D68 072003	S.B. Athar *et al.* (CLEO Collab.)
AUBERT	03B	PRL 90 091801	B. Aubert *et al.* (BaBar Collab.)
AUBERT	03C	PR D67 072002	B. Aubert *et al.* (BaBar Collab.)
AUBERT	03D	PRL 90 181803	B. Aubert *et al.* (BaBar Collab.)
AUBERT	03E	PRL 90 181801	B. Aubert *et al.* (BaBar Collab.)
AUBERT	03H	PR D67 091101R	B. Aubert *et al.* (BaBar Collab.)
AUBERT	03I	PR D67 092003	B. Aubert *et al.* (BaBar Collab.)
AUBERT	03J	PRL 90 221801	B. Aubert *et al.* (BaBar Collab.)
AUBERT	03K	PRL 90 231801	B. Aubert *et al.* (BaBar Collab.)
AUBERT	03L	PRL 91 021801	B. Aubert *et al.* (BaBar Collab.)
AUBERT	03N	PRL 91 061802	B. Aubert *et al.* (BaBar Collab.)
AUBERT	03O	PRL 91 071801	B. Aubert *et al.* (BaBar Collab.)
AUBERT	03Q	PRL 91 131801	B. Aubert *et al.* (BaBar Collab.)
AUBERT	03S	PRL 91 241801	B. Aubert *et al.* (BaBar Collab.)
AUBERT	03T	PRL 91 201802	B. Aubert *et al.* (BaBar Collab.)
AUBERT	03V	PRL 91 171802	B. Aubert *et al.* (BaBar Collab.)
AUBERT	03W	PRL 91 161801	B. Aubert *et al.* (BaBar Collab.)
AUBERT	03X	PR D68 092001	B. Aubert *et al.* (BaBar Collab.)
BORNHEIM	03	PR D68 052002	A. Bornheim *et al.* (CLEO Collab.)
CHANG	03	PR D68 111101	M.-C. Chang *et al.* (BELLE Collab.)
CHEN	03B	PRL 91 201801	K.-F. Chen *et al.* (BELLE Collab.)
CSORNA	03	PR D67 112002	S.E. Csorna *et al.* (CLEO Collab.)
EISENSTEIN	03	PR D68 017101	B.I. Eisenstein *et al.* (CLEO Collab.)
FANG	03	PRL 90 071801	F. Fang *et al.* (BELLE Collab.)
GABYSHEV	03	PRL 90 121802	N. Gabyshev *et al.* (BELLE Collab.)
HASTINGS	03	PR D67 052004	N.C. Hastings *et al.* (BELLE Collab.)
ISHIKAWA	03	PRL 91 261601	A. Ishikawa *et al.* (BELLE Collab.)
KROKOVNY	03	PRL 90 141802	P. Krokovny *et al.* (BELLE Collab.)
KROKOVNY	03B	PRL 91 262002	P. Krokovny *et al.* (BELLE Collab.)
LEE	03	PRL 91 261801	S.H. Lee *et al.* (BELLE Collab.)
SATPATHY	03	PL B553 159	A. Satpathy *et al.* (BELLE Collab.)
WANG	03	PRL 90 201802	M.-Z. Wang *et al.* (BELLE Collab.)
ZHENG	03	PR D67 092004	Y. Zheng *et al.* (BELLE Collab.)
ABE	02	PRL 88 021801	K. Abe *et al.* (BELLE Collab.)
ABE	02E	PL B526 258	K. Abe *et al.* (BELLE Collab.)
ABE	02F	PL B526 247	K. Abe *et al.* (BELLE Collab.)
ABE	02H	PRL 88 171801	K. Abe *et al.* (BELLE Collab.)
ABE	02J	PRL 88 052002	K. Abe *et al.* (BELLE Collab.)
ABE	02K	PRL 88 181803	K. Abe *et al.* (BELLE Collab.)
ABE	02M	PRL 89 071801	K. Abe *et al.* (BELLE Collab.)
ABE	02N	PL B538 11	K. Abe *et al.* (BELLE Collab.)
ABE	02O	PR D65 091103R	K. Abe *et al.* (BELLE Collab.)
ABE	02Q	PRL 89 122001	K. Abe *et al.* (BELLE Collab.)
ABE	02U	PR D66 032007	K. Abe *et al.* (BELLE Collab.)
ABE	02W	PRL 89 151802	K. Abe *et al.* (BELLE Collab.)
ABE	02Z	PR D66 071102R	K. Abe *et al.* (BELLE Collab.)
ACOSTA	02C	PR D65 092009	D. Acosta *et al.* (CDF Collab.)
ACOSTA	02G	PR D66 112002	D. Acosta *et al.* (CDF Collab.)
AFFOLDER	02B	PRL 88 071801	T. Affolder *et al.* (CDF Collab.)
AHMED	02B	PR D66 031101R	S. Ahmed *et al.* (CLEO Collab.)
ASNER	02	PR D65 031103R	D.M. Asner *et al.* (CLEO Collab.)
AUBERT	02	PR D65 032001	B. Aubert *et al.* (BaBar Collab.)
AUBERT	02C	PRL 88 101805	B. Aubert *et al.* (BaBar Collab.)
AUBERT	02D	PR D65 051502R	B. Aubert *et al.* (BaBar Collab.)
AUBERT	02E	PR D65 051101R	B. Aubert *et al.* (BaBar Collab.)
AUBERT	02H	PRL 89 011802	B. Aubert *et al.* (BaBar Collab.)
Also	02O	PRL 89 169903 (erratum)	B. Aubert *et al.* (BaBar Collab.)
AUBERT	02I	PRL 88 221802	B. Aubert *et al.* (BaBar Collab.)
AUBERT	02J	PRL 88 221803	B. Aubert *et al.* (BaBar Collab.)
AUBERT	02K	PRL 88 231801	B. Aubert *et al.* (BaBar Collab.)
AUBERT	02L	PRL 88 241801	B. Aubert *et al.* (BaBar Collab.)
AUBERT	02M	PRL 89 061801	B. Aubert *et al.* (BaBar Collab.)
AUBERT	02N	PR D66 032003	B. Aubert *et al.* (BaBar Collab.)
AUBERT	02P	PRL 89 201802	B. Aubert *et al.* (BaBar Collab.)
AUBERT	02Q	PRL 89 281802	B. Aubert *et al.* (BaBar Collab.)
BRIERE	02	PRL 89 081803	R. Briere *et al.* (CLEO Collab.)
CASEY	02	PR D66 092002	B.C.K. Casey *et al.* (BELLE Collab.)
CHEN	02B	PL B546 196	K.-F. Chen *et al.* (BELLE Collab.)
COAN	02	PRL 88 062001	T.E. Coan *et al.* (CLEO Collab.)
Also	02B	PRL 88 069902 (erratum)	T.E. Coan *et al.* (CLEO Collab.)
DRUTSKOY	02	PL B542 171	A. Drutskoy *et al.* (BELLE Collab.)
DYTMAN	02	PR D66 091101R	S.A. Dytman *et al.* (CLEO Collab.)
ECKHART	02	PRL 89 251801	E. Eckhart *et al.* (CLEO Collab.)
EDWARDS	02	PR D65 012002	K.W. Edwards *et al.* (CLEO Collab.)
GABYSHEV	02	PR D66 091102R	N. Gabyshev *et al.* (BELLE Collab.)
GODANG	02	PRL 88 021802	R. Godang *et al.* (CLEO Collab.)
GORDON	02	PL B542 183	A. Gordon *et al.* (BELLE Collab.)
HARA	02	PRL 89 251803	K. Hara *et al.* (BELLE Collab.)
KROKOVNY	02	PRL 89 231804	P. Krokovny *et al.* (BELLE Collab.)
MAHAPATRA	02	PRL 88 101803	R. Mahapatra *et al.* (CLEO Collab.)
NISHIDA	02	PRL 89 231801	S. Nishida *et al.* (BELLE Collab.)
TOMURA	02	PL B542 207	T. Tomura *et al.* (BELLE Collab.)
ABASHIAN	01	PRL 86 2509	A. Abashian *et al.* (BELLE Collab.)
ABE	01D	PRL 86 3228	K. Abe *et al.* (BELLE Collab.)
ABE	01G	PRL 87 091802	K. Abe *et al.* (BELLE Collab.)
ABE	01H	PRL 87 101801	K. Abe *et al.* (BELLE Collab.)
ABE	01I	PRL 87 111801	K. Abe *et al.* (BELLE Collab.)
ABE	01K	PR D64 071101	K. Abe *et al.* (BELLE Collab.)
ABE	01L	PRL 87 161601	K. Abe *et al.* (BELLE Collab.)
ABE	01M	PL B517 309	K. Abe *et al.* (BELLE Collab.)
ABREU	01H	PL B510 55	P. Abreu *et al.* (DELPHI Collab.)
ALEXANDER	01B	PR D64 092001	J.P. Alexander *et al.* (CLEO Collab.)
AMMAR	01B	PRL 87 271801	R. Ammar *et al.* (CLEO Collab.)
ANDERSON	01	PRL 86 2732	S. Anderson *et al.* (CLEO Collab.)
ANDERSON	01B	PRL 87 181803	S. Anderson *et al.* (CLEO Collab.)
AUBERT	01	PRL 86 2515	B. Aubert *et al.* (BaBar Collab.)
AUBERT	01B	PRL 87 091801	B. Aubert *et al.* (BaBar Collab.)
AUBERT	01D	PRL 87 151801	B. Aubert *et al.* (BaBar Collab.)
AUBERT	01E	PRL 87 151802	B. Aubert *et al.* (BaBar Collab.)
AUBERT	01F	PRL 87 201803	B. Aubert *et al.* (BaBar Collab.)
AUBERT	01G	PRL 87 221802	B. Aubert *et al.* (BaBar Collab.)
AUBERT	01H	PRL 87 241801	B. Aubert *et al.* (BaBar Collab.)
AUBERT	01I	PRL 87 241803	B. Aubert *et al.* (BaBar Collab.)
BARATE	01D	EPJ C20 431	R. Barate *et al.* (ALEPH Collab.)
BRIERE	01	PRL 86 3718	R.A. Biere *et al.* (CLEO Collab.)
EDWARDS	01	PRL 86 30	K.W. Edwards *et al.* (CLEO Collab.)
JAFFE	01	PRL 86 5000	D. Jaffe *et al.* (CLEO Collab.)
RICHICHI	01	PR D63 031103R	S.J. Richichi *et al.* (CLEO Collab.)
ABBIENDI	00Q	PL B482 15	G. Abbiendi *et al.* (OPAL Collab.)

Meson Particle Listings

B^0, $B^\pm/B^0$ ADMIXTURE

ABBIENDI,G 00B PL B493 266 G. Abbiendi *et al.* (OPAL Collab.)
ABE 00C PR D62 071101R K. Abe *et al.* (SLD Collab.)
AFFOLDER 00C PR D61 072005 T. Affolder *et al.* (CDF Collab.)
AFFOLDER 00N PRL 85 4668 T. Affolder *et al.* (CDF Collab.)
AHMED 00B PR D62 112003 S. Ahmed *et al.* (CLEO Collab.)
ANASTASSOV 00 PRL 84 1393 A. Anastassov *et al.* (CLEO Collab.)
ARTUSO 00 PRL 84 4292 M. Artuso *et al.* (CLEO Collab.)
AVERY 00 PR D62 051101 P. Avery *et al.* (CLEO Collab.)
BARATE 00Q PL B492 259 R. Barate *et al.* (ALEPH Collab.)
BARATE 00R PL B492 275 R. Barate *et al.* (ALEPH Collab.)
BEHRENS 00 PR D61 052001 B.H. Behrens *et al.* (CLEO Collab.)
BEHRENS 00B PL B490 36 B.H. Behrens *et al.* (CLEO Collab.)
BERGFELD 00B PR D62 091102R T. Bergfeld *et al.* (CLEO Collab.)
CHEN 00 PRL 85 525 S. Chen *et al.* (CLEO Collab.)
COAN 00 PRL 84 5283 T.E. Coan *et al.* (CLEO Collab.)
CRONIN-HEN... 00 PRL 85 515 D. Cronin-Hennessy *et al.* (CLEO Collab.)
CSORNA 00 PR D61 111101 S.E. Csorna *et al.* (CLEO Collab.)
JESSOP 00 PRL 85 2881 C.P. Jessop *et al.* (CLEO Collab.)
LIPELES 00 PR D62 032005 E. Lipeles *et al.* (CLEO Collab.)
RICHICHI 00 PRL 85 520 S.J. Richichi *et al.* (CLEO Collab.)
ABBIENDI 99J EPJ C12 609 G. Abbiendi *et al.* (OPAL Collab.)
ABE 99K PR D60 051101 F. Abe *et al.* (CDF Collab.)
ABE 99Q PR D60 072003 F. Abe *et al.* (CDF Collab.)
AFFOLDER 99B PRL 83 3378 T. Affolder *et al.* (CDF Collab.)
AFFOLDER 99C PR D60 112004 T. Affolder *et al.* (CDF Collab.)
ARTUSO 99 PRL 82 3020 M. Artuso *et al.* (CLEO Collab.)
BARTELT 99 PRL 82 3746 J. Bartelt *et al.* (CLEO Collab.)
COAN 99 PR D59 111101 T.E. Coan *et al.* (CLEO Collab.)
ABBOTT 98B PL B423 419 B. Abbott *et al.* (D0 Collab.)
ABE 98 PR D57 R3811 F. Abe *et al.* (CDF Collab.)
ABE 98B PR D57 5382 F. Abe *et al.* (CDF Collab.)
ABE 98C PRL 80 2057 F. Abe *et al.* (CDF Collab.)
Also 99C PR D59 032001 F. Abe *et al.* (CDF Collab.)
ABE 98O PR D58 072001 F. Abe *et al.* (CDF Collab.)
ABE 98Q PR D58 092002 F. Abe *et al.* (CDF Collab.)
ABE 98U PRL 81 5513 F. Abe *et al.* (CDF Collab.)
ABE 98V PRL 81 5742 F. Abe *et al.* (CDF Collab.)
ACCIARRI 98D EPJ C5 195 M. Acciarri *et al.* (L3 Collab.)
ACCIARRI 98S PL B438 417 M. Acciarri *et al.* (L3 Collab.)
ACKERSTAFF 98Z EPJ C5 379 K. Ackerstaff *et al.* (OPAL Collab.)
BARATE 98Q EPJ C4 387 R. Barate *et al.* (ALEPH Collab.)
BEHRENS 98 PRL 80 3710 B.H. Behrens *et al.* (CLEO Collab.)
BERGFELD 98 PRL 81 272 T. Bergfeld *et al.* (CLEO Collab.)
BRANDENB... 98 PRL 80 2762 G. Brandenburg *et al.* (CLEO Collab.)
GODANG 98 PRL 80 3456 R. Godang *et al.* (CLEO Collab.)
NEMATI 98 PR D57 5363 B. Nemati *et al.* (CLEO Collab.)
ABE 97J PRL 79 590 K. Abe *et al.* (SLD Collab.)
ABREU 97F ZPHY C74 19 P. Abreu *et al.* (DELPHI Collab.)
Also 97K ZPHY C75 579 erratum P. Abreu *et al.* (DELPHI Collab.)
ABREU 97N ZPHY C76 579 P. Abreu *et al.* (DELPHI Collab.)
ACCIARRI 97B PL B391 474 M. Acciarri *et al.* (L3 Collab.)
ACCIARRI 97C PL B391 481 M. Acciarri *et al.* (L3 Collab.)
ACKERSTAFF 97G PL B395 128 K. Ackerstaff *et al.* (OPAL Collab.)
ACKERSTAFF 97U ZPHY C76 401 K. Ackerstaff *et al.* (OPAL Collab.)
ACKERSTAFF 97V ZPHY C76 417 K. Ackerstaff *et al.* (OPAL Collab.)
ARTUSO 97 PL B399 321 M. Artuso *et al.* (CLEO Collab.)
ASNER 97 PRL 79 799 D. Asner *et al.* (CLEO Collab.)
ATHANAS 97 PRL 79 2208 M. Athanas *et al.* (CLEO Collab.)
BUSKULIC 97 PL B395 373 D. Buskulic *et al.* (ALEPH Collab.)
BUSKULIC 97D ZPHY C75 397 D. Buskulic *et al.* (ALEPH Collab.)
FU 97 PRL 79 3125 X. Fu *et al.* (CLEO Collab.)
JESSOP 97 PRL 79 4533 C.P. Jessop *et al.* (CLEO Collab.)
ABE 96B PR D53 3496 F. Abe *et al.* (CDF Collab.)
ABE 96C PRL 76 4462 F. Abe *et al.* (CDF Collab.)
ABE 96H PRL 76 2015 F. Abe *et al.* (CDF Collab.)
ABE 96L PRL 76 4675 F. Abe *et al.* (CDF Collab.)
ABE 96Q PR D54 6596 F. Abe *et al.* (CDF Collab.)
ABREU 96P ZPHY C71 539 P. Abreu *et al.* (DELPHI Collab.)
ABREU 96Q ZPHY C72 17 P. Abreu *et al.* (DELPHI Collab.)
ACCIARRI 96E PL B383 487 M. Acciarri *et al.* (L3 Collab.)
ADAM 96D ZPHY C72 207 W. Adam *et al.* (DELPHI Collab.)
ALBRECHT 96D PL B374 256 H. Albrecht *et al.* (ARGUS Collab.)
ALEXANDER 96T PRL 77 5000 J.P. Alexander *et al.* (CLEO Collab.)
ALEXANDER 96V ZPHY C72 377 G. Alexander *et al.* (OPAL Collab.)
ASNER 96 PR D53 1039 D.M. Asner *et al.* (CLEO Collab.)
BARISH 96B PRL 76 1570 B.C. Barish *et al.* (CLEO Collab.)
BISHAI 96 PL B369 186 M. Bishai *et al.* (CLEO Collab.)
BUSKULIC 96J ZPHY C71 31 D. Buskulic *et al.* (ALEPH Collab.)
BUSKULIC 96V PL B384 471 D. Buskulic *et al.* (ALEPH Collab.)
DUBOSCQ 96 PRL 76 3898 J.E. Duboscq *et al.* (CLEO Collab.)
GIBAUT 96 PR D53 4734 D. Gibaut *et al.* (CLEO Collab.)
PDG 96 PR D54 1 R.M. Barnett *et al.*
ABE 95Z PRL 75 3068 F. Abe *et al.* (CDF Collab.)
ABREU 95N PL B357 255 P. Abreu *et al.* (DELPHI Collab.)
ABREU 95Q ZPHY C68 13 P. Abreu *et al.* (DELPHI Collab.)
ACCIARRI 95H PL B363 127 M. Acciarri *et al.* (L3 Collab.)
ACCIARRI 95I PL B363 137 M. Acciarri *et al.* (L3 Collab.)
ADAM 95 ZPHY C68 363 W. Adam *et al.* (DELPHI Collab.)
AKERS 95J ZPHY C66 555 R. Akers *et al.* (OPAL Collab.)
AKERS 95T ZPHY C67 379 R. Akers *et al.* (OPAL Collab.)
ALEXANDER 95 PL B341 435 J. Alexander *et al.* (CLEO Collab.)
Also 95C PL B347 469 (erratum) J. Alexander *et al.* (CLEO Collab.)
BARISH 95 PR D51 1014 B.C. Barish *et al.* (CLEO Collab.)
BUSKULIC 95N PL B359 236 D. Buskulic *et al.* (ALEPH Collab.)
ABE 94D PRL 72 3456 F. Abe *et al.* (CDF Collab.)
ABREU 94M PL B338 409 P. Abreu *et al.* (DELPHI Collab.)
AKERS 94C PL B327 411 R. Akers *et al.* (OPAL Collab.)
AKERS 94H PL B336 585 R. Akers *et al.* (OPAL Collab.)
AKERS 94J PL B337 196 R. Akers *et al.* (OPAL Collab.)
AKERS 94L PL B337 393 R. Akers *et al.* (OPAL Collab.)
ALAM 94 PR D50 43 M.S. Alam *et al.* (CLEO Collab.)
ALBRECHT 94 PL B324 249 H. Albrecht *et al.* (ARGUS Collab.)
ALBRECHT 94G PL B340 217 H. Albrecht *et al.* (ARGUS Collab.)
AMMAR 94 PR D49 5701 R. Ammar *et al.* (CLEO Collab.)
ATHANAS 94 PRL 73 3503 M. Athanas *et al.* (CLEO Collab.)
Also 95 PRL 74 3090 (erratum) M. Athanas *et al.* (CLEO Collab.)
BUSKULIC 94B PL B322 441 D. Buskulic *et al.* (ALEPH Collab.)
PDG 94 PR D50 1173 L. Montanet *et al.* (CERN, LBL, BOST+)
PROCARIO 94 PRL 73 1472 M. Procario *et al.* (CLEO Collab.)
STONE 94 HEPSY 93-11 S. Stone
Published in B Decays, 2nd Edition, World Scientific, Singapore
ABREU 93D ZPHY C57 181 P. Abreu *et al.* (DELPHI Collab.)
ABREU 93G PL B312 253 P. Abreu *et al.* (DELPHI Collab.)
ACTON 93C PL B307 247 P.D. Acton *et al.* (OPAL Collab.)
ALBRECHT 93 ZPHY C57 533 H. Albrecht *et al.* (ARGUS Collab.)
ALBRECHT 93E ZPHY C60 11 H. Albrecht *et al.* (ARGUS Collab.)
ALEXANDER 93B PL B319 365 J. Alexander *et al.* (CLEO Collab.)
AMMAR 93 PRL 71 674 R. Ammar *et al.* (CLEO Collab.)
BARTELT 93 PRL 71 1680 J.E. Bartelt *et al.* (CLEO Collab.)
BATTLE 93 PRL 71 3922 M. Battle *et al.* (CLEO Collab.)
BEAN 93B PRL 70 2681 A. Bean *et al.* (CLEO Collab.)
BUSKULIC 93D PL B307 194 D. Buskulic *et al.* (ALEPH Collab.)
Also 94H PL B325 537 (errata) D. Buskulic *et al.* (ALEPH Collab.)
BUSKULIC 93K PL B313 498 D. Buskulic *et al.* (ALEPH Collab.)
SANGHERA 93 PR D47 791 S. Sanghera *et al.* (CLEO Collab.)
ALBRECHT 92C PL B275 195 H. Albrecht *et al.* (ARGUS Collab.)
ALBRECHT 92G ZPHY C54 1 H. Albrecht *et al.* (ARGUS Collab.)
ALBRECHT 92L ZPHY C55 357 H. Albrecht *et al.* (ARGUS Collab.)
BORTOLETTO 92 PR D45 21 D. Bortoletto *et al.* (CLEO Collab.)
HENDERSON 92 PR D45 2212 S. Henderson *et al.* (CLEO Collab.)
KRAMER 92 PL B279 181 G. Kramer, W.F. Palmer (HAMB, OSU)
ALBAJAR 91C PL B262 163 C. Albajar *et al.* (UA1 Collab.)
ALBAJAR 91E PL B273 540 C. Albajar *et al.* (UA1 Collab.)
ALBRECHT 91B PL B254 288 H. Albrecht *et al.* (ARGUS Collab.)
ALBRECHT 91C PL B255 297 H. Albrecht *et al.* (ARGUS Collab.)
ALBRECHT 91E PL B262 148 H. Albrecht *et al.* (ARGUS Collab.)
BERKELMAN 91 ARNPS 41 1 K. Berkelman, S. Stone (CORN, SYRA)
"Decays of B Mesons"
FULTON 91 PR D43 651 R. Fulton *et al.* (CLEO Collab.)
ALBRECHT 90B PL B241 278 H. Albrecht *et al.* (ARGUS Collab.)
ALBRECHT 90J ZPHY C48 543 H. Albrecht *et al.* (ARGUS Collab.)
ANTREASYAN 90B ZPHY C48 553 D. Antreasyan *et al.* (Crystal Ball Collab.)
BORTOLETTO 90 PRL 64 2117 D. Bortoletto *et al.* (CLEO Collab.)
ELSEN 90 ZPHY C46 349 E. Elsen *et al.* (JADE Collab.)
ROSNER 90 PR D42 3732 J.L. Rosner
WAGNER 90 PRL 64 1095 S.R. Wagner *et al.* (Mark II Collab.)
ALBRECHT 89C PL B219 121 H. Albrecht *et al.* (ARGUS Collab.)
ALBRECHT 89G PL B229 304 H. Albrecht *et al.* (ARGUS Collab.)
ALBRECHT 89J PL B229 175 H. Albrecht *et al.* (ARGUS Collab.)
ALBRECHT 89L PL B232 554 H. Albrecht *et al.* (ARGUS Collab.)
ARTUSO 89 PRL 62 2233 M. Artuso *et al.* (CLEO Collab.)
AVERILL 89 PR D39 123 D.A. Averill *et al.* (HRS Collab.)
AVERY 89B PL B223 470 P. Avery *et al.* (CLEO Collab.)
BEBEK 89 PRL 62 8 C. Bebek *et al.* (CLEO Collab.)
BORTOLETTO 89 PRL 62 2436 D. Bortoletto *et al.* (CLEO Collab.)
BORTOLETTO 89B PRL 63 1667 D. Bortoletto *et al.* (CLEO Collab.)
ALBRECHT 88F PL B209 119 H. Albrecht *et al.* (ARGUS Collab.)
ALBRECHT 88K PL B215 424 H. Albrecht *et al.* (ARGUS Collab.)
ALBRECHT 87C PL B185 218 H. Albrecht *et al.* (ARGUS Collab.)
ALBRECHT 87D PL B199 451 H. Albrecht *et al.* (ARGUS Collab.)
ALBRECHT 87I PL B192 245 H. Albrecht *et al.* (ARGUS Collab.)
ALBRECHT 87J PL B197 452 H. Albrecht *et al.* (ARGUS Collab.)
AVERY 87 PL B183 429 P. Avery *et al.* (CLEO Collab.)
BEAN 87B PRL 58 183 A. Bean *et al.* (CLEO Collab.)
BEBEK 87 PR D36 1289 C. Bebek *et al.* (CLEO Collab.)
ALAM 86 PR D34 3279 M.S. Alam *et al.* (CLEO Collab.)
ALBRECHT 86F PL B182 95 H. Albrecht *et al.* (ARGUS Collab.)
PDG 86 PL 170B M. Aguilar-Benitez *et al.* (CERN, CIT+)
CHEN 85 PR D31 2386 A. Chen *et al.* (CLEO Collab.)
HAAS 85 PRL 55 1248 J. Haas *et al.* (CLEO Collab.)
AVERY 84 PRL 53 1309 P. Avery *et al.* (CLEO Collab.)
GILES 84 PR D30 2279 R. Giles *et al.* (CLEO Collab.)
BEHRENDS 83 PRL 50 881 S. Behrends *et al.* (CLEO Collab.)

$B^\pm/B^0$ ADMIXTURE

B DECAY MODES

The branching fraction measurements are for an admixture of B mesons at the $\Upsilon(4S)$. The values quoted assume that $B(\Upsilon(4S) \to B\overline{B}) = 100\%$.

For inclusive branching fractions, *e.g.*, $B \to D^\pm$ anything, the values usually are multiplicities, not branching fractions. They can be greater than one.

$\overline{B}$ modes are charge conjugates of the modes below. Reactions indicate the weak decay vertex and do not include mixing.

	Mode		Fraction (Γ_i/Γ)			Scale factor/ Confidence level
	Semileptonic and leptonic modes					
Γ_1	$B \to e^+\nu_e$ anything	[a]	(10.73	± 0.28)	%	
Γ_2	$B \to \overline{p}e^+\nu_e$ anything		< 5.9			$\times 10^{-4}$ CL=90%
Γ_3	$B \to \mu^+\nu_\mu$ anything	[a]				
Γ_4	$B \to \ell^+\nu_\ell$ anything	[a,b]	(10.73	± 0.28)	%	
Γ_5	$B \to D^-\ell^+\nu_\ell$ anything	[b]	(2.8	± 0.9)	%	
Γ_6	$B \to \overline{D}^0\ell^+\nu_\ell$ anything	[b]	(7.2	± 1.5)	%	
Γ_7	$B \to D^{*-}\ell^+\nu_\ell$ anything					
Γ_8	$B \to D^{*0}\ell^+\nu_\ell$ anything					
Γ_9	$B \to \overline{D}^{**}\ell^+\nu_\ell$	[b,c]	(2.7	± 0.7)	%	
Γ_{10}	$B \to \overline{D}_1(2420)\ell^+\nu_\ell$ anything		(7.4	± 1.6)	$\times 10^{-3}$	
Γ_{11}	$B \to D\pi\ell^+\nu_\ell$ anything + $D^*\pi\ell^+\nu_\ell$ anything		(2.6	± 0.5)	%	S=1.5
Γ_{12}	$B \to D\pi\ell^+\nu_\ell$ anything		(1.5	± 0.6)	%	
Γ_{13}	$B \to D^*\pi\ell^+\nu_\ell$ anything		(1.9	± 0.4)	%	
Γ_{14}	$B \to \overline{D}_2^*(2460)\ell^+\nu_\ell$ anything		< 6.5		$\times 10^{-3}$	CL=95%
Γ_{15}	$B \to D^{*-}\pi^+\ell^+\nu_\ell$ anything		(1.00	± 0.34)	%	
Γ_{16}	$B \to D_s^-\ell^+\nu_\ell$ anything	[b]	< 9		$\times 10^{-3}$	CL=90%
Γ_{17}	$B \to D_s^-\ell^+\nu_\ell K^+$ anything	[b]	< 6		$\times 10^{-3}$	CL=90%
Γ_{18}	$B \to D_s^-\ell^+\nu_\ell K^0$ anything	[b]	< 9		$\times 10^{-3}$	CL=90%
Γ_{19}	$B \to \ell^+\nu_\ell$ noncharmed	[b]				
Γ_{20}	$B \to K^+\ell^+\nu_\ell$ anything	[b]	(6.2	± 0.6)	%	
Γ_{21}	$B \to K^-\ell^+\nu_\ell$ anything	[b]	(10	± 4)	$\times 10^{-3}$	
Γ_{22}	$B \to K^0/\overline{K}^0\ell^+\nu_\ell$ anything	[b]	(4.5	± 0.5)	%	

D, D^*, or D_s modes

Γ_{23}	$B \to$	$D^{\pm}$ anything		(23.5	$\pm$ 1.9	) %		
Γ_{24}	$B \to$	$D^0/\overline{D}^0$ anything		(64.0	$\pm$ 3.0	) %		S=1.1
Γ_{25}	$B \to$	$D^*(2010)^{\pm}$ anything		(22.5	$\pm$ 1.5	) %		
Γ_{26}	$B \to$	$D^*(2007)^0$ anything		(26.0	$\pm$ 2.7	) %		
Γ_{27}	$B \to$	$D_s^{\pm}$ anything	[d]	(10.5	$\pm$ 2.6	) %		
Γ_{28}	$B \to$	$D_s^{*\pm}$ anything		(7.9	$\pm$ 2.2	) %		
Γ_{29}	$B \to$	$D_s^{*\pm}\overline{D}^{(*)}$		(4.2	$\pm$ 1.2	) %		
Γ_{30}	$B \to$	$\overline{D}D_{sJ}(2317)$		seen				
Γ_{31}	$B \to$	$\overline{D}D_{sJ}(2457)$		seen				
Γ_{32}	$B \to$	$D^{(*)}\overline{D}^{(*)}K^0 + D^{(*)}\overline{D}^{(*)}K^{\pm}$	[d,e]	(7.1	$^{+2.7}_{-1.7}$	) %		
Γ_{33}	$b \to$	$c\overline{c}s$		(22	$\pm$ 4	) %		
Γ_{34}	$B \to$	$D_s^{(*)}\overline{D}^{(*)}$	[d,e]	(4.9	$\pm$ 1.2	) %		
Γ_{35}	$B \to$	$D^*D^*(2010)^{\pm}$	[d]	< 5.9			$\times 10^{-3}$	CL=90%
Γ_{36}	$B \to$	$DD^*(2010)^{\pm} + D^*D^{\pm}$	[d]	< 5.5			$\times 10^{-3}$	CL=90%
Γ_{37}	$B \to$	$DD^{\pm}$	[d]	< 3.1			$\times 10^{-3}$	CL=90%
Γ_{38}	$B \to$	$D_s^{(*)\pm}\overline{D}^{(*)}X(n\pi^{\pm})$	[d,e]	(9	$^{+5}_{-4}$	) %		
Γ_{39}	$B \to$	$D^*(2010)\gamma$		< 1.1			$\times 10^{-3}$	CL=90%
Γ_{40}	$B \to$	$D_s^+\pi^-$, $D_s^{*+}\pi^-$, $D_s^+\rho^-$, $D_s^{*+}\rho^-$, $D_s^+\pi^0$, $D_s^{*+}\pi^0$, $D_s^+\eta$, $D_s^{*+}\eta$, $D_s^+\rho^0$, $D_s^{*+}\rho^0$, $D_s^+\omega$, $D_s^{*+}\omega$	[d]	< 5			$\times 10^{-4}$	CL=90%
Γ_{41}	$B \to$	$D_{s1}(2536)^+$ anything		< 9.5			$\times 10^{-3}$	CL=90%

Charmonium modes

Γ_{42}	$B \to$	$J/\psi(1S)$ anything		(1.094	$\pm$ 0.032) %			S=1.1
Γ_{43}	$B \to$	$J/\psi(1S)$(direct) anything		(7.8	$\pm$ 0.4	) $\times 10^{-3}$		S=1.1
Γ_{44}	$B \to$	$\psi(2S)$ anything		(3.07	$\pm$ 0.21	) $\times 10^{-3}$		
Γ_{45}	$B \to$	$\chi_{c1}(1P)$ anything		(3.86	$\pm$ 0.27	) $\times 10^{-3}$		
Γ_{46}	$B \to$	$\chi_{c1}(1P)$(direct) anything		(3.34	$\pm$ 0.28	) $\times 10^{-3}$		
Γ_{47}	$B \to$	$\chi_{c2}(1P)$ anything		(1.3	$\pm$ 0.4	) $\times 10^{-3}$		S=1.9
Γ_{48}	$B \to$	$\chi_{c2}(1P)$(direct) anything		(1.65	$\pm$ 0.31	) $\times 10^{-3}$		
Γ_{49}	$B \to$	$\eta_c(1S)$ anything		< 9			$\times 10^{-3}$	CL=90%

K or K^* modes

Γ_{50}	$B \to$	$K^{\pm}$ anything	[d]	(78.9	$\pm$ 2.5	) %		
Γ_{51}	$B \to$	K^+ anything		(66	$\pm$ 5	) %		
Γ_{52}	$B \to$	K^- anything		(13	$\pm$ 4	) %		
Γ_{53}	$B \to$	$K^0/\overline{K}^0$ anything	[d]	(64	$\pm$ 4	) %		
Γ_{54}	$B \to$	$K^*(892)^{\pm}$ anything		(18	$\pm$ 6	) %		
Γ_{55}	$B \to$	$K^*(892)^0/\overline{K}^*(892)^0$ anything	[d]	(14.6	$\pm$ 2.6	) %		
Γ_{56}	$B \to$	$K^*(892)\gamma$		(4.2	$\pm$ 0.6	) $\times 10^{-5}$		
Γ_{57}	$B \to$	$K_1(1400)\gamma$		< 1.27			$\times 10^{-4}$	CL=90%
Γ_{58}	$B \to$	$K_2^*(1430)\gamma$		(1.7	$^{+0.6}_{-0.5}$	) $\times 10^{-5}$		
Γ_{59}	$B \to$	$K_2(1770)\gamma$		< 1.2			$\times 10^{-3}$	CL=90%
Γ_{60}	$B \to$	$K_3^*(1780)\gamma$		< 3.0			$\times 10^{-3}$	CL=90%
Γ_{61}	$B \to$	$K_4^*(2045)\gamma$		< 1.0			$\times 10^{-3}$	CL=90%
Γ_{62}	$B \to$	$K\eta'(958)$		(8.3	$\pm$ 1.1	) $\times 10^{-5}$		
Γ_{63}	$B \to$	$K^*(892)\eta'(958)$		< 2.2			$\times 10^{-5}$	CL=90%
Γ_{64}	$B \to$	$K\eta$		< 5.2			$\times 10^{-6}$	CL=90%
Γ_{65}	$B \to$	$K^*(892)\eta$		(1.8	$\pm$ 0.5	) $\times 10^{-5}$		
Γ_{66}	$B \to$	$K\phi\phi$		(2.3	$\pm$ 0.9	) $\times 10^{-6}$		
Γ_{67}	$B \to$	$\overline{b} \to \overline{s}\gamma$		(3.3	$\pm$ 0.4	) $\times 10^{-4}$		
Γ_{68}	$B \to$	$\overline{b} \to \overline{s}$gluon		< 6.8		%		CL=90%
Γ_{69}	$B \to$	η anything		< 4.4			$\times 10^{-4}$	CL=90%
Γ_{70}	$B \to$	η' anything		(4.6	$\pm$ 1.3	) $\times 10^{-4}$		

Light unflavored meson modes

Γ_{71}	$B \to$	$\rho\gamma$		< 1.9			$\times 10^{-6}$	CL=90%
Γ_{72}	$B \to$	$\pi^{\pm}$ anything	[d,f]	(358	$\pm$ 7	) %		
Γ_{73}	$B \to$	π^0 anything		(235	$\pm$11	) %		
Γ_{74}	$B \to$	η anything		(17.6	$\pm$ 1.6	) %		
Γ_{75}	$B \to$	ρ^0 anything		(21	$\pm$ 5	) %		
Γ_{76}	$B \to$	ω anything		< 81		%		CL=90%
Γ_{77}	$B \to$	ϕ anything		(3.5	$\pm$ 0.7	) %		S=1.8
Γ_{78}	$B \to$	$\phi K^*(892)$		< 2.2			$\times 10^{-5}$	CL=90%

Baryon modes

Γ_{79}	$B \to$	$\Lambda_c^+ / \overline{\Lambda}_c^-$ anything		(6.4	$\pm$ 1.1	) %		
Γ_{80}	$B \to$	Λ_c^+ anything						
Γ_{81}	$B \to$	$\overline{\Lambda}_c^-$ anything						
Γ_{82}	$B \to$	$\overline{\Lambda}_c^- e^+$ anything		< 3.2			$\times 10^{-3}$	CL=90%
Γ_{83}	$B \to$	$\overline{\Lambda}_c^- p$ anything		(3.6	$\pm$ 0.7	) %		
Γ_{84}	$B \to$	$\overline{\Lambda}_c^- p e^+ \nu_e$		< 1.5			$\times 10^{-3}$	CL=90%
Γ_{85}	$B \to$	$\overline{\Sigma}_c^{--}$ anything		(4.2	$\pm$ 2.4	) $\times 10^{-3}$		
Γ_{86}	$B \to$	$\overline{\Sigma}_c^-$ anything		< 9.6			$\times 10^{-3}$	CL=90%
Γ_{87}	$B \to$	$\overline{\Sigma}_c^0$ anything		(4.6	$\pm$ 2.4	) $\times 10^{-3}$		
Γ_{88}	$B \to$	$\overline{\Sigma}_c^0 N(N = p$ or $n)$		< 1.5			$\times 10^{-3}$	CL=90%
Γ_{89}	$B \to$	Ξ_c^0 anything $\times$ B($\Xi_c^0 \to \Xi^-\pi^+$)		(1.4	$\pm$ 0.5	) $\times 10^{-4}$		
Γ_{90}	$B \to$	Ξ_c^+ anything $\times$ B($\Xi_c^+ \to \Xi^-\pi^+\pi^+$)		(4.5	$^{+1.3}_{-1.2}$	) $\times 10^{-4}$		
Γ_{91}	$B \to$	$p/\overline{p}$ anything	[d]	(8.0	$\pm$ 0.4	) %		
Γ_{92}	$B \to$	$p/\overline{p}$(direct) anything	[d]	(5.5	$\pm$ 0.5	) %		
Γ_{93}	$B \to$	$\Lambda/\overline{\Lambda}$ anything	[d]	(4.0	$\pm$ 0.5	) %		
Γ_{94}	$B \to$	Λ anything						
Γ_{95}	$B \to$	$\overline{\Lambda}$ anything						
Γ_{96}	$B \to$	$\Xi^-/\overline{\Xi}^+$ anything	[d]	(2.7	$\pm$ 0.6	) $\times 10^{-3}$		
Γ_{97}	$B \to$	baryons anything		(6.8	$\pm$ 0.6	) %		
Γ_{98}	$B \to$	$p\overline{p}$ anything		(2.47	$\pm$ 0.23	) %		
Γ_{99}	$B \to$	$\Lambda\overline{p}/\overline{\Lambda}p$ anything	[d]	(2.5	$\pm$ 0.4	) %		
Γ_{100}	$B \to$	$\Lambda\overline{\Lambda}$ anything		< 5			$\times 10^{-3}$	CL=90%

Lepton Family number (LF) violating modes or $\Delta B = 1$ weak neutral current ($B1$) modes

Γ_{101}	$B \to$	se^+e^-	$B1$		(5.0	$\pm$ 2.6	) $\times 10^{-6}$	
Γ_{102}	$B \to$	$s\mu^+\mu^-$	$B1$		(7.9	$^{+3.0}_{-2.6}$	) $\times 10^{-6}$	
Γ_{103}	$B \to$	$s\ell^+\ell^-$	$B1$	[b]	(6.1	$^{+2.0}_{-1.8}$	) $\times 10^{-6}$	
Γ_{104}	$B \to$	Ke^+e^-	$B1$		(4.8	$^{+1.5}_{-1.3}$	) $\times 10^{-7}$	
Γ_{105}	$B \to$	$K^*(892)e^+e^-$	$B1$		(1.5	$\pm$ 0.5	) $\times 10^{-6}$	
Γ_{106}	$B \to$	$K\mu^+\mu^-$	$B1$		(4.8	$\pm$ 1.2	) $\times 10^{-7}$	
Γ_{107}	$B \to$	$K^*(892)\mu^+\mu^-$	$B1$		(1.17	$^{+0.37}_{-0.33}$	) $\times 10^{-6}$	
Γ_{108}	$B \to$	$K\ell^+\ell^-$	$B1$		(5.4	$\pm$ 0.8	) $\times 10^{-7}$	
Γ_{109}	$B \to$	$K^*(892)\ell^+\ell^-$	$B1$		(1.05	$\pm$ 0.20	) $\times 10^{-6}$	
Γ_{110}	$B \to$	$e^{\pm}\mu^{\mp}s$	LF	[d]	< 2.2		$\times 10^{-5}$	CL=90%
Γ_{111}	$B \to$	$\pi e^{\pm}\mu^{\mp}$	LF		< 1.6		$\times 10^{-6}$	CL=90%
Γ_{112}	$B \to$	$\rho e^{\pm}\mu^{\mp}$	LF		< 3.2		$\times 10^{-6}$	CL=90%
Γ_{113}	$B \to$	$Ke^{\pm}\mu^{\mp}$	LF		< 1.6		$\times 10^{-6}$	CL=90%
Γ_{114}	$B \to$	$K^*(892)e^{\pm}\mu^{\mp}$	LF		< 6.2		$\times 10^{-6}$	CL=90%

[a] These values are model dependent. See 'Note on Semileptonic Decays' in the B^+ Particle Listings.

[b] An ℓ indicates an e or a μ mode, not a sum over these modes.

[c] D^{**} stands for the sum of the $D(1\,^1P_1)$, $D(1\,^3P_0)$, $D(1\,^3P_1)$, $D(1\,^3P_2)$, $D(2\,^1S_0)$, and $D(2\,^1S_1)$ resonances.

[d] The value is for the sum of the charge states or particle/antiparticle states indicated.

[e] $D^{(*)}\overline{D}^{(*)}$ stands for the sum of $D^*\overline{D}^*$, $D^*\overline{D}$, $D\overline{D}^*$, and $D\overline{D}$.

[f] Inclusive branching fractions have a multiplicity definition and can be greater than 100%.

$B^{\pm}/B^0$ ADMIXTURE BRANCHING RATIOS

$\Gamma(\ell^+\nu_\ell\,\text{anything})/\Gamma_{\text{total}}$ Γ_4/Γ

These branching fraction values are model dependent.

"OUR EVALUATION" is an average using rescaled values of the data listed below. The average and rescaling were performed by the Heavy Flavor Averaging Group (HFAG) and are described at http://www.slac.stanford.edu/xorg/hfag/. The averaging/rescaling procedure takes into account corrections between the measurements.

VALUE	DOCUMENT ID		TECN	COMMENT
0.1073±0.0028 OUR EVALUATION				
0.1064±0.0023 OUR AVERAGE Includes data from the 2 datablocks that follow this one.				
• • • We do not use the following data for averages, fits, limits, etc. • • •				
0.108 ±0.002 ±0.0056	[1] HENDERSON	92	CLEO	$e^+e^- \to \Upsilon(4S)$

[1] HENDERSON 92 measurement employs e and μ. The systematic error contains 0.004 in quadrature from model dependence. The authors average a variation of the Isgur, Scora, Grinstein, and Wise model with that of the Altarelli-Cabibbo-Corbo-Maiani-Martinelli model for semileptonic decays to correct the acceptance.

$\Gamma(e^+\nu_e\,\text{anything})/\Gamma_{\text{total}}$ Γ_1/Γ

These branching fraction values are model dependent.

"OUR EVALUATION" is an average using rescaled values of the data listed below. The average and rescaling were performed by the Heavy Flavor Averaging Group (HFAG) and are described at http://www.slac.stanford.edu/xorg/hfag/. The averaging/rescaling procedure takes into account corrections between the measurements.

VALUE	DOCUMENT ID		TECN	COMMENT
The data in this block is included in the average printed for a previous datablock.				
0.1073±0.0028 OUR EVALUATION				
0.1064±0.0023 OUR AVERAGE				
0.1087±0.0018±0.0030	[2] AUBERT	03	BABR	$e^+e^- \to \Upsilon(4S)$
0.109 ±0.0012±0.0049	[3] ABE	02Y	BELL	$e^+e^- \to \Upsilon(4S)$
0.1049±0.0017±0.0043	[4] BARISH	96B	CLE2	$e^+e^- \to \Upsilon(4S)$
0.097 ±0.005 ±0.004	[5] ALBRECHT	93H	ARG	$e^+e^- \to \Upsilon(4S)$
• • • We do not use the following data for averages, fits, limits, etc. • • •				
0.100 ±0.004 ±0.003	[6] YANAGISAWA	91	CSB2	$e^+e^- \to \Upsilon(4S)$
0.103 ±0.006 ±0.002	[7] ALBRECHT	90H	ARG	$e^+e^- \to \Upsilon(4S)$
0.117 ±0.004 ±0.010	[8] WACHS	89	CBAL	Direct e at $\Upsilon(4S)$
0.120 ±0.007 ±0.005	CHEN	84	CLEO	Direct e at $\Upsilon(4S)$
0.132 ±0.008 ±0.014	[9] KLOPFEN...	83B	CUSB	Direct e at $\Upsilon(4S)$

[2] Uses the high-momentum lepton tag method. They also report $|V_{cb}| = 0.0423 \pm 0.0007(\text{exp}) \pm 0.0020(\text{theo.})$.

[3] Uses the high-momentum lepton tag method. ABE 02Y also reports $|V_{cb}| = 0.0408 \pm 0.0010(\text{exp}) \pm 0.0025(\text{theo.})$. The second error is due to uncertainties of theoretical inputs.

[4] BARISH 96B analysis performed using tagged semileptonic decays of the B. This technique is almost model independent for the lepton branching ratio.

[5] ALBRECHT 93H analysis performed using tagged semileptonic decays of the B. This technique is almost model independent for the lepton branching ratio.

[6] YANAGISAWA 91 also measures an average semileptonic branching ratio at the $\Upsilon(5S)$ of 9.6–10.5% depending on assumptions about the relative production of different B meson species.

[7] ALBRECHT 90H uses the model of ALTARELLI 82 to correct over all lepton momenta. 0.099 ± 0.006 is obtained using ISGUR 89B.

[8] Using data above $p(e) = 2.4$ GeV, WACHS 89 determine $\sigma(B \to e\nu\text{up})/\sigma(B \to e\nu\text{charm}) < 0.065$ at 90% CL.

[9] Ratio $\sigma(b \to e\nu\text{up})/\sigma(b \to e\nu\text{charm}) < 0.055$ at CL = 90%.

$\Gamma(\mu^+\nu_\mu\,\text{anything})/\Gamma_{\text{total}}$ Γ_3/Γ

These branching fraction values are model dependent. See the note on "Semileptonic Decays of B Mesons at the beginning of the B^+ Particle Listings.

VALUE	DOCUMENT ID		TECN	COMMENT
The data in this block is included in the average printed for a previous datablock.				
• • • We do not use the following data for averages, fits, limits, etc. • • •				
0.100±0.006±0.002	[10] ALBRECHT	90H	ARG	$e^+e^- \to \Upsilon(4S)$
0.108±0.006±0.01	CHEN	84	CLEO	Direct μ at $\Upsilon(4S)$
0.112±0.009±0.01	LEVMAN	84	CUSB	Direct μ at $\Upsilon(4S)$

[10] ALBRECHT 90H uses the model of ALTARELLI 82 to correct over all lepton momenta. 0.097 ± 0.006 is obtained using ISGUR 89B.

$\Gamma(\overline{p}e^+\nu_e\,\text{anything})/\Gamma_{\text{total}}$ Γ_2/Γ

VALUE	CL%	DOCUMENT ID		TECN	COMMENT
<5.9 $\times 10^{-4}$	90	[11] ADAM	03B	CLE2	$e^+e^- \to \Upsilon(4S)$
• • • We do not use the following data for averages, fits, limits, etc. • • •					
<0.0016	90	ALBRECHT	90H	ARG	$e^+e^- \to \Upsilon(4S)$

[11] Based on $V-A$ model.

$\Gamma(D^-\ell^+\nu_\ell\,\text{anything})/\Gamma(\ell^+\nu_\ell\,\text{anything})$ Γ_5/Γ_4

$\ell = e$ or μ.

VALUE	DOCUMENT ID		TECN	COMMENT
0.26±0.07±0.04	[12] FULTON	91	CLEO	$e^+e^- \to \Upsilon(4S)$

[12] FULTON 91 uses $B(D^+ \to K^-\pi^+\pi^+) = (9.1 \pm 1.3 \pm 0.4)\%$ as measured by MARK III.

$\Gamma(\overline{D}^0\ell^+\nu_\ell\,\text{anything})/\Gamma(\ell^+\nu_\ell\,\text{anything})$ Γ_6/Γ_4

$\ell = e$ or μ.

VALUE	DOCUMENT ID		TECN	COMMENT
0.67±0.09±0.10	[13] FULTON	91	CLEO	$e^+e^- \to \Upsilon(4S)$

[13] FULTON 91 uses $B(D^0 \to K^-\pi^+) = (4.2 \pm 0.4 \pm 0.4)\%$ as measured by MARK III.

$\Gamma(D^{*-}\ell^+\nu_\ell\,\text{anything})/\Gamma_{\text{total}}$ Γ_7/Γ

VALUE (units 10^{-2})	DOCUMENT ID		TECN	COMMENT
• • • We do not use the following data for averages, fits, limits, etc. • • •				
0.6±0.3±0.1	[14] BARISH	95	CLE2	$e^+e^- \to \Upsilon(4S)$

[14] BARISH 95 use $B(D^0 \to K^-\pi^+) = (3.91 \pm 0.08 \pm 0.17)\%$ and $B(D^{*+} \to D^0\pi^+) = (68.1 \pm 1.0 \pm 1.3)\%$.

$\Gamma(D^{*0}\ell^+\nu_\ell\,\text{anything})/\Gamma_{\text{total}}$ Γ_8/Γ

VALUE (units 10^{-2})	DOCUMENT ID		TECN	COMMENT
• • • We do not use the following data for averages, fits, limits, etc. • • •				
0.6±0.6±0.1	[15] BARISH	95	CLE2	$e^+e^- \to \Upsilon(4S)$

[15] BARISH 95 use $B(D^0 \to K^-\pi^+) = (3.91 \pm 0.08 \pm 0.17)\%$, $B(D^{*+} \to D^0\pi^+) = (68.1 \pm 1.0 \pm 1.3)\%$, $B(D^{*0} \to D^0\pi^0) = (63.6 \pm 2.3 \pm 3.3)\%$.

$\Gamma(\overline{D}^{**}\ell^+\nu_\ell)/\Gamma_{\text{total}}$ Γ_9/Γ

D^{**} stands for the sum of the $D(1\,^1P_1)$, $D(1\,^3P_0)$, $D(1\,^3P_1)$, $D(1\,^3P_2)$, $D(2\,^1S_0)$, and $D(2\,^1S_1)$ resonances. $\ell = e$ or μ, not sum over e and μ modes.

VALUE	CL%	EVTS	DOCUMENT ID		TECN	COMMENT
0.027±0.005±0.005		63	[16] ALBRECHT	93	ARG	$e^+e^- \to \Upsilon(4S)$
• • • We do not use the following data for averages, fits, limits, etc. • • •						
<0.028	95		[17] BARISH	95	CLE2	$e^+e^- \to \Upsilon(4S)$

[16] ALBRECHT 93 assumes the GISW model to correct for unseen modes. Using the BHKT model, the result becomes 0.023 ± 0.006 ± 0.004. Assumes $B(D^{*+} \to D^0\pi^+) = 68.1\%$, $B(D^0 \to K^-\pi^+) = 3.65\%$, $B(D^0 \to K^-\pi^+\pi^-\pi^+) = 7.5\%$. We have taken their average e and μ value.

[17] BARISH 95 use $B(D^0 \to K^-\pi^+) = (3.91 \pm 0.08 \pm 0.17)\%$, assume all nonresonant channels are zero, and use GISW model for relative abundances of D^{**} states.

$\Gamma(\overline{D}_1(2420)\ell^+\nu_\ell\,\text{anything})/\Gamma_{\text{total}}$ Γ_{10}/Γ

VALUE	DOCUMENT ID		TECN	COMMENT
0.0074±0.0016	[18] BUSKULIC	97B	ALEP	$e^+e^- \to Z$
• • • We do not use the following data for averages, fits, limits, etc. • • •				
seen	[19] BUSKULIC	95B	ALEP	Repl. by BUSKULIC 97B

[18] BUSKULIC 97B assumes $B(D_1(2420) \to D^*\pi) = 1$, $B(D_1(2420) \to D^*\pi^\pm) = 2/3$, and $B(b \to B) = 0.378 \pm 0.022$.

[19] BUSKULIC 95B reports $f_B \times B(B \to \overline{D}_1(2420)^0\ell^+\nu_\ell\,\text{anything}) \times B(\overline{D}_1(2420)^0 \to \overline{D}^*(2010)^-\pi^+) = (2.04 \pm 0.58 \pm 0.34)10^{-3}$, where f_B is the production fraction for a single B charge state.

$[\Gamma(D\pi\ell^+\nu_\ell\,\text{anything}) + \Gamma(D^*\pi\ell^+\nu_\ell\,\text{anything})]/\Gamma_{\text{total}}$ Γ_{11}/Γ

VALUE	DOCUMENT ID		TECN	COMMENT
0.026 ±0.005 OUR AVERAGE Error includes scale factor of 1.5.				
0.0340±0.0052±0.0032	[20] ABREU	00R	DLPH	$e^+e^- \to Z$
0.0226±0.0029±0.0033	[21] BUSKULIC	97B	ALEP	$e^+e^- \to Z$

[20] Assumes no contribution from B_s and b baryons. Further assumes contributions from single pion ($D\pi$ and $D^*\pi$) states only, allowing isospin conservation to relate the relative π^0 and π^+ rates.

[21] BUSKULIC 97B assumes $B(b \to B) = 0.378 \pm 0.022$ and uses isospin invariance by assuming that all observed $D^0\pi^+$, $D^{*0}\pi^+$, $D^+\pi^-$, and $D^{*+}\pi^-$ are from D^{**} states. A correction has been applied to account for the production of B_s^0 and Λ_b^0.

$\Gamma(D\pi\ell^+\nu_\ell\,\text{anything})/\Gamma_{\text{total}}$ Γ_{12}/Γ

VALUE	DOCUMENT ID		TECN	COMMENT
0.0154±0.0061	ABREU	00R	DLPH	$e^+e^- \to Z$

$\Gamma(D^*\pi\ell^+\nu_\ell\,\text{anything})/\Gamma_{\text{total}}$ Γ_{13}/Γ

VALUE	DOCUMENT ID		TECN	COMMENT
0.0186±0.0038	ABREU	00R	DLPH	$e^+e^- \to Z$

$\Gamma(\overline{D}_2^*(2460)\ell^+\nu_\ell\,\text{anything})/\Gamma_{\text{total}}$ Γ_{14}/Γ

VALUE	CL%	DOCUMENT ID		TECN	COMMENT
<0.0065	95	[22] BUSKULIC	97B	ALEP	$e^+e^- \to Z$
• • • We do not use the following data for averages, fits, limits, etc. • • •					
not seen		[23] BUSKULIC	95B	ALEP	$e^+e^- \to Z$

[22] A revised number based on BUSKULIC 97B which assumes $B(D_2^*(2460) \to D^*\pi^\pm) = 0.20$ and $B(b \to B) = 0.378 \pm 0.022$.

[23] BUSKULIC 95B reports $f_B \times B(B \to \overline{D}_2^*(2460)^0\ell^+\nu_\ell\,\text{anything}) \times B(\overline{D}_2^*(2460)^0 \to \overline{D}^*(2010)^-\pi^+) \leq 0.81 \times 10^{-3}$ at CL=95%, where f_B is the production fraction for a single B charge state.

$\Gamma(D^{*-}\pi^+\ell^+\nu_\ell \text{ anything})/\Gamma_{\text{total}}$ Γ_{15}/Γ

Includes resonant and nonresonant contributions.

VALUE (units 10^{-3})	DOCUMENT ID		TECN	COMMENT
$10.0 \pm 2.7 \pm 2.1$	[24] BUSKULIC	95B	ALEP	$e^+e^- \to Z$

[24] BUSKULIC 95B reports $f_B \times B(B \to \overline{D}^*(2010)^-\pi^+\ell^+\nu_\ell \text{ anything}) = (3.7 \pm 1.0 \pm 0.7)10^{-3}$. Above value assumes $f_B = 0.37 \pm 0.03$.

$\Gamma(D_s^-\ell^+\nu_\ell \text{ anything})/\Gamma_{\text{total}}$ Γ_{16}/Γ

VALUE	CL%	DOCUMENT ID		TECN	COMMENT
<0.009	90	[25] ALBRECHT	93E	ARG	$e^+e^- \to \Upsilon(4S)$

[25] ALBRECHT 93E reports < 0.012 for $B(D_s^+ \to \phi\pi^+) = 0.027$. We rescale to our best value $B(D_s^+ \to \phi\pi^+) = 0.036$.

$\Gamma(D_s^-\ell^+\nu_\ell K^+ \text{ anything})/\Gamma_{\text{total}}$ Γ_{17}/Γ

VALUE	CL%	DOCUMENT ID		TECN	COMMENT
<0.006	90	[26] ALBRECHT	93E	ARG	$e^+e^- \to \Upsilon(4S)$

[26] ALBRECHT 93E reports < 0.008 for $B(D_s^+ \to \phi\pi^+) = 0.027$. We rescale to our best value $B(D_s^+ \to \phi\pi^+) = 0.036$.

$\Gamma(D_s^-\ell^+\nu_\ell K^0 \text{ anything})/\Gamma_{\text{total}}$ Γ_{18}/Γ

VALUE	CL%	DOCUMENT ID		TECN	COMMENT
<0.009	90	[27] ALBRECHT	93E	ARG	$e^+e^- \to \Upsilon(4S)$

[27] ALBRECHT 93E reports < 0.012 for $B(D_s^+ \to \phi\pi^+) = 0.027$. We rescale to our best value $B(D_s^+ \to \phi\pi^+) = 0.036$.

$\Gamma(\ell^+\nu_\ell \text{ noncharmed})/\Gamma(\ell^+\nu_\ell \text{ anything})$ Γ_{19}/Γ_4

ℓ denotes e or μ, not the sum. These experiments measure this ratio in very limited momentum intervals.

VALUE	CL%	EVTS	DOCUMENT ID		TECN	COMMENT
			[28] ALBRECHT	94C	ARG	$e^+e^- \to \Upsilon(4S)$
		107	[29] BARTELT	93B	CLE2	$e^+e^- \to \Upsilon(4S)$
		77	[30] ALBRECHT	91C	ARG	$e^+e^- \to \Upsilon(4S)$
		76	[31] FULTON	90	CLEO	$e^+e^- \to \Upsilon(4S)$
• • • We do not use the following data for averages, fits, limits, etc. • • •						
		41	[32] ALBRECHT	90	ARG	$e^+e^- \to \Upsilon(4S)$
<0.04	90		[33] BEHRENDS	87	CLEO	$e^+e^- \to \Upsilon(4S)$
<0.04	90		CHEN	84	CLEO	Direct e at $\Upsilon(4S)$
<0.055	90		KLOPFEN...	83B	CUSB	Direct e at $\Upsilon(4S)$

[28] ALBRECHT 94C find $\Gamma(b \to c)/\Gamma(b \to \text{all}) = 0.99 \pm 0.02 \pm 0.04$.

[29] BARTELT 93B (CLEO II) measures an excess of $107 \pm 15 \pm 11$ leptons in the lepton momentum interval 2.3–2.6 GeV/c which is attributed to $b \to u\ell\nu_\ell$. This corresponds to a model-dependent partial branching ratio ΔB_{ub} between $(1.15 \pm 0.16 \pm 0.15) \times 10^{-4}$, as evaluated using the KS model (KOERNER 88), and $(1.54 \pm 0.22 \pm 0.20) \times 10^{-4}$ using the ACCMM model (ARTUSO 93). The corresponding values of $|V_{ub}|/|V_{cb}|$ are 0.056 ± 0.006 and 0.076 ± 0.008, respectively.

[30] ALBRECHT 91C result supersedes ALBRECHT 90. Two events are fully reconstructed providing evidence for the $b \to u$ transition. Using the model of ALTARELLI 82, they obtain $|V_{ub}/V_{cb}| = 0.11 \pm 0.012$ from 77 leptons in the 2.3–2.6 GeV momentum range.

[31] FULTON 90 observe 76 ± 20 excess e and μ (lepton) events in the momentum interval $p = 2.4$–2.6 GeV signaling the presence of the $b \to u$ transition. The average branching ratio, $(1.8 \pm 0.4 \pm 0.3) \times 10^{-4}$, corresponds to a model-dependent measurement of approximately $|V_{ub}/V_{cb}| = 0.1$ using $B(b \to c\ell\nu) = 10.2 \pm 0.2 \pm 0.7\%$.

[32] ALBRECHT 90 observes 41 ± 10 excess e and μ (lepton) events in the momentum interval $p = 2.3$–2.6 GeV signaling the presence of the $b \to u$ transition. The events correspond to a model-dependent measurement of $|V_{ub}/V_{cb}| = 0.10 \pm 0.01$.

[33] The quoted possible limits range from 0.018 to 0.04 for the ratio, depending on which model or momentum range is chosen. We select the most conservative limit they have calculated. This corresponds to a limit on $|V_{ub}|/|V_{cb}| < 0.20$. While the endpoint technique employed is more robust than their previous results in CHEN 84, these results do not provide a numerical improvement in the limit.

$\Gamma(K^+\ell^+\nu_\ell \text{ anything})/\Gamma(\ell^+\nu_\ell \text{ anything})$ Γ_{20}/Γ_4

ℓ denotes e or μ, not the sum.

VALUE	DOCUMENT ID		TECN	COMMENT
0.58 ± 0.05 OUR AVERAGE				
$0.594 \pm 0.021 \pm 0.056$	ALBRECHT	94C	ARG	$e^+e^- \to \Upsilon(4S)$
$0.54 \pm 0.07 \pm 0.06$	[34] ALAM	87B	CLEO	$e^+e^- \to \Upsilon(4S)$

[34] ALAM 87B measurement relies on lepton-kaon correlations.

$\Gamma(K^-\ell^+\nu_\ell \text{ anything})/\Gamma(\ell^+\nu_\ell \text{ anything})$ Γ_{21}/Γ_4

ℓ denotes e or μ, not the sum.

VALUE	DOCUMENT ID		TECN	COMMENT
0.092 ± 0.035 OUR AVERAGE				
$0.086 \pm 0.011 \pm 0.044$	ALBRECHT	94C	ARG	$e^+e^- \to \Upsilon(4S)$
$0.10 \pm 0.05 \pm 0.02$	[35] ALAM	87B	CLEO	$e^+e^- \to \Upsilon(4S)$

[35] ALAM 87B measurement relies on lepton-kaon correlations.

$\Gamma(K^0/\overline{K}^0\ell^+\nu_\ell \text{ anything})/\Gamma(\ell^+\nu_\ell \text{ anything})$ Γ_{22}/Γ_4

ℓ denotes e or μ, not the sum. Sum over K^0 and $\overline{K}^0$ states.

VALUE	DOCUMENT ID		TECN	COMMENT
0.42 ± 0.05 OUR AVERAGE				
$0.452 \pm 0.038 \pm 0.056$	[36] ALBRECHT	94C	ARG	$e^+e^- \to \Upsilon(4S)$
$0.39 \pm 0.06 \pm 0.04$	[37] ALAM	87B	CLEO	$e^+e^- \to \Upsilon(4S)$

[36] ALBRECHT 94C assume a $K^0/\overline{K}^0$ multiplicity twice that of K_S^0.

[37] ALAM 87B measurement relies on lepton-kaon correlations.

$\langle n_c \rangle$

VALUE	DOCUMENT ID		TECN	COMMENT
1.10 ± 0.05	[38] GIBBONS	97B	CLE2	$e^+e^- \to \Upsilon(4S)$
• • • We do not use the following data for averages, fits, limits, etc. • • •				
$0.98 \pm 0.16 \pm 0.12$	[39] ALAM	87B	CLEO	$e^+e^- \to \Upsilon(4S)$

[38] GIBBONS 97B from charm counting using $B(D_s^+ \to \phi\pi) = 0.036 \pm 0.009$ and $B(\Lambda_c^+ \to pK^-\pi^+) = 0.044 \pm 0.006$.

[39] From the difference between K^- and K^+ widths. ALAM 87B measurement relies on lepton-kaon correlations. It does not consider the possibility of $B\overline{B}$ mixing. We have thus removed it from the average.

$\Gamma(D^{\pm} \text{ anything})/\Gamma_{\text{total}}$ Γ_{23}/Γ

VALUE	EVTS	DOCUMENT ID		TECN	COMMENT
0.235 ± 0.019 OUR AVERAGE					
$0.234 \pm 0.012 \pm 0.015$		[40] GIBBONS	97B	CLE2	$e^+e^- \to \Upsilon(4S)$
$0.25 \pm 0.04 \pm 0.02$		[41] BORTOLETTO	92	CLEO	$e^+e^- \to \Upsilon(4S)$
$0.23 \pm 0.05 \pm 0.01$		[42] ALBRECHT	91H	ARG	$e^+e^- \to \Upsilon(4S)$
• • • We do not use the following data for averages, fits, limits, etc. • • •					
$0.21 \pm 0.05 \pm 0.01$	20k	[43] BORTOLETTO	87	CLEO	Sup. by BORTOLETTO 92

[40] GIBBONS 97B reports $[B(B \to D^{\pm} \text{ anything}) \times B(D^+ \to K^-\pi^+\pi^+)] = 0.0216 \pm 0.0008 \pm 0.00082$. We divide by our best value $B(D^+ \to K^-\pi^+\pi^+) = (9.2 \pm 0.6) \times 10^{-2}$. Our first error is their experiment's error and our second error is the systematic error from using our best value.

[41] BORTOLETTO 92 reports $[B(B \to D^{\pm} \text{ anything}) \times B(D^+ \to K^-\pi^+\pi^+)] = 0.0226 \pm 0.0030 \pm 0.0018$. We divide by our best value $B(D^+ \to K^-\pi^+\pi^+) = (9.2 \pm 0.6) \times 10^{-2}$. Our first error is their experiment's error and our second error is the systematic error from using our best value.

[42] ALBRECHT 91H reports $[B(B \to D^{\pm} \text{ anything}) \times B(D^+ \to K^-\pi^+\pi^+)] = 0.0209 \pm 0.0027 \pm 0.0040$. We divide by our best value $B(D^+ \to K^-\pi^+\pi^+) = (9.2 \pm 0.6) \times 10^{-2}$. Our first error is their experiment's error and our second error is the systematic error from using our best value.

[43] BORTOLETTO 87 reports $[B(B \to D^{\pm} \text{ anything}) \times B(D^+ \to K^-\pi^+\pi^+)] = 0.019 \pm 0.004 \pm 0.002$. We divide by our best value $B(D^+ \to K^-\pi^+\pi^+) = (9.2 \pm 0.6) \times 10^{-2}$. Our first error is their experiment's error and our second error is the systematic error from using our best value.

$\Gamma(D^0/\overline{D}^0 \text{ anything})/\Gamma_{\text{total}}$ Γ_{24}/Γ

VALUE	EVTS	DOCUMENT ID		TECN	COMMENT
0.640 ± 0.030 OUR AVERAGE		Error includes scale factor of 1.1.			
$0.660 \pm 0.025 \,^{+0.016}_{-0.015}$		[44] GIBBONS	97B	CLE2	$e^+e^- \to \Upsilon(4S)$
$0.61 \pm 0.05 \pm 0.01$		[45] BORTOLETTO	92	CLEO	$e^+e^- \to \Upsilon(4S)$
$0.51 \pm 0.08 \pm 0.01$		[46] ALBRECHT	91H	ARG	$e^+e^- \to \Upsilon(4S)$
• • • We do not use the following data for averages, fits, limits, etc. • • •					
$0.55 \pm 0.07 \pm 0.01$	21k	[47] BORTOLETTO	87	CLEO	$e^+e^- \to \Upsilon(4S)$
$0.63 \pm 0.19 \,^{+0.02}_{-0.01}$		[48] GREEN	83	CLEO	Repl. by BORTOLETTO 87

[44] GIBBONS 97B reports $[B(B \to D^0/\overline{D}^0 \text{ anything}) \times B(D^0 \to K^-\pi^+)] = 0.0251 \pm 0.0006 \pm 0.00075$. We divide by our best value $B(D^0 \to K^-\pi^+) = (3.80 \pm 0.09) \times 10^{-2}$. Our first error is their experiment's error and our second error is the systematic error from using our best value.

[45] BORTOLETTO 92 reports $[B(B \to D^0/\overline{D}^0 \text{ anything}) \times B(D^0 \to K^-\pi^+)] = 0.0233 \pm 0.0012 \pm 0.0014$. We divide by our best value $B(D^0 \to K^-\pi^+) = (3.80 \pm 0.09) \times 10^{-2}$. Our first error is their experiment's error and our second error is the systematic error from using our best value.

[46] ALBRECHT 91H reports $[B(B \to D^0/\overline{D}^0 \text{ anything}) \times B(D^0 \to K^-\pi^+)] = 0.0194 \pm 0.0015 \pm 0.0025$. We divide by our best value $B(D^0 \to K^-\pi^+) = (3.80 \pm 0.09) \times 10^{-2}$. Our first error is their experiment's error and our second error is the systematic error from using our best value.

[47] BORTOLETTO 87 reports $[B(B \to D^0/\overline{D}^0 \text{ anything}) \times B(D^0 \to K^-\pi^+)] = 0.0210 \pm 0.0015 \pm 0.0021$. We divide by our best value $B(D^0 \to K^-\pi^+) = (3.80 \pm 0.09) \times 10^{-2}$. Our first error is their experiment's error and our second error is the systematic error from using our best value.

[48] GREEN 83 reports $[B(B \to D^0/\overline{D}^0 \text{ anything}) \times B(D^0 \to K^-\pi^+)] = 0.024 \pm 0.006 \pm 0.004$. We divide by our best value $B(D^0 \to K^-\pi^+) = (3.80 \pm 0.09) \times 10^{-2}$. Our first error is their experiment's error and our second error is the systematic error from using our best value.

$\Gamma(D^*(2010)^{\pm} \text{ anything})/\Gamma_{\text{total}}$ Γ_{25}/Γ

VALUE	EVTS	DOCUMENT ID		TECN	COMMENT
0.225 ± 0.015 OUR AVERAGE					
$0.247 \pm 0.019 \pm 0.01$		[49] GIBBONS	97B	CLE2	$e^+e^- \to \Upsilon(4S)$
$0.205 \pm 0.019 \pm 0.007$		[50] ALBRECHT	96D	ARG	$e^+e^- \to \Upsilon(4S)$
$0.230 \pm 0.028 \pm 0.009$		[51] BORTOLETTO	92	CLEO	$e^+e^- \to \Upsilon(4S)$
• • • We do not use the following data for averages, fits, limits, etc. • • •					
$0.283 \pm 0.053 \pm 0.002$		[52] ALBRECHT	91H	ARG	Sup. by ALBRECHT 96D
$0.22 \pm 0.04 \,^{+0.07}_{-0.04}$	5200	[53] BORTOLETTO	87	CLEO	$e^+e^- \to \Upsilon(4S)$
$0.27 \pm 0.06 \,^{+0.08}_{-0.06}$	510	[54] CSORNA	85	CLEO	Repl. by BORTOLETTO 87

[49] GIBBONS 97B reports $B(B \to D^*(2010)^+ \text{anything}) = 0.239 \pm 0.015 \pm 0.014 \pm 0.009$ using CLEO measured D and D^* branching fractions. We rescale to our PDG 96 values of D and D^* branching ratios. Our first error is their experiment's error and our second error is the systematic error from using our best value.

[50] ALBRECHT 96D reports $B(B \to D^*(2010)^+ \text{anything}) 0.196 \pm 0.019$ using CLEO measured $B(D^*(2010)^+ \to D^0\pi^+) = 0.681 \pm 0.01 \pm 0.013$, $B(D^0 \to K^-\pi^+) = 0.0401 \pm 0.0014$, $B(D^0 \to K^-\pi^+\pi^+\pi^-) = 0.081 \pm 0.005$., We rescale to our PDG 96 values of D and D^* branching ratios. Our first error is their experiment's error and our second error is the systematic error from using our best value.

[51] BORTOLETTO 92 reports $B(B \to D^*(2010)^+ \text{anything}) = 0.25 \pm 0.03 \pm 0.04$ using MARK II $B(D^*(2010)^+ \to D^0\pi^+) = 0.57 \pm 0.06$ and $B(D^0 \to K^-\pi^+) = 0.042 \pm 0.008$. We rescale to our PDG 96 values of D and D^* branching ratios. Our first error is their experiment's error and our second error is the systematic error from using our best value.

[52] ALBRECHT 91H reports $0.348 \pm 0.060 \pm 0.035$ for $B(D^*(2010)^+ \to D^0\pi^+) = 0.55 \pm 0.04$. We rescale to our best value $B(D^*(2010)^+ \to D^0\pi^+) = (67.7 \pm 0.5) \times 10^{-2}$. Our first error is their experiment's error and our second error is the systematic error from using our best value. Uses the PDG 90 $B(D^0 \to K^-\pi^+) = 0.0371 \pm 0.0025$.

[53] BORTOLETTO 87 uses old MARK III (BALTRUSAITIS 86E) branching ratios $B(D^0 \to K^-\pi^+) = 0.056 \pm 0.004 \pm 0.003$ and also assumes $B(D^*(2010)^+ \to D^0\pi^+) = 0.60^{+0.08}_{-0.15}$. The product branching ratio for $B(B \to D^*(2010)^+) B(D^*(2010)^+ \to D^0\pi^+)$ is $0.13 \pm 0.02 \pm 0.012$. Superseded by BORTOLETTO 92.

[54] $V-A$ momentum spectrum used to extrapolate below $p = 1$ GeV. We correct the value assuming $B(D^0 \to K^-\pi^+) = 0.042 \pm 0.006$ and $B(D^{*+} \to D^0\pi^+) = 0.6^{+0.08}_{-0.15}$. The product branching fraction is $B(B \to D^{*+}X) \cdot B(D^{*+} \to \pi^+ D^0) \cdot B(D^0 \to K^-\pi^+) = (68 \pm 15 \pm 9) \times 10^{-4}$.

$\Gamma(D^*(2007)^0 \text{anything})/\Gamma_{\text{total}}$ Γ_{26}/Γ

VALUE	DOCUMENT ID		TECN	COMMENT
$0.260 \pm 0.023 \pm 0.015$	[55] GIBBONS	97B	CLE2	$e^+e^- \to \Upsilon(4S)$

[55] GIBBONS 97B reports $B(B \to D^*(2007)^0 \text{anything}) 0.247 \pm 0.012 \pm 0.018 \pm 0.018$ using CLEO measured D and D^* branching fractions. We rescale to our PDG 96 values of D and D^* branching ratios. Our first error is their experiment's error and our second error is the systematic error from using our best value.

$\Gamma(D_s^{\pm} \text{anything})/\Gamma_{\text{total}}$ Γ_{27}/Γ

VALUE	EVTS	DOCUMENT ID		TECN	COMMENT
0.105 ± 0.026 OUR AVERAGE					
$0.109 \pm 0.006^{+0.026}_{-0.027}$		[56] AUBERT	02G	BABR	$e^+e^- \to \Upsilon(4S)$
$0.117 \pm 0.009^{+0.028}_{-0.029}$		[57] GIBAUT	96	CLE2	$e^+e^- \to \Upsilon(4S)$
$0.081 \pm 0.014^{+0.019}_{-0.020}$		[58] ALBRECHT	92G	ARG	$e^+e^- \to \Upsilon(4S)$
$0.085 \pm 0.013^{+0.020}_{-0.021}$	257	[59] BORTOLETTO	90	CLEO	$e^+e^- \to \Upsilon(4S)$
$0.105 \pm 0.028^{+0.025}_{-0.026}$		[60] HAAS	86	CLEO	$e^+e^- \to \Upsilon(4S)$
• • • We do not use the following data for averages, fits, limits, etc. • • •					
$0.116 \pm 0.030 \pm 0.028$		[61] ALBRECHT	87H	ARG	$e^+e^- \to \Upsilon(4S)$

[56] AUBERT 02G reports $[B(B \to D_s^{\pm} \text{anything}) \times B(D_s^+ \to \phi\pi^+)] = 0.00393 \pm 0.00007 \pm 0.00021$. We divide by our best value $B(D_s^+ \to \phi\pi^+) = (3.6 \pm 0.9) \times 10^{-2}$. Our first error is their experiment's error and our second error is the systematic error from using our best value.

[57] GIBAUT 96 reports $0.1211 \pm 0.0039 \pm 0.0088$ for $B(D_s^+ \to \phi\pi^+) = 0.035$. We rescale to our best value $B(D_s^+ \to \phi\pi^+) = (3.6 \pm 0.9) \times 10^{-2}$. Our first error is their experiment's error and our second error is the systematic error from using our best value.

[58] ALBRECHT 92G reports $[B(B \to D_s^{\pm} \text{anything}) \times B(D_s^+ \to \phi\pi^+)] = 0.00292 \pm 0.00039 \pm 0.00031$. We divide by our best value $B(D_s^+ \to \phi\pi^+) = (3.6 \pm 0.9) \times 10^{-2}$. Our first error is their experiment's error and our second error is the systematic error from using our best value.

[59] BORTOLETTO 90 reports $[B(B \to D_s^{\pm} \text{anything}) \times B(D_s^+ \to \phi\pi^+)] = 0.00306 \pm 0.00047$. We divide by our best value $B(D_s^+ \to \phi\pi^+) = (3.6 \pm 0.9) \times 10^{-2}$. Our first error is their experiment's error and our second error is the systematic error from using our best value.

[60] HAAS 86 reports $[B(B \to D_s^{\pm} \text{anything}) \times B(D_s^+ \to \phi\pi^+)] = 0.0038 \pm 0.0010$. We divide by our best value $B(D_s^+ \to \phi\pi^+) = (3.6 \pm 0.9) \times 10^{-2}$. Our first error is their experiment's error and our second error is the systematic error from using our best value. $64 \pm 22\%$ decays are 2-body.

[61] ALBRECHT 87H reports $[B(B \to D_s^{\pm} \text{anything}) \times B(D_s^+ \to \phi\pi^+)] = 0.0042 \pm 0.0009 \pm 0.0006$. We divide by our best value $B(D_s^+ \to \phi\pi^+) = (3.6 \pm 0.9) \times 10^{-2}$. Our first error is their experiment's error and our second error is the systematic error from using our best value. $46 \pm 16\%$ of $B \to D_s X$ decays are 2-body. Superseded by ALBRECHT 92G.

$\Gamma(D_s^{*\pm} \text{anything})/\Gamma_{\text{total}}$ Γ_{28}/Γ

VALUE	DOCUMENT ID		TECN	COMMENT
$0.079 \pm 0.011 \pm 0.019$	[62] AUBERT	02G	BABR	$e^+e^- \to \Upsilon(4S)$

[62] AUBERT 02G reports $[B(B \to D_s^{*\pm} \text{anything}) \times B(D_s^+ \to \phi\pi^+)] = 0.00284 \pm 0.00029 \pm 0.00025$. We divide by our best value $B(D_s^+ \to \phi\pi^+) = (3.6 \pm 0.9) \times 10^{-2}$. Our first error is their experiment's error and our second error is the systematic error from using our best value.

$\Gamma(D_s^{*\pm}\overline{D}^{(*)})/\Gamma(D_s^{*\pm} \text{anything})$ Γ_{29}/Γ_{28}

Sum over modes

VALUE	DOCUMENT ID		TECN	COMMENT
$0.533 \pm 0.037 \pm 0.037$	AUBERT	02G	BABR	$e^+e^- \to \Upsilon(4S)$

$\Gamma(\overline{D}D_{sJ}(2317))/\Gamma_{\text{total}}$ Γ_{30}/Γ

VALUE	DOCUMENT ID		TECN	COMMENT
seen	[63] KROKOVNY	03B	BELL	$e^+e^- \to \Upsilon(4S)$

[63] The product branching ratio for $B(B \to \overline{D}D_{sJ}(2317)^+) \times B(D_{sJ}(2317)^+ \to D_s\pi^0)$ is measured to be $(8.5^{+2.1}_{-1.9} \pm 2.6) \times 10^{-4}$.

$\Gamma(\overline{D}D_{sJ}(2457))/\Gamma_{\text{total}}$ Γ_{31}/Γ

VALUE	DOCUMENT ID		TECN	COMMENT
seen	[64] KROKOVNY	03B	BELL	$e^+e^- \to \Upsilon(4S)$

[64] The product branching ratio for $B(B \to \overline{D}D_{sJ}(2457)^+) \times B(D_{sJ}(2457)^+ \to D_s^{*+}\pi^0, D_s^+\gamma)$ are measured to be $(17.8^{+4.5}_{-3.9} \pm 5.3) \times 10^{-4}$ and $(6.7^{+1.3}_{-1.2} \pm 2.0) \times 10^{-4}$, respectively.

$[\Gamma(D^{(*)}\overline{D}^{(*)}K^0) + \Gamma(D^{(*)}\overline{D}^{(*)}K^{\pm})]/\Gamma_{\text{total}}$ Γ_{32}/Γ

VALUE	DOCUMENT ID		TECN	COMMENT
$0.071^{+0.025}_{-0.015}{}^{+0.010}_{-0.009}$	[65] BARATE	98Q	ALEP	$e^+e^- \to Z$

[65] The systematic error includes the uncertainties due to the charm branching ratios.

$\Gamma(c\overline{c}s)/\Gamma_{\text{total}}$ Γ_{33}/Γ

VALUE	DOCUMENT ID		TECN	COMMENT
0.219 ± 0.037	[66] COAN	98	CLE2	$e^+e^- \to \Upsilon(4S)$

[66] COAN 98 uses D-ℓ correlation.

$\Gamma(D_s^{(*)}\overline{D}^{(*)})/\Gamma(D_s^{\pm} \text{anything})$ Γ_{34}/Γ_{27}

Sum over modes.

VALUE	DOCUMENT ID		TECN	COMMENT
0.469 ± 0.017 OUR AVERAGE				
$0.464 \pm 0.013 \pm 0.015$	AUBERT	02G	BABR	$e^+e^- \to \Upsilon(4S)$
$0.56^{+0.21}_{-0.15}{}^{+0.09}_{-0.08}$	[67] BARATE	98Q	ALEP	$e^+e^- \to Z$
$0.457 \pm 0.019 \pm 0.037$	GIBAUT	96	CLE2	$e^+e^- \to \Upsilon(4S)$
$0.58 \pm 0.07 \pm 0.09$	ALBRECHT	92G	ARG	$e^+e^- \to \Upsilon(4S)$
0.56 ± 0.10	BORTOLETTO	90	CLEO	$e^+e^- \to \Upsilon(4S)$

[67] BARATE 98Q measures $B(B \to D_s(*)\overline{D}(*)) = 0.056^{+0.021}_{-0.015}{}^{+0.009}_{-0.008}{}^{+0.019}_{-0.011}$, where the third error results from the uncertainty on the different D branching ratios and is dominated by the uncertainty on $B(D_s^+ \to \phi\pi^+)$. We divide $B(B \to D_s(*)\overline{D}(*))$ by our best value of $B(B \to D_s \text{anything}) = 0.1 \pm 0.025$.

$\Gamma(D^*D^*(2010)^{\pm})/\Gamma_{\text{total}}$ Γ_{35}/Γ

VALUE	CL%	DOCUMENT ID		TECN	COMMENT
$<5.9 \times 10^{-3}$	90	BARATE	98Q	ALEP	$e^+e^- \to Z$

$[\Gamma(DD^*(2010)^{\pm}) + \Gamma(D^*D^{\pm})]/\Gamma_{\text{total}}$ Γ_{36}/Γ

VALUE	CL%	DOCUMENT ID		TECN	COMMENT
$<5.5 \times 10^{-3}$	90	BARATE	98Q	ALEP	$e^+e^- \to Z$

$\Gamma(DD^{\pm})/\Gamma_{\text{total}}$ Γ_{37}/Γ

VALUE	CL%	DOCUMENT ID		TECN	COMMENT
$<3.1 \times 10^{-3}$	90	BARATE	98Q	ALEP	$e^+e^- \to Z$

$\Gamma(D_s^{(*)\pm}\overline{D}^{(*)}X(n\pi^{\pm}))/\Gamma_{\text{total}}$ Γ_{38}/Γ

VALUE	DOCUMENT ID		TECN	COMMENT
$0.094^{+0.040}_{-0.031}{}^{+0.034}_{-0.024}$	[68] BARATE	98Q	ALEP	$e^+e^- \to Z$

[68] The systematic error includes the uncertainties due to the charm branching ratios.

$\Gamma(D^*(2010)\gamma)/\Gamma_{\text{total}}$ Γ_{39}/Γ

VALUE	CL%	DOCUMENT ID		TECN	COMMENT
$<1.1 \times 10^{-3}$	90	[69] LESIAK	92	CBAL	$e^+e^- \to \Upsilon(4S)$

[69] LESIAK 92 set a limit on the inclusive process $B(b \to s\gamma) < 2.8 \times 10^{-3}$ at 90% CL for the range of masses of 892–2045 MeV, independent of assumptions about s-quark hadronization.

$\Gamma(D_s^+\pi^-, D_s^{*+}\pi^-, D_s^+\rho^-, D_s^{*+}\rho^-, D_s^+\pi^0, D_s^{*+}\pi^0, D_s^+\eta, D_s^{*+}\eta, D_s^+\rho^0, D_s^{*+}\rho^0, D_s^+\omega, D_s^{*+}\omega)/\Gamma_{\text{total}}$ Γ_{40}/Γ

Sum over modes.

VALUE	CL%	DOCUMENT ID		TECN	COMMENT
<0.0005	90	[70] ALEXANDER	93B	CLE2	$e^+e^- \to \Upsilon(4S)$

[70] ALEXANDER 93B reports $< 4.8 \times 10^{-4}$ for $B(D_s^+ \to \phi\pi^+) = 0.037$. We rescale to our best value $B(D_s^+ \to \phi\pi^+) = 0.036$. This branching ratio limit provides a model-dependent upper limit $|V_{ub}|/|V_{cb}| < 0.16$ at CL=90%.

$\Gamma(D_{s1}(2536)^+ \text{anything})/\Gamma_{\text{total}}$ Γ_{41}/Γ

$D_{s1}(2536)^+$ is the narrow P-wave D_s^+ meson with $J^P = 1^+$.

VALUE	CL%	DOCUMENT ID		TECN	COMMENT
< 0.0095	90	[71] BISHAI	98	CLE2	$e^+e^- \to \Upsilon(4S)$

[71] Assuming factorization, the decay constant $f_{D_{s1}^+}$ is at least a factor of 2.5 times smaller than $f_{D_s^+}$.

$\Gamma(J/\psi(1S) \text{anything})/\Gamma_{\text{total}}$ Γ_{42}/Γ

VALUE (units 10^{-2})	EVTS	DOCUMENT ID		TECN	COMMENT
1.094 ± 0.032 OUR AVERAGE		Error includes scale factor of 1.1.			
1.057 ± 0.012 ± 0.040		[72] AUBERT	03F	BABR	$e^+e^- \to \Upsilon(4S)$
1.121 ± 0.013 ± 0.042		ANDERSON	02	CLE2	$e^+e^- \to \Upsilon(4S)$
1.30 ± 0.45 ± 0.02	27	[73] MASCHMANN	90	CBAL	$e^+e^- \to \Upsilon(4S)$
1.24 ± 0.27 ± 0.02	120	[74] ALBRECHT	87D	ARG	$e^+e^- \to \Upsilon(4S)$
1.37 ± 0.25 ± 0.02	52	[75] ALAM	86	CLEO	$e^+e^- \to \Upsilon(4S)$
• • • We do not use the following data for averages, fits, limits, etc. • • •					
1.13 ± 0.06 ± 0.02	1489	[76] BALEST	95B	CLE2	$e^+e^- \to \Upsilon(4S)$
$1.4\ ^{+0.6}_{-0.5}$	7	[77] ALBRECHT	85H	ARG	$e^+e^- \to \Upsilon(4S)$
1.1 ± 0.21 ± 0.23	46	[78] HAAS	85	CLEO	Repl. by ALAM 86

[72] AUBERT 03F also reports the momentum distribution and helicity of $J/\psi \to \ell^+\ell^-$ in the $\Upsilon(4S)$ center-of-mass frame.

[73] MASCHMANN 90 reports 1.12 ± 0.33 ± 0.25 for $B(J/\psi(1S) \to e^+e^-) = 0.069 \pm 0.009$. We rescale to our best value $B(J/\psi(1S) \to e^+e^-) = (5.93 \pm 0.10) \times 10^{-2}$. Our first error is their experiment's error and our second error is the systematic error from using our best value.

[74] ALBRECHT 87D reports 1.07 ± 0.16 ± 0.22 for $B(J/\psi(1S) \to e^+e^-) = 0.069 \pm 0.009$. We rescale to our best value $B(J/\psi(1S) \to e^+e^-) = (5.93 \pm 0.10) \times 10^{-2}$. Our first error is their experiment's error and our second error is the systematic error from using our best value. ALBRECHT 87D find the branching ratio for J/ψ not from $\psi(2S)$ to be 0.0081 ± 0.0023.

[75] ALAM 86 reports 1.09 ± 0.16 ± 0.21 for $B(J/\psi(1S) \to \mu^+\mu^-) = 0.074 \pm 0.012$. We rescale to our best value $B(J/\psi(1S) \to \mu^+\mu^-) = (5.88 \pm 0.10) \times 10^{-2}$. Our first error is their experiment's error and our second error is the systematic error from using our best value.

[76] BALEST 95B reports 1.12 ± 0.04 ± 0.06 for $B(J/\psi(1S) \to e^+e^-) = 0.0599 \pm 0.0025$. We rescale to our best value $B(J/\psi(1S) \to e^+e^-) = (5.93 \pm 0.10) \times 10^{-2}$. Our first error is their experiment's error and our second error is the systematic error from using our best value.. They measure $J/\psi(1S) \to e^+e^-$ and $\mu^+\mu^-$ and use PDG 1994 values for the branching fractions. The rescaling is the same for either mode so we use e^+e^-.

[77] Statistical and systematic errors were added in quadrature. ALBRECHT 85H also report a CL = 90% limit of 0.007 for $B \to J/\psi(1S) + X$ where $m_X < 1$ GeV.

[78] Dimuon and dielectron events used.

$\Gamma(J/\psi(1S) \text{(direct) anything})/\Gamma_{\text{total}}$ Γ_{43}/Γ

VALUE	DOCUMENT ID		TECN	COMMENT
0.0078 ± 0.0004 OUR AVERAGE	Error includes scale factor of 1.1.			
0.00740 ± 0.00023 ± 0.00043	[79] AUBERT	03F	BABR	$e^+e^- \to \Upsilon(4S)$
0.00813 ± 0.00017 ± 0.00037	[80] ANDERSON	02	CLE2	$e^+e^- \to \Upsilon(4S)$
• • • We do not use the following data for averages, fits, limits, etc. • • •				
0.0080 ± 0.0008	[81] BALEST	95B	CLE2	$e^+e^- \to \Upsilon(4S)$

[79] AUBERT 03F also reports the helicity of $J/\psi \to \ell^+\ell^-$ produced directly in B decay.

[80] Also reports the measurement of $J/\psi \to \ell^+\ell^-$ polarization produced directly from B decay.

[81] BALEST 95B assume PDG 1994 values for sub mode branching ratios. $J/\psi(1S)$ mesons are reconstructed in $J/\psi(1S) \to e^+e^-$ and $J/\psi(1S) \to \mu^+\mu^-$. The $B \to J/\psi(1S)X$ branching ratio contains $J/\psi(1S)$ mesons directly from B decays and also from feeddown through $\psi(2S) \to J/\psi(1S)$, $\chi_{c1}(1P) \to J/\psi(1S)$, or $\chi_{c2}(1P) \to J/\psi(1S)$. Using the measured inclusive rates, BALEST 95B corrects for the feeddown and finds the $B \to J/\psi(1S)$ (direct) X branching ratio.

$\Gamma(\psi(2S) \text{anything})/\Gamma_{\text{total}}$ Γ_{44}/Γ

VALUE	EVTS	DOCUMENT ID		TECN	COMMENT
0.00307 ± 0.00021 OUR AVERAGE					
0.00297 ± 0.00020 ± 0.00020		AUBERT	03F	BABR	$e^+e^- \to \Upsilon(4S)$
0.00316 ± 0.00014 ± 0.00028		[82] ANDERSON	02	CLE2	$e^+e^- \to \Upsilon(4S)$
0.0046 ± 0.0017 ± 0.0011	8	ALBRECHT	87D	ARG	$e^+e^- \to \Upsilon(4S)$
• • • We do not use the following data for averages, fits, limits, etc. • • •					
0.0034 ± 0.0004 ± 0.0003	240	[83] BALEST	95B	CLE2	$e^+e^- \to \Upsilon(4S)$

[82] Also reports the measurement of $\psi(2S) \to \ell^+\ell^-$ polarization produced directly from B decay.

[83] BALEST 95B assume PDG 1994 values for sub mode branching ratios. They find $B(B \to \psi(2S)X,\ \psi(2S) \to \ell^+\ell^-) = 0.30 \pm 0.05 \pm 0.04$ and $B(B \to \psi(2S)X,\ \psi(2S) \to J/\psi(1S)\pi^+\pi^-) = 0.37 \pm 0.05 \pm 0.05$. Weighted average is quoted for $B(B \to \psi(2S)X)$.

$\Gamma(\chi_{c1}(1P) \text{anything})/\Gamma_{\text{total}}$ Γ_{45}/Γ

VALUE	EVTS	DOCUMENT ID		TECN	COMMENT
0.00386 ± 0.00027 OUR AVERAGE					
0.00367 ± 0.00035 ± 0.00044		AUBERT	03F	BABR	$e^+e^- \to \Upsilon(4S)$
0.00363 ± 0.00022 ± 0.00034		[84] ABE	02L	BELL	$e^+e^- \to \Upsilon(4S)$
0.00435 ± 0.00029 ± 0.00040		ANDERSON	02	CLE2	$e^+e^- \to \Upsilon(4S)$
• • • We do not use the following data for averages, fits, limits, etc. • • •					
0.0036 ± 0.0004 ± 0.0004		[85] CHEN	01	CLE2	$e^+e^- \to \Upsilon(4S)$
0.0040 ± 0.0006 ± 0.0004	112	[86] BALEST	95B	CLE2	Repl. by CHEN 01
0.0105 ± 0.0035 ± 0.0025		[87] ALBRECHT	92E	ARG	$e^+e^- \to \Upsilon(4S)$

[84] ABE 02L uses PDG 01 values for $B(J/\psi(1S) \to \ell^+\ell^-)$ and $B(\chi_{c1,c2} \to J/\psi(1S)\gamma)$.

[85] CHEN 01 reports 0.00414 ± 0.00031 ± 0.00040 for $B(\chi_{c1}(1P) \to \gamma J/\psi(1S)) = 0.273 \pm 0.016$. We rescale to our best value $B(\chi_{c1}(1P) \to \gamma J/\psi(1S)) = (31.6 \pm 3.3) \times 10^{-2}$. Our first error is their experiment's error and our second error is the systematic error from using our best value. Assumes equal production of B^+ and B^0 at the $\Upsilon(4S)$.

[86] BALEST 95B assume $B(\chi_{c1}(1P) \to J/\psi(1S)\gamma) = (27.3 \pm 1.6) \times 10^{-2}$, the PDG 1994 value. Fit to ψ-photon invariant mass distribution allows for a $\chi_{c1}(1P)$ and a $\chi_{c2}(1P)$ component.

[87] ALBRECHT 92E assumes no $\chi_{c2}(1P)$ production.

$\Gamma(\chi_{c1}(1P) \text{(direct) anything})/\Gamma_{\text{total}}$ Γ_{46}/Γ

VALUE	DOCUMENT ID		TECN	COMMENT
0.00334 ± 0.00028 OUR AVERAGE				
0.00341 ± 0.00035 ± 0.00042	AUBERT	03F	BABR	$e^+e^- \to \Upsilon(4S)$
0.00332 ± 0.00022 ± 0.00034	[88] ABE	02L	BELL	$e^+e^- \to \Upsilon(4S)$
0.0033 ± 0.0004 ± 0.0003	[89] CHEN	01	CLE2	$e^+e^- \to \Upsilon(4S)$
• • • We do not use the following data for averages, fits, limits, etc. • • •				
0.0037 ± 0.0007	[90] BALEST	95B	CLE2	Repl. by CHEN 01

[88] ABE 02L uses PDG 01 values for $B(J/\psi(1S) \to \ell^+\ell^-)$ and $B(\chi_{c1,c2} \to J/\psi(1S)\gamma)$.

[89] CHEN 01 reports 0.00383 ± 0.00031 ± 0.00040 for $B(\chi_{c1}(1P) \to \gamma J/\psi(1S)) = 0.273 \pm 0.016$. We rescale to our best value $B(\chi_{c1}(1P) \to \gamma J/\psi(1S)) = (31.6 \pm 3.3) \times 10^{-2}$. Our first error is their experiment's error and our second error is the systematic error from using our best value. Assumes equal production of B^+ and B^0 at the $\Upsilon(4S)$.

[90] BALEST 95B assume PDG 1994 values. $J/\psi(1S)$ mesons are reconstructed in the e^+e^- and $\mu^+\mu^-$ modes. The $B \to \chi_{c1}(1P)X$ branching ratio contains $\chi_{c1}(1P)$ mesons directly from B decays and also from feeddown through $\psi(2S) \to \chi_{c1}(1P)\gamma$. Using the measured inclusive rates, BALEST 95B corrects for the feeddown and finds the $B \to \chi_{c1}(1P)$ (direct) X branching ratio.

$\Gamma(\chi_{c2}(1P) \text{anything})/\Gamma_{\text{total}}$ Γ_{47}/Γ

VALUE (units 10^{-4})	CL%	EVTS	DOCUMENT ID		TECN	COMMENT
13 ± 4 OUR AVERAGE			Error includes scale factor of 1.9. See the ideogram below.			
21.0 ± 4.5 ± 3.1			AUBERT	03F	BABR	$e^+e^- \to \Upsilon(4S)$
$18.0\ ^{+2.3}_{-2.8} \pm 2.6$			[91] ABE	02L	BELL	$e^+e^- \to \Upsilon(4S)$
6.5 ± 3.3 ± 0.6			[92] CHEN	01	CLE2	$e^+e^- \to \Upsilon(4S)$
• • • We do not use the following data for averages, fits, limits, etc. • • •						
< 38	90	35	[93] BALEST	95B	CLE2	Repl. by CHEN 01

[91] ABE 02L uses PDG 01 values for $B(J/\psi(1S) \to \ell^+\ell^-)$ and $B(\chi_{c1,c2} \to J/\psi(1S)\gamma)$.

[92] CHEN 01 reports 9.8 ± 4.8 ± 1.5 for $B(\chi_{c2}(1P) \to \gamma J/\psi(1S)) = 0.135 \pm 0.011$. We rescale to our best value $B(\chi_{c2}(1P) \to \gamma J/\psi(1S)) = (20.2 \pm 1.7) \times 10^{-2}$. Our first error is their experiment's error and our second error is the systematic error from using our best value. Assumes equal production of B^+ and B^0 at the $\Upsilon(4S)$.

[93] BALEST 95B assume $B(\chi_{c2}(1P) \to J/\psi(1S)\gamma) = (13.5 \pm 1.1) \times 10^{-2}$, the PDG 1994 value. $J/\psi(1S)$ mesons are reconstructed in the e^+e^- and $\mu^+\mu^-$ modes, and PDG 1994 branching fractions are used. If interpreted as signal, the 35 ± 13 events correspond to $B(B \to \chi_{c2}(1P)X) = (0.25 \pm 0.10 \pm 0.03) \times 10^{-2}$.

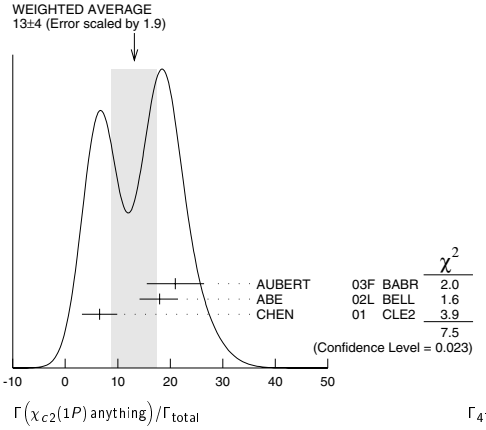

$\Gamma(\chi_{c2}(1P) \text{anything})/\Gamma_{\text{total}}$ Γ_{47}/Γ

$\Gamma(\chi_{c2}(1P) \text{(direct) anything})/\Gamma_{\text{total}}$ Γ_{48}/Γ

VALUE	DOCUMENT ID		TECN	COMMENT
0.00165 ± 0.00031 OUR AVERAGE				
0.00190 ± 0.00045 ± 0.00029	AUBERT	03F	BABR	$e^+e^- \to \Upsilon(4S)$
$0.00153\ ^{+0.00023}_{-0.00028} \pm 0.00027$	[94] ABE	02L	BELL	$e^+e^- \to \Upsilon(4S)$

[94] ABE 02L uses PDG 01 values for $B(J/\psi(1S) \to \ell^+\ell^-)$ and $B(\chi_{c1,c2} \to J/\psi(1S)\gamma)$.

$\Gamma(\eta_c(1S)\text{anything})/\Gamma_{\text{total}}$ Γ_{49}/Γ

VALUE	CL%	DOCUMENT ID		TECN	COMMENT
< 0.009	90	[95] BALEST	95B	CLE2	$e^+e^- \to \Upsilon(4S)$

[95] BALEST 95B assume PDG 1994 values for sub mode branching ratios. $J/\psi(1S)$ mesons are reconstructed in $J/\psi(1S) \to e^+e^-$ and $J/\psi(1S) \to \mu^+\mu^-$. Search region $2960 < m_{\eta_c(1S)} < 3010$ MeV/c^2.

$\Gamma(K^{\pm}\text{anything})/\Gamma_{\text{total}}$ Γ_{50}/Γ

VALUE	DOCUMENT ID		TECN	COMMENT
0.789 ± 0.025 OUR AVERAGE				
0.82 ± 0.01 ± 0.05	ALBRECHT	94C	ARG	$e^+e^- \to \Upsilon(4S)$
0.775 ± 0.015 ± 0.025	[96] ALBRECHT	93I	ARG	$e^+e^- \to \Upsilon(4S)$
0.85 ± 0.07 ± 0.09	ALAM	87B	CLEO	$e^+e^- \to \Upsilon(4S)$
• • • We do not use the following data for averages, fits, limits, etc. • • •				
seen	[97] BRODY	82	CLEO	$e^+e^- \to \Upsilon(4S)$
seen	[98] GIANNINI	82	CUSB	$e^+e^- \to \Upsilon(4S)$

[96] ALBRECHT 93I value is not independent of the sum of $B \to K^+$ anything and $B \to K^-$ anything ALBRECHT 94C values.

[97] Assuming $\Upsilon(4S) \to B\overline{B}$, a total of $3.38 \pm 0.34 \pm 0.68$ kaons per $\Upsilon(4S)$ decay is found (the second error is systematic). In the context of the standard B-decay model, this leads to a value for (b-quark $\to$ c-quark)/(b-quark $\to$ all) of $1.09 \pm 0.33 \pm 0.13$.

[98] GIANNINI 82 at CESR-CUSB observed 1.58 ± 0.35 K^0 per hadronic event much higher than 0.82 ± 0.10 below threshold. Consistent with predominant $b \to cX$ decay.

$\Gamma(K^+\text{anything})/\Gamma_{\text{total}}$ Γ_{51}/Γ

VALUE	DOCUMENT ID		TECN	COMMENT
0.66 ± 0.05	[99] ALBRECHT	94C	ARG	$e^+e^- \to \Upsilon(4S)$
• • • We do not use the following data for averages, fits, limits, etc. • • •				
0.620 ± 0.013 ± 0.038	[100] ALBRECHT	94C	ARG	$e^+e^- \to \Upsilon(4S)$
0.66 ± 0.05 ± 0.07	[100] ALAM	87B	CLEO	$e^+e^- \to \Upsilon(4S)$

[99] Measurement relies on lepton-kaon correlations. It is for the weak decay vertex and does not include mixing of the neutral B meson. Mixing effects were corrected for by assuming a mixing parameter r of (18.1 ± 4.3)%.

[100] Measurement relies on lepton-kaon correlations. It includes production through mixing of the neutral B meson.

$\Gamma(K^-\text{anything})/\Gamma_{\text{total}}$ Γ_{52}/Γ

VALUE	DOCUMENT ID		TECN	COMMENT
0.13 ± 0.04	[101] ALBRECHT	94C	ARG	$e^+e^- \to \Upsilon(4S)$
• • • We do not use the following data for averages, fits, limits, etc. • • •				
0.165 ± 0.011 ± 0.036	[102] ALBRECHT	94C	ARG	$e^+e^- \to \Upsilon(4S)$
0.19 ± 0.05 ± 0.02	[102] ALAM	87B	CLEO	$e^+e^- \to \Upsilon(4S)$

[101] Measurement relies on lepton-kaon correlations. It is for the weak decay vertex and does not include mixing of the neutral B meson. Mixing effects were corrected for by assuming a mixing parameter r of (18.1 ± 4.3)%.

[102] Measurement relies on lepton-kaon correlations. It includes production through mixing of the neutral B meson.

$\Gamma(K^0/\overline{K}^0\text{anything})/\Gamma_{\text{total}}$ Γ_{53}/Γ

VALUE	DOCUMENT ID		TECN	COMMENT
0.64 ± 0.04 OUR AVERAGE				
0.642 ± 0.010 ± 0.042	[103] ALBRECHT	94C	ARG	$e^+e^- \to \Upsilon(4S)$
0.63 ± 0.06 ± 0.06	ALAM	87B	CLEO	$e^+e^- \to \Upsilon(4S)$

[103] ALBRECHT 94C assume a $K^0/\overline{K}^0$ multiplicity twice that of K^0_S.

$\Gamma(K^*(892)^{\pm}\text{anything})/\Gamma_{\text{total}}$ Γ_{54}/Γ

VALUE	DOCUMENT ID		TECN	COMMENT
0.182 ± 0.054 ± 0.024	ALBRECHT	94J	ARG	$e^+e^- \to \Upsilon(4S)$

$\Gamma(K^*(892)^0/\overline{K}^*(892)^0\text{anything})/\Gamma_{\text{total}}$ Γ_{55}/Γ

VALUE	DOCUMENT ID		TECN	COMMENT
0.146 ± 0.016 ± 0.020	ALBRECHT	94J	ARG	$e^+e^- \to \Upsilon(4S)$

$\Gamma(K^*(892)\gamma)/\Gamma_{\text{total}}$ Γ_{56}/Γ

VALUE (units 10^{-5})	CL%	DOCUMENT ID		TECN	COMMENT
4.24 ± 0.54 ± 0.32		[104] COAN	00	CLE2	$e^+e^- \to \Upsilon(4S)$
• • • We do not use the following data for averages, fits, limits, etc. • • •					
< 150	90	[105] LESIAK	92	CBAL	$e^+e^- \to \Upsilon(4S)$
< 24	90	ALBRECHT	88H	ARG	$e^+e^- \to \Upsilon(4S)$

[104] An average of $B(B^+ \to K^*(892)^+\gamma)$ and $B(B^0 \to K^*(892)^0\gamma)$ measurements reported in COAN 00 by assuming full correlated systematic errors.

[105] LESIAK 92 set a limit on the inclusive process $B(b \to s\gamma) < 2.8 \times 10^{-3}$ at 90% CL for the range of masses of 892–2045 MeV, independent of assumptions about s-quark hadronization.

$\Gamma(K_1(1400)\gamma)/\Gamma_{\text{total}}$ Γ_{57}/Γ

VALUE	CL%	DOCUMENT ID		TECN	COMMENT
< 12.7 × 10⁻⁵	90	[106] COAN	00	CLE2	$e^+e^- \to \Upsilon(4S)$
• • • We do not use the following data for averages, fits, limits, etc. • • •					
< 1.6 × 10⁻³	90	[107] LESIAK	92	CBAL	$e^+e^- \to \Upsilon(4S)$
< 4.1 × 10⁻⁴	90	ALBRECHT	88H	ARG	$e^+e^- \to \Upsilon(4S)$

[106] Assumes equal production of B^+ and B^0 at the $\Upsilon(4S)$.

[107] LESIAK 92 set a limit on the inclusive process $B(b \to s\gamma) < 2.8 \times 10^{-3}$ at 90% CL for the range of masses of 892–2045 MeV, independent of assumptions about s-quark hadronization.

$\Gamma(K_2^*(1430)\gamma)/\Gamma_{\text{total}}$ Γ_{58}/Γ

VALUE (units 10^{-5})	CL%	DOCUMENT ID		TECN	COMMENT
$1.66^{+0.59}_{-0.53} \pm 0.13$		[108] COAN	00	CLE2	$e^+e^- \to \Upsilon(4S)$
• • • We do not use the following data for averages, fits, limits, etc. • • •					
< 83	90	ALBRECHT	88H	ARG	$e^+e^- \to \Upsilon(4S)$

[108] COAN 00 obtains a fitted signal yield of $15.9^{+5.7}_{-5.2}$ events. A search for contamination by $K^*(1410)$ yielded a rate consistent with 0; the central value assumes no contamination.

$\Gamma(K_2(1770)\gamma)/\Gamma_{\text{total}}$ Γ_{59}/Γ

VALUE	CL%	DOCUMENT ID		TECN	COMMENT
< 1.2 × 10⁻³	90	[109] LESIAK	92	CBAL	$e^+e^- \to \Upsilon(4S)$

[109] LESIAK 92 set a limit on the inclusive process $B(b \to s\gamma) < 2.8 \times 10^{-3}$ at 90% CL for the range of masses of 892–2045 MeV, independent of assumptions about s-quark hadronization.

$\Gamma(K_3^*(1780)\gamma)/\Gamma_{\text{total}}$ Γ_{60}/Γ

VALUE	CL%	DOCUMENT ID		TECN	COMMENT
< 3.0 × 10⁻³	90	ALBRECHT	88H	ARG	$e^+e^- \to \Upsilon(4S)$

$\Gamma(K_4^*(2045)\gamma)/\Gamma_{\text{total}}$ Γ_{61}/Γ

VALUE	CL%	DOCUMENT ID		TECN	COMMENT
< 1.0 × 10⁻³	90	[110] LESIAK	92	CBAL	$e^+e^- \to \Upsilon(4S)$

[110] LESIAK 92 set a limit on the inclusive process $B(b \to s\gamma) < 2.8 \times 10^{-3}$ at 90% CL for the range of masses of 892–2045 MeV, independent of assumptions about s-quark hadronization.

$\Gamma(K\eta'(958))/\Gamma_{\text{total}}$ Γ_{62}/Γ

VALUE	DOCUMENT ID		TECN	COMMENT
$(8.3^{+0.9}_{-0.8} \pm 0.7) \times 10^{-5}$	[111] RICHICHI	00	CLE2	$e^+e^- \to \Upsilon(4S)$

[111] Assumes equal production of B^+ and B^0 at the $\Upsilon(4S)$.

$\Gamma(K^*(892)\eta'(958))/\Gamma_{\text{total}}$ Γ_{63}/Γ

VALUE	CL%	DOCUMENT ID		TECN	COMMENT
< 2.2 × 10⁻⁵	90	[112] RICHICHI	00	CLE2	$e^+e^- \to \Upsilon(4S)$

[112] Assumes equal production of B^+ and B^0 at the $\Upsilon(4S)$.

$\Gamma(K\eta)/\Gamma_{\text{total}}$ Γ_{64}/Γ

VALUE	CL%	DOCUMENT ID		TECN	COMMENT
< 5.2 × 10⁻⁶	90	[113] RICHICHI	00	CLE2	$e^+e^- \to \Upsilon(4S)$

[113] Assumes equal production of B^+ and B^0 at the $\Upsilon(4S)$.

$\Gamma(K^*(892)\eta)/\Gamma_{\text{total}}$ Γ_{65}/Γ

VALUE	DOCUMENT ID		TECN	COMMENT
$(1.80^{+0.49}_{-0.43} \pm 0.18) \times 10^{-5}$	[114] RICHICHI	00	CLE2	$e^+e^- \to \Upsilon(4S)$

[114] Assumes equal production of B^+ and B^0 at the $\Upsilon(4S)$.

$\Gamma(K\phi\phi)/\Gamma_{\text{total}}$ Γ_{66}/Γ

VALUE (units 10^{-6})	DOCUMENT ID		TECN	COMMENT
$2.3^{+0.9}_{-0.8} \pm 0.3$	[115] HUANG	03	BELL	$e^+e^- \to \Upsilon(4S)$

[115] Assumes equal production of charged and neutral B meson pairs and isospin symmetry.

$\Gamma(\overline{b} \to \overline{s}\gamma)/\Gamma_{\text{total}}$ Γ_{67}/Γ

VALUE (units 10^{-4})	DOCUMENT ID		TECN	COMMENT
3.3 ± 0.4 OUR AVERAGE				
$3.36 \pm 0.53^{+0.65}_{-0.68}$	[116] ABE	01F	BELL	$e^+e^- \to \Upsilon(4S)$
$3.21 \pm 0.43^{+0.32}_{-0.29}$	[117] CHEN	01C	CLE2	$e^+e^- \to \Upsilon(4S)$
• • • We do not use the following data for averages, fits, limits, etc. • • •				
2.32 ± 0.57 ± 0.35	ALAM	95	CLE2	Repl. by CHEN 01C

[116] ABE 01F reports their systematic errors $\pm 0.42^{+0.50}_{-0.54}$, where the second error is due to the theoretical uncertainty. We combine them in quadrature.

[117] We have combined the experimental systematic theoretical uncertainties in quadrature. Also determined the first and second moments of the photon energy spectrum above 2.0 GeV: $\langle E_\gamma \rangle = 2.346 \pm 0.032 \pm 0.011$ GeV and $\langle E_\gamma^2 \rangle - \langle E_\gamma \rangle^2 = 0.0226 \pm 0.0066 \pm 0.0020$ GeV^2.

$\Gamma(\overline{b} \to \overline{s}\text{gluon})/\Gamma_{\text{total}}$ Γ_{68}/Γ

VALUE	CL%	EVTS	DOCUMENT ID		TECN	COMMENT
< 0.068	90		[118] COAN	98	CLE2	$e^+e^- \to \Upsilon(4S)$
• • • We do not use the following data for averages, fits, limits, etc. • • •						
< 0.08	2		[119] ALBRECHT	95D	ARG	$e^+e^- \to \Upsilon(4S)$

[118] COAN 98 uses D-ℓ correlation.

[119] ALBRECHT 95D use full reconstruction of one B decay as tag. Two candidate events for charmless B decay can be interpreted as either $b \to s$gluon or $b \to u$ transition. If interpreted as $b \to s$gluon they find a branching ratio of ~ 0.026 or the upper limit quoted above. Result is highly model dependent.

$\Gamma(\eta\,\text{anything})/\Gamma_{\text{total}}$ Γ_{69}/Γ

VALUE	CL%	DOCUMENT ID		TECN	COMMENT
$<4.4\times10^{-4}$	90	[120] BROWDER	98	CLE2	$e^+e^-\to\Upsilon(4S)$

[120] BROWDER 98 search for high momentum $B\to\eta X_s$ between 2.1 and 2.7 GeV/c.

$\Gamma(\eta'\,\text{anything})/\Gamma_{\text{total}}$ Γ_{70}/Γ

VALUE	DOCUMENT ID		TECN	COMMENT
$(4.6\pm1.1\pm0.6)\times10^{-4}$	[121] BONVICINI	03	CLE2	$e^+e^-\to\Upsilon(4S)$
• • • We do not use the following data for averages, fits, limits, etc. • • •				
$(6.2\pm1.6^{+1.3}_{-2.0})\times10^{-4}$	[122] BROWDER	98	CLE2	$e^+e^-\to\Upsilon(4S)$

[121] BONVICINI 03 observed a signal of 61.2 ± 13.9 events in $B\to\eta' X_{nc}$ production for high momentum η' between 2.0 and 2.7 GeV/c in the $\Upsilon(4S)$ center-of-mass frame. The X_{nc} denotes "charmless" hadronic states recoiling against η'. The second error combines systematic and background subtraction uncertainties in quadrature.

[122] BROWDER 98 observed a signal of 39.0 ± 11.6 events in high momentum $B\to\eta' X_s$ production between 2.0 and 2.7 GeV/c. The branching fraction is based on the interpretation of $b\to sg$, where the last error includes additional uncertainties due to the color-suppressed $b\to$ backgrounds.

$\Gamma(\rho\gamma)/\Gamma_{\text{total}}$ Γ_{71}/Γ

VALUE	CL%	DOCUMENT ID		TECN	COMMENT
$<1.9\times10^{-6}$	90	[123] AUBERT	04C	BABR	$e^+e^-\to\Upsilon(4S)$
• • • We do not use the following data for averages, fits, limits, etc. • • •					
$<1.4\times10^{-5}$	90	[124] COAN	00	CLE2	$e^+e^-\to\Upsilon(4S)$

[123] Assumes $\Gamma(B\to\rho\gamma)=\Gamma(B^+\to\rho^+\gamma)=2\,\Gamma(B^0\to\rho^0\gamma)$ and uses lifetime ratio of ${}^{\tau}B^+/{}^{\tau}B^0=1.083\pm0.017$.

[124] COAN 00 reports $B(B\to\rho\gamma)/B(B\to K^*(892)\gamma)<0.32$ at 90%CL and scaled by the central value of $B(B\to K^*(892)\gamma)=(4.24\pm0.54\pm0.32)\times10^{-5}$.

$\Gamma(\pi^{\pm}\,\text{anything})/\Gamma_{\text{total}}$ Γ_{72}/Γ

VALUE	DOCUMENT ID		TECN	COMMENT
$3.585\pm0.025\pm0.070$	[125] ALBRECHT	93I	ARG	$e^+e^-\to\Upsilon(4S)$

[125] ALBRECHT 93 excludes $\pi^{\pm}$ from K^0_S and Λ decays. If included, they find 4.105 ± 0.025 ± 0.080.

$\Gamma(\pi^0\,\text{anything})/\Gamma_{\text{total}}$ Γ_{73}/Γ

VALUE	DOCUMENT ID		TECN	COMMENT
$2.35\pm0.02\pm0.11$	[126] ABE	01J	BELL	$e^+e^-\to\Upsilon(4S)$

[126] From fully inclusive π^0 yield with no corrections from decays of K^0_S or other particles.

$\Gamma(\eta\,\text{anything})/\Gamma_{\text{total}}$ Γ_{74}/Γ

VALUE	DOCUMENT ID		TECN	COMMENT
$0.176\pm0.011\pm0.012$	KUBOTA	96	CLE2	$e^+e^-\to\Upsilon(4S)$

$\Gamma(\rho^0\,\text{anything})/\Gamma_{\text{total}}$ Γ_{75}/Γ

VALUE	DOCUMENT ID		TECN	COMMENT
$0.208\pm0.042\pm0.032$	ALBRECHT	94J	ARG	$e^+e^-\to\Upsilon(4S)$

$\Gamma(\omega\,\text{anything})/\Gamma_{\text{total}}$ Γ_{76}/Γ

VALUE	CL%	DOCUMENT ID		TECN	COMMENT
<0.81	90	ALBRECHT	94J	ARG	$e^+e^-\to\Upsilon(4S)$

$\Gamma(\phi\,\text{anything})/\Gamma_{\text{total}}$ Γ_{77}/Γ

VALUE	DOCUMENT ID		TECN	COMMENT
0.035 ±0.007 OUR AVERAGE	Error includes scale factor of 1.8.			
$0.0390\pm0.0030\pm0.0035$	ALBRECHT	94J	ARG	$e^+e^-\to\Upsilon(4S)$
$0.023\ \pm0.006\ \pm0.005$	BORTOLETTO	86	CLEO	$e^+e^-\to\Upsilon(4S)$

$\Gamma(\phi K^*(892))/\Gamma_{\text{total}}$ Γ_{78}/Γ

VALUE	CL%	DOCUMENT ID		TECN
$<2.2\times10^{-5}$	90	[127] BERGFELD	98	CLE2

[127] Assumes equal production of B^+ and B^0 at the $\Upsilon(4S)$.

$\Gamma(\Lambda_c^+/\overline{\Lambda}_c^-\,\text{anything})/\Gamma_{\text{total}}$ Γ_{79}/Γ

VALUE	CL%	DOCUMENT ID		TECN	COMMENT
$0.064\pm0.008\pm0.008$		[128] CRAWFORD	92	CLEO	$e^+e^-\to\Upsilon(4S)$
• • • We do not use the following data for averages, fits, limits, etc. • • •					
$0.14\ \pm0.09$		[129] ALBRECHT	88E	ARG	$e^+e^-\to\Upsilon(4S)$
<0.112	90	[130] ALAM	87	CLEO	$e^+e^-\to\Upsilon(4S)$

[128] CRAWFORD 92 result derived from lepton baryon correlations. Assumes all charmed baryons in B^0 and $B^{\pm}$ decay are Λ_c.

[129] ALBRECHT 88E measured $B(B\to\Lambda_c^+X)\cdot B(\Lambda_c^+\to pK^-\pi^+)=(0.30\pm0.12\pm0.06)\%$ and used $B(\Lambda_c^+\to pK^-\pi^+)=(2.2\pm1.0)\%$ from ABRAMS 80 to obtain above number.

[130] Assuming all baryons result from charmed baryons, ALAM 86 conclude the branching fraction is 7.4 ± 2.9%. The limit given above is model independent.

$\Gamma(\Lambda_c^+\,\text{anything})/\Gamma(\overline{\Lambda}_c^-\,\text{anything})$ Γ_{80}/Γ_{81}

VALUE	DOCUMENT ID		TECN	COMMENT
$0.19\pm0.13\pm0.04$	[131] AMMAR	97	CLE2	$e^+e^-\to\Upsilon(4S)$

[131] AMMAR 97 uses a high-momentum lepton tag ($P_\ell>1.4$ GeV/c^2).

$\Gamma(\overline{\Lambda}_c^-e^+\,\text{anything})/\Gamma(\Lambda_c^+/\overline{\Lambda}_c^-\,\text{anything})$ Γ_{82}/Γ_{79}

VALUE	CL%	DOCUMENT ID		TECN	COMMENT
<0.05	90	[132] BONVICINI	98	CLE2	$e^+e^-\to\Upsilon(4S)$

[132] BONVICINI 98 uses the electron with momentum above 0.6 GeV/c.

$\Gamma(\overline{\Lambda}_c^-p\,\text{anything})/\Gamma(\Lambda_c^+/\overline{\Lambda}_c^-\,\text{anything})$ Γ_{83}/Γ_{79}

VALUE	DOCUMENT ID		TECN	COMMENT
$0.57\pm0.05\pm0.05$	BONVICINI	98	CLE2	$e^+e^-\to\Upsilon(4S)$

$\Gamma(\overline{\Lambda}_c^-pe^+\nu_e)/\Gamma(\overline{\Lambda}_c^-p\,\text{anything})$ Γ_{84}/Γ_{83}

VALUE	CL%	DOCUMENT ID		TECN	COMMENT
<0.04	90	[133] BONVICINI	98	CLE2	$e^+e^-\to\Upsilon(4S)$

[133] BONVICINI 98 uses the electron with momentum above 0.6 GeV/c.

$\Gamma(\overline{\Sigma}_c^{--}\,\text{anything})/\Gamma_{\text{total}}$ Γ_{85}/Γ

VALUE	EVTS	DOCUMENT ID		TECN	COMMENT
$0.0042\pm0.0021\pm0.0011$	77	[134] PROCARIO	94	CLE2	$e^+e^-\to\Upsilon(4S)$

[134] PROCARIO 94 reports $[B(B\to\overline{\Sigma}_c^{--}\,\text{anything})\times B(\Lambda_c^+\to pK^-\pi^+)]=0.00021\pm0.00008\pm0.00007$. We divide by our best value $B(\Lambda_c^+\to pK^-\pi^+)=(5.0\pm1.3)\times10^{-2}$. Our first error is their experiment's error and our second error is the systematic error from using our best value.

$\Gamma(\overline{\Sigma}_c^-\,\text{anything})/\Gamma_{\text{total}}$ Γ_{86}/Γ

VALUE	CL%	DOCUMENT ID		TECN	COMMENT
<0.010	90	[135] PROCARIO	94	CLE2	$e^+e^-\to\Upsilon(4S)$

[135] PROCARIO 94 reports $[B(B\to\overline{\Sigma}_c^-\,\text{anything})\times B(\Lambda_c^+\to pK^-\pi^+)]=<0.00048$. We divide by our best value $B(\Lambda_c^+\to pK^-\pi^+)=0.050$.

$\Gamma(\overline{\Sigma}_c^0\,\text{anything})/\Gamma_{\text{total}}$ Γ_{87}/Γ

VALUE	EVTS	DOCUMENT ID		TECN	COMMENT
$0.0046\pm0.0021\pm0.0012$	76	[136] PROCARIO	94	CLE2	$e^+e^-\to\Upsilon(4S)$

[136] PROCARIO 94 reports $[B(B\to\overline{\Sigma}_c^0\,\text{anything})\times B(\Lambda_c^+\to pK^-\pi^+)]=0.00023\pm0.00008\pm0.00007$. We divide by our best value $B(\Lambda_c^+\to pK^-\pi^+)=(5.0\pm1.3)\times10^{-2}$. Our first error is their experiment's error and our second error is the systematic error from using our best value.

$\Gamma(\overline{\Sigma}_c^0N(N=p\text{ or }n))/\Gamma_{\text{total}}$ Γ_{88}/Γ

VALUE	CL%	DOCUMENT ID		TECN	COMMENT
<0.0015	90	[137] PROCARIO	94	CLE2	$e^+e^-\to\Upsilon(4S)$

[137] PROCARIO 94 reports <0.0017 for $B(\Lambda_c^+\to pK^-\pi^+)=0.043$. We rescale to our best value $B(\Lambda_c^+\to pK^-\pi^+)=0.050$.

$\Gamma(\Xi_c^0\,\text{anything}\times B(\Xi_c^0\to\Xi^-\pi^+))/\Gamma_{\text{total}}$ Γ_{89}/Γ

VALUE (units 10^{-3})	DOCUMENT ID		TECN	COMMENT
$0.144\pm0.048\pm0.021$	[138] BARISH	97	CLE2	$e^+e^-\to\Upsilon(4S)$

[138] BARISH 97 find 79 ± 27 Ξ_c^0 events.

$\Gamma(\Xi_c^+\,\text{anything}\times B(\Xi_c^+\to\Xi^-\pi^+\pi^+))/\Gamma_{\text{total}}$ Γ_{90}/Γ

VALUE (units 10^{-3})	DOCUMENT ID		TECN	COMMENT
$0.453\pm0.096^{+0.085}_{-0.065}$	[139] BARISH	97	CLE2	$e^+e^-\to\Upsilon(4S)$

[139] BARISH 97 find 125 ± 28 Ξ_c^+ events.

$\Gamma(p/\overline{p}\,\text{anything})/\Gamma_{\text{total}}$ Γ_{91}/Γ

Includes p and $\overline{p}$ from Λ and $\overline{\Lambda}$ decay.

VALUE	EVTS	DOCUMENT ID		TECN	COMMENT
0.080±0.004 OUR AVERAGE					
$0.080\pm0.005\pm0.005$		ALBRECHT	93I	ARG	$e^+e^-\to\Upsilon(4S)$
$0.080\pm0.005\pm0.003$		CRAWFORD	92	CLEO	$e^+e^-\to\Upsilon(4S)$
$0.082\pm0.005^{+0.013}_{-0.010}$	2163	[140] ALBRECHT	89K	ARG	$e^+e^-\to\Upsilon(4S)$
• • • We do not use the following data for averages, fits, limits, etc. • • •					
>0.021		[141] ALAM	83B	CLEO	$e^+e^-\to\Upsilon(4S)$

[140] ALBRECHT 89K include direct and nondirect protons.

[141] ALAM 83B reported their result as $>0.036\pm0.006\pm0.009$. Data are consistent with equal yields of p and $\overline{p}$. Using assumed yields below cut, $B(B\to p+X)=0.03$ not including protons from Λ decays.

$\Gamma(p/\overline{p}(\text{direct})\,\text{anything})/\Gamma_{\text{total}}$ Γ_{92}/Γ

VALUE	EVTS	DOCUMENT ID		TECN	COMMENT
0.055±0.005 OUR AVERAGE					
$0.055\pm0.005\pm0.0035$		ALBRECHT	93I	ARG	$e^+e^-\to\Upsilon(4S)$
$0.056\pm0.006\pm0.005$		CRAWFORD	92	CLEO	$e^+e^-\to\Upsilon(4S)$
0.055 ± 0.016	1220	[142] ALBRECHT	89K	ARG	$e^+e^-\to\Upsilon(4S)$

[142] ALBRECHT 89K subtract contribution of Λ decay from the inclusive proton yield.

Meson Particle Listings

$B^{\pm}/B^{0}$ ADMIXTURE

$\Gamma(\Lambda/\overline{\Lambda}\text{anything})/\Gamma_{\text{total}}$ Γ_{93}/Γ

VALUE	EVTS	DOCUMENT ID		TECN	COMMENT
0.040 ± 0.005 OUR AVERAGE					
0.038 ± 0.004 ± 0.006	2998	CRAWFORD	92	CLEO	$e^+e^- \to \Upsilon(4S)$
0.042 ± 0.005 ± 0.006	943	ALBRECHT	89K	ARG	$e^+e^- \to \Upsilon(4S)$
• • • We do not use the following data for averages, fits, limits, etc. • • •					
0.022 ± 0.003 ± 0.0022		[143] ACKERSTAFF	97N	OPAL	$e^+e^- \to Z$
> 0.011		[144] ALAM	83B	CLEO	$e^+e^- \to \Upsilon(4S)$

[143] ACKERSTAFF 97N assumes $B(b \to B) = 0.868 \pm 0.041$, *i.e.*, an admixture of B^0, $B^{\pm}$, and B_s.

[144] ALAM 83B reported their result as $> 0.022 \pm 0.007 \pm 0.004$. Values are for $(B(\Lambda X)+B(\overline{\Lambda} X))/2$. Data are consistent with equal yields of p and $\overline{p}$. Using assumed yields below cut, $B(B \to \Lambda X) = 0.03$.

$\Gamma(\Lambda\text{anything})/\Gamma(\overline{\Lambda}\text{anything})$ Γ_{94}/Γ_{95}

VALUE	DOCUMENT ID		TECN	COMMENT
0.43 ± 0.09 ± 0.07	[145] AMMAR	97	CLE2	$e^+e^- \to \Upsilon(4S)$

[145] AMMAR 97 uses a high-momentum lepton tag ($P_\ell > 1.4$ GeV/c^2).

$\Gamma(\Xi^-/\overline{\Xi}^+\text{anything})/\Gamma_{\text{total}}$ Γ_{96}/Γ

VALUE	EVTS	DOCUMENT ID		TECN	COMMENT
0.0027 ± 0.0006 OUR AVERAGE					
0.0027 ± 0.0005 ± 0.0004	147	CRAWFORD	92	CLEO	$e^+e^- \to \Upsilon(4S)$
0.0028 ± 0.0014	54	ALBRECHT	89K	ARG	$e^+e^- \to \Upsilon(4S)$

$\Gamma(\text{baryons anything})/\Gamma_{\text{total}}$ Γ_{97}/Γ

VALUE	DOCUMENT ID		TECN	COMMENT
0.068 ± 0.005 ± 0.003	[146] ALBRECHT	92O	ARG	$e^+e^- \to \Upsilon(4S)$
• • • We do not use the following data for averages, fits, limits, etc. • • •				
0.076 ± 0.014	[147] ALBRECHT	89K	ARG	$e^+e^- \to \Upsilon(4S)$

[146] ALBRECHT 92O result is from simultaneous analysis of p and Λ yields, $p\overline{p}$ and $\Lambda\overline{p}$ correlations, and various lepton-baryon and lepton-baryon-antibaryon correlations. Supersedes ALBRECHT 89K.

[147] ALBRECHT 89K obtain this result by adding their their measurements (5.5 ± 1.6)% for direct protons and (4.2 ± 0.5 ± 0.6)% for inclusive Λ production. They then assume (5.5 ± 1.6)% for neutron production and add it in also. Since each B decay has two baryons, they divide by 2 to obtain (7.6 ± 1.4)%.

$\Gamma(p\overline{p}\text{anything})/\Gamma_{\text{total}}$ Γ_{98}/Γ

Includes p and $\overline{p}$ from Λ and $\overline{\Lambda}$ decay.

VALUE	EVTS	DOCUMENT ID		TECN	COMMENT
0.0247 ± 0.0023 OUR AVERAGE					
0.024 ± 0.001 ± 0.004		CRAWFORD	92	CLEO	$e^+e^- \to \Upsilon(4S)$
0.025 ± 0.002 ± 0.002	918	ALBRECHT	89K	ARG	$e^+e^- \to \Upsilon(4S)$

$\Gamma(p\overline{p}\text{anything})/\Gamma(p/\overline{p}\text{anything})$ Γ_{98}/Γ_{91}

Includes p and $\overline{p}$ from Λ and $\overline{\Lambda}$ decay.

VALUE	DOCUMENT ID		TECN	COMMENT
• • • We do not use the following data for averages, fits, limits, etc. • • •				
0.30 ± 0.02 ± 0.05	[148] CRAWFORD	92	CLEO	$e^+e^- \to \Upsilon(4S)$

[148] CRAWFORD 92 value is not independent of their $\Gamma(p\overline{p}\text{anything})/\Gamma_{\text{total}}$ value.

$\Gamma(\Lambda\overline{p}/\overline{\Lambda}p\text{anything})/\Gamma_{\text{total}}$ Γ_{99}/Γ

Includes p and $\overline{p}$ from Λ and $\overline{\Lambda}$ decay.

VALUE	EVTS	DOCUMENT ID		TECN	COMMENT
0.025 ± 0.004 OUR AVERAGE					
0.029 ± 0.005 ± 0.005		CRAWFORD	92	CLEO	$e^+e^- \to \Upsilon(4S)$
0.023 ± 0.004 ± 0.003	165	ALBRECHT	89K	ARG	$e^+e^- \to \Upsilon(4S)$

$\Gamma(\Lambda\overline{p}/\overline{\Lambda}p\text{anything})/\Gamma(\Lambda/\overline{\Lambda}\text{anything})$ Γ_{99}/Γ_{93}

Includes p and $\overline{p}$ from Λ and $\overline{\Lambda}$ decay.

VALUE	DOCUMENT ID		TECN	COMMENT
• • • We do not use the following data for averages, fits, limits, etc. • • •				
0.76 ± 0.11 ± 0.08	[149] CRAWFORD	92	CLEO	$e^+e^- \to \Upsilon(4S)$

[149] CRAWFORD 92 value is not independent of their $[\Gamma(\Lambda\overline{p}\text{anything})+\Gamma(\overline{\Lambda}p\text{anything})]/\Gamma_{\text{total}}$ value.

$\Gamma(\Lambda\overline{\Lambda}\text{anything})/\Gamma_{\text{total}}$ Γ_{100}/Γ

VALUE	CL%	EVTS	DOCUMENT ID		TECN	COMMENT
< 0.005	90		CRAWFORD	92	CLEO	$e^+e^- \to \Upsilon(4S)$
• • • We do not use the following data for averages, fits, limits, etc. • • •						
< 0.0088	90	12	ALBRECHT	89K	ARG	$e^+e^- \to \Upsilon(4S)$

$\Gamma(\Lambda\overline{\Lambda}\text{anything})/\Gamma(\Lambda/\overline{\Lambda}\text{anything})$ Γ_{100}/Γ_{93}

VALUE	CL%	DOCUMENT ID		TECN	COMMENT
• • • We do not use the following data for averages, fits, limits, etc. • • •					
< 0.13	90	[150] CRAWFORD	92	CLEO	$e^+e^- \to \Upsilon(4S)$

[150] CRAWFORD 92 value is not independent of their $\Gamma(\Lambda\overline{\Lambda}\text{anything})/\Gamma_{\text{total}}$ value.

$\Gamma(se^+e^-)/\Gamma_{\text{total}}$ Γ_{101}/Γ

Test for $\Delta B = 1$ weak neutral current. Allowed by higher-order electroweak interactions.

VALUE (units 10^{-6})	CL%	DOCUMENT ID		TECN	COMMENT
$\mathbf{5.0 \pm 2.3^{+1.3}_{-1.1}}$		[151] KANEKO	03	BELL	$e^+e^- \to \Upsilon(4S)$
• • • We do not use the following data for averages, fits, limits, etc. • • •					
< 57	90	GLENN	98	CLEO	$e^+e^- \to \Upsilon(4S)$
< 50000	90	BEBEK	81	CLEO	$e^+e^- \to \Upsilon(4S)$

[151] KANEKO 03 requires $M(e^+e^-) > 0.2$ GeV/c^2.

$\Gamma(s\mu^+\mu^-)/\Gamma_{\text{total}}$ Γ_{102}/Γ

Test for $\Delta B = 1$ weak neutral current. Allowed by higher-order electroweak interactions.

VALUE (units 10^{-6})	CL%	DOCUMENT ID		TECN	COMMENT
$\mathbf{7.9 \pm 2.1^{+2.1}_{-1.5}}$		KANEKO	03	BELL	$e^+e^- \to \Upsilon(4S)$
• • • We do not use the following data for averages, fits, limits, etc. • • •					
< 58	90	GLENN	98	CLEO	$e^+e^- \to \Upsilon(4S)$
< 17000	90	CHADWICK	81	CLEO	$e^+e^- \to \Upsilon(4S)$

$[\Gamma(se^+e^-) + \Gamma(s\mu^+\mu^-)]/\Gamma_{\text{total}}$ $(\Gamma_{101}+\Gamma_{102})/\Gamma$

Test for $\Delta B = 1$ weak neutral current. Allowed by higher-order electroweak interactions.

VALUE	CL%	DOCUMENT ID		TECN	COMMENT
< 4.2 × 10^{-5}	90	GLENN	98	CLEO	$e^+e^- \to \Upsilon(4S)$
• • • We do not use the following data for averages, fits, limits, etc. • • •					
< 0.0024	90	[152] BEAN	87	CLEO	Repl. by GLENN 98
< 0.0062	90	[153] AVERY	84	CLEO	Repl. by BEAN 87

[152] BEAN 87 reports $[(\mu^+\mu^-)+(e^+e^-)]/2$ and we converted it.

[153] Determine ratio of B^+ to B^0 semileptonic decays to be in the range 0.25–2.9.

$\Gamma(s\ell^+\ell^-)/\Gamma_{\text{total}}$ Γ_{103}/Γ

Test for $\Delta B = 1$ weak neutral current.

VALUE	DOCUMENT ID		TECN	COMMENT
$\mathbf{(6.1 \pm 1.4^{+1.4}_{-1.1}) \times 10^{-6}}$	[154] KANEKO	03	BELL	$e^+e^- \to \Upsilon(4S)$

[154] KANEKO 03 requires $M(e^+e^-) > 0.2$ GeV/c^2.

$\Gamma(Ke^+e^-)/\Gamma_{\text{total}}$ Γ_{104}/Γ

Test for $\Delta B = 1$ weak neutral current. Allowed by higher-order electroweak interactions.

VALUE (units 10^{-7})	CL%	DOCUMENT ID		TECN	COMMENT
$\mathbf{4.8^{+1.5}_{-1.3} \pm 0.3}$		[155] ISHIKAWA	03	BELL	$e^+e^- \to \Upsilon(4S)$
• • • We do not use the following data for averages, fits, limits, etc. • • •					
< 13	90	ABE	02	BELL	Repl. by ISHIKAWA 03

[155] Assumes equal production of B^0 and B^+ at $\Upsilon(4S)$. The second error is a total of systematic uncertainties including model dependence.

$\Gamma(K^*(892)e^+e^-)/\Gamma_{\text{total}}$ Γ_{105}/Γ

Test for $\Delta B = 1$ weak neutral current. Allowed by higher-order electroweak interactions.

VALUE (units 10^{-6})	CL%	DOCUMENT ID		TECN	COMMENT
$\mathbf{1.49^{+0.52}_{-0.46} \pm 0.12 \pm 0.13}$		[156] ISHIKAWA	03	BELL	$e^+e^- \to \Upsilon(4S)$
• • • We do not use the following data for averages, fits, limits, etc. • • •					
< 5.6	90	ABE	02	BELL	Repl. by ISHIKAWA 03

[156] Assumes equal production of B^0 and B^+ at $\Upsilon(4S)$. The second error is a total of systematic uncertainties including model dependence.

$\Gamma(K\mu^+\mu^-)/\Gamma_{\text{total}}$ Γ_{106}/Γ

Test for $\Delta B = 1$ weak neutral current. Allowed by higher-order electroweak interactions.

VALUE	DOCUMENT ID		TECN	COMMENT
$\mathbf{(4.8\ ^{+1.2}_{-1.1}\ \pm 0.4\ ) \times 10^{-7}}$	[157] ISHIKAWA	03	BELL	$e^+e^- \to \Upsilon(4S)$
• • • We do not use the following data for averages, fits, limits, etc. • • •				
$(0.99^{+0.40+0.13}_{-0.32-0.14}) \times 10^{-6}$	ABE	02	BELL	Repl. by ISHIKAWA 03

[157] Assumes equal production of B^0 and B^+ at $\Upsilon(4S)$. The second error is a total of systematic uncertainties including model dependence.

$\Gamma(K^*(892)\mu^+\mu^-)/\Gamma_{\text{total}}$ Γ_{107}/Γ

Test for $\Delta B = 1$ weak neutral current. Allowed by higher-order electroweak interactions.

VALUE (units 10^{-6})	CL%	DOCUMENT ID		TECN	COMMENT
$\mathbf{1.17^{+0.36}_{-0.31} \pm 0.10}$		[158] ISHIKAWA	03	BELL	$e^+e^- \to \Upsilon(4S)$
• • • We do not use the following data for averages, fits, limits, etc. • • •					
< 3.1	90	ABE	02	BELL	Repl. by ISHIKAWA 03

[158] Assumes equal production of B^0 and B^+ at $\Upsilon(4S)$. The second error is a total of systematic uncertainties including model dependence.

$\Gamma(K\ell^+\ell^-)/\Gamma_{total}$ Γ_{108}/Γ

Test for $\Delta B = 1$ weak neutral current. Allowed by higher-order electroweak interactions.

VALUE (units 10^{-6})	CL%	DOCUMENT ID		TECN	COMMENT
0.54 ± 0.08 OUR AVERAGE					
$0.65^{+0.14}_{-0.13}\pm0.04$		[159] AUBERT	03U	BABR	$e^+e^- \to \Upsilon(4S)$
$0.48^{+0.10}_{-0.09}\pm0.03$		[160] ISHIKAWA	03	BELL	$e^+e^- \to \Upsilon(4S)$
• • • We do not use the following data for averages, fits, limits, etc. • • •					
$0.75^{+0.25}_{-0.21}\pm0.06$		[161] ABE	02	BELL	Repl. by ISHIKAWA 03
<0.51	90	[162] AUBERT	02L	BABR	$e^+e^- \to \Upsilon(4S)$
<1.7	90	[163] ANDERSON	01B	CLE2	$e^+e^- \to \Upsilon(4S)$

[159] Assumes all four $B \to K\ell^+\ell^-$ modes having equal partial widths in the fit.
[160] Assumes equal production rate for charge and neutral B meson pairs, isospin invariance, lepton universality for $B \to K\ell^+\ell^-$, and $B(B \to K^*(892)\mu^+\mu^-) = 1.33$. The second error is total systematic uncertainties including model dependence.
[161] Assumes lepton universality.
[162] Assumes equal production of B^+ and B^0 at the $\Upsilon(4S)$.
[163] The result is for di-lepton masses above 0.5 GeV.

$\Gamma(K^*(892)\ell^+\ell^-)/\Gamma_{total}$ Γ_{109}/Γ

Test for $\Delta B = 1$ weak neutral current. Allowed by higher-order electroweak interactions.

VALUE (units 10^{-6})	CL%	DOCUMENT ID		TECN	COMMENT
1.05 ± 0.20 OUR AVERAGE					
$0.88^{+0.33}_{-0.29}\pm0.10$		[164] AUBERT	03U	BABR	$e^+e^- \to \Upsilon(4S)$
$1.15^{+0.26}_{-0.24}\pm0.08$		[165] ISHIKAWA	03	BELL	$e^+e^- \to \Upsilon(4S)$
• • • We do not use the following data for averages, fits, limits, etc. • • •					
<3.1	90	[166,167] AUBERT	02L	BABR	Repl. by AUBERT 03U
<3.3	90	[168] ANDERSON	01B	CLE2	$e^+e^- \to \Upsilon(4S)$

[164] Assumes the partial width ratio of electron and muon modes to be $\Gamma(B \to K^*(892)e^+e^-)/\Gamma(B \to K^*(892)\mu^+\mu^-) = 1.33$.
[165] Assumes equal production rate for charge and neutral B meson pairs, isospin invariance, lepton universality for $B \to K\ell^+\ell^-$, and $B(B \to K^*(892)\mu^+\mu^-) = 1.33$. The second error is total systematic uncertainties including model dependence.
[166] Assumes equal production of B^+ and B^0 at the $\Upsilon(4S)$.
[167] For averaging $K^*(892)\mu^+\mu^-$ and $K^*(892)e^+e^-$ modes, AUBERT 02L assumed $B(B \to K^*(892)e^+e^-)/B(B \to K^*(892)\mu^+\mu^-) = 1.2$.
[168] The result is for di-lepton masses above 0.5 GeV.

$\Gamma(e^\pm\mu^\mp s)/\Gamma_{total}$ Γ_{110}/Γ

Test for lepton family number conservation. Allowed by higher-order electroweak interactions.

VALUE	CL%	DOCUMENT ID		TECN	COMMENT
$<2.2\times10^{-5}$	90	GLENN	98	CLEO	$e^+e^- \to \Upsilon(4S)$

$\Gamma(\pi e^\pm\mu^\mp)/\Gamma_{total}$ Γ_{111}/Γ

Test of lepton family number conservation.

VALUE	CL%	DOCUMENT ID		TECN	COMMENT
$<1.6\times10^{-6}$	90	[169] EDWARDS	02B	CLE2	$e^+e^- \to \Upsilon(4S)$

[169] Assumes equal production of B^+ and B^0 at the $\Upsilon(4S)$.

$\Gamma(\rho e^\pm\mu^\mp)/\Gamma_{total}$ Γ_{112}/Γ

Test of lepton family number conservation.

VALUE	CL%	DOCUMENT ID		TECN	COMMENT
$<3.2\times10^{-6}$	90	[170] EDWARDS	02B	CLE2	$e^+e^- \to \Upsilon(4S)$

[170] Assumes equal production of B^+ and B^0 at the $\Upsilon(4S)$.

$\Gamma(Ke^\pm\mu^\mp)/\Gamma_{total}$ Γ_{113}/Γ

Test of lepton family number conservation.

VALUE	CL%	DOCUMENT ID		TECN	COMMENT
$<1.6\times10^{-6}$	90	[171] EDWARDS	02B	CLE2	$e^+e^- \to \Upsilon(4S)$

[171] Assumes equal production of B^+ and B^0 at the $\Upsilon(4S)$.

$\Gamma(K^*(892)e^\pm\mu^\mp)/\Gamma_{total}$ Γ_{114}/Γ

Test of lepton family number conservation.

VALUE	CL%	DOCUMENT ID		TECN	COMMENT
$<6.2\times10^{-6}$	90	[172] EDWARDS	02B	CLE2	$e^+e^- \to \Upsilon(4S)$

[172] Assumes equal production of B^+ and B^0 at the $\Upsilon(4S)$.

CP VIOLATION

A_{CP} is defined as

$$\frac{B(B \to \overline{f}) - B(\overline{B} \to f)}{B(B \to \overline{f}) + B(\overline{B} \to f)},$$

the CP-violation charge asymmetry of inclusive $B^\pm$ and B^0 decay.

$A_{CP}(B \to K^*(892)\gamma)$

VALUE	DOCUMENT ID		TECN	COMMENT
-0.01 ±0.07 OUR AVERAGE				
$-0.044\pm0.076\pm0.012$	[173] AUBERT	02C	BABR	$e^+e^- \to \Upsilon(4S)$
$+0.08$ ±0.13 ±0.03	[174] COAN	00	CLE2	$e^+e^- \to \Upsilon(4S)$

[173] A 90% CL range is $-0.170 < A_{CP} < 0.082$.
[174] Assumes equal production of B^+ and B^0 at the $\Upsilon(4S)$.

$A_{CP}(B \to s\gamma)$

VALUE	DOCUMENT ID		TECN	COMMENT
$-0.079\pm0.108\pm0.022$	[175] COAN	01	CLE2	$e^+e^- \to \Upsilon(4S)$

[175] Corresponds to $-0.27 < A_{CP} < 0.10$ at 90% CL.

$B \to X_c\ell\nu$ HADRONIC MASS MOMENTS

$\langle M_X^2 - \overline{M}_D^2 \rangle$ (First Moments)

VALUE (GeV^2)	DOCUMENT ID		TECN	COMMENT
$0.251\pm0.023\pm0.062$	[176] CRONIN-HEN...01B		CLE2	$e^+e^- \to \Upsilon(4S)$

[176] The leptons are required to have $P_l > 1.5$ GeV/c.

$\langle M_X^2 - \overline{M}_X^2 \rangle$ (Second Moments)

VALUE (GeV^4)	DOCUMENT ID		TECN	COMMENT
$0.576\pm0.048\pm0.168$	[177] CRONIN-HEN...01B		CLE2	$e^+e^- \to \Upsilon(4S)$

[177] The leptons are required to have $P_l > 1.5$ GeV/c.

$\langle (M_X^2 - \overline{M}_D^2)^2 \rangle$ (Second Moments)

VALUE (GeV^4)	DOCUMENT ID		TECN	COMMENT
$0.639\pm0.056\pm0.178$	[178] CRONIN-HEN...01B		CLE2	$e^+e^- \to \Upsilon(4S)$

[178] The leptons are required to have $P_l > 1.5$ GeV/c.

$B \to X_c\ell\nu$ LEPTON MOMENTUM MOMENTS

R_0 ($\Gamma_{E_l>1.7GeV}$ / $\Gamma_{E_l>1.5GeV}$)

VALUE	DOCUMENT ID		TECN	COMMENT
$0.6187\pm0.0014\pm0.0016$	[179] MAHMOOD	03	CLE2	$e^+e^- \to \Upsilon(4S)$

[179] The leptons are required to have $E_l > 1.5$ GeV in the B rest frame.

R_1 ($\langle E_l \rangle_{E_l>1.5GeV}$)

VALUE	DOCUMENT ID		TECN	COMMENT
$1.7810\pm0.0007\pm0.0009$	[180] MAHMOOD	03	CLE2	$e^+e^- \to \Upsilon(4S)$

[180] The leptons are required to have $E_l > 1.5$ GeV in the B rest frame.

$B^\pm/B^0$ ADMIXTURE REFERENCES

AUBERT	04C	PRL 92 111801	B. Aubert *et al.*	(BaBar Collab.)
ADAM	03B	PR D68 012004	N.E. Adam *et al.*	(CLEO Collab.)
AUBERT	03	PR D67 031101R	B. Aubert *et al.*	(BaBar Collab.)
AUBERT	03F	PR D67 032002	B. Aubert *et al.*	(BaBar Collab.)
AUBERT	03U	PRL 91 221802	B. Aubert *et al.*	(BaBar Collab.)
BONVICINI	03	PR D68 011101R	G. Bonvicini *et al.*	(CLEO Collab.)
HUANG	03	PRL 91 241802	H.-C. Huang *et al.*	(BELLE Collab.)
ISHIKAWA	03	PRL 91 261601	A. Ishikawa *et al.*	(BELLE Collab.)
KANEKO	03	PRL 90 021801	J. Kaneko *et al.*	(BELLE Collab.)
KROKOVNY	03B	PRL 91 262002	P. Krokovny *et al.*	(BELLE Collab.)
MAHMOOD	03	PR D67 072001	A.H. Mahmood *et al.*	(CLEO Collab.)
ABE	02	PRL 88 021801	K. Abe *et al.*	(BELLE Collab.)
ABE	02L	PRL 89 011803	K. Abe *et al.*	(BELLE Collab.)
ABE	02Y	PL B547 181	K. Abe *et al.*	(BELLE Collab.)
ANDERSON	02	PRL 89 282001	S. Anderson *et al.*	(CLEO Collab.)
AUBERT	02C	PRL 88 101805	B. Aubert *et al.*	(BaBar Collab.)
AUBERT	02G	PR D65 091104R	B. Aubert *et al.*	(BaBar Collab.)
AUBERT	02L	PRL 88 241801	B. Aubert *et al.*	(BaBar Collab.)
EDWARDS	02B	PR D65 111102R	K.W. Edwards *et al.*	(CLEO Collab.)
ABE	01F	PL B511 151	K. Abe *et al.*	(BELLE Collab.)
ABE	01J	PR D64 072001	K. Abe *et al.*	(BELLE Collab.)
ANDERSON	01B	PRL 87 181803	S. Anderson *et al.*	(CLEO Collab.)
CHEN	01	PR D63 031102	S. Chen *et al.*	(CLEO Collab.)
CHEN	01C	PRL 87 251807	S. Chen *et al.*	(CLEO Collab.)
COAN	01	PRL 86 5661	T.E. Coan *et al.*	(CLEO Collab.)
CRONIN-HEN...	01B	PRL 87 251808	D. Cronin-Hennessy *et al.*	(CLEO Collab.)
PDG	01	Unofficial 2001 WWW edition		
ABREU	00R	PL B475 407	P. Abreu *et al.*	(DELPHI Collab.)
COAN	00	PRL 84 5283	T.E. Coan *et al.*	(CLEO Collab.)
RICHICHI	00	PRL 85 520	S.J. Richichi *et al.*	(CLEO Collab.)
BARATE	98Q	EPJ C4 387	R. Barate *et al.*	(ALEPH Collab.)
BERGFELD	98	PRL 81 272	T. Bergfeld *et al.*	(CLEO Collab.)
BISHAI	98	PR D57 3847	M. Bishai *et al.*	(CLEO Collab.)
BONVICINI	98	PR D57 6604	G. Bonvicini *et al.*	(CLEO Collab.)
BROWDER	98	PRL 81 1786	T.E. Browder *et al.*	(CLEO Collab.)
COAN	98	PRL 80 1150	T.E. Coan *et al.*	(CLEO Collab.)
GLENN	98	PRL 80 2289	S. Glenn *et al.*	(CLEO Collab.)
ACKERSTAFF	97N	ZPHY C74 423	K. Ackerstaff *et al.*	(OPAL Collab.)
AMMAR	97	PR D55 13	R. Ammar *et al.*	(CLEO Collab.)
BARISH	97	PRL 79 3599	B. Barish *et al.*	(CLEO Collab.)
BUSKULIC	97B	ZPHY C73 601	D. Buskulic *et al.*	(ALEPH Collab.)
GIBBONS	97B	PR D56 3783	L. Gibbons *et al.*	(CLEO Collab.)
ALBRECHT	96D	PL B374 256	H. Albrecht *et al.*	(ARGUS Collab.)
BARISH	96B	PRL 76 1570	B.C. Barish *et al.*	(CLEO Collab.)
GIBAUT	96	PR D53 4734	D. Gibaut *et al.*	(CLEO Collab.)
KUBOTA	96	PR D53 6033	Y. Kubota *et al.*	(CLEO Collab.)
PDG	96	PR D54 1	R. M. Barnett *et al.*	
ALAM	95	PRL 74 2885	M.S. Alam *et al.*	(CLEO Collab.)
ALBRECHT	95D	PL B353 554	H. Albrecht *et al.*	(ARGUS Collab.)
BALEST	95B	PR D52 2661	R. Balest *et al.*	(CLEO Collab.)
BARISH	95	PR D51 1014	B.C. Barish *et al.*	(CLEO Collab.)
BUSKULIC	95B	PL B345 103	D. Buskulic *et al.*	(ALEPH Collab.)
ALBRECHT	94C	ZPHY C62 371	H. Albrecht *et al.*	(ARGUS Collab.)
ALBRECHT	94J	ZPHY C61 1	H. Albrecht *et al.*	(ARGUS Collab.)
PROCARIO	94	PRL 73 1472	M. Procario *et al.*	(CLEO Collab.)
ALBRECHT	93	ZPHY C57 533	H. Albrecht *et al.*	(ARGUS Collab.)
ALBRECHT	93E	ZPHY C60 11	H. Albrecht *et al.*	(ARGUS Collab.)
ALBRECHT	93H	PL B318 397	H. Albrecht *et al.*	(ARGUS Collab.)
ALBRECHT	93I	ZPHY C58 191	H. Albrecht *et al.*	(ARGUS Collab.)
ALEXANDER	93B	PL B319 365	J. Alexander *et al.*	(CLEO Collab.)
ARTUSO	93	PL B311 307	M. Artuso	(SYRA)
BARTELT	93B	PRL 71 4111	J.E. Bartelt *et al.*	(CLEO Collab.)
ALBRECHT	92E	PL B277 209	H. Albrecht *et al.*	(ARGUS Collab.)

Meson Particle Listings

$B^{\pm}/B^0$ ADMIXTURE, $B^{\pm}/B^0/B_s^0/b$-baryon ADMIXTURE

ALBRECHT	92G	ZPHY C54 1	H. Albrecht *et al.*	(ARGUS Collab.)
ALBRECHT	92O	ZPHY C56 1	H. Albrecht *et al.*	(ARGUS Collab.)
BORTOLETTO	92	PR D45 21	D. Bortoletto *et al.*	(CLEO Collab.)
CRAWFORD	92	PR D45 752	G. Crawford *et al.*	(CLEO Collab.)
HENDERSON	92	PR D45 2212	S. Henderson *et al.*	(CLEO Collab.)
LESIAK	92	ZPHY C55 33	T. Lesiak *et al.*	(Crystal Ball Collab.)
ALBRECHT	91C	PL B255 297	H. Albrecht *et al.*	(ARGUS Collab.)
ALBRECHT	91H	ZPHY C52 353	H. Albrecht *et al.*	(ARGUS Collab.)
FULTON	91	PR D43 651	R. Fulton *et al.*	(CLEO Collab.)
YANAGISAWA	91	PRL 66 2436	C. Yanagisawa *et al.*	(CUSB II Collab.)
ALBRECHT	90	PL B234 409	H. Albrecht *et al.*	(ARGUS Collab.)
ALBRECHT	90H	PL B249 359	H. Albrecht *et al.*	(ARGUS Collab.)
BORTOLETTO	90	PRL 64 2117	D. Bortoletto *et al.*	(CLEO Collab.)
Also	92	PR D45 21	D. Bortoletto *et al.*	(CLEO Collab.)
FULTON	90	PRL 64 16	R. Fulton *et al.*	(CLEO Collab.)
MASCHMANN	90	ZPHY C46 555	W.S. Maschmann *et al.*	(Crystal Ball Collab.)
PDG	90	PL B239	J.J. Hernandez *et al.*	(IFIC, BOST, CIT+)
ALBRECHT	89K	ZPHY C42 519	H. Albrecht *et al.*	(ARGUS Collab.)
ISGUR	89B	PR D39 799	N. Isgur *et al.*	(TNTO, CIT)
WACHS	89	ZPHY C42 33	K. Wachs *et al.*	(Crystal Ball Collab.)
ALBRECHT	88E	PL B210 263	H. Albrecht *et al.*	(ARGUS Collab.)
ALBRECHT	88H	PL B210 258	H. Albrecht *et al.*	(ARGUS Collab.)
KOERNER	88	ZPHY C38 511	J.G. Korner, G.A. Schuler	(MANZ, DESY)
ALAM	87	PRL 59 22	M.S. Alam *et al.*	(CLEO Collab.)
ALAM	87B	PRL 58 1814	M.S. Alam *et al.*	(CLEO Collab.)
ALBRECHT	87D	PL B199 451	H. Albrecht *et al.*	(ARGUS Collab.)
ALBRECHT	87H	PL B187 425	H. Albrecht *et al.*	(ARGUS Collab.)
BEAN	87	PR D35 3533	A. Bean *et al.*	(CLEO Collab.)
BEHRENDS	87	PRL 59 407	S. Behrends *et al.*	(CLEO Collab.)
BORTOLETTO	87	PR D35 19	D. Bortoletto *et al.*	(CLEO Collab.)
ALAM	86	PR D34 3279	M.S. Alam *et al.*	(CLEO Collab.)
BALTRUSAIT...	86E	PRL 56 2140	R.M. Baltrusaitis *et al.*	(Mark III Collab.)
BORTOLETTO	86	PRL 56 800	D. Bortoletto *et al.*	(CLEO Collab.)
HAAS	86	PRL 56 2781	J. Haas *et al.*	(CLEO Collab.)
ALBRECHT	85H	PL 162B 395	H. Albrecht *et al.*	(ARGUS Collab.)
CSORNA	85	PRL 54 1894	S.E. Csorna *et al.*	(CLEO Collab.)
HAAS	85	PRL 55 1248	J. Haas *et al.*	(CLEO Collab.)
AVERY	84	PRL 53 1309	P. Avery *et al.*	(CLEO Collab.)
CHEN	84	PRL 52 1084	A. Chen *et al.*	(CLEO Collab.)
LEVMAN	84	PL 141B 271	G.M. Levman *et al.*	(CUSB Collab.)
ALAM	83B	PRL 51 1143	M.S. Alam *et al.*	(CLEO Collab.)
GREEN	83	PRL 51 347	J. Green *et al.*	(CLEO Collab.)
KLOPFEN...	83B	PL 130B 444	C. Klopfenstein *et al.*	(CUSB Collab.)
ALTARELLI	82	NP B208 365	G. Altarelli *et al.*	(ROMA, INFN, FRAS)
BRODY	82	PRL 48 1070	A.D. Brody *et al.*	(CLEO Collab.)
GIANNINI	82	NP B206 1	G. Giannini *et al.*	(CUSB Collab.)
BEBEK	81	PRL 46 84	C. Bebek *et al.*	(CLEO Collab.)
CHADWICK	81	PRL 46 88	K. Chadwick *et al.*	(CLEO Collab.)
ABRAMS	80	PRL 44 10	G.S. Abrams *et al.*	(SLAC, LBL)

$B^{\pm}/B^0/B_s^0/b$-baryon ADMIXTURE

$B^{\pm}/B^0/B_s^0/b$-baryon ADMIXTURE MEAN LIFE

Each measurement of the B mean life is an average over an admixture of various bottom mesons and baryons which decay weakly. Different techniques emphasize different admixtures of produced particles, which could result in a different B mean life.

"OUR EVALUATION" is an average using rescaled values of the data listed below. The average and rescaling were performed by the Heavy Flavor Averaging Group (HFAG) and are described at http://www.slac.stanford.edu/xorg/hfag/. The averaging/rescaling procedure takes into account corrections between the measurements and asymmetric lifetime errors, but ignores the small differences due to different techniques.

VALUE (10^{-12} s)	*EVTS*	*DOCUMENT ID*		*TECN*	*COMMENT*
1.564 ± 0.014 OUR EVALUATION					
$1.533 \pm 0.015\ ^{+0.035}_{-0.031}$		[1] ABE	98B	CDF	$p\overline{p}$ at 1.8 TeV
$1.549 \pm 0.009 \pm 0.015$		[2] ACCIARRI	98	L3	$e^+e^- \to Z$
$1.611 \pm 0.010 \pm 0.027$		[3] ACKERSTAFF	97F	OPAL	$e^+e^- \to Z$
$1.582 \pm 0.011 \pm 0.027$		[3] ABREU	96E	DLPH	$e^+e^- \to Z$
$1.533 \pm 0.013 \pm 0.022$	19.8k	[4] BUSKULIC	96F	ALEP	$e^+e^- \to Z$
$1.564 \pm 0.030 \pm 0.036$		[5] ABE,K	95B	SLD	$e^+e^- \to Z$
$1.542 \pm 0.021 \pm 0.045$		[6] ABREU	94L	DLPH	$e^+e^- \to Z$
$1.523 \pm 0.034 \pm 0.038$	5372	[7] ACTON	93L	OPAL	$e^+e^- \to Z$
$1.511 \pm 0.022 \pm 0.078$		[8] BUSKULIC	93O	ALEP	$e^+e^- \to Z$
• • • We do not use the following data for averages, fits, limits, etc. • • •					
$1.575 \pm 0.010 \pm 0.026$		[9] ABREU	96E	DLPH	$e^+e^- \to Z$
$1.50\ ^{+0.24}_{-0.21} \pm 0.03$		[10] ABREU	94P	DLPH	$e^+e^- \to Z$
$1.46 \pm 0.06 \pm 0.06$	5344	[11] ABE	93J	CDF	Repl. by ABE 98B
$1.23\ ^{+0.14}_{-0.13} \pm 0.15$	188	[12] ABREU	93D	DLPH	Sup. by ABREU 94L
$1.49 \pm 0.11 \pm 0.12$	253	[13] ABREU	93G	DLPH	Sup. by ABREU 94L
$1.51\ ^{+0.16}_{-0.14} \pm 0.11$	130	[14] ACTON	93C	OPAL	$e^+e^- \to Z$
$1.535 \pm 0.035 \pm 0.028$	7357	[7] ADRIANI	93K	L3	Repl. by ACCIARRI 98
1.28 ± 0.10		[15] ABREU	92	DLPH	Sup. by ABREU 94L
$1.37 \pm 0.07 \pm 0.06$	1354	[16] ACTON	92	OPAL	Sup. by ACTON 93L
$1.49 \pm 0.03 \pm 0.06$		[17] BUSKULIC	92F	ALEP	Sup. by BUSKULIC 96F
$1.35\ ^{+0.19}_{-0.17} \pm 0.05$		[18] BUSKULIC	92G	ALEP	$e^+e^- \to Z$
$1.32 \pm 0.08 \pm 0.09$	1386	[19] ADEVA	91H	L3	Sup. by ADRIANI 93K
$1.32\ ^{+0.31}_{-0.25} \pm 0.15$	37	[20] ALEXANDER	91G	OPAL	$e^+e^- \to Z$
$1.29 \pm 0.06 \pm 0.10$	2973	[21] DECAMP	91C	ALEP	Sup. by BUSKULIC 92F
$1.36\ ^{+0.25}_{-0.23}$		[22] HAGEMANN	90	JADE	$E_{cm}^{ee} = 35$ GeV
1.13 ± 0.15		[23] LYONS	90	RVUE	
$1.35 \pm 0.10 \pm 0.24$		BRAUNSCH...	89B	TASS	$E_{cm}^{ee} = 35$ GeV
$0.98 \pm 0.12 \pm 0.13$		ONG	89	MRK2	$E_{cm}^{ee} = 29$ GeV
$1.17\ ^{+0.27}_{-0.22} \pm 0.17$		KLEM	88	DLCO	$E_{cm}^{ee} = 29$ GeV
$1.29 \pm 0.20 \pm 0.21$		[24] ASH	87	MAC	$E_{cm}^{ee} = 29$ GeV
$1.02\ ^{+0.42}_{-0.39}$ 301		[25] BROM	87	HRS	$E_{cm}^{ee} = 29$ GeV

[1] Measured using inclusive $J/\psi(1S) \to \mu^+\mu^-$ vertex.
[2] ACCIARRI 98 uses inclusively reconstructed secondary vertex and lepton impact parameter.
[3] ACKERSTAFF 97F uses inclusively reconstructed secondary vertices.
[4] BUSKULIC 96F analyzed using 3D impact parameter.
[5] ABE,K 95B uses an inclusive topological technique.
[6] ABREU 94L uses charged particle impact parameters. Their result from inclusively reconstructed secondary vertices is superseded by ABREU 96E.
[7] ACTON 93L and ADRIANI 93K analyzed using lepton (e and μ) impact parameter at Z.
[8] BUSKULIC 93O analyzed using dipole method.
[9] Combines ABREU 96E secondary vertex result with ABREU 94L impact parameter result.
[10] From proper time distribution of $b \to J/\psi(1S)$ anything.
[11] ABE 93J analyzed using $J/\psi(1S) \to \mu\mu$ vertices.
[12] ABREU 93D data analyzed using $D/D^*\ell$ anything event vertices.
[13] ABREU 93G data analyzed using charged and neutral vertices.
[14] ACTON 93C analysed using $D/D^*\ell$ anything event vertices.
[15] ABREU 92 is combined result of muon and hadron impact parameter analyses. Hadron tracks gave $(12.7 \pm 0.4 \pm 1.2) \times 10^{-13}$ s for an admixture of B species weighted by production fraction and mean charge multiplicity, while muon tracks gave $(13.0 \pm 1.0 \pm 0.8) \times 10^{-13}$ s for an admixture weighted by production fraction and semileptonic branching fraction.
[16] ACTON 92 is combined result of muon and electron impact parameter analyses.
[17] BUSKULIC 92F uses the lepton impact parameter distribution for data from the 1991 run.
[18] BUSKULIC 92G use $J/\psi(1S)$ tags to measure the average b lifetime. This is comparable to other methods only if the $J/\psi(1S)$ branching fractions of the different b-flavored hadrons are in the same ratio.
[19] Using $Z \to e^+X$ or μ^+X, ADEVA 91H determined the average lifetime for an admixture of B hadrons from the impact parameter distribution of the lepton.
[20] Using $Z \to J/\psi(1S)X$, $J/\psi(1S) \to \ell^+\ell^-$, ALEXANDER 91G determined the average lifetime for an admixture of B hadrons from the decay point of the $J/\psi(1S)$.
[21] Using $Z \to eX$ or μX, DECAMP 91C determines the average lifetime for an admixture of B hadrons from the signed impact parameter distribution of the lepton.
[22] HAGEMANN 90 uses electrons and muons in an impact parameter analysis.
[23] LYONS 90 combine the results of the B lifetime measurements of ONG 89, BRAUNSCHWEIG 89B, KLEM 88, and ASH 87, and JADE data by private communication. They use statistical techniques which include variation of the error with the mean life, and possible correlations between the systematic errors. This result is not independent of the measured results used in our average.
[24] We have combined an overall scale error of 15% in quadrature with the systematic error of ±0.7 to obtain ±2.1 systematic error.
[25] Statistical and systematic errors were combined by BROM 87.

CHARGED b-HADRON ADMIXTURE MEAN LIFE

VALUE (10^{-12} s)	*DOCUMENT ID*		*TECN*	*COMMENT*
1.72 ± 0.08 ± 0.06	[26] ADAM	95	DLPH	$e^+e^- \to Z$

[26] ADAM 95 data analyzed using vertex-charge technique to tag b-hadron charge.

NEUTRAL b-HADRON ADMIXTURE MEAN LIFE

VALUE (10^{-12} s)	*DOCUMENT ID*		*TECN*	*COMMENT*
1.58 ± 0.11 ± 0.09	[27] ADAM	95	DLPH	$e^+e^- \to Z$

[27] ADAM 95 data analyzed using vertex-charge technique to tag b-hadron charge.

MEAN LIFE RATIO $\tau_{\text{charged } b\text{-hadron}}/\tau_{\text{neutral } b\text{-hadron}}$

VALUE	*DOCUMENT ID*		*TECN*	*COMMENT*
$\mathbf{1.09^{+0.11}_{-0.10} \pm 0.08}$	[28] ADAM	95	DLPH	$e^+e^- \to Z$

[28] ADAM 95 data analyzed using vertex-charge technique to tag b-hadron charge.

$|\Delta\tau_b|/\tau_{b,\overline{b}}$

$\tau_{b,\overline{b}}$ and $|\Delta\tau_b|$ are the mean life average and difference between b and $\overline{b}$ hadrons.

VALUE	*DOCUMENT ID*		*TECN*	*COMMENT*
−0.001 ± 0.012 ± 0.008	[29] ABBIENDI	99J	OPAL	$e^+e^- \to Z$

[29] Data analyzed using both the jet charge and the charge of secondary vertex in the opposite hemisphere.

$\overline{b}$ PRODUCTION FRACTIONS AND DECAY MODES

The branching fraction measurements are for an admixture of B mesons and baryons at energies above the $\Upsilon(4S)$. Only the highest energy results (LEP, Tevatron, S$p\overline{p}$S) are used in the branching fraction averages. In the following, we assume that the production fractions are the same at the LEP and at the Tevatron.

For inclusive branching fractions, *e.g.*, $B \rightarrow D^{\pm}$ anything, the values usually are multiplicities, not branching fractions. They can be greater than one.

The modes below are listed for a $\overline{b}$ initial state. b modes are their charge conjugates. Reactions indicate the weak decay vertex and do not include mixing.

Mode	Fraction (Γ_j/Γ)	Scale factor/ Confidence level

PRODUCTION FRACTIONS

The production fractions for weakly decaying b-hadrons at high energy have been calculated from the best values of mean lives, mixing parameters, and branching fractions in this edition by the Heavy Flavor Averaging Group (HFAG) as described in the note "B^0-$\overline{B}^0$ Mixing" in the B^0 Particle Listings. Values assume

$$B(\overline{b} \rightarrow B^+) = B(\overline{b} \rightarrow B^0)$$
$$B(\overline{b} \rightarrow B^+) + B(\overline{b} \rightarrow B^0) + B(\overline{b} \rightarrow B_s^0) + B(b \rightarrow b\text{-baryon}) = 100\ \%.$$

The notation for production fractions varies in the literature (f_d, d_{B^0}, $f(b \rightarrow \overline{B}^0)$, $Br(b \rightarrow \overline{B}^0)$). We use our own branching fraction notation here, $B(\overline{b} \rightarrow B^0)$.

Γ_1	B^+		(39.7 ± 1.0) %	
Γ_2	B^0		(39.7 ± 1.0) %	
Γ_3	B_s^0		(10.7 ± 1.1) %	
Γ_4	b-baryon		(9.9 ± 1.7) %	
Γ_5	B_c		—	

DECAY MODES

Semileptonic and leptonic modes

Γ_6	ν anything		(23.1 ± 1.5) %	
Γ_7	$\ell^+ \nu_\ell$ anything	[a]	(10.68 ± 0.22) %	
Γ_8	$e^+ \nu_e$ anything		(10.86 ± 0.35) %	
Γ_9	$\mu^+ \nu_\mu$ anything		(10.95 $^{+0.29}_{-0.25}$) %	
Γ_{10}	$D^- \ell^+ \nu_\ell$ anything	[a]	(2.3 ± 0.4) %	S=1.7
Γ_{11}	$D^- \pi^+ \ell^+ \nu_\ell$ anything		(4.9 ± 1.9) $\times 10^{-3}$	
Γ_{12}	$D^- \pi^- \ell^+ \nu_\ell$ anything		(2.6 ± 1.6) $\times 10^{-3}$	
Γ_{13}	$\overline{D}^0 \ell^+ \nu_\ell$ anything	[a]	(6.90 ± 0.35) %	
Γ_{14}	$\overline{D}^0 \pi^- \ell^+ \nu_\ell$ anything		(1.07 ± 0.27) %	
Γ_{15}	$\overline{D}^0 \pi^+ \ell^+ \nu_\ell$ anything		(2.3 ± 1.6) $\times 10^{-3}$	
Γ_{16}	$D^{*-} \ell^+ \nu_\ell$ anything	[a]	(2.75 ± 0.19) %	
Γ_{17}	$D^{*-} \pi^+ \ell^+ \nu_\ell$ anything		(4.8 ± 1.0) $\times 10^{-3}$	
Γ_{18}	$D^{*-} \pi^- \ell^+ \nu_\ell$ anything		(6 ± 7) $\times 10^{-4}$	
Γ_{19}	$\overline{D}_j^0 \ell^+ \nu_\ell$ anything	[a,b]		
Γ_{20}	$D_j^- \ell^+ \nu_\ell$ anything	[a,b]	seen	
Γ_{21}	$\overline{D}_2^*(2460)^0 \ell^+ \nu_\ell$ anything			
Γ_{22}	$D_2^*(2460)^- \ell^+ \nu_\ell$ anything		seen	
Γ_{23}	charmless $\ell \overline{\nu}_\ell$	[a]	(1.7 ± 0.5) $\times 10^{-3}$	
Γ_{24}	$\tau^+ \nu_\tau$ anything		(2.48 ± 0.26) %	
Γ_{25}	$D^{*-} \tau \nu_\tau$ anything		(9 ± 4) $\times 10^{-3}$	
Γ_{26}	$\overline{c} \rightarrow \ell^- \overline{\nu}_\ell$ anything	[a]	(8.0 ± 0.4) %	
Γ_{27}	$c \rightarrow \ell^+ \nu$ anything		(1.6 $^{+0.4}_{-0.5}$) %	

Charmed meson and baryon modes

Γ_{28}	$\overline{D}^0$ anything		(61.0 ± 3.2) %	
Γ_{29}	$D^0 D_s^{\pm}$ anything	[c]	(9.1 $^{+3.9}_{-2.8}$) %	
Γ_{30}	$D^{\mp} D_s^{\pm}$ anything	[c]	(4.0 $^{+2.3}_{-1.8}$) %	
Γ_{31}	$\overline{D}^0 D^0$ anything	[c]	(5.1 $^{+2.0}_{-1.8}$) %	
Γ_{32}	$D^0 D^{\pm}$ anything	[c]	(2.7 $^{+1.8}_{-1.6}$) %	
Γ_{33}	$D^{\pm} D^{\mp}$ anything	[c]	< 9 $\times 10^{-3}$	CL=90%
Γ_{34}	D^0 anything			
Γ_{35}	D^+ anything			
Γ_{36}	D^- anything		(23.1 ± 2.2) %	
Γ_{37}	$D^*(2010)^+$ anything		(17.3 ± 2.0) %	
Γ_{38}	$D_1(2420)^0$ anything		(5.0 ± 1.5) %	
Γ_{39}	$D^*(2010)^{\mp} D_s^{\pm}$ anything	[c]	(3.3 $^{+1.6}_{-1.3}$) %	
Γ_{40}	$D^0 D^*(2010)^{\pm}$ anything	[c]	(3.0 $^{+1.1}_{-0.9}$) %	
Γ_{41}	$D^*(2010)^{\pm} D^{\mp}$ anything	[c]	(2.5 $^{+1.2}_{-1.0}$) %	
Γ_{42}	$D^*(2010)^{\pm} D^*(2010)^{\mp}$ anything	[c]	(1.2 ± 0.4) %	
Γ_{43}	$D_2^*(2460)^0$ anything		(4.7 ± 2.7) %	
Γ_{44}	D_s^- anything		(18 ± 5) %	
Γ_{45}	D_s^+ anything		(10.1 ± 3.1) %	
Γ_{46}	Λ_c^+ anything		(9.7 ± 2.9) %	
Γ_{47}	$\overline{c}/c$ anything	[d]	(116.6 ± 3.3) %	

Charmonium modes

Γ_{48}	$J/\psi(1S)$ anything	(1.16 ± 0.10) %	
Γ_{49}	$\psi(2S)$ anything	(4.8 ± 2.4) $\times 10^{-3}$	
Γ_{50}	$\chi_{c1}(1P)$ anything	(1.5 ± 0.5) %	

K or K^* modes

Γ_{51}	$\overline{s}\gamma$		(3.1 ± 1.1) $\times 10^{-4}$	
Γ_{52}	$\overline{s}\overline{\nu}\nu$		< 6.4 $\times 10^{-4}$	CL=90%
Γ_{53}	$K^{\pm}$ anything		(74 ± 6) %	
Γ_{54}	K_S^0 anything		(29.0 ± 2.9) %	

Pion modes

Γ_{55}	$\pi^{\pm}$ anything		(397 ±21) %	
Γ_{56}	π^0 anything	[d]	(278 ±60) %	
Γ_{57}	ϕ anything		(2.82 ± 0.23) %	

Baryon modes

Γ_{58}	$p/\overline{p}$ anything		(13.1 ± 1.1) %	

Other modes

Γ_{59}	charged anything	[d]	(497 ± 7) %	
Γ_{60}	hadron$^+$ hadron$^-$		(1.7 $^{+1.0}_{-0.7}$) $\times 10^{-5}$	
Γ_{61}	charmless		(7 ±21) $\times 10^{-3}$	

Baryon modes

Γ_{62}	$\Lambda/\overline{\Lambda}$ anything		(5.9 ± 0.6) %	
Γ_{63}	b-baryon anything		(10.2 ± 2.8) %	

$\Delta B = 1$ weak neutral current ($B1$) modes

Γ_{64}	$e^+ e^-$ anything				
Γ_{65}	$\mu^+ \mu^-$ anything	$B1$	< 3.2	$\times 10^{-4}$	CL=90%
Γ_{66}	$\nu\overline{\nu}$ anything				

[a] An ℓ indicates an e or a μ mode, not a sum over these modes.

[b] D_j represents an unresolved mixture of pseudoscalar and tensor D^{**} (P-wave) states.

[c] The value is for the sum of the charge states or particle/antiparticle states indicated.

[d] Inclusive branching fractions have a multiplicity definition and can be greater than 100%.

$B^{\pm}/B^0/B_s^0/b$-baryon ADMIXTURE BRANCHING RATIOS

$\Gamma(B^+)/\Gamma_{total}$ Γ_1/Γ

"OUR EVALUATION" is an average using rescaled values of the data listed below and from the best values of mean lives, mixing parameters, and branching fractions in this edition by the Heavy Flavor Averaging Group (AFAG) as described at http://www.slac.stanford.edu/xorg/hfag/.

VALUE	DOCUMENT ID		TECN	COMMENT
0.397 ±0.010 OUR EVALUATION				
0.4099 ± 0.0082 ± 0.0111	[30] ABDALLAH	03K	DLPH	$e^+ e^- \rightarrow Z$

[30] The analysis is based on a neural network, to estimate the charge of the weakly-decaying b hadron by distinguishing its decay products from particles produced at the primary vertex.

$\Gamma(B_s^0)/[\Gamma(B^+) + \Gamma(B^0)]$ $\Gamma_3/(\Gamma_1+\Gamma_2)$

VALUE	DOCUMENT ID		TECN	COMMENT
0.21 ±0.04 OUR AVERAGE				
0.213 ± 0.068	[31] AFFOLDER	00E	CDF	$p\overline{p}$ at 1.8 TeV
0.21 $\pm 0.036 ^{+0.038}_{-0.030}$	[32] ABE	99P	CDF	$\overline{p}p$ at 1.8 TeV

[31] AFFOLDER 00E uses several electron-charm final states in $b \rightarrow c e^- X$.

[32] ABE 99P uses the numbers of $K^*(892)^0$, $K^*(892)^+$, and $\phi(1020)$ events produced in association with the double semileptonic decays $b \rightarrow c \mu^- X$ with $c \rightarrow s \mu^+ X$.

$\Gamma(b\text{-baryon})/[\Gamma(B^+)+\Gamma(B^0)]$ $\Gamma_4/(\Gamma_1+\Gamma_2)$

VALUE	DOCUMENT ID		TECN	COMMENT
0.118±0.042	[33] AFFOLDER	00E	CDF	$p\overline{p}$ at 1.8 TeV

[33] AFFOLDER 00E uses several electron-charm final states in $b \to c e^-$ X.

$\Gamma(\nu\text{anything})/\Gamma_{\text{total}}$ Γ_6/Γ

VALUE	DOCUMENT ID		TECN	COMMENT
0.2308±0.0077±0.0124	[34,35] ACCIARRI	96C	L3	$e^+e^- \to Z$

[34] ACCIARRI 96C assumes relative b semileptonic decay rates $e{:}\mu{:}\tau$ of 1:1:0.25. Based on missing-energy spectrum.
[35] Assumes Standard Model value for R_B.

$\Gamma(\ell^+\nu_\ell\text{anything})/\Gamma_{\text{total}}$ Γ_7/Γ

"OUR EVALUATION" is an average of the data listed below performed by the LEP Electroweak Working Group as described in the "Note on the Z boson" in the Z Particle Listings.

VALUE	DOCUMENT ID		TECN	COMMENT
0.1068±0.0022 OUR EVALUATION				
0.1064±0.0016 OUR AVERAGE				
0.1070±0.0010±0.0035	[36] HEISTER	02G	ALEP	$e^+e^- \to Z$
0.1070±0.0008 $^{+0.0037}_{-0.0049}$	[37] ABREU	01L	DLPH	$e^+e^- \to Z$
0.1083±0.0010 $^{+0.0028}_{-0.0024}$	[38] ABBIENDI	00E	OPAL	$e^+e^- \to Z$
0.1016±0.0013±0.0030	[39] ACCIARRI	00	L3	$e^+e^- \to Z$
0.1085±0.0012±0.0047	[40,41] ACCIARRI	96C	L3	$e^+e^- \to Z$
• • • We do not use the following data for averages, fits, limits, etc. • • •				
0.1106±0.0039±0.0022	[42] ABREU	95D	DLPH	$e^+e^- \to Z$
0.114 ±0.003 ±0.004	[43] BUSKULIC	94G	ALEP	$e^+e^- \to Z$
0.100 ±0.007 ±0.007	[44] ABREU	93C	DLPH	$e^+e^- \to Z$
0.105 ±0.006 ±0.005	[45] AKERS	93B	OPAL	Repl. by ABBIENDI 00E

[36] Uses the combination of lepton transverse momentum spectrum and the correlation between the charge of the lepton and opposite jet charge. The first error is statistic and the second error is the total systematic error including the modeling.
[37] The experimental systematic and model uncertainties are combined in quadrature.
[38] ABBIENDI 00E result is determined by comparing the distribution of several kinematic variables of leptonic events in a lifetime tagged $Z \to b\overline{b}$ sample using artificial neural network techniques. The first error is statistic; the second error is the total systematic error.
[39] ACCIARRI 00 result obtained from a combined fit of $R_b = \Gamma(Z \to b\overline{b})/\Gamma(Z \to \text{hadrons})$ and $B(b \to \ell\nu X)$, using double-tagging method.
[40] ACCIARRI 96C result obtained by a fit to the single lepton spectrum.
[41] Assumes Standard Model value for R_B.
[42] ABREU 95D give systematic errors ±0.0019 (model) and 0.0012 (R_c). We combine these in quadrature.
[43] BUSKULIC 94G uses e and μ events. This value is from a global fit to the lepton p and p_T (relative to jet) spectra which also determines the b and c production fractions, the fragmentation functions, and the forward-backward asymmetries. This branching ratio depends primarily on the ratio of dileptons to single leptons at high p_T, but the lower p_T portion of the lepton spectrum is included in the global fit to reduce the model dependence. The model dependence is ±0.0026 and is included in the systematic error.
[44] ABREU 93C event count includes ee events. Combining ee, $\mu\mu$, and $e\mu$ events, they obtain 0.100 ± 0.007 ± 0.007.
[45] AKERS 93B analysis performed using single and dilepton events.

$\Gamma(e^+\nu_e\text{anything})/\Gamma_{\text{total}}$ Γ_8/Γ

VALUE	EVTS	DOCUMENT ID		TECN	COMMENT
0.1086±0.0035 OUR AVERAGE					
0.1078±0.0008 $^{+0.0050}_{-0.0046}$		[46] ABBIENDI	00E	OPAL	$e^+e^- \to Z$
0.1089±0.0020±0.0051		[47,48] ACCIARRI	96C	L3	$e^+e^- \to Z$
0.107 ±0.015 ±0.007	260	[49] ABREU	93C	DLPH	$e^+e^- \to Z$
0.138 ±0.032 ±0.008		[50] ADEVA	91C	L3	$e^+e^- \to Z$
• • • We do not use the following data for averages, fits, limits, etc. • • •					
0.086 ±0.027 ±0.008		[51] ABE	93E	VNS	E_{cm}^{ee} = 58 GeV
0.109 $^{+0.014}_{-0.013}$ ±0.0055	2719	[52] AKERS	93B	OPAL	Repl. by ABBIENDI 00E
0.111 ±0.028 ±0.026		BEHREND	90D	CELL	E_{cm}^{ee} = 43 GeV
0.150 ±0.011 ±0.022		BEHREND	90D	CELL	E_{cm}^{ee} = 35 GeV
0.112 ±0.009 ±0.011		ONG	88	MRK2	E_{cm}^{ee} = 29 GeV
0.149 $^{+0.022}_{-0.019}$		PAL	86	DLCO	E_{cm}^{ee} = 29 GeV
0.110 ±0.018 ±0.010		AIHARA	85	TPC	E_{cm}^{ee} = 29 GeV
0.111 ±0.034 ±0.040		ALTHOFF	84J	TASS	E_{cm}^{ee} = 34.6 GeV
0.146 ±0.028		KOOP	84	DLCO	Repl. by PAL 86
0.116 ±0.021 ±0.017		NELSON	83	MRK2	E_{cm}^{ee} = 29 GeV

[46] ABBIENDI 00E result is determined by comparing the distribution of several kinematic variables of leptonic events in a lifetime tagged $Z \to b\overline{b}$ sample using artificial neural network techniques. The first error is statistic; the second error is the total systematic error.
[47] ACCIARRI 96C result obtained by a fit to the single lepton spectrum.
[48] Assumes Standard Model value for R_B.
[49] ABREU 93C event count includes ee events. Combining ee, $\mu\mu$, and $e\mu$ events, they obtain 0.100 ± 0.007 ± 0.007.
[50] ADEVA 91C measure the average $B(b \to eX)$ branching ratio using single and double tagged b enhanced Z events. Combining e and μ results, they obtain 0.113 ± 0.010 ± 0.006. Constraining the initial number of b quarks by the Standard Model prediction (378 ± 3 MeV) for the decay of the Z into $b\overline{b}$, the electron result gives 0.112 ± 0.004 ± 0.008. They obtain 0.119 ± 0.003 ± 0.006 when e and μ results are combined. Used to measure the $b\overline{b}$ width itself, this electron result gives 370 ± 12 ± 24 MeV and combined with the muon result gives 385 ± 7 ± 22 MeV.
[51] ABE 93E experiment also measures forward-backward asymmetries and fragmentation functions for b and c.
[52] AKERS 93B analysis performed using single and dilepton events.

$\Gamma(\mu^+\nu_\mu\text{anything})/\Gamma_{\text{total}}$ Γ_9/Γ

VALUE	EVTS	DOCUMENT ID		TECN	COMMENT
0.1095 $^{+0.0029}_{-0.0025}$ OUR AVERAGE					
0.1096±0.0008 $^{+0.0034}_{-0.0027}$		[53] ABBIENDI	00E	OPAL	$e^+e^- \to Z$
0.1082±0.0015±0.0059		[54,55] ACCIARRI	96C	L3	$e^+e^- \to Z$
0.110 ±0.012 ±0.007	656	[56] ABREU	93C	DLPH	$e^+e^- \to Z$
0.113 ±0.012 ±0.006		[57] ADEVA	91C	L3	$e^+e^- \to Z$
• • • We do not use the following data for averages, fits, limits, etc. • • •					
0.122 ±0.006 ±0.007		[55] UENO	96	AMY	e^+e^- at 57.9 GeV
0.101 $^{+0.010}_{-0.009}$ ±0.0055	4248	[58] AKERS	93B	OPAL	Repl. by ABBIENDI 00E
0.104 ±0.023 ±0.016		BEHREND	90D	CELL	E_{cm}^{ee} = 43 GeV
0.148 ±0.010 ±0.016		BEHREND	90D	CELL	E_{cm}^{ee} = 35 GeV
0.118 ±0.012 ±0.010		ONG	88	MRK2	E_{cm}^{ee} = 29 GeV
0.117 ±0.016 ±0.015		BARTEL	87	JADE	E_{cm}^{ee} = 34.6 GeV
0.114 ±0.018 ±0.025		BARTEL	85J	JADE	Repl. by BARTEL 87
0.117 ±0.028 ±0.010		ALTHOFF	84G	TASS	E_{cm}^{ee} = 34.5 GeV
0.105 ±0.015 ±0.013		ADEVA	83B	MRKJ	E_{cm}^{ee} = 33–38.5 GeV
0.155 $^{+0.054}_{-0.029}$		FERNANDEZ	83D	MAC	E_{cm}^{ee} = 29 GeV

[53] ABBIENDI 00E result is determined by comparing the distribution of several kinematic variables of leptonic events in a lifetime tagged $Z \to b\overline{b}$ sample using artificial neural network techniques. The first error is statistic; the second error is the total systematic error.
[54] ACCIARRI 96C result obtained by a fit to the single lepton spectrum.
[55] Assumes Standard Model value for R_B.
[56] ABREU 93C event count includes $\mu\mu$ events. Combining ee, $\mu\mu$, and $e\mu$ events, they obtain 0.100 ± 0.007 ± 0.007.
[57] ADEVA 91C measure the average $B(b \to eX)$ branching ratio using single and double tagged b enhanced Z events. Combining e and μ results, they obtain 0.113 ± 0.010 ± 0.006. Constraining the initial number of b quarks by the Standard Model prediction (378 ± 3 MeV) for the decay of the Z into $b\overline{b}$, the muon result gives 0.123 ± 0.003 ± 0.006. They obtain 0.119 ± 0.003 ± 0.006 when e and μ results are combined. Used to measure the $b\overline{b}$ width itself, this muon result gives 394 ± 9 ± 22 MeV and combined with the electron result gives 385 ± 7 ± 22 MeV.
[58] AKERS 93B analysis performed using single and dilepton events.

$\Gamma(D^-\ell^+\nu_\ell\text{anything})/\Gamma_{\text{total}}$ Γ_{10}/Γ

VALUE	DOCUMENT ID		TECN	COMMENT
0.023 ±0.004 OUR AVERAGE	Error includes scale factor of 1.7.			
0.0272±0.0028±0.0018	[59] ABREU	00R	DLPH	$e^+e^- \to Z$
0.0198±0.0025±0.0013	[60] AKERS	95Q	OPAL	$e^+e^- \to Z$

[59] ABREU 00R reports their experiment's uncertainties ±0.0019 ± 0.0016 ± 0.0018, where the first error is statistical, the second is systematic, and the third is the uncertainty due to the D branching fraction. We combine first two in quadrature.
[60] AKERS 95Q reports $[B(\overline{b} \to D^-\ell^+\nu_\ell\text{anything}) \times B(D^+ \to K^-\pi^+\pi^+)] = (1.82 \pm 0.20 \pm 0.12) \times 10^{-3}$. We divide by our best value $B(D^+ \to K^-\pi^+\pi^+) = (9.2 \pm 0.6) \times 10^{-2}$. Our first error is their experiment's error and our second error is the systematic error from using our best value.

$\Gamma(D^-\pi^+\ell^+\nu_\ell\text{anything})/\Gamma_{\text{total}}$ Γ_{11}/Γ

VALUE	DOCUMENT ID		TECN	COMMENT
0.0049±0.0018±0.0007	ABREU	00R	DLPH	$e^+e^- \to Z$

$\Gamma(D^-\pi^-\ell^+\nu_\ell\text{anything})/\Gamma_{\text{total}}$ Γ_{12}/Γ

VALUE	DOCUMENT ID		TECN	COMMENT
0.0026±0.0015±0.0004	ABREU	00R	DLPH	$e^+e^- \to Z$

$\Gamma(\overline{D}^0\ell^+\nu_\ell\text{anything})/\Gamma_{\text{total}}$ Γ_{13}/Γ

VALUE	DOCUMENT ID		TECN	COMMENT
0.0690±0.0035 OUR AVERAGE				
0.0704±0.0040±0.0017	[61] ABREU	00R	DLPH	$e^+e^- \to Z$
0.066 ±0.006 $^{+0.002}_{-0.001}$	[62] AKERS	95Q	OPAL	$e^+e^- \to Z$

[61] ABREU 00R reports their experiment's uncertainties ±0.0034 ± 0.0036 ± 0.0017, where the first error is statistical, the second is systematic, and the third is the uncertainty due to the D branching fraction. We combine first two in quadrature.
[62] AKERS 95Q reports $[B(\overline{b} \to \overline{D}^0\ell^+\nu_\ell\text{anything}) \times B(D^0 \to K^-\pi^+)] = (2.52 \pm 0.14 \pm 0.17) \times 10^{-3}$. We divide by our best value $B(D^0 \to K^-\pi^+) = (3.80 \pm 0.09) \times 10^{-2}$. Our first error is their experiment's error and our second error is the systematic error from using our best value.

$\Gamma(\overline{D}^0\pi^-\ell^+\nu_\ell\text{anything})/\Gamma_{\text{total}}$ Γ_{14}/Γ

VALUE	DOCUMENT ID		TECN	COMMENT
0.0107±0.0025±0.0011	ABREU	00R	DLPH	$e^+e^- \to Z$

$\Gamma(\overline{D}^0\pi^+\ell^+\nu_\ell\text{anything})/\Gamma_{\text{total}}$ Γ_{15}/Γ

VALUE	DOCUMENT ID		TECN	COMMENT
0.0023±0.0015±0.0004	ABREU	00R	DLPH	$e^+e^- \to Z$

$\Gamma(D^{*-}\ell^+\nu_\ell \text{ anything})/\Gamma_{\text{total}}$ Γ_{16}/Γ

VALUE	DOCUMENT ID	TECN	COMMENT
0.0275 ± 0.0019 OUR AVERAGE			
0.0275 ± 0.0021 ± 0.0009	[63] ABREU	00R DLPH	$e^+e^- \to Z$
0.0276 ± 0.0027 ± 0.0011	[64] AKERS	95Q OPAL	$e^+e^- \to Z$

[63] ABREU 00R reports their experiment's uncertainties ±0.0017 ± 0.0013 ± 0.0009, where the first error is statistical, the second is systematic, and the third is the uncertainty due to the D branching fraction. We combine first two in quadrature.

[64] AKERS 95Q reports $[B(\overline{b} \to D^* \ell^+ \nu_\ell X) \times B(D^{*+} \to D^0\pi^+) \times B(D^0 \to K^-\pi^+)] = ((7.53 \pm 0.47 \pm 0.56) \times 10^{-4})$ and uses $B(D^{*+} \to D^0\pi^+) = 0.681 \pm 0.013$ and $B(D^0 \to K^-\pi^+) = 0.0401 \pm 0.0014$ to obtain the above result. The first error is the experiments error and the second error is the systematic error from the D^{*+} and D^0 branching ratios.

$\Gamma(D^{*-}\pi^-\ell^+\nu_\ell \text{ anything})/\Gamma_{\text{total}}$ Γ_{17}/Γ

VALUE	DOCUMENT ID	TECN	COMMENT
0.0048 ± 0.0009 ± 0.0005	ABREU	00R DLPH	$e^+e^- \to Z$

$\Gamma(D^{*-}\pi^-\ell^+\nu_\ell \text{ anything})/\Gamma_{\text{total}}$ Γ_{18}/Γ

VALUE	DOCUMENT ID	TECN	COMMENT
0.0006 ± 0.0007 ± 0.0002	ABREU	00R DLPH	$e^+e^- \to Z$

$\Gamma(\overline{D}{}^0_1\ell^+\nu_\ell \text{ anything})/\Gamma_{\text{total}}$ Γ_{19}/Γ

D_j represents an unresolved mixture of pseudoscalar and tensor D^{**} (P-wave) states.

VALUE	DOCUMENT ID	TECN	COMMENT
seen	[65] ABBIENDI	03M OPAL	$e^+e^- \to Z$
• • • We do not use the following data for averages, fits, limits, etc. • • •			
seen	[66] AKERS	95Q OPAL	Repl. by ABBIENDI 03M

[65] The product branching ratio for decays into the $\overline{D}{}^0_1$ state is measured to be $B(b \to \overline{D}{}^0_1\ell^+\nu_\ell X) \times B(\overline{D}{}^0_1 \to D^{*-}\pi^+) = (2.64 \pm 0.79 \pm 0.39) \times 10^{-3}$.

[66] AKERS 95Q quotes the product branching ratio $B(\overline{b} \to \overline{D}{}^0_j\ell^+\nu_\ell X)\, B(\overline{D}{}^0_j \to D^{*+}\pi^-) = ((6.1 \pm 1.3 \pm 1.3) \times 10^{-3})$.

$\Gamma(D_j^-\ell^+\nu_\ell \text{ anything})/\Gamma_{\text{total}}$ Γ_{20}/Γ

D_j represents an unresolved mixture of pseudoscalar and tensor D^{**} (P-wave) states.

VALUE	DOCUMENT ID	TECN	COMMENT
seen	[67] AKERS	95Q OPAL	$e^+e^- \to Z$

[67] AKERS 95Q quotes the product branching ratio $B(\overline{b} \to D_j^-\ell^+\nu_\ell \text{anything})\, B(D_j^- \to D^0\pi^-) = ((7.0 \pm 1.9^{+1.2}_{-1.3}) \times 10^{-3})$.

$\Gamma(\overline{D}{}^*_2(2460)^0\ell^+\nu_\ell \text{ anything})/\Gamma_{\text{total}}$ Γ_{21}/Γ

VALUE	DOCUMENT ID	TECN	COMMENT
not seen	[68] ABBIENDI	03M OPAL	$e^+e^- \to Z$
• • • We do not use the following data for averages, fits, limits, etc. • • •			
seen	[69] AKERS	95Q OPAL	Repl. by ABBIENDI 03M

[68] No evidence is found for such decay and set a limit on $B(b \to \overline{D}{}^*_2(2460)^0\ell^+\nu_\ell X) \times B(\overline{D}{}^*_2(2460)^0 \to D^{*-}\pi^+) < 1.4 \times 10^{-3}$ at 90% CL.

[69] AKERS 95Q quotes the product branching ratio $B(\overline{b} \to \overline{D}{}^*_2(2460)^0\ell^+\nu_\ell \text{anything})\, B(D^*_2(2460)^0 \to D^+\pi^-) = (1.6 \pm 0.7 \pm 0.3) \times 10^{-3}$.

$\Gamma(D^*_2(2460)^-\ell^+\nu_\ell \text{ anything})/\Gamma_{\text{total}}$ Γ_{22}/Γ

VALUE	DOCUMENT ID	TECN	COMMENT
seen	[70] AKERS	95Q OPAL	$e^+e^- \to Z$

[70] AKERS 95Q quotes the product branching ratio $B(\overline{b} \to D^*_2(2460)\ell^+\nu_\ell \text{anything})\, B(D^*_2(2460)^+ \to D^0\pi^-) = 4.2 \pm 1.3^{+0.7}_{-1.2}$.

$\Gamma(\text{charmless } \ell\overline{\nu}_\ell)/\Gamma_{\text{total}}$ Γ_{23}/Γ

"OUR EVALUATION" is an average of the data listed below performed by the LEP Heavy Flavour Steering Group. The averaging procedure takes into account correlations between the measurements.

VALUE	DOCUMENT ID	TECN	COMMENT
0.00171 ± 0.00052 OUR EVALUATION			
0.0017 ± 0.0004 OUR AVERAGE			
0.00163 ± 0.00053 $^{+0.00055}_{-0.00062}$	[71] ABBIENDI	01R OPAL	$e^+e^- \to Z$
0.00157 ± 0.00035 ± 0.00055	[72] ABREU	00D DLPH	$e^+e^- \to Z$
0.00173 ± 0.00055 ± 0.00055	[73] BARATE	99G ALEP	$e^+e^- \to Z$
0.0033 ± 0.0010 ± 0.0017	[74] ACCIARRI	98K L3	$e^+e^- \to Z$

[71] Obtained from the best fit of the MC simulated events to the data based on the $b \to X_u\ell\nu$ neutral network output distributions.

[72] ABREU 00D result obtained from a fit to the numbers of decays in $b \to u$ enriched and depleted samples and their lepton spectra, and assuming $|V_{cb}| = 0.0384 \pm 0.0033$ and $\tau_b = 1.564 \pm 0.014$ ps.

[73] Uses lifetime tagged $b\overline{b}$ sample.

[74] ACCIARRI 98K assumes $R_b = 0.2174 \pm 0.0009$ at Z decay.

$\Gamma(\tau^+\nu_\tau \text{ anything})/\Gamma_{\text{total}}$ Γ_{24}/Γ

VALUE (units 10^{-2})	EVTS	DOCUMENT ID	TECN	COMMENT
2.48 ± 0.26 OUR AVERAGE				
2.78 ± 0.18 ± 0.51		[75] ABBIENDI	01Q OPAL	$e^+e^- \to Z$
2.43 ± 0.20 ± 0.25		[76] BARATE	01E ALEP	$e^+e^- \to Z$
1.7 ± 0.5 ± 1.1		[77,78] ACCIARRI	96C L3	$e^+e^- \to Z$
2.4 ± 0.7 ± 0.8	1032	[79] ACCIARRI	94C L3	$e^+e^- \to Z$
• • • We do not use the following data for averages, fits, limits, etc. • • •				
2.75 ± 0.30 ± 0.37	405	[80] BUSKULIC	95 ALEP	Repl. by BARATE 01E
4.08 ± 0.76 ± 0.62		BUSKULIC	93B ALEP	Repl. by BUSKULIC 95

[75] ABBIENDI 01Q uses a missing energy technique.

[76] The energy-flow and b-tagging algorithms were used.

[77] ACCIARRI 96C result obtained from missing energy spectrum.

[78] Assumes Standard Model value for R_B.

[79] This is a direct result using tagged $b\overline{b}$ events at the Z, but species are not separated.

[80] BUSKULIC 95 uses missing-energy technique.

$\Gamma(D^{*-}\tau\nu_\tau \text{ anything})/\Gamma_{\text{total}}$ Γ_{25}/Γ

VALUE	DOCUMENT ID	TECN	COMMENT
(0.88 ± 0.31 ± 0.28) × 10^{-2}	[81] BARATE	01E ALEP	$e^+e^- \to Z$

[81] The energy-flow and b-tagging algorithms were used.

$\Gamma(\overline{b} \to \overline{c} \to \ell^-\overline{\nu}_\ell \text{anything})/\Gamma_{\text{total}}$ Γ_{26}/Γ

"OUR EVALUATION" is an average of the data listed below performed by the LEP Electroweak Working Group as described in the "Note on the Z boson" in the Z Particle Listings.

VALUE	DOCUMENT ID	TECN	COMMENT
0.0801 ± 0.0036 OUR EVALUATION			
0.0817 ± 0.0020 OUR AVERAGE			
0.0818 ± 0.0015 $^{+0.0024}_{-0.0026}$	[82] HEISTER	02G ALEP	$e^+e^- \to Z$
0.0798 ± 0.0022 $^{+0.0025}_{-0.0029}$	[83] ABREU	01L DLPH	$e^+e^- \to Z$
0.0840 ± 0.0016 $^{+0.0039}_{-0.0036}$	[84] ABBIENDI	00E OPAL	$e^+e^- \to Z$
• • • We do not use the following data for averages, fits, limits, etc. • • •			
0.0770 ± 0.0097 ± 0.0046	[85] ABREU	95D DLPH	$e^+e^- \to Z$
0.082 ± 0.003 ± 0.012	[86] BUSKULIC	94G ALEP	$e^+e^- \to Z$
0.077 ± 0.004 ± 0.007	[87] AKERS	93B OPAL	Repl. by ABBIENDI 00E

[82] Uses the combination of lepton transverse momentum spectrum and the correlation between the charge of the lepton and opposite jet charge. The first error is statistic and the second error is the total systematic error including the modeling.

[83] The experimental systematic and model uncertainties are combined in quadrature.

[84] ABBIENDI 00E result is determined by comparing the distribution of several kinematic variables of leptonic events in a lifetime tagged $Z \to b\overline{b}$ sample using artificial neural network techniques. The first error is statistic; the second error is the total systematic error.

[85] ABREU 95D give systematic errors ±0.0033 (model) and 0.0032 (R_c). We combine these in quadrature. This result is from the same global fit as their $\Gamma(\overline{b} \to \ell^+\nu_\ell X)$ data.

[86] BUSKULIC 94G uses e and μ events. This value is from the same global fit as their $\Gamma(\overline{b} \to \ell^+\nu_\ell \text{anything})/\Gamma_{\text{total}}$ data.

[87] AKERS 93B analysis performed using single and dilepton events.

$\Gamma(c \to \ell^+\nu \text{anything})/\Gamma_{\text{total}}$ Γ_{27}/Γ

VALUE	DOCUMENT ID	TECN	COMMENT
0.0161 ± 0.0020 $^{+0.0034}_{-0.0047}$	[88] ABREU	01L DLPH	$e^+e^- \to Z$

[88] The experimental systematic and model uncertainties are combined in quadrature.

$\Gamma(\overline{D}{}^0 \text{anything})/\Gamma_{\text{total}}$ Γ_{28}/Γ

VALUE	DOCUMENT ID	TECN	COMMENT
0.610 ± 0.029 $^{+0.015}_{-0.014}$	[89] BUSKULIC	96Y ALEP	$e^+e^- \to Z$

[89] BUSKULIC 96Y reports 0.605 ± 0.024 ± 0.016 for $B(D^0 \to K^-\pi^+) = 0.0383$. We rescale to our best value $B(D^0 \to K^-\pi^+) = (3.80 \pm 0.09) \times 10^{-2}$. Our first error is their experiment's error and our second error is the systematic error from using our best value.

$\Gamma(D^0 D_s^\pm \text{anything})/\Gamma_{\text{total}}$ Γ_{29}/Γ

VALUE	DOCUMENT ID	TECN	COMMENT
0.091 $^{+0.020}_{-0.018}$ $^{+0.034}_{-0.022}$	[90] BARATE	98Q ALEP	$e^+e^- \to Z$

[90] The systematic error includes the uncertainties due to the charm branching ratios.

$\Gamma(D^\mp D_s^\pm \text{anything})/\Gamma_{\text{total}}$ Γ_{30}/Γ

VALUE	DOCUMENT ID	TECN	COMMENT
0.040 $^{+0.017}_{-0.014}$ $^{+0.016}_{-0.011}$	[91] BARATE	98Q ALEP	$e^+e^- \to Z$

[91] The systematic error includes the uncertainties due to the charm branching ratios.

$[\Gamma(D^0 D_s^\pm \text{anything}) + \Gamma(D^\mp D_s^\pm \text{anything})]/\Gamma_{\text{total}}$ $(\Gamma_{29}+\Gamma_{30})/\Gamma$

VALUE	DOCUMENT ID	TECN	COMMENT
0.131 $^{+0.026}_{-0.022}$ $^{+0.048}_{-0.031}$	[92] BARATE	98Q ALEP	$e^+e^- \to Z$

[92] The systematic error includes the uncertainties due to the charm branching ratios.

$\Gamma(\overline{D}^0 D^0 \text{anything})/\Gamma_{\text{total}}$ Γ_{31}/Γ

VALUE	DOCUMENT ID		TECN	COMMENT
$0.051^{+0.016}_{-0.014}\pm0.012$	[93] BARATE	98Q	ALEP	$e^+e^- \to Z$

[93] The systematic error includes the uncertainties due to the charm branching ratios.

$\Gamma(D^0 D^{\pm} \text{anything})/\Gamma_{\text{total}}$ Γ_{32}/Γ

VALUE	DOCUMENT ID		TECN	COMMENT
$0.027^{+0.015}_{-0.013}\pm0.010$	[94] BARATE	98Q	ALEP	$e^+e^- \to Z$

[94] The systematic error includes the uncertainties due to the charm branching ratios.

$[\Gamma(\overline{D}^0 D^0 \text{anything}) + \Gamma(D^0 D^{\pm} \text{anything})]/\Gamma_{\text{total}}$ $(\Gamma_{31}+\Gamma_{32})/\Gamma$

VALUE	DOCUMENT ID		TECN	COMMENT
$0.078^{+0.020}_{-0.018}\pm0.018$	[95] BARATE	98Q	ALEP	$e^+e^- \to Z$

[95] The systematic error includes the uncertainties due to the charm branching ratios.

$\Gamma(D^{\pm} D^{\mp} \text{anything})/\Gamma_{\text{total}}$ Γ_{33}/Γ

VALUE	CL%	DOCUMENT ID		TECN	COMMENT
<0.009	90	BARATE	98Q	ALEP	$e^+e^- \to Z$

$[\Gamma(D^0 \text{anything}) + \Gamma(D^+ \text{anything})]/\Gamma_{\text{total}}$ $(\Gamma_{34}+\Gamma_{35})/\Gamma$

VALUE	DOCUMENT ID		TECN	COMMENT
$0.093\pm0.017\pm0.014$	[96] ABDALLAH	03E	DLPH	$e^+e^- -> Z$

[96] The second error is the total of systematic uncertainties including the branching fractions used in the measurement.

$\Gamma(D^- \text{anything})/\Gamma_{\text{total}}$ Γ_{36}/Γ

VALUE	DOCUMENT ID		TECN	COMMENT
$0.231\pm0.016\pm0.015$	[97] BUSKULIC	96Y	ALEP	$e^+e^- \to Z$

[97] BUSKULIC 96Y reports $0.234 \pm 0.013 \pm 0.010$ for $B(D^+ \to K^-\pi^+\pi^+) = 0.091$. We rescale to our best value $B(D^+ \to K^-\pi^+\pi^+) = (9.2 \pm 0.6) \times 10^{-2}$. Our first error is their experiment's error and our second error is the systematic error from using our best value.

$\Gamma(D^*(2010)^+ \text{anything})/\Gamma_{\text{total}}$ Γ_{37}/Γ

VALUE	DOCUMENT ID		TECN	COMMENT
$0.173\pm0.016\pm0.012$	[98] ACKERSTAFF	98E	OPAL	$e^+e^- \to Z$

[98] Uses lepton tags to select $Z \to b\overline{b}$ events.

$\Gamma(D_1(2420)^0 \text{anything})/\Gamma_{\text{total}}$ Γ_{38}/Γ

VALUE	DOCUMENT ID		TECN	COMMENT
$0.050\pm0.014\pm0.006$	[99] ACKERSTAFF	97W	OPAL	$e^+e^- \to Z$

[99] ACKERSTAFF 97W assumes $B(D_2^*(2460)^0 \to D^{*+}\pi^-) = 0.21 \pm 0.04$ and $\Gamma_{b\overline{b}}/\Gamma_{\text{hadrons}} = 0.216$ at Z decay.

$\Gamma(D^*(2010)^{\mp} D_s^{\pm} \text{anything})/\Gamma_{\text{total}}$ Γ_{39}/Γ

VALUE	DOCUMENT ID		TECN	COMMENT
$0.033^{+0.010}_{-0.009}\pm0.012$	[100] BARATE	98Q	ALEP	$e^+e^- \to Z$

[100] The systematic error includes the uncertainties due to the charm branching ratios.

$\Gamma(D^0 D^*(2010)^{\pm} \text{anything})/\Gamma_{\text{total}}$ Γ_{40}/Γ

VALUE	DOCUMENT ID		TECN	COMMENT
$0.030^{+0.009}_{-0.008}\pm0.007$	[101] BARATE	98Q	ALEP	$e^+e^- \to Z$

[101] The systematic error includes the uncertainties due to the charm branching ratios.

$\Gamma(D^*(2010)^{\pm} D^{\mp} \text{anything})/\Gamma_{\text{total}}$ Γ_{41}/Γ

VALUE	DOCUMENT ID		TECN	COMMENT
$0.025^{+0.010}_{-0.009}\pm0.006$	[102] BARATE	98Q	ALEP	$e^+e^- \to Z$

[102] The systematic error includes the uncertainties due to the charm branching ratios.

$\Gamma(D^*(2010)^{\pm} D^*(2010)^{\mp} \text{anything})/\Gamma_{\text{total}}$ Γ_{42}/Γ

VALUE	DOCUMENT ID		TECN	COMMENT
$0.012^{+0.004}_{-0.003}\pm0.002$	[103] BARATE	98Q	ALEP	$e^+e^- \to Z$

[103] The systematic error includes the uncertainties due to the charm branching ratios.

$\Gamma(D_2^*(2460)^0 \text{anything})/\Gamma_{\text{total}}$ Γ_{43}/Γ

VALUE	DOCUMENT ID		TECN	COMMENT
$0.047\pm0.024\pm0.013$	[104] ACKERSTAFF	97W	OPAL	$e^+e^- \to Z$

[104] ACKERSTAFF 97W assumes $B(D_2^*(2460)^0 \to D^{*+}\pi^-) = 0.21 \pm 0.04$ and $\Gamma_{b\overline{b}}/\Gamma_{\text{hadrons}} = 0.216$ at Z decay.

$\Gamma(D_s^- \text{anything})/\Gamma_{\text{total}}$ Γ_{44}/Γ

VALUE	DOCUMENT ID		TECN	COMMENT
$0.18\pm0.02\pm0.04$	[105] BUSKULIC	96Y	ALEP	$e^+e^- \to Z$

[105] BUSKULIC 96Y reports $0.183 \pm 0.019 \pm 0.009$ for $B(D_s^+ \to \phi\pi^+) = 0.036$. We rescale to our best value $B(D_s^+ \to \phi\pi^+) = (3.6 \pm 0.9) \times 10^{-2}$. Our first error is their experiment's error and our second error is the systematic error from using our best value.

$\Gamma(D_s^+ \text{anything})/\Gamma_{\text{total}}$ Γ_{45}/Γ

VALUE	DOCUMENT ID		TECN	COMMENT
$0.101\pm0.010\pm0.029$	[106] ABDALLAH	03E	DLPH	$e^+e^- -> Z$

[106] The second error is the total of systematic uncertainties including the branching fractions used in the measurement.

$\Gamma(b \to \Lambda_c^+ \text{anything})/\Gamma_{\text{total}}$ Γ_{46}/Γ

VALUE	DOCUMENT ID		TECN	COMMENT
$0.097\pm0.013\pm0.025$	[107] BUSKULIC	96Y	ALEP	$e^+e^- \to Z$

[107] BUSKULIC 96Y reports $0.110 \pm 0.014 \pm 0.006$ for $B(\Lambda_c^+ \to pK^-\pi^+) = 0.044$. We rescale to our best value $B(\Lambda_c^+ \to pK^-\pi^+) = (5.0 \pm 1.3) \times 10^{-2}$. Our first error is their experiment's error and our second error is the systematic error from using our best value.

$\Gamma(\overline{c}/c \text{ anything})/\Gamma_{\text{total}}$ Γ_{47}/Γ

VALUE	DOCUMENT ID		TECN	COMMENT
1.166 ± 0.033 OUR AVERAGE				
$1.166\pm0.031\pm0.080$	[108] ABREU	00	DLPH	$e^+e^- \to Z$
1.147 ± 0.041	[109] ABREU	98D	DLPH	$e^+e^- \to Z$
$1.230\pm0.036\pm0.065$	[110] BUSKULIC	96Y	ALEP	$e^+e^- \to Z$

[108] Evaluated via summation of exclusive and inclusive channels.
[109] ABREU 98D results are extracted from a fit to the b-tagging probability distribution based on the impact parameter.
[110] BUSKULIC 96Y assumes PDG 96 production fractions for B^0, B^+, B_s, b baryons, and PDG 96 branching ratios for charm decays. This is sum of their inclusive $\overline{D}^0$, D^-, $\overline{D}_s$, and Λ_c branching ratios, corrected to include inclusive Ξ_c and charmonium.

$\Gamma(J/\psi(1S) \text{anything})/\Gamma_{\text{total}}$ Γ_{48}/Γ

VALUE (units 10^{-2})	CL%	EVTS	DOCUMENT ID		TECN	COMMENT
1.16 ± 0.10 OUR AVERAGE						
$1.12\pm0.12\pm0.10$			[111] ABREU	94P	DLPH	$e^+e^- \to Z$
$1.16\pm0.16\pm0.14$		121	[112] ADRIANI	93J	L3	$e^+e^- \to Z$
$1.21\pm0.13\pm0.08$			BUSKULIC	92G	ALEP	$e^+e^- \to Z$
• • • We do not use the following data for averages, fits, limits, etc. • • •						
$1.3\ \pm0.2\ \pm0.2$			[113] ADRIANI	92	L3	$e^+e^- \to Z$
<4.9	90		MATTEUZZI	83	MRK2	E_{cm}^{ee}= 29 GeV

[111] ABREU 94P is an inclusive measurement from b decays at the Z. Uses $J/\psi(1S) \to e^+e^-$ and $\mu^+\mu^-$ channels. Assumes $\Gamma(Z \to b\overline{b})/\Gamma_{\text{hadron}}$=0.22.
[112] ADRIANI 93J is an inclusive measurement from b decays at the Z. Uses $J/\psi(1S) \to \mu^+\mu^-$ and $J/\psi(1S) \to e^+e^-$ channels.
[113] ADRIANI 92 measurement is an inclusive result for $B(Z \to J/\psi(1S)X) = (4.1 \pm 0.7 \pm 0.3) \times 10^{-3}$ which is used to extract the b-hadron contribution to $J/\psi(1S)$ production.

$\Gamma(\psi(2S) \text{anything})/\Gamma_{\text{total}}$ Γ_{49}/Γ

VALUE	DOCUMENT ID		TECN	COMMENT
$0.0048\pm0.0022\pm0.0010$	[114] ABREU	94P	DLPH	$e^+e^- \to Z$

[114] ABREU 94P is an inclusive measurement from b decays at the Z. Uses $\psi(2S) \to J/\psi(1S)\pi^+\pi^-$, $J/\psi(1S) \to \mu^+\mu^-$ channels. Assumes $\Gamma(Z \to b\overline{b})/\Gamma_{\text{hadron}}$=0.22.

$\Gamma(\chi_{c1}(1P) \text{anything})/\Gamma_{\text{total}}$ Γ_{50}/Γ

VALUE	EVTS	DOCUMENT ID		TECN	COMMENT
0.015 ± 0.005 OUR AVERAGE					
$0.012^{+0.006}_{-0.005}\pm0.001$		[115] ABREU	94P	DLPH	$e^+e^- \to Z$
$0.021\pm0.008\pm0.002$	19	[116] ADRIANI	93J	L3	$e^+e^- \to Z$

[115] ABREU 94P reports $0.014 \pm 0.006^{+0.004}_{-0.002}$ for $B(\chi_{c1}(1P) \to \gamma J/\psi(1S)) = 0.273 \pm 0.016$. We rescale to our best value $B(\chi_{c1}(1P) \to \gamma J/\psi(1S)) = (31.6 \pm 3.3) \times 10^{-2}$. Our first error is their experiment's error and our second error is the systematic error from using our best value. Assumes no $\chi_{c2}(1P)$ and $\Gamma(Z \to b\overline{b})/\Gamma_{\text{hadron}}$=0.22.
[116] ADRIANI 93J reports $0.024 \pm 0.009 \pm 0.002$ for $B(\chi_{c1}(1P) \to \gamma J/\psi(1S)) = 0.273 \pm 0.016$. We rescale to our best value $B(\chi_{c1}(1P) \to \gamma J/\psi(1S)) = (31.6 \pm 3.3) \times 10^{-2}$. Our first error is their experiment's error and our second error is the systematic error from using our best value.

$\Gamma(\chi_{c1}(1P) \text{anything})/\Gamma(J/\psi(1S) \text{anything})$ Γ_{50}/Γ_{48}

VALUE	EVTS	DOCUMENT ID		TECN	COMMENT
• • • We do not use the following data for averages, fits, limits, etc. • • •					
1.92 ± 0.82	121	[117] ADRIANI	93J	L3	$e^+e^- \to Z$

[117] ADRIANI 93J is a ratio of inclusive measurements from b decays at the Z using only the $J/\psi(1S) \to \mu^+\mu^-$ channel since some systematics cancel.

$\Gamma(\overline{3}\gamma)/\Gamma_{\text{total}}$ Γ_{51}/Γ

VALUE (units 10^{-4})	CL%	DOCUMENT ID		TECN	COMMENT
$3.11\pm0.80\pm0.72$		[118] BARATE	98I	ALEP	$e^+e^- \to Z$
• • • We do not use the following data for averages, fits, limits, etc. • • •					
< 5.4	90	[119] ADAM	96D	DLPH	$e^+e^- \to Z$
<12	90	[120] ADRIANI	93L	L3	$e^+e^- \to Z$

[118] BARATE 98I uses lifetime tagged $Z \to b\overline{b}$ sample.
[119] ADAM 96D assumes $f_{B^0} = f_{B^-} = 0.39$ and $f_{B_s} = 0.12$.
[120] ADRIANI 93L result is for $\overline{b} \to \overline{3}\gamma$ is performed inclusively.

$\Gamma(\overline{s}\nu\overline{\nu})/\Gamma_{total}$ Γ_{52}/Γ

VALUE	CL%	DOCUMENT ID		TECN	COMMENT
$<6.4\times10^{-4}$	90	[121] BARATE	01E	ALEP	$e^+e^-\to Z$

[121] The energy-flow and b-tagging algorithms were used.

$\Gamma(K^{\pm}\text{anything})/\Gamma_{total}$ Γ_{53}/Γ

VALUE	DOCUMENT ID		TECN	COMMENT
0.74 ± 0.06 OUR AVERAGE				
$0.72\pm0.02\pm0.06$	BARATE	98V	ALEP	$e^+e^-\to Z$
$0.88\pm0.05\pm0.18$	ABREU	95C	DLPH	$e^+e^-\to Z$

$\Gamma(K_S^0\text{anything})/\Gamma_{total}$ Γ_{54}/Γ

VALUE	DOCUMENT ID		TECN	COMMENT
$0.290\pm0.011\pm0.027$	ABREU	95C	DLPH	$e^+e^-\to Z$

$\Gamma(\pi^{\pm}\text{anything})/\Gamma_{total}$ Γ_{55}/Γ

VALUE	DOCUMENT ID		TECN	COMMENT
$3.97\pm0.02\pm0.21$	BARATE	98V	ALEP	$e^+e^-\to Z$

$\Gamma(\pi^0\text{anything})/\Gamma_{total}$ Γ_{56}/Γ

VALUE	DOCUMENT ID		TECN	COMMENT
$2.78\pm0.15\pm0.60$	[122] ADAM	96	DLPH	$e^+e^-\to Z$

[122] ADAM 96 measurement obtained from a fit to the rapidity distribution of $\pi^{0's}$ in $Z\to b\overline{b}$ events.

$\Gamma(\phi\text{anything})/\Gamma_{total}$ Γ_{57}/Γ

VALUE	DOCUMENT ID		TECN	COMMENT
$0.0282\pm0.0013\pm0.0019$	ABBIENDI	00Z	OPAL	$e^+e^-\to Z$

$\Gamma(p/\overline{p}\text{anything})/\Gamma_{total}$ Γ_{58}/Γ

VALUE	DOCUMENT ID		TECN	COMMENT
0.131 ± 0.011 OUR AVERAGE				
$0.131\pm0.004\pm0.011$	BARATE	98V	ALEP	$e^+e^-\to Z$
$0.141\pm0.018\pm0.056$	ABREU	95C	DLPH	$e^+e^-\to Z$

$\Gamma(\text{charged anything})/\Gamma_{total}$ Γ_{59}/Γ

VALUE	DOCUMENT ID		TECN	COMMENT
$4.97\pm0.03\pm0.06$	[123] ABREU	98H	DLPH	$e^+e^-\to Z$
• • • We do not use the following data for averages, fits, limits, etc. • • •				
$5.84\pm0.04\pm0.38$	ABREU	95C	DLPH	Repl. by ABREU 98H

[123] ABREU 98H measurement excludes the contribution from K^0 and Λ decay.

$\Gamma(\text{hadron}^+\,\text{hadron}^-)/\Gamma_{total}$ Γ_{60}/Γ

VALUE (units 10^{-5})	DOCUMENT ID		TECN	COMMENT
$1.7^{+1.0}_{-0.7}\pm0.2$	[124,125] BUSKULIC	96V	ALEP	$e^+e^-\to Z$

[124] BUSKULIC 96V assumes PDG 96 production fractions for B^0, B^+, B_s, b baryons.

[125] Average branching fraction of weakly decaying B hadrons into two long-lived charged hadrons, weighted by their production cross section and lifetimes.

$\Gamma(\text{charmless})/\Gamma_{total}$ Γ_{61}/Γ

VALUE	DOCUMENT ID		TECN	COMMENT
0.007 ± 0.021	[126] ABREU	98D	DLPH	$e^+e^-\to Z$

[126] ABREU 98D results are extracted from a fit to the b-tagging probability distribution based on the impact parameter. The expected hidden charm contribution of 0.026 ± 0.004 has been subtracted.

$\Gamma(\Lambda/\overline{\Lambda}\text{anything})/\Gamma_{total}$ Γ_{62}/Γ

VALUE	DOCUMENT ID		TECN	COMMENT
0.059 ± 0.006 OUR AVERAGE				
$0.0587\pm0.0046\pm0.0048$	ACKERSTAFF	97N	OPAL	$e^+e^-\to Z$
$0.059\pm0.007\pm0.009$	ABREU	95C	DLPH	$e^+e^-\to Z$

$\Gamma(b\text{-baryon anything})/\Gamma_{total}$ Γ_{63}/Γ

VALUE	DOCUMENT ID		TECN	COMMENT
$0.102\pm0.007\pm0.027$	[127] BARATE	98V	ALEP	$e^+e^-\to Z$

[127] BARATE 98V assumes $B(B_s\to pX)=8\pm4\%$ and $B(b\text{-baryon}\to pX)=58\pm6\%$.

$\Gamma(\mu^+\mu^-\text{anything})/\Gamma_{total}$ Γ_{65}/Γ

Test for $\Delta B=1$ weak neutral current.

VALUE	CL%	DOCUMENT ID		TECN	COMMENT
$<3.2\times10^{-4}$	90	ABBOTT	98B	D0	$p\overline{p}$ 1.8 TeV
• • • We do not use the following data for averages, fits, limits, etc. • • •					
$<5.0\times10^{-5}$	90	[128] ALBAJAR	91C	UA1	$E_{cm}^{p\overline{p}}=630$ GeV
<0.02	95	ALTHOFF	84G	TASS	$E_{cm}^{ee}=34.5$ GeV
<0.007	95	ADEVA	83	MRKJ	$E_{cm}^{ee}=30$–38 GeV
<0.007	95	BARTEL	83B	JADE	$E_{cm}^{ee}=33$–37 GeV

[128] Both ABBOTT 98B and GLENN 98 claim that the efficiency quoted in ALBAJAR 91C was overestimated by a large factor.

$[\Gamma(e^+e^-\text{anything})+\Gamma(\mu^+\mu^-\text{anything})]/\Gamma_{total}$ $(\Gamma_{64}+\Gamma_{65})/\Gamma$

Test for $\Delta B=1$ weak neutral current.

VALUE	CL%	DOCUMENT ID		TECN	COMMENT
• • • We do not use the following data for averages, fits, limits, etc. • • •					
<0.008	90	MATTEUZZI	83	MRK2	$E_{cm}^{ee}=29$ GeV

$\Gamma(\nu\overline{\nu}\text{anything})/\Gamma_{total}$ Γ_{66}/Γ

VALUE	DOCUMENT ID		TECN	COMMENT
• • • We do not use the following data for averages, fits, limits, etc. • • •				
$<3.9\times10^{-4}$	[129] GROSSMAN	96	RVUE	$e^+e^-\to Z$

[129] GROSSMAN 96 limit is derived from the ALEPH BUSKULIC 95 limit $B(B^+\to\tau^+\nu_\tau)<1.8\times10^{-3}$ at CL=90% using conservative simplifying assumptions.

χ_b AT HIGH ENERGY

For a discussion of B-$\overline{B}$ mixing, see the note on B^0-$\overline{B}^0$ Mixing" in the B^0 Particle Listings.

χ_b is the average B-$\overline{B}$ mixing parameter at high-energy $\chi_b=f'_d\chi_d+f'_s\chi_s$ where f'_d and f'_s are the fractions of B^0 and B_s^0 hadrons in an unbiased sample of semileptonic b-hadron decays.

"OUR EVALUATION" is an average of the data listed below. Performed by the LEP Electroweak Working Group as described in the "Note on the Z boson" in the Z Particle Listings.

VALUE	CL%	EVTS	DOCUMENT ID		TECN	COMMENT
0.1257 ± 0.0042 OUR EVALUATION						
0.127 ± 0.004 OUR AVERAGE						
$0.1312\pm0.0049\pm0.0042$			[130] ABBIENDI	04E	OPAL	$e^+e^-\to Z$
$0.127\pm0.013\pm0.006$			[131] ABREU	01L	DLPH	$e^+e^-\to Z$
$0.1192\pm0.0068\pm0.0051$			[132] ACCIARRI	99D	L3	$e^+e^-\to Z$
$0.131\pm0.020\pm0.016$			[133] ABE	97I	CDF	$p\overline{p}$ 1.8 TeV
$0.121\pm0.016\pm0.006$			[134] ABREU	94J	DLPH	$e^+e^-\to Z$
$0.114\pm0.014\pm0.008$			[135] BUSKULIC	94G	ALEP	$e^+e^-\to Z$
0.129 ± 0.022			[136] BUSKULIC	92B	ALEP	$e^+e^-\to Z$
$0.176\pm0.031\pm0.032$		1112	[137] ABE	91G	CDF	$p\overline{p}$ 1.8 TeV
$0.148\pm0.029\pm0.017$			[138] ALBAJAR	91D	UA1	$p\overline{p}$ 630 GeV
• • • We do not use the following data for averages, fits, limits, etc. • • •						
$0.1107\pm0.0062\pm0.0055$			[139] ALEXANDER	96	OPAL	Rep. by ABBIENDI 04E
$0.136\pm0.037\pm0.040$			[140] UENO	96	AMY	e^+e^- at 57.9 GeV
$0.144\pm0.014\,^{+0.017}_{-0.011}$			[141] ABREU	94F	DLPH	Sup. by ABREU 94J
0.131 ± 0.014			[142] ABREU	94J	DLPH	$e^+e^-\to Z$
$0.123\pm0.012\pm0.008$			ACCIARRI	94D	L3	Repl. by ACCIARRI 99D
$0.157\pm0.020\pm0.032$			[143] ALBAJAR	94	UA1	$\sqrt{s}=630$ GeV
$0.121\,^{+0.044}_{-0.040}\pm0.017$		1665	[144] ABREU	93C	DLPH	Sup. by ABREU 94J
$0.143\,^{+0.022}_{-0.021}\pm0.007$			[145] AKERS	93B	OPAL	Sup. by ALEXANDER 96
$0.145\,^{+0.041}_{-0.035}\pm0.018$			[146] ACTON	92C	OPAL	$e^+e^-\to Z$
$0.121\pm0.017\pm0.006$			[147] ADEVA	92C	L3	Sup. by ACCIARRI 94D
$0.132\pm0.22\,^{+0.015}_{-0.012}$		823	[148] DECAMP	91	ALEP	$e^+e^-\to Z$
$0.178\,^{+0.049}_{-0.040}\pm0.020$			[149] ADEVA	90P	L3	$e^+e^-\to Z$
$0.17\,^{+0.15}_{-0.08}$			[150,151] WEIR	90	MRK2	e^+e^- 29 GeV
$0.21\,^{+0.29}_{-0.15}$			[150] BAND	88	MAC	$E_{cm}^{ee}=29$ GeV
>0.02	90		[150] BAND	88	MAC	$E_{cm}^{ee}=29$ GeV
0.121 ± 0.047			[150,152] ALBAJAR	87C	UA1	Repl. by ALBAJAR 91D
<0.12	90		[150,153] SCHAAD	85	MRK2	$E_{cm}^{ee}=29$ GeV

[130] The average B mixing parameter is determined simultaneously with b and c forward-backward asymmetries in the fit.

[131] The experimental systematic and model uncertainties are combined in quadrature.

[132] ACCIARRI 99D uses maximum-likelihood fits to extract χ_b as well as the A_{FB}^b in $Z\to b\overline{b}$ events containing prompt leptons.

[133] Uses di-muon events.

[134] This ABREU 94J result is from 5182 $\ell\ell$ and 279 $\Lambda\ell$ events. The systematic error includes 0.004 for model dependence.

[135] BUSKULIC 94G data analyzed using ee, $e\mu$, and $\mu\mu$ events.

[136] BUSKULIC 92B uses a jet charge technique combined with electrons and muons.

[137] ABE 91G measurement of χ is done with $e\mu$ and ee events.

[138] ALBAJAR 91D measurement of χ is done with dimuons.

[139] ALEXANDER 96 uses a maximum likelihood fit to simultaneously extract χ as well as the forward-backward asymmetries in $e^+e^-\to Z\to b\overline{b}$ and $c\overline{c}$.

[140] UENO 96 extracted χ from the energy dependence of the forward-backward asymmetry.

[141] ABREU 94F uses the average electric charge sum of the jets recoiling against a b-quark jet tagged by a high p_T muon. The result is for $\overline{\chi}=f_d\chi_d+0.9f_s\chi_s$.

[142] This ABREU 94J result combines $\ell\ell$, $\Lambda\ell$, and jet-charge ℓ (ABREU 94F) analyses. It is for $\overline{\chi}=f_d\chi_d+0.96f_s\chi_s$.

[143] ALBAJAR 94 uses dimuon events. Not independent of ALBAJAR 91D.

Meson Particle Listings

$B^{\pm}/B^0/B_s^0/b$-baryon ADMIXTURE, V_{cb} and V_{ub} CKM Matrix Elements

[144] ABREU 93C data analyzed using ee, $e\mu$, and $\mu\mu$ events.
[145] AKERS 93B analysis performed using dilepton events.
[146] ACTON 92C uses electrons and muons. Superseded by AKERS 93B.
[147] ADEVA 92C uses electrons and muons.
[148] DECAMP 91 done with opposite and like-sign dileptons. Superseded by BUSKULIC 92B.
[149] ADEVA 90P measurement uses ee, $\mu\mu$, and $e\mu$ events from 118k events at the Z. Superseded by ADEVA 92C.
[150] These experiments are not in the average because the combination of B_s and B_d mesons which they see could differ from those at higher energy.
[151] The WEIR 90 measurement supersedes the limit obtained in SCHAAD 85. The 90% CL are 0.06 and 0.38.
[152] ALBAJAR 87C measured $\chi = (\overline{B}^0 \rightarrow B^0 \rightarrow \mu^+ X)$ divided by the average production weighted semileptonic branching fraction for B hadrons at 546 and 630 GeV.
[153] Limit is average probability for hadron containing B quark to produce a positive lepton.

$B^{\pm}/B^0/B_s^0/b$-baryon ADMIXTURE REFERENCES

ABBIENDI	04E	PL B577 18	G. Abbiendi *et al.*	(OPAL Collab.)
ABBIENDI	03M	EPJ C30 467	G. Abbiendi *et al.*	(OPAL Collab.)
ABDALLAH	03E	PL B561 26	J. Abdallah *et al.*	(DELPHI Collab.)
ABDALLAH	03K	PL B576 29	J. Abdallah *et al.*	(DELPHI Collab.)
HEISTER	02G	EPJ C22 613	A. Heister *et al.*	(ALEPH Collab.)
ABBIENDI	01Q	PL B520 1	G. Abbiendi *et al.*	(OPAL Collab.)
ABBIENDI	01R	EPJ C21 399	G. Abbiendi *et al.*	(OPAL Collab.)
ABREU	01L	EPJ C20 455	P. Abreu *et al.*	(DELPHI Collab.)
BARATE	01E	EPJ C19 213	R. Barate *et al.*	(ALEPH Collab.)
ABBIENDI	00E	EPJ C13 225	G. Abbiendi *et al.*	(OPAL Collab.)
ABBIENDI	00Z	PL B492 13	G. Abbiendi *et al.*	(OPAL Collab.)
ABREU	00	EPJ C12 225	P. Abreu *et al.*	(DELPHI Collab.)
ABREU	00D	PL B478 14	P. Abreu *et al.*	(DELPHI Collab.)
ABREU	00R	PL B475 407	P. Abreu *et al.*	(DELPHI Collab.)
ACCIARRI	00	EPJ C13 47	M. Acciarri *et al.*	(L3 Collab.)
AFFOLDER	00E	PRL 84 1663	T. Affolder *et al.*	(CDF Collab.)
ABBIENDI	99J	EPJ C12 609	G. Abbiendi *et al.*	(OPAL Collab.)
ABE	99P	PR D60 092005	F. Abe *et al.*	(CDF Collab.)
ACCIARRI	99D	PL B448 152	M. Acciarri *et al.*	(L3 Collab.)
BARATE	99G	EPJ C6 555	R. Barate *et al.*	(ALEPH Collab.)
ABBOTT	98B	PL B423 419	B. Abbott *et al.*	(D0 Collab.)
ABE	98B	PR D57 5382	F. Abe *et al.*	(CDF Collab.)
ABREU	98D	PL B426 193	P. Abreu *et al.*	(DELPHI Collab.)
ABREU	98H	PL B425 399	P. Abreu *et al.*	(DELPHI Collab.)
ACCIARRI	98	PL B416 220	M. Acciarri *et al.*	(L3 Collab.)
ACCIARRI	98K	PL B436 174	M. Acciarri *et al.*	(L3 Collab.)
ACKERSTAFF	98E	EPJ C1 439	K. Ackerstaff *et al.*	(OPAL Collab.)
BARATE	98I	PL B429 169	R. Barate *et al.*	(ALEPH Collab.)
BARATE	98Q	EPJ C4 387	R. Barate *et al.*	(ALEPH Collab.)
BARATE	98V	EPJ C5 205	R. Barate *et al.*	(ALEPH Collab.)
GLENN	98	PRL 80 2289	S. Glenn *et al.*	(CLEO Collab.)
ABE	97I	PR D55 2546	F. Abe *et al.*	(CDF Collab.)
ACKERSTAFF	97F	ZPHY C73 397	K. Ackerstaff *et al.*	(OPAL Collab.)
ACKERSTAFF	97N	ZPHY C74 423	K. Ackerstaff *et al.*	(OPAL Collab.)
ACKERSTAFF	97W	ZPHY C76 425	K. Ackerstaff *et al.*	(OPAL Collab.)
ABREU	96E	PL B377 195	P. Abreu *et al.*	(DELPHI Collab.)
ACCIARRI	96C	ZPHY C71 379	M. Acciarri *et al.*	(L3 Collab.)
ADAM	96	ZPHY C69 561	W. Adam *et al.*	(DELPHI Collab.)
ADAM	96D	ZPHY C72 207	W. Adam *et al.*	(DELPHI Collab.)
ALEXANDER	96	ZPHY C70 357	G. Alexander *et al.*	(OPAL Collab.)
BUSKULIC	96F	PL B369 151	D. Buskulic *et al.*	(ALEPH Collab.)
BUSKULIC	96V	PL B384 471	D. Buskulic *et al.*	(ALEPH Collab.)
BUSKULIC	96Y	PL B388 648	D. Buskulic *et al.*	(ALEPH Collab.)
GROSSMAN	96	NP B465 369	Y. Grossman, Z. Ligeti, E. Nardi	(REHO, CIT)
Also	96B	NP B480 753 (erratum)	Y. Grossman, Z. Ligeti, E. Nardi	
PDG	96	PR D54 1	R. M. Barnett *et al.*	
UENO	96	PL B381 365	K. Ueno *et al.*	(AMY Collab.)
ABE,K	95B	PRL 75 3624	K. Abe *et al.*	(SLD Collab.)
ABREU	95C	PL B347 447	P. Abreu *et al.*	(DELPHI Collab.)
ABREU	95D	ZPHY C66 323	P. Abreu *et al.*	(DELPHI Collab.)
ADAM	95	ZPHY C68 363	W. Adam *et al.*	(DELPHI Collab.)
AKERS	95Q	ZPHY C67 57	R. Akers *et al.*	(OPAL Collab.)
BUSKULIC	95	PL B343 444	D. Buskulic *et al.*	(ALEPH Collab.)
ABREU	94F	PL B322 459	P. Abreu *et al.*	(DELPHI Collab.)
ABREU	94J	PL B332 488	P. Abreu *et al.*	(DELPHI Collab.)
ABREU	94L	ZPHY C63 3	P. Abreu *et al.*	(DELPHI Collab.)
ABREU	94P	PL B341 109	P. Abreu *et al.*	(DELPHI Collab.)
ACCIARRI	94C	PL B332 201	M. Acciarri *et al.*	(L3 Collab.)
ACCIARRI	94D	PL B335 542	M. Acciarri *et al.*	(L3 Collab.)
ALBAJAR	94	ZPHY C61 41	C. Albajar *et al.*	(UA1 Collab.)
BUSKULIC	94G	ZPHY C62 179	D. Buskulic *et al.*	(ALEPH Collab.)
ABE	93E	PL B313 288	K. Abe *et al.*	(VENUS Collab.)
ABE	93J	PRL 71 3421	F. Abe *et al.*	(CDF Collab.)
ABREU	93C	PL B301 145	P. Abreu *et al.*	(DELPHI Collab.)
ABREU	93D	ZPHY C57 181	P. Abreu *et al.*	(DELPHI Collab.)
ABREU	93G	PL B312 253	P. Abreu *et al.*	(DELPHI Collab.)
ACTON	93C	PL B307 247	P.D. Acton *et al.*	(OPAL Collab.)
ACTON	93L	ZPHY C60 217	P.D. Acton *et al.*	(OPAL Collab.)
ADRIANI	93J	PL B317 467	O. Adriani *et al.*	(L3 Collab.)
ADRIANI	93K	PL B317 474	O. Adriani *et al.*	(L3 Collab.)
ADRIANI	93L	PL B317 637	O. Adriani *et al.*	(L3 Collab.)
AKERS	93B	ZPHY C60 199	R. Akers *et al.*	(OPAL Collab.)
BUSKULIC	93B	PL B298 479	D. Buskulic *et al.*	(ALEPH Collab.)
BUSKULIC	93O	PL B314 459	D. Buskulic *et al.*	(ALEPH Collab.)
ABREU	92	ZPHY C53 567	P. Abreu *et al.*	(DELPHI Collab.)
ACTON	92	PL B274 513	D.P. Acton *et al.*	(OPAL Collab.)
ACTON	92C	PL B276 379	D.P. Acton *et al.*	(OPAL Collab.)
ADEVA	92C	PL B288 395	B. Adeva *et al.*	(L3 Collab.)
ADRIANI	92	PL B288 412	O. Adriani *et al.*	(L3 Collab.)
BUSKULIC	92B	PL B284 177	D. Buskulic *et al.*	(ALEPH Collab.)
BUSKULIC	92F	PL B295 174	D. Buskulic *et al.*	(ALEPH Collab.)
BUSKULIC	92G	PL B295 396	D. Buskulic *et al.*	(ALEPH Collab.)
ABE	91G	PRL 67 3351	F. Abe *et al.*	(CDF Collab.)
ADEVA	91C	PL B261 177	B. Adeva *et al.*	(L3 Collab.)
ADEVA	91H	PL B270 111	B. Adeva *et al.*	(L3 Collab.)
ALBAJAR	91C	PL B262 163	C. Albajar *et al.*	(UA1 Collab.)
ALBAJAR	91D	PL B262 171	C. Albajar *et al.*	(UA1 Collab.)
ALEXANDER	91G	PL B266 485	G. Alexander *et al.*	(OPAL Collab.)
DECAMP	91	PL B258 236	D. Decamp *et al.*	(ALEPH Collab.)
DECAMP	91C	PL B257 492	D. Decamp *et al.*	(ALEPH Collab.)
ADEVA	90P	PL B252 703	B. Adeva *et al.*	(L3 Collab.)
BEHREND	90D	ZPHY C47 333	H.J. Behrend *et al.*	(CELLO Collab.)
HAGEMANN	90	ZPHY C48 401	J. Hagemann *et al.*	(JADE Collab.)
LYONS	90	PR D41 982	L. Lyons, A.J. Martin, D.H. Saxon	(OXF, BRIS+)
WEIR	90	PL B240 289	A.J. Weir *et al.*	(Mark II Collab.)
BRAUNSCH...	89B	ZPHY C44 1	R. Braunschweig *et al.*	(TASSO Collab.)
ONG	89	PRL 62 1236	R.A. Ong *et al.*	(Mark II Collab.)
BAND	88	PL B200 221	H.R. Band *et al.*	(MAC Collab.)
KLEM	88	PR D37 41	D.E. Klem *et al.*	(DELCO Collab.)
ONG	88	PRL 60 2587	R.A. Ong *et al.*	(Mark II Collab.)
ALBAJAR	87C	PL B186 247	C. Albajar *et al.*	(UA1 Collab.)
ASH	87	PRL 58 640	W.W. Ash *et al.*	(MAC Collab.)
BARTEL	87	ZPHY C33 339	W. Bartel *et al.*	(JADE Collab.)
BROM	87	PL B195 301	J.M. Brom *et al.*	(HRS Collab.)
PAL	86	PR D33 2708	T. Pal *et al.*	(DELCO Collab.)
AIHARA	85	ZPHY C27 39	H. Aihara *et al.*	(TPC Collab.)
BARTEL	85J	PL 163B 277	W. Bartel *et al.*	(JADE Collab.)
SCHAAD	85	PL 160B 188	T. Schaad *et al.*	(Mark II Collab.)
ALTHOFF	84G	ZPHY C22 219	M. Althoff *et al.*	(TASSO Collab.)
ALTHOFF	84J	PL 146B 443	M. Althoff *et al.*	(TASSO Collab.)
KOOP	84	PRL 52 970	D.E. Koop *et al.*	(DELCO Collab.)
ADEVA	83	PRL 50 799	B. Adeva *et al.*	(Mark-J Collab.)
ADEVA	83B	PRL 51 443	B. Adeva *et al.*	(Mark-J Collab.)
BARTEL	83B	PL 132B 241	W. Bartel *et al.*	(JADE Collab.)
FERNANDEZ	83D	PRL 50 2054	E. Fernandez *et al.*	(MAC Collab.)
MATTEUZZI	83	PL 129B 141	C. Matteuzzi *et al.*	(Mark II Collab.)
NELSON	83	PRL 50 1542	M.E. Nelson *et al.*	(Mark II Collab.)

V_{cb} and V_{ub} CKM Matrix Elements

OMITTED FROM SUMMARY TABLE

DETERMINATION OF $|V_{cb}|$

Updated December 2003 by M. Artuso (Syracuse University) and E. Barberio (University of Melbourne).

I. Introduction

In the framework of the Standard Model, the quark sector is characterized by a rich pattern of flavor-changing transitions, described by the Cabibbo-Kobayashi-Maskawa (CKM) matrix (see CKM review [1]). This report focuses on the quark mixing parameter $|V_{cb}|$.

Two different methods have been used to extract this parameter from data: the **exclusive** measurement, where $|V_{cb}|$ is extracted by studying $B \to D^{\star}\ell\nu$ or $B \to D\ell\nu$ decay processes; and the **inclusive** measurement, which uses the semileptonic width of b-hadron decays ($B \to X\ell\overline{\nu}$). Theoretical estimates play a crucial role in extracting $|V_{cb}|$, and an understanding of their uncertainties is very important.

II. $|V_{cb}|$ determination from exclusive channels

The exclusive $|V_{cb}|$ determination is obtained studying $B \to D^{\star}\ell\nu$ or $B \to D\ell\nu$ decays, using Heavy Quark Effective Theory (HQET), an exact theory in the limit of infinite quark masses. Currently, the $B \to D\ell\nu$ transition provides a less precise value, and is used as a check.

The decay $B \to D^{\star}\ell\nu$ in HQET: HQET predicts that the differential partial decay width for this process, $d\Gamma/dw$, is related to $|V_{cb}|$ through:

$$\frac{d\Gamma}{dw}(B \to D^{\star}\ell\nu) = \frac{G_F^2|V_{cb}|^2}{48\pi^3}\mathcal{K}(w)\mathcal{F}(w)^2, \qquad (1)$$

where w is the inner product of the B and $D^{\star}$ meson 4-velocities, $\mathcal{K}(w)$ is a known phase-space factor, and the form factor $\mathcal{F}(w)$ is generally expressed as the product of a normalization constant, $\mathcal{F}(1)$, and a function, $g(w)$, constrained by experimental studies of the helicity amplitudes characterizing this decay [2] and dispersion relations [3].

There are several different corrections to the infinite mass value $\mathcal{F}(1) = 1$ [4]:

$$\mathcal{F}(1) = \eta_{\rm QED}\eta_A\left[1 + \delta_{1/m_Q^2} + ...\right], \qquad (2)$$

here and in the following discussion of exclusive semileptonic decays, m_Q is a generic notation for m_c or m_b. By virtue

of Luke's theorem [5], the first term in the non-perturbative expansion in powers of $1/m_Q$ vanishes. QED corrections up to leading-logarithmic order give $\eta_{\rm QED} \approx 1.007$ [6] and QCD radiative corrections to two loops give $\eta_A = 0.960 \pm 0.007$ [7]. Different estimates of the $1/m_Q^2$ corrections, involving terms proportional to $1/m_b^2$, $1/m_c^2$, and $1/(m_b m_c)$, have been performed in a quark model [8,10], with OPE sum rules [11], and, more recently, with an HQET based lattice gauge calculation [12]. The value from this quenched lattice HQET calculation is $\mathcal{F}(1) = 0.913^{+0.024}_{-0.017} \pm 0.016^{+0.003}_{-0.014}{}^{+0.000}_{-0.016}{}^{+0.006}_{-0.014}$. The errors quoted reflect the statistical accuracy, the matching error, the lattice finite size, the uncertainty in the quark masses, and an estimate of the error induced by the quenched approximation, respectively. The central value obtained with OPE sum rules is similar, $0.900 \pm 0.015 \pm 0.025 \pm 0.025$ [11], where the three errors parameterize different sources of theoretical uncertainty. Here we will use $\mathcal{F}(1) = 0.91 \pm 0.04$ [13], a value that is consistent with all the three determinations discussed above. We have chosen not to rely solely on the value of $\mathcal{F}(1)$ coming from the lattice, because of the difficulties of quantifying the uncertainty induced by the quenched approximation. Recent developments give confidence that this limitation will be overcome in the next few years [15]. Technical advances, such as new improved staggered discretization, may lead to precise value of some "gold-plated" lattice quantities, such as $\mathcal{F}(1)$ in $B \to D^\star \ell \overline{\nu}$. The stated theoretical accuracy will be checked by comparing predicted and measured values of a large number of non-perturbative quantities [17].

The analytical expression of $g(w)$, the universal form factor related to the Isgur-Wise function [18], is not known a-priori, and this introduces an additional uncertainty in the determination of $\mathcal{F}(1)|V_{cb}|$. First measurements of $|V_{cb}|$ were performed assuming a linear approximation for $g(w)$. It has been shown [19] that this assumption is not justified, and that linear fits systematically underestimate the extrapolation at zero recoil ($w = 1$) by about 3%. Most of this effect is related to the curvature of the form factor, and does not depend strongly upon the details of the chosen non-linear shape [19]. All recent published results use a non-linear shape for $g(w)$, approximated with an expansion near $w = 1$ [20]. $g(w)$ is parameterized in terms of the variable ρ^2, which is the slope of the form factor at zero recoil given in Ref. 20.

Experimental techniques to study the decay $B \to D^\star \ell \nu$:

The decay $B \to D^\star \ell \nu$ has been studied in experiments performed at center-of-mass energies equal to the $\Upsilon(4S)$ mass and the Z^0 mass. At the $\Upsilon(4S)$, experiments have the advantage that the w resolution is quite good. The dominant systematic uncertainties arise from background estimation and from the slow pion efficiency evaluation. This efficiency for charged pions is very low near w=1 and increases rapidly as w increases, while for neutral pions it drops slowly. CLEO [22] studies both $D^{\star +}$ and $D^{\star o}$ channels, while Belle [23] and BaBar [24] have so far presented only results based on $D^{\star +} \ell \nu$. In addition, kinematic constraints enable $\Upsilon(4S)$ experiments to identify the final state, including the $D^\star$, without a large contamination from the poorly known semileptonic decays including a hadronic system heavier than $D^\star$, commonly identified as '$D^{\star\star}$'. At LEP, B's are produced with a large momentum (about 30 GeV on average). The large boost produces a broadening in the reconstructed ν 4-momentum, needed to determine w, thus giving a relatively poor resolution and limited physics background rejection capabilities. On the other hand, LEP experiments benefit from an efficiency that is only mildly dependent upon w.

Experiments determine the product $(\mathcal{F}(1) \cdot |V_{cb}|)^2$ by fitting the measured $d\Gamma/dw$ distribution. Measurements have been published by CLEO [22], Belle [23], DELPHI [25], ALEPH [26], and OPAL [27]. Most recently, a preliminary measurement from BaBar has been presented [24]. At LEP, the dominant source of systematic error is the uncertainty on the contribution to $d\Gamma/dw$ from semileptonic B decays with final states including a hadron system heavier than the $D^\star$. This component includes both narrow orbitally excited charmed mesons and non-resonant or broad species. The existence of narrow resonant states is well established [1], and a signal of a broad resonance has been seen by CLEO [28], and, most recently, by Belle [29], but the decay characteristics of these states in b-hadron semileptonic decays have large uncertainties. The average of ALEPH [30], Belle [33], CLEO [31], and DELPHI [32] narrow state branching fractions show that the ratio $R_{\star\star} = \dfrac{\mathrm{B}(\overline{B} \to D_2^\star \ell \overline{\nu})}{\mathrm{B}(\overline{B} \to D_1 \ell \overline{\nu})}$ is smaller than one (< 0.6 at 95% C.L. [34]), in disagreement with HQET models where an infinite quark mass is assumed [35], but in agreement with models which take into account finite quark mass corrections [36]. Hence, LEP experiments use the treatment of narrow $D^{\star\star}$ proposed in [36], which accounts for $\mathcal{O}(1/m_c)$ corrections and provides several possible approximations of the form factors that depend on five different expansion schemes, and on three input parameters. To calculate the systematic errors, each proposed scheme is tested, with the relevant input parameters varied over a range consistent with the experimental limit on $R_{\star\star}$. The quoted systematic error is the maximal difference from the central value obtained with this method. Broad resonances or other non-resonant terms may not be modelled correctly with this approach.

To combine the published data, the central values and the errors of $\mathcal{F}(1)|V_{cb}|$ and ρ^2 are re-scaled to the same set of input parameters and their quoted uncertainties [21]. The $\mathcal{F}(1)|V_{cb}|$ values used for this average are extracted using the parametrization in Ref. 22, based on the experimental determinations of the vector and axial form factor ratios R_1 and R_2 [38]. The LEP data, which originally used theoretical values for these ratios, are re-scaled accordingly [37]. Table 1 summarizes the corrected data. The averaging procedure [37] takes into account statistical and systematic correlations between $\mathcal{F}(1)|V_{cb}|$ and ρ^2. Averaging the measurements in Table 1, we get:

$$\mathcal{F}(1)|V_{cb}| = (38.2 \pm 0.5 \pm 0.9) \times 10^{-3}$$

and

$$\rho^2 = 1.56 \pm 0.05 \pm 0.13, \qquad (3)$$

with χ^2 per degree of freedom of 22/12. The error ellipses for the corrected measurements and for the world average are shown in Figure 1. They are the product between the 1 σ error of $\mathcal{F}(1)|V_{cb}|$, ρ^2, and the correlation between the two. Since this is a 2 parameter fit, the ellipses correspond to about 37% CL contours. The χ^2 per degree of freedom is 1.8. We have not rescaled the errors.

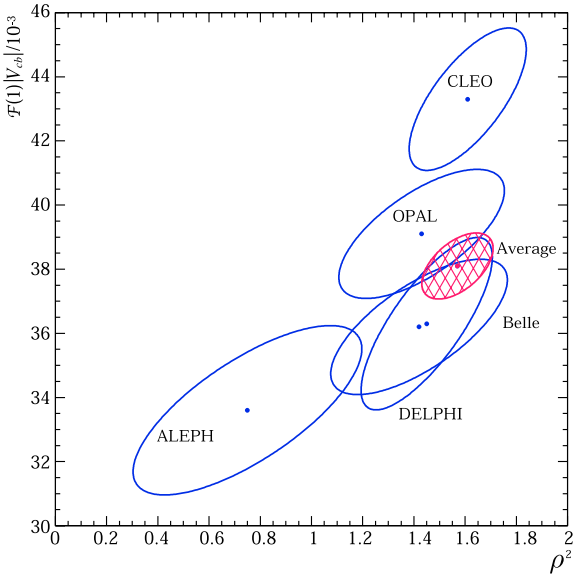

Figure 1: The error ellipses for the corrected measurements and world average for $\mathcal{F}(1)|V_{cb}|$ vs ρ^2. The ellipses are the product between the 1 σ error of $\mathcal{F}(1)|V_{cb}|$, ρ^2, and the correlation between the two. Consequently the ellipses correspond to about 37% CL. See full-color version on color pages at end of book.

The main contributions to the $\mathcal{F}(1)|V_{cb}|$ systematic error are from the uncertainty on the $B \to D^{**}\ell\nu$ shape and B($b \to B_d$), fully correlated among the LEP experiments, the branching fraction of D and $D^\star$ decays, fully correlated among all the experiments, and the slow pion reconstruction from Belle and CLEO which are uncorrelated, The main contribution to the ρ^2 systematic error is from the uncertainties in the measured values of R_1 and R_2, fully correlated among experiments. Because of the large contribution of this uncertainty to the non-diagonal terms of the covariance matrix, the averaged ρ^2 is higher than one would naively expect.

Using $\mathcal{F}(1) = 0.91 \pm 0.04$ [13], we get $|V_{cb}| = (42.0 \pm 1.1_{\rm exp} \pm 1.8_{\rm theo}) \times 10^{-3}$. The dominant error is theoretical, and there are good prospects to reduce it in the next few years [14], [17].

Table 1: Experimental results from $B \to D^\star\ell\nu$ analyses after the correction to common inputs and world average. The LEP numbers are corrected to use R_1 and R_2 from CLEO data. ρ^2 is the slope of the form factor at zero recoil as defined in Ref. 20. $\rm Corr_{stat}$ is the statistical correlation between $\mathcal{F}(1)|V_{cb}|$ and ρ^2. (* Average of two measurements.)

Exp.	$\mathcal{F}(1)\lvert V_{cb}\rvert(\times 10^3)$	ρ^2	$\rm Corr_{stat}$
ALEPH	$33.6 \pm 2.1 \pm 1.6$	$0.75 \pm 0.25 \pm 0.37$	94%
DELPHI*	$36.2 \pm 1.1 \pm 1.8$	$1.42 \pm 0.10 \pm 0.33$	92%
OPAL*	$39.1 \pm 0.9 \pm 1.8$	$1.43 \pm 0.12 \pm 0.31$	89%
Belle	$36.3 \pm 1.9 \pm 1.9$	$1.45 \pm 0.16 \pm 0.20$	91%
CLEO	$43.3 \pm 1.3 \pm 1.8$	$1.61 \pm 0.09 \pm 0.21$	87%
BaBar	$34.1 \pm 0.2 \pm 1.3$	$1.23 \pm 0.02 \pm 0.28$	92%
World average	$38.2 \pm 0.5 \pm 0.9$	$1.56 \pm 0.05 \pm 0.13$	53%

The decay $B \to D\ell\nu$: The study of the decay $B \to D\ell\nu$ poses new challenges both from the theoretical and experimental point of view.

The differential decay rate for $B \to D\ell\nu$ can be expressed as:

$$\frac{d\Gamma_D}{dw}(B \to D\ell\nu) = \frac{G_F^2|V_{cb}|^2}{48\pi^3}\mathcal{K}_{\mathcal{D}}(w)\mathcal{G}(w)^2, \qquad (4)$$

where w is the inner product of the B and D meson 4-velocities, $\mathcal{K}_{\mathcal{D}}(w)$ is the phase space, and the form factor $\mathcal{G}(w)$ is generally expressed as the product of a normalization factor, $\mathcal{G}(1)$, and a function, $g_D(w)$, constrained by dispersion relations [3].

The strategy to extract $\mathcal{G}(1)|V_{cb}|$ is identical to that used for the $B \to D^\star\ell\nu$ decay. However, in this case there is no suppression of $1/m_Q$ (*i.e.*, no Luke theorem) and corrections and QCD effects on $\mathcal{G}(1)$ are calculated with less accuracy than $\mathcal{F}(1)$ [39,40]. Moreover, $d\Gamma_D/dw$ is more heavily suppressed near $w = 1$ than $d\Gamma_{D^*}/dw$, due to the helicity mismatch between initial and final states. This channel is also much more challenging from the experimental point of view as it is hard to isolate from the dominant $B \to D^\star\ell\nu$ background, as well as from fake D–ℓ combinations. Thus, the extraction of $|V_{cb}|$ from this channel is less precise than the one from the $B \to D^\star\ell\nu$ decay. Nevertheless, the $B \to D\ell\nu$ channel provides a consistency check, and allows a test of heavy-quark symmetry [40] through the measurement of the form factor $\mathcal{G}(w)$, as HQET predicts the ratio $\mathcal{G}(w)/\mathcal{F}(w)$ to be very close to one.

Belle [41] and ALEPH [26] studied the $\overline{B}^0 \to D^+\ell^-\overline{\nu}$ channel, while CLEO [42] studied both $B^+ \to D^0\ell^+\overline{\nu}$ and $\overline{B}^0 \to D^+\ell^-\overline{\nu}$ decays. Averaging the data in Table 2 [37], we get $\mathcal{G}(1)|V_{cb}| = (41.8 \pm 3.7) \times 10^{-3}$ and $\rho_D^2 = 1.15 \pm 0.16$, where ρ_D^2 is the slope of the form factor at zero recoil given in Ref. 20.

Table 2: Experimental results after the correction to common inputs and world average. ρ_D^2 is the slope of the form factor at zero recoil given in Ref. 20.

Exp.	$\mathcal{G}(1)\lvert V_{cb}\rvert(\times 10^3)$	ρ_D^2
ALEPH	$39.3 \pm 10.0 \pm 6.5$	$0.97 \pm 0.98 \pm 0.38$
Belle	$41.8 \pm 4.4 \pm 5.2$	$1.12 \pm 0.22 \pm 0.14$
CLEO	$44.4 \pm 5.8 \pm 3.5$	$1.27 \pm 0.25 \pm 0.14$
World average	$41.8 \pm 2.5 \pm 2.7$	$1.15 \pm 0.13 \pm 0.09$

The theoretical predictions for $\mathcal{G}(1)$ are consistent: 1.03 ± 0.07 [43], and 1.02 ± 0.08 [40]. A quenched lattice calculation gives $\mathcal{G}(1) = 1.058^{+0.021}_{-0.017}$ [44], where the errors do not include the uncertainties induced by the quenching approximation and lattice spacing. An unquenched value should be available in the next few years [15]. A recent study of the decay $B \to D\ell\overline{\nu}$ in the context of heavy quark sum rules [16] argues that this channel can provide an alternative very precise determination of $|V_{cb}|$. *Ref. [16] uses heavy quark sum rules to relate exclusive form factors and inclusive semileptonic width and argues that in the approximation $\mu_\pi^2 - \mu_G^2 << \mu_\pi^2$, many power corrections vanish to all orders in $1/m_Q$. The parameter μ_π^2 represents the expectation value of the leading local heavy quark kinetic operator and μ_G^2 parameterizes the corresponding expectation value of the chromomagnetic operator. A more extensive discussion of the theoretical treatment of inclusive semileptonic decays is given in the next section.

Using $\mathcal{G}(1) = 1.04 \pm 0.06$, we get $|V_{cb}| = (40.2 \pm 3.6_{\rm exp} \pm 2.3_{\rm theo}) \times 10^{-3}$, consistent with the value extracted from $B \to D^\star\ell\nu$ decay, but with a larger uncertainty.

The experiments have also measured the differential decay rate distribution to extract the ratio $\mathcal{G}(w)/\mathcal{F}(w)$. The data are compatible with a universal from factor as predicted by HQET.

III. $|V_{cb}|$ determination from inclusive B semileptonic decays

Alternatively, $|V_{cb}|$ can be extracted from the inclusive semileptonic width, requiring measurements of both the B lifetimes and the semileptonic branching fraction B($B \to X_c\ell\nu$) [45,46]. In this case, quark-hadron duality bridges the gap between theoretical calculations and experimental observables [47]. The modern theoretical formulation based on the Operator Product Expansion (OPE) determines the inclusive decay amplitudes in inverse powers of $1/m_Q$ [45]. Non-perturbative corrections to the leading term, given by the spectator decay amplitude, arise only to order $1/m_b^2$. Quark-hadron duality is an important *ab initio* assumption in these calculations [47]. As M. Shifman put it [47], "It is fair to say that (short of the full solution of QCD) understanding and controlling the accuracy of the quark-hadron duality is one of the most important and challenging problem for the QCD practitioner today." In other words, as pointed out by Shifman and Buchalla [49], "duality violation parameterize our ignorance." Models can give estimates of the uncertainty induced by duality violations [48], [50]. These models need to have a clear physical interpretation and must be tested, in their key features, against experimental data [47]. The models quoted before imply different power suppression of duality violations. This issue needs to be resolved with further theoretical effort in defining clear and unambiguous quantitative tests of duality violations complemented by an experimental program to validate them.

The coefficients of the $1/m_b$ power terms are expectation values of operators that include non-perturbative physics. Relationships that are valid up to $1/m_b^2$ include four such parameters: the expectation value of the kinetic operator, corresponding to the average of the square of the heavy-quark momentum inside the hadron, the expectation value of the chromomagnetic operator, and the heavy-quark masses (m_b and m_c). The expectation value of the kinetic operator is introduced in the literature as μ_π^2 [45,46] or $-\lambda_1$ [51,52], and the expectation value of the chromomagnetic operator as μ_G^2 [45,46], or $3\lambda_2$ [51,52]. The two notations reflect a difference in the approach used to handle the energy scale μ used to separate long-distance from short-distance physics. HQET is most commonly renormalized in a mass-independent scheme, thus making the quark masses the pole masses of the underlying theory (QCD). The second group of authors prefer the definition of the non-perturbative operators using a mass scale $\mu \approx 1$ GeV.

The semileptonic width expression in Ref. 53 has been used to extract $|V_{cb}|$ from the semileptonic branching fraction measured by CLEO, and to measure the heavy-quark expansion (HQE) parameters $\overline{\Lambda}$ and λ_1, as discussed below. The most recent version of the alternative formulation can be found in Ref. 9.

The quark masses are related to the corresponding meson masses through [8]:

$$m_b = \overline{M}_B - \overline{\Lambda} + \frac{\lambda_1}{2\overline{M}_B}, \qquad (5)$$

where $\overline{M}_B$ is the spin averaged $B - B^\star$ mass ($\overline{M}_B = 5.3134$ GeV/c^2). A similar equation relates m_c and $\overline{M}_D$. The parameter $\overline{\Lambda}$ represents the energy of the light quark and gluons. From the equations relating m_b and m_c to the corresponding spin-averaged meson masses, experimentalists usually derive the constraint on m_c to be used in the theoretical formulae. It has been pointed out [9] that it may be opportune to replace this constraint with an independent experimental determination of m_c.

HQE and moments in semileptonic decays:

Experimental determinations of the HQE parameters are important in several respects. In particular, redundant determinations of these parameters may uncover inconsistencies, or point to violation of some important assumptions inherent in these calculations. The parameter λ_2 can be extracted from

the $B^\star - B$ mass splitting, whereas the other parameters need more elaborate measurements.

The CLEO collaboration determines the parameter $\overline{\Lambda}$ from the first moment of the γ energy in the decay $b \to s\gamma$, which gives the average energy of the γ emitted in this transition. Using the formalism of Ref. 53, they obtain $\overline{\Lambda} = 0.35 \pm 0.07 \pm 0.10$ GeV [54].

The parameter λ_1 can be determined from of the first moment of the mass M_X of the hadronic system recoiling against the $\ell - \overline{\nu}$ pair. The relationship between the first moment of $M_1 \equiv < M_X^2 - M_D^2 >$ and the parameters $\overline{\Lambda}$ and λ_1 is given in Ref. 55.

The measured value for $< M_X^2 - M_D^2 >$ [55] is 0.251 ± 0.066 GeV^2. This constraint, combined with the measurement of the mean photon energy in $b \to s\gamma$, implies a value of $\lambda_1 = -0.24 \pm 0.11$ GeV^2, to order $1/M_B^3$ and $\beta_0 \alpha_s^2$ in ($\overline{\rm MS}$).

The shape of the lepton spectrum provides further constraints on OPE. Moments of the lepton momentum with a cut $p_\ell^{CM} \geq 1.5$ GeV/c have been measured by the CLEO collaboration [62]. The two approaches give consistent results, although the technique used to extract the OPE parameters has still relatively large uncertainties associated with the $1/m_b^3$ form factors. The sensitivity to $1/m_b^3$ corrections depends upon which moments are considered. Bauer and Trott [61] have performed an extensive study of the sensitivity of lepton energy moments to non-perturbative effects. In particular, they have proposed "duality moments," very insensitive to neglected higher order terms. The comparison between the CLEO measurement of these moments [62] and the predicted values shows a very impressive agreement:

$$D_3 \equiv \frac{\int_{1.6\,\mathrm{GeV}} E_\ell^{0.7} \frac{d\Gamma}{dE_\ell} dE_\ell}{\int_{1.5\,\mathrm{GeV}} E_\ell^{1.5} \frac{d\Gamma}{dE_\ell} dE_\ell} = \begin{cases} 0.5190 \pm 0.0007 & \text{(T)} \\ 0.5193 \pm 0.0008 & \text{(E)} \end{cases}$$

$$D_4 \equiv \frac{\int_{1.6\,\mathrm{GeV}} E_\ell^{2.3} \frac{d\Gamma}{dE_\ell} dE_\ell}{\int_{1.5\,\mathrm{GeV}} E_\ell^{2.9} \frac{d\Gamma}{dE_\ell} dE_\ell} = \begin{cases} 0.6034 \pm 0.0008 & \text{(T)} \\ 0.6036 \pm 0.0006 & \text{(E)} \end{cases} \qquad (6)$$

(where "T" and "E" denote theory and experiment, respectively).

More recently, both CLEO and BaBar explored the moments of the hadronic mass M_X^2 with lower lepton momentum cuts. In order to identify the desired semileptonic decay from background processes including cascade decays, continuum leptons and fake leptons, CLEO performs a fit for the contributions of signal and backgrounds to the full three-dimensional differential decay rate distribution as a function of the reconstructed quantities q^2, M_X^2, $\cos\theta_{W\ell}$. The signal includes the components $B \to D\ell\overline{\nu}$, $B \to D^\star\ell\overline{\nu}$, $B \to D^{\star\star}\ell\overline{\nu}$, $B \to X_c\ell\overline{\nu}$ non-resonant, and $B \to X_u\ell\overline{\nu}$. The backgrounds considered are: secondary leptons, continuum leptons and fake leptons. BaBar uses a sample where the hadronic decay of one B is fully reconstructed and the charged lepton from the other B is identified. In this case the main sources of systematic errors are the uncertainties related to the detector modelling and reconstruction.

Figure 2 shows the extracted $< M_X^2 - \overline{M}_D^2 >$ moments as a function of the minimum lepton momentum cut from these two measurements, as well as the original measurement with $p_\ell \geq 1.5$ GeV/c. The results are compared with theory bands that reflect experimental errors, $1/m_b^3$ correction uncertainties and uncertainties in the higher order QCD radiative corrections [56]. The CLEO and BaBar results are consistent and show an improved agreement with theoretical predictions with respect to earlier preliminary results [57]. Moments of the M_X distribution without an explicit lepton momentum cut have been extracted from preliminary DELPHI data [58] and give consistent results.

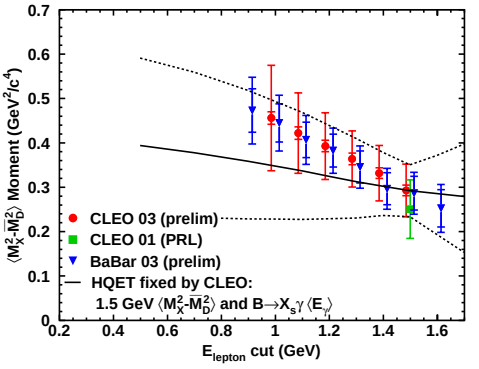

Figure 2: The results of the recent CLEO analysis [59] compared to previous measurements [55,60] and the HQET prediction. The theory bands shown in the figure reflect the variation of the experimental errors on the two constraints, the variation of the third-order HQET parameters by the scale $(0.5\ \mathrm{GeV})^3$, and variation of the size of the higher order QCD radiative corrections [56]. See full-color version on color pages at end of book.

Experimental determination of the semileptonic branching fraction:

The value of B($B \to X_c\ell\nu$) has been measured both at the $\Upsilon(4S)$ and LEP.

Experiments taking data at the Υ(4S) center-of-mass energy determine the inclusive semileptonic branching fraction through a lepton tagged sample. In this approach, a di-lepton sample is studied, and the charge correlation between the two leptons is used to disentangle leptons coming from the direct decay $B \to X_c\ell\nu$ and the dominant background at low lepton momenta, the cascade decay $B \to X_c \to X_s\ell\nu$. This method was pioneered by the ARGUS collaboration [63] to measure the electron spectrum from $B \to X_c\ell\nu$ down to 0.6 GeV/c. Thus,

it reduces the model dependence of the extracted semileptonic branching fraction very substantially. Experimental data are summarized in Table 3. The systematic error is dominated by experimental uncertainties: lepton identification efficiency, fake rate determination, and tracking efficiencies contribute to 3% of this overall error. The remaining error is a sum of several small corrections associated with the uncertainty in the mixing parameter, and additional background estimates [64]. BaBar [65] and Belle [66] have studied the inclusive electron spectrum with the same technique.

Table 3: B($b \to \ell$) measurement from experiments at $\Upsilon(4S)$ center-of-mass energy and their average. The errors quoted reflect statistical, and systematic uncertainties. These measurements are largely model independent.

Experiment	B($b \to \ell\nu$)%
ARGUS	$9.75 \pm 0.50 \pm 0.39$
CLEO	$10.49 \pm 0.17 \pm 0.43$
Belle	$10.96 \pm 0.12 \pm 0.50$
BaBar	$10.91 \pm 0.18 \pm 0.29$
Υ(4S) Average	10.73 ± 0.28

Combining $\Upsilon(4S)$ results [1], we obtain: B($b \to X\ell\nu$) = (10.73±0.28)%. Upon subtracting B($b \to u\ell\nu$) = (0.17±0.05)%, we get: B($b \to X_c\ell\nu$) = (10.56 ± 0.28)%. Using τ_{B^+}, τ_{B^0} [1], and the ratio between charged and neutral B pair production $f_{+-}/f_{00} = 1.044 \pm 0.05$ [21], we obtain the semileptonic width $\Gamma(b \to X_c\ell\nu) = (0.434 \pm 0.011 \pm 0.003) \times 10^{-10}$ MeV, where the second error includes the uncertainties from B($b \to u\ell\nu$), and the model dependence. A common value for the ratio f_{+-}/f_{00} between B^+B^- and $B^0\overline{B}^0$ final states produced at the $\Upsilon(4S)$ is used here. This parameter is very sensitive to the precise value of the center-of-mass energy and beam energy spread [70] and thus as more precise data become available, it is important to check that it is appropriate to average f_{+-}/f_{00} at different machines.

At LEP, B^0, B^-, B_s, and b baryons are produced, so the measured inclusive semileptonic branching ratio is an average over the different hadron species. Assuming that the semileptonic widths of all b hadrons are equal, the following relation holds:

$$\begin{aligned}\mathrm{B}(b \to X_c l\nu)_{\mathrm{LEP}} = & \\ & f_{B^0}\frac{\Gamma(B^0 \to X_c l\nu)}{\Gamma(B^0)} + f_{B^-}\frac{\Gamma(B^- \to X_c l\nu)}{\Gamma(B^-)} \\ & + f_{B_s}\frac{\Gamma(B_s \to X_c l\nu)}{\Gamma(B_s)} + f_{\Lambda_b}\frac{\Gamma(\Lambda_b \to X_c l\nu)}{\Gamma(\Lambda_b)} \\ & = \Gamma(B \to X_c\ell\nu)\tau_b \ , \end{aligned} \quad (7)$$

where τ_b is the average b-hadron lifetime. Taking into account the present precision of LEP measurements of b-baryon semileptonic branching ratios and lifetimes, the estimate uncertainty for a possible difference for the width of b baryons is 0.13%. The average LEP value for B($b \to X\ell\nu$) = (10.59 ± 0.30)% is taken from a fit [71], which combines the semileptonic branching ratios, the B^0–$\overline{B}^0$ mixing parameter $\overline{\chi}_b$, and $R_b = \Gamma(Z \to b\bar{b})/\Gamma(Z \to \mathrm{had})$. Ref. 72 shows that the main contribution to the model uncertainty is the composition of the semileptonic width, including the narrow, wide and non-resonant D^{**} states. B_s and b baryons are about 20% of the total signal, and their contribution to the uncertainty of the spectrum is small. In this average, we use the modelling error quoted by Ref. 72, rather than the error from the combined fit, as the ALEPH procedure is based on more recent information. The dominant errors in the combined branching fraction are the modelling of semileptonic decays (2.6%) and the detector related items (1.3%).

Subtracting B($b \to u\ell\nu$) from the LEP semileptonic branching fraction, we get: B($b \to X_c\ell\nu$) = (10.52±0.32)%, and using τ_b [1]: $\Gamma(b \to X_c\ell\nu) = (0.439 \pm 0.010 \pm 0.011) \times 10^{-10}$ MeV, where the systematic error 0.011×10^{-10}MeV reflects the B($b \to u\ell\nu$) uncertainty and the model dependence.

Combining the LEP and the $\Upsilon(4S)$ semileptonic widths, we get: $\Gamma(b \to X_c\ell\nu) = (0.44 \pm 0.01) \times 10^{-10}$ MeV, which is used in the formula of Ref. 55 to get:

$$|V_{cb}|_{\mathrm{incl}} = (41.0 \pm 0.5_{\mathrm{exp}} \pm 0.5_{\lambda_1,\overline{\Lambda}} \pm 0.8_{\mathrm{theo}}) \times 10^{-3} \ , \quad (8)$$

where the first error is experimental, and the second is from the measured value of λ_1 and $\overline{\Lambda}$, assumed to be universal up to higher orders. The third error is from $1/m_b^3$ corrections and from the ambiguity in the α_s scale definition. The error on the average b-hadron lifetime is assumed to be uncorrelated with the error on the semileptonic branching ratio.

IV. Conclusions

The values of $|V_{cb}|$ obtained both from the inclusive and exclusive method agree within errors. The value of $|V_{cb}|$ obtained from the analysis of the $B \to D^*\ell\nu$ decay is:

$$|V_{cb}|_{\mathrm{exclusive}} = (42.0 \pm 1.1_{\mathrm{exp}} \pm 1.9_{\mathrm{theo}}) \times 10^{-3} \ , \quad (9)$$

where the first error is experimental and the second error is from the $1/m_Q^2$ corrections to $\mathcal{F}(1)$. The value of $|V_{cb}|$, obtained from inclusive semileptonic branching fractions is:

$$|V_{cb}|_{\mathrm{incl}} = (41.0 \pm 0.5_{\mathrm{exp}} \pm 0.5_{\lambda_1,\overline{\Lambda}} \pm 0.8_{\mathrm{theo}}) \times 10^{-3}. \quad (10)$$

In addition, non-quantified uncertainties are associated with a possible quark-hadron duality violations when using the inclusive method. A first conservative assessment of these uncertainties may be obtained from the difference between the two values of $|V_{cb}|$ extracted from $B \to D^*\ell\overline{\nu}$ and from inclusive measurements. These data imply about 6% uncertainty for non-quantified assumptions in the inclusive determination. This result is largely affected by the quantified theoretical errors in the two determinations and thus does not give a very stringent bound.

High precision tests of lattice gauge theory calculations and more refined experimental assessments of quark-hadron duality in inclusive semileptonic decays are needed to achieve the ultimate accuracy in our knowledge of V_{cb}.

References

1. See "The Cabibbo-Kobayashi-Maskawa Quark-Mixing Matrix" by F.J. Gilman, K. Kleinknecht, and B. Renk in this *Review* .
2. J. Duboscq *et al.* (CLEO), Phys. Rev. Lett. **76**, 3898 (1996).
3. C. Glenn Boyd, B. Grinstein, and R.F. Lebed, Phys. Lett. **B353**, 306 (1995).
4. P.F. Harrison and H.R. Quinn, editors, *The BaBar Physics Book*, SLAC-R-504 (1998) and references therein.
5. M. Luke, Phys. Lett. **B252**, 447 (1990).
6. A. Sirlin, Nucl. Phys. **B196**, 83 (1982).
7. A. Czarnecki, Phys. Rev. Lett. **76**, 4124 (1993).
8. A.F. Falk and M. Neubert, Phys. Rev. **D47**, 2965 (1993) and Phys. Rev. **D47**, 2982 (1993).
9. D. Benson *et al.*, Nucl. Phys. **B665**, 367 (2003).
10. T. Mannel, Phys. Rev. **D50**, 428 (1994).
11. M. Shifman, N.G. Uraltsev, and A. Vainshtein, Phys. Rev. **D51**, 2217 (1995).
12. J.N. Simone *et al.*, Nucl. Phys. Proc. Suppl. **83**, 334 (2000).
13. Working Group 1 Summary, CKM Workshop, CERN, CH (2002); `http://ckm-workshop.web.cern.ch/ckm-workshop/`.
14. R.A. Briere *et al.* (CLEO), CLNS 01/1742 (2001).
15. C.T.H. Davies *et al.*, `hep-lat/0304004` (2003).
16. N. Uraltsev, `hep-ph/0312001` (2003).
17. A.S. Kronfeld, `hep-lat/0310063` (2003).
18. N. Isgur and M.B. Wise, Phys. Lett. **B232**, 113 (1989) and Phys. Lett. **B237**, 527 (1990).
19. S. Stone, in *B Decays, 2nd Edition*, S. Stone editor (1994), 283.
20. I. Caprini, L. Lellouch, and M. Neubert, Nucl. Phys. **B530**, 153 (1998); C.G. Boyd, B. Grinstein, R.F. Lebed, Phys. Rev. **56**, 6895 (1997).
21. The Heavy Flavor Averaging Group (HFAG); `http://www.slac.stanford.edu/xorg/hfag/semi/`.
22. R.A. Brierie *et al.* (CLEO), Phys. Rev. Lett. **89**, 081803 (2002).
23. K. Abe *et al.* (Belle), Phys. Lett. **B526**, 247 (2002).
24. B. Aubert *et al.* (BaBar), `hep-ex/0308027`.
25. P. Abreu *et al.* (DELPHI), Phys. Lett. **B510**, 55 (2001); P. Abreu *et al.* (DELPHI), accepted by EPJC..
26. D. Buskulic *et al.* (ALEPH), Phys. Lett. **B395**, 373 (1997).
27. G. Abbiendi *et al.* (OPAL), Phys. Lett. **B482**, 15 (2000).
28. S. Anderson *et al.* (CLEO), Nucl. Phys. **A663**, 647 (2000).
29. K. Abe *et al.* (Belle) Phys. Lett. **B570**, 205 (2003).
30. D. Buskulic *et al.* (ALEPH), Z. Phys. **C73**, 601 (1997).
31. A. Anastassov *et al.* (CLEO), Phys. Rev. Lett. **80**, 4127 (1998).
32. D. Block *et al.* (DELPHI), Contributed Paper to *ICHEP 2000*, DELPHI 2000-106 Conf. 45 (2000).
33. K. Abe *et al.* (Belle), submitted to Phys. Rev. D..
34. ALEPH, CDF, DELPHI, L3, OPAL, SLD, CERN-EP/2001-050.
35. V. Morenas *et al.*, Phys. Rev. **D56**, 5668 (1997); M.Q. Huang and Y.B. Dai, Phys. Rev. **D59**, 34018 (1999); M.Oda *et al.*, `hep-ph/0005102` (2000).
36. A.K. Leibovich *et al.*, Phys. Rev. **D57**, 308 (1998); Phys. Rev. Lett. **78**, 3995 (1997).
37. LEP V_{cb} Working Group, Internal Note, `http://lepvcb.web.cern.ch/LEPVCB/`.
38. J.E. Duboscq *et al.* (CLEO), Phys. Rev. Lett. **76**, 3898 (1996).
39. M. Neubert, Phys. Lett. **B264**, 455 (1991).
40. Z. Ligeti, Y. Nir, and M. Neubert, Phys. Rev. **D49**, 1302 (1994); Z. Ligeti, `hep-ph/9908432`.
41. K. Abe *et al.* (Belle), Phys. Lett. **B526**, 258 (2002).
42. J. Bartelt *et al.* (CLEO), Phys. Rev. Lett. **82**, 3746 (1999).
43. D. Scora and N. Isgur, Phys. Rev. **D52**, 2783 (1995).
44. S. Hashimoto *et al.*, Phys. Rev. **D61**, 014502 (1999).
45. I. Bigi, M. Shifman, and N. Uraltsev, Ann. Rev. Nuc. Part. Sci. **47**, 591 (1997).
46. A.V. Manohar and M.B. Wise, Phys. Rev. **D49**, 110 (1994); A.F. Falk, Lectures presented at TASI-2000, `hep-ph/0007339`.
47. M. Shifman in Boris Ioffe Festshrift *At the frontier of Particle Physics/Handbook of QCD*, World Scientific, Singapore (2001).
48. Le Yaouanc *et al.*, Phys. Lett. **B488**, 153 (2000); A. Le Yaouanc *et al.*, Phys. Rev. **D62**, 74007 (2000); A. Le Yaouanc *et al.*, Phys. Lett. **B517**, 135 (2001).
49. G. Buchalla, `hep-ph/0202092` (2002) and references therein.
50. N. Isgur, Phys. Lett. **B448**, 111 (1999).
51. M. Gremm and N. Kapustin, Phys. Rev. **D55**, 6924 (1997).
52. A. Falk, M. Luke, and M.J. Savage, Phys. Rev. **D33**, 2491 (1996).
53. A. Falk and M. Luke, Phys. Rev. **D57**, 424 (1998).
54. S. Chen *et al.*, Phys. Rev. Lett. **87**, 251807 (2001).
55. D. Cronin-Hennessy *et al.* (CLEO), Phys. Rev. Lett. **87**, 251808 (2001).
56. C. W. Bauer *et al.*, Phys. Rev. **D67**, 054012 (2003).
57. V. G. Luth (BABAR), SLAC-PUB-9695 *Prepared for 31st International Conference on High Energy Physics* (ICHEP 2002), Amsterdam, The Netherlands, 24-31 Jul 2002.
58. M. Battaglia *et al.*, Phys. Lett. **B56**, 41 (2003).
59. G. S. Huang *et al.*, (CLEO), `hep-ex/0307081`.
60. B. Aubert *et al.* (BABAR), `hep-ex/0307046` .
61. C.S. Bauer and M. Trott, Phys. Rev. **D67**, 014021 (2003).
62. A. Mahmood *et al.* (CLEO), Phys. Rev. **D67**, 072001 (2003).
63. H.Albrecht *et al.* (ARGUS), Phys. Lett. **B318**, 397 (1993).
64. B.C. Barish *et al.* (CLEO), Phys. Rev. Lett. **76**, 1570 (1996); S. Henderson *et al.* (CLEO), Phys. Rev. **D45**, 2212 (1992).
65. B. Aubert *et al.* (BaBar), Phys. Rev. **D67**, 031101 (2003).
66. K. Abe *et al.* (Belle), Phys. Lett. **B547**, 181 (2002).

67. J.P. Alexander *et al.* (CLEO), Phys. Rev. Lett. **86**, 2737 (2001).
68. B. Aubert *et al.* (BaBar), Phys. Rev. **D65**, 032001 (2002).
69. N. Hastings *et al.* (Belle), Phys. Rev. **D67**, 052004 (2003).
70. M. Voloshin, Mod. Phys. Lett. A **18**, 1783 (2003).
71. LEP/SLD Electroweak Heavy Flavor Results Winter 2001 Conferences; http://lepewwg.web.cern.ch/LEPEWWG/heavy/.
72. A. Heister *et al.* (ALEPH), Eur. Phys. J. **C22**, 613 (2002).
73. P. Abreu *et al.* (DELPHI), Eur. Phys. J. **C20**, 455 (2001).
74. M. Acciari *et al.* (L3), Z. Phys. **C71**, 379 (1996); M. Acciari *et al.* (L3), Eur. Phys. J. **C13**, 47 (2000).
75. G. Abbiendi *et al.* (OPAL), Eur. Phys. J. **C13**, 225 (2000).

V_{cb} MEASUREMENTS

For the discussion of V_{cb} measurements, which is not repeated here, see the review on "Determination of $|V_{cb}|$."

The CKM matrix element $|V_{cb}|$ can be determined by studying the rate of the semileptonic decay $B \to D^{(*)}\ell\nu$ as a function of the recoil kinematics of $D^{(*)}$ mesons. Taking advantage of theoretical constraints on the normalization and a linear ω dependence of the form factors provided by Heavy Quark Effective Theory (HQET), the $|V_{cb}|\times F(\omega)$ and ρ^2 (a^2) can be simultaneously extracted from data, where ω is the scalar product of the two-meson four velocities, $F(1)$ is the form factor at zero recoil (ω=1) and ρ^2 is the slope, sometimes denoted as a^2. Using the theoretical input of $F(1)$, a value of $|V_{cb}|$ can be obtained.

"OUR EVALUATION" is an average using rescaled values of the data listed below. The average and rescaling were performed by the Heavy Flavor Averaging Group (HFAG) and are described at http://www.slac.stanford.edu/xorg/hfag/. The averaging/rescaling procedure takes into account corrections between the measurements.

$|V_{cb}| \times F(1)$ (from $B^0 \to D^{*-}\ell^+\nu$)

VALUE	DOCUMENT ID		TECN	COMMENT
0.0381 ± 0.0011 OUR EVALUATION	with ρ^2=1.55 ± 0.15 and a correlation 0.88. The fitted χ^2 is 21.9 for 10 degrees of freedom.			
0.0371 ± 0.0019 OUR AVERAGE	Error includes scale factor of 1.7. See the ideogram below.			
0.0431 ± 0.0013 ± 0.0018	[1] ADAM	03	CLE2	$e^+e^- \to \Upsilon(4S)$
0.0354 ± 0.0019 ± 0.0018	[2] ABE	02F	BELL	$e^+e^- \to \Upsilon(4S)$
0.0355 ± 0.0014 $^{+0.0023}_{-0.0024}$	[3] ABREU	01H	DLPH	$e^+e^- \to Z$
0.0371 ± 0.0010 ± 0.0020	[4] ABBIENDI	00Q	OPAL	$e^+e^- \to Z$
0.0319 ± 0.0018 ± 0.0019	[5] BUSKULIC	97	ALEP	$e^+e^- \to Z$
• • • We do not use the following data for averages, fits, limits, etc. • • •				
0.0431 ± 0.0013 ± 0.0018	[6] BRIERE	02	CLE2	$e^+e^- \to \Upsilon(4S)$
0.0328 ± 0.0019 ± 0.0022	ACKERSTAFF	97G	OPAL	Repl. by ABBIENDI 00Q
0.0350 ± 0.0019 ± 0.0023	[7] ABREU	96P	DLPH	Repl. by ABREU 01H
0.0351 ± 0.0019 ± 0.0020	[8] BARISH	95	CLE2	Repl. by ADAM 03
0.0314 ± 0.0023 ± 0.0025	BUSKULIC	95N	ALEP	Repl. by BUSKULIC 97

[1] Average of the $B^0 \to D^*(2010)^-\ell^+\nu$ and $B^+ \to \overline{D}{}^*(2007))\ell^+\nu$ modes with ρ^2 = 1.61 ± 0.09 ± 0.21 and f_{+-} = 0.521 ± 0.012.

[2] Measured using exclusive $B^0 \to D^*(892)^-e^+\nu$ decays with ρ^2= 1.35 ± 0.17 ± 0.19 and a correlation of 0.91.

[3] ABREU 01H measured using about 5000 partial reconstructed D^* sample with a ρ^2=1.34 ± 0.14 $^{+0.24}_{-0.22}$.

[4] ABBIENDI 00Q: measured using both inclusively and exclusively reconstructed $D^{*\pm}$ samples with a ρ^2=1.21 ± 0.12 ± 0.20. The statistical and systematic correlations between $|V_{cb}|\times F(1)$ and ρ^2 are 0.90 and 0.54 respectively.

[5] BUSKULIC 97: measured using exclusively reconstructed $D^{*\pm}$ with a a^2=0.31 ± 0.17 ± 0.08. The statistical correlation is 0.92.

[6] BRIERE 02 result is based on the same analysis and data sample reported in ADAM 03.

[7] ABREU 96P: measured using both inclusively and exclusively reconstructed $D^{*\pm}$ samples.

[8] BARISH 95: measured using both exclusive reconstructed $B^0 \to D^{*-}\ell^+\nu$ and $B^+ \to D^{*0}\ell^+\nu$ samples. They report their experiment's uncertainties ±0.0019 ± 0.0018 ± 0.0008, where the first error is statistical, the second is systematic, and the third is the uncertainty in the lifetimes. We combine the last two in quadrature.

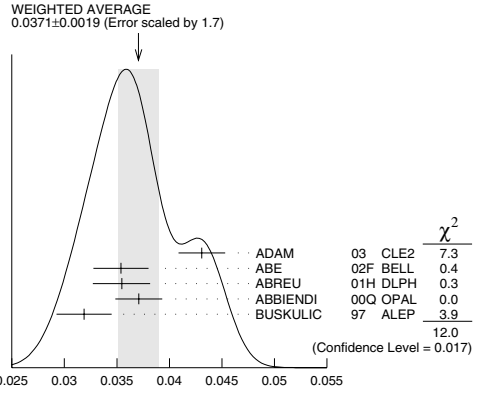

$|V_{cb}| \times F(1)$ (from $B \to D^-\ell^+\nu$)

VALUE	DOCUMENT ID		TECN	COMMENT
0.0418 ± 0.0037 OUR EVALUATION	with ρ^2=1.15 ± 0.16 and a correlation of 0.93. The fitted χ^2 is 0.3 for 4 degrees of freedom.			
0.039 ± 0.004 OUR AVERAGE				
0.0411 ± 0.0044 ± 0.0052	[9] ABE	02E	BELL	$e^+e^- \to \Upsilon(4S)$
0.0416 ± 0.0047 ± 0.0037	[10] BARTELT	99	CLE2	$e^+e^- \to \Upsilon(4S)$
0.0278 ± 0.0068 ± 0.0065	[11] BUSKULIC	97	ALEP	$e^+e^- \to Z$
• • • We do not use the following data for averages, fits, limits, etc. • • •				
0.0337 ± 0.0044 $^{+0.0072}_{-0.0049}$	[12] ATHANAS	97	CLE2	Repl. by BARTELT 99

[9] Using the missing energy and momentum to extract kinematic information about the undetected neutrino in the $B^0 \to D^-\ell^+\nu$ decay.

[10] BARTELT 99: measured using both exclusive reconstructed $B^0 \to D^-\ell^+\nu$ and $B^+ \to D^0\ell^+\nu$ samples.

[11] BUSKULIC 97: measured using exclusively reconstructed $D^{\pm}$ with a a^2= − 0.05 ± 0.53 ± 0.38. The statistical correlation is 0.99.

[12] ATHANAS 97: measured using both exclusive reconstructed $B^0 \to D^-\ell^+\nu$ and $B^+ \to D^0\ell^+\nu$ samples with a ρ^2=0.59 ± 0.22 ± 0.12 $^{+0.59}_{-0}$. They report their experiment's uncertainties ±0.0044 ± 0.0048 $^{+0.0053}_{-0.0012}$, where the first error is statistical, the second is systematic, and the third is the uncertainty due to the form factor model variations. We combine the last two in quadrature.

DETERMINATION OF V_{ub}

Updated December 2003 by M. Battaglia (University of California, Berkeley and LBNL) and L. Gibbons (Cornell University, Ithaca) .

The precise determination of the magnitude of V_{ub} with a robust, well-understood uncertainty remains one of the key goals of the heavy flavor physics programs, both experimentally and theoretically. Because $|V_{ub}|$, the smallest element in the CKM mixing matrix, provides a bound on the upper vertex of one of the triangles representing the unitarity property of the CKM matrix, it plays a crucial role in the examination of the unitarity constraints and the fundamental questions on which the constraints can bear (see the minireviews on the CKM matrix [1] and on CP violation [2] for details). Investigation of these issues require measurements that are precise and that have well-understood uncertainties.

The charmless semi-leptonic (s.l.) decay channel $b \to u\ell\overline{\nu}$ provides the cleanest path for the determination of $|V_{ub}|$. However, the theory for the heavy-to-light $b \to u$ transition cannot be as well constrained as that for the heavy-to-heavy $b \to c$ transition used in the determination of $|V_{cb}|$ (see the $|V_{cb}|$ minireview [3]). The extraction of $|V_{ub}|$ and the interplay between experimental measurements and their theoretical interpretation are further complicated by the large background from

$b \to c\ell\overline{\nu}$ decay, which has a rate about 60 times higher than that for charmless s.l. decay. Measurements based both on exclusive decay channels and on inclusive techniques have been, and are being, pursued.

The last several years have seen significant developments in both the theoretical framework and the experimental techniques used in the study of $b \to u\ell\overline{\nu}$. The inclusive theory has progressed significantly in categorization of the corrections to the base theory still needed, in their relative importance in different regions of phase space, and in the determination of some of them. Recent work on exclusive processes bolsters confidence in the current uncertainties for the form factor calculations needed to extract $|V_{ub}|$. Experimentally, we have new inclusive and exclusive measurements that minimize dependence on detailed modeling of the signal process to separate signal from the $b \to c\ell\overline{\nu}$ background, have well-defined sensitivities in particular regions of phase space and have improved signal-to-background ratios. These improvements provide us with a first opportunity to develop a method for a robust determination of $|V_{ub}|$ with complete error estimates, including constraints on hitherto unquantified contributions. We review the current determinations of $|V_{ub}|$, focusing primarily on these recent developments. An average of the inclusive information from all regions of phase space remains, unfortunately, beyond our reach because of the potentially sizable corrections for which we lack estimates. Rather, we combine the inclusive results to obtain a central value and, in particular, a more complete evaluation of the uncertainty than has been possible in the past.

Inclusive measurements of $b \to u\ell\overline{\nu}$:

Theoretically, issues regarding the calculation of the total semileptonic partial width $\Gamma(B \to X_u\ell\nu)$ via the operator product expansion (OPE) are well-understood [4–9]. The OPE is both a nonperturbative power series in $1/m_b$ and a perturbative expansion in α_s. At order $1/m_b^2$, it predicts

$$\Gamma(B \to X_u\ell\nu) = \frac{G_F^2|V_{ub}|^2}{192\pi^3}\, m_b^5 \times \left[1 - \frac{9\lambda_2 - \lambda_1}{2m_b^2} + \ldots - \mathcal{O}(\frac{\alpha_s}{\pi})\right] , \quad (1)$$

where λ_2 parameterizes the hyperfine interaction between the heavy quark and the light degrees of freedom and λ_1 is related to the Fermi momentum of the heavy quark. The perturbative corrections are known to order α_s^2 [10]. The OPE is alternatively expressed in terms of the nonperturbative parameters μ_π^2 and μ_G^2, which are closely related to λ_1 and λ_2, respectively, but differ significantly in their infrared treatment. Within the OPE, the importance of a proper field theoretic treatment of the parameters is paramount both for the total rate and for the restricted phase space studies discussed below. The treatment of the quark mass and its associated uncertainties are particularly important given the strong mass dependance of the width. Such considerations have led to useful definitions like the kinematic mass, which are discussed in detail in Ref. 11 and Ref. 12.

The error induced by uncertainties in the nonperturbative parameters $\lambda_{1,2}$ is relatively small, and an evaluation [13] by the LEP VUB working group yielded

$$|V_{ub}| = 0.00445 \left(\frac{\mathrm{B}(b \to u\ell\overline{\nu})}{0.002}\frac{1.55\mathrm{ps}}{\tau_b}\right)^{1/2} \times (1 \pm 0.020_{\mathrm{OPE}} \pm 0.052_{m_b}) \ . \quad (2)$$

The quoted uncertainty is dominated by the uncertainty in the b quark mass, for which $m_b^{1S}(1\ \mathrm{GeV}) = 4.58 \pm 0.09$ GeV was assumed. The value and uncertainty are in good agreement with a recent survey [14]. No weak annihilation uncertainties (discussed below) are included in the quoted OPE error. Use of the quark-level OPE for prediction of moments of the true inclusive spectra has generated concern regarding potential violation of the underlying assumption of global quark-hadron duality. This concern has been confronted by theoretical wisdom [15] supporting global duality for the inclusive $b \to u\ell\overline{\nu}$ transition, and new data both support this assumption and allow placement of quantitative limits on the violation. In particular, the exclusive and inclusive extractions of $|V_{cb}|$ agree to $(0.8 \pm 1.6) \times 10^{-3}$ [3]. Taking the uncertainty as an upper bound on the global duality violation for $|V_{ub}|$ shows that it should not exceed $\simeq$4%. Using this as bound as an uncertainty estimate for duality effects in the partial width prediction brings the total uncertainty on $|V_{ub}|$ to 6.8%. The agreement of the OPE parameters extracted using moments of different distributions in s.l. decays further supports the small scale for duality violation effects.

While theoretically the total inclusive rate would allow determination of $|V_{ub}|$ to better than 10%, experimentally the much more copious $b \to c\ell\overline{\nu}$ process makes a measurement over the full phase space unrealizable. To overcome this background, inclusive $b \to u\ell\overline{\nu}$ measurements utilize restricted regions of phase space in which the $b \to c\ell\overline{\nu}$ process is kinematically highly suppressed. The background is forbidden in the regions of large charged lepton energy $E_\ell > (M_B^2 - M_D^2)/(2M_B)$ (the endpoint), low hadronic mass $M_X < M_D$ and large dilepton mass $q^2 > (M_B - M_D)^2$. Extraction of $|V_{ub}|$ from such a measurement requires knowledge of the fraction of the total $b \to u\ell\overline{\nu}$ rate that lies within the utilized region of phase space, which complicates the theoretical issues and uncertainty considerably. Ref. 16 and Ref. 17 discuss the issues in detail.

CLEO [18], BaBar [19], and Belle [20] have all presented recent measurements of the $b \to u\ell\overline{\nu}$ rate near the endpoint. The results, which are for integrated ranges in the $\Upsilon(4S)$ rest frame, are summarized in Table 1. Experimentally, these measurements must contend with a large background from continuum e^+e^- annihilation processes. Suppression of these backgrounds introduces significant efficiency variation with the q^2 of the decay, which introduces model dependence. Greater awareness of this issue has resulted in more sophisticated suppression methods in these recent measurements and thus in over a factor of three reduction in the model dependence of the measured rates relative to earlier measurements [21, 22]. Future measurements, either using fully-reconstructed B-tag samples

that would remove the problem or a modest q^2 binning, would essentially eliminate the remaining model dependence.

Table 1: Partial branching fractions for $b \to u\ell\overline{\nu}$ within the charged lepton momentum range ($\Upsilon(4S)$ frame) from 2.6 GeV/c down to the indicated minimum. The estimated fraction f_E of the total $b \to u\ell\overline{\nu}$ rate expected to lie in that range is also given. The dagger (†) indicates the quantity that received the QED radiative correction appropriate to the indicated mix of electrons and muons, which has not always been treated self-consistently in the literature.

$p_\ell^{\min}$ (GeV/c)	$\Delta\mathcal{B}_u(p)$ (10^{-4})	f_E	
2.0	$4.22 \pm 0.33 \pm 1.78$	$\dagger 0.266 \pm 0.041 \pm 0.024$	CLEO (e,μ)
2.1	$3.28 \pm 0.23 \pm 0.73$	$\dagger 0.198 \pm 0.035 \pm 0.020$	CLEO (e,μ)
2.2	$2.30 \pm 0.15 \pm 0.35$	$\dagger 0.130 \pm 0.024 \pm 0.015$	CLEO (e,μ)
2.3	$1.43 \pm 0.10 \pm 0.13$	$\dagger 0.074 \pm 0.014 \pm 0.009$	CLEO (e,μ)
	$\dagger 1.52 \pm 0.14 \pm 0.14$	$0.078 \pm 0.015 \pm 0.009$	BaBar (e)
	$1.19 \pm 0.11 \pm 0.10$	$\dagger 0.072 \pm 0.014 \pm 0.008$	Belle (e)
2.4	$0.64 \pm 0.07 \pm 0.05$	$\dagger 0.037 \pm 0.007 \pm 0.003$	CLEO (e,μ)

BaBar [23] and Belle [24] have presented new analyses of the low M_X region [25–28]. They also utilize a moderate (only $\sim 10\%$ loss) $p_\ell > 1.0$ GeV/c requirement. This technique was pioneered by Delphi at LEP [29], but the achievable resolution and signal-to-background ratio were lower compared to those obtained at the B factories. Because of experimental resolution on M_X, the $b \to c\ell\overline{\nu}$ background smears below its theoretical lower limit of $M_X = M_D$, so experiments must impose more stringent M_X requirements which are theoretically more problematic. The BaBar and Belle analyses are based on "B-tag" samples of fully reconstructed hadronic decays and $D^{(*)}\ell\nu$ decays, respectively. In both cases, M_X is calculated directly from the particles remaining after removal of tag and lepton contributions. The BaBar analysis, in particular, reveals a beautiful $b \to u\ell\overline{\nu}$ signal with an unsurpassed signal to background ratio of about 2:1 in the region $M_X < 1.55$ GeV/c, which rivals that of current exclusive analyses. This analysis demonstrates the anticipated power of a large fully reconstructed sample, both in the signal to background levels and in the excellent resolution that can be achieved. The efficiency versus M_X appears reasonably uniform, and the signal yield fitting procedure minimizes the dependence of the extracted rate on the modeling of the detailed $b \to u\ell\overline{\nu}$ dynamics. Both allow for improved determination of $|V_{ub}|$ as theory advances.

Determination of the fraction of the $b \to u\ell\overline{\nu}$ rate in the p_ℓ endpoint or the low M_X region requires resummation of the OPE to all orders in $E_X\Lambda_{\rm QCD}/M_X^2$ [30–34]. The resummation results, at leading-twist order, in a nonperturbative shape function $f(k_+)$, where $k_+ = k^0 + k_\parallel$ and $k^\mu = p_b^\mu - m_b v^\mu$ is the residual b quark momentum after the "mechanical" portion of momentum is subtracted off. Spatial components $k_\parallel$ and $k_\perp$ are defined relative to the $m_b v^\mu - q^\mu$ (roughly the recoiling u quark) direction. At this order, effects such as the "jiggling" of $k_\perp$ are ignored and the differential partial width is given by the convolution of the shape function with the parton level differential distribution. Because the shape function depends only on parameters of the B meson, this leading order description holds for any B decay to a light quark. It holds, in particular, for $B \to s\gamma$, which can provides an estimation of $f(k_+)$ via the shape of the photon energy (E_γ) spectrum [31, 32]. In addition to the increased uncertainty on $|V_{ub}|$ from the m_b and b quark kinetic energy contributions that results from the restriction of phase space, higher twist contributions and unknown power corrections of order $\Lambda_{\rm QCD}/M_B$ [35, 36] also contribute to the uncertainty, as will be discussed further below.

Ideally, $|V_{ub}|$ would be determined without introduction of an intermediate extracted shape function through the use of appropriately weighted spectra [32,37–41]. This would avoid introduction of an element of model dependence. For the lepton spectrum, for example, one would take

$$\left|\frac{V_{ub}}{V_{tb}V_{ts}^*}\right|^2 = \frac{3\alpha}{\pi}\,K_{\rm pert}\frac{\widehat{\Gamma}_u(E_0)}{\widehat{\Gamma}_s(E_0)} + O(\Lambda_{\rm QCD}/M_B)\ , \qquad (3)$$

where $K_{\rm pert}$ is a calculable perturbative kernel, and $\widehat{\Gamma}_u(E_0)$ and $\widehat{\Gamma}_s(E_0)$ are appropriately weighted integrals over, respectively, the lepton energy and photon energy spectra above the minimum cutoff energy E_0. Practical application of this approach awaits measurement of the lepton momentum spectrum in the B, not the $\Upsilon(4S)$, rest frame, which B-tag methods will permit in the future. Similar expressions exist for integration over the low hadronic mass region [38,41], so, in principle, current M_X analyses should be able to take such an approach. Experimental efficiency and lepton momentum cutoffs must, however, be incorporated into the integrals. To date, experiments have instead introduced intermediate shape functions of a variety of forms into the inclusive analyses, as discussed below.

A third way to isolate the charmless s.l. signal is to use a selection based on the q^2 of the leptonic system. Restriction of phase space to regions of large q^2 also restores the validity of the OPE [42,43] and suppresses shape function effects. Taking only the region kinematically forbidden to $b \to c\ell\overline{\nu}$, $q^2 > (M_B - M_D)^2$, unfortunately introduces a low mass scale [44,45] into the OPE and the $1/m^3$ uncertainties blow up to be of order $(\Lambda_{\rm QCD}/m_c)^3$. However, a combination of M_X with looser q^2 requirements can suppress both $b \to c\ell\overline{\nu}$ background experimentally and shape function effects theoretically. Furthermore, the q^2 requirement moves the parton level pole away from the experimentally feasible M_X requirement. The shape function effects, while suppressed, cannot be neglected. One drawback of the q^2 requirement is the elimination of higher energy hadronic final states, which may exacerbate duality concerns.

A recent Belle analysis [46] has been performed in this region. Belle employs a $p_\ell > 1.2$ GeV/c requirement in the $\Upsilon(4S)$ rest frame, and an "annealing" procedure to separate reconstructed particles into signal and "other B" halves. They

then examine the integrated rate in the region $M_X < 1.7$ GeV and $q^2 > 8$ GeV^2 to extract $|V_{ub}|$, which again has the desired effect of minimizing dependence of the analysis on detailed $b \to u\ell\overline{\nu}$ modeling. The signal to background ratio of the annealing technique, about 1:6 for the Belle analysis, is significantly degraded relative to that of the hadronic B-tag technique. As we mentioned in the previous review, control of background subtractions of this size requires extreme care and careful scrutiny of the associated systematic issues. Belle finds the rate $\Delta\mathcal{B}$ in that region of phase space to be

$$\Delta\mathcal{B} = (7.37 \pm 0.89_{\rm stat} \pm 1.12_{\rm sys} \pm 0.55_{c\ell\nu} \pm 0.24_{u\ell\nu}) \times 10^{-4} \ . \quad (4)$$

An analysis of this restricted region of phase space, for which the shape function influence is significantly reduced [42], with the significantly cleaner B tag technique should be a priority for both B experiments.

Each analysis discussed here has relied on an intermediate shape function to evaluate the fraction of the inclusive rate that lies in its restricted region of phase space. The endpoint analyses have used rate fractions [18] based on intermediate shape functions derived from the CLEO $b \to s\gamma$ photon spectrum. Several two-parameter ansaetze [47,48], $F[\Lambda^{SF}, \lambda_1^{SF}]$, were implemented as the form of the shape function. These parameters are related to the HQET parameters of similar name, and play a similar role in evaluation of the rates. At this time, however, we do not know the precise relationship between the shape function parameters, or the moments of the shape function, and the HQET nonperturbative parameters $\overline{\Lambda}$ and λ_1 [49,50]. The fact that Λ^{SF} and λ_1^{SF} depend on the functional ansatz while the HQET parameters depend on the renormalization scheme underscores the current ambiguity.

With the limited E_γ statistics available, there exists a strong correlation between the two parameters because of the interplay between the effective b quark mass (controlled by Λ^{SF}) and the effective b quark kinetic energy (controlled by λ_1^{SF}) in determining the *mean* of the E_γ spectrum. No external constraints that could break the correlation, such as $m_b^{(1S)}$ or measured $b \to c\ell\overline{\nu}$ moments, have been input into the $b \to s\gamma$ fits because of their unknown relationship to the shape function parameters. The resulting effective m_b mass range contributing to the uncertainties ($\pm$200 MeV) is therefore much larger than the current m_b uncertainty. Given the current independence of the shape function and m_b determinations and the broad effective m_b range sampled in the shape function, we do not consider it necessary to treat the E_γ-derived phase space fractions and the partial width (Eq. (2)) as positively correlated [46]. As the data statistics increase, it will become possible to constrain the shape function parameters directly from distributions in $b \to u\ell\overline{\nu}$, such as the M_X spectrum, thus removing the uncertainties introduced from their derivation from another class of decays. Furthermore, once the renormalization behaviour of the shape function and the relationship of its moments to the HQET parameters becomes known, the powerful constraints from the kinematic mass of the b quark and from moments information in the $b \to c\ell\nu$ system can be incorporated into a shape function derivation based either on $b \to s\gamma$ or $b \to u\ell\overline{\nu}$.

Two alternate approaches to the shape function evaluation have been taken in experimental studies so far. In their low-M_X analysis [23], BaBar has evaluated the phase space fraction using the same $f(k_+)$ parameterizations noted above, but has substituted HQET parameters derived from studies of spectral moments of the $b \to s\gamma$ and $b \to c\ell\overline{\nu}$ processes. The Belle M_X-q^2 analysis [46](discussed below) uses the calculation of Bauer *et al.* [42] based on a form with a single parameter $a = \Lambda^{SF}/\lambda_1^{SF}$, which was estimated from the $m_b^{(1S)}$ mass and from typical estimates for λ_1. The uncertainties in the different rate fractions in the momentum endpoint, the low M_X and the M_X-q^2 regions are strongly correlated, and the values and uncertainties are sensitive to the theoretical assumptions made. Hence, a common theoretical scheme must be chosen for meaningful comparison of the extracted values of $|V_{ub}|$. Given the *ad hoc* nature of the association of shape function parameters with the HQET parameters in the $\overline{MS}$ or the $\Upsilon(1S)$ mass scheme [7], and the difficulty in evaluating the uncertainty in such an association, we have chosen to extract $|V_{ub}|$ from all of the measurements discussed using the $b \to s\gamma$-derived shape function.

Table 2: Summary of inclusive $|V_{ub}|$ measurements. The last five measurements are incorporated into the analysis presented below. The errors in the first group are the experimental and theoretical uncertainties. The errors in the second group are from the statistical, experimental systematic, E_γ-based rate fraction, and $\Gamma_{\rm tot}$ uncertainties. The two groups are *not* directly comparable as they have not been evaluated with identical theoretical inputs.

	$\lvert V_{ub}\rvert(10^{-3})$	
ALEPH [53]	$4.12 \pm 0.67 \pm 0.76$	neural net
L3 [54]	$5.70 \pm 1.00 \pm 1.40$	cut and count
DELPHI	$4.07 \pm 0.65 \pm 0.61$	M_X
OPAL [55]	$4.00 \pm 0.71 \pm 0.71$	neural net
LEP Avg.	$4.09 \pm 0.37 \pm 0.56$	
CLEO [56]	$4.05 \pm 0.61 \pm 0.65$	$d\Gamma/dq^2 dM_X^2 dE_\ell$
Belle	$5.00 \pm 0.64 \pm 0.53$	M_X, $D^{(*)}\ell\nu$ tag
CLEO	$4.11 \pm 0.13 \pm 0.31 \pm 0.46 \pm 0.28$	$2.2 < p < 2.6$
BaBar	$4.31 \pm 0.20 \pm 0.20 \pm 0.49 \pm 0.30$	$2.3 < p < 2.6$
Belle	$3.99 \pm 0.17 \pm 0.16 \pm 0.45 \pm 0.27$	$2.3 < p < 2.6$
Belle	$4.63 \pm 0.28 \pm 0.39 \pm 0.48 \pm 0.32$	$M_X < 1.7$, $q^2 > 8$
BaBar	$4.79 \pm 0.29 \pm 0.28 \pm 0.60 \pm 0.33$	$M_X < 1.55$

The full set of inclusive $|V_{ub}|$ results is summarized in Table 2, which is an updated version of the Heavy Flavors Averaging Group summary [51]. All endpoint results have QED radiative corrections applied correctly. The listed uncertainties do not include contributions for potentially large theoretical corrections that have been categorized but remain incalculable (see below). The last five results in the table, which we will use

below, have been updated to a common framework based on the CLEO E_γ-derived shape function. The rate fractions [52] for the BaBar M_X analysis (f_M) and the Belle $M_X - q^2$ analysis f_{qM} are $f_M = 0.55 \pm 0.14$ and $f_{qM} = 0.33 \pm 0.07$. The central values for these and for the endpoint fractions (Table 1) correspond to an exponential shape function ansatz [48] and $(\lambda_1^{SF}, \overline{\Lambda}^{SF}) = (-0.342, 0.545)$, with small corrections related to background subtractions in the $b \to s\gamma$ spectrum. The errors are dominated by the statistical uncertainty in the $f(k_+)$ fit to the E_γ spectrum, but include contributions from experimental systematics, α_s uncertainties and modeling. Incorporation of results beyond those used here will require significant input from the experimental analyses, and is left to the HFAG.

Combining inclusive information:

Evaluation of the total uncertainty on $|V_{ub}|$ remains problematic because of a variety of theoretical complications. A recent review [16] discusses these issues in detail. There are three main contributions. The first arises from subleading (higher twist) contributions to the shape function resummation [57–61]. These involve incorporation of effects such as the variation of $k_\perp$, and are not universal for all B decay processes. Hence with the use of $b \to s\gamma$ to obtain a shape function, there are two contributions, one from subleading contributions to the use of a shape function in $b \to u\ell\overline{\nu}$ process itself, and the second from the different corrections in $b \to s\gamma$ from which the shape function is obtained. These contributions are potentially large, since they are of order $\Lambda_{\rm QCD}/m_b$. Indeed, a partial estimate of these effects [59] for the momentum endpoint region finds corrections that are similar in size to the total uncertainties of those analyses. Recent work indicates that the subleading contributions for $u\ell\nu$ and $s\gamma$ may partially cancel in the low M_X and the low M_X-high q^2 regions [61].

The second contribution, from "weak annihilation" processes, is formally of order $(\Lambda_{\rm QCD}/m_b)^3$ but receives a large multiplicative enhancement of $16\pi^2$ [62,63]. The contribution, which requires factorization violation to be nonzero, is expected to be localized near $q^2 \sim m_b^2$, and this localization can result in a further enhancement of the effect on $|V_{ub}|$. For the endpoint region, which sees about 10% of the total rate, an effect on the total rate of 2-3% (corresponding to factorization violation of about 10%), produces an effect on the measured rate of 20-30%.

Finally, there are unknown contributions from potential violation of local quark hadron duality. The true differential distribution cannot be predicted via the OPE—the resonant substructure is not described. However, spectra integrated over a sufficiently broad range should be better described.

The problems just outlined present a challenge to the averaging of the various inclusive results. Results with a potentially large bias might be included with neither a correction nor an appropriate uncertainty due to these effects. The resulting $|V_{ub}|$ determination would be potentially biased and the attached uncertainty unreliable. This motivated us not to provide an average result in the first edition of this review two years ago.

As an alternative, we here choose measurements in the region of phase space that appears to have the best compromise of the affects discussed to obtain an estimate of $|V_{ub}|$. Measurements from the other regions of phase space, which have increased sensitivity to one or more of the corrections, then provide limits on the uncertainties from these effects and thereby allow as complete as possible an estimation of the theoretical uncertainty, as first proposed by Ref. 52. At this time, the low M_X, high q^2 region appears to be the best motivated choice. It has reduced (though by no means negligible) corrections from the shape function and thus also from the subleading contributions to the shape function. Yet it integrates over a sufficient fraction of the spectrum to dilute weak annihilation contributions and concerns on local quark hadron duality.

While this choice is at present subjective, it offers the advantage of a reduction of the shape function influence coupled with the ability to bound the remaining theoretical uncertainties. In the opinion of the reviewers, this is a reasonable tradeoff for the statistical loss relative to the low M_X region. We expect that each experiment will perform an improved combination of information from the different regions of phase space where the experimental and theoretical correlations can be made manifest more straightforwardly.

We further stress that we view all three regions as equally crucial in this combination of information, as a more complete evaluation of the inclusive uncertainty than has previously existed is necessary for proper use of the inclusive results. The choice of the phase space region should not be misconstrued as a preference of experimental technique. Indeed, we look forward to a similar (or improved) analysis when a sample of clean results based on fully tagged B samples have been obtained for all regions of phase space.

At present only Belle [46] has contributed a result for this region of phase space, so for now we take this result as the "central value":

$$|V_{ub}|/10^{-3} = 4.63 \pm 0.28_{\rm stat} \pm 0.39_{\rm sys} \pm 0.48_{\rm f_{qM}} \pm 0.32_{\Gamma \rm thy} \pm \sigma_{\rm WA} \pm \sigma_{\rm SSF} \pm \sigma_{\rm LQD} \ . \quad (5)$$

Additional measurements by the B factories of the rate in this region of phase space will soon improve the experimental uncertainties.

We must determine the last three uncertainties for weak annihilation (WA), subleading shape function corrections (SSF) and local quark hadron duality (LQD). The measurements from other regions of phase space are crucial for this task.

We assume that the WA contribution is largely contained within each of the $p_\ell > 2.2$ GeV/c, the $M_X < 1.55$ GeV and the combined $M_X < 1.7$ GeV, $q^2 > 8$ GeV^2 regions. The contribution will be most diluted in the low M_X region, with the rate fraction $f_M = 0.55 \pm 0.14$, and most concentrated in the endpoint region, with the rate fraction $f_e = 0.14 \pm 0.03$ (without radiative corrections). It is simple to show that for a neglected WA contribution, a comparison of $|V_{ub}|$ from these

two regions would predict the bias in the M_X, q^2 region (with rate fraction $f_{qM} = 0.33 \pm 0.07$) to be

$$[(1 - f_{qM})/f_{qM}][f_e f_M/(f_M - f_e)] \approx 0.39 \qquad (6)$$

of the observed difference. Comparison of the endpoint result from CLEO and the low M_X result from BaBar, taking into consideration the almost total correlation in the shape function and Γ_{tot} uncertainties, yields $\Delta|V_{ub}|/10^{-3} = 0.69 \pm 0.53$. There is not sufficient sensitivity to draw conclusions regarding the presence of a WA component, but we can place a bound. We take the larger of the error and central value and scale according to Eq. (6) to obtain

$$\sigma_{\rm WA} \approx 0.27 \ . \qquad (7)$$

To estimate the uncertainty from the subleading corrections to the shape function, we assume that subleading corrections will scale like the fractional change in the predicted rate ($\Delta\Gamma/\Gamma$) with and without convolution of the parton-level expression with the shape function. As the base comparison, we take the low M_X region, with $(\Delta\Gamma/\Gamma)_M = 0.15$, and compare to the combined M_X, q^2 region, with $(\Delta\Gamma/\Gamma)_{qM} = -0.075$). The shifts again depend on the shape function modeling, and the quoted values correspond to the $f(k_+)$ from the best fit to the CLEO E_γ spectrum . The theory uncertainties are again correlated, and we find $\Delta|V_{ub}|/10^{-3} = 0.16 \pm 0.63$. Scaling the uncertainty of the comparison by $|(\Delta\Gamma/\Gamma)_{qM}/(\Delta\Gamma/\Gamma)_M| = 0.49$, we have

$$\sigma_{\rm SSF} \approx 0.31 \ . \qquad (8)$$

Finally, we must make an estimate of the local duality uncertainty. We assume that a potential violation will scale with the fraction of rate f in a given region as $(1 - f)/f$. This form ranges from no "local" violation for integration of the full phase space ($f = 1$), to large uncertainty for use of a very localized region of phase space ($f \to 0$). The estimate derives from comparison of the CLEO $p_\ell > 2.2$ GeV/c analysis ($f \sim 0.14 \pm 0.03$) to the average of the BaBar and Belle $p_\ell > 2.3$ GeV/c analyses ($f \sim 0.07 \pm 0.02$). The subleading correction estimates of Ref. 59 are applied to minimize potential cancelation between duality violation and subleading corrections. This yields $(|V_{ub}|^{2.3} - |V_{ub}|^{2.2} + 0.27)/10^{-3} = 0.29 \pm 0.38$, where the 0.27 is the estimate of the relative subleading correction. With our scaling assumption, we then apply a scale factor s of

$$s = \frac{(1 - f_{qM})/f_{qM}}{(1 - f_{2.3})/f_{2.3} - (1 - f_{2.2})/f_{2.2}} \approx 0.29 \qquad (9)$$

to the uncertainty in this difference estimate. Our local duality estimate therefore is

$$\sigma_{\rm LQD} \sim 0.11.$$

From this analysis, we finally obtain

$$|V_{ub}|/10^{-3} = 4.63 \pm 0.28_{\rm stat} \pm 0.39_{\rm sys} \pm 0.48_{f_{qM}} \pm 0.32_{\Gamma\rm thy} \pm 0.27_{\rm WA} \pm 0.31_{\rm SSF} \pm 0.11_{\rm LQD} \ , \qquad (10)$$

for a total theory error of 15% and total precision of 18%. Given that the uncertainties are dominated by experimental limits, addition in quadrature seems appropriate. Note that these estimates apply *only* in the combined low M_X, high q^2 region of phase space. The limits presented here can be improved both in robustness, through more sophisticated scaling estimates, and in magnitude, through additional and improved $|V_{ub}|$ measurements and through inputs from other sources. The consistency of the values of $|V_{ub}|$ extracted with different inclusive methods and the stability of the results over changes in the selected region of phase space will provide increasing confidence in the reliability of the extracted results and of their estimated uncertainties. Improvement of the $b \to s\gamma$ photon energy spectrum is key until a self-consistent extraction of the shape function from $b \to u\ell\overline{\nu}$ transition becomes available. Comparisons of the D^0 versus D_s semileptonic widths and of the rates for charged versus neutral B mesons can provide estimates of the weak annihilation contributions [63]. Finally, improved theoretical guidance concerning the scaling of the effects over phase space would allow development of a simultaneous extraction of $|V_{ub}|$ and the corrections, with all experimental information contributing directly to $|V_{ub}|$.

Exclusive measurements of $b \to u\ell\overline{\nu}$:

Reconstruction of exclusive $b \to u\ell\overline{\nu}$ channels provides powerful kinematic constraints for suppression of the $b \to c\ell\overline{\nu}$ background. For this suppression to be effective, an estimate of the four momentum of the undetected neutrino must be provided. The measurements to date have made use of detector hermeticity and the well-determined beam parameters to define a missing momentum that is used as the neutrino momentum. Signal-to-background ratios (S/B) of order two have been achieved in these channels.

To extract $|V_{ub}|$ from an exclusive channel, the form factors for that channel must be known. The form factor normalization dominates the uncertainty on $|V_{ub}|$. The q^2-dependence of the form factors, which is needed to determine the experimental efficiency, also contributes to the uncertainty, but at a much reduced level. For example, the requirement of a stiff lepton for background reduction in these analyses introduces a q^2-dependence to the efficiency. In the limit of a massless charged lepton (a reasonable limit for the electron and muon decay channels), the $B \to \pi\ell\nu$ decay depends on one form factor $f_1(q^2)$:

$$\frac{d\Gamma(B^0 \to \pi^-\ell^+\nu)}{dy\, d\cos\theta_\ell} = |V_{ub}|^2 \frac{G_F^2 p_\pi^3 M_B^2}{32\pi^3} \sin^2\theta_\ell |f_1(q^2)|^2 \ , \qquad (11)$$

where $y = q^2/M_B^2$ and θ_ℓ is the angle between the charged lepton direction in the virtual W ($\ell + \nu$) rest frame and the direction of the virtual W. For the vector meson final states ρ and ω, three form factors A_1, A_2, and V are necessary (see *e.g.* reference [64]).

Calculation of these form factors constitutes a considerable theoretical industry, with a variety of techniques now being employed. Form factors based on lattice QCD calculations [65–77] and on light cone sum rules [78–87] currently have uncertainties in the 15% to 20% range. A variety of quark model calculations

exists [88–102]. Finally, a number of other approaches [103–109], such as dispersive bounds and experimentally-constrained models based on Heavy Quark Symmetry, seek to improve the q^2 range where the form factors can be estimated, without introducing significant model dependence.

Of particular interest are the light cone sum rules (LCSR) and lattice QCD (LQCD) calculations, which minimize modeling assumptions as they are QCD-based calculations and provide a much firmer basis compared to the quark model calculations for systematic evaluation of the uncertainties. The calculations used in the current results have been summarized nicely in Ref. 11. The LCSR are expected to be valid in the region $q^2 \lesssim 16$ GeV^2. The light cone sum rules calculations use quark-hadron duality to estimate some spectral densities, and offer a "canonical" contribution to the related uncertainty of 10% with no known means of rigorously limiting that uncertainty. The theory community is currently debating the size of potential contributions to the form factors missing from the LCSR approach [110–114] that have been revealed using the newly-developed soft collinear effective theory (SCET) [115–118]. The

$B \to \rho\ell\nu$ form factors, in particular, could be appreciably overestimated, biasing $|V_{ub}|$ low. Two exclusive results will therefore be presented in this review, one based on the full set of exclusive results, and the second based only on results in the $q^2 > 16$ GeV^2 region for $B \to \rho\ell\nu$.

The LQCD calculations that can be applied to experimental $B \to X_u\ell\nu$ decay remain, to date, in the "quenched" approximation (no light quark loops in the propagators), which limits the ultimate precision to the 15% to 20% range. The q^2 range accessible to these calculations has been $q^2 \gtrsim 16$ GeV^2. Significant progress has been made towards unquenched lattice QCD calculations, and a recent comparison [119] of a range unquenched results to experiment shows much better agreement (few percent) than the corresponding quenched results. Work has begun on the unquenched form factors needed for $|V_{ub}|$, though the initial results have been limited to valence quarks closer to the strange quark mass. Nevertheless, initial results [120,121] are compatible with the 15% to 20% uncertainties used for the quenching uncertainty, lending them some validity.

The exclusive $|V_{ub}|$ results are summarized in Table 3. These include a simultaneous measurement of the $B \to \pi\ell\overline{\nu}$ and the $B \to \rho\ell\overline{\nu}$ transitions by CLEO [122], and measurement of the $B \to \rho\ell\overline{\nu}$ rate by CLEO [123] and BaBar [124]. All measurements employ the missing energy and momentum to estimate the neutrino momentum. With that technique, the major background results from $b \to c\ell\overline{\nu}$ decays in events that cannot be properly reconstructed (for example, because of additional neutrinos in the event) and hence which overestimate the neutrino energy. All measurements also employ the isospin relations

$$\Gamma(B^0 \to \pi^-\ell^+\nu) = 2\Gamma(B^+ \to \pi^0\ell^+\nu)$$

and

$$\Gamma(B^0 \to \rho^-\ell^+\nu) = 2\Gamma(B^+ \to \rho^0\ell^+\nu) \qquad (12)$$

to combine the charged and neutral decays. These relationships can be distorted by $\rho-\omega$ mixing [125], and all results discussed here allow for this possibility in their systematic evaluation.

In the combined π and ρ measurement, strict event quality requirements were made that resulted in a low efficiency, but a relatively low background to signal ratio over a fairly broad lepton momentum range. The ρ-only analyses employ looser event cleanliness requirements, resulting in a much higher efficiency. The efficiency gain comes at the price of an increased background, and the analyses are primarily sensitive to signal with lepton momenta above 2.3 GeV/c, which is near (and beyond) the kinematic endpoint for $b \to c\ell\overline{\nu}$ decays which are therefore highly suppressed.

The combined π and ρ analysis of CLEO employs relatively loose lepton selection criteria and extracts rates independently in three separate q^2 intervals. Form factor dependence of the rates is then evaluated using models and calculations that exhibit a broad variation in $d\Gamma/dq^2$, which shows that this approach has eliminated model dependence of the rates in $\pi\ell\nu$, and significantly reduced it in $\rho\ell\nu$. To further reduce modeling uncertainties, CLEO then extracts $|V_{ub}|$ using only the LQCD and LCSR QCD-based calculations restricted to their respective valid q^2 ranges, thereby eliminating modeling used for extrapolation. Averages of the CLEO results, with and without the low q^2 region for $\rho\ell\nu$ are listed in Table 3.

A more complete review of recent $B \to X_u\ell\nu$ branching fractions, including analyses too incomplete for inclusion in this $|V_{ub}|$ summary, can be found in Reference [126]. Of note is the recent evidence presented for $B \to \omega\ell\nu$ by Belle [127].

With all results resting on use of detector hermeticity, the potential for significant correlation among the dominant experimental systematics exists [126]. Results from the three measurements have been averaged here assuming full correlation in these systematics. The $\rho\ell\nu$-only results [123,124], which depend more heavily on modeling even for the LCSR and LQCD calculations, are deweighted by 5% in the average. This yields

$$|V_{ub}| = (3.27 \pm 0.13 \pm 0.19^{+0.51}_{-0.45}) \times 10^{-3} \qquad (13)$$

where the errors arise from statistical, experimental systematic and form factor uncertainties, respectively. While similar in precision to the exclusive result in the previous $|V_{ub}|$ minireview, this result relies much less heavily on modeling. Should the LCSR form factors prove to be overestimated, we also provide an average excluding any result using information for $q^2 < 16$ GeV^2 in the $\rho\ell\nu$ modes, with the result

$$|V_{ub}| = (3.26 \pm 0.19 \pm 0.15 \pm 0.04^{+0.54}_{-0.39}) \times 10^{-3}\ , \qquad (14)$$

where the errors arise from statistical, experimental systematic $\rho\ell\nu$ form factor uncertainties, and LQCD and LCSR (treated as correlated), respectively.

Table 3: Summary of all exclusive $|V_{ub}|$ measurements. For the CLEO 00 and BaBar 01 measurements, the errors arise from statistical, experimental systematic and form factor modeling uncertainties, respectively. For the CLEO 03 measurements, the errors arise from statistical, experimental systematic, $\rho\ell\nu$ form factor, and LQCD and LCSR calculation uncertainties, respectively. In the CLEO 03 averages, the LQCD and LCSR uncertainties have been treated as correlated.

mode	$\lvert V_{ub}\rvert(10^{-3})$	q^2 range	FF
CLEO 00 $\rho\ell\nu$	$3.23 \pm 0.24^{+0.23}_{-0.26} \pm 0.58$	all	model survey
BaBar 01 $\rho\ell\nu$	$3.64 \pm 0.22 \pm 0.25^{+0.39}_{-0.56}$	all	model survey
CLEO 03 $\pi\ell\nu$	$3.33 \pm 0.24 \pm 0.15 \pm 0.06\ ^{+0.57}_{-0.40}$	$q^2 < 16$ GeV^2	LCSR
CLEO 03 $\pi\ell\nu$	$2.88 \pm 0.55 \pm 0.30 \pm 0.18\ ^{+0.45}_{-0.35}$	$q^2 > 16$ GeV^2	LQCD
CLEO 03 $\pi\ell\nu$	$3.24 \pm 0.22 \pm 0.13 \pm 0.09^{+0.55}_{-0.39}$	average	
CLEO 03 $\rho\ell\nu$	$2.67 \pm 0.27\ ^{+0.38}_{-0.42} \pm 0.17\ ^{+0.47}_{-0.35}$	$q^2 < 16$ GeV^2	LCSR
CLEO 03 $\rho\ell\nu$	$3.34 \pm 0.32\ ^{+0.27}_{-0.36} \pm 0.47\ ^{+0.50}_{-0.40}$	$q^2 > 16$ GeV^2	LQCD
CLEO 03 $\rho\ell\nu$	$3.00 \pm 0.21^{+0.29}_{-0.35} \pm 0.28^{+0.49}_{-0.38}$	average	
CLEO 03 $\pi + \rho$	$3.17 \pm 0.17^{+0.16}_{-0.17} \pm 0.03^{+0.53}_{-0.39}$	average	
CLEO 03 $\pi + \rho$	$3.26 \pm 0.19 \pm 0.15 \pm 0.04^{+0.54}_{-0.39}$	average	no $\rho\ell\nu$ LCSR

The future for exclusive determinations of $|V_{ub}|$ appears promising. Unquenched lattice calculations are appearing, with very encouraging results. These calculations will eliminate the primary source of uncontrolled uncertainty in these calculations, and have already provided some validity to the quenching uncertainty estimate used in the results presented here. Simultaneously, the B factories are performing very well, and very large samples of events in which one B meson has been fully reconstructed are already being used. This will allow a more robust determination of the neutrino momentum, and should allow a significant reduction of backgrounds and experimental systematic uncertainties. The high statistics should also allow more detailed measurements of $d\Gamma/dq^2$, which have already provided a sorely-needed litmus test for the form factor calculations and reduced the form factor shape contribution to the uncertainty on $|V_{ub}|$. Should theory allow use of the full range of q^2 in the extraction of $|V_{ub}|$ [128], the B factories have already logged data sufficient for a 5% statistical determination of $|V_{ub}|$.

For both lattice and the B factories, $\pi\ell\nu$ appears to be a golden mode for future precise determination of $|V_{ub}|$. The one caveat is management of contributions from the B^* pole, but recent work [76] suggests that this problem can be successfully overcome. $B \to \eta\ell\nu$ will provide a valuable cross check. The $\rho\ell\nu$ mode will be more problematic for high precision: the broad width introduces both experimental and theoretical difficulties. Experiments must, for example, assess potential nonresonant $\pi\pi$ contributions, but only crude arguments based on isospin and quark-popping have been brought to bear to date. Theoretically, no calculation, including lattice, has dealt with the width of the ρ. When the lattice calculations become unquenched, the ρ will become unstable and the $\pi\pi$ final state must be faced by the calculations. The methodology for accommodation of high-energy two particle final states on the lattice has yet to be developed. The $\omega\ell\nu$ mode may provide a more tractable alternative to the ρ mode because of the relative narrowness of the ω resonance. Agreement between accurate $|V_{ub}|$ determinations from $\pi\ell\nu$ and from $\omega\ell\nu$ will provide added confidence in both.

Combined results:

The experimental bounds provided for the outstanding uncertainties in the inclusive $|V_{ub}|$ measurements in the low M_X, high q^2 region and theoretical work which clarifies the reliability of the LCSR and quenched LQCD form factors make possible comparison of the inclusive and exclusive determinations of $|V_{ub}|$. Results agree to better than 1.5 times the quadratic combination of the quoted uncertainties. Therefore it becomes feasible to propose an average the inclusive and exclusive results, which have comparable accuracies.

The uncertainties have been combined in quadrature, using the larger (upward) error for the exclusive numbers. The proposed average of the inclusive and exclusive results, with all the exclusive data considered, is

$$|V_{ub}| = (3.67 \pm 0.47) \times 10^{-3}\ . \qquad (15)$$

Including in the average only the exclusive analyses based on data with $q^2 > 16$ GeV^2 in the $\rho\ell\nu$ mode, the average becomes $|V_{ub}| = (3.70 \pm 0.49) \times 10^{-3}$, so exclusion of this region, if appropriate, has only a minor effect.

The procedure proposed here results in a value of $|V_{ub}|$ with a 13% uncertainty. With the experimental and theoretical progress expected over the next few years an improvement of the accuracy at the 10% level, and possibly below, appears now realizable.

References

1. See the "CKM Quark Mixing Matrix" by F.J. Gilman, K. Kleinknecht, and B. Renk in this *Review*.
2. See the "*CP* Violation in Meson Decays" by D. Kirkby and Y. Nir in this *Review*.

3. See the "Determination of $|V_{cb}|$" review by M. Artuso and E. Barberio in this *Review*.
4. I.I.Y. Bigi *et al.*, Int. J. Mod. Phys. A **9**, 2467 (1994).
5. M. Neubert, Int. J. Mod. Phys. A **11**, 4173 (1996).
6. I.I. Bigi, M.A. Shifman, and N. Uraltsev, Ann. Rev. Nucl. Part. Sci. **47**, 591 (1997).
7. A.H. Hoang, Z. Ligeti, and A.V. Manohar, Phys. Rev. Lett. **82**, 277 (1999).
8. I.I. Bigi, UND-HEP-BIG-99-05, hep-ph/9907270.
9. Z. Ligeti, FERMILAB-Conf-99/213-T, hep-ph/9908432.
10. T. van Ritbergen, Phys. Lett. B **454**, 353 (1999) [hep-ph/9903226].
11. M. Battaglia *et al.*, arXiv:hep-ph/0304132.
12. Proceedings of the Second Workshop on the CKM Unitarity Triangle, Durham, 2003, edited by P. Ball, J. Flynn, P. Kluit, and A. Stocchi, eConf C0304052 (2003).
13. The LEP VUB Working Group, Note LEPVUB-01/01.
14. A.X. El-Khadra and M. Luke, Ann. Rev. Nucl. Sci. **52**, 201 (2002).
15. I.I.Y. Bigi and N. Uraltsev, Int. J. Mod. Phys. A **16**, 5201 (2001).
16. M. Luke, eConf **C0304052**, WG107 (2003) [arXiv:hep-ph/0307378].
17. Z. Ligeti, arXiv:hep-ph/0309219.
18. A. Bornheim *et al.* [CLEO Collab.], Phys. Rev. Lett. **88**, 231803 (2002).
19. B. Aubert *et al.* [BABAR Collab.], arXiv:hep-ex/0207081.
20. K. Abe *et al.* [BELLE Collab.], BELLE-CONF-0325, 2003.
21. R. Fulton *et al.* [CLEO Collab.], Phys. Rev. Lett. **64**, 16, (1990);
J. Bartelt *et al.*, Phys. Rev. Lett. **71**, 4111 (1993).
22. H. Albrecht *et al.* [ARGUS Collab.] Phys. Lett. **B234**, 409 (1990) and Phys. Lett. **B255**, 297 (1991).
23. B. Aubert *et al.* [BABAR Collab.], arXiv:hep-ex/0307062.
24. C. Schwanda (*for the BELLE Collab.*) to appear in the "Proceedings of the International Europhysics Conference on High Energy Physics—EPS 2003," Aachen, Germany, July, 2003.
25. V. Barger, C.S. Kim, and R.J.N. Phillips, Phys. Lett. **B251**, 629 (1990).
26. A.F. Falk, Z. Ligeti, and M.B. Wise, Phys. Lett. **B406**, 225 (1997).
27. I.I. Bigi, R.D. Dikeman, and N. Uraltsev, Eur. Phys. J. **C4**, 453 (1998).
28. F. De Fazio and M. Neubert, JHEP **9906**, 017 (1999).
29. P. Abreu *et al.* [DELPHI Collab.], Phys. Lett. **B478**, 14 (2000).
30. M. Neubert, Phys. Rev. D **49**, 3392 (1994).
31. I. Bigi *et al.*, Int. J. Mod. Phys. **A9**, 2467 (1994).
32. M. Neubert Phys. Rev. **D49**, 4623 (1994).
33. U. Aglietti and G. Ricciardi, Nucl. Phys. B **587**, 363 (2000).
34. R.D. Dikeman, M.A. Shifman, and N.G. Uraltsev, Int. J. Mod. Phys. A **11**, 571 (1996).
35. A.K. Leibovich, in *Proc. of the 5th International Symposium on Radiative Corrections (RADCOR 2000)* ed. Howard E. Haber, [arXiv:hep-ph/0011181].
36. M. Neubert, Phys. Lett. **B513**, 88 (2001).
37. A.K. Leibovich, I. Low, and I.Z. Rothstein, Phys. Rev. D **61**, 053006 (2000).
38. A.K. Leibovich, I. Low, and I.Z. Rothstein, Phys. Lett. B **486**, 86 (2000).
39. M. Neubert, Phys. Lett. B **513**, 88 (2001).
40. A.K. Leibovich, I. Low, and I.Z. Rothstein, Phys. Lett. B **513**, 83 (2001).
41. I. Bigi and N. Uraltsev, Int. J. Mod. Phys. A **17**, 4709 (2002).
42. C.W. Bauer, Z. Ligeti, and M.E. Luke, Phys. Rev. D **64**, 113004 (2001).
43. C.W. Bauer, Z. Ligeti, and M.E. Luke, Phys. Lett. B **479**, 395 (2000).
44. M. Neubert, JHEP **0007**, 022 (2000).
45. M. Neubert and T. Becher, Phys. Lett. B **535**, 127 (2002).
46. H. Kakuno *et al.* [BELLE Collab.], arXiv:hep-ex/0311048.
47. I.I. Bigi *et al.*, Phys. Lett. **B328**, 431 (1994).
48. A.L. Kagan and M. Neubert, Eur. Phys. J. **C7**, 5 (1999).
49. M. Neubert, private communications and CLNS-04/1858 (in preparation).
50. C.W. Bauer and A.V. Manohar, arXiv:hep-ph/0312109.
51. www.slac.stanford.edu/xorg/hfag/semi/summer03-lp/summer03.shtml.
52. L. Gibbons, to appear in "Proceedings of the 9th International Conference on B-Physics at Hadron Machines - BEAUTY 2003", Carnegie-Mellon University, 2003, arXiv:hep-ex/0402009.
53. R. Barate *et al.* [ALEPH Collab.], Eur. Phys. J. **C6**, 555 (1999).
54. M. Acciarri *et al.* [L3 Collab.], Phys. Lett. **B436**, 174 (1998).
55. G. Abbiendi *et al.* [OPAL Collab.], Eur. Phys. J. **C21** 399 (2001).
56. A. Bornheim *et al.* [CLEO Collab.], CLEO-CONF-02-08, 2002.
57. A.K. Leibovich, Z. Ligeti, and M.B. Wise, Phys. Lett. B **539**, 242 (2002).
58. C.W. Bauer, M. Luke, and T. Mannel, Phys. Lett. B **543**, 261 (2002).
59. M. Neubert, Phys. Lett. B **543**, 269 (2002).
60. C.W. Bauer, M.E. Luke, and T. Mannel, Phys. Rev. D **68**, 094001 (2003).
61. C.N. Burrell, M.E. Luke, and A.R. Williamson, arXiv:hep-ph/0312366.
62. I.I. Bigi and N.G. Uraltsev, Nucl. Phys. B **423** (1994) 33 [hep-ph/9310285].
63. M.B. Voloshin, Phys. Lett. B **515**, 74 (2001).
64. F.J. Gilman and R.L. Singleton, Phys. Rev. **D41**, 142 (1990).
65. A. Abada *et al.*, Nucl. Phys. B **416** (1994) 675.
66. C.R. Allton *et al.* [APE Collab.], Phys. Lett. B **345**, 513 (1995).
67. L. Del Debbio *et al.* [UKQCD Collab.], Phys. Lett. B **416**, 392 (1998).
68. S. Hashimoto *et al.*, Phys. Rev. D **58**, 014502 (1998).
69. S.M. Ryan *et al.*, Nucl. Phys. Proc. Suppl. **73**, 390 (1999).

70. S.M. Ryan *et al.*, Nucl. Phys. Proc. Suppl. **83**, 328 (2000).
71. L. Lellouch, [arXiv:hep-ph/9912353].
72. K.C. Bowler *et al.* [UKQCD Collab.], Phys. Lett. B **486**, 111 (2000).
73. D. Becirevic and A.B. Kaidalov, Phys. Lett. B **478**, 417 (2000).
74. S. Aoki *et al.* [JLQCD Collab.], Nucl. Phys. Proc. Suppl. **94**, 329 (2001).
75. A. Abada *et al.*, Nucl. Phys. B **619**, 565 (2001).
76. A.X. El-Khadra *et al.*, Phys. Rev. D **64**, 014502 (2001).
77. S. Aoki *et al.* [JLQCD Collab.], Phys. Rev. D **64**, 114505 (2001).
78. P. Ball and V.M. Braun, Phys. Rev. D **55**, 5561 (1997).
79. P. Ball and V.M. Braun, Phys. Rev. D **58**, 094016 (1998).
80. A. Khodjamirian *et al.*, Phys. Lett. B **410**, 275 (1997).
81. A. Khodjamirian *et al.*, Phys. Rev. D **62**, 114002 (2000).
82. A.P. Bakulev, S.V. Mikhailov, and R. Ruskov, [arXiv:hep-ph/0006216].
83. T. Huang, Z. Li, and X. Wu, [arXiv:hep-ph/0011161].
84. W.Y. Wang and Y.L. Wu, Phys. Lett. B **515**, 57 (2001).
85. W.Y. Wang and Y.L. Wu, Phys. Lett. B **519**, 219 (2001).
86. P. Ball and R. Zwicky, JHEP **0110**, 019 (2001).
87. J.G. Korner, C. Liu, and C.T. Yan, Phys. Rev. D **66**, 076007 (2002).
88. M. Wirbel, B. Stech, and M. Bauer, Z. Phys. C **29**, 637 (1985).
89. J.G. Korner and G.A. Schuler, Z. Phys. C **38**, 511 (1988) [Erratum-ibid. C **41**, 690 (1988)].
90. N. Isgur *et al.*, Phys. Rev. D **39**, 799 (1989).
91. D. Scora and N. Isgur, Phys. Rev. D **52**, 2783 (1995).
92. D. Melikhov, Phys. Rev. D **53**, 2460 (1996).
93. M. Beyer and D. Melikhov, Phys. Lett. B **436**, 344 (1998).
94. R.N. Faustov, V.O. Galkin, and A.Y. Mishurov, Phys. Rev. D **53**, 6302 (1996).
95. N.B. Demchuk *et al.*, Phys. Atom. Nucl. **60**, 1292 (1997) [Yad. Fiz. **60N8**, 1429 (1997)].
96. I.L. Grach, I.M. Narodetsky, and S. Simula, Phys. Lett. B **385**, 317 (1996).
97. Riazuddin, T.A. Al-Aithan, and A.H.S. Gilani, Int. J. Mod. Phys. A **17**, 4927 (2002).
98. D. Melikhov and B. Stech, Phys. Rev. D **62**, 014006 (2000).
99. T. Feldmann and P. Kroll, Eur. Phys. J. C **12**, 99 (2000).
100. J.M. Flynn and J. Nieves, Phys. Lett. B **505**, 82 (2001).
101. M. Beneke and T. Feldmann, Nucl. Phys. B **592**, 3 (2001).
102. H.M. Choi and C.R. Ji, Phys. Lett. B **460**, 461 (1999).
103. C.S. Huang, C. Liu, and C.T. Yan, Phys. Rev. D **62**, 054019 (2000).
104. T. Kurimoto, H.n. Li, and A.I. Sanda, Phys. Rev. D **65**, 014007 (2002).
105. Z. Ligeti and M.B. Wise, Phys. Rev. D **53**, 4937 (1996).
106. E.M. Aitala *et al.* [E791 Collab.], Phys. Rev. Lett. **80**, 1393 (1998).
107. G. Burdman and J. Kambor, Phys. Rev. D **55**, 2817 (1997).
108. L. Lellouch, Nucl. Phys. B **479**, 353 (1996).
109. T. Mannel and B. Postler, Nucl. Phys. B **535**, 372 (1998).
110. C.W. Bauer, D. Pirjol, and I.W. Stewart, Phys. Rev. D **67**, 071502 (2003).
111. B.O. Lange, arXiv:hep-ph/0310139.
112. P. Ball, arXiv:hep-ph/0308249.
113. M. Beneke and T. Feldmann, arXiv:hep-ph/0311335.
114. B.O. Lange and M. Neubert, arXiv:hep-ph/0311345.
115. C.W. Bauer, S. Fleming, and M.E. Luke, Phys. Rev. D **63**, 014006 (2001).
116. C.W. Bauer *et al.*, Phys. Rev. D **63**, 114020 (2001).
117. C.W. Bauer and I.W. Stewart, Phys. Lett. B **516**, 134 (2001).
118. C.W. Bauer, D. Pirjol, and I.W. Stewart, Phys. Rev. D **65**, 054022 (2002).
119. C.T.H. Davies *et al.* [HPQCD Collab.], arXiv:hep-lat/0304004.
120. C. Bernard *et al.* [MILC Collab.], arXiv:hep-lat/0309055.
121. M. Okamoto *et al.*, arXiv:hep-lat/0309107.
122. S.B. Athar *et al.* [CLEO Collab.], Phys. Rev. D **68**, 072003 (2003).
123. B.H. Behrens *et al.* [CLEO Collab.], Phys. Rev. **D61**, 052001 (2000).
124. B. Aubert *et al.* [BABAR Collab.], Phys. Rev. Lett. **90**, 181801 (2003).
125. J.L. Diaz-Cruz, G. Lopez Castro, and J.H. Munoz, Phys. Rev. D **54**, 2388 (1996).
126. L. Gibbons, eConf **C0304052**, WG105 (2003) [arXiv:hep-ex/0307065].
127. K. Abe *et al.* [Belle Collab.], arXiv:hep-ex/0307075.
128. K.M. Foley and G.P. Lepage, Nucl. Phys. Proc. Suppl. **119**, 635 (2003).

V_{ub} MEASUREMENTS

For the discussion of V_{ub} measurements, which is not repeated here, see the review on "Determination of $|V_{ub}|$."

The CKM matrix element $|V_{ub}|$ can be determined by studying the rate of the charmless semileptonic decay $b \to u\ell\nu$. Measurements based on exclusive decay channels and on inclusive techniques can be found in the previous *B* Listings, which will not repeat here.

V_{cb} and V_{ub} CKM Matrix Elements REFERENCES

ADAM	03	PR D67 032001	N.E. Adam *et al.*	(CLEO Collab.)
ABE	02E	PL B526 258	K. Abe *et al.*	(BELLE Collab.)
ABE	02F	PL B526 247	K. Abe *et al.*	(BELLE Collab.)
BRIERE	02	PRL 89 081803	R. Briere *et al.*	(CLEO Collab.)
ABREU	01H	PL B510 55	P. Abreu *et al.*	(DELPHI Collab.)
ABBIENDI	00Q	PL B482 15	G. Abbiendi *et al.*	(OPAL Collab.)
BARTELT	99	PRL 82 3746	J. Bartelt *et al.*	(CLEO Collab.)
ACKERSTAFF	97G	PL B395 128	K. Ackerstaff *et al.*	(OPAL Collab.)
ATHANAS	97	PRL 79 2208	M. Athanas *et al.*	(CLEO Collab.)
BUSKULIC	97	PL B395 373	D. Buskulic *et al.*	(ALEPH Collab.)
ABREU	96P	ZPHY C71 539	P. Abreu *et al.*	(DELPHI Collab.)
BARISH	95	PR D51 1014	B.C. Barish *et al.*	(CLEO Collab.)
BUSKULIC	95N	PL B359 236	D. Buskulic *et al.*	(ALEPH Collab.)

B^*

$I(J^P) = \frac{1}{2}(1^-)$

I, J, P need confirmation. Quantum numbers shown are quark-model predictions.

B^* MASS

From mass difference below and the average of our B masses $(m_{B^\pm} + m_{B^0})/2$.

VALUE (MeV)	DOCUMENT ID
5325.0±0.6 OUR FIT	

$m_{B^*} - m_B$

VALUE (MeV)	EVTS	DOCUMENT ID		TECN	COMMENT
45.78±0.35 OUR FIT					
45.78±0.35 OUR AVERAGE					
46.2 ±0.3 ±0.8		[1] ACKERSTAFF	97M	OPAL	$e^+e^- \to Z$
45.3 ±0.35±0.87	4227	[1] BUSKULIC	96D	ALEP	E_{cm}^{ee}= 88–94 GeV
45.5 ±0.3 ±0.8		[1] ABREU	95R	DLPH	E_{cm}^{ee}= 88–94 GeV
46.3 ±1.9	1378	[1] ACCIARRI	95B	L3	E_{cm}^{ee}= 88–94 GeV
46.4 ±0.3 ±0.8		[2] AKERIB	91	CLE2	$e^+e^- \to \gamma X$
45.6 ±0.8		[2] WU	91	CSB2	$e^+e^- \to \gamma X, \gamma \ell X$
45.4 ±1.0		[3] LEE-FRANZINI	90	CSB2	$e^+e^- \to \Upsilon(5S)$
• • • We do not use the following data for averages, fits, limits, etc. • • •					
52 ±2 ±4	1400	[4] HAN	85	CUSB	$e^+e^- \to \gamma e X$

[1] u, d, s flavor averaged.

[2] These papers report E_γ in the B^* center of mass. The $m_{B^*} - m_B$ is 0.2 MeV higher. E_{cm} = 10.61–10.7 GeV. Admixture of B^0 and B^+ mesons, but not B_s.

[3] LEE-FRANZINI 90 value is for an admixture of B^0 and B^+. They measure 46.7 ± 0.4 ± 0.2 MeV for an admixture of B^0, B^+, and B_s, and use the shape of the photon line to separate the above value.

[4] HAN 85 is for E_{cm} = 10.6–11.2 GeV, giving an admixture of B^0, B^+, and B_s.

$|(m_{B^{*+}} - m_{B^+}) - (m_{B^{*0}} - m_{B^0})|$

VALUE (MeV)	CL%	DOCUMENT ID		TECN	COMMENT
<6	95	ABREU	95R	DLPH	E_{cm}^{ee}= 88–94 GeV

B^* DECAY MODES

	Mode	Fraction (Γ_i/Γ)
Γ_1	$B\gamma$	dominant

B^* REFERENCES

ACKERSTAFF	97M	ZPHY C74 413	K. Ackerstaff *et al.*	(OPAL Collab.)
BUSKULIC	96D	ZPHY C69 393	D. Buskulic *et al.*	(ALEPH Collab.)
ABREU	95R	ZPHY C68 353	P. Abreu *et al.*	(DELPHI Collab.)
ACCIARRI	95B	PL B345 589	M. Acciarri *et al.*	(L3 Collab.)
AKERIB	91	PRL 67 1692	D.S. Akerib *et al.*	(CLEO Collab.)
WU	91	PL B273 177	Q.W. Wu *et al.*	(CUSB II Collab.)
LEE-FRANZINI	90	PRL 65 2947	J. Lee-Franzini *et al.*	(CUSB II Collab.)
HAN	85	PRL 55 36	K. Han *et al.*	(COLU, LSU, MPIM, STON)

$B_J^*(5732)$ or B^{**}

$I(J^P) = ?(?^?)$

I, J, P need confirmation.

OMITTED FROM SUMMARY TABLE

Signal can be interpreted as stemming from several narrow and broad resonances. Needs confirmation.

$B_J^*(5732)$ MASS

VALUE (MeV)	EVTS	DOCUMENT ID		TECN	COMMENT
5698± 8 OUR AVERAGE Error includes scale factor of 1.2.					
5710±20		[1] AFFOLDER	01F	CDF	$p\overline{p}$ at 1.8 TeV
5695^{+17}_{-19}		[2] BARATE	98L	ALEP	$e^+e^- \to Z$
5704± 4±10	1944	[3] BUSKULIC	96D	ALEP	E_{cm}^{ee}= 88–94 GeV
5732± 5±20	2157	ABREU	95B	DLPH	E_{cm}^{ee}= 88–94 GeV
5681±11	1738	AKERS	95E	OPAL	E_{cm}^{ee}= 88–94 GeV
• • • We do not use the following data for averages, fits, limits, etc. • • •					
5713± 2		[4] ACCIARRI	99N	L3	$e^+e^- \to Z$

[1] AFFOLDER 01F uses the reconstructed B meson through semileptonic decay channels. The fraction of light B mesons that are produced at L=1 B^{**} states is measured to be 0.28 ± 0.06 ± 0.03.

[2] BARATE 98L uses fully reconstructed B mesons to search for B^{**} production in the $B\pi^\pm$ system. In the framework of heavy quark symmetry (HQS), they also measured the mass of B_2^* to be 5739^{+8+6}_{-11-4} MeV/c^2 and the relative production rate of $B(b \to B_2^* \to B^{(*)}\pi)/B(b \to B_{u,d}) = (31 \pm 9^{+6}_{-5})\%$.

[3] Using $m_{B\pi} - m_B$ = 424 ± 4 ± 10 MeV.

[4] ACCIARRI 99N uses inclusive reconstructed B mesons to search for B^{**} production in the $B^{(*)}\pi^\pm$ system. In the framework of HQET, they measured the mass of B_1^* and B_2^* to be 5670±10±13 MeV and 5768±5±6 with the $B(b \to B^{**}) = (32 \pm 3 \pm 6) \times 10^{-2}$. They also reported the evidence for the existence of an excited B-meson state or mixture of states in the region 5.9–6.0 GeV.

$B_J^*(5732)$ WIDTH

VALUE (MeV)	EVTS	DOCUMENT ID		TECN	COMMENT
128±18 OUR AVERAGE					
145±28	2157	ABREU	95B	DLPH	E_{cm}^{ee}= 88–94 GeV
116±24	1738	AKERS	95E	OPAL	E_{cm}^{ee}= 88–94 GeV

$B_J^*(5732)$ DECAY MODES

	Mode	Fraction (Γ_i/Γ)
Γ_1	$B^*\pi + B\pi$	dominant
Γ_2	$B^*\pi$(X)	[a] (85 ± 29) %

[a] X refers to decay modes with or without additional accompanying decay particles.

$B_J^*(5732)$ BRANCHING RATIOS

X refers to decay modes with or without additional accompanying decay particles.

$\Gamma(B^*\pi(X))/\Gamma_{total}$ Γ_2/Γ

VALUE	DOCUMENT ID		TECN	COMMENT
$\mathbf{0.85^{+0.26}_{-0.27} \pm 0.12}$	ABBIENDI	02E	OPAL	$e^+e^- \to Z$

$B_J^*(5732)$ REFERENCES

ABBIENDI	02E	EPJ C23 437	G. Abbiendi *et al.*	(OPAL Collab.)
AFFOLDER	01F	PR D64 072002	T. Affolder *et al.*	(CDF Collab.)
ACCIARRI	99N	PL B465 323	M. Acciarri *et al.*	(L3 Collab.)
BARATE	98L	PL B425 215	R. Barate *et al.*	(ALEPH Collab.)
BUSKULIC	96D	ZPHY C69 393	D. Buskulic *et al.*	(ALEPH Collab.)
ABREU	95B	PL B345 598	P. Abreu *et al.*	(DELPHI Collab.)
AKERS	95E	ZPHY C66 19	R. Akers *et al.*	(OPAL Collab.)

BOTTOM, STRANGE MESONS ($B = \pm 1$, $S = \mp 1$)

$B_s^0 = s\overline{b}$, $\overline{B}_s^0 = \overline{s}b$, similarly for B_s^*'s

B_s^0

$I(J^P) = 0(0^-)$

I, J, P need confirmation. Quantum numbers shown are quark-model predictions.

B_s^0 MASS

VALUE (MeV)	EVTS	DOCUMENT ID		TECN	COMMENT
5369.6± 2.4 OUR FIT					
5369.6± 2.4 OUR AVERAGE					
5369.9± 2.3±1.3	32	[1] ABE	96B	CDF	$p\overline{p}$ at 1.8 TeV
5374 ±16 ±2	3	ABREU	94D	DLPH	$e^+e^- \to Z$
5359 ±19 ±7	1	[1] AKERS	94J	OPAL	$e^+e^- \to Z$
5368.6± 5.6±1.5	2	BUSKULIC	93G	ALEP	$e^+e^- \to Z$
• • • We do not use the following data for averages, fits, limits, etc. • • •					
5370 ±40	6	[2] AKERS	94J	OPAL	$e^+e^- \to Z$
5383.3± 4.5±5.0	14	ABE	93F	CDF	Repl by ABE 96B

[1] From the decay $B_s \to J/\psi(1S)\phi$.
[2] From the decay $B_s \to D_s^- \pi^+$.

$m_{B_s^0} - m_B$

m_B is the average of our B masses $(m_{B^\pm} + m_{B^0})/2$.

VALUE (MeV)	CL%	DOCUMENT ID		TECN	COMMENT
90.4±2.4 OUR FIT					
89.7±2.7±1.2		ABE	96B	CDF	$p\overline{p}$ at 1.8 TeV
• • • We do not use the following data for averages, fits, limits, etc. • • •					
80 to 130	68	LEE-FRANZINI 90		CSB2	$e^+e^- \to \Upsilon(5S)$

$m_{B_{sH}^0} - m_{B_{sL}^0}$

See the B_s^0-$\overline{B}_s^0$ MIXING section near the end of these B_s^0 Listings.

B_s^0 MEAN LIFE

"OUR EVALUATION" is an average using rescaled values of the data listed below. The average and rescaling were performed by the Heavy Flavor Averaging Group (HFAG) and are described at http://www.slac.stanford.edu/xorg/hfag/. The averaging/rescaling procedure takes into account corrections between the measurements and asymmetric lifetime errors.

VALUE (10^{-12} s)	EVTS	DOCUMENT ID		TECN	COMMENT
1.461±0.057 OUR EVALUATION					
$1.42\ ^{+0.14}_{-0.13} \pm 0.03$		[3] ABREU	00Y	DLPH	$e^+e^- \to Z$
$1.53\ ^{+0.16}_{-0.15} \pm 0.07$		[4] ABREU,P	00G	DLPH	$e^+e^- \to Z$
$1.36 \pm 0.09\ ^{+0.06}_{-0.05}$		[5] ABE	99D	CDF	$p\overline{p}$ at 1.8 TeV
$1.34\ ^{+0.23}_{-0.19} \pm 0.05$		[6] ABE	98B	CDF	$p\overline{p}$ at 1.8 TeV
$1.72\ ^{+0.20}_{-0.19}\ ^{+0.18}_{-0.17}$		[7] ACKERSTAFF	98F	OPAL	$e^+e^- \to Z$
$1.50\ ^{+0.16}_{-0.15} \pm 0.04$		[5] ACKERSTAFF	98G	OPAL	$e^+e^- \to Z$
$1.47 \pm 0.14 \pm 0.08$		[4] BARATE	98C	ALEP	$e^+e^- \to Z$
$1.60 \pm 0.26\ ^{+0.13}_{-0.15}$		[8] ABREU	96F	DLPH	$e^+e^- \to Z$
$1.54\ ^{+0.14}_{-0.13} \pm 0.04$		[5] BUSKULIC	96M	ALEP	$e^+e^- \to Z$
• • • We do not use the following data for averages, fits, limits, etc. • • •					
1.51 ± 0.11		[9] BARATE	98C	ALEP	$e^+e^- \to Z$
$1.34\ ^{+0.23}_{-0.19} \pm 0.05$		[10] ABE	96N	CDF	Repl. by ABE 98B
$1.56\ ^{+0.29}_{-0.26}\ ^{+0.08}_{-0.07}$		[5] ABREU	96F	DLPH	Repl. by ABREU 00Y
$1.65\ ^{+0.34}_{-0.31} \pm 0.12$		[4] ABREU	96F	DLPH	Repl. by ABREU 00Y
$1.76 \pm 0.20\ ^{+0.15}_{-0.10}$		[11] ABREU	96F	DLPH	Repl. by ABREU 00Y
1.67 ± 0.14		[12] ABREU	96F	DLPH	$e^+e^- \to Z$
$1.61\ ^{+0.30}_{-0.29}\ ^{+0.18}_{-0.16}$	90	[4] BUSKULIC	96E	ALEP	Repl. by BARATE 98C
$1.42\ ^{+0.27}_{-0.23} \pm 0.11$	76	[5] ABE	95R	CDF	Repl. by ABE 99D
$1.74\ ^{+1.08}_{-0.69} \pm 0.07$	8	[13] ABE	95R	CDF	Sup. by ABE 96N
$1.54\ ^{+0.25}_{-0.21} \pm 0.06$	79	[5] AKERS	95G	OPAL	Repl. by ACKERSTAFF 98G
$1.59\ ^{+0.17}_{-0.15} \pm 0.03$	134	[5] BUSKULIC	95O	ALEP	Sup. by BUSKULIC 96M
0.96 ± 0.37	41	[14] ABREU	94E	DLPH	Sup. by ABREU 96F
$1.92\ ^{+0.45}_{-0.35} \pm 0.04$	31	[5] BUSKULIC	94C	ALEP	Sup. by BUSKULIC 95O
$1.13\ ^{+0.35}_{-0.26} \pm 0.09$	22	[5] ACTON	93H	OPAL	Sup. by AKERS 95G

[3] Uses $D_s^- \ell^+$, and $\phi\ell^+$ vertices.
[4] Measured using D_s hadron vertices.
[5] Measured using $D_s^- \ell^+$ vertices.
[6] Measured using fully reconstructed $B_s \to J/\psi(1S)\phi$ decay.
[7] ACKERSTAFF 98F use fully reconstructed $D_s^- \to \phi\pi^-$ and $D_s^- \to K^{*0}K^-$ in the inclusive B_s^0 decay.
[8] Measured using inclusive D_s vertices.
[9] Combined results from $D_s^- \ell^+$ and D_s hadron.
[10] ABE 96N uses 58 ± 12 exclusive $B_s \to J/\psi(1S)\phi$ events.
[11] Measured using $\phi\ell$ vertices.
[12] Combined result for the four ABREU 96F methods.
[13] Exclusive reconstruction of $B_s \to \psi\phi$.
[14] ABREU 94E uses the flight-distance distribution of D_s vertices, ϕ-lepton vertices, and $D_s\mu$ vertices.

B_{sL}^0 MEAN LIFE

B_{sL}^0 is a long-lived CP-even state of two B_s^0 CP eigenstates.

VALUE (10^{-12} s)	DOCUMENT ID		TECN	COMMENT
1.27±0.33±0.08	[15] BARATE	00K	ALEP	$e^+e^- \to Z$

[15] Uses $\phi\phi$ correlations from $B_s^0 \to D_s^{(*)+} D_s^{(*)-}$.

$|\Delta\Gamma_{B_s^0}|/\Gamma_{B_s^0}$

$\Gamma_{B_s^0}$ and $|\Delta\Gamma_{B_s^0}|$ are the decay rate average and difference between two B_s^0 CP eigenstates.

The second "OUR EVALUATION," < 0.54 (CL=95%), is an average of all available B_s semi-leptonic lifetime measurements with the $\Delta\Gamma_{B_s^0}/\Gamma_s$ analyses performed by the Heavy Flavor Averaging Group (HFAG) as described in our "Review on B-$\overline{B}$ Mixing" in the B^0 Section of these Listings.

The first "OUR EVALUATION," < 0.29 (CL=95%), also provided by the HFAG, including the assumption of $\Gamma_s = \frac{1}{\tau_{B_d}}$.

VALUE	CL%	DOCUMENT ID		TECN	COMMENT
<0.29 (CL = 95%) OUR EVALUATION		First			
<0.54 (CL = 95%) OUR EVALUATION		Second			
<0.46	95	[16] ABREU	00Y	DLPH	$e^+e^- \to Z$
<0.69	95	[17] ABREU,P	00G	DLPH	$e^+e^- \to Z$
$0.25^{+0.21}_{-0.14}$		[18] BARATE	00K	ALEP	$e^+e^- \to Z$
<0.83	95	[19] ABE	99D	CDF	$p\overline{p}$ at 1.8 TeV
<0.67	95	[20] ACCIARRI	98S	L3	$e^+e^- \to Z$

[16] Uses $D_s^- \ell^+$, and $\phi\ell^+$ vertices.
[17] Measured using D_s hadron vertices.
[18] Uses $\phi\phi$ correlations from $B_s^0 \to D_s^{(*)+} D_s^{(*)-}$.
[19] ABE 99D assumes $\tau_{B_s^0} = 1.55 \pm 0.05$ ps.
[20] ACCIARRI 98S assumes $\tau_{B_s^0} = 1.49 \pm 0.06$ ps and PDG 98 values of b production fraction.

B_s^0 DECAY MODES

These branching fractions all scale with $B(\overline{b} \to B_s^0)$, the LEP B_s^0 production fraction. The first four were evaluated using $B(\overline{b} \to B_s^0) = (10.7 \pm 1.4)\%$ and the rest assume $B(\overline{b} \to B_s^0) = 12\%$.

The branching fraction $B(B_s^0 \to D_s^- \ell^+ \nu_\ell \text{anything})$ is not a pure measurement since the measured product branching fraction $B(\overline{b} \to B_s^0) \times B(B_s^0 \to D_s^- \ell^+ \nu_\ell \text{anything})$ was used to determine $B(\overline{b} \to B_s^0)$, as described in the note on "Production and Decay of b-Flavored Hadrons."

For inclusive branching fractions, *e.g.*, $B \to D^\pm$ anything, the values usually are multiplicities, not branching fractions. They can be greater than one.

	Mode	Fraction (Γ_i/Γ)		Confidence level
Γ_1	D_s^- anything	(94 $\pm$30) %		
Γ_2	$D_s^- \ell^+ \nu_\ell$ anything	[a] (7.9 $\pm$ 2.4) %		
Γ_3	$D_s^- \pi^+$	< 13	%	
Γ_4	$D_s^{(*)+} D_s^{(*)-}$	(23 $^{+21}_{-13}$) %		
Γ_5	$J/\psi(1S)\phi$	(9.3 $\pm$ 3.3)	$\times 10^{-4}$	
Γ_6	$J/\psi(1S)\pi^0$	< 1.2	$\times 10^{-3}$	90%
Γ_7	$J/\psi(1S)\eta$	< 3.8	$\times 10^{-3}$	90%
Γ_8	$\psi(2S)\phi$	seen		
Γ_9	$\pi^+\pi^-$	< 1.7	$\times 10^{-4}$	90%
Γ_{10}	$\pi^0\pi^0$	< 2.1	$\times 10^{-4}$	90%
Γ_{11}	$\eta\pi^0$	< 1.0	$\times 10^{-3}$	90%
Γ_{12}	$\eta\eta$	< 1.5	$\times 10^{-3}$	90%
Γ_{13}	$\rho^0\rho^0$	< 3.20	$\times 10^{-4}$	90%
Γ_{14}	$\phi\rho^0$	< 6.17	$\times 10^{-4}$	90%
Γ_{15}	$\phi\phi$	< 1.183	$\times 10^{-3}$	90%
Γ_{16}	$\pi^+ K^-$	< 2.1	$\times 10^{-4}$	90%
Γ_{17}	$K^+ K^-$	< 5.9	$\times 10^{-5}$	90%
Γ_{18}	$\overline{K}^*(892)^0\rho^0$	< 7.67	$\times 10^{-4}$	90%
Γ_{19}	$\overline{K}^*(892)^0 K^*(892)^0$	< 1.681	$\times 10^{-3}$	90%
Γ_{20}	$\phi K^*(892)^0$	< 1.013	$\times 10^{-3}$	90%
Γ_{21}	$p\overline{p}$	< 5.9	$\times 10^{-5}$	90%
Γ_{22}	$\gamma\gamma$	< 1.48	$\times 10^{-4}$	90%
Γ_{23}	$\phi\gamma$	< 1.2	$\times 10^{-4}$	90%

Lepton Family number (LF) violating modes or $\Delta B = 1$ weak neutral current ($B1$) modes

Γ_{24}	$\mu^+\mu^-$	$B1$	< 2.0	$\times 10^{-6}$	90%
Γ_{25}	e^+e^-	$B1$	< 5.4	$\times 10^{-5}$	90%
Γ_{26}	$e^\pm\mu^\mp$	LF [b]	< 6.1	$\times 10^{-6}$	90%
Γ_{27}	$\phi(1020)\mu^+\mu^-$	$B1$	< 4.7	$\times 10^{-5}$	90%
Γ_{28}	$\phi\nu\overline{\nu}$	$B1$	< 5.4	$\times 10^{-3}$	90%

[a] Not a pure measurement. See note at head of B_s^0 Decay Modes.

[b] The value is for the sum of the charge states or particle/antiparticle states indicated.

B_s^0 BRANCHING RATIOS

$\Gamma(D_s^- \text{anything})/\Gamma_{\text{total}}$ Γ_1/Γ

VALUE	EVTS	DOCUMENT ID		TECN	COMMENT
0.93 $\pm$ 0.30 OUR AVERAGE					
0.81 $\pm$ 0.24 $\pm$ 0.22	90	[21] BUSKULIC	96E	ALEP	$e^+e^- \to Z$
1.56 $\pm$ 0.58 $\pm$ 0.44	147	[22] ACTON	92N	OPAL	$e^+e^- \to Z$

[21] BUSKULIC 96E separate $c\overline{c}$ and $b\overline{b}$ sources of D_s^+ mesons using a lifetime tag, subtract generic $\overline{b} \to W^+ \to D_s^+$ events, and obtain $B(\overline{b} \to B_s^0) \times B(B_s^0 \to D_s^- \text{anything}) = 0.088 \pm 0.020 \pm 0.020$ assuming $B(D_s \to \phi\pi) = (3.5 \pm 0.4) \times 10^{-2}$ and PDG 1994 values for the relative partial widths to other D_s channels. We evaluate using our current values $B(\overline{b} \to B_s^0) = 0.107 \pm 0.014$ and $B(D_s \to \phi\pi) = 0.036 \pm 0.009$. Our first error is their experiment's and our second error is that due to $B(\overline{b} \to B_s^0)$ and $B(D_s \to \phi\pi)$.

[22] ACTON 92N assume that excess of 147 ± 48 D_s^0 events over that expected from B^0, B^+, and $c\overline{c}$ is all from B_s^0 decay. The product branching fraction is measured to be $B(\overline{b} \to B_s^0) B(B_s^0 \to D_s^- \text{anything}) \times B(D_s^- \to \phi\pi^-) = (5.9 \pm 1.9 \pm 1.1) \times 10^{-3}$. We evaluate using our current values $B(\overline{b} \to B_s^0) = 0.107 \pm 0.014$ and $B(D_s \to \phi\pi) = 0.036 \pm 0.009$. Our first error is their experiment's and our second error is that due to $B(\overline{b} \to B_s^0)$ and $B(D_s \to \phi\pi)$.

$\Gamma(D_s^- \ell^+ \nu_\ell \text{anything})/\Gamma_{\text{total}}$ Γ_2/Γ

The values and averages in this section serve only to show what values result if one assumes our $B(\overline{b} \to B_s^0)$. They cannot be thought of as measurements since the underlying product branching fractions were also used to determine $B(\overline{b} \to B_s^0)$ as described in the note on "Production and Decay of b-Flavored Hadrons."

VALUE	EVTS	DOCUMENT ID		TECN	COMMENT
0.079 $\pm$ 0.024 OUR AVERAGE					
0.076 $\pm$ 0.012 $\pm$ 0.021	134	[23] BUSKULIC	95O	ALEP	$e^+e^- \to Z$
0.107 $\pm$ 0.043 $\pm$ 0.029		[24] ABREU	92M	DLPH	$e^+e^- \to Z$
0.103 $\pm$ 0.036 $\pm$ 0.028	18	[25] ACTON	92N	OPAL	$e^+e^- \to Z$
• • • We do not use the following data for averages, fits, limits, etc. • • •					
0.13 $\pm$0.04 $\pm$0.04	27	[26] BUSKULIC	92E	ALEP	$e^+e^- \to Z$

[23] BUSKULIC 95O use $D_s\ell$ correlations. The measured product branching ratio is $B(\overline{b} \to B_s) \times B(B_s \to D_s^- \ell^+ \nu_\ell \text{anything}) = (0.82 \pm 0.09^{+0.13}_{-0.14})\%$ assuming $B(D_s \to \phi\pi) = (3.5 \pm 0.4) \times 10^{-2}$ and PDG 1994 values for the relative partial widths to the six other D_s channels used in this analysis. Combined with results from $\Upsilon(4S)$ experiments this can be used to extract $B(\overline{b} \to B_s) = (11.0 \pm 1.2^{+2.5}_{-2.6})\%$. We evaluate using our current values $B(\overline{b} \to B_s^0) = 0.107 \pm 0.014$ and $B(D_s \to \phi\pi) = 0.036 \pm 0.009$. Our first error is their experiment's and our second error is that due to $B(\overline{b} \to B_s^0)$ and $B(D_s \to \phi\pi)$.

[24] ABREU 92M measured muons only and obtained product branching ratio $B(Z \to b\text{or } \overline{b}) \times B(\overline{b} \to B_s) \times B(B_s \to D_s \mu^+ \nu_\mu \text{anything}) \times B(D_s \to \phi\pi) = (18 \pm 8) \times 10^{-5}$. We evaluate using our current values $B(\overline{b} \to B_s^0) = 0.107 \pm 0.014$ and $B(D_s \to \phi\pi) = 0.036 \pm 0.009$. Our first error is their experiment's and our second error is that due to $B(\overline{b} \to B_s^0)$ and $B(D_s \to \phi\pi)$. We use $B(Z \to b\text{or } \overline{b}) = 2B(Z \to b\overline{b}) = 2 \times (0.2212 \pm 0.0019)$.

[25] ACTON 92N is measured using $D_s \to \phi\pi^+$ and $K^*(892)^0 K^+$ events. The product branching fraction measured is measured to be $B(\overline{b} \to B_s^0) B(B_s^0 \to D_s^- \ell^+ \nu_\ell \text{anything}) \times B(D_s^- \to \phi\pi^-) = (3.9 \pm 1.1 \pm 0.8) \times 10^{-4}$. We evaluate using our current values $B(\overline{b} \to B_s^0) = 0.107 \pm 0.014$ and $B(D_s \to \phi\pi) = 0.036 \pm 0.009$. Our first error is their experiment's and our second error is that due to $B(\overline{b} \to B_s^0)$ and $B(D_s \to \phi\pi)$.

[26] BUSKULIC 92E is measured using $D_s \to \phi\pi^+$ and $K^*(892)^0 K^+$ events. They use $2.7 \pm 0.7\%$ for the $\phi\pi^+$ branching fraction. The average product branching fraction is measured to be $B(\overline{b} \to B_s^0) B(B_s^0 \to D_s^- \ell^+ \nu_\ell \text{anything}) = 0.020 \pm 0.0055^{+0.005}_{-0.006}$. We evaluate using our current values $B(\overline{b} \to B_s^0) = 0.107 \pm 0.014$ and $B(D_s \to \phi\pi) = 0.036 \pm 0.009$. Our first error is their experiment's and our second error is that due to $B(\overline{b} \to B_s^0)$ and $B(D_s \to \phi\pi)$. Superseded by BUSKULIC 95O.

$\Gamma(D_s^- \pi^+)/\Gamma_{\text{total}}$ Γ_3/Γ

VALUE	EVTS	DOCUMENT ID		TECN	COMMENT
< 0.13	6	[27] AKERS	94J	OPAL	$e^+e^- \to Z$
• • • We do not use the following data for averages, fits, limits, etc. • • •					
seen	1	BUSKULIC	93G	ALEP	$e^+e^- \to Z$

[27] AKERS 94J sees ≤ 6 events and measures the limit on the product branching fraction $f(\overline{b} \to B_s^0) \cdot B(B_s^0 \to D_s^- \pi^+) < 1.3\%$ at CL = 90%. We divide by our current value $B(\overline{b} \to B_s^0) = 0.105$.

$\Gamma(D_s^{(*)+} D_s^{(*)-})/\Gamma_{\text{total}}$ Γ_4/Γ

VALUE	CL%	DOCUMENT ID		TECN	COMMENT
0.23 $\pm$0.10 $^{+0.19}_{-0.09}$		[28] BARATE	00K	ALEP	$e^+e^- \to Z$
• • • We do not use the following data for averages, fits, limits, etc. • • •					
< 0.218	90	BARATE	98Q	ALEP	$e^+e^- \to Z$

[28] Uses $\phi\phi$ correlations from $B_s^0 \to D_s^{(*)+} D_s^{(*)-}$.

$\Gamma(J/\psi(1S)\phi)/\Gamma_{\text{total}}$ Γ_5/Γ

VALUE (units 10^{-3})	EVTS	DOCUMENT ID		TECN	COMMENT
0.93 $\pm$ 0.28 $\pm$ 0.17		[29] ABE	96Q	CDF	$p\overline{p}$
• • • We do not use the following data for averages, fits, limits, etc. • • •					
< 6	1	[30] AKERS	94J	OPAL	$e^+e^- \to Z$
seen	14	[31] ABE	93F	CDF	$p\overline{p}$ at 1.8 TeV
seen	1	[32] ACTON	92N	OPAL	Sup. by AKERS 94J

[29] ABE 96Q assumes $f_U = f_d$ and $f_s/f_U = 0.40 \pm 0.06$. Uses $B \to J/\psi(1S) K$ and $B \to J/\psi(1S) K^*$ branching fractions from PDG 94. They quote two systematic errors, ± 0.10 and ± 0.14 where the latter is the uncertainty in f_s. We combine in quadrature.

[30] AKERS 94J sees one event and measures the limit on the product branching fraction $f(\overline{b} \to B_s^0) \cdot B(B_s^0 \to J/\psi(1S)\phi) < 7 \times 10^{-4}$ at CL = 90%. We divide by $B(\overline{b} \to B_s^0) = 0.112$.

[31] ABE 93F measured using $J/\psi(1S) \to \mu^+\mu^-$ and $\phi \to K^+K^-$.

[32] In ACTON 92N a limit on the product branching fraction is measured to be $f(\overline{b} \to B_s^0) \cdot B(B_s^0 \to J/\psi(1S)\phi) \leq 0.22 \times 10^{-2}$.

$\Gamma(J/\psi(1S)\pi^0)/\Gamma_{\text{total}}$ Γ_6/Γ

VALUE	CL%	DOCUMENT ID		TECN
< 1.2 $\times 10^{-3}$	90	[33] ACCIARRI	97C	L3

[33] ACCIARRI 97C assumes B^0 production fraction ($39.5 \pm 4.0\%$) and B_s ($12.0 \pm 3.0\%$).

Meson Particle Listings

B_s^0

$\Gamma(J/\psi(1S)\eta)/\Gamma_{total}$ Γ_7/Γ

VALUE	CL%	DOCUMENT ID		TECN
$<3.8\times10^{-3}$	90	[34] ACCIARRI	97C	L3

[34] ACCIARRI 97C assumes B^0 production fraction (39.5 ± 4.0%) and B_s (12.0 ± 3.0%).

$\Gamma(\psi(2S)\phi)/\Gamma_{total}$ Γ_8/Γ

VALUE	EVTS	DOCUMENT ID		TECN	COMMENT
seen	1	BUSKULIC	93G	ALEP	$e^+e^-\to Z$

$\Gamma(\pi^+\pi^-)/\Gamma_{total}$ Γ_9/Γ

VALUE	CL%	DOCUMENT ID		TECN	COMMENT
$<1.7\times10^{-4}$	90	[35] BUSKULIC	96V	ALEP	$e^+e^-\to Z$
• • • We do not use the following data for averages, fits, limits, etc. • • •					
$<2.32\times10^{-4}$	90	[36] ABE	00C	SLD	$e^+e^-\to Z$

[35] BUSKULIC 96V assumes PDG 96 production fractions for B^0, B^+, B_s, b baryons.

[36] ABE 00C assumes B($Z\to b\overline{b}$)=(21.7 ± 0.1)% and the B fractions $f_{B^0}=f_{B^+}=(39.7^{+1.8}_{-2.2})$% and $f_{B_s}=(10.5^{+1.8}_{-2.2})$%.

$\Gamma(\pi^0\pi^0)/\Gamma_{total}$ Γ_{10}/Γ

VALUE	CL%	DOCUMENT ID		TECN	COMMENT
$<2.1\times10^{-4}$	90	[37] ACCIARRI	95H	L3	$e^+e^-\to Z$

[37] ACCIARRI 95H assumes $f_{B^0}=39.5\pm4.0$ and $f_{B_s}=12.0\pm3.0$%.

$\Gamma(\eta\pi^0)/\Gamma_{total}$ Γ_{11}/Γ

VALUE	CL%	DOCUMENT ID		TECN	COMMENT
$<1.0\times10^{-3}$	90	[38] ACCIARRI	95H	L3	$e^+e^-\to Z$

[38] ACCIARRI 95H assumes $f_{B^0}=39.5\pm4.0$ and $f_{B_s}=12.0\pm3.0$%.

$\Gamma(\eta\eta)/\Gamma_{total}$ Γ_{12}/Γ

VALUE	CL%	DOCUMENT ID		TECN	COMMENT
$<1.5\times10^{-3}$	90	[39] ACCIARRI	95H	L3	$e^+e^-\to Z$

[39] ACCIARRI 95H assumes $f_{B^0}=39.5\pm4.0$ and $f_{B_s}=12.0\pm3.0$%.

$\Gamma(\rho^0\rho^0)/\Gamma_{total}$ Γ_{13}/Γ

VALUE	CL%	DOCUMENT ID		TECN	COMMENT
$<3.20\times10^{-4}$	90	[40] ABE	00C	SLD	$e^+e^-\to Z$

[40] ABE 00C assumes B($Z\to b\overline{b}$)=(21.7 ± 0.1)% and the B fractions $f_{B^0}=f_{B^+}=(39.7^{+1.8}_{-2.2})$% and $f_{B_s}=(10.5^{+1.8}_{-2.2})$%.

$\Gamma(\phi\rho^0)/\Gamma_{total}$ Γ_{14}/Γ

VALUE	CL%	DOCUMENT ID		TECN	COMMENT
$<6.17\times10^{-4}$	90	[41] ABE	00C	SLD	$e^+e^-\to Z$

[41] ABE 00C assumes B($Z\to b\overline{b}$)=(21.7 ± 0.1)% and the B fractions $f_{B^0}=f_{B^+}=(39.7^{+1.8}_{-2.2})$% and $f_{B_s}=(10.5^{+1.8}_{-2.2})$%.

$\Gamma(\phi\phi)/\Gamma_{total}$ Γ_{15}/Γ

VALUE	CL%	DOCUMENT ID		TECN	COMMENT
$<11.83\times10^{-4}$	90	[42] ABE	00C	SLD	$e^+e^-\to Z$

[42] ABE 00C assumes B($Z\to b\overline{b}$)=(21.7 ± 0.1)% and the B fractions $f_{B^0}=f_{B^+}=(39.7^{+1.8}_{-2.2})$% and $f_{B_s}=(10.5^{+1.8}_{-2.2})$%.

$\Gamma(\pi^+K^-)/\Gamma_{total}$ Γ_{16}/Γ

VALUE	CL%	DOCUMENT ID		TECN	COMMENT
$<2.1\times10^{-4}$	90	[43] BUSKULIC	96V	ALEP	$e^+e^-\to Z$
• • • We do not use the following data for averages, fits, limits, etc. • • •					
$<2.61\times10^{-4}$	90	[44] ABE	00C	SLD	$e^+e^-\to Z$
$<2.6\times10^{-4}$	90	[45] AKERS	94L	OPAL	$e^+e^-\to Z$

[43] BUSKULIC 96V assumes PDG 96 production fractions for B^0, B^+, B_s, b baryons.

[44] ABE 00C assumes B($Z\to b\overline{b}$)=(21.7 ± 0.1)% and the B fractions $f_{B^0}=f_{B^+}=(39.7^{+1.8}_{-2.2})$% and $f_{B_s}=(10.5^{+1.8}_{-2.2})$%.

[45] Assumes B($Z\to b\overline{b}$) = 0.217 and B_d^0 (B_s^0) fraction 39.5% (12%).

$\Gamma(K^+K^-)/\Gamma_{total}$ Γ_{17}/Γ

VALUE	CL%	DOCUMENT ID		TECN	COMMENT
$<5.9\times10^{-5}$	90	[46] BUSKULIC	96V	ALEP	$e^+e^-\to Z$
• • • We do not use the following data for averages, fits, limits, etc. • • •					
$<2.83\times10^{-4}$	90	[47] ABE	00C	SLD	$e^+e^-\to Z$
$<1.4\times10^{-4}$	90	[48] AKERS	94L	OPAL	$e^+e^-\to Z$

[46] BUSKULIC 96V assumes PDG 96 production fractions for B^0, B^+, B_s, b baryons.

[47] ABE 00C assumes B($Z\to b\overline{b}$)=(21.7 ± 0.1)% and the B fractions $f_{B^0}=f_{B^+}=(39.7^{+1.8}_{-2.2})$% and $f_{B_s}=(10.5^{+1.8}_{-2.2})$%.

[48] Assumes B($Z\to b\overline{b}$) = 0.217 and B_d^0 (B_s^0) fraction 39.5% (12%).

$\Gamma(\overline{K}^*(892)^0\rho^0)/\Gamma_{total}$ Γ_{18}/Γ

VALUE	CL%	DOCUMENT ID		TECN	COMMENT
$<7.67\times10^{-4}$	90	[49] ABE	00C	SLD	$e^+e^-\to Z$

[49] ABE 00C assumes B($Z\to b\overline{b}$)=(21.7 ± 0.1)% and the B fractions $f_{B^0}=f_{B^+}=(39.7^{+1.8}_{-2.2})$% and $f_{B_s}=(10.5^{+1.8}_{-2.2})$%.

$\Gamma(\overline{K}^*(892)^0K^*(892)^0)/\Gamma_{total}$ Γ_{19}/Γ

VALUE	CL%	DOCUMENT ID		TECN	COMMENT
$<16.81\times10^{-4}$	90	[50] ABE	00C	SLD	$e^+e^-\to Z$

[50] ABE 00C assumes B($Z\to b\overline{b}$)=(21.7 ± 0.1)% and the B fractions $f_{B^0}=f_{B^+}=(39.7^{+1.8}_{-2.2})$% and $f_{B_s}=(10.5^{+1.8}_{-2.2})$%.

$\Gamma(\phi K^*(892)^0)/\Gamma_{total}$ Γ_{20}/Γ

VALUE	CL%	DOCUMENT ID		TECN	COMMENT
$<10.13\times10^{-4}$	90	[51] ABE	00C	SLD	$e^+e^-\to Z$

[51] ABE 00C assumes B($Z\to b\overline{b}$)=(21.7 ± 0.1)% and the B fractions $f_{B^0}=f_{B^+}=(39.7^{+1.8}_{-2.2})$% and $f_{B_s}=(10.5^{+1.8}_{-2.2})$%.

$\Gamma(p\overline{p})/\Gamma_{total}$ Γ_{21}/Γ

VALUE	CL%	DOCUMENT ID		TECN	COMMENT
$<5.9\times10^{-5}$	90	[52] BUSKULIC	96V	ALEP	$e^+e^-\to Z$

[52] BUSKULIC 96V assumes PDG 96 production fractions for B^0, B^+, B_s, b baryons.

$\Gamma(\gamma\gamma)/\Gamma_{total}$ Γ_{22}/Γ

VALUE	CL%	DOCUMENT ID		TECN	COMMENT
$<14.8\times10^{-5}$	90	[53] ACCIARRI	95I	L3	$e^+e^-\to Z$

[53] ACCIARRI 95I assumes $f_{B^0}=39.5\pm4.0$ and $f_{B_s}=12.0\pm3.0$%.

$\Gamma(\phi\gamma)/\Gamma_{total}$ Γ_{23}/Γ

VALUE	CL%	DOCUMENT ID		TECN	COMMENT
$<1.2\times10^{-4}$	90	ACOSTA	02G	CDF	$p\overline{p}$ at 1.8 TeV
• • • We do not use the following data for averages, fits, limits, etc. • • •					
$<7\times10^{-4}$	90	[54] ADAM	96D	DLPH	$e^+e^-\to Z$

[54] ADAM 96D assumes $f_{B^0}=f_{B^-}=0.39$ and $f_{B_s}=0.12$.

$\Gamma(\mu^+\mu^-)/\Gamma_{total}$ Γ_{24}/Γ

Test for $\Delta B=1$ weak neutral current.

VALUE	CL%	DOCUMENT ID		TECN	COMMENT
$<2.0\times10^{-6}$	90	[55] ABE	98	CDF	$p\overline{p}$ at 1.8 TeV
• • • We do not use the following data for averages, fits, limits, etc. • • •					
$<3.8\times10^{-5}$	90	[56] ACCIARRI	97B	L3	$e^+e^-\to Z$
$<8.4\times10^{-6}$	90	[57] ABE	96L	CDF	Repl. by ABE 98

[55] ABE 98 assumes production of $\sigma(B^0)=\sigma(B^+)$ and $\sigma(B_s)/\sigma(B^0)=1/3$. They normalize to their measured $\sigma(B^0, p_T(B)>6, |y|<1.0)=2.39\pm0.32\pm0.44\,\mu$b.

[56] ACCIARRI 97B assume PDG 96 production fractions for B^+, B^0, B_s, and Λ_b.

[57] ABE 96L assumes B^+/B_s production ratio 3/1. They normalize to their measured $\sigma(B^+, p_T(B)>6$ GeV/c, $|y|<1)=2.39\pm0.54\,\mu$b.

$\Gamma(e^+e^-)/\Gamma_{total}$ Γ_{25}/Γ

Test for $\Delta B=1$ weak neutral current.

VALUE	CL%	DOCUMENT ID		TECN	COMMENT
$<5.4\times10^{-5}$	90	[58] ACCIARRI	97B	L3	$e^+e^-\to Z$

[58] ACCIARRI 97B assume PDG 96 production fractions for B^+, B^0, B_s, and Λ_b.

$\Gamma(e^\pm\mu^\mp)/\Gamma_{total}$ Γ_{26}/Γ

Test of lepton family number conservation.

VALUE	CL%	DOCUMENT ID		TECN	COMMENT
$<6.1\times10^{-6}$	90	ABE	98V	CDF	$p\overline{p}$ at 1.8 TeV
• • • We do not use the following data for averages, fits, limits, etc. • • •					
$<4.1\times10^{-5}$	90	[59] ACCIARRI	97B	L3	$e^+e^-\to Z$

[59] ACCIARRI 97B assume PDG 96 production fractions for B^+, B^0, B_s, and Λ_b.

$\Gamma(\phi(1020)\mu^+\mu^-)/\Gamma_{total}$ Γ_{27}/Γ

Test for $\Delta B=1$ weak neutral current.

VALUE	CL%	DOCUMENT ID		TECN	COMMENT
$<4.7\times10^{-5}$	90	ACOSTA	02D	CDF	$p\overline{p}$ at 1.8 TeV

$\Gamma(\phi\nu\overline{\nu})/\Gamma_{total}$ Γ_{28}/Γ

Test for $\Delta B=1$ weak neutral current.

VALUE	CL%	DOCUMENT ID		TECN	COMMENT
$<5.4\times10^{-3}$	90	[60] ADAM	96D	DLPH	$e^+e^-\to Z$

[60] ADAM 96D assumes $f_{B^0}=f_{B^-}=0.39$ and $f_{B_s}=0.12$.

POLARIZATION IN B_s^0 DECAY

Γ_L/Γ in $B_s^0 \to J/\psi(1S)\phi$

VALUE	EVTS	DOCUMENT ID		TECN	COMMENT
0.59±0.12 OUR AVERAGE					
0.61±0.14±0.02		[61] AFFOLDER	00N	CDF	$p\overline{p}$ at 1.8 TeV
$0.56\pm0.21^{+0.02}_{-0.04}$	19	ABE	95Z	CDF	$p\overline{p}$ at 1.8 TeV

[61] AFFOLDER 00N measurements are based on 40 B_s^0 candidates obtained from a data sample of 89 pb^{-1}. The P-wave fraction is found to be 0.23 ± 0.19 ± 0.04.

B_s^0-$\overline{B}_s^0$ MIXING

For a discussion of B_s^0-$\overline{B}_s^0$ mixing see the note on "B^0-$\overline{B}^0$ Mixing" in the B^0 Particle Listings above.

χ_s is a measure of the time-integrated B_s^0-$\overline{B}_s^0$ mixing probability that produced $B_s^0(\overline{B}_s^0)$ decays as a $\overline{B}_s^0(B_s^0)$. Mixing violates $\Delta B \neq 2$ rule.

$$\chi_s = \frac{x_s^2}{2(1+x_s^2)}$$

$$x_s = \frac{\Delta m_{B_s^0}}{\Gamma_{B_s^0}} = (m_{B_{sH}^0} - m_{B_{sL}^0})\,\tau_{B_s^0},$$

where H, L stand for heavy and light states of two B_s^0 CP eigenstates and $\tau_{B_s^0} = \frac{1}{0.5(\Gamma_{B_{sH}^0}+\Gamma_{B_{sL}^0})}$.

$\Delta m_{B_s^0} = m_{B_{sH}^0} - m_{B_{sL}^0}$

$\Delta m_{B_s^0}$ is a measure of 2π times the B_s^0-$\overline{B}_s^0$ oscillation frequency in time-dependent mixing experiments.

"OUR EVALUATION" is an average using rescaled values of the data listed below. The average and rescaling were performed by the Heavy Flavor Averaging Group (HFAG) and are described at http://www.slac.stanford.edu/xorg/hfag/. The averaging/rescaling procedure takes into account corrections between the measurements.

VALUE (10^{12} $\hbar$ s^{-1})	CL%	DOCUMENT ID		TECN	COMMENT
>14.4 (CL = 95%) OUR EVALUATION					
> 5.0	95	[62] ABDALLAH	03B	DLPH	$e^+e^- \to Z$
>10.3	95	[63] ABE	03	SLD	$e^+e^- \to Z$
>10.9	95	[64] HEISTER	03E	ALEP	$e^+e^- \to Z$
> 5.3	95	[65] ABE	02V	SLD	$e^+e^- \to Z$
> 1.0	95	[66] ABBIENDI	01D	OPAL	$e^+e^- \to Z$
> 7.4	95	[67] ABREU	00Y	DLPH	$e^+e^- \to Z$
> 4.0	95	[68] ABREU,P	00G	DLPH	$e^+e^- \to Z$
> 5.2	95	[69] ABBIENDI	99S	OPAL	$e^+e^- \to Z$
> 5.8	95	[70] ABE	99J	CDF	$p\overline{p}$ at 1.8 TeV
• • • We do not use the following data for averages, fits, limits, etc. • • •					
<96	95	[71] ABE	99D	CDF	$p\overline{p}$ at 1.8 TeV
> 9.6	95	[72] BARATE	99J	ALEP	$e^+e^- \to Z$
> 7.9	95	[73] BARATE	98C	ALEP	Repl. by BARATE 99J
> 3.1	95	[74] ACKERSTAFF	97U	OPAL	Repl. by ABBIENDI 99S
> 2.2	95	[75] ACKERSTAFF	97V	OPAL	Repl. by ABBIENDI 99S
> 6.5	95	[76] ADAM	97	DLPH	Repl. by ABREU 00Y
> 6.6	95	[77] BUSKULIC	96M	ALEP	Repl. by BARATE 98C
> 2.2	95	[75] AKERS	95J	OPAL	Sup. by ACKERSTAFF 97V
> 5.7	95	[78] BUSKULIC	95J	ALEP	$e^+e^- \to Z$
> 1.8	95	[75] BUSKULIC	94B	ALEP	$e^+e^- \to Z$

[62] Events with a high transverse momentum lepton were removed and an inclusively reconstructed vertex was required.

[63] ABE 03 uses the novel "charge dipole" technique to reconstruct separate secondary and tertiary vertices originating from the $B \to D$ decay chain. The analysis excludes $\Delta m_s < 4.9\ ps^{-1}$ and $7.9 < \Delta m_s < 10.3\ ps^{-1}$.

[64] Three analyses based on complementary event selections: (1) fully-reconstructed hadronic decays; (2) semileptonic decays with D_s exclusively reconstructed; (3) inclusive semileptonic decays.

[65] ABE 02V uses exclusively reconstructed D_s^- mesons and excludes $\Delta m_s < 1.4\ ps^{-1}$ and $2.4 < \Delta m_s < 5.3\ ps^{-1}$ at 95%CL.

[66] Uses fully or partially reconstructed $D_s\ell$ vertices and a mixing tag as a flavor tagging.

[67] Uses $D_s^-\ell^+$, and $\phi\ell^+$ vertices, and a multi-variable discriminant as a flavor tagging.

[68] Uses inclusive D_s vertices and fully reconstructed B_s decays and a multi-variable discriminant as a flavor tagging.

[69] Uses ℓ-$Q_{\rm hem}$ and ℓ-ℓ.

[70] ABE 99J uses $\phi\ell$-ℓ correlation.

[71] ABE 99D assumes $\tau_{B_s^0} = 1.55 \pm 0.05$ ps and $\Delta\Gamma/\Delta m = (5.6 \pm 2.6) \times 10^{-3}$.

[72] BARATE 99J uses combination of an inclusive lepton and D_s^--based analyses.

[73] BARATE 98C combines results from $D_s h$-$\ell/Q_{\rm hem}$, $D_s h$-K in the same side, $D_s\ell$-$\ell/Q_{\rm hem}$ and $D_s\ell$-K in the same side.

[74] Uses ℓ-$Q_{\rm hem}$.

[75] Uses ℓ-ℓ.

[76] ADAM 97 combines results from $D_s\ell$-$Q_{\rm hem}$, ℓ-$Q_{\rm hem}$, and ℓ-ℓ.

[77] BUSKULIC 96M uses D_s lepton correlations and lepton, kaon, and jet charge tags.

[78] BUSKULIC 95J uses ℓ-$Q_{\rm hem}$. They find $\Delta m_s > 5.6$ [> 6.1] for f_s=10% [12%]. We interpolate to our central value f_s=10.5%.

$x_s = \Delta m_{B_s^0}/\Gamma_{B_s^0}$

This is derived by the Heavy Flavor Averaging Group (HFAG) from the results on $\Delta m_{B_s^0}$ and "OUR EVALUATION" of the B_s^0 mean lifetime.

VALUE	CL%	DOCUMENT ID
>20.6 (CL = 95%) OUR EVALUATION		

χ_s

This B_s^0-$\overline{B}_s^0$ integrated mixing parameter is derived from x_s above.

VALUE	CL%	DOCUMENT ID
>0.49883 (CL = 95%) OUR EVALUATION		

B_s^0 REFERENCES

ABDALLAH	03B	EPJ C28 155	J. Abdallah *et al.*	(DELPHI Collab.)
ABE	03	PR D67 012006	K. Abe *et al.*	(SLD Collab.)
HEISTER	03E	EPJ C29 143	A. Heister *et al.*	(ALEPH Collab.)
ABE	02V	PR D66 032009	K. Abe *et al.*	(SLD Collab.)
ACOSTA	02D	PR D65 111101R	D. Acosta *et al.*	(CDF Collab.)
ACOSTA	02G	PR D66 112002	D. Acosta *et al.*	(CDF Collab.)
ABBIENDI	01D	EPJ C19 241	G. Abbiendi *et al.*	(OPAL Collab.)
ABE	00C	PR D62 071101R	K. Abe *et al.*	(SLD Collab.)
ABREU	00Y	EPJ C16 555	P. Abreu *et al.*	(DELPHI Collab.)
ABREU,P	00G	EPJ C18 229	P. Abreu *et al.*	(DELPHI Collab.)
AFFOLDER	00N	PRL 85 4668	T. Affolder *et al.*	(CDF Collab.)
BARATE	00K	PL B486 286	R. Barate *et al.*	(ALEPH Collab.)
ABBIENDI	99S	EPJ C11 587	G. Abbiendi *et al.*	(OPAL Collab.)
ABE	99D	PR D59 032004	F. Abe *et al.*	(CDF Collab.)
ABE	99J	PRL 82 3576	F. Abe *et al.*	(CDF Collab.)
BARATE	99J	EPJ C7 553	R. Barate *et al.*	(ALEPH Collab.)
Also	00	EPJ C12 181 (erratum)	R. Barate *et al.*	(ALEPH Collab.)
ABE	98	PR D57 R3811	F. Abe *et al.*	(CDF Collab.)
ABE	98B	PR D57 5382	F. Abe *et al.*	(CDF Collab.)
ABE	98V	PRL 81 5742	F. Abe *et al.*	(CDF Collab.)
ACCIARRI	98S	PL B438 417	M. Acciarri *et al.*	(L3 Collab.)
ACKERSTAFF	98F	EPJ C2 407	K. Ackerstaff *et al.*	(OPAL Collab.)
ACKERSTAFF	98G	PL B426 161	K. Ackerstaff *et al.*	(OPAL Collab.)
BARATE	98C	EPJ C4 367	R. Barate *et al.*	(ALEPH Collab.)
BARATE	98Q	EPJ C4 387	R. Barate *et al.*	(ALEPH Collab.)
PDG	98	EPJ C3 1	C. Caso *et al.*	
ACCIARRI	97B	PL B391 474	M. Acciarri *et al.*	(L3 Collab.)
ACCIARRI	97C	PL B391 481	M. Acciarri *et al.*	(L3 Collab.)
ACKERSTAFF	97U	ZPHY C76 401	K. Ackerstaff *et al.*	(OPAL Collab.)
ACKERSTAFF	97V	ZPHY C76 417	K. Ackerstaff *et al.*	(OPAL Collab.)
ADAM	97	PL B414 382	W. Adam *et al.*	(DELPHI Collab.)
ABE	96B	PR D53 3496	F. Abe *et al.*	(CDF Collab.)
ABE	96L	PRL 76 4675	F. Abe *et al.*	(CDF Collab.)
ABE	96N	PRL 77 1945	F. Abe *et al.*	(CDF Collab.)
ABE	96Q	PR D54 6596	F. Abe *et al.*	(CDF Collab.)
ABREU	96F	ZPHY C71 11	P. Abreu *et al.*	(DELPHI Collab.)
ADAM	96D	ZPHY C72 207	W. Adam *et al.*	(DELPHI Collab.)
BUSKULIC	96E	ZPHY C69 585	D. Buskulic *et al.*	(ALEPH Collab.)
BUSKULIC	96M	PL B377 205	D. Buskulic *et al.*	(ALEPH Collab.)
BUSKULIC	96V	PL B384 471	D. Buskulic *et al.*	(ALEPH Collab.)
PDG	96	PR D54 1	R. M. Barnett *et al.*	
ABE	95R	PRL 74 4988	F. Abe *et al.*	(CDF Collab.)
ABE	95Z	PRL 75 3068	F. Abe *et al.*	(CDF Collab.)
ACCIARRI	95H	PL B363 127	M. Acciarri *et al.*	(L3 Collab.)
ACCIARRI	95I	PL B363 137	M. Acciarri *et al.*	(L3 Collab.)
AKERS	95G	PL B350 273	R. Akers *et al.*	(OPAL Collab.)
AKERS	95J	ZPHY C66 555	R. Akers *et al.*	(OPAL Collab.)
BUSKULIC	95J	PL B356 409	D. Buskulic *et al.*	(ALEPH Collab.)
BUSKULIC	95O	PL B361 221	D. Buskulic *et al.*	(ALEPH Collab.)
ABREU	94D	PL B324 500	P. Abreu *et al.*	(DELPHI Collab.)
ABREU	94E	ZPHY C61 407	P. Abreu *et al.*	(DELPHI Collab.)
Also	92M	PL B289 199	P. Abreu *et al.*	(DELPHI Collab.)
AKERS	94J	PL B337 196	R. Akers *et al.*	(OPAL Collab.)
AKERS	94L	PL B337 393	R. Akers *et al.*	(OPAL Collab.)
BUSKULIC	94B	PL B322 441	D. Buskulic *et al.*	(ALEPH Collab.)
BUSKULIC	94C	PL B322 275	D. Buskulic *et al.*	(ALEPH Collab.)
PDG	94	PR D50 1173	L. Montanet *et al.*	(CERN, LBL, BOST+)
ABE	93F	PRL 71 1685	F. Abe *et al.*	(CDF Collab.)
ACTON	93H	PL B312 501	P.D. Acton *et al.*	(OPAL Collab.)
BUSKULIC	93G	PL B311 425	D. Buskulic *et al.*	(ALEPH Collab.)
ABREU	92M	PL B289 199	P. Abreu *et al.*	(DELPHI Collab.)
ACTON	92N	PL B295 357	P.D. Acton *et al.*	(OPAL Collab.)
BUSKULIC	92E	PL B294 145	D. Buskulic *et al.*	(ALEPH Collab.)
LEE-FRANZINI	90	PRL 65 2947	J. Lee-Franzini *et al.*	(CUSB II Collab.)

Meson Particle Listings

B_s^*, $B_{sJ}^*(5850)$

B_s^*

$I(J^P) = 0(1^-)$

OMITTED FROM SUMMARY TABLE

I, J, P need confirmation. Quantum numbers shown are quark-model predictions.

B_s^* MASS

From mass difference below and the B_s^0 mass.

VALUE (MeV)	DOCUMENT ID
5416.6±3.5 OUR FIT	

$m_{B_s^*} - m_{B_s}$

VALUE (MeV)	DOCUMENT ID	TECN	COMMENT
47.0±2.6 OUR FIT			
47.0±2.6	[1] LEE-FRANZINI 90	CSB2	$e^+e^- \to \Upsilon(5S)$

[1] LEE-FRANZINI 90 measure 46.7 ± 0.4 ± 0.2 MeV for an admixture of B^0, B^+, and B_S. They use the shape of the photon line to separate the above value for B_S.

$\left|(m_{B_s^*} - m_{B_s}) - (m_{B^*} - m_B)\right|$

VALUE (MeV)	CL%	DOCUMENT ID		TECN	COMMENT
<6	95	ABREU	95R	DLPH	E_{cm}^{ee} = 88–94 GeV

B_s^* DECAY MODES

	Mode	Fraction (Γ_i/Γ)
Γ_1	$B_s\gamma$	dominant

B_s^* REFERENCES

ABREU 95R ZPHY C68 353 P. Abreu *et al.* (DELPHI Collab.)
LEE-FRANZINI 90 PRL 65 2947 J. Lee-Franzini *et al.* (CUSB II Collab.)

$B_{sJ}^*(5850)$

$I(J^P) = ?(?^?)$

I, J, P need confirmation.

OMITTED FROM SUMMARY TABLE

Signal can be interpreted as coming from $\overline{b}s$ states. Needs confirmation.

$B_{sJ}^*(5850)$ MASS

VALUE (MeV)	EVTS	DOCUMENT ID		TECN	COMMENT
5853±15	141	AKERS	95E	OPAL	E_{cm}^{ee} = 88–94 GeV

$B_{sJ}^*(5850)$ WIDTH

VALUE (MeV)	EVTS	DOCUMENT ID		TECN	COMMENT
47±22	141	AKERS	95E	OPAL	E_{cm}^{ee} = 88–94 GeV

$B_{sJ}^*(5850)$ REFERENCES

AKERS 95E ZPHY C66 19 R. Akers *et al.* (OPAL Collab.)

BOTTOM, CHARMED MESONS ($B = C = \pm 1$)

$B_c^+ = c\overline{b}$, $B_c^- = \overline{c}b$, similarly for B_c^{*}'s

$B_c^\pm$

$I(J^P) = 0(0^-)$

I, J, P need confirmation.

Quantum numbers shown are quark-model predictions.

$B_c^\pm$ MASS

VALUE (GeV)	DOCUMENT ID		TECN	COMMENT
6.4 ±0.39±0.13	[1] ABE	98M	CDF	$p\overline{p}$ 1.8 TeV
• • • We do not use the following data for averages, fits, limits, etc. • • •				
6.32±0.06	[2] ACKERSTAFF	98O	OPAL	$e^+e^- \to Z$

[1] ABE 98M observed $20.4^{+6.2}_{-5.5}$ events in the $B_c^+ \to J/\psi(1s)\ell\nu_\ell$ with a significance of > 4.8 standard deviations. The mass value is estimated from $m(J/\psi(1S)\ell)$.

[2] ACKERSTAFF 98O observed 2 candidate events in the $B_c \to J/\psi(1S)\pi^+$ channel with an estimated background of 0.63 ± 0.20 events.

$B_c^\pm$ MEAN LIFE

VALUE (10^{-12} s)	DOCUMENT ID		TECN	COMMENT
$0.46^{+0.18}_{-0.16}$ ±0.03	[3] ABE	98M	CDF	$p\overline{p}$ 1.8 TeV

[3] The lifetime is measured from the $J/\psi(1S)\ell$ decay vertices.

B_c^+ DECAY MODES × B($\overline{b} \to B_c$)

B_c^- modes are charge conjugates of the modes below.

	Mode	Fraction (Γ_i/Γ)	Confidence level
	The following quantities are not pure branching ratios; rather the fraction $\Gamma_i/\Gamma \times$ B($\overline{b} \to B_c$).		
Γ_1	$J/\psi(1S)\ell^+\nu_\ell$ anything	$(5.2^{+2.4}_{-2.1}) \times 10^{-5}$	
Γ_2	$J/\psi(1S)\pi^+$	$< 8.2 \times 10^{-5}$	90%
Γ_3	$J/\psi(1S)\pi^+\pi^+\pi^-$	$< 5.7 \times 10^{-4}$	90%
Γ_4	$J/\psi(1S)a_1(1260)$	$< 1.2 \times 10^{-3}$	90%
Γ_5	$D^*(2010)^+\overline{D}^0$	$< 6.2 \times 10^{-3}$	90%

B_c^+ BRANCHING RATIOS

$\Gamma(J/\psi(1S)\ell^+\nu_\ell \text{ anything})/\Gamma_{\text{total}} \times$ B($\overline{b} \to B_c$) — $\Gamma_1/\Gamma \times$ B

VALUE	CL%	DOCUMENT ID		TECN	COMMENT
$(5.2^{+2.4}_{-2.1}) \times 10^{-5}$		[4] ABE	98M	CDF	$p\overline{p}$ 1.8 TeV
• • • We do not use the following data for averages, fits, limits, etc. • • •					
$< 1.6 \times 10^{-4}$	90	[5] ACKERSTAFF	98O	OPAL	$e^+e^- \to Z$
$< 1.9 \times 10^{-4}$	90	[6] ABREU	97E	DLPH	$e^+e^- \to Z$
$< 1.2 \times 10^{-4}$	90	[7] BARATE	97H	ALEP	$e^+e^- \to Z$

[4] ABE 98M result is derived from the measurement of $[\sigma(B_c)\times$B$(B_c \to J/\psi(1S)\ell\nu_\ell)]$ / $[\sigma(B^+)\times$B$(B^+ \to J/\psi(1S)K^+)] = 0.132^{+0.041}_{-0.037}(\text{stat}) \pm 0.031(\text{sys})^{+0.032}_{-0.020}(\text{lifetime})$ by using PDG 98 values of B$(b \to B^+)$ and B$(B^+ \to J/\psi(1S)K^+)$.

[5] ACKERSTAFF 98O reports B$(Z \to B_c X)$/B$(Z \to q\overline{q})\times$B$(B_c \to J/\psi(1S)\ell\nu_\ell) < 6.95 \times 10^{-5}$ at 90%CL. We rescale to our PDG 98 values of B$(Z \to b\overline{b})$.

[6] ABREU 97E value listed is for an assumed $\tau_{B_c} = 0.4$ ps and improves to 1.6×10^{-4} for $\tau_{B_c} = 1.4$ ps.

[7] BARATE 97H reports B$(Z \to B_c X)$/B$(Z \to q\overline{q})\cdot$B$(B_c \to J/\psi(1S)\ell\nu_\ell) < 5.2\times 10^{-5}$ at 90%CL. We rescale to our PDG 96 values of B$(Z \to b\overline{b})$. A $B_c^+ \to J/\psi(1S)\mu^+\nu_\mu$ candidate event is found, compared to all the known background sources 2×10^{-3}, which gives $m_{B_c} = 5.96^{+0.25}_{-0.19}$ GeV and $\tau_{B_c} = 1.77 \pm 0.17$ ps.

$\Gamma(J/\psi(1S)\pi^+)/\Gamma_{\text{total}} \times$ B($\overline{b} \to B_c$) — $\Gamma_2/\Gamma \times$ B

VALUE	CL%	DOCUMENT ID		TECN	COMMENT
$< 8.2 \times 10^{-5}$	90	[8] BARATE	97H	ALEP	$e^+e^- \to Z$
• • • We do not use the following data for averages, fits, limits, etc. • • •					
$< 2.4 \times 10^{-4}$	90	[9] ACKERSTAFF	98O	OPAL	$e^+e^- \to Z$
$< 3.4 \times 10^{-4}$	90	[10] ABREU	97E	DLPH	$e^+e^- \to Z$
$< 2.0 \times 10^{-5}$	95	[11] ABE	96R	CDF	$p\overline{p}$ 1.8 TeV

[8] BARATE 97H reports B$(Z \to B_c X)$/B$(Z \to q\overline{q})\cdot$B$(B_c \to J/\psi(1S)\pi) < 3.6\times 10^{-5}$ at 90%CL. We rescale to our PDG 96 values of B$(Z \to b\overline{b})$.

[9] ACKERSTAFF 98O reports B$(Z \to B_c X)$/B$(Z \to q\overline{q})\times$B$(B_c \to J/\psi(1S)\pi^+) < 1.06 \times 10^{-4}$ at 90%CL. We rescale to our PDG 98 values of B$(Z \to b\overline{b})$.

[10] ABREU 97E value listed is for an assumed $\tau_{B_c} = 0.4$ ps and improves to 2.7×10^{-4} for $\tau_{B_c} = 1.4$ ps.

[11] ABE 96R reports B$(b \to B_c X)$/B$(b \to B^+ X)\cdot$B$(B_c^+ \to J/\psi(1S)\pi^+)$/B$(B^+ \to J/\psi(1S)K^+) < 0.053$ at 95%CL for $\tau_{B_c} = 0.8$ ps. It changes from 0.15 to 0.04 for $0.17 \text{ ps} < \tau_{B_c} < 1.6$ ps. We rescale to our PDG 96 values of B$(b \to B^+) = 0.378 \pm 0.022$ and B$(B^+ \to J/\psi(1S)K^+) = 0.00101 \pm 0.00014$.

$\Gamma(J/\psi(1S)\pi^+\pi^+\pi^-)/\Gamma_{\text{total}} \times$ B($\overline{b} \to B_c$) — $\Gamma_3/\Gamma \times$ B

VALUE	CL%	DOCUMENT ID		TECN	COMMENT
$< 5.7 \times 10^{-4}$	90	[12] ABREU	97E	DLPH	$e^+e^- \to Z$

[12] ABREU 97E value listed is independent of 0.4 ps$< \tau_{B_c} < 1.4$ ps.

$\Gamma(J/\psi(1S)a_1(1260))/\Gamma_{\text{total}} \times$ B($\overline{b} \to B_c$) — $\Gamma_4/\Gamma \times$ B

VALUE	CL%	DOCUMENT ID		TECN	COMMENT
$< 1.2 \times 10^{-3}$	90	[13] ACKERSTAFF	98O	OPAL	$e^+e^- \to Z$

[13] ACKERSTAFF 98O reports B$(Z \to B_c X)$/B$(Z \to q\overline{q})\times$B$(B_c \to J/\psi(1S)a_1(1260)) < 5.29 \times 10^{-4}$ at 90%CL. We rescale to our PDG 98 values of B$(Z \to b\overline{b})$.

$\Gamma(D^*(2010)^+\overline{D}^0)/\Gamma_{\text{total}} \times$ B($\overline{b} \to B_c$) — $\Gamma_5/\Gamma \times$ B

VALUE	CL%	DOCUMENT ID		TECN	COMMENT
$< 6.2 \times 10^{-3}$	90	[14] BARATE	98Q	ALEP	$e^+e^- \to Z$

[14] BARATE 98Q reports B$(Z \to B_c X)\times$B$(B_c \to D^*(2010)^+\overline{D}^0) < 1.9 \times 10^{-3}$ at 90%CL. We rescale to our PDG 98 values of B$(Z \to b\overline{b})$.

$B_c^\pm$ REFERENCES

ABE	98M	PRL 81 2432	F. Abe *et al.*	(CDF Collab.)
Also	98R	PR D58 112004	F. Abe *et al.*	(CDF Collab.)
ACKERSTAFF	98O	PL B420 157	K. Ackerstaff *et al.*	(OPAL Collab.)
BARATE	98Q	EPJ C4 387	R. Barate *et al.*	(ALEPH Collab.)
PDG	98	EPJ C3 1	C. Caso *et al.*	
ABREU	97E	PL B398 207	P. Abreu *et al.*	(DELPHI Collab.)
BARATE	97H	PL B402 213	R. Barate *et al.*	(ALEPH Collab.)
ABE	96R	PRL 77 5176	F. Abe *et al.*	(CDF Collab.)
PDG	96	PR D54 1	R. M. Barnett *et al.*	

$c\overline{c}$ MESONS

THE CHARMONIUM SYSTEM

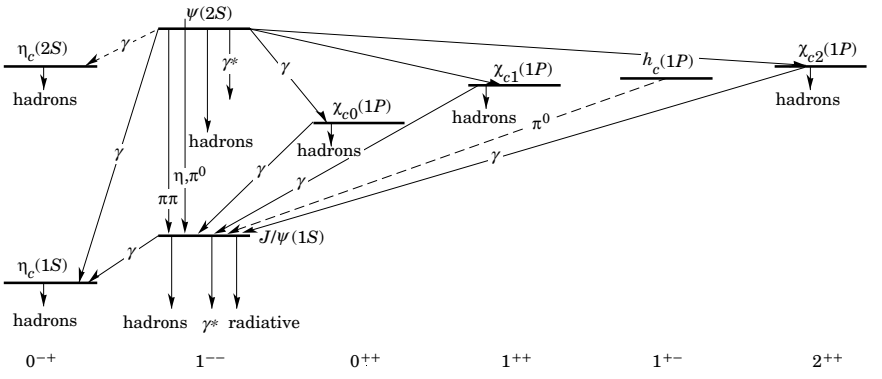

The current state of knowledge of the charmonium system and transitions, as interpreted by the charmonium model. Uncertain states and transitions are indicated by dashed lines. The notation γ^* refers to decay processes involving intermediate virtual photons, including decays to e^+e^- and $\mu^+\mu^-$.

$\eta_c(1S)$

$I^G(J^{PC}) = 0^+(0^{-+})$

$\eta_c(1S)$ MASS

VALUE (MeV)	EVTS	DOCUMENT ID		TECN	COMMENT
2979.6± 1.2 OUR AVERAGE		Error includes scale factor of 1.7. See the ideogram below.			
2984.1± 2.1± 1.0	190	[4] AMBROGIANI	03	E835	$\overline{p}p \to \eta_c \to \gamma\gamma$
2977.5± 1.0± 1.2		[1] BAI	03	BES	$J/\psi \to \gamma\eta_c$
2979.6± 2.3± 1.6	182± 25	FANG	03	BELL	$B \to \eta_c K$
2976.3± 2.3± 1.2		[5,6,7] BAI	00F	BES	$J/\psi \to \gamma\eta_c$ and $\psi(2S) \to \gamma\eta_c$
2980.4± 2.3± 0.6		BRANDENB...	00B	CLE2	$\gamma\gamma \to \eta_c \to K^\pm K^0_S \pi^\mp$
2999 ± 8	25	ABREU	98O	DLPH	$e^+e^- \to e^+e^-$ +hadrons
2988.3 $^{+\ 3.3}_{-\ 3.1}$		ARMSTRONG	95F	E760	$\overline{p}p \to \gamma\gamma$
2974.4± 1.9		[5] BISELLO	91	DM2	$J/\psi \to \eta_c\gamma$
2969 ± 4 ± 4	80	BAI	90B	MRK3	$J/\psi \to \gamma K^+K^-K^+K^-$
2982.6 $^{+\ 2.7}_{-\ 2.3}$	12	BAGLIN	87B	SPEC	$\overline{p}p \to \gamma\gamma$
2980.2± 1.6		[5] BALTRUSAIT...	86	MRK3	$J/\psi \to \eta_c\gamma$
2984 ± 2.3± 4.0		GAISER	86	CBAL	$J/\psi \to \gamma$X, $\psi(2S) \to \gamma$X
2982 ± 8	18	[2] HIMEL	80B	MRK2	e^+e^-
• • • We do not use the following data for averages, fits, limits, etc. • • •					
2976.6± 2.9± 1.3	140	[5,6] BAI	00F	BES	$J/\psi \to \gamma\eta_c$
2975.8± 3.9± 1.2		[5,6] BAI	99B	BES	Sup. by BAI 00F
2956 ±12 ±12		BAI	90B	MRK3	$J/\psi \to \gamma K^+K^-K^0_S K^0_L$
2976 ± 8		[3] BALTRUSAIT...	84	MRK3	$J/\psi \to 2\phi\gamma$
2980 ± 9		[2] PARTRIDGE	80B	CBAL	e^+e^-

[1] From a simultaneous fit of five decay modes of the η_c.
[2] Mass adjusted by us to correspond to $J/\psi(1S)$ mass = 3097 MeV.
[3] $\eta_c \to \phi\phi$.

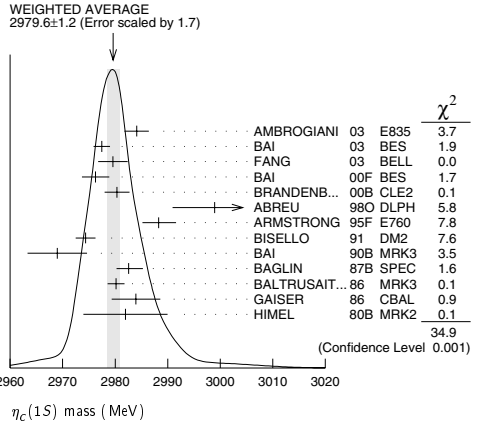

[4] Using mass of $\psi(2S) = 3686.00$ MeV.
[5] Average of several decay modes.
[6] Using an η_c width of 13.2 MeV.
[7] Weighted average of the $\psi(2S)$ and $J/\psi(1S)$ samples.

$\eta_c(1S)$ WIDTH

VALUE (MeV)	CL%	EVTS	DOCUMENT ID		TECN	COMMENT
17.3 $^{+\ 2.7}_{-\ 2.5}$ OUR AVERAGE			Error includes scale factor of 1.1.			
20.4 $^{+\ 7.7}_{-\ 6.7}$ ± 2.0		190	AMBROGIANI	03	E835	$\overline{p}p \to \eta_c \to \gamma\gamma$
17.0± 3.7± 7.4			[8] BAI	03	BES	$J/\psi \to \gamma\eta_c$
29 ± 8 ± 6		182± 25	FANG	03	BELL	$B \to \eta_c K$
11.0± 8.1± 4.1			[10] BAI	00F	BES	$J/\psi \to \gamma\eta_c$ and $\psi(2S) \to \gamma\eta_c$
27.0± 5.8± 1.4			BRANDENB...	00B	CLE2	$\gamma\gamma \to \eta_c \to K^\pm K^0_S \pi^\mp$
23.9 $^{+12.6}_{-\ 7.1}$			ARMSTRONG	95F	E760	$\overline{p}p \to \gamma\gamma$
7.0 $^{+\ 7.5}_{-\ 7.0}$		12	BAGLIN	87B	SPEC	$\overline{p}p \to \gamma\gamma$
10.1 $^{+33.0}_{-\ 8.2}$		23	[9] BALTRUSAIT...	86	MRK3	$J/\psi \to \gamma p\overline{p}$
11.5 ± 4.5			GAISER	86	CBAL	$J/\psi \to \gamma$X, $\psi(2S) \to \gamma$X
• • • We do not use the following data for averages, fits, limits, etc. • • •						

<40	90	18	HIMEL	80B	MRK2	e^+e^-
<20	90		PARTRIDGE	80B	CBAL	e^+e^-

[8] From a simultaneous fit of five decay modes of the η_c.

[9] Positive and negative errors correspond to 90% confidence level.

[10] From a fit to the 4-prong invariant mass in $\psi(2S) \to \gamma\eta_c$ and $J/\psi(1S) \to \gamma\eta_c$ decays.

$\eta_c(1S)$ DECAY MODES

	Mode	Fraction (Γ_i/Γ)		Confidence level
	Decays involving hadronic resonances			
Γ_1	$\eta'(958)\pi\pi$	(4.1 ±1.7) %		
Γ_2	$\rho\rho$	(2.6 ±0.9) %		
Γ_3	$K^*(892)^0 K^-\pi^+ +$ c.c.	(2.0 ±0.7) %		
Γ_4	$K^*(892)\overline{K}^*(892)$	(8.5 ±3.1) $\times 10^{-3}$		
Γ_5	$\phi K^+ K^-$	(2.9 ±1.4) $\times 10^{-3}$		
Γ_6	$\phi\phi$	(2.6 ±0.9) $\times 10^{-3}$		
Γ_7	$a_0(980)\pi$	< 2	%	90%
Γ_8	$a_2(1320)\pi$	< 2	%	90%
Γ_9	$K^*(892)\overline{K}+$ c.c.	< 1.28	%	90%
Γ_{10}	$f_2(1270)\eta$	< 1.1	%	90%
Γ_{11}	$\omega\omega$	< 3.1	$\times 10^{-3}$	90%
	Decays into stable hadrons			
Γ_{12}	$K\overline{K}\pi$	(5.7 ±1.6) %		
Γ_{13}	$\eta\pi\pi$	(4.9 ±1.8) %		
Γ_{14}	$\pi^+\pi^- K^+ K^-$	(1.5 ±0.6) %		
Γ_{15}	$2(K^+K^-)$	(1.5 ±0.7) $\times 10^{-3}$		
Γ_{16}	$2(\pi^+\pi^-)$	(1.20±0.30) %		
Γ_{17}	$p\overline{p}$	(1.3 ±0.4) $\times 10^{-3}$		
Γ_{18}	$K\overline{K}\eta$	< 3.1	%	90%
Γ_{19}	$\pi^+\pi^- p\overline{p}$	< 1.2	%	90%
Γ_{20}	$\Lambda\overline{\Lambda}$	< 2	$\times 10^{-3}$	90%
	Radiative decays			
Γ_{21}	$\gamma\gamma$	(4.3 ±1.5) $\times 10^{-4}$		

$\eta_c(1S)$ PARTIAL WIDTHS

$\Gamma(\gamma\gamma)$ Γ_{21}

VALUE (keV)	EVTS	DOCUMENT ID		TECN	COMMENT
7.4± 0.9± 2.1 OUR EVALUATION		Treating systematic errors as corrected.			
$7.0^{+1.0}_{-0.9}$ OUR AVERAGE					
13.9± 2.0± 3.0	41	[19] ABDALLAH	03J	DLPH	$\gamma\gamma \to \eta_c$
$3.8^{+1.1}_{-1.0}{}^{+1.9}_{-1.0}$	190	[11] AMBROGIANI	03	E835	$\overline{p}p \to \eta_c \to \gamma\gamma$
7.6± 0.8± 2.3		[12] BRANDENB...	00B	CLE2	$\gamma\gamma \to \eta_c \to K^\pm K^0_S \pi^\mp$
6.9± 1.7± 2.1	76	[13] ACCIARRI	99T	L3	$e^+e^- \to e^+e^-\eta_c$
27 ±16 ±10	5	[12] SHIRAI	98	AMY	58 e^+e^-
$6.7^{+2.4}_{-1.7}$± 2.3		[14] ARMSTRONG	95F	E760	$\overline{p}p \to \gamma\gamma$
11.3± 4.2		[15] ALBRECHT	94H	ARG	$e^+e^- \to e^+e^-\eta_c$
$5.9^{+2.1}_{-1.8}$± 1.9		[11] CHEN	90B	CLEO	$e^+e^- \to e^+e^-\eta_c$
$6.4^{+5.0}_{-3.4}$		[16] AIHARA	88D	TPC	$e^+e^- \to e^+e^-$X
$4.3^{+3.4}_{-3.7}$± 2.4		[14] BAGLIN	87B	SPEC	$\overline{p}p \to \gamma\gamma$
28 ±15		[12,17] BERGER	86	PLUT	$\gamma\gamma \to K\overline{K}\pi$
• • • We do not use the following data for averages, fits, limits, etc. • • •					
8.0± 2.3± 2.4	17	[18] ADRIANI	93N	L3	$e^+e^- \to e^+e^-\eta_c$

[11] Normalized to the sum of $B(\eta_c \to K^\pm K^0_S \pi^\mp)$, $B(\eta_c \to K^+K^-\pi^+\pi^-)$, and $B(\eta_c \to 2\pi^+2\pi^-)$.

[12] Normalized to $B(\eta_c \to K^\pm K^0_S \pi^\mp)$.

[13] Normalized to the sum of 9 branching ratios.

[14] Normalized to $B(\eta_c \to p\overline{p}) = (1.2 \pm 0.4) \times 10^{-3}$.

[15] Normalized to the sum of $B(\eta_c \to K^\pm K^0_S \pi^\mp)$, $B(\eta_c \to \phi\phi)$, $B(\eta_c \to K^+K^-\pi^+\pi^-)$, and $B(\eta_c \to 2\pi^+2\pi^-)$.

[16] Normalized to the sum of $B(\eta_c \to K^\pm K^0_S \pi^\mp)$, $B(\eta_c \to 2K^+2K^-)$, $B(\eta_c \to K^+K^-\pi^+\pi^-)$, and $B(\eta_c \to 2\pi^+2\pi^-)$.

[17] Re-evaluated by AIHARA 88D.

[18] Superseded by ACCIARRI 99T.

[19] Average of $K^0_S K^\pm\pi^\mp$, $\pi^+\pi^- K^+K^-$, and $2(K^+K^-)$ decay modes.

$\eta_c(1S)\,\Gamma(i)\Gamma(\gamma\gamma)/\Gamma(\text{total})$

$\Gamma(K\overline{K}\pi) \times \Gamma(\gamma\gamma)/\Gamma_{\text{total}}$ $\Gamma_{12}\Gamma_{21}/\Gamma$

VALUE (keV)	CL%	EVTS	DOCUMENT ID		TECN	COMMENT
0.48 ±0.06 OUR AVERAGE			Error includes scale factor of 1.3. See the ideogram below.			
0.60 ±0.12 ±0.09		41	[20,21] ABDALLAH	03J	DLPH	$\gamma\gamma \to K^0_S K^\pm\pi^\mp$
0.418±0.044±0.022			[21] BRANDENB...	00B	CLE2	$\gamma\gamma \to \eta_c \to K^\pm K^0_S \pi^\mp$
1.47 ±0.87 ±0.27			[21] SHIRAI	98	AMY	$\gamma\gamma \to \eta_c \to K^\pm K^0_S \pi^\mp$
0.84 ±0.21			[21] ALBRECHT	94H	ARG	$\gamma\gamma \to K^\pm K^0_S \pi^\mp$
$0.60^{+0.23}_{-0.20}$			[21] CHEN	90B	CLEO	$\gamma\gamma \to \eta_c K^\pm K^0_S \pi^\mp$
1.06 ±0.41 ±0.27		11	[21] BRAUNSCH...	89	TASS	$\gamma\gamma \to K\overline{K}\pi$
1.5 $^{+0.60}_{-0.45}$ ±0.3		7	[21] BERGER	86	PLUT	$\gamma\gamma \to K\overline{K}\pi$
• • • We do not use the following data for averages, fits, limits, etc. • • •						
<0.63	95		[21] BEHREND	89	CELL	$\gamma\gamma \to K^0_S K^\pm\pi^\mp$
<4.4	95		ALTHOFF	85B	TASS	$\gamma\gamma \to K\overline{K}\pi$

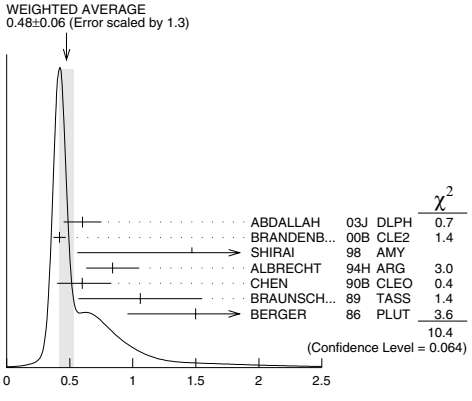

$\Gamma(K\overline{K}\pi) \times \Gamma(\gamma\gamma)/\Gamma_{\text{total}}$ $\Gamma_{12}\Gamma_{21}/\Gamma$

$\Gamma(\pi^+\pi^- K^+K^-) \times \Gamma(\gamma\gamma)/\Gamma_{\text{total}}$ $\Gamma_{14}\Gamma_{21}/\Gamma$

VALUE (keV)	EVTS	DOCUMENT ID		TECN	COMMENT
0.21±0.07 OUR AVERAGE					
0.28±0.10±0.06	42	[22] ABDALLAH	03J	DLPH	$\gamma\gamma \to \pi^+\pi^- K^+K^-$
0.17±0.08±0.02	13.9± 6.6	ALBRECHT	94H	ARG	$\gamma\gamma \to \pi^+\pi^- K^+K^-$

$\Gamma(2(K^+K^-)) \times \Gamma(\gamma\gamma)/\Gamma_{\text{total}}$ $\Gamma_{15}\Gamma_{21}/\Gamma$

VALUE (keV)	EVTS	DOCUMENT ID		TECN	COMMENT
0.28 ±0.07 OUR AVERAGE					
0.35 ±0.09 ±0.06	46	[23] ABDALLAH	03J	DLPH	$\gamma\gamma \to 2(K^+K^-)$
0.231±0.090±0.023	9.1 ± 3.3	[24] ALBRECHT	94H	ARG	$\gamma\gamma \to 2(K^+K^-)$

$\Gamma(2(\pi^+\pi^-)) \times \Gamma(\gamma\gamma)/\Gamma_{\text{total}}$ $\Gamma_{16}\Gamma_{21}/\Gamma$

VALUE (keV)	EVTS	DOCUMENT ID	TECN	COMMENT
0.18±0.07±0.02	21.4 ± 8.6	ALBRECHT 94H	ARG	$\gamma\gamma \to 2(\pi^+\pi^-)$

[20] Calculated by us from the value reported in ABDALLAH 03J, which uses $B(\eta_c \to K^0_S K^\pm\pi^\mp) = (1.5 \pm 0.4)\%$.

[21] We have multiplied $K^\pm K^0_S \pi^\mp$ measurement by 3 to obtain $K\overline{K}\pi$.

[22] Calculated by us from the value reported in ABDALLAH 03J, which uses $B(\eta_c \to \pi^+\pi^- K^+K^-) = (2.0 \pm 0.7)\%$.

[23] Calculated by us from the value reported in ABDALLAH 03J, which uses $B(\eta_c \to 2(K^+K^-)) = (2.1 \pm 1.2)\%$.

[24] Incudes all topological modes except $\eta_c \to \phi\phi$.

$\eta_c(1S)$ BRANCHING RATIOS

HADRONIC DECAYS

$\Gamma(\eta'(958)\pi\pi)/\Gamma_{\text{total}}$ Γ_1/Γ

VALUE	EVTS	DOCUMENT ID		TECN	COMMENT
0.041±0.017	14	[25] BALTRUSAIT...86		MRK3	$J/\psi \to \eta_c\gamma$

$\Gamma(\rho\rho)/\Gamma_{\text{total}}$ Γ_2/Γ

VALUE (units 10^{-3})	CL%	EVTS	DOCUMENT ID		TECN	COMMENT
26 ± 9 OUR EVALUATION (Treating systematicerrors as correlated.)						
25 ± 8 OUR AVERAGE						
26.0 ± 2.4 ± 8.8		113	[25] BISELLO	91	DM2	$J/\psi \to \gamma\rho^0\rho^0$
23.6 ± 10.6 ± 8.2		32	[25] BISELLO	91	DM2	$J/\psi \to \gamma\rho^+\rho^-$
• • • We do not use the following data for averages, fits, limits, etc. • • •						
< 14	90		[25] BALTRUSAIT...86		MRK3	$J/\psi \to \eta_c\gamma$

$\Gamma(K^*(892)^0 K^-\pi^+ + \text{c.c.})/\Gamma_{\text{total}}$ Γ_3/Γ

VALUE	EVTS	DOCUMENT ID		TECN	COMMENT
0.02 ± 0.007	63	[25] BALTRUSAIT...86		MRK3	$J/\psi \to \eta_c\gamma$

$\Gamma(K^*(892)\overline{K}^*(892))/\Gamma_{\text{total}}$ Γ_4/Γ

VALUE (units 10^{-4})	EVTS	DOCUMENT ID		TECN	COMMENT
85 ± 31 OUR AVERAGE					
82 ± 28 ± 27	14	[25] BISELLO	91	DM2	$e^+e^- \to \gamma K^+K^-\pi^+\pi^-$
90 ± 50	9	[25] BALTRUSAIT...86		MRK3	$J/\psi \to \eta_c\gamma$

$\Gamma(K^*(892)\overline{K} + \text{c.c.})/\Gamma_{\text{total}}$ Γ_9/Γ

VALUE	CL%	DOCUMENT ID		TECN	COMMENT
< 0.0128	90	BISELLO	91	DM2	$J/\psi \to \gamma K^0_S K^\pm\pi^\mp$
< 0.0132	90	[25] BISELLO	91	DM2	$J/\psi \to \gamma K^+K^-\pi^0$

$\Gamma(\phi K^+K^-)/\Gamma_{\text{total}}$ Γ_5/Γ

VALUE (units 10^{-3})	EVTS	DOCUMENT ID		TECN	COMMENT
$\mathbf{2.9^{+0.9}_{-0.8} \pm 1.1}$	$14.1^{+4.4}_{-3.7}$	[26] HUANG	03	BELL	$B^+ \to (\phi K^+K^-)\,K^+$

$\Gamma(\phi\phi)/\Gamma_{\text{total}}$ Γ_6/Γ

VALUE (units 10^{-4})	EVTS	DOCUMENT ID		TECN	COMMENT
26 ± 9 OUR EVALUATION (Treating systematic errors as correlated.)					
28 ± 5 OUR AVERAGE					
26 ± 9	357 ± 64	[25] BAI	04	BES	$J/\psi \to \gamma K^+K^-K^+K^-$
$18^{+8}_{-6} \pm 7$	$7.0^{+3.0}_{-2.3}$	[26] HUANG	03	BELL	$B^+ \to (\phi\phi)\,K^+$
31 ± 7 ± 10	19	[25] BISELLO	91	DM2	$J/\psi \to \gamma K^+K^-K^+K^-$
$30^{+18}_{-12} \pm 10$	5	[25] BISELLO	91	DM2	$J/\psi \to \gamma K^+K^-K^0_S K^0_L$
74 ± 18 ± 24	80	[25] BAI	90B	MRK3	$J/\psi \to \gamma K^+K^-K^+K^-$
67 ± 21 ± 24		[25] BAI	90B	MRK3	$J/\psi \to \gamma K^+K^-K^0_S K^0_L$

$\Gamma(a_0(980)\pi)/\Gamma_{\text{total}}$ Γ_7/Γ

VALUE	CL%	DOCUMENT ID		TECN	COMMENT
< 0.02	90	[25,27] BALTRUSAIT...86		MRK3	$J/\psi \to \eta_c\gamma$

$\Gamma(a_2(1320)\pi)/\Gamma_{\text{total}}$ Γ_8/Γ

VALUE	CL%	DOCUMENT ID		TECN	COMMENT
< 0.02	90	[25] BALTRUSAIT...86		MRK3	$J/\psi \to \eta_c\gamma$

$\Gamma(f_2(1270)\eta)/\Gamma_{\text{total}}$ Γ_{10}/Γ

VALUE	CL%	DOCUMENT ID		TECN	COMMENT
< 0.011	90	[25] BALTRUSAIT...86		MRK3	$J/\psi \to \eta_c\gamma$

$\Gamma(\omega\omega)/\Gamma_{\text{total}}$ Γ_{11}/Γ

VALUE	CL%	DOCUMENT ID		TECN	COMMENT
< 0.0031	90	[25] BALTRUSAIT...86		MRK3	$J/\psi \to \eta_c\gamma$
• • • We do not use the following data for averages, fits, limits, etc. • • •					
< 0.0063		[25] BISELLO	91	DM2	$J/\psi \to \eta_c\omega\omega$

$\Gamma(K\overline{K}\pi)/\Gamma_{\text{total}}$ Γ_{12}/Γ

VALUE	CL%	EVTS	DOCUMENT ID		TECN	COMMENT
0.057 ± 0.016 OUR EVALUATION (Treating systematic errors as correlated.)						
0.056 ± 0.008 OUR AVERAGE						
0.051 ± 0.021		609 ± 71	[25] BAI	04	BES	$J/\psi \to \gamma K^\pm\pi^\mp K^0_S$
0.0690 ± 0.0142 ± 0.0132		33	[25] BISELLO	91	DM2	$J/\psi \to \gamma K^+K^-\pi^0$
0.0543 ± 0.0094 ± 0.0094		68	[25] BISELLO	91	DM2	$J/\psi \to \gamma K^\pm\pi^\mp K^0_S$
0.048 ± 0.017		95	[25,28] BALTRUSAIT...86		MRK3	$J/\psi \to \eta_c\gamma$
$0.161^{+0.092}_{-0.073}$			[29] HIMEL	80B	MRK2	$\psi(2S) \to \eta_c\gamma$
• • • We do not use the following data for averages, fits, limits, etc. • • •						
< 0.107	90		[25] PARTRIDGE	80B	CBAL	$J/\psi \to \eta_c\gamma$

$\Gamma(\eta\pi\pi)/\Gamma_{\text{total}}$ Γ_{13}/Γ

VALUE	EVTS	DOCUMENT ID		TECN	COMMENT
0.049 ± 0.018 OUR EVALUATION					
0.047 ± 0.015 OUR AVERAGE					
0.054 ± 0.020	75	[25] BALTRUSAIT...86		MRK3	$J/\psi \to \eta_c\gamma$
0.037 ± 0.013 ± 0.020	18	[25] PARTRIDGE	80B	CBAL	$J/\psi \to \eta\pi^+\pi^-\gamma$

$\Gamma(\pi^+\pi^-K^+K^-)/\Gamma_{\text{total}}$ Γ_{14}/Γ

VALUE	EVTS	DOCUMENT ID		TECN	COMMENT
0.015 ± 0.006 OUR EVALUATION					
0.0142 ± 0.0033 OUR AVERAGE					
0.012 ± 0.004	413 ± 54	[25] BAI	04	BES	$J/\psi \to \gamma K^+K^-\pi^+\pi^-$
0.021 ± 0.007	110	[25] BALTRUSAIT...86		MRK3	$J/\psi \to \eta_c\gamma$
$0.014^{+0.022}_{-0.009}$		[29] HIMEL	80B	MRK2	$\psi(2S) \to \eta_c\gamma$

$\Gamma(2(\pi^+\pi^-))/\Gamma_{\text{total}}$ Γ_{16}/Γ

VALUE	EVTS	DOCUMENT ID		TECN	COMMENT
0.012 ± 0.003 OUR EVALUATION					
0.0115 ± 0.0026 OUR AVERAGE					
0.010 ± 0.005	542 ± 75	[25] BAI	04	BES	$J/\psi \to \gamma 2(\pi^+\pi^-)$
0.0105 ± 0.0017 ± 0.0034	137	[25] BISELLO	91	DM2	$J/\psi \to \gamma 2\pi^+2\pi^-$
0.013 ± 0.006	25	[25] BALTRUSAIT...86		MRK3	$J/\psi \to \eta_c\gamma$
$0.020^{+0.015}_{-0.010}$		[29] HIMEL	80B	MRK2	$\psi(2S) \to \eta_c\gamma$

$\Gamma(2(K^+K^-))/\Gamma_{\text{total}}$ Γ_{15}/Γ

VALUE	EVTS	DOCUMENT ID		TECN	COMMENT
0.0015 ± 0.0007 OUR AVERAGE					
$0.0014^{+0.0005}_{-0.0004} \pm 0.0006$	$14.5^{+4.6}_{-3.0}$	[26] HUANG	03	BELL	$B^+ \to 2(K^+K^-)\,K^+$
0.021 ± 0.010 ± 0.006		[30] ALBRECHT	94H	ARG	$\gamma\gamma \to K^+K^-K^+K^-$

$\Gamma(p\overline{p})/\Gamma_{\text{total}}$ Γ_{17}/Γ

VALUE (units 10^{-4})	EVTS	DOCUMENT ID		TECN	COMMENT
13 ± 4 OUR EVALUATION (Treating systematic errors as correlated.)					
12.5 ± 3.2 OUR AVERAGE					
15 ± 6	213 ± 33	[25] BAI	04	BES	$J/\psi \to \gamma p\overline{p}$
10 ± 3 ± 4	18	[25] BISELLO	91	DM2	$J/\psi \to \gamma p\overline{p}$
11 ± 6	23	[25] BALTRUSAIT...86		MRK3	$J/\psi \to \eta_c\gamma$
29^{+29}_{-15}		[29] HIMEL	80B	MRK2	$\psi(2S) \to \eta_c\gamma$

$\Gamma(K\overline{K}\eta)/\Gamma_{\text{total}}$ Γ_{18}/Γ

VALUE	CL%	DOCUMENT ID		TECN	COMMENT
< 0.031	90	[25] BALTRUSAIT...86		MRK3	$J/\psi \to \eta_c\gamma$

$\Gamma(\pi^+\pi^-p\overline{p})/\Gamma_{\text{total}}$ Γ_{19}/Γ

VALUE	CL%	DOCUMENT ID		TECN	COMMENT
< 0.012	90	HIMEL	80B	MRK2	$\psi(2S) \to \eta_c\gamma$

$\Gamma(\Lambda\overline{\Lambda})/\Gamma_{\text{total}}$ Γ_{20}/Γ

VALUE	CL%	DOCUMENT ID		TECN	COMMENT
< 0.002	90	[25] BISELLO	91	DM2	$e^+e^- \to \gamma\Lambda\overline{\Lambda}$

$\Gamma_i\Gamma_f/\Gamma^2_{\text{total}}$ in $p\overline{p} \to \eta_c(1S) \to \phi\phi$ $\Gamma_{17}\Gamma_6/\Gamma^2$

VALUE (units 10^{-5})	DOCUMENT ID		TECN	COMMENT
$\mathbf{4.0^{+3.5}_{-3.2}}$	BAGLIN	89	SPEC	$\overline{p}p \to K^+K^-K^+K^-$

[25] The quoted branching ratios use $B(J/\psi(1S) \to \gamma\eta_c(1S)) = 0.0127 \pm 0.0036$. Where relevant, the error in this branching ratio is treated as a common systematic in computing averages.

[26] Using $B(B^+ \to \eta_c K^+) = (1.25 \pm 0.12^{+0.10}_{-0.12}) \times 10^{-3}$ from FANG 03 and $B(\eta_c \to K\overline{K}\pi) = (5.5 \pm 1.7) \times 10^{-2}$.

[27] We are assuming $B(a_0(980) \to \eta\pi) > 0.5$.

[28] Average from $K^+K^-\pi^0$ and $K^\pm K^0_S\pi^\mp$ decay channels.

[29] Estimated using $B(\psi(2S) \to \gamma\eta_c(1S)) = 0.0028 \pm 0.0006$.

[30] Normalized to the sum of $B(\eta_c \to K^\pm K^0_S\pi^\mp)$, $B(\eta_c \to \phi\phi)$, $B(\eta_c \to K^+K^-\pi^+\pi^-)$, and $B(\eta_c \to 2\pi^+2\pi^-)$.

RADIATIVE DECAYS

$\Gamma(\gamma\gamma)/\Gamma_{\text{total}}$ Γ_{21}/Γ

VALUE (units 10^{-4})	CL%	DOCUMENT ID		TECN	COMMENT
• • • We do not use the following data for averages, fits, limits, etc. • • •					
$2.80^{+0.67}_{-0.58} \pm 1.0$		[31] ARMSTRONG	95F	E760	$\overline{p}p \to \gamma\gamma$
< 9	90	[25] BISELLO	91	DM2	$J/\psi \to \gamma\gamma\gamma$
$6^{+4}_{-3} \pm 4$		[31] BAGLIN	87B	SPEC	$\overline{p}p \to \gamma\gamma$
< 18	90	[32] BLOOM	83	CBAL	$J/\psi \to \eta_c\gamma$

[31] Not independent from the values of the total and two-photon width quoted by the same experiment.

[32] Using $B(J/\psi(1S) \to \gamma\eta_c(1S)) = 0.0127 \pm 0.0036$.

$\Gamma_i\Gamma_f/\Gamma^2_{\rm total}$ in $p\overline{p}\to\eta_c(1S)\to\gamma\gamma$ $\quad\Gamma_{17}\Gamma_{21}/\Gamma^2$

VALUE (units 10^{-6})	EVTS	DOCUMENT ID		TECN	COMMENT
0.26 ±0.05 OUR AVERAGE		Error includes scale factor of 1.4.			
$0.224^{+0.038}_{-0.037}\pm0.020$	190	AMBROGIANI	03	E835	$\overline{p}p\to\eta_c\to\gamma\gamma$
$0.336^{+0.080}_{-0.070}$		ARMSTRONG	95F	E760	$\overline{p}p\to\gamma\gamma$
$0.68\ ^{+0.42}_{-0.31}$	12	BAGLIN	87B	SPEC	$\overline{p}p\to\gamma\gamma$

$\eta_c(1S)$ REFERENCES

BAI	04	PL B578 16	J.Z. Bai *et al.*	(BES Collab.)
ABDALLAH	03J	EPJ C31 481	J. Abdallah *et al.*	(DELPHI Collab.)
AMBROGIANI	03	PL B566 45	M. Ambrogiani *et al.*	(FNAL E835 Collab.)
BAI	03	PL B555 174	J.Z. Bai *et al.*	(BES Collab.)
FANG	03	PRL 90 071801	F. Fang *et al.*	(BELLE Collab.)
HUANG	03	PRL 91 241802	H.-C. Huang *et al.*	(BELLE Collab.)
BAI	00F	PR D62 072001	J.Z. Bai *et al.*	(BES Collab.)
BRANDENB...	00B	PRL 85 3095	G. Brandenburg *et al.*	(CLEO Collab.)
ACCIARRI	99T	PL B461 155	M. Acciarri *et al.*	(L3 Collab.)
BAI	99B	PR D60 072001	J.Z. Bai *et al.*	(BES Collab.)
ABREU	98O	PL B441 479	P. Abreu *et al.*	(DELPHI Collab.)
SHIRAI	98	PL B424 405	M. Shirai *et al.*	(AMY Collab.)
ARMSTRONG	95F	PR D52 4839	T.A. Armstrong *et al.*	(FNAL, FERR, GENO+)
ALBRECHT	94H	PL B338 390	H. Albrecht *et al.*	(ARGUS Collab.)
ADRIANI	93N	PL B318 575	O. Adriani *et al.*	(L3 Collab.)
BISELLO	91	NP B350 1	D. Bisello *et al.*	(DM2 Collab.)
BAI	90B	PRL 65 1309	Z. Bai *et al.*	(Mark III Collab.)
CHEN	90B	PL B243 169	W.Y. Chen *et al.*	(CLEO Collab.)
BAGLIN	89	PL B231 557	C. Baglin, S. Baird, G. Bassompierre	(R704 Collab.)
BEHREND	89	ZPHY C42 367	H.J. Behrend *et al.*	(CELLO Collab.)
BRAUNSCH...	89	ZPHY C41 533	W. Braunschweig *et al.*	(TASSO Collab.)
AIHARA	88D	PRL 60 2355	H. Aihara *et al.*	(TPC Collab.)
BAGLIN	87B	PL B187 191	C. Baglin *et al.*	(R704 Collab.)
BALTRUSAIT...	86	PR D33 629	R.M. Baltrusaitis *et al.*	(Mark III Collab.)
BERGER	86	PL 167B 120	C. Berger *et al.*	(PLUTO Collab.)
GAISER	86	PR D34 711	J. Gaiser *et al.*	(Crystal Ball Collab.)
ALTHOFF	85B	ZPHY C29 189	M. Althoff *et al.*	(TASSO Collab.)
BALTRUSAIT...	84	PRL 52 2126	R.M. Baltrusaitis *et al.*	(CIT, UCSC+) J/P
BLOOM	83	ARNS 33 143	E.D. Bloom, C. Peck	(SLAC, CIT)
HIMEL	80B	PRL 45 1146	T.M. Himel *et al.*	(SLAC, LBL, UCB)
PARTRIDGE	80B	PRL 45 1150	R. Partridge *et al.*	(CIT, HARV, PRIN+)

OTHER RELATED PAPERS

ARMSTRONG	89	PL B221 216	T.A. Armstrong *et al.*	(CERN, CDEF, BIRM+)

$J/\psi(1S)$

$I^G(J^{PC}) = 0^-(1^{--})$

$J/\psi(1S)$ MASS

VALUE (MeV)	EVTS	DOCUMENT ID		TECN	COMMENT
3096.916±0.011 OUR AVERAGE					
3096.917±0.010±0.007		AULCHENKO	03	KEDR	$e^+e^-\to$ hadrons
3096.89 ±0.09	502	[1] ARTAMONOV	00	OLYA	$e^+e^-\to$ hadrons
3096.91 ±0.03 ±0.01		[2] ARMSTRONG	93B	E760	$\overline{p}p\to e^+e^-$
3096.95 ±0.1 ±0.3	193	BAGLIN	87	SPEC	$\overline{p}p\to e^+e^-X$
• • • We do not use the following data for averages, fits, limits, etc. • • •					
3097.5 ±0.3		GRIBUSHIN	96	FMPS	515 π^- Be $\to 2\mu X$
3098.4 ±2.0	38k	LEMOIGNE	82	GOLI	190 π^- Be $\to 2\mu$
3096.93 ±0.09	502	[3] ZHOLENTZ	80	REDE	e^+e^-
3097.0 ±1		[4] BRANDELIK	79C	DASP	e^+e^-

[1] Reanalysis of ZHOLENTZ 80 using new electron mass (COHEN 87) and radiative corrections (KURAEV 85).

[2] Mass central value and systematic error recalculated by us according to Eq. (16) in ARMSTRONG 93B, using the value for the $\psi(2S)$ mass from AULCHENKO 03.

[3] Superseded by ARTAMONOV 00.

[4] From a simultaneous fit to e^+e^-, $\mu^+\mu^-$ and hadronic channels assuming $\Gamma(e^+e^-) = \Gamma(\mu^+\mu^-)$.

$J/\psi(1S)$ WIDTH

VALUE (keV)	EVTS	DOCUMENT ID		TECN	COMMENT
91.0± 3.2 OUR AVERAGE					
94.7± 4.4	7.8k	[5] AUBERT	04	BABR	$e^+e^-\to\mu^+\mu^-\gamma$
84.4± 8.9		BAI	95B	BES	e^+e^-
99 ±12 ±6		ARMSTRONG	93B	E760	$\overline{p}p\to e^+e^-$
$85.5^{+6.1}_{-5.8}$		[6] HSUEH	92	RVUE	See Υ mini-review

[5] From a direct measurement of $\Gamma(e^+e^-)\times B(\mu^+\mu^-)$.

[6] Using data from COFFMAN 92, BALDINI-CELIO 75, BOYARSKI 75, ESPOSITO 75B, BRANDELIK 79C.

$J/\psi(1S)$ DECAY MODES

	Mode	Fraction (Γ_i/Γ)	Scale factor/ Confidence level
Γ_1	hadrons	(87.7 ±0.5) %	
Γ_2	virtual$\gamma\to$ hadrons	(17.0 ±2.0) %	
Γ_3	e^+e^-	(5.93±0.10) %	
Γ_4	$\mu^+\mu^-$	(5.88±0.10) %	

Decays involving hadronic resonances

Γ_5	$\rho\pi$		(1.27±0.09) %		
Γ_6	$\rho^0\pi^0$		(4.2 ±0.5) $\times10^{-3}$		
Γ_7	$a_2(1320)\rho$		(1.09±0.22) %		
Γ_8	$\omega\pi^+\pi^+\pi^-\pi^-$		(8.5 ±3.4) $\times10^{-3}$		
Γ_9	$\omega\pi^+\pi^-$		(7.2 ±1.0) $\times10^{-3}$		
Γ_{10}	$\omega f_2(1270)$		(4.3 ±0.6) $\times10^{-3}$		
Γ_{11}	$K^*(892)^0\overline{K}{}^*_2(1430)^0$ + c.c.		(6.7 ±2.6) $\times10^{-3}$		
Γ_{12}	$\omega K^*(892)\overline{K}$ + c.c.		(5.3 ±2.0) $\times10^{-3}$		
Γ_{13}	$K^+\overline{K}{}^*(892)^-$ + c.c.		(5.0 ±0.4) $\times10^{-3}$		
Γ_{14}	$K^0\overline{K}{}^*(892)^0$ + c.c.		(4.2 ±0.4) $\times10^{-3}$		
Γ_{15}	$K_1(1400)^\pm K^\mp$		(3.8 ±1.4) $\times10^{-3}$		
Γ_{16}	$\omega\pi^0\pi^0$		(3.4 ±0.8) $\times10^{-3}$		
Γ_{17}	$b_1(1235)^\pm\pi^\mp$	[a]	(3.0 ±0.5) $\times10^{-3}$		
Γ_{18}	$\omega K^\pm K^0_S\pi^\mp$	[a]	(2.9 ±0.7) $\times10^{-3}$		
Γ_{19}	$b_1(1235)^0\pi^0$		(2.3 ±0.6) $\times10^{-3}$		
Γ_{20}	$\phi K^*(892)\overline{K}$ + c.c.		(2.04±0.28) $\times10^{-3}$		
Γ_{21}	$\omega K\overline{K}$		(1.9 ±0.4) $\times10^{-3}$		
Γ_{22}	$\omega f_0(1710)\to\omega K\overline{K}$		(4.8 ±1.1) $\times10^{-4}$		
Γ_{23}	$\phi2(\pi^+\pi^-)$		(1.60±0.32) $\times10^{-3}$		
Γ_{24}	$\Delta(1232)^{++}\overline{p}\pi^-$		(1.6 ±0.5) $\times10^{-3}$		
Γ_{25}	$\omega\eta$		(1.58±0.16) $\times10^{-3}$		
Γ_{26}	$\phi K\overline{K}$		(1.54±0.21) $\times10^{-3}$		
Γ_{27}	$\phi f_0(1710)\to\phi K\overline{K}$		(3.6 ±0.6) $\times10^{-4}$		
Γ_{28}	$p\overline{p}\omega$		(1.30±0.25) $\times10^{-3}$		S=1.3
Γ_{29}	$\Delta(1232)^{++}\overline{\Delta}(1232)^{--}$		(1.10±0.29) $\times10^{-3}$		
Γ_{30}	$\Sigma(1385)^-\overline{\Sigma}(1385)^+$ (or c.c.)	[a]	(1.03±0.13) $\times10^{-3}$		
Γ_{31}	$p\overline{p}\eta'(958)$		(9 ±4) $\times10^{-4}$		S=1.7
Γ_{32}	$\phi f'_2(1525)$		(8 ±4) $\times10^{-4}$		S=2.7
Γ_{33}	$\phi\pi^+\pi^-$		(8.0 ±1.2) $\times10^{-4}$		
Γ_{34}	$\phi K^\pm K^0_S\pi^\mp$	[a]	(7.2 ±0.9) $\times10^{-4}$		
Γ_{35}	$\omega f_1(1420)$		(6.8 ±2.4) $\times10^{-4}$		
Γ_{36}	$\phi\eta$		(6.5 ±0.7) $\times10^{-4}$		
Γ_{37}	$\Xi(1530)^-\overline{\Xi}{}^+$		(5.9 ±1.5) $\times10^{-4}$		
Γ_{38}	$pK^-\overline{\Sigma}(1385)^0$		(5.1 ±3.2) $\times10^{-4}$		
Γ_{39}	$\omega\pi^0$		(4.2 ±0.6) $\times10^{-4}$		S=1.4
Γ_{40}	$\phi\eta'(958)$		(3.3 ±0.4) $\times10^{-4}$		
Γ_{41}	$\phi f_0(980)$		(3.2 ±0.9) $\times10^{-4}$		S=1.9
Γ_{42}	$\Xi(1530)^0\overline{\Xi}{}^0$		(3.2 ±1.4) $\times10^{-4}$		
Γ_{43}	$\Sigma(1385)^-\overline{\Sigma}{}^+$ (or c.c.)	[a]	(3.1 ±0.5) $\times10^{-4}$		
Γ_{44}	$\phi f_1(1285)$		(2.6 ±0.5) $\times10^{-4}$		S=1.1
Γ_{45}	$\rho\eta$		(1.93±0.23) $\times10^{-4}$		
Γ_{46}	$\omega\eta'(958)$		(1.67±0.25) $\times10^{-4}$		
Γ_{47}	$\omega f_0(980)$		(1.4 ±0.5) $\times10^{-4}$		
Γ_{48}	$\rho\eta'(958)$		(1.05±0.18) $\times10^{-4}$		
Γ_{49}	$p\overline{p}\phi$		(4.5 ±1.5) $\times10^{-5}$		
Γ_{50}	$a_2(1320)^\pm\pi^\mp$	[a]	< 4.3	$\times10^{-3}$	CL=90%
Γ_{51}	$K\overline{K}{}^*_2(1430)$ + c.c.		< 4.0	$\times10^{-3}$	CL=90%
Γ_{52}	$K_1(1270)^\pm K^\mp$		< 3.0	$\times10^{-3}$	CL=90%
Γ_{53}	$K^*_2(1430)^0\overline{K}{}^*_2(1430)^0$		< 2.9	$\times10^{-3}$	CL=90%
Γ_{54}	$K^*(892)^0\overline{K}{}^*(892)^0$		< 5	$\times10^{-4}$	CL=90%
Γ_{55}	$\phi f_2(1270)$		< 3.7	$\times10^{-4}$	CL=90%
Γ_{56}	$p\overline{p}\rho$		< 3.1	$\times10^{-4}$	CL=90%
Γ_{57}	$\phi\eta(1405)\to\phi\eta\pi\pi$		< 2.5	$\times10^{-4}$	CL=90%
Γ_{58}	$\omega f'_2(1525)$		< 2.2	$\times10^{-4}$	CL=90%
Γ_{59}	$\Sigma(1385)^0\overline{\Lambda}$		< 2	$\times10^{-4}$	CL=90%
Γ_{60}	$\Delta(1232)^+\overline{p}$		< 1	$\times10^{-4}$	CL=90%
Γ_{61}	$\Sigma^0\overline{\Lambda}$		< 9	$\times10^{-5}$	CL=90%
Γ_{62}	$\phi\pi^0$		< 6.8	$\times10^{-6}$	CL=90%

Decays into stable hadrons

Γ_{63}	$2(\pi^+\pi^-)\pi^0$	(3.37±0.26) %		
Γ_{64}	$3(\pi^+\pi^-)\pi^0$	(2.9 ±0.6) %		
Γ_{65}	$\pi^+\pi^-\pi^0$	(1.50±0.20) %		
Γ_{66}	$\pi^+\pi^-\pi^0K^+K^-$	(1.20±0.30) %		
Γ_{67}	$4(\pi^+\pi^-)\pi^0$	(9.0 ±3.0) $\times10^{-3}$		
Γ_{68}	$\pi^+\pi^-K^+K^-$	(7.2 ±2.3) $\times10^{-3}$		
Γ_{69}	$K\overline{K}\pi$	(6.1 ±1.0) $\times10^{-3}$		
Γ_{70}	$p\overline{p}\pi^+\pi^-$	(6.0 ±0.5) $\times10^{-3}$		S=1.3
Γ_{71}	$2(\pi^+\pi^-)$	(4.0 ±1.0) $\times10^{-3}$		
Γ_{72}	$3(\pi^+\pi^-)$	(4.0 ±2.0) $\times10^{-3}$		
Γ_{73}	$n\overline{n}\pi^+\pi^-$	(4 ±4) $\times10^{-3}$		
Γ_{74}	$\Sigma^0\overline{\Sigma}{}^0$	(1.27±0.17) $\times10^{-3}$		
Γ_{75}	$2(\pi^+\pi^-)K^+K^-$	(3.1 ±1.3) $\times10^{-3}$		
Γ_{76}	$p\overline{p}\pi^+\pi^-\pi^0$	[b]	(2.3 ±0.9) $\times10^{-3}$	S=1.9

Γ_{77}	$p\overline{p}$		$(2.12\pm0.10)\times10^{-3}$		
Γ_{78}	$p\overline{p}\eta$		$(2.09\pm0.18)\times10^{-3}$		
Γ_{79}	$p\overline{n}\pi^-$		$(2.00\pm0.10)\times10^{-3}$		
Γ_{80}	$n\overline{n}$		$(2.2\pm0.4)\times10^{-3}$		
Γ_{81}	$\Xi^-\overline{\Xi}^-$		$(1.8\pm0.4)\times10^{-3}$		S=1.8
Γ_{82}	$\Lambda\overline{\Lambda}$		$(1.30\pm0.12)\times10^{-3}$		S=1.1
Γ_{83}	$p\overline{p}\pi^0$		$(1.09\pm0.09)\times10^{-3}$		
Γ_{84}	$\Lambda\overline{\Sigma}^-\pi^+$ (or c.c.)	[a]	$(1.06\pm0.12)\times10^{-3}$		
Γ_{85}	$pK^-\overline{\Lambda}$		$(8.9\pm1.6)\times10^{-4}$		
Γ_{86}	$2(K^+K^-)$		$(9.2\pm3.3)\times10^{-4}$		S=1.3
Γ_{87}	$pK^-\overline{\Sigma}^0$		$(2.9\pm0.8)\times10^{-4}$		
Γ_{88}	K^+K^-		$(2.37\pm0.31)\times10^{-4}$		
Γ_{89}	$K^0_S K^0_L$		$(1.46\pm0.26)\times10^{-4}$		S=2.7
Γ_{90}	$\Lambda\overline{\Lambda}\pi^0$		$(2.2\pm0.6)\times10^{-4}$		
Γ_{91}	$\pi^+\pi^-$		$(1.47\pm0.23)\times10^{-4}$		
Γ_{92}	$\Lambda\overline{\Sigma}+$ c.c.		$<1.5\times10^{-4}$		CL=90%
Γ_{93}	$K^0_S K^0_S$		$<5.2\times10^{-6}$		CL=90%

Radiative decays

Γ_{94}	$\gamma\eta_c(1S)$		(1.3 ± 0.4) %		
Γ_{95}	$\gamma\pi^+\pi^-2\pi^0$		$(8.3\pm3.1)\times10^{-3}$		
Γ_{96}	$\gamma\eta\pi\pi$		$(6.1\pm1.0)\times10^{-3}$		
Γ_{97}	$\gamma\eta(1405/1475)\to\gamma K\overline{K}\pi$	[c]	$(2.8\pm0.6)\times10^{-3}$		S=1.6
Γ_{98}	$\gamma\eta(1405/1475)\to\gamma\gamma\rho^0$		$(6.4\pm1.4)\times10^{-5}$		
Γ_{99}	$\gamma\eta(1405/1475)\to\gamma\eta\pi^+\pi^-$		$(3.0\pm0.5)\times10^{-4}$		
Γ_{100}	$\gamma\rho\rho$		$(4.5\pm0.8)\times10^{-3}$		
Γ_{101}	$\gamma\eta_2(1870)\to\gamma\pi^+\pi^-$		$(6.2\pm2.4)\times10^{-4}$		
Γ_{102}	$\gamma\eta'(958)$		$(4.31\pm0.30)\times10^{-3}$		
Γ_{103}	$\gamma2\pi^+2\pi^-$		$(2.8\pm0.5)\times10^{-3}$		S=1.9
Γ_{104}	$\gamma K^+K^-\pi^+\pi^-$		$(2.1\pm0.6)\times10^{-3}$		
Γ_{105}	$\gamma f_4(2050)$		$(2.7\pm0.7)\times10^{-3}$		
Γ_{106}	$\gamma\omega\omega$		$(1.59\pm0.33)\times10^{-3}$		
Γ_{107}	$\gamma\eta(1405/1475)\to\gamma\rho^0\rho^0$		$(1.7\pm0.4)\times10^{-3}$		S=1.3
Γ_{108}	$\gamma f_2(1270)$		$(1.38\pm0.14)\times10^{-3}$		
Γ_{109}	$\gamma f_0(1710)\to\gamma K\overline{K}$		$(8.5^{+1.2}_{-0.9})\times10^{-4}$		S=1.2
Γ_{110}	$\gamma f_0(1710)\to\gamma\pi\pi$				
Γ_{111}	$\gamma\eta$		$(8.6\pm0.8)\times10^{-4}$		
Γ_{112}	$\gamma f_1(1420)\to\gamma K\overline{K}\pi$		$(7.9\pm1.3)\times10^{-4}$		
Γ_{113}	$\gamma f_1(1285)$		$(6.1\pm0.8)\times10^{-4}$		
Γ_{114}	$\gamma f_1(1510)\to\gamma\eta\pi^+\pi^-$		$(4.5\pm1.2)\times10^{-4}$		
Γ_{115}	$\gamma f'_2(1525)$		$(4.5^{+0.7}_{-0.4})\times10^{-4}$		
Γ_{116}	$\gamma f_2(1950)\to\gamma K^*(892)\overline{K}^*(892)$		$(7.0\pm2.2)\times10^{-4}$		
Γ_{117}	$\gamma K^*(892)\overline{K}^*(892)$		$(4.0\pm1.3)\times10^{-3}$		
Γ_{118}	$\gamma\phi\phi$		$(4.0\pm1.2)\times10^{-4}$		S=2.1
Γ_{119}	$\gamma p\overline{p}$		$(3.8\pm1.0)\times10^{-4}$		
Γ_{120}	$\gamma\eta(2225)$		$(2.9\pm0.6)\times10^{-4}$		
Γ_{121}	$\gamma\eta(1760)\to\gamma\rho^0\rho^0$		$(1.3\pm0.9)\times10^{-4}$		
Γ_{122}	$\gamma(K\overline{K}\pi)_{J^PC=0^-+}$		$(7\pm4)\times10^{-4}$		S=2.1
Γ_{123}	$\gamma\pi^0$		$(3.9\pm1.3)\times10^{-5}$		
Γ_{124}	$\gamma p\overline{p}\pi^+\pi^-$		$<7.9\times10^{-4}$		CL=90%
Γ_{125}	$\gamma\gamma$		$<5\times10^{-4}$		CL=90%
Γ_{126}	$\gamma\Lambda\overline{\Lambda}$		$<1.3\times10^{-4}$		CL=90%
Γ_{127}	3γ		$<5.5\times10^{-5}$		CL=90%
Γ_{128}	$\gamma f_0(2200)$				
Γ_{129}	$\gamma f_J(2220)$		$>2.50\times10^{-3}$		CL=99.9%
Γ_{130}	$\gamma f_J(2220)\to\gamma\pi\pi$		$(8\pm4)\times10^{-5}$		
Γ_{131}	$\gamma f_J(2220)\to\gamma K\overline{K}$		$(8.1\pm3.0)\times10^{-5}$		
Γ_{132}	$\gamma f_J(2220)\to\gamma p\overline{p}$		$(1.5\pm0.8)\times10^{-5}$		
Γ_{133}	$\gamma f_0(1500)$		$>(5.7\pm0.8)\times10^{-4}$		
Γ_{134}	γe^+e^-		$(8.8\pm1.4)\times10^{-3}$		

Lepton Family number (LF) violating modes

Γ_{135}	$e^\pm\mu^\mp$	LF	$<1.1\times10^{-6}$		CL=90%

[a] The value is for the sum of the charge states or particle/antiparticle states indicated.

[b] Includes $p\overline{p}\pi^+\pi^-\gamma$ and excludes $p\overline{p}\eta$, $p\overline{p}\omega$, $p\overline{p}\eta'$.

[c] See the "Note on the $\eta(1405)$" in the $\eta(1405)$ Particle Listings.

$J/\psi(1S)$ PARTIAL WIDTHS

Γ(hadrons) — Γ_1

VALUE (keV)	DOCUMENT ID		TECN	COMMENT
• • • We do not use the following data for averages, fits, limits, etc. • • •				
74.1 ± 8.1	BAI	95B	BES	e^+e^-
59 ±24	BALDINI-...	75	FRAG	e^+e^-
59 ±14	BOYARSKI	75	MRK1	e^+e^-
50 ±25	ESPOSITO	75B	FRAM	e^+e^-

Γ(virtual $\gamma\to$ hadrons) — Γ_2

VALUE (keV)	DOCUMENT ID		TECN	COMMENT
12 ±2	[7] BOYARSKI	75	MRK1	e^+e^-

[7] Included in Γ(hadrons).

$\Gamma(e^+e^-)$ — Γ_3

VALUE (keV)	EVTS	DOCUMENT ID		TECN	COMMENT
5.40±0.15±0.07 OUR EVALUATION					
• • • We do not use the following data for averages, fits, limits, etc. • • •					
5.61±0.20	7.8k	[8] AUBERT	04	BABR	$e^+e^-\to\mu^+\mu^-\gamma$
5.14±0.39		BAI	95B	BES	e^+e^-
$5.36^{+0.29}_{-0.28}$		[9] HSUEH	92	RVUE	See Υ mini-review
4.72±0.35		ALEXANDER	89	RVUE	See Υ mini-review
4.4 ±0.6		[9] BRANDELIK	79C	DASP	e^+e^-
4.6 ±0.8		[10] BALDINI-...	75	FRAG	e^+e^-
4.8 ±0.6		BOYARSKI	75	MRK1	e^+e^-
4.6 ±1.0		ESPOSITO	75B	FRAM	e^+e^-

[8] From a direct measurement of $\Gamma(e^+e^-)\times B(\mu^+\mu^-)$.

[9] From a simultaneous fit to e^+e^-, $\mu^+\mu^-$, and hadronic channels assuming $\Gamma(e^+e^-)=\Gamma(\mu^+\mu^-)$.

[10] Assuming equal partial widths for e^+e^- and $\mu^+\mu^-$.

$\Gamma(\mu^+\mu^-)$ — Γ_4

VALUE (keV)	DOCUMENT ID		TECN	COMMENT
• • • We do not use the following data for averages, fits, limits, etc. • • •				
5.13±0.52	BAI	95B	BES	e^+e^-
4.8 ±0.6	BOYARSKI	75	MRK1	e^+e^-
5 ±1	ESPOSITO	75B	FRAM	e^+e^-

$\Gamma(\gamma\gamma)$ — Γ_{125}

VALUE (eV)	CL%	DOCUMENT ID		TECN	COMMENT
<5.4	90	BRANDELIK	79C	DASP	e^+e^-

$J/\psi(1S)\ \Gamma(i)\Gamma(e^+e^-)/\Gamma$(total)

This combination of a partial width with the partial width into e^+e^- and with the total width is obtained from the integrated cross section into channel$_i$ in the e^+e^- annihilation.

Γ(hadrons) × $\Gamma(e^+e^-)/\Gamma_{\rm total}$ — $\Gamma_1\Gamma_3/\Gamma$

VALUE (keV)	DOCUMENT ID		TECN	COMMENT
• • • We do not use the following data for averages, fits, limits, etc. • • •				
4 ±0.8	[11] BALDINI-...	75	FRAG	e^+e^-
3.9±0.8	[11] ESPOSITO	75B	FRAM	e^+e^-

$\Gamma(e^+e^-)\times\Gamma(e^+e^-)/\Gamma_{\rm total}$ — $\Gamma_3\Gamma_3/\Gamma$

VALUE (keV)	DOCUMENT ID		TECN	COMMENT
• • • We do not use the following data for averages, fits, limits, etc. • • •				
0.35±0.02	BRANDELIK	79C	DASP	e^+e^-
0.32±0.07	[11] BALDINI-...	75	FRAG	e^+e^-
0.34±0.09	[11] ESPOSITO	75B	FRAM	e^+e^-
0.36±0.10	[11] FORD	75	SPEC	e^+e^-

$\Gamma(\mu^+\mu^-)\times\Gamma(e^+e^-)/\Gamma_{\rm total}$ — $\Gamma_4\Gamma_3/\Gamma$

VALUE (keV)	EVTS	DOCUMENT ID		TECN	COMMENT
0.3301±0.0077±0.0073	7.8k	AUBERT	04	BABR	$e^+e^-\to\mu^+\mu^-\gamma$
• • • We do not use the following data for averages, fits, limits, etc. • • •					
0.51 ±0.09		DASP	75	DASP	e^+e^-
0.38 ±0.05		[11] ESPOSITO	75B	FRAM	e^+e^-

$\Gamma(p\overline{p})\times\Gamma(e^+e^-)/\Gamma_{\rm total}$ — $\Gamma_{77}\Gamma_3/\Gamma$

VALUE (eV)	DOCUMENT ID		TECN	COMMENT
9.7±1.7	[12] ARMSTRONG	93B	E760	$\overline{p}p\to e^+e^-$

[11] Data redundant with branching ratios or partial widths above.

[12] Using $\Gamma_{\rm total}=85.5^{+6.1}_{-5.8}$ MeV.

$J/\psi(1S)$ BRANCHING RATIOS

For the first four branching ratios, see also the partial widths, and (partial widths) $\times\ \Gamma(e^+e^-)/\Gamma_{total}$ above.

$\Gamma(\text{hadrons})/\Gamma_{total}$ Γ_1/Γ

VALUE	DOCUMENT ID		TECN	COMMENT
0.877 ± 0.005 OUR AVERAGE				
0.878 ± 0.005	BAI	95B	BES	e^+e^-
0.86 ± 0.02	BOYARSKI	75	MRK1	e^+e^-

$\Gamma(\text{virtual}\,\gamma \to \text{hadrons})/\Gamma_{total}$ Γ_2/Γ

VALUE	DOCUMENT ID		TECN	COMMENT
0.17 ± 0.02	[13] BOYARSKI	75	MRK1	e^+e^-

[13] Included in $\Gamma(\text{hadrons})/\Gamma_{total}$.

$\Gamma(e^+e^-)/\Gamma_{total}$ Γ_3/Γ

VALUE	DOCUMENT ID		TECN	COMMENT
0.0593 ± 0.0010 OUR AVERAGE				
0.0590 ± 0.0005 ± 0.0010	BAI	98D	BES	$\psi(2S) \to J/\psi\pi^+\pi^-$
0.0609 ± 0.0033	BAI	95B	BES	e^+e^-
0.0592 ± 0.0015 ± 0.0020	COFFMAN	92	MRK3	$\psi(2S) \to J/\psi\pi^+\pi^-$
0.069 ± 0.009	BOYARSKI	75	MRK1	e^+e^-

$\Gamma(\mu^+\mu^-)/\Gamma_{total}$ Γ_4/Γ

VALUE	DOCUMENT ID		TECN	COMMENT
0.0588 ± 0.0010 OUR AVERAGE				
0.0584 ± 0.0006 ± 0.0010	BAI	98D	BES	$\psi(2S) \to J/\psi\pi^+\pi^-$
0.0608 ± 0.0033	BAI	95B	BES	e^+e^-
0.0590 ± 0.0015 ± 0.0019	COFFMAN	92	MRK3	$\psi(2S) \to J/\psi\pi^+\pi^-$
0.069 ± 0.009	BOYARSKI	75	MRK1	e^+e^-

$\Gamma(e^+e^-)/\Gamma(\mu^+\mu^-)$ Γ_3/Γ_4

VALUE	DOCUMENT ID		TECN	COMMENT
• • • We do not use the following data for averages, fits, limits, etc. • • •				
1.00 ± 0.07	BAI	95B	BES	e^+e^-
1.00 ± 0.05	BOYARSKI	75	MRK1	e^+e^-
0.91 ± 0.15	ESPOSITO	75B	FRAM	e^+e^-
0.93 ± 0.10	FORD	75	SPEC	e^+e^-

HADRONIC DECAYS

$\Gamma(\rho\pi)/\Gamma_{total}$ Γ_5/Γ

VALUE	EVTS	DOCUMENT ID		TECN	COMMENT
0.0127 ± 0.0009 OUR AVERAGE					
0.0121 ± 0.0020		BAI	96D	BES	$e^+e^- \to \rho\pi$
0.0142 ± 0.0001 ± 0.0019		COFFMAN	88	MRK3	e^+e^-
0.013 ± 0.003	150	FRANKLIN	83	MRK2	e^+e^-
0.016 ± 0.004	183	ALEXANDER	78	PLUT	e^+e^-
0.0133 ± 0.0021		BRANDELIK	78B	DASP	e^+e^-
0.010 ± 0.002	543	BARTEL	76	CNTR	e^+e^-
0.013 ± 0.003	153	JEAN-MARIE	76	MRK1	e^+e^-

$\Gamma(\rho^0\pi^0)/\Gamma(\rho\pi)$ Γ_6/Γ_5

VALUE	DOCUMENT ID		TECN	COMMENT
0.328 ± 0.005 ± 0.027	COFFMAN	88	MRK3	e^+e^-
• • • We do not use the following data for averages, fits, limits, etc. • • •				
0.35 ± 0.08	ALEXANDER	78	PLUT	e^+e^-
0.32 ± 0.08	BRANDELIK	78B	DASP	e^+e^-
0.39 ± 0.11	BARTEL	76	CNTR	e^+e^-
0.37 ± 0.09	JEAN-MARIE	76	MRK1	e^+e^-

$\Gamma(a_2(1320)\rho)/\Gamma_{total}$ Γ_7/Γ

VALUE (units 10^{-3})	EVTS	DOCUMENT ID		TECN	COMMENT
10.9 ± 2.2 OUR AVERAGE					
11.7 ± 0.7 ± 2.5	7584	AUGUSTIN	89	DM2	$J/\psi \to \rho^0\rho^\pm\pi^\mp$
8.4 ± 4.5	36	VANNUCCI	77	MRK1	$e^+e^- \to 2(\pi^+\pi^-)\pi^0$

$\Gamma(\omega\pi^+\pi^+\pi^-\pi^-)/\Gamma_{total}$ Γ_8/Γ

VALUE (units 10^{-4})	EVTS	DOCUMENT ID		TECN	COMMENT
85 ± 34	140	VANNUCCI	77	MRK1	$e^+e^- \to 3(\pi^+\pi^-)\pi^0$

$\Gamma(\omega\pi^+\pi^-)/\Gamma_{total}$ Γ_9/Γ

VALUE (units 10^{-3})	EVTS	DOCUMENT ID		TECN	COMMENT
7.2 ± 1.0 OUR AVERAGE					
7.0 ± 1.6	18058	AUGUSTIN	89	DM2	$J/\psi \to 2(\pi^+\pi^-)\pi^0$
7.8 ± 1.6	215	BURMESTER	77D	PLUT	e^+e^-
6.8 ± 1.9	348	VANNUCCI	77	MRK1	$e^+e^- \to 2(\pi^+\pi^-)\pi^0$

$\Gamma(\omega\pi^+\pi^-)/\Gamma(2(\pi^+\pi^-)\pi^0)$ Γ_9/Γ_{63}

VALUE	DOCUMENT ID		TECN	COMMENT
• • • We do not use the following data for averages, fits, limits, etc. • • •				
0.3	[14] JEAN-MARIE	76	MRK1	e^+e^-

[14] Final state $(\pi^+\pi^-)\pi^0$ under the assumption that $\pi\pi$ is isospin 0.

$\Gamma(K^*(892)^0\overline{K}_2^*(1430)^0 + \text{c.c.})/\Gamma_{total}$ Γ_{11}/Γ

VALUE (units 10^{-4})	EVTS	DOCUMENT ID		TECN	COMMENT
67 ± 26	40	VANNUCCI	77	MRK1	$e^+e^- \to \pi^+\pi^- K^+K^-$

$\Gamma(\omega K^*(892)\overline{K} + \text{c.c.})/\Gamma_{total}$ Γ_{12}/Γ

VALUE (units 10^{-4})	EVTS	DOCUMENT ID		TECN	COMMENT
53 ± 14 ± 14	530 ± 140	BECKER	87	MRK3	$e^+e^- \to$ hadrons

$\Gamma(\omega f_2(1270))/\Gamma_{total}$ Γ_{10}/Γ

VALUE (units 10^{-3})	EVTS	DOCUMENT ID		TECN	COMMENT
4.3 ± 0.6 OUR AVERAGE					
4.3 ± 0.2 ± 0.6	5860	AUGUSTIN	89	DM2	e^+e^-
4.0 ± 1.6	70	BURMESTER	77D	PLUT	e^+e^-
• • • We do not use the following data for averages, fits, limits, etc. • • •					
1.9 ± 0.8	81	VANNUCCI	77	MRK1	$e^+e^- \to 2(\pi^+\pi^-)\pi^0$

$\Gamma(K^+\overline{K}^*(892)^- + \text{c.c.})/\Gamma_{total}$ Γ_{13}/Γ

VALUE (units 10^{-3})	EVTS	DOCUMENT ID		TECN	COMMENT
5.0 ± 0.4 OUR AVERAGE					
4.57 ± 0.17 ± 0.70	2285	JOUSSET	90	DM2	$J/\psi \to$ hadrons
5.26 ± 0.13 ± 0.53		COFFMAN	88	MRK3	$J/\psi \to K^\pm K_S^0\pi^\mp$, $K^+K^-\pi^0$
• • • We do not use the following data for averages, fits, limits, etc. • • •					
2.6 ± 0.6	24	FRANKLIN	83	MRK2	$J/\psi \to K^+K^-\pi^0$
3.2 ± 0.6	48	VANNUCCI	77	MRK1	$J/\psi \to K^\pm K_S^0\pi^\mp$
4.1 ± 1.2	39	BRAUNSCH...	76	DASP	$J/\psi \to K^\pm$X

$\Gamma(K^0\overline{K}^*(892)^0 + \text{c.c.})/\Gamma_{total}$ Γ_{14}/Γ

VALUE (units 10^{-3})	EVTS	DOCUMENT ID		TECN	COMMENT
4.2 ± 0.4 OUR AVERAGE					
3.96 ± 0.15 ± 0.60	1192	JOUSSET	90	DM2	$J/\psi \to$ hadrons
4.33 ± 0.12 ± 0.45		COFFMAN	88	MRK3	$J/\psi \to K^\pm K_S^0\pi^\mp$
• • • We do not use the following data for averages, fits, limits, etc. • • •					
2.7 ± 0.6	45	VANNUCCI	77	MRK1	$J/\psi \to K^\pm K_S^0\pi^\mp$

$\Gamma(K^0\overline{K}^*(892)^0 + \text{c.c.})/\Gamma(K^+\overline{K}^*(892)^- + \text{c.c.})$ Γ_{14}/Γ_{13}

VALUE	DOCUMENT ID		TECN	COMMENT
0.82 ± 0.05 ± 0.09	COFFMAN	88	MRK3	$J/\psi \to K\overline{K}^*(892) + \text{c.c.}$

$\Gamma(K_1(1400)^\pm K^\mp)/\Gamma_{total}$ Γ_{15}/Γ

VALUE (units 10^{-3})	DOCUMENT ID		TECN	COMMENT
3.8 ± 0.8 ± 1.2	[15] BAI	99C	BES	e^+e^-

[15] Assuming $B(K_1(1400) \to K^*\pi) = 0.94 \pm 0.06$

$\Gamma(\omega\pi^0\pi^0)/\Gamma_{total}$ Γ_{16}/Γ

VALUE (units 10^{-3})	EVTS	DOCUMENT ID		TECN	COMMENT
3.4 ± 0.3 ± 0.7	509	AUGUSTIN	89	DM2	$J/\psi \to \pi^+\pi^- 3\pi^0$

$\Gamma(b_1(1235)^\pm\pi^\mp)/\Gamma_{total}$ Γ_{17}/Γ

VALUE (units 10^{-4})	EVTS	DOCUMENT ID		TECN	COMMENT
30 ± 5 OUR AVERAGE					
31 ± 6	4600	AUGUSTIN	89	DM2	$J/\psi \to 2(\pi^+\pi^-)\pi^0$
29 ± 7	87	BURMESTER	77D	PLUT	e^+e^-

$\Gamma(\omega K^\pm K_S^0\pi^\mp)/\Gamma_{total}$ Γ_{18}/Γ

VALUE (units 10^{-4})	EVTS	DOCUMENT ID		TECN	COMMENT
29.5 ± 1.4 ± 7.0	879 ± 41	BECKER	87	MRK3	$e^+e^- \to$ hadrons

$\Gamma(b_1(1235)^0\pi^0)/\Gamma_{total}$ Γ_{19}/Γ

VALUE (units 10^{-4})	EVTS	DOCUMENT ID		TECN	COMMENT
23 ± 3 ± 5	229	AUGUSTIN	89	DM2	e^+e^-

$\Gamma(\phi K^*(892)\overline{K} + \text{c.c.})/\Gamma_{total}$ Γ_{20}/Γ

VALUE (units 10^{-4})	EVTS	DOCUMENT ID		TECN	COMMENT
20.4 ± 2.8 OUR AVERAGE					
20.7 ± 2.4 ± 3.0		FALVARD	88	DM2	$J/\psi \to$ hadrons
20 ± 3 ± 3	155 ± 20	BECKER	87	MRK3	$e^+e^- \to$ hadrons

$\Gamma(\omega K\overline{K})/\Gamma_{total}$ Γ_{21}/Γ

VALUE (units 10^{-4})	EVTS	DOCUMENT ID		TECN	COMMENT
19 ± 4 OUR AVERAGE					
19.8 ± 2.1 ± 3.9		[16] FALVARD	88	DM2	$J/\psi \to$ hadrons
16 ± 10	22	FELDMAN	77	MRK1	e^+e^-

[16] Addition of ωK^+K^- and $\omega K^0\overline{K}^0$ branching ratios.

$\Gamma(\omega f_0(1710) \to \omega K\overline{K})/\Gamma_{total}$ Γ_{22}/Γ

VALUE (units 10^{-4})	DOCUMENT ID		TECN	COMMENT
4.8 ± 1.1 ± 0.3	[17,18] FALVARD	88	DM2	$J/\psi \to$ hadrons

[17] Includes unknown branching fraction $f_0(1710) \to K\overline{K}$.

[18] Addition of $f_0(1710) \to K^+K^-$ and $f_0(1710) \to K^0\overline{K}^0$ branching ratios.

$\Gamma(\phi 2(\pi^+\pi^-))/\Gamma_{total}$ Γ_{23}/Γ

VALUE (units 10^{-4})	DOCUMENT ID		TECN	COMMENT
16.0 ± 1.0 ± 3.0	FALVARD	88	DM2	$J/\psi \to$ hadrons

$\Gamma(\Delta(1232)^{++}\overline{p}\pi^-)/\Gamma_{total}$ Γ_{24}/Γ

VALUE (units 10^{-3})	EVTS	DOCUMENT ID		TECN	COMMENT
1.58 ± 0.23 ± 0.40	332	EATON	84	MRK2	e^+e^-

$\Gamma(\omega\eta)/\Gamma_{total}$ Γ_{25}/Γ

VALUE (units 10^{-3})	EVTS	DOCUMENT ID		TECN	COMMENT
1.58 ± 0.16 OUR AVERAGE					
1.43 ± 0.10 ± 0.21	378	JOUSSET	90	DM2	$J/\psi \to$ hadrons
1.71 ± 0.08 ± 0.20		COFFMAN	88	MRK3	$e^+e^- \to 3\pi\eta$

$\Gamma(\phi K\overline{K})/\Gamma_{total}$ Γ_{26}/Γ

VALUE (units 10^{-4})	EVTS	DOCUMENT ID		TECN	COMMENT
15.4 ± 2.1 OUR AVERAGE					
$48\ ^{+20}_{-16} \pm 6$	$9.0^{+3.7}_{-3.0}$	[30,31] HUANG	03	BELL	$B^+ \to (\phi K^+K^-)\,K^+$
14.6 ± 0.8 ± 2.1		[19] FALVARD	88	DM2	$J/\psi \to$ hadrons
18 ± 8	14	FELDMAN	77	MRK1	e^+e^-

[19] Addition of ϕK^+K^- and $\phi K^0\overline{K}^0$ branching ratios.

$\Gamma(\phi f_0(1710) \to \phi K\overline{K})/\Gamma_{total}$ Γ_{27}/Γ

VALUE (units 10^{-4})	DOCUMENT ID		TECN	COMMENT
3.6 ± 0.2 ± 0.6	[20,21] FALVARD	88	DM2	$J/\psi \to$ hadrons

[20] Including interference with $f_2'(1525)$.
[21] Includes unknown branching fraction $f_0(1710) \to K\overline{K}$.

$\Gamma(p\overline{p}\omega)/\Gamma_{total}$ Γ_{28}/Γ

VALUE (units 10^{-3})	EVTS	DOCUMENT ID		TECN	COMMENT
1.30 ± 0.25 OUR AVERAGE Error includes scale factor of 1.3.					
1.10 ± 0.17 ± 0.18	486	EATON	84	MRK2	e^+e^-
1.6 ± 0.3	77	PERUZZI	78	MRK1	e^+e^-

$\Gamma(\Delta(1232)^{++}\overline{\Delta}(1232)^{--})/\Gamma_{total}$ Γ_{29}/Γ

VALUE (units 10^{-3})	EVTS	DOCUMENT ID		TECN	COMMENT
1.10 ± 0.09 ± 0.28	233	EATON	84	MRK2	e^+e^-

$\Gamma(\Sigma(1385)^-\overline{\Sigma}(1385)^+ \text{(or c.c.)})/\Gamma_{total}$ Γ_{30}/Γ

VALUE (units 10^{-3})	EVTS	DOCUMENT ID		TECN	COMMENT
1.03 ± 0.13 OUR AVERAGE					
1.00 ± 0.04 ± 0.21	631 ± 25	HENRARD	87	DM2	$e^+e^- \to \Sigma^{*-}$
1.19 ± 0.04 ± 0.25	754 ± 27	HENRARD	87	DM2	$e^+e^- \to \Sigma^{*+}$
0.86 ± 0.18 ± 0.22	56	EATON	84	MRK2	$e^+e^- \to \Sigma^{*-}$
1.03 ± 0.24 ± 0.25	68	EATON	84	MRK2	$e^+e^- \to \Sigma^{*+}$

$\Gamma(p\overline{p}\eta'(958))/\Gamma_{total}$ Γ_{31}/Γ

VALUE (units 10^{-3})	EVTS	DOCUMENT ID		TECN	COMMENT
0.9 ± 0.4 OUR AVERAGE Error includes scale factor of 1.7.					
0.68 ± 0.23 ± 0.17	19	EATON	84	MRK2	e^+e^-
1.8 ± 0.6	19	PERUZZI	78	MRK1	e^+e^-

$\Gamma(\phi f_2'(1525))/\Gamma_{total}$ Γ_{32}/Γ

VALUE (units 10^{-4})	EVTS	DOCUMENT ID		TECN	COMMENT
8 ± 4 OUR AVERAGE Error includes scale factor of 2.7.					
12.3 ± 0.6 ± 2.0		[22,23] FALVARD	88	DM2	$J/\psi \to$ hadrons
4.8 ± 1.8	46	[22] GIDAL	81	MRK2	$J/\psi \to K^+K^-K^+K^-$

[22] Re-evaluated using $B(f_2'(1525) \to K\overline{K}) = 0.713$.
[23] Including interference with $f_0(1710)$.

$\Gamma(\phi\pi^+\pi^-)/\Gamma_{total}$ Γ_{33}/Γ

VALUE (units 10^{-3})	EVTS	DOCUMENT ID		TECN	COMMENT
0.80 ± 0.12 OUR AVERAGE					
0.78 ± 0.03 ± 0.12		FALVARD	88	DM2	$J/\psi \to$ hadrons
2.1 ± 0.9	23	FELDMAN	77	MRK1	e^+e^-

$\Gamma(\phi K^\pm K^0_S\pi^\mp)/\Gamma_{total}$ Γ_{34}/Γ

VALUE (units 10^{-4})	EVTS	DOCUMENT ID		TECN	COMMENT
7.2 ± 0.9 OUR AVERAGE					
7.4 ± 0.9 ± 1.1		FALVARD	88	DM2	$J/\psi \to$ hadrons
7 ± 0.6 ± 1.0	163 ± 15	BECKER	87	MRK3	$e^+e^- \to$ hadrons

$\Gamma(\omega f_1(1420))/\Gamma_{total}$ Γ_{35}/Γ

VALUE (units 10^{-4})	EVTS	DOCUMENT ID		TECN	COMMENT
$\mathbf{6.8^{+1.9}_{-1.6} \pm 1.7}$	111^{+31}_{-26}	BECKER	87	MRK3	$e^+e^- \to$ hadrons

$\Gamma(\phi\eta)/\Gamma_{total}$ Γ_{36}/Γ

VALUE (units 10^{-3})	EVTS	DOCUMENT ID		TECN	COMMENT
0.65 ± 0.07 OUR AVERAGE					
0.64 ± 0.04 ± 0.11	346	JOUSSET	90	DM2	$J/\psi \to$ hadrons
0.661 ± 0.045 ± 0.078		COFFMAN	88	MRK3	$e^+e^- \to K^+K^-\eta$

$\Gamma(\Xi(1530)^-\overline{\Xi}^+)/\Gamma_{total}$ Γ_{37}/Γ

VALUE (units 10^{-3})	EVTS	DOCUMENT ID		TECN	COMMENT
0.59 ± 0.09 ± 0.12	75 ± 11	HENRARD	87	DM2	e^+e^-

$\Gamma(pK^-\overline{\Sigma}(1385)^0)/\Gamma_{total}$ Γ_{38}/Γ

VALUE (units 10^{-3})	EVTS	DOCUMENT ID		TECN	COMMENT
0.51 ± 0.26 ± 0.18	89	EATON	84	MRK2	e^+e^-

$\Gamma(\omega\pi^0)/\Gamma_{total}$ Γ_{39}/Γ

VALUE (units 10^{-3})	EVTS	DOCUMENT ID		TECN	COMMENT
0.42 ± 0.06 OUR AVERAGE Error includes scale factor of 1.4.					
0.360 ± 0.028 ± 0.054	222	JOUSSET	90	DM2	$J/\psi \to$ hadrons
0.482 ± 0.019 ± 0.064		COFFMAN	88	MRK3	$e^+e^- \to \pi^0\pi^+\pi^-\pi^0$

$\Gamma(\phi\eta'(958))/\Gamma_{total}$ Γ_{40}/Γ

VALUE (units 10^{-3})	CL%	EVTS	DOCUMENT ID		TECN	COMMENT
0.33 ± 0.04 OUR AVERAGE						
0.41 ± 0.03 ± 0.08		167	JOUSSET	90	DM2	$J/\psi \to$ hadrons
0.308 ± 0.034 ± 0.036			COFFMAN	88	MRK3	$e^+e^- \to K^+K^-\eta'$
• • • We do not use the following data for averages, fits, limits, etc. • • •						
<1.3	90		VANNUCCI	77	MRK1	e^+e^-

$\Gamma(\phi f_0(980))/\Gamma_{total}$ Γ_{41}/Γ

VALUE (units 10^{-4})	EVTS	DOCUMENT ID		TECN	COMMENT
3.2 ± 0.9 OUR AVERAGE Error includes scale factor of 1.9.					
4.6 ± 0.4 ± 0.8		[24] FALVARD	88	DM2	$J/\psi \to$ hadrons
2.6 ± 0.6	50	[24] GIDAL	81	MRK2	$J/\psi \to K^+K^-K^+K^-$

[24] Assuming $B(f_0(980) \to \pi\pi) = 0.78$.

$\Gamma(\Xi(1530)^0\overline{\Xi}^0)/\Gamma_{total}$ Γ_{42}/Γ

VALUE (units 10^{-3})	EVTS	DOCUMENT ID		TECN	COMMENT
0.32 ± 0.12 ± 0.07	24 ± 9	HENRARD	87	DM2	e^+e^-

$\Gamma(\Sigma(1385)^-\overline{\Sigma}^+ \text{(or c.c.)})/\Gamma_{total}$ Γ_{43}/Γ

VALUE (units 10^{-3})	EVTS	DOCUMENT ID		TECN	COMMENT
0.31 ± 0.05 OUR AVERAGE					
0.30 ± 0.03 ± 0.07	74 ± 8	HENRARD	87	DM2	$e^+e^- \to \Sigma^{*-}$
0.34 ± 0.04 ± 0.07	77 ± 9	HENRARD	87	DM2	$e^+e^- \to \Sigma^{*+}$
0.29 ± 0.11 ± 0.10	26	EATON	84	MRK2	$e^+e^- \to \Sigma^{*-}$
0.31 ± 0.11 ± 0.11	28	EATON	84	MRK2	$e^+e^- \to \Sigma^{*+}$

$\Gamma(\phi f_1(1285))/\Gamma_{total}$ Γ_{44}/Γ

VALUE (units 10^{-4})	EVTS	DOCUMENT ID		TECN	COMMENT
2.6 ± 0.5 OUR AVERAGE Error includes scale factor of 1.1.					
3.2 ± 0.6 ± 0.4		JOUSSET	90	DM2	$J/\psi \to \phi 2(\pi^+\pi^-)$
2.1 ± 0.5 ± 0.4	25	[25] JOUSSET	90	DM2	$J/\psi \to \phi\eta\pi^+\pi^-$
• • • We do not use the following data for averages, fits, limits, etc. • • •					
0.6 ± 0.2 ± 0.1	16 ± 6	BECKER	87	MRK3	$J/\psi \to \phi K\overline{K}\pi$

[25] We attribute to the $f_1(1285)$ the signal observed in the $\pi^+\pi^-\eta$ invariant mass distribution at 1297 Mev.

$\Gamma(\rho\eta)/\Gamma_{total}$ Γ_{45}/Γ

VALUE (units 10^{-3})	EVTS	DOCUMENT ID		TECN	COMMENT
0.193 ± 0.023 OUR AVERAGE					
0.194 ± 0.017 ± 0.029	299	JOUSSET	90	DM2	$J/\psi \to$ hadrons
0.193 ± 0.013 ± 0.029		COFFMAN	88	MRK3	$e^+e^- \to \pi^+\pi^-\eta$

$\Gamma(\omega\eta'(958))/\Gamma_{total}$ Γ_{46}/Γ

VALUE (units 10^{-3})	EVTS	DOCUMENT ID		TECN	COMMENT
0.167 ± 0.025 OUR AVERAGE					
$0.18\ ^{+0.10}_{-0.08} \pm 0.03$	6	JOUSSET	90	DM2	$J/\psi \to$ hadrons
0.166 ± 0.017 ± 0.019		COFFMAN	88	MRK3	$e^+e^- \to 3\pi\eta'$

$\Gamma(\omega f_0(980))/\Gamma_{total}$ Γ_{47}/Γ

VALUE (units 10^{-4})	DOCUMENT ID		TECN	COMMENT
1.41 ± 0.27 ± 0.47	[26] AUGUSTIN	89	DM2	$J/\psi \to 2(\pi^+\pi^-)\pi^0$

[26] Assuming $B(f_0(980) \to \pi\pi) = 0.78$.

$\Gamma(\rho\eta'(958))/\Gamma_{total}$ Γ_{48}/Γ

VALUE (units 10^{-3})	EVTS	DOCUMENT ID		TECN	COMMENT
0.105 ± 0.018 OUR AVERAGE					
0.083 ± 0.030 ± 0.012	19	JOUSSET	90	DM2	$J/\psi \to$ hadrons
0.114 ± 0.014 ± 0.016		COFFMAN	88	MRK3	$J/\psi \to \pi^+\pi^-\eta'$

$\Gamma(p\overline{p}\phi)/\Gamma_{total}$ Γ_{49}/Γ

VALUE (units 10^{-4})	DOCUMENT ID		TECN	COMMENT
0.45 ± 0.13 ± 0.07	FALVARD	88	DM2	$J/\psi \to$ hadrons

$\Gamma(a_2(1320)^{\pm}\pi^{\mp})/\Gamma_{total}$ Γ_{50}/Γ

VALUE (units 10^{-4})	CL%	DOCUMENT ID		TECN	COMMENT
< 43	90	BRAUNSCH...	76	DASP	e^+e^-

$\Gamma(K\overline{K}_2^*(1430) + \text{c.c.})/\Gamma_{total}$ Γ_{51}/Γ

VALUE (units 10^{-4})	CL%	DOCUMENT ID		TECN	COMMENT
< 40	90	VANNUCCI	77	MRK1	$e^+e^- \to K^0\overline{K}_2^{*0}$
• • • We do not use the following data for averages, fits, limits, etc. • • •					
< 66	90	BRAUNSCH...	76	DASP	$e^+e^- \to K^{\pm}\overline{K}_2^{*\mp}$

$\Gamma(K_1(1270)^{\pm}K^{\mp})/\Gamma_{total}$ Γ_{52}/Γ

VALUE (units 10^{-3})	CL%	DOCUMENT ID		TECN	COMMENT
< 3.0	90	[27] BAI	99C	BES	e^+e^-

[27] Assuming B($K_1(1270) \to K\rho$)=0.42 ± 0.06

$\Gamma(K_2^*(1430)^0\overline{K}_2^*(1430)^0)/\Gamma_{total}$ Γ_{53}/Γ

VALUE (units 10^{-4})	CL%	DOCUMENT ID		TECN	COMMENT
< 29	90	VANNUCCI	77	MRK1	$e^+e^- \to \pi^+\pi^- K^+K^-$

$\Gamma(K^*(892)^0\overline{K}^*(892)^0)/\Gamma_{total}$ Γ_{54}/Γ

VALUE (units 10^{-4})	CL%	DOCUMENT ID		TECN	COMMENT
< 5	90	VANNUCCI	77	MRK1	$e^+e^- \to \pi^+\pi^- K^+K^-$

$\Gamma(\phi f_2(1270))/\Gamma_{total}$ Γ_{55}/Γ

VALUE (units 10^{-4})	CL%	DOCUMENT ID		TECN	COMMENT
< 3.7	90	VANNUCCI	77	MRK1	$e^+e^- \to \pi^+\pi^- K^+K^-$
• • • We do not use the following data for averages, fits, limits, etc. • • •					
< 4.5	90	FALVARD	88	DM2	$J/\psi \to$ hadrons

$\Gamma(p\overline{p}\rho)/\Gamma_{total}$ Γ_{56}/Γ

VALUE (units 10^{-3})	CL%	DOCUMENT ID		TECN	COMMENT
< 0.31	90	EATON	84	MRK2	$e^+e^- \to$ hadrons γ

$\Gamma(\phi\eta(1405) \to \phi\eta\pi\pi)/\Gamma_{total}$ Γ_{57}/Γ

VALUE (units 10^{-4})	CL%	DOCUMENT ID		TECN	COMMENT
< 2.5	90	[28] FALVARD	88	DM2	$J/\psi \to$ hadrons

[28] Includes unknown branching fraction $\eta(1405) \to \eta\pi\pi$.

$\Gamma(\omega f_2'(1525))/\Gamma_{total}$ Γ_{58}/Γ

VALUE (units 10^{-4})	CL%	DOCUMENT ID		TECN	COMMENT
< 2.2	90	[29] VANNUCCI	77	MRK1	$e^+e^- \to \pi^+\pi^-\pi^0 K^+K^-$
• • • We do not use the following data for averages, fits, limits, etc. • • •					
< 2.8	90	[29] FALVARD	88	DM2	$J/\psi \to$ hadrons

[29] Re-evaluated assuming B($f_2'(1525) \to K\overline{K}$) = 0.713.

$\Gamma(\Sigma(1385)^0\overline{\Lambda})/\Gamma_{total}$ Γ_{59}/Γ

VALUE (units 10^{-3})	CL%	DOCUMENT ID		TECN	COMMENT
< 0.2	90	HENRARD	87	DM2	e^+e^-

$\Gamma(\Delta(1232)^+\overline{p})/\Gamma_{total}$ Γ_{60}/Γ

VALUE (units 10^{-3})	CL%	DOCUMENT ID		TECN	COMMENT
< 0.1	90	HENRARD	87	DM2	e^+e^-

$\Gamma(\Sigma^0\overline{\Lambda})/\Gamma_{total}$ Γ_{61}/Γ

VALUE (units 10^{-4})	CL%	DOCUMENT ID		TECN	COMMENT
< 0.9	90	HENRARD	87	DM2	e^+e^-

$\Gamma(\phi\pi^0)/\Gamma_{total}$ Γ_{62}/Γ

VALUE (units 10^{-4})	CL%	DOCUMENT ID		TECN	COMMENT
< 0.068	90	COFFMAN	88	MRK3	$e^+e^- \to K^+K^-\pi^0$

[30] We have multiplied K^+K^- measurement by 2 to obtain $K\overline{K}$.

[31] Using B($B^+ \to J/\psi K^+$) = (1.01 ± 0.05) × 10^{-3}.

STABLE HADRONS

$\Gamma(2(\pi^+\pi^-)\pi^0)/\Gamma_{total}$ Γ_{63}/Γ

VALUE	EVTS	DOCUMENT ID		TECN	COMMENT
0.0337 ± 0.0026 OUR AVERAGE					
0.0325 ± 0.0049	46055	AUGUSTIN	89	DM2	$J/\psi \to 2(\pi^+\pi^-)\pi^0$
0.0317 ± 0.0042	147	FRANKLIN	83	MRK2	$e^+e^- \to$ hadrons
0.0364 ± 0.0052	1500	BURMESTER	77D	PLUT	e^+e^-
0.04 ± 0.01	675	JEAN-MARIE	76	MRK1	e^+e^-

$\Gamma(3(\pi^+\pi^-)\pi^0)/\Gamma_{total}$ Γ_{64}/Γ

VALUE	EVTS	DOCUMENT ID		TECN	COMMENT
0.029 ± 0.006 OUR AVERAGE					
0.028 ± 0.009	11	FRANKLIN	83	MRK2	$e^+e^- \to$ hadrons
0.029 ± 0.007	181	JEAN-MARIE	76	MRK1	e^+e^-

$\Gamma(\pi^+\pi^-\pi^0)/\Gamma_{total}$ Γ_{65}/Γ

VALUE	EVTS	DOCUMENT ID		TECN	COMMENT
0.015 ± 0.002	168	FRANKLIN	83	MRK2	e^+e^-

$\Gamma(\pi^+\pi^-\pi^0 K^+K^-)/\Gamma_{total}$ Γ_{66}/Γ

VALUE	EVTS	DOCUMENT ID		TECN	COMMENT
0.012 ± 0.003	309	VANNUCCI	77	MRK1	e^+e^-

$\Gamma(4(\pi^+\pi^-)\pi^0)/\Gamma_{total}$ Γ_{67}/Γ

VALUE (units 10^{-4})	EVTS	DOCUMENT ID		TECN	COMMENT
90 ± 30	13	JEAN-MARIE	76	MRK1	e^+e^-

$\Gamma(\pi^+\pi^- K^+K^-)/\Gamma_{total}$ Γ_{68}/Γ

VALUE (units 10^{-4})	EVTS	DOCUMENT ID		TECN	COMMENT
72 ± 23	205	VANNUCCI	77	MRK1	e^+e^-

$\Gamma(K\overline{K}\pi)/\Gamma_{total}$ Γ_{69}/Γ

VALUE (units 10^{-4})	EVTS	DOCUMENT ID		TECN	COMMENT
61 ± 10 OUR AVERAGE					
55.2 ± 12.0	25	FRANKLIN	83	MRK2	$e^+e^- \to K^+K^-\pi^0$
78.0 ± 21.0	126	VANNUCCI	77	MRK1	$e^+e^- \to K_S^0 K^{\pm}\pi^{\mp}$

$\Gamma(p\overline{p}\pi^+\pi^-)/\Gamma_{total}$ Γ_{70}/Γ

VALUE (units 10^{-3})	EVTS	DOCUMENT ID		TECN	COMMENT
6.0 ± 0.5 OUR AVERAGE Error includes scale factor of 1.3. See the ideogram below.					
6.46 ± 0.17 ± 0.43	1435	EATON	84	MRK2	e^+e^-
3.8 ± 1.6	48	BESCH	81	BONA	e^+e^-
5.5 ± 0.6	533	PERUZZI	78	MRK1	e^+e^-

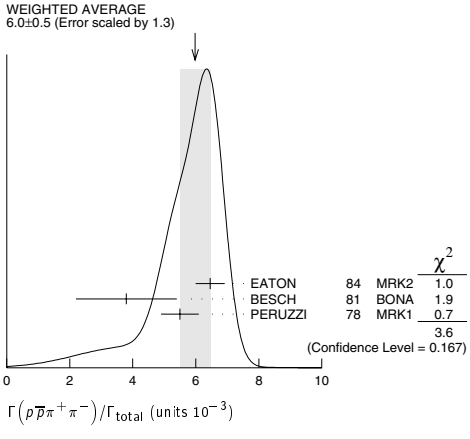

$\Gamma(2(\pi^+\pi^-))/\Gamma_{total}$ Γ_{71}/Γ

VALUE	EVTS	DOCUMENT ID		TECN	COMMENT
0.004 ± 0.001	76	JEAN-MARIE	76	MRK1	e^+e^-

$\Gamma(3(\pi^+\pi^-))/\Gamma_{total}$ Γ_{72}/Γ

VALUE (units 10^{-4})	EVTS	DOCUMENT ID		TECN	COMMENT
40 ± 20	32	JEAN-MARIE	76	MRK1	e^+e^-

$\Gamma(n\overline{n}\pi^+\pi^-)/\Gamma_{total}$ Γ_{73}/Γ

VALUE (units 10^{-3})	EVTS	DOCUMENT ID		TECN	COMMENT
3.8 ± 3.6	5	BESCH	81	BONA	e^+e^-

$\Gamma(\Sigma^0\overline{\Sigma}^0)/\Gamma_{total}$ Γ_{74}/Γ

VALUE (units 10^{-3})	EVTS	DOCUMENT ID		TECN	COMMENT
1.27 ± 0.17 OUR AVERAGE					
1.06 ± 0.04 ± 0.23	884 ± 30	PALLIN	87	DM2	$e^+e^- \to \Sigma^0\overline{\Sigma}^0$
1.58 ± 0.16 ± 0.25	90	EATON	84	MRK2	$e^+e^- \to \Sigma^0\overline{\Sigma}^0$
1.3 ± 0.4	52	PERUZZI	78	MRK1	$e^+e^- \to \Sigma^0\overline{\Sigma}^0$
• • • We do not use the following data for averages, fits, limits, etc. • • •					
2.4 ± 2.6	3	BESCH	81	BONA	$e^+e^- \to \Sigma^+\overline{\Sigma}^-$

$\Gamma(2(\pi^+\pi^-)K^+K^-)/\Gamma_{total}$ Γ_{75}/Γ

VALUE (units 10^{-4})	EVTS	DOCUMENT ID		TECN	COMMENT
31 ± 13	30	VANNUCCI	77	MRK1	e^+e^-

$\Gamma(p\overline{p}\pi^+\pi^-\pi^0)/\Gamma_{total}$ Γ_{76}/Γ

Including $p\overline{p}\pi^+\pi^-\gamma$ and excluding ω, η, η'

VALUE (units 10^{-3})	EVTS	DOCUMENT ID		TECN	COMMENT
2.3 ±0.9 OUR AVERAGE		Error includes scale factor of 1.9.			
3.36±0.65±0.28	364	EATON	84	MRK2	e^+e^-
1.6 ±0.6	39	PERUZZI	78	MRK1	e^+e^-

$\Gamma(p\overline{p})/\Gamma_{total}$ Γ_{77}/Γ

VALUE (units 10^{-3})	EVTS	DOCUMENT ID		TECN	COMMENT
2.12±0.10 OUR AVERAGE					
1.97±0.22	99	BALDINI	98	FENI	e^+e^-
1.91±0.04±0.30		PALLIN	87	DM2	e^+e^-
2.16±0.07±0.15	1420	EATON	84	MRK2	e^+e^-
2.5 ±0.4	133	BRANDELIK	79C	DASP	e^+e^-
2.0 ±0.5		BESCH	78	BONA	e^+e^-
2.2 ±0.2	331	[32] PERUZZI	78	MRK1	e^+e^-
• • • We do not use the following data for averages, fits, limits, etc. • • •					
2.0 ±0.3	48	ANTONELLI	93	SPEC	e^+e^-

[32] Assuming angular distribution $(1+\cos^2\theta)$.

$\Gamma(p\overline{p}\eta)/\Gamma_{total}$ Γ_{78}/Γ

VALUE (units 10^{-3})	EVTS	DOCUMENT ID		TECN	COMMENT
2.09±0.18 OUR AVERAGE					
2.03±0.13±0.15	826	EATON	84	MRK2	e^+e^-
2.5 ±1.2		BRANDELIK	79C	DASP	e^+e^-
2.3 ±0.4	197	PERUZZI	78	MRK1	e^+e^-

$\Gamma(p\overline{n}\pi^-)/\Gamma_{total}$ Γ_{79}/Γ

VALUE (units 10^{-3})	EVTS	DOCUMENT ID		TECN	COMMENT
2.00±0.10 OUR AVERAGE					
2.02±0.07±0.16	1288	EATON	84	MRK2	$e^+e^- \to p\pi^-$
1.93±0.07±0.16	1191	EATON	84	MRK2	$e^+e^- \to \overline{p}\pi^+$
1.7 ±0.7	32	BESCH	81	BONA	$e^+e^- \to p\pi^-$
1.6 ±1.2	5	BESCH	81	BONA	$e^+e^- \to \overline{p}\pi^+$
2.16±0.29	194	PERUZZI	78	MRK1	$e^+e^- \to p\pi^-$
2.04±0.27	204	PERUZZI	78	MRK1	$e^+e^- \to \overline{p}\pi^+$

$\Gamma(\Xi\overline{\Xi})/\Gamma_{total}$ Γ_{81}/Γ

VALUE (units 10^{-3})	EVTS	DOCUMENT ID		TECN	COMMENT
1.8 ±0.4 OUR AVERAGE		Error includes scale factor of 1.8. See the ideogram below.			
1.40±0.12±0.24	132 ± 11	HENRARD	87	DM2	$e^+e^- \to \Xi^-\overline{\Xi}^+$
2.28±0.16±0.40	194	EATON	84	MRK2	$e^+e^- \to \Xi^-\overline{\Xi}^+$
3.2 ±0.8	71	PERUZZI	78	MRK1	e^+e^-

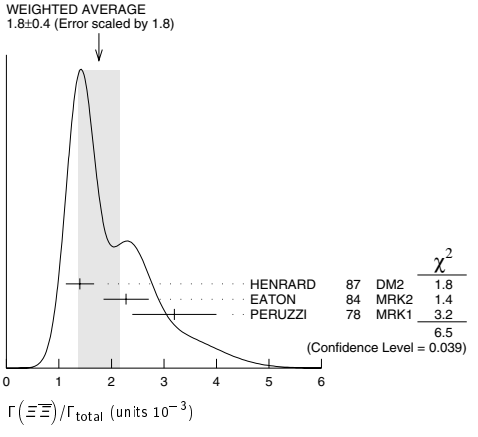

$\Gamma(n\overline{n})/\Gamma_{total}$ Γ_{80}/Γ

VALUE (units 10^{-2})	EVTS	DOCUMENT ID		TECN	COMMENT
0.22 ±0.04 OUR AVERAGE					
0.231±0.049	79	BALDINI	98	FENI	e^+e^-
0.18 ±0.09		BESCH	78	BONA	e^+e^-
• • • We do not use the following data for averages, fits, limits, etc. • • •					
0.190±0.055	40	ANTONELLI	93	SPEC	e^+e^-

$\Gamma(\Lambda\overline{\Lambda})/\Gamma_{total}$ Γ_{82}/Γ

VALUE (units 10^{-3})	EVTS	DOCUMENT ID		TECN	COMMENT
1.30±0.12 OUR AVERAGE		Error includes scale factor of 1.1.			
1.08±0.06±0.24	631	BAI	98G	BES	e^+e^-
1.38±0.05±0.20	1847	PALLIN	87	DM2	e^+e^-
1.58±0.08±0.19	365	EATON	84	MRK2	e^+e^-
2.6 ±1.6	5	BESCH	81	BONA	e^+e^-
1.1 ±0.2	196	PERUZZI	78	MRK1	e^+e^-

$\Gamma(p\overline{p}\pi^0)/\Gamma_{total}$ Γ_{83}/Γ

VALUE (units 10^{-3})	EVTS	DOCUMENT ID		TECN	COMMENT
1.09±0.09 OUR AVERAGE					
1.13±0.09±0.09	685	EATON	84	MRK2	e^+e^-
1.4 ±0.4		BRANDELIK	79C	DASP	e^+e^-
1.00±0.15	109	PERUZZI	78	MRK1	e^+e^-

$\Gamma(\Lambda\overline{\Sigma}^-\pi^+ (\text{or c.c.}))/\Gamma_{total}$ Γ_{84}/Γ

VALUE (units 10^{-3})	EVTS	DOCUMENT ID		TECN	COMMENT
1.06±0.12 OUR AVERAGE					
0.90±0.06±0.16	225 ± 15	HENRARD	87	DM2	$e^+e^- \to \Lambda\overline{\Sigma}^+\pi^-$
1.11±0.06±0.20	342 ± 18	HENRARD	87	DM2	$e^+e^- \to \Lambda\overline{\Sigma}^-\pi^+$
1.53±0.17±0.38	135	EATON	84	MRK2	$e^+e^- \to \Lambda\overline{\Sigma}^+\pi^-$
1.38±0.21±0.35	118	EATON	84	MRK2	$e^+e^- \to \Lambda\overline{\Sigma}^-\pi^+$

$\Gamma(pK^-\overline{\Lambda})/\Gamma_{total}$ Γ_{85}/Γ

VALUE (units 10^{-3})	EVTS	DOCUMENT ID		TECN	COMMENT
0.89±0.07±0.14	307	EATON	84	MRK2	e^+e^-

$\Gamma(2(K^+K^-))/\Gamma_{total}$ Γ_{86}/Γ

VALUE (units 10^{-4})	EVTS	DOCUMENT ID		TECN	COMMENT
9.2±3.3 OUR AVERAGE		Error includes scale factor of 1.3.			
$14\ ^{+5}_{-4}\ \pm2$	$11.0\ ^{+4.3}_{-3.5}$	[31] HUANG	03	BELL	$B^+ \to 2(K^+K^-)\,K^+$
7 ±3		VANNUCCI	77	MRK1	e^+e^-

$\Gamma(pK^-\overline{\Sigma}^0)/\Gamma_{total}$ Γ_{87}/Γ

VALUE (units 10^{-3})	EVTS	DOCUMENT ID		TECN	COMMENT
0.29±0.06±0.05	90	EATON	84	MRK2	e^+e^-

$\Gamma(K^+K^-)/\Gamma_{total}$ Γ_{88}/Γ

VALUE (units 10^{-4})	EVTS	DOCUMENT ID		TECN	COMMENT
2.37±0.31 OUR AVERAGE					
2.39±0.24±0.22	107	BALTRUSAIT...85D		MRK3	e^+e^-
2.2 ±0.9	6	BRANDELIK	79C	DASP	e^+e^-

$\Gamma(K^0_S K^0_L)/\Gamma_{total}$ Γ_{89}/Γ

VALUE (units 10^{-4})	EVTS	DOCUMENT ID		TECN	COMMENT
1.46±0.26 OUR AVERAGE		Error includes scale factor of 2.7. See the ideogram below.			
1.82±0.04±0.13	2155 ± 45	[34] BAI	04A	BES2	$J/\psi \to K^0_S K^0_L \to \pi^+\pi^- X$
1.18±0.12±0.18		JOUSSET	90	DM2	$J/\psi \to$ hadrons
1.01±0.16±0.09	74	BALTRUSAIT...85D		MRK3	e^+e^-

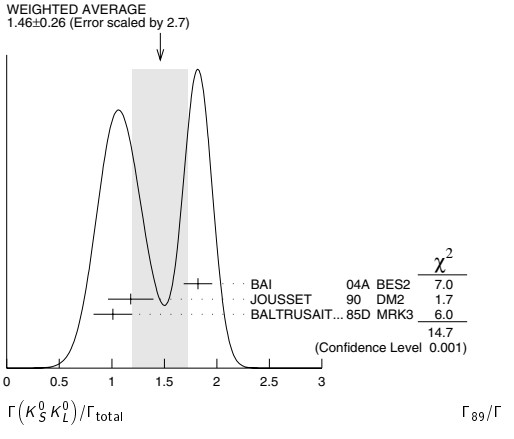

$\Gamma(\Lambda\overline{\Lambda}\pi^0)/\Gamma_{total}$ Γ_{90}/Γ

VALUE (units 10^{-3})	EVTS	DOCUMENT ID		TECN	COMMENT
0.22±0.06 OUR AVERAGE					
0.23±0.07±0.08	11	BAI	98G	BES	e^+e^-
0.22±0.05±0.05	19 ± 4	HENRARD	87	DM2	e^+e^-

$\Gamma(\pi^+\pi^-)/\Gamma_{total}$ Γ_{91}/Γ

VALUE (units 10^{-4})	EVTS	DOCUMENT ID		TECN	COMMENT
1.47±0.23 OUR AVERAGE					
1.58±0.20±0.15	84	BALTRUSAIT...85D		MRK3	e^+e^-
1.0 ±0.5	5	BRANDELIK	78B	DASP	e^+e^-
1.6 ±1.6	1	VANNUCCI	77	MRK1	e^+e^-

$\Gamma(\Lambda\overline{\Sigma}+\text{c.c.})/\Gamma_{total}$ Γ_{92}/Γ

VALUE (units 10^{-3})	CL%	DOCUMENT ID		TECN	COMMENT
<0.15	90	PERUZZI	78	MRK1	$e^+e^- \to \Lambda X$

$\Gamma(K_S^0 K_S^0)/\Gamma_{total}$ Γ_{93}/Γ

VALUE (units 10^{-4})	CL%	DOCUMENT ID		TECN	COMMENT
< 0.052	90	[33] BALTRUSAIT...85C		MRK3	e^+e^-

[33] Forbidden by *CP*.

[34] Using $B(K_S^0 \to \pi^+\pi^-) = 0.6868 \pm 0.0027$.

RADIATIVE DECAYS

$\Gamma(\gamma\eta_c(1S))/\Gamma_{total}$ Γ_{94}/Γ

VALUE	EVTS	DOCUMENT ID		TECN	COMMENT
0.0127 ± 0.0036		GAISER	86	CBAL	$J/\psi \to \gamma X$
• • • We do not use the following data for averages, fits, limits, etc. • • •					
seen	16	BALTRUSAIT...84		MRK3	$J/\psi \to 2\phi\gamma$

$\Gamma(\gamma\pi^+\pi^- 2\pi^0)/\Gamma_{total}$ Γ_{95}/Γ

VALUE (units 10^{-3})	DOCUMENT ID		TECN	COMMENT
8.3 ± 0.2 ± 3.1	[35] BALTRUSAIT...86B		MRK3	$J/\psi \to 4\pi\gamma$

[35] 4π mass less than 2.0 GeV.

$\Gamma(\gamma\eta\pi\pi)/\Gamma_{total}$ Γ_{96}/Γ

VALUE (units 10^{-3})	DOCUMENT ID		TECN	COMMENT
6.1 ± 1.0 OUR AVERAGE				
5.85 ± 0.3 ± 1.05	[36] EDWARDS	83B	CBAL	$J/\psi \to \eta\pi^+\pi^-$
7.8 ± 1.2 ± 2.4	[36] EDWARDS	83B	CBAL	$J/\psi \to \eta 2\pi^0$

[36] Broad enhancement at 1700 MeV.

$\Gamma(\gamma\eta(1405/1475) \to \gamma K\overline{K}\pi)/\Gamma_{total}$ Γ_{97}/Γ

VALUE (units 10^{-3})	DOCUMENT ID		TECN	COMMENT
2.8 ± 0.6 OUR AVERAGE Error includes scale factor of 1.6. See the ideogram below.				
1.66 ± 0.1 ± 0.58	[37,38] BAI	00D	BES	$J/\psi \to \gamma K^\pm K_S^0 \pi^\mp$
3.8 ± 0.3 ± 0.6	[39] AUGUSTIN	90	DM2	$J/\psi \to \gamma K\overline{K}\pi$
4.0 ± 0.7 ± 1.0	[39] EDWARDS	82E	CBAL	$J/\psi \to K^+K^-\pi^0\gamma$
4.3 ± 1.7	[39,40] SCHARRE	80	MRK2	e^+e^-
• • • We do not use the following data for averages, fits, limits, etc. • • •				
1.78 ± 0.21 ± 0.33	[39,41,42] AUGUSTIN	92	DM2	$J/\psi \to \gamma K\overline{K}\pi$
0.83 ± 0.13 ± 0.18	[39,43,44] AUGUSTIN	92	DM2	$J/\psi \to \gamma K\overline{K}\pi$
$0.66^{+0.17+0.24}_{-0.16-0.15}$	[39,42,45] BAI	90C	MRK3	$J/\psi \to \gamma K_S^0 K^\pm\pi^\mp$
$1.03^{+0.21+0.26}_{-0.18-0.19}$	[39,44,46] BAI	90C	MRK3	$J/\psi \to \gamma K_S^0 K^\pm\pi^\mp$

[37] Interference with the $J/\psi(1S)$ radiative transition to the broad $K\overline{K}\pi$ pseudoscalar state around 1800 is $(0.15 \pm 0.01 \pm 0.05) \times 10^{-3}$.

[38] Interference with $J/\psi \to \gamma f_1(1420)$ is $(-0.03 \pm 0.01 \pm 0.01) \times 10^{-3}$.

[39] Includes unknown branching fraction $\eta(1405) \to K\overline{K}\pi$.

[40] Corrected for spin-zero hypothesis for $\eta(1405)$.

[41] From fit to the $a_0(980)\pi$ 0^{-+} partial wave.

[42] $a_0(980)\pi$ mode.

[43] From fit to the $K^*(892)K$ 0^{-+} partial wave.

[44] K^*K mode.

[45] From $a_0(980)\pi$ final state.

[46] From $K^*(890)K$ final state.

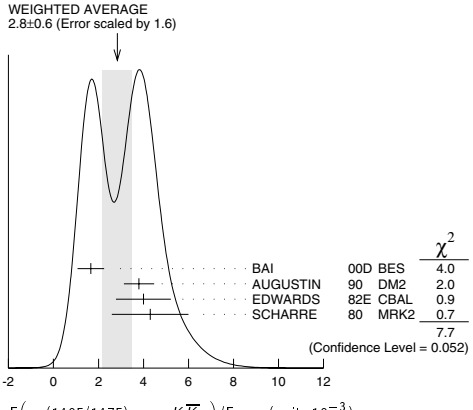

$\Gamma(\gamma\eta(1405/1475) \to \gamma\gamma\rho^0)/\Gamma_{total}$ Γ_{98}/Γ

VALUE (units 10^{-5})	DOCUMENT ID		TECN	COMMENT
6.4 ± 1.2 ± 0.7	[47] COFFMAN	90	MRK3	$J/\psi \to \gamma\gamma\pi^+\pi^-$

[47] Includes unknown branching fraction $\eta(1405) \to \gamma\rho^0$.

$\Gamma(\gamma\eta(1405/1475) \to \eta\pi^+\pi^-)/\Gamma_{total}$ Γ_{99}/Γ

VALUE (units 10^{-4})	EVTS	DOCUMENT ID		TECN	COMMENT
3.0 ± 0.5 OUR AVERAGE					
2.6 ± 0.7 ± 0.4		BAI	99	BES	$J/\psi \to \gamma\eta\pi^+\pi^-$
3.38 ± 0.33 ± 0.64		[48] BOLTON	92B	MRK3	$J/\psi \to \gamma\eta\pi^+\pi^-$
• • • We do not use the following data for averages, fits, limits, etc. • • •					
7.0 ± 0.6 ± 1.1	261	[49] AUGUSTIN	90	DM2	$J/\psi \to \gamma\eta\pi^+\pi^-$

[48] Via $a_0(980)\pi$.

[49] Includes unknown branching fraction to $\eta\pi^+\pi^-$.

$\Gamma(\gamma\rho\rho)/\Gamma_{total}$ Γ_{100}/Γ

VALUE (units 10^{-3})	CL%	DOCUMENT ID		TECN	COMMENT
4.5 ± 0.8 OUR AVERAGE					
4.7 ± 0.3 ± 0.9		[50] BALTRUSAIT...86B		MRK3	$J/\psi \to 4\pi\gamma$
3.75 ± 1.05 ± 1.20		[51] BURKE	82	MRK2	$J/\psi \to 4\pi\gamma$
• • • We do not use the following data for averages, fits, limits, etc. • • •					
< 0.09	90	[52] BISELLO	89B		$J/\psi \to 4\pi\gamma$

[50] 4π mass less than 2.0 GeV.

[51] 4π mass less than 2.0 GeV. We have multiplied $2\rho^0$ measurement by 3 to obtain 2ρ.

[52] 4π mass in the range 2.0–25 GeV.

$\Gamma(\gamma\eta_2(1870) \to \gamma\pi^+\pi^-)/\Gamma_{total}$ Γ_{101}/Γ

VALUE (units 10^{-4})	DOCUMENT ID		TECN	COMMENT
6.2 ± 2.2 ± 0.9	BAI	99	BES	$J/\psi \to \gamma\eta\pi^+\pi^-$

$\Gamma(\gamma\eta'(958))/\Gamma_{total}$ Γ_{102}/Γ

VALUE (units 10^{-3})	EVTS	DOCUMENT ID		TECN	COMMENT
4.31 ± 0.30 OUR AVERAGE					
4.50 ± 0.14 ± 0.53		BOLTON	92B	MRK3	$J/\psi \to \gamma\pi^+\pi^-\eta, \eta \to \gamma\gamma$
4.30 ± 0.31 ± 0.71		BOLTON	92B	MRK3	$J/\psi \to \gamma\pi^+\pi^-\eta, \eta \to \pi^+\pi^-\pi^0$
4.04 ± 0.16 ± 0.85	622	AUGUSTIN	90	DM2	$J/\psi \to \gamma\eta\pi^+\pi^-$
4.39 ± 0.09 ± 0.66	2420	AUGUSTIN	90	DM2	$J/\psi \to \gamma\gamma\pi^+\pi^-$
4.1 ± 0.3 ± 0.6		BLOOM	83	CBAL	$e^+e^- \to 3\gamma +$ hadrons
• • • We do not use the following data for averages, fits, limits, etc. • • •					
2.9 ± 1.1	6	BRANDELIK	79C	DASP	$e^+e^- \to 3\gamma$
2.4 ± 0.7	57	BARTEL	76	CNTR	$e^+e^- \to 2\gamma\rho$

$\Gamma(\gamma 2\pi^+ 2\pi^-)/\Gamma_{total}$ Γ_{103}/Γ

VALUE (units 10^{-3})	DOCUMENT ID		TECN	COMMENT
2.8 ± 0.5 OUR AVERAGE Error includes scale factor of 1.9. See the ideogram below.				
4.32 ± 0.14 ± 0.73	[53] BISELLO	89B	DM2	$J/\psi \to 4\pi\gamma$
2.08 ± 0.13 ± 0.35	[54] BISELLO	89B	DM2	$J/\psi \to 4\pi\gamma$
3.05 ± 0.08 ± 0.45	[54] BALTRUSAIT...86B		MRK3	$J/\psi \to 4\pi\gamma$
4.85 ± 0.45 ± 1.20	[55] BURKE	82	MRK2	e^+e^-

[53] 4π mass less than 3.0 GeV.

[54] 4π mass less than 2.0 GeV.

[55] 4π mass less than 2.5 GeV.

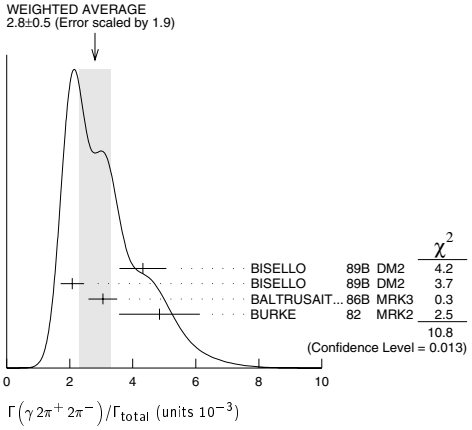

$\Gamma(\gamma K^+K^-\pi^+\pi^-)/\Gamma_{total}$ Γ_{104}/Γ

VALUE (units 10^{-3})	EVTS	DOCUMENT ID		TECN	COMMENT
2.1 ± 0.1 ± 0.6	1516	BAI	00B	BES	$J/\psi \to \gamma K^+K^0\pi^+\pi^-$

$\Gamma(\gamma f_4(2050))/\Gamma_{total}$ Γ_{105}/Γ

VALUE (units 10^{-3})	DOCUMENT ID		TECN	COMMENT
2.7 ± 0.5 ± 0.5	[56] BALTRUSAIT...87		MRK3	$J/\psi \to \gamma\pi^+\pi^-$

[56] Assuming branching fraction $f_4(2050) \to \pi\pi/$ total = 0.167.

$\Gamma(\gamma\omega\omega)/\Gamma_{\text{total}}$ Γ_{106}/Γ

VALUE (units 10^{-3})	EVTS	DOCUMENT ID		TECN	COMMENT
1.59±0.33 OUR AVERAGE					
1.41±0.2 ±0.42	120 ± 17	BISELLO	87	SPEC	e^+e^-, hadrons γ
1.76±0.09±0.45		BALTRUSAIT...85C		MRK3	$e^+e^- \to$ hadrons γ

$\Gamma(\gamma\eta(1405/1475) \to \gamma\rho^0\rho^0)/\Gamma_{\text{total}}$ Γ_{107}/Γ

VALUE (units 10^{-3})	DOCUMENT ID		TECN	COMMENT
1.7 ±0.4 OUR AVERAGE Error includes scale factor of 1.3.				
2.1 ±0.4	BUGG	95	MRK3	$J/\psi \to \gamma\pi^+\pi^-\pi^+\pi^-$
1.36±0.38 [57,58]	BISELLO	89B	DM2	$J/\psi \to 4\pi\gamma$

[57] Estimated by us from various fits.
[58] Includes unknown branching fraction to $\rho^0\rho^0$.

$\Gamma(\gamma f_2(1270))/\Gamma_{\text{total}}$ Γ_{108}/Γ

VALUE (units 10^{-3})	EVTS	DOCUMENT ID		TECN	CHG	COMMENT
1.38±0.14 OUR AVERAGE						
1.33±0.05±0.20		[59] AUGUSTIN	87	DM2		$J/\psi \to \gamma\pi^+\pi^-$
1.36±0.09±0.23		[59] BALTRUSAIT...87		MRK3		$J/\psi \to \gamma\pi^+\pi^-$
1.48±0.25±0.30	178	EDWARDS	82B	CBAL		$e^+e^- \to 2\pi^0\gamma$
2.0 ±0.7	35	ALEXANDER	78	PLUT	0	e^+e^-
1.2 ±0.6	30	[60] BRANDELIK	78B	DASP		$e^+e^- \to \pi^+\pi^-\gamma$

[59] Estimated using B($f_2(1270) \to \pi\pi$)=0.843 ± 0.012. The errors do not contain the uncertainty in the $f_2(1270)$ decay.
[60] Restated by us to take account of spread of E1, M2, E3 transitions.

$\Gamma(\gamma f_0(1710) \to \gamma K\overline{K})/\Gamma_{\text{total}}$ Γ_{109}/Γ

VALUE (units 10^{-4})	CL%	DOCUMENT ID		TECN	COMMENT
8.5 $^{+1.2}_{-0.9}$ OUR AVERAGE Error includes scale factor of 1.2.					
9.62±029 $^{+3.51}_{-1.86}$		[61] BAI	03G	BES	$J/\psi \to \gamma K\overline{K}$
5.0 ± 0.8 $^{+1.8}_{-0.4}$		[62,63] BAI	96C	BES	$J/\psi \to \gamma K^+K^-$
9.2 ± 1.4±1.4		[63] AUGUSTIN	88	DM2	$J/\psi \to \gamma K^+K^-$
10.4 ± 1.2±1.6		[63] AUGUSTIN	88	DM2	$J/\psi \to \gamma K^0_S K^0_S$
9.6 ± 1.2±1.8		[63] BALTRUSAIT...87		MRK3	$J/\psi \to \gamma K^+K^-$
• • • We do not use the following data for averages, fits, limits, etc. • • •					
1.6 ± 0.2 $^{+0.6}_{-0.2}$		[63,64] BAI	96C	BES	$J/\psi \to \gamma K^+K^-$
< 0.8	90	[65] BISELLO	89B		$J/\psi \to 4\pi\gamma$
1.6 ± 0.4±0.3		[66] BALTRUSAIT...87		MRK3	$J/\psi \to \gamma\pi^+\pi^-$
3.8 ± 1.6		[67] EDWARDS	82D	CBAL	$e^+e^- \to \eta\eta\gamma$

[61] Includes unknown branching ratio to K^+K^- or $K^0_S K^0_S$.
[62] Assuming $J^P = 2^+$ for $f_0(1710)$.
[63] Includes unknown branching fraction to K^+K^- or $K^0_S K^0_S$. We have multiplied K^+K^- measurement by 2, and $K^0_S K^0_S$ by 4 to obtain $K\overline{K}$ result.
[64] Assuming $J^P = 0^+$ for $f_0(1710)$.
[65] Includes unknown branching fraction to $\rho^0\rho^0$.
[66] Includes unknown branching fraction to $\pi^+\pi^-$.
[67] Includes unknown branching fraction to $\eta\eta$.

$\Gamma(\gamma f_0(1710) \to \gamma\pi\pi)/\Gamma_{\text{total}}$ Γ_{110}/Γ

VALUE (units 10^{-4})	DOCUMENT ID		TECN	COMMENT
• • • We do not use the following data for averages, fits, limits, etc. • • •				
2.5±1.6±0.8	BAI	98H	BES	$J/\psi \to \gamma\pi^0\pi^0$

$\Gamma(\gamma\eta)/\Gamma_{\text{total}}$ Γ_{111}/Γ

VALUE (units 10^{-3})	EVTS	DOCUMENT ID		TECN	COMMENT
0.86±0.08 OUR AVERAGE					
0.88±0.08±0.11		BLOOM	83	CBAL	e^+e^-
0.82±0.10		BRANDELIK	79C	DASP	e^+e^-
1.3 ±0.4	21	BARTEL	77	CNTR	e^+e^-

$\Gamma(\gamma f_1(1420) \to \gamma K\overline{K}\pi)/\Gamma_{\text{total}}$ Γ_{112}/Γ

VALUE (units 10^{-3})	DOCUMENT ID		TECN	COMMENT
0.79±0.13 OUR AVERAGE				
0.68±0.04±0.24	BAI	00D	BES	$J/\psi \to \gamma K^\pm K^0_S \pi^\mp$
0.76±0.15±0.21	[68,69] AUGUSTIN	92	DM2	$J/\psi \to \gamma K\overline{K}\pi$
0.87±0.14 $^{+0.14}_{-0.11}$	[68] BAI	90C	MRK3	$J/\psi \to \gamma K^0_S K^\pm \pi^\mp$

[68] Included unknown branching fraction $f_1(1420) \to K\overline{K}\pi$.
[69] From fit to the $K^*(892)K$ 1^{++} partial wave.

$\Gamma(\gamma f_1(1285))/\Gamma_{\text{total}}$ Γ_{113}/Γ

VALUE (units 10^{-3})	DOCUMENT ID		TECN	COMMENT
0.61 ±0.08 OUR AVERAGE				
0.61 ±0.04 ±0.21	[70] BAI	00D	BES	$J/\psi \to \gamma K^\pm K^0_S \pi^\mp$
0.45 ±0.09 ±0.17	[71] BAI	99	BES	$J/\psi \to \gamma\eta\pi^+\pi^-$
0.625±0.063±0.103	[72] BOLTON	92	MRK3	$J/\psi \to \gamma f_1(1285)$
0.70 ±0.08 ±0.16	[73] BOLTON	92B	MRK3	$J/\psi \to \gamma\eta\pi^+\pi^-$

[70] Assuming $\Gamma(f_1(1285) \to K\overline{K}\pi)/\Gamma_{\text{total}}$ =0.09 ± 0.04.
[71] Assuming $\Gamma(f_1(1285) \to \eta\pi\pi)/\Gamma_{\text{total}}$ =0.5 ± 0.18.
[72] Obtained summing the sequential decay channels
B($J/\psi \to \gamma f_1(1285), f_1(1285) \to \pi\pi\pi\pi$) = (1.44 ± 0.39 ± 0.27) × 10^{-4};
B($J/\psi \to \gamma f_1(1285), f_1(1285) \to a_0(980)\pi, a_0(980) \to \eta\pi$) = (3.90 ± 0.42 ± 0.87) × 10^{-4};
B($J/\psi \to \gamma f_1(1285), f_1(1285) \to a_0(980)\pi, a_0(980) \to K\overline{K}$) = (0.66 ± 0.26 ± 0.29) × 10^{-4};
B($J/\psi \to \gamma f_1(1285), f_1(1285) \to \gamma\rho^0$) = (0.25 ± 0.07 ± 0.03) × 10^{-4}.
[73] Using B($f_1(1285) \to a_0(980)\pi$) = 0.37, and including unknown branching ratio for $a_0(980) \to \eta\pi$.

$\Gamma(\gamma f_1(1510) \to \gamma\eta\pi^+\pi^-)/\Gamma_{\text{total}}$ Γ_{114}/Γ

VALUE (units 10^{-4})	DOCUMENT ID		TECN	COMMENT
4.5±1.0±0.7	BAI	99	BES	$J/\psi \to \gamma\eta\pi^+\pi^-$

$\Gamma(\gamma f_2'(1525))/\Gamma_{\text{total}}$ Γ_{115}/Γ

VALUE (units 10^{-4})	CL%	EVTS	DOCUMENT ID		TECN	COMMENT
4.5 $^{+0.7}_{-0.4}$ OUR AVERAGE						
3.85±0.17 $^{+1.91}_{-0.73}$			[74] BAI	03G	BES	$J/\psi \to \gamma K\overline{K}$
3.6 ±0.4 $^{+1.4}_{-0.4}$			[74] BAI	96C	BES	$J/\psi \to \gamma K^+K^-$
5.6 ±1.4 ±0.9			[74] AUGUSTIN	88	DM2	$J/\psi \to \gamma K^+K^-$
4.5 ±0.4 ±0.9			[74] AUGUSTIN	88	DM2	$J/\psi \to \gamma K^0_S K^0_S$
6.8 ±1.6 ±1.4			[74] BALTRUSAIT...87		MRK3	$J/\psi \to \gamma K^+K^-$
• • • We do not use the following data for averages, fits, limits, etc. • • •						
<3.4	90	4	[75] BRANDELIK	79C	DASP	$e^+e^- \to \pi^+\pi^-\gamma$
<2.3	90	3	ALEXANDER	78	PLUT	$e^+e^- \to K^+K^-\gamma$

[74] Using B($f_2'(1525) \to K\overline{K}$) = 0.888.
[75] Assuming isotropic production and decay of the $f_2'(1525)$ and isospin.

$\Gamma(\gamma f_2(1950) \to \gamma K^*(892)\overline{K}^*(892))/\Gamma_{\text{total}}$ Γ_{116}/Γ

VALUE (units 10^{-3})	DOCUMENT ID		TECN	COMMENT
0.7 ±0.1 ±0.2	BAI	00B	BES	$J/\psi \to \gamma K^+K^0\pi^+\pi^-$

$\Gamma(\gamma K^*(892)\overline{K}^*(892))/\Gamma_{\text{total}}$ Γ_{117}/Γ

VALUE (units 10^{-3})	EVTS	DOCUMENT ID		TECN	COMMENT
4.0±0.3±1.3	320	[76] BAI	00B	BES	$J/\psi \to \gamma K^+K^0\pi^+\pi^-$

[76] Summed over all charges.

$\Gamma(\gamma\phi\phi)/\Gamma_{\text{total}}$ Γ_{118}/Γ

VALUE (units 10^{-4})	EVTS	DOCUMENT ID		TECN	COMMENT
4.0±1.2 OUR AVERAGE Error includes scale factor of 2.1. See the ideogram below.					
7.5±0.6±1.2	168	BAI	90B	MRK3	$J/\psi \to \gamma 4K$
3.4±0.8±0.6	33 ± 7	[77] BISELLO	90	DM2	$J/\psi \to \gamma K^+K^-K^0_S K^0_L$
3.1±0.7±0.4		[77] BISELLO	86B	DM2	$J/\psi \to \gamma K^+K^-K^+K^-$

[77] $\phi\phi$ mass less than 2.9 GeV, η_C excluded.

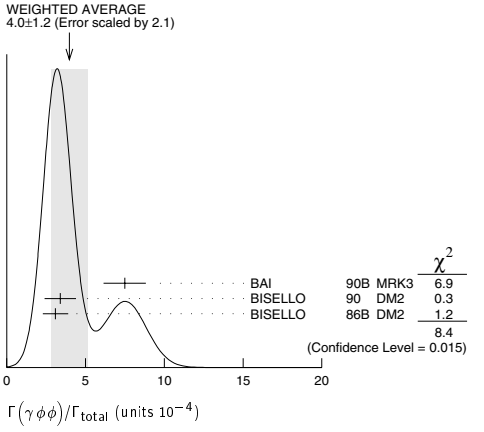

$\Gamma(\gamma p\overline{p})/\Gamma_{total}$ Γ_{119}/Γ

VALUE (units 10^{-3})	CL%	EVTS	DOCUMENT ID		TECN	COMMENT
$0.38\pm0.07\pm0.07$		49	EATON	84	MRK2	e^+e^-
• • • We do not use the following data for averages, fits, limits, etc. • • •						
<0.11	90		PERUZZI	78	MRK1	e^+e^-

$\Gamma(\gamma\eta(2225))/\Gamma_{total}$ Γ_{120}/Γ

VALUE (units 10^{-3})	DOCUMENT ID		TECN	COMMENT
0.29 ± 0.06 OUR AVERAGE				
$0.33\pm0.08\pm0.05$	[78] BAI	90B	MRK3	$J/\psi\to\gamma K^+K^-K^+K^-$
$0.27\pm0.06\pm0.06$	[78] BAI	90B	MRK3	$J/\psi\to\gamma K^+K^-K^0_SK^0_L$
$0.24^{+0.15}_{-0.10}$	[79,80] BISELLO	89B	DM2	$J/\psi\to4\pi\gamma$

[78] Includes unknown branching fraction to $\phi\phi$.
[79] Estimated by us from various fits.
[80] Includes unknown branching fraction to $\rho^0\rho^0$.

$\Gamma(\gamma\eta(1760)\to\gamma\rho^0\rho^0)/\Gamma_{total}$ Γ_{121}/Γ

VALUE (units 10^{-3})	DOCUMENT ID		TECN	COMMENT
0.13 ± 0.09	[81,82] BISELLO	89B	DM2	$J/\psi\to4\pi\gamma$

[81] Estimated by us from various fits.
[82] Includes unknown branching fraction to $\rho^0\rho^0$.

$\Gamma(\gamma(K\overline{K}\pi)_{J^PC=0^-+})/\Gamma_{total}$ Γ_{122}/Γ

VALUE (units 10^{-3})	DOCUMENT ID		TECN	COMMENT
0.7 ± 0.4 OUR AVERAGE Error includes scale factor of 2.1.				
$0.58\pm0.03\pm0.20$	[83] BAI	00D	BES	$J/\psi\to\gamma K^\pm K^0_S\pi^\mp$
$2.1\pm0.1\pm0.7$	[84] BAI	00D	BES	$J/\psi\to\gamma K^\pm K^0_S\pi^\mp$

[83] For a broad structure around 1800 MeV.
[84] For a broad structure around 2040 MeV.

$\Gamma(\gamma\pi^0)/\Gamma_{total}$ Γ_{123}/Γ

VALUE (units 10^{-3})	EVTS	DOCUMENT ID		TECN	COMMENT
0.039 ± 0.013 OUR AVERAGE					
$0.036\pm0.011\pm0.007$		BLOOM	83	CBAL	e^+e^-
0.073 ± 0.047	10	BRANDELIK	79C	DASP	e^+e^-

$\Gamma(\gamma p\overline{p}\pi^+\pi^-)/\Gamma_{total}$ Γ_{124}/Γ

VALUE (units 10^{-3})	CL%	DOCUMENT ID		TECN	COMMENT
<0.79	90	EATON	84	MRK2	e^+e^-

$\Gamma(\gamma\gamma)/\Gamma_{total}$ Γ_{125}/Γ

VALUE (units 10^{-3})	CL%	DOCUMENT ID		TECN	COMMENT
<0.5	90	BARTEL	77	CNTR	e^+e^-

$\Gamma(\gamma\lambda\overline{\lambda})/\Gamma_{total}$ Γ_{126}/Γ

VALUE (units 10^{-3})	CL%	DOCUMENT ID		TECN	COMMENT
<0.13	90	HENRARD	87	DM2	e^+e^-
• • • We do not use the following data for averages, fits, limits, etc. • • •					
<0.16	90	BAI	98G	BES	e^+e^-

$\Gamma(3\gamma)/\Gamma_{total}$ Γ_{127}/Γ

VALUE (units 10^{-3})	CL%	DOCUMENT ID		TECN	COMMENT
<0.055	90	PARTRIDGE	80	CBAL	e^+e^-

$\Gamma(\gamma f_0(2200))/\Gamma_{total}$ Γ_{128}/Γ

VALUE (units 10^{-4})	DOCUMENT ID		TECN	COMMENT
• • • We do not use the following data for averages, fits, limits, etc. • • •				
1.5	[85] AUGUSTIN	88	DM2	$J/\psi\to\gamma K^0_SK^0_S$

[85] Includes unknown branching fraction to $K^0_SK^0_S$.

$\Gamma(\gamma f_J(2220))/\Gamma_{total}$ Γ_{129}/Γ

VALUE (units 10^{-5})	CL%	EVTS	DOCUMENT ID		TECN	COMMENT
>250	99.9		[86] HASAN	96	SPEC	$\overline{p}p\to\pi^+\pi^-$
• • • We do not use the following data for averages, fits, limits, etc. • • •						
>300			[87] BAI	96B	BES	$e^+e^-\to\gamma\overline{p}p,\ K\overline{K}$
<2.3	95		[88] AUGUSTIN	88	DM2	$J/\psi\to\gamma K^+K^-$
<1.6	95		[88] AUGUSTIN	88	DM2	$J/\psi\to\gamma K^0_SK^0_S$
$12.4^{+6.4}_{-5.2}\pm2.8$		23	[88] BALTRUSAIT...	86D	MRK3	$J/\psi\to\gamma K^0_SK^0_S$
$8.4^{+3.4}_{-2.8}\pm1.6$		93	[88] BALTRUSAIT...	86D	MRK3	$J/\psi\to\gamma K^+K^-$

[86] Using BAI 96B.
[87] Using BARNES 93.
[88] Includes unknown branching fraction to K^+K^- or $K^0_SK^0_S$.

$\Gamma(\gamma f_J(2220)\to\gamma\pi\pi)/\Gamma_{total}$ Γ_{130}/Γ

VALUE (units 10^{-4})	DOCUMENT ID		TECN	COMMENT
$0.84\pm0.26\pm0.30$	BAI	96B	BES	$e^+e^-\to J/\psi\to\gamma\pi^+\pi^-$
• • • We do not use the following data for averages, fits, limits, etc. • • •				
$1.4\pm0.8\pm0.4$	BAI	98H	BES	$J/\psi\to\gamma\pi^0\pi^0$

$\Gamma(\gamma f_J(2220)\to\gamma K\overline{K})/\Gamma_{total}$ Γ_{131}/Γ

VALUE (units 10^{-5})	DOCUMENT ID		TECN	COMMENT
8.1 ± 3.0 OUR AVERAGE				
$6.6\pm2.9\pm2.4$	BAI	96B	BES	$e^+e^-\to J/\psi\to\gamma K^+K^-$
$10.8\pm4.0\pm3.2$	BAI	96B	BES	$e^+e^-\to J/\psi\to\gamma K^0_SK^0_S$

$\Gamma(\gamma f_J(2220)\to\gamma p\overline{p})/\Gamma_{total}$ Γ_{132}/Γ

VALUE (units 10^{-5})	DOCUMENT ID		TECN	COMMENT
$1.5\pm0.6\pm0.5$	BAI	96B	BES	$e^+e^-\to J/\psi\to\gamma p\overline{p}$

$\Gamma(\gamma f_0(1500))/\Gamma_{total}$ Γ_{133}/Γ

VALUE (units 10^{-4})	DOCUMENT ID		TECN	COMMENT
$>5.7\pm0.8$	[89,90] BUGG	95	MRK3	$J/\psi\to\gamma\pi^+\pi^-\pi^+\pi^-$

[89] Including unknown branching ratio for $f_0(1500)\to\pi^+\pi^-\pi^+\pi^-$.
[90] Assuming that $f_0(1500)$ decays only to two S-wave dipions.

$\Gamma(\gamma e^+e^-)/\Gamma_{total}$ Γ_{134}/Γ

VALUE (units 10^{-3})	DOCUMENT ID		TECN	COMMENT
$8.8\pm1.3\pm0.4$	[91] ARMSTRONG	96	E760	$\overline{p}p\to e^+e^-\gamma$

[91] For $E_\gamma > 100$ MeV.

LEPTON FAMILY NUMBER (LF) VIOLATING MODES

$\Gamma(e^\pm\mu^\mp)/\Gamma_{total}$ Γ_{135}/Γ

VALUE (units 10^{-6})	CL%	DOCUMENT ID		TECN	COMMENT
<1.1	90	BAI	03D	BES	$e^+e^-\to J/\psi$

$J/\psi(1S)$ REFERENCES

AUBERT	04	PR D69 011103	B. Aubert *et al.*	(BaBar Collab.)
BAI	04A	PR D69 012003	J.Z. Bai *et al.*	(BES Collab.)
AULCHENKO	03	PL B573 63	V.M. Aulchenko *et al.*	(KEDR Collab.)
BAI	03D	PL B561 49	J.Z. Bai *et al.*	(BES Collab.)
BAI	03G	PR D68 052003	J.Z. Bai *et al.*	(BES Collab.)
HUANG	03	PRL 91 241802	H.-C. Huang *et al.*	(BELLE Collab.)
ARTAMONOV	00	PL B474 427	A.S. Artamonov *et al.*	
BAI	00B	PL B472 200	J.Z. Bai *et al.*	(BES Collab.)
BAI	00D	PL B476 25	J.Z. Bai *et al.*	(BES Collab.)
BAI	99	PL B446 356	J.Z. Bai *et al.*	(BES Collab.)
BAI	99C	PRL 83 1918	J.Z. Bai *et al.*	(BES Collab.)
BAI	98D	PR D58 092006	J.Z. Bai *et al.*	(BES Collab.)
BAI	98G	PL B424 213	J.Z. Bai *et al.*	(BES Collab.)
BAI	98H	PRL 81 1179	J.Z. Bai *et al.*	(BES Collab.)
BALDINI	98	PL B444 111	R. Baldini *et al.*	(FENICE Collab.)
ARMSTRONG	96	PR D54 7067	T.A. Armstrong *et al.*	(E760 Collab.)
BAI	96B	PRL 76 3502	J.Z. Bai *et al.*	(BES Collab.)
BAI	96C	PRL 77 3959	J.Z. Bai *et al.*	(BES Collab.)
BAI	96D	PR D54 1221	J.Z. Bai *et al.*	(BES Collab.)
GRIBUSHIN	96	PR D53 4723	A. Gribushin *et al.*	(E672 Collab., E706 Collab.)
HASAN	96	PL B388 376	A. Hasan, D.V. Bugg	(BRUN, LOQM)
BAI	95B	PL B355 374	J.Z. Bai *et al.*	(BES Collab.)
BUGG	95	PL B353 378	D.V. Bugg *et al.*	(LOQM, PNPI, WASH)
ANTONELLI	93	PL B301 317	A. Antonelli *et al.*	(FENICE Collab.)
ARMSTRONG	93B	PR D47 772	T.A. Armstrong *et al.*	(FNAL E760 Collab.)
BARNES	93	PL B309 469	P.D. Barnes, P. Birien, W.H. Breunlich	
AUGUSTIN	92	PR D46 1951	J.E. Augustin, G. Cosme	(DM2 Collab.)
BOLTON	92	PL B278 495	T. Bolton *et al.*	(Mark III Collab.)
BOLTON	92B	PRL 69 1328	T. Bolton *et al.*	(Mark III Collab.)
COFFMAN	92	PRL 68 282	D.M. Coffman *et al.*	(Mark III Collab.)
HSUEH	92	PR D45 R2181	S. Hsueh, S. Palestini	(FNAL, TORI)
AUGUSTIN	90	PR D42 10	J.E. Augustin *et al.*	(DM2 Collab.)
BAI	90B	PRL 65 1309	Z. Bai *et al.*	(Mark III Collab.)
BAI	90C	PRL 65 2507	Z. Bai *et al.*	(Mark III Collab.)
BISELLO	90	PL B241 617	D. Bisello *et al.*	(DM2 Collab.)
COFFMAN	90	PR D41 1410	D.M. Coffman *et al.*	(Mark III Collab.)
JOUSSET	90	PR D41 1389	J. Jousset *et al.*	(DM2 Collab.)
ALEXANDER	89	NP B320 45	J.P. Alexander *et al.*	(LBL, MICH, SLAC)
AUGUSTIN	89	NP B320 1	J.E. Augustin, G. Cosme	(DM2 Collab.)
BISELLO	89B	PR D39 701	G. Busetto *et al.*	(DM2 Collab.)
AUGUSTIN	88	PRL 60 2238	J.E. Augustin *et al.*	(DM2 Collab.)
COFFMAN	88	PR D38 2695	D.M. Coffman *et al.*	(Mark III Collab.)
FALVARD	88	PR D38 2706	A. Falvard *et al.*	(CLER, FRAS, LALO+)
AUGUSTIN	87	ZPHY C36 369	J.E. Augustin *et al.*	(LALO, CLER, FRAS+)
BAGLIN	87	NP B286 592	C. Baglin *et al.*	(LAPP, CERN, GENO, LYON+)
BALTRUSAIT...	87	PR D35 2077	R.M. Baltrusaitis *et al.*	(Mark III Collab.)
BECKER	87	PRL 59 186	J.J. Becker *et al.*	(Mark III Collab.)
BISELLO	87	PL B192 239	D. Bisello *et al.*	(PADO, CLER, FRAS+)
COHEN	87	RMP 59 1121	E.R. Cohen, B.N. Taylor	(RISC, NBS)
HENRARD	87	NP B292 670	P. Henrard *et al.*	(CLER, FRAS, LALO+)
PALLIN	87	NP B292 653	D. Pallin *et al.*	(CLER, FRAS, LALO, PADO)
BALTRUSAIT...	86B	PR D33 1222	R.M. Baltrusaitis *et al.*	(Mark III Collab.)
BALTRUSAIT...	86D	PRL 56 107	R.M. Baltrusaitis	(CIT, UCSC, ILL, SLAC+)
BISELLO	86B	PL B179 294	D. Bisello *et al.*	(DM2 Collab.)
GAISER	86	PR D34 711	J. Gaiser *et al.*	(Crystal Ball Collab.)
BALTRUSAIT...	85C	PRL 55 1723	R.M. Baltrusaitis *et al.*	(CIT, UCSC+)
BALTRUSAIT...	85D	PR D32 566	R.M. Baltrusaitis *et al.*	(CIT, UCSC+)
KURAEV	85	SJNP 41 466	E.A. Kuraev, V.S. Fadin	(NOVO)

Translated from YAF 41 733.

BALTRUSAIT...	84	PRL 52 2126	R.M. Baltrusaitis *et al.*	(CIT, UCSC+)
EATON	84	PR D29 804	M.W. Eaton *et al.*	(LBL, SLAC)
BLOOM	83	ARNS 33 143	E.D. Bloom, C. Peck	(SLAC, CIT)
EDWARDS	83B	PRL 51 859	C. Edwards *et al.*	(CIT, HARV, PRIN+)
FRANKLIN	83	PRL 51 963	M.E.B. Franklin *et al.*	(LBL, SLAC)
BURKE	82	PRL 49 632	D.L. Burke *et al.*	(LBL, SLAC)
EDWARDS	82B	PR D25 3065	C. Edwards *et al.*	(CIT, HARV, PRIN+)
EDWARDS	82D	PRL 48 458	C. Edwards *et al.*	(CIT, HARV, PRIN+)
Also	83	ARNS 33 143	E.D. Bloom, C. Peck	(SLAC, CIT)
EDWARDS	82E	PRL 49 259	C. Edwards *et al.*	(CIT, HARV, PRIN+)
LEMOIGNE	82	PL 113B 509	Y. Lemoigne *et al.*	(SACL, LOIC, SHMP+)
BESCH	81	ZPHY C8 1	H.J. Besch *et al.*	(BONN, DESY, MANZ)
GIDAL	81	PL 107B 153	G. Gidal *et al.*	(SLAC, LBL)
PARTRIDGE	80	PRL 44 712	R. Partridge *et al.*	(CIT, HARV, PRIN+)
SCHARRE	80	PL 97B 329	D.L. Scharre *et al.*	(SLAC, LBL)
ZHOLENTZ	80	PL 96B 214	A.A. Zholents *et al.*	(NOVO)
Also	81	SJNP 34 814 Translated from YAF 34 1471.	A.A. Zholents *et al.*	(NOVO)
BRANDELIK	79C	ZPHY C1 233	R. Brandelik *et al.*	(DASP Collab.)
ALEXANDER	78	PL 72B 493	G. Alexander *et al.*	(DESY, HAMB, SIEG+)
BESCH	78	PL 78B 347	H.J. Besch *et al.*	(BONN, DESY, MANZ)
BRANDELIK	78B	PL 74B 292	R. Brandelik *et al.*	(DASP Collab.)
PERUZZI	78	PR D17 2901	I. Peruzzi *et al.*	(SLAC, LBL)
BARTEL	77	PL 66B 489	W. Bartel *et al.*	(DESY, HEIDP)
BURMESTER	77D	PL 72B 135	J. Burmester *et al.*	(DESY, HAMB, SIEG+)
FELDMAN	77	PRPL 33C 285	G.J. Feldman, M.L. Perl	(LBL, SLAC)
VANNUCCI	77	PR D15 1814	F. Vannucci *et al.*	(SLAC, LBL)
BARTEL	76	PL 64B 483	W. Bartel *et al.*	(DESY, HEIDP)
BRAUNSCH...	76	PL 63B 487	W. Braunschweig *et al.*	(DASP Collab.)
JEAN-MARIE	76	PRL 36 291	B. Jean-Marie *et al.*	(SLAC, LBL) IG
BALDINI-...	75	PL 58B 471	R. Baldini-Cello *et al.*	(FRAS, ROMA)
BOYARSKI	75	PRL 34 1357	A.M. Boyarski *et al.*	(SLAC, LBL) JPC
DASP	75	PL 56B 491	W. Braunschweig *et al.*	(DASP Collab.)
ESPOSITO	75B	LNC 14 73	B. Esposito *et al.*	(FRAS, NAPL, PADO+)
FORD	75	PRL 34 604	R.L. Ford *et al.*	(SLAC, PENN)

OTHER RELATED PAPERS

DATTA	03B	PL B567 273	A. Datta, P.J. O'Donnel	
LI	03C	EPJ C28 335	D.M. Li *et al.*	
LI	03D	IJMP A18 3335	D.M. Li *et al.*	
BAI	01B	PR B510 75	J.Z. Bai *et al.*	(BEPC BES Collab.)
CHEN	98	PRL 80 5060	Y.Q. Chen, E. Braaten	
SUZUKI	98	PR D57 5717	M. Suzuki	
BARATE	83	PL 121B 449	R. Barate *et al.*	(SACL, LOIC, SHMP, IND)
ABRAMS	74	PRL 33 1453	G.S. Abrams *et al.*	(LBL, SLAC)
ASH	74	LNC 11 705	W.W. Ash *et al.*	(FRAS, UMD, NAPL, PADO+)
AUBERT	74	PRL 33 1404	J.J. Aubert *et al.*	(MIT, BNL)
AUGUSTIN	74	PRL 33 1406	J.E. Augustin *et al.*	(SLAC, LBL)
BACCI	74	PRL 33 1408	C. Bacci *et al.*	(FRAS)
Also	74B	PRL 33 1649 (erratum)	C. Bacci	
BALDINI-...	74	LNC 11 711	R. Baldini-Cello *et al.*	(FRAS, ROMA)
BARBIELLINI	74	LNC 11 718	G. Barbiellini *et al.*	(FRAS, NAPL, PISA+)
BRAUNSCH...	74	PL 53B 393	W. Braunschweig *et al.*	(DASP Collab.)
CHRISTENS...	70	PRL 25 1523	J.C. Christenson *et al.*	(COLU, BNL, CERN)

BRANCHING RATIOS OF $\psi(2S)$ AND $\chi_{c0,1,2}$

Written March 2002 by J.J. Hernández-Rey (IFIC, Valencia), S. Navas (University of Granada), and C. Patrignani (INFN, Genova). Updated Nov 2003

Since 2002, the treatment of the branching ratios of the $\psi(2S)$ and $\chi_{c0,1,2}$ has undergone an important restructuring.

When measuring a branching ratio experimentally, it is not always possible to normalize the number of events observed in the corresponding decay mode to the total number of particles produced. Therefore, the experimenters sometimes report the number of observed decays with respect to another decay mode of the same or another particle in the relevant decay chain. This is actually equivalent to measuring combinations of branching fractions of several decay modes.

To extract the branching ratio of a given decay mode, the collaborations use some previously reported measurements of the required branching ratios. However, the values are frequently taken from the *Review of Particle Physics* (RPP), which in turn uses the branching ratio reported by the experiment in the following edition, giving rise either to correlations or to plain vicious circles.

One of these inconsistencies within the $\psi(2S)$ decays was reported in Ref. 10. To obtain the branching ratios of the decay modes $\psi(2S) \to J/\psi(1S)\,\pi^+\,\pi^-$, $\psi(2S) \to J/\psi(1S)\,\pi^0\,\pi^0$, and $\psi(2S) \to J/\psi(1S)\,\eta$, E760 Collaboration [2] used the value of $\mathrm{B}(\psi(2S) \to J/\psi(1S)\ anything)$ given in Ref. 6, obtained with a fit that included the above decays. The values obtained in this way in Ref. 2 were subsequently used in the 1998 edition of RPP [7] as new entries in the same fit.

A more subtle correlation, among others, was pointed out in Ref. 5. BES Collaboration [3] obtained the value of $B(\chi_{c0} \to p\,\overline{p})$ in e^+e^- collisions from the number of observed decays $\psi(2S) \to \gamma\,\chi_{c0} \to \gamma\,p\,\overline{p}$, and the total number of $\psi(2S)$ produced, which was estimated in turn from the observed number of decays of the type $\psi(2S) \to J/\psi(1S)\,\pi^+\,\pi^-$ [4]. To this end, they used the values of the branching ratios of $\psi(2S) \to J/\psi(1S)\,\pi^+\,\pi^-$ and $\psi(2S) \to \gamma\,\chi_{c0}$ given in the 1996 edition of RPP [6]. On the other hand, in $p\,\overline{p}$ collision experiments (*e.g.*, E835 Collaboration [1]), the value of $\mathrm{B}(\psi(2S) \to \gamma\,\chi_{c0})$ was entered inversely in the determination of $\mathrm{B}(\chi_{c0} \to p\,\overline{p})$ from a measurement of $\Gamma(\chi_{c0} \to p\,\overline{p}) \times \mathrm{B}(\chi_{c0} \to \gamma\,J/\psi(1S))$, since it was used to derive $\mathrm{B}(\chi_{c0} \to \gamma\,J/\psi(1S))$. Therefore, a hidden correlation was introduced in RPP when quoting the values of the corresponding unfolded magnitudes for both types of experiments.

The way to avoid these dependencies and correlations is to extract the branching ratios through a fit that uses the truly measured combinations of branching fractions and partial widths. This fit, in fact, should involve decays from the four concerned particles, $\psi(2S)$, χ_{c0}, χ_{c1}, and χ_{c2}, and occasionally some combinations of branching ratios of more than one of them. This is what is done since the 2002 edition [9].

The PDG policy is to quote the results of the collaborations in a manner as close as possible to what appears in their original publications. However, in order to avoid the problems mentioned above, we had in some cases to work out the values originally measured, using the number of events and detection efficiencies given by the collaborations, or rescaling back the published results. The information was sometimes spread over several articles, and some articles referred to papers still unpublished, which in turn contained the relevant numbers in footnotes.

Even though the experimental collaborations are entitled to extract whatever branching ratios they consider appropriate by using other published results, we would like to encourage them to also quote explicitly in their articles the actual quantities measured, so that they can be used directly in averages and fits of different experimental determinations.

To inform the reader how we computed some of the values used in this edition of RPP, we use footnotes to indicate the branching ratios actually given by the experiments and the quantities they use to derive them from the true combination of branching ratios actually measured.

None of the branching ratios of the $\chi_{c0,1,2}$ are measured independently of the $\psi(2S)$ radiative decays. We tried to identify those branching ratios which can be correlated in a non-trivial way, and although we cannot preclude the existence of other cases, we are confident that the most relevant correlations have already been removed. Nevertheless, correlations in the errors of different quantities measured by the same experiment have not been taken into account.

The relatively high χ^2 of the fit, 1.5 per d.o.f., can be traced back to a few specific discrepancies in the data. No rescaling of errors has been applied.

FIT INFORMATION

This is an overall fit to 4 total widths, 1 partial width, 6 combinations of partial widths, 6 branching ratios, and 28 combinations of branching ratios. Of the latter, 13 involve decays of more than one particle. The overall fit uses 88 measurements to determine 24 parameters. The overall fit has a χ^2 of 95.8 for 64 degrees of freedom.

	Mode	Value
1	$\Gamma(\chi_{c0})$ (MeV)	10.1 ± 0.8
2	$\mathcal{B}(\chi_{c0} \to \gamma J/\psi)$	$(1.18 \pm 0.14) \times 10^{-2}$
3	$\mathcal{B}(\chi_{c0} \to p\bar{p})$	$(2.24 \pm 0.27) \times 10^{-4}$
4	$\mathcal{B}(\chi_{c0} \to \gamma\gamma)$	$(2.6 \pm 0.5) \times 10^{-4}$
5	$\mathcal{B}(\chi_{c0} \to 2\pi^+ 2\pi^-)$	$(2.58 \pm 0.31) \times 10^{-2}$
6	$\mathcal{B}(\chi_{c0} \to \pi\pi)$	$(7.4 \pm 0.8) \times 10^{-3}$
7	$\Gamma(\chi_{c1})$ (MeV)	0.91 ± 0.13
8	$\mathcal{B}(\chi_{c1} \to \gamma J/\psi)$	0.316 ± 0.033
9	$\mathcal{B}(\chi_{c1} \to p\bar{p})$	$(0.72 \pm 0.13) \times 10^{-4}$
10	$\Gamma(\chi_{c2})$ (MeV)	2.11 ± 0.16
11	$\mathcal{B}(\chi_{c2} \to \gamma J/\psi)$	0.202 ± 0.017
12	$\mathcal{B}(\chi_{c2} \to p\bar{p})$	$(0.68 \pm 0.07) \times 10^{-4}$
13	$\mathcal{B}(\chi_{c2} \to \gamma\gamma)$	$(2.46 \pm 0.23) \times 10^{-4}$
14	$\mathcal{B}(\chi_{c2} \to 2\pi^+ 2\pi^-)$	$(1.48 \pm 0.21) \times 10^{-2}$
15	$\Gamma(\psi')$ (keV)	281 ± 17
16	$\mathcal{B}(\psi' \to J/\psi\, \pi^+\pi^-)$	0.317 ± 0.011
17	$\mathcal{B}(\psi' \to J/\psi\, \pi^0\pi^0)$	0.188 ± 0.012
18	$\mathcal{B}(\psi' \to J/\psi\, \eta)$	$(3.16 \pm 0.22) \times 10^{-2}$
19	$\mathcal{B}(\psi' \to \gamma\, \chi_{c0})$	$(8.6 \pm 0.7) \times 10^{-2}$
20	$\mathcal{B}(\psi' \to \gamma\, \chi_{c1})$	$(8.4 \pm 0.8) \times 10^{-2}$
21	$\mathcal{B}(\psi' \to \gamma\, \chi_{c2})$	$(6.4 \pm 0.6) \times 10^{-2}$
22	$\mathcal{B}(\psi' \to e^+ e^-)$	$(75.5 \pm 3.1) \times 10^{-4}$
23	$\mathcal{B}(\psi' \to \mu^+ \mu^-)$	$(73 \pm 8) \times 10^{-4}$
24	$\mathcal{B}(\psi' \to \tau^+ \tau^-)$	$(28 \pm 7) \times 10^{-4}$

The following *off-diagonal* array elements are the correlation coefficients $< \delta x_i \delta x_j > / (\delta x_i \cdot \delta x_j)$, in percent, from the fit to the corresponding parameter x_i.

2	−8											
3	7	−81										
4	−21	18	−13									
5	−8	24	−24	−27								
6	−6	47	−52	−3	46							
7	0	0	0	0	0	0						
8	0	0	0	0	0	0	−12					
9	0	0	0	0	1	0	−65	−42				
10	0	0	0	0	0	0	0	0	0			
11	0	0	0	0	0	0	0	0	0	−43		
12	0	0	0	0	0	0	0	0	0	−30	−41	
13	0	0	0	0	−1	−1	0	0	0	−34	16	2
14	0	0	0	−1	3	3	0	0	1	−25	40	−10
15	0	1	0	2	−6	−5	1	−1	−1	0	1	−1
16	−1	−3	0	−7	17	15	−2	−1	3	−1	−3	3
17	0	−1	0	−3	8	7	−1	0	1	0	−1	1
18	0	0	0	−1	2	2	0	0	0	0	−1	1
19	7	−44	41	9	−63	−65	0	0	0	0	0	0
20	0	0	0	0	0	0	12	−84	33	0	0	0
21	0	0	0	0	1	1	0	0	0	35	−77	30
22	−1	−2	0	−5	12	10	−2	2	1	−1	−1	2
23	0	−1	0	−2	5	5	−1	0	1	0	−1	1
24	0	0	0	−1	2	2	0	0	0	0	0	0
	1	2	3	4	5	6	7	8	9	10	11	12

14	−8										
15	1	−5									
16	−3	17	−33								
17	−2	8	−27	48							
18	−1	2	−8	14	13						
19	0	3	−5	15	7	2					
20	0	0	−1	2	1	0	0				
21	−8	−51	−2	5	3	1	1	0			
22	−2	11	−40	69	69	21	10	2	5		
23	−1	5	−10	30	17	5	4	1	2	22	
24	0	3	−5	15	7	2	2	0	1	10	4
	13	14	15	16	17	18	19	20	21	22	23

References

1. M. Ambrogiani *et al.*, Phys. Rev. Lett. **83**, 2902 (1999).
2. T.A. Armstrong *et al.*, Phys. Rev. **D55**, 1153 (1997).
3. J.Z. Bai *et al.*, Phys. Rev. Lett. **81**, 3091 (1998).
4. J.Z. Bai *et al.*, Phys. Rev. **D58**, 092006–1 (1998).
5. C. Patrignani, Phys. Rev. **D64**, 034017 (2001).
6. Particle Data Group, R.M. Barnett *et al.*, Phys. Rev. **D54**, 1 (1996).
7. Particle Data Group, C. Caso *et al.*, Eur. Phys. J. **C3**, 1 (1998).
8. Particle Data Group, D.E. Groom *et al.*, Eur. Phys. J. **C15**, 1 (2000).
9. Particle Data Group, K.Hagiwara *et al.*, Phys. Rev. **D68**, 010001 (2002).
10. Y.F. Gu and X.H. Li, Phys. Lett. **B449**, 361 (1999).

$\chi_{c0}(1P)$

$I^G(J^{PC}) = 0^+(0^{++})$

$\chi_{c0}(1P)$ MASS

VALUE (MeV)	EVTS	DOCUMENT ID		TECN	COMMENT
3415.19 ± 0.34 OUR AVERAGE					
$3414.7\ ^{+\ 0.7}_{-\ 0.6} \pm 0.2$		[1] ANDREOTTI	03	E835	$\overline{p}p \to \chi_{c0} \to \pi^0\pi^0$
3415.4 ± 0.4 ± 0.2	392	[1] BAGNASCO	02	E835	$\overline{p}p \to \chi_{c0} \to J/\psi\gamma$
3416.5 ± 3.0		EISENSTEIN	01	CLE2	$e^+e^- \to e^+e^-\chi_{c0}$
$3417.4\ ^{+\ 1.8}_{-\ 1.9} \pm 0.2$		[1] AMBROGIANI	99B	E835	$\overline{p}p \to e^+e^-\gamma$
3414.1 ± 0.6 ± 0.8		BAI	99B	BES	$\psi(2S) \to \gamma X$
3417.8 ± 0.4 ± 4		[1] GAISER	86	CBAL	$\psi(2S) \to \gamma X$
3422 ± 10		[2] BARTEL	78B	CNTR	$e^+e^- \to J/\psi 2\gamma$
3416 ± 3 ± 4		[2] TANENBAUM	78	MRK1	e^+e^-
3415 ± 9		[2] BIDDICK	77	CNTR	$e^+e^- \to \gamma X$

[1] Using mass of $\psi(2S) = 3686.0$ MeV.
[2] Mass value shifted by us by amount appropriate for $\psi(2S)$ mass = 3686 MeV and $J/\psi(1S)$ mass = 3097 MeV.

$\chi_{c0}(1P)$ WIDTH

VALUE (MeV)	EVTS	DOCUMENT ID		TECN	COMMENT
10.1 ± 0.8 OUR FIT					
10.2 ± 0.9 OUR AVERAGE Error includes scale factor of 1.2.					
$8.6^{+1.7}_{-1.3} \pm 0.1$		ANDREOTTI	03	E835	$\overline{p}p \to \chi_{c0} \to \pi^0\pi^0$
9.8 ± 1.0 ± 0.1	392	BAGNASCO	02	E835	$\overline{p}p \to \chi_{c0} \to J/\psi\gamma$
$16.6^{+5.2}_{-3.7} \pm 0.1$		AMBROGIANI	99B	E835	$\overline{p}p \to e^+e^-\gamma$
14.3 ± 2.0 ± 3.0		BAI	98I	BES	$\psi(2S) \to \gamma\pi^+\pi^-$
13.5 ± 3.3 ± 4.2		GAISER	86	CBAL	$\psi(2S) \to \gamma X, \gamma\pi^0\pi^0$

$\chi_{c0}(1P)$ DECAY MODES

	Mode	Fraction (Γ_i/Γ)	Confidence level
	Hadronic decays		
Γ_1	$2(\pi^+\pi^-)$	(2.58 ± 0.31) %	
Γ_2	$\pi^+\pi^- K^+K^-$	(2.1 ± 0.5) %	
Γ_3	$\rho^0\pi^+\pi^-$	(1.6 ± 0.5) %	
Γ_4	$3(\pi^+\pi^-)$	(1.27 ± 0.22) %	
Γ_5	$K^+\overline{K}^*(892)^0\pi^- +$ c.c.	(1.2 ± 0.4) %	
Γ_6	K^+K^-	(6.0 ± 0.9) × 10^{-3}	
Γ_7	$\pi\pi$	(7.4 ± 0.8) × 10^{-3}	
Γ_8	$\eta\eta$	(2.1 ± 1.1) × 10^{-3}	
Γ_9	$K^+K^-K^+K^-$	(2.3 ± 0.5) × 10^{-3}	
Γ_{10}	$K^0_S K^0_S$	(2.1 ± 0.6) × 10^{-3}	
Γ_{11}	$\pi^+\pi^- p\overline{p}$	(2.2 ± 0.8) × 10^{-3}	
Γ_{12}	$\phi\phi$	(1.0 ± 0.6) × 10^{-3}	
Γ_{13}	$p\overline{p}$	(2.24 ± 0.27) × 10^{-4}	
Γ_{14}	$\Lambda\overline{\Lambda}$	(4.7 ± 1.6) × 10^{-4}	
Γ_{15}	$K^0_S K^+\pi^-$ + c.c.	< 8 × 10^{-4}	90%
	Radiative decays		
Γ_{16}	$\gamma J/\psi(1S)$	(1.18 ± 0.14) %	
Γ_{17}	$\gamma\gamma$	(2.6 ± 0.5) × 10^{-4}	

$\chi_{c0}(1P)$ PARTIAL WIDTHS

$\chi_{c0}(1P)$ Γ(i)$\Gamma(\gamma J/\psi(1S))/\Gamma$(total)

$\Gamma(p\overline{p}) \times \Gamma(\gamma J/\psi(1S))/\Gamma_{\text{total}}$ $\Gamma_{13}\Gamma_{16}/\Gamma$

VALUE (eV)	EVTS	DOCUMENT ID		TECN	COMMENT
26.8 ± 2.9 OUR FIT					
• • • We do not use the following data for averages, fits, limits, etc. • • •					
26.6 ± 2.6 ± 1.4	392	[3,4] BAGNASCO	02	E835	$\overline{p}p \to \chi_{c0} \to J/\psi\gamma$
$48.7^{+11.3}_{-8.9} \pm 2.4$		[3,4] AMBROGIANI	99B	E835	$\overline{p}p \to \gamma J/\psi$

$\Gamma(\gamma\gamma) \times \Gamma(2(\pi^+\pi^-))/\Gamma_{\text{total}}$ $\Gamma_{17}\Gamma_1/\Gamma$

VALUE (eV)	DOCUMENT ID		TECN	COMMENT
67 ± 14 OUR FIT				
75 ± 13 ± 8	EISENSTEIN	01	CLE2	$e^+e^- \to e^+e^-\chi_{c0}$

[3] Calculated by us using $B(J/\psi(1S) \to e^+e^-) = 0.0593 \pm 0.0010$.
[4] Values in $(\Gamma(p\overline{p}) \times \Gamma(\gamma J/\psi(1S))/\Gamma_{\text{total}})$ and $(\Gamma(p\overline{p}) \times \Gamma(\gamma J/\psi(1S))/\Gamma^2_{\text{total}})$ are not independent. The latter is used in the fit since it is less correlated to the total width.

$\chi_{c0}(1P)$ BRANCHING RATIOS

HADRONIC DECAYS

$\Gamma(2(\pi^+\pi^-))/\Gamma_{\text{total}}$ Γ_1/Γ

VALUE	DOCUMENT ID
0.0258 ± 0.0031 OUR FIT	

$\Gamma(\pi^+\pi^- K^+K^-)/\Gamma_{\text{total}}$ Γ_2/Γ

VALUE (units 10^{-3})	DOCUMENT ID		TECN	COMMENT
21 ± 5 OUR EVALUATION Treating systematic error as correlated.				
21 ± 6 OUR AVERAGE Error includes scale factor of 1.9.				
15.6 ± 0.7 ± 3.9	[5] BAI	99B	BES	$\psi(2S) \to \gamma\chi_{c0}$
27.4 ± 3.7 ± 2.7	[5] TANENBAUM	78	MRK1	$\psi(2S) \to \gamma\chi_{c0}$

$\Gamma(\rho^0\pi^+\pi^-)/\Gamma_{\text{total}}$ Γ_3/Γ

VALUE	DOCUMENT ID		TECN	COMMENT
0.016 ± 0.005	[6] TANENBAUM	78	MRK1	$\psi(2S) \to \gamma\chi_{c0}$

$\Gamma(3(\pi^+\pi^-))/\Gamma_{\text{total}}$ Γ_4/Γ

VALUE (units 10^{-3})	DOCUMENT ID		TECN	COMMENT
12.7 ± 2.2 OUR EVALUATION Treating systematic error as correlated.				
12.7 ± 2.0 OUR AVERAGE				
12.4 ± 1.1 ± 2.3	[5] BAI	99B	BES	$\psi(2S) \to \gamma\chi_{c0}$
13.3 ± 3.0 ± 1.3	[5] TANENBAUM	78	MRK1	$\psi(2S) \to \gamma\chi_{c0}$

$\Gamma(K^+\overline{K}^*(892)^0\pi^- + \text{c.c.})/\Gamma_{\text{total}}$ Γ_5/Γ

VALUE	DOCUMENT ID		TECN	COMMENT
0.012 ± 0.004	[6] TANENBAUM	78	MRK1	$\psi(2S) \to \gamma\chi_{c0}$

$\Gamma(K^+K^-)/\Gamma_{\text{total}}$ Γ_6/Γ

VALUE (units 10^{-3})	EVTS	DOCUMENT ID		TECN	COMMENT
6.0 ± 0.4 ± 0.8	774 ± 38	[5] BAI	98I	BES	$\psi(2S) \to \gamma\chi_{c0}$
• • • We do not use the following data for averages, fits, limits, etc. • • •					
6 ± 3		[6] BRANDELIK	79B	DASP	$\psi(2S) \to \gamma\chi_{c0}$
9 ± 4		[6] TANENBAUM	78	MRK1	$\psi(2S) \to \gamma\chi_{c0}$

$\Gamma(K^0_S K^0_S)/\Gamma_{\text{total}}$ Γ_{10}/Γ

VALUE (units 10^{-3})	DOCUMENT ID		TECN	COMMENT
2.08 ± 0.30 ± 0.54	[5] BAI	99B	BES	$\psi(2S) \to \gamma\chi_{c0}$

$\Gamma(\pi\pi)/\Gamma_{\text{total}}$ Γ_7/Γ

VALUE (units 10^{-3})	DOCUMENT ID
7.4 ± 0.8 OUR FIT	

$\Gamma(K^+K^-K^+K^-)/\Gamma_{\text{total}}$ Γ_9/Γ

VALUE (units 10^{-3})	DOCUMENT ID		TECN	COMMENT
2.27 ± 0.28 ± 0.40	[5] BAI	99B	BES	$\psi(2S) \to \gamma\chi_{c0}$

$\Gamma(\pi^+\pi^- p\overline{p})/\Gamma_{\text{total}}$ Γ_{11}/Γ

VALUE (units 10^{-3})	DOCUMENT ID		TECN	COMMENT
2.2 ± 0.8 OUR EVALUATION Treating systematic error as correlated.				
2.2 ± 1.1 OUR AVERAGE Error includes scale factor of 1.9.				
1.66 ± 0.22 ± 0.58	[5] BAI	99B	BES	$\psi(2S) \to \gamma\chi_{c0}$
4.4 ± 1.2 ± 0.4	[5] TANENBAUM	78	MRK1	$\psi(2S) \to \gamma\chi_{c0}$

$\Gamma(\phi\phi)/\Gamma_{\text{total}}$ Γ_{12}/Γ

VALUE (units 10^{-3})	DOCUMENT ID		TECN	COMMENT
1.0 ± 0.4 ± 0.4	[5] BAI	99B	BES	$\psi(2S) \to \gamma\chi_{c0}$

$\Gamma(\eta\eta)/\Gamma_{\text{total}}$ Γ_8/Γ

VALUE (units 10^{-3})	EVTS	DOCUMENT ID		TECN	COMMENT
2.1 ± 0.9 ± 0.6	12.7 ± 5.3	[5] BAI	03C	BES	$\psi(2S) \to \gamma\eta\eta \to 5\gamma$
• • • We do not use the following data for averages, fits, limits, etc. • • •					
2.5 ± 0.8 ± 0.8		[7] LEE	85	CBAL	$\psi' \to$ photons

$\Gamma(\eta\eta)/\Gamma(\pi\pi)$ Γ_8/Γ_7

VALUE	DOCUMENT ID		TECN	COMMENT
• • • We do not use the following data for averages, fits, limits, etc. • • •				
0.24 ± 0.10 ± 0.08	[8] BAI	03C	BES	$\psi(2S) \to 5\gamma$

$\Gamma(K^0_S K^+\pi^- + \text{c.c.})/\Gamma_{\text{total}}$ Γ_{15}/Γ

VALUE (units 10^{-3})	CL%	DOCUMENT ID		TECN	COMMENT
< 0.8	90	[5] BAI	99B	BES	$\psi(2S) \to \gamma\chi_{c0}$

$\Gamma(p\overline{p})/\Gamma_{\text{total}}$ Γ_{13}/Γ

VALUE (units 10^{-4})	DOCUMENT ID
2.24 ± 0.27 OUR FIT	

$\Gamma(\Lambda\overline{\Lambda})/\Gamma_{\rm total}$ Γ_{14}/Γ

VALUE (units 10^{-4})	EVTS	DOCUMENT ID		TECN	COMMENT
4.7±1.3±1.0	$15.2^{+4.2}_{-4.0}$	[5] BAI	03E	BES	$\psi(2S) \to \gamma\chi_{c0} \to \gamma\Lambda\overline{\Lambda}$

$\Gamma(p\overline{p}) \times \Gamma(\pi\pi)/\Gamma^2_{\rm total}$ $\Gamma_{13}\Gamma_7/\Gamma^2$

VALUE (units 10^{-7})	DOCUMENT ID		TECN	COMMENT
16.7±1.9 OUR FIT				
15.3±2.4±0.8	[9] ANDREOTTI	03	E835	$\overline{p}p \to \chi_{c0} \to \pi^0\pi^0$

[5] Rescaled by us using $B(\psi(2S) \to \gamma\chi_{c0}) = (8.6 \pm 0.7)\%$ and $B(\psi(2S) \to J/\psi(1S)\pi^+\pi^-) = 0.317 \pm 0.011$.

[6] Calculated using $B(\psi(2S) \to \gamma\chi_{c0}(1P)) = 0.094$; the errors do not contain the uncertainty in the $\psi(2S)$ decay.

[7] Calculated using $B(\psi(2S) \to \gamma\chi_{c0}(1P)) = 0.093 \pm 0.008$.

[8] We have multiplied $\pi^0\pi^0$ measurement by 3 to obtain $\pi\pi$.

[9] We have multiplied $B(p\overline{p})\cdot B(\pi^0\pi^0)$ measurement by 3 to obtain $B(p\overline{p})\cdot B(\pi\pi)$.

RADIATIVE DECAYS

$\Gamma(\gamma J/\psi(1S))/\Gamma_{\rm total}$ Γ_{16}/Γ

VALUE (units 10^{-4})	DOCUMENT ID
118±14 OUR FIT	

$\Gamma(\gamma\gamma)/\Gamma_{\rm total}$ Γ_{17}/Γ

VALUE (units 10^{-4})	DOCUMENT ID
2.6±0.5 OUR FIT	

$\Gamma(\gamma\gamma)/\Gamma(\gamma J/\psi(1S))$ Γ_{17}/Γ_{16}

VALUE (units 10^{-2})	DOCUMENT ID		TECN	COMMENT
2.2 ±0.6 OUR FIT				
1.45±0.74	[10] AMBROGIANI	00B	E835	$\overline{p}p \to \chi_{c2} \to \gamma\gamma, \gamma J/\psi$

$\Gamma(p\overline{p}) \times \Gamma(\gamma J/\psi(1S))/\Gamma^2_{\rm total}$ $\Gamma_{13}\Gamma_{16}/\Gamma^2$

VALUE (units 10^{-7})	EVTS	DOCUMENT ID		TECN	COMMENT
26.5±2.0 OUR FIT					
27.5±2.1 OUR AVERAGE					
27.2±1.9±1.3	392	[10,11] BAGNASCO	02	E835	$\overline{p}p \to \chi_{c0} \to J/\psi\gamma$
$29.3^{+5.7}_{-4.7}\pm1.5$	89	[10,11] AMBROGIANI	99B		$\overline{p}p \to \chi_{c0} \to J/\psi\gamma$

[10] Calculated by us using $B(J/\psi(1S) \to e^+e^-) = 0.0593 \pm 0.0010$.

[11] Values in $(\Gamma(p\overline{p}) \times \Gamma(\gamma J/\psi(1S))/\Gamma_{\rm total})$ and $(\Gamma(p\overline{p}) \times \Gamma(\gamma J/\psi(1S))/\Gamma^2_{\rm total})$ are not independent. The latter is used in the fit since it is less correlated to the total width.

$\chi_{c0}(1P)$ CROSS-PARTICLE BRANCHING RATIOS

$B(\chi_{c0}(1P) \to p\overline{p}) \times \frac{\Gamma(\psi(2S) \to \gamma\chi_{c0}(1P))}{\Gamma(\psi(2S) \to J/\psi(1S)\pi^+\pi^-)}$

VALUE (units 10^{-5})	DOCUMENT ID		TECN	COMMENT
6.1±1.1 OUR FIT				
4.6±1.9	[12] BAI	98I	BES	$\psi(2S) \to \gamma\chi_{c0} \to \gamma\overline{p}p$

$B(\chi_{c0}(1P) \to \gamma J/\psi(1S)) \times B(\psi(2S) \to \gamma\chi_{c0}(1P))$

VALUE (units 10^{-2})	DOCUMENT ID		TECN	COMMENT
0.101±0.012 OUR FIT				
0.073±0.018 OUR AVERAGE				
0.069±0.018	[13] OREGLIA	82	CBAL	$\psi(2S) \to \gamma\chi_{c0}$
0.4 ±0.3	[14] BRANDELIK	79B	DASP	$\psi(2S) \to \gamma\chi_{c0}$
0.16 ±0.11	[14] BARTEL	78B	CNTR	$\psi(2S) \to \gamma\chi_{c0}$
3.3 ±1.7	[15] BIDDICK	77	CNTR	$e^+e^- \to \gamma X$

$B(\chi_{c0}(1P) \to \gamma\gamma) \times B(\psi(2S) \to \gamma\chi_{c0}(1P))$

VALUE (units 10^{-5})	DOCUMENT ID		TECN	COMMENT
2.2±0.5 OUR FIT				
3.7±1.8±1.0	LEE	85	CBAL	$\psi(2S) \to \gamma\chi_{c0}$

$B(\chi_{c0}(1P) \to \pi\pi) \times \frac{\Gamma(\psi(2S) \to \gamma\chi_{c0}(1P))}{\Gamma(\psi(2S) \to J/\psi(1S)\pi^+\pi^-)}$

VALUE (units 10^{-4})	EVTS	DOCUMENT ID		TECN	COMMENT
20.1±2.1 OUR FIT					
20.7±1.7 OUR AVERAGE					
23.9±2.7±4.1	96.9± 11.1	[16] BAI	03C	BES	$\psi(2S) \to \gamma\chi_{c0} \to \gamma\pi^0\pi^0$
20.2±1.1±1.5	720± 32	[17] BAI	98I	BES	$\psi(2S) \to \gamma\chi_{c0} \to \gamma\pi^+\pi^-$

$B(\chi_{c0}(1P) \to 2(\pi^+\pi^-)) \times \frac{\Gamma(\psi(2S) \to \gamma\chi_{c0}(1P))}{\Gamma(\psi(2S) \to J/\psi(1S)\pi^+\pi^-)}$

VALUE (units 10^{-3})	DOCUMENT ID		TECN	COMMENT
7.0±0.8 OUR FIT				
6.9±2.4 OUR AVERAGE Error includes scale factor of 3.8.				
4.4±0.1±0.9	[18] BAI	99B	BES	$\psi(2S) \to \gamma\chi_{c0}$
9.3±0.9	[19] TANENBAUM	78	MRK1	$\psi(2S) \to \gamma\chi_{c0}$

[12] Calculated by us. The value for $B(\chi_{c0} \to p\overline{p})$ reported in BAI 98I is derived using $B(\psi(2S) \to \gamma\chi_{c0}) = (9.3 \pm 0.8)\%$ and $B(\psi(2S) \to J/\psi(1S)\pi^+\pi^-) = (32.4 \pm 2.6)\%$ [BAI 98D].

[13] Recalculated by us using $B(J/\psi(1S) \to \ell^+\ell^-) = 0.1181 \pm 0.0020$.

[14] Recalculated by us using $B(J/\psi(1S) \to \mu^+\mu^-) = 0.0588 \pm 0.0010$.

[15] Assumes isotropic gamma distribution.

[16] We have multiplied $\pi^0\pi^0$ measurement by 3 to obtain $\pi\pi$.

[17] Calculated by us. The value for $B(\chi_{c0} \to \pi^+\pi^-)$ reported in BAI 98I is derived using $B(\psi' \to \gamma\chi_{c0}) = (9.3 \pm 0.8)\%$ and $B(\psi' \to J/\psi\pi^+\pi^-) = (32.4 \pm 2.6)\%$ [BAI 98D]. We have multiplied $\pi^+\pi^-$ measurement by 3/2 to obtain $\pi\pi$.

[18] Calculated by us. The value for $B(\chi_{c0} \to 2\pi^+2\pi^-)$ reported in BAI 99B is derived using $B(\psi(2S) \to \gamma\chi_{c0}) = (9.3 \pm 0.8)\%$ and $B(\psi(2S) \to J/\psi(1S)\pi^+\pi^-) = (32.4 \pm 2.6)\%$ [BAI 98D].

[19] The value $B(\psi(1S) \to \gamma\chi_{c0}) \times B(\chi_{c0} \to 2\pi^+2\pi^-)$ reported in TANENBAUM 78 is derived using $B(\psi(2S) \to J/\psi(1S)\pi^+\pi^-) \times B(J/\psi(1S) \to \ell^+\ell^-) = (4.6 \pm 0.7)\%$. Calculated by us using $B(J/\psi(1S) \to \ell^+\ell^-) = 0.1181 \pm 0.0020$.

$\chi_{c0}(1P)$ REFERENCES

ANDREOTTI	03	PRL 91 091801	M. Andreotti *et al.*	(FNAL E835 Collab.)
BAI	03C	PR D67 032004	J.Z. Bai *et al.*	(BES Collab.)
BAI	03E	PR D67 112001	J.Z. Bai *et al.*	(BES Collab.)
BAGNASCO	02	PL B533 237	S. Bagnasco *et al.*	(FNAL E835 Collab.)
EISENSTEIN	01	PRL 87 061801	B.I. Eisenstein *et al.*	(CLEO Collab.)
AMBROGIANI	00B	PR D62 052002	M. Ambrogiani *et al.*	(FNAL E835 Collab.)
AMBROGIANI	99B	PRL 83 2902	M. Ambrogiani *et al.*	(FNAL E835 Collab.)
BAI	99B	PR D60 072001	J.Z. Bai *et al.*	(BES Collab.)
BAI	98D	PR D58 092006	J.Z. Bai *et al.*	(BES Collab.)
BAI	98I	PRL 81 3091	J.Z. Bai *et al.*	(BES Collab.)
GAISER	86	PR D34 711	J. Gaiser *et al.*	(Crystal Ball Collab.)
LEE	85	SLAC 282	R.A. Lee	(SLAC)
OREGLIA	82	PR D25 2259	M.J. Oreglia *et al.*	(SLAC, CIT, HARV+)
BRANDELIK	79B	NP B160 426	R. Brandelik *et al.*	(DASP Collab.)
BARTEL	78B	PL 79B 492	W. Bartel *et al.*	(DESY, HEIDP)
TANENBAUM	78	PR D17 1731	W.M. Tanenbaum *et al.*	(SLAC, LBL)
Also	82	Private Comm.	G. Trilling	(LBL, UCB)
BIDDICK	77	PRL 38 1324	C.J. Biddick *et al.*	(UCSD, UMD, PAVI+)

OTHER RELATED PAPERS

BARBERIS	00G	PL B485 357	D. Barberis *et al.*	(Omega Expt.)
ACCIARRI	99T	PL B461 155	M. Acciarri *et al.*	(L3 Collab.)
CHEN	90B	PL B243 169	W.Y. Chen *et al.*	(CLEO Collab.)
AIHARA	88D	PRL 60 2355	H. Aihara *et al.*	(TPC Collab.)
FELDMAN	75B	PRL 35 821	G.J. Feldman *et al.*	(LBL, SLAC)
Also	75C	PRL 35 1189	G.J. Feldman	
Erratum.				
TANENBAUM	75	PRL 35 1323	W.M. Tanenbaum *et al.*	(LBL, SLAC)

$\chi_{c1}(1P)$

$I^G(J^{PC}) = 0^+(1^{++})$

See the Review on "$\psi(2S)$ and χ_c branching ratios" before the $\chi_{c0}(1P)$ Listings.

$\chi_{c1}(1P)$ MASS

VALUE (MeV)	EVTS	DOCUMENT ID		TECN	COMMENT
3510.59± 0.10 OUR AVERAGE		Error includes scale factor of 1.1.			
3509.4 ± 0.9		BAI	99B	BES	$\psi(2S) \to \gamma X$
3510.61± 0.04±0.09	513	[1] ARMSTRONG	92	E760	$\overline{p}p \to e^+e^-\gamma$
3511.3 ± 0.4 ±0.4	30	BAGLIN	86B	SPEC	$\overline{p}p \to e^+e^-X$
3512.3 ± 0.3 ±4.0		[2] GAISER	86	CBAL	$\psi(2S) \to \gamma X$
3507.4 ± 1.7	91	[3] LEMOIGNE	82	GOLI	190 π^- Be $\to \gamma 2\mu$
3510.4 ± 0.6		OREGLIA	82	CBAL	$e^+e^- \to J/\psi 2\gamma$
3510.1 ± 1.1	254	[4] HIMEL	80	MRK2	$e^+e^- \to J/\psi 2\gamma$
3509 ±11	21	BRANDELIK	79B	DASP	$e^+e^- \to J/\psi 2\gamma$
3507 ± 3		[4] BARTEL	78B	CNTR	$e^+e^- \to J/\psi 2\gamma$
3505.0 ± 4 ±4		[4,5] TANENBAUM	78	MRK1	e^+e^-
3513 ± 7	367	[4] BIDDICK	77	CNTR	$\psi(2S) \to \gamma X$
• • • We do not use the following data for averages, fits, limits, etc. • • •					
3500 ±10	40	TANENBAUM	75	MRK1	Hadrons γ

[1] Mass central value and systematic error recalculated by us according to Eq. (16) in ARMSTRONG 93B, using the value for the $\psi(2S)$ mass from AULCHENKO 03.

[2] Using mass of $\psi(2S) = 3686.0$ MeV.

[3] $J/\psi(1S)$ mass constrained to 3097 MeV.

[4] Mass value shifted by us by amount appropriate for $\psi(2S)$ mass = 3686 MeV and $J/\psi(1S)$ mass = 3097 MeV.

[5] From a simultaneous fit to radiative and hadronic decay channels.

$\chi_{c1}(1P)$ WIDTH

VALUE (MeV)	CL%	EVTS	DOCUMENT ID		TECN	COMMENT
0.91 ± 0.13 OUR FIT						
0.88 ± 0.11 ± 0.08		513	ARMSTRONG	92	E760	$\overline{p}p \rightarrow e^+e^-\gamma$
• • • We do not use the following data for averages, fits, limits, etc. • • •						
< 1.3	95		BAGLIN	86B	SPEC	$\overline{p}p \rightarrow e^+e^-X$
< 3.8	90		GAISER	86	CBAL	$\psi(2S) \rightarrow \gamma X$

$\chi_{c1}(1P)$ DECAY MODES

	Mode	Fraction (Γ_i/Γ)
	Hadronic decays	
Γ_1	$3(\pi^+\pi^-)$	$(6.2 \pm 1.6) \times 10^{-3}$
Γ_2	$2(\pi^+\pi^-)$	$(8.2 \pm 2.9) \times 10^{-3}$
Γ_3	$\pi^+\pi^- K^+ K^-$	$(4.9 \pm 1.1) \times 10^{-3}$
Γ_4	$\rho^0\pi^+\pi^-$	$(3.9 \pm 3.5) \times 10^{-3}$
Γ_5	$K^+\overline{K}^*(892)^0\pi^- +$ c.c.	$(3.2 \pm 2.1) \times 10^{-3}$
Γ_6	$K^0_S K^+\pi^- +$ c.c.	$(2.5 \pm 0.7) \times 10^{-3}$
Γ_7	$\pi^+\pi^- p\overline{p}$	$(5.3 \pm 2.1) \times 10^{-4}$
Γ_8	$K^+K^-K^+K^-$	$(4.2 \pm 1.9) \times 10^{-4}$
Γ_9	$p\overline{p}$	$(7.2 \pm 1.3) \times 10^{-5}$
Γ_{10}	$\Lambda\overline{\Lambda}$	$(2.6 \pm 1.2) \times 10^{-4}$
Γ_{11}	$\pi^+\pi^- + K^+K^-$	$< 2.1 \times 10^{-3}$
	Radiative decays	
Γ_{12}	$\gamma J/\psi(1S)$	(31.6 ± 3.3) %
Γ_{13}	$\gamma\gamma$	

$\chi_{c1}(1P)$ PARTIAL WIDTHS

$\chi_{c1}(1P)$ Γ(i)$\Gamma(\gamma J/\psi(1S))/\Gamma$(total)

$\Gamma(p\overline{p}) \times \Gamma(\gamma J/\psi(1S))/\Gamma_{\text{total}}$ $\Gamma_9\Gamma_{12}/\Gamma$

VALUE (eV)	DOCUMENT ID		TECN	COMMENT
20.9 ± 2.2 OUR FIT				
21.3 ± 2.2 OUR AVERAGE				
21.8 ± 1.5 ± 2.2	[6] ARMSTRONG	92	E760	$\overline{p}p \rightarrow e^+e^-\gamma$
$19.9^{+4.4}_{-4.0}$	[6] BAGLIN	86B	SPEC	$\overline{p}p \rightarrow e^+e^-X$

[6] Calculated by us using $B(J/\psi(1S) \rightarrow e^+e^-) = 0.0593 \pm 0.0010$.

$\chi_{c1}(1P)$ BRANCHING RATIOS

HADRONIC DECAYS

$\Gamma(3(\pi^+\pi^-))/\Gamma_{\text{total}}$ Γ_1/Γ

VALUE (units 10^{-3})	DOCUMENT ID		TECN	COMMENT
6.2 ± 1.6 OUR EVALUATION	Treating systematic error as correlated.			
6.2 ± 1.3 OUR AVERAGE				
5.8 ± 0.7 ± 1.1	[7] BAI	99B	BES	$\psi(2S) \rightarrow \gamma\chi_{c1}$
17.2 ± 6.4 ± 1.7	[7] TANENBAUM	78	MRK1	$\psi(2S) \rightarrow \gamma\chi_{c1}$

$\Gamma(2(\pi^+\pi^-))/\Gamma_{\text{total}}$ Γ_2/Γ

VALUE (units 10^{-3})	DOCUMENT ID		TECN	COMMENT
8.2 ± 2.9 OUR EVALUATION	Treating systematic error as correlated.			
8 ± 4 OUR AVERAGE	Error includes scale factor of 1.5.			
4.9 ± 2.2 ± 2.8	[7] BAI	99B	BES	$\psi(2S) \rightarrow \gamma\chi_{c1}$
13.5 ± 4.5 ± 1.3	[7] TANENBAUM	78	MRK1	$\psi(2S) \rightarrow \gamma\chi_{c1}$

$\Gamma(\pi^+\pi^- K^+K^-)/\Gamma_{\text{total}}$ Γ_3/Γ

VALUE (units 10^{-3})	DOCUMENT ID		TECN	COMMENT
4.9 ± 1.1 OUR EVALUATION	Treating systematic error as correlated.			
4.9 ± 1.1 OUR AVERAGE				
4.5 ± 0.4 ± 1.1	[7] BAI	99B	BES	$\psi(2S) \rightarrow \gamma\chi_{c1}$
7.9 ± 3.2 ± 0.8	[7] TANENBAUM	78	MRK1	$\psi(2S) \rightarrow \gamma\chi_{c1}$

$\Gamma(\rho^0\pi^+\pi^-)/\Gamma_{\text{total}}$ Γ_4/Γ

VALUE (units 10^{-4})	DOCUMENT ID		TECN	COMMENT
39 ± 35	[8] TANENBAUM	78	MRK1	$\psi(2S) \rightarrow \gamma\chi_{c1}$

$\Gamma(K^+\overline{K}^*(892)^0\pi^- + \text{c.c.})/\Gamma_{\text{total}}$ Γ_5/Γ

VALUE (units 10^{-4})	DOCUMENT ID		TECN	COMMENT
32 ± 21	[8] TANENBAUM	78	MRK1	$\psi(2S) \rightarrow \gamma\chi_{c1}$

$\Gamma(K^0_S K^+\pi^- + \text{c.c.})/\Gamma_{\text{total}}$ Γ_6/Γ

VALUE (units 10^{-3})	DOCUMENT ID		TECN	COMMENT
2.5 ± 0.4 ± 0.6	[7] BAI	99B	BES	$\psi(2S) \rightarrow \gamma\chi_{c1}$

$\Gamma(\pi^+\pi^- p\overline{p})/\Gamma_{\text{total}}$ Γ_7/Γ

VALUE (units 10^{-3})	DOCUMENT ID		TECN	COMMENT
0.53 ± 0.21 OUR EVALUATION	Treating systematic error as correlated.			
0.53 ± 0.21 OUR AVERAGE				
0.49 ± 0.13 ± 0.17	[7] BAI	99B	BES	$\psi(2S) \rightarrow \gamma\chi_{c1}$
1.16 ± 0.82 ± 0.11	[7] TANENBAUM	78	MRK1	$\psi(2S) \rightarrow \gamma\chi_{c1}$

$\Gamma(K^+K^-K^+K^-)/\Gamma_{\text{total}}$ Γ_8/Γ

VALUE (units 10^{-3})	DOCUMENT ID		TECN	COMMENT
0.42 ± 0.15 ± 0.12	[7] BAI	99B	BES	$\psi(2S) \rightarrow \gamma\chi_{c1}$

$\Gamma(p\overline{p})/\Gamma_{\text{total}}$ Γ_9/Γ

VALUE (units 10^{-4})	DOCUMENT ID
0.72 ± 0.13 OUR FIT	

$\Gamma(\Lambda\overline{\Lambda})/\Gamma_{\text{total}}$ Γ_{10}/Γ

VALUE (units 10^{-4})	EVTS	DOCUMENT ID		TECN	COMMENT
2.6 ± 1.0 ± 0.6	$9.0^{+3.5}_{-3.1}$	[7] BAI	03E	BES	$\psi(2S) \rightarrow \gamma\chi_{c1} \rightarrow \gamma\Lambda\overline{\Lambda}$

$[\Gamma(\pi^+\pi^-) + \Gamma(K^+K^-)]/\Gamma_{\text{total}}$ Γ_{11}/Γ

VALUE (units 10^{-4})	CL%	DOCUMENT ID		TECN	COMMENT
< 21		[8] FELDMAN	77	MRK1	$\psi(2S) \rightarrow \gamma\chi_{c1}$
• • • We do not use the following data for averages, fits, limits, etc. • • •					
< 38	90	[8] BRANDELIK	79B	DASP	$\psi(2S) \rightarrow \gamma\chi_{c1}$

[7] Rescaled by us using $B(\psi(2S) \rightarrow \gamma\chi_{c1}) = (8.4 \pm 0.8)\%$ and $B(\psi(2S) \rightarrow J/\psi(1S)\pi^+\pi^-) = 0.317 \pm 0.011$.

[8] Estimated using $B(\psi(2S) \rightarrow \gamma\chi_{c1}(1P)) = 0.087$. The errors do not contain the uncertainty in the $\psi(2S)$ decay.

RADIATIVE DECAYS

$\Gamma(\gamma J/\psi(1S))/\Gamma_{\text{total}}$ Γ_{12}/Γ

VALUE	DOCUMENT ID
0.316 ± 0.033 OUR FIT	

$\Gamma(\gamma\gamma)/\Gamma_{\text{total}}$ Γ_{13}/Γ

VALUE	CL%	DOCUMENT ID		TECN	COMMENT
• • • We do not use the following data for averages, fits, limits, etc. • • •					
< 0.0015	90	[9] YAMADA	77	DASP	$e^+e^- \rightarrow 3\gamma$

[9] Estimated using $B(\psi(2S) \rightarrow \gamma\chi_{c1}(1P)) = 0.087$. The errors do not contain the uncertainty in the $\psi(2S)$ decay.

$\chi_{c1}(1P)$ CROSS-PARTICLE BRANCHING RATIOS

$$B(\chi_{c1}(1P) \rightarrow p\overline{p}) \times \frac{\Gamma(\psi(2S) \rightarrow \gamma\chi_{c1}(1P))}{\Gamma(\psi(2S) \rightarrow J/\psi(1S)\pi^+\pi^-)}$$

VALUE (units 10^{-5})	DOCUMENT ID		TECN	COMMENT
1.9 ± 0.5 OUR FIT				
1.1 ± 1.0	[10] BAI	98I	BES	$\psi(2S) \rightarrow \gamma\chi_{c1} \rightarrow \gamma p\overline{p}$

$$B(\chi_{c1}(1P) \rightarrow \gamma J/\psi(1S)) \times B(\psi(2S) \rightarrow \gamma\chi_{c1}(1P))$$

VALUE (units 10^{-2})	DOCUMENT ID		TECN	COMMENT
2.67 ± 0.15 OUR FIT				
2.66 ± 0.16 OUR AVERAGE				
2.56 ± 0.12 ± 0.20	GAISER	86	CBAL	$\psi(2S) \rightarrow \gamma X$
2.78 ± 0.30	[11] OREGLIA	82	CBAL	$\psi(2S) \rightarrow \gamma\chi_{c1}$
2.2 ± 0.5	[12] BRANDELIK	79B	DASP	$\psi(2S) \rightarrow \gamma\chi_{c1}$
2.9 ± 0.5	[12] BARTEL	78B	CNTR	$\psi(2S) \rightarrow \gamma\chi_{c1}$
5.0 ± 1.5	[13] BIDDICK	77	CNTR	$e^+e^- \rightarrow \gamma X$
2.8 ± 0.9	[11] WHITAKER	76	MRK1	e^+e^-

$$B(\chi_{c1}(1P) \rightarrow \gamma J/\psi(1S)) \times \frac{\Gamma(\psi(2S) \rightarrow \gamma\chi_{c1}(1P))}{\Gamma(\psi(2S) \rightarrow J/\psi(1S)\pi^+\pi^-)}$$

VALUE (units 10^{-2})	DOCUMENT ID		TECN	COMMENT
8.4 ± 0.6 OUR FIT				
8.5 ± 2.1	[14] HIMEL	80	MRK2	$\psi(2S) \rightarrow \gamma\chi_{c1}$

[10] Calculated by us. The value for $B(\chi_{c1} \rightarrow p\overline{p})$ reported in BAI 98I is derived using $B(\psi(2S) \rightarrow \gamma\chi_{c1}) = (8.7 \pm 0.8)\%$ and $B(\psi(2S) \rightarrow J/\psi(1S)\pi^+\pi^-) = (32.4 \pm 2.6)\%$ [BAI 98D].

[11] Recalculated by us using $B(J/\psi(1S) \rightarrow \ell^+\ell^-) = 0.1181 \pm 0.0020$.

[12] Recalculated by us using $B(J/\psi(1S) \rightarrow \mu^+\mu^-) = 0.0588 \pm 0.0010$.

[13] Assumes isotropic gamma distribution.

[14] The value for $B(\psi(2S) \rightarrow \gamma\chi_{c1}) \times B(\chi_{c1} \rightarrow \gamma J/\psi(1S))$ quoted in HIMEL 80 is derived using $B(\psi(2S) \rightarrow J/\psi(1S)\pi^+\pi^-) = (33 \pm 3)\%$ and $B(J/\psi(1S) \rightarrow \ell^+\ell^-) = 0.138 \pm 0.018$. Calculated by us using $B(J/\psi(1S) \rightarrow \ell^+\ell^-) = 0.1181 \pm 0.0020$.

MULTIPOLE AMPLITUDES IN $\chi_{c1}(1P) \to \gamma J/\psi(1S)$

$a_2 = M2/\sqrt{E1^2 + M2^2}$ Magnetic quadrupole fractional transition amplitude

VALUE	EVTS	DOCUMENT ID		TECN	COMMENT
$-0.002^{+0.008}_{-0.017}$ OUR AVERAGE					
$0.002 \pm 0.032 \pm 0.004$	2090	AMBROGIANI	02	E835	$p\overline{p} \to \chi_{c1} \to J/\psi\gamma$
$-0.002^{+0.008}_{-0.020}$	921	OREGLIA	82	CBAL	$\psi(2S) \to \chi_{c1}\gamma \to J/\psi\gamma\gamma$

$\chi_{c1}(1P)$ REFERENCES

AULCHENKO	03	PL B573 63	V.M. Aulchenko *et al.*	(KEDR Collab.)
BAI	03E	PR D67 112001	J.Z. Bai *et al.*	(BES Collab.)
AMBROGIANI	02	PR D65 052002	M. Ambrogiani *et al.*	(FNAL E835 Collab.)
BAI	99B	PR D60 072001	J.Z. Bai *et al.*	(BES Collab.)
BAI	98D	PR D58 092006	J.Z. Bai *et al.*	(BES Collab.)
BAI	98I	PRL 81 3091	J.Z. Bai *et al.*	(BES Collab.)
ARMSTRONG	93B	PR D47 772	T.A. Armstrong *et al.*	(FNAL E760 Collab.)
ARMSTRONG	92	NP B373 35	T.A. Armstrong *et al.*	(FNAL, FERR, GENO+)
Also	92B	PRL 68 1468	T.A. Armstrong *et al.*	(FNAL, FERR, GENO+)
BAGLIN	86B	PL B172 455	C. Baglin	(LAPP, CERN, GENO, LYON, OSLO+)
GAISER	86	PR D34 711	J. Gaiser *et al.*	(Crystal Ball Collab.)
LEMOIGNE	82	PL 113B 509	Y. Lemoigne *et al.*	(SACL, LOIC, SHMP+)
OREGLIA	82	PR D25 2259	M.J. Oreglia *et al.*	(SLAC, CIT, HARV+)
Also	82B	Private Comm.	M.J. Oreglia	(EFI)
HIMEL	80	PRL 44 920	T. Himel *et al.*	(LBL, SLAC)
Also	82	Private Comm.	G. Trilling	(LBL, UCB)
BRANDELIK	79B	NP B160 426	R. Brandelik *et al.*	(DASP Collab.)
BARTEL	78B	PL 79B 492	W. Bartel *et al.*	(DESY, HEIDP)
TANENBAUM	78	PR D17 1731	W.M. Tanenbaum *et al.*	(SLAC, LBL)
Also	82	Private Comm.	G. Trilling	(LBL, UCB)
BIDDICK	77	PRL 38 1324	C.J. Biddick *et al.*	(UCSD, UMD, PAVI+)
FELDMAN	77	PRPL 33C 285	G.J. Feldman, M.L. Perl	(LBL, SLAC)
YAMADA	77	Hamburg Conf. 69	S. Yamada	(DASP Collab.)
WHITAKER	76	PRL 37 1596	J.S. Whitaker *et al.*	(SLAC, LBL)
TANENBAUM	75	PRL 35 1323	W.M. Tanenbaum *et al.*	(LBL, SLAC)

OTHER RELATED PAPERS

BARBERIS	00G	PL B485 357	D. Barberis *et al.*	(Omega Expt.)
BARATE	83	PL 121B 449	R. Barate *et al.*	(SACL, LOIC, SHMP, IND)
BRAUNSCH...	75B	PL 57B 407	W. Braunschweig *et al.*	(DASP Collab.)
SIMPSON	75	PRL 35 699	J.W. Simpson *et al.*	(STAN, PENN)

$h_c(1P)$

$I^G(J^{PC}) = ?^?(?^{??})$

OMITTED FROM SUMMARY TABLE

Needs confirmation.

$h_c(1P)$ MASS

VALUE (MeV)	EVTS	DOCUMENT ID		TECN	COMMENT
3526.21 ± 0.25 OUR AVERAGE					
$3526.28 \pm 0.18 \pm 0.19$	59	[1] ARMSTRONG	92D	E760	$\overline{p}p \to J/\psi\pi^0$
$3525.4 \pm 0.8 \pm 0.4$	5	BAGLIN	86	SPEC	$\overline{p}p \to J/\psi X$
• • • We do not use the following data for averages, fits, limits, etc. • • •					
3527 ± 8	42	ANTONIAZZI	94	E705	300 $\pi^\pm$, pLi $\to J/\psi\pi^0 X$

[1] Mass central value and systematic error recalculated by us according to Eq. (16) in ARMSTRONG 93B, using the value for the $\psi(2S)$ mass from AULCHENKO 03.

$h_c(1P)$ WIDTH

VALUE (MeV)	CL%	EVTS	DOCUMENT ID		TECN	COMMENT
< 1.1	90	59	ARMSTRONG	92D	E760	$\overline{p}p \to J/\psi\pi^0$

$h_c(1P)$ DECAY MODES

	Mode	Fraction (Γ_i/Γ)
Γ_1	$J/\psi(1S)\pi^0$	seen
Γ_2	$J/\psi(1S)\pi\pi$	not seen
Γ_3	$p\overline{p}$	

$\Gamma(J/\psi(1S)\pi\pi)/\Gamma(J/\psi(1S)\pi^0)$ Γ_2/Γ_1

VALUE	CL%	DOCUMENT ID		TECN	COMMENT
< 0.18	90	ARMSTRONG	92D	E760	$\overline{p}p \to J/\psi\pi^0$

$h_c(1P)$ REFERENCES

AULCHENKO	03	PL B573 63	V.M. Aulchenko *et al.*	(KEDR Collab.)
ANTONIAZZI	94	PR D50 4258	L. Antoniazzi *et al.*	(E705 Collab.)
ARMSTRONG	93B	PR D47 772	T.A. Armstrong *et al.*	(FNAL E760 Collab.)
ARMSTRONG	92D	PRL 69 2337	T.A. Armstrong *et al.*	(FNAL, FERR, GENO+)
BAGLIN	86	PL B171 135	C. Baglin *et al.*	(LAPP, CERN, TORI, STRB+)

OTHER RELATED PAPERS

EICHTEN	02	PRL 89 162002	E.J. Eichten, K. Lane, C. Quigg	

$\chi_{c2}(1P)$

$I^G(J^{PC}) = 0^+(2^{++})$

See the Review on "$\psi(2S)$ and χ_c branching ratios" before the $\chi_{c0}(1P)$ Listings.

$\chi_{c2}(1P)$ MASS

VALUE (MeV)	EVTS	DOCUMENT ID		TECN	COMMENT
3556.26 ± 0.11 OUR AVERAGE					
3559.9 ± 2.9		EISENSTEIN	01	CLE2	$e^+e^- \to e^+e^-\chi_{c2}$
3556.4 ± 0.7		BAI	99B	BES	$\psi(2S) \to \gamma X$
$3556.24 \pm 0.07 \pm 0.09$	585	[1] ARMSTRONG	92	E760	$\overline{p}p \to e^+e^-\gamma$
$3556.9 \pm 0.4 \pm 0.5$	50	BAGLIN	86B	SPEC	$\overline{p}p \to e^+e^- X$
3557.8 ± 0.2 ±4		[2] GAISER	86	CBAL	$\psi(2S) \to \gamma X$
3553.4 ± 2.2	66	[3] LEMOIGNE	82	GOLI	190 π^- Be $\to \gamma 2\mu$
3555.9 ± 0.7		[4] OREGLIA	82	CBAL	$e^+e^- \to J/\psi 2\gamma$
3557 ± 1.5	69	[5] HIMEL	80	MRK2	$e^+e^- \to J/\psi 2\gamma$
3551 ±11	15	BRANDELIK	79B	DASP	$e^+e^- \to J/\psi 2\gamma$
3553 ± 4		[5] BARTEL	78B	CNTR	$e^+e^- \to J/\psi 2\gamma$
3553 ± 4 ±4		[5,6] TANENBAUM	78	MRK1	e^+e^-
3563 ± 7	360	[5] BIDDICK	77	CNTR	$e^+e^- \to \gamma X$
• • • We do not use the following data for averages, fits, limits, etc. • • •					
3543 ±10	4	WHITAKER	76	MRK1	$e^+e^- \to J/\psi 2\gamma$

[1] Mass central value and systematic error recalculated by us according to Eq. (16) in ARMSTRONG 93B, using the value for the $\psi(2S)$ mass from AULCHENKO 03.
[2] Using mass of $\psi(2S) = 3686.0$ MeV.
[3] $J/\psi(1S)$ mass constrained to 3097 MeV.
[4] Assuming $\psi(2S)$ mass = 3686 MeV and $J/\psi(1S)$ mass = 3097 MeV.
[5] Mass value shifted by us by amount appropriate for $\psi(2S)$ mass = 3686 MeV and $J/\psi(1S)$ mass = 3097 MeV.
[6] From a simultaneous fit to radiative and hadronic decay channels.

$\chi_{c2}(1P)$ WIDTH

VALUE (MeV)	EVTS	DOCUMENT ID		TECN	COMMENT
2.11 ± 0.16 OUR FIT					
2.00 ± 0.18 OUR AVERAGE					
$1.98 \pm 0.17 \pm 0.07$	585	ARMSTRONG	92	E760	$\overline{p}p \to e^+e^-\gamma$
$2.6\ ^{+1.4}_{-1.0}$	50	BAGLIN	86B	SPEC	$\overline{p}p \to e^+e^- X$
$2.8\ ^{+2.1}_{-2.0}$		[7] GAISER	86	CBAL	$\psi(2S) \to \gamma X$

[7] Errors correspond to 90% confidence level; authors give only width range.

$\chi_{c2}(1P)$ DECAY MODES

	Mode	Fraction (Γ_i/Γ)	Confidence level
	Hadronic decays		
Γ_1	$2(\pi^+\pi^-)$	(1.48 ± 0.21) %	
Γ_2	$\pi^+\pi^- K^+K^-$	(1.24 ± 0.33) %	
Γ_3	$3(\pi^+\pi^-)$	(1.07 ± 0.24) %	
Γ_4	$\rho^0\pi^+\pi^-$	$(7 \pm 4) \times 10^{-3}$	
Γ_5	$K^+\overline{K}^*(892)^0\pi^- +$ c.c.	$(4.8 \pm 2.8) \times 10^{-3}$	
Γ_6	$\phi\phi$	$(2.4 \pm 0.9) \times 10^{-3}$	
Γ_7	$\pi^+\pi^-$	$(1.77 \pm 0.27) \times 10^{-3}$	
Γ_8	$\pi^0\pi^0$	$(1.1 \pm 0.7) \times 10^{-3}$	
Γ_9	$\eta\eta$	$< 1.5 \times 10^{-3}$	90%
Γ_{10}	$K^+K^-K^+K^-$	$(1.8 \pm 0.5) \times 10^{-3}$	
Γ_{11}	$\pi^+\pi^- p\overline{p}$	$(1.7 \pm 0.4) \times 10^{-3}$	
Γ_{12}	K^+K^-	$(9.4 \pm 2.1) \times 10^{-4}$	
Γ_{13}	$K^0_S K^0_S$	$(7.2 \pm 2.7) \times 10^{-4}$	
Γ_{14}	$p\overline{p}$	$(6.8 \pm 0.7) \times 10^{-5}$	
Γ_{15}	$\Lambda\overline{\Lambda}$	$(3.4 \pm 1.7) \times 10^{-4}$	
Γ_{16}	$J/\psi(1S)\pi^+\pi^-\pi^0$	< 1.5 %	90%
Γ_{17}	$K^0_S K^+\pi^-$ + c.c.	$< 1.3 \times 10^{-3}$	90%
	Radiative decays		
Γ_{18}	$\gamma J/\psi(1S)$	(20.2 ± 1.7) %	
Γ_{19}	$\gamma\gamma$	$(2.46 \pm 0.23) \times 10^{-4}$	

$\chi_{c2}(1P)$ PARTIAL WIDTHS

$\chi_{c2}(1P)$ Γ(i)$\Gamma(\gamma J/\psi(1S))/\Gamma$(total)

$\Gamma(p\overline{p}) \times \Gamma(\gamma J/\psi(1S))/\Gamma_{\text{total}}$ $\Gamma_{14}\Gamma_{18}/\Gamma$

VALUE (eV)	DOCUMENT ID		TECN	COMMENT
29.0 ± 2.4 OUR FIT				
28.9 ± 2.5 OUR AVERAGE				
28.2 ± 2.6	[8] ARMSTRONG	92	E760	$\overline{p}p \to e^+e^-\gamma$
36 ±8	[8] BAGLIN	86B	SPEC	$\overline{p}p \to e^+e^- X$

$\Gamma(\gamma\gamma) \times \Gamma(\gamma J/\psi(1S))/\Gamma_{\text{total}}$ $\Gamma_{19}\Gamma_{18}/\Gamma$

VALUE (eV)	EVTS	DOCUMENT ID		TECN	COMMENT
105 ± 12 OUR FIT					
121 ± 13 OUR AVERAGE					
114 ± 11 ± 9	136 ± 13.3	[9] ABE	02T	BELL	$e^+e^- \to e^+e^-\chi_{c2}$
139 ± 55 ± 21		[10] ACCIARRI	99E	L3	$e^+e^- \to e^+e^-\chi_{c2}$
242 ± 65 ± 51		[11] ACKER...,K...	98	OPAL	$e^+e^- \to e^+e^-\chi_{c2}$
150 ± 42 ± 36		[12] DOMINICK	94	CLE2	$e^+e^- \to e^+e^-\chi_{c2}$
470 ± 240 ± 120		[13] BAUER	93	TPC	$e^+e^- \to e^+e^-\chi_{c2}$

$\Gamma(\gamma\gamma) \times \Gamma(2(\pi^+\pi^-))/\Gamma_{\text{total}}$ $\Gamma_{19}\Gamma_{1}/\Gamma$

VALUE (eV)	DOCUMENT ID		TECN	COMMENT
7.7 ± 1.1 OUR FIT				
6.4 ± 1.8 ± 0.8	EISENSTEIN	01	CLE2	$e^+e^- \to e^+e^-\chi_{c2}$

[8] Calculated by us using $B(J/\psi(1S) \to e^+e^-) = 0.0593 \pm 0.0010$.
[9] Using $B(J/\psi \to \ell^+\ell^-) = 0.1181 \pm 0.0020$. All systematic errors added in quadrature.
[10] The value for $\Gamma(\chi_{c2} \to \gamma\gamma)$ reported in ACCIARRI 99E is derived using $B(\chi_{c2} \to \gamma J/\psi(1S)) \times B(J/\psi(1S) \to \ell^+\ell^-) = 0.0162 \pm 0.0014$. Calculated by us using $B(J/\psi(1S) \to \ell^+\ell^-) = 0.1181 \pm 0.0020$.
[11] The value for $\Gamma(\chi_{c2} \to \gamma\gamma)$ reported in ACKERSTAFF,K 98 is derived using $B(\chi_{c2} \to \gamma J/\psi(1S)) = 0.135 \pm 0.011$ and $B(J/\psi(1S) \to \ell^+\ell^-) = 0.1203 \pm 0.0038$. Calculated by us using $B(J/\psi(1S) \to \ell^+\ell^-) = 0.1181 \pm 0.0020$.
[12] The value for $\Gamma(\chi_{c2} \to \gamma\gamma)$ reported in DOMINICK 94 is derived using $B(\chi_{c2} \to \gamma J/\psi(1S)) = 0.135 \pm 0.011$, $B(J/\psi(1S) \to e^+e^-) = 0.0627 \pm 0.0020$, and $B(J/\psi(1S) \to \mu^+\mu^-) = 0.0597 \pm 0.0025$. Calculated by us using $B(J/\psi(1S) \to \ell^+\ell^-) = 0.1181 \pm 0.0020$.
[13] The value for $\Gamma(\chi_{c2} \to \gamma\gamma)$ reported in BAUER 93 is derived using $B(\chi_{c2} \to \gamma J/\psi(1S)) = 0.135 \pm 0.011$, $B(J/\psi(1S) \to e^+e^-) = 0.0627 \pm 0.0020$, and $B(J/\psi(1S) \to \mu^+\mu^-) = 0.0597 \pm 0.0025$. Calculated by us using $B(J/\psi(1S) \to \ell^+\ell^-) = 0.1181 \pm 0.0020$.

$\chi_{c2}(1P)$ BRANCHING RATIOS

HADRONIC DECAYS

$\Gamma(2(\pi^+\pi^-))/\Gamma_{\text{total}}$ Γ_1/Γ

VALUE	DOCUMENT ID
0.0148 ± 0.0021 OUR FIT	

$\Gamma(\pi^+\pi^-K^+K^-)/\Gamma_{\text{total}}$ Γ_2/Γ

VALUE (units 10^{-3})	DOCUMENT ID		TECN	COMMENT
12.4 ± 3.3 OUR EVALUATION Treating systematic error as correlated.				
12 ± 4 OUR AVERAGE Error includes scale factor of 2.1.				
9.4 ± 0.7 ± 2.3	[14] BAI	99B	BES	$\psi(2S) \to \gamma\chi_{c2}$
18.7 ± 3.3 ± 1.8	[14] TANENBAUM	78	MRK1	$\psi(2S) \to \gamma\chi_{c2}$

$\Gamma(3(\pi^+\pi^-))/\Gamma_{\text{total}}$ Γ_3/Γ

VALUE (units 10^{-3})	DOCUMENT ID		TECN	COMMENT
10.7 ± 2.4 OUR EVALUATION Treating systematic error as correlated.				
10.7 ± 2.4 OUR AVERAGE				
10.7 ± 1.2 ± 2.2	[14] BAI	99B	BES	$\psi(2S) \to \gamma\chi_{c2}$
10.8 ± 7.4 ± 1.0	[14] TANENBAUM	78	MRK1	$\psi(2S) \to \gamma\chi_{c2}$

$\Gamma(\rho^0\pi^+\pi^-)/\Gamma_{\text{total}}$ Γ_4/Γ

VALUE (units 10^{-4})	DOCUMENT ID		TECN	COMMENT
68 ± 40	[15] TANENBAUM	78	MRK1	$\psi(2S) \to \gamma\chi_{c2}$

$\Gamma(K^+\overline{K}{}^*(892)^0\pi^- + \text{c.c.})/\Gamma_{\text{total}}$ Γ_5/Γ

VALUE (units 10^{-4})	DOCUMENT ID		TECN	COMMENT
48 ± 28	[15] TANENBAUM	78	MRK1	$\psi(2S) \to \gamma\chi_{c2}$

$\Gamma(\phi\phi)/\Gamma_{\text{total}}$ Γ_6/Γ

VALUE (units 10^{-3})	DOCUMENT ID		TECN	COMMENT
2.4 ± 0.6 ± 0.7	[14] BAI	99B	BES	$\psi(2S) \to \gamma\chi_{c2}$

$\Gamma(\pi^+\pi^-)/\Gamma_{\text{total}}$ Γ_7/Γ

VALUE (units 10^{-3})	EVTS	DOCUMENT ID		TECN	COMMENT
1.77 ± 0.17 ± 0.21	185 ± 16	[14] BAI	98I	BES	$\psi(2S) \to \gamma\chi_{c2}$
• • • We do not use the following data for averages, fits, limits, etc. • • •					
1.9 ± 1.0	4	[15] BRANDELIK	79C	DASP	$\psi(2S) \to \gamma\chi_{c2}$

$\Gamma(\pi^0\pi^0)/\Gamma_{\text{total}}$ Γ_8/Γ

VALUE (units 10^{-3})	EVTS	DOCUMENT ID		TECN	COMMENT
1.08 ± 0.30 ± 0.61	20.8 ± 5.8	[14] BAI	03C	BES	$\psi(2S) \to \gamma\pi^0\pi^0 \to 5\gamma$
• • • We do not use the following data for averages, fits, limits, etc. • • •					
1.1 ± 0.2 ± 0.2		[16] LEE	85	CBAL	$\psi' \to$ photons

$[\Gamma(\pi^+\pi^-) + \Gamma(K^+K^-)]/\Gamma_{\text{total}}$ $(\Gamma_7+\Gamma_{12})/\Gamma$

VALUE (units 10^{-4})	DOCUMENT ID		TECN	COMMENT
24 ± 10	[15] TANENBAUM	78	MRK1	$\psi(2S) \to \gamma\chi_{c2}$

$\Gamma(K^+K^-K^+K^-)/\Gamma_{\text{total}}$ Γ_{10}/Γ

VALUE (units 10^{-3})	DOCUMENT ID		TECN	COMMENT
1.75 ± 0.31 ± 0.34	[14] BAI	99B	BES	$\psi(2S) \to \gamma\chi_{c2}$

$\Gamma(\pi^+\pi^-p\overline{p})/\Gamma_{\text{total}}$ Γ_{11}/Γ

VALUE (units 10^{-3})	DOCUMENT ID		TECN	COMMENT
1.7 ± 0.4 OUR EVALUATION Treating systematic error as correlated.				
1.7 ± 0.6 OUR AVERAGE Error includes scale factor of 1.3.				
1.46 ± 0.24 ± 0.40	[14] BAI	99B	BES	$\psi(2S) \to \gamma\chi_{c2}$
3.30 ± 1.28 ± 0.32	[14] TANENBAUM	78	MRK1	$\psi(2S) \to \gamma\chi_{c2}$

$\Gamma(K^+K^-)/\Gamma_{\text{total}}$ Γ_{12}/Γ

VALUE (units 10^{-3})	EVTS	DOCUMENT ID		TECN	COMMENT
0.94 ± 0.17 ± 0.13	115 ± 13	[14] BAI	98I	BES	$\psi(2S) \to \gamma\chi_{c2}$
• • • We do not use the following data for averages, fits, limits, etc. • • •					
1.5 ± 1.1	2	[15] BRANDELIK	79C	DASP	$\psi(2S) \to \gamma\chi_{c2}$

$\Gamma(K^0_SK^0_S)/\Gamma_{\text{total}}$ Γ_{13}/Γ

VALUE (units 10^{-3})	DOCUMENT ID		TECN	COMMENT
0.72 ± 0.20 ± 0.18	[14] BAI	99B	BES	$\psi(2S) \to \gamma\chi_{c2}$

$\Gamma(p\overline{p})/\Gamma_{\text{total}}$ Γ_{14}/Γ

VALUE (units 10^{-4})	DOCUMENT ID
0.68 ± 0.07 OUR FIT	

$\Gamma(\Lambda\overline{\Lambda})/\Gamma_{\text{total}}$ Γ_{15}/Γ

VALUE (units 10^{-4})	EVTS	DOCUMENT ID		TECN	COMMENT
3.4 ± 1.5 ± 0.7	$8.3^{+3.7}_{-3.4}$	[14] BAI	03E	BES	$\psi(2S) \to \gamma\chi_{c2} \to \gamma\Lambda\overline{\Lambda}$

$\Gamma(\eta\eta)/\Gamma_{\text{total}}$ Γ_9/Γ

VALUE (units 10^{-4})	CL%	DOCUMENT ID		TECN	COMMENT
< 15	90	[14] BAI	03C	BES	$\psi(2S) \to \gamma\eta\eta \to 5\gamma$
• • • We do not use the following data for averages, fits, limits, etc. • • •					
7.9 ± 4.1 ± 2.4		[16] LEE	85	CBAL	$\psi' \to$ photons

$\Gamma(J/\psi(1S)\pi^+\pi^-\pi^0)/\Gamma_{\text{total}}$ Γ_{16}/Γ

VALUE	CL%	DOCUMENT ID		TECN	COMMENT
< 0.015	90	BARATE	81	SPEC	190 GeV π^- Be $\to 2\pi\,2\mu$

$\Gamma(K^0_SK^+\pi^- + \text{c.c.})/\Gamma_{\text{total}}$ Γ_{17}/Γ

VALUE (units 10^{-3})	CL%	DOCUMENT ID		TECN	COMMENT
< 1.3	90	[14] BAI	99B	BES	$\psi(2S) \to \gamma\chi_{c2}$

[14] Rescaled by us using $B(\psi(2S) \to \gamma\chi_{c2}) = (6.4 \pm 0.6)\%$ and $B(\psi(2S) \to J/\psi(1S)\pi^+\pi^-) = 0.317 \pm 0.011$.
[15] Estimated using $B(\psi(2S) \to \gamma\chi_{c2}(1P)) = 0.078$; the errors do not contain the uncertainty in the $\psi(2S)$ decay.
[16] Calculated using $B(\psi(2S) \to \gamma\chi_{c2}(1P)) = 0.078 \pm 0.008$.

RADIATIVE DECAYS

$\Gamma(\gamma J/\psi(1S))/\Gamma_{\text{total}}$ Γ_{18}/Γ

VALUE	DOCUMENT ID
0.202 ± 0.017 OUR FIT	

$\Gamma(\gamma\gamma)/\Gamma_{\text{total}}$ Γ_{19}/Γ

VALUE (units 10^{-4})	DOCUMENT ID
2.46 ± 0.23 OUR FIT	

$\Gamma(\gamma\gamma)/\Gamma(\gamma J/\psi(1S))$ Γ_{19}/Γ_{18}

VALUE (units 10^{-3})	DOCUMENT ID		TECN	COMMENT
1.21 ± 0.16 OUR FIT				
0.99 ± 0.18	[17] AMBROGIANI	00B	E835	$\overline{p}p \to \chi_{c2} \to \gamma\gamma, \gamma J/\psi$

$\Gamma(\gamma\gamma) \times \Gamma(p\overline{p})/\Gamma^2_{\text{total}}$ $\Gamma_{19}\Gamma_{14}/\Gamma^2$

VALUE (units 10^{-8})	DOCUMENT ID		TECN	COMMENT
1.66 ± 0.24 OUR FIT				
1.7 ± 0.4 OUR AVERAGE				
1.60 ± 0.42	ARMSTRONG	93	E760	$\overline{p}p \to \gamma\gamma X$
9.9 ± 4.5	BAGLIN	87B	SPEC	$\overline{p}p \to \gamma\gamma X$

[17] Calculated by us using $B(J/\psi(1S) \to e^+e^-) = 0.0593 \pm 0.0010$.

$\chi_{c2}(1P)$ CROSS-PARTICLE BRANCHING RATIOS

$$B(\chi_{c2}(1P) \to p\overline{p}) \times \frac{\Gamma(\psi(2S) \to \gamma\chi_{c2}(1P))}{\Gamma(\psi(2S) \to J/\psi(1S)\pi^+\pi^-)}$$

VALUE (units 10^{-5})	DOCUMENT ID		TECN	COMMENT
1.38 ± 0.23 OUR FIT				
1.4 ± 1.1	[18] BAI	98I	BES	$\psi(2S) \to \gamma\chi_{c2} \to \gamma\overline{p}p$

$B(\chi_{c2}(1P) \to \gamma J/\psi(1S)) \times B(\psi(2S) \to \gamma\chi_{c2}(1P))$

VALUE (units 10^{-2})	DOCUMENT ID		TECN	COMMENT
1.30±0.08 OUR FIT				
1.20±0.13 OUR AVERAGE	Error includes scale factor of 1.5. See the ideogram below.			
0.99±0.10±0.08	GAISER	86	CBAL	$\psi(2S) \to \gamma X$
1.47±0.17	[19] OREGLIA	82	CBAL	$\psi(2S) \to \gamma\chi_{c2}$
1.8 ±0.5	[20] BRANDELIK	79B	DASP	$\psi(2S) \to \gamma\chi_{c2}$
1.2 ±0.2	[20] BARTEL	78B	CNTR	$\psi(2S) \to \gamma\chi_{c2}$
2.2 ±1.2	[21] BIDDICK	77	CNTR	$e^+e^- \to \gamma X$
1.2 ±0.7	[19] WHITAKER	76	MRK1	e^+e^-

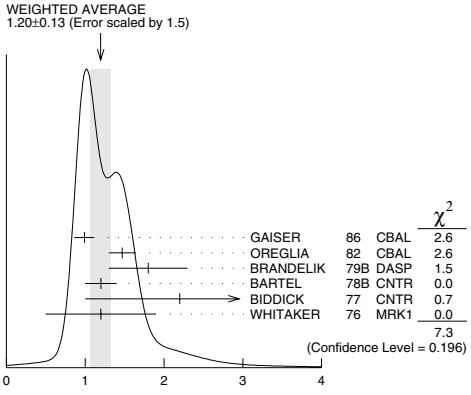

$B(\chi_{c2}(1P) \to \gamma J/\psi(1S)) \times B(\psi(2S) \to \gamma\chi_{c2}(1P))$

$B(\chi_{c2}(1P) \to \gamma J/\psi(1S)) \times \dfrac{\Gamma(\psi(2S) \to \gamma\chi_{c2}(1P))}{\Gamma(\psi(2S) \to J/\psi(1S)\pi^+\pi^-)}$

VALUE (units 10^{-2})	DOCUMENT ID		TECN	COMMENT
4.11±0.29 OUR FIT				
3.9 ±1.2	[22] HIMEL	80	MRK2	$\psi(2S) \to \gamma\chi_{c2}$

$B(\chi_{c2}(1P) \to \gamma\gamma) \times B(\psi(2S) \to \gamma\chi_{c2}(1P))$

VALUE (units 10^{-5})	DOCUMENT ID		TECN	COMMENT
1.58±0.19 OUR FIT				
7.0 ±2.1 ±2.0	LEE	85	CBAL	$\psi(2S) \to \gamma\chi_{c2}$

$B(\chi_{c2}(1P) \to 2(\pi^+\pi^-)) \times \dfrac{\Gamma(\psi(2S) \to \gamma\chi_{c2}(1P))}{\Gamma(\psi(2S) \to J/\psi(1S)\pi^+\pi^-)}$

VALUE (units 10^{-3})	DOCUMENT ID		TECN	COMMENT
3.0±0.4 OUR FIT				
3.1±1.0 OUR AVERAGE	Error includes scale factor of 2.5.			
2.3±0.1±0.5	[23] BAI	99B	BES	$\psi(2S) \to \gamma\chi_{c2}$
4.3±0.6	[24] TANENBAUM	78	MRK1	$\psi(2S) \to \gamma\chi_{c2}$

[18] Calculated by us. The value for $B(\chi_{c2} \to p\overline{p})$ reported in BAI 98I is derived using $B(\psi(2S) \to \gamma\chi_{c2}) = (7.8 \pm 0.8)\%$ and $B(\psi(2S) \to J/\psi(1S)\pi^+\pi^-) = (32.4 \pm 2.6)\%$ [BAI 98D].

[19] Recalculated by us using $B(J/\psi(1S) \to \ell^+\ell^-) = 0.1181 \pm 0.0020$.

[20] Recalculated by us using $B(J/\psi(1S) \to \mu^+\mu^-) = 0.0588 \pm 0.0010$.

[21] Assumes isotropic gamma distribution.

[22] The value for $B(\psi(2S) \to \gamma\chi_{c2}) \times B(\chi_{c2} \to \gamma J/\psi(1S))$ reported in HIMEL 80 is derived using $B(\psi(2S) \to J/\psi(1S)\pi^+\pi^-) = (33 \pm 3)\%$ and $B(J/\psi(1S) \to \ell^+\ell^-) = 0.138 \pm 0.018$. Calculated by us using $B(J/\psi(1S) \to \ell^+\ell^-) = (0.1181 \pm 0.0020)$.

[23] Calculated by us. The value for $B(\chi_{c2} \to 2\pi^+2\pi^-)$ reported in BAI 99B is derived using $B(\psi(2S) \to \gamma\chi_{c2}) = (7.8 \pm 0.8)\%$ and $B(\psi(2S) \to J/\psi(1S)\pi^+\pi^-) = (32.4 \pm 2.6)\%$ [BAI 98D].

[24] The value for $B(\psi(2S) \to \gamma\chi_{c2}) \times B(\chi_{c2} \to 2\pi^+\pi^-)$ reported in TANENBAUM 78 is derived using $B(\psi(2S) \to J/\psi(1S)\pi^+\pi^-) \times B(J/\psi(1S)\ell^+\ell^-) = (4.6 \pm 0.7)\%$. Calculated by us using $B(J/\psi(1S) \to \ell^+\ell^-) = 0.1181 \pm 0.0020$.

MULTIPOLE AMPLITUDES IN $\chi_{c2}(1P) \to \gamma J/\psi(1S)$ RADIATIVE DECAY

$a_2 = M2/\sqrt{E1^2 + M2^2 + E3^2}$ Magnetic quadrupole fractional transition amplitude

VALUE	EVTS	DOCUMENT ID		TECN	COMMENT
−0.13 ±0.05 OUR AVERAGE		Error includes scale factor of 1.4. See the ideogram below.			
$-0.093^{+0.039}_{-0.041} \pm 0.006$	5908	[25] AMBROGIANI	02	E835	$p\overline{p} \to \chi_{c2} \to J/\psi\gamma$
−0.14 ±0.06	1904	[25] ARMSTRONG	93E	E760	$p\overline{p} \to \chi_{c2} \to J/\psi\gamma$
$-0.333^{+0.116}_{-0.292}$	441	[25] OREGLIA	82	CBAL	$\psi(2S) \to \chi_{c1}\gamma \to J/\psi\gamma\gamma$

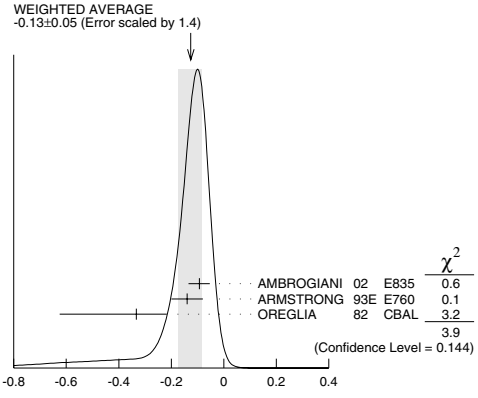

$a_2 = M2/\sqrt{E1^2 + M2^2 + E3^2}$

$a_3 = M2/\sqrt{E1^2 + M2^2 + E3^2}$ Electric octupole fractional transition amplitude

VALUE	EVTS	DOCUMENT ID		TECN	COMMENT
$\mathbf{0.011^{+0.041}_{-0.033}}$ **OUR AVERAGE**					
$0.020^{+0.055}_{-0.044} \pm 0.009$	5908	AMBROGIANI	02	E835	$p\overline{p} \to \chi_{c2} \to J/\psi\gamma$
$0.00^{+0.06}_{-0.05}$	1904	ARMSTRONG	93E	E760	$p\overline{p} \to \chi_{c2} \to J/\psi\gamma$

[25] Assuming $a_3 = 0$.

$\chi_{c2}(1P)$ REFERENCES

AULCHENKO	03	PL B573 63	V.M. Aulchenko *et al.* (KEDR Collab.)
BAI	03C	PR D67 032004	J.Z. Bai *et al.* (BES Collab.)
BAI	03E	PR D67 112001	J.Z. Bai *et al.* (BES Collab.)
ABE	02T	PL B540 33	K. Abe *et al.* (BELLE Collab.)
AMBROGIANI	02	PR D65 052002	M. Ambrogiani *et al.* (FNAL E835 Collab.)
EISENSTEIN	01	PRL 87 061801	B.I. Eisenstein *et al.* (CLEO Collab.)
AMBROGIANI	00B	PR D62 052002	M. Ambrogiani *et al.* (FNAL E835 Collab.)
ACCIARRI	99E	PL B453 73	M. Acciarri *et al.* (L3 Collab.)
BAI	99B	PR D60 072001	J.Z. Bai *et al.* (BES Collab.)
ACKER...K...	98	PL B439 197	K. Ackerstaff *et al.* (OPAL Collab.)
BAI	98D	PR D58 092006	J.Z. Bai *et al.* (BES Collab.)
BAI	98I	PRL 81 3091	J.Z. Bai *et al.* (BES Collab.)
DOMINICK	94	PR D50 4265	J. Dominick *et al.* (CLEO Collab.)
ARMSTRONG	93	PRL 70 2988	T.A. Armstrong *et al.* (FNAL E760 Collab.)
ARMSTRONG	93B	PR D47 772	T.A. Armstrong *et al.* (FNAL E760 Collab.)
ARMSTRONG	93E	PR D48 3037	T.A. Armstrong *et al.* (FNAL-E760 Collab.)
BAUER	93	PL B302 345	D.A. Bauer *et al.* (TPC Collab.)
ARMSTRONG	92	NP B373 35	T.A. Armstrong *et al.* (FNAL, FERR, GENO+)
Also	92B	PRL 68 1468	T.A. Armstrong *et al.* (FNAL, FERR, GENO+)
BAGLIN	87B	PL B187 191	C. Baglin *et al.* (R704 Collab.)
BAGLIN	86B	PL B172 455	C. Baglin (LAPP, CERN, GENO, LYON, OSLO+)
GAISER	86	PR D34 711	J. Gaiser *et al.* (Crystal Ball Collab.)
LEE	85	SLAC 282	R.A. Lee (SLAC)
LEMOIGNE	82	PL 113B 509	Y. Lemoigne *et al.* (SACL, LOIC, SHMP+)
OREGLIA	82	PR D25 2259	M.J. Oreglia *et al.* (SLAC, CIT, HARV+)
Also	82B	Private Comm.	M.J. Oreglia (EFI)
BARATE	81	PR D24 2994	R. Barate *et al.* (SACL, LOIC, SHMP, CERN+)
HIMEL	80	PRL 44 920	T. Himel *et al.* (LBL, SLAC)
Also	82	Private Comm.	G. Trilling (LBL, UCB)
BRANDELIK	79B	NP B160 426	R. Brandelik *et al.* (DASP Collab.)
BRANDELIK	79C	ZPHY C1 233	R. Brandelik *et al.* (DASP Collab.)
BARTEL	78B	PL 79B 492	W. Bartel *et al.* (DESY, HEIDP)
TANENBAUM	78	PR D17 1731	W.M. Tanenbaum *et al.* (SLAC, LBL)
Also	82	Private Comm.	G. Trilling (LBL, UCB)
BIDDICK	77	PRL 38 1324	C.J. Biddick *et al.* (UCSD, UMD, PAVI+)
WHITAKER	76	PRL 37 1596	J.S. Whitaker *et al.* (SLAC, LBL)

OTHER RELATED PAPERS

BARBERIS	00G	PL B485 357	D. Barberis *et al.* (Omega Expt.)
ACCIARRI	99T	PL B461 155	M. Acciarri *et al.* (L3 Collab.)
CHEN	90B	PL B243 169	W.Y. Chen *et al.* (CLEO Collab.)
AIHARA	88D	PRL 60 2355	H. Aihara *et al.* (TPC Collab.)
BARATE	83	PL 121B 449	R. Barate *et al.* (SACL, LOIC, SHMP, IND)
FELDMAN	75B	PRL 35 821	G.J. Feldman *et al.* (LBL, SLAC)
Also	75C	PRL 35 1189	G.J. Feldman
Erratum.			
TANENBAUM	75	PRL 35 1323	W.M. Tanenbaum *et al.* (LBL, SLAC)

Meson Particle Listings

$\chi_{c2}(1P)$, $\eta_c(2S)$, $\psi(2S)$

$\eta_c(2S)$

$I^G(J^{PC}) = 0^+(0^{-+})$

OMITTED FROM SUMMARY TABLE

Needs confirmation. Quantum numbers are quark model predictions.

$\eta_c(2S)$ MASS

VALUE (MeV)	EVTS	DOCUMENT ID		TECN	COMMENT
3654± 6±8	39 ± 11	CHOI	02	BELL	$B \to K K_S K^- \pi^+$
• • • We do not use the following data for averages, fits, limits, etc. • • •					
3622±12	42	[1] ABE,K	02	BELL	10.6 $e^+e^- \to J/\psi + X$
3594± 5		[2] EDWARDS	82C	CBAL	$e^+e^- \to \gamma X$

[1] From a fit of the J/ψ recoil mass spectrum. Systematic errors not estimated.
[2] Assuming mass of $\psi(2S) = 3686$ MeV.

$\eta_c(2S)$ WIDTH

VALUE (MeV)	CL%	EVTS	DOCUMENT ID		TECN	COMMENT
• • • We do not use the following data for averages, fits, limits, etc. • • •						
<55	90	39 ± 11	[3] CHOI	02	BELL	$B \to K K_S K^- \pi^+$
< 8.0	95		[4] EDWARDS	82C	CBAL	$e^+e^- \to \gamma X$

[3] For a mass value of 3654 ± 6 MeV
[4] For a mass value of 3594 ± 5 MeV

$\eta_c(2S)$ DECAY MODES

	Mode
Γ_1	hadrons
Γ_2	$K\overline{K}\pi$
Γ_3	$p\overline{p}$
Γ_4	$\gamma\gamma$

$\eta_c(2S)$ $\Gamma(i)\Gamma(\gamma\gamma)/\Gamma^2(\text{total})$

$\Gamma(p\overline{p}) \times \Gamma(\gamma\gamma)/\Gamma^2_{\text{total}}$ $\Gamma_3\Gamma_4/\Gamma^2$

VALUE (units 10^{-8})	CL%	DOCUMENT ID		TECN	COMMENT
< 5.6	90	[5,6,7] AMBROGIANI	01	E835	$\overline{p}p \to \gamma\gamma$
• • • We do not use the following data for averages, fits, limits, etc. • • •					
< 8.0	90	[5,6,8] AMBROGIANI	01	E835	$\overline{p}p \to \gamma\gamma$
<12.0	90	[6,8] AMBROGIANI	01	E835	$\overline{p}p \to \gamma\gamma$

[5] Including the measurements of of ARMSTRONG 95F in the AMBROGIANI 01 analysis.
[6] For a total width Γ=5 MeV.
[7] For the resonance mass region 3589–3599 MeV/c^2.
[8] For the resonance mass region 3575–3660 MeV/c^2.

$\eta_c(2S)$ BRANCHING RATIOS

$\Gamma(\text{hadrons})/\Gamma_{\text{total}}$ Γ_1/Γ

VALUE	DOCUMENT ID		TECN	COMMENT
• • • We do not use the following data for averages, fits, limits, etc. • • •				
not seen	ABREU	98O	DLPH	$e^+e^- \to e^+e^-$ +hadrons
seen	[9] EDWARDS	82C	CBAL	$e^+e^- \to \gamma X$

$\Gamma(K\overline{K}\pi)/\Gamma_{\text{total}}$ Γ_2/Γ

VALUE	EVTS	DOCUMENT ID		TECN	COMMENT
seen	39 ± 11	[10] CHOI	02	BELL	$B \to K K_S K^- \pi^+$

$\Gamma(\gamma\gamma)/\Gamma_{\text{total}}$ Γ_4/Γ

VALUE	CL%	DOCUMENT ID		TECN	COMMENT
• • • We do not use the following data for averages, fits, limits, etc. • • •					
<0.01	90	LEE	85	CBAL	$\psi' \to$ photons

[9] For a mass value of 3594 ± 5 MeV
[10] For a mass value of 3654 ± 6 MeV

$\eta_c(2S)$ REFERENCES

ABE,K	02	PRL 89 142001	K. Abe *et al.*	(BELLE Collab.)
CHOI	02	PRL 89 102001	S.-K. Choi *et al.*	(BELLE Collab.)
AMBROGIANI	01	PR D64 052003	M. Ambrogiani *et al.*	(FNAL E835 Collab.)
ABREU	98O	PL B441 479	P. Abreu *et al.*	(DELPHI Collab.)
ARMSTRONG	95F	PR D52 4839	T.A. Armstrong *et al.*	(FNAL, FERR, GENO+)
LEE	85	SLAC 282	R.A. Lee	(SLAC)
EDWARDS	82C	PRL 48 70	C. Edwards *et al.*	(CIT, HARV, PRIN+)

OTHER RELATED PAPERS

BADALIAN	03	PR D67 071901	A.M. Badalian, B.L.G. Bakker	
EICHTEN	02	PRL 89 162002	E.J. Eichten, K. Lane, C. Quigg	
ACCIARRI	99T	PL B461 155	M. Acciarri *et al.*	(L3 Collab.)
OREGLIA	82	PR D25 2259	M.J. Oreglia *et al.*	(SLAC, CIT, HARV+)
PORTER	81	SLAC Summer Inst. 355	F.C. Porter *et al.*	(CIT, HARV, PRIN+)
BARTEL	78B	PL 79B 492	W. Bartel *et al.*	(DESY, HEIDP)

$\psi(2S)$

$I^G(J^{PC}) = 0^-(1^{--})$

See the Review on "$\psi(2S)$ and χ_c branching ratios" before the $\chi_{c0}(1P)$ Listings.

$\psi(2S)$ MASS

VALUE (MeV)	EVTS	DOCUMENT ID		TECN	COMMENT
3686.093±0.034 OUR AVERAGE		Error includes scale factor of 1.4. See the ideogram below.			
3686.111±0.025±0.009		AULCHENKO	03	KEDR	$e^+e^- \to$ hadrons
3685.95 ±0.10	413	[1] ARTAMONOV	00	OLYA	$e^+e^- \to$ hadrons
3685.98 ±0.09 ±0.04		[2] ARMSTRONG	93B	E760	$\overline{p}p \to e^+e^-$
• • • We do not use the following data for averages, fits, limits, etc. • • •					
3684 ±2		GRIBUSHIN	96	FMPS	515 π^- Be $\to 2\mu X$
3683 ±5	77	ANTONIAZZI	94	E705	300 $\pi^\pm$, p Li $\to J/\psi\pi^+\pi^-$ X
3686.00 ±0.10	413	[3] ZHOLENTZ	80	OLYA	e^+e^-

[1] Reanalysis of ZHOLENTZ 80 using new electron mass (COHEN 87) and radiative corrections (KURAEV 85).
[2] Mass central value and systematic error recalculated by us according to Eq. (16) in ARMSTRONG 93B, using the value for the $J/\psi(1S)$ mass from AULCHENKO 03.
[3] Superseded by ARTAMONOV 00.

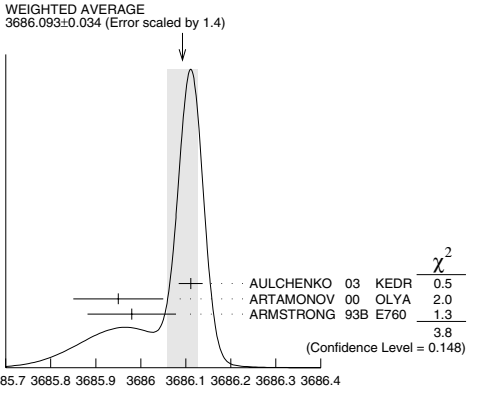

$m_{\psi(2S)} - m_{J/\psi(1S)}$

VALUE (MeV)	DOCUMENT ID		TECN	COMMENT
589.188±0.028 OUR AVERAGE				
589.194±0.027±0.011	[4] AULCHENKO	03	KEDR	$e^+e^- \to$ hadrons
589.7 ±1.2	LEMOIGNE	82	GOLI	190 π^- Be $\to 2\mu$
589.07 ±0.13	[4] ZHOLENTZ	80	OLYA	e^+e^-
588.7 ±0.8	LUTH	75	MRK1	
• • • We do not use the following data for averages, fits, limits, etc. • • •				
588 ±1	[5] BAI	98E	BES	e^+e^-

[4] Redundant with data in mass above.
[5] Systematic errors not evaluated.

$\psi(2S)$ WIDTH

VALUE (keV)	DOCUMENT ID		TECN	COMMENT
281±17 OUR FIT				
277±22 OUR AVERAGE				
264±27	[6] BAI	02B	BES	e^+e^-
306±36±16	ARMSTRONG	93B	E760	$\overline{p}p \to e^+e^-$

[6] From a simultaneous fit to the hadronic and $\mu^+\mu^-$ cross section, assuming $\Gamma = \Gamma_h + \Gamma_e + \Gamma_\mu + \Gamma_\tau$ and lepton universality.

$\psi(2S)$ DECAY MODES

	Mode	Fraction (Γ_i/Γ)	Scale factor/ Confidence level
Γ_1	hadrons	(97.85±0.13) %	
Γ_2	virtual $\gamma \to$ hadrons	(2.16±0.35) %	S=2.1
Γ_3	e^+e^-	(7.55±0.31) $\times 10^{-3}$	
Γ_4	$\mu^+\mu^-$	(7.3 ±0.8) $\times 10^{-3}$	
Γ_5	$\tau^+\tau^-$	(2.8 ±0.7) $\times 10^{-3}$	

Decays into $J/\psi(1S)$ and anything

Γ_6	$J/\psi(1S)$ anything	(57.6 ±2.0) %		
Γ_7	$J/\psi(1S)$ neutrals	(24.6 ±1.2) %		
Γ_8	$J/\psi(1S)\pi^+\pi^-$	(31.7 ±1.1) %		
Γ_9	$J/\psi(1S)\pi^0\pi^0$	(18.8 ±1.2) %		
Γ_{10}	$J/\psi(1S)\eta$	(3.16±0.22) %		
Γ_{11}	$J/\psi(1S)\pi^0$	(9.6 ±2.1) $\times 10^{-4}$		

Hadronic decays

Γ_{12}	$3(\pi^+\pi^-)\pi^0$	(3.5 ±1.6) $\times 10^{-3}$		
Γ_{13}	$2(\pi^+\pi^-)\pi^0$	(3.0 ±0.8) $\times 10^{-3}$		
Γ_{14}	$\rho a_2(1320)$	< 2.3 $\times 10^{-4}$		CL=90%
Γ_{15}	$\omega\pi^+\pi^-$	(4.8 ±0.9) $\times 10^{-4}$		
Γ_{16}	$b_1^\pm\pi^\mp$	(3.2 ±0.8) $\times 10^{-4}$		
Γ_{17}	$\omega f_2(1270)$	< 1.5 $\times 10^{-4}$		CL=90%
Γ_{18}	$\pi^+\pi^- K^+K^-$	(1.6 ±0.4) $\times 10^{-3}$		
Γ_{19}	$K^*(892)\overline{K}_2^*(1430)^0$	< 1.2 $\times 10^{-4}$		CL=90%
Γ_{20}	$K_1(1270)^\pm K^\mp$	(1.00±0.28) $\times 10^{-3}$		
Γ_{21}	$\pi^+\pi^- p\overline{p}$	(8.0 ±2.0) $\times 10^{-4}$		
Γ_{22}	$K^+\overline{K}^*(892)^0\pi^-$ + c.c.	(6.7 ±2.5) $\times 10^{-4}$		
Γ_{23}	$2(\pi^+\pi^-)$	(4.5 ±1.0) $\times 10^{-4}$		
Γ_{24}	$\rho^0\pi^+\pi^-$	(4.2 ±1.5) $\times 10^{-4}$		
Γ_{25}	ωK^+K^-	(1.5 ±0.4) $\times 10^{-4}$		
Γ_{26}	$\omega p\overline{p}$	(8.0 ±3.2) $\times 10^{-5}$		
Γ_{27}	$\overline{p}p$	(2.07±0.31) $\times 10^{-4}$		
Γ_{28}	$\Lambda\overline{\Lambda}$	(1.81±0.34) $\times 10^{-4}$		
Γ_{29}	$3(\pi^+\pi^-)$	(1.5 ±1.0) $\times 10^{-4}$		
Γ_{30}	$\overline{p}p\pi^0$	(1.4 ±0.5) $\times 10^{-4}$		
Γ_{31}	$\Delta^{++}\overline{\Delta}^{--}$	(1.28±0.35) $\times 10^{-4}$		
Γ_{32}	$\Sigma^0\overline{\Sigma}^0$	(1.2 ±0.6) $\times 10^{-4}$		
Γ_{33}	$\Sigma^{*+}\overline{\Sigma}^{*-}$	(1.1 ±0.4) $\times 10^{-4}$		
Γ_{34}	K^+K^-	(1.0 ±0.7) $\times 10^{-4}$		
Γ_{35}	$K_S^0K_L^0$	(5.2 ±0.7) $\times 10^{-5}$		
Γ_{36}	$\pi^+\pi^-\pi^0$	(8 ±5) $\times 10^{-5}$		
Γ_{37}	$\rho\pi$	< 8.3 $\times 10^{-5}$		CL=90%
Γ_{38}	$\pi^+\pi^-$	(8 ±5) $\times 10^{-5}$		
Γ_{39}	$\Xi^-\overline{\Xi}^+$	(9.4 ±3.1) $\times 10^{-5}$		
Γ_{40}	$K_1(1400)^\pm K^\mp$	< 3.1 $\times 10^{-4}$		CL=90%
Γ_{41}	$\Xi^{*0}\overline{\Xi}^{*0}$	< 8.1 $\times 10^{-5}$		CL=90%
Γ_{42}	$\Omega^-\overline{\Omega}^+$	< 7.3 $\times 10^{-5}$		CL=90%
Γ_{43}	$K^+K^-\pi^0$	< 2.96 $\times 10^{-5}$		CL=90%
Γ_{44}	$K^+\overline{K}^*(892)^-$ + c.c.	< 5.4 $\times 10^{-5}$		CL=90%
Γ_{45}	$\phi\pi^+\pi^-$	(1.50±0.28) $\times 10^{-4}$		
Γ_{46}	$\phi f_0(980) \to \pi^+\pi^-$	(6.0 ±2.2) $\times 10^{-5}$		
Γ_{47}	ϕK^+K^-	(6.0 ±2.2) $\times 10^{-5}$		
Γ_{48}	$\phi p\overline{p}$	< 2.6 $\times 10^{-5}$		CL=90%
Γ_{49}	$\phi f_2'(1525)$	< 4.5 $\times 10^{-5}$		CL=90%

Radiative decays

Γ_{50}	$\gamma\chi_{c0}(1P)$	(8.6 ±0.7) %		
Γ_{51}	$\gamma\chi_{c1}(1P)$	(8.4 ±0.8) %		
Γ_{52}	$\gamma\chi_{c2}(1P)$	(6.4 ±0.6) %		
Γ_{53}	$\gamma\eta_c(1S)$	(2.8 ±0.6) $\times 10^{-3}$		
Γ_{54}	$\gamma\eta_c(2S)$			
Γ_{55}	$\gamma\pi^0$			
Γ_{56}	$\gamma\eta'(958)$	(1.5 ±0.4) $\times 10^{-4}$		
Γ_{57}	$\gamma f_2(1270)$	(2.1 ±0.4) $\times 10^{-4}$		
Γ_{58}	$\gamma f_0(1710) \to \gamma\pi\pi$	(3.0 ±1.3) $\times 10^{-5}$		
Γ_{59}	$\gamma f_0(1710) \to \gamma K\overline{K}$	(6.0 ±1.6) $\times 10^{-5}$		
Γ_{60}	$\gamma\gamma$	< 1.5 $\times 10^{-4}$		CL=90%
Γ_{61}	$\gamma\eta$	< 9 $\times 10^{-5}$		CL=90%
Γ_{62}	$\gamma\eta(1405) \to \gamma K\overline{K}\pi$	< 1.2 $\times 10^{-4}$		CL=90%

$\psi(2S)$ PARTIAL WIDTHS

Γ(hadrons) Γ_1

VALUE (keV)	DOCUMENT ID		TECN	COMMENT
• • • We do not use the following data for averages, fits, limits, etc. • • •				
258±26	BAI	02B	BES	e^+e^-
224±56	LUTH	75	MRK1	e^+e^-

$\Gamma(e^+e^-)$ Γ_3

VALUE (keV)	DOCUMENT ID		TECN	COMMENT
2.12±0.12 OUR FIT				
2.14±0.21	ALEXANDER	89	RVUE	See Υ mini-review
• • • We do not use the following data for averages, fits, limits, etc. • • •				
2.44±0.21	[8] BAI	02B	BES	e^+e^-
2.0 ±0.3	BRANDELIK	79C	DASP	e^+e^-
2.1 ±0.3	[7] LUTH	75	MRK1	e^+e^-

[7] From a simultaneous fit to e^+e^-, $\mu^+\mu^-$, and hadronic channels assuming $\Gamma(e^+e^-) = \Gamma(\mu^+\mu^-)$.

$\Gamma(\gamma\gamma)$ Γ_{60}

VALUE (eV)	CL%	DOCUMENT ID	TECN	COMMENT
<43	90	BRANDELIK 79C	DASP	e^+e^-

[8] From a simultaneous fit to e^+e^-, $\mu^+\mu^-$, and hadronic channel, assuming $\Gamma_e = \Gamma_\mu = \Gamma_\tau/0.38847$.

$\psi(2S)$ Γ(i)$\Gamma(e^+e^-)/\Gamma$(total)

This combination of a partial width with the partial width into e^+e^- and with the total width is obtained from the integrated cross section into channel$_i$ in the e^+e^- annihilation. We list only data that have not been used to determine the partial width Γ(i) or the branching ratio Γ(i)/total.

Γ(hadrons) × $\Gamma(e^+e^-)/\Gamma_{\rm total}$ $\Gamma_1\Gamma_3/\Gamma$

VALUE (keV)	DOCUMENT ID		TECN	COMMENT
• • • We do not use the following data for averages, fits, limits, etc. • • •				
2.2±0.4	ABRAMS	75	MRK1	e^+e^-

$\Gamma(e^+e^-)$ × $\Gamma(J/\psi(1S)\pi^+\pi^-)/\Gamma_{\rm total}$ $\Gamma_3\Gamma_8/\Gamma$

VALUE (keV)	DOCUMENT ID		TECN	COMMENT
0.67±0.05 OUR FIT				
0.68±0.09	[9] BAI	98E	BES	e^+e^-

[9] The value of $\Gamma(e^+e^-)$ quoted in BAI 98E is derived using $B(\psi(2S) \to J/\psi(1S)\pi^+\pi^-) = (32.4 \pm 2.6)\times 10^{-2}$ and $B(J/\psi(1S) \to \ell^+\ell^-) = 0.1203 \pm 0.0038$. Recalculated by us using $B(J/\psi(1S) \to \ell^+\ell^-) = 0.1181 \pm 0.0020$.

$\psi(2S)$ BRANCHING RATIOS

Γ(hadrons)/$\Gamma_{\rm total}$ Γ_1/Γ

VALUE	DOCUMENT ID		TECN	COMMENT
0.9785±0.0013 OUR AVERAGE				
0.9779±0.0015	[10] BAI	02B	BES	e^+e^-
0.981 ±0.003	[10] LUTH	75	MRK1	e^+e^-

Γ(virtual $\gamma \to$ hadrons)/$\Gamma_{\rm total}$ Γ_2/Γ

VALUE	DOCUMENT ID		TECN	COMMENT
0.0216±0.0035 OUR AVERAGE	Error includes scale factor of 2.1.			
0.0199±0.0019	[11] BAI	02B	BES	e^+e^-
0.029 ±0.004	[11] LUTH	75	MRK1	e^+e^-

$\Gamma(e^+e^-)/\Gamma_{\rm total}$ Γ_3/Γ

VALUE (units 10^{-4})	DOCUMENT ID		TECN	COMMENT
75.5± 3.1 OUR FIT				
• • • We do not use the following data for averages, fits, limits, etc. • • •				
88 ±13	[12] FELDMAN	77	RVUE	e^+e^-

$\Gamma(\mu^+\mu^-)/\Gamma_{\rm total}$ Γ_4/Γ

VALUE (units 10^{-4})	DOCUMENT ID
73±8 OUR FIT	

$\Gamma(\tau^+\tau^-)/\Gamma_{\rm total}$ Γ_5/Γ

VALUE (units 10^{-4})	DOCUMENT ID
28±7 OUR FIT	

$\Gamma(\mu^+\mu^-)/\Gamma(e^+e^-)$ Γ_4/Γ_3

VALUE	DOCUMENT ID		TECN	COMMENT
0.97±0.13 OUR FIT				
• • • We do not use the following data for averages, fits, limits, etc. • • •				
0.89±0.16	BOYARSKI	75C	MRK1	e^+e^-

[10] Includes cascade decay into $J/\psi(1S)$.

[11] Included in Γ(hadrons)/$\Gamma_{\rm total}$.

[12] From an overall fit assuming equal partial widths for e^+e^- and $\mu^+\mu^-$. For a measurement of the ratio see the entry $\Gamma(\mu^+\mu^-)/\Gamma(e^+e^-)$ below. Includes LUTH 75, HILGER 75, BURMESTER 77.

DECAYS INTO $J/\psi(1S)$ AND ANYTHING

$\Gamma(J/\psi(1S)$ anything$)/\Gamma_{\rm total}$ Γ_6/Γ

VALUE	DOCUMENT ID		TECN	COMMENT
0.576±0.020 OUR FIT				
0.55 ±0.07 OUR AVERAGE				
0.51 ±0.12	BRANDELIK	79C	DASP	$e^+e^- \to \mu^+\mu^-$X
0.57 ±0.08	ABRAMS	75B	MRK1	$e^+e^- \to \mu^+\mu^-$X

$\Gamma(J/\psi(1S)\text{neutrals})/\Gamma_{\text{total}}$ Γ_7/Γ

VALUE	DOCUMENT ID
0.246±0.012 OUR FIT	

$\Gamma(J/\psi(1S)\pi^+\pi^-)/\Gamma_{\text{total}}$ Γ_8/Γ

VALUE	DOCUMENT ID		TECN	COMMENT
0.317±0.011 OUR FIT				
0.323±0.013 OUR AVERAGE				
0.323±0.014	BAI	02B	BES	e^+e^-
0.32 ±0.04	ABRAMS	75B	MRK1	$e^+e^- \to J/\psi\pi^+\pi^-$

$\Gamma(J/\psi(1S)\pi^0\pi^0)/\Gamma_{\text{total}}$ Γ_9/Γ

VALUE	DOCUMENT ID
0.188±0.012 OUR FIT	

$\Gamma(J/\psi(1S)\eta)/\Gamma_{\text{total}}$ Γ_{10}/Γ

VALUE	EVTS	DOCUMENT ID		TECN	COMMENT
0.0316±0.0022 OUR FIT					
0.029 ±0.005 OUR AVERAGE Error includes scale factor of 2.0. See the ideogram below.					
0.0255±0.0029	386	[13] OREGLIA	80	CBAL	$e^+e^- \to J/\psi\,2\gamma$
0.045 ±0.012	17	[14] BRANDELIK	79B	DASP	$e^+e^- \to J/\psi\,2\gamma$
0.042 ±0.006	164	[14] BARTEL	78B	CNTR	e^+e^-
• • • We do not use the following data for averages, fits, limits, etc. • • •					
0.043 ±0.008	44	TANENBAUM	76	MRK1	e^+e^-

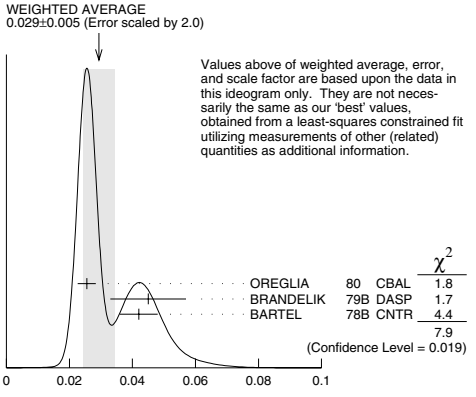

$\Gamma(J/\psi(1S)\eta)/\Gamma_{\text{total}}$

$\Gamma(J/\psi(1S)\pi^0)/\Gamma_{\text{total}}$ Γ_{11}/Γ

VALUE (units 10^{-4})	EVTS	DOCUMENT ID		TECN	COMMENT
9.6±2.1 OUR AVERAGE					
14 ±6	7	HIMEL	80	MRK2	e^+e^-
9 ±2 ±1	23	[13] OREGLIA	80	CBAL	$\psi(2S) \to J/\psi\,2\gamma$

$\Gamma(J/\psi(1S)\text{neutrals})/\Gamma(J/\psi(1S)\pi^+\pi^-)$ Γ_7/Γ_8

VALUE	DOCUMENT ID		TECN	COMMENT
0.777±0.032 OUR FIT				
0.73 ±0.09	TANENBAUM	76	MRK1	e^+e^-

$\Gamma(J/\psi(1S)\pi^+\pi^-)/\Gamma(J/\psi(1S)\text{anything})$ Γ_8/Γ_6

VALUE	DOCUMENT ID		TECN	COMMENT
0.549±0.011 OUR FIT				
0.496±0.037	ARMSTRONG	97	E760	$\overline{p}p \to \psi(2S)$

$\Gamma(J/\psi(1S)\pi^0\pi^0)/\Gamma(J/\psi(1S)\text{anything})$ Γ_9/Γ_6

VALUE	DOCUMENT ID		TECN	COMMENT
0.327±0.012 OUR FIT				
0.327±0.014 OUR AVERAGE				
0.328±0.013±0.008	AMBROGIANI	00A	E835	$p\overline{p} \to \psi(2S)$
0.323±0.033	ARMSTRONG	97	E760	$\overline{p}p \to \psi(2S)$

$\Gamma(J/\psi(1S)\pi^0\pi^0)/\Gamma(J/\psi(1S)\pi^+\pi^-)$ Γ_9/Γ_8

VALUE	DOCUMENT ID		TECN	COMMENT
0.59±0.05 OUR FIT				
• • • We do not use the following data for averages, fits, limits, etc. • • •				
0.53±0.06	TANENBAUM	76	MRK1	e^+e^-
0.64±0.15	[15] HILGER	75	SPEC	e^+e^-

$\Gamma(J/\psi(1S)\eta)/\Gamma(J/\psi(1S)\text{anything})$ Γ_{10}/Γ_6

VALUE	DOCUMENT ID		TECN	COMMENT
0.055±0.004 OUR FIT				
0.069±0.008 OUR AVERAGE				
0.072±0.009	AMBROGIANI	00A	E835	$p\overline{p} \to \psi(2S)$
0.061±0.015	ARMSTRONG	97	E760	$\overline{p}p \to \psi(2S)$

$\Gamma(J/\psi(1S)\eta)/\Gamma(J/\psi(1S)\pi^+\pi^-)$ Γ_{10}/Γ_8

VALUE	DOCUMENT ID		TECN	COMMENT
0.100±0.008 OUR FIT				
0.091±0.021	[16] HIMEL	80	MRK2	$e^+e^- \to \psi(2S)X$

$\Gamma(e^+e^-)/\Gamma(J/\psi(1S)\text{anything})$ Γ_3/Γ_6

VALUE	DOCUMENT ID		TECN	COMMENT
0.0131±0.0010 OUR FIT				
0.0131±0.0006 OUR AVERAGE Error includes scale factor of 1.8.				
0.0128±0.0003±0.0002	[17] AMBROGIANI	00A	E835	$p\overline{p} \to \psi(2S)$
0.0144±0.0008±0.0002	[17] ARMSTRONG	97	E760	$\overline{p}p \to \psi(2S)$

$\Gamma(e^+e^-)/\Gamma(J/\psi(1S)\pi^+\pi^-)$ Γ_3/Γ_8

VALUE	DOCUMENT ID		TECN	COMMENT
0.0238±0.0017 OUR FIT				
0.0252±0.0028±0.0011	[17] AUBERT	02B	BABR	e^+e^-

$\Gamma(\mu^+\mu^-)/\Gamma(J/\psi(1S)\text{anything})$ Γ_4/Γ_6

VALUE	DOCUMENT ID		TECN	COMMENT
0.0127±0.0033 OUR FIT				
0.014 ±0.003	HILGER	75	SPEC	e^+e^-

$\Gamma(\mu^+\mu^-)/\Gamma(J/\psi(1S)\pi^+\pi^-)$ Γ_4/Γ_8

VALUE	DOCUMENT ID		TECN	COMMENT
0.0231±0.0030 OUR FIT				
0.0224±0.0029 OUR AVERAGE				
0.0216±0.0026±0.0014	[18] AUBERT	02B	BABR	e^+e^-
0.0327±0.0077±0.0072	[18] GRIBUSHIN	96	FMPS	515 π^- Be $\to 2\mu X$

$\Gamma(\tau^+\tau^-)/\Gamma(J/\psi(1S)\pi^+\pi^-)$ Γ_5/Γ_8

VALUE (units 10^{-3})	DOCUMENT ID		TECN	COMMENT
8.7 ±2.2 OUR FIT				
8.73±1.39±1.57	BAI	02	BES	e^+e^-

[13] Recalculated by us using $B(J/\psi(1S) \to \ell^+\ell^-) = 0.1181 \pm 0.0020$.
[14] Recalculated by us using $B(J/\psi(1S) \to \mu^+\mu^-) = 0.0588 \pm 0.0010$.
[15] Ignoring the $J/\psi(1S)\eta$ and $J/\psi(1S)\gamma\gamma$ decays.
[16] The value for $B(\psi(2S) \to J/\psi(1s)\eta)$ reported in HIMEL 80 is derived using $B(\psi(2S)) \to J/\psi(1S)\pi^+\pi^-) = (33\pm3)\%$ and $B(J/\psi(1S) \to \ell^+\ell^-) = 0.138\pm0.018$. Calculated by us using $B(J/\psi(1S) \to \ell^+\ell^-) = (0.1181 \pm 0.0020)$.
[17] Using $B(J/\psi(1S) \to e^+e^-) = 0.0593 \pm 0.0010$.
[18] Using $B(J/\psi(1S) \to \mu^+\mu^-) = 0.0588 \pm 0.0010$.

HADRONIC DECAYS

$\Gamma(3(\pi^+\pi^-)\pi^0)/\Gamma_{\text{total}}$ Γ_{12}/Γ

VALUE (units 10^{-4})	EVTS	DOCUMENT ID		TECN	COMMENT
35±16	6	FRANKLIN	83	MRK2	$e^+e^- \to$ hadrons

$\Gamma(2(\pi^+\pi^-)\pi^0)/\Gamma_{\text{total}}$ Γ_{13}/Γ

VALUE (units 10^{-4})	EVTS	DOCUMENT ID		TECN	COMMENT
30±8	42	FRANKLIN	83	MRK2	e^+e^-

$\Gamma(\omega\pi^+\pi^-)/\Gamma_{\text{total}}$ Γ_{15}/Γ

VALUE (units 10^{-4})	EVTS	DOCUMENT ID		TECN	COMMENT
4.8±0.6±0.7	100±22	[19] BAI	03B	BES	$\psi(2S) \to 2(\pi^+\pi^-)\pi^0$

$\Gamma(b_1^\pm\pi^\mp)/\Gamma_{\text{total}}$ Γ_{16}/Γ

VALUE (units 10^{-4})	EVTS	DOCUMENT ID		TECN	COMMENT
3.2±0.6±0.5	61±11	[19,20] BAI	03B	BES	$\psi(2S) \to 2(\pi^+\pi^-)\pi^0$
• • • We do not use the following data for averages, fits, limits, etc. • • •					
5.2±0.8±1.0		[20] BAI	99C	BES	Repl. by BAI 03B

$\Gamma(\omega f_2(1270))/\Gamma_{\text{total}}$ Γ_{17}/Γ

VALUE (units 10^{-4})	CL%	DOCUMENT ID		TECN	COMMENT
<1.5	90	[19] BAI	03B	BES	$\psi(2S) \to 2(\pi^+\pi^-)\pi^0$
• • • We do not use the following data for averages, fits, limits, etc. • • •					
<1.7	90	BAI	98J	BES	Repl. by BAI 03B

$\Gamma(\pi^+\pi^- K^+K^-)/\Gamma_{\text{total}}$ Γ_{18}/Γ

VALUE (units 10^{-4})	DOCUMENT ID		TECN	COMMENT
16±4	[21] TANENBAUM	78	MRK1	e^+e^-

$\Gamma(K_1(1270)^\pm K^\mp)/\Gamma_{\text{total}}$ Γ_{20}/Γ

VALUE (units 10^{-4})	DOCUMENT ID		TECN	COMMENT
10.0±1.8±2.1	[22] BAI	99C	BES	e^+e^-

$\Gamma(\pi^+\pi^-\rho\overline{p})/\Gamma_{total}$ Γ_{21}/Γ

VALUE (units 10^{-4})	DOCUMENT ID		TECN	COMMENT
8 ±2	[21] TANENBAUM	78	MRK1	e^+e^-

$\Gamma(K^+\overline{K}^*(892)^0\pi^- + c.c.)/\Gamma_{total}$ Γ_{22}/Γ

VALUE (units 10^{-4})	DOCUMENT ID		TECN	COMMENT
6.7±2.5	TANENBAUM	78	MRK1	e^+e^-

$\Gamma(\omega K^+K^-)/\Gamma_{total}$ Γ_{25}/Γ

VALUE (units 10^{-4})	EVTS	DOCUMENT ID		TECN	COMMENT
1.5 ±0.3 ±0.2	23.0± 5.2	[19] BAI	03B	BES	$\psi(2S) \to K^+K^-\pi^+\pi^-\pi^0$

$\Gamma(\omega p\overline{p})/\Gamma_{total}$ Γ_{26}/Γ

VALUE (units 10^{-4})	EVTS	DOCUMENT ID		TECN	COMMENT
0.8 ±0.3 ±0.1	14.9± 0.1	[19] BAI	03B	BES	$\psi(2S) \to p\overline{p}\pi^+\pi^-\pi^0$

$\Gamma(2(\pi^+\pi^-))/\Gamma_{total}$ Γ_{23}/Γ

VALUE (units 10^{-4})	DOCUMENT ID		TECN	COMMENT
4.5±1.0	TANENBAUM	78	MRK1	e^+e^-

$\Gamma(\rho^0\pi^+\pi^-)/\Gamma_{total}$ Γ_{24}/Γ

VALUE (units 10^{-4})	DOCUMENT ID		TECN	COMMENT
4.2±1.5	TANENBAUM	78	MRK1	e^+e^-

$\Gamma(\rho a_2(1320))/\Gamma_{total}$ Γ_{14}/Γ

VALUE (units 10^{-4})	CL%	DOCUMENT ID		TECN	COMMENT
<2.3	90	BAI	98J	BES	e^+e^-

$\Gamma(\overline{p}p)/\Gamma_{total}$ Γ_{27}/Γ

VALUE (units 10^{-4})	EVTS	DOCUMENT ID		TECN	COMMENT
2.07±0.31 OUR AVERAGE					
2.16±0.15±0.36	201	[23] BAI	01	BES	$e^+e^- \to \psi(2S)$
1.4 ±0.8	4	BRANDELIK	79C	DASP	e^+e^-
2.3 ±0.7		FELDMAN	77	MRK1	e^+e^-

$\Gamma(\Lambda\overline{\Lambda})/\Gamma_{total}$ Γ_{28}/Γ

VALUE (units 10^{-4})	CL%	EVTS	DOCUMENT ID		TECN	COMMENT
1.81±0.20±0.27		80	[23] BAI	01	BES	$e^+e^- \to \psi(2S)$
• • • We do not use the following data for averages, fits, limits, etc. • • •						
<4	90		FELDMAN	77	MRK1	e^+e^-

$\Gamma(3(\pi^+\pi^-))/\Gamma_{total}$ Γ_{29}/Γ

VALUE (units 10^{-4})	DOCUMENT ID		TECN	COMMENT
1.5±1.0	[21] TANENBAUM	78	MRK1	e^+e^-

$\Gamma(\overline{p}p\pi^0)/\Gamma_{total}$ Γ_{30}/Γ

VALUE (units 10^{-4})	EVTS	DOCUMENT ID		TECN	COMMENT
1.4±0.5	9	FRANKLIN	83	MRK2	e^+e^-

$\Gamma(K^+K^-)/\Gamma_{total}$ Γ_{34}/Γ

VALUE (units 10^{-4})	CL%	DOCUMENT ID		TECN	COMMENT
1.0±0.7		BRANDELIK	79C	DASP	e^+e^-
• • • We do not use the following data for averages, fits, limits, etc. • • •					
<0.5	90	FELDMAN	77	MRK1	e^+e^-

$\Gamma(K_S^0K_L^0)/\Gamma_{total}$ Γ_{35}/Γ

VALUE (units 10^{-5})	EVTS	DOCUMENT ID		TECN	COMMENT
5.24±0.47±0.48	156± 14	[24] BAI	04B	BES2	$\psi(2S) \to K_S^0K_L^0 \to \pi^+\pi^-X$

$\Gamma(\pi^+\pi^-)/\Gamma_{total}$ Γ_{38}/Γ

VALUE (units 10^{-4})	CL%	DOCUMENT ID		TECN	COMMENT
0.8±0.5		BRANDELIK	79C	DASP	e^+e^-
• • • We do not use the following data for averages, fits, limits, etc. • • •					
<0.5	90	FELDMAN	77	MRK1	e^+e^-

$\Gamma(\pi^+\pi^-\pi^0)/\Gamma_{total}$ Γ_{36}/Γ

VALUE (units 10^{-4})	EVTS	DOCUMENT ID		TECN	COMMENT
0.85±0.46	4	FRANKLIN	83	MRK2	$e^+e^- \to$ hadrons

$\Gamma(\Delta^{++}\overline{\Delta}^{--})/\Gamma_{total}$ Γ_{31}/Γ

VALUE (units 10^{-5})	EVTS	DOCUMENT ID		TECN	COMMENT
12.8±1.0±3.4	157	[23] BAI	01	BES	$e^+e^- \to \psi(2S)$

$\Gamma(\Sigma^0\overline{\Sigma}^0)/\Gamma_{total}$ Γ_{32}/Γ

VALUE (units 10^{-5})	EVTS	DOCUMENT ID		TECN	COMMENT
12±4±4	8	[23] BAI	01	BES	$e^+e^- \to \psi(2S)$

$\Gamma(\Sigma^{*+}\overline{\Sigma}^{*-})/\Gamma_{total}$ Γ_{33}/Γ

VALUE (units 10^{-5})	EVTS	DOCUMENT ID		TECN	COMMENT
11±3±3	14	[23] BAI	01	BES	$e^+e^- \to \psi(2S)$

$\Gamma(K_1(1400)^\pm K^\mp)/\Gamma_{total}$ Γ_{40}/Γ

VALUE (units 10^{-4})	CL%	DOCUMENT ID		TECN	COMMENT
<3.1	90	[25] BAI	99C	BES	e^+e^-

$\Gamma(\Xi^-\overline{\Xi}^+)/\Gamma_{total}$ Γ_{39}/Γ

VALUE (units 10^{-5})	CL%	EVTS	DOCUMENT ID		TECN	COMMENT
9.4±2.7±1.5		12	[23] BAI	01	BES	$e^+e^- \to \psi(2S)$
• • • We do not use the following data for averages, fits, limits, etc. • • •						
<20	90		FELDMAN	77	MRK1	e^+e^-

$\Gamma(\Xi^{*0}\overline{\Xi}^{*0})/\Gamma_{total}$ Γ_{41}/Γ

VALUE (units 10^{-5})	CL%	DOCUMENT ID		TECN	COMMENT
<8.1	90	[23] BAI	01	BES	$e^+e^- \to \psi(2S)$

$\Gamma(\Omega^-\overline{\Omega}^+)/\Gamma_{total}$ Γ_{42}/Γ

VALUE (units 10^{-5})	CL%	DOCUMENT ID		TECN	COMMENT
<7.3	90	[23] BAI	01	BES	$e^+e^- \to \psi(2S)$

$\Gamma(\rho\pi)/\Gamma_{total}$ Γ_{37}/Γ

VALUE (units 10^{-4})	CL%	EVTS	DOCUMENT ID		TECN	COMMENT
< 0.83	90	1	FRANKLIN	83	MRK2	e^+e^-
• • • We do not use the following data for averages, fits, limits, etc. • • •						
<10	90		BARTEL	76	CNTR	e^+e^-
<10	90		[26] ABRAMS	75	MRK1	e^+e^-

$\Gamma(K^+K^-\pi^0)/\Gamma_{total}$ Γ_{43}/Γ

VALUE (units 10^{-5})	CL%	EVTS	DOCUMENT ID		TECN	COMMENT
<2.96	90	1	FRANKLIN	83	MRK2	$e^+e^- \to$ hadrons

$\Gamma(K^+\overline{K}^*(892)^- + c.c.)/\Gamma_{total}$ Γ_{44}/Γ

VALUE (units 10^{-5})	CL%	DOCUMENT ID		TECN	COMMENT
<5.4	90	FRANKLIN	83	MRK2	$e^+e^- \to$ hadrons

$\Gamma(K^*(892)\overline{K}_2^*(1430)^0)/\Gamma_{total}$ Γ_{19}/Γ

VALUE (units 10^{-4})	CL%	DOCUMENT ID		TECN	COMMENT
<1.2	90	BAI	98J	BES	e^+e^-

$\Gamma(\phi\pi^+\pi^-)/\Gamma_{total}$ Γ_{45}/Γ

VALUE (units 10^{-4})	EVTS	DOCUMENT ID		TECN	COMMENT
1.5 ±0.2 ±0.2	51.5 ± 8.3	[19] BAI	03B	BES	$\psi(2S) \to K^+K^-\pi^+\pi^-$

$\Gamma(\phi f_0(980) \to \pi^+\pi^-)/\Gamma_{total}$ Γ_{46}/Γ

VALUE (units 10^{-4})	EVTS	DOCUMENT ID		TECN	COMMENT
0.6 ±0.2 ±0.1	18.4 ± 6.4	[19] BAI	03B	BES	$\psi(2S) \to K^+K^-\pi^+\pi^-$

$\Gamma(\phi K^+K^-)/\Gamma_{total}$ Γ_{47}/Γ

VALUE (units 10^{-4})	EVTS	DOCUMENT ID		TECN	COMMENT
0.6 ±0.2 ±0.1	16.1 ± 5.0	[19] BAI	03B	BES	$\psi(2S) \to 2(K^+K^-)$

$\Gamma(\phi p\overline{p})/\Gamma_{total}$ Γ_{48}/Γ

VALUE (units 10^{-4})	CL%	DOCUMENT ID		TECN	COMMENT
<0.26	90	[19] BAI	03B	BES	$\psi(2S) \to K^+K^-p\overline{p}$

$\Gamma(\phi f_2'(1525))/\Gamma_{total}$ Γ_{49}/Γ

VALUE (units 10^{-4})	CL%	DOCUMENT ID		TECN	COMMENT
<0.45	90	BAI	98J	BES	$e^+e^- \to 2(K^+K^-)$

[19] Normalized to $B(\psi(2S) \to J/\psi\pi^+\pi^-) = 0.305 \pm 0.016$.
[20] Assuming $B(b_1 \to \omega\pi)=1$.
[21] Assuming entirely strong decay.
[22] Assuming $B(K_1(1270) \to K\rho)=0.42 \pm 0.06$
[23] Estimated using $B(\psi(2S) \to J/\psi\pi^+\pi^-)= 0.310 \pm 0.028$.
[24] Using $B(K_S^0 \to \pi^+\pi^-) = 0.6860 \pm 0.0027$.
[25] Assuming $B(K_1(1400) \to K^*\pi)=0.94 \pm 0.06$
[26] Final state $\rho^0\pi^0$.

RADIATIVE DECAYS

$\Gamma(\gamma\chi_{c0}(1P))/\Gamma_{total}$ Γ_{50}/Γ

VALUE (units 10^{-2})	DOCUMENT ID		TECN	COMMENT
8.6±0.7 OUR FIT				
9.3±0.8 OUR AVERAGE				
9.9±0.5±0.8	[27] GAISER	86	CBAL	$e^+e^- \to \gamma X$
7.2±2.3	[27] BIDDICK	77	CNTR	$e^+e^- \to \gamma X$
7.5±2.6	[27] WHITAKER	76	MRK1	e^+e^-

Meson Particle Listings

$\psi(2S)$, $\psi(3770)$

$\Gamma(\gamma\chi_{c1}(1P))/\Gamma_{total}$ Γ_{51}/Γ

VALUE (units 10^{-2})	DOCUMENT ID		TECN	COMMENT
8.4 ± 0.8 OUR FIT				
8.7 ± 0.8 OUR AVERAGE				
9.0 ± 0.5 ± 0.7	[28] GAISER	86	CBAL	$e^+e^- \to \gamma X$
7.1 ± 1.9	[29] BIDDICK	77	CNTR	$e^+e^- \to \gamma X$

$\Gamma(\gamma\chi_{c2}(1P))/\Gamma_{total}$ Γ_{52}/Γ

VALUE (units 10^{-2})	DOCUMENT ID		TECN	COMMENT
6.4 ± 0.6 OUR FIT				
7.8 ± 0.8 OUR AVERAGE				
8.0 ± 0.5 ± 0.7	[30] GAISER	86	CBAL	$e^+e^- \to \gamma X$
7.0 ± 2.0	[29] BIDDICK	77	CNTR	$e^+e^- \to \gamma X$

$\Gamma(\gamma\eta_c(1S))/\Gamma_{total}$ Γ_{53}/Γ

VALUE (units 10^{-2})	DOCUMENT ID		TECN	COMMENT
0.28 ± 0.06	GAISER	86	CBAL	$e^+e^- \to \gamma X$

$\Gamma(\gamma\eta_c(2S))/\Gamma_{total}$ Γ_{54}/Γ

VALUE (units 10^{-2})	CL%	DOCUMENT ID		TECN	COMMENT
• • • We do not use the following data for averages, fits, limits, etc. • • •					
0.2 to 1.3	95	EDWARDS	82C	CBAL	$e^+e^- \to \gamma X$

$\Gamma(\gamma\pi^0)/\Gamma_{total}$ Γ_{55}/Γ

VALUE (units 10^{-4})	CL%	DOCUMENT ID		TECN	COMMENT
• • • We do not use the following data for averages, fits, limits, etc. • • •					
< 54	95	[31] LIBERMAN	75	SPEC	e^+e^-
< 100	90	WIIK	75	DASP	e^+e^-

$\Gamma(\gamma\eta'(958))/\Gamma_{total}$ Γ_{56}/Γ

VALUE (units 10^{-4})	CL%	EVTS	DOCUMENT ID		TECN	COMMENT
1.54 ± 0.31 ± 0.20		~ 43	BAI	98F	BES	$\psi(2S) \to \pi^+\pi^- 2\gamma$, $\pi^+\pi^- 3\gamma$
• • • We do not use the following data for averages, fits, limits, etc. • • •						
< 60	90		[32] BRAUNSCH...	77	DASP	e^+e^-
< 11	90		[33] BARTEL	76	CNTR	e^+e^-

$\Gamma(\gamma f_2(1270))/\Gamma_{total}$ Γ_{57}/Γ

VALUE (units 10^{-4})	EVTS	DOCUMENT ID		TECN	COMMENT
2.12 ± 0.19 ± 0.32	[34,35]	BAI	03C	BES	$\psi(2S) \to \gamma\pi\pi$
• • • We do not use the following data for averages, fits, limits, etc. • • •					
2.08 ± 0.19 ± 0.33	200.6 ± 18.8	[34] BAI	03C	BES	$\psi(2S) \to \gamma\pi^+\pi^-$
2.90 ± 1.08 ± 1.07	29.9 ± 11.1	[34] BAI	03C	BES	$\psi(2S) \to \gamma\pi^0\pi^0$

$\Gamma(\gamma f_0(1710) \to \gamma\pi\pi)/\Gamma_{total}$ Γ_{58}/Γ

VALUE (units 10^{-4})	EVTS	DOCUMENT ID		TECN	COMMENT
0.301 ± 0.041 ± 0.124	35.6 ± 4.8	[34] BAI	03C	BES	$\psi(2S) \to \gamma\pi^+\pi^-$

$\Gamma(\gamma f_0(1710) \to \gamma K\overline{K})/\Gamma_{total}$ Γ_{59}/Γ

VALUE (units 10^{-4})	CL%	EVTS	DOCUMENT ID		TECN	COMMENT
0.604 ± 0.090 ± 0.132		39.6 ± 5.9	[34,36] BAI	03C	BES	$\psi(2S) \to \gamma K^+K^-$
• • • We do not use the following data for averages, fits, limits, etc. • • •						
< 1.56	90	6.8 ± 3.1	[34,36] BAI	03C	BES	$\psi(2S) \to \gamma K^0_S K^0_S$

$\Gamma(\gamma\eta)/\Gamma_{total}$ Γ_{61}/Γ

VALUE (units 10^{-4})	CL%	DOCUMENT ID		TECN	COMMENT
< 0.9	90	BAI	98F	BES	$\psi(2S) \to \pi^+\pi^- 3\gamma$
• • • We do not use the following data for averages, fits, limits, etc. • • •					
< 2	90	YAMADA	77	DASP	$e^+e^- \to 3\gamma$

$\Gamma(\gamma\eta(1405) \to \gamma K\overline{K}\pi)/\Gamma_{total}$ Γ_{62}/Γ

VALUE (units 10^{-3})	CL%	DOCUMENT ID		TECN	COMMENT
< 0.12	90	[37] SCHARRE	80	MRK1	e^+e^-

[27] Angular distribution $(1+\cos^2\theta)$ assumed.
[28] Angular distribution $(1-0.189\cos^2\theta)$ assumed.
[29] Valid for isotropic distribution of the photon.
[30] Angular distribution $(1-0.052\cos^2\theta)$ assumed.
[31] Restated by us using $B(\psi(2S) \to \mu^+\mu^-) = 0.0077$.
[32] Restated by us using total decay width 228 keV.
[33] The value is normalized to the branching ratio for $\Gamma(J/\psi(1S)\eta)/\Gamma_{total}$.
[34] Normalized to $B(\psi(2S) \to J/\psi\pi^+\pi^-) = 0.305 \pm 0.016$.
[35] Combining the results from $\pi^+\pi^-$ and $\pi^0\pi^0$ decay modes.
[36] Includes unknown branching fractions to K^+K^- or $K^0_S K^0_S$. We have multiplied the K^+K^- result by a factor of 2 and the $K^0_S K^0_S$ result by a factor of 4 to obtain the $K\overline{K}$ result.
[37] Includes unknown branching fraction $\eta(1405) \to K\overline{K}\pi$.

$\psi(2S)$ CROSS-PARTICLE BRANCHING RATIOS

For measurements involving $B(\psi(2S) \to \gamma\chi_{cJ}(1P))\times B(\chi_{cJ}(1P) \to X)$ see the corresponding entries in the $\chi_{cJ}(1P)$ sections.

$\psi(2S)$ REFERENCES

BAI	04B	PRL 92 052001	J.Z. Bai *et al.*	(BES2 Collab.)
AULCHENKO	03	PL B573 63	V.M. Aulchenko *et al.*	(KEDR Collab.)
BAI	03B	PR D67 052002	J.Z. Bai *et al.*	(BES Collab.)
BAI	03C	PR D67 032004	J.Z. Bai *et al.*	(BES Collab.)
AUBERT	02B	PR D65 031101R	B. Aubert *et al.*	(BaBar Collab.)
BAI	02	PR D65 052004	J.Z. Bai *et al.*	(BES Collab.)
BAI	02B	PL B550 24	J.Z. Bai *et al.*	(BES Collab.)
BAI	01	PR D63 032002	J.Z. Bai *et al.*	(BES Collab.)
AMBROGIANI	00A	PR D62 032004	M. Ambrogiani *et al.*	(FNAL E835 Collab.)
ARTAMONOV	00	PL B474 427	A.S. Artamonov *et al.*	
BAI	99C	PRL 83 1918	J.Z. Bai *et al.*	(BES Collab.)
BAI	98E	PR D57 3854	J.Z. Bai *et al.*	(BES Collab.)
BAI	98F	PR D58 097101	J.Z. Bai *et al.*	(BES Collab.)
BAI	98J	PRL 81 5080	J.Z. Bai *et al.*	(BES Collab.)
ARMSTRONG	97	PR D55 1153	T.A. Armstrong *et al.*	(E760 Collab.)
GRIBUSHIN	96	PR D53 4723	A. Gribushin *et al.*	(E672 Collab., E706 Collab.)
ANTONIAZZI	94	PR D50 4258	L. Antoniazzi *et al.*	(E705 Collab.)
ARMSTRONG	93B	PR D47 772	T.A. Armstrong *et al.*	(FNAL E760 Collab.)
ALEXANDER	89	NP B320 45	J.P. Alexander *et al.*	(LBL, MICH, SLAC)
COHEN	87	RMP 59 1121	E.R. Cohen, B.N. Taylor	(RISC, NBS)
GAISER	86	PR D34 711	J. Gaiser *et al.*	(Crystal Ball Collab.)
KURAEV	85	SJNP 41 466 Translated from YAF 41 733.	E.A. Kuraev, V.S. Fadin	(NOVO)
FRANKLIN	83	PRL 51 963	M.E.B. Franklin *et al.*	(LBL, SLAC)
EDWARDS	82C	PRL 48 70	C. Edwards *et al.*	(CIT, HARV, PRIN+)
LEMOIGNE	82	PL 113B 509	Y. Lemoigne *et al.*	(SACL, LOIC, SHMP+)
HIMEL	80	PRL 44 920	T. Himel *et al.*	(LBL, SLAC)
OREGLIA	80	PRL 45 959	M.J. Oreglia *et al.*	(SLAC, CIT, HARV+)
SCHARRE	80	PL 97B 329	D.L. Scharre *et al.*	(SLAC, LBL)
ZHOLENTZ	80	PL 96B 214	A.A. Zholentz *et al.*	(NOVO)
Also	81	SJNP 34 814 Translated from YAF 34 1471.	A.A. Zholents *et al.*	(NOVO)
BRANDELIK	79B	NP B160 426	R. Brandelik *et al.*	(DASP Collab.)
BRANDELIK	79C	ZPHY C1 233	R. Brandelik *et al.*	(DASP Collab.)
BARTEL	78B	PL 79B 492	W. Bartel *et al.*	(DESY, HEIDP)
TANENBAUM	78	PR D17 1731	W.M. Tanenbaum *et al.*	(SLAC, LBL)
BIDDICK	77	PRL 38 1324	C.J. Biddick *et al.*	(UCSD, UMD, PAVI+)
BRAUNSCH...	77	PL 67B 249	W. Braunschweig *et al.*	(DASP Collab.)
BURMESTER	77	PL 66B 395	J. Burmester *et al.*	(DESY, HAMB, SIEG+)
FELDMAN	77	PRPL 33C 285	G.J. Feldman, M.L. Perl	(LBL, SLAC)
YAMADA	77	Hamburg Conf. 69	S. Yamada	(DASP Collab.)
BARTEL	76	PL 64B 483	W. Bartel *et al.*	(DESY, HEIDP)
TANENBAUM	76	PRL 36 402	W.M. Tanenbaum *et al.*	(SLAC, LBL) IG
WHITAKER	76	PRL 37 1596	J.S. Whitaker *et al.*	(SLAC, LBL)
ABRAMS	75	Stanford Symp. 25	G.S. Abrams	(LBL)
ABRAMS	75B	PRL 34 1181	G.S. Abrams *et al.*	(LBL, SLAC)
BOYARSKI	75C	Palermo Conf. 54	A.M. Boyarski *et al.*	(SLAC, LBL)
HILGER	75	PRL 35 625	E. Hilger *et al.*	(STAN, PENN)
LIBERMAN	75	Stanford Symp. 55	A.D. Liberman	(STAN)
LUTH	75	PRL 35 1124	V. Luth *et al.*	(SLAC, LBL) JPC
WIIK	75	Stanford Symp. 69	B.H. Wiik	(DESY)

OTHER RELATED PAPERS

CHEN	98	PRL 80 5060	Y.Q. Chen, E. Braaten	
SUZUKI	98	PR D57 5717	M. Suzuki	
BARATE	83	PL 121B 449	R. Barate *et al.*	(SACL, LOIC, SHMP, IND)
AUBERT	75B	PRL 33 1624	J.J. Aubert *et al.*	(MIT, BNL)
BRAUNSCH...	75B	PL 57B 407	W. Braunschweig *et al.*	(DASP Collab.)
CAMERINI	75	PRL 35 483	U. Camerini *et al.*	(WISC, SLAC)
FELDMAN	75B	PRL 35 821	G.J. Feldman *et al.*	(LBL, SLAC)
GRECO	75	PL 56B 367	M. Greco, G. Pancheri-Srivastava, Y. Srivastava	
JACKSON	75	NIM 128 13	J.D. Jackson, D.L. Scharre	(LBL)
SIMPSON	75	PRL 35 699	J.W. Simpson *et al.*	(STAN, PENN)
ABRAMS	74	PRL 33 1453	G.S. Abrams *et al.*	(LBL, SLAC)

$\psi(3770)$ $I^G(J^{PC}) = 0^-(1^{--})$

$\psi(3770)$ MASS

VALUE (MeV)	DOCUMENT ID		TECN	COMMENT
3770.0 ± 2.4 OUR EVALUATION	Error includes scale factor of 1.8. From $m_{\psi(2S)}$ and mass difference below.			
• • • We do not use the following data for averages, fits, limits, etc. • • •				
3766.1 ± 2.0	[1] SCHINDLER	80	MRK2	e^+e^-
3772.1 ± 2.0	[1] BACINO	78	DLCO	e^+e^-
3774.1 ± 3.0	[1] RAPIDIS	77	MRK1	e^+e^-

[1] Recalculated by us from $m_{\psi(2S)} = 3686.093 \pm 0.034$ MeV and mass difference below.

$m_{\psi(3770)} - m_{\psi(2S)}$

VALUE (MeV)	DOCUMENT ID		TECN	COMMENT
83.9 ± 2.4 OUR AVERAGE	Error includes scale factor of 1.8. See the ideogram below.			
80 ± 2	SCHINDLER	80	MRK2	e^+e^-
86 ± 2	[2] BACINO	78	DLCO	e^+e^-
88 ± 3	RAPIDIS	77	MRK1	e^+e^-

[2] SPEAR $\psi(2S)$ mass subtracted (see SCHINDLER 80).

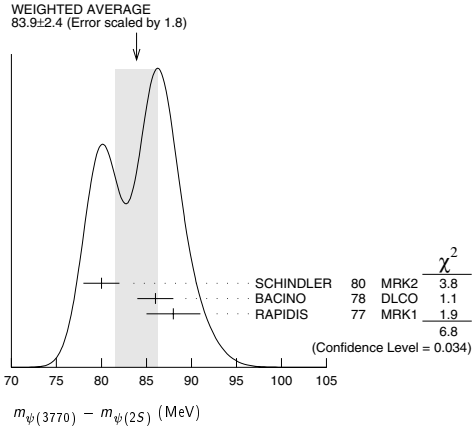

$\psi(3770)$ WIDTH

VALUE (MeV)	DOCUMENT ID		TECN	COMMENT
23.6±2.7 OUR FIT Error includes scale factor of 1.1.				
25.3±2.9 OUR AVERAGE				
24 ±5	SCHINDLER	80	MRK2	e^+e^-
24 ±5	BACINO	78	DLCO	e^+e^-
28 ±5	RAPIDIS	77	MRK1	e^+e^-

$\psi(3770)$ DECAY MODES

	Mode	Fraction (Γ_i/Γ)	Scale factor
Γ_1	$D\overline{D}$	dominant	
Γ_2	e^+e^-	$(1.12\pm0.17)\times10^{-5}$	1.2

$\psi(3770)$ PARTIAL WIDTHS

$\Gamma(e^+e^-)$ Γ_2

VALUE (keV)	DOCUMENT ID		TECN	COMMENT
0.26 ±0.04 OUR FIT Error includes scale factor of 1.2.				
0.24 ±0.05 OUR AVERAGE Error includes scale factor of 1.2.				
0.276±0.050	SCHINDLER	80	MRK2	e^+e^-
0.18 ±0.06	BACINO	78	DLCO	e^+e^-
• • • We do not use the following data for averages, fits, limits, etc. • • •				
0.37 ±0.09	[3] RAPIDIS	77	MRK1	e^+e^-

[3] See also $\Gamma(e^+e^-)/\Gamma_{total}$ below.

$\psi(3770)$ BRANCHING RATIOS

$\Gamma(D\overline{D})/\Gamma_{total}$ Γ_1/Γ

VALUE	DOCUMENT ID		TECN	COMMENT
dominant	PERUZZI	77	MRK1	$e^+e^- \to D\overline{D}$

$\Gamma(e^+e^-)/\Gamma_{total}$ Γ_2/Γ

VALUE (units 10^{-5})	DOCUMENT ID		TECN	COMMENT
1.12±0.17 OUR FIT Error includes scale factor of 1.2.				
1.3 ±0.2	RAPIDIS	77	MRK1	e^+e^-

$\psi(3770)$ REFERENCES

SCHINDLER	80	PR D21 2716	R.H. Schindler *et al.*	(Mark II Collab.)
BACINO	78	PRL 40 671	W.J. Bacino *et al.*	(SLAC, UCLA, UCI)
PERUZZI	77	PRL 39 1301	I. Peruzzi *et al.*	(Mark I Collab.)
RAPIDIS	77	PRL 39 526	P.A. Rapidis *et al.*	(Mark I Collab.)

$\psi(3836)$

$I^G(J^{PC}) = 0^-(2^{--})$

OMITTED FROM SUMMARY TABLE

Quantum numbers are not established.

Seen in $\pi^\pm$Li interactions by ANTONIAZZI 94 as a peak in the invariant mass of the $J/\psi(1S)\pi^+\pi^-$ system. Possibly seen also in pLi interactions. Interpretation as a $^3D_2$ (2^{--}) charmonium state favored. Not seen by BAI 98E in e^+e^- interactions. Needs confirmation.

$\psi(3836)$ MASS

VALUE (MeV)	EVTS	DOCUMENT ID		TECN	COMMENT
3836±13	58 ± 21	ANTONIAZZI	94	E705	$\pi^\pm\text{Li} \to J/\psi\pi^+\pi^- X$

$\psi(3836)$ DECAY MODES

	Mode	Fraction (Γ_i/Γ)
Γ_1	$J/\psi(1S)\pi^+\pi^-$	seen

$\psi(3836)$ REFERENCES

BAI	98E	PR D57 3854	J.Z. Bai *et al.*	(BES Collab.)
ANTONIAZZI	94	PR D50 4258	L. Antoniazzi *et al.*	(E705 Collab.)

$X(3872)$

$I^G(J^P) = ?^?(?^?)$

OMITTED FROM SUMMARY TABLE

Seen by CHOI 03 in $B \to K\pi^+\pi^- J/\psi(1S)$ decays as a narrow peak in the invariant mass distribution of the $\pi^+\pi^- J/\psi(1S)$ final state, but not seen in the $\gamma\chi_{c1}$ final state of these decays. Possibly absent in the invariant mass spectrum of the final state $\pi^+\pi^- J/\psi(1S)$ in e^+e^- collisions. Interpretation as a 1^{--} charmonium state not favored.

Quantum numbers are not established.

$X(3872)$ MASS

VALUE (MeV)	EVTS	DOCUMENT ID		TECN	COMMENT
3872.0±0.6±0.5	36	CHOI	03	BELL	$B \to K\pi^+\pi^- J/\psi$

$X(3872)$ WIDTH

VALUE (MeV)	CL%	EVTS	DOCUMENT ID		TECN	COMMENT
<2.3	90	36	CHOI	03	BELL	$B \to K\pi^+\pi^- J/\psi$

$X(3872)$ DECAY MODES

	Mode	Fraction (Γ_i/Γ)
Γ_1	e^+e^-	
Γ_2	$\pi^+\pi^- J/\psi(1S)$	seen
Γ_3	$\gamma\chi_{c1}$	

$X(3872)$ PARTIAL WIDTHS

$\Gamma(e^+e^-)$ Γ_1

VALUE (keV)	CL%	DOCUMENT ID		TECN	COMMENT
• • • We do not use the following data for averages, fits, limits, etc. • • •					
<0.28	90	[1] YUAN	04	RVUE	$e^+e^- \to \pi^+\pi^- J/\psi$

[1] Using BAI 98E data on $e^+e^- \to \pi^+\pi^-\ell^+\ell^-$. Assuming that $\Gamma(\pi^+\pi^- J/\psi)$ of $X(3872)$ is the same as that of $\psi(2S)$ (85.4 keV).

$X(3872)$ $\Gamma(i)\Gamma(e^+e^-)/\Gamma(total)$

$\Gamma(e^+e^-) \times \Gamma(\pi^+\pi^- J/\psi(1S))/\Gamma_{total}$ $\Gamma_1\Gamma_2/\Gamma$

VALUE (eV)	CL%	DOCUMENT ID		TECN	COMMENT
• • • We do not use the following data for averages, fits, limits, etc. • • •					
<10	90	[2] YUAN	04	RVUE	$e^+e^- \to \pi^+\pi^- J/\psi$

[2] Using BAI 98E data on $e^+e^- \to \pi^+\pi^-\ell^+\ell^-$. From theoretical calculation of the production cross section and using $B(J/\psi \to \mu^+\mu^-) = (5.88 \pm 0.10)\%$.

Meson Particle Listings

$X(3872)$, $\psi(4040)$, $\psi(4160)$, $\psi(4415)$

X(3872) BRANCHING RATIOS

$\Gamma(\gamma\chi_{c1})/\Gamma(\pi^+\pi^- J/\psi(1S))$ Γ_3/Γ_2

VALUE	CL%	DOCUMENT ID		TECN	COMMENT
< 0.89	90	CHOI	03	BELL	$B \to K\pi^+\pi^- J/\psi$

X(3872) REFERENCES

YUAN	04	PL B579 74	C.Z. Yuan *et al.*	
CHOI	03	PRL 91 262001	S.-K. Choi *et al.*	(BELLE Collab.)
BAI	98E	PR D57 3854	J.Z. Bai *et al.*	(BES Collab.)

OTHER RELATED PAPERS

CLOSE	04	PL B578 119	F.E. Close, P.R. Page
PAKVASA	04	PL B579 67	S. Pakvasa, M. Suzuki
VOLOSHIN	04	PL B579 316	M.B. Voloshin

$\psi(4040)$

$I^G(J^{PC}) = 0^-(1^{--})$

ψ(4040) MASS

VALUE (MeV)	DOCUMENT ID		TECN	COMMENT
4040±10	BRANDELIK	78C	DASP	e^+e^-

ψ(4040) WIDTH

VALUE (MeV)	DOCUMENT ID		TECN	COMMENT
52±10	BRANDELIK	78C	DASP	e^+e^-

ψ(4040) DECAY MODES

	Mode	Fraction (Γ_i/Γ)
Γ_1	e^+e^-	$(1.4\pm0.4)\times10^{-5}$
Γ_2	$D^0\overline{D}^0$	seen
Γ_3	$D^*(2007)^0\overline{D}^0 + \text{c.c.}$	seen
Γ_4	$D^*(2007)^0\overline{D}^*(2007)^0$	seen
Γ_5	$J/\psi(1S)$hadrons	
Γ_6	$\mu^+\mu^-$	

ψ(4040) PARTIAL WIDTHS

$\Gamma(e^+e^-)$ Γ_1

VALUE (keV)	DOCUMENT ID		TECN	COMMENT
0.75±0.15	BRANDELIK	78C	DASP	e^+e^-

ψ(4040) BRANCHING RATIOS

$\Gamma(e^+e^-)/\Gamma_{total}$ Γ_1/Γ

VALUE (units 10^{-5})	DOCUMENT ID		TECN	COMMENT
• • • We do not use the following data for averages, fits, limits, etc. • • •				
~ 1.0	FELDMAN	77	MRK1	e^+e^-

$\Gamma(D^0\overline{D}^0)/\Gamma(D^*(2007)^0\overline{D}^0 + \text{c.c.})$ Γ_2/Γ_3

VALUE	DOCUMENT ID		TECN	COMMENT
0.05 ±0.03	[1] GOLDHABER	77	MRK1	e^+e^-

$\Gamma(D^*(2007)^0\overline{D}^*(2007)^0)/\Gamma(D^*(2007)^0\overline{D}^0 + \text{c.c.})$ Γ_4/Γ_3

VALUE	DOCUMENT ID		TECN	COMMENT
32.0±12.0	[1] GOLDHABER	77	MRK1	e^+e^-

[1] Phase-space factor (p^3) explicitly removed.

ψ(4040) REFERENCES

BRANDELIK	78C	PL 76B 361	R. Brandelik *et al.*	(DASP Collab.)
Also	79C	ZPHY C1 233	R. Brandelik *et al.*	(DASP Collab.)
FELDMAN	77	PRPL 33C 285	G.J. Feldman, M.L. Perl	(LBL, SLAC)
GOLDHABER	77	PL 69B 503	G. Goldhaber *et al.*	(Mark I Collab.)

OTHER RELATED PAPERS

HEIKKILA	84	PR D29 110	K. Heikkila, N.A. Tornqvist, S. Ono	(HELS, AACHT)
ONO	84	ZPHY C26 307	S. Ono	(ORSAY)
SIEGRIST	82	PR D26 969	J.L. Siegrist *et al.*	(SLAC, LBL)
AUGUSTIN	75	PRL 34 764	J.E. Augustin *et al.*	(SLAC, LBL)
BACCI	75	PL 58B 481	C. Bacci *et al.*	(ROMA, FRAS)
BOYARSKI	75B	PRL 34 762	A.M. Boyarski *et al.*	(SLAC, LBL)
ESPOSITO	75	PL 58B 478	B. Esposito *et al.*	(FRAS, NAPL, PADO+)

$\psi(4160)$

$I^G(J^{PC}) = 0^-(1^{--})$

ψ(4160) MASS

VALUE (MeV)	DOCUMENT ID		TECN	COMMENT
4159±20	BRANDELIK	78C	DASP	e^+e^-

ψ(4160) WIDTH

VALUE (MeV)	DOCUMENT ID		TECN	COMMENT
78±20	BRANDELIK	78C	DASP	e^+e^-

ψ(4160) DECAY MODES

	Mode	Fraction (Γ_i/Γ)
Γ_1	e^+e^-	$(10\pm4)\times10^{-6}$

ψ(4160) PARTIAL WIDTHS

$\Gamma(e^+e^-)$ Γ_1

VALUE (keV)	DOCUMENT ID		TECN	COMMENT
0.77±0.23	BRANDELIK	78C	DASP	e^+e^-

ψ(4160) REFERENCES

BRANDELIK	78C	PL 76B 361	R. Brandelik *et al.*	(DASP Collab.)

OTHER RELATED PAPERS

IDDIR	98	PL B433 125	F. Iddir *et al.*
ONO	84	ZPHY C26 307	S. Ono (ORSAY)
BURMESTER	77	PL 66B 395	J. Burmester *et al.* (DESY, HAMB, SIEG+)

$\psi(4415)$

$I^G(J^{PC}) = 0^-(1^{--})$

ψ(4415) MASS

VALUE (MeV)	DOCUMENT ID		TECN	COMMENT
4415± 6 OUR AVERAGE				
4417±10	BRANDELIK	78C	DASP	e^+e^-
4414± 7	SIEGRIST	76	MRK1	e^+e^-

ψ(4415) WIDTH

VALUE (MeV)	DOCUMENT ID		TECN	COMMENT
43±15 OUR AVERAGE Error includes scale factor of 1.8.				
66±15	BRANDELIK	78C	DASP	e^+e^-
33±10	SIEGRIST	76	MRK1	e^+e^-

ψ(4415) DECAY MODES

	Mode	Fraction (Γ_i/Γ)
Γ_1	hadrons	dominant
Γ_2	e^+e^-	$(1.1\pm0.4)\times10^{-5}$

ψ(4415) PARTIAL WIDTHS

$\Gamma(e^+e^-)$ Γ_2

VALUE (keV)	DOCUMENT ID		TECN	COMMENT
0.47±0.10 OUR AVERAGE				
0.49±0.13	BRANDELIK	78C	DASP	e^+e^-
0.44±0.14	SIEGRIST	76	MRK1	e^+e^-

ψ(4415) BRANCHING RATIOS

$\Gamma(\text{hadrons})/\Gamma_{total}$ Γ_1/Γ

VALUE	DOCUMENT ID		TECN	COMMENT
dominant	SIEGRIST	76	MRK1	e^+e^-

ψ(4415) REFERENCES

BRANDELIK	78C	PL 76B 361	R. Brandelik *et al.*	(DASP Collab.)
SIEGRIST	76	PRL 36 700	J.L. Siegrist *et al.*	(LBL, SLAC)

OTHER RELATED PAPERS

BURMESTER	77	PL 66B 395	J. Burmester *et al.*	(DESY, HAMB, SIEG+)
LUTH	77	PL 70B 120	V. Luth *et al.*	(LBL, SLAC)

$b\bar{b}$ MESONS

THE BOTTOMONIUM SYSTEM

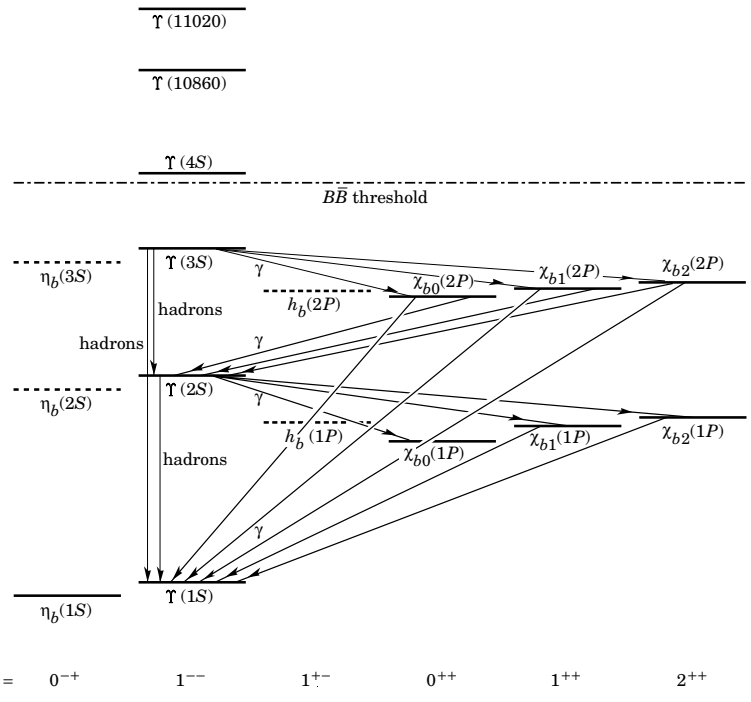

The level scheme of the $b\bar{b}$ states showing experimentally established states with solid lines. Singlet states are called η_b and h_b, triplet states Υ and χ_{bJ}. In parentheses it is sufficient to give the radial quantum number and the orbital angular momentum to specify the states with all their quantum numbers. *E.g.*, $h_b(2P)$ means 2^1P_1 with $n = 2$, $L = 1$, $S = 0$, $J = 1$, $PC = +-$. If found, D-wave states would be called $\eta_b(nD)$ and $\Upsilon_J(nD)$, with J = 1,2,3 and $n = 1, 2, 3, 4, \cdots$. For the χ_b states, the spins of only the $\chi_{b2}(1P)$ and $\chi_{b1}(1P)$ have been experimentally established. The spins of the other χ_b are given as the preferred values, based on the quarkonium models. The figure also shows the observed hadronic and radiative transitions.

WIDTH DETERMINATIONS OF THE Υ STATES

As is the case for the $J/\psi(1S)$ and $\psi(2S)$, the full widths of the $b\bar{b}$ states $\Upsilon(1S)$, $\Upsilon(2S)$, and $\Upsilon(3S)$ are not directly measurable, since they are much narrower than the energy resolution of the e^+e^- storage rings where these states are produced. The common indirect method to determine Γ starts from

$$\Gamma = \Gamma_{\ell\ell}/B_{\ell\ell} \ , \tag{1}$$

where $\Gamma_{\ell\ell}$ is one leptonic partial width and $B_{\ell\ell}$ is the corresponding branching fraction (ℓ = e, μ, or τ). One then assumes e-μ-τ universality and uses

$$\Gamma_{\ell\ell} = \Gamma_{ee}$$

$$B_{\ell\ell} = \text{average of } B_{ee},\ B_{\mu\mu},\ \text{and } B_{\tau\tau} \ . \tag{2}$$

The electronic partial width Γ_{ee} is also not directly measurable at e^+e^- storage rings, only in the combination $\Gamma_{ee}\Gamma_{\rm had}/\Gamma$, where $\Gamma_{\rm had}$ is the hadronic partial width and

$$\Gamma_{\rm had} + 3\Gamma_{ee} = \Gamma \ . \tag{3}$$

This combination is obtained experimentally from the energy-integrated hadronic cross section

$$\int_{\text{resonance}} \sigma(e^+e^- \to \Upsilon \to \text{hadrons})dE$$

$$= \frac{6\pi^2}{M^2}\frac{\Gamma_{ee}\Gamma_{\rm had}}{\Gamma}C_r = \frac{6\pi^2}{M^2}\frac{\Gamma_{ee}^{(0)}\Gamma_{\rm had}}{\Gamma}C_r^{(0)} \ , \tag{4}$$

where M is the Υ mass, and C_r and $C_r^{(0)}$ are radiative correction factors. C_r is used for obtaining Γ_{ee} as defined in Eq. (1), and contains corrections from all orders of QED for describing $(b\bar{b}) \to e^+e^-$. The lowest order QED value $\Gamma_{ee}^{(0)}$, relevant for comparison with potential-model calculations, is defined by the

lowest order QED graph (Born term) alone, and is about 7% lower than Γ_{ee}.

The Listings give experimental results on B_{ee}, $B_{\mu\mu}$, $B_{\tau\tau}$, and $\Gamma_{ee}\Gamma_{\rm had}/\Gamma$. The entries of the last quantity have been re-evaluated consistently using the correction procedure of KURAEV 85. The partial width Γ_{ee} is obtained from the average values for $\Gamma_{ee}\Gamma_{\rm had}/\Gamma$ and $B_{\ell\ell}$ using

$$\Gamma_{ee} = \frac{\Gamma_{ee}\Gamma_{\rm had}}{\Gamma(1-3B_{\ell\ell})} \ . \qquad (5)$$

The total width Γ is then obtained from Eq. (1). We do not list Γ_{ee} and Γ values of individual experiments. The Γ_{ee} values in the Meson Summary Table are also those defined in Eq. (1).

$\eta_b(1S)$

$I^G(J^{PC}) = 0^+(0^{-+})$

OMITTED FROM SUMMARY TABLE

Quantum numbers shown are quark-model predictions. One event is observed with the expected background of one. Needs confirmation.

$\eta_b(1S)$ MASS

VALUE (MeV)	DOCUMENT ID		TECN	COMMENT
• • • We do not use the following data for averages, fits, limits, etc. • • •				
$9300 \pm 20 \pm 20$	HEISTER	02D	ALEP	181–209 e^+e^-

$\eta_b(1S)$ DECAY MODES

	Mode	Fraction (Γ_i/Γ)
Γ_1	$3h^+3h^-$	seen
Γ_2	$2h^+2h^-$	not seen
Γ_3	$\gamma\gamma$	seen

$\eta_b(1S)$ Γ(i)$\Gamma(\gamma\gamma)/\Gamma$(total)

$\Gamma(3h^+3h^-) \times \Gamma(\gamma\gamma)/\Gamma_{\rm total}$ $\Gamma_1\Gamma_3/\Gamma$

VALUE (eV)	CL%	DOCUMENT ID		TECN	COMMENT
• • • We do not use the following data for averages, fits, limits, etc. • • •					
<132	95	HEISTER	02D	ALEP	181–209 e^+e^-

$\Gamma(2h^+2h^-) \times \Gamma(\gamma\gamma)/\Gamma_{\rm total}$ $\Gamma_2\Gamma_3/\Gamma$

VALUE (eV)	CL%	DOCUMENT ID		TECN	COMMENT
• • • We do not use the following data for averages, fits, limits, etc. • • •					
<48	95	HEISTER	02D	ALEP	181–209 e^+e^-

$\eta_b(1S)$ REFERENCES

HEISTER 02D PL B530 56 A. Heister *et al.* (ALEPH Collab.)

$\Upsilon(1S)$

$I^G(J^{PC}) = 0^-(1^{--})$

$\Upsilon(1S)$ MASS

VALUE (MeV)	DOCUMENT ID		TECN	COMMENT
9460.30 ± 0.26 OUR AVERAGE	Error includes scale factor of 3.3.			
$9460.51 \pm 0.09 \pm 0.05$	[1] ARTAMONOV	00	MD1	$e^+e^- \to$ hadrons
$9459.97 \pm 0.11 \pm 0.07$	MACKAY	84	REDE	$e^+e^- \to$ hadrons
• • • We do not use the following data for averages, fits, limits, etc. • • •				
$9460.60 \pm 0.09 \pm 0.05$	[2,3] BARU	92B	REDE	$e^+e^- \to$ hadrons
9460.59 ± 0.12	BARU	86	REDE	$e^+e^- \to$ hadrons
9460.6 ± 0.4	[3,4] ARTAMONOV	84	REDE	$e^+e^- \to$ hadrons

[1] Reanalysis of BARU 92B and ARTAMONOV 84 using new electron mass (COHEN 87).
[2] Superseding BARU 86.
[3] Superseded by ARTAMONOV 00.
[4] Value includes data of ARTAMONOV 82.

$\Upsilon(1S)$ WIDTH

VALUE (keV)	DOCUMENT ID
53.0 ± 1.5 OUR EVALUATION	See the Note on Width Determinations of the Υ states

$\Upsilon(1S)$ DECAY MODES

	Mode	Fraction (Γ_i/Γ)	Confidence level
Γ_1	$\tau^+\tau^-$	$(2.67^{+0.14}_{-0.16})$ %	
Γ_2	e^+e^-	(2.38 ± 0.11) %	
Γ_3	$\mu^+\mu^-$	(2.48 ± 0.06) %	
	Hadronic decays		
Γ_4	$\eta'(958)$anything	$(2.8 \pm 0.4) \times 10^{-3}$	
Γ_5	$J/\psi(1S)$anything	$(1.1 \pm 0.4) \times 10^{-3}$	
Γ_6	$\rho\pi$	$< 2 \times 10^{-4}$	90%
Γ_7	$\pi^+\pi^-$	$< 5 \times 10^{-4}$	90%
Γ_8	K^+K^-	$< 5 \times 10^{-4}$	90%
Γ_9	$p\overline{p}$	$< 5 \times 10^{-4}$	90%
Γ_{10}	$\pi^0\pi^+\pi^-$	$< 1.84 \times 10^{-5}$	90%
Γ_{11}	$D^*(2010)^\pm$anything		
	Radiative decays		
Γ_{12}	$\gamma\pi^+\pi^-$	$(6.3 \pm 1.8) \times 10^{-5}$	
Γ_{13}	$\gamma\pi^0\pi^0$	$(1.7 \pm 0.7) \times 10^{-5}$	
Γ_{14}	$\gamma 2h^+2h^-$	$(7.0 \pm 1.5) \times 10^{-4}$	
Γ_{15}	$\gamma 3h^+3h^-$	$(5.4 \pm 2.0) \times 10^{-4}$	
Γ_{16}	$\gamma 4h^+4h^-$	$(7.4 \pm 3.5) \times 10^{-4}$	
Γ_{17}	$\gamma\pi^+\pi^-K^+K^-$	$(2.9 \pm 0.9) \times 10^{-4}$	
Γ_{18}	$\gamma 2\pi^+2\pi^-$	$(2.5 \pm 0.9) \times 10^{-4}$	
Γ_{19}	$\gamma 3\pi^+3\pi^-$	$(2.5 \pm 1.2) \times 10^{-4}$	
Γ_{20}	$\gamma 2\pi^+2\pi^-K^+K^-$	$(2.4 \pm 1.2) \times 10^{-4}$	
Γ_{21}	$\gamma\pi^+\pi^-p\overline{p}$	$(1.5 \pm 0.6) \times 10^{-4}$	
Γ_{22}	$\gamma 2\pi^+2\pi^-p\overline{p}$	$(4 \pm 6) \times 10^{-5}$	
Γ_{23}	$\gamma 2K^+2K^-$	$(2.0 \pm 2.0) \times 10^{-5}$	
Γ_{24}	$\gamma\eta'(958)$	$< 1.6 \times 10^{-5}$	90%
Γ_{25}	$\gamma\eta$	$< 2.1 \times 10^{-5}$	90%
Γ_{26}	$\gamma f_2'(1525)$	$< 1.4 \times 10^{-4}$	90%
Γ_{27}	$\gamma f_2(1270)$	$(8 \pm 4) \times 10^{-5}$	
Γ_{28}	$\gamma\eta(1405)$	$< 8.2 \times 10^{-5}$	90%
Γ_{29}	$\gamma f_0(1710) \to \gamma K\overline{K}$	$< 2.6 \times 10^{-4}$	90%
Γ_{30}	$\gamma f_0(2200) \to \gamma K^+K^-$	$< 2 \times 10^{-4}$	90%
Γ_{31}	$\gamma f_J(2220) \to \gamma K^+K^-$	$< 1.5 \times 10^{-5}$	90%
Γ_{32}	$\gamma f_J(2220) \to \gamma\pi^+\pi^-$	$< 1.2 \times 10^{-5}$	90%
Γ_{33}	$\gamma f_J(2220) \to \gamma p\overline{p}$	$< 1.6 \times 10^{-5}$	90%
Γ_{34}	$\gamma\eta(2225) \to \gamma\phi\phi$	$< 3 \times 10^{-3}$	90%
Γ_{35}	γX (X = pseudoscalar with $m < 7.2$ GeV)	$< 3 \times 10^{-5}$	90%
Γ_{36}	$\gamma X\overline{X}$ ($X\overline{X}$ = vectors with $m < 3.1$ GeV)	$< 1 \times 10^{-3}$	90%

$\Upsilon(1S)$ Γ(i)$\Gamma(e^+e^-)/\Gamma$(total)

$\Gamma(e^+e^-) \times \Gamma(\mu^+\mu^-)/\Gamma_{\rm total}$ $\Gamma_2\Gamma_3/\Gamma$

VALUE (eV)	DOCUMENT ID		TECN	COMMENT
31.2 ± 1.6 ± 1.7	KOBEL	92	CBAL	$e^+e^- \to \mu^+\mu^-$

Γ(hadrons) $\times \Gamma(e^+e^-)/\Gamma_{\rm total}$ $\Gamma_0\Gamma_2/\Gamma$

VALUE (keV)	DOCUMENT ID		TECN	COMMENT
1.216 ± 0.027 OUR AVERAGE				
$1.187 \pm 0.023 \pm 0.031$	[5] BARU	92B	MD1	$e^+e^- \to$ hadrons
$1.23 \pm 0.02 \pm 0.05$	[5] JAKUBOWSKI	88	CBAL	$e^+e^- \to$ hadrons
$1.37 \pm 0.06 \pm 0.09$	[6] GILES	84B	CLEO	$e^+e^- \to$ hadrons
$1.23 \pm 0.08 \pm 0.04$	[6] ALBRECHT	82	DASP	$e^+e^- \to$ hadrons
$1.13 \pm 0.07 \pm 0.11$	[6] NICZYPORUK	82	LENA	$e^+e^- \to$ hadrons
1.09 ± 0.25	[6] BOCK	80	CNTR	$e^+e^- \to$ hadrons
1.35 ± 0.14	[7] BERGER	79	PLUT	$e^+e^- \to$ hadrons

[5] Radiative corrections evaluated following KURAEV 85.
[6] Radiative corrections reevaluated by BUCHMUELLER 88 following KURAEV 85.
[7] Radiative corrections reevaluated by ALEXANDER 89 using $B(\mu\mu) = 0.026$.

$\Upsilon(1S)$ PARTIAL WIDTHS

$\Gamma(e^+e^-)$ Γ_2

VALUE (keV)	DOCUMENT ID
1.314 ± 0.029 OUR EVALUATION	

$\Upsilon(1S)$ BRANCHING RATIOS

$\Gamma(\tau^+\tau^-)/\Gamma_{total}$ Γ_1/Γ

VALUE	EVTS	DOCUMENT ID		TECN	COMMENT
$0.0267^{+0.0014}_{-0.0016}$ OUR AVERAGE					
$0.0261 \pm 0.0012^{+0.0009}_{-0.0013}$	25k	CINABRO	94B	CLE2	$e^+e^- \to \tau^+\tau^-$
$0.027 \pm 0.004 \pm 0.002$		[8] ALBRECHT	85C	ARG	$\Upsilon(2S) \to \pi^+\pi^-\tau^+\tau^-$
$0.034 \pm 0.004 \pm 0.004$		GILES	83	CLEO	$e^+e^- \to \tau^+\tau^-$

[8] Using $B(\Upsilon(1S) \to e e) = B(\Upsilon(1S) \to \mu\mu) = 0.0256$; not used for width evaluations.

$\Gamma(\mu^+\mu^-)/\Gamma_{total}$ Γ_3/Γ

VALUE	EVTS	DOCUMENT ID		TECN	COMMENT
0.0248 ± 0.0006 OUR AVERAGE					
$0.0249 \pm 0.0008 \pm 0.0013$		ALEXANDER	98	CLE2	$\Upsilon(2S) \to \pi^+\pi^-\mu^+\mu^-$
$0.0212 \pm 0.0020 \pm 0.0010$		[9] BARU	92	MD1	$e^+e^- \to \mu^+\mu^-$
$0.0231 \pm 0.0012 \pm 0.0010$		[9] KOBEL	92	CBAL	$e^+e^- \to \mu^+\mu^-$
$0.0252 \pm 0.0007 \pm 0.0007$		CHEN	89B	CLEO	$e^+e^- \to \mu^+\mu^-$
$0.0261 \pm 0.0009 \pm 0.0011$		KAARSBERG	89	CSB2	$e^+e^- \to \mu^+\mu^-$
$0.0230 \pm 0.0025 \pm 0.0013$	86	ALBRECHT	87	ARG	$\Upsilon(2S) \to \pi^+\pi^-\mu^+\mu^-$
$0.029 \pm 0.003 \pm 0.002$	864	BESSON	84	CLEO	$\Upsilon(2S) \to \pi^+\pi^-\mu^+\mu^-$
$0.027 \pm 0.003 \pm 0.003$		ANDREWS	83	CLEO	$e^+e^- \to \mu^+\mu^-$
$0.032 \pm 0.013 \pm 0.003$		ALBRECHT	82	DASP	$e^+e^- \to \mu^+\mu^-$
$0.038 \pm 0.015 \pm 0.002$		NICZYPORUK	82	LENA	$e^+e^- \to \mu^+\mu^-$
$0.014^{+0.034}_{-0.014}$		BOCK	80	CNTR	$e^+e^- \to \mu^+\mu^-$
0.022 ± 0.020		BERGER	79	PLUT	$e^+e^- \to \mu^+\mu^-$

[9] Taking into account interference between the resonance and continuum.

$\Gamma(e^+e^-)/\Gamma_{total}$ Γ_2/Γ

VALUE	EVTS	DOCUMENT ID		TECN	COMMENT
0.0238 ± 0.0011 OUR AVERAGE					
$0.0229 \pm 0.0008 \pm 0.0011$		ALEXANDER	98	CLE2	$\Upsilon(2S) \to \pi^+\pi^- e^+e^-$
$0.0242 \pm 0.0014 \pm 0.0014$	307	ALBRECHT	87	ARG	$\Upsilon(2S) \to \pi^+\pi^- e^+e^-$
$0.028 \pm 0.003 \pm 0.002$	826	BESSON	84	CLEO	$\Upsilon(2S) \to \pi^+\pi^- e^+e^-$
0.051 ± 0.030		BERGER	80C	PLUT	$e^+e^- \to e^+e^-$

$\Gamma(\eta'(958)\text{anything})/\Gamma_{total}$ Γ_4/Γ

VALUE	DOCUMENT ID		TECN	COMMENT
$0.028 \pm 0.004 \pm 0.002$	ARTUSO	03	CLE2	$\Upsilon(1S) \to \eta'$ anything

$\Gamma(J/\psi(1S)\text{anything})/\Gamma_{total}$ Γ_5/Γ

VALUE (units 10^{-3})	CL%	DOCUMENT ID		TECN	COMMENT
< 0.68	90	ALBRECHT	92J	ARG	$e^+e^- \to e^+e^-X$, $e^+e^- \to \mu^+\mu^-X$
1.1 $\pm 0.4 \pm 0.2$		[10] FULTON	89	CLEO	$e^+e^- \to \mu^+\mu^-X$
• • • We do not use the following data for averages, fits, limits, etc. • • •					
< 1.7	90	MASCHMANN	90	CBAL	$e^+e^- \to$ hadrons
< 20	90	NICZYPORUK	83	LENA	

[10] Using $B((J/\psi) \to \mu^+\mu^-) = (6.9 \pm 0.9)\%$.

$\Gamma(\pi^+\pi^-)/\Gamma_{total}$ Γ_7/Γ

VALUE (units 10^{-4})	CL%	DOCUMENT ID		TECN	COMMENT
<5	90	BARU	92	MD1	$\Upsilon(1S) \to \pi^+\pi^-$

$\Gamma(K^+K^-)/\Gamma_{total}$ Γ_8/Γ

VALUE (units 10^{-4})	CL%	DOCUMENT ID		TECN	COMMENT
<5	90	BARU	92	MD1	$\Upsilon(1S) \to K^+K^-$

$\Gamma(p\overline{p})/\Gamma_{total}$ Γ_9/Γ

VALUE (units 10^{-4})	CL%	DOCUMENT ID		TECN	COMMENT
<5	90	[11] BARU	96	MD1	$\Upsilon(1S) \to p\overline{p}$

[11] Supersedes BARU 92 in this node.

$\Gamma(\pi^0\pi^+\pi^-)/\Gamma_{total}$ Γ_{10}/Γ

VALUE (units 10^{-5})	CL%	DOCUMENT ID		TECN	COMMENT
<1.84	90	ANASTASSOV	99	CLE2	$e^+e^- \to$ hadrons

$\Gamma(\gamma X)/\Gamma_{total}$ Γ_{35}/Γ

(X = pseudoscalar with $m <$ 7.2 GeV)

VALUE (units 10^{-5})	CL%	DOCUMENT ID		TECN	COMMENT
<3	90	[12] BALEST	95	CLEO	$e^+e^- \to \gamma + X$

[12] For a noninteracting pseudoscalar X with mass < 7.2 GeV.

$\Gamma(\gamma X\overline{X})/\Gamma_{total}$ Γ_{36}/Γ

($X\overline{X}$ = vectors with $m <$ 3.1 GeV)

VALUE (units 10^{-3})	CL%	DOCUMENT ID		TECN	COMMENT
<1	90	[13] BALEST	95	CLEO	$e^+e^- \to \gamma + X\overline{X}$

[13] For a noninteracting vector X with mass < 3.1 GeV.

$\Gamma(\gamma\pi^+\pi^-)/\Gamma_{total}$ Γ_{12}/Γ

VALUE (units 10^{-5})	DOCUMENT ID		TECN	COMMENT
$6.3 \pm 1.2 \pm 1.3$	[14] ANASTASSOV	99	CLE2	$e^+e^- \to$ hadrons

[14] For $m_{\pi\pi} > 1$ GeV.

$\Gamma(\gamma\pi^0\pi^0)/\Gamma_{total}$ Γ_{13}/Γ

VALUE (units 10^{-5})	DOCUMENT ID		TECN	COMMENT
$1.7 \pm 0.6 \pm 0.3$	[15] ANASTASSOV	99	CLE2	$e^+e^- \to$ hadrons

[15] For $m_{\pi\pi} > 1$ GeV.

$\Gamma(\gamma 2\pi^+2\pi^-)/\Gamma_{total}$ Γ_{18}/Γ

VALUE (units 10^{-4})	EVTS	DOCUMENT ID		TECN	COMMENT
$2.5 \pm 0.7 \pm 0.5$	26 ± 7	FULTON	90B	CLEO	$e^+e^- \to$ hadrons

$\Gamma(\gamma\pi^+\pi^- K^+K^-)/\Gamma_{total}$ Γ_{17}/Γ

VALUE (units 10^{-4})	EVTS	DOCUMENT ID		TECN	COMMENT
$2.9 \pm 0.7 \pm 0.6$	29 ± 8	FULTON	90B	CLEO	$e^+e^- \to$ hadrons

$\Gamma(\gamma\pi^+\pi^- p\overline{p})/\Gamma_{total}$ Γ_{21}/Γ

VALUE (units 10^{-4})	EVTS	DOCUMENT ID		TECN	COMMENT
$1.5 \pm 0.5 \pm 0.3$	22 ± 6	FULTON	90B	CLEO	$e^+e^- \to$ hadrons

$\Gamma(\gamma 2K^+2K^-)/\Gamma_{total}$ Γ_{23}/Γ

VALUE (units 10^{-4})	EVTS	DOCUMENT ID		TECN	COMMENT
0.2 ± 0.2	2 ± 2	FULTON	90B	CLEO	$e^+e^- \to$ hadrons

$\Gamma(\gamma 3\pi^+3\pi^-)/\Gamma_{total}$ Γ_{19}/Γ

VALUE (units 10^{-4})	EVTS	DOCUMENT ID		TECN	COMMENT
$2.5 \pm 0.9 \pm 0.8$	17 ± 5	FULTON	90B	CLEO	$e^+e^- \to$ hadrons

$\Gamma(\gamma 2\pi^+2\pi^- K^+K^-)/\Gamma_{total}$ Γ_{20}/Γ

VALUE (units 10^{-4})	EVTS	DOCUMENT ID		TECN	COMMENT
$2.4 \pm 0.9 \pm 0.8$	18 ± 7	FULTON	90B	CLEO	$e^+e^- \to$ hadrons

$\Gamma(\gamma 2\pi^+2\pi^- p\overline{p})/\Gamma_{total}$ Γ_{22}/Γ

VALUE (units 10^{-4})	EVTS	DOCUMENT ID		TECN	COMMENT
$0.4 \pm 0.4 \pm 0.4$	7 ± 6	FULTON	90B	CLEO	$e^+e^- \to$ hadrons

$\Gamma(\gamma 2h^+2h^-)/\Gamma_{total}$ Γ_{14}/Γ

VALUE (units 10^{-4})	EVTS	DOCUMENT ID		TECN	COMMENT
$7.0 \pm 1.1 \pm 1.0$	80 ± 12	FULTON	90B	CLEO	$e^+e^- \to$ hadrons

$\Gamma(\gamma 3h^+3h^-)/\Gamma_{total}$ Γ_{15}/Γ

VALUE (units 10^{-4})	EVTS	DOCUMENT ID		TECN	COMMENT
$5.4 \pm 1.5 \pm 1.3$	39 ± 11	FULTON	90B	CLEO	$e^+e^- \to$ hadrons

$\Gamma(\gamma 4h^+4h^-)/\Gamma_{total}$ Γ_{16}/Γ

VALUE (units 10^{-4})	EVTS	DOCUMENT ID		TECN	COMMENT
$7.4 \pm 2.5 \pm 2.5$	36 ± 12	FULTON	90B	CLEO	$e^+e^- \to$ hadrons

$\Gamma(\rho\pi)/\Gamma_{total}$ Γ_6/Γ

VALUE (units 10^{-4})	CL%	DOCUMENT ID		TECN	COMMENT
< 2	90	FULTON	90B		$\Upsilon(1S) \to \rho^0\pi^0$
• • • We do not use the following data for averages, fits, limits, etc. • • •					
<10	90	BLINOV	90	MD1	$\Upsilon(1S) \to \rho^0\pi^0$
<21	90	NICZYPORUK	83	LENA	$\Upsilon(1S) \to \rho^0\pi^0$

$\Gamma(D^*(2010)^\pm\text{anything})/\Gamma_{total}$ Γ_{11}/Γ

VALUE (units 10^{-3})	CL%	DOCUMENT ID		TECN	COMMENT
<19	90	[16] ALBRECHT	92J	ARG	$e^+e^- \to D^0\pi^\pm X$

[16] For $x_p > 0.2$.

Meson Particle Listings

$\Upsilon(1S)$, $\chi_{b0}(1P)$

$\Gamma(\gamma\eta(1405))/\Gamma_{total}$ Γ_{28}/Γ

VALUE (units 10^{-5})	CL%	DOCUMENT ID		TECN	COMMENT
< 8.2	90	[17] FULTON	90B	CLEO	$\Upsilon(1S) \to \gamma K^{\pm}\pi^{\mp}K^0_S$

[17] Includes unknown branching ratio of $\eta(1405) \to K^{\pm}\pi^{\mp}K^0_S$.

$\Gamma(\gamma\eta'(958))/\Gamma_{total}$ Γ_{24}/Γ

VALUE (units 10^{-5})	CL%	DOCUMENT ID		TECN	COMMENT
< 1.6	90	RICHICHI	01B	CLE2	$\Upsilon(1S) \to \gamma\eta' \to \gamma\eta\pi^+\pi^-$
• • • We do not use the following data for averages, fits, limits, etc. • • •					
<130	90	SCHMITT	88	CBAL	$\Upsilon(1S) \to \gamma X$

$\Gamma(\gamma\eta)/\Gamma_{total}$ Γ_{25}/Γ

VALUE (units 10^{-5})	CL%	DOCUMENT ID		TECN	COMMENT
< 2.1	90	MASEK	02	CLEO	$\Upsilon(1S) \to \gamma\eta$
• • • We do not use the following data for averages, fits, limits, etc. • • •					
<28.2	90	MASEK	02	CLEO	$\eta \to \gamma\gamma$
< 6.7	90	MASEK	02	CLEO	$\eta \to \pi^0\pi^0\pi^0$
< 2.6	90	MASEK	02	CLEO	$\eta \to \pi^+\pi^-\pi^0$
<35	90	SCHMITT	88	CBAL	$\Upsilon(1S) \to \gamma X$

$\Gamma(\gamma f_2'(1525))/\Gamma_{total}$ Γ_{26}/Γ

VALUE (units 10^{-5})	CL%	DOCUMENT ID		TECN	COMMENT
<14	90	[18] FULTON	90B	CLEO	$\Upsilon(1S) \to \gamma K^+K^-$
• • • We do not use the following data for averages, fits, limits, etc. • • •					
<19.4	90	[18] ALBRECHT	89	ARG	$\Upsilon(1S) \to \gamma K^+K^-$

[18] Assuming $B(f_2'(1525) \to K\overline{K}) = 0.71$.

$\Gamma(\gamma f_0(1710) \to \gamma K\overline{K})/\Gamma_{total}$ Γ_{29}/Γ

VALUE (units 10^{-4})	CL%	DOCUMENT ID		TECN	COMMENT
< 2.6	90	[19] ALBRECHT	89	ARG	$\Upsilon(1S) \to \gamma K^+K^-$
• • • We do not use the following data for averages, fits, limits, etc. • • •					
< 6.3	90	[19] FULTON	90B	CLEO	$\Upsilon(1S) \to \gamma K^+K^-$
<19	90	[19] FULTON	90B	CLEO	$\Upsilon(1S) \to \gamma K^0_S K^0_S$
< 8	90	[20] ALBRECHT	89	ARG	$\Upsilon(1S) \to \gamma\pi^+\pi^-$
<24	90	[21] SCHMITT	88	CBAL	$\Upsilon(1S) \to \gamma X$

[19] Assuming $B(f_0(1710) \to K\overline{K}) = 0.38$.
[20] Assuming $B(f_0(1710) \to \pi\pi) = 0.04$.
[21] Assuming $B(f_0(1710) \to \eta\eta) = 0.18$.

$\Gamma(\gamma f_2(1270))/\Gamma_{total}$ Γ_{27}/Γ

VALUE (units 10^{-5})	CL%	DOCUMENT ID		TECN	COMMENT
$8.1 \pm 2.3^{+2.9}_{-2.7}$		[22] ANASTASSOV	99	CLE2	$e^+e^- \to$ hadrons
• • • We do not use the following data for averages, fits, limits, etc. • • •					
<21	90	[22] FULTON	90B	CLEO	$\Upsilon(1S) \to \gamma\pi^+\pi^-$
<13	90	[22] ALBRECHT	89	ARG	$\Upsilon(1S) \to \gamma\pi^+\pi^-$
<81	90	SCHMITT	88	CBAL	$\Upsilon(1S) \to \gamma X$

[22] Using $B(f_2(1270) \to \pi\pi) = 0.84$.

$\Gamma(\gamma f_J(2220) \to \gamma K^+K^-)/\Gamma_{total}$ Γ_{31}/Γ

VALUE (units 10^{-5})	CL%	DOCUMENT ID		TECN	COMMENT
< 1.6	90	MASEK	02	CLEO	$\Upsilon(1S) \to \gamma K^+K^-$
< 1.5	90	[23] FULTON	90B	CLEO	$\Upsilon(1S) \to \gamma K^+K^-$
• • • We do not use the following data for averages, fits, limits, etc. • • •					
< 2.9	90	[23] ALBRECHT	89	ARG	$\Upsilon(1S) \to \gamma K^+K^-$
<20	90	[23] BARU	89	MD1	$\Upsilon(1S) \to \gamma K^+K^-$

[23] Including unknown branching ratio of $f_J(2220) \to K^+K^-$.

$\Gamma(\gamma f_J(2220) \to \gamma\pi^+\pi^-)/\Gamma_{total}$ Γ_{32}/Γ

VALUE (units 10^{-5})	CL%	DOCUMENT ID		TECN	COMMENT
<1.2	90	MASEK	02	CLEO	$\Upsilon(1S) \to \gamma\pi^+\pi^-$

$\Gamma(\gamma f_J(2220) \to \gamma p\overline{p})/\Gamma_{total}$ Γ_{33}/Γ

VALUE (units 10^{-5})	CL%	DOCUMENT ID		TECN	COMMENT
<1.6	90	MASEK	02	CLEO	$\Upsilon(1S) \to \gamma p\overline{p}$

$\Gamma(\gamma\eta(2225) \to \gamma\phi\phi)/\Gamma_{total}$ Γ_{34}/Γ

VALUE	CL%	DOCUMENT ID		TECN	COMMENT
<0.003	90	[24] BARU	89	MD1	$\Upsilon(1S) \to \gamma K^+K^-K^+K^-$

[24] Assuming that the $\eta(2225)$ decays only into $\phi\phi$.

$\Gamma(\gamma f_0(2200) \to \gamma K^+K^-)/\Gamma_{total}$ Γ_{30}/Γ

VALUE	CL%	DOCUMENT ID		TECN	COMMENT
<0.0002	90	[25] BARU	89	MD1	$\Upsilon(1S) \to \gamma K^+K^-$

[25] Assuming that the $f_0(2200)$ decays only into K^+K^-.

$\Upsilon(1S)$ REFERENCES

ARTUSO	03	PR D67 052003	M. Artuso *et al.*	(CLEO Collab.)
MASEK	02	PR D65 072002	G. Masek *et al.*	(CLEO Collab.)
RICHICHI	01B	PRL 87 141801	S.J. Richichi *et al.*	(CLEO Collab.)
ARTAMONOV	00	PL B474 427	A.S. Artamonov *et al.*	
ANASTASSOV	99	PRL 82 286	A. Anastassov *et al.*	(CLEO Collab.)
ALEXANDER	98	PR D58 052004	J.P. Alexander *et al.*	(CLEO Collab.)
BARU	96	PRPL 267 71	S.E. Baru *et al.*	(NOVO)
BALEST	95	PR D51 2053	R. Balest *et al.*	(CLEO Collab.)
CINABRO	94B	PL B340 129	D. Cinabro *et al.*	(CLEO Collab.)
ALBRECHT	92J	ZPHY C55 25	H. Albrecht *et al.*	(ARGUS Collab.)
BARU	92	ZPHY C54 229	S.E. Baru *et al.*	(NOVO)
BARU	92B	ZPHY C56 547	S.E. Baru *et al.*	(NOVO)
KOBEL	92	ZPHY C53 193	M. Kobel *et al.*	(Crystal Ball Collab.)
BLINOV	90	PL B245 311	A.E. Blinov *et al.*	(NOVO)
FULTON	90B	PR D41 1401	R. Fulton *et al.*	(CLEO Collab.)
MASCHMANN	90	ZPHY C46 555	W.S. Maschmann *et al.*	(Crystal Ball Collab.)
ALBRECHT	89	ZPHY C42 349	H. Albrecht *et al.*	(ARGUS Collab.)
ALEXANDER	89	NP B320 45	J.P. Alexander *et al.*	(LBL, MICH, SLAC)
BARU	89	ZPHY C42 505	S.E. Baru *et al.*	(NOVO)
CHEN	89B	PR D39 3528	W.Y. Chen *et al.*	(CLEO Collab.)
FULTON	89	PL B224 445	R. Fulton *et al.*	(CLEO Collab.)
KAARSBERG	89	PRL 62 2077	T.M. Kaarsberg *et al.*	(CUSB Collab.)
BUCHMUEL...	88	HE e^+e^- Physics 412 Editors: A. Ali and P. Soeding, World Scientific, Singapore	W. Buchmueller, S. Cooper	(HANN, DESY, MIT)
JAKUBOWSKI	88	ZPHY C40 49	Z. Jakubowski *et al.*	(Crystal Ball Collab.) IGJPC
SCHMITT	88	ZPHY C40 199	P. Schmitt *et al.*	(Crystal Ball Collab.)
ALBRECHT	87	ZPHY C35 283	H. Albrecht *et al.*	(ARGUS Collab.)
COHEN	87	RMP 59 1121	E.R. Cohen, B.N. Taylor	(RISC, NBS)
BARU	86	ZPHY C30 551	S.E. Baru *et al.*	(NOVO)
ALBRECHT	85C	PL 154B 452	H. Albrecht *et al.*	(ARGUS Collab.)
KURAEV	85	SJNP 41 466 Translated from YAF 41 733.	E.A. Kuraev, V.S. Fadin	(NOVO)
ARTAMONOV	84	PL 137B 272	A.S. Artamonov *et al.*	(NOVO)
BESSON	84	PR D30 1433	D. Besson *et al.*	(CLEO Collab.)
GILES	84B	PR D29 1285	R. Giles *et al.*	(CLEO Collab.)
MACKAY	84	PR D29 2483	W.W. MacKay *et al.*	(CUSB Collab.)
ANDREWS	83	PRL 50 807	D.E. Andrews *et al.*	(CLEO Collab.)
GILES	83	PRL 50 877	R. Giles *et al.*	(HARV, OSU, ROCH, RUTG+)
NICZYPORUK	83	ZPHY C17 197	B. Niczyporuk *et al.*	(LENA Collab.)
ALBRECHT	82	PL 116B 383	H. Albrecht *et al.*	(DESY, DORT, HEIDH+)
ARTAMONOV	82	PL 118B 225	A.S. Artamonov *et al.*	(NOVO)
NICZYPORUK	82	ZPHY C15 299	B. Niczyporuk *et al.*	(LENA Collab.)
BERGER	80C	PL 93B 497	C. Berger *et al.*	(PLUTO Collab.)
BOCK	80	ZPHY C6 125	P. Bock *et al.*	(HEIDP, MPIM, DESY, HAMB)
BERGER	79	ZPHY C1 343	C. Berger *et al.*	(PLUTO Collab.)

OTHER RELATED PAPERS

KOENIGS...	86	DESY 86/136	K. Koenigsmann	(DESY)
ALBRECHT	84	PL 134B 137	H. Albrecht *et al.*	(ARGUS Collab.)
ARTAMONOV	84	PL 137B 272	A.S. Artamonov *et al.*	(NOVO)
ARTAMONOV	82	PL 118B 225	A.S. Artamonov *et al.*	(NOVO)
BERGER	78	PL 76B 243	C. Berger *et al.*	(PLUTO Collab.)
BIENLEIN	78	PL 78B 360	J.K. Bienlein *et al.*	(DESY, HAMB, HEIDP+)
DARDEN	78	PL 76B 246	C.W. Darden *et al.*	(DESY, DORT, HEIDH+)
GARELICK	78	PR D18 945	D.A. Garelick *et al.*	(NEAS, WASH, TUFTS)
KAPLAN	78	PRL 40 435	D.M. Kaplan *et al.*	(STON, FNAL, COLU)
YOH	78	PRL 41 684	J.K. Yoh *et al.*	(COLU, FNAL, STON)
COBB	77	PL 72B 273	J.H. Cobb *et al.*	(BNL, CERN, SYRA, YALE)
HERB	77	PRL 39 252	S.W. Herb *et al.*	(COLU, FNAL, STON)
INNES	77	PRL 39 1240	W.R. Innes *et al.*	(COLU, FNAL, STON)

$\chi_{b0}(1P)$

$I^G(J^{PC}) = 0^+(0^{++})$
J needs confirmation.

Observed in radiative decay of the $\Upsilon(2S)$, therefore $C = +$. Branching ratio requires E1 transition, M1 is strongly disfavored, therefore $P = +$.

$\chi_{b0}(1P)$ MASS

VALUE (MeV)	DOCUMENT ID		TECN	COMMENT
9859.9±1.0 OUR AVERAGE				
9860.0±0.8±1.2	[1] EDWARDS	99	CLE2	$\Upsilon(2S) \to \gamma\chi(1P)$
9859.9±0.5±1.4	[1] ALBRECHT	85E	ARG	$\Upsilon(2S) \to$ conv.γX
9858.1±1.6±2.7	[1] NERNST	85	CBAL	$\Upsilon(2S) \to \gamma X$
9864.0±7 ±1	[1] HAAS	84	CLEO	$\Upsilon(2S) \to$ conv.γX
• • • We do not use the following data for averages, fits, limits, etc. • • •				
9872.8±0.7±5.0	[1] KLOPFEN...	83	CUSB	$\Upsilon(2S) \to \gamma X$

[1] From γ energy below, assuming $\Upsilon(2S)$ mass = 10023.3 MeV.

γ ENERGY IN $\Upsilon(2S)$ DECAY

VALUE (MeV)	DOCUMENT ID		TECN	COMMENT
162.1±1.0 OUR AVERAGE				
162.0±0.8±1.2	EDWARDS	99	CLE2	$\Upsilon(2S) \to \gamma\chi(1P)$
162.1±0.5±1.4	ALBRECHT	85E	ARG	$\Upsilon(2S) \to$ conv.γX
163.8±1.6±2.7	NERNST	85	CBAL	$\Upsilon(2S) \to \gamma X$
158.0±7 ±1	HAAS	84	CLEO	$\Upsilon(2S) \to$ conv.γX
• • • We do not use the following data for averages, fits, limits, etc. • • •				
149.4±0.7±5.0	KLOPFEN...	83	CUSB	$\Upsilon(2S) \to \gamma X$

$\chi_{b0}(1P)$ DECAY MODES

	Mode	Fraction (Γ_j/Γ)	Confidence level
Γ_1	$\gamma\Upsilon(1S)$	<6 %	90%

$\chi_{b0}(1P)$ BRANCHING RATIOS

$\Gamma(\gamma\,\Upsilon(1S))/\Gamma_{total}$ Γ_1/Γ

VALUE	CL%	DOCUMENT ID		TECN	COMMENT
< 0.06	90	WALK	86	CBAL	$\Upsilon(2S) \to \gamma\gamma\ell^+\ell^-$
• • • We do not use the following data for averages, fits, limits, etc. • • •					
< 0.11	90	PAUSS	83	CUSB	$\Upsilon(2S) \to \gamma\gamma\ell^+\ell^-$

$\chi_{b0}(1P)$ REFERENCES

EDWARDS	99	PR D59 032003	K.W. Edwards *et al.*	(CLEO Collab.)
WALK	86	PR D34 2611	W.S. Walk *et al.*	(Crystal Ball Collab.)
ALBRECHT	85E	PL 160B 331	H. Albrecht *et al.*	(ARGUS Collab.)
NERNST	85	PRL 54 2195	R. Nernst *et al.*	(Crystal Ball Collab.)
HAAS	84	PRL 52 799	J. Haas *et al.*	(CLEO Collab.)
KLOPFEN...	83	PRL 51 160	C. Klopfenstein *et al.*	(CUSB Collab.)
PAUSS	83	PL 130B 439	F. Pauss *et al.*	(MPIM, COLU, CORN, LSU+)

$\chi_{b1}(1P)$

$I^G(J^{PC}) = 0^+(1^{++})$
J needs confirmation.

Observed in radiative decay of the $\Upsilon(2S)$, therefore $C = +$. Branching ratio requires E1 transition, M1 is strongly disfavored, therefore $P = +$. $J = 1$ from SKWARNICKI 87.

$\chi_{b1}(1P)$ MASS

VALUE (MeV)		DOCUMENT ID		TECN	COMMENT
9892.7 ± 0.6 OUR AVERAGE	Error includes scale factor of 1.1.				
9893.7 ± 0.4 ± 0.6	[1]	EDWARDS	99	CLE2	$\Upsilon(2S) \to \gamma\chi(1P)$
9890.7 ± 0.9 ± 1.3	[1]	WALK	86	CBAL	$\Upsilon(2S) \to \gamma\gamma\ell^+\ell^-$
9890.7 ± 0.3 ± 1.1	[1]	ALBRECHT	85E	ARG	$\Upsilon(2S) \to$ conv.γX
9891.8 ± 0.8 ± 2.4	[1]	NERNST	85	CBAL	$\Upsilon(2S) \to \gamma$X
9893.5 ± 0.8 ± 1.0	[1]	HAAS	84	CLEO	$\Upsilon(2S) \to$ conv.γX
9894.4 ± 0.4 ± 3.0	[1]	KLOPFEN...	83	CUSB	$\Upsilon(2S) \to \gamma$X
9892 ± 3	[1]	PAUSS	83	CUSB	$\Upsilon(2S) \to \gamma\gamma\ell^+\ell^-$

[1] From γ energy below, assuming $\Upsilon(2S)$ mass = 10023.3 MeV.

γ ENERGY IN $\Upsilon(2S)$ DECAY

VALUE (MeV)	DOCUMENT ID		TECN	COMMENT
129.8 ± 0.5 OUR AVERAGE	Error includes scale factor of 1.1.			
128.8 ± 0.4 ± 0.6	EDWARDS	99	CLE2	$\Upsilon(2S) \to \gamma\chi(1P)$
131.7 ± 0.9 ± 1.3	WALK	86	CBAL	$\Upsilon(2S) \to \gamma\gamma\ell^+\ell^-$
131.7 ± 0.3 ± 1.1	ALBRECHT	85E	ARG	$\Upsilon(2S) \to$ conv.γX
130.6 ± 0.8 ± 2.4	NERNST	85	CBAL	$\Upsilon(2S) \to \gamma$X
129 ± 0.8 ± 1	HAAS	84	CLEO	$\Upsilon(2S) \to$ conv.γX
128.1 ± 0.4 ± 3.0	KLOPFEN...	83	CUSB	$\Upsilon(2S) \to \gamma$X
130.6 ± 3.0	PAUSS	83	CUSB	$\Upsilon(2S) \to \gamma\gamma\ell^+\ell^-$

$\chi_{b1}(1P)$ DECAY MODES

	Mode	Fraction (Γ_j/Γ)
Γ_1	$\gamma\,\Upsilon(1S)$	(35 ± 8) %

$\chi_{b1}(1P)$ BRANCHING RATIOS

$\Gamma(\gamma\,\Upsilon(1S))/\Gamma_{total}$ Γ_1/Γ

VALUE	DOCUMENT ID		TECN	COMMENT
0.35 ± 0.08 OUR AVERAGE				
0.32 ± 0.06 ± 0.07	WALK	86	CBAL	$\Upsilon(2S) \to \gamma\gamma\ell^+\ell^-$
0.47 ± 0.18	KLOPFEN...	83	CUSB	$\Upsilon(2S) \to \gamma\gamma\ell^+\ell^-$

$\chi_{b1}(1P)$ REFERENCES

EDWARDS	99	PR D59 032003	K.W. Edwards *et al.*	(CLEO Collab.)
SKWARNICKI	87	PRL 58 972	T. Skwarnicki *et al.*	(Crystal Ball Collab.) J
WALK	86	PR D34 2611	W.S. Walk *et al.*	(Crystal Ball Collab.)
ALBRECHT	85E	PL 160B 331	H. Albrecht *et al.*	(ARGUS Collab.)
NERNST	85	PRL 54 2195	R. Nernst *et al.*	(Crystal Ball Collab.)
HAAS	84	PRL 52 799	J. Haas *et al.*	(CLEO Collab.)
KLOPFEN...	83	PRL 51 160	C. Klopfenstein *et al.*	(CUSB Collab.)
PAUSS	83	PL 130B 439	F. Pauss *et al.*	(MPIM, COLU, CORN, LSU+)

$\chi_{b2}(1P)$

$I^G(J^{PC}) = 0^+(2^{++})$
J needs confirmation.

Observed in radiative decay of the $\Upsilon(2S)$, therefore $C = +$. Branching ratio requires E1 transition, M1 is strongly disfavored, therefore $P = +$. $J = 2$ from SKWARNICKI 87.

$\chi_{b2}(1P)$ MASS

VALUE (MeV)		DOCUMENT ID		TECN	COMMENT
9912.6 ± 0.5 OUR AVERAGE	Error includes scale factor of 1.1.				
9911.9 ± 0.3 ± 0.6	[1]	EDWARDS	99	CLE2	$\Upsilon(2S) \to \gamma\chi(1P)$
9915.7 ± 1.1 ± 1.3	[1]	WALK	86	CBAL	$\Upsilon(2S) \to \gamma\gamma\ell^+\ell^-$
9912.1 ± 0.3 ± 0.9	[1]	ALBRECHT	85E	ARG	$\Upsilon(2S) \to$ conv.γX
9912.3 ± 0.8 ± 2.2	[1]	NERNST	85	CBAL	$\Upsilon(2S) \to \gamma$X
9913.2 ± 0.7 ± 1.0	[1]	HAAS	84	CLEO	$\Upsilon(2S) \to$ conv.γX
9914.5 ± 0.3 ± 2.0	[1]	KLOPFEN...	83	CUSB	$\Upsilon(2S) \to \gamma$X
9914 ± 4	[1]	PAUSS	83	CUSB	$\Upsilon(2S) \to \gamma\gamma\ell^+\ell^-$

[1] From γ energy below, assuming $\Upsilon(2S)$ mass = 10023.3 MeV.

γ ENERGY IN $\Upsilon(2S)$ DECAY

VALUE (MeV)	DOCUMENT ID		TECN	COMMENT
110.1 ± 0.5 OUR AVERAGE	Error includes scale factor of 1.1.			
110.8 ± 0.3 ± 0.6	EDWARDS	99	CLE2	$\Upsilon(2S) \to \gamma\chi(1P)$
107.0 ± 1.1 ± 1.3	WALK	86	CBAL	$\Upsilon(2S) \to \gamma\gamma\ell^+\ell^-$
110.6 ± 0.3 ± 0.9	ALBRECHT	85E	ARG	$\Upsilon(2S) \to$ conv.γX
110.4 ± 0.8 ± 2.2	NERNST	85	CBAL	$\Upsilon(2S) \to \gamma$X
109.5 ± 0.7 ± 1.0	HAAS	84	CLEO	$\Upsilon(2S) \to$ conv.γX
108.2 ± 0.3 ± 2.0	KLOPFEN...	83	CUSB	$\Upsilon(2S) \to \gamma$X
108.8 ± 4.0	PAUSS	83	CUSB	$\Upsilon(2S) \to \gamma\gamma\ell^+\ell^-$

$\chi_{b2}(1P)$ DECAY MODES

	Mode	Fraction (Γ_j/Γ)
Γ_1	$\gamma\,\Upsilon(1S)$	(22 ± 4) %

$\chi_{b2}(1P)$ BRANCHING RATIOS

$\Gamma(\gamma\,\Upsilon(1S))/\Gamma_{total}$ Γ_1/Γ

VALUE	DOCUMENT ID		TECN	COMMENT
0.22 ± 0.04 OUR AVERAGE				
0.27 ± 0.06 ± 0.06	WALK	86	CBAL	$\Upsilon(2S) \to \gamma\gamma\ell^+\ell^-$
0.20 ± 0.05	KLOPFEN...	83	CUSB	$\Upsilon(2S) \to \gamma\gamma\ell^+\ell^-$

$\chi_{b2}(1P)$ REFERENCES

EDWARDS	99	PR D59 032003	K.W. Edwards *et al.*	(CLEO Collab.)
SKWARNICKI	87	PRL 58 972	T. Skwarnicki *et al.*	(Crystal Ball Collab.) J
WALK	86	PR D34 2611	W.S. Walk *et al.*	(Crystal Ball Collab.)
ALBRECHT	85E	PL 160B 331	H. Albrecht *et al.*	(ARGUS Collab.)
NERNST	85	PRL 54 2195	R. Nernst *et al.*	(Crystal Ball Collab.)
HAAS	84	PRL 52 799	J. Haas *et al.*	(CLEO Collab.)
KLOPFEN...	83	PRL 51 160	C. Klopfenstein *et al.*	(CUSB Collab.)
PAUSS	83	PL 130B 439	F. Pauss *et al.*	(MPIM, COLU, CORN, LSU+)

$\Upsilon(2S)$

$I^G(J^{PC}) = 0^-(1^{--})$

$\Upsilon(2S)$ MASS

VALUE (GeV)		DOCUMENT ID		TECN	COMMENT
10.02326 ± 0.00031 OUR AVERAGE					
10.0235 ± 0.0005	[1]	ARTAMONOV	00	MD1	$e^+e^- \to$ hadrons
10.0231 ± 0.0004		BARBER	84	REDE	$e^+e^- \to$ hadrons
• • • We do not use the following data for averages, fits, limits, etc. • • •					
10.0236 ± 0.0005	[2,3]	BARU	86B	REDE	$e^+e^- \to$ hadrons

[1] Reanalysis of BARU 86B using new electron mass (COHEN 87).
[2] Reanalysis of ARTAMONOV 84.
[3] Superseded by ARTAMONOV 00.

$\Upsilon(2S)$ WIDTH

VALUE (keV)	DOCUMENT ID
43 ± 6 OUR EVALUATION	See the Note on Width Determinations of the Υ states

$\Upsilon(2S)$ DECAY MODES

	Mode	Fraction (Γ_i/Γ)	Confidence level
Γ_1	$\Upsilon(1S)\pi^+\pi^-$	(18.8 ±0.6) %	
Γ_2	$\Upsilon(1S)\pi^0\pi^0$	(9.0 ±0.8) %	
Γ_3	$\tau^+\tau^-$	(1.7 ±1.6) %	
Γ_4	$\mu^+\mu^-$	(1.31±0.21) %	
Γ_5	e^+e^-	(1.34±0.20) %	
Γ_6	$\Upsilon(1S)\pi^0$	< 1.1 $\times 10^{-3}$	90%
Γ_7	$\Upsilon(1S)\eta$	< 2 $\times 10^{-3}$	90%
Γ_8	$J/\psi(1S)$anything	< 6 $\times 10^{-3}$	90%
	Radiative decays		
Γ_9	$\gamma\chi_{b1}(1P)$	(6.8 ±0.7) %	
Γ_{10}	$\gamma\chi_{b2}(1P)$	(7.0 ±0.6) %	
Γ_{11}	$\gamma\chi_{b0}(1P)$	(3.8 ±0.6) %	
Γ_{12}	$\gamma f_0(1710)$	< 5.9 $\times 10^{-4}$	90%
Γ_{13}	$\gamma f_2'(1525)$	< 5.3 $\times 10^{-4}$	90%
Γ_{14}	$\gamma f_2(1270)$	< 2.41 $\times 10^{-4}$	90%
Γ_{15}	$\gamma f_J(2220)$		

$\Upsilon(2S)$ $\Gamma(i)\Gamma(e^+e^-)/\Gamma(\text{total})$

$\Gamma(e^+e^-) \times \Gamma(\mu^+\mu^-)/\Gamma_{\text{total}}$ $\Gamma_5\Gamma_4/\Gamma$

VALUE (eV)	DOCUMENT ID		TECN	COMMENT
6.5 ±1.5 ±1.0	KOBEL	92	CBAL	$e^+e^- \to \mu^+\mu^-$

$\Gamma(\text{hadrons}) \times \Gamma(e^+e^-)/\Gamma_{\text{total}}$ $\Gamma_0\Gamma_5/\Gamma$

VALUE (keV)	DOCUMENT ID		TECN	COMMENT
0.553±0.023 OUR AVERAGE				
0.552±0.031±0.017	[4] BARU	96	MD1	$e^+e^- \to$ hadrons
0.54 ±0.04 ±0.02	[4] JAKUBOWSKI	88	CBAL	$e^+e^- \to$ hadrons
0.58 ±0.03 ±0.04	[5] GILES	84B	CLEO	$e^+e^- \to$ hadrons
0.60 ±0.12 ±0.07	[5] ALBRECHT	82	DASP	$e^+e^- \to$ hadrons
0.54 ±0.07 $^{+0.09}_{-0.05}$	[5] NICZYPORUK	81C	LENA	$e^+e^- \to$ hadrons
0.41 ±0.18	[5] BOCK	80	CNTR	$e^+e^- \to$ hadrons

[4] Radiative corrections evaluated following KURAEV 85.
[5] Radiative corrections reevaluated by BUCHMUELLER 88 following KURAEV 85.

$\Upsilon(2S)$ PARTIAL WIDTHS

$\Gamma(e^+e^-)$ Γ_5

VALUE (keV)	DOCUMENT ID
0.576±0.024 OUR EVALUATION	

$\Upsilon(2S)$ BRANCHING RATIOS

$\Gamma(J/\psi(1S)\text{anything})/\Gamma_{\text{total}}$ Γ_8/Γ

VALUE	CL%	DOCUMENT ID		TECN	COMMENT
<0.006	90	MASCHMANN	90	CBAL	$e^+e^- \to$ hadrons

$\Gamma(\Upsilon(1S)\pi^+\pi^-)/\Gamma_{\text{total}}$ Γ_1/Γ

VALUE	EVTS	DOCUMENT ID		TECN	COMMENT
0.188±0.006 OUR AVERAGE					
0.192±0.002±0.010	52.6k	[6] ALEXANDER	98	CLE2	$\pi^+\pi^-\ell^+\ell^-$, $\pi^+\pi^-$ MM
0.181±0.005±0.010	11.6k	ALBRECHT	87	ARG	$e^+e^- \to \pi^+\pi^-$ MM
0.169±0.040		GELPHMAN	85	CBAL	$e^+e^- \to e^+e^-\pi^+\pi^-$
0.191±0.012±0.006		BESSON	84	CLEO	$\pi^+\pi^-$ MM
0.189±0.026		FONSECA	84	CUSB	$e^+e^- \to \ell^+\ell^-\pi^+\pi^-$
0.21 ±0.07	7	NICZYPORUK	81B	LENA	$e^+e^- \to \ell^+\ell^-\pi^+\pi^-$

[6] Using B($\Upsilon(1S) \to e^+e^-$) = (2.52 ± 0.17)% and B($\Upsilon(1S) \to \mu^+\mu^-$) = (2.48 ± 0.07)%.

$\Gamma(\Upsilon(1S)\pi^0\pi^0)/\Gamma_{\text{total}}$ Γ_2/Γ

VALUE	EVTS	DOCUMENT ID		TECN	COMMENT
0.090±0.008 OUR AVERAGE					
0.092±0.006±0.008	275	[7] ALEXANDER	98	CLE2	$e^+e^- \to \ell^+\ell^-\pi^0\pi^0$
0.095±0.019±0.019	25	ALBRECHT	87	ARG	$e^+e^- \to \pi^0\pi^0\ell^+\ell^-$
0.080±0.015		GELPHMAN	85	CBAL	$e^+e^- \to \ell^+\ell^-\pi^0\pi^0$
0.103±0.023		FONSECA	84	CUSB	$e^+e^- \to \ell^+\ell^-\pi^0\pi^0$

[7] Using B($\Upsilon(1S) \to e^+e^-$) = (2.52 ± 0.17)% and B($\Upsilon(1S) \to \mu^+\mu^-$) = (2.48 ± 0.07)%.

$\Gamma(\tau^+\tau^-)/\Gamma_{\text{total}}$ Γ_3/Γ

VALUE	DOCUMENT ID		TECN	COMMENT
0.017±0.015±0.006	HAAS	84B	CLEO	$e^+e^- \to \tau^+\tau^-$

$\Gamma(\mu^+\mu^-)/\Gamma_{\text{total}}$ Γ_4/Γ

VALUE	CL%	DOCUMENT ID		TECN	COMMENT
0.0131±0.0021 OUR AVERAGE					
0.0122±0.0028±0.0019		[8] KOBEL	92	CBAL	$e^+e^- \to \mu^+\mu^-$
0.0138±0.0025±0.0015		KAARSBERG	89	CSB2	$e^+e^- \to \mu^+\mu^-$
0.009 ±0.006 ±0.006		[9] ALBRECHT	85	ARG	$e^+e^- \to \mu^+\mu^-$
0.018 ±0.008 ±0.005		HAAS	84B	CLEO	$e^+e^- \to \mu^+\mu^-$
• • • We do not use the following data for averages, fits, limits, etc. • • •					
<0.038	90	NICZYPORUK	81C	LENA	$e^+e^- \to \mu^+\mu^-$

[8] Taking into account interference between the resonance and continuum.
[9] Re-evaluated using B($\Upsilon(1S) \to \mu^+\mu^-$) = 0.026.

$\Gamma(\Upsilon(1S)\pi^0)/\Gamma_{\text{total}}$ Γ_6/Γ

VALUE	CL%	DOCUMENT ID		TECN	COMMENT
<0.0011	90	ALEXANDER	98	CLE2	$e^+e^- \to \ell^+\ell^-\gamma\gamma$
• • • We do not use the following data for averages, fits, limits, etc. • • •					
<0.008	90	LURZ	87	CBAL	$e^+e^- \to \ell^+\ell^-\gamma\gamma$

$\Gamma(\Upsilon(1S)\eta)/\Gamma_{\text{total}}$ Γ_7/Γ

VALUE	CL%	DOCUMENT ID		TECN	COMMENT
<0.002	90	FONSECA	84	CUSB	
• • • We do not use the following data for averages, fits, limits, etc. • • •					
<0.0028	90	ALEXANDER	98	CLE2	$e^+e^- \to \ell^+\ell^-\eta$
<0.005	90	ALBRECHT	87	ARG	$e^+e^- \to \pi^+\pi^-\ell^+\ell^-$ MM
<0.007	90	LURZ	87	CBAL	$e^+e^- \to \ell^+\ell^-(\gamma\gamma, 3\pi^0)$
<0.010	90	BESSON	84	CLEO	

$\Gamma(\gamma\chi_{b1}(1P))/\Gamma_{\text{total}}$ Γ_9/Γ

VALUE	DOCUMENT ID		TECN	COMMENT
0.068±0.007 OUR AVERAGE				
0.069±0.005±0.009	EDWARDS	99	CLE2	$\Upsilon(2S) \to \gamma\chi(1P)$
0.091±0.018±0.022	ALBRECHT	85E	ARG	$e^+e^- \to \gamma$conv. X
0.065±0.007±0.012	NERNST	85	CBAL	$e^+e^- \to \gamma$X
0.080±0.017±0.016	HAAS	84	CLEO	$e^+e^- \to \gamma$conv. X
0.059±0.014	KLOPFEN...	83	CUSB	$e^+e^- \to \gamma$X

$\Gamma(\gamma\chi_{b2}(1P))/\Gamma_{\text{total}}$ Γ_{10}/Γ

VALUE	DOCUMENT ID		TECN	COMMENT
0.070±0.006 OUR AVERAGE				
0.074±0.005±0.008	EDWARDS	99	CLE2	$\Upsilon(2S) \to \gamma\chi(1P)$
0.098±0.021±0.024	ALBRECHT	85E	ARG	$e^+e^- \to \gamma$conv. X
0.058±0.007±0.010	NERNST	85	CBAL	$e^+e^- \to \gamma$X
0.102±0.018±0.021	HAAS	84	CLEO	$e^+e^- \to \gamma$conv. X
0.061±0.014	KLOPFEN...	83	CUSB	$e^+e^- \to \gamma$X

$\Gamma(\gamma\chi_{b0}(1P))/\Gamma_{\text{total}}$ Γ_{11}/Γ

VALUE	DOCUMENT ID		TECN	COMMENT
0.038±0.006 OUR AVERAGE				
0.034±0.005±0.006	EDWARDS	99	CLE2	$\Upsilon(2S) \to \gamma\chi(1P)$
0.064±0.014±0.016	ALBRECHT	85E	ARG	$e^+e^- \to \gamma$conv. X
0.036±0.008±0.009	NERNST	85	CBAL	$e^+e^- \to \gamma$X
0.044±0.023±0.009	HAAS	84	CLEO	$e^+e^- \to \gamma$conv. X
• • • We do not use the following data for averages, fits, limits, etc. • • •				
0.035±0.014	KLOPFEN...	83	CUSB	$e^+e^- \to \gamma$X

$\Gamma(\gamma f_0(1710))/\Gamma_{\text{total}}$ Γ_{12}/Γ

VALUE (units 10^{-5})	CL%	DOCUMENT ID		TECN	COMMENT
<59	90	[10] ALBRECHT	89	ARG	$\Upsilon(2S) \to \gamma K^+K^-$
• • • We do not use the following data for averages, fits, limits, etc. • • •					
< 5.9	90	[11] ALBRECHT	89	ARG	$\Upsilon(2S) \to \gamma\pi^+\pi^-$

[10] Re-evaluated assuming B($f_0(1710) \to K^+K^-$) = 0.19.
[11] Includes unknown branching ratio of $f_0(1710) \to \pi^+\pi^-$.

$\Gamma(\gamma f_2'(1525))/\Gamma_{\text{total}}$ Γ_{13}/Γ

VALUE (units 10^{-5})	CL%	DOCUMENT ID		TECN	COMMENT
<53	90	[12] ALBRECHT	89	ARG	$\Upsilon(2S) \to \gamma K^+K^-$

[12] Re-evaluated assuming B($f_2'(1525) \to K\overline{K}$) = 0.71.

$\Gamma(\gamma f_2(1270))/\Gamma_{\text{total}}$ Γ_{14}/Γ

VALUE (units 10^{-5})	CL%	DOCUMENT ID		TECN	COMMENT
<24.1	90	[13] ALBRECHT	89	ARG	$\Upsilon(2S) \to \gamma\pi^+\pi^-$

[13] Using B($f_2(1270) \to \pi\pi$) = 0.84.

$\Gamma(\gamma f_J(2220))/\Gamma_{\text{total}}$ Γ_{15}/Γ

VALUE (units 10^{-5})	CL%	DOCUMENT ID		TECN	COMMENT
• • • We do not use the following data for averages, fits, limits, etc. • • •					
<6.8	90	[14] ALBRECHT	89	ARG	$\Upsilon(2S) \to \gamma K^+K^-$

[14] Includes unknown branching ratio of $f_J(2220) \to K^+K^-$.

$\Upsilon(2S)$ REFERENCES

ARTAMONOV	00	PL B474 427	A.S. Artamonov *et al.*	
EDWARDS	99	PR D59 032003	K.W. Edwards *et al.*	(CLEO Collab.)
ALEXANDER	98	PR D58 052004	J.P. Alexander *et al.*	(CLEO Collab.)
BARU	96	PRPL 267 71	S.E. Baru *et al.*	(NOVO)
KOBEL	92	ZPHY C53 193	M. Kobel *et al.*	(Crystal Ball Collab.)
MASCHMANN	90	ZPHY C46 555	W.S. Maschmann *et al.*	(Crystal Ball Collab.)
ALBRECHT	89	ZPHY C42 349	H. Albrecht *et al.*	(ARGUS Collab.)
KAARSBERG	89	PRL 62 2077	T.M. Kaarsberg *et al.*	(CUSB Collab.)
BUCHMUEL...	88	HE e^+e^- Physics 412 Editors: A. Ali and P. Soeding, World Scientific, Singapore	W. Buchmueller, S. Cooper	(HANN, DESY, MIT)
JAKUBOWSKI	88	ZPHY C40 49	Z. Jakubowski *et al.*	(Crystal Ball Collab.) IGJPC
ALBRECHT	87	ZPHY C35 283	H. Albrecht *et al.*	(ARGUS Collab.)
COHEN	87	RMP 59 1121	E.R. Cohen, B.N. Taylor	(RISC, NBS)
LURZ	87	ZPHY C36 383	B. Lurz *et al.*	(Crystal Ball Collab.)
BARU	86B	ZPHY C32 622	S.E. Baru *et al.*	(NOVO)
ALBRECHT	85	ZPHY C28 45	H. Albrecht *et al.*	(ARGUS Collab.)
ALBRECHT	85E	PL 160B 331	H. Albrecht *et al.*	(ARGUS Collab.)
GELPHMAN	85	PR D11 2893	D. Gelphman *et al.*	(Crystal Ball Collab.)
KURAEV	85	SJNP 41 466 Translated from YAF 41 733.	E.A. Kuraev, V.S. Fadin	(NOVO)
NERNST	85	PRL 54 2195	R. Nernst *et al.*	(Crystal Ball Collab.)
ARTAMONOV	84	PL 137B 272	A.S. Artamonov *et al.*	(NOVO)
BARBER	84	PL 135B 498	D.P. Barber *et al.*	
BESSON	84	PR D30 1433	D. Besson *et al.*	(CLEO Collab.)
FONSECA	84	NP B242 31	V. Fonseca *et al.*	(CUSB Collab.)
GILES	84B	PR D29 1285	R. Giles *et al.*	(CLEO Collab.)
HAAS	84	PRL 52 799	J. Haas *et al.*	(CLEO Collab.)
HAAS	84B	PR D30 1996	J. Haas *et al.*	(CLEO Collab.)
KLOPFEN...	83	PRL 51 160	C. Klopfenstein *et al.*	(CUSB Collab.)
ALBRECHT	82	PL 116B 383	H. Albrecht *et al.*	(DESY, DORT, HEIDH+)
NICZYPORUK	81B	PL 100B 95	B. Niczyporuk *et al.*	(LENA Collab.)
NICZYPORUK	81C	PL 99B 169	B. Niczyporuk *et al.*	(LENA Collab.)
BOCK	80	ZPHY C6 125	P. Bock *et al.*	(HEIDP, MPIM, DESY, HAMB)

OTHER RELATED PAPERS

ALEXANDER	89	NP B320 45	J.P. Alexander *et al.*	(LBL, MICH, SLAC)
WALK	86	PR D34 2611	W.S. Walk *et al.*	(Crystal Ball Collab.)
ALBRECHT	84	PL 134B 137	H. Albrecht *et al.*	(ARGUS Collab.)
ARTAMONOV	84	PL 137B 272	A.S. Artamonov *et al.*	(NOVO)
ANDREWS	83	PRL 50 807	D.E. Andrews *et al.*	(CLEO Collab.)
GREEN	82	PRL 49 617	J. Green *et al.*	(CLEO Collab.)
BIENLEIN	78	PL 78B 360	J.K. Bienlein *et al.*	(DESY, HAMB, HEIDP+)
DARDEN	78	PL 76B 246	C.W. Darden *et al.*	(DESY, DORT, HEIDH+)
KAPLAN	78	PRL 40 435	D.M. Kaplan *et al.*	(STON, FNAL, COLU)
YOH	78	PRL 41 684	J.K. Yoh *et al.*	(COLU, FNAL, STON)
COBB	77	PL 72B 273	J.H. Cobb *et al.*	(BNL, CERN, SYRA, YALE)
HERB	77	PRL 39 252	S.W. Herb *et al.*	(COLU, FNAL, STON)
INNES	77	PRL 39 1240	W.R. Innes *et al.*	(COLU, FNAL, STON)

$\chi_{b0}(2P)$

$I^G(J^{PC}) = 0^+(0^{++})$
J needs confirmation.

Observed in radiative decay of the $\Upsilon(3S)$, therefore $C = +$. Branching ratio requires E1 transition, M1 is strongly disfavored, therefore $P = +$.

$\chi_{b0}(2P)$ MASS

VALUE (GeV)	DOCUMENT ID		TECN	COMMENT
10.2321 ± 0.0006 OUR AVERAGE				
10.2312 ± 0.0008 ± 0.0012	[1] HEINTZ	92	CSB2	$e^+e^- \to \gamma X, \ell^+\ell^-\gamma\gamma$
10.2323 ± 0.0007	[2] MORRISON	91	CLE2	$e^+e^- \to \gamma X$

[1] From the average photon energy for inclusive and exclusive events and assuming $\Upsilon(3S)$ mass = 10355.3 ± 0.5 MeV. Supersedes HEINTZ 91 and NARAIN 91.
[2] From γ energy below assuming $\Upsilon(3S)$ mass = 10355.3 ± 0.5 MeV. The error on the $\Upsilon(3S)$ mass is not included in the individual measurements. It is included in the final average.

γ ENERGY IN $\Upsilon(3S)$ DECAY

VALUE (MeV)	EVTS	DOCUMENT ID		TECN	COMMENT
122.8 ± 0.5 OUR AVERAGE Error includes scale factor of 1.1.					
123.0 ± 0.8	4959	[3] HEINTZ	92	CSB2	$e^+e^- \to \gamma X$
124.6 ± 1.4	17	[4] HEINTZ	92	CSB2	$e^+e^- \to \ell^+\ell^-\gamma\gamma$
122.3 ± 0.3 ± 0.6	9903	MORRISON	91	CLE2	$e^+e^- \to \gamma X$

[3] A systematic uncertainty on the energy scale of 0.9% not included. Supersedes NARAIN 91.
[4] A systematic uncertainty on the energy scale of 0.9% not included. Supersedes HEINTZ 91.

$\chi_{b0}(2P)$ DECAY MODES

	Mode	Fraction (Γ_i/Γ)
Γ_1	$\gamma\,\Upsilon(2S)$	(4.6 ± 2.1) %
Γ_2	$\gamma\,\Upsilon(1S)$	(9 ± 6) × 10^{-3}

$\chi_{b0}(2P)$ BRANCHING RATIOS

$\Gamma(\gamma\,\Upsilon(2S))/\Gamma_{\text{total}}$ **Γ_1/Γ**

VALUE	CL%	DOCUMENT ID		TECN	COMMENT
< 0.089	90	[5] CRAWFORD	92B	CLE2	$e^+e^- \to \ell^+\ell^-\gamma\gamma$
0.046 ± 0.020 ± 0.007		[6] HEINTZ	92	CSB2	$e^+e^- \to \ell^+\ell^-\gamma\gamma$

[5] Using B($\Upsilon(2S) \to \mu^+\mu^-$) = (1.37 ± 0.26)%, B($\Upsilon(3S) \to \gamma\gamma\,\Upsilon(2S)$)×2 B($\Upsilon(2S) \to \mu^+\mu^-$) < 1.19 × 10^{-4}, and B($\Upsilon(3S) \to \chi_{b0}(2P)\gamma$) = 0.049.
[6] Using B($\Upsilon(2S) \to \mu^+\mu^-$) = (1.44 ± 0.10)%, B($\Upsilon(3S) \to \gamma\chi_{b0}(2P)$) = (6.0 ± 0.4 ± 0.6)% and assuming $e\mu$ universality. Supersedes HEINTZ 91.

$\Gamma(\gamma\,\Upsilon(1S))/\Gamma_{\text{total}}$ **Γ_2/Γ**

VALUE	CL%	DOCUMENT ID		TECN	COMMENT
< 0.025	90	[7] CRAWFORD	92B	CLE2	$e^+e^- \to \ell^+\ell^-\gamma\gamma$
0.009 ± 0.006 ± 0.001		[8] HEINTZ	92	CSB2	$e^+e^- \to \ell^+\ell^-\gamma\gamma$

[7] Using B($\Upsilon(1S) \to \mu^+\mu^-$) = (2.57 ± 0.07)%, B($\Upsilon(3S) \to \gamma\gamma\,\Upsilon(1S)$)×2 B($\Upsilon(1S) \to \mu^+\mu^-$) < 0.63 × 10^{-4}, and B($\Upsilon(3S) \to \chi_{b0}(2P)\gamma$) = 0.049.
[8] Using B($\Upsilon(1S) \to \mu^+\mu^-$) = (2.57 ± 0.07)%, B($\Upsilon(3S) \to \gamma\chi_{b0}(2P)$) = (6.0 ± 0.4 ± 0.6)% and assuming $e\mu$ universality. Supersedes HEINTZ 91.

$\chi_{b0}(2P)$ REFERENCES

CRAWFORD	92B	PL B294 139	G. Crawford, R. Fulton	(CLEO Collab.)
HEINTZ	92	PR D46 1928	U. Heintz *et al.*	(CUSB II Collab.)
HEINTZ	91	PRL 66 1563	U. Heintz *et al.*	(CUSB Collab.)
MORRISON	91	PRL 67 1696	R.J. Morrison *et al.*	(CLEO Collab.)
NARAIN	91	PRL 66 3113	M. Narain *et al.*	(CUSB Collab.)

OTHER RELATED PAPERS

EIGEN	82	PRL 49 1616	G. Eigen *et al.*	(CUSB Collab.)
HAN	82	PRL 49 1612	K. Han *et al.*	(CUSB Collab.)

$\chi_{b1}(2P)$

$I^G(J^{PC}) = 0^+(1^{++})$
J needs confirmation.

Observed in radiative decay of the $\Upsilon(3S)$, therefore $C = +$. Branching ratio requires E1 transition, M1 is strongly disfavored, therefore $P = +$.

$\chi_{b1}(2P)$ MASS

VALUE (GeV)	DOCUMENT ID		TECN	COMMENT
10.2552 ± 0.0005 OUR AVERAGE				
10.2547 ± 0.0004 ± 0.0010	[1] HEINTZ	92	CSB2	$e^+e^- \to \gamma X, \ell^+\ell^-\gamma\gamma$
10.2553 ± 0.0005	[2] MORRISON	91	CLE2	$e^+e^- \to \gamma X$

[1] From the average photon energy for inclusive and exclusive events and assuming $\Upsilon(3S)$ mass = 10355.3 ± 0.5 MeV. Supersedes HEINTZ 91 and NARAIN 91.
[2] From γ energy below assuming $\Upsilon(3S)$ mass = 10355.3 ± 0.5 MeV. The error on the $\Upsilon(3S)$ mass is not included in the individual measurements. It is included in the final evaluation.

$m_{\chi_{b1}(2P)} - m_{\chi_{b0}(2P)}$

VALUE (MeV)	DOCUMENT ID		TECN	COMMENT
23.5 ± 0.7 ± 0.7	[3] HEINTZ	92	CSB2	$e^+e^- \to \gamma X, \ell^+\ell^-\gamma\gamma$

[3] From the average photon energy for inclusive and exclusive events. Supersedes NARAIN 91.

γ ENERGY IN $\Upsilon(3S)$ DECAY

VALUE (MeV)	EVTS	DOCUMENT ID		TECN	COMMENT
99.90 ± 0.26 OUR AVERAGE					
99 ± 1	169	CRAWFORD	92B	CLE2	$e^+e^- \to \ell^+\ell^-\gamma\gamma$
100.1 ± 0.4	11147	[4] HEINTZ	92	CSB2	$e^+e^- \to \gamma X$
100.2 ± 0.5	223	[5] HEINTZ	92	CSB2	$e^+e^- \to \ell^+\ell^-\gamma\gamma$
99.5 ± 0.1 ± 0.5	25759	MORRISON	91	CLE2	$e^+e^- \to \gamma X$

[4] A systematic uncertainty on the energy scale of 0.9% not included. Supersedes NARAIN 91.
[5] A systematic uncertainty on the energy scale of 0.9% not included. Supersedes HEINTZ 91.

$\chi_{b1}(2P)$ DECAY MODES

	Mode	Fraction (Γ_i/Γ)	Scale factor
Γ_1	$\gamma\,\Upsilon(2S)$	(21 ± 4) %	1.5
Γ_2	$\gamma\,\Upsilon(1S)$	(8.5 ± 1.3) %	1.3

$\chi_{b1}(2P)$ BRANCHING RATIOS

$\Gamma(\gamma\,\Upsilon(2S))/\Gamma_{\text{total}}$ **Γ_1/Γ**

VALUE	DOCUMENT ID		TECN	COMMENT
0.21 ± 0.04 OUR AVERAGE Error includes scale factor of 1.5.				
0.356 ± 0.042 ± 0.092	[6] CRAWFORD	92B	CLE2	$e^+e^- \to \ell^+\ell^-\gamma\gamma$
0.199 ± 0.020 ± 0.022	[7] HEINTZ	92	CSB2	$e^+e^- \to \ell^+\ell^-\gamma\gamma$

[6] Using B($\Upsilon(2S) \to \mu^+\mu^-$) = (1.37 ± 0.26)%, B($\Upsilon(3S) \to \gamma\gamma\,\Upsilon(2S)$)×2 B($\Upsilon(2S) \to \mu^+\mu^-$) = (10.23 ± 1.20 ± 1.26)×10^{-4}, and B($\Upsilon(3S) \to \gamma\chi_{b1}(2P)$) = $0.105^{+0.003}_{-0.002}$ ± 0.013.
[7] Using B($\Upsilon(2S) \to \mu^+\mu^-$) = (1.44 ± 0.10)%, B($\Upsilon(3S) \to \gamma\chi_{b1}(2P)$) = (11.5 ± 0.5 ± 0.5)% and assuming $e\mu$ universality. Supersedes HEINTZ 91.

$\Gamma(\gamma\,\Upsilon(1S))/\Gamma_{\rm total}$ Γ_2/Γ

VALUE	DOCUMENT ID		TECN	COMMENT
0.085 ± 0.013 OUR AVERAGE	Error includes scale factor of 1.3.			
0.120 ± 0.021 ± 0.021	[8] CRAWFORD	92B	CLE2	$e^+e^- \to \ell^+\ell^-\gamma\gamma$
0.080 ± 0.009 ± 0.007	[9] HEINTZ	92	CSB2	$e^+e^- \to \ell^+\ell^-\gamma\gamma$

[8] Using $B(\Upsilon(1S) \to \mu^+\mu^-) = (2.57 \pm 0.07)\%$, $B(\Upsilon(3S) \to \gamma\gamma\Upsilon(1S)) \times 2\ B(\Upsilon(1S) \to \mu^+\mu^-) = (6.47 \pm 1.12 \pm 0.82) \times 10^{-4}$ and $B(\Upsilon(3S) \to \gamma\chi_{b1}(2P)) = 0.105^{+0.003}_{-0.002} \pm 0.013$.
[9] Using $B(\Upsilon(1S) \to \mu^+\mu^-) = (2.57 \pm 0.07)\%$, $B(\Upsilon(3S) \to \gamma\chi_{b1}(2P)) = (11.5 \pm 0.5 \pm 0.5)\%$ and assuming $e\mu$ universality. Supersedes HEINTZ 91.

$\chi_{b1}(2P)$ REFERENCES

CRAWFORD	92B	PL B294 139	G. Crawford, R. Fulton	(CLEO Collab.)
HEINTZ	92	PR D46 1928	U. Heintz *et al.*	(CUSB II Collab.)
HEINTZ	91	PRL 66 1563	U. Heintz *et al.*	(CUSB Collab.)
MORRISON	91	PRL 67 1696	R.J. Morrison *et al.*	(CLEO Collab.)
NARAIN	91	PRL 66 3113	M. Narain *et al.*	(CUSB Collab.)

OTHER RELATED PAPERS

EIGEN	82	PRL 49 1616	G. Eigen *et al.*	(CUSB Collab.)
HAN	82	PRL 49 1612	K. Han *et al.*	(CUSB Collab.)

$\chi_{b2}(2P)$

$I^G(J^{PC}) = 0^+(2^{++})$
J needs confirmation.

Observed in radiative decay of the $\Upsilon(3S)$, therefore $C = +$. Branching ratio requires E1 transition, M1 is strongly disfavored, therefore $P = +$.

$\chi_{b2}(2P)$ MASS

VALUE (GeV)	DOCUMENT ID		TECN	COMMENT
10.2685 ± 0.0004 OUR AVERAGE				
10.2681 ± 0.0004 ± 0.0010	[1] HEINTZ	92	CSB2	$e^+e^- \to \gamma X, \ell^+\ell^-\gamma\gamma$
10.2685 ± 0.0004	[2] MORRISON	91	CLE2	$e^+e^- \to \gamma X$

[1] From the average photon energy for inclusive and exclusive events and assuming $\Upsilon(3S)$ mass = 10355.3 ± 0.5 MeV. Supersedes HEINTZ 91 and NARAIN 91.
[2] From γ energy below, assuming $\Upsilon(3S)$ mass = 10355.3 ± 0.5 MeV. The error on the $\Upsilon(3S)$ mass is not included in the individual measurements. It is included in the final average.

$m_{\chi_{b2}(2P)} - m_{\chi_{b1}(2P)}$

VALUE (MeV)	DOCUMENT ID		TECN	COMMENT
13.5 ± 0.4 ± 0.5	[3] HEINTZ	92	CSB2	$e^+e^- \to \gamma X, \ell^+\ell^-\gamma\gamma$

[3] From the average photon energy for inclusive and exclusive events. Supersedes NARAIN 91.

γ ENERGY IN $\Upsilon(3S)$ DECAY

VALUE (MeV)	EVTS	DOCUMENT ID		TECN	COMMENT
86.64 ± 0.23 OUR AVERAGE					
86 ± 1	101	CRAWFORD	92B	CLE2	$e^+e^- \to \ell^+\ell^-\gamma\gamma$
86.7 ± 0.4	10319	[4] HEINTZ	92	CSB2	$e^+e^- \to \gamma X$
86.9 ± 0.4	157	[5] HEINTZ	92	CSB2	$e^+e^- \to \ell^+\ell^-\gamma\gamma$
86.4 ± 0.1 ± 0.4	30741	MORRISON	91	CLE2	$e^+e^- \to \gamma X$

[4] A systematic uncertainty on the energy scale of 0.9% not included. Supersedes NARAIN 91.
[5] A systematic uncertainty on the energy scale of 0.9% not included. Supersedes HEINTZ 91.

$\chi_{b2}(2P)$ DECAY MODES

	Mode	Fraction (Γ_i/Γ)
Γ_1	$\gamma\,\Upsilon(2S)$	(16.2 ± 2.4) %
Γ_2	$\gamma\,\Upsilon(1S)$	(7.1 ± 1.0) %

$\chi_{b2}(2P)$ BRANCHING RATIOS

$\Gamma(\gamma\,\Upsilon(2S))/\Gamma_{\rm total}$ Γ_1/Γ

VALUE	DOCUMENT ID		TECN	COMMENT
0.162 ± 0.024 OUR AVERAGE				
0.135 ± 0.025 ± 0.035	[6] CRAWFORD	92B	CLE2	$e^+e^- \to \ell^+\ell^-\gamma\gamma$
0.173 ± 0.021 ± 0.019	[7] HEINTZ	92	CSB2	$e^+e^- \to \ell^+\ell^-\gamma\gamma$

[6] Using $B(\Upsilon(2S) \to \mu^+\mu^-) = (1.37 \pm 0.26)\%$, $B(\Upsilon(3S) \to \gamma\gamma\Upsilon(2S)) \times 2\ B(\Upsilon(2S) \to \mu^+\mu^-) = (4.98 \pm 0.94 \pm 0.62) \times 10^{-4}$, and $B(\Upsilon(3S) \to \gamma\chi_{b2}(2P)) = 0.135 \pm 0.003 \pm 0.017$.
[7] Using $B(\Upsilon(2S) \to \mu^+\mu^-) = (1.44 \pm 0.10)\%$, $B(\Upsilon(3S) \to \gamma\chi_{b2}(2P)) = (11.1 \pm 0.5 \pm 0.4)\%$ and assuming $e\mu$ universality. Supersedes HEINTZ 91.

$\Gamma(\gamma\,\Upsilon(1S))/\Gamma_{\rm total}$ Γ_2/Γ

VALUE	DOCUMENT ID		TECN	COMMENT
0.071 ± 0.010 OUR AVERAGE				
0.072 ± 0.014 ± 0.013	[8] CRAWFORD	92B	CLE2	$e^+e^- \to \ell^+\ell^-\gamma\gamma$
0.070 ± 0.010 ± 0.006	[9] HEINTZ	92	CSB2	$e^+e^- \to \ell^+\ell^-\gamma\gamma$

[8] Using $B(\Upsilon(1S) \to \mu^+\mu^-) = (2.57 \pm 0.07)\%$, $B(\Upsilon(3S) \to \gamma\gamma\Upsilon(2S)) \times 2\ B(\Upsilon(1S) \to \mu^+\mu^-) = (5.03 \pm 0.94 \pm 0.63) \times 10^{-4}$, and $B(\Upsilon(3S) \to \gamma\chi_{b2}(2P)) = 0.135 \pm 0.003 \pm 0.017$.
[9] Using $B(\Upsilon(1S) \to \mu^+\mu^-) = (2.57 \pm 0.07)\%$, $B(\Upsilon(3S) \to \gamma\chi_{b2}(2P)) = (11.1 \pm 0.5 \pm 0.4)\%$ and assuming $e\mu$ universality. Supersedes HEINTZ 91.

$\chi_{b2}(2P)$ REFERENCES

CRAWFORD	92B	PL B294 139	G. Crawford, R. Fulton	(CLEO Collab.)
HEINTZ	92	PR D46 1928	U. Heintz *et al.*	(CUSB II Collab.)
HEINTZ	91	PRL 66 1563	U. Heintz *et al.*	(CUSB Collab.)
MORRISON	91	PRL 67 1696	R.J. Morrison *et al.*	(CLEO Collab.)
NARAIN	91	PRL 66 3113	M. Narain *et al.*	(CUSB Collab.)

OTHER RELATED PAPERS

EIGEN	82	PRL 49 1616	G. Eigen *et al.*	(CUSB Collab.)
HAN	82	PRL 49 1612	K. Han *et al.*	(CUSB Collab.)

$\Upsilon(3S)$

$I^G(J^{PC}) = 0^-(1^{--})$

$\Upsilon(3S)$ MASS

VALUE (GeV)	DOCUMENT ID		TECN	COMMENT
10.3552 ± 0.0005	[1] ARTAMONOV	00	MD1	$e^+e^- \to$ hadrons
• • • We do not use the following data for averages, fits, limits, etc. • • •				
10.3553 ± 0.0005	[2,3] BARU	86B	REDE	$e^+e^- \to$ hadrons

[1] Reanalysis of BARU 86B using new electron mass (COHEN 87).
[2] Reanalysis of ARTAMONOV 84.
[3] Superseded by ARTAMONOV 00.

$\Upsilon(3S)$ WIDTH

VALUE (keV)	DOCUMENT ID
26.3 ± 3.4 OUR EVALUATION	See the Note on Width Determinations of the Υ states

$\Upsilon(3S)$ DECAY MODES

	Mode	Fraction (Γ_i/Γ)	Scale factor/ Confidence level
Γ_1	$\Upsilon(2S)$anything	(10.6 ± 0.8) %	
Γ_2	$\Upsilon(2S)\pi^+\pi^-$	(2.8 ± 0.6) %	S=2.2
Γ_3	$\Upsilon(2S)\pi^0\pi^0$	(2.00 ± 0.32) %	
Γ_4	$\Upsilon(2S)\gamma\gamma$	(5.0 ± 0.7) %	
Γ_5	$\Upsilon(1S)\pi^+\pi^-$	(4.48 ± 0.21) %	
Γ_6	$\Upsilon(1S)\pi^0\pi^0$	(2.06 ± 0.28) %	
Γ_7	$\Upsilon(1S)\eta$	< 2.2 $\times 10^{-3}$	CL=90%
Γ_8	$\mu^+\mu^-$	(1.81 ± 0.17) %	
Γ_9	e^+e^-	seen	
	Radiative decays		
Γ_{10}	$\gamma\chi_{b2}(2P)$	(11.4 ± 0.8) %	S=1.3
Γ_{11}	$\gamma\chi_{b1}(2P)$	(11.3 ± 0.6) %	
Γ_{12}	$\gamma\chi_{b0}(2P)$	(5.4 ± 0.6) %	S=1.1

$\Upsilon(3S)$ $\Gamma(i)\Gamma(e^+e^-)/\Gamma(\text{total})$

$\Gamma(\text{hadrons}) \times \Gamma(e^+e^-)/\Gamma_{\rm total}$ $\Gamma_0\Gamma_9/\Gamma$

VALUE (keV)	DOCUMENT ID		TECN	COMMENT
0.45 ± 0.03 ± 0.03	[4] GILES	84B	CLEO	$e^+e^- \to$ hadrons

[4] Radiative corrections reevaluated by BUCHMUELLER 88 following KURAEV 85.

$\Upsilon(3S)$ BRANCHING RATIOS

$\Gamma(\Upsilon(2S)\text{anything})/\Gamma_{\rm total}$ Γ_1/Γ

VALUE	EVTS	DOCUMENT ID		TECN	COMMENT
0.106 ± 0.008 OUR AVERAGE					
0.1023 ± 0.0105	4625	[5,6,7] BUTLER	94B	CLE2	$e^+e^- \to \ell^+\ell^-$X
0.111 ± 0.012	4891	[6,7,8] BROCK	91	CLEO	$e^+e^- \to \pi^+\pi^-$X, $\pi^+\pi^-\ell^+\ell^-$

$\Gamma(\Upsilon(2S)\pi^+\pi^-)/\Gamma_{total}$ Γ_2/Γ

VALUE	EVTS	DOCUMENT ID		TECN	COMMENT
0.028 ±0.006 OUR AVERAGE Error includes scale factor of 2.2. See the ideogram below.					
0.0312±0.0049	980	[5,9] BUTLER	94B	CLE2	$e^+e^- \to \pi^+\pi^-\ell^+\ell^-$
0.0482±0.0065±0.0053	138	[8] WU	93	CUSB	$\Upsilon(3S) \to \pi^+\pi^-\ell^+\ell^-$
0.0213±0.0038	974	[8] BROCK	91	CLEO	$e^+e^- \to \pi^+\pi^- X,\ \pi^+\pi^-\ell^+\ell^-$
• • • We do not use the following data for averages, fits, limits, etc. • • •					
0.031 ±0.020	5	MAGERAS	82	CUSB	$\Upsilon(3S) \to \pi^+\pi^-\ell^+\ell^-$

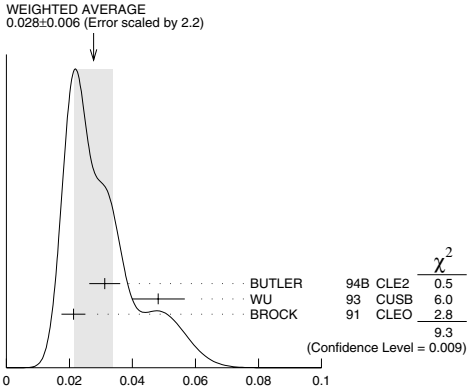

$\Gamma(\Upsilon(2S)\pi^0\pi^0)/\Gamma_{total}$ Γ_3/Γ

VALUE	EVTS	DOCUMENT ID		TECN	COMMENT
0.0200±0.0032 OUR AVERAGE					
0.0216±0.0039		[9,10] BUTLER	94B	CLE2	$e^+e^- \to \ell^+\ell^-\pi^0\pi^0$
0.017 ±0.005 ±0.002	10	[11] HEINTZ	92	CSB2	$e^+e^- \to \ell^+\ell^-\pi^0\pi^0$

$\Gamma(\Upsilon(2S)\gamma\gamma)/\Gamma_{total}$ Γ_4/Γ

VALUE	DOCUMENT ID		TECN	COMMENT
0.0502±0.0069	[9] BUTLER	94B	CLE2	$e^+e^- \to \ell^+\ell^-2\gamma$

$\Gamma(\Upsilon(1S)\pi^+\pi^-)/\Gamma_{total}$ Γ_5/Γ

VALUE	EVTS	DOCUMENT ID		TECN	COMMENT
0.0448±0.0021 OUR AVERAGE					
0.0452±0.0035	11830	[6] BUTLER	94B	CLE2	$e^+e^- \to \pi^+\pi^- X,\ \pi^+\pi^-\ell^+\ell^-$
0.0446±0.0034±0.0050	451	[6] WU	93	CUSB	$\Upsilon(3S) \to \pi^+\pi^-\ell^+\ell^-$
0.0446±0.0030	11221	[6] BROCK	91	CLEO	$e^+e^- \to \pi^+\pi^- X,\ \pi^+\pi^-\ell^+\ell^-$
• • • We do not use the following data for averages, fits, limits, etc. • • •					
0.049 ±0.010	22	GREEN	82	CLEO	$\Upsilon(3S) \to \pi^+\pi^-\ell^+\ell^-$
0.039 ±0.013	26	MAGERAS	82	CUSB	$\Upsilon(3S) \to \pi^+\pi^-\ell^+\ell^-$

$\Gamma(\Upsilon(1S)\pi^0\pi^0)/\Gamma_{total}$ Γ_6/Γ

VALUE	EVTS	DOCUMENT ID		TECN	COMMENT
0.0206±0.0028 OUR AVERAGE					
0.0199±0.0034	56	[6] BUTLER	94B	CLE2	$e^+e^- \to \ell^+\ell^-\pi^0\pi^0$
0.022 ±0.004 ±0.003	33	[12] HEINTZ	92	CSB2	$e^+e^- \to \ell^+\ell^-\pi^0\pi^0$

$\Gamma(\Upsilon(1S)\eta)/\Gamma_{total}$ Γ_7/Γ

VALUE	CL%	DOCUMENT ID		TECN	COMMENT
<0.0022	90	BROCK	91	CLEO	$e^+e^- \to \pi^+\pi^-\pi^0\ell^+\ell^-$

$\Gamma(\mu^+\mu^-)/\Gamma_{total}$ Γ_8/Γ

VALUE	EVTS	DOCUMENT ID		TECN	COMMENT
0.0181±0.0017 OUR AVERAGE					
0.0202±0.0019±0.0033		CHEN	89B	CLEO	$e^+e^- \to \mu^+\mu^-$
0.0173±0.0015±0.0011		KAARSBERG	89	CSB2	$e^+e^- \to \mu^+\mu^-$
0.033 ±0.013 ±0.007	1096	ANDREWS	83	CLEO	$e^+e^- \to \mu^+\mu^-$

$\Gamma(\gamma\chi_{b2}(2P))/\Gamma_{total}$ Γ_{10}/Γ

VALUE	EVTS	DOCUMENT ID		TECN	COMMENT
0.114±0.008 OUR AVERAGE Error includes scale factor of 1.3.					
0.111±0.005±0.004	10319	[13] HEINTZ	92	CSB2	$e^+e^- \to \gamma X$
0.135±0.003±0.017	30741	MORRISON	91	CLE2	$e^+e^- \to \gamma X$

$\Gamma(\gamma\chi_{b1}(2P))/\Gamma_{total}$ Γ_{11}/Γ

VALUE	EVTS	DOCUMENT ID		TECN	COMMENT
0.113±0.006 OUR AVERAGE					
0.115±0.005±0.005	11147	[13] HEINTZ	92	CSB2	$e^+e^- \to \gamma X$
$0.105^{+0.003}_{-0.002}\pm0.013$	25759	MORRISON	91	CLE2	$e^+e^- \to \gamma X$

$\Gamma(\gamma\chi_{b0}(2P))/\Gamma_{total}$ Γ_{12}/Γ

VALUE	EVTS	DOCUMENT ID		TECN	COMMENT
0.054±0.006 OUR AVERAGE Error includes scale factor of 1.1.					
0.060±0.004±0.006	4959	[13] HEINTZ	92	CSB2	$e^+e^- \to \gamma X$
$0.049^{+0.003}_{-0.004}\pm0.006$	9903	MORRISON	91	CLE2	$e^+e^- \to \gamma X$

[5] Using $B(\Upsilon(2S) \to \Upsilon(1S)\gamma\gamma) = (0.038 \pm 0.007)\%$, and $B(\Upsilon(2S) \to \Upsilon(1S)\pi^0\pi^0) = (1/2)B(\Upsilon(2S) \to \Upsilon(1S)\pi^+\pi^-)$.
[6] Using $B(\Upsilon(1S) \to \mu^+\mu^-) = (2.48 \pm 0.06)\%$. With the assumption of $e\mu$ universality.
[7] Using $B(\Upsilon(2S) \to \Upsilon(1S)\pi^+\pi^-) = (18.5 \pm 0.8)\%$.
[8] Using $B(\Upsilon(2S) \to \mu^+\mu^-) = (1.31 \pm 0.21)\%$, $B(\Upsilon(2S) \to \Upsilon(1S)\gamma\gamma)\times 2B(\Upsilon(1S) \to \mu^+\mu^-) = (0.188 \pm 0.035)\%$, and $B(\Upsilon(2S) \to \Upsilon(1S)\pi^0\pi^0)\times 2B(\Upsilon(1S) \to \mu^+\mu^-) = (0.436 \pm 0.056)\%$. With the assumption of $e\mu$ universality.
[9] From the exclusive mode.
[10] $B(\Upsilon(2S) \to \mu^+\mu^-) = (1.31 \pm 0.21)\%$ and assuming $e\mu$ universality.
[11] $B(\Upsilon(2S) \to \mu^+\mu^-) = (1.44 \pm 0.10)\%$ and assuming $e\mu$ universality. Supersedes HEINTZ 91.
[12] Using $B(\Upsilon(1S) \to \mu^+\mu^-) = (2.57 \pm 0.07)\%$ and assuming $e\mu$ universality. Supersedes HEINTZ 91.
[13] Supersedes NARAIN 91.

$\Upsilon(3S)$ REFERENCES

ARTAMONOV	00	PL B474 427	A.S. Artamonov *et al.*	
BUTLER	94B	PR D49 40	F. Butler *et al.*	(CLEO Collab.)
WU	93	PL B301 307	Q.W. Wu *et al.*	(CUSB Collab.)
HEINTZ	92	PR D46 1928	U. Heintz *et al.*	(CUSB II Collab.)
BROCK	91	PR D43 1448	I.C. Brock *et al.*	(CLEO Collab.)
HEINTZ	91	PRL 66 1563	U. Heintz *et al.*	(CUSB Collab.)
MORRISON	91	PRL 67 1696	R.J. Morrison *et al.*	(CLEO Collab.)
NARAIN	91	PRL 66 3113	M. Narain *et al.*	(CUSB Collab.)
CHEN	89B	PR D39 3528	W.Y. Chen *et al.*	(CLEO Collab.)
KAARSBERG	89	PRL 62 2077	T.M. Kaarsberg *et al.*	(CUSB Collab.)
BUCHMUEL...	88	HE e^+e^- Physics 412 Editors: A. Ali and P. Soeding, World Scientific, Singapore	W. Buchmueller, S. Cooper	(HANN, DESY, MIT)
COHEN	87	RMP 59 1121	E.R. Cohen, B.N. Taylor	(RISC, NBS)
BARU	86B	ZPHY C32 622	S.E. Baru *et al.*	(NOVO)
KURAEV	85	SJNP 41 466 Translated from YAF 41 733.	E.A. Kuraev, V.S. Fadin	(NOVO)
ARTAMONOV	84	PL 137B 272	A.S. Artamonov *et al.*	(NOVO)
GILES	84B	PR D29 1285	R. Giles *et al.*	(CLEO Collab.)
ANDREWS	83	PRL 50 807	D.E. Andrews *et al.*	(CLEO Collab.)
GREEN	82	PRL 49 617	J. Green *et al.*	(CLEO Collab.)
MAGERAS	82	PL 118B 453	G. Mageras *et al.*	(COLU, CORN, LSU+)

OTHER RELATED PAPERS

ROSNER	03	PR D67 097504	J.L. Rosner	
ALEXANDER	89	NP B320 45	J.P. Alexander *et al.*	(LBL, MICH, SLAC)
ARTAMONOV	84	PL 137B 272	A.S. Artamonov *et al.*	(NOVO)
GILES	84B	PR D29 1285	R. Giles *et al.*	(CLEO Collab.)
HAN	82	PRL 49 1612	K. Han *et al.*	(CUSB Collab.)
PETERSON	82	PL 114B 277	D. Peterson *et al.*	(CUSB Collab.)
KAPLAN	78	PRL 40 435	D.M. Kaplan *et al.*	(STON, FNAL, COLU)
YOH	78	PRL 41 684	J.K. Yoh *et al.*	(COLU, FNAL, STON)
COBB	77	PL 72B 273	J.H. Cobb *et al.*	(BNL, CERN, SYRA, YALE)
HERB	77	PRL 39 252	S.W. Herb *et al.*	(COLU, FNAL, STON)
INNES	77	PRL 39 1240	W.R. Innes *et al.*	(COLU, FNAL, STON)

$\Upsilon(4S)$ or $\Upsilon(10580)$

$I^G(J^{PC}) = 0^-(1^{--})$

$\Upsilon(4S)$ MASS

VALUE (GeV)	DOCUMENT ID		TECN	COMMENT
10.5800±0.0035	[1] BEBEK	87	CLEO	$e^+e^- \to$ hadrons
• • • We do not use the following data for averages, fits, limits, etc. • • •				
10.5774±0.0010	[2] LOVELOCK	85	CUSB	$e^+e^- \to$ hadrons

[1] Reanalysis of BESSON 85.
[2] No systematic error given.

$\Upsilon(4S)$ WIDTH

VALUE (MeV)	DOCUMENT ID		TECN	COMMENT
20±2 ±4	BESSON	85	CLEO	$e^+e^- \to$ hadrons
• • • We do not use the following data for averages, fits, limits, etc. • • •				
25±2.5	LOVELOCK	85	CUSB	$e^+e^- \to$ hadrons

$\Upsilon(4S)$ DECAY MODES

	Mode	Fraction (Γ_i/Γ)	Confidence level
Γ_1	$B\overline{B}$	> 96 %	95%
Γ_2	B^+B^-		
Γ_3	$B^0\overline{B}^0$		
Γ_4	non-$B\overline{B}$	< 4 %	95%
Γ_5	e^+e^-	$(2.8\pm0.7)\times10^{-5}$	
Γ_6	$J/\psi(1S)$anything	$< 1.9\times10^{-4}$	95%
Γ_7	D^{*+}anything + c.c.	< 7.4 %	90%
Γ_8	ϕanything	$< 2.3\times10^{-3}$	90%
Γ_9	$\Upsilon(1S)$anything	$< 4\times10^{-3}$	90%
Γ_{10}	$\Upsilon(1S)\pi^+\pi^-$	$< 1.2\times10^{-4}$	90%
Γ_{11}	$\Upsilon(2S)\pi^+\pi^-$	$< 3.9\times10^{-4}$	90%

$\Upsilon(4S)$ PARTIAL WIDTHS

$\Gamma(e^+e^-)$ Γ_5

VALUE (keV)	DOCUMENT ID	TECN	COMMENT
0.248±0.031 OUR AVERAGE	Error includes scale factor of 1.3. See the ideogram below.		
0.28 ±0.05 ±0.01	[3] ALBRECHT	95E ARG	$e^+e^-\to$ hadrons
0.192±0.007±0.038	BESSON	85 CLEO	$e^+e^-\to$ hadrons
0.283±0.037	LOVELOCK	85 CUSB	$e^+e^-\to$ hadrons

[3] Using LEYAOUANC 77 parametrization of $\Gamma(s)$.

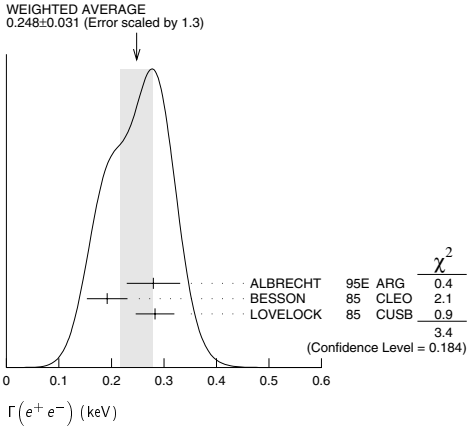

$\Upsilon(4S)$ BRANCHING RATIOS

$\Gamma(B^+B^-)/\Gamma(B^0\overline{B}^0)$ Γ_2/Γ_3

VALUE	DOCUMENT ID	TECN	COMMENT
1.029±0.054±0.045	[4] ATHAR 02	CLEO	$e^+e^-\to B\overline{B}$
• • • We do not use the following data for averages, fits, limits, etc. • • •			
1.02 ±0.14	[5] ALEXANDER 01	CLEO	$e^+e^-\to B\overline{B}$

[4] Using also data from ALEXANDER 01 and assuming $\tau_{B^+}/\tau_{B^0} = 1.086 \pm 0.017$.

[5] Assuming isospin conservation with $(\tau_{B^+})/(\tau_{B^0}) = 1.09^{+0.11}_{-0.10} \pm 0.08$. Superseded by ATHAR 02.

$\Gamma(e^+e^-)/\Gamma_{\rm total}$ Γ_5/Γ

VALUE (units 10^{-5})	DOCUMENT ID	TECN	COMMENT
2.77±0.50±0.49	[6] ALBRECHT 95E	ARG	$e^+e^-\to$ hadrons

[6] Using LEYAOUANC 77 parametrization of $\Gamma(s)$.

$[\Gamma(D^{*+}\text{anything}) + \Gamma(\text{c.c.})]/\Gamma_{\rm total}$ Γ_7/Γ

VALUE	CL%	DOCUMENT ID	TECN	COMMENT
<0.074	90	[7] ALEXANDER 90C	CLEO	e^+e^-

[7] For $x > 0.473$.

$\Gamma(\phi\text{anything})/\Gamma_{\rm total}$ Γ_8/Γ

VALUE	CL%	DOCUMENT ID	TECN	COMMENT
<0.0023	90	[8] ALEXANDER 90C	CLEO	e^+e^-

[8] For $x > 0.52$.

$\Gamma(J/\psi(1S)\text{anything})/\Gamma_{\rm total}$ Γ_6/Γ

VALUE (units 10^{-4})	CL%	DOCUMENT ID	TECN	COMMENT
<1.9	95	[9] ABE 02D	BELL	$e^+e^-\to J/\psi X\to \ell^+\ell^- X$
• • • We do not use the following data for averages, fits, limits, etc. • • •				
<4.7	90	[9] AUBERT 01C	BABR	$e^+e^-\to J/\psi X\to \ell^+\ell^- X$

[9] Uses $B(J/\psi\to e^+e^-) = 0.0593 \pm 0.0010$ and $B(J/\psi\to\mu^+\mu^-) = 0.0588 \pm 0.0010$.

$\Gamma(\Upsilon(1S)\text{anything})/\Gamma_{\rm total}$ Γ_9/Γ

VALUE	CL%	DOCUMENT ID	TECN	COMMENT
<0.004	90	ALEXANDER 90C	CLEO	e^+e^-

$\Gamma(\Upsilon(1S)\pi^+\pi^-)/\Gamma_{\rm total}$ Γ_{10}/Γ

VALUE (units 10^{-4})	CL%	DOCUMENT ID	TECN	COMMENT
<1.2	90	GLENN 99	CLE2	e^+e^-

$\Gamma(\Upsilon(2S)\pi^+\pi^-)/\Gamma_{\rm total}$ Γ_{11}/Γ

VALUE (units 10^{-4})	CL%	DOCUMENT ID	TECN	COMMENT
<3.9	90	GLENN 99	CLE2	e^+e^-

$\Gamma(\text{non-}B\overline{B})/\Gamma_{\rm total}$ Γ_4/Γ

VALUE	CL%	DOCUMENT ID	TECN	COMMENT
<0.04	95	BARISH 96B	CLEO	e^+e^-

$\Upsilon(4S)$ REFERENCES

ABE	02D	PRL 88 052001	K. Abe *et al.*	(BELLE Collab.)
ATHAR	02	PR D66 052003	S.B. Athar *et al.*	(CLEO Collab.)
ALEXANDER	01	PRL 86 2737	J.P. Alexander *et al.*	(CLEO Collab.)
AUBERT	01C	PRL 87 162002	B. Aubert *et al.*	(BaBar Collab.)
GLENN	99	PR D59 052003	S. Glenn *et al.*	
BARISH	96B	PRL 76 1570	B.C. Barish *et al.*	(CLEO Collab.)
ALBRECHT	95E	ZPHY C65 619	H. Albrecht *et al.*	(ARGUS Collab.)
ALEXANDER	90C	PRL 64 2226	J. Alexander *et al.*	(CLEO Collab.)
BEBEK	87	PR D36 1289	C. Bebek *et al.*	(CLEO Collab.)
BESSON	85	PRL 54 381	D. Besson *et al.*	(CLEO Collab.)
LOVELOCK	85	PRL 54 377	D.M.J. Lovelock *et al.*	(CUSB Collab.)
LEYAOUANC	77	PL B71 397	A. Le Yaouanc *et al.*	(ORSAY)

OTHER RELATED PAPERS

ABE	01J	PR D64 072001	K. Abe *et al.*	(BELLE Collab.)
HENDERSON	92	PR D45 2212	S. Henderson *et al.*	(CLEO Collab.)
ANDREWS	80B	PRL 45 219	D. Andrews *et al.*	(CLEO Collab.)
FINOCCHI...	80	PRL 45 222	G. Finocchiaro *et al.*	(CUSB Collab.)

$\Upsilon(10860)$ $I^G(J^{PC}) = 0^-(1^{--})$

$\Upsilon(10860)$ MASS

VALUE (GeV)	DOCUMENT ID	TECN	COMMENT
10.865±0.008 OUR AVERAGE	Error includes scale factor of 1.1.		
10.868±0.006±0.005	BESSON 85	CLEO	$e^+e^-\to$ hadrons
10.845±0.020	LOVELOCK 85	CUSB	$e^+e^-\to$ hadrons

$\Upsilon(10860)$ WIDTH

VALUE (MeV)	DOCUMENT ID	TECN	COMMENT
110±13 OUR AVERAGE			
112±17±23	BESSON 85	CLEO	$e^+e^-\to$ hadrons
110±15	LOVELOCK 85	CUSB	$e^+e^-\to$ hadrons

$\Upsilon(10860)$ DECAY MODES

	Mode	Fraction (Γ_i/Γ)
Γ_1	e^+e^-	$(2.8\pm0.7)\times10^{-6}$

$\Upsilon(10860)$ PARTIAL WIDTHS

$\Gamma(e^+e^-)$ Γ_1

VALUE (keV)	DOCUMENT ID	TECN	COMMENT
0.31 ±0.07 OUR AVERAGE	Error includes scale factor of 1.3.		
0.22 ±0.05 ±0.07	BESSON 85	CLEO	$e^+e^-\to$ hadrons
0.365±0.070	LOVELOCK 85	CUSB	$e^+e^-\to$ hadrons

$\Upsilon(10860)$ REFERENCES

BESSON	85	PRL 54 381	D. Besson *et al.*	(CLEO Collab.)
LOVELOCK	85	PRL 54 377	D.M.J. Lovelock *et al.*	(CUSB Collab.)

See key on page 323

$\Upsilon(11020)$

$I^G(J^{PC}) = 0^-(1^{--})$

$\Upsilon(11020)$ MASS

VALUE (GeV)	DOCUMENT ID		TECN	COMMENT
11.019±0.008 OUR AVERAGE				
11.019±0.005±0.007	BESSON	85	CLEO	$e^+e^- \to$ hadrons
11.020±0.030	LOVELOCK	85	CUSB	$e^+e^- \to$ hadrons

$\Upsilon(11020)$ WIDTH

VALUE (MeV)	DOCUMENT ID		TECN	COMMENT
79±16 OUR AVERAGE				
61±13±22	BESSON	85	CLEO	$e^+e^- \to$ hadrons
90±20	LOVELOCK	85	CUSB	$e^+e^- \to$ hadrons

$\Upsilon(11020)$ DECAY MODES

	Mode	Fraction (Γ_i/Γ)
Γ_1	e^+e^-	$(1.6\pm0.5)\times10^{-6}$

$\Upsilon(11020)$ PARTIAL WIDTHS

$\Gamma(e^+e^-)$ Γ_1

VALUE (keV)	DOCUMENT ID		TECN	COMMENT
0.130±0.030 OUR AVERAGE				
0.095±0.03 ±0.035	BESSON	85	CLEO	$e^+e^- \to$ hadrons
0.156±0.040	LOVELOCK	85	CUSB	$e^+e^- \to$ hadrons

$\Upsilon(11020)$ REFERENCES

BESSON	85	PRL 54 381	D. Besson *et al.*	(CLEO Collab.)
LOVELOCK	85	PRL 54 377	D.M.J. Lovelock *et al.*	(CUSB Collab.)

NON-$q\overline{q}$ CANDIDATES

We include here mini-reviews and reference lists on gluonium and other non-$q\overline{q}$ candidates. See also the section on Further States for possible bound states.

NON-$q\overline{q}$ MESONS

Revised December 2003 by C. Amsler (University of Zürich).

The constituent quark model describes the observed meson spectrum as bound $q\overline{q}$ states grouped into SU(N) flavor multiplets (see our review on the quark model). However, the self-coupling of gluons in QCD suggests that additional mesons made of bound gluons (glueballs), or $q\overline{q}$-pairs with an excited gluon (hybrids), may exist. Multiquark color singlet states like $qq\overline{qq}$ or $qqq\overline{qqq}$ have also been predicted (JAFFE 77). Among the signatures naively expected for glueballs are (i) no place in $q\overline{q}$ nonets, (ii) enhanced production in gluon-rich channels such as central production and radiative $J/\psi(1S)$ decay, (iii) decay branching fractions incompatible with SU(N) predictions for $q\overline{q}$ states, and (iv) reduced $\gamma\gamma$ couplings. However, mixing effects with isoscalar $q\overline{q}$ mesons (AMSLER 96, ANISOVICH 97, WEINGARTEN 97, CLOSE 01B) and decay form factors (BARNES 97) may obscure these simple signatures.

Lattice calculations (BALI 93, SEXTON 95, MORNINGSTAR 99), QCD sum rules, flux tube, and constituent glue models agree that the lightest glueballs have quantum numbers $J^{PC} = 0^{++}$ and 2^{++}. On the lattice, the scale parameter (estimated from the string tension in heavy quark mesons) gives by extrapolation to zero lattice spacing a mass of 1611 $\pm$ 163 MeV for the ground state (0^{++}) glueball, while the first excited state (2^{++}) has a mass of 2232 $\pm$ 310 MeV (MICHAEL 97). Hence, the low-mass glueballs lie in the same mass region as ordinary isoscalar $q\overline{q}$ states, that is, in the mass range of the $1^3P_0(0^{++})$, 2^3P_2, 3^3P_2, and $1^3F_2(2^{++})$ $q\overline{q}$ states. The 0^{-+} state and exotic glueballs (with non-$q\overline{q}$ quantum numbers such as 0^{--}, 0^{+-}, 1^{-+}, 2^{+-}, *etc.*) are expected above 2 GeV (MORNINGSTAR 99).

The lattice calculations assume that the quark masses are infinite, and therefore neglect $q\overline{q}$ loops. However, one expects that glueballs will mix with nearby $q\overline{q}$ states of the same quantum numbers. The presence of a glueball mixed with $q\overline{q}$ would still lead to a supernumerary isoscalar in the SU(3) classification of $q\overline{q}$ mesons.

For earlier experimental searches, we refer to the Notes in the 1996 and 1998 issues of this *Review*. For a detailed recent review on exotic mesons, see AMSLER 04.

We first deal with non-$q\overline{q}$ candidates in the scalar sector. Five isoscalar resonances are well established: the very broad $f_0(600)$ (or σ), the $f_0(980)$, the broad $f_0(1370)$, and the comparatively narrow $f_0(1500)$ and $f_0(1710)$ (see the Note on "Scalar Mesons," and also AMSLER 98). The $f_0(1500)$ was observed in many experiments, *e.g.*, in π^-p reactions, in $\overline{p}p$ annihilations, in central collisions, in $J/\psi(1S)$ radiative decays, and in D_s decays (see the Meson Particle Listings). The $f_0(1710)$ decays mainly into $K\overline{K}$. This points to a mostly $s\overline{s}$ structure, although no signal was reported earlier in $K^-p \to K_SK_S\Lambda$ interactions (ASTON 88D). However, the assumption was that the spin would be 2. Also, the $f_0(1710)$ is not observed in $p\overline{p}$ annihilation (AMSLER 02), as expected from the OZI rule for an $s\overline{s}$ state.

In $\gamma\gamma$ collisions leading to K_SK_S (ACCIARRI 01H) and K^+K^- (ABE 04), a signal is observed at the $f_0(1710)$ mass. Spin 2 is preferred, but the isospin cannot be determined, hence, the signal is possibly coming from $a_2(1700)$. A spin 0 component from the $s\overline{s}$ $f_0(1710)$ is compatible with data.

On the other hand, $f_0(1500)$ is not observed in $\gamma\gamma \to K_SK_S$ nor $\pi^+\pi^-$ (BARATE 00E). The upper limit from $\pi^+\pi^-$ excludes a large $u\overline{u}+d\overline{d}$ content, and points to a mainly $s\overline{s}$ meson (AMSLER 02B). This is, however, in contradiction with the small $K\overline{K}$ decay branching ratio of $f_0(1500)$ (ABELE 96B,98, BARBERIS 99D). Hence, this state is hard to accommodate as a $q\overline{q}$ meson.

Since $f_0(1370)$ does not couple strongly to $s\overline{s}$ either (BARBERIS 99D), $f_0(1370)$ or $f_0(1500)$ appear to be supernumerary. Note that $f_0(1370)$ and $f_0(1500)$ have rather different 4π decay patterns. The former decays dominantly into two S-wave dipions, and the latter mostly into $\pi(1300)\pi$ (ABELE 01,01B). The narrow width of $f_0(1500)$, and its enhanced production at low transverse momentum transfer in central collisions (CLOSE 97,98B, KIRK 00) also favor $f_0(1500)$ to be non-$q\overline{q}$. In AMSLER 96, the ground state scalar nonet is made of $a_0(1450)$, $f_0(1370)$, $K_0^*(1430)$, and $f_0(1710)$. The isoscalars $f_0(1370)$ and $f_0(1710)$ contain a small fraction of glue, while $f_0(1500)$ is mostly gluonic. The light scalars $f_0(600)$, $f_0(980)$, $a_0(980)$, and $\kappa(800)$ are four-quark states or two-meson resonances (see AMSLER 04 for a review). In the mixing scheme of CLOSE 01B, which uses all recent data in central production and $p\overline{p}$ annihilation, glue is shared between $f_0(1370)$ and $f_0(1500)$, while $f_0(1710)$ remains mainly $s\overline{s}$.

Alternative mixing schemes have been proposed (see for example TORNQVIST 96, ANISOVICH 97, BOGLIONE 97, WEINGARTEN 97, MINKOWSKI 99).

As mentioned above, $a_0(980)$ and $f_0(980)$ could be four-quark states (JAFFE 77, ALFORD 00) or $K\overline{K}$ molecular states (WEINSTEIN 90, LOCHER 98) due to their strong affinity for $K\overline{K}$, in spite of their masses being very close to threshold. For $q\overline{q}$ states, the expected $\gamma\gamma$ widths (OLLER 97B, DELBOURGO 99) are not significantly larger than for molecular states (BARNES 85). A better filter is radiative $\phi(1020)$ decay to $a_0(980)$ and $f_0(980)$. Recent data (ALOISIO 02C, 02D) favor these mesons to be four-quark states (ACHASOV 00F). The $f_0(980)$ is strongly produced in D_s^+ decay (FRABETTI 97, AITALA 01A). Assuming a dominant Cabibbo favored $c \to s$ decay suggests a large $s\overline{s}$ component. However, the mainly $u\overline{u}+d\overline{d}$ $f_0(1370)$ is also strongly produced in D_s^+ decay, indicating that other graphs must contribute (CHENG 03B).

Two very narrow states, $D_{sJ}(2317)^{*\pm}$ and $D_{sJ}(2460)^{*\pm}$, were observed recently at the B-factories (AUBERT 03G, BESSON 03), the former with preferred spin 0^+, the latter with 1^+. They lie far below the predicted masses for the two expected

broad P-wave $c\overline{s}$ mesons. These states have hence been interpreted as four-quark states (CHENG 03C, TERASAKI 03) or DK (DK^*) molecules (BARNES 03). However, strong cusp effects due to the nearby closed DK, respectively DK^* thresholds, could shift their masses downwards and quench the observed widths, an effect similar to that occuring for the $a_0(980)$ and $f_0(980)$ mesons, which lie just below the $K\overline{K}$ threshold.

We now turn to the 2^{++} sector. The isoscalar $1^3P_2(2^{++})$ $q\overline{q}$ mesons, $f_2(1270)$, and $f_2'(1525)$, are well known. Above the $f_2'(1525)$, none of the reported isoscalars can be definitely assigned to the 2^3P_2, 3^3P_2, or 1^3F_2 nonets, and therefore, the identification of the 2^{++} glueball is premature. Three states appear to be solid. The $f_2(1565)$ observed in $\overline{p}p$ annihilation at rest (MAY 90, BERTIN 98) is perhaps the same state as $f_2(1640)$, reported to decay into $\omega\omega$ (ALDE 90, BAKER 99) and 4π (ADAMO 92). This could be one of the 2^3P_2 isoscalars or a nucleon-antinucleon resonance. The broad $f_2(1950)$ is observed by several experiments, *e.g.*, in central production (BARBERIS 00C) and in $\overline{p}p$ annihilation in flight (AMSLER 02). The large $\phi\phi$ cross section in $\overline{p}p$ just above threshold (EVANGELISTA 98) could be due to the production of the 2^{++} glueball, in accord with earlier observations in π^-N reactions (BOOTH 86, ETKIN 88) and in central collisions (BARBERIS 98).

There is no evidence for a narrow meson, $f_J(2220)$ (possibly a tensor) in $\overline{p}p$ annihilation (see the Note under the $f_J(2220)$ section). The measured partial width to $\overline{p}p$ in radiative $J/\psi(1S)$ decay (BAI 96B) is too large and inconsistent with the upper limit from $\overline{p}p$ annihilation into $\pi\pi$ (AMSLER 01).

Let us now deal with hybrid states. Hybrids may be viewed as $q\overline{q}$ mesons with a vibrating gluon flux tube. In contrast to glueballs, they can have isospin 0 and 1. The mass spectrum of hybrids with exotic (non-$q\overline{q}$) quantum numbers was predicted by ISGUR 85, while CLOSE 95 also deals with non-exotic quantum numbers. The ground state hybrids with quantum numbers (0^{-+}, 1^{-+}, 1^{--}, and 2^{-+}) are expected around 1.7 to 1.9 GeV. Lattice calculations predict that the hybrid with exotic quantum numbers 1^{-+} lies at a mass of 1.9 ± 0.2 GeV (LACOCK 97, BERNARD 97). Most hybrids are rather broad, but some can be as narrow as 100 MeV (PAGE 99). They prefer to decay into a pair of S- and P-wave mesons.

A $J^{PC} = 1^{-+}$ exotic meson, $\pi_1(1400)$, was reported in $\pi^-p \to \eta\pi^-p$ (THOMPSON 97, CHUNG 99). It was observed as an interference between the angular momentum $L = 1$ and $L = 2$ $\eta\pi$ amplitudes, leading to a forward/backward asymmetry in the $\eta\pi$ angular distribution. This state was reported earlier in π^-p reactions (ALDE 88B), but ambiguous solutions in the partial-wave analysis were pointed out by PROKOSHKIN 95B,95C. A resonating 1^{-+} contribution to the $\eta\pi$ P wave is also required in the Dalitz plot analysis of $\overline{p}n$ annihilation into $\pi^-\pi^0\eta$ (ABELE 98B), and in $\overline{p}p$ annihilation into $\pi^0\pi^0\eta$ (ABELE 99). Mass and width are consistent with THOMPSON 97.

Another 1^{-+} state, $\pi_1(1600)$, decaying into $\rho\pi$ (ADAMS 98B) and $\eta'\pi$ (IVANOV 01), was reported in the reaction $\pi^-p \to \pi^-\rho^0(\pi^-\eta')n$. It was already observed earlier in the decay modes $\rho\pi$, $\eta'\pi$, and $b_1(1235)\pi$, but not $\eta\pi$ (GOUZ 92). A strong enhancement in the 1^{-+} $\eta'\pi$ wave, compared to $\eta\pi$, was reported at this mass by BELADIDZE 93. DONNACHIE 98 suggests that a Deck-generated $\eta\pi$ background from final state rescattering in $\pi_1(1600)$ decay could mimic $\pi_1(1400)$. However, this mechanism is absent in $\overline{p}p$ annihilation. The $\eta\pi\pi$ data require $\pi_1(1400)$ and cannot accommodate a state at 1600 MeV (DUENNWEBER 99).

Thus, we now have evidence for two 1^{-+} exotics, $\pi_1(1400)$ and $\pi_1(1600)$, while the flux tube model and the lattice concur to predict a mass of about 1.9 GeV, where a signal had been reported earlier (LEE 94). As isovectors, $\pi_1(1400)$ and $\pi_1(1600)$ cannot be glueballs. The coupling to $\eta\pi$ of the former points to a four-quark state (see also CHUNG 02C), while the strong $\eta'\pi$ coupling of the latter is favored for hybrid states (CLOSE 87B, IDDIR 01). Its mass is not far below the lattice prediction.

Finally, 0^{-+}, 1^{--}, and 2^{-+} hybrids were also reported. The $\pi(1800)$ decays mostly to a pair of S- and P-wave mesons (AMELIN 95B), in line with expectations for a 0^{-+} hybrid meson. This meson is also rather narrow if interpreted as the second radial excitation of the pion. The evidence for 1^{--} hybrids required in e^+e^- annihilation and in τ decays has been discussed by DONNACHIE 99. The $\rho(1900)$ seems too narrow for a $q\overline{q}$ radial excitation. A candidate for the 2^{-+} hybrid, the $\eta_2(1870)$, was reported in $\gamma\gamma$ interactions (KARCH 92), in $\overline{p}p$ annihilation (ADOMEIT 96), and in central production (BARBERIS 97B). The near degeneracy of $\eta_2(1645)$ and $\pi_2(1670)$ suggests ideal mixing in the 2^{-+} $q\overline{q}$ nonet, and hence, the second isoscalar should be mainly $s\overline{s}$. However, $\eta_2(1870)$ decays mainly to $a_2(1320)\pi$ and $f_2(1270)\pi$ (ADOMEIT 96), with a relative rate compatible with a hybrid state (CLOSE 95).

Meson Particle Listings

Non-$q\overline{q}$ Candidates,

Non-$q\overline{q}$ Candidates

OMITTED FROM SUMMARY TABLE

NON-$q\overline{q}$ CANDIDATES REFERENCES

ABE 04 EPJ C32 323 K. Abe *et al.* (BELLE Collab.)
AMSLER 04 PRPL 389 61 C. Amsler, N.A. Tornqvist
AUBERT 03G PRL 90 242001 B. Aubert *et al.* (BaBar Collab.)
BARNES 03 PR D68 054006 T. Barnes *et al.*
BESSON 03 PR D68 032002 D. Besson *et al.* (CLEO Collab.)
CHENG 03B PR D67 054021 H.Y. Cheng
CHENG 03C PL B566 193 H.-Y. Cheng, W.-S. Hou
TERASAKI 03 PR D68 011501 K. Terasaki
ALOISIO 02C PL B536 209 A. Aloisio *et al.* (KLOE Collab.)
ALOISIO 02D PL B537 21 A. Aloisio *et al.* (KLOE Collab.)
AMSLER 02 EPJ C23 29 C. Amsler *et al.*
AMSLER 02B PL B541 22 C. Amsler
CHUNG 02C EPL A15 539 S.U. Chung, E. Klempt, J.G. Korener
ABELE 01 EPJ C19 667 A. Abele *et al.* (Crystal Barrel Collab.)
ABELE 01B EPJ C21 261 A. Abele *et al.* (Crystal Barrel Collab.)
ACCIARRI 01H PL B501 173 M. Acciarri *et al.* (L3 Collab.)
AITALA 01A PRL 86 765 E.M. Aitala *et al.* (FNAL E791 Collab.)
AMSLER 01 PL B520 175 C. Amsler *et al.* (Crystal Barrel Collab.)
CLOSE 01B EPJ C21 531 F.E. Close, A. Kirk
IDDIR 01 PL B507 183 F. Iddir, A.S. Safir
IVANOV 01 PRL 86 3977 E.I. Ivanov *et al.*
ACHASOV 00F PL B479 53 M.N. Achasov *et al.* (Novosibirsk SND Collab.)
ALFORD 00 NP B578 367 M. Alford, R.L. Jaffe
BARATE 00E PL B472 189 R. Barate *et al.* (ALEPH Collab.)
BARBERIS 00C PL B471 440 D. Barberis *et al.* (WA 102 Collab.)
KIRK 00 PL B489 29 A. Kirk
ABELE 99 PL B446 349 A. Abele *et al.* (Crystal Barrel Collab.)
BAKER 99 PL B449 114 C.A. Baker *et al.*
BARBERIS 99D PL B462 462 D. Barberis *et al.* (Omega Expt.)
CHUNG 99 PR D60 092001 S.U. Chung *et al.* (BNL E852 Collab.)
DELBOURGO 99 PL B446 332 R. Delbourgo, D. Liu, M. Scadron
DONNACHIE 99 PR D60 114011 A. Donnachie, Yu.S. Kalashnikova
DUENNWEBER 99 NP A 663 + 664, 592C W. Duennweber
Proc. XV Particles and Nuclei Int. Conf., Uppsala
MINKOWSKI 99 EPJ C9 283 P. Minkowski, W. Ochs
MORNINGSTAR 99 PR D60 034509 C.J. Morningstar, M. Peardon
PAGE 99 PR D59 034016 P.R. Page, E.S. Swanson, A.P. Szczepaniak
ABELE 98B PL B423 175 A. Abele *et al.* (Crystal Barrel Collab.)
ADAMS 98B PRL 81 5760 G.S. Adams *et al.* (MPS Collab.)
AMSLER 98 RMP 70 1293 C. Amsler
BARBERIS 98 PL B432 436 D. Barberis *et al.* (Omega Expt.)
BERTIN 98 PR D57 55 A. Bertin *et al.* (OBELIX Collab.)
CLOSE 98B PL B419 387 F.E. Close
DONNACHIE 98 PR D58 114012 A. Donnachie *et al.*
EVANGELISTA 98 PR D57 5370 C. Evangelista *et al.* (JETSET Collab.)
LOCHER 98 EPJ C4 317 M.P. Locher *et al.* (PSI)
ANISOVICH 97 PL B395 123 A.V. Anisovich, A.V. Sarantsev (PNPI)
BARBERIS 97B PL B413 217 D. Barberis *et al.* (WA 102 Collab.)
BARNES 97 PR D55 4157 T. Barnes *et al.* (ORNL, RAL, MCHS)
BERNARD 97 PR D56 7039 C. Bernard *et al.* (MILC Collab.)
BOGLIONE 97 PRL 79 1998 M. Boglione *et al.*
CLOSE 97 PL B397 333 F. Close *et al.* (RAL, BIRM)
FRABETTI 97 PL B391 235 P.L. Frabetti *et al.* (FNAL E687 Collab.)
LACOCK 97 PL B401 308 P. Lacock *et al.* (EDIN, LIVP)
MICHAEL 97 Hadron 97 Conf. C. Michael
AIP Conf. Proc. 432 657
OLLER 97B Hadron 97 Conf. J.A. Oller, E. Oset
AIP Conf. Proc. 432 413
THOMPSON 97 PRL 79 1630 D.R. Thompson *et al.* (E852 Collab.)
WEINGARTEN 97 NPPS 53 232 D. Weingarten
ABELE 96B PL B385 425 A. Abele *et al.* (Crystal Barrel Collab.)
ADOMEIT 96 ZPHY C71 227 J. Adomeit *et al.* (Crystal Barrel Collab.)
AMSLER 96 PR D53 295 C. Amsler, F.E. Close (ZURI, RAL)
BAI 96B PRL 76 3502 J.Z. Bai *et al.* (BES Collab.)
TORNQVIST 96 PRL 76 1575 N.A. Tornqvist, M. Roos (HELS)
AMELIN 95B PL B356 595 D.V. Amelin *et al.* (SERP, TBIL)
CLOSE 95 NP B443 233 F.E. Close, P.R. Page (RAL)
PROKOSHKIN 95B PAN 58 606 Y.D. Prokoshkin, S.A. Sadovsky (SERP)
Translated from YAF 58 662.
PROKOSHKIN 95C PAN 58 853 Y.D. Prokoshkin, S.A. Sadovsky (SERP)
Translated from YAF 58 921.
SEXTON 95 PRL 75 4563 J. Sexton *et al.* (IBM)
LEE 94 PL B323 227 J.H. Lee *et al.* (BNL, IND, KYUN, MASD+)
BALI 93 PL B309 378 G.S. Bali *et al.* (LIVP)
BELADIDZE 93 PL B313 276 G.M. Beladidze *et al.* (VES Collab.)
ADAMO 92 PL B287 368 A. Adamo *et al.* (OBELIX Collab.)
GOUZ 92 Dallas HEP 92, p. 572 Yu.P. Gouz *et al.* (VES Collab.)
Proceedings XXVI Int. Conf. on High Energy Physics
KARCH 92 ZPHY C54 33 K. Karch *et al.* (Crystal Ball Collab.)
ALDE 90 PL B241 600 D.M. Alde *et al.* (SERP, BELG, LANL, LAPP+)
MAY 90 ZPHY C46 203 B. May *et al.* (ASTERIX Collab.)
WEINSTEIN 90 PR D41 2236 J. Weinstein, N. Isgur (TNTO)
ALDE 88B PL B205 397 D.M. Alde *et al.* (SERP, BELG, LANL, LAPP)
ASTON 88D NP B301 525 D. Aston *et al.* (SLAC, NAGO, CINC, INUS)
ETKIN 88 PL B201 568 A. Etkin *et al.* (BNL, CUNY)
CLOSE 87B PL B196 245 F.E. Close, H.J. Lipkin
BOOTH 86 NP B273 677 P.S.L. Booth *et al.* (LIVP, GLAS, CERN)
BARNES 85 PL B165 434 T. Barnes
ISGUR 85 PRL 54 869 N. Isgur, R. Kokoski, J. Paton (TNTO)
JAFFE 77 PR D15 267,281 R. Jaffe (MIT)

N BARYONS
($S = 0$, $I = 1/2$)

p, $N^+ = uud$; n, $N^0 = udd$

p

$I(J^P) = \frac{1}{2}(\frac{1}{2}^+)$ Status: ****

p MASS (atomic mass units u)

The mass is known much more precisely in u (atomic mass units) than in MeV. See the next data block.

VALUE (u)	DOCUMENT ID		TECN	COMMENT
1.00727646688 ± 0.00000000013	MOHR	04	RVUE	2002 CODATA value
• • • We do not use the following data for averages, fits, limits, etc. • • •				
1.00727646688 ± 0.00000000013	MOHR	99	RVUE	1998 CODATA value
1.007276470 ± 0.000000012	COHEN	87	RVUE	1986 CODATA value

p MASS (MeV)

The mass is known much more precisely in u (atomic mass units) than in MeV. The conversion from u to MeV, 1 u = 931.494043±0.000080 MeV/c^2 (MOHR 04, the 2002 CODATA value), involves the relatively poorly known electronic charge.

VALUE (MeV)	DOCUMENT ID		TECN	COMMENT
938.272029 ± 0.000080	MOHR	04	RVUE	2002 CODATA value
• • • We do not use the following data for averages, fits, limits, etc. • • •				
938.271998 ± 0.000038	MOHR	99	RVUE	1998 CODATA value
938.27231 ± 0.00028	COHEN	87	RVUE	1986 CODATA value
938.2796 ± 0.0027	COHEN	73	RVUE	1973 CODATA value

$|m_p - m_{\overline{p}}|/m_p$

A test of *CPT* invariance. Note that the comparison of the $\overline{p}$ and p charge-to-mass ratio, given in the next data block, is much better determined.

VALUE	CL%	DOCUMENT ID		TECN	COMMENT
< 1.0 × 10^{-8}	90	[1] HORI	03	SPEC	$\overline{p}e^-$ ^{4}He and $\overline{p}e^-$ ^{3}He
• • • We do not use the following data for averages, fits, limits, etc. • • •					
< 6 × 10^{-8}	90	[1] HORI	01	SPEC	$\overline{p}e^-$ He atom
< 5 × 10^{-7}		[2] TORII	99	SPEC	$\overline{p}e^-$ He atom

[1] HORI 01 and HORI 03 use the more-precisely-known constraint on the $\overline{p}$ charge-to-mass ratio of GABRIELSE 99 (see below) to get their results. Their results are not independent of the HORI 01 and HORI 03 values for $|q_p + q_{\overline{p}}|/e$, below.

[2] TORII 99 uses the more-precisely-known constraint on the $\overline{p}$ charge-to-mass ratio of GABRIELSE 95 (see below) to get this result. This is not independent of the TORII 99 value for $|q_p + q_{\overline{p}}|/e$, below.

$\overline{p}/p$ CHARGE-TO-MASS RATIO, $\left|\frac{q_{\overline{p}}}{m_{\overline{p}}}\right|/\left(\frac{q_p}{m_p}\right)$

A test of *CPT* invariance. Listed here are measurements involving the *inertial* masses. For a discussion of what may be inferred about the ratio of $\overline{p}$ and p *gravitational* masses, see ERICSON 90; they obtain an upper bound of 10^{-6}–10^{-7} for violation of the equivalence principle for $\overline{p}$s.

VALUE	DOCUMENT ID		TECN	COMMENT
0.99999999991 ± 0.00000000009	GABRIELSE	99	TRAP	Penning trap
• • • We do not use the following data for averages, fits, limits, etc. • • •				
1.0000000015 ± 0.0000000011	[3] GABRIELSE	95	TRAP	Penning trap
1.000000023 ± 0.000000042	[4] GABRIELSE	90	TRAP	Penning trap

[3] Equation (2) of GABRIELSE 95 should read $M(\overline{p})/M(p) = 0.999\,999\,9985\,(11)$ (G. Gabrielse, private communication).

[4] GABRIELSE 90 also measures $m_{\overline{p}}/m_{e^-} = 1836.152660 \pm 0.000083$ and $m_p/m_{e^-} = 1836.152680 \pm 0.000088$. Both are completely consistent with the 1986 CODATA (COHEN 87) value for m_p/m_{e^-} of 1836.152701 ± 0.000037.

$\left(\left|\frac{q_{\overline{p}}}{m_{\overline{p}}}\right| - \frac{q_p}{m_p}\right)/\frac{q_p}{m_p}$

A test of *CPT* invariance. Taken from the $\overline{p}/p$ charge-to-mass ratio, above.

VALUE	DOCUMENT ID
(−9 ± 9) × 10^{-11} OUR EVALUATION	

$|q_p + q_{\overline{p}}|/e$

A test of *CPT* invariance. Note that the comparison of the $\overline{p}$ and p charge-to-mass ratios given above is much better determined. See also a similar test involving the electron.

VALUE	CL%	DOCUMENT ID		TECN	COMMENT
< 1.0 × 10^{-8}	90	[5] HORI	03	SPEC	$\overline{p}e^-$ ^{4}He and $\overline{p}e^-$ ^{3}He
• • • We do not use the following data for averages, fits, limits, etc. • • •					
< 6 × 10^{-8}	90	[5] HORI	01	SPEC	$\overline{p}e^-$ He atom
< 5 × 10^{-7}		[6] TORII	99	SPEC	$\overline{p}e^-$ He atom
< 2 × 10^{-5}		[7] HUGHES	92	RVUE	

[5] HORI 01 and HORI 03 use the more-precisely-known constraint on the $\overline{p}$ charge-to-mass ratio of GABRIELSE 99 (see above) to get their results. Their results are not independent of the HORI 01 and HORI 03 values for $|m_p - m_{\overline{p}}|/m_p$, above.

[6] TORII 99 uses the more-precisely-known constraint on the $\overline{p}$ charge-to-mass ratio of GABRIELSE 95 (see above) to get this result. This is not independent of the TORII 99 value for $|m_p - m_{\overline{p}}|/m_p$, above.

[7] HUGHES 92 uses recent measurements of Rydberg-energy and cyclotron-frequency ratios.

$|q_p + q_e|/e$

See DYLLA 73 for a summary of experiments on the neutrality of matter. See also "*n* CHARGE" in the neutron Listings.

VALUE	DOCUMENT ID		COMMENT
< 1.0 × 10^{-21}	[8] DYLLA	73	Neutrality of SF_6
• • • We do not use the following data for averages, fits, limits, etc. • • •			
< 3.2 × 10^{-20}	[9] SENGUPTA	00	binary pulsar
< 0.8 × 10^{-21}	MARINELLI	84	Magnetic levitation

[8] Assumes that $q_n = q_p + q_e$.

[9] SENGUPTA 00 uses the difference between the observed rate of of rotational energy loss by the binary pulsar PSR B1913+16 and the rate predicted by general relativity to set this limit. See the paper for assumptions.

p MAGNETIC MOMENT

See the "Note on Baryon Magnetic Moments" in the Λ Listings.

VALUE (μ_N)	DOCUMENT ID		TECN	COMMENT
2.79284351 ± 0.00000028	MOHR	04	RVUE	2002 CODATA value
• • • We do not use the following data for averages, fits, limits, etc. • • •				
2.792847337 ± 0.000000029	MOHR	99	RVUE	1998 CODATA value
2.792847386 ± 0.000000063	COHEN	87	RVUE	1986 CODATA value
2.7928456 ± 0.0000011	COHEN	73	RVUE	1973 CODATA value

$\overline{p}$ MAGNETIC MOMENT

A few early results have been omitted.

VALUE (μ_N)	DOCUMENT ID		TECN	COMMENT
−2.800 ± 0.008 OUR AVERAGE				
−2.8005 ± 0.0090	KREISSL	88	CNTR	$\overline{p}$ ^{208}Pb 11→10 X-ray
−2.817 ± 0.048	ROBERTS	78	CNTR	
−2.791 ± 0.021	HU	75	CNTR	Exotic atoms

$(\mu_p + \mu_{\overline{p}})/\mu_p$

A test of *CPT* invariance. Calculated from the p and $\overline{p}$ magnetic moments, above.

VALUE	DOCUMENT ID
(−2.6 ± 2.9) × 10^{-3} OUR EVALUATION	

p ELECTRIC DIPOLE MOMENT

A nonzero value is forbidden by both T invariance and P invariance.

VALUE (10^{-23} ecm)	EVTS	DOCUMENT ID		TECN	COMMENT
< 0.54		[10] DMITRIEV	03		Uses ^{199}Hg atom EDM
• • • We do not use the following data for averages, fits, limits, etc. • • •					
− 3.7 ± 6.3		CHO	89	NMR	Tl F molecules
< 400		DZUBA	85	THEO	Uses ^{129}Xe moment
130 ± 200		[11] WILKENING	84		
900 ± 1400		[12] WILKENING	84		
700 ± 900	1G	HARRISON	69	MBR	Molecular beam

[10] DMITRIEV 03 calculates this limit from the limit on the electric dipole moment of the ^{199}Hg atom.

[11] This WILKENING 84 value includes a finite-size effect and a magnetic effect.

[12] This WILKENING 84 value is more cautious than the other and excludes the finite-size effect, which relies on uncertain nuclear integrals.

Baryon Particle Listings

p

p ELECTRIC POLARIZABILITY α_p

VALUE (10^{-4} fm^3)	DOCUMENT ID		TECN	COMMENT
12.0 ±0.6 OUR AVERAGE				
12.1 ±1.1 ±0.5	[13] BEANE	03		EFT + γp
$11.82 \pm 0.98^{+0.52}_{-0.98}$	[14] BLANPIED	01	LEGS	$p(\vec{\gamma},\gamma)$, $p(\vec{\gamma},\pi^0)$, $p(\vec{\gamma},\pi^+)$
11.9 ±0.5 ±1.3	[15] OLMOSDEL...	01	CNTR	γp Compton scattering
12.1 ±0.8 ±0.5	[16] MACGIBBON	95	RVUE	global average
• • • We do not use the following data for averages, fits, limits, etc. • • •				
11.7 ±0.8 ±0.7	[17] BARANOV	01	RVUE	Global average
12.5 ±0.6 ±0.9	MACGIBBON	95	CNTR	γp Compton scattering
9.8 ±0.4 ±1.1	HALLIN	93	CNTR	γp Compton scattering
$10.62^{+1.25+1.07}_{-1.19-1.03}$	ZIEGER	92	CNTR	γp Compton scattering
10.9 ±2.2 ±1.3	[18] FEDERSPIEL	91	CNTR	γp Compton scattering

[13] BEANE 03 uses effective field theory and low-energy γp and γd Compton-scattering data. It also gets for the isoscalar polarizabilities $\alpha_N = (9.0 \pm 1.5^{+3.6}_{-0.8}) \times 10^{-4}$ fm^3 and $\beta_N = (1.7 \pm 1.5^{+1.4}_{-0.6}) \times 10^{-4}$ fm^3.

[14] BLANPIED 01 gives $\alpha_p + \beta_p$ and $\alpha_p - \beta_p$. The separate α_p and β_p are provided to us by A. Sandorfi. The first error above is statistics plus systematics; the second is from the model.

[15] This OLMOSDELEON 01 result uses the TAPS data alone, and does not use the (re-evaluated) sum-rule constraint that $\alpha + \beta = (13.8 \pm 0.4) \times 10^{-4}$ fm^3. See the paper for a discussion.

[16] MACGIBBON 95 combine the results of ZIEGER 92, FEDERSPIEL 91, and their own experiment to get a "global average" in which model errors and systematic errors are treated in a consistent way. See MACGIBBON 95 for a discussion.

[17] BARANOV 01 combines the results of 10 experiments from 1958 through 1995 to get a global average that takes into account both systematic and model errors and does not use the theoretical constraint on the sum $\alpha_p + \beta_p$.

[18] FEDERSPIEL 91 obtains for the (static) electric polarizability α_p, defined in terms of the induced electric dipole moment by $\mathbf{D} = 4\pi\epsilon_0\alpha_p\mathbf{E}$, the value $(7.0 \pm 2.2 \pm 1.3) \times 10^{-4}$ fm^3.

p MAGNETIC POLARIZABILITY β_p

The electric and magnetic polarizabilities are subject to a dispersion sum-rule constraint $\overline{\alpha} + \overline{\beta} = (14.2 \pm 0.5) \times 10^{-4}$ fm^3. Errors here are anticorrelated with those on $\overline{\alpha}_p$ due to this constraint.

VALUE (10^{-4} fm^3)	DOCUMENT ID		TECN	COMMENT
1.9 ±0.5 OUR AVERAGE				
3.4 ±1.1 ±0.1	[19] BEANE	03		EFT + γp
$1.43 \pm 0.98^{+0.52}_{-0.98}$	[20] BLANPIED	01	LEGS	$p(\vec{\gamma},\gamma)$, $p(\vec{\gamma},\pi^0)$, $p(\vec{\gamma},\pi^+)$
1.2 ±0.7 ±0.5	[21] OLMOSDEL...	01	CNTR	γp Compton scattering
2.1 ±0.8 ±0.5	[22] MACGIBBON	95	RVUE	global average
• • • We do not use the following data for averages, fits, limits, etc. • • •				
2.3 ±0.9 ±0.7	[23] BARANOV	01	RVUE	Global average
1.7 ±0.6 ±0.9	MACGIBBON	95	CNTR	γp Compton scattering
4.4 ±0.4 ±1.1	HALLIN	93	CNTR	γp Compton scattering
$3.58^{+1.19+1.03}_{-1.25-1.07}$	ZIEGER	92	CNTR	γp Compton scattering
3.3 ±2.2 ±1.3	FEDERSPIEL	91	CNTR	γp Compton scattering

[19] BEANE 03 uses effective field theory and low-energy γp and γd Compton-scattering data. It also gets for the isoscalar polarizabilities $\alpha_N = (9.0 \pm 1.5^{+3.6}_{-0.8}) \times 10^{-4}$ fm^3 and $\beta_N = (1.7 \pm 1.5^{+1.4}_{-0.6}) \times 10^{-4}$ fm^3.

[20] BLANPIED 01 gives $\alpha_p + \beta_p$ and $\alpha_p - \beta_p$. The separate α_p and β_p are provided to us by A. Sandorfi. The first error above is statistics plus systematics; the second is from the model.

[21] This OLMOSDELEON 01 result uses the TAPS data alone, and does not use the (re-evaluated) sum-rule constraint that $\alpha + \beta = (13.8 \pm 0.4) \times 10^{-4}$ fm^3. See the paper for a discussion.

[22] MACGIBBON 95 combine the results of ZIEGER 92, FEDERSPIEL 91, and their own experiment to get a "global average" in which model errors and systematic errors are treated in a consistent way. See MACGIBBON 95 for a discussion.

[23] BARANOV 01 combines the results of 10 experiments from 1958 through 1995 to get a global average that takes into account both systematic and model errors and does not use the theoretical constraint on the sum $\alpha_p + \beta_p$.

p CHARGE RADIUS

VALUE (fm)	DOCUMENT ID		COMMENT
0.870±0.008 OUR AVERAGE			
0.830±0.040±0.040	[24] ESCHRICH	01	$ep \to ep$
0.883±0.014	MELNIKOV	00	1S Lamb Shift in H
0.865±0.020	MCCORD	91	$ep \to ep$
0.862±0.012	SIMON	80	$ep \to ep$
0.880±0.030	BORKOWSKI	74	$ep \to ep$
• • • We do not use the following data for averages, fits, limits, etc. • • •			
0.880±0.015	ROSENFELDR...	00	ep + Coul. corrections
0.847±0.008	MERGELL	96	ep + disp. relations
0.877±0.024	WONG	94	reanalysis of Mainz ep data
0.810±0.020	AKIMOV	72	$ep \to ep$
0.800±0.025	FREREJACQ...	66	$ep \to ep$ (CH_2 tgt.)
0.805±0.011	HAND	63	$ep \to ep$

[24] ESCHRICH 01 actually gives $\langle r^2 \rangle = (0.69 \pm 0.06 \pm 0.06)$ fm^2.

p MEAN LIFE

A test of baryon conservation. See the "p Partial Mean Lives" section below for limits for identified final states. The limits here are to "anything" or are for "disappearance" modes of a bound proton (p) or (n). See also the 3ν modes in the "Partial Mean Lives" section. Table 1 of BACK 03 is a nice summary.

LIMIT (years)	PARTICLE	CL%	DOCUMENT ID		TECN	COMMENT
$>2.1 \times 10^{29}$	p	90	[25] AHMED	04	SNO	$p \to$ invisible
$>1.9 \times 10^{29}$	n	90	[25] AHMED	04	SNO	$n \to$ invisible
• • • We do not use the following data for averages, fits, limits, etc. • • •						
$>1.8 \times 10^{25}$	n	90	[26] BACK	03	BORX	
$>1.1 \times 10^{26}$	p	90	[26] BACK	03	BORX	
$>3.5 \times 10^{28}$	p	90	[27] ZDESENKO	03		$p \to$ invisible
$>1 \times 10^{28}$	p	90	[28] AHMAD	02	SNO	$p \to$ invisible
$>4 \times 10^{23}$	p	95	TRETYAK	01		$d \to n$ + ?
$>1.9 \times 10^{24}$	p	90	[29] BERNABEI	00B	DAMA	
$>1.6 \times 10^{25}$	p, n		[30,31] EVANS	77		
$>3 \times 10^{23}$	p		[31] DIX	70	CNTR	
$>3 \times 10^{23}$	p, n		[31,32] FLEROV	58		

[25] AHMED 04 looks for γ rays from the de-excitation of a residual ^{15}O* or ^{15}N* following the disappearance of a neutron or proton in ^{16}O.

[26] BACK 03 looks for decays of unstable nuclides left after N decays of parent ^{12}C, ^{13}C, ^{16}O nuclei. These are "invisible channel" limits.

[27] ZDESENKO 03 gets this limit on proton disappearance in deuterium by analyzing SNO data in AHMAD 02.

[28] AHMAD 02 (see its footnote 7) looks for neutrons left behind after the disappearance of the proton in deuterons.

[29] BERNABEI 00B looks for the decay of a $^{128}_{53}$I nucleus following the disappearance of a proton in the otherwise-stable $^{129}_{54}$Xe nucleus.

[30] EVANS 77 looks for the daughter nuclide ^{129}Xe from possible ^{130}Te decays in ancient Te ore samples.

[31] This mean-life limit has been obtained from a half-life limit by dividing the latter by ln(2) = 0.693.

[32] FLEROV 58 looks for the spontaneous fission of a ^{232}Th nucleus after the disappearance of one of its nucleons.

$\overline{p}$ MEAN LIFE

Of the two astrophysical limits here, that of GEER 00D involves considerably more refinements in its modeling. The other limits come from direct observations of stored antiprotons. See also "$\overline{p}$ Partial Mean Lives" after "p Partial Mean Lives," below, for exclusive-mode limits. The best (lifetime/branching fraction) limit there is 7×10^5 years, for $\overline{p} \to e^-\gamma$. We advance only the exclusive-mode limits to our Summary Tables.

LIMIT (years)	CL%	EVTS	DOCUMENT ID		TECN	COMMENT
• • • We do not use the following data for averages, fits, limits, etc. • • •						
$>8 \times 10^5$	90		[33] GEER	00D		$\overline{p}/p$ ratio, cosmic rays
>0.28			GABRIELSE	90	TRAP	Penning trap
>0.08	90	1	BELL	79	CNTR	Storage ring
$>1 \times 10^7$			GOLDEN	79	SPEC	$\overline{p}/p$ ratio, cosmic rays
$>3.7 \times 10^{-3}$			BREGMAN	78	CNTR	Storage ring

[33] GEER 00D uses agreement between a model of galactic $\overline{p}$ production and propagation and the observed $\overline{p}/p$ cosmic-ray spectrum to set this limit.

p DECAY MODES

See the "Note on Nucleon Decay" in our 1994 edition (Phys. Rev. **D50**, 1673) for a short review.

The "partial mean life" limits tabulated here are the limits on τ/B_i, where τ is the total mean life and B_i is the branching fraction for the mode in question. For N decays, p and n indicate proton and neutron partial lifetimes.

	Mode	Partial mean life (10^{30} years)	Confidence level
	Antilepton + meson		
τ_1	$N \to e^+\pi$	>158 (n), >1600 (p)	90%
τ_2	$N \to \mu^+\pi$	>100 (n), >473 (p)	90%
τ_3	$N \to \nu\pi$	>112 (n), >25 (p)	90%
τ_4	$p \to e^+\eta$	>313	90%
τ_5	$p \to \mu^+\eta$	>126	90%
τ_6	$n \to \nu\eta$	>158	90%
τ_7	$N \to e^+\rho$	>217 (n), >75 (p)	90%
τ_8	$N \to \mu^+\rho$	>228 (n), >110 (p)	90%
τ_9	$N \to \nu\rho$	>19 (n), >162 (p)	90%
τ_{10}	$p \to e^+\omega$	>107	90%
τ_{11}	$p \to \mu^+\omega$	>117	90%
τ_{12}	$n \to \nu\omega$	>108	90%
τ_{13}	$N \to e^+K$	>17 (n), >150 (p)	90%

τ_{14}	$p \to e^+ K^0_S$	> 120	90%
τ_{15}	$p \to e^+ K^0_L$	> 51	90%
τ_{16}	$N \to \mu^+ K$	> 26 (n), > 120 (p)	90%
τ_{17}	$p \to \mu^+ K^0_S$	> 150	90%
τ_{18}	$p \to \mu^+ K^0_L$	> 83	90%
τ_{19}	$N \to \nu K$	> 86 (n), > 670 (p)	90%
τ_{20}	$n \to \nu K^0_S$	> 51	90%
τ_{21}	$p \to e^+ K^*(892)^0$	> 84	90%
τ_{22}	$N \to \nu K^*(892)$	> 78 (n), > 51 (p)	90%

Antilepton + mesons

τ_{23}	$p \to e^+ \pi^+ \pi^-$	> 82	90%
τ_{24}	$p \to e^+ \pi^0 \pi^0$	> 147	90%
τ_{25}	$n \to e^+ \pi^- \pi^0$	> 52	90%
τ_{26}	$p \to \mu^+ \pi^+ \pi^-$	> 133	90%
τ_{27}	$p \to \mu^+ \pi^0 \pi^0$	> 101	90%
τ_{28}	$n \to \mu^+ \pi^- \pi^0$	> 74	90%
τ_{29}	$n \to e^+ K^0 \pi^-$	> 18	90%

Lepton + meson

τ_{30}	$n \to e^- \pi^+$	> 65	90%
τ_{31}	$n \to \mu^- \pi^+$	> 49	90%
τ_{32}	$n \to e^- \rho^+$	> 62	90%
τ_{33}	$n \to \mu^- \rho^+$	> 7	90%
τ_{34}	$n \to e^- K^+$	> 32	90%
τ_{35}	$n \to \mu^- K^+$	> 57	90%

Lepton + mesons

τ_{36}	$p \to e^- \pi^+ \pi^+$	> 30	90%
τ_{37}	$n \to e^- \pi^+ \pi^0$	> 29	90%
τ_{38}	$p \to \mu^- \pi^+ \pi^+$	> 17	90%
τ_{39}	$n \to \mu^- \pi^+ \pi^0$	> 34	90%
τ_{40}	$p \to e^- \pi^+ K^+$	> 75	90%
τ_{41}	$p \to \mu^- \pi^+ K^+$	> 245	90%

Antilepton + photon(s)

τ_{42}	$p \to e^+ \gamma$	> 670	90%
τ_{43}	$p \to \mu^+ \gamma$	> 478	90%
τ_{44}	$n \to \nu \gamma$	> 28	90%
τ_{45}	$p \to e^+ \gamma \gamma$	> 100	90%
τ_{46}	$n \to \nu \gamma \gamma$	> 219	90%

Three (or more) leptons

τ_{47}	$p \to e^+ e^+ e^-$	> 793	90%
τ_{48}	$p \to e^+ \mu^+ \mu^-$	> 359	90%
τ_{49}	$p \to e^+ \nu \nu$	> 17	90%
τ_{50}	$n \to e^+ e^- \nu$	> 257	90%
τ_{51}	$n \to \mu^+ e^- \nu$	> 83	90%
τ_{52}	$n \to \mu^+ \mu^- \nu$	> 79	90%
τ_{53}	$p \to \mu^+ e^+ e^-$	> 529	90%
τ_{54}	$p \to \mu^+ \mu^+ \mu^-$	> 675	90%
τ_{55}	$p \to \mu^+ \nu \nu$	> 21	90%
τ_{56}	$p \to e^- \mu^+ \mu^+$	> 6	90%
τ_{57}	$n \to 3\nu$	> 0.0005	90%
τ_{58}	$n \to 5\nu$		

Inclusive modes

τ_{59}	$N \to e^+$ anything	> 0.6 (n, p)	90%
τ_{60}	$N \to \mu^+$ anything	> 12 (n, p)	90%
τ_{61}	$N \to \nu$ anything		
τ_{62}	$N \to e^+ \pi^0$ anything	> 0.6 (n, p)	90%
τ_{63}	$N \to$ 2 bodies, ν-free		

$\Delta B = 2$ dinucleon modes

The following are lifetime limits per iron nucleus.

τ_{64}	$pp \to \pi^+ \pi^+$	> 0.7	90%
τ_{65}	$pn \to \pi^+ \pi^0$	> 2	90%
τ_{66}	$nn \to \pi^+ \pi^-$	> 0.7	90%
τ_{67}	$nn \to \pi^0 \pi^0$	> 3.4	90%
τ_{68}	$pp \to e^+ e^+$	> 5.8	90%
τ_{69}	$pp \to e^+ \mu^+$	> 3.6	90%
τ_{70}	$pp \to \mu^+ \mu^+$	> 1.7	90%
τ_{71}	$pn \to e^+ \overline{\nu}$	> 2.8	90%
τ_{72}	$pn \to \mu^+ \overline{\nu}$	> 1.6	90%
τ_{73}	$nn \to \nu_e \overline{\nu}_e$	> 0.000049	90%
τ_{74}	$nn \to \nu_\mu \overline{\nu}_\mu$		
τ_{75}	$pp \to$ neutrinos	> 0.00005	90%

$\overline{p}$ DECAY MODES

	Mode	Partial mean life (years)	Confidence level
τ_{76}	$\overline{p} \to e^- \gamma$	$> 7 \times 10^5$	90%
τ_{77}	$\overline{p} \to \mu^- \gamma$	$> 5 \times 10^4$	90%
τ_{78}	$\overline{p} \to e^- \pi^0$	$> 4 \times 10^5$	90%
τ_{79}	$\overline{p} \to \mu^- \pi^0$	$> 5 \times 10^4$	90%
τ_{80}	$\overline{p} \to e^- \eta$	$> 2 \times 10^4$	90%
τ_{81}	$\overline{p} \to \mu^- \eta$	$> 8 \times 10^3$	90%
τ_{82}	$\overline{p} \to e^- K^0_S$	> 900	90%
τ_{83}	$\overline{p} \to \mu^- K^0_S$	$> 4 \times 10^3$	90%
τ_{84}	$\overline{p} \to e^- K^0_L$	$> 9 \times 10^3$	90%
τ_{85}	$\overline{p} \to \mu^- K^0_L$	$> 7 \times 10^3$	90%
τ_{86}	$\overline{p} \to e^- \gamma \gamma$	$> 2 \times 10^4$	90%
τ_{87}	$\overline{p} \to \mu^- \gamma \gamma$	$> 2 \times 10^4$	90%
τ_{88}	$\overline{p} \to e^- \rho$		
τ_{89}	$\overline{p} \to e^- \omega$	> 200	90%
τ_{90}	$\overline{p} \to e^- K^*(892)^0$		

p PARTIAL MEAN LIVES

The "partial mean life" limits tabulated here are the limits on τ / B_i, where τ is the total mean life for the proton and B_i is the branching fraction for the mode in question.

Decaying particle: p = proton, n = bound neutron. The same event may appear under more than one partial decay mode. Background estimates may be accurate to a factor of two.

Antilepton + meson

$\tau(N \to e^+ \pi)$ τ_1

LIMIT (10^{30} years)	PARTICLE	CL%	EVTS	BKGD EST	DOCUMENT ID		TECN
> 158	***n***	**90**	**3**	**5**	MCGREW	99	IMB3
>1600	***p***	**90**	**0**	**0.1**	SHIOZAWA	98	SKAM
• • • We do not use the following data for averages, fits, limits, etc. • • •							
> 540	p	90	0	0.2	MCGREW	99	IMB3
> 70	p	90	0	0.5	BERGER	91	FREJ
> 70	n	90	0	≤ 0.1	BERGER	91	FREJ
> 550	p	90	0	0.7	[34] BECKER-SZ...	90	IMB3
> 260	p	90	0	<0.04	HIRATA	89C	KAMI
> 130	n	90	0	<0.2	HIRATA	89C	KAMI
> 310	p	90	0	0.6	SEIDEL	88	IMB
> 100	n	90	0	1.6	SEIDEL	88	IMB
> 1.3	n	90	0		BARTELT	87	SOUD
> 1.3	p	90	0		BARTELT	87	SOUD
> 250	p	90	0	0.3	HAINES	86	IMB
> 31	n	90	8	9	HAINES	86	IMB
> 64	p	90	0	<0.4	ARISAKA	85	KAMI
> 26	n	90	0	<0.7	ARISAKA	85	KAMI
> 82	p (free)	90	0	0.2	BLEWITT	85	IMB
> 250	p	90	0	0.2	BLEWITT	85	IMB
> 25	n	90	4	4	PARK	85	IMB
> 15	p, n	90	0		BATTISTONI	84	NUSX
> 0.5	p	90	1	0.3	[35] BARTELT	83	SOUD
> 0.5	n	90	1	0.3	[35] BARTELT	83	SOUD
> 5.8	p	90	2		[36] KRISHNA...	82	KOLR
> 5.8	n	90	2		[36] KRISHNA...	82	KOLR
> 0.1	n	90			[37] GURR	67	CNTR

[34] This BECKER-SZENDY 90 result includes data from SEIDEL 88.
[35] Limit based on zero events.
[36] We have calculated 90% CL limit from 1 confined event.
[37] We have converted half-life to 90% CL mean life.

$\tau(N \to \mu^+ \pi)$ τ_2

LIMIT (10^{30} years)	PARTICLE	CL%	EVTS	BKGD EST	DOCUMENT ID		TECN
>473	***p***	**90**	**0**	**0.6**	MCGREW	99	IMB3
>100	***n***	**90**	**0**	**<0.2**	HIRATA	89C	KAMI
• • • We do not use the following data for averages, fits, limits, etc. • • •							
> 90	n	90	1	1.9	MCGREW	99	IMB3
> 81	p	90	0	0.2	BERGER	91	FREJ
> 35	n	90	1	1.0	BERGER	91	FREJ
>230	p	90	0	<0.07	HIRATA	89C	KAMI
>270	p	90	0	0.5	SEIDEL	88	IMB
> 63	n	90	0	0.5	SEIDEL	88	IMB
> 76	p	90	2	1	HAINES	86	IMB
> 23	n	90	8	7	HAINES	86	IMB
> 46	p	90	0	<0.7	ARISAKA	85	KAMI
> 20	n	90	0	<0.4	ARISAKA	85	KAMI
> 59	p (free)	90	0	0.2	BLEWITT	85	IMB
>100	p	90	1	0.4	BLEWITT	85	IMB
> 38	n	90	1	4	PARK	85	IMB
> 10	p, n	90	0		BATTISTONI	84	NUSX
> 1.3	p, n	90	0		ALEKSEEV	81	BAKS

$\tau(N \to \nu\pi)$ τ_3

LIMIT (10^{30} years)	PARTICLE	CL%	EVTS	BKGD EST	DOCUMENT ID		TECN
> 16	***p***	**90**	**6**	**6.7**	WALL	00B	SOU2
>112	***n***	**90**	**6**	**6.6**	MCGREW	99	IMB3
• • • We do not use the following data for averages, fits, limits, etc. • • •							
> 39	*n*	90	4	3.8	WALL	00B	SOU2
> 10	*p*	90	15	20.3	MCGREW	99	IMB3
> 13	*n*	90	1	1.2	BERGER	89	FREJ
> 10	*p*	90	11	14	BERGER	89	FREJ
> 25	*p*	90	32	32.8	[38] HIRATA	89C	KAMI
>100	*n*	90	1	3	HIRATA	89C	KAMI
> 6	*n*	90	73	60	HAINES	86	IMB
> 2	*p*	90	16	13	KAJITA	86	KAMI
> 40	*n*	90	0	1	KAJITA	86	KAMI
> 7	*n*	90	28	19	PARK	85	IMB
> 7	*n*	90	0		BATTISTONI	84	NUSX
> 2	*p*	90	$\leq$ 3		BATTISTONI	84	NUSX
> 5.8	*p*	90	1		[39] KRISHNA...	82	KOLR
> 0.3	*p*	90	2		[40] CHERRY	81	HOME
> 0.1	*p*	90			[41] GURR	67	CNTR

[38] In estimating the background, this HIRATA 89C limit (as opposed to the later limits of WALL 00B and MCGREW 99) does not take into account present understanding that the flux of ν_μ originating in the upper atmosphere is depleted. Doing so would reduce the limit here.
[39] We have calculated 90% CL limit from 1 confined event.
[40] We have converted 2 possible events to 90% CL limit.
[41] We have converted half-life to 90% CL mean life.

$\tau(p \to e^+\eta)$ τ_4

LIMIT (10^{30} years)	PARTICLE	CL%	EVTS	BKGD EST	DOCUMENT ID		TECN
>313	***p***	**90**	**0**	**0.2**	MCGREW	99	IMB3
• • • We do not use the following data for averages, fits, limits, etc. • • •							
> 81	*p*	90	1	1.7	WALL	00B	SOU2
> 44	*p*	90	0	0.1	BERGER	91	FREJ
>140	*p*	90	0	<0.04	HIRATA	89C	KAMI
>100	*p*	90	0	0.6	SEIDEL	88	IMB
>200	*p*	90	5	3.3	HAINES	86	IMB
> 64	*p*	90	0	<0.8	ARISAKA	85	KAMI
> 64	*p* (free)	90	5	6.5	BLEWITT	85	IMB
>200	*p*	90	5	4.7	BLEWITT	85	IMB
> 1.2	*p*	90	2		[42] CHERRY	81	HOME

[42] We have converted 2 possible events to 90% CL limit.

$\tau(p \to \mu^+\eta)$ τ_5

LIMIT (10^{30} years)	PARTICLE	CL%	EVTS	BKGD EST	DOCUMENT ID		TECN
>126	***p***	**90**	**3**	**2.8**	MCGREW	99	IMB3
• • • We do not use the following data for averages, fits, limits, etc. • • •							
> 89	*p*	90	0	1.6	WALL	00B	SOU2
> 26	*p*	90	1	0.8	BERGER	91	FREJ
> 69	*p*	90	1	<0.08	HIRATA	89C	KAMI
> 1.3	*p*	90	0	0.7	PHILLIPS	89	HPW
> 34	*p*	90	1	1.5	SEIDEL	88	IMB
> 46	*p*	90	7	6	HAINES	86	IMB
> 26	*p*	90	1	<0.8	ARISAKA	85	KAMI
> 17	*p* (free)	90	6	6	BLEWITT	85	IMB
> 46	*p*	90	7	8	BLEWITT	85	IMB

$\tau(n \to \nu\eta)$ τ_6

LIMIT (10^{30} years)	PARTICLE	CL%	EVTS	BKGD EST	DOCUMENT ID		TECN
>158	***n***	**90**	**0**	**1.2**	MCGREW	99	IMB3
• • • We do not use the following data for averages, fits, limits, etc. • • •							
> 71	*n*	90	2	3.7	WALL	00B	SOU2
> 29	*n*	90	0	0.9	BERGER	89	FREJ
> 54	*n*	90	2	0.9	HIRATA	89C	KAMI
> 16	*n*	90	3	2.1	SEIDEL	88	IMB
> 25	*n*	90	7	6	HAINES	86	IMB
> 30	*n*	90	0	0.4	KAJITA	86	KAMI
> 18	*n*	90	4	3	PARK	85	IMB
> 0.6	*n*	90	2		[43] CHERRY	81	HOME

[43] We have converted 2 possible events to 90% CL limit.

$\tau(N \to e^+\rho)$ τ_7

LIMIT (10^{30} years)	PARTICLE	CL%	EVTS	BKGD EST	DOCUMENT ID		TECN
>217	***n***	**90**	**4**	**4.8**	MCGREW	99	IMB3
> 75	***p***	**90**	**2**	**2.7**	HIRATA	89C	KAMI
• • • We do not use the following data for averages, fits, limits, etc. • • •							
> 29	*p*	90	0	2.2	BERGER	91	FREJ
> 41	*n*	90	0	1.4	BERGER	91	FREJ
> 58	*n*	90	0	1.9	HIRATA	89C	KAMI
> 38	*n*	90	2	4.1	SEIDEL	88	IMB
> 1.2	*p*	90	0		BARTELT	87	SOUD
> 1.5	*n*	90	0		BARTELT	87	SOUD
> 17	*p*	90	7	7	HAINES	86	IMB
> 14	*n*	90	9	4	HAINES	86	IMB
> 12	*p*	90	0	<1.2	ARISAKA	85	KAMI
> 6	*n*	90	2	<1	ARISAKA	85	KAMI
> 6.7	*p* (free)	90	6	6	BLEWITT	85	IMB
> 17	*p*	90	7	7	BLEWITT	85	IMB
> 12	*n*	90	4	2	PARK	85	IMB
> 0.6	*n*	90	1	0.3	[44] BARTELT	83	SOUD
> 0.5	*p*	90	1	0.3	[44] BARTELT	83	SOUD
> 9.8	*p*	90	1		[45] KRISHNA...	82	KOLR
> 0.8	*p*	90	2		[46] CHERRY	81	HOME

[44] Limit based on zero events.
[45] We have calculated 90% CL limit from 0 confined events.
[46] We have converted 2 possible events to 90% CL limit.

$\tau(N \to \mu^+\rho)$ τ_8

LIMIT (10^{30} years)	PARTICLE	CL%	EVTS	BKGD EST	DOCUMENT ID		TECN
>228	***n***	**90**	**3**	**9.5**	MCGREW	99	IMB3
>110	***p***	**90**	**0**	**1.7**	HIRATA	89C	KAMI
• • • We do not use the following data for averages, fits, limits, etc. • • •							
> 12	*p*	90	0	0.5	BERGER	91	FREJ
> 22	*n*	90	0	1.1	BERGER	91	FREJ
> 23	*n*	90	1	1.8	HIRATA	89C	KAMI
> 4.3	*p*	90	0	0.7	PHILLIPS	89	HPW
> 30	*p*	90	0	0.5	SEIDEL	88	IMB
> 11	*n*	90	1	1.1	SEIDEL	88	IMB
> 16	*p*	90	4	4.5	HAINES	86	IMB
> 7	*n*	90	6	5	HAINES	86	IMB
> 12	*p*	90	0	<0.7	ARISAKA	85	KAMI
> 5	*n*	90	1	<1.2	ARISAKA	85	KAMI
> 5.5	*p* (free)	90	4	5	BLEWITT	85	IMB
> 16	*p*	90	4	5	BLEWITT	85	IMB
> 9	*n*	90	1	2	PARK	85	IMB

$\tau(N \to \nu\rho)$ τ_9

LIMIT (10^{30} years)	PARTICLE	CL%	EVTS	BKGD EST	DOCUMENT ID		TECN
>162	***p***	**90**	**18**	**21.7**	MCGREW	99	IMB3
> 19	***n***	**90**	**0**	**0.5**	SEIDEL	88	IMB
• • • We do not use the following data for averages, fits, limits, etc. • • •							
> 9	*n*	90	4	2.4	BERGER	89	FREJ
> 24	*p*	90	0	0.9	BERGER	89	FREJ
> 27	*p*	90	5	1.5	HIRATA	89C	KAMI
> 13	*n*	90	4	3.6	HIRATA	89C	KAMI
> 13	*p*	90	1	1.1	SEIDEL	88	IMB
> 8	*p*	90	6	5	HAINES	86	IMB
> 2	*n*	90	15	10	HAINES	86	IMB
> 11	*p*	90	2	1	KAJITA	86	KAMI
> 4	*n*	90	2	2	KAJITA	86	KAMI
> 4.1	*p* (free)	90	6	7	BLEWITT	85	IMB
> 8.4	*p*	90	6	5	BLEWITT	85	IMB
> 2	*n*	90	7	3	PARK	85	IMB
> 0.9	*p*	90	2		[47] CHERRY	81	HOME
> 0.6	*n*	90	2		[47] CHERRY	81	HOME

[47] We have converted 2 possible events to 90% CL limit.

$\tau(p \to e^+\omega)$ τ_{10}

LIMIT (10^{30} years)	PARTICLE	CL%	EVTS	BKGD EST	DOCUMENT ID		TECN
>107	***p***	**90**	**7**	**10.8**	MCGREW	99	IMB3
• • • We do not use the following data for averages, fits, limits, etc. • • •							
> 17	*p*	90	0	1.1	BERGER	91	FREJ
> 45	*p*	90	2	1.45	HIRATA	89C	KAMI
> 26	*p*	90	1	1.0	SEIDEL	88	IMB
> 1.5	*p*	90	0		BARTELT	87	SOUD
> 37	*p*	90	6	5.3	HAINES	86	IMB
> 25	*p*	90	1	<1.4	ARISAKA	85	KAMI
> 12	*p* (free)	90	6	7.5	BLEWITT	85	IMB
> 37	*p*	90	6	5.7	BLEWITT	85	IMB
> 0.6	*p*	90	1	0.3	[48] BARTELT	83	SOUD
> 9.8	*p*	90	1		[49] KRISHNA...	82	KOLR
> 2.8	*p*	90	2		[50] CHERRY	81	HOME

[48] Limit based on zero events.
[49] We have calculated 90% CL limit from 0 confined events.
[50] We have converted 2 possible events to 90% CL limit.

$\tau(p \to \mu^+ \omega)$ τ_{11}

LIMIT (10^{30} years)	PARTICLE	CL%	EVTS	BKGD EST	DOCUMENT ID		TECN
>117	**p**	**90**	**11**	**12.1**	MCGREW	99	IMB3
• • • We do not use the following data for averages, fits, limits, etc. • • •							
> 11	p	90	0	1.0	BERGER	91	FREJ
> 57	p	90	2	1.9	HIRATA	89C	KAMI
> 4.4	p	90	0	0.7	PHILLIPS	89	HPW
> 10	p	90	2	1.3	SEIDEL	88	IMB
> 23	p	90	2	1	HAINES	86	IMB
> 6.5	p (free)	90	9	8.7	BLEWITT	85	IMB
> 23	p	90	8	7	BLEWITT	85	IMB

$\tau(n \to \nu \omega)$ τ_{12}

LIMIT (10^{30} years)	PARTICLE	CL%	EVTS	BKGD EST	DOCUMENT ID		TECN
>108	**n**	**90**	**12**	**22.5**	MCGREW	99	IMB3
• • • We do not use the following data for averages, fits, limits, etc. • • •							
> 17	n	90	1	0.7	BERGER	89	FREJ
> 43	n	90	3	2.7	HIRATA	89C	KAMI
> 6	n	90	2	1.3	SEIDEL	88	IMB
> 12	n	90	6	6	HAINES	86	IMB
> 18	n	90	2	2	KAJITA	86	KAMI
> 16	n	90	1	2	PARK	85	IMB
> 2.0	n	90	2		[51] CHERRY	81	HOME

[51] We have converted 2 possible events to 90% CL limit.

$\tau(N \to e^+ K)$ τ_{13}

LIMIT (10^{30} years)	PARTICLE	CL%	EVTS	BKGD EST	DOCUMENT ID		TECN
> 17	**n**	**90**	**35**	**29.4**	MCGREW	99	IMB3
>150	**p**	**90**	**0**	**<0.27**	HIRATA	89C	KAMI
• • • We do not use the following data for averages, fits, limits, etc. • • •							
> 85	p	90	3	4.9	WALL	00	SOU2
> 31	p	90	23	25.2	MCGREW	99	IMB3
> 60	p	90	0		BERGER	91	FREJ
> 70	p	90	0	1.8	SEIDEL	88	IMB
> 77	p	90	5	4.5	HAINES	86	IMB
> 38	p	90	0	<0.8	ARISAKA	85	KAMI
> 24	p (free)	90	7	8.5	BLEWITT	85	IMB
> 77	p	90	5	4	BLEWITT	85	IMB
> 1.3	p	90	0		ALEKSEEV	81	BAKS
> 1.3	n	90	0		ALEKSEEV	81	BAKS

$\tau(p \to e^+ K^0_S)$ τ_{14}

LIMIT (10^{30} years)	PARTICLE	CL%	EVTS	BKGD EST	DOCUMENT ID		TECN
>120	**p**	**90**	**1**	**1.3**	WALL	00	SOU2
• • • We do not use the following data for averages, fits, limits, etc. • • •							
> 76	p	90	0	0.5	BERGER	91	FREJ

$\tau(p \to e^+ K^0_L)$ τ_{15}

LIMIT (10^{30} years)	PARTICLE	CL%	EVTS	BKGD EST	DOCUMENT ID		TECN
>51	**p**	**90**	**2**	**3.5**	WALL	00	SOU2
• • • We do not use the following data for averages, fits, limits, etc. • • •							
>44	p	90	0	≤ 0.1	BERGER	91	FREJ

$\tau(N \to \mu^+ K)$ τ_{16}

LIMIT (10^{30} years)	PARTICLE	CL%	EVTS	BKGD EST	DOCUMENT ID		TECN
>120	**p**	**90**	**0**	**<1.2**	WALL	00	SOU2
>120	**p**	**90**	**4**	**7.2**	MCGREW	99	IMB3
> 26	**n**	**90**	**20**	**28.4**	MCGREW	99	IMB3
>120	**p**	**90**	**1**	**0.4**	HIRATA	89C	KAMI
• • • We do not use the following data for averages, fits, limits, etc. • • •							
> 54	p	90	0		BERGER	91	FREJ
> 3.0	p	90	0	0.7	PHILLIPS	89	HPW
> 19	p	90	3	2.5	SEIDEL	88	IMB
> 1.5	p	90	0		[52] BARTELT	87	SOUD
> 1.1	n	90	0		BARTELT	87	SOUD
> 40	p	90	7	6	HAINES	86	IMB
> 19	p	90	1	<1.1	ARISAKA	85	KAMI
> 6.7	p (free)	90	11	13	BLEWITT	85	IMB
> 40	p	90	7	8	BLEWITT	85	IMB
> 6	p	90	1		BATTISTONI	84	NUSX
> 0.6	p	90	0		[53] BARTELT	83	SOUD
> 0.4	n	90	0		[53] BARTELT	83	SOUD
> 5.8	p	90	2		[54] KRISHNA...	82	KOLR
> 2.0	p	90	0		CHERRY	81	HOME
> 0.2	n	90			[55] GURR	67	CNTR

[52] BARTELT 87 limit applies to $p \to \mu^+ K^0_S$.

[53] Limit based on zero events.

[54] We have calculated 90% CL limit from 1 confined event.

[55] We have converted half-life to 90% CL mean life.

$\tau(p \to \mu^+ K^0_S)$ τ_{17}

LIMIT (10^{30} years)	PARTICLE	CL%	EVTS	BKGD EST	DOCUMENT ID		TECN
>150	**p**	**90**	**0**	**<0.8**	WALL	00	SOU2
• • • We do not use the following data for averages, fits, limits, etc. • • •							
> 64	p	90	0	1.2	BERGER	91	FREJ

$\tau(p \to \mu^+ K^0_L)$ τ_{18}

LIMIT (10^{30} years)	PARTICLE	CL%	EVTS	BKGD EST	DOCUMENT ID		TECN
>83	**p**	**90**	**0**	**0.4**	WALL	00	SOU2
• • • We do not use the following data for averages, fits, limits, etc. • • •							
>44	p	90	0	≤ 0.1	BERGER	91	FREJ

$\tau(N \to \nu K)$ τ_{19}

LIMIT (10^{30} years)	PARTICLE	CL%	EVTS	BKGD EST	DOCUMENT ID		TECN
>670	**p**	**90**			HAYATO	99	SKAM
> 86	**n**	**90**	**0**	**2.4**	HIRATA	89C	KAMI
• • • We do not use the following data for averages, fits, limits, etc. • • •							
> 26	n	90	16	9.1	WALL	00	SOU2
>151	p	90	15	21.4	MCGREW	99	IMB3
> 30	n	90	34	34.1	MCGREW	99	IMB3
> 43	p	90	1	1.54	[56] ALLISON	98	SOU2
> 15	n	90	1	1.8	BERGER	89	FREJ
> 15	p	90	1	1.8	BERGER	89	FREJ
>100	p	90	9	7.3	HIRATA	89C	KAMI
> 0.28	p	90	0	0.7	PHILLIPS	89	HPW
> 0.3	p	90	0		BARTELT	87	SOUD
> 0.75	n	90	0		[57] BARTELT	87	SOUD
> 10	p	90	6	5	HAINES	86	IMB
> 15	n	90	3	5	HAINES	86	IMB
> 28	p	90	3	3	KAJITA	86	KAMI
> 32	n	90	0	1.4	KAJITA	86	KAMI
> 1.8	p (free)	90	6	11	BLEWITT	85	IMB
> 9.6	p	90	6	5	BLEWITT	85	IMB
> 10	n	90	2	2	PARK	85	IMB
> 5	n	90	0		BATTISTONI	84	NUSX
> 2	p	90	0		BATTISTONI	84	NUSX
> 0.3	n	90	0		[58] BARTELT	83	SOUD
> 0.1	p	90	0		[58] BARTELT	83	SOUD
> 5.8	p	90	1		[59] KRISHNA...	82	KOLR
> 0.3	n	90	2		[60] CHERRY	81	HOME

[56] This ALLISON 98 limit is with no background subtraction; with subtraction the limit becomes $> 46 \times 10^{30}$ years.

[57] BARTELT 87 limit applies to $n \to \nu K^0_S$.

[58] Limit based on zero events.

[59] We have calculated 90% CL limit from 1 confined event.

[60] We have converted 2 possible events to 90% CL limit.

$\tau(n \to \nu K^0_S)$ τ_{20}

LIMIT (10^{30} years)	PARTICLE	CL%	EVTS	BKGD EST	DOCUMENT ID		TECN
>51	**n**	**90**	**16**	**9.1**	WALL	00	SOU2

$\tau(p \to e^+ K^*(892)^0)$ τ_{21}

LIMIT (10^{30} years)	PARTICLE	CL%	EVTS	BKGD EST	DOCUMENT ID		TECN
>84	**p**	**90**	**38**	**52.0**	MCGREW	99	IMB3
• • • We do not use the following data for averages, fits, limits, etc. • • •							
>10	p	90	0	0.8	BERGER	91	FREJ
>52	p	90	2	1.55	HIRATA	89C	KAMI
>10	p	90	1	<1	ARISAKA	85	KAMI

$\tau(N \to \nu K^*(892))$ τ_{22}

LIMIT (10^{30} years)	PARTICLE	CL%	EVTS	BKGD EST	DOCUMENT ID		TECN
>51	**p**	**90**	**7**	**9.1**	MCGREW	99	IMB3
>78	**n**	**90**	**40**	**50**	MCGREW	99	IMB3
• • • We do not use the following data for averages, fits, limits, etc. • • •							
>22	n	90	0	2.1	BERGER	89	FREJ
>17	p	90	0	2.4	BERGER	89	FREJ
>20	p	90	5	2.1	HIRATA	89C	KAMI
>21	n	90	4	2.4	HIRATA	89C	KAMI
>10	p	90	7	6	HAINES	86	IMB
> 5	n	90	8	7	HAINES	86	IMB
> 8	p	90	3	2	KAJITA	86	KAMI
> 6	n	90	2	1.6	KAJITA	86	KAMI
> 5.8	p (free)	90	10	16	BLEWITT	85	IMB
> 9.6	p	90	7	6	BLEWITT	85	IMB
> 7	n	90	1	4	PARK	85	IMB
> 2.1	p	90	1		[61] BATTISTONI	82	NUSX

[61] We have converted 1 possible event to 90% CL limit.

Antilepton + mesons

$\tau(p \to e^+\pi^+\pi^-)$ τ_{23}

LIMIT (10^{30} years)	PARTICLE	CL%	EVTS	BKGD EST	DOCUMENT ID		TECN
>82	**p**	**90**	**16**	**23.1**	MCGREW	99	IMB3
• • • We do not use the following data for averages, fits, limits, etc. • • •							
>21	p	90	0	2.2	BERGER	91	FREJ

$\tau(p \to e^+\pi^0\pi^0)$ τ_{24}

LIMIT (10^{30} years)	PARTICLE	CL%	EVTS	BKGD EST	DOCUMENT ID		TECN
>147	**p**	**90**	**2**	**0.8**	MCGREW	99	IMB3
• • • We do not use the following data for averages, fits, limits, etc. • • •							
> 38	p	90	1	0.5	BERGER	91	FREJ

$\tau(n \to e^+\pi^-\pi^0)$ τ_{25}

LIMIT (10^{30} years)	PARTICLE	CL%	EVTS	BKGD EST	DOCUMENT ID		TECN
>52	**n**	**90**	**38**	**34.2**	MCGREW	99	IMB3
• • • We do not use the following data for averages, fits, limits, etc. • • •							
>32	n	90	1	0.8	BERGER	91	FREJ

$\tau(p \to \mu^+\pi^+\pi^-)$ τ_{26}

LIMIT (10^{30} years)	PARTICLE	CL%	EVTS	BKGD EST	DOCUMENT ID		TECN
>133	**p**	**90**	**25**	**38.0**	MCGREW	99	IMB3
• • • We do not use the following data for averages, fits, limits, etc. • • •							
> 17	p	90	1	2.6	BERGER	91	FREJ
> 3.3	p	90	0	0.7	PHILLIPS	89	HPW

$\tau(p \to \mu^+\pi^0\pi^0)$ τ_{27}

LIMIT (10^{30} years)	PARTICLE	CL%	EVTS	BKGD EST	DOCUMENT ID		TECN
>101	**p**	**90**	**3**	**1.6**	MCGREW	99	IMB3
• • • We do not use the following data for averages, fits, limits, etc. • • •							
> 33	p	90	1	0.9	BERGER	91	FREJ

$\tau(n \to \mu^+\pi^-\pi^0)$ τ_{28}

LIMIT (10^{30} years)	PARTICLE	CL%	EVTS	BKGD EST	DOCUMENT ID		TECN
>74	**n**	**90**	**17**	**20.8**	MCGREW	99	IMB3
• • • We do not use the following data for averages, fits, limits, etc. • • •							
>33	n	90	0	1.1	BERGER	91	FREJ

$\tau(n \to e^+K^0\pi^-)$ τ_{29}

LIMIT (10^{30} years)	PARTICLE	CL%	EVTS	BKGD EST	DOCUMENT ID		TECN
>18	**n**	**90**	**1**	**0.2**	BERGER	91	FREJ

Lepton + meson

$\tau(n \to e^-\pi^+)$ τ_{30}

LIMIT (10^{30} years)	PARTICLE	CL%	EVTS	BKGD EST	DOCUMENT ID		TECN
>65	**n**	**90**	**0**	**1.6**	SEIDEL	88	IMB
• • • We do not use the following data for averages, fits, limits, etc. • • •							
>55	n	90	0	1.09	BERGER	91B	FREJ
>16	n	90	9	7	HAINES	86	IMB
>25	n	90	2	4	PARK	85	IMB

$\tau(n \to \mu^-\pi^+)$ τ_{31}

LIMIT (10^{30} years)	PARTICLE	CL%	EVTS	BKGD EST	DOCUMENT ID		TECN
>49	**n**	**90**	**0**	**0.5**	SEIDEL	88	IMB
• • • We do not use the following data for averages, fits, limits, etc. • • •							
>33	n	90	0	1.40	BERGER	91B	FREJ
> 2.7	n	90	0	0.7	PHILLIPS	89	HPW
>25	n	90	7	6	HAINES	86	IMB
>27	n	90	2	3	PARK	85	IMB

$\tau(n \to e^-\rho^+)$ τ_{32}

LIMIT (10^{30} years)	PARTICLE	CL%	EVTS	BKGD EST	DOCUMENT ID		TECN
>62	**n**	**90**	**2**	**4.1**	SEIDEL	88	IMB
• • • We do not use the following data for averages, fits, limits, etc. • • •							
>12	n	90	13	6	HAINES	86	IMB
>12	n	90	5	3	PARK	85	IMB

$\tau(n \to \mu^-\rho^+)$ τ_{33}

LIMIT (10^{30} years)	PARTICLE	CL%	EVTS	BKGD EST	DOCUMENT ID		TECN
>7	**n**	**90**	**1**	**1.1**	SEIDEL	88	IMB
• • • We do not use the following data for averages, fits, limits, etc. • • •							
>2.6	n	90	0	0.7	PHILLIPS	89	HPW
>9	n	90	7	5	HAINES	86	IMB
>9	n	90	2	2	PARK	85	IMB

$\tau(n \to e^-K^+)$ τ_{34}

LIMIT (10^{30} years)	PARTICLE	CL%	EVTS	BKGD EST	DOCUMENT ID		TECN
>32	**n**	**90**	**3**	**2.96**	BERGER	91B	FREJ
• • • We do not use the following data for averages, fits, limits, etc. • • •							
> 0.23	n	90	0	0.7	PHILLIPS	89	HPW

$\tau(n \to \mu^-K^+)$ τ_{35}

LIMIT (10^{30} years)	PARTICLE	CL%	EVTS	BKGD EST	DOCUMENT ID		TECN
>57	**n**	**90**	**0**	**2.18**	BERGER	91B	FREJ
• • • We do not use the following data for averages, fits, limits, etc. • • •							
> 4.7	n	90	0	0.7	PHILLIPS	89	HPW

Lepton + mesons

$\tau(p \to e^-\pi^+\pi^+)$ τ_{36}

LIMIT (10^{30} years)	PARTICLE	CL%	EVTS	BKGD EST	DOCUMENT ID		TECN
>30	**p**	**90**	**1**	**2.50**	BERGER	91B	FREJ
• • • We do not use the following data for averages, fits, limits, etc. • • •							
> 2.0	p	90	0	0.7	PHILLIPS	89	HPW

$\tau(n \to e^-\pi^+\pi^0)$ τ_{37}

LIMIT (10^{30} years)	PARTICLE	CL%	EVTS	BKGD EST	DOCUMENT ID		TECN
>29	**n**	**90**	**1**	**0.78**	BERGER	91B	FREJ

$\tau(p \to \mu^-\pi^+\pi^+)$ τ_{38}

LIMIT (10^{30} years)	PARTICLE	CL%	EVTS	BKGD EST	DOCUMENT ID		TECN
>17	**p**	**90**	**1**	**1.72**	BERGER	91B	FREJ
• • • We do not use the following data for averages, fits, limits, etc. • • •							
> 7.8	p	90	0	0.7	PHILLIPS	89	HPW

$\tau(n \to \mu^-\pi^+\pi^0)$ τ_{39}

LIMIT (10^{30} years)	PARTICLE	CL%	EVTS	BKGD EST	DOCUMENT ID		TECN
>34	**n**	**90**	**0**	**0.78**	BERGER	91B	FREJ

$\tau(p \to e^-\pi^+K^+)$ τ_{40}

LIMIT (10^{30} years)	PARTICLE	CL%	EVTS	BKGD EST	DOCUMENT ID		TECN
>75	**p**	**90**	**81**	**127.2**	MCGREW	99	IMB3
• • • We do not use the following data for averages, fits, limits, etc. • • •							
>20	p	90	3	2.50	BERGER	91B	FREJ

$\tau(p \to \mu^-\pi^+K^+)$ τ_{41}

LIMIT (10^{30} years)	PARTICLE	CL%	EVTS	BKGD EST	DOCUMENT ID		TECN
>245	**p**	**90**	**3**	**4.0**	MCGREW	99	IMB3
• • • We do not use the following data for averages, fits, limits, etc. • • •							
> 5	p	90	2	0.78	BERGER	91B	FREJ

Antilepton + photon(s)

$\tau(p \to e^+\gamma)$ τ_{42}

LIMIT (10^{30} years)	PARTICLE	CL%	EVTS	BKGD EST	DOCUMENT ID		TECN
>670	**p**	**90**	**0**	**0.1**	MCGREW	99	IMB3
• • • We do not use the following data for averages, fits, limits, etc. • • •							
>133	p	90	0	0.3	BERGER	91	FREJ
>460	p	90	0	0.6	SEIDEL	88	IMB
>360	p	90	0	0.3	HAINES	86	IMB
> 87	p (free)	90	0	0.2	BLEWITT	85	IMB
>360	p	90	0	0.2	BLEWITT	85	IMB
> 0.1	p	90			[62] GURR	67	CNTR

[62] We have converted half-life to 90% CL mean life.

$\tau(p \to \mu^+\gamma)$ τ_{43}

LIMIT (10^{30} years)	PARTICLE	CL%	EVTS	BKGD EST	DOCUMENT ID		TECN
>478	**p**	**90**	**0**	**0.1**	MCGREW	99	IMB3
• • • We do not use the following data for averages, fits, limits, etc. • • •							
>155	p	90	0	0.1	BERGER	91	FREJ
>380	p	90	0	0.5	SEIDEL	88	IMB
> 97	p	90	3	2	HAINES	86	IMB
> 61	p (free)	90	0	0.2	BLEWITT	85	IMB
>280	p	90	0	0.6	BLEWITT	85	IMB
> 0.3	p	90			[63] GURR	67	CNTR

[63] We have converted half-life to 90% CL mean life.

$\tau(n \to \nu\gamma)$ [τ44]

LIMIT (10^{30} years)	PARTICLE	CL%	EVTS	BKGD EST	DOCUMENT ID		TECN
>28	***n***	**90**	**163**	**144.7**	MCGREW	99	IMB3
• • • We do not use the following data for averages, fits, limits, etc. • • •							
>24	*n*	90	10	6.86	BERGER	91B	FREJ
> 9	*n*	90	73	60	HAINES	86	IMB
>11	*n*	90	28	19	PARK	85	IMB

$\tau(p \to e^+\gamma\gamma)$ [τ45]

LIMIT (10^{30} years)	PARTICLE	CL%	EVTS	BKGD EST	DOCUMENT ID		TECN
>100	***p***	**90**	**1**	**0.8**	BERGER	91	FREJ

$\tau(n \to \nu\gamma\gamma)$ [τ46]

LIMIT (10^{30} years)	PARTICLE	CL%	EVTS	BKGD EST	DOCUMENT ID		TECN
>219	***n***	**90**	**5**	**7.5**	MCGREW	99	IMB3

Three (or more) leptons

$\tau(p \to e^+e^+e^-)$ [τ47]

LIMIT (10^{30} years)	PARTICLE	CL%	EVTS	BKGD EST	DOCUMENT ID		TECN
>793	***p***	**90**	**0**	**0.5**	MCGREW	99	IMB3
• • • We do not use the following data for averages, fits, limits, etc. • • •							
>147	*p*	90	0	0.1	BERGER	91	FREJ
>510	*p*	90	0	0.3	HAINES	86	IMB
> 89	*p* (free)	90	0	0.5	BLEWITT	85	IMB
>510	*p*	90	0	0.7	BLEWITT	85	IMB

$\tau(p \to e^+\mu^+\mu^-)$ [τ48]

LIMIT (10^{30} years)	PARTICLE	CL%	EVTS	BKGD EST	DOCUMENT ID		TECN
>359	***p***	**90**	**1**	**0.9**	MCGREW	99	IMB3
• • • We do not use the following data for averages, fits, limits, etc. • • •							
> 81	*p*	90	0	0.16	BERGER	91	FREJ
> 5.0	*p*	90	0	0.7	PHILLIPS	89	HPW

$\tau(p \to e^+\nu\nu)$ [τ49]

LIMIT (10^{30} years)	PARTICLE	CL%	EVTS	BKGD EST	DOCUMENT ID		TECN
>17	***p***	**90**	**152**	**153.7**	MCGREW	99	IMB3
• • • We do not use the following data for averages, fits, limits, etc. • • •							
>11	*p*	90	11	6.08	BERGER	91B	FREJ

$\tau(n \to e^+e^-\nu)$ [τ50]

LIMIT (10^{30} years)	PARTICLE	CL%	EVTS	BKGD EST	DOCUMENT ID		TECN
>257	***n***	**90**	**5**	**7.5**	MCGREW	99	IMB3
• • • We do not use the following data for averages, fits, limits, etc. • • •							
> 74	*n*	90	0	< 0.1	BERGER	91B	FREJ
> 45	*n*	90	5	5	HAINES	86	IMB
> 26	*n*	90	4	3	PARK	85	IMB

$\tau(n \to \mu^+e^-\nu)$ [τ51]

LIMIT (10^{30} years)	PARTICLE	CL%	EVTS	BKGD EST	DOCUMENT ID		TECN
>83	***n***	**90**	**25**	**29.4**	MCGREW	99	IMB3
• • • We do not use the following data for averages, fits, limits, etc. • • •							
>47	*n*	90	0	< 0.1	BERGER	91B	FREJ

$\tau(n \to \mu^+\mu^-\nu)$ [τ52]

LIMIT (10^{30} years)	PARTICLE	CL%	EVTS	BKGD EST	DOCUMENT ID		TECN
>79	***n***	**90**	**100**	**145**	MCGREW	99	IMB3
• • • We do not use the following data for averages, fits, limits, etc. • • •							
>42	*n*	90	0	1.4	BERGER	91B	FREJ
> 5.1	*n*	90	0	0.7	PHILLIPS	89	HPW
>16	*n*	90	14	7	HAINES	86	IMB
>19	*n*	90	4	7	PARK	85	IMB

$\tau(p \to \mu^+e^+e^-)$ [τ53]

LIMIT (10^{30} years)	PARTICLE	CL%	EVTS	BKGD EST	DOCUMENT ID		TECN
>529	***p***	**90**	**0**	**1.0**	MCGREW	99	IMB3
• • • We do not use the following data for averages, fits, limits, etc. • • •							
> 91	*p*	90	0	≤ 0.1	BERGER	91	FREJ

$\tau(p \to \mu^+\mu^+\mu^-)$ [τ54]

LIMIT (10^{30} years)	PARTICLE	CL%	EVTS	BKGD EST	DOCUMENT ID		TECN
>675	***p***	**90**	**0**	**0.3**	MCGREW	99	IMB3
• • • We do not use the following data for averages, fits, limits, etc. • • •							
>119	*p*	90	0	0.2	BERGER	91	FREJ
> 10.5	*p*	90	0	0.7	PHILLIPS	89	HPW
>190	*p*	90	1	0.1	HAINES	86	IMB
> 44	*p* (free)	90	1	0.7	BLEWITT	85	IMB
>190	*p*	90	1	0.9	BLEWITT	85	IMB
> 2.1	*p*	90	1		[64] BATTISTONI	82	NUSX

[64] We have converted 1 possible event to 90% CL limit.

$\tau(p \to \mu^+\nu\nu)$ [τ55]

LIMIT (10^{30} years)	PARTICLE	CL%	EVTS	BKGD EST	DOCUMENT ID		TECN
>21	***p***	**90**	**7**	**11.23**	BERGER	91B	FREJ

$\tau(p \to e^-\mu^+\mu^+)$ [τ56]

LIMIT (10^{30} years)	PARTICLE	CL%	EVTS	BKGD EST	DOCUMENT ID		TECN
>6.0	***p***	**90**	**0**	**0.7**	PHILLIPS	89	HPW

$\tau(n \to 3\nu)$ [τ57]

See also the "to anything" and "disappearance" limits for bound nucleons in the "*p* Mean Life" data block just in front of the list of possible *p* decay modes.

LIMIT (10^{30} years)	PARTICLE	CL%	EVTS	BKGD EST	DOCUMENT ID		TECN
>0.00049	***n***	**90**	**2**	**2**	[65] SUZUKI	93B	KAMI
• • • We do not use the following data for averages, fits, limits, etc. • • •							
>0.0023	*n*	90			[66] GLICENSTEIN	97	KAMI
>0.00003	*n*	90	11	6.1	[67] BERGER	91B	FREJ
>0.00012	*n*	90	7	11.2	[67] BERGER	91B	FREJ
>0.0005	*n*	90	0		LEARNED	79	RVUE

[65] The SUZUKI 93B limit applies to any of $\nu_e\nu_e\overline{\nu}_e$, $\nu_\mu\nu_\mu\overline{\nu}_\mu$, or $\nu_\tau\nu_\tau\overline{\nu}_\tau$.

[66] GLICENSTEIN 97 uses Kamioka data and the idea that the disappearance of the neutron's magnetic moment should produce radiation.

[67] The first BERGER 91B limit is for $n \to \nu_e\nu_e\overline{\nu}_e$, the second is for $n \to \nu_\mu\nu_\mu\overline{\nu}_\mu$.

$\tau(n \to 5\nu)$ [τ58]

LIMIT (10^{30} years)	PARTICLE	CL%	EVTS	BKGD EST	DOCUMENT ID		TECN
• • • We do not use the following data for averages, fits, limits, etc. • • •							
>0.0017	*n*	90			[68] GLICENSTEIN	97	KAMI

[68] GLICENSTEIN 97 uses Kamioka data and the idea that the disappearance of the neutron's magnetic moment should produce radiation.

Inclusive modes

$\tau(N \to e^+\text{anything})$ [τ59]

LIMIT (10^{30} years)	PARTICLE	CL%	EVTS	BKGD EST	DOCUMENT ID		TECN
>0.6	***p, n***	**90**			[69] LEARNED	79	RVUE

[69] The electron may be primary or secondary.

$\tau(N \to \mu^+\text{anything})$ [τ60]

LIMIT (10^{30} years)	PARTICLE	CL%	EVTS	BKGD EST	DOCUMENT ID		TECN
>12	***p, n***	**90**	**2**		[70,71] CHERRY	81	HOME
• • • We do not use the following data for averages, fits, limits, etc. • • •							
> 1.8	*p, n*	90			[71] COWSIK	80	CNTR
> 6	*p, n*	90			[71] LEARNED	79	RVUE

[70] We have converted 2 possible events to 90% CL limit.

[71] The muon may be primary or secondary.

$\tau(N \to \nu\text{anything})$ [τ61]

Anything = π, ρ, K, etc.

LIMIT (10^{30} years)	PARTICLE	CL%	EVTS	BKGD EST	DOCUMENT ID		TECN
• • • We do not use the following data for averages, fits, limits, etc. • • •							
>0.0002	*p, n*	90	0		LEARNED	79	RVUE

$\tau(N \to e^+\pi^0\text{anything})$ [τ62]

LIMIT (10^{30} years)	PARTICLE	CL%	EVTS	BKGD EST	DOCUMENT ID		TECN
>0.6	***p, n***	**90**	**0**		LEARNED	79	RVUE

$\tau(N \to 2\text{bodies, }\nu\text{-free})$ [τ63]

LIMIT (10^{30} years)	PARTICLE	CL%	EVTS	BKGD EST	DOCUMENT ID		TECN
• • • We do not use the following data for averages, fits, limits, etc. • • •							
>1.3	*p, n*	90	0		ALEKSEEV	81	BAKS

$\Delta B = 2$ dinucleon modes

$\tau(pp \to \pi^+\pi^+)$ τ_{64}

LIMIT (10^{30} years)	CL%	EVTS	BKGD EST	DOCUMENT ID		TECN	COMMENT
>0.7	90	4	2.34	BERGER	91B	FREJ	τ per iron nucleus

$\tau(pn \to \pi^+\pi^0)$ τ_{65}

LIMIT (10^{30} years)	CL%	EVTS	BKGD EST	DOCUMENT ID		TECN	COMMENT
>2.0	90	0	0.31	BERGER	91B	FREJ	τ per iron nucleus

$\tau(nn \to \pi^+\pi^-)$ τ_{66}

LIMIT (10^{30} years)	CL%	EVTS	BKGD EST	DOCUMENT ID		TECN	COMMENT
>0.7	90	4	2.18	BERGER	91B	FREJ	τ per iron nucleus

$\tau(nn \to \pi^0\pi^0)$ τ_{67}

LIMIT (10^{30} years)	CL%	EVTS	BKGD EST	DOCUMENT ID		TECN	COMMENT
>3.4	90	0	0.78	BERGER	91B	FREJ	τ per iron nucleus

$\tau(pp \to e^+e^+)$ τ_{68}

LIMIT (10^{30} years)	CL%	EVTS	BKGD EST	DOCUMENT ID		TECN	COMMENT
>5.8	90	0	<0.1	BERGER	91B	FREJ	τ per iron nucleus

$\tau(pp \to e^+\mu^+)$ τ_{69}

LIMIT (10^{30} years)	CL%	EVTS	BKGD EST	DOCUMENT ID		TECN	COMMENT
>3.6	90	0	<0.1	BERGER	91B	FREJ	τ per iron nucleus

$\tau(pp \to \mu^+\mu^+)$ τ_{70}

LIMIT (10^{30} years)	CL%	EVTS	BKGD EST	DOCUMENT ID		TECN	COMMENT
>1.7	90	0	0.62	BERGER	91B	FREJ	τ per iron nucleus

$\tau(pn \to e^+\overline{\nu})$ τ_{71}

LIMIT (10^{30} years)	CL%	EVTS	BKGD EST	DOCUMENT ID		TECN	COMMENT
>2.8	90	5	9.67	BERGER	91B	FREJ	τ per iron nucleus

$\tau(pn \to \mu^+\overline{\nu})$ τ_{72}

LIMIT (10^{30} years)	CL%	EVTS	BKGD EST	DOCUMENT ID		TECN	COMMENT
>1.6	90	4	4.37	BERGER	91B	FREJ	τ per iron nucleus

$\tau(nn \to \nu_e\overline{\nu}_e)$ τ_{73}

We include "invisible" modes here.

LIMIT (10^{30} years)	CL%	EVTS	BKGD EST	CL%	DOCUMENT ID		TECN	COMMENT
>0.000049				90	[72] BACK	03	BORX	
• • • We do not use the following data for averages, fits, limits, etc. • • •								
>0.000012	90				[73] BERNABEI	00B	DAMA	
>0.000012	90	5	9.7		BERGER	91B	FREJ	τ per iron nucleus

[72] BACK 03 looks for decays of unstable nuclides left after NN decays of parent ^{12}C, ^{13}C, ^{16}O nuclei. These are "invisible channel" limits.

[73] BERNABEI 00B looks for the decay of a $^{127}_{54}$Xe nucleus following the disappearance of an nn pair in the otherwise-stable $^{129}_{54}$Xe nucleus. The limit here applies as well to $nn \to \nu_\mu\overline{\nu}_\mu$, $nn \to \nu_\tau\overline{\nu}_\tau$, or any "disappearance" mode.

$\tau(nn \to \nu_\mu\overline{\nu}_\mu)$ τ_{74}

LIMIT (10^{30} years)	CL%	EVTS	BKGD EST	DOCUMENT ID		TECN	COMMENT
• • • We do not use the following data for averages, fits, limits, etc. • • •							
>0.000006	90	4	4.4	BERGER	91B	FREJ	τ per iron nucleus

$\tau(pp \to \text{neutrinos})$ τ_{75}

We include "invisible" modes here.

LIMIT (10^{30} years)	CL%	EVTS	BKGD EST	CL%	DOCUMENT ID		TECN
>0.00005				90	[74] BACK	03	BORX
• • • We do not use the following data for averages, fits, limits, etc. • • •							
>0.00000055	90				[75] BERNABEI	00B	DAMA

[74] BACK 03 looks for decays of unstable nuclides left after NN decays of parent ^{12}C, ^{13}C, ^{16}O nuclei. These are "invisible channel" limits.

[75] BERNABEI 00B looks for the decay of a $^{127}_{52}$Te nucleus following the disappearance of a pp pair in the otherwise-stable $^{129}_{54}$Xe nucleus. Note that the decay doesn't conserve charge as well as baryon number.

$\overline{p}$ PARTIAL MEAN LIVES

The "partial mean life" limits tabulated here are the limits on $\overline{\tau}/B_i$, where $\overline{\tau}$ is the total mean life for the antiproton and B_i is the branching fraction for the mode in question.

$\tau(\overline{p} \to e^-\gamma)$ τ_{76}

VALUE (years)	CL%	DOCUMENT ID		TECN	COMMENT
> 7×10^5	90	GEER	00	APEX	8.9 GeV/c $\overline{p}$ beam
• • • We do not use the following data for averages, fits, limits, etc. • • •					
>1848	95	GEER	94	CALO	8.9 GeV/c $\overline{p}$ beam

$\tau(\overline{p} \to \mu^-\gamma)$ τ_{77}

VALUE (years)	CL%	DOCUMENT ID		TECN	COMMENT
>5 $\times 10^4$	90	GEER	00	APEX	8.9 GeV/c $\overline{p}$ beam
• • • We do not use the following data for averages, fits, limits, etc. • • •					
>5.0×10^4	90	HU	98B	APEX	8.9 GeV/c $\overline{p}$ beam

$\tau(\overline{p} \to e^-\pi^0)$ τ_{78}

VALUE (years)	CL%	DOCUMENT ID		TECN	COMMENT
> 4×10^5	90	GEER	00	APEX	8.9 GeV/c $\overline{p}$ beam
• • • We do not use the following data for averages, fits, limits, etc. • • •					
>554	95	GEER	94	CALO	8.9 GeV/c $\overline{p}$ beam

$\tau(\overline{p} \to \mu^-\pi^0)$ τ_{79}

VALUE (years)	CL%	DOCUMENT ID		TECN	COMMENT
>5 $\times 10^4$	90	GEER	00	APEX	8.9 GeV/c $\overline{p}$ beam
• • • We do not use the following data for averages, fits, limits, etc. • • •					
>4.8×10^4	90	HU	98B	APEX	8.9 GeV/c $\overline{p}$ beam

$\tau(\overline{p} \to e^-\eta)$ τ_{80}

VALUE (years)	CL%	DOCUMENT ID		TECN	COMMENT
> 2×10^4	90	GEER	00	APEX	8.9 GeV/c $\overline{p}$ beam
• • • We do not use the following data for averages, fits, limits, etc. • • •					
>171	95	GEER	94	CALO	8.9 GeV/c $\overline{p}$ beam

$\tau(\overline{p} \to \mu^-\eta)$ τ_{81}

VALUE (years)	CL%	DOCUMENT ID		TECN	COMMENT
>8 $\times 10^3$	90	GEER	00	APEX	8.9 GeV/c $\overline{p}$ beam
• • • We do not use the following data for averages, fits, limits, etc. • • •					
>7.9×10^3	90	HU	98B	APEX	8.9 GeV/c $\overline{p}$ beam

$\tau(\overline{p} \to e^- K^0_S)$ τ_{82}

VALUE (years)	CL%	DOCUMENT ID		TECN	COMMENT
>900	90	GEER	00	APEX	8.9 GeV/c $\overline{p}$ beam
• • • We do not use the following data for averages, fits, limits, etc. • • •					
> 29	95	GEER	94	CALO	8.9 GeV/c $\overline{p}$ beam

$\tau(\overline{p} \to \mu^- K^0_S)$ τ_{83}

VALUE (years)	CL%	DOCUMENT ID		TECN	COMMENT
>4 $\times 10^3$	90	GEER	00	APEX	8.9 GeV/c $\overline{p}$ beam
• • • We do not use the following data for averages, fits, limits, etc. • • •					
>4.3×10^3	90	HU	98B	APEX	8.9 GeV/c $\overline{p}$ beam

$\tau(\overline{p} \to e^- K^0_L)$ τ_{84}

VALUE (years)	CL%	DOCUMENT ID		TECN	COMMENT
>9 $\times 10^3$	90	GEER	00	APEX	8.9 GeV/c $\overline{p}$ beam
• • • We do not use the following data for averages, fits, limits, etc. • • •					
>9	95	GEER	94	CALO	8.9 GeV/c $\overline{p}$ beam

$\tau(\overline{p} \to \mu^- K^0_L)$ τ_{85}

VALUE (years)	CL%	DOCUMENT ID		TECN	COMMENT
>7 $\times 10^3$	90	GEER	00	APEX	8.9 GeV/c $\overline{p}$ beam
• • • We do not use the following data for averages, fits, limits, etc. • • •					
>6.5×10^3	90	HU	98B	APEX	8.9 GeV/c $\overline{p}$ beam

$\tau(\overline{p} \to e^-\gamma\gamma)$ τ_{86}

VALUE (years)	CL%	DOCUMENT ID		TECN	COMMENT
>2×10^4	90	GEER	00	APEX	8.9 GeV/c $\overline{p}$ beam

$\tau(\overline{p} \to \mu^-\gamma\gamma)$ τ_{87}

VALUE (years)	CL%	DOCUMENT ID		TECN	COMMENT
>2 $\times 10^4$	90	GEER	00	APEX	8.9 GeV/c $\overline{p}$ beam
• • • We do not use the following data for averages, fits, limits, etc. • • •					
>2.3×10^4	90	HU	98B	APEX	8.9 GeV/c $\overline{p}$ beam

$\tau(\overline{p} \to e^-\rho)$ τ_{88}

VALUE (years)	CL%	DOCUMENT ID		TECN	COMMENT
• • • We do not use the following data for averages, fits, limits, etc. • • •					
>200	90	[76] GEER	00	APEX	8.9 GeV/c $\overline{p}$ beam

[76] This GEER 00 measurement has been withdrawn; see GEER 00C.

$\tau(\overline{p} \to e^- \omega)$ [789]

VALUE (years)	CL%	DOCUMENT ID		TECN	COMMENT
>200	90	GEER	00	APEX	8.9 GeV/c $\overline{p}$ beam

$\tau(\overline{p} \to e^- K^*(892)^0)$ [790]

VALUE (years)	CL%	DOCUMENT ID		TECN	COMMENT
• • • We do not use the following data for averages, fits, limits, etc. • • •					
$>1 \times 10^3$	90	[77] GEER	00	APEX	8.9 GeV/c $\overline{p}$ beam

[77] This GEER 00 measurement has been withdrawn; see GEER 00C.

p REFERENCES

AHMED	04	PRL 92 102004	S.N. Ahmed *et al.*	(SNO Collab.)
MOHR	04	RMP (to be publ.) physics.nist.gov/constants	P.J. Mohr, B.N. Taylor	(NIST)
BACK	03	PL B563 23	H.O. Back *et al.*	(BOREXINO Collab.)
BEANE	03	PL B567 200	S.R. Beane *et al.*	
DMITRIEV	03	PRL 91 212303	V.F. Dmitriev, R.A. Senkov	(NOVO)
HORI	03	PRL 91 123401	M. Hori *et al.*	(CERN ASACUSA Collab.)
ZDESENKO	03	PL B553 135	Yu.G. Zdesenko, V.I. Tretyak	(KIEV)
AHMAD	02	PRL 89 011301	Q.R. Ahmad *et al.*	(SNO Collab.)
BARANOV	01	PPN 32 376 Translated from FECAY 32 699.	P.S. Baranov *et al.*	
BLANPIED	01	PR C64 025203	G. Blanpied *et al.*	(BNL LEGS Collab.)
ESCHRICH	01	PL B522 233	I. Eschrich *et al.*	(FNAL SELEX Collab.)
HORI	01	PRL 87 093401	M. Hori *et al.*	(CERN ASACUSA Collab.)
OLMOSDEL...	01	EPJ A10 207	V. Olmos de Leon *et al.*	(MAMI TAPS Collab.)
TRETYAK	01	PL B505 59	V.I. Tretyak, Yu.G. Zdesenko	(KIEV)
BERNABEI	00B	PL B493 12	R. Bernabei *et al.*	(Gran Sasso DAMA Collab.)
GEER	00	PRL 84 590	S. Geer *et al.*	(FNAL APEX Collab.)
Also	00B	PR D62 052004	S. Geer *et al.*	(FNAL APEX Collab.)
Also	00C	PRL 85 3546 (erratum)	S. Geer *et al.*	(FNAL APEX Collab.)
GEER	00C	PRL 85 3546 (erratum)	S. Geer *et al.*	(FNAL APEX Collab.)
GEER	00D	APJ 532 648	S.H. Geer, D.C. Kennedy	
MELNIKOV	00	PRL 84 1673	K. Melnikov *et al.*	(SLAC, KARL)
ROSENFELDR...	00	PL B479 381	R. Rosenfelder	
SENGUPTA	00	PL B484 275	S. Sengupta	
WALL	00	PR D61 072004	D. Wall *et al.*	(Soudan-2 Collab.)
WALL	00B	PR D62 092003	D. Wall *et al.*	(Soudan-2 Collab.)
GABRIELSE	99	PRL 82 3198	G. Gabrielse *et al.*	
HAYATO	99	PRL 83 1529	Y. Hayato *et al.*	(Super-Kamiokande Collab.)
MCGREW	99	PR D59 052004	C. McGrew *et al.*	(IMB-3 Collab.)
MOHR	99	JPCRD 28 1713	P.J. Mohr, B.N. Taylor	(NIST)
Also	00	RMP 72 351	P.J. Mohr, B.N. Taylor	(NIST)
TORII	99	PR A59 223	H.A. Torii *et al.*	(CERN-PS-205 Collab.)
ALLISON	98	PL B427 217	W.W.M. Allison *et al.*	(Soudan-2 Collab.)
HU	98B	PR D58 111101	M. Hu *et al.*	(FNAL APEX Collab.)
SHIOZAWA	98	PRL 81 3319	M. Shiozawa *et al.*	(Super-Kamiokande Collab.)
GLICENSTEIN	97	PL B411 326	J.F. Glicenstein	(SACL)
MERGELL	96	NP A596 367	P. Mergell *et al.*	(MANZ, BONN)
GABRIELSE	95	PRL 74 3544	G. Gabrielse *et al.*	(HARV, MANZ, SEOUL)
MACGIBBON	95	PR C52 2097	B.E. MacGibbon *et al.*	(ILL, SASK, INRM)
GEER	94	PRL 72 1596	S. Geer *et al.*	(FNAL, UCLA, PSU)
WONG	94	IJMP E3 821	C.W. Wong	(UCLA)
HALLIN	93	PR C48 1497	E.L. Hallin *et al.*	(SASK, BOST, ILL)
SUZUKI	93B	PL B311 357	Y. Suzuki *et al.*	(KAMIOKANDE Collab.)
HUGHES	92	PRL 69 578	R.J. Hughes, B.I. Deutch	(LANL, AARH)
ZIEGER	92	PL B278 34	A. Zieger *et al.*	(MPCM)
Also	92B	PL B281 417 (erratum)	A. Zieger *et al.*	(MPCM)
BERGER	91	ZPHY C50 385	C. Berger *et al.*	(FREJUS Collab.)
BERGER	91B	PL B269 227	C. Berger *et al.*	(FREJUS Collab.)
FEDERSPIEL	91	PRL 67 1511	F.J. Federspiel *et al.*	(ILL)
MCCORD	91	NIM B56/57 496	M. McCord *et al.*	
BECKER-SZ...	90	PR D42 2974	R.A. Becker-Szendy *et al.*	(IMB-3 Collab.)
ERICSON	90	PRL 11 295	T.E.O. Ericson, A. Richter	(CERN, DARM)
GABRIELSE	90	PRL 65 1317	G. Gabrielse *et al.*	(HARV, MANZ, WASH+)
BERGER	89	NP B313 509	C. Berger *et al.*	(FREJUS Collab.)
CHO	89	PRL 63 2559	D. Cho, K. Sangster, E.A. Hinds	(YALE)
HIRATA	89C	PL B220 308	K.S. Hirata *et al.*	(Kamiokande Collab.)
PHILLIPS	89	PL B224 348	T.J. Phillips *et al.*	(HPW Collab.)
KREISSL	88	ZPHY C37 557	A. Kreissl *et al.*	(CERN PS176 Collab.)
SEIDEL	88	PRL 61 2522	S. Seidel *et al.*	(IMB Collab.)
BARTELT	87	PR D36 1990	J.E. Bartelt *et al.*	(Soudan Collab.)
Also	89	PR D40 1701 erratum	J.E. Bartelt *et al.*	(Soudan Collab.)
COHEN	87	RMP 59 1121	E.R. Cohen, B.N. Taylor	(RISC, NBS)
HAINES	86	PRL 57 1986	T.J. Haines *et al.*	(IMB Collab.)
KAJITA	86	JPSJ 55 711	T. Kajita *et al.*	(Kamiokande Collab.)
ARISAKA	85	JPSJ 54 3213	K. Arisaka *et al.*	(Kamiokande Collab.)
BLEWITT	85	PRL 55 2114	G.B. Blewitt *et al.*	(IMB Collab.)
DZUBA	85	PL 154B 93	V.A. Dzuba, V.V. Flambaum, P.G. Silvestrov	(NOVO)
PARK	85	PRL 54 22	H.S. Park *et al.*	(IMB Collab.)
BATTISTONI	84	PL 133B 454	G. Battistoni *et al.*	(NUSEX Collab.)
MARINELLI	84	PL 137B 439	M. Marinelli, G. Morpurgo	(GENO)
WILKENING	84	PR A29 425	D.A. Wilkening, N.F. Ramsey, D.J. Larson	(HARV+)
BARTELT	83	PRL 50 651	J.E. Bartelt *et al.*	(MINN, ANL)
BATTISTONI	82	PL 118B 461	G. Battistoni *et al.*	(NUSEX Collab.)
KRISHNA...	82	PL 115B 349	M.R. Krishnaswamy *et al.*	(TATA, OSKC+)
ALEKSEEV	81	JETPL 33 651 Translated from ZETFP 33 664.	E.N. Alekseev *et al.*	(PNPI)
CHERRY	81	PRL 47 1507	M.L. Cherry *et al.*	(PENN, BNL)
COWSIK	80	PR D22 2204	R. Cowsik, V.S. Narasimham	(TATA)
SIMON	80	NP A333 381	G.G. Simon *et al.*	
BELL	79	PL 86B 215	M. Bell *et al.*	(CERN)
GOLDEN	79	PRL 43 1196	R.L. Golden *et al.*	(NASA, PSL)
LEARNED	79	PRL 43 907	J.G. Learned, F. Reines, A. Soni	(UCI)
BREGMAN	78	PL 78B 174	M. Bregman *et al.*	(CERN)
ROBERTS	78	PR D17 358	B.L. Roberts	(WILL, RHEL)
EVANS	77	Science 197 989	J.C. Evans Jr., R.I. Steinberg	(BNL, PENN)
HU	75	NP A254 403	E. Hu *et al.*	(COLU, YALE)
BORKOWSKI	74	NP A222 269	F. Borkowski *et al.*	
COHEN	73	JPCRD 2 664	E.R. Cohen, B.N. Taylor	(RISC, NBS)
DYLLA	73	PR A7 1224	H.F. Dylla, J.G. King	(MIT)
AKIMOV	72	JETP 35 651 Translated from ZETF 62 1231.	Yu.K. Akimov *et al.*	(YERE)
DIX	70	Thesis Case	F.W. Dix	(CASE)
HARRISON	69	PRL 22 1263	G.E. Harrison, P.G.H. Sandars, S.J. Wright	(OXF)
GURR	67	PR 158 1321	H.S. Gurr *et al.*	(CASE, WITW)
FREREJACQ...	66	PR 141 1308	D. Frerejacque *et al.*	
HAND	63	RMP 35 335	L.N. hand *et al.*	
FLEROV	58	DOKL 3 79	G.N. Flerov *et al.*	(ASCI)

n

$I(J^P) = \frac{1}{2}(\frac{1}{2}^+)$ Status: ****

We have omitted some results that have been superseded by later experiments. See our earlier editions.

n MASS (atomic mass units u)

The mass is known much more precisely in u (atomic mass units) than in MeV. See the next data block.

VALUE (u)	DOCUMENT ID		TECN	COMMENT
1.00866491560 ± 0.00000000055	MOHR	04	RVUE	2002 CODATA value
• • • We do not use the following data for averages, fits, limits, etc. • • •				
1.008664915 78 ± 0.000000000055	MOHR	99	RVUE	1998 CODATA value
1.008665904 ± 0.000000014	COHEN	87	RVUE	1986 CODATA value

n MASS (MeV)

The mass is known much more precisely in u (atomic mass units) than in MeV. The conversion from u to MeV, 1 u = 931.494043±0.000080 MeV/c^2 (MOHR 04, the 2002 CODATA value), involves the relatively poorly known electronic charge.

VALUE (MeV)	DOCUMENT ID		TECN	COMMENT
939.565360 ± 0.000081	MOHR	04	RVUE	2002 CODATA value
• • • We do not use the following data for averages, fits, limits, etc. • • •				
939.565331 ± 0.000037	[1] KESSLER	99	SPEC	$np \to d\gamma$
939.565330 ± 0.000038	MOHR	99	RVUE	1998 CODATA value
939.56565 ± 0.00028	[2,3] DIFILIPPO	94	TRAP	Penning trap
939.56563 ± 0.00028	COHEN	87	RVUE	1986 CODATA value
939.56564 ± 0.00028	[3,4] GREENE	86	SPEC	$np \to d\gamma$
939.5731 ± 0.0027	[3] COHEN	73	RVUE	1973 CODATA value

[1] We use the 1998 CODATA u-to-MeV conversion factor (see the heading above) to get this mass in MeV from the much more precisely measured KESSLER 99 value of 1.00866491637 ± 0.00000000082 u.

[2] The mass is known much more precisely in u: m = 1.0086649235 ± 0.0000000023 u. We use the 1986 CODATA conversion factor to get the mass in MeV.

[3] These determinations are not independent of the $m_n - m_p$ measurements below.

[4] The mass is known much more precisely in u: m = 1.008664919 ± 0.000000014 u.

$\overline{n}$ MASS

VALUE (MeV)	EVTS	DOCUMENT ID		TECN	COMMENT
939.485 ± 0.051	59	[5] CRESTI	86	HBC	$\overline{p}p \to \overline{n}n$

[5] This is a corrected result (see the erratum). The error is statistical. The maximum systematic error is 0.029 MeV.

$(m_n - m_{\overline{n}})/m_n$

A test of CPT invariance. Calculated from the n and $\overline{n}$ masses, above.

VALUE	DOCUMENT ID
(9±5) × 10^{-5} OUR EVALUATION	

$m_n - m_p$

VALUE (MeV)	DOCUMENT ID		TECN	COMMENT
1.2933317 ± 0.0000005	[6] MOHR	04	RVUE	2002 CODATA value
• • • We do not use the following data for averages, fits, limits, etc. • • •				
1.2933318 ± 0.0000005	[7] MOHR	99	RVUE	1998 CODATA value
1.293318 ± 0.000009	[8] COHEN	87	RVUE	1986 CODATA value
1.2933328 ± 0.0000072	GREENE	86	SPEC	$np \to d\gamma$
1.293429 ± 0.000036	COHEN	73	RVUE	1973 CODATA value

[6] Calculated by us from the MOHR 04 ratio m_n/m_p = 1.00137841870 ± 0.0000000058. In u, $m_n - m_p$ = (1.3884487 ± 0.0000006) × 10^{-3} u.

[7] Calculated by us from the MOHR 99 ratio m_n/m_p = 1.00137841887 ± 0.0000000058. In u, $m_n - m_p$ = (1.3884489 ± 0.0000006) × 10^{-3} u.

[8] Calculated by us from the COHEN 87 ratio m_n/m_p = 1.001378404 ± 0.000000009. In u, $m_n - m_p$ = 0.001388434 ± 0.000000009 u.

n MEAN LIFE

We now compile only direct measurements of the lifetime, not those inferred from decay correlation measurements. For the average, we only use measurements with an error less than 10 s.

Limits on lifetimes for *bound* neutrons are given in the section "*p* PARTIAL MEAN LIVES."

For an early review, see EROZOLIMSKII 89 and papers that follow it in an issue of NIM devoted to the "Proceedings of the International Workshop on Fundamental Physics with Slow Neutrons" (Grenoble 1989). For later reviews and/or commentary, see FREEDMAN 90, SCHRECKENBACH 92, and PENDLEBURY 93.

VALUE (s)	DOCUMENT ID		TECN	COMMENT
885.7± 0.8 OUR AVERAGE				
886.8± 1.2± 3.2	DEWEY	03	CNTR	In-beam *n*, *p* trap
885.4± 0.9± 0.4	ARZUMANOV	00	CNTR	UCN double bottle
889.2± 3.0± 3.8	BYRNE	96	CNTR	Penning trap
882.6± 2.7	[9] MAMPE	93	CNTR	Gravitational trap
888.4± 3.1± 1.1	NESVIZHEV...	92	CNTR	Gravitational trap
887.6± 3.0	MAMPE	89	CNTR	Gravitational trap
891 ± 9	SPIVAK	88	CNTR	Beam
• • • We do not use the following data for averages, fits, limits, etc. • • •				
888.4± 2.9	ALFIMENKOV	90	CNTR	See NESVIZHEVSKII 92
893.6± 3.8± 3.7	BYRNE	90	CNTR	See BYRNE 96
878 ±27 ±14	KOSSAKOW...	89	TPC	Pulsed beam
877 ±10	PAUL	89	CNTR	Storage ring
876 ±10 ±19	LAST	88	SPEC	Pulsed beam
903 ±13	KOSVINTSEV	86	CNTR	Gravitational trap
937 ±18	[10] BYRNE	80	CNTR	
875 ±95	KOSVINTSEV	80	CNTR	
881 ± 8	BONDAREN...	78	CNTR	See SPIVAK 88
918 ±14	CHRISTENSEN	72	CNTR	

[9] IGNATOVICH 95 calls into question some of the corrections and averaging procedures used by MAMPE 93. The response, BONDARENKO 96, denies the validity of the criticisms.

[10] This measurement has been withdrawn (J. Byrne, private communication, 1990).

n MAGNETIC MOMENT

See the "Note on Baryon Magnetic Moments" in the Λ Listings.

VALUE (μ_N)	DOCUMENT ID		TECN	COMMENT
−1.91304273±0.00000045	MOHR	04	RVUE	2002 CODATA value
• • • We do not use the following data for averages, fits, limits, etc. • • •				
−1.91304272±0.00000045	MOHR	99	RVUE	1998 CODATA value
−1.91304275±0.00000045	COHEN	87	RVUE	1986 CODATA value
−1.91304277±0.00000048	[11] GREENE	82	MRS	

[11] GREENE 82 measures the moment to be $(1.04187564 \pm 0.00000026) \times 10^{-3}$ Bohr magnetons. The value above is obtained by multiplying this by $m_p/m_e = 1836.152701 \pm 0.000037$ (the 1986 CODATA value from COHEN 87).

n ELECTRIC DIPOLE MOMENT

A nonzero value is forbidden by both *T* invariance and *P* invariance. A number of early results have been omitted. See RAMSEY 90 and GOLUB 94 for reviews.

VALUE (10^{-25} *e* cm)	CL%	DOCUMENT ID		TECN	COMMENT
< 0.63	90	[12] HARRIS	99	MRS	$d = (-0.1 \pm 0.36) \times 10^{-25}$
• • • We do not use the following data for averages, fits, limits, etc. • • •					
< 0.97	90	ALTAREV	96	MRS	$(+0.26 \pm 0.40 \pm 0.16) \times 10^{-25}$
< 1.1	95	ALTAREV	92	MRS	See ALTAREV 96
< 1.2	95	SMITH	90	MRS	See HARRIS 99
< 2.6	95	ALTAREV	86	MRS	$d = (-1.4 \pm 0.6) \times 10^{-25}$
0.3 ±4.8		PENDLEBURY	84	MRS	Ultracold neutrons
< 6	90	ALTAREV	81	MRS	$d = (2.1 \pm 2.4) \times 10^{-25}$
<16	90	ALTAREV	79	MRS	$d = (4.0 \pm 7.5) \times 10^{-25}$

[12] This HARRIS 99 result includes the result of SMITH 90. However, the averaging of the results of these two experiments has been criticized by LAMOREAUX 00.

n MEAN-SQUARE CHARGE RADIUS

The mean-square charge radius of the neutron, $\langle r_n^2 \rangle$, is related to the neutron-electron scattering length b_{ne} by $\langle r_n^2 \rangle = 3(m_e a_0/m_n) b_{ne}$, where m_e and m_n are the masses of the electron and neutron, and a_0 is the Bohr radius. Numerically, $\langle r_n^2 \rangle = 86.34\, b_{ne}$, if we use a_0 for a nucleus with infinite mass.

VALUE (fm^2)	DOCUMENT ID		COMMENT
−0.1161±0.0022 OUR AVERAGE	Error includes scale factor of 1.3. See the ideogram below.		
−0.115 ±0.002 ±0.003	KOPECKY	97	*ne* scattering (Pb)
−0.124 ±0.003 ±0.005	KOPECKY	97	*ne* scattering (Bi)
−0.114 ±0.003	KOESTER	95	*ne* scattering (Pb, Bi)
−0.134 ±0.009	ALEKSANDR...	86	*ne* scattering (Bi)
−0.115 ±0.003	[13] KROHN	73	*ne* scattering (Ne, Ar, Kr, Xe)
• • • We do not use the following data for averages, fits, limits, etc. • • •			
−0.113 ±0.003 ±0.004	KOPECKY	95	*ne* scattering (Pb)
−0.114 ±0.003	KOESTER	86	*ne* scattering (Pb, Bi)
−0.118 ±0.002	KOESTER	76	*ne* scattering (Pb)
−0.120 ±0.002	KOESTER	76	*ne* scattering (Bi)
−0.116 ±0.003	KROHN	66	*ne* scattering (Ne, Ar, Kr, Xe)

[13] This value is as corrected by KOESTER 76.

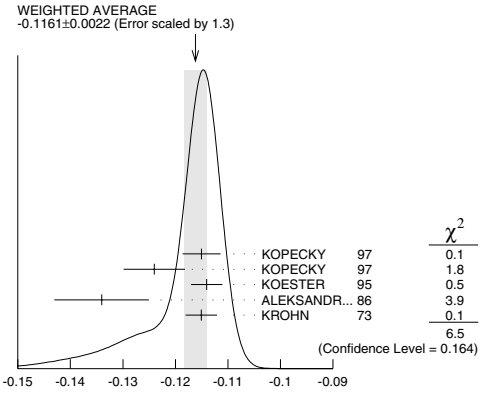

n mean-square charge radius

n ELECTRIC POLARIZABILITY α_n

Following is the electric polarizability α_n defined in terms of the induced electric dipole moment by $\mathbf{D} = 4\pi\epsilon_0\alpha_n\mathbf{E}$. For a review, see SCHMIEDMAYER 89.

VALUE (10^{-4} fm^3)	DOCUMENT ID		TECN	COMMENT
11.6± 1.5 OUR AVERAGE				
$12.5 \pm 1.8^{+1.6}_{-1.3}$	[14] KOSSERT	03	CNTR	$\gamma d \to \gamma pn$
8.8± 2.4±3.0	[15] LUNDIN	03	CNTR	$\gamma d \to \gamma d$
12.0± 1.5±2.0	SCHMIEDM...	91	CNTR	*n* Pb transmission
$10.7^{+3.3}_{-10.7}$	ROSE	90B	CNTR	$\gamma d \to \gamma np$
• • • We do not use the following data for averages, fits, limits, etc. • • •				
13.6	[16] KOLB	00	CNTR	$\gamma d \to \gamma np$
0.0± 5.0	[17] KOESTER	95	CNTR	*n* Pb, *n* Bi transmission
$11.7^{+4.3}_{-11.7}$	ROSE	90	CNTR	See ROSE 90B
8 ±10	KOESTER	88	CNTR	*n* Pb, *n* Bi transmission
12 ±10	SCHMIEDM...	88	CNTR	*n* Pb, *n* C transmission

[14] KOSSERT 03 gets $\alpha_n - \beta_n = (9.8 \pm 3.6^{+2.1}_{-1.1} \pm 2.2) \times 10^{-4}$ fm^3, and uses $\alpha_n + \beta_n = (15.2 \pm 0.5) \times 10^{-4}$ fm^3 from OLMOSDELEON 01. Thus the errors on α_n and β_n are anti-correlated.

[15] LUNDIN 03 measures $\alpha_N - \beta_N = (6.4 \pm 2.4) \times 10^{-4}$ fm^3 and uses accurate values for α_p and α_p and a precise sum-rule result for $\alpha_n + \beta_n$. The second error is a model uncertainty, and errors on α_n and β_n are anticorrelated.

[16] KOLB 00 obtains this value with a lower limit of 7.6×10^{-4} fm^3 but no upper limit from this experiment alone. Combined with results of ROSE 90, the 1-σ range is $(7.6–14.0) \times 10^{-4}$ fm^3.

[17] KOESTER 95 uses natural Pb and the isotopes 208, 207, and 206. See this paper for a discussion of methods used by various groups to extract α_n from data.

n MAGNETIC POLARIZABILITY β_n

VALUE (10^{-4} fm^3)	DOCUMENT ID		TECN	COMMENT
3.7±2.0 OUR AVERAGE				
$2.7 \pm 1.8^{+1.3}_{-1.6}$	[18] KOSSERT	03	CNTR	$\gamma d \to \gamma pn$
6.5±2.4±3.0	[19] LUNDIN	03	CNTR	$\gamma d \to \gamma d$
• • • We do not use the following data for averages, fits, limits, etc. • • •				
1.6	[20] KOLB	00	CNTR	$\gamma d \to \gamma np$

[18] KOSSERT 03 gets $\alpha_n - \beta_n = (9.8 \pm 3.6^{+2.1}_{-1.1} \pm 2.2) \times 10^{-4}$ fm^3, and uses $\alpha_n + \beta_n = (15.2 \pm 0.5) \times 10^{-4}$ fm^3 from OLMOSDELEON 01. Thus the errors on α_n and β_n are anti-correlated.

[19] LUNDIN 03 measures $\alpha_N - \beta_N = (6.4 \pm 2.4) \times 10^{-4}$ fm^3 and uses accurate values for α_p and α_p and a precise sum-rule result for $\alpha_n + \beta_n$. The second error is a model uncertainty, and errors on α_n and β_n are anticorrelated.

[20] KOLB 00 obtains this value with an upper limit of 7.6×10^{-4} fm^3 but no lower limit from this experiment alone. Combined with results of ROSE 90, the 1-σ range is $(1.2–7.6) \times 10^{-4}$ fm^3.

See key on page 323

n CHARGE

See also "$|q_p + q_e|/e$" in the proton Listings.

VALUE (10^{-21} e)	DOCUMENT ID		TECN	COMMENT
− 0.4 ± 1.1	[21] BAUMANN	88		Cold n deflection
• • • We do not use the following data for averages, fits, limits, etc. • • •				
− 15 ± 22	[22] GAEHLER	82	CNTR	Cold n deflection

[21] The BAUMANN 88 error ±1.1 gives the 68% CL limits about the the value − 0.4.
[22] The GAEHLER 82 error ±22 gives the 90% CL limits about the the value − 15.

LIMIT ON $n\overline{n}$ OSCILLATIONS

Mean Time for $n\overline{n}$ Transition in Vacuum

A test of ΔB=2 baryon number nonconservation. MOHAPATRA 80 and MOHAPATRA 89 discuss the theoretical motivations for looking for $n\overline{n}$ oscillations. DOVER 83 and DOVER 85 give phenomenological analyses. The best limits come from looking for the decay of neutrons bound in nuclei. However, these analyses require model-dependent corrections for nuclear effects. See KABIR 83, DOVER 89, ALBERICO 91, and GAL 00 for discussions. Direct searches for $n \to \overline{n}$ transitions using reactor neutrons are cleaner but give somewhat poorer limits. We include limits for both free and bound neutrons in the Summary Table.

VALUE (s)	CL%	DOCUMENT ID		TECN	COMMENT
$>1.3\times10^{8}$	90	CHUNG	02B	SOU2	n bound in iron
$>8.6\times10^{7}$	90	BALDO-...	94	CNTR	Reactor (free) neutrons
• • • We do not use the following data for averages, fits, limits, etc. • • •					
$>1\times10^{7}$	90	BALDO-...	90	CNTR	See BALDO-CEOLIN 94
$>1.2\times10^{8}$	90	BERGER	90	FREJ	n bound in iron
$>4.9\times10^{5}$	90	BRESSI	90	CNTR	Reactor neutrons
$>4.7\times10^{5}$	90	BRESSI	89	CNTR	See BRESSI 90
$>1.2\times10^{8}$	90	TAKITA	86	CNTR	n bound in oxygen
$>1\times10^{6}$	90	FIDECARO	85	CNTR	Reactor neutrons
$>8.8\times10^{7}$	90	PARK	85B	CNTR	
$>3\times10^{7}$		BATTISTONI	84	NUSX	
$>2.7\times10^{7}-1.1\times10^{8}$		JONES	84	CNTR	
$>2\times10^{7}$		CHERRY	83	CNTR	

n DECAY MODES

	Mode	Fraction (Γ_i/Γ)	Confidence level
Γ_1	$pe^-\overline{\nu}_e$	100 %	
Γ_2	hydrogen-atom $\overline{\nu}_e$		
Γ_3	$pe^-\overline{\nu}_e\gamma$	[a] $< 6.9\times10^{-3}$	90%
	Charge conservation (Q) violating mode		
Γ_4	$p\nu_e\overline{\nu}_e$	Q $< 8\times10^{-27}$	68%

[a] This limit is for γ energies between 35 and 100 keV.

n BRANCHING RATIOS

Γ(hydrogen-atom $\overline{\nu}_e$)/Γ_{total} Γ_2/Γ

VALUE	CL%	DOCUMENT ID		TECN
• • • We do not use the following data for averages, fits, limits, etc. • • •				
$<3\times10^{-2}$	95	[23] GREEN	90	RVUE

[23] GREEN 90 infers that τ(hydrogen-atom $\overline{\nu}_e$) > 3×10^4 s by comparing neutron lifetime measurements made in storage experiments with those made in β-decay experiments. However, the result depends sensitively on the lifetime measurements, and does not of course take into account more recent measurements of same.

$\Gamma(pe^-\overline{\nu}_e\gamma)/\Gamma_{total}$ Γ_3/Γ

VALUE	CL%	DOCUMENT ID		TECN	COMMENT
$<6.9\times10^{-3}$	90	[24] BECK	02	CNTR	Cold n

[24] This BECK 02 limit is for γ energies between 35 and 100 keV.

$\Gamma(p\nu_e\overline{\nu}_e)/\Gamma_{total}$ Γ_4/Γ

Forbidden by charge conservation.

VALUE	CL%	DOCUMENT ID		TECN	COMMENT
$<8\times10^{-27}$	68	[25] NORMAN	96	RVUE	^{71}Ga → ^{71}Ge neutrals
• • • We do not use the following data for averages, fits, limits, etc. • • •					
$<9.7\times10^{-18}$	90	ROY	83	CNTR	^{113}Cd → ^{113m}Inneut.
$<7.9\times10^{-21}$		VAIDYA	83	CNTR	^{87}Rb → ^{87m}Srneut.
$<9\times10^{-24}$	90	BARABANOV	80	CNTR	^{71}Ga → ^{71}GeX
$<3\times10^{-19}$		NORMAN	79	CNTR	^{87}Rb → ^{87m}Srneut.

[25] NORMAN 96 gets this limit by attributing SAGE and GALLEX counting rates to the charge-nonconserving transition ^{71}Ga → ^{71}Ge+neutrals rather than to solar-neutrino reactions.

BARYON DECAY PARAMETERS

Written 1996 by E.D. Commins (University of California, Berkeley).

Baryon semileptonic decays

The typical spin-1/2 baryon semileptonic decay is described by a matrix element, the hadronic part of which may be written as:

$$\overline{B}_f \left[f_1(q^2)\gamma_\lambda + i\, f_2(q^2)\sigma_{\lambda\mu}q^\mu + g_1(q^2)\gamma_\lambda\gamma_5 + g_3(q^2)\gamma_5 q_\lambda \right] B_i \ . \quad (1)$$

Here B_i and $\overline{B}_f$ are spinors describing the initial and final baryons, and $q = p_i - p_f$, while the terms in f_1, f_2, g_1, and g_3 account for vector, induced tensor ("weak magnetism"), axial vector, and induced pseudoscalar contributions [1]. Second-class current contributions are ignored here. In the limit of zero momentum transfer, f_1 reduces to the vector coupling constant g_V, and g_1 reduces to the axial-vector coupling constant g_A. The latter coefficients are related by Cabibbo's theory [2], generalized to six quarks (and three mixing angles) by Kobayashi and Maskawa [3]. The g_3 term is negligible for transitions in which an $e^\pm$ is emitted, and gives a very small correction, which can be estimated by PCAC [4], for $\mu^\pm$ modes. Recoil effects include weak magnetism, and are taken into account adequately by considering terms of first order in

$$\delta = \frac{m_i - m_f}{m_i + m_f} \ , \quad (2)$$

where m_i and m_f are the masses of the initial and final baryons.

The experimental quantities of interest are the total decay rate, the lepton-neutrino angular correlation, the asymmetry coefficients in the decay of a polarized initial baryon, and the polarization of the decay baryon in its own rest frame for an unpolarized initial baryon. Formulae for these quantities are derived by standard means [5] and are analogous to formulae for nuclear beta decay [6]. We use the notation of Ref. 6 in the Listings for neutron beta decay. For comparison with experiments at higher q^2, it is necessary to modify the form factors at $q^2 = 0$ by a "dipole" q^2 dependence, and for high-precision comparisons to apply appropriate radiative corrections [7].

The ratio g_A/g_V may be written as

$$g_A/g_V = |g_A/g_V|\, e^{i\phi_{AV}} \ . \quad (3)$$

The presence of a "triple correlation" term in the transition probability, proportional to $\mathrm{Im}(g_A/g_V)$ and of the form

$$\boldsymbol{\sigma}_i \cdot (\mathbf{p}_\ell \times \mathbf{p}_\nu) \quad (4)$$

for initial baryon polarization or

$$\boldsymbol{\sigma}_f \cdot (\mathbf{p}_\ell \times \mathbf{p}_\nu) \quad (5)$$

for final baryon polarization, would indicate failure of time-reversal invariance. The phase angle ϕ has been measured precisely only in neutron decay (and in ^{19}Ne nuclear beta decay), and the results are consistent with T invariance.

Hyperon nonleptonic decays

The amplitude for a spin-1/2 hyperon decaying into a spin-1/2 baryon and a spin-0 meson may be written in the form

$$M = G_F m_\pi^2 \cdot \overline{B}_f (A - B\gamma_5) B_i \ , \tag{6}$$

where A and B are constants [1]. The transition rate is proportional to

$$R = 1 + \gamma\, \hat{\omega}_f \cdot \hat{\omega}_i + (1-\gamma)(\hat{\omega}_f \cdot \hat{\mathbf{n}})(\hat{\omega}_i \cdot \hat{\mathbf{n}}) + \alpha(\hat{\omega}_f \cdot \hat{\mathbf{n}} + \hat{\omega}_i \cdot \hat{\mathbf{n}}) + \beta \hat{\mathbf{n}} \cdot (\hat{\omega}_f \times \hat{\omega}_i) \ , \tag{7}$$

where $\hat{\mathbf{n}}$ is a unit vector in the direction of the final baryon momentum, and $\hat{\omega}_i$ and $\hat{\omega}_f$ are unit vectors in the directions of the initial and final baryon spins. (The sign of the last term in the above equation was incorrect in our 1988 and 1990 editions.) The parameters α, β, and γ are defined as

$$\alpha = 2\,\mathrm{Re}(s^* p)/(|s|^2 + |p|^2) \ ,$$
$$\beta = 2\,\mathrm{Im}(s^* p)/(|s|^2 + |p|^2) \ ,$$
$$\gamma = (|s|^2 - |p|^2)/(|s|^2 + |p|^2) \ , \tag{8}$$

where $s = A$ and $p = |\mathbf{p}_f| B/(E_f + m_f)$; here E_f and $\mathbf{p}_f$ are the energy and momentum of the final baryon. The parameters α, β, and γ satisfy

$$\alpha^2 + \beta^2 + \gamma^2 = 1 \ . \tag{9}$$

If the hyperon polarization is $\mathbf{P}_Y$, the polarization $\mathbf{P}_B$ of the decay baryons is

$$\mathbf{P}_B = \frac{(\alpha + \mathbf{P}_Y \cdot \hat{\mathbf{n}})\hat{\mathbf{n}} + \beta(\mathbf{P}_Y \times \hat{\mathbf{n}}) + \gamma \hat{\mathbf{n}} \times (\mathbf{P}_Y \times \hat{\mathbf{n}})}{1 + \alpha \mathbf{P}_Y \cdot \hat{\mathbf{n}}} \ . \tag{10}$$

Here $\mathbf{P}_B$ is defined in the rest system of the baryon, obtained by a Lorentz transformation along $\hat{\mathbf{n}}$ from the hyperon rest frame, in which $\hat{\mathbf{n}}$ and $\mathbf{P}_Y$ are defined.

An additional useful parameter ϕ is defined by

$$\beta = (1 - \alpha^2)^{1/2} \sin\phi \ . \tag{11}$$

In the Listings, we compile α and ϕ for each decay, since these quantities are most closely related to experiment and are essentially uncorrelated. When necessary, we have changed the signs of reported values to agree with our sign conventions. In the Baryon Summary Table, we give α, ϕ, and Δ (defined below) with errors, and also give the value of γ without error.

Time-reversal invariance requires, in the absence of final-state interactions, that s and p be relatively real, and therefore that $\beta = 0$. However, for the decays discussed here, the final-state interaction is strong. Thus

$$s = |s|\, e^{i\delta_s} \text{ and } p = |p|\, e^{i\delta_p} \ , \tag{12}$$

where δ_s and δ_p are the pion-baryon s- and p-wave strong interaction phase shifts. We then have

$$\beta = \frac{-2|s|\,|p|}{|s|^2 + |p|^2} \sin(\delta_s - \delta_p) \ . \tag{13}$$

One also defines $\Delta = -\tan^{-1}(\beta/\alpha)$. If T invariance holds, $\Delta = \delta_s - \delta_p$. For $\Lambda \to p\pi^-$ decay, the value of Δ may be compared with the s- and p-wave phase shifts in low-energy $\pi^- p$ scattering, and the results are consistent with T invariance.

See also the note on "Radiative Hyperon Decays" in the Ξ^0 Listings in this *Review*.

References

1. E.D. Commins and P.H. Bucksbaum, *Weak Interactions of Leptons and Quarks* (Cambridge University Press, Cambridge, England, 1983).
2. N. Cabibbo, Phys. Rev. Lett. **10**, 531 (1963).
3. M. Kobayashi and T. Maskawa, Prog. Theor. Phys. **49**, 652 (1973).
4. M.L. Goldberger and S.B. Treiman, Phys. Rev. **111**, 354 (1958).
5. P.H. Frampton and W.K. Tung, Phys. Rev. **D3**, 1114 (1971).
6. J.D. Jackson, S.B. Treiman, and H.W. Wyld, Jr., Phys. Rev. **106**, 517 (1957), and Nucl. Phys. **4**, 206 (1957).
7. Y. Yokoo, S. Suzuki, and M. Morita, Prog. Theor. Phys. **50**, 1894 (1973).

$n \to p e^- \bar{\nu}_e$ DECAY PARAMETERS

See the above "Note on Baryon Decay Parameters." For discussions of recent results, see the references cited at the beginning of the section on the neutron mean life. For discussions of the values of the weak coupling constants g_A and g_V obtained using the neutron lifetime and asymmetry parameter A, comparisons with other methods of obtaining these constants, and implications for particle physics and for astrophysics, see DUBBERS 91 and WOOLCOCK 91. For tests of the $V-A$ theory of neutron decay, see EROZOLIMSKII 91B and MOSTOVOI 96.

$\lambda \equiv g_A / g_V$

VALUE	DOCUMENT ID		TECN	COMMENT
−1.2695 ± 0.0029 OUR AVERAGE	Error includes scale factor of 2.0. See the ideogram below.			
−1.2739 ± 0.0019	[26] ABELE	02	SPEC	Cold n, polarized, A
−1.2686 ± 0.0046 ± 0.007	[27] MOSTOVOI	01	CNTR	A and B × polarizations
−1.266 ± 0.004	LIAUD	97	TPC	Cold n, polarized, A
−1.2594 ± 0.0038	[28] YEROZLIM...	97	CNTR	Cold n, polarized, A
−1.262 ± 0.005	BOPP	86	SPEC	Cold n, polarized, A
• • • We do not use the following data for averages, fits, limits, etc. • • •				
−1.274 ± 0.003	ABELE	97D	SPEC	Cold n, polarized, A
−1.266 ± 0.004	SCHRECK...	95	TPC	See LIAUD 97
−1.2544 ± 0.0036	EROZOLIM...	91	CNTR	See YEROZOLIMSKY 97
−1.226 ± 0.042	MOSTOVOY	83	RVUE	
−1.261 ± 0.012	EROZOLIM...	79	CNTR	Cold n, polarized, A
−1.259 ± 0.017	[29] STRATOWA	78	CNTR	p recoil spectrum, a
−1.263 ± 0.015	EROZOLIM...	77	CNTR	See EROZOLIMSKII 79
−1.250 ± 0.036	[29] DOBROZE...	75	CNTR	See STRATOWA 78
−1.258 ± 0.015	[30] KROHN	75	CNTR	Cold n, polarized, A
−1.263 ± 0.016	[31] KROPF	74	RVUE	n decay alone
−1.250 ± 0.009	[31] KROPF	74	RVUE	n decay + nuclear ft

[26] This is the combined result of ABELE 02 and ABELE 97D.
[27] MOSTOVOI 01 measures the two P-odd correlations A and B, or rather SA and SB, where S is the n polarization, in free neutron decay.
[28] YEROZOLIMSKY 97 makes a correction to the EROZOLIMSKII 91 value.
[29] These experiments measure the absolute value of g_A/g_V only.
[30] KROHN 75 includes events of CHRISTENSEN 70.
[31] KROPF 74 reviews all data through 1972.

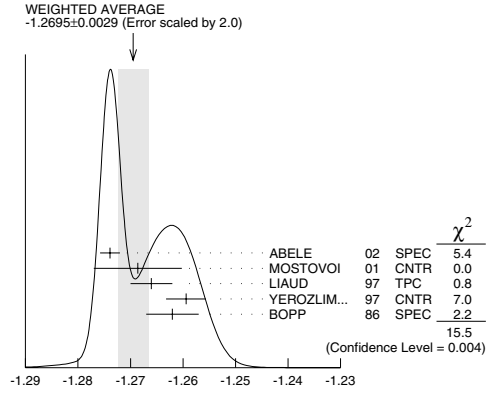

$\lambda \equiv g_A / g_V$

β ASYMMETRY PARAMETER *A*

This is the neutron-spin electron-momentum correlation coefficient. Unless otherwise noted, the values are corrected for radiative effects and weak magnetism.

VALUE	DOCUMENT ID		TECN	COMMENT
−0.1173±0.0013 OUR AVERAGE	Error includes scale factor of 2.3. See the ideogram below.			
−0.1189±0.0007	[32] ABELE	02	SPEC	Cold *n*, polarized
−0.1160±0.0009±0.0012	LIAUD	97	TPC	Cold *n*, polarized
−0.1135±0.0014	[33] YEROZLIM...	97	CNTR	Cold *n*, polarized
−0.1146±0.0019	BOPP	86	SPEC	Cold *n*, polarized
• • • We do not use the following data for averages, fits, limits, etc. • • •				
−0.1168±0.0017	[34] MOSTOVOI	01	CNTR	Inferred
−0.1189±0.0012	ABELE	97D	SPEC	Cold *n*, polarized
−0.1160±0.0009±0.0011	SCHRECK...	95	TPC	See LIAUD 97
−0.1116±0.0014	EROZOLIM...	91	CNTR	See YEROZOLIMSKY 97
−0.114 ±0.005	[35] EROZOLIM...	79	CNTR	Cold *n*, polarized
−0.113 ±0.006	[35] KROHN	75	CNTR	Cold *n*, polarized

[32] This is the combined result of ABELE 02 and ABELE 97D.
[33] YEROZOLIMSKY 97 makes a correction to the EROZOLIMSKII 91 value.
[34] MOSTOVOI 01 calculates this from its measurement of $\lambda = g_A/g_V$ above.
[35] These results are not corrected for radiative effects and weak magnetism, but the corrections are small compared to the errors.

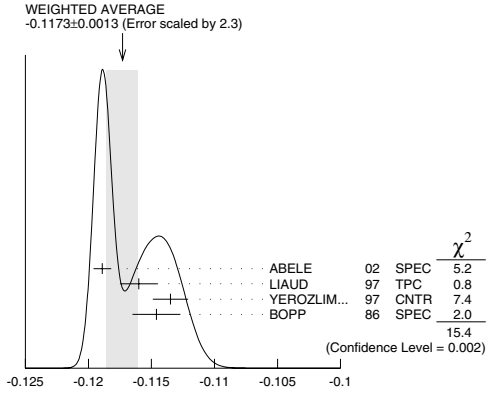

β asymmetry parameter *A*

ν_e ASYMMETRY PARAMETER *B*

This is the neutron-spin antineutrino-momentum correlation coefficient.

VALUE	DOCUMENT ID		TECN	COMMENT
0.983 ±0.004 OUR AVERAGE				
0.9801±0.0046	SEREBROV	98	CNTR	Cold *n*, polarized
0.9894±0.0083	KUZNETSOV	95	CNTR	Cold *n*, polarized
0.995 ±0.034	CHRISTENSEN	70	CNTR	Cold *n*, polarized
1.00 ±0.05	EROZOLIM...	70C	CNTR	Cold *n*, polarized
• • • We do not use the following data for averages, fits, limits, etc. • • •				
0.9876±0.0004	[36] MOSTOVOI	01	CNTR	Inferred

[36] MOSTOVOI 01 calculates this from its measurement of $\lambda = g_A/g_V$ above.

e-ν_e ANGULAR CORRELATION COEFFICIENT *a*

VALUE	DOCUMENT ID		TECN	COMMENT
−0.103 ±0.004 OUR AVERAGE				
−0.1054±0.0055	BYRNE	02	SPEC	Proton recoil spectrum
−0.1017±0.0051	STRATOWA	78	CNTR	Proton recoil spectrum
−0.091 ±0.039	GRIGOREV	68	SPEC	Proton recoil spectrum
• • • We do not use the following data for averages, fits, limits, etc. • • •				
−0.1045±0.0014	[37] MOSTOVOI	01	CNTR	Inferred

[37] MOSTOVOI 01 calculates this from its measurement of $\lambda = g_A/g_V$ above.

ϕ_{AV}, PHASE OF g_A RELATIVE TO g_V

Time reversal invariance requires this to be 0 or 180°. This is related to *D* given in the next data block and $\lambda \equiv g_A/g_V$ by $\sin(\phi_{AV}) = D(1+3\lambda^2)/2\lambda$.

VALUE (°)	DOCUMENT ID		TECN	COMMENT
180.08±0.10 OUR AVERAGE				
180.08±0.13	LISING	00	CNTR	Polarized >93%
179.71±0.39	EROZOLIM...	78	CNTR	Cold *n*, polarized
180.35±0.43	EROZOLIM...	74	CNTR	Cold *n*, polarized
180.14±0.22	STEINBERG	74	CNTR	Cold *n*, polarized
• • • We do not use the following data for averages, fits, limits, etc. • • •				
181.1 ±1.3	[38] KROPF	74	RVUE	*n* decay

[38] KROPF 74 reviews all data through 1972.

TRIPLE CORRELATION COEFFICIENT *D*

These are measurements of the component of *n* spin perpendicular to the decay plane in β decay. Should be zero if *T* invariance is not violated.

VALUE	DOCUMENT ID		TECN	COMMENT
(−0.6 ±1.0) × 10⁻³ OUR AVERAGE				
−0.0006±0.0012±0.0005	LISING	00	CNTR	Polarized >93%
+0.0022±0.0030	EROZOLIM...	78	CNTR	Cold *n*, polarized
−0.0027±0.0050	[39] EROZOLIM...	74	CNTR	Cold *n*, polarized
−0.0011±0.0017	STEINBERG	74	CNTR	Cold *n*, polarized

[39] EROZOLIMSKII 78 says asymmetric proton losses and nonuniform beam polarization may give a systematic error up to 0.003, thus increasing the EROZOLIMSKII 74 error to 0.005. STEINBERG 74 and STEINBERG 76 estimate these systematic errors to be insignificant in their experiment.

n REFERENCES

We have omitted some papers that have been superseded by later experiments. See our earlier editions.

MOHR	04	RMP (to be publ.)	P.J. Mohr, B.N. Taylor	(NIST)
physics.nist.gov/constants				
DEWEY	03	PRL 91 152302	M.S. Dewey *et al.*	(NIST, TULN, IND+)
KOSSERT	03	EPJ A16 259	K. Kossert *et al.*	(Mainz MAMI Collab.)
Also	02	PRL 88 162301	K. Kossert *et al.*	(Mainz MAMI Collab.)
LUNDIN	03	PRL 90 192501	M. Lundin *et al.*	
ABELE	02	PRL 88 211801	H. Abele *et al.*	(PERKEO-II Collab.)
BECK	02	JETPL 76 332	M. Beck *et al.*	(LEUV, SUSS, KIAE, PNPI)
		Translated from ZETFP 76 392.		
BYRNE	02	JPG 28 1325	J. Byrne *et al.*	
CHUNG	02B	PR D66 032004	J. Chung *et al.*	(SOUDAN-2 Collab.)
MOSTOVOI	01	PAN 64 1955	Yu.A. Mostovoi *et al.*	
		Translated from YAF 64 2040.		
OLMOSDEL...	01	EPJ A10 207	V. Olmos de Leon *et al.*	(MAMI TAPS Collab.)
ARZUMANOV	00	PL B483 15	S. Arzumanov *et al.*	
GAL	00	PR C61 028201	A. Gal	
KOLB	00	PRL 85 1388	N.R. Kolb *et al.*	
LAMOREAUX	00	PR D61 051301R	S.K. Lamoreaux, R. Golub	
LISING	00	PR C62 055501	L.J. Lising *et al.*	(NIST emiT Collab.)
HARRIS	99	PRL 82 904	P.G. Harris *et al.*	
KESSLER	99	PL A255 221	E.G. Kessler Jr *et al.*	
MOHR	99	JPCRD 28 1713	P.J. Mohr, B.N. Taylor	(NIST)
Also	00	RMP 72 351	P.J. Mohr, B.N. Taylor	(NIST)
SEREBROV	98	JETP 86 1074	A.P. Serebrov *et al.*	
		Translated from ZETF 113 1963.		
ABELE	97D	PL B407 212	H. Abele *et al.*	(HEIDP, ILLG)
KOPECKY	97	PR C56 2229	S. Kopecky *et al.*	
LIAUD	97	NP A612 53	P. Liaud *et al.*	(ILLG, LAPP)
YEROZLIM...	97	PL B412 240	B.G. Erozolimsky *et al.*	(HARV, PNPI, KIAE)
ALTAREV	96	PAN 59 1152	I.S. Altarev *et al.*	(PNPI)
		Translated from YAF 59 1204.		
BONDAREN...	96	JETPL 64 416	A.N. Bondarenko *et al.*	(KIAE)
		Translated from ZETFP 64 382.		
BYRNE	96	EPL 33 187	J. Byrne *et al.*	(SUSS, ILLG)
MOSTOVOI	96	PAN 59 968	Y.A. Mostovoy	(KIAE)
		Translated from YAF 59 1013.		
NORMAN	96	PR D53 4086	E.B. Norman, J.N. Bahcall, M. Goldhaber	(LBL+)
IGNATOVICH	95	JETPL 62 1	V.K. Ignatovich	(JINR)
		Translated from ZETFP 62 3.		
KOESTER	95	PR C51 3363	L. Koester *et al.*	(+)
KOPECKY	95	PRL 74 2427	S. Kopecky *et al.*	
KUZNETSOV	95	PRL 75 794	I.A. Kuznetsov *et al.*	(PNPI, KIAE, HARV+)
SCHRECK...	95	PL B349 427	K. Schreckenbach *et al.*	(MUNT, ILLG, LAPP)
BALDO-...	94	ZPHY C63 409	M. Baldo-Ceolin *et al.*	(HEID, ILLG, PADO+)
DIFILIPPO	94	PRL 73 1481	F. DiFilippo *et al.*	(MIT)
Also	93	PRL 71 1998	V. Natarajan *et al.*	(MIT)
GOLUB	94	PRPL 237C 1	R. Golub, K. Lamoreaux	(HAHN, WASH)
MAMPE	93	JETPL 57 82	B. Mampe *et al.*	(KIAE)
		Translated from ZETFP 57 77.		
PENDLEBURY	93	ARNPS 43 687	J.M. Pendlebury	(ILLG)
ALTAREV	92	PL B276 242	I.S. Altarev *et al.*	(PNPI)
NESVIZHEV...	92	JETP 75 405	V.V. Nesvizhevsky *et al.*	(PNPI, JINR)
		Translated from ZETF 102 740.		
SCHRECK...	92	JPG 18 1	K. Schreckenbach, W. Mampe	(ILLG)
ALBERICO	91	NP A523 488	W.M. Alberico, A. de Pace, M. Pignone	(TORI)
DUBBERS	91	NP A527 239c	D. Dubbers	(ILLG)
Also	90	EPL 11 195	D. Dubbers, W. Mampe, J. Dohner	(ILLG, HEID)
EROZOLIM...	91	PL B263 33	B.G. Erozolimsky *et al.*	(PNPI, KIAE)
Also	90	SJNP 52 999	B.G. Erozolimsky *et al.*	(PNPI, KIAE)
		Translated from YAF 52 1583.		
EROZOLIM...	91B	SJNP 53 260	B.G. Erozolimsky, Y.A. Mostovoy	(KIAE)
		Translated from YAF 53 418.		
SCHMIEDM...	91	PRL 66 1015	J. Schmiedmayer *et al.*	(TUW, ORNL)
WOOLCOCK	91	MPL A6 2579	W.S. Woolcock	(CANB)
ALFIMENKOV	90	JETPL 52 373	V.P. Alfimenkov *et al.*	(PNPI, JINR)
		Translated from ZETFP 52 984.		

BALDO-...	90	PL B236 95	M. Baldo-Ceolin *et al.*	(PADO, PAVI, HEIDP+)
BERGER	90	PL B240 237	C. Berger *et al.*	(FREJUS Collab.)
BRESSI	90	NC 103A 731	G. Bressi *et al.*	(PAVI, ROMA, MILA)
BYRNE	90	PRL 65 289	J. Byrne *et al.*	(SUSS, NBS, SCOT, CBNM)
FREEDMAN	90	CNPP A19 209	S.J. Freedman	(ANL)
GREEN	90	JPG 16 L75	K. Green, D. Thompson	(RAL)
RAMSEY	90	ARNPS 40 1	N.F. Ramsey	(HARV)
ROSE	90	PL B234 460	K.W. Rose *et al.*	(GOET, MPCM, MANZ)
ROSE	90B	NP A514 621	K.W. Rose *et al.*	(GOET, MPCM)
SMITH	90	PL B234 191	K.F. Smith *et al.*	(SUSS, RAL, HARV+)
BRESSI	89	ZPHY C43 175	G. Bressi *et al.*	(INFN, MILA, PAVI, ROMA)
DOVER	89	NIM A284 13	C.B. Dover, A. Gal, J.M. Richard	(BNL, HEBR+)
EROZOLIM...	89	NIM A284 89	B.G. Erozolimsky	(PNPI)
KOSSAKOW...	89	NP A503 473	R. Kossakowski *et al.*	(LAPP, SAVO, ISNG+)
MAMPE	89	PRL 63 593	W. Mampe *et al.*	(ILLG, RISL, SUSS, URI)
MOHAPATRA	89	NIM A284 1	R.N. Mohapatra	(UMD)
PAUL	89	ZPHY C45 25	W. Paul *et al.*	(BONN, WUPP, MPIH, ILLG)
SCHMIEDM...	89	NIM A284 137	J. Schmiedmayer, H. Rauch, P. Riehs	(WIEN)
BAUMANN	88	PR D37 3107	J. Baumann *et al.*	(BAYR, MUNI, ILLG)
KOESTER	88	ZPHY A329 229	L. Koester, W. Waschkowski, J. Meier	(MUNI, MUNT)
LAST	88	PRL 60 995	I. Last *et al.*	(HEIDP, ILLG, ANL)
SCHMIEDM...	88	PRL 61 1065	J. Schmiedmayer, H. Rauch, P. Riehs	(TUW)
Also	88B	PRL 61 2509 erratum	J. Schmiedmayer, H. Rauch, P. Riehs	(TUW)
SPIVAK	88	JETP 67 1735 Translated from ZETF 94 1.	P.E. Spivak	(KIAE)
COHEN	87	RMP 59 1121	E.R. Cohen, B.N. Taylor	(RISC, NBS)
ALEKSANDR...	86	SJNP 44 900 Translated from YAF 44 1384.	Yu.A. Aleksandrov *et al.*	
ALTAREV	86	JETPL 44 460 Translated from ZETFP 44 360.	I.S. Altarev *et al.*	(PNPI)
BOPP	86	PRL 56 919	P. Bopp *et al.*	(HEIDP, ANL, ILLG)
Also	88	ZPHY C37 179	E. Klempt *et al.*	(HEIDP, ANL, ILLG)
CRESTI	86	PL B177 206	M. Cresti *et al.*	(PADO)
Also	88	PL B200 587 erratum	M. Cresti *et al.*	(PADO)
GREENE	86	PRL 56 819	G.L. Greene *et al.*	(NBS, ILLG)
KOESTER	86	Physica B137 282	L. Koester *et al.*	
KOSVINTSEV	86	JETPL 44 571 Translated from ZETFP 44 444.	Y.Y. Kosvintsev, V.I. Morozov, G.I. Terekhov	(KIAE)
TAKITA	86	PR D34 902	M. Takita *et al.*	(KEK, TOKY+)
DOVER	85	PR C31 1423	C.B. Dover, A. Gal, J.M. Richard	(BNL)
FIDECARO	85	PL 156B 122	G. Fidecaro *et al.*	(CERN, ILLG, PADO+)
PARK	85B	NP B252 261	H.S. Park *et al.*	(IMB Collab.)
BATTISTONI	84	PL 133B 454	G. Battistoni *et al.*	(NUSEX Collab.)
JONES	84	PRL 52 720	T.W. Jones *et al.*	(IMB Collab.)
PENDLEBURY	84	PL 136B 327	J.M. Pendlebury *et al.*	(SUSS, HARV, RAL+)
CHERRY	83	PRL 50 1354	M.L. Cherry *et al.*	(PENN, BNL)
DOVER	83	PR D27 1090	C.B. Dover, A. Gal, J.M. Richard	(BNL)
KABIR	83	PRL 51 231	P.K. Kabir	(HARV)
MOSTOVOY	83	JETPL 37 196 Translated from ZETFP 37 162.	Y.A. Mostovoy	(KIAE)
ROY	83	PR D28 1770	A. Roy *et al.*	(TATA)
VAIDYA	83	PR D27 486	S.C. Vaidya *et al.*	(TATA)
GAEHLER	82	PR D25 2887	R. Gahler, J. Kalus, W. Mampe	(BAYR, ILLG)
GREENE	82	Metrologia 18 93	G.L. Greene *et al.*	(YALE, HARV, ILLG+)
ALTAREV	81	PL 102B 13	I.S. Altarev *et al.*	(PNPI)
BARABANOV	80	JETPL 32 359 Translated from ZETFP 32 384.	I.R. Barabanov *et al.*	(PNPI)
BYRNE	80	PL 92B 274	J. Byrne *et al.*	(SUSS, RL)
KOSVINTSEV	80	JETPL 31 236 Translated from ZETFP 31 257.	Y.Y. Kosvintsev *et al.*	(JINR)
MOHAPATRA	80	PRL 44 1316	R.N. Mohapatra, R.E. Marshak	(CUNY, VPI)
ALTAREV	79	JETPL 29 730 Translated from ZETFP 29 794.	I.S. Altarev *et al.*	(PNPI)
EROZOLIM...	79	SJNP 30 356 Translated from YAF 30 692.	B.G. Erozolimsky *et al.*	(KIAE)
NORMAN	79	PRL 43 1226	E.B. Norman, A.G. Seamster	(WASH)
BONDAREN...	78	JETPL 28 303 Translated from ZETFP 28 328.	L.N. Bondarenko *et al.*	(KIAE)
Also	82	Smolenice Conf.	P.G. Bondarenko	(KIAE)
EROZOLIM...	78	SJNP 28 48 Translated from YAF 28 98.	B.G. Erozolimsky *et al.*	(KIAE)
STRATOWA	78	PR D18 3970	C. Stratowa, R. Dobrozemsky, P. Weinzierl	(SEIB)
EROZOLIM...	77	JETPL 23 663 Translated from ZETFP 23 720.	B.G. Erozolimsky *et al.*	(KIAE)
KOESTER	76	PRL 36 1021	L. Koester *et al.*	
STEINBERG	76	PR D13 2469	R.I. Steinberg *et al.*	(YALE, ISNG)
DOBROZE...	75	PR D11 510	R. Dobrozemsky *et al.*	(SEIB)
KROHN	75	PL 55B 175	V.E. Krohn, G.R. Ringo	(ANL)
EROZOLIM...	74	JETPL 20 345 Translated from ZETFP 20 745.	B.G. Erozolimsky *et al.*	
KROPF	74	ZPHY 267 129	H. Kropf, E. Paul	(LINZ)
Also	70	NP A154 160	H. Paul	(VIEN)
STEINBERG	74	PRL 33 41	R.I. Steinberg *et al.*	(YALE, ISNG)
COHEN	73	JPCRD 2 664	E.R. Cohen, B.N. Taylor	(RISC, NBS)
KROHN	73	PR D8 1305	V.E. Krohn, G.R. Ringo	
CHRISTENSEN	72	PR D5 1628	C.J. Christensen *et al.*	(RISO)
CHRISTENSEN	70	PR C1 1693	C.J. Christensen, V.E. Krohn, G.R. Ringo	(ANL)
EROZOLIM...	70C	PL 33B 351	B.G. Erozolimsky *et al.*	(KIAE)
GRIGOREV	68	SJNP 6 239 Translated from YAF 6 329.	V.K. Grigoriev *et al.*	(ITEP)
KROHN	66	PR 148 1303	V.E. Krohn, G.R. Ringo	

N AND Δ RESONANCES

I. Introduction

The excited states of the nucleon have been studied in a large number of formation and production experiments. The conventional (*i.e.,* Breit-Wigner) masses, pole positions, widths, and elasticities of the N and Δ resonances in the Baryon Summary Table come largely from partial-wave analyses of πN total, elastic, and charge-exchange scattering data. Partial-wave analyses have also been performed on much smaller data sets to get $N\eta$, ΛK, and ΣK branching fractions. Other branching fractions come from isobar-model analyses of $\pi N \to N\pi\pi$ data. Finally, many $N\gamma$ branching fractions have been determined from photoproduction experiments (see Sec. III).

Table 1 lists all the N and Δ entries in the Baryon Listings and gives our evaluation of the status of each, both overall and channel by channel. Only the "established" resonances (overall status 3 or 4 stars) appear in the Baryon Summary Table. We generally consider a resonance to be established only if it has been seen in at least two independent analyses of elastic scattering and if the relevant partial-wave amplitudes do not behave erratically or have large errors.

Table 1. The status of the N and Δ resonances. Only those with an overall status of *** or **** are included in the main Baryon Summary Table.

			Status as seen in —						
Particle	$L_{2I\,2J}$	Overall status	$N\pi$	$N\eta$	ΛK	ΣK	$\Delta\pi$	$N\rho$	$N\gamma$
$N(939)$	P_{11}	****							
$N(1440)$	P_{11}	****	****	*			***	*	***
$N(1520)$	D_{13}	****	****	*			****	****	****
$N(1535)$	S_{11}	****	****	****			*	**	***
$N(1650)$	S_{11}	****	****	*	***	**	***	**	***
$N(1675)$	D_{15}	****	****	*	*		****	*	****
$N(1680)$	F_{15}	****	****				****	****	****
$N(1700)$	D_{13}	***	***	*	**	*	**	*	**
$N(1710)$	P_{11}	***	***	**	**	*	**	*	***
$N(1720)$	P_{13}	****	****	*	**	*	*	**	**
$N(1900)$	P_{13}	**	**					*	
$N(1990)$	F_{17}	**	**	*	*	*			*
$N(2000)$	F_{15}	**	**	*	*	*	*	**	
$N(2080)$	D_{13}	**	**	*	*				*
$N(2090)$	S_{11}	*	*						
$N(2100)$	P_{11}	*	*	*					
$N(2190)$	G_{17}	****	****	*	*	*		*	*
$N(2200)$	D_{15}	**	**	*	*				
$N(2220)$	H_{19}	****	****	*					
$N(2250)$	G_{19}	****	****	*					
$N(2600)$	$I_{1\,11}$	***	***						
$N(2700)$	$K_{1\,13}$	**	**						
$\Delta(1232)$	P_{33}	****	****	F					****
$\Delta(1600)$	P_{33}	***	***	o			***	*	**
$\Delta(1620)$	S_{31}	****	****	r			****	****	***
$\Delta(1700)$	D_{33}	****	****	b		*	***	**	***
$\Delta(1750)$	P_{31}	*	*	i					
$\Delta(1900)$	S_{31}	**	**	d		*	*	**	*
$\Delta(1905)$	F_{35}	****	****	d		*	**	**	***
$\Delta(1910)$	P_{31}	****	****	e		*	*	*	*
$\Delta(1920)$	P_{33}	***	***	n		*	**		*
$\Delta(1930)$	D_{35}	***	***			*			**
$\Delta(1940)$	D_{33}	*	*	F					
$\Delta(1950)$	F_{37}	****	****	o		*	****	*	****
$\Delta(2000)$	F_{35}	**		r				**	
$\Delta(2150)$	S_{31}	*	*	b					
$\Delta(2200)$	G_{37}	*	*	i					
$\Delta(2300)$	H_{39}	**	**	d					
$\Delta(2350)$	D_{35}	*	*	d					
$\Delta(2390)$	F_{37}	*	*	e					
$\Delta(2400)$	G_{39}	**	**	n					
$\Delta(2420)$	$H_{3\,11}$	****	****						*
$\Delta(2750)$	$I_{3\,13}$	**	**						
$\Delta(2950)$	$K_{3\,15}$	**	**						

****	Existence is certain, and properties are at least fairly well explored.
***	Existence ranges from very likely to certain, but further confirmation is desirable and/or quantum numbers, branching fractions, *etc.* are not well determined.
**	Evidence of existence is only fair.
*	Evidence of existence is poor.

While no new elastic partial-wave analyses have been published since our last edition, a comprehensive set of resonance parameters has been extracted from a multi-channel analysis of transition amplitudes and data for πN scattering to six

baryon-meson final states [1]. This work has determined both Breit-Wigner and pole parameters for resonances up to about 2 GeV.

The interested reader will find further discussions in the proceedings of two recent conferences [2, 3], and in two older reviews [4, 5].

II. Using the N and Δ listings

Written 2002 by G. Höhler (University of Karlsruhe) and R.L Workman, (George Washington University)

In the inelastic region, a resonance is associated with a cluster of poles on different Riemann sheets. If one of these poles is located near the real axis and far enough from branch points, it will be strongly dominant. If one of the final-state particles itself has a strong decay, it is also necessary to consider branch points in the lower half plane that belong to thresholds for two-particle final states; see for example Refs. 6 and 7.

Our Particle Listings and Summary Tables include pole parameters for the N and Δ resonances. However, the Breit-Wigner parameters are most often quoted and are used in model-based studies of the baryons and associated reaction dynamics. Problems associated with this choice were discussed in our 2000 edition [8]. Here we just point out that the use of Breit-Wigner parameters for complicated structures, such as the N(1440), should be avoided. In this case, the method used in Ref. 7 is suitable for the analysis.

In the search for "missing" quark-model states, indications of new structures occasionally are found. Often these are associated (if possible) with the one- and two-star states listed in Table 1. We caution against this: The status of the one- and two-star states found in the Karlsruhe-Helsinki (KH80) [4] and Carnegie-Mellon/Berkeley (CMB80) [9] fits is now doubtful. Predictions for π^+p spin-rotation parameters from those fits are in significant disagreement with recent ITEP/PNPI measurements [10], whereas the predictions of Ref. 11 are good. This discrepancy has been associated in Ref. 10 with the behavior of a zero trajectory at a "critical point" (see Sec. 2.1.1 of Ref. 4) near a pion lab momentum of 0.8 GeV/c. According to Ref. 10, the effect on the 4-star resonances $\Delta(1905)$ and $\Delta(1950)$ is small, but the effect on the 3-star resonances $\Delta(1920)$ and $\Delta(1930)$ is large. For a study of the approximation made in Ref. 10 and of problems with some higher resonances, the detailed treatment of zero trajectories in Ref. 12 is relevant. This problem should also be considered in any multi-channel analysis that uses the KH80 and CMB80 amplitudes as input.

III. Electromagnetic interactions

Revised 2003 by R.L. Workman (George Washington University)

Nearly all the entries in the Listings concerning electromagnetic properties of the N and Δ resonances are $N\gamma$ couplings. These couplings, the helicity amplitudes $A_{1/2}$ and $A_{3/2}$, have been obtained in partial-wave analyses of single-pion photoproduction, η photoproduction, and Compton scattering. Most photoproduction analyses have taken the existence, masses, and widths of the resonances from the $\pi N \to \pi N$ analyses, and have only determined the $N\gamma$ couplings. This approach is only applicable to resonances with a significant $N\pi$ coupling. A brief description of the various methods of analysis of photoproduction data may be found in our 1992 edition [13].

Our Listings omit a number of analyses that are now obsolete. Most of the older results may be found in our 1982 edition [14]. The errors quoted for the couplings in the Listings are calculated in different ways in different analyses and therefore should be used with care. In general, the systematic differences between the analyses caused by using different parameterization schemes are probably more indicative of the true uncertainties than are the quoted errors.

Probably the most reliable analyses, for most resonances, are ARAI 80, CRAWFORD 80, AWAJI 81, FUJII 81, CRAWFORD 83, and ARNDT 96. There is an update to the Crawford analysis [2]. The errors we give on $N\gamma$ couplings are a combination of the stated statistical errors on the analyses and the systematic differences between them. The analyses are given equal weight, except ARNDT 96 is weighted, rather arbitrarily, by a factor of two because its data set is at least 50% larger than those of the other analyses and contains many new high-quality measurements. The $\Delta(1232)$ and $N(1535)$ are special cases and are discussed in the 2002 *Review* [15].

The Baryon Summary Table gives $N\gamma$ branching fractions for those resonances whose couplings are considered to be reasonably well established. The $N\gamma$ partial width Γ_γ is given in terms of the helicity amplitudes $A_{1/2}$ and $A_{3/2}$ by

$$\Gamma_\gamma = \frac{k^2}{\pi}\frac{2M_N}{(2J+1)M_R}\left[|A_{1/2}|^2 + |A_{3/2}|^2\right] \quad .$$

Here M_N and M_R are the nucleon and resonance masses, J is the resonance spin, and k is the photon c.m. decay momentum.

See our 2002 *Review* for some further discussion [15].

IV. Non-qqq baryon candidates

Revised 2003 by R.L. Workman (George Washington University).

The standard quark-model assignments for baryons are outlined in Sec. 13.3, "Baryons: qqq states." Just as with mesons (see the note on "Non-$q\overline{q}$ mesons"), there have been suggestions that non-qqq baryons might exist, such as hybrid ($qqqg$) baryons, unstable meson-nucleon bound states [16], or pentaquarks ($qqqq\overline{q}$). If hybrid states exist, they will be more difficult to verify than hybrid mesons. Possibilities are listed in Ref. [17] and in our 2000 edition. No hybrid baryon has yet been clearly established. Other unconventional quark configurations include the H dibaryon ($uuddss$). Recent searches for the H dibaryon at BNL [18, 19]. KEK [20], and Fermilab [21] have reported null results.

Recent experiments at a number of labs have reported sharp structures in nK^+ and pK^0 invariant mass distributions, evidence for an S=+1 resonance with a mass of 1540 MeV and a

very narrow width (see our note on "A Possible Exotic Baryon Resonance"). This would be a pentaquark candidate. Evidence for a pentaquark state with hidden strangeness ($qqqs\overline{s}$) has also been reported [22].

Narrow structures continue to be seen in proton-proton and proton-nucleus scattering [23]. However, a number of high-precision searches for such states has found no structure of statistical significance [24]. A clear understanding of this growing set of experiments remains elusive.

References

1. G. Penner and U. Mosel, Phys. Rev. **C66**, 055211 (2002).
2. Proceedings of the Workshop on the Physics of Excited Nucleons (NSTAR2001), eds. D. Drechsel and L. Tiator (World Scientific, Singapore, 2001).
3. Proceedings of the 9th International Conference on the Structure of Baryons, eds. C. Carlson and B. Mecking (World Scientific, Singapore, 2003).
4. G. Höhler, Pion-Nucleon Scattering, Landolt-Börnstein Vol. I/9b2 (1983), ed. H. Schopper, Springer Verlag.
5. A.J.G. Hey and R.L. Kelly, Phys. Reports **96**, 71 (1983).
6. W.R. Frazier and A.W. Hendry, Phys. Rev. **134**, B1307 (1964).
7. R.E. Cutkosky and S. Wang, Phys. Rev. **D42**, 235 (1990).
8. D.E. Groom *et al.*, Eur. Phys. J. **C15**, 1 (2000).
9. R.E. Cutkosky *et al.*, Baryon 1980, *IV International Conference on Baryon Resonances*, Toronto, ed. N. Isgur, p. 19.
10. I.G. Alekseev *et al.*, Phys. Rev. **C55**, 2049 (1997); Phys. Lett. **B485**, 32 (2000); Eur. Phys. J. **A12**, 117 (2001).
11. R.A. Arndt *et al.*, Phys. Rev. **C52**, 2120 (1995).
12. I. Sabba-Stefanescu, Progress of Physics **35**, 573 (1987).
13. K. Hikasa *et al.*, Phys. Rev. **D45**, S1 (1992).
14. M. Roos *et al.*, Phys. Lett. **B111**, 1 (1982).
15. K. Hagiwara *et al.*, Phys. Rev. **D66**, 010001 (2002).
16. S. Pakvasa and S.F. Tuan, Phys. Lett. **B459**, 301 (1999); N. Kaiser, T. Waas, and W. Weise, Nucl. Phys. **A612**, 297 (1997); N. Kaiser, P.B. Siegel, and W. Weise, Phys. Lett. **B362**, 23 (1995).
17. P.R. Page, *Proceedings of the Conference on Excited Nucleons and Hadronic Structure (NSTAR 2000)*, eds. V. Burkert *et al.* (World Scientific, Singapore, 2001), p. 171.
18. K. Yamamoto *et al.*, Phys. Lett. **B478**, 401 (2000).
19. F. Merrill *et al.*, Phys. Rev. **C63**, 035206 (2001).
20. K. Ahn *et al.*, Phys. Rev. **C62**, 055201 (2000).
21. A. Alavi-Harati *et al.*, Phys. Rev. Lett. **84**, 2593 (2000).
22. Yu.M. Antipov *et al.*, PAN **65**, 2070 (2002).
23. B. Tatischeff *et al.*, Eur. Phys. J. **A17**, 245 (2003); L.V. Fil'kov *et al.*, Phys. Rev. **C61**, 044004 (2000); Yu. A. Troyan *et al.*, PAN **63**, 1562 (2000); A.S. Khrykin *et al.*, Phys. Rev. **C64**, 034002 (2001).
24. X. Jiang *et al.*, Phys. Rev. **C67**, 028201 (2003); W. Brodowski *et al.*, Phys. Lett. **B550**, 147 (2002); P.A. Zolnierczuk *et al.*, Phys. Lett. **B549**, 301 (2002); U. Siodlaczek *et al.*, Eur. Phys. J. **A9**, 309 (2000).

$N(1440)$ P_{11}

$I(J^P) = \frac{1}{2}(\frac{1}{2}^+)$ Status: ****

Most of the results published before 1975 are now obsolete and have been omitted. They may be found in our 1982 edition, Physics Letters **111B** (1982).

$N(1440)$ BREIT-WIGNER MASS

VALUE (MeV)	DOCUMENT ID		TECN	COMMENT
1430 to 1470 (≈ 1440) OUR ESTIMATE				
1462±10	MANLEY	92	IPWA	$\pi N \to \pi N$ & $N\pi\pi$
1440±30	CUTKOSKY	80	IPWA	$\pi N \to \pi N$
1410±12	HOEHLER	79	IPWA	$\pi N \to \pi N$
• • • We do not use the following data for averages, fits, limits, etc. • • •				
1518± 5	PENNER	02C	DPWA	Multichannel
1479±80	VRANA	00	DPWA	Multichannel
1463± 7	ARNDT	96	IPWA	$\gamma N \to \pi N$
1467	ARNDT	95	DPWA	$\pi N \to N\pi$
1421±18	BATINIC	95	DPWA	$\pi N \to N\pi$, $N\eta$
1465	LI	93	IPWA	$\gamma N \to \pi N$
1471	CUTKOSKY	90	IPWA	$\pi N \to \pi N$
1411	CRAWFORD	80	DPWA	$\gamma N \to \pi N$
1472	[1] BAKER	79	DPWA	$\pi^- p \to n\eta$
1417	BARBOUR	78	DPWA	$\gamma N \to \pi N$
1460	BERENDS	77	IPWA	$\gamma N \to \pi N$
1380	[2] LONGACRE	77	IPWA	$\pi N \to N\pi\pi$
1390	[3] LONGACRE	75	IPWA	$\pi N \to N\pi\pi$

$N(1440)$ BREIT-WIGNER WIDTH

VALUE (MeV)	DOCUMENT ID		TECN	COMMENT
250 to 450 (≈ 350) OUR ESTIMATE				
391± 34	MANLEY	92	IPWA	$\pi N \to \pi N$ & $N\pi\pi$
545±170	CUTKOSKY	90	IPWA	$\pi N \to \pi N$
340± 70	CUTKOSKY	80	IPWA	$\pi N \to \pi N$
135± 10	HOEHLER	79	IPWA	$\pi N \to \pi N$
• • • We do not use the following data for averages, fits, limits, etc. • • •				
668± 41	PENNER	02C	DPWA	Multichannel
490±120	VRANA	00	DPWA	Multichannel
360± 20	ARNDT	96	IPWA	$\gamma N \to \pi N$
440	ARNDT	95	DPWA	$\pi N \to N\pi$
250± 63	BATINIC	95	DPWA	$\pi N \to N\pi$, $N\eta$
315	LI	93	IPWA	$\gamma N \to \pi N$
334	CRAWFORD	80	DPWA	$\gamma N \to \pi N$
113	[1] BAKER	79	DPWA	$\pi^- p \to n\eta$
331	BARBOUR	78	DPWA	$\gamma N \to \pi N$
279	BERENDS	77	IPWA	$\gamma N \to \pi N$
200	[2] LONGACRE	77	IPWA	$\pi N \to N\pi\pi$
200	[3] LONGACRE	75	IPWA	$\pi N \to N\pi\pi$

$N(1440)$ POLE POSITION

REAL PART

VALUE (MeV)	DOCUMENT ID		TECN	COMMENT
1345 to 1385 (≈ 1365) OUR ESTIMATE				
1346	[4] ARNDT	95	DPWA	$\pi N \to N\pi$
1385	[5] HOEHLER	93	SPED	$\pi N \to \pi N$
1370	CUTKOSKY	90	IPWA	$\pi N \to \pi N$
1375±30	CUTKOSKY	80	IPWA	$\pi N \to \pi N$
• • • We do not use the following data for averages, fits, limits, etc. • • •				
1383	VRANA	00	DPWA	Multichannel
1360	[6] ARNDT	91	DPWA	$\pi N \to \pi N$ Soln SM90
1381 or 1379	[7] LONGACRE	78	IPWA	$\pi N \to N\pi\pi$
1360 or 1333	[2] LONGACRE	77	IPWA	$\pi N \to N\pi\pi$

$-2\times$IMAGINARY PART

VALUE (MeV)	DOCUMENT ID		TECN	COMMENT
160 to 260 (≈ 210) OUR ESTIMATE				
176	[4] ARNDT	95	DPWA	$\pi N \to N\pi$
164	[5] HOEHLER	93	SPED	$\pi N \to \pi N$
228	CUTKOSKY	90	IPWA	$\pi N \to \pi N$
180±40	CUTKOSKY	80	IPWA	$\pi N \to \pi N$
• • • We do not use the following data for averages, fits, limits, etc. • • •				
316	VRANA	00	DPWA	Multichannel
252	[6] ARNDT	91	DPWA	$\pi N \to \pi N$ Soln SM90
209 or 210	[7] LONGACRE	78	IPWA	$\pi N \to N\pi\pi$
167 or 234	[2] LONGACRE	77	IPWA	$\pi N \to N\pi\pi$

$N(1440)$ ELASTIC POLE RESIDUE

MODULUS $|r|$

VALUE (MeV)	DOCUMENT ID		TECN	COMMENT
42	[4] ARNDT	95	DPWA	$\pi N \to \pi N$
40	HOEHLER	93	SPED	$\pi N \to \pi N$
74	CUTKOSKY	90	IPWA	$\pi N \to \pi N$
52 ± 5	CUTKOSKY	80	IPWA	$\pi N \to \pi N$
• • • We do not use the following data for averages, fits, limits, etc. • • •				
109	[6] ARNDT	91	DPWA	$\pi N \to \pi N$ Soln SM90

PHASE θ

VALUE (°)	DOCUMENT ID		TECN	COMMENT
-101	[4] ARNDT	95	DPWA	$\pi N \to \pi N$
-84	CUTKOSKY	90	IPWA	$\pi N \to \pi N$
-100 ± 35	CUTKOSKY	80	IPWA	$\pi N \to \pi N$
• • • We do not use the following data for averages, fits, limits, etc. • • •				
-93	[6] ARNDT	91	DPWA	$\pi N \to \pi N$ Soln SM90

$N(1440)$ DECAY MODES

The following branching fractions are our estimates, not fits or averages.

	Mode	Fraction (Γ_i/Γ)
Γ_1	$N\pi$	60–70 %
Γ_2	$N\eta$	
Γ_3	$N\pi\pi$	30–40 %
Γ_4	$\Delta\pi$	20–30 %
Γ_5	$\Delta(1232)\pi$, P-wave	
Γ_6	$N\rho$	<8 %
Γ_7	$N\rho$, S=1/2, P-wave	
Γ_8	$N\rho$, S=3/2, P-wave	
Γ_9	$N(\pi\pi)^{I=0}_{S\text{-wave}}$	5–10 %
Γ_{10}	$p\gamma$	0.035–0.048 %
Γ_{11}	$p\gamma$, helicity=1/2	0.035–0.048 %
Γ_{12}	$n\gamma$	0.009–0.032 %
Γ_{13}	$n\gamma$, helicity=1/2	0.009–0.032 %

$N(1440)$ BRANCHING RATIOS

$\Gamma(N\pi)/\Gamma_{\text{total}}$ Γ_1/Γ

VALUE	DOCUMENT ID		TECN	COMMENT
0.6 to 0.7 OUR ESTIMATE				
0.69 ± 0.03	MANLEY	92	IPWA	$\pi N \to \pi N$ & $N\pi\pi$
0.68 ± 0.04	CUTKOSKY	80	IPWA	$\pi N \to \pi N$
0.51 ± 0.05	HOEHLER	79	IPWA	$\pi N \to \pi N$
• • • We do not use the following data for averages, fits, limits, etc. • • •				
0.57 ± 0.01	PENNER	02C	DPWA	Multichannel
0.72 ± 0.05	VRANA	00	DPWA	Multichannel
0.68	ARNDT	95	DPWA	$\pi N \to N\pi$
0.56 ± 0.08	BATINIC	95	DPWA	$\pi N \to N\pi$, $N\eta$

$(\Gamma_i\Gamma_f)^{1/2}/\Gamma_{\text{total}}$ in $N\pi \to N(1440) \to N\eta$ $(\Gamma_1\Gamma_2)^{1/2}/\Gamma$

VALUE	DOCUMENT ID		TECN	COMMENT
• • • We do not use the following data for averages, fits, limits, etc. • • •				
seen	[1] BAKER	79	DPWA	$\pi^- p \to n\eta$
$+0.328$	[8] FELTESSE	75	DPWA	1488–1745 MeV

$\Gamma(N\eta)/\Gamma_{\text{total}}$ Γ_2/Γ

VALUE	DOCUMENT ID		TECN	COMMENT
0.00 ± 0.01	VRANA	00	DPWA	Multichannel

Note: Signs of couplings from $\pi N \to N\pi\pi$ analyses were changed in the 1986 edition to agree with the baryon-first convention; the overall phase ambiguity is resolved by choosing a negative sign for the $\Delta(1620)$ S_{31} coupling to $\Delta(1232)\pi$.

$(\Gamma_i\Gamma_f)^{1/2}/\Gamma_{\text{total}}$ in $N\pi \to N(1440) \to \Delta(1232)\pi$, P-wave $(\Gamma_1\Gamma_5)^{1/2}/\Gamma$

VALUE	DOCUMENT ID		TECN	COMMENT
+0.37 to +0.41 OUR ESTIMATE				
$+0.39 \pm 0.02$	MANLEY	92	IPWA	$\pi N \to \pi N$ & $N\pi\pi$
+0.41	[2,9] LONGACRE	77	IPWA	$\pi N \to N\pi\pi$
+0.37	[3] LONGACRE	75	IPWA	$\pi N \to N\pi\pi$

$\Gamma(\Delta(1232)\pi$, P-wave$)/\Gamma_{\text{total}}$ Γ_5/Γ

VALUE	DOCUMENT ID		TECN	COMMENT
0.16 ± 0.01	VRANA	00	DPWA	Multichannel

$(\Gamma_i\Gamma_f)^{1/2}/\Gamma_{\text{total}}$ in $N\pi \to N(1440) \to N\rho$, S=1/2, P-wave $(\Gamma_1\Gamma_7)^{1/2}/\Gamma$

VALUE	DOCUMENT ID		TECN	COMMENT
±0.07 to ±0.25 OUR ESTIMATE				
-0.11	[2,9] LONGACRE	77	IPWA	$\pi N \to N\pi\pi$
+0.23	[3] LONGACRE	75	IPWA	$\pi N \to N\pi\pi$

$\Gamma(N\rho, S$=1/2, P-wave$)/\Gamma_{\text{total}}$ Γ_7/Γ

VALUE	DOCUMENT ID		TECN	COMMENT
0.00 ± 0.01	VRANA	00	DPWA	Multichannel

$(\Gamma_i\Gamma_f)^{1/2}/\Gamma_{\text{total}}$ in $N\pi \to N(1440) \to N\rho$, S=3/2, P-wave $(\Gamma_1\Gamma_8)^{1/2}/\Gamma$

VALUE	DOCUMENT ID		TECN	COMMENT
+0.18	[2,9] LONGACRE	77	IPWA	$\pi N \to N\pi\pi$

$(\Gamma_i\Gamma_f)^{1/2}/\Gamma_{\text{total}}$ in $N\pi \to N(1440) \to N(\pi\pi)^{I=0}_{S\text{-wave}}$ $(\Gamma_1\Gamma_9)^{1/2}/\Gamma$

VALUE	DOCUMENT ID		TECN	COMMENT
±0.17 to ±0.25 OUR ESTIMATE				
$+0.24 \pm 0.03$	MANLEY	92	IPWA	$\pi N \to \pi N$ & $N\pi\pi$
-0.18	[2,9] LONGACRE	77	IPWA	$\pi N \to N\pi\pi$
-0.23	[3] LONGACRE	75	IPWA	$\pi N \to N\pi\pi$

$\Gamma(N(\pi\pi)^{I=0}_{S\text{-wave}})/\Gamma_{\text{total}}$ Γ_9/Γ

VALUE	DOCUMENT ID		TECN	COMMENT
0.12 ± 0.01	VRANA	00	DPWA	Multichannel

$N(1440)$ PHOTON DECAY AMPLITUDES

$N(1440) \to p\gamma$, helicity-1/2 amplitude $A_{1/2}$

VALUE ($\text{GeV}^{-1/2}$)	DOCUMENT ID		TECN	COMMENT
−0.065 ±0.004 OUR ESTIMATE				
-0.063 ± 0.005	ARNDT	96	IPWA	$\gamma N \to \pi N$
-0.069 ± 0.018	CRAWFORD	83	IPWA	$\gamma N \to \pi N$
-0.063 ± 0.008	AWAJI	81	DPWA	$\gamma N \to \pi N$
-0.069 ± 0.004	ARAI	80	DPWA	$\gamma N \to \pi N$ (fit 1)
-0.066 ± 0.004	ARAI	80	DPWA	$\gamma N \to \pi N$ (fit 2)
-0.079 ± 0.009	BRATASHEV...	80	DPWA	$\gamma N \to \pi N$
-0.068 ± 0.015	CRAWFORD	80	DPWA	$\gamma N \to \pi N$
-0.0584 ± 0.0148	ISHII	80	DPWA	Compton scattering
• • • We do not use the following data for averages, fits, limits, etc. • • •				
-0.087	PENNER	02D	DPWA	Multichannel
-0.085 ± 0.003	LI	93	IPWA	$\gamma N \to \pi N$
-0.129	[10] WADA	84	DPWA	Compton scattering
-0.075 ± 0.015	BARBOUR	78	DPWA	$\gamma N \to \pi N$
-0.125	[11] NOELLE	78		$\gamma N \to \pi N$
-0.076	BERENDS	77	IPWA	$\gamma N \to \pi N$
-0.087 ± 0.006	FELLER	76	DPWA	$\gamma N \to \pi N$

$N(1440) \to n\gamma$, helicity-1/2 amplitude $A_{1/2}$

VALUE ($\text{GeV}^{-1/2}$)	DOCUMENT ID		TECN	COMMENT
+0.040±0.010 OUR ESTIMATE				
0.045 ± 0.015	ARNDT	96	IPWA	$\gamma N \to \pi N$
0.037 ± 0.010	AWAJI	81	DPWA	$\gamma N \to \pi N$
0.030 ± 0.003	FUJII	81	DPWA	$\gamma N \to \pi N$
0.023 ± 0.009	ARAI	80	DPWA	$\gamma N \to \pi N$ (fit 1)
0.019 ± 0.012	ARAI	80	DPWA	$\gamma N \to \pi N$ (fit 2)
0.056 ± 0.015	CRAWFORD	80	DPWA	$\gamma N \to \pi N$
-0.029 ± 0.035	TAKEDA	80	DPWA	$\gamma N \to \pi N$
• • • We do not use the following data for averages, fits, limits, etc. • • •				
0.121	PENNER	02D	DPWA	Multichannel
0.085 ± 0.006	LI	93	IPWA	$\gamma N \to \pi N$
$+0.059 \pm 0.016$	BARBOUR	78	DPWA	$\gamma N \to \pi N$
0.062	[11] NOELLE	78		$\gamma N \to \pi N$

$N(1440)$ FOOTNOTES

[1] BAKER 79 finds a coupling of the $N(1440)$ to the $N\eta$ channel near (but slightly below) threshold.

[2] LONGACRE 77 pole positions are from a search for poles in the unitarized T-matrix; the first (second) value uses, in addition to $\pi N \to N\pi\pi$ data, elastic amplitudes from a Saclay (CERN) partial-wave analysis. The other LONGACRE 77 values are from eyeball fits with Breit-Wigner circles to the T-matrix amplitudes.

[3] From method II of LONGACRE 75: eyeball fits with Breit-Wigner circles to the T-matrix amplitudes.

[4] ARNDT 95 also finds a second-sheet pole with real part = 1383 MeV, $-2\times$imaginary part = 210 MeV, and residue with modulus 92 MeV and phase = $-54°$.

[5] See HOEHLER 93 for a detailed discussion of the evidence for and the pole parameters of N and Δ resonances as determined from Argand diagrams of πN elastic partial-wave amplitudes and from plots of the speeds with which the amplitudes traverse the diagrams.

[6] ARNDT 91 (Soln SM90) also finds a second-sheet pole with real part = 1413 MeV, $-2\times$ imaginary part = 256 MeV, and residue = $(78-153i)$ MeV.

[7] LONGACRE 78 values are from a search for poles in the unitarized T-matrix. The first (second) value uses, in addition to $\pi N \to N\pi\pi$ data, elastic amplitudes from a Saclay (CERN) partial-wave analysis.

[8] An alternative which cannot be distinguished from this is to have a P_{13} resonance with M = 1530 MeV, Γ = 79 MeV, and elasticity = +0.271.

[9] LONGACRE 77 considers this coupling to be well determined.

[10] WADA 84 is inconsistent with other analyses; see the Note on N and Δ Resonances.

[11] Converted to our conventions using M = 1486 MeV, Γ = 613 MeV from NOELLE 78.

$N(1440)$ REFERENCES

For early references, see Physics Letters **111B** 70 (1982).

PENNER	02C	PR C66 055211	G. Penner, U. Mosel	(GIES)
PENNER	02D	PR C66 055212	G. Penner, U. Mosel	(GIES)
VRANA	00	PRPL 328 181	T.P. Vrana, S.A. Dytman,, T.-S.H. Lee	(PITT+)
ARNDT	96	PR C53 430	R.A. Arndt, I.I. Strakovsky, R.L. Workman	(VPI)
ARNDT	95	PR C52 2120	R.A. Arndt *et al.*	(VPI, BRCO)
BATINIC	95	PR C51 2310	M. Batinić *et al.*	(BOSK, UCLA)
Also	98	PR C57 1004 (erratum)	M. Batinić *et al.*	
HOEHLER	93	πN Newsletter 9 1	G. Hohler	(KARL)
LI	93	PR C47 2759	Z.J. Li *et al.*	(VPI)
MANLEY	92	PR D45 4002	D.M. Manley, E.M. Saleski	(KENT) IJP
Also	84	PR D30 904	D.M. Manley *et al.*	(VPI)
ARNDT	91	PR D43 2131	R.A. Arndt *et al.*	(VPI, TELE) IJP
CUTKOSKY	90	PR D42 235	R.E. Cutkosky, S. Wang	(CMU)
WADA	84	NP B247 313	Y. Wada *et al.*	(INUS)
CRAWFORD	83	NP B211 1	R.L. Crawford, W.T. Morton	(GLAS)
PDG	82	PL 111B	M. Roos *et al.*	(HELS, CIT, CERN)
AWAJI	81	Bonn Conf. 352	N. Awaji, R. Kajikawa	(NAGO)
Also	82	NP B197 365	K. Fujii *et al.*	(NAGO)
FUJII	81	NP B187 53	K. Fujii *et al.*	(NAGO, OSAK)
ARAI	80	Toronto Conf. 93	I. Arai	(INUS)
Also	82	NP B194 251	I. Arai, H. Fujii	(INUS)
BRATASHEV...	80	NP B166 525	A.S. Bratashevsky *et al.*	(KFTI)
CRAWFORD	80	Toronto Conf. 107	R.L. Crawford	(GLAS)
CUTKOSKY	80	Toronto Conf. 19	R.E. Cutkosky *et al.*	(CMU, LBL) IJP
Also	79	PR D20 2839	R.E. Cutkosky *et al.*	(CMU, LBL) IJP
ISHII	80	NP B165 189	T. Ishii *et al.*	(KYOT, INUS)
TAKEDA	80	NP B168 17	H. Takeda *et al.*	(TOKY, INUS)
BAKER	79	NP B156 93	R.D. Baker *et al.*	(RHEL) IJP
HOEHLER	79	PDAT 12-1	G. Hohler *et al.*	(KARLT) IJP
Also	80	Toronto Conf. 3	R. Koch	(KARLT) IJP
BARBOUR	78	NP B141 253	I.M. Barbour, R.L. Crawford, N.H. Parsons	(GLAS)
LONGACRE	78	PR D17 1795	R.S. Longacre *et al.*	(LBL, SLAC)
NOELLE	78	PTP 60 778	P. Noelle	(NAGO)
BERENDS	77	NP B136 317	F.A. Berends, A. Donnachie	(LEID, MCHS) IJP
LONGACRE	77	NP B122 493	R.S. Longacre, J. Dolbeau	(SACL) IJP
Also	76	NP B108 365	J. Dolbeau *et al.*	(SACL) IJP
FELLER	76	NP B104 219	P. Feller *et al.*	(NAGO, OSAK) IJP
FELTESSE	75	NP B93 242	J. Feltesse *et al.*	(SACL) IJP
LONGACRE	75	PL 55B 415	R.S. Longacre *et al.*	(LBL, SLAC) IJP

$N(1520)$ D_{13}

$I(J^P) = \frac{1}{2}(\frac{3}{2}^-)$ Status: ****

Most of the results published before 1975 are now obsolete and have been omitted. They may be found in our 1982 edition, Physics Letters **111B** (1982).

$N(1520)$ BREIT-WIGNER MASS

VALUE (MeV)	*DOCUMENT ID*		*TECN*	*COMMENT*
1515 to 1530 (≈ 1520) OUR ESTIMATE				
1524 ± 4	MANLEY	92	IPWA	$\pi N \to \pi N$ & $N\pi\pi$
1525 ± 10	CUTKOSKY	80	IPWA	$\pi N \to \pi N$
1519 ± 4	HOEHLER	79	IPWA	$\pi N \to \pi N$
• • • We do not use the following data for averages, fits, limits, etc. • • •				
1509 ± 1	PENNER	02C	DPWA	Multichannel
1518 ± 3	VRANA	00	DPWA	Multichannel
1516 ± 10	ARNDT	96	IPWA	$\gamma N \to \pi N$
1515	ARNDT	95	DPWA	$\pi N \to N\pi$
1526 ± 18	BATINIC	95	DPWA	$\pi N \to N\pi$, $N\eta$
1510	LI	93	IPWA	$\gamma N \to \pi N$
1504	CRAWFORD	80	DPWA	$\gamma N \to \pi N$
1503	BARBOUR	78	DPWA	$\gamma N \to \pi N$
1510	BERENDS	77	IPWA	$\gamma N \to \pi N$
1510	[1] LONGACRE	77	IPWA	$\pi N \to N\pi\pi$
1520	[2] LONGACRE	75	IPWA	$\pi N \to N\pi\pi$

$N(1520)$ BREIT-WIGNER WIDTH

VALUE (MeV)	*DOCUMENT ID*		*TECN*	*COMMENT*
110 to 135 (≈ 120) OUR ESTIMATE				
124 ± 8	MANLEY	92	IPWA	$\pi N \to \pi N$ & $N\pi\pi$
120 ± 15	CUTKOSKY	80	IPWA	$\pi N \to \pi N$
114 ± 7	HOEHLER	79	IPWA	$\pi N \to \pi N$
• • • We do not use the following data for averages, fits, limits, etc. • • •				
100 ± 2	PENNER	02C	DPWA	Multichannel
124 ± 4	VRANA	00	DPWA	Multichannel
106 ± 4	ARNDT	96	IPWA	$\gamma N \to \pi N$
106	ARNDT	95	DPWA	$\pi N \to N\pi$
143 ± 32	BATINIC	95	DPWA	$\pi N \to N\pi$, $N\eta$
120	LI	93	IPWA	$\gamma N \to \pi N$
124	CRAWFORD	80	DPWA	$\gamma N \to \pi N$
183	BAKER	79	DPWA	$\pi^- p \to n\eta$
135	BARBOUR	78	DPWA	$\gamma N \to \pi N$
105	BERENDS	77	IPWA	$\gamma N \to \pi N$
110	[1] LONGACRE	77	IPWA	$\pi N \to N\pi\pi$
150	[2] LONGACRE	75	IPWA	$\pi N \to N\pi\pi$

$N(1520)$ POLE POSITION

REAL PART

VALUE (MeV)	*DOCUMENT ID*		*TECN*	*COMMENT*
1505 to 1515 (≈ 1510) OUR ESTIMATE				
1515	ARNDT	95	DPWA	$\pi N \to N\pi$
1510	[3] HOEHLER	93	ARGD	$\pi N \to \pi N$
1510 ± 5	CUTKOSKY	80	IPWA	$\pi N \to \pi N$
• • • We do not use the following data for averages, fits, limits, etc. • • •				
1504	VRANA	00	DPWA	Multichannel
1511	ARNDT	91	DPWA	$\pi N \to \pi N$ Soln SM90
1514 or 1511	[4] LONGACRE	78	IPWA	$\pi N \to N\pi\pi$
1508 or 1505	[1] LONGACRE	77	IPWA	$\pi N \to N\pi\pi$

$-2\times$IMAGINARY PART

VALUE (MeV)	*DOCUMENT ID*		*TECN*	*COMMENT*
110 to 120 (≈ 115) OUR ESTIMATE				
110	ARNDT	95	DPWA	$\pi N \to N\pi$
120	[3] HOEHLER	93	ARGD	$\pi N \to \pi N$
114 ± 10	CUTKOSKY	80	IPWA	$\pi N \to \pi N$
• • • We do not use the following data for averages, fits, limits, etc. • • •				
112	VRANA	00	DPWA	Multichannel
108	ARNDT	91	DPWA	$\pi N \to \pi N$ Soln SM90
146 or 137	[4] LONGACRE	78	IPWA	$\pi N \to N\pi\pi$
109 or 107	[1] LONGACRE	77	IPWA	$\pi N \to N\pi\pi$

$N(1520)$ ELASTIC POLE RESIDUE

MODULUS $|r|$

VALUE (MeV)	*DOCUMENT ID*		*TECN*	*COMMENT*
34	ARNDT	95	DPWA	$\pi N \to N\pi$
32	HOEHLER	93	ARGD	$\pi N \to \pi N$
35 ± 2	CUTKOSKY	80	IPWA	$\pi N \to \pi N$
• • • We do not use the following data for averages, fits, limits, etc. • • •				
33	ARNDT	91	DPWA	$\pi N \to \pi N$ Soln SM90

PHASE θ

VALUE (°)	*DOCUMENT ID*		*TECN*	*COMMENT*
7	ARNDT	95	DPWA	$\pi N \to N\pi$
− 8	HOEHLER	93	ARGD	$\pi N \to \pi N$
− 12 ± 5	CUTKOSKY	80	IPWA	$\pi N \to \pi N$
• • • We do not use the following data for averages, fits, limits, etc. • • •				
− 10	ARNDT	91	DPWA	$\pi N \to \pi N$ Soln SM90

$N(1520)$ DECAY MODES

The following branching fractions are our estimates, not fits or averages.

	Mode	Fraction (Γ_j/Γ)
Γ_1	$N\pi$	50–60 %
Γ_2	$N\eta$	$(2.3 \pm 0.4) \times 10^{-3}$
Γ_3	$N\pi\pi$	40–50 %
Γ_4	$\Delta\pi$	15–25 %
Γ_5	$\Delta(1232)\pi$, S-wave	5–12 %
Γ_6	$\Delta(1232)\pi$, D-wave	10–14 %
Γ_7	$N\rho$	15–25 %
Γ_8	$N\rho$, S=1/2, D-wave	
Γ_9	$N\rho$, S=3/2, S-wave	
Γ_{10}	$N\rho$, S=3/2, D-wave	
Γ_{11}	$N(\pi\pi)^{I=0}_{S\text{-wave}}$	< 8 %
Γ_{12}	$p\gamma$	0.46–0.56 %
Γ_{13}	$p\gamma$, helicity=1/2	0.001–0.034 %
Γ_{14}	$p\gamma$, helicity=3/2	0.44–0.53 %
Γ_{15}	$n\gamma$	0.30–0.53 %
Γ_{16}	$n\gamma$, helicity=1/2	0.04–0.10 %
Γ_{17}	$n\gamma$, helicity=3/2	0.25–0.45 %

$N(1520)$ BRANCHING RATIOS

$\Gamma(N\pi)/\Gamma_{\text{total}}$ Γ_1/Γ

VALUE	*DOCUMENT ID*		*TECN*	*COMMENT*
0.5 to 0.6 OUR ESTIMATE				
0.59 ± 0.03	MANLEY	92	IPWA	$\pi N \to \pi N$ & $N\pi\pi$
0.58 ± 0.03	CUTKOSKY	80	IPWA	$\pi N \to \pi N$
0.54 ± 0.03	HOEHLER	79	IPWA	$\pi N \to \pi N$
• • • We do not use the following data for averages, fits, limits, etc. • • •				
0.56 ± 0.01	PENNER	02C	DPWA	Multichannel
0.63 ± 0.02	VRANA	00	DPWA	Multichannel
0.61	ARNDT	95	DPWA	$\pi N \to N\pi$
0.46 ± 0.06	BATINIC	95	DPWA	$\pi N \to N\pi$, $N\eta$

$\Gamma(N\eta)/\Gamma_{total}$ Γ_2/Γ

VALUE	DOCUMENT ID		TECN	COMMENT
0.0023±0.0004 OUR AVERAGE				
0.0023±0.0004	PENNER	02C	DPWA	Multichannel
0.00 ±0.01	VRANA	00	DPWA	Multichannel
• • • We do not use the following data for averages, fits, limits, etc. • • •				
0.0008±0.0001	TIATOR	99	DPWA	$\gamma p \rightarrow p\eta$
0.001 ±0.002	BATINIC	95	DPWA	$\pi N \rightarrow N\pi$, $N\eta$

$(\Gamma_i\Gamma_f)^{1/2}/\Gamma_{total}$ in $N\pi \rightarrow N(1520) \rightarrow N\eta$ $(\Gamma_1\Gamma_2)^{1/2}/\Gamma$

VALUE	DOCUMENT ID		TECN	COMMENT
• • • We do not use the following data for averages, fits, limits, etc. • • •				
0.02	BAKER	79	DPWA	$\pi^- p \rightarrow n\eta$
+0.011	FELTESSE	75	DPWA	Soln A; see BAKER 79

Note: Signs of couplings from $\pi N \rightarrow N\pi\pi$ analyses were changed in the 1986 edition to agree with the baryon-first convention; the overall phase ambiguity is resolved by choosing a negative sign for the $\Delta(1620)$ S_{31} coupling to $\Delta(1232)\pi$.

$(\Gamma_i\Gamma_f)^{1/2}/\Gamma_{total}$ in $N\pi \rightarrow N(1520) \rightarrow \Delta(1232)\pi$, S-wave $(\Gamma_1\Gamma_5)^{1/2}/\Gamma$

VALUE	DOCUMENT ID		TECN	COMMENT
−0.26 to −0.20 OUR ESTIMATE				
−0.18±0.05	MANLEY	92	IPWA	$\pi N \rightarrow \pi N$ & $N\pi\pi$
−0.26	[1,5] LONGACRE	77	IPWA	$\pi N \rightarrow N\pi\pi$
−0.24	[2] LONGACRE	75	IPWA	$\pi N \rightarrow N\pi\pi$

$\Gamma(\Delta(1232)\pi$, S-wave$)/\Gamma_{total}$ Γ_5/Γ

VALUE	DOCUMENT ID		TECN	COMMENT
0.15±0.02	VRANA	00	DPWA	Multichannel

$(\Gamma_i\Gamma_f)^{1/2}/\Gamma_{total}$ in $N\pi \rightarrow N(1520) \rightarrow \Delta(1232)\pi$, D-wave $(\Gamma_1\Gamma_6)^{1/2}/\Gamma$

VALUE	DOCUMENT ID		TECN	COMMENT
−0.28 to −0.24 OUR ESTIMATE				
−0.29±0.03	MANLEY	92	IPWA	$\pi N \rightarrow \pi N$ & $N\pi\pi$
−0.21	[1,5] LONGACRE	77	IPWA	$\pi N \rightarrow N\pi\pi$
−0.30	[2] LONGACRE	75	IPWA	$\pi N \rightarrow N\pi\pi$

$\Gamma(\Delta(1232)\pi$, D-wave$)/\Gamma_{total}$ Γ_6/Γ

VALUE	DOCUMENT ID		TECN	COMMENT
0.11±0.02	VRANA	00	DPWA	Multichannel

$(\Gamma_i\Gamma_f)^{1/2}/\Gamma_{total}$ in $N\pi \rightarrow N(1520) \rightarrow N\rho$, S=3/2, S-wave $(\Gamma_1\Gamma_9)^{1/2}/\Gamma$

VALUE	DOCUMENT ID		TECN	COMMENT
−0.35 to −0.31 OUR ESTIMATE				
−0.35±0.03	MANLEY	92	IPWA	$\pi N \rightarrow \pi N$ & $N\pi\pi$
−0.35	[1,5] LONGACRE	77	IPWA	$\pi N \rightarrow N\pi\pi$
−0.24	[2] LONGACRE	75	IPWA	$\pi N \rightarrow N\pi\pi$

$\Gamma(N\rho$, S=3/2, S-wave$)/\Gamma_{total}$ Γ_9/Γ

VALUE	DOCUMENT ID		TECN	COMMENT
0.09±0.01	VRANA	00	DPWA	Multichannel

$(\Gamma_i\Gamma_f)^{1/2}/\Gamma_{total}$ in $N\pi \rightarrow N(1520) \rightarrow N(\pi\pi)^{I=0}_{S\text{-wave}}$ $(\Gamma_1\Gamma_{11})^{1/2}/\Gamma$

VALUE	DOCUMENT ID		TECN	COMMENT
−0.22 to −0.06 OUR ESTIMATE				
−0.13	[1,5] LONGACRE	77	IPWA	$\pi N \rightarrow N\pi\pi$
−0.17	[2] LONGACRE	75	IPWA	$\pi N \rightarrow N\pi\pi$

$\Gamma(N(\pi\pi)^{I=0}_{S\text{-wave}})/\Gamma_{total}$ Γ_{11}/Γ

VALUE	DOCUMENT ID		TECN	COMMENT
0.01±0.01	VRANA	00	DPWA	Multichannel

$N(1520)$ PHOTON DECAY AMPLITUDES

$N(1520) \rightarrow p\gamma$, helicity-1/2 amplitude $A_{1/2}$

VALUE (GeV$^{-1/2}$)	DOCUMENT ID		TECN	COMMENT
−0.024 ±0.009 OUR ESTIMATE				
−0.038 ±0.003	AHRENS	02	DPWA	$\gamma N \rightarrow \pi N$
−0.020 ±0.007	ARNDT	96	IPWA	$\gamma N \rightarrow \pi N$
−0.028 ±0.014	CRAWFORD	83	IPWA	$\gamma N \rightarrow \pi N$
−0.007 ±0.004	AWAJI	81	DPWA	$\gamma N \rightarrow \pi N$
−0.032 ±0.005	ARAI	80	DPWA	$\gamma N \rightarrow \pi N$ (fit 1)
−0.032 ±0.004	ARAI	80	DPWA	$\gamma N \rightarrow \pi N$ (fit 2)
−0.031 ±0.009	BRATASHEV...	80	DPWA	$\gamma N \rightarrow \pi N$
−0.019 ±0.007	CRAWFORD	80	DPWA	$\gamma N \rightarrow \pi N$
−0.0430±0.0063	ISHII	80	DPWA	Compton scattering
• • • We do not use the following data for averages, fits, limits, etc. • • •				
−0.003	PENNER	02D	DPWA	Multichannel
−0.052 ±0.010 ±0.007	[6] MUKHOPAD...	98		$\gamma p \rightarrow \eta p$
−0.020 ±0.002	LI	93	IPWA	$\gamma N \rightarrow \pi N$
−0.012	WADA	84	DPWA	Compton scattering
−0.016 ±0.008	BARBOUR	78	DPWA	$\gamma N \rightarrow \pi N$
−0.008	[7] NOELLE	78		$\gamma N \rightarrow \pi N$
−0.021	BERENDS	77	IPWA	$\gamma N \rightarrow \pi N$
−0.005 ±0.005	FELLER	76	DPWA	$\gamma N \rightarrow \pi N$

$N(1520) \rightarrow p\gamma$, helicity-3/2 amplitude $A_{3/2}$

VALUE (GeV$^{-1/2}$)	DOCUMENT ID		TECN	COMMENT
+0.166 ±0.005 OUR ESTIMATE				
0.147 ±0.010	AHRENS	02	DPWA	$\gamma N \rightarrow \pi N$
0.167 ±0.005	ARNDT	96	IPWA	$\gamma N \rightarrow \pi N$
0.156 ±0.022	CRAWFORD	83	IPWA	$\gamma N \rightarrow \pi N$
0.168 ±0.013	AWAJI	81	DPWA	$\gamma N \rightarrow \pi N$
0.178 ±0.003	ARAI	80	DPWA	$\gamma N \rightarrow \pi N$ (fit 1)
0.162 ±0.003	ARAI	80	DPWA	$\gamma N \rightarrow \pi N$ (fit 2)
0.166 ±0.005	BRATASHEV...	80	DPWA	$\gamma N \rightarrow \pi N$
0.167 ±0.010	CRAWFORD	80	DPWA	$\gamma N \rightarrow \pi N$
0.1695±0.0014	ISHII	80	DPWA	Compton scattering
• • • We do not use the following data for averages, fits, limits, etc. • • •				
0.151	PENNER	02D	DPWA	Multichannel
0.130 ±0.020 ±0.015	[6] MUKHOPAD...	98		$\gamma p \rightarrow \eta p$
0.167 ±0.002	LI	93	IPWA	$\gamma N \rightarrow \pi N$
0.168	WADA	84	DPWA	Compton scattering
+0.157 ±0.007	BARBOUR	78	DPWA	$\gamma N \rightarrow \pi N$
0.206	[7] NOELLE	78		$\gamma N \rightarrow \pi N$
+0.075	BERENDS	77	IPWA	$\gamma N \rightarrow \pi N$
+0.164 ±0.008	FELLER	76	DPWA	$\gamma N \rightarrow \pi N$

$N(1520) \rightarrow n\gamma$, helicity-1/2 amplitude $A_{1/2}$

VALUE (GeV$^{-1/2}$)	DOCUMENT ID		TECN	COMMENT
−0.059±0.009 OUR ESTIMATE				
−0.048±0.008	ARNDT	96	IPWA	$\gamma N \rightarrow \pi N$
−0.066±0.013	AWAJI	81	DPWA	$\gamma N \rightarrow \pi N$
−0.067±0.004	FUJII	81	DPWA	$\gamma N \rightarrow \pi N$
−0.076±0.006	ARAI	80	DPWA	$\gamma N \rightarrow \pi N$ (fit 1)
−0.071±0.011	ARAI	80	DPWA	$\gamma N \rightarrow \pi N$ (fit 2)
−0.056±0.011	CRAWFORD	80	DPWA	$\gamma N \rightarrow \pi N$
−0.050±0.014	TAKEDA	80	DPWA	$\gamma N \rightarrow \pi N$
• • • We do not use the following data for averages, fits, limits, etc. • • •				
−0.084	PENNER	02D	DPWA	Multichannel
−0.058±0.003	LI	93	IPWA	$\gamma N \rightarrow \pi N$
−0.055±0.014	BARBOUR	78	DPWA	$\gamma N \rightarrow \pi N$
−0.060	[7] NOELLE	78		$\gamma N \rightarrow \pi N$

$N(1520) \rightarrow n\gamma$, helicity-3/2 amplitude $A_{3/2}$

VALUE (GeV$^{-1/2}$)	DOCUMENT ID		TECN	COMMENT
−0.139±0.011 OUR ESTIMATE				
−0.140±0.010	ARNDT	96	IPWA	$\gamma N \rightarrow \pi N$
−0.124±0.009	AWAJI	81	DPWA	$\gamma N \rightarrow \pi N$
−0.158±0.003	FUJII	81	DPWA	$\gamma N \rightarrow \pi N$
−0.147±0.008	ARAI	80	DPWA	$\gamma N \rightarrow \pi N$ (fit 1)
−0.148±0.009	ARAI	80	DPWA	$\gamma N \rightarrow \pi N$ (fit 2)
−0.144±0.015	CRAWFORD	80	DPWA	$\gamma N \rightarrow \pi N$
−0.118±0.011	TAKEDA	80	DPWA	$\gamma N \rightarrow \pi N$
• • • We do not use the following data for averages, fits, limits, etc. • • •				
−0.159	PENNER	02D	DPWA	Multichannel
−0.131±0.003	LI	93	IPWA	$\gamma N \rightarrow \pi N$
−0.141±0.015	BARBOUR	78	DPWA	$\gamma N \rightarrow \pi N$
−0.127	[7] NOELLE	78		$\gamma N \rightarrow \pi N$

$N(1520)$ FOOTNOTES

[1] LONGACRE 77 pole positions are from a search for poles in the unitarized T-matrix; the first (second) value uses, in addition to $\pi N \rightarrow N\pi\pi$ data, elastic amplitudes from a Saclay (CERN) partial-wave analysis. The other LONGACRE 77 values are from eyeball fits with Breit-Wigner circles to the T-matrix amplitudes.

[2] From method II of LONGACRE 75: eyeball fits with Breit-Wigner circles to the T-matrix amplitudes.

[3] See HOEHLER 93 for a detailed discussion of the evidence for and the pole parameters of N and Δ resonances as determined from Argand diagrams of πN elastic partial-wave amplitudes and from plots of the speeds with which the amplitudes traverse the diagrams.

[4] LONGACRE 78 values are from a search for poles in the unitarized T-matrix. The first (second) value uses, in addition to $\pi N \rightarrow N\pi\pi$ data, elastic amplitudes from a Saclay (CERN) partial-wave analysis.

[5] LONGACRE 77 considers this coupling to be well determined.

[6] MUKHOPADHYAY 98 uses an effective Lagrangian approach to analyze η photoproduction data. The *ratio* of the $A_{3/2}$ and $A_{1/2}$ amplitudes is determined, with less model dependence than the amplitudes themselves, to be $A_{3/2}/A_{1/2} = -2.5 \pm 0.5 \pm 0.4$.

[7] Converted to our conventions using M = 1528 MeV, Γ = 187 MeV from NOELLE 78.

$N(1520)$ REFERENCES

For early references, see Physics Letters **111B** 70 (1982). For very early references, see Reviews of Modern Physics **37** 633 (1965).

AHRENS	02	PRL 88 232002	J. Ahrens *et al.*	(Mainz MAMI GDH/A2 Collab.)
PENNER	02C	PR C66 055211	G. Penner, U. Mosel	(GIES)
PENNER	02D	PR C66 055212	G. Penner, U. Mosel	(GIES)
VRANA	00	PRPL 328 181	T.P. Vrana, S.A. Dytman,, T.-S.H. Lee	(PITT+)
TIATOR	99	PR C60 035210	L. Tiator *et al.*	
MUKHOPAD...	98	PL B444 7	N.C. Mukhopadhyay, N. Mathur	
ARNDT	96	PR C53 430	R.A. Arndt, I.I. Strakovsky, R.L. Workman	(VPI)
ARNDT	95	PR C52 2120	R.A. Arndt *et al.*	(VPI, BRCO)
BATINIC	95	PR C51 2310	M. Batinic *et al.*	(BOSK, UCLA)
Also	98	PR C57 1004 (erratum)	M. Batinic *et al.*	
HOEHLER	93	πN Newsletter 9 1	G. Hohler	(KARL)
LI	93	PR C47 2759	Z.J. Li *et al.*	(VPI)

MANLEY	92	PR D45 4002	D.M. Manley, E.M. Saleski	(KENT) IJP
Also	84	PR D30 904	D.M. Manley *et al.*	(VPI)
ARNDT	91	PR D43 2131	R.A. Arndt *et al.*	(VPI, TELE) IJP
WADA	84	NP B247 313	Y. Wada *et al.*	(INUS)
CRAWFORD	83	NP B211 1	R.L. Crawford, W.T. Morton	(GLAS)
PDG	82	PL 111B	M. Roos *et al.*	(HELS, CIT, CERN)
AWAJI	81	Bonn Conf. 352	N. Awaji, R. Kajikawa	(NAGO)
Also	82	NP B197 365	K. Fujii *et al.*	(NAGO)
FUJII	81	NP B187 53	K. Fujii *et al.*	(NAGO, OSAK)
ARAI	80	Toronto Conf. 93	I. Arai	(INUS)
Also	82	NP B194 251	I. Arai, H. Fujii	(INUS)
BRATASHEV...	80	NP B166 525	A.S. Bratashevsky *et al.*	(KFTI)
CRAWFORD	80	Toronto Conf. 107	R.L. Crawford	(GLAS)
CUTKOSKY	80	Toronto Conf. 19	R.E. Cutkosky *et al.*	(CMU, LBL) IJP
Also	79	PR D20 2839	R.E. Cutkosky *et al.*	(CMU, LBL) IJP
ISHII	80	NP B165 189	T. Ishii *et al.*	(KYOT, INUS)
TAKEDA	80	NP B168 17	H. Takeda *et al.*	(TOKY, INUS)
BAKER	79	NP B156 93	R.D. Baker *et al.*	(RHEL) IJP
HOEHLER	79	PDAT 12-1	G. Hohler *et al.*	(KARLT) IJP
Also	80	Toronto Conf. 3	R. Koch	(KARLT) IJP
BARBOUR	78	NP B141 253	I.M. Barbour, R.L. Crawford, N.H. Parsons	(GLAS)
LONGACRE	78	PR D17 1795	R.S. Longacre *et al.*	(LBL, SLAC)
NOELLE	78	PTP 60 778	P. Noelle	(NAGO)
BERENDS	77	NP B136 317	F.A. Berends, A. Donnachie	(LEID, MCHS) IJP
LONGACRE	77	NP B122 493	R.S. Longacre, J. Dolbeau	(SACL) IJP
Also	76	NP B108 365	J. Dolbeau *et al.*	(SACL) IJP
FELLER	76	NP B104 219	P. Feller *et al.*	(NAGO, OSAK) IJP
FELTESSE	75	NP B93 242	J. Feltesse *et al.*	(SACL) IJP
LONGACRE	75	PL 55B 415	R.S. Longacre *et al.*	(LBL, SLAC) IJP

$N(1535)$ S_{11}

$I(J^P) = \frac{1}{2}(\frac{1}{2}^-)$ Status: ****

Most of the results published before 1975 are now obsolete and have been omitted. They may be found in our 1982 edition, Physics Letters **111B** (1982).

$N(1535)$ BREIT-WIGNER MASS

VALUE (MeV)	*DOCUMENT ID*		*TECN*	*COMMENT*
1520 to 1555 (≈ 1535) OUR ESTIMATE				
1534 ± 7	MANLEY	92	IPWA	$\pi N \to \pi N$ & $N\pi\pi$
1550 ±40	CUTKOSKY	80	IPWA	$\pi N \to \pi N$
1526 ± 7	HOEHLER	79	IPWA	$\pi N \to \pi N$
• • • We do not use the following data for averages, fits, limits, etc. • • •				
1526 ± 2	PENNER	02C	DPWA	Multichannel
1530 ±10	BAI	01B	BES	$J/\psi \to p\overline{p}\eta$
1522 ±11	THOMPSON	01	CLAS	$\gamma^* p \to p\eta$
1542 ± 3	VRANA	00	DPWA	Multichannel
1532 ± 5	ARMSTRONG	99B	DPWA	$\gamma^* p \to p\eta$
1549.0± 2.1	ABAEV	96	DPWA	$\pi^- p \to \eta n$
1525 ±10	ARNDT	96	IPWA	$\gamma N \to \pi N$
1535	ARNDT	95	DPWA	$\pi N \to N\pi$
1542 ± 6	BATINIC	95	DPWA	$\pi N \to N\pi$, $N\eta$
1537	BATINIC	95B	DPWA	$\pi N \to N\pi$, $N\eta$
1544 ±13	KRUSCHE	95	DPWA	$\gamma p \to p\eta$
1518	LI	93	IPWA	$\gamma N \to \pi N$
1513	CRAWFORD	80	DPWA	$\gamma N \to \pi N$
1511	BARBOUR	78	DPWA	$\gamma N \to \pi N$
1500	BERENDS	77	IPWA	$\gamma N \to \pi N$
1547 ± 6	BHANDARI	77	DPWA	Uses $N\eta$ cusp
1520	[1] LONGACRE	77	IPWA	$\pi N \to N\pi\pi$
1510	[2] LONGACRE	75	IPWA	$\pi N \to N\pi\pi$

$N(1535)$ BREIT-WIGNER WIDTH

VALUE (MeV)	*DOCUMENT ID*		*TECN*	*COMMENT*
100 to 200 (≈ 150) OUR ESTIMATE				
148.2± 8.1	GREEN	97	DPWA	$\pi N \to \pi N$, ηN
151 ±27	MANLEY	92	IPWA	$\pi N \to \pi N$ & $N\pi\pi$
240 ±80	CUTKOSKY	80	IPWA	$\pi N \to \pi N$
120 ±20	HOEHLER	79	IPWA	$\pi N \to \pi N$
• • • We do not use the following data for averages, fits, limits, etc. • • •				
129 ± 8	PENNER	02C	DPWA	Multichannel
95 ±25	BAI	01B	BES	$J/\psi \to p\overline{p}\eta$
143 ±18	THOMPSON	01	CLAS	$\gamma^* p \to p\eta$
112 ±19	VRANA	00	DPWA	Multichannel
154 ±20	ARMSTRONG	99B	DPWA	$\gamma^* p \to p\eta$
212 ±20	[3] KRUSCHE	97	DPWA	$\gamma N \to \eta N$
168.8±11.6	ABAEV	96	DPWA	$\pi^- p \to \eta n$
103 ± 5	ARNDT	96	IPWA	$\gamma N \to \pi N$
66	ARNDT	95	DPWA	$\pi N \to N\pi$
150 ±15	BATINIC	95	DPWA	$\pi N \to N\pi$, $N\eta$
145	BATINIC	95B	DPWA	$\pi N \to N\pi$, $N\eta$
200 ±40	KRUSCHE	95	DPWA	$\gamma p \to p\eta$
84	LI	93	IPWA	$\gamma N \to \pi N$
136	CRAWFORD	80	DPWA	$\gamma N \to \pi N$
180	BAKER	79	DPWA	$\pi^- p \to n\eta$
132	BARBOUR	78	DPWA	$\gamma N \to \pi N$
57	BERENDS	77	IPWA	$\gamma N \to \pi N$
139 ±33	BHANDARI	77	DPWA	Uses $N\eta$ cusp
135	[1] LONGACRE	77	IPWA	$\pi N \to N\pi\pi$
100	[2] LONGACRE	75	IPWA	$\pi N \to N\pi\pi$

$N(1535)$ POLE POSITION

REAL PART

VALUE (MeV)	*DOCUMENT ID*		*TECN*	*COMMENT*
1495 to 1515 (≈ 1505) OUR ESTIMATE				
1510±10	[4] ARNDT	98	DPWA	$\pi N \to \pi N$, ηN
1501	ARNDT	95	DPWA	$\pi N \to N\pi$
1487	[5] HOEHLER	93	SPED	$\pi N \to \pi N$
1510±50	CUTKOSKY	80	IPWA	$\pi N \to \pi N$
• • • We do not use the following data for averages, fits, limits, etc. • • •				
1525	VRANA	00	DPWA	Multichannel
1499	ARNDT	91	DPWA	$\pi N \to \pi N$ Soln SM90
1496 or 1499	[6] LONGACRE	78	IPWA	$\pi N \to N\pi\pi$
1519± 4	BHANDARI	77	DPWA	Uses $N\eta$ cusp
1525 or 1527	[1] LONGACRE	77	IPWA	$\pi N \to N\pi\pi$

−2×IMAGINARY PART

VALUE (MeV)	*DOCUMENT ID*		*TECN*	*COMMENT*
90 to 250 (≈ 170) OUR ESTIMATE				
170±30	[4] ARNDT	98	DPWA	$\pi N \to \pi N$, ηN
124	ARNDT	95	DPWA	$\pi N \to N\pi$
260±80	CUTKOSKY	80	IPWA	$\pi N \to \pi N$
• • • We do not use the following data for averages, fits, limits, etc. • • •				
102	VRANA	00	DPWA	Multichannel
110	ARNDT	91	DPWA	$\pi N \to \pi N$ Soln SM90
103 or 105	[6] LONGACRE	78	IPWA	$\pi N \to N\pi\pi$
140±32	BHANDARI	77	DPWA	Uses $N\eta$ cusp
135 or 123	[1] LONGACRE	77	IPWA	$\pi N \to N\pi\pi$

$N(1535)$ ELASTIC POLE RESIDUE

MODULUS $|r|$

VALUE (MeV)	*DOCUMENT ID*		*TECN*	*COMMENT*
31	ARNDT	95	DPWA	$\pi N \to N\pi$
120±40	CUTKOSKY	80	IPWA	$\pi N \to \pi N$
• • • We do not use the following data for averages, fits, limits, etc. • • •				
23	ARNDT	91	DPWA	$\pi N \to \pi N$ Soln SM90

PHASE θ

VALUE (°)	*DOCUMENT ID*		*TECN*	*COMMENT*
−12	ARNDT	95	DPWA	$\pi N \to N\pi$
+15±45	CUTKOSKY	80	IPWA	$\pi N \to \pi N$
• • • We do not use the following data for averages, fits, limits, etc. • • •				
−13	ARNDT	91	DPWA	$\pi N \to \pi N$ Soln SM90

$N(1535)$ DECAY MODES

The following branching fractions are our estimates, not fits or averages.

	Mode	Fraction (Γ_i/Γ)
Γ_1	$N\pi$	35–55 %
Γ_2	$N\eta$	30–55 %
Γ_3	$N\pi\pi$	1–10 %
Γ_4	$\Delta\pi$	<1 %
Γ_5	$\Delta(1232)\pi$, D-wave	
Γ_6	$N\rho$	<4 %
Γ_7	$N\rho$, S=1/2, S-wave	
Γ_8	$N\rho$, S=3/2, D-wave	
Γ_9	$N(\pi\pi)^{I=0}_{S\text{-wave}}$	<3 %
Γ_{10}	$N(1440)\pi$	<7 %
Γ_{11}	$p\gamma$	0.15–0.35 %
Γ_{12}	$p\gamma$, helicity=1/2	0.15–0.35 %
Γ_{13}	$n\gamma$	0.004–0.29 %
Γ_{14}	$n\gamma$, helicity=1/2	0.004–0.29 %

$N(1535)$ BRANCHING RATIOS

$\Gamma(N\pi)/\Gamma_{\text{total}}$ Γ_1/Γ

VALUE	*DOCUMENT ID*		*TECN*	*COMMENT*
0.35 to 0.55 OUR ESTIMATE				
0.394±0.009	GREEN	97	DPWA	$\pi N \to \pi N$, ηN
0.51 ±0.05	MANLEY	92	IPWA	$\pi N \to \pi N$ & $N\pi\pi$
0.50 ±0.10	CUTKOSKY	80	IPWA	$\pi N \to \pi N$
0.38 ±0.04	HOEHLER	79	IPWA	$\pi N \to \pi N$
• • • We do not use the following data for averages, fits, limits, etc. • • •				
0.36 ±0.01	PENNER	02C	DPWA	Multichannel
0.35 ±0.08	VRANA	00	DPWA	Multichannel
0.330±0.011	ABAEV	96	DPWA	$\pi^- p \to \eta n$
0.31	ARNDT	95	DPWA	$\pi N \to N\pi$
0.34 ±0.09	BATINIC	95	DPWA	$\pi N \to N\pi$, $N\eta$
0.297±0.026	BHANDARI	77	DPWA	Uses $N\eta$ cusp

$\Gamma(N\eta)/\Gamma_{total}$ Γ_2/Γ

VALUE	CL%	DOCUMENT ID		TECN	COMMENT
+0.30 to 0.55 OUR ESTIMATE					
0.529±0.010 OUR AVERAGE					
0.53 ±0.01		PENNER	02C	DPWA	Multichannel
0.51 ±0.05		VRANA	00	DPWA	Multichannel
• • • We do not use the following data for averages, fits, limits, etc. • • •					
> 0.45	95	[7] ARMSTRONG	99B	DPWA	$p\,(e,e'p)\,\eta$
0.568±0.011		GREEN	97	DPWA	$\pi N \to \pi N, \eta N$
0.591±0.017		ABAEV	96	DPWA	$\pi^- p \to \eta n$
0.63 ±0.07		BATINIC	95	DPWA	$\pi N \to N\pi, N\eta$

$(\Gamma_i\Gamma_f)^{1/2}/\Gamma_{total}$ in $N\pi \to N(1535) \to N\eta$ $(\Gamma_1\Gamma_2)^{1/2}/\Gamma$

VALUE	DOCUMENT ID		TECN	COMMENT
+0.44 to +0.50 OUR ESTIMATE				
+0.47±0.02	MANLEY	92	IPWA	$\pi N \to \pi N$ & $N\pi\pi$
• • • We do not use the following data for averages, fits, limits, etc. • • •				
+0.33	BAKER	79	DPWA	$\pi^- p \to n\eta$
+0.48	FELTESSE	75	DPWA	1488–1745 MeV

Note: Signs of couplings from $\pi N \to N\pi\pi$ analyses were changed in the 1986 edition to agree with the baryon-first convention; the overall phase ambiguity is resolved by choosing a negative sign for the $\Delta(1620)$ S_{31} coupling to $\Delta(1232)\pi$.

$(\Gamma_i\Gamma_f)^{1/2}/\Gamma_{total}$ in $N\pi \to N(1535) \to \Delta(1232)\pi$, D-wave $(\Gamma_1\Gamma_5)^{1/2}/\Gamma$

VALUE	DOCUMENT ID		TECN	COMMENT
−0.04 to +0.06 OUR ESTIMATE				
+0.00±0.04	MANLEY	92	IPWA	$\pi N \to \pi N$ & $N\pi\pi$
0.00	[1] LONGACRE	77	IPWA	$\pi N \to N\pi\pi$
+0.06	[2] LONGACRE	75	IPWA	$\pi N \to N\pi\pi$

$\Gamma(\Delta(1232)\pi,\ D\text{-wave})/\Gamma_{total}$ Γ_5/Γ

VALUE	DOCUMENT ID	TECN	COMMENT
0.01±0.01	VRANA	00	DPWA Multichannel

$(\Gamma_i\Gamma_f)^{1/2}/\Gamma_{total}$ in $N\pi \to N(1535) \to N\rho$, S=1/2, S-wave $(\Gamma_1\Gamma_7)^{1/2}/\Gamma$

VALUE	DOCUMENT ID		TECN	COMMENT
−0.14 to −0.06 OUR ESTIMATE				
−0.10±0.03	MANLEY	92	IPWA	$\pi N \to \pi N$ & $N\pi\pi$
−0.10	[1] LONGACRE	77	IPWA	$\pi N \to N\pi\pi$
−0.09	[2] LONGACRE	75	IPWA	$\pi N \to N\pi\pi$

$\Gamma(N\rho,\ S$=1/2, S-wave$)/\Gamma_{total}$ Γ_7/Γ

VALUE	DOCUMENT ID	TECN	COMMENT
0.02±0.01	VRANA	00	DPWA Multichannel

$\Gamma(N\rho,\ S$=3/2, D-wave$)/\Gamma_{total}$ Γ_8/Γ

VALUE	DOCUMENT ID	TECN	COMMENT
0.00±0.01	VRANA	00	DPWA Multichannel

$(\Gamma_i\Gamma_f)^{1/2}/\Gamma_{total}$ in $N\pi \to N(1535) \to N(\pi\pi)^{I=0}_{S\text{-wave}}$ $(\Gamma_1\Gamma_9)^{1/2}/\Gamma$

VALUE	DOCUMENT ID		TECN	COMMENT
+0.03 to +0.13 OUR ESTIMATE				
+0.07±0.04	MANLEY	92	IPWA	$\pi N \to \pi N$ & $N\pi\pi$
+0.08	[1] LONGACRE	77	IPWA	$\pi N \to N\pi\pi$
+0.09	[2] LONGACRE	75	IPWA	$\pi N \to N\pi\pi$

$\Gamma(N(\pi\pi)^{I=0}_{S\text{-wave}})/\Gamma_{total}$ Γ_9/Γ

VALUE	DOCUMENT ID	TECN	COMMENT
0.02±0.01	VRANA	00	DPWA Multichannel

$(\Gamma_i\Gamma_f)^{1/2}/\Gamma_{total}$ in $N\pi \to N(1535) \to N(1440)\pi$ $(\Gamma_1\Gamma_{10})^{1/2}/\Gamma$

VALUE	DOCUMENT ID	TECN	COMMENT
+0.10±0.05	MANLEY	92	IPWA $\pi N \to \pi N$ & $N\pi\pi$

$\Gamma(N(1440)\pi)/\Gamma_{total}$ Γ_{10}/Γ

VALUE	DOCUMENT ID		TECN	COMMENT
0.08±0.02	[8] STAROSTIN	03		$\pi^- p \to n3\pi^0$
0.10±0.09	VRANA	00	DPWA	Multichannel

$N(1535)$ PHOTON DECAY AMPLITUDES

$N(1535) \to p\gamma$, helicity-1/2 amplitude $A_{1/2}$

VALUE (GeV$^{-1/2}$)	DOCUMENT ID		TECN	COMMENT
+0.090 ±0.030 OUR ESTIMATE				
0.120 ±0.011 ±0.015	[3] KRUSCHE	97	DPWA	$\gamma N \to \eta N$
0.060 ±0.015	ARNDT	96	IPWA	$\gamma N \to \pi N$
0.097 ±0.006	BENMERROU...	95	DPWA	$\gamma N \to N\eta$
0.095 ±0.011	[9] BENMERROU...	91		$\gamma p \to p\eta$
0.053 ±0.015	CRAWFORD	83	IPWA	$\gamma N \to \pi N$
0.077 ±0.021	AWAJI	81	DPWA	$\gamma N \to \pi N$
0.083 ±0.007	ARAI	80	DPWA	$\gamma N \to \pi N$ (fit 1)
0.080 ±0.007	ARAI	80	DPWA	$\gamma N \to \pi N$ (fit 2)
0.029 ±0.007	BRATASHEV...	80	DPWA	$\gamma N \to \pi N$
0.065 ±0.016	CRAWFORD	80	DPWA	$\gamma N \to \pi N$
0.0704±0.0091	ISHII	80	DPWA	Compton scattering
• • • We do not use the following data for averages, fits, limits, etc. • • •				
0.090	PENNER	02D	DPWA	Multichannel
0.110 to 0.140	KRUSCHE	95	DPWA	$\gamma p \to p\eta$
0.125 ±0.025	KRUSCHE	95C	IPWA	$\gamma d \to \eta N(N)$
0.061 ±0.003	LI	93	IPWA	$\gamma N \to \pi N$
0.055	WADA	84	DPWA	Compton scattering
+0.082 ±0.019	BARBOUR	78	DPWA	$\gamma N \to \pi N$
0.046	[10] NOELLE	78		$\gamma N \to \pi N$
+0.034	BERENDS	77	IPWA	$\gamma N \to \pi N$
+0.070 ±0.004	FELLER	76	DPWA	$\gamma N \to \pi N$

$N(1535) \to n\gamma$, helicity-1/2 amplitude $A_{1/2}$

VALUE (GeV$^{-1/2}$)	DOCUMENT ID		TECN	COMMENT
−0.046±0.027 OUR ESTIMATE				
−0.020±0.035	ARNDT	96	IPWA	$\gamma N \to \pi N$
0.035±0.014	AWAJI	81	DPWA	$\gamma N \to \pi N$
−0.062±0.003	FUJII	81	DPWA	$\gamma N \to \pi N$
−0.075±0.019	ARAI	80	DPWA	$\gamma N \to \pi N$ (fit 1)
−0.075±0.018	ARAI	80	DPWA	$\gamma N \to \pi N$ (fit 2)
−0.098±0.026	CRAWFORD	80	DPWA	$\gamma N \to \pi N$
−0.011±0.017	TAKEDA	80	DPWA	$\gamma N \to \pi N$
• • • We do not use the following data for averages, fits, limits, etc. • • •				
−0.024	PENNER	02D	DPWA	Multichannel
−0.100±0.030	KRUSCHE	95C	IPWA	$\gamma d \to \eta N(N)$
−0.046±0.005	LI	93	IPWA	$\gamma N \to \pi N$
−0.112±0.034	BARBOUR	78	DPWA	$\gamma N \to \pi N$
−0.048	[10] NOELLE	78		$\gamma N \to \pi N$

$N(1535) \to N\gamma$, ratio $A^n_{1/2}/A^p_{1/2}$

VALUE (GeV$^{-1/2}$)	DOCUMENT ID	TECN
• • • We do not use the following data for averages, fits, limits, etc. • • •		
−0.84±0.15	MUKHOPAD... 95B	IPWA

$N(1535)$ FOOTNOTES

[1] LONGACRE 77 pole positions are from a search for poles in the unitarized T-matrix; the first (second) value uses, in addition to $\pi N \to N\pi\pi$ data, elastic amplitudes from a Saclay (CERN) partial-wave analysis. The other LONGACRE 77 values are from eyeball fits with Breit-Wigner circles to the T-matrix amplitudes.

[2] From method II of LONGACRE 75: eyeball fits with Breit-Wigner circles to the T-matrix amplitudes.

[3] KRUSCHE 97 fits with the mass fixed at 1544 MeV.

[4] ARNDT 98 also lists pole residues, which display more model dependence than do the associated pole positions.

[5] See HOEHLER 93 for a detailed discussion of the evidence for and the pole parameters of N and Δ resonances as determined from Argand diagrams of πN elastic partial-wave amplitudes and from plots of the speeds with which the amplitudes traverse the diagrams.

[6] LONGACRE 78 values are from a search for poles in the unitarized T-matrix. The first (second) value uses, in addition to $\pi N \to N\pi\pi$ data, elastic amplitudes from a Saclay (CERN) partial-wave analysis.

[7] The best value ARMSTRONG 99B obtains is $\simeq 0.55$; this assumes S_{11} dominance in the reaction $p(e,\ e'\ p)\ \eta$ at $Q^2 = 4$ (GeV/c)^2.

[8] This STAROSTIN 03 value is an estimate made using simplest assumptions.

[9] BENMERROUCHE 91 uses an effective Lagrangian approach to analyze η photoproduction data.

[10] Converted to our conventions using M = 1548 MeV, Γ = 73 MeV from NOELLE 78.

$N(1535)$ REFERENCES

For early references, see Physics Letters **111B** 70 (1982).

STAROSTIN	03	PR C67 068201	A. Starostin *et al.*	(BNL Crystal Ball Collab.)
PENNER	02C	PR C66 055211	G. Penner, U. Mosel	(GIES)
PENNER	02D	PR C66 055212	G. Penner, U. Mosel	(GIES)
BAI	01B	PL B510 75	J.Z. Bai *et al.*	(BEPC BES Collab.)
THOMPSON	01	PRL 86 1702	R. Thompson *et al.*	(Jefferson CLAS Collab.)
VRANA	00	PRPL 328 181	T.P. Vrana, S.A. Dytman,, T.-S.H. Lee	(PITT+)
ARMSTRONG	99B	PR D60 052004	C.S. Armstrong *et al.*	
ARNDT	98	PR C58 3636	R.A. Arndt *et al.*	
GREEN	97	PR C55 R2167	A.M. Green, S. Wycech	(HELS, WINR)
KRUSCHE	97	PL B397 171	B. Krusche *et al.*	(GIES, RPI, SASK)
ABAEV	96	PR C53 385	V.V. Abaev, B.M.K. Nefkens	(UCLA)
ARNDT	96	PR C53 430	R.A. Arndt, I.I. Strakovsky, R.L. Workman	(VPI)
ARNDT	95	PR C52 2120	R.A. Arndt *et al.*	(VPI, BRCO)
BATINIC	95	PR C51 2310	M. Batinic *et al.*	(BOSK, UCLA)
Also	98	PR C57 1004 (erratum)	M. Batinic *et al.*	
BATINIC	95B	PR C52 2188	M. Batinic, I. Slaus, A. Svarc	(BOSK)
BENMERROU...	95	PR D51 3237	M. Benmerrouche, N.C. Mukhopadhyay, J.F. Zhang	
KRUSCHE	95	PRL 74 3736	B. Krusche *et al.*	(GIES, MANZ, GLAS+)
KRUSCHE	95C	PL B358 40	B. Krusche *et al.*	(GIES, MANZ, GLAS+)
MUKHOPAD...	95B	PL B364 1	N.C. Mukhopadhyay, J.F. Zhang, M. Benmerrouche	
HOEHLER	93	πN Newsletter 9 1	G. Hohler	(KARL)
LI	93	PR C47 2759	Z.I. Li *et al.*	(VPI)
MANLEY	92	PR D45 4002	D.M. Manley, E.M. Saleski	(KENT) IJP
Also	84	PR D30 904	D.M. Manley *et al.*	(VPI)
ARNDT	91	PR D43 2131	R.A. Arndt *et al.*	(VPI, TELE) IJP
BENMERROU...	91	PRL 67 1070	M. Benmerrouche, N.C. Mukhopadhyay	(RPI)
WADA	84	NP B247 313	Y. Wada *et al.*	(INUS)
CRAWFORD	83	NP B211 1	R.L. Crawford, W.T. Morton	(GLAS)
PDG	82	PL 111B	M. Roos *et al.*	(HELS, CIT, CERN)
AWAJI	81	Bonn Conf. 352	N. Awaji, R. Kajikawa	(NAGO)
Also	82	NP B197 365	K. Fujii *et al.*	(NAGO)
FUJII	81	NP B187 53	K. Fujii *et al.*	(NAGO, OSAK)
ARAI	80	Toronto Conf. 93	I. Arai	(INUS)
Also	82	NP B194 251	I. Arai, H. Fujii	(INUS)

BRATASHEV...	80	NP B166 525	A.S. Bratashevsky *et al.*	(KFTI)
CRAWFORD	80	Toronto Conf. 107	R.L. Crawford	(GLAS)
CUTKOSKY	80	Toronto Conf. 19	R.E. Cutkosky *et al.*	(CMU, LBL) IJP
Also	79	PR D20 2839	R.E. Cutkosky *et al.*	(CMU, LBL) IJP
ISHII	80	NP B165 189	T. Ishii *et al.*	(KYOT, INUS)
TAKEDA	80	NP B168 17	H. Takeda *et al.*	(TOKY, INUS)
BAKER	79	NP B156 93	R.D. Baker *et al.*	(RHEL) IJP
HOEHLER	79	PDAT 12-1	G. Hohler *et al.*	(KARLT) IJP
Also	80	Toronto Conf. 3	R. Koch	(KARLT) IJP
BARBOUR	78	NP B141 253	I.M. Barbour, R.L. Crawford, N.H. Parsons	(GLAS)
LONGACRE	78	PR D17 1795	R.S. Longacre *et al.*	(LBL, SLAC)
NOELLE	78	PTP 60 778	P. Noelle	(NAGO)
BERENDS	77	NP B136 317	F.A. Berends, A. Donnachie	(LEID, MCHS) IJP
BHANDARI	77	PR D15 192	R. Bhandari, Y.A. Chao	(CMU) IJP
LONGACRE	77	NP B122 493	R.S. Longacre, J. Dolbeau	(SACL) IJP
Also	76	NP B108 365	J. Dolbeau *et al.*	(SACL) IJP
FELLER	76	NP B104 219	P. Feller *et al.*	(NAGO, OSAK) IJP
FELTESSE	75	NP B93 242	J. Feltesse *et al.*	(SACL) IJP
LONGACRE	75	PL 55B 415	R.S. Longacre *et al.*	(LBL, SLAC) IJP

$N(1650)$ S_{11}

$I(J^P) = \frac{1}{2}(\frac{1}{2}^-)$ Status: ****

Most of the results published before 1975 are now obsolete and have been omitted. They may be found in our 1982 edition, Physics Letters **111B** (1982).

$N(1650)$ BREIT-WIGNER MASS

VALUE (MeV)		*DOCUMENT ID*		*TECN*	*COMMENT*
1640 to 1680 (≈ 1650) OUR ESTIMATE					
1659 ± 9		MANLEY	92	IPWA	$\pi N \to \pi N$ & $N\pi\pi$
1650 ± 30		CUTKOSKY	80	IPWA	$\pi N \to \pi N$
1670 ± 8		HOEHLER	79	IPWA	$\pi N \to \pi N$
• • • We do not use the following data for averages, fits, limits, etc. • • •					
1665 ± 2		PENNER	02C	DPWA	Multichannel
1647 ± 20		BAI	01B	BES	$J/\psi \to p\overline{p}\eta$
1689 ± 12		VRANA	00	DPWA	Multichannel
1677 ± 8		ARNDT	96	IPWA	$\gamma N \to \pi N$
1667		ARNDT	95	DPWA	$\pi N \to N\pi$
1712	[1]	ARNDT	95	DPWA	$\pi N \to N\pi$
1669 ± 17		BATINIC	95	DPWA	$\pi N \to N\pi$, $N\eta$
1713 ± 27	[2]	BATINIC	95	DPWA	$\pi N \to N\pi$, $N\eta$
1674		LI	93	IPWA	$\gamma N \to \pi N$
1688		CRAWFORD	80	DPWA	$\gamma N \to \pi N$
1672		MUSETTE	80	IPWA	$\pi^- p \to \Lambda K^0$
1680		SAXON	80	DPWA	$\pi^- p \to \Lambda K^0$
1680		BAKER	78	DPWA	$\pi^- p \to \Lambda K^0$
1694		BARBOUR	78	DPWA	$\gamma N \to \pi N$
1700 ± 5	[3]	BAKER	77	IPWA	$\pi^- p \to \Lambda K^0$
1680	[3]	BAKER	77	DPWA	$\pi^- p \to \Lambda K^0$
1700	[4]	LONGACRE	77	IPWA	$\pi N \to N\pi\pi$
1675		KNASEL	75	DPWA	$\pi^- p \to \Lambda K^0$
1660	[5]	LONGACRE	75	IPWA	$\pi N \to N\pi\pi$

$N(1650)$ BREIT-WIGNER WIDTH

VALUE (MeV)		*DOCUMENT ID*		*TECN*	*COMMENT*
145 to 190 (≈ 150) OUR ESTIMATE					
167.9 ± 9.4		GREEN	97	DPWA	$\pi N \to \pi N$, ηN
173 ± 12		MANLEY	92	IPWA	$\pi N \to \pi N$ & $N\pi\pi$
150 ± 40		CUTKOSKY	80	IPWA	$\pi N \to \pi N$
180 ± 20		HOEHLER	79	IPWA	$\pi N \to \pi N$
• • • We do not use the following data for averages, fits, limits, etc. • • •					
138 ± 7		PENNER	02C	DPWA	Multichannel
145 $^{+80}_{-45}$		BAI	01B	BES	$J/\psi \to p\overline{p}\eta$
202 ± 40		VRANA	00	DPWA	Multichannel
160 ± 12		ARNDT	96	IPWA	$\gamma N \to \pi N$
90		ARNDT	95	DPWA	$\pi N \to N\pi$
184	[1]	ARNDT	95	DPWA	$\pi N \to N\pi$
215 ± 32		BATINIC	95	DPWA	$\pi N \to N\pi$, $N\eta$
279 ± 54	[2]	BATINIC	95	DPWA	$\pi N \to N\pi$, $N\eta$
225		LI	93	IPWA	$\gamma N \to \pi N$
183		CRAWFORD	80	DPWA	$\gamma N \to \pi N$
179		MUSETTE	80	IPWA	$\pi^- p \to \Lambda K^0$
120		SAXON	80	DPWA	$\pi^- p \to \Lambda K^0$
90		BAKER	78	DPWA	$\pi^- p \to \Lambda K^0$
193		BARBOUR	78	DPWA	$\gamma N \to \pi N$
130 ± 10	[3]	BAKER	77	IPWA	$\pi^- p \to \Lambda K^0$
90	[3]	BAKER	77	DPWA	$\pi^- p \to \Lambda K^0$
170	[4]	LONGACRE	77	IPWA	$\pi N \to N\pi\pi$
170		KNASEL	75	DPWA	$\pi^- p \to \Lambda K^0$
130	[5]	LONGACRE	75	IPWA	$\pi N \to N\pi\pi$

$N(1650)$ POLE POSITION

REAL PART

VALUE (MeV)		*DOCUMENT ID*		*TECN*	*COMMENT*
1640 to 1680 (≈ 1660) OUR ESTIMATE					
1660 ± 10	[6]	ARNDT	98	DPWA	$\pi N \to \pi N$, ηN
1673		ARNDT	95	DPWA	$\pi N \to N\pi$
1689	[1]	ARNDT	95	DPWA	$\pi N \to N\pi$
1670	[7]	HOEHLER	93	ARGD	$\pi N \to \pi N$
1640 ± 20		CUTKOSKY	80	IPWA	$\pi N \to \pi N$
• • • We do not use the following data for averages, fits, limits, etc. • • •					
1663		VRANA	00	DPWA	Multichannel
1657		ARNDT	91	DPWA	$\pi N \to \pi N$ Soln SM90
1648 or 1651	[8]	LONGACRE	78	IPWA	$\pi N \to N\pi\pi$
1699 or 1698	[4]	LONGACRE	77	IPWA	$\pi N \to N\pi\pi$

−2×IMAGINARY PART

VALUE (MeV)		*DOCUMENT ID*		*TECN*	*COMMENT*
150 to 170 (≈ 160) OUR ESTIMATE					
140 ± 20	[6]	ARNDT	98	DPWA	$\pi N \to \pi N$, ηN
82		ARNDT	95	DPWA	$\pi N \to N\pi$
192	[1]	ARNDT	95	DPWA	$\pi N \to N\pi$
163	[7]	HOEHLER	93	ARGD	$\pi N \to \pi N$
150 ± 30		CUTKOSKY	80	IPWA	$\pi N \to \pi N$
• • • We do not use the following data for averages, fits, limits, etc. • • •					
240		VRANA	00	DPWA	Multichannel
160		ARNDT	91	DPWA	$\pi N \to \pi N$ Soln SM90
117 or 119	[8]	LONGACRE	78	IPWA	$\pi N \to N\pi\pi$
174 or 173	[4]	LONGACRE	77	IPWA	$\pi N \to N\pi\pi$

$N(1650)$ ELASTIC POLE RESIDUE

MODULUS $|r|$

VALUE (MeV)		*DOCUMENT ID*		*TECN*	*COMMENT*
22		ARNDT	95	DPWA	$\pi N \to N\pi$
72	[1]	ARNDT	95	DPWA	$\pi N \to N\pi$
39		HOEHLER	93	ARGD	$\pi N \to \pi N$
60 ± 10		CUTKOSKY	80	IPWA	$\pi N \to \pi N$
• • • We do not use the following data for averages, fits, limits, etc. • • •					
54		ARNDT	91	DPWA	$\pi N \to \pi N$ Soln SM90

PHASE θ

VALUE (°)		*DOCUMENT ID*		*TECN*	*COMMENT*
29		ARNDT	95	DPWA	$\pi N \to N\pi$
−85	[1]	ARNDT	95	DPWA	$\pi N \to N\pi$
−37		HOEHLER	93	ARGD	$\pi N \to \pi N$
−75 ± 25		CUTKOSKY	80	IPWA	$\pi N \to \pi N$
• • • We do not use the following data for averages, fits, limits, etc. • • •					
−38		ARNDT	91	DPWA	$\pi N \to \pi N$ Soln SM90

$N(1650)$ DECAY MODES

The following branching fractions are our estimates, not fits or averages.

	Mode	Fraction (Γ_i/Γ)
Γ_1	$N\pi$	55–90 %
Γ_2	$N\eta$	3–10 %
Γ_3	ΛK	3–11 %
Γ_4	ΣK	
Γ_5	$N\pi\pi$	10–20 %
Γ_6	$\Delta\pi$	1–7 %
Γ_7	$\Delta(1232)\pi$, D-wave	
Γ_8	$N\rho$	4–12 %
Γ_9	$N\rho$, S=1/2, S-wave	
Γ_{10}	$N\rho$, S=3/2, D-wave	
Γ_{11}	$N(\pi\pi)^{I=0}_{S\text{-wave}}$	< 4 %
Γ_{12}	$N(1440)\pi$	< 5 %
Γ_{13}	$p\gamma$	0.04–0.18 %
Γ_{14}	$p\gamma$, helicity=1/2	0.04–0.18 %
Γ_{15}	$n\gamma$	0.003–0.17 %
Γ_{16}	$n\gamma$, helicity=1/2	0.003–0.17 %

$N(1650)$ BRANCHING RATIOS

$\Gamma(N\pi)/\Gamma_{\text{total}}$ Γ_1/Γ

VALUE	*DOCUMENT ID*		*TECN*	*COMMENT*
0.55 to 0.90 OUR ESTIMATE				
0.735 ± 0.011	GREEN	97	DPWA	$\pi N \to \pi N$, ηN
0.89 ± 0.07	MANLEY	92	IPWA	$\pi N \to \pi N$ & $N\pi\pi$
0.65 ± 0.10	CUTKOSKY	80	IPWA	$\pi N \to \pi N$
0.61 ± 0.04	HOEHLER	79	IPWA	$\pi N \to \pi N$

• • • We do not use the following data for averages, fits, limits, etc. • • •

0.65 ±0.04	PENNER	02C	DPWA	Multichannel
0.74 ±0.02	VRANA	00	DPWA	Multichannel
0.99	ARNDT	95	DPWA	$\pi N \to N\pi$
0.27	[1] ARNDT	95	DPWA	$\pi N \to N\pi$
0.94 ±0.07	BATINIC	95	DPWA	$\pi N \to N\pi$, $N\eta$
0.49 ±0.21	[2] BATINIC	95	DPWA	$\pi N \to N\pi$, $N\eta$

$\Gamma(N\eta)/\Gamma_{total}$ Γ_2/Γ

VALUE	DOCUMENT ID	TECN	COMMENT
0.023±0.022 OUR AVERAGE	Error includes scale factor of 4.3.		
0.010±0.006	PENNER	02C	DPWA Multichannel
0.06 ±0.01	VRANA	00	DPWA Multichannel
• • • We do not use the following data for averages, fits, limits, etc. • • •			
0.06 ±0.05	BATINIC	95	DPWA $\pi N \to N\pi$, $N\eta$
0.02 ±0.03	[2] BATINIC	95	DPWA $\pi N \to N\pi$, $N\eta$

$(\Gamma_i\Gamma_f)^{1/2}/\Gamma_{total}$ in $N\pi \to N(1650) \to N\eta$ $(\Gamma_1\Gamma_2)^{1/2}/\Gamma$

VALUE	DOCUMENT ID	TECN	COMMENT
• • • We do not use the following data for averages, fits, limits, etc. • • •			
−0.09	[9] BAKER	79	DPWA $\pi^- p \to n\eta$

$\Gamma(\Lambda K)/\Gamma_{total}$ Γ_3/Γ

VALUE	DOCUMENT ID	TECN	COMMENT
0.027±0.004	PENNER	02C	DPWA Multichannel

$(\Gamma_i\Gamma_f)^{1/2}/\Gamma_{total}$ in $N\pi \to N(1650) \to \Lambda K$ $(\Gamma_1\Gamma_3)^{1/2}/\Gamma$

VALUE	DOCUMENT ID	TECN	COMMENT
−0.27 to −0.17 OUR ESTIMATE			
−0.22	BELL	83	DPWA $\pi^- p \to \Lambda K^0$
−0.22	SAXON	80	DPWA $\pi^- p \to \Lambda K^0$
• • • We do not use the following data for averages, fits, limits, etc. • • •			
−0.25	[10] BAKER	78	DPWA See SAXON 80
−0.23±0.01	[3] BAKER	77	IPWA $\pi^- p \to \Lambda K^0$
−0.25	[3] BAKER	77	DPWA $\pi^- p \to \Lambda K^0$
0.12	KNASEL	75	DPWA $\pi^- p \to \Lambda K^0$

$(\Gamma_i\Gamma_f)^{1/2}/\Gamma_{total}$ in $N\pi \to N(1650) \to \Sigma K$ $(\Gamma_1\Gamma_4)^{1/2}/\Gamma$

VALUE	DOCUMENT ID	TECN	COMMENT
• • • We do not use the following data for averages, fits, limits, etc. • • •			
−0.254	LIVANOS	80	DPWA $\pi p \to \Sigma K$
0.066 to 0.137	[11] DEANS	75	DPWA $\pi N \to \Sigma K$
0.20	KNASEL	75	DPWA

Note: Signs of couplings from $\pi N \to N\pi\pi$ analyses were changed in the 1986 edition to agree with the baryon-first convention; the overall phase ambiguity is resolved by choosing a negative sign for the $\Delta(1620)$ S_{31} coupling to $\Delta(1232)\pi$.

$(\Gamma_i\Gamma_f)^{1/2}/\Gamma_{total}$ in $N\pi \to N(1650) \to \Delta(1232)\pi$, D-wave $(\Gamma_1\Gamma_7)^{1/2}/\Gamma$

VALUE	DOCUMENT ID	TECN	COMMENT
+0.15 to 0.23 OUR ESTIMATE			
+0.12±0.04	MANLEY	92	IPWA $\pi N \to \pi N$ & $N\pi\pi$
+0.29	[4,12] LONGACRE	77	IPWA $\pi N \to N\pi\pi$
+0.15	[5] LONGACRE	75	IPWA $\pi N \to N\pi\pi$

$\Gamma(\Delta(1232)\pi,\ D\text{-wave})/\Gamma_{total}$ Γ_7/Γ

VALUE	DOCUMENT ID	TECN	COMMENT
0.02±0.01	VRANA	00	DPWA Multichannel

$(\Gamma_i\Gamma_f)^{1/2}/\Gamma_{total}$ in $N\pi \to N(1650) \to N\rho$, S=1/2, S-wave $(\Gamma_1\Gamma_9)^{1/2}/\Gamma$

VALUE	DOCUMENT ID	TECN	COMMENT
±0.03 to ±0.19 OUR ESTIMATE			
−0.01±0.09	MANLEY	92	IPWA $\pi N \to \pi N$ & $N\pi\pi$
+0.17	[4,12] LONGACRE	77	IPWA $\pi N \to N\pi\pi$
−0.16	[5] LONGACRE	75	IPWA $\pi N \to N\pi\pi$

$\Gamma(N\rho,\ S$=1/2, S-wave$)/\Gamma_{total}$ Γ_9/Γ

VALUE	DOCUMENT ID	TECN	COMMENT
0.01±0.01	VRANA	00	DPWA Multichannel

$(\Gamma_i\Gamma_f)^{1/2}/\Gamma_{total}$ in $N\pi \to N(1650) \to N\rho$, S=3/2, D-wave $(\Gamma_1\Gamma_{10})^{1/2}/\Gamma$

VALUE	DOCUMENT ID	TECN	COMMENT
+0.17 to +0.29 OUR ESTIMATE			
+0.16±0.06	MANLEY	92	IPWA $\pi N \to \pi N$ & $N\pi\pi$
+0.29	[4,12] LONGACRE	77	IPWA $\pi N \to N\pi\pi$

$\Gamma(N\rho,\ S$=3/2, D-wave$)/\Gamma_{total}$ Γ_{10}/Γ

VALUE	DOCUMENT ID	TECN	COMMENT
0.13±0.03	VRANA	00	DPWA Multichannel

$(\Gamma_i\Gamma_f)^{1/2}/\Gamma_{total}$ in $N\pi \to N(1650) \to N(\pi\pi)^{I=0}_{S\text{-wave}}$ $(\Gamma_1\Gamma_{11})^{1/2}/\Gamma$

VALUE	DOCUMENT ID	TECN	COMMENT
+0.04 to +0.18 OUR ESTIMATE			
+0.12±0.08	MANLEY	92	IPWA $\pi N \to \pi N$ & $N\pi\pi$
0.00	[4,12] LONGACRE	77	IPWA $\pi N \to N\pi\pi$
+0.25	[5] LONGACRE	75	IPWA $\pi N \to N\pi\pi$

$\Gamma(N(\pi\pi)^{I=0}_{S\text{-wave}})/\Gamma_{total}$ Γ_{11}/Γ

VALUE	DOCUMENT ID	TECN	COMMENT
0.01±0.01	VRANA	00	DPWA Multichannel

$(\Gamma_i\Gamma_f)^{1/2}/\Gamma_{total}$ in $N\pi \to N(1650) \to N(1440)\pi$ $(\Gamma_1\Gamma_{12})^{1/2}/\Gamma$

VALUE	DOCUMENT ID	TECN	COMMENT
+0.11±0.06	MANLEY	92	IPWA $\pi N \to \pi N$ & $N\pi\pi$

$\Gamma(N(1440)\pi)/\Gamma_{total}$ Γ_{12}/Γ

VALUE	DOCUMENT ID	TECN	COMMENT
0.03±0.01	VRANA	00	DPWA Multichannel

$N(1650)$ PHOTON DECAY AMPLITUDES

$N(1650) \to p\gamma$, helicity-1/2 amplitude $A_{1/2}$

VALUE (GeV$^{-1/2}$)	DOCUMENT ID	TECN	COMMENT
+0.053±0.016 OUR ESTIMATE			
0.069±0.005	ARNDT	96	IPWA $\gamma N \to \pi N$
0.033±0.015	CRAWFORD	83	IPWA $\gamma N \to \pi N$
0.050±0.010	AWAJI	81	DPWA $\gamma N \to \pi N$
0.065±0.005	ARAI	80	DPWA $\gamma N \to \pi N$ (fit 1)
0.061±0.005	ARAI	80	DPWA $\gamma N \to \pi N$ (fit 2)
0.031±0.017	CRAWFORD	80	DPWA $\gamma N \to \pi N$
• • • We do not use the following data for averages, fits, limits, etc. • • •			
0.049	PENNER	02D	DPWA Multichannel
0.068±0.003	LI	93	IPWA $\gamma N \to \pi N$
0.091	WADA	84	DPWA Compton scattering
+0.048±0.017	BARBOUR	78	DPWA $\gamma N \to \pi N$
+0.068±0.009	FELLER	76	DPWA $\gamma N \to \pi N$

$N(1650) \to n\gamma$, helicity-1/2 amplitude $A_{1/2}$

VALUE (GeV$^{-1/2}$)	DOCUMENT ID	TECN	COMMENT
−0.015±0.021 OUR ESTIMATE			
−0.015±0.005	ARNDT	96	IPWA $\gamma N \to \pi N$
−0.008±0.004	AWAJI	81	DPWA $\gamma N \to \pi N$
0.004±0.004	FUJII	81	DPWA $\gamma N \to \pi N$
0.010±0.020	ARAI	80	DPWA $\gamma N \to \pi N$ (fit 1)
0.008±0.019	ARAI	80	DPWA $\gamma N \to \pi N$ (fit 2)
−0.068±0.040	CRAWFORD	80	DPWA $\gamma N \to \pi N$
−0.011±0.011	TAKEDA	80	DPWA $\gamma N \to \pi N$
• • • We do not use the following data for averages, fits, limits, etc. • • •			
−0.011	PENNER	02D	DPWA Multichannel
−0.002±0.002	LI	93	IPWA $\gamma N \to \pi N$
−0.045±0.024	BARBOUR	78	DPWA $\gamma N \to \pi N$

$N(1650)$ $\gamma p \to \Lambda K^+$ AMPLITUDES

$(\Gamma_i\Gamma_f)^{1/2}/\Gamma_{total}$ in $p\gamma \to N(1650) \to \Lambda K^+$ (E_{0+} amplitude)

VALUE (units 10^{-3})	DOCUMENT ID	TECN
• • • We do not use the following data for averages, fits, limits, etc. • • •		
7.8 ±0.3	WORKMAN	90 DPWA
8.13	TANABE	89 DPWA

$p\gamma \to N(1650) \to \Lambda K^+$ phase angle θ (E_{0+} amplitude)

VALUE (degrees)	DOCUMENT ID	TECN
• • • We do not use the following data for averages, fits, limits, etc. • • •		
−107 ±3	WORKMAN	90 DPWA
−107.8	TANABE	89 DPWA

$N(1650)$ FOOTNOTES

[1] ARNDT 95 finds two distinct states.

[2] BATINIC 95 finds two distinct states. This second resonance was associated with the $N(2090)$ S_{11}.

[3] The two BAKER 77 entries are from an IPWA using the Barrelet-zero method and from a conventional energy-dependent analysis.

[4] LONGACRE 77 pole positions are from a search for poles in the unitarized T-matrix; the first (second) value uses, in addition to $\pi N \to N\pi\pi$ data, elastic amplitudes from a Saclay (CERN) partial-wave analysis. The other LONGACRE 77 values are from eyeball fits with Breit-Wigner circles to the T-matrix amplitudes.

[5] From method II of LONGACRE 75: eyeball fits with Breit-Wigner circles to the T-matrix amplitudes.

[6] ARNDT 98 also lists pole residues, which display more model dependence than do the associated pole positions.

[7] See HOEHLER 93 for a detailed discussion of the evidence for and the pole parameters of N and Δ resonances as determined from Argand diagrams of πN elastic partial-wave amplitudes and from plots of the speeds with which the amplitudes traverse the diagrams.

[8] LONGACRE 78 values are from a search for poles in the unitarized T-matrix. The first (second) value uses, in addition to $\pi N \rightarrow N\pi\pi$ data, elastic amplitudes from a Saclay (CERN) partial-wave analysis.
[9] BAKER 79 fixed this coupling during fitting, but the negative sign relative to the $N(1535)$ is well determined.
[10] The overall phase of BAKER 78 couplings has been changed to agree with previous conventions. Superseded by SAXON 80.
[11] The range given for DEANS 75 is from the four best solutions.
[12] LONGACRE 77 considers this coupling to be well determined.

$N(1650)$ REFERENCES

For early references, see Physics Letters **111B** 70 (1982).

PENNER	02C	PR C66 055211	G. Penner, U. Mosel	(GIES)
PENNER	02D	PR C66 055212	G. Penner, U. Mosel	(GIES)
BAI	01B	PL B510 75	J.Z. Bai *et al.*	(BEPC BES Collab.)
VRANA	00	PRPL 328 181	T.P. Vrana, S.A. Dytman,, T.-S.H. Lee	(PITT+)
ARNDT	98	PR C58 3636	R.A. Arndt *et al.*	
GREEN	97	PR C55 R2167	A.M. Green, S. Wycech	(HELS, WINR)
ARNDT	96	PR C53 430	R.A. Arndt, I.I. Strakovsky, R.L. Workman	(VPI)
ARNDT	95	PR C52 2120	R.A. Arndt *et al.*	(VPI, BRCO)
BATINIC	95	PR C51 2310	M. Batinić *et al.*	(BOSK, UCLA)
Also	98	PR C57 1004 (erratum)	M. Batinić *et al.*	
HOEHLER	93	πN Newsletter 9 1	G. Hohler	(KARL)
LI	93	PR C47 2759	Z.J. Li *et al.*	(VPI)
MANLEY	92	PR D45 4002	D.M. Manley, E.M. Saleski	(KENT) IJP
Also	84	PR D30 904	D.M. Manley *et al.*	(VPI)
ARNDT	91	PR D43 2131	R.A. Arndt *et al.*	(VPI, TELE) IJP
WORKMAN	90	PR C42 781	R.L. Workman	(VPI)
TANABE	89	PR C39 741	H. Tanabe, M. Kohno, C. Bennhold	(MANZ)
Also	89	NC 102A 193	M. Kohno, H. Tanabe, C. Bennhold	(MANZ)
WADA	84	NP B247 313	Y. Wada *et al.*	(INUS)
BELL	83	NP B222 389	K.W. Bell *et al.*	(RL) IJP
CRAWFORD	83	NP B211 1	R.L. Crawford, W.T. Morton	(GLAS)
PDG	82	PL 111B	M. Roos *et al.*	(HELS, CIT, CERN)
AWAJI	81	Bonn Conf. 352	N. Awaji, R. Kajikawa	(NAGO)
Also	82	NP B197 365	K. Fujii *et al.*	(NAGO)
FUJII	81	NP B187 53	K. Fujii *et al.*	(NAGO, OSAK)
ARAI	80	Toronto Conf. 93	I. Arai	(INUS)
Also	82	NP B194 251	I. Arai, H. Fujii	(INUS)
CRAWFORD	80	Toronto Conf. 107	R.L. Crawford	(GLAS)
CUTKOSKY	80	Toronto Conf. 19	R.E. Cutkosky *et al.*	(CMU, LBL) IJP
Also	79	PR D20 2839	R.E. Cutkosky *et al.*	(CMU, LBL) IJP
LIVANOS	80	Toronto Conf. 35	P. Livanos *et al.*	(SACL) IJP
MUSETTE	80	NC 57A 37	M. Musette	(BRUX) IJP
SAXON	80	NP B162 522	D.H. Saxon *et al.*	(RHEL, BRIS) IJP
TAKEDA	80	NP B168 17	H. Takeda *et al.*	(TOKY, INUS)
BAKER	79	NP B156 93	R.D. Baker *et al.*	(RHEL) IJP
HOEHLER	79	PDAT 12-1	G. Hohler *et al.*	(KARLT) IJP
Also	80	Toronto Conf. 3	R. Koch	(KARLT) IJP
BAKER	78	NP B141 29	R.D. Baker *et al.*	(RL, CAVE) IJP
BARBOUR	78	NP B141 253	I.M. Barbour, R.L. Crawford, N.H. Parsons	(GLAS)
LONGACRE	78	PR D17 1795	R.S. Longacre *et al.*	(LBL, SLAC)
BAKER	77	NP B126 365	R.D. Baker *et al.*	(RHEL) IJP
LONGACRE	77	NP B122 493	R.S. Longacre, J. Dolbeau	(SACL) IJP
Also	76	NP B108 365	J. Dolbeau *et al.*	(SACL) IJP
FELLER	76	NP B104 219	P. Feller *et al.*	(NAGO, OSAK) IJP
DEANS	75	NP B96 90	S.R. Deans *et al.*	(SFLA, ALAH) IJP
KNASEL	75	PR D11 1	T.M. Knasel *et al.*	(CHIC, WUSL, OSU+) IJP
LONGACRE	75	PL 55B 415	R.S. Longacre *et al.*	(LBL, SLAC) IJP

$N(1675)$ D_{15} $I(J^P) = \frac{1}{2}(\frac{5}{2}^-)$ Status: ****

Most of the results published before 1975 are now obsolete and have been omitted. They may be found in our 1982 edition, Physics Letters **111B** (1982).

$N(1675)$ BREIT-WIGNER MASS

VALUE (MeV)	*DOCUMENT ID*		*TECN*	*COMMENT*
1670 to 1685 (≈ 1675) OUR ESTIMATE				
1676± 2	MANLEY	92	IPWA	$\pi N \rightarrow \pi N$ & $N\pi\pi$
1675±10	CUTKOSKY	80	IPWA	$\pi N \rightarrow \pi N$
1679± 8	HOEHLER	79	IPWA	$\pi N \rightarrow \pi N$
• • • We do not use the following data for averages, fits, limits, etc. • • •				
1685± 4	VRANA	00	DPWA	Multichannel
1673± 5	ARNDT	96	IPWA	$\gamma N \rightarrow \pi N$
1673	ARNDT	95	DPWA	$\pi N \rightarrow N\pi$
1683±19	BATINIC	95	DPWA	$\pi N \rightarrow N\pi$, $N\eta$
1666	LI	93	IPWA	$\gamma N \rightarrow \pi N$
1685	CRAWFORD	80	DPWA	$\gamma N \rightarrow \pi N$
1670	SAXON	80	DPWA	$\pi^- p \rightarrow \Lambda K^0$
1680	BARBOUR	78	DPWA	$\gamma N \rightarrow \pi N$
1650	[1] LONGACRE	77	IPWA	$\pi N \rightarrow N\pi\pi$
1660	[2] LONGACRE	75	IPWA	$\pi N \rightarrow N\pi\pi$

$N(1675)$ BREIT-WIGNER WIDTH

VALUE (MeV)	*DOCUMENT ID*		*TECN*	*COMMENT*
140 to 180 (≈ 150) OUR ESTIMATE				
159± 7	MANLEY	92	IPWA	$\pi N \rightarrow \pi N$ & $N\pi\pi$
160±20	CUTKOSKY	80	IPWA	$\pi N \rightarrow \pi N$
120±15	HOEHLER	79	IPWA	$\pi N \rightarrow \pi N$
• • • We do not use the following data for averages, fits, limits, etc. • • •				
131±10	VRANA	00	DPWA	Multichannel
154± 7	ARNDT	96	IPWA	$\gamma N \rightarrow \pi N$
154	ARNDT	95	DPWA	$\pi N \rightarrow N\pi$
142±23	BATINIC	95	DPWA	$\pi N \rightarrow N\pi$, $N\eta$
136	LI	93	IPWA	$\gamma N \rightarrow \pi N$
191	CRAWFORD	80	DPWA	$\gamma N \rightarrow \pi N$
40	SAXON	80	DPWA	$\pi^- p \rightarrow \Lambda K^0$
88	BAKER	79	DPWA	$\pi^- p \rightarrow n\eta$
192	BARBOUR	78	DPWA	$\gamma N \rightarrow \pi N$
130	[1] LONGACRE	77	IPWA	$\pi N \rightarrow N\pi\pi$
150	[2] LONGACRE	75	IPWA	$\pi N \rightarrow N\pi\pi$

$N(1675)$ POLE POSITION

REAL PART

VALUE (MeV)	*DOCUMENT ID*		*TECN*	*COMMENT*
1655 to 1665 (≈ 1660) OUR ESTIMATE				
1663	ARNDT	95	DPWA	$\pi N \rightarrow N\pi$
1656	[3] HOEHLER	93	ARGD	$\pi N \rightarrow \pi N$
1660±10	CUTKOSKY	80	IPWA	$\pi N \rightarrow \pi N$
• • • We do not use the following data for averages, fits, limits, etc. • • •				
1674	VRANA	00	DPWA	Multichannel
1655	ARNDT	91	DPWA	$\pi N \rightarrow \pi N$ Soln SM90
1663 or 1668	[4] LONGACRE	78	IPWA	$\pi N \rightarrow N\pi\pi$
1649 or 1650	[1] LONGACRE	77	IPWA	$\pi N \rightarrow N\pi\pi$

$-2\times$IMAGINARY PART

VALUE (MeV)	*DOCUMENT ID*		*TECN*	*COMMENT*
125 to 155 (≈ 140) OUR ESTIMATE				
152	ARNDT	95	DPWA	$\pi N \rightarrow N\pi$
126	[3] HOEHLER	93	ARGD	$\pi N \rightarrow \pi N$
140±10	CUTKOSKY	80	IPWA	$\pi N \rightarrow \pi N$
• • • We do not use the following data for averages, fits, limits, etc. • • •				
120	VRANA	00	DPWA	Multichannel
124	ARNDT	91	DPWA	$\pi N \rightarrow \pi N$ Soln SM90
146 or 171	[4] LONGACRE	78	IPWA	$\pi N \rightarrow N\pi\pi$
127 or 127	[1] LONGACRE	77	IPWA	$\pi N \rightarrow N\pi\pi$

$N(1675)$ ELASTIC POLE RESIDUE

MODULUS $|r|$

VALUE (MeV)	*DOCUMENT ID*		*TECN*	*COMMENT*
29	ARNDT	95	DPWA	$\pi N \rightarrow N\pi$
23	HOEHLER	93	ARGD	$\pi N \rightarrow \pi N$
31±5	CUTKOSKY	80	IPWA	$\pi N \rightarrow \pi N$
• • • We do not use the following data for averages, fits, limits, etc. • • •				
28	ARNDT	91	DPWA	$\pi N \rightarrow \pi N$ Soln SM90

PHASE θ

VALUE (°)	*DOCUMENT ID*		*TECN*	*COMMENT*
− 6	ARNDT	95	DPWA	$\pi N \rightarrow N\pi$
−22	HOEHLER	93	ARGD	$\pi N \rightarrow \pi N$
−30±10	CUTKOSKY	80	IPWA	$\pi N \rightarrow \pi N$
• • • We do not use the following data for averages, fits, limits, etc. • • •				
−17	ARNDT	91	DPWA	$\pi N \rightarrow \pi N$ Soln SM90

$N(1675)$ DECAY MODES

The following branching fractions are our estimates, not fits or averages.

	Mode	Fraction (Γ_j/Γ)
Γ_1	$N\pi$	40–50 %
Γ_2	$N\eta$	(0.0±1.0) %
Γ_3	ΛK	<1 %
Γ_4	ΣK	
Γ_5	$N\pi\pi$	50–60 %
Γ_6	$\Delta\pi$	50–60 %
Γ_7	$\Delta(1232)\pi$, D-wave	
Γ_8	$\Delta(1232)\pi$, G-wave	
Γ_9	$N\rho$	< 1–3 %
Γ_{10}	$N\rho$, S=1/2, D-wave	
Γ_{11}	$N\rho$, S=3/2, D-wave	
Γ_{12}	$N\rho$, S=3/2, G-wave	
Γ_{13}	$N(\pi\pi)^{I=0}_{S\text{-wave}}$	
Γ_{14}	$p\gamma$	0.004–0.023 %
Γ_{15}	$p\gamma$, helicity=1/2	0.0–0.015 %
Γ_{16}	$p\gamma$, helicity=3/2	0.0–0.011 %
Γ_{17}	$n\gamma$	0.02–0.12 %
Γ_{18}	$n\gamma$, helicity=1/2	0.006–0.046 %
Γ_{19}	$n\gamma$, helicity=3/2	0.01–0.08 %

$N(1675)$ BRANCHING RATIOS

$\Gamma(N\pi)/\Gamma_{total}$ Γ_1/Γ

VALUE	DOCUMENT ID		TECN	COMMENT
0.4 to 0.5 OUR ESTIMATE				
0.47±0.02	MANLEY	92	IPWA	$\pi N \to \pi N$ & $N\pi\pi$
0.38±0.05	CUTKOSKY	80	IPWA	$\pi N \to \pi N$
0.38±0.03	HOEHLER	79	IPWA	$\pi N \to \pi N$
• • • We do not use the following data for averages, fits, limits, etc. • • •				
0.35±0.01	VRANA	00	DPWA	Multichannel
0.38	ARNDT	95	DPWA	$\pi N \to N\pi$
0.31±0.06	BATINIC	95	DPWA	$\pi N \to N\pi$, $N\eta$

$\Gamma(N\eta)/\Gamma_{total}$ Γ_2/Γ

VALUE	DOCUMENT ID		TECN	COMMENT
0.00 ±0.01	VRANA	00	DPWA	Multichannel
• • • We do not use the following data for averages, fits, limits, etc. • • •				
0.001±0.001	BATINIC	95	DPWA	$\pi N \to N\pi$, $N\eta$

$(\Gamma_i\Gamma_f)^{1/2}/\Gamma_{total}$ in $N\pi \to N(1675) \to N\eta$ $(\Gamma_1\Gamma_2)^{1/2}/\Gamma$

VALUE	DOCUMENT ID		TECN	COMMENT
• • • We do not use the following data for averages, fits, limits, etc. • • •				
−0.07	BAKER	79	DPWA	$\pi^- p \to n\eta$
+0.009	FELTESSE	75	DPWA	Soln A; see BAKER 79

$(\Gamma_i\Gamma_f)^{1/2}/\Gamma_{total}$ in $N\pi \to N(1675) \to \Lambda K$ $(\Gamma_1\Gamma_3)^{1/2}/\Gamma$

VALUE	DOCUMENT ID		TECN	COMMENT
±0.04 to ±0.08 OUR ESTIMATE				
−0.01	BELL	83	DPWA	$\pi^- p \to \Lambda K^0$
+0.036	[5] SAXON	80	DPWA	$\pi^- p \to \Lambda K^0$
• • • We do not use the following data for averages, fits, limits, etc. • • •				
−0.034±0.006	DEVENISH	74B		Fixed-t dispersion rel.

$(\Gamma_i\Gamma_f)^{1/2}/\Gamma_{total}$ in $N\pi \to N(1675) \to \Sigma K$ $(\Gamma_1\Gamma_4)^{1/2}/\Gamma$

VALUE	DOCUMENT ID		TECN	COMMENT
• • • We do not use the following data for averages, fits, limits, etc. • • •				
<0.003	[6] DEANS	75	DPWA	$\pi N \to \Sigma K$

Note: Signs of couplings from $\pi N \to N\pi\pi$ analyses were changed in the 1986 edition to agree with the baryon-first convention; the overall phase ambiguity is resolved by choosing a negative sign for the $\Delta(1620)$ S_{31} coupling to $\Delta(1232)\pi$.

$(\Gamma_i\Gamma_f)^{1/2}/\Gamma_{total}$ in $N\pi \to N(1675) \to \Delta(1232)\pi$, D-wave $(\Gamma_1\Gamma_7)^{1/2}/\Gamma$

VALUE	DOCUMENT ID		TECN	COMMENT
+0.46 to +0.50 OUR ESTIMATE				
+0.496±0.003	MANLEY	92	IPWA	$\pi N \to \pi N$ & $N\pi\pi$
+0.46	[1,7] LONGACRE	77	IPWA	$\pi N \to N\pi\pi$
+0.50	[2] LONGACRE	75	IPWA	$\pi N \to N\pi\pi$
• • • We do not use the following data for averages, fits, limits, etc. • • •				
+0.5	[8] NOVOSELLER	78	IPWA	$\pi N \to N\pi\pi$

$\Gamma(\Delta(1232)\pi$, D-wave$)/\Gamma_{total}$ Γ_7/Γ

VALUE	DOCUMENT ID		TECN	COMMENT
0.63±0.02	VRANA	00	DPWA	Multichannel

$(\Gamma_i\Gamma_f)^{1/2}/\Gamma_{total}$ in $N\pi \to N(1675) \to N\rho$, S=1/2, D-wave $(\Gamma_1\Gamma_{10})^{1/2}/\Gamma$

VALUE	DOCUMENT ID		TECN	COMMENT
+0.04±0.02	MANLEY	92	IPWA	$\pi N \to \pi N$ & $N\pi\pi$

$\Gamma(N\rho$, S=1/2, D-wave$)/\Gamma_{total}$ Γ_{10}/Γ

VALUE	DOCUMENT ID		TECN	COMMENT
0.00±0.01	VRANA	00	DPWA	Multichannel

$(\Gamma_i\Gamma_f)^{1/2}/\Gamma_{total}$ in $N\pi \to N(1675) \to N\rho$, S=3/2, D-wave $(\Gamma_1\Gamma_{11})^{1/2}/\Gamma$

VALUE	DOCUMENT ID		TECN	COMMENT
−0.12 to −0.06 OUR ESTIMATE				
−0.03±0.02	MANLEY	92	IPWA	$\pi N \to \pi N$ & $N\pi\pi$
−0.15	[1,7] LONGACRE	77	IPWA	$\pi N \to N\pi\pi$

$\Gamma(N\rho$, S=3/2, D-wave$)/\Gamma_{total}$ Γ_{11}/Γ

VALUE	DOCUMENT ID		TECN	COMMENT
0.01±0.01	VRANA	00	DPWA	Multichannel

$(\Gamma_i\Gamma_f)^{1/2}/\Gamma_{total}$ in $N\pi \to N(1675) \to N(\pi\pi)^{I=0}_{S\text{-wave}}$ $(\Gamma_1\Gamma_{13})^{1/2}/\Gamma$

VALUE	DOCUMENT ID		TECN	COMMENT
+0.03	[1,7] LONGACRE	77	IPWA	$\pi N \to N\pi\pi$

$N(1675)$ PHOTON DECAY AMPLITUDES

$N(1675) \to p\gamma$, helicity-1/2 amplitude $A_{1/2}$

VALUE (GeV$^{-1/2}$)	DOCUMENT ID		TECN	COMMENT
+0.019±0.008 OUR ESTIMATE				
0.015±0.010	ARNDT	96	IPWA	$\gamma N \to \pi N$
0.021±0.011	CRAWFORD	83	IPWA	$\gamma N \to \pi N$
0.034±0.005	AWAJI	81	DPWA	$\gamma N \to \pi N$
0.006±0.005	ARAI	80	DPWA	$\gamma N \to \pi N$ (fit 1)
0.006±0.004	ARAI	80	DPWA	$\gamma N \to \pi N$ (fit 2)
0.023±0.015	CRAWFORD	80	DPWA	$\gamma N \to \pi N$
• • • We do not use the following data for averages, fits, limits, etc. • • •				
0.012±0.002	LI	93	IPWA	$\gamma N \to \pi N$
+0.022±0.010	BARBOUR	78	DPWA	$\gamma N \to \pi N$
+0.034±0.004	FELLER	76	DPWA	$\gamma N \to \pi N$

$N(1675) \to p\gamma$, helicity-3/2 amplitude $A_{3/2}$

VALUE (GeV$^{-1/2}$)	DOCUMENT ID		TECN	COMMENT
+0.015±0.009 OUR ESTIMATE				
0.010±0.007	ARNDT	96	IPWA	$\gamma N \to \pi N$
0.015±0.009	CRAWFORD	83	IPWA	$\gamma N \to \pi N$
0.024±0.008	AWAJI	81	DPWA	$\gamma N \to \pi N$
0.030±0.004	ARAI	80	DPWA	$\gamma N \to \pi N$ (fit 1)
0.029±0.004	ARAI	80	DPWA	$\gamma N \to \pi N$ (fit 2)
0.003±0.012	CRAWFORD	80	DPWA	$\gamma N \to \pi N$
• • • We do not use the following data for averages, fits, limits, etc. • • •				
0.021±0.002	LI	93	IPWA	$\gamma N \to \pi N$
+0.015±0.006	BARBOUR	78	DPWA	$\gamma N \to \pi N$
+0.019±0.009	FELLER	76	DPWA	$\gamma N \to \pi N$

$N(1675) \to n\gamma$, helicity-1/2 amplitude $A_{1/2}$

VALUE (GeV$^{-1/2}$)	DOCUMENT ID		TECN	COMMENT
−0.043±0.012 OUR ESTIMATE				
−0.049±0.010	ARNDT	96	IPWA	$\gamma N \to \pi N$
−0.057±0.024	AWAJI	81	DPWA	$\gamma N \to \pi N$
−0.033±0.004	FUJII	81	DPWA	$\gamma N \to \pi N$
−0.039±0.017	ARAI	80	DPWA	$\gamma N \to \pi N$ (fit 1)
−0.025±0.027	ARAI	80	DPWA	$\gamma N \to \pi N$ (fit 2)
−0.059±0.015	CRAWFORD	80	DPWA	$\gamma N \to \pi N$
−0.021±0.011	TAKEDA	80	DPWA	$\gamma N \to \pi N$
• • • We do not use the following data for averages, fits, limits, etc. • • •				
−0.060±0.003	LI	93	IPWA	$\gamma N \to \pi N$
−0.066±0.020	BARBOUR	78	DPWA	$\gamma N \to \pi N$

$N(1675) \to n\gamma$, helicity-3/2 amplitude $A_{3/2}$

VALUE (GeV$^{-1/2}$)	DOCUMENT ID		TECN	COMMENT
−0.058±0.013 OUR ESTIMATE				
−0.051±0.010	ARNDT	96	IPWA	$\gamma N \to \pi N$
−0.077±0.018	AWAJI	81	DPWA	$\gamma N \to \pi N$
−0.069±0.004	FUJII	81	DPWA	$\gamma N \to \pi N$
−0.066±0.026	ARAI	80	DPWA	$\gamma N \to \pi N$ (fit 1)
−0.071±0.022	ARAI	80	DPWA	$\gamma N \to \pi N$ (fit 2)
−0.059±0.020	CRAWFORD	80	DPWA	$\gamma N \to \pi N$
−0.030±0.012	TAKEDA	80	DPWA	$\gamma N \to \pi N$
• • • We do not use the following data for averages, fits, limits, etc. • • •				
−0.074±0.003	LI	93	IPWA	$\gamma N \to \pi N$
−0.073±0.014	BARBOUR	78	DPWA	$\gamma N \to \pi N$

$N(1675)$ FOOTNOTES

[1] LONGACRE 77 pole positions are from a search for poles in the unitarized T-matrix; the first (second) value uses, in addition to $\pi N \to N\pi\pi$ data, elastic amplitudes from a Saclay (CERN) partial-wave analysis. The other LONGACRE 77 values are from eyeball fits with Breit-Wigner circles to the T-matrix amplitudes.

[2] From method II of LONGACRE 75: eyeball fits with Breit-Wigner circles to the T-matrix amplitudes.

[3] See HOEHLER 93 for a detailed discussion of the evidence for and the pole parameters of N and Δ resonances as determined from Argand diagrams of πN elastic partial-wave amplitudes and from plots of the speeds with which the amplitudes traverse the diagrams.

[4] LONGACRE 78 values are from a search for poles in the unitarized T-matrix. The first (second) value uses, in addition to $\pi N \to N\pi\pi$ data, elastic amplitudes from a Saclay (CERN) partial-wave analysis.

[5] SAXON 80 finds the coupling phase is near 90°.

[6] The range given is from the four best solutions. DEANS 75 disagrees with $\pi^+ p \to \Sigma^+ K^+$ data of WINNIK 77 around 1920 MeV.

[7] LONGACRE 77 considers this coupling to be well determined.

[8] A Breit-Wigner fit to the HERNDON 75 IPWA.

$N(1675)$ REFERENCES

For early references, see Physics Letters **111B** 70 (1982).

VRANA	00	PRPL 328 181	T.P. Vrana, S.A. Dytman,, T.-S.H. Lee	(PITT+)
ARNDT	96	PR C53 430	R.A. Arndt, I.I. Strakovsky, R.L. Workman	(VPI)
ARNDT	95	PR C52 2120	R.A. Arndt *et al.*	(VPI, BRCO)
BATINIC	95	PR C51 2310	M. Batinic *et al.*	(BOSK, UCLA)
Also	98	PR C57 1004 (erratum)	M. Batinic *et al.*	
HOEHLER	93	πN Newsletter 9 1	G. Hohler	(KARL)
LI	93	PR C47 2759	Z.J. Li *et al.*	(VPI)
MANLEY	92	PR D45 4002	D.M. Manley, E.M. Saleski	(KENT) IJP
Also	84	PR D30 904	D.M. Manley *et al.*	(VPI)
ARNDT	91	PR D43 2131	R.A. Arndt *et al.*	(VPI, TELE) IJP
BELL	83	NP B222 389	K.W. Bell *et al.*	(RL) IJP
CRAWFORD	83	NP B211 1	R.L. Crawford, W.T. Morton	(GLAS)
PDG	82	PL 111B	M. Roos *et al.*	(HELS, CIT, CERN)
AWAJI	81	Bonn Conf. 352	N. Awaji, R. Kajikawa	(NAGO)
Also	82	NP B197 365	K. Fujii *et al.*	(NAGO)
FUJII	81	NP B187 53	K. Fujii *et al.*	(NAGO, OSAK)
ARAI	80	Toronto Conf. 93	I. Arai	(INUS)
Also	82	NP B194 251	I. Arai, H. Fujii	(INUS)
CRAWFORD	80	Toronto Conf. 107	R.L. Crawford	(GLAS)
CUTKOSKY	80	Toronto Conf. 19	R.E. Cutkosky *et al.*	(CMU, LBL) IJP
Also	79	PR D20 2839	R.E. Cutkosky *et al.*	(CMU, LBL) IJP
SAXON	80	NP B162 522	D.H. Saxon *et al.*	(RHEL, BRIS) IJP
TAKEDA	80	NP B168 17	H. Takeda *et al.*	(TOKY, INUS)
BAKER	79	NP B156 93	R.D. Baker *et al.*	(RHEL) IJP
HOEHLER	79	PDAT 12-1	G. Hohler *et al.*	(KARLT) IJP
Also	80	Toronto Conf. 3	R. Koch	(KARLT) IJP
BARBOUR	78	NP B141 253	I.M. Barbour, R.L. Crawford, N.H. Parsons	(GLAS)
LONGACRE	78	PR D17 1795	R.S. Longacre *et al.*	(LBL, SLAC)
NOVOSELLER	78	NP B137 509	D.E. Novoseller	(CIT) IJP
Also	78B	NP B137 445	D.E. Novoseller	(CIT) IJP
LONGACRE	77	NP B122 493	R.S. Longacre, J. Dolbeau	(SACL) IJP
Also	76	NP B108 365	J. Dolbeau *et al.*	(SACL) IJP
WINNIK	77	NP B128 66	M. Winnik *et al.*	(HAIF) I
FELLER	76	NP B104 219	P. Feller *et al.*	(NAGO, OSAK) IJP
DEANS	75	NP B96 90	S.R. Deans *et al.*	(SFLA, ALAH) IJP
FELTESSE	75	NP B93 242	J. Feltesse *et al.*	(SACL) IJP
HERNDON	75	PR D11 3183	D. Herndon *et al.*	(LBL, SLAC)
LONGACRE	75	PL 55B 415	R.S. Longacre *et al.*	(LBL, SLAC) IJP
DEVENISH	74B	NP B81 330	R.C.E. Devenish, C.D. Froggatt, B.R. Martin	(DESY+)

$N(1680)$ F_{15}

$I(J^P) = \frac{1}{2}(\frac{5}{2}^+)$ Status: ****

Most of the results published before 1975 are now obsolete and have been omitted. They may be found in our 1982 edition, Physics Letters **111B** (1982).

$N(1680)$ BREIT-WIGNER MASS

VALUE (MeV)		*DOCUMENT ID*		*TECN*	*COMMENT*
1675 to 1690 (≈ 1680) OUR ESTIMATE					
1684± 4		MANLEY	92	IPWA	$\pi N \to \pi N$ & $N\pi\pi$
1680±10		CUTKOSKY	80	IPWA	$\pi N \to \pi N$
1684± 3		HOEHLER	79	IPWA	$\pi N \to \pi N$
• • • We do not use the following data for averages, fits, limits, etc. • • •					
1679± 3		VRANA	00	DPWA	Multichannel
1679± 5		ARNDT	96	IPWA	$\gamma N \to \pi N$
1678		ARNDT	95	DPWA	$\pi N \to N\pi$
1674±12		BATINIC	95	DPWA	$\pi N \to N\pi$, $N\eta$
1682		CRAWFORD	80	DPWA	$\gamma N \to \pi N$
1680		BARBOUR	78	DPWA	$\gamma N \to \pi N$
1660	[1]	LONGACRE	77	IPWA	$\pi N \to N\pi\pi$
1685		KNASEL	75	DPWA	$\pi^- p \to \Lambda K^0$
1670	[2]	LONGACRE	75	IPWA	$\pi N \to N\pi\pi$

$N(1680)$ BREIT-WIGNER WIDTH

VALUE (MeV)		*DOCUMENT ID*		*TECN*	*COMMENT*
120 to 140 (≈ 130) OUR ESTIMATE					
139± 8		MANLEY	92	IPWA	$\pi N \to \pi N$ & $N\pi\pi$
120±10		CUTKOSKY	80	IPWA	$\pi N \to \pi N$
128± 8		HOEHLER	79	IPWA	$\pi N \to \pi N$
• • • We do not use the following data for averages, fits, limits, etc. • • •					
128± 9		VRANA	00	DPWA	Multichannel
124± 4		ARNDT	96	IPWA	$\gamma N \to \pi N$
126		ARNDT	95	DPWA	$\pi N \to N\pi$
126±20		BATINIC	95	DPWA	$\pi N \to N\pi$, $N\eta$
121		CRAWFORD	80	DPWA	$\gamma N \to \pi N$
119		BARBOUR	78	DPWA	$\gamma N \to \pi N$
150	[1]	LONGACRE	77	IPWA	$\pi N \to N\pi\pi$
155		KNASEL	75	DPWA	$\pi^- p \to \Lambda K^0$
130	[2]	LONGACRE	75	IPWA	$\pi N \to N\pi\pi$

$N(1680)$ POLE POSITION

REAL PART

VALUE (MeV)		*DOCUMENT ID*		*TECN*	*COMMENT*
1665 to 1675 (≈ 1670) OUR ESTIMATE					
1670		ARNDT	95	DPWA	$\pi N \to N\pi$
1673	[3]	HOEHLER	93	ARGD	$\pi N \to \pi N$
1667±5		CUTKOSKY	80	IPWA	$\pi N \to \pi N$
• • • We do not use the following data for averages, fits, limits, etc. • • •					
1667		VRANA	00	DPWA	Multichannel
1670		ARNDT	91	DPWA	$\pi N \to \pi N$ Soln SM90
1668 or 1674	[4]	LONGACRE	78	IPWA	$\pi N \to N\pi\pi$
1656 or 1653	[1]	LONGACRE	77	IPWA	$\pi N \to N\pi\pi$

$-2\times$IMAGINARY PART

VALUE (MeV)		*DOCUMENT ID*		*TECN*	*COMMENT*
105 to 135 (≈ 120) OUR ESTIMATE					
120		ARNDT	95	DPWA	$\pi N \to N\pi$
135	[3]	HOEHLER	93	ARGD	$\pi N \to \pi N$
110±10		CUTKOSKY	80	IPWA	$\pi N \to \pi N$
• • • We do not use the following data for averages, fits, limits, etc. • • •					
122		VRANA	00	DPWA	Multichannel
116		ARNDT	91	DPWA	$\pi N \to \pi N$ Soln SM90
132 or 137	[4]	LONGACRE	78	IPWA	$\pi N \to N\pi\pi$
145 or 143	[1]	LONGACRE	77	IPWA	$\pi N \to N\pi\pi$

$N(1680)$ ELASTIC POLE RESIDUE

MODULUS $|r|$

VALUE (MeV)	*DOCUMENT ID*		*TECN*	*COMMENT*
40	ARNDT	95	DPWA	$\pi N \to N\pi$
44	HOEHLER	93	ARGD	$\pi N \to \pi N$
34±2	CUTKOSKY	80	IPWA	$\pi N \to \pi N$
• • • We do not use the following data for averages, fits, limits, etc. • • •				
37	ARNDT	91	DPWA	$\pi N \to \pi N$ Soln SM90

PHASE θ

VALUE (°)	*DOCUMENT ID*		*TECN*	*COMMENT*
+ 1	ARNDT	95	DPWA	$\pi N \to N\pi$
− 17	HOEHLER	93	ARGD	$\pi N \to \pi N$
− 25±5	CUTKOSKY	80	IPWA	$\pi N \to \pi N$
• • • We do not use the following data for averages, fits, limits, etc. • • •				
− 14	ARNDT	91	DPWA	$\pi N \to \pi N$ Soln SM90

$N(1680)$ DECAY MODES

The following branching fractions are our estimates, not fits or averages.

	Mode	Fraction (Γ_i/Γ)
Γ_1	$N\pi$	60–70 %
Γ_2	$N\eta$	(0.0±1.0) %
Γ_3	ΛK	
Γ_4	ΣK	
Γ_5	$N\pi\pi$	30–40 %
Γ_6	$\Delta\pi$	5–15 %
Γ_7	$\Delta(1232)\pi$, P-wave	6–14 %
Γ_8	$\Delta(1232)\pi$, F-wave	<2 %
Γ_9	$N\rho$	3–15 %
Γ_{10}	$N\rho$, S=1/2, F-wave	
Γ_{11}	$N\rho$, S=3/2, P-wave	<12 %
Γ_{12}	$N\rho$, S=3/2, F-wave	1–5 %
Γ_{13}	$N(\pi\pi)^{I=0}_{S\text{-wave}}$	5–20 %
Γ_{14}	$p\gamma$	0.21–0.32 %
Γ_{15}	$p\gamma$, helicity=1/2	0.001–0.011 %
Γ_{16}	$p\gamma$, helicity=3/2	0.20–0.32 %
Γ_{17}	$n\gamma$	0.021–0.046 %
Γ_{18}	$n\gamma$, helicity=1/2	0.004–0.029 %
Γ_{19}	$n\gamma$, helicity=3/2	0.01–0.024 %

$N(1680)$ BRANCHING RATIOS

$\Gamma(N\pi)/\Gamma_{\text{total}}$ Γ_1/Γ

VALUE	*DOCUMENT ID*		*TECN*	*COMMENT*
0.6 to 0.7 OUR ESTIMATE				
0.70±0.03	MANLEY	92	IPWA	$\pi N \to \pi N$ & $N\pi\pi$
0.62±0.05	CUTKOSKY	80	IPWA	$\pi N \to \pi N$
0.65±0.02	HOEHLER	79	IPWA	$\pi N \to \pi N$
• • • We do not use the following data for averages, fits, limits, etc. • • •				
0.69±0.02	VRANA	00	DPWA	Multichannel
0.68	ARNDT	95	DPWA	$\pi N \to N\pi$
0.69±0.04	BATINIC	95	DPWA	$\pi N \to N\pi$, $N\eta$

$(\Gamma_i\Gamma_f)^{1/2}/\Gamma_{\text{total}}$ in $N\pi \to N(1680) \to N\eta$ $(\Gamma_1\Gamma_2)^{1/2}/\Gamma$

VALUE	*DOCUMENT ID*		*TECN*	*COMMENT*
• • • We do not use the following data for averages, fits, limits, etc. • • •				
not seen	BAKER	79	DPWA	$\pi^- p \to n\eta$

$\Gamma(N\eta)/\Gamma_{\text{total}}$ Γ_2/Γ

VALUE	DOCUMENT ID		TECN	COMMENT
0.00 ±0.01	VRANA	00	DPWA	Multichannel
• • • We do not use the following data for averages, fits, limits, etc. • • •				
$0.0015\ ^{+0.0035}_{-0.0010}$	TIATOR	99	DPWA	$\gamma p \to p\eta$
0.01 ±0.004	BATINIC	95	DPWA	$\pi N \to N\pi$, $N\eta$
0.0005 or 0.001	[5] CARRERAS	70	MPWA	t pole + resonance
0.0004	[5] BOTKE	69	MPWA	t pole + resonance
0.003 ±0.002	[5] DEANS	69	MPWA	t pole + resonance

$\Gamma(N\eta)/\Gamma(N\pi)$ Γ_2/Γ_1

VALUE	DOCUMENT ID		TECN	COMMENT
• • • We do not use the following data for averages, fits, limits, etc. • • •				
<0.027	HEUSCH	66	RVUE	π^0, η photoproduction

$(\Gamma_i\Gamma_f)^{1/2}/\Gamma_{\text{total}}$ in $N\pi \to N(1680) \to \Lambda K$ $(\Gamma_1\Gamma_3)^{1/2}/\Gamma$

Coupling to ΛK not required in the analyses of BAKER 77, SAXON 80, or BELL 83.

VALUE	DOCUMENT ID		TECN	COMMENT
• • • We do not use the following data for averages, fits, limits, etc. • • •				
0.01	KNASEL	75	DPWA	$\pi^- p \to \Lambda K^0$
−0.009±0.009	DEVENISH	74B		Fixed-t dispersion rel.

$(\Gamma_i\Gamma_f)^{1/2}/\Gamma_{\text{total}}$ in $N\pi \to N(1680) \to \Sigma K$ $(\Gamma_1\Gamma_4)^{1/2}/\Gamma$

VALUE	DOCUMENT ID		TECN	COMMENT
• • • We do not use the following data for averages, fits, limits, etc. • • •				
<0.001	[6] DEANS	75	DPWA	$\pi N \to \Sigma K$

Note: Signs of couplings from $\pi N \to N\pi\pi$ analyses were changed in the 1986 edition to agree with the baryon-first convention; the overall phase ambiguity is resolved by choosing a negative sign for the $\Delta(1620)$ S_{31} coupling to $\Delta(1232)\pi$.

$(\Gamma_i\Gamma_f)^{1/2}/\Gamma_{\text{total}}$ in $N\pi \to N(1680) \to \Delta(1232)\pi$, P-wave $(\Gamma_1\Gamma_7)^{1/2}/\Gamma$

VALUE	DOCUMENT ID		TECN	COMMENT
−0.31 to −0.21 OUR ESTIMATE				
−0.26±0.04	MANLEY	92	IPWA	$\pi N \to \pi N$ & $N\pi\pi$
−0.27	[1,7] LONGACRE	77	IPWA	$\pi N \to N\pi\pi$
−0.25	[2] LONGACRE	75	IPWA	$\pi N \to N\pi\pi$
• • • We do not use the following data for averages, fits, limits, etc. • • •				
−0.38	[8] NOVOSELLER	78	IPWA	$\pi N \to N\pi\pi$

$\Gamma(\Delta(1232)\pi$, P-wave$)/\Gamma_{\text{total}}$ Γ_7/Γ

VALUE	DOCUMENT ID		TECN	COMMENT
0.14±0.03	VRANA	00	DPWA	Multichannel

$(\Gamma_i\Gamma_f)^{1/2}/\Gamma_{\text{total}}$ in $N\pi \to N(1680) \to \Delta(1232)\pi$, F-wave $(\Gamma_1\Gamma_8)^{1/2}/\Gamma$

VALUE	DOCUMENT ID		TECN	COMMENT
+0.03 to +0.11 OUR ESTIMATE				
+0.07±0.03	MANLEY	92	IPWA	$\pi N \to \pi N$ & $N\pi\pi$
+0.07	[1,7] LONGACRE	77	IPWA	$\pi N \to N\pi\pi$
+0.08	[2] LONGACRE	75	IPWA	$\pi N \to N\pi\pi$
• • • We do not use the following data for averages, fits, limits, etc. • • •				
+0.05	[8] NOVOSELLER	78	IPWA	$\pi N \to N\pi\pi$

$\Gamma(\Delta(1232)\pi$, F-wave$)/\Gamma_{\text{total}}$ Γ_8/Γ

VALUE	DOCUMENT ID		TECN	COMMENT
0.01±0.01	VRANA	00	DPWA	Multichannel

$(\Gamma_i\Gamma_f)^{1/2}/\Gamma_{\text{total}}$ in $N\pi \to N(1680) \to N\rho$, S=3/2, P-wave $(\Gamma_1\Gamma_{11})^{1/2}/\Gamma$

VALUE	DOCUMENT ID		TECN	COMMENT
−0.30 to −0.10 OUR ESTIMATE				
−0.20±0.05	MANLEY	92	IPWA	$\pi N \to \pi N$ & $N\pi\pi$
−0.23	[1,7] LONGACRE	77	IPWA	$\pi N \to N\pi\pi$
−0.30	[2] LONGACRE	75	IPWA	$\pi N \to N\pi\pi$
• • • We do not use the following data for averages, fits, limits, etc. • • •				
−0.34	[8] NOVOSELLER	78	IPWA	$\pi N \to N\pi\pi$

$\Gamma(N\rho$, S=3/2, P-wave$)/\Gamma_{\text{total}}$ Γ_{11}/Γ

VALUE	DOCUMENT ID		TECN	COMMENT
0.05±0.01	VRANA	00	DPWA	Multichannel

$(\Gamma_i\Gamma_f)^{1/2}/\Gamma_{\text{total}}$ in $N\pi \to N(1680) \to N\rho$, S=3/2, F-wave $(\Gamma_1\Gamma_{12})^{1/2}/\Gamma$

VALUE	DOCUMENT ID		TECN	COMMENT
−0.18 to −0.10 OUR ESTIMATE				
−0.13±0.03	MANLEY	92	IPWA	$\pi N \to \pi N$ & $N\pi\pi$
−0.15	[1,7] LONGACRE	77	IPWA	$\pi N \to N\pi\pi$

$\Gamma(N\rho$, S=3/2, F-wave$)/\Gamma_{\text{total}}$ Γ_{12}/Γ

VALUE	DOCUMENT ID		TECN	COMMENT
0.03±0.01	VRANA	00	DPWA	Multichannel

$(\Gamma_i\Gamma_f)^{1/2}/\Gamma_{\text{total}}$ in $N\pi \to N(1680) \to N(\pi\pi)^{I=0}_{S\text{-wave}}$ $(\Gamma_1\Gamma_{13})^{1/2}/\Gamma$

VALUE	DOCUMENT ID		TECN	COMMENT
+0.25 to +0.35 OUR ESTIMATE				
+0.29±0.04	MANLEY	92	IPWA	$\pi N \to \pi N$ & $N\pi\pi$
+0.31	[1,7] LONGACRE	77	IPWA	$\pi N \to N\pi\pi$
+0.30	[2] LONGACRE	75	IPWA	$\pi N \to N\pi\pi$
• • • We do not use the following data for averages, fits, limits, etc. • • •				
+0.42	[8] NOVOSELLER	78	IPWA	$\pi N \to N\pi\pi$

$\Gamma(N(\pi\pi)^{I=0}_{S\text{-wave}})/\Gamma_{\text{total}}$ Γ_{13}/Γ

VALUE	DOCUMENT ID		TECN	COMMENT
0.09±0.01	VRANA	00	DPWA	Multichannel

$N(1680)$ PHOTON DECAY AMPLITUDES

$N(1680) \to p\gamma$, helicity-1/2 amplitude $A_{1/2}$

VALUE (GeV$^{-1/2}$)	DOCUMENT ID		TECN	COMMENT
−0.015±0.006 OUR ESTIMATE				
−0.010±0.004	ARNDT	96	IPWA	$\gamma N \to \pi N$
−0.017±0.018	CRAWFORD	83	IPWA	$\gamma N \to \pi N$
−0.009±0.006	AWAJI	81	DPWA	$\gamma N \to \pi N$
−0.028±0.003	ARAI	80	DPWA	$\gamma N \to \pi N$ (fit 1)
−0.026±0.003	ARAI	80	DPWA	$\gamma N \to \pi N$ (fit 2)
−0.018±0.014	CRAWFORD	80	DPWA	$\gamma N \to \pi N$
• • • We do not use the following data for averages, fits, limits, etc. • • •				
−0.006±0.002	LI	93	IPWA	$\gamma N \to \pi N$
−0.005±0.015	BARBOUR	78	DPWA	$\gamma N \to \pi N$
−0.009±0.002	FELLER	76	DPWA	$\gamma N \to \pi N$

$N(1680) \to p\gamma$, helicity-3/2 amplitude $A_{3/2}$

VALUE (GeV$^{-1/2}$)	DOCUMENT ID		TECN	COMMENT
+0.133±0.012 OUR ESTIMATE				
0.145±0.005	ARNDT	96	IPWA	$\gamma N \to \pi N$
0.132±0.010	CRAWFORD	83	IPWA	$\gamma N \to \pi N$
0.115±0.008	AWAJI	81	DPWA	$\gamma N \to \pi N$
0.115±0.003	ARAI	80	DPWA	$\gamma N \to \pi N$ (fit 1)
0.122±0.003	ARAI	80	DPWA	$\gamma N \to \pi N$ (fit 2)
0.141±0.014	CRAWFORD	80	DPWA	$\gamma N \to \pi N$
• • • We do not use the following data for averages, fits, limits, etc. • • •				
0.154±0.002	LI	93	IPWA	$\gamma N \to \pi N$
+0.138±0.021	BARBOUR	78	DPWA	$\gamma N \to \pi N$
+0.121±0.010	FELLER	76	DPWA	$\gamma N \to \pi N$

$N(1680) \to n\gamma$, helicity-1/2 amplitude $A_{1/2}$

VALUE (GeV$^{-1/2}$)	DOCUMENT ID		TECN	COMMENT
+0.029±0.010 OUR ESTIMATE				
0.030±0.005	ARNDT	96	IPWA	$\gamma N \to \pi N$
0.017±0.014	AWAJI	81	DPWA	$\gamma N \to \pi N$
0.032±0.003	FUJII	81	DPWA	$\gamma N \to \pi N$
0.026±0.005	ARAI	80	DPWA	$\gamma N \to \pi N$ (fit 1)
0.028±0.014	ARAI	80	DPWA	$\gamma N \to \pi N$ (fit 2)
0.044±0.012	CRAWFORD	80	DPWA	$\gamma N \to \pi N$
0.025±0.010	TAKEDA	80	DPWA	$\gamma N \to \pi N$
• • • We do not use the following data for averages, fits, limits, etc. • • •				
0.022±0.002	LI	93	IPWA	$\gamma N \to \pi N$
+0.037±0.010	BARBOUR	78	DPWA	$\gamma N \to \pi N$

$N(1680) \to n\gamma$, helicity-3/2 amplitude $A_{3/2}$

VALUE (GeV$^{-1/2}$)	DOCUMENT ID		TECN	COMMENT
−0.033±0.009 OUR ESTIMATE				
−0.040±0.015	ARNDT	96	IPWA	$\gamma N \to \pi N$
−0.033±0.013	AWAJI	81	DPWA	$\gamma N \to \pi N$
−0.023±0.005	FUJII	81	DPWA	$\gamma N \to \pi N$
−0.024±0.009	ARAI	80	DPWA	$\gamma N \to \pi N$ (fit 1)
−0.029±0.017	ARAI	80	DPWA	$\gamma N \to \pi N$ (fit 2)
−0.033±0.015	CRAWFORD	80	DPWA	$\gamma N \to \pi N$
−0.035±0.012	TAKEDA	80	DPWA	$\gamma N \to \pi N$
• • • We do not use the following data for averages, fits, limits, etc. • • •				
−0.048±0.002	LI	93	IPWA	$\gamma N \to \pi N$
−0.038±0.018	BARBOUR	78	DPWA	$\gamma N \to \pi N$

$N(1680)$ FOOTNOTES

[1] LONGACRE 77 pole positions are from a search for poles in the unitarized T-matrix; the first (second) value uses, in addition to $\pi N \to N\pi\pi$ data, elastic amplitudes from a Saclay (CERN) partial-wave analysis. The other LONGACRE 77 values are from eyeball fits with Breit-Wigner circles to the T-matrix amplitudes.

[2] From method II of LONGACRE 75: eyeball fits with Breit-Wigner circles to the T-matrix amplitudes.

[3] See HOEHLER 93 for a detailed discussion of the evidence for and the pole parameters of N and Δ resonances as determined from Argand diagrams of πN elastic partial-wave amplitudes and from plots of the speeds with which the amplitudes traverse the diagrams.

[4] LONGACRE 78 values are from a search for poles in the unitarized T-matrix. The first (second) value uses, in addition to $\pi N \to N\pi\pi$ data, elastic amplitudes from a Saclay (CERN) partial-wave analysis.

[5] The parametrization used may be double counting.

[6] The range given is from 3 of 4 best solutions; not present in solution 1. DEANS 75 disagrees with $\pi^+ p \rightarrow \Sigma^+ K^+$ data of WINNIK 77 around 1920 MeV.
[7] LONGACRE 77 considers this coupling to be well determined.
[8] A Breit-Wigner fit to the HERNDON 75 IPWA.

$N(1680)$ REFERENCES

For early references, see Physics Letters **111B** 70 (1982). For very early references, see Reviews of Modern Physics **37** 633 (1965).

VRANA	00	PRPL 328 181	T.P. Vrana, S.A. Dytman,, T.-S.H. Lee	(PITT+)
TIATOR	99	PR C60 035210	L. Tiator *et al.*	
ARNDT	96	PR C53 430	R.A. Arndt, I.I. Strakovsky, R.L. Workman	(VPI)
ARNDT	95	PR C52 2120	R.A. Arndt *et al.*	(VPI, BRCO)
BATINIC	95	PR C51 2310	M. Batinic *et al.*	(BOSK, UCLA)
Also	98	PR C57 1004 (erratum)	M. Batinic *et al.*	
HOEHLER	93	πN Newsletter 9 1	G. Hohler	(KARL)
LI	93	PR C47 2759	Z.J. Li *et al.*	(VPI)
MANLEY	92	PR D45 4002	D.M. Manley, E.M. Saleski	(KENT) IJP
Also	84	PR D30 904	D.M. Manley *et al.*	(VPI)
ARNDT	91	PR D43 2131	R.A. Arndt *et al.*	(VPI, TELE) IJP
BELL	83	NP B222 389	K.W. Bell *et al.*	(RL) IJP
CRAWFORD	83	NP B211 1	R.L. Crawford, W.T. Morton	(GLAS)
PDG	82	PL 111B	M. Roos *et al.*	(HELS, CIT, CERN)
AWAJI	81	Bonn Conf. 352	N. Awaji, R. Kajikawa	(NAGO)
Also	82	NP B197 365	K. Fujii *et al.*	(NAGO)
FUJII	81	NP B187 53	K. Fujii *et al.*	(NAGO, OSAK)
ARAI	80	Toronto Conf. 93	I. Arai	(INUS)
Also	82	NP B194 251	I. Arai, H. Fujii	(INUS)
CRAWFORD	80	Toronto Conf. 107	R.L. Crawford	(GLAS)
CUTKOSKY	80	Toronto Conf. 19	R.E. Cutkosky *et al.*	(CMU, LBL) IJP
Also	79	PR D20 2839	R.E. Cutkosky *et al.*	(CMU, LBL) IJP
SAXON	80	NP B162 522	D.H. Saxon *et al.*	(RHEL, BRIS) IJP
TAKEDA	80	NP B168 17	H. Takeda *et al.*	(TOKY, INUS)
BAKER	79	NP B156 93	R.D. Baker *et al.*	(RHEL) IJP
HOEHLER	79	PDAT 12-1	G. Hohler *et al.*	(KARLT) IJP
Also	80	Toronto Conf. 3	R. Koch	(KARLT) IJP
BARBOUR	78	NP B141 253	I.M. Barbour, R.L. Crawford, N.H. Parsons	(GLAS)
LONGACRE	78	PR D17 1795	R.S. Longacre *et al.*	(LBL, SLAC)
NOVOSELLER	78	NP B137 509	D.E. Novoseller	(CIT) IJP
Also	78B	NP B137 445	D.E. Novoseller	(CIT) IJP
BAKER	77	NP B126 365	R.D. Baker *et al.*	(RHEL) IJP
LONGACRE	77	NP B122 493	R.S. Longacre, J. Dolbeau	(SACL) IJP
Also	76	NP B108 365	J. Dolbeau *et al.*	(SACL) IJP
WINNIK	77	NP B128 66	M. Winnik *et al.*	(HAIF) I
FELLER	76	NP B104 219	P. Feller *et al.*	(NAGO, OSAK) IJP
DEANS	75	NP B96 90	S.R. Deans *et al.*	(SFLA, ALAH) IJP
HERNDON	75	PR D11 3183	D. Herndon *et al.*	(LBL, SLAC)
KNASEL	75	PR D11 1	T.M. Knasel *et al.*	(CHIC, WUSL, OSU+) IJP
LONGACRE	75	PL 55B 415	R.S. Longacre *et al.*	(LBL, SLAC) IJP
DEVENISH	74B	NP B81 330	R.C.E. Devenish, C.D. Froggatt, B.R. Martin	(DESY+)
CARRERAS	70	NP B16 35	B. Carreras, A. Donnachie	(DARE, MCHS)
BOTKE	69	PR 180 1417	J.C. Botke	(UCSB)
DEANS	69	PR 185 1797	S.R. Deans, J.W. Wooten	(SFLA)
HEUSCH	66	PRL 17 1019	C.A. Heusch, C.Y. Prescott, R.F. Dashen	(CIT)

$N(1700)$ D_{13}

$I(J^P) = \frac{1}{2}(\frac{3}{2}^-)$ Status: ***

Most of the results published before 1975 are now obsolete and have been omitted. They may be found in our 1982 edition, Physics Letters **111B** (1982).

The various partial-wave analyses do not agree very well.

$N(1700)$ BREIT-WIGNER MASS

VALUE (MeV)	*DOCUMENT ID*		*TECN*	*COMMENT*
1650 to 1750 (≈ 1700) OUR ESTIMATE				
1737±44	MANLEY	92	IPWA	$\pi N \rightarrow \pi N$ & $N\pi\pi$
1675±25	CUTKOSKY	80	IPWA	$\pi N \rightarrow \pi N$
1731±15	HOEHLER	79	IPWA	$\pi N \rightarrow \pi N$
• • • We do not use the following data for averages, fits, limits, etc. • • •				
1736±33	VRANA	00	DPWA	Multichannel
1791±46	BATINIC	95	DPWA	$\pi N \rightarrow N\pi$, $N\eta$
1709	CRAWFORD	80	DPWA	$\gamma N \rightarrow \pi N$
1650	SAXON	80	DPWA	$\pi^- p \rightarrow \Lambda K^0$
1690 to 1710	BAKER	78	DPWA	$\pi^- p \rightarrow \Lambda K^0$
1719	BARBOUR	78	DPWA	$\gamma N \rightarrow \pi N$
1670±10	[1] BAKER	77	IPWA	$\pi^- p \rightarrow \Lambda K^0$
1690	[1] BAKER	77	DPWA	$\pi^- p \rightarrow \Lambda K^0$
1660	[2] LONGACRE	77	IPWA	$\pi N \rightarrow N\pi\pi$
1710	[3] LONGACRE	75	IPWA	$\pi N \rightarrow N\pi\pi$

$N(1700)$ BREIT-WIGNER WIDTH

VALUE (MeV)	*DOCUMENT ID*		*TECN*	*COMMENT*
50 to 150 (≈ 100) OUR ESTIMATE				
250±220	MANLEY	92	IPWA	$\pi N \rightarrow \pi N$ & $N\pi\pi$
90± 40	CUTKOSKY	80	IPWA	$\pi N \rightarrow \pi N$
110± 30	HOEHLER	79	IPWA	$\pi N \rightarrow \pi N$
• • • We do not use the following data for averages, fits, limits, etc. • • •				
175±133	VRANA	00	DPWA	Multichannel
215± 60	BATINIC	95	DPWA	$\pi N \rightarrow N\pi$, $N\eta$
166	CRAWFORD	80	DPWA	$\gamma N \rightarrow \pi N$
70	SAXON	80	DPWA	$\pi^- p \rightarrow \Lambda K^0$
70 to 100	BAKER	78	DPWA	$\pi^- p \rightarrow \Lambda K^0$
126	BARBOUR	78	DPWA	$\gamma N \rightarrow \pi N$
90± 25	[1] BAKER	77	IPWA	$\pi^- p \rightarrow \Lambda K^0$
100	[1] BAKER	77	DPWA	$\pi^- p \rightarrow \Lambda K^0$
600	[2] LONGACRE	77	IPWA	$\pi N \rightarrow N\pi\pi$
300	[3] LONGACRE	75	IPWA	$\pi N \rightarrow N\pi\pi$

$N(1700)$ POLE POSITION

REAL PART

VALUE (MeV)	*DOCUMENT ID*		*TECN*	*COMMENT*
1630 to 1730 (≈ 1680) OUR ESTIMATE				
1700	[4] HOEHLER	93	SPED	$\pi N \rightarrow \pi N$
1660±30	CUTKOSKY	80	IPWA	$\pi N \rightarrow \pi N$
• • • We do not use the following data for averages, fits, limits, etc. • • •				
1704	VRANA	00	DPWA	Multichannel
not seen	ARNDT	91	DPWA	$\pi N \rightarrow \pi N$ Soln SM90
1710 or 1678	[5] LONGACRE	78	IPWA	$\pi N \rightarrow N\pi\pi$
1616 or 1613	[2] LONGACRE	77	IPWA	$\pi N \rightarrow N\pi\pi$

$-2\times$IMAGINARY PART

VALUE (MeV)	*DOCUMENT ID*		*TECN*	*COMMENT*
50 to 150 (≈ 100) OUR ESTIMATE				
120	[4] HOEHLER	93	SPED	$\pi N \rightarrow \pi N$
90±40	CUTKOSKY	80	IPWA	$\pi N \rightarrow \pi N$
• • • We do not use the following data for averages, fits, limits, etc. • • •				
156	VRANA	00	DPWA	Multichannel
not seen	ARNDT	91	DPWA	$\pi N \rightarrow \pi N$ Soln SM90
607 or 567	[5] LONGACRE	78	IPWA	$\pi N \rightarrow N\pi\pi$
577 or 575	[2] LONGACRE	77	IPWA	$\pi N \rightarrow N\pi\pi$

$N(1700)$ ELASTIC POLE RESIDUE

MODULUS $|r|$

VALUE (MeV)	*DOCUMENT ID*	*TECN*	*COMMENT*
5	HOEHLER	93 SPED	$\pi N \rightarrow \pi N$
6±3	CUTKOSKY	80 IPWA	$\pi N \rightarrow \pi N$

PHASE θ

VALUE (°)	*DOCUMENT ID*	*TECN*	*COMMENT*
0±50	CUTKOSKY	80 IPWA	$\pi N \rightarrow \pi N$

$N(1700)$ DECAY MODES

The following branching fractions are our estimates, not fits or averages.

	Mode	Fraction (Γ_i/Γ)
Γ_1	$N\pi$	5–15 %
Γ_2	$N\eta$	(0.0±1.0) %
Γ_3	ΛK	<3 %
Γ_4	ΣK	
Γ_5	$N\pi\pi$	85–95 %
Γ_6	$\Delta\pi$	
Γ_7	$\Delta(1232)\pi$, S-wave	
Γ_8	$\Delta(1232)\pi$, D-wave	
Γ_9	$N\rho$	<35 %
Γ_{10}	$N\rho$, S=1/2, D-wave	
Γ_{11}	$N\rho$, S=3/2, S-wave	
Γ_{12}	$N\rho$, S=3/2, D-wave	
Γ_{13}	$N(\pi\pi)^{I=0}_{S\text{-wave}}$	
Γ_{14}	$p\gamma$	0.01–0.05 %
Γ_{15}	$p\gamma$, helicity=1/2	0.0–0.024 %
Γ_{16}	$p\gamma$, helicity=3/2	0.002–0.026 %
Γ_{17}	$n\gamma$	0.01–0.13 %
Γ_{18}	$n\gamma$, helicity=1/2	0.0–0.09 %
Γ_{19}	$n\gamma$, helicity=3/2	0.01–0.05 %

$N(1700)$ BRANCHING RATIOS

$\Gamma(N\pi)/\Gamma_{\text{total}}$ Γ_1/Γ

VALUE	*DOCUMENT ID*		*TECN*	*COMMENT*
0.05 to 0.15 OUR ESTIMATE				
0.01±0.02	MANLEY	92	IPWA	$\pi N \rightarrow \pi N$ & $N\pi\pi$
0.11±0.05	CUTKOSKY	80	IPWA	$\pi N \rightarrow \pi N$
0.08±0.03	HOEHLER	79	IPWA	$\pi N \rightarrow \pi N$
• • • We do not use the following data for averages, fits, limits, etc. • • •				
0.04±0.02	VRANA	00	DPWA	Multichannel
0.04±0.05	BATINIC	95	DPWA	$\pi N \rightarrow N\pi$, $N\eta$

$\Gamma(N\eta)/\Gamma_{total}$ Γ_2/Γ

VALUE	DOCUMENT ID		TECN	COMMENT
0.00 ±0.01	VRANA	00	DPWA	Multichannel
• • • We do not use the following data for averages, fits, limits, etc. • • •				
0.10 ±0.06	BATINIC	95	DPWA	$\pi N \to N\pi,\ N\eta$

$(\Gamma_i\Gamma_f)^{1/2}/\Gamma_{total}$ in $N\pi \to N(1700) \to \Lambda K$ $(\Gamma_1\Gamma_3)^{1/2}/\Gamma$

VALUE	DOCUMENT ID		TECN	COMMENT
−0.06 to +0.04 OUR ESTIMATE				
−0.012	BELL	83	DPWA	$\pi^- p \to \Lambda K^0$
−0.012	SAXON	80	DPWA	$\pi^- p \to \Lambda K^0$
• • • We do not use the following data for averages, fits, limits, etc. • • •				
−0.04	[6] BAKER	78	DPWA	See SAXON 80
−0.03 ±0.004	[1] BAKER	77	IPWA	$\pi^- p \to \Lambda K^0$
−0.03	[1] BAKER	77	DPWA	$\pi^- p \to \Lambda K^0$
+0.026±0.019	DEVENISH	74B		Fixed-t dispersion rel.

$(\Gamma_i\Gamma_f)^{1/2}/\Gamma_{total}$ in $N\pi \to N(1700) \to \Sigma K$ $(\Gamma_1\Gamma_4)^{1/2}/\Gamma$

VALUE	DOCUMENT ID		TECN	COMMENT
• • • We do not use the following data for averages, fits, limits, etc. • • •				
not seen	LIVANOS	80	DPWA	$\pi p \to \Sigma K$
<0.017	[7] DEANS	75	DPWA	$\pi N \to \Sigma K$

Note: Signs of couplings from $\pi N \to N\pi\pi$ analyses were changed in the 1986 edition to agree with the baryon-first convention; the overall phase ambiguity is resolved by choosing a negative sign for the $\Delta(1620)$ S_{31} coupling to $\Delta(1232)\pi$.

$(\Gamma_i\Gamma_f)^{1/2}/\Gamma_{total}$ in $N\pi \to N(1700) \to \Delta(1232)\pi$, S-wave $(\Gamma_1\Gamma_7)^{1/2}/\Gamma$

VALUE	DOCUMENT ID		TECN	COMMENT
0.00 to ±0.08 OUR ESTIMATE				
+0.02±0.03	MANLEY	92	IPWA	$\pi N \to \pi N$ & $N\pi\pi$
0.00	[2] LONGACRE	77	IPWA	$\pi N \to N\pi\pi$
−0.16	[3] LONGACRE	75	IPWA	$\pi N \to N\pi\pi$

$\Gamma(\Delta(1232)\pi,\ S\text{-wave})/\Gamma_{total}$ Γ_7/Γ

VALUE	DOCUMENT ID		TECN	COMMENT
0.11±0.01	VRANA	00	DPWA	Multichannel

$(\Gamma_i\Gamma_f)^{1/2}/\Gamma_{total}$ in $N\pi \to N(1700) \to \Delta(1232)\pi$, D-wave $(\Gamma_1\Gamma_8)^{1/2}/\Gamma$

VALUE	DOCUMENT ID		TECN	COMMENT
±0.04 to ±0.20 OUR ESTIMATE				
+0.10±0.09	MANLEY	92	IPWA	$\pi N \to \pi N$ & $N\pi\pi$
−0.12	[2] LONGACRE	77	IPWA	$\pi N \to N\pi\pi$
+0.14	[3] LONGACRE	75	IPWA	$\pi N \to N\pi\pi$

$\Gamma(\Delta(1232)\pi,\ D\text{-wave})/\Gamma_{total}$ Γ_8/Γ

VALUE	DOCUMENT ID		TECN	COMMENT
0.79±0.56	VRANA	00	DPWA	Multichannel

$(\Gamma_i\Gamma_f)^{1/2}/\Gamma_{total}$ in $N\pi \to N(1700) \to N\rho$, S=3/2, S-wave $(\Gamma_1\Gamma_{11})^{1/2}/\Gamma$

VALUE	DOCUMENT ID		TECN	COMMENT
±0.01 to ±0.13 OUR ESTIMATE				
−0.04±0.06	MANLEY	92	IPWA	$\pi N \to \pi N$ & $N\pi\pi$
−0.07	[2] LONGACRE	77	IPWA	$\pi N \to N\pi\pi$
+0.07	[3] LONGACRE	75	IPWA	$\pi N \to N\pi\pi$

$\Gamma(N\rho,\ S$=3/2, S-wave$)/\Gamma_{total}$ Γ_{11}/Γ

VALUE	DOCUMENT ID		TECN	COMMENT
0.07±0.01	VRANA	00	DPWA	Multichannel

$(\Gamma_i\Gamma_f)^{1/2}/\Gamma_{total}$ in $N\pi \to N(1700) \to N(\pi\pi)^{I=0}_{S\text{-wave}}$ $(\Gamma_1\Gamma_{13})^{1/2}/\Gamma$

VALUE	DOCUMENT ID		TECN	COMMENT
±0.02 to ±0.28 OUR ESTIMATE				
+0.02±0.02	MANLEY	92	IPWA	$\pi N \to \pi N$ & $N\pi\pi$
0.00	[2] LONGACRE	77	IPWA	$\pi N \to N\pi\pi$
+0.2	[3] LONGACRE	75	IPWA	$\pi N \to N\pi\pi$

$\Gamma(N(\pi\pi)^{I=0}_{S\text{-wave}})/\Gamma_{total}$ Γ_{13}/Γ

VALUE	DOCUMENT ID		TECN	COMMENT
0.00±0.01	VRANA	00	DPWA	Multichannel

$N(1700)$ PHOTON DECAY AMPLITUDES

$N(1700) \to p\gamma$, helicity-1/2 amplitude $A_{1/2}$

VALUE (GeV$^{-1/2}$)	DOCUMENT ID		TECN	COMMENT
−0.018±0.013 OUR ESTIMATE				
−0.016±0.014	CRAWFORD	83	IPWA	$\gamma N \to \pi N$
−0.002±0.013	AWAJI	81	DPWA	$\gamma N \to \pi N$
−0.028±0.007	ARAI	80	DPWA	$\gamma N \to \pi N$ (fit 1)
−0.029±0.006	ARAI	80	DPWA	$\gamma N \to \pi N$ (fit 2)
−0.024±0.019	CRAWFORD	80	DPWA	$\gamma N \to \pi N$
• • • We do not use the following data for averages, fits, limits, etc. • • •				
−0.033±0.021	BARBOUR	78	DPWA	$\gamma N \to \pi N$
−0.014±0.025	FELLER	76	DPWA	$\gamma N \to \pi N$

$N(1700) \to p\gamma$, helicity-3/2 amplitude $A_{3/2}$

VALUE (GeV$^{-1/2}$)	DOCUMENT ID		TECN	COMMENT
−0.002±0.024 OUR ESTIMATE				
−0.009±0.012	CRAWFORD	83	IPWA	$\gamma N \to \pi N$
0.029±0.014	AWAJI	81	DPWA	$\gamma N \to \pi N$
−0.002±0.005	ARAI	80	DPWA	$\gamma N \to \pi N$ (fit 1)
0.014±0.005	ARAI	80	DPWA	$\gamma N \to \pi N$ (fit 2)
−0.017±0.014	CRAWFORD	80	DPWA	$\gamma N \to \pi N$
• • • We do not use the following data for averages, fits, limits, etc. • • •				
−0.014±0.025	BARBOUR	78	DPWA	$\gamma N \to \pi N$
0.0 ±0.014	FELLER	76	DPWA	$\gamma N \to \pi N$

$N(1700) \to n\gamma$, helicity-1/2 amplitude $A_{1/2}$

VALUE (GeV$^{-1/2}$)	DOCUMENT ID		TECN	COMMENT
0.000±0.050 OUR ESTIMATE				
0.006±0.024	AWAJI	81	DPWA	$\gamma N \to \pi N$
−0.002±0.013	FUJII	81	DPWA	$\gamma N \to \pi N$
−0.052±0.030	ARAI	80	DPWA	$\gamma N \to \pi N$ (fit 1)
−0.055±0.030	ARAI	80	DPWA	$\gamma N \to \pi N$ (fit 2)
0.052±0.035	CRAWFORD	80	DPWA	$\gamma N \to \pi N$
• • • We do not use the following data for averages, fits, limits, etc. • • •				
+0.050±0.042	BARBOUR	78	DPWA	$\gamma N \to \pi N$

$N(1700) \to n\gamma$, helicity-3/2 amplitude $A_{3/2}$

VALUE (GeV$^{-1/2}$)	DOCUMENT ID		TECN	COMMENT
−0.003±0.044 OUR ESTIMATE				
−0.033±0.017	AWAJI	81	DPWA	$\gamma N \to \pi N$
0.018±0.018	FUJII	81	DPWA	$\gamma N \to \pi N$
−0.037±0.036	ARAI	80	DPWA	$\gamma N \to \pi N$ (fit 1)
−0.035±0.024	ARAI	80	DPWA	$\gamma N \to \pi N$ (fit 2)
0.041±0.030	CRAWFORD	80	DPWA	$\gamma N \to \pi N$
• • • We do not use the following data for averages, fits, limits, etc. • • •				
+0.035±0.030	BARBOUR	78	DPWA	$\gamma N \to \pi N$

$N(1700)$ $\gamma p \to \Lambda K^+$ AMPLITUDES

$(\Gamma_i\Gamma_f)^{1/2}/\Gamma_{total}$ in $p\gamma \to N(1700) \to \Lambda K^+$ (E_{2-} amplitude)

VALUE (units 10^{-3})	DOCUMENT ID		TECN
• • • We do not use the following data for averages, fits, limits, etc. • • •			
4.09	TANABE	89	DPWA

$(\Gamma_i\Gamma_f)^{1/2}/\Gamma_{total}$ in $p\gamma \to N(1700) \to \Lambda K^+$ (M_{2-} amplitude)

VALUE (units 10^{-3})	DOCUMENT ID		TECN
• • • We do not use the following data for averages, fits, limits, etc. • • •			
−7.09	TANABE	89	DPWA

$p\gamma \to N(1700) \to \Lambda K^+$ phase angle θ (E_{2-} amplitude)

VALUE (degrees)	DOCUMENT ID		TECN
• • • We do not use the following data for averages, fits, limits, etc. • • •			
−35.9	TANABE	89	DPWA

$N(1700)$ FOOTNOTES

[1] The two BAKER 77 entries are from an IPWA using the Barrelet-zero method and from a conventional energy-dependent analysis.

[2] LONGACRE 77 pole positions are from a search for poles in the unitarized T-matrix; the first (second) value uses, in addition to $\pi N \to N\pi\pi$ data, elastic amplitudes from a Saclay (CERN) partial-wave analysis. The other LONGACRE 77 values are from eyeball fits with Breit-Wigner circles to the T-matrix amplitudes.

[3] From method II of LONGACRE 75: eyeball fits with Breit-Wigner circles to the T-matrix amplitudes.

[4] See HOEHLER 93 for a detailed discussion of the evidence for and the pole parameters of N and Δ resonances as determined from Argand diagrams of πN elastic partial-wave amplitudes and from plots of the speeds with which the amplitudes traverse the diagrams.

[5] LONGACRE 78 values are from a search for poles in the unitarized T-matrix. The first (second) value uses, in addition to $\pi N \to N\pi\pi$ data, elastic amplitudes from a Saclay (CERN) partial-wave analysis.

[6] The overall phase of BAKER 78 couplings has been changed to agree with previous conventions.

[7] The range given is from the four best solutions.

$N(1700)$ REFERENCES

For early references, see Physics Letters **111B** 70 (1982).

VRANA	00	PRPL 328 181	T.P. Vrana, S.A. Dytman,, T.-S.H. Lee (PITT+)
BATINIC	95	PR C51 2310	M. Batinic *et al.* (BOSK, UCLA)
Also	98	PR C57 1004 (erratum)	M. Batinic *et al.*
HOEHLER	93	πN Newsletter 9 1	G. Hohler (KARL)
MANLEY	92	PR D45 4002	D.M. Manley, E.M. Saleski (KENT) IJP
Also	84	PR D30 904	D.M. Manley *et al.* (VPI)
ARNDT	91	PR D43 2131	R.A. Arndt *et al.* (VPI, TELE) IJP
TANABE	89	PR C39 741	H. Tanabe, M. Kohno, C. Bennhold (MANZ)
Also	89	NC 102A 193	M. Kohno, H. Tanabe, C. Bennhold (MANZ)
BELL	83	NP B222 389	K.W. Bell *et al.* (RL) IJP
CRAWFORD	83	NP B211 1	R.L. Crawford, W.T. Morton (GLAS)
PDG	82	PL 111B	M. Roos *et al.* (HELS, CIT, CERN)
AWAJI	81	Bonn Conf. 352	N. Awaji, R. Kajikawa (NAGO)
Also	82	NP B197 365	K. Fujii *et al.* (NAGO)
FUJII	81	NP B187 53	K. Fujii *et al.* (NAGO, OSAK)

ARAI	80	Toronto Conf. 93	I. Arai	(INUS)
Also	82	NP B194 251	I. Arai, H. Fujii	(INUS)
CRAWFORD	80	Toronto Conf. 107	R.L. Crawford	(GLAS)
CUTKOSKY	80	Toronto Conf. 19	R.E. Cutkosky *et al.*	(CMU, LBL) IJP
Also	79	PR D20 2839	R.E. Cutkosky *et al.*	(CMU, LBL) IJP
LIVANOS	80	Toronto Conf. 35	P. Livanos *et al.*	(SACL) IJP
SAXON	80	NP B162 522	D.H. Saxon *et al.*	(RHEL, BRIS) IJP
HOEHLER	79	PDAT 12-1	G. Hohler *et al.*	(KARLT) IJP
Also	80	Toronto Conf. 3	R. Koch	(KARLT) IJP
BAKER	78	NP B141 29	R.D. Baker *et al.*	(RL, CAVE) IJP
BARBOUR	78	NP B141 253	I.M. Barbour, R.L. Crawford, N.H. Parsons	(GLAS)
LONGACRE	78	PR D17 1795	R.S. Longacre *et al.*	(LBL, SLAC)
BAKER	77	NP B126 365	R.D. Baker *et al.*	(RHEL) IJP
LONGACRE	77	NP B122 493	R.S. Longacre, J. Dolbeau	(SACL) IJP
Also	76	NP B108 365	J. Dolbeau *et al.*	(SACL) IJP
FELLER	76	NP B104 219	P. Feller *et al.*	(NAGO, OSAK) IJP
DEANS	75	NP B96 90	S.R. Deans *et al.*	(SFLA, ALAH) IJP
LONGACRE	75	PL 55B 415	R.S. Longacre *et al.*	(LBL, SLAC) IJP
DEVENISH	74B	NP B81 330	R.C.E. Devenish, C.D. Froggatt, B.R. Martin	(DESY+)

$N(1710)$ P_{11}

$I(J^P) = \frac{1}{2}(\frac{1}{2}^+)$ Status: ***

Most of the results published before 1975 are now obsolete and have been omitted. They may be found in our 1982 edition, Physics Letters **111B** (1982).

The various partial-wave analyses do not agree very well.

$N(1710)$ BREIT-WIGNER MASS

VALUE (MeV)	DOCUMENT ID		TECN	COMMENT
1680 to 1740 (≈ 1710) OUR ESTIMATE				
1717±28	MANLEY	92	IPWA	$\pi N \to \pi N$ & $N\pi\pi$
1700±50	CUTKOSKY	80	IPWA	$\pi N \to \pi N$
1723± 9	HOEHLER	79	IPWA	$\pi N \to \pi N$
• • • We do not use the following data for averages, fits, limits, etc. • • •				
1752± 3	PENNER	02C	DPWA	Multichannel
1699±65	VRANA	00	DPWA	Multichannel
1720±10	ARNDT	96	IPWA	$\gamma N \to \pi N$
1766±34	[1] BATINIC	95	DPWA	$\pi N \to N\pi$, $N\eta$
1706	CUTKOSKY	90	IPWA	$\pi N \to \pi N$
1692	CRAWFORD	80	DPWA	$\gamma N \to \pi N$
1730	SAXON	80	DPWA	$\pi^- p \to \Lambda K^0$
1690	BAKER	79	DPWA	$\pi^- p \to n\eta$
1650 to 1680	BAKER	78	DPWA	$\pi^- p \to \Lambda K^0$
1721	BARBOUR	78	DPWA	$\gamma N \to \pi N$
1625±10	[2] BAKER	77	IPWA	$\pi^- p \to \Lambda K^0$
1650	[2] BAKER	77	DPWA	$\pi^- p \to \Lambda K^0$
1720	[3] LONGACRE	77	IPWA	$\pi N \to N\pi\pi$
1670	KNASEL	75	DPWA	$\pi^- p \to \Lambda K^0$
1710	[4] LONGACRE	75	IPWA	$\pi N \to N\pi\pi$

$N(1710)$ BREIT-WIGNER WIDTH

VALUE (MeV)	DOCUMENT ID		TECN	COMMENT
50 to 250 (≈ 100) OUR ESTIMATE				
480±230	MANLEY	92	IPWA	$\pi N \to \pi N$ & $N\pi\pi$
93± 30	CUTKOSKY	90	IPWA	$\pi N \to \pi N$
90± 30	CUTKOSKY	80	IPWA	$\pi N \to \pi N$
120± 15	HOEHLER	79	IPWA	$\pi N \to \pi N$
• • • We do not use the following data for averages, fits, limits, etc. • • •				
386± 59	PENNER	02C	DPWA	Multichannel
143±100	VRANA	00	DPWA	Multichannel
105± 10	ARNDT	96	IPWA	$\gamma N \to \pi N$
185± 61	BATINIC	95	DPWA	$\pi N \to N\pi$, $N\eta$
540	BELL	83	DPWA	$\pi^- p \to \Lambda K^0$
200	CRAWFORD	80	DPWA	$\gamma N \to \pi N$
550	SAXON	80	DPWA	$\pi^- p \to \Lambda K^0$
97	BAKER	79	DPWA	$\pi^- p \to n\eta$
90 to 150	BAKER	78	DPWA	$\pi^- p \to \Lambda K^0$
167	BARBOUR	78	DPWA	$\gamma N \to \pi N$
160± 6	[2] BAKER	77	IPWA	$\pi^- p \to \Lambda K^0$
95	[2] BAKER	77	DPWA	$\pi^- p \to \Lambda K^0$
120	[3] LONGACRE	77	IPWA	$\pi N \to N\pi\pi$
174	KNASEL	75	DPWA	$\pi^- p \to \Lambda K^0$
75	[4] LONGACRE	75	IPWA	$\pi N \to N\pi\pi$

$N(1710)$ POLE POSITION

REAL PART

VALUE (MeV)	DOCUMENT ID		TECN	COMMENT
1670 to 1770 (≈ 1720) OUR ESTIMATE				
1770	ARNDT	95	DPWA	$\pi N \to N\pi$
1690	[5] HOEHLER	93	SPED	$\pi N \to \pi N$
1698	CUTKOSKY	90	IPWA	$\pi N \to \pi N$
1690±20	CUTKOSKY	80	IPWA	$\pi N \to \pi N$
• • • We do not use the following data for averages, fits, limits, etc. • • •				
1679	VRANA	00	DPWA	Multichannel
1636	ARNDT	91	DPWA	$\pi N \to \pi N$ Soln SM90
1708 or 1712	[6] LONGACRE	78	IPWA	$\pi N \to N\pi\pi$
1720 or 1711	[3] LONGACRE	77	IPWA	$\pi N \to N\pi\pi$

−2×IMAGINARY PART

VALUE (MeV)	DOCUMENT ID		TECN	COMMENT
80 to 380 (≈ 230) OUR ESTIMATE				
378	ARNDT	95	DPWA	$\pi N \to N\pi$
200	[5] HOEHLER	93	SPED	$\pi N \to \pi N$
88	CUTKOSKY	90	IPWA	$\pi N \to \pi N$
80±20	CUTKOSKY	80	IPWA	$\pi N \to \pi N$
• • • We do not use the following data for averages, fits, limits, etc. • • •				
132	VRANA	00	DPWA	Multichannel
544	ARNDT	91	DPWA	$\pi N \to \pi N$ Soln SM90
17 or 22	[6] LONGACRE	78	IPWA	$\pi N \to N\pi\pi$
123 or 115	[3] LONGACRE	77	IPWA	$\pi N \to N\pi\pi$

$N(1710)$ ELASTIC POLE RESIDUE

MODULUS $|r|$

VALUE (MeV)	DOCUMENT ID		TECN	COMMENT
37	ARNDT	95	DPWA	$\pi N \to N\pi$
15	HOEHLER	93	SPED	$\pi N \to \pi N$
9	CUTKOSKY	90	IPWA	$\pi N \to \pi N$
8±2	CUTKOSKY	80	IPWA	$\pi N \to \pi N$
• • • We do not use the following data for averages, fits, limits, etc. • • •				
149	ARNDT	91	DPWA	$\pi N \to \pi N$ Soln SM90

PHASE θ

VALUE (°)	DOCUMENT ID		TECN	COMMENT
−167	ARNDT	95	DPWA	$\pi N \to N\pi$
−167	CUTKOSKY	90	IPWA	$\pi N \to \pi N$
175±35	CUTKOSKY	80	IPWA	$\pi N \to \pi N$
• • • We do not use the following data for averages, fits, limits, etc. • • •				
149	ARNDT	91	DPWA	$\pi N \to \pi N$ Soln SM90

$N(1710)$ DECAY MODES

The following branching fractions are our estimates, not fits or averages.

	Mode	Fraction (Γ_i/Γ)
Γ_1	$N\pi$	10–20 %
Γ_2	$N\eta$	(6.2±1.0) %
Γ_3	$N\omega$	(13.0±2.0) %
Γ_4	ΛK	5–25 %
Γ_5	ΣK	
Γ_6	$N\pi\pi$	40–90 %
Γ_7	$\Delta\pi$	15–40 %
Γ_8	$\Delta(1232)\pi$, P-wave	
Γ_9	$N\rho$	5–25 %
Γ_{10}	$N\rho$, S=1/2, P-wave	
Γ_{11}	$N\rho$, S=3/2, P-wave	
Γ_{12}	$N(\pi\pi)^{I=0}_{S\text{-wave}}$	10–40 %
Γ_{13}	$p\gamma$	0.002–0.05%
Γ_{14}	$p\gamma$, helicity=1/2	0.002–0.05%
Γ_{15}	$n\gamma$	0.0–0.02%
Γ_{16}	$n\gamma$, helicity=1/2	0.0–0.02%

$N(1710)$ BRANCHING RATIOS

$\Gamma(N\pi)/\Gamma_{\text{total}}$ Γ_1/Γ

VALUE	DOCUMENT ID		TECN	COMMENT
0.10 to 0.20 OUR ESTIMATE				
0.09±0.04	MANLEY	92	IPWA	$\pi N \to \pi N$ & $N\pi\pi$
0.20±0.04	CUTKOSKY	80	IPWA	$\pi N \to \pi N$
0.12±0.04	HOEHLER	79	IPWA	$\pi N \to \pi N$
• • • We do not use the following data for averages, fits, limits, etc. • • •				
0.14±0.08	PENNER	02C	DPWA	Multichannel
0.27±0.13	VRANA	00	DPWA	Multichannel
0.08±0.14	BATINIC	95	DPWA	$\pi N \to N\pi$, $N\eta$

$\Gamma(N\eta)/\Gamma_{\text{total}}$ Γ_2/Γ

VALUE	DOCUMENT ID		TECN	COMMENT
0.062±0.010 OUR AVERAGE				
0.36 ±0.11	PENNER	02C	DPWA	Multichannel
0.06 ±0.01	VRANA	00	DPWA	Multichannel
• • • We do not use the following data for averages, fits, limits, etc. • • •				
0.16 ±0.10	BATINIC	95	DPWA	$\pi N \to N\pi$, $N\eta$

$(\Gamma_i\Gamma_f)^{1/2}/\Gamma_{\text{total}}$ in $N\pi \to N(1710) \to N\eta$ $(\Gamma_1\Gamma_2)^{1/2}/\Gamma$

VALUE	DOCUMENT ID		TECN	COMMENT
• • • We do not use the following data for averages, fits, limits, etc. • • •				
0.22	BAKER	79	DPWA	$\pi^- p \to n\eta$
+0.383	FELTESSE	75	DPWA	Soln A; see BAKER 79

$\Gamma(N\omega)/\Gamma_{total}$ Γ_3/Γ

VALUE	DOCUMENT ID		TECN	COMMENT
0.13 ±0.02	PENNER	02C	DPWA	Multichannel

$(\Gamma_i\Gamma_f)^{1/2}/\Gamma_{total}$ in $N\pi \to N(1710) \to \Lambda K$ $(\Gamma_1\Gamma_4)^{1/2}/\Gamma$

VALUE	DOCUMENT ID		TECN	COMMENT
+0.12 to +0.18 OUR ESTIMATE				
+0.16	BELL	83	DPWA	$\pi^- p \to \Lambda K^0$
+0.14	SAXON	80	DPWA	$\pi^- p \to \Lambda K^0$
• • • We do not use the following data for averages, fits, limits, etc. • • •				
−0.12	[7] BAKER	78	DPWA	See SAXON 80
−0.05 ±0.03	[2] BAKER	77	IPWA	$\pi^- p \to \Lambda K^0$
−0.10	[2] BAKER	77	DPWA	$\pi^- p \to \Lambda K^0$
0.10	KNASEL	75	DPWA	$\pi^- p \to \Lambda K^0$

$\Gamma(\Lambda K)/\Gamma_{total}$ Γ_4/Γ

VALUE	DOCUMENT ID		TECN	COMMENT
0.05 ±0.02	PENNER	02C	DPWA	Multichannel
0.1 ±0.1	VRANA	00	DPWA	Multichannel

$\Gamma(\Sigma K)/\Gamma_{total}$ Γ_5/Γ

VALUE	DOCUMENT ID		TECN	COMMENT
• • • We do not use the following data for averages, fits, limits, etc. • • •				
0.07 ±0.07	PENNER	02C	DPWA	Multichannel

$(\Gamma_i\Gamma_f)^{1/2}/\Gamma_{total}$ in $N\pi \to N(1710) \to \Sigma K$ $(\Gamma_1\Gamma_5)^{1/2}/\Gamma$

VALUE	DOCUMENT ID		TECN	COMMENT
• • • We do not use the following data for averages, fits, limits, etc. • • •				
−0.034	LIVANOS	80	DPWA	$\pi p \to \Sigma K$
0.075 to 0.203	[8] DEANS	75	DPWA	$\pi N \to \Sigma K$

Note: Signs of couplings from $\pi N \to N\pi\pi$ analyses were changed in the 1986 edition to agree with the baryon-first convention; the overall phase ambiguity is resolved by choosing a negative sign for the $\Delta(1620)$ S_{31} coupling to $\Delta(1232)\pi$.

$(\Gamma_i\Gamma_f)^{1/2}/\Gamma_{total}$ in $N\pi \to N(1710) \to \Delta(1232)\pi$, P-wave $(\Gamma_1\Gamma_8)^{1/2}/\Gamma$

VALUE	DOCUMENT ID		TECN	COMMENT
±0.16 to ±0.22 OUR ESTIMATE				
−0.21 ±0.04	MANLEY	92	IPWA	$\pi N \to \pi N$ & $N\pi\pi$
−0.17	[3] LONGACRE	77	IPWA	$\pi N \to N\pi\pi$
+0.20	[4] LONGACRE	75	IPWA	$\pi N \to N\pi\pi$

$\Gamma(\Delta(1232)\pi$, P-wave$)/\Gamma_{total}$ Γ_8/Γ

VALUE	DOCUMENT ID		TECN	COMMENT
0.39 ±0.08	VRANA	00	DPWA	Multichannel

$(\Gamma_i\Gamma_f)^{1/2}/\Gamma_{total}$ in $N\pi \to N(1710) \to N\rho$, S=1/2, P-wave $(\Gamma_1\Gamma_{10})^{1/2}/\Gamma$

VALUE	DOCUMENT ID		TECN	COMMENT
±0.09 to ±0.19 OUR ESTIMATE				
+0.05 ±0.06	MANLEY	92	IPWA	$\pi N \to \pi N$ & $N\pi\pi$
+0.19	[3] LONGACRE	77	IPWA	$\pi N \to N\pi\pi$
−0.20	[4] LONGACRE	75	IPWA	$\pi N \to N\pi\pi$

$\Gamma(N\rho$, S=1/2, P-wave$)/\Gamma_{total}$ Γ_{10}/Γ

VALUE	DOCUMENT ID		TECN	COMMENT
0.17 ±0.01	VRANA	00	DPWA	Multichannel

$(\Gamma_i\Gamma_f)^{1/2}/\Gamma_{total}$ in $N\pi \to N(1710) \to N\rho$, S=3/2, P-wave $(\Gamma_1\Gamma_{11})^{1/2}/\Gamma$

VALUE	DOCUMENT ID		TECN	COMMENT
+0.31	[3] LONGACRE	77	IPWA	$\pi N \to N\pi\pi$

$(\Gamma_i\Gamma_f)^{1/2}/\Gamma_{total}$ in $N\pi \to N(1710) \to N(\pi\pi)^{I=0}_{S\text{-wave}}$ $(\Gamma_1\Gamma_{12})^{1/2}/\Gamma$

VALUE	DOCUMENT ID		TECN	COMMENT
±0.14 to ±0.22 OUR ESTIMATE				
+0.04 ±0.05	MANLEY	92	IPWA	$\pi N \to \pi N$ & $N\pi\pi$
−0.26	[3] LONGACRE	77	IPWA	$\pi N \to N\pi\pi$
−0.28	[4] LONGACRE	75	IPWA	$\pi N \to N\pi\pi$

$\Gamma(N(\pi\pi)^{I=0}_{S\text{-wave}})/\Gamma_{total}$ Γ_{12}/Γ

VALUE	DOCUMENT ID		TECN	COMMENT
0.01 ±0.01	VRANA	00	DPWA	Multichannel

$N(1710)$ PHOTON DECAY AMPLITUDES

$N(1710) \to p\gamma$, helicity-1/2 amplitude $A_{1/2}$

VALUE (GeV$^{-1/2}$)	DOCUMENT ID		TECN	COMMENT
+0.009±0.022 OUR ESTIMATE				
0.007±0.015	ARNDT	96	IPWA	$\gamma N \to \pi N$
0.006±0.018	CRAWFORD	83	IPWA	$\gamma N \to \pi N$
0.028±0.009	AWAJI	81	DPWA	$\gamma N \to \pi N$
−0.009±0.006	ARAI	80	DPWA	$\gamma N \to \pi N$ (fit 1)
−0.012±0.005	ARAI	80	DPWA	$\gamma N \to \pi N$ (fit 2)
0.015±0.025	CRAWFORD	80	DPWA	$\gamma N \to \pi N$
• • • We do not use the following data for averages, fits, limits, etc. • • •				
0.044	PENNER	02D	DPWA	Multichannel
−0.037±0.002	LI	93	IPWA	$\gamma N \to \pi N$
+0.001±0.039	BARBOUR	78	DPWA	$\gamma N \to \pi N$
+0.053±0.019	FELLER	76	DPWA	$\gamma N \to \pi N$

$N(1710) \to n\gamma$, helicity-1/2 amplitude $A_{1/2}$

VALUE (GeV$^{-1/2}$)	DOCUMENT ID		TECN	COMMENT
−0.002±0.014 OUR ESTIMATE				
−0.002±0.015	ARNDT	96	IPWA	$\gamma N \to \pi N$
0.000±0.018	AWAJI	81	DPWA	$\gamma N \to \pi N$
−0.001±0.003	FUJII	81	DPWA	$\gamma N \to \pi N$
0.005±0.013	ARAI	80	DPWA	$\gamma N \to \pi N$ (fit 1)
0.011±0.021	ARAI	80	DPWA	$\gamma N \to \pi N$ (fit 2)
−0.017±0.020	CRAWFORD	80	DPWA	$\gamma N \to \pi N$
• • • We do not use the following data for averages, fits, limits, etc. • • •				
−0.024	PENNER	02D	DPWA	Multichannel
0.052±0.003	LI	93	IPWA	$\gamma N \to \pi N$
−0.028±0.045	BARBOUR	78	DPWA	$\gamma N \to \pi N$

$N(1710)$ $\gamma p \to \Lambda K^+$ AMPLITUDES

$(\Gamma_i\Gamma_f)^{1/2}/\Gamma_{total}$ in $p\gamma \to N(1710) \to \Lambda K^+$ (M_{1-} amplitude)

VALUE (units 10^{-3})	DOCUMENT ID		TECN
• • • We do not use the following data for averages, fits, limits, etc. • • •			
−10.6 ±0.4	WORKMAN	90	DPWA
− 7.21	TANABE	89	DPWA

$p\gamma \to N(1710) \to \Lambda K^+$ phase angle θ (M_{1-} amplitude)

VALUE (degrees)	DOCUMENT ID		TECN
• • • We do not use the following data for averages, fits, limits, etc. • • •			
215 ±3	WORKMAN	90	DPWA
176.3	TANABE	89	DPWA

$N(1710)$ FOOTNOTES

[1] BATINIC 95 finds a second state with a 6 MeV mass difference.
[2] The two BAKER 77 entries are from an IPWA using the Barrelet-zero method and from a conventional energy-dependent analysis.
[3] LONGACRE 77 pole positions are from a search for poles in the unitarized T-matrix; the first (second) value uses, in addition to $\pi N \to N\pi\pi$ data, elastic amplitudes from a Saclay (CERN) partial-wave analysis. The other LONGACRE 77 values are from eyeball fits with Breit-Wigner circles to the T-matrix amplitudes.
[4] From method II of LONGACRE 75: eyeball fits with Breit-Wigner circles to the T-matrix amplitudes.
[5] See HOEHLER 93 for a detailed discussion of the evidence for and the pole parameters of N and Δ resonances as determined from Argand diagrams of πN elastic partial-wave amplitudes and from plots of the speeds with which the amplitudes traverse the diagrams.
[6] LONGACRE 78 values are from a search for poles in the unitarized T-matrix. The first (second) value uses, in addition to $\pi N \to N\pi\pi$ data, elastic amplitudes from a Saclay (CERN) partial-wave analysis.
[7] The overall phase of BAKER 78 couplings has been changed to agree with previous conventions.
[8] The range given for DEANS 75 is from the four best solutions.

$N(1710)$ REFERENCES

For early references, see Physics Letters **111B** 70 (1982).

PENNER	02C	PR C66 055211	G. Penner, U. Mosel	(GIES)
PENNER	02D	PR C66 055212	G. Penner, U. Mosel	(GIES)
VRANA	00	PRPL 328 181	T.P. Vrana, S.A. Dytman,, T.-S.H. Lee	(PITT+)
ARNDT	96	PR C53 430	R.A. Arndt, I.I. Strakovsky, R.L. Workman	(VPI)
ARNDT	95	PR C52 2120	R.A. Arndt *et al.*	(VPI, BRCO)
BATINIC	95	PR C51 2310	M. Batinic *et al.*	(BOSK, UCLA)
Also	98	PR C57 1004 (erratum)	M. Batinic *et al.*	
HOEHLER	93	πN Newsletter 9 1	G. Hohler	(KARL)
LI	93	PR C47 2759	Z.J. Li *et al.*	(VPI)
MANLEY	92	PR D45 4002	D.M. Manley, E.M. Saleski	(KENT) IJP
Also	84	PR D30 904	D.M. Manley *et al.*	(VPI)
ARNDT	91	PR D43 2131	R.A. Arndt *et al.*	(VPI, TELE) IJP
CUTKOSKY	90	PR D42 235	R.E. Cutkosky, S. Wang	(CMU)
WORKMAN	90	PR C42 781	R.L. Workman	(VPI)
TANABE	89	PR C39 741	H. Tanabe, M. Kohno, C. Bennhold	(MANZ)
Also	89	NC 102A 193	M. Kohno, H. Tanabe, C. Bennhold	(MANZ)
BELL	83	NP B222 389	K.W. Bell *et al.*	(RL) IJP
CRAWFORD	83	NP B211 1	R.L. Crawford, W.T. Morton	(GLAS)
PDG	82	PL 111B	M. Roos *et al.*	(HELS, CIT, CERN)
AWAJI	81	Bonn Conf. 352	N. Awaji, R. Kajikawa	(NAGO)
Also	82	NP B197 365	K. Fujii *et al.*	(NAGO)
FUJII	81	NP B187 53	K. Fujii *et al.*	(NAGO, OSAK)
ARAI	80	Toronto Conf. 93	I. Arai	(INUS)
Also	82	NP B194 251	I. Arai, H. Fujii	(INUS)
CRAWFORD	80	Toronto Conf. 107	R.L. Crawford	(GLAS)
CUTKOSKY	80	Toronto Conf. 19	R.E. Cutkosky *et al.*	(CMU, LBL) IJP
Also	79	PR D20 2839	R.E. Cutkosky *et al.*	(CMU, LBL) IJP
LIVANOS	80	Toronto Conf. 35	P. Livanos *et al.*	(SACL) IJP
SAXON	80	NP B162 522	D.H. Saxon *et al.*	(RHEL, BRIS) IJP
BAKER	79	NP B156 93	R.D. Baker *et al.*	(RHEL) IJP
HOEHLER	79	PDAT 12-1	G. Hohler *et al.*	(KARLT) IJP
Also	80	Toronto Conf. 3	R. Koch	(KARLT) IJP
BAKER	78	NP B141 29	R.D. Baker *et al.*	(RL, CAVE) IJP
BARBOUR	78	NP B141 253	I.M. Barbour, R.L. Crawford, N.H. Parsons	(GLAS)

LONGACRE	78	PR D17 1795	R.S. Longacre *et al.*	(LBL, SLAC)
BAKER	77	NP B126 365	R.D. Baker *et al.*	(RHEL) IJP
LONGACRE	77	NP B122 493	R.S. Longacre, J. Dolbeau	(SACL) IJP
Also	76	NP B108 365	J. Dolbeau *et al.*	(SACL) IJP
FELLER	76	NP B104 219	P. Feller *et al.*	(NAGO, OSAK) IJP
DEANS	75	NP B96 90	S.R. Deans *et al.*	(SFLA, ALAH) IJP
FELTESSE	75	NP B93 242	J. Feltesse *et al.*	(SACL) IJP
KNASEL	75	PR D11 1	T.M. Knasel *et al.*	(CHIC, WUSL, OSU+) IJP
LONGACRE	75	PL 55B 415	R.S. Longacre *et al.*	(LBL, SLAC) IJP

$N(1720)$ P_{13}

$I(J^P) = \frac{1}{2}(\frac{3}{2}^+)$ Status: ****

Most of the results published before 1975 are now obsolete and have been omitted. They may be found in our 1982 edition, Physics Letters **111B** (1982).

RIPANI 03, in a study of $ep \to e'p\pi^+\pi^-$, finds some evidence for another P_{13} resonance in this region.

$N(1720)$ BREIT-WIGNER MASS

VALUE (MeV)	DOCUMENT ID		TECN	COMMENT
1650 to 1750 (≈ 1720) OUR ESTIMATE				
1717± 31	MANLEY	92	IPWA	$\pi N \to \pi N$ & $N\pi\pi$
1700± 50	CUTKOSKY	80	IPWA	$\pi N \to \pi N$
1710± 20	HOEHLER	79	IPWA	$\pi N \to \pi N$
• • • We do not use the following data for averages, fits, limits, etc. • • •				
1705± 10	PENNER	02C	DPWA	Multichannel
1716±112	VRANA	00	DPWA	Multichannel
1713± 10	ARNDT	96	IPWA	$\gamma N \to \pi N$
1820	ARNDT	95	DPWA	$\pi N \to N\pi$
1711± 26	BATINIC	95	DPWA	$\pi N \to N\pi$, $N\eta$
1720	LI	93	IPWA	$\gamma N \to \pi N$
1785	CRAWFORD	80	DPWA	$\gamma N \to \pi N$
1690	SAXON	80	DPWA	$\pi^- p \to \Lambda K^0$
1710 to 1790	BAKER	78	DPWA	$\pi^- p \to \Lambda K^0$
1809	BARBOUR	78	DPWA	$\gamma N \to \pi N$
1640± 10	[1] BAKER	77	IPWA	$\pi^- p \to \Lambda K^0$
1710	[1] BAKER	77	DPWA	$\pi^- p \to \Lambda K^0$
1750	[2] LONGACRE	77	IPWA	$\pi N \to N\pi\pi$
1850	KNASEL	75	DPWA	$\pi^- p \to \Lambda K^0$
1720	[3] LONGACRE	75	IPWA	$\pi N \to N\pi\pi$

$N(1720)$ BREIT-WIGNER WIDTH

VALUE (MeV)	DOCUMENT ID		TECN	COMMENT
100 to 200 (≈ 150) OUR ESTIMATE				
380±180	MANLEY	92	IPWA	$\pi N \to \pi N$ & $N\pi\pi$
125± 70	CUTKOSKY	80	IPWA	$\pi N \to \pi N$
190± 30	HOEHLER	79	IPWA	$\pi N \to \pi N$
• • • We do not use the following data for averages, fits, limits, etc. • • •				
237± 73	PENNER	02C	DPWA	Multichannel
121± 39	VRANA	00	DPWA	Multichannel
153± 15	ARNDT	96	IPWA	$\gamma N \to \pi N$
354	ARNDT	95	DPWA	$\pi N \to N\pi$
235± 51	BATINIC	95	DPWA	$\pi N \to N\pi$, $N\eta$
200	LI	93	IPWA	$\gamma N \to \pi N$
308	CRAWFORD	80	DPWA	$\gamma N \to \pi N$
120	SAXON	80	DPWA	$\pi^- p \to \Lambda K^0$
447	BAKER	79	DPWA	$\pi^- p \to n\eta$
300 to 400	BAKER	78	DPWA	$\pi^- p \to \Lambda K^0$
285	BARBOUR	78	DPWA	$\gamma N \to \pi N$
200± 50	[1] BAKER	77	IPWA	$\pi^- p \to \Lambda K^0$
500	[1] BAKER	77	DPWA	$\pi^- p \to \Lambda K^0$
130	[2] LONGACRE	77	IPWA	$\pi N \to N\pi\pi$
327	KNASEL	75	DPWA	$\pi^- p \to \Lambda K^0$
150	[3] LONGACRE	75	IPWA	$\pi N \to N\pi\pi$

$N(1720)$ POLE POSITION

REAL PART

VALUE (MeV)	DOCUMENT ID		TECN	COMMENT
1650 to 1750 (≈ 1700) OUR ESTIMATE				
1717	ARNDT	95	DPWA	$\pi N \to N\pi$
1686	[4] HOEHLER	93	SPED	$\pi N \to \pi N$
1680±30	CUTKOSKY	80	IPWA	$\pi N \to \pi N$
• • • We do not use the following data for averages, fits, limits, etc. • • •				
1692	VRANA	00	DPWA	Multichannel
1675	ARNDT	91	DPWA	$\pi N \to \pi N$ Soln SM90
1716 or 1716	[5] LONGACRE	78	IPWA	$\pi N \to N\pi\pi$
1745 or 1748	[2] LONGACRE	77	IPWA	$\pi N \to N\pi\pi$

−2×IMAGINARY PART

VALUE (MeV)	DOCUMENT ID		TECN	COMMENT
110 to 390 (≈ 250) OUR ESTIMATE				
388	ARNDT	95	DPWA	$\pi N \to N\pi$
187	[4] HOEHLER	93	SPED	$\pi N \to \pi N$
120±40	CUTKOSKY	80	IPWA	$\pi N \to \pi N$
• • • We do not use the following data for averages, fits, limits, etc. • • •				
94	VRANA	00	DPWA	Multichannel
114	ARNDT	91	DPWA	$\pi N \to \pi N$ Soln SM90
124 or 126	[5] LONGACRE	78	IPWA	$\pi N \to N\pi\pi$
135 or 123	[2] LONGACRE	77	IPWA	$\pi N \to N\pi\pi$

$N(1720)$ ELASTIC POLE RESIDUE

MODULUS $|r|$

VALUE (MeV)	DOCUMENT ID		TECN	COMMENT
39	ARNDT	95	DPWA	$\pi N \to N\pi$
15	HOEHLER	93	SPED	$\pi N \to \pi N$
8±2	CUTKOSKY	80	IPWA	$\pi N \to \pi N$
• • • We do not use the following data for averages, fits, limits, etc. • • •				
11	ARNDT	91	DPWA	$\pi N \to \pi N$ Soln SM90

PHASE θ

VALUE (°)	DOCUMENT ID		TECN	COMMENT
− 70	ARNDT	95	DPWA	$\pi N \to N\pi$
−160±30	CUTKOSKY	80	IPWA	$\pi N \to \pi N$
• • • We do not use the following data for averages, fits, limits, etc. • • •				
−130	ARNDT	91	DPWA	$\pi N \to \pi N$ Soln SM90

$N(1720)$ DECAY MODES

The following branching fractions are our estimates, not fits or averages.

	Mode	Fraction (Γ_j/Γ)
Γ_1	$N\pi$	10–20 %
Γ_2	$N\eta$	(4.0±1.0) %
Γ_3	ΛK	1–15 %
Γ_4	ΣK	
Γ_5	$N\pi\pi$	>70 %
Γ_6	$\Delta\pi$	
Γ_7	$\Delta(1232)\pi$, P-wave	
Γ_8	$N\rho$	70–85 %
Γ_9	$N\rho$, S=1/2, P-wave	
Γ_{10}	$N\rho$, S=3/2, P-wave	
Γ_{11}	$N(\pi\pi)^{I=0}_{S\text{-wave}}$	
Γ_{12}	$p\gamma$	0.003–0.10 %
Γ_{13}	$p\gamma$, helicity=1/2	0.003–0.08 %
Γ_{14}	$p\gamma$, helicity=3/2	0.001–0.03 %
Γ_{15}	$n\gamma$	0.002–0.39 %
Γ_{16}	$n\gamma$, helicity=1/2	0.0–0.002 %
Γ_{17}	$n\gamma$, helicity=3/2	0.001–0.39 %

$N(1720)$ BRANCHING RATIOS

$\Gamma(N\pi)/\Gamma_{\text{total}}$ Γ_1/Γ

VALUE	DOCUMENT ID		TECN	COMMENT
0.10 to 0.20 OUR ESTIMATE				
0.13±0.05	MANLEY	92	IPWA	$\pi N \to \pi N$ & $N\pi\pi$
0.10±0.04	CUTKOSKY	80	IPWA	$\pi N \to \pi N$
0.14±0.03	HOEHLER	79	IPWA	$\pi N \to \pi N$
• • • We do not use the following data for averages, fits, limits, etc. • • •				
0.17±0.02	PENNER	02C	DPWA	Multichannel
0.05±0.05	VRANA	00	DPWA	Multichannel
0.16	ARNDT	95	DPWA	$\pi N \to N\pi$
0.18±0.04	BATINIC	95	DPWA	$\pi N \to N\pi$, $N\eta$

$\Gamma(N\eta)/\Gamma_{\text{total}}$ Γ_2/Γ

VALUE	DOCUMENT ID		TECN	COMMENT
0.04 ±0.01	VRANA	00	DPWA	Multichannel
• • • We do not use the following data for averages, fits, limits, etc. • • •				
0.002±0.002	PENNER	02C	DPWA	Multichannel
0.002±0.01	BATINIC	95	DPWA	$\pi N \to N\pi$, $N\eta$

$(\Gamma_j\Gamma_f)^{1/2}/\Gamma_{\text{total}}$ in $N\pi \to N(1720) \to N\eta$ $(\Gamma_1\Gamma_2)^{1/2}/\Gamma$

VALUE	DOCUMENT ID		TECN	COMMENT
• • • We do not use the following data for averages, fits, limits, etc. • • •				
− 0.08	BAKER	79	DPWA	$\pi^- p \to n\eta$

$\Gamma(\Lambda K)/\Gamma_{\text{total}}$ Γ_3/Γ

VALUE	DOCUMENT ID		TECN	COMMENT
0.09 ±0.03	PENNER	02C	DPWA	Multichannel

$(\Gamma_i\Gamma_f)^{1/2}/\Gamma_{total}$ in $N\pi \to N(1720) \to \Lambda K$ $(\Gamma_1\Gamma_3)^{1/2}/\Gamma$

VALUE	DOCUMENT ID		TECN	COMMENT
−0.14 to −0.06 OUR ESTIMATE				
−0.09	BELL	83	DPWA	$\pi^- p \to \Lambda K^0$
−0.11	SAXON	80	DPWA	$\pi^- p \to \Lambda K^0$
• • • We do not use the following data for averages, fits, limits, etc. • • •				
−0.09	[6] BAKER	78	DPWA	See SAXON 80
−0.06 ± 0.02	[1] BAKER	77	IPWA	$\pi^- p \to \Lambda K^0$
−0.09	[1] BAKER	77	DPWA	$\pi^- p \to \Lambda K^0$

$(\Gamma_i\Gamma_f)^{1/2}/\Gamma_{total}$ in $N\pi \to N(1720) \to \Sigma K$ $(\Gamma_1\Gamma_4)^{1/2}/\Gamma$

VALUE	DOCUMENT ID		TECN	COMMENT
• • • We do not use the following data for averages, fits, limits, etc. • • •				
0.051 to 0.087	[7] DEANS	75	DPWA	$\pi N \to \Sigma K$

Note: Signs of couplings from $\pi N \to N\pi\pi$ analyses were changed in the 1986 edition to agree with the baryon-first convention; the overall phase ambiguity is resolved by choosing a negative sign for the $\Delta(1620)$ S_{31} coupling to $\Delta(1232)\pi$.

$(\Gamma_i\Gamma_f)^{1/2}/\Gamma_{total}$ in $N\pi \to N(1720) \to \Delta(1232)\pi$, P-wave $(\Gamma_1\Gamma_7)^{1/2}/\Gamma$

VALUE	DOCUMENT ID		TECN	COMMENT
±0.27 to ±0.37 OUR ESTIMATE				
−0.17	[2] LONGACRE	77	IPWA	$\pi N \to N\pi\pi$

$(\Gamma_i\Gamma_f)^{1/2}/\Gamma_{total}$ in $N\pi \to N(1720) \to N\rho$, S=1/2, P-wave $(\Gamma_1\Gamma_9)^{1/2}/\Gamma$

VALUE	DOCUMENT ID		TECN	COMMENT
+0.34 ± 0.05	MANLEY	92	IPWA	$\pi N \to \pi N$ & $N\pi\pi$
−0.26	[2] LONGACRE	77	IPWA	$\pi N \to N\pi\pi$
+0.40	[3] LONGACRE	75	IPWA	$\pi N \to N\pi\pi$

$\Gamma(N\rho, S$=1/2, P-wave$)/\Gamma_{total}$ Γ_9/Γ

VALUE	DOCUMENT ID		TECN	COMMENT
0.91 ± 0.01	VRANA	00	DPWA	Multichannel

$(\Gamma_i\Gamma_f)^{1/2}/\Gamma_{total}$ in $N\pi \to N(1720) \to N\rho$, S=3/2, P-wave $(\Gamma_1\Gamma_{10})^{1/2}/\Gamma$

VALUE	DOCUMENT ID		TECN	COMMENT
+0.15	[2] LONGACRE	77	IPWA	$\pi N \to N\pi\pi$

$(\Gamma_i\Gamma_f)^{1/2}/\Gamma_{total}$ in $N\pi \to N(1720) \to N(\pi\pi)^{I=0}_{S\text{-wave}}$ $(\Gamma_1\Gamma_{11})^{1/2}/\Gamma$

VALUE	DOCUMENT ID		TECN	COMMENT
−0.19	[2] LONGACRE	77	IPWA	$\pi N \to N\pi\pi$

$N(1720)$ PHOTON DECAY AMPLITUDES

$N(1720) \to p\gamma$, helicity-1/2 amplitude $A_{1/2}$

VALUE (GeV$^{-1/2}$)	DOCUMENT ID		TECN	COMMENT
+0.018±0.030 OUR ESTIMATE				
−0.015 ± 0.015	ARNDT	96	IPWA	$\gamma N \to \pi N$
0.044 ± 0.066	CRAWFORD	83	IPWA	$\gamma N \to \pi N$
−0.004 ± 0.007	AWAJI	81	DPWA	$\gamma N \to \pi N$
0.051 ± 0.009	ARAI	80	DPWA	$\gamma N \to \pi N$ (fit 1)
0.071 ± 0.010	ARAI	80	DPWA	$\gamma N \to \pi N$ (fit 2)
0.038 ± 0.050	CRAWFORD	80	DPWA	$\gamma N \to \pi N$
• • • We do not use the following data for averages, fits, limits, etc. • • •				
−0.053	PENNER	02D	DPWA	Multichannel
0.012 ± 0.003	LI	93	IPWA	$\gamma N \to \pi N$
+0.111 ± 0.047	BARBOUR	78	DPWA	$\gamma N \to \pi N$

$N(1720) \to p\gamma$, helicity-3/2 amplitude $A_{3/2}$

VALUE (GeV$^{-1/2}$)	DOCUMENT ID		TECN	COMMENT
−0.019±0.020 OUR ESTIMATE				
0.007 ± 0.010	ARNDT	96	IPWA	$\gamma N \to \pi N$
−0.024 ± 0.006	CRAWFORD	83	IPWA	$\gamma N \to \pi N$
−0.040 ± 0.016	AWAJI	81	DPWA	$\gamma N \to \pi N$
−0.058 ± 0.010	ARAI	80	DPWA	$\gamma N \to \pi N$ (fit 1)
−0.011 ± 0.011	ARAI	80	DPWA	$\gamma N \to \pi N$ (fit 2)
−0.014 ± 0.040	CRAWFORD	80	DPWA	$\gamma N \to \pi N$
• • • We do not use the following data for averages, fits, limits, etc. • • •				
0.027	PENNER	02D	DPWA	Multichannel
−0.022 ± 0.003	LI	93	IPWA	$\gamma N \to \pi N$
−0.063 ± 0.032	BARBOUR	78	DPWA	$\gamma N \to \pi N$

$N(1720) \to n\gamma$, helicity-1/2 amplitude $A_{1/2}$

VALUE (GeV$^{-1/2}$)	DOCUMENT ID		TECN	COMMENT
+0.001±0.015 OUR ESTIMATE				
0.007 ± 0.015	ARNDT	96	IPWA	$\gamma N \to \pi N$
0.002 ± 0.005	AWAJI	81	DPWA	$\gamma N \to \pi N$
−0.019 ± 0.033	ARAI	80	DPWA	$\gamma N \to \pi N$ (fit 1)
0.001 ± 0.038	ARAI	80	DPWA	$\gamma N \to \pi N$ (fit 2)
−0.003 ± 0.034	CRAWFORD	80	DPWA	$\gamma N \to \pi N$
• • • We do not use the following data for averages, fits, limits, etc. • • •				
−0.004	PENNER	02D	DPWA	Multichannel
0.050 ± 0.004	LI	93	IPWA	$\gamma N \to \pi N$
+0.007 ± 0.020	BARBOUR	78	DPWA	$\gamma N \to \pi N$

$N(1720) \to n\gamma$, helicity-3/2 amplitude $A_{3/2}$

VALUE (GeV$^{-1/2}$)	DOCUMENT ID		TECN	COMMENT
−0.029±0.061 OUR ESTIMATE				
−0.005 ± 0.025	ARNDT	96	IPWA	$\gamma N \to \pi N$
−0.015 ± 0.019	AWAJI	81	DPWA	$\gamma N \to \pi N$
−0.139 ± 0.039	ARAI	80	DPWA	$\gamma N \to \pi N$ (fit 1)
−0.134 ± 0.044	ARAI	80	DPWA	$\gamma N \to \pi N$ (fit 2)
0.018 ± 0.028	CRAWFORD	80	DPWA	$\gamma N \to \pi N$
• • • We do not use the following data for averages, fits, limits, etc. • • •				
0.003	PENNER	02D	DPWA	Multichannel
−0.017 ± 0.004	LI	93	IPWA	$\gamma N \to \pi N$
+0.051 ± 0.051	BARBOUR	78	DPWA	$\gamma N \to \pi N$

$N(1720)$ $\gamma p \to \Lambda K^+$ AMPLITUDES

$(\Gamma_i\Gamma_f)^{1/2}/\Gamma_{total}$ in $p\gamma \to N(1720) \to \Lambda K^+$ (E_{1+} amplitude)

VALUE (units 10^{-3})	DOCUMENT ID		TECN
• • • We do not use the following data for averages, fits, limits, etc. • • •			
10.2 ± 0.2	WORKMAN	90	DPWA
9.52	TANABE	89	DPWA

$p\gamma \to N(1720) \to \Lambda K^+$ phase angle θ (E_{1+} amplitude)

VALUE (degrees)	DOCUMENT ID		TECN
• • • We do not use the following data for averages, fits, limits, etc. • • •			
−124 ± 2	WORKMAN	90	DPWA
−103.4	TANABE	89	DPWA

$(\Gamma_i\Gamma_f)^{1/2}/\Gamma_{total}$ in $p\gamma \to N(1720) \to \Lambda K^+$ (M_{1+} amplitude)

VALUE (units 10^{-3})	DOCUMENT ID		TECN
• • • We do not use the following data for averages, fits, limits, etc. • • •			
−4.5 ± 0.2	WORKMAN	90	DPWA
3.18	TANABE	89	DPWA

$N(1720)$ FOOTNOTES

[1] The two BAKER 77 entries are from an IPWA using the Barrelet-zero method and from a conventional energy-dependent analysis.

[2] LONGACRE 77 pole positions are from a search for poles in the unitarized T-matrix; the first (second) value uses, in addition to $\pi N \to N\pi\pi$ data, elastic amplitudes from a Saclay (CERN) partial-wave analysis. The other LONGACRE 77 values are from eyeball fits with Breit-Wigner circles to the T-matrix amplitudes.

[3] From method II of LONGACRE 75: eyeball fits with Breit-Wigner circles to the T-matrix amplitudes.

[4] See HOEHLER 93 for a detailed discussion of the evidence for and the pole parameters of N and Δ resonances as determined from Argand diagrams of πN elastic partial-wave amplitudes and from plots of the speeds with which the amplitudes traverse the diagrams.

[5] LONGACRE 78 values are from a search for poles in the unitarized T-matrix. The first (second) value uses, in addition to $\pi N \to N\pi\pi$ data, elastic amplitudes from a Saclay (CERN) partial-wave analysis.

[6] The overall phase of BAKER 78 couplings has been changed to agree with previous conventions.

[7] The range given is from the four best solutions. DEANS 75 disagrees with $\pi^+ p \to \Sigma^+ K^+$ data of WINNIK 77 around 1920 MeV.

$N(1720)$ REFERENCES

For early references, see Physics Letters **111B** 70 (1982).

RIPANI	03	PRL 91 022002	M. Ripani *et al.* (Jefferson Lab CLAS Collab.)
PENNER	02C	PR C66 055211	G. Penner, U. Mosel (GIES)
PENNER	02D	PR C66 055212	G. Penner, U. Mosel (GIES)
VRANA	00	PRPL 328 181	T.P. Vrana, S.A. Dytman,, T.-S.H. Lee (PITT+)
ARNDT	96	PR C53 430	R.A. Arndt, I.I. Strakovsky, R.L. Workman (VPI)
ARNDT	95	PR C52 2120	R.A. Arndt *et al.* (VPI, BRCO)
BATINIC	95	PR C51 2310	M. Batinic *et al.* (BOSK, UCLA)
Also	98	PR C57 1004 (erratum)	M. Batinic *et al.*
HOEHLER	93	πN Newsletter 9 1	G. Hohler (KARL)
LI	93	PR C47 2759	Z.J. Li *et al.* (VPI)
MANLEY	92	PR D45 4002	D.M. Manley, E.M. Saleski (KENT) IJP
Also	84	PR D30 904	D.M. Manley *et al.* (VPI)
ARNDT	91	PR D43 2131	R.A. Arndt *et al.* (VPI, TELE) IJP
WORKMAN	90	PR C42 781	R.L. Workman (VPI)
TANABE	89	PR C39 741	H. Tanabe, M. Kohno, C. Bennhold (MANZ)
Also	89	NC 102A 193	M. Kohno, H. Tanabe, C. Bennhold (MANZ)
BELL	83	NP B222 389	K.W. Bell *et al.* (RL) IJP
CRAWFORD	83	NP B211 1	R.L. Crawford, W.T. Morton (GLAS)
PDG	82	PL 111B	M. Roos *et al.* (HELS, CIT, CERN)
AWAJI	81	Bonn Conf. 352	N. Awaji, R. Kajikawa (NAGO)
Also	82	NP B197 365	K. Fujii *et al.* (NAGO)
ARAI	80	Toronto Conf. 93	I. Arai (INUS)
Also	82	NP B194 251	I. Arai, H. Fujii (INUS)
CRAWFORD	80	Toronto Conf. 107	R.L. Crawford (GLAS)
CUTKOSKY	80	Toronto Conf. 19	R.E. Cutkosky *et al.* (CMU, LBL) IJP
Also	79	PR D20 2839	R.E. Cutkosky *et al.* (CMU, LBL) IJP
SAXON	80	NP B162 522	D.H. Saxon *et al.* (RHEL, BRIS) IJP
BAKER	79	NP B156 93	R.D. Baker *et al.* (RHEL) IJP
HOEHLER	79	PDAT 12-1	G. Hohler *et al.* (KARLT) IJP
Also	80	Toronto Conf. 3	R. Koch (KARLT) IJP
BAKER	78	NP B141 29	R.D. Baker *et al.* (RL, CAVE) IJP
BARBOUR	78	NP B141 253	I.M. Barbour, R.L. Crawford, N.H. Parsons (GLAS)
LONGACRE	78	PR D17 1795	R.S. Longacre *et al.* (LBL, SLAC)
BAKER	77	NP B126 365	R.D. Baker *et al.* (RHEL) IJP
LONGACRE	77	NP B122 493	R.S. Longacre, J. Dolbeau (SACL) IJP
Also	76	NP B108 365	J. Dolbeau *et al.* (SACL) IJP
WINNIK	77	NP B128 66	M. Winnik *et al.* (HAIF) I
DEANS	75	NP B96 90	S.R. Deans *et al.* (SFLA, ALAH) IJP
KNASEL	75	PR D11 1	T.M. Knasel *et al.* (CHIC, WUSL, OSU+) IJP
LONGACRE	75	PL 55B 415	R.S. Longacre *et al.* (LBL, SLAC) IJP

$N(1900)$ P_{13}

$I(J^P) = \frac{1}{2}(\frac{3}{2}^+)$ Status: **

OMITTED FROM SUMMARY TABLE

$N(1900)$ BREIT-WIGNER MASS

VALUE (MeV)	DOCUMENT ID		TECN	COMMENT
≈ 1900 OUR ESTIMATE				
1879 ± 17	MANLEY	92	IPWA	$\pi N \to \pi N$ & $N\pi\pi$
• • • We do not use the following data for averages, fits, limits, etc. • • •				
1951 ± 53	PENNER	02C	DPWA	Multichannel

$N(1900)$ BREIT-WIGNER WIDTH

VALUE (MeV)	DOCUMENT ID		TECN	COMMENT
498 ± 78	MANLEY	92	IPWA	$\pi N \to \pi N$ & $N\pi\pi$
• • • We do not use the following data for averages, fits, limits, etc. • • •				
622 ± 42	PENNER	02C	DPWA	Multichannel

$N(1900)$ DECAY MODES

	Mode	Fraction (Γ_i/Γ)
Γ_1	$N\pi$	
Γ_2	$N\pi\pi$	
Γ_3	$N\rho$, S=1/2, P-wave	
Γ_4	$N\eta$	(14 ± 5) %
Γ_5	$N\omega$	(39 ± 9) %
Γ_6	ΛK	
Γ_7	ΣK	

$N(1900)$ BRANCHING RATIOS

$\Gamma(N\pi)/\Gamma_{total}$ Γ_1/Γ

VALUE	DOCUMENT ID		TECN	COMMENT
0.26 ± 0.06	MANLEY	92	IPWA	$\pi N \to \pi N$ & $N\pi\pi$
• • • We do not use the following data for averages, fits, limits, etc. • • •				
0.16 ± 0.02	PENNER	02C	DPWA	Multichannel

$\Gamma(N\eta)/\Gamma_{total}$ Γ_4/Γ

VALUE	DOCUMENT ID		TECN	COMMENT
0.14 ± 0.05	PENNER	02C	DPWA	Multichannel

$\Gamma(N\omega)/\Gamma_{total}$ Γ_5/Γ

VALUE	DOCUMENT ID		TECN	COMMENT
0.39 ± 0.09	PENNER	02C	DPWA	Multichannel

$(\Gamma_i\Gamma_f)^{1/2}/\Gamma_{total}$ in $N\pi \to N(1900) \to N\rho$, S=1/2, P-wave $(\Gamma_1\Gamma_3)^{1/2}/\Gamma$

VALUE	DOCUMENT ID		TECN	COMMENT
− 0.34 ± 0.03	MANLEY	92	IPWA	$\pi N \to \pi N$ & $N\pi\pi$

$\Gamma(\Lambda K)/\Gamma_{total}$ Γ_6/Γ

VALUE	DOCUMENT ID		TECN	COMMENT
• • • We do not use the following data for averages, fits, limits, etc. • • •				
0.001 ± 0.001	PENNER	02C	DPWA	Multichannel

$\Gamma(\Sigma K)/\Gamma_{total}$ Γ_7/Γ

VALUE	DOCUMENT ID		TECN	COMMENT
• • • We do not use the following data for averages, fits, limits, etc. • • •				
0.01 ± 0.01	PENNER	02C	DPWA	Multichannel

$N(1900)$ PHOTON DECAY AMPLITUDES

$N(1900) \to p\gamma$, helicity-1/2 amplitude $A_{1/2}$

VALUE (GeV$^{-1/2}$)	DOCUMENT ID		TECN	COMMENT
• • • We do not use the following data for averages, fits, limits, etc. • • •				
− 0.017	PENNER	02D	DPWA	Multichannel

$N(1900) \to p\gamma$, helicity-3/2 amplitude $A_{3/2}$

VALUE (GeV$^{-1/2}$)	DOCUMENT ID		TECN	COMMENT
• • • We do not use the following data for averages, fits, limits, etc. • • •				
0.031	PENNER	02D	DPWA	Multichannel

$N(1900) \to n\gamma$, helicity-1/2 amplitude $A_{1/2}$

VALUE (GeV$^{-1/2}$)	DOCUMENT ID		TECN	COMMENT
• • • We do not use the following data for averages, fits, limits, etc. • • •				
− 0.016	PENNER	02D	DPWA	Multichannel

$N(1900) \to n\gamma$, helicity-3/2 amplitude $A_{3/2}$

VALUE (GeV$^{-1/2}$)	DOCUMENT ID		TECN	COMMENT
• • • We do not use the following data for averages, fits, limits, etc. • • •				
− 0.002	PENNER	02D	DPWA	Multichannel

$N(1900)$ REFERENCES

PENNER	02C	PR C66 055211	G. Penner, U. Mosel	(GIES)
PENNER	02D	PR C66 055212	G. Penner, U. Mosel	(GIES)
MANLEY	92	PR D45 4002	D.M. Manley, E.M. Saleski	(KENT)
Also	84	PR D30 904	D.M. Manley *et al.*	(VPI)

$N(1990)$ F_{17}

$I(J^P) = \frac{1}{2}(\frac{7}{2}^+)$ Status: **

OMITTED FROM SUMMARY TABLE

Most of the results published before 1975 are now obsolete and have been omitted. They may be found in our 1982 edition, Physics Letters **111B** (1982).

The various analyses do not agree very well with one another.

$N(1990)$ BREIT-WIGNER MASS

VALUE (MeV)	DOCUMENT ID		TECN	COMMENT
≈ 1990 OUR ESTIMATE				
2086 ± 28	MANLEY	92	IPWA	$\pi N \to \pi N$ & $N\pi\pi$
2018	CRAWFORD	80	DPWA	$\gamma N \to \pi N$
1970 ± 50	CUTKOSKY	80	IPWA	$\pi N \to \pi N$
2005 ± 150	HOEHLER	79	IPWA	$\pi N \to \pi N$
1999	BARBOUR	78	DPWA	$\gamma N \to \pi N$
• • • We do not use the following data for averages, fits, limits, etc. • • •				
2311 ± 16	VRANA	00	DPWA	Multichannel

$N(1990)$ BREIT-WIGNER WIDTH

VALUE (MeV)	DOCUMENT ID		TECN	COMMENT
535 ± 120	MANLEY	92	IPWA	$\pi N \to \pi N$ & $N\pi\pi$
295	CRAWFORD	80	DPWA	$\gamma N \to \pi N$
350 ± 120	CUTKOSKY	80	IPWA	$\pi N \to \pi N$
350 ± 100	HOEHLER	79	IPWA	$\pi N \to \pi N$
216	BARBOUR	78	DPWA	$\gamma N \to \pi N$
• • • We do not use the following data for averages, fits, limits, etc. • • •				
205 ± 72	VRANA	00	DPWA	Multichannel

$N(1990)$ POLE POSITION

REAL PART

VALUE (MeV)	DOCUMENT ID		TECN	COMMENT
1900 ± 30	CUTKOSKY	80	IPWA	$\pi N \to \pi N$
• • • We do not use the following data for averages, fits, limits, etc. • • •				
2301	VRANA	00	DPWA	Multichannel
not seen	ARNDT	91	DPWA	$\pi N \to \pi N$ Soln SM90

$-2\times$IMAGINARY PART

VALUE (MeV)	DOCUMENT ID		TECN	COMMENT
260 ± 60	CUTKOSKY	80	IPWA	$\pi N \to \pi N$
• • • We do not use the following data for averages, fits, limits, etc. • • •				
202	VRANA	00	DPWA	Multichannel
not seen	ARNDT	91	DPWA	$\pi N \to \pi N$ Soln SM90

$N(1990)$ ELASTIC POLE RESIDUE

MODULUS $|r|$

VALUE (MeV)	DOCUMENT ID		TECN	COMMENT
9 ± 3	CUTKOSKY	80	IPWA	$\pi N \to \pi N$

PHASE θ

VALUE (°)	DOCUMENT ID		TECN	COMMENT
− 60 ± 30	CUTKOSKY	80	IPWA	$\pi N \to \pi N$

$N(1990)$ DECAY MODES

	Mode
Γ_1	$N\pi$
Γ_2	$N\eta$
Γ_3	ΛK
Γ_4	ΣK
Γ_5	$N\pi\pi$
Γ_6	$p\gamma$, helicity=1/2
Γ_7	$p\gamma$, helicity=3/2
Γ_8	$n\gamma$, helicity=1/2
Γ_9	$n\gamma$, helicity=3/2

$N(1990)$ BRANCHING RATIOS

$\Gamma(N\pi)/\Gamma_{total}$ Γ_1/Γ

VALUE	DOCUMENT ID		TECN	COMMENT
0.06 ± 0.02	MANLEY	92	IPWA	$\pi N \to \pi N$ & $N\pi\pi$
0.06 ± 0.02	CUTKOSKY	80	IPWA	$\pi N \to \pi N$
0.04 ± 0.02	HOEHLER	79	IPWA	$\pi N \to \pi N$
• • • We do not use the following data for averages, fits, limits, etc. • • •				
0.22 ± 0.11	VRANA	00	DPWA	Multichannel

$(\Gamma_i\Gamma_f)^{1/2}/\Gamma_{total}$ in $N\pi \to N(1990) \to N\eta$ $(\Gamma_1\Gamma_2)^{1/2}/\Gamma$

VALUE	DOCUMENT ID		TECN	COMMENT
-0.043	BAKER	79	DPWA	$\pi^- p \to n\eta$

$\Gamma(N\eta)/\Gamma_{total}$ Γ_2/Γ

VALUE	DOCUMENT ID		TECN	COMMENT
0.00 ± 0.01	VRANA	00	DPWA	Multichannel

$(\Gamma_i\Gamma_f)^{1/2}/\Gamma_{total}$ in $N\pi \to N(1990) \to \Lambda K$ $(\Gamma_1\Gamma_3)^{1/2}/\Gamma$

VALUE	DOCUMENT ID		TECN	COMMENT
$+0.01$	BELL	83	DPWA	$\pi^- p \to \Lambda K^0$
not seen	SAXON	80	DPWA	$\pi^- p \to \Lambda K^0$
-0.021 ± 0.033	DEVENISH	74B		Fixed-t dispersion rel.

$(\Gamma_i\Gamma_f)^{1/2}/\Gamma_{total}$ in $N\pi \to N(1990) \to \Sigma K$ $(\Gamma_1\Gamma_4)^{1/2}/\Gamma$

VALUE	DOCUMENT ID		TECN	COMMENT
0.010 to 0.023	[1] DEANS	75	DPWA	$\pi N \to \Sigma K$
0.06	LANGBEIN	73	IPWA	$\pi N \to \Sigma K$ (sol. 1)

$(\Gamma_i\Gamma_f)^{1/2}/\Gamma_{total}$ in $N\pi \to N(1990) \to N\pi\pi$ $(\Gamma_1\Gamma_5)^{1/2}/\Gamma$

VALUE	DOCUMENT ID		TECN	COMMENT
not seen	LONGACRE	75	IPWA	$\pi N \to N\pi\pi$

$N(1990)$ PHOTON DECAY AMPLITUDES

$N(1990) \to p\gamma$, helicity-1/2 amplitude $A_{1/2}$

VALUE (GeV$^{-1/2}$)	DOCUMENT ID		TECN	COMMENT
0.030 ± 0.029	AWAJI	81	DPWA	$\gamma N \to \pi N$
0.001 ± 0.040	CRAWFORD	80	DPWA	$\gamma N \to \pi N$
• • • We do not use the following data for averages, fits, limits, etc. • • •				
0.040	BARBOUR	78	DPWA	$\gamma N \to \pi N$

$N(1990) \to p\gamma$, helicity-3/2 amplitude $A_{3/2}$

VALUE (GeV$^{-1/2}$)	DOCUMENT ID		TECN	COMMENT
0.086 ± 0.060	AWAJI	81	DPWA	$\gamma N \to \pi N$
0.004 ± 0.025	CRAWFORD	80	DPWA	$\gamma N \to \pi N$
• • • We do not use the following data for averages, fits, limits, etc. • • •				
$+0.004$	BARBOUR	78	DPWA	$\gamma N \to \pi N$

$N(1990) \to n\gamma$, helicity-1/2 amplitude $A_{1/2}$

VALUE (GeV$^{-1/2}$)	DOCUMENT ID		TECN	COMMENT
-0.001	AWAJI	81	DPWA	$\gamma N \to \pi N$
-0.078 ± 0.030	CRAWFORD	80	DPWA	$\gamma N \to \pi N$
• • • We do not use the following data for averages, fits, limits, etc. • • •				
-0.069	BARBOUR	78	DPWA	$\gamma N \to \pi N$

$N(1990) \to n\gamma$, helicity-3/2 amplitude $A_{3/2}$

VALUE (GeV$^{-1/2}$)	DOCUMENT ID		TECN	COMMENT
-0.178	AWAJI	81	DPWA	$\gamma N \to \pi N$
-0.116 ± 0.045	CRAWFORD	80	DPWA	$\gamma N \to \pi N$
• • • We do not use the following data for averages, fits, limits, etc. • • •				
-0.072	BARBOUR	78	DPWA	$\gamma N \to \pi N$

$N(1990)$ FOOTNOTES

[1] The range given for DEANS 75 is from the four best solutions.

$N(1990)$ REFERENCES

For early references, see Physics Letters **111B** 70 (1982).

VRANA	00	PRPL 328 181	T.P. Vrana, S.A. Dytman, T.-S.H. Lee	(PITT+)
MANLEY	92	PR D45 4002	D.M. Manley, E.M. Saleski	(KENT) IJP
Also	84	PR D30 904	D.M. Manley *et al.*	(VPI)
ARNDT	91	PR D43 2131	R.A. Arndt *et al.*	(VPI, TELE) IJP
BELL	83	NP B222 389	K.W. Bell *et al.*	(RL) IJP
PDG	82	PL 111B	M. Roos *et al.*	(HELS, CIT, CERN)
AWAJI	81	Bonn Conf. 352	N. Awaji, R. Kajikawa	(NAGO)
Also	82	NP B197 365	K. Fujii *et al.*	(NAGO)
CRAWFORD	80	Toronto Conf. 107	R.L. Crawford	(GLAS)
CUTKOSKY	80	Toronto Conf. 19	R.E. Cutkosky *et al.*	(CMU, LBL) IJP
Also	79	PR D20 2839	R.E. Cutkosky *et al.*	(CMU, LBL) IJP
SAXON	80	NP B162 522	D.H. Saxon *et al.*	(RHEL, BRIS) IJP
BAKER	79	NP B156 93	R.D. Baker *et al.*	(RHEL) IJP
HOEHLER	79	PDAT 12-1	G. Hohler *et al.*	(KARLT) IJP
Also	80	Toronto Conf. 3	R. Koch	(KARLT) IJP
BARBOUR	78	NP B141 253	I.M. Barbour, R.L. Crawford, N.H. Parsons	(GLAS)
DEANS	75	NP B96 90	S.R. Deans *et al.*	(SFLA, ALAH) IJP
LONGACRE	75	PL 55B 415	R.S. Longacre *et al.*	(LBL, SLAC) IJP
DEVENISH	74B	NP B81 330	R.C.E. Devenish, C.D. Froggatt, B.R. Martin	(DESY+)
LANGBEIN	73	NP B53 251	W. Langbein, F. Wagner	(MUNI) IJP

$N(2000)$ F_{15}

$I(J^P) = \frac{1}{2}(\frac{5}{2}^+)$ Status: **

OMITTED FROM SUMMARY TABLE

Older results have been retained simply because there is little information at all about this possible state.

$N(2000)$ BREIT-WIGNER MASS

VALUE (MeV)	DOCUMENT ID		TECN	COMMENT
≈ 2000 OUR ESTIMATE				
1903 ± 87	MANLEY	92	IPWA	$\pi N \to \pi N$ & $N\pi\pi$
1882 ± 10	HOEHLER	79	IPWA	$\pi N \to \pi N$
2025	AYED	76	IPWA	$\pi N \to \pi N$
1970	[1] LANGBEIN	73	IPWA	$\pi N \to \Sigma K$ (sol. 2)
2175	ALMEHED	72	IPWA	$\pi N \to \pi N$
1930	DEANS	72	MPWA	$\gamma p \to \Lambda K$ (sol. D)
• • • We do not use the following data for averages, fits, limits, etc. • • •				
1814	ARNDT	95	DPWA	$\pi N \to N\pi$

$N(2000)$ BREIT-WIGNER WIDTH

VALUE (MeV)	DOCUMENT ID		TECN	COMMENT
490 ± 310	MANLEY	92	IPWA	$\pi N \to \pi N$ & $N\pi\pi$
95 ± 20	HOEHLER	79	IPWA	$\pi N \to \pi N$
157	AYED	76	IPWA	$\pi N \to \pi N$
170	[1] LANGBEIN	73	IPWA	$\pi N \to \Sigma K$ (sol. 2)
150	ALMEHED	72	IPWA	$\pi N \to \pi N$
112	DEANS	72	MPWA	$\gamma p \to \Lambda K$ (sol. D)
• • • We do not use the following data for averages, fits, limits, etc. • • •				
176	ARNDT	95	DPWA	$\pi N \to N\pi$

$N(2000)$ DECAY MODES

	Mode
Γ_1	$N\pi$
Γ_2	$N\eta$
Γ_3	ΛK
Γ_4	ΣK
Γ_5	$N\pi\pi$
Γ_6	$\Delta(1232)\pi$, P-wave
Γ_7	$N\rho$, S=3/2, P-wave
Γ_8	$N\rho$, S=3/2, F-wave
Γ_9	$p\gamma$

$N(2000)$ BRANCHING RATIOS

$\Gamma(N\pi)/\Gamma_{total}$ Γ_1/Γ

VALUE	DOCUMENT ID		TECN	COMMENT
0.08 ± 0.05	MANLEY	92	IPWA	$\pi N \to \pi N$ & $N\pi\pi$
0.04 ± 0.02	HOEHLER	79	IPWA	$\pi N \to \pi N$
0.08	AYED	76	IPWA	$\pi N \to \pi N$
0.25	ALMEHED	72	IPWA	$\pi N \to \pi N$
• • • We do not use the following data for averages, fits, limits, etc. • • •				
0.10	ARNDT	95	DPWA	$\pi N \to N\pi$

$(\Gamma_i\Gamma_f)^{1/2}/\Gamma_{total}$ in $N\pi \to N(2000) \to N\eta$ $(\Gamma_1\Gamma_2)^{1/2}/\Gamma$

VALUE	DOCUMENT ID		TECN	COMMENT
$+0.03$	BAKER	79	DPWA	$\pi^- p \to n\eta$

$(\Gamma_i\Gamma_f)^{1/2}/\Gamma_{total}$ in $N\pi \to N(2000) \to \Lambda K$ $(\Gamma_1\Gamma_3)^{1/2}/\Gamma$

VALUE	DOCUMENT ID		TECN	COMMENT
not seen	SAXON	80	DPWA	$\pi^- p \to \Lambda K^0$

$(\Gamma_i\Gamma_f)^{1/2}/\Gamma_{total}$ in $N\pi \to N(2000) \to \Sigma K$ $(\Gamma_1\Gamma_4)^{1/2}/\Gamma$

VALUE	DOCUMENT ID		TECN	COMMENT
0.022	[2] DEANS	75	DPWA	$\pi N \to \Sigma K$
0.05	[1] LANGBEIN	73	IPWA	$\pi N \to \Sigma K$ (sol. 2)

$(\Gamma_i\Gamma_f)^{1/2}/\Gamma_{total}$ in $N\pi \to N(2000) \to \Delta(1232)\pi$, P-wave $(\Gamma_1\Gamma_6)^{1/2}/\Gamma$

VALUE	DOCUMENT ID		TECN	COMMENT
$+0.10\pm0.06$	MANLEY	92	IPWA	$\pi N \to \pi N$ & $N\pi\pi$

$(\Gamma_i\Gamma_f)^{1/2}/\Gamma_{total}$ in $N\pi \to N(2000) \to N\rho$, S=3/2, P-wave $(\Gamma_1\Gamma_7)^{1/2}/\Gamma$

VALUE	DOCUMENT ID		TECN	COMMENT
-0.22 ± 0.08	MANLEY	92	IPWA	$\pi N \to \pi N$ & $N\pi\pi$

$(\Gamma_i\Gamma_f)^{1/2}/\Gamma_{total}$ in $N\pi \to N(2000) \to N\rho$, S=3/2, F-wave $(\Gamma_1\Gamma_8)^{1/2}/\Gamma$

VALUE	DOCUMENT ID		TECN	COMMENT
$+0.11\pm0.06$	MANLEY	92	IPWA	$\pi N \to \pi N$ & $N\pi\pi$

$(\Gamma_i\Gamma_f)^{1/2}/\Gamma_{total}$ in $p\gamma \to N(2000) \to \Lambda K$ $(\Gamma_9\Gamma_3)^{1/2}/\Gamma$

VALUE	DOCUMENT ID		TECN	COMMENT
0.0022	DEANS	72	MPWA	$\gamma p \to \Lambda K$ (sol. D)

$N(2000)$ FOOTNOTES

[1] Not seen in solution 1 of LANGBEIN 73.
[2] Value given is from solution 1 of DEANS 75; not present in solutions 2, 3, or 4.

$N(2000)$ REFERENCES

ARNDT	95	PR C52 2120	R.A. Arndt *et al.*	(VPI, BRCO)
MANLEY	92	PR D45 4002	D.M. Manley, E.M. Saleski	(KENT) IJP
Also	84	PR D30 904	D.M. Manley *et al.*	(VPI)
SAXON	80	NP B162 522	D.H. Saxon *et al.*	(RHEL, BRIS) IJP
BAKER	79	NP B156 93	R.D. Baker *et al.*	(RHEL) IJP
HOEHLER	79	PDAT 12-1	G. Hohler *et al.*	(KARLT) IJP
Also	80	Toronto Conf. 3	R. Koch	(KARLT) IJP
AYED	76	Thesis CEA-N-1921	R. Ayed	(SACL) IJP
DEANS	75	NP B96 90	S.R. Deans *et al.*	(SFLA, ALAH) IJP
LANGBEIN	73	NP B53 251	W. Langbein, F. Wagner	(MUNI) IJP
ALMEHED	72	NP B40 157	S. Almehed, C. Lovelace	(LUND, RUTG) IJP
DEANS	72	PR D6 1906	S.R. Deans *et al.*	(SFLA) IJP

$N(2080)$ D_{13}

$I(J^P) = \frac{1}{2}(\frac{3}{2}^-)$ Status: $**$

OMITTED FROM SUMMARY TABLE

There is some evidence for two resonances in this wave between 1800 and 2200 MeV (see CUTKOSKY 80). However, the solution of HOEHLER 79 is quite different.

Most of the results published before 1975 are now obsolete and have been omitted. They may be found in our 1982 edition, Physics Letters **111B** (1982).

$N(2080)$ BREIT-WIGNER MASS

VALUE (MeV)	DOCUMENT ID		TECN	COMMENT
≈ 2080 OUR ESTIMATE				
1804 ± 55	MANLEY	92	IPWA	$\pi N \to \pi N$ & $N\pi\pi$
1920	BELL	83	DPWA	$\pi^- p \to \Lambda K^0$
1880 ± 100	[1] CUTKOSKY	80	IPWA	$\pi N \to \pi N$
2060 ± 80	[1] CUTKOSKY	80	IPWA	$\pi N \to \pi N$
1900	SAXON	80	DPWA	$\pi^- p \to \Lambda K^0$
2081 ± 20	HOEHLER	79	IPWA	$\pi N \to \pi N$
• • • We do not use the following data for averages, fits, limits, etc. • • •				
1946 ± 1	PENNER	02C	DPWA	Multichannel
1895	MART	00	DPWA	$\gamma p \to \Lambda K^+$
2003 ± 18	VRANA	00	DPWA	Multichannel
1986 ± 75	BATINIC	95	DPWA	$\pi N \to N\pi, N\eta$
1880	BAKER	79	DPWA	$\pi^- p \to n\eta$

$N(2080)$ BREIT-WIGNER WIDTH

VALUE (MeV)	DOCUMENT ID		TECN	COMMENT
450 ± 185	MANLEY	92	IPWA	$\pi N \to \pi N$ & $N\pi\pi$
320	BELL	83	DPWA	$\pi^- p \to \Lambda K^0$
180 ± 60	[1] CUTKOSKY	80	IPWA	$\pi N \to \pi N$ (lower m)
300 ± 100	[1] CUTKOSKY	80	IPWA	$\pi N \to \pi N$ (higher m)
240	SAXON	80	DPWA	$\pi^- p \to \Lambda K^0$
265 ± 40	HOEHLER	79	IPWA	$\pi N \to \pi N$
• • • We do not use the following data for averages, fits, limits, etc. • • •				
859 ± 7	PENNER	02C	DPWA	Multichannel
372	MART	00	DPWA	$\gamma p \to \Lambda K^+$
1070 ± 858	VRANA	00	DPWA	Multichannel
1050 ± 225	BATINIC	95	DPWA	$\pi N \to N\pi, N\eta$
87	BAKER	79	DPWA	$\pi^- p \to n\eta$

$N(2080)$ POLE POSITION

REAL PART

VALUE (MeV)	DOCUMENT ID		TECN	COMMENT
1880 ± 100	[1] CUTKOSKY	80	IPWA	$\pi N \to \pi N$ (lower m)
2050 ± 70	[1] CUTKOSKY	80	IPWA	$\pi N \to \pi N$ (higher m)
• • • We do not use the following data for averages, fits, limits, etc. • • •				
1824	VRANA	00	DPWA	Multichannel
not seen	ARNDT	91	DPWA	$\pi N \to \pi N$ Soln SM90

$-2\times$IMAGINARY PART

VALUE (MeV)	DOCUMENT ID		TECN	COMMENT
160 ± 80	[1] CUTKOSKY	80	IPWA	$\pi N \to \pi N$ (lower m)
200 ± 80	[1] CUTKOSKY	80	IPWA	$\pi N \to \pi N$ (higher m)
• • • We do not use the following data for averages, fits, limits, etc. • • •				
614	VRANA	00	DPWA	Multichannel
not seen	ARNDT	91	DPWA	$\pi N \to \pi N$ Soln SM90

$N(2080)$ ELASTIC POLE RESIDUE

MODULUS $|r|$

VALUE (MeV)	DOCUMENT ID		TECN	COMMENT
10 ± 5	[1] CUTKOSKY	80	IPWA	$\pi N \to \pi N$ (lower m)
30 ± 20	[1] CUTKOSKY	80	IPWA	$\pi N \to \pi N$ (higher m)

PHASE θ

VALUE (°)	DOCUMENT ID		TECN	COMMENT
100 ± 80	[1] CUTKOSKY	80	IPWA	$\pi N \to \pi N$ (lower m)
0 ± 100	[1] CUTKOSKY	80	IPWA	$\pi N \to \pi N$ (higher m)

$N(2080)$ DECAY MODES

	Mode	Fraction (Γ_j/Γ)	Scale factor
Γ_1	$N\pi$		
Γ_2	$N\eta$	(3.5 ± 3.5) %	2.5
Γ_3	$N\omega$	(21 ± 7) %	
Γ_4	ΛK		
Γ_5	ΣK	(7 ± 4) $\times 10^{-3}$	
Γ_6	$N\pi\pi$		
Γ_7	$\Delta(1232)\pi$, S-wave		
Γ_8	$\Delta(1232)\pi$, D-wave		
Γ_9	$N\rho$, S=3/2, S-wave		
Γ_{10}	$N(\pi\pi)^{I=0}_{S\text{-wave}}$		
Γ_{11}	$p\gamma$, helicity=1/2		
Γ_{12}	$p\gamma$, helicity=3/2		
Γ_{13}	$n\gamma$, helicity=1/2		
Γ_{14}	$n\gamma$, helicity=3/2		
Γ_{15}	$p\gamma$		

$N(2080)$ BRANCHING RATIOS

$\Gamma(N\pi)/\Gamma_{total}$ Γ_1/Γ

VALUE	DOCUMENT ID		TECN	COMMENT
0.23 ± 0.03	MANLEY	92	IPWA	$\pi N \to \pi N$ & $N\pi\pi$
0.10 ± 0.04	[1] CUTKOSKY	80	IPWA	$\pi N \to \pi N$ (lower m)
0.14 ± 0.07	[1] CUTKOSKY	80	IPWA	$\pi N \to \pi N$ (higher m)
0.06 ± 0.02	HOEHLER	79	IPWA	$\pi N \to \pi N$
• • • We do not use the following data for averages, fits, limits, etc. • • •				
0.12 ± 0.02	PENNER	02C	DPWA	Multichannel
0.13 ± 0.03	VRANA	00	DPWA	Multichannel
0.09 ± 0.02	BATINIC	95	DPWA	$\pi N \to N\pi, N\eta$

$\Gamma(N\eta)/\Gamma_{total}$ Γ_2/Γ

VALUE	DOCUMENT ID		TECN	COMMENT
0.035 ± 0.035 OUR AVERAGE	Error includes scale factor of 2.5.			
0.07 ± 0.02	PENNER	02C	DPWA	Multichannel
0.00 ± 0.02	VRANA	00	DPWA	Multichannel
• • • We do not use the following data for averages, fits, limits, etc. • • •				
0.07 ± 0.04	BATINIC	95	DPWA	$\pi N \to N\pi, N\eta$

$(\Gamma_i\Gamma_f)^{1/2}/\Gamma_{total}$ in $N\pi \to N(2080) \to N\eta$ $(\Gamma_1\Gamma_2)^{1/2}/\Gamma$

VALUE	DOCUMENT ID		TECN	COMMENT
0.065	BAKER	79	DPWA	$\pi^- p \to n\eta$

$\Gamma(N\omega)/\Gamma_{total}$ Γ_3/Γ

VALUE	DOCUMENT ID		TECN	COMMENT
0.21 ± 0.07	PENNER	02C	DPWA	Multichannel

$\Gamma(\Lambda K)/\Gamma_{total}$ Γ_4/Γ

VALUE	DOCUMENT ID		TECN	COMMENT
• • • We do not use the following data for averages, fits, limits, etc. • • •				
0.002 ± 0.002	PENNER	02C	DPWA	Multichannel

$(\Gamma_i\Gamma_f)^{1/2}/\Gamma_{total}$ in $N\pi \to N(2080) \to \Lambda K$ $(\Gamma_1\Gamma_4)^{1/2}/\Gamma$

VALUE	DOCUMENT ID		TECN	COMMENT
+ 0.04	BELL	83	DPWA	$\pi^- p \to \Lambda K^0$
+ 0.03	SAXON	80	DPWA	$\pi^- p \to \Lambda K^0$

$\Gamma(\Sigma K)/\Gamma_{total}$ Γ_5/Γ

VALUE	DOCUMENT ID		TECN	COMMENT
0.007 ± 0.004	PENNER	02C	DPWA	Multichannel

$(\Gamma_i\Gamma_f)^{1/2}/\Gamma_{total}$ in $N\pi \to N(2080) \to \Sigma K$ $(\Gamma_1\Gamma_5)^{1/2}/\Gamma$

VALUE	DOCUMENT ID		TECN	COMMENT
0.014 to 0.037	[2] DEANS	75	DPWA	$\pi N \to \Sigma K$

$(\Gamma_i\Gamma_f)^{1/2}/\Gamma_{total}$ in $N\pi \to N(2080) \to \Delta(1232)\pi$, S-wave $(\Gamma_1\Gamma_7)^{1/2}/\Gamma$

VALUE	DOCUMENT ID		TECN	COMMENT
− 0.09 ± 0.09	MANLEY	92	IPWA	$\pi N \to \pi N$ & $N\pi\pi$

$\Gamma(\Delta(1232)\pi$, S-wave$)/\Gamma_{total}$ Γ_7/Γ

VALUE	DOCUMENT ID		TECN	COMMENT
0.40±0.10	VRANA	00	DPWA	Multichannel

$(\Gamma_i\Gamma_f)^{1/2}/\Gamma_{total}$ in $N\pi \to N(2080) \to \Delta(1232)\pi$, D-wave $(\Gamma_1\Gamma_8)^{1/2}/\Gamma$

VALUE	DOCUMENT ID		TECN	COMMENT
+0.22±0.07	MANLEY	92	IPWA	$\pi N \to \pi N$ & $N\pi\pi$

$\Gamma(\Delta(1232)\pi$, D-wave$)/\Gamma_{total}$ Γ_8/Γ

VALUE	DOCUMENT ID		TECN	COMMENT
0.17±0.10	VRANA	00	DPWA	Multichannel

$(\Gamma_i\Gamma_f)^{1/2}/\Gamma_{total}$ in $N\pi \to N(2080) \to N\rho$, S=3/2, S-wave $(\Gamma_1\Gamma_9)^{1/2}/\Gamma$

VALUE	DOCUMENT ID		TECN	COMMENT
−0.24±0.06	MANLEY	92	IPWA	$\pi N \to \pi N$ & $N\pi\pi$

$\Gamma(N\rho$, S=3/2, S-wave$)/\Gamma_{total}$ Γ_9/Γ

VALUE	DOCUMENT ID		TECN	COMMENT
0.06±0.06	VRANA	00	DPWA	Multichannel

$(\Gamma_i\Gamma_f)^{1/2}/\Gamma_{total}$ in $N\pi \to N(2080) \to N(\pi\pi)^{I=0}_{S\text{-wave}}$ $(\Gamma_1\Gamma_{10})^{1/2}/\Gamma$

VALUE	DOCUMENT ID		TECN	COMMENT
+0.25±0.06	MANLEY	92	IPWA	$\pi N \to \pi N$ & $N\pi\pi$

$\Gamma(N(\pi\pi)^{I=0}_{S\text{-wave}})/\Gamma_{total}$ Γ_{10}/Γ

VALUE	DOCUMENT ID		TECN	COMMENT
0.24±0.24	VRANA	00	DPWA	Multichannel

$(\Gamma_i\Gamma_f)^{1/2}/\Gamma_{total}$ in $p\gamma \to N(2080) \to N\eta$ $(\Gamma_{15}\Gamma_2)^{1/2}/\Gamma$

VALUE	DOCUMENT ID		TECN	COMMENT
0.0037	HICKS	73	MPWA	$\gamma p \to p\eta$

$N(2080)$ PHOTON DECAY AMPLITUDES

$N(2080) \to p\gamma$, helicity-1/2 amplitude $A_{1/2}$

VALUE (GeV$^{-1/2}$)	DOCUMENT ID		TECN	COMMENT
−0.020±0.008	AWAJI	81	DPWA	$\gamma N \to \pi N$
• • • We do not use the following data for averages, fits, limits, etc. • • •				
0.012	PENNER	02D	DPWA	Multichannel
0.026±0.052	DEVENISH	74	DPWA	$\gamma N \to \pi N$

$N(2080) \to p\gamma$, helicity-3/2 amplitude $A_{3/2}$

VALUE (GeV$^{-1/2}$)	DOCUMENT ID		TECN	COMMENT
0.017±0.011	AWAJI	81	DPWA	$\gamma N \to \pi N$
• • • We do not use the following data for averages, fits, limits, etc. • • •				
−0.010	PENNER	02D	DPWA	Multichannel
0.128±0.057	DEVENISH	74	DPWA	$\gamma N \to \pi N$

$N(2080) \to n\gamma$, helicity-1/2 amplitude $A_{1/2}$

VALUE (GeV$^{-1/2}$)	DOCUMENT ID		TECN	COMMENT
0.007±0.013	AWAJI	81	DPWA	$\gamma N \to \pi N$
• • • We do not use the following data for averages, fits, limits, etc. • • •				
0.023	PENNER	02D	DPWA	Multichannel
0.053±0.083	DEVENISH	74	DPWA	$\gamma N \to \pi N$

$N(2080) \to n\gamma$, helicity-3/2 amplitude $A_{3/2}$

VALUE (GeV$^{-1/2}$)	DOCUMENT ID		TECN	COMMENT
−0.053±0.034	AWAJI	81	DPWA	$\gamma N \to \pi N$
• • • We do not use the following data for averages, fits, limits, etc. • • •				
−0.009	PENNER	02D	DPWA	Multichannel
0.100±0.141	DEVENISH	74	DPWA	$\gamma N \to \pi N$

$N(2080)$ $\gamma p \to \Lambda K^+$ AMPLITUDES

$(\Gamma_i\Gamma_f)^{1/2}/\Gamma_{total}$ in $p\gamma \to N(2080) \to \Lambda K^+$ (E_{2-} amplitude)

VALUE (units 10^{-3})	DOCUMENT ID		TECN	COMMENT
• • • We do not use the following data for averages, fits, limits, etc. • • •				
$2.29^{+0.7}_{-0.2}$	MART	00	DPWA	$\gamma p \to \Lambda K^+$
5.5 ±0.3	WORKMAN	90	DPWA	
4.09	TANABE	89	DPWA	

$p\gamma \to N(2080) \to \Lambda K^+$ phase angle θ (E_{2-} amplitude)

VALUE (degrees)	DOCUMENT ID		TECN
• • • We do not use the following data for averages, fits, limits, etc. • • •			
−48 ±5	WORKMAN	90	DPWA
−35.9	TANABE	89	DPWA

$(\Gamma_i\Gamma_f)^{1/2}/\Gamma_{total}$ in $p\gamma \to N(2080) \to \Lambda K^+$ (M_{2-} amplitude)

VALUE (units 10^{-3})	DOCUMENT ID		TECN
• • • We do not use the following data for averages, fits, limits, etc. • • •			
−6.7 ±0.2	WORKMAN	90	DPWA
−4.09	TANABE	89	DPWA

$N(2080)$ FOOTNOTES

[1] CUTKOSKY 80 finds a lower mass D_{13} resonance, as well as one in this region. Both are listed here.

[2] The range given for DEANS 75 is from the four best solutions. Disagrees with $\pi^+ p \to \Sigma^+ K^+$ data of WINNIK 77 around 1920 MeV.

$N(2080)$ REFERENCES

For early references, see Physics Letters **111B** 70 (1982).

PENNER	02C	PR C66 055211	G. Penner, U. Mosel	(GIES)
PENNER	02D	PR C66 055212	G. Penner, U. Mosel	(GIES)
MART	00	PR C61 012201	T. Mart, C. Bennhold	
VRANA	00	PRPL 328 181	T.P. Vrana, S.A. Dytman,, T.-S.H. Lee	(PITT+)
BATINIC	95	PR C51 2310	M. Batinic *et al.*	(BOSK, UCLA)
Also	98	PR C57 1004 (erratum)	M. Batinic *et al.*	
MANLEY	92	PR D45 4002	D.M. Manley, E.M. Saleski	(KENT) IJP
Also	84	PR D30 904	D.M. Manley *et al.*	(VPI)
ARNDT	91	PR D43 2131	R.A. Arndt *et al.*	(VPI, TELE) IJP
WORKMAN	90	PR C42 781	R.L. Workman	(VPI)
TANABE	89	PR C39 741	H. Tanabe, M. Kohno, C. Bennhold	(MANZ)
Also	89	NC 102A 193	M. Kohno, H. Tanabe, C. Bennhold	(MANZ)
BELL	83	NP B222 389	K.W. Bell *et al.*	(RL) IJP
PDG	82	PL 111B	M. Roos *et al.*	(HELS, CIT, CERN)
AWAJI	81	Bonn Conf. 352	N. Awaji, R. Kajikawa	(NAGO)
Also	82	NP B197 365	K. Fujii *et al.*	(NAGO)
CUTKOSKY	80	Toronto Conf. 19	R.E. Cutkosky *et al.*	(CMU, LBL) IJP
Also	79	PR D20 2839	R.E. Cutkosky *et al.*	(CMU, LBL) IJP
SAXON	80	NP B162 522	D.H. Saxon *et al.*	(RHEL, BRIS) IJP
BAKER	79	NP B156 93	R.D. Baker *et al.*	(RHEL) IJP
HOEHLER	79	PDAT 12-1	G. Hohler *et al.*	(KARLT) IJP
Also	80	Toronto Conf. 3	R. Koch	(KARLT) IJP
WINNIK	77	NP B128 66	M. Winnik *et al.*	(HAIF) I
DEANS	75	NP B96 90	S.R. Deans *et al.*	(SFLA, ALAH) IJP
DEVENISH	74	PL 52B 227	R.C.E. Devenish, D.H. Lyth, W.A. Rankin	(DESY+) IJP
HICKS	73	PR D7 2614	H.R. Hicks *et al.*	(CMU, ORNL, SFLA) IJP

$N(2090)$ S_{11}

$I(J^P) = \frac{1}{2}(\frac{1}{2}^-)$ Status: *

OMITTED FROM SUMMARY TABLE

Any structure in the S_{11} wave above 1800 MeV is listed here. A few early results that are now obsolete have been omitted.

$N(2090)$ BREIT-WIGNER MASS

VALUE (MeV)	DOCUMENT ID		TECN	COMMENT
≈ 2090 OUR ESTIMATE				
1928±59	MANLEY	92	IPWA	$\pi N \to \pi N$ & $N\pi\pi$
2180±80	CUTKOSKY	80	IPWA	$\pi N \to \pi N$
1880±20	HOEHLER	79	IPWA	$\pi N \to \pi N$
• • • We do not use the following data for averages, fits, limits, etc. • • •				
1822±43	VRANA	00	DPWA	Multichannel
$1897\pm50^{+30}_{-2}$	PLOETZKE	98	SPEC	$\gamma p \to p\eta'(958)$

$N(2090)$ BREIT-WIGNER WIDTH

VALUE (MeV)	DOCUMENT ID		TECN	COMMENT
414±157	MANLEY	92	IPWA	$\pi N \to \pi N$ & $N\pi\pi$
350±100	CUTKOSKY	80	IPWA	$\pi N \to \pi N$
95± 30	HOEHLER	79	IPWA	$\pi N \to \pi N$
• • • We do not use the following data for averages, fits, limits, etc. • • •				
248±185	VRANA	00	DPWA	Multichannel
$396\pm155^{+35}_{-45}$	PLOETZKE	98	SPEC	$\gamma p \to p\eta'(958)$

$N(2090)$ POLE POSITION

REAL PART

VALUE (MeV)	DOCUMENT ID		TECN	COMMENT
2150±70	CUTKOSKY	80	IPWA	$\pi N \to \pi N$
1937 or 1949	[1] LONGACRE	78	IPWA	$\pi N \to N\pi\pi$
• • • We do not use the following data for averages, fits, limits, etc. • • •				
1795	VRANA	00	DPWA	Multichannel

−2×IMAGINARY PART

VALUE (MeV)	DOCUMENT ID		TECN	COMMENT
350±100	CUTKOSKY	80	IPWA	$\pi N \to \pi N$
139 or 131	[1] LONGACRE	78	IPWA	$\pi N \to N\pi\pi$
• • • We do not use the following data for averages, fits, limits, etc. • • •				
220	VRANA	00	DPWA	Multichannel

$N(2090)$ ELASTIC POLE RESIDUE

MODULUS $|r|$

VALUE (MeV)	DOCUMENT ID		TECN	COMMENT
40 ± 20	CUTKOSKY	80	IPWA	$\pi N \rightarrow \pi N$

PHASE θ

VALUE (°)	DOCUMENT ID		TECN	COMMENT
0 ± 90	CUTKOSKY	80	IPWA	$\pi N \rightarrow \pi N$

$N(2090)$ DECAY MODES

	Mode
Γ_1	$N\pi$
Γ_2	$N\eta$
Γ_3	ΛK
Γ_4	$N\pi\pi$
Γ_5	$\Delta\pi$
Γ_6	$\Delta(1232)\pi$, D-wave
Γ_7	$N\rho$
Γ_8	$N\rho$, S=1/2, S-wave
Γ_9	$N\rho$, S=3/2, D-wave
Γ_{10}	$N(\pi\pi)^{I=0}_{S\text{-wave}}$
Γ_{11}	$N(1440)\pi$

$N(2090)$ BRANCHING RATIOS

$\Gamma(N\pi)/\Gamma_{\text{total}}$ Γ_1/Γ

VALUE	DOCUMENT ID		TECN	COMMENT
0.10 ± 0.10	MANLEY	92	IPWA	$\pi N \rightarrow \pi N$ & $N\pi\pi$
0.18 ± 0.08	CUTKOSKY	80	IPWA	$\pi N \rightarrow \pi N$
0.09 ± 0.05	HOEHLER	79	IPWA	$\pi N \rightarrow \pi N$
• • • We do not use the following data for averages, fits, limits, etc. • • •				
0.17 ± 0.03	VRANA	00	DPWA	Multichannel

$\Gamma(N\eta)/\Gamma_{\text{total}}$ Γ_2/Γ

VALUE	DOCUMENT ID		TECN	COMMENT
0.41 ± 0.04	VRANA	00	DPWA	Multichannel

$(\Gamma_i\Gamma_f)^{1/2}/\Gamma_{\text{total}}$ in $N\pi \rightarrow N(2090) \rightarrow \Lambda K$ $(\Gamma_1\Gamma_3)^{1/2}/\Gamma$

VALUE	DOCUMENT ID		TECN	COMMENT
not seen	SAXON	80	DPWA	$\pi^- p \rightarrow \Lambda K^0$

$\Gamma(\Delta(1232)\pi$, D-wave$)/\Gamma_{\text{total}}$ Γ_6/Γ

VALUE	DOCUMENT ID		TECN	COMMENT
0.01 ± 0.01	VRANA	00	DPWA	Multichannel

$\Gamma(N\rho$, S=1/2, S-wave$)/\Gamma_{\text{total}}$ Γ_8/Γ

VALUE	DOCUMENT ID		TECN	COMMENT
0.36 ± 0.01	VRANA	00	DPWA	Multichannel

$\Gamma(N\rho$, S=3/2, D-wave$)/\Gamma_{\text{total}}$ Γ_9/Γ

VALUE	DOCUMENT ID		TECN	COMMENT
0.01 ± 0.01	VRANA	00	DPWA	Multichannel

$\Gamma(N(\pi\pi)^{I=0}_{S\text{-wave}})/\Gamma_{\text{total}}$ Γ_{10}/Γ

VALUE	DOCUMENT ID		TECN	COMMENT
0.02 ± 0.01	VRANA	00	DPWA	Multichannel

$\Gamma(N(1440)\pi)/\Gamma_{\text{total}}$ Γ_{11}/Γ

VALUE	DOCUMENT ID		TECN	COMMENT
0.02 ± 0.01	VRANA	00	DPWA	Multichannel

$N(2090)$ FOOTNOTES

[1] LONGACRE 78 values are from a search for poles in the unitarized T-matrix. The first (second) value uses, in addition to $\pi N \rightarrow N\pi\pi$ data, elastic amplitudes from a Saclay (CERN) partial-wave analysis.

$N(2090)$ REFERENCES

VRANA	00	PRPL 328 181	T.P. Vrana, S.A. Dytman,, T.-S.H. Lee	(PITT+)
PLOETZKE	98	PL B444 555	R. Ploetzke *et al.*	(Bonn SAPHIR Collab.)
MANLEY	92	PR D45 4002	D.M. Manley, E.M. Saleski	(KENT) IJP
Also	84	PR D30 904	D.M. Manley *et al.*	(VPI)
CUTKOSKY	80	Toronto Conf. 19	R.E. Cutkosky *et al.*	(CMU, LBL) IJP
Also	79	PR D20 2839	R.E. Cutkosky *et al.*	(CMU, LBL)
SAXON	80	NP B162 522	D.H. Saxon *et al.*	(RHEL, BRIS) IJP
HOEHLER	79	PDAT 12-1	G. Hohler *et al.*	(KARLT) IJP
Also	80	Toronto Conf. 3	R. Koch	(KARLT) IJP
LONGACRE	78	PR D17 1795	R.S. Longacre *et al.*	(LBL, SLAC)

$N(2100)$ P_{11}

$I(J^P) = \frac{1}{2}(\frac{1}{2}^+)$ Status: *

OMITTED FROM SUMMARY TABLE

$N(2100)$ BREIT-WIGNER MASS

VALUE (MeV)	DOCUMENT ID		TECN	COMMENT
$\approx$ 2100 OUR ESTIMATE				
1885 ± 30	MANLEY	92	IPWA	$\pi N \rightarrow \pi N$ & $N\pi\pi$
2125 ± 75	CUTKOSKY	80	IPWA	$\pi N \rightarrow \pi N$
2050 ± 20	HOEHLER	79	IPWA	$\pi N \rightarrow \pi N$
• • • We do not use the following data for averages, fits, limits, etc. • • •				
2084 ± 93	VRANA	00	DPWA	Multichannel
$1986 \pm 26^{+10}_{-30}$	PLOETZKE	98	SPEC	$\gamma p \rightarrow p\eta'(958)$
2203 ± 70	BATINIC	95	DPWA	$\pi N \rightarrow N\pi$, $N\eta$

$N(2100)$ BREIT-WIGNER WIDTH

VALUE (MeV)	DOCUMENT ID		TECN	COMMENT
113 ± 44	MANLEY	92	IPWA	$\pi N \rightarrow \pi N$ & $N\pi\pi$
260 ± 100	CUTKOSKY	80	IPWA	$\pi N \rightarrow \pi N$
200 ± 30	HOEHLER	79	IPWA	$\pi N \rightarrow \pi N$
• • • We do not use the following data for averages, fits, limits, etc. • • •				
1077 ± 643	VRANA	00	DPWA	Multichannel
$296 \pm 100^{+60}_{-10}$	PLOETZKE	98	SPEC	$\gamma p \rightarrow p\eta'(958)$
418 ± 171	BATINIC	95	DPWA	$\pi N \rightarrow N\pi$, $N\eta$

$N(2100)$ POLE POSITION

REAL PART

VALUE (MeV)	DOCUMENT ID		TECN	COMMENT
2120 ± 40	CUTKOSKY	80	IPWA	$\pi N \rightarrow \pi N$
• • • We do not use the following data for averages, fits, limits, etc. • • •				
1810	VRANA	00	DPWA	Multichannel
not seen	ARNDT	91	DPWA	$\pi N \rightarrow \pi N$ Soln SM90

$-2\times$IMAGINARY PART

VALUE (MeV)	DOCUMENT ID		TECN	COMMENT
240 ± 80	CUTKOSKY	80	IPWA	$\pi N \rightarrow \pi N$
• • • We do not use the following data for averages, fits, limits, etc. • • •				
622	VRANA	00	DPWA	Multichannel
not seen	ARNDT	91	DPWA	$\pi N \rightarrow \pi N$ Soln SM90

$N(2100)$ ELASTIC POLE RESIDUE

MODULUS $|r|$

VALUE (MeV)	DOCUMENT ID		TECN	COMMENT
14 ± 7	CUTKOSKY	80	IPWA	$\pi N \rightarrow \pi N$

PHASE θ

VALUE (°)	DOCUMENT ID		TECN	COMMENT
35 ± 25	CUTKOSKY	80	IPWA	$\pi N \rightarrow \pi N$

$N(2100)$ DECAY MODES

	Mode	Fraction (Γ_i/Γ)
Γ_1	$N\pi$	
Γ_2	$N\eta$	(61 ± 60) %
Γ_3	ΛK	
Γ_4	$N\pi\pi$	
Γ_5	$\Delta(1232)\pi$, P-wave	
Γ_6	$N\rho$, S=1/2, P-wave	
Γ_7	$N(\pi\pi)^{I=0}_{S\text{-wave}}$	

$N(2100)$ BRANCHING RATIOS

$\Gamma(N\pi)/\Gamma_{\text{total}}$ Γ_1/Γ

VALUE	DOCUMENT ID		TECN	COMMENT
0.15 ± 0.06	MANLEY	92	IPWA	$\pi N \rightarrow \pi N$ & $N\pi\pi$
0.12 ± 0.03	CUTKOSKY	80	IPWA	$\pi N \rightarrow \pi N$
0.10 ± 0.04	HOEHLER	79	IPWA	$\pi N \rightarrow \pi N$
• • • We do not use the following data for averages, fits, limits, etc. • • •				
0.02 ± 0.05	VRANA	00	DPWA	Multichannel
0.11 ± 0.07	BATINIC	95	DPWA	$\pi N \rightarrow N\pi$, $N\eta$

$\Gamma(N\eta)/\Gamma_{\text{total}}$ Γ_2/Γ

VALUE	DOCUMENT ID		TECN	COMMENT
0.61 ± 0.61	VRANA	00	DPWA	Multichannel
• • • We do not use the following data for averages, fits, limits, etc. • • •				
0.86 ± 0.07	BATINIC	95	DPWA	$\pi N \rightarrow N\pi$, $N\eta$

$\Gamma(\Lambda K)/\Gamma_{total}$ Γ_3/Γ

VALUE	DOCUMENT ID		TECN	COMMENT
0.21 ± 0.20	VRANA	00	DPWA	Multichannel

$(\Gamma_i\Gamma_f)^{1/2}/\Gamma_{total}$ in $N\pi \to N(2100) \to \Delta(1232)\pi$, P-wave $(\Gamma_1\Gamma_5)^{1/2}/\Gamma$

VALUE	DOCUMENT ID		TECN	COMMENT
-0.19 ± 0.08	MANLEY	92	IPWA	$\pi N \to \pi N$ & $N\pi\pi$

$\Gamma(\Delta(1232)\pi$, P-wave$)/\Gamma_{total}$ Γ_5/Γ

VALUE	DOCUMENT ID		TECN	COMMENT
0.02 ± 0.01	VRANA	00	DPWA	Multichannel

$\Gamma(N\rho$, S=1/2, P-wave$)/\Gamma_{total}$ Γ_6/Γ

VALUE	DOCUMENT ID		TECN	COMMENT
0.04 ± 0.01	VRANA	00	DPWA	Multichannel

$\Gamma(N(\pi\pi)^{I=0}_{S\text{-wave}})/\Gamma_{total}$ Γ_7/Γ

VALUE	DOCUMENT ID		TECN	COMMENT
0.10 ± 0.01	VRANA	00	DPWA	Multichannel

$N(2100)$ REFERENCES

VRANA	00	PRPL 328 181	T.P. Vrana, S.A. Dytman,, T.-S.H. Lee	(PITT+)
PLOETZKE	98	PL B444 555	R. Ploetzke *et al.*	(Bonn SAPHIR Collab.)
BATINIC	95	PR C51 2310	M. Batinic *et al.*	(BOSK, UCLA)
Also	98	PR C57 1004 (erratum)	M. Batinic *et al.*	
MANLEY	92	PR D45 4002	D.M. Manley, E.M. Saleski	(KENT) IJP
Also	84	PR D30 904	D.M. Manley *et al.*	(VPI)
ARNDT	91	PR D43 2131	R.A. Arndt *et al.*	(VPI, TELE) IJP
CUTKOSKY	80	Toronto Conf. 19	R.E. Cutkosky *et al.*	(CMU, LBL) IJP
Also	79	PR D20 2839	R.E. Cutkosky *et al.*	(CMU, LBL)
HOEHLER	79	PDAT 12-1	G. Hohler *et al.*	(KARLT) IJP
Also	80	Toronto Conf. 3	R. Koch	(KARLT) IJP

$N(2190)$ G_{17}

$I(J^P) = \frac{1}{2}(\frac{7}{2}^-)$ Status: ****

Most of the results published before 1975 are now obsolete and have been omitted. They may be found in our 1982 edition, Physics Letters **111B** (1982).

$N(2190)$ BREIT-WIGNER MASS

VALUE (MeV)	DOCUMENT ID		TECN	COMMENT
2100 to 2200 ($\approx$ 2190) OUR ESTIMATE				
2127 ± 9	MANLEY	92	IPWA	$\pi N \to \pi N$ & $N\pi\pi$
2200 ± 70	CUTKOSKY	80	IPWA	$\pi N \to \pi N$
2140 ± 12	HOEHLER	79	IPWA	$\pi N \to \pi N$
2140 ± 40	HENDRY	78	MPWA	$\pi N \to \pi N$
• • • We do not use the following data for averages, fits, limits, etc. • • •				
2168 ± 18	VRANA	00	DPWA	Multichannel
2131	ARNDT	95	DPWA	$\pi N \to N\pi$
2198 ± 68	BATINIC	95	DPWA	$\pi N \to N\pi$, $N\eta$
2098	CRAWFORD	80	DPWA	$\gamma N \to \pi N$
2180	SAXON	80	DPWA	$\pi^- p \to \Lambda K^0$
2140	BAKER	79	DPWA	$\pi^- p \to n\eta$
2117	BARBOUR	78	DPWA	$\gamma N \to \pi N$

$N(2190)$ BREIT-WIGNER WIDTH

VALUE (MeV)	DOCUMENT ID		TECN	COMMENT
350 to 550 ($\approx$ 450) OUR ESTIMATE				
550 ± 50	MANLEY	92	IPWA	$\pi N \to \pi N$ & $N\pi\pi$
500 ± 150	CUTKOSKY	80	IPWA	$\pi N \to \pi N$
390 ± 30	HOEHLER	79	IPWA	$\pi N \to \pi N$
270 ± 50	HENDRY	78	MPWA	$\pi N \to \pi N$
• • • We do not use the following data for averages, fits, limits, etc. • • •				
453 ± 101	VRANA	00	DPWA	Multichannel
476	ARNDT	95	DPWA	$\pi N \to N\pi$
805 ± 140	BATINIC	95	DPWA	$\pi N \to N\pi$, $N\eta$
238	CRAWFORD	80	DPWA	$\gamma N \to \pi N$
80	SAXON	80	DPWA	$\pi^- p \to \Lambda K^0$
319	BAKER	79	DPWA	$\pi^- p \to n\eta$
220	BARBOUR	78	DPWA	$\gamma N \to \pi N$

$N(2190)$ POLE POSITION

REAL PART

VALUE (MeV)	DOCUMENT ID		TECN	COMMENT
1950 to 2150 ($\approx$ 2050) OUR ESTIMATE				
2030	ARNDT	95	DPWA	$\pi N \to N\pi$
2042	[1] HOEHLER	93	SPED	$\pi N \to \pi N$
2100 ± 50	CUTKOSKY	80	IPWA	$\pi N \to \pi N$
• • • We do not use the following data for averages, fits, limits, etc. • • •				
2107	VRANA	00	DPWA	Multichannel
2060	ARNDT	91	DPWA	$\pi N \to \pi N$ Soln SM90

$-2\times$IMAGINARY PART

VALUE (MeV)	DOCUMENT ID		TECN	COMMENT
350 to 550 ($\approx$ 450) OUR ESTIMATE				
460	ARNDT	95	DPWA	$\pi N \to N\pi$
482	[1] HOEHLER	93	SPED	$\pi N \to \pi N$
400 ± 160	CUTKOSKY	80	IPWA	$\pi N \to \pi N$
• • • We do not use the following data for averages, fits, limits, etc. • • •				
380	VRANA	00	DPWA	Multichannel
464	ARNDT	91	DPWA	$\pi N \to \pi N$ Soln SM90

$N(2190)$ ELASTIC POLE RESIDUE

MODULUS $|r|$

VALUE (MeV)	DOCUMENT ID		TECN	COMMENT
46	ARNDT	95	DPWA	$\pi N \to N\pi$
45	HOEHLER	93	SPED	$\pi N \to \pi N$
25 ± 10	CUTKOSKY	80	IPWA	$\pi N \to \pi N$
• • • We do not use the following data for averages, fits, limits, etc. • • •				
54	ARNDT	91	DPWA	$\pi N \to \pi N$ Soln SM90

PHASE θ

VALUE (°)	DOCUMENT ID		TECN	COMMENT
-23	ARNDT	95	DPWA	$\pi N \to N\pi$
-30 ± 50	CUTKOSKY	80	IPWA	$\pi N \to \pi N$
• • • We do not use the following data for averages, fits, limits, etc. • • •				
-44	ARNDT	91	DPWA	$\pi N \to \pi N$ Soln SM90

$N(2190)$ DECAY MODES

The following branching fractions are our estimates, not fits or averages.

	Mode	Fraction (Γ_i/Γ)
Γ_1	$N\pi$	10–20 %
Γ_2	$N\eta$	(0.0 ± 1.0) %
Γ_3	ΛK	
Γ_4	ΣK	
Γ_5	$N\pi\pi$	
Γ_6	$N\rho$	
Γ_7	$N\rho$, S=3/2, D-wave	
Γ_8	$p\gamma$, helicity=1/2	
Γ_9	$p\gamma$, helicity=3/2	
Γ_{10}	$n\gamma$, helicity=1/2	
Γ_{11}	$n\gamma$, helicity=3/2	

$N(2190)$ BRANCHING RATIOS

$\Gamma(N\pi)/\Gamma_{total}$ Γ_1/Γ

VALUE	DOCUMENT ID		TECN	COMMENT
0.1 to 0.2 OUR ESTIMATE				
0.22 ± 0.01	MANLEY	92	IPWA	$\pi N \to \pi N$ & $N\pi\pi$
0.12 ± 0.06	CUTKOSKY	80	IPWA	$\pi N \to \pi N$
0.14 ± 0.02	HOEHLER	79	IPWA	$\pi N \to \pi N$
0.16 ± 0.04	HENDRY	78	MPWA	$\pi N \to \pi N$
• • • We do not use the following data for averages, fits, limits, etc. • • •				
0.20 ± 0.04	VRANA	00	DPWA	Multichannel
0.23	ARNDT	95	DPWA	$\pi N \to N\pi$
0.19 ± 0.05	BATINIC	95	DPWA	$\pi N \to N\pi$, $N\eta$

$\Gamma(N\eta)/\Gamma_{total}$ Γ_2/Γ

VALUE	DOCUMENT ID		TECN	COMMENT
0.00 ±0.01	VRANA	00	DPWA	Multichannel
• • • We do not use the following data for averages, fits, limits, etc. • • •				
0.001 ± 0.003	BATINIC	95	DPWA	$\pi N \to N\pi$, $N\eta$

$(\Gamma_i\Gamma_f)^{1/2}/\Gamma_{total}$ in $N\pi \to N(2190) \to N\eta$ $(\Gamma_1\Gamma_2)^{1/2}/\Gamma$

VALUE	DOCUMENT ID		TECN	COMMENT
• • • We do not use the following data for averages, fits, limits, etc. • • •				
$+0.052$	BAKER	79	DPWA	$\pi^- p \to n\eta$

$(\Gamma_i\Gamma_f)^{1/2}/\Gamma_{total}$ in $N\pi \to N(2190) \to \Lambda K$ $(\Gamma_1\Gamma_3)^{1/2}/\Gamma$

VALUE	DOCUMENT ID		TECN	COMMENT
-0.02	BELL	83	DPWA	$\pi^- p \to \Lambda K^0$
-0.02	SAXON	80	DPWA	$\pi^- p \to \Lambda K^0$

$(\Gamma_i\Gamma_f)^{1/2}/\Gamma_{total}$ in $N\pi \to N(2190) \to \Sigma K$ $(\Gamma_1\Gamma_4)^{1/2}/\Gamma$

VALUE	DOCUMENT ID		TECN	COMMENT
• • • We do not use the following data for averages, fits, limits, etc. • • •				
0.014 to 0.019	[2] DEANS	75	DPWA	$\pi N \to \Sigma K$

$(\Gamma_i\Gamma_f)^{1/2}/\Gamma_{total}$ in $N\pi \to N(2190) \to N\rho$, S=3/2, D-wave $(\Gamma_1\Gamma_7)^{1/2}/\Gamma$

VALUE	DOCUMENT ID		TECN	COMMENT
-0.25 ± 0.03	MANLEY	92	IPWA	$\pi N \to \pi N$ & $N\pi\pi$

$\Gamma(N\rho, S$=3/2, D-wave$)/\Gamma_{total}$ Γ_7/Γ

VALUE	DOCUMENT ID		TECN	COMMENT
0.29 ± 0.28	VRANA	00	DPWA	Multichannel

$N(2190)$ PHOTON DECAY AMPLITUDES

$N(2190) \to p\gamma$, helicity-1/2 amplitude $A_{1/2}$

VALUE (GeV$^{-1/2}$)	DOCUMENT ID		TECN	COMMENT
• • • We do not use the following data for averages, fits, limits, etc. • • •				
-0.055	CRAWFORD	80	DPWA	$\gamma N \to \pi N$
-0.030	BARBOUR	78	DPWA	$\gamma N \to \pi N$

$N(2190) \to p\gamma$, helicity-3/2 amplitude $A_{3/2}$

VALUE (GeV$^{-1/2}$)	DOCUMENT ID		TECN	COMMENT
• • • We do not use the following data for averages, fits, limits, etc. • • •				
0.081	CRAWFORD	80	DPWA	$\gamma N \to \pi N$
$+0.180$	BARBOUR	78	DPWA	$\gamma N \to \pi N$

$N(2190) \to n\gamma$, helicity-1/2 amplitude $A_{1/2}$

VALUE (GeV$^{-1/2}$)	DOCUMENT ID		TECN	COMMENT
• • • We do not use the following data for averages, fits, limits, etc. • • •				
-0.042	CRAWFORD	80	DPWA	$\gamma N \to \pi N$
-0.085	BARBOUR	78	DPWA	$\gamma N \to \pi N$

$N(2190) \to n\gamma$, helicity-3/2 amplitude $A_{3/2}$

VALUE (GeV$^{-1/2}$)	DOCUMENT ID		TECN	COMMENT
• • • We do not use the following data for averages, fits, limits, etc. • • •				
-0.126	CRAWFORD	80	DPWA	$\gamma N \to \pi N$
$+0.007$	BARBOUR	78	DPWA	$\gamma N \to \pi N$

$N(2190)$ $\gamma p \to \Lambda K^+$ AMPLITUDES

$(\Gamma_i\Gamma_f)^{1/2}/\Gamma_{total}$ in $p\gamma \to N(2190) \to \Lambda K^+$ (E_{4-} amplitude)

VALUE (units 10^{-3})	DOCUMENT ID		TECN
• • • We do not use the following data for averages, fits, limits, etc. • • •			
2.5 ± 1.0	WORKMAN	90	DPWA
2.04	TANABE	89	DPWA

$p\gamma \to N(2190) \to \Lambda K^+$ phase angle θ (E_{4-} amplitude)

VALUE (degrees)	DOCUMENT ID		TECN
• • • We do not use the following data for averages, fits, limits, etc. • • •			
-4 ± 9	WORKMAN	90	DPWA
-27.5	TANABE	89	DPWA

$(\Gamma_i\Gamma_f)^{1/2}/\Gamma_{total}$ in $p\gamma \to N(2190) \to \Lambda K^+$ (M_{4-} amplitude)

VALUE (units 10^{-3})	DOCUMENT ID		TECN
• • • We do not use the following data for averages, fits, limits, etc. • • •			
-7.0 ± 0.7	WORKMAN	90	DPWA
-5.78	TANABE	89	DPWA

$N(2190)$ FOOTNOTES

[1] See HOEHLER 93 for a detailed discussion of the evidence for and the pole parameters of N and Δ resonances as determined from Argand diagrams of πN elastic partial-wave amplitudes and from plots of the speeds with which the amplitudes traverse the diagrams.
[2] The range given for DEANS 75 is from the four best solutions. Disagrees with $\pi^+ p \to \Sigma^+ K^+$ data of WINNIK 77 around 1920 MeV.

$N(2190)$ REFERENCES

For early references, see Physics Letters **111B** 70 (1982).

VRANA	00	PRPL 328 181	T.P. Vrana, S.A. Dytman,, T.-S.H. Lee	(PITT+)
ARNDT	95	PR C52 2120	R.A. Arndt *et al.*	(VPI, BRCO)
BATINIC	95	PR C51 2310	M. Batinic *et al.*	(BOSK, UCLA)
Also	98	PR C57 1004 (erratum)	M. Batinic *et al.*	
HOEHLER	93	πN Newsletter 9 1	G. Hohler	(KARL)
MANLEY	92	PR D45 4002	D.M. Manley, E.M. Saleski	(KENT) IJP
Also	84	PR D30 904	D.M. Manley *et al.*	(VPI)
ARNDT	91	PR D43 2131	R.A. Arndt *et al.*	(VPI, TELE) IJP
WORKMAN	90	PR C42 781	R.L. Workman	(VPI)
TANABE	89	PR C39 741	H. Tanabe, M. Kohno, C. Bennhold	(MANZ)
Also	89	NC 102A 193	M. Kohno, H. Tanabe, C. Bennhold	(MANZ)
BELL	83	NP B222 389	K.W. Bell *et al.*	(RL) IJP
PDG	82	PL 111B	M. Roos *et al.*	(HELS, CIT, CERN)
CRAWFORD	80	Toronto Conf. 107	R.L. Crawford	(GLAS)
CUTKOSKY	80	Toronto Conf. 19	R.E. Cutkosky *et al.*	(CMU, LBL) IJP
Also	79	PR D20 2839	R.E. Cutkosky *et al.*	(CMU, LBL) IJP
SAXON	80	NP B162 522	D.H. Saxon *et al.*	(RHEL, BRIS) IJP
BAKER	79	NP B156 93	R.D. Baker *et al.*	(RHEL) IJP
HOEHLER	79	PDAT 12-1	G. Hohler *et al.*	(KARLT) IJP
Also	80	Toronto Conf. 3	R. Koch	(KARLT) IJP
BARBOUR	78	NP B141 253	I.M. Barbour, R.L. Crawford, N.H. Parsons	(GLAS)
HENDRY	78	PRL 41 222	A.W. Hendry	(IND, LBL) IJP
Also	81	ANP 136 1	A.W. Hendry	(IND)
WINNIK	77	NP B128 66	M. Winnik *et al.*	(HAIF) I
DEANS	75	NP B96 90	S.R. Deans *et al.*	(SFLA, ALAH) IJP

$N(2200)$ D_{15}

$I(J^P) = \frac{1}{2}(\frac{5}{2}^-)$ Status: **

OMITTED FROM SUMMARY TABLE

The mass is not well determined. A few early results have been omitted.

$N(2200)$ BREIT-WIGNER MASS

VALUE (MeV)	DOCUMENT ID		TECN	COMMENT
≈ 2200 OUR ESTIMATE				
1900	BELL	83	DPWA	$\pi^- p \to \Lambda K^0$
2180 ± 80	CUTKOSKY	80	IPWA	$\pi N \to \pi N$
1920	SAXON	80	DPWA	$\pi^- p \to \Lambda K^0$
2228 ± 30	HOEHLER	79	IPWA	$\pi N \to \pi N$
• • • We do not use the following data for averages, fits, limits, etc. • • •				
2240 ± 65	BATINIC	95	DPWA	$\pi N \to N\pi$, $N\eta$

$N(2200)$ BREIT-WIGNER WIDTH

VALUE (MeV)	DOCUMENT ID		TECN	COMMENT
130	BELL	83	DPWA	$\pi^- p \to \Lambda K^0$
400 ± 100	CUTKOSKY	80	IPWA	$\pi N \to \pi N$
220	SAXON	80	DPWA	$\pi^- p \to \Lambda K^0$
310 ± 50	HOEHLER	79	IPWA	$\pi N \to \pi N$
• • • We do not use the following data for averages, fits, limits, etc. • • •				
761 ± 139	BATINIC	95	DPWA	$\pi N \to N\pi$, $N\eta$

$N(2200)$ POLE POSITION

REAL PART

VALUE (MeV)	DOCUMENT ID		TECN	COMMENT
2100 ± 60	CUTKOSKY	80	IPWA	$\pi N \to \pi N$

$-2\times$IMAGINARY PART

VALUE (MeV)	DOCUMENT ID		TECN	COMMENT
360 ± 80	CUTKOSKY	80	IPWA	$\pi N \to \pi N$

$N(2200)$ ELASTIC POLE RESIDUE

MODULUS $|r|$

VALUE (MeV)	DOCUMENT ID		TECN	COMMENT
20 ± 10	CUTKOSKY	80	IPWA	$\pi N \to \pi N$

PHASE θ

VALUE (°)	DOCUMENT ID		TECN	COMMENT
-90 ± 50	CUTKOSKY	80	IPWA	$\pi N \to \pi N$

$N(2200)$ DECAY MODES

	Mode
Γ_1	$N\pi$
Γ_2	$N\eta$
Γ_3	ΛK

$N(2200)$ BRANCHING RATIOS

$\Gamma(N\pi)/\Gamma_{total}$ Γ_1/Γ

VALUE	DOCUMENT ID		TECN	COMMENT
0.10 ± 0.03	CUTKOSKY	80	IPWA	$\pi N \to \pi N$
0.07 ± 0.02	HOEHLER	79	IPWA	$\pi N \to \pi N$
• • • We do not use the following data for averages, fits, limits, etc. • • •				
0.08 ± 0.04	BATINIC	95	DPWA	$\pi N \to N\pi$, $N\eta$

$\Gamma(N\eta)/\Gamma_{total}$ Γ_2/Γ

VALUE	DOCUMENT ID		TECN	COMMENT
• • • We do not use the following data for averages, fits, limits, etc. • • •				
0.001 ± 0.01	BATINIC	95	DPWA	$\pi N \to N\pi$, $N\eta$

$(\Gamma_i\Gamma_f)^{1/2}/\Gamma_{total}$ in $N\pi \to N(2200) \to N\eta$ $(\Gamma_1\Gamma_2)^{1/2}/\Gamma$

VALUE	DOCUMENT ID		TECN	COMMENT
0.066	BAKER	79	DPWA	$\pi^- p \to n\eta$

$(\Gamma_i\Gamma_f)^{1/2}/\Gamma_{total}$ in $N\pi \to N(2200) \to \Lambda K$ $(\Gamma_1\Gamma_3)^{1/2}/\Gamma$

VALUE	DOCUMENT ID		TECN	COMMENT
-0.03	BELL	83	DPWA	$\pi^- p \to \Lambda K^0$
-0.05	SAXON	80	DPWA	$\pi^- p \to \Lambda K^0$

$N(2200)$ REFERENCES

BATINIC	95	PR C51 2310	M. Batinic *et al.*	(BOSK, UCLA)
Also	98	PR C57 1004 (erratum)	M. Batinic *et al.*	
BELL	83	NP B222 389	K.W. Bell *et al.*	(RL) IJP
CUTKOSKY	80	Toronto Conf. 19	R.E. Cutkosky *et al.*	(CMU, LBL) IJP
Also	79	PR D20 2839	R.E. Cutkosky *et al.*	(CMU, LBL)
SAXON	80	NP B162 522	D.H. Saxon *et al.*	(RHEL, BRIS) IJP
BAKER	79	NP B156 93	R.D. Baker *et al.*	(RHEL) IJP
HOEHLER	79	PDAT 12-1	G. Hohler *et al.*	(KARLT) IJP
Also	80	Toronto Conf. 3	R. Koch	(KARLT) IJP

$N(2200)$ H_{19}

$I(J^P) = \frac{1}{2}(\frac{9}{2}^+)$ Status: ****

Most of the results published before 1975 are now obsolete and have been omitted. They may be found in our 1982 edition, Physics Letters **111B** (1982).

$N(2220)$ BREIT-WIGNER MASS

VALUE (MeV)	DOCUMENT ID		TECN	COMMENT
2180 to 2310 (≈ 2220) OUR ESTIMATE				
2230± 80	CUTKOSKY	80	IPWA	$\pi N \to \pi N$
2205± 10	HOEHLER	79	IPWA	$\pi N \to \pi N$
2300±100	HENDRY	78	MPWA	$\pi N \to \pi N$
• • • We do not use the following data for averages, fits, limits, etc. • • •				
2258	ARNDT	95	DPWA	$\pi N \to N\pi$
2050	BAKER	79	DPWA	$\pi^- p \to n\eta$

$N(2220)$ BREIT-WIGNER WIDTH

VALUE (MeV)	DOCUMENT ID		TECN	COMMENT
320 to 550 (≈ 400) OUR ESTIMATE				
500±150	CUTKOSKY	80	IPWA	$\pi N \to \pi N$
365± 30	HOEHLER	79	IPWA	$\pi N \to \pi N$
450±150	HENDRY	78	MPWA	$\pi N \to \pi N$
• • • We do not use the following data for averages, fits, limits, etc. • • •				
334	ARNDT	95	DPWA	$\pi N \to N\pi$

$N(2220)$ POLE POSITION

REAL PART

VALUE (MeV)	DOCUMENT ID		TECN	COMMENT
2100 to 2240 (≈ 2170) OUR ESTIMATE				
2203	ARNDT	95	DPWA	$\pi N \to N\pi$
2135	[1] HOEHLER	93	ARGD	$\pi N \to \pi N$
2160±80	CUTKOSKY	80	IPWA	$\pi N \to \pi N$
• • • We do not use the following data for averages, fits, limits, etc. • • •				
2253	ARNDT	91	DPWA	$\pi N \to \pi N$ Soln SM90

−2×IMAGINARY PART

VALUE (MeV)	DOCUMENT ID		TECN	COMMENT
370 to 570 (≈ 470) OUR ESTIMATE				
536	ARNDT	95	DPWA	$\pi N \to N\pi$
400	[1] HOEHLER	93	ARGD	$\pi N \to \pi N$
480±100	CUTKOSKY	80	IPWA	$\pi N \to \pi N$
• • • We do not use the following data for averages, fits, limits, etc. • • •				
640	ARNDT	91	DPWA	$\pi N \to \pi N$ Soln SM90

$N(2220)$ ELASTIC POLE RESIDUE

MODULUS $|r|$

VALUE (MeV)	DOCUMENT ID		TECN	COMMENT
68	ARNDT	95	DPWA	$\pi N \to N\pi$
40	HOEHLER	93	ARGD	$\pi N \to \pi N$
45 ± 20	CUTKOSKY	80	IPWA	$\pi N \to \pi N$
• • • We do not use the following data for averages, fits, limits, etc. • • •				
85	ARNDT	91	DPWA	$\pi N \to \pi N$ Soln SM90

PHASE θ

VALUE (°)	DOCUMENT ID		TECN	COMMENT
−43	ARNDT	95	DPWA	$\pi N \to N\pi$
−50	HOEHLER	93	ARGD	$\pi N \to \pi N$
−45 ± 25	CUTKOSKY	80	IPWA	$\pi N \to \pi N$
• • • We do not use the following data for averages, fits, limits, etc. • • •				
−62	ARNDT	91	DPWA	$\pi N \to \pi N$ Soln SM90

$N(2220)$ DECAY MODES

The following branching fractions are our estimates, not fits or averages.

	Mode	Fraction (Γ_i/Γ)
Γ_1	$N\pi$	10–20 %
Γ_2	$N\eta$	
Γ_3	ΛK	

$N(2220)$ BRANCHING RATIOS

$\Gamma(N\pi)/\Gamma_{\text{total}}$ Γ_1/Γ

VALUE	DOCUMENT ID		TECN	COMMENT
0.1 to 0.2 OUR ESTIMATE				
0.15 ±0.03	CUTKOSKY	80	IPWA	$\pi N \to \pi N$
0.18 ±0.015	HOEHLER	79	IPWA	$\pi N \to \pi N$
0.12 ±0.04	HENDRY	78	MPWA	$\pi N \to \pi N$
• • • We do not use the following data for averages, fits, limits, etc. • • •				
0.26	ARNDT	95	DPWA	$\pi N \to N\pi$

$(\Gamma_i\Gamma_f)^{1/2}/\Gamma_{\text{total}}$ in $N\pi \to N(2220) \to N\eta$ $(\Gamma_1\Gamma_2)^{1/2}/\Gamma$

VALUE	DOCUMENT ID		TECN	COMMENT
• • • We do not use the following data for averages, fits, limits, etc. • • •				
0.034	BAKER	79	DPWA	$\pi^- p \to n\eta$

$(\Gamma_i\Gamma_f)^{1/2}/\Gamma_{\text{total}}$ in $N\pi \to N(2220) \to \Lambda K$ $(\Gamma_1\Gamma_3)^{1/2}/\Gamma$

VALUE	DOCUMENT ID		TECN	COMMENT
not required	BELL	83	DPWA	$\pi^- p \to \Lambda K^0$
not seen	SAXON	80	DPWA	$\pi^- p \to \Lambda K^0$

$N(2220)$ FOOTNOTES

[1] See HOEHLER 93 for a detailed discussion of the evidence for and the pole parameters of N and Δ resonances as determined from Argand diagrams of πN elastic partial-wave amplitudes and from plots of the speeds with which the amplitudes traverse the diagrams.

$N(2220)$ REFERENCES

For early references, see Physics Letters **111B** 70 (1982).

ARNDT	95	PR C52 2120	R.A. Arndt *et al.*	(VPI, BRCO)
HOEHLER	93	πN Newsletter 9 1	G. Hohler	(KARL)
ARNDT	91	PR D43 2131	R.A. Arndt *et al.*	(VPI, TELE) IJP
BELL	83	NP B222 389	K.W. Bell *et al.*	(RL) IJP
PDG	82	PL 111B	M. Roos *et al.*	(HELS, CIT, CERN)
CUTKOSKY	80	Toronto Conf. 19	R.E. Cutkosky *et al.*	(CMU, LBL) IJP
Also	79	PR D20 2839	R.E. Cutkosky *et al.*	(CMU, LBL) IJP
SAXON	80	NP B162 522	D.H. Saxon *et al.*	(RHEL, BRIS) IJP
BAKER	79	NP B156 93	R.D. Baker *et al.*	(RHEL) IJP
HOEHLER	79	PDAT 12-1	G. Hohler *et al.*	(KARLT) IJP
Also	80	Toronto Conf. 3	R. Koch	(KARLT) IJP
HENDRY	78	PRL 41 222	A.W. Hendry	(IND, LBL) IJP
Also	81	ANP 136 1	A.W. Hendry	(IND)

$N(2250)$ G_{19}

$I(J^P) = \frac{1}{2}(\frac{9}{2}^-)$ Status: ****

$N(2250)$ BREIT-WIGNER MASS

VALUE (MeV)	DOCUMENT ID		TECN	COMMENT
2170 to 2310 (≈ 2250) OUR ESTIMATE				
2250± 80	CUTKOSKY	80	IPWA	$\pi N \to \pi N$
2268± 15	HOEHLER	79	IPWA	$\pi N \to \pi N$
2200±100	HENDRY	78	MPWA	$\pi N \to \pi N$
• • • We do not use the following data for averages, fits, limits, etc. • • •				
2291	ARNDT	95	DPWA	$\pi N \to N\pi$

$N(2250)$ BREIT-WIGNER WIDTH

VALUE (MeV)	DOCUMENT ID		TECN	COMMENT
290 to 470 (≈ 400) OUR ESTIMATE				
480±120	CUTKOSKY	80	IPWA	$\pi N \to \pi N$
300± 40	HOEHLER	79	IPWA	$\pi N \to \pi N$
350±100	HENDRY	78	MPWA	$\pi N \to \pi N$
• • • We do not use the following data for averages, fits, limits, etc. • • •				
772	ARNDT	95	DPWA	$\pi N \to N\pi$

$N(2250)$ POLE POSITION

REAL PART

VALUE (MeV)	DOCUMENT ID		TECN	COMMENT
2080 to 2200 (≈ 2140) OUR ESTIMATE				
2087	ARNDT	95	DPWA	$\pi N \to N\pi$
2187	[1] HOEHLER	93	SPED	$\pi N \to \pi N$
2150±50	CUTKOSKY	80	IPWA	$\pi N \to \pi N$
• • • We do not use the following data for averages, fits, limits, etc. • • •				
2243	ARNDT	91	DPWA	$\pi N \to \pi N$ Soln SM90

−2×IMAGINARY PART

VALUE (MeV)	DOCUMENT ID		TECN	COMMENT
280 to 680 (≈ 480) OUR ESTIMATE				
680	ARNDT	95	DPWA	$\pi N \to N\pi$
388	[1] HOEHLER	93	SPED	$\pi N \to \pi N$
360±100	CUTKOSKY	80	IPWA	$\pi N \to \pi N$
• • • We do not use the following data for averages, fits, limits, etc. • • •				
650	ARNDT	91	DPWA	$\pi N \to \pi N$ Soln SM90

$N(2250)$ ELASTIC POLE RESIDUE

MODULUS $|r|$

VALUE (MeV)	DOCUMENT ID		TECN	COMMENT
24	ARNDT	95	DPWA	$\pi N \to N\pi$
21	HOEHLER	93	SPED	$\pi N \to \pi N$
20 ± 6	CUTKOSKY	80	IPWA	$\pi N \to \pi N$
• • • We do not use the following data for averages, fits, limits, etc. • • •				
47	ARNDT	91	DPWA	$\pi N \to \pi N$ Soln SM90

PHASE θ

VALUE (°)	DOCUMENT ID		TECN	COMMENT
-44	ARNDT	95	DPWA	$\pi N \to N\pi$
-50 ± 20	CUTKOSKY	80	IPWA	$\pi N \to \pi N$
• • • We do not use the following data for averages, fits, limits, etc. • • •				
-37	ARNDT	91	DPWA	$\pi N \to \pi N$ Soln SM90

$N(2250)$ DECAY MODES

The following branching fractions are our estimates, not fits or averages.

	Mode	Fraction (Γ_i/Γ)
Γ_1	$N\pi$	5–15 %
Γ_2	$N\eta$	
Γ_3	ΛK	

$N(2250)$ BRANCHING RATIOS

$\Gamma(N\pi)/\Gamma_{\text{total}}$ Γ_1/Γ

VALUE	DOCUMENT ID		TECN	COMMENT
0.05 to 0.15 OUR ESTIMATE				
0.10 ± 0.02	CUTKOSKY	80	IPWA	$\pi N \to \pi N$
0.10 ± 0.02	HOEHLER	79	IPWA	$\pi N \to \pi N$
0.09 ± 0.02	HENDRY	78	MPWA	$\pi N \to \pi N$
• • • We do not use the following data for averages, fits, limits, etc. • • •				
0.10	ARNDT	95	DPWA	$\pi N \to N\pi$

$(\Gamma_i\Gamma_f)^{1/2}/\Gamma_{\text{total}}$ in $N\pi \to N(2250) \to N\eta$ $(\Gamma_1\Gamma_2)^{1/2}/\Gamma$

VALUE	DOCUMENT ID		TECN	COMMENT
• • • We do not use the following data for averages, fits, limits, etc. • • •				
-0.043	BAKER	79	DPWA	$\pi^- p \to n\eta$

$(\Gamma_i\Gamma_f)^{1/2}/\Gamma_{\text{total}}$ in $N\pi \to N(2250) \to \Lambda K$ $(\Gamma_1\Gamma_3)^{1/2}/\Gamma$

VALUE	DOCUMENT ID		TECN	COMMENT
-0.02	BELL	83	DPWA	$\pi^- p \to \Lambda K^0$
not seen	SAXON	80	DPWA	$\pi^- p \to \Lambda K^0$

$N(2250)$ FOOTNOTES

[1] See HOEHLER 93 for a detailed discussion of the evidence for and the pole parameters of N and Δ resonances as determined from Argand diagrams of πN elastic partial-wave amplitudes and from plots of the speeds with which the amplitudes traverse the diagrams.

$N(2250)$ REFERENCES

ARNDT	95	PR C52 2120	R.A. Arndt *et al.*	(VPI, BRCO)
HOEHLER	93	πN Newsletter 9 1	G. Hohler	(KARL)
ARNDT	91	PR D43 2131	R.A. Arndt *et al.*	(VPI, TELE) IJP
BELL	83	NP B222 389	K.W. Bell *et al.*	(RL) IJP
CUTKOSKY	80	Toronto Conf. 19	R.E. Cutkosky *et al.*	(CMU, LBL) IJP
Also	79	PR D20 2839	R.E. Cutkosky *et al.*	(CMU, LBL) IJP
SAXON	80	NP B162 522	D.H. Saxon *et al.*	(RHEL, BRIS) IJP
BAKER	79	NP B156 93	R.D. Baker *et al.*	(RHEL) IJP
HOEHLER	79	PDAT 12-1	G. Hohler *et al.*	(KARLT) IJP
Also	80	Toronto Conf. 3	R. Koch	(KARLT) IJP
HENDRY	78	PRL 41 222	A.W. Hendry	(IND, LBL) IJP
Also	81	ANP 136 1	A.W. Hendry	(IND)

$N(2600)$ $I_{1,11}$

$I(J^P) = \frac{1}{2}(\frac{11}{2}^-)$ Status: ***

$N(2600)$ BREIT-WIGNER MASS

VALUE (MeV)	DOCUMENT ID		TECN	COMMENT
2550 to 2750 (≈ 2600) OUR ESTIMATE				
2577 ± 50	HOEHLER	79	IPWA	$\pi N \to \pi N$
2700 ± 100	HENDRY	78	MPWA	$\pi N \to \pi N$

$N(2600)$ BREIT-WIGNER WIDTH

VALUE (MeV)	DOCUMENT ID		TECN	COMMENT
500 to 800 (≈ 650) OUR ESTIMATE				
400 ± 100	HOEHLER	79	IPWA	$\pi N \to \pi N$
900 ± 100	HENDRY	78	MPWA	$\pi N \to \pi N$

$N(2600)$ DECAY MODES

	Mode	Fraction (Γ_i/Γ)
Γ_1	$N\pi$	5–10 %

$N(2600)$ BRANCHING RATIOS

$\Gamma(N\pi)/\Gamma_{\text{total}}$ Γ_1/Γ

VALUE	DOCUMENT ID		TECN	COMMENT
0.05 to 0.1 OUR ESTIMATE				
0.05 ± 0.01	HOEHLER	79	IPWA	$\pi N \to \pi N$
0.08 ± 0.02	HENDRY	78	MPWA	$\pi N \to \pi N$

$N(2600)$ REFERENCES

HOEHLER	79	PDAT 12-1	G. Hohler *et al.*	(KARLT) IJP
Also	80	Toronto Conf. 3	R. Koch	(KARLT) IJP
HENDRY	78	PRL 41 222	A.W. Hendry	(IND, LBL) IJP
Also	81	ANP 136 1	A.W. Hendry	(IND)

$N(2700)$ $K_{1,13}$

$I(J^P) = \frac{1}{2}(\frac{13}{2}^+)$ Status: **

OMITTED FROM SUMMARY TABLE

$N(2700)$ BREIT-WIGNER MASS

VALUE (MeV)	DOCUMENT ID		TECN	COMMENT
≈ 2700 OUR ESTIMATE				
2612 ± 45	HOEHLER	79	IPWA	$\pi N \to \pi N$
3000 ± 100	HENDRY	78	MPWA	$\pi N \to \pi N$

$N(2700)$ BREIT-WIGNER WIDTH

VALUE (MeV)	DOCUMENT ID		TECN	COMMENT
350 ± 50	HOEHLER	79	IPWA	$\pi N \to \pi N$
900 ± 150	HENDRY	78	MPWA	$\pi N \to \pi N$

$N(2700)$ DECAY MODES

	Mode
Γ_1	$N\pi$

$N(2700)$ BRANCHING RATIOS

$\Gamma(N\pi)/\Gamma_{\text{total}}$ Γ_1/Γ

VALUE	DOCUMENT ID		TECN	COMMENT
0.04 ± 0.01	HOEHLER	79	IPWA	$\pi N \to \pi N$
0.07 ± 0.02	HENDRY	78	MPWA	$\pi N \to \pi N$

$N(2700)$ REFERENCES

HOEHLER	79	PDAT 12-1	G. Hohler *et al.*	(KARLT) IJP
Also	80	Toronto Conf. 3	R. Koch	(KARLT) IJP
HENDRY	78	PRL 41 222	A.W. Hendry	(IND, LBL) IJP
Also	81	ANP 136 1	A.W. Hendry	(IND)

See key on page 323

$N(\sim 3000$ Region) Partial-Wave Analyses

OMITTED FROM SUMMARY TABLE

We list here miscellaneous high-mass candidates for isospin-1/2 resonances found in partial-wave analyses.

Our 1982 edition had an $N(3245)$, an $N(3690)$, and an $N(3755)$, each a narrow peak seen in a production experiment. Since nothing has been heard from them since the 1960's, we declare them to be dead. There was also an $N(3030)$, deduced from total cross-section and 180° elastic cross-section measurements; it is the KOCH 80 $L_{1,15}$ state below.

$N(\sim 3000)$ BREIT-WIGNER MASS

VALUE (MeV)	*DOCUMENT ID*		*TECN*	*COMMENT*
≈ 3000 OUR ESTIMATE				
2600	KOCH	80	IPWA	$\pi N \to \pi N\ D_{13}$
3100	KOCH	80	IPWA	$\pi N \to \pi N\ L_{1,15}$ wave
3500	KOCH	80	IPWA	$\pi N \to \pi N\ M_{1,17}$ wave
3500 to 4000	KOCH	80	IPWA	$\pi N \to \pi N\ N_{1,19}$ wave
3500 ± 200	HENDRY	78	MPWA	$\pi N \to \pi N\ L_{1,15}$ wave
3800 ± 200	HENDRY	78	MPWA	$\pi N \to \pi N\ M_{1,17}$ wave
4100 ± 200	HENDRY	78	MPWA	$\pi N \to \pi N\ N_{1,19}$ wave

$N(\sim 3000)$ BREIT-WIGNER WIDTH

VALUE (MeV)	*DOCUMENT ID*		*TECN*	*COMMENT*
1300 ± 200	HENDRY	78	MPWA	$\pi N \to \pi N\ L_{1,15}$ wave
1600 ± 200	HENDRY	78	MPWA	$\pi N \to \pi N\ M_{1,17}$ wave
1900 ± 300	HENDRY	78	MPWA	$\pi N \to \pi N\ N_{1,19}$ wave

$N(\sim 3000)$ DECAY MODES

	Mode
Γ_1	$N\pi$

$N(\sim 3000)$ BRANCHING RATIOS

$\Gamma(N\pi)/\Gamma_{\text{total}}$					Γ_1/Γ
VALUE	*DOCUMENT ID*		*TECN*	*COMMENT*	
0.055 ± 0.02	HENDRY	78	MPWA	$\pi N \to \pi N\ L_{1,15}$ wave	
0.040 ± 0.015	HENDRY	78	MPWA	$\pi N \to \pi N\ M_{1,17}$ wave	
0.030 ± 0.015	HENDRY	78	MPWA	$\pi N \to \pi N\ N_{1,19}$ wave	

$N(\sim 3000)$ REFERENCES

KOCH	80	Toronto Conf. 3	R. Koch	(KARLT) IJP
HENDRY	78	PRL 41 222	A.W. Hendry	(IND, LBL) IJP
Also	81	ANP 136 1	A.W. Hendry	(IND) IJP

Δ BARYONS
(S = 0, I = 3/2)

$\Delta^{++} = uuu$, $\Delta^{+} = uud$, $\Delta^{0} = udd$, $\Delta^{-} = ddd$

Δ(1232) P_{33}

$I(J^P) = \frac{3}{2}(\frac{3}{2}^+)$ Status: ****

Most of the results published before 1977 are now obsolete and have been omitted. They may be found in our 1982 edition, Physics Letters **111B** (1982).

Δ(1232) BREIT-WIGNER MASSES

MIXED CHARGES

VALUE (MeV)	DOCUMENT ID		TECN	COMMENT
1230 to 1234 (≈ 1232) OUR ESTIMATE				
1231±1	MANLEY	92	IPWA	$\pi N \to \pi N$ & $N\pi\pi$
1232±3	CUTKOSKY	80	IPWA	$\pi N \to \pi N$
1233±2	HOEHLER	79	IPWA	$\pi N \to \pi N$
• • • We do not use the following data for averages, fits, limits, etc. • • •				
1228±1	PENNER	02C	DPWA	Multichannel
1234±5	VRANA	00	DPWA	Multichannel
1233	ARNDT	95	DPWA	$\pi N \to N\pi$

Δ(1232)++ MASS

VALUE (MeV)	DOCUMENT ID		TECN	COMMENT
• • • We do not use the following data for averages, fits, limits, etc. • • •				
1231.88±0.29	BERNICHA	96		Fit to PEDRONI 78
1230.5 ±0.2	ABAEV	95	IPWA	$\pi N \to \pi N$
1230.9 ±0.3	KOCH	80B	IPWA	$\pi N \to \pi N$
1231.1 ±0.2	PEDRONI	78		$\pi N \to \pi N$ 70–370 MeV

Δ(1232)+ MASS

VALUE (MeV)	DOCUMENT ID		TECN	COMMENT
• • • We do not use the following data for averages, fits, limits, etc. • • •				
1231.6	CRAWFORD	80	DPWA	$\gamma N \to \pi N$
1234.9±1.4	MIROSHNIC...	79		Fit photoproduction
1231.2	BARBOUR	78	DPWA	$\gamma N \to \pi N$
1231.8	BERENDS	75	IPWA	$\gamma p \to \pi N$

Δ(1232)0 MASS

VALUE (MeV)	DOCUMENT ID		TECN	COMMENT
• • • We do not use the following data for averages, fits, limits, etc. • • •				
1234.35±0.75	BERNICHA	96		Fit to PEDRONI 78
1233.1 ±0.3	ABAEV	95	IPWA	$\pi N \to \pi N$
1233.6 ±0.5	KOCH	80B	IPWA	$\pi N \to \pi N$
1233.8 ±0.2	PEDRONI	78		$\pi N \to \pi N$ 70–370 MeV

$m_{\Delta^0} - m_{\Delta^{++}}$

VALUE (MeV)	DOCUMENT ID		TECN	COMMENT
• • • We do not use the following data for averages, fits, limits, etc. • • •				
2.25±0.68	BERNICHA	96		Fit to PEDRONI 78
2.6 ±0.4	ABAEV	95	IPWA	$\pi N \to \pi N$
2.7 ±0.3	[3] PEDRONI	78		See the masses

Δ(1232) BREIT-WIGNER WIDTHS

MIXED CHARGES

VALUE (MeV)	DOCUMENT ID		TECN	COMMENT
115 to 125 (≈ 120) OUR ESTIMATE				
118± 4	MANLEY	92	IPWA	$\pi N \to \pi N$ & $N\pi\pi$
120± 5	CUTKOSKY	80	IPWA	$\pi N \to \pi N$
116± 5	HOEHLER	79	IPWA	$\pi N \to \pi N$
• • • We do not use the following data for averages, fits, limits, etc. • • •				
106± 1	PENNER	02C	DPWA	Multichannel
112±18	VRANA	00	DPWA	Multichannel
114	ARNDT	95	DPWA	$\pi N \to N\pi$

Δ(1232)++ WIDTH

VALUE (MeV)	DOCUMENT ID		TECN	COMMENT
• • • We do not use the following data for averages, fits, limits, etc. • • •				
109.07±0.48	BERNICHA	96		Fit to PEDRONI 78
111.0 ±1.0	KOCH	80B	IPWA	$\pi N \to \pi N$
111.3 ±0.5	PEDRONI	78		$\pi N \to \pi N$ 70–370 MeV

Δ(1232)+ WIDTH

VALUE (MeV)	DOCUMENT ID		TECN	COMMENT
• • • We do not use the following data for averages, fits, limits, etc. • • •				
111.2	CRAWFORD	80	DPWA	$\gamma N \to \pi N$
131.1±2.4	MIROSHNIC...	79		Fit photoproduction
111.0	BARBOUR	78	DPWA	$\gamma N \to \pi N$

Δ(1232)0 WIDTH

VALUE (MeV)	DOCUMENT ID		TECN	COMMENT
• • • We do not use the following data for averages, fits, limits, etc. • • •				
117.58±1.16	BERNICHA	96		Fit to PEDRONI 78
113.0 ±1.5	KOCH	80B	IPWA	$\pi N \to \pi N$
117.9 ±0.9	PEDRONI	78		$\pi N \to \pi N$ 70–370 MeV

Δ0-Δ++ WIDTH DIFFERENCE

VALUE (MeV)	DOCUMENT ID		TECN	COMMENT
• • • We do not use the following data for averages, fits, limits, etc. • • •				
8.45±1.11	BERNICHA	96		Fit to PEDRONI 78
5.1 ±1.0	ABAEV	95	IPWA	$\pi N \to \pi N$
6.6 ±1.0	PEDRONI	78		See the widths

Δ(1232) POLE POSITIONS

REAL PART, MIXED CHARGES

VALUE (MeV)	DOCUMENT ID		TECN	COMMENT
1209 to 1211 (≈ 1210) OUR ESTIMATE				
1211	ARNDT	95	DPWA	$\pi N \to N\pi$
1209	[4] HOEHLER	93	ARGD	$\pi N \to \pi N$
1210±1	CUTKOSKY	80	IPWA	$\pi N \to \pi N$
• • • We do not use the following data for averages, fits, limits, etc. • • •				
1217	VRANA	00	DPWA	Multichannel
1210	ARNDT	91	DPWA	$\pi N \to \pi N$ Soln SM90

−2×IMAGINARY PART, MIXED CHARGES

VALUE (MeV)	DOCUMENT ID		TECN	COMMENT
98 to 102 (≈ 100) OUR ESTIMATE				
100	ARNDT	95	DPWA	$\pi N \to N\pi$
100	[4] HOEHLER	93	ARGD	$\pi N \to \pi N$
100±2	CUTKOSKY	80	IPWA	$\pi N \to \pi N$
• • • We do not use the following data for averages, fits, limits, etc. • • •				
96	VRANA	00	DPWA	Multichannel
100	ARNDT	91	DPWA	$\pi N \to \pi N$ Soln SM90

REAL PART, Δ(1232)++

VALUE (MeV)	DOCUMENT ID		COMMENT
• • • We do not use the following data for averages, fits, limits, etc. • • •			
1212.50±0.24	BERNICHA	96	Fit to PEDRONI 78
1209.6 ±0.5	[5] VASAN	76B	Fit to CARTER 73
1210.5 to 1210.8	[6] VASAN	76B	Fit to CARTER 73

−2×IMAGINARY PART, Δ(1232)++

VALUE (MeV)	DOCUMENT ID		COMMENT
• • • We do not use the following data for averages, fits, limits, etc. • • •			
97.37±0.42	BERNICHA	96	Fit to PEDRONI 78
100.8 ±1.0	[5] VASAN	76B	Fit to CARTER 73
99.8 to 100	[6] VASAN	76B	Fit to CARTER 73

REAL PART, Δ(1232)+

VALUE (MeV)	DOCUMENT ID		TECN	COMMENT
• • • We do not use the following data for averages, fits, limits, etc. • • •				
1211 ±1 to 1212 ±1	HANSTEIN	96	DPWA	$\gamma N \to \pi N$
1206.9±0.9 to 1210.5 ±1.8	MIROSHNIC...	79		Fit photoproduction
1208.0±2.0	CAMPBELL	76		Fit photoproduction

−2×IMAGINARY PART, Δ(1232)+

VALUE (MeV)	DOCUMENT ID		TECN	COMMENT
• • • We do not use the following data for averages, fits, limits, etc. • • •				
102 ±2 to 99 ± 2	[1] HANSTEIN	96	DPWA	$\gamma N \to \pi N$
111.2±2.0 to 116.6 ± 2.2	MIROSHNIC...	79		Fit photoproduction
106 ±4	CAMPBELL	76		Fit photoproduction

[1] The second (lower) value of HANSTEIN 96 here goes with the second (higher) value of the real part in the preceding data block.

REAL PART, Δ(1232)0

VALUE (MeV)	DOCUMENT ID		COMMENT
• • • We do not use the following data for averages, fits, limits, etc. • • •			
1213.20±0.66	BERNICHA	96	Fit to PEDRONI 78
1210.75±0.6	[5] VASAN	76B	Fit to CARTER 73
1210.2	[6] VASAN	76B	Fit to CARTER 73

−2×IMAGINARY PART, Δ(1232)⁰

VALUE (MeV)	DOCUMENT ID		COMMENT
• • • We do not use the following data for averages, fits, limits, etc. • • •			
104.10 ±1.01	BERNICHA	96	Fit to PEDRONI 78
105.6 ±1.2	[5] VASAN	76B	Fit to CARTER 73
105.8 to 106.2	[6] VASAN	76B	Fit to CARTER 73

Δ(1232) ELASTIC POLE RESIDUES

ABSOLUTE VALUE, MIXED CHARGES

VALUE (MeV)	DOCUMENT ID		TECN	COMMENT
50	HOEHLER	93	ARGD	$\pi N \to \pi N$
53 ± 2	CUTKOSKY	80	IPWA	$\pi N \to \pi N$
• • • We do not use the following data for averages, fits, limits, etc. • • •				
38	[7] ARNDT	95	DPWA	$\pi N \to N\pi$
52	ARNDT	91	DPWA	$\pi N \to \pi N$ Soln SM90

PHASE, MIXED CHARGES

VALUE (°)	DOCUMENT ID		TECN	COMMENT
−48	HOEHLER	93	ARGD	$\pi N \to \pi N$
−47 ±1	CUTKOSKY	80	IPWA	$\pi N \to \pi N$
• • • We do not use the following data for averages, fits, limits, etc. • • •				
−22	[7] ARNDT	95	DPWA	$\pi N \to N\pi$
−31	ARNDT	91	DPWA	$\pi N \to \pi N$ Soln SM90

ABSOLUTE VALUE, Δ(1232)⁺⁺

VALUE (MeV)	DOCUMENT ID		COMMENT
• • • We do not use the following data for averages, fits, limits, etc. • • •			
52.4 to 53.2	[5] VASAN	76B	Fit to CARTER 73
52.1 to 52.4	[6] VASAN	76B	Fit to CARTER 73

PHASE, Δ(1232)⁺⁺

VALUE (rad)	DOCUMENT ID		COMMENT
• • • We do not use the following data for averages, fits, limits, etc. • • •			
−0.822 to −0.833	[5] VASAN	76B	Fit to CARTER 73
−0.823 to −0.830	[6] VASAN	76B	Fit to CARTER 73

ABSOLUTE VALUE, Δ(1232)⁰

VALUE (MeV)	DOCUMENT ID		COMMENT
• • • We do not use the following data for averages, fits, limits, etc. • • •			
54.8 to 55.0	[5] VASAN	76B	Fit to CARTER 73
55.2 to 55.3	[6] VASAN	76B	Fit to CARTER 73

PHASE, Δ(1232)⁰

VALUE (rad)	DOCUMENT ID		COMMENT
• • • We do not use the following data for averages, fits, limits, etc. • • •			
−0.840 to −0.847	[5] VASAN	76B	Fit to CARTER 73
−0.848 to −0.856	[6] VASAN	76B	Fit to CARTER 73

Δ(1232) DECAY MODES

The following branching fractions are our estimates, not fits or averages.

	Mode	Fraction (Γ_i/Γ)
Γ_1	$N\pi$	>99 %
Γ_2	$N\gamma$	0.52–0.60 %
Γ_3	$N\gamma$, helicity=1/2	0.11–0.13 %
Γ_4	$N\gamma$, helicity=3/2	0.41–0.47 %

Δ(1232) BRANCHING RATIOS

$\Gamma(N\pi)/\Gamma_{total}$ Γ_1/Γ

VALUE	DOCUMENT ID		TECN	COMMENT
0.993 to 0.995 OUR ESTIMATE				
1.0	MANLEY	92	IPWA	$\pi N \to \pi N$ & $N\pi\pi$
1.0	CUTKOSKY	80	IPWA	$\pi N \to \pi N$
1.0	HOEHLER	79	IPWA	$\pi N \to \pi N$
• • • We do not use the following data for averages, fits, limits, etc. • • •				
1.00	PENNER	02C	DPWA	Multichannel
1.00 ±0.01	VRANA	00	DPWA	Multichannel
1.0	ARNDT	95	DPWA	$\pi N \to N\pi$

Δ(1232) PHOTON DECAY AMPLITUDES

Δ(1232) → $N\gamma$, helicity-1/2 amplitude $A_{1/2}$

VALUE (GeV$^{-1/2}$)	DOCUMENT ID		TECN	COMMENT
−0.135 ±0.006 OUR ESTIMATE				
−0.129 ±0.001	ARNDT	02	DPWA	$\gamma p \to N\pi$
−0.1357 ±0.0013 ±0.0037	BLANPIED	01	LEGS	$\gamma p \to p\gamma,\ p\pi^0,\ n\pi^+$
−0.131 ±0.001	BECK	00	IPWA	$\vec{\gamma} p \to p\pi^0,\ n\pi^+$
−0.1294 ±0.0013	HANSTEIN	98	IPWA	$\gamma N \to \pi N$
−0.135 ±0.005	ARNDT	97	IPWA	$\gamma N \to \pi N$
−0.1278 ±0.0012	DAVIDSON	97	DPWA	$\gamma N \to \pi N$
−0.141 ±0.005	ARNDT	96	IPWA	$\gamma N \to \pi N$
−0.135 ±0.016	DAVIDSON	91B	FIT	$\gamma N \to \pi N$
−0.145 ±0.015	CRAWFORD	83	IPWA	$\gamma N \to \pi N$
−0.138 ±0.004	AWAJI	81	DPWA	$\gamma N \to \pi N$
−0.147 ±0.001	ARAI	80	DPWA	$\gamma N \to \pi N$ (fit 1)
−0.145 ±0.001	ARAI	80	DPWA	$\gamma N \to \pi N$ (fit 2)
−0.136 ±0.006	CRAWFORD	80	DPWA	$\gamma N \to \pi N$
• • • We do not use the following data for averages, fits, limits, etc. • • •				
−0.128	PENNER	02D	DPWA	Multichannel
−0.1312	HANSTEIN	98	DPWA	$\gamma N \to \pi N$
−0.143 ±0.004	LI	93	IPWA	$\gamma N \to \pi N$
−0.140 ±0.007	DAVIDSON	90	FIT	See DAVIDSON 91B
−0.142 ±0.007	BARBOUR	78	DPWA	$\gamma N \to \pi N$
−0.140	[8] NOELLE	78		$\gamma N \to \pi N$
−0.141 ±0.004	FELLER	76	DPWA	$\gamma N \to \pi N$

Δ(1232) → $N\gamma$, helicity-3/2 amplitude $A_{3/2}$

VALUE (GeV$^{-1/2}$)	DOCUMENT ID		TECN	COMMENT
−0.250 ±0.008 OUR ESTIMATE				
−0.243 ±0.001	ARNDT	02	DPWA	$\gamma p \to N\pi$
−0.2669 ±0.0016 ±0.0078	BLANPIED	01	LEGS	$\gamma p \to p\gamma,\ p\pi^0,\ n\pi^+$
−0.251 ±0.001	BECK	00	IPWA	$\vec{\gamma} p \to p\pi^0,\ n\pi^+$
−0.2466 ±0.0013	HANSTEIN	98	IPWA	$\gamma N \to \pi N$
−0.250 ±0.008	ARNDT	97	IPWA	$\gamma N \to \pi N$
−0.2524 ±0.0013	DAVIDSON	97	DPWA	$\gamma N \to \pi N$
−0.261 ±0.005	ARNDT	96	IPWA	$\gamma N \to \pi N$
−0.251 ±0.033	DAVIDSON	91B	FIT	$\gamma N \to \pi N$
−0.263 ±0.026	CRAWFORD	83	IPWA	$\gamma N \to \pi N$
−0.259 ±0.006	AWAJI	81	DPWA	$\gamma N \to \pi N$
−0.264 ±0.002	ARAI	80	DPWA	$\gamma N \to \pi N$ (fit 1)
−0.261 ±0.002	ARAI	80	DPWA	$\gamma N \to \pi N$ (fit 2)
−0.247 ±0.010	CRAWFORD	80	DPWA	$\gamma N \to \pi N$
• • • We do not use the following data for averages, fits, limits, etc. • • •				
−0.247	PENNER	02D	DPWA	Multichannel
−0.2522	HANSTEIN	98	DPWA	$\gamma N \to \pi N$
−0.262 ±0.004	LI	93	IPWA	$\gamma N \to \pi N$
−0.254 ±0.011	DAVIDSON	90	FIT	See DAVIDSON 91B
−0.271 ±0.010	BARBOUR	78	DPWA	$\gamma N \to \pi N$
−0.247	[8] NOELLE	78		$\gamma N \to \pi N$
−0.256 ±0.003	FELLER	76	DPWA	$\gamma N \to \pi N$

Δ(1232) → $N\gamma$, E_2/M_1 ratio

VALUE	DOCUMENT ID		TECN	COMMENT
−0.025 ±0.005 OUR ESTIMATE				
−0.020 ±0.002	ARNDT	02	DPWA	$\gamma p \to N\pi$
−0.0307 ±0.0026 ±0.0024	BLANPIED	01	LEGS	$\gamma p \to p\gamma,\ p\pi^0,\ n\pi^+$
−0.016 ±0.004 ±0.002	GALLER	01	DPWA	$\gamma p \to \gamma p$
−0.025 ±0.001 ±0.002	BECK	00	IPWA	$\vec{\gamma} p \to p\pi^0,\ n\pi^+$
−0.0254 ±0.0010	HANSTEIN	98	DPWA	$\gamma N \to \pi N$
−0.015 ±0.005	[9] ARNDT	97	IPWA	$\gamma N \to \pi N$
−0.0319 ±0.0024	DAVIDSON	97	DPWA	$\gamma N \to \pi N$
• • • We do not use the following data for averages, fits, limits, etc. • • •				
−0.026	PENNER	02D	DPWA	Multichannel
−0.0233 ±0.0017	HANSTEIN	98	IPWA	$\gamma N \to \pi N$
−0.025 ±0.002 ±0.002	BECK	97	IPWA	$\gamma N \to \pi N$
−0.030 ±0.003 ±0.002	BLANPIED	97	DPWA	$\gamma N \to \pi N,\ \gamma N$
−0.027 ±0.003 ±0.001	KHANDAKER	95	DPWA	$\gamma N \to \pi N$
−0.015 ±0.005	WORKMAN	92	IPWA	$\gamma N \to \pi N$
−0.0157 ±0.0072	DAVIDSON	91B	FIT	$\gamma N \to \pi N$
−0.0107 ±0.0037	DAVIDSON	90	FIT	$\gamma N \to \pi N$
−0.015 ±0.002	DAVIDSON	86	FIT	$\gamma N \to \pi N$
+0.037 ±0.004	TANABE	85	FIT	$\gamma N \to \pi N$

Δ(1232) → $N\gamma$, absolute value of E_2/M_1 ratio at pole

VALUE	DOCUMENT ID		TECN	COMMENT
• • • We do not use the following data for averages, fits, limits, etc. • • •				
0.065 ±0.007	ARNDT	97	DPWA	$\gamma N \to \pi N$
0.058	HANSTEIN	96	DPWA	$\gamma N \to \pi N$

Δ(1232) → $N\gamma$, phase of E_2/M_1 ratio at pole

VALUE	DOCUMENT ID		TECN	COMMENT
• • • We do not use the following data for averages, fits, limits, etc. • • •				
−122 ±5	ARNDT	97	DPWA	$\gamma N \to \pi N$
−127.2	HANSTEIN	96	DPWA	$\gamma N \to \pi N$

Δ(1232) MAGNETIC MOMENTS

Δ(1232)++ MAGNETIC MOMENT

The values are extracted from UCLA and SIN data on $\pi^+ p$ bremsstrahlung using a variety of different theoretical approximations and methods. Our estimate is *only* a rough guess of the range we expect the moment to lie within.

VALUE (μ_N)	DOCUMENT ID		TECN	COMMENT
3.7 to 7.5 OUR ESTIMATE				
• • • We do not use the following data for averages, fits, limits, etc. • • •				
6.14 ± 0.51	LOPEZCAST...	01	DPWA	$\pi^+ p \to \pi^+ p\gamma$
4.52 ± 0.50 ± 0.45	BOSSHARD	91		$\pi^+ p \to \pi^+ p\gamma$ (SIN data)
3.7 to 4.2	LIN	91B		$\pi^+ p \to \pi^+ p\gamma$ (from UCLA data)
4.6 to 4.9	LIN	91B		$\pi^+ p \to \pi^+ p\gamma$ (from SIN data)
5.6 to 7.5	WITTMAN	88		$\pi^+ p \to \pi^+ p\gamma$ (from UCLA data)
6.9 to 9.8	HELLER	87		$\pi^+ p \to \pi^+ p\gamma$ (from UCLA data)
4.7 to 6.7	NEFKENS	78		$\pi^+ p \to \pi^+ p\gamma$ (UCLA data)

Δ(1232)+ MAGNETIC MOMENT

VALUE (μ_N)	DOCUMENT ID		COMMENT
• • • We do not use the following data for averages, fits, limits, etc. • • •			
$2.7^{+1.0}_{-1.3} \pm 1.5 \pm 3$	[2] KOTULLA	02	$\gamma p \to p\pi^0\gamma'$

[2] The second error is systematic, the third is an estimate of theoretical uncertainties.

Δ(1232) FOOTNOTES

[3] Using $\pi^\pm d$ as well, PEDRONI 78 determine $(M^- - M^{++}) + (M^0 - M^+)/3 = 4.6 \pm 0.2$ MeV.

[4] See HOEHLER 93 for a detailed discussion of the evidence for and the pole parameters of N and Δ resonances as determined from Argand diagrams of πN elastic partial-wave amplitudes and from plots of the speeds with which the amplitudes traverse the diagrams.

[5] This VASAN 76B value is from fits to the coulomb-barrier-corrected CARTER 73 phase shift.

[6] This VASAN 76B value is from fits to the CARTER 73 nuclear phase shift without coulomb barrier corrections.

[7] This ARNDT 95 value is in error, as pointed out by HOHLER 01. The corrected value is in line with the ARNDT 91 value (R.A. Arndt, private communication).

[8] Converted to our conventions using $M = 1232$ MeV, $\Gamma = 110$ MeV from NOELLE 78.

[9] This ARNDT 97 value is very sensitive to the database being fitted. The result is from a fit to the full pion photoproduction database, apart from the BLANPIED 97 cross-section measurements.

Δ(1232) REFERENCES

For early references, see Physics Letters **111B** 70 (1982).

ARNDT	02	PR C66 055213	R. A. Arndt *et al.*	(GWU)
KOTULLA	02	PRL 89 272001	M. Kotulla *et al.*	(MAMI TAPS Collab.)
PENNER	02C	PR C66 055211	G. Penner, U. Mosel	(GIES)
PENNER	02D	PR C66 055212	G. Penner, U. Mosel	(GIES)
BLANPIED	01	PR C64 025203	G. Blanpied *et al.*	(BNL LEGS Collab.)
GALLER	01	PL B503 245	G. Galler *et al.*	(Mainz LARA Collab.)
HOHLER	01	NSTAR 2001 185	G. Hohler	(KARL)
LOPEZCAST...	01	PL B517 339	G. Lopez Castro, A. Mariano	
Also	02	NP A697 440	G. Lopez Castro, A. Mariano	
BECK	00	PR C61 035204	R. Beck *et al.*	(Mainz Microtron DAPHNE Col.)
VRANA	00	PRPL 328 181	T.P. Vrana, S.A. Dytman, T.-S.H. Lee	(PITT+)
HANSTEIN	98	NP A632 561	O. Hanstein, D. Drechsel, L. Tiator	
ARNDT	97	PR C56 577	R.A. Arndt, I.I. Strakovsky, R.L. Workman	(VPI)
BECK	97	PRL 78 606	R. Beck *et al.*	(MANZ, SACL, PAVI, GLAS)
Also	97B	PRL 79 4510	R.L. Beck, H.P. Krahn	(MANZ)
Also	97C	PRL 79 4512	R.L. Beck, H.P. Krahn	(MANZ)
Also	97D	PRL 79 4515 (erratum)	R.L. Beck *et al.*	(MANZ, SACL, PAVI, GLAS)
BLANPIED	97	PRL 79 4337	G.S. Blanpied *et al.*	(LEGS Collab.)
DAVIDSON	97	PRL 79 4509	R.M. Davidson, N.C.A. Mukhopadhyay	(RPI)
ARNDT	96	PR C53 430	R.A. Arndt, I.I. Strakovsky, R.L. Workman	(VPI)
BERNICHA	96	NP A597 623	A. Bernicha, G. Lopez Castro, J. Pestieau	(LOUV+)
HANSTEIN	96	PL B385 45	O. Hanstein, D. Drechsel, L. Tiator	(MANZ)
ABAEV	95	ZPHY A352 85	V.V. Abaev, S.P. Kruglov	(PNPI)
ARNDT	95	PR C52 2120	R.A. Arndt *et al.*	(VPI, BRCO)
KHANDAKER	95	PR D51 3966	M. Khandaker, A.M. Sandorfi	(BNL, VPI)
HOEHLER	93	πN Newsletter 9 1	G. Hohler	(KARL)
LI	93	PR C47 2759	Z.J. Li *et al.*	(VPI)
MANLEY	92	PR D45 4002	D.M. Manley, E.M. Saleski	(KENT) IJP
Also	84	PR D30 904	D.M. Manley *et al.*	(VPI)
WORKMAN	92	PR C46 1546	R.L. Workman, R.A. Arndt, Z.J. Li	(VPI)
ARNDT	91	PR D43 2131	R.A. Arndt *et al.*	(VPI, TELE) IJP
BOSSHARD	91	PR D44 1962	A. Bosshard *et al.*	(ZURI, LBL, VILL+)
Also	90	PRL 64 2619	A. Bosshard *et al.*	(CATH, LAUS, LBL+)
DAVIDSON	91B	PR D43 71	R.M. Davidson, N.C. Mukhopadhyay, R.S. Wittman	
LIN	91B	PR C44 1819	D.H. Lin, M.K. Liou, Z.M. Ding	(CUNY, CSOK)
Also	91	PR C43 R930	D. Lin, M.K. Liou	(CUNY)
DAVIDSON	90	PR D42 20	R.M. Davidson, N.C. Mukhopadhyay	(RPI)
WITTMAN	88	PR C37 2075	R. Wittman	(TRIU)
HELLER	87	PR C35 718	L. Heller *et al.*	(LANL, MIT, ILL)
DAVIDSON	86	PRL 56 804	R.M. Davidson, N.C. Mukhopadhyay, R. Wittman	(RPI)
TANABE	85	PR C31 1876	H. Tanabe, K. Ohta	(KOMAB)
CRAWFORD	83	NP B211 1	R.L. Crawford, W.T. Morton	(GLAS)
PDG	82	PL 111B	M. Roos *et al.*	(HELS, CIT, CERN)
AWAJI	81	Bonn Conf. 352	N. Awaji, R. Kajikawa	(NAGO)
Also	82	NP B197 365	K. Fujii *et al.*	(NAGO)
ARAI	80	Toronto Conf. 93	I. Arai	(INUS)
Also	82	NP B194 251	I. Arai, H. Fujii	(INUS)
CRAWFORD	80	Toronto Conf. 107	R.L. Crawford	(GLAS)
CUTKOSKY	80	Toronto Conf. 19	R.E. Cutkosky *et al.*	(CMU, LBL) IJP
Also	79	PR D20 2839	R.E. Cutkosky *et al.*	(CMU, LBL)
KOCH	80B	NP A336 331	R. Koch, E. Pietarinen	(KARLT) IJP
HOEHLER	79	PDAT 12-1	G. Hohler *et al.*	(KARLT) IJP
Also	80	Toronto Conf. 3	R. Koch	(KARLT) IJP
MIROSHNIC...	79	SJNP 29 94	I.I. Miroshnichenko *et al.*	(KFTI) IJP
		Translated from YAF 29 188.		
BARBOUR	78	NP B141 253	I.M. Barbour, R.L. Crawford, N.H. Parsons	(GLAS)
NEFKENS	78	PR D18 3911	B.M.K. Nefkens *et al.*	(UCLA, CATH) IJP
NOELLE	78	PTP 60 778	P. Noelle	(NAGO)
PEDRONI	78	NP A300 321	E. Pedroni *et al.*	(SIN, ISNG, KARLE+) IJP
CAMPBELL	76	PR D14 2431	R.R. Campbell, G.L. Shaw, J.S. Ball	(BOIS, UCI+) IJP
FELLER	76	NP B104 219	P. Feller *et al.*	(NAGO, OSAK) IJP
VASAN	76B	NP B106 535	S.S. Vasan	(CMU) IJP
Also	76	NP B106 526	S.S Vasan	(CMU) IJP
BERENDS	75	NP B84 342	F.A. Berends, A. Donnachie	(LEID, MCHS)
CARTER	73	NP B58 378	J.R. Carter, D.V. Bugg, J.R. Carter	(CAVE, LOQM) IJP

Δ(1600) P_{33}

$I(J^P) = \frac{3}{2}(\frac{3}{2}^+)$ Status: ***

Most of the results published before 1975 are now obsolete and have been omitted. They may be found in our 1982 edition, Physics Letters **111B** (1982).

The various analyses are not in good agreement.

Δ(1600) BREIT-WIGNER MASS

VALUE (MeV)	DOCUMENT ID		TECN	COMMENT
1550 to 1700 (≈ 1600) OUR ESTIMATE				
1706 ± 10	MANLEY	92	IPWA	$\pi N \to \pi N$ & $N\pi\pi$
1600 ± 50	CUTKOSKY	80	IPWA	$\pi N \to \pi N$
1522 ± 13	HOEHLER	79	IPWA	$\pi N \to \pi N$
• • • We do not use the following data for averages, fits, limits, etc. • • •				
1667 ± 1	PENNER	02C	DPWA	Multichannel
1687 ± 44	VRANA	00	DPWA	Multichannel
1672 ± 15	ARNDT	96	IPWA	$\gamma N \to \pi N$
1706	LI	93	IPWA	$\gamma N \to \pi N$
1690	BARNHAM	80	IPWA	$\pi N \to N\pi\pi$
1560	[1] LONGACRE	77	IPWA	$\pi N \to N\pi\pi$
1640	[2] LONGACRE	75	IPWA	$\pi N \to N\pi\pi$

Δ(1600) BREIT-WIGNER WIDTH

VALUE (MeV)	DOCUMENT ID		TECN	COMMENT
250 to 450 (≈ 350) OUR ESTIMATE				
430 ± 73	MANLEY	92	IPWA	$\pi N \to \pi N$ & $N\pi\pi$
300 ± 100	CUTKOSKY	80	IPWA	$\pi N \to \pi N$
220 ± 40	HOEHLER	79	IPWA	$\pi N \to \pi N$
• • • We do not use the following data for averages, fits, limits, etc. • • •				
397 ± 10	PENNER	02C	DPWA	Multichannel
493 ± 75	VRANA	00	DPWA	Multichannel
315 ± 20	ARNDT	96	IPWA	$\gamma N \to \pi N$
215	LI	93	IPWA	$\gamma N \to \pi N$
250	BARNHAM	80	IPWA	$\pi N \to N\pi\pi$
180	[1] LONGACRE	77	IPWA	$\pi N \to N\pi\pi$
300	[2] LONGACRE	75	IPWA	$\pi N \to N\pi\pi$

Δ(1600) POLE POSITION

REAL PART

VALUE (MeV)	DOCUMENT ID		TECN	COMMENT
1500 to 1700 (≈ 1600) OUR ESTIMATE				
1675	ARNDT	95	DPWA	$\pi N \to N\pi$
1550	[3] HOEHLER	93	SPED	$\pi N \to \pi N$
1550 ± 40	CUTKOSKY	80	IPWA	$\pi N \to \pi N$
• • • We do not use the following data for averages, fits, limits, etc. • • •				
1599	VRANA	00	DPWA	Multichannel
1612	ARNDT	91	DPWA	$\pi N \to \pi N$ Soln SM90
1609 or 1610	[4] LONGACRE	78	IPWA	$\pi N \to N\pi\pi$
1541 or 1542	[1] LONGACRE	77	IPWA	$\pi N \to N\pi\pi$

−2×IMAGINARY PART

VALUE (MeV)	DOCUMENT ID		TECN	COMMENT
200 to 400 (≈ 300) OUR ESTIMATE				
386	ARNDT	95	DPWA	$\pi N \to N\pi$
200 ± 60	CUTKOSKY	80	IPWA	$\pi N \to \pi N$
• • • We do not use the following data for averages, fits, limits, etc. • • •				
312	VRANA	00	DPWA	Multichannel
230	ARNDT	91	DPWA	$\pi N \to \pi N$ Soln SM90
323 or 325	[4] LONGACRE	78	IPWA	$\pi N \to N\pi\pi$
178 or 178	[1] LONGACRE	77	IPWA	$\pi N \to N\pi\pi$

Δ(1600) ELASTIC POLE RESIDUE

MODULUS |r|

VALUE (MeV)	DOCUMENT ID		TECN	COMMENT
52	ARNDT	95	DPWA	$\pi N \to N\pi$
17 ± 4	CUTKOSKY	80	IPWA	$\pi N \to \pi N$
• • • We do not use the following data for averages, fits, limits, etc. • • •				
16	ARNDT	91	DPWA	$\pi N \to \pi N$ Soln SM90

PHASE θ

VALUE (°)	DOCUMENT ID		TECN	COMMENT
+ 14	ARNDT	95	DPWA	$\pi N \to N\pi$
−150 ± 30	CUTKOSKY	80	IPWA	$\pi N \to \pi N$
• • • We do not use the following data for averages, fits, limits, etc. • • •				
− 73	ARNDT	91	DPWA	$\pi N \to \pi N$ Soln SM90

Δ(1600) DECAY MODES

The following branching fractions are our estimates, not fits or averages.

	Mode	Fraction (Γ_i/Γ)
Γ_1	$N\pi$	10–25 %
Γ_2	ΣK	
Γ_3	$N\pi\pi$	75–90 %
Γ_4	$\Delta\pi$	40–70 %
Γ_5	$\Delta(1232)\pi$, P-wave	
Γ_6	$\Delta(1232)\pi$, F-wave	
Γ_7	$N\rho$	<25 %
Γ_8	$N\rho$, S=1/2, P-wave	
Γ_9	$N\rho$, S=3/2, P-wave	
Γ_{10}	$N\rho$, S=3/2, F-wave	
Γ_{11}	$N(1440)\pi$	10–35 %
Γ_{12}	$N(1440)\pi$, P-wave	
Γ_{13}	$N\gamma$	0.001–0.02 %
Γ_{14}	$N\gamma$, helicity=1/2	0.0–0.02 %
Γ_{15}	$N\gamma$, helicity=3/2	0.001–0.005 %

Δ(1600) BRANCHING RATIOS

$\Gamma(N\pi)/\Gamma_{total}$ Γ_1/Γ

VALUE	DOCUMENT ID		TECN	COMMENT
0.10 to 0.25 OUR ESTIMATE				
0.12 ± 0.02	MANLEY	92	IPWA	$\pi N \to \pi N$ & $N\pi\pi$
0.18 ± 0.04	CUTKOSKY	80	IPWA	$\pi N \to \pi N$
0.21 ± 0.06	HOEHLER	79	IPWA	$\pi N \to \pi N$
• • • We do not use the following data for averages, fits, limits, etc. • • •				
0.13 ± 0.01	PENNER	02C	DPWA	Multichannel
0.28 ± 0.05	VRANA	00	DPWA	Multichannel

$(\Gamma_i\Gamma_f)^{1/2}/\Gamma_{total}$ in $N\pi \to \Delta(1600) \to \Sigma K$ $(\Gamma_1\Gamma_2)^{1/2}/\Gamma$

VALUE	DOCUMENT ID		TECN	COMMENT
−0.36 to −0.28 OUR ESTIMATE				
• • • We do not use the following data for averages, fits, limits, etc. • • •				
0.006 to 0.042	[5] DEANS	75	DPWA	$\pi N \to \Sigma K$

Note: Signs of couplings from $\pi N \to N\pi\pi$ analyses were changed in the 1986 edition to agree with the baryon-first convention; the overall phase ambiguity is resolved by choosing a negative sign for the Δ(1620) S_{31} coupling to Δ(1232)π.

$(\Gamma_i\Gamma_f)^{1/2}/\Gamma_{total}$ in $N\pi \to \Delta(1600) \to \Delta(1232)\pi$, P-wave $(\Gamma_1\Gamma_5)^{1/2}/\Gamma$

VALUE	DOCUMENT ID		TECN	COMMENT
+0.27 to +0.33 OUR ESTIMATE				
+ 0.29 ± 0.02	MANLEY	92	IPWA	$\pi N \to \pi N$ & $N\pi\pi$
+ 0.24 ± 0.05	BARNHAM	80	IPWA	$\pi N \to N\pi\pi$
+ 0.34	[1,6] LONGACRE	77	IPWA	$\pi N \to N\pi\pi$
+ 0.30	[2] LONGACRE	75	IPWA	$\pi N \to N\pi\pi$

$\Gamma(\Delta(1232)\pi$, P-wave$)/\Gamma_{total}$ Γ_5/Γ

VALUE	DOCUMENT ID		TECN	COMMENT
0.59 ± 0.10	VRANA	00	DPWA	Multichannel

$(\Gamma_i\Gamma_f)^{1/2}/\Gamma_{total}$ in $N\pi \to \Delta(1600) \to \Delta(1232)\pi$, F-wave $(\Gamma_1\Gamma_6)^{1/2}/\Gamma$

VALUE	DOCUMENT ID		TECN	COMMENT
−0.15 to −0.03 OUR ESTIMATE				
− 0.07	[1,6] LONGACRE	77	IPWA	$\pi N \to N\pi\pi$

$(\Gamma_i\Gamma_f)^{1/2}/\Gamma_{total}$ in $N\pi \to \Delta(1600) \to N\rho$, S=1/2, P-wave $(\Gamma_1\Gamma_8)^{1/2}/\Gamma$

VALUE	DOCUMENT ID		TECN	COMMENT
+ 0.10	[1,6] LONGACRE	77	IPWA	$\pi N \to N\pi\pi$

$(\Gamma_i\Gamma_f)^{1/2}/\Gamma_{total}$ in $N\pi \to \Delta(1600) \to N\rho$, S=3/2, P-wave $(\Gamma_1\Gamma_9)^{1/2}/\Gamma$

VALUE	DOCUMENT ID		TECN	COMMENT
+ 0.10	[1,6] LONGACRE	77	IPWA	$\pi N \to N\pi\pi$

$(\Gamma_i\Gamma_f)^{1/2}/\Gamma_{total}$ in $N\pi \to \Delta(1600) \to N(1440)\pi$, P-wave $(\Gamma_1\Gamma_{12})^{1/2}/\Gamma$

VALUE	DOCUMENT ID		TECN	COMMENT
+0.15 to +0.23 OUR ESTIMATE				
+ 0.16 ± 0.02	MANLEY	92	IPWA	$\pi N \to \pi N$ & $N\pi\pi$
+ 0.23 ± 0.04	BARNHAM	80	IPWA	$\pi N \to N\pi\pi$

$\Gamma(N(1440)\pi)/\Gamma_{total}$ Γ_{11}/Γ

VALUE	DOCUMENT ID		TECN	COMMENT
0.13 ± 0.04	VRANA	00	DPWA	Multichannel

Δ(1600) PHOTON DECAY AMPLITUDES

Δ(1600) → $N\gamma$, helicity-1/2 amplitude $A_{1/2}$

VALUE (GeV$^{-1/2}$)	DOCUMENT ID		TECN	COMMENT
−0.023 ± 0.020 OUR ESTIMATE				
− 0.018 ± 0.015	ARNDT	96	IPWA	$\gamma N \to \pi N$
− 0.039 ± 0.030	CRAWFORD	83	IPWA	$\gamma N \to \pi N$
− 0.046 ± 0.013	AWAJI	81	DPWA	$\gamma N \to \pi N$
0.005 ± 0.020	CRAWFORD	80	DPWA	$\gamma N \to \pi N$
• • • We do not use the following data for averages, fits, limits, etc. • • •				
0.0	PENNER	02D	DPWA	Multichannel
− 0.026 ± 0.002	LI	93	IPWA	$\gamma N \to \pi N$
− 0.200	[7] WADA	84	DPWA	Compton scattering
0.000 ± 0.030	BARBOUR	78	DPWA	$\gamma N \to \pi N$
0.0 ± 0.020	FELLER	76	DPWA	$\gamma N \to \pi N$

Δ(1600) → $N\gamma$, helicity-3/2 amplitude $A_{3/2}$

VALUE (GeV$^{-1/2}$)	DOCUMENT ID		TECN	COMMENT
−0.009 ± 0.021 OUR ESTIMATE				
− 0.025 ± 0.015	ARNDT	96	IPWA	$\gamma N \to \pi N$
− 0.013 ± 0.014	CRAWFORD	83	IPWA	$\gamma N \to \pi N$
0.025 ± 0.031	AWAJI	81	DPWA	$\gamma N \to \pi N$
− 0.009 ± 0.020	CRAWFORD	80	DPWA	$\gamma N \to \pi N$
• • • We do not use the following data for averages, fits, limits, etc. • • •				
− 0.024	PENNER	02D	DPWA	Multichannel
− 0.016 ± 0.002	LI	93	IPWA	$\gamma N \to \pi N$
0.023	WADA	84	DPWA	Compton scattering
0.000 ± 0.045	BARBOUR	78	DPWA	$\gamma N \to \pi N$
0.0 ± 0.015	FELLER	76	DPWA	$\gamma N \to \pi N$

Δ(1600) FOOTNOTES

[1] LONGACRE 77 pole positions are from a search for poles in the unitarized T-matrix; the first (second) value uses, in addition to $\pi N \to N\pi\pi$ data, elastic amplitudes from a Saclay (CERN) partial-wave analysis. The other LONGACRE 77 values are from eyeball fits with Breit-Wigner circles to the T-matrix amplitudes.

[2] From method II of LONGACRE 75: eyeball fits with Breit-Wigner circles to the T-matrix amplitudes.

[3] See HOEHLER 93 for a detailed discussion of the evidence for and the pole parameters of N and Δ resonances as determined from Argand diagrams of πN elastic partial-wave amplitudes and from plots of the speeds with which the amplitudes traverse the diagrams.

[4] LONGACRE 78 values are from a search for poles in the unitarized T-matrix. The first (second) value uses, in addition to $\pi N \to N\pi\pi$ data, elastic amplitudes from a Saclay (CERN) partial-wave analysis.

[5] The range given is from the four best solutions. DEANS 75 disagrees with $\pi^+ p \to \Sigma^+ K^+$ data of WINNIK 77 around 1920 MeV.

[6] LONGACRE 77 considers this coupling to be well determined.

[7] WADA 84 is inconsistent with other analyses — see the Note on N and Δ Resonances.

Δ(1600) REFERENCES

For early references, see Physics Letters **111B** 70 (1982).

PENNER	02C	PR C66 055211	G. Penner, U. Mosel	(GIES)
PENNER	02D	PR C66 055212	G. Penner, U. Mosel	(GIES)
VRANA	00	PRPL 328 181	T.P. Vrana, S.A. Dytman,, T.-S.H. Lee	(PITT+)
ARNDT	96	PR C53 430	R.A. Arndt, I.I. Strakovsky, R.L. Workman	(VPI)
ARNDT	95	PR C52 2120	R.A. Arndt *et al.*	(VPI, BRCO)
HOEHLER	93	πN Newsletter 9 1	G. Hohler	(KARL)
LI	93	PR C47 2759	Z.J. Li *et al.*	(VPI)
MANLEY	92	PR D45 4002	D.M. Manley, E.M. Saleski	(KENT) IJP
Also	84	PR D30 904	D.M. Manley *et al.*	(VPI)
ARNDT	91	PR D43 2131	R.A. Arndt *et al.*	(VPI, TELE) IJP
WADA	84	NP B247 313	Y. Wada *et al.*	(INUS)
CRAWFORD	83	NP B211 1	R.L. Crawford, W.T. Morton	(GLAS)
PDG	82	PL 111B	M. Roos *et al.*	(HELS, CIT, CERN)
AWAJI	81	Bonn Conf. 352	N. Awaji, R. Kajikawa	(NAGO)
Also	82	NP B197 365	K. Fujii *et al.*	(NAGO)
BARNHAM	80	NP B168 243	K.W.J. Barnham *et al.*	(LOIC)
CRAWFORD	80	Toronto Conf. 107	R.L. Crawford	(GLAS)
CUTKOSKY	80	Toronto Conf. 19	R.E. Cutkosky *et al.*	(CMU, LBL) IJP
Also	79	PR D20 2839	R.E. Cutkosky *et al.*	(CMU, LBL) IJP
HOEHLER	79	PDAT 12-1	G. Hohler *et al.*	(KARLT) IJP
Also	80	Toronto Conf. 3	R. Koch	(KARLT) IJP
BARBOUR	78	NP B141 253	I.M. Barbour, R.L. Crawford, N.H. Parsons	(GLAS)
LONGACRE	78	PR D17 1795	R.S. Longacre *et al.*	(LBL, SLAC)
LONGACRE	77	NP B122 493	R.S. Longacre, J. Dolbeau	(SACL) IJP
Also	76	NP B108 365	J. Dolbeau *et al.*	(SACL) IJP
WINNIK	77	NP B128 66	M. Winnik *et al.*	(HAIF) I
FELLER	76	NP B104 219	P. Feller *et al.*	(NAGO, OSAK) IJP
DEANS	75	NP B96 90	S.R. Deans *et al.*	(SFLA, ALAH) IJP
LONGACRE	75	PL 55B 415	R.S. Longacre *et al.*	(LBL, SLAC) IJP

Baryon Particle Listings

$\Delta(1620)$

$\Delta(1620)$ S_{31}

$I(J^P) = \frac{3}{2}(\frac{1}{2}^-)$ Status: ****

Most of the results published before 1975 are now obsolete and have been omitted. They may be found in our 1982 edition, Physics Letters **111B** (1982).

$\Delta(1620)$ BREIT-WIGNER MASS

VALUE (MeV)		DOCUMENT ID		TECN	COMMENT
1615 to 1675 (≈ 1620) OUR ESTIMATE					
1672 ± 7		MANLEY	92	IPWA	$\pi N \to \pi N$ & $N\pi\pi$
1620 ±20		CUTKOSKY	80	IPWA	$\pi N \to \pi N$
1610 ± 7		HOEHLER	79	IPWA	$\pi N \to \pi N$
• • • We do not use the following data for averages, fits, limits, etc. • • •					
1612 ± 2		PENNER	02C	DPWA	Multichannel
1617 ±15		VRANA	00	DPWA	Multichannel
1672 ± 5		ARNDT	96	IPWA	$\gamma N \to \pi N$
1617		ARNDT	95	DPWA	$\pi N \to N\pi$
1669		LI	93	IPWA	$\gamma N \to \pi N$
1620		BARNHAM	80	IPWA	$\pi N \to N\pi\pi$
1712.8± 6.0	[1]	CHEW	80	BPWA	$\pi^+ p \to \pi^+ p$
1786.7± 2.0	[1]	CHEW	80	BPWA	$\pi^+ p \to \pi^+ p$
1657		CRAWFORD	80	DPWA	$\gamma N \to \pi N$
1662		BARBOUR	78	DPWA	$\gamma N \to \pi N$
1580	[2]	LONGACRE	77	IPWA	$\pi N \to N\pi\pi$
1600	[3]	LONGACRE	75	IPWA	$\pi N \to N\pi\pi$

$\Delta(1620)$ BREIT-WIGNER WIDTH

VALUE (MeV)		DOCUMENT ID		TECN	COMMENT
120 to 180 (≈ 150) OUR ESTIMATE					
154 ±37		MANLEY	92	IPWA	$\pi N \to \pi N$ & $N\pi\pi$
140 ±20		CUTKOSKY	80	IPWA	$\pi N \to \pi N$
139 ±18		HOEHLER	79	IPWA	$\pi N \to \pi N$
• • • We do not use the following data for averages, fits, limits, etc. • • •					
202 ± 7		PENNER	02C	DPWA	Multichannel
143 ±42		VRANA	00	DPWA	Multichannel
147 ± 8		ARNDT	96	IPWA	$\gamma N \to \pi N$
108		ARNDT	95	DPWA	$\pi N \to N\pi$
184		LI	93	IPWA	$\gamma N \to \pi N$
120		BARNHAM	80	IPWA	$\pi N \to N\pi\pi$
228.3±18.0	[1]	CHEW	80	BPWA	$\pi^+ p \to \pi^+ p$ (lower mass)
30.0± 6.4	[1]	CHEW	80	BPWA	$\pi^+ p \to \pi^+ p$ (higher mass)
161		CRAWFORD	80	DPWA	$\gamma N \to \pi N$
180		BARBOUR	78	DPWA	$\gamma N \to \pi N$
120	[2]	LONGACRE	77	IPWA	$\pi N \to N\pi\pi$
150	[3]	LONGACRE	75	IPWA	$\pi N \to N\pi\pi$

$\Delta(1620)$ POLE POSITION

REAL PART

VALUE (MeV)		DOCUMENT ID		TECN	COMMENT
1580 to 1620 (≈ 1600) OUR ESTIMATE					
1585		ARNDT	95	DPWA	$\pi N \to N\pi$
1608	[4]	HOEHLER	93	SPED	$\pi N \to \pi N$
1600±15		CUTKOSKY	80	IPWA	$\pi N \to \pi N$
• • • We do not use the following data for averages, fits, limits, etc. • • •					
1607		VRANA	00	DPWA	Multichannel
1587		ARNDT	91	DPWA	$\pi N \to \pi N$ Soln SM90
1583 or 1583	[5]	LONGACRE	78	IPWA	$\pi N \to N\pi\pi$
1575 or 1572	[2]	LONGACRE	77	IPWA	$\pi N \to N\pi\pi$

−2×IMAGINARY PART

VALUE (MeV)		DOCUMENT ID		TECN	COMMENT
100 to 130 (≈ 115) OUR ESTIMATE					
104		ARNDT	95	DPWA	$\pi N \to N\pi$
116	[4]	HOEHLER	93	SPED	$\pi N \to \pi N$
120±20		CUTKOSKY	80	IPWA	$\pi N \to \pi N$
• • • We do not use the following data for averages, fits, limits, etc. • • •					
148		VRANA	00	DPWA	Multichannel
120		ARNDT	91	DPWA	$\pi N \to \pi N$ Soln SM90
143 or 149	[5]	LONGACRE	78	IPWA	$\pi N \to N\pi\pi$
119 or 128	[2]	LONGACRE	77	IPWA	$\pi N \to N\pi\pi$

$\Delta(1620)$ ELASTIC POLE RESIDUE

MODULUS $|r|$

VALUE (MeV)	DOCUMENT ID		TECN	COMMENT
14	ARNDT	95	DPWA	$\pi N \to N\pi$
19	HOEHLER	93	SPED	$\pi N \to \pi N$
15 ± 2	CUTKOSKY	80	IPWA	$\pi N \to \pi N$
• • • We do not use the following data for averages, fits, limits, etc. • • •				
15	ARNDT	91	DPWA	$\pi N \to \pi N$ Soln SM90

PHASE θ

VALUE (°)	DOCUMENT ID		TECN	COMMENT
−121	ARNDT	95	DPWA	$\pi N \to N\pi$
− 95	HOEHLER	93	SPED	$\pi N \to \pi N$
−110±20	CUTKOSKY	80	IPWA	$\pi N \to \pi N$
• • • We do not use the following data for averages, fits, limits, etc. • • •				
−125	ARNDT	91	DPWA	$\pi N \to \pi N$ Soln SM90

$\Delta(1620)$ DECAY MODES

The following branching fractions are our estimates, not fits or averages.

	Mode	Fraction (Γ_j/Γ)
Γ_1	$N\pi$	20–30 %
Γ_2	$N\pi\pi$	70–80 %
Γ_3	$\Delta\pi$	30–60 %
Γ_4	$\Delta(1232)\pi$, D-wave	
Γ_5	$N\rho$	7–25 %
Γ_6	$N\rho$, S=1/2, S-wave	
Γ_7	$N\rho$, S=3/2, D-wave	
Γ_8	$N(1440)\pi$	
Γ_9	$N\gamma$	0.004–0.044 %
Γ_{10}	$N\gamma$, helicity=1/2	0.004–0.044 %

$\Delta(1620)$ BRANCHING RATIOS

$\Gamma(N\pi)/\Gamma_{\text{total}}$ Γ_1/Γ

VALUE	DOCUMENT ID		TECN	COMMENT
0.2 to 0.3 OUR ESTIMATE				
0.09±0.02	MANLEY	92	IPWA	$\pi N \to \pi N$ & $N\pi\pi$
0.25±0.03	CUTKOSKY	80	IPWA	$\pi N \to \pi N$
0.35±0.06	HOEHLER	79	IPWA	$\pi N \to \pi N$
• • • We do not use the following data for averages, fits, limits, etc. • • •				
0.34±0.01	PENNER	02C	DPWA	Multichannel
0.45±0.05	VRANA	00	DPWA	Multichannel
0.29	ARNDT	95	DPWA	$\pi N \to N\pi$
0.60	[1] CHEW	80	BPWA	$\pi^+ p \to \pi^+ p$ (lower mass)
0.36	[1] CHEW	80	BPWA	$\pi^+ p \to \pi^+ p$ (higher mass)

Note: Signs of couplings from $\pi N \to N\pi\pi$ analyses were changed in the 1986 edition to agree with the baryon-first convention; the overall phase ambiguity is resolved by choosing a negative sign for the $\Delta(1620)$ S_{31} coupling to $\Delta(1232)\pi$.

$(\Gamma_i\Gamma_f)^{1/2}/\Gamma_{\text{total}}$ in $N\pi \to \Delta(1620) \to \Delta(1232)\pi$, D-wave $(\Gamma_1\Gamma_4)^{1/2}/\Gamma$

VALUE	DOCUMENT ID		TECN	COMMENT
−0.36 to −0.28 OUR ESTIMATE				
−0.24±0.03	MANLEY	92	IPWA	$\pi N \to \pi N$ & $N\pi\pi$
−0.33±0.06	BARNHAM	80	IPWA	$\pi N \to N\pi\pi$
−0.39	[2,6] LONGACRE	77	IPWA	$\pi N \to N\pi\pi$
−0.40	[3] LONGACRE	75	IPWA	$\pi N \to N\pi\pi$

$\Gamma(\Delta(1232)\pi, D\text{-wave})/\Gamma_{\text{total}}$ Γ_4/Γ

VALUE	DOCUMENT ID		TECN	COMMENT
0.39±0.02	VRANA	00	DPWA	Multichannel

$(\Gamma_i\Gamma_f)^{1/2}/\Gamma_{\text{total}}$ in $N\pi \to \Delta(1620) \to N\rho$, S=1/2, S-wave $(\Gamma_1\Gamma_6)^{1/2}/\Gamma$

VALUE	DOCUMENT ID		TECN	COMMENT
+0.12 to +0.22 OUR ESTIMATE				
+0.15±0.02	MANLEY	92	IPWA	$\pi N \to \pi N$ & $N\pi\pi$
+0.40±0.10	BARNHAM	80	IPWA	$\pi N \to N\pi\pi$
+0.08	[2,6] LONGACRE	77	IPWA	$\pi N \to N\pi\pi$
+0.28	[3] LONGACRE	75	IPWA	$\pi N \to N\pi\pi$

$\Gamma(N\rho, S$=1/2, S-wave$)/\Gamma_{\text{total}}$ Γ_6/Γ

VALUE	DOCUMENT ID		TECN	COMMENT
0.14±0.03	VRANA	00	DPWA	Multichannel

$(\Gamma_i\Gamma_f)^{1/2}/\Gamma_{\text{total}}$ in $N\pi \to \Delta(1620) \to N\rho$, S=3/2, D-wave $(\Gamma_1\Gamma_7)^{1/2}/\Gamma$

VALUE	DOCUMENT ID		TECN	COMMENT
−0.15 to −0.03 OUR ESTIMATE				
−0.06±0.02	MANLEY	92	IPWA	$\pi N \to \pi N$ & $N\pi\pi$
−0.13	[2,6] LONGACRE	77	IPWA	$\pi N \to N\pi\pi$

$\Gamma(N\rho, S$=3/2, D-wave$)/\Gamma_{\text{total}}$ Γ_7/Γ

VALUE	DOCUMENT ID		TECN	COMMENT
0.02±0.01	VRANA	00	DPWA	Multichannel

$(\Gamma_i\Gamma_f)^{1/2}/\Gamma_{\text{total}}$ in $N\pi \to \Delta(1620) \to N(1440)\pi$ $(\Gamma_1\Gamma_8)^{1/2}/\Gamma$

VALUE	DOCUMENT ID		TECN	COMMENT
0.11±0.05	BARNHAM	80	IPWA	$\pi N \to N\pi\pi$

$\Gamma(N(1440)\pi)/\Gamma_{total}$ Γ_8/Γ

VALUE	DOCUMENT ID		TECN	COMMENT
0.00±0.01	VRANA	00	DPWA	Multichannel

$\Delta(1620)$ PHOTON DECAY AMPLITUDES

$\Delta(1620) \rightarrow N\gamma$, helicity-1/2 amplitude $A_{1/2}$

VALUE (GeV$^{-1/2}$)	DOCUMENT ID		TECN	COMMENT
+0.027±0.011 OUR ESTIMATE				
0.035±0.020	ARNDT	96	IPWA	$\gamma N \rightarrow \pi N$
0.035±0.010	CRAWFORD	83	IPWA	$\gamma N \rightarrow \pi N$
0.010±0.015	AWAJI	81	DPWA	$\gamma N \rightarrow \pi N$
−0.022±0.007	ARAI	80	DPWA	$\gamma N \rightarrow \pi N$ (fit 1)
−0.026±0.008	ARAI	80	DPWA	$\gamma N \rightarrow \pi N$ (fit 2)
0.021±0.020	CRAWFORD	80	DPWA	$\gamma N \rightarrow \pi N$
0.126±0.021	TAKEDA	80	DPWA	$\gamma N \rightarrow \pi N$
• • • We do not use the following data for averages, fits, limits, etc. • • •				
−0.050	PENNER	02D	DPWA	Multichannel
0.042±0.003	LI	93	IPWA	$\gamma N \rightarrow \pi N$
0.066	WADA	84	DPWA	Compton scattering
+0.034±0.028	BARBOUR	78	DPWA	$\gamma N \rightarrow \pi N$
−0.005±0.016	FELLER	76	DPWA	$\gamma N \rightarrow \pi N$

$\Delta(1620)$ FOOTNOTES

[1] CHEW 80 reports two S_{31} resonances at somewhat higher masses than other analyses. Problems with this analysis are discussed in section 2.1.11 of HOEHLER 83.

[2] LONGACRE 77 pole positions are from a search for poles in the unitarized T-matrix; the first (second) value uses, in addition to $\pi N \rightarrow N\pi\pi$ data, elastic amplitudes from a Saclay (CERN) partial-wave analysis. The other LONGACRE 77 values are from eyeball fits with Breit-Wigner circles to the T-matrix amplitudes.

[3] From method II of LONGACRE 75: eyeball fits with Breit-Wigner circles to the T-matrix amplitudes.

[4] See HOEHLER 93 for a detailed discussion of the evidence for and the pole parameters of N and Δ resonances as determined from Argand diagrams of πN elastic partial-wave amplitudes and from plots of the speeds with which the amplitudes traverse the diagrams.

[5] LONGACRE 78 values are from a search for poles in the unitarized T-matrix. The first (second) value uses, in addition to $\pi N \rightarrow N\pi\pi$ data, elastic amplitudes from a Saclay (CERN) partial-wave analysis.

[6] LONGACRE 77 considers this coupling to be well determined.

$\Delta(1620)$ REFERENCES

For early references, see Physics Letters **111B** 70 (1982).

PENNER	02C	PR C66 055211	G. Penner, U. Mosel	(GIES)
PENNER	02D	PR C66 055212	G. Penner, U. Mosel	(GIES)
VRANA	00	PRPL 328 181	T.P. Vrana, S.A. Dytman,, T.-S.H. Lee	(PITT+)
ARNDT	96	PR C53 430	R.A. Arndt, I.I. Strakovsky, R.L. Workman	(VPI)
ARNDT	95	PR C52 2120	R.A. Arndt *et al.*	(VPI, BRCO)
HOEHLER	93	πN Newsletter 9 1	G. Hohler	(KARL)
LI	93	PR C47 2759	Z.J. Li *et al.*	(VPI)
MANLEY	92	PR D45 4002	D.M. Manley, E.M. Saleski	(KENT) IJP
Also	84	PR D30 904	D.M. Manley *et al.*	(VPI)
ARNDT	91	PR D43 2131	R.A. Arndt *et al.*	(VPI, TELE) IJP
WADA	84	NP B247 313	Y. Wada *et al.*	(INUS)
CRAWFORD	83	NP B211 1	R.L. Crawford, W.T. Morton	(GLAS)
HOEHLER	83	Landolt-Boernstein 1/9B2	G. Hohler	(KARLT)
PDG	82	PL 111B	M. Roos *et al.*	(HELS, CIT, CERN)
AWAJI	81	Bonn Conf. 352	N. Awaji, R. Kajikawa	(NAGO)
Also	82	NP B197 365	K. Fujii *et al.*	(NAGO)
ARAI	80	Toronto Conf. 93	I. Arai	(INUS)
Also	82	NP B194 251	I. Arai, H. Fujii	(INUS)
BARNHAM	80	NP B168 243	K.W.J. Barnham *et al.*	(LOIC)
CHEW	80	Toronto Conf. 123	D.M. Chew	(LBL) IJP
CRAWFORD	80	Toronto Conf. 107	R.L. Crawford	(GLAS)
CUTKOSKY	80	Toronto Conf. 19	R.E. Cutkosky *et al.*	(CMU, LBL) IJP
Also	79	PR D20 2839	R.E. Cutkosky *et al.*	(CMU, LBL) IJP
TAKEDA	80	NP B168 17	H. Takeda *et al.*	(TOKY, INUS)
HOEHLER	79	PDAT 12-1	G. Hohler *et al.*	(KARLT) IJP
Also	80	Toronto Conf. 3	R. Koch	(KARLT) IJP
BARBOUR	78	NP B141 253	I.M. Barbour, R.L. Crawford, N.H. Parsons	(GLAS)
LONGACRE	78	PR D17 1795	R.S. Longacre *et al.*	(LBL, SLAC)
LONGACRE	77	NP B122 493	R.S. Longacre, J. Dolbeau	(SACL) IJP
Also	76	NP B108 365	J. Dolbeau *et al.*	(SACL) IJP
FELLER	76	NP B104 219	P. Feller *et al.*	(NAGO, OSAK) IJP
LONGACRE	75	PL 55B 415	R.S. Longacre *et al.*	(LBL, SLAC) IJP

$\Delta(1700)$ D_{33}

$I(J^P) = \frac{3}{2}(\frac{3}{2}^-)$ Status: ****

Most of the results published before 1975 are now obsolete and have been omitted. They may be found in our 1982 edition, Physics Letters **111B** (1982).

$\Delta(1700)$ BREIT-WIGNER MASS

VALUE (MeV)	DOCUMENT ID		TECN	COMMENT
1670 to 1770 (≈ 1700) OUR ESTIMATE				
1762 ±44	MANLEY	92	IPWA	$\pi N \rightarrow \pi N$ & $N\pi\pi$
1710 ±30	CUTKOSKY	80	IPWA	$\pi N \rightarrow \pi N$
1680 ±70	HOEHLER	79	IPWA	$\pi N \rightarrow \pi N$
• • • We do not use the following data for averages, fits, limits, etc. • • •				
1678 ± 1	PENNER	02C	DPWA	Multichannel
1732 ±23	VRANA	00	DPWA	Multichannel
1690 ±15	ARNDT	96	IPWA	$\gamma N \rightarrow \pi N$
1680	ARNDT	95	DPWA	$\pi N \rightarrow N\pi$
1655	LI	93	IPWA	$\gamma N \rightarrow \pi N$
1650	BARNHAM	80	IPWA	$\pi N \rightarrow N\pi\pi$
$1718.4^{+13.1}_{-13.0}$	[1] CHEW	80	BPWA	$\pi^+ p \rightarrow \pi^+ p$
1622	CRAWFORD	80	DPWA	$\gamma N \rightarrow \pi N$
1629	BARBOUR	78	DPWA	$\gamma N \rightarrow \pi N$
1600	[2] LONGACRE	77	IPWA	$\pi N \rightarrow N\pi\pi$
1680	[3] LONGACRE	75	IPWA	$\pi N \rightarrow N\pi\pi$

$\Delta(1700)$ BREIT-WIGNER WIDTH

VALUE (MeV)	DOCUMENT ID		TECN	COMMENT
200 to 400 (≈ 300) OUR ESTIMATE				
600 ±250	MANLEY	92	IPWA	$\pi N \rightarrow \pi N$ & $N\pi\pi$
280 ± 80	CUTKOSKY	80	IPWA	$\pi N \rightarrow \pi N$
230 ± 80	HOEHLER	79	IPWA	$\pi N \rightarrow \pi N$
• • • We do not use the following data for averages, fits, limits, etc. • • •				
606 ± 15	PENNER	02C	DPWA	Multichannel
119 ± 70	VRANA	00	DPWA	Multichannel
285 ± 20	ARNDT	96	IPWA	$\gamma N \rightarrow \pi N$
272	ARNDT	95	DPWA	$\pi N \rightarrow N\pi$
348	LI	93	IPWA	$\gamma N \rightarrow \pi N$
160	BARNHAM	80	IPWA	$\pi N \rightarrow N\pi\pi$
193.3± 26.0	[1] CHEW	80	BPWA	$\pi^+ p \rightarrow \pi^+ p$
209	CRAWFORD	80	DPWA	$\gamma N \rightarrow \pi N$
216	BARBOUR	78	DPWA	$\gamma N \rightarrow \pi N$
200	[2] LONGACRE	77	IPWA	$\pi N \rightarrow N\pi\pi$
240	[3] LONGACRE	75	IPWA	$\pi N \rightarrow N\pi\pi$

$\Delta(1700)$ POLE POSITION

REAL PART

VALUE (MeV)	DOCUMENT ID		TECN	COMMENT
1620 to 1700 (≈ 1660) OUR ESTIMATE				
1655	ARNDT	95	DPWA	$\pi N \rightarrow N\pi$
1651	[4] HOEHLER	93	SPED	$\pi N \rightarrow \pi N$
1675 ±25	CUTKOSKY	80	IPWA	$\pi N \rightarrow \pi N$
• • • We do not use the following data for averages, fits, limits, etc. • • •				
1726	VRANA	00	DPWA	Multichannel
1646	ARNDT	91	DPWA	$\pi N \rightarrow \pi N$ Soln SM90
1681 or 1672	[5] LONGACRE	78	IPWA	$\pi N \rightarrow N\pi\pi$
1600 or 1594	[2] LONGACRE	77	IPWA	$\pi N \rightarrow N\pi\pi$

−2×IMAGINARY PART

VALUE (MeV)	DOCUMENT ID		TECN	COMMENT
150 to 250 (≈ 200) OUR ESTIMATE				
242	ARNDT	95	DPWA	$\pi N \rightarrow N\pi$
159	[4] HOEHLER	93	SPED	$\pi N \rightarrow \pi N$
220±40	CUTKOSKY	80	IPWA	$\pi N \rightarrow \pi N$
• • • We do not use the following data for averages, fits, limits, etc. • • •				
118	VRANA	00	DPWA	Multichannel
208	ARNDT	91	DPWA	$\pi N \rightarrow \pi N$ Soln SM90
245 or 241	[5] LONGACRE	78	IPWA	$\pi N \rightarrow N\pi\pi$
208 or 201	[2] LONGACRE	77	IPWA	$\pi N \rightarrow N\pi\pi$

$\Delta(1700)$ ELASTIC POLE RESIDUE

MODULUS $|r|$

VALUE (MeV)	DOCUMENT ID		TECN	COMMENT
16	ARNDT	95	DPWA	$\pi N \rightarrow N\pi$
10	HOEHLER	93	SPED	$\pi N \rightarrow \pi N$
13±3	CUTKOSKY	80	IPWA	$\pi N \rightarrow \pi N$
• • • We do not use the following data for averages, fits, limits, etc. • • •				
13	ARNDT	91	DPWA	$\pi N \rightarrow \pi N$ Soln SM90

PHASE θ

VALUE (°)	DOCUMENT ID		TECN	COMMENT
−12	ARNDT	95	DPWA	$\pi N \to \pi N$
−20 ± 25	CUTKOSKY	80	IPWA	$\pi N \to \pi N$
• • • We do not use the following data for averages, fits, limits, etc. • • •				
−22	ARNDT	91	DPWA	$\pi N \to \pi N$ Soln SM90

Δ(1700) DECAY MODES

The following branching fractions are our estimates, not fits or averages.

	Mode	Fraction (Γ_i/Γ)
Γ_1	$N\pi$	10–20 %
Γ_2	ΣK	
Γ_3	$N\pi\pi$	80–90 %
Γ_4	$\Delta\pi$	30–60 %
Γ_5	$\Delta(1232)\pi$, S-wave	25–50 %
Γ_6	$\Delta(1232)\pi$, D-wave	1–7 %
Γ_7	$N\rho$	30–55 %
Γ_8	$N\rho$, S=1/2, D-wave	
Γ_9	$N\rho$, S=3/2, S-wave	5–20 %
Γ_{10}	$N\rho$, S=3/2, D-wave	
Γ_{11}	$N\gamma$	0.12–0.26 %
Γ_{12}	$N\gamma$, helicity=1/2	0.08–0.16 %
Γ_{13}	$N\gamma$, helicity=3/2	0.025–0.12 %

Δ(1700) BRANCHING RATIOS

$\Gamma(N\pi)/\Gamma_{total}$ Γ_1/Γ

VALUE	DOCUMENT ID		TECN	COMMENT
0.10 to 0.20 OUR ESTIMATE				
0.14 ± 0.06	MANLEY	92	IPWA	$\pi N \to \pi N$ & $N\pi\pi$
0.12 ± 0.03	CUTKOSKY	80	IPWA	$\pi N \to \pi N$
0.20 ± 0.03	HOEHLER	79	IPWA	$\pi N \to \pi N$
• • • We do not use the following data for averages, fits, limits, etc. • • •				
0.14 ± 0.01	PENNER	02C	DPWA	Multichannel
0.05 ± 0.01	VRANA	00	DPWA	Multichannel
0.16	ARNDT	95	DPWA	$\pi N \to \pi N$
0.16	[1] CHEW	80	BPWA	$\pi^+ p \to \pi^+ p$

$(\Gamma_i\Gamma_f)^{1/2}/\Gamma_{total}$ in $N\pi \to \Delta(1700) \to \Sigma K$ $(\Gamma_1\Gamma_2)^{1/2}/\Gamma$

VALUE	DOCUMENT ID		TECN	COMMENT
• • • We do not use the following data for averages, fits, limits, etc. • • •				
0.002	LIVANOS	80	DPWA	$\pi p \to \Sigma K$
0.001 to 0.011	[6] DEANS	75	DPWA	$\pi N \to \Sigma K$

Note: Signs of couplings from $\pi N \to N\pi\pi$ analyses were changed in the 1986 edition to agree with the baryon-first convention; the overall phase ambiguity is resolved by choosing a negative sign for the Δ(1620) S_{31} coupling to $\Delta(1232)\pi$.

$(\Gamma_i\Gamma_f)^{1/2}/\Gamma_{total}$ in $N\pi \to \Delta(1700) \to \Delta(1232)\pi$, S-wave $(\Gamma_1\Gamma_5)^{1/2}/\Gamma$

VALUE	DOCUMENT ID		TECN	COMMENT
+0.21 to +0.29 OUR ESTIMATE				
+0.32 ± 0.06	MANLEY	92	IPWA	$\pi N \to \pi N$ & $N\pi\pi$
+0.18 ± 0.04	BARNHAM	80	IPWA	$\pi N \to N\pi\pi$
+0.30	[2,7] LONGACRE	77	IPWA	$\pi N \to N\pi\pi$
+0.24	[3] LONGACRE	75	IPWA	$\pi N \to N\pi\pi$

$\Gamma(\Delta(1232)\pi$, S-wave$)/\Gamma_{total}$ Γ_5/Γ

VALUE	DOCUMENT ID	TECN	COMMENT
0.90 ± 0.02	VRANA 00	DPWA	Multichannel

$(\Gamma_i\Gamma_f)^{1/2}/\Gamma_{total}$ in $N\pi \to \Delta(1700) \to \Delta(1232)\pi$, D-wave $(\Gamma_1\Gamma_6)^{1/2}/\Gamma$

VALUE	DOCUMENT ID		TECN	COMMENT
+0.05 to +0.11 OUR ESTIMATE				
+0.08 ± 0.03	MANLEY	92	IPWA	$\pi N \to \pi N$ & $N\pi\pi$
0.14 ± 0.04	BARNHAM	80	IPWA	$\pi N \to N\pi\pi$
+0.05	[2,7] LONGACRE	77	IPWA	$\pi N \to N\pi\pi$
+0.10	[3] LONGACRE	75	IPWA	$\pi N \to N\pi\pi$

$\Gamma(\Delta(1232)\pi$, D-wave$)/\Gamma_{total}$ Γ_6/Γ

VALUE	DOCUMENT ID	TECN	COMMENT
0.04 ± 0.01	VRANA 00	DPWA	Multichannel

$(\Gamma_i\Gamma_f)^{1/2}/\Gamma_{total}$ in $N\pi \to \Delta(1700) \to N\rho$, S=1/2, D-wave $(\Gamma_1\Gamma_8)^{1/2}/\Gamma$

VALUE	DOCUMENT ID		TECN	COMMENT
+0.17 ± 0.05	BARNHAM	80	IPWA	$\pi N \to N\pi\pi$

$(\Gamma_i\Gamma_f)^{1/2}/\Gamma_{total}$ in $N\pi \to \Delta(1700) \to N\rho$, S=3/2, S-wave $(\Gamma_1\Gamma_9)^{1/2}/\Gamma$

VALUE	DOCUMENT ID		TECN	COMMENT
±0.11 to ±0.19 OUR ESTIMATE				
+0.10 ± 0.03	MANLEY	92	IPWA	$\pi N \to \pi N$ & $N\pi\pi$
+0.04	[2,7] LONGACRE	77	IPWA	$\pi N \to N\pi\pi$
−0.30	[3] LONGACRE	75	IPWA	$\pi N \to N\pi\pi$

$\Gamma(N\rho$, S=3/2, S-wave$)/\Gamma_{total}$ Γ_9/Γ

VALUE	DOCUMENT ID	TECN	COMMENT
0.01 ± 0.01	VRANA 00	DPWA	Multichannel

$(\Gamma_i\Gamma_f)^{1/2}/\Gamma_{total}$ in $N\pi \to \Delta(1700) \to N\rho$, S=3/2, D-wave $(\Gamma_1\Gamma_{10})^{1/2}/\Gamma$

VALUE	DOCUMENT ID		TECN	COMMENT
0.18 ± 0.07	BARNHAM	80	IPWA	$\pi N \to N\pi\pi$

Δ(1700) PHOTON DECAY AMPLITUDES

Δ(1700) → $N\gamma$, helicity-1/2 amplitude $A_{1/2}$

VALUE (GeV$^{-1/2}$)	DOCUMENT ID		TECN	COMMENT
+0.104 ± 0.015 OUR ESTIMATE				
0.090 ± 0.025	ARNDT	96	IPWA	$\gamma N \to \pi N$
0.111 ± 0.017	CRAWFORD	83	IPWA	$\gamma N \to \pi N$
0.089 ± 0.033	AWAJI	81	DPWA	$\gamma N \to \pi N$
0.112 ± 0.006	ARAI	80	DPWA	$\gamma N \to \pi N$ (fit 1)
0.130 ± 0.006	ARAI	80	DPWA	$\gamma N \to \pi N$ (fit 2)
0.123 ± 0.022	CRAWFORD	80	DPWA	$\gamma N \to \pi N$
• • • We do not use the following data for averages, fits, limits, etc. • • •				
0.096	PENNER	02D	DPWA	Multichannel
0.121 ± 0.004	LI	93	IPWA	$\gamma N \to \pi N$
+0.130 ± 0.037	BARBOUR	78	DPWA	$\gamma N \to \pi N$
+0.072 ± 0.033	FELLER	76	DPWA	$\gamma N \to \pi N$

Δ(1700) → $N\gamma$, helicity-3/2 amplitude $A_{3/2}$

VALUE (GeV$^{-1/2}$)	DOCUMENT ID		TECN	COMMENT
+0.085 ± 0.022 OUR ESTIMATE				
0.097 ± 0.020	ARNDT	96	IPWA	$\gamma N \to \pi N$
0.107 ± 0.015	CRAWFORD	83	IPWA	$\gamma N \to \pi N$
0.060 ± 0.015	AWAJI	81	DPWA	$\gamma N \to \pi N$
0.047 ± 0.007	ARAI	80	DPWA	$\gamma N \to \pi N$ (fit 1)
0.050 ± 0.007	ARAI	80	DPWA	$\gamma N \to \pi N$ (fit 2)
0.102 ± 0.015	CRAWFORD	80	DPWA	$\gamma N \to \pi N$
• • • We do not use the following data for averages, fits, limits, etc. • • •				
0.154	PENNER	02D	DPWA	Multichannel
0.115 ± 0.004	LI	93	IPWA	$\gamma N \to \pi N$
+0.098 ± 0.036	BARBOUR	78	DPWA	$\gamma N \to \pi N$
+0.087 ± 0.023	FELLER	76	DPWA	$\gamma N \to \pi N$

Δ(1700) FOOTNOTES

[1] Problems with CHEW 80 are discussed in section 2.1.11 of HOEHLER 83.
[2] LONGACRE 77 pole positions are from a search for poles in the unitarized T-matrix; the first (second) value uses, in addition to $\pi N \to N\pi\pi$ data, elastic amplitudes from a Saclay (CERN) partial-wave analysis. The other LONGACRE 77 values are from eyeball fits with Breit-Wigner circles to the T-matrix amplitudes.
[3] From method II of LONGACRE 75: eyeball fits with Breit-Wigner circles to the T-matrix amplitudes.
[4] See HOEHLER 93 for a detailed discussion of the evidence for and the pole parameters of N and Δ resonances as determined from Argand diagrams of πN elastic partial-wave amplitudes and from plots of the speeds with which the amplitudes traverse the diagrams.
[5] LONGACRE 78 values are from a search for poles in the unitarized T-matrix. The first (second) value uses, in addition to $\pi N \to N\pi\pi$ data, elastic amplitudes from a Saclay (CERN) partial-wave analysis.
[6] The range given is from the four best solutions. DEANS 75 disagrees with $\pi^+ p \to \Sigma^+ K^+$ data of WINNIK 77 around 1920 MeV.
[7] LONGACRE 77 considers this coupling to be well determined.

Δ(1700) REFERENCES

For early references, see Physics Letters **111B** 70 (1982).

PENNER	02C	PR C66 055211	G. Penner, U. Mosel	(GIES)
PENNER	02D	PR C66 055212	G. Penner, U. Mosel	(GIES)
VRANA	00	PRPL 328 181	T.P. Vrana, S.A. Dytman,, T.-S.H. Lee	(PITT+)
ARNDT	96	PR C53 430	R.A. Arndt, I.I. Strakovsky, R.L. Workman	(VPI)
ARNDT	95	PR C52 2120	R.A. Arndt *et al.*	(VPI, BRCO)
HOEHLER	93	πN Newsletter 9 1	G. Hohler	(KARL)
LI	93	PR C47 2759	Z.J. Li *et al.*	(VPI)
MANLEY	92	PR D45 4002	D.M. Manley, E.M. Saleski	(KENT) IJP
Also	84	PR D30 904	D.M. Manley *et al.*	(VPI)
ARNDT	91	PR D43 2131	R.A. Arndt *et al.*	(VPI, TELE) IJP
CRAWFORD	83	NP B211 1	R.L. Crawford, W.T. Morton	(GLAS)
HOEHLER	83	Landolt-Boernstein 1/9B2	G. Hohler	(KARLT)
PDG	82	PL 111B	M. Roos *et al.*	(HELS, CIT, CERN)
AWAJI	81	Bonn Conf. 352	N. Awaji, R. Kajikawa	(NAGO)
Also	82	NP B197 365	K. Fujii *et al.*	(NAGO)
ARAI	80	Toronto Conf. 93	I. Arai	(INUS)
Also	82	NP B194 251	I. Arai, H. Fujii	(INUS)
BARNHAM	80	NP B168 243	K.W.J. Barnham *et al.*	(LOIC)
CHEW	80	Toronto Conf. 123	D.M. Chew	(LBL) IJP

CRAWFORD	80	Toronto Conf. 107	R.L. Crawford	(GLAS)
CUTKOSKY	80	Toronto Conf. 19	R.E. Cutkosky *et al.*	(CMU, LBL) IJP
Also	79	PR D20 2839	R.E. Cutkosky *et al.*	(CMU, LBL) IJP
LIVANOS	80	Toronto Conf. 35	P. Livanos *et al.*	(SACL) IJP
HOEHLER	79	PDAT 12-1	G. Höhler *et al.*	(KARLT) IJP
Also	80	Toronto Conf. 3	R. Koch	(KARLT) IJP
BARBOUR	78	NP B141 253	I.M. Barbour, R.L. Crawford, N.H. Parsons	(GLAS)
LONGACRE	78	PR D17 1795	R.S. Longacre *et al.*	(LBL, SLAC)
LONGACRE	77	NP B122 493	R.S. Longacre, J. Dolbeau	(SACL) IJP
Also	76	NP B108 365	J. Dolbeau *et al.*	(SACL) IJP
WINNIK	77	NP B128 66	M. Winnik *et al.*	(HAIF) I
FELLER	76	NP B104 219	P. Feller *et al.*	(NAGO, OSAK) IJP
DEANS	75	NP B96 90	S.R. Deans *et al.*	(SFLA, ALAH) IJP
LONGACRE	75	PL 55B 415	R.S. Longacre *et al.*	(LBL, SLAC) IJP

Δ(1750) P_{31}

$I(J^P) = \frac{3}{2}(\frac{1}{2}^+)$ Status: *

OMITTED FROM SUMMARY TABLE

Δ(1750) BREIT-WIGNER MASS

VALUE (MeV)	DOCUMENT ID		TECN	COMMENT
≈ 1750 OUR ESTIMATE				
1744 ±36	MANLEY	92	IPWA	$\pi N \to \pi N$ & $N\pi\pi$
• • • We do not use the following data for averages, fits, limits, etc. • • •				
1712 ± 1	PENNER	02C	DPWA	Multichannel
1721 ±61	VRANA	00	DPWA	Multichannel
1715.2±21.0	[1] CHEW	80	BPWA	$\pi^+ p \to \pi^+ p$
1778.4± 9.0	[1] CHEW	80	BPWA	$\pi^+ p \to \pi^+ p$

Δ(1750) BREIT-WIGNER WIDTH

VALUE (MeV)	DOCUMENT ID		TECN	COMMENT
300 ±120	MANLEY	92	IPWA	$\pi N \to \pi N$ & $N\pi\pi$
• • • We do not use the following data for averages, fits, limits, etc. • • •				
643 ± 17	PENNER	02C	DPWA	Multichannel
70 ± 50	VRANA	00	DPWA	Multichannel
93.3± 55.0	[1] CHEW	80	BPWA	$\pi^+ p \to \pi^+ p$
23.0± 29.0	[1] CHEW	80	BPWA	$\pi^+ p \to \pi^+ p$

Δ(1750) POLE POSITION

REAL PART

VALUE (MeV)	DOCUMENT ID		TECN	COMMENT
• • • We do not use the following data for averages, fits, limits, etc. • • •				
1714	VRANA	00	DPWA	Multichannel

−2×IMAGINARY PART

VALUE (MeV)	DOCUMENT ID		TECN	COMMENT
• • • We do not use the following data for averages, fits, limits, etc. • • •				
68	VRANA	00	DPWA	Multichannel

Δ(1750) DECAY MODES

	Mode
Γ_1	$N\pi$
Γ_2	$N\pi\pi$
Γ_3	$N(1440)\pi$
Γ_4	ΣK

Δ(1750) BRANCHING RATIOS

$\Gamma(N\pi)/\Gamma_{total}$ Γ_1/Γ

VALUE	DOCUMENT ID		TECN	COMMENT
0.08±0.03	MANLEY	92	IPWA	$\pi N \to \pi N$ & $N\pi\pi$
• • • We do not use the following data for averages, fits, limits, etc. • • •				
0.01±0.01	PENNER	02C	DPWA	Multichannel
0.06±0.09	VRANA	00	DPWA	Multichannel
0.18	[1] CHEW	80	BPWA	$\pi^+ p \to \pi^+ p$
0.20	[1] CHEW	80	BPWA	$\pi^+ p \to \pi^+ p$

$(\Gamma_i\Gamma_f)^{1/2}/\Gamma_{total}$ in $N\pi \to \Delta(1700) \to N(1440)\pi$ $(\Gamma_1\Gamma_3)^{1/2}/\Gamma$

VALUE	DOCUMENT ID		TECN	COMMENT
+0.15±0.03	MANLEY	92	IPWA	$\pi N \to \pi N$ & $N\pi\pi$

$\Gamma(N(1440)\pi)/\Gamma_{total}$ Γ_3/Γ

VALUE	DOCUMENT ID		TECN	COMMENT
0.83±0.01	VRANA	00	DPWA	Multichannel

$\Gamma(\Sigma K)/\Gamma_{total}$ Γ_4/Γ

VALUE	DOCUMENT ID		TECN	COMMENT
• • • We do not use the following data for averages, fits, limits, etc. • • •				
0.001±0.001	PENNER	02C	DPWA	Multichannel

Δ(1750) PHOTON DECAY AMPLITUDES

Δ(1750) → $N\gamma$, helicity-1/2 amplitude $A_{1/2}$

VALUE (GeV$^{-1/2}$)	DOCUMENT ID		TECN	COMMENT
• • • We do not use the following data for averages, fits, limits, etc. • • •				
0.053	PENNER	02D	DPWA	Multichannel

Δ(1750) FOOTNOTES

[1] CHEW 80 reports four resonances in the P_{31} wave — see also the Δ(1910). Problems with this analysis are discussed in section 2.1.11 of HOEHLER 83.

Δ(1750) REFERENCES

PENNER	02C	PR C66 055211	G. Penner, U. Mosel	(GIES)
PENNER	02D	PR C66 055212	G. Penner, U. Mosel	(GIES)
VRANA	00	PRPL 328 181	T.P. Vrana, S.A. Dytman,, T.-S.H. Lee	(PITT+)
MANLEY	92	PR D45 4002	D.M. Manley, E.M. Saleski	(KENT)
Also	84	PR D30 904	D.M. Manley *et al.*	(VPI)
HOEHLER	83	Landolt-Boernstein 1/9B2	G. Höhler	(KARLT)
CHEW	80	Toronto Conf. 123	D.M. Chew	(LBL)

Δ(1900) S_{31}

$I(J^P) = \frac{3}{2}(\frac{1}{2}^-)$ Status: **

OMITTED FROM SUMMARY TABLE

Δ(1900) BREIT-WIGNER MASS

VALUE (MeV)	DOCUMENT ID		TECN	COMMENT
1850 to 1950 (≈ 1900) OUR ESTIMATE				
1920 ±24	MANLEY	92	IPWA	$\pi N \to \pi N$ & $N\pi\pi$
1890 ±50	CUTKOSKY	80	IPWA	$\pi N \to \pi N$
1908 ±30	HOEHLER	79	IPWA	$\pi N \to \pi N$
• • • We do not use the following data for averages, fits, limits, etc. • • •				
1802 ±87	VRANA	00	DPWA	Multichannel
1918.5±23.0	CHEW	80	BPWA	$\pi^+ p \to \pi^+ p$
1803	CRAWFORD	80	DPWA	$\gamma N \to \pi N$

Δ(1900) BREIT-WIGNER WIDTH

VALUE (MeV)	DOCUMENT ID		TECN	COMMENT
140 to 240 (≈ 200) OUR ESTIMATE				
263 ±39	MANLEY	92	IPWA	$\pi N \to \pi N$ & $N\pi\pi$
170 ±50	CUTKOSKY	80	IPWA	$\pi N \to \pi N$
140 ±40	HOEHLER	79	IPWA	$\pi N \to \pi N$
• • • We do not use the following data for averages, fits, limits, etc. • • •				
48 ±45	VRANA	00	DPWA	Multichannel
93.5±54.0	CHEW	80	BPWA	$\pi^+ p \to \pi^+ p$
137	CRAWFORD	80	DPWA	$\gamma N \to \pi N$

Δ(1900) POLE POSITION

REAL PART

VALUE (MeV)	DOCUMENT ID		TECN	COMMENT
1780	[1] HOEHLER	93	SPED	$\pi N \to \pi N$
1870±40	CUTKOSKY	80	IPWA	$\pi N \to \pi N$
• • • We do not use the following data for averages, fits, limits, etc. • • •				
1795	VRANA	00	DPWA	Multichannel
not seen	ARNDT	91	DPWA	$\pi N \to \pi N$ Soln SM90
2029 or 2025	[2] LONGACRE	78	IPWA	$\pi N \to N\pi\pi$

−2×IMAGINARY PART

VALUE (MeV)	DOCUMENT ID		TECN	COMMENT
180±50	CUTKOSKY	80	IPWA	$\pi N \to \pi N$
• • • We do not use the following data for averages, fits, limits, etc. • • •				
58	VRANA	00	DPWA	Multichannel
not seen	ARNDT	91	DPWA	$\pi N \to \pi N$ Soln SM90
164 or 163	[2] LONGACRE	78	IPWA	$\pi N \to N\pi\pi$

Δ(1900) ELASTIC POLE RESIDUE

MODULUS $|r|$

VALUE (MeV)	DOCUMENT ID		TECN	COMMENT
10±3	CUTKOSKY	80	IPWA	$\pi N \to \pi N$

PHASE θ

VALUE (°)	DOCUMENT ID		TECN	COMMENT
+20±40	CUTKOSKY	80	IPWA	$\pi N \to \pi N$

Baryon Particle Listings

$\Delta(1900)$, $\Delta(1905)$

$\Delta(1900)$ DECAY MODES

The following branching fractions are our estimates, not fits or averages.

	Mode	Fraction (Γ_i/Γ)
Γ_1	$N\pi$	10–30 %
Γ_2	ΣK	
Γ_3	$N\pi\pi$	
Γ_4	$\Delta\pi$	
Γ_5	$\Delta(1232)\pi$, D-wave	
Γ_6	$N\rho$	
Γ_7	$N\rho$, S=1/2, S-wave	
Γ_8	$N\rho$, S=3/2, D-wave	
Γ_9	$N(1440)\pi$, S-wave	
Γ_{10}	$N\gamma$, helicity=1/2	

$\Delta(1900)$ BRANCHING RATIOS

$\Gamma(N\pi)/\Gamma_{total}$ Γ_1/Γ

VALUE	DOCUMENT ID		TECN	COMMENT
0.1 to 0.3 OUR ESTIMATE				
0.41 ± 0.04	MANLEY	92	IPWA	$\pi N \to \pi N$ & $N\pi\pi$
0.10 ± 0.03	CUTKOSKY	80	IPWA	$\pi N \to \pi N$
0.08 ± 0.04	HOEHLER	79	IPWA	$\pi N \to \pi N$
• • • We do not use the following data for averages, fits, limits, etc. • • •				
0.33 ± 0.10	VRANA	00	DPWA	Multichannel
0.28	CHEW	80	BPWA	$\pi^+ p \to \pi^+ p$

$(\Gamma_i\Gamma_f)^{1/2}/\Gamma_{total}$ in $N\pi \to \Delta(1900) \to \Sigma K$ $(\Gamma_1\Gamma_2)^{1/2}/\Gamma$

VALUE	DOCUMENT ID		TECN	COMMENT
<0.03	CANDLIN	84	DPWA	$\pi^+ p \to \Sigma^+ K^+$
• • • We do not use the following data for averages, fits, limits, etc. • • •				
0.076	[3] DEANS	75	DPWA	$\pi N \to \Sigma K$
0.11	LANGBEIN	73	IPWA	$\pi N \to \Sigma K$ (sol. 1)
0.12	LANGBEIN	73	IPWA	$\pi N \to \Sigma K$ (sol. 2)

$(\Gamma_i\Gamma_f)^{1/2}/\Gamma_{total}$ in $N\pi \to \Delta(1900) \to \Delta(1232)\pi$, D-wave $(\Gamma_1\Gamma_5)^{1/2}/\Gamma$

VALUE	DOCUMENT ID		TECN	COMMENT
$+0.25\pm0.07$	MANLEY	92	IPWA	$\pi N \to \pi N$ & $N\pi\pi$

$\Gamma(\Delta(1232)\pi$, D-wave$)/\Gamma_{total}$ Γ_5/Γ

VALUE	DOCUMENT ID		TECN	COMMENT
0.28 ± 0.01	VRANA	00	DPWA	Multichannel

$(\Gamma_i\Gamma_f)^{1/2}/\Gamma_{total}$ in $N\pi \to \Delta(1900) \to N\rho$, S=1/2, S-wave $(\Gamma_1\Gamma_7)^{1/2}/\Gamma$

VALUE	DOCUMENT ID		TECN	COMMENT
-0.14 ± 0.11	MANLEY	92	IPWA	$\pi N \to \pi N$ & $N\pi\pi$

$\Gamma(N\rho$, S=1/2, S-wave$)/\Gamma_{total}$ Γ_7/Γ

VALUE	DOCUMENT ID		TECN	COMMENT
0.30 ± 0.02	VRANA	00	DPWA	Multichannel

$(\Gamma_i\Gamma_f)^{1/2}/\Gamma_{total}$ in $N\pi \to \Delta(1900) \to N\rho$, S=3/2, D-wave $(\Gamma_1\Gamma_8)^{1/2}/\Gamma$

VALUE	DOCUMENT ID		TECN	COMMENT
-0.37 ± 0.07	MANLEY	92	IPWA	$\pi N \to \pi N$ & $N\pi\pi$

$\Gamma(N\rho$, S=3/2, D-wave$)/\Gamma_{total}$ Γ_8/Γ

VALUE	DOCUMENT ID		TECN	COMMENT
0.05 ± 0.01	VRANA	00	DPWA	Multichannel

$(\Gamma_i\Gamma_f)^{1/2}/\Gamma_{total}$ in $N\pi \to \Delta(1900) \to N(1440)\pi$, S-wave $(\Gamma_1\Gamma_9)^{1/2}/\Gamma$

VALUE	DOCUMENT ID		TECN	COMMENT
-0.16 ± 0.11	MANLEY	92	IPWA	$\pi N \to \pi N$ & $N\pi\pi$

$\Gamma(N(1440)\pi$, S-wave$)/\Gamma_{total}$ Γ_9/Γ

VALUE	DOCUMENT ID		TECN	COMMENT
0.04 ± 0.01	VRANA	00	DPWA	Multichannel

$\Delta(1900)$ PHOTON DECAY AMPLITUDES

$\Delta(1900) \to N\gamma$, helicity-1/2 amplitude $A_{1/2}$

VALUE (GeV$^{-1/2}$)	DOCUMENT ID		TECN	COMMENT
-0.004 ± 0.016	CRAWFORD	83	IPWA	$\gamma N \to \pi N$
0.029 ± 0.008	AWAJI	81	DPWA	$\gamma N \to \pi N$
• • • We do not use the following data for averages, fits, limits, etc. • • •				
-0.006 to -0.025	CRAWFORD	80	DPWA	$\gamma N \to \pi N$

$\Delta(1900)$ FOOTNOTES

[1] See HOEHLER 93 for a detailed discussion of the evidence for and the pole parameters of N and Δ resonances as determined from Argand diagrams of πN elastic partial-wave amplitudes and from plots of the speeds with which the amplitudes traverse the diagrams.

[2] LONGACRE 78 values are from a search for poles in the unitarized T-matrix. The first (second) value uses, in addition to $\pi N \to N\pi\pi$ data, elastic amplitudes from a Saclay (CERN) partial-wave analysis.

[3] The value given is from solution 1; the resonance is not present in solutions 2, 3, or 4.

$\Delta(1900)$ REFERENCES

For early references, see Physics Letters **111B** 70 (1982).

VRANA	00	PRPL 328 181	T.P. Vrana, S.A. Dytman,, T.-S.H. Lee	(PITT+)
HOEHLER	93	πN Newsletter 9 1	G. Hohler	(KARL)
MANLEY	92	PR D45 4002	D.M. Manley, E.M. Saleski	(KENT) IJP
Also	84	PR D30 904	D.M. Manley *et al.*	(VPI)
ARNDT	91	PR D43 2131	R.A. Arndt *et al.*	(VPI, TELE) IJP
CANDLIN	84	NP B238 477	D.J. Candlin *et al.*	(EDIN, RAL, LOWC)
CRAWFORD	83	NP B211 1	R.L. Crawford, W.T. Morton	(GLAS)
AWAJI	81	Bonn Conf. 352	N. Awaji, R. Kajikawa	(NAGO)
Also	82	NP B197 365	K. Fujii *et al.*	(NAGO)
CHEW	80	Toronto Conf. 123	D.M. Chew	(LBL) IJP
CRAWFORD	80	Toronto Conf. 107	R.L. Crawford	(GLAS)
CUTKOSKY	80	Toronto Conf. 19	R.E. Cutkosky *et al.*	(CMU, LBL) IJP
Also	79	PR D20 2839	R.E. Cutkosky *et al.*	(CMU, LBL) IJP
HOEHLER	79	PDAT 12-1	G. Hohler *et al.*	(KARLT) IJP
Also	80	Toronto Conf. 3	R. Koch	(KARLT) IJP
LONGACRE	78	PR D17 1795	R.S. Longacre *et al.*	(LBL, SLAC)
DEANS	75	NP B96 90	S.R. Deans *et al.*	(SFLA, ALAH) IJP
LANGBEIN	73	NP B53 251	W. Langbein, F. Wagner	(MUNI) IJP

$\Delta(1905)$ F_{35}

$I(J^P) = \frac{3}{2}(\frac{5}{2}^+)$ Status: ****

Most of the results published before 1975 are now obsolete and have been omitted. They may be found in our 1982 edition, Physics Letters **111B** (1982).

$\Delta(1905)$ BREIT-WIGNER MASS

VALUE (MeV)	DOCUMENT ID		TECN	COMMENT
1870 to 1920 (≈ 1905) OUR ESTIMATE				
$1881\ \pm18$	MANLEY	92	IPWA	$\pi N \to \pi N$ & $N\pi\pi$
$1910\ \pm30$	CUTKOSKY	80	IPWA	$\pi N \to \pi N$
$1905\ \pm20$	HOEHLER	79	IPWA	$\pi N \to \pi N$
• • • We do not use the following data for averages, fits, limits, etc. • • •				
$1873\ \pm77$	VRANA	00	DPWA	Multichannel
$1895\ \pm\ 8$	ARNDT	96	IPWA	$\gamma N \to \pi N$
1850	ARNDT	95	DPWA	$\pi N \to N\pi$
$1960\ \pm40$	CANDLIN	84	DPWA	$\pi^+ p \to \Sigma^+ K^+$
$1787.0^{+\ 6.0}_{-\ 5.7}$	CHEW	80	BPWA	$\pi^+ p \to \pi^+ p$
1880	CRAWFORD	80	DPWA	$\gamma N \to \pi N$
1892	BARBOUR	78	DPWA	$\gamma N \to \pi N$
1830	[1] LONGACRE	75	IPWA	$\pi N \to N\pi\pi$

$\Delta(1905)$ BREIT-WIGNER WIDTH

VALUE (MeV)	DOCUMENT ID		TECN	COMMENT
280 to 440 (≈ 350) OUR ESTIMATE				
$327\ \pm\ 51$	MANLEY	92	IPWA	$\pi N \to \pi N$ & $N\pi\pi$
$400\ \pm100$	CUTKOSKY	80	IPWA	$\pi N \to \pi N$
$260\ \pm\ 20$	HOEHLER	79	IPWA	$\pi N \to \pi N$
• • • We do not use the following data for averages, fits, limits, etc. • • •				
$461\ \pm111$	VRANA	00	DPWA	Multichannel
$354\ \pm\ 10$	ARNDT	96	IPWA	$\gamma N \to \pi N$
294	ARNDT	95	DPWA	$\pi N \to N\pi$
$270\ \pm\ 40$	CANDLIN	84	DPWA	$\pi^+ p \to \Sigma^+ K^+$
$66.0^{+\ 24.0}_{-\ 16.0}$	CHEW	80	BPWA	$\pi^+ p \to \pi^+ p$
193	CRAWFORD	80	DPWA	$\gamma N \to \pi N$
159	BARBOUR	78	DPWA	$\gamma N \to \pi N$
220	[1] LONGACRE	75	IPWA	$\pi N \to N\pi\pi$

$\Delta(1905)$ POLE POSITION

REAL PART

VALUE (MeV)	DOCUMENT ID		TECN	COMMENT
1800 to 1860 (≈ 1830) OUR ESTIMATE				
1832	ARNDT	95	DPWA	$\pi N \to N\pi$
1829	[2] HOEHLER	93	SPED	$\pi N \to \pi N$
1830 ± 40	CUTKOSKY	80	IPWA	$\pi N \to \pi N$
• • • We do not use the following data for averages, fits, limits, etc. • • •				
1793	VRANA	00	DPWA	Multichannel
1794	ARNDT	91	DPWA	$\pi N \to \pi N$ Soln SM90
1813 or 1808	[3] LONGACRE	78	IPWA	$\pi N \to N\pi\pi$

−2×IMAGINARY PART

VALUE (MeV)	DOCUMENT ID		TECN	COMMENT
230 to 330 (≈ 280) OUR ESTIMATE				
254	ARNDT	95	DPWA	$\pi N \to N\pi$
303	[2] HOEHLER	93	SPED	$\pi N \to \pi N$
280 ± 60	CUTKOSKY	80	IPWA	$\pi N \to \pi N$
• • • We do not use the following data for averages, fits, limits, etc. • • •				
302	VRANA	00	DPWA	Multichannel
230	ARNDT	91	DPWA	$\pi N \to \pi N$ Soln SM90
193 or 187	[3] LONGACRE	78	IPWA	$\pi N \to N\pi\pi$

Δ(1905) ELASTIC POLE RESIDUE

MODULUS |r|

VALUE (MeV)	DOCUMENT ID		TECN	COMMENT
12	ARNDT	95	DPWA	$\pi N \to N\pi$
25	HOEHLER	93	SPED	$\pi N \to \pi N$
25 ± 8	CUTKOSKY	80	IPWA	$\pi N \to \pi N$
• • • We do not use the following data for averages, fits, limits, etc. • • •				
14	ARNDT	91	DPWA	$\pi N \to \pi N$ Soln SM90

PHASE θ

VALUE (°)	DOCUMENT ID		TECN	COMMENT
− 4	ARNDT	95	DPWA	$\pi N \to N\pi$
−50 ± 20	CUTKOSKY	80	IPWA	$\pi N \to \pi N$
• • • We do not use the following data for averages, fits, limits, etc. • • •				
−40	ARNDT	91	DPWA	$\pi N \to \pi N$ Soln SM90

Δ(1905) DECAY MODES

The following branching fractions are our estimates, not fits or averages.

	Mode	Fraction (Γ_i/Γ)
Γ_1	$N\pi$	5–15 %
Γ_2	ΣK	
Γ_3	$N\pi\pi$	85–95 %
Γ_4	$\Delta\pi$	<25 %
Γ_5	$\Delta(1232)\pi$, *P*-wave	
Γ_6	$\Delta(1232)\pi$, *F*-wave	
Γ_7	$N\rho$	>60 %
Γ_8	$N\rho$, *S*=3/2, *P*-wave	
Γ_9	$N\rho$, *S*=3/2, *F*-wave	
Γ_{10}	$N\rho$, *S*=1/2, *F*-wave	
Γ_{11}	$N\gamma$	0.01–0.03 %
Γ_{12}	$N\gamma$, helicity=1/2	0.0–0.1 %
Γ_{13}	$N\gamma$, helicity=3/2	0.004–0.03 %

Δ(1905) BRANCHING RATIOS

$\Gamma(N\pi)/\Gamma_{total}$ Γ_1/Γ

VALUE	DOCUMENT ID		TECN	COMMENT
0.05 to 0.15 OUR ESTIMATE				
0.12 ± 0.03	MANLEY	92	IPWA	$\pi N \to \pi N$ & $N\pi\pi$
0.08 ± 0.03	CUTKOSKY	80	IPWA	$\pi N \to \pi N$
0.15 ± 0.02	HOEHLER	79	IPWA	$\pi N \to \pi N$
• • • We do not use the following data for averages, fits, limits, etc. • • •				
0.09 ± 0.01	VRANA	00	DPWA	Multichannel
0.12	ARNDT	95	DPWA	$\pi N \to N\pi$
0.11	CHEW	80	BPWA	$\pi^+ p \to \pi^+ p$

$(\Gamma_i\Gamma_f)^{1/2}/\Gamma_{total}$ in $N\pi \to \Delta(1905) \to \Sigma K$ $(\Gamma_1\Gamma_2)^{1/2}/\Gamma$

VALUE	DOCUMENT ID		TECN	COMMENT
− 0.015 ± 0.003	CANDLIN	84	DPWA	$\pi^+ p \to \Sigma^+ K^+$
• • • We do not use the following data for averages, fits, limits, etc. • • •				
− 0.013	LIVANOS	80	DPWA	$\pi p \to \Sigma K$
0.021 to 0.054	[4] DEANS	75	DPWA	$\pi N \to \Sigma K$

Note: Signs of couplings from $\pi N \to N\pi\pi$ analyses were changed in the 1986 edition to agree with the baryon-first convention; the overall phase ambiguity is resolved by choosing a negative sign for the Δ(1620) S_{31} coupling to Δ(1232)π.

$(\Gamma_i\Gamma_f)^{1/2}/\Gamma_{total}$ in $N\pi \to \Delta(1905) \to \Delta(1232)\pi$, *P*-wave $(\Gamma_1\Gamma_5)^{1/2}/\Gamma$

VALUE	DOCUMENT ID		TECN	COMMENT
− 0.04 ± 0.05	MANLEY	92	IPWA	$\pi N \to \pi N$ & $N\pi\pi$

$\Gamma(\Delta(1232)\pi$, *P*-wave$)/\Gamma_{total}$ Γ_5/Γ

VALUE	DOCUMENT ID		TECN	COMMENT
0.23 ± 0.01	VRANA	00	DPWA	Multichannel

$(\Gamma_i\Gamma_f)^{1/2}/\Gamma_{total}$ in $N\pi \to \Delta(1905) \to \Delta(1232)\pi$, *F*-wave $(\Gamma_1\Gamma_6)^{1/2}/\Gamma$

VALUE	DOCUMENT ID		TECN	COMMENT
+ 0.02 ± 0.03	MANLEY	92	IPWA	$\pi N \to \pi N$ & $N\pi\pi$
+ 0.20	[1] LONGACRE	75	IPWA	$\pi N \to N\pi\pi$
• • • We do not use the following data for averages, fits, limits, etc. • • •				
+ 0.17	[5] NOVOSELLER	78	IPWA	$\pi N \to N\pi\pi$
+ 0.06	[6] NOVOSELLER	78	IPWA	$\pi N \to N\pi\pi$

$\Gamma(\Delta(1232)\pi$, *F*-wave$)/\Gamma_{total}$ Γ_6/Γ

VALUE	DOCUMENT ID		TECN	COMMENT
0.44 ± 0.01	VRANA	00	DPWA	Multichannel

$(\Gamma_i\Gamma_f)^{1/2}/\Gamma_{total}$ in $N\pi \to \Delta(1905) \to N\rho$, *S*=3/2, *P*-wave $(\Gamma_1\Gamma_8)^{1/2}/\Gamma$

VALUE	DOCUMENT ID		TECN	COMMENT
+ 0.030 to + 0.36 OUR ESTIMATE				
+ 0.33 ± 0.03	MANLEY	92	IPWA	$\pi N \to \pi N$ & $N\pi\pi$
+ 0.33	[1] LONGACRE	75	IPWA	$\pi N \to N\pi\pi$
• • • We do not use the following data for averages, fits, limits, etc. • • •				
+ 0.26	[5] NOVOSELLER	78	IPWA	$\pi N \to N\pi\pi$
+ 0.11 to + 0.33	[7] NOVOSELLER	78	IPWA	$\pi N \to N\pi\pi$

$\Gamma(N\rho$, *S*=3/2, *P*-wave$)/\Gamma_{total}$ Γ_8/Γ

VALUE	DOCUMENT ID		TECN	COMMENT
0.24 ± 0.01	VRANA	00	DPWA	Multichannel

Δ(1905) PHOTON DECAY AMPLITUDES

Δ(1905) → $N\gamma$, helicity-1/2 amplitude $A_{1/2}$

VALUE (GeV$^{-1/2}$)	DOCUMENT ID		TECN	COMMENT
+ 0.026 ± 0.011 OUR ESTIMATE				
0.022 ± 0.005	ARNDT	96	IPWA	$\gamma N \to \pi N$
0.021 ± 0.010	CRAWFORD	83	IPWA	$\gamma N \to \pi N$
0.043 ± 0.020	AWAJI	81	DPWA	$\gamma N \to \pi N$
0.022 ± 0.010	ARAI	80	DPWA	$\gamma N \to \pi N$ (fit 1)
0.031 ± 0.009	ARAI	80	DPWA	$\gamma N \to \pi N$ (fit 2)
0.024 ± 0.014	CRAWFORD	80	DPWA	$\gamma N \to \pi N$
• • • We do not use the following data for averages, fits, limits, etc. • • •				
0.055 ± 0.004	LI	93	IPWA	$\gamma N \to \pi N$
+ 0.033 ± 0.018	BARBOUR	78	DPWA	$\gamma N \to \pi N$

Δ(1905) → $N\gamma$, helicity-3/2 amplitude $A_{3/2}$

VALUE (GeV$^{-1/2}$)	DOCUMENT ID		TECN	COMMENT
− 0.045 ± 0.020 OUR ESTIMATE				
− 0.045 ± 0.005	ARNDT	96	IPWA	$\gamma N \to \pi N$
− 0.056 ± 0.028	CRAWFORD	83	IPWA	$\gamma N \to \pi N$
− 0.025 ± 0.023	AWAJI	81	DPWA	$\gamma N \to \pi N$
− 0.029 ± 0.007	ARAI	80	DPWA	$\gamma N \to \pi N$ (fit 1)
− 0.045 ± 0.006	ARAI	80	DPWA	$\gamma N \to \pi N$ (fit 2)
− 0.072 ± 0.035	CRAWFORD	80	DPWA	$\gamma N \to \pi N$
• • • We do not use the following data for averages, fits, limits, etc. • • •				
0.002 ± 0.003	LI	93	IPWA	$\gamma N \to \pi N$
− 0.055 ± 0.019	BARBOUR	78	DPWA	$\gamma N \to \pi N$

Δ(1905) FOOTNOTES

[1] From method II of LONGACRE 75: eyeball fits with Breit-Wigner circles to the T-matrix amplitudes.

[2] See HOEHLER 93 for a detailed discussion of the evidence for and the pole parameters of *N* and Δ resonances as determined from Argand diagrams of πN elastic partial-wave amplitudes and from plots of the speeds with which the amplitudes traverse the diagrams.

[3] LONGACRE 78 values are from a search for poles in the unitarized T-matrix. The first (second) value uses, in addition to $\pi N \to N\pi\pi$ data, elastic amplitudes from a Saclay (CERN) partial-wave analysis.

[4] The range given for DEANS 75 is from the four best solutions.

[5] A Breit-Wigner fit to the HERNDON 75 IPWA.

[6] A Breit-Wigner fit to the NOVOSELLER 78B IPWA.

[7] A Breit-Wigner fit to the NOVOSELLER 78B IPWA; the phase is near 90°.

Δ(1905) REFERENCES

For early references, see Physics Letters **111B** 70 (1982).

VRANA	00	PRPL 328 181	T.P. Vrana, S.A. Dytman,, T.-S.H. Lee (PITT+)
ARNDT	96	PR C53 430	R.A. Arndt, I.I. Strakovsky, R.L. Workman (VPI)
ARNDT	95	PR C52 2120	R.A. Arndt *et al.* (VPI, BRCO)
HOEHLER	93	πN Newsletter 9 1	G. Hohler (KARL)
LI	93	PR C47 2759	Z.I. Li *et al.* (VPI)
MANLEY	92	PR D45 4002	D.M. Manley, E.M. Saleski (KENT) IJP
Also	84	PR D30 904	D.M. Manley *et al.* (VPI)
ARNDT	91	PR D43 2131	R.A. Arndt *et al.* (VPI, TELE) IJP
CANDLIN	84	NP B238 477	D.J. Candlin *et al.* (EDIN, RAL, LOWC)
CRAWFORD	83	NP B211 1	R.L. Crawford, W.T. Morton (GLAS)
PDG	82	PL 111B	M. Roos *et al.* (HELS, CIT, CERN)
AWAJI	81	Bonn Conf. 352	N. Awaji, R. Kajikawa (NAGO)
Also	82	NP B197 365	K. Fujii *et al.* (NAGO)
ARAI	80	Toronto Conf. 93	I. Arai (INUS)
Also	82	NP B194 251	I. Arai, H. Fujii (INUS)

CHEW	80	Toronto Conf. 123	D.M. Chew	(LBL) IJP
CRAWFORD	80	Toronto Conf. 107	R.L. Crawford	(GLAS)
CUTKOSKY	80	Toronto Conf. 19	R.E. Cutkosky *et al.*	(CMU, LBL) IJP
Also	79	PR D20 2839	R.E. Cutkosky *et al.*	(CMU, LBL) IJP
LIVANOS	80	Toronto Conf. 35	P. Livanos *et al.*	(SACL) IJP
HOEHLER	79	PDAT 12-1	G. Hohler *et al.*	(KARLT) IJP
Also	80	Toronto Conf. 3	R. Koch	(KARLT) IJP
BARBOUR	78	NP B141 253	I.M. Barbour, R.L. Crawford, N.H. Parsons	(GLAS)
LONGACRE	78	PR D17 1795	R.S. Longacre *et al.*	(LBL, SLAC)
NOVOSELLER	78	NP B137 509	D.E. Novoseller	(CIT) IJP
NOVOSELLER	78B	NP B137 445	D.E. Novoseller	(CIT) IJP
DEANS	75	NP B96 90	S.R. Deans *et al.*	(SFLA, ALAH) IJP
HERNDON	75	PR D11 3183	D. Herndon *et al.*	(LBL, SLAC)
LONGACRE	75	PL 55B 415	R.S. Longacre *et al.*	(LBL, SLAC) IJP

$\Delta(1910)$ P_{31}

$I(J^P) = \frac{3}{2}(\frac{1}{2}^+)$ Status: ****

Most of the results published before 1975 are now obsolete and have been omitted. They may be found in our 1982 edition, Physics Letters **111B** (1982).

$\Delta(1910)$ BREIT-WIGNER MASS

VALUE (MeV)	*DOCUMENT ID*		*TECN*	*COMMENT*
1870 to 1920 (≈ 1910) OUR ESTIMATE				
1882 ±10	MANLEY	92	IPWA	$\pi N \to \pi N$ & $N\pi\pi$
1910 ±40	CUTKOSKY	80	IPWA	$\pi N \to \pi N$
1888 ±20	HOEHLER	79	IPWA	$\pi N \to \pi N$
• • • We do not use the following data for averages, fits, limits, etc. • • •				
1995 ±12	VRANA	00	DPWA	Multichannel
2152	ARNDT	95	DPWA	$\pi N \to N\pi$
1960.1 ±21.0	[1] CHEW	80	BPWA	$\pi^+ p \to \pi^+ p$
2121.4 $^{+13.0}_{-14.3}$	[1] CHEW	80	BPWA	$\pi^+ p \to \pi^+ p$
1921	CRAWFORD	80	DPWA	$\gamma N \to \pi N$
1899	BARBOUR	78	DPWA	$\gamma N \to \pi N$
1790	[2] LONGACRE	77	IPWA	$\pi N \to N\pi\pi$

$\Delta(1910)$ BREIT-WIGNER WIDTH

VALUE (MeV)	*DOCUMENT ID*		*TECN*	*COMMENT*
190 to 270 (≈ 250) OUR ESTIMATE				
239 ± 25	MANLEY	92	IPWA	$\pi N \to \pi N$ & $N\pi\pi$
225 ± 50	CUTKOSKY	80	IPWA	$\pi N \to \pi N$
280 ± 50	HOEHLER	79	IPWA	$\pi N \to \pi N$
• • • We do not use the following data for averages, fits, limits, etc. • • •				
713 ±465	VRANA	00	DPWA	Multichannel
760	ARNDT	95	DPWA	$\pi N \to N\pi$
152.9± 60.0	[1] CHEW	80	BPWA	$\pi^+ p \to \pi^+ p$
172.2± 37.0	[1] CHEW	80	BPWA	$\pi^+ p \to \pi^+ p$
351	CRAWFORD	80	DPWA	$\gamma N \to \pi N$
230	BARBOUR	78	DPWA	$\gamma N \to \pi N$
170	[2] LONGACRE	77	IPWA	$\pi N \to N\pi\pi$

$\Delta(1910)$ POLE POSITION

REAL PART

VALUE (MeV)	*DOCUMENT ID*		*TECN*	*COMMENT*
1830 to 1880 (≈ 1855) OUR ESTIMATE				
1810	ARNDT	95	DPWA	$\pi N \to N\pi$
1874	[3] HOEHLER	93	SPED	$\pi N \to \pi N$
1880±30	CUTKOSKY	80	IPWA	$\pi N \to \pi N$
• • • We do not use the following data for averages, fits, limits, etc. • • •				
1880	VRANA	00	DPWA	Multichannel
1950	ARNDT	91	DPWA	$\pi N \to \pi N$ Soln SM90
1792 or 1801	[2] LONGACRE	77	IPWA	$\pi N \to N\pi\pi$

−2×IMAGINARY PART

VALUE (MeV)	*DOCUMENT ID*		*TECN*	*COMMENT*
200 to 500 (≈ 350) OUR ESTIMATE				
494	ARNDT	95	DPWA	$\pi N \to N\pi$
283	[3] HOEHLER	93	SPED	$\pi N \to \pi N$
200±40	CUTKOSKY	80	IPWA	$\pi N \to \pi N$
• • • We do not use the following data for averages, fits, limits, etc. • • •				
496	VRANA	00	DPWA	Multichannel
398	ARNDT	91	DPWA	$\pi N \to \pi N$ Soln SM90
172 or 165	[2] LONGACRE	77	IPWA	$\pi N \to N\pi\pi$

$\Delta(1910)$ ELASTIC POLE RESIDUE

MODULUS $|r|$

VALUE (MeV)	*DOCUMENT ID*		*TECN*	*COMMENT*
53	ARNDT	95	DPWA	$\pi N \to N\pi$
38	HOEHLER	93	SPED	$\pi N \to \pi N$
20±4	CUTKOSKY	80	IPWA	$\pi N \to \pi N$
• • • We do not use the following data for averages, fits, limits, etc. • • •				
37	ARNDT	91	DPWA	$\pi N \to \pi N$ Soln SM90

PHASE θ

VALUE (°)	*DOCUMENT ID*		*TECN*	*COMMENT*
−176	ARNDT	95	DPWA	$\pi N \to N\pi$
− 90±30	CUTKOSKY	80	IPWA	$\pi N \to \pi N$
• • • We do not use the following data for averages, fits, limits, etc. • • •				
− 91	ARNDT	91	DPWA	$\pi N \to \pi N$ Soln SM90

$\Delta(1910)$ DECAY MODES

The following branching fractions are our estimates, not fits or averages.

	Mode	Fraction (Γ_i/Γ)
Γ_1	$N\pi$	15–30 %
Γ_2	ΣK	
Γ_3	$N\pi\pi$	
Γ_4	$\Delta\pi$	
Γ_5	$\Delta(1232)\pi$, *P*-wave	
Γ_6	$N\rho$	
Γ_7	$N\rho$, S=3/2, *P*-wave	
Γ_8	$N(1440)\pi$	
Γ_9	$N(1440)\pi$, *P*-wave	
Γ_{10}	$N\gamma$	0.0–0.2 %
Γ_{11}	$N\gamma$, helicity=1/2	0.0–0.2 %

$\Delta(1910)$ BRANCHING RATIOS

$\Gamma(N\pi)/\Gamma_{total}$ Γ_1/Γ

VALUE	*DOCUMENT ID*		*TECN*	*COMMENT*
0.15 to 0.3 OUR ESTIMATE				
0.23±0.08	MANLEY	92	IPWA	$\pi N \to \pi N$ & $N\pi\pi$
0.19±0.03	CUTKOSKY	80	IPWA	$\pi N \to \pi N$
0.24±0.06	HOEHLER	79	IPWA	$\pi N \to \pi N$
• • • We do not use the following data for averages, fits, limits, etc. • • •				
0.29±0.21	VRANA	00	DPWA	Multichannel
0.26	ARNDT	95	DPWA	$\pi N \to N\pi$
0.17	[1] CHEW	80	BPWA	$\pi^+ p \to \pi^+ p$
0.40	[1] CHEW	80	BPWA	$\pi^+ p \to \pi^+ p$

$(\Gamma_i\Gamma_f)^{1/2}/\Gamma_{total}$ in $N\pi \to \Delta(1910) \to \Sigma K$ $(\Gamma_1\Gamma_2)^{1/2}/\Gamma$

VALUE	*DOCUMENT ID*		*TECN*	*COMMENT*
< 0.03	CANDLIN	84	DPWA	$\pi^+ p \to \Sigma^+ K^+$
• • • We do not use the following data for averages, fits, limits, etc. • • •				
− 0.019	LIVANOS	80	DPWA	$\pi p \to \Sigma K$
0.082 to 0.184	[4] DEANS	75	DPWA	$\pi N \to \Sigma K$

Note: Signs of couplings from $\pi N \to N\pi\pi$ analyses were changed in the 1986 edition to agree with the baryon-first convention; the overall phase ambiguity is resolved by choosing a negative sign for the $\Delta(1620)$ S_{31} coupling to $\Delta(1232)\pi$.

$(\Gamma_i\Gamma_f)^{1/2}/\Gamma_{total}$ in $N\pi \to \Delta(1910) \to \Delta(1232)\pi$, *P*-wave $(\Gamma_1\Gamma_5)^{1/2}/\Gamma$

VALUE	*DOCUMENT ID*		*TECN*	*COMMENT*
+0.06	[2] LONGACRE	77	IPWA	$\pi N \to N\pi\pi$

$(\Gamma_i\Gamma_f)^{1/2}/\Gamma_{total}$ in $N\pi \to \Delta(1910) \to N\rho$, S=3/2, *P*-wave $(\Gamma_1\Gamma_7)^{1/2}/\Gamma$

VALUE	*DOCUMENT ID*		*TECN*	*COMMENT*
+0.29	[2] LONGACRE	77	IPWA	$\pi N \to N\pi\pi$
• • • We do not use the following data for averages, fits, limits, etc. • • •				
+0.17	[5] NOVOSELLER	78	IPWA	$\pi N \to N\pi\pi$

$(\Gamma_i\Gamma_f)^{1/2}/\Gamma_{total}$ in $N\pi \to \Delta(1910) \to N(1440)\pi$, *P*-wave $(\Gamma_1\Gamma_9)^{1/2}/\Gamma$

VALUE	*DOCUMENT ID*		*TECN*	*COMMENT*
− 0.39±0.04	MANLEY	92	IPWA	$\pi N \to \pi N$ & $N\pi\pi$

$\Gamma(N(1440)\pi)/\Gamma_{total}$ Γ_8/Γ

VALUE	*DOCUMENT ID*		*TECN*	*COMMENT*
0.56±0.07	VRANA	00	DPWA	Multichannel

$\Delta(1910)$ PHOTON DECAY AMPLITUDES

$\Delta(1910) \to N\gamma$, helicity-1/2 amplitude $A_{1/2}$

VALUE (GeV$^{-1/2}$)	*DOCUMENT ID*		*TECN*	*COMMENT*
+0.003±0.014 OUR ESTIMATE				
− 0.002±0.008	ARNDT	96	IPWA	$\gamma N \to \pi N$
0.014±0.030	CRAWFORD	83	IPWA	$\gamma N \to \pi N$
0.025±0.011	AWAJI	81	DPWA	$\gamma N \to \pi N$
− 0.012±0.005	ARAI	80	DPWA	$\gamma N \to \pi N$ (fit 1)
− 0.031±0.004	ARAI	80	DPWA	$\gamma N \to \pi N$ (fit 2)
− 0.005±0.030	CRAWFORD	80	DPWA	$\gamma N \to \pi N$
• • • We do not use the following data for averages, fits, limits, etc. • • •				
0.032±0.003	LI	93	IPWA	$\gamma N \to \pi N$
− 0.035±0.021	BARBOUR	78	DPWA	$\gamma N \to \pi N$

Δ(1910) FOOTNOTES

[1] CHEW 80 reports four resonances in the P_{31} wave — see also the Δ(1750). Problems with this analysis are discussed in section 2.1.11 of HOEHLER 83.

[2] LONGACRE 77 pole positions are from a search for poles in the unitarized T-matrix; the first (second) value uses, in addition to $\pi N \rightarrow N\pi\pi$ data, elastic amplitudes from a Saclay (CERN) partial-wave analysis. The other LONGACRE 77 values are from eyeball fits with Breit-Wigner circles to the T-matrix amplitudes.

[3] See HOEHLER 93 for a detailed discussion of the evidence for and the pole parameters of N and Δ resonances as determined from Argand diagrams of πN elastic partial-wave amplitudes and from plots of the speeds with which the amplitudes traverse the diagrams.

[4] The range given for DEANS 75 is from the four best solutions.

[5] Evidence for this coupling is weak; see NOVOSELLER 78. This coupling assumes the mass is near 1820 MeV.

Δ(1910) REFERENCES

For early references, see Physics Letters **111B** 70 (1982).

VRANA	00	PRPL 328 181	T.P. Vrana, S.A. Dytman,, T.-S.H. Lee	(PITT+)
ARNDT	96	PR C53 430	R.A. Arndt, I.I. Strakovsky, R.L. Workman	(VPI)
ARNDT	95	PR C52 2120	R.A. Arndt *et al.*	(VPI, BRCO)
HOEHLER	93	πN Newsletter 9 1	G. Hohler	(KARL)
LI	93	PR C47 2759	Z.J. Li *et al.*	(VPI)
MANLEY	92	PR D45 4002	D.M. Manley, E.M. Saleski	(KENT) IJP
Also	84	PR D30 904	D.M. Manley *et al.*	(VPI)
ARNDT	91	PR D43 2131	R.A. Arndt *et al.*	(VPI, TELE) IJP
CANDLIN	84	NP B238 477	D.J. Candlin *et al.*	(EDIN, RAL, LOWC)
CRAWFORD	83	NP B211 1	R.L. Crawford, W.T. Morton	(GLAS)
HOEHLER	83	Landolt-Boernstein 1/9B2	G. Hohler	(KARLT)
PDG	82	PL 111B	M. Roos *et al.*	(HELS, CIT, CERN)
AWAJI	81	Bonn Conf. 352	N. Awaji, R. Kajikawa	(NAGO)
Also	82	NP B197 365	K. Fujii *et al.*	(NAGO)
ARAI	80	Toronto Conf. 93	I. Arai	(INUS)
Also	82	NP B194 251	I. Arai, H. Fujii	(INUS)
CHEW	80	Toronto Conf. 123	D.M. Chew	(LBL) IJP
CRAWFORD	80	Toronto Conf. 107	R.L. Crawford	(GLAS)
CUTKOSKY	80	Toronto Conf. 19	R.E. Cutkosky *et al.*	(CMU, LBL) IJP
Also	79	PR D20 2839	R.E. Cutkosky *et al.*	(CMU, LBL) IJP
LIVANOS	80	Toronto Conf. 35	P. Livanos *et al.*	(SACL) IJP
HOEHLER	79	PDAT 12-1	G. Hohler *et al.*	(KARLT) IJP
Also	80	Toronto Conf. 3	R. Koch	(KARLT) IJP
BARBOUR	78	NP B141 253	I.M. Barbour, R.L. Crawford, N.H. Parsons	(GLAS)
NOVOSELLER	78	NP B137 509	D.E. Novoseller	(CIT) IJP
Also	78B	NP B137 445	D.E. Novoseller	(CIT) IJP
LONGACRE	77	NP B122 493	R.S. Longacre, J. Dolbeau	(SACL) IJP
Also	76	NP B108 365	J. Dolbeau *et al.*	(SACL) IJP
DEANS	75	NP B96 90	S.R. Deans *et al.*	(SFLA, ALAH) IJP

Δ(1920) P_{33}

$I(J^P) = \frac{3}{2}(\frac{3}{2}^+)$ Status: ***

Most of the results published before 1975 are now obsolete and have been omitted. They may be found in our 1982 edition, Physics Letters **111B** (1982).

Δ(1920) BREIT-WIGNER MASS

VALUE (MeV)	DOCUMENT ID		TECN	COMMENT
1900 to 1970 (≈ 1920) OUR ESTIMATE				
2014 ± 16	MANLEY	92	IPWA	$\pi N \rightarrow \pi N$ & $N\pi\pi$
1920 ± 80	CUTKOSKY	80	IPWA	$\pi N \rightarrow \pi N$
1868 ± 10	HOEHLER	79	IPWA	$\pi N \rightarrow \pi N$
• • • We do not use the following data for averages, fits, limits, etc. • • •				
2057 ± 1	PENNER	02C	DPWA	Multichannel
1889 ±100	VRANA	00	DPWA	Multichannel
1840 ± 40	CANDLIN	84	DPWA	$\pi^+ p \rightarrow \Sigma^+ K^+$
1955.0± 13.0	[1] CHEW	80	BPWA	$\pi^+ p \rightarrow \pi^+ p$
$2065.0^{+\ 13.6}_{-\ 12.9}$	[1] CHEW	80	BPWA	$\pi^+ p \rightarrow \pi^+ p$

Δ(1920) BREIT-WIGNER WIDTH

VALUE (MeV)	DOCUMENT ID		TECN	COMMENT
150 to 300 (≈ 200) OUR ESTIMATE				
152 ± 55	MANLEY	92	IPWA	$\pi N \rightarrow \pi N$ & $N\pi\pi$
300 ±100	CUTKOSKY	80	IPWA	$\pi N \rightarrow \pi N$
220 ± 80	HOEHLER	79	IPWA	$\pi N \rightarrow \pi N$
• • • We do not use the following data for averages, fits, limits, etc. • • •				
525 ± 32	PENNER	02C	DPWA	Multichannel
123 ± 53	VRANA	00	DPWA	Multichannel
200 ± 40	CANDLIN	84	DPWA	$\pi^+ p \rightarrow \Sigma^+ K^+$
88.3± 35.0	[1] CHEW	80	BPWA	$\pi^+ p \rightarrow \pi^+ p$
62.0± 44.0	[1] CHEW	80	BPWA	$\pi^+ p \rightarrow \pi^+ p$

Δ(1920) POLE POSITION

REAL PART

VALUE (MeV)	DOCUMENT ID		TECN	COMMENT
1850 to 1950 (≈ 1900) OUR ESTIMATE				
1900	[2] HOEHLER	93	SPED	$\pi N \rightarrow \pi N$
1900±80	CUTKOSKY	80	IPWA	$\pi N \rightarrow \pi N$
• • • We do not use the following data for averages, fits, limits, etc. • • •				
1880	VRANA	00	DPWA	Multichannel
not seen	ARNDT	91	DPWA	$\pi N \rightarrow \pi N$ Soln SM90

−2×IMAGINARY PART

VALUE (MeV)	DOCUMENT ID		TECN	COMMENT
200 to 400 (≈ 300) OUR ESTIMATE				
300±100	CUTKOSKY	80	IPWA	$\pi N \rightarrow \pi N$
• • • We do not use the following data for averages, fits, limits, etc. • • •				
120	VRANA	00	DPWA	Multichannel
not seen	ARNDT	91	DPWA	$\pi N \rightarrow \pi N$ Soln SM90

Δ(1920) ELASTIC POLE RESIDUE

MODULUS $|r|$

VALUE (MeV)	DOCUMENT ID		TECN	COMMENT
24±4	CUTKOSKY	80	IPWA	$\pi N \rightarrow \pi N$

PHASE θ

VALUE (°)	DOCUMENT ID		TECN	COMMENT
−150±30	CUTKOSKY	80	IPWA	$\pi N \rightarrow \pi N$

Δ(1920) DECAY MODES

The following branching fractions are our estimates, not fits or averages.

	Mode	Fraction (Γ_i/Γ)
Γ_1	$N\pi$	5–20 %
Γ_2	ΣK	(2.10 ± 0.30) %
Γ_3	$N\pi\pi$	
Γ_4	$\Delta(1232)\pi$, P-wave	
Γ_5	$N(1440)\pi$, P-wave	
Γ_6	$N\gamma$, helicity=1/2	
Γ_7	$N\gamma$, helicity=3/2	

Δ(1920) BRANCHING RATIOS

$\Gamma(N\pi)/\Gamma_{total}$ Γ_1/Γ

VALUE	DOCUMENT ID		TECN	COMMENT
0.05 to 0.2 OUR ESTIMATE				
0.02±0.02	MANLEY	92	IPWA	$\pi N \rightarrow \pi N$ & $N\pi\pi$
0.20±0.05	CUTKOSKY	80	IPWA	$\pi N \rightarrow \pi N$
0.14±0.04	HOEHLER	79	IPWA	$\pi N \rightarrow \pi N$
• • • We do not use the following data for averages, fits, limits, etc. • • •				
0.15±0.01	PENNER	02C	DPWA	Multichannel
0.05±0.04	VRANA	00	DPWA	Multichannel
0.24	[1] CHEW	80	BPWA	$\pi^+ p \rightarrow \pi^+ p$
0.18	[1] CHEW	80	BPWA	$\pi^+ p \rightarrow \pi^+ p$

$(\Gamma_i\Gamma_f)^{1/2}/\Gamma_{total}$ in $N\pi \rightarrow \Delta(1920) \rightarrow \Sigma K$ $(\Gamma_1\Gamma_2)^{1/2}/\Gamma$

VALUE	DOCUMENT ID		TECN	COMMENT
−0.052±0.015	CANDLIN	84	DPWA	$\pi^+ p \rightarrow \Sigma^+ K^+$
• • • We do not use the following data for averages, fits, limits, etc. • • •				
−0.049	LIVANOS	80	DPWA	$\pi p \rightarrow \Sigma K$
0.048 to 0.120	[3] DEANS	75	DPWA	$\pi N \rightarrow \Sigma K$

$\Gamma(\Sigma K)/\Gamma_{total}$ Γ_2/Γ

VALUE	DOCUMENT ID		TECN	COMMENT
0.021 ±0.003	PENNER	02C	DPWA	Multichannel

$(\Gamma_i\Gamma_f)^{1/2}/\Gamma_{total}$ in $N\pi \rightarrow \Delta(1920) \rightarrow \Delta(1232)\pi$, P-wave $(\Gamma_1\Gamma_4)^{1/2}/\Gamma$

VALUE	DOCUMENT ID		TECN	COMMENT
−0.13±0.04	MANLEY	92	IPWA	$\pi N \rightarrow \pi N$ & $N\pi\pi$
0.3	[4] NOVOSELLER	78	IPWA	$\pi N \rightarrow N\pi\pi$
0.27	[5] NOVOSELLER	78	IPWA	$\pi N \rightarrow N\pi\pi$

$\Gamma(\Delta(1232)\pi, P\text{-wave})/\Gamma_{total}$ Γ_4/Γ

VALUE	DOCUMENT ID		TECN	COMMENT
0.41±0.03	VRANA	00	DPWA	Multichannel

$(\Gamma_i\Gamma_f)^{1/2}/\Gamma_{total}$ in $N\pi \rightarrow \Delta(1920) \rightarrow N(1440)\pi$, P-wave $(\Gamma_1\Gamma_5)^{1/2}/\Gamma$

VALUE	DOCUMENT ID		TECN	COMMENT
+0.06±0.07	MANLEY	92	IPWA	$\pi N \rightarrow \pi N$ & $N\pi\pi$

$\Gamma(N(1440)\pi, P\text{-wave})/\Gamma_{total}$ Γ_5/Γ

VALUE	DOCUMENT ID		TECN	COMMENT
0.53±0.08	VRANA	00	DPWA	Multichannel

Δ(1920) PHOTON DECAY AMPLITUDES

Δ(1920) → $N\gamma$, helicity-1/2 amplitude $A_{1/2}$

VALUE (GeV$^{-1/2}$)	DOCUMENT ID		TECN	COMMENT
0.040±0.014	AWAJI	81	DPWA	$\gamma N \rightarrow \pi N$
• • • We do not use the following data for averages, fits, limits, etc. • • •				
−0.007	PENNER	02D	DPWA	Multichannel

Δ(1920) → Nγ, helicity-3/2 amplitude $A_{3/2}$

VALUE ($GeV^{-1/2}$)	DOCUMENT ID		TECN	COMMENT
0.023±0.017	AWAJI	81	DPWA	$\gamma N \to \pi N$
• • • We do not use the following data for averages, fits, limits, etc. • • •				
−0.001	PENNER	02D	DPWA	Multichannel

Δ(1920) FOOTNOTES

[1] CHEW 80 reports two P_{33} resonances in this mass region. Problems with this analysis are discussed in section 2.1.11 of HOEHLER 83.
[2] See HOEHLER 93 for a detailed discussion of the evidence for and the pole parameters of N and Δ resonances as determined from Argand diagrams of πN elastic partial-wave amplitudes and from plots of the speeds with which the amplitudes traverse the diagrams.
[3] The range given for DEANS 75 is from the four best solutions.
[4] A Breit-Wigner fit to the HERNDON 75 IPWA; the phase is near −90°.
[5] A Breit-Wigner fit to the NOVOSELLER 78B IPWA; the phase is near −90°.

Δ(1920) REFERENCES

For early references, see Physics Letters **111B** 70 (1982).

PENNER	02C	PR C66 055211	G. Penner, U. Mosel	(GIES)
PENNER	02D	PR C66 055212	G. Penner, U. Mosel	(GIES)
VRANA	00	PRPL 328 181	T.P. Vrana, S.A. Dytman,, T.-S.H. Lee	(PITT+)
HOEHLER	93	πN Newsletter 9 1	G. Hohler	(KARL)
MANLEY	92	PR D45 4002	D.M. Manley, E.M. Saleski	(KENT) IJP
Also	84	PR D30 904	D.M. Manley *et al.*	(VPI)
ARNDT	91	PR D43 2131	R.A. Arndt *et al.*	(VPI, TELE) IJP
CANDLIN	84	NP B238 477	D.J. Candlin *et al.*	(EDIN, RAL, LOWC)
HOEHLER	83	Landolt-Boernstein 1/9B2	G. Hohler	(KARLT)
PDG	82	PL 111B	M. Roos *et al.*	(HELS, CIT, CERN)
AWAJI	81	Bonn Conf. 352	N. Awaji, R. Kajikawa	(NAGO)
Also	82	NP B197 365	K. Fujii *et al.*	(NAGO)
CHEW	80	Toronto Conf. 123	D.M. Chew	(LBL) IJP
CUTKOSKY	80	Toronto Conf. 19	R.E. Cutkosky *et al.*	(CMU, LBL) IJP
Also	79	PR D20 2839	R.E. Cutkosky *et al.*	(CMU, LBL) IJP
LIVANOS	80	Toronto Conf. 35	P. Livanos *et al.*	(SACL) IJP
HOEHLER	79	PDAT 12-1	G. Hohler *et al.*	(KARLT) IJP
Also	80	Toronto Conf. 3	R. Koch	(KARLT) IJP
NOVOSELLER	78	NP B137 509	D.E. Novoseller	(CIT)
NOVOSELLER	78B	NP B137 445	D.E. Novoseller	(CIT)
DEANS	75	NP B96 90	S.R. Deans *et al.*	(SFLA, ALAH) IJP
HERNDON	75	PR D11 3183	D. Herndon *et al.*	(LBL, SLAC)

Δ(1930) D_{35}

$I(J^P) = \frac{3}{2}(\frac{5}{2}^-)$ Status: ***

Most of the results published before 1975 are now obsolete and have been omitted. They may be found in our 1982 edition, Physics Letters **111B** (1982).

The various analyses are not in good agreement.

Δ(1930) BREIT-WIGNER MASS

VALUE (MeV)	DOCUMENT ID		TECN	COMMENT
1920 to 1970 (≈ 1930) OUR ESTIMATE				
1956 ± 22	MANLEY	92	IPWA	$\pi N \to \pi N$ & $N\pi\pi$
1940 ± 30	CUTKOSKY	80	IPWA	$\pi N \to \pi N$
1901 ± 15	HOEHLER	79	IPWA	$\pi N \to \pi N$
• • • We do not use the following data for averages, fits, limits, etc. • • •				
1932 ±100	VRANA	00	DPWA	Multichannel
1955 ± 15	ARNDT	96	IPWA	$\gamma N \to \pi N$
2056	ARNDT	95	DPWA	$\pi N \to N\pi$
1963	LI	93	IPWA	$\gamma N \to \pi N$
$1910.0^{+15.0}_{-17.2}$	CHEW	80	BPWA	$\pi^+ p \to \pi^+ p$
2000	CRAWFORD	80	DPWA	$\gamma N \to \pi N$
2024	BARBOUR	78	DPWA	$\gamma N \to \pi N$

Δ(1930) BREIT-WIGNER WIDTH

VALUE (MeV)	DOCUMENT ID		TECN	COMMENT
250 to 450 (≈ 350) OUR ESTIMATE				
530 ±140	MANLEY	92	IPWA	$\pi N \to \pi N$ & $N\pi\pi$
320 ± 60	CUTKOSKY	80	IPWA	$\pi N \to \pi N$
195 ± 60	HOEHLER	79	IPWA	$\pi N \to \pi N$
• • • We do not use the following data for averages, fits, limits, etc. • • •				
316 ±237	VRANA	00	DPWA	Multichannel
350 ± 20	ARNDT	96	IPWA	$\gamma N \to \pi N$
590	ARNDT	95	DPWA	$\pi N \to N\pi$
260	LI	93	IPWA	$\gamma N \to \pi N$
$74.8^{+17.0}_{-16.0}$	CHEW	80	BPWA	$\pi^+ p \to \pi^+ p$
442	CRAWFORD	80	DPWA	$\gamma N \to \pi N$
462	BARBOUR	78	DPWA	$\gamma N \to \pi N$

Δ(1930) POLE POSITION

REAL PART

VALUE (MeV)	DOCUMENT ID		TECN	COMMENT
1840 to 1940 (≈ 1890) OUR ESTIMATE				
1913	ARNDT	95	DPWA	$\pi N \to N\pi$
1850	[1] HOEHLER	93	SPED	$\pi N \to \pi N$
1890±50	CUTKOSKY	80	IPWA	$\pi N \to \pi N$
• • • We do not use the following data for averages, fits, limits, etc. • • •				
1883	VRANA	00	DPWA	Multichannel
2018	ARNDT	91	DPWA	$\pi N \to \pi N$ Soln SM90

−2×IMAGINARY PART

VALUE (MeV)	DOCUMENT ID		TECN	COMMENT
200 to 300 (≈ 250) OUR ESTIMATE				
246	ARNDT	95	DPWA	$\pi N \to N\pi$
180	[1] HOEHLER	93	SPED	$\pi N \to \pi N$
260±60	CUTKOSKY	80	IPWA	$\pi N \to \pi N$
• • • We do not use the following data for averages, fits, limits, etc. • • •				
250	VRANA	00	DPWA	Multichannel
398	ARNDT	91	DPWA	$\pi N \to \pi N$ Soln SM90

Δ(1930) ELASTIC POLE RESIDUE

MODULUS |r|

VALUE (MeV)	DOCUMENT ID		TECN	COMMENT
8	ARNDT	95	DPWA	$\pi N \to N\pi$
20	HOEHLER	93	SPED	$\pi N \to \pi N$
18±6	CUTKOSKY	80	IPWA	$\pi N \to \pi N$
• • • We do not use the following data for averages, fits, limits, etc. • • •				
15	ARNDT	91	DPWA	$\pi N \to \pi N$ Soln SM90

PHASE θ

VALUE (°)	DOCUMENT ID		TECN	COMMENT
−47	ARNDT	95	DPWA	$\pi N \to N\pi$
−20±40	CUTKOSKY	80	IPWA	$\pi N \to \pi N$
• • • We do not use the following data for averages, fits, limits, etc. • • •				
−24	ARNDT	91	DPWA	$\pi N \to \pi N$ Soln SM90

Δ(1930) DECAY MODES

The following branching fractions are our estimates, not fits or averages.

	Mode	Fraction (Γ_i/Γ)
Γ_1	$N\pi$	10–20 %
Γ_2	ΣK	
Γ_3	$N\pi\pi$	
Γ_4	$N\gamma$	0.0–0.02 %
Γ_5	$N\gamma$, helicity=1/2	0.0–0.01 %
Γ_6	$N\gamma$, helicity=3/2	0.0–0.01 %

Δ(1930) BRANCHING RATIOS

$\Gamma(N\pi)/\Gamma_{total}$ Γ_1/Γ

VALUE	DOCUMENT ID		TECN	COMMENT
0.1 to 0.2 OUR ESTIMATE				
0.18±0.02	MANLEY	92	IPWA	$\pi N \to \pi N$ & $N\pi\pi$
0.14±0.04	CUTKOSKY	80	IPWA	$\pi N \to \pi N$
0.04±0.03	HOEHLER	79	IPWA	$\pi N \to \pi N$
• • • We do not use the following data for averages, fits, limits, etc. • • •				
0.09±0.08	VRANA	00	DPWA	Multichannel
0.11	ARNDT	95	DPWA	$\pi N \to N\pi$
0.11	CHEW	80	BPWA	$\pi^+ p \to \pi^+ p$

$(\Gamma_i\Gamma_f)^{1/2}/\Gamma_{total}$ in $N\pi \to \Delta(1930) \to \Sigma K$ $(\Gamma_1\Gamma_2)^{1/2}/\Gamma$

VALUE	DOCUMENT ID		TECN	COMMENT
< 0.015	CANDLIN	84	DPWA	$\pi^+ p \to \Sigma^+ K^+$
• • • We do not use the following data for averages, fits, limits, etc. • • •				
−0.031	LIVANOS	80	DPWA	$\pi p \to \Sigma K$
0.018 to 0.035	[2] DEANS	75	DPWA	$\pi N \to \Sigma K$

$(\Gamma_i\Gamma_f)^{1/2}/\Gamma_{total}$ in $N\pi \to \Delta(1930) \to N\pi\pi$ $(\Gamma_1\Gamma_3)^{1/2}/\Gamma$

VALUE	DOCUMENT ID		TECN	COMMENT
not seen	LONGACRE	75	IPWA	$\pi N \to N\pi\pi$

$\Delta(1930)$ PHOTON DECAY AMPLITUDES

$\Delta(1930) \rightarrow N\gamma$, helicity-1/2 amplitude $A_{1/2}$

VALUE ($GeV^{-1/2}$)	DOCUMENT ID		TECN	COMMENT
-0.009 ± 0.028 OUR ESTIMATE				
-0.007 ± 0.010	ARNDT	96	IPWA	$\gamma N \rightarrow \pi N$
0.009 ± 0.009	AWAJI	81	DPWA	$\gamma N \rightarrow \pi N$
-0.030 ± 0.047	CRAWFORD	80	DPWA	$\gamma N \rightarrow \pi N$
• • • We do not use the following data for averages, fits, limits, etc. • • •				
-0.019 ± 0.001	LI	93	IPWA	$\gamma N \rightarrow \pi N$
-0.062 ± 0.064	BARBOUR	78	DPWA	$\gamma N \rightarrow \pi N$

$\Delta(1930) \rightarrow N\gamma$, helicity-3/2 amplitude $A_{3/2}$

VALUE ($GeV^{-1/2}$)	DOCUMENT ID		TECN	COMMENT
-0.018 ± 0.028 OUR ESTIMATE				
0.005 ± 0.010	ARNDT	96	IPWA	$\gamma N \rightarrow \pi N$
-0.025 ± 0.011	AWAJI	81	DPWA	$\gamma N \rightarrow \pi N$
-0.033 ± 0.060	CRAWFORD	80	DPWA	$\gamma N \rightarrow \pi N$
• • • We do not use the following data for averages, fits, limits, etc. • • •				
0.009 ± 0.001	LI	93	IPWA	$\gamma N \rightarrow \pi N$
$+0.019\pm0.054$	BARBOUR	78	DPWA	$\gamma N \rightarrow \pi N$

$\Delta(1930)$ FOOTNOTES

[1] See HOEHLER 93 for a detailed discussion of the evidence for and the pole parameters of N and Δ resonances as determined from Argand diagrams of πN elastic partial-wave amplitudes and from plots of the speeds with which the amplitudes traverse the diagrams.
[2] The range given for DEANS 75 is from the four best solutions.

$\Delta(1930)$ REFERENCES

For early references, see Physics Letters **111B** 70 (1982).

VRANA	00	PRPL 328 181	T.P. Vrana, S.A. Dytman,, T.-S.H. Lee	(PITT+)
ARNDT	96	PR C53 430	R.A. Arndt, I.I. Strakovsky, R.L. Workman	(VPI)
ARNDT	95	PR C52 2120	R.A. Arndt *et al.*	(VPI, BRCO)
HOEHLER	93	πN Newsletter 9 1	G. Hohler	(KARL)
LI	93	PR C47 2759	Z.J. Li *et al.*	(VPI)
MANLEY	92	PR D45 4002	D.M. Manley, E.M. Saleski	(KENT) IJP
Also	84	PR D30 904	D.M. Manley *et al.*	(VPI)
ARNDT	91	PR D43 2131	R.A. Arndt *et al.*	(VPI, TELE) IJP
CANDLIN	84	NP B238 477	D.J. Candlin *et al.*	(EDIN, RAL, LOWC)
PDG	82	PL 111B	M. Roos *et al.*	(HELS, CIT, CERN)
AWAJI	81	Bonn Conf. 352	N. Awaji, R. Kajikawa	(NAGO)
Also	82	NP B197 365	K. Fujii *et al.*	(NAGO)
CHEW	80	Toronto Conf. 123	D.M. Chew	(LBL) IJP
CRAWFORD	80	Toronto Conf. 107	R.L. Crawford	(GLAS)
CUTKOSKY	80	Toronto Conf. 19	R.E. Cutkosky *et al.*	(CMU, LBL) IJP
Also	79	PR D20 2839	R.E. Cutkosky *et al.*	(CMU, LBL) IJP
LIVANOS	80	Toronto Conf. 35	P. Livanos *et al.*	(SACL) IJP
HOEHLER	79	PDAT 12-1	G. Hohler *et al.*	(KARL) IJP
Also	80	Toronto Conf. 3	R. Koch	(KARL) IJP
BARBOUR	78	NP B141 253	I.M. Barbour, R.L. Crawford, N.H. Parsons	(GLAS)
DEANS	75	NP B96 90	S.R. Deans *et al.*	(SFLA, ALAH) IJP
LONGACRE	75	PL 55B 415	R.S. Longacre *et al.*	(LBL, SLAC) IJP

$\Delta(1940)$ D_{33}

$I(J^P) = \frac{3}{2}(\frac{3}{2}^-)$ Status: *

OMITTED FROM SUMMARY TABLE

$\Delta(1940)$ BREIT-WIGNER MASS

VALUE (MeV)	DOCUMENT ID		TECN	COMMENT
≈ 1940 OUR ESTIMATE				
2057 ± 110	MANLEY	92	IPWA	$\pi N \rightarrow \pi N$ & $N\pi\pi$
2058.1 ± 34.5	CHEW	80	BPWA	$\pi^+ p \rightarrow \pi^+ p$
1940 ± 100	CUTKOSKY	80	IPWA	$\pi N \rightarrow \pi N$

$\Delta(1940)$ BREIT-WIGNER WIDTH

VALUE (MeV)	DOCUMENT ID		TECN	COMMENT
460 ± 320	MANLEY	92	IPWA	$\pi N \rightarrow \pi N$ & $N\pi\pi$
198.4 ± 45.5	CHEW	80	BPWA	$\pi^+ p \rightarrow \pi^+ p$
200 ± 100	CUTKOSKY	80	IPWA	$\pi N \rightarrow \pi N$

$\Delta(1940)$ POLE POSITION

REAL PART

VALUE (MeV)	DOCUMENT ID		TECN	COMMENT
1900 ± 100	CUTKOSKY	80	IPWA	$\pi N \rightarrow \pi N$
1915 or 1926	[1] LONGACRE	78	IPWA	$\pi N \rightarrow N\pi\pi$

$-2\times$IMAGINARY PART

VALUE (MeV)	DOCUMENT ID		TECN	COMMENT
200 ± 60	CUTKOSKY	80	IPWA	$\pi N \rightarrow \pi N$
190 or 186	[1] LONGACRE	78	IPWA	$\pi N \rightarrow N\pi\pi$

$\Delta(1940)$ ELASTIC POLE RESIDUE

MODULUS $|r|$

VALUE (MeV)	DOCUMENT ID		TECN	COMMENT
8 ± 3	CUTKOSKY	80	IPWA	$\pi N \rightarrow \pi N$

PHASE θ

VALUE ($^\circ$)	DOCUMENT ID		TECN	COMMENT
135 ± 45	CUTKOSKY	80	IPWA	$\pi N \rightarrow \pi N$

$\Delta(1940)$ DECAY MODES

	Mode
Γ_1	$N\pi$
Γ_2	ΣK
Γ_3	$N\pi\pi$
Γ_4	$\Delta(1232)\pi$, S-wave
Γ_5	$\Delta(1232)\pi$, D-wave
Γ_6	$N\rho$, S=3/2, S-wave
Γ_7	$N\gamma$, helicity=1/2
Γ_8	$N\gamma$, helicity=3/2

$\Delta(1940)$ BRANCHING RATIOS

$\Gamma(N\pi)/\Gamma_{total}$ **Γ_1/Γ**

VALUE	DOCUMENT ID		TECN	COMMENT
0.18 ± 0.12	MANLEY	92	IPWA	$\pi N \rightarrow \pi N$ & $N\pi\pi$
0.18	CHEW	80	BPWA	$\pi^+ p \rightarrow \pi^+ p$
0.05 ± 0.02	CUTKOSKY	80	IPWA	$\pi N \rightarrow \pi N$

$(\Gamma_i\Gamma_f)^{1/2}/\Gamma_{total}$ in $N\pi \rightarrow \Delta(1940) \rightarrow \Sigma K$ **$(\Gamma_1\Gamma_2)^{1/2}/\Gamma$**

VALUE	DOCUMENT ID		TECN	COMMENT
<0.015	CANDLIN	84	DPWA	$\pi^+ p \rightarrow \Sigma^+ K^+$

$(\Gamma_i\Gamma_f)^{1/2}/\Gamma_{total}$ in $N\pi \rightarrow \Delta(1940) \rightarrow \Delta(1232)\pi$, S-wave **$(\Gamma_1\Gamma_4)^{1/2}/\Gamma$**

VALUE	DOCUMENT ID		TECN	COMMENT
$+0.11\pm0.10$	MANLEY	92	IPWA	$\pi N \rightarrow \pi N$ & $N\pi\pi$

$(\Gamma_i\Gamma_f)^{1/2}/\Gamma_{total}$ in $N\pi \rightarrow \Delta(1940) \rightarrow \Delta(1232)\pi$, D-wave **$(\Gamma_1\Gamma_5)^{1/2}/\Gamma$**

VALUE	DOCUMENT ID		TECN	COMMENT
$+0.27\pm0.16$	MANLEY	92	IPWA	$\pi N \rightarrow \pi N$ & $N\pi\pi$

$(\Gamma_i\Gamma_f)^{1/2}/\Gamma_{total}$ in $N\pi \rightarrow \Delta(1940) \rightarrow N\rho$, S=3/2, S-wave **$(\Gamma_1\Gamma_6)^{1/2}/\Gamma$**

VALUE	DOCUMENT ID		TECN	COMMENT
$+0.25\pm0.10$	MANLEY	92	IPWA	$\pi N \rightarrow \pi N$ & $N\pi\pi$

$\Delta(1940)$ PHOTON DECAY AMPLITUDES

$\Delta(1940) \rightarrow N\gamma$, helicity-1/2 amplitude $A_{1/2}$

VALUE ($GeV^{-1/2}$)	DOCUMENT ID		TECN	COMMENT
-0.036 ± 0.058	AWAJI	81	DPWA	$\gamma N \rightarrow \pi N$

$\Delta(1940) \rightarrow N\gamma$, helicity-3/2 amplitude $A_{3/2}$

VALUE ($GeV^{-1/2}$)	DOCUMENT ID		TECN	COMMENT
-0.031 ± 0.012	AWAJI	81	DPWA	$\gamma N \rightarrow \pi N$

$\Delta(1940)$ FOOTNOTES

[1] LONGACRE 78 values are from a search for poles in the unitarized T-matrix. The first (second) value uses, in addition to $\pi N \rightarrow N\pi\pi$ data, elastic amplitudes from a Saclay (CERN) partial-wave analysis.

$\Delta(1940)$ REFERENCES

MANLEY	92	PR D45 4002	D.M. Manley, E.M. Saleski	(KENT) IJP
Also	84	PR D30 904	D.M. Manley *et al.*	(VPI)
CANDLIN	84	NP B238 477	D.J. Candlin *et al.*	(EDIN, RAL, LOWC)
AWAJI	81	Bonn Conf. 352	N. Awaji, R. Kajikawa	(NAGO)
Also	82	NP B197 365	K. Fujii *et al.*	(NAGO)
CHEW	80	Toronto Conf. 123	D.M. Chew	(LBL) IJP
CUTKOSKY	80	Toronto Conf. 19	R.E. Cutkosky *et al.*	(CMU, LBL) IJP
Also	79	PR D20 2839	R.E. Cutkosky *et al.*	(CMU, LBL)
LONGACRE	78	PR D17 1795	R.S. Longacre *et al.*	(LBL, SLAC)

Δ(1950) F_{37}

$I(J^P) = \frac{3}{2}(\frac{7}{2}^+)$ Status: ****

Most of the results published before 1975 are now obsolete and have been omitted. They may be found in our 1982 edition, Physics Letters **111B** (1982).

Δ(1950) BREIT-WIGNER MASS

VALUE (MeV)	DOCUMENT ID		TECN	COMMENT
1940 to 1960 (≈ 1950) OUR ESTIMATE				
1945 ± 2	MANLEY	92	IPWA	$\pi N \to \pi N$ & $N\pi\pi$
1950 ±15	CUTKOSKY	80	IPWA	$\pi N \to \pi N$
1913 ± 8	HOEHLER	79	IPWA	$\pi N \to \pi N$
• • • We do not use the following data for averages, fits, limits, etc. • • •				
1936 ± 5	VRANA	00	DPWA	Multichannel
1947 ± 9	ARNDT	96	IPWA	$\gamma N \to \pi N$
1921	ARNDT	95	DPWA	$\pi N \to N\pi$
1940	LI	93	IPWA	$\gamma N \to \pi N$
1925 ±20	CANDLIN	84	DPWA	$\pi^+ p \to \Sigma^+ K^+$
$1855.0^{+11.0}_{-10.0}$	CHEW	80	BPWA	$\pi^+ p \to \pi^+ p$
1902	CRAWFORD	80	DPWA	$\gamma N \to \pi N$
1912	BARBOUR	78	DPWA	$\gamma N \to \pi N$
1925	[1] LONGACRE	75	IPWA	$\pi N \to N\pi\pi$

Δ(1950) BREIT-WIGNER WIDTH

VALUE (MeV)	DOCUMENT ID		TECN	COMMENT
290 to 350 (≈ 300) OUR ESTIMATE				
300 ± 7	MANLEY	92	IPWA	$\pi N \to \pi N$ & $N\pi\pi$
340 ±50	CUTKOSKY	80	IPWA	$\pi N \to \pi N$
224 ±10	HOEHLER	79	IPWA	$\pi N \to \pi N$
• • • We do not use the following data for averages, fits, limits, etc. • • •				
245 ±12	VRANA	00	DPWA	Multichannel
302 ± 9	ARNDT	96	IPWA	$\gamma N \to \pi N$
232	ARNDT	95	DPWA	$\pi N \to N\pi$
306	LI	93	IPWA	$\gamma N \to \pi N$
330 ±40	CANDLIN	84	DPWA	$\pi^+ p \to \Sigma^+ K^+$
$157.2^{+22.0}_{-19.0}$	CHEW	80	BPWA	$\pi^+ p \to \pi^+ p$
225	CRAWFORD	80	DPWA	$\gamma N \to \pi N$
198	BARBOUR	78	DPWA	$\gamma N \to \pi N$
240	[1] LONGACRE	75	IPWA	$\pi N \to N\pi\pi$

Δ(1950) POLE POSITION

REAL PART

VALUE (MeV)	DOCUMENT ID		TECN	COMMENT
1880 to 1890 (≈ 1885) OUR ESTIMATE				
1880	ARNDT	95	DPWA	$\pi N \to N\pi$
1878	[2] HOEHLER	93	ARGD	$\pi N \to \pi N$
1890±15	CUTKOSKY	80	IPWA	$\pi N \to \pi N$
• • • We do not use the following data for averages, fits, limits, etc. • • •				
1910	VRANA	00	DPWA	Multichannel
1884	ARNDT	91	DPWA	$\pi N \to \pi N$ Soln SM90
1924 or 1924	[3] LONGACRE	78	IPWA	$\pi N \to N\pi\pi$

−2×IMAGINARY PART

VALUE (MeV)	DOCUMENT ID		TECN	COMMENT
210 to 270 (≈ 240) OUR ESTIMATE				
236	ARNDT	95	DPWA	$\pi N \to N\pi$
230	[2] HOEHLER	93	ARGD	$\pi N \to \pi N$
260±40	CUTKOSKY	80	IPWA	$\pi N \to \pi N$
• • • We do not use the following data for averages, fits, limits, etc. • • •				
230	VRANA	00	DPWA	Multichannel
238	ARNDT	91	DPWA	$\pi N \to \pi N$ Soln SM90
258 or 258	[3] LONGACRE	78	IPWA	$\pi N \to N\pi\pi$

Δ(1950) ELASTIC POLE RESIDUE

MODULUS $|r|$

VALUE (MeV)	DOCUMENT ID		TECN	COMMENT
54	ARNDT	95	DPWA	$\pi N \to N\pi$
47	HOEHLER	93	ARGD	$\pi N \to \pi N$
50±7	CUTKOSKY	80	IPWA	$\pi N \to \pi N$
• • • We do not use the following data for averages, fits, limits, etc. • • •				
61	ARNDT	91	DPWA	$\pi N \to \pi N$ Soln SM90

PHASE θ

VALUE (°)	DOCUMENT ID		TECN	COMMENT
−17	ARNDT	95	DPWA	$\pi N \to N\pi$
−32	HOEHLER	93	ARGD	$\pi N \to \pi N$
−33±8	CUTKOSKY	80	IPWA	$\pi N \to \pi N$
• • • We do not use the following data for averages, fits, limits, etc. • • •				
−23	ARNDT	91	DPWA	$\pi N \to \pi N$ Soln SM90

Δ(1950) DECAY MODES

The following branching fractions are our estimates, not fits or averages.

	Mode	Fraction (Γ_i/Γ)
Γ_1	$N\pi$	35–40 %
Γ_2	ΣK	
Γ_3	$N\pi\pi$	
Γ_4	$\Delta\pi$	20–30 %
Γ_5	$\Delta(1232)\pi$, F-wave	
Γ_6	$\Delta(1232)\pi$, H-wave	
Γ_7	$N\rho$	<10 %
Γ_8	$N\rho$, S=1/2, F-wave	
Γ_9	$N\rho$, S=3/2, F-wave	
Γ_{10}	$N\gamma$	0.08–0.13 %
Γ_{11}	$N\gamma$, helicity=1/2	0.03–0.055 %
Γ_{12}	$N\gamma$, helicity=3/2	0.05–0.075 %

Δ(1950) BRANCHING RATIOS

$\Gamma(N\pi)/\Gamma_{total}$ Γ_1/Γ

VALUE	DOCUMENT ID		TECN	COMMENT
0.35 to 0.4 OUR ESTIMATE				
0.38±0.01	MANLEY	92	IPWA	$\pi N \to \pi N$ & $N\pi\pi$
0.39±0.04	CUTKOSKY	80	IPWA	$\pi N \to \pi N$
0.38±0.02	HOEHLER	79	IPWA	$\pi N \to \pi N$
• • • We do not use the following data for averages, fits, limits, etc. • • •				
0.44±0.01	VRANA	00	DPWA	Multichannel
0.49	ARNDT	95	DPWA	$\pi N \to N\pi$
0.44	CHEW	80	BPWA	$\pi^+ p \to \pi^+ p$

$(\Gamma_i\Gamma_f)^{1/2}/\Gamma_{total}$ in $N\pi \to \Delta(1950) \to \Sigma K$ $(\Gamma_1\Gamma_2)^{1/2}/\Gamma$

VALUE	DOCUMENT ID		TECN	COMMENT
−0.053±0.005	CANDLIN	84	DPWA	$\pi^+ p \to \Sigma^+ K^+$
• • • We do not use the following data for averages, fits, limits, etc. • • •				
0.022 to 0.040	[4] DEANS	75	DPWA	$\pi N \to \Sigma K$

Note: Signs of couplings from $\pi N \to N\pi\pi$ analyses were changed in the 1986 edition to agree with the baryon-first convention; the overall phase ambiguity is resolved by choosing a negative sign for the Δ(1620) S_{31} coupling to $\Delta(1232)\pi$.

$(\Gamma_i\Gamma_f)^{1/2}/\Gamma_{total}$ in $N\pi \to \Delta(1950) \to \Delta(1232)\pi$, F-wave $(\Gamma_1\Gamma_5)^{1/2}/\Gamma$

VALUE	DOCUMENT ID		TECN	COMMENT
+0.28 to +0.32 OUR ESTIMATE				
+0.27±0.02	MANLEY	92	IPWA	$\pi N \to \pi N$ & $N\pi\pi$
+0.32	[1] LONGACRE	75	IPWA	$\pi N \to N\pi\pi$
• • • We do not use the following data for averages, fits, limits, etc. • • •				
0.21	[5] NOVOSELLER	78	IPWA	$\pi N \to N\pi\pi$
0.38	[6] NOVOSELLER	78	IPWA	$\pi N \to N\pi\pi$

$\Gamma(\Delta(1232)\pi$, F-wave$)/\Gamma_{total}$ Γ_5/Γ

VALUE	DOCUMENT ID		TECN	COMMENT
0.36±0.01	VRANA	00	DPWA	Multichannel

$(\Gamma_i\Gamma_f)^{1/2}/\Gamma_{total}$ in $N\pi \to \Delta(1950) \to N\rho$, S=3/2, F-wave $(\Gamma_1\Gamma_9)^{1/2}/\Gamma$

VALUE	DOCUMENT ID		TECN	COMMENT
+0.24	[1] LONGACRE	75	IPWA	$\pi N \to N\pi\pi$
• • • We do not use the following data for averages, fits, limits, etc. • • •				
0.24	[7] NOVOSELLER	78	IPWA	$\pi N \to N\pi\pi$
0.43	[8] NOVOSELLER	78	IPWA	$\pi N \to N\pi\pi$

Δ(1950) PHOTON DECAY AMPLITUDES

Δ(1950) → $N\gamma$, helicity-1/2 amplitude $A_{1/2}$

VALUE (GeV$^{-1/2}$)	DOCUMENT ID		TECN	COMMENT
−0.076±0.012 OUR ESTIMATE				
−0.079±0.006	ARNDT	96	IPWA	$\gamma N \to \pi N$
−0.068±0.007	AWAJI	81	DPWA	$\gamma N \to \pi N$
−0.091±0.005	ARAI	80	DPWA	$\gamma N \to \pi N$ (fit 1)
−0.083±0.005	ARAI	80	DPWA	$\gamma N \to \pi N$ (fit 2)
−0.067±0.014	CRAWFORD	80	DPWA	$\gamma N \to \pi N$
• • • We do not use the following data for averages, fits, limits, etc. • • •				
−0.102±0.003	LI	93	IPWA	$\gamma N \to \pi N$
−0.058±0.013	BARBOUR	78	DPWA	$\gamma N \to \pi N$

Δ(1950) → Nγ, helicity-3/2 amplitude $A_{3/2}$

VALUE (GeV$^{-1/2}$)	DOCUMENT ID		TECN	COMMENT
−0.097±0.010 OUR ESTIMATE				
−0.103±0.006	ARNDT	96	IPWA	$\gamma N \to \pi N$
−0.094±0.016	AWAJI	81	DPWA	$\gamma N \to \pi N$
−0.101±0.005	ARAI	80	DPWA	$\gamma N \to \pi N$ (fit 1)
−0.100±0.005	ARAI	80	DPWA	$\gamma N \to \pi N$ (fit 2)
−0.082±0.017	CRAWFORD	80	DPWA	$\gamma N \to \pi N$
• • • We do not use the following data for averages, fits, limits, etc. • • •				
−0.115±0.003	LI	93	IPWA	$\gamma N \to \pi N$
−0.075±0.020	BARBOUR	78	DPWA	$\gamma N \to \pi N$

Δ(1950) FOOTNOTES

[1] From method II of LONGACRE 75: eyeball fits with Breit-Wigner circles to the T-matrix amplitudes.
[2] See HOEHLER 93 for a detailed discussion of the evidence for and the pole parameters of N and Δ resonances as determined from Argand diagrams of πN elastic partial-wave amplitudes and from plots of the speeds with which the amplitudes traverse the diagrams.
[3] LONGACRE 78 values are from a search for poles in the unitarized T-matrix. The first (second) value uses, in addition to $\pi N \to N\pi\pi$ data, elastic amplitudes from a Saclay (CERN) partial-wave analysis.
[4] The range given is from the four best solutions. DEANS 75 disagrees with $\pi^+ p \to \Sigma^+ K^+$ data of WINNIK 77 around 1920 MeV.
[5] A Breit-Wigner fit to the HERNDON 75 IPWA; the phase is near −60°.
[6] A Breit-Wigner fit to the NOVOSELLER 78B IPWA; the phase is near −60°.
[7] A Breit-Wigner fit to the HERNDON 75 IPWA; the phase is near 120°.
[8] A Breit-Wigner fit to the NOVOSELLER 78B IPWA; the phase is near 120°.

Δ(1950) REFERENCES

VRANA	00	PRPL 328 181	T.P. Vrana, S.A. Dytman,, T.-S.H. Lee	(PITT+)
ARNDT	96	PR C53 430	R.A. Arndt, I.I. Strakovsky, R.L. Workman	(VPI)
ARNDT	95	PR C52 2120	R.A. Arndt *et al.*	(VPI, BRCO)
HOEHLER	93	πN Newsletter 9 1	G. Hohler	(KARL)
LI	93	PR C47 2759	Z.J. Li *et al.*	(VPI)
MANLEY	92	PR D45 4002	D.M. Manley, E.M. Saleski	(KENT) IJP
Also	84	PR D30 904	D.M. Manley *et al.*	(VPI)
ARNDT	91	PR D43 2131	R.A. Arndt *et al.*	(VPI, TELE) IJP
CANDLIN	84	NP B238 477	D.J. Candlin *et al.*	(EDIN, RAL, LOWC)
PDG	82	PL 111B	M. Roos *et al.*	(HELS, CIT, CERN)
AWAJI	81	Bonn Conf. 352	N. Awaji, R. Kajikawa	(NAGO)
Also	82	NP B197 365	K. Fujii *et al.*	(NAGO)
ARAI	80	Toronto Conf. 93	I. Arai	(INUS)
Also	82	NP B194 251	I. Arai, H. Fujii	(INUS)
CHEW	80	Toronto Conf. 123	D.M. Chew	(LBL) IJP
CRAWFORD	80	Toronto Conf. 107	R.L. Crawford	(GLAS)
CUTKOSKY	80	Toronto Conf. 19	R.E. Cutkosky *et al.*	(CMU, LBL) IJP
Also	79	PR D20 2839	R.E. Cutkosky *et al.*	(CMU, LBL) IJP
HOEHLER	79	PDAT 12-1	G. Hohler *et al.*	(KARLT) IJP
Also	80	Toronto Conf. 3	R. Koch	(KARLT) IJP
BARBOUR	78	NP B141 253	I.M. Barbour, R.L. Crawford, N.H. Parsons	(GLAS)
LONGACRE	78	PR D17 1795	R.S. Longacre *et al.*	(LBL, SLAC)
NOVOSELLER	78	NP B137 509	D.E. Novoseller	(CIT) IJP
NOVOSELLER	78B	NP B137 445	D.E. Novoseller	(CIT) IJP
WINNIK	77	NP B128 66	M. Winnik *et al.*	(HAIF) I
DEANS	75	NP B96 90	S.R. Deans *et al.*	(SFLA, ALAH) IJP
HERNDON	75	PR D11 3183	D. Herndon *et al.*	(LBL, SLAC)
LONGACRE	75	PL 55B 415	R.S. Longacre *et al.*	(LBL, SLAC) IJP

Δ(2000) F_{35}

$I(J^P) = \frac{3}{2}(\frac{5}{2}^+)$ Status: **

OMITTED FROM SUMMARY TABLE

Δ(2000) BREIT-WIGNER MASS

VALUE (MeV)	DOCUMENT ID		TECN	COMMENT
≈ 2000 OUR ESTIMATE				
1724± 61	VRANA	00	DPWA	Multichannel
1752± 32	MANLEY	92	IPWA	$\pi N \to \pi N$ & $N\pi\pi$
2200±125	CUTKOSKY	80	IPWA	$\pi N \to \pi N$

Δ(2000) BREIT-WIGNER WIDTH

VALUE (MeV)	DOCUMENT ID		TECN	COMMENT
138± 68	VRANA	00	DPWA	Multichannel
251± 93	MANLEY	92	IPWA	$\pi N \to \pi N$ & $N\pi\pi$
400±125	CUTKOSKY	80	IPWA	$\pi N \to \pi N$

Δ(2000) POLE POSITION

REAL PART

VALUE (MeV)	DOCUMENT ID		TECN	COMMENT
1697	VRANA	00	DPWA	Multichannel
2150±100	CUTKOSKY	80	IPWA	$\pi N \to \pi N$

−2×IMAGINARY PART

VALUE (MeV)	DOCUMENT ID		TECN	COMMENT
112	VRANA	00	DPWA	Multichannel
350±100	CUTKOSKY	80	IPWA	$\pi N \to \pi N$

Δ(2000) ELASTIC POLE RESIDUE

MODULUS $|r|$

VALUE (MeV)	DOCUMENT ID		TECN	COMMENT
16±5	CUTKOSKY	80	IPWA	$\pi N \to \pi N$

PHASE θ

VALUE (°)	DOCUMENT ID		TECN	COMMENT
150±90	CUTKOSKY	80	IPWA	$\pi N \to \pi N$

Δ(2000) DECAY MODES

	Mode
Γ_1	$N\pi$
Γ_2	$N\pi\pi$
Γ_3	$\Delta(1232)\pi$, P-wave
Γ_4	$\Delta(1232)\pi$, F-wave
Γ_5	$N\rho$, S=3/2, P-wave

Δ(2000) BRANCHING RATIOS

$\Gamma(N\pi)/\Gamma_{total}$ Γ_1/Γ

VALUE	DOCUMENT ID		TECN	COMMENT
0.00±0.01	VRANA	00	DPWA	Multichannel
0.02±0.01	MANLEY	92	IPWA	$\pi N \to \pi N$ & $N\pi\pi$
0.07±0.04	CUTKOSKY	80	IPWA	$\pi N \to \pi N$

$(\Gamma_i\Gamma_f)^{1/2}/\Gamma_{total}$ in $N\pi \to \Delta(2000) \to \Delta(1232)\pi$, P-wave $(\Gamma_1\Gamma_3)^{1/2}/\Gamma$

VALUE	DOCUMENT ID		TECN	COMMENT
+0.07±0.03	MANLEY	92	IPWA	$\pi N \to \pi N$ & $N\pi\pi$

$\Gamma(\Delta(1232)\pi$, P-wave$)/\Gamma_{total}$ Γ_3/Γ

VALUE	DOCUMENT ID		TECN	COMMENT
0.00±0.01	VRANA	00	DPWA	Multichannel

$(\Gamma_i\Gamma_f)^{1/2}/\Gamma_{total}$ in $N\pi \to \Delta(2000) \to \Delta(1232)\pi$, F-wave $(\Gamma_1\Gamma_4)^{1/2}/\Gamma$

VALUE	DOCUMENT ID		TECN	COMMENT
+0.09±0.04	MANLEY	92	IPWA	$\pi N \to \pi N$ & $N\pi\pi$

$\Gamma(\Delta(1232)\pi$, F-wave$)/\Gamma_{total}$ Γ_4/Γ

VALUE	DOCUMENT ID		TECN	COMMENT
0.40±0.01	VRANA	00	DPWA	Multichannel

$(\Gamma_i\Gamma_f)^{1/2}/\Gamma_{total}$ in $N\pi \to \Delta(2000) \to N\rho$, S=3/2, P-wave $(\Gamma_1\Gamma_5)^{1/2}/\Gamma$

VALUE	DOCUMENT ID		TECN	COMMENT
−0.06±0.01	MANLEY	92	IPWA	$\pi N \to \pi N$ & $N\pi\pi$

$\Gamma(N\rho$, S=3/2, P-wave$)/\Gamma_{total}$ Γ_5/Γ

VALUE	DOCUMENT ID		TECN	COMMENT
0.60±0.60	VRANA	00	DPWA	Multichannel

Δ(2000) REFERENCES

VRANA	00	PRPL 328 181	T.P. Vrana, S.A. Dytman,, T.-S.H. Lee	(PITT+)
MANLEY	92	PR D45 4002	D.M. Manley, E.M. Saleski	(KENT) IJP
Also	84	PR D30 904	D.M. Manley *et al.*	(VPI)
CUTKOSKY	80	Toronto Conf. 19	R.E. Cutkosky *et al.*	(CMU, LBL)
Also	79	PR D20 2839	R.E. Cutkosky *et al.*	(CMU, LBL)

Δ(2150) S_{31}

$I(J^P) = \frac{3}{2}(\frac{1}{2}^-)$ Status: *

OMITTED FROM SUMMARY TABLE

Δ(2150) BREIT-WIGNER MASS

VALUE (MeV)	DOCUMENT ID		TECN	COMMENT
≈ 2150 OUR ESTIMATE				
2047.4± 27.0	[1] CHEW	80	BPWA	$\pi^+ p \to \pi^+ p$
2203.2± 8.4	[1] CHEW	80	BPWA	$\pi^+ p \to \pi^+ p$
2150 ±100	CUTKOSKY	80	IPWA	$\pi N \to \pi N$

Δ(2150) BREIT-WIGNER WIDTH

VALUE (MeV)	DOCUMENT ID		TECN	COMMENT
121.6± 62.0	[1] CHEW	80	BPWA	$\pi^+ p \to \pi^+ p$
120.5± 45.0	[1] CHEW	80	BPWA	$\pi^+ p \to \pi^+ p$
200 ±100	CUTKOSKY	80	IPWA	$\pi N \to \pi N$

Δ(2150) POLE POSITION

REAL PART

VALUE (MeV)	DOCUMENT ID		TECN	COMMENT
2140±80	CUTKOSKY	80	IPWA	$\pi N \to \pi N$

$-2\times$IMAGINARY PART

VALUE (MeV)	DOCUMENT ID		TECN	COMMENT
200 ± 80	CUTKOSKY	80	IPWA	$\pi N \to \pi N$

$\Delta(2150)$ ELASTIC POLE RESIDUE

MODULUS $|r|$

VALUE (MeV)	DOCUMENT ID		TECN	COMMENT
7 ± 2	CUTKOSKY	80	IPWA	$\pi N \to \pi N$

PHASE θ

VALUE (°)	DOCUMENT ID		TECN	COMMENT
-60 ± 90	CUTKOSKY	80	IPWA	$\pi N \to \pi N$

$\Delta(2150)$ DECAY MODES

	Mode
Γ_1	$N\pi$
Γ_2	ΣK

$\Delta(2150)$ BRANCHING RATIOS

$\Gamma(N\pi)/\Gamma_{\text{total}}$ Γ_1/Γ

VALUE	DOCUMENT ID		TECN	COMMENT
0.41	[1] CHEW	80	BPWA	$\pi^+ p \to \pi^+ p$
0.37	[1] CHEW	80	BPWA	$\pi^+ p \to \pi^+ p$
0.08 ± 0.02	CUTKOSKY	80	IPWA	$\pi N \to \pi N$

$(\Gamma_i\Gamma_f)^{1/2}/\Gamma_{\text{total}}$ in $N\pi \to \Delta(2150) \to \Sigma K$ $(\Gamma_1\Gamma_2)^{1/2}/\Gamma$

VALUE	DOCUMENT ID		TECN	COMMENT
<0.03	CANDLIN	84	DPWA	$\pi^+ p \to \Sigma^+ K^+$

$\Delta(2150)$ FOOTNOTES

[1] CHEW 80 reports two S_{31} resonances in this mass region. Problems with this analysis are discussed in section 2.1.11 of HOEHLER 83.

$\Delta(2150)$ REFERENCES

CANDLIN	84	NP B238 477	D.J. Candlin *et al.*	(EDIN, RAL, LOWC)
HOEHLER	83	Landolt-Boernstein 1/9B2	G. Hohler	(KARLT)
CHEW	80	Toronto Conf. 123	D.M. Chew	(LBL) IJP
CUTKOSKY	80	Toronto Conf. 19	R.E. Cutkosky *et al.*	(CMU, LBL) IJP
Also	79	PR D20 2839	R.E. Cutkosky *et al.*	(CMU, LBL)

$\Delta(2200)$ G_{37}

$I(J^P) = \frac{3}{2}(\frac{7}{2}^-)$ Status: *

OMITTED FROM SUMMARY TABLE

The various analyses are not in good agreement.

$\Delta(2200)$ BREIT-WIGNER MASS

VALUE (MeV)	DOCUMENT ID		TECN	COMMENT
≈ 2200 OUR ESTIMATE				
2200 ± 80	CUTKOSKY	80	IPWA	$\pi N \to \pi N$
2215 ± 60	HOEHLER	79	IPWA	$\pi N \to \pi N$
2280 ± 80	HENDRY	78	MPWA	$\pi N \to \pi N$
• • • We do not use the following data for averages, fits, limits, etc. • • •				
2280 ± 40	CANDLIN	84	DPWA	$\pi^+ p \to \Sigma^+ K^+$

$\Delta(2200)$ BREIT-WIGNER WIDTH

VALUE (MeV)	DOCUMENT ID		TECN	COMMENT
450 ± 100	CUTKOSKY	80	IPWA	$\pi N \to \pi N$
400 ± 100	HOEHLER	79	IPWA	$\pi N \to \pi N$
400 ± 150	HENDRY	78	MPWA	$\pi N \to \pi N$
• • • We do not use the following data for averages, fits, limits, etc. • • •				
400 ± 50	CANDLIN	84	DPWA	$\pi^+ p \to \Sigma^+ K^+$

$\Delta(2200)$ POLE POSITION

REAL PART

VALUE (MeV)	DOCUMENT ID		TECN	COMMENT
2100 ± 50	CUTKOSKY	80	IPWA	$\pi N \to \pi N$

$-2\times$IMAGINARY PART

VALUE (MeV)	DOCUMENT ID		TECN	COMMENT
340 ± 80	CUTKOSKY	80	IPWA	$\pi N \to \pi N$

$\Delta(2200)$ ELASTIC POLE RESIDUE

MODULUS $|r|$

VALUE (MeV)	DOCUMENT ID		TECN	COMMENT
8 ± 3	CUTKOSKY	80	IPWA	$\pi N \to \pi N$

PHASE θ

VALUE (°)	DOCUMENT ID		TECN	COMMENT
-70 ± 40	CUTKOSKY	80	IPWA	$\pi N \to \pi N$

$\Delta(2200)$ DECAY MODES

	Mode
Γ_1	$N\pi$
Γ_2	ΣK

$\Delta(2200)$ BRANCHING RATIOS

$\Gamma(N\pi)/\Gamma_{\text{total}}$ Γ_1/Γ

VALUE	DOCUMENT ID		TECN	COMMENT
0.06 ± 0.02	CUTKOSKY	80	IPWA	$\pi N \to \pi N$
0.05 ± 0.02	HOEHLER	79	IPWA	$\pi N \to \pi N$
0.09 ± 0.02	HENDRY	78	MPWA	$\pi N \to \pi N$

$(\Gamma_i\Gamma_f)^{1/2}/\Gamma_{\text{total}}$ in $N\pi \to \Delta(2200) \to \Sigma K$ $(\Gamma_1\Gamma_2)^{1/2}/\Gamma$

VALUE	DOCUMENT ID		TECN	COMMENT
-0.014 ± 0.005	CANDLIN	84	DPWA	$\pi^+ p \to \Sigma^+ K^+$

$\Delta(2200)$ REFERENCES

CANDLIN	84	NP B238 477	D.J. Candlin *et al.*	(EDIN, RAL, LOWC)
CUTKOSKY	80	Toronto Conf. 19	R.E. Cutkosky *et al.*	(CMU, LBL) IJP
Also	79	PR D20 2839	R.E. Cutkosky *et al.*	(CMU, LBL) IJP
HOEHLER	79	PDAT 12-1	G. Hohler *et al.*	(KARLT) IJP
Also	80	Toronto Conf. 3	R. Koch	(KARLT) IJP
HENDRY	78	PRL 41 222	A.W. Hendry	(IND, LBL) IJP
Also	81	ANP 136 1	A.W. Hendry	(IND)

$\Delta(2300)$ H_{39}

$I(J^P) = \frac{3}{2}(\frac{9}{2}^+)$ Status: **

OMITTED FROM SUMMARY TABLE

$\Delta(2300)$ BREIT-WIGNER MASS

VALUE (MeV)	DOCUMENT ID		TECN	COMMENT
≈ 2300 OUR ESTIMATE				
2204.5 ± 3.4	CHEW	80	BPWA	$\pi^+ p \to \pi^+ p$
2400 ± 125	CUTKOSKY	80	IPWA	$\pi N \to \pi N$
2217 ± 80	HOEHLER	79	IPWA	$\pi N \to \pi N$
2450 ± 100	HENDRY	78	MPWA	$\pi N \to \pi N$
• • • We do not use the following data for averages, fits, limits, etc. • • •				
2400	CANDLIN	84	DPWA	$\pi^+ p \to \Sigma^+ K^+$

$\Delta(2300)$ BREIT-WIGNER WIDTH

VALUE (MeV)	DOCUMENT ID		TECN	COMMENT
32.3 ± 1.0	CHEW	80	BPWA	$\pi^+ p \to \pi^+ p$
425 ± 150	CUTKOSKY	80	IPWA	$\pi N \to \pi N$
300 ± 100	HOEHLER	79	IPWA	$\pi N \to \pi N$
500 ± 200	HENDRY	78	MPWA	$\pi N \to \pi N$
• • • We do not use the following data for averages, fits, limits, etc. • • •				
200	CANDLIN	84	DPWA	$\pi^+ p \to \Sigma^+ K^+$

$\Delta(2300)$ POLE POSITION

REAL PART

VALUE (MeV)	DOCUMENT ID		TECN	COMMENT
2370 ± 80	CUTKOSKY	80	IPWA	$\pi N \to \pi N$

$-2\times$IMAGINARY PART

VALUE (MeV)	DOCUMENT ID		TECN	COMMENT
420 ± 160	CUTKOSKY	80	IPWA	$\pi N \to \pi N$

$\Delta(2300)$ ELASTIC POLE RESIDUE

MODULUS $|r|$

VALUE (MeV)	DOCUMENT ID		TECN	COMMENT
10 ± 4	CUTKOSKY	80	IPWA	$\pi N \to \pi N$

PHASE θ

VALUE (°)	DOCUMENT ID		TECN	COMMENT
-20 ± 30	CUTKOSKY	80	IPWA	$\pi N \to \pi N$

$\Delta(2300)$ DECAY MODES

	Mode
Γ_1	$N\pi$
Γ_2	ΣK

Δ(2300) BRANCHING RATIOS

Γ(Nπ)/Γ_total — Γ1/Γ

VALUE	DOCUMENT ID		TECN	COMMENT
0.05	CHEW	80	BPWA	$\pi^+ p \rightarrow \pi^+ p$
0.06±0.02	CUTKOSKY	80	IPWA	$\pi N \rightarrow \pi N$
0.03±0.02	HOEHLER	79	IPWA	$\pi N \rightarrow \pi N$
0.08±0.02	HENDRY	78	MPWA	$\pi N \rightarrow \pi N$

(Γ_i Γ_f)^½/Γ_total in Nπ → Δ(2300) → ΣK — (Γ1Γ2)^½/Γ

VALUE	DOCUMENT ID		TECN	COMMENT
−0.017	CANDLIN	84	DPWA	$\pi^+ p \rightarrow \Sigma^+ K^+$

Δ(2300) REFERENCES

CANDLIN	84	NP B238 477	D.J. Candlin *et al.*	(EDIN, RAL, LOWC)
CHEW	80	Toronto Conf. 123	D.M. Chew	(LBL) IJP
CUTKOSKY	80	Toronto Conf. 19	R.E. Cutkosky *et al.*	(CMU, LBL) IJP
Also	79	PR D20 2839	R.E. Cutkosky *et al.*	(CMU, LBL)
HOEHLER	79	PDAT 12-1	G. Hohler *et al.*	(KARLT) IJP
Also	80	Toronto Conf. 3	R. Koch	(KARLT) IJP
HENDRY	78	PRL 41 222	A.W. Hendry	(IND, LBL) IJP
Also	81	ANP 136 1	A.W. Hendry	(IND)

Δ(2350) D_{35}

$I(J^P) = \frac{3}{2}(\frac{5}{2}^-)$ Status: *

OMITTED FROM SUMMARY TABLE

Δ(2350) BREIT-WIGNER MASS

VALUE (MeV)	DOCUMENT ID		TECN	COMMENT
≈ 2350 OUR ESTIMATE				
2171 ± 18	MANLEY	92	IPWA	$\pi N \rightarrow \pi N$ & $N\pi\pi$
2400±125	CUTKOSKY	80	IPWA	$\pi N \rightarrow \pi N$
2305 ± 26	HOEHLER	79	IPWA	$\pi N \rightarrow \pi N$
• • • We do not use the following data for averages, fits, limits, etc. • • •				
2459±100	VRANA	00	DPWA	Multichannel

Δ(2350) BREIT-WIGNER WIDTH

VALUE (MeV)	DOCUMENT ID		TECN	COMMENT
264 ± 51	MANLEY	92	IPWA	$\pi N \rightarrow \pi N$ & $N\pi\pi$
400±150	CUTKOSKY	80	IPWA	$\pi N \rightarrow \pi N$
300 ± 70	HOEHLER	79	IPWA	$\pi N \rightarrow \pi N$
• • • We do not use the following data for averages, fits, limits, etc. • • •				
480±360	VRANA	00	DPWA	Multichannel

Δ(2350) POLE POSITION

REAL PART

VALUE (MeV)	DOCUMENT ID		TECN	COMMENT
2400±125	CUTKOSKY	80	IPWA	$\pi N \rightarrow \pi N$
• • • We do not use the following data for averages, fits, limits, etc. • • •				
2427	VRANA	00	DPWA	Multichannel

−2×IMAGINARY PART

VALUE (MeV)	DOCUMENT ID		TECN	COMMENT
400±150	CUTKOSKY	80	IPWA	$\pi N \rightarrow \pi N$
• • • We do not use the following data for averages, fits, limits, etc. • • •				
458	VRANA	00	DPWA	Multichannel

Δ(2350) ELASTIC POLE RESIDUE

MODULUS |r|

VALUE (MeV)	DOCUMENT ID		TECN	COMMENT
15 ± 8	CUTKOSKY	80	IPWA	$\pi N \rightarrow \pi N$

PHASE θ

VALUE (°)	DOCUMENT ID		TECN	COMMENT
−70±70	CUTKOSKY	80	IPWA	$\pi N \rightarrow \pi N$

Δ(2350) DECAY MODES

	Mode
Γ_1	$N\pi$
Γ_2	ΣK

Δ(2350) BRANCHING RATIOS

Γ(Nπ)/Γ_total — Γ1/Γ

VALUE	DOCUMENT ID		TECN	COMMENT
0.020±0.003	MANLEY	92	IPWA	$\pi N \rightarrow \pi N$ & $N\pi\pi$
0.20 ±0.10	CUTKOSKY	80	IPWA	$\pi N \rightarrow \pi N$
0.04 ±0.02	HOEHLER	79	IPWA	$\pi N \rightarrow \pi N$
• • • We do not use the following data for averages, fits, limits, etc. • • •				
0.07 ±0.14	VRANA	00	DPWA	Multichannel

(Γ_i Γ_f)^½/Γ_total in Nπ → Δ(2350) → ΣK — (Γ1Γ2)^½/Γ

VALUE	DOCUMENT ID		TECN	COMMENT
<0.015	CANDLIN	84	DPWA	$\pi^+ p \rightarrow \Sigma^+ K^+$

Δ(2350) REFERENCES

VRANA	00	PRPL 328 181	T.P. Vrana, S.A. Dytman,, T.-S.H. Lee	(PITT+)
MANLEY	92	PR D45 4002	D.M. Manley, E.M. Saleski	(KENT) IJP
Also	84	PR D30 904	D.M. Manley *et al.*	(VPI)
CANDLIN	84	NP B238 477	D.J. Candlin *et al.*	(EDIN, RAL, LOWC)
CUTKOSKY	80	Toronto Conf. 19	R.E. Cutkosky *et al.*	(CMU, LBL) IJP
Also	79	PR D20 2839	R.E. Cutkosky *et al.*	(CMU, LBL)
HOEHLER	79	PDAT 12-1	G. Hohler *et al.*	(KARLT) IJP
Also	80	Toronto Conf. 3	R. Koch	(KARLT) IJP

Δ(2390) F_{37}

$I(J^P) = \frac{3}{2}(\frac{7}{2}^+)$ Status: *

OMITTED FROM SUMMARY TABLE

Δ(2390) BREIT-WIGNER MASS

VALUE (MeV)	DOCUMENT ID		TECN	COMMENT
≈ 2390 OUR ESTIMATE				
2350±100	CUTKOSKY	80	IPWA	$\pi N \rightarrow \pi N$
2425 ± 60	HOEHLER	79	IPWA	$\pi N \rightarrow \pi N$

Δ(2390) BREIT-WIGNER WIDTH

VALUE (MeV)	DOCUMENT ID		TECN	COMMENT
300±100	CUTKOSKY	80	IPWA	$\pi N \rightarrow \pi N$
300 ± 80	HOEHLER	79	IPWA	$\pi N \rightarrow \pi N$

Δ(2390) POLE POSITION

REAL PART

VALUE (MeV)	DOCUMENT ID		TECN	COMMENT
2350±100	CUTKOSKY	80	IPWA	$\pi N \rightarrow \pi N$

−2×IMAGINARY PART

VALUE (MeV)	DOCUMENT ID		TECN	COMMENT
260±100	CUTKOSKY	80	IPWA	$\pi N \rightarrow \pi N$

Δ(2390) ELASTIC POLE RESIDUE

MODULUS |r|

VALUE (MeV)	DOCUMENT ID		TECN	COMMENT
12±6	CUTKOSKY	80	IPWA	$\pi N \rightarrow \pi N$

PHASE θ

VALUE (°)	DOCUMENT ID		TECN	COMMENT
−90±60	CUTKOSKY	80	IPWA	$\pi N \rightarrow \pi N$

Δ(2390) DECAY MODES

	Mode
Γ_1	$N\pi$
Γ_2	ΣK

Δ(2390) BRANCHING RATIOS

Γ(Nπ)/Γ_total — Γ1/Γ

VALUE	DOCUMENT ID		TECN	COMMENT
0.08±0.04	CUTKOSKY	80	IPWA	$\pi N \rightarrow \pi N$
0.07±0.04	HOEHLER	79	IPWA	$\pi N \rightarrow \pi N$

(Γ_i Γ_f)^½/Γ_total in Nπ → Δ(2390) → ΣK — (Γ1Γ2)^½/Γ

VALUE	DOCUMENT ID		TECN	COMMENT
<0.015	CANDLIN	84	DPWA	$\pi^+ p \rightarrow \Sigma^+ K^+$

Δ(2390) REFERENCES

CANDLIN	84	NP B238 477	D.J. Candlin *et al.*	(EDIN, RAL, LOWC)
CUTKOSKY	80	Toronto Conf. 19	R.E. Cutkosky *et al.*	(CMU, LBL) IJP
Also	79	PR D20 2839	R.E. Cutkosky *et al.*	(CMU, LBL)
HOEHLER	79	PDAT 12-1	G. Hohler *et al.*	(KARLT) IJP
Also	80	Toronto Conf. 3	R. Koch	(KARLT) IJP

$\Delta(2400)$ G_{39}

$I(J^P) = \frac{3}{2}(\frac{9}{2}^-)$ Status: **

OMITTED FROM SUMMARY TABLE

$\Delta(2400)$ BREIT-WIGNER MASS

VALUE (MeV)	DOCUMENT ID		TECN	COMMENT
≈ 2400 OUR ESTIMATE				
2300 ± 100	CUTKOSKY	80	IPWA	$\pi N \to \pi N$
2468 ± 50	HOEHLER	79	IPWA	$\pi N \to \pi N$
2200 ± 100	HENDRY	78	MPWA	$\pi N \to \pi N$

$\Delta(2400)$ BREIT-WIGNER WIDTH

VALUE (MeV)	DOCUMENT ID		TECN	COMMENT
330 ± 100	CUTKOSKY	80	IPWA	$\pi N \to \pi N$
480 ± 100	HOEHLER	79	IPWA	$\pi N \to \pi N$
450 ± 200	HENDRY	78	MPWA	$\pi N \to \pi N$

$\Delta(2400)$ POLE POSITION

REAL PART

VALUE (MeV)	DOCUMENT ID		TECN	COMMENT
2260 ± 60	CUTKOSKY	80	IPWA	$\pi N \to \pi N$

$-2\times$IMAGINARY PART

VALUE (MeV)	DOCUMENT ID		TECN	COMMENT
320 ± 160	CUTKOSKY	80	IPWA	$\pi N \to \pi N$

$\Delta(2400)$ ELASTIC POLE RESIDUE

MODULUS $|r|$

VALUE (MeV)	DOCUMENT ID		TECN	COMMENT
8 ± 4	CUTKOSKY	80	IPWA	$\pi N \to \pi N$

PHASE θ

VALUE (°)	DOCUMENT ID		TECN	COMMENT
− 25 ± 15	CUTKOSKY	80	IPWA	$\pi N \to \pi N$

$\Delta(2400)$ DECAY MODES

	Mode
Γ_1	$N\pi$
Γ_2	ΣK

$\Delta(2400)$ BRANCHING RATIOS

$\Gamma(N\pi)/\Gamma_{total}$ Γ_1/Γ

VALUE	DOCUMENT ID		TECN	COMMENT
0.05 ± 0.02	CUTKOSKY	80	IPWA	$\pi N \to \pi N$
0.06 ± 0.03	HOEHLER	79	IPWA	$\pi N \to \pi N$
0.10 ± 0.03	HENDRY	78	MPWA	$\pi N \to \pi N$

$(\Gamma_i\Gamma_f)^{1/2}/\Gamma_{total}$ in $N\pi \to \Delta(2400) \to \Sigma K$ $(\Gamma_1\Gamma_2)^{1/2}/\Gamma$

VALUE	DOCUMENT ID		TECN	COMMENT
< 0.015	CANDLIN	84	DPWA	$\pi^+ p \to \Sigma^+ K^+$

$\Delta(2400)$ REFERENCES

CANDLIN	84	NP B238 477	D.J. Candlin *et al.*	(EDIN, RAL, LOWC)
CUTKOSKY	80	Toronto Conf. 19	R.E. Cutkosky *et al.*	(CMU, LBL) IJP
Also	79	PR D20 2839	R.E. Cutkosky *et al.*	(CMU, LBL)
HOEHLER	79	PDAT 12-1	G. Hohler *et al.*	(KARLT) IJP
Also	80	Toronto Conf. 3	R. Koch	(KARLT) IJP
HENDRY	78	PRL 41 222	A.W. Hendry	(IND, LBL) IJP
Also	81	ANP 136 1	A.W. Hendry	(IND)

$\Delta(2420)$ $H_{3,11}$

$I(J^P) = \frac{3}{2}(\frac{11}{2}^+)$ Status: ****

Most of the results published before 1975 are now obsolete and have been omitted. They may be found in our 1982 edition, Physics Letters **111B** (1982).

$\Delta(2420)$ BREIT-WIGNER MASS

VALUE (MeV)	DOCUMENT ID		TECN	COMMENT
2300 to 2500 (≈ 2420) OUR ESTIMATE				
2400 ±125	CUTKOSKY	80	IPWA	$\pi N \to \pi N$
2416 ± 17	HOEHLER	79	IPWA	$\pi N \to \pi N$
2400 ± 60	HENDRY	78	MPWA	$\pi N \to \pi N$
• • • We do not use the following data for averages, fits, limits, etc. • • •				
2400	CANDLIN	84	DPWA	$\pi^+ p \to \Sigma^+ K^+$
2358.0 ± 9.0	CHEW	80	BPWA	$\pi^+ p \to \pi^+ p$

$\Delta(2420)$ BREIT-WIGNER WIDTH

VALUE (MeV)	DOCUMENT ID		TECN	COMMENT
300 to 500 (≈ 400) OUR ESTIMATE				
450 ±150	CUTKOSKY	80	IPWA	$\pi N \to \pi N$
340 ± 28	HOEHLER	79	IPWA	$\pi N \to \pi N$
460 ±100	HENDRY	78	MPWA	$\pi N \to \pi N$
• • • We do not use the following data for averages, fits, limits, etc. • • •				
400	CANDLIN	84	DPWA	$\pi^+ p \to \Sigma^+ K^+$
202.2 ± 45.0	CHEW	80	BPWA	$\pi^+ p \to \pi^+ p$

$\Delta(2420)$ POLE POSITION

REAL PART

VALUE (MeV)	DOCUMENT ID		TECN	COMMENT
2260 to 2400 (≈ 2330) OUR ESTIMATE				
2300	[1] HOEHLER	93	ARGD	$\pi N \to \pi N$
2360 ± 100	CUTKOSKY	80	IPWA	$\pi N \to \pi N$

$-2\times$IMAGINARY PART

VALUE (MeV)	DOCUMENT ID		TECN	COMMENT
350 to 750 (≈ 550) OUR ESTIMATE				
620	[1] HOEHLER	93	ARGD	$\pi N \to \pi N$
420 ± 100	CUTKOSKY	80	IPWA	$\pi N \to \pi N$

$\Delta(2420)$ ELASTIC POLE RESIDUE

MODULUS $|r|$

VALUE (MeV)	DOCUMENT ID		TECN	COMMENT
39	HOEHLER	93	ARGD	$\pi N \to \pi N$
18 ± 6	CUTKOSKY	80	IPWA	$\pi N \to \pi N$

PHASE θ

VALUE (°)	DOCUMENT ID		TECN	COMMENT
− 60	HOEHLER	93	ARGD	$\pi N \to \pi N$
− 30 ± 40	CUTKOSKY	80	IPWA	$\pi N \to \pi N$

$\Delta(2420)$ DECAY MODES

The following branching fractions are our estimates, not fits or averages.

	Mode	Fraction (Γ_i/Γ)
Γ_1	$N\pi$	5–15 %
Γ_2	ΣK	

$\Delta(2420)$ BRANCHING RATIOS

$\Gamma(N\pi)/\Gamma_{total}$ Γ_1/Γ

VALUE	DOCUMENT ID		TECN	COMMENT
0.05 to 0.15 OUR ESTIMATE				
0.08 ± 0.03	CUTKOSKY	80	IPWA	$\pi N \to \pi N$
0.08 ± 0.015	HOEHLER	79	IPWA	$\pi N \to \pi N$
0.11 ± 0.02	HENDRY	78	MPWA	$\pi N \to \pi N$
• • • We do not use the following data for averages, fits, limits, etc. • • •				
0.22	CHEW	80	BPWA	$\pi^+ p \to \pi^+ p$

$(\Gamma_i\Gamma_f)^{1/2}/\Gamma_{total}$ in $N\pi \to \Delta(2420) \to \Sigma K$ $(\Gamma_1\Gamma_2)^{1/2}/\Gamma$

VALUE	DOCUMENT ID		TECN	COMMENT
− 0.016	CANDLIN	84	DPWA	$\pi^+ p \to \Sigma^+ K^+$

$\Delta(2420)$ FOOTNOTES

[1] See HOEHLER 93 for a detailed discussion of the evidence for and the pole parameters of N and Δ resonances as determined from Argand diagrams of πN elastic partial-wave amplitudes and from plots of the speeds with which the amplitudes traverse the diagrams.

$\Delta(2420)$ REFERENCES

HOEHLER	93	πN Newsletter 9 1	G. Hohler	(KARL)
CANDLIN	84	NP B238 477	D.J. Candlin *et al.*	(EDIN, RAL, LOWC)
PDG	82	PL 111B	M. Roos *et al.*	(HELS, CIT, CERN)
CHEW	80	Toronto Conf. 123	D.M. Chew	(LBL) IJP
CUTKOSKY	80	Toronto Conf. 19	R.E. Cutkosky *et al.*	(CMU, LBL) IJP
Also	79	PR D20 2839	R.E. Cutkosky *et al.*	(CMU, LBL)
HOEHLER	79	PDAT 12-1	G. Hohler *et al.*	(KARLT) IJP
Also	80	Toronto Conf. 3	R. Koch	(KARLT) IJP
HENDRY	78	PRL 41 222	A.W. Hendry	(IND, LBL) IJP
Also	81	ANP 136 1	A.W. Hendry	(IND)

$\Delta(2750)$ $I_{3,13}$

$I(J^P) = \frac{3}{2}(\frac{13}{2}^-)$ Status: $**$

OMITTED FROM SUMMARY TABLE

$\Delta(2750)$ BREIT-WIGNER MASS

VALUE (MeV)	DOCUMENT ID		TECN	COMMENT
≈ 2750 OUR ESTIMATE				
2794 ± 80	HOEHLER	79	IPWA	$\pi N \to \pi N$
2650 ± 100	HENDRY	78	MPWA	$\pi N \to \pi N$

$\Delta(2750)$ BREIT-WIGNER WIDTH

VALUE (MeV)	DOCUMENT ID		TECN	COMMENT
350 ± 100	HOEHLER	79	IPWA	$\pi N \to \pi N$
500 ± 100	HENDRY	78	MPWA	$\pi N \to \pi N$

$\Delta(2750)$ DECAY MODES

	Mode
Γ_1	$N\pi$

$\Delta(2750)$ BRANCHING RATIOS

$\Gamma(N\pi)/\Gamma_{total}$ Γ_1/Γ

VALUE	DOCUMENT ID		TECN	COMMENT
0.04 ± 0.015	HOEHLER	79	IPWA	$\pi N \to \pi N$
0.05 ± 0.01	HENDRY	78	MPWA	$\pi N \to \pi N$

$\Delta(2750)$ REFERENCES

HOEHLER	79	PDAT 12-1	G. Hohler *et al.*	(KARLT) IJP
Also	80	Toronto Conf. 3	R. Koch	(KARLT) IJP
HENDRY	78	PRL 41 222	A.W. Hendry	(IND, LBL) IJP
Also	81	ANP 136 1	A.W. Hendry	(IND)

$\Delta(2950)$ $K_{3,15}$

$I(J^P) = \frac{3}{2}(\frac{15}{2}^+)$ Status: $**$

OMITTED FROM SUMMARY TABLE

$\Delta(2950)$ BREIT-WIGNER MASS

VALUE (MeV)	DOCUMENT ID		TECN	COMMENT
≈ 2950 OUR ESTIMATE				
2990 ± 100	HOEHLER	79	IPWA	$\pi N \to \pi N$
2850 ± 100	HENDRY	78	MPWA	$\pi N \to \pi N$

$\Delta(2950)$ BREIT-WIGNER WIDTH

VALUE (MeV)	DOCUMENT ID		TECN	COMMENT
330 ± 100	HOEHLER	79	IPWA	$\pi N \to \pi N$
700 ± 200	HENDRY	78	MPWA	$\pi N \to \pi N$

$\Delta(2950)$ DECAY MODES

	Mode
Γ_1	$N\pi$

$\Delta(2950)$ BRANCHING RATIOS

$\Gamma(N\pi)/\Gamma_{total}$ Γ_1/Γ

VALUE	DOCUMENT ID		TECN	COMMENT
0.04 ± 0.02	HOEHLER	79	IPWA	$\pi N \to \pi N$
0.03 ± 0.01	HENDRY	78	MPWA	$\pi N \to \pi N$

$\Delta(2950)$ REFERENCES

HOEHLER	79	PDAT 12-1	G. Hohler *et al.*	(KARLT) IJP
Also	80	Toronto Conf. 3	R. Koch	(KARLT) IJP
HENDRY	78	PRL 41 222	A.W. Hendry	(IND, LBL) IJP
Also	81	ANP 136 1	A.W. Hendry	(IND)

$\Delta(\sim 3000$ Region) Partial-Wave Analyses

OMITTED FROM SUMMARY TABLE

We list here miscellaneous high-mass candidates for isospin-3/2 resonances found in partial-wave analyses.

Our 1982 edition also had a $\Delta(2850)$ and a $\Delta(3230)$. The evidence for them was deduced from total cross-section and 180° elastic cross-section measurements. The $\Delta(2850)$ has been resolved into the $\Delta(2750)$ $I_{3,13}$ and $\Delta(2950)$ $K_{3,15}$. The $\Delta(3230)$ is perhaps related to the $K_{3,13}$ of HENDRY 78 and to the $L_{3,17}$ of KOCH 80.

$\Delta(\sim 3000)$ BREIT-WIGNER MASS

VALUE (MeV)	DOCUMENT ID		TECN	COMMENT
≈ 3000 OUR ESTIMATE				
3300	[1] KOCH	80	IPWA	$\pi N \to \pi N$ $L_{3,17}$ wave
3500	[1] KOCH	80	IPWA	$\pi N \to \pi N$ $M_{3,19}$ wave
2850 ± 150	HENDRY	78	MPWA	$\pi N \to \pi N$ $I_{3,11}$ wave
3200 ± 200	HENDRY	78	MPWA	$\pi N \to \pi N$ $K_{3,13}$ wave
3300 ± 200	HENDRY	78	MPWA	$\pi N \to \pi N$ $L_{3,17}$ wave
3700 ± 200	HENDRY	78	MPWA	$\pi N \to \pi N$ $M_{3,19}$ wave
4100 ± 300	HENDRY	78	MPWA	$\pi N \to \pi N$ $N_{3,21}$ wave

$\Delta(\sim 3000)$ BREIT-WIGNER WIDTH

VALUE (MeV)	DOCUMENT ID		TECN	COMMENT
700 ± 200	HENDRY	78	MPWA	$\pi N \to \pi N$ $I_{3,11}$ wave
1000 ± 300	HENDRY	78	MPWA	$\pi N \to \pi N$ $K_{3,13}$ wave
1100 ± 300	HENDRY	78	MPWA	$\pi N \to \pi N$ $L_{3,17}$ wave
1300 ± 400	HENDRY	78	MPWA	$\pi N \to \pi N$ $M_{3,19}$ wave
1600 ± 500	HENDRY	78	MPWA	$\pi N \to \pi N$ $N_{3,21}$ wave

$\Delta(\sim 3000)$ DECAY MODES

	Mode
Γ_1	$N\pi$

$\Delta(\sim 3000)$ BRANCHING RATIOS

$\Gamma(N\pi)/\Gamma_{total}$ Γ_1/Γ

VALUE	DOCUMENT ID		TECN	COMMENT
0.06 ± 0.02	HENDRY	78	MPWA	$\pi N \to \pi N$ $I_{3,11}$ wave
0.045 ± 0.02	HENDRY	78	MPWA	$\pi N \to \pi N$ $K_{3,13}$ wave
0.03 ± 0.01	HENDRY	78	MPWA	$\pi N \to \pi N$ $L_{3,17}$ wave
0.025 ± 0.01	HENDRY	78	MPWA	$\pi N \to \pi N$ $M_{3,19}$ wave
0.018 ± 0.01	HENDRY	78	MPWA	$\pi N \to \pi N$ $N_{3,21}$ wave

$\Delta(\sim 3000)$ FOOTNOTES

[1] In addition, KOCH 80 reports some evidence for an S_{31} $\Delta(2700)$ and a P_{33} $\Delta(2800)$.

$\Delta(\sim 3000)$ REFERENCES

KOCH	80	Toronto Conf. 3	R. Koch	(KARLT) IJP
HENDRY	78	PRL 41 222	A.W. Hendry	(IND, LBL) IJP
Also	81	ANP 136 1	A.W. Hendry	(IND)

EXOTIC BARYONS

Minimum quark content: $\Theta^+ = uudd\overline{s}$, $\Phi^{--} = ssdd\overline{u}$, $\Phi^+ = ssuu\overline{d}$.

$\Theta(1540)^+$

$I(J^P) = 0(?^?)$ Status: ***

A POSSIBLE EXOTIC BARYON RESONANCE

Written November 2003 by G. Trilling (LBNL).

I. Introduction

The well-established baryon states can be understood as combinations of three valence quarks. In this discussion, we confine ourselves to baryon states constructed from combinations of u, d, and s quarks. The three-quark combinations are members of SU(3) singlets, octets, and decuplets. Baryon states that cannot be constructed with triplets of u, d, and s quarks are called exotic.

Do there exist in nature baryon states constructed from more complicated quark configurations? The simplest might consist of four quarks plus an antiquark. In a 1997 paper [1], Diakonov *et al.* proposed, on the basis of a chiral soliton model, the existence of a low-mass anti-decuplet of such baryons, with spin 1/2 and even parity, and with specific estimates for the masses and widths. Figure 1, from their paper, shows this proposed anti-decuplet. The baryons at the three corners of the triangle are exotic: their isospin and strangeness cannot be obtained by any triplet combination of u, d, and s quarks. The other baryons of the anti-decuplet are made up of combinations such as, for example, $uudd\overline{d}$ and $uuds\overline{s}$ (relevant to the charged $N(1710)$ in Fig. 1). These two combinations have the same isospin and strangeness as uud, and the corresponding baryons are therefore not exotic. Diakonov *et al.* estimated the masses and widths of the four isospin multiplets in the anti-decuplet of Fig. 1. They assumed equal mass spacings between multiplets, with a calculated spacing of 180 MeV. Associating the $S = 0$ isospin doublet with the $N(1710)$, an $I = J = 1/2$, P-wave πN resonance listed in our Tables, they predicted a mass of 1530 MeV for the $S = +1$ exotic Z^+ isosinglet. They also estimated its total decay width to be 15 MeV or less.

Before 2003, there was no evidence for a narrow $S = +1$ baryon resonance, but that situation has now changed. In 2003, several groups searched old or new data for evidence of a K^+n or K^0p resonance in the neighborhood of the predicted 1530 MeV and reported positive results. On the other hand, attempts to find this exotic state in other fairly extensive older published data have so far yielded no supporting evidence. We first consider the new positive results, and then review some of the relevant older information. One point of nomenclature: the Z^+ is now universally called the Θ^+.

II. Recent results

We discuss the results from seven different experiments. Five are photo- or electroproduction experiments using carbon, deuterium, or hydrogen targets, one is a K^+n charge-exchange experiment in a liquid-xenon bubble chamber, and one involves a compilation of neutrino bubble-chamber data with hydrogen, deuterium, and neon fills. As an example, we show in Fig. 2 the nK^+ mass spectrum from the first of two CLAS photoproduction experiments discussed below [2]. The structure at 1540 MeV is interpreted as a possible Θ^+ signal with a significance of 5.2 σ.

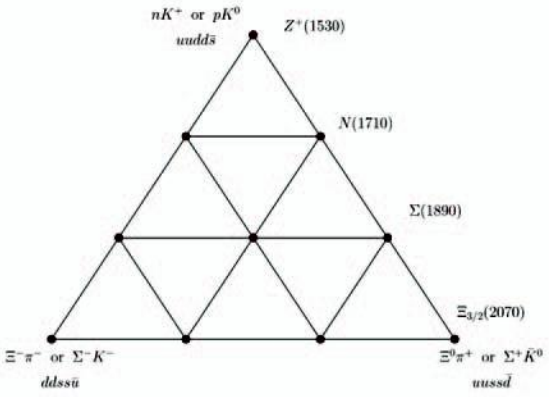

Figure 1: Proposed anti-decuplet of baryons (from [1]).

The LEPS experiment — The LEPS experiment [3] was carried out at the Laser-Electron-Photon facility at the Spring-8 Synchrotron Radiation Facility in Japan during 2000–2001. A photon beam with tagged energies between 1.5 and 2.4 GeV was incident on a scintillator target; for the Θ^+ search, the reaction $\gamma n \to nK^+K^-$, with carbon from the scintillator as the neutron target, was identified and measured in the LEPS spectrometer. The goal was to search for a nK^+ mass enhancement. Cuts were made to remove a large number of $\phi \to K^+K^-$ decays and possible backgrounds from $\gamma p \to pK^+K^-$ in the same carbon target. Corrections were made for the Fermi momentum of the target nucleon, relevant to the reconstruction since the final-state neutron is not detected. After cuts, the final sample consists of 109 events. There is a peak at 1540 MeV, consisting of 19 events above a background of 17. The significance is claimed to be 4.6 σ, the mass 1540 ± 10 MeV, and the width less than 25 MeV at 90% confidence.

The DIANA experiment — The DIANA experiment [4], run in 1986, was a xenon bubble-chamber exposure to a K^+ beam. The K^+ momentum at the bubble-chamber entry was 750 MeV/c, decreasing through ionization loss all the way to rest at the back of the chamber. Only those interactions produced by K^+ of momenta below 550 MeV/c were considered in the analysis, which focused on charge-exchange events, $K^+\mathrm{Xe} \to K^0_S pX$, with the K^0_S decaying into $\pi^+\pi^-$. After cuts to remove

See key on page 323

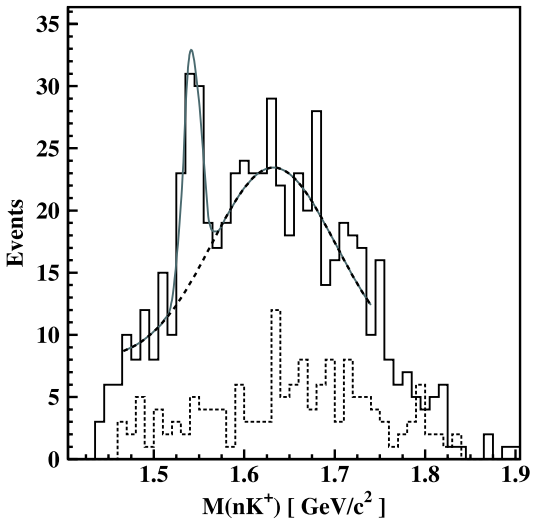

Figure 2: Invariant nK^+ mass spectrum from the reaction $\gamma d \to K^+K^-pn$ after cuts. The dotted histogram shows events associated with $\Lambda(1520) \to K^-p$ production (from [2]).

low-momentum protons and K^0_S, and cuts on K^0_S and proton directions (said to reduce the effects of rescatterings in nuclear matter), a sharp peak in the pK^0_S mass spectrum at 1539 ± 2 MeV, consisting of a signal of 29 events over a background of 44 events, was observed. The quoted statistical significance is 4.4 σ, and the width upper limit is 9 MeV.

The CLAS experiments — The first of the CLAS experiments [2], run in 1999 at Jefferson Lab, studied the nK^+ mass spectrum from the reaction $\gamma d \to npK^+K^-$, produced by a tagged photon beam of energies between 1.5 and 2.9 GeV. The events of interest are really $\gamma n \to nK^+K^-$, but reconstruction requires a detectable proton; hence only events with a rescattering that changes the spectator into a detectable proton are useful. With removal of $\phi \to K^+K^-$ and $\Lambda(1520) \to pK^-$ events, and an imposed upper limit of 1 GeV/c on the K^+ momentum, the spectrum shown in Fig. 2, with a signal of 43 events over a background of about 54 events, is observed. The mass is 1542 ± 5 MeV, the quoted significance is 5.2 σ, and the observed width of 21 MeV is consistent with the instrumental resolution.

Another CLAS experiment [5] studied the reaction $\gamma p \to n\pi^+K^+K^-$, a four-body final state, with photons of energies between 3 and 5.5 GeV. After a ϕ mass cut, the nK^+ mass distribution for 14,000 events shows no significant structure. To enrich the sample, angular requirements that select events with forward π^+ and backward K^+ are imposed. These cuts remove about 95% of the events, leaving a peak in the nK^+ mass at 1555 ± 10 MeV. The fit yields a signal of 41 events over a background of about 35 events, with a quoted significance of 7.8 σ. The observed width of 26 MeV is consistent with the resolution.

The SAPHIR experiment — The 1997–1998 data from the SAPHIR experiment [6], run at the ELSA facility in Bonn, allow study of the reaction $\gamma p \to nK^+K^0_S$, with an incident tagged photon beam with energy between 0.9 and 2.6 GeV. To enhance the Θ^+ signal, a requirement that $\cos\theta_{\rm cm} > 0.5$, where $\theta_{\rm cm}$ is the angle between the beam and the K^0_S in the center of mass, is imposed. A signal of about 55 events over a background of about 56 is observed in the nK^+ mass spectrum at a mass of $1540 \pm 4 \pm 2$ MeV. The quoted significance is 4.8 σ, and the width is less than 25 MeV. Because there is no significant signal in the pK^+ spectrum observed in a separate experiment to study $\gamma p \to pK^+K^-$, the authors conclude that the Θ^+ must have $I = 0$.

A compendium of neutrino experiments — Asratyan *et al.* [7] have analyzed a database of some 120,000 ν and $\overline{\nu}$ charged-current events from the BEBC (CERN) and 15-foot (Fermilab) bubble chambers; the fills were hydrogen, deuterium, or neon. Some of the runs had mean incident energies of about 40 GeV and others about 110 GeV. The authors looked for final states with a proton (momentum between 300 and 900 MeV/c), and a K^0_S decay, both originating from the same vertex. The goal was to search for evidence of the Θ^+ in the pK^0_S mass spectra. A signal consisting of an excess of about 27 events over a background of about 8 events, at 1533 ± 5 MeV, was observed in the combined neon and deuterium data. The quoted significance is 6.7 σ, and the width is less than 20 MeV. There is one concern here: the K^0_S can have $S = +1$ or -1, and there are numerous $S = -1$ baryon resonances. The authors argue that, since there is no established $S = -1$, $I = 1$ narrow resonance near 1530 MeV, the observed structure must be taken as evidence for the Θ^+.

The HERMES experiment — In the HERMES experiment [8], a 27.6 GeV positron beam from the HERA storage ring is incident on a deuterium target in a search for Θ^+ in quasi-real inclusive photoproduction. The analysis selects final states with a proton and $K^0_S \to \pi^+\pi^-$ decay. In the resulting pK^0_S mass spectrum, an enhancement at a mass of $1528 \pm 2.6 \pm 2.1$ MeV is observed. Depending on the background model, the significance is said to be 4-to-6 σ and the width may be larger than expected from just the measurement uncertainty of 4.3-to-6.2 MeV (one standard deviation).

III. Information based on earlier data

There are a number of old experiments that may be relevant to the search for a Θ^+. We consider three sets of experiments:

(1) Studies of K^+p and K^+d interactions leading to $KN\pi$ final states. One looks for an enhancement in nK^+ and pK^0 mass distributions.

(2) Studies of $\pi^- p$ interactions leading to $K\overline{K}N$ final states, again looking for structure in the KN mass distributions.

(3) Measurements of $K^+ d$ total and charge-exchange cross sections as functions of incident momentum, looking for a cross section peak in the neighborhood of 440 MeV/c.

The Berthon *et al.* pK^0 mass spectra [12] show no indication of structure near 1540 MeV for incident momenta of 1210, 1290, 1380 MeV/c, but there is just a hint at 1690 MeV/c. Inspection of the corresponding Dalitz plot, however (see Fig. 3), indicates that any small population excess is likely

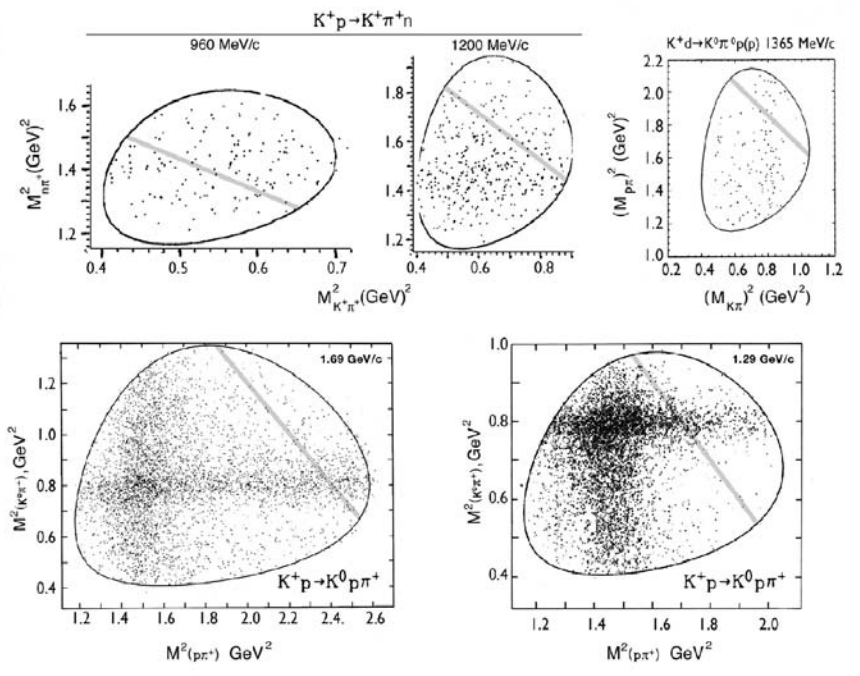

Dalitz plots for $K^+N \to KN\pi$ reactions studied in hydrogen and deuterium bubble chambers. References, going clockwise starting at upper left, are [9], [9], [13], [12] and [12]. The diagonal lines show where one would expect to see the $\Theta(1540)^+$.

K^+p and $K^+d \to KN\pi$ — One might expect that an $S = +1$ initial state would increase the likelihood of producing an $S = +1$ resonance in the final state. Published results for the reactions $K^+p \to pK^0\pi^+$, $pK^+\pi^0$, and $nK^+\pi^+$, studied in bubble chambers at incident momenta of 960, 1200, 1210, 1290, 1360, 1380, 1520, 1585, 1690, and 2650 MeV/c [9–12], have been examined with some care. In most cases, only Dalitz plots are available, but Berthon *et al.* [12] also supplies pK^0_S mass spectra with very substantial statistics. In these final states, the $K^*(892)$ and $\Delta(1232)$ dominate, and most features of the KN spectra are simply reflections of these resonances. Study of all the available Dalitz plots, especially away from the known resonance bands, shows no indication of a population increase near a pK^0 or nK^+ mass of 1540 MeV. Figure 3 shows some representative Dalitz plots, with the diagonal lines corresponding to a 1540 MeV KN resonance. For a strongly decaying spin-1/2 state, the distribution of points along the lines should be uniform.

related to overlap with the K^* resonance band. Similarly, the $K^+d \to KN\pi(N)$ Dalitz plots (see Fig. 3) from Hirata *et al.* [13] are also dominated by the same known resonance bands.

It is important to note that these bubble-chamber data have no acceptance issue, and that they have not been subjected to any cuts, unlike the claimed signal populations, where cuts have been made that enhance the Θ^+ signal relative to background.

$\pi^- p \to nK^+K^-$ and $pK^0_S K^-$ — Dahl at al. [14] used the Berkeley 72-in hydrogen bubble chamber to study the reactions $\pi^- p \to nK^+K^-$ and $\pi^- p \to pK^-K^0_S$ at momenta from 1.5 to 4.2 GeV/c. Their paper provides the relevant nK^+ and pK^0_S mass spectra, as well as Dalitz plots for three momentum groupings: 1.6–2.3, 2.9–3.3, and 3.8–4.2 GeV/c. Of the six relevant mass spectra, only one, nK^+ at 3.8–4.2 GeV/c, has the slightest hint of structure at low mass, but that structure is actually centered at about 1600 MeV with a width of roughly

200 MeV. There is simply no evidence in these data for a narrow KN resonance at 1540 MeV.

K^+d cross section data — An $I = 0$ KN resonance should manifest itself through increases in the K^+n charge-exchange and total cross sections at the resonance cm energy near 1540 MeV, corresponding for a neutron at rest to an incident K^+ momentum of 442 MeV/c. Since free-neutron targets are not available, K^+d cross-section measurements are required, and proper account must be taken of the Fermi momentum of the bound neutron. The distribution of the Fermi momentum in deuterium peaks near 50 MeV/c, and for a fixed incident K^+ momentum leads to a cm energy distribution with a full width of about 30 MeV. This number is, as shown below, much larger than any reasonable estimate of the Θ^+ width, and also is larger than the typical spread of incident momentum at any measurement point.

It is straightforward to calculate the resonance cross section averaged over the Fermi momentum distribution, as determined by the deuteron wave function. The result can be written as $\sigma_R = AB_iB_f\Gamma$, where B_i and B_f are the initial and final Θ^+ branching ratios relevant to the reaction under study, and Γ is the full width. The coefficient A is the product of several factors, including the result of the Fermi-motion averaging process. For an incident K^+ momentum close to the resonant value for a stationary neutron target (442 MeV/c), and for a Θ^+ having spin 1/2 and isospin 0, the value of A is 3.6 mb/MeV [15].

We first apply this result to K^+d charge exchange, $K^+d \to K^0pp$, using the measurements from Slater *et al.* [16] at incident momenta of 376 and 530 MeV/c, and Damerell *et al.* [17] at 434, 526, and 604 MeV/c. The 434 MeV/c measurement is close to the resonance value, and the others are sufficiently distant that, even with the Fermi smearing, their resonance contributions are small. We estimate the resonance part of the 434-MeV/c cross section by subtracting from it a background estimated from interpolations and extrapolations of the cross sections at the other momenta. These subtractions yield numbers smaller than the estimated errors of 0.3 mb. There is therefore no evidence for a significant resonant contribution, and we estimate a conservative upper limit for σ_R of 1 mb. Here $B_i = B_f = 1/2$ in the above formula, and we deduce an upper limit for Γ of 1.1 MeV.

A similar analysis can be applied to the K^+d total cross section, using the data of Bowen *et al.* [18] at 366, 440, and 506 MeV/c. The 440 MeV/c point is very close to the resonance value, and the other two points are sufficiently distant to avoid the inclusion of resonance contributions arising from Fermi smearing. Subtraction of a linearly interpolated background cross section from the measured value at 440 MeV/c leads to an excess of 0.6 ± 0.3 mb. The fact that this difference deviates from zero should not be taken as evidence for the Θ^+: it can simply reflect deviation from linearity in the momentum dependence of the cross section. We take 1.5 mb as a conservative upper limit to the resonance cross section. Here B_i=1/2 and B_f =1, and the upper limit on Γ is 0.8 MeV.

Finally, we consider the $I = 0$ KN total cross sections reported by Bowen *et al.* [18] and Carroll *et al.* [19] at 440 MeV/c, and take the even more conservative approach of considering the full cross section at that momentum as resonant. The Carroll and Bowen measurements disagree by about 3 mb, and we use Carroll's larger value of 13 mb. With $B_i = B_f = 1$, the upper limit for Γ is 3.6 MeV.

These width limits are predicated on the Θ^+ mass being in the range of 1533–1543 MeV, corresponding closely to incident momenta at which the K^+d charge-exchange and total cross sections have been measured. For masses of 1528 or 1548 MeV, the upper limits would increase by a factor of 1.6.

IV. Width estimate from xenon experiment

The results of the DIANA xenon charge-exchange experiment [4] have been analyzed by Cahn and Trilling [15] on the assumption that, near the resonance, one is observing charge exchange on a single nucleon. Associating the observed signal and background populations with resonant and non-resonant charge-exchange cross sections, they deduce a Θ^+ width of 0.9 ± 0.3 MeV, where the quoted error is statistical. The systematic uncertainty is difficult to evaluate.

V. Results from partial-wave analysis

Motivated by the newly reported results, Arndt *et al.* [20] have recently reanalyzed K^+N scattering data in the 1540 MeV cm energy region. They have considered possible structure not only in the P_{01} partial wave, but also in other S, P, and D waves. An immediate result was that the addition of resonances of widths above 5 MeV resulted in an enormous increase in the χ^2 of their fit to data. Indeed, they found no χ^2 improvement in their fit from the addition of resonances in S, P, or D waves unless the inserted structures had widths of 1 MeV or less. They conclude that Θ^+ widths larger than a few MeV are excluded, but that the existence of a Θ^+ in the P_{01} state with a width of 1 MeV or less is possible. These results are stronger than, although consistent with, a 6-MeV upper limit given by Nussinov [21] and a 5-MeV limit by Haidenbauer and Krein [22], and are consistent with the limits quoted in Secs. III and IV above.

VI. Comments on all these results

What can we conclude from these various results and observations? One general principle should apply: For claims of major new discoveries, the burden of proof is greater than for research results that fall within the boundaries of what is already established. Has this burden been met well enough to claim the discovery of an exotic baryon resonance?

Measured in terms of claimed numbers of standard deviations, the results are impressive. In some cases [5, 6, 7], inspection of the published plots suggests that the backgrounds may be somewhat underestimated (background fits seem to

be normalized below the observed backgrounds), reducing perhaps the real significance of the results. Nevertheless, there are substantial indications that something interesting is being observed. However, that something seems to behave rather differently from the known non-exotic resonances. As one example, the $\Lambda(1520)$ decays by D-wave to $\overline{K}N$ with a partial width of 7.2 MeV, much larger than the upper limits based on measured cross sections and partial-wave analyses for the presumed P-wave $\Theta(1540)^+$.

There are some further concerns about the new evidence for the Θ^+. In most cases, the signal does not appear in a significant way until various cuts are made, often reducing the data sample by a large factor. Because all but the xenon and neutrino experiments involve spectrometers of finite acceptance, it is difficult for the reader of these papers to know what role kinematics and reflections from other resonances may have played in determining the results, especially since the cuts were likely chosen to optimize observed signal to background.

One of the most powerful tools for understanding resonances in three-body final states has been the use of Dalitz plots to study correlations and reflections, yet there are no published Dalitz plots in any of the new papers that involve three-body final states [2, 3, 6]. The possible importance of reflections has been emphasized in a recent paper by Dzierba *et al.* [23].

In three of the papers, the Θ^+ production is from a nucleus (carbon, xenon, or neon): the decay products may be created inside the nucleus, and may further interact before leaving the nucleus, raising some uncertainties about the interpretation of the final state. In short, most of the new papers are relatively brief, and yet, given the potential importance of the results, the work cries for more complete description and discussion.

There is the further problem that there seems to be no evidence for the Θ^+ in the rather extensive existing K^+N charge-exchange and total cross section data, in the $KN\pi$ and $K\overline{K}N$ final states produced by incident kaons and pions over a range of energies, and in the results of K^+N partial wave analyses. All the observations may be consistent with a Θ^+ having a width of 1 MeV or less, but then there are two further questions: Why the very small width for a strong decay, and why is the very narrow Θ^+ so readily produced in photoproduction experiments?

There is one other tantalizing piece of information. Alt *et al.* [24] have recently claimed to see, at the 4 σ level, another exotic baryon, an $S = -2$, $Q = -2$ $ddss\bar{u}$ state (see the lower left corner of Fig. 1) decaying into $\Xi^-\pi^-$ with a mass of 1862 ± 2 MeV and a width of less than 18 MeV. This mass agrees with neither the Diakonov *et al.* prediction of 2070 MeV [1] nor a later prediction of 1750 MeV from Jaffe and Wilczek [25]. Nevertheless, this observation is additional support for the existence of exotic baryons.

VII. Future Needs

What experiments do we need to establish fully the Θ^+, recognizing the fact that its width may be very small? One can suggest two experiments:

(1) Confirmation with high statistics, much improved effective mass resolution, and excellent particle identification, of the photoproduction results, through study of such reactions as $\gamma p \to nK^+K^0_S$, $\gamma n \to pK^0_SK^-$, and $\gamma n \to nK^+K^-$.

(2) Measurement in the 400–500 MeV/c incident momentum range of the $K^+d \to K^0_Sp(p)$ charge-exchange cross section as a function of the final-state K^0_Sp mass. This requires measurement of the K^0_S decay and reconstruction of the K^0_Sp mass with the best possible resolution, in order to demonstrate resonant behavior undiluted by target Fermi motion or beam-momentum spread.

References

1. D. Diakonov, V. Petrov, and M. Polyakov, Z. Phys. **A359**, 305 (1997).
2. S. Stepanyan *et al.*, Phys. Rev. Lett. **91**, 252001 (2003).
3. T. Nakano *et al.*, Phys. Rev. Lett. **91**, 012002 (2003); see also T. Nakano, AAPPS Bulletin **13**, 2 (2003).
4. V.V. Barmin *et al.*, Phys. Atom. Nucl. **66**, 1715 (2003).
5. V. Kubarovsky *et al.*, Phys. Rev. Lett. **92**, 032001 (2004).
6. J. Barth *et al.*, Phys. Lett. **B572**, 127 (2003);; see also J. Barth *et al.*, hep-ex/0307083 (2003).
7. A.E. Asratyan, hep-ex/0309042 (2003).
8. A. Airapetian *et al.*, hep-ex/0312044 (2003).
9. R. Bland *et al.*, Nucl. Phys. **B13**, 595 (1969).
10. S. Loken *et al.*, Phys. Rev. **D6**, 2346 (1972).
11. R. Newman *et al.*, Phys. Rev. **158**, 1310 (1967).
12. A. Berthon *et al.*, Nucl. Phys. **B63**, 54 (1973).
13. A.A. Hirata *et al.*, Nucl. Phys. **B33**, 525 (1971).
14. O. Dahl *et al.*, Phys. Rev. **163**, 1377 (1967).
15. R.N. Cahn and G.H. Trilling, Phys. Rev. **D69**, 011501R (2004).
16. W. Slater *et al.*, Phys. Rev. Lett. **7**, 378 (1961).
17. C.J.S. Damerell *et al.*, Nucl. Phys. **B94**, 374 (1975).
18. T. Bowen *et al.*, Phys. Rev. **D2**, 2599 (1970).
19. A.S. Carroll *et al.*, Phys. Lett. **45B**, 531 (1973).
20. R.A. Arndt, I.I. Strakovsky, and R.L. Workman, Phys. Rev. **C68**, 042201R (2003).
21. S. Nussinov, hep-ph/0307357 (2003).
22. J. Haidenbauer and G. Krein, Phys. Rev. **C68**, 052201 (2003).
23. A.R. Dzierba *et al.*, hep-ph/0311125 (2003).
24. C. Alt *et al.*, Phys. Rev. Lett. **92**, 042003 (2004).
25. R. Jaffe and F. Wilczek, Phys. Rev. Lett. **91**, 232003 (2003).

$\Theta(1540)^+$ MASS

As is done through the *Review*, papers are listed by year, with the latest year first, and within each year they are listed alphabetically. NAKANO 03 was the earliest paper.

It is difficult to deny a status of three stars and a place in the Summary Tables for a state that six experiments claim to have seen. Nevertheless, as discussed in the above note, we believe it reasonable to have some reservations about the existence of this state on the basis of the present evidence.

VALUE (MeV)	*EVTS*	*DOCUMENT ID*		*TECN*	*COMMENT*
1539.2± 1.6 OUR AVERAGE					
1533 ± 5	27	[1] ASRATYAN	04	BC	$\nu, \overline{\nu}$ in p,d,Ne, BEBC and 15-ft
1555 ±10	41	[2] KUBAROVSKY	04	CLAS	$\gamma p \to \pi^+K^-K^+n$
1539 ± 2	29	[3] BARMIN	03	XEBC	$K^+\mathrm{Xe} \to K^0p\,\mathrm{Xe}'$
1540 ± 4 ±2	63	[4] BARTH	03	SPHR	$\gamma p \to nK^+K^0_S$
1540 ±10	19	[5] NAKANO	03	LEPS	$\gamma\,{}^{12}\mathrm{C} \to K^+K^-n\,\mathrm{X}$
1542 ± 5	43	[6] STEPANYAN	03	CLAS	$\gamma d \to K^+K^-pn$

$\Theta(1540)^+$ WIDTH

VALUE (MeV)	CL%	DOCUMENT ID		TECN	COMMENT
0.9 ±0.3		[7] CAHN	04		$K^+ n \to K^0 p$ in xenon
• • • We do not use the following data for averages, fits, limits, etc. • • •					
< 20		ASRATYAN	04	BC	$\nu, \overline{\nu}$ in p,d,Ne, BEBC and 15-ft
< 26		KUBAROVSKY	04	CLAS	$\gamma p \to \pi^+ K^- K^+ n$
$\lesssim 1$		[8] ARNDT	03	DPWA	$K^+ N$ partial-wave reanalysis
< 9	90	BARMIN	03	XEBC	K^+Xe $\to K^0 p$ Xe$'$
< 25	90	BARTH	03	SPHR	$\gamma p \to n K^+ K^0_S$
< 25	90	NAKANO	03	LEPS	$\gamma\, ^{12}$C $\to K^+ K^- n$ X
< 21		STEPANYAN	03	CLAS	$\gamma d \to K^+ K^- p n$

$\Theta(1540)^+$ DECAY MODES

NK is the only strong decay mode allowed for a strangeness S=+1 resonance of this mass.

	Mode	Fraction (Γ_i/Γ)
Γ_1	KN	100%

$\Theta(1540)^+$ FOOTNOTES

[1] ASRATYAN 04 analyzes old BEBC and 15-ft bubble-chamber data and estimates a peak of 27 $K^0 p$ events (mostly from $\nu, \overline{\nu}$ in Ne) above a background of 8 events and claims a statistical significance of 6.7 standard deviations.

[2] KUBAROVSKY 04 estimates a peak of 41 $K^+ n$ events and claims a statistical significance of 7.8 ± 1.0 standard deviations.

[3] BARMIN 03 estimates a peak of 29 $K^0 p$ events above a background of 44 events and claims a statistical significance of 4.4 standard deviations.

[4] BARTH 03 estimates a peak of 63 ± 13 $K^+ n$ events and claims a significance of 4.8 standard deviations.

[5] NAKANO 03 estimates a peak of 19.0 ± 2.8 $K^+ n$ events above a background of 17.0 ± 2.8 events and claims a significance of $4.6^{+1.2}_{-1.0}$ standard deviations.

[6] STEPANYAN 03 estimates a peak of 43 $K^+ n$ events above a background of 54 events and claims a statistical significance of 5.2 ± 0.5 standard deviations.

[7] CAHN 04 uses the integrated $K^+ n \to K^0 p$ cross section from the DIANA experiment in xenon (BARMIN 03); some assumptions are needed. Other estimates, based on measured $K^+ d$ cross sections, give upper limits in the 1–4 MeV range.

[8] ARNDT 03 introduces a test resonance in various partial waves in a reanalysis of $K^+ N$ elastic-scattering data and finds that a width of more than an MeV or so would greatly increase the χ^2 of the fit.

$\Theta(1540)^+$ REFERENCES

ASRATYAN	04	hep-ex/0309042	A.E. Asratyan, A. Dolgolenko, M. Kubantsev	(ITEP)
		PAN (accepted)		
CAHN	04	PR D69 011501R	R.N. Cahn, G.H. Trilling	(LBNL)
KUBAROVSKY	04	PRL 92 032001	V. Kubarovsky *et al.*	(Jefferson Lab CLAS Collab.)
ARNDT	03	PR C68 042201R	R.A. Arndt, I.I. Strakovsky, R.L. Workman	(GWU)
BARMIN	03	PAN 66 1715	V.V. Barmin *et al.*	(ITEP DIANA Collab.)
		Translated from YAF 66 1763.		
BARTH	03	PL B572 127	J. Barth *et al.*	(Bonn SAPHIR Collab.)
NAKANO	03	PRL 91 012002	T. Nakano *et al.*	(SPring-8 LEPS Collab.)
STEPANYAN	03	PRL 91 252001	S. Stepanyan *et al.*	(Jefferson Lab CLAS Collab.)

$\Phi(1860)$

$I(J^P) = \frac{3}{2}(?^?)$ Status: *

OMITTED FROM SUMMARY TABLE

A peak seen in the $\Xi^- \pi^-$ invariant-mass spectrum. Confirmation is needed. The minimum quark content would be $ssd\overline{u}$.

$\Phi(1860)$ MASS

VALUE (MeV)	EVTS	DOCUMENT ID		TECN	COMMENT
1862 ±2	36	[1] ALT	04	NA49	pp, $\sqrt{s} = 17.2$ GeV

$\Phi(1860)$ WIDTH

VALUE (MeV)	CL%	DOCUMENT ID		TECN	COMMENT
<18	90	[1] ALT	04	NA49	pp, $\sqrt{s} = 17.2$ GeV

[1] ALT 04 estimates a peak of 38 $\Xi^- \pi^-$ events above a background of 43 events and claims a significance of 4.2 standard deviations. Combining $\Xi^- \pi^-$, $\Xi^- \pi^+$, $\overline{\Xi}^+ \pi^+$, and $\overline{\Xi}^+ \pi^-$ events, ALT 04 estimates a peak of 69 over a background of 75, for 5.8 σ. However, when the number of bins searched in is taken into account, the significance then falls to 4.2 σ.

$\Phi(1860)$ REFERENCES

ALT	04	PRL 92 042003	C. Alt *et al.*	(CERN NA49 Collab.)

Λ BARYONS
($S = -1$, $I = 0$)

$\Lambda^0 = uds$

Λ $I(J^P) = 0(\frac{1}{2}^+)$ Status: ****

We have omitted some results that have been superseded by later experiments. See our earlier editions.

Λ MASS

The fit uses Λ, Σ^+, Σ^0, Σ^- mass and mass-difference measurements.

VALUE (MeV)	EVTS	DOCUMENT ID		TECN	COMMENT
1115.683±0.006 OUR FIT					
1115.683±0.006 OUR AVERAGE					
1115.678±0.006±0.006	20k	HARTOUNI	94	SPEC	pp 27.5 GeV/c
1115.690±0.008±0.006	18k	[1] HARTOUNI	94	SPEC	pp 27.5 GeV/c
• • • We do not use the following data for averages, fits, limits, etc. • • •					
1115.59 ±0.08	935	HYMAN	72	HEBC	
1115.39 ±0.12	195	MAYEUR	67	EMUL	
1115.6 ±0.4		LONDON	66	HBC	
1115.65 ±0.07	488	[2] SCHMIDT	65	HBC	
1115.44 ±0.12		[3] BHOWMIK	63	RVUE	

[1] We assume CPT invariance: this is the $\overline{\Lambda}$ mass as measured by HARTOUNI 94. See below for the fractional mass difference, testing CPT.

[2] The SCHMIDT 65 masses have been reevaluated using our April 1973 proton and $K^\pm$ and $\pi^\pm$ masses. P. Schmidt, private communication (1974).

[3] The mass has been raised 35 keV to take into account a 46 keV increase in the proton mass and an 11 keV decrease in the $\pi^\pm$ mass (note added Reviews of Modern Physics **39** 1 (1967)).

$(m_\Lambda - m_{\overline{\Lambda}}) / m_\Lambda$

A test of CPT invariance.

VALUE (units 10^{-5})	EVTS	DOCUMENT ID		TECN	COMMENT
− 0.1 ± 1.1 OUR AVERAGE		Error includes scale factor of 1.6. See the ideogram below.			
+ 1.3 ± 1.2	31k	[4] RYBICKI	96	NA32	π^- Cu, 230 GeV
− 1.08± 0.90		HARTOUNI	94	SPEC	pp 27.5 GeV/c
4.5 ± 5.4		CHIEN	66	HBC	6.9 GeV/c $\overline{p}p$
• • • We do not use the following data for averages, fits, limits, etc. • • •					
− 26 ±13		BADIER	67	HBC	2.4 GeV/c $\overline{p}p$

[4] RYBICKI 96 is an analysis of old ACCMOR (NA32) data.

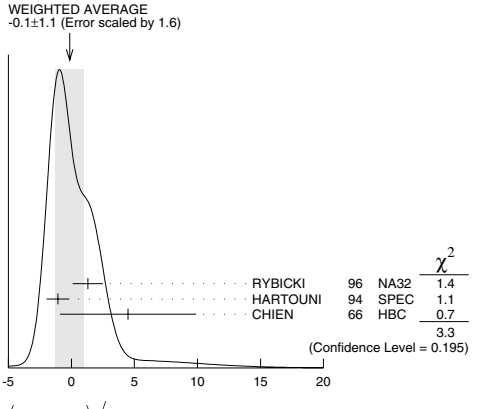

Λ MEAN LIFE

Measurements with an error $\geq 0.1 \times 10^{-10}$ s have been omitted altogether, and only the latest high-statistics measurements are used for the average.

VALUE (10^{-10} s)	EVTS	DOCUMENT ID		TECN	COMMENT
2.632±0.020 OUR AVERAGE		Error includes scale factor of 1.6. See the ideogram below.			
2.69 ±0.03	53k	ZECH	77	SPEC	Neutral hyperon beam
2.611±0.020	34k	CLAYTON	75	HBC	0.96–1.4 GeV/c K^-p
2.626±0.020	36k	POULARD	73	HBC	0.4–2.3 GeV/c K^-p
• • • We do not use the following data for averages, fits, limits, etc. • • •					
2.69 ±0.05	6582	ALTHOFF	73B	OSPK	$\pi^+ n \to \Lambda K^+$
2.54 ±0.04	4572	BALTAY	71B	HBC	K^-p at rest
2.535±0.035	8342	GRIMM	68	HBC	
2.47 ±0.08	2600	HEPP	68	HBC	
2.35 ±0.09	916	BURAN	66	HLBC	
$2.452^{+0.056}_{-0.054}$	2213	ENGELMANN	66	HBC	
2.59 ±0.09	794	HUBBARD	64	HBC	
2.59 ±0.07	1378	SCHWARTZ	64	HBC	
2.36 ±0.06	2239	BLOCK	63	HEBC	

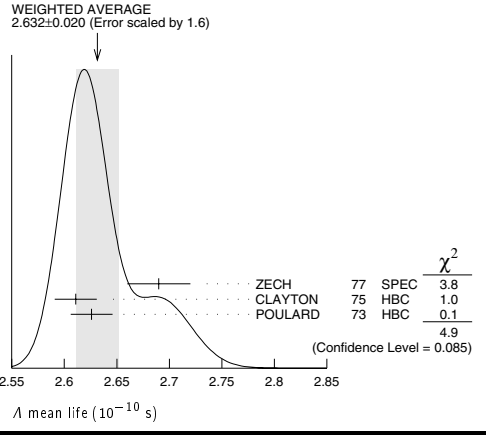

$(\tau_\Lambda - \tau_{\overline{\Lambda}}) / \tau_\Lambda$

A test of CPT invariance.

VALUE	DOCUMENT ID		TECN	COMMENT
−0.001 ±0.009 OUR AVERAGE				
−0.0018±0.0066±0.0056	BARNES	96	CNTR	LEAR $\overline{p}p \to \overline{\Lambda}\Lambda$
0.044 ±0.085	BADIER	67	HBC	2.4 GeV/c $\overline{p}p$

BARYON MAGNETIC MOMENTS

Written 1994 by C.G. Wohl (LBNL).

The figure below shows the measured magnetic moments of the stable baryons. It also shows the predictions of the simplest quark model, using the measured p, n, and Λ moments as input. In this model, the moments are [1]

$$\mu_p = (4\mu_u - \mu_d)/3 \qquad \mu_n = (4\mu_d - \mu_u)/3$$
$$\mu_{\Sigma^+} = (4\mu_u - \mu_s)/3 \qquad \mu_{\Sigma^-} = (4\mu_d - \mu_s)/3$$
$$\mu_{\Xi^0} = (4\mu_s - \mu_u)/3 \qquad \mu_{\Xi^-} = (4\mu_s - \mu_d)/3$$
$$\mu_\Lambda = \mu_s \qquad \mu_{\Sigma^0} = (2\mu_u + 2\mu_d - \mu_s)/3$$
$$\mu_{\Omega^-} = 3\mu_s$$

and the $\Sigma^0 \to \Lambda$ transition moment is

$$\mu_{\Sigma^0\Lambda} = (\mu_d - \mu_u)/\sqrt{3}\ .$$

The quark moments that result from this model are $\mu_u = +1.852\,\mu_N$, $\mu_d = -0.972\,\mu_N$, and $\mu_s = -0.613\,\mu_N$. The corresponding effective quark masses, taking the quarks to be Dirac point particles, where $\mu = q\hbar/2m$, are 338, 322, and 510 MeV. As the figure shows, the model gives a good first approximation to the experimental moments. For efforts to make a better model, we refer to the literature [2].

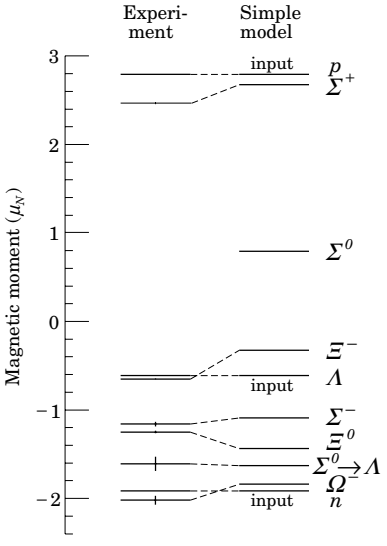

References

1. See, for example, D.H. Perkins, *Introduction to High Energy Physics* (Addison-Wesley, Reading, MA, 1987), or D. Griffiths, *Introduction to Elementary Particles* (Harper & Row, New York, 1987).
2. See, for example, J. Franklin, Phys. Rev. **D29**, 2648 (1984); H.J. Lipkin, Nucl. Phys. **B241**, 477 (1984); K. Suzuki, H. Kumagai, and Y. Tanaka, Europhys. Lett. **2**, 109 (1986); S.K. Gupta and S.B. Khadkikar, Phys. Rev. **D36**, 307 (1987); M.I. Krivoruchenko, Sov. J. Nucl. Phys. **45**, 109 (1987); L. Brekke and J.L. Rosner, Comm. Nucl. Part. Phys. **18**, 83 (1988); K.-T. Chao, Phys. Rev. **D41**, 920 (1990) and references cited therein Also, see references cited in discussions of results in the experimental papers..

Λ MAGNETIC MOMENT

See the "Note on Baryon Magnetic Moments" above. Measurements with an error $\geq 0.15\ \mu_N$ have been omitted.

VALUE (μ_N)	EVTS	DOCUMENT ID		TECN	COMMENT
−0.613 ±0.004 OUR AVERAGE					
−0.606 ±0.015	200k	COX	81	SPEC	
−0.6138±0.0047	3M	SCHACHIN...	78	SPEC	
−0.59 ±0.07	350k	HELLER	77	SPEC	
−0.57 ±0.05	1.2M	BUNCE	76	SPEC	
−0.66 ±0.07	1300	DAHL-JENSEN	71	EMUL	200 kG field

Λ ELECTRIC DIPOLE MOMENT

A nonzero value is forbidden by both T invariance and P invariance.

VALUE (10^{-16} ecm)	CL%	DOCUMENT ID		TECN
< 1.5	95	[5] PONDROM	81	SPEC
• • • We do not use the following data for averages, fits, limits, etc. • • •				
<100	95	[6] BARONI	71	EMUL
<500	95	GIBSON	66	EMUL

[5] PONDROM 81 measures $(-3.0 \pm 7.4) \times 10^{-17}$ e-cm.
[6] BARONI 71 measures $(-5.9 \pm 2.9) \times 10^{-15}$ e-cm.

Λ DECAY MODES

	Mode	Fraction (Γ_i/Γ)
Γ_1	$p\pi^-$	(63.9 ±0.5) %
Γ_2	$n\pi^0$	(35.8 ±0.5) %
Γ_3	$n\gamma$	(1.75±0.15) × 10^{-3}
Γ_4	$p\pi^-\gamma$	[a] (8.4 ±1.4) × 10^{-4}
Γ_5	$pe^-\overline{\nu}_e$	(8.32±0.14) × 10^{-4}
Γ_6	$p\mu^-\overline{\nu}_\mu$	(1.57±0.35) × 10^{-4}

[a] See the Listings below for the pion momentum range used in this measurement.

CONSTRAINED FIT INFORMATION

An overall fit to 5 branching ratios uses 20 measurements and one constraint to determine 5 parameters. The overall fit has a $\chi^2 = 10.5$ for 16 degrees of freedom.

The following *off-diagonal* array elements are the correlation coefficients $\langle \delta x_i \delta x_j \rangle / (\delta x_i \cdot \delta x_j)$, in percent, from the fit to the branching fractions, $x_i \equiv \Gamma_i/\Gamma_{total}$. The fit constrains the x_i whose labels appear in this array to sum to one.

x_2	−100			
x_3	−2	−1		
x_5	46	−46	−1	
x_6	0	0	0	0
	x_1	x_2	x_3	x_5

Λ BRANCHING RATIOS

$\Gamma(p\pi^-)/\Gamma(N\pi)$ — $\Gamma_1/(\Gamma_1+\Gamma_2)$

VALUE	EVTS	DOCUMENT ID		TECN	COMMENT
0.641±0.005 OUR FIT					
0.640±0.005 OUR AVERAGE					
0.646±0.008	4572	BALTAY	71B	HBC	K^-p at rest
0.635±0.007	6736	DOYLE	69	HBC	$\pi^-p \to \Lambda K^0$
0.643±0.016	903	HUMPHREY	62	HBC	
0.624±0.030		CRAWFORD	59B	HBC	$\pi^-p \to \Lambda K^0$

$\Gamma(n\pi^0)/\Gamma(N\pi)$ — $\Gamma_2/(\Gamma_1+\Gamma_2)$

VALUE	EVTS	DOCUMENT ID		TECN
0.359±0.005 OUR FIT				
0.310±0.028 OUR AVERAGE				
0.35 ±0.05		BROWN	63	HLBC
0.291±0.034	75	CHRETIEN	63	HLBC

$\Gamma(n\gamma)/\Gamma_{total}$ — Γ_3/Γ

VALUE (units 10^{-3})	EVTS	DOCUMENT ID		TECN	COMMENT
1.75±0.15 OUR FIT					
1.75±0.15	1816	LARSON	93	SPEC	K^-p at rest
• • • We do not use the following data for averages, fits, limits, etc. • • •					
$1.78 \pm 0.24 \pm^{0.14}_{0.16}$	287	NOBLE	92	SPEC	See LARSON 93

$\Gamma(n\gamma)/\Gamma(n\pi^0)$ — Γ_3/Γ_2

VALUE (units 10^{-3})	EVTS	DOCUMENT ID		TECN	COMMENT
• • • We do not use the following data for averages, fits, limits, etc. • • •					
2.86±0.74±0.57	24	BIAGI	86	SPEC	SPS hyperon beam

$\Gamma(p\pi^-\gamma)/\Gamma(p\pi^-)$ — Γ_4/Γ_1

VALUE (units 10^{-3})	EVTS	DOCUMENT ID		TECN	COMMENT
1.32±0.22	72	BAGGETT	72C	HBC	π^- < 95 MeV/c

$\Gamma(pe^-\overline{\nu}_e)/\Gamma(p\pi^-)$ — Γ_5/Γ_1

VALUE (units 10^{-3})	EVTS	DOCUMENT ID		TECN	COMMENT
1.301±0.019 OUR FIT					
1.301±0.019 OUR AVERAGE					
1.335±0.056	7111	BOURQUIN	83	SPEC	SPS hyperon beam
1.313±0.024	10k	WISE	80	SPEC	
1.23 ±0.11	544	LINDQUIST	77	SPEC	$\pi^-p \to K^0\Lambda$
1.27 ±0.07	1089	KATZ	73	HBC	
1.31 ±0.06	1078	ALTHOFF	71	OSPK	
1.17 ±0.13	86	[7] CANTER	71	HBC	K^-p at rest
1.20 ±0.12	143	[8] MALONEY	69	HBC	
1.17 ±0.18	120	[8] BAGLIN	64	FBC	K^- freon 1.45 GeV/c
1.23 ±0.20	150	[8] ELY	63	FBC	
• • • We do not use the following data for averages, fits, limits, etc. • • •					
1.32 ±0.15	218	[7] LINDQUIST	71	OSPK	See LINDQUIST 77

[7] Changed by us from $\Gamma(pe^-\overline{\nu}_e)/\Gamma(N\pi)$ assuming the authors used $\Gamma(p\pi^-)/\Gamma_{total} = 2/3$.
[8] Changed by us from $\Gamma(pe^-\overline{\nu}_e)/\Gamma(N\pi)$ because $\Gamma(pe^-\nu)/\Gamma(p\pi^-)$ is the directly measured quantity.

$\Gamma(p\mu^-\overline{\nu}_\mu)/\Gamma(N\pi)$ $\Gamma_6/(\Gamma_1+\Gamma_2)$

VALUE (units 10^{-4})	EVTS	DOCUMENT ID		TECN	COMMENT
1.57±0.35 OUR FIT					
1.57±0.35 OUR AVERAGE					
1.4 ±0.5	14	BAGGETT	72B	HBC	K^-p at rest
2.4 ±0.8	9	CANTER	71B	HBC	K^-p at rest
1.3 ±0.7	3	LIND	64	RVUE	
1.5 ±1.2	2	RONNE	64	FBC	

Λ DECAY PARAMETERS

See the "Note on Baryon Decay Parameters" in the neutron Listings. Some early results have been omitted.

α_- FOR $\Lambda \to p\pi^-$

VALUE	EVTS	DOCUMENT ID		TECN	COMMENT
0.642±0.013 OUR AVERAGE					
0.584±0.046	8500	ASTBURY	75	SPEC	
0.649±0.023	10325	CLELAND	72	OSPK	
0.67 ±0.06	3520	DAUBER	69	HBC	From Ξ decay
0.645±0.017	10130	OVERSETH	67	OSPK	Λ from π^-p
0.62 ±0.07	1156	CRONIN	63	CNTR	Λ from π^-p

ϕ ANGLE FOR $\Lambda \to p\pi^-$ $(\tan\phi = \beta/\gamma)$

VALUE (°)	EVTS	DOCUMENT ID	TECN	COMMENT
− 6.5± 3.5 OUR AVERAGE				
− 7.0± 4.5	10325	CLELAND	72 OSPK	Λ from π^-p
− 8.0± 6.0	10130	OVERSETH	67 OSPK	Λ from π^-p
13.0±17.0	1156	CRONIN	63 OSPK	Λ from π^-p

$\alpha_0/\alpha_- = \alpha(\Lambda \to n\pi^0)/\alpha(\Lambda \to p\pi^-)$

VALUE	EVTS	DOCUMENT ID		TECN	COMMENT
1.01 ±0.07 OUR AVERAGE					
1.000±0.068	4760	[9] OLSEN	70	OSPK	$\pi^+n \to \Lambda K^+$
1.10 ±0.27		CORK	60	CNTR	

[9] OLSEN 70 compares proton and neutron distributions from Λ decay.

$[\alpha_-(\Lambda)+\alpha_+(\overline{\Lambda})]/[\alpha_-(\Lambda)-\alpha_+(\overline{\Lambda})]$

Zero if *CP* is conserved; α_- and α_+ are the asymmetry parameters for $\Lambda \to p\pi^-$ and $\overline{\Lambda} \to \overline{p}\pi^+$ decay. See also the Ξ^- for a similar test involving the decay chain $\Xi^- \to \Lambda\pi^-$, $\Lambda \to p\pi^-$ and the corresponding antiparticle chain.

VALUE	EVTS	DOCUMENT ID		TECN	COMMENT
0.012±0.021 OUR AVERAGE					
+0.013±0.022	96k	BARNES	96	CNTR	LEAR $\overline{p}p \to \overline{\Lambda}\Lambda$
+0.01 ±0.10	770	TIXIER	88	DM2	$J/\psi \to \Lambda\overline{\Lambda}$
−0.02 ±0.14	10k	[10] CHAUVAT	85	CNTR	pp, $\overline{p}p$ ISR
• • • We do not use the following data for averages, fits, limits, etc. • • •					
−0.07 ±0.09	4063	BARNES	87	CNTR	See BARNES 96

[10] CHAUVAT 85 actually gives $\alpha_+(\overline{\Lambda})/\alpha_-(\Lambda) = -1.04 \pm 0.29$. Assumes polarization is same in $\overline{p}p \to \overline{\Lambda}X$ and $pp \to \Lambda X$. Tests of this assumption, based on *C*-invariance and fragmentation, are satisfied by the data.

g_A/g_V FOR $\Lambda \to pe^-\overline{\nu}_e$

Measurements with fewer than 500 events have been omitted. Where necessary, signs have been changed to agree with our conventions, which are given in the "Note on Baryon Decay Parameters" in the neutron Listings. The measurements all assume that the form factor $g_2 = 0$. See also the footnote on DWORKIN 90.

VALUE	EVTS	DOCUMENT ID		TECN	COMMENT
−0.718±0.015 OUR AVERAGE					
−0.719±0.016±0.012	37k	[11] DWORKIN	90	SPEC	$e\nu$ angular corr.
−0.70 ±0.03	7111	BOURQUIN	83	SPEC	$\Xi \to \Lambda\pi^-$
−0.734±0.031	10k	[12] WISE	81	SPEC	$e\nu$ angular correl.
• • • We do not use the following data for averages, fits, limits, etc. • • •					
−0.63 ±0.06	817	ALTHOFF	73	OSPK	Polarized Λ

[11] The tabulated result assumes the weak-magnetism coupling $w \equiv g_W(0)/g_V(0)$ to be 0.97, as given by the CVC hypothesis and as assumed by the other listed measurements. However, DWORKIN 90 *measures* w to be 0.15 ± 0.30, and then $g_A/g_V = -0.731 \pm 0.016$.

[12] This experiment measures only the absolute value of g_A/g_V.

Λ REFERENCES

We have omitted some papers that have been superseded by later experiments. See our earlier editions.

BARNES	96	PR C54 1877	P.D. Barnes *et al.*	(CERN PS-185 Collab.)
RYBICKI	96	APP B27 2155	K. Rybicki	
HARTOUNI	94	PRL 72 1322	E.P. Hartouni *et al.*	(BNL E766 Collab.)
Also	94B	PRL 72 2821 (erratum)	E.P. Hartouni *et al.*	(BNL E766 Collab.)
LARSON	93	PR D47 799	K.D. Larson *et al.*	(BNL-811 Collab.)
NOBLE	92	PRL 69 414	A.J. Noble *et al.*	(BIRM, BOST, BRCO+)
DWORKIN	90	PR D41 780	J. Dworkin *et al.*	(MICH, WISC, RUTG+)
TIXIER	88	PL B212 523	M.H. Tixier *et al.*	(DM2 Collab.)
BARNES	87	PL B199 147	P.D. Barnes *et al.*	(CMU, SACL, LANL+)
BIAGI	86	ZPHY C30 201	S.F. Biagi *et al.*	(BRIS, CERN, GEVA+)
CHAUVAT	85	PL 163B 273	P. Chauvat *et al.*	(CERN, CLER, UCLA+)
BOURQUIN	83	ZPHY C21 1	M.H. Bourquin *et al.*	(BRIS, GEVA, HEIDP+)
COX	81	PRL 46 877	P.T. Cox *et al.*	(MICH, WISC, RUTG, MINN+)
PONDROM	81	PR D23 814	L. Pondrom *et al.*	(WISC, MICH, RUTG+)
WISE	81	PL 98B 123	J.E. Wise *et al.*	(MASA, BNL)
WISE	80	PL 91B 165	J.E. Wise *et al.*	(MASA, BNL)
SCHACHIN...	78	PRL 41 1348	L. Schachinger *et al.*	(MICH, RUTG, WISC)
HELLER	77	PL 68B 480	K. Heller *et al.*	(MICH, WISC, HEIDH)
LINDQUIST	77	PR D16 2104	J. Lindquist *et al.*	(EFI, OSU, ANL)
Also	76	JPG 2 L211	J. Lindquist *et al.*	(EFI, WUSL, OSU+)
ZECH	77	NP B124 413	G. Zech *et al.*	(SIEG, CERN, DORT, HEIDH)
BUNCE	76	PRL 36 1113	G.R.M. Bunce *et al.*	(WISC, MICH, RUTG)
ASTBURY	75	NP B99 30	P. Astbury *et al.*	(LOIC, CERN, ETH+)
CLAYTON	75	NP B95 130	E.F. Clayton *et al.*	(LOIC, RHEL)
ALTHOFF	73	PL 43B 237	K.H. Althoff *et al.*	(CERN, HEID)
ALTHOFF	73B	NP B66 29	K.H. Althoff *et al.*	(CERN, HEID)
KATZ	73	Thesis MDDP-TR-74-044	C.N. Katz	(UMD)
POULARD	73	PL 46B 135	G. Poulard, A. Givernaud, A.C. Borg	(SACL)
BAGGETT	72B	ZPHY 252 362	M.J. Baggett *et al.*	(HEID)
BAGGETT	72C	PL 42B 379	M.J. Baggett *et al.*	(HEID)
CLELAND	72	NP B40 221	W.E. Cleland *et al.*	(CERN, GEVA, LUND)
HYMAN	72	PR D5 1063	L.G. Hyman *et al.*	(ANL, CMU)
ALTHOFF	71	PL 37B 531	K.H. Althoff *et al.*	(CERN, HEID)
BALTAY	71B	PR D4 670	C. Baltay *et al.*	(COLU, BING)
BARONI	71	LNC 2 1256	G. Baroni, S. Petrera, G. Romano	(ROMA)
CANTER	71	PRL 26 868	J. Canter *et al.*	(STON, COLU)
CANTER	71B	PRL 27 59	J. Canter *et al.*	(STON, COLU)
DAHL-JENSEN	71	NC 3A 1	E. Dahl-Jensen *et al.*	(CERN, ANKA, LAUS+)
LINDQUIST	71	PRL 27 612	J. Lindquist *et al.*	(EFI, WUSL, OSU+)
OLSEN	70	PRL 24 843	S.L. Olsen *et al.*	(WISC, MICH)
DAUBER	69	PR 179 1262	P.M. Dauber *et al.*	(LRL)
DOYLE	69	Thesis UCRL 18139	J.C. Doyle	(LRL)
MALONEY	69	PRL 23 425	J.E. Maloney, B. Sechi-Zorn	(UMD)
GRIMM	68	NC 54A 187	H.J. Grimm	(HEID)
HEPP	68	ZPHY 214 71	V. Hepp, H. Schleich	(HEID)
BADIER	67	PL 25B 152	J. Badier *et al.*	(EPOL)
MAYEUR	67	U.Libr.Brux.Bul. 32	C. Mayeur, E. Tompa, J.H. Wickens	(BELG, LOUC)
OVERSETH	67	PRL 19 391	O.E. Overseth, R.F. Roth	(MICH, PRIN)
PDG	67	RMP 39 1	A.H. Rosenfeld *et al.*	(LRL, CERN, YALE)
BURAN	66	PL 20 318	T. Buran *et al.*	(OSLO)
CHIEN	66	PR 152 1171	C.Y. Chien *et al.*	(YALE, BNL)
ENGELMANN	66	NC 45A 1038	R. Engelmann *et al.*	(HEID, REHO)
GIBSON	66	NC 45A 882	W.M. Gibson, K. Green	(BRIS)
LONDON	66	PR 143 1034	G.W. London *et al.*	(BNL, SYRA)
SCHMIDT	65	PR 140B 1328	P. Schmidt	(COLU)
BAGLIN	64	NC 35 977	C. Baglin *et al.*	(EPOL, CERN, LOUC, RHEL+)
HUBBARD	64	PR 135B 183	J.R. Hubbard *et al.*	(LRL)
LIND	64	PR 135B 1483	V.G. Lind *et al.*	(WISC)
RONNE	64	PL 11 357	B.E. Ronne *et al.*	(CERN, EPOL, LOUC+)
SCHWARTZ	64	Thesis UCRL 11360	J.A. Schwartz	(LRL)
BHOWMIK	63	NC 28 1494	B. Bhowmik, D.P. Goyal	(DELH)
BLOCK	63	PR 130 766	M.M. Block *et al.*	(NWES, BGNA, SYRA+)
BROWN	63	PR 130 769	J.L. Brown *et al.*	(LRL, MICH)
CHRETIEN	63	PR 131 2208	M. Chretien *et al.*	(BRAN, BROW, HARV+)
CRONIN	63	PR 129 1795	J.W. Cronin, O.E. Overseth	(PRIN)
ELY	63	PR 131 868	R.P. Ely *et al.*	(LRL)
HUMPHREY	62	PR 127 1305	W.E. Humphrey, R.R. Ross	(LRL)
CORK	60	PR 120 1000	B. Cork *et al.*	(LRL, PRIN, BNL)
CRAWFORD	59B	PRL 2 266	F.S. Crawford *et al.*	(LRL)

Λ AND Σ RESONANCES

Introduction: This was a big year for these resonances: two papers—see the $\Lambda(1405)$ and $\Lambda(1670)$. The field remains at a standstill and will only be revived if a kaon factory is built. What follows is a much abbreviated version of the note on Λ and Σ Resonances from our 1990 edition [1]. In particular, see that edition for some representative Argand plots from partial-wave analyses.

Table 1 is an attempt to evaluate the status, both overall and channel by channel, of each Λ and Σ resonance in the Particle Listings. The evaluations are of course partly subjective. A blank indicates there is no evidence at all: either the relevant couplings are small or the resonance does not really exist. The main Baryon Summary Table includes only the established resonances (overall status 3 or 4 stars). A number of the 1- and 2-star entries may eventually disappear, but there are certainly many resonances yet to be discovered underlying the established ones.

Sign conventions for resonance couplings: In terms of the isospin-0 and -1 elastic scattering amplitudes A_0 and A_1, the amplitude for $K^- p \to \overline{K}^0 n$ scattering is $\pm(A_1 - A_0)/2$, where the sign depends on conventions used in conjunction with the Clebsch-Gordan coefficients (such as, is the baryon or the meson the "first" particle). If this reaction is partial-wave analyzed and if the overall phase is chosen so that, say, the $\Sigma(1775) D_{15}$ amplitude at resonance points along the positive imaginary axis (points "up"), then any Σ at resonance will point "up" and any Λ at resonance will point "down" (along the negative imaginary axis). Thus the phase at resonance determines the isospin. The above ignores background amplitudes in the resonating partial waves.

That is the basic idea. In a similar but somewhat more complicated way, the phases of the $\overline{K}N \to \Lambda\pi$ and $\overline{K}N \to \Sigma\pi$ amplitudes for a resonating wave help determine the SU(3) multiplet to which the resonance belongs. Again, a convention has to be adopted for some overall arbitrary phases: which way is "up"? Our convention is that of Levi-Setti [2] and is shown in Fig. 1, which also compares experimental results with theoretical predictions for the signs of several resonances. In the Listings, a + or − sign in front of a measurement of an inelastic resonance coupling indicates the sign (the *absence* of a sign means that the sign is not determined, *not* that it is positive). For more details, see Appendix II of our 1982 edition [3].

Errors on masses and widths: The errors quoted on resonance parameters from partial-wave analyses are often only statistical, and the parameters can change by more than these errors when a different parametrization of the waves is used. Furthermore, the different analyses use more or less the same data, so it is not really appropriate to treat the different determinations of the resonance parameters as independent or to average them together. In any case, the spread of the masses, widths, and branching fractions from the different analyses is certainly a better indication of the uncertainties than are the quoted errors. In the Baryon Summary Table, we usually give a range reflecting the spread of the values rather than a particular value with error.

For three states, the $\Lambda(1520)$, the $\Lambda(1820)$, and the $\Sigma(1775)$, there is enough information to make an overall fit to the various branching fractions. It is then necessary to use the quoted errors, but the errors obtained from the fit should not be taken seriously.

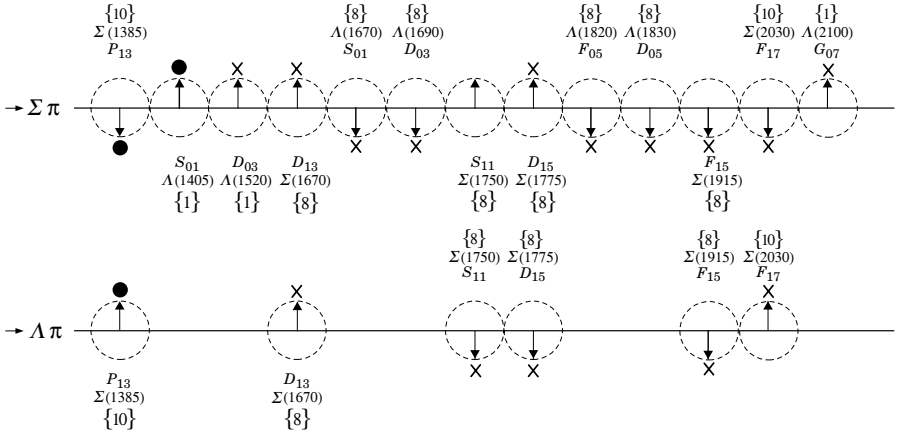

Figure 1. The signs of the imaginary parts of resonating amplitudes in the $\overline{K}N \to \Lambda\pi$ and $\Sigma\pi$ channels. The signs of the $\Sigma(1385)$ and $\Lambda(1405)$, marked with a •, are set by convention, and then the others are determined relative to them. The signs required by the SU(3) assignments of the resonances are shown with an arrow, and the experimentally determined signs are shown with an ×.

Table 1. The status of the Λ and Σ resonances. Only those with an overall status of *** or **** are included in the main Baryon Summary Table.

Particle	$L_{I\,2J}$	Overall status	Status as seen in — $N\overline{K}$	$\Lambda\pi$	$\Sigma\pi$	Other channels
$\Lambda(1116)$	P_{01}	****		F		$N\pi$(weakly)
$\Lambda(1405)$	S_{01}	****	****	o	****	
$\Lambda(1520)$	D_{03}	****	****	r	****	$\Lambda\pi\pi$, $\Lambda\gamma$
$\Lambda(1600)$	P_{01}	***	***	b	**	
$\Lambda(1670)$	S_{01}	****	****	i	****	$\Lambda\eta$
$\Lambda(1690)$	D_{03}	****	****	d	****	$\Lambda\pi\pi$, $\Sigma\pi\pi$
$\Lambda(1800)$	S_{01}	***	***	d	**	$N\overline{K}^*$, $\Sigma(1385)\pi$
$\Lambda(1810)$	P_{01}	***	***	e	**	$N\overline{K}^*$
$\Lambda(1820)$	F_{05}	****	****	n	****	$\Sigma(1385)\pi$
$\Lambda(1830)$	D_{05}	****	***	F	****	$\Sigma(1385)\pi$
$\Lambda(1890)$	P_{03}	****	****	o	**	$N\overline{K}^*$, $\Sigma(1385)\pi$
$\Lambda(2000)$		*		r	*	$\Lambda\omega$, $N\overline{K}^*$
$\Lambda(2020)$	F_{07}	*	*	b	*	
$\Lambda(2100)$	G_{07}	****	****	i	***	$\Lambda\omega$, $N\overline{K}^*$
$\Lambda(2110)$	F_{05}	***	**	d	*	$\Lambda\omega$, $N\overline{K}^*$
$\Lambda(2325)$	D_{03}	*	*	d		$\Lambda\omega$
$\Lambda(2350)$		***	***	e	*	
$\Lambda(2585)$		**	**	n		
$\Sigma(1193)$	P_{11}	****				$N\pi$(weakly)
$\Sigma(1385)$	P_{13}	****		****	****	
$\Sigma(1480)$		*	*	*	*	
$\Sigma(1560)$		**		**	**	
$\Sigma(1580)$	D_{13}	**	*	*		
$\Sigma(1620)$	S_{11}	**	**	*	*	
$\Sigma(1660)$	P_{11}	***	***	*	**	
$\Sigma(1670)$	D_{13}	****	****	****	****	several others
$\Sigma(1690)$		**	*	**	*	$\Lambda\pi\pi$
$\Sigma(1750)$	S_{11}	***	***	**	*	$\Sigma\eta$
$\Sigma(1770)$	P_{11}	*				
$\Sigma(1775)$	D_{15}	****	****	****	***	several others
$\Sigma(1840)$	P_{13}	*	*	**	*	
$\Sigma(1880)$	P_{11}	**	**	**		$N\overline{K}^*$
$\Sigma(1915)$	F_{15}	****	***	****	***	$\Sigma(1385)\pi$
$\Sigma(1940)$	D_{13}	***	*	***	**	quasi-2-body
$\Sigma(2000)$	S_{11}	*		*		$N\overline{K}^*$, $\Lambda(1520)\pi$
$\Sigma(2030)$	F_{17}	****	****	****	**	several others
$\Sigma(2070)$	F_{15}	*	*		*	
$\Sigma(2080)$	P_{13}	**		**		
$\Sigma(2100)$	G_{17}	*		*	*	
$\Sigma(2250)$		***	***	*	*	
$\Sigma(2455)$		**	*			
$\Sigma(2620)$		**	*			
$\Sigma(3000)$		*	*	*		
$\Sigma(3170)$		*				multi-body

**** Existence is certain, and properties are at least fairly well explored.
*** Existence ranges from very likely to certain, but further confirmation is desirable and/or quantum numbers, branching fractions, *etc.* are not well determined.
** Evidence of existence is only fair.
* Evidence of existence is poor.

Production experiments: Partial-wave analyses of course separate partial waves, whereas a peak in a cross section or an invariant mass distribution usually cannot be disentangled from background and analyzed for its quantum numbers; and more than one resonance may be contributing to the peak. Results from partial-wave analyses and from production experiments are generally kept separate in the Listings, and in the Baryon Summary Table results from production experiments are used only for the low-mass states. The $\Sigma(1385)$ and $\Lambda(1405)$ of course lie below the $\overline{K}N$ threshold and nearly everything about them is learned from production experiments; and production and formation experiments agree quite well in the case of $\Lambda(1520)$ and results have been combined. There is some disagreement between production and formation experiments in the 1600–1700 MeV region: see the note on the $\Sigma(1670)$.

References

1. Particle Data Group, Phys. Lett. **B239**, VIII.64 (1990).
2. R. Levi-Setti, in *Proceedings of the Lund International Conference on Elementary Particles* (Lund, 1969), p. 339.
3. Particle Data Group, Phys. Lett. **111B** (1982).

Λ(1405) S_{01}

$I(J^P) = 0(\frac{1}{2}^-)$ Status: ****

See the note on "The Λ(1405)" in our 2000 edition (Eur. Phys. J. **C15**, p. 748 (2000)).

Λ(1405) MASS

PRODUCTION EXPERIMENTS

VALUE (MeV)	EVTS	DOCUMENT ID		TECN	COMMENT
1406.5 ± 4.0		[1] DALITZ	91		M-matrix fit
• • • We do not use the following data for averages, fits, limits, etc. • • •					
1391 ± 1	700	[1] HEMINGWAY	85	HBC	K^-p 4.2 GeV/c
~ 1405	400	[2] THOMAS	73	HBC	π^-p 1.69 GeV/c
1405	120	BARBARO-...	68B	DBC	K^-d 2.1–2.7 GeV/c
1400 ± 5	67	BIRMINGHAM	66	HBC	K^-p 3.5 GeV/c
1382 ± 8		ENGLER	65	HDBC	π^-p, π^+d 1.68 GeV/c
1400 ±24		MUSGRAVE	65	HBC	$\overline{p}p$ 3–4 GeV/c
1410		ALEXANDER	62	HBC	π^-p 2.1 GeV/c
1405		ALSTON	62	HBC	K^-p 1.2–0.5 GeV/c
1405		ALSTON	61B	HBC	K^-p 1.15 GeV/c

EXTRAPOLATIONS BELOW $N\overline{K}$ THRESHOLD

VALUE (MeV)	DOCUMENT ID		TECN	COMMENT
• • • We do not use the following data for averages, fits, limits, etc. • • •				
1407.56 or 1407.50	[3] KIMURA	00		potential model
1411	[4] MARTIN	81		K-matrix fit
1406	[5] CHAO	73	DPWA	0–range fit (sol. B)
1421	MARTIN	70	RVUE	Constant K-matrix
1416 ±4	MARTIN	69	HBC	Constant K-matrix
1403 ±3	KIM	67	HBC	K-matrix fit
1407.5 ±1.2	[6] KITTEL	66	HBC	0–effective-range fit
1410.7 ±1.0	KIM	65	HBC	0–effective-range fit
1409.6 ±1.7	[6] SAKITT	65	HBC	0–effective-range fit

Λ(1405) WIDTH

PRODUCTION EXPERIMENTS

VALUE (MeV)	EVTS	DOCUMENT ID		TECN	COMMENT
50 ± 2		[1] DALITZ	91		M-matrix fit
• • • We do not use the following data for averages, fits, limits, etc. • • •					
32 ± 1	700	[1] HEMINGWAY	85	HBC	K^-p 4.2 GeV/c
45 to 55	400	[2] THOMAS	73	HBC	π^-p 1.69 GeV/c
35	120	BARBARO-...	68B	DBC	K^-d 2.1–2.7 GeV/c
50 ±10	67	BIRMINGHAM	66	HBC	K^-p 3.5 GeV/c
89 ±20		ENGLER	65	HDBC	
60 ±20		MUSGRAVE	65	HBC	
35 ± 5		ALEXANDER	62	HBC	
50		ALSTON	62	HBC	
20		ALSTON	61B	HBC	

EXTRAPOLATIONS BELOW $N\overline{K}$ THRESHOLD

VALUE (MeV)	DOCUMENT ID		TECN	COMMENT
• • • We do not use the following data for averages, fits, limits, etc. • • •				
50.24 or 50.26	[3] KIMURA	00		potential model
30	[4] MARTIN	81		K-matrix fit
55	[5,7] CHAO	73	DPWA	0–range fit (sol. B)
20	MARTIN	70	RVUE	Constant K-matrix
29 ±6	MARTIN	69	HBC	Constant K-matrix
50 ±5	KIM	67	HBC	K-matrix fit
34.1 ±4.1	[6] KITTEL	66	HBC	
37.0 ±3.2	KIM	65	HBC	
28.2 ±4.1	[6] SAKITT	65	HBC	

Λ(1405) DECAY MODES

	Mode	Fraction (Γ_i/Γ)
Γ_1	$\Sigma\pi$	100 %
Γ_2	$\Lambda\gamma$	
Γ_3	$\Sigma^0\gamma$	
Γ_4	$N\overline{K}$	

Λ(1405) PARTIAL WIDTHS

$\Gamma(\Lambda\gamma)$ Γ_2

VALUE (keV)	DOCUMENT ID		COMMENT
• • • We do not use the following data for averages, fits, limits, etc. • • •			
27 ± 8	BURKHARDT	91	Isobar model fit

$\Gamma(\Sigma^0\gamma)$ Γ_3

VALUE (keV)	DOCUMENT ID		COMMENT
• • • We do not use the following data for averages, fits, limits, etc. • • •			
10 ± 4 or 23 ± 7	BURKHARDT	91	Isobar model fit

Λ(1405) BRANCHING RATIOS

$\Gamma(N\overline{K})/\Gamma(\Sigma\pi)$ Γ_4/Γ_1

VALUE	CL%	DOCUMENT ID		TECN	COMMENT
• • • We do not use the following data for averages, fits, limits, etc. • • •					
< 3	95	HEMINGWAY	85	HBC	K^-p 4.2 GeV/c

Λ(1405) FOOTNOTES

[1] DALITZ 91 fits the HEMINGWAY 85 data.
[2] THOMAS 73 data is fit by CHAO 73 (see next section).
[3] The KIMURA 00 values are from fits A and B from a coupled-channel potential model using low-energy $\overline{K}N$ and $\Sigma\pi$ data, kaonic-hydrogen x-ray measurements, and our Λ(1405) mass and width. The results bear mainly on the *nature* of the Λ(1405): three-quark state or $\overline{K}N$ bound state.
[4] The MARTIN 81 fit includes the $K^\pm p$ forward scattering amplitudes and the dispersion relations they must satisfy.
[5] See also the accompanying paper of THOMAS 73.
[6] Data of SAKITT 65 are used in the fit by KITTEL 66.
[7] An asymmetric shape, with $\Gamma/2 = 41$ MeV below resonance, 14 MeV above.

Λ(1405) REFERENCES

KIMURA	00	PR C62 015206	M. Kimura *et al.*	
BURKHARDT	91	PR C44 607	H. Burkhardt, J. Lowe	(NOTT, UNM, BIRM)
DALITZ	91	JPG 17 289	R.H. Dalitz, A. Deloff	(OXFTP, WINR)
HEMINGWAY	85	NP B253 742	R.J. Hemingway	(CERN) J
MARTIN	81	NP B179 33	A.D. Martin	(DURH)
CHAO	73	NP B56 46	Y.A. Chao *et al.*	(RHEL, CMU, LOUC)
THOMAS	73	NP B56 15	D.W. Thomas *et al.*	(CMU) J
MARTIN	70	NP B16 479	A.D. Martin, G.G. Ross	(DURH)
MARTIN	69	PR 183 1352	B.R. Martin, M. Sakitt	(LOUC, BNL)
Also	69B	PR 183 1345	B.R. Martin, M. Sakitt	(LOUC, BNL)
BARBARO-...	68B	PRL 21 573	A. Barbaro-Galtieri *et al.*	(LRL, SLAC)
KIM	67	PRL 19 1074	J.K. Kim	(YALE)
BIRMINGHAM	66	PR 152 1148	M. Haque *et al.*	(BIRM, GLAS, LOIC, OXF+)
KITTEL	66	PL 21 349	W. Kittel, G. Otter, I. Wacek	(VIEN)
ENGLER	65	PRL 15 224	A. Engler *et al.*	(CMU, BNL) IJ
KIM	65	PRL 14 29	J.K. Kim	(COLU)
MUSGRAVE	65	NC 35 735	B. Musgrave *et al.*	(BIRM, CERN, EPOL+)
SAKITT	65	PR 139B 719	M. Sakitt *et al.*	(UMD, LRL)
ALEXANDER	62	PRL 8 447	G. Alexander *et al.*	(LRL) I
ALSTON	62	CERN Conf. 311	M.H. Alston *et al.*	(LRL) I
ALSTON	61B	PRL 6 698	M.H. Alston *et al.*	(LRL) I

OTHER RELATED PAPERS

IWASAKI	97	PRL 78 3067	M. Iwasaki *et al.*	(KEK 228 Collab.)
FINK	90	PR C41 2720	P.J.Jr. Fink *et al.*	(IBMY, ORST, ANSM)
LEINWEBER	90	ANP 198 203	D.B. Leinweber	(MCMS)
MUELLER-GR...	90	NP A513 557	A. Mueller-Groeling, K. Holinde, J. Speth	(JULI)
BARRETT	89	NC 102A 179	R.C. Barrett	(SURR)
BATTY	89	NC 102A 255	C.J. Batty, A. Gal	(RAL, HEBR)
CAPSTICK	89	Excited Baryons 88, p.32	S. Capstick	(GUEL)
LOWE	89	NC 102A 167	J. Lowe	(BIRM)
WHITEHOUSE	89	PRL 63 1352	D.A. Whitehouse *et al.*	(BIRM, BOST, BRCO+)
SIEGEL	88	PRL C38 2221	P.B. Siegel, W. Weise	(REGE)
WORKMAN	88	PR D37 3117	R.L. Workman, H.W. Fearing	(TRIU)
SCHNICK	87	PRL 58 1719	J. Schnick, R.H. Landau	(ORST)
CAPSTICK	86	PR D34 2809	S. Capstick, N. Isgur	(TNTO)
JENNINGS	86	PL B176 229	B.K. Jennings	(TRIU)
MALTMAN	86	PR D34 1372	K. Maltman, N. Isgur	(LANL, TNTO)
ZHONG	86	PL B171 471	Y.S. Zhong *et al.*	(ADLD, TRIU, SURR)
BURKHARDT	85	NP A440 653	H. Burkhardt, J. Lowe, A.S. Rosenthal	(NOTT+)
DAREWYCH	85	PR D32 1765	J.W. Darewych, R. Koniuk, N. Isgur	(YORKC, TNTO)
VEIT	85	PR D31 1033	E.A. Veit *et al.*	(TRIU, ADLD, SURR)
KIANG	84	PR C30 1638	D. Kiang *et al.*	(DALH, MCMS)
MILLER	84	Conference paper	D.J. Miller	(LOUC)
		Conf. Intersections between Particle and Nuclear Physics, p. 783		
VANDIJK	84	PR D30 937	W. van Dijk	(MCMS)
VEIT	84	PL 137B 415	E.A. Veit *et al.*	(TRIU, SURR, CERN)
DALITZ	82	Heid. Conf.	R.H. Dalitz *et al.*	(OXFTP)
		Heidelberg Conf., p. 201		
DALITZ	81	Kaon Conf.	R.H. Dalitz, J.G. McGinley	(OXFTP)
		Low and Intermediate Energy Kaon-Nucleon Physics, p.381		
MARTIN	81B	Kaon Conf.	A.D. Martin	(DURH)
		Low and Intermediate Energy Kaon-Nucelon Physics, p. 97		
OADES	77	NC 42A 462	G.C. Oades, G. Rasche	(AARH, ZURI)
SHAW	73	Purdue Conf. 417	G.L. Shaw	(UCI)
BARBARO-...	72	LBL-555	A. Barbaro-Galtieri	(LBL)
DOBSON	72	PR D6 3256	P.N. Dobson, R. McElhaney	(HAWA)
RAJASEKA...	72	PR D5 610	G. Rajasekaran	(TATA)
		Earlier papers also cited in RAJASEKARAN 72.		
CLINE	71	PRL 26 1194	D. Cline, R. Laumann, J. Mapp	(WISC)
MARTIN	71	PL 35B 62	A.D. Martin, A.D. Martin, G.G. Ross	(DURH, LOUC+)
DALITZ	67	PR 153 1617	R.H. Dalitz, T.C. Wong, G. Rajasekaran	(OXFTP+)
DONALD	66	PL 22 711	R.A. Donald *et al.*	(LIVP)
KADYK	66	PRL 17 599	J.A. Kadyk *et al.*	(LRL)
ABRAMS	65	PR 139B 454	G.S. Abrams, B. Sechi-Zorn	(UMD)

Λ(1520) D_{03}

$I(J^P) = 0(\frac{3}{2}^-)$ Status: ****

Discovered by FERRO-LUZZI 62; the elaboration in WATSON 63 is the classic paper on the Breit-Wigner analysis of a multichannel resonance.

The measurements of the mass, width, and elasticity published before 1975 are now obsolete and have been omitted. They were last listed in our 1982 edition Physics Letters **111B** (1982).

Production and formation experiments agree quite well, so they are listed together here.

Λ(1520) MASS

VALUE (MeV)	EVTS	DOCUMENT ID		TECN	COMMENT
1519.5 ±1.0 OUR ESTIMATE					
1519.50±0.18 OUR AVERAGE					
1517.3 ±1.5	300	BARBER	80D	SPEC	$\gamma p \to \Lambda(1520)K^+$
1519 ±1		GOPAL	80	DPWA	$\overline{K}N \to \overline{K}N$
1517.8 ±1.2	5k	BARLAG	79	HBC	K^-p 4.2 GeV/c
1520.0 ±0.5		ALSTON-...	78	DPWA	$\overline{K}N \to \overline{K}N$
1519.7 ±0.3	4k	CAMERON	77	HBC	K^-p 0.96–1.36 GeV/c
1519 ±1		GOPAL	77	DPWA	$\overline{K}N$ multichannel
1519.4 ±0.3	2000	CORDEN	75	DBC	K^-d 1.4–1.8 GeV/c

Λ(1520) WIDTH

VALUE (MeV)	EVTS	DOCUMENT ID		TECN	COMMENT
15.6 ±1.0 OUR ESTIMATE					
15.59±0.27 OUR AVERAGE					
16.3 ±3.3	300	BARBER	80D	SPEC	$\gamma p \to \Lambda(1520)K^+$
16 ±1		GOPAL	80	DPWA	$\overline{K}N \to \overline{K}N$
14 ±3	677	[1] BARLAG	79	HBC	K^-p 4.2 GeV/c
15.4 ±0.5		ALSTON-...	78	DPWA	$\overline{K}N \to \overline{K}N$
16.3 ±0.5	4k	CAMERON	77	HBC	K^-p 0.96–1.36 GeV/c
15.0 ±0.5		GOPAL	77	DPWA	$\overline{K}N$ multichannel
15.5 ±1.6	2000	CORDEN	75	DBC	K^-d 1.4–1.8 GeV/c

Λ(1520) DECAY MODES

	Mode	Fraction (Γ_i/Γ)
Γ_1	$N\overline{K}$	45 ± 1%
Γ_2	$\Sigma\pi$	42 ± 1%
Γ_3	$\Lambda\pi\pi$	10 ± 1%
Γ_4	$\Sigma(1385)\pi$	
Γ_5	$\Sigma(1385)\pi(\to \Lambda\pi\pi)$	
Γ_6	$\Lambda(\pi\pi)S$-wave	
Γ_7	$\Sigma\pi\pi$	0.9 ± 0.1%
Γ_8	$\Lambda\gamma$	0.8 ± 0.2%
Γ_9	$\Sigma^0\gamma$	

CONSTRAINED FIT INFORMATION

An overall fit to 9 branching ratios uses 24 measurements and one constraint to determine 6 parameters. The overall fit has a $\chi^2 = 16.5$ for 19 degrees of freedom.

The following *off-diagonal* array elements are the correlation coefficients $\langle \delta x_i \delta x_j \rangle / (\delta x_i \cdot \delta x_j)$, in percent, from the fit to the branching fractions, $x_i \equiv \Gamma_i/\Gamma_{\text{total}}$. The fit constrains the x_i whose labels appear in this array to sum to one.

x_2	−63				
x_3	−32	−33			
x_7	−4	−3	−1		
x_8	−9	−8	−4	0	
x_9	−24	−21	−10	−1	−2
	x_1	x_2	x_3	x_7	x_8

Λ(1520) BRANCHING RATIOS

See "Sign conventions for resonance couplings" in the Note on Λ and Σ Resonances.

Γ(NK̄)/Γ_total — Γ1/Γ

VALUE	DOCUMENT ID		TECN	COMMENT
0.45 ±0.01 OUR ESTIMATE				
0.448±0.007 OUR FIT Error includes scale factor of 1.2.				
0.455±0.011 OUR AVERAGE				
0.47 ±0.02	GOPAL	80	DPWA	$\overline{K}N \to \overline{K}N$
0.45 ±0.03	ALSTON-...	78	DPWA	$\overline{K}N \to \overline{K}N$
0.448±0.014	CORDEN	75	DBC	K^-d 1.4–1.8 GeV/c
• • • We do not use the following data for averages, fits, limits, etc. • • •				
0.47 ±0.01	GOPAL	77	DPWA	See GOPAL 80
0.42	MAST	76	HBC	$K^-p \to \overline{K}^0 n$

Γ(Σπ)/Γ_total — Γ2/Γ

VALUE	DOCUMENT ID		TECN	COMMENT
0.42 ±0.01 OUR ESTIMATE				
0.421±0.007 OUR FIT Error includes scale factor of 1.2.				
0.423±0.011 OUR AVERAGE				
0.426±0.014	CORDEN	75	DBC	K^-d 1.4–1.8 GeV/c
0.418±0.017	BARBARO-...	69B	HBC	K^-p 0.28–0.45 GeV/c
• • • We do not use the following data for averages, fits, limits, etc. • • •				
0.46	KIM	71	DPWA	K-matrix analysis

Γ(Σπ)/Γ(NK̄) — Γ2/Γ1

VALUE	DOCUMENT ID		TECN	COMMENT
0.940±0.026 OUR FIT Error includes scale factor of 1.3.				
0.95 ±0.04 OUR AVERAGE Error includes scale factor of 1.7. See the ideogram below.				
0.98 ±0.03	[2] GOPAL	77	DPWA	$\overline{K}N$ multichannel
0.82 ±0.08	BURKHARDT	69	HBC	K^-p 0.8–1.2 GeV/c
1.06 ±0.14	SCHEUER	68	DBC	K^-N 3 GeV/c
0.96 ±0.20	DAHL	67	HBC	π^-p 1.6–4 GeV/c
0.73 ±0.11	DAUBER	67	HBC	K^-p 2 GeV/c
• • • We do not use the following data for averages, fits, limits, etc. • • •				
1.06 ±0.12	BERTHON	74	HBC	Quasi-2-body σ
1.72 ±0.78	MUSGRAVE	65	HBC	

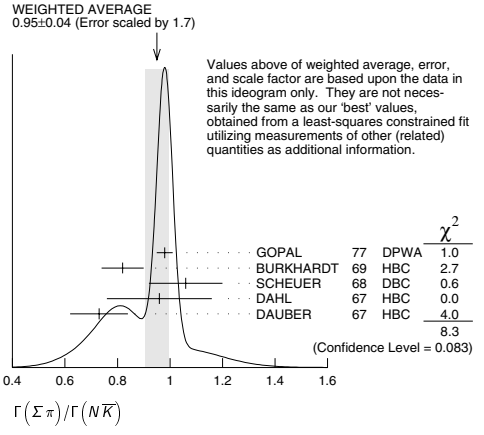

Γ(Λππ)/Γ_total — Γ3/Γ

VALUE	DOCUMENT ID		TECN	COMMENT
0.10 ±0.01 OUR ESTIMATE				
0.095±0.005 OUR FIT Error includes scale factor of 1.2.				
0.096±0.008 OUR AVERAGE Error includes scale factor of 1.6.				
0.091±0.006	CORDEN	75	DBC	K^-d 1.4–1.8 GeV/c
0.11 ±0.01	[3] MAST	73B	IPWA	$K^-p \to \Lambda\pi\pi$

Γ(Λππ)/Γ(NK̄) — Γ3/Γ1

VALUE	DOCUMENT ID		TECN	COMMENT
0.213±0.012 OUR FIT Error includes scale factor of 1.2.				
0.202±0.021 OUR AVERAGE				
0.22 ±0.03	BURKHARDT	69	HBC	K^-p 0.8–1.2 GeV/c
0.19 ±0.04	SCHEUER	68	DBC	K^-N 3 GeV/c
0.17 ±0.05	DAHL	67	HBC	π^-p 1.6–4 GeV/c
0.21 ±0.18	DAUBER	67	HBC	K^-p 2 GeV/c
• • • We do not use the following data for averages, fits, limits, etc. • • •				
0.27 ±0.13	BERTHON	74	HBC	Quasi-2-body σ
0.2	KIM	71	DPWA	K-matrix analysis

Γ(Σπ)/Γ(Λππ) — Γ2/Γ3

VALUE	DOCUMENT ID		TECN	COMMENT
4.42±0.25 OUR FIT Error includes scale factor of 1.2.				
3.9 ±0.6 OUR AVERAGE				
3.9 ±1.0	UHLIG	67	HBC	K^-p 0.9–1.0 GeV/c
3.3 ±1.1	BIRMINGHAM	66	HBC	K^-p 3.5 GeV/c
4.5 ±1.0	ARMENTEROS	65C	HBC	

Γ(Σ(1385)π)/Γ_total — Γ4/Γ

VALUE	DOCUMENT ID		TECN	COMMENT
0.041±0.005	CHAN	72	HBC	$K^-p \to \Lambda\pi\pi$

Γ(Σ(1385)π(→ Λππ))/Γ(Λππ) — Γ5/Γ3

The Λππ mode is largely due to Σ(1385)π. Only the values of (Σ(1385)π) / (Λ2π) given by MAST 73B and CORDEN 75 are based on real 3-body partial-wave analyses. The discrepancy between the two results is essentially due to the different hypotheses made concerning the shape of the $(\pi\pi)_{S\text{-wave}}$ state.

VALUE	DOCUMENT ID		TECN	COMMENT
0.58±0.22	CORDEN	75	DBC	K^-d 1.4–1.8 GeV/c
0.82±0.10	[4] MAST	73B	IPWA	$K^-p \to \Lambda\pi\pi$
• • • We do not use the following data for averages, fits, limits, etc. • • •				
0.39±0.10	[5] BURKHARDT	71	HBC	$K^-p \to (\Lambda\pi\pi)\pi$

Γ(Λ(ππ)_S-wave)/Γ(Λππ) — Γ6/Γ3

VALUE	DOCUMENT ID		TECN	COMMENT
0.20±0.08	CORDEN	75	DBC	K^-d 1.4–1.8 GeV/c

Γ(Σππ)/Γ_total — Γ7/Γ

VALUE	DOCUMENT ID		TECN	COMMENT
0.009 ±0.001 OUR ESTIMATE				
0.0086±0.0005 OUR FIT				
0.0086±0.0005 OUR AVERAGE				
0.007 ±0.002	[6] CORDEN	75	DBC	K^-d 1.4–1.8 GeV/c
0.0085±0.0006	[7] MAST	73	MPWA	$K^-p \to \Sigma\pi\pi$
0.010 ±0.0015	BARBARO-...	69B	HBC	K^-p 0.28–0.45 GeV/c

Γ(Λγ)/Γ_total — Γ8/Γ

VALUE	EVTS	DOCUMENT ID		TECN	COMMENT
0.008 ±0.002 OUR ESTIMATE					
0.0079±0.0014 OUR FIT					
0.0080±0.0014	238	MAST	68B	HBC	Using Γ(NK̄)/Γ_total = 0.45

Γ(Σ⁰γ)/Γ_total — Γ9/Γ

VALUE	DOCUMENT ID		TECN	COMMENT
0.0195±0.0034 OUR FIT				
0.02 ±0.0035	[8] MAST	68B	HBC	Not measured; see note

Λ(1520) FOOTNOTES

[1] From the best-resolution sample of Λππ events only.
[2] The $\overline{K}N \to \Sigma\pi$ amplitude at resonance is +0.46 ± 0.01.
[3] Assumes $\Gamma(N\overline{K})/\Gamma_{\text{total}} = 0.46 \pm 0.02$.
[4] Both Σ(1385)π DS_{03} and Σ(ππ) DP_{03} contribute.
[5] The central bin (1514–1524 MeV) gives 0.74 ± 0.10; other bins are lower by 2-to-5 standard deviations.
[6] Much of the Σππ decay proceeds via Σ(1385)π.
[7] Assumes $\Gamma(N\overline{K})/\Gamma_{\text{total}} = 0.46$.
[8] Calculated from $\Gamma(\Lambda\gamma)/\Gamma_{\text{total}}$, assuming SU(3). Needed to constrain the sum of all the branching ratios to be unity.

Λ(1520) REFERENCES

PDG	82	PL 111B	M. Roos *et al.*	(HELS, CIT, CERN)
BARBER	80D	ZPHY C7 17	D.P. Barber *et al.*	(DARE, LANC, SHEF)
GOPAL	80	Toronto Conf. 159	G.P. Gopal	(RHEL) IJP
BARLAG	79	NP B149 220	S.J.M. Barlag *et al.*	(AMST, CERN, NIJM+)
ALSTON-...	78	PR D18 182	M. Alston-Garnjost *et al.*	(LBL, MTHO+) IJP
Also	77	PRL 38 1007	M. Alston-Garnjost *et al.*	(LBL, MTHO+) IJP
CAMERON	77	NP B131 399	W. Cameron *et al.*	(RHEL, LOIC) IJP
GOPAL	77	NP B119 362	G.P. Gopal *et al.*	(LOIC, RHEL) IJP
MAST	76	PR D14 13	T.S. Mast *et al.*	(LBL)
CORDEN	75	NP B84 306	M.J. Corden *et al.*	(BIRM)
BERTHON	74	NC 21A 146	A. Berthon *et al.*	(CDEF, RHEL, SACL+)
MAST	73	PR D7 3212	T.S. Mast *et al.*	(LBL) IJP
MAST	73B	PR D7 5	T.S. Mast *et al.*	(LBL) IJP
CHAN	72	PRL 28 256	S.B. Chan *et al.*	(MASA, YALE)
BURKHARDT	71	NP B27 64	E. Burkhardt *et al.*	(HEID, CERN, SACL)
KIM	71	PRL 27 356	J.K. Kim	(HARV) IJP
Also	70	Duke Conf. 161 Hyperon Resonances, 1970	J.K. Kim	(HARV) IJP
BARBARO-...	69B	Lund Conf. 352	A. Barbaro-Galtieri *et al.*	(LRL)
Also	70	Duke Conf. 95 Hyperon Resonances 1970	R.D. Tripp	(LRL)
BURKHARDT	69	NP B14 106	E. Burkhardt *et al.*	(HEID, EFI, CERN+)
MAST	68B	PRL 21 1715	T.S. Mast *et al.*	(LRL)
SCHEUER	68	NP B8 503	J.C. Scheuer *et al.*	(SABRE Collab.)
DAHL	67	PR 163 1377	O.I. Dahl *et al.*	(LRL)
DAUBER	67	PL 24B 525	P.M. Dauber *et al.*	(UCLA)
UHLIG	67	PR 155 1448	R.P. Uhlig *et al.*	(UMD, NRL)
BIRMINGHAM	66	PR 152 1148	M. Haque *et al.*	(BIRM, GLAS, LOIC, OXF+)
ARMENTEROS	65C	PL 19 338	R. Armenteros *et al.*	(CERN, HEID, SACL)
MUSGRAVE	65	NC 35 735	B. Musgrave *et al.*	(BIRM, CERN, EPOL+)
WATSON	63	PR 131 2248	M.B. Watson, M. Ferro-Luzzi, R.D. Tripp	(LRL) IJP
FERRO-LUZZI	62	PRL 8 28	M. Ferro-Luzzi, R.D. Tripp, M.B. Watson	(LRL) IJP

$\Lambda(1600)$ P_{01}

$I(J^P) = 0(\frac{1}{2}^+)$ Status: ***

See also the $\Lambda(1810)$ P_{01}. There are quite possibly two P_{01} states in this region.

$\Lambda(1600)$ MASS

VALUE (MeV)	DOCUMENT ID		TECN	COMMENT
1560 to 1700 (≈ 1600) OUR ESTIMATE				
1568± 20	GOPAL	80	DPWA	$\overline{K}N \to \overline{K}N$
1703±100	ALSTON-...	78	DPWA	$\overline{K}N \to \overline{K}N$
1573± 25	GOPAL	77	DPWA	$\overline{K}N$ multichannel
1596± 6	KANE	74	DPWA	$K^-p \to \Sigma\pi$
1620± 10	LANGBEIN	72	IPWA	$\overline{K}N$ multichannel
• • • We do not use the following data for averages, fits, limits, etc. • • •				
1572 or 1617	[1] MARTIN	77	DPWA	$\overline{K}N$ multichannel
1646± 7	[2] CARROLL	76	DPWA	Isospin-0 total σ
1570	KIM	71	DPWA	K-matrix analysis

$\Lambda(1600)$ WIDTH

VALUE (MeV)	DOCUMENT ID		TECN	COMMENT
50 to 250 (≈ 150) OUR ESTIMATE				
116± 20	GOPAL	80	DPWA	$\overline{K}N \to \overline{K}N$
593±200	ALSTON-...	78	DPWA	$\overline{K}N \to \overline{K}N$
147± 50	GOPAL	77	DPWA	$\overline{K}N$ multichannel
175± 20	KANE	74	DPWA	$K^-p \to \Sigma\pi$
60± 10	LANGBEIN	72	IPWA	$\overline{K}N$ multichannel
• • • We do not use the following data for averages, fits, limits, etc. • • •				
247 or 271	[1] MARTIN	77	DPWA	$\overline{K}N$ multichannel
20	[2] CARROLL	76	DPWA	Isospin-0 total σ
50	KIM	71	DPWA	K-matrix analysis

$\Lambda(1600)$ DECAY MODES

	Mode	Fraction (Γ_i/Γ)
Γ_1	$N\overline{K}$	15–30 %
Γ_2	$\Sigma\pi$	10–60 %

The above branching fractions are our estimates, not fits or averages.

$\Lambda(1600)$ BRANCHING RATIOS

See "Sign conventions for resonance couplings" in the Note on Λ and Σ Resonances.

$\Gamma(N\overline{K})/\Gamma_{total}$ Γ_1/Γ

VALUE	DOCUMENT ID		TECN	COMMENT
0.15 to 0.30 OUR ESTIMATE				
0.23±0.04	GOPAL	80	DPWA	$\overline{K}N \to \overline{K}N$
0.14±0.05	ALSTON-...	78	DPWA	$\overline{K}N \to \overline{K}N$
0.25±0.15	LANGBEIN	72	IPWA	$\overline{K}N$ multichannel
• • • We do not use the following data for averages, fits, limits, etc. • • •				
0.24±0.04	GOPAL	77	DPWA	See GOPAL 80
0.30 or 0.29	[1] MARTIN	77	DPWA	$\overline{K}N$ multichannel

$(\Gamma_i\Gamma_f)^{1/2}/\Gamma_{total}$ in $N\overline{K} \to \Lambda(1600) \to \Sigma\pi$ $(\Gamma_1\Gamma_2)^{1/2}/\Gamma$

VALUE	DOCUMENT ID		TECN	COMMENT
−0.16±0.04	GOPAL	77	DPWA	$\overline{K}N$ multichannel
−0.33±0.11	KANE	74	DPWA	$K^-p \to \Sigma\pi$
0.28±0.09	LANGBEIN	72	IPWA	$\overline{K}N$ multichannel
• • • We do not use the following data for averages, fits, limits, etc. • • •				
−0.39 or −0.39	[1] MARTIN	77	DPWA	$\overline{K}N$ multichannel
not seen	HEPP	76B	DPWA	$K^-N \to \Sigma\pi$

$\Lambda(1600)$ FOOTNOTES

[1] The two MARTIN 77 values are from a T-matrix pole and from a Breit-Wigner fit.
[2] A total cross-section bump with $(J+1/2)\ \Gamma_{el}\ /\ \Gamma_{total} = 0.04$.

$\Lambda(1600)$ REFERENCES

GOPAL	80	Toronto Conf. 159	G.P. Gopal	(RHEL) IJP
ALSTON-...	78	PR D18 182	M. Alston-Garnjost *et al.*	(LBL, MTHO+) IJP
Also	77	PRL 38 1007	M. Alston-Garnjost *et al.*	(LBL, MTHO+) IJP
GOPAL	77	NP B119 362	G.P. Gopal *et al.*	(LOIC, RHEL) IJP
MARTIN	77	NP B127 349	B.R. Martin, M.K. Pidcock, R.G. Moorhouse	(LOUC+) IJP
Also	77B	NP B126 266	B.R. Martin, M.K. Pidcock	(LOUC)
Also	77C	NP B126 285	B.R. Martin, M.K. Pidcock	(LOUC) IJP
CARROLL	76	PRL 37 806	A.S. Carroll *et al.*	(BNL) I
HEPP	76B	PL 65B 487	V. Hepp *et al.*	(CERN, HEIDH, MPIM) IJP
KANE	74	LBL-2452	D.F. Kane	(LBL) IJP
LANGBEIN	72	NP B47 477	W. Langbein, F. Wagner	(MPIM) IJP
KIM	71	PRL 27 356	J.K. Kim	(HARV) IJP

$\Lambda(1670)$ S_{01}

$I(J^P) = 0(\frac{1}{2}^-)$ Status: ****

The measurements of the mass, width, and elasticity published before 1974 are now obsolete and have been omitted. They were last listed in our 1982 edition Physics Letters **111B** (1982).

$\Lambda(1670)$ MASS

VALUE (MeV)	DOCUMENT ID		TECN	COMMENT
1660 to 1680 (≈ 1670) OUR ESTIMATE				
1677.5±0.8	[1] GARCIA-REC...	03	DPWA	$\overline{K}N$ multichannel
1673 ±2	MANLEY	02	DPWA	$\overline{K}N$ multichannel
1670.8±1.7	KOISO	85	DPWA	$K^-p \to \Sigma\pi$
1667 ±5	GOPAL	80	DPWA	$\overline{K}N \to \overline{K}N$
1671 ±3	ALSTON-...	78	DPWA	$\overline{K}N \to \overline{K}N$
1670 ±5	GOPAL	77	DPWA	$\overline{K}N$ multichannel
1675 ±2	HEPP	76B	DPWA	$K^-N \to \Sigma\pi$
1679 ±1	KANE	74	DPWA	$K^-p \to \Sigma\pi$
1665 ±5	PREVOST	74	DPWA	$K^-N \to \Sigma(1385)\pi$
• • • We do not use the following data for averages, fits, limits, etc. • • •				
1668.9±2.0	ABAEV	96	DPWA	$K^-p \to \Lambda\eta$
1664	[2] MARTIN	77	DPWA	$\overline{K}N$ multichannel

$\Lambda(1670)$ WIDTH

VALUE (MeV)	DOCUMENT ID		TECN	COMMENT
25 to 50 (≈ 35) OUR ESTIMATE				
29.2± 1.4	[1] GARCIA-REC...	03	DPWA	$\overline{K}N$ multichannel
23 ± 6	MANLEY	02	DPWA	$\overline{K}N$ multichannel
34.1± 3.7	KOISO	85	DPWA	$K^-p \to \Sigma\pi$
29 ± 5	GOPAL	80	DPWA	$\overline{K}N \to \overline{K}N$
29 ± 5	ALSTON-...	78	DPWA	$\overline{K}N \to \overline{K}N$
45 ±10	GOPAL	77	DPWA	$\overline{K}N$ multichannel
46 ± 5	HEPP	76B	DPWA	$K^-N \to \Sigma\pi$
40 ± 3	KANE	74	DPWA	$K^-p \to \Sigma\pi$
19 ± 5	PREVOST	74	DPWA	$K^-N \to \Sigma(1385)\pi$
• • • We do not use the following data for averages, fits, limits, etc. • • •				
21.1± 3.6	ABAEV	96	DPWA	$K^-p \to \Lambda\eta$
12	[2] MARTIN	77	DPWA	$\overline{K}N$ multichannel

$\Lambda(1670)$ DECAY MODES

	Mode	Fraction (Γ_i/Γ)
Γ_1	$N\overline{K}$	20–30 %
Γ_2	$\Sigma\pi$	25–55 %
Γ_3	$\Lambda\eta$	10–25 %
Γ_4	$\Sigma(1385)\pi$	

The above branching fractions are our estimates, not fits or averages.

$\Lambda(1670)$ BRANCHING RATIOS

See "Sign conventions for resonance couplings" in the Note on Λ and Σ Resonances.

$\Gamma(N\overline{K})/\Gamma_{total}$ Γ_1/Γ

VALUE	DOCUMENT ID		TECN	COMMENT
0.20 to 0.30 OUR ESTIMATE				
0.37±0.07	MANLEY	02	DPWA	$\overline{K}N$ multichannel
0.18±0.03	GOPAL	80	DPWA	$\overline{K}N \to \overline{K}N$
0.17±0.03	ALSTON-...	78	DPWA	$\overline{K}N \to \overline{K}N$
• • • We do not use the following data for averages, fits, limits, etc. • • •				
0.20±0.03	GOPAL	77	DPWA	See GOPAL 80
0.15	[2] MARTIN	77	DPWA	$\overline{K}N$ multichannel

$\Gamma(\Lambda\eta)/\Gamma_{total}$ Γ_3/Γ

VALUE	DOCUMENT ID		TECN	COMMENT
• • • We do not use the following data for averages, fits, limits, etc. • • •				
0.30±0.08	ABAEV	96	DPWA	$K^-p \to \Lambda\eta$

$(\Gamma_i\Gamma_f)^{1/2}/\Gamma_{total}$ in $N\overline{K} \to \Lambda(1670) \to \Sigma\pi$ $(\Gamma_1\Gamma_2)^{1/2}/\Gamma$

VALUE	DOCUMENT ID		TECN	COMMENT
−0.38±0.03	MANLEY	02	DPWA	$\overline{K}N$ multichannel
−0.26±0.02	KOISO	85	DPWA	$K^-p \to \Sigma\pi$
−0.31±0.03	GOPAL	77	DPWA	$\overline{K}N$ multichannel
−0.29±0.03	HEPP	76B	DPWA	$K^-N \to \Sigma\pi$
−0.23±0.03	LONDON	75	HLBC	$K^-p \to \Sigma^0\pi^0$
−0.27±0.02	KANE	74	DPWA	$K^-p \to \Sigma\pi$
• • • We do not use the following data for averages, fits, limits, etc. • • •				
−0.13	[2] MARTIN	77	DPWA	$\overline{K}N$ multichannel

$(\Gamma_i\Gamma_f)^{1/2}/\Gamma_{total}$ in $N\overline{K} \to \Lambda(1670) \to \Lambda\eta$ $(\Gamma_1\Gamma_3)^{1/2}/\Gamma$

VALUE	DOCUMENT ID		TECN	COMMENT
$+0.24 \pm 0.04$	MANLEY	02	DPWA	$\overline{K}N$ multichannel
$+0.20 \pm 0.05$	BAXTER	73	DPWA	$K^- p \to$ neutrals
• • • We do not use the following data for averages, fits, limits, etc. • • •				
0.24	KIM	71	DPWA	K-matrix analysis
0.26	ARMENTEROS	69C	HBC	
0.20 or 0.23	BERLEY	65	HBC	

$(\Gamma_i\Gamma_f)^{1/2}/\Gamma_{total}$ in $N\overline{K} \to \Lambda(1670) \to \Sigma(1385)\pi$ $(\Gamma_1\Gamma_4)^{1/2}/\Gamma$

VALUE	DOCUMENT ID		TECN	COMMENT
-0.17 ± 0.06	MANLEY	02	DPWA	$\overline{K}N$ multichannel
-0.18 ± 0.05	PREVOST	74	DPWA	$K^- N \to \Sigma(1385)\pi$

$\Lambda(1670)$ FOOTNOTES

[1] GARCIA-RECIO 03 gives pole, not Breit-Wigner, parameters, but the narrow width of the $\Lambda(1670)$ means there will be little difference.
[2] MARTIN 77 obtains identical resonance parameters from a T-matrix pole and from a Breit-Wigner fit.

$\Lambda(1670)$ REFERENCES

GARCIA-REC...	03	PR D67 076009	C. Garcia-Recio *et al.*	(GRAN, VALE)
MANLEY	02	PRL 88 012002	D.M. Manley *et al.*	(BNL Crystal Ball Collab.)
ABAEV	96	PR C53 385	V.V. Abaev, B.M.K. Nefkens	(UCLA)
KOISO	85	NP A433 619	H. Koiso *et al.*	(TOKY, MASA)
PDG	82	PL 111B	M. Roos *et al.*	(HELS, CIT, CERN)
GOPAL	80	Toronto Conf. 159	G.P. Gopal	(RHEL) IJP
ALSTON-...	78	PR D18 182	M. Alston-Garnjost *et al.*	(LBL, MTHO+) IJP
Also	77	PRL 38 1007	M. Alston-Garnjost *et al.*	(LBL, MTHO+) IJP
GOPAL	77	NP B119 362	G.P. Gopal *et al.*	(LOIC, RHEL) IJP
MARTIN	77	NP B127 349	B.R. Martin, M.K. Pidcock, R.G. Moorhouse	(LOUC+) IJP
Also	77B	NP B126 266	B.R. Martin, M.K. Pidcock	(LOUC)
Also	77C	NP B126 285	B.R. Martin, M.K. Pidcock	(LOUC) IJP
HEPP	76B	PL 65B 487	V. Hepp *et al.*	(CERN, HEIDH, MPIM) IJP
LONDON	75	NP B85 289	G.W. London *et al.*	(BNL, CERN, EPOL+)
KANE	74	LBL-2452	D.F. Kane	(LBL) IJP
PREVOST	74	NP B69 246	J. Prevost *et al.*	(SACL, CERN, HEID)
BAXTER	73	NP B67 125	D.F. Baxter *et al.*	(OXF) IJP
KIM	71	PRL 27 356	J.K. Kim	(HARV) IJP
Also	70	Duke Conf. 161 Hyperon Resonances, 1970	J.K. Kim	(HARV) IJP
ARMENTEROS	69C	Lund Paper 229 Values are quoted in LEVI-SETTI 69.	R. Armenteros *et al.*	(CERN, HEID, SACL) IJP
BERLEY	65	PRL 15 641	D. Berley *et al.*	(BNL) IJP

$\Lambda(1690)$ D_{03}

$I(J^P) = 0(\frac{3}{2}^-)$ Status: ****

The measurements of the mass, width, and elasticity published before 1974 are now obsolete and have been omitted. They were last listed in our 1982 edition Physics Letters **111B** (1982).

$\Lambda(1690)$ MASS

VALUE (MeV)	DOCUMENT ID		TECN	COMMENT
1685 to 1695 (≈ 1690) OUR ESTIMATE				
1695.7 ± 2.6	KOISO	85	DPWA	$K^- p \to \Sigma\pi$
1690 ± 5	GOPAL	80	DPWA	$\overline{K}N \to \overline{K}N$
1692 ± 5	ALSTON-...	78	DPWA	$\overline{K}N \to \overline{K}N$
1690 ± 5	GOPAL	77	DPWA	$\overline{K}N$ multichannel
1690 ± 3	HEPP	76B	DPWA	$K^- N \to \Sigma\pi$
1689 ± 1	KANE	74	DPWA	$K^- p \to \Sigma\pi$
• • • We do not use the following data for averages, fits, limits, etc. • • •				
1687 or 1689	[1] MARTIN	77	DPWA	$\overline{K}N$ multichannel
1692 ± 4	CARROLL	76	DPWA	Isospin-0 total σ

$\Lambda(1690)$ WIDTH

VALUE (MeV)	DOCUMENT ID		TECN	COMMENT
50 to 70 (≈ 60) OUR ESTIMATE				
67.2 ± 5.6	KOISO	85	DPWA	$K^- p \to \Sigma\pi$
61 ± 5	GOPAL	80	DPWA	$\overline{K}N \to \overline{K}N$
64 ± 10	ALSTON-...	78	DPWA	$\overline{K}N \to \overline{K}N$
60 ± 5	GOPAL	77	DPWA	$\overline{K}N$ multichannel
82 ± 8	HEPP	76B	DPWA	$K^- N \to \Sigma\pi$
60 ± 4	KANE	74	DPWA	$K^- p \to \Sigma\pi$
• • • We do not use the following data for averages, fits, limits, etc. • • •				
62 or 62	[1] MARTIN	77	DPWA	$\overline{K}N$ multichannel
38	CARROLL	76	DPWA	Isospin-0 total σ

$\Lambda(1690)$ DECAY MODES

	Mode	Fraction (Γ_i/Γ)
Γ_1	$N\overline{K}$	20–30 %
Γ_2	$\Sigma\pi$	20–40 %
Γ_3	$\Lambda\pi\pi$	~ 25 %
Γ_4	$\Sigma\pi\pi$	~ 20 %
Γ_5	$\Lambda\eta$	
Γ_6	$\Sigma(1385)\pi$, *S*-wave	

The above branching fractions are our estimates, not fits or averages.

$\Lambda(1690)$ BRANCHING RATIOS

The sum of all the quoted branching ratios is more than 1.0. The two-body ratios are from partial-wave analyses, and thus probably are more reliable than the three-body ratios, which are determined from bumps in cross sections. Of the latter, the $\Sigma\pi\pi$ bump looks more significant. (The error given for the $\Lambda\pi\pi$ ratio looks unreasonably small.) Hardly any of the $\Sigma\pi\pi$ decay can be via $\Sigma(1385)$, for then seven times as much $\Lambda\pi\pi$ decay would be required. See "Sign conventions for resonance couplings" in the Note on Λ and Σ Resonances.

$\Gamma(N\overline{K})/\Gamma_{total}$ Γ_1/Γ

VALUE	DOCUMENT ID		TECN	COMMENT
0.2 to 0.3 OUR ESTIMATE				
0.23 ± 0.03	GOPAL	80	DPWA	$\overline{K}N \to \overline{K}N$
0.22 ± 0.03	ALSTON-...	78	DPWA	$\overline{K}N \to \overline{K}N$
• • • We do not use the following data for averages, fits, limits, etc. • • •				
0.24 ± 0.03	GOPAL	77	DPWA	See GOPAL 80
0.28 or 0.26	[1] MARTIN	77	DPWA	$\overline{K}N$ multichannel

$(\Gamma_i\Gamma_f)^{1/2}/\Gamma_{total}$ in $N\overline{K} \to \Lambda(1690) \to \Sigma\pi$ $(\Gamma_1\Gamma_2)^{1/2}/\Gamma$

VALUE	DOCUMENT ID		TECN	COMMENT
-0.34 ± 0.02	KOISO	85	DPWA	$K^- p \to \Sigma\pi$
-0.25 ± 0.03	GOPAL	77	DPWA	$\overline{K}N$ multichannel
-0.29 ± 0.03	HEPP	76B	DPWA	$K^- N \to \Sigma\pi$
-0.28 ± 0.03	LONDON	75	HLBC	$K^- p \to \Sigma^0\pi^0$
-0.28 ± 0.02	KANE	74	DPWA	$K^- p \to \Sigma\pi$
• • • We do not use the following data for averages, fits, limits, etc. • • •				
-0.30 or -0.28	[1] MARTIN	77	DPWA	$\overline{K}N$ multichannel

$(\Gamma_i\Gamma_f)^{1/2}/\Gamma_{total}$ in $N\overline{K} \to \Lambda(1690) \to \Lambda\eta$ $(\Gamma_1\Gamma_5)^{1/2}/\Gamma$

VALUE	DOCUMENT ID		TECN	COMMENT
0.00 ± 0.03	BAXTER	73	DPWA	$K^- p \to$ neutrals

$(\Gamma_i\Gamma_f)^{1/2}/\Gamma_{total}$ in $N\overline{K} \to \Lambda(1690) \to \Lambda\pi\pi$ $(\Gamma_1\Gamma_3)^{1/2}/\Gamma$

VALUE	DOCUMENT ID		TECN	COMMENT
• • • We do not use the following data for averages, fits, limits, etc. • • •				
0.25 ± 0.02	[2] BARTLEY	68	HDBC	$K^- p \to \Lambda\pi\pi$

$(\Gamma_i\Gamma_f)^{1/2}/\Gamma_{total}$ in $N\overline{K} \to \Lambda(1690) \to \Sigma\pi\pi$ $(\Gamma_1\Gamma_4)^{1/2}/\Gamma$

VALUE	DOCUMENT ID		TECN	COMMENT
0.21	ARMENTEROS	68C	HDBC	$K^- N \to \Sigma\pi\pi$

$(\Gamma_i\Gamma_f)^{1/2}/\Gamma_{total}$ in $N\overline{K} \to \Lambda(1690) \to \Sigma(1385)\pi$, *S*-wave $(\Gamma_1\Gamma_6)^{1/2}/\Gamma$

VALUE	DOCUMENT ID		TECN	COMMENT
$+0.27 \pm 0.04$	PREVOST	74	DPWA	$K^- N \to \Sigma(1385)\pi$

$\Lambda(1690)$ FOOTNOTES

[1] The two MARTIN 77 values are from a T-matrix pole and from a Breit-Wigner fit. Another D_{03} Λ at 1966 MeV is also suggested by MARTIN 77, but is very uncertain.
[2] BARTLEY 68 uses only cross-section data. The enhancement is not seen by PREVOST 71.

$\Lambda(1690)$ REFERENCES

KOISO	85	NP A433 619	H. Koiso *et al.*	(TOKY, MASA)
PDG	82	PL 111B	M. Roos *et al.*	(HELS, CIT, CERN)
GOPAL	80	Toronto Conf. 159	G.P. Gopal	(RHEL) IJP
ALSTON-...	78	PR D18 182	M. Alston-Garnjost *et al.*	(LBL, MTHO+) IJP
Also	77	PRL 38 1007	M. Alston-Garnjost *et al.*	(LBL, MTHO+) IJP
GOPAL	77	NP B119 362	G.P. Gopal *et al.*	(LOIC, RHEL) IJP
MARTIN	77	NP B127 349	B.R. Martin, M.K. Pidcock, R.G. Moorhouse	(LOUC+) IJP
Also	77B	NP B126 266	B.R. Martin, M.K. Pidcock	(LOUC)
Also	77C	NP B126 285	B.R. Martin, M.K. Pidcock	(LOUC) IJP
CARROLL	76	PRL 37 806	A.S. Carroll *et al.*	(BNL) I
HEPP	76B	PL 65B 487	V. Hepp *et al.*	(CERN, HEIDH, MPIM) IJP
LONDON	75	NP B85 289	G.W. London *et al.*	(BNL, CERN, EPOL+)
KANE	74	LBL-2452	D.F. Kane	(LBL) IJP
PREVOST	74	NP B69 246	J. Prevost *et al.*	(SACL, CERN, HEID)
BAXTER	73	NP B67 125	D.F. Baxter *et al.*	(OXF) IJP
PREVOST	71	Amsterdam Conf.	J. Prevost	(CERN, HEID, SACL)
ARMENTEROS	68C	NP B8 216	R. Armenteros *et al.*	(CERN, HEID, SACL) I
BARTLEY	68	PRL 21 1111	J.H. Bartley *et al.*	(TUFTS, FSU, BRAN) I

$\Lambda(1800)$ S_{01}

$I(J^P) = 0(\frac{1}{2}^-)$ Status: ***

This is the second resonance in the S_{01} wave, the first being the $\Lambda(1670)$.

$\Lambda(1800)$ MASS

VALUE (MeV)	DOCUMENT ID		TECN	COMMENT
1720 to 1850 (≈ 1800) OUR ESTIMATE				
1845 ± 10	MANLEY	02	DPWA	$\overline{K}N$ multichannel
1841 ± 10	GOPAL	80	DPWA	$\overline{K}N \to \overline{K}N$
1725 ± 20	ALSTON-...	78	DPWA	$\overline{K}N \to \overline{K}N$
1825 ± 20	GOPAL	77	DPWA	$\overline{K}N$ multichannel
1830 ± 20	LANGBEIN	72	IPWA	$\overline{K}N$ multichannel
• • • We do not use the following data for averages, fits, limits, etc. • • •				
1767 or 1842	[1] MARTIN	77	DPWA	$\overline{K}N$ multichannel
1780	KIM	71	DPWA	K-matrix analysis
1872 ± 10	BRICMAN	70B	DPWA	$\overline{K}N \to \overline{K}N$

$\Lambda(1800)$ WIDTH

VALUE (MeV)	DOCUMENT ID		TECN	COMMENT
200 to 400 (≈ 300) OUR ESTIMATE				
518 ± 84	MANLEY	02	DPWA	$\overline{K}N$ multichannel
228 ± 20	GOPAL	80	DPWA	$\overline{K}N \to \overline{K}N$
185 ± 20	ALSTON-...	78	DPWA	$\overline{K}N \to \overline{K}N$
230 ± 20	GOPAL	77	DPWA	$\overline{K}N$ multichannel
70 ± 15	LANGBEIN	72	IPWA	$\overline{K}N$ multichannel
• • • We do not use the following data for averages, fits, limits, etc. • • •				
435 or 473	[1] MARTIN	77	DPWA	$\overline{K}N$ multichannel
40	KIM	71	DPWA	K-matrix analysis
100 ± 20	BRICMAN	70B	DPWA	$\overline{K}N \to \overline{K}N$

$\Lambda(1800)$ DECAY MODES

	Mode	Fraction (Γ_i/Γ)
Γ_1	$N\overline{K}$	25–40 %
Γ_2	$\Sigma\pi$	seen
Γ_3	$\Sigma(1385)\pi$	seen
Γ_4	$N\overline{K}^*(892)$	seen
Γ_5	$N\overline{K}^*(892)$, S=1/2, S-wave	
Γ_6	$N\overline{K}^*(892)$, S=3/2, D-wave	

The above branching fractions are our estimates, not fits or averages.

$\Lambda(1800)$ BRANCHING RATIOS

See "Sign conventions for resonance couplings" in the Note on Λ and Σ Resonances.

$\Gamma(N\overline{K})/\Gamma_{total}$ Γ_1/Γ

VALUE	DOCUMENT ID		TECN	COMMENT
0.25 to 0.40 OUR ESTIMATE				
0.24 ± 0.10	MANLEY	02	DPWA	$\overline{K}N$ multichannel
0.36 ± 0.04	GOPAL	80	DPWA	$\overline{K}N \to \overline{K}N$
0.28 ± 0.05	ALSTON-...	78	DPWA	$\overline{K}N \to \overline{K}N$
0.35 ± 0.15	LANGBEIN	72	IPWA	$\overline{K}N$ multichannel
• • • We do not use the following data for averages, fits, limits, etc. • • •				
0.37 ± 0.05	GOPAL	77	DPWA	See GOPAL 80
1.21 or 0.70	[1] MARTIN	77	DPWA	$\overline{K}N$ multichannel
0.80	KIM	71	DPWA	K-matrix analysis
0.18 ± 0.02	BRICMAN	70B	DPWA	$\overline{K}N \to \overline{K}N$

$(\Gamma_i\Gamma_f)^{1/2}/\Gamma_{total}$ in $N\overline{K} \to \Lambda(1800) \to \Sigma\pi$ $(\Gamma_1\Gamma_2)^{1/2}/\Gamma$

VALUE	DOCUMENT ID		TECN	COMMENT
− 0.08 ± 0.05	GOPAL	77	DPWA	$\overline{K}N$ multichannel
• • • We do not use the following data for averages, fits, limits, etc. • • •				
− 0.74 or − 0.43	[1] MARTIN	77	DPWA	$\overline{K}N$ multichannel
0.24	KIM	71	DPWA	K-matrix analysis

$(\Gamma_i\Gamma_f)^{1/2}/\Gamma_{total}$ in $N\overline{K} \to \Lambda(1800) \to \Sigma(1385)\pi$ $(\Gamma_1\Gamma_3)^{1/2}/\Gamma$

VALUE	DOCUMENT ID		TECN	COMMENT
+ 0.056 ± 0.028	[2] CAMERON	78	DPWA	$K^-p \to \Sigma(1385)\pi$

$(\Gamma_i\Gamma_f)^{1/2}/\Gamma_{total}$ in $N\overline{K} \to \Lambda(1800) \to N\overline{K}^*(892)$, S=1/2, S-wave $(\Gamma_1\Gamma_5)^{1/2}/\Gamma$

VALUE	DOCUMENT ID		TECN	COMMENT
− 0.17 ± 0.03	[2] CAMERON	78B	DPWA	$K^-p \to N\overline{K}^*$

$(\Gamma_i\Gamma_f)^{1/2}/\Gamma_{total}$ in $N\overline{K} \to \Lambda(1800) \to N\overline{K}^*(892)$, S=3/2, D-wave $(\Gamma_1\Gamma_6)^{1/2}/\Gamma$

VALUE	DOCUMENT ID		TECN	COMMENT
− 0.13 ± 0.04	CAMERON	78B	DPWA	$K^-p \to N\overline{K}^*$

$\Lambda(1800)$ FOOTNOTES

[1] The two MARTIN 77 values are from a T-matrix pole and from a Breit-Wigner fit.
[2] The published sign has been changed to be in accord with the baryon-first convention.

$\Lambda(1800)$ REFERENCES

MANLEY	02	PRL 88 012002	D.M. Manley *et al.*	(BNL Crystal Ball Collab.)
GOPAL	80	Toronto Conf. 159	G.P. Gopal	(RHEL) IJP
ALSTON-...	78	PR D18 182	M. Alston-Garnjost *et al.*	(LBL, MTHO+) IJP
Also	77	PRL 38 1007	M. Alston-Garnjost *et al.*	(LBL, MTHO+) IJP
CAMERON	78	NP B143 189	W. Cameron *et al.*	(RHEL, LOIC) IJP
CAMERON	78B	NP B146 327	W. Cameron *et al.*	(RHEL, LOIC) IJP
GOPAL	77	NP B119 362	G.P. Gopal *et al.*	(LOIC, RHEL) IJP
MARTIN	77	NP B127 349	B.R. Martin, M.K. Pidcock, R.G. Moorhouse	(LOUC+) IJP
Also	77B	NP B126 266	B.R. Martin, M.K. Pidcock	(LOUC)
Also	77C	NP B126 285	B.R. Martin, M.K. Pidcock	(LOUC) IJP
LANGBEIN	72	NP B47 477	W. Langbein, F. Wagner	(MPIM) IJP
KIM	71	PRL 27 356	J.K. Kim	(HARV) IJP
Also	70	Duke Conf. 161 Hyperon Resonances, 1970	J.K. Kim	(HARV) IJP
BRICMAN	70B	PL 33B 511	C. Bricman, M. Ferro-Luzzi, J.P. Lagnaux	(CERN) IJP

$\Lambda(1810)$ P_{01}

$I(J^P) = 0(\frac{1}{2}^+)$ Status: ***

Almost all the recent analyses contain a P_{01} state, and sometimes two of them, but the masses, widths, and branching ratios vary greatly. See also the $\Lambda(1600)$ P_{01}.

$\Lambda(1810)$ MASS

VALUE (MeV)	DOCUMENT ID		TECN	COMMENT
1750 to 1850 (≈ 1810) OUR ESTIMATE				
1841 ± 20	GOPAL	80	DPWA	$\overline{K}N \to \overline{K}N$
1853 ± 20	GOPAL	77	DPWA	$\overline{K}N$ multichannel
1735 ± 5	CARROLL	76	DPWA	Isospin-0 total σ
1746 ± 10	PREVOST	74	DPWA	$K^-N \to \Sigma(1385)\pi$
1780 ± 20	LANGBEIN	72	IPWA	$\overline{K}N$ multichannel
• • • We do not use the following data for averages, fits, limits, etc. • • •				
1861 or 1953	[1] MARTIN	77	DPWA	$\overline{K}N$ multichannel
1755	KIM	71	DPWA	K-matrix analysis
1800	ARMENTEROS	70	HBC	$\overline{K}N \to \overline{K}N$
1750	ARMENTEROS	70	HBC	$\overline{K}N \to \Sigma\pi$
1690 ± 10	BARBARO-...	70	HBC	$\overline{K}N \to \Sigma\pi$
1740	BAILEY	69	DPWA	$\overline{K}N \to \overline{K}N$
1745	ARMENTEROS	68B	HBC	$\overline{K}N \to \overline{K}N$

$\Lambda(1810)$ WIDTH

VALUE (MeV)	DOCUMENT ID		TECN	COMMENT
50 to 250 (≈ 150) OUR ESTIMATE				
164 ± 20	GOPAL	80	DPWA	$\overline{K}N \to \overline{K}N$
90 ± 20	CAMERON	78B	DPWA	$K^-p \to N\overline{K}^*$
166 ± 20	GOPAL	77	DPWA	$\overline{K}N$ multichannel
46 ± 20	PREVOST	74	DPWA	$K^-N \to \Sigma(1385)\pi$
120 ± 10	LANGBEIN	72	IPWA	$\overline{K}N$ multichannel
• • • We do not use the following data for averages, fits, limits, etc. • • •				
535 or 585	[1] MARTIN	77	DPWA	$\overline{K}N$ multichannel
28	CARROLL	76	DPWA	Isospin-0 total σ
35	KIM	71	DPWA	K-matrix analysis
30	ARMENTEROS	70	HBC	$\overline{K}N \to \overline{K}N$
70	ARMENTEROS	70	HBC	$\overline{K}N \to \Sigma\pi$
22	BARBARO-...	70	HBC	$\overline{K}N \to \Sigma\pi$
300	BAILEY	69	DPWA	$\overline{K}N \to \overline{K}N$
147	ARMENTEROS	68B	HBC	

$\Lambda(1810)$ DECAY MODES

	Mode	Fraction (Γ_i/Γ)
Γ_1	$N\overline{K}$	20–50 %
Γ_2	$\Sigma\pi$	10–40 %
Γ_3	$\Sigma(1385)\pi$	seen
Γ_4	$N\overline{K}^*(892)$	30–60 %
Γ_5	$N\overline{K}^*(892)$, S=1/2, P-wave	
Γ_6	$N\overline{K}^*(892)$, S=3/2, P-wave	

The above branching fractions are our estimates, not fits or averages.

$\Lambda(1810)$ BRANCHING RATIOS

See "Sign conventions for resonance couplings" in the Note on Λ and Σ Resonances.

$\Gamma(N\overline{K})/\Gamma_{total}$ Γ_1/Γ

VALUE	DOCUMENT ID		TECN	COMMENT
0.2 to 0.5 OUR ESTIMATE				
0.24 ± 0.04	GOPAL	80	DPWA	$\overline{K}N \to \overline{K}N$
0.36 ± 0.05	LANGBEIN	72	IPWA	$\overline{K}N$ multichannel

Baryon Particle Listings

Λ(1810), Λ(1820)

• • • We do not use the following data for averages, fits, limits, etc. • • •

0.21±0.04	GOPAL	77	DPWA	See GOPAL 80
0.52 or 0.49	[1] MARTIN	77	DPWA	$\overline{K}N$ multichannel
0.30	KIM	71	DPWA	K-matrix analysis
0.15	ARMENTEROS	70	DPWA	$\overline{K}N \to \overline{K}N$
0.55	BAILEY	69	DPWA	$\overline{K}N \to \overline{K}N$
0.4	ARMENTEROS	68B	DPWA	$\overline{K}N \to \overline{K}N$

$(\Gamma_i\Gamma_f)^{1/2}/\Gamma_{total}$ in $N\overline{K} \to \Lambda(1810) \to \Sigma\pi$ $(\Gamma_1\Gamma_2)^{1/2}/\Gamma$

VALUE	DOCUMENT ID	TECN	COMMENT
−0.24±0.04	GOPAL	77	DPWA $\overline{K}N$ multichannel

• • • We do not use the following data for averages, fits, limits, etc. • • •

+0.25 or +0.23	[1] MARTIN	77	DPWA	$\overline{K}N$ multichannel
< 0.01	LANGBEIN	72	IPWA	$\overline{K}N$ multichannel
0.17	KIM	71	DPWA	K-matrix analysis
+0.20	[2] ARMENTEROS	70	DPWA	$\overline{K}N \to \Sigma\pi$
−0.13±0.03	BARBARO-...	70	DPWA	$\overline{K}N \to \Sigma\pi$

$(\Gamma_i\Gamma_f)^{1/2}/\Gamma_{total}$ in $N\overline{K} \to \Lambda(1810) \to \Sigma(1385)\pi$ $(\Gamma_1\Gamma_3)^{1/2}/\Gamma$

VALUE	DOCUMENT ID	TECN	COMMENT
+0.18±0.10	PREVOST	74	DPWA $K^-N \to \Sigma(1385)\pi$

$(\Gamma_i\Gamma_f)^{1/2}/\Gamma_{total}$ in $N\overline{K} \to \Lambda(1810) \to N\overline{K}^*(892)$, S=1/2, P-wave $(\Gamma_1\Gamma_5)^{1/2}/\Gamma$

VALUE	DOCUMENT ID	TECN	COMMENT
−0.14±0.03	[2] CAMERON	78B	DPWA $K^-p \to N\overline{K}^*$

$(\Gamma_i\Gamma_f)^{1/2}/\Gamma_{total}$ in $N\overline{K} \to \Lambda(1810) \to N\overline{K}^*(892)$, S=3/2, P-wave $(\Gamma_1\Gamma_6)^{1/2}/\Gamma$

VALUE	DOCUMENT ID	TECN	COMMENT
+0.35±0.06	CAMERON	78B	DPWA $K^-p \to N\overline{K}^*$

Λ(1810) FOOTNOTES

[1] The two MARTIN 77 values are from a T-matrix pole and from a Breit-Wigner fit.
[2] The published sign has been changed to be in accord with the baryon-first convention.

Λ(1810) REFERENCES

GOPAL	80	Toronto Conf. 159	G.P. Gopal	(RHEL) IJP
CAMERON	78B	NP B146 327	W. Cameron *et al.*	(RHEL, LOIC) IJP
GOPAL	77	NP B119 362	G.P. Gopal *et al.*	(LOIC, RHEL) IJP
MARTIN	77	NP B127 349	B.R. Martin, M.K. Pidcock, R.G. Moorhouse	(LOUC+) IJP
Also	77B	NP B126 266	B.R. Martin, M.K. Pidcock	(LOUC)
Also	77C	NP B126 285	B.R. Martin, M.K. Pidcock	(LOUC) IJP
CARROLL	76	PRL 37 806	A.S. Carroll *et al.*	(BNL) I
PREVOST	74	NP B69 246	J. Prevost *et al.*	(SACL, CERN, HEID)
LANGBEIN	72	NP B47 477	W. Langbein, F. Wagner	(MPIM) IJP
KIM	71	PRL 27 356	J.K. Kim	(HARV) IJP
Also	70	Duke Conf. 161 Hyperon Resonances, 1970	J.K. Kim	(HARV) IJP
ARMENTEROS	70	Duke Conf. 123 Hyperon Resonances, 1970	R. Armenteros *et al.*	(CERN, HEID, SACL) IJP
BARBARO-...	70	Duke Conf. 173 Hyperon Resonances, 1970	A. Barbaro-Galtieri	(LRL) IJP
BAILEY	69	Thesis UCRL 50617	J.M. Bailey	(LLL) IJP
ARMENTEROS	68B	NP B8 195	R. Armenteros *et al.*	(CERN, HEID, SACL) IJP

Λ(1820) F_{05}

$I(J^P) = 0(\frac{5}{2}^+)$ Status: ****

This resonance is the cornerstone for all partial-wave analyses in this region. Most of the results published before 1973 are now obsolete and have been omitted. They may be found in our 1982 edition Physics Letters **111B** (1982).

Most of the quoted errors are statistical only; the systematic errors due to the particular parametrizations used in the partial-wave analyses are not included. For this reason we do not calculate weighted averages for the mass and width.

Λ(1820) MASS

VALUE (MeV)	DOCUMENT ID	TECN	COMMENT
1815 to 1825 (≈ 1820) OUR ESTIMATE			
1823±3	GOPAL	80	DPWA $\overline{K}N \to \overline{K}N$
1819±2	ALSTON-...	78	DPWA $\overline{K}N \to \overline{K}N$
1822±2	GOPAL	77	DPWA $\overline{K}N$ multichannel
1821±2	KANE	74	DPWA $K^-p \to \Sigma\pi$

• • • We do not use the following data for averages, fits, limits, etc. • • •

1830	DECLAIS	77	DPWA	$\overline{K}N \to \overline{K}N$
1817 or 1819	[1] MARTIN	77	DPWA	$\overline{K}N$ multichannel

Λ(1820) WIDTH

VALUE (MeV)	DOCUMENT ID	TECN	COMMENT
70 to 90 (≈ 80) OUR ESTIMATE			
77±5	GOPAL	80	DPWA $\overline{K}N \to \overline{K}N$
72±5	ALSTON-...	78	DPWA $\overline{K}N \to \overline{K}N$
81±5	GOPAL	77	DPWA $\overline{K}N$ multichannel
87±3	KANE	74	DPWA $K^-p \to \Sigma\pi$

• • • We do not use the following data for averages, fits, limits, etc. • • •

82	DECLAIS	77	DPWA	$\overline{K}N \to \overline{K}N$
76 or 76	[1] MARTIN	77	DPWA	$\overline{K}N$ multichannel

Λ(1820) DECAY MODES

	Mode	Fraction (Γ_j/Γ)
Γ_1	$N\overline{K}$	55–65 %
Γ_2	$\Sigma\pi$	8–14 %
Γ_3	$\Sigma(1385)\pi$	5–10 %
Γ_4	$\Sigma(1385)\pi$, P-wave	
Γ_5	$\Sigma(1385)\pi$, F-wave	
Γ_6	$\Lambda\eta$	
Γ_7	$\Sigma\pi\pi$	

The above branching fractions are our estimates, not fits or averages.

Λ(1820) BRANCHING RATIOS

Errors quoted do not include uncertainties in the parametrizations used in the partial-wave analyses and are thus too small. See also "Sign conventions for resonance couplings" in the Note on Λ and Σ Resonances.

$\Gamma(N\overline{K})/\Gamma_{total}$ Γ_1/Γ

VALUE	DOCUMENT ID	TECN	COMMENT
0.55 to 0.65 OUR ESTIMATE			
0.58±0.02	GOPAL	80	DPWA $\overline{K}N \to \overline{K}N$
0.60±0.03	ALSTON-...	78	DPWA $\overline{K}N \to \overline{K}N$

• • • We do not use the following data for averages, fits, limits, etc. • • •

0.51	DECLAIS	77	DPWA	$\overline{K}N \to \overline{K}N$
0.57±0.02	GOPAL	77	DPWA	See GOPAL 80
0.59 or 0.58	[1] MARTIN	77	DPWA	$\overline{K}N$ multichannel

$(\Gamma_i\Gamma_f)^{1/2}/\Gamma_{total}$ in $N\overline{K} \to \Lambda(1820) \to \Sigma\pi$ $(\Gamma_1\Gamma_2)^{1/2}/\Gamma$

VALUE	DOCUMENT ID	TECN	COMMENT
−0.28±0.03	GOPAL	77	DPWA $\overline{K}N$ multichannel
−0.28±0.01	KANE	74	DPWA $K^-p \to \Sigma\pi$

• • • We do not use the following data for averages, fits, limits, etc. • • •

−0.25 or −0.25	[1] MARTIN	77	DPWA	$\overline{K}N$ multichannel

$(\Gamma_i\Gamma_f)^{1/2}/\Gamma_{total}$ in $N\overline{K} \to \Lambda(1820) \to \Lambda\eta$ $(\Gamma_1\Gamma_6)^{1/2}/\Gamma$

VALUE	DOCUMENT ID	TECN
$-0.096^{+0.040}_{-0.020}$	RADER	73 MPWA

$\Gamma(\Sigma\pi\pi)/\Gamma_{total}$ Γ_7/Γ

VALUE	DOCUMENT ID	TECN	COMMENT
no clear signal	[2] ARMENTEROS	68C	HDBC $K^-N \to \Sigma\pi\pi$

$(\Gamma_i\Gamma_f)^{1/2}/\Gamma_{total}$ in $N\overline{K} \to \Lambda(1820) \to \Sigma(1385)\pi$, P-wave $(\Gamma_1\Gamma_4)^{1/2}/\Gamma$

VALUE	DOCUMENT ID	TECN	COMMENT
−0.167±0.054	[3] CAMERON	78	DPWA $K^-p \to \Sigma(1385)\pi$
+0.27 ±0.03	PREVOST	74	DPWA $K^-N \to \Sigma(1385)\pi$

$(\Gamma_i\Gamma_f)^{1/2}/\Gamma_{total}$ in $N\overline{K} \to \Lambda(1820) \to \Sigma(1385)\pi$, F-wave $(\Gamma_1\Gamma_5)^{1/2}/\Gamma$

VALUE	DOCUMENT ID	TECN	COMMENT
+0.065±0.029	[3] CAMERON	78	DPWA $K^-p \to \Sigma(1385)\pi$

Λ(1820) FOOTNOTES

[1] The two MARTIN 77 values are from a T-matrix pole and from a Breit-Wigner fit.
[2] There is a suggestion of a bump, enough to be consistent with what is expected from $\Sigma(1385) \to \Sigma\pi$ decay.
[3] The published sign has been changed to be in accord with the baryon-first convention.

Λ(1820) REFERENCES

PDG	82	PL 111B	M. Roos *et al.*	(HELS, CIT, CERN)
GOPAL	80	Toronto Conf. 159	G.P. Gopal	(RHEL) IJP
ALSTON-...	78	PR D18 182	M. Alston-Garnjost *et al.*	(LBL, MTHO+) IJP
Also	77	PRL 38 1007	M. Alston-Garnjost *et al.*	(LBL, MTHO+) IJP
CAMERON	78	NP B143 189	W. Cameron *et al.*	(RHEL, LOIC) IJP
DECLAIS	77	CERN 77-16	Y. Declais *et al.*	(CAEN, CERN) IJP
GOPAL	77	NP B119 362	G.P. Gopal *et al.*	(LOIC, RHEL) IJP
MARTIN	77	NP B127 349	B.R. Martin, M.K. Pidcock, R.G. Moorhouse	(LOUC+) IJP
Also	77B	NP B126 266	B.R. Martin, M.K. Pidcock	(LOUC)
Also	77C	NP B126 285	B.R. Martin, M.K. Pidcock	(LOUC) IJP
KANE	74	LBL-2452	D.F. Kane	(LBL) IJP
PREVOST	74	NP B69 246	J. Prevost *et al.*	(SACL, CERN, HEID)
RADER	73	NC 16A 178	R.K. Rader *et al.*	(SACL, HEID, CERN+)
ARMENTEROS	68C	NP B8 216	R. Armenteros *et al.*	(CERN, HEID, SACL) I

Λ(1830) D_{05}

$I(J^P) = 0(\frac{5}{2}^-)$ Status: ****

For results published before 1973 (they are now obsolete), see our 1982 edition Physics Letters **111B** (1982).

The best evidence for this resonance is in the $\Sigma\pi$ channel.

Λ(1830) MASS

VALUE (MeV)	DOCUMENT ID		TECN	COMMENT
1810 to 1830 (≈ 1830) OUR ESTIMATE				
1831±10	GOPAL	80	DPWA	$\overline{K}N \to \overline{K}N$
1825±10	GOPAL	77	DPWA	$\overline{K}N$ multichannel
1825± 1	KANE	74	DPWA	$K^-p \to \Sigma\pi$
• • • We do not use the following data for averages, fits, limits, etc. • • •				
1817 or 1818	[1] MARTIN	77	DPWA	$\overline{K}N$ multichannel

Λ(1830) WIDTH

VALUE (MeV)	DOCUMENT ID		TECN	COMMENT
60 to 110 (≈ 95) OUR ESTIMATE				
100±10	GOPAL	80	DPWA	$\overline{K}N \to \overline{K}N$
94±10	GOPAL	77	DPWA	$\overline{K}N$ multichannel
119± 3	KANE	74	DPWA	$K^-p \to \Sigma\pi$
• • • We do not use the following data for averages, fits, limits, etc. • • •				
56 or 56	[1] MARTIN	77	DPWA	$\overline{K}N$ multichannel

Λ(1830) DECAY MODES

	Mode	Fraction (Γ_i/Γ)
Γ_1	$N\overline{K}$	3–10 %
Γ_2	$\Sigma\pi$	35–75 %
Γ_3	$\Sigma(1385)\pi$	>15 %
Γ_4	$\Sigma(1385)\pi$, D-wave	
Γ_5	$\Lambda\eta$	

The above branching fractions are our estimates, not fits or averages.

Λ(1830) BRANCHING RATIOS

See "Sign conventions for resonance couplings" in the Note on Λ and Σ Resonances.

$\Gamma(N\overline{K})/\Gamma_{total}$ Γ_1/Γ

VALUE	DOCUMENT ID		TECN	COMMENT
0.03 to 0.10 OUR ESTIMATE				
0.08±0.03	GOPAL	80	DPWA	$\overline{K}N \to \overline{K}N$
0.02±0.02	ALSTON-...	78	DPWA	$\overline{K}N \to \overline{K}N$
• • • We do not use the following data for averages, fits, limits, etc. • • •				
0.04±0.03	GOPAL	77	DPWA	See GOPAL 80
0.04 or 0.04	[1] MARTIN	77	DPWA	$\overline{K}N$ multichannel

$(\Gamma_i\Gamma_f)^{1/2}/\Gamma_{total}$ in $N\overline{K} \to \Lambda(1830) \to \Sigma\pi$ $(\Gamma_1\Gamma_2)^{1/2}/\Gamma$

VALUE	DOCUMENT ID		TECN	COMMENT
−0.17±0.03	GOPAL	77	DPWA	$\overline{K}N$ multichannel
−0.15±0.01	KANE	74	DPWA	$K^-p \to \Sigma\pi$
• • • We do not use the following data for averages, fits, limits, etc. • • •				
−0.17 or −0.17	[1] MARTIN	77	DPWA	$\overline{K}N$ multichannel

$(\Gamma_i\Gamma_f)^{1/2}/\Gamma_{total}$ in $N\overline{K} \to \Lambda(1830) \to \Lambda\eta$ $(\Gamma_1\Gamma_5)^{1/2}/\Gamma$

VALUE	DOCUMENT ID		TECN
−0.044±0.020	RADER	73	MPWA

$(\Gamma_i\Gamma_f)^{1/2}/\Gamma_{total}$ in $N\overline{K} \to \Lambda(1830) \to \Sigma(1385)\pi$ $(\Gamma_1\Gamma_3)^{1/2}/\Gamma$

VALUE	DOCUMENT ID		TECN	COMMENT
+0.141±0.014	[2] CAMERON	78	DPWA	$K^-p \to \Sigma(1385)\pi$
+0.13 ±0.03	PREVOST	74	DPWA	$K^-N \to \Sigma(1385)\pi$

Λ(1830) FOOTNOTES

[1] The two MARTIN 77 values are from a T-matrix pole and from a Breit-Wigner fit.
[2] The CAMERON 78 upper limit on G-wave decay is 0.03. The published sign has been changed to be in accord with the baryon-first convention.

Λ(1830) REFERENCES

PDG	82	PL 111B	M. Roos *et al.*	(HELS, CIT, CERN)
GOPAL	80	Toronto Conf. 159	G.P. Gopal	(RHEL) IJP
ALSTON-...	78	PR D18 182	M. Alston-Garnjost *et al.*	(LBL, MTHO+) IJP
Also	77	PRL 38 1007	M. Alston-Garnjost *et al.*	(LBL, MTHO+) IJP
CAMERON	78	NP B143 189	W. Cameron *et al.*	(RHEL, LOIC) IJP
GOPAL	77	NP B119 362	G.P. Gopal *et al.*	(LOIC, RHEL) IJP
MARTIN	77	NP B127 349	B.R. Martin, M.K. Pidcock, R.G. Moorhouse	(LOUC+) IJP
Also	77B	NP B126 266	B.R. Martin, M.K. Pidcock	(LOUC)
Also	77C	NP B126 285	B.R. Martin, M.K. Pidcock	(LOUC) IJP
KANE	74	LBL-2452	D.F. Kane	(LBL) IJP
PREVOST	74	NP B69 246	J. Prevost *et al.*	(SACL, CERN, HEID)
RADER	73	NC 16A 178	R.K. Rader *et al.*	(SACL, HEID, CERN+)

Λ(1890) P_{03}

$I(J^P) = 0(\frac{3}{2}^+)$ Status: ****

For results published before 1974 (they are now obsolete), see our 1982 edition Physics Letters **111B** (1982).

The $J^P = 3/2^+$ assignment is consistent with all available data (including polarization) and recent partial-wave analyses. The dominant inelastic modes remain unknown.

Λ(1890) MASS

VALUE (MeV)	DOCUMENT ID		TECN	COMMENT
1850 to 1910 (≈ 1890) OUR ESTIMATE				
1897± 5	GOPAL	80	DPWA	$\overline{K}N \to \overline{K}N$
1908±10	ALSTON-...	78	DPWA	$\overline{K}N \to \overline{K}N$
1900± 5	GOPAL	77	DPWA	$\overline{K}N$ multichannel
1894±10	HEMINGWAY	75	DPWA	$K^-p \to \overline{K}N$
• • • We do not use the following data for averages, fits, limits, etc. • • •				
1856 or 1868	[1] MARTIN	77	DPWA	$\overline{K}N$ multichannel
1900	[2] NAKKASYAN	75	DPWA	$K^-p \to \Lambda\omega$

Λ(1890) WIDTH

VALUE (MeV)	DOCUMENT ID		TECN	COMMENT
60 to 200 (≈ 100) OUR ESTIMATE				
74±10	GOPAL	80	DPWA	$\overline{K}N \to \overline{K}N$
119±20	ALSTON-...	78	DPWA	$\overline{K}N \to \overline{K}N$
72±10	GOPAL	77	DPWA	$\overline{K}N$ multichannel
107±10	HEMINGWAY	75	DPWA	$K^-p \to \overline{K}N$
• • • We do not use the following data for averages, fits, limits, etc. • • •				
191 or 193	[1] MARTIN	77	DPWA	$\overline{K}N$ multichannel
100	[2] NAKKASYAN	75	DPWA	$K^-p \to \Lambda\omega$

Λ(1890) DECAY MODES

	Mode	Fraction (Γ_i/Γ)
Γ_1	$N\overline{K}$	20–35 %
Γ_2	$\Sigma\pi$	3–10 %
Γ_3	$\Sigma(1385)\pi$	seen
Γ_4	$\Sigma(1385)\pi$, P-wave	
Γ_5	$\Sigma(1385)\pi$, F-wave	
Γ_6	$N\overline{K}^*(892)$	seen
Γ_7	$N\overline{K}^*(892)$, S=1/2, P-wave	
Γ_8	$\Lambda\omega$	

The above branching fractions are our estimates, not fits or averages.

Λ(1890) BRANCHING RATIOS

See "Sign conventions for resonance couplings" in the Note on Λ and Σ Resonances.

$\Gamma(N\overline{K})/\Gamma_{total}$ Γ_1/Γ

VALUE	DOCUMENT ID		TECN	COMMENT
0.20 to 0.35 OUR ESTIMATE				
0.20±0.02	GOPAL	80	DPWA	$\overline{K}N \to \overline{K}N$
0.34±0.05	ALSTON-...	78	DPWA	$\overline{K}N \to \overline{K}N$
0.24±0.04	HEMINGWAY	75	DPWA	$K^-p \to \overline{K}N$
• • • We do not use the following data for averages, fits, limits, etc. • • •				
0.18±0.02	GOPAL	77	DPWA	See GOPAL 80
0.36 or 0.34	[1] MARTIN	77	DPWA	$\overline{K}N$ multichannel

$(\Gamma_i\Gamma_f)^{1/2}/\Gamma_{total}$ in $N\overline{K} \to \Lambda(1890) \to \Sigma\pi$ $(\Gamma_1\Gamma_2)^{1/2}/\Gamma$

VALUE	DOCUMENT ID		TECN	COMMENT
−0.09±0.03	GOPAL	77	DPWA	$\overline{K}N$ multichannel
• • • We do not use the following data for averages, fits, limits, etc. • • •				
+0.15 or +0.14	[1] MARTIN	77	DPWA	$\overline{K}N$ multichannel

$(\Gamma_i\Gamma_f)^{1/2}/\Gamma_{total}$ in $N\overline{K} \to \Lambda(1890) \to \Lambda\omega$ $(\Gamma_1\Gamma_8)^{1/2}/\Gamma$

VALUE	DOCUMENT ID		TECN	COMMENT
seen	BACCARI	77	IPWA	$K^-p \to \Lambda\omega$
0.032	[2] NAKKASYAN	75	DPWA	$K^-p \to \Lambda\omega$

$(\Gamma_i\Gamma_f)^{1/2}/\Gamma_{total}$ in $N\overline{K} \to \Lambda(1890) \to \Sigma(1385)\pi$, P-wave $(\Gamma_1\Gamma_4)^{1/2}/\Gamma$

VALUE	DOCUMENT ID		TECN	COMMENT
<0.03	CAMERON	78	DPWA	$K^-p \to \Sigma(1385)\pi$

$(\Gamma_i\Gamma_f)^{1/2}/\Gamma_{total}$ in $N\overline{K} \to \Lambda(1890) \to \Sigma(1385)\pi$, F-wave $(\Gamma_1\Gamma_5)^{1/2}/\Gamma$

VALUE	DOCUMENT ID		TECN	COMMENT
−0.126±0.055	[3] CAMERON	78	DPWA	$K^-p \to \Sigma(1385)\pi$

Baryon Particle Listings

Λ(1890), Λ(2000), Λ(2020)

$(\Gamma_i\Gamma_f)^{1/2}/\Gamma_{total}$ in $N\overline{K} \to \Lambda(1890) \to N\overline{K}^*(892)$ $(\Gamma_1\Gamma_6)^{1/2}/\Gamma$

VALUE	DOCUMENT ID		TECN	COMMENT
-0.07 ± 0.03	[3,4] CAMERON	78B	DPWA	$K^- p \to N\overline{K}^*$

Λ(1890) FOOTNOTES

[1] The two MARTIN 77 values are from a T-matrix pole and from a Breit-Wigner fit.
[2] Found in one of two best solutions.
[3] The published sign has been changed to be in accord with the baryon-first convention.
[4] Upper limits on the P_3 and F_3 waves are each 0.03.

Λ(1890) REFERENCES

PDG	82	PL 111B	M. Roos *et al.*	(HELS, CIT, CERN)
GOPAL	80	Toronto Conf. 159	G.P. Gopal	(RHEL) IJP
ALSTON-...	78	PR D18 182	M. Alston-Garnjost *et al.*	(LBL, MTHO+) IJP
Also	77	PRL 38 1007	M. Alston-Garnjost *et al.*	(LBL, MTHO+) IJP
CAMERON	78	NP B143 189	W. Cameron *et al.*	(RHEL, LOIC) IJP
CAMERON	78B	NP B146 327	W. Cameron *et al.*	(RHEL, LOIC) IJP
BACCARI	77	NC 41A 96	B. Baccari *et al.*	(SACL, CDEF) IJP
GOPAL	77	NP B119 362	G.P. Gopal *et al.*	(LOIC, RHEL) IJP
MARTIN	77	NP B127 349	B.R. Martin, M.K. Pidcock, R.G. Moorhouse	(LOUC+) IJP
Also	77B	NP B126 266	B.R. Martin, M.K. Pidcock	(LOUC)
Also	77C	NP B126 285	B.R. Martin, M.K. Pidcock	(LOUC) IJP
HEMINGWAY	75	NP B91 12	R.J. Hemingway *et al.*	(CERN, HEIDH, MPIM) IJP
NAKKASYAN	75	NP B93 85	A. Nakkasyan	(CERN) IJP

Λ(2000) $I(J^P) = 0(?^?)$ Status: *

OMITTED FROM SUMMARY TABLE

We list here all the ambiguous resonance possibilities with a mass around 2 GeV. The proposed quantum numbers are D_3 (BARBARO-GALTIERI 70 in $\Sigma\pi$), D_3+F_5, P_3+D_5, or P_1+D_3 (BRANDSTETTER 72 in $\Lambda\omega$), and S_1 (CAMERON 78B in $N\overline{K}^*$). The first two of the above analyses should now be considered obsolete. See also NAKKASYAN 75.

Λ(2000) MASS

VALUE (MeV)	DOCUMENT ID		TECN	COMMENT
≈ 2000 OUR ESTIMATE				
2030 ± 30	CAMERON	78B	DPWA	$K^- p \to N\overline{K}^*$
1935 to 1971	[1] BRANDSTET...	72	DPWA	$K^- p \to \Lambda\omega$
1951 to 2034	[1] BRANDSTET...	72	DPWA	$K^- p \to \Lambda\omega$
2010 ± 30	BARBARO-...	70	DPWA	$K^- p \to \Sigma\pi$

Λ(2000) WIDTH

VALUE (MeV)	DOCUMENT ID		TECN	COMMENT
125 ± 25	CAMERON	78B	DPWA	$K^- p \to N\overline{K}^*$
180 to 240	[1] BRANDSTET...	72	DPWA	(lower mass)
73 to 154	[1] BRANDSTET...	72	DPWA	(higher mass)
130 ± 50	BARBARO-...	70	DPWA	$K^- p \to \Sigma\pi$

Λ(2000) DECAY MODES

	Mode
Γ_1	$N\overline{K}$
Γ_2	$\Sigma\pi$
Γ_3	$\Lambda\omega$
Γ_4	$N\overline{K}^*(892)$, S=1/2, S-wave
Γ_5	$N\overline{K}^*(892)$, S=3/2, D-wave

Λ(2000) BRANCHING RATIOS

See "Sign conventions for resonance couplings" in the Note on Λ and Σ Resonances.

$(\Gamma_i\Gamma_f)^{1/2}/\Gamma_{total}$ in $N\overline{K} \to \Lambda(2000) \to \Sigma\pi$ $(\Gamma_1\Gamma_2)^{1/2}/\Gamma$

VALUE	DOCUMENT ID		TECN	COMMENT
-0.20 ± 0.04	BARBARO-...	70	DPWA	$K^- p \to \Sigma\pi$

$(\Gamma_i\Gamma_f)^{1/2}/\Gamma_{total}$ in $N\overline{K} \to \Lambda(2000) \to \Lambda\omega$ $(\Gamma_1\Gamma_3)^{1/2}/\Gamma$

VALUE	DOCUMENT ID		TECN	COMMENT
0.17 to 0.25	[1] BRANDSTET...	72	DPWA	(lower mass)
0.04 to 0.15	[1] BRANDSTET...	72	DPWA	(higher mass)

$(\Gamma_i\Gamma_f)^{1/2}/\Gamma_{total}$ in $N\overline{K} \to \Lambda(2000) \to N\overline{K}^*(892)$, S=1/2, S-wave $(\Gamma_1\Gamma_4)^{1/2}/\Gamma$

VALUE	DOCUMENT ID		TECN	COMMENT
-0.12 ± 0.03	[2] CAMERON	78B	DPWA	$K^- p \to N\overline{K}^*$

$(\Gamma_i\Gamma_f)^{1/2}/\Gamma_{total}$ in $N\overline{K} \to \Lambda(2000) \to N\overline{K}^*(892)$, S=3/2, D-wave $(\Gamma_1\Gamma_5)^{1/2}/\Gamma$

VALUE	DOCUMENT ID		TECN	COMMENT
$+0.09 \pm 0.03$	CAMERON	78B	DPWA	$K^- p \to N\overline{K}^*$

Λ(2000) FOOTNOTES

[1] The parameters quoted here are ranges from the three best fits; the lower state probably has $J \leq 3/2$, and the higher one probably has $J \leq 5/2$.
[2] The published sign has been changed to be in accord with the baryon-first convention.

Λ(2000) REFERENCES

CAMERON	78B	NP B146 327	W. Cameron *et al.*	(RHEL, LOIC) IJP
NAKKASYAN	75	NP B93 85	A. Nakkasyan	(CERN) IJP
BRANDSTET...	72	NP B39 13	A.A. Brandstetter *et al.*	(RHEL, CDEF+)
BARBARO-...	70	Duke Conf. 173 Hyperon Resonances, 1970	A. Barbaro-Galtieri	(LRL) IJP

Λ(2020) F_{07} $I(J^P) = 0(\frac{7}{2}^+)$ Status: *

OMITTED FROM SUMMARY TABLE

In LITCHFIELD 71, need for the state rests solely on a possibly inconsistent polarization measurement at 1.784 GeV/c. HEMINGWAY 75 does not require this state. GOPAL 77 does not need it in either $N\overline{K}$ or $\Sigma\pi$. With new $K^- n$ angular distributions included, DECLAIS 77 sees it. However, this and other new data are included in GOPAL 80 and the state is not required. BACCARI 77 weakly supports it.

Λ(2020) MASS

VALUE (MeV)	DOCUMENT ID		TECN	COMMENT
≈ 2020 OUR ESTIMATE				
2140	BACCARI	77	DPWA	$K^- p \to \Lambda\omega$
2117	DECLAIS	77	DPWA	$\overline{K}N \to \overline{K}N$
2100 ± 30	LITCHFIELD	71	DPWA	$K^- p \to \overline{K}N$
2020 ± 20	BARBARO-...	70	DPWA	$K^- p \to \Sigma\pi$

Λ(2020) WIDTH

VALUE (MeV)	DOCUMENT ID		TECN	COMMENT
128	BACCARI	77	DPWA	$K^- p \to \Lambda\omega$
167	DECLAIS	77	DPWA	$\overline{K}N \to \overline{K}N$
120 ± 30	LITCHFIELD	71	DPWA	$K^- p \to \overline{K}N$
160 ± 30	BARBARO-...	70	DPWA	$K^- p \to \Sigma\pi$

Λ(2020) DECAY MODES

	Mode
Γ_1	$N\overline{K}$
Γ_2	$\Sigma\pi$
Γ_3	$\Lambda\omega$

Λ(2020) BRANCHING RATIOS

See "Sign conventions for resonance couplings" in the Note on Λ and Σ Resonances.

$\Gamma(N\overline{K})/\Gamma_{total}$ Γ_1/Γ

VALUE	DOCUMENT ID		TECN	COMMENT
0.05	DECLAIS	77	DPWA	$\overline{K}N \to \overline{K}N$
0.05 ± 0.02	LITCHFIELD	71	DPWA	$K^- p \to \overline{K}N$

$(\Gamma_i\Gamma_f)^{1/2}/\Gamma_{total}$ in $N\overline{K} \to \Lambda(2020) \to \Sigma\pi$ $(\Gamma_1\Gamma_2)^{1/2}/\Gamma$

VALUE	DOCUMENT ID		TECN	COMMENT
-0.15 ± 0.02	BARBARO-...	70	DPWA	$K^- p \to \Sigma\pi$

$(\Gamma_i\Gamma_f)^{1/2}/\Gamma_{total}$ in $N\overline{K} \to \Lambda(2020) \to \Lambda\omega$ $(\Gamma_1\Gamma_3)^{1/2}/\Gamma$

VALUE	DOCUMENT ID		TECN	COMMENT
<0.05	BACCARI	77	DPWA	$K^- p \to \Lambda\omega$

Λ(2020) REFERENCES

GOPAL	80	Toronto Conf. 159	G.P. Gopal	(RHEL)
BACCARI	77	NC 41A 96	B. Baccari *et al.*	(SACL, CDEF) IJP
DECLAIS	77	CERN 77-16	Y. Declais *et al.*	(CAEN, CERN) IJP
GOPAL	77	NP B119 362	G.P. Gopal *et al.*	(LOIC, RHEL)
HEMINGWAY	75	NP B91 12	R.J. Hemingway *et al.*	(CERN, HEIDH, MPIM) IJP
LITCHFIELD	71	NP B30 125	P.J. Litchfield *et al.*	(RHEL, CDEF, SACL) IJP
BARBARO-...	70	Duke Conf. 173 Hyperon Resonances, 1970	A. Barbaro-Galtieri	(LRL) IJP

Λ(2100) G_{07}

$I(J^P) = 0(\frac{7}{2}^-)$ Status: ****

Discovered by COOL 66 and by WOHL 66. Most of the results published before 1973 are now obsolete and have been omitted. They may be found in our 1982 edition Physics Letters **111B** (1982).

This entry only includes results from partial-wave analyses. Parameters of peaks seen in cross sections and in invariant-mass distributions around 2100 MeV used to be listed in a separate entry immediately following. It may be found in our 1986 edition Physics Letters **170B** (1986).

Λ(2100) MASS

VALUE (MeV)	DOCUMENT ID		TECN	COMMENT
2090 to 2110 (≈ 2100) OUR ESTIMATE				
2104±10	GOPAL	80	DPWA	$\overline{K}N \to \overline{K}N$
2106±30	DEBELLEFON	78	DPWA	$\overline{K}N \to \overline{K}N$
2110±10	GOPAL	77	DPWA	$\overline{K}N$ multichannel
2105±10	HEMINGWAY	75	DPWA	$K^-p \to \overline{K}N$
2115±10	KANE	74	DPWA	$K^-p \to \Sigma\pi$
• • • We do not use the following data for averages, fits, limits, etc. • • •				
2094	BACCARI	77	DPWA	$K^-p \to \Lambda\omega$
2094	DECLAIS	77	DPWA	$\overline{K}N \to \overline{K}N$
2110 or 2089	[1] NAKKASYAN	75	DPWA	$K^-p \to \Lambda\omega$

Λ(2100) WIDTH

VALUE (MeV)	DOCUMENT ID		TECN	COMMENT
100 to 250 (≈ 200) OUR ESTIMATE				
157±40	DEBELLEFON	78	DPWA	$\overline{K}N \to \overline{K}N$
250±30	GOPAL	77	DPWA	$\overline{K}N$ multichannel
241±30	HEMINGWAY	75	DPWA	$K^-p \to \overline{K}N$
152±15	KANE	74	DPWA	$K^-p \to \Sigma\pi$
• • • We do not use the following data for averages, fits, limits, etc. • • •				
98	BACCARI	77	DPWA	$K^-p \to \Lambda\omega$
250	DECLAIS	77	DPWA	$\overline{K}N \to \overline{K}N$
244 or 302	[1] NAKKASYAN	75	DPWA	$K^-p \to \Lambda\omega$

Λ(2100) DECAY MODES

	Mode	Fraction (Γ_i/Γ)
Γ_1	$N\overline{K}$	25–35 %
Γ_2	$\Sigma\pi$	∼ 5 %
Γ_3	$\Lambda\eta$	<3 %
Γ_4	ΞK	<3 %
Γ_5	$\Lambda\omega$	<8 %
Γ_6	$N\overline{K}^*(892)$	10–20 %
Γ_7	$N\overline{K}^*(892)$, S=1/2, G-wave	
Γ_8	$N\overline{K}^*(892)$, S=3/2, D-wave	

The above branching fractions are our estimates, not fits or averages.

Λ(2100) BRANCHING RATIOS

See "Sign conventions for resonance couplings" in the Note on Λ and Σ Resonances.

$\Gamma(N\overline{K})/\Gamma_{total}$ Γ_1/Γ

VALUE	DOCUMENT ID		TECN	COMMENT
0.25 to 0.35 OUR ESTIMATE				
0.34±0.03	GOPAL	80	DPWA	$\overline{K}N \to \overline{K}N$
0.24±0.06	DEBELLEFON	78	DPWA	$\overline{K}N \to \overline{K}N$
0.31±0.03	HEMINGWAY	75	DPWA	$K^-p \to \overline{K}N$
• • • We do not use the following data for averages, fits, limits, etc. • • •				
0.29	DECLAIS	77	DPWA	$\overline{K}N \to \overline{K}N$
0.30±0.03	GOPAL	77	DPWA	See GOPAL 80

$(\Gamma_i\Gamma_f)^{1/2}/\Gamma_{total}$ in $N\overline{K} \to \Lambda(2100) \to \Sigma\pi$ $(\Gamma_1\Gamma_2)^{1/2}/\Gamma$

VALUE	DOCUMENT ID		TECN	COMMENT
+0.12±0.04	GOPAL	77	DPWA	$\overline{K}N$ multichannel
+0.11±0.01	KANE	74	DPWA	$K^-p \to \Sigma\pi$

$(\Gamma_i\Gamma_f)^{1/2}/\Gamma_{total}$ in $N\overline{K} \to \Lambda(2100) \to \Lambda\eta$ $(\Gamma_1\Gamma_3)^{1/2}/\Gamma$

VALUE	DOCUMENT ID		TECN	COMMENT
−0.050±0.020	RADER	73	MPWA	$K^-p \to \Lambda\eta$

$(\Gamma_i\Gamma_f)^{1/2}/\Gamma_{total}$ in $N\overline{K} \to \Lambda(2100) \to \Xi K$ $(\Gamma_1\Gamma_4)^{1/2}/\Gamma$

VALUE	DOCUMENT ID		TECN	COMMENT
0.035±0.018	LITCHFIELD	71	DPWA	$K^-p \to \Xi K$
• • • We do not use the following data for averages, fits, limits, etc. • • •				
0.003	MULLER	69B	DPWA	$K^-p \to \Xi K$
0.05	TRIPP	67	RVUE	$K^-p \to \Xi K$

$(\Gamma_i\Gamma_f)^{1/2}/\Gamma_{total}$ in $N\overline{K} \to \Lambda(2100) \to \Lambda\omega$ $(\Gamma_1\Gamma_5)^{1/2}/\Gamma$

VALUE	DOCUMENT ID		TECN	COMMENT
−0.070	[2] BACCARI	77	DPWA	GD_{37} wave
+0.011	[2] BACCARI	77	DPWA	GG_{17} wave
+0.008	[2] BACCARI	77	DPWA	GG_{37} wave
0.122 or 0.154	[1] NAKKASYAN	75	DPWA	$K^-p \to \Lambda\omega$

$(\Gamma_i\Gamma_f)^{1/2}/\Gamma_{total}$ in $N\overline{K} \to \Lambda(2100) \to N\overline{K}^*(892)$, S=3/2, D-wave $(\Gamma_1\Gamma_8)^{1/2}/\Gamma$

VALUE	DOCUMENT ID		TECN	COMMENT
+0.21±0.04	CAMERON	78B	DPWA	$K^-p \to N\overline{K}^*$

$(\Gamma_i\Gamma_f)^{1/2}/\Gamma_{total}$ in $N\overline{K} \to \Lambda(2100) \to N\overline{K}^*(892)$, S=1/2, G-wave $(\Gamma_1\Gamma_7)^{1/2}/\Gamma$

VALUE	DOCUMENT ID		TECN	COMMENT
−0.04±0.03	[3] CAMERON	78B	DPWA	$K^-p \to N\overline{K}^*$

Λ(2100) FOOTNOTES

[1] The NAKKASYAN 75 values are from the two best solutions found. Each has the Λ(2100) and one additional resonance (P_3 or F_5).

[2] Note that the three for BACCARI 77 entries are for three different waves.

[3] The published sign has been changed to be in accord with the baryon-first convention. The upper limit on the G_3 wave is 0.03.

Λ(2100) REFERENCES

PDG	86	PL 170B	M. Aguilar-Benitez *et al.*	(CERN, CIT+)
PDG	82	PL 111B	M. Roos *et al.*	(HELS, CIT, CERN)
GOPAL	80	Toronto Conf. 159	G.P. Gopal	(RHEL) IJP
CAMERON	78B	NP B146 327	W. Cameron *et al.*	(RHEL, LOIC) IJP
DEBELLEFON	78	NC 42A 403	A. de Bellefon *et al.*	(CDEF, SACL) IJP
BACCARI	77	NC 41A 96	B. Baccari *et al.*	(SACL, CDEF) IJP
DECLAIS	77	CERN 77-16	Y. Declais *et al.*	(CAEN, CERN) IJP
GOPAL	77	NP B119 362	G.P. Gopal *et al.*	(LOIC, RHEL) IJP
HEMINGWAY	75	NP B91 12	R.J. Hemingway *et al.*	(CERN, HEIDH, MPIM) IJP
NAKKASYAN	75	NP B93 85	A. Nakkasyan	(CERN) IJP
KANE	74	LBL-2452	D.F. Kane	(LBL) IJP
RADER	73	NC 16A 178	R.K. Rader *et al.*	(SACL, HEID, CERN+)
LITCHFIELD	71	NP B30 125	P.J. Litchfield *et al.*	(RHEL, CDEF, SACL) IJP
MULLER	69B	Thesis UCRL 19372	R.A. Muller	(LRL)
TRIPP	67	NP B3 10	R.D. Tripp *et al.*	(LRL, SLAC, CERN+)
COOL	66	PRL 16 1228	R.L. Cool *et al.*	(BNL)
WOHL	66	PRL 17 107	C.G. Wohl, F.T. Solmitz, M.L. Stevenson	(LRL) IJP

Λ(2110) F_{05}

$I(J^P) = 0(\frac{5}{2}^+)$ Status: ***

For results published before 1974 (they are now obsolete), see our 1982 edition Physics Letters **111B** (1982). All the references have been retained.

This resonance is in the Baryon Summary Table, but the evidence for it could be better.

Λ(2110) MASS

VALUE (MeV)	DOCUMENT ID		TECN	COMMENT
2090 to 2140 (≈ 2110) OUR ESTIMATE				
2092±25	GOPAL	80	DPWA	$\overline{K}N \to \overline{K}N$
2125±25	CAMERON	78B	DPWA	$K^-p \to N\overline{K}^*$
2106±50	DEBELLEFON	78	DPWA	$\overline{K}N \to \overline{K}N$
2140±20	DEBELLEFON	77	DPWA	$K^-p \to \Sigma\pi$
2100±50	GOPAL	77	DPWA	$\overline{K}N$ multichannel
2112± 7	KANE	74	DPWA	$K^-p \to \Sigma\pi$
• • • We do not use the following data for averages, fits, limits, etc. • • •				
2137	BACCARI	77	DPWA	$K^-p \to \Lambda\omega$
2103	[1] NAKKASYAN	75	DPWA	$K^-p \to \Lambda\omega$

Λ(2110) WIDTH

VALUE (MeV)	DOCUMENT ID		TECN	COMMENT
150 to 250 (≈ 200) OUR ESTIMATE				
245±25	GOPAL	80	DPWA	$\overline{K}N \to \overline{K}N$
160±30	CAMERON	78B	DPWA	$K^-p \to N\overline{K}^*$
251±50	DEBELLEFON	78	DPWA	$\overline{K}N \to \overline{K}N$
140±20	DEBELLEFON	77	DPWA	$K^-p \to \Sigma\pi$
200±50	GOPAL	77	DPWA	$\overline{K}N$ multichannel
190±30	KANE	74	DPWA	$K^-p \to \Sigma\pi$
• • • We do not use the following data for averages, fits, limits, etc. • • •				
132	BACCARI	77	DPWA	$K^-p \to \Lambda\omega$
391	[1] NAKKASYAN	75	DPWA	$K^-p \to \Lambda\omega$

Baryon Particle Listings

$\Lambda(2110)$, $\Lambda(2325)$, $\Lambda(2350)$

$\Lambda(2110)$ DECAY MODES

	Mode	Fraction (Γ_i/Γ)
Γ_1	$N\overline{K}$	5–25 %
Γ_2	$\Sigma\pi$	10–40 %
Γ_3	$\Lambda\omega$	seen
Γ_4	$\Sigma(1385)\pi$	seen
Γ_5	$\Sigma(1385)\pi$, P-wave	
Γ_6	$N\overline{K}^*(892)$	10–60 %
Γ_7	$N\overline{K}^*(892)$, S=1/2, F-wave	

The above branching fractions are our estimates, not fits or averages.

$\Lambda(2110)$ BRANCHING RATIOS

See "Sign conventions for resonance couplings" in the Note on Λ and Σ Resonances.

$\Gamma(N\overline{K})/\Gamma_{\text{total}}$ Γ_1/Γ

VALUE	DOCUMENT ID		TECN	COMMENT
0.05 to 0.25 OUR ESTIMATE				
0.07 ± 0.03	GOPAL	80	DPWA	$\overline{K}N\to\overline{K}N$
0.27 ± 0.06	[2] DEBELLEFON	78	DPWA	$\overline{K}N\to\overline{K}N$
• • • We do not use the following data for averages, fits, limits, etc. • • •				
0.07 ± 0.03	GOPAL	77	DPWA	See GOPAL 80

$(\Gamma_i\Gamma_f)^{1/2}/\Gamma_{\text{total}}$ in $N\overline{K}\to\Lambda(2110)\to\Sigma\pi$ $(\Gamma_1\Gamma_2)^{1/2}/\Gamma$

VALUE	DOCUMENT ID		TECN	COMMENT
$+0.14\pm0.01$	DEBELLEFON	77	DPWA	$K^-p\to\Sigma\pi$
$+0.20\pm0.03$	KANE	74	DPWA	$K^-p\to\Sigma\pi$
• • • We do not use the following data for averages, fits, limits, etc. • • •				
$+0.10\pm0.03$	GOPAL	77	DPWA	$\overline{K}N$ multichannel

$(\Gamma_i\Gamma_f)^{1/2}/\Gamma_{\text{total}}$ in $N\overline{K}\to\Lambda(2110)\to\Lambda\omega$ $(\Gamma_1\Gamma_3)^{1/2}/\Gamma$

VALUE	DOCUMENT ID		TECN	COMMENT
<0.05	BACCARI	77	DPWA	$K^-p\to\Lambda\omega$
0.112	[1] NAKKASYAN	75	DPWA	$K^-p\to\Lambda\omega$

$(\Gamma_i\Gamma_f)^{1/2}/\Gamma_{\text{total}}$ in $N\overline{K}\to\Lambda(2110)\to\Sigma(1385)\pi$ $(\Gamma_1\Gamma_4)^{1/2}/\Gamma$

VALUE	DOCUMENT ID		TECN	COMMENT
$+0.071\pm0.025$	[3] CAMERON	78	DPWA	$K^-p\to\Sigma(1385)\pi$

$(\Gamma_i\Gamma_f)^{1/2}/\Gamma_{\text{total}}$ in $N\overline{K}\to\Lambda(2110)\to N\overline{K}^*(892)$ $(\Gamma_1\Gamma_6)^{1/2}/\Gamma$

VALUE	DOCUMENT ID		TECN	COMMENT
-0.17 ± 0.04	[4] CAMERON	78B	DPWA	$K^-p\to N\overline{K}^*$

$\Lambda(2110)$ FOOTNOTES

[1] Found in one of two best solutions.
[2] The published error of 0.6 was a misprint.
[3] The CAMERON 78 upper limit on F-wave decay is 0.03. The sign here has been changed to be in accord with the baryon-first convention.
[4] The published sign has been changed to be in accord with the baryon-first convention. The CAMERON 78B upper limits on the P_3 and F_3 waves are each 0.03.

$\Lambda(2110)$ REFERENCES

PDG	82	PL 111B	M. Roos *et al.*	(HELS, CIT, CERN)
GOPAL	80	Toronto Conf. 159	G.P. Gopal	(RHEL) IJP
CAMERON	78	NP B143 189	W. Cameron *et al.*	(RHEL, LOIC) IJP
CAMERON	78B	NP B146 327	W. Cameron *et al.*	(RHEL, LOIC) IJP
DEBELLEFON	78	NC 42A 403	A. de Bellefon *et al.*	(CDEF, SACL) IJP
BACCARI	77	NC 41A 96	B. Baccari *et al.*	(SACL, CDEF) IJP
DEBELLEFON	77	NC 37A 175	A. de Bellefon *et al.*	(CDEF, SACL) IJP
GOPAL	77	NP B119 362	G.P. Gopal *et al.*	(LOIC, RHEL) IJP
NAKKASYAN	75	NP B93 85	A. Nakkasyan	(CERN) IJP
KANE	74	LBL-2452	D.F. Kane	(LBL) IJP

$\Lambda(2325)$ D_{03}

$I(J^P) = 0(\frac{3}{2}^-)$ Status: *

OMITTED FROM SUMMARY TABLE

BACCARI 77 finds this state with either $J^P = 3/2^-$ or $3/2^+$ in a energy-dependent partial-wave analyses of $K^-p\to\Lambda\omega$ from 2070 to 2436 MeV. A subsequent semi-energy-independent analysis from threshold to 2436 MeV selects $3/2^-$. DEBELLEFON 78 (same group) also sees this state in an energy-dependent partial-wave analysis of $K^-p\to\overline{K}N$ data, and finds $J^P = 3/2^-$ or $3/2^+$. They again prefer $J^P = 3/2^-$, but only on the basis of model-dependent considerations.

$\Lambda(2325)$ MASS

VALUE (MeV)	DOCUMENT ID		TECN	COMMENT
≈ 2325 OUR ESTIMATE				
2342 ± 30	DEBELLEFON	78	DPWA	$\overline{K}N\to\overline{K}N$
2327 ± 20	BACCARI	77	DPWA	$K^-p\to\Lambda\omega$

$\Lambda(2325)$ WIDTH

VALUE (MeV)	DOCUMENT ID		TECN	COMMENT
177 ± 40	DEBELLEFON	78	DPWA	$\overline{K}N\to\overline{K}N$
160 ± 40	BACCARI	77	IPWA	$K^-p\to\Lambda\omega$

$\Lambda(2325)$ DECAY MODES

	Mode
Γ_1	$N\overline{K}$
Γ_2	$\Lambda\omega$

$\Lambda(2325)$ BRANCHING RATIOS

$\Gamma(N\overline{K})/\Gamma_{\text{total}}$ Γ_1/Γ

VALUE	DOCUMENT ID		TECN	COMMENT
0.19 ± 0.06	DEBELLEFON	78	DPWA	$\overline{K}N\to\overline{K}N$

$(\Gamma_i\Gamma_f)^{1/2}/\Gamma_{\text{total}}$ in $N\overline{K}\to\Lambda(2325)\to\Lambda\omega$ $(\Gamma_1\Gamma_2)^{1/2}/\Gamma$

VALUE	DOCUMENT ID		TECN	COMMENT
0.06 ± 0.02	[1] BACCARI	77	IPWA	DS_{33} wave
0.05 ± 0.02	[1] BACCARI	77	DPWA	DD_{13} wave
0.08 ± 0.03	[1] BACCARI	77	DPWA	DD_{33} wave

$\Lambda(2325)$ FOOTNOTES

[1] Note that the three BACCARI 77 entries are for three different waves.

$\Lambda(2325)$ REFERENCES

DEBELLEFON	78	NC 42A 403	A. de Bellefon *et al.*	(CDEF, SACL) IJP
BACCARI	77	NC 41A 96	B. Baccari *et al.*	(SACL, CDEF) IJP

$\Lambda(2350)$ H_{09}

$I(J^P) = 0(\frac{9}{2}^+)$ Status: ***

DAUM 68 favors $J^P = 7/2^-$ or $9/2^+$. BRICMAN 70 favors $9/2^+$. LASINSKI 71 suggests three states in this region using a Pomeron + resonances model. There are now also three formation experiments from the College de France-Saclay group, DEBELLEFON 77, BACCARI 77, and DEBELLEFON 78, which find $9/2^+$ in energy-dependent partial-wave analyses of $\overline{K}N\to\Sigma\pi$, $\Lambda\omega$, and $N\overline{K}$.

$\Lambda(2350)$ MASS

VALUE (MeV)	DOCUMENT ID		TECN	COMMENT
2340 to 2370 (≈ 2350) OUR ESTIMATE				
2370 ± 50	DEBELLEFON	78	DPWA	$\overline{K}N\to\overline{K}N$
2365 ± 20	DEBELLEFON	77	DPWA	$K^-p\to\Sigma\pi$
2358 ± 6	BRICMAN	70	CNTR	Total, charge exchange
• • • We do not use the following data for averages, fits, limits, etc. • • •				
2372	BACCARI	77	DPWA	$K^-p\to\Lambda\omega$
2344 ± 15	COOL	70	CNTR	K^-p, K^-d total
2360 ± 20	LU	70	CNTR	$\gamma p\to K^+Y^*$
2340 ± 7	BUGG	68	CNTR	K^-p, K^-d total

Λ(2350) WIDTH

VALUE (MeV)	DOCUMENT ID		TECN	COMMENT
100 to 250 (≈ 150) OUR ESTIMATE				
204 ± 50	DEBELLEFON	78	DPWA	$\overline{K}N \rightarrow \overline{K}N$
110 ± 20	DEBELLEFON	77	DPWA	$K^- p \rightarrow \Sigma\pi$
324 ± 30	BRICMAN	70	CNTR	Total, charge exchange
• • • We do not use the following data for averages, fits, limits, etc. • • •				
257	BACCARI	77	DPWA	$K^- p \rightarrow \Lambda\omega$
190	COOL	70	CNTR	$K^- p$, $K^- d$ total
55	LU	70	CNTR	$\gamma p \rightarrow K^+ Y^*$
140 ± 20	BUGG	68	CNTR	$K^- p$, $K^- d$ total

Λ(2350) DECAY MODES

	Mode	Fraction (Γ_i/Γ)
Γ_1	$N\overline{K}$	~ 12 %
Γ_2	$\Sigma\pi$	~ 10 %
Γ_3	$\Lambda\omega$	

The above branching fractions are our estimates, not fits or averages.

Λ(2350) BRANCHING RATIOS

See "Sign conventions for resonance couplings" in the Note on Λ and Σ Resonances.

$\Gamma(N\overline{K})/\Gamma_{total}$ — **Γ_1/Γ**

VALUE	DOCUMENT ID		TECN	COMMENT
~ 0.12 OUR ESTIMATE				
0.12 ± 0.04	DEBELLEFON	78	DPWA	$\overline{K}N \rightarrow \overline{K}N$

$(\Gamma_i\Gamma_f)^{1/2}/\Gamma_{total}$ in $N\overline{K} \rightarrow \Lambda(2350) \rightarrow \Sigma\pi$ — **$(\Gamma_1\Gamma_2)^{1/2}/\Gamma$**

VALUE	DOCUMENT ID		TECN	COMMENT
− 0.11 ± 0.02	DEBELLEFON	77	DPWA	$K^- p \rightarrow \Sigma\pi$

$(\Gamma_i\Gamma_f)^{1/2}/\Gamma_{total}$ in $N\overline{K} \rightarrow \Lambda(2350) \rightarrow \Lambda\omega$ — **$(\Gamma_1\Gamma_3)^{1/2}/\Gamma$**

VALUE	DOCUMENT ID		TECN	COMMENT
< 0.05	BACCARI	77	DPWA	$K^- p \rightarrow \Lambda\omega$

Λ(2350) REFERENCES

DEBELLEFON	78	NC 42A 403	A. de Bellefon *et al.*	(CDEF, SACL) IJP
BACCARI	77	NC 41A 96	B. Baccari *et al.*	(SACL, CDEF) IJP
DEBELLEFON	77	NC 37A 175	A. de Bellefon *et al.*	(CDEF, SACL) IJP
LASINSKI	71	NP B29 125	T.A. Lasinski	(EFI) IJP
BRICMAN	70	PL 31B 152	C. Bricman *et al.*	(CERN, CAEN, SACL)
COOL	70	PR D1 1887	R.L. Cool *et al.*	(BNL) I
Also	66	PRL 16 1228	R.L. Cool *et al.*	(BNL) I
LU	70	PR D2 1846	D.C. Lu *et al.*	(YALE)
BUGG	68	PR 168 1466	D.V. Bugg *et al.*	(RHEL, BIRM, CAVE) I
DAUM	68	NP B7 19	C. Daum *et al.*	(CERN) JP

Λ(2585) Bumps

$I(J^P) = 0(?^?)$ Status: **

OMITTED FROM SUMMARY TABLE

Λ(2585) MASS (BUMPS)

VALUE (MeV)	DOCUMENT ID		TECN	COMMENT
≈ 2585 OUR ESTIMATE				
2585 ± 45	ABRAMS	70	CNTR	$K^- p$, $K^- d$ total
2530 ± 25	LU	70	CNTR	$\gamma p \rightarrow K^+ Y^*$

Λ(2585) WIDTH (BUMPS)

VALUE (MeV)	DOCUMENT ID		TECN	COMMENT
300	ABRAMS	70	CNTR	$K^- p$, $K^- d$ total
150	LU	70	CNTR	$\gamma p \rightarrow K^+ Y^*$

Λ(2585) DECAY MODES (BUMPS)

	Mode
Γ_1	$N\overline{K}$

Λ(2585) BRANCHING RATIOS (BUMPS)

$(J+\frac{1}{2})\times\Gamma(N\overline{K})/\Gamma_{total}$ — **Γ_1/Γ**

J is not known, so only $(J+\frac{1}{2}) \times \Gamma(N\overline{K})/\Gamma_{total}$ can be given.

VALUE	DOCUMENT ID		TECN	COMMENT
1	ABRAMS	70	CNTR	$K^- p$, $K^- d$ total
0.12 ± 0.12	[1] BRICMAN	70	CNTR	Total, charge exchange

Λ(2585) FOOTNOTES (BUMPS)

[1] The resonance is at the end of the region analyzed — no clear signal.

Λ(2585) REFERENCES (BUMPS)

ABRAMS	70	PR D1 1917	R.J. Abrams *et al.*	(BNL) I
Also	66	PRL 16 1228	R.L. Cool *et al.*	(BNL) I
BRICMAN	70	PL 31B 152	C. Bricman *et al.*	(CERN, CAEN, SACL)
LU	70	PR D2 1846	D.C. Lu *et al.*	(YALE)

Σ BARYONS
$(S = -1, I = 1)$

$\Sigma^+ = uus, \quad \Sigma^0 = uds, \quad \Sigma^- = dds$

Σ^+

$I(J^P) = 1(\frac{1}{2}^+)$ Status: ****

We have omitted some results that have been superseded by later experiments. See our earlier editions.

Σ^+ MASS

The fit uses Σ^+, Σ^0, Σ^-, and Λ mass and mass-difference measurements.

VALUE (MeV)	EVTS	DOCUMENT ID		TECN	COMMENT
1189.37 ± 0.07 OUR FIT	Error includes scale factor of 2.2.				
1189.37 ± 0.06 OUR AVERAGE	Error includes scale factor of 1.8. See the ideogram below.				
1189.33 ± 0.04	607	[1] BOHM	72	EMUL	
1189.16 ± 0.12		HYMAN	67	HEBC	
1189.61 ± 0.08	4205	SCHMIDT	65	HBC	See note with Λ mass
1189.48 ± 0.22	58	[2] BHOWMIK	64	EMUL	
1189.38 ± 0.15	144	[2] BARKAS	63	EMUL	

[1] BOHM 72 is updated with our 1973 K^-, π^-, and π^0 masses (Reviews of Modern Physics **45** No. 2 Pt. II (1973)).

[2] These masses have been raised 30 keV to take into account a 46 keV increase in the proton mass and a 21 keV decrease in the π^0 mass (note added 1967 edition, Reviews of Modern Physics **39** 1 (1967)).

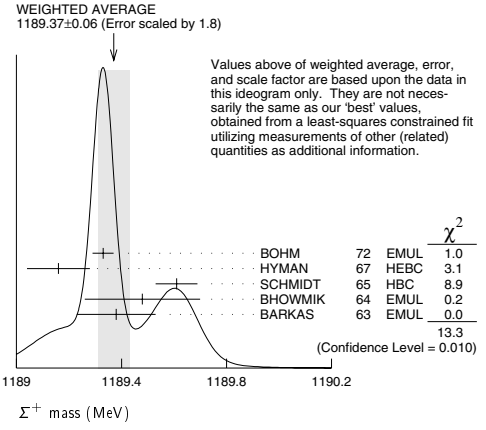

Σ^+ MEAN LIFE

Measurements with fewer than 1000 events have been omitted.

VALUE (10^{-10} s)	EVTS	DOCUMENT ID		TECN	COMMENT
0.8018 ± 0.0026 OUR AVERAGE					
0.8038 ± 0.0040 ± 0.0014		BARBOSA	00	E761	hyperons, 375 GeV
0.8043 ± 0.0080 ± 0.0014		[3] BARBOSA	00	E761	hyperons, 375 GeV
0.798 ± 0.005	30k	MARRAFFINO	80	HBC	K^-p 0.42–0.5 GeV/c
0.807 ± 0.013	5719	CONFORTO	76	HBC	K^-p 1–1.4 GeV/c
0.795 ± 0.010	20k	EISELE	70	HBC	K^-p at rest
0.803 ± 0.008	10664	BARLOUTAUD	69	HBC	K^-p 0.4–1.2 GeV/c
0.83 ± 0.032	1300	[4] CHANG	66	HBC	

[3] This is a measurement of the $\overline{\Sigma}^-$ lifetime. Here we assume *CPT* invariance; see below for the fractional Σ^+-$\overline{\Sigma}^-$ lifetime difference obtained by BARBOSA 00.

[4] We have increased the CHANG 66 error of 0.018; see our 1970 edition, Reviews of Modern Physics **42** No. 1 (1970).

$(\tau_{\Sigma^+} - \tau_{\overline{\Sigma}^-}) / \tau_{\Sigma^+}$

A test of *CPT* invariance.

VALUE	DOCUMENT ID		TECN	COMMENT
(−6 ± 12) × 10^{-4}	BARBOSA	00	E761	hyperons, 375 GeV

Σ^+ MAGNETIC MOMENT

See the "Note on Baryon Magnetic Moments" in the Λ Listings. Measurements with an error $\geq$ 0.1 μ_N have been omitted.

VALUE (μ_N)	EVTS	DOCUMENT ID		TECN	COMMENT
2.458 ± 0.010 OUR AVERAGE	Error includes scale factor of 2.1. See the ideogram below.				
2.4613 ± 0.0034 ± 0.0040	250k	MORELOS	93	SPEC	pCu 800 GeV
2.428 ± 0.036 ± 0.007	12k	[5] MORELOS	93	SPEC	pCu 800 GeV
2.479 ± 0.012 ± 0.022	137k	WILKINSON	87	SPEC	pBe 400 GeV
2.4040 ± 0.0198	44k	[6] ANKENBRA...	83	CNTR	pCu 400 GeV

[5] We assume *CPT* invariance: this is (minus) the $\overline{\Sigma}^-$ magnetic moment as measured by MORELOS 93. See below for the moment difference testing *CPT*.

[6] ANKENBRANDT 83 gives the value 2.38 ± 0.02μ_N. MORELOS 93 uses the same hyperon magnet and channel and claims to determine the field integral better, leading to the revised value given here.

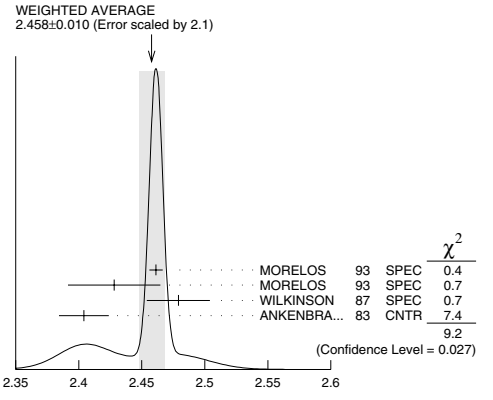

$(\mu_{\Sigma^+} + \mu_{\overline{\Sigma}^-}) / \mu_{\Sigma^+}$

A test of *CPT* invariance.

VALUE	DOCUMENT ID		TECN	COMMENT
0.014 ± 0.015	[7] MORELOS	93	SPEC	pCu 800 GeV

[7] This is our calculation from the MORELOS 93 measurements of the Σ^+ and $\overline{\Sigma}^-$ magnetic moments given above. The statistical error on $\mu_{\overline{\Sigma}^-}$ dominates the error here.

Σ^+ DECAY MODES

	Mode		Fraction (Γ_i/Γ)		Confidence level
Γ_1	$p\pi^0$		(51.57 ± 0.30) %		
Γ_2	$n\pi^+$		(48.31 ± 0.30) %		
Γ_3	$p\gamma$		(1.23 ± 0.05) × 10^{-3}		
Γ_4	$n\pi^+\gamma$	[a]	(4.5 ± 0.5) × 10^{-4}		
Γ_5	$\Lambda e^+\nu_e$		(2.0 ± 0.5) × 10^{-5}		
	$\Delta S = \Delta Q$ (SQ) violating modes or $\Delta S = 1$ weak neutral current ($S1$) modes				
Γ_6	$ne^+\nu_e$	SQ	< 5	× 10^{-6}	90%
Γ_7	$n\mu^+\nu_\mu$	SQ	< 3.0	× 10^{-5}	90%
Γ_8	pe^+e^-	$S1$	< 7	× 10^{-6}	

[a] See the Listings below for the pion momentum range used in this measurement.

CONSTRAINED FIT INFORMATION

An overall fit to 2 branching ratios uses 14 measurements and one constraint to determine 3 parameters. The overall fit has a χ^2 = 7.7 for 12 degrees of freedom.

The following *off-diagonal* array elements are the correlation coefficients $\langle \delta x_i \delta x_j \rangle / (\delta x_i \cdot \delta x_j)$, in percent, from the fit to the branching fractions, $x_i \equiv \Gamma_i/\Gamma_{\text{total}}$. The fit constrains the x_i whose labels appear in this array to sum to one.

x_2	−100		
x_3	12	−14	
	x_1	x_2	

Σ^+ BRANCHING RATIOS

$\Gamma(n\pi^+)/\Gamma(N\pi)$ $\Gamma_2/(\Gamma_1+\Gamma_2)$

VALUE	EVTS	DOCUMENT ID		TECN	COMMENT
0.4836±0.0030 OUR FIT					
0.4836±0.0030 OUR AVERAGE					
0.4828±0.0036	10k	[8] MARRAFFINO	80	HBC	K^-p 0.42–0.5 GeV/c
0.488 ±0.008	1861	NOWAK	78	HBC	
0.484 ±0.015	537	TOVEE	71	EMUL	
0.488 ±0.010	1331	BARLOUTAUD	69	HBC	K^-p 0.4–1.2 GeV/c
0.46 ±0.02	534	CHANG	66	HBC	
0.490 ±0.024	308	HUMPHREY	62	HBC	

[8] MARRAFFINO 80 actually gives $\Gamma(p\pi^0)/\Gamma(\text{total}) = 0.5172 \pm 0.0036$.

$\Gamma(p\gamma)/\Gamma(p\pi^0)$ Γ_3/Γ_1

VALUE (units 10^{-3})	EVTS	DOCUMENT ID		TECN	COMMENT
2.38±0.10 OUR FIT					
2.38±0.10 OUR AVERAGE					
2.32±0.11±0.10	32k	TIMM	95	E761	Σ^+ 375 GeV
$2.81\pm0.39^{+0.21}_{-0.43}$	408	HESSEY	89	CNTR	$K^-p \to \Sigma^+\pi^-$ at rest
2.52±0.28	190	[9] KOBAYASHI	87	CNTR	$\pi^+p \to \Sigma^+K^+$
$2.46^{+0.30}_{-0.35}$	155	BIAGI	85	CNTR	CERN hyperon beam
2.11±0.38	46	MANZ	80	HBC	$K^-p \to \Sigma^+\pi^-$
2.1 ±0.3	45	ANG	69B	HBC	K^-p at rest
2.76±0.51	31	GERSHWIN	69B	HBC	$K-p \to \Sigma^+\pi^-$
3.7 ±0.8	24	BAZIN	65	HBC	K^-p at rest

[9] KOBAYASHI 87 actually gives $\Gamma(p\gamma)/\Gamma(\text{total}) = (1.30 \pm 0.15) \times 10^{-3}$.

$\Gamma(n\pi^+\gamma)/\Gamma(n\pi^+)$ Γ_4/Γ_2

The π^+ momentum cuts differ, so we do not average the results but simply use the latest value in the Summary Table.

VALUE (units 10^{-3})	EVTS	DOCUMENT ID		TECN	COMMENT
0.93±0.10	180	EBENHOH	73	HBC	$\pi^+ < 150$ MeV/c
• • • We do not use the following data for averages, fits, limits, etc. • • •					
0.27±0.05	29	ANG	69B	HBC	$\pi^+ < 110$ MeV/c
~ 1.8		BAZIN	65B	HBC	$\pi^+ < 116$ MeV/c

$\Gamma(\Lambda e^+\nu_e)/\Gamma_{\text{total}}$ Γ_5/Γ

VALUE (units 10^{-5})	EVTS	DOCUMENT ID		TECN	COMMENT
2.0±0.5 OUR AVERAGE					
1.6±0.7	5	BALTAY	69	HBC	K^-p at rest
2.9±1.0	10	EISELE	69	HBC	K^-p at rest
2.0±0.8	6	BARASH	67	HBC	K^-p at rest

$\Gamma(ne^+\nu_e)/\Gamma(n\pi^+)$ Γ_6/Γ_2

Test of $\Delta S = \Delta Q$ rule. Experiments with an effective denominator less than 100,000 have been omitted.

EFFECTIVE DENOM.	EVTS	DOCUMENT ID		TECN	COMMENT
< 1.1 × 10^{-5} OUR LIMIT Our 90% CL limit = (2.3 events)/(effective denominator sum). [Number of events increased to 2.3 for a 90% confidence level.]					
111000	0	[10] EBENHOH	74	HBC	K^-p at rest
105000	0	[10] SECHI-ZORN	73	HBC	K^-p at rest

[10] Effective denominator calculated by us.

$\Gamma(n\mu^+\nu_\mu)/\Gamma(n\pi^+)$ Γ_7/Γ_2

Test of $\Delta S = \Delta Q$ rule.

EFFECTIVE DENOM.	EVTS	DOCUMENT ID		TECN
< 6.2 × 10^{-5} OUR LIMIT Our 90% CL limit = (6.7 events)/(effective denominator sum). [Number of events increased to 6.7 for a 90% confidence level.]				
33800	0	BAGGETT	69B	HBC
62000	2	[11] EISELE	69B	HBC
10150	0	[12] COURANT	64	HBC
1710	0	[12] NAUENBERG	64	HBC
120	1	GALTIERI	62	EMUL

[11] Effective denominator calculated by us.
[12] Effective denominator taken from EISELE 67.

$\Gamma(pe^+e^-)/\Gamma_{\text{total}}$ Γ_8/Γ

VALUE (units 10^{-6})	DOCUMENT ID		TECN	COMMENT
<7	[13] ANG	69B	HBC	K^-p at rest

[13] ANG 69B found three pe^+e^- events in agreement with $\gamma \to e^+e^-$ conversion from $\Sigma^+ \to p\gamma$. The limit given here is for neutral currents.

$\Gamma(\Sigma^+ \to ne^+\nu_e)/\Gamma(\Sigma^- \to ne^-\overline{\nu}_e)$

VALUE	CL%	EVTS	DOCUMENT ID		TECN	COMMENT
<0.009 OUR LIMIT Our 90% CL limit, using $\Gamma(ne^+\nu_e)/\Gamma(n\pi^+)$ above.						
• • • We do not use the following data for averages, fits, limits, etc. • • •						
<0.019	90	0	EBENHOH	74	HBC	K^-p at rest
<0.018	90	0	SECHI-ZORN	73	HBC	K^-p at rest
<0.12	95	0	COLE	71	HBC	K^-p at rest
<0.03	90	0	EISELE	69B	HBC	See EBENHOH 74

$\Gamma(\Sigma^+ \to n\mu^+\nu_\mu)/\Gamma(\Sigma^- \to n\mu^-\overline{\nu}_\mu)$

VALUE	EVTS	DOCUMENT ID		TECN	COMMENT
<0.12 OUR LIMIT Our 90% CL limit, using $\Gamma(n\mu^+\nu_\mu)/\Gamma(n\pi^+)$ above.					
• • • We do not use the following data for averages, fits, limits, etc. • • •					
$0.06^{+0.045}_{-0.03}$	2	EISELE	69B	HBC	K^-p at rest

$\Gamma(\Sigma^+ \to n\ell^+\nu)/\Gamma(\Sigma^- \to n\ell^-\overline{\nu})$

Test of $\Delta S = \Delta Q$ rule.

VALUE	EVTS	DOCUMENT ID		TECN
<0.043 OUR LIMIT Our 90% CL limit, using $\left[\Gamma(ne^+\nu_e) + \Gamma(n\mu^+\nu_\mu)\right]/\Gamma(n\pi^+)$.				
• • • We do not use the following data for averages, fits, limits, etc. • • •				
<0.08	1	NORTON	69	HBC
<0.034	0	BAGGETT	67	HBC

Σ^+ DECAY PARAMETERS

See the "Note on Baryon Decay Parameters" in the neutron Listings. A few early results have been omitted.

α_0 FOR $\Sigma^+ \to p\pi^0$

VALUE	EVTS	DOCUMENT ID		TECN	COMMENT
$\mathbf{-0.980^{+0.017}_{-0.015}}$ **OUR FIT**					
$\mathbf{-0.980^{+0.017}_{-0.013}}$ **OUR AVERAGE**					
$-0.945^{+0.055}_{-0.042}$	1259	[14] LIPMAN	73	OSPK	$\pi^+p \to \Sigma^+$
−0.940±0.045	16k	BELLAMY	72	ASPK	$\pi^+p \to \Sigma^+K^+$
$-0.98^{+0.05}_{-0.02}$	1335	[15] HARRIS	70	OSPK	$\pi^+p \to \Sigma^+K^+$
−0.999±0.022	32k	BANGERTER	69	HBC	K^-p 0.4 GeV/c

[14] Decay protons scattered off aluminum.
[15] Decay protons scattered off carbon.

ϕ_0 ANGLE FOR $\Sigma^+ \to p\pi^0$ $(\tan\phi_0 = \beta/\gamma)$

VALUE (°)	EVTS	DOCUMENT ID		TECN	COMMENT
36 ±34 OUR AVERAGE					
$38.1^{+35.7}_{-37.1}$	1259	[16] LIPMAN	73	OSPK	$\pi^+p \to \Sigma^+K^+$
22 ±90		[17] HARRIS	70	OSPK	$\pi^+p \to \Sigma^+K^+$

[16] Decay proton scattered off aluminum.
[17] Decay protons scattered off carbon.

α_+ / α_0

Older results have been omitted.

VALUE	EVTS	DOCUMENT ID		TECN	COMMENT
−0.069±0.013 OUR FIT					
−0.073±0.021	23k	MARRAFFINO	80	HBC	K^-p 0.42–0.5 GeV/c

α_+ FOR $\Sigma^+ \to n\pi^+$

VALUE	EVTS	DOCUMENT ID		TECN	COMMENT
0.068±0.013 OUR FIT					
0.066±0.016 OUR AVERAGE					
0.037±0.049	4101	BERLEY	70B	HBC	
0.069±0.017	35k	BANGERTER	69	HBC	K^-p 0.4 GeV/c

ϕ_+ ANGLE FOR $\Sigma^+ \to n\pi^+$ $(\tan\phi_+ = \beta/\gamma)$

VALUE (°)	EVTS	DOCUMENT ID		TECN	COMMENT
167±20 OUR AVERAGE Error includes scale factor of 1.1.					
184±24	1054	[18] BERLEY	70B	HBC	
143±29	560	BANGERTER	69B	HBC	K^-p 0.4 GeV/c

[18] Changed from 176 to 184° to agree with our sign convention.

α_γ FOR $\Sigma^+ \to p\gamma$

VALUE	EVTS	DOCUMENT ID		TECN	COMMENT
−0.76 ±0.08 OUR AVERAGE					
−0.720±0.086±0.045	35k	[19] FOUCHER	92	SPEC	Σ^+ 375 GeV
−0.86 ±0.13 ±0.04	190	KOBAYASHI	87	CNTR	$\pi^+p \to \Sigma^+K^+$
$-0.53^{+0.38}_{-0.36}$	46	MANZ	80	HBC	$K^-p \to \Sigma^+\pi^-$
$-1.03^{+0.52}_{-0.42}$	61	GERSHWIN	69B	HBC	$K^-p \to \Sigma^+\pi^-$

[19] See TIMM 95 for a detailed description of the analysis.

Σ^+ REFERENCES

We have omitted some papers that have been superseded by later experiments. See our earlier editions.

BARBOSA	00	PR D61 031101R	R.F. Barbosa *et al.*	(FNAL E761 Collab.)
TIMM	95	PR D51 4638	S. Timm *et al.*	(FNAL E761 Collab.)
MORELOS	93	PRL 71 3417	A. Morelos *et al.*	(FNAL E761 Collab.)
FOUCHER	92	PRL 68 3004	M. Foucher *et al.*	(FNAL E761 Collab.)
HESSEY	89	ZPHY C42 175	N.P. Hessey *et al.*	(BNL-811 Collab.)
KOBAYASHI	87	PRL 59 868	M. Kobayashi *et al.*	(KYOT)
WILKINSON	87	PRL 58 855	C.A. Wilkinson *et al.*	(WISC, MICH, RUTG+)
BIAGI	85	ZPHY C28 495	S.F. Biagi *et al.*	(CERN WA62 Collab.)
ANKENBRA...	83	PRL 51 863	C.M. Ankenbrandt *et al.*	(FNAL, IOWA, ISU+)
MANZ	80	PL 96B 217	A. Manz *et al.*	(MPIM, VAND)
MARRAFFINO	80	PR D21 2501	J. Marraffino *et al.*	(VAND, MPIM)
NOWAK	78	NP B139 61	R.J. Nowak *et al.*	(LOUC, BELG, DURH+)
CONFORTO	76	NP B105 189	B. Conforto *et al.*	(RHEL, LOIC)
EBENHOH	74	ZPHY 266 367	H. Ebenhoh *et al.*	(HEIDT)
EBENHOH	73	ZPHY 264 413	W. Ebenhoh *et al.*	(HEIDT)
LIPMAN	73	PL 43B 89	N.H. Lipman *et al.*	(RHEL, SUSS, LOWC)
PDG	73	RMP 45 No. 2 Pt. II	T.A. Lasinski *et al.*	(LBL, BRAN, CERN+)
SECHI-ZORN	73	PR D8 12	B. Sechi-Zorn, G.A. Snow	(UMD)
BELLAMY	72	PL 39B 299	E.H. Bellamy *et al.*	(LOWC, RHEL, SUSS)
BOHM	72	NP B48 1	G. Bohm *et al.*	(BERL, KIDR, BRUX, IASD+)
Also	73	IIHE-73.2 Nov	G. Bohm	(BERL, KIDR, BRUX, IASD, DUUC+)
COLE	71	PR D4 631	J. Cole *et al.*	(STON, COLU)
TOVEE	71	NP B33 493	D.N. Tovee *et al.*	(LOUC, KIDR, BERL+)
BERLEY	70B	PR D1 2015	D. Berley *et al.*	(BNL, MASA, YALE)
EISELE	70	ZPHY 238 372	F. Eisele *et al.*	(HEID)
HARRIS	70	PRL 24 165	F. Harris *et al.*	(MICH, WISC)
PDG	70	RMP 42 No. 1	A. Barbaro-Galtieri *et al.*	(LRL, BRAN+)
ANG	69B	ZPHY 228 151	G. Ang *et al.*	(HEID)
BAGGETT	69B	Thesis MDDP-TR-973	N.V. Baggett	(UMD)
BALTAY	69	PRL 22 615	C. Baltay *et al.*	(COLU, STON)
BANGERTER	69	Thesis UCRL 19244	R.O. Bangerter	(LRL)
BANGERTER	69B	PR 187 1821	R.O. Bangerter *et al.*	(LRL)
BARLOUTAUD	69	NP B14 153	R. Barloutaud *et al.*	(SACL, CERN, HEID)
EISELE	69	ZPHY 221 1	F. Eisele *et al.*	(HEID)
Also	64	PRL 13 291	W. Willis *et al.*	(BNL, CERN, HEID, UMD)
EISELE	69B	ZPHY 221 401	F. Eisele *et al.*	(HEID)
GERSHWIN	69B	PR 188 2077	L.K. Gershwin *et al.*	(LRL)
Also	69	Thesis UCRL 19246	L.K. Gershwin	(LRL)
NORTON	69	Thesis Nevis 175	H. Norton	(COLU)
BAGGETT	67	PRL 19 1458	N. Baggett *et al.*	(UMD)
Also	68	Vienna Abs. 374	N.V. Baggett, B. Kehoe	(UMD)
Also	68B	Private Comm.	N.V. Baggett	(UMD)
BARASH	67	PRL 19 181	N. Barash *et al.*	(UMD)
EISELE	67	ZPHY 205 409	F. Eisele *et al.*	(HEID)
HYMAN	67	PL 25B 376	L.G. Hyman *et al.*	(ANL, CMU, NWES)
PDG	67	RMP 39 1	A.H. Rosenfeld *et al.*	(LRL, CERN, YALE)
CHANG	66	PR 151 1081	C.Y. Chang	(COLU)
Also	65	Thesis Nevis 145	C.Y. Chang	(COLU)
BAZIN	65	PRL 14 154	M. Bazin *et al.*	(PRIN, COLU)
BAZIN	65B	PR 140B 1358	M. Bazin *et al.*	(PRIN, RUTG, COLU)
SCHMIDT	65	PR 140B 1328	P. Schmidt	(COLU)
BHOWMIK	64	NP 53 22	B. Bhowmik *et al.*	(DELH)
COURANT	64	PR 136B 1791	H. Courant *et al.*	(CERN, HEID, UMD+)
NAUENBERG	64	PRL 12 679	U. Nauenberg *et al.*	(COLU, RUTG, PRIN)
BARKAS	63	PRL 11 26	W.H. Barkas, J.N. Dyer, H.H. Heckman	(LRL)
Also	61	Thesis UCRL 9450	J.N. Dyer	(LRL)
GALTIERI	62	PRL 9 26	A. Barbaro-Galtieri *et al.*	(LRL)
HUMPHREY	62	PR 127 1305	W.E. Humphrey, R.R. Ross	(LRL)

Σ^0

$I(J^P) = 1(\frac{1}{2}^+)$ Status: ****

COURANT 63 and ALFF-STEINBERGER 65, using $\Sigma^0 \to \Lambda e^+ e^-$ decays (Dalitz decays), determined the Σ^0 parity to be positive, given that $J = 1/2$ and that certain very reasonable assumptions about form factors are true. The results of experiments involving the Primakoff effect, from which the Σ^0 mean life and $\Sigma^0 \to \Lambda$ transition magnetic moment come (see below), strongly support $J = 1/2$.

Σ^0 MASS

The fit uses Σ^+, Σ^0, Σ^-, and Λ mass and mass-difference measurements.

VALUE (MeV)	EVTS	DOCUMENT ID	TECN	COMMENT
1192.642 ± 0.024 OUR FIT				
• • • We do not use the following data for averages, fits, limits, etc. • • •				
1192.65 ± 0.020 ± 0.014	3327	[1] WANG	97 SPEC	$\Sigma^0 \to \Lambda\gamma \to (p\pi^-)(e^+e^-)$

[1] This WANG 97 result is redundant with the Σ^0-Λ mass-difference measurement below.

$m_{\Sigma^-} - m_{\Sigma^0}$

VALUE (MeV)	EVTS	DOCUMENT ID	TECN	COMMENT
4.807 ± 0.035 OUR FIT Error includes scale factor of 1.1.				
4.86 ± 0.08 OUR AVERAGE Error includes scale factor of 1.2.				
4.87 ± 0.12	37	DOSCH	65 HBC	
5.01 ± 0.12	12	SCHMIDT	65 HBC	See note with Λ mass
4.75 ± 0.1	18	BURNSTEIN	64 HBC	

$m_{\Sigma^0} - m_{\Lambda}$

VALUE (MeV)	EVTS	DOCUMENT ID	TECN	COMMENT
76.959 ± 0.023 OUR FIT				
76.966 ± 0.020 ± 0.013	3327	WANG	97 SPEC	$\Sigma^0 \to \Lambda\gamma \to (p\pi^-)(e^+e^-)$
• • • We do not use the following data for averages, fits, limits, etc. • • •				
76.23 ± 0.55	109	COLAS	75 HLBC	$\Sigma^0 \to \Lambda\gamma$
76.63 ± 0.28	208	SCHMIDT	65 HBC	See note with Λ mass

Σ^0 MEAN LIFE

These lifetimes are deduced from measurements of the cross sections for the Primakoff process $\Lambda \to \Sigma^0$ in nuclear Coulomb fields. An alternative expression of the same information is the Σ^0-Λ transition magnetic moment given in the following section. The relation is $(\mu_{\Sigma\Lambda}/\mu_N)^2\,\tau = 1.92951 \times 10^{-19}$ s (see DEVLIN 86).

VALUE (10^{-20} s)	DOCUMENT ID		TECN	COMMENT
7.4 ± 0.7 OUR EVALUATION Using $\mu_{\Sigma\Lambda}$ (see the above note).				
$6.5^{+1.7}_{-1.1}$	[2] DEVLIN	86	SPEC	Primakoff effect
7.6 ± 0.5 ± 0.7	[3] PETERSEN	86	SPEC	Primakoff effect
• • • We do not use the following data for averages, fits, limits, etc. • • •				
5.8 ± 1.3	[2] DYDAK	77	SPEC	See DEVLIN 86

[2] DEVLIN 86 is a recalculation of the results of DYDAK 77 removing a numerical approximation made in that work.
[3] An additional uncertainty of the Primakoff formalism is estimated to be < 5%.

$|\mu(\Sigma^0 \to \Lambda)|$ TRANSITION MAGNETIC MOMENT

See the note in the Σ^0 mean-life section above. Also, see the "Note on Baryon Magnetic Moments" in the Λ Listings.

VALUE (μ_N)	DOCUMENT ID		TECN	COMMENT
1.61 ± 0.08 OUR AVERAGE				
$1.72^{+0.17}_{-0.19}$	[4] DEVLIN	86	SPEC	Primakoff effect
1.59 ± 0.05 ± 0.07	[5] PETERSEN	86	SPEC	Primakoff effect
• • • We do not use the following data for averages, fits, limits, etc. • • •				
$1.82^{+0.25}_{-0.18}$	[4] DYDAK	77	SPEC	See DEVLIN 86

[4] DEVLIN 86 is a recalculation of the results of DYDAK 77 removing a numerical approximation made in that work.
[5] An additional uncertainty of the Primakoff formalism is estimated to be < 2.5%.

Σ^0 DECAY MODES

	Mode	Fraction (Γ_i/Γ)	Confidence level
Γ_1	$\Lambda\gamma$	100 %	
Γ_2	$\Lambda\gamma\gamma$	< 3 %	90%
Γ_3	$\Lambda e^+ e^-$	[a] 5×10^{-3}	

[a] A theoretical value using QED.

Σ^0 BRANCHING RATIOS

$\Gamma(\Lambda\gamma\gamma)/\Gamma_{total}$ Γ_2/Γ

VALUE	CL%	DOCUMENT ID		TECN
< 0.03	90	COLAS	75	HLBC

$\Gamma(\Lambda e^+ e^-)/\Gamma_{total}$ Γ_3/Γ

See COURANT 63 and ALFF-STEINBERGER 65 for measurements of the invariant-mass spectrum of the Dalitz pairs.

VALUE	DOCUMENT ID		COMMENT
0.00545	FEINBERG	58	Theoretical QED calculation

Σ^0 REFERENCES

WANG	97	PR D56 2544	M.H.L.S. Wang *et al.*	(BNL-E766 Collab.)
DEVLIN	86	PR D34 1626	T. Devlin, P.C. Petersen, A. Beretvas	(RUTG)
PETERSEN	86	PRL 57 949	P.C. Petersen *et al.*	(RUTG, WISC, MICH+)
DYDAK	77	NP B118 1	F. Dydak *et al.*	(CERN, DORT, HEIDH)
COLAS	75	NP B91 253	J. Colas *et al.*	(ORSAY)
ALFF-...	65	PR 137B 1105	C. Alff-Steinberger *et al.*	(COLU, RUTG+) P
DOSCH	65	PL 14 239	H.C. Dosch *et al.*	(HEID)
SCHMIDT	65	PR 140B 1328	P. Schmidt	(COLU)
BURNSTEIN	64	PRL 13 66	R.A. Burnstein *et al.*	(UMD)
COURANT	63	PRL 10 409	H. Courant *et al.*	(CERN, UMD) P
FEINBERG	58	PR 109 1019	G. Feinberg	(BNL)

Σ^- $I(J^P) = 1(\frac{1}{2}^+)$ Status: ****

We have omitted some results that have been superseded by later experiments. See our earlier editions.

Σ^- MASS

The fit uses Σ^+, Σ^0, Σ^-, and Λ mass and mass-difference measurements.

VALUE (MeV)	EVTS	DOCUMENT ID		TECN	COMMENT
1197.449±0.030 OUR FIT	Error includes scale factor of 1.2.				
1197.45 ±0.04 OUR AVERAGE	Error includes scale factor of 1.2.				
1197.417±0.040		GUREV	93	SPEC	Σ^- C atom, crystal diff.
1197.532±0.057		GALL	88	CNTR	Σ^- Pb, Σ^- W atoms
1197.43 ±0.08	3000	SCHMIDT	65	HBC	See note with Λ mass
• • • We do not use the following data for averages, fits, limits, etc. • • •					
1197.24 ±0.15		[1] DUGAN	75	CNTR	Exotic atoms

[1] GALL 88 concludes that the DUGAN 75 mass needs to be reevaluated.

$m_{\Sigma^-} - m_{\Sigma^+}$

VALUE (MeV)	EVTS	DOCUMENT ID	TECN
8.08±0.08 OUR FIT	Error includes scale factor of 1.9.		
8.09±0.16 OUR AVERAGE			
7.91±0.23	86	BOHM	72 EMUL
8.25±0.25	2500	DOSCH	65 HBC
8.25±0.40	87	BARKAS	63 EMUL

$m_{\Sigma^-} - m_{\Lambda}$

VALUE (MeV)	EVTS	DOCUMENT ID		TECN	COMMENT
81.766±0.030 OUR FIT	Error includes scale factor of 1.2.				
81.69 ±0.07 OUR AVERAGE					
81.64 ±0.09	2279	HEPP	68	HBC	
81.80 ±0.13	85	SCHMIDT	65	HBC	See note with Λ mass
81.70 ±0.19		BURNSTEIN	64	HBC	

Σ^- MEAN LIFE

Measurements with an error $\geq 0.2 \times 10^{-10}$ s have been omitted.

VALUE (10^{-10} s)	EVTS	DOCUMENT ID		TECN	COMMENT
1.479±0.011 OUR AVERAGE	Error includes scale factor of 1.3. See the ideogram below.				
1.480±0.014	16k	MARRAFFINO	80	HBC	K^-p 0.42–0.5 GeV/c
1.49 ±0.03	8437	CONFORTO	76	HBC	K^-p 1–1.4 GeV/c
1.463±0.039	2400	ROBERTSON	72	HBC	K^-p 0.25 GeV/c
1.42 ±0.05	1383	BAKKER	71	DBC	$K^-N \to \Sigma^-\pi\pi$
$1.41\ ^{+0.09}_{-0.08}$		TOVEE	71	EMUL	
1.485±0.022	100k	EISELE	70	HBC	K^-p at rest
1.472±0.016	10k	BARLOUTAUD	69	HBC	K^-p 0.4–1.2 GeV/c
1.38 ±0.07	506	WHITESIDE	68	HBC	K^-p at rest
1.666±0.075	3267	[2] CHANG	66	HBC	K^-p at rest
1.58 ±0.06	1208	HUMPHREY	62	HBC	K^-p at rest

[2] We have increased the CHANG 66 error of 0.018; see our 1970 edition, Reviews of Modern Physics **42** No. 1 (1970).

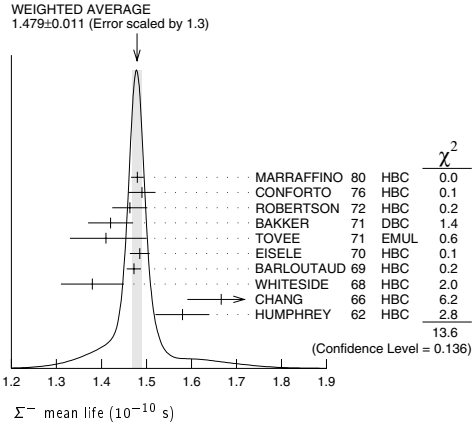

Σ^- mean life (10^{-10} s)

Σ^- MAGNETIC MOMENT

See the "Note on Baryon Magnetic Moments" in the Λ Listings. Measurements with an error ≥ 0.3 μ_N have been omitted.

VALUE (μ_N)	EVTS	DOCUMENT ID		TECN	COMMENT
−1.160±0.025 OUR AVERAGE	Error includes scale factor of 1.7. See the ideogram below.				
−1.105±0.029±0.010		HERTZOG	88	CNTR	Σ^- Pb, Σ^- W atoms
−1.166±0.014±0.010	671k	ZAPALAC	86	SPEC	$ne^-\nu$, $n\pi^-$ decays
−1.23 ±0.03 ±0.03		WAH	85	CNTR	p Cu → Σ^- X
• • • We do not use the following data for averages, fits, limits, etc. • • •					
−0.89 ±0.14	516k	DECK	83	SPEC	p Be → Σ^- X

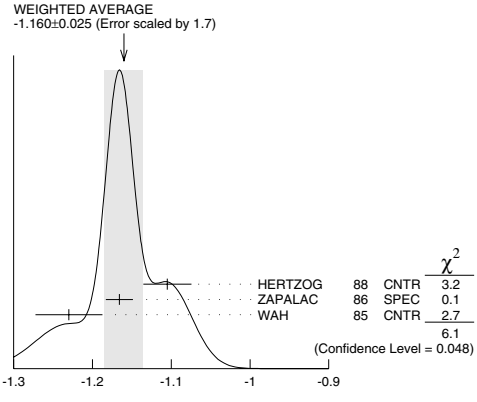

Σ^- magnetic moment (μ_N)

Σ^- CHARGE RADIUS

VALUE (fm)	DOCUMENT ID		TECN	COMMENT
0.780±0.080±0.060	[3] ESCHRICH	01	SELX	$\Sigma^-e \to \Sigma^-e$

[3] ESCHRICH 01 actually gives $\langle r^2 \rangle = (0.61 \pm 0.12 \pm 0.09)$ fm^2.

Σ^- DECAY MODES

	Mode	Fraction (Γ_i/Γ)
Γ_1	$n\pi^-$	(99.848±0.005) %
Γ_2	$n\pi^-\gamma$	[a] (4.6 ±0.6) × 10^{-4}
Γ_3	$ne^-\overline{\nu}_e$	(1.017±0.034) × 10^{-3}
Γ_4	$n\mu^-\overline{\nu}_\mu$	(4.5 ±0.4) × 10^{-4}
Γ_5	$\Lambda e^-\overline{\nu}_e$	(5.73 ±0.27) × 10^{-5}

[a] See the Listings below for the pion momentum range used in this measurement.

CONSTRAINED FIT INFORMATION

An overall fit to 3 branching ratios uses 16 measurements and one constraint to determine 4 parameters. The overall fit has a $\chi^2 = 8.7$ for 13 degrees of freedom.

The following *off-diagonal* array elements are the correlation coefficients $\langle \delta x_i \delta x_j \rangle / (\delta x_i \cdot \delta x_j)$, in percent, from the fit to the branching fractions, $x_i \equiv \Gamma_i/\Gamma_{\text{total}}$. The fit constrains the x_i whose labels appear in this array to sum to one.

	x_1	x_3	x_4
x_3	−64		
x_4	−77	0	
x_5	−5	0	0

Σ^- BRANCHING RATIOS

$\Gamma(n\pi^-\gamma)/\Gamma(n\pi^-)$ Γ_2/Γ_1

The π^+ momentum cuts differ, so we do not average the results but simply use the latest value for the Summary Table.

VALUE (units 10^{-3})	EVTS	DOCUMENT ID		TECN	COMMENT
0.46±0.06	292	EBENHOH	73	HBC	$\pi^+ < 150$ MeV/c
• • • We do not use the following data for averages, fits, limits, etc. • • •					
0.10±0.02	23	ANG	69B	HBC	$\pi^- < 110$ MeV/c
~ 1.1		BAZIN	65B	HBC	$\pi^- < 166$ MeV/c

$\Gamma(ne^-\overline{\nu}_e)/\Gamma(n\pi^-)$ Γ_3/Γ_1

Measurements with an error $\geq 0.2\times10^{-3}$ have been omitted.

VALUE (units 10^{-3})	EVTS	DOCUMENT ID		TECN	COMMENT
1.019±0.035 OUR FIT					
$1.019^{+0.031}_{-0.036}$ OUR AVERAGE					
0.96 ±0.05	2847	BOURQUIN	83C	SPEC	SPS hyperon beam
$1.09^{+0.06}_{-0.08}$	601	[4] EBENHOH	74	HBC	K^-p at rest
$1.05^{+0.07}_{-0.13}$	455	[4] SECHI-ZORN	73	HBC	K^-p at rest
0.97 ±0.15	57	COLE	71	HBC	K^-p at rest
1.11 ±0.09	180	BIERMAN	68	HBC	

[4] An additional negative systematic error is included for internal radiative corrections and latest form factors; see BOURQUIN 83C.

$\Gamma(n\mu^-\overline{\nu}_\mu)/\Gamma(n\pi^-)$ Γ_4/Γ_1

VALUE (units 10^{-3})	EVTS	DOCUMENT ID		TECN	COMMENT
0.45±0.04 OUR FIT					
0.45±0.04 OUR AVERAGE					
0.38±0.11	13	COLE	71	HBC	K^-p at rest
0.43±0.06	72	ANG	69	HBC	K^-p at rest
0.43±0.09	56	BAGGETT	69	HBC	K^-p at rest
0.56±0.20	11	BAZIN	65B	HBC	K^-p at rest
0.66±0.15	22	COURANT	64	HBC	

$\Gamma(\Lambda e^-\overline{\nu}_e)/\Gamma(n\pi^-)$ Γ_5/Γ_1

VALUE (units 10^{-4})	EVTS	DOCUMENT ID		TECN	COMMENT
0.574±0.027 OUR FIT					
0.574±0.027 OUR AVERAGE					
0.561±0.031	1620	[5] BOURQUIN	82	SPEC	SPS hyperon beam
0.63 ±0.11	114	THOMPSON	80	ASPK	Hyperon beam
0.52 ±0.09	31	BALTAY	69	HBC	K^-p at rest
0.69 ±0.12	31	EISELE	69	HBC	K^-p at rest
0.64 ±0.12	35	BARASH	67	HBC	K^-p at rest
0.75 ±0.28	11	COURANT	64	HBC	K^-p at rest

[5] The value is from BOURQUIN 83B, and includes radiation corrections and new acceptance.

Σ^- DECAY PARAMETERS

See the "Note on Baryon Decay Parameters" in the neutron Listings. Older, outdated results have been omitted.

α_- FOR $\Sigma^- \to n\pi^-$

VALUE	EVTS	DOCUMENT ID		TECN	COMMENT
−0.068±0.008 OUR AVERAGE					
−0.062±0.024	28k	HANSL	78	HBC	$K^-p \to \Sigma^-\pi^+$
−0.067±0.011	60k	BOGERT	70	HBC	K^-p 0.4 GeV/c
−0.071±0.012	51k	BANGERTER	69	HBC	K^-p 0.4 GeV/c

ϕ ANGLE FOR $\Sigma^- \to n\pi^-$ $(\tan\phi = \beta\,/\,\gamma)$

VALUE (°)	EVTS	DOCUMENT ID		TECN	COMMENT
10±15 OUR AVERAGE					
+ 5±23	1092	[6] BERLEY	70B	HBC	n rescattering
14±19	1385	BANGERTER	69B	HBC	K^-p 0.4 GeV/c

[6] BERLEY 70B changed from −5 to +5° to agree with our sign convention.

g_A/g_V FOR $\Sigma^- \to ne^-\overline{\nu}_e$

Measurements with fewer than 500 events have been omitted. Where necessary, signs have been changed to agree with our conventions, which are given in the "Note on Baryon Decay Parameters" in the neutron Listings. What is actually listed is $|g_1/f_1 - 0.237 g_2/f_1|$. This reduces to $g_A/g_V \equiv g_1(0)/f_1(0)$ on making the usual assumption that $g_2 = 0$. See also the note on HSUEH 88.

VALUE	EVTS	DOCUMENT ID		TECN	COMMENT
0.340±0.017 OUR AVERAGE					
+0.327±0.007±0.019	50k	[7] HSUEH	88	SPEC	Σ^- 250 GeV
+0.34 ±0.05	4456	[8] BOURQUIN	83C	SPEC	SPS hyperon beam
0.385±0.037	3507	[9] TANENBAUM	74	ASPK	
• • • We do not use the following data for averages, fits, limits, etc. • • •					
0.29 ±0.07	25k	HSUEH	85	SPEC	See HSUEH 88
$0.17^{+0.07}_{-0.09}$	519	DECAMP	77	ELEC	Hyperon beam

[7] The sign is, *with our conventions*, unambiguously positive. The value assumes, as usual, that $g_2 = 0$. If g_2 is included in the fit, than (with our sign convention) $g_2 = -0.56 \pm 0.37$, with a corresponding reduction of g_A/g_V to $+0.20 \pm 0.08$.

[8] BOURQUIN 83C favors the positive sign by at least 2.6 standard deviations.

[9] TANENBAUM 74 gives 0.435 ± 0.035, assuming no q^2 dependence in g_A and g_V. The listed result allows q^2 dependence, and is taken from HSUEH 88.

$f_2(0)/f_1(0)$ FOR $\Sigma^- \to ne^-\overline{\nu}_e$

The signs have been changed to be in accord with our conventions, given in the "Note on Baryon Decay Parameters" in the neutron Listings.

VALUE	EVTS	DOCUMENT ID		TECN	COMMENT
0.97±0.14 OUR AVERAGE					
+0.96±0.07±0.13	50k	HSUEH	88	SPEC	Σ^- 250 GeV
+1.02±0.34	4456	BOURQUIN	83C	SPEC	SPS hyperon beam

TRIPLE CORRELATION COEFFICIENT D for $\Sigma^- \to ne^-\overline{\nu}_e$

The coefficient D of the term $D\,\mathbf{P}\cdot(\mathbf{p}_e\times\mathbf{p}_\nu)$ in the $\Sigma^- \to ne^-\overline{\nu}$ decay angular distribution. A nonzero value would indicate a violation of time-reversal invariance.

VALUE	EVTS	DOCUMENT ID		TECN	COMMENT
0.11±0.10	50k	HSUEH	88	SPEC	Σ^- 250 GeV

g_V/g_A FOR $\Sigma^- \to \Lambda e^-\overline{\nu}_e$

For the sign convention, see the "Note on Baryon Decay Parameters" in the neutron Listings. The value is predicted to be zero by conserved vector current theory. The values averaged assume CVC-SU(3) weak magnetism term.

VALUE	EVTS	DOCUMENT ID		TECN	COMMENT
0.01 ±0.10 OUR AVERAGE		Error includes scale factor of 1.5. See the ideogram below.			
−0.034±0.080	1620	[10] BOURQUIN	82	SPEC	SPS hyperon beam
−0.29 ±0.29	114	THOMPSON	80	ASPK	BNL hyperon beam
−0.17 ±0.35	55	TANENBAUM	75B	SPEC	BNL hyperon beam
+0.45 ±0.20	186	[10,11] FRANZINI	72	HBC	

[10] The sign has been changed to agree with our convention.

[11] The FRANZINI 72 value includes the events of earlier papers.

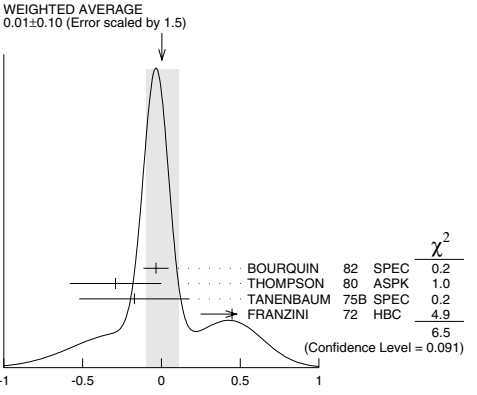

g_V/g_A for $\Sigma^- \to \Lambda e^-\overline{\nu}_e$

g_{WM}/g_A FOR $\Sigma^- \to \Lambda e^-\overline{\nu}_e$

The values quoted assume the CVC prediction $g_V = 0$.

VALUE	EVTS	DOCUMENT ID		TECN	COMMENT
2.4 ±1.7 OUR AVERAGE					
1.75±3.5	114	THOMPSON	80	ASPK	BNL hyperon beam
3.5 ±4.5	55	TANENBAUM	75B	SPEC	BNL hyperon beam
2.4 ±2.1	186	FRANZINI	72	HBC	

Σ^- REFERENCES

We have omitted some papers that have been superseded by later experiments. See our earlier editions.

ESCHRICH	01	PL B522 233	I. Eschrich *et al.* (FNAL SELEX Collab.)
GUREV	93	JETPL 57 400 Translated from ZETFP 57 389.	M.P. Gurev *et al.* (PNPI)
GALL	88	PRL 60 186	K.P. Gall *et al.* (BOST, MIT, WILL, CIT+)
HERTZOG	88	PR D37 1142	D.W. Hertzog *et al.* (WILL, BOST, MIT+)
HSUEH	88	PR D38 2056	S.Y. Hsueh *et al.* (CHIC, ELMT, FNAL+)
ZAPALAC	86	PRL 57 1526	G. Zapalac *et al.* (EFI, ELMT, FNAL+)
HSUEH	85	PRL 54 2399	S.Y. Hsueh *et al.* (CHIC, ELMT, FNAL+)
WAH	85	PRL 55 2551	Y.W. Wah *et al.* (FNAL, IOWA, ISU)
BOURQUIN	83B	ZPHY C21 27	M.H. Bourquin *et al.* (BRIS, GEVA, HEIDP+)
BOURQUIN	83C	ZPHY C21 17	M.H. Bourquin *et al.* (BRIS, GEVA, HEIDP+)
DECK	83	PR D28 1	L. Deck *et al.* (RUTG, WISC, MICH, MINN)
BOURQUIN	82	ZPHY C12 307	M.H. Bourquin *et al.* (BRIS, GEVA, HEIDP+)
MARRAFFINO	80	PR D21 2501	J. Marraffino *et al.* (VAND, MPIM)
THOMPSON	80	PR D21 25	J.A. Thompson *et al.* (PITT, BNL)
HANSL	78	NP B132 45	T. Hansl *et al.* (MPIM, VAND)
DECAMP	77	PL 66B 295	D. Decamp *et al.* (LALO, EPOL)
CONFORTO	76	NP B105 189	B. Conforto *et al.* (RHEL, LOIC)
DUGAN	75	NP A254 396	G. Dugan *et al.* (COLU, YALE)
TANENBAUM	75B	PR D12 1871	W. Tanenbaum *et al.* (YALE, FNAL, BNL)
EBENHOH	74	ZPHY 266 367	H. Ebenhoh *et al.* (HEIDT)
TANENBAUM	74	PRL 33 175	W. Tanenbaum *et al.* (YALE, FNAL, BNL)
EBENHOH	73	ZPHY 264 413	W. Ebenhoh *et al.* (HEIDT)
SECHI-ZORN	73	PR D8 12	B. Sechi-Zorn, G.A. Snow (UMD)
BOHM	72	NP B48 1	G. Bohm *et al.* (BERL, KIDR, BRUX, IASD+)
FRANZINI	72	PR D6 2417	P. Franzini *et al.* (COLU, HEID, UMD+)
ROBERTSON	72	Thesis UMI 78-00877	R.M. Robertson (IIT)
BAKKER	71	LNC 1 37	A.M. Bakker *et al.* (SABRE Collab.)
COLE	71	PR D4 631	J. Cole *et al.* (STON, COLU)
Also	69	Thesis Nevis 175	H. Norton (COLU)
TOVEE	71	NP B33 493	D.N. Tovee *et al.* (LOUC, KIDR, BERL+)
BERLEY	70B	PR D1 2015	D. Berley *et al.* (BNL, MASA, YALE)
BOGERT	70	PR D2 6	D.V. Bogert *et al.* (BNL, MASA, YALE)
EISELE	70	ZPHY 238 372	F. Eisele *et al.* (HEID)
PDG	70	RMP 42 No. 1	A. Barbaro-Galtieri *et al.* (LRL, BRAN+)
ANG	69	ZPHY 223 103	G. Ang *et al.* (HEID)
ANG	69B	ZPHY 228 151	G. Ang *et al.* (HEID)

BAGGETT	69	PRL 23 249	N.V. Baggett, B. Kehoe, G.A. Snow	(UMD)
BALTAY	69	PRL 22 615	C. Baltay *et al.*	(COLU, STON)
BANGERTER	69	Thesis UCRL 19244	R.O. Bangerter	(LRL)
BANGERTER	69B	PR 187 1821	R.O. Bangerter *et al.*	(LRL)
BARLOUTAUD	69	NP B14 153	R. Barloutaud *et al.*	(SACL, CERN, HEID)
EISELE	69	ZPHY 221 1	F. Eisele *et al.*	(HEID)
BIERMAN	68	PRL 20 1459	E. Bierman *et al.*	(PRIN)
HEPP	68	ZPHY 214 71	V. Hepp, H. Schleich	(HEID)
WHITESIDE	68	NC 54A 537	H. Whiteside, J. Gollub	(OBER)
BARASH	67	PRL 19 181	N. Barash *et al.*	(UMD)
CHANG	66	PR 151 1081	C.Y. Chang	(COLU)
BAZIN	65B	PR 140B 1358	M. Bazin *et al.*	(PRIN, RUTG, COLU)
DOSCH	65	PL 14 239	H.C. Dosch *et al.*	(HEID)
Also	66	PR 151 1081	C.Y. Chang	(COLU)
SCHMIDT	65	PR 140B 1328	P. Schmidt	(COLU)
BURNSTEIN	64	PRL 13 66	R.A. Burnstein *et al.*	(UMD)
COURANT	64	PR 136B 1791	H. Courant *et al.*	(CERN, HEID, UMD+)
BARKAS	63	PRL 11 26	W.H. Barkas, J.N. Dyer, H.H. Heckman	(LRL)
HUMPHREY	62	PR 127 1305	W.E. Humphrey, R.R. Ross	(LRL)

$\Sigma(1385)\ P_{13}$

$I(J^P) = 1(\frac{3}{2}^+)$ Status: ****

Discovered by ALSTON 60. Early measurements of the mass and width for combined charge states have been omitted. They may be found in our 1984 edition Reviews of Modern Physics **56** No. 2 Pt. II (1984).

We average only the most significant determinations. We do not average results from inclusive experiments with large backgrounds or results which are not accompanied by some discussion of experimental resolution. Nevertheless systematic differences between experiments remain. (See the ideograms in the Listings below.) These differences could arise from interference effects that change with production mechanism and/or beam momentum. They can also be accounted for in part by differences in the parametrizations employed. (See BORENSTEIN 74 for a discussion on this point.) Thus BORENSTEIN 74 uses a Breit-Wigner with energy-independent width, since a P-wave was found to give unsatisfactory fits. CAMERON 78 uses the same form. On the other hand HOLMGREN 77 obtains a good fit to their $\Lambda\pi$ spectrum with a P-wave Breit-Wigner, but includes the partial width for the $\Sigma\pi$ decay mode in the parametrization. AGUILAR-BENITEZ 81D gives masses and widths for five different Breit-Wigner shapes. The results vary considerably. Only the best-fit S-wave results are given here.

$\Sigma(1385)$ MASSES

$\Sigma(1385)^+$ MASS

VALUE (MeV)	EVTS	DOCUMENT ID		TECN	COMMENT
1382.8±0.4 OUR AVERAGE		Error includes scale factor of 2.0. See the ideogram below.			
1384.1±0.7	1897	BAUBILLIER	84	HBC	$K^- p$ 8.25 GeV/c
1384.5±0.5	5256	AGUILAR-...	81D	HBC	$K^- p \to \Lambda\pi\pi$ 4.2 GeV/c
1383.0±0.4	9361	AGUILAR-...	81D	HBC	$K^- p \to \Lambda 3\pi$ 4.2 GeV/c
1381.9±0.3	6900	CAMERON	78	HBC	$K^- p$ 0.96–1.36 GeV/c
1381 ±1	6846	BORENSTEIN	74	HBC	$K^- p$ 2.18 GeV/c
1383.5±0.85	2300	HABIBI	73	HBC	$K^- p \to \Lambda\pi\pi$
1382 ±2	400	AGUILAR-...	72B	HBC	$K^- p \to \Lambda\pi$'s
1384.4±1.0	1260	SIEGEL	67	HBC	$K^- p$ 2.1 GeV/c
1382 ±1	750	ARMENTEROS	65B	HBC	$K^- p$ 0.9–1.2 GeV/c
1381.0±1.6	859	HUWE	64	HBC	$K^- p$ 1.22 GeV/c
• • • We do not use the following data for averages, fits, limits, etc. • • •					
1385.1±1.2	600	BAKER	80	HYBR	$\pi^+ p$ 7 GeV/c
1383.2±1.0	750	BAKER	80	HYBR	$K^- p$ 7 GeV/c
1381 ±2	7k	[1] BAUBILLIER	79B	HBC	$K^- p$ 8.25 GeV/c
1391 ±2	2k	CAUTIS	79	HYBR	$\pi^+ p/K^- p$ 11.5 GeV
1390 ±2	100	[1] SUGAHARA	79B	HBC	$\pi^- p$ 6 GeV/c
1385 ±3	22k	[1,2] BARREIRO	77B	HBC	$K^- p$ 4.2 GeV/c
1385 ±1	2594	HOLMGREN	77	HBC	See AGUILAR 81D
1380 ±2		[1] BARDADIN-...	75	HBC	$K^- p$ 14.3 GeV/c
1382 ±1	3740	[3] BERTHON	74	HBC	$K^- p$ 1263–1843 MeV/c
1390 ±6	46	AGUILAR-...	70B	HBC	$K^- p \to \Sigma\pi$'s 4 GeV/c
1383 ±8	62	[4] BIRMINGHAM	66	HBC	$K^- p$ 3.5 GeV/c
1378 ±5	135	LONDON	66	HBC	$K^- p$ 2.24 GeV/c
1384.3±1.9	250	[4] SMITH	65	HBC	$K^- p$ 1.8 GeV/c
1382.6±2.1	250	[4] SMITH	65	HBC	$K^- p$ 1.95 GeV/c
1375.0±3.9	170	COOPER	64	HBC	$K^- p$ 1.45 GeV/c
1376.0±3.9	154	[4] ELY	61	HLBC	$K^- p$ 1.11 GeV/c

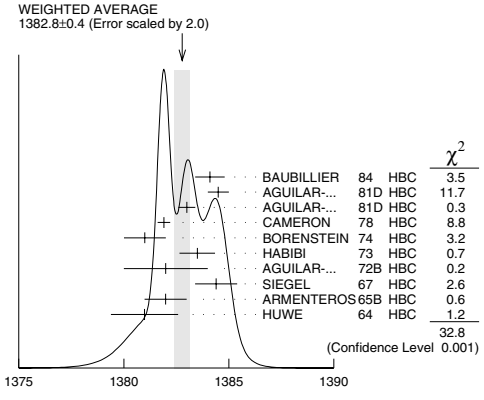

$\Sigma(1385)^+$ mass (MeV)

$\Sigma(1385)^0$ MASS

VALUE (MeV)	EVTS	DOCUMENT ID		TECN	COMMENT
1383.7±1.0 OUR AVERAGE		Error includes scale factor of 1.4. See the ideogram below.			
1384.1±0.8	5722	AGUILAR-...	81D	HBC	$K^- p \to \Lambda 3\pi$ 4.2 GeV/c
1380 ±2	3100	[5] BORENSTEIN	74	HBC	$K^- p \to \Lambda 3\pi$ 2.18 GeV/c
1385.1±2.5	240	[4] THOMAS	73	HBC	$\pi^- p \to \Lambda\pi^0 K^0$
• • • We do not use the following data for averages, fits, limits, etc. • • •					
1389 ±3	500	[6] BAUBILLIER	79B	HBC	$K^- p$ 8.25 GeV/c

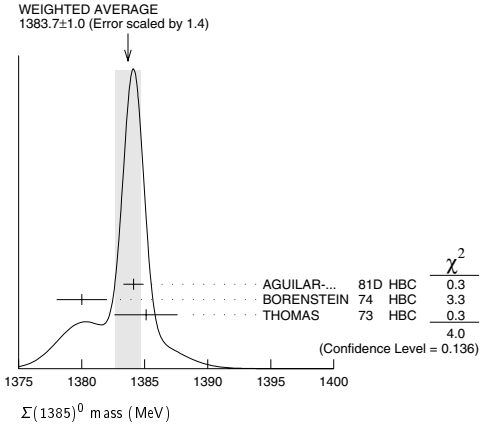

$\Sigma(1385)^0$ mass (MeV)

$\Sigma(1385)^-$ MASS

VALUE (MeV)	EVTS	DOCUMENT ID		TECN	COMMENT
1387.2±0.5 OUR AVERAGE		Error includes scale factor of 2.2. See the ideogram below.			
1388.3±1.7	620	AGUILAR-...	81D	HBC	$K^- p \to \Lambda\pi\pi$ 4.2 GeV/c
1384.9±0.8	3346	AGUILAR-...	81D	HBC	$K^- p \to \Lambda 3\pi$ 4.2 GeV/c
1387.6±0.3	9720	CAMERON	78	HBC	$K^- p$ 0.96–1.36 GeV/c
1383 ±2	2303	BORENSTEIN	74	HBC	$K^- p$ 2.18 GeV/c
1390.7±1.2	1900	HABIBI	73	HBC	$K^- p \to \Lambda\pi\pi$
1387.1±1.9	630	[4] THOMAS	73	HBC	$\pi^- p \to \Lambda\pi^- K^+$
1390.7±2.0	370	SIEGEL	67	HBC	$K^- p$ 2.1 GeV/c
1384 ±1	1380	ARMENTEROS	65B	HBC	$K^- p$ 0.9–1.2 GeV/c
1385.3±1.9	1086	[4] HUWE	64	HBC	$K^- p$ 1.15–1.30 GeV/c
• • • We do not use the following data for averages, fits, limits, etc. • • •					
1383 ±1	4.5k	[1] BAUBILLIER	79B	HBC	$K^- p$ 8.25 GeV/c
1380 ±6	150	[1] SUGAHARA	79B	HBC	$\pi^- p$ 6 GeV/c
1387 ±3	12k	[1,2] BARREIRO	77B	HBC	$K^- p$ 4.2 GeV/c
1391 ±3	193	HOLMGREN	77	HBC	See AGUILAR 81D
1383 ±2		[1] BARDADIN-...	75	HBC	$K^- p$ 14.3 GeV/c
1389 ±1	3060	[3] BERTHON	74	HBC	$K^- p$ 1263–1843 MeV/c
1389 ±9	15	LONDON	66	HBC	$K^- p$ 2.24 GeV/c
1391.5±2.6	120	[4] SMITH	65	HBC	$K^- p$ 1.8 GeV/c
1399.8±2.2	58	[4] SMITH	65	HBC	$K^- p$ 1.95 GeV/c
1392.0±6.2	200	COOPER	64	HBC	$K^- p$ 1.45 GeV/c
1382 ±3	93	DAHL	61	DBC	$K^- d$ 0.45 GeV/c
1376.0±4.4	224	[4] ELY	61	HLBC	$K^- p$ 1.11 GeV/c

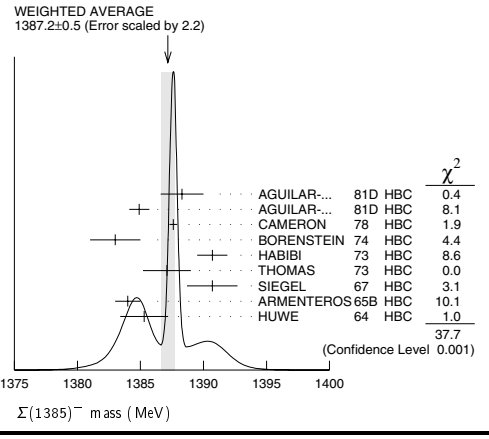

$m_{\Sigma(1385)^-} - m_{\Sigma(1385)^+}$

VALUE (MeV)	CL%	DOCUMENT ID		TECN	COMMENT
• • • We do not use the following data for averages, fits, limits, etc. • • •					
−2 to +6	95	[7] BORENSTEIN	74	HBC	$K^- p$ 2.18 GeV/c
7.2±1.4		[7] HABIBI	73	HBC	$K^- p \to \Lambda\pi\pi$
6.3±2.0		[7] SIEGEL	67	HBC	$K^- p$ 2.1 GeV/c
11 ±9		[7] LONDON	66	HBC	$K^- p$ 2.24 GeV/c
9 ±6		LONDON	66	HBC	$\Lambda 3\pi$ events
2.0±1.5		[7] ARMENTEROS	65B	HBC	$K^- p$ 0.9–1.2 GeV/c
7.2±2.1		[7] SMITH	65	HBC	$K^- p$ 1.8 GeV/c
17.2±2.0		[7] SMITH	65	HBC	$K^- p$ 1.95 GeV/c
17 ±7		[7] COOPER	64	HBC	$K^- p$ 1.45 GeV/c
4.3±2.2		[7] HUWE	64	HBC	$K^- p$ 1.22 GeV/c
0.0±4.2		[7] ELY	61	HLBC	$K^- p$ 1.11 GeV/c

$m_{\Sigma(1385)^0} - m_{\Sigma(1385)^+}$

VALUE (MeV)	CL%	DOCUMENT ID		TECN	COMMENT
• • • We do not use the following data for averages, fits, limits, etc. • • •					
−4 to +4	95	[7] BORENSTEIN	74	HBC	$K^- p$ 2.18 GeV/c

$m_{\Sigma(1385)^-} - m_{\Sigma(1385)^0}$

VALUE (MeV)	DOCUMENT ID		TECN	COMMENT
• • • We do not use the following data for averages, fits, limits, etc. • • •				
2.0±2.4	[7] THOMAS	73	HBC	$\pi^- p \to \Lambda\pi^- K^+$

$\Sigma(1385)$ WIDTHS

$\Sigma(1385)^+$ WIDTH

VALUE (MeV)	EVTS	DOCUMENT ID		TECN	COMMENT
35.8± 0.8 OUR AVERAGE					
37.2± 2.0	1897	BAUBILLIER	84	HBC	$K^- p$ 8.25 GeV/c
35.1± 1.7	5256	AGUILAR-...	81D	HBC	$K^- p \to \Lambda\pi\pi$ 4.2 GeV/c
37.5± 2.0	9361	AGUILAR-...	81D	HBC	$K^- p \to \Lambda 3\pi$ 4.2 GeV/c
35.5± 1.9	6900	CAMERON	78	HBC	$K^- p$ 0.96–1.36 GeV/c
34.0± 1.6	6846	[8] BORENSTEIN	74	HBC	$K^- p$ 2.18 GeV/c
38.3± 3.2	2300	[9] HABIBI	73	HBC	$K^- p \to \Lambda\pi\pi$
32.5± 6.0	400	AGUILAR-...	72B	HBC	$K^- p \to \Lambda\pi$'s
36 ± 4	1260	[9] SIEGEL	67	HBC	$K^- p$ 2.1 GeV/c
32.0± 4.7	750	[9] ARMENTEROS	65B	HBC	$K^- p$ 0.95–1.20 GeV/c
46.5± 6.4	859	[9] HUWE	64	HBC	$K^- p$ 1.15–1.30 GeV/c
• • • We do not use the following data for averages, fits, limits, etc. • • •					
40 ± 3	600	BAKER	80	HYBR	$\pi^+ p$ 7 GeV/c
37 ± 2	750	BAKER	80	HYBR	$K^- p$ 7 GeV/c
37 ± 2	7k	[1] BAUBILLIER	79B	HBC	$K^- p$ 8.25 GeV/c
30 ± 4	2k	CAUTIS	79	HYBR	$\pi^+ p/K^- p$ 11.5 GeV
30 ± 6	100	[1] SUGAHARA	79B	HBC	$\pi^- p$ 6 GeV/c
43 ± 5	22k	[1,2] BARREIRO	77B	HBC	$K^- p$ 4.2 GeV/c
34 ± 2	2594	HOLMGREN	77	HBC	See AGUILAR 81D
40.0± 3.2		[1] BARDADIN-...	75	HBC	$K^- p$ 14.3 GeV/c
48 ± 3	3740	[3] BERTHON	74	HBC	$K^- p$ 1263–1843 MeV/c
33 ±20	46	[9] AGUILAR-...	70B	HBC	$K^- p \to \Sigma\pi$'s 4 GeV/c
25 ±32	62	[9] BIRMINGHAM	66	HBC	$K^- p$ 3.5 GeV/c
30.3± 7.5	250	[9] SMITH	65	HBC	$K^- p$ 1.8 GeV/c
33.1± 8.3	250	[9] SMITH	65	HBC	$K^- p$ 1.95 GeV/c
51 ±16	170	[9] COOPER	64	HBC	$K^- p$ 1.45 GeV/c
48 ±16	154	[9] ELY	61	HLBC	$K^- p$ 1.11 GeV/c

$\Sigma(1385)^0$ WIDTH

VALUE (MeV)	EVTS	DOCUMENT ID		TECN	COMMENT
36 ± 5 OUR AVERAGE					
34.8± 5.6	5722	AGUILAR-...	81D	HBC	$K^- p \to \Lambda 3\pi$ 4.2 GeV/c
39.3±10.2	240	[9] THOMAS	73	HBC	$\pi^- p \to \Lambda\pi^0 K^0$
• • • We do not use the following data for averages, fits, limits, etc. • • •					
53 ± 8	3100	[10] BORENSTEIN	74	HBC	$K^- p \to \Lambda 3\pi$ 2.18 GeV/c
30 ± 9	106	CURTIS	63	OSPK	$\pi^- p$ 1.5 GeV/c

$\Sigma(1385)^-$ WIDTH

VALUE (MeV)	EVTS	DOCUMENT ID		TECN	COMMENT
39.4± 2.1 OUR AVERAGE Error includes scale factor of 1.7. See the ideogram below.					
38.4±10.7	620	AGUILAR-...	81D	HBC	$K^- p \to \Lambda\pi\pi$ 4.2 GeV/c
34.6± 4.2	3346	AGUILAR-...	81D	HBC	$K^- p \to \Lambda 3\pi$ 4.2 GeV/c
39.2± 1.7	9720	CAMERON	78	HBC	$K^- p$ 0.96–1.36 GeV/c
35 ± 3	2303	[8] BORENSTEIN	74	HBC	$K^- p$ 2.18 GeV/c
51.9± 4.8	1900	[9] HABIBI	73	HBC	$K^- p \to \Lambda\pi\pi$
48.2± 7.7	630	[9] THOMAS	73	HBC	$\pi^- p \to \Lambda\pi^- K^0$
31.0± 6.5	370	[9] SIEGEL	67	HBC	$K^- p$ 2.1 GeV/c
38.0± 4.1	1382	[9] ARMENTEROS	65B	HBC	$K^- p$ 0.95–1.20 GeV/c
62 ± 7	1086	HUWE	64	HBC	$K^- p$ 1.15–1.30 GeV/c
• • • We do not use the following data for averages, fits, limits, etc. • • •					
44 ± 4	4.5k	[1] BAUBILLIER	79B	HBC	$K^- p$ 8.25 GeV/c
58 ± 4	150	[1] SUGAHARA	79B	HBC	$\pi^- p$ 6 GeV/c
45 ± 5	12k	[1,2] BARREIRO	77B	HBC	$K^- p$ 4.2 GeV/c
35 ±10	193	HOLMGREN	77	HBC	See AGUILAR 81D
47 ± 6		[1] BARDADIN-...	75	HBC	$K^- p$ 14.3 GeV/c
40 ± 3	3060	[3] BERTHON	74	HBC	$K^- p$ 1263–1843 MeV/c
29.2±10.6	120	[9] SMITH	65	HBC	$K^- p$ 1.80 GeV/c
17.1± 8.9	58	[9] SMITH	65	HBC	$K^- p$ 1.95 GeV/c
88 ±24	200	[9] COOPER	64	HBC	$K^- p$ 1.45 GeV/c
40		DAHL	61	DBC	$K^- d$ 0.45 GeV/c
66 ±18	224	[9] ELY	61	HLBC	$K^- p$ 1.11 GeV/c

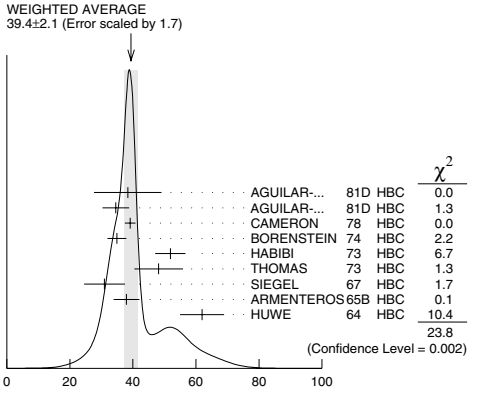

$\Sigma(1385)$ POLE POSITIONS

$\Sigma(1385)^+$ REAL PART

VALUE	DOCUMENT ID	COMMENT
1379±1	LICHTENBERG74	Extrapolates HABIBI 73

$\Sigma(1385)^+$ −IMAGINARY PART

VALUE	DOCUMENT ID	COMMENT
17.5±1.5	LICHTENBERG74	Extrapolates HABIBI 73

$\Sigma(1385)^-$ REAL PART

VALUE	DOCUMENT ID	COMMENT
1383±1	LICHTENBERG74	Extrapolates HABIBI 73

$\Sigma(1385)^-$ −IMAGINARY PART

VALUE	DOCUMENT ID	COMMENT
22.5±1.5	LICHTENBERG74	Extrapolates HABIBI 73

$\Sigma(1385)$ DECAY MODES

	Mode	Fraction (Γ_i/Γ)
Γ_1	$\Lambda\pi$	88±2 %
Γ_2	$\Sigma\pi$	12±2 %
Γ_3	$\Lambda\gamma$	
Γ_4	$\Sigma\gamma$	
Γ_5	$N\overline{K}$	

The above branching fractions are our estimates, not fits or averages.

$\Sigma(1385)$ BRANCHING RATIOS

$\Gamma(\Sigma\pi)/\Gamma(\Lambda\pi)$ Γ_2/Γ_1

VALUE	DOCUMENT ID		TECN	CHG	COMMENT
0.135 ± 0.011 OUR AVERAGE					
0.20 ± 0.06	DIONISI	78B	HBC	±	$K^-p \to Y^*K\overline{K}$
0.16 ± 0.03	BERTHON	74	HBC	+	K^-p 1.26–1.84 GeV/c
0.11 ± 0.02	BERTHON	74	HBC	−	K^-p 1.26–1.84 GeV/c
0.21 ± 0.05	BORENSTEIN	74	HBC	+	$K^-p \to \Lambda\pi^+\pi^-$, $\Sigma^0\pi^+\pi^-$
0.18 ± 0.04	MAST	73	MPWA	±	$K^-p \to \Lambda\pi^+\pi^-$, $\Sigma^0\pi^+\pi^-$
0.10 ± 0.05	THOMAS	73	HBC	−	$\pi^-p \to \Lambda K\pi$, $\Sigma K\pi$
0.16 ± 0.07	AGUILAR-...	72B	HBC	+	K^-p 3.9, 4.6 GeV/c
0.13 ± 0.04	COLLEY	71B	DBC	−0	K^-N 1.5 GeV/c
0.13 ± 0.04	PAN	69	HBC	+	$\pi^+p \to \Lambda K\pi$, $\Sigma K\pi$
0.08 ± 0.06	LONDON	66	HBC	+	K^-p 2.24 GeV/c
0.163 ± 0.041	ARMENTEROS	65B	HBC	±	K^-p 0.95–1.20 GeV/c
0.09 ± 0.04	HUWE	64	HBC	±	K^-p 1.2–1.7 GeV
• • • We do not use the following data for averages, fits, limits, etc. • • •					
< 0.04	ALSTON	62	HBC	±0	K^-p 1.15 GeV/c
0.04 ± 0.04	BASTIEN	61	HBC	±	

$\Gamma(\Lambda\gamma)/\Gamma_{\text{total}}$ Γ_3/Γ

VALUE	EVTS	DOCUMENT ID		TECN	COMMENT
• • • We do not use the following data for averages, fits, limits, etc. • • •					
0.17 ± 0.17	1	MEISNER	72	HBC	1 event only

$\Gamma(\Lambda\gamma)/\Gamma(\Lambda\pi)$ Γ_3/Γ_1

VALUE	CL%	DOCUMENT ID		TECN	COMMENT
• • • We do not use the following data for averages, fits, limits, etc. • • •					
< 0.06	90	COLAS	75	HLBC	K^-p 575–970 MeV

$\Gamma(\Sigma\gamma)/\Gamma(\Lambda\pi)$ Γ_4/Γ_1

VALUE	CL%	DOCUMENT ID		TECN	COMMENT
• • • We do not use the following data for averages, fits, limits, etc. • • •					
< 0.05	90	COLAS	75	HLBC	K^-p 575–970 MeV

$(\Gamma_i\Gamma_f)^{1/2}/\Gamma_{\text{total}}$ in $N\overline{K} \to \Sigma(1385) \to \Lambda\pi$ $(\Gamma_5\Gamma_1)^{1/2}/\Gamma$

VALUE	DOCUMENT ID		CHG	COMMENT
+0.586 ± 0.319	[11] DEVENISH	74B	0	Fixed-t dispersion rel.

$\Sigma(1385)$ FOOTNOTES

[1] From fit to inclusive $\Lambda\pi$ spectrum.
[2] Includes data of HOLMGREN 77.
[3] The errors are statistical only. The resolution is not unfolded.
[4] The error is enlarged to $\Gamma/\sqrt{N}$. See the note on the $K^*(892)$ mass in the 1984 edition.
[5] From a fit to $\Lambda\pi^0$ with the width fixed at 34 MeV.
[6] From fit to inclusive $\Lambda\pi^0$ spectrum with the width fixed at 40 MeV.
[7] Redundant with data in the mass Listings.
[8] Results from $\Lambda\pi^+\pi^-$ and $\Lambda\pi^+\pi^-\pi^0$ combined by us.
[9] The error is enlarged to $4\Gamma/\sqrt{N}$. See the note on the $K^*(892)$ mass in the 1984 edition.
[10] Consistent with +, 0, and − widths equal.
[11] An extrapolation of the parametrized amplitude below threshold.

$\Sigma(1385)$ REFERENCES

BAUBILLIER	84	ZPHY C23 213	M. Baubillier *et al.*	(BIRM, CERN, GLAS+)
PDG	84	RMP 56 No. 2 Pt. II	C.G. Wohl *et al.*	(LBL, CIT, CERN)
AGUILAR-...	81D	AFIS A77 144	M. Aguilar-Benitez, J. Salicio	(MADR)
BAKER	80	NP B166 207	P.A. Baker *et al.*	(LOIC)
BAUBILLIER	79B	NP B148 18	M. Baubillier *et al.*	(BIRM, CERN, GLAS+)
CAUTIS	79	NP B156 507	C.V. Cautis *et al.*	(SLAC)
SUGAHARA	79B	NP B156 237	R. Sugahara *et al.*	(KEK, OSKC, KINK)
CAMERON	78	NP B143 189	W. Cameron *et al.*	(RHEL, LOIC)
DIONISI	78B	PL 78B 154	C. Dionisi, R. Armenteros, J. Diaz	(CERN, AMST+)
BARREIRO	77B	NP B126 319	F. Barreiro *et al.*	(CERN, AMST, NIJM)
HOLMGREN	77	NP B119 261	S.O. Holmgren *et al.*	(CERN, AMST, NIJM)
BARDADIN-...	75	NP B98 418	M. Bardadin-Otwinowska *et al.*	(SACL, EPOL+)
COLAS	75	NP B91 253	J. Colas *et al.*	(ORSAY)
BERTHON	74	NC 21A 146	A. Berthon *et al.*	(CDEF, RHEL, SACL+)
BORENSTEIN	74	PR D9 3006	S.R. Borenstein *et al.*	(BNL, MICH)
DEVENISH	74B	NP B81 330	R.C.E. Devenish, C.D. Froggatt, B.R. Martin	(DESY+)
LICHTENBERG	74	PR D10 3865	D.B. Lichtenberg	(IND)
Also	74B	Private Comm.	D.B. Lichtenberg	(IND)
HABIBI	73	Thesis Nevis 199	M. Habibi	(COLU)
Also	73	Purdue Conf. 387	C. Baltay *et al.*	(COLU, BING)
MAST	73	PR D7 3212	T.S. Mast *et al.*	(LBL) IJP
Also	73B	PR D7 5	T.S. Mast *et al.*	(LBL) IJP
THOMAS	73	NP B56 15	D.W. Thomas *et al.*	(CMU) JP
AGUILAR-...	72B	PR D6 29	M. Aguilar-Benitez *et al.*	(BNL)
MEISNER	72	NC 12A 62	G.W. Meisner	(UNC, LBL)
COLLEY	71B	NP B31 61	D.C. Colley *et al.*	(BIRM, EDIN, GLAS+)
AGUILAR-...	70B	PRL 25 58	M. Aguilar-Benitez *et al.*	(BNL, SYRA)
PAN	69	PRL 23 808	Y.L. Pan, F.L. Forman	(PENN) I
SIEGEL	67	Thesis UCRL 18041	D.M. Siegel	(LRL)
BIRMINGHAM	66	PR 152 1148	M. Haque *et al.*	(BIRM, GLAS, LOIC, OXF+)
LONDON	66	PR 143 1034	G.W. London *et al.*	(BNL, SYRA) J
ARMENTEROS	65B	PL 19 75	R. Armenteros *et al.*	(CERN, HEID, SACL)
SMITH	65	Thesis UCLA	L.T. Smith	(UCLA)
COOPER	64	PL 8 365	W.A. Cooper *et al.*	(CERN, AMST)
HUWE	64	Thesis UCRL 11291	D.O. Huwe	(LRL) JP
Also	69	PR 180 1824	D.O. Huwe	(LRL)
CURTIS	63	PR 132 1771	L.J. Curtis *et al.*	(MICH) J
ALSTON	62	CERN Conf. 311	M.H. Alston *et al.*	(LRL)
BASTIEN	61	PRL 6 702	P.L. Bastien, M. Ferro-Luzzi, A.H. Rosenfeld	(LRL)
DAHL	61	PRL 6 142	O.I. Dahl *et al.*	(LRL)
ELY	61	PRL 7 461	R.P. Ely *et al.*	(LRL) J
ALSTON	60	PRL 5 520	M.H. Alston *et al.*	(LRL) I

$\Sigma(1480)$ Bumps

$I(J^P) = 1(?^?)$ Status: *

OMITTED FROM SUMMARY TABLE

These are peaks seen in $\Lambda\pi$ and $\Sigma\pi$ spectra in the reaction $\pi^+p \to (Y\pi)K^+$ at 1.7 GeV/c. Also, the Y polarization oscillates in the same region.

MILLER 70 suggests a possible alternate explanation in terms of a reflection of $N(1675) \to \Lambda K$ decay. However, such an explanation for the $(\Sigma^+\pi^0)K^+$ channel in terms of $\Delta(1650) \to \Sigma K$ decay seems unlikely (see PAN 70). In addition such reflections would also have to account for the oscillation of the Y polarization in the 1480 MeV region.

HANSON 71, with less data than PAN 70, can neither confirm nor deny the existence of this state. MAST 75 sees no structure in this region in $K^-p \to \Lambda\pi^0$.

ENGELEN 80 performs a multichannel analysis of $K^-p \to p\overline{K}^0\pi^-$ at 4.2 GeV/c. They observe a 3.5 standard-deviation signal at 1480 MeV in $p\overline{K}^0$ which cannot be explained as a reflection of any competing channel.

$\Sigma(1480)$ MASS (PRODUCTION EXPERIMENTS)

VALUE (MeV)	EVTS	DOCUMENT ID		TECN	CHG	COMMENT
≈ 1480 OUR ESTIMATE						
1480	120	ENGELEN	80	HBC	+	$K^-p \to (p\overline{K}^0)\pi^-$
1485 ± 10		CLINE	73	MPWA	−	$K^-d \to (\Lambda\pi^-)p$
1479 ± 10		PAN	70	HBC	+	$\pi^+p \to (\Lambda\pi^+)K^+$
1465 ± 15		PAN	70	HBC	+	$\pi^+p \to (\Sigma\pi)K^+$

$\Sigma(1480)$ WIDTH (PRODUCTION EXPERIMENTS)

VALUE (MeV)	EVTS	DOCUMENT ID		TECN	CHG	COMMENT
80 ± 20	120	ENGELEN	80	HBC	+	$K^-p \to (p\overline{K}^0)\pi^-$
40 ± 20		CLINE	73	MPWA	−	$K^-d \to (\Lambda\pi^-)p$
31 ± 15		PAN	70	HBC	+	$\pi^+p \to (\Lambda\pi^+)K^+$
30 ± 20		PAN	70	HBC	+	$\pi^+p \to (\Sigma\pi)K^+$

$\Sigma(1480)$ DECAY MODES (PRODUCTION EXPERIMENTS)

	Mode
Γ_1	$N\overline{K}$
Γ_2	$\Lambda\pi$
Γ_3	$\Sigma\pi$

$\Sigma(1480)$ BRANCHING RATIOS (PRODUCTION EXPERIMENTS)

$\Gamma(\Sigma\pi)/\Gamma(\Lambda\pi)$ Γ_3/Γ_2

VALUE	DOCUMENT ID		TECN	CHG
0.82 ± 0.51	PAN	70	HBC	+

$\Gamma(N\overline{K})/\Gamma(\Lambda\pi)$ Γ_1/Γ_2

VALUE	DOCUMENT ID		TECN	CHG
0.72 ± 0.50	PAN	70	HBC	+

$\Gamma(N\overline{K})/\Gamma_{\text{total}}$ Γ_1/Γ

VALUE	DOCUMENT ID		TECN	COMMENT
small	CLINE	73	MPWA	$K^-d\to(\Lambda\pi^-)p$

$\Sigma(1480)$ REFERENCES (PRODUCTION EXPERIMENTS)

ENGELEN	80	NP B167 61	J.J. Engelen *et al.*	(NIJM, AMST, CERN+)
MAST	75	PR D11 3078	T.S. Mast *et al.*	(LBL)
CLINE	73	LNC 6 205	D. Cline, R. Laumann, J. Mapp	(WISC) IJP
HANSON	71	PR D4 1296	P. Hanson, G.E. Kalmus, J. Louie	(LBL) I
MILLER	70	Duke Conf. 229	D.H. Miller	(PURD)
		Hyperon Resonances, 1970		
PAN	70	PR D2 49	Y.L. Pan *et al.*	(PENN)
Also	69	PRL 23 808	Y.L. Pan, F.L. Forman	(PENN) I
Also	69B	PRL 23 806	Y.L. Pan, F.L. Forman	(PENN) I

$\Sigma(1560)$ Bumps

$I(J^P) = 1(?^?)$ Status: **

OMITTED FROM SUMMARY TABLE

This entry lists peaks reported in mass spectra around 1560 MeV without implying that they are necessarily related.

DIONISI 78B observes a 6 standard-deviation enhancement at 1553 MeV in the charged $\Lambda/\Sigma\pi$ mass spectra from $K^-p\to(\Lambda/\Sigma)\pi K\overline{K}$ at 4.2 GeV/c. In a CERN ISR experiment, LOCKMAN 78 reports a narrow 6 standard-deviation enhancement at 1572 MeV in $\Lambda\pi^\pm$ from the reaction $pp\to\Lambda\pi^+\pi^-X$. These enhancements are unlikely to be associated with the $\Sigma(1580)$ (which has not been confirmed by several recent experiments – see the next entry in the Listings).

CARROLL 76 observes a bump at 1550 MeV (as well as one at 1580 MeV) in the isospin-1 $\overline{K}N$ total cross section, but uncertainties in cross section measurements outside the mass range of the experiment preclude estimating its significance.

See also MEADOWS 80 for a review of this state.

$\Sigma(1560)$ MASS (PRODUCTION EXPERIMENTS)

VALUE (MeV)	EVTS	DOCUMENT ID		TECN	CHG	COMMENT
≈ 1560 OUR ESTIMATE						
1553 ± 7	121	DIONISI	78B	HBC	±	$K^-p\to(Y\pi)K\overline{K}$
1572 ± 4	40	LOCKMAN	78	SPEC	±	$pp\to\Lambda\pi^+\pi^-X$

$\Sigma(1560)$ WIDTH (PRODUCTION EXPERIMENTS)

VALUE (MeV)	EVTS	DOCUMENT ID		TECN	CHG	COMMENT
79 ± 30	121	DIONISI	78B	HBC	±	$K^-p\to(Y\pi)K\overline{K}$
15 ± 6	40	[1] LOCKMAN	78	SPEC	±	$pp\to\Lambda\pi^+\pi^-X$

$\Sigma(1560)$ DECAY MODES (PRODUCTION EXPERIMENTS)

	Mode	Fraction (Γ_i/Γ)
Γ_1	$\Lambda\pi$	seen
Γ_2	$\Sigma\pi$	

$\Sigma(1560)$ BRANCHING RATIOS (PRODUCTION EXPERIMENTS)

$\Gamma(\Sigma\pi)/[\Gamma(\Lambda\pi)+\Gamma(\Sigma\pi)]$ $\Gamma_2/(\Gamma_1+\Gamma_2)$

VALUE	DOCUMENT ID		TECN	CHG	COMMENT
0.35 ± 0.12	DIONISI	78B	HBC	±	$K^-p\to(Y\pi)K\overline{K}$

$\Gamma(\Lambda\pi)/\Gamma_{\text{total}}$ Γ_1/Γ

VALUE	DOCUMENT ID		TECN	CHG	COMMENT
seen	LOCKMAN	78	SPEC	±	$pp\to\Lambda\pi^+\pi^-X$

$\Sigma(1560)$ FOOTNOTES (PRODUCTION EXPERIMENTS)

[1] The width observed by LOCKMAN 78 is consistent with experimental resolution.

$\Sigma(1560)$ REFERENCES (PRODUCTION EXPERIMENTS)

MEADOWS	80	Toronto Conf. 283	B.T. Meadows	(CINC)
DIONISI	78B	PL 78B 154	C. Dionisi, R. Armenteros, J. Diaz	(CERN, AMST+) I
LOCKMAN	78	Saclay DPHPE 78-01	W. Lockman *et al.*	(UCLA, SACL)
CARROLL	76	PRL 37 806	A.S. Carroll *et al.*	(BNL) I

$\Sigma(1580)$ D_{13}

$I(J^P) = 1(\frac{3}{2}^-)$ Status: **

OMITTED FROM SUMMARY TABLE

Seen in the isospin-1 $\overline{K}N$ cross section at BNL (LI 73, CARROLL 76) and in a partial-wave analysis of $K^-p\to\Lambda\pi^0$ for c.m. energies 1560–1600 MeV by LITCHFIELD 74. LITCHFIELD 74 finds $J^P=3/2^-$. Not seen by ENGLER 78 or by CAMERON 78C (with larger statistics in $K^0_Lp\to\Lambda\pi^+$ and $\Sigma^0\pi^+$).

$\Sigma(1580)$ MASS

VALUE (MeV)	DOCUMENT ID		TECN	COMMENT
≈ 1580 OUR ESTIMATE				
1583 ± 4	[1] CARROLL	76	DPWA	Isospin-1 total σ
1582 ± 4	[2] LITCHFIELD	74	DPWA	$K^-p\to\Lambda\pi^0$

$\Sigma(1580)$ WIDTH

VALUE (MeV)	DOCUMENT ID		TECN	COMMENT
15	[1] CARROLL	76	DPWA	Isospin-1 total σ
11 ± 4	[2] LITCHFIELD	74	DPWA	$K^-p\to\Lambda\pi^0$

$\Sigma(1580)$ DECAY MODES

	Mode
Γ_1	$N\overline{K}$
Γ_2	$\Lambda\pi$
Γ_3	$\Sigma\pi$

$\Sigma(1580)$ BRANCHING RATIOS

See "Sign conventions for resonance couplings" in the Note on Λ and Σ Resonances.

$\Gamma(N\overline{K})/\Gamma_{\text{total}}$ Γ_1/Γ

VALUE	DOCUMENT ID		TECN	COMMENT
$+0.03\pm0.01$	[2] LITCHFIELD	74	DPWA	$\overline{K}N$ multichannel

$(\Gamma_i\Gamma_f)^{1/2}/\Gamma_{\text{total}}$ in $N\overline{K}\to\Sigma(1580)\to\Lambda\pi$ $(\Gamma_1\Gamma_2)^{1/2}/\Gamma$

VALUE	DOCUMENT ID		TECN	COMMENT
not seen	CAMERON	78C	HBC	$K^0_Lp\to\Lambda\pi^+$
not seen	ENGLER	78	HBC	$K^0_Lp\to\Lambda\pi^+$
$+0.10\pm0.02$	[2] LITCHFIELD	74	DPWA	$K^-p\to\Lambda\pi^0$

$(\Gamma_i\Gamma_f)^{1/2}/\Gamma_{\text{total}}$ in $N\overline{K}\to\Sigma(1580)\to\Sigma\pi$ $(\Gamma_1\Gamma_3)^{1/2}/\Gamma$

VALUE	DOCUMENT ID		TECN	COMMENT
not seen	CAMERON	78C	HBC	$K^0_Lp\to\Sigma^0\pi^+$
not seen	ENGLER	78	HBC	$K^0_Lp\to\Sigma^0\pi^+$
$+0.03\pm0.04$	[2] LITCHFIELD	74	DPWA	$\overline{K}N$ multichannel

$\Sigma(1580)$ FOOTNOTES

[1] CARROLL 76 sees a total-cross-section bump with $(J+1/2)\ \Gamma_{el}/\Gamma_{total}=0.06$.

[2] The main effect observed by LITCHFIELD 74 is in the $\Lambda\pi$ final state; the $\overline{K}N$ and $\Sigma\pi$ couplings are estimated from a multichannel fit including total-cross-section data of LI 73.

$\Sigma(1580)$ REFERENCES

CAMERON	78C	NP B132 189	W. Cameron *et al.*	(BGNA, EDIN, GLAS+) I
ENGLER	78	PR D18 3061	A. Engler *et al.*	(CMU, ANL)
CARROLL	76	PRL 37 806	A.S. Carroll *et al.*	(BNL) I
LITCHFIELD	74	PL 51B 509	P.J. Litchfield	(CERN) IJP
LI	73	Purdue Conf. 283	K.K. Li	(BNL) I

$\Sigma(1620)$ S_{11}

$I(J^P) = 1(\frac{1}{2}^-)$ Status: **

OMITTED FROM SUMMARY TABLE

The S_{11} state at 1697 MeV reported by VANHORN 75 is tentatively listed under the $\Sigma(1750)$. CARROLL 76 sees two bumps in the isospin-1 total cross section near this mass.

Production experiments are listed separately in the next entry.

$\Sigma(1620)$ MASS

VALUE (MeV)	DOCUMENT ID		TECN	COMMENT
≈ 1620 OUR ESTIMATE				
1600 ± 6	[1] MORRIS	78	DPWA	$K^- n \to \Lambda\pi^-$
1608 ± 5	[2] CARROLL	76	DPWA	Isospin-1 total σ
1633 ± 10	[3] CARROLL	76	DPWA	Isospin-1 total σ
1630 ± 10	LANGBEIN	72	IPWA	$\overline{K}N$ multichannel
1620	KIM	71	DPWA	K-matrix analysis

$\Sigma(1620)$ WIDTH

VALUE (MeV)	DOCUMENT ID		TECN	COMMENT
87 ± 19	[1] MORRIS	78	DPWA	$K^- n \to \Lambda\pi^-$
15	[2] CARROLL	76	DPWA	Isospin-1 total σ
10	[3] CARROLL	76	DPWA	Isospin-1 total σ
65 ± 20	LANGBEIN	72	IPWA	$\overline{K}N$ multichannel
40	KIM	71	DPWA	K-matrix analysis

$\Sigma(1620)$ DECAY MODES

	Mode
Γ_1	$N\overline{K}$
Γ_2	$\Lambda\pi$
Γ_3	$\Sigma\pi$

$\Sigma(1620)$ BRANCHING RATIOS

$\Gamma(N\overline{K})/\Gamma_{total}$ — **Γ_1/Γ**

VALUE	DOCUMENT ID		TECN	COMMENT
0.22 ± 0.02	LANGBEIN	72	IPWA	$\overline{K}N$ multichannel
0.05	KIM	71	DPWA	K-matrix analysis

$(\Gamma_i\Gamma_f)^{1/2}/\Gamma_{total}$ in $N\overline{K} \to \Sigma(1620) \to \Lambda\pi$ — **$(\Gamma_1\Gamma_2)^{1/2}/\Gamma$**

VALUE	DOCUMENT ID		TECN	COMMENT
0.12 ± 0.02	[1] MORRIS	78	DPWA	$K^- n \to \Lambda\pi^-$
not seen	BAILLON	75	IPWA	$\overline{K}N \to \Lambda\pi$
0.15	KIM	71	DPWA	K-matrix analysis

$(\Gamma_i\Gamma_f)^{1/2}/\Gamma_{total}$ in $N\overline{K} \to \Sigma(1620) \to \Sigma\pi$ — **$(\Gamma_1\Gamma_3)^{1/2}/\Gamma$**

VALUE	DOCUMENT ID		TECN	COMMENT
not seen	HEPP	76B	DPWA	$K^- N \to \Sigma\pi$
0.40 ± 0.06	LANGBEIN	72	IPWA	$\overline{K}N$ multichannel
0.08	KIM	71	DPWA	K-matrix analysis

$\Sigma(1620)$ FOOTNOTES

[1] MORRIS 78 obtains an equally good fit without including this resonance.
[2] Total cross-section bump with $(J+1/2)\ \Gamma_{el}\ /\ \Gamma_{total}$ is 0.06 seen by CARROLL 76.
[3] Total cross-section bump with $(J+1/2)\ \Gamma_{el}\ /\ \Gamma_{total}$ is 0.04 seen by CARROLL 76.

$\Sigma(1620)$ REFERENCES

MORRIS	78	PR D17 55	W.A. Morris *et al.*	(FSU) IJP
CARROLL	76	PRL 37 806	A.S. Carroll *et al.*	(BNL) I
HEPP	76B	PL 65B 487	V. Hepp *et al.*	(CERN, HEIDH, MPIM) IJP
BAILLON	75	NP B94 39	P.H. Baillon, P.J. Litchfield	(CERN, RHEL) IJP
VANHORN	75	NP B87 145	A.J. van Horn	(LBL) IJP
Also	75B	NP B87 157	A.J. van Horn	(LBL) IJP
LANGBEIN	72	NP B47 477	W. Langbein, F. Wagner	(MPIM) IJP
KIM	71	PRL 27 356	J.K. Kim	(HARV) IJP
Also	70	Duke Conf. 161 Hyperon Resonances, 1970	J.K. Kim	(HARV) IJP

$\Sigma(1620)$ Production Experiments

$I(J^P) = 1(?^?)$

OMITTED FROM SUMMARY TABLE

Formation experiments are listed separately in the previous entry.

The results of CRENNELL 69B at 3.9 GeV/c are not confirmed by SABRE 70 at 3.0 GeV/c. However, at 4.5 GeV/c, AMMANN 70 sees a peak at 1642 MeV which on the basis of branching ratios they do not associate with the $\Sigma(1670)$. See MILLER 70 for a review of these conflicts.

$\Sigma(1620)$ MASS (PRODUCTION EXPERIMENTS)

VALUE (MeV)	EVTS	DOCUMENT ID		TECN	CHG	COMMENT
≈ 1620 OUR ESTIMATE						
1642 ± 12		AMMANN	70	DBC		$K^- N$ 4.5 GeV/c
1618 ± 3	20	BLUMENFELD	69	HBC	+	$K^0_L p$
1619 ± 8		CRENNELL	69B	DBC	±	$K^- N \to \Lambda\pi\pi\pi$
• • • We do not use the following data for averages, fits, limits, etc. • • •						
1616 ± 8		CRENNELL	68	DBC	±	See CRENNELL 69B

$\Sigma(1620)$ WIDTH (PRODUCTION EXPERIMENTS)

VALUE (MeV)	EVTS	DOCUMENT ID		TECN	CHG	COMMENT
55 ± 24		AMMANN	70	DBC		$K^- N$ 4.5 GeV/c
30 ± 10	20	BLUMENFELD	69	HBC	+	
72^{+22}_{-15}		CRENNELL	69B	DBC	±	
• • • We do not use the following data for averages, fits, limits, etc. • • •						
66 ± 16		CRENNELL	68	DBC	±	See CRENNELL 69B

$\Sigma(1620)$ DECAY MODES (PRODUCTION EXPERIMENTS)

	Mode
Γ_1	$N\overline{K}$
Γ_2	$\Lambda\pi$
Γ_3	$\Sigma\pi$
Γ_4	$\Lambda\pi\pi$
Γ_5	$\Sigma(1385)\pi$
Γ_6	$\Lambda(1405)\pi$

$\Sigma(1620)$ BRANCHING RATIOS (PRODUCTION EXPERIMENTS)

$\Gamma(\Lambda\pi\pi)/\Gamma(\Lambda\pi)$ — **Γ_4/Γ_2**

VALUE	EVTS	DOCUMENT ID		TECN	CHG
~ 2.5	14	BLUMENFELD	69	HBC	+

$\Gamma(N\overline{K})/\Gamma(\Lambda\pi)$ — **Γ_1/Γ_2**

VALUE	DOCUMENT ID		TECN	CHG	COMMENT
0.4 ± 0.4	AMMANN	70	DBC		$K^- p$ 4.5 GeV/c
0.0 ± 0.1	CRENNELL	68	DBC	+	See CRENNELL 69B

$\Gamma(\Lambda\pi)/\Gamma_{total}$ — **Γ_2/Γ**

VALUE	DOCUMENT ID		TECN	CHG
large	CRENNELL	68	DBC	±

$\Gamma(\Sigma(1385)\pi)/\Gamma(\Lambda\pi)$ — **Γ_5/Γ_2**

VALUE	CL%	DOCUMENT ID		TECN	CHG	COMMENT
< 0.3	95	AMMANN	70	DBC		$K^- p$ 4.5 GeV/c
0.2 ± 0.1		CRENNELL	68	DBC	±	

$\Gamma(\Sigma\pi)/\Gamma(\Lambda\pi)$ — **Γ_3/Γ_2**

VALUE	CL%	DOCUMENT ID		TECN	COMMENT
< 1.1	95	AMMANN	70	DBC	$K^- N$ 4.5 GeV/c

$\Gamma(\Lambda(1405)\pi)/\Gamma(\Lambda\pi)$ — **Γ_6/Γ_2**

VALUE	DOCUMENT ID		TECN	COMMENT
0.7 ± 0.4	AMMANN	70	DBC	$K^- p$ 4.5 GeV/c

$\Sigma(1620)$ REFERENCES (PRODUCTION EXPERIMENTS)

AMMANN	70	PRL 24 327	A.C. Ammann *et al.*	(PURD, IND)
Also	73	PR D7 1345	A.C. Ammann *et al.*	(PURD, IUPU)
MILLER	70	Duke Conf. 229	D.H. Miller	(PURD)
Hyperon Resonances, 1970				
SABRE	70	NP B16 201	R. Barloutaud *et al.*	(SABRE Collab.)
BLUMENFELD	69	PL 29B 58	B.J. Blumenfeld, G.R. Kalbfleisch	(BNL) I
CRENNELL	69B	Lund Paper 183	D.J. Crennell *et al.*	(BNL, CUNY) I
Results are quoted in LEVI-SETTI 69C.				
Also	69C	Lund Conf.	R. Levi-Setti	(EFI)
CRENNELL	68	PRL 21 648	D.J. Crennell *et al.*	(BNL, CUNY) I

$\Sigma(1660)$ P_{11}

$I(J^P) = 1(\frac{1}{2}^+)$ Status: ***

For results published before 1974 (they are now obsolete), see our 1982 edition Physics Letters **111B** (1982).

$\Sigma(1660)$ MASS

VALUE (MeV)		DOCUMENT ID		TECN	COMMENT
1630 to 1690 (≈ 1660) OUR ESTIMATE					
1665.1	±11.2	[1] KOISO	85	DPWA	$K^- p \to \Sigma\pi$
1670	±10	GOPAL	80	DPWA	$\overline{K}N \to \overline{K}N$
1679	±10	ALSTON-...	78	DPWA	$\overline{K}N \to \overline{K}N$
1676	±15	GOPAL	77	DPWA	$\overline{K}N$ multichannel
1668	±25	VANHORN	75	DPWA	$K^- p \to \Lambda\pi^0$
1670	±20	KANE	74	DPWA	$K^- p \to \Sigma\pi$
• • • We do not use the following data for averages, fits, limits, etc. • • •					
1565	or 1597	[2] MARTIN	77	DPWA	$\overline{K}N$ multichannel
1660	±30	[3] BAILLON	75	IPWA	$\overline{K}N \to \Lambda\pi$
1671	± 2	[4] PONTE	75	DPWA	$K^- p \to \Lambda\pi^0$

$\Sigma(1660)$ WIDTH

VALUE (MeV)		DOCUMENT ID		TECN	COMMENT
40 to 200 (≈ 100) OUR ESTIMATE					
81.5	± 22.2	[1] KOISO	85	DPWA	$K^- p \to \Sigma\pi$
152	± 20	GOPAL	80	DPWA	$\overline{K}N \to \overline{K}N$
38	± 10	ALSTON-...	78	DPWA	$\overline{K}N \to \overline{K}N$
120	± 20	GOPAL	77	DPWA	$\overline{K}N$ multichannel
230	$^{+165}_{-60}$	VANHORN	75	DPWA	$K^- p \to \Lambda\pi^0$
250	±110	KANE	74	DPWA	$K^- p \to \Sigma\pi$
• • • We do not use the following data for averages, fits, limits, etc. • • •					
202	or 217	[2] MARTIN	77	DPWA	$\overline{K}N$ multichannel
80	± 40	[3] BAILLON	75	IPWA	$\overline{K}N \to \Lambda\pi$
81	± 10	[4] PONTE	75	DPWA	$K^- p \to \Lambda\pi^0$

$\Sigma(1660)$ DECAY MODES

	Mode	Fraction (Γ_i/Γ)
Γ_1	$N\overline{K}$	10–30 %
Γ_2	$\Lambda\pi$	seen
Γ_3	$\Sigma\pi$	seen

$\Sigma(1660)$ BRANCHING RATIOS

See "Sign conventions for resonance couplings" in the Note on Λ and Σ Resonances.

$\Gamma(N\overline{K})/\Gamma_{total}$ Γ_1/Γ

VALUE	DOCUMENT ID		TECN	COMMENT
0.1 to 0.3 OUR ESTIMATE				
0.12 ± 0.03	GOPAL	80	DPWA	$\overline{K}N \to \overline{K}N$
0.10 ± 0.05	ALSTON-...	78	DPWA	$\overline{K}N \to \overline{K}N$
• • • We do not use the following data for averages, fits, limits, etc. • • •				
< 0.04	GOPAL	77	DPWA	See GOPAL 80
0.27 or 0.29	[2] MARTIN	77	DPWA	$\overline{K}N$ multichannel

$(\Gamma_i\Gamma_f)^{1/2}/\Gamma_{total}$ in $N\overline{K} \to \Sigma(1660) \to \Lambda\pi$ $(\Gamma_1\Gamma_2)^{1/2}/\Gamma$

VALUE	DOCUMENT ID		TECN	COMMENT
< 0.04	GOPAL	77	DPWA	$\overline{K}N$ multichannel
$0.12^{+0.12}_{-0.04}$	VANHORN	75	DPWA	$K^- p \to \Lambda\pi^0$
• • • We do not use the following data for averages, fits, limits, etc. • • •				
−0.10 or −0.11	[2] MARTIN	77	DPWA	$\overline{K}N$ multichannel
−0.04 ± 0.02	[3] BAILLON	75	IPWA	$\overline{K}N \to \Lambda\pi$
+0.16 ± 0.01	[4] PONTE	75	DPWA	$K^- p \to \Lambda\pi^0$

$(\Gamma_i\Gamma_f)^{1/2}/\Gamma_{total}$ in $N\overline{K} \to \Sigma(1660) \to \Sigma\pi$ $(\Gamma_1\Gamma_3)^{1/2}/\Gamma$

VALUE	DOCUMENT ID		TECN	COMMENT
−0.13 ± 0.04	[1] KOISO	85	DPWA	$K^- p \to \Sigma\pi$
−0.16 ± 0.03	GOPAL	77	DPWA	$\overline{K}N$ multichannel
−0.11 ± 0.01	KANE	74	DPWA	$K^- p \to \Sigma\pi$
• • • We do not use the following data for averages, fits, limits, etc. • • •				
−0.34 or −0.37	[2] MARTIN	77	DPWA	$\overline{K}N$ multichannel
not seen	HEPP	76B	DPWA	$K^- N \to \Sigma\pi$

$\Sigma(1660)$ FOOTNOTES

[1] The evidence of KOISO 85 is weak.
[2] The two MARTIN 77 values are from a T-matrix pole and from a Breit-Wigner fit.
[3] From solution 1 of BAILLON 75; not present in solution 2.
[4] From solution 2 of PONTE 75; not present in solution 1.

$\Sigma(1660)$ REFERENCES

KOISO	85	NP A433 619	H. Koiso *et al.*	(TOKY, MASA)
PDG	82	PL 111B	M. Roos *et al.*	(HELS, CIT, CERN)
GOPAL	80	Toronto Conf. 159	G.P. Gopal	(RHEL) IJP
ALSTON-...	78	PR D18 182	M. Alston-Garnjost *et al.*	(LBL, MTHO+) IJP
Also	77	PRL 38 1007	M. Alston-Garnjost *et al.*	(LBL, MTHO+) IJP
GOPAL	77	NP B119 362	G.P. Gopal *et al.*	(LOIC, RHEL) IJP
MARTIN	77	NP B127 349	B.R. Martin, M.K. Pidcock, R.G. Moorhouse	(LOUC+) IJP
Also	77B	NP B126 266	B.R. Martin, M.K. Pidcock	(LOUC) IJP
Also	77C	NP B126 285	B.R. Martin, M.K. Pidcock	(LOUC) IJP
HEPP	76B	PL 65B 487	V. Hepp *et al.*	(CERN, HEIDH, MPIM) IJP
BAILLON	75	NP B94 39	P.H. Baillon, P.J. Litchfield	(CERN, RHEL) IJP
PONTE	75	PR D12 2597	R.A. Ponte *et al.*	(MASA, TENN, UCR) IJP
VANHORN	75	NP B87 145	A.J. van Horn	(LBL) IJP
Also	75B	NP B87 157	A.J. van Horn	(LBL) IJP
KANE	74	LBL-2452	D.F. Kane	(LBL) IJP

THE $\Sigma(1670)$ REGION

Production experiments: The measured $\Sigma\pi/\Sigma\pi\pi$ branching ratio for the $\Sigma(1670)$ produced in the reaction $K^- p \to \pi^- \Sigma(1670)^+$ is strongly dependent on momentum transfer. This was first discovered by EBERHARD 69, who suggested that there exist two Σ resonances with the same mass and quantum numbers: one with a large $\Sigma\pi\pi$ (mainly $\Lambda(1405)\pi$) branching fraction produced peripherally, and the other with a large $\Sigma\pi$ branching fraction produced at larger angles. The experimental results have been confirmed by AGUILAR-BENITEZ 70, ASPELL 74, ESTES 74, and TIMMERMANS 76. If, in fact, there are two resonances, the most likely quantum numbers for both the $\Sigma\pi$ and the $\Lambda(1405)\pi$ states are D_{13}. There is also possibly a third Σ in this region, the $\Sigma(1690)$ in the Listings, the main evidence for which is a large $\Lambda\pi/\Sigma\pi$ branching ratio. These topics have been reviewed by EBERHARD 73 and by MILLER 70.

Formation experiments: Two states are also observed near this mass in formation experiments. One of these, the $\Sigma(1670)D_{13}$, has the same quantum numbers as those observed in production and has a large $\Sigma\pi/\Sigma\pi\pi$ branching ratio; it may well be the $\Sigma(1670)$ produced at larger angles (see TIMMERMANS 76). The other state, the $\Sigma(1660)P_{11}$, has different quantum numbers, its $\Sigma\pi/\Sigma\pi\pi$ branching ratio is unknown, and its relation to the produced $\Sigma(1670)$ states is obscure.

$\Sigma(1670)$ D_{13}

$I(J^P) = 1(\frac{3}{2}^-)$ Status: ****

For most results published before 1974 (they are now obsolete), see our 1982 edition Physics Letters **111B** (1982).

Results from production experiments are listed separately in the next entry.

$\Sigma(1670)$ MASS

VALUE (MeV)	DOCUMENT ID		TECN	COMMENT
1665 to 1685 (≈ 1670) OUR ESTIMATE				
1665.1 ± 4.1	KOISO	85	DPWA	$K^- p \to \Sigma\pi$
1682 ± 5	GOPAL	80	DPWA	$\overline{K}N \to \overline{K}N$
1679 ±10	ALSTON-...	78	DPWA	$\overline{K}N \to \overline{K}N$
1670 ± 5	GOPAL	77	DPWA	$\overline{K}N$ multichannel
1670 ± 6	HEPP	76B	DPWA	$K^- N \to \Sigma\pi$
1685 ±20	BAILLON	75	IPWA	$\overline{K}N \to \Lambda\pi$
1659 $^{+12}_{-5}$	VANHORN	75	DPWA	$K^- p \to \Lambda\pi^0$
1670 ± 2	KANE	74	DPWA	$K^- p \to \Sigma\pi$
• • • We do not use the following data for averages, fits, limits, etc. • • •				
1667 or 1668	[1] MARTIN	77	DPWA	$\overline{K}N$ multichannel
1650	DEBELLEFON	76	IPWA	$K^- p \to \Lambda\pi^0$
1671 ± 3	PONTE	75	DPWA	$K^- p \to \Lambda\pi^0$ (sol. 1)
1655 ± 2	PONTE	75	DPWA	$K^- p \to \Lambda\pi^0$ (sol. 2)

$\Sigma(1670)$ WIDTH

VALUE (MeV)	DOCUMENT ID		TECN	COMMENT
40 to 80 (≈ 60) OUR ESTIMATE				
65.0 ± 7.3	KOISO	85	DPWA	$K^- p \to \Sigma\pi$
79 ±10	GOPAL	80	DPWA	$\overline{K}N \to \overline{K}N$
56 ±20	ALSTON-...	78	DPWA	$\overline{K}N \to \overline{K}N$
50 ± 5	GOPAL	77	DPWA	$\overline{K}N$ multichannel
56 ± 3	HEPP	76B	DPWA	$K^- N \to \Sigma\pi$
85 ±25	BAILLON	75	IPWA	$\overline{K}N \to \Lambda\pi$
32 ±11	VANHORN	75	DPWA	$K^- p \to \Lambda\pi^0$
79 ± 6	KANE	74	DPWA	$K^- p \to \Sigma\pi$
• • • We do not use the following data for averages, fits, limits, etc. • • •				
46 or 46	[1] MARTIN	77	DPWA	$\overline{K}N$ multichannel
80	DEBELLEFON	76	IPWA	$K^- p \to \Lambda\pi^0$
44 ±11	PONTE	75	DPWA	$K^- p \to \Lambda\pi^0$ (sol. 1)
76 ± 5	PONTE	75	DPWA	$K^- p \to \Lambda\pi^0$ (sol. 2)

$\Sigma(1670)$ DECAY MODES

	Mode	Fraction (Γ_i/Γ)
Γ_1	$N\overline{K}$	7–13 %
Γ_2	$\Lambda\pi$	5–15 %
Γ_3	$\Sigma\pi$	30–60 %
Γ_4	$\Lambda\pi\pi$	
Γ_5	$\Sigma\pi\pi$	
Γ_6	$\Sigma(1385)\pi$	
Γ_7	$\Sigma(1385)\pi$, S-wave	
Γ_8	$\Lambda(1405)\pi$	
Γ_9	$\Lambda(1520)\pi$	

The above branching fractions are our estimates, not fits or averages.

$\Sigma(1670)$ BRANCHING RATIOS

See "Sign conventions for resonance couplings" in the Note on Λ and Σ Resonances.

$\Gamma(N\overline{K})/\Gamma_{total}$ Γ_1/Γ

VALUE	DOCUMENT ID		TECN	COMMENT
0.07 to 0.13 OUR ESTIMATE				
0.10 ± 0.03	GOPAL	80	DPWA	$\overline{K}N \to \overline{K}N$
0.11 ± 0.03	ALSTON-...	78	DPWA	$\overline{K}N \to \overline{K}N$
• • • We do not use the following data for averages, fits, limits, etc. • • •				
0.08 ± 0.03	GOPAL	77	DPWA	See GOPAL 80
0.07 or 0.07	[1] MARTIN	77	DPWA	$\overline{K}N$ multichannel

$(\Gamma_i\Gamma_f)^{1/2}/\Gamma_{total}$ in $N\overline{K} \to \Sigma(1670) \to \Lambda\pi$ $(\Gamma_1\Gamma_2)^{1/2}/\Gamma$

VALUE	DOCUMENT ID		TECN	COMMENT
0.17 ± 0.03	[2] MORRIS	78	DPWA	$K^- n \to \Lambda\pi^-$
0.13 ± 0.02	[2] MORRIS	78	DPWA	$K^- n \to \Lambda\pi^-$
+0.10 ± 0.02	GOPAL	77	DPWA	$\overline{K}N$ multichannel
+0.06 ± 0.02	BAILLON	75	IPWA	$\overline{K}N \to \Lambda\pi$
+0.09 ± 0.02	VANHORN	75	DPWA	$K^- p \to \Lambda\pi^0$
+0.018 ± 0.060	DEVENISH	74B		Fixed-t dispersion rel.
• • • We do not use the following data for averages, fits, limits, etc. • • •				
+0.08 or +0.08	[1] MARTIN	77	DPWA	$\overline{K}N$ multichannel
+0.05	DEBELLEFON	76	IPWA	$K^- p \to \Lambda\pi^0$
0.08 ± 0.01	PONTE	75	DPWA	$K^- p \to \Lambda\pi^0$ (sol. 1)
0.17 ± 0.01	PONTE	75	DPWA	$K^- p \to \Lambda\pi^0$ (sol. 2)

$(\Gamma_i\Gamma_f)^{1/2}/\Gamma_{total}$ in $N\overline{K} \to \Sigma(1670) \to \Sigma\pi$ $(\Gamma_1\Gamma_3)^{1/2}/\Gamma$

VALUE	DOCUMENT ID		TECN	COMMENT
+0.20 ± 0.02	KOISO	85	DPWA	$K^- p \to \Sigma\pi$
+0.21 ± 0.02	GOPAL	77	DPWA	$\overline{K}N$ multichannel
+0.20 ± 0.01	HEPP	76B	DPWA	$K^- N \to \Sigma\pi$
+0.21 ± 0.03	KANE	74	DPWA	$K^- p \to \Sigma\pi$
• • • We do not use the following data for averages, fits, limits, etc. • • •				
+0.18 or +0.17	[1] MARTIN	77	DPWA	$\overline{K}N$ multichannel

$\Gamma(\Lambda\pi\pi)/\Gamma_{total}$ Γ_4/Γ

VALUE	DOCUMENT ID	TECN	COMMENT
• • • We do not use the following data for averages, fits, limits, etc. • • •			
<0.11	ARMENTEROS68E	HBC	$K^- p$ (Γ_1=0.09)

$(\Gamma_i\Gamma_f)^{1/2}/\Gamma_{total}$ in $N\overline{K} \to \Sigma(1670) \to \Sigma(1385)\pi$, S-wave $(\Gamma_1\Gamma_7)^{1/2}/\Gamma$

VALUE	DOCUMENT ID		TECN	COMMENT
+0.11 ± 0.03	PREVOST	74	DPWA	$K^- N \to \Sigma(1385)\pi$
• • • We do not use the following data for averages, fits, limits, etc. • • •				
0.17 ± 0.02	[3] SIMS	68	DBC	$K^- N \to \Lambda\pi\pi$

$\Gamma(\Sigma\pi\pi)/\Gamma_{total}$ Γ_5/Γ

VALUE	DOCUMENT ID		TECN	COMMENT
• • • We do not use the following data for averages, fits, limits, etc. • • •				
<0.14	[4] ARMENTEROS68E		HBC	$K^- p$, $K^- d$ (Γ_1=0.09)

$\Gamma(\Lambda(1405)\pi)/\Gamma_{total}$ Γ_8/Γ

VALUE	DOCUMENT ID	TECN	COMMENT
• • • We do not use the following data for averages, fits, limits, etc. • • •			
<0.06	ARMENTEROS68E	HBC	$K^- p$, $K^- d$ (Γ_1=0.09)

$\Gamma_i\Gamma_f/\Gamma^2_{total}$ in $N\overline{K} \to \Sigma(1670) \to \Lambda(1405)\pi$ $\Gamma_1\Gamma_8/\Gamma^2$

VALUE	DOCUMENT ID		TECN	COMMENT
0.007 ± 0.002	[5] BRUCKER	70	DBC	$K^- N \to \Sigma\pi\pi$
• • • We do not use the following data for averages, fits, limits, etc. • • •				
<0.03	BERLEY	69	HBC	$K^- p$ 0.6–0.82 GeV/c

$\Gamma(\Lambda(1405)\pi)/\Gamma(\Sigma(1385)\pi)$ Γ_8/Γ_6

VALUE	DOCUMENT ID	TECN	COMMENT
0.23 ± 0.08	BRUCKER	70 DBC	$K^- N \to \Sigma\pi\pi$

$(\Gamma_i\Gamma_f)^{1/2}/\Gamma_{total}$ in $N\overline{K} \to \Sigma(1670) \to \Lambda(1520)\pi$ $(\Gamma_1\Gamma_9)^{1/2}/\Gamma$

VALUE	DOCUMENT ID		TECN	COMMENT
0.081 ± 0.016	[6] CAMERON	77	DPWA	P-wave decay

$\Sigma(1670)$ FOOTNOTES

[1] The two MARTIN 77 values are from a T-matrix pole and from a Breit-Wigner fit.
[2] Results are with and without an S_{11} $\Sigma(1620)$ in the fit.
[3] SIMS 68 uses only cross-section data. Result used as upper limit only.
[4] Ratio only for $\Sigma 2\pi$ system in $I = 1$, which cannot be $\Sigma(1385)$.
[5] Assuming the $\Lambda(1405)\pi$ cross-section bump is due only to $3/2^-$ resonance.
[6] The CAMERON 77 upper limit on F-wave decay is 0.03.

$\Sigma(1670)$ REFERENCES

KOISO	85	NP A433 619	H. Koiso *et al.* (TOKY, MASA)
PDG	82	PL 111B	M. Roos *et al.* (HELS, CIT, CERN)
GOPAL	80	Toronto Conf. 159	G.P. Gopal (RHEL) IJP
ALSTON-...	78	PR D18 182	M. Alston-Garnjost *et al.* (LBL, MTHO+) IJP
Also	77	PRL 38 1007	M. Alston-Garnjost *et al.* (LBL, MTHO+) IJP
MORRIS	78	PR D17 55	W.A. Morris *et al.* (FSU) IJP
CAMERON	77	NP B131 399	W. Cameron *et al.* (RHEL, LOIC) IJP
GOPAL	77	NP B119 362	G.P. Gopal *et al.* (LOIC, RHEL) IJP
MARTIN	77	NP B127 349	B.R. Martin, M.K. Pidcock, R.G. Moorhouse (LOUC+) IJP
Also	77B	NP B126 266	B.R. Martin, M.K. Pidcock (LOUC)
Also	77C	NP B126 285	B.R. Martin, M.K. Pidcock (LOUC) IJP
DEBELLEFON	76	NP B109 129	A. de Bellefon, A. Berthon (CDEF) IJP
HEPP	76B	PL 65B 487	V. Hepp *et al.* (CERN, HEIDH, MPIM) IJP
BAILLON	75	NP B94 39	P.H. Baillon, P.J. Litchfield (CERN, RHEL) IJP
PONTE	75	PR D12 2597	R.A. Ponte *et al.* (MASA, TENN, UCR) IJP
VANHORN	75	NP B87 145	A.J. van Horn (LBL) IJP
Also	75B	NP B87 157	A.J. van Horn (LBL) IJP
DEVENISH	74B	NP B81 330	R.C.E. Devenish, C.D. Froggatt, B.R. Martin (DESY+)
KANE	74	LBL-2452	D.F. Kane (LBL) IJP
PREVOST	74	NP B69 246	J. Prevost *et al.* (SACL, CERN, HEID)
BRUCKER	70	Duke Conf. 155 Hyperon Resonances, 1970	E.B. Brucker *et al.* (FSU) I
BERLEY	69	PL 30B 430	D. Berley *et al.* (BNL)
ARMENTEROS	68E	PL 28B 521	R. Armenteros *et al.* (CERN, HEID, SACL) I
SIMS	68	PRL 21 1413	W.H. Sims *et al.* (FSU, TUFTS, BRAN)

Baryon Particle Listings

$\Sigma(1670)$, $\Sigma(1670)$ Bumps

$\Sigma(1670)$ Bumps

$I(J^P) = 1(?^?)$

OMITTED FROM SUMMARY TABLE

Formation experiments are listed separately in the preceding entry.

Probably there are two states at the same mass with the same quantum numbers, one decaying to $\Sigma\pi$ and $\Lambda\pi$, the other to $\Lambda(1405)\pi$. See the note in front of the preceding entry.

$\Sigma(1670)$ MASS (PRODUCTION EXPERIMENTS)

VALUE (MeV)	EVTS	DOCUMENT ID		TECN	CHG	COMMENT
≈ 1670 OUR ESTIMATE						
1670 ± 4		[1] CARROLL	76	DPWA		Isospin-1 total σ
1675 ± 10		[2] HEPP	76	DBC	−	K^-N 1.6–1.75 GeV/c
1665 ± 1		APSELL	74	HBC		K^-p 2.87 GeV/c
1688 ± 2 or 1683 ± 5	1200	BERTHON	74	HBC	0	Quasi-2-body σ
1670 ± 6		AGUILAR-...	70B	HBC		$K^-p \to \Sigma\pi\pi$ 4 GeV
1668 ± 10		AGUILAR-...	70B	HBC		$K^-p \to \Sigma 3\pi$ 4 GeV
1660 ± 10		ALVAREZ	63	HBC	+	K^-p 1.51 GeV/c
• • • We do not use the following data for averages, fits, limits, etc. • • •						
1668 ± 10	150	[3] FERRERSORIA	81	OMEG	−	π^-p 9,12 GeV/c
1655 to 1677		TIMMERMANS	76	HBC	+	K^-p 4.2 GeV/c
1665 ± 5		BUGG	68	CNTR		K^-p, d total σ
1661 ± 9	70	PRIMER	68	HBC	+	See BARNES 69E
1685		ALEXANDER	62C	HBC	−0	π^-p 2–2.2 GeV/c

$\Sigma(1670)$ WIDTH (PRODUCTION EXPERIMENTS)

VALUE (MeV)	EVTS	DOCUMENT ID		TECN	CHG	COMMENT
67.0 ± 2.4		APSELL	74	HBC		K^-p 2.87 GeV/c
110 ± 12		AGUILAR-...	70B	HBC		$K^-p \to \Sigma\pi\pi$ 4 GeV
$135\ ^{+40}_{-30}$		AGUILAR-...	70B	HBC		$K^-p \to \Sigma 3\pi$ 4 GeV
40 ± 10		ALVAREZ	63	HBC	+	
• • • We do not use the following data for averages, fits, limits, etc. • • •						
90 ± 20	150	[3] FERRERSORIA	81	OMEG	−	π^-p 9,12 GeV/c
52		[1] CARROLL	76	DPWA		Isospin-1 total σ
48 to 63		TIMMERMANS	76	HBC	+	K^-p 4.2 GeV/c
30 ± 15		BUGG	68	CNTR		
60 ± 20	70	PRIMER	68	HBC	+	See BARNES 69E
45		ALEXANDER	62C	HBC	−0	

$\Sigma(1670)$ DECAY MODES (PRODUCTION EXPERIMENTS)

	Mode
Γ_1	$N\overline{K}$
Γ_2	$\Lambda\pi$
Γ_3	$\Sigma\pi$
Γ_4	$\Lambda\pi\pi$
Γ_5	$\Sigma\pi\pi$
Γ_6	$\Sigma(1385)\pi$
Γ_7	$\Lambda(1405)\pi$

$\Sigma(1670)$ BRANCHING RATIOS (PRODUCTION EXPERIMENTS)

$\Gamma(N\overline{K})/\Gamma(\Sigma\pi)$ — **Γ_1/Γ_3**

VALUE	EVTS	DOCUMENT ID		TECN	CHG	COMMENT
< 0.03		TIMMERMANS	76	HBC	+	K^-p 4.2 GeV/c
< 0.10		BERTHON	74	HBC	0	Quasi-2-body σ
< 0.2		AGUILAR-...	70B	HBC		
< 0.26		BARNES	69E	HBC	+	K^-p 3.9–5 GeV/c
0.025		BUGG	68	CNTR	0	Assuming $J = 3/2$
< 0.24	0	PRIMER	68	HBC	+	K^-p 4.6–5 GeV/c
< 0.6		LONDON	66	HBC	+	K^-p 2.25 GeV/c
< 0.19	0	ALVAREZ	63	HBC	+	K^-p 1.15 GeV/c
≥ 0.5 ± 0.25		SMITH	63	HBC	−0	

$\Gamma(\Lambda\pi)/\Gamma(\Sigma\pi)$ — **Γ_2/Γ_3**

VALUE	EVTS	DOCUMENT ID		TECN	CHG	COMMENT
0.76 ± 0.09		ESTES	74	HBC	0	K^-p 2.1,2.6 GeV/c
0.45 ± 0.15		BARNES	69E	HBC	+	K^-p 3.9–5 GeV/c
0.15 ± 0.07		HUWE	69	HBC	+	
0.11 ± 0.06	33	BUTTON-...	68	HBC	+	K^-p 1.7 GeV/c
• • • We do not use the following data for averages, fits, limits, etc. • • •						
≤ 0.45 ± 0.07		TIMMERMANS	76	HBC	+	K^-p 4.2 GeV/c
0.55 ± 0.11		BERTHON	74	HBC	0	Quasi-2-body σ
0	0	PRIMER	68	HBC	+	See BARNES 69E
< 0.6		LONDON	66	HBC	+	K^-p 2.25 GeV/c
1.2	130	ALVAREZ	63	HBC	+	K^-p 1.15 GeV/c
1.2		SMITH	63	HBC	−0	

$\Gamma(\Lambda\pi\pi)/\Gamma(\Sigma\pi)$ — **Γ_4/Γ_3**

VALUE	EVTS	DOCUMENT ID		TECN	CHG	COMMENT
< 0.6		LONDON	66	HBC	+	K^-p 2.25 GeV/c
0.56	90	ALVAREZ	63	HBC	+	K^-p 1.15 GeV/c
0.17		SMITH	63	HBC	−0	

$\Gamma(\Sigma\pi\pi)/\Gamma(\Sigma\pi)$ — **Γ_5/Γ_3**

VALUE	EVTS	DOCUMENT ID		TECN	CHG	COMMENT
largest at small angles		ESTES	74	HBC	0	K^-p 2.1,2.6 GeV/c
• • • We do not use the following data for averages, fits, limits, etc. • • •						
< 0.2		[2] HEPP	76	DBC	−	K^-N 1.6–1.75 GeV/c
0.56	180	ALVAREZ	63	HBC	+	K^-p 1.15 GeV/c

$\Gamma(\Lambda(1405)\pi)/\Gamma(\Sigma\pi)$ — **Γ_7/Γ_3**

VALUE	EVTS	DOCUMENT ID		TECN	CHG	COMMENT
1.8 ± 0.3 to 0.02 ± 0.07		[3,4] TIMMERMANS	76	HBC	+	K^-p 4.2 GeV/c
largest at small angles		ESTES	74	HBC	±	K^-p 2.1,2.6 GeV/c
3.0 ± 1.6	50	LONDON	66	HBC	+	K^-p 2.25 GeV/c
• • • We do not use the following data for averages, fits, limits, etc. • • •						
0.58 ± 0.20	17	PRIMER	68	HBC	+	See BARNES 69E

$\Gamma(\Sigma\pi)/\Gamma(\Sigma\pi\pi)$ — **Γ_3/Γ_5**

VALUE	DOCUMENT ID		TECN	CHG	COMMENT
varies with prod. angle	[5] APSELL	74	HBC	+	K^-p 2.87 GeV/c
1.39 ± 0.16	BERTHON	74	HBC	0	Quasi-2-body σ
2.5 to 0.24	[4] EBERHARD	69	HBC		K^-p 2.6 GeV/c
< 0.4	BIRMINGHAM	66	HBC	+	K^-p 3.5 GeV/c
0.30 ± 0.15	LONDON	66	HBC	+	K^-p 2.25 GeV/c

$\Gamma(\Lambda(1405)\pi)/\Gamma(\Sigma\pi\pi)$ — **Γ_7/Γ_5**

VALUE	DOCUMENT ID		TECN	CHG	COMMENT
0.97 ± 0.08	TIMMERMANS	76	HBC		K^-p 4.2 GeV/c
1.00 ± 0.02	APSELL	74	HBC		K^-p 2.87 GeV/c
$0.90\ ^{+0.10}_{-0.16}$	EBERHARD	65	HBC	+	K^-p 2.45 GeV/c

$\Gamma(\Lambda(1405)\pi)/\Gamma(\Sigma(1385)\pi)$ — **Γ_7/Γ_6**

VALUE	DOCUMENT ID		TECN	CHG	COMMENT
< 0.8	EBERHARD	65	HBC	+	K^-p 2.45 GeV/c

$\Gamma(\Lambda\pi\pi)/\Gamma(\Sigma\pi\pi)$ — **Γ_4/Γ_5**

VALUE	DOCUMENT ID		TECN	CHG	COMMENT
0.35 ± 0.2	BIRMINGHAM	66	HBC	+	K^-p 3.5 GeV/c

$\Gamma(\Lambda\pi)/\Gamma(\Sigma\pi\pi)$ — **Γ_2/Γ_5**

VALUE	DOCUMENT ID		TECN	CHG	COMMENT
< 0.2	BIRMINGHAM	66	HBC	+	K^-p 3.5 GeV/c

$\Gamma(\Lambda\pi)/[\Gamma(\Lambda\pi)+\Gamma(\Sigma\pi)]$ — **$\Gamma_2/(\Gamma_2+\Gamma_3)$**

VALUE	DOCUMENT ID		TECN
< 0.6	AGUILAR-...	70B	HBC

$\Gamma(\Sigma(1385)\pi)/\Gamma(\Sigma\pi)$ — **Γ_6/Γ_3**

VALUE	DOCUMENT ID		TECN	COMMENT
≤ 0.21 ± 0.05	TIMMERMANS	76	HBC	K^-p 4.2 GeV/c

$\Sigma(1670)$ QUANTUM NUMBERS (PRODUCTION EXPERIMENTS)

VALUE	EVTS	DOCUMENT ID		TECN	CHG	COMMENT
$J^P = 3/2^-$	400	BUTTON-...	68	HBC	±	$\Sigma^0\pi$
$J^P = 3/2^-$		EBERHARD	67	HBC	+	$\Lambda(1405)\pi$
$J^P = 3/2^+$		LEVEQUE	65	HBC		$\Lambda(1405)\pi$

$\Sigma(1670)$ FOOTNOTES

[1] Total cross-section bump with $(J+1/2)\ \Gamma_{el}\ /\ \Gamma_{total} = 0.23$.
[2] Enhancements in $\Sigma\pi$ and $\Sigma\pi\pi$ cross sections.
[3] Backward production in the $\Lambda\pi^- K^+$ final state.
[4] Depending on production angle.
[5] APSELL 74, ESTES 74, and TIMMERMANS 76 find strong branching ratio dependence on production angle, as in earlier production experiments.

$\Sigma(1670)$ REFERENCES (PRODUCTION EXPERIMENTS)

FERRERSORIA	81	NP B178 373	A. Ferrer Soria *et al.*	(CERN, CDEF, EPOL+)
CARROLL	76	PRL 37 806	A.S. Carroll *et al.*	(BNL) I
HEPP	76	NP B115 82	V. Hepp *et al.*	(CERN, HEID, MPIM) I
TIMMERMANS	76	NP B112 77	J.J.M. Timmermans *et al.*	(NIJM, CERN+) JP
APSELL	74	PR D10 1419	S.P. Apsell *et al.*	(BRAN, UMD, SYRA+) I
BERTHON	74	NC 21A 146	A. Berthon *et al.*	(CDEF, RHEL, SACL+)
ESTES	74	Thesis LBL-3827	R.D. Estes	(LBL)
AGUILAR-...	70B	PRL 25 58	M. Aguilar-Benitez *et al.*	(BNL, SYRA)
BARNES	69E	BNL 13823	V.E. Barnes *et al.*	(BNL, SYRA)
EBERHARD	69	PRL 22 200	P.H. Eberhard *et al.*	(LRL)
HUWE	69	PR 180 1824	D.O. Huwe	(LRL)
BUGG	68	PR 168 1466	D.V. Bugg *et al.*	(RHEL, BIRM, CAVE) I
BUTTON-...	68	PRL 21 1123	J. Button-Shafer	(MASA, LRL) JP
PRIMER	68	PRL 20 610	M. Primer *et al.*	(SYRA, BNL)
EBERHARD	67	PR 163 1446	P. Eberhard *et al.*	(LRL, ILL) IJP
BIRMINGHAM	66	PR 152 1148	M. Haque *et al.*	(BIRM, GLAS, LOIC, OXF+)
LONDON	66	PR 143 1034	G.W. London *et al.*	(BNL, SYRA) IJ
EBERHARD	65	PRL 14 466	P.H. Eberhard *et al.*	(LRL, ILL) I
LEVEQUE	65	PL 18 69	A. Leveque *et al.*	(SACL, EPOL, GLAS+) JP
ALVAREZ	63	PRL 10 184	L.W. Alvarez *et al.*	(LRL) I
SMITH	63	Athens Conf. 67	G.A. Smith	(LRL)
ALEXANDER	62C	CERN Conf. 320	G. Alexander *et al.*	(LRL) I

$\Sigma(1690)$ Bumps

$I(J^P) = 1(?^?)$ Status: **

OMITTED FROM SUMMARY TABLE

See the note preceding the $\Sigma(1670)$ Listings. Seen in production experiments only, mainly in $\Lambda\pi$.

$\Sigma(1690)$ MASS (PRODUCTION EXPERIMENTS)

VALUE (MeV)	EVTS	DOCUMENT ID		TECN	CHG	COMMENT
≈ 1690 OUR ESTIMATE						
1698 ± 20	70	[1] GODDARD	79	HBC	+	$\pi^+ p$ 10.3 GeV/c
1707 ± 20	40	[2] GODDARD	79	HBC	+	$\pi^+ p$ 10.3 GeV/c
1698 ± 20	15	ADERHOLZ	69	HBC	+	$\pi^+ p$ 8 GeV/c
1682 ± 2	46	BLUMENFELD	69	HBC	+	$K^0_L p$
1700 ± 20		MOTT	69	HBC	+	$K^- p$ 5.5 GeV/c
1694 ± 24	60	[3] PRIMER	68	HBC	+	$K^- p$ 4.6–5 GeV/c
1700 ± 6		[4] SIMS	68	HBC	–	$K^- N \to \Lambda\pi\pi$
1715 ± 12	30	COLLEY	67	HBC	+	$K^- p$ 6 GeV/c

$\Sigma(1690)$ WIDTH (PRODUCTION EXPERIMENTS)

VALUE (MeV)	EVTS	DOCUMENT ID		TECN	CHG	COMMENT
240 ± 60	70	[1] GODDARD	79	HBC	+	$\pi^+ p$ 10.3 GeV/c
130^{+100}_{-60}	40	[2] GODDARD	79	HBC	+	$\pi^+ p$ 10.3 GeV/c
142 ± 40	15	ADERHOLZ	69	HBC	+	$\pi^+ p$ 8 GeV/c
25 ± 10	46	BLUMENFELD	69	HBC	+	$K^0_L p$
130 ± 25		MOTT	69	HBC	+	$K^- p$ 5.5 GeV/c
105 ± 35	60	[3] PRIMER	68	HBC	+	$K^- p$ 4.6–5 GeV/c
62 ± 14		[4] SIMS	68	HBC	–	$K^- N \to \Lambda\pi\pi$
100 ± 35	30	COLLEY	67	HBC	+	$K^- p$ 6 GeV/c

$\Sigma(1690)$ DECAY MODES (PRODUCTION EXPERIMENTS)

	Mode
Γ_1	$N\overline{K}$
Γ_2	$\Lambda\pi$
Γ_3	$\Sigma\pi$
Γ_4	$\Sigma(1385)\pi$
Γ_5	$\Lambda\pi\pi$ (including $\Sigma(1385)\pi$)

$\Sigma(1690)$ BRANCHING RATIOS (PRODUCTION EXPERIMENTS)

$\Gamma(N\overline{K})/\Gamma(\Lambda\pi)$ — **Γ_1/Γ_2**

VALUE	EVTS	DOCUMENT ID		TECN	CHG	COMMENT
small		GODDARD	79	HBC	+	$\pi^+ p$ 10.2 GeV/c
< 0.2		MOTT	69	HBC	+	$K^- p$ 5.5 GeV/c
0.4 ± 0.25	18	COLLEY	67	HBC	+	6/30 events

$\Gamma(\Sigma\pi)/\Gamma(\Lambda\pi)$ — **Γ_3/Γ_2**

VALUE	CL%	DOCUMENT ID		TECN	CHG	COMMENT
small		GODDARD	79	HBC	+	$\pi^+ p$ 10.2 GeV/c
< 0.4	90	MOTT	69	HBC	+	$K^- p$ 5.5 GeV/c
0.3 ± 0.3		COLLEY	67	HBC	+	4/30 events

$\Gamma(\Sigma(1385)\pi)/\Gamma(\Lambda\pi)$ — **Γ_4/Γ_2**

VALUE	DOCUMENT ID		TECN	CHG	COMMENT
< 0.5	MOTT	69	HBC	+	$K^- p$ 5.5 GeV/c

$\Gamma(\Lambda\pi\pi(\text{including}\ \Sigma(1385)\pi))/\Gamma(\Lambda\pi)$ — **Γ_5/Γ_2**

VALUE	DOCUMENT ID		TECN	CHG	COMMENT
2.0 ± 0.6	BLUMENFELD	69	HBC	+	31/15 events
0.5 ± 0.25	COLLEY	67	HBC	+	15/30 events

$\Gamma(\Sigma(1385)\pi)/\Gamma(\Lambda\pi\pi(\text{including}\ \Sigma(1385)\pi))$ — **Γ_4/Γ_5**

VALUE	DOCUMENT ID		TECN	CHG	COMMENT
large	SIMS	68	HBC	–	$K^- N \to \Lambda\pi\pi$
small	COLLEY	67	HBC	+	$K^- p$ 6 GeV/c

$\Sigma(1690)$ FOOTNOTES (PRODUCTION EXPERIMENTS)

[1] From $\pi^+ p \to (\Lambda\pi^+) K^+$. $J > 1/2$ is not required by the data.
[2] From $\pi^+ p \to (\Lambda\pi^+)(K\pi)^+$. $J > 1/2$ is indicated, but large background precludes a definite conclusion.
[3] See the $\Sigma(1670)$ Listings. AGUILAR-BENITEZ 70B with three times the data of PRIMER 68 find no evidence for the $\Sigma(1690)$.
[4] This analysis, which is difficult and requires several assumptions and shows no unambiguous $\Sigma(1690)$ signal, suggests $J^P = 5/2^+$. Such a state would lead all previously known Y^* trajectories.

$\Sigma(1690)$ REFERENCES (PRODUCTION EXPERIMENTS)

GODDARD	79	PR D19 1350	M.C. Goddard *et al.*	(TNTO, BNL) IJ
AGUILAR-...	70B	PRL 25 58	M. Aguilar-Benitez *et al.*	(BNL, SYRA)
ADERHOLZ	69	NP B11 259	M. Aderholz *et al.*	(AACH3, BERL, CERN+) I
BLUMENFELD	69	PL 29B 58	B.J. Blumenfeld, G.R. Kalbfleisch	(BNL) I
MOTT	69	PR 177 1966	J. Mott *et al.*	(NWES, ANL) I
Also	67	PRL 18 266	M. Derrick *et al.*	(ANL, NWES) I
PRIMER	68	PRL 20 610	M. Primer *et al.*	(SYRA, BNL) I
SIMS	68	PRL 21 1413	W.H. Sims *et al.*	(FSU, TUFTS, BRAN) I
COLLEY	67	PL 24B 489	D.C. Colley	(BIRM, GLAS, LOIC, MUNI, OXF+) I

$\Sigma(1750)$ S_{11}

$I(J^P) = 1(\frac{1}{2}^-)$ Status: ***

For most results published before 1974 (they are now obsolete), see our 1982 edition Physics Letters **111B** (1982).

There is evidence for this state in many partial-wave analyses, but with wide variations in the mass, width, and couplings. The latest analyses indicated significant couplings to $N\overline{K}$ and $\Lambda\pi$, as well as to $\Sigma\eta$ whose threshold is at 1746 MeV (JONES 74).

$\Sigma(1750)$ MASS

VALUE (MeV)	DOCUMENT ID		TECN	COMMENT
1730 to 1800 (≈ 1750) OUR ESTIMATE				
1756 ± 10	GOPAL	80	DPWA	$\overline{K}N \to \overline{K}N$
1770 ± 10	ALSTON-...	78	DPWA	$\overline{K}N \to \overline{K}N$
1770 ± 15	GOPAL	77	DPWA	$\overline{K}N$ multichannel
• • • We do not use the following data for averages, fits, limits, etc. • • •				
1800 or 1813	[1] MARTIN	77	DPWA	$\overline{K}N$ multichannel
1715 ± 10	[2] CARROLL	76	DPWA	Isospin-1 total σ
1730	DEBELLEFON	76	IPWA	$K^- p \to \Lambda\pi^0$
1780 ± 30	BAILLON	75	IPWA	$\overline{K}N \to \Lambda\pi$ (sol. 1)
1700 ± 30	BAILLON	75	IPWA	$\overline{K}N \to \Lambda\pi$ (sol. 2)
1697^{+20}_{-10}	VANHORN	75	DPWA	$K^- p \to \Lambda\pi^0$
1785 ± 12	CHU	74	DBC	Fits $\sigma(K^- n \to \Sigma^- \eta)$
1760 ± 5	[3] JONES	74	HBC	Fits $\sigma(K^- p \to \Sigma^0 \eta)$
1739 ± 10	PREVOST	74	DPWA	$K^- N \to \Sigma(1385)\pi$

$\Sigma(1750)$ WIDTH

VALUE (MeV)	DOCUMENT ID		TECN	COMMENT
60 to 160 (≈ 90) OUR ESTIMATE				
64 ± 10	GOPAL	80	DPWA	$\overline{K}N \to \overline{K}N$
161 ± 20	ALSTON-...	78	DPWA	$\overline{K}N \to \overline{K}N$
60 ± 10	GOPAL	77	DPWA	$\overline{K}N$ multichannel

Baryon Particle Listings

$\Sigma(1750)$, $\Sigma(1770)$

• • • We do not use the following data for averages, fits, limits, etc. • • •

117 or 119	[1] MARTIN	77	DPWA	$\overline{K}N$ multichannel
10	[2] CARROLL	76	DPWA	Isospin-1 total σ
110	DEBELLEFON	76	IPWA	$K^- p \rightarrow \Lambda\pi^0$
140 ± 30	BAILLON	75	IPWA	$\overline{K}N \rightarrow \Lambda\pi$ (sol. 1)
160 ± 50	BAILLON	75	IPWA	$\overline{K}N \rightarrow \Lambda\pi$ (sol. 2)
66^{+14}_{-12}	VANHORN	75	DPWA	$K^- p \rightarrow \Lambda\pi^0$
89 ± 33	CHU	74	DBC	Fits $\sigma(K^- n \rightarrow \Sigma^-\eta)$
92 ± 7	[3] JONES	74	HBC	Fits $\sigma(K^- p \rightarrow \Sigma^0\eta)$
108 ± 20	PREVOST	74	DPWA	$K^- N \rightarrow \Sigma(1385)\pi$

$\Sigma(1750)$ DECAY MODES

	Mode	Fraction (Γ_i/Γ)
Γ_1	$N\overline{K}$	10–40 %
Γ_2	$\Lambda\pi$	seen
Γ_3	$\Sigma\pi$	<8 %
Γ_4	$\Sigma\eta$	15–55 %
Γ_5	$\Sigma(1385)\pi$	
Γ_6	$\Lambda(1520)\pi$	

The above branching fractions are our estimates, not fits or averages.

$\Sigma(1750)$ BRANCHING RATIOS

See "Sign conventions for resonance couplings" in the Note on Λ and Σ Resonances.

$\Gamma(N\overline{K})/\Gamma_{\text{total}}$ — Γ_1/Γ

VALUE	DOCUMENT ID		TECN	COMMENT
0.1 to 0.4 OUR ESTIMATE				
0.14 ± 0.03	GOPAL	80	DPWA	$\overline{K}N \rightarrow \overline{K}N$
0.33 ± 0.05	ALSTON-...	78	DPWA	$\overline{K}N \rightarrow \overline{K}N$
• • • We do not use the following data for averages, fits, limits, etc. • • •				
0.15 ± 0.03	GOPAL	77	DPWA	See GOPAL 80
0.06 or 0.05	[1] MARTIN	77	DPWA	$\overline{K}N$ multichannel

$(\Gamma_i\Gamma_f)^{1/2}/\Gamma_{\text{total}}$ in $N\overline{K} \rightarrow \Sigma(1750) \rightarrow \Lambda\pi$ — $(\Gamma_1\Gamma_2)^{1/2}/\Gamma$

VALUE	DOCUMENT ID		TECN	COMMENT
$0.04\ \pm0.03$	GOPAL	77	DPWA	$\overline{K}N$ multichannel
• • • We do not use the following data for averages, fits, limits, etc. • • •				
-0.10 or -0.09	[1] MARTIN	77	DPWA	$\overline{K}N$ multichannel
-0.12	DEBELLEFON	76	IPWA	$K^- p \rightarrow \Lambda\pi^0$
$-0.12\ \pm0.02$	BAILLON	75	IPWA	$\overline{K}N \rightarrow \Lambda\pi$ (sol. 1)
$-0.13\ \pm0.03$	BAILLON	75	IPWA	$\overline{K}N \rightarrow \Lambda\pi$ (sol. 2)
$-0.13\ \pm0.04$	VANHORN	75	DPWA	$K^- p \rightarrow \Lambda\pi^0$
-0.120 ± 0.077	DEVENISH	74B		Fixed-t dispersion rel.

$(\Gamma_i\Gamma_f)^{1/2}/\Gamma_{\text{total}}$ in $N\overline{K} \rightarrow \Sigma(1750) \rightarrow \Sigma\pi$ — $(\Gamma_1\Gamma_3)^{1/2}/\Gamma$

VALUE	DOCUMENT ID		TECN	COMMENT
-0.09 ± 0.05	GOPAL	77	DPWA	$\overline{K}N$ multichannel
• • • We do not use the following data for averages, fits, limits, etc. • • •				
$+0.06$ or $+0.06$	[1] MARTIN	77	DPWA	$\overline{K}N$ multichannel
0.13 ± 0.02	LANGBEIN	72	IPWA	$\overline{K}N$ multichannel

$(\Gamma_i\Gamma_f)^{1/2}/\Gamma_{\text{total}}$ in $N\overline{K} \rightarrow \Sigma(1750) \rightarrow \Sigma\eta$ — $(\Gamma_1\Gamma_4)^{1/2}/\Gamma$

VALUE	DOCUMENT ID		TECN	COMMENT
0.23 ± 0.01	[3] JONES	74	HBC	Fits $\sigma(K^- p \rightarrow \Sigma^0\eta)$
• • • We do not use the following data for averages, fits, limits, etc. • • •				
seen	CLINE	69	DBC	Threshold bump

$(\Gamma_i\Gamma_f)^{1/2}/\Gamma_{\text{total}}$ in $N\overline{K} \rightarrow \Sigma(1750) \rightarrow \Sigma(1385)\pi$ — $(\Gamma_1\Gamma_5)^{1/2}/\Gamma$

VALUE	DOCUMENT ID		TECN	COMMENT
$+0.18\pm0.15$	PREVOST	74	DPWA	$K^- N \rightarrow \Sigma(1385)\pi$

$(\Gamma_i\Gamma_f)^{1/2}/\Gamma_{\text{total}}$ in $N\overline{K} \rightarrow \Sigma(1750) \rightarrow \Lambda(1520)\pi$ — $(\Gamma_1\Gamma_6)^{1/2}/\Gamma$

VALUE	DOCUMENT ID		TECN	COMMENT
• • • We do not use the following data for averages, fits, limits, etc. • • •				
0.032 ± 0.021	CAMERON	77	DPWA	P-wave decay

$\Sigma(1750)$ FOOTNOTES

[1] The two MARTIN 77 values are from a T-matrix pole and from a Breit-Wigner fit.
[2] A total cross-section bump with $(J{+}1/2)\ \Gamma_{el}\ /\ \Gamma_{total} = 0.30$.
[3] An S-wave Breit-Wigner fit to the threshold cross section with no background and errors statistical only.

$\Sigma(1750)$ REFERENCES

PDG	82	PL 111B	M. Roos *et al.*	(HELS, CIT, CERN)
GOPAL	80	Toronto Conf. 159	G.P. Gopal	(RHEL) IJP
ALSTON-...	78	PR D18 182	M. Alston-Garnjost *et al.*	(LBL, MTHO+) IJP
Also	77	PRL 38 1007	M. Alston-Garnjost *et al.*	(LBL, MTHO+) IJP
CAMERON	77	NP B131 399	W. Cameron *et al.*	(RHEL, LOIC) IJP
GOPAL	77	NP B119 362	G.P. Gopal *et al.*	(LOIC, RHEL) IJP
MARTIN	77	NP B127 349	B.R. Martin, M.K. Pidcock, R.G. Moorhouse	(LOUC+) IJP
Also	77B	NP B126 266	B.R. Martin, M.K. Pidcock	(LOUC)
Also	77C	NP B126 285	B.R. Martin, M.K. Pidcock	(LOUC) IJP
CARROLL	76	PRL 37 806	A.S. Carroll *et al.*	(BNL) I
DEBELLEFON	76	NP B109 129	A. de Bellefon, A. Berthon	(CDEF) IJP
BAILLON	75	NP B94 39	P.H. Baillon, P.J. Litchfield	(CERN, RHEL) IJP
VANHORN	75	NP B87 145	A.J. van Horn	(LBL) IJP
Also	75B	NP B87 157	A.J. van Horn	(LBL) IJP
CHU	74	NC 20A 35	R.Y.L. Chu *et al.*	(PLAT, TUFTS, BRAN) IJP
DEVENISH	74B	NP B81 330	R.C.E. Devenish, C.D. Froggatt, B.R. Martin	(DESY+)
JONES	74	NP B73 141	M.D. Jones	(CHIC) IJP
PREVOST	74	NP B69 246	J. Prevost *et al.*	(SACL, CERN, HEID)
LANGBEIN	72	NP B47 477	W. Langbein, F. Wagner	(MPIM) IJP
CLINE	69	LNC 2 407	D. Cline, R. Laumann, J. Mapp	(WISC)

$\Sigma(1770)$ P_{11}

$I(J^P) = 1(\frac{1}{2}^+)$ Status: *

OMITTED FROM SUMMARY TABLE

Evidence for this state now rests solely on solution 1 of BAILLON 75, (see the footnotes) but the $\Lambda\pi$ partial-wave amplitudes of this solution are in disagreement with amplitudes from most other $\Lambda\pi$ analyses.

$\Sigma(1770)$ MASS

VALUE (MeV)	DOCUMENT ID		TECN	COMMENT
≈ 1770 OUR ESTIMATE				
1738 ± 10	[1] GOPAL	77	DPWA	$\overline{K}N$ multichannel
1770 ± 20	[2] BAILLON	75	IPWA	$\overline{K}N \rightarrow \Lambda\pi$
1772	[3] KANE	72	DPWA	$K^- p \rightarrow \Sigma\pi$

$\Sigma(1770)$ WIDTH

VALUE (MeV)	DOCUMENT ID		TECN	COMMENT
72 ± 10	[1] GOPAL	77	DPWA	$\overline{K}N$ multichannel
80 ± 30	[2] BAILLON	75	IPWA	$\overline{K}N \rightarrow \Lambda\pi$
80	[3] KANE	72	DPWA	$K^- p \rightarrow \Sigma\pi$

$\Sigma(1770)$ DECAY MODES

	Mode
Γ_1	$N\overline{K}$
Γ_2	$\Lambda\pi$
Γ_3	$\Sigma\pi$

$\Sigma(1770)$ BRANCHING RATIOS

See "Sign conventions for resonance couplings" in the Note on Λ and Σ Resonances.

$\Gamma(N\overline{K})/\Gamma_{\text{total}}$ — Γ_1/Γ

VALUE	DOCUMENT ID		TECN	COMMENT
0.14 ± 0.04	[1] GOPAL	77	DPWA	$\overline{K}N$ multichannel

$(\Gamma_i\Gamma_f)^{1/2}/\Gamma_{\text{total}}$ in $N\overline{K} \rightarrow \Sigma(1770) \rightarrow \Lambda\pi$ — $(\Gamma_1\Gamma_2)^{1/2}/\Gamma$

VALUE	DOCUMENT ID		TECN	COMMENT
< 0.04	GOPAL	77	DPWA	$\overline{K}N$ multichannel
-0.08 ± 0.02	[2] BAILLON	75	IPWA	$\overline{K}N \rightarrow \Lambda\pi$

$(\Gamma_i\Gamma_f)^{1/2}/\Gamma_{\text{total}}$ in $N\overline{K} \rightarrow \Sigma(1770) \rightarrow \Sigma\pi$ — $(\Gamma_1\Gamma_3)^{1/2}/\Gamma$

VALUE	DOCUMENT ID		TECN	COMMENT
< 0.04	GOPAL	77	DPWA	$\overline{K}N$ multichannel
-0.108	[3] KANE	72	DPWA	$K^- p \rightarrow \Sigma\pi$

$\Sigma(1770)$ FOOTNOTES

[1] Required to fit the isospin-1 total cross section of CARROLL 76 in the $\overline{K}N$ channel. The addition of new $K^- p$ polarization and $K^- n$ differential cross-section data in GOPAL 80 find it to be more consistent with the $\Sigma(1660)$ P_{11}.
[2] From solution 1 of BAILLON 75; not present in solution 2.
[3] Not required in KANE 74, which supersedes KANE 72.

$\Sigma(1770)$ REFERENCES

GOPAL	80	Toronto Conf. 159	G.P. Gopal	(RHEL)
GOPAL	77	NP B119 362	G.P. Gopal *et al.*	(LOIC, RHEL) IJP
CARROLL	76	PRL 37 806	A.S. Carroll *et al.*	(BNL) I
BAILLON	75	NP B94 39	P.H. Baillon, P.J. Litchfield	(CERN, RHEL) IJP
KANE	74	LBL-2452	D.F. Kane	(LBL) IJP
KANE	72	PR D5 1583	D.F.J. Kane	(LBL)

$\Sigma(1775)$ D_{15}

$I(J^P) = 1(\frac{5}{2}^-)$ Status: ****

Discovered by GALTIERI 63, this resonance plays the same role as cornerstone for isospin-1 analyses in this region as the $\Lambda(1820)$ does in the isospin-0 channel.

For most results published before 1974 (they are now obsolete), see our 1982 edition Physics Letters **111B** (1982).

$\Sigma(1775)$ MASS

VALUE (MeV)	DOCUMENT ID		TECN	COMMENT
1770 to 1780 (≈ 1775) OUR ESTIMATE				
1778± 5	GOPAL	80	DPWA	$\overline{K}N \to \overline{K}N$
1777± 5	ALSTON-...	78	DPWA	$\overline{K}N \to \overline{K}N$
1774± 5	GOPAL	77	DPWA	$\overline{K}N$ multichannel
1775±10	BAILLON	75	IPWA	$\overline{K}N \to \Lambda\pi$
1774±10	VANHORN	75	DPWA	$K^-p \to \Lambda\pi^0$
1772± 6	KANE	74	DPWA	$K^-p \to \Sigma\pi$
• • • We do not use the following data for averages, fits, limits, etc. • • •				
1772 or 1777	[1] MARTIN	77	DPWA	$\overline{K}N$ multichannel
1765	DEBELLEFON	76	IPWA	$K^-p \to \Lambda\pi^0$

$\Sigma(1775)$ WIDTH

VALUE (MeV)	DOCUMENT ID		TECN	COMMENT
105 to 135 (≈ 120) OUR ESTIMATE				
137±10	GOPAL	80	DPWA	$\overline{K}N \to \overline{K}N$
116±10	ALSTON-...	78	DPWA	$\overline{K}N \to \overline{K}N$
130±10	GOPAL	77	DPWA	$\overline{K}N$ multichannel
125±15	BAILLON	75	IPWA	$\overline{K}N \to \Lambda\pi$
146±18	VANHORN	75	DPWA	$K^-p \to \Lambda\pi^0$
154±10	KANE	74	DPWA	$K^-p \to \Sigma\pi$
• • • We do not use the following data for averages, fits, limits, etc. • • •				
102 or 103	[1] MARTIN	77	DPWA	$\overline{K}N$ multichannel
120	DEBELLEFON	76	IPWA	$K^-p \to \Lambda\pi^0$

$\Sigma(1775)$ DECAY MODES

	Mode	Fraction (Γ_i/Γ)
Γ_1	$N\overline{K}$	37–43%
Γ_2	$\Lambda\pi$	14–20%
Γ_3	$\Sigma\pi$	2–5%
Γ_4	$\Sigma(1385)\pi$	8–12%
Γ_5	$\Sigma(1385)\pi$, D-wave	
Γ_6	$\Lambda(1520)\pi$	17–23%
Γ_7	$\Sigma\pi\pi$	

The above branching fractions are our estimates, not fits or averages.

CONSTRAINED FIT INFORMATION

An overall fit to 8 branching ratios uses 16 measurements and one constraint to determine 5 parameters. The overall fit has a $\chi^2 = 63.9$ for 12 degrees of freedom.

The following *off-diagonal* array elements are the correlation coefficients $\langle \delta x_i \delta x_j \rangle / (\delta x_i \cdot \delta x_j)$, in percent, from the fit to the branching fractions, $x_i \equiv \Gamma_i/\Gamma_{\text{total}}$. The fit constrains the x_i whose labels appear in this array to sum to one.

x_2	−30			
x_3	−17	−21		
x_4	−37	−49	−14	
x_6	−81	6	8	16
	x_1	x_2	x_3	x_4

$\Sigma(1775)$ BRANCHING RATIOS

See "Sign conventions for resonance couplings" in the Note on Λ and Σ Resonances. Also, the errors quoted do not include uncertainties due to the parametrization used in the partial-wave analyses and are thus too small.

$\Gamma(N\overline{K})/\Gamma_{\text{total}}$ Γ_1/Γ

VALUE	DOCUMENT ID		TECN	COMMENT
0.37 to 0.43 OUR ESTIMATE				
0.45 ±0.04 OUR FIT Error includes scale factor of 3.1.				
0.391±0.017 OUR AVERAGE				
0.40 ±0.02	GOPAL	80	DPWA	$\overline{K}N \to \overline{K}N$
0.37 ±0.03	ALSTON-...	78	DPWA	$\overline{K}N \to \overline{K}N$
• • • We do not use the following data for averages, fits, limits, etc. • • •				
0.41 ±0.03	GOPAL	77	DPWA	See GOPAL 80
0.37 or 0.36	[1] MARTIN	77	DPWA	$\overline{K}N$ multichannel

$(\Gamma_i\Gamma_f)^{1/2}/\Gamma_{\text{total}}$ in $N\overline{K} \to \Sigma(1775) \to \Lambda\pi$ $(\Gamma_1\Gamma_2)^{1/2}/\Gamma$

VALUE	DOCUMENT ID		TECN	COMMENT
0.305±0.018 OUR FIT Error includes scale factor of 2.4.				
−0.262±0.015 OUR AVERAGE				
−0.28 ±0.03	GOPAL	77	DPWA	$\overline{K}N$ multichannel
−0.25 ±0.02	BAILLON	75	IPWA	$\overline{K}N \to \Lambda\pi$
$-0.28\ ^{+0.04}_{-0.05}$	VANHORN	75	DPWA	$K^-p \to \Lambda\pi^0$
−0.259±0.048	DEVENISH	74B		Fixed-t dispersion rel.
• • • We do not use the following data for averages, fits, limits, etc. • • •				
−0.29 or −0.28	[1] MARTIN	77	DPWA	$\overline{K}N$ multichannel
−0.30	DEBELLEFON	76	IPWA	$K^-p \to \Lambda\pi^0$

$(\Gamma_i\Gamma_f)^{1/2}/\Gamma_{\text{total}}$ in $N\overline{K} \to \Sigma(1775) \to \Sigma\pi$ $(\Gamma_1\Gamma_3)^{1/2}/\Gamma$

VALUE	DOCUMENT ID		TECN	COMMENT
0.105±0.025 OUR FIT Error includes scale factor of 3.1.				
0.098±0.016 OUR AVERAGE Error includes scale factor of 1.8.				
+0.13 ±0.02	GOPAL	77	DPWA	$\overline{K}N$ multichannel
0.09 ±0.01	KANE	74	DPWA	$K^-p \to \Sigma\pi$
• • • We do not use the following data for averages, fits, limits, etc. • • •				
+0.08 or +0.08	[1] MARTIN	77	DPWA	$\overline{K}N$ multichannel

$(\Gamma_i\Gamma_f)^{1/2}/\Gamma_{\text{total}}$ in $N\overline{K} \to \Sigma(1775) \to \Lambda(1520)\pi$ $(\Gamma_1\Gamma_6)^{1/2}/\Gamma$

VALUE	DOCUMENT ID		TECN	COMMENT
$\mathbf{0.315\ ^{+0.010}_{-0.009}}$ **OUR FIT** Error includes scale factor of 1.5.				
0.303±0.009 OUR AVERAGE Signs on measurements were ignored.				
−0.305±0.010	[2] CAMERON	77	DPWA	$K^-p \to \Lambda(1520)\pi^0$
0.31 ±0.02	BARLETTA	72	DPWA	$K^-p \to \Lambda(1520)\pi^0$
0.27 ±0.03	ARMENTEROS	65C	HBC	$K^-p \to \Lambda(1520)\pi^0$

$(\Gamma_i\Gamma_f)^{1/2}/\Gamma_{\text{total}}$ in $N\overline{K} \to \Sigma(1775) \to \Sigma(1385)\pi$ $(\Gamma_1\Gamma_4)^{1/2}/\Gamma$

VALUE	DOCUMENT ID		TECN	COMMENT
0.211±0.022 OUR FIT Error includes scale factor of 2.8.				
0.188±0.010 OUR AVERAGE Signs on measurements were ignored.				
−0.184±0.011	[3] CAMERON	78	DPWA	$K^-p \to \Sigma(1385)\pi$
+0.20 ±0.02	PREVOST	74	DPWA	$K^-N \to \Sigma(1385)\pi$
• • • We do not use the following data for averages, fits, limits, etc. • • •				
0.32 ±0.06	SIMS	68	DBC	$K^-N \to \Lambda\pi\pi$
0.24 ±0.03	ARMENTEROS	67C	HBC	$K^-p \to \Lambda\pi\pi$

$\Gamma(\Lambda\pi)/\Gamma(N\overline{K})$ Γ_2/Γ_1

VALUE	DOCUMENT ID		TECN	COMMENT
0.46±0.09 OUR FIT Error includes scale factor of 2.9.				
0.33±0.05	UHLIG	67	HBC	K^-p 0.9 GeV/c

$\Gamma(\Sigma\pi\pi)/\Gamma_{\text{total}}$ Γ_7/Γ

VALUE	DOCUMENT ID		TECN	COMMENT
• • • We do not use the following data for averages, fits, limits, etc. • • •				
0.12	[4] ARMENTEROS	68C	HDBC	$K^-N \to \Sigma\pi\pi$

$\Gamma(\Sigma(1385)\pi)/\Gamma(N\overline{K})$ Γ_4/Γ_1

VALUE	DOCUMENT ID		TECN	COMMENT
0.22±0.07 OUR FIT Error includes scale factor of 3.6.				
0.25±0.09	UHLIG	67	HBC	K^-p 0.9 GeV/c

$\Gamma(\Lambda(1520)\pi)/\Gamma(N\overline{K})$ Γ_6/Γ_1

VALUE	DOCUMENT ID		TECN	COMMENT
0.49±0.11 OUR FIT Error includes scale factor of 3.5.				
0.28±0.05	UHLIG	67	HBC	K^-p 0.9 GeV/c

$\Sigma(1775)$ FOOTNOTES

[1] The two MARTIN 77 values are from a T-matrix pole and from a Breit-Wigner fit.

[2] This rate combines P-wave- and F-wave decays. The CAMERON 77 results for the separate P-wave- and F-wave decays are -0.303 ± 0.010 and -0.037 ± 0.014. The published signs have been changed here to be in accord with the baryon-first convention.

[3] The CAMERON 78 upper limit on G-wave decay is 0.03.

[4] For about 3/4 of this, the $\Sigma\pi$ system has $I = 0$ and is almost entirely $\Lambda(1520)$. For the rest, the $\Sigma\pi$ has $I = 1$, which is about what is expected from the known $\Sigma(1775) \to \Sigma(1385)\pi$ rate, as seen in $\Lambda\pi\pi$.

$\Sigma(1775)$ REFERENCES

PDG	82	PL 111B	M. Roos *et al.*	(HELS, CIT, CERN)
GOPAL	80	Toronto Conf. 159	G.P. Gopal	(RHEL) IJP
ALSTON-...	78	PR D18 182	M. Alston-Garnjost *et al.*	(LBL, MTHO+) IJP
Also	77	PRL 38 1007	M. Alston-Garnjost *et al.*	(LBL, MTHO+) IJP
CAMERON	78	NP B143 189	W. Cameron *et al.*	(RHEL, LOIC) IJP
CAMERON	77	NP B131 399	W. Cameron *et al.*	(RHEL, LOIC) IJP
GOPAL	77	NP B119 362	G.P. Gopal *et al.*	(LOIC, RHEL) IJP
MARTIN	77	NP B127 349	B.R. Martin, M.K. Pidcock, R.G. Moorhouse	(LOUC+) IJP
Also	77B	NP B126 266	B.R. Martin, M.K. Pidcock	(LOUC)
Also	77C	NP B126 285	B.R. Martin, M.K. Pidcock	(LOUC) IJP
DEBELLEFON	76	NP B109 129	A. de Bellefon, A. Berthon	(CDEF) IJP
BAILLON	75	NP B94 39	P.H. Baillon, P.J. Litchfield	(CERN, RHEL) IJP
VANHORN	75	NP B87 145	A.J. van Horn	(LBL) IJP
Also	75B	NP B87 157	A.J. van Horn	(LBL) IJP

Baryon Particle Listings

$\Sigma(1775)$, $\Sigma(1840)$, $\Sigma(1880)$

DEVENISH	74B	NP B81 330	R.C.E. Devenish, C.D. Froggatt, B.R. Martin	(DESY+)
KANE	74	LBL-2452	D.F. Kane	(LBL) IJP
PREVOST	74	NP B69 246	J. Prevost *et al.*	(SACL, CERN, HEID)
BARLETTA	72	NP B40 45	W.A. Barletta	(EFI) IJP
Also	66	PRL 17 841	S. Fenster *et al.*	(CHIC, ANL, CERN) IJP
ARMENTEROS	68C	NP B8 216	R. Armenteros *et al.*	(CERN, HEID, SACL) I
SIMS	68	PRL 21 1413	W.H. Sims *et al.*	(FSU, TUFTS, BRAN)
ARMENTEROS	67C	ZPHY 202 486	R. Armenteros *et al.*	(CERN, HEID, SACL)
UHLIG	67	PR 155 1448	R.P. Uhlig *et al.*	(UMD, NRL)
ARMENTEROS	65C	PL 19 338	R. Armenteros *et al.*	(CERN, HEID, SACL) IJP
GALTIERI	63	PL 6 296	A. Galtieri, A. Hussain, R. Tripp	(LRL) IJ

$\Sigma(1840)$ P_{13}

$I(J^P) = 1(\frac{3}{2}^+)$ Status: *

OMITTED FROM SUMMARY TABLE

For the time being, we list together here all resonance claims in the P_{13} wave between 1700 and 1900 MeV.

$\Sigma(1840)$ MASS

VALUE (MeV)	DOCUMENT ID		TECN	COMMENT
≈ 1840 OUR ESTIMATE				
1798 or 1802	[1] MARTIN	77	DPWA	$\overline{K}N$ multichannel
1720 ± 30	[2] BAILLON	75	IPWA	$\overline{K}N \to \Lambda\pi$
1925 ± 200	VANHORN	75	DPWA	$K^- p \to \Lambda\pi^0$
1840 ± 10	LANGBEIN	72	IPWA	$\overline{K}N$ multichannel

$\Sigma(1840)$ WIDTH

VALUE (MeV)	DOCUMENT ID		TECN	COMMENT
93 or 93	[1] MARTIN	77	DPWA	$\overline{K}N$ multichannel
120 ± 30	[2] BAILLON	75	IPWA	$\overline{K}N \to \Lambda\pi$
65^{+50}_{-20}	VANHORN	75	DPWA	$K^- p \to \Lambda\pi^0$
120 ± 10	LANGBEIN	72	IPWA	$\overline{K}N$ multichannel

$\Sigma(1840)$ DECAY MODES

	Mode
Γ_1	$N\overline{K}$
Γ_2	$\Lambda\pi$
Γ_3	$\Sigma\pi$

$\Sigma(1840)$ BRANCHING RATIOS

See "Sign conventions for resonance couplings" in the Note on Λ and Σ Resonances.

$\Gamma(N\overline{K})/\Gamma_{total}$ Γ_1/Γ

VALUE	DOCUMENT ID		TECN	COMMENT
0 or 0	[1] MARTIN	77	DPWA	$\overline{K}N$ multichannel
0.37 ± 0.13	LANGBEIN	72	IPWA	$\overline{K}N$ multichannel

$(\Gamma_i\Gamma_f)^{1/2}/\Gamma_{total}$ in $N\overline{K} \to \Sigma(1840) \to \Lambda\pi$ $(\Gamma_1\Gamma_2)^{1/2}/\Gamma$

VALUE	DOCUMENT ID		TECN	COMMENT
+ 0.03 or + 0.03	[1] MARTIN	77	DPWA	$\overline{K}N$ multichannel
+ 0.11 ± 0.02	[2] BAILLON	75	IPWA	$\overline{K}N \to \Lambda\pi$
+ 0.06 ± 0.04	VANHORN	75	DPWA	$K^- p \to \Lambda\pi^0$
+ 0.122 ± 0.078	DEVENISH	74B		Fixed-t dispersion rel.
0.20 ± 0.04	LANGBEIN	72	IPWA	$\overline{K}N$ multichannel

$(\Gamma_i\Gamma_f)^{1/2}/\Gamma_{total}$ in $N\overline{K} \to \Sigma(1840) \to \Sigma\pi$ $(\Gamma_1\Gamma_3)^{1/2}/\Gamma$

VALUE	DOCUMENT ID		TECN	COMMENT
− 0.04 or − 0.04	[1] MARTIN	77	DPWA	$\overline{K}N$ multichannel
0.15 ± 0.04	LANGBEIN	72	IPWA	$\overline{K}N$ multichannel

$\Sigma(1840)$ FOOTNOTES

[1] The two MARTIN 77 values are from a T-matrix pole and from a Breit-Wigner fit.
[2] From solution 1 of BAILLON 75; not present in solution 2.

$\Sigma(1840)$ REFERENCES

MARTIN	77	NP B127 349	B.R. Martin, M.K. Pidcock, R.G. Moorhouse	(LOUC+) IJP
Also	77B	NP B126 266	B.R. Martin, M.K. Pidcock	(LOUC)
Also	77C	NP B126 285	B.R. Martin, M.K. Pidcock	(LOUC) IJP
BAILLON	75	NP B94 39	P.H. Baillon, P.J. Litchfield	(CERN, RHEL) IJP
VANHORN	75	NP B87 145	A.J. van Horn	(LBL) IJP
Also	75B	NP B87 157	A.J. van Horn	(LBL) IJP
DEVENISH	74B	NP B81 330	R.C.E. Devenish, C.D. Froggatt, B.R. Martin	(DESY+)
LANGBEIN	72	NP B47 477	W. Langbein, F. Wagner	(MPIM) IJP

$\Sigma(1880)$ P_{11}

$I(J^P) = 1(\frac{1}{2}^+)$ Status: **

OMITTED FROM SUMMARY TABLE

A P_{11} resonance is suggested by several partial-wave analyses, but with wide variations in the mass and other parameters. We list here all claims which lie well above the P_{11} $\Sigma(1770)$.

$\Sigma(1880)$ MASS

VALUE (MeV)	DOCUMENT ID		TECN	COMMENT
≈ 1880 OUR ESTIMATE				
1826 ± 20	GOPAL	80	DPWA	$\overline{K}N \to \overline{K}N$
1870 ± 10	CAMERON	78B	DPWA	$K^- p \to N\overline{K}^*$
1847 or 1863	[1] MARTIN	77	DPWA	$\overline{K}N$ multichannel
1960 ± 30	[2] BAILLON	75	IPWA	$\overline{K}N \to \Lambda\pi$
1985 ± 50	VANHORN	75	DPWA	$K^- p \to \Lambda\pi^0$
1898	[3] LEA	73	DPWA	Multichannel K-matrix
~ 1850	ARMENTEROS	70	IPWA	$\overline{K}N \to \overline{K}N$
1950 ± 50	BARBARO-...	70	DPWA	$K^- N \to \Lambda\pi$
1920 ± 30	LITCHFIELD	70	DPWA	$K^- N \to \Lambda\pi$
1850	BAILEY	69	DPWA	$\overline{K}N \to \overline{K}N$
1882 ± 40	SMART	68	DPWA	$K^- N \to \Lambda\pi$

$\Sigma(1880)$ WIDTH

VALUE (MeV)	DOCUMENT ID		TECN	COMMENT
86 ± 15	GOPAL	80	DPWA	$\overline{K}N \to \overline{K}N$
80 ± 10	CAMERON	78B	DPWA	$K^- p \to N\overline{K}^*$
216 or 220	[1] MARTIN	77	DPWA	$\overline{K}N$ multichannel
260 ± 40	[2] BAILLON	75	IPWA	$\overline{K}N \to \Lambda\pi$
220 ± 140	VANHORN	75	DPWA	$K^- p \to \Lambda\pi^0$
222	[3] LEA	73	DPWA	Multichannel K-matrix
~ 30	ARMENTEROS	70	IPWA	$\overline{K}N \to \overline{K}N$
200 ± 50	BARBARO-...	70	DPWA	$K^- N \to \Lambda\pi$
170 ± 40	LITCHFIELD	70	DPWA	$K^- N \to \Lambda\pi$
200	BAILEY	69	DPWA	$\overline{K}N \to \overline{K}N$
222 ± 150	SMART	68	DPWA	$K^- N \to \Lambda\pi$

$\Sigma(1880)$ DECAY MODES

	Mode
Γ_1	$N\overline{K}$
Γ_2	$\Lambda\pi$
Γ_3	$\Sigma\pi$
Γ_4	$N\overline{K}^*(892)$, S=1/2, P-wave
Γ_5	$N\overline{K}^*(892)$, S=3/2, P-wave

$\Sigma(1880)$ BRANCHING RATIOS

See "Sign conventions for resonance couplings" in the Note on Λ and Σ Resonances.

$\Gamma(N\overline{K})/\Gamma_{total}$ Γ_1/Γ

VALUE	DOCUMENT ID		TECN	COMMENT
0.06 ± 0.02	GOPAL	80	DPWA	$\overline{K}N \to \overline{K}N$
0.27 or 0.27	[1] MARTIN	77	DPWA	$\overline{K}N$ multichannel
0.31	[3] LEA	73	DPWA	Multichannel K-matrix
0.20	ARMENTEROS	70	IPWA	$\overline{K}N \to \overline{K}N$
0.22	BAILEY	69	DPWA	$\overline{K}N \to \overline{K}N$

$(\Gamma_i\Gamma_f)^{1/2}/\Gamma_{total}$ in $N\overline{K} \to \Sigma(1880) \to \Lambda\pi$ $(\Gamma_1\Gamma_2)^{1/2}/\Gamma$

VALUE	DOCUMENT ID		TECN	COMMENT
− 0.24 or − 0.24	[1] MARTIN	77	DPWA	$\overline{K}N$ multichannel
− 0.12 ± 0.02	[2] BAILLON	75	IPWA	$\overline{K}N \to \Lambda\pi$
$+0.05\ ^{+0.07}_{-0.02}$	VANHORN	75	DPWA	$K^- p \to \Lambda\pi^0$
− 0.169 ± 0.119	DEVENISH	74B		Fixed-t dispersion rel.
− 0.30	[3] LEA	73	DPWA	Multichannel K-matrix
− 0.09 ± 0.04	BARBARO-...	70	DPWA	$K^- N \to \Lambda\pi$
− 0.14 ± 0.03	LITCHFIELD	70	DPWA	$K^- N \to \Lambda\pi$
− 0.11 ± 0.03	SMART	68	DPWA	$K^- N \to \Lambda\pi$

$(\Gamma_i\Gamma_f)^{1/2}/\Gamma_{total}$ in $N\overline{K} \to \Sigma(1880) \to \Sigma\pi$ $(\Gamma_1\Gamma_3)^{1/2}/\Gamma$

VALUE	DOCUMENT ID		TECN	COMMENT
+ 0.30 or + 0.29 not seen	[1] MARTIN	77	DPWA	$\overline{K}N$ multichannel
	[3] LEA	73	DPWA	Multichannel K-matrix

$(\Gamma_i\Gamma_f)^{1/2}/\Gamma_{total}$ in $N\overline{K} \to \Sigma(1880) \to N\overline{K}^*(892)$, S=1/2, P-wave $(\Gamma_1\Gamma_4)^{1/2}/\Gamma$

VALUE	DOCUMENT ID		TECN	COMMENT
− 0.05 ± 0.03	[4] CAMERON	78B	DPWA	$K^- p \to N\overline{K}^*$

$(\Gamma_i\Gamma_f)^{1/2}/\Gamma_{total}$ in $N\overline{K} \to \Sigma(1880) \to N\overline{K}^*(892)$, S=3/2, P-wave $(\Gamma_1\Gamma_5)^{1/2}/\Gamma$

VALUE	DOCUMENT ID		TECN	COMMENT
$+0.11 \pm 0.03$	CAMERON	78B	DPWA	$K^- p \to N\overline{K}^*$

$\Sigma(1880)$ FOOTNOTES

[1] The two MARTIN 77 values are from a T-matrix pole and from a Breit-Wigner fit.
[2] From solution 1 of BAILLON 75; not present in solution 2.
[3] Only unconstrained states from table 1 of LEA 73 are listed.
[4] The published sign has been changed to be in accord with the baryon-first convention.

$\Sigma(1880)$ REFERENCES

GOPAL	80	Toronto Conf. 159	G.P. Gopal	(RHEL) IJP
CAMERON	78B	NP B146 327	W. Cameron *et al.*	(RHEL, LOIC) IJP
MARTIN	77	NP B127 349	B.R. Martin, M.K. Pidcock, R.G. Moorhouse	(LOUC+) IJP
Also	77B	NP B126 266	B.R. Martin, M.K. Pidcock	(LOUC)
Also	77C	NP B126 285	B.R. Martin, M.K. Pidcock	(LOUC) IJP
BAILLON	75	NP B94 39	P.H. Baillon, P.J. Litchfield	(CERN, RHEL) IJP
VANHORN	75	NP B87 145	A.J. van Horn	(LBL) IJP
Also	75B	NP B87 157	A.J. van Horn	(LBL) IJP
DEVENISH	74B	NP B81 330	R.C.E. Devenish, C.D. Froggatt, B.R. Martin	(DESY+)
LEA	73	NP B56 77	A.T. Lea *et al.*	(RHEL, LOUC, GLAS, AARH) IJP
ARMENTEROS	70	Duke Conf. 123 Hyperon Resonances, 1970	R. Armenteros *et al.*	(CERN, HEID, SACL) IJP
BARBARO-...	70	Duke Conf. 173 Hyperon Resonances, 1970	A. Barbaro-Galtieri	(LRL) IJP
LITCHFIELD	70	NP B22 269	P.J. Litchfield	(RHEL) IJP
BAILEY	69	Thesis UCRL 50617	J.M. Bailey	(LLL) IJP
SMART	68	PR 169 1330	W.M. Smart	(LRL) IJP

$\Sigma(1915)$ F_{15}

$I(J^P) = 1(\frac{5}{2}^+)$ Status: ****

Discovered by COOL 66. For results published before 1974 (they are now obsolete), see our 1982 edition Physics Letters **111B** (1982).

This entry only includes results from partial-wave analyses. Parameters of peaks seen in cross sections and invariant-mass distributions in this region used to be listed in in a separate entry immediately following. They may be found in our 1986 edition Physics Letters **170B** (1986).

$\Sigma(1915)$ MASS

VALUE (MeV)	DOCUMENT ID		TECN	COMMENT
1900 to 1935 (≈ 1915) OUR ESTIMATE				
1937 ± 20	ALSTON-...	78	DPWA	$\overline{K}N \to \overline{K}N$
1894 ± 5	[1] CORDEN	77C		$K^- n \to \Sigma\pi$
1909 ± 5	[1] CORDEN	77C		$K^- n \to \Sigma\pi$
1920 ± 10	GOPAL	77	DPWA	$\overline{K}N$ multichannel
1900 ± 4	[2] CORDEN	76	DPWA	$K^- n \to \Lambda\pi^-$
1920 ± 30	BAILLON	75	IPWA	$\overline{K}N \to \Lambda\pi$
1914 ± 10	HEMINGWAY	75	DPWA	$K^- p \to \overline{K}N$
1920^{+15}_{-20}	VANHORN	75	DPWA	$K^- p \to \Lambda\pi^0$
1920 ± 5	KANE	74	DPWA	$K^- p \to \Sigma\pi$
• • • We do not use the following data for averages, fits, limits, etc. • • •				
not seen	DECLAIS	77	DPWA	$\overline{K}N \to \overline{K}N$
1925 or 1933	[3] MARTIN	77	DPWA	$\overline{K}N$ multichannel
1915	DEBELLEFON	76	IPWA	$K^- p \to \Lambda\pi^0$

$\Sigma(1915)$ WIDTH

VALUE (MeV)	DOCUMENT ID		TECN	COMMENT
80 to 160 (≈ 120) OUR ESTIMATE				
161 ± 20	ALSTON-...	78	DPWA	$\overline{K}N \to \overline{K}N$
107 ± 14	[1] CORDEN	77C		$K^- n \to \Sigma\pi$
85 ± 13	[1] CORDEN	77C		$K^- n \to \Sigma\pi$
130 ± 10	GOPAL	77	DPWA	$\overline{K}N$ multichannel
75 ± 14	[2] CORDEN	76	DPWA	$K^- n \to \Lambda\pi^-$
70 ± 20	BAILLON	75	IPWA	$\overline{K}N \to \Lambda\pi$
85 ± 15	HEMINGWAY	75	DPWA	$K^- p \to \overline{K}N$
102 ± 18	VANHORN	75	DPWA	$K^- p \to \Lambda\pi^0$
162 ± 25	KANE	74	DPWA	$K^- p \to \Sigma\pi$
• • • We do not use the following data for averages, fits, limits, etc. • • •				
171 or 173	[3] MARTIN	77	DPWA	$\overline{K}N$ multichannel
60	DEBELLEFON	76	IPWA	$K^- p \to \Lambda\pi^0$

$\Sigma(1915)$ DECAY MODES

	Mode	Fraction (Γ_j/Γ)
Γ_1	$N\overline{K}$	5–15 %
Γ_2	$\Lambda\pi$	seen
Γ_3	$\Sigma\pi$	seen
Γ_4	$\Sigma(1385)\pi$	<5 %
Γ_5	$\Sigma(1385)\pi$, P-wave	
Γ_6	$\Sigma(1385)\pi$, F-wave	

The above branching fractions are our estimates, not fits or averages.

$\Sigma(1915)$ BRANCHING RATIOS

See "Sign conventions for resonance couplings" in the Note on Λ and Σ Resonances.

$\Gamma(N\overline{K})/\Gamma_{total}$ Γ_1/Γ

VALUE	DOCUMENT ID		TECN	COMMENT
0.05 to 0.15 OUR ESTIMATE				
0.03 ± 0.02	[4] GOPAL	80	DPWA	$\overline{K}N \to \overline{K}N$
0.14 ± 0.05	ALSTON-...	78	DPWA	$\overline{K}N \to \overline{K}N$
0.11 ± 0.04	HEMINGWAY	75	DPWA	$K^- p \to \overline{K}N$
• • • We do not use the following data for averages, fits, limits, etc. • • •				
0.05 ± 0.03	GOPAL	77	DPWA	See GOPAL 80
0.08 or 0.08	[3] MARTIN	77	DPWA	$\overline{K}N$ multichannel

$(\Gamma_i\Gamma_f)^{1/2}/\Gamma_{total}$ in $N\overline{K} \to \Sigma(1915) \to \Lambda\pi$ $(\Gamma_1\Gamma_2)^{1/2}/\Gamma$

VALUE	DOCUMENT ID		TECN	COMMENT
-0.09 ± 0.03	GOPAL	77	DPWA	$\overline{K}N$ multichannel
-0.10 ± 0.01	[2] CORDEN	76	DPWA	$K^- n \to \Lambda\pi^-$
-0.06 ± 0.02	BAILLON	75	IPWA	$\overline{K}N \to \Lambda\pi$
-0.09 ± 0.02	VANHORN	75	DPWA	$K^- p \to \Lambda\pi^0$
-0.087 ± 0.056	DEVENISH	74B		Fixed-t dispersion rel.
• • • We do not use the following data for averages, fits, limits, etc. • • •				
-0.09 or -0.09	[3] MARTIN	77	DPWA	$\overline{K}N$ multichannel
-0.10	DEBELLEFON	76	IPWA	$K^- p \to \Lambda\pi^0$

$(\Gamma_i\Gamma_f)^{1/2}/\Gamma_{total}$ in $N\overline{K} \to \Sigma(1915) \to \Sigma\pi$ $(\Gamma_1\Gamma_3)^{1/2}/\Gamma$

VALUE	DOCUMENT ID		TECN	COMMENT
-0.17 ± 0.01	[1] CORDEN	77C		$K^- n \to \Sigma\pi$
-0.15 ± 0.02	[1] CORDEN	77C		$K^- n \to \Sigma\pi$
-0.19 ± 0.03	GOPAL	77	DPWA	$\overline{K}N$ multichannel
-0.16 ± 0.03	KANE	74	DPWA	$K^- p \to \Sigma\pi$
• • • We do not use the following data for averages, fits, limits, etc. • • •				
-0.05 or -0.05	[3] MARTIN	77	DPWA	$\overline{K}N$ multichannel

$(\Gamma_i\Gamma_f)^{1/2}/\Gamma_{total}$ in $N\overline{K} \to \Sigma(1915) \to \Sigma(1385)\pi$, P-wave $(\Gamma_1\Gamma_5)^{1/2}/\Gamma$

VALUE	DOCUMENT ID		TECN	COMMENT
<0.01	CAMERON	78	DPWA	$K^- p \to \Sigma(1385)\pi$

$(\Gamma_i\Gamma_f)^{1/2}/\Gamma_{total}$ in $N\overline{K} \to \Sigma(1915) \to \Sigma(1385)\pi$, F-wave $(\Gamma_1\Gamma_6)^{1/2}/\Gamma$

VALUE	DOCUMENT ID		TECN	COMMENT
$+0.039 \pm 0.009$	[5] CAMERON	78	DPWA	$K^- p \to \Sigma(1385)\pi$

$\Sigma(1915)$ FOOTNOTES

[1] The two entries for CORDEN 77C are from two different acceptable solutions.
[2] Preferred solution 3; see CORDEN 76 for other possibilities.
[3] The two MARTIN 77 values are from a T-matrix pole and from a Breit-Wigner fit.
[4] The mass and width are fixed to the GOPAL 77 values due to the low elasticity.
[5] The published sign has been changed to be in accord with the baryon-first convention.

$\Sigma(1915)$ REFERENCES

PDG	86	PL 170B	M. Aguilar-Benitez *et al.*	(CERN, CIT+)
PDG	82	PL 111B	M. Roos *et al.*	(HELS, CIT, CERN)
GOPAL	80	Toronto Conf. 159	G.P. Gopal	(RHEL) IJP
ALSTON-...	78	PR D18 182	M. Alston-Garnjost *et al.*	(LBL, MTHO+) IJP
Also	77	PRL 38 1007	M. Alston-Garnjost *et al.*	(LBL, MTHO+) IJP
CAMERON	78	NP B143 189	W. Cameron *et al.*	(RHEL, LOIC) IJP
CORDEN	77C	NP B125 61	M.J. Corden *et al.*	(BIRM) IJP
DECLAIS	77	CERN 77-16	Y. Declais *et al.*	(CAEN, CERN) IJP
GOPAL	77	NP B119 362	G.P. Gopal *et al.*	(LOIC, RHEL) IJP
MARTIN	77	NP B127 349	B.R. Martin, M.K. Pidcock, R.G. Moorhouse	(LOUC+) IJP
Also	77B	NP B126 266	B.R. Martin, M.K. Pidcock	(LOUC)
Also	77C	NP B126 285	B.R. Martin, M.K. Pidcock	(LOUC) IJP
CORDEN	76	NP B104 382	M.J. Corden *et al.*	(BIRM) IJP
DEBELLEFON	76	NP B109 129	A. de Bellefon, A. Berthon	(CDEF) IJP
BAILLON	75	NP B94 39	P.H. Baillon, P.J. Litchfield	(CERN, RHEL) IJP
HEMINGWAY	75	NP B91 12	R.J. Hemingway *et al.*	(CERN, HEIDH, MPIM) IJP
VANHORN	75	NP B87 145	A.J. van Horn	(LBL) IJP
Also	75B	NP B87 157	A.J. van Horn	(LBL) IJP
DEVENISH	74B	NP B81 330	R.C.E. Devenish, C.D. Froggatt, B.R. Martin	(DESY+)
KANE	74	LBL-2452	D.F. Kane	(LBL) IJP
COOL	66	PRL 16 1228	R.L. Cool *et al.*	(BNL)

$\Sigma(1940)$ D_{13}

$I(J^P) = 1(\frac{3}{2}^-)$ Status: ***

For results published before 1974 (they are now obsolete), see our 1982 edition Physics Letters **111B** (1982).

Not all analyses require this state. It is not required by the GOYAL 77 analysis of $K^- n \to (\Sigma\pi)^-$ nor by the GOPAL 80 analysis of $K^- n \to K^- n$. See also HEMINGWAY 75.

$\Sigma(1940)$ MASS

VALUE (MeV)	DOCUMENT ID		TECN	COMMENT
1900 to 1950 (≈ 1940) OUR ESTIMATE				
1920±50	GOPAL	77	DPWA	$\overline{K}N$ multichannel
1950±30	BAILLON	75	IPWA	$\overline{K}N \to \Lambda\pi$
1949^{+40}_{-60}	VANHORN	75	DPWA	$K^- p \to \Lambda\pi^0$
1935±80	KANE	74	DPWA	$K^- p \to \Sigma\pi$
1940±20	LITCHFIELD	74B	DPWA	$K^- p \to \Lambda(1520)\pi^0$
1950±20	LITCHFIELD	74C	DPWA	$K^- p \to \Delta(1232)\overline{K}$
• • • We do not use the following data for averages, fits, limits, etc. • • •				
1886 or 1893	[1] MARTIN	77	DPWA	$\overline{K}N$ multichannel
1940	DEBELLEFON	76	IPWA	$K^- p \to \Lambda\pi^0$, F_{17} wave

$\Sigma(1940)$ WIDTH

VALUE (MeV)	DOCUMENT ID		TECN	COMMENT
150 to 300 (≈ 220) OUR ESTIMATE				
170±25	CAMERON	78B	DPWA	$K^- p \to N\overline{K}^*$
300±80	GOPAL	77	DPWA	$\overline{K}N$ multichannel
150±75	BAILLON	75	IPWA	$\overline{K}N \to \Lambda\pi$
160^{+70}_{-40}	VANHORN	75	DPWA	$K^- p \to \Lambda\pi^0$
330±80	KANE	74	DPWA	$K^- p \to \Sigma\pi$
60±20	LITCHFIELD	74B	DPWA	$K^- p \to \Lambda(1520)\pi^0$
70^{+30}_{-20}	LITCHFIELD	74C	DPWA	$K^- p \to \Delta(1232)\overline{K}$
• • • We do not use the following data for averages, fits, limits, etc. • • •				
157 or 159	[1] MARTIN	77	DPWA	$\overline{K}N$ multichannel

$\Sigma(1940)$ DECAY MODES

	Mode	Fraction (Γ_i/Γ)
Γ_1	$N\overline{K}$	<20 %
Γ_2	$\Lambda\pi$	seen
Γ_3	$\Sigma\pi$	seen
Γ_4	$\Sigma(1385)\pi$	seen
Γ_5	$\Sigma(1385)\pi$, S-wave	
Γ_6	$\Lambda(1520)\pi$	seen
Γ_7	$\Lambda(1520)\pi$, P-wave	
Γ_8	$\Lambda(1520)\pi$, F-wave	
Γ_9	$\Delta(1232)\overline{K}$	seen
Γ_{10}	$\Delta(1232)\overline{K}$, S-wave	
Γ_{11}	$\Delta(1232)\overline{K}$, D-wave	
Γ_{12}	$N\overline{K}^*(892)$	seen
Γ_{13}	$N\overline{K}^*(892)$, S=3/2, S-wave	

$\Sigma(1940)$ BRANCHING RATIOS

See "Sign conventions for resonance couplings" in the Note on Λ and Σ Resonances.

$\Gamma(N\overline{K})/\Gamma_{total}$ Γ_1/Γ

VALUE	DOCUMENT ID		TECN	COMMENT
<0.2 OUR ESTIMATE				
<0.04	GOPAL	77	DPWA	$\overline{K}N$ multichannel
0.14 or 0.13	[1] MARTIN	77	DPWA	$\overline{K}N$ multichannel

$(\Gamma_i\Gamma_f)^{1/2}/\Gamma_{total}$ in $N\overline{K} \to \Sigma(1940) \to \Lambda\pi$ $(\Gamma_1\Gamma_2)^{1/2}/\Gamma$

VALUE	DOCUMENT ID		TECN	COMMENT
−0.06 ±0.03	GOPAL	77	DPWA	$\overline{K}N$ multichannel
−0.04 ±0.02	BAILLON	75	IPWA	$\overline{K}N \to \Lambda\pi$
$-0.05\ ^{+0.03}_{-0.02}$	VANHORN	75	DPWA	$K^- p \to \Lambda\pi^0$
−0.153±0.070	DEVENISH	74B		Fixed-t dispersion rel.
• • • We do not use the following data for averages, fits, limits, etc. • • •				
−0.15 or −0.14	[1] MARTIN	77	DPWA	$\overline{K}N$ multichannel

$(\Gamma_i\Gamma_f)^{1/2}/\Gamma_{total}$ in $N\overline{K} \to \Sigma(1940) \to \Sigma\pi$ $(\Gamma_1\Gamma_3)^{1/2}/\Gamma$

VALUE	DOCUMENT ID		TECN	COMMENT
−0.08±0.04	GOPAL	77	DPWA	$\overline{K}N$ multichannel
−0.14±0.04	KANE	74	DPWA	$K^- p \to \Sigma\pi$
• • • We do not use the following data for averages, fits, limits, etc. • • •				
+0.16 or +0.16	[1] MARTIN	77	DPWA	$\overline{K}N$ multichannel

$(\Gamma_i\Gamma_f)^{1/2}/\Gamma_{total}$ in $N\overline{K} \to \Sigma(1940) \to \Lambda(1520)\pi$, P-wave $(\Gamma_1\Gamma_7)^{1/2}/\Gamma$

VALUE	DOCUMENT ID		TECN	COMMENT
< 0.03	CAMERON	77	DPWA	$K^- p \to \Lambda(1520)\pi^0$
−0.11±0.04	LITCHFIELD	74B	DPWA	$K^- p \to \Lambda(1520)\pi^0$

$(\Gamma_i\Gamma_f)^{1/2}/\Gamma_{total}$ in $N\overline{K} \to \Sigma(1940) \to \Lambda(1520)\pi$, F-wave $(\Gamma_1\Gamma_8)^{1/2}/\Gamma$

VALUE	DOCUMENT ID		TECN	COMMENT
0.062±0.021	CAMERON	77	DPWA	$K^- p \to \Lambda(1520)\pi^0$
−0.08 ±0.04	LITCHFIELD	74B	DPWA	$K^- p \to \Lambda(1520)\pi^0$

$(\Gamma_i\Gamma_f)^{1/2}/\Gamma_{total}$ in $N\overline{K} \to \Sigma(1940) \to \Delta(1232)\overline{K}$, S-wave $(\Gamma_1\Gamma_{10})^{1/2}/\Gamma$

VALUE	DOCUMENT ID		TECN	COMMENT
−0.16±0.05	LITCHFIELD	74C	DPWA	$K^- p \to \Delta(1232)\overline{K}$

$(\Gamma_i\Gamma_f)^{1/2}/\Gamma_{total}$ in $N\overline{K} \to \Sigma(1940) \to \Delta(1232)\overline{K}$, D-wave $(\Gamma_1\Gamma_{11})^{1/2}/\Gamma$

VALUE	DOCUMENT ID		TECN	COMMENT
−0.14±0.05	LITCHFIELD	74C	DPWA	$K^- p \to \Delta(1232)\overline{K}$

$(\Gamma_i\Gamma_f)^{1/2}/\Gamma_{total}$ in $N\overline{K} \to \Sigma(1940) \to \Sigma(1385)\pi$ $(\Gamma_1\Gamma_4)^{1/2}/\Gamma$

VALUE	DOCUMENT ID		TECN	COMMENT
+0.066±0.025	[2] CAMERON	78	DPWA	$K^- p \to \Sigma(1385)\pi$

$(\Gamma_i\Gamma_f)^{1/2}/\Gamma_{total}$ in $N\overline{K} \to \Sigma(1940) \to N\overline{K}^*(892)$ $(\Gamma_1\Gamma_{12})^{1/2}/\Gamma$

VALUE	DOCUMENT ID		TECN	COMMENT
−0.09±0.02	[3] CAMERON	78B	DPWA	$K^- p \to N\overline{K}^*$

$\Sigma(1940)$ FOOTNOTES

[1] The two MARTIN 77 values are from a T-matrix pole and from a Breit-Wigner fit.
[2] The published sign has been changed to be in accord with the baryon-first convention.
[3] Upper limits on the D_1 and D_3 waves are each 0.03.

$\Sigma(1940)$ REFERENCES

PDG	82	PL 111B	M. Roos *et al.*	(HELS, CIT, CERN)
GOPAL	80	Toronto Conf. 159	G.P. Gopal	(RHEL)
CAMERON	78	NP B143 189	W. Cameron *et al.*	(RHEL, LOIC) IJP
CAMERON	78B	NP B146 327	W. Cameron *et al.*	(RHEL, LOIC) IJP
CAMERON	77	NP B131 399	W. Cameron *et al.*	(RHEL, LOIC) IJP
GOPAL	77	NP B119 362	G.P. Gopal *et al.*	(LOIC, RHEL) IJP
GOYAL	77	PR D16 2746	D.P. Goyal, A.V. Sodhi	(DELH)
MARTIN	77	NP B127 349	B.R. Martin, M.K. Pidcock, R.G. Moorhouse	(LOUC+) IJP
Also	77B	NP B126 266	B.R. Martin, M.K. Pidcock	(LOUC)
Also	77C	NP B126 285	B.R. Martin, M.K. Pidcock	(LOUC) IJP
DEBELLEFON	76	NP B109 129	A. de Bellefon, A. Berthon	(CDEF) IJP
BAILLON	75	NP B94 39	P.H. Baillon, P.J. Litchfield	(CERN, RHEL) IJP
HEMINGWAY	75	NP B91 12	R.J. Hemingway *et al.*	(CERN, HEIDH, MPIM) IJP
VANHORN	75	NP B87 145	A.J. van Horn	(LBL) IJP
Also	75B	NP B87 157	A.J. van Horn	(LBL) IJP
DEVENISH	74B	NP B81 330	R.C.E. Devenish, C.D. Froggatt, B.R. Martin	(DESY+)
KANE	74	LBL-2452	D.F. Kane	(LBL) IJP
LITCHFIELD	74B	NP B74 19	P.J. Litchfield *et al.*	(CERN, HEIDH) IJP
LITCHFIELD	74C	NP B74 39	P.J. Litchfield *et al.*	(CERN, HEIDH) IJP

$\Sigma(2000)$ S_{11}

$I(J^P) = 1(\frac{1}{2}^-)$ Status: *

OMITTED FROM SUMMARY TABLE

We list here all reported S_{11} states lying above the $\Sigma(1750)$ S_{11}.

$\Sigma(2000)$ MASS

VALUE (MeV)	DOCUMENT ID		TECN	COMMENT
≈ 2000 OUR ESTIMATE				
1944±15	GOPAL	80	DPWA	$\overline{K}N \to \overline{K}N$
1955±15	GOPAL	77	DPWA	$\overline{K}N$ multichannel
1755 or 1834	[1] MARTIN	77	DPWA	$\overline{K}N$ multichannel
2004±40	VANHORN	75	DPWA	$K^- p \to \Lambda\pi^0$

$\Sigma(2000)$ WIDTH

VALUE (MeV)	DOCUMENT ID		TECN	COMMENT
215±25	GOPAL	80	DPWA	$\overline{K}N \to \overline{K}N$
170±40	GOPAL	77	DPWA	$\overline{K}N$ multichannel
413 or 450	[1] MARTIN	77	DPWA	$\overline{K}N$ multichannel
116±40	VANHORN	75	DPWA	$K^- p \to \Lambda\pi^0$

$\Sigma(2000)$ DECAY MODES

	Mode
Γ_1	$N\overline{K}$
Γ_2	$\Lambda\pi$
Γ_3	$\Sigma\pi$
Γ_4	$\Lambda(1520)\pi$
Γ_5	$N\overline{K}^*(892)$, S=1/2, S-wave
Γ_6	$N\overline{K}^*(892)$, S=3/2, D-wave

$\Sigma(2000)$ BRANCHING RATIOS

See "Sign conventions for resonance couplings" in the Note on Λ and Σ Resonances.

$\Gamma(N\overline{K})/\Gamma_{total}$ Γ_1/Γ

VALUE	DOCUMENT ID		TECN	COMMENT
0.51 ± 0.05	GOPAL	80	DPWA	$\overline{K}N \to \overline{K}N$
0.44 ± 0.05	GOPAL	77	DPWA	See GOPAL 80
0.62 or 0.57	[1] MARTIN	77	DPWA	$\overline{K}N$ multichannel

$(\Gamma_i\Gamma_f)^{1/2}/\Gamma_{total}$ in $N\overline{K} \to \Sigma(2000) \to \Lambda\pi$ $(\Gamma_1\Gamma_2)^{1/2}/\Gamma$

VALUE	DOCUMENT ID		TECN	COMMENT
0.08 ± 0.03	GOPAL	77	DPWA	$\overline{K}N$ multichannel
-0.19 or -0.18	[1] MARTIN	77	DPWA	$\overline{K}N$ multichannel
not seen	BAILLON	75	IPWA	$\overline{K}N \to \Lambda\pi$
$+0.07^{+0.02}_{-0.01}$	VANHORN	75	DPWA	$K^-p \to \Lambda\pi^0$

$(\Gamma_i\Gamma_f)^{1/2}/\Gamma_{total}$ in $N\overline{K} \to \Sigma(2000) \to \Sigma\pi$ $(\Gamma_1\Gamma_3)^{1/2}/\Gamma$

VALUE	DOCUMENT ID		TECN	COMMENT
$+0.20\pm0.04$	GOPAL	77	DPWA	$\overline{K}N$ multichannel
$+0.26$ or $+0.24$	[1] MARTIN	77	DPWA	$\overline{K}N$ multichannel

$(\Gamma_i\Gamma_f)^{1/2}/\Gamma_{total}$ in $N\overline{K} \to \Sigma(2000) \to \Lambda(1520)\pi$ $(\Gamma_1\Gamma_4)^{1/2}/\Gamma$

VALUE	DOCUMENT ID		TECN	COMMENT
$+0.081\pm0.021$	[2] CAMERON	77	DPWA	P-wave decay

$(\Gamma_i\Gamma_f)^{1/2}/\Gamma_{total}$ in $N\overline{K} \to \Sigma(2000) \to N\overline{K}^*(892)$, S=1/2, S-wave $(\Gamma_1\Gamma_5)^{1/2}/\Gamma$

VALUE	DOCUMENT ID		TECN	COMMENT
$+0.10\pm0.02$	[2] CAMERON	78B	DPWA	$K^-p \to N\overline{K}^*$

$(\Gamma_i\Gamma_f)^{1/2}/\Gamma_{total}$ in $N\overline{K} \to \Sigma(2000) \to N\overline{K}^*(892)$, S=3/2, D-wave $(\Gamma_1\Gamma_6)^{1/2}/\Gamma$

VALUE	DOCUMENT ID		TECN	COMMENT
-0.07 ± 0.03	CAMERON	78B	DPWA	$K^-p \to N\overline{K}^*$

$\Sigma(2000)$ FOOTNOTES

[1] The two MARTIN 77 values are from a T-matrix pole and from a Breit-Wigner fit.
[2] The published sign has been changed to be in accord with the baryon-first convention.

$\Sigma(2000)$ REFERENCES

GOPAL	80	Toronto Conf. 159	G.P. Gopal	(RHEL) IJP
CAMERON	78B	NP B146 327	W. Cameron *et al.*	(RHEL, LOIC) IJP
CAMERON	77	NP B131 399	W. Cameron *et al.*	(RHEL, LOIC) IJP
GOPAL	77	NP B119 362	G.P. Gopal *et al.*	(LOIC, RHEL) IJP
MARTIN	77	NP B127 349	B.R. Martin, M.K. Pidcock, R.G. Moorhouse	(LOUC+) IJP
Also	77B	NP B126 266	B.R. Martin, M.K. Pidcock	(LOUC)
Also	77C	NP B126 285	B.R. Martin, M.K. Pidcock	(LOUC) IJP
BAILLON	75	NP B94 39	P.H. Baillon, P.J. Litchfield	(CERN, RHEL) IJP
VANHORN	75	NP B87 145	A.J. van Horn	(LBL) IJP
Also	75B	NP B87 157	A.J. van Horn	(LBL) IJP

$\Sigma(2030)$ F_{17}

$I(J^P) = 1(\frac{7}{2}^+)$ Status: ****

Discovered by COOL 66 and by WOHL 66. For most results published before 1974 (they are now obsolete), see our 1982 edition Physics Letters **111B** (1982).

This entry only includes results from partial-wave analyses. Parameters of peaks seen in cross sections and invariant-mass distributions around 2030 MeV may be found in our 1984 edition, Reviews of Modern Physics **56** No. 2 Pt. II (1984).

$\Sigma(2030)$ MASS

VALUE (MeV)	DOCUMENT ID		TECN	COMMENT
2025 to 2040 (≈ 2030) OUR ESTIMATE				
2036 ± 5	GOPAL	80	DPWA	$\overline{K}N \to \overline{K}N$
2038 ± 10	CORDEN	77B		$K^-N \to N\overline{K}^*$
2040 ± 5	GOPAL	77	DPWA	$\overline{K}N$ multichannel
2030 ± 3	[1] CORDEN	76	DPWA	$K^-n \to \Lambda\pi^-$
2035 ± 15	BAILLON	75	IPWA	$\overline{K}N \to \Lambda\pi$
2038 ± 10	HEMINGWAY	75	DPWA	$K^-p \to \overline{K}N$
2042 ± 11	VANHORN	75	DPWA	$K^-p \to \Lambda\pi^0$
2020 ± 6	KANE	74	DPWA	$K^-p \to \Sigma\pi$
2035 ± 10	LITCHFIELD	74B	DPWA	$K^-p \to \Lambda(1520)\pi^0$
2020 ± 30	LITCHFIELD	74C	DPWA	$K^-p \to \Delta(1232)\overline{K}$
2025 ± 10	LITCHFIELD	74D	DPWA	$K^-p \to \Lambda(1820)\pi^0$
• • • We do not use the following data for averages, fits, limits, etc. • • •				
2027 to 2057	GOYAL	77	DPWA	$K^-N \to \Sigma\pi$
2030	DEBELLEFON	76	IPWA	$K^-p \to \Lambda\pi^0$

$\Sigma(2030)$ WIDTH

VALUE (MeV)	DOCUMENT ID		TECN	COMMENT
150 to 200 (≈ 180) OUR ESTIMATE				
172 ± 10	GOPAL	80	DPWA	$\overline{K}N \to \overline{K}N$
137 ± 40	CORDEN	77B		$K^-N \to N\overline{K}^*$
190 ± 10	GOPAL	77	DPWA	$\overline{K}N$ multichannel
201 ± 9	[1] CORDEN	76	DPWA	$K^-n \to \Lambda\pi^-$
180 ± 20	BAILLON	75	IPWA	$\overline{K}N \to \Lambda\pi$
172 ± 15	HEMINGWAY	75	DPWA	$K^-p \to \overline{K}N$
178 ± 13	VANHORN	75	DPWA	$K^-p \to \Lambda\pi^0$
111 ± 5	KANE	74	DPWA	$K^-p \to \Sigma\pi$
160 ± 20	LITCHFIELD	74B	DPWA	$K^-p \to \Lambda(1520)\pi^0$
200 ± 30	LITCHFIELD	74C	DPWA	$K^-p \to \Delta(1232)\overline{K}$
• • • We do not use the following data for averages, fits, limits, etc. • • •				
260	DECLAIS	77	DPWA	$\overline{K}N \to \overline{K}N$
126 to 195	GOYAL	77	DPWA	$K^-N \to \Sigma\pi$
160	DEBELLEFON	76	IPWA	$K^-p \to \Lambda\pi^0$
70 to 125	LITCHFIELD	74D	DPWA	$K^-p \to \Lambda(1820)\pi^0$

$\Sigma(2030)$ DECAY MODES

	Mode	Fraction (Γ_i/Γ)
Γ_1	$N\overline{K}$	17–23 %
Γ_2	$\Lambda\pi$	17–23 %
Γ_3	$\Sigma\pi$	5–10 %
Γ_4	ΞK	<2 %
Γ_5	$\Sigma(1385)\pi$	5–15 %
Γ_6	$\Sigma(1385)\pi$, F-wave	
Γ_7	$\Lambda(1520)\pi$	10–20 %
Γ_8	$\Lambda(1520)\pi$, D-wave	
Γ_9	$\Lambda(1520)\pi$, G-wave	
Γ_{10}	$\Delta(1232)\overline{K}$	10–20 %
Γ_{11}	$\Delta(1232)\overline{K}$, F-wave	
Γ_{12}	$\Delta(1232)\overline{K}$, H-wave	
Γ_{13}	$N\overline{K}^*(892)$	<5 %
Γ_{14}	$N\overline{K}^*(892)$, S=1/2, F-wave	
Γ_{15}	$N\overline{K}^*(892)$, S=3/2, F-wave	
Γ_{16}	$\Lambda(1820)\pi$, P-wave	

The above branching fractions are our estimates, not fits or averages.

$\Sigma(2030)$ BRANCHING RATIOS

See "Sign conventions for resonance couplings" in the Note on Λ and Σ Resonances.

$\Gamma(N\overline{K})/\Gamma_{total}$ Γ_1/Γ

VALUE	DOCUMENT ID		TECN	COMMENT
0.17 to 0.23 OUR ESTIMATE				
0.19 ± 0.03	GOPAL	80	DPWA	$\overline{K}N\to\overline{K}N$
0.18 ± 0.03	HEMINGWAY	75	DPWA	$K^-p\to\overline{K}N$
• • • We do not use the following data for averages, fits, limits, etc. • • •				
0.15	DECLAIS	77	DPWA	$\overline{K}N\to\overline{K}N$
0.24 ± 0.02	GOPAL	77	DPWA	See GOPAL 80

$(\Gamma_i\Gamma_f)^{1/2}/\Gamma_{total}$ in $N\overline{K}\to\Sigma(2030)\to\Lambda\pi$ $(\Gamma_1\Gamma_2)^{1/2}/\Gamma$

VALUE	DOCUMENT ID		TECN	COMMENT
$+0.18\ \pm0.02$	GOPAL	77	DPWA	$\overline{K}N$ multichannel
$+0.20\ \pm0.01$	[1] CORDEN	76	DPWA	$K^-n\to\Lambda\pi^-$
$+0.18\ \pm0.02$	BAILLON	75	IPWA	$\overline{K}N\to\Lambda\pi$
$+0.20\ \pm0.01$	VANHORN	75	DPWA	$K^-p\to\Lambda\pi^0$
$+0.195\pm0.053$	DEVENISH	74B		Fixed-t dispersion rel.
• • • We do not use the following data for averages, fits, limits, etc. • • •				
0.20	DEBELLEFON	76	IPWA	$K^-p\to\Lambda\pi^0$

$(\Gamma_i\Gamma_f)^{1/2}/\Gamma_{total}$ in $N\overline{K}\to\Sigma(2030)\to\Sigma\pi$ $(\Gamma_1\Gamma_3)^{1/2}/\Gamma$

VALUE	DOCUMENT ID		TECN	COMMENT
$-0.09\ \pm0.01$	[2] CORDEN	77C		$K^-n\to\Sigma\pi$
$-0.06\ \pm0.01$	[2] CORDEN	77C		$K^-n\to\Sigma\pi$
$-0.15\ \pm0.03$	GOPAL	77	DPWA	$\overline{K}N$ multichannel
$-0.10\ \pm0.01$	KANE	74	DPWA	$K^-p\to\Sigma\pi$
• • • We do not use the following data for averages, fits, limits, etc. • • •				
-0.085 ± 0.02	[3] GOYAL	77	DPWA	$K^-N\to\Sigma\pi$

$(\Gamma_i\Gamma_f)^{1/2}/\Gamma_{total}$ in $N\overline{K}\to\Sigma(2030)\to\Xi K$ $(\Gamma_1\Gamma_4)^{1/2}/\Gamma$

VALUE	DOCUMENT ID		TECN	COMMENT
0.023	MULLER	69B	DPWA	$K^-p\to\Xi K$
<0.05	BURGUN	68	DPWA	$K^-p\to\Xi K$
<0.05	TRIPP	67	RVUE	$K^-p\to\Xi K$

$(\Gamma_i\Gamma_f)^{1/2}/\Gamma_{total}$ in $N\overline{K}\to\Sigma(2030)\to\Lambda(1820)\pi$, P-wave $(\Gamma_1\Gamma_{16})^{1/2}/\Gamma$

VALUE	DOCUMENT ID		TECN	COMMENT
0.14 ± 0.02	CORDEN	75B	DBC	$K^-n\to N\overline{K}\pi^-$
0.18 ± 0.04	LITCHFIELD	74D	DPWA	$K^-p\to\Lambda(1820)\pi^0$

$(\Gamma_i\Gamma_f)^{1/2}/\Gamma_{total}$ in $N\overline{K}\to\Sigma(2030)\to\Lambda(1520)\pi$, D-wave $(\Gamma_1\Gamma_8)^{1/2}/\Gamma$

VALUE	DOCUMENT ID		TECN	COMMENT
$+0.114\pm0.010$	[4] CAMERON	77	DPWA	$K^-p\to\Lambda(1520)\pi^0$
$0.14\ \pm0.03$	LITCHFIELD	74B	DPWA	$K^-p\to\Lambda(1520)\pi^0$
• • • We do not use the following data for averages, fits, limits, etc. • • •				
$0.10\ \pm0.03$	[5] CORDEN	75B	DBC	$K^-n\to N\overline{K}\pi^-$

$(\Gamma_i\Gamma_f)^{1/2}/\Gamma_{total}$ in $N\overline{K}\to\Sigma(2030)\to\Lambda(1520)\pi$, G-wave $(\Gamma_1\Gamma_9)^{1/2}/\Gamma$

VALUE	DOCUMENT ID		TECN	COMMENT
$+0.146\pm0.010$	[4] CAMERON	77	DPWA	$K^-p\to\Lambda(1520)\pi^0$
$0.02\ \pm0.02$	LITCHFIELD	74B	DPWA	$K^-p\to\Lambda(1520)\pi^0$

$(\Gamma_i\Gamma_f)^{1/2}/\Gamma_{total}$ in $N\overline{K}\to\Sigma(2030)\to\Delta(1232)\overline{K}$, F-wave $(\Gamma_1\Gamma_{11})^{1/2}/\Gamma$

VALUE	DOCUMENT ID		TECN	COMMENT
0.16 ± 0.03	LITCHFIELD	74C	DPWA	$K^-p\to\Delta(1232)\overline{K}$
• • • We do not use the following data for averages, fits, limits, etc. • • •				
0.17 ± 0.03	[5] CORDEN	75B	DBC	$K^-n\to N\overline{K}\pi^-$

$(\Gamma_i\Gamma_f)^{1/2}/\Gamma_{total}$ in $N\overline{K}\to\Sigma(2030)\to\Delta(1232)\overline{K}$, H-wave $(\Gamma_1\Gamma_{12})^{1/2}/\Gamma$

VALUE	DOCUMENT ID		TECN	COMMENT
0.00 ± 0.02	LITCHFIELD	74C	DPWA	$K^-p\to\Delta(1232)\overline{K}$

$(\Gamma_i\Gamma_f)^{1/2}/\Gamma_{total}$ in $N\overline{K}\to\Sigma(2030)\to\Sigma(1385)\pi$ $(\Gamma_1\Gamma_5)^{1/2}/\Gamma$

VALUE	DOCUMENT ID		TECN	COMMENT
$+0.153\pm0.026$	[4] CAMERON	78	DPWA	$K^-p\to\Sigma(1385)\pi$

$(\Gamma_i\Gamma_f)^{1/2}/\Gamma_{total}$ in $N\overline{K}\to\Sigma(2030)\to N\overline{K}^*(892)$, S=1/2, F-wave $(\Gamma_1\Gamma_{14})^{1/2}/\Gamma$

VALUE	DOCUMENT ID		TECN	COMMENT
$+0.06\pm0.03$	[4] CAMERON	78B	DPWA	$K^-p\to N\overline{K}^*$
-0.02 ± 0.01	CORDEN	77B		$K^-d\to NN\overline{K}^*$

$(\Gamma_i\Gamma_f)^{1/2}/\Gamma_{total}$ in $N\overline{K}\to\Sigma(2030)\to N\overline{K}^*(892)$, S=3/2, F-wave $(\Gamma_1\Gamma_{15})^{1/2}/\Gamma$

VALUE	DOCUMENT ID		TECN	COMMENT
$+0.04\pm0.03$	[6] CAMERON	78B	DPWA	$K^-p\to N\overline{K}^*$
-0.12 ± 0.02	CORDEN	77B		$K^-d\to NN\overline{K}^*$

$\Sigma(2030)$ FOOTNOTES

[1] Preferred solution 3; see CORDEN 76 for other possibilities.
[2] The two entries for CORDEN 77C are from two different acceptable solutions.
[3] This coupling is extracted from unnormalized data.
[4] The published sign has been changed to be in accord with the baryon-first convention.
[5] An upper limit.
[6] The upper limit on the G_3 wave is 0.03.

$\Sigma(2030)$ REFERENCES

PDG	84	RMP 56 No. 2 Pt. II	C.G. Wohl *et al.*	(LBL, CIT, CERN)
PDG	82	PL 111B	M. Roos *et al.*	(HELS, CIT, CERN)
GOPAL	80	Toronto Conf. 159	G.P. Gopal	(RHEL) IJP
CAMERON	78	NP B143 189	W. Cameron *et al.*	(RHEL, LOIC) IJP
CAMERON	78B	NP B146 327	W. Cameron *et al.*	(RHEL, LOIC) IJP
CAMERON	77	NP B131 399	W. Cameron *et al.*	(RHEL, LOIC) IJP
CORDEN	77B	NP B121 365	M.J. Corden *et al.*	(BIRM) IJP
CORDEN	77C	NP B125 61	M.J. Corden *et al.*	(BIRM) IJP
DECLAIS	77	CERN 77-16	Y. Declais *et al.*	(CAEN, CERN) IJP
GOPAL	77	NP B119 362	G.P. Gopal *et al.*	(LOIC, RHEL) IJP
GOYAL	77	PR D16 2746	D.P. Goyal, A.V. Sodhi	(DELH) IJP
CORDEN	76	NP B104 382	M.J. Corden *et al.*	(BIRM) IJP
DEBELLEFON	76	NP B109 129	A. de Bellefon, A. Berthon	(CDEF) IJP
BAILLON	75	NP B94 39	P.H. Baillon, P.J. Litchfield	(CERN, RHEL) IJP
CORDEN	75B	NP B92 365	M.J. Corden *et al.*	(BIRM) IJP
HEMINGWAY	75	NP B91 12	R.J. Hemingway *et al.*	(CERN, HEIDH, MPIM) IJP
VANHORN	75	NP B87 145	A.J. van Horn	(LBL) IJP
Also	75B	NP B87 157	A.J. van Horn	(LBL) IJP
DEVENISH	74B	NP B81 330	R.C.E. Devenish, C.D. Froggatt, B.R. Martin	(DESY+)
KANE	74	LBL-2452	D.F. Kane	(LBL) IJP
LITCHFIELD	74B	NP B74 19	P.J. Litchfield *et al.*	(CERN, HEIDH) IJP
LITCHFIELD	74C	NP B74 39	P.J. Litchfield *et al.*	(CERN, HEIDH) IJP
LITCHFIELD	74D	NP B74 12	P.J. Litchfield *et al.*	(CERN, HEIDH) IJP
MULLER	69B	Thesis UCRL 19372	R.A. Muller	(LRL)
BURGUN	68	NP B8 447	G. Burgun *et al.*	(SACL, CDEF, RHEL)
TRIPP	67	NP B3 10	R.D. Tripp *et al.*	(LRL, SLAC, CERN+)
COOL	66	PRL 16 1228	R.L. Cool *et al.*	(BNL)
WOHL	66	PRL 17 107	C.G. Wohl, F.T. Solmitz, M.L. Stevenson	(LRL) IJP

$\Sigma(2070)$ F_{15}

$I(J^P) = 1(\frac{5}{2}^+)$ Status: *

OMITTED FROM SUMMARY TABLE

This state suggested by BERTHON 70B finds support in GOPAL 80 with new K^-p polarization and K^-n angular distributions. The very broad state seen in KANE 72 is not required in the later (KANE 74) analysis of $\overline{K}N\to\Sigma\pi$.

$\Sigma(2070)$ MASS

VALUE (MeV)	DOCUMENT ID		TECN	COMMENT
≈ 2070 OUR ESTIMATE				
2051 ± 25	GOPAL	80	DPWA	$\overline{K}N\to\overline{K}N$
2057	KANE	72	DPWA	$K^-p\to\Sigma\pi$
2070 ± 10	BERTHON	70B	DPWA	$K^-p\to\Sigma\pi$

$\Sigma(2070)$ WIDTH

VALUE (MeV)	DOCUMENT ID		TECN	COMMENT
300 ± 30	GOPAL	80	DPWA	$\overline{K}N\to\overline{K}N$
906	KANE	72	DPWA	$K^-p\to\Sigma\pi$
140 ± 20	BERTHON	70B	DPWA	$K^-p\to\Sigma\pi$

$\Sigma(2070)$ DECAY MODES

	Mode
Γ_1	$N\overline{K}$
Γ_2	$\Sigma\pi$

$\Sigma(2070)$ BRANCHING RATIOS

See "Sign conventions for resonance couplings" in the Note on Λ and Σ Resonances.

$\Gamma(N\overline{K})/\Gamma_{total}$ Γ_1/Γ

VALUE	DOCUMENT ID		TECN	COMMENT
0.08 ± 0.03	GOPAL	80	DPWA	$\overline{K}N\to\overline{K}N$

$(\Gamma_i\Gamma_f)^{1/2}/\Gamma_{total}$ in $N\overline{K}\to\Sigma(2070)\to\Sigma\pi$ $(\Gamma_1\Gamma_2)^{1/2}/\Gamma$

VALUE	DOCUMENT ID		TECN	COMMENT
$+0.104$	KANE	72	DPWA	$K^-p\to\Sigma\pi$
$+0.12\ \pm0.02$	BERTHON	70B	DPWA	$K^-p\to\Sigma\pi$

$\Sigma(2070)$ REFERENCES

GOPAL	80	Toronto Conf. 159	G.P. Gopal	(RHEL) IJP
KANE	74	LBL-2452	D.F. Kane	(LBL)
KANE	72	PR D5 1583	D.F.J. Kane	(LBL)
BERTHON	70B	NP B24 417	A. Berthon *et al.*	(CDEF, RHEL, SACL) IJP

$\Sigma(2080)$ P_{13}

$I(J^P) = 1(\frac{3}{2}^+)$ Status: **

OMITTED FROM SUMMARY TABLE

Suggested by some but not all partial-wave analyses across this region.

$\Sigma(2080)$ MASS

VALUE (MeV)	DOCUMENT ID		TECN	COMMENT
≈ 2080 OUR ESTIMATE				
2091 ± 7	[1] CORDEN	76	DPWA	$K^- n \to \Lambda\pi^-$
2070 to 2120	DEBELLEFON	76	IPWA	$K^- p \to \Lambda\pi^0$
2120 ± 40	BAILLON	75	IPWA	$\overline{K}N \to \Lambda\pi$ (sol. 1)
2140 ± 40	BAILLON	75	IPWA	$\overline{K}N \to \Lambda\pi$ (sol. 2)
2082 ± 4	COX	70	DPWA	See CORDEN 76
2070 ± 30	LITCHFIELD	70	DPWA	$K^- N \to \Lambda\pi$

$\Sigma(2080)$ WIDTH

VALUE (MeV)	DOCUMENT ID		TECN	COMMENT
186 ± 48	[1] CORDEN	76	DPWA	$K^- n \to \Lambda\pi^-$
100	DEBELLEFON	76	IPWA	$K^- p \to \Lambda\pi^0$
240 ± 50	BAILLON	75	IPWA	$\overline{K}N \to \Lambda\pi$ (sol. 1)
200 ± 50	BAILLON	75	IPWA	$\overline{K}N \to \Lambda\pi$ (sol. 2)
87 ± 20	COX	70	DPWA	See CORDEN 76
250 ± 40	LITCHFIELD	70	DPWA	$K^- N \to \Lambda\pi$

$\Sigma(2080)$ DECAY MODES

	Mode
Γ_1	$N\overline{K}$
Γ_2	$\Lambda\pi$

$\Sigma(2080)$ BRANCHING RATIOS

See "Sign conventions for resonance couplings" in the Note on Λ and Σ Resonances.

$(\Gamma_i\Gamma_f)^{1/2}/\Gamma_{total}$ in $N\overline{K} \to \Sigma(2080) \to \Lambda\pi$ **$(\Gamma_1\Gamma_2)^{1/2}/\Gamma$**

VALUE	DOCUMENT ID		TECN	COMMENT
−0.10 ± 0.03	[1] CORDEN	76	DPWA	$K^- n \to \Lambda\pi^-$
−0.10	DEBELLEFON	76	IPWA	$K^- p \to \Lambda\pi^0$
−0.13 ± 0.04	BAILLON	75	IPWA	$\overline{K}N \to \Lambda\pi$ (sol. 1 and 2)
−0.16 ± 0.03	COX	70	DPWA	See CORDEN 76
−0.09 ± 0.03	LITCHFIELD	70	DPWA	$K^- N \to \Lambda\pi$

$\Sigma(2080)$ FOOTNOTES

[1] Preferred solution 3; see CORDEN 76 for other possibilities, including a D_{15} at this mass.

$\Sigma(2080)$ REFERENCES

CORDEN	76	NP B104 382	M.J. Corden *et al.*	(BIRM) IJP
DEBELLEFON	76	NP B109 129	A. de Bellefon, A. Berthon	(CDEF) IJP
Also	75	NP B90 1	A. de Bellefon *et al.*	(CDEF, SACL) IJP
BAILLON	75	NP B94 39	P.H. Baillon, P.J. Litchfield	(CERN, RHEL) IJP
COX	70	NP B19 61	G.F. Cox *et al.*	(BIRM, EDIN, GLAS, LOIC) IJP
LITCHFIELD	70	NP B22 269	P.J. Litchfield	(RHEL) IJP

$\Sigma(2100)$ G_{17}

$I(J^P) = 1(\frac{7}{2}^-)$ Status: *

OMITTED FROM SUMMARY TABLE

$\Sigma(2100)$ MASS

VALUE (MeV)	DOCUMENT ID		TECN	COMMENT
≈ 2100 OUR ESTIMATE				
2060 ± 20	BARBARO-...	70	DPWA	$K^- p \to \Lambda\pi^0$
2120 ± 30	BARBARO-...	70	DPWA	$K^- p \to \Sigma\pi$

$\Sigma(2100)$ WIDTH

VALUE (MeV)	DOCUMENT ID		TECN	COMMENT
70 ± 30	BARBARO-...	70	DPWA	$K^- p \to \Lambda\pi^0$
135 ± 30	BARBARO-...	70	DPWA	$K^- p \to \Sigma\pi$

$\Sigma(2100)$ DECAY MODES

	Mode
Γ_1	$N\overline{K}$
Γ_2	$\Lambda\pi$
Γ_3	$\Sigma\pi$

$\Sigma(2100)$ BRANCHING RATIOS

See "Sign conventions for resonance couplings" in the Note on Λ and Σ Resonances.

$(\Gamma_i\Gamma_f)^{1/2}/\Gamma_{total}$ in $N\overline{K} \to \Sigma(2100) \to \Lambda\pi$ **$(\Gamma_1\Gamma_2)^{1/2}/\Gamma$**

VALUE	DOCUMENT ID		TECN	COMMENT
−0.07 ± 0.02	BARBARO-...	70	DPWA	$K^- p \to \Lambda\pi^0$

$(\Gamma_i\Gamma_f)^{1/2}/\Gamma_{total}$ in $N\overline{K} \to \Sigma(2100) \to \Sigma\pi$ **$(\Gamma_1\Gamma_3)^{1/2}/\Gamma$**

VALUE	DOCUMENT ID		TECN	COMMENT
+0.13 ± 0.02	BARBARO-...	70	DPWA	$K^- p \to \Sigma\pi$

$\Sigma(2100)$ REFERENCES

BARBARO-...	70	Duke Conf. 173 Hyperon Resonances, 1970	A. Barbaro-Galtieri	(LRL) IJP

$\Sigma(2250)$

$I(J^P) = 1(?^?)$ Status: ***

Results from partial-wave analyses are too weak to warrant separating them from the production and cross-section experiments. LASINSKI 71 in $\overline{K}N$ using a Pomeron + resonances model, and DEBELLEFON 76, DEBELLEFON 77, and DEBELLEFON 78 in energy-dependent partial-wave analyses of $\overline{K}N \to \Lambda\pi$, $\Sigma\pi$, and $N\overline{K}$, respectively, suggest two resonances around this mass.

$\Sigma(2250)$ MASS

VALUE (MeV)	DOCUMENT ID		TECN	COMMENT
2210 to 2280 (≈ 2250) OUR ESTIMATE				
2270 ± 50	DEBELLEFON	78	DPWA	D_5 wave
2210 ± 30	DEBELLEFON	78	DPWA	G_9 wave
2275 ± 20	DEBELLEFON	77	DPWA	D_5 wave
2215 ± 20	DEBELLEFON	77	DPWA	G_9 wave
2300 ± 30	[1] DEBELLEFON	75B	HBC	$K^- p \to \Xi^{*0} K^0$
2251^{+30}_{-20}	VANHORN	75	DPWA	$K^- p \to \Lambda\pi^0$, F_5 wave
2280 ± 14	AGUILAR-...	70B	HBC	$K^- p$ 3.9, 4.6 GeV/c
2237 ± 11	BRICMAN	70	CNTR	Total, charge exchange
2255 ± 10	COOL	70	CNTR	$K^- p$, $K^- d$ total
2250 ± 7	BUGG	68	CNTR	$K^- p$, $K^- d$ total
• • • We do not use the following data for averages, fits, limits, etc. • • •				
2260	DEBELLEFON	76	IPWA	D_5 wave
2215	DEBELLEFON	76	IPWA	G_9 wave
2250 ± 20	LU	70	CNTR	$\gamma p \to K^+ Y^*$
2245	BLANPIED	65	CNTR	$\gamma p \to K^+ Y^*$
2299 ± 6	BOCK	65	HBC	$\overline{p}p$ 5.7 GeV/c

$\Sigma(2250)$ WIDTH

VALUE (MeV)	DOCUMENT ID		TECN	COMMENT
60 to 150 (≈ 100) OUR ESTIMATE				
120±40	DEBELLEFON	78	DPWA	D_5 wave
80±20	DEBELLEFON	78	DPWA	G_9 wave
70±20	DEBELLEFON	77	DPWA	D_5 wave
60±20	DEBELLEFON	77	DPWA	G_9 wave
130±20	[1] DEBELLEFON	75B	HBC	$K^- p \rightarrow \Xi^{*0} K^0$
192±30	VANHORN	75	DPWA	$K^- p \rightarrow \Lambda\pi^0$, F_5 wave
100±20	AGUILAR-...	70B	HBC	$K^- p$ 3.9, 4.6 GeV/c
164±50	BRICMAN	70	CNTR	Total, charge exchange
230±20	BUGG	68	CNTR	$K^- p$, $K^- d$ total
• • • We do not use the following data for averages, fits, limits, etc. • • •				
100	DEBELLEFON	76	IPWA	D_5 wave
140	DEBELLEFON	76	IPWA	G_9 wave
170	COOL	70	CNTR	$K^- p$, $K^- d$ total
125	LU	70	CNTR	$\gamma p \rightarrow K^+ Y^*$
150	BLANPIED	65	CNTR	$\gamma p \rightarrow K^+ Y^*$
21^{+17}_{-21}	BOCK	65	HBC	$\overline{p}p$ 5.7 GeV/c

$\Sigma(2250)$ DECAY MODES

	Mode	Fraction (Γ_i/Γ)
Γ_1	$N\overline{K}$	<10 %
Γ_2	$\Lambda\pi$	seen
Γ_3	$\Sigma\pi$	seen
Γ_4	$N\overline{K}\pi$	
Γ_5	$\Xi(1530)K$	

The above branching fractions are our estimates, not fits or averages.

$\Sigma(2250)$ BRANCHING RATIOS

See "Sign conventions for resonance couplings" in the Note on Λ and Σ Resonances.

$\Gamma(N\overline{K})/\Gamma_{total}$ — Γ_1/Γ

VALUE	DOCUMENT ID		TECN	COMMENT
<0.1 OUR ESTIMATE				
0.08±0.02	DEBELLEFON	78	DPWA	D_5 wave
0.02±0.01	DEBELLEFON	78	DPWA	G_9 wave

$(J+\frac{1}{2})\times\Gamma(N\overline{K})/\Gamma_{total}$ — Γ_1/Γ

VALUE	DOCUMENT ID		TECN	COMMENT
• • • We do not use the following data for averages, fits, limits, etc. • • •				
0.16±0.12	BRICMAN	70	CNTR	Total, charge exchange
0.42	COOL	70	CNTR	$K^- p$, $K^- d$ total
0.47	BUGG	68	CNTR	

$(\Gamma_i\Gamma_f)^{1/2}/\Gamma_{total}$ in $N\overline{K} \rightarrow \Sigma(2250) \rightarrow \Lambda\pi$ — $(\Gamma_1\Gamma_2)^{1/2}/\Gamma$

VALUE	DOCUMENT ID		TECN	COMMENT
−0.16±0.03	VANHORN	75	DPWA	$K^- p \rightarrow \Lambda\pi^0$, F_5 wave
• • • We do not use the following data for averages, fits, limits, etc. • • •				
+0.11	DEBELLEFON	76	IPWA	D_5 wave
−0.10	DEBELLEFON	76	IPWA	G_9 wave
−0.18	BARBARO-...	70	DPWA	$K^- p \rightarrow \Lambda\pi^0$, G_9 wave

$(\Gamma_i\Gamma_f)^{1/2}/\Gamma_{total}$ in $N\overline{K} \rightarrow \Sigma(2250) \rightarrow \Sigma\pi$ — $(\Gamma_1\Gamma_3)^{1/2}/\Gamma$

VALUE	DOCUMENT ID		TECN	COMMENT
+0.06±0.02	DEBELLEFON	77	DPWA	D_5 wave
−0.03±0.02	DEBELLEFON	77	DPWA	G_9 wave
+0.07	BARBARO-...	70	DPWA	$K^- p \rightarrow \Sigma\pi$, G_9 wave

$\Gamma(N\overline{K})/\Gamma(\Sigma\pi)$ — Γ_1/Γ_3

VALUE	DOCUMENT ID		TECN	COMMENT
• • • We do not use the following data for averages, fits, limits, etc. • • •				
<0.18	BARNES	69	HBC	1 standard dev. limit

$\Gamma(\Lambda\pi)/\Gamma(\Sigma\pi)$ — Γ_2/Γ_3

VALUE	DOCUMENT ID		TECN	COMMENT
• • • We do not use the following data for averages, fits, limits, etc. • • •				
<0.18	BARNES	69	HBC	1 standard dev. limit

$(\Gamma_i\Gamma_f)^{1/2}/\Gamma_{total}$ in $N\overline{K} \rightarrow \Sigma(2250) \rightarrow \Xi(1530)K$ — $(\Gamma_1\Gamma_5)^{1/2}/\Gamma$

VALUE	DOCUMENT ID		TECN	COMMENT
0.18±0.04	[1] DEBELLEFON	75B	HBC	$K^- p \rightarrow \Xi^{*0} K^0$

$\Sigma(2250)$ FOOTNOTES

[1] Seen in the (initial and final state) D_5 wave. Isospin not determined.

$\Sigma(2250)$ REFERENCES

DEBELLEFON	78	NC 42A 403	A. de Bellefon *et al.* (CDEF, SACL) IJP
DEBELLEFON	77	NC 37A 175	A. de Bellefon *et al.* (CDEF, SACL) IJP
DEBELLEFON	76	NP B109 129	A. de Bellefon, A. Berthon (CDEF) IJP
Also	75	NP B90 1	A. de Bellefon *et al.* (CDEF, SACL) IJP
DEBELLEFON	75B	NC 28A 289	A. de Bellefon *et al.* (CDEF, SACL)
VANHORN	75	NP B87 145	A.J. van Horn (LBL) IJP
Also	75B	NP B87 157	A.J. van Horn (LBL) IJP
LASINSKI	71	NP B29 125	T.A. Lasinski (EFI) IJP
AGUILAR-...	70B	PRL 25 58	M. Aguilar-Benítez *et al.* (BNL, SYRA)
BARBARO-...	70	Duke Conf. 173 Hyperon Resonances, 1970	A. Barbaro-Galtieri (LRL) IJP
BRICMAN	70	PL 31B 152	C. Bricman *et al.* (CERN, CAEN, SACL)
COOL	70	PR D1 1887	R.L. Cool *et al.* (BNL) I
Also	66	PRL 16 1228	R.L. Cool *et al.* (BNL) I
LU	70	PR D2 1846	D.C. Lu *et al.* (YALE)
BARNES	69	PRL 22 479	V.E. Barnes *et al.* (BNL, SYRA)
BUGG	68	PR 168 1466	D.V. Bugg *et al.* (RHEL, BIRM, CAVE) I
BLANPIED	65	PRL 14 741	W.A. Blanpied *et al.* (YALE, CEA)
BOCK	65	PL 17 166	R.K. Bock *et al.* (CERN, SACL)

$\Sigma(2455)$ Bumps

$I(J^P) = 1(?^?)$ Status: **

OMITTED FROM SUMMARY TABLE

There is also some slight evidence for Y^* states in this mass region from the reaction $\gamma p \rightarrow K^+ X$ — see GREENBERG 68.

$\Sigma(2455)$ MASS

VALUE (MeV)	DOCUMENT ID		TECN	COMMENT
≈ 2455 OUR ESTIMATE				
2455±10	ABRAMS	70	CNTR	$K^- p$, $K^- d$ total
2455± 7	BUGG	68	CNTR	$K^- p$, $K^- d$ total

$\Sigma(2455)$ WIDTH

VALUE (MeV)	DOCUMENT ID		TECN	COMMENT
140	ABRAMS	70	CNTR	$K^- p$, $K^- d$ total
100±20	BUGG	68	CNTR	

$\Sigma(2455)$ DECAY MODES

	Mode
Γ_1	$N\overline{K}$

$\Sigma(2455)$ BRANCHING RATIOS

$(J+\frac{1}{2})\times\Gamma(N\overline{K})/\Gamma_{total}$ — Γ_1/Γ

VALUE	DOCUMENT ID		TECN	COMMENT
0.39	ABRAMS	70	CNTR	$K^- p$, $K^- d$ total
0.05±0.05	[1] BRICMAN	70	CNTR	Total, charge exchange
0.3	BUGG	68	CNTR	

$\Sigma(2455)$ FOOTNOTES

[1] Fit of total cross section given by BRICMAN 70 is poor in this region.

$\Sigma(2455)$ REFERENCES

ABRAMS	70	PR D1 1917	R.J. Abrams *et al.* (BNL) I
Also	67E	PRL 19 678	R.J. Abrams *et al.* (BNL)
BRICMAN	70	PL 31B 152	C. Bricman *et al.* (CERN, CAEN, SACL)
BUGG	68	PR 168 1466	D.V. Bugg *et al.* (RHEL, BIRM, CAVE) I
GREENBERG	68	PRL 20 221	J.S. Greenberg *et al.* (YALE)

$\Sigma(2620)$ Bumps

$I(J^P) = 1(?^?)$ Status: **

OMITTED FROM SUMMARY TABLE

$\Sigma(2620)$ MASS

VALUE (MeV)	DOCUMENT ID		TECN	COMMENT
≈ 2620 OUR ESTIMATE				
2542 ± 22	DIBIANCA	75	DBC	$K^- N \to \Xi K \pi$
2620 ± 15	ABRAMS	70	CNTR	$K^- p$, $K^- d$ total

$\Sigma(2620)$ WIDTH

VALUE (MeV)	DOCUMENT ID		TECN	COMMENT
221 ± 81	DIBIANCA	75	DBC	$K^- N \to \Xi K \pi$
175	ABRAMS	70	CNTR	$K^- p$, $K^- d$ total

$\Sigma(2620)$ DECAY MODES

	Mode
Γ_1	$N\overline{K}$

$\Sigma(2620)$ BRANCHING RATIOS

$(J+\frac{1}{2})\times\Gamma(N\overline{K})/\Gamma_{total}$ Γ_1/Γ

VALUE	DOCUMENT ID		TECN	COMMENT
0.32	ABRAMS	70	CNTR	$K^- p$, $K^- d$ total
0.36 ± 0.12	BRICMAN	70	CNTR	Total, charge exchange

$\Sigma(2620)$ REFERENCES

DIBIANCA	75	NP B98 137	F.A. Dibianca, R.J. Endorf	(CMU)
ABRAMS	70	PR D1 1917	R.J. Abrams *et al.*	(BNL) I
Also	67E	PRL 19 678	R.J. Abrams *et al.*	(BNL)
BRICMAN	70	PL 31B 152	C. Bricman *et al.*	(CERN, CAEN, SACL)

$\Sigma(3000)$ Bumps

$I(J^P) = 1(?^?)$ Status: *

OMITTED FROM SUMMARY TABLE

Seen as an enhancement in $\Lambda\pi$ and $\overline{K}N$ invariant mass spectra and in the missing mass of neutrals recoiling against a K^0.

$\Sigma(3000)$ MASS

VALUE (MeV)	DOCUMENT ID		TECN	CHG	COMMENT
≈ 3000 OUR ESTIMATE					
3000	EHRLICH	66	HBC	0	$\pi^- p$ 7.91 GeV/c

$\Sigma(3000)$ DECAY MODES

	Mode
Γ_1	$N\overline{K}$
Γ_2	$\Lambda\pi$

$\Sigma(3000)$ REFERENCES

EHRLICH	66	PR 152 1194	R. Ehrlich, W. Selove, H. Yuta		(PENN) I

$\Sigma(3170)$ Bumps

$I(J^P) = 1(?^?)$ Status: *

OMITTED FROM SUMMARY TABLE

Seen by AMIRZADEH 79 as a narrow 6.5-standard-deviation enhancement in the reaction $K^- p \to Y^{*+}\pi^-$ using data from independent high statistics bubble chamber experiments at 8.25 and 6.5 GeV/c. The dominant decay modes are multibody, multistrange final states and the production is via isospin-3/2 baryon exchange. Isospin 1 is favored.

Not seen in a $K^- p$ experiment in LASS at 11 GeV/c (ASTON 85B).

$\Sigma(3170)$ MASS (PRODUCTION EXPERIMENTS)

VALUE (MeV)	EVTS	DOCUMENT ID		TECN	COMMENT
≈ 3170 OUR ESTIMATE					
3170 ± 5	35	AMIRZADEH	79	HBC	$K^- p \to Y^{*+}\pi^-$

$\Sigma(3170)$ WIDTH (PRODUCTION EXPERIMENTS)

VALUE (MeV)	EVTS	DOCUMENT ID		TECN	COMMENT
< 20	35	[1] AMIRZADEH	79	HBC	$K^- p \to Y^{*+}\pi^-$

$\Sigma(3170)$ DECAY MODES (PRODUCTION EXPERIMENTS)

	Mode	Fraction (Γ_i/Γ)
Γ_1	$\Lambda K\overline{K}\pi$'s	seen
Γ_2	$\Sigma K\overline{K}\pi$'s	seen
Γ_3	$\Xi K\pi$'s	seen

$\Sigma(3170)$ BRANCHING RATIOS (PRODUCTION EXPERIMENTS)

$\Gamma(\Lambda K\overline{K}\pi\text{'s})/\Gamma_{total}$ Γ_1/Γ

VALUE	DOCUMENT ID		TECN	COMMENT
seen	AMIRZADEH	79	HBC	$K^- p \to Y^{*+}\pi^-$

$\Gamma(\Sigma K\overline{K}\pi\text{'s})/\Gamma_{total}$ Γ_2/Γ

VALUE	DOCUMENT ID		TECN	COMMENT
seen	AMIRZADEH	79	HBC	$K^- p \to Y^{*+}\pi^-$

$\Gamma(\Xi K\pi\text{'s})/\Gamma_{total}$ Γ_3/Γ

VALUE	DOCUMENT ID		TECN	COMMENT
seen	AMIRZADEH	79	HBC	$K^- p \to Y^{*+}\pi^-$

$\Sigma(3170)$ FOOTNOTES (PRODUCTION EXPERIMENTS)

[1] Observed width consistent with experimental resolution.

$\Sigma(3170)$ REFERENCES (PRODUCTION EXPERIMENTS)

ASTON	85B	PR D32 2270	D. Aston *et al.*	(SLAC, CARL, CNRC, CINC)
AMIRZADEH	79	PL 89B 125	J. Amirzadeh *et al.*	(BIRM, CERN, GLAS+) I
Also	80	Toronto Conf. 263	J.B. Kinson *et al.*	(BIRM, CERN, GLAS+) I

Ξ BARYONS
($S = -2$, $I = 1/2$)

$\Xi^0 = uss$, $\Xi^- = dss$

Ξ^0

$I(J^P) = \frac{1}{2}(\frac{1}{2}^+)$ Status: ****

The parity has not actually been measured, but + is of course expected.

Ξ^0 MASS

The fit uses the Ξ^0, Ξ^-, and $\overline{\Xi}^+$ mass and mass difference measurements.

VALUE (MeV)	EVTS	DOCUMENT ID		TECN	COMMENT
1314.83±0.20 OUR FIT					
1314.82±0.20 OUR AVERAGE					
1314.82±0.06±0.20	3120	FANTI	00	NA48	p Be, 450 GeV
1315.2 ±0.92	49	WILQUET	72	HLBC	
1313.4 ±1.8	1	PALMER	68	HBC	

$m_{\Xi^-} - m_{\Xi^0}$

The fit uses the Ξ^0, Ξ^-, and $\overline{\Xi}^+$ mass and mass difference measurements.

VALUE (MeV)	EVTS	DOCUMENT ID		TECN	COMMENT
6.48±0.24 OUR FIT					
6.3 ±0.7 OUR AVERAGE					
6.9 ±2.2	29	LONDON	66	HBC	
6.1 ±0.9	88	PJERROU	65B	HBC	
6.8 ±1.6	23	JAUNEAU	63	FBC	
• • • We do not use the following data for averages, fits, limits, etc. • • •					
6.1 ±1.6	45	CARMONY	64B	HBC	See PJERROU 65B

Ξ^0 MEAN LIFE

VALUE (10^{-10} s)	EVTS	DOCUMENT ID		TECN	COMMENT
2.90±0.09 OUR AVERAGE					
2.83±0.16	6300	[1] ZECH	77	SPEC	Neutral hyperon beam
$2.88^{+0.21}_{-0.19}$	652	BALTAY	74	HBC	1.75 GeV/c K^-p
$2.90^{+0.32}_{-0.27}$	157	[2] MAYEUR	72	HLBC	2.1 GeV/c K^-
$3.07^{+0.22}_{-0.20}$	340	DAUBER	69	HBC	
3.0 ±0.5	80	PJERROU	65B	HBC	
$2.5\ ^{+0.4}_{-0.3}$	101	HUBBARD	64	HBC	
$3.9\ ^{+1.4}_{-0.8}$	24	JAUNEAU	63	FBC	
• • • We do not use the following data for averages, fits, limits, etc. • • •					
$3.5\ ^{+1.0}_{-0.8}$	45	CARMONY	64B	HBC	See PJERROU 65B

[1] The ZECH 77 result is $\tau_{\Xi^0} = [2.77-(\tau_\Lambda - 2.69)] \times 10^{-10}$ s, in which we use $\tau_\Lambda = 2.63 \times 10^{-10}$ s.
[2] The MAYEUR 72 value is modified by the erratum.

Ξ^0 MAGNETIC MOMENT

See the "Note on Baryon Magnetic Moments" in the Λ Listings.

VALUE (μ_N)	EVTS	DOCUMENT ID		TECN
−1.250±0.014 OUR AVERAGE				
−1.253±0.014	270k	COX	81	SPEC
−1.20 ±0.06	42k	BUNCE	79	SPEC

Ξ^0 DECAY MODES

	Mode	Fraction (Γ_i/Γ)	Scale factor/ Confidence level
Γ_1	$\Lambda\pi^0$	(99.522±0.032) %	S=1.7
Γ_2	$\Lambda\gamma$	(1.18 ±0.30) $\times 10^{-3}$	S=2.0
Γ_3	$\Sigma^0\gamma$	(3.33 ±0.10) $\times 10^{-3}$	
Γ_4	$\Sigma^+ e^- \overline{\nu}_e$	(2.7 ±0.4) $\times 10^{-4}$	
Γ_5	$\Sigma^+ \mu^- \overline{\nu}_\mu$	< 1.1 $\times 10^{-3}$	CL=90%

$\Delta S = \Delta Q$ (SQ) violating modes or $\Delta S = 2$ forbidden ($S2$) modes

Γ_6	$\Sigma^- e^+ \nu_e$	SQ	< 9	$\times 10^{-4}$	CL=90%
Γ_7	$\Sigma^- \mu^+ \nu_\mu$	SQ	< 9	$\times 10^{-4}$	CL=90%
Γ_8	$p\pi^-$	$S2$	< 4	$\times 10^{-5}$	CL=90%
Γ_9	$pe^-\overline{\nu}_e$	$S2$	< 1.3	$\times 10^{-3}$	
Γ_{10}	$p\mu^-\overline{\nu}_\mu$	$S2$	< 1.3	$\times 10^{-3}$	

CONSTRAINED FIT INFORMATION

An overall fit to 3 branching ratios uses 6 measurements and one constraint to determine 4 parameters. The overall fit has a $\chi^2 = 4.4$ for 3 degrees of freedom.

The following *off-diagonal* array elements are the correlation coefficients $\langle \delta x_i \delta x_j \rangle / (\delta x_i \cdot \delta x_j)$, in percent, from the fit to the branching fractions, $x_i \equiv \Gamma_i/\Gamma_{\rm total}$. The fit constrains the x_i whose labels appear in this array to sum to one.

x_2	−94		
x_3	−31	−1	
x_4	−12	0	0
	x_1	x_2	x_3

Ξ^0 BRANCHING RATIOS

$\Gamma(\Lambda\gamma)/\Gamma(\Lambda\pi^0)$ Γ_2/Γ_1

VALUE (units 10^{-3})	EVTS	DOCUMENT ID		TECN	COMMENT
1.19±0.30 OUR FIT Error includes scale factor of 2.0.					
1.19±0.30 OUR AVERAGE Error includes scale factor of 2.0.					
1.91±0.34±0.19	31	[3] FANTI	00	NA48	p Be, 450 GeV
1.06±0.12±0.11	116	JAMES	90	SPEC	FNAL hyperons

[3] FANTI 00 used our 1998 value of 99.5% for the $\Xi^0 \to \Lambda\pi^0$ branching fraction to get $\Gamma(\Xi^0 \to \Lambda\gamma)/\Gamma_{\rm total} = (1.90 \pm 0.34 \pm 0.19) \times 10^{-3}$. We adjust slightly to go back to what was directly measured.

$\Gamma(\Sigma^0\gamma)/\Gamma(\Lambda\pi^0)$ Γ_3/Γ_1

VALUE (units 10^{-3})	EVTS	DOCUMENT ID		TECN	COMMENT
3.35±0.10 OUR FIT					
3.35±0.10 OUR AVERAGE					
3.34±0.05±0.09	4045	ALAVI-HARATI	01C	KTEV	p nucleus, 800 GeV
3.16±0.76±0.32	17	[4] FANTI	00	NA48	p Be, 450 GeV
3.56±0.42±0.10	85	TEIGE	89	SPEC	FNAL hyperons

[4] FANTI 00 used our 1998 value of 99.5% for the $\Xi^0 \to \Lambda\pi^0$ branching fraction to get $\Gamma(\Xi^0 \to \Sigma^0\gamma)/\Gamma_{\rm total} = (3.14 \pm 0.76 \pm 0.32) \times 10^{-3}$. We adjust slightly to go back to what was directly measured.

$\Gamma(\Sigma^+ e^- \overline{\nu}_e)/\Gamma_{\rm total}$ Γ_4/Γ

VALUE (units 10^{-4})	EVTS	DOCUMENT ID		TECN	COMMENT
2.7 ±0.4 OUR FIT					
2.71±0.22±0.31	176	AFFOLDER	99	KTEV	p nucleus 800 GeV

$\Gamma(\Sigma^+ \mu^- \overline{\nu}_\mu)/\Gamma(\Lambda\pi^0)$ Γ_5/Γ_1

VALUE (units 10^{-3})	CL%	EVTS	DOCUMENT ID		TECN	COMMENT
<1.1	90	0	YEH	74	HBC	Effective denom.=2100
• • • We do not use the following data for averages, fits, limits, etc. • • •						
<1.5			DAUBER	69	HBC	
<7			HUBBARD	66	HBC	

$\Gamma(\Sigma^- e^+ \nu_e)/\Gamma(\Lambda\pi^0)$ Γ_6/Γ_1

Test of $\Delta S = \Delta Q$ rule.

VALUE (units 10^{-3})	CL%	EVTS	DOCUMENT ID		TECN	COMMENT
<0.9	90	0	YEH	74	HBC	Effective denom.=2500
• • • We do not use the following data for averages, fits, limits, etc. • • •						
<1.5			DAUBER	69	HBC	
<6			HUBBARD	66	HBC	

$\Gamma(\Sigma^- \mu^+ \nu_\mu)/\Gamma(\Lambda\pi^0)$ Γ_7/Γ_1

Test of $\Delta S = \Delta Q$ rule.

VALUE (units 10^{-3})	CL%	EVTS	DOCUMENT ID		TECN	COMMENT
<0.9	90	0	YEH	74	HBC	Effective denom.=2500
• • • We do not use the following data for averages, fits, limits, etc. • • •						
<1.5			DAUBER	69	HBC	
<6			HUBBARD	66	HBC	

$\Gamma(p\pi^-)/\Gamma(\Lambda\pi^0)$ Γ_8/Γ_1

ΔS=2. Forbidden in first-order weak interaction.

VALUE (units 10^{-5})	CL%	EVTS	DOCUMENT ID		TECN	COMMENT
< 3.6	90		GEWENIGER	75	SPEC	
• • • We do not use the following data for averages, fits, limits, etc. • • •						
<180	90	0	YEH	74	HBC	Effective denom.=1300
< 90			DAUBER	69	HBC	
<500			HUBBARD	66	HBC	

$\Gamma(pe^-\overline{\nu}_e)/\Gamma(\Lambda\pi^0)$ Γ_9/Γ_1

ΔS=2. Forbidden in first-order weak interaction.

VALUE (units 10^{-3})	CL%	EVTS	DOCUMENT ID		TECN	COMMENT
<1.3			DAUBER	69	HBC	
• • • We do not use the following data for averages, fits, limits, etc. • • •						
<3.4	90	0	YEH	74	HBC	Effective denom.=670
<6			HUBBARD	66	HBC	

$\Gamma(p\mu^-\overline{\nu}_\mu)/\Gamma(\Lambda\pi^0)$ Γ_{10}/Γ_1

ΔS=2. Forbidden in first-order weak interaction.

VALUE (units 10^{-3})	CL%	EVTS	DOCUMENT ID		TECN	COMMENT
<1.3			DAUBER	69	HBC	
• • • We do not use the following data for averages, fits, limits, etc. • • •						
<3.5	90	0	YEH	74	HBC	Effective denom.=664
<6			HUBBARD	66	HBC	

Ξ^0 DECAY PARAMETERS

See the "Note on Baryon Decay Parameters" in the neutron Listings.

$\alpha(\Xi^0)$ $\alpha_-(\Lambda)$

VALUE	EVTS	DOCUMENT ID		TECN	COMMENT
−0.264±0.013 OUR AVERAGE Error includes scale factor of 2.1. See the ideogram below.					
−0.260±0.004±0.005	300k	HANDLER	82	SPEC	FNAL hyperons
−0.317±0.027	6075	BUNCE	78	SPEC	FNAL hyperons
−0.35 ±0.06	505	BALTAY	74	HBC	K^-p 1.75 GeV/c
−0.28 ±0.06	739	DAUBER	69	HBC	K^-p 1.7–2.6 GeV/c

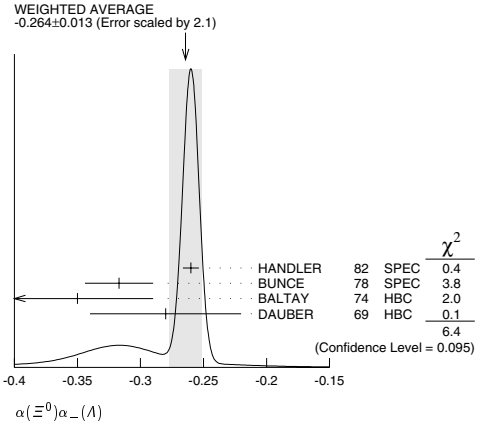

α FOR $\Xi^0 \rightarrow \Lambda\pi^0$

The above average, $\alpha(\Xi^0)\alpha_-(\Lambda) = -0.264 \pm 0.013$, where the error includes a scale factor of 2.1, divided by our current average $\alpha_-(\Lambda) = 0.642 \pm 0.013$, gives the following value for $\alpha(\Xi^0)$.

VALUE	DOCUMENT ID
−0.411±0.022 OUR EVALUATION	Error includes scale factor of 2.1.

ϕ ANGLE FOR $\Xi^0 \rightarrow \Lambda\pi^0$ $(\tan\phi = \beta/\gamma)$

VALUE (°)	EVTS	DOCUMENT ID		TECN	COMMENT
21±12 OUR AVERAGE					
16±17	652	BALTAY	74	HBC	1.75 GeV/c K^-p
38±19	739	[5] DAUBER	69	HBC	
− 8±30	146	[6] BERGE	66	HBC	

[5] DAUBER 69 uses $\alpha_\Lambda = 0.647 \pm 0.020$.

[6] The errors have been multiplied by 1.2 due to approximations used for the Ξ polarization; see DAUBER 69 for a discussion.

RADIATIVE HYPERON DECAYS

Written September 2003 by J.D. Jackson (LBNL).

The weak radiative decays of spin-1/2 hyperons, $B_i \rightarrow B_f\gamma$, yield information about matrix elements (form factors) similar to that gained from weak hadronic decays. For a polarized spin-1/2 hyperon decaying radiatively via a $\Delta Q = 0$, $\Delta S = 1$ transition, the angular distribution of the direction $\hat{\mathbf{p}}$ of the final spin-1/2 baryon in the hyperon rest frame is

$$\frac{dN}{d\Omega} = \frac{N}{4\pi}\,(1 + \alpha_\gamma\,\mathbf{P}_i\cdot\hat{\mathbf{p}})\ . \qquad (1)$$

Here $\mathbf{P}_i$ is the polarization of the decaying hyperon, and α_γ is the asymmetry parameter. In terms of the form factors $F_1(q^2)$, $F_2(q^2)$, and $G(q^2)$ of the effective hadronic weak electromagnetic vertex,

$$F_1(q^2)\gamma_\lambda + iF_2(q^2)\sigma_{\lambda\mu}q^\mu + G(q^2)\gamma_\lambda\gamma_5\ ,$$

α_γ is

$$\alpha_\gamma = \frac{2\,\mathrm{Re}[G(0)F_M^*(0)]}{|G(0)|^2 + |F_M(0)|^2}\ , \qquad (2)$$

where $F_M = (m_i - m_f)[F_2 - F_1/(m_i + m_f)]$. If the decaying hyperon is unpolarized, the decay baryon has a longitudinal polarization given by $P_f = -\alpha_\gamma$ [1].

The angular distribution for the weak hadronic decay, $B_i \rightarrow B_f\pi$, has the same form as Eq. (1), but of course with a different asymmetry parameter, α_π. Now, however, if the decaying hyperon is unpolarized, the decay baryon has a longitudinal polarization given by $P_f = +\alpha_\pi$ [2,3]. The difference of sign is because the spins of the pion and photon are different.

$\Xi^0 \rightarrow \Lambda\gamma$ decay—The radiative decay $\Xi^0 \rightarrow \Lambda\gamma$ of an unpolarized Ξ^0 uses the hadronic decay $\Lambda \rightarrow p\pi^-$ as the analyzer. As noted above, the longitudinal polarization of the Λ will be $P_\Lambda = -\alpha_{\Xi\Lambda\gamma}$. Let α_- be the $\Lambda \rightarrow p\pi^-$ asymmetry parameter and $\theta_{\Lambda p}$ be the angle, as seen in the Λ rest frame, between the Λ line of flight and the proton momentum. Then the hadronic version of Eq. (1) applied to the $\Lambda \rightarrow p\pi^-$ decay gives

$$\frac{dN}{d\cos\theta_{\Lambda p}} = \frac{N}{2}\,(1 - \alpha_{\Xi\Lambda\gamma}\,\alpha_-\cos\theta_{\Lambda p}) \qquad (3)$$

for the angular distribution of the proton in the Λ frame. The only published measurement of $\alpha_{\Xi\Lambda\gamma}$ [4] got the sign wrong, as explained in an erratum 12 years later [5]. The corrected result is $\alpha_{\Xi\Lambda\gamma} = -0.43 \pm 0.44$.

$\Xi^0 \rightarrow \Sigma^0\gamma$ decay—The asymmetry parameter here, $\alpha_{\Xi\Sigma\gamma}$, is measured by following the decay chain $\Xi^0 \rightarrow \Sigma^0\gamma$, $\Sigma^0 \rightarrow \Lambda\gamma$, $\Lambda \rightarrow p\pi^-$. Again, for an unpolarized Ξ^0, the longitudinal polarization of the Σ^0 will be $P_\Sigma = -\alpha_{\Xi\Sigma\gamma}$. In the $\Sigma^0 \rightarrow \Lambda\gamma$ decay, a parity-conserving magnetic-dipole transition, the polarization of the Σ^0 is transferred to the Λ, as may be seen as follows. Let $\theta_{\Sigma\Lambda}$ be the angle seen in the Σ^0 rest frame between the Σ^0 line of flight and the Λ momentum. For Σ^0 helicity $+1/2$, the probability amplitudes for positive and negative spin states of the Σ^0 *along the Λ momentum* are $\cos(\theta_{\Sigma\Lambda}/2)$ and $\sin(\theta_{\Sigma\Lambda}/2)$. Then the amplitude for a negative helicity photon and a negative helicity Λ is $\cos(\theta_{\Sigma\Lambda}/2)$, while the amplitude for positive helicities for the photon and Λ is $\sin(\theta_{\Sigma\Lambda}/2)$. For Σ^0 helicity $-1/2$, the amplitudes are interchanged. If the Σ^0 has

longitudinal polarization P_Σ, the probabilities for Λ helicities $\pm 1/2$ are therefore

$$p(\pm 1/2) = \frac{1}{2}(1 \mp P_\Sigma)\cos^2(\theta_{\Sigma\Lambda}/2) + \frac{1}{2}(1 \pm P_\Sigma)\sin^2(\theta_{\Sigma\Lambda}/2) \ , \quad (4)$$

and the longitudinal polarization of the Λ is

$$P_\Lambda = -P_\Sigma \cos\theta_{\Sigma\Lambda} = +\alpha_{\Xi\Sigma\gamma}\cos\theta_{\Sigma\Lambda} \ . \quad (5)$$

Using Eq. (1) for the $\Lambda \to p\pi^-$ decay again, we get for the joint angular distribution of the $\Sigma^0 \to \Lambda\gamma$, $\Lambda \to p\pi^-$ chain,

$$\frac{d^2N}{d\cos\theta_{\Sigma\Lambda}\, d\cos\theta_{\Lambda p}} = \frac{N}{4}\left(1 + \alpha_{\Xi\Sigma\gamma}\cos\theta_{\Sigma\Lambda}\,\alpha_-\cos\theta_{\Lambda p}\right) \ . \quad (6)$$

The KTeV collaboration recently measured $\alpha_{\Xi\Sigma\gamma}$ to be -0.63 ± 0.09 [6]. The only other measurement has been withdrawn [7].

References

1. R.E. Behrends, Phys. Rev. **111**, 1691 (1958); see Eq. (7) or (8).
2. In ancient times, the signs of the asymmetry term in the angular distributions of radiative and hadronic decays of polarized hyperons were sometimes opposite. For roughly 40 years, however, the overwhelming convention has been to make them the same. The aim, not always achieved, is to remove ambiguities.
3. For the definition of α_π, see the note on "Baryon Decay Parameters," in the Neutron Listings in this *Review*..
4. C. James *et al.*, Phys. Rev. Lett. **64**, 843 (1990).
5. C. James *et al.*, Phys. Rev. Lett. **89**, 169901 (2002) (erratum). The various sign conventions spelled out here are discussed.
6. A. Alavi-Harati *et al.*, Phys. Rev. Lett. **86**, 3239 (2001).
7. S. Teige *et al.*, Phys. Rev. Lett. **63**, 2717 (1989); erratum, Phys. Rev. Lett. **89**, 169902 (2002).

α FOR $\Xi^0 \to \Lambda\gamma$

See the note above on "Radiative Hyperon Decays."

VALUE	EVTS	DOCUMENT ID		TECN	COMMENT
-0.43 ± 0.44	87	[7] JAMES	90	SPEC	FNAL hyperons

[7] The sign has been changed; see the erratum (JAMES 02, under JAMES 90).

α FOR $\Xi^0 \to \Sigma^0\gamma$

See the note above on "Radiative Hyperon Decays."

VALUE	EVTS	DOCUMENT ID		TECN	COMMENT
$-0.63 \pm 0.08 \pm 0.05$	4045	ALAVI-HARATI	01C	KTEV	p nucleus, 800 GeV
• • • We do not use the following data for averages, fits, limits, etc. • • •					
$+0.20 \pm 0.32 \pm 0.05$	85	[8] TEIGE	89	SPEC	FNAL hyperons

[8] This result has been withdrawn, due to an error. See the erratum (TEIGE 02, under TEIGE 89).

$g_1(0)/f_1(0)$ FOR $\Xi^0 \to \Sigma^+ e^- \bar{\nu}_e$

VALUE	EVTS	DOCUMENT ID		TECN	COMMENT
$+1.32^{+0.21}_{-0.17} \pm 0.05$	487	[9] ALAVI-HARATI	01I	KTEV	p nucleus, 800 GeV

[9] ALAVI-HARATI 01I assumes here that the second-class current is zero and that the weak-magnetism term takes its exact SU(3) value.

$g_2(0)/f_1(0)$ FOR $\Xi^0 \to \Sigma^+ e^- \bar{\nu}_e$

VALUE	EVTS	DOCUMENT ID		TECN	COMMENT
$-1.7^{+2.1}_{-2.0} \pm 0.5$	487	[10] ALAVI-HARATI	01I	KTEV	p nucleus, 800 GeV

[10] ALAVI-HARATI 01I thus assumes that $g_2 = 0$ in calculating g_1/f_1, above.

$f_2(0)/f_1(0)$ FOR $\Xi^0 \to \Sigma^+ e^- \bar{\nu}_e$

VALUE	EVTS	DOCUMENT ID		TECN	COMMENT
$2.0 \pm 1.2 \pm 0.5$	487	ALAVI-HARATI	01I	KTEV	p nucleus, 800 GeV

Ξ^0 REFERENCES

JAMES	02	PRL 89 169901 (erratum)	C. James *et al.* (MINN, MICH, WISC, RUTG)
TEIGE	02	PRL 89 169902 (erratum)	S. Teige *et al.* (RUTG, MICH, MINN)
ALAVI-HARATI	01C	PRL 86 3239	A. Alavi-Harati *et al.* (FNAL KTeV Collab.)
ALAVI-HARATI	01I	PRL 87 132001	A. Alavi-Harati *et al.* (FNAL KTeV Collab.)
FANTI	00	EPJ C12 69	V. Fanti *et al.* (CERN NA48 Collab.)
AFFOLDER	99	PRL 82 3751	A. Affolder *et al.* (FNAL KTeV Collab.)
JAMES	90	PRL 64 843	C. James *et al.* (MINN, MICH, WISC, RUTG)
Also	02	PRL 89 169901 (erratum)	C. James *et al.* (MINN, MICH, WISC, RUTG)
TEIGE	89	PRL 63 2717	S. Teige *et al.* (RUTG, MICH, MINN)
Also	02	PRL 89 169902 (erratum)	S. Teige *et al.* (RUTG, MICH, MINN)
HANDLER	82	PR D25 639	R. Handler *et al.* (WISC, MICH, MINN+)
COX	81	PRL 46 877	P.T. Cox *et al.* (MICH, WISC, RUTG, MINN+)
BUNCE	79	PL 86B 386	G.R.M. Bunce *et al.* (BNL, MICH, RUTG+)
BUNCE	78	PR D18 633	G.R.M. Bunce *et al.* (WISC, MICH, RUTG)
ZECH	77	NP B124 413	G. Zech *et al.* (SIEG, CERN, DORT, HEIDH)
GEWENIGER	75	PL 57B 193	C. Geweniger *et al.* (CERN, HEIDH)
BALTAY	74	PR D9 49	C. Baltay *et al.* (COLU, BING) J
YEH	74	PR D10 3545	N. Yeh *et al.* (BING, COLU)
MAYEUR	72	NP B47 333	C. Mayeur *et al.* (BRUX, CERN, TUFTS, LOUC)
Also	73	NP B53 268 erratum	C. Mayeur
WILQUET	72	PL 42B 372	G. Wilquet *et al.* (BRUX, CERN, TUFTS+)
DAUBER	69	PR 179 1262	P.M. Dauber *et al.* (LRL)
PALMER	68	PL 26B 323	R.B. Palmer *et al.* (BNL, SYRA)
BERGE	66	PR 147 945	J.P. Berge *et al.* (LRL)
HUBBARD	66	Thesis UCRL 11510	J.R. Hubbard (LRL)
LONDON	66	PR 143 1034	G.W. London *et al.* (BNL, SYRA)
PJERROU	65B	PRL 14 275	G.M. Pjerrou *et al.* (UCLA)
Also	65	Thesis	G.M. Pjerrou (UCLA)
CARMONY	64B	PRL 12 482	D.D. Carmony *et al.* (UCLA)
HUBBARD	64	PR 135B 183	J.R. Hubbard *et al.* (LRL)
JAUNEAU	63	PL 4 49	L. Jauneau *et al.* (EPOL, CERN, LOUC+)
Also	63C	Siena Conf. 1 1	L. Jauneau *et al.* (EPOL, CERN, LOUC+)

Ξ^-

$I(J^P) = \frac{1}{2}(\frac{1}{2}^+)$ Status: ****

The parity has not actually been measured, but + is of course expected.

We have omitted some results that have been superseded by later experiments. See our earlier editions.

Ξ^- MASS

The fit uses the Ξ^-, $\overline{\Xi}^+$, and Ξ^0 mass and mass difference measurements. It assumes the Ξ^- and $\overline{\Xi}^+$ masses are the same.

VALUE (MeV)	EVTS	DOCUMENT ID		TECN	COMMENT
1321.31 ± 0.13 OUR FIT					
1321.34 ± 0.14 OUR AVERAGE					
1321.46 ± 0.34	632	DIBIANCA	75	DBC	4.9 GeV/c K^-d
1321.12 ± 0.41	268	WILQUET	72	HLBC	
1321.87 ± 0.51	195	[1] GOLDWASSER	70	HBC	5.5 GeV/c K^-p
1321.67 ± 0.52	6	CHIEN	66	HBC	6.9 GeV/c $\overline{p}p$
1321.4 ± 1.1	299	LONDON	66	HBC	
1321.3 ± 0.4	149	PJERROU	65B	HBC	
1321.1 ± 0.3	241	[2] BADIER	64	HBC	
1321.4 ± 0.4	517	[2] JAUNEAU	63D	FBC	
1321.1 ± 0.65	62	[2] SCHNEIDER	63	HBC	

[1] GOLDWASSER 70 uses $m_\Lambda = 1115.58$ MeV.
[2] These masses have been increased 0.09 MeV because the Λ mass increased.

$\overline{\Xi}^+$ MASS

The fit uses the Ξ^-, $\overline{\Xi}^+$, and Ξ^0 mass and mass difference measurements. It assumes the Ξ^- and $\overline{\Xi}^+$ masses are the same.

VALUE (MeV)	EVTS	DOCUMENT ID		TECN	COMMENT
1321.31 ± 0.13 OUR FIT					
1321.20 ± 0.33 OUR AVERAGE					
1321.6 ± 0.8	35	VOTRUBA	72	HBC	10 GeV/c K^+p
1321.2 ± 0.4	34	STONE	70	HBC	
1320.69 ± 0.93	5	CHIEN	66	HBC	6.9 GeV/c $\overline{p}p$

$(m_{\Xi^-} - m_{\overline{\Xi}^+}) / m_{\Xi^-}$

A test of *CPT* invariance. We calculate this from the *average* Ξ^- and $\overline{\Xi}^+$ masses above.

VALUE	DOCUMENT ID
$(1.1 \pm 2.7) \times 10^{-4}$ OUR EVALUATION	

Ξ^- MEAN LIFE

Measurements with an error $> 0.2 \times 10^{-10}$ s or with systematic errors not included have been omitted.

VALUE (10^{-10} s)	EVTS	DOCUMENT ID		TECN	COMMENT
1.639 ± 0.015 OUR AVERAGE					
1.652 ± 0.051	32k	BOURQUIN	84	SPEC	Hyperon beam
1.665 ± 0.065	41k	BOURQUIN	79	SPEC	Hyperon beam
1.609 ± 0.028	4286	HEMINGWAY	78	HBC	4.2 GeV/c K^-p
1.67 ± 0.08		DIBIANCA	75	DBC	4.9 GeV/c K^-d
1.63 ± 0.03	4303	BALTAY	74	HBC	1.75 GeV/c K^-p

$1.73\ ^{+0.08}_{-0.07}$	680	MAYEUR	72	HLBC	2.1 GeV/c K^-
$1.61\ \pm0.04$	2610	DAUBER	69	HBC	
$1.80\ \pm0.16$	299	LONDON	66	HBC	
$1.70\ \pm0.12$	246	PJERROU	65B	HBC	
$1.69\ \pm0.07$	794	HUBBARD	64	HBC	
$1.86\ ^{+0.15}_{-0.14}$	517	JAUNEAU	63D	FBC	

Ξ^+ MEAN LIFE

VALUE (10^{-10} s)	EVTS	DOCUMENT ID		TECN	COMMENT
1.6 ±0.3	34	STONE	70	HBC	
• • • We do not use the following data for averages, fits, limits, etc. • • •					
$1.55\ ^{+0.35}_{-0.20}$	35	[3] VOTRUBA	72	HBC	10 GeV/c K^+p
$1.9\ ^{+0.7}_{-0.5}$	12	[3] SHEN	67	HBC	
1.51 ± 0.55	5	[3] CHIEN	66	HBC	6.9 GeV/c $\overline{p}p$

[3] The error is statistical only.

$(\tau_{\Xi^-} - \tau_{\overline{\Xi}^+}) / \tau_{\Xi^-}$

A test of *CPT* invariance. Calculated from the Ξ^- and $\overline{\Xi}^+$ mean lives, above.

VALUE	DOCUMENT ID
0.02±0.18 OUR EVALUATION	

Ξ^- MAGNETIC MOMENT

See the "Note on Baryon Magnetic Moments" in the Λ Listings.

VALUE (μ_N)	EVTS	DOCUMENT ID		TECN	COMMENT
−0.6507±0.0025 OUR AVERAGE					
-0.6505 ± 0.0025	4.36M	DURYEA	92	SPEC	800 GeV p Be
$-0.661\ \pm0.036\ \pm0.036$	44k	TROST	89	SPEC	Ξ^- ~ 250 GeV
$-0.69\ \pm0.04$	218k	RAMEIKA	84	SPEC	400 GeV p Be
• • • We do not use the following data for averages, fits, limits, etc. • • •					
$-0.674\ \pm0.021\ \pm0.020$	122k	HO	90	SPEC	See DURYEA 92
$-2.1\ \pm0.8$	2436	COOL	74	OSPK	1.8 GeV/c K^-p
$-0.1\ \pm2.1$	2724	BINGHAM	70B	OSPK	1.8 GeV/c K^-p

$\overline{\Xi}^+$ MAGNETIC MOMENT

See the "Note on Baryon Magnetic Moments" in the Λ Listings.

VALUE (μ_N)	EVTS	DOCUMENT ID		TECN	COMMENT
+0.657±0.028±0.020	70k	HO	90	SPEC	800 GeV pBe

$(\mu_{\Xi^-} + \mu_{\overline{\Xi}^+}) / |\mu_{\Xi^-}|$

A test of *CPT* invariance. We calculate this from the Ξ^- and $\overline{\Xi}^+$ magnetic moments above.

VALUE	DOCUMENT ID
+0.01±0.05 OUR EVALUATION	

Ξ^- DECAY MODES

	Mode		Fraction (Γ_i/Γ)		Confidence level
Γ_1	$\Lambda\pi^-$		(99.887±0.035) %		
Γ_2	$\Sigma^-\gamma$		(1.27 ±0.23)	$\times10^{-4}$	
Γ_3	$\Lambda e^-\overline{\nu}_e$		(5.63 ±0.31)	$\times10^{-4}$	
Γ_4	$\Lambda\mu^-\overline{\nu}_\mu$		(3.5 $^{+3.5}_{-2.2}$)	$\times10^{-4}$	
Γ_5	$\Sigma^0 e^-\overline{\nu}_e$		(8.7 ±1.7)	$\times10^{-5}$	
Γ_6	$\Sigma^0\mu^-\overline{\nu}_\mu$	<	8	$\times10^{-4}$	90%
Γ_7	$\Xi^0 e^-\overline{\nu}_e$	<	2.3	$\times10^{-3}$	90%
	$\Delta S = 2$ forbidden ($S2$) modes				
Γ_8	$n\pi^-$	$S2$	< 1.9	$\times10^{-5}$	90%
Γ_9	$ne^-\overline{\nu}_e$	$S2$	< 3.2	$\times10^{-3}$	90%
Γ_{10}	$n\mu^-\overline{\nu}_\mu$	$S2$	< 1.5	%	90%
Γ_{11}	$p\pi^-\pi^-$	$S2$	< 4	$\times10^{-4}$	90%
Γ_{12}	$p\pi^- e^-\overline{\nu}_e$	$S2$	< 4	$\times10^{-4}$	90%
Γ_{13}	$p\pi^-\mu^-\overline{\nu}_\mu$	$S2$	< 4	$\times10^{-4}$	90%
Γ_{14}	$p\mu^-\mu^-$	L	< 4	$\times10^{-4}$	90%

CONSTRAINED FIT INFORMATION

An overall fit to 4 branching ratios uses 5 measurements and one constraint to determine 5 parameters. The overall fit has a $\chi^2 = 1.0$ for 1 degrees of freedom.

The following *off-diagonal* array elements are the correlation coefficients $\langle\delta x_i\delta x_j\rangle/(\delta x_i\cdot\delta x_j)$, in percent, from the fit to the branching fractions, $x_i \equiv \Gamma_i/\Gamma_{\rm total}$. The fit constrains the x_i whose labels appear in this array to sum to one.

x_2	−6			
x_3	−8	0		
x_4	−99	0	−1	
x_5	−5	0	0	0
	x_1	x_2	x_3	x_4

Ξ^- BRANCHING RATIOS

A number of early results have been omitted.

$\Gamma(\Sigma^-\gamma)/\Gamma(\Lambda\pi^-)$ Γ_2/Γ_1

VALUE (units 10^{-4})	EVTS	DOCUMENT ID		TECN	COMMENT
1.27±0.24 OUR FIT					
1.27±0.23 OUR AVERAGE					
$1.22\pm0.23\pm0.06$	211	[4] DUBBS	94	E761	Ξ^- 375 GeV
2.27 ± 1.02	9	BIAGI	87B	SPEC	SPS hyperon beam

[4] DUBBS 94 also finds weak evidence that the asymmetry parameter α_γ is positive ($\alpha_\gamma = 1.0 \pm 1.3$).

$\Gamma(\Lambda e^-\overline{\nu}_e)/\Gamma(\Lambda\pi^-)$ Γ_3/Γ_1

VALUE (units 10^{-3})	EVTS	DOCUMENT ID		TECN	COMMENT
0.564±0.031 OUR FIT					
0.564±0.031	2857	BOURQUIN	83	SPEC	SPS hyperon beam
• • • We do not use the following data for averages, fits, limits, etc. • • •					
$0.30\ \pm0.13$	11	THOMPSON	80	ASPK	Hyperon beam

$\Gamma(\Lambda\mu^-\overline{\nu}_\mu)/\Gamma(\Lambda\pi^-)$ Γ_4/Γ_1

VALUE (units 10^{-3})	CL%	EVTS	DOCUMENT ID		TECN	COMMENT
$0.35\ ^{+0.35}_{-0.22}$ **OUR FIT**						
0.35±0.35		1	YEH	74	HBC	Effective denom.=2859
• • • We do not use the following data for averages, fits, limits, etc. • • •						
< 2.3	90	0	THOMPSON	80	ASPK	Effective denom.=1017
< 1.3			DAUBER	69	HBC	
<12			BERGE	66	HBC	

$\Gamma(\Sigma^0 e^-\overline{\nu}_e)/\Gamma(\Lambda\pi^-)$ Γ_5/Γ_1

VALUE (units 10^{-3})	EVTS	DOCUMENT ID		TECN	COMMENT
0.087±0.017 OUR FIT					
0.087±0.017	154	BOURQUIN	83	SPEC	SPS hyperon beam

$\Gamma(\Sigma^0\mu^-\overline{\nu}_\mu)/\Gamma(\Lambda\pi^-)$ Γ_6/Γ_1

VALUE (units 10^{-3})	CL%	EVTS	DOCUMENT ID		TECN	COMMENT
<0.76	90	0	YEH	74	HBC	Effective denom.=3026
• • • We do not use the following data for averages, fits, limits, etc. • • •						
<5			BERGE	66	HBC	

$[\Gamma(\Lambda e^-\overline{\nu}_e) + \Gamma(\Sigma^0 e^-\overline{\nu}_e)]/\Gamma(\Lambda\pi^-)$ $(\Gamma_3+\Gamma_5)/\Gamma_1$

VALUE (units 10^{-3})	EVTS	DOCUMENT ID		TECN	COMMENT
• • • We do not use the following data for averages, fits, limits, etc. • • •					
0.651 ± 0.031	3011	[5] BOURQUIN	83	SPEC	SPS hyperon beam
$0.68\ \pm0.22$	17	[6] DUCLOS	71	OSPK	

[5] See the separate BOURQUIN 83 values for $\Gamma(\Lambda e^-\overline{\nu}_e)/\Gamma(\Lambda\pi^-)$ and $\Gamma(\Sigma^0 e^-\overline{\nu}_e)/\Gamma(\Lambda\pi^-)$ above.

[6] DUCLOS 71 cannot distinguish Σ^0's from Λ's. The Cabibbo theory predicts the Σ^0 rate is about a factor 6 smaller than the Λ rate.

$\Gamma(\Xi^0 e^-\overline{\nu}_e)/\Gamma(\Lambda\pi^-)$ Γ_7/Γ_1

VALUE (units 10^{-3})	CL%	EVTS	DOCUMENT ID		TECN	COMMENT
<2.3	90	0	YEH	74	HBC	Effective denom.=1000

$\Gamma(n\pi^-)/\Gamma(\Lambda\pi^-)$ Γ_8/Γ_1

ΔS=2. Forbidden in first-order weak interaction.

VALUE (units 10^{-3})	CL%	EVTS	DOCUMENT ID		TECN	COMMENT
<0.019	90		BIAGI	82B	SPEC	SPS hyperon beam
• • • We do not use the following data for averages, fits, limits, etc. • • •						
<3.0	90	0	YEH	74	HBC	Effective denom.=760
<1.1			DAUBER	69	HBC	
<5.0			FERRO-LUZZI	63	HBC	

Baryon Particle Listings

Ξ^-

$\Gamma(ne^-\overline{\nu}_e)/\Gamma(\Lambda\pi^-)$ Γ_9/Γ_1

$\Delta S=2$. Forbidden in first-order weak interaction.

VALUE (units 10^{-3})	CL%	EVTS	DOCUMENT ID		TECN	COMMENT
< 3.2	90	0	YEH	74	HBC	Effective denom.=715
• • • We do not use the following data for averages, fits, limits, etc. • • •						
<10	90		BINGHAM	65	RVUE	

$\Gamma(n\mu^-\overline{\nu}_\mu)/\Gamma(\Lambda\pi^-)$ Γ_{10}/Γ_1

$\Delta S=2$. Forbidden in first-order weak interaction.

VALUE (units 10^{-3})	CL%	EVTS	DOCUMENT ID		TECN	COMMENT
<15.3	90	0	YEH	74	HBC	Effective denom.=150

$\Gamma(p\pi^-\pi^-)/\Gamma(\Lambda\pi^-)$ Γ_{11}/Γ_1

$\Delta S=2$. Forbidden in first-order weak interaction.

VALUE (units 10^{-4})	CL%	EVTS	DOCUMENT ID		TECN	COMMENT
<3.7	90	0	YEH	74	HBC	Effective denom.=6200

$\Gamma(p\pi^-e^-\overline{\nu}_e)/\Gamma(\Lambda\pi^-)$ Γ_{12}/Γ_1

$\Delta S=2$. Forbidden in first-order weak interaction.

VALUE (units 10^{-4})	CL%	EVTS	DOCUMENT ID		TECN	COMMENT
<3.7	90	0	YEH	74	HBC	Effective denom.=6200

$\Gamma(p\pi^-\mu^-\overline{\nu}_\mu)/\Gamma(\Lambda\pi^-)$ Γ_{13}/Γ_1

$\Delta S=2$. Forbidden in first-order weak interaction.

VALUE (units 10^{-4})	CL%	EVTS	DOCUMENT ID		TECN	COMMENT
<3.7	90	0	YEH	74	HBC	Effective denom.=6200

$\Gamma(p\mu^-\mu^-)/\Gamma(\Lambda\pi^-)$ Γ_{14}/Γ_1

A $\Delta L=2$ decay, forbidden by total lepton number conservation.

VALUE (units 10^{-4})	CL%	DOCUMENT ID		TECN	COMMENT
<3.7	90	[7] LITTENBERG	92B	HBC	Uses YEH 74 data

[7] This LITTENBERG 92B limit and the identical YEH 74 limits for the preceding three modes all result from nonobservance of any 3-prong decays of the Ξ^-. One could as well apply the limit to the *sum* of the four modes.

Ξ^- DECAY PARAMETERS

See the "Note on Baryon Decay Parameters" in the neutron Listings.

$\alpha(\Xi^-)\alpha_-(\Lambda)$

VALUE	EVTS	DOCUMENT ID		TECN	COMMENT
−0.294 ±0.005 OUR AVERAGE Error includes scale factor of 1.7. See the ideogram below.					
−0.2963±0.0042	189k	LUK	00	E756	p Be, 800 GeV
−0.2894±0.0073	63k	[8] LUK	00	E756	p Be, 800 GeV
−0.303 ±0.004 ±0.004	192k	RAMEIKA	86	SPEC	400 GeV p Be
−0.257 ±0.020	11k	ASTON	85B	LASS	11 GeV/c K^-p
−0.260 ±0.017	21k	BENSINGER	85	MPS	5 GeV/c K^-p
−0.299 ±0.007	150k	BIAGI	82	SPEC	SPS hyperon beam
−0.315 ±0.026	9046	CLELAND	80C	ASPK	BNL hyperon beam
−0.239 ±0.021	6599	HEMINGWAY	78	HBC	4.2 GeV/c K^-p
−0.243 ±0.025	4303	BALTAY	74	HBC	1.75 GeV/c K^-p
−0.252 ±0.032	2436	COOL	74	OSPK	1.8 GeV/c K^-p
−0.253 ±0.028	2781	DAUBER	69	HBC	

[8] This LUK 00 value is for $\alpha(\overline{\Xi}^+)\,\alpha_+(\overline{\Lambda})$. We assume CP conservation here by including it in the average for $\alpha(\Xi^-)\,\alpha_-(\Lambda)$. But see the second data block below for the CP test.

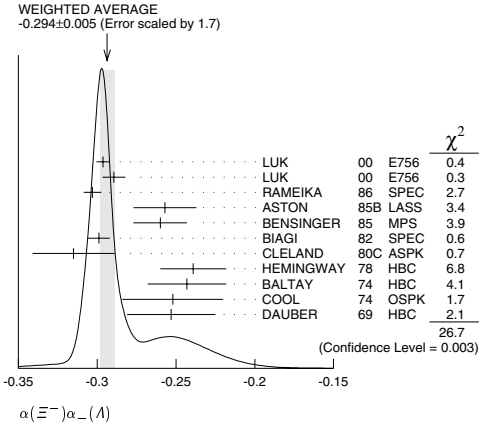

α FOR $\Xi^- \to \Lambda\pi^-$

The above average, $\alpha(\Xi^-)\,\alpha_-(\Lambda) = -0.293 \pm 0.007$, where the error includes a scale factor of 1.8, divided by our current average $\alpha_-(\Lambda) = 0.642 \pm 0.013$, gives the following value for $\alpha(\Xi^-)$.

VALUE	DOCUMENT ID
−0.458±0.012 OUR EVALUATION	Error includes scale factor of 1.8.

$\frac{[\alpha(\Xi^-)\alpha_-(\Lambda)-\alpha(\overline{\Xi}^+)\alpha_+(\overline{\Lambda})]}{[\alpha(\Xi^-)\alpha_-(\Lambda)+\alpha(\overline{\Xi}^+)\alpha_+(\overline{\Lambda})]}$

This is zero if CP is conserved. The α's are the decay-asymmetry parameters for $\Xi^- \to \Lambda\pi^-$ and $\Lambda \to p\pi^-$ and for $\overline{\Xi}^+ \to \overline{\Lambda}\pi^+$ and $\overline{\Lambda} \to \overline{p}\pi^-$.

VALUE	EVTS	DOCUMENT ID		TECN	COMMENT
+0.012±0.014	252k	LUK	00	E756	p Be, 800 GeV

ϕ ANGLE FOR $\Xi^- \to \Lambda\pi^-$ $(\tan\phi = \beta/\gamma)$

VALUE (°)	EVTS	DOCUMENT ID		TECN	COMMENT
− 0.4 ± 2.3 OUR AVERAGE					
− 1.61± 2.66±0.37	1.35M	[9] CHAKRAVO...	03	E756	p Be, 800 GeV
5 ±10	11k	ASTON	85B	LASS	K^-p
14.7 ±16.0	21k	[10] BENSINGER	85	MPS	5 GeV/c K^-p
11 ± 9	4303	BALTAY	74	HBC	1.75 GeV/c K^-p
5 ±16	2436	COOL	74	OSPK	1.8 GeV/c K^-p
− 14 ±11	2781	DAUBER	69	HBC	Uses $\alpha_\Lambda = 0.647\pm0.020$
0 ±12	1004	[11] BERGE	66	HBC	
• • • We do not use the following data for averages, fits, limits, etc. • • •					
− 26 ±30	2724	BINGHAM	70B	OSPK	
0 ±20.4	364	[11] LONDON	66	HBC	Using $\alpha_\Lambda = 0.62$
54 ±30	356	[11] CARMONY	64B	HBC	

[9] From this result and α_Ξ, CHAKRAVORTY 03 obtains $\beta_\Xi = -0.025\pm0.042\pm0.006$ and $\gamma_\Xi = 0.889\pm0.001\pm0.007$. And the strong P-S phase difference is $(3.17\pm5.28\pm0.73)^\circ$.

[10] BENSINGER 85 used $\alpha_\Lambda = 0.642 \pm 0.013$.

[11] The errors have been multiplied by 1.2 due to approximations used for the Ξ polarization; see DAUBER 69 for a discussion.

g_A / g_V FOR $\Xi^- \to \Lambda e^-\overline{\nu}_e$

VALUE	EVTS	DOCUMENT ID		TECN	COMMENT
−0.25±0.05	1992	[12] BOURQUIN	83	SPEC	SPS hyperon beam

[12] BOURQUIN 83 assumes that $g_2 = 0$. Also, the sign has been changed to agree with our conventions, given in the "Note on Baryon Decay Parameters" in the neutron Listings.

Ξ^- REFERENCES

We have omitted some papers that have been superseded by later experiments. See our earlier editions.

CHAKRAVO...	03	PRL 91 031601	A. Chakravorty *et al.* (FNAL E756 Collab.)
LUK	00	PRL 85 4860	K.B. Luk *et al.* (FNAL E756 Collab.)
DUBBS	94	PRL 72 808	T. Dubbs *et al.* (FNAL E761 Collab.)
DURYEA	92	PRL 68 768	J. Duryea *et al.* (MINN, FNAL, MICH, RUTG)
LITTENBERG	92B	PR D46 R892	L.S. Littenberg, R.E. Shrock (BNL, STON)
HO	90	PRL 65 1713	P.M. Ho *et al.* (MICH, FNAL, MINN, RUTG)
Also	91	PR D44 3402	P.M. Ho *et al.* (MICH, FNAL, MINN, RUTG)
TROST	89	PR D40 1703	L.H. Trost *et al.* (FNAL-715 Collab.)
BIAGI	87B	ZPHY C35 143	S.F. Biagi *et al.* (BRIS, CERN, GEVA+)
RAMEIKA	86	PR D33 3172	R. Rameika *et al.* (RUTG, MICH, WISC+)
ASTON	85B	PR D32 2270	D. Aston *et al.* (SLAC, CARL, CNRC, CINC)
BENSINGER	85	NP B252 561	J.R. Bensinger *et al.* (CHIC, ELMT, FNAL+)
BOURQUIN	84	NP B241 1	M.H. Bourquin *et al.* (BRIS, GEVA, HEIDP+)
RAMEIKA	84	PRL 52 581	R. Rameika *et al.* (RUTG, MICH, WISC+)
BOURQUIN	83	ZPHY C21 1	M.H. Bourquin *et al.* (BRIS, GEVA, HEIDP+)
BIAGI	82	PL 112B 265	S.F. Biagi *et al.* (BRIS, CAVE, GEVA+)
BIAGI	82B	PL 112B 277	S.F. Biagi *et al.* (LOQM, GEVA, RL+)
CLELAND	80C	PR D21 12	W.E. Cleland *et al.* (PITT, BNL)
THOMPSON	80	PR D21 25	J.A. Thompson *et al.* (PITT, BNL)
BOURQUIN	79	PL 87B 297	M.H. Bourquin *et al.* (BRIS, GEVA, HEIDP+)
HEMINGWAY	78	NP B142 205	R.J. Hemingway *et al.* (CERN, ZEEM, NIJM+)
DIBIANCA	75	NP B98 137	F.A. DiBianca, R.J. Endorf (CMU)
BALTAY	74	PR D9 49	C. Baltay *et al.* (COLU, BING) J
COOL	74	PR D10 792	R.L. Cool *et al.* (BNL)
Also	72	PRL 29 1630	R.L. Cool *et al.* (BNL)
YEH	74	PR D10 3545	N. Yeh *et al.* (BING, COLU)
MAYEUR	72	NP B47 333	C. Mayeur *et al.* (BRUX, CERN, TUFTS, LOUC)
VOTRUBA	72	NP B45 77	M.F. Votruba, A. Safder, T.M. Ratcliffe (BIRM+)
WILQUET	72	PL 42B 372	G. Wilquet *et al.* (BRUX, CERN, TUFTS+)
DUCLOS	71	NP B32 493	J. Duclos *et al.* (CERN)
BINGHAM	70B	PR D1 3010	G.M. Bingham *et al.* (UCSD, WASH)
GOLDWASSER	70	PR D1 1960	E.L. Goldwasser, P.F. Schultz (ILL)
STONE	70	PL 32B 515	S.L. Stone *et al.* (ROCH)
DAUBER	69	PR 179 1262	P.M. Dauber *et al.* (LRL) J
SHEN	67	PL 25B 443	B.C. Shen, A. Firestone, G. Goldhaber (UCB+)
BERGE	66	PR 147 945	J.P. Berge *et al.* (LRL)
CHIEN	66	PR 152 1171	C.Y. Chien *et al.* (YALE, BNL)
LONDON	66	PR 143 1034	G.W. London *et al.* (BNL, SYRA)
BINGHAM	65	PRSL 285 202	H.H. Bingham (CERN)
PJERROU	65B	PRL 14 275	G.M. Pjerrou *et al.* (UCLA)
Also	65	Thesis	G.M. Pjerrou (UCLA)
BADIER	64	Dubna Conf. 1 593	J. Badier *et al.* (EPOL, SACL, ZEEM)
CARMONY	64B	PRL 12 482	D.D. Carmony *et al.* (UCLA) J
HUBBARD	64	PR 135B 183	J.R. Hubbard *et al.* (LRL)
FERRO-LUZZI	63	PR 130 1568	M. Ferro-Luzzi *et al.* (LRL)
JAUNEAU	63D	Siena Conf. 4	L. Jauneau *et al.* (EPOL, CERN, LOUC+)
Also	63B	PL 5 261	L. Jauneau *et al.* (EPOL, CERN, LOUC+)
SCHNEIDER	63	PL 4 360	J. Schneider (CERN)

Ξ RESONANCES

The accompanying table gives our evaluation of the present status of the Ξ resonances. Not much is known about Ξ resonances. This is because (1) they can only be produced as a part of a final state, and so the analysis is more complicated than if direct formation were possible, (2) the production cross sections are small (typically a few μb), and (3) the final states are topologically complicated and difficult to study with electronic techniques. Thus early information about Ξ resonances came entirely from bubble chamber experiments, where the numbers of events are small, and only in the 1980's did electronic experiments make any significant contributions. However, nothing of significance on Ξ resonances has been added since our 1988 edition.

For a detailed earlier review, see Meadows [1].

Table 1. The status of the Ξ resonances. Only those with an overall status of *** or **** are included in the Baryon Summary Table.

Particle	$L_{2I\,2J}$	Overall status	Status as seen in — Ξπ	AK	ΣK	Ξ(1530)π	Other channels
Ξ(1318)	P_{11}	****					Decays weakly
Ξ(1530)	P_{13}	****	****				
Ξ(1620)		*	*				
Ξ(1690)		***		***	**		
Ξ(1820)	D_{13}	***	**	***	**	**	
Ξ(1950)		***	**	**		*	
Ξ(2030)	1	***		**	***		
Ξ(2120)		*		*			
Ξ(2250)		**					3-body decays
Ξ(2370)	1	**					3-body decays
Ξ(2500)		*		*	*		3-body decays

**** Existence is certain, and properties are at least fairly well explored.
*** Existence ranges from very likely to certain, but further confirmation is desirable and/or quantum numbers, branching fractions, *etc.* are not well determined.
** Evidence of existence is only fair.
* Evidence of existence is poor.

Reference

1. B.T. Meadows, in *Proceedings of the IVth International Conference on Baryon Resonances* (Toronto, 1980), ed. N. Isgur, p. 283.

Ξ(1530) P_{13}

$I(J^P) = \frac{1}{2}(\frac{3}{2}^+)$ Status: ****

This is the only Ξ resonance whose properties are all reasonably well known. Spin-parity $3/2^+$ is favored by the data.

We use only those determinations of the mass and width that are accompanied by some discussion of systematics and resolution.

Ξ(1530) MASSES

Ξ(1530)^0 MASS

VALUE (MeV)	EVTS	DOCUMENT ID		TECN	COMMENT
1531.80±0.32 OUR FIT Error includes scale factor of 1.3.					
1531.78±0.34 OUR AVERAGE Error includes scale factor of 1.4. See the ideogram below.					
1532.2 ±0.7		DEBELLEFON	75B	HBC	$K^-p \to \Xi^-\overline{K}\pi$
1533 ±1		ROSS	73B	HBC	$K^-p \to \Xi\overline{K}\pi(\pi)$
1531.4 ±0.8	59	BADIER	72	HBC	K^-p 3.95 GeV/c
1532.0 ±0.4	1262	BALTAY	72	HBC	K^-p 1.75 GeV/c
1531.3 ±0.6	324	BORENSTEIN	72	HBC	K^-p 2.2 GeV/c
1532.3 ±0.7	286	KIRSCH	72	HBC	K^-p 2.87 GeV/c
1528.7 ±1.1	76	LONDON	66	HBC	K^-p 2.24 GeV/c
• • • We do not use the following data for averages, fits, limits, etc. • • •					
1532.1 ±0.4	1244	ASTON	85B	LASS	K^-p 11 GeV/c
1532.1 ±0.6	2700	[1] BAUBILLIER	81B	HBC	K^-p 8.25 GeV/c
1530 ±1	450	BIAGI	81	SPEC	SPS hyperon beam
1527 ±6	80	SIXEL	79	HBC	K^-p 10 GeV/c
1535 ±4	100	SIXEL	79	HBC	K^-p 16 GeV/c
1533.6 ±1.4	97	BERTHON	74	HBC	Quasi-2-body σ

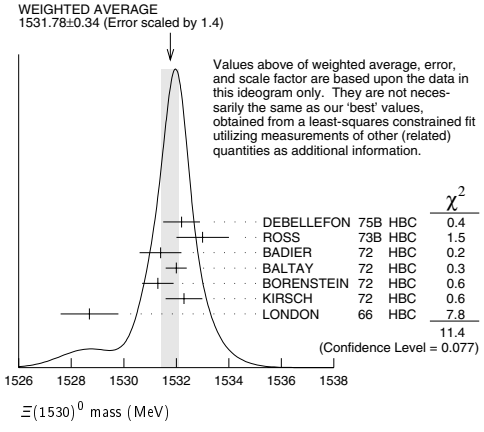

Ξ(1530)$^-$ MASS

VALUE (MeV)	EVTS	DOCUMENT ID		TECN	COMMENT
1535.0±0.6 OUR FIT					
1535.2±0.8 OUR AVERAGE					
1534.5 ±1.2		DEBELLEFON	75B	HBC	$K^-p \to \Xi^-\overline{K}\pi$
1535.3 ±2.0		ROSS	73B	HBC	$K^-p \to \Xi\overline{K}\pi(\pi)$
1536.2 ±1.6	185	KIRSCH	72	HBC	K^-p 2.87 GeV/c
1535.7 ±3.2	38	LONDON	66	HBC	K^-p 2.24 GeV/c
• • • We do not use the following data for averages, fits, limits, etc. • • •					
1540 ±3	48	BERTHON	74	HBC	Quasi-2-body σ
1534.7 ±1.1	334	BALTAY	72	HBC	K^-p 1.75 GeV/c

$m_{\Xi(1530)^-} - m_{\Xi(1530)}$

VALUE (MeV)	DOCUMENT ID		TECN	COMMENT
3.2±0.6 OUR FIT				
2.9±0.9 OUR AVERAGE				
2.7±1.0	BALTAY	72	HBC	K^-p 1.75 GeV/c
2.0±3.2	MERRILL	66	HBC	K^-p 1.7–2.7 GeV/c
5.7±3.0	PJERROU	65B	HBC	K^-p 1.8–1.95 GeV/c
• • • We do not use the following data for averages, fits, limits, etc. • • •				
3.9±1.8	[2] KIRSCH	72	HBC	K^-p 2.87 GeV/c
7 ±4	[2] LONDON	66	HBC	K^-p 2.24 GeV/c

Ξ(1530) WIDTHS

Ξ(1530)^0 WIDTH

VALUE (MeV)	EVTS	DOCUMENT ID		TECN	COMMENT
9.1±0.5 OUR AVERAGE					
9.5 ±1.2		DEBELLEFON	75B	HBC	$K^-p \to \Xi^-\overline{K}\pi$
9.1 ±2.4		ROSS	73B	HBC	$K^-p \to \Xi\overline{K}\pi(\pi)$
11 ±2		BADIER	72	HBC	K^-p 3.95 GeV/c
9.0±0.7		BALTAY	72	HBC	K^-p 1.75 GeV/c
8.4±1.4		BORENSTEIN	72	HBC	$\Xi^-\pi^+$
11.0±1.8		KIRSCH	72	HBC	$\Xi^-\pi^+$
7 ±7		BERGE	66	HBC	K^-p 1.5–1.7 GeV/c
8.5±3.5		LONDON	66	HBC	K^-p 2.24 GeV/c
7 ±2		SCHLEIN	63B	HBC	K^-p 1.8, 1.95 GeV/c
• • • We do not use the following data for averages, fits, limits, etc. • • •					
12.8±1.0	2700	[1] BAUBILLIER	81B	HBC	K^-p 8.25 GeV/c
19 ±6	80	[3] SIXEL	79	HBC	K^-p 10 GeV/c
14 ±5	100	[3] SIXEL	79	HBC	K^-p 16 GeV/c

Ξ(1530)$^-$ WIDTH

VALUE (MeV)	DOCUMENT ID		TECN	COMMENT
$9.9^{+1.7}_{-1.9}$ OUR AVERAGE				
9.6±2.8	DEBELLEFON	75B	HBC	$K^-p \to \Xi^-\overline{K}\pi$
8.3±3.6	ROSS	73B	HBC	$K^-p \to \Xi\overline{K}\pi(\pi)$
$7.8^{+3.5}_{-7.8}$	BALTAY	72	HBC	K^-p 1.75 GeV/c
16.2±4.6	KIRSCH	72	HBC	$\Xi^-\pi^0$, $\Xi^0\pi^-$

Baryon Particle Listings

Ξ(1530), Ξ(1620), Ξ(1690)

Ξ(1530) POLE POSITIONS

Ξ(1530)^0 REAL PART

VALUE	DOCUMENT ID	COMMENT
1531.6 ± 0.4	LICHTENBERG74	Using HABIBI 73

Ξ(1530)^0 IMAGINARY PART

VALUE	DOCUMENT ID	COMMENT
4.45 ± 0.35	LICHTENBERG74	Using HABIBI 73

Ξ(1530)$^-$ REAL PART

VALUE	DOCUMENT ID	COMMENT
1534.4 ± 1.1	LICHTENBERG74	Using HABIBI 73

Ξ(1530)$^-$ IMAGINARY PART

VALUE	DOCUMENT ID	COMMENT
$3.9^{+1.75}_{-3.9}$	LICHTENBERG74	Using HABIBI 73

Ξ(1530) DECAY MODES

	Mode	Fraction (Γ_i/Γ)	Confidence level
Γ_1	$\Xi\pi$	100 %	
Γ_2	$\Xi\gamma$	< 4 %	90%

Ξ(1530) BRANCHING RATIOS

$\Gamma(\Xi\gamma)/\Gamma_{total}$ Γ_2/Γ

VALUE	CL%	DOCUMENT ID	TECN	COMMENT
< 0.04	90	KALBFLEISCH 75	HBC	K^-p 2.18 GeV/c

Ξ(1530) FOOTNOTES

[1] BAUBILLIER 81B is a fit to the inclusive spectrum. The resolution (5 MeV) is not unfolded.
[2] Redundant with data in the mass Listings.
[3] SIXEL 79 doesn't unfold the experimental resolution of 15 MeV.

Ξ(1530) REFERENCES

ASTON	85B	PR D32 2270	D. Aston *et al.*	(SLAC, CARL, CNRC, CINC)
BAUBILLIER	81B	NP B192 1	M. Baubillier *et al.*	(BIRM, CERN, GLAS+)
BIAGI	81	ZPHY C9 305	S.F. Biagi *et al.*	(BRIS, CAVE, GEVA+)
SIXEL	79	NP B159 125	P. Sixel *et al.*	(AACH3, BERL, CERN, LOIC+)
DEBELLEFON	75B	NC 28A 289	A. de Bellefon *et al.*	(CDEF, SACL)
KALBFLEISCH	75	PR D11 987	G.R. Kalbfleisch, R.C. Strand, J.W. Chapman	(BNL+)
BERTHON	74	NC 21A 146	A. Berthon *et al.*	(CDEF, RHEL, SACL+)
LICHTENBERG	74	PR D10 3865	D.B. Lichtenberg	(IND)
Also	74B	Private Comm.	D.B. Lichtenberg	(IND)
HABIBI	73	Thesis Nevis 199	M. Habibi	(COLU)
ROSS	73B	Purdue Conf. 355	R.T. Ross, J.L. Lloyd, D. Radojicic	(OXF)
BADIER	72	NP B37 429	J. Badier *et al.*	(EPOL)
BALTAY	72	PL 42B 129	C. Baltay *et al.*	(COLU, BING)
BORENSTEIN	72	PR D5 1559	S.R. Borenstein *et al.*	(BNL, MICH) I
KIRSCH	72	NP B40 349	L.E. Kirsch *et al.*	(BRAN, UMD, SYRA+) I
BERGE	66	PR 147 945	J.P. Berge *et al.*	(LRL) I
LONDON	66	PR 143 1034	G.W. London *et al.*	(BNL, SYRA) IJ
MERRILL	66	Thesis UCRL 16455	D.W. Merrill	(LRL) JP
PJERROU	65B	PRL 14 275	G.M. Pjerrou *et al.*	(UCLA)
SCHLEIN	63B	PRL 11 167	P.E. Schlein *et al.*	(UCLA) IJP

OTHER RELATED PAPERS

MAZZUCATO	81	NP B178 1	M. Mazzucato *et al.*	(AMST, CERN, NIJM+)
BRIEFEL	77	PR D16 2706	E. Briefel *et al.*	(BRAN, UMD, SYRA+)
BRIEFEL	75	PR D12 1859	E. Briefel *et al.*	(BRAN, UMD, SYRA+)
HUNGERBU...	74	PR D10 2051	V. Hungerbuhler *et al.*	(YALE, FNAL, BNL+)
BUTTON-...	66	PR 142 883	J. Button-Shafer *et al.*	(LRL) JP

Ξ(1620)

$I(J^P) = \frac{1}{2}(?^?)$ Status: *

J, *P* need confirmation.

OMITTED FROM SUMMARY TABLE

What little evidence there is consists of weak signals in the $\Xi\pi$ channel. A number of other experiments (e.g., BORENSTEIN 72 and HASSALL 81) have looked for but not seen any effect.

Ξ(1620) MASS

VALUE (MeV)	EVTS	DOCUMENT ID	TECN	COMMENT
≈ 1620 OUR ESTIMATE				
1624 ± 3	31	BRIEFEL 77	HBC	K^-p 2.87 GeV/c
1633 ± 12	34	DEBELLEFON 75B	HBC	$K^-p \to \Xi^-\overline{K}\pi$
1606 ± 6	29	ROSS 72	HBC	K^-p 3.1–3.7 GeV/c

Ξ(1620) WIDTH

VALUE (MeV)	EVTS	DOCUMENT ID	TECN	COMMENT
22.5	31	[1] BRIEFEL 77	HBC	K^-p 2.87 GeV/c
40 ± 15	34	DEBELLEFON 75B	HBC	$K^-p \to \Xi^-\overline{K}\pi$
21 ± 7	29	ROSS 72	HBC	$K^-p \to \Xi^-\pi^+K^{*0}(892)$

Ξ(1620) DECAY MODES

	Mode
Γ_1	$\Xi\pi$

Ξ(1620) FOOTNOTES

[1] The fit is insensitive to values between 15 and 30 MeV.

Ξ(1620) REFERENCES

HASSALL	81	NP B189 397	J.K. Hassall *et al.*	(CAVE, MSU)
BRIEFEL	77	PR D16 2706	E. Briefel *et al.*	(BRAN, UMD, SYRA+)
Also	70	Duke Conf. 317	E. Briefel *et al.*	(BRAN, UMD, SYRA+)
Hyperon Resonances, 1970				
Also	75	PR D12 1859	E. Briefel *et al.*	(BRAN, UMD, SYRA+)
DEBELLEFON	75B	NC 28A 289	A. de Bellefon *et al.*	(CDEF, SACL)
BORENSTEIN	72	PR D5 1559	S.R. Borenstein *et al.*	(BNL, MICH) I
ROSS	72	PL 38B 177	R.T. Ross *et al.*	(OXF) I

OTHER RELATED PAPERS

HUNGERBU...	74	PR D10 2051	V. Hungerbuhler *et al.*	(YALE, FNAL, BNL+)
SCHMIDT	73	Purdue Conf. 363	P.E. Schmidt	(BRAN)
KALBFLEISCH	70	Duke Conf. 331	G.R. Kalbfleisch	(BNL) I
Hyperon Resonances 1970				
APSELL	69	PRL 23 884	S.P. Apsell *et al.*	(BRAN, UMD, SYRA+)
BARTSCH	69	PL 28B 439	J. Bartsch *et al.*	(AACH, BERL, CERN+)

Ξ(1690)

$I(J^P) = \frac{1}{2}(?^?)$ Status: ***

DIONISI 78 sees a threshold enhancement in both the neutral and negatively charged $\Sigma\overline{K}$ mass spectra in $K^-p \to (\Sigma\overline{K})K\pi$ at 4.2 GeV/c. The data from the $\Sigma\overline{K}$ channels alone cannot distinguish between a resonance and a large scattering length. Weaker evidence at the same mass is seen in the corresponding $\Lambda\overline{K}$ channels, and a coupled-channel analysis yields results consistent with a new Ξ.

BIAGI 81 sees an enhancement at 1700 MeV in the diffractively produced ΛK^- system. A peak is also observed in the $\Lambda\overline{K}^0$ mass spectrum at 1660 MeV that is consistent with a 1720 MeV resonance decaying to $\Sigma^0\overline{K}^0$, with the γ from the Σ^0 decay not detected.

BIAGI 87 provides further confirmation of this state in diffractive dissociation of Ξ^- into ΛK^-. The significance claimed is 6.7 standard deviations.

ADAMOVICH 98 sees a peak of 1400 ± 300 events in the $\Xi^-\pi^+$ spectrum produced by 345 GeV/c Σ^--nucleus interactions.

Ξ(1690) MASSES

MIXED CHARGES

VALUE (MeV)	DOCUMENT ID
1690±10 OUR ESTIMATE	This is only an educated guess; the error given is larger than the error on the average of the published values.

Ξ(1690)^0 MASS

VALUE (MeV)	EVTS	DOCUMENT ID	TECN	COMMENT
1686 ± 4	1400	ADAMOVICH 98	WA89	Σ^- nucleus, 345 GeV/c
1699 ± 5	175	[1] DIONISI 78	HBC	K^-p 4.2 GeV/c
1684 ± 5	183	[2] DIONISI 78	HBC	K^-p 4.2 GeV/c

Ξ(1690)$^-$ MASS

VALUE (MeV)	EVTS	DOCUMENT ID	TECN	COMMENT
1691.1 ± 1.9 ± 2.0	104	BIAGI 87	SPEC	Ξ^- Be 116 GeV
1700 ± 10	150	[3] BIAGI 81	SPEC	Ξ^- H 100, 135 GeV
1694 ± 6	45	[4] DIONISI 78	HBC	K^-p 4.2 GeV/c

Ξ(1690) WIDTHS

MIXED CHARGES

VALUE (MeV)	DOCUMENT ID
< 30 OUR ESTIMATE	

Ξ(1690)^0 WIDTH

VALUE (MeV)	EVTS	DOCUMENT ID	TECN	COMMENT
10 ± 6	1400	ADAMOVICH 98	WA89	Σ^- nucleus, 345 GeV/c
44 ± 23	175	[1] DIONISI 78	HBC	K^-p 4.2 GeV/c
20 ± 4	183	[2] DIONISI 78	HBC	K^-p 4.2 GeV/c

Ξ(1690)$^-$ WIDTH

VALUE (MeV)	CL%	EVTS	DOCUMENT ID	TECN	COMMENT
< 8	90	104	BIAGI 87	SPEC	Ξ^- Be 116 GeV
47 ± 14		150	[3] BIAGI 81	SPEC	Ξ^- H 100, 135 GeV
26 ± 6		45	[4] DIONISI 78	HBC	K^-p 4.2 GeV/c

Ξ(1690) DECAY MODES

	Mode	Fraction (Γ_i/Γ)
Γ_1	$\Lambda\overline{K}$	seen
Γ_2	$\Sigma\overline{K}$	seen
Γ_3	$\Xi\pi$	seen
Γ_4	$\Xi^-\pi^+\pi^0$	
Γ_5	$\Xi^-\pi^+\pi^-$	possibly seen
Γ_6	$\Xi(1530)\pi$	

Ξ(1690) BRANCHING RATIOS

$\Gamma(\Lambda\overline{K})/\Gamma_{total}$ Γ_1/Γ

VALUE	EVTS	DOCUMENT ID		TECN	CHG	COMMENT
seen	104	BIAGI	87	SPEC	–	Ξ^- Be 116 GeV

$\Gamma(\Sigma\overline{K})/\Gamma(\Lambda\overline{K})$ Γ_2/Γ_1

VALUE	EVTS	DOCUMENT ID		TECN	CHG	COMMENT
0.75 ± 0.39	75	ABE	02C	BELL		$e^+e^-\approx\Upsilon(4S)$
$2.7\ \pm0.9$		DIONISI	78	HBC	0	K^-p 4.2 GeV/c
$3.1\ \pm1.4$		DIONISI	78	HBC	–	K^-p 4.2 GeV/c

$\Gamma(\Xi\pi)/\Gamma(\Sigma\overline{K})$ Γ_3/Γ_2

VALUE	DOCUMENT ID		TECN	CHG	COMMENT
<0.09	DIONISI	78	HBC	0	K^-p 4.2 GeV/c

$\Gamma(\Xi\pi)/\Gamma_{total}$ Γ_3/Γ

VALUE	DOCUMENT ID		TECN	COMMENT
seen	ADAMOVICH	98	WA89	Σ^- nucleus, 345 GeV/c

$\Gamma(\Xi^-\pi^+\pi^0)/\Gamma(\Sigma\overline{K})$ Γ_4/Γ_2

VALUE	DOCUMENT ID		TECN	CHG	COMMENT
<0.04	DIONISI	78	HBC	0	K^-p 4.2 GeV/c

$\Gamma(\Xi^-\pi^+\pi^-)/\Gamma_{total}$ Γ_5/Γ

VALUE	EVTS	DOCUMENT ID		TECN	CHG	COMMENT
possibly seen	4	BIAGI	87	SPEC	–	Ξ^- Be 116 GeV

$\Gamma(\Xi^-\pi^+\pi^-)/\Gamma(\Sigma\overline{K})$ Γ_5/Γ_2

VALUE	DOCUMENT ID		TECN	CHG	COMMENT
<0.03	DIONISI	78	HBC	–	K^-p 4.2 GeV/c

$\Gamma(\Xi(1530)\pi)/\Gamma(\Sigma\overline{K})$ Γ_6/Γ_2

VALUE	DOCUMENT ID		TECN	CHG	COMMENT
<0.06	DIONISI	78	HBC	–	K^-p 4.2 GeV/c

Ξ(1690) FOOTNOTES

[1] From a fit to the Σ^+K^- spectrum.
[2] From a coupled-channel analysis of the Σ^+K^- and $\Lambda\overline{K}^0$ spectra.
[3] A fit to the inclusive spectrum from $\Xi^-N\rightarrow\Lambda K^-X$.
[4] From a coupled-channel analysis of the Σ^0K^- and ΛK^- spectra.

Ξ(1690) REFERENCES

ABE	02C	PL B524 33	K. Abe *et al.*	(KEK BELLE Collab.)
ADAMOVICH	98	EPJ C5 621	M.I. Adamovich *et al.*	(CERN WA89 Collab.)
BIAGI	87	ZPHY C34 15	S.F. Biagi *et al.*	(BRIS, CERN, GEVA+) I
BIAGI	81	ZPHY C9 305	S.F. Biagi *et al.*	(BRIS, CAVE, GEVA+)
DIONISI	78	PL 80B 145	C. Dionisi *et al.*	(CERN, AMST, NIJM+) I

Ξ(1820) D_{13}

$I(J^P) = \frac{1}{2}(\frac{3}{2}^-)$ Status: ***

The clearest evidence is an 8-standard-deviation peak in ΛK^- seen by GAY 76C. TEODORO 78 favors J=3/2, but cannot make a parity discrimination. BIAGI 87C is consistent with J=3/2 and favors negative parity for this J value.

Ξ(1820) MASS

We only average the measurements that appear to us to be most significant and best determined.

VALUE (MeV)	EVTS	DOCUMENT ID		TECN	CHG	COMMENT
1823 ± 5 OUR ESTIMATE						
1823.4 ± 1.4 OUR AVERAGE						
$1819.4\pm3.1\pm2.0$	280	[1] BIAGI	87	SPEC	0	Ξ^- Be → (ΛK^-) X
$1826\ \pm3\ \pm1$	54	BIAGI	87C	SPEC	0	Ξ^- Be → ($\Lambda\overline{K}^0$) X
$1822\ \pm6$		JENKINS	83	MPS	–	$K^-p\rightarrow K^+$ (MM)
$1830\ \pm6$	300	BIAGI	81	SPEC	–	SPS hyperon beam
$1823\ \pm2$	130	GAY	76C	HBC	–	K^-p 4.2 GeV/c
• • • We do not use the following data for averages, fits, limits, etc. • • •						
$1817\ \pm3$		ADAMOVICH	99B	WA89		Σ^- nucleus, 345 GeV
$1797\ \pm19$	74	BRIEFEL	77	HBC	0	K^-p 2.87 GeV/c
$1829\ \pm9$	68	BRIEFEL	77	HBC	−0	$\Xi(1530)\pi$
$1860\ \pm14$	39	BRIEFEL	77	HBC	–	$\Sigma^-\overline{K}^0$
$1870\ \pm9$	44	BRIEFEL	77	HBC	0	$\Lambda\overline{K}^0$
$1813\ \pm4$	57	BRIEFEL	77	HBC	–	ΛK^-
$1807\ \pm27$		DIBIANCA	75	DBC	−0	$\Xi\pi\pi$, $\Xi^*\pi$
$1762\ \pm8$	28	[2] BADIER	72	HBC	−0	$\Xi\pi$, $\Xi\pi\pi$, YK
$1838\ \pm5$	38	[2] BADIER	72	HBC	−0	$\Xi\pi$, $\Xi\pi\pi$, YK
$1830\ \pm10$	25	[3] CRENNELL	70B	DBC	−0	3.6, 3.9 GeV/c
$1826\ \pm12$		[4] CRENNELL	70B	DBC	−0	3.6, 3.9 GeV/c
$1830\ \pm10$	40	ALITTI	69	HBC	–	Λ, $\Sigma\overline{K}$
$1814\ \pm4$	30	BADIER	65	HBC	0	$\Lambda\overline{K}^0$
$1817\ \pm7$	29	SMITH	65C	HBC	−0	$\Lambda\overline{K}^0$, ΛK^-
1770		HALSTEINSLID	63	FBC	−0	K^- freon 3.5 GeV/c

Ξ(1820) WIDTH

VALUE (MeV)	EVTS	DOCUMENT ID		TECN	CHG	COMMENT
$24\ ^{+15}_{-10}$ OUR ESTIMATE						
24 ± 6 OUR AVERAGE Error includes scale factor of 1.5. See the ideogram below.						
24.6 ± 5.3	280	[1] BIAGI	87	SPEC	0	Ξ^- Be → (ΛK^-) X
$12\ \pm14\ \pm1.7$	54	BIAGI	87C	SPEC	0	Ξ^- Be → ($\Lambda\overline{K}^0$) X
$72\ \pm20$	300	BIAGI	81	SPEC	–	SPS hyperon beam
$21\ \pm7$	130	GAY	76C	HBC	–	K^-p 4.2 GeV/c
• • • We do not use the following data for averages, fits, limits, etc. • • •						
$23\ \pm13$		ADAMOVICH	99B	WA89		Σ^- nucleus, 345 GeV
$99\ \pm57$	74	BRIEFEL	77	HBC	0	K^-p 2.87 GeV/c
$52\ \pm34$	68	BRIEFEL	77	HBC	−0	$\Xi(1530)\pi$
$72\ \pm17$	39	BRIEFEL	77	HBC	–	$\Sigma^-\overline{K}^0$
$44\ \pm11$	44	BRIEFEL	77	HBC	0	$\Lambda\overline{K}^0$
$26\ \pm11$	57	BRIEFEL	77	HBC	–	ΛK^-
$85\ \pm58$		DIBIANCA	75	DBC	−0	$\Xi\pi\pi$, $\Xi^*\pi$
$51\ \pm13$		[2] BADIER	72	HBC	−0	Lower mass
$58\ \pm13$		[2] BADIER	72	HBC	−0	Higher mass
$103\ ^{+38}_{-24}$		[3] CRENNELL	70B	DBC	−0	3.6, 3.9 GeV/c
$48\ ^{+36}_{-19}$		[4] CRENNELL	70B	DBC	−0	3.6, 3.9 GeV/c
$55\ ^{+40}_{-20}$		ALITTI	69	HBC	–	Λ, $\Sigma\overline{K}$
$12\ \pm4$		BADIER	65	HBC	0	$\Lambda\overline{K}^0$
$30\ \pm7$		SMITH	65B	HBC	−0	$\Lambda\overline{K}$
<80		HALSTEINSLID	63	FBC	−0	K^- freon 3.5 GeV/c

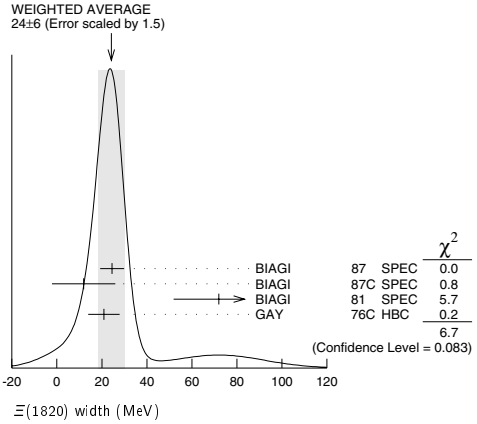

Ξ(1820) DECAY MODES

	Mode	Fraction (Γ_i/Γ)
Γ_1	$\Lambda\overline{K}$	large
Γ_2	$\Sigma\overline{K}$	small
Γ_3	$\Xi\pi$	small
Γ_4	$\Xi(1530)\pi$	small
Γ_5	$\Xi\pi\pi$ (not $\Xi(1530)\pi$)	

Baryon Particle Listings

Ξ(1820), Ξ(1950)

Ξ(1820) BRANCHING RATIOS

The dominant modes seem to be $\Lambda\overline{K}$ and (perhaps) $\Xi(1530)\pi$, but the branching fractions are very poorly determined.

$\Gamma(\Lambda\overline{K})/\Gamma_{total}$ Γ_1/Γ

VALUE	DOCUMENT ID		TECN	CHG	COMMENT
0.30±0.15	ALITTI	69	HBC	–	K^-p 3.9–5 GeV/c

$\Gamma(\Xi\pi)/\Gamma_{total}$ Γ_3/Γ

VALUE	DOCUMENT ID		TECN	CHG	COMMENT
0.10±0.10	ALITTI	69	HBC	–	K^-p 3.9–5 GeV/c

$\Gamma(\Xi\pi)/\Gamma(\Lambda\overline{K})$ Γ_3/Γ_1

VALUE	CL%	DOCUMENT ID		TECN	CHG	COMMENT
<0.36	95	GAY	76C	HBC	–	K^-p 4.2 GeV/c
0.20±0.20		BADIER	65	HBC	0	K^-p 3 GeV/c

$\Gamma(\Xi\pi)/\Gamma(\Xi(1530)\pi)$ Γ_3/Γ_4

VALUE	DOCUMENT ID		TECN	CHG	COMMENT
$1.5^{+0.6}_{-0.4}$	APSELL	70	HBC	0	K^-p 2.87 GeV/c

$\Gamma(\Sigma\overline{K})/\Gamma_{total}$ Γ_2/Γ

VALUE	DOCUMENT ID		TECN	CHG	COMMENT
0.30±0.15	ALITTI	69	HBC	–	K^-p 3.9–5 GeV/c
• • • We do not use the following data for averages, fits, limits, etc. • • •					
<0.02	TRIPP	67	RVUE		Use SMITH 65C

$\Gamma(\Sigma\overline{K})/\Gamma(\Lambda\overline{K})$ Γ_2/Γ_1

VALUE	DOCUMENT ID		TECN	CHG	COMMENT
0.24±0.10	GAY	76C	HBC	–	K^-p 4.2 GeV/c

$\Gamma(\Xi(1530)\pi)/\Gamma_{total}$ Γ_4/Γ

VALUE	DOCUMENT ID		TECN	CHG	COMMENT
0.30±0.15	ALITTI	69	HBC	–	K^-p 3.9–5 GeV/c
• • • We do not use the following data for averages, fits, limits, etc. • • •					
seen	ASTON	85B	LASS		K^-p 11 GeV/c
not seen	[5] HASSALL	81	HBC		K^-p 6.5 GeV/c
<0.25	[6] DAUBER	69	HBC		K^-p 2.7 GeV/c

$\Gamma(\Xi(1530)\pi)/\Gamma(\Lambda\overline{K})$ Γ_4/Γ_1

VALUE	DOCUMENT ID		TECN	CHG	COMMENT
0.38±0.27 OUR AVERAGE Error includes scale factor of 2.3.					
1.0 ±0.3	GAY	76C	HBC	–	K^-p 4.2 GeV/c
0.26±0.13	SMITH	65C	HBC	−0	K^-p 2.45–2.7 GeV/c

$\Gamma(\Xi\pi\pi(\text{not }\Xi(1530)\pi))/\Gamma(\Lambda\overline{K})$ Γ_5/Γ_1

VALUE	DOCUMENT ID		TECN	CHG	COMMENT
0.30±0.20	BIAGI	87	SPEC	–	Ξ^- Be 116 GeV
• • • We do not use the following data for averages, fits, limits, etc. • • •					
<0.14	[7] BADIER	65	HBC	0	1 st. dev. limit
>0.1	SMITH	65C	HBC	−0	K^-p 2.45–2.7 GeV/c

$\Gamma(\Xi\pi\pi(\text{not }\Xi(1530)\pi))/\Gamma(\Xi(1530)\pi)$ Γ_5/Γ_4

VALUE	DOCUMENT ID		TECN	CHG	COMMENT
consistent with zero	GAY	76C	HBC	–	K^-p 4.2 GeV/c
• • • We do not use the following data for averages, fits, limits, etc. • • •					
0.3±0.5	[8] APSELL	70	HBC	0	K^-p 2.87 GeV/c

Ξ(1820) FOOTNOTES

[1] BIAGI 87 also sees weak signals in the in the $\Xi^-\pi^+\pi^-$ channel at 1782.6 ± 1.4 MeV (Γ = 6.0 ± 1.5 MeV) and 1831.9 ± 2.8 MeV (Γ = 9.6 ± 9.9 MeV).

[2] BADIER 72 adds all channels and divides the peak into lower and higher mass regions. The data can also be fitted with a single Breit-Wigner of mass 1800 MeV and width 150 MeV.

[3] From a fit to inclusive $\Xi\pi$, $\Xi\pi\pi$, and ΛK^- spectra.

[4] From a fit to inclusive $\Xi\pi$ and $\Xi\pi\pi$ spectra only.

[5] Including $\Xi\pi\pi$.

[6] DAUBER 69 uses in part the same data as SMITH 65C.

[7] For the decay mode $\Xi^-\pi^+\pi^0$ only. This limit includes $\Xi(1530)\pi$.

[8] Or less. Upper limit for the 3-body decay.

Ξ(1820) REFERENCES

ADAMOVICH	99B	EPJ C11 271	M.I. Adamovich *et al.*	(CERN WA89 Collab.)
BIAGI	87	ZPHY C34 15	S.F. Biagi *et al.*	(BRIS, CERN, GEVA+)
BIAGI	87C	ZPHY C34 175	S.F. Biagi *et al.*	(BRIS, CERN, GEVA+) JP
ASTON	85B	PR D32 2270	D. Aston *et al.*	(SLAC, CARL, CNRC, CINC)
JENKINS	83	PRL 51 951	C.M. Jenkins *et al.*	(FSU, BRAN, LBL+)
BIAGI	81	ZPHY C9 305	S.F. Biagi *et al.*	(BRIS, CAVE, GEVA+)
HASSALL	81	NP B189 397	J.K. Hassall *et al.*	(CAVE, MSU)
TEODORO	78	PL 77B 451	D. Teodoro *et al.*	(AMST, CERN, NIJM+) JP
BRIEFEL	77	PR D16 2706	E. Briefel *et al.*	(BRAN, UMD, SYRA+)
Also	69	PRL 23 884	S.P. Apsell *et al.*	(BRAN, UMD, SYRA+)
GAY	76C	PL 62B 477	J.B. Gay *et al.*	(AMST, CERN, NIJM) IJ
DIBIANCA	75	NP B98 137	F.A. Dibianca, R.J. Endorf	(CMU)
BADIER	72	NP B37 429	J. Badier *et al.*	(EPOL)
APSELL	70	PRL 24 777	S.P. Apsell *et al.*	(BRAN, UMD, SYRA+) I
CRENNELL	70B	PR D1 847	D.J. Crennell *et al.*	(BNL)
ALITTI	69	PRL 22 79	J. Alitti *et al.*	(BNL, SYRA) I
DAUBER	69	PR 179 1262	P.M. Dauber *et al.*	(LRL)
TRIPP	67	NP B3 10	R.D. Tripp *et al.*	(LRL, SLAC, CERN+)
BADIER	65	PL 16 171	J. Badier *et al.*	(EPOL, SACL, AMST) I
SMITH	65B	Athens Conf. 251	G.A. Smith, J.S. Lindsey	(LRL)
SMITH	65C	PRL 14 25	G.A. Smith *et al.*	(LRL) IJP
HALSTEINSLID	63	Siena Conf. 1 73	A. Halsteinslid *et al.*	(BERG, CERN, EPOL+) I

OTHER RELATED PAPERS

TEODORO	78	PL 77B 451	D. Teodoro *et al.*	(AMST, CERN, NIJM+) JP
BRIEFEL	75	PR D12 1859	E. Briefel *et al.*	(BRAN, UMD, SYRA+)
SCHMIDT	73	Purdue Conf. 363	P.E. Schmidt	(BRAN)
MERRILL	68	PR 167 1202	D.W. Merrill, J. Button-Shafer	(LRL)
SMITH	64	PRL 13 61	G.A. Smith *et al.*	(LRL) IJP

Ξ(1950)

$I(J^P) = \frac{1}{2}(?^?)$ Status: ***

We list here everything reported between 1875 and 2000 MeV. The accumulated evidence for a Ξ near 1950 MeV seems strong enough to include a Ξ(1950) in the main Baryon Table, but not much can be said about its properties. In fact, there may be more than one Ξ near this mass.

Ξ(1950) MASS

VALUE (MeV)	EVTS	DOCUMENT ID		TECN	COMMENT
1950±15 OUR ESTIMATE					
1955 ± 6		ADAMOVICH	99B	WA89	Σ^- nucleus, 345 GeV
1944 ± 9	129	BIAGI	87	SPEC	Ξ^- Be → $(\Xi^-\pi^+)\pi^-$X
1963 ± 5±2	63	BIAGI	87C	SPEC	Ξ^- Be → $(\Lambda\overline{K}^0)$ X
1937 ± 7	150	BIAGI	81	SPEC	SPS hyperon beam
1961 ±18	139	BRIEFEL	77	HBC	2.87 $K^-p \to \Xi^-\pi^+$X
1936 ±22	44	BRIEFEL	77	HBC	2.87 $K^-p \to \Xi^0\pi^-$X
1964 ±10	56	BRIEFEL	77	HBC	$\Xi(1530)\pi$
1900 ±12		DIBIANCA	75	DBC	$\Xi\pi$
1952 ±11	25	ROSS	73C		$(\Xi\pi)^-$
1956 ± 6	29	BADIER	72	HBC	$\Xi\pi$, $\Xi\pi\pi$, YK
1955 ±14	21	GOLDWASSER	70	HBC	$\Xi\pi$
1894 ±18	66	DAUBER	69	HBC	$\Xi\pi$
1930 ±20	27	ALITTI	68	HBC	$\Xi^-\pi^+$
1933 ±16	35	BADIER	65	HBC	$\Xi^-\pi^+$

Ξ(1950) WIDTH

VALUE (MeV)	EVTS	DOCUMENT ID		TECN	COMMENT
60±20 OUR ESTIMATE					
68±22		ADAMOVICH	99B	WA89	Σ^- nucleus, 345 GeV
100±31	129	BIAGI	87	SPEC	Ξ^- Be → $(\Xi^-\pi^+)\pi^-$X
25±15±1.2	63	BIAGI	87C	SPEC	Ξ^- Be → $(\Lambda\overline{K}^0)$ X
60± 8	150	BIAGI	81	SPEC	SPS hyperon beam
159±57	139	BRIEFEL	77	HBC	2.87 $K^-p \to \Xi^-\pi^+$X
87±26	44	BRIEFEL	77	HBC	2.87 $K^-p \to \Xi^0\pi^-$X
60±39	56	BRIEFEL	77	HBC	$\Xi(1530)\pi$
63±78		DIBIANCA	75	DBC	$\Xi\pi$
38±10		ROSS	73C		$(\Xi\pi)^-$
35±11	29	BADIER	72	HBC	$\Xi\pi$, $\Xi\pi\pi$, YK
56±26	21	GOLDWASSER	70	HBC	$\Xi\pi$
98±23	66	DAUBER	69	HBC	$\Xi\pi$
80±40	27	ALITTI	68	HBC	$\Xi^-\pi^+$
140±35	35	BADIER	65	HBC	$\Xi^-\pi^+$

Ξ(1950) DECAY MODES

	Mode	Fraction (Γ_i/Γ)
Γ_1	$\Lambda\overline{K}$	seen
Γ_2	$\Sigma\overline{K}$	possibly seen
Γ_3	$\Xi\pi$	seen
Γ_4	$\Xi(1530)\pi$	
Γ_5	$\Xi\pi\pi$(not $\Xi(1530)\pi$)	

$\Xi(1950)$ BRANCHING RATIOS

$\Gamma(\Sigma\overline{K})/\Gamma(\Lambda\overline{K})$ Γ_2/Γ_1

VALUE	CL%	EVTS	DOCUMENT ID		TECN	COMMENT
<2.3	90	0	BIAGI	87C	SPEC	Ξ^- Be 116 GeV

$\Gamma(\Sigma\overline{K})/\Gamma_{total}$ Γ_2/Γ

VALUE	EVTS	DOCUMENT ID		TECN	COMMENT
possibly seen	17	HASSALL	81	HBC	K^-p 6.5 GeV/c

$\Gamma(\Xi\pi)/\Gamma(\Xi(1530)\pi)$ Γ_3/Γ_4

VALUE	DOCUMENT ID		TECN
$2.8^{+0.7}_{-0.6}$	APSELL	70	HBC

$\Gamma(\Xi\pi\pi(\text{not }\Xi(1530)\pi))/\Gamma(\Xi(1530)\pi)$ Γ_5/Γ_4

VALUE	DOCUMENT ID		TECN
0.0 ± 0.3	APSELL	70	HBC

$\Xi(1950)$ REFERENCES

ADAMOVICH	99B	EPJ C11 271	M.I. Adamovich *et al.*	(CERN WA89 Collab.)
BIAGI	87	ZPHY C34 15	S.F. Biagi *et al.*	(BRIS, CERN, GEVA+)
BIAGI	87C	ZPHY C34 175	S.F. Biagi *et al.*	(BRIS, CERN, GEVA+)
BIAGI	81	ZPHY C9 305	S.F. Biagi *et al.*	(BRIS, CAVE, GEVA+)
HASSALL	81	NP B189 397	J.K. Hassall *et al.*	(CAVE, MSU)
BRIEFEL	77	PR D16 2706	E. Briefel *et al.*	(BRAN, UMD, SYRA+)
Also	70	Duke Conf. 317	E. Briefel *et al.*	(BRAN, UMD, SYRA+)
Hyperon Resonances, 1970				
DIBIANCA	75	NP B98 137	F.A. Dibianca, R.J. Endorf	(CMU)
ROSS	73C	Purdue Conf. 345	R.T. Ross, J.L. Lloyd, D. Radojicic	(OXF)
BADIER	72	NP B37 429	J. Badier *et al.*	(EPOL)
APSELL	70	PRL 24 777	S.P. Apsell *et al.*	(BRAN, UMD, SYRA+) I
GOLDWASSER	70	PR D1 1960	E.L. Goldwasser, P.F. Schultz	(ILL)
DAUBER	69	PR 179 1262	P.M. Dauber *et al.*	(LRL) I
ALITTI	68	PRL 21 1119	J. Alitti *et al.*	(BNL, SYRA) I
BADIER	65	PL 16 171	J. Badier *et al.*	(EPOL, SACL, AMST) I

$\Xi(2030)$

$I(J^P) = \frac{1}{2}(\geq\frac{5}{2}^?)$ Status: ***

The evidence for this state has been much improved by HEMINGWAY 77, who see an eight standard deviation enhancement in $\Sigma\overline{K}$ and a weaker coupling to $\Lambda\overline{K}$. ALITTI 68 and HEMINGWAY 77 observe no signals in the $\Xi\pi\pi$ (or $\Xi(1530)\pi$) channel, in contrast to DIBIANCA 75. The decay $(\Lambda/\Sigma)\overline{K}\pi$ reported by BARTSCH 69 is also not confirmed by HEMINGWAY 77.

A moments analysis of the HEMINGWAY 77 data indicates at a level of three standard deviations that $J \geq 5/2$.

$\Xi(2030)$ MASS

VALUE (MeV)	EVTS	DOCUMENT ID		TECN	CHG	COMMENT
2025 ± 5 OUR ESTIMATE						
2025.1 ± 2.4 OUR AVERAGE		Error includes scale factor of 1.3. See the ideogram below.				
2022 ± 7		JENKINS	83	MPS	–	$K^-p \to K^+$ MM
2024 ± 2	200	HEMINGWAY	77	HBC	–	K^-p 4.2 GeV/c
2044 ± 8		DIBIANCA	75	DBC	−0	$\Xi\pi\pi$, $\Xi^*\pi$
2019 ± 7	15	ROSS	73C	HBC	−0	$\Sigma\overline{K}$
2030 ±10	42	ALITTI	69	HBC	–	K^-p 3.9–5 GeV/c
2058 ±17	40	BARTSCH	69	HBC	−0	K^-p 10 GeV/c

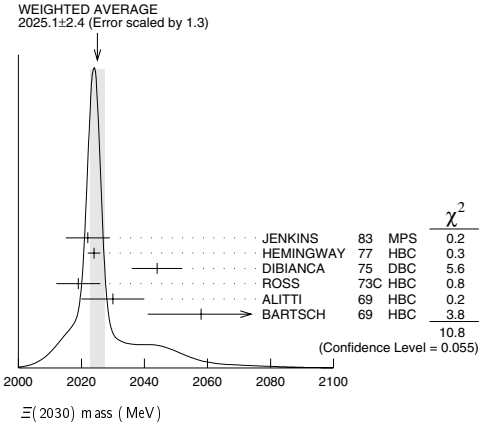

$\Xi(2030)$ WIDTH

VALUE (MeV)	EVTS	DOCUMENT ID		TECN	CHG	COMMENT
20^{+15}_{-5} OUR ESTIMATE						
21 ± 6 OUR AVERAGE		Error includes scale factor of 1.3. See the ideogram below.				
16± 5	200	HEMINGWAY	77	HBC	–	K^-p 4.2 GeV/c
60±24		DIBIANCA	75	DBC	−0	$\Xi\pi\pi$, $\Xi^*\pi$
33±17	15	ROSS	73C	HBC	−0	$\Sigma\overline{K}$
45^{+40}_{-20}		ALITTI	69	HBC	–	K^-p 3.9–5 GeV/c
57±30		BARTSCH	69	HBC	−0	K^-p 10 GeV/c

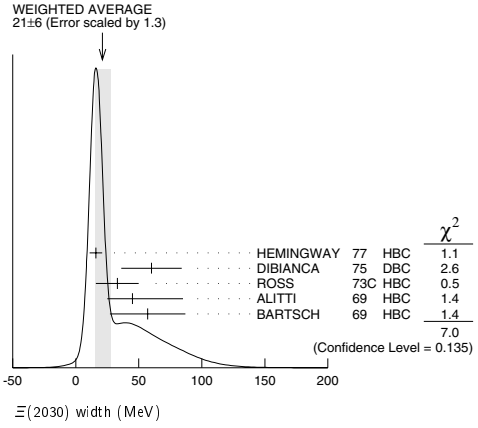

$\Xi(2030)$ DECAY MODES

	Mode	Fraction (Γ_i/Γ)
Γ_1	$\Lambda\overline{K}$	~ 20 %
Γ_2	$\Sigma\overline{K}$	~ 80 %
Γ_3	$\Xi\pi$	small
Γ_4	$\Xi(1530)\pi$	small
Γ_5	$\Xi\pi\pi$(not $\Xi(1530)\pi$)	small
Γ_6	$\Lambda\overline{K}\pi$	small
Γ_7	$\Sigma\overline{K}\pi$	small

$\Xi(2030)$ BRANCHING RATIOS

$\Gamma(\Xi\pi)/[\Gamma(\Lambda\overline{K})+\Gamma(\Sigma\overline{K})+\Gamma(\Xi\pi)+\Gamma(\Xi(1530)\pi)]$ $\Gamma_3/(\Gamma_1+\Gamma_2+\Gamma_3+\Gamma_4)$

VALUE	DOCUMENT ID		TECN	CHG	COMMENT
• • • We do not use the following data for averages, fits, limits, etc. • • •					
<0.30	ALITTI	69	HBC	–	1 standard dev. limit

$\Gamma(\Xi\pi)/\Gamma(\Sigma\overline{K})$ Γ_3/Γ_2

VALUE	CL%	DOCUMENT ID		TECN	CHG	COMMENT
<0.19	95	HEMINGWAY	77	HBC	–	K^-p 4.2 GeV/c

$\Gamma(\Lambda\overline{K})/[\Gamma(\Lambda\overline{K})+\Gamma(\Sigma\overline{K})+\Gamma(\Xi\pi)+\Gamma(\Xi(1530)\pi)]$ $\Gamma_1/(\Gamma_1+\Gamma_2+\Gamma_3+\Gamma_4)$

VALUE	DOCUMENT ID		TECN	CHG	COMMENT
0.25 ± 0.15	ALITTI	69	HBC	–	K^-p 3.9–5 GeV/c

$\Gamma(\Lambda\overline{K})/\Gamma(\Sigma\overline{K})$ Γ_1/Γ_2

VALUE	DOCUMENT ID		TECN	CHG	COMMENT
0.22 ± 0.09	HEMINGWAY	77	HBC	–	K^-p 4.2 GeV/c

$\Gamma(\Sigma\overline{K})/[\Gamma(\Lambda\overline{K})+\Gamma(\Sigma\overline{K})+\Gamma(\Xi\pi)+\Gamma(\Xi(1530)\pi)]$ $\Gamma_2/(\Gamma_1+\Gamma_2+\Gamma_3+\Gamma_4)$

VALUE	DOCUMENT ID		TECN	CHG	COMMENT
0.75 ± 0.20	ALITTI	69	HBC	–	K^-p 3.9–5 GeV/c

$\Gamma(\Xi(1530)\pi)/[\Gamma(\Lambda\overline{K})+\Gamma(\Sigma\overline{K})+\Gamma(\Xi\pi)+\Gamma(\Xi(1530)\pi)]$ $\Gamma_4/(\Gamma_1+\Gamma_2+\Gamma_3+\Gamma_4)$

VALUE	DOCUMENT ID		TECN	CHG	COMMENT
• • • We do not use the following data for averages, fits, limits, etc. • • •					
<0.15	ALITTI	69	HBC	–	1 standard dev. limit

$[\Gamma(\Xi(1530)\pi)+\Gamma(\Xi\pi\pi(\text{not }\Xi(1530)\pi))]/\Gamma(\Sigma\overline{K})$ $(\Gamma_4+\Gamma_5)/\Gamma_2$

VALUE	CL%	DOCUMENT ID		TECN	CHG	COMMENT
<0.11	95	[1] HEMINGWAY	77	HBC	–	K^-p 4.2 GeV/c

$\Gamma(\Lambda\overline{K}\pi)/\Gamma_{total}$ Γ_6/Γ

VALUE	DOCUMENT ID		TECN	COMMENT
• • • We do not use the following data for averages, fits, limits, etc. • • •				
seen	BARTSCH	69	HBC	K^-p 10 GeV

$\Gamma(\Lambda\overline{K}\pi)/\Gamma(\Sigma\overline{K})$ Γ_6/Γ_2

VALUE	CL%	DOCUMENT ID		TECN	CHG	COMMENT
<0.32	95	HEMINGWAY	77	HBC	–	K^-p 4.2 GeV/c

$\Gamma(\Sigma\overline{K}\pi)/\Gamma_{total}$ Γ_7/Γ

VALUE	DOCUMENT ID		TECN	COMMENT
• • • We do not use the following data for averages, fits, limits, etc. • • •				
seen	BARTSCH	69	HBC	K^-p 10 GeV

$\Gamma(\Sigma\overline{K}\pi)/\Gamma(\Sigma\overline{K})$ Γ_7/Γ_2

VALUE	CL%	DOCUMENT ID		TECN	CHG	COMMENT
<0.04	95	[2] HEMINGWAY	77	HBC	–	K^-p 4.2 GeV/c

$\Xi(2030)$ FOOTNOTES

[1] For the decay mode $\Xi^-\pi^+\pi^-$ only.
[2] For the decay mode $\Sigma^\pm K^-\pi^\mp$ only.

$\Xi(2030)$ REFERENCES

JENKINS	83	PRL 51 951	C.M. Jenkins *et al.*	(FSU, BRAN, LBL+)
HEMINGWAY	77	PL 68B 197	R.J. Hemingway *et al.*	(AMST, CERN, NIJM+) IJ
Also	76C	PL 62B 477	J.B. Gay *et al.*	(AMST, CERN, NIJM)
DIBIANCA	75	NP B98 137	F.A. Dibianca, R.J. Endorf	(CMU)
ROSS	73C	Purdue Conf. 345	R.T. Ross, J.L. Lloyd, D. Radojicic	(OXF)
ALITTI	69	PRL 22 79	J. Alitti *et al.*	(BNL, SYRA) I
BARTSCH	69	PL 28B 439	J. Bartsch *et al.*	(AACH, BERL, CERN+)
ALITTI	68	PRL 21 1119	J. Alitti *et al.*	(BNL, SYRA)

$\Xi(2120)$

$I(J^P) = \frac{1}{2}(?^?)$ Status: *
J, P need confirmation.

OMITTED FROM SUMMARY TABLE

$\Xi(2120)$ MASS

VALUE (MeV)	EVTS	DOCUMENT ID		TECN	COMMENT
≈ 2120 OUR ESTIMATE					
2137 ± 4	18	[1] CHLIAPNIK...	79	HBC	K^+p 32 GeV/c
2123 ± 7		[2] GAY	76C	HBC	K^-p 4.2 GeV/c

$\Xi(2120)$ WIDTH

VALUE (MeV)	EVTS	DOCUMENT ID		TECN	COMMENT
<20	18	[1] CHLIAPNIK...	79	HBC	K^+p 32 GeV/c
25 ± 12		[2] GAY	76C	HBC	K^-p 4.2 GeV/c

$\Xi(2120)$ DECAY MODES

	Mode	Fraction (Γ_i/Γ)
Γ_1	$\Lambda\overline{K}$	seen

$\Xi(2120)$ BRANCHING RATIOS

$\Gamma(\Lambda\overline{K})/\Gamma_{total}$ Γ_1/Γ

VALUE	DOCUMENT ID		TECN	COMMENT
seen	[1] CHLIAPNIK...	79	HBC	$K^+p \to (\overline{\Lambda}K^+)$ X
seen	[2] GAY	76C	HBC	K^-p 4.2 GeV/c

$\Xi(2120)$ FOOTNOTES

[1] CHLIAPNIKOV 79 does not uniquely identify the K^+ in the $(\overline{\Lambda}K^+)$ X final state. It also reports bumps with fewer events at 2240, 2540, and 2830 MeV.
[2] GAY 76C sees a 4-standard deviation signal. However, HEMINGWAY 77, with more events from the same experiment points out that the signal is greatly reduced if a cut is made on the 4-momentum u. This suggests an anomalous production mechanism if the $\Xi(2120)$ is real.

$\Xi(2120)$ REFERENCES

CHLIAPNIK...	79	NP B158 253	P.V. Chliapnikov *et al.*	(CERN, BELG, MONS)
HEMINGWAY	77	PL 68B 197	R.J. Hemingway *et al.*	(AMST, CERN, NIJM+)
GAY	76C	PL 62B 477	J.B. Gay *et al.*	(AMST, CERN, NIJM)

$\Xi(2250)$

$I(J^P) = \frac{1}{2}(?^?)$ Status: **
J, P need confirmation.

OMITTED FROM SUMMARY TABLE

The evidence for this state is mixed. BARTSCH 69 sees a bump of not much statistical significance in $\Lambda\overline{K}\pi$, $\Sigma\overline{K}\pi$, and $\Xi\pi\pi$ mass spectra. GOLDWASSER 70 sees a narrower bump in $\Xi\pi\pi$ at a higher mass. Not seen by HASSALL 81 with 45 events/μb at 6.5 GeV/c. Seen by JENKINS 83. Perhaps seen by BIAGI 87.

$\Xi(2250)$ MASS

VALUE (MeV)	EVTS	DOCUMENT ID		TECN	CHG	COMMENT
≈ 2250 OUR ESTIMATE						
2189 ± 7	66	BIAGI	87	SPEC	–	Ξ^-Be → ($\Xi^-\pi^+\pi^-$) X
2214 ± 5		JENKINS	83	MPS	–	$K^-p \to K^+$ MM
2295 ± 15	18	GOLDWASSER	70	HBC	–	K^-p 5.5 GeV/c
2244 ± 52	35	BARTSCH	69	HBC		K^-p 10 GeV/c

$\Xi(2250)$ WIDTH

VALUE (MeV)	EVTS	DOCUMENT ID		TECN	CHG	COMMENT
46 ± 27	66	BIAGI	87	SPEC	–	Ξ^-Be → ($\Xi^-\pi^+\pi^-$) X
<30		GOLDWASSER	70	HBC	–	K^-p 5.5 GeV/c
130 ± 80		BARTSCH	69	HBC		

$\Xi(2250)$ DECAY MODES

	Mode
Γ_1	$\Xi\pi\pi$
Γ_2	$\Lambda\overline{K}\pi$
Γ_3	$\Sigma\overline{K}\pi$

$\Xi(2250)$ REFERENCES

BIAGI	87	ZPHY C34 15	S.F. Biagi *et al.*	(BRIS, CERN, GEVA+)
JENKINS	83	PRL 51 951	C.M. Jenkins *et al.*	(FSU, BRAN, LBL+)
HASSALL	81	NP B189 397	J.K. Hassall *et al.*	(CAVE, MSU)
GOLDWASSER	70	PR D1 1960	E.L. Goldwasser, P.F. Schultz	(ILL)
BARTSCH	69	PL 28B 439	J. Bartsch *et al.*	(AACH, BERL, CERN+)

$\Xi(2370)$

$I(J^P) = \frac{1}{2}(?^?)$ Status: **
J, P need confirmation.

OMITTED FROM SUMMARY TABLE

$\Xi(2370)$ MASS

VALUE (MeV)	EVTS	DOCUMENT ID		TECN	CHG	COMMENT
≈ 2370 OUR ESTIMATE						
2356 ± 10		JENKINS	83	MPS	–	$K^-p \to K^+$ MM
2370	50	HASSALL	81	HBC	−0	K^-p 6.5 GeV/c
2373 ± 8	94	AMIRZADEH	80	HBC	−0	K^-p 8.25 GeV/c
2392 ± 27		DIBIANCA	75	DBC		$\Xi2\pi$

$\Xi(2370)$ WIDTH

VALUE (MeV)	EVTS	DOCUMENT ID		TECN	CHG	COMMENT
80	50	HASSALL	81	HBC	−0	K^-p 6.5 GeV/c
80 ± 25	94	AMIRZADEH	80	HBC	−0	K^-p 8.25 GeV/c
75 ± 69		DIBIANCA	75	DBC		$\Xi2\pi$

$\Xi(2370)$ DECAY MODES

	Mode	Fraction (Γ_i/Γ)
Γ_1	$\Lambda\overline{K}\pi$ Includes $\Gamma_4+\Gamma_6$.	seen
Γ_2	$\Sigma\overline{K}\pi$ Includes $\Gamma_5+\Gamma_6$.	seen
Γ_3	Ω^-K	
Γ_4	$\Lambda\overline{K}^*(892)$	
Γ_5	$\Sigma\overline{K}^*(892)$	
Γ_6	$\Sigma(1385)\overline{K}$	

$\Xi(2370)$ BRANCHING RATIOS

$\Gamma(\Lambda\overline{K}\pi)/\Gamma_{total}$ Γ_1/Γ

VALUE	DOCUMENT ID		TECN	CHG	COMMENT
seen	AMIRZADEH	80	HBC	−0	K^-p 8.25 GeV/c

$\Gamma(\Sigma\overline{K}\pi)/\Gamma_{\text{total}}$ Γ_2/Γ

VALUE	DOCUMENT ID		TECN	CHG	COMMENT
seen	AMIRZADEH	80	HBC	−0	K^-p 8.25 GeV/c

$[\Gamma(\Lambda\overline{K}\pi)+\Gamma(\Sigma\overline{K}\pi)]/\Gamma_{\text{total}}$ $(\Gamma_1+\Gamma_2)/\Gamma$

VALUE	EVTS	DOCUMENT ID		TECN	CHG	COMMENT
seen	50	HASSALL	81	HBC	−0	K^-p 6.5 GeV/c

$\Gamma(\Omega^-K)/\Gamma_{\text{total}}$ Γ_3/Γ

VALUE	DOCUMENT ID		TECN	CHG	COMMENT
0.09±0.04	[1] KINSON	80	HBC	–	K^-p 8.25 GeV/c

$[\Gamma(\Lambda\overline{K}^*(892))+\Gamma(\Sigma\overline{K}^*(892))]/\Gamma_{\text{total}}$ $(\Gamma_4+\Gamma_5)/\Gamma$

VALUE	DOCUMENT ID		TECN	CHG	COMMENT
0.22±0.13	[1] KINSON	80	HBC	–	K^-p 8.25 GeV/c

$\Gamma(\Sigma(1385)\overline{K})/\Gamma_{\text{total}}$ Γ_6/Γ

VALUE	DOCUMENT ID		TECN	CHG	COMMENT
0.12±0.08	[1] KINSON	80	HBC	–	K^-p 8.25 GeV/c

$\Xi(2370)$ FOOTNOTES

[1] KINSON 80 is a reanalysis of AMIRZADEH 80 with 50% more events.

$\Xi(2370)$ REFERENCES

JENKINS	83	PRL 51 951	C.M. Jenkins *et al.*	(FSU, BRAN, LBL+)
HASSALL	81	NP B189 397	J.K. Hassall *et al.*	(CAVE, MSU)
AMIRZADEH	80	PL 90B 324	J. Amirzadeh *et al.*	(BIRM, CERN, GLAS+) I
KINSON	80	Toronto Conf. 263	J.B. Kinson *et al.*	(BIRM, CERN, GLAS+) I
DIBIANCA	75	NP B98 137	F.A. Dibianca, R.J. Endorf	(CMU)

$\Xi(2500)$

$I(J^P) = \frac{1}{2}(?^?)$ Status: * J, P need confirmation.

OMITTED FROM SUMMARY TABLE

The ALITTI 69 peak might be instead the $\Xi(2370)$ or might be neither the $\Xi(2370)$ nor the $\Xi(2500)$.

$\Xi(2500)$ MASS

VALUE (MeV)	EVTS	DOCUMENT ID		TECN	CHG	COMMENT
≈ 2500 OUR ESTIMATE						
2505±10		JENKINS	83	MPS	–	$K^-p \to K^+$ MM
2430±20	30	ALITTI	69	HBC	–	K^-p 4.6–5 GeV/c
2500±10	45	BARTSCH	69	HBC	−0	K^-p 10 GeV/c

$\Xi(2500)$ WIDTH

VALUE (MeV)	DOCUMENT ID		TECN	CHG
150^{+60}_{-40}	ALITTI	69	HBC	–
59±27	BARTSCH	69	HBC	−0

$\Xi(2500)$ DECAY MODES

	Mode	Fraction (Γ_i/Γ)
Γ_1	$\Xi\pi$	
Γ_2	$\Lambda\overline{K}$	
Γ_3	$\Sigma\overline{K}$	
Γ_4	$\Xi\pi\pi$	seen
Γ_5	$\Xi(1530)\pi$	
Γ_6	$\Lambda\overline{K}\pi + \Sigma\overline{K}\pi$	seen

$\Xi(2500)$ BRANCHING RATIOS

$\Gamma(\Xi\pi)/[\Gamma(\Xi\pi)+\Gamma(\Lambda\overline{K})+\Gamma(\Sigma\overline{K})+\Gamma(\Xi(1530)\pi)]$ $\Gamma_1/(\Gamma_1+\Gamma_2+\Gamma_3+\Gamma_5)$

VALUE	DOCUMENT ID		TECN	COMMENT
<0.5	ALITTI	69	HBC	1 standard dev. limit

$\Gamma(\Lambda\overline{K})/[\Gamma(\Xi\pi)+\Gamma(\Lambda\overline{K})+\Gamma(\Sigma\overline{K})+\Gamma(\Xi(1530)\pi)]$ $\Gamma_2/(\Gamma_1+\Gamma_2+\Gamma_3+\Gamma_5)$

VALUE	DOCUMENT ID		TECN	CHG
0.5±0.2	ALITTI	69	HBC	–

$\Gamma(\Sigma\overline{K})/[\Gamma(\Xi\pi)+\Gamma(\Lambda\overline{K})+\Gamma(\Sigma\overline{K})+\Gamma(\Xi(1530)\pi)]$ $\Gamma_3/(\Gamma_1+\Gamma_2+\Gamma_3+\Gamma_5)$

VALUE	DOCUMENT ID		TECN	CHG
0.5±0.2	ALITTI	69	HBC	–

$\Gamma(\Xi(1530)\pi)/[\Gamma(\Xi\pi)+\Gamma(\Lambda\overline{K})+\Gamma(\Sigma\overline{K})+\Gamma(\Xi(1530)\pi)]$ $\Gamma_5/(\Gamma_1+\Gamma_2+\Gamma_3+\Gamma_5)$

VALUE	DOCUMENT ID		TECN	COMMENT
<0.2	ALITTI	69	HBC	1 standard dev. limit

$\Gamma(\Xi\pi\pi)/\Gamma_{\text{total}}$ Γ_4/Γ

VALUE	DOCUMENT ID		TECN	CHG
seen	BARTSCH	69	HBC	−0

$[\Gamma(\Lambda\overline{K}\pi)+\Gamma(\Sigma\overline{K}\pi)]/\Gamma_{\text{total}}$ Γ_6/Γ

VALUE	DOCUMENT ID		TECN	CHG
seen	BARTSCH	69	HBC	−0

$\Xi(2500)$ REFERENCES

JENKINS	83	PRL 51 951	C.M. Jenkins *et al.*	(FSU, BRAN, LBL+)
ALITTI	69	PRL 22 79	J. Alitti *et al.*	(BNL, SYRA) I
BARTSCH	69	PL 28B 439	J. Bartsch *et al.*	(AACH, BERL, CERN+)

Ω BARYONS
($S = -3$, $I = 0$)

$\Omega^- = sss$

Ω^-

$I(J^P) = 0(\frac{3}{2}^+)$ Status: ****

The unambiguous discovery in both production and decay was by BARNES 64. The quantum numbers have not actually been measured, but follow from the assignment of the particle to the baryon decuplet. DEUTSCHMANN 78 and BAUBILLIER 78 rule out $J = 1/2$ and find consistency with $J = 3/2$.

We have omitted some results that have been superseded by later experiments. See our earlier editions.

Ω^- MASS

The fit assumes the Ω^- and $\overline{\Omega}^+$ masses are the same, and averages them together.

VALUE (MeV)	EVTS	DOCUMENT ID		TECN	COMMENT
1672.45 ± 0.29 OUR FIT					
1672.43 ± 0.32 OUR AVERAGE					
1673 ± 1	100	HARTOUNI	85	SPEC	80–280 GeV K^0_L C
1673.0 ± 0.8	41	BAUBILLIER	78	HBC	8.25 GeV/c K^-p
1671.7 ± 0.6	27	HEMINGWAY	78	HBC	4.2 GeV/c K^-p
1673.4 ± 1.7	4	[1] DIBIANCA	75	DBC	4.9 GeV/c K^-d
1673.3 ± 1.0	3	PALMER	68	HBC	K^-p 4.6, 5 GeV/c
1671.8 ± 0.8	3	SCHULTZ	68	HBC	K^-p 5.5 GeV/c
1674.2 ± 1.6	5	SCOTTER	68	HBC	K^-p 6 GeV/c
1672.1 ± 1.0	1	[2] FRY	55	EMUL	
• • • We do not use the following data for averages, fits, limits, etc. • • •					
1671.43 ± 0.78	13	[3] DEUTSCH...	73	HBC	K^-p 10 GeV/c
1671.9 ± 1.2	6	[3] SPETH	69	HBC	See DEUTSCHMANN 73 → $\Xi^-\pi^0$
1673.0 ± 8.0	1	ABRAMS	64	HBC	
1670.6 ± 1.0	1	[2] FRY	55B	EMUL	
1615	1	[4] EISENBERG	54	EMUL	

[1] DIBIANCA 75 gives a mass for each event. We quote the average.

[2] The FRY 55 and FRY 55B events were identified as Ω^- by ALVAREZ 73. The masses assume decay to ΛK^- at rest. For FRY 55B, decay from an atomic orbit could Doppler shift the K^- energy and the resulting Ω^- mass by several MeV. This shift is negligible for FRY 55 because the Ω decay is approximately perpendicular to its orbital velocity, as is known because the Λ strikes the nucleus (L.Alvarez, private communication 1973). We have calculated the error assuming that the orbital n is 4 or larger.

[3] Excluded from the average; the Ω^- lifetimes measured by the experiments differ significantly from other measurements.

[4] The EISENBERG 54 mass was calculated for decay in flight. ALVAREZ 73 has shown that the Ω interacted with an Ag nucleus to give $K^-\,\Xi$Ag.

$\overline{\Omega}^+$ MASS

The fit assumes the Ω^- and $\overline{\Omega}^+$ masses are the same, and averages them together.

VALUE (MeV)	EVTS	DOCUMENT ID		TECN	COMMENT
1672.45 ± 0.29 OUR FIT					
1672.5 ± 0.7 OUR AVERAGE					
1672 ± 1	72	HARTOUNI	85	SPEC	80–280 GeV K^0_L C
1673.1 ± 1.0	1	FIRESTONE	71B	HBC	12 GeV/c K^+d

$(m_{\Omega^-} - m_{\overline{\Omega}^+}) / m_{\Omega^-}$

A test of CPT invariance.

VALUE	DOCUMENT ID		TECN	COMMENT
$(-1.44 \pm 7.98) \times 10^{-5}$	CHAN	98	E756	p Be, 800 GeV

Ω^- MEAN LIFE

Measurements with an error > 0.1×10^{-10} s have been omitted. The fit assumes the Ω^- and $\overline{\Omega}^+$ mean lives are the same, and averages them together.

VALUE (10^{-10} s)	EVTS	DOCUMENT ID		TECN	COMMENT
0.821 ± 0.011 OUR FIT					
0.821 ± 0.011 OUR AVERAGE					
0.817 ± 0.013 ± 0.018	6934	CHAN	98	E756	p Be, 800 GeV
0.811 ± 0.037	1096	LUK	88	SPEC	pBe 400 GeV
0.823 ± 0.013	12k	BOURQUIN	84	SPEC	SPS hyperon beam
• • • We do not use the following data for averages, fits, limits, etc. • • •					
0.822 ± 0.028	2437	BOURQUIN	79B	SPEC	See BOURQUIN 84

$\overline{\Omega}^+$ MEAN LIFE

The fit assumes the Ω^- and $\overline{\Omega}^+$ mean lives are the same, and averages them together.

VALUE (10^{-10} s)	EVTS	DOCUMENT ID		TECN	COMMENT
0.821 ± 0.011 OUR FIT					
0.823 ± 0.031 ± 0.022	1801	CHAN	98	E756	p Be, 800 GeV

$(\tau_{\Omega^-} - \tau_{\overline{\Omega}^+}) / \tau_{\Omega^-}$

A test of CPT invariance. Our calculation, from the preceding two data blocks.

VALUE	DOCUMENT ID
-0.002 ± 0.040 OUR ESTIMATE	

Ω^- MAGNETIC MOMENT

VALUE (μ_N)	EVTS	DOCUMENT ID		TECN	COMMENT
−2.02 ± 0.05 OUR AVERAGE					
−2.024 ± 0.056	235k	WALLACE	95	SPEC	Ω^- 300–550 GeV
−1.94 ± 0.17 ± 0.14	25k	DIEHL	91	SPEC	Spin-transfer production

Ω^- DECAY MODES

	Mode	Fraction (Γ_i/Γ)	Confidence level
Γ_1	ΛK^-	(67.8 ± 0.7) %	
Γ_2	$\Xi^0\pi^-$	(23.6 ± 0.7) %	
Γ_3	$\Xi^-\pi^0$	(8.6 ± 0.4) %	
Γ_4	$\Xi^-\pi^+\pi^-$	$(4.3^{+3.4}_{-1.3}) \times 10^{-4}$	
Γ_5	$\Xi(1530)^0\pi^-$	$(6.4^{+5.1}_{-2.0}) \times 10^{-4}$	
Γ_6	$\Xi^0 e^- \overline{\nu}_e$	(5.6 ± 2.8) $\times 10^{-3}$	
Γ_7	$\Xi^-\gamma$	< 4.6 $\times 10^{-4}$	90%
	$\Delta S = 2$ forbidden ($S2$) modes		
Γ_8	$\Lambda\pi^-$ $S2$	< 1.9 $\times 10^{-4}$	90%

Ω^- BRANCHING RATIOS

The BOURQUIN 84 values (which include results of BOURQUIN 79B, a separate experiment) are much more accurate than any other results, and so the other results have been omitted.

$\Gamma(\Lambda K^-)/\Gamma_{total}$ Γ_1/Γ

VALUE	EVTS	DOCUMENT ID		TECN	COMMENT
0.678 ± 0.007	14k	BOURQUIN	84	SPEC	SPS hyperon beam
• • • We do not use the following data for averages, fits, limits, etc. • • •					
0.686 ± 0.013	1920	BOURQUIN	79B	SPEC	See BOURQUIN 84

$\Gamma(\Xi^0\pi^-)/\Gamma_{total}$ Γ_2/Γ

VALUE	EVTS	DOCUMENT ID		TECN	COMMENT
0.236 ± 0.007	1947	BOURQUIN	84	SPEC	SPS hyperon beam
• • • We do not use the following data for averages, fits, limits, etc. • • •					
0.234 ± 0.013	317	BOURQUIN	79B	SPEC	See BOURQUIN 84

$\Gamma(\Xi^-\pi^0)/\Gamma_{total}$ Γ_3/Γ

VALUE	EVTS	DOCUMENT ID		TECN	COMMENT
0.086 ± 0.004	759	BOURQUIN	84	SPEC	SPS hyperon beam
• • • We do not use the following data for averages, fits, limits, etc. • • •					
0.080 ± 0.008	145	BOURQUIN	79B	SPEC	See BOURQUIN 84

$\Gamma(\Xi^-\pi^+\pi^-)/\Gamma_{total}$ Γ_4/Γ

VALUE (units 10^{-4})	EVTS	DOCUMENT ID		TECN	COMMENT
$4.3^{+3.4}_{-1.3}$	4	BOURQUIN	84	SPEC	SPS hyperon beam

$\Gamma(\Xi(1530)^0\pi^-)/\Gamma_{total}$ Γ_5/Γ

VALUE (units 10^{-4})	EVTS	DOCUMENT ID		TECN	COMMENT
$6.4^{+5.1}_{-2.0}$	4	[5] BOURQUIN	84	SPEC	SPS hyperon beam
• • • We do not use the following data for averages, fits, limits, etc. • • •					
~ 20	1	BOURQUIN	79B	SPEC	See BOURQUIN 84

[5] The same 4 events as in the previous mode, with the isospin factor to take into account $\Xi(1530)^0 \to \Xi^0\pi^0$ decays included.

$\Gamma(\Xi^0 e^- \overline{\nu}_e)/\Gamma_{total}$ Γ_6/Γ

VALUE (units 10^{-3})	EVTS	DOCUMENT ID		TECN	COMMENT
5.6 ± 2.8	14	BOURQUIN	84	SPEC	SPS hyperon beam
• • • We do not use the following data for averages, fits, limits, etc. • • •					
~ 10	3	BOURQUIN	79B	SPEC	See BOURQUIN 84

$\Gamma(\Xi^-\gamma)/\Gamma_{total}$ Γ_7/Γ

VALUE (units 10^{-4})	CL%	EVTS	DOCUMENT ID		TECN	COMMENT
< 4.6	90	0	ALBUQUERQ...94		E761	Ω^- 375 GeV
• • • We do not use the following data for averages, fits, limits, etc. • • •						
< 22	90	9	BOURQUIN	84	SPEC	SPS hyperon beam
< 31	90	0	BOURQUIN	79B	SPEC	See BOURQUIN 84

$\Gamma(\Lambda\pi^-)/\Gamma_{total}$ Γ_8/Γ

ΔS=2. Forbidden in first-order weak interaction.

VALUE (units 10^{-4})	CL%	EVTS	DOCUMENT ID		TECN	COMMENT
< 1.9	90	0	BOURQUIN	84	SPEC	SPS hyperon beam
• • • We do not use the following data for averages, fits, limits, etc. • • •						
< 13	90	0	BOURQUIN	79B	SPEC	See BOURQUIN 84

Ω^- DECAY PARAMETERS

α FOR $\Omega^- \to \Lambda K^-$

Some early results have been omitted.

VALUE	EVTS	DOCUMENT ID		TECN	COMMENT
−0.026 ± 0.023 OUR AVERAGE					
−0.028 ± 0.047	6953	CHAN	98	E756	p Be, 800 GeV
−0.034 ± 0.079	1743	LUK	88	SPEC	pBe 400 GeV
−0.025 ± 0.028	12k	BOURQUIN	84	SPEC	SPS hyperon beam

α FOR $\overline{\Omega}^+ \to \overline{\Lambda} K^+$

VALUE	EVTS	DOCUMENT ID		TECN	COMMENT
+0.017 ± 0.077	1823	CHAN	98	E756	p Be, 800 GeV

$[\alpha(\Omega^- \to \Lambda K^-) + \alpha(\overline{\Omega}^+ \to \overline{\Lambda} K^+)]/2$

Zero if CP is conserved. Calculated from the preceding two datablocks.

VALUE	DOCUMENT ID
−0.004 ± 0.040 OUR ESTIMATE	

α FOR $\Omega^- \to \Xi^0\pi^-$

VALUE	EVTS	DOCUMENT ID		TECN	COMMENT
+0.09 ± 0.14	1630	BOURQUIN	84	SPEC	SPS hyperon beam

α FOR $\Omega^- \to \Xi^-\pi^0$

VALUE	EVTS	DOCUMENT ID		TECN	COMMENT
+0.05 ± 0.21	614	BOURQUIN	84	SPEC	SPS hyperon beam

Ω^- REFERENCES

We have omitted some papers that have been superseded by later experiments. See our earlier editions.

CHAN	98	PR D58 072002	A.W. Chan *et al.*	(FNAL E756 Collab.)
WALLACE	95	PRL 74 3732	N.B. Wallace *et al.*	(MINN, ARIZ, MICH+)
ALBUQUERQ...	94	PR D50 R18	I.F. Albuquerque *et al.*	(FNAL E761 Collab.)
DIEHL	91	PRL 67 804	H.T. Diehl *et al.*	(RUTG, FNAL, MICH+)
LUK	88	PR D38 19	K.B. Luk *et al.*	(RUTG, WISC, MICH, MINN)
HARTOUNI	85	PRL 54 628	E.P. Hartouni *et al.*	(COLU, ILL, FNAL)
BOURQUIN	84	NP B241 1	M.H. Bourquin *et al.*	(BRIS, GEVA, HEIDP+)
Also	79	PL 87B 297	M.H. Bourquin *et al.*	(BRIS, GEVA, HEIDP+)
BOURQUIN	79B	PL 88B 192	M.H. Bourquin *et al.*	(BRIS, GEVA, HEIDP+)
BAUBILLIER	78	PL 78B 342	M. Baubillier *et al.*	(BIRM, CERN, GLAS+) J
DEUTSCH...	78	PL 73B 96	M. Deutschmann *et al.*	(AACH3, BERL, CERN+) J
HEMINGWAY	78	NP B142 205	R.J. Hemingway *et al.*	(CERN, ZEEM, NIJM+)
DIBIANCA	75	NP B98 137	F.A. Dibianca, R.J. Endorf	(CMU)
ALVAREZ	73	PR D8 702	L.W. Alvarez	(LBL)
DEUTSCH...	73	NP B61 102	M. Deutschmann *et al.*	(ABCLV Collab.)
FIRESTONE	71B	PRL 26 410	I. Firestone *et al.*	(LRL)
SPETH	69	PL 29B 252	R. Speth *et al.*	(AACH, BERL, CERN, LOIC+)
PALMER	68	PL 26B 323	R.B. Palmer *et al.*	(BNL, SYRA)
SCHULTZ	68	PR 168 1509	P.F. Schultz *et al.*	(ILL, ANL, NWES+)
SCOTTER	68	PL 26B 474	D. Scotter *et al.*	(BIRM, GLAS, LOIC+)
ABRAMS	64	PRL 13 670	G.S. Abrams *et al.*	(UMD, NRL)
BARNES	64	PRL 12 204	V.E. Barnes *et al.*	(BNL)
FRY	55	PR 97 1189	W.F. Fry, J. Schneps, M.S. Swami	(WISC)
FRY	55B	NC 2 346	W.F. Fry, J. Schneps, M.S. Swami	(WISC)
EISENBERG	54	PR 96 541	Y. Eisenberg	(CORN)

$\Omega(2250)^-$

$I(J^P) = 0(?^?)$ Status: ***

$\Omega(2250)^-$ MASS

VALUE (MeV)	EVTS	DOCUMENT ID		TECN	COMMENT
2252 ± 9 OUR AVERAGE					
2253 ± 13	44	ASTON	87B	LASS	K^-p 11 GeV/c
2251 ± 9 ± 8	78	BIAGI	86B	SPEC	SPS Ξ^- beam

$\Omega(2250)^-$ WIDTH

VALUE (MeV)	EVTS	DOCUMENT ID		TECN	COMMENT
55 ± 18 OUR AVERAGE					
81 ± 38	44	ASTON	87B	LASS	K^-p 11 GeV/c
48 ± 20	78	BIAGI	86B	SPEC	SPS Ξ^- beam

$\Omega(2250)^-$ DECAY MODES

	Mode	Fraction (Γ_i/Γ)
Γ_1	$\Xi^-\pi^+K^-$	seen
Γ_2	$\Xi(1530)^0K^-$	seen

$\Omega(2250)^-$ BRANCHING RATIOS

$\Gamma(\Xi(1530)^0K^-)/\Gamma(\Xi^-\pi^+K^-)$ Γ_2/Γ_1

VALUE	EVTS	DOCUMENT ID		TECN	COMMENT
~ 1.0	44	ASTON	87B	LASS	K^-p 11 GeV/c
0.70 ± 0.20	49	BIAGI	86B	SPEC	Ξ^- Be 116 GeV/c

$\Omega(2250)^-$ REFERENCES

ASTON	87B	PL B194 579	D. Aston *et al.*	(SLAC, NAGO, CINC, INUS)
BIAGI	86B	ZPHY C31 33	S.F. Biagi *et al.*	(LOQM, GEVA, RAL+)

$\Omega(2380)^-$

Status: **

OMITTED FROM SUMMARY TABLE

$\Omega(2380)^-$ MASS

VALUE (MeV)	EVTS	DOCUMENT ID		TECN	COMMENT
≈ 2380 OUR ESTIMATE					
2384 ± 9 ± 8	45	BIAGI	86B	SPEC	SPS Ξ^- beam

$\Omega(2380)^-$ WIDTH

VALUE (MeV)	EVTS	DOCUMENT ID		TECN	COMMENT
26 ± 23	45	BIAGI	86B	SPEC	SPS Ξ^- beam

$\Omega(2380)^-$ DECAY MODES

	Mode	Fraction (Γ_i/Γ)
Γ_1	$\Xi^-\pi^+K^-$	
Γ_2	$\Xi(1530)^0K^-$	seen
Γ_3	$\Xi^-\overline{K}^*(892)^0$	

$\Omega(2380)^-$ BRANCHING RATIOS

$\Gamma(\Xi(1530)^0K^-)/\Gamma(\Xi^-\pi^+K^-)$ Γ_2/Γ_1

VALUE	CL%	EVTS	DOCUMENT ID		TECN	COMMENT
< 0.44	90	9	BIAGI	86B	SPEC	Ξ^- Be 116 GeV/c

$\Gamma(\Xi^-\overline{K}^*(892)^0)/\Gamma(\Xi^-\pi^+K^-)$ Γ_3/Γ_1

VALUE	EVTS	DOCUMENT ID		TECN	COMMENT
0.5 ± 0.3	21	BIAGI	86B	SPEC	Ξ^- Be 116 GeV/c

$\Omega(2380)^-$ REFERENCES

BIAGI	86B	ZPHY C31 33	S.F. Biagi *et al.*	(LOQM, GEVA, RAL+)

$\Omega(2470)^-$

Status: **

OMITTED FROM SUMMARY TABLE

A peak in the $\Omega^-\pi^+\pi^-$ mass spectrum with a signal significance claimed to be at least 5.5 standard deviations. There is no reason to seriously doubt the existence of this state, but unless the evidence is overwhelming we usually wait for confirmation from a second experiment before elevating peaks to the Summary Table.

$\Omega(2470)^-$ MASS

VALUE (MeV)	EVTS	DOCUMENT ID		TECN	COMMENT
2474±12	59	ASTON	88G	LASS	K^-p 11 GeV/c

$\Omega(2470)^-$ WIDTH

VALUE (MeV)	EVTS	DOCUMENT ID		TECN	COMMENT
72±33	59	ASTON	88G	LASS	K^-p 11 GeV/c

$\Omega(2470)^-$ DECAY MODES

	Mode
Γ_1	$\Omega^-\pi^+\pi^-$

$\Omega(2470)^-$ REFERENCES

ASTON 88G PL B215 799 D. Aston *et al.* (SLAC, NAGO, CINC, INUS)

See key on page 323

CHARMED BARYONS
($C = +1$)

$\Lambda_c^+ = udc$, $\Sigma_c^{++} = uuc$, $\Sigma_c^+ = udc$, $\Sigma_c^0 = ddc$,
$\Xi_c^+ = usc$, $\Xi_c^0 = dsc$, $\Omega_c^0 = ssc$

CHARMED BARYONS

Revised August 2003 by C.G. Wohl (LBNL).

There are eleven known charmed baryons, each with one c quark.* Figure 1(a) shows the mass spectrum, and for comparison Fig. 1(b) shows the spectrum of the lightest strange baryons. The Λ_c and Σ_c spectra ought to look much like the Λ and Σ spectra, since a Λ_c or a Σ_c is obtained from a Λ or a Σ by changing the s quark to a c quark. However, a Ξ or an Ω has more than one s quark, only *one* of which is changed to a c quark to make a Ξ_c or an Ω_c. Thus the Ξ_c and Ω_c spectra ought to be richer than the Ξ or Ω spectra.**

Before discussing the observed spectra, we review the theory of SU(4) multiplets, which tells us what charmed baryons we should expect to find; this is essential, because the spin-parity values given in Fig. 1(a) have not been measured but have been assigned in accord with expectations of the theory.

SU(4) multiplets—Baryons made from u, d, s, and c quarks belong to SU(4) multiplets. The multiplet numerology, analogous to $3\times3\times3 = 10+8_1+8_2+1$ for the subset of baryons made from just u, d, and s quarks, is $4\times4\times4 = 20+20'_1+20'_2+\bar{4}$. Figure 2(a) shows the 20-plet whose bottom level is an SU(3) decuplet, such as the decuplet that includes the $\Delta(1232)$. Figure 2(b) shows the $20'$-plet whose bottom level is an SU(3) octet, such as the octet that includes the nucleon. Figure 2(c) shows the $\bar{4}$ multiplet, an inverted tetrahedron. One level up in each multiplet are the baryons with one c quark. All the baryons in a given multiplet have the same spin and parity. Each N or Δ or SU(3)-singlet-Λ resonance calls for another $20'$- or 20- or $\bar{4}$-plet, respectively.

The flavor symmetries shown in Fig. 2 are of course very badly broken, but the figure is the simplest way to see what charmed baryons should exist. For example, from Fig. 2(b), we expect to find, in the same $J^P = 1/2^+$ $20'$-plet as the nucleon, a Λ_c, a Σ_c, *two* Ξ_c's, and an Ω_c. Note that this Ω_c is not in the same SU(4) multiplet as the famous $J^P = 3/2^+$ Ω^-.

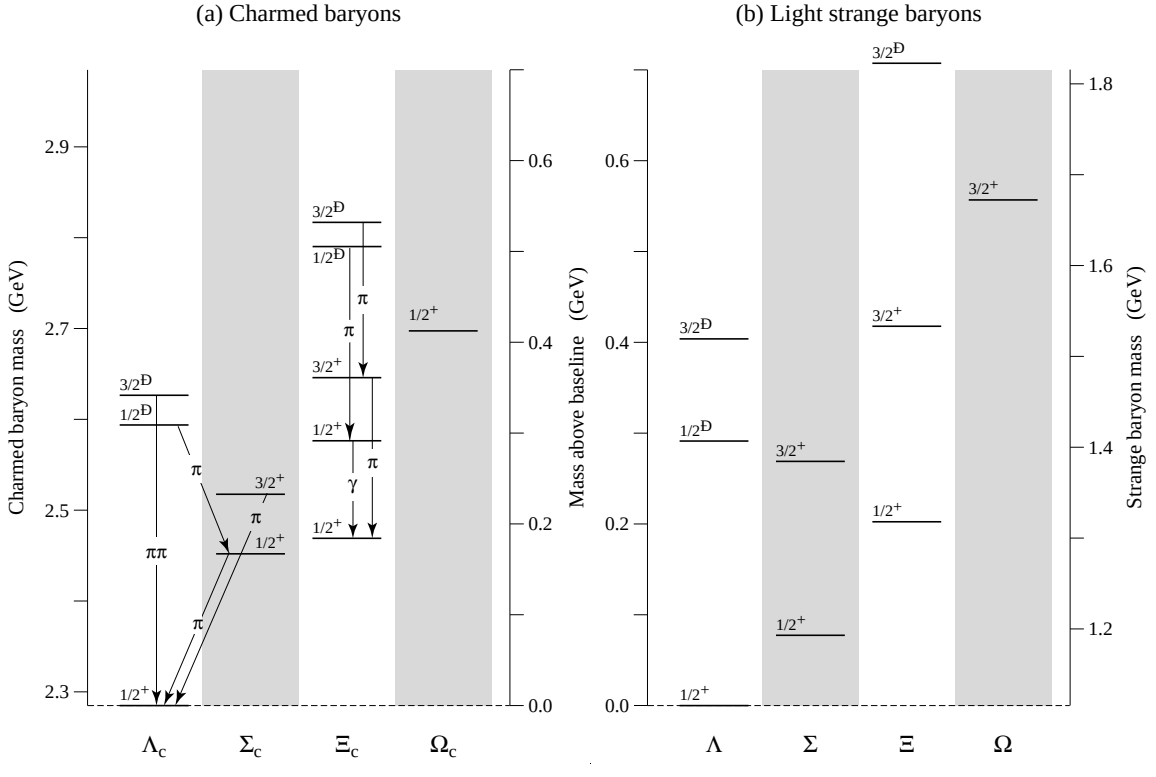

Figure 1. (a) The known charmed baryons, and (b) the lightest strange baryons. The baseline masses are $m(\Lambda_c) = 2284.9$ MeV and $m(\Lambda) = 1115.7$ MeV. Isospin splittings are not shown. Note that there are two $J^P = 1/2^+$ Ξ_c states, and that the Ω_c does not have $J = 3/2$. In fact, none of the J^P values of the charmed baryons has been measured (except perhaps for the $1/2^+\Lambda_c$), but they are all very likely as shown—see the discussion.

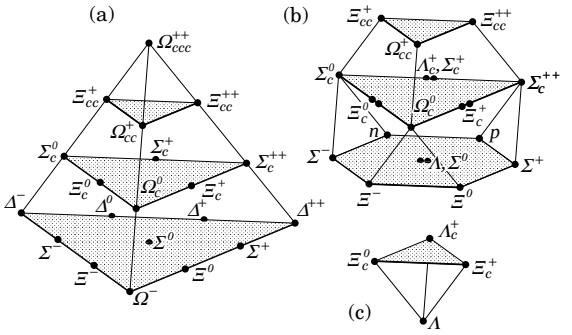

Figure 2: SU(4) multiplets of baryons made of u, d, s, and c quarks. (a) The 20-plet with an SU(3) decuplet on the lowest level. (b) The $20'$-plet with an SU(3) octet on the lowest level. (c) The $\overline{4}$-plet.

Figure 3 shows in more detail the middle level of the $20'$-plet of Fig. 2(b); it splits apart into two SU(3) multiplets, a $\overline{3}$ and a 6. The states of the $\overline{3}$ are antisymmetric under the interchange of the two light quarks (the u, d, and s quarks), whereas the states of the 6 are symmetric under this interchange. We use a prime to distinguish the Ξ_c in the 6 from the one in the $\overline{3}$.

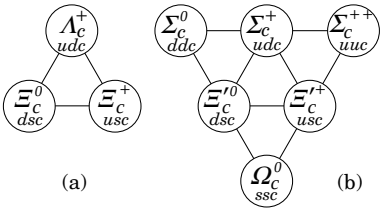

Figure 3: The SU(3) multiplets on the second level of the SU(4) multiplet of Fig. 2(b).

The observed spectra—(1) The parity of the lightest Λ_c is defined to be positive (as are the parities of the p, n, and Λ); the limited evidence about its spin is consistent with $J = 1/2$. However, none of the other J^P quantum numbers given in Fig. 1(a) has been measured. Models using spin-spin and spin-orbit interactions between the quarks, with parameters determined using a few of the masses as input, lead to the J^P assignments shown.† There are no surprises: the $J^P = 1/2^+$ states come first, then the $J^P = 3/2^+$ states ...

(2) There is, however, strong evidence that at least some of the J^P assignments in Fig. 1(a) are correct. As is well known, the successive mass differences between the $J^P = 3/2^+$ particles, the $\Delta(1232)^-$, $\Sigma(1385)^-$, $\Xi(1535)^-$, and Ω^-, which lie along the lower left edge of the 20-plet in Fig. 2(a), should be equal according to SU(3); and indeed experimentally they nearly are. Similarly, the successive mass differences between the $J^P = 1/2^+$ $\Sigma_c(2455)^0$, $\Xi_c'^0$, and Ω_c^0,‡ the particles along the left edge of Fig. 3(b), should be equal—assuming, of course, that they *do* all have the same J^P. And the observed differences are 126.6 ± 3.3 MeV and 118.7 ± 4.1 MeV—not perfect, but close. By the same reasoning, since the mass difference between the presumed $J^P = 3/2^+$ $\Sigma_c(2520)^0$ and $\Xi_c(2645)^0$ is 127.0 ± 2.3 MeV, the $3/2^+$ Ω_c^0 should be at about 2772 MeV.

(3) Other evidence comes from the decay of the $\Lambda_c(2593)$. The only allowed strong decay is $\Lambda_c(2593)^+ \to \Lambda_c^+\pi\pi$, and this appears to be dominated by the submode $\Sigma_c(2455)\pi$, despite little available phase space for the latter (the 'Q' is about 2 MeV, the c.m. decay momentum about 20 MeV/c). Thus the decay is almost certainly s-wave, which, assuming that the $\Sigma_c(2455)$ does indeed have $J^P = 1/2^+$, makes $J^P = 1/2^-$ for the $\Lambda_c(2593)$.

(4) The heavier charmed baryons, such as the $J^P = 1/2^-$ and $3/2^-$ Λ_c's, have much narrower widths than do their strange counterparts, such as the $\Lambda(1405)$ and $\Lambda(1520)$. The clean Λ_c spectrum has in fact been taken to settle the decades-long discussion about the nature of the $\Lambda(1405)$—true 3-quark state or mere $\overline{K}N$ threshold effect?—unambiguously in favor of the first interpretation (which is not to say that the proximity of the $\overline{K}N$ threshold has no effect on the $\Lambda(1405)$). In fact, models of baryon-resonance spectroscopy should now *start* with the narrow charmed baryons, and work back to those broad old resonances.

Footnotes:

* There is evidence for two more baryons with one c quark—a $\Lambda_c(2765)^+$ and a $\Lambda_c(2880)^+$—and for a baryon with *two* c quarks—a Ξ_{cc}^+ at 3519 MeV. However, they have not yet been promoted to the Summary Table. See the Particle Listings.

** For example, there are three Ω_c^0 states (properly symmetrized states of ssc, scs, and css) corresponding to each Ω^- (sss) state.

† This is not the place to discuss the details of the models, nor to attempt a guide to the literature. See the discovery papers of the various charmed baryons for references to the models that lead to the quantum-number assignments.

‡ A reminder about the Particle Data Group naming scheme: A particle that decays strongly has its mass as part of its name; otherwise it doesn't. Thus $\Sigma(1385)$ and $\Sigma_c(2455)$ but Ω^- and Ξ_c'.

Λ_c^+ $I(J^P) = 0(\frac{1}{2}^+)$ Status: ****

The parity of the Λ_c^+ is defined to be positive (as are the parities of the proton, neutron, and Λ). The spin J has not actually been measured yet. Results of an analysis of $pK^-\pi^+$ decays (JEZABEK 92) are consistent with the expected $J = 1/2$. The quark content is udc.

We have omitted some results that have been superseded by later experiments. The omitted results may be found in earlier editions.

Λ_c^+ MASS

Measurements with an error greater than 5 MeV or that are otherwise obsolete have been omitted.

The fit also includes Σ_c–Λ_c^+ and Λ_c^{*+}–Λ_c^+ mass-difference measurements, but this doesn't affect the Λ_c^+ mass.

VALUE (MeV)	EVTS	DOCUMENT ID		TECN	COMMENT
2284.9±0.6 OUR FIT					
2284.9±0.6 OUR AVERAGE					
2284.7±0.6±0.7	1134	AVERY	91	CLEO	Six modes
2281.7±2.7±2.6	29	ALVAREZ	90B	NA14	$pK^-\pi^+$
2285.8±0.6±1.2	101	BARLAG	89	NA32	$pK^-\pi^+$
2284.7±2.3±0.5	5	AGUILAR-...	88B	LEBC	$pK^-\pi^+$
2283.1±1.7±2.0	628	ALBRECHT	88C	ARG	$pK^-\pi^+$, $p\overline{K}^0$, $\Lambda 3\pi$
2286.2±1.7±0.7	97	ANJOS	88B	E691	$pK^-\pi^+$
2281 ±3	2	JONES	87	HBC	$pK^-\pi^+$
2283 ±3	3	BOSETTI	82	HBC	$pK^-\pi^+$
2290 ±3	1	CALICCHIO	80	HYBR	$pK^-\pi^+$

Λ_c^+ MEAN LIFE

Measurements with an error $\geq 100 \times 10^{-15}$ s or with fewer than 20 events have been omitted.

VALUE (10^{-15} s)	EVTS	DOCUMENT ID		TECN	COMMENT
200 ± 6 OUR AVERAGE Error includes scale factor of 1.6. See the ideogram below.					
204.6± 3.4± 2.5	8034	LINK	02C	FOCS	$pK^-\pi^+$
198.1± 7.0± 5.6	1630	KUSHNIR...	01	SELX	$\Lambda_c^+ \to pK^-\pi^+$
179.6± 6.9± 4.4	4749	MAHMOOD	01	CLE2	$e^+e^- \approx \Upsilon(4S)$
215 ±16 ± 8	1340	FRABETTI	93D	E687	γBe, $\Lambda_c^+ \to pK^-\pi^+$
• • • We do not use the following data for averages, fits, limits, etc. • • •					
180 ±30 ±30	29	ALVAREZ	90	NA14	γ, $\Lambda_c^+ \to pK^-\pi^+$
200 ±30 ±30	90	FRABETTI	90	E687	γBe, $\Lambda_c^+ \to pK^-\pi^+$
196 $^{+23}_{-20}$	101	BARLAG	89	NA32	$pK^-\pi^+$ + c.c.
220 ±30 ±20	97	ANJOS	88B	E691	$pK^-\pi^+$ + c.c.

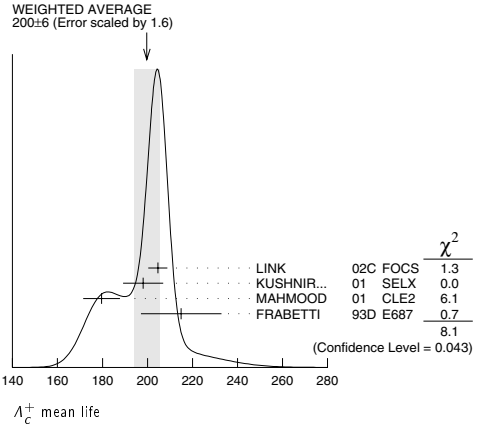

Λ_c^+ mean life

Λ_c^+ DECAY MODES

Nearly all branching fractions of the Λ_c^+ are measured relative to the $pK^-\pi^+$ mode, but there are no model-independent measurements of this branching fraction. We explain how we arrive at our value of $B(\Lambda_c^+ \to pK^-\pi^+)$ in a Note at the beginning of the branching-ratio measurements, below. When this branching fraction is eventually well determined, all the other branching fractions will slide up or down proportionally as the true value differs from the value we use here.

	Mode		Fraction (Γ_i/Γ)	Scale factor/ Confidence level
	Hadronic modes with a p: $S = -1$ final states			
Γ_1	$p\overline{K}^0$		(2.3 ± 0.6) %	
Γ_2	$pK^-\pi^+$	[a]	(5.0 ± 1.3) %	
Γ_3	$p\overline{K}^*(892)^0$	[b]	(1.6 ± 0.5) %	
Γ_4	$\Delta(1232)^{++}K^-$		(8.6 ± 3.0) $\times 10^{-3}$	
Γ_5	$\Lambda(1520)\pi^+$	[b]	(5.9 ± 2.1) $\times 10^{-3}$	
Γ_6	$pK^-\pi^+$ nonresonant		(2.8 ± 0.8) %	
Γ_7	$p\overline{K}^0\pi^0$		(3.3 ± 1.0) %	
Γ_8	$p\overline{K}^0\eta$		(1.2 ± 0.4) %	
Γ_9	$p\overline{K}^0\pi^+\pi^-$		(2.6 ± 0.7) %	
Γ_{10}	$pK^-\pi^+\pi^0$		(3.4 ± 1.0) %	
Γ_{11}	$pK^*(892)^-\pi^+$	[b]	(1.1 ± 0.5) %	
Γ_{12}	$p(K^-\pi^+)_{\text{nonresonant}}\pi^0$		(3.6 ± 1.2) %	
Γ_{13}	$\Delta(1232)\overline{K}^*(892)$		seen	
Γ_{14}	$pK^-\pi^+\pi^+\pi^-$		(1.1 ± 0.8) $\times 10^{-3}$	
Γ_{15}	$pK^-\pi^+\pi^0\pi^0$		(8 ± 4) $\times 10^{-3}$	
Γ_{16}	$pK^-\pi^+\pi^0\pi^0\pi^0$			
	Hadronic modes with a p: $S = 0$ final states			
Γ_{17}	$p\pi^+\pi^-$		(3.5 ± 2.0) $\times 10^{-3}$	
Γ_{18}	$pf_0(980)$	[b]	(2.8 ± 1.9) $\times 10^{-3}$	
Γ_{19}	$p\pi^+\pi^+\pi^-\pi^-$		(1.8 ± 1.2) $\times 10^{-3}$	
Γ_{20}	pK^+K^-		(7.7 ± 3.5) $\times 10^{-4}$	
Γ_{21}	$p\phi$	[b]	(8.2 ± 2.7) $\times 10^{-4}$	
Γ_{22}	pK^+K^- non-ϕ		(3.5 ± 1.7) $\times 10^{-4}$	
	Hadronic modes with a hyperon: $S = -1$ final states			
Γ_{23}	$\Lambda\pi^+$		(9.0 ± 2.8) $\times 10^{-3}$	
Γ_{24}	$\Lambda\pi^+\pi^0$		(3.6 ± 1.3) %	
Γ_{25}	$\Lambda\rho^+$		< 5 %	CL=95%
Γ_{26}	$\Lambda\pi^+\pi^+\pi^-$		(3.3 ± 1.0) %	
Γ_{27}	$\Lambda\pi^+\pi^+\pi^-\pi^0$ total		(1.8 ± 0.8) %	
Γ_{28}	$\Lambda\pi^+\eta$		(1.8 ± 0.6) %	
Γ_{29}	$\Sigma(1385)^+\eta$	[b]	(8.5 ± 3.3) $\times 10^{-3}$	
Γ_{30}	$\Lambda\pi^+\omega$	[b]	(1.2 ± 0.5) %	
Γ_{31}	$\Lambda\pi^+\pi^+\pi^-\pi^0$, no η or ω		< 7 $\times 10^{-3}$	CL=90%
Γ_{32}	$\Lambda K^+\overline{K}^0$		(6.0 ± 2.1) $\times 10^{-3}$	
Γ_{33}	$\Xi(1690)^0K^+$, $\Xi(1690)^0 \to \Lambda\overline{K}^0$		(1.6 ± 0.8) $\times 10^{-3}$	
Γ_{34}	$\Sigma^0\pi^+$		(9.9 ± 3.2) $\times 10^{-3}$	
Γ_{35}	$\Sigma^+\pi^0$		(1.00 ± 0.34) %	
Γ_{36}	$\Sigma^+\eta$		(5.5 ± 2.3) $\times 10^{-3}$	
Γ_{37}	$\Sigma^+\pi^+\pi^-$		(3.6 ± 1.0) %	
Γ_{38}	$\Sigma^+\rho^0$		< 1.4 %	CL=95%
Γ_{39}	$\Sigma^-\pi^+\pi^+$		(1.9 ± 0.8) %	
Γ_{40}	$\Sigma^0\pi^+\pi^0$		(1.8 ± 0.8) %	
Γ_{41}	$\Sigma^0\pi^+\pi^+\pi^-$		(1.1 ± 0.4) %	
Γ_{42}	$\Sigma^+\pi^+\pi^-\pi^0$		—	
Γ_{43}	$\Sigma^+\omega$	[b]	(2.7 ± 1.0) %	
Γ_{44}	$\Sigma^+K^+K^-$		(2.8 ± 0.8) $\times 10^{-3}$	
Γ_{45}	$\Sigma^+\phi$	[b]	(3.2 ± 1.0) $\times 10^{-3}$	
Γ_{46}	$\Xi(1690)^0K^+$, $\Xi(1690)^0 \to \Sigma^+K^-$		(8.2 ± 3.1) $\times 10^{-4}$	
Γ_{47}	$\Sigma^+K^+K^-$ nonresonant		< 7 $\times 10^{-4}$	CL=90%
Γ_{48}	Ξ^0K^+		(3.9 ± 1.4) $\times 10^{-3}$	
Γ_{49}	$\Xi^-K^+\pi^+$		(4.9 ± 1.7) $\times 10^{-3}$	
Γ_{50}	$\Xi(1530)^0K^+$	[b]	(2.6 ± 1.0) $\times 10^{-3}$	
	Hadronic modes with a hyperon: $S = 0$ final states			
Γ_{51}	ΛK^+		(6.7 ± 2.5) $\times 10^{-4}$	
Γ_{52}	Σ^0K^+		(5.6 ± 2.4) $\times 10^{-4}$	
Γ_{53}	$\Sigma^+K^+\pi^-$		(1.7 ± 0.7) $\times 10^{-3}$	
Γ_{54}	$\Sigma^+K^*(892)^0$	[b]	(2.8 ± 1.1) $\times 10^{-3}$	
Γ_{55}	$\Sigma^-K^+\pi^+$		< 1.0 $\times 10^{-3}$	CL=90%
	Semileptonic modes			
Γ_{56}	$\Lambda\ell^+\nu_\ell$	[c]	(2.0 ± 0.6) %	
Γ_{57}	$\Lambda e^+\nu_e$		(2.1 ± 0.6) %	
Γ_{58}	$\Lambda\mu^+\nu_\mu$		(2.0 ± 0.7) %	

Inclusive modes

Γ_{59}	e^+ anything	(4.5 ± 1.7) %		
Γ_{60}	pe^+ anything	(1.8 ± 0.9) %		
Γ_{61}	Λe^+ anything			
Γ_{62}	p anything	(50 ±16) %		
Γ_{63}	p anything (no Λ)	(12 ±19) %		
Γ_{64}	p hadrons			
Γ_{65}	n anything	(50 ±16) %		
Γ_{66}	n anything (no Λ)	(29 ±17) %		
Γ_{67}	Λ anything	(35 ±11) %		S=1.4
Γ_{68}	$\Sigma^\pm$ anything	[d] (10 ± 5) %		
Γ_{69}	3prongs	(24 ± 8) %		

$\Delta C = 1$ weak neutral current ($C1$) modes, or Lepton number (L) violating modes

Γ_{70}	$p\mu^+\mu^-$	$C1$	< 3.4	$\times 10^{-4}$	CL=90%
Γ_{71}	$\Sigma^-\mu^+\mu^+$	L	< 7.0	$\times 10^{-4}$	CL=90%

[a] See the note on "Λ_c^+ Branching Fractions" below.

[b] This branching fraction includes all the decay modes of the final-state resonance.

[c] An ℓ indicates an e or a μ mode, not a sum over these modes.

[d] The value is for the sum of the charge states or particle/antiparticle states indicated.

CONSTRAINED FIT INFORMATION

An overall fit to 6 branching ratios uses 9 measurements and one constraint to determine 5 parameters. The overall fit has a χ^2 = 2.1 for 5 degrees of freedom.

The following *off-diagonal* array elements are the correlation coefficients $\langle \delta x_i \delta x_j \rangle / (\delta x_i \cdot \delta x_j)$, in percent, from the fit to the branching fractions, $x_i \equiv \Gamma_i/\Gamma_{\rm total}$. The fit constrains the x_i whose labels appear in this array to sum to one.

x_{37}	91		
x_{44}	87	93	
x_{45}	84	90	84
	x_2	x_{37}	x_{44}

Λ_c^+ BRANCHING FRACTIONS

Revised 2002 by P.R. Burchat (Stanford University).

Most Λ_c^+ branching fractions are measured relative to the decay mode $\Lambda_c^+ \to pK^-\pi^+$. However, there are no completely model-independent measurements of the absolute branching fraction for $\Lambda_c^+ \to pK^-\pi^+$. Here we describe the measurements that have been used to extract $\mathrm{B}(\Lambda_c^+ \to pK^-\pi^+)$, the model-dependence of the results, and the method we have used to average the results.

ARGUS (ALBRECHT 88C) and CLEO (CRAWFORD 92) measure $\mathrm{B}(\overline{B} \to \Lambda_c^+ \mathrm{X}) \cdot \mathrm{B}(\Lambda_c^+ \to pK^-\pi^+)$ to be $(0.30 \pm 0.12 \pm 0.06)\%$ and $(0.273 \pm 0.051 \pm 0.039)\%$. Under the assumptions that decays of $\overline{B}$ mesons to baryons are dominated by $\overline{B} \to \Lambda_c^+ \mathrm{X}$ and that $\Lambda_c^+ \mathrm{X}$ final states other than $\Lambda_c^+ \overline{N} \mathrm{X}$ can be neglected, they also measure $\mathrm{B}(\overline{B} \to \Lambda_c^+ \mathrm{X})$ to be $(6.8 \pm 0.5 \pm 0.3)\%$ (ALBRECHT 92O) and $(6.4 \pm 0.8 \pm 0.8)\%$ (CRAWFORD 92). Combining these results, we get $\mathrm{B}(\Lambda_c^+ \to pK^-\pi^+) = (4.14 \pm 0.91)\%$. However, the assumption that $\overline{B}$ decay modes to baryons other than $\Lambda_c^+ \overline{N} \mathrm{X}$ are negligible is not on solid ground experimentally or theoretically [2]. Therefore, the branching fraction for $\Lambda_c^+ \to pK^-\pi^+$ given above may be low by some undetermined amount.

A second type of model-dependent determination of $\mathrm{B}(\Lambda_c^+ \to pK^-\pi^+)$ is based on measurements by ARGUS (ALBRECHT 91G) and CLEO (BERGFELD 94) of $\sigma(e^+e^- \to \Lambda_c^+ \mathrm{X}) \cdot \mathrm{B}(\Lambda_c^+ \to \Lambda \ell^+ \nu_\ell) = (4.15 \pm 1.03 \pm 1.18)$ pb and $(4.77 \pm 0.25 \pm 0.66)$ pb. ARGUS (ALBRECHT 96E) and CLEO (AVERY 91) have also measured $\sigma(e^+e^- \to \Lambda_c^+ \mathrm{X}) \cdot \mathrm{B}(\Lambda_c^+ \to pK^-\pi^+)$. The weighted average is (11.2 ± 1.3) pb.

From these measurements, we extract $R \equiv \mathrm{B}(\Lambda_c^+ \to pK^-\pi^+)/\mathrm{B}(\Lambda_c^+ \to \Lambda \ell^+ \nu_\ell) = 2.40 \pm 0.43$. We estimate the $\Lambda_c^+ \to pK^-\pi^+$ branching fraction from the equation

$$\mathrm{B}(\Lambda_c^+ \to pK^-\pi^+) = R\, f\, F\, \frac{\Gamma(D \to \mathrm{X}\ell^+\nu_\ell)}{1 + |V_{cd}/V_{cs}|^2} \cdot \tau(\Lambda_c^+) \ , \quad (1)$$

where $f = \mathrm{B}(\Lambda_c^+ \to \Lambda \ell^+ \nu_\ell)/\mathrm{B}(\Lambda_c^+ \to X_s \ell^+ \nu_\ell)$ and $F = \Gamma(\Lambda_c^+ \to X_s \ell^+ \nu_\ell)/\Gamma(D^0 \to X_s \ell^+ \nu_\ell)$. When we use $1 + |V_{cd}/V_{cs}|^2 = 1.05$ and the world averages $\Gamma(D \to \mathrm{X}\ell^+\nu_\ell) = (0.166 \pm 0.006) \times 10^{12}\ \mathrm{s}^{-1}$ and $\tau(\Lambda_c^+) = (0.192 \pm 0.005) \times 10^{-12}$ s, we calculate $\mathrm{B}(\Lambda_c^+ \to pK^-\pi^+) = (7.3 \pm 1.4)\% \cdot f\, F$. Theoretical estimates for f and F are near 1.0 with significant uncertainties.

So, we have two results with significant model-dependence: $\mathrm{B}(\Lambda_c^+ \to pK^-\pi^+) = (4.14 \pm 0.91)\%$ from $\overline{B}$ decays, and $\mathrm{B}(\Lambda_c^+ \to pK^-\pi^+) = (7.3 \pm 1.4)\% \cdot f\, F$ from semileptonic Λ_c^+ decays. If we set $f\, F = 1.0$ in the second result, and assign an uncertainty of 30% to each result to account for the unknown model-dependence, we get the consistent results $\mathrm{B}(\Lambda_c^+ \to pK^-\pi^+) = (4.14 \pm 0.91 \pm 1.24)\%$ and $\mathrm{B}(\Lambda_c^+ \to pK^-\pi^+) = (7.3 \pm 1.4 \pm 2.2)\%$. The weighted average of these two results is $\mathrm{B}(\Lambda_c^+ \to pK^-\pi^+) = (5.0 \pm 1.3)\%$, where the uncertainty contains both the experimental uncertainty and the 30% estimate of model dependence in each result. We assigned the value $(5.0 \pm 1.3)\%$ to the $\Lambda_c^+ \to pK^-\pi^+$ branching fraction in our 2000 *Review* [1].

A third type of measurement of $\mathrm{B}(\Lambda_c^+ \to pK^-\pi^+)$ has been published by CLEO (JAFFE 00). Under the assumption that a $\overline{D}$ meson and an antiproton in opposite hemispheres is evidence for a Λ_c^+ in the hemisphere of the $\overline{p}$, the fraction of such $\overline{D}\,\overline{p}$ events with a $\Lambda_c^+ \to pK^-\pi^+$ decay can be used to determine the $\Lambda_c^+ \to pK^-\pi^+$ branching fraction. CLEO measures $\mathrm{B}(\Lambda_c^+ \to pK^-\pi^+) = (5.0 \pm 1.3)\%$, which is coincidentally exactly the same value as our PDG 00 average given above. The quoted uncertainty includes significant contributions from model-dependent effects (*e.g.,* differences between the $\overline{p}$ momentum spectrum in events with a Λ_c^+ and $\overline{p}$ in the same hemisphere, and with a $\overline{D}$ and $\overline{p}$ in opposite hemispheres; extrapolation of the Λ_c^+ and $\overline{D}$ momentum spectrum below the minimum value used for rejecting B decay products; and our limited understanding of backgrounds such as $D\overline{D}N\overline{p}$ events).

We have chosen to continue to assign the value $(5.0 \pm 1.3)\%$ to the $\Lambda_c^+ \to pK^-\pi^+$ branching fraction (given as PDG 02 below). As was noted earlier, most of the other Λ_c^+ decay modes are measured relative to this mode.

New methods for measuring the Λ_c^+ absolute branching fractions have been proposed [2,3].

References

1. D.E. Groom *et al.* (Particle Data Group), *Review of Particle Physics*, Eur. Phys. J. **C15**, 1 (2000).
2. I. Dunietz, Phys. Rev. **D58**, 094010 (1998).
3. P. Migliozzi *et al.*, Phys. Lett. **B462**, 217 (1999).

Λ_c^+ BRANCHING RATIOS

Hadronic modes with a p: $S = -1$ final states

$\Gamma(p\overline{K}^0)/\Gamma(pK^-\pi^+)$ Γ_1/Γ_2

VALUE	EVTS	DOCUMENT ID		TECN	COMMENT
0.47 ± 0.04 OUR AVERAGE					
0.46 ± 0.02 ± 0.04	1025	ALAM	98	CLE2	$e^+e^- \approx \Upsilon(4S)$
0.44 ± 0.07 ± 0.05	133	AVERY	91	CLEO	e^+e^- 10.5 GeV
0.55 ± 0.17 ± 0.14	45	ANJOS	90	E691	γBe 70–260 GeV
0.62 ± 0.15 ± 0.03	73	ALBRECHT	88C	ARG	e^+e^- 10 GeV

$\Gamma(pK^-\pi^+)/\Gamma_{total}$ Γ_2/Γ

See the note on "Λ_c^+ Branching Fractions" above.

VALUE	EVTS	DOCUMENT ID		TECN	COMMENT
0.050 ± 0.013 OUR FIT					
0.050 ± 0.013		PDG	02		See note at top of ratios
• • • We do not use the following data for averages, fits, limits, etc. • • •					
0.050 ± 0.005 ± 0.012	1205	[1] JAFFE	00	CLE2	e^+e^- 10.52–10.58 GeV
0.041 ± 0.010		[2,3] ALBRECHT	92O	ARG	$e^+e^- \approx \Upsilon(4S)$
0.044 ± 0.012		[2,4] CRAWFORD	92	CLEO	e^+e^- 10.5 GeV

[1] JAFFE 00 assumes that a $\overline{D}$ meson and an antiproton in opposite hemispheres tags for a Λ_c^+ in the hemisphere of the $\overline{p}$. The fraction of such $\overline{D}p$ events with a $\Lambda_c^+ \to pK^-\pi^+$ decay then gives the $pK^-\pi^+$ branching fraction. See the paper for assumptions, caveats, etc.

[2] To extract $\Gamma(pK^-\pi^+)/\Gamma_{total}$, we use $B(\overline{B} \to \Lambda_c^+ X)\cdot B(\Lambda_c^+ \to pK^-\pi^+) = (0.28 \pm 0.06)\%$, which is the average of measurements from ARGUS (ALBRECHT 88C) and CLEO (CRAWFORD 92).

[3] ALBRECHT 92O measures $B(\overline{B} \to \Lambda_c^+ X) = (6.8 \pm 0.5 \pm 0.3)\%$.

[4] CRAWFORD 92 measures $B(\overline{B} \to \Lambda_c^+ X) = (6.4 \pm 0.8 \pm 0.8)\%$.

$\Gamma(p\overline{K}^*(892)^0)/\Gamma(pK^-\pi^+)$ Γ_3/Γ_2

Unseen decay modes of the $\overline{K}^*(892)^0$ are included.

VALUE	EVTS	DOCUMENT ID		TECN	COMMENT
0.31 ± 0.04 OUR AVERAGE					
0.29 ± 0.04 ± 0.03		[5] AITALA	00	E791	π^- N, 500 GeV
$0.35^{+0.06}_{-0.07} \pm 0.03$	39	BOZEK	93	NA32	π^- Cu 230 GeV
0.42 ± 0.24	12	BASILE	81B	CNTR	$pp \to \Lambda_c^+ e^- X$
• • • We do not use the following data for averages, fits, limits, etc. • • •					
0.35 ± 0.11		BARLAG	90D	NA32	See BOZEK 93

[5] AITALA 00 makes a coherent 5-dimensional amplitude analysis of 946 ± 38 $\Lambda_c^+ \to pK^-\pi^+$ decays.

$\Gamma(\Delta(1232)^{++}K^-)/\Gamma(pK^-\pi^+)$ Γ_4/Γ_2

VALUE	EVTS	DOCUMENT ID		TECN	COMMENT
0.17 ± 0.04 OUR AVERAGE Error includes scale factor of 1.1.					
0.18 ± 0.03 ± 0.03		[6] AITALA	00	E791	π^- N, 500 GeV
$0.12^{+0.04}_{-0.05} \pm 0.05$	14	BOZEK	93	NA32	π^- Cu 230 GeV
0.40 ± 0.17	17	BASILE	81B	CNTR	$pp \to \Lambda_c^+ e^- X$

[6] AITALA 00 makes a coherent 5-dimensional amplitude analysis of 946 ± 38 $\Lambda_c^+ \to pK^-\pi^+$ decays.

$\Gamma(\Lambda(1520)\pi^+)/\Gamma(pK^-\pi^+)$ Γ_5/Γ_2

Unseen decay modes of the $\Lambda(1520)$ are included.

VALUE	EVTS	DOCUMENT ID		TECN	COMMENT
$\mathbf{0.119^{+0.032}_{-0.028}}$ **OUR AVERAGE**					
$0.15 \pm 0.04 \pm 0.02$		[7] AITALA	00	E791	π^- N, 500 GeV
$0.09^{+0.04}_{-0.03} \pm 0.02$	12	BOZEK	93	NA32	π^- Cu 230 GeV

[7] AITALA 00 makes a coherent 5-dimensional amplitude analysis of 946 ± 38 $\Lambda_c^+ \to pK^-\pi^+$ decays.

$\Gamma(pK^-\pi^+\text{nonresonant})/\Gamma(pK^-\pi^+)$ Γ_6/Γ_2

VALUE	EVTS	DOCUMENT ID		TECN	COMMENT
0.55 ± 0.06 OUR AVERAGE					
0.55 ± 0.06 ± 0.04		[8] AITALA	00	E791	π^- N, 500 GeV
$0.56^{+0.07}_{-0.09} \pm 0.05$	71	BOZEK	93	NA32	π^- Cu 230 GeV

[8] AITALA 00 makes a coherent 5-dimensional amplitude analysis of 946 ± 38 $\Lambda_c^+ \to pK^-\pi^+$ decays.

$\Gamma(p\overline{K}^0\pi^0)/\Gamma(pK^-\pi^+)$ Γ_7/Γ_2

VALUE	EVTS	DOCUMENT ID		TECN	COMMENT
0.66 ± 0.05 ± 0.07	774	ALAM	98	CLE2	$e^+e^- \approx \Upsilon(4S)$

$\Gamma(p\overline{K}^0\eta)/\Gamma(pK^-\pi^+)$ Γ_8/Γ_2

Unseen decay modes of the η are included.

VALUE	EVTS	DOCUMENT ID		TECN	COMMENT
0.25 ± 0.04 ± 0.04	57	AMMAR	95	CLE2	$e^+e^- \approx \Upsilon(4S)$

$\Gamma(p\overline{K}^0\pi^+\pi^-)/\Gamma(pK^-\pi^+)$ Γ_9/Γ_2

VALUE	EVTS	DOCUMENT ID		TECN	COMMENT
0.51 ± 0.06 OUR AVERAGE					
0.52 ± 0.04 ± 0.05	985	ALAM	98	CLE2	$e^+e^- \approx \Upsilon(4S)$
0.43 ± 0.12 ± 0.04	83	AVERY	91	CLEO	e^+e^- 10.5 GeV
0.98 ± 0.36 ± 0.08	12	BARLAG	90D	NA32	π^- 230 GeV

$\Gamma(pK^-\pi^+\pi^0)/\Gamma(pK^-\pi^+)$ Γ_{10}/Γ_2

VALUE	EVTS	DOCUMENT ID		TECN	COMMENT
0.67 ± 0.04 ± 0.11	2606	ALAM	98	CLE2	$e^+e^- \approx \Upsilon(4S)$

$\Gamma(pK^*(892)^-\pi^+)/\Gamma(p\overline{K}^0\pi^+\pi^-)$ Γ_{11}/Γ_9

Unseen decay modes of the $K^*(892)^-$ are included.

VALUE	EVTS	DOCUMENT ID		TECN	COMMENT
0.44 ± 0.14	17	ALEEV	94	BIS2	nN 20–70 GeV

$\Gamma(pK^-\pi^+)_{nonresonant}\pi^0)/\Gamma(pK^-\pi^+)$ Γ_{12}/Γ_2

VALUE	EVTS	DOCUMENT ID		TECN	COMMENT
0.73 ± 0.12 ± 0.05	67	BOZEK	93	NA32	π^- Cu 230 GeV

$\Gamma(\Delta(1232)\overline{K}^*(892))/\Gamma_{total}$ Γ_{13}/Γ

VALUE	EVTS	DOCUMENT ID		TECN	COMMENT
seen	35	AMENDOLIA	87	SPEC	γGe-Si

$\Gamma(pK^-\pi^+\pi^+\pi^-)/\Gamma(pK^-\pi^+)$ Γ_{14}/Γ_2

VALUE	EVTS	DOCUMENT ID		TECN	COMMENT
0.022 ± 0.015		BARLAG	90D	NA32	π^- 230 GeV

$\Gamma(pK^-\pi^+\pi^0\pi^0)/\Gamma(pK^-\pi^+)$ Γ_{15}/Γ_2

VALUE	EVTS	DOCUMENT ID		TECN	COMMENT
0.16 ± 0.07 ± 0.03	15	BOZEK	93	NA32	π^- Cu 230 GeV

$\Gamma(pK^-\pi^+\pi^0\pi^0\pi^0)/\Gamma(pK^-\pi^+)$ Γ_{16}/Γ_2

VALUE	EVTS	DOCUMENT ID		TECN	COMMENT
• • • We do not use the following data for averages, fits, limits, etc. • • •					
0.10 ± 0.06 ± 0.02	8	BOZEK	93	NA32	π^- Cu 230 GeV

Hadronic modes with a p: $S = 0$ final states

$\Gamma(p\pi^+\pi^-)/\Gamma(pK^-\pi^+)$ Γ_{17}/Γ_2

VALUE	EVTS	DOCUMENT ID		TECN	COMMENT
0.069 ± 0.036		BARLAG	90D	NA32	π^- 230 GeV

$\Gamma(pf_0(980))/\Gamma(pK^-\pi^+)$ Γ_{18}/Γ_2

Unseen decay modes of the $f_0(980)$ are included.

VALUE	EVTS	DOCUMENT ID		TECN	COMMENT
0.055 ± 0.036		BARLAG	90D	NA32	π^- 230 GeV

$\Gamma(p\pi^+\pi^+\pi^-\pi^-)/\Gamma(pK^-\pi^+)$ Γ_{19}/Γ_2

VALUE	EVTS	DOCUMENT ID		TECN	COMMENT
0.036 ± 0.023		BARLAG	90D	NA32	π^- 230 GeV

$\Gamma(pK^+K^-)/\Gamma(pK^-\pi^+)$ Γ_{20}/Γ_2

VALUE	EVTS	DOCUMENT ID		TECN	COMMENT
0.015 ± 0.006 OUR AVERAGE Error includes scale factor of 2.1.					
0.014 ± 0.002 ± 0.002	676	ABE	02C	BELL	$e^+e^- \approx \Upsilon(4S)$
0.039 ± 0.009 ± 0.007	214	ALEXANDER	96C	CLE2	$e^+e^- \approx \Upsilon(4S)$
• • • We do not use the following data for averages, fits, limits, etc. • • •					
0.096 ± 0.029 ± 0.010	30	FRABETTI	93H	E687	γBe, $\overline{E}_\gamma$ 220 GeV
0.048 ± 0.027		BARLAG	90D	NA32	π^- 230 GeV

$\Gamma(p\phi)/\Gamma(pK^-\pi^+)$ Γ_{21}/Γ_2

Unseen decay modes of the ϕ are included.

VALUE	EVTS	DOCUMENT ID		TECN	COMMENT
0.0164 ± 0.0032 OUR AVERAGE Error includes scale factor of 1.2.					
0.015 ± 0.002 ± 0.002	345	ABE	02C	BELL	$e^+e^- \approx \Upsilon(4S)$
0.024 ± 0.006 ± 0.003	54	ALEXANDER	96C	CLE2	$e^+e^- \approx \Upsilon(4S)$
• • • We do not use the following data for averages, fits, limits, etc. • • •					
0.040 ± 0.027		BARLAG	90D	NA32	π^- 230 GeV

$\Gamma(p\phi)/\Gamma(pK^+K^-)$ Γ_{21}/Γ_{20}

Unseen decay modes of the ϕ are included.

VALUE	CL%	DOCUMENT ID		TECN	COMMENT
• • • We do not use the following data for averages, fits, limits, etc. • • •					
< 0.58	90	FRABETTI	93H	E687	γBe, $\overline{E}_\gamma$ 220 GeV

$\Gamma(pK^+K^-\text{non-}\phi)/\Gamma(pK^-\pi^+)$ Γ_{22}/Γ_2

VALUE	EVTS	DOCUMENT ID		TECN	COMMENT
0.007 ± 0.002 ± 0.002	344	ABE	02C	BELL	$e^+e^- \approx \Upsilon(4S)$

Hadronic modes with a hyperon: $S = -1$ final states

$\Gamma(\Lambda\pi^+)/\Gamma(pK^-\pi^+)$ Γ_{23}/Γ_2

VALUE	CL%	EVTS	DOCUMENT ID		TECN	COMMENT
0.180 ± 0.032 OUR AVERAGE						
0.18 ± 0.03 ± 0.04			ALBRECHT	92	ARG	e^+e^- ≈ 10.4 GeV
0.18 ± 0.03 ± 0.03		87	AVERY	91	CLEO	e^+e^- 10.5 GeV
• • • We do not use the following data for averages, fits, limits, etc. • • •						
< 0.33	90		ANJOS	90	E691	γBe 70–260 GeV
< 0.16	90		ALBRECHT	88C	ARG	e^+e^- 10 GeV

$\Gamma(\Lambda\pi^+\pi^0)/\Gamma(pK^-\pi^+)$ Γ_{24}/Γ_2

VALUE	EVTS	DOCUMENT ID		TECN	COMMENT
0.73 ± 0.09 ± 0.16	464	AVERY	94	CLE2	e^+e^- ≈ $\Upsilon(3S), \Upsilon(4S)$

$\Gamma(\Lambda\rho^+)/\Gamma(pK^-\pi^+)$ Γ_{25}/Γ_2

VALUE	CL%	DOCUMENT ID		TECN	COMMENT
< 0.95	95	AVERY	94	CLE2	e^+e^- ≈ $\Upsilon(3S), \Upsilon(4S)$

$\Gamma(\Lambda\pi^+\pi^+\pi^-)/\Gamma(pK^-\pi^+)$ Γ_{26}/Γ_2

VALUE	EVTS	DOCUMENT ID		TECN	COMMENT
0.66 ± 0.11 OUR AVERAGE					
0.65 ± 0.11 ± 0.12	289	AVERY	91	CLEO	e^+e^- 10.5 GeV
0.82 ± 0.29 ± 0.27	44	ANJOS	90	E691	γBe 70–260 GeV
0.94 ± 0.41 ± 0.13	10	BARLAG	90D	NA32	π^- 230 GeV
0.61 ± 0.16 ± 0.04	105	ALBRECHT	88C	ARG	e^+e^- 10 GeV

$\Gamma(p\overline{K}^0\pi^+\pi^-)/\Gamma(\Lambda\pi^+\pi^+\pi^-)$ Γ_9/Γ_{26}

VALUE	EVTS	DOCUMENT ID		TECN	COMMENT
• • • We do not use the following data for averages, fits, limits, etc. • • •					
2.6 ± 1.2		ALEEV	96	SPEC	n nucleus, 50 GeV/c
4.3 ± 1.2	130	ALEEV	84	BIS2	nC 40–70 GeV

$\Gamma(\Lambda\pi^+\pi^+\pi^-\pi^0\text{total})/\Gamma(pK^-\pi^+)$ Γ_{27}/Γ_2

VALUE	EVTS	DOCUMENT ID		TECN	COMMENT
0.36 ± 0.09 ± 0.09	50	[9] CRONIN-HEN..03		CLE3	e^+e^- ≈ $\Upsilon(4S)$

[9] CRONIN-HENNESSY 03 finds this channel to be dominately $\Lambda\eta\pi^+$ and $\Lambda\omega\pi^+$; see below.

$\Gamma(\Lambda\pi^+\eta)/\Gamma(pK^-\pi^+)$ Γ_{28}/Γ_2

Unseen decay modes of the η are included.

VALUE	EVTS	DOCUMENT ID		TECN	COMMENT
0.36 ± 0.07 OUR AVERAGE					
0.41 ± 0.17 ± 0.10	11	CRONIN-HEN..03		CLE3	e^+e^- ≈ $\Upsilon(4S)$
0.35 ± 0.05 ± 0.06	116	AMMAR	95	CLE2	e^+e^- ≈ $\Upsilon(4S)$

$\Gamma(\Sigma(1385)^+\eta)/\Gamma(pK^-\pi^+)$ Γ_{29}/Γ_2

Unseen decay modes of the $\Sigma(1385)^+$ are included.

VALUE	EVTS	DOCUMENT ID		TECN	COMMENT
0.17 ± 0.04 ± 0.03	54	AMMAR	95	CLE2	e^+e^- ≈ $\Upsilon(4S)$

$\Gamma(\Lambda\pi^+\omega)/\Gamma(pK^-\pi^+)$ Γ_{30}/Γ_2

Unseen decay modes of the ω are included.

VALUE	EVTS	DOCUMENT ID		TECN	COMMENT
0.24 ± 0.06 ± 0.06	32	CRONIN-HEN..03		CLE3	e^+e^- ≈ $\Upsilon(4S)$

$\Gamma(\Lambda\pi^+\pi^+\pi^-\pi^0, \text{no}\,\eta\,\text{or}\,\omega)/\Gamma(pK^-\pi^+)$ Γ_{31}/Γ_2

VALUE	CL%	DOCUMENT ID		TECN	COMMENT
< 0.13	90	CRONIN-HEN..03		CLE3	e^+e^- ≈ $\Upsilon(4S)$

$\Gamma(\Lambda K^+\overline{K}^0)/\Gamma(pK^-\pi^+)$ Γ_{32}/Γ_2

VALUE	EVTS	DOCUMENT ID		TECN	COMMENT
0.12 ± 0.02 ± 0.02	59	AMMAR	95	CLE2	e^+e^- ≈ $\Upsilon(4S)$

$\Gamma(\Xi(1690)^0K^+, \Xi(1690)^0 \to \Lambda\overline{K}^0)/\Gamma(\Lambda K^+\overline{K}^0)$ Γ_{33}/Γ_{32}

VALUE	EVTS	DOCUMENT ID		TECN	COMMENT
0.26 ± 0.08 ± 0.03	93	ABE	02C	BELL	e^+e^- ≈ $\Upsilon(4S)$

$\Gamma(\Sigma^0\pi^+)/\Gamma(pK^-\pi^+)$ Γ_{34}/Γ_2

VALUE	EVTS	DOCUMENT ID		TECN	COMMENT
0.20 ± 0.04 OUR AVERAGE					
0.21 ± 0.02 ± 0.04	196	AVERY	94	CLE2	e^+e^- ≈ $\Upsilon(3S), \Upsilon(4S)$
0.17 ± 0.06 ± 0.04		ALBRECHT	92	ARG	e^+e^- ≈ 10.4 GeV

$\Gamma(\Sigma^+\pi^0)/\Gamma(pK^-\pi^+)$ Γ_{35}/Γ_2

VALUE	EVTS	DOCUMENT ID		TECN	COMMENT
0.20 ± 0.03 ± 0.03	93	KUBOTA	93	CLE2	e^+e^- ≈ $\Upsilon(4S)$

$\Gamma(\Sigma^+\eta)/\Gamma(pK^-\pi^+)$ Γ_{36}/Γ_2

VALUE	EVTS	DOCUMENT ID		TECN	COMMENT
0.11 ± 0.03 ± 0.02	26	AMMAR	95	CLE2	e^+e^- ≈ $\Upsilon(4S)$

$\Gamma(\Sigma^+\pi^+\pi^-)/\Gamma(pK^-\pi^+)$ Γ_{37}/Γ_2

VALUE	EVTS	DOCUMENT ID		TECN	COMMENT
0.73 ± 0.08 OUR FIT					
0.68 ± 0.09 OUR AVERAGE					
0.74 ± 0.07 ± 0.09	487	KUBOTA	93	CLE2	e^+e^- ≈ $\Upsilon(4S)$
$0.54^{+0.18}_{-0.15}$	11	BARLAG	92	NA32	π^- Cu 230 GeV

$\Gamma(\Sigma^+\rho^0)/\Gamma(pK^-\pi^+)$ Γ_{38}/Γ_2

VALUE	CL%	DOCUMENT ID		TECN	COMMENT
< 0.27	95	KUBOTA	93	CLE2	e^+e^- ≈ $\Upsilon(4S)$

$\Gamma(\Sigma^-\pi^+\pi^+)/\Gamma(\Sigma^+\pi^+\pi^-)$ Γ_{39}/Γ_{37}

VALUE	EVTS	DOCUMENT ID		TECN	COMMENT
0.53 ± 0.15 ± 0.07	56	FRABETTI	94E	E687	γBe, $\overline{E}_\gamma$ 220 GeV

$\Gamma(\Sigma^0\pi^+\pi^0)/\Gamma(pK^-\pi^+)$ Γ_{40}/Γ_2

VALUE	EVTS	DOCUMENT ID		TECN	COMMENT
0.36 ± 0.09 ± 0.10	117	AVERY	94	CLE2	e^+e^- ≈ $\Upsilon(3S), \Upsilon(4S)$

$\Gamma(\Sigma^0\pi^+\pi^+\pi^-)/\Gamma(pK^-\pi^+)$ Γ_{41}/Γ_2

VALUE	EVTS	DOCUMENT ID		TECN	COMMENT
0.21 ± 0.05 ± 0.05	90	AVERY	94	CLE2	e^+e^- ≈ $\Upsilon(3S), \Upsilon(4S)$

$\Gamma(\Sigma^+\omega)/\Gamma(pK^-\pi^+)$ Γ_{43}/Γ_2

Unseen decay modes of the ω are included.

VALUE	EVTS	DOCUMENT ID		TECN	COMMENT
0.54 ± 0.13 ± 0.06	107	KUBOTA	93	CLE2	e^+e^- ≈ $\Upsilon(4S)$

$\Gamma(\Sigma^+K^+K^-)/\Gamma(pK^-\pi^+)$ Γ_{44}/Γ_2

VALUE	EVTS	DOCUMENT ID		TECN	COMMENT
0.057 ± 0.008 OUR FIT					
0.070 ± 0.011 ± 0.011	59	AVERY	93	CLE2	e^+e^- ≈ 10.5 GeV

$\Gamma(\Sigma^+K^+K^-)/\Gamma(\Sigma^+\pi^+\pi^-)$ Γ_{44}/Γ_{37}

VALUE	EVTS	DOCUMENT ID		TECN	COMMENT
0.078 ± 0.009 OUR FIT					
0.074 ± 0.009 OUR AVERAGE					
0.076 ± 0.007 ± 0.009	246	ABE	02C	BELL	e^+e^- ≈ $\Upsilon(4S)$
0.071 ± 0.011 ± 0.011	103	LINK	02G	FOCS	γ nucleus, ≈ 180 GeV

$\Gamma(\Sigma^+\phi)/\Gamma(pK^-\pi^+)$ Γ_{45}/Γ_2

Unseen decay modes of the ϕ are included.

VALUE	EVTS	DOCUMENT ID		TECN	COMMENT
0.063 ± 0.011 OUR FIT					
0.069 ± 0.023 ± 0.016	26	AVERY	93	CLE2	e^+e^- ≈ 10.5 GeV

$\Gamma(\Sigma^+\phi)/\Gamma(\Sigma^+\pi^+\pi^-)$ Γ_{45}/Γ_{37}

Unseen decay modes of the ϕ are included.

VALUE	EVTS	DOCUMENT ID		TECN	COMMENT
0.087 ± 0.012 OUR FIT					
0.086 ± 0.012 OUR AVERAGE					
0.085 ± 0.012 ± 0.012	129	ABE	02C	BELL	e^+e^- ≈ $\Upsilon(4S)$
0.087 ± 0.016 ± 0.006	57	LINK	02G	FOCS	γ nucleus, ≈ 180 GeV

$\Gamma(\Xi(1690)^0K^+, \Xi(1690)^0 \to \Sigma^+K^-)/\Gamma(\Sigma^+\pi^+\pi^-)$ Γ_{46}/Γ_{37}

VALUE	EVTS	DOCUMENT ID		TECN	COMMENT
0.023 ± 0.005 OUR AVERAGE					
0.023 ± 0.005 ± 0.005	75	ABE	02C	BELL	e^+e^- ≈ $\Upsilon(4S)$
0.022 ± 0.006 ± 0.006	34	LINK	02G	FOCS	γ nucleus, ≈ 180 GeV

$\Gamma(\Sigma^+K^+K^-\text{nonresonant})/\Gamma(\Sigma^+\pi^+\pi^-)$ Γ_{47}/Γ_{37}

VALUE	CL%	DOCUMENT ID		TECN	COMMENT
< 0.018	90	ABE	02C	BELL	e^+e^- ≈ $\Upsilon(4S)$
• • • We do not use the following data for averages, fits, limits, etc. • • •					
< 0.028	90	LINK	02G	FOCS	γ nucleus, ≈ 180 GeV

$\Gamma(\Xi^0K^+)/\Gamma(pK^-\pi^+)$ Γ_{48}/Γ_2

VALUE	EVTS	DOCUMENT ID		TECN	COMMENT
0.078 ± 0.013 ± 0.013	56	AVERY	93	CLE2	e^+e^- ≈ 10.5 GeV

$\Gamma(\Xi^-K^+\pi^+)/\Gamma(pK^-\pi^+)$ Γ_{49}/Γ_2

VALUE	EVTS	DOCUMENT ID		TECN	COMMENT
0.098 ± 0.021 OUR AVERAGE		Error includes scale factor of 1.3. See the ideogram below.			
0.14 ± 0.03 ± 0.02	34	ALBRECHT	95B	ARG	e^+e^- ≈ 10.4 GeV
0.079 ± 0.013 ± 0.014	60	AVERY	93	CLE2	e^+e^- ≈ 10.5 GeV
0.15 ± 0.04 ± 0.03	30	AVERY	91	CLEO	e^+e^- 10.5 GeV

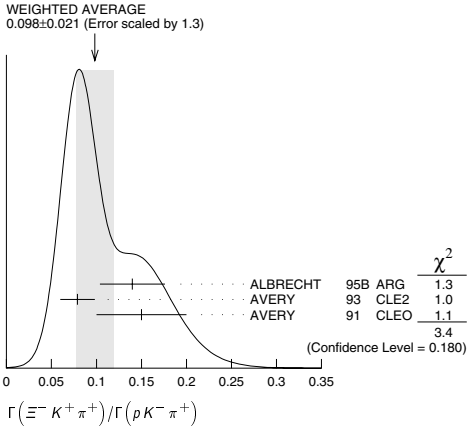

$\Gamma(\Xi(1530)^0 K^+)/\Gamma(pK^-\pi^+)$ Γ_{50}/Γ_2

Unseen decay modes of the $\Xi(1530)^0$ are included.

VALUE	EVTS	DOCUMENT ID		TECN	COMMENT
0.052±0.014 OUR AVERAGE					
0.05 ±0.02 ±0.01	11	ALBRECHT	95B	ARG	e^+e^- ≈ 10.4 GeV
0.053±0.016±0.010	24	AVERY	93	CLE2	e^+e^- ≈ 10.5 GeV

Hadronic modes with a hyperon: $S = 0$ final states

$\Gamma(\Lambda K^+)/\Gamma(\Lambda\pi^+)$ Γ_{51}/Γ_{23}

VALUE	EVTS	DOCUMENT ID		TECN	COMMENT
0.074±0.010±0.012	265	ABE	02C	BELL	e^+e^- ≈ $\Upsilon(4S)$

$\Gamma(\Sigma^0 K^+)/\Gamma(\Sigma^0\pi^+)$ Γ_{52}/Γ_{34}

VALUE	EVTS	DOCUMENT ID		TECN	COMMENT
0.056±0.014±0.008	75	ABE	02C	BELL	e^+e^- ≈ $\Upsilon(4S)$

$\Gamma(\Sigma^+ K^+\pi^-)/\Gamma(\Sigma^+\pi^+\pi^-)$ Γ_{53}/Γ_{37}

VALUE	EVTS	DOCUMENT ID		TECN	COMMENT
0.047±0.011±0.008	105	ABE	02C	BELL	e^+e^- ≈ $\Upsilon(4S)$

$\Gamma(\Sigma^+ K^*(892)^0)/\Gamma(\Sigma^+\pi^+\pi^-)$ Γ_{54}/Γ_{37}

Unseen decay modes of the $K^*(892)^0$ are included.

VALUE	EVTS	DOCUMENT ID		TECN	COMMENT
0.078±0.018±0.013	49	LINK	02G	FOCS	γ nucleus, ≈ 180 GeV

$\Gamma(\Sigma^- K^+\pi^+)/\Gamma(\Sigma^+ K^*(892)^0)$ Γ_{55}/Γ_{54}

VALUE	CL%	DOCUMENT ID		TECN	COMMENT
<0.35	90	LINK	02G	FOCS	γ nucleus, ≈ 180 GeV

Semileptonic modes

$\Gamma(\Lambda\ell^+\nu_\ell)/\Gamma(pK^-\pi^+)$ Γ_{56}/Γ_2

We average here the averages of the next two data blocks.

VALUE	DOCUMENT ID		COMMENT
0.41±0.05 OUR AVERAGE			
0.42±0.07	PDG	02	Our $\Gamma(\Lambda e^+\nu_e)/\Gamma(pK^-\pi^+)$
0.39±0.08	PDG	02	Our $\Gamma(\Lambda\mu^+\nu_\mu)/\Gamma(pK^-\pi^+)$

$\Gamma(\Lambda e^+\nu_e)/\Gamma(pK^-\pi^+)$ Γ_{57}/Γ_2

VALUE	DOCUMENT ID		TECN	COMMENT
0.42±0.07 OUR AVERAGE				
0.43±0.08	[10,11] BERGFELD	94	CLE2	e^+e^- ≈ $\Upsilon(4S)$
0.38±0.14	[11,12] ALBRECHT	91G	ARG	e^+e^- ≈ 10.4 GeV

[10] BERGFELD 94 measures $\sigma(e^+e^- \to \Lambda_c^+ X)\cdot B(\Lambda_c^+ \to \Lambda e^+\nu_e) = (4.87 \pm 0.28 \pm 0.69)$ pb.

[11] To extract $\Gamma(\Lambda_c^+ \to \Lambda e^+\nu_e)/\Gamma(\Lambda_c^+ \to pK^-\pi^+)$, we use $\sigma(e^+e^- \to \Lambda_c^+ X)\cdot B(\Lambda_c \to pK^-\pi^+) = (11.2 \pm 1.3)$ pb, which is the weighted average of measurements from ARGUS (ALBRECHT 96E) and CLEO (AVERY 91).

[12] ALBRECHT 91G measures $\sigma(e^+e^- \to \Lambda_c^+ X)\cdot B(\Lambda_c^+ \to \Lambda e^+\nu_e) = (4.20 \pm 1.28 \pm 0.71)$ pb.

$\Gamma(\Lambda\mu^+\nu_\mu)/\Gamma(pK^-\pi^+)$ Γ_{58}/Γ_2

VALUE	DOCUMENT ID		TECN	COMMENT
0.39±0.08 OUR AVERAGE				
0.40±0.09	[13,14] BERGFELD	94	CLE2	e^+e^- ≈ $\Upsilon(4S)$
0.35±0.20	[14,15] ALBRECHT	91G	ARG	e^+e^- ≈ 10.4 GeV

[13] BERGFELD 94 measures $\sigma(e^+e^- \to \Lambda_c^+ X)\cdot B(\Lambda_c^+ \to \Lambda\mu^+\nu_\mu) = (4.43 \pm 0.51 \pm 0.64)$ pb.

[14] To extract $\Gamma(\Lambda_c^+ \to \Lambda\mu^+\nu_\mu)/\Gamma(\Lambda_c^+ \to pK^-\pi^+)$, we use $\sigma(e^+e^- \to \Lambda_c^+ X)\cdot B(\Lambda_c \to pK^-\pi^+) = (11.2 \pm 1.3)$ pb, which is the weighted average of measurements from ARGUS (ALBRECHT 96E) and CLEO (AVERY 91).

[15] ALBRECHT 91G measures $\sigma(e^+e^- \to \Lambda_c^+ X)\cdot B(\Lambda_c^+ \to \Lambda\mu^+\nu_\mu) = (3.91 \pm 2.02 \pm 0.90)$ pb.

Inclusive modes

$\Gamma(e^+ \text{anything})/\Gamma_{\text{total}}$ Γ_{59}/Γ

VALUE	DOCUMENT ID		TECN	COMMENT
0.045±0.017	VELLA	82	MRK2	e^+e^- 4.5–6.8 GeV

$\Gamma(pe^+ \text{anything})/\Gamma_{\text{total}}$ Γ_{60}/Γ

VALUE	DOCUMENT ID		TECN	COMMENT
0.018±0.009	[16] VELLA	82	MRK2	e^+e^- 4.5–6.8 GeV

[16] VELLA 82 includes protons from Λ decay.

$\Gamma(\Lambda e^+ \text{anything})/\Gamma_{\text{total}}$ Γ_{61}/Γ

VALUE	DOCUMENT ID		TECN	COMMENT
• • • We do not use the following data for averages, fits, limits, etc. • • •				
0.011±0.008	[17] VELLA	82	MRK2	e^+e^- 4.5–6.8 GeV

[17] VELLA 82 includes Λ's from Σ^0 decay.

$\Gamma(p \text{ anything})/\Gamma_{\text{total}}$ Γ_{62}/Γ

VALUE	DOCUMENT ID		TECN	COMMENT
0.50±0.08±0.14	[18] CRAWFORD	92	CLEO	e^+e^- 10.5 GeV

[18] This CRAWFORD 92 value includes protons from Λ decay. The value is model dependent, but account is taken of this in the systematic error.

$\Gamma(p \text{ anything (no } \Lambda))/\Gamma_{\text{total}}$ Γ_{63}/Γ

VALUE	DOCUMENT ID		TECN	COMMENT
0.12±0.10±0.16	CRAWFORD	92	CLEO	e^+e^- 10.5 GeV

$\Gamma(n \text{ anything})/\Gamma_{\text{total}}$ Γ_{65}/Γ

VALUE	DOCUMENT ID		TECN	COMMENT
0.50±0.08±0.14	[19] CRAWFORD	92	CLEO	e^+e^- 10.5 GeV

[19] This CRAWFORD 92 value includes neutrons from Λ decay. The value is model dependent, but account is taken of this in the systematic error.

$\Gamma(n \text{ anything (no } \Lambda))/\Gamma_{\text{total}}$ Γ_{66}/Γ

VALUE	DOCUMENT ID		TECN	COMMENT
0.29±0.09±0.15	CRAWFORD	92	CLEO	e^+e^- 10.5 GeV

$\Gamma(p \text{ hadrons})/\Gamma_{\text{total}}$ Γ_{64}/Γ

VALUE	DOCUMENT ID		TECN	COMMENT
• • • We do not use the following data for averages, fits, limits, etc. • • •				
0.41±0.24	ADAMOVICH	87	EMUL	γA 20–70 GeV/c

$\Gamma(\Lambda \text{ anything})/\Gamma_{\text{total}}$ Γ_{67}/Γ

VALUE	EVTS	DOCUMENT ID		TECN	COMMENT
0.35±0.11 OUR AVERAGE Error includes scale factor of 1.4. See the ideogram below.					
0.59±0.10±0.12		CRAWFORD	92	CLEO	e^+e^- 10.5 GeV
0.49±0.24		ADAMOVICH	87	EMUL	γA 20–70 GeV/c
0.23±0.10	8	[20] ABE	86	HYBR	20 GeV γp

[20] ABE 86 includes Λ's from Σ^0 decay.

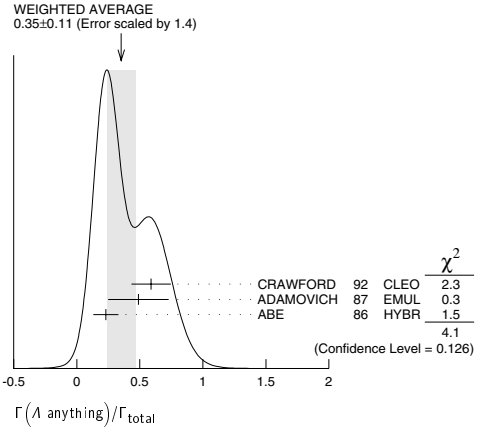

$\Gamma(\Sigma^{\pm}\text{anything})/\Gamma_{\text{total}}$ Γ_{68}/Γ

VALUE	EVTS	DOCUMENT ID		TECN	COMMENT
0.1 ±0.05	5	ABE	86	HYBR	20 GeV γp

$\Gamma(3\text{prongs})/\Gamma_{\text{total}}$ Γ_{69}/Γ

VALUE	DOCUMENT ID		TECN	COMMENT
0.24±0.07±0.04	KAYIS-TOPAK.03		CHRS	ν_μ emulsion, $\overline{E}$=27 GeV

Rare or forbidden modes

$\Gamma(p\mu^+\mu^-)/\Gamma_{\text{total}}$ Γ_{70}/Γ

A test for the ΔC=1 weak neutral current. Allowed by higher-order electroweak interactions.

VALUE	CL%	EVTS	DOCUMENT ID		TECN	COMMENT
$<3.4\times10^{-4}$	90	0	KODAMA	95	E653	π^- emulsion 600 GeV

$\Gamma(\Sigma^-\mu^+\mu^+)/\Gamma_{\text{total}}$ Γ_{71}/Γ

A test of lepton-number conservation.

VALUE	CL%	EVTS	DOCUMENT ID		TECN	COMMENT
$<7.0\times10^{-4}$	90	0	KODAMA	95	E653	π^- emulsion 600 GeV

Λ_c^+ DECAY PARAMETERS

See the note on "Baryon Decay Parameters" in the neutron Listings.

α FOR $\Lambda_c^+ \to \Lambda\pi^+$

VALUE	EVTS	DOCUMENT ID		TECN	COMMENT
−0.98±0.19 OUR AVERAGE					
$-0.94\pm0.21\pm0.12$	414	[21] BISHAI	95	CLE2	$e^+e^-\approx\Upsilon(4S)$
-0.96 ± 0.42		ALBRECHT	92	ARG	$e^+e^-\approx10.4$ GeV
$-1.1\ \pm0.4$	86	AVERY	90B	CLEO	$e^+e^-\approx10.6$ GeV

[21] BISHAI 95 actually gives $\alpha=-0.94^{+0.21}_{-0.06}{}^{+0.12}_{-0.06}$, chopping the errors at the physical limit -1.0. However, for $\alpha\approx-1.0$, some experiments should *get* unphysical values ($\alpha<-1.0$), and for averaging with other measurements such values (or errors that extend below -1.0) should *not* be chopped.

α FOR $\Lambda_c^+ \to \Sigma^+\pi^0$

VALUE	EVTS	DOCUMENT ID		TECN	COMMENT
−0.45±0.31±0.06	89	BISHAI	95	CLE2	$e^+e^-\approx\Upsilon(4S)$

α FOR $\Lambda_c^+ \to \Lambda\ell^+\nu_\ell$

The experiments don't cover the complete (or same incomplete) $M(\Lambda\ell^+)$ range, but we average them together anyway.

VALUE	EVTS	DOCUMENT ID		TECN	COMMENT
$-0.82^{+0.11}_{-0.07}$ OUR AVERAGE					
$-0.82^{+0.09}_{-0.06}{}^{+0.06}_{-0.03}$	700	[22] CRAWFORD	95	CLE2	$e^+e^-\approx\Upsilon(4S)$
$-0.91\pm0.42\pm0.25$		[23] ALBRECHT	94B	ARG	$e^+e^-\approx10$ GeV
• • • We do not use the following data for averages, fits, limits, etc. • • •					
$-0.89^{+0.17}_{-0.11}{}^{+0.09}_{-0.05}$	350	[24] BERGFELD	94	CLE2	See CRAWFORD 95

[22] CRAWFORD 95 measures the form-factor ratio $R\equiv f_2/f_1$ for $\Lambda_c^+\to\Lambda e^+\nu_e$ events to be $-0.25\pm0.14\pm0.08$ and from this calculates α, averaged over q^2, to be the above.
[23] ALBRECHT 94B uses Λe^+ and $\Lambda\mu^+$ events in the mass range $1.85<M(\Lambda\ell^+)<2.20$ GeV.
[24] BERGFELD 94 uses Λe^+ events.

Λ_c^+ REFERENCES

We have omitted some papers that have been superseded by later experiments. The omitted papers may be found in our 1992 edition (Physical Review **D45**, 1 June, Part II) or in earlier editions.

CRONIN-HEN...03	PR D67 012001	D. Cronin-Hennessy *et al.*		(CLEO Collab.)
KAYIS-TOPAK...03	PL B555 156	A. Kayis-Topaksu *et al.*		(CERN CHORUS Collab.)
ABE	02C	PL B524 33	K. Abe *et al.*	(KEK BELLE Collab.)
LINK	02C	PRL 88 161801	J.M. Link *et al.*	(FNAL FOCUS Collab.)
LINK	02G	PL B540 25	J.M. Link *et al.*	(FNAL FOCUS Collab.)
PDG	02	PR D66 010001	K. Hagiwara *et al.*	
KUSHNIR...	01	PRL 86 5243	A. Kushnirenko *et al.*	(FNAL SELEX Collab.)
MAHMOOD	01	PRL 86 2232	A.H. Mahmood *et al.*	(CLEO Collab.)
AITALA	00	PL B471 449	E.M. Aitala *et al.*	(FNAL E791 Collab.)
JAFFE	00	PR D62 072005	D.E. Jaffe *et al.*	(CLEO Collab.)
ALAM	98	PR D57 4667	M.S. Alam *et al.*	(CLEO Collab.)
ALBRECHT	96E	PRPL 276 223	H. Albrecht *et al.*	(ARGUS Collab.)
ALEEV	96	JINRRC 3-77 31	A.N. Aleev *et al.*	(Serpukhov EXCHARM Collab.)
ALEXANDER	96C	PR D53 R1013	J.P. Alexander *et al.*	(CLEO Collab.)
ALBRECHT	95B	PL B342 397	H. Albrecht *et al.*	(ARGUS Collab.)
AMMAR	95	PRL 74 3534	R. Ammar *et al.*	(CLEO Collab.)
BISHAI	95	PL B350 256	M. Bishai *et al.*	(CLEO Collab.)
CRAWFORD	95	PRL 75 624	G. Crawford *et al.*	(CLEO Collab.)
KODAMA	95	PL B345 85	K. Kodama *et al.*	(FNAL E653 Collab.)
ALBRECHT	94B	PL B326 320	H. Albrecht *et al.*	(ARGUS Collab.)
ALEEV	94	PAN 57 1370	A.N. Aleev *et al.*	(Serpukhov BIS-2 Collab.)
		Translated from YF 57 1443.		
AVERY	94	PL B325 257	P. Avery *et al.*	(CLEO Collab.)
BERGFELD	94	PL B323 219	T. Bergfeld *et al.*	(CLEO Collab.)
FRABETTI	94E	PL B328 193	P.L. Frabetti *et al.*	(FNAL E687 Collab.)
AVERY	93	PRL 71 2391	P. Avery *et al.*	(CLEO Collab.)
BOZEK	93	PL B312 247	A. Bozek *et al.*	(CERN NA32 Collab.)
FRABETTI	93D	PRL 70 1755	P.L. Frabetti *et al.*	(FNAL E687 Collab.)
FRABETTI	93H	PL B314 477	P.L. Frabetti *et al.*	(FNAL E687 Collab.)
KUBOTA	93	PRL 71 3255	Y. Kubota *et al.*	(CLEO Collab.)
ALBRECHT	92	PL B274 239	H. Albrecht *et al.*	(ARGUS Collab.)
ALBRECHT	92O	ZPHY C56 1	H. Albrecht *et al.*	(ARGUS Collab.)
BARLAG	92	PL B283 465	S. Barlag *et al.*	(ACCMOR Collab.)
CRAWFORD	92	PR D45 752	G. Crawford *et al.*	(CLEO Collab.)
JEZABEK	92	PL B286 175	M. Jezabek, K. Rybicki, R. Rylko	(CRAC)
ALBRECHT	91G	PL B269 234	H. Albrecht *et al.*	(ARGUS Collab.)
AVERY	91	PR D43 3599	P. Avery *et al.*	(CLEO Collab.)
ALVAREZ	90	ZPHY C47 539	M.P. Alvarez *et al.*	(CERN NA14/2 Collab.)
ALVAREZ	90B	PL B246 256	M.P. Alvarez *et al.*	(CERN NA14/2 Collab.)
ANJOS	90	PR D41 801	J.C. Anjos *et al.*	(FNAL E691 Collab.)
AVERY	90B	PRL 65 2842	P. Avery *et al.*	(CLEO Collab.)
BARLAG	90D	ZPHY C48 29	S. Barlag *et al.*	(ACCMOR Collab.)
FRABETTI	90	PL B251 639	P.L. Frabetti *et al.*	(FNAL E687 Collab.)
BARLAG	89	PL B218 374	S. Barlag *et al.*	(ACCMOR Collab.)
AGUILAR-...	88B	ZPHY C40 321	M. Aguilar-Benitez *et al.*	(LEBC-EHS Collab.)
Also	87	PL B189 254	M. Aguilar-Benitez *et al.*	(LEBC-EHS Collab.)
Also	87B	PL B199 462	M. Aguilar-Benitez *et al.*	(LEBC-EHS Collab.)
Also	88	SJNP 48 833	M. Begalli *et al.*	(LEBC-EHS Collab.)
		Translated from YAF 48 1310.		
ALBRECHT	88C	PL B207 109	H. Albrecht *et al.*	(ARGUS Collab.)
ANJOS	88B	PRL 60 1379	J.C. Anjos *et al.*	(FNAL E691 Collab.)
ADAMOVICH	87	EPL 4 887	M.I. Adamovich *et al.*	(Photon Emulsion Collab.)
Also	87	SJNP 46 447	F. Viaggi *et al.*	(Photon Emulsion Collab.)
		Translated from YAF 46 799.		
AMENDOLIA	87	ZPHY C36 513	S.R. Amendolia *et al.*	(CERN NA1 Collab.)
JONES	87	ZPHY C36 593	G.T. Jones *et al.*	(CERN WA21 Collab.)
ABE	86	PR D33 1	K. Abe *et al.*	
ALEEV	84	ZPHY C23 333	A.N. Aleev *et al.*	(BIS-2 Collab.)
BOSETTI	82	PL 109B 234	P.C. Bosetti *et al.*	(AACH3, BONN, CERN+)
VELLA	82	PRL 48 1515	E. Vella *et al.*	(SLAC, LBL, UCB)
BASILE	81B	NC 62A 14	M. Basile *et al.*	(CERN, BGNA, PGIA, FRAS)
CALICCHIO	80	PL 93B 521	M. Calicchio *et al.*	(BARI, BIRM, BRUX+)

OTHER RELATED PAPERS

MIGLIOZZI	99	PL B462 217	P. Migliozzi *et al.*	
DUNIETZ	98	PR D58 094010	I. Dunietz	

$\Lambda_c(2593)^+$

$I(J^P) = 0(\frac{1}{2}^-)$ Status: ***

Seen in $\Lambda_c^+\pi^+\pi^-$ but not in $\Lambda_c^+\pi^0$, so this is indeed an excited Λ_c^+ rather than a Σ_c^+. The $\Lambda_c^+\pi^+\pi^-$ mode is largely, and perhaps entirely, $\Sigma_c\pi$, which is just at threshold; thus (assuming, as has not yet been proven, that the Σ_c has $J^P=1/2^+$) the J^P here is almost certainly $1/2^-$. This result is in accord with the theoretical expectation that this is the charm counterpart of the strange $\Lambda(1405)$.

$\Lambda_c(2593)^+$ MASS

The mass is obtained from the $\Lambda_c(2593)^+-\Lambda_c^+$ mass-difference measurements below.

VALUE (MeV)	DOCUMENT ID
2593.9±0.8 OUR FIT	

$\Lambda_c(2593)^+ - \Lambda_c^+$ MASS DIFFERENCE

VALUE (MeV)	EVTS	DOCUMENT ID		TECN	COMMENT
308.9±0.6 OUR FIT Error includes scale factor of 1.1.					
308.9±0.6 OUR AVERAGE Error includes scale factor of 1.1.					
309.7±0.9±0.4	19	ALBRECHT	97	ARG	$e^+e^-\approx10$ GeV
309.2±0.7±0.3	14	[1] FRABETTI	96	E687	γBe, $\overline{E}_\gamma\approx220$ GeV
307.5±0.4±1.0	112	[2] EDWARDS	95	CLE2	$e^+e^-\approx10.5$ GeV

[1] FRABETTI 96 claims a signal of 13.9 ± 4.5 events.
[2] EDWARDS 95 claims a signal of 112.5 ± 16.5 events in $\Lambda_c^+\pi^+\pi^-$.

$\Lambda_c(2593)^+$ WIDTH

VALUE (MeV)	EVTS	DOCUMENT ID	TECN	COMMENT
$3.6^{+2.0}_{-1.3}$ OUR AVERAGE				
$2.9^{+2.9}_{-2.1}{}^{+1.8}_{-1.4}$	19	ALBRECHT	97 ARG	$e^+e^-\approx10$ GeV
$3.9^{+1.4}_{-1.2}{}^{+2.0}_{-1.0}$	112	EDWARDS	95 CLE2	$e^+e^-\approx10.5$ GeV

$\Lambda_c(2593)^+$ DECAY MODES

$\Lambda_c^+\pi\pi$ and its submode $\Sigma_c(2455)\pi$ — the latter just barely — are the only strong decays allowed to an excited Λ_c^+ having this mass; and the submode seems to dominate.

	Mode	Fraction (Γ_i/Γ)
Γ_1	$\Lambda_c^+\pi^+\pi^-$	[a] ≈ 67 %
Γ_2	$\Sigma_c(2455)^{++}\pi^-$	24 ± 7 %
Γ_3	$\Sigma_c(2455)^0\pi^+$	24 ± 7 %
Γ_4	$\Lambda_c^+\pi^+\pi^-$ 3-body	18 ± 10 %
Γ_5	$\Lambda_c^+\pi^0$	[b] not seen
Γ_6	$\Lambda_c^+\gamma$	not seen

[a] Assuming isospin conservation, so that the other third is $\Lambda_c^+\pi^0\pi^0$.

[b] A test that the isospin is indeed 0, so that the particle is indeed a Λ_c^+.

$\Lambda_c(2593)^+$ BRANCHING RATIOS

$\Gamma(\Sigma_c(2455)^{++}\pi^-)/\Gamma(\Lambda_c^+\pi^+\pi^-)$ Γ_2/Γ_1

VALUE	DOCUMENT ID		TECN	COMMENT
0.36±0.10 OUR AVERAGE				
0.37±0.12±0.13	ALBRECHT	97	ARG	$e^+e^-\approx$ 10 GeV
0.36±0.09±0.09	EDWARDS	95	CLE2	$e^+e^-\approx$ 10.5 GeV

$\Gamma(\Sigma_c(2455)^0\pi^+)/\Gamma(\Lambda_c^+\pi^+\pi^-)$ Γ_3/Γ_1

VALUE	DOCUMENT ID		TECN	COMMENT
0.37±0.10 OUR AVERAGE				
0.29±0.10±0.11	ALBRECHT	97	ARG	$e^+e^-\approx$ 10 GeV
0.42±0.09±0.09	EDWARDS	95	CLE2	$e^+e^-\approx$ 10.5 GeV

$[\Gamma(\Sigma_c(2455)^{++}\pi^-)+\Gamma(\Sigma_c(2455)^0\pi^+)]/\Gamma(\Lambda_c^+\pi^+\pi^-)$ $(\Gamma_2+\Gamma_3)/\Gamma_1$

VALUE	CL%	DOCUMENT ID		TECN	COMMENT
• • • We do not use the following data for averages, fits, limits, etc. • • •					
$0.66^{+0.13}_{-0.16}\pm0.07$		ALBRECHT	97	ARG	$e^+e^-\approx$ 10 GeV
>0.51	90	[3] FRABETTI	96	E687	γBe, $\overline{E}_\gamma\approx$ 220 GeV

[3] The results of FRABETTI 96 are consistent with this ratio being 100%.

$\Gamma(\Lambda_c^+\pi^0)/\Gamma(\Lambda_c^+\pi^+\pi^-)$ Γ_5/Γ_1

$\Lambda_c^+\pi^0$ decay is forbidden by isospin conservation if this state is in fact a Λ_c.

VALUE	CL%	DOCUMENT ID		TECN	COMMENT
<3.53	90	EDWARDS	95	CLE2	$e^+e^-\approx$ 10.5 GeV

$\Gamma(\Lambda_c^+\gamma)/\Gamma(\Lambda_c^+\pi^+\pi^-)$ Γ_6/Γ_1

VALUE	CL%	DOCUMENT ID		TECN	COMMENT
<0.98	90	EDWARDS	95	CLE2	$e^+e^-\approx$ 10.5 GeV

$\Lambda_c(2593)^+$ REFERENCES

ALBRECHT	97	PL B402 207	H. Albrecht *et al.*	(ARGUS Collab.)
FRABETTI	96	PL B365 461	P.L. Frabetti *et al.*	(FNAL E687 Collab.)
EDWARDS	95	PRL 74 3331	K.W. Edwards *et al.*	(CLEO Collab.)

$\Lambda_c(2625)^+$

$I(J^P) = 0(\frac{3}{2}^-)$ Status: ***

Seen in $\Lambda_c^+\pi^+\pi^-$ but not in $\Lambda_c^+\pi^0$ so this is indeed an excited Λ_c^+ rather than a Σ_c^+. The spin-parity has not been measured but is expected to be $3/2^-$: this is presumably the charm counterpart of the strange $\Lambda(1520)$.

$\Lambda_c(2625)^+$ MASS

The mass is obtained from the $\Lambda_c(2625)^+$–Λ_c^+ mass-difference measurements below.

VALUE (MeV)	EVTS	DOCUMENT ID		TECN	COMMENT
2626.6±0.8 OUR FIT Error includes scale factor of 1.2.					
• • • We do not use the following data for averages, fits, limits, etc. • • •					
2626.6±0.5±1.5	42	[1] ALBRECHT	93F	ARG	See ALBRECHT 97

[1] ALBRECHT 93F claims a signal of 42.4 ± 8.8 events.

$\Lambda_c(2625)^+ - \Lambda_c^+$ MASS DIFFERENCE

VALUE (MeV)	EVTS	DOCUMENT ID		TECN	COMMENT
341.7±0.6 OUR FIT Error includes scale factor of 1.6.					
341.7±0.6 OUR AVERAGE Error includes scale factor of 1.6. See the ideogram below.					
342.1±0.5±0.5	51	ALBRECHT	97	ARG	$e^+e^-\approx$ 10 GeV
342.2±0.2±0.5	245	[2] EDWARDS	95	CLE2	$e^+e^-\approx$ 10.5 GeV
340.4±0.6±0.3	40	[3] FRABETTI	94	E687	γBe, $\overline{E}_\gamma$ = 220 GeV

[2] EDWARDS 95 claims a signal of 244.6 ± 19.0 events in $\Lambda_c^+\pi^+\pi^-$.

[3] FRABETTI 94 claims a signal of 39.7 ± 8.7 events.

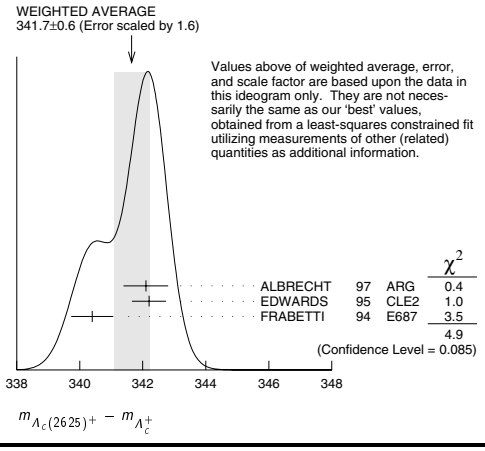

$\Lambda_c(2625)^+$ WIDTH

VALUE (MeV)	CL%	EVTS	DOCUMENT ID		TECN	COMMENT
<1.9	90	245	EDWARDS	95	CLE2	$e^+e^-\approx$ 10.5 GeV
• • • We do not use the following data for averages, fits, limits, etc. • • •						
<3.2	90		ALBRECHT	93F	ARG	$e^+e^-\approx\Upsilon(4S)$

$\Lambda_c(2625)^+$ DECAY MODES

$\Lambda_c^+\pi\pi$ and its submode $\Sigma(2455)\pi$ are the only strong decays allowed to an excited Λ_c^+ having this mass.

	Mode		Fraction (Γ_i/Γ)	Confidence level
Γ_1	$\Lambda_c^+\pi^+\pi^-$	[a]	≈ 67%	
Γ_2	$\Sigma_c(2455)^{++}\pi^-$		<5	90%
Γ_3	$\Sigma_c(2455)^0\pi^+$		<5	90%
Γ_4	$\Lambda_c^+\pi^+\pi^-$ 3-body		large	
Γ_5	$\Lambda_c^+\pi^0$	[b]	not seen	
Γ_6	$\Lambda_c^+\gamma$		not seen	

[a] Assuming isospin conservation, so that the other third is $\Lambda_c^+\pi^0\pi^0$.

[b] A test that the isospin is indeed 0, so that the particle is indeed a Λ_c^+.

$\Lambda_c(2625)^+$ BRANCHING RATIOS

$\Gamma(\Sigma_c(2455)^{++}\pi^-)/\Gamma(\Lambda_c^+\pi^+\pi^-)$ Γ_2/Γ_1

VALUE	CL%	DOCUMENT ID		TECN	COMMENT
<0.08	90	EDWARDS	95	CLE2	$e^+e^-\approx$ 10.5 GeV

$\Gamma(\Sigma_c(2455)^0\pi^+)/\Gamma(\Lambda_c^+\pi^+\pi^-)$ Γ_3/Γ_1

VALUE	CL%	DOCUMENT ID		TECN	COMMENT
<0.07	90	EDWARDS	95	CLE2	$e^+e^-\approx$ 10.5 GeV

$[\Gamma(\Sigma_c(2455)^{++}\pi^-)+\Gamma(\Sigma_c(2455)^0\pi^+)]/\Gamma(\Lambda_c^+\pi^+\pi^-)$ $(\Gamma_2+\Gamma_3)/\Gamma_1$

VALUE	CL%	EVTS	DOCUMENT ID		TECN	COMMENT
• • • We do not use the following data for averages, fits, limits, etc. • • •						
<0.36	90		FRABETTI	94	E687	γBe, $\overline{E}_\gamma$ = 220 GeV
0.46±0.14		21	ALBRECHT	93F	ARG	$e^+e^-\approx\Upsilon(4S)$

$\Gamma(\Lambda_c^+\pi^+\pi^-$ 3-body$)/\Gamma(\Lambda_c^+\pi^+\pi^-)$ Γ_4/Γ_1

VALUE	EVTS	DOCUMENT ID		TECN	COMMENT
• • • We do not use the following data for averages, fits, limits, etc. • • •					
0.54±0.14	16	ALBRECHT	93F	ARG	$e^+e^-\approx\Upsilon(4S)$

$\Gamma(\Lambda_c^+\pi^0)/\Gamma(\Lambda_c^+\pi^+\pi^-)$ Γ_5/Γ_1

$\Lambda_c^+\pi^0$ decay is forbidden by isospin conservation if this state is in fact a Λ_c.

VALUE	CL%	DOCUMENT ID		TECN	COMMENT
<0.91	90	EDWARDS	95	CLE2	$e^+e^-\approx$ 10.5 GeV

$\Gamma(\Lambda_c^+\gamma)/\Gamma(\Lambda_c^+\pi^+\pi^-)$ Γ_6/Γ_1

VALUE	CL%	DOCUMENT ID		TECN	COMMENT
<0.52	90	EDWARDS	95	CLE2	$e^+e^-\approx$ 10.5 GeV

$\Lambda_c(2625)^+$ REFERENCES

ALBRECHT	97	PL B402 207	H. Albrecht *et al.*	(ARGUS Collab.)
EDWARDS	95	PRL 74 3331	K.W. Edwards *et al.*	(CLEO Collab.)
FRABETTI	94	PRL 72 961	P.L. Frabetti *et al.*	(FNAL E687 Collab.)
ALBRECHT	93F	PL B317 227	H. Albrecht *et al.*	(ARGUS Collab.)

$\Lambda_c(2765)^+$ or $\Sigma_c(2765)$

$I(J^P) = ?(?^?)$ Status: *

OMITTED FROM SUMMARY TABLE

A broad, statistically significant peak (997^{+141}_{-129} events) seen in $\Lambda_c^+\pi^+\pi^-$. However, nothing at all is known about its quantum numbers, including whether it is a Λ_c^+ or a Σ_c, or whether the width might be due to overlapping states.

$\Lambda_c(2765)^+$ MASS

The mass is obtained from the $\Lambda_c(2765)^+ - \Lambda_c^+$ mass-difference measurement below.

VALUE (MeV)	DOCUMENT ID
2765.0±2.5 OUR FIT	

$\Lambda_c(2765)^+ - \Lambda_c^+$ MASS DIFFERENCE

VALUE (MeV)	EVTS	DOCUMENT ID		TECN	COMMENT
480.1±2.4 OUR FIT					
480.1±2.4	997	ARTUSO	01	CLE2	$e^+e^- \approx \Upsilon(4S)$

$\Lambda_c(2765)^+$ WIDTH

VALUE (MeV)	DOCUMENT ID		TECN	COMMENT
50	ARTUSO	01	CLE2	$e^+e^- \approx \Upsilon(4S)$

$\Lambda_c(2765)^+$ DECAY MODES

	Mode	Fraction (Γ_i/Γ)
Γ_1	$\Lambda_c^+\pi^+\pi^-$	seen

$\Lambda_c(2765)^+$ REFERENCES

ARTUSO	01	PRL 86 4479	M. Artuso *et al.*	(CLEO Collab.)

$\Lambda_c(2880)^+$

$I(J^P) = ?(?^?)$ Status: **

OMITTED FROM SUMMARY TABLE

A narrow, statistically significant peak (350^{+57}_{-55} events) seen in $\Lambda_c^+\pi^+\pi^-$. However, nothing is known about its quantum numbers—it could even be a Σ_c instead of a Λ_c^+—and it occurs in a mass region where several states are expected. ARTUSO 01 guesses, based on the narrow width, that it might be a $J^P = 1/2^-$ $\Lambda_{c0}'^+$, where the subscript 0 indicates that the two light quarks are in a $J^P = 0^-$ state.

$\Lambda_c(2880)^+$ MASS

The mass is obtained from the $\Lambda_c(2880)^+ - \Lambda_c^+$ mass-difference measurement below.

VALUE (MeV)	DOCUMENT ID
2880.9±2.3 OUR FIT	

$\Lambda_c(2880)^+ - \Lambda_c^+$ MASS DIFFERENCE

VALUE (MeV)	EVTS	DOCUMENT ID		TECN	COMMENT
596.0±2.2 OUR FIT					
596 ±1 ±2	350	ARTUSO	01	CLE2	$e^+e^- \approx \Upsilon(4S)$

$\Lambda_c(2880)^+$ WIDTH

VALUE (MeV)	CL%	DOCUMENT ID		TECN	COMMENT
<8	90	ARTUSO	01	CLE2	$e^+e^- \approx \Upsilon(4S)$

$\Lambda_c(2880)^+$ DECAY MODES

	Mode	Fraction (Γ_i/Γ)
Γ_1	$\Lambda_c^+\pi^+\pi^-$	seen
Γ_2	$\Sigma_c(2455)\pi$	seen
Γ_3	$\Sigma_c(2520)\pi$	not seen

$\Lambda_c(2880)^+$ BRANCHING RATIOS

$\Gamma(\Sigma_c(2455)\pi)/\Gamma(\Lambda_c^+\pi^+\pi^-)$ **Γ_2/Γ_1**

VALUE	EVTS	DOCUMENT ID		TECN	COMMENT
0.31±0.06±0.03	96	ARTUSO	01	CLE2	$e^+e^- \approx \Upsilon(4S)$

$\Gamma(\Sigma_c(2520)\pi)/\Gamma(\Lambda_c^+\pi^+\pi^-)$ **Γ_3/Γ_1**

VALUE	CL%	DOCUMENT ID		TECN	COMMENT
<0.11	90	ARTUSO	01	CLE2	$e^+e^- \approx \Upsilon(4S)$

$\Lambda_c(2880)^+$ REFERENCES

ARTUSO	01	PRL 86 4479	M. Artuso *et al.*	(CLEO Collab.)

$\Sigma_c(2455)$

$I(J^P) = 1(\frac{1}{2}^+)$ Status: ****

Neither J nor P has been measured; $1/2^+$ is the quark model prediction.

$\Sigma_c(2455)$ MASSES

The masses are obtained from the mass-difference measurements that follow.

$\Sigma_c(2455)^{++}$ MASS

VALUE (MeV)	DOCUMENT ID
2452.5±0.6 OUR FIT	

$\Sigma_c(2455)^+$ MASS

VALUE (MeV)	DOCUMENT ID
2451.3±0.7 OUR FIT	

$\Sigma_c(2455)^0$ MASS

VALUE (MeV)	DOCUMENT ID
2452.2±0.6 OUR FIT	

$\Sigma_c(2455) - \Lambda_c^+$ MASS DIFFERENCES

$m_{\Sigma_c^{++}} - m_{\Lambda_c^+}$

VALUE (MeV)	EVTS	DOCUMENT ID		TECN	COMMENT
167.58± 0.12 OUR FIT					
167.57± 0.13 OUR AVERAGE					
167.4 ± 0.1 ±0.2	2k	ARTUSO	02	CLE2	$e^+e^- \approx \Upsilon(4S)$
167.35± 0.19±0.12	461	LINK	00C	FOCS	γ nucleus, $\overline{E}_\gamma$ 180 GeV
167.76± 0.29±0.15	122	AITALA	96B	E791	π^- N, 500 GeV
167.6 ± 0.6 ±0.6	56	FRABETTI	96	E687	γBe, $\overline{E}_\gamma \approx$ 220 GeV
168.2 ± 0.3 ±0.2	126	CRAWFORD	93	CLE2	$e^+e^- \approx \Upsilon(4S)$
167.8 ± 0.4 ±0.3	54	BOWCOCK	89	CLEO	e^+e^- 10 GeV
168.2 ± 0.5 ±1.6	92	ALBRECHT	88D	ARG	e^+e^- 10 GeV
167.4 ± 0.5 ±2.0	46	DIESBURG	87	SPEC	nA ~ 600 GeV
• • • We do not use the following data for averages, fits, limits, etc. • • •					
167 ± 1	2	JONES	87	HBC	νp in BEBC
166 ± 1	1	BOSETTI	82	HBC	See JONES 87
168 ± 3	6	BALTAY	79	HLBC	ν Ne-H in 15-ft
166 ±15	1	CAZZOLI	75	HBC	νp in BNL 7-ft

$m_{\Sigma_c^+} - m_{\Lambda_c^+}$

VALUE (MeV)	EVTS	DOCUMENT ID		TECN	COMMENT
166.4±0.4 OUR FIT					
166.4±0.2±0.3	661	AMMAR	01	CLE2	$e^+e^- \approx \Upsilon(4S)$
• • • We do not use the following data for averages, fits, limits, etc. • • •					
168.5±0.4±0.2	111	CRAWFORD	93	CLE2	See AMMAR 01
168 ±3	1	CALICCHIO	80	HBC	νp in BEBC-TST

$m_{\Sigma_c^0} - m_{\Lambda_c^+}$

VALUE (MeV)	EVTS	DOCUMENT ID		TECN	COMMENT
167.32±0.12 OUR FIT					
167.29±0.13 OUR AVERAGE					
167.2 ±0.1 ±0.2	2k	ARTUSO	02	CLE2	$e^+e^- \approx \Upsilon(4S)$
167.38±0.21±0.13	362	LINK	00C	FOCS	γ nucleus, $\overline{E}_\gamma$ 180 GeV
167.38±0.29±0.15	143	AITALA	96B	E791	π^- N, 500 GeV
167.8 ±0.6 ±0.2		ALEEV	96	SPEC	n nucleus, 50 GeV/c
166.6 ±0.5 ±0.6	69	FRABETTI	96	E687	γBe, $\overline{E}_\gamma \approx$ 220 GeV
167.1 ±0.3 ±0.2	124	CRAWFORD	93	CLE2	$e^+e^- \approx \Upsilon(4S)$
168.4 ±1.0 ±0.3	14	ANJOS	89D	E691	γBe 90–260 GeV

• • • We do not use the following data for averages, fits, limits, etc. • • •

167.9 ±0.5 ±0.3	48	[1] BOWCOCK	89	CLEO	e^+e^- 10 GeV
167.0 ±0.5 ±1.6	70	[1] ALBRECHT	88D	ARG	e^+e^- 10 GeV
178.2 ±0.4 ±2.0	85	[2] DIESBURG	87	SPEC	nA ~ 600 GeV
163 ±2	1	AMMAR	86	EMUL	νA

[1] This result enters the fit through $m_{\Sigma_c^{++}} - m_{\Sigma_c^0}$ given below.

[2] See the note on DIESBURG 87 in the $m_{\Sigma_c^{++}} - m_{\Sigma_c^0}$ section below.

$\Sigma_c(2455)$ MASS DIFFERENCES

$m_{\Sigma_c^{++}} - m_{\Sigma_c^0}$

VALUE (MeV)	DOCUMENT ID		TECN	COMMENT
0.26±0.11 OUR FIT				
0.26±0.14 OUR AVERAGE	Error includes scale factor of 1.2.			
+ 0.2 ±0.1 ±0.1	ARTUSO	02	CLE2	$e^+e^- \approx \Upsilon(4S)$
− 0.03±0.28±0.11	LINK	00C	FOCS	γ nucleus, $\overline{E}_\gamma$ 180 GeV
+ 0.38±0.40±0.15	AITALA	96B	E791	π^- N, 500 GeV
+ 1.1 ±0.4 ±0.1	CRAWFORD	93	CLE2	$e^+e^- \approx \Upsilon(4S)$
− 0.1 ±0.6 ±0.1	BOWCOCK	89	CLEO	e^+e^- 10 GeV
+ 1.2 ±0.7 ±0.3	ALBRECHT	88D	ARG	e^+e^- ~ 10 GeV
• • • We do not use the following data for averages, fits, limits, etc. • • •				
−10.8 ±2.9	[3] DIESBURG	87	SPEC	nA ~ 600 GeV

[3] DIESBURG 87 is completely incompatible with the other experiments, which is surprising since it agrees with them about $m_{\Sigma_c(2455)^{++}} - m_{\Lambda_c^+}$. We go with the majority here.

$m_{\Sigma_c^+} - m_{\Sigma_c^0}$

VALUE (MeV)	DOCUMENT ID		TECN	COMMENT
−0.9±0.4 OUR FIT				
• • • We do not use the following data for averages, fits, limits, etc. • • •				
1.4±0.5±0.3	CRAWFORD	93	CLE2	See AMMAR 01

$\Sigma_c(2455)$ WIDTHS

$\Sigma_c(2455)^{++}$ WIDTH

VALUE (MeV)	EVTS	DOCUMENT ID		TECN	COMMENT
2.23±0.30 OUR AVERAGE					
2.3 ±0.2 ±0.3	2k	ARTUSO	02	CLE2	$e^+e^- \approx \Upsilon(4S)$
$2.05^{+0.41}_{-0.38}\pm0.38$	1110	LINK	02	FOCS	γ nucleus, $\overline{E}_\gamma \approx$ 180 GeV

$\Sigma_c(2455)^+$ WIDTH

VALUE (MeV)	CL%	EVTS	DOCUMENT ID		TECN	COMMENT
<4.6	90	661	AMMAR	01	CLE2	$e^+e^- \approx \Upsilon(4S)$

$\Sigma_c(2455)^0$ WIDTH

VALUE (MeV)	EVTS	DOCUMENT ID		TECN	COMMENT
2.2 ±0.4 OUR AVERAGE Error includes scale factor of 1.4.					
2.5 ±0.2 ±0.3	2k	ARTUSO	02	CLE2	$e^+e^- \approx \Upsilon(4S)$
$1.55^{+0.41}_{-0.37}\pm0.38$	913	LINK	02	FOCS	γ nucleus, $\overline{E}_\gamma \approx$ 180 GeV

$\Sigma_c(2455)$ DECAY MODES

$\Lambda_c^+\pi$ is the only strong decay allowed to a Σ_c having this mass.

	Mode	Fraction (Γ_j/Γ)
Γ_1	$\Lambda_c^+\pi$	≈ 100 %

$\Sigma_c(2455)$ REFERENCES

ARTUSO	02	PR D65 071101R	M. Artuso *et al.*	(CLEO Collab.)
LINK	02	PL B525 205	J.M. Link *et al.*	(FNAL FOCUS Collab.)
AMMAR	01	PRL 86 1167	R. Ammar *et al.*	(CLEO Collab.)
LINK	00C	PL B488 218	J.M. Link *et al.*	(FNAL FOCUS Collab.)
AITALA	96B	PL B379 292	E.M. Aitala *et al.*	(FNAL E791 Collab.)
ALEEV	96	JINRRC 3-77 31	A.N. Aleev *et al.*	(Serpukhov EXCHARM Collab.)
FRABETTI	96	PL B365 461	P.L. Frabetti *et al.*	(FNAL E687 Collab.)
CRAWFORD	93	PRL 71 3259	G. Crawford *et al.*	(CLEO Collab.)
ANJOS	89D	PRL 62 1721	J.C. Anjos *et al.*	(FNAL E691 Collab.)
BOWCOCK	89	PRL 62 1240	T.J.V. Bowcock *et al.*	(CLEO Collab.)
ALBRECHT	88D	PL B211 489	H. Albrecht *et al.*	(ARGUS Collab.)
DIESBURG	87	PRL 59 2711	M. Diesburg *et al.*	(FNAL E400 Collab.)
JONES	87	ZPHY C36 593	G.T. Jones *et al.*	(CERN WA21 Collab.)
AMMAR	86	JETPL 43 515 Translated from ZETFP 43 401.	R. Ammar *et al.*	(ITEP)
BOSETTI	82	PL 109B 234	P.C. Bosetti *et al.*	(AACH3, BONN, CERN+)
CALICCHIO	80	PL 93B 521	M. Calicchio *et al.*	(BARI, BIRM, BRUX+)
BALTAY	79	PRL 42 1721	C. Baltay *et al.*	(COLU, BNL) I
CAZZOLI	75	PRL 34 1125	E.G. Cazzoli *et al.*	(BNL)

$\Sigma_c(2520)$

$I(J^P) = 1(\frac{3}{2}^+)$ Status: ***

Seen in the $\Lambda_c^+\pi^\pm$ mass spectrum. The natural assignment is that this is the $J^P = 3/2^+$ excitation of the $\Sigma_c(2455)$, the charm counterpart of the $\Sigma(1385)$, but neither J nor P has been measured.

$\Sigma_c(2520)$ MASSES

The masses are obtained from the mass-difference measurements that follow.

$\Sigma_c(2520)^{++}$ MASS

VALUE (MeV)	EVTS	DOCUMENT ID		TECN	COMMENT
2519.4±1.5 OUR FIT					
• • • We do not use the following data for averages, fits, limits, etc. • • •					
2530 ±5 ±5	6	[1] AMMOSOV	93	HLBC	$\nu p \to \mu^- \Sigma_c(2530)^{++}$

[1] AMMOSOV 93 sees a cluster of 6 events and estimates the background to be 1 event.

$\Sigma_c(2520)^+$ MASS

VALUE (MeV)	DOCUMENT ID
2515.9±2.4 OUR FIT	

$\Sigma_c(2520)^0$ MASS

VALUE (MeV)	DOCUMENT ID
2517.5±1.4 OUR FIT	

$\Sigma_c(2520)$ MASS DIFFERENCES

$m_{\Sigma_c(2520)^{++}} - m_{\Lambda_c^+}$

VALUE (MeV)	EVTS	DOCUMENT ID		TECN	COMMENT
234.5±1.4 OUR FIT					
234.5±1.1±0.8	677	BRANDENB...	97	CLE2	$e^+e^- \approx \Upsilon(4S)$

$m_{\Sigma_c(2520)^+} - m_{\Lambda_c^+}$

VALUE (MeV)	EVTS	DOCUMENT ID		TECN	COMMENT
231.0±2.3 OUR FIT					
231.0±1.1±2.0	327	AMMAR	01	CLE2	$e^+e^- \approx \Upsilon(4S)$

$m_{\Sigma_c(2520)^0} - m_{\Lambda_c^+}$

VALUE (MeV)	EVTS	DOCUMENT ID		TECN	COMMENT
232.6±1.3 OUR FIT					
232.6±1.0±0.8	504	BRANDENB...	97	CLE2	$e^+e^- \approx \Upsilon(4S)$

$m_{\Sigma_c(2520)^{++}} - m_{\Sigma_c(2520)^0}$

VALUE (MeV)	DOCUMENT ID		TECN	COMMENT
1.9±1.7 OUR FIT				
1.9±1.4±1.0	[2] BRANDENB...	97	CLE2	$e^+e^- \approx \Upsilon(4S)$

[2] This BRANDENBURG 97 result is redundant with measurements in earlier entries.

$\Sigma_c(2520)$ WIDTHS

$\Sigma_c(2520)^{++}$ WIDTH

VALUE (MeV)	EVTS	DOCUMENT ID		TECN	COMMENT
$\mathbf{17.9^{+3.8}_{-3.2}\pm4.0}$	677	BRANDENB...	97	CLE2	$e^+e^- \approx \Upsilon(4S)$

$\Sigma_c(2520)^+$ WIDTH

VALUE (MeV)	CL%	EVTS	DOCUMENT ID		TECN	COMMENT
<17	90	327	AMMAR	01	CLE2	$e^+e^- \approx \Upsilon(4S)$

$\Sigma_c(2520)^0$ WIDTH

VALUE (MeV)	EVTS	DOCUMENT ID		TECN	COMMENT
$\mathbf{13.0^{+3.7}_{-3.0}\pm4.0}$	504	BRANDENB...	97	CLE2	$e^+e^- \approx \Upsilon(4S)$

$\Sigma_c(2520)$ DECAY MODES

$\Lambda_c^+\pi$ is the only strong decay allowed to a Σ_c having this mass.

	Mode	Fraction (Γ_j/Γ)
Γ_1	$\Lambda_c^+\pi$	≈ 100 %

$\Sigma_c(2520)$ REFERENCES

AMMAR	01	PRL 86 1167	R. Ammar *et al.*	(CLEO Collab.)
BRANDENB...	97	PRL 78 2304	G. Brandenburg *et al.*	(CLEO Collab.)
AMMOSOV	93	JETPL 58 247 Translated from ZETFP 58 241.	V.V. Ammosov *et al.*	(SERP)

Ξ_c^+ $I(J^P) = \frac{1}{2}(\frac{1}{2}^+)$ Status: ***

According to the quark model, the Ξ_c^+ (quark content usc) and Ξ_c^0 form an isospin doublet, and the spin-parity ought to be $J^P = 1/2^+$. None of I, J, or P has actually been measured.

Ξ_c^+ MASS

The fit uses the Ξ_c^+ and Ξ_c^0 mass and mass-difference measurements.

VALUE (MeV)	EVTS	DOCUMENT ID		TECN	COMMENT
2466.3± 1.4 OUR FIT					
2466.4± 1.5 OUR AVERAGE					
2465.8± 1.9± 2.5	90	FRABETTI	98	E687	γ Be, $\overline{E}_\gamma$= 220 GeV
2467.0± 1.6± 2.0	147	EDWARDS	96	CLE2	e^+e^- ≈ $\Upsilon(4S)$
2465.1± 3.6± 1.9	30	ALBRECHT	90F	ARG	e^+e^- at $\Upsilon(4S)$
2467 ± 3 ± 4	23	ALAM	89	CLEO	e^+e^- 10.6 GeV
2466.5± 2.7± 1.2	5	BARLAG	89C	ACCM	π^- Cu 230 GeV
• • • We do not use the following data for averages, fits, limits, etc. • • •					
2464.4± 2.0± 1.4	30	FRABETTI	93B	E687	See FRABETTI 98
2459 ± 5 ±30	56	[1] COTEUS	87	SPEC	nA ≃ 600 GeV
2460 ±25	82	BIAGI	83	SPEC	Σ^- Be 135 GeV

[1] Although COTEUS 87 claims to agree well with BIAGI 83 on the mass and width, there appears to be a discrepancy between the two experiments. BIAGI 83 sees a single peak (stated significance about 6 standard deviations) in the $\Lambda K^-\pi^+\pi^+$ mass spectrum. COTEUS 87 sees *two* peaks in the same spectrum, one at the Ξ_c^+ mass, the other 75 MeV lower. The latter is attributed to $\Xi_c^+ \to \Sigma^0 K^-\pi^+\pi^+ \to (\Lambda\gamma)K^-\pi^+\pi^+$, with the γ unseen. The *combined* significance of the double peak is stated to be 5.5 standard deviations. But the absence of any trace of a lower peak in BIAGI 83 seems to us to throw into question the interpretation of the lower peak of COTEUS 87.

Ξ_c^+ MEAN LIFE

VALUE (10^{-15} s)	EVTS	DOCUMENT ID		TECN	COMMENT
442± 26 OUR AVERAGE Error includes scale factor of 1.3. See the ideogram below.					
503± 47± 18	250	MAHMOOD	02	CLE2	e^+e^- ≈ $\Upsilon(4S)$
439± 22± 9	532	LINK	01D	FOCS	γ nucleus, $\overline{E}_\gamma$ ≈ 180 GeV
340^{+70}_{-50} ± 20	56	FRABETTI	98	E687	γ Be, $\overline{E}_\gamma$= 220 GeV
400^{+180}_{-120} ±100	102	COTEUS	87	SPEC	nA ≃ 600 GeV
$480^{+210}_{-150}{}^{+200}_{-100}$	53	BIAGI	85C	SPEC	Σ^- Be 135 GeV
• • • We do not use the following data for averages, fits, limits, etc. • • •					
410^{+110}_{-80} ± 20	30	FRABETTI	93B	E687	See FRABETTI 98
200^{+110}_{-60}	6	BARLAG	89C	ACCM	π^- (K^-) Cu 230 GeV

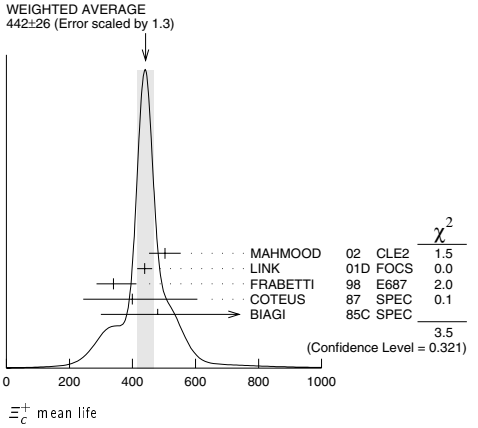

Ξ_c^+ DECAY MODES

Mode	Fraction (Γ_i/Γ)	Confidence level

No absolute branching fractions have been measured. The following are branching *ratios* relative to $\Xi^-\pi^+\pi^+$.

Cabibbo-favored ($S = -2$) decays

Γ_1	$\Lambda\overline{K}^0\pi^+$		—	
Γ_2	$\Sigma(1385)^+\overline{K}^0$	[a,b]	1.0 ±0.5	
Γ_3	$\Lambda K^-\pi^+\pi^+$	[a]	0.34±0.12	
Γ_4	$\Lambda\overline{K}^*(892)^0\pi^+$	[a,b]	<0.2	90%
Γ_5	$\Sigma(1385)^+K^-\pi^+$	[a,b]	<0.3	90%
Γ_6	$\Sigma^+K^-\pi^+$	[a]	0.94±0.11	
Γ_7	$\Sigma^+\overline{K}^*(892)^0$	[a,b]	0.81±0.15	
Γ_8	$\Sigma^0K^-\pi^+\pi^+$	[a]	0.29±0.16	
Γ_9	$\Xi^0\pi^+$	[a]	0.55±0.16	
Γ_{10}	$\Xi^-\pi^+\pi^+$	[a]	DEFINED AS 1	
Γ_{11}	$\Xi(1530)^0\pi^+$	[a,b]	<0.1	90%
Γ_{12}	$\Xi^0\pi^+\pi^0$	[a]	2.34±0.68	
Γ_{13}	$\Xi^0\pi^+\pi^+\pi^-$	[a]	1.74±0.50	
Γ_{14}	$\Xi^0e^+\nu_e$	[a]	$2.3\ ^{+0.7}_{-0.9}$	
Γ_{15}	$\Omega^-K^+\pi^+$	[a]	0.07±0.04	

Cabibbo-suppressed decays

Γ_{16}	$pK^-\pi^+$	[a]	0.21±0.03	
Γ_{17}	$p\overline{K}^*(892)^0$	[a,b]	0.12±0.02	
Γ_{18}	$\Sigma^+K^+K^-$	[a]	0.15±0.07	
Γ_{19}	$\Sigma^+\phi$	[a,b]	<0.11	90%
Γ_{20}	$\Xi(1690)^0K^+$ $\times$B($\Xi(1690)^0 \to \Sigma^+K^-$)	[a]	<0.05	90%

[a] No absolute branching fractions have been measured. The following are branching *ratios* relative to $\Xi^-\pi^+\pi^+$.

[b] This branching fraction includes all the decay modes of the final-state resonance.

Ξ_c^+ BRANCHING RATIOS

Cabibbo-favored ($S = -2$) decays

$\Gamma(\Sigma(1385)^+\overline{K}^0)/\Gamma(\Xi^-\pi^+\pi^+)$ Γ_2/Γ_{10}

Unseen decay modes of the $\Sigma(1385)^+$ are included.

VALUE	EVTS	DOCUMENT ID		TECN	COMMENT
1.00±0.49±0.24	20	LINK	03E	FOCS	< 1.72, 90% CL

$\Gamma(\Lambda K^-\pi^+\pi^+)/\Gamma_{total}$ Γ_3/Γ

VALUE	EVTS	DOCUMENT ID		TECN	COMMENT
• • • We do not use the following data for averages, fits, limits, etc. • • •					
seen	56	COTEUS	87	SPEC	nA ≃ 600 GeV
seen	82	[2] BIAGI	83	SPEC	Σ^- Be 135 GeV

[2] BIAGI 85B looks for but does not see the Ξ_c^+ in $pK^-\overline{K}^0\pi^+$ ($\Gamma(pK^-\overline{K}^0\pi^+)$ / $\Gamma(\Lambda K^-\pi^+\pi^+)$ <0.08 with 90% CL), $p2K^-2\pi^+$ ($\Gamma(p2K^-2\pi^+)$ / $\Gamma(\Lambda K^-\pi^+\pi^+)$ <0.03, 90% CL), $\Omega^-K^+\pi^+$, $\Lambda K^{*0}\pi^+$, and $\Sigma(1385)^+K^-\pi^+$.

$\Gamma(\Lambda K^-\pi^+\pi^+)/\Gamma(\Xi^-\pi^+\pi^+)$ Γ_3/Γ_{10}

VALUE	EVTS	DOCUMENT ID		TECN	COMMENT
0.34±0.12 OUR AVERAGE Error includes scale factor of 1.5.					
0.28±0.06±0.06	58	LINK	03E	FOCS	γ nucleus, $\overline{E}_\gamma$ ≈ 180 GeV
0.58±0.16±0.07	61	BERGFELD	96	CLE2	e^+e^- ≈ $\Upsilon(4S)$

$\Gamma(\Lambda\overline{K}^*(892)^0\pi^+)/\Gamma(\Lambda K^-\pi^+\pi^+)$ Γ_4/Γ_3

Unseen decay modes of the $\overline{K}^*(892)^0$ are included.

VALUE	CL%	DOCUMENT ID		TECN	COMMENT
<0.5	90	BERGFELD	96	CLE2	e^+e^- ≈ $\Upsilon(4S)$

$\Gamma(\Sigma(1385)^+K^-\pi^+)/\Gamma(\Lambda K^-\pi^+\pi^+)$ Γ_5/Γ_3

Unseen decay modes of the $\Sigma(1385)^+$ are included.

VALUE	CL%	DOCUMENT ID		TECN	COMMENT
<0.7	90	BERGFELD	96	CLE2	e^+e^- ≈ $\Upsilon(4S)$

$\Gamma(\Sigma^+K^-\pi^+)/\Gamma(\Xi^-\pi^+\pi^+)$ Γ_6/Γ_{10}

VALUE	EVTS	DOCUMENT ID		TECN	COMMENT
0.94±0.11 OUR AVERAGE					
0.91±0.11±0.04	251	LINK	03E	FOCS	γ nucleus, $\overline{E}_\gamma$ ≈ 180 GeV
1.18±0.26±0.17	119	BERGFELD	96	CLE2	e^+e^- ≈ $\Upsilon(4S)$
• • • We do not use the following data for averages, fits, limits, etc. • • •					
0.92±0.20±0.07	[3]	JUN	00	SELX	Σ^- nucleus, 600 GeV

[3] This JUN 00 result is redundant with other results given below.

$\Gamma(\Sigma^+\overline{K}^*(892)^0)/\Gamma(\Xi^-\pi^+\pi^+)$ Γ_7/Γ_{10}

Unseen decay modes of the $\overline{K}^*(892)^0$ are included.

VALUE	EVTS	DOCUMENT ID		TECN	COMMENT
0.81 ± 0.15 OUR AVERAGE					
0.78 ± 0.16 ± 0.06	119	LINK	03E	FOCS	γ nucleus, $\overline{E}_\gamma \approx 180$ GeV
0.92 ± 0.27 ± 0.14	61	BERGFELD	96	CLE2	$e^+e^- \approx \Upsilon(4S)$
• • • We do not use the following data for averages, fits, limits, etc. • • •					
seen	59	AVERY	95	CLE2	$e^+e^- \approx \Upsilon(4S)$

$\Gamma(\Sigma^0 K^-\pi^+\pi^+)/\Gamma(\Lambda K^-\pi^+\pi^+)$ Γ_8/Γ_3

VALUE	EVTS	DOCUMENT ID		TECN	COMMENT
0.84 ± 0.36	47	[4] COTEUS	87	SPEC	$nA \simeq 600$ GeV

[4] See, however, the note on the COTEUS 87 Ξ_c^+ mass measurement.

$\Gamma(\Xi^0\pi^+)/\Gamma(\Xi^-\pi^+\pi^+)$ Γ_9/Γ_{10}

VALUE	EVTS	DOCUMENT ID		TECN	COMMENT
0.55 ± 0.13 ± 0.09	39	EDWARDS	96	CLE2	$e^+e^- \approx \Upsilon(4S)$

$\Gamma(\Xi^-\pi^+\pi^+)/\Gamma_{\text{total}}$ Γ_{10}/Γ

VALUE	EVTS	DOCUMENT ID		TECN	COMMENT
• • • We do not use the following data for averages, fits, limits, etc. • • •					
seen	131	BERGFELD	96	CLE2	$e^+e^- \approx \Upsilon(4S)$
seen	160	AVERY	95	CLE2	$e^+e^- \approx \Upsilon(4S)$
seen	30	FRABETTI	93B	E687	γ Be, $\overline{E}_\gamma = 220$ GeV
seen	30	ALBRECHT	90F	ARG	e^+e^- at $\Upsilon(4S)$
seen	23	ALAM	89	CLEO	e^+e^- 10.6 GeV

$\Gamma(\Xi(1530)^0\pi^+)/\Gamma(\Xi^-\pi^+\pi^+)$ Γ_{11}/Γ_{10}

Unseen decay modes of the $\Xi(1530)^0$ are included.

VALUE	CL%	DOCUMENT ID		TECN	COMMENT
< 0.1	90	LINK	03E	FOCS	γ nucleus, $\overline{E}_\gamma \approx 180$ GeV
• • • We do not use the following data for averages, fits, limits, etc. • • •					
< 0.2	90	BERGFELD	96	CLE2	$e^+e^- \approx \Upsilon(4S)$

$\Gamma(\Xi^0\pi^+\pi^0)/\Gamma(\Xi^-\pi^+\pi^+)$ Γ_{12}/Γ_{10}

VALUE	EVTS	DOCUMENT ID		TECN	COMMENT
2.34 ± 0.57 ± 0.37	81	EDWARDS	96	CLE2	$e^+e^- \approx \Upsilon(4S)$

$\Gamma(\Xi(1530)^0\pi^+)/\Gamma(\Xi^0\pi^+\pi^0)$ Γ_{11}/Γ_{12}

VALUE	CL%	DOCUMENT ID		TECN	COMMENT
• • • We do not use the following data for averages, fits, limits, etc. • • •					
< 0.3	90	EDWARDS	96	CLE2	$e^+e^- \approx \Upsilon(4S)$

$\Gamma(\Xi^0\pi^+\pi^+\pi^-)/\Gamma(\Xi^-\pi^+\pi^+)$ Γ_{13}/Γ_{10}

VALUE	EVTS	DOCUMENT ID		TECN	COMMENT
1.74 ± 0.42 ± 0.27	57	EDWARDS	96	CLE2	$e^+e^- \approx \Upsilon(4S)$

$\Gamma(\Xi^0 e^+\nu_e)/\Gamma(\Xi^-\pi^+\pi^+)$ Γ_{14}/Γ_{10}

VALUE	EVTS	DOCUMENT ID		TECN	COMMENT
2.3 ± 0.6 $^{+0.3}_{-0.6}$	41	ALEXANDER	95B	CLE2	$e^+e^- \approx \Upsilon(4S)$

$\Gamma(\Omega^- K^+\pi^+)/\Gamma(\Xi^-\pi^+\pi^+)$ Γ_{15}/Γ_{10}

VALUE	EVTS	DOCUMENT ID		TECN	COMMENT
0.07 ± 0.03 ± 0.03	14	LINK	03E	FOCS	< 0.12, 90% CL

Cabibbo-suppressed decays

$\Gamma(pK^-\pi^+)/\Gamma(\Sigma^+K^-\pi^+)$ Γ_{16}/Γ_6

VALUE	EVTS	DOCUMENT ID		TECN	COMMENT
0.22 ± 0.06 ± 0.03	76	JUN	00	SELX	Σ^- nucleus, 600 GeV

$\Gamma(pK^-\pi^+)/\Gamma(\Xi^-\pi^+\pi^+)$ Γ_{16}/Γ_{10}

VALUE	EVTS	DOCUMENT ID		TECN	COMMENT
0.214 ± 0.034 OUR AVERAGE					
0.234 ± 0.047 ± 0.022	202	LINK	01B	FOCS	γ nucleus
0.20 ± 0.04 ± 0.02	76	JUN	00	SELX	Σ^- nucleus, 600 GeV

$\Gamma(p\overline{K}^*(892)^0)/\Gamma(pK^-\pi^+)$ Γ_{17}/Γ_{16}

Unseen decay modes of the $\overline{K}^*(892)^0$ are included.

VALUE	DOCUMENT ID		TECN	COMMENT
0.54 ± 0.09 ± 0.05	LINK	01B	FOCS	γ nucleus

$\Gamma(\Sigma^+K^+K^-)/\Gamma(\Sigma^+K^-\pi^+)$ Γ_{18}/Γ_6

VALUE	EVTS	DOCUMENT ID		TECN	COMMENT
0.16 ± 0.06 ± 0.01	17	LINK	03E	FOCS	γ nucleus, $\overline{E}_\gamma \approx 180$ GeV

$\Gamma(\Sigma^+\phi)/\Gamma(\Sigma^+K^-\pi^+)$ Γ_{19}/Γ_6

Unseen decay modes of the ϕ are included.

VALUE	CL%	DOCUMENT ID		TECN	COMMENT
< 0.12	90	LINK	03E	FOCS	γ nucleus, $\overline{E}_\gamma \approx 180$ GeV

$\Gamma(\Xi(1690)^0 K^+ \times B(\Xi(1690)^0 \to \Sigma^+K^-))/\Gamma(\Sigma^+K^-\pi^+)$ Γ_{20}/Γ_6

VALUE	CL%	DOCUMENT ID		TECN	COMMENT
< 0.05	90	LINK	03E	FOCS	γ nucleus, $\overline{E}_\gamma \approx 180$ GeV

Ξ_c^+ REFERENCES

LINK	03E	PL B571 139	J.M. Link *et al.*	(FNAL FOCUS Collab.)
MAHMOOD	02	PR D65 031102	A.H. Mahmood *et al.*	(CLEO Collab.)
LINK	01B	PL B512 277	J.M. Link *et al.*	(FNAL FOCUS Collab.)
LINK	01D	PL B523 53	J.M. Link *et al.*	(FNAL FOCUS Collab.)
JUN	00	PRL 84 1857	S.Y. Jun *et al.*	(FNAL SELEX Collab.)
FRABETTI	98	PL B427 211	P.L. Frabetti *et al.*	(FNAL E687 Collab.)
BERGFELD	96	PL B365 431	T. Bergfeld *et al.*	(CLEO Collab.)
EDWARDS	96	PL B373 261	K.W. Edwards *et al.*	(CLEO Collab.)
ALEXANDER	95B	PRL 74 3113	J. Alexander *et al.*	(CLEO Collab.)
Also	95E	PRL 75 4155 (erratum)	J. Alexander *et al.*	(CLEO Collab.)
AVERY	95	PRL 75 4364	P. Avery *et al.*	(CLEO Collab.)
FRABETTI	93B	PRL 70 1381	P.L. Frabetti *et al.*	(FNAL E687 Collab.)
ALBRECHT	90F	PL B247 121	H. Albrecht *et al.*	(ARGUS Collab.)
ALAM	89	PL B226 401	M.S. Alam *et al.*	(CLEO Collab.)
BARLAG	89C	PL B233 522	S. Barlag *et al.*	(ACCMOR Collab.)
COTEUS	87	PRL 59 1530	P. Coteus *et al.*	(FNAL E400 Collab.)
BIAGI	85B	ZPHY C28 175	S.F. Biagi *et al.*	(CERN WA62 Collab.)
BIAGI	85C	PL 150B 230	S.F. Biagi *et al.*	(CERN WA62 Collab.)
BIAGI	83	PL 122B 455	S.F. Biagi *et al.*	(CERN WA62 Collab.)

Ξ_c^0

$I(J^P) = \frac{1}{2}(\frac{1}{2}^+)$ Status: ***

According to the quark model, the Ξ_c^0 (quark content dsc) and Ξ_c^+ form an isospin doublet, and the spin-parity ought to be $J^P = 1/2^+$. None of I, J, or P has actually been measured.

Ξ_c^0 MASS

The fit uses the Ξ_c^0 and Ξ_c^+ mass and mass-difference measurements.

VALUE (MeV)	EVTS	DOCUMENT ID		TECN	COMMENT
2471.8 ± 1.4 OUR FIT					
2471.8 ± 1.4 OUR AVERAGE					
2470.0 ± 2.8 ± 2.6	85	FRABETTI	98B	E687	γ Be, $\overline{E}_\gamma = 220$ GeV
2469 ± 2 ± 3	9	HENDERSON	92B	CLEO	$\Omega^- K^+$
2472.1 ± 2.7 ± 1.6	54	ALBRECHT	90F	ARG	e^+e^- at $\Upsilon(4S)$
2473.3 ± 1.9 ± 1.2	4	BARLAG	90	ACCM	π^- (K^-) Cu 230 GeV
2472 ± 3 ± 4	19	ALAM	89	CLEO	e^+e^- 10.6 GeV
• • • We do not use the following data for averages, fits, limits, etc. • • •					
2462.1 ± 3.1 ± 1.4	42	[1] FRABETTI	93C	E687	See FRABETTI 98B
2471 ± 3 ± 4	14	AVERY	89	CLEO	See ALAM 89

[1] The FRABETTI 93C mass is well below the other measurements.

$\Xi_c^0 - \Xi_c^+$ MASS DIFFERENCE

VALUE (MeV)	DOCUMENT ID		TECN	COMMENT
5.5 ± 1.8 OUR FIT				
6.3 ± 2.3 OUR AVERAGE				
+7.0 ± 4.5 ± 2.2	ALBRECHT	90F	ARG	e^+e^- at $\Upsilon(4S)$
+6.8 ± 3.3 ± 0.5	BARLAG	90	ACCM	π^- (K^-) Cu 230 GeV
+5 ± 4 ± 1	ALAM	89	CLEO	$\Xi_c^0 \to \Xi^-\pi^+$, $\Xi_c^+ \to \Xi^-\pi^+\pi^+$

Ξ_c^0 MEAN LIFE

VALUE (10^{-15} s)	EVTS	DOCUMENT ID		TECN	COMMENT
112 $^{+13}_{-10}$ OUR AVERAGE					
118 $^{+14}_{-12}$ ± 5	110	LINK	02H	FOCS	γ nucleus, ≈ 180 GeV
101 $^{+25}_{-17}$ ± 5	42	FRABETTI	93C	E687	γBe, $\overline{E}_\gamma$= 220 GeV
82 $^{+59}_{-30}$	4	BARLAG	90	ACCM	π^- (K^-) Cu 230 GeV

Ξ_c^0 DECAY MODES

	Mode	Fraction (Γ_i/Γ)
Γ_1	$\Lambda\overline{K}^0$	seen
Γ_2	$\Lambda\overline{K}^0\pi^+\pi^-$	seen
Γ_3	$\Lambda K^-\pi^+\pi^+\pi^-$	seen
Γ_4	$\Xi^-\pi^+$	seen
Γ_5	$\Xi^-\pi^+\pi^+\pi^-$	seen
Γ_6	$pK^-\overline{K}^*(892)^0$	seen
Γ_7	$\Omega^- K^+$	seen
Γ_8	$\Xi^- e^+\nu_e$	seen
Γ_9	$\Xi^-\ell^+$ anything	seen

Baryon Particle Listings

Ξ_c^0, $\Xi_c^{\prime+}$, $\Xi_c^{\prime0}$, $\Xi_c(2645)$

Ξ_c^0 BRANCHING RATIOS

$\Gamma(\Lambda\overline{K}^0)/\Gamma_{total}$ Γ_1/Γ

VALUE	EVTS	DOCUMENT ID		TECN	COMMENT
seen	7	ALBRECHT	95B	ARG	$e^+e^-\approx 10.4$ GeV

$\Gamma(\Lambda\overline{K}^0\pi^+\pi^-)/\Gamma_{total}$ Γ_2/Γ

VALUE	DOCUMENT ID		TECN	COMMENT
seen	FRABETTI	98B	E687	γ Be, $\overline{E}_\gamma = 220$ GeV

$\Gamma(\Lambda K^-\pi^+\pi^+\pi^-)/\Gamma_{total}$ Γ_3/Γ

VALUE	DOCUMENT ID		TECN	COMMENT
seen	FRABETTI	98B	E687	γ Be, $\overline{E}_\gamma = 220$ GeV

$\Gamma(\Xi^-\pi^+)/\Gamma(\Xi^-\pi^+\pi^+\pi^-)$ Γ_4/Γ_5

VALUE	DOCUMENT ID		TECN	COMMENT
$0.30\pm0.12\pm0.05$	ALBRECHT	90F	ARG	e^+e^- at $\Upsilon(4S)$

$\Gamma(pK^-\overline{K}^*(892)^0)/\Gamma_{total}$ Γ_6/Γ

VALUE	DOCUMENT ID		TECN	COMMENT
seen	BARLAG	90	ACCM	π^- (K^-) Cu 230 GeV

$\Gamma(\Omega^-K^+)/\Gamma(\Xi^-\pi^+)$ Γ_7/Γ_4

VALUE	EVTS	DOCUMENT ID		TECN	COMMENT
$0.50\pm0.21\pm0.05$	9	HENDERSON	92B	CLEO	$e^+e^-\approx 10.6$ GeV

$\Gamma(\Xi^-e^+\nu_e)/\Gamma(\Xi^-\pi^+)$ Γ_8/Γ_4

VALUE	EVTS	DOCUMENT ID		TECN	COMMENT
$3.1\pm1.0^{+0.3}_{-0.5}$	54	ALEXANDER	95B	CLE2	$e^+e^-\approx \Upsilon(4S)$

$\Gamma(\Xi^-\ell^+\text{anything})/\Gamma(\Xi^-\pi^+)$ Γ_9/Γ_4

The ratio is for the *average* (not the sum) of the Ξ^-e^+ anything and $\Xi^-\mu^+$ anything modes.

VALUE	EVTS	DOCUMENT ID		TECN	COMMENT
$0.96\pm0.43\pm0.18$	18	ALBRECHT	93B	ARG	$e^+e^-\approx 10.4$ GeV

$\Gamma(\Xi^-\ell^+\text{anything})/\Gamma(\Xi^-\pi^+\pi^+\pi^-)$ Γ_9/Γ_5

The ratio is for the *average* (not the sum) of the Ξ^-e^+ anything and $\Xi^-\mu^+$ anything modes.

VALUE	EVTS	DOCUMENT ID		TECN	COMMENT
$0.29\pm0.12\pm0.04$	18	ALBRECHT	93B	ARG	$e^+e^-\approx 10.4$ GeV

Ξ_c^0 DECAY PARAMETERS

See the note on "Baryon Decay Parameters" in the neutron Listings.

α FOR $\Xi_c^0 \to \Xi^-\pi^+$

VALUE	EVTS	DOCUMENT ID		TECN	COMMENT
$-0.56\pm0.39^{+0.10}_{-0.09}$	138	CHAN	01	CLE2	$e^+e^-\approx \Upsilon(4S)$

Ξ_c^0 REFERENCES

LINK	02H	PL B541 211	J.M. Link *et al.*	(FNAL FOCUS Collab.)
CHAN	01	PR D63 111102R	S. Chan *et al.*	(CLEO Collab.)
FRABETTI	98B	PL B426 403	P.L. Frabetti *et al.*	(FNAL E687 Collab.)
ALBRECHT	95B	PL B342 397	H. Albrecht *et al.*	(ARGUS Collab.)
ALEXANDER	95B	PRL 74 3113	J. Alexander *et al.*	(CLEO Collab.)
Also	95E	PRL 75 4155 (erratum)	J. Alexander *et al.*	(CLEO Collab.)
ALBRECHT	93B	PL B303 368	H. Albrecht *et al.*	(ARGUS Collab.)
FRABETTI	93C	PRL 70 2058	P.L. Frabetti *et al.*	(FNAL E687 Collab.)
HENDERSON	92B	PL B283 161	S. Henderson *et al.*	(CLEO Collab.)
ALBRECHT	90F	PL B247 121	H. Albrecht *et al.*	(ARGUS Collab.)
BARLAG	90	PL B236 495	S. Barlag *et al.*	(ACCMOR Collab.)
ALAM	89	PL B226 401	M.S. Alam *et al.*	(CLEO Collab.)
AVERY	89	PRL 62 863	P. Avery *et al.*	(CLEO Collab.)

$\Xi_c^{\prime+}$

$I(J^P) = \frac{1}{2}(\frac{1}{2}^+)$ Status: ***

The $\Xi_c^{\prime+}$ and $\Xi_c^{\prime0}$ presumably complete the SU(3) sextet whose other members are the Σ_c^{++}, Σ_c^+, Σ_c^0, and Ω_c^0: see Fig. 3 in the Note on Charmed Baryons just before the the Λ_c^+ Listings. The quantum numbers given above come from this presumption but have not been measured.

$\Xi_c^{\prime+}$ MASS

The mass is obtained from the mass-difference measurement that follows.

VALUE (MeV)	DOCUMENT ID
2574.1±3.3 OUR FIT	

$\Xi_c^{\prime+} - \Xi_c^+$ MASS DIFFERENCE

VALUE (MeV)	EVTS	DOCUMENT ID		TECN	COMMENT
107.8±3.0 OUR FIT					
107.8±1.7±2.5	25	JESSOP	99	CLE2	$e^+e^-\approx \Upsilon(4S)$

$\Xi_c^{\prime+}$ DECAY MODES

The $\Xi_c^{\prime+}-\Xi_c^+$ mass difference is too small for any strong decay to occur.

	Mode	Fraction (Γ_j/Γ)
Γ_1	$\Xi_c^+\gamma$	seen

$\Xi_c^{\prime+}$ REFERENCES

JESSOP 99 PRL 82 492 C.P. Jessop *et al.* (CLEO Collab.)

$\Xi_c^{\prime0}$

$I(J^P) = \frac{1}{2}(\frac{1}{2}^+)$ Status: ***

See the note in the Listing for the $\Xi_c^{\prime+}$, above.

$\Xi_c^{\prime0}$ MASS

The mass is obtained from the mass-difference measurement that follows.

VALUE (MeV)	DOCUMENT ID
2578.8±3.2 OUR FIT	

$\Xi_c^{\prime0} - \Xi_c^0$ MASS DIFFERENCE

VALUE (MeV)	EVTS	DOCUMENT ID		TECN	COMMENT
107.0±2.9 OUR FIT					
107.0±1.4±2.5	28	JESSOP	99	CLE2	$e^+e^-\approx \Upsilon(4S)$

$\Xi_c^{\prime0}$ DECAY MODES

The $\Xi_c^{\prime0} - \Xi_c^0$ mass difference is too small for any strong decay to occur.

	Mode	Fraction (Γ_j/Γ)
Γ_1	$\Xi_c^0\gamma$	seen

$\Xi_c^{\prime0}$ REFERENCES

JESSOP 99 PRL 82 492 C.P. Jessop *et al.* (CLEO Collab.)

$\Xi_c(2645)$

$I(J^P) = \frac{1}{2}(\frac{3}{2}^+)$ Status: ***

A narrow peak seen in the $\Xi_c\pi$ mass spectrum. The natural assignment is that this is the $J^P = 3/2^+$ excitation of the Ξ_c in the same SU(4) multiplet as the $\Delta(1232)$, but the quantum numbers have not been measured.

$\Xi_c(2645)$ MASSES

The masses are obtained from the mass-difference measurements that follow.

$\Xi_c(2645)^+$ MASS

VALUE (MeV)	DOCUMENT ID
2647.4±2.0 OUR FIT Error includes scale factor of 1.2.	

$\Xi_c(2645)^0$ MASS

VALUE (MeV)	DOCUMENT ID
2644.5±1.8 OUR FIT	

$\Xi_c(2645) - \Xi_c$ MASS DIFFERENCES

$m_{\Xi_c(2645)^+} - m_{\Xi_c^0}$

VALUE (MeV)	EVTS	DOCUMENT ID		TECN	COMMENT
175.6±1.4 OUR FIT Error includes scale factor of 1.7.					
175.6±1.4 OUR AVERAGE Error includes scale factor of 1.7.					
$177.1\pm0.5\pm1.1$	47	FRABETTI	98B	E687	γ Be, $\overline{E}_\gamma = 220$ GeV
$174.3\pm0.5\pm1.0$	34	GIBBONS	96	CLE2	$e^+e^-\approx \Upsilon(4S)$

$m_{\Xi_c(2645)^0} - m_{\Xi_c^+}$

VALUE (MeV)	EVTS	DOCUMENT ID		TECN	COMMENT
178.2±1.1 OUR FIT					
178.2±0.5±1.0	55	AVERY	95	CLE2	$e^+e^- \approx \Upsilon(4S)$

$\Xi_c(2645)$ WIDTHS

$\Xi_c(2645)^+$ WIDTH

VALUE (MeV)	CL%	DOCUMENT ID		TECN	COMMENT
<3.1	90	GIBBONS	96	CLE2	$e^+e^- \approx \Upsilon(4S)$

$\Xi_c(2645)^0$ WIDTH

VALUE (MeV)	CL%	EVTS	DOCUMENT ID		TECN	COMMENT
<5.5	90	55	AVERY	95	CLE2	$e^+e^- \approx \Upsilon(4S)$

$\Xi_c(2645)$ DECAY MODES

$\Xi_c\pi$ is the only strong decay allowed to a Ξ_c resonance having this mass.

	Mode	Fraction (Γ_i/Γ)
Γ_1	$\Xi_c^0\pi^+$	seen
Γ_2	$\Xi_c^+\pi^-$	seen

$\Xi_c(2645)$ REFERENCES

FRABETTI	98B	PL B426 403	P.L. Frabetti *et al.*	(FNAL E687 Collab.)
GIBBONS	96	PRL 77 810	L.K. Gibbons *et al.*	(CLEO Collab.)
AVERY	95	PRL 75 4364	P. Avery *et al.*	(CLEO Collab.)

$\Xi_c(2790)$

$I(J^P) = \frac{1}{2}(\frac{1}{2}^-)$ Status: ***

A peak seen in the $\Xi_c'\pi$ mass spectrum. The simplest assignment, based on the mass, width, and decay mode, is that this belongs in the same SU(4) multiplet as the $\Lambda(1405)$ and the $\Lambda_c(2593)^+$, but the spin and parity have not been measured.

$\Xi_c(2790)$ MASSES

The masses are obtained from the mass-difference measurements that follow.

$\Xi_c(2790)^+$ MASS

VALUE (MeV)	DOCUMENT ID
2790.0±3.5 OUR FIT	

$\Xi_c(2790)^0$ MASS

VALUE (MeV)	DOCUMENT ID
2790±4 OUR FIT	

$\Xi_c(2790) - \Xi_c$ MASS DIFFERENCES

$m_{\Xi_c(2790)^+} - m_{\Xi_c^0}$

VALUE (MeV)	EVTS	DOCUMENT ID		TECN	COMMENT
318.2±3.2 OUR FIT					
318.2±1.3±2.9	18	CSORNA	01	CLEO	$e^+e^- \approx \Upsilon(4S)$

$m_{\Xi_c(2790)^0} - m_{\Xi_c^+}$

VALUE (MeV)	EVTS	DOCUMENT ID		TECN	COMMENT
324.0±3.3 OUR FIT					
324.0±1.3±3.0	14	CSORNA	01	CLEO	$e^+e^- \approx \Upsilon(4S)$

$\Xi_c(2790)$ WIDTHS

$\Xi_c(2790)^+$ WIDTH

VALUE (MeV)	CL%	DOCUMENT ID		TECN	COMMENT
<15	90	CSORNA	01	CLEO	$e^+e^- \approx \Upsilon(4S)$

$\Xi_c(2790)^0$ WIDTH

VALUE (MeV)	CL%	DOCUMENT ID		TECN	COMMENT
<12	90	CSORNA	01	CLEO	$e^+e^- \approx \Upsilon(4S)$

$\Xi_c(2790)$ DECAY MODES

	Mode	Fraction (Γ_i/Γ)
Γ_1	$\Xi_c'\pi$	seen

$\Xi_c(2790)$ REFERENCES

CSORNA	01	PRL 86 4243	S.E. Csorna *et al.*	(CLEO Collab.)

$\Xi_c(2815)$

$I(J^P) = \frac{1}{2}(\frac{3}{2}^-)$ Status: ***

A narrow peak seen in the $\Xi_c\pi\pi$ mass spectrum. The simplest assignment is that this belongs to the same SU(4) multiplet as the $\Lambda(1520)$ and the $\Lambda_c(2625)$, but the spin and parity have not been measured.

$\Xi_c(2815)$ MASSES

The masses are obtained from the mass-difference measurements that follow.

$\Xi_c(2815)^+$ MASS

VALUE (MeV)	DOCUMENT ID
2814.9±1.8 OUR FIT	

$\Xi_c(2815)^0$ MASS

VALUE (MeV)	DOCUMENT ID
2819.0±2.5 OUR FIT	

$\Xi_c(2815) - \Xi_c$ MASS DIFFERENCES

$m_{\Xi_c(2815)^+} - m_{\Xi_c^+}$

VALUE (MeV)	EVTS	DOCUMENT ID		TECN	COMMENT
348.6±1.2 OUR FIT					
348.6±0.6±1.0	20	ALEXANDER	99B	CLE2	$e^+e^- \approx \Upsilon(4S)$

$m_{\Xi_c(2815)^0} - m_{\Xi_c^0}$

VALUE (MeV)	EVTS	DOCUMENT ID		TECN	COMMENT
347.2±2.1 OUR FIT					
347.2±0.7±2.0	9	ALEXANDER	99B	CLE2	$e^+e^- \approx \Upsilon(4S)$

$\Xi_c(2815)$ WIDTHS

$\Xi_c(2815)^+$ WIDTH

VALUE (MeV)	CL%	DOCUMENT ID		TECN	COMMENT
<3.5	90	ALEXANDER	99B	CLE2	$e^+e^- \approx \Upsilon(4S)$

$\Xi_c(2815)^0$ WIDTH

VALUE (MeV)	CL%	DOCUMENT ID		TECN	COMMENT
<6.5	90	ALEXANDER	99B	CLE2	$e^+e^- \approx \Upsilon(4S)$

$\Xi_c(2815)$ DECAY MODES

The $\Xi_c\pi\pi$ modes are consistent with being entirely via $\Xi_c(2645)\pi$.

	Mode	Fraction (Γ_i/Γ)
Γ_1	$\Xi_c^+\pi^+\pi^-$	seen
Γ_2	$\Xi_c^0\pi^+\pi^-$	seen

$\Xi_c(2815)$ REFERENCES

ALEXANDER	99B	PRL 83 3390	J.P. Alexander *et al.*	(CLEO Collab.)

Ω_c^0

$I(J^P) = 0(\frac{1}{2}^+)$ Status: ***

The quantum numbers have not been measured, but are simply assigned in accord with the quark model, in which the Ω_c^0 is the ssc ground state.

Ω_c^0 MASS

VALUE (MeV)	EVTS	DOCUMENT ID		TECN	COMMENT
2697.5± 2.6 OUR AVERAGE		Error includes scale factor of 1.2.			
2694.6± 2.6±1.9	40	[1] CRONIN-HEN..01		CLE2	$e^+e^- \approx$ 10.6 GeV
2699.9± 1.5±2.5	42	[2] FRABETTI	94H	E687	γBe, $\overline{E}_\gamma$= 221 GeV
• • • We do not use the following data for averages, fits, limits, etc. • • •					
2705.9± 3.3±2.0	10	[3] FRABETTI	93	E687	γBe, $\overline{E}_\gamma$= 221 GeV
2719.0± 7.0±2.5	11	[4] ALBRECHT	92H	ARG	$e^+e^- \approx$ 10.6 GeV
2740 ±20	3	BIAGI	85B	SPEC	Σ^-Be 135 GeV/c

[1] CRONIN-HENNESSY 01 sees 40.4 ± 9.0 events in a sum over five channels.
[2] FRABETTI 94H claims a signal of 42.5 ± 8.8 $\Sigma^+K^-K^-\pi^+$ events. The background is about 24 events.
[3] FRABETTI 93 claims a signal of 10.3 ± 3.9 $\Omega^-\pi^+$ events above a background of 5.8 events.
[4] ALBRECHT 92H claims a signal of 11.5 ± 4.3 $\Xi^-K^-\pi^+\pi^+$ events. The background is about 5 events.

Baryon Particle Listings

Ω_c^0

Ω_c^0 MEAN LIFE

VALUE (10^{-15} s)	EVTS	DOCUMENT ID		TECN	COMMENT
69 ± 12 OUR AVERAGE					
72 ± 11 ± 11	64	LINK	03C	FOCS	$\Omega^-\pi^+$, $\Xi^-K^-\pi^+\pi^+$
$55^{+13}_{-11}{}^{+18}_{-23}$	86	ADAMOVICH	95B	WA89	$\Omega^-\pi^-\pi^+\pi^+$, $\Xi^-K^-\pi^+\pi^+$
86^{+27}_{-20} ± 28	25	FRABETTI	95D	E687	$\Sigma^+K^-K^-\pi^+$

Ω_c^0 DECAY MODES

No absolute branching fractions have been measured.

	Mode	Fraction (Γ_i/Γ)
Γ_1	$\Sigma^+K^-K^-\pi^+$	seen
Γ_2	$\Xi^0K^-\pi^+$	seen
Γ_3	$\Xi^-K^-\pi^+\pi^+$	seen
Γ_4	$\Omega^-e^+\nu_e$	seen
Γ_5	$\Omega^-\pi^+$	seen
Γ_6	$\Omega^-\pi^+\pi^0$	seen
Γ_7	$\Omega^-\pi^-\pi^+\pi^+$	seen

Ω_c^0 BRANCHING RATIOS

$\Gamma(\Sigma^+K^-K^-\pi^+)/\Gamma_{total}$ — Γ_1/Γ

VALUE	EVTS	DOCUMENT ID		TECN	COMMENT
seen	42	FRABETTI	94H	E687	γBe, $\overline{E}_\gamma$ = 221 GeV

$\Gamma(\Sigma^+K^-K^-\pi^+)/\Gamma(\Omega^-\pi^+)$ — Γ_1/Γ_5

VALUE	CL%	DOCUMENT ID		TECN	COMMENT
• • • We do not use the following data for averages, fits, limits, etc. • • •					
< 4.8	90	CRONIN-HEN..	01	CLE2	e^+e^- ≈ 10.6 GeV

$\Gamma(\Xi^0K^-\pi^+)/\Gamma(\Omega^-\pi^+)$ — Γ_2/Γ_5

VALUE	EVTS	DOCUMENT ID		TECN	COMMENT
4.0 ± 2.5 ± 0.4	9	CRONIN-HEN..	01	CLE2	e^+e^- ≈ 10.6 GeV

$\Gamma(\Xi^-K^-\pi^+\pi^+)/\Gamma_{total}$ — Γ_3/Γ

VALUE	EVTS	DOCUMENT ID		TECN	COMMENT
seen	11	ALBRECHT	92H	ARG	e^+e^- ≈ 10.6 GeV
seen	3	BIAGI	85B	SPEC	Σ^- Be 135 GeV/c

$\Gamma(\Xi^-K^-\pi^+\pi^+)/\Gamma(\Omega^-\pi^+)$ — Γ_3/Γ_5

VALUE	CL%	EVTS	DOCUMENT ID		TECN	COMMENT
1.6 ± 1.1 ± 0.4		7	CRONIN-HEN..	01	CLE2	e^+e^- ≈ 10.6 GeV
• • • We do not use the following data for averages, fits, limits, etc. • • •						
< 2.8	90		FRABETTI	93	E687	γBe, $\overline{E}_\gamma$ = 221 GeV

$\Gamma(\Omega^-\pi^+)/\Gamma(\Omega^-e^+\nu_e)$ — Γ_5/Γ_4

VALUE	EVTS	DOCUMENT ID		TECN	COMMENT
0.41 ± 0.19 ± 0.04	11	AMMAR	02	CLE2	e^+e^- ≈ $\Upsilon(4S)$

$\Gamma(\Omega^-\pi^+)/\Gamma_{total}$ — Γ_5/Γ

VALUE	EVTS	DOCUMENT ID		TECN	COMMENT
seen	13	CRONIN-HEN..	01	CLE2	e^+e^- ≈ 10.6 GeV
seen	10	FRABETTI	93	E687	γBe, $\overline{E}_\gamma$ = 221 GeV

$\Gamma(\Omega^-\pi^+\pi^0)/\Gamma(\Omega^-\pi^+)$ — Γ_6/Γ_5

VALUE	EVTS	DOCUMENT ID		TECN	COMMENT
4.2 ± 2.2 ± 0.9	12	CRONIN-HEN..	01	CLE2	e^+e^- ≈ 10.6 GeV

$\Gamma(\Omega^-\pi^-\pi^+\pi^+)/\Gamma(\Omega^-\pi^+)$ — Γ_7/Γ_5

VALUE	CL%	DOCUMENT ID		TECN	COMMENT
seen		ADAMOVICH	95B	WA89	Σ^- 340 GeV
• • • We do not use the following data for averages, fits, limits, etc. • • •					
< 0.56	90	CRONIN-HEN..	01	CLE2	e^+e^- ≈ 10.6 GeV
< 1.6	90	FRABETTI	93	E687	γBe, $\overline{E}_\gamma$ = 221 GeV

Ω_c^0 REFERENCES

LINK	03C	PL B561 41	J.M. Link *et al.*	(FNAL FOCUS Collab.)
AMMAR	02	PRL 89 171803	R. Ammar *et al.*	(CLEO Collab.)
CRONIN-HEN...	01	PRL 86 3730	D. Cronin-Hennessy *et al.*	(CLEO Collab.)
ADAMOVICH	95B	PL B358 151	M.I. Adamovich *et al.*	(CERN WA89 Collab.)
FRABETTI	95D	PL B357 678	P.L. Frabetti *et al.*	(FNAL E687 Collab.)
FRABETTI	94H	PL B338 106	P.L. Frabetti *et al.*	(FNAL E687 Collab.)
FRABETTI	93	PL B300 190	P.L. Frabetti *et al.*	(FNAL E687 Collab.)
ALBRECHT	92H	PL B288 367	H. Albrecht *et al.*	(ARGUS Collab.)
BIAGI	85B	ZPHY C28 175	S.F. Biagi *et al.*	(CERN WA62 Collab.)

See key on page 323

DOUBLY-CHARMED BARYONS ($C = +2$)

$\Xi_{cc}^{++} = ucc$, $\Xi_{cc}^{+} = dcc$, $\Omega_{cc}^{+} = scc$

Ξ_{cc}^{+}

$I(J^P) = ?(?^?)$ Status: *

OMITTED FROM SUMMARY TABLE

MATTSON 02 claims "an excess of 15.9 events over an expected background of 6.1 ± 0.5 events, a statistical significance of 6.3σ" in the $\Lambda_c^+ K^- \pi^+$ invariant-mass spectrum. The probability that the peak is a fluctuation increases from 1.0×10^{-6} to 1.1×10^{-4} when the number of bins searched is considered.

See the paper for various other tests made of the significance of the signal. Confirmation is needed before the state can be considered to be established.

Ξ_{cc}^{+} MASS

VALUE (MeV)	EVTS	DOCUMENT ID		TECN	COMMENT
3519 ±1	16	[1] MATTSON	02	SELX	Σ^- nucleus, $\approx$ 600 GeV

[1] This error is statistical; MATTSON 02 does not give a systematic uncertainty on the mass.

Ξ_{cc}^{+} MEAN LIFE

VALUE (10^{-15} s)	CL%	DOCUMENT ID		TECN	COMMENT
< 33	90	MATTSON	02	SELX	Σ^- nucleus, $\approx$ 600 GeV

Ξ_{cc}^{+} REFERENCES

MATTSON 02 PRL 89 112001 M. Mattson *et al.* (FNAL SELEX Collab.)

BOTTOM BARYONS ($B = -1$)

$\Lambda_b^0 = udb$, $\Xi_b^0 = usb$, $\Xi_b^- = dsb$

Λ_b^0

$I(J^P) = 0(\frac{1}{2}^+)$ Status: ***

In the quark model, a Λ_b^0 is an isospin-0 udb state. The lowest Λ_b^0 ought to have $J^P = 1/2^+$. None of I, J, or P have actually been measured.

Λ_b^0 MASS

VALUE (MeV)	EVTS	DOCUMENT ID		TECN	COMMENT
5624± 9 OUR AVERAGE Error includes scale factor of 1.8. See the ideogram below.					
5621± 4± 3		[1] ABE	97B	CDF	$p\overline{p}$ at 1.8 TeV
5668± 16± 8	4	[2] ABREU	96N	DLPH	$e^+e^- \to Z$
5614± 21± 4	4	[2] BUSKULIC	96L	ALEP	$e^+e^- \to Z$
• • • We do not use the following data for averages, fits, limits, etc. • • •					
not seen		[3] ABE	93B	CDF	Sup. by ABE 97B
5640± 50± 30	16	[4] ALBAJAR	91E	UA1	$p\overline{p}$ 630 GeV
5640^{+100}_{-210}	52	BARI	91	SFM	$\Lambda_b^0 \to pD^0\pi^-$
5650^{+150}_{-200}	90	BARI	91	SFM	$\Lambda_b^0 \to \Lambda_c^+\pi^+\pi^-\pi^-$

[1] ABE 97B observed 38 events above a background 18 ± 1.6 events in the mass range 5.60–5.65 GeV/c^2, a significance of > 3.4 standard deviations.

[2] Uses 4 fully reconstructed Λ_b events.

[3] ABE 93B states that, based on the signal claimed by ALBAJAR 91E, CDF should have found 30 ± 23 $\Lambda_b^0 \to J/\psi(1S)\Lambda$ events. Instead, CDF found not more than 2 events.

[4] ALBAJAR 91E claims 16 ± 5 events above a background of 9 ± 1 events, a significance of about 5 standard deviations.

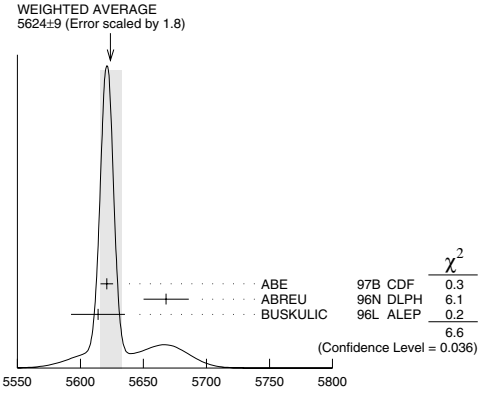

Λ_b^0 MEAN LIFE

These are actually measurements of the average lifetime of weakly decaying b baryons weighted by generally unknown production rates, branching fractions, and detection efficiencies. Presumably, the mix is mainly Λ_b^0, with some Ξ_b^0 and Ξ_b^-.

See b-baryon Admixture section for data on b-baryon mean life average over species of b-baryon particles.

"OUR EVALUATION" is an average using rescaled values of the data listed below. The average and rescaling were performed by the Heavy Flavor Averaging Group (HFAG) and are described at http://www.slac.stanford.edu/xorg/hfag/. The averaging/rescaling procedure takes into account corrections between the measurements and asymmetric lifetime errors.

VALUE (10^{-12} s)	EVTS	DOCUMENT ID		TECN	COMMENT
1.229±0.080 OUR EVALUATION					
$1.11\ ^{+0.19}_{-0.18}\ \pm 0.05$		[5] ABREU	99W	DLPH	$e^+e^- \to Z$
$1.29\ ^{+0.24}_{-0.22}\ \pm 0.06$		[5] ACKERSTAFF	98G	OPAL	$e^+e^- \to Z$
1.21 ±0.11		[5] BARATE	98D	ALEP	$e^+e^- \to Z$
1.32 ±0.15 ±0.07		ABE	96M	CDF	Excess $\Lambda_c\ell^-$, decay lengths
• • • We do not use the following data for averages, fits, limits, etc. • • •					
$1.19\ ^{+0.21}_{-0.18}\ ^{+0.07}_{-0.08}$		ABREU	96D	DLPH	Repl. by ABREU 99W
$1.14\ ^{+0.22}_{-0.19}\ \pm 0.07$	69	AKERS	95K	OPAL	Repl. by ACKERSTAFF 98G
$1.02\ ^{+0.23}_{-0.18}\ \pm 0.06$	44	BUSKULIC	95L	ALEP	Repl. by BARATE 98D

[5] Measured using $\Lambda_c\ell^-$ and $\Lambda\ell^+\ell^-$.

Λ_b^0 DECAY MODES

These branching fractions are actually an average over weakly decaying b-baryons weighted by their production rates in Z decay (or high-energy $p\overline{p}$), branching ratios, and detection efficiencies. They scale with the LEP b-baryon production fraction $B(b \to b\text{-baryon})$ and are evaluated for our value $B(b \to b\text{-baryon}) = (9.9 \pm 1.7)\%$.

The branching fractions $B(b\text{-baryon} \to \Lambda\ell^-\overline{\nu}_\ell \text{anything})$ and $B(\Lambda_b^0 \to \Lambda_c^+\ell^-\overline{\nu}_\ell \text{anything})$ are not pure measurements because the underlying measured products of these with $B(b \to b\text{-baryon})$ were used to determine $B(b \to b\text{-baryon})$, as described in the note "Production and Decay of b-Flavored Hadrons."

For inclusive branching fractions, *e.g.*, $B \to D^\pm$ anything, the values usually are multiplicities, not branching fractions. They can be greater than one.

	Mode	Fraction (Γ_i/Γ)		Confidence level
Γ_1	$J/\psi(1S)\Lambda$	$(4.7 \pm 2.8) \times 10^{-4}$		
Γ_2	$pD^0\pi^-$			
Γ_3	$\Lambda_c^+\pi^-$	seen		
Γ_4	$\Lambda_c^+ a_1(1260)^-$	seen		
Γ_5	$\Lambda_c^+\pi^+\pi^-\pi^-$			
Γ_6	$\Lambda K^0 2\pi^+ 2\pi^-$			
Γ_7	$\Lambda_c^+\ell^-\overline{\nu}_\ell$ anything	[a] (9.2 ± 2.1) %		
Γ_8	$p\pi^-$	< 5.0	$\times 10^{-5}$	90%
Γ_9	pK^-	< 5.0	$\times 10^{-5}$	90%
Γ_{10}	$\Lambda\gamma$	< 1.3	$\times 10^{-3}$	90%

[a] Not a pure measurement. See note at head of Λ_b^0 Decay Modes.

Λ_b^0 BRANCHING RATIOS

$\Gamma(J/\psi(1S)\Lambda)/\Gamma_{total}$ Γ_1/Γ

VALUE (units 10^{-4})	EVTS	DOCUMENT ID		TECN	COMMENT
4.7± 2.1± 1.9		[6] ABE	97B	CDF	$p\overline{p}$ at 1.8 TeV
• • • We do not use the following data for averages, fits, limits, etc. • • •					
182. ±111. ±31.	16	[7] ALBAJAR	91E	UA1	$J/\psi(1S) \to \mu^+\mu^-$

[6] ABE 97B reports $(0.037 \pm 0.017(\text{stat}) \pm 0.007(\text{sys}))\%$ for $B(b \to b\text{-baryon}) = 0.1$ and for $B(B^0 \to J/\psi(1S)K_S^0) = 0.037\%$. We rescale to our PDG 98 best value $B(b \to b\text{-baryon}) = (10.1^{+3.9}_{-3.1})\%$ and $B(B^0 \to J/\psi(1S)K_S^0) = (0.044 \pm 0.006)\%$. Our first error is their experiments's error and our second error is the systematic error from using our best value.

[7] ALBAJAR 91E reports 180 ± 110 for $B(\overline{b} \to b\text{-baryon}) = 0.10$. We rescale to our best value $B(\overline{b} \to b\text{-baryon}) = (9.9 \pm 1.7) \times 10^{-2}$. Our first error is their experiment's error and our second error is the systematic error from using our best value.

$\Gamma(pD^0\pi^-)/\Gamma_{total}$ Γ_2/Γ

VALUE	EVTS	DOCUMENT ID		TECN	COMMENT
• • • We do not use the following data for averages, fits, limits, etc. • • •					
seen	52	BARI	91	SFM	$D^0 \to K^-\pi^+$
seen		BASILE	81	SFM	$D^0 \to K^-\pi^+$

$\Gamma(\Lambda_c^+\pi^-)/\Gamma_{total}$ Γ_3/Γ

VALUE	EVTS	DOCUMENT ID		TECN	COMMENT
seen	3	ABREU	96N	DLPH	$\Lambda_c^+ \to pK^-\pi^+$
seen	4	BUSKULIC	96L	ALEP	$\Lambda_c^+ \to pK^-\pi^+$, $p\overline{K}^0$, $\Lambda\pi^+\pi^+\pi^-$

$\Gamma(\Lambda_c^+ a_1(1260)^-)/\Gamma_{total}$ Γ_4/Γ

VALUE	EVTS	DOCUMENT ID		TECN	COMMENT
seen	1	ABREU	96N	DLPH	$\Lambda_c^+ \to pK^-\pi^+$, $a_1^- \to \rho^0\pi^- \to \pi^+\pi^-\pi^-$

$\Gamma(\Lambda_c^+\pi^+\pi^-\pi^-)/\Gamma_{total}$ Γ_5/Γ

VALUE	EVTS	DOCUMENT ID		TECN	COMMENT
• • • We do not use the following data for averages, fits, limits, etc. • • •					
seen	90	BARI	91	SFM	$\Lambda_c^+ \to pK^-\pi^+$

$\Gamma(\Lambda K^0 2\pi^+ 2\pi^-)/\Gamma_{total}$ Γ_6/Γ

VALUE	EVTS	DOCUMENT ID		TECN	COMMENT
• • • We do not use the following data for averages, fits, limits, etc. • • •					
seen	4	[8] ARENTON	86	FMPS	$\Lambda K_S^0 2\pi^+ 2\pi^-$

[8] See the footnote to the ARENTON 86 mass value.

$\Gamma(\Lambda_c^+ \ell^- \overline{\nu}_\ell \text{anything})/\Gamma_{total}$ Γ_7/Γ

The values and averages in this section serve only to show what values result if one assumes our B($b \to$ b-baryon). They cannot be thought of as measurements since the underlying product branching fractions were also used to determine B($b \to$ b-baryon) as described in the note on "Production and Decay of b-Flavored Hadrons."

VALUE	EVTS	DOCUMENT ID		TECN	COMMENT
0.092±0.021 OUR AVERAGE					
$0.087 \pm 0.016 \pm 0.015$		[9] BARATE	98D	ALEP	$e^+e^- \to Z$
$0.119^{+0.041}_{-0.034} \pm 0.020$	29	[10] ABREU	95S	DLPH	$e^+e^- \to Z$
• • • We do not use the following data for averages, fits, limits, etc. • • •					
$0.076 \pm 0.019 \pm 0.013$	55	[11] BUSKULIC	95L	ALEP	Repl. by BARATE 98D
$0.15 \pm 0.06 \pm 0.03$	21	[12] BUSKULIC	92E	ALEP	$\Lambda_c^+ \to pK^-\pi^+$

[9] BARATE 98D reports [B($\Lambda_b^0 \to \Lambda_c^+ \ell^- \overline{\nu}_\ell$ anything) × B($\overline{b} \to$ b-baryon)] = $0.0086 \pm 0.0007 \pm 0.0014$. We divide by our best value B($\overline{b} \to$ b-baryon) = $(9.9 \pm 1.7) \times 10^{-2}$. Our first error is their experiment's error and our second error is the systematic error from using our best value. Measured using $\Lambda_c \ell^-$ and $\Lambda \ell^+ \ell^-$.

[10] ABREU 95S reports [B($\Lambda_b^0 \to \Lambda_c^+ \ell^- \overline{\nu}_\ell$ anything) × B($\overline{b} \to$ b-baryon)] = $0.0118 \pm 0.0026^{+0.0031}_{-0.0021}$. We divide by our best value B($\overline{b} \to$ b-baryon) = $(9.9 \pm 1.7) \times 10^{-2}$. Our first error is their experiment's error and our second error is the systematic error from using our best value.

[11] BUSKULIC 95L reports [B($\Lambda_b^0 \to \Lambda_c^+ \ell^- \overline{\nu}_\ell$ anything) × B($\overline{b} \to$ b-baryon)] = $0.00755 \pm 0.0014 \pm 0.0012$. We divide by our best value B($\overline{b} \to$ b-baryon) = $(9.9 \pm 1.7) \times 10^{-2}$. Our first error is their experiment's error and our second error is the systematic error from using our best value.

[12] BUSKULIC 92E reports [B($\Lambda_b^0 \to \Lambda_c^+ \ell^- \overline{\nu}_\ell$ anything) × B($\overline{b} \to$ b-baryon)] = $0.015 \pm 0.0035 \pm 0.0045$. We divide by our best value B($\overline{b} \to$ b-baryon) = $(9.9 \pm 1.7) \times 10^{-2}$. Our first error is their experiment's error and our second error is the systematic error from using our best value. Superseded by BUSKULIC 95L.

$\Gamma(p\pi^-)/\Gamma_{total}$ Γ_8/Γ

VALUE	CL%	DOCUMENT ID		TECN	COMMENT
$< 5.0 \times 10^{-5}$	90	[13] BUSKULIC	96V	ALEP	$e^+e^- \to Z$

[13] BUSKULIC 96V assumes PDG 96 production fractions for B^0, B^+, B_s, b baryons.

$\Gamma(pK^-)/\Gamma_{total}$ Γ_9/Γ

VALUE	CL%	DOCUMENT ID		TECN	COMMENT
$< 5.0 \times 10^{-5}$	90	[14] BUSKULIC	96V	ALEP	$e^+e^- \to Z$
• • • We do not use the following data for averages, fits, limits, etc. • • •					
$< 3.6 \times 10^{-4}$	90	[15] ADAM	96D	DLPH	$e^+e^- \to Z$

[14] BUSKULIC 96V assumes PDG 96 production fractions for B^0, B^+, B_s, b baryons.

[15] ADAM 96D assumes $f_{B^0} = f_{B^-} = 0.39$ and $f_{B_s} = 0.12$.

$\Gamma(\Lambda\gamma)/\Gamma_{total}$ Γ_{10}/Γ

VALUE	CL%	DOCUMENT ID		TECN	COMMENT
$< 1.3 \times 10^{-3}$	90	ACOSTA	02G	CDF	$p\overline{p}$ at 1.8 TeV

Λ_b^0 REFERENCES

ACOSTA	02G	PR D66 112002	D. Acosta *et al.*	(CDF Collab.)
ABREU	99W	EPJ C10 185	P. Abreu *et al.*	(DELPHI Collab.)
ACKERSTAFF	98G	PL B426 161	K. Ackerstaff *et al.*	(OPAL Collab.)
BARATE	98D	EPJ C2 197	R. Barate *et al.*	(ALEPH Collab.)
PDG	98	EPJ C3 1	C. Caso *et al.*	
ABE	97B	PR D55 1142	F. Abe *et al.*	(CDF Collab.)
ABE	96M	PRL 77 1439	F. Abe *et al.*	(CDF Collab.)
ABREU	96D	ZPHY C71 199	P. Abreu *et al.*	(DELPHI Collab.)
ABREU	96N	PL B374 351	P. Abreu *et al.*	(DELPHI Collab.)
ADAM	96D	ZPHY C72 207	W. Adam *et al.*	(DELPHI Collab.)
BUSKULIC	96L	PL B380 442	D. Buskulic *et al.*	(ALEPH Collab.)
BUSKULIC	96V	PL B384 471	D. Buskulic *et al.*	(ALEPH Collab.)
PDG	96	PR D54 1	R. M. Barnett *et al.*	
ABREU	95S	ZPHY C68 375	P. Abreu *et al.*	(DELPHI Collab.)
AKERS	95K	PL B353 402	R. Akers *et al.*	(OPAL Collab.)
BUSKULIC	95L	PL B357 685	D. Buskulic *et al.*	(ALEPH Collab.)
ABE	93B	PR D47 R2639	F. Abe *et al.*	(CDF Collab.)
BUSKULIC	92E	PL B294 145	D. Buskulic *et al.*	(ALEPH Collab.)
ALBAJAR	91E	PL B273 540	C. Albajar *et al.*	(UA1 Collab.)
BARI	91	NC 104A 1787	G. Bari *et al.*	(CERN R422 Collab.)
ARENTON	86	NP B274 707	M.W. Arenton *et al.*	(ARIZ, NDAM, VAND)
BASILE	81	LNC 31 97	M. Basile *et al.*	(CERN R415 Collab.)

Ξ_b^0, Ξ_b^-

$I(J^P) = \frac{1}{2}(\frac{1}{2}^+)$ Status: *

OMITTED FROM SUMMARY TABLE

ABREU 95V observe an excess of same-sign $\Xi^\mp \ell^\mp$ events in jets, which they interpret as $\Xi_b \to \Xi^- \ell^- \overline{\nu}_\ell$X. They find that the probability for these events to come from non-b-baryon decays is less than 5×10^{-4} and that Λ_b decays can account for less than 10% of these events.

In the quark model, Ξ_b^0 and Ξ_b^- are an isodoublet (usb, dsb) state; the lowest Ξ_b^0 and Ξ_b^- ought to have $J^P = 1/2^+$. None of I, J, or P have actually been measured.

Ξ_b MEAN LIFE

This is actually a measurement of the average lifetime of b-baryons that decay to a jet containing a same-sign $\Xi^\mp \ell^\mp$ pair. Presumably the mix is mainly Ξ_b, with some Λ_b.

"OUR EVALUATION" is an average using rescaled values of the data listed below. The average and rescaling were performed by the Heavy Flavor Averaging Group (HFAG) and are described at http://www.slac.stanford.edu/xorg/hfag/. The averaging/rescaling procedure takes into account corrections between the measurements and asymmetric lifetime errors.

VALUE (10^{-12} s)	EVTS	DOCUMENT ID		TECN	COMMENT
$1.39^{+0.34}_{-0.28}$ OUR EVALUATION					
$1.35^{+0.37}_{-0.28}{}^{+0.15}_{-0.17}$		BUSKULIC	96T	ALEP	Excess $\Xi^- \ell^-$, impact parameters
$1.5 \ ^{+0.7}_{-0.4} \pm 0.3$	8	ABREU	95V	DLPH	Excess $\Xi^- \ell^-$, decay lengths

Ξ_b DECAY MODES

	Mode	Fraction (Γ_i/Γ)
Γ_1	$\Xi^- \ell^- \overline{\nu}_\ell$ anything	seen

Ξ_b BRANCHING RATIOS

$\Gamma(\Xi^- \ell^- \overline{\nu}_\ell \text{anything})/\Gamma_{total}$ Γ_1/Γ

VALUE	DOCUMENT ID		TECN	COMMENT
seen	[1] BUSKULIC	96T	ALEP	Excess $\Xi^- \ell^-$ over $\Xi^- \ell^+$
seen	ABREU	95V	DLPH	Excess $\Xi^- \ell^-$ over $\Xi^- \ell^+$

[1] BUSKULIC 96T measures [B($b \to \Xi_b$) × B($\Xi_b \to \Xi^- \ell^- \overline{\nu}_\ell$ anything)] = $(5.4 \pm 1.1 \pm 0.8) \times 10^{-4}$ per lepton species, averaged over e and μ.

Ξ_b REFERENCES

BUSKULIC	96T	PL B384 449	D. Buskulic *et al.*	(ALEPH Collab.)
ABREU	95V	ZPHY C68 541	P. Abreu *et al.*	(DELPHI Collab.)

b-baryon ADMIXTURE (Λ_b, Ξ_b, Σ_b, Ω_b)

b-baryon ADMIXTURE MEAN LIFE

Each measurement of the b-baryon mean life is an average over an admixture of various b baryons which decay weakly. Different techniques emphasize different admixtures of produced particles, which could result in a different b-baryon mean life. More b-baryon flavor specific channels are not included in the measurement.

"OUR EVALUATION" is an average using rescaled values of the data listed below. The average and rescaling were performed by the Heavy Flavor Averaging Group (HFAG) and are described at http://www.slac.stanford.edu/xorg/hfag/. The averaging/rescaling procedure takes into account corrections between the measurements and asymmetric lifetime errors.

VALUE (10^{-12} s)	EVTS	DOCUMENT ID		TECN	COMMENT
1.208±0.051 OUR EVALUATION					
$1.16 \pm 0.20 \pm 0.08$		[1] ABREU	99W	DLPH	$e^+e^- \to Z$
$1.19 \pm 0.14 \pm 0.07$		[2] ABREU	99W	DLPH	$e^+e^- \to Z$
$1.20 \pm 0.08 \pm 0.06$		[3] BARATE	98D	ALEP	$e^+e^- \to Z$
$1.10 \ ^{+0.19}_{-0.17} \pm 0.09$		ABREU	96D	DLPH	Excess $\Lambda\mu^-$ impact parameters
$1.16 \pm 0.11 \pm 0.06$		AKERS	96	OPAL	Excess $\Lambda\ell^-$, decay lengths and impact parameters

Baryon Particle Listings

b-baryon ADMIXTURE (Λ_b, Ξ_b, Σ_b, Ω_b)

• • • We do not use the following data for averages, fits, limits, etc. • • •

$1.14 \pm 0.08 \pm 0.04$		[4] ABREU	99W	DLPH	$e^+e^- \to Z$	
$1.46 \,^{+0.22}_{-0.21} \,^{+0.07}_{-0.09}$		ABREU	96D	DLPH	Repl. by ABREU 99W	
$1.27 \,^{+0.35}_{-0.29} \pm 0.09$		ABREU	95S	DLPH	Repl. by ABREU 99W	
$1.05 \,^{+0.12}_{-0.11} \pm 0.09$	290	BUSKULIC	95L	ALEP	Repl. by BARATE 98D	
$1.04 \,^{+0.48}_{-0.38} \pm 0.10$	11	[5] ABREU	93F	DLPH	Excess $\Lambda\mu^-$, decay lengths	
$1.05 \,^{+0.23}_{-0.20} \pm 0.08$	157	[6] AKERS	93	OPAL	Excess $\Lambda\ell^-$, decay lengths	
$1.12 \,^{+0.32}_{-0.29} \pm 0.16$	101	[7] BUSKULIC	92I	ALEP	Excess $\Lambda\ell^-$, impact parameters	

[1] Measured using $\Lambda\ell^-$ decay length.
[2] Measured using $p\ell^-$ decay length.
[3] Measured using the excess of $\Lambda\ell^-$, lepton impact parameter.
[4] This ABREU 99W result is the combined result of the $\Lambda\ell^-$, $p\ell^-$, and excess $\Lambda\mu^-$ impact parameter measurements.
[5] ABREU 93F superseded by ABREU 96D.
[6] AKERS 93 superseded by AKERS 96.
[7] BUSKULIC 92I superseded by BUSKULIC 95L.

b-baryon ADMIXTURE DECAY MODES (Λ_b, Ξ_b, Σ_b, Ω_b)

These branching fractions are actually an average over weakly decaying b-baryons weighted by their production rates in Z decay (or high-energy $p\overline{p}$), branching ratios, and detection efficiencies. They scale with the LEP b-baryon production fraction $B(b \to b\text{-baryon})$ and are evaluated for our value $B(b \to b\text{-baryon}) = (9.9 \pm 1.7)\%$.

The branching fractions $B(b\text{-baryon} \to \Lambda\ell^-\overline{\nu}_\ell \text{ anything})$ and $B(\Lambda_b^0 \to \Lambda_c^+\ell^-\overline{\nu}_\ell \text{ anything})$ are not pure measurements because the underlying measured products of these with $B(b \to b\text{-baryon})$ were used to determine $B(b \to b\text{-baryon})$, as described in the note "Production and Decay of b-Flavored Hadrons."

For inclusive branching fractions, *e.g.*, $B \to D^\pm$ anything, the values usually are multiplicities, not branching fractions. They can be greater than one.

	Mode	Fraction (Γ_i/Γ)
Γ_1	$p\mu^-\overline{\nu}$ anything	$(4.9^{+2.1}_{-1.8})\%$
Γ_2	$p\ell\overline{\nu}_\ell$ anything	$(4.8 \pm 1.1)\%$
Γ_3	p anything	$(60 \pm 20)\%$
Γ_4	$\Lambda\ell^-\overline{\nu}_\ell$ anything	$(3.2 \pm 0.6)\%$
Γ_5	$\Lambda\ell^+\nu_\ell$ anything	
Γ_6	Λ anything	
Γ_7	$\Lambda_c^+\ell^-\overline{\nu}_\ell$ anything	
Γ_8	$\Lambda/\overline{\Lambda}$ anything	$(33 \pm 7)\%$
Γ_9	$\Xi^-\ell^-\overline{\nu}_\ell$ anything	$(5.6 \pm 1.5) \times 10^{-3}$

b-baryon ADMIXTURE (Λ_b, Ξ_b, Σ_b, Ω_b) BRANCHING RATIOS

$\Gamma(p\mu^-\overline{\nu}\text{anything})/\Gamma_{\text{total}}$ Γ_1/Γ

VALUE	EVTS	DOCUMENT ID		TECN	COMMENT
$\mathbf{0.049^{+0.019}_{-0.016} \pm 0.008}$	125	[8] ABREU	95S	DLPH	$e^+e^- \to Z$

[8] ABREU 95S reports $[B(b\text{-baryon} \to p\mu^-\overline{\nu}\text{anything}) \times B(\overline{b} \to b\text{-baryon})] = 0.0049 \pm 0.0011^{+0.0015}_{-0.0011}$. We divide by our best value $B(\overline{b} \to b\text{-baryon}) = (9.9 \pm 1.7) \times 10^{-2}$. Our first error is their experiment's error and our second error is the systematic error from using our best value.

$\Gamma(p\ell\overline{\nu}_\ell\text{anything})/\Gamma_{\text{total}}$ Γ_2/Γ

VALUE	DOCUMENT ID		TECN	COMMENT
$\mathbf{0.048 \pm 0.008 \pm 0.008}$	[9] BARATE	98V	ALEP	$e^+e^- \to Z$

[9] BARATE 98V reports $[B(b\text{-baryon} \to p\ell\overline{\nu}_\ell\text{anything}) \times B(\overline{b} \to b\text{-baryon})] = (4.72 \pm 0.66 \pm 0.44) \times 10^{-3}$. We divide by our best value $B(\overline{b} \to b\text{-baryon}) = (9.9 \pm 1.7) \times 10^{-2}$. Our first error is their experiment's error and our second error is the systematic error from using our best value.

$\Gamma(p\ell\overline{\nu}_\ell\text{anything})/\Gamma(p\text{anything})$ Γ_2/Γ_3

VALUE	DOCUMENT ID		TECN	COMMENT
$\mathbf{0.080 \pm 0.012 \pm 0.014}$	BARATE	98V	ALEP	$e^+e^- \to Z$

$\Gamma(\Lambda\ell^-\overline{\nu}_\ell\text{anything})/\Gamma_{\text{total}}$ Γ_4/Γ

The values and averages in this section serve only to show what values result if one assumes our $B(b \to b\text{-baryon})$. They cannot be thought of as measurements since the underlying product branching fractions were also used to determine $B(b \to b\text{-baryon})$ as described in the note on "Production and Decay of b-Flavored Hadrons."

VALUE	EVTS	DOCUMENT ID		TECN	COMMENT
0.032 ± 0.006 OUR AVERAGE					
$0.033 \pm 0.004 \pm 0.006$		[10] BARATE	98D	ALEP	$e^+e^- \to Z$
$0.029 \pm 0.003 \pm 0.005$		[11] AKERS	96	OPAL	Excess of $\Lambda\ell^-$ over $\Lambda\ell^+$
$0.030 \pm 0.007 \pm 0.005$	262	[12] ABREU	95S	DLPH	Excess of $\Lambda\ell^-$ over $\Lambda\ell^+$
$0.062 \pm 0.012 \pm 0.011$	290	[13] BUSKULIC	95L	ALEP	Excess of $\Lambda\ell^-$ over $\Lambda\ell^+$
• • • We do not use the following data for averages, fits, limits, etc. • • •					
seen	157	[14] AKERS	93	OPAL	Excess of $\Lambda\ell^-$ over $\Lambda\ell^+$
$0.071 \pm 0.021 \pm 0.012$	101	[15] BUSKULIC	92I	ALEP	Excess of $\Lambda\ell^-$ over $\Lambda\ell^+$

[10] BARATE 98D reports $[B(b\text{-baryon} \to \Lambda\ell^-\overline{\nu}_\ell\text{anything}) \times B(\overline{b} \to b\text{-baryon})] = 0.00326 \pm 0.00016 \pm 0.00039$. We divide by our best value $B(\overline{b} \to b\text{-baryon}) = (9.9 \pm 1.7) \times 10^{-2}$. Our first error is their experiment's error and our second error is the systematic error from using our best value. Measured using the excess of $\Lambda\ell^-$, lepton impact parameter.

[11] AKERS 96 reports $[B(b\text{-baryon} \to \Lambda\ell^-\overline{\nu}_\ell\text{anything}) \times B(\overline{b} \to b\text{-baryon})] = 0.00291 \pm 0.00023 \pm 0.00025$. We divide by our best value $B(\overline{b} \to b\text{-baryon}) = (9.9 \pm 1.7) \times 10^{-2}$. Our first error is their experiment's error and our second error is the systematic error from using our best value.

[12] ABREU 95S reports $[B(b\text{-baryon} \to \Lambda\ell^-\overline{\nu}_\ell\text{anything}) \times B(\overline{b} \to b\text{-baryon})] = 0.0030 \pm 0.0006 \pm 0.0004$. We divide by our best value $B(\overline{b} \to b\text{-baryon}) = (9.9 \pm 1.7) \times 10^{-2}$. Our first error is their experiment's error and our second error is the systematic error from using our best value.

[13] BUSKULIC 95L reports $[B(b\text{-baryon} \to \Lambda\ell^-\overline{\nu}_\ell\text{anything}) \times B(\overline{b} \to b\text{-baryon})] = 0.0061 \pm 0.0006 \pm 0.0010$. We divide by our best value $B(\overline{b} \to b\text{-baryon}) = (9.9 \pm 1.7) \times 10^{-2}$. Our first error is their experiment's error and our second error is the systematic error from using our best value.

[14] AKERS 93 superseded by AKERS 96.

[15] BUSKULIC 92I reports $[B(b\text{-baryon} \to \Lambda\ell^-\overline{\nu}_\ell\text{anything}) \times B(\overline{b} \to b\text{-baryon})] = 0.0070 \pm 0.0010 \pm 0.0018$. We divide by our best value $B(\overline{b} \to b\text{-baryon}) = (9.9 \pm 1.7) \times 10^{-2}$. Our first error is their experiment's error and our second error is the systematic error from using our best value. Superseded by BUSKULIC 95L.

$\Gamma(\Lambda\ell^+\nu_\ell\text{anything})/\Gamma(\Lambda\text{anything})$ Γ_5/Γ_6

VALUE	DOCUMENT ID		TECN	COMMENT
$\mathbf{0.080 \pm 0.012 \pm 0.008}$	ABBIENDI	99L	OPAL	$e^+e^- \to Z$
• • • We do not use the following data for averages, fits, limits, etc. • • •				
$0.070 \pm 0.012 \pm 0.007$	ACKERSTAFF	97N	OPAL	Repl. by ABBIENDI 99L

$\Gamma(\Lambda/\overline{\Lambda}\text{anything})/\Gamma_{\text{total}}$ Γ_8/Γ

VALUE	DOCUMENT ID		TECN	COMMENT
0.33 ± 0.07 OUR AVERAGE				
$0.35 \pm 0.05 \pm 0.06$	[16] ABBIENDI	99L	OPAL	$e^+e^- \to Z$
$0.23^{+0.13}_{-0.08} \pm 0.04$	[17] ABREU	95C	DLPH	$e^+e^- \to Z$
• • • We do not use the following data for averages, fits, limits, etc. • • •				
$0.40 \pm 0.06 \pm 0.07$	[18] ACKERSTAFF	97N	OPAL	Repl. by ABBIENDI 99L

[16] ABBIENDI 99L reports $[B(b\text{-baryon} \to \Lambda/\overline{\Lambda}\text{anything}) \times B(\overline{b} \to b\text{-baryon})] = 0.035 \pm 0.0032 \pm 0.0035$. We divide by our best value $B(\overline{b} \to b\text{-baryon}) = (9.9 \pm 1.7) \times 10^{-2}$. Our first error is their experiment's error and our second error is the systematic error from using our best value.

[17] ABREU 95C reports $0.28^{+0.17}_{-0.12}$ for $B(\overline{b} \to b\text{-baryon}) = 0.08 \pm 0.02$. We rescale to our best value $B(\overline{b} \to b\text{-baryon}) = (9.9 \pm 1.7) \times 10^{-2}$. Our first error is their experiment's error and our second error is the systematic error from using our best value.

[18] ACKERSTAFF 97N reports $[B(b\text{-baryon} \to \Lambda/\overline{\Lambda}\text{anything}) \times B(\overline{b} \to b\text{-baryon})] = 0.0393 \pm 0.0046 \pm 0.0037$. We divide by our best value $B(\overline{b} \to b\text{-baryon}) = (9.9 \pm 1.7) \times 10^{-2}$. Our first error is their experiment's error and our second error is the systematic error from using our best value.

$\Gamma(\Xi^-\ell^-\overline{\nu}_\ell\text{anything})/\Gamma_{\text{total}}$ Γ_9/Γ

VALUE	DOCUMENT ID		TECN	COMMENT
0.0056 ± 0.0015 OUR AVERAGE				
$0.0055 \pm 0.0014 \pm 0.0009$	[19] BUSKULIC	96T	ALEP	Excess $\Xi^-\ell^-$ over $\Xi^-\ell^+$
$0.0060 \pm 0.0023 \pm 0.0010$	[20] ABREU	95V	DLPH	Excess $\Xi^-\ell^-$ over $\Xi^-\ell^+$

[19] BUSKULIC 96T reports $[B(b\text{-baryon} \to \Xi^-\ell^-\overline{\nu}_\ell\text{anything}) \times B(\overline{b} \to b\text{-baryon})] = 0.00054 \pm 0.00011 \pm 0.00008$. We divide by our best value $B(\overline{b} \to b\text{-baryon}) = (9.9 \pm 1.7) \times 10^{-2}$. Our first error is their experiment's error and our second error is the systematic error from using our best value.

[20] ABREU 95V reports $[B(b\text{-baryon} \to \Xi^-\ell^-\overline{\nu}_\ell\text{anything}) \times B(\overline{b} \to b\text{-baryon})] = 0.00059 \pm 0.00021 \pm 0.0001$. We divide by our best value $B(\overline{b} \to b\text{-baryon}) = (9.9 \pm 1.7) \times 10^{-2}$. Our first error is their experiment's error and our second error is the systematic error from using our best value.

See key on page 323

b-baryon ADMIXTURE (Λ_b, Ξ_b, Σ_b, Ω_b) REFERENCES

ABBIENDI	99L	EPJ C9 1	G. Abbiendi *et al.*	(OPAL Collab.)
ABREU	99W	EPJ C10 185	P. Abreu *et al.*	(DELPHI Collab.)
BARATE	98D	EPJ C2 197	R. Barate *et al.*	(ALEPH Collab.)
BARATE	98V	EPJ C5 205	R. Barate *et al.*	(ALEPH Collab.)
ACKERSTAFF	97N	ZPHY C74 423	K. Ackerstaff *et al.*	(OPAL Collab.)
ABREU	96D	ZPHY C71 199	P. Abreu *et al.*	(DELPHI Collab.)
AKERS	96	ZPHY C69 195	R. Akers *et al.*	(OPAL Collab.)
BUSKULIC	96T	PL B384 449	D. Buskulic *et al.*	(ALEPH Collab.)
ABREU	95C	PL B347 447	P. Abreu *et al.*	(DELPHI Collab.)
ABREU	95S	ZPHY C68 375	P. Abreu *et al.*	(DELPHI Collab.)
ABREU	95V	ZPHY C68 541	P. Abreu *et al.*	(DELPHI Collab.)
BUSKULIC	95L	PL B357 685	D. Buskulic *et al.*	(ALEPH Collab.)
ABREU	93F	PL B311 379	P. Abreu *et al.*	(DELPHI Collab.)
AKERS	93	PL B316 435	R. Akers *et al.*	(OPAL Collab.)
BUSKULIC	92I	PL B297 449	D. Buskulic *et al.*	(ALEPH Collab.)

SEARCHES*

Notes in the Search Listings

* See the Boson Particle Listings for searches for Higgs bosons, other heavy bosons, and axions and other very light bosons; the Lepton Particle Listings for searches for heavy leptons and for neutrino mixing; the Quark Particle Listings for free quark searches; and the Meson Particle Listings for searches for top and fourth-generation hadrons.

SEARCHES FOR MONOPOLES, SUPERSYMMETRY, TECHNICOLOR, COMPOSITENESS, EXTRA DIMENSIONS, etc.

Magnetic Monopole Searches

MAGNETIC MONOPOLE SEARCHES

Revised December 1997 by D.E. Groom (LBNL).

"At the present time (1975) there is no experimental evidence for the existence of magnetic charges or monopoles, but chiefly because of an early, brilliant theoretical argument by Dirac, the search for monopoles is renewed whenever a new energy region is opened up in high energy physics or a new source of matter, such as rocks from the moon, becomes available [1]." Dirac argued that a monopole anywhere in the universe results in electric charge quantization everywhere, and leads to the prediction of a least magnetic charge $g = e/2\alpha$, the Dirac charge [2]. Recently monopoles have become indispensable in many gauge theories, which endow them with a variety of extraordinarily large masses. The discovery by a candidate event in a single superconducting loop in 1982 [6] stimulated an enormous experimental effort to search for supermassive magnetic monopoles [3,4,5].

Monopole detectors have predominantly used either induction or ionization. Induction experiments measure the monopole magnetic charge and are independent of monopole electric charge, mass, and velocity. Monopole candidate events in single semiconductor loops [6,7] have been detected by this method, but no two-loop coincidence has been observed. Ionization experiments rely on a magnetic charge producing more ionization than an electrical charge with the same velocity. In the case of supermassive monopoles, time-of-flight measurements indicating $v \ll c$ has also been a frequently sought signature.

Cosmic rays are the most likely source of massive monopoles, since accelerator energies are insufficient to produce them. Evidence for such monopoles may also be obtained from astrophysical observations.

Jackson's 1975 assessment remains true. The search is somewhat abated by the lack of success in the 1980's and the decrease of interest in grand unified gauge theories.

References

1. J. D. Jackson, *Classical Electrodynamics*, 2nd edition (John Wiley & Sons, New York, 1975).
2. P.A.M. Dirac, Proc. Royal Soc. London **A133**, 60 (1931).
3. J. Preskill, Ann. Rev. Nucl. and Part. Sci. **34**, 461 (1984).
4. G. Giacomelli, La Rivista del Nuovo Cimento **7**, N. 12, 1 (1984).
5. Phys. Rep. **140**, 323 (1986).
6. B. Cabrera, Phys. Rev. Lett. **48**, 1378 (1982) .
7. A.D. Caplin *et al.*, Nature **321**, 402 (1986) .

Monopole Production Cross Section — Accelerator Searches

X-SECT (cm^2)	MASS (GeV)	CHG ($|g|$)	ENERGY (GeV)	BEAM	EVTS	DOCUMENT ID		TECN
< 0.6E−36	>265	1	1800	$p\overline{p}$	0	[1] KALBFLEISCH	04	INDU
< 0.2E−36	>355	2	1800	$p\overline{p}$	0	[1] KALBFLEISCH	04	INDU
< 0.07E−36	>410	3	1800	$p\overline{p}$	0	[1] KALBFLEISCH	04	INDU
< 0.2E−36	>375	6	1800	$p\overline{p}$	0	[1] KALBFLEISCH	04	INDU
< 0.7E−36	>295	1	1800	$p\overline{p}$	0	[2,3] KALBFLEISCH	00	INDU
< 7.8E−36	>260	2	1800	$p\overline{p}$	0	[2,3] KALBFLEISCH	00	INDU
< 2.3E−36	>325	3	1800	$p\overline{p}$	0	[2,4] KALBFLEISCH	00	INDU
< 0.11E−36	>420	6	1800	$p\overline{p}$	0	[2,4] KALBFLEISCH	00	INDU
<0.65E−33	<3.3	≥ 2	11A	^{197}Au	0	[5] HE	97	
<1.90E−33	<8.1	≥ 2	160A	^{208}Pb	0	[5] HE	97	
<3.E−37	<45.0	1.0	88–94	e^+e^-	0	PINFOLD	93	PLAS
<3.E−37	<41.6	2.0	88–94	e^+e^-	0	PINFOLD	93	PLAS
<7.E−35	<44.9	0.2–1.0	89–93	e^+e^-	0	KINOSHITA	92	PLAS
<2.E−34	<850	≥ 0.5	1800	$p\overline{p}$	0	BERTANI	90	PLAS
<1.2E−33	<800	≥ 1	1800	$p\overline{p}$	0	PRICE	90	PLAS
<1.E−37	<29	1	50–61	e^+e^-	0	KINOSHITA	89	PLAS
<1.E−37	<18	2	50–61	e^+e^-	0	KINOSHITA	89	PLAS
<1.E−38	<17	<1	35	e^+e^-	0	BRAUNSCH...	88B	CNTR
<8.E−37	<24	1	50–52	e^+e^-	0	KINOSHITA	88	PLAS
<1.3E−35	<22	2	50–52	e^+e^-	0	KINOSHITA	88	PLAS
<9.E−37	<4	<0.15	10.6	e^+e^-	0	GENTILE	87	CLEO
<3.E−32	<800	≥ 1	1800	$p\overline{p}$	0	PRICE	87	PLAS
<3.E−38		<3	29	e^+e^-	0	FRYBERGER	84	PLAS
<1.E−31		1,3	540	$p\overline{p}$	0	AUBERT	83B	PLAS
<4.E−38	<10	<6	34	e^+e^-	0	MUSSET	83	PLAS
<8.E−36	<20		52	pp	0	[6] DELL	82	CNTR
<9.E−37	<30	<3	29	e^+e^-	0	KINOSHITA	82	PLAS
<1.E−37	<20	<24	63	pp	0	CARRIGAN	78	CNTR
<1.E−37	<30	<3	56	pp	0	HOFFMANN	78	PLAS
			62	pp	0	[6] DELL	76	SPRK
<4.E−33			300	p	0	[6] STEVENS	76B	SPRK
<1.E−40	<5	<2	70	p	0	[7] ZRELOV	76	CNTR
<2.E−30			300	n	0	[6] BURKE	75	OSPK
<1.E−38			8	ν	0	[8] CARRIGAN	75	HLBC
<5.E−43	<12	<10	400	p	0	EBERHARD	75B	INDU
<2.E−36	<30	<3	60	pp	0	GIACOMELLI	75	PLAS
<5.E−42	<13	<24	400	p	0	CARRIGAN	74	CNTR
<6.E−42	<12	<24	300	p	0	CARRIGAN	73	CNTR
<2.E−36		1	0.001	γ	0	[7] BARTLETT	72	CNTR
<1.E−41	<5		70	p	0	GUREVICH	72	EMUL
<1.E−40	<3	<2	28	p	0	AMALDI	63	EMUL
<2.E−40	<3	<2	30	p	0	PURCELL	63	CNTR
<1.E−35	<3	<4	28	p	0	FIDECARO	61	CNTR
<2.E−35	<1	1	6	p	0	BRADNER	59	EMUL

[1] KALBFLEISCH 04 reports searches for stopped magnetic monopoles in Be, Al, and Pb samples obtained from discarded material from the upgrading of DØ and CDF. A large-aperture warm-bore cryogenic detector was used. The approach was an extension of the methods of KALBFLEISCH 00. Results are model dependent.
[2] KALBFLEISCH 00 used an induction method to search for stopped monopoles in pieces of the DØ (FNAL) beryllium beam pipe and in extensions to the drift chamber aluminum support cylinder. Results are model dependent.
[3] KALBFLEISCH 00 result is for aluminum.
[4] KALBFLEISCH 00 result is for beryllium.
[5] HE 97 used a lead target and barium phosphate glass detectors. Cross-section limits are well below those predicted via the Drell-Yan mechanism.
[6] Multiphoton events.
[7] Cherenkov radiation polarization.
[8] Re-examines CERN neutrino experiments.

Monopole Production — Other Accelerator Searches

MASS (GeV)	CHG ($|g|$)	SPIN	ENERGY (GeV)	BEAM	DOCUMENT ID		TECN
> 610	≥ 1	0	1800	$p\overline{p}$	[9] ABBOTT	98K	D0
> 870	≥ 1	1/2	1800	$p\overline{p}$	[9] ABBOTT	98K	D0
>1580	≥ 1	1	1800	$p\overline{p}$	[9] ABBOTT	98K	D0
> 510			88–94	e^+e^-	[10] ACCIARRI	95C	L3

[9] ABBOTT 98K search for heavy pointlike Dirac monopoles via central production of a pair of photons with high transverse energies.
[10] ACCIARRI 95C finds a limit $B(Z \to \gamma\gamma\gamma) < 0.8 \times 10^{-5}$ (which is possible via a monopole loop) at 95% CL and sets the mass limit via a cross section model.

Monopole Flux — Cosmic Ray Searches

"Caty" in the charge column indicates a search for monopole-catalyzed nucleon decay. The absence of an entry usually means a track-etch experiment.

FLUX ($cm^{-2}sr^{-1}s^{-1}$)	MASS (GeV)	CHG ($|g|$)	COMMENTS ($\beta = v/c$)	EVTS	DOCUMENT ID		TECN
<1.4E−16		1	$1.1E-4 < \beta < 1$	0	[11] AMBROSIO	02B	MCRO
<3E−16		Caty	$1.1E-4 < \beta < 5E-3$	0	[12] AMBROSIO	02C	MCRO

$<1.5E-15$		1	$5E-3<\beta<0.99$	0	[13] AMBROSIO 02D MCRO
$<1E-15$		1	1.1×10^{-4}–0.1	0	[14] AMBROSIO 97 MCRO
$<5.6E-15$		1	(0.18–3.0)E−3	0	[15] AHLEN 94 MCRO
$<2.7E-15$		Caty	$\beta\sim1\times10^{-3}$	0	[16] BECKER-SZ... 94 IMB
$<8.7E-15$		1	>2.E−3	0	THRON 92 SOUD
$<4.4E-12$		1	all β	0	GARDNER 91 INDU
$<7.2E-13$		1	all β	0	HUBER 91 INDU
$<3.7E-15$	>E12	1	β=1.E−4	0	[17] ORITO 91 PLAS
$<3.2E-16$	>E10	1	$\beta>0.05$	0	[17] ORITO 91 PLAS
$<3.2E-16$	>E10–E12	2, 3		0	[17] ORITO 91 PLAS
$<3.8E-13$		1	all β	0	BERMON 90 INDU
$<5.E-16$		Caty	$\beta<1.E-3$	0	[16] BEZRUKOV 90 CHER
$<1.8E-14$		1	$\beta>1.1E-4$	0	[18] BUCKLAND 90 HEPT
$<1E-18$			$3.E-4<\beta<1.5E-3$	0	[19] GHOSH 90 MICA
$<7.2E-13$		1	all β	0	HUBER 90 INDU
$<5.E-12$	>E7	1	$3.E-4<\beta<5.E-3$	0	BARISH 87 CNTR
$<1.E-13$		Caty	$1.E-5<\beta<1$	0	[16] BARTELT 87 SOUD
$<1.E-10$		1	all β	0	EBISU 87 INDU
$<2.E-13$			$1.E-4<\beta<6.E-4$	0	MASEK 87 HEPT
$<2.E-14$			$4.E-5<\beta<2.E-4$	0	NAKAMURA 87 PLAS
$<2.E-14$			$1.E-3<\beta<1$	0	NAKAMURA 87 PLAS
$<5.E-14$			$9.E-4<\beta<1.E-2$	0	SHEPKO 87 CNTR
$<2.E-13$			$4.E-4<\beta<1$	0	TSUKAMOTO 87 CNTR
$<5.E-14$		1	all β	1	[20] CAPLIN 86 INDU
$<5.E-12$		1		0	CROMAR 86 INDU
$<1.E-13$		1	$7.E-4<\beta$	0	HARA 86 CNTR
$<7.E-11$		1	all β	0	INCANDELA 86 INDU
$<1.E-18$			$4.E-4<\beta<1.E-3$	0	[19] PRICE 86 MICA
$<5.E-12$		1		0	BERMON 85 INDU
$<6.E-12$		1		0	CAPLIN 85 INDU
$<6.E-10$		1		0	EBISU 85 INDU
$<3.E-15$		Caty	$5.E-5\le\beta\le1.E-3$	0	[16] KAJITA 85 KAMI
$<2.E-21$		Caty	$\beta<1.E-3$	0	[16,21] KAJITA 85 KAMI
$<3.E-15$		Caty	$1.E-3<\beta<1.E-1$	0	[16] PARK 85B CNTR
$<5.E-12$		1	$1.E-4<\beta<1$	0	BATTISTONI 84 NUSX
$<7.E-12$		1		0	INCANDELA 84 INDU
$<7.E-13$		1	$3.E-4<\beta$	0	[18] KAJINO 84 CNTR
$<2.E-12$		1	$3.E-4<\beta<1.E-1$	0	KAJINO 84B CNTR
$<6.E-13$		1	$5.E-4<\beta<1$	0	KAWAGOE 84 CNTR
$<2.E-14$			$1.E-3<\beta$	0	[16] KRISHNA... 84 CNTR
$<4.E-13$		1	$6.E-4<\beta<2.E-3$	0	LISS 84 CNTR
$<1.E-16$			$3.E-4<\beta<1.E-3$	0	[19] PRICE 84 MICA
$<1.E-13$		1	$1.E-4<\beta$	0	PRICE 84B PLAS
$<4.E-13$		1	$6.E-4<\beta<2.E-3$	0	TARLE 84 CNTR
				7	[22] ANDERSON 83 EMUL
$<4.E-13$		1	$1.E-2<\beta<1.E-3$	0	BARTELT 83B CNTR
$<1.E-12$		1	$7.E-3<\beta<1$	0	BARWICK 83 PLAS
$<3.E-13$		1	$1.E-3<\beta<4.E-1$	0	BONARELLI 83 CNTR
$<3.E-12$		Caty	$5.E-4<\beta<5.E-2$	0	[16] BOSETTI 83 CNTR
$<4.E-11$		1		0	CABRERA 83 INDU
$<5.E-15$		1	$1.E-2<\beta<1$	0	DOKE 83 PLAS
$<8.E-15$		Caty	$1.E-4<\beta<1.E-1$	0	[16] ERREDE 83 IMB
$<5.E-12$		1	$1.E-4<\beta<3.E-2$	0	GROOM 83 CNTR
$<2.E-12$			$6.E-4<\beta<1$	0	MASHIMO 83 CNTR
$<1.E-13$		1	β=3.E−3	0	ALEXEYEV 82 CNTR
$<2.E-12$		1	$7.E-3<\beta<6.E-1$	0	BONARELLI 82 CNTR
6.E−10		1	all β	1	[23] CABRERA 82 INDU
$<2.E-11$			$1.E-2<\beta<1.E-1$	0	MASHIMO 82 CNTR
$<2.E-15$			concentrator	0	BARTLETT 81 PLAS
$<1.E-13$	>1		$1.E-3<\beta$	0	KINOSHITA 81B PLAS
$<5.E-11$	<E17		$3.E-4<\beta<1.E-3$	0	ULLMAN 81 CNTR
$<2.E-11$			concentrator	0	BARTLETT 78 PLAS
1.E−1	>200	2		1	[24] PRICE 75 PLAS
$<2.E-13$		>2		0	FLEISCHER 71 PLAS
$<1.E-19$		>2	obsidian, mica	0	FLEISCHER 69C PLAS
$<5.E-15$	<15	<3	concentrator	0	CARITHERS 66 ELEC
$<2.E-11$		<1–3	concentrator	0	MALKUS 51 EMUL

[11] AMBROSIO 02B direct search final result for $m\ge10^{17}$ GeV, based upon 4.2 to 9.5 years of running, depending upon the subsystem. Limit with CR39 track-etch detector extends the limit from $\beta=4\times10^{-5}$ (3.1×10^{-16} cm^{-2} sr^{-1} s^{-1}) to $\beta=1\times10^{-4}$ (2.1×10^{-16} cm^{-2} sr^{-1} s^{-1}). Limit curve in paper is piecewise continuous due to different detection techniques for different β ranges.

[12] AMBROSIO 02C limit for catalysis of nucleon decay with catalysis cross section of $\approx$ 1 mb. The flux limit increases by $\sim$ 3 at the higher β limit, and increases to 1×10^{-14} cm^{-2} sr^{-1} s^{-1} if the catalysis cross section is 0.01 mb. Based upon 71193 hr of data with the streamer detector, with an acceptance of 4250 m^2 sr.

[13] AMBROSIO 02D result for "more than two years of data." Ionization search using several subsystems. Limit curve as a function of β not given. Included in AMBROSIO 02B.

[14] AMBROSIO 97 global MACRO 90%CL is 0.78×10^{-15} at $\beta=1.1\times10^{-4}$, goes through a minimum at 0.61×10^{-15} near $\beta=(1.1–2.7)\times10^{-3}$, then rises to 0.84×10^{-15} at $\beta=0.1$. The global limit in this region is below the Parker bound at 10^{-15}. Less stringent limits are established for $4\times10^{-5}<\beta<1\times10^{-4}$. Limits set by various triggers and different subdetectors are given in the paper. All limits assume a catalysis cross section smaller than a few mb.

[15] AHLEN 94 limit for dyons extends down to β=0.9E−4 and a limit of 1.3E−14 extends to β = 0.8E−4. Also see comment by PRICE 94 and reply of BARISH 94. One loophole in the AHLEN 94 result is that in the case of monopoles catalyzing nucleon decay, relativisitic particles could veto the events. See AMBROSIO 97 for additional results.

[16] Catalysis of nucleon decay; sensitive to assumed catalysis cross section.

[17] ORITO 91 limits are functions of velocity. Lowest limits are given here.

[18] Used DKMPR mechanism and Penning effect.

[19] Assumes monopole attaches fermion nucleus.

[20] Limit from combining data of CAPLIN 86, BERMON 85, INCANDELA 84, and CABRERA 83. For a discussion of controversy about CAPLIN 86 observed event, see GUY 87. Also see SCHOUTEN 87.

[21] Based on lack of high- energy solar neutrinos from catalysis in the sun.

[22] Anomalous long-range α (^{4}He) tracks.

[23] CABRERA 82 candidate event has single Dirac charge within $\pm$5%.

[24] ALVAREZ 75, FLEISCHER 75, and FRIEDLANDER 75 explain as fragmenting nucleus. EBERHARD 75 and ROSS 76 discuss conflict with other experiments. HAGSTROM 77 reinterprets as antinucleus. PRICE 78 reassesses.

Monopole Flux — Astrophysics

FLUX (cm^{-2} sr^{-1} s^{-1})	MASS (GeV)	CHG ($\lvert g\rvert$)	COMMENTS ($\lvert\beta=v/c\rvert$)	EVTS	DOCUMENT ID		TECN
$<1.3E-20$			faint white dwarf		[25] FREESE	99	ASTR
$<1.E-16$	E17	1	galactic field	0	[26] ADAMS	93	COSM
$<1.E-23$			Jovian planets		[25] ARAFUNE	85	ASTR
$<1.E-16$	E15		solar trapping	0	BRACCI	85B	ASTR
$<1.E-18$		1		0	[25] HARVEY	84	COSM
$<3.E-23$			neutron stars		KOLB	84	ASTR
$<7.E-22$			pulsars	0	[25] FREESE	83B	ASTR
$<1.E-18$	<E18	1	intergalactic field	0	[25] REPHAELI	83	COSM
$<1.E-23$			neutron stars	0	[25] DIMOPOUL...	82	COSM
$<5.E-22$			neutron stars	0	[25] KOLB	82	COSM
$<5.E-15$	>E21		galactic halo		SALPETER	82	COSM
$<1.E-12$	E19	1	β=3.E−3	0	[27] TURNER	82	COSM
$<1.E-16$		1	galactic field	0	PARKER	70	COSM

[25] Catalysis of nucleon decay.

[26] ADAMS 93 limit based on "survival and growth of a small galactic seed field" is 10^{-16} ($m/10^{17}$ GeV) cm^{-2} s^{-1} sr^{-1}. Above 10^{17} GeV, limit 10^{-16} (10^{17} GeV/m) cm^{-2} s^{-1} sr^{-1} (from requirement that monopole density does not overclose the universe) is more stringent.

[27] Re-evaluates PARKER 70 limit for GUT monopoles.

Monopole Density — Matter Searches

DENSITY	CHG ($\lvert g\rvert$)	MATERIAL	EVTS	DOCUMENT ID		TECN
$<6.9E-6$/gram	>1/3	Meteorites and other	0	JEON	95	INDU
$<2.E-7$/gram	>0.6	Fe ore	0	[28] EBISU	87	INDU
$<4.6E-6$/gram	> 0.5	deep schist	0	KOVALIK	86	INDU
$<1.6E-6$/gram	> 0.5	manganese nodules	0	[29] KOVALIK	86	INDU
$<1.3E-6$/gram	> 0.5	seawater	0	KOVALIK	86	INDU
>1.E+14/gram	>1/3	iron aerosols	>1	MIKHAILOV	83	SPEC
$<6.E-4$/gram		air, seawater	0	CARRIGAN	76	CNTR
$<5.E-1$/gram	>0.04	11 materials	0	CABRERA	75	INDU
$<2.E-4$/gram	>0.05	moon rock	0	ROSS	73	INDU
$<6.E-7$/gram	<140	seawater	0	KOLM	71	CNTR
$<1.E-2$/gram	<120	manganese nodules	0	FLEISCHER	69	PLAS
$<1.E-4$/gram	>0	manganese	0	FLEISCHER	69B	PLAS
$<2.E-3$/gram	<1–3	magnetite, meteor	0	GOTO	63	EMUL
$<2.E-2$/gram		meteorite	0	PETUKHOV	63	CNTR

[28] Mass 1×10^{14}–1×10^{17} GeV.

[29] KOVALIK 86 examined 498 kg of schist from two sites which exhibited clear minearalogic evidence of having been buried at least 20 km deep and held below the Curie temperature.

Monopole Density — Astrophysics

DENSITY	CHG ($\lvert g\rvert$)	MATERIAL	EVTS	DOCUMENT ID		TECN
$<1.E-9$/gram	1	sun, catalysis	0	[30] ARAFUNE	83	COSM
$<6.E-33$/nucl	1	moon wake	0	SCHATTEN	83	ELEC
$<2.E-28$/nucl		earth heat	0	CARRIGAN	80	COSM
$<2.E-4$/prot		42cm absorption	0	BRODERICK	79	COSM
$<2.E-13$/m^3		moon wake	0	SCHATTEN	70	ELEC

[30] Catalysis of nucleon decay.

REFERENCES FOR Magnetic Monopole Searches

KALBFLEISCH	04	PR D69 052002	G.R. Kalbfleisch *et al.*	(OKLA)
AMBROSIO	02B	EPJ C25 511	M. Ambrosio *et al.*	(MACRO Collab.)
AMBROSIO	02C	EPJ C26 163	M. Ambrosio *et al.*	(MACRO Collab.)
AMBROSIO	02D	ASP 18 27	M. Ambrosio *et al.*	(MACRO Collab.)
KALBFLEISCH	00	PRL 85 5292	G.R. Kalbfleisch *et al.*	
FREESE	99	PR D59 063007	K. Freese, E. Krasteva	
ABBOTT	98K	PRL 81 524	B. Abbott *et al.*	(D0 Collab.)
AMBROSIO	97	PL B406 249	M. Ambrosio *et al.*	(MACRO Collab.)
HE	97	PRL 79 3134	Y.D. He	(UCB)
ACCIARRI	95C	PL B345 609	M. Acciarri *et al.*	(L3 Collab.)
JEON	95	PRL 75 1443	H. Jeon, M.J. Longo	(MICH)
Also	96	PRL 76 159 (errata)	H. Jeon, M.J. Longo	
AHLEN	94	PRL 72 608	S.P. Ahlen *et al.*	(MACRO Collab.)
BARISH	94	PRL 73 1306	B.C. Barish, G. Giacomelli, J.T. Hong	(CIT+)
BECKER-SZ...	94	PR D49 2169	R.A. Becker-Szendy *et al.*	(IMB Collab.)
PRICE	94	PRL 73 1305	P.B. Price	(UCB)
ADAMS	93	PRL 70 2511	F.C. Adams *et al.*	(MICH, FNAL)
PINFOLD	93	PL B316 407	J.L. Pinfold *et al.*	(ALBE, HARV, MONT+)
KINOSHITA	92	PR D46 R881	K. Kinoshita *et al.*	(HARV, BGNA, REHO)
THRON	92	PR D46 4846	J.L. Thron *et al.*	(SOUDAN-2 Collab.)
GARDNER	91	PR D44 622	R.D. Gardner *et al.*	(STAN)
HUBER	91	PR D44 636	M.E. Huber *et al.*	(STAN)

ORITO	91	PRL 66 1951	S. Orito *et al.*	(ICEPP, WASCR, NIHO, ICRR)
BERMON	90	PRL 64 839	S. Bermon *et al.*	(IBM, BNL)
BERTANI	90	EPL 12 613	M. Bertani *et al.*	(BGNA, INFN)
BEZRUKOV	90	SJNP 52 54	L.B. Bezrukov *et al.*	(INRM)
		Translated from YAF 52 86.		
BUCKLAND	90	PR D41 2726	K.N. Buckland *et al.*	(UCSD)
GHOSH	90	EPL 12 25	D.C. Ghosh, S. Chatterjea	(JADA)
HUBER	90	PRL 64 835	M.E. Huber *et al.*	(STAN)
PRICE	90	PRL 65 149	P.B. Price, J. Guiru, K. Kinoshita	(UCB, HARV)
KINOSHITA	89	PL B228 543	K. Kinoshita *et al.*	(HARV, TISA, KEK+)
BRAUNSCH...	88B	ZPHY C38 543	R. Braunschweig *et al.*	(TASSO Collab.)
KINOSHITA	88	PRL 60 1610	K. Kinoshita *et al.*	(HARV, TISA, KEK+)
BARISH	87	PR D36 2641	B.C. Barish, G. Liu, C. Lane	(CIT)
BARTELT	87	PR D36 1990	J.E. Bartelt *et al.*	(Soudan Collab.)
Also	89	PR D40 1701 erratum	J.E. Bartelt *et al.*	(Soudan Collab.)
EBISU	87	PR D36 3359	T. Ebisu, T. Watanabe	(KOBE)
Also	85	JPG 11 883	T. Ebisu, T. Watanabe	(KOBE)
GENTILE	87	PR D35 1081	T. Gentile *et al.*	(CLEO Collab.)
GUY	87	NAT 325 463	J. Guy	(LOIC)
MASEK	87	PR D35 2758	G.E. Masek *et al.*	(UCSD)
NAKAMURA	87	PL B183 395	S. Nakamura *et al.*	(INUS, WASCR, NIHO)
PRICE	87	PRL 59 2523	P.B. Price, R. Guoxiao, K. Kinoshita	(UCB, HARV)
SCHOUTEN	87	JPE 20 850	J.C. Schouten *et al.*	(LOIC)
SHEPKO	87	PR D35 2917	M.J. Shepko *et al.*	(TAMU)
TSUKAMOTO	87	EPL 3 39	T. Tsukamoto *et al.*	(ICRR)
CAPLIN	86	NAT 321 402	A.D. Caplin *et al.*	(LOIC)
Also	87	JPE 20 850	J.C. Schouten *et al.*	(LOIC)
Also	87	NAT 325 463	J. Guy	(LOIC)
CROMAR	86	PRL 56 2561	M.W. Cromar, A.F. Clark, F.R. Fickett	(NBSB)
HARA	86	PRL 56 553	T. Hara *et al.*	(ICRR, KYOT, KEK, KOBE+)
INCANDELA	86	PR D34 2637	J. Incandela *et al.*	(CHIC, FNAL, MICH)
KOVALIK	86	PR A33 1183	J.M. Kovalik, J.L. Kirschvink	(CIT)
PRICE	86	PRL 56 1226	P.B. Price, M.H. Salamon	(UCB)
ARAFUNE	85	PR D32 2586	J. Arafune, M. Fukugita, S. Yanagita	(ICRR, KYOTU+)
BERMON	85	PRL 55 1850	S. Bermon *et al.*	(IBM)
BRACCI	85B	NP B258 726	L. Bracci, G. Fiorentini, G. Mezzorani	(PISA+)
Also	85	LNC 42 123	L. Bracci, G. Fiorentini	(PISA)
CAPLIN	85	NAT 317 234	A.D. Caplin *et al.*	(LOIC)
EBISU	85	JPG 11 883	T. Ebisu, T. Watanabe	(KOBE)
KAJITA	85	JPSJ 54 4065	T. Kajita *et al.*	(ICRR, KEK, NIIG)
PARK	85B	NP B252 261	H.S. Park *et al.*	(IMB Collab.)
BATTISTONI	84	PL 133B 454	G. Battistoni *et al.*	(NUSEX Collab.)
FRYBERGER	84	PR D29 1524	D. Fryberger *et al.*	(SLAC, UCB)
HARVEY	84	NP B236 255	J.A. Harvey	(PRIN)
INCANDELA	84	PRL 53 2067	J. Incandela *et al.*	(CHIC, FNAL, MICH)
KAJINO	84	PRL 52 1373	F. Kajino *et al.*	(ICRR)
KAJINO	84B	JPG 10 447	F. Kajino *et al.*	(ICRR)
KAWAGOE	84	LNC 41 315	K. Kawagoe *et al.*	(TOKY)
KOLB	84	APJ 286 702	E.W. Kolb, M.S. Turner	(FNAL, CHIC)
KRISHNA...	84	PL 142B 99	M.R. Krishnaswamy *et al.*	(TATA, OSKC+)
LISS	84	PR D30 884	T.M. Liss, S.P. Ahlen, G. Tarle	(UCB, IND+)
PRICE	84	PRL 52 1265	P.B. Price *et al.*	(ROMA, UCB, IND+)
PRICE	84B	PL 140B 112	P.B. Price	(CERN)
TARLE	84	PRL 52 90	G. Tarle, S.P. Ahlen, T.M. Liss	(UCB, MICH+)
ANDERSON	83	PR D28 2308	S.N. Anderson *et al.*	(WASH)
ARAFUNE	83	PL 133B 380	J. Arafune, M. Fukugita	(ICRR, KYOTU)
AUBERT	83B	PL 120B 465	B. Aubert *et al.*	(CERN, LAPP)
BARTELT	83B	PRL 50 655	J.E. Bartelt *et al.*	(MINN, ANL)
BARWICK	83	PR D28 2338	S.W. Barwick, K. Kinoshita, P.B. Price	(UCB)
BONARELLI	83	PL 126B 137	R. Bonarelli, P. Capiluppi, I. d'Antone	(BGNA)
BOSETTI	83	PL 133B 265	P.C. Bosetti *et al.*	(AACH3, HAWA, TOKY)
CABRERA	83	PRL 51 1933	B. Cabrera *et al.*	(STAN)
DOKE	83	PL 129B 370	T. Doke *et al.*	(WASU, RIKK, TTAM, RIKEN)
ERREDE	83	PRL 51 245	S.M. Errede *et al.*	(IMB Collab.)
FREESE	83B	PRL 51 1625	K. Freese, M.S. Turner, D.N. Schramm	(CHIC)
GROOM	83	PRL 50 573	D.E. Groom *et al.*	(UTAH, STAN)
MASHIMO	83	PL 128B 327	T. Mashimo *et al.*	(ICEPP)
MIKHAILOV	83	PL 130B 331	V.F. Mikhailov	(KAZA)
MUSSET	83	PL 128B 333	P. Musset, M. Price, E. Lohrmann	(CERN, HAMB)
REPHAELI	83	PL 121B 115	Y. Rephaeli, M.S. Turner	(CHIC)
SCHATTEN	83	PR D27 1525	K.H. Schatten	(NASA)
ALEXEYEV	82	LNC 35 413	E.N. Alekseev *et al.*	(INRM)
BONARELLI	82	PL 112B 100	R. Bonarelli *et al.*	(BGNA)
CABRERA	82	PRL 48 1378	B. Cabrera	(STAN)
DELL	82	NP B209 45	G.F. Dell *et al.*	(BNL, ADEL, ROMA)
DIMOPOUL...	82	PL 119B 320	S. Dimopoulos, J. Preskill, F. Wilczek	(HARV+)
KINOSHITA	82	PRL 48 77	K. Kinoshita, P.B. Price, D. Fryberger	(UCB+)
KOLB	82	PRL 49 1373	E.W. Kolb, S.A. Colgate, J.A. Harvey	(LASL, PRIN)
MASHIMO	82	JPSJ 51 3067	T. Mashimo, K. Kawagoe, M. Koshiba	(INUS)
SALPETER	82	PRL 49 1114	E.E. Salpeter, S.L. Shapiro, I. Wasserman	(CORN)
TURNER	82	PR D26 1296	M.S. Turner, E.N. Parker, T.J. Bogdan	(CHIC)
BARTLETT	81	PR D24 612	D.F. Bartlett *et al.*	(COLO, GESC)
KINOSHITA	81B	PR D24 1707	K. Kinoshita, P.B. Price	(UCB)
ULLMAN	81	PRL 47 289	J.D. Ullman	(LEHM, BNL)
CARRIGAN	80	NAT 288 348	R.A. Carrigan	(FNAL)
BRODERICK	79	PR D19 1046	J.J. Broderick *et al.*	(VPI)
BARTLETT	78	PR D18 2253	D.F. Bartlett, D. Soo, M.G. White	(COLO, PRIN)
CARRIGAN	78	PR D17 1754	R.A. Carrigan, B.P. Strauss, G. Giacomelli	(FNAL+)
HOFFMANN	78	LNC 23 357	H. Hoffmann *et al.*	(CERN, ROMA)
PRICE	78	PR D18 1382	P.B. Price *et al.*	(UCB, HOUS)
HAGSTROM	77	PRL 38 729	R. Hagstrom	(LBL)
CARRIGAN	76	PR D13 1823	R.A. Carrigan, F.A. Nezrick, B.P. Strauss	(FNAL)
DELL	76	LNC 15 269	G.F. Dell *et al.*	(CERN, BNL, ROMA, ADEL)
ROSS	76	LBL-4665	R.R. Ross	(LBL)
STEVENS	76B	PR D14 2207	D.M. Stevens *et al.*	(VPI, BNL)
ZRELOV	76	CZJP B26 1306	V.P. Zrelov *et al.*	(JINR)
ALVAREZ	75	LBL-4260	L.W. Alvarez	(LBL)
BURKE	75	PL 60B 113	D.L. Burke *et al.*	(MICH)
CABRERA	75	Thesis	B. Cabrera	(STAN)
CARRIGAN	75	NP B91 279	R.A. Carrigan, F.A. Nezrick	(FNAL)
Also	71	PR D3 56	R.A. Carrigan, F.A. Nezrick	(FNAL)
EBERHARD	75	PR D11 3099	P.H. Eberhard *et al.*	(LBL, MPIM)
EBERHARD	75B	LBL-4289	P.H. Eberhard	(LBL)
FLEISCHER	75	PRL 35 1412	R.L. Fleischer, R.N.F. Walker	(GESC, WUSL)
FRIEDLANDER	75	PRL 35 1167	M.W. Friedlander	(WUSL)
GIACOMELLI	75	NC 28A 21	G. Giacomelli *et al.*	(BGNA, CERN, SACL+)
PRICE	75	PRL 35 487	P.B. Price *et al.*	(UCB, HOUS)
CARRIGAN	74	PR D10 3867	R.A. Carrigan, F.A. Nezrick, B.P. Strauss	(FNAL)
CARRIGAN	73	PR D8 3717	R.A. Carrigan, F.A. Nezrick, B.P. Strauss	(FNAL)
ROSS	73	PR D8 698	R.R. Ross *et al.*	(LBL, SLAC)
Also	71	PR D4 3260	P.H. Eberhard *et al.*	(LBL, SLAC)
Also	70	Science 167 701	L.W. Alvarez *et al.*	(LBL, SLAC)
BARTLETT	72	PR D6 1817	D.F. Bartlett, M.D. Lahana	(COLO)
GUREVICH	72	PL 38B 549	I.I. Gurevich *et al.*	(KIAE, NOVO, SERP)
Also	72B	JETP 34 917	L.M. Barkov, I.I. Gurevich, M.S. Zolotorev	(KIAE+)
		Translated from ZETF 61 1721.		
Also	70	PL 31B 394	I.I. Gurevich *et al.*	(KIAE, NOVO, SERP)
FLEISCHER	71	PR D4 24	R.L. Fleischer *et al.*	(GESC)
KOLM	71	PR D4 1285	H.H. Kolm, F. Villa, A. Odian	(MIT, SLAC)
PARKER	70	APJ 160 383	E.N. Parker	(CHIC)
SCHATTEN	70	PR D1 2245	K.H. Schatten	(NASA)
FLEISCHER	69	PR 177 2029	R.L. Fleischer *et al.*	(GESC, FSU)
FLEISCHER	69B	PR 184 1393	R.L. Fleischer *et al.*	(GESC, UNCS, GSCO)
FLEISCHER	69C	PR 184 1398	R.L. Fleischer, P.B. Price, R.T. Woods	(GESC)
Also	70C	JAP 41 958	R.L. Fleischer *et al.*	(GESC)
CARITHERS	66	PR 149 1070	W.C.J. Carithers, R.J. Stefanski, R.K. Adair	
AMALDI	63	NC 28 773	E. Amaldi *et al.*	(ROMA, UCSD, CERN)
GOTO	63	PR 132 387	E. Goto, H.H. Kolm, K.W. Ford	(TOKY, MIT, BRAN)
PETUKHOV	63	NP 49 87	V.A. Petukhov, M.N. Yakimenko	(LEBD)
PURCELL	63	PR 129 2326	E.M. Purcell *et al.*	(HARV, BNL)
FIDECARO	61	NC 22 657	M. Fidecaro, G. Finocchiaro, G. Giacomelli	(CERN)
BRADNER	59	PR 114 603	H. Bradner, W.M. Isbell	(LBL)
MALKUS	51	PR 83 899	W.V.R. Malkus	(CHIC)

OTHER RELATED PAPERS

GROOM	86	PRPL 140 323	D.E. Groom	(UTAH)
Review				

Supersymmetric Particle Searches

SUPERSYMMETRY

Revised September 2003 by H.E. Haber (Univ. of California, Santa Cruz) Part I, and by M. Schmitt (Northwestern Univ.) Part II.

This review is divided into two parts:

Supersymmetry, Part I (Theory)

I.1. Introduction
I.2. Structure of the MSSM
I.3. Parameters of the MSSM
I.4. The supersymmetric-particle sector
I.5. The Higgs sector of the MSSM
I.6. Reducing the MSSM parameter freedom
I.7. The constrained MSSMs: mSUGRA, GMSB, and SGUTs
I.8. Beyond the MSSM

Supersymmetry, Part II (Experiment)

II.1. Introduction
II.2. Common supersymmetry scenarios
II.3. Experimental issues
II.4. Supersymmetry searches in e^+e^- colliders
II.5. Supersymmetry searches at proton machines
II.6. Supersymmetry searches at HERA and fixed-target experiments
II.7. Conclusions

SUPERSYMMETRY, PART I (THEORY)

(by H.E. Haber)

I.1. Introduction: Supersymmetry (SUSY) is a generalization of the space-time symmetries of quantum field theory that transforms fermions into bosons and vice versa. It also provides a framework for the unification of particle physics and gravity [1–4], which is governed by the Planck scale, $M_{\rm P} \approx 10^{19}$ GeV (defined to be the energy scale where the gravitational interactions of elementary particles become comparable to the gauge interactions). In particular, it is possible that supersymmetry will ultimately explain the origin of the large hierarchy of energy scales from the W and Z masses to the Planck scale. The stability of this hierarchy in the presence of radiative corrections is not possible in the Standard Model, but can be maintained in supersymmetric theories.

If supersymmetry were an exact symmetry of nature, then particles and their superpartners (which differ in spin by half

a unit) would be degenerate in mass. Since this is not observed in data, supersymmetry cannot be an exact symmetry and must be broken. Nevertheless, the stability of the hierarchy of scales mentioned above can still be maintained if the supersymmetry breaking is *soft* [5] and the corresponding supersymmetry-breaking mass terms are no larger than a few TeV. (In softly-broken supersymmetry, the theory behaves like an unbroken supersymmetric theory at energy scales much larger than the size of the supersymmetry-breaking masses.) The most interesting theories of this type are theories of "low-energy" (or "weak-scale") supersymmetry, where the effective scale of supersymmetry breaking is tied to the scale of electroweak symmetry breaking [6–8]. The latter is characterized by the Standard Model Higgs vacuum expectation value, $v = 246$ GeV.

At present, there are no unambiguous experimental results that require the existence of low-energy supersymmetry. However, one tantalizing clue may be the observed unification of the three gauge couplings at an energy scale close to the Planck scale. The unification of gauge couplings does not occur in the Standard Model, but is achievable in the minimal supersymmetric extension of the Standard Model, and provides an additional motivation for seriously considering the low-energy supersymmetric framework [9]. If experimentation at future colliders uncovers evidence for supersymmetry, this would have a profound effect on the study of TeV-scale physics, and the development of a more fundamental theory of mass and symmetry-breaking phenomena in particle physics.

I.2. Structure of the MSSM: The minimal supersymmetric extension of the Standard Model (MSSM) consists of taking the Standard Model and adding the corresponding supersymmetric partners [3,10]. In addition, the MSSM contains two hypercharge $Y = \pm 1$ Higgs doublets, which is the minimal structure for the Higgs sector of an anomaly-free supersymmetric extension of the Standard Model. The supersymmetric structure of the theory also requires (at least) two Higgs doublets to generate mass for both "up"-type and "down"-type quarks (and charged leptons) [11,12]. All renormalizable supersymmetric interactions consistent with (global) B–L conservation (B =baryon number and L =lepton number) are included. Finally, the most general soft-supersymmetry-breaking terms are added [5]. To generate nonzero neutrino masses, extra structure is needed as discussed briefly in section I.8.

If supersymmetry is associated with the origin of the scale of electroweak interactions, then the mass parameters introduced by the soft-supersymmetry-breaking must be generally of order 1 TeV or below [13] (although models have been proposed in which some supersymmetric particle masses can be larger, in the range of 1–10 TeV [14]). Some lower bounds on these parameters exist due to the absence of supersymmetric-particle production at current accelerators [15]. Additional constraints arise from limits on the contributions of virtual supersymmetric particle exchange to a variety of Standard Model processes [16,17].

For example, the Standard Model global fit to precision electroweak data is quite good [18]. If all supersymmetric particle masses are significantly heavier than m_Z (in practice, masses greater than 300 GeV are sufficient [19]), then the effects of the supersymmetric particles decouple in loop-corrections to electroweak observables [20]. In this case, the Standard Model global fit to precision data and the corresponding MSSM fit yield similar results. On the other hand, regions of parameter space with light supersymmetric particle masses (just above the present day experimental limits) can in some cases generate significant one-loop corrections, resulting in a slight improvement or worsening of the overall global fit to the electroweak data depending on the choice of the MSSM parameters [21]. Thus, the precision electroweak data provide some constraints on the magnitude of the soft-supersymmetry-breaking terms.

There are a number of other low-energy measurements that are especially sensitive to the effects of new physics through virtual loops. For example, the virtual exchange of supersymmetric particles can contribute to the muon anomalous magnetic moment, $a_\mu \equiv \frac{1}{2}(g-2)_\mu$, and to the inclusive decay rate for $b \to s\gamma$. The most recent theoretical analysis of $(g-2)_\mu$ finds only a small deviation (less than two standard deviations) of the theoretical prediction from the experimentally observed value [22]. The theoretical prediction for $\Gamma(b \to s\gamma)$ agrees quite well (within the error bars) to the experimental observation [23]. In both cases, supersymmetric corrections could have generated an observable shift from the Standard Model prediction in some regions of the MSSM parameter space [23–25]. The absence of a significant deviation places interesting constraints on the low-energy supersymmetry parameters.

As a consequence of B–L invariance, the MSSM possesses a multiplicative R-parity invariance, where $R = (-1)^{3(B-L)+2S}$ for a particle of spin S [26]. Note that this implies that all the ordinary Standard Model particles have even R parity, whereas the corresponding supersymmetric partners have odd R parity. The conservation of R parity in scattering and decay processes has a crucial impact on supersymmetric phenomenology. For example, starting from an initial state involving ordinary (R-even) particles, it follows that supersymmetric particles must be produced in pairs. In general, these particles are highly unstable and decay into lighter states. However, R-parity invariance also implies that the lightest supersymmetric particle (LSP) is absolutely stable, and must eventually be produced at the end of a decay chain initiated by the decay of a heavy unstable supersymmetric particle.

In order to be consistent with cosmological constraints, a stable LSP is almost certainly electrically and color neutral [27]. (There are some model circumstances in which a colored gluino LSP is allowed [28], but we do not consider this possibility further here.) Consequently, the LSP in an R-parity-conserving theory is weakly interacting with ordinary matter, *i.e.*, it behaves like a stable heavy neutrino and will escape collider detectors without being directly observed. Thus, the canonical signature for conventional R-parity-conserving supersymmetric

theories is missing (transverse) energy, due to the escape of the LSP. Moreover, the LSP is a prime candidate for "cold dark matter" [29], a potentially important component of the non-baryonic dark matter that is required in many models of cosmology and galaxy formation [30]. Further aspects of dark matter can be found in Ref. [31].

In the MSSM, supersymmetry breaking is accomplished by including the most general renormalizable soft-supersymmetry-breaking terms consistent with the $SU(3)\times SU(2)\times U(1)$ gauge symmetry and R-parity invariance. These terms parameterize our ignorance of the fundamental mechanism of supersymmetry breaking. If supersymmetry breaking occurs spontaneously, then a massless Goldstone fermion called the *goldstino* ($\widetilde{G}$) must exist. The goldstino would then be the LSP and could play an important role in supersymmetric phenomenology [32]. However, the goldstino is a physical degree of freedom only in models of spontaneously broken global supersymmetry. If the supersymmetry is a local symmetry, then the theory must incorporate gravity; the resulting theory is called supergravity. In models of spontaneously broken supergravity, the goldstino is "absorbed" by the *gravitino* ($\widetilde{g}_{3/2}$), the spin-3/2 partner of the graviton [33]. By this super-Higgs mechanism, the goldstino is removed from the physical spectrum and the gravitino acquires a mass ($m_{3/2}$).

It is very difficult (perhaps impossible) to construct a realistic model of spontaneously-broken low-energy supersymmetry where the supersymmetry breaking arises solely as a consequence of the interactions of the particles of the MSSM. A more viable scheme posits a theory consisting of at least two distinct sectors: a "hidden" sector consisting of particles that are completely neutral with respect to the Standard Model gauge group, and a "visible" sector consisting of the particles of the MSSM. There are no renormalizable tree-level interactions between particles of the visible and hidden sectors. Supersymmetry breaking is assumed to occur in the hidden sector, and to then be transmitted to the MSSM by some mechanism. Two theoretical scenarios have been examined in detail: gravity-mediated and gauge-mediated supersymmetry breaking.

Supergravity models provide a natural mechanism for transmitting the supersymmetry breaking of the hidden sector to the particle spectrum of the MSSM. In models of *gravity-mediated* supersymmetry breaking, gravity is the messenger of supersymmetry breaking [34,35]. More precisely, supersymmetry breaking is mediated by effects of gravitational strength (suppressed by an inverse power of the Planck mass). In this scenario, the gravitino mass is of order the electroweak-symmetry-breaking scale, while its couplings are roughly gravitational in strength [1,36]. Such a gravitino would play no role in supersymmetric phenomenology at colliders.

In *gauge-mediated* supersymmetry breaking, supersymmetry breaking is transmitted to the MSSM via gauge forces. A typical structure of such models involves a hidden sector where supersymmetry is broken, a "messenger sector" consisting of particles (messengers) with $SU(3)\times SU(2)\times U(1)$ quantum numbers, and the visible sector consisting of the fields of the MSSM [37,38]. The direct coupling of the messengers to the hidden sector generates a supersymmetry breaking spectrum in the messenger sector. Finally, supersymmetry breaking is transmitted to the MSSM via the virtual exchange of the messengers. If this approach is extended to incorporate gravitational phenomena, then supergravity effects will also contribute to supersymmetry breaking. However, in models of gauge-mediated supersymmetry breaking, one usually chooses the model parameters in such a way that the virtual exchange of the messengers dominates the effects of the direct gravitational interactions between the hidden and visible sectors. In this scenario, the gravitino mass is typically in the eV to keV range, and is therefore the LSP. The helicity $\pm\frac{1}{2}$ components of $\widetilde{g}_{3/2}$ behave approximately like the goldstino; its coupling to the particles of the MSSM is significantly stronger than a coupling of gravitational strength.

During the last few years, new approaches to supersymmetry breaking have been proposed, based on theories in which the number of space dimensions is greater than three. This is not a new idea-consistent superstring theories are formulated in ten spacetime dimensions, and the associated M-theory is based in eleven spacetime dimensions [39]. Nevertheless, in all approaches considered above, the string scale and the inverse size of the extra dimensions are assumed to be at or near the Planck scale, below which an effective four spacetime dimensional broken supersymmetric field theory emerges. More recently, a number of supersymmetry-breaking mechanisms have been proposed that are inherently extra-dimensional. In some cases, the size of the extra dimensions can be significantly larger than $M_{\rm P}^{-1}$; in some cases of order $(\mathrm{TeV})^{-1}$ or even larger [40,41]. For example, in one approach, the fields of the MSSM live on some brane (a lower-dimensional manifold existing in a higher dimensional spacetime), while the sector of the theory that breaks supersymmetry lives on a second separated brane. Two examples of this approach are anomaly-mediated supersymmetry breaking of Ref. [42] and gaugino-mediated supersymmetry breaking of Ref. [43]; in both cases supersymmetry-breaking is transmitted through fields that live in the bulk (the higher dimensional space between the two branes). This setup has some features in common with both gravity-mediated and gauge-mediated supersymmetry breaking (*e.g.*, a hidden and visible sector and messengers). In another approach, one starts with a higher dimensional theory, which is compactified to four spacetime dimensions. In this approach, supersymmetry is broken by boundary conditions on the compactified space that distinguish between fermions and bosons [44](the so-called Scherk-Schwarz mechanism [45]). The phenomenology of such models can be strikingly different from the usual MSSM [46]. These approaches clearly deserve further investigation, although they will not be discussed further here.

I.3. Parameters of the MSSM: The parameters of the MSSM are conveniently described by considering separately

the supersymmetry-conserving sector and the supersymmetry-breaking sector. A careful discussion of the conventions used in defining the MSSM parameters can be found in Ref. [47]. For simplicity, consider the case of one generation of quarks, leptons, and their scalar superpartners. The parameters of the supersymmetry-conserving sector consist of: (i) gauge couplings: g_s, g, and g', corresponding to the Standard Model gauge group SU(3)×SU(2)×U(1) respectively; (ii) a supersymmetry-conserving Higgs mass parameter μ; and (iii) Higgs-fermion Yukawa coupling constants: λ_u, λ_d, and λ_e (corresponding to the coupling of one generation of quarks, leptons, and their superpartners to the Higgs bosons and higgsinos).

The supersymmetry-breaking sector contains the following set of parameters: (i) gaugino Majorana masses M_3, M_2, and M_1 associated with the SU(3), SU(2), and U(1) subgroups of the Standard Model; (ii) five scalar squared-mass parameters for the squarks and sleptons, $M^2_{\widetilde{Q}}$, $M^2_{\widetilde{U}}$, $M^2_{\widetilde{D}}$, $M^2_{\widetilde{L}}$, and $M^2_{\widetilde{E}}$ [corresponding to the five electroweak gauge multiplets, *i.e.*, superpartners of $(u,d)_L$, u^c_L, d^c_L, $(\nu,\ e^-)_L$, and e^c_L, where the superscript c indicates a charge-conjugated fermion]; (iii) Higgs-squark-squark and Higgs-slepton-slepton trilinear interaction terms, with coefficients A_u, A_d, and A_e (these are the so-called "A parameters"); and (iv) three scalar Higgs squared-mass parameters-two of which (m_1^2 and m_2^2) contribute to the diagonal Higgs squared-masses, given by $m_1^2+|\mu|^2$ and $m_2^2+|\mu|^2$, and a third which contributes to the off-diagonal Higgs squared-mass term, $m_{12}^2 \equiv B\mu$ (which defines the "B-parameter"). These three squared-mass parameters can be re-expressed in terms of the two Higgs vacuum expectation values, v_d and v_u (also called v_1 and v_2, respectively, in the literature), and one physical Higgs mass. Here, v_d (v_u) is the vacuum expectation value of the Higgs field which couples exclusively to down-type (up-type) quarks and leptons. Note that $v_d^2+v_u^2 = 4m_W^2/g^2 = (246\ \mathrm{GeV})^2$ is fixed by the W mass and the gauge coupling, whereas the ratio

$$\tan\beta = v_u/v_d \qquad (1)$$

is a free parameter of the model.

The total number of degrees of freedom of the MSSM is quite large, primarily due to the parameters of the soft-supersymmetry-breaking sector. In particular, in the case of three generations of quarks, leptons, and their superpartners, $M^2_{\widetilde{Q}}$, $M^2_{\widetilde{U}}$, $M^2_{\widetilde{D}}$, $M^2_{\widetilde{L}}$, and $M^2_{\widetilde{E}}$ are hermitian 3×3 matrices, and the A parameters are complex 3×3 matrices. In addition, M_1, M_2, M_3, B, and μ are in general complex. Finally, as in the Standard Model, the Higgs-fermion Yukawa couplings, λ_f ($f=u$, d, and e), are complex 3×3 matrices that are related to the quark and lepton mass matrices via: $M_f = \lambda_f v_f/\sqrt{2}$, where $v_e \equiv v_d$ (with v_u and v_d as defined above). However, not all these parameters are physical. Some of the MSSM parameters can be eliminated by expressing interaction eigenstates in terms of the mass eigenstates, with an appropriate redefinition of the MSSM fields to remove unphysical degrees of freedom. The analysis of Ref. [48] shows that the MSSM possesses 124 independent parameters. Of these, 18 parameters correspond to Standard Model parameters (including the QCD vacuum angle θ_{QCD}), one corresponds to a Higgs sector parameter (the analogue of the Standard Model Higgs mass), and 105 are genuinely new parameters of the model. The latter include: five real parameters and three CP-violating phases in the gaugino/higgsino sector, 21 squark and slepton masses, 36 real mixing angles to define the squark and slepton mass eigenstates, and 40 CP-violating phases that can appear in squark and slepton interactions. The most general R-parity-conserving minimal supersymmetric extension of the Standard Model (without additional theoretical assumptions) will be denoted henceforth as MSSM-124 [49].

I.4. The supersymmetric-particle sector: Consider the sector of supersymmetric particles (*sparticles*) in the MSSM. The supersymmetric partners of the gauge and Higgs bosons are fermions, whose names are obtained by appending "ino" at the end of the corresponding Standard Model particle name. The *gluino* is the color octet Majorana fermion partner of the gluon with mass $M_{\widetilde{g}} = |M_3|$. The supersymmetric partners of the electroweak gauge and Higgs bosons (the *gauginos* and *higgsinos*) can mix. As a result, the physical mass eigenstates are model-dependent linear combinations of these states, called *charginos* and *neutralinos*, which are obtained by diagonalizing the corresponding mass matrices. The chargino-mass matrix depends on M_2, μ, $\tan\beta$, and m_W [50].

The corresponding chargino-mass eigenstates are denoted by $\widetilde{\chi}_1^+$ and $\widetilde{\chi}_2^+$, with masses

$$M^2_{\widetilde{\chi}_1^+,\widetilde{\chi}_2^+} = \tfrac{1}{2}\Big\{ |\mu|^2+|M_2|^2+2m_W^2 \mp \Big[\big(|\mu|^2+|M_2|^2+2m_W^2\big)^2 - 4|\mu|^2|M_2|^2 - 4m_W^4\sin^2 2\beta + 8m_W^2\sin 2\beta\,\mathrm{Re}(\mu M_2)\Big]^{1/2}\Big\}, \qquad (2)$$

where the states are ordered such that $M_{\widetilde{\chi}_1^+} \le M_{\widetilde{\chi}_2^+}$. If CP-violating effects are neglected (in which case, M_2 and μ are real parameters), then one can choose a convention where $\tan\beta$ and M_2 are positive. (Note that the relative sign of M_2 and μ is meaningful. The sign of μ is convention-dependent; the reader is warned that both sign conventions appear in the literature.) The sign convention for μ implicit in Eq. (2) is used by the LEP collaborations [15] in their plots of exclusion contours in the M_2 vs. μ plane derived from the non-observation of $e^+e^- \to \widetilde{\chi}_1^+\widetilde{\chi}_1^-$.

The neutralino mass matrix depends on M_1, M_2, μ, $\tan\beta$, m_Z, and the weak mixing angle θ_W [50]. The corresponding neutralino eigenstates are usually denoted by $\widetilde{\chi}_i^0$ ($i=1,\ldots4$), according to the convention that $M_{\widetilde{\chi}_1^0} \le M_{\widetilde{\chi}_2^0} \le M_{\widetilde{\chi}_3^0} \le M_{\widetilde{\chi}_4^0}$. If a chargino or neutralino eigenstate approximates a particular gaugino or higgsino state, it is convenient to employ the corresponding nomenclature. Specifically, if M_1 and M_2 are small compared to m_Z and $|\mu|$, then the lightest neutralino $\widetilde{\chi}_1^0$ would be nearly a pure *photino*, $\widetilde{\gamma}$, the supersymmetric partner of the photon. If M_1 and m_Z are small compared to M_2 and $|\mu|$, then the lightest neutralino would be nearly a pure *bino*,

$\widetilde{B}$, the supersymmetric partner of the weak hypercharge gauge boson. If M_2 and m_Z are small compared to M_1 and $|\mu|$, then the lightest chargino pair and neutralino would constitute a triplet of roughly mass-degenerate pure *winos*, $\widetilde{W}^{\pm}$, and $\widetilde{W}_3^0$, the supersymmetric partners of the weak SU(2) gauge bosons. Finally, if $|\mu|$ and m_Z are small compared to M_1 and M_2, then the lightest neutralino would be nearly a pure *higgsino*. Each of the above cases leads to a strikingly different phenomenology.

The supersymmetric partners of the quarks and leptons are spin-zero bosons: the *squarks*, charged *sleptons*, and *sneutrinos*. For simplicity, only the one-generation case is illustrated below (using first-generation notation). For a given fermion f, there are two supersymmetric partners, $\widetilde{f}_L$ and $\widetilde{f}_R$, which are scalar partners of the corresponding left- and right-handed fermion. (There is no $\widetilde{\nu}_R$ in the MSSM.) However, in general, $\widetilde{f}_L$ and $\widetilde{f}_R$ are not mass-eigenstates, since there is $\widetilde{f}_L$-$\widetilde{f}_R$ mixing which is proportional in strength to the corresponding element of the scalar squared-mass matrix [51]

$$M^2_{LR} = \begin{cases} m_d(A_d - \mu\tan\beta), & \text{for "down"-type } f \\ m_u(A_u - \mu\cot\beta), & \text{for "up"-type } f, \end{cases} \qquad (3)$$

where m_d (m_u) is the mass of the appropriate "down" ("up") type quark or lepton. The signs of the A parameters are also convention-dependent; see Ref. [47]. Due to the appearance of the *fermion* mass in Eq. (3), one expects M_{LR} to be small compared to the diagonal squark and slepton masses, with the possible exception of the top-squark, since m_t is large, and the bottom-squark and tau-slepton if $\tan\beta \gg 1$.

The (diagonal) L- and R-type squark and slepton squared-masses are given by

$$\begin{aligned} M^2_{\widetilde{f}_L} &= M^2_{\widetilde{F}} + m_f^2 + (T_{3f} - e_f \sin^2\theta_W) m_Z^2 \cos 2\beta\,, \\ M^2_{\widetilde{f}_R} &= M^2_{\widetilde{R}} + m_f^2 + e_f \sin^2\theta_W m_Z^2 \cos 2\beta\,, \end{aligned} \qquad (4)$$

where $M^2_{\widetilde{F}} \equiv M^2_{\widetilde{Q}}$ [$M^2_{\widetilde{L}}$] for $\widetilde{u}_L$ and $\widetilde{d}_L$ [$\widetilde{\nu}_L$ and $\widetilde{e}_L$], and $M^2_{\widetilde{R}} \equiv M^2_{\widetilde{U}}$, $M^2_{\widetilde{D}}$, and $M^2_{\widetilde{E}}$ for $\widetilde{u}_R$, $\widetilde{d}_R$, and $\widetilde{e}_R$, respectively. In addition, $e_f = \frac{2}{3}$, $-\frac{1}{3}$, 0, -1 for $f = u$, d, ν, and e, respectively, $T_{3f} = \frac{1}{2}$ [$-\frac{1}{2}$] for up-type [down-type] squarks and sleptons, and m_f is the corresponding quark or lepton mass. Squark and slepton mass eigenstates, generically called $\widetilde{f}_1$ and $\widetilde{f}_2$ (these are linear combinations of $\widetilde{f}_L$ and $\widetilde{f}_R$), are obtained by diagonalizing the corresponding 2×2 squared-mass matrices.

In the case of three generations, the general analysis is more complicated. The scalar squared-masses [$M^2_{\widetilde{F}}$ and $M^2_{\widetilde{R}}$ in Eq. (4)], the fermion masses m_f, and the A parameters are now 3×3 matrices as noted in Section I.3. Thus, to obtain the squark and slepton mass eigenstates, one must diagonalize 6×6 mass matrices. As a result, intergenerational mixing is possible, although there are some constraints from the nonobservation of FCNC's [16,17]. In practice, because off-diagonal scalar mixing is appreciable only for the third generation, this additional complication can usually be neglected.

It should be noted that all mass formulae quoted in this section are tree-level results. One-loop corrections will modify all these results, and eventually must be included in any precision study of supersymmetric phenomenology [52].

I.5. The Higgs sector of the MSSM: Next, consider the MSSM Higgs sector [11,12,53]. Despite the large number of potential CP-violating phases among the MSSM-124 parameters, the tree-level MSSM Higgs sector is automatically CP-conserving. That is, unphysical phases can be absorbed into the definition of the Higgs fields such that $\tan\beta$ is a real parameter (conventionally chosen to be positive). Moreover, the physical neutral Higgs scalars are CP eigenstates. The model contains five physical Higgs particles: a charged Higgs boson pair ($H^{\pm}$), two CP-even neutral Higgs bosons (denoted by h^0 and H^0 where $m_h \leq m_H$), and one CP-odd neutral Higgs boson (A^0).

The properties of the Higgs sector are determined by the Higgs potential, which is made up of quadratic terms [whose squared-mass coefficients were mentioned above Eq. (1)] and quartic interaction terms whose coefficients are dimensionless couplings. The quartic interaction terms are manifestly supersymmetric at tree-level (and are modified by supersymmetry-breaking effects only at the loop level). In general, the quartic couplings arise from two sources: (i) the supersymmetric generalization of the scalar potential (the so-called "F-terms"), and (ii) interaction terms related by supersymmetry to the coupling of the scalar fields and the gauge fields, whose coefficients are proportional to the corresponding gauge couplings (the so-called "D-terms"). In the MSSM, F-term contributions to the quartic couplings are absent (although such terms may be present in extensions of the MSSM, *e.g.*, models with Higgs singlets). As a result, the strengths of the MSSM quartic Higgs interactions are fixed in terms of the gauge couplings. Due to the resulting constraint on the form of the two-Higgs-doublet scalar potential, all the tree-level MSSM Higgs-sector parameters depend only on two quantities: $\tan\beta$ [defined in Eq. (1)] and one Higgs mass (usually taken to be m_A). From these two quantities, one can predict the values of the remaining Higgs boson masses, an angle α (which measures the component of the original $Y = \pm 1$ Higgs doublet states in the physical CP-even neutral scalars), and the Higgs boson self-couplings.

When one-loop radiative corrections are incorporated, additional parameters of the supersymmetric model enter via virtual loops. The impact of these corrections can be significant [54]. For example, at tree-level, MSSM-124 predicts $m_h \leq m_Z|\cos 2\beta| \leq m_Z$ [11,12]. If this prediction were unmodified, it would be in conflict with the MSSM Higgs mass bounds obtained at LEP [55]. However, when radiative corrections are included, the light Higgs-mass upper bound may be significantly increased. The qualitative behavior of the radiative corrections can be most easily seen in the large top-squark mass limit, where in addition, both the splitting of the two diagonal entries [Eq. (4)] and the two off-diagonal entries [Eq. (3)]

of the top-squark squared-mass matrix are small in comparison to the average of the two top-squark squared-masses, $M_S^2 \equiv \frac{1}{2}(M_{\tilde{t}_1}^2 + M_{\tilde{t}_2}^2)$. In this case (assuming $m_A > m_Z$), the upper bound on the lightest CP-even Higgs mass at one-loop is approximately given by

$$m_h^2 \lesssim m_Z^2 + \frac{3g^2 m_t^4}{8\pi^2 m_W^2}\left\{\ln\left(M_S^2/m_t^2\right) + \frac{X_t^2}{M_S^2}\left(1 - \frac{X_t^2}{12M_S^2}\right)\right\}, \quad (5)$$

where $X_t \equiv A_t - \mu\cot\beta$ is the top-squark mixing factor [see Eq. (3)]. A more complete treatment of the radiative corrections [56] shows that Eq. (5) somewhat overestimates the true upper bound of m_h. These more refined computations, which incorporate renormalization group improvement and the leading two-loop contributions, yield $m_h \lesssim 130$ GeV (with an accuracy of a few GeV) for $m_t = 175$ GeV and $M_S \lesssim 2$ TeV [56].

In addition, one-loop radiative corrections can introduce CP-violating effects in the Higgs sector, which depend on some of the CP-violating phases among the MSSM-124 parameters [57]. Although these effects are more model-dependent, they can have a non-trivial impact on the Higgs searches at future colliders.

I.6. Reducing the MSSM parameter freedom: In Sections I.4 and I.5 we surveyed the parameters that comprise the MSSM-124. However in its most general form, the MSSM-124 is not a phenomenologically-viable theory over most of its parameter space. This conclusion follows from the observation that a generic point in the MSSM-124 parameter space exhibits: (i) no conservation of the separate lepton numbers L_e, L_μ, and L_τ; (ii) unsuppressed FCNC's; and (iii) new sources of CP violation that are inconsistent with the experimental bounds. For example, the MSSM contains many new sources of CP violation [58]. In particular, some combination of the complex phases of the gaugino-mass parameters, the A parameters, and μ must be less than of order 10^{-2}–10^{-3} (for a supersymmetry-breaking scale of 100 GeV) to avoid generating electric dipole moments for the neutron, electron, and atoms in conflict with observed data [59,60]. As a result of the phenomenological deficiencies listed above, almost the entire MSSM-124 parameter space is ruled out! This theory is viable only at very special "exceptional" points of the full parameter space.

The MSSM-124 is also theoretically incomplete since it provides no explanation for the origin of the supersymmetry-breaking parameters (and in particular, why these parameters should conform to the exceptional points of the parameter space mentioned above). Moreover, there is no understanding of the choice of parameters that leads to the breaking of the electroweak symmetry. What is needed ultimately is a fundamental theory of supersymmetry breaking, which would provide a rationale for some set of soft-supersymmetry breaking terms that would be consistent with the phenomenological constraints referred to above. Presumably, the number of independent parameters characterizing such a theory would be considerably less than 124.

In the absence of a fundamental theory of supersymmetry breaking, there are two general approaches for reducing the parameter freedom of MSSM-124. In the low-energy approach, an attempt is made to elucidate the nature of the exceptional points in the MSSM-124 parameter space that are phenomenologically viable. Consider the following two possible choices. First, one can assume that $M_{\tilde{Q}}^2$, $M_{\tilde{U}}^2$, $M_{\tilde{D}}^2$, $M_{\tilde{L}}^2$, $M_{\tilde{E}}^2$, and the matrix A parameters are generation-independent (horizontal universality [7,48,61]). Alternatively, one can simply require that all the aforementioned matrices are flavor diagonal in a basis where the quark and lepton mass matrices are diagonal (flavor alignment [62]). In either case, L_e, L_μ, and L_τ are separately conserved, while tree-level FCNC's are automatically absent. In both cases, the number of free parameters characterizing the MSSM is substantially less than 124. Both scenarios are phenomenologically viable, although there is no strong theoretical basis for either scenario.

In the high-energy approach, one treats the parameters of the MSSM as running parameters and imposes a particular structure on the soft-supersymmetry-breaking terms at a common high-energy scale (such as the Planck scale, M_P). Using the renormalization group equations, one can then derive the low-energy MSSM parameters. The initial conditions (at the appropriate high-energy scale) for the renormalization group equations depend on the mechanism by which supersymmetry breaking is communicated to the effective low energy theory. Examples of this scenario are provided by models of gravity-mediated and gauge-mediated supersymmetry breaking (see Section I.2). One bonus of such an approach is that one of the diagonal Higgs squared-mass parameters is typically driven negative by renormalization group evolution. Thus, electroweak symmetry breaking is generated radiatively, and the resulting electroweak symmetry-breaking scale is intimately tied to the scale of low-energy supersymmetry breaking.

One prediction of the high-energy approach that arises in most grand unified supergravity models and gauge-mediated supersymmetry-breaking models is the unification of the (tree-level) gaugino mass parameters at some high-energy scale M_X, *i.e.*,

$$M_1(M_X) = M_2(M_X) = M_3(M_X) = m_{1/2}\,. \quad (6)$$

Consequently, the effective low-energy gaugino mass parameters (at the electroweak scale) are related:

$$M_3 = (g_s^2/g^2)M_2\,, \qquad M_1 = (5g'^2/3g^2)M_2 \simeq 0.5M_2\,. \quad (7)$$

In this case, the chargino and neutralino masses and mixing angles depend only on three unknown parameters: the gluino mass, μ, and $\tan\beta$. If in addition $|\mu| \gg M_1$, m_Z, then the lightest neutralino is nearly a pure bino, an assumption often made in supersymmetric particle searches at colliders.

In a certain class of supergravity models, tree-level masses for the gauginos are absent. The gaugino mass parameters arise at one-loop and do not satisfy Eq. (7). In this case, one finds a model-independent contribution to the gaugino mass

whose origin can be traced to the super-conformal (super-Weyl) anomaly, which is common to all supergravity models [42]. This approach is called *anomaly-mediated* supersymmetry breaking. Eq. (7) is then replaced (in the one-loop approximation) by:

$$M_i \simeq \frac{b_i g_i^2}{16\pi^2} m_{3/2}\,, \tag{8}$$

where $m_{3/2}$ is the gravitino mass (assumed to be of order 1 TeV), and b_i are the coefficients of the MSSM gauge beta-functions corresponding to the corresponding U(1), SU(2) and SU(3) gauge groups: $(b_1, b_2, b_3) = (\frac{33}{5}, 1, -3)$. Eq. (8) yields $M_1 \simeq 2.8 M_2$ and $M_3 \simeq -8.3 M_2$, which implies that over most of the MSSM parameter space the lightest chargino pair and neutralino make up a nearly mass-degenerate triplet of winos. (For example, if $|\mu| \gg m_Z$, then Eq. (8) implies that $M_{\widetilde{\chi}_1^\pm} \simeq M_{\widetilde{\chi}_1^0} \simeq M_2$ [63].) The corresponding supersymmetric phenomenology differs significantly from the standard phenomenology based on Eq. (7), and is explored in detail in Ref. [64]. Anomaly-mediated supersymmetry breaking also generates (approximate) flavor-diagonal squark and slepton mass matrices. However, this yields negative squared-mass contributions for the sleptons in the MSSM. This fatal flaw may be possible to cure in approaches beyond the minimal supersymmetric model [65]. Alternatively, one may conclude that anomaly-mediation is not the sole source of supersymmetry-breaking in the slepton sector.

I.7. The constrained MSSMs: mSUGRA, GMSB, and SGUTs: One way to guarantee the absence of significant FCNC's mediated by virtual supersymmetric-particle exchange is to posit that the diagonal soft-supersymmetry-breaking scalar squared-masses are universal at some energy scale. In models of gauge-mediated supersymmetry breaking, scalar squared-masses are expected to be flavor-independent since gauge forces are flavor-blind. In the *minimal* supergravity (mSUGRA) framework [1–3], the soft-supersymmetry-breaking parameters at the Planck scale take a particularly simple form in which the scalar squared-masses and the A parameters are flavor-diagonal and universal [34]:

$$\begin{aligned}
&M^2_{\widetilde{Q}}(M_{\rm P}) = M^2_{\widetilde{U}}(M_{\rm P}) = M^2_{\widetilde{D}}(M_{\rm P}) = m_0^2 \mathbf{1}\,,\\
&M^2_{\widetilde{L}}(M_{\rm P}) = M^2_{\widetilde{E}}(M_{\rm P}) = m_0^2 \mathbf{1}\,,\\
&m_1^2(M_{\rm P}) = m_2^2(M_{\rm P}) = m_0^2\,,\\
&A_U(M_{\rm P}) = A_D(M_{\rm P}) = A_L(M_{\rm P}) = A_0 \mathbf{1}\,,
\end{aligned} \tag{9}$$

where $\mathbf{1}$ is a 3×3 identity matrix in generation space. Renormalization group evolution is then used to derive the values of the supersymmetric parameters at the low-energy (electroweak) scale. For example, to compute squark and slepton masses, one must use the *low-energy* values for $M^2_{\widetilde{F}}$ and $M^2_{\widetilde{R}}$ in Eq. (4). Through the renormalization group running with boundary conditions specified in Eq. (7) and Eq. (9), one can show that the low-energy values of $M^2_{\widetilde{F}}$ and $M^2_{\widetilde{R}}$ depend primarily on m_0^2 and $m_{1/2}^2$. A number of useful approximate analytic expressions for superpartner masses in terms of the mSUGRA parameters can be found in Ref. [66].

Clearly, in the mSUGRA approach, the MSSM-124 parameter freedom has been significantly reduced. For example, typical mSUGRA models give low-energy values for the scalar mass parameters that satisfy $M_{\widetilde{L}} \approx M_{\widetilde{E}} < M_{\widetilde{Q}} \approx M_{\widetilde{U}} \approx M_{\widetilde{D}}$, with the squark mass parameters somewhere between a factor of 1–3 larger than the slepton mass parameters (*e.g.*, see Ref. [66]). More precisely, the low-energy values of the squark mass parameters of the first two generations are roughly degenerate, while $M_{\widetilde{Q}_3}$ and $M_{\widetilde{U}_3}$ are typically reduced by a factor of 1–3 from the values of the first and second generation squark mass parameters, because of renormalization effects due to the heavy top quark mass.

As a result, one typically finds that four flavors of squarks (with two squark eigenstates per flavor) and $\widetilde{b}_R$ are nearly mass-degenerate. The $\widetilde{b}_L$ mass and the diagonal $\widetilde{t}_L$ and $\widetilde{t}_R$ masses are reduced compared to the common squark mass of the first two generations. (If $\tan\beta \gg 1$, then the pattern of third generation squark masses is somewhat altered; *e.g.*, see Ref. [67].) In addition, there are six flavors of nearly mass-degenerate sleptons (with two slepton eigenstates per flavor for the charged sleptons and one per flavor for the sneutrinos); the sleptons are expected to be somewhat lighter than the mass-degenerate squarks. Finally, third generation squark masses and tau-slepton masses are sensitive to the strength of the respective $\widetilde{f}_L$–$\widetilde{f}_R$ mixing, as discussed below Eq. (3).

Due to the implicit $m_{1/2}$ dependence in the low-energy values of $M^2_{\widetilde{Q}}$, $M^2_{\widetilde{U}}$, and $M^2_{\widetilde{D}}$, there is a tendency for the gluino in mSUGRA models to be lighter than the first- and second-generation squarks. Moreover, the LSP is typically the lightest neutralino, $\widetilde{\chi}_1^0$, which is dominated by its bino component. However, there are some regions of mSUGRA parameter space where the above conclusions do not hold. For example, one can reject those mSUGRA parameter regimes in which the LSP is a chargino. In general, if one imposes the constraints of supersymmetric particle searches and those of cosmology (say, by requiring the LSP to be a suitable dark matter candidate), one obtains significant restrictions to the mSUGRA parameter space. A recent compilation of benchmark mSUGRA points consistent with present data from particle physics and cosmology can be found in Ref. [68].

One can count the number of independent parameters in the mSUGRA framework. In addition to 18 Standard Model parameters (excluding the Higgs mass), one must specify m_0, $m_{1/2}$, A_0, and Planck-scale values for μ and B-parameters (denoted by μ_0 and B_0). In principle, A_0, B_0, and μ_0 can be complex, although in the mSUGRA approach, these parameters are taken (arbitrarily) to be real. As previously noted, renormalization group evolution is used to compute the low-energy values of the mSUGRA parameters, which then fixes all the parameters of the low-energy MSSM. In particular, the two Higgs vacuum expectation values (or equivalently, m_Z and $\tan\beta$) can be expressed as a function of the Planck-scale supergravity

parameters. The simplest procedure is to remove μ_0 and B_0 in favor of m_Z and $\tan\beta$ (the sign of μ_0 is not fixed in this process). In this case, the MSSM spectrum and its interaction strengths are determined by five parameters: m_0, A_0, $m_{1/2}$, $\tan\beta$, and the sign of μ_0, in addition to the 18 parameters of the Standard Model. However, the mSUGRA approach is probably too simplistic. Theoretical considerations suggest that the universality of Planck-scale soft-supersymmetry-breaking parameters is not generic [69]. In particular, it is easy to write down effective operators at the Planck scale that do not respect flavor universality, and it is difficult to find a theoretical principle that would forbid them.

In contrast, in gauge-mediated supersymmetry breaking, universality of the fundamental soft-supersymmetry-breaking squark and slepton squared-mass parameters is guaranteed because the supersymmetry-breaking is communicated to the sector of MSSM fields via gauge interactions. In the minimal gauge-mediated supersymmetry-breaking (GMSB) approach, there is one effective mass scale, Λ, that determines all low-energy scalar and gaugino mass parameters through loop-effects (while the resulting A parameters are suppressed). In order that the resulting superpartner masses be of order 1 TeV or less, one must have $\Lambda \sim 100$ TeV. The origin of the μ and B-parameters is quite model-dependent, and lies somewhat outside the ansatz of gauge-mediated supersymmetry breaking. The simplest models of this type are even more restrictive than mSUGRA, with two fewer degrees of freedom. However, minimal GMSB is not a fully realized model. The sector of supersymmetry-breaking dynamics can be very complex, and no complete model of gauge-mediated supersymmetry yet exists that is both simple and compelling.

It was noted in Section I.2 that the gravitino is the LSP in GMSB models. Thus, in such models, the next-to-lightest supersymmetric particle (NLSP) plays a crucial role in the phenomenology of supersymmetric particle production and decay. Note that unlike the LSP, the NLSP can be charged. In GMSB models, the most likely candidates for the NLSP are $\widetilde{\chi}^0_1$ and $\widetilde{\tau}^\pm_R$. The NLSP will decay into its superpartner plus a gravitino (*e.g.*, $\widetilde{\chi}^0_1 \to \gamma\widetilde{g}_{3/2}$, $\widetilde{\chi}^0_1 \to Z\widetilde{g}_{3/2}$ or $\widetilde{\tau}^\pm_R \to \tau^\pm\widetilde{g}_{3/2}$), with lifetimes and branching ratios that depend on the model parameters.

Different choices for the identity of the NLSP and its decay rate lead to a variety of distinctive supersymmetric phenomenologies [38,70]. For example, a long-lived $\widetilde{\chi}^0_1$-NLSP that decays outside collider detectors leads to supersymmetric decay chains with missing energy in association with leptons and/or hadronic jets (this case is indistinguishable from the canonical phenomenology of the $\widetilde{\chi}^0_1$-LSP). On the other hand, if $\widetilde{\chi}^0_1 \to \gamma\widetilde{g}_{3/2}$ is the dominant decay mode, and the decay occurs inside the detector, then nearly *all* supersymmetric particle decay chains would contain a photon. In contrast, the case of a $\widetilde{\tau}^\pm_R$-NLSP would lead either to a new long-lived charged particle (*i.e.*, the $\widetilde{\tau}^\pm_R$) or to supersymmetric particle decay chains with τ leptons.

Finally, grand unification [71] can impose additional constraints on the MSSM parameters. Perhaps one of the most compelling hints for low-energy supersymmetry is the unification of $SU(3)\times SU(2)\times U(1)$ gauge couplings predicted by models of supersymmetric grand unified theories (SGUTs) [7,9,72] (with the supersymmetry-breaking scale of order 1 TeV or below). Gauge coupling unification, which takes place at an energy scale of order 10^{16} GeV, is quite robust [73]. For example, successful unification depends weakly on the details of the theory at the unification scale. In particular, given the low-energy values of the electroweak couplings $g(m_Z)$ and $g'(m_Z)$, one can predict $\alpha_s(m_Z)$ by using the MSSM renormalization group equations to extrapolate to higher energies, and by imposing the unification condition on the three gauge couplings at some high-energy scale, $M_{\rm X}$. This procedure, which fixes $M_{\rm X}$, can be successful (*i.e.*, three running couplings will meet at a single point) only for a unique value of $\alpha_s(m_Z)$. The extrapolation depends somewhat on the low-energy supersymmetric spectrum (so-called low-energy "threshold effects"), and on the SGUT spectrum (high-energy threshold effects), which can somewhat alter the evolution of couplings. Ref. [74] summarizes the comparison of present data with the expectations of SGUTs, and shows that the measured value of $\alpha_s(m_Z)$ is in good agreement with the predictions of supersymmetric grand unification for a reasonable choice of supersymmetric threshold corrections.

Additional SGUT predictions arise through the unification of the Higgs-fermion Yukawa couplings (λ_f). There is some evidence that $\lambda_b = \lambda_\tau$ leads to good low-energy phenomenology [75], and an intriguing possibility that $\lambda_b = \lambda_\tau = \lambda_t$ may be phenomenologically viable [67,76] in the parameter regime where $\tan\beta \simeq m_t/m_b$. Finally, grand unification imposes constraints on the soft-supersymmetry-breaking parameters. For example, gaugino-mass unification leads to the relations given by Eq. (7). Diagonal squark and slepton soft-supersymmetry-breaking scalar masses may also be unified, which is analogous to the unification of Higgs-fermion Yukawa couplings.

In the absence of a fundamental theory of supersymmetry breaking, further progress will require a detailed knowledge of the supersymmetric-particle spectrum in order to determine the nature of the high-energy parameters. Of course, any of the theoretical assumptions described in this section could be wrong and must eventually be tested experimentally.

I.8. Beyond the MSSM: Non-minimal models of low-energy supersymmetry can also be constructed. One approach is to add new structure beyond the Standard Model at the TeV scale or below. The supersymmetric extension of such a theory would be a non-minimal extension of the MSSM. Possible new structures include: (i) the supersymmetric generalization of the see-saw model of neutrino masses [77,78]; (ii) an enlarged electroweak gauge group beyond $SU(2)\times U(1)$ [79]; (iii) the addition of new, possibly exotic, matter multiplets [*e.g.*, a vector-like color triplet with electric charge $\frac{1}{3}e$; such states sometimes occur as low-energy remnants in E_6 grand unification models]; and/or (iv) the addition of low-energy $SU(3)\times SU(2)\times U(1)$

singlets [80]. A possible theoretical motivation for such new structure arises from the study of phenomenologically viable string theory ground states [81].

A second approach is to retain the minimal particle content of the MSSM but remove the assumption of R-parity invariance. The most general R-parity-violating (RPV) theory involving the MSSM spectrum introduces many new parameters to both the supersymmetry-conserving and the supersymmetry-breaking sectors. Each new interaction term violates either B or L conservation. For example, consider new scalar-fermion Yukawa couplings derived from the following interactions:

$$(\lambda_L)_{pmn}\widehat{L}_p\widehat{L}_m\widehat{E}^c_n+(\lambda'_L)_{pmn}\widehat{L}_p\widehat{Q}_m\widehat{D}^c_n+(\lambda_B)_{pmn}\widehat{U}^c_p\widehat{D}^c_m\widehat{D}^c_n\,, \quad (10)$$

where p, m, and n are generation indices, and gauge group indices are suppressed. In the notation above, $\widehat{Q}$, $\widehat{U}^c$, $\widehat{D}^c$, $\widehat{L}$, and $\widehat{E}^c$ respectively represent $(u,d)_L$, u^c_L, d^c_L, $(\nu,\, e^-)_L$, and e^c_L and the corresponding superpartners. The Yukawa interactions are obtained from Eq. (10) by taking all possible combinations involving two fermions and one scalar superpartner. Note that the term in Eq. (10) proportional to λ_B violates B, while the other two terms violate L. Even if all the terms of Eq. (10) are absent, there is one more possible supersymmetric source of R-parity violation. In the notation of Eq. (10), one can add a term of the form $(\mu_L)_p\widehat{H}_u\widehat{L}_p$, where $\widehat{H}_u$ represents the $Y=1$ Higgs doublet and its higgsino superpartner. This term is the RPV generalization of the supersymmetry-conserving Higgs mass parameter μ of the MSSM, in which the $Y=-1$ Higgs/higgsino super-multiplet $\widehat{H}_d$ is replaced by the lepton/slepton super-multiplet $\widehat{L}_p$. The RPV-parameters $(\mu_L)_p$ also violate L.

Phenomenological constraints on various low-energy B- and L-violating processes can be used to derive limits on each of the coefficients $(\lambda_L)_{pmn}$, $(\lambda'_L)_{pmn}$, and $(\lambda_B)_{pmn}$ taken one at a time [82]. If more than one coefficient is simultaneously non-zero, then the limits are, in general, more complicated. All possible RPV terms cannot be simultaneously present and unsuppressed; otherwise the proton decay rate would be many orders of magnitude larger than the present experimental bound. One way to avoid proton decay is to impose B or L invariance (either one alone would suffice). Otherwise, one must accept the requirement that certain RPV coefficients must be extremely suppressed.

One particularly interesting class of RPV models is one in which B is conserved, but L is violated. It is possible to enforce baryon number conservation, while allowing for lepton number violating interactions by imposing a discrete baryon $\mathbf{Z_3}$ symmetry on the low-energy theory [83], in place of the standard $\mathbf{Z_2}$ R parity. In these models, supersymmetric phenomenology exhibits features that are quite distinct from that of the MSSM. The LSP is no longer stable, which implies that not all supersymmetric decay chains must yield missing-energy events at colliders. Both $\Delta L=1$ and $\Delta L=2$ phenomena are allowed (if L is violated), leading to neutrino masses and mixing [84], neutrinoless double-beta decay [85], sneutrino-antisneutrino mixing [78,86,87], and s-channel resonant production of the sneutrino in e^+e^- collisions [88]. Since the distinction between the Higgs and matter super-multiplets is lost, R-parity violation permits the mixing of sleptons and Higgs bosons, the mixing of neutrinos and neutralinos, and the mixing of charged leptons and charginos, leading to more complicated mass matrices and mass eigenstates than in the MSSM. Note that if $\lambda'_L \neq 0$, then squarks can behave as leptoquarks since the following processes are allowed: $e^+\overline{u}_m \to \overline{\widetilde{d}}_n \to e^+\overline{u}_m, \overline{\nu}\overline{d}_m$, and $e^+d_m \to \widetilde{u}_n \to e^+d_m$. (As above, m and n are generation labels, so that $d_2=s$, $d_3=b$, *etc.*)

Of course, R-parity-violation can also enter via the soft-supersymmetry-breaking terms, leading to an explosion of unknown parameters (well beyond the 124 of the MSSM in the most general case). As in the MSSM, one can consider constrained versions of RPV supersymmetry, in which simplified assumptions are made about the structure of the supersymmetry breaking terms at some high energy scale. Moreover, one can make additional assumptions regarding the RPV parameters. For example, in the bilinear RPV model [89], the trilinear RPV terms of Eq. (10) (and the corresponding supersymmetry-breaking "A-parameters") are absent, and the only source of R-parity violation arises from $(\mu_L)_p$ and L-violating soft-supersymmetry-breaking "B-parameters" and squared-mass terms.

With the overwhelming evidence for neutrino masses and mixing [90], it is clear that any viable supersymmetric model of fundamental particles must incorporate some form of L violation in the low-energy theory [91]. The supersymmetric generalization of the see-saw mechanism and RPV supersymmetry provide two possible frameworks for non-zero neutrino masses. For example, Ref. [92] demonstrates how one can fit both the solar and atmospheric neutrino data in the bilinear RPV supersymmetric model. In addition, experimental and theoretical constraints from collider physics also places some non-trivial restrictions on general R-parity-violating alternatives to the MSSM (see Refs. [82] and [93] for further details).

References

1. H.P. Nilles, Phys. Reports **110**, 1 (1984).
2. P. Nath, R. Arnowitt, and A.H. Chamseddine, *Applied $N=1$ Supergravity* (World Scientific, Singapore, 1984).
3. S.P. Martin, in *Perspectives on Supersymmetry*, ed. G.L. Kane (World Scientific, Singapore, 1998) pp. 1–98.
4. S. Weinberg, *The Quantum Theory of Fields, Volume III: Supersymmetry* (Cambridge University Press, Cambridge, UK, 2000).
5. L. Girardello and M. Grisaru, Nucl. Phys. **B194**, 65 (1982);
   L.J. Hall and L. Randall, Phys. Rev. Lett. **65**, 2939 (1990);
   I. Jack and D.R.T. Jones, Phys. Lett. **B457**, 101 (1999).
6. E. Witten, Nucl. Phys. **B188**, 513 (1981).
7. S. Dimopoulos and H. Georgi, Nucl. Phys. **B193**, 150 (1981).
8. L. Susskind, Phys. Reports **104**, 181 (1984);

N. Sakai, Z. Phys. **C11**, 153 (1981);
R.K. Kaul, Phys. Lett. **109B**, 19 (1982).

9. For a review, see R.N. Mohapatra, in *Particle Physics 1999*, ICTP Summer School in Particle Physics, Trieste, Italy, 21 June—9 July, 1999, eds. G. Senjanovic and A.Yu. Smirnov (World Scientific, Singapore, 2000) pp. 336–394.
10. H.E. Haber and G.L. Kane, Phys. Reports **117**, 75 (1985).
11. K. Inoue *et al.*, Prog. Theor. Phys. **68**, 927 (1982) [erratum: **70,** 330 (1983)]; **71,** 413 (1984);
R. Flores and M. Sher, Ann. Phys. (NY) **148**, 95 (1983).
12. J.F. Gunion and H.E. Haber, Nucl. Phys. **B272**, 1 (1986) [erratum: **B402**, 567 (1993)].
13. See, *e.g.*, R. Barbieri and G.F. Giudice, Nucl. Phys. **B305**, 63 (1988);
G.W. Anderson and D.J. Castano, Phys. Lett. **B347**, 300 (1995); Phys. Rev. **D52**, 1693 (1995); Phys. Rev. **D53**, 2403 (1996);
J.L. Feng, K.T. Matchev, and T. Moroi, Phys. Rev. **D61**, 075005 (2000).
14. S. Dimopoulos and G.F. Giudice, Phys. Lett. **B357**, 573 (1995);
A. Pomarol and D. Tommasini, Nucl. Phys. **B466**, 3 (1996);
A.G. Cohen, D.B. Kaplan, and A.E. Nelson, Phys. Lett. **B388**, 588 (1996);
J.L. Feng, K.T. Matchev, and T. Moroi, Phys. Rev. Lett. **84**, 2322 (2000).
15. M. Schmitt, "Supersymmetry Part II (Experiment)," immediately following, in the printed version of the *Review of Particle Physics* (see also the Particle Listings immediately following).
16. See, *e.g.*, F. Gabbiani *et al.*, Nucl. Phys. **B477**, 321 (1996).
17. For a recent review and references to the original literature, see: A. Masiero and O. Vives, New Journal of Physics **4**, 4.1 (2002).
18. J. Erler and P. Langacker, "Electroweak Model and Constraints on New Physics," in the section on Reviews, Tables, and Plots in this *Review*.
19. P.H. Chankowski and S. Pokorski, in *Perspectives on Supersymmetry*, ed. G.L. Kane (World Scientific, Singapore, 1998) pp. 402–422.
20. A. Dobado, M.J. Herrero, and S. Penaranda, Eur. Phys. J. **C7**, 313 (1999); **C12**, 673 (2000); **C17**, 487 (2000).
21. G. Altarelli *et al.*, JHEP **0106**, 018 (2001);
W. de Boer and C. Sander, in the Proceedings of the 10th International Conference on Supersymmetry and Unification of Fundamental Interactions (SUSY-02), DESY Hamburg, Germany, 17–23 June 2002, edited by P. Nath and P.M. Zerwas, (DESY publications, Hamburg, Germany) pp. 1121–1126;
S. Heinemeyer and G. Weiglein, `hep-ph/0307177`, to appear in the Proceedings of the workshop "Electroweak precision data and the Higgs mass," DESY Zeuthen, February 2003.
22. M. Davier *et al.*, preprint LAL 03-50 (2003) [`hep-ph/0308213`].
23. For a recent review and references to the literature, see T. Hurth, `hep-ph/0212304`, to be published in Rev. Mod. Phys. .
24. See, *e.g.*, M. Ciuchini *et al.*, Phys. Rev. **D67**, 075016 (2003).
25. U. Chattopadhyay and P. Nath, Phys. Rev. **D66**, 093001 (2002);
S.P. Martin and J.D. Wells, Phys. Rev. **D67**, 015002 (2003).
26. P. Fayet, Phys. Lett. **69B**, 489 (1977);
G. Farrar and P. Fayet, Phys. Lett. **76B**, 575 (1978).
27. J. Ellis *et al.*, Nucl. Phys. **B238**, 453 (1984).
28. S. Raby, Phys. Lett. **B422**, 158 (1998);
S. Raby and K. Tobe, Nucl. Phys. **B539**, 3 (1999);
A. Mafi and S. Raby, Phys. Rev. **D62**, 035003 (2000).
29. G. Jungman, M. Kamionkowski, and K. Griest, Phys. Reports **267**, 195 (1996).
30. A.R. Liddle and D.H. Lyth, Phys. Reports **213**, 1 (1993).
31. N.J.C. Spooner and M. Srednicki, in the section on "Dark Matter" in the *Review of Particle Physics*.
32. P. Fayet, Phys. Lett. **84B**, 421 (1979); Phys. Lett. **86B**, 272 (1979).
33. S. Deser and B. Zumino, Phys. Rev. Lett. **38**, 1433 (1977).
34. L.J. Hall, J. Lykken, and S. Weinberg, Phys. Rev. **D27**, 2359 (1983).
35. S.K. Soni and H.A. Weldon, Phys. Lett. **126B**, 215 (1983);
Y. Kawamura, H. Murayama, and M. Yamaguchi, Phys. Rev. **D51**, 1337 (1995).
36. A.B. Lahanas and D.V. Nanopoulos, Phys. Reports **145**, 1 (1987).
37. M. Dine and A.E. Nelson, Phys. Rev. **D48**, 1277 (1993);
M. Dine, A.E. Nelson, and Y. Shirman, Phys. Rev. **D51**, 1362 (1995);
M. Dine *et al.*, Phys. Rev. **D53**, 2658 (1996).
38. G.F. Giudice, and R. Rattazzi, Phys. Reports **322**, 419 (1999).
39. J. Polchinski, *String Theory, Volumes I and II* (Cambridge University Press, Cambridge, UK, 1998).
40. For a review of recent developments in models and the phenomenology of large extra dimensions, see J. Hewett and J. March-Russell, in the section on "Extra Dimensions" in the *Review of Particle Physics*.
41. These ideas are reviewed in: V.A. Rubakov, Sov. Phys. Usp. **44**, 871 (2001);
Y.A. Kubyshin, Lectures given at the 11th International School on Particles and Cosmology, Karbardino-Balkaria, Russia, 18–24 April 2001, `hep-ph/0111027`.
42. L. Randall and R. Sundrum, Nucl. Phys. **B557**, 79 (1999).
43. Z. Chacko, M.A. Luty, and E. Ponton, JHEP **0007**, 036 (2000);
D.E. Kaplan, G.D. Kribs, and M. Schmaltz, Phys. Rev. **D62**, 035010 (2000);
Z. Chacko *et al.*, JHEP **0001**, 003 (2000).
44. M. Quiros, to appear in the Proceedings of the 2002 Theoretical Advanced Study Institute (TASI-02), Boulder, CO, 3–28 June 2002 [`hep-ph/0302189`].
45. J. Scherk and J.H. Schwarz, Phys. Lett. **82B**, 60 (1979); Nucl. Phys. **B153**, 61 (1979).
46. See, *e.g.*, R. Barbieri, L.J. Hall, and Y. Nomura, Phys. Rev. **D66**, 045025 (2002); Nucl. Phys. **B624**, 63 (2002).
47. H.E. Haber, in *Recent Directions in Particle Theory, Proceedings of the 1992 Theoretical Advanced Study Institute in Particle Physics*, eds. J. Harvey and J. Polchinski (World Scientific, Singapore, 1993) pp. 589–686.
48. S. Dimopoulos and D. Sutter, Nucl. Phys. **B452**, 496 (1995);

D.W. Sutter, Stanford Ph. D. thesis, hep-ph/9704390.

49. H.E. Haber, Nucl. Phys. B (Proc. Suppl.) **62A-C**, 469 (1998).
50. Explicit forms for the chargino and neutralino mass matrices can be found in Appendix A of Ref. [12]; see also Ref. [47].
51. J. Ellis and S. Rudaz, Phys. Lett. **128B**, 248 (1983).
52. D.M. Pierce *et al.*, Nucl. Phys. **B491**, 3 (1997).
53. J.F. Gunion *et al.*, *The Higgs Hunter's Guide* (Perseus Publishing, Cambridge, MA, 1990);
M. Carena and H.E. Haber, Prog. in Part. Nucl. Phys. **50**, 63 (2003).
54. H.E. Haber and R. Hempfling, Phys. Rev. Lett. **66**, 1815 (1991);
Y. Okada, M. Yamaguchi, and T. Yanagida, Prog. Theor. Phys. **85**, 1 (1991);
J. Ellis, G. Ridolfi, and F. Zwirner, Phys. Lett. **B257**, 83 (1991).
55. ALEPH, DELPHI, L3 and OPAL Collaborations [LEP Higgs Working Group for Higgs boson searches], Phys. Lett. **B565**, 61 (2003).
56. See, *e.g.*, G. Degrassi *et al.*, Eur. Phys. J. **C28**, 133 (2003) and references contained therein.
57. A. Pilaftsis and C.E.M. Wagner, Nucl. Phys. **B553**, 3 (1999);
D.A. Demir, Phys. Rev. **D60**, 055006 (1999);
S.Y. Choi, M. Drees, and J.S. Lee, Phys. Lett. **B481**, 57 (2000);
M. Carena *et al.*, Nucl. Phys. **B586**, 92 (2000); Phys. Lett. **B495**, 155 (2000); Nucl. Phys. **B625**, 345 (2002).
58. S. Khalil, Int. J. Mod. Phys. **A18**, 1697 (2003).
59. W. Fischler, S. Paban, and S. Thomas, Phys. Lett. **B289**, 373 (1992);
S.M. Barr, Int. J. Mod. Phys. **A8**, 209 (1993);
T. Ibrahim and P. Nath, Phys. Rev. **D58**, 111301 (1998) [erratum: **D60**, 099902 (1999)];
M. Brhlik, G.J. Good, and G.L. Kane, Phys. Rev. **D59**, 115004 (1999).
60. A. Masiero and L. Silvestrini, in *Perspectives on Supersymmetry*, ed. G.L. Kane (World Scientific, Singapore, 1998) pp. 423–441.
61. H. Georgi, Phys. Lett. **169B**, 231 (1986);
L.J. Hall, V.A. Kostelecky, and S. Raby, Nucl. Phys. **B267**, 415 (1986).
62. Y. Nir and N. Seiberg, Phys. Lett. **B309**, 337 (1993);
S. Dimopoulos, G.F. Giudice, and N. Tetradis, Nucl. Phys. **B454**, 59 (1995);
G.F. Giudice *et al.*, JHEP **12**, 027 (1998);
J.L. Feng and T. Moroi, Phys. Rev. **D61**, 095004 (2000).
63. J.F. Gunion and H.E. Haber, Phys. Rev. **D37**, 2515 (1988).
64. J.L. Feng *et al.*, Phys. Rev. Lett. **83**, 1731 (1999);
T. Gherghetta, G.F. Giudice, and J.D. Wells, Nucl. Phys. **B559**, 27 (1999);
J.F. Gunion and S. Mrenna, Phys. Rev. **D62**, 015002 (2000).
65. See, *e.g.*, B. Murakami and J.D. Wells, Phys. Rev. **D68**, 035006 (2003) and references contained therein.
66. M. Drees and S.P. Martin, in *Electroweak Symmetry Breaking and New Physics at the TeV Scale*, eds. T. Barklow *et al.* (World Scientific, Singapore, 1996) pp. 146–215.
67. M. Carena *et al.*, Nucl. Phys. **B426**, 269 (1994).
68. M. Battaglia *et al.*, CERN-TH/2003-138 [hep-ph/0306219].
69. L.E. Ibáñez and D. Lüst, Nucl. Phys. **B382**, 305 (1992);
B. de Carlos, J.A. Casas, and C. Munoz, Phys. Lett. **B299**, 234 (1993);
V. Kaplunovsky and J. Louis, Phys. Lett. **B306**, 269 (1993);
A. Brignole, L.E. Ibáñez, and C. Munoz, Nucl. Phys. **B422**, 125 (1994) [erratum: **B436**, 747 (1995)].
70. For a review and guide to the literature, see J.F. Gunion and H.E. Haber, in *Perspectives on Supersymmetry*, ed. G.L. Kane (World Scientific, Singapore, 1998) pp. 235–255.
71. S. Raby , in the section on "Grand Unified Theories" in the *Review of Particle Physics*.
72. M.B. Einhorn and D.R.T. Jones, Nucl. Phys. **B196**, 475 (1982);
W.J. Marciano and G. Senjanovic, Phys. Rev. **D25**, 3092 (1982).
73. D.M. Ghilencea and G.G. Ross, Nucl. Phys. **B606**, 101 (2001).
74. S. Pokorski, Acta Phys. Polon. **B30**, 1759 (1999);
For a review, see N. Polonsky, *Supersymmetry: Structure and phenomena. Extensions of the standard model*, Lect. Notes Phys. **M68**, 1 (2001).
75. H. Arason *et al.*, Phys. Rev. Lett. **67**, 2933 (1991);
Phys. Rev. **D46**, 3945 (1992);
V. Barger, M.S. Berger, and P. Ohmann, Phys. Rev. **D47**, 1093 (1993);
M. Carena, S. Pokorski, and C.E.M. Wagner, Nucl. Phys. **B406**, 59 (1993);
P. Langacker and N. Polonsky, Phys. Rev. **D49**, 1454 (1994).
76. M. Olechowski and S. Pokorski, Phys. Lett. **B214**, 393 (1988);
B. Ananthanarayan, G. Lazarides, and Q. Shafi, Phys. Rev. **D44**, 1613 (1991);
S. Dimopoulos, L.J. Hall, and S. Raby, Phys. Rev. Lett. **68**, 1984 (1992);
L.J. Hall, R. Rattazzi, and U. Sarid, Phys. Rev. **D50**, 7048 (1994);
R. Rattazzi and U. Sarid, Phys. Rev. **D53**, 1553 (1996).
77. J. Hisano *et al.*, Phys. Lett. **B357**, 579 (1995);
J. Hisano *et al.*, Phys. Rev. **D53**, 2442 (1996);
J. Ellis *et al.*, Phys. Rev. **D66**, 115013 (2002).
78. Y. Grossman and H.E. Haber, Phys. Rev. Lett. **78**, 3438 (1997).
79. J.L. Hewett and T.G. Rizzo, Phys. Reports **183**, 193 (1989).
80. See, *e.g.*, U. Ellwanger, M. Rausch de Traubenberg, and C.A. Savoy, Nucl. Phys. **B492**, 21 (1997);
U. Ellwanger and C. Hugonie, Eur. Phys. J. **C25**, 297 (2002) and references contained therein.
81. K.R. Dienes, Phys. Reports **287**, 447 (1997).
82. H. Dreiner, in *Perspectives on Supersymmetry*, ed. G.L. Kane (World Scientific, Singapore, 1998) pp. 462–479.
83. L.E. Ibáñez and G.G. Ross, Nucl. Phys. **B368**, 3 (1992);
L.E. Ibáñez, Nucl. Phys. **B398**, 301 (1993).
84. For a review, see J.C. Romao, Nucl. Phys. Proc. Suppl. **81**, 231 (2000).
85. R.N. Mohapatra, Phys. Rev. **D34**, 3457 (1986);
K.S. Babu and R.N. Mohapatra, Phys. Rev. Lett. **75**, 2276 (1995);

M. Hirsch, H.V. Klapdor-Kleingrothaus, and S.G. Kovalenko, Phys. Rev. Lett. **75**, 17 (1995); Phys. Rev. **D53**, 1329 (1996).

86. M. Hirsch, H.V. Klapdor-Kleingrothaus, and S.G. Kovalenko, Phys. Lett. **B398**, 311 (1997).
87. Y. Grossman and H.E. Haber, Phys. Rev. **D59**, 093008 (1999).
88. S. Dimopoulos and L.J. Hall, Phys. Lett. **B207**, 210 (1988);
J. Kalinowski *et al.*, Phys. Lett. **B406**, 314 (1997);
J. Erler, J.L. Feng, and N. Polonsky, Phys. Rev. Lett. **78**, 3063 (1997).
89. A study of the phenomenology of bilinear R-parity-breaking supersymmetry and a guide to the literature can be found in D.A. Restrepo Quintero, `hep-ph/0111198`.
90. See the section on neutrinos in "Particle Listings" in the *Review of Particle Physics*.
91. For a recent review of neutrino masses in supersymmetry, see B. Mukhopadhyaya, `hep-ph/0301278`.
92. See, *e.g.*, M. Hirsch *et al.*, Phys. Rev. **D62**, 113008 (2000) [erratum: **D65**, 119901 (2002)];
M.A. Diaz, *et al.*, Phys. Rev. **D68**, 013009 (2003).
93. M. Bisset *et al.*, Phys. Rev. **D62**, 035001 (2000);
R. Barbier *et al.*, Report of the group on the R-parity violation, `hep-ph/9810232` (1998).

SUPERSYMMETRY, PART II (EXPERIMENT)

Revised September, 2003 by M. Schmitt (Northwestern University)

II.1. Introduction: The theoretical strong points of supersymmetry (SUSY) have motivated many searches for supersymmetric particles. Many of these have been based on the canonical missing-energy signature caused by the escape of weakly-interacting LSP's ('lightest supersymmetric particles'). Other scenarios also have been investigated, widening the range of topologies and experimental signatures in which new physics might be found. Unfortunately, no convincing evidence for the production of supersymmetric particles has been found.

Theoretical aspects of supersymmetry have been covered in Part I of this review by H.E. Haber (see also Ref. 1, 2); we use his notations and terminology.

II.2. Common supersymmetry scenarios: In the 'canonical' scenario [1], supersymmetric particles are pair-produced and decay directly or via cascades to the LSP. It follows that there are always at least two LSP's per event. If R-parity, the quantum number which distinguishes SM and SUSY particles, is conserved, the LSP is stable. For most typical choices of model parameters, the lightest neutralino is the LSP. Since the neutralino is neutral and colorless, interacting only weakly with matter, it will escape detection, giving signal events the characteristic appearance of "missing energy." In e^+e^- machines, the total visible energy and total visible momentum can be well measured. Since the electron beam energy has a very small spread, the missing energy ($E^{\rm miss} = \sqrt{s} - E^{\rm vis}$) and the missing momentum ($\vec{p}^{\ \rm miss} = -\vec{p}^{\ \rm vis}$) are well correlated with the net energy and momentum of the LSP's. In proton colliders, the distribution of the energy and longitudinal momentum of the partons (quarks and gluons inside the (anti-)protons) is very broad, so in practice only the transverse momentum is useful. It is calculated from the vector sum of energy deposits registered in the calorimetry and is called "missing transverse energy" ($\not\!\!E_T$). Collimated jets, isolated leptons or photons, and appropriate kinematic and topological cuts provide additional handles for reducing backgrounds.

The conservation of R-parity is not required in supersymmetry, however, and in some searches it is assumed that supersymmetric particles decay via interactions which violate R-parity (RPV). For the most part the production of superpartners is unchanged, but the missing-energy signature is lost. Depending on the choice of the R-parity–violating interaction, SUSY events are characterized by an excess of leptons or hadronic jets, and in many cases it is relatively easy to suppress SM backgrounds [3]. A distinction is made between "indirect" RPV, in which the LSP decays close to the interaction point but no other decays are modified, and "direct" RPV, in which the supersymmetric particles decay to SM particles, producing no LSP's. The LSP's themselves provide a visible signal by virtue or their decay to ordinary fermions. Note that the cosmological constraint which requires stable LSP's to be charge and color neutral no longer applies when there R-parity is violated.

In models assuming gauge-mediated supersymmetry breaking (GMSB) [4], the gravitino, $\widetilde{g}_{3/2}$, is a weakly-interacting fermion with a mass so small that it can be neglected when considering the event kinematics. It is the LSP, and the lightest neutralino, $\widetilde{\chi}^0_1$, decays to it radiatively, possibly with a long lifetime. With few exceptions the decays and production of other superpartners are the same as in the canonical scenario, so when the neutralino lifetime is not too long, the event topologies are augmented by the presence of energetic and isolated photons. If the lifetime is so long that the neutralino decays outside the detector, the event topologies are the same as in the canonical scenario. In some variants of this theory the right-sleptons are lighter than the lightest neutralino, and they decay to a lepton and a gravitino. The most important case of this type is the channel $\widetilde{\tau}_R \to \tau\widetilde{G}$. The lifetime of the $\widetilde{\tau}_R$ can vary over a wide range depending on model parameters, leading to new exotic signatures, including quasi-stable, heavily ionizing charged particles.

Finally, there is another phenomenologically important scenario in which the gluino $\widetilde{g}$ is assumed to be relatively light ($M_{\widetilde{g}} < 5$ GeV/c^2). Experimental evidence does not support the hypothesis, however, as discussed further in the review by H. Murayama.

II.3. Experimental issues: When given no signal for supersymmetric particles, experimenters are obliged to derive limits on their production. The most general formulation of supersymmetry is so flexible that few universal bounds can be obtained. Often more restricted forms of the theory are evoked for which predictions are more definite. The most popular of

these is minimal supergravity ('mSUGRA'). As explained in Part I of this review, parameter freedom is drastically reduced by requiring related parameters to be equal at the unification scale, M_X. Thus, the gaugino masses are equal with value $m_{1/2}$, and the slepton, squark, and Higgs masses depend on a *common* scalar mass parameter, m_0. In the individual experimental analyses, only some of these assumptions are necessary. For example, the gluino and squark searches at proton machines constrain mainly M_3 and a scalar mass parameter m_0 for the squark masses, while the chargino, neutralino, and slepton searches at e^+e^- colliders constrain M_2 and a scalar mass parameter m_0 for the slepton masses. In addition, results from the Higgs searches can be used to constrain $m_{1/2}$ and m_0 as a function of $\tan\beta$. (The full analysis involves large radiative corrections coming from squark mixing, which is where the dependence on $m_{1/2}$ and m_0 enter.) In the mSUGRA framework, all the scalar mass parameters m_0 are the same and the three gaugino mass parameters are proportional to $m_{1/2}$, so limits from squarks, sleptons, charginos, gluinos, and Higgs all can be used together to constrain the parameter space. A slightly less constrained model allows the Higgs sector to be independent of the sfermion sector, while still requiring that the scalar mass parameter m_0 is the same for sleptons and squarks and that the gaugino mass parameter $m_{1/2}$ is the same for charginos, neutralinos and gluinos. This model is called the 'constrained MSSM' (cMSSM) [5,6].

While the mSUGRA framework is convenient, it is based on several highly specific theoretical assumptions, so limits presented in this framework cannot easily be applied to other supersymmetric models. It has been possible in some instances to reduce the model dependence of experimental results by combining several searches. When model-independent results are impossible, the underlying assumptions and their consequences are (or should be) carefully delineated.

In the analysis of data from hadron collider experiments, the experimenter considers several supersymmetric processes simultaneously. In contrast to experiments at e^+e^- colliders, it does not makes sense to talk about one process at a time due to the very broad mass range spanned. This makes the utilization of some sort of organizing device, such as a constrained version of the MSSM, practically unavoidable.

II.4. Supersymmetry searches at e^+e^- colliders:

The large electron-positron collider (LEP) at CERN ran at energies ranging from the Z peak up to $\sqrt{s} = 209$ GeV/c^2. Each experiment (ALEPH, DELPHI, L3, OPAL) accumulated large data sets at a series of energies, as detailed in [7]. For the limits discussed here, the most relevant data samples include 180 pb^{-1} at 189 GeV/c^2, and 220 pb^{-1} at higher energies, of which 140 pb^{-1} was delivered above 206 GeV/c^2. Since the last edition of this review, several of the searches at the highest energies have been finalized.

Running at the Z pole, the LEP experiments and SLD at SLAC excluded many supersymmetric particles up to about half the Z mass. These limits come mainly from the comparison of the measured Z widths to SM expectations, and are relatively insensitive to the details of SUSY particle decays [8]. The data taken at higher energies allow much stronger limits to be set, although the complex interplay of masses, cross sections, and branching ratios allow for a few exceptions to simple general limits.

The main signals come from SUSY particles with charge, weak isospin, or large Yukawa couplings. The gauge fermions (charginos and neutralinos) generally are produced with large cross sections, while the scalar particles (sleptons and squarks) are suppressed near threshold by kinematic factors.

The various SUSY particles considered at LEP typically decay directly to SM particles and LSP's, so signatures consist of some combination of jets, leptons, possibly photons, and missing energy. Consequently the search criteria are geared toward a few distinct topologies. Although they may be optimized for one specific signal, they are often efficient for others. For example, acoplanar jets are expected in both $\tilde{t}_1\bar{\tilde{t}}_1$ and $\tilde{\chi}_1^0\tilde{\chi}_2^0$ production, and acoplanar leptons for both $\tilde{\ell}^+\tilde{\ell}^-$ and $\tilde{\chi}^+\tilde{\chi}^-$.

Backgrounds come mainly from three sources. First, there are the so-called 'two-photon interactions,' in which the beam electrons emit photons which combine to produce a low mass hadronic or leptonic system leaving little visible energy in the detector. Since the electrons are seldom deflected through large angles, $p_T^{\rm miss}$ is low. Second, there is difermion production, usually accompanied by large initial-state radiation induced by the Z pole, which gives events that are well balanced with respect to the beam direction. Finally, there is four-fermion production through states with one or two resonating bosons (W^+W^-, ZZ, $We\nu$, Ze^+e^-, etc.) which can give events with large $E^{\rm miss}$ and $p_T^{\rm miss}$ due to neutrinos and electrons lost down the beam pipe.

In the canonical case, $E^{\rm miss}$ and $p_T^{\rm miss}$ are large enough to eliminate most of these backgrounds. The e^+e^- initial state is well defined so searches utilize both transverse and longitudinal momentum components. It is possible to measure the missing mass ($M_{\rm miss} = \{(\sqrt{s}-E_{\rm vis})^2 - \vec{p}^{\,2}_{\rm vis}\}^{1/2}$) which is small if $p_T^{\rm miss}$ is caused by a single neutrino or an undetected electron or photon, and large when there are two massive LSP's. The four-fermion processes cannot be entirely eliminated, however, and a non-negligible irreducible background is expected. Fortunately, the uncertainties for these backgrounds are not large.

High efficiencies are easily achieved when the mass of the LSP ($M_{\rm LSP}$) is less than the parent particle ($M_{\rm parent}$) by at least 10 GeV/c^2 and greater than about 10 GeV/c^2. Difficulties arise when the mass difference $\Delta M = M_{\rm parent} - M_{\rm LSP}$ is smaller than 10 GeV/c^2 as the signal resembles background from two-photon interactions. A very light LSP is challenging also since, kinematically speaking, it plays a role similar to a neutrino, so that, for example, a signal for charginos of mass ~ 80 GeV/c^2 is difficult to distinguish from the production of W^+W^- pairs. The lower signal efficiency obtained in these two extreme cases

has been offset by the large integrated luminosities delivered, so mass limits are not degraded.

Charginos and Neutralinos: The phenomenology of charginos and neutralinos depends on their field content: they tend to be 'gaugino-like' (for $M_2 \ll |\mu|$) or 'higgsino-like' ($|\mu| \ll M_2$), with a 'mixed' field content available only for a relatively small region of parameter space. The cross section for gauginos varies with the masses of sleptons exchanged in the t-channel. In particular, chargino production can be suppressed by more than an order of magnitude for particular values of $M_{\tilde{\nu}_e}$. The gaugino branching ratios also depend on the sfermion sector. When the sfermion masses are larger than ~ 200 GeV/c^2, the chargino and neutralino branching ratios are close to those of the W and Z bosons. Enhancements of leptonic branching ratios are important when sleptons are light. Light squarks are excluded by hadron collider experiments and are not considered. Cross sections and branching ratios for higgsinos are, in contrast, insensitive to the masses of the sfermions.

In the gaugino-like region, the lightest chargino mass is driven by M_2 and the lightest neutralino mass by M_1. For many popular models (such as 'supergravity'), M_1 and M_2 unify at a GUT scale, with $M_1 \approx M_2/2$ at the electroweak scale. Consequently, the mass difference $\Delta M = M_{\tilde{\chi}^\pm} - M_{\tilde{\chi}^0_1}$ is not very small and selection efficiencies are high. However, as explained in the theoretical section of this review, this unification scheme is not required by Supersymmetry, and it is important to consider both $M_1 \approx M_2$ and $M_1 \ll M_2$. In the higgsino-like region, chargino and neutralino masses are all close to $|\mu|$, and hence, small mass differences of order 5 GeV/c^2 are typical. In the mixed region of moderate, negative μ, $\Delta M \approx M_W$, and cuts designed to reject W background lead to lower efficiencies.

Chargino masses have been excluded up to 103 GeV/c^2. However, this limit can be degraded when the sneutrino is lighter than ~ 200 GeV/c^2. Thanks to the large integrated luminosity and the combination of four experiments [7], the impact for $M_{\tilde{\nu}_e} \gtrsim 100$ GeV/c^2 is less than a GeV/c^2. The limit is also weakened when the mass difference is small ($\Delta M = M_{\tilde{\chi}^\pm} - M_{\tilde{\chi}^0_1} \lesssim 3$ GeV/c^2), as in the higgsino region; however, in this case the associated production of neutralino pairs $\tilde{\chi}^0_1\tilde{\chi}^0_2$ is large and the problem of small mass differences ($M_{\tilde{\chi}^0_2} - M_{\tilde{\chi}^0_1}$) less severe. Experimental sensitivity now extends down to mass differences of 3 GeV/c^2, corresponding to M_2 above 2 TeV/c^2.

For a summary of the interplay of chargino field content and sfermion masses, see Fig. 1.

The possibility of extremely small mass differences has been raised in several theoretical papers which propose models rather different from supergravity [9]. The DELPHI Collaboration was the first to engineer searches to cover this scenario [10], and other collaborations have followed suit [11]. For $\Delta M \sim 1$ GeV/c^2, the signal can be distinguished from two-photon background on the basis of isolated photons detected

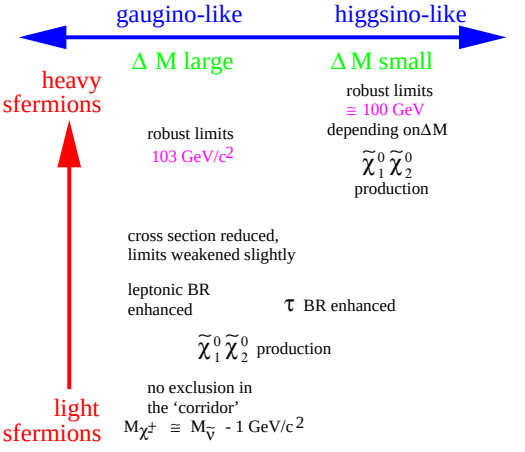

Figure 1: Heuristic diagram of the interplay of chargino field content and sfermion masses. See full-color version on color pages at end of book.

at low angles: hard initial-state radiation sometimes accompanies the signal process but is absent for the background. For $\Delta M \sim 0.2$ GeV/c^2, the chargino acquires a non-negligible lifetime and decays at a significant distance from the interaction point, producing tracks which do not extrapolate back to the interaction point. When $\Delta M < m_\pi$, the lifetime is so long that the chargino appears as a heavily ionizing particle which exits the tracking detector before decaying. The bounds on the chargino mass vary from 68 to 88 GeV/c^2 depending on the assumed sneutrino mass; the limit is 92 GeV/c^2 from the combination of the four LEP experiments when $M_{\tilde{\nu}_e} > 500$ GeV/c^2 [7].

The limits from chargino and neutralino production are most often used to constrain M_2 and μ for fixed $\tan\beta$. For large $|\mu|$ (the gaugino case), chargino bounds limit M_2, and vice versa (the Higgsino case). When $\tan\beta$ is not large, the region of parameter space with $\mu < 0$ and $|\mu| \sim M_2$ corresponds to 'mixed' field content, and the limits on M_2 and $|\mu|$ are relatively modest, especially when electron sneutrinos are light. This is the weak point when inferring an indirect limit on the LSP mass [12].

When the sleptons are light, branching ratios to leptons are enhanced, especially to τ's via $\tilde{\tau}$'s when there is non-negligible mixing of $\tilde{\tau}_R$ and $\tilde{\tau}_L$. These effects are greatest when the chargino has a large gaugino component. The weakest bounds are found for small negative μ and small $\tan\beta$, as the cross section is reduced with respect to larger $|\mu|$, the impact of $\tilde{\tau}$ mixing can be large, and the efficiency is not optimal because ΔM is large. If sneutrinos are lighter than the chargino, then two-body decays $\tilde{\chi}^+ \to \ell^+\tilde{\nu}$ dominate, and in the 'corridor' $0 < M_{\tilde{\chi}^\pm} - M_{\tilde{\nu}} \lesssim 3$ GeV/c^2 the acceptance is so low that no

direct exclusion is possible [13]. However, in the context of the cMSSM it is possible to cover this region with slepton and neutralino searches.

Sleptons: Sleptons and squarks are produced via γ^* and Z^* exchange. For selectrons there is an important contribution from t-channel neutralino exchange which generally increases the cross section. Even though the cross section is suppressed near threshold, the large luminosity at LEP has allowed mass limits to be placed close to the kinematic threshold [14]. For equal masses, the cross section for the R state is smaller than for the L state, so limits are set conservatively for the production of R-sleptons only. In grand unified theories the masses of the R and L states are linked, and usually the R state is lighter, especially when $\tan\beta$ is large. For $\tilde{\tau}$ sleptons, mixing can be important.

The simplest slepton topology results from $\tilde{\ell} \to \ell\widetilde{\chi}^0_1$, though for some particular parameter choices, branching ratios for decays to $\widetilde{\chi}^0_2$ reach a few percent. Combined mass limits have been obtained by the LEP SUSY working group [7]. For $\tilde{\mu}_R$, the limit is 95 GeV/c^2. The limit for $\tilde{e}_R$ is 4 GeV/c^2 higher due to the higher cross section coming from $\widetilde{\chi}^0$ exchange. Since the selection of τ's is relatively difficult, the limit is expected to be lower, and the actual limit is 86 GeV/c^2. These limits hold provided the slepton is at least 10 GeV/c^2 heavier than the neutralino.

Assuming a common scalar mass term m_0, as in the cMSSM, the masses of the R and L-sleptons can be related as a function of $\tan\beta$, and one finds $m_{\tilde{\ell}_L} > m_{\tilde{\ell}_R}$ by a few GeV/c^2. Consequently, in associated $\tilde{e}_L\tilde{e}_R$ production, the special case of a neutralino close in mass to the right-selectron still results in a viable signature: a single energetic electron. ALEPH and L3 have used this to close the gap $M_{\tilde{e}_R} - M_{\widetilde{\chi}} \to 0$, and place an absolute limit $M_{\widetilde{e}_R} > 73$ GeV/c^2 [15,16].

Squarks: Although the Tevatron experiments had placed general limits on squark masses far beyond the reach of LEP, a light top squark ('stop') could still have been found since the interaction eigenstates can mix to give a large splitting between the mass eigenstates. While theoretically less natural, light sbottoms also have been considered. LEP limits on stop and sbottom masses vary with the mixing angle because the cross section does: for $\theta_{\widetilde{t}} = 56°$ and $\theta_{\widetilde{b}} = 67°$ the contribution from Z exchange is "turned off." In fact the variation in mass limits is only a couple of GeV/c^2 due to the large luminosity used for these searches [7].

The stop decay $\widetilde{t}_1 \to c\widetilde{\chi}^0_1$ proceeds through loops, giving a lifetime long enough to allow the top squark to form supersymmetric hadrons which provide a pair of jets and missing energy. The conservative limit is $M_{\widetilde{t}_1} > 95$ GeV/c^2, valid for $\Delta M > 5$ GeV/c^2. If sneutrinos are light, the decay $\widetilde{t}_1 \to b\ell\widetilde{\nu}$ dominates, giving two leptons in addition to jets, and the limit is 96 GeV/c^2. The same signature obtains when sleptons are light. A somewhat more difficult case comes when $\widetilde{\tau}$'s are light [17,18,16]. Four-fermion final states ($b\,f\,\bar{f}'\,\widetilde{\chi}^0_1$) dominate when charginos are light, a topology covered by ALEPH [18]. Access to very small ΔM is possible due to the visibility of the decay products of the c and b hadrons [19], in which case conservative limit is $M_{\widetilde{t}_1} > 59$ GeV/c^2 is obtained. A comparison to results from the Tevatron is given below.

The electric charge of the sbottoms is smaller than that of stops, so the cross section is considerably lower. The only decay channel considered is $\widetilde{b}_1 \to b\widetilde{\chi}^0_1$. Use of b-jet tagging helps retain sensitivity: the bound is $M_{\widetilde{b}} > 96$ GeV/c^2. It has been pointed out that very light bottoms squarks ($M_{\widetilde{b}} < 5$ GeV/c^2) which are decoupled from the Z are not generally excluded by LEP searches. Ther is, however, a constraint from a CLEO analysis [20] applicable when the sbottoms always decay semileptonically.

The results from the search for acoplanar jets and missing energy has been interpreted as a limit on the production of generic squarks [21,16,7]. A comparison with Tevatron results is given below.

The Lightest Neutralino: In canonical SUSY scenarios the lightest neutralino leaves no signal in the detector. Nonetheless, the tight correspondences among the neutralino and chargino masses allow an indirect limit on $M_{\widetilde{\chi}^0_1}$ to be derived [12,22]. The key assumption is that the gaugino mass parameters M_1 and M_2 unify at the GUT scale, which leads to a definite relation between them at the electroweak scale: $M_1 = \frac{5}{3}\tan^2\theta_W M_2$. Assuming slepton masses to be high, the bound on $M_{\widetilde{\chi}^0_1}$ is derived from the results of chargino and neutralino searches, and the limit is $M_{\widetilde{\chi}^0_1} > 39$ GeV/c^2 [23,11].

When sleptons are lighter than ~ 200 GeV/c^2, all the effects of light sneutrinos on both the production and decay of charginos and heavier neutralinos must be taken into account. Although the bounds from charginos are weakened, useful additional constraints from slepton and higher-mass neutralino searches rule out the possibility of a light neutralino. A combined limit has been obtained in the cMSSM for any $\tan\beta$: $M_{\widetilde{\chi}^0_1} > 37$ GeV/c^2 [23]. The results of Higgs searches can be brought into play on the basis of mSUGRA mass relations, to very good effect. They exclude large regions at low m_0 and $m_{1/2}$ for low $\tan\beta$, and strengthen the neutralino bound to $M_{\widetilde{\chi}^0_1} > 45$ GeV/c^2 [7].

There is a special case for light neutralinos not excluded by collider experiments: when the $\widetilde{\chi}^0_1$ is a pure bino, the constraints from the invisible Z width and from the cross section for γ+invisible are ineffective [24]. If one does not assume any relation between M_1 and M_2 then the constraints from chargino searches can be evaded also. Thus a bino of mass $\mathcal{O}(0.1$ MeV/$c^2)$ is not excluded by collider experiments.

Gauge-Mediated Scenarios: All of the limits above obtain in supergravity models. In models with gauge-mediated supersymmetry breaking (GMSB), however, the phenomenology is rather different, and several interesting new topologies are expected. They can be classified on the basis of the 'next-to-lightest supersymmetric particle' (NLSP) which can be either

the lightest neutralino or charged sleptons, in particular, $\widetilde{\tau}_R$. The gravitino is the LSP, with mass well below a keV.

In the case in which $\widetilde{\chi}_1^0$ is the NLSP, high energy photons are present from the decay $\widetilde{\chi}_1^0 \to \gamma\,\widetilde{g}_{3/2}$. They facilitate the separation of signal and background, so for gauginos and sfermions, the resulting limits are very similar to the canonical case. The pair production of $\widetilde{\chi}_1^0$'s provides an additional search channel consisting of two acollinear photons and missing energy. The mass limit derived is 99 GeV/c^2, from ALEPH, assuming the neutralino lifetime is negligible [25]. A more general limit of 54 GeV/c^2 is set by combining searches for photons which do not point back to the interaction point with indirect limits derived from slepton and chargino searches [26]. Also, single-photon production has been used to constrain the processes $e^+e^- \to \widetilde{g}_{3/2}\widetilde{\chi}_1^0$ and $e^+e^- \to \widetilde{g}_{3/2}\widetilde{g}_{3/2}$.

When sleptons are the NLSP, there are two possibilities: all three flavors enter more or less equally, or, due to significant mixing, the lightest stau dominates. Considering first three flavors of sleptons, the topology depends strongly on the slepton lifetime which is determined by the scale parameter $\sqrt{F}$. For very short lifetimes, the decay $\widetilde{\ell}_R \to \ell\widetilde{g}_{3/2}$ corresponds to the searches described above with a very light neutralino. When the sleptons have some lifetime, the leptons will have impact parameters which help to reject backgrounds. For even longer lifetimes, the apparatus can actually resolve the decay vertex, consisting of an incoming slepton and an outgoing lepton – a track with a 'kink' in the tracking volume. Finally, if the lifetime is long, the experimental signature is a pair of collinear, heavily ionizing tracks. By combining searches for all of these signatures, limits of approximately 82 GeV/c^2 for staus can be placed independent of the slepton lifetime [27,26].

When, due to mixing, the lightest stau is significantly lighter than the other sleptons, special topologies may result. For example, 4τ final states result from neutralino pair production. No evidence for a signal was found [27,28].

R-parity Violation: If R-parity is not conserved, searches based on missing energy are not viable. The three possible RPV interaction terms ($LL\overline{E}$, $LQ\overline{D}$, $\overline{U}\,\overline{D}\,\overline{D}$) violate lepton or baryon number, consequently precisely measured SM processes constrain products of dissimilar terms. Collider searches assume only one of the many possible terms dominates; given this assumption, searches for charginos and neutralinos, sleptons and squarks have been performed. At LEP all sets of generational indices (λ_{ijk}, λ'_{ijk}, λ''_{ijk}) have been considered. Signatures of indirect and also direct RPV have been utilized. Rather exotic topologies can occur, such as six-lepton final states in slepton production with $LL\overline{E}$ dominating, or ten-jet final states in chargino production with $\overline{U}\,\overline{D}\,\overline{D}$ dominating; entirely new search criteria keyed to an excess of leptons and/or jets have been devised [29]. Searches with a wide scope have found no evidence for supersymmetry with R-parity violation, and limits are as constraining as in the canonical scenario. In fact, the direct exclusion of pair-produced $\widetilde{\chi}_1^0$'s rules out some parameter space not accessible in the canonical case.

II.5. Supersymmetry searches at hadron machines: While the LEP experiments can investigate a wide range of scenarios and cover corners of theoretical parameter space, they cannot match the mass reach of the Tevatron experiments (CDF and DØ). Although the full $p\bar{p}$ energy is never available for annihilation, the cross sections for supersymmetric particle production are large due to color factors and strong coupling. Each experiment has analyzed approximately 110 pb^{-1} of data at $\sqrt{s}$ = 1.8 TeV during Run I, which ended in 1996. Now Run IIa is underway, with an expected 2 fb^{-1} to be logged by 2006.

The main source of signals for supersymmetry are squarks and gluinos, in contradistinction to LEP. Pairs of squarks or gluinos are produced in s, t and u-channel processes. These particles decay directly or via cascades to at least two $\widetilde{\chi}_1^0$'s. The number of observed hadronic jets depends on whether the gluino or the squark is heavier, with the latter occurring naturally in mSUGRA models. The possibility of cascade decays through charginos or heavier neutralinos also enriches the possibilities of the search. The u, d, s, c, and (usually) b squarks are assumed to have similar masses; the search results are reported in terms of their average mass $M_{\widetilde{q}}$ and the gluino mass $M_{\widetilde{g}}$.

The spread of partonic energies in hadron machines is very large, so one has to consider the possible presence of several SUSY signals in one data set. A search in a given topology, such as ≥ 3 jets+$\not\!\!E_T$, can capture events from $\widetilde{q}$'s, $\widetilde{g}$'s and even $\widetilde{\chi}^{(\pm,0)}$, with or without cascade decays. Applying experimental bounds on one production mechanism while ignoring the rest would be invalid, so the experimenters must find a relatively simple way of organizing the full phenomenology. Traditionally, they have turned to mSUGRA, in part because the fundamental parameters m_0 and $m_{1/2}$ can be fairly easily related to the squark, gluino and gaugino masses which determine the event kinematics and hence the signal acceptance.

Backgrounds at the Tevatron are relatively much higher than at LEP. There are essentially two types. First, ordinary multijet events can appear to have missing energy due to measurement errors. While large mismeasurements are rare, there are very many di-jet and tri-jet 'QCD' events. This background must be estimated directly from control samples. Second, much rarer processes yield energetic neutrinos which produce a genuine missing energy signature. Examples include the production of W and Z bosons with initial-state jets, of boson pairs, and of the top quark. Estimates for these backgrounds commonly are based on theoretical cross sections, although in some analyses direct measurements are used to reduce uncertainties.

Squarks and Gluinos: The classic searches [30] rely on large missing transverse energy $\not\!\!E_T$ caused by the escaping neutralinos. Jets with high transverse energy are also required as evidence of a hard interaction; care is taken to distinguish

genuine $\not\!\!E_T$ from fluctuations in the jet energy measurement. Backgrounds from W, Z and top production can be reduced by rejecting events with identified leptons. Uncertainties in the rates of these processes can be reduced by normalizing related samples, such as events with two jets and one or more leptons. The tails of more ordinary hard-scattering processes accompanied by multiple gluon emission are estimated directly using simulations normalized using the data.

The bounds traditionally are derived for the $(M_{\tilde{g}}, M_{\tilde{q}})$ plane. The most recent analysis by the CDF Collaboration places significantly stronger bounds that previous analyses [31]. The removal of instrumental backgrounds is keyed more directly to the detector, which, together with specific topological cuts against poorly reconstructed multijet backgrounds, leaves gauge boson and $t\bar{t}$ backgrounds dominant. The estimates for these are tied directly to CDF measurements, which greatly reduces systematic uncertainties. The signal region is loosely specified by demanding high $\not\!\!E_T$ and H_T, the scalar sum of the $\not\!\!E_T$ of the second and third jets, and $\not\!\!E_T$. The number of isolated tracks allows the experimentalist to switch between a background-dominated sample and one which could contain SUSY events. As a measure of analysis rigor, the region expected to be potentially rich in SUSY events is ignored as the event counts in background-dominated samples are examined. No excess is observed, and the cuts on $\not\!\!E_T$ and H_T are tuned to obtain the exclusion shown in Fig. 2.

If squarks are heavier than gluinos, then $M_{\tilde{g}} \gtrsim 195$ GeV/c^2. If they all have the same mass, then that mass is at least 300 GeV/c^2. If the squarks are much lighter than the gluino (in which case they decay via $\tilde{q} \to q\tilde{\chi}_1^0$), the bound on the gluino mass is generally high, much more than 300 GeV/c^2. A small region in which the neutralino-squark mass difference is small, is covered by the LEP experiments (see Fig. 2).

Since these results are expressed in terms of the physical masses relevant to the production process and experimental signature, the excluded region depends primarily on the assumption of nearly equal squark masses with only a small dependence on other parameters such as μ and $\tan\beta$. Direct constraints on the theoretical parameters m_0 and $m_{1/2} \approx 0.34\, M_3$ have been obtained by DØ assuming the mass relations of the mSUGRA model (see the first paper in [30]. These bounds do not carry significantly more information than contained in the region above the diagonal of Fig. 2. It is interesting to note that, if the LEP limits on chargino production are interpreted in this context as an indirect limit on gluinos, then roughly one obtains $M_{\tilde{g}} > 310$ GeV/c^2 [6].

Gauginos: In the context of the mSUGRA model, which fixes $|\mu|$ by the requirement of radiative electroweak symmetry breaking, the lightest chargino and neutralinos are dominantly gaugino. They may be produced directly by annihilation ($q\overline{q} \to \tilde{\chi}_i^{\pm}\tilde{\chi}_j^0$) or in the decays of heavier squarks ($\tilde{q} \to q'\tilde{\chi}_i^{\pm}$, $q\tilde{\chi}_j^0$). They decay to energetic leptons ($\tilde{\chi}^{\pm} \to \ell^{\pm}\nu^{(*)}\tilde{\chi}_1^0$ and $\tilde{\chi}_2^0 \to \ell^+\ell^-\tilde{\chi}_1^0$) and the branching ratio can be high for some parameter

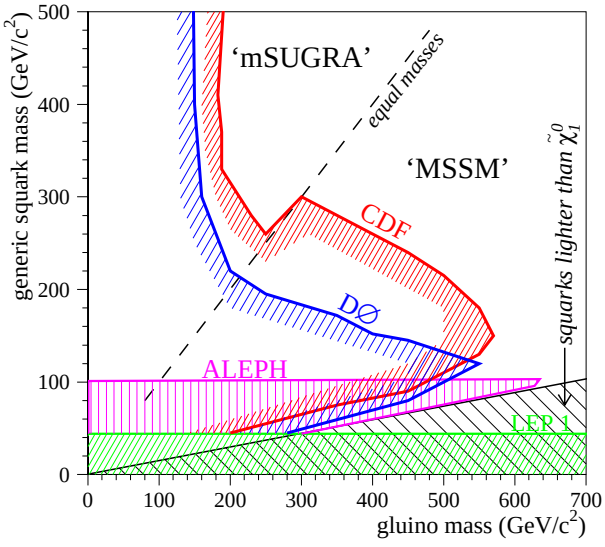

Figure 2: Regions in the $M_{\tilde{g}}$-$M_{\tilde{q}}$ plane excluded by searches for jets and missing energy at CDF, DØ, and LEP. See full-color version on color pages at end of book.

choices. The presence of energetic leptons has been exploited in two ways: the 'trilepton' signature and the 'dilepton' signature.

The search for trileptons is most effective for the associated production of $\tilde{\chi}_1^{\pm}\tilde{\chi}_2^0$ [32]. The requirement of three energetic leptons (e or μ), augmented by simple angular cuts against Drell-Yan production and cosmic rays, isolation requirements against semileptonic decays of heavy mesons, and significant $\not\!\!E_T$ reduce backgrounds to a very small level. The bounds have been derived in the context of mSUGRA models, which generally predict modest leptonic branching ratios for charginos and neutralinos. Consequently, in this framework, the results are not competitive with the LEP bounds. When $\tan\beta$ is large, final states with τ's are enhanced, and existing searches are inefficient. Nonetheless the search is completely independent of the jets+$\not\!\!E_T$ search and could be more effective in particular models with light sleptons, for example.

The dilepton signal is geared more for the production of gauginos in gluino and squark cascades [33]. Jets are required as expected from the rest of the decay chain; the leptons should be well separated from the jets in order to avoid backgrounds from heavy quark decays. Drell-Yan events are rejected with simple cuts on the relative azimuthal angle of the leptons and their transverse momentum and by a cut on $\not\!\!E_T$. The Majorana nature of the gluino can be exploited by requiring two leptons with the same charge, thereby greatly reducing the background. In this scenario limits on squarks and gluinos are comparable to those from the jets+ $\not\!\!E_T$ when couched in an mSUGRA context.

DØ tried to find squarks tagged by $\widetilde{\chi}_2^0 \to \widetilde{\chi}_1^0\gamma$, where the $\widetilde{\chi}_2^0$ appear in cascade decays [34]. The branching ratio can be large for a selected set of model parameters leading to a Higgsino-like $\widetilde{\chi}_1^0$ and a gaugino-like $\widetilde{\chi}_2^0$. DØ assumed a branching ratio of 100% to place the limits $M_{\widetilde{g}} > 240$ GeV/c^2 for heavy squarks, and $M_{\widetilde{g}} > 310$ GeV/c^2 for squarks of the same mass as the gluino.

Stops and Sbottoms: The top squark is unique among the squarks because its SM partner is so massive: large off-diagonal terms in the squared-mass matrix lead to large mixing effects and a mass eigenstate possibly much lighter than all the others. This can also happen for bottom squarks for rather special parameter choices. Hence, special analyses have been developed for $\widetilde{t}_1$'s and $\widetilde{b}_1$'s among all the squarks.

Top squarks are pair-produced with no dependence on the mixing angle, in contrast to LEP. The searches are based on two final states: $c\not{E}_T$ and $b\ell\not{E}_T$, and it is assumed that one or the other dominates. Theoretical calculations show that if chargino and slepton masses are well above $M_{\widetilde{t}_1}$, then the loop-induced FCNC decay $\widetilde{t}_1 \to c\widetilde{\chi}^0$ dominates. If $M_{\widetilde{\chi}^\pm} < M_{\widetilde{t}_1}$, then $\widetilde{t}_1 \to b\widetilde{\chi}^\pm$ is the main decay mode, and the experimenters assume $BR(\widetilde{\chi}^\pm \to \ell\nu\widetilde{\chi}^0) = BR(W \to \ell\nu)$. When charginos are heavy but $M_{\widetilde{\nu}} < M_{\widetilde{t}_1}$, leptonic final states again are favored via $\widetilde{t}_1 \to b\ell\widetilde{\nu}$. In this case the branching ratio is assumed to be 1/3 for each lepton flavor. In fact, all these channels compete, and the assumption of a 100% branching ratio is not general. Furthermore, four-body decays to $b\ell\nu\widetilde{\chi}$ should not be neglected, for which limits would be reported in the $(M_{\widetilde{t}}, M_{\widetilde{\chi}})$ plane [36].

CDF have obtained a result for the $c\not{E}_T$ final state [37]. They employed their vertex detector to select charm jets. After a lepton veto and $\not{E}_T$ requirement, this result surpasses the prior result from DØ [38]. The vertex detector was also used to tag b-quark jets for the final state $b\ell\not{E}_T$. In this case, CDF went beyond simple event counting and applied a likelihood test to the shapes of kinematic distributions. Like the first DØ result, however, this search did not exclude any signal in the channel $\widetilde{t}_1 \to b\widetilde{\chi}^\pm$, and covered a small region for $\widetilde{t}_1 \to b\ell\widetilde{\nu}$. A new result from DØ is much more performant [39] and significantly extends the parameter space excluded by LEP searches. Finally, CDF considered the possibility $t \to \widetilde{t}_1\widetilde{\chi}$ followed by $\widetilde{t}_1 \to b\widetilde{\chi}^+$ [40]. Such events would remain in the top event sample and can be discriminated using a multivariate technique. No events were found compatible with the kinematics of SUSY decays, and limits on $BR(t \to \widetilde{t}_1\widetilde{\chi})$ were derived in a fairly limited range of stop and chargino masses.

The search for light $\widetilde{b}_1 \to b\widetilde{\chi}$ follows the $\widetilde{t}_1$ search in the charm channel [37]. The CDF search tightens the requirements for a jet with heavy flavor to good effect. An earlier DØ result tagged b-jets through semileptonic decays to muons [41].

A summary of the searches for stops is shown in Fig. 3. Given the modest luminosity and small detection efficiencies, the mass reach of the Tevatron searches is impressive. New data would likely extend this reach (as would the combination of results from the two experiments). Unfortunately, the region with $M_{\widetilde{\chi}^0} > M_{\widetilde{t}_1} + 20$ GeV/c^2 will remain inaccessible in Run 2, due to the necessity of requiring a minimum missing energy in the experimental trigger.

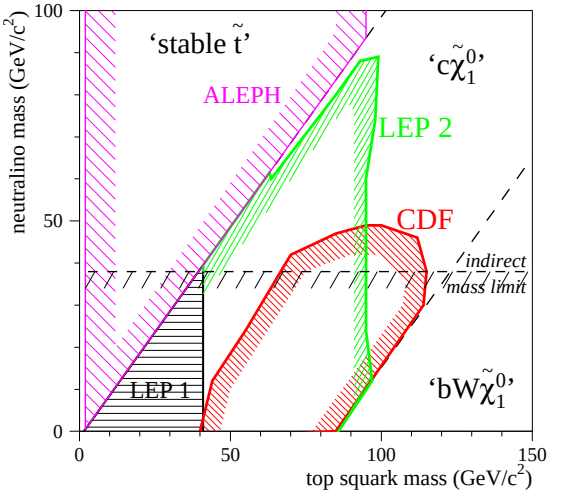

Figure 3: Regions excluded in the $(M_{\widetilde{t}_1}, M_{\widetilde{\chi}})$ plane. The results for the $c\widetilde{\chi}_1^0$ decay mode are displayed from LEP and CDF. A DELPHI result for stable stops is indicated for $M_{\widetilde{t}_1} < M_{\widetilde{\chi}}$. Finally, the indirect limit on $M_{\widetilde{\chi}}$ is also shown. There is effectively no exclusion in the region where $\widetilde{t}_1 \to bW\widetilde{\chi}_1^0$. See full-color version on color pages at end of book.

R-Parity Violation: The CDF and DØ collaborations have searched for supersymmetry in certain RPV scenarios [42] in which the lightest neutralino decays to a lepton and two quarks. DØ considered all possible production processes as a function of mSUGRA parameters. Their trilepton search amounts to strong bounds on these parameters, stronger than the limits from their search for two electrons and jets. CDF used their same-sign dielectron and jets topology to look for gluino and squark (including stop) production and obtained some specific upper limits on cross sections corresponding to $M_{\widetilde{q}} > 200$ GeV/c^2 and $M_{\widetilde{t}_1} > 120$ GeV/c^2. They also completed a search for R-parity violating stop decays, $\widetilde{t}_1 \to b\tau$ in which one tau decays leptonically and the other hadronically, giving the limit $M_{\widetilde{t}_1} > 122$ GeV/c^2 [43].

Gauge-Mediated Models: Interest in GMSB models was spurred by an anomalous '$ee\gamma\gamma\not{E}_T$' event found by the CDF Collaboration [44]. Some of these models predict large inclusive signals for $p\overline{p} \to \gamma\gamma + X$ given kinematic constraints derived from the properties of the CDF event. The photons arise from

the decay $\widetilde{\chi}_1^0 \to \gamma\widetilde{g}_{3/2}$ and the 'superlight' gravitino has a mass much smaller than the charged fermions. DØ examined their sample of $\gamma\gamma\not{E}_T$ events and reported limits on neutralino and chargino production corresponding to $M_{\widetilde{\chi}_1^0} > 75$ GeV/c^2 [45]. CDF experimenters carried out a systematic survey of events with photons and SM particles (leptons, jets, missing energy) and found no signal confirming the interpretation of the original anomalous event [44,46]. They also looked for evidence of light gravitino pairs without additional SUSY particles. The invisible gravitinos are tagged by a high-E_T jet from the initial state; this is the so-called 'monojet' signature [47]. The limit $\sqrt{F} > 215$ GeV/c^2 is placed on the fundamental parameter of this model.

DØ also reported limits on $\widetilde{q}$ and $\widetilde{g}$ production in this same scenario [35]. If $\widetilde{q}$ and $\widetilde{g}$ have similar masses, then that mass is great than 310 GeV/c^2.

In GMSB models, a heavy 'sGoldstino' is possible, which may have sizable branching ratios to photon pairs. CDF looked for narrow diphoton resonances and placed a limit $\sqrt{F} > 1$ TeV/c^2, depending on assumed mass of the sGoldstino [48].

The Search for $B_s \to \mu^+\mu^-$: Indirect evidence for SUSY could come from measurements of rare processes, especially those which are highly suppressed in the Standard Model. For example, the branching fraction for the flavor-changing neutral decay $B_s \to \mu^+\mu^-$ is only 3×10^{-9} [49]. In the MSSM, however, it can be greatly enhanced due to Higgsino and possibly gluino contributions, and in fact, $\mathcal{B}(B_s \to \mu^+\mu^-) \propto \tan^6\beta$ [50]. The exact value for the branching fraction is highly model dependent, but in mSUGRA values as high as 0.5×10^{-7} can be obtained for $\tan\beta = 55$.

CDF found no evidence for $B_s \to \mu^+\mu^-$ in their Run I data, and placed the upper limit $\mathcal{B}(B_s \to \mu^+\mu^-) < 20 \times 10^{-7}$ at 90% C.L. [51]. The sensitivity will be substantially improved for Run II due to a much higher trigger acceptance and better vertex reconstruction. Recent preliminary results from Run II have strengthened the bound to 9.5×10^{-7} (CDF, 113 pb^{-1}) and 16×10^{-7} (DØ, $\sim$ 100 pb^{-1}), both at 90% C.L. [52]. The sensitivity for an integrated luminosity of 4 fb^{-1} could reach, optimistically, 0.5×10^{-7} [53].

Table 1: Lower limits on supersymmetric particle masses. 'GMSB' refers to models with gauge-mediated supersymmetry breaking, and 'RPV' refers to models allowing R-parity violation.

particle		Condition	Lower limit (GeV/c^2)	Source
$\widetilde{\chi}_1^\pm$	gaugino	$M_{\widetilde{\nu}} > 200$ GeV/c^2	103	LEP 2
		$M_{\widetilde{\nu}} > M_{\widetilde{\chi}^\pm}$	85	LEP 2
		any $M_{\widetilde{\nu}}$	45	Z width
	Higgsino	$M_2 < 1$ TeV/c^2	99	LEP 2
	GMSB		150	DØ isolated photons
	RPV	$LL\overline{E}$ worst case	87	LEP 2
		$LQ\overline{D}$ $m_0 > 500$ GeV/c^2	88	LEP 2
$\widetilde{\chi}_1^0$	indirect	any $\tan\beta$, $M_{\widetilde{\nu}} > 500$ GeV/c^2	39	LEP 2
		any $\tan\beta$, any m_0	36	LEP 2
		any $\tan\beta$, any m_0, SUGRA Higgs	59	LEP 2 combined
	GMSB		93	LEP 2 combined
	RPV	$LL\overline{E}$ worst case	23	LEP 2
$\widetilde{e}_R$	$e\widetilde{\chi}_1^0$	$\Delta M > 10$ GeV/c^2	99	LEP 2 combined
$\widetilde{\mu}_R$	$\mu\widetilde{\chi}_1^0$	$\Delta M > 10$ GeV/c^2	95	LEP 2 combined
$\widetilde{\tau}_R$	$\tau\widetilde{\chi}_1^0$	$M_{\widetilde{\chi}_1^0} < 20$ GeV/c^2	80	LEP 2 combined
$\widetilde{\nu}$			43	Z width
$\widetilde{\mu}_R$, $\widetilde{\tau}_R$		stable	86	LEP 2 combined
$\widetilde{t}_1$	$c\widetilde{\chi}_1^0$	any $\theta_{\rm mix}$, $\Delta M > 10$ GeV/c^2	95	LEP 2 combined
		any $\theta_{\rm mix}$, $M_{\widetilde{\chi}_1^0} \sim \frac{1}{2}M_{\widetilde{t}}$	115	CDF
		any $\theta_{\rm mix}$ and any ΔM	59	ALEPH
	$b\ell\widetilde{\nu}$	any $\theta_{\rm mix}$, $\Delta M > 7$ GeV/c^2	96	LEP 2 combined
$\widetilde{g}$	any $M_{\widetilde{q}}$		195	CDF jets+$\not{E}_T$
$\widetilde{q}$	$M_{\widetilde{q}} = M_{\widetilde{g}}$		300	CDF jets+$\not{E}_T$

If the decay $B_s \to \mu^+\mu^-$ is observed, then a general lower bound on $\tan\beta$ can be derived [54]. It is also worth noting that, if a signal is observed at the Tevatron, then models based on anomaly-mediated or gauge-mediated supersymmetry breaking would not be favored [50,54].

II.7. Searches at HERA: The initial state for collisions at HERA includes an electron (or positron) and a proton, which provides a special opportunity to probe RPV scenarios with a dominant λ'_{1jk} coupling [55]. The H1 and ZEUS experiments have searched for the resonant production of squarks. The most up-to-date results include the search by H1 based on 37 pb^{-1} of e^+p data [56]. Both R_p-violating and conserving decays of the squark were covered by a combination of seven different topologies. Bounds are placed on the R_p-violating coupling as a function of the squark mass. Completely general limits on the squark mass are impossible. However, in the constrained MSSM, and assuming $M_{\widetilde{\chi}^0_1} > 30$ GeV/c^2, the limit $M_{\tilde{u}_L} > 160$ GeV/c^2 can be placed (235 GeV/c^2 for the third generation). See Ref. [56] for more details, and the Particle Listings for a list of previous results from both H1 and ZEUS.

II.8. Conclusions: A huge variety of searches for supersymmetry have been carried out at LEP, the Tevatron, and in fixed-target experiments. Despite all the effort, no inarguable signal has been found, forcing the experimenters to derive limits. We have tried to summarize the interesting cases in Table 1. At the present time there is little room for SUSY particles lighter than M_Z. The LEP collaborations have analyzed all their data, so prospects for the immediate future pass to the Tevatron collaborations. If still no sign of supersymmetry is found, definitive tests will be made at the LHC.

References

1. H.E. Haber and G. Kane, Phys. Reports **117**, 75 (1985);
H.P. Nilles, Phys. Reports **110**, 1 (1984);
M. Chen, C. Dionisi, M. Martinez, and X. Tata, Phys. Reports **159**, 201 (1988).
2. H.E. Haber, Nucl. Phys. (Proc. Supp.) **B62**, 469 (1998);
S. Dawson, *SUSY and Such*, hep-ph/9612229.
3. H. Dreiner, *An Introduction to Explicit R-parity Violation*, in **Perspectives on Supersymmetry**, ed. by G.L. Kane, World Scientific, 1997, p.462;
G. Bhattacharyya, Nucl. Phys. Proc. Suppl. **A52**, 83 (1997);
V. Barger, G.F. Giudice, and T. Han, Phys. Rev. **D40**, 1987 (1989);
S. Dawson, Nucl. Phys. **B261**, 297 (1985).
4. M. Dine, Nucl. Phys. Proc. Suppl. **52A**, 201(1997);
K.S. Babu, C. Kolda, and F. Wilczek, Phys. Rev. Lett. **77**, 3070 (1996);
S. Dimopoulos *et al.*, Phys. Rev. Lett. **76**, 3494 (1996);
S. Dimopoulos, S. Thomas, J.D. Wells, Phys. Rev. **D54**, 3283 (1996), and Nucl. Phys. **B488**, 39 (1997);
D.R. Stump, M. Wiest, C.P. Yuan, Phys. Rev. **D54**, 1936 (1996);
M. Dine, A. Nelson, and Y. Shirman Phys. Rev. **D51**, 1362 (1995);
D.A. Dicus, S. Nandi, and J. Woodside, Phys. Rev. **D41**, 2347 (1990) and Phys. Rev. **D43**, 2951 (1990);
P. Fayet, Phys. Lett. **B175**, 471 (1986);
J. Ellis, K. Enqvist, and D.V. Nanopoulos, Phys. Lett. **B151**, 357 (1985), and Phys. Lett. **B147**, 99 (1984);
P. Fayet, Phys. Lett. **B69**, 489 (1977) and Phys. Lett. **B70**, 461 (1977).
5. F. Gianotti, New Jour. Phys. **4**,63(2002).
6. A. Lipniacka, hep-ph/0112280.
7. **LEPSUSYWG, ALEPH, DELPHI, L3** and **OPAL** Collab., Preliminary results from the combination of LEP data, prepared by the LEP SUSY Working Group. LEPSUSYWG/02-01.1, 02-02.1, 02-04.1, 02-05.1, 02-06.2, 02-07.1, 02-08.1, 02-09.2, 02-10.1, 01-03.1, 01-07.1 See also http://www.cern.ch/lepsusy/.
8. J.-F. Grivaz, *Supersymmetric Particle Searches at LEP*, in **Perspectives on Supersymmetry**, *ibid.*, p.179;
M. Drees and X. Tata, Phys. Rev. **D43**, 2971 (1991).
9. J. L. Feng and T. Moroi, Phys. Rev. **D61**, 095004 (2000);
L. Randall and R. Sundrum, Nucl. Phys. **B557**, 79 (1999).
10. **DELPHI**: Eur. Phys. J. **C11**, 1 (1999).
11. **ALEPH**: Phys. Lett. **B533**, 223 (2002);
OPAL: hep-ex/0210043;
L3: Phys. Lett. **B482**, 31 (2000).
12. **ALEPH**: Z. Phys. **C72**, 549 (1996) and Eur. Phys. J. **C11**, 193 (1999).
13. **ALEPH**: Eur. Phys. J. **C2**, 417 (1998).
14. **ALEPH**: Phys. Lett. **B526**, 206 (2002);
OPAL: hep-ex/0309014;
DELPHI: Eur. Phys. J. **C19**, 29 (2001);
L3: Phys. Lett. **B471**, 280 (1999).
15. **ALEPH**: Phys. Lett. **B544**, 73 (2002).
16. **L3**: hep-ex/0310007.
17. **OPAL**: Phys. Lett. **B545**, 272 (2002) Err. *ibid.* **B548**,258(2002).
18. **ALEPH**: Phys. Lett. **B537**, 5 (2002).
19. **ALEPH**: Phys. Lett. **B488**, 234 (2000).
20. **CLEO**: Phys. Rev. **D63**, 051101 (2001).
21. **ALEPH**: Phys. Lett. **B469**, 303 (1999).
22. **OPAL**: Eur. Phys. J. **C8**, 255 (1999);
L3: Eur. Phys. J. **C4**, 207 (1998).
23. **ALEPH**: Phys. Lett. **B499**, 67 (2001).
24. H. K. Dreiner *et al.*, hep-ph/0304289;
D. Choudhury, *et al.*, Phys. Rev. **D61**, 095009 (2000).
25. **ALEPH**: Eur. Phys. J. **C28**, 1 (2003).
26. **ALEPH**: Eur. Phys. J. **C25**, 339 (2002).
27. **DELPHI**: Eur. Phys. J. **C27**, 153 (2003);
DELPHI: Phys. Lett. **B503**, 34 (2001);
ALEPH: Eur. Phys. J. **C16**, 71 (1999).
28. **DELPHI**: Eur. Phys. J. **C7**, 595 (1999).
29. **ALEPH**: Eur. Phys. J. **C19**, 415 (2001) and Eur. Phys. J. **C13**, 29 (2000);
OPAL: Eur. Phys. J. **C12**, 1 (2000) and Eur. Phys. J. **C11**, 619 (1999);
DELPHI: Phys. Lett. **B502**, 24 (2001);
L3: Eur. Phys. J. **C19**, 397 (2001) and Phys. Lett. **B524**, 65 (2002).
30. **DØ**: Phys. Rev. Lett. **83**, 4937 (1999) and Phys. Rev. Lett. **75**, 618 (1995);
CDF: Phys. Rev. **D56**, 1357 (1997) and Phys. Rev. Lett. **76**, 2006 (1996).

31. **CDF**: Phys. Rev. Lett. **88**, 041801 (2002).
32. **DØ**: Phys. Rev. Lett. **80**, 1591 (1998);
CDF: Phys. Rev. Lett. **80**, 5275 (1998).
33. **DØ**: Phys. Rev. **D63**, 091102 (2001);
CDF: Phys. Rev. Lett. **76**, 2006 (1996) and Phys. Rev. Lett. **87**, 251803 (2001).
34. **DØ**: Phys. Rev. Lett. **82**, 29 (1999).
35. **DØ**: Phys. Rev. Lett. **78**, 2070 (1997).
36. A. Djouadi *et al.*, Phys. Rev. **D71**, 095006 (2000) and Phys. Rev. **D63**, 115005 (2001).
37. **CDF**: Phys. Rev. Lett. **84**, 5704 (2000).
38. **DØ**: Phys. Rev. Lett. **76**, 2222 (1996).
39. **DØ**: Phys. Rev. Lett. **88**, 171802 (2002).
40. **CDF**: Phys. Rev. **D63**, 091101 (2001).
41. **DØ**: Phys. Rev. **D60**, 031101 (1999).
42. **CDF**: Phys. Rev. Lett. **83**, 2133 (1999) and Phys. Rev. Lett. **87**, 251803 (2001);
DØ: Phys. Rev. **D62**, 071701 (2000) and Phys. Rev. Lett. **83**, 4476 (1999).
43. **CDF**: hep-ex/0305010.
44. **CDF**: Phys. Rev. **D59**, 092002 (1999).
45. **DØ**: Phys. Rev. Lett. **78**, 2070 (1997).
46. **CDF**: Phys. Rev. Lett. **81**, 1791 (1998).
47. **CDF**: Phys. Rev. Lett. **85**, 1378 (2000).
48. **CDF**: Phys. Rev. Lett. **81**, 1791 (1998).
49. Andrzej J. Buras, hep-ph/9806471 and references therein.
50. A. Dedes, H.K. Dreiner, U. Nierste and P. Richardson, hep-ph/0207026.
51. **CDF**: Phys. Rev. Lett. **57**, 3811 (1998).
52. Prelim. results from **CDF** and **DØ** were reported by M.Schmitt at Lepton-Photon, 2003, at FNAL.
53. R. Arnowitt, B.Dutta, T.Kamon and M.Tanaka, Phys. Lett. **B538**, 121 (2002).
54. G.L.Kane, C.Kolda and J.E.Lennon, hep-ph/0310042.
55. M. Kuze and Y. Sirois, Prog. in Part. Nucl. Phys. **50**, 1 (2003).
56. **H1**: Eur. Phys. J. **C20**, 639 (2001);
H1: Phys. Lett. **B568**, 35 (2003).

SUPERSYMMETRIC MODEL ASSUMPTIONS

The exclusion of particle masses within a mass range (m_1, m_2) will be denoted with the notation "none m_1–m_2" in the VALUE column of the following Listings.

Most of the results shown below, unless stated otherwise, are based on the Minimal Supersymmetric Standard Model (MSSM), as described in the Note on Supersymmetry. Unless otherwise indicated, this includes the assumption of common gaugino and scalar masses at the scale of Grand Unification (GUT), and use of the resulting relations in the spectrum and decay branching ratios. It is also assumed that R-parity (R) is conserved. Unless otherwise indicated, the results also assume that:

1) The $\widetilde{\chi}_1^0$ is the lighest supersymmetric particle (LSP)
2) $m_{\widetilde{f}_L} = m_{\widetilde{f}_R}$, where $\widetilde{f}_{L,R}$ refer to the scalar partners of left- and right-handed fermions.

Limits involving different assumptions are identified in the Comments or in the Footnotes. We summarize here the notations used in this Chapter to characterize some of the most common deviations from the MSSM (for further details, see the Note on Supersymmetry).

Theories with R-parity violation ($\not{R}$) are characterised by a superpotential of the form: $\lambda_{ijk} L_i L_j e^c_k + \lambda'_{ijk} L_i Q_j d^c_k + \lambda''_{ijk} u^c_i d^c_j d^c_k$, where i, j, k are generation indices. The presence of any of these couplings is often identified in the following by the symbols $LL\overline{E}$, $LQ\overline{D}$, and $\overline{UDD}$. Mass limits in the presence of $\not{R}$ will often refer to "direct" and "indirect" decays. Direct refers to $\not{R}$ decays of the particle in consideration. Indirect refers to cases where $\not{R}$ appears in the decays of the LSP.

In several models, most notably in theories with so-called Gauge Mediated Supersymmetry Breaking (GMSB), the gravitino ($\widetilde{G}$) is the LSP. It is usually much lighter than any other massive particle in the spectrum, and $m_{\widetilde{G}}$ is then neglected in all decay processes involving gravitinos. In these scenarios, particles other than the neutralino are sometimes considered as the next-to-lighest supersymmetric particle (NLSP), and are assumed to decay to their even-R partner plus $\widetilde{G}$. If the lifetime is short enough for the decay to take place within the detector, $\widetilde{G}$ is assumed to be undetected and to give rise to missing energy ($\not{E}$) or missing transverse energy ($\not{E}_T$) signatures.

When needed, specific assumptions on the eigenstate content of $\widetilde{\chi}^0$ and $\widetilde{\chi}^\pm$ states are indicated, using the notation $\widetilde{\gamma}$ (photino), $\widetilde{H}$ (higgsino), $\widetilde{W}$ (wino), and $\widetilde{Z}$ (zino) to signal that the limit of pure states was used. The terms gaugino is also used, to generically indicate wino-like charginos and zino-like neutralinos.

$\widetilde{\chi}_1^0$ (Lightest Neutralino) MASS LIMIT

$\widetilde{\chi}_1^0$ is often assumed to be the lightest supersymmetric particle (LSP). See also the $\widetilde{\chi}_2^0$, $\widetilde{\chi}_3^0$, $\widetilde{\chi}_4^0$ section below.

We have divided the $\widetilde{\chi}_1^0$ listings below into five sections:

1) Accelerator limits for stable $\widetilde{\chi}_1^0$,
2) Bounds on $\widetilde{\chi}_1^0$ from dark matter searches,
3) Bounds on $\widetilde{\chi}_1^0$ elastic cross sections from dark matter searches,
4) Other bounds on $\widetilde{\chi}_1^0$ from astrophysics and cosmology, and
5) Bounds on unstable $\widetilde{\chi}_1^0$.

Accelerator limits for stable $\widetilde{\chi}_1^0$

Unless otherwise stated, results in this section assume spectra, production rates, decay modes, and branching ratios as evaluated in the MSSM, with gaugino and sfermion mass unification at the GUT scale. These papers generally study production of $\widetilde{\chi}_i^0 \widetilde{\chi}_j^0$ ($i \geq 1$, $j \geq 2$), $\widetilde{\chi}_1^+ \widetilde{\chi}_1^-$, and (in the case of hadronic collisions) $\widetilde{\chi}_1^+ \widetilde{\chi}_2^0$ pairs. The mass limits on $\widetilde{\chi}_1^0$ are either direct, or follow indirectly from the constraints set by the non-observation of $\widetilde{\chi}_1^\pm$ and $\widetilde{\chi}_2^0$ states on the gaugino and higgsino MSSM parameters M_2 and μ. In some cases, information is used from the nonobservation of slepton decays.

Obsolete limits obtained from e^+e^- collisions up to $\sqrt{s}$=184 GeV have been removed from this compilation and can be found in the 2000 Edition (The European Physical Journal **C15** 1 (2000)) of this Review. $\Delta m_0 = m_{\widetilde{\chi}_2^0} - m_{\widetilde{\chi}_1^0}$.

VALUE (GeV)	CL%	DOCUMENT ID		TECN	COMMENT
>39.2	95	[1] ABDALLAH	03M	DLPH	all tanβ, $m_{\tilde{\nu}}$ >500 GeV
>46	95	[2] ABDALLAH	03M	DLPH	all tanβ, all Δm_0, all m_0
>37	95	[3] BARATE	01	ALEP	all tanβ, all m_0
>31.6	95	[4] ABBIENDI	00H	OPAL	all tanβ, all Δm_0 >5 GeV, all m_0
>32.5	95	[5] ACCIARRI	00D	L3	tanβ > 0.7, Δm_0 > 3 GeV, all m_0
• • • We do not use the following data for averages, fits, limits, etc. • • •					
		[6] ABBOTT	98C	D0	$p\overline{p} \rightarrow \tilde{\chi}_1^{\pm}\tilde{\chi}_2^0$
>41	95	[7] ABE	98J	CDF	$p\overline{p} \rightarrow \tilde{\chi}_1^{\pm}\tilde{\chi}_2^0$

[1] ABDALLAH 03M uses data from $\sqrt{s}$ = 192–208 GeV. A limit on the mass of $\tilde{\chi}_1^0$ is derived from direct searches for neutralinos combined with the chargino search. Neutralinos are searched in the production of $\tilde{\chi}_1^0\tilde{\chi}_2^0$, $\tilde{\chi}_1^0\tilde{\chi}_3^0$, as well as $\tilde{\chi}_2^0\tilde{\chi}_3^0$ and $\tilde{\chi}_2^0\tilde{\chi}_4^0$ giving rise to cascade decays, and $\tilde{\chi}_1^0\tilde{\chi}_2^0$ and $\tilde{\chi}_1^0\tilde{\chi}_2^0$, followed by the decay $\tilde{\chi}_2^0 \rightarrow \tilde{\tau}\tau$. The results hold for the parameter space defined by values of $M_2 < 1$ TeV, $|\mu| \leq 2$ TeV with the $\tilde{\chi}_1^0$ as LSP. The limit is obtained for tanβ = 1 and large m_0, where $\tilde{\chi}_2^0\tilde{\chi}_4^0$ and chargino pair production are important. If the constraint from Higgs searches is also imposed, the limit improves to 49.0 GeV in the M_h^{max} scenario with m_t=174.3 GeV. These limits update the results of ABREU 00J.

[2] ABDALLAH 03M uses data from $\sqrt{s}$ = 192–208 GeV. An indirect limit on the mass of $\tilde{\chi}_1^0$ is derived by constraining the MSSM parameter space by the results from direct searches for neutralinos (including cascade decays and $\tilde{\tau}\tau$ final states), for charginos (for all $\Delta m_{\pm}$) and for sleptons, stop and sbottom. The results hold for the full parameter space defined by values of $M_2 < 1$ TeV, $|\mu| \leq 2$ TeV with the $\tilde{\chi}_1^0$ as LSP. Constraints from the Higgs search in the M_h^{max} scenario assuming m_t=174.3 GeV are included. The limit is obtained for tanβ ≥5 when stau mixing leads to mass degeneracy between $\tilde{\tau}_1$ and $\tilde{\chi}_1^0$ and the limit is based on $\tilde{\chi}_2^0$ production followed by its decay to $\tilde{\tau}_1\tau$. In the pathological scenario where m_0 and $|\mu|$ are large, so that the $\tilde{\chi}_2^0$ production cross section is negligible, and where there is mixing in the stau sector but not in stop nor sbottom, the limit is based on charginos with soft decay products and an ISR photon. The limit then degrades to 39 GeV. See Figs 40–42 for the dependence of the limit on tanβ and $m_{\tilde{\nu}}$. These limits update the results of ABREU 00W.

[3] BARATE 01 data collected at 189 to 202 GeV. Updates earlier analyses of sleptons and squarks from BARATE 99Q, and of charginos and neutralinos from BARATE 98X and BARATE 99P. The limit is based on the direct search for charginos and neutralinos and the constraints from the slepton search and Z^0 width measurements, as discussed in BARATE 99P, assuming a negligible mixing in the stau sector. The limit improves to 48 GeV under the assumption of MSUGRA with unification of the Higgs and sfermion masses, when direct constraints on the Higgs mass from BARATE 01C are used and $m_{\tilde{\tau}} - m_{\tilde{\chi}_1^0} > 5$ GeV to avoid degeneracy at large tanβ. These limits include and update the results of BARATE 99P.

[4] ABBIENDI 00H data collected at $\sqrt{s}$=189 GeV. The results hold over the full parameter space defined by $0 \leq M_2 \leq 2$ TeV, $|\mu| \leq 500$ GeV, $m_0 \leq 500$ GeV, $A = \pm M_2, \pm m_0$, and 0. The minimum mass limit is reached for tanβ=1. The results of ABBIENDI 99F are used to constrain regions of parameter space dominated by radiative $\tilde{\chi}_2^0 \rightarrow \tilde{\chi}_1^0\gamma$ decays. The limit improves to 48.5 GeV for m_0=500 GeV and tanβ=35. See their Table and Figs 4–5 for the tanβ and m_0 dependence of the limits. Updates ABBIENDI 99G.

[5] ACCIARRI 00D data collected at $\sqrt{s}$=189 GeV. The results hold over the full parameter space defined by $0.7 \leq \tan\beta \leq 60$, $0 \leq M_2 \leq 2$ TeV, $m_0 \leq 500$ GeV, $|\mu| \leq 2$ TeV The minimum mass limit is reached for tanβ=1 and large m_0. The results of slepton searches from ACCIARRI 99W are used to help set constraints in the region of small m_0. The limit improves to 48 GeV for $m_0 \gtrsim 200$ GeV and tanβ $\gtrsim$ 10. See their Figs. 6–8 for the tanβ and m_0 dependence of the limits. Updates ACCIARRI 98F.

[6] ABBOTT 98C searches for trilepton final states (ℓ=e,μ). See footnote to ABBOTT 98C in the Chargino Section for details on the assumptions. Assuming a negligible decay rate of $\tilde{\chi}_1^{\pm}$ and $\tilde{\chi}_2^0$ to quarks, they obtain $m_{\tilde{\chi}_2^0} \gtrsim 51$ GeV.

[7] ABE 98J searches for trilepton final states (ℓ=e,μ). See footnote to ABE 98J in the Chargino Section for details on the assumptions. The quoted result corresponds to the best limit within the selected range of parameters, obtained for $m_{\tilde{q}} > m_{\tilde{g}}$, tanβ=2, and μ=− 600 GeV.

Bounds on $\tilde{\chi}_1^0$ from dark matter searches

These papers generally exclude regions in the $M_2-\mu$ parameter plane assuming that $\tilde{\chi}_1^0$ is the dominant form of dark matter in the galactic halo. These limits are based on the lack of detection in laboratory experiments or by the absence of a signal in underground neutrino detectors. The latter signal is expected if $\tilde{\chi}_1^0$ accumulates in the Sun or the Earth and annihilates into high-energy ν's.

VALUE	DOCUMENT ID		TECN
• • • We do not use the following data for averages, fits, limits, etc. • • •			
	[8] AMBROSIO	99	MCRO
	[9] LOSECCO	95	RVUE
	[10] MORI	93	KAMI
	[11] BOTTINO	92	COSM
	[12] BOTTINO	91	RVUE
	[13] GELMINI	91	COSM
	[14] KAMIONKOW..	91	RVUE
	[15] MORI	91B	KAMI
none 4–15 GeV	[16] OLIVE	88	COSM

[8] AMBROSIO 99 set new neutrino flux limits which can be used to limit the parameter space in supersymmetric models based on neutralino annihilation in the Sun and the Earth.

[9] LOSECCO 95 reanalyzed the IMB data and places lower limit on $m_{\tilde{\chi}_1^0}$ of 18 GeV if the LSP is a photino and 10 GeV if the LSP is a higgsino based on LSP annihilation in the sun producing high-energy neutrinos and the limits on neutrino fluxes from the IMB detector.

[10] MORI 93 excludes some region in $M_2-\mu$ parameter space depending on tanβ and lightest scalar Higgs mass for neutralino dark matter $m_{\tilde{\chi}^0} > m_{W^{\pm}}$, using limits on upgoing muons produced by energetic neutrinos from neutralino annihilation in the Sun and the Earth.

[11] BOTTINO 92 excludes some region $M_2-\mu$ parameter space assuming that the lightest neutralino is the dark matter, using upgoing muons at Kamiokande, direct searches by Ge detectors, and by LEP experiments. The analysis includes top radiative corrections on Higgs parameters and employs two different hypotheses for nucleon-Higgs coupling. Effects of rescaling in the local neutralino density according to the neutralino relic abundance are taken into account.

[12] BOTTINO 91 excluded a region in $M_2-\mu$ plane using upgoing muon data from Kamioka experiment, assuming that the dark matter surrounding us is composed of neutralinos and that the Higgs boson is not too heavy.

[13] GELMINI 91 exclude a region in $M_2-\mu$ plane using dark matter searches.

[14] KAMIONKOWSKI 91 excludes a region in the $M_2-\mu$ plane using IMB limit on upgoing muons originated by energetic neutrinos from neutralino annihilation in the sun, assuming that the dark matter is composed of neutralinos and that $m_{H_1^0} \lesssim 50$ GeV. See Fig. 8 in the paper.

[15] MORI 91B exclude a part of the region in the $M_2-\mu$ plane with $m_{\tilde{\chi}_1^0} \lesssim 80$ GeV using a limit on upgoing muons originated by energetic neutrinos from neutralino annihilation in the earth, assuming that the dark matter surrounding us is composed of neutralinos and that $m_{H_1^0} \lesssim 80$ GeV.

[16] OLIVE 88 result assumes that photinos make up the dark matter in the galactic halo. Limit is based on annihilations in the sun and is due to an absence of high energy neutrinos detected in underground experiments. The limit is model dependent.

$\tilde{\chi}_1^0$-p elastic cross section

Experimental results on the $\tilde{\chi}_1^0$-p elastic cross section are evaluated at $m_{\tilde{\chi}_1^0}$=100 GeV. The experimental results on the cross section are often mass dependent. Therefore, the mass and cross section results are also given where the limit is strongest, when appropriate. Results are quoted separately for spin-dependent interactions (based on an effective 4-Fermi Lagrangian of the form $\overline{\chi}\gamma^{\mu}\gamma^5\chi\overline{q}\gamma_{\mu}\gamma^5 q$) and spin-independent interactions ($\overline{\chi}\chi\overline{q}q$). For calculational details see GRIEST 88B, ELLIS 88D, BARBIERI 89C, DREES 93B, ARNOWITT 96, BERGSTROM 96, and BAER 97 in addition to the theory papers listed in the Tables. For a description of the theoretical assumptions and experimental techniques underlying most of the listed papers, see the review on "Dark matter" in this "Review of Particle Properties," and references therein. Most of the following papers use galactic halo and nuclear interaction assumptions from (LEWIN 96).

Spin-dependent interactions

VALUE (pb)	DOCUMENT ID		TECN	COMMENT
• • • We do not use the following data for averages, fits, limits, etc. • • •				
< 0.8	[17] AHMED	03	NAIA	NaI Spin Dep.
< 40	[18] TAKEDA	03	BOLO	NaF Spin Dep.
< 10	[19] ANGLOHER	02	CRES	Saphire
8×10^{-7} to 2×10^{-5}	ELLIS	01C	THEO	tanβ ≤ 10
< 3.8	[21] BERNABEI	00D	DAMA	Xe
< 15	[22] COLLAR	00	SMPL	F
< 0.8	SPOONER	00	UKDM	NaI
< 4.8	[23] BELLI	99C	DAMA	F
<100	[24] OOTANI	99	BOLO	LiF
< 0.6	BERNABEI	98C	DAMA	Xe
< 5	[23] BERNABEI	97	DAMA	F

[17] The strongest upper limit is 0.75 pb and occurs at $m_{\chi} \approx 70$ GeV.

[18] The strongest upper limit is 30 pb and occurs at $m_{\chi} \approx 20$ GeV.

[19] The strongest upper limit is 8 pb and occurs at $m_{\chi} \simeq 30$ GeV.

[20] ELLIS 01C calculates the χ-p elastic scattering cross section in the framework of N=1 supergravity models with radiative breaking of the electroweak gauge symmetry. In models with nonuniversal Higgs masses, the upper limit to the cross section is 6×10^{-4}.

[21] The strongest upper limit is 3 pb and occurs at $m_{\chi} \simeq 60$ GeV. The limits are for inelastic scattering $X^0 + {}^{129}\mathrm{Xe} \rightarrow X^0 + {}^{129}\mathrm{Xe}^*$ (39.58 keV).

[22] The strongest upper limit is 9 pb and occurs at $m_{\chi} \simeq 30$ GeV.

[23] The strongest upper limit is 4.4 pb and occurs at $m_{\chi} \simeq 60$ GeV.

[24] The strongest upper limit is about 35 pb and occurs at $m_{\chi} \simeq 15$ GeV.

Spin-independent interactions

VALUE (pb)	DOCUMENT ID		TECN	COMMENT
• • • We do not use the following data for averages, fits, limits, etc. • • •				
$< 2 \times 10^{-5}$	[25] AHMED	03	NAIA	NaI Spin Indep.
$< 1.4 \times 10^{-5}$	[26] KLAPDOR-K...	03	HDMS	Ge
$< 6 \times 10^{-6}$	[27] ABRAMS	02	CDMS	Ge
$< 1.4 \times 10^{-6}$	[28] BENOIT	02	EDEL	Ge
10^{-12} to 7×10^{-6}	KIM	02B	THEO	
$< 3 \times 10^{-5}$	[29] MORALES	02B	CSME	Ge
$<10^{-5}$	[30] MORALES	02C	IGEX	Ge
$<10^{-6}$	BALTZ	01	THEO	

$< 3 \times 10^{-5}$	[31] BAUDIS	01	HDMS	Ge
$< 4.5 \times 10^{-6}$	BENOIT	01	EDEL	Ge
$< 7 \times 10^{-6}$	[32] BOTTINO	01	THEO	
$< 10^{-8}$	[33] CORSETTI	01	THEO	$\tan\beta \leq 25$
5×10^{-10} to 1.5×10^{-8}	[34] ELLIS	01C	THEO	$\tan\beta \leq 10$
$< 4 \times 10^{-6}$	[33] GOMEZ	01	THEO	
2×10^{-10} to 10^{-7}	[33] LAHANAS	01	THEO	
$< 3 \times 10^{-6}$	ABUSAIDI	00	CDMS	Ge, Si
$< 6 \times 10^{-7}$	[35] ACCOMANDO	00	THEO	
	[36] BERNABEI	00	DAMA	NaI
2.5×10^{-9} to 3.5×10^{-8}	[37] FENG	00	THEO	$\tan\beta$=10
$< 1.5 \times 10^{-5}$	MORALES	00	IGEX	Ge
$< 4 \times 10^{-5}$	SPOONER	00	UKDM	NaI
$< 7 \times 10^{-6}$	BAUDIS	99	HDMO	^{76}Ge
	[38] BERNABEI	99	DAMA	NaI
	[39] BERNABEI	98	DAMA	NaI
$< 7 \times 10^{-6}$	BERNABEI	98C	DAMA	Xe

[25] The strongest upper limit is 1.8×10^{-5} pb and occurs at $m_\chi \approx 80$ GeV.

[26] The strongest upper limit is 7×10^{-6} pb and occurs at $m_\chi \simeq 30$ GeV.

[27] ABRAMS 02 is incompatible with the DAMA most likely value at the 99.9% CL. The strongest upper limit is 3×10^{-6} pb and occurs at $m_\chi \simeq 30$ GeV.

[28] BENOIT 02 excludes the central result of DAMA at the 99.8%CL.

[29] The strongest upper limit is 2×10^{-5} pb and occurs at $m_\chi \simeq 40$ GeV.

[30] The strongest upper limit is 7×10^{-6} pb and occurs at $m_\chi \simeq 46$ GeV.

[31] The strongest upper limit is 1.8×10^{-5} pb and occurs at $m_\chi \simeq 32$ GeV

[32] BOTTINO 01 calculates the χ-p elastic scattering cross section in the framework of the following supersymmetric models: N=1 supergravity with the radiative breaking of the electroweak gauge symmetry, N=1 supergravity with nonuniversal scalar masses and an effective MSSM model at the electroweak scale.

[33] Calculates the χ-p elastic scattering cross section in the framework of N=1 supergravity models with radiative breaking of the electroweak gauge symmetry.

[34] ELLIS 01C calculates the χ-p elastic scattering cross section in the framework of N=1 supergravity models with radiative breaking of the electroweak gauge symmetry. ELLIS 02B find a range 2×10^{-8}–1.5×10^{-7} at $\tan\beta$=50. In models with nonuniversal Higgs masses, the upper limit to the cross section is 4×10^{-7}.

[35] ACCOMANDO 00 calculate the χ-p elastic scattering cross section in the framework of minimal N=1 supergravity models with radiative breaking of the electroweak gauge symmetry. The limit is relaxed by at least an order of magnitude when models with nonuniversal scalar masses are considered. A subset of the authors in ARNOWITT 02 updated the limit to $< 9 \times 10^{-8}$ ($\tan\beta < 55$).

[36] BERNABEI 00 search for annual modulation of the WIMP signal. The data favor the hypothesis of annual modulation at 4σ and are consistent, for a particular model framework quoted there, with m_{χ^0}=44 $^{+12}_{-9}$ GeV and a spin-independent χ^0-proton cross section of $(5.4 \pm 1.0) \times 10^{-6}$ pb. See also BERNABEI 01 and BERNABEI 00C.

[37] FENG 00 calculate the χ-p elastic scattering cross section in the framework of N=1 supergravity models with radiative breaking of the electroweak gauge symmetry with a particular emphasis on focus point models. At $\tan\beta$=50, the range is 8×10^{-8}–4×10^{-7}.

[38] BERNABEI 99 search for annual modulation of the WIMP signal. The data favor the hypothesis of annual modulation at 99.6%CL and are consistent, for the particular model framework considered there, with m_{χ^0}=59 $^{+17}_{-14}$ GeV and spin-independent χ^0-proton cross section of $(7.0^{+0.4}_{-1.2}) \times 10^{-6}$ pb (1 σ errors).

[39] BERNABEI 98 search for annual modulation of the WIMP signal. The data are consistent, for the particular model framework considered there, with m_{χ^0}=59 $^{+36}_{-19}$ GeV and spin-independent χ^0-proton cross section of $(1.0^{+0.1}_{-0.4}) \times 10^{-5}$ pb (1 σ errors).

Other bounds on $\tilde{\chi}_1^0$ from astrophysics and cosmology

Most of these papers generally exclude regions in the $M_2 - \mu$ parameter plane by requiring that the $\tilde{\chi}_1^0$ contribution to the overall cosmological density is less than some maximal value to avoid overclosure of the Universe. Those not based on the cosmological density are indicated. Many of these papers also include LEP and/or other bounds.

VALUE	DOCUMENT ID		TECN	COMMENT
>46 GeV	[40] ELLIS	00	RVUE	
• • • We do not use the following data for averages, fits, limits, etc. • • •				
	[41] BAER	03	COSM	
> 6 GeV	[42] BOTTINO	03	COSM	
	[41] CHATTOPAD...	03	COSM	
	[43] ELLIS	03	COSM	
	[44] ELLIS	03B	COSM	
	[41] ELLIS	03C	COSM	
	[45] ELLIS	03D	COSM	
> 18 GeV	[42] HOOPER	03	COSM	$\Omega_\chi = 0.05$–0.3
	[41] LAHANAS	03	COSM	
	[46] BAER	02	COSM	
	[47] ELLIS	02	COSM	
	[48] LAHANAS	02	COSM	
	[49] BARGER	01C	COSM	
	[46] DJOUADI	01	COSM	
	[50] ELLIS	01B	COSM	
	[46] ROSZKOWSKI	01	COSM	
< 600 GeV	[43] BOEHM	00B	COSM	
	[51] FENG	00	COSM	
	[52] LAHANAS	00	COSM	
	[53] ELLIS	98B	COSM	
	[54] EDSJO	97	COSM	Co-annihilation
	[55] BAER	96	COSM	
	[56] BEREZINSKY	95	COSM	
	[57] FALK	95	COSM	CP-violating phases
	[58] DREES	93	COSM	Minimal supergravity
	[59] FALK	93	COSM	Sfermion mixing
	[58] KELLEY	93	COSM	Minimal supergravity
	[60] MIZUTA	93	COSM	Co-annihilation
	[61] LOPEZ	92	COSM	Minimal supergravity, m_0=A=0
	[62] MCDONALD	92	COSM	
	[63] GRIEST	91	COSM	
	[64] NOJIRI	91	COSM	Minimal supergravity
	[65] OLIVE	91	COSM	
	[66] ROSZKOWSKI	91	COSM	
	[67] GRIEST	90	COSM	
	[65] OLIVE	89	COSM	
none 100 eV – 15 GeV	SREDNICKI	88	COSM	$\tilde{\gamma}$; $m_{\tilde{f}}$=100 GeV
none 100 eV–5 GeV	ELLIS	84	COSM	$\tilde{\gamma}$; for $m_{\tilde{f}}$=100 GeV
	GOLDBERG	83	COSM	$\tilde{\gamma}$
	[68] KRAUSS	83	COSM	$\tilde{\gamma}$
	VYSOTSKII	83	COSM	$\tilde{\gamma}$

[40] ELLIS 00 updates ELLIS 98. Uses LEP e^+e^- data at $\sqrt{s}$=202 and 204 GeV to improve bound on neutralino mass to 51 GeV when scalar mass universality is assumed and 46 GeV when Higgs mass universality is relaxed. Limits on $\tan\beta$ improve to > 2.7 ($\mu > 0$), > 2.2 ($\mu < 0$) when scalar mass universality is assumed and > 1.9 (both signs of μ) when Higgs mass universality is relaxed.

[41] BAER 03, CHATTOPADHYAY 03, ELLIS 03C and LAHANAS 03 place constraints on the SUSY parameter space in the framework of N=1 supergravity models with radiative breaking of the electroweak gauge symmetry based on WMAP results for the cold dark matter density.

[42] BOTTINO 03 (see also BOTTINO 03A) and HOOPER 03 do not assume gaugino or scalar mass unification.

[43] BOEHM 00B and ELLIS 03 place constraints on the SUSY parameter space in the framework of minimal N=1 supergravity models with radiative breaking of the electroweak gauge symmetry. Includes the effect of χ-$\tilde{t}$ co-annihilations.

[44] BEREZINSKY 95 and ELLIS 03B places constraints on the SUSY parameter space in the framework of N=1 supergravity models with radiative breaking of the electroweak gauge symmetry but non-Universal Higgs masses.

[45] ELLIS 03D places constraints on the SUSY parameter space in the framework of N=1 supergravity models with radiative breaking of the electroweak gauge symmetry including supersymmetry breaking relations between A and B parameters.

[46] DJOUADI 01, ROSZKOWSKI 01, and BAER 02 place constraints on the SUSY parameter space in the framework of minimal N=1 supergravity models with radiative breaking of the electroweak gauge symmetry.

[47] ELLIS 02 places constraints on the soft supersymmetry breaking masses in the framework of minimal N=1 supergravity models with radiative breaking of the electroweak gauge symmetry.

[48] LAHANAS 02 places constraints on the SUSY parameter space in the framework of minimal N=1 supergravity models with radiative breaking of the electroweak gauge symmetry. Focuses on the role of pseudo-scalar Higgs exchange.

[49] BARGER 01C use the cosmic relic density inferred from recent CMB measurements to constrain the parameter space in the framework of minimal N=1 supergravity models with radiative breaking of the electroweak gauge symmetry.

[50] ELLIS 01B places constraints on the SUSY parameter space in the framework of minimal N=1 supergravity models with radiative breaking of the electroweak gauge symmetry. Focuses on models with large $\tan\beta$.

[51] FENG 00 explores cosmologically allowed regions of MSSM parameter space with multi-TeV masses.

[52] LAHANAS 00 use the new cosmological data which favor a cosmological constant and its implications on the relic density to constrain the parameter space in the framework of minimal N=1 supergravity models with radiative breaking of the electroweak gauge symmetry.

[53] ELLIS 98B assumes a universal scalar mass and radiative supersymmetry breaking with universal gaugino masses. The upper limit to the LSP mass is increased due to the inclusion of $\chi - \tilde{\tau}_R$ coannihilations.

[54] EDSJO 97 included all coannihilation processes between neutralinos and charginos for any neutralino mass and composition.

[55] Notes the location of the neutralino Z resonance and h resonance annihilation corridors in minimal supergravity models with radiative electroweak breaking.

[56] BEREZINSKY 95 and ELLIS 02C places constraints on the SUSY parameter space in the framework of N=1 supergravity models with radiative breaking of the electroweak gauge symmetry but non-Universal Higgs masses.

[57] Mass of the bino (=LSP) is limited to $m_{\tilde{B}} \lesssim 350$ GeV for $m_t = 174$ GeV.

[58] DREES 93, KELLEY 93 compute the cosmic relic density of the LSP in the framework of minimal N=1 supergravity models with radiative breaking of the electroweak gauge symmetry.

[59] FALK 93 relax the upper limit to the LSP mass by considering sfermion mixing in the MSSM.

[60] MIZUTA 93 include coannihilations to compute the relic density of Higgsino dark matter.

[61] LOPEZ 92 calculate the relic LSP density in a minimal SUSY GUT model.

[62] MCDONALD 92 calculate the relic LSP density in the MSSM including exact tree-level annihilation cross sections for all two-body final states.

[63] GRIEST 91 improve relic density calculations to account for coannihilations, pole effects, and threshold effects.

[64] NOJIRI 91 uses minimal supergravity mass relations between squarks and sleptons to narrow cosmologically allowed parameter space.

[65] Mass of the bino (=LSP) is limited to $m_{\tilde{B}} \lesssim 350$ GeV for $m_t \leq 200$ GeV. Mass of the higgsino (=LSP) is limited to $m_{\tilde{H}} \lesssim 1$ TeV for $m_t \leq 200$ GeV.

[66] ROSZKOWSKI 91 calculates LSP relic density in mixed gaugino/higgsino region.

[67] Mass of the bino (=LSP) is limited to $m_{\widetilde{B}} \lesssim 550$ GeV. Mass of the higgsino (=LSP) is limited to $m_{\widetilde{H}} \lesssim 3.2$ TeV.

[68] KRAUSS 83 finds $m_{\widetilde{\gamma}}$ not 30 eV to 2.5 GeV. KRAUSS 83 takes into account the gravitino decay. Find that limits depend strongly on reheated temperature. For example a new allowed region $m_{\widetilde{\gamma}}$ = 4–20 MeV exists if $m_{\text{gravitino}}$ <40 TeV. See figure 2.

Unstable $\widetilde{\chi}_1^0$ (Lightest Neutralino) MASS LIMIT

Unless otherwise stated, results in this section assume spectra and production rates as evaluated in the MSSM. Unless otherwise stated, the goldstino or gravitino mass $m_{\widetilde{G}}$ is assumed to be negligible relative to all other masses. In the following, $\widetilde{G}$ is assumed to be undetected and to give rise to a missing energy ($\not{E}$) signature.

VALUE (GeV)	CL%	DOCUMENT ID		TECN	COMMENT
• • • We do not use the following data for averages, fits, limits, etc. • • •					
>89	95	[69] ABDALLAH	03D	DLPH	$e^+e^- \to \widetilde{\chi}_1^0\widetilde{\chi}_1^0$, GMSB, $m(\widetilde{G})$ < 1 eV
		[70] HEISTER	03C	ALEP	$e^+e^- \to \widetilde{B}\widetilde{B}$, $(\widetilde{B} \to \gamma\widetilde{G})$
		[71] HEISTER	03C	ALEP	$e^+e^- \to \widetilde{G}\widetilde{\chi}_1^0$, $(\widetilde{\chi}_1^0 \to \widetilde{G}\gamma)$
>39.9	95	[72] ACHARD	02	L3	$\not{R}$, MSUGRA
>92	95	[73] HEISTER	02R	ALEP	short lifetime
>54	95	[73] HEISTER	02R	ALEP	any lifetime
>85	95	[74] ABBIENDI	01	OPAL	$e^+e^- \to \widetilde{\chi}_1^0\widetilde{\chi}_1^0$, GMSB, tan$\beta$=2
>76	95	[74] ABBIENDI	01	OPAL	$e^+e^- \to \widetilde{\chi}_1^0\widetilde{\chi}_1^0$, GMSB, tan$\beta$=20
none 10–32	95	[75] ABREU	01D	DLPH	$\not{R}(\overline{UDD})$, all m_0, $0.5 \le \tan\beta \le 30$
>32.5	95	[76] ACCIARRI	01	L3	$\not{R}$, all m_0, $0.7 \le \tan\beta \le 40$
		[77] ADAMS	01	NTEV	$\widetilde{\chi}^0 \to \mu\mu\nu$, $\not{R}$, $LL\overline{E}$
		[78] ABBIENDI,G	00D	OPAL	$e^+e^- \to \widetilde{G}\widetilde{\chi}_1^0$ $(\widetilde{\chi}_1^0 \to \gamma\widetilde{G})$
none 45–88.3	95	[79] ABBIENDI,G	00D	OPAL	$e^+e^- \to \widetilde{B}\widetilde{B}$, $(\widetilde{B} \to \gamma\widetilde{G})$
none 10–30	95	[80] ABREU	00U	DLPH	$\not{R}$ ($LL\overline{E}$), all m_0, $1 \le \tan\beta \le 30$
		[81] ABREU	00Z	DLPH	$e^+e^- \to \widetilde{G}\widetilde{\chi}_1^0$ $(\widetilde{\chi}_1^0 \to \widetilde{G}\gamma)$
>83.5	95	[82] ABREU	00Z	DLPH	$e^+e^- \to \widetilde{B}\widetilde{B}$ $(\widetilde{B} \to \widetilde{G}\gamma)$
>29	95	[83] ABBIENDI	99T	OPAL	$e^+e^- \to \widetilde{\chi}_1^0\widetilde{\chi}_1^0$, $\not{R}$, m_0=500 GeV, tan$\beta > 1.2$
>65	95	[84] ABE	99I	CDF	$p\overline{p} \to \widetilde{\chi}\widetilde{\chi}$, $\widetilde{\chi}=\widetilde{\chi}_{1,2}^{\pm}$, $\widetilde{\chi}_1^0 \to \gamma\widetilde{G}$
		[85] ACCIARRI	99R	L3	$e^+e^- \to \widetilde{G}\widetilde{\chi}_1^0$, $\widetilde{\chi}_1^0 \to \widetilde{G}\gamma$
>88.2	95	[86] ACCIARRI	99R	L3	$e^+e^- \to \widetilde{\chi}_1^0\widetilde{\chi}_1^0$, $\widetilde{\chi}_1^0 \to \widetilde{G}\gamma$
>29	95	[87] BARATE	99E	ALEP	$\not{R}$, $LQ\overline{D}$, tanβ=1.41, m_0=500 GeV
>77	95	[88] ABBOTT	98	D0	$p\overline{p} \to \widetilde{\chi}\widetilde{\chi}$, $\widetilde{\chi}=\widetilde{\chi}_{1,2}^{\pm}$, $\widetilde{\chi}_1^0 \to \gamma\widetilde{G}$
		[89] ABREU	98	DLPH	$e^+e^- \to \widetilde{\chi}_1^0\widetilde{\chi}_1^0$ $(\widetilde{\chi}_1^0 \to \gamma\widetilde{G})$
>23	95	[90] BARATE	98S	ALEP	$\not{R}$, $LL\overline{E}$
		[91] ELLIS	97	THEO	$e^+e^- \to \widetilde{\chi}_1^0\widetilde{\chi}_1^0$, $\widetilde{\chi}_1^0 \to \gamma\widetilde{G}$
		[92] CABIBBO	81	COSM	

[69] ABDALLAH 03D use data from $\sqrt{s}$= 161-208 GeV. They look for 4-tau + $\not{E}$ final states, expected in GMSB when the $\widetilde{\tau}_1$ is the NLSP, and 4-lepton + $\not{E}$ final states, expected in the co-NLSP scenario, and assuming a short-lived $\widetilde{\chi}_1^0$ ($m(\widetilde{G})$ < 1 eV). Limits are computed in the plane ($m(\widetilde{\tau}_1)$,$m(\widetilde{\chi}_1^0)$) from a scan of the GMSB parameters space, after combining these results with the search for slepton pair production from the same paper to cover prompt decays and for the case of $\widetilde{\chi}_1^0$ NLSP from ABREU 00Z. The limit above is reached for a single generation of messengers and when the $\widetilde{\tau}_1$ is the NLSP. Stronger limits are obtained when more messenger generations are assumed or when the other sleptons are co-NLSP, see their Fig. 10. Supersedes the results of ABREU 01G.

[70] HEISTER 03C use the data from $\sqrt{s}$= 189-209 GeV to search for $\gamma\not{E}_T$ final states with non-pointing photons and $\gamma\gamma$ $\not{E}_T$ events. Interpreted in the framework of Minimal GMSB, a lower bound on the $\widetilde{\chi}_1^0$ mass is obtained as function of its lifetime. For a laboratory lifetime of less than 3 ns, the limit at 95% CL is 98.8 GeV. For other lifetimes, see their Fig. 5. These results are interpreted in a more general GMSB framework in HEISTER 02R.

[71] HEISTER 03C use the data from $\sqrt{s}$= 189-209 GeV to search for $\gamma\not{E}_T$ final states. They obtained an upper bound on the cross section for the process $e^+e^- \to \widetilde{G}\widetilde{\chi}_1^0$, followed by the prompt decay $\widetilde{\chi}_1^0 \to \gamma\widetilde{G}$, shown in their Fig. 4. These results supersede BARATE 98H.

[72] ACHARD 02 searches for the production of sparticles in the case of $\not{R}$ prompt decays with $LL\overline{E}$ or $\overline{UDD}$ couplings at $\sqrt{s}$=189–208 GeV. The search is performed for direct and indirect decays, assuming one coupling at the time to be nonzero. The MSUGRA limit results from a scan over the MSSM parameter space with the assumption of gaugino and scalar mass unification at the GUT scale, imposing simultaneously the exclusions from neutralino, chargino, sleptons, and squarks analyses. The limit holds for $\overline{UDD}$ couplings and increases to 40.2 GeV for $LL\overline{E}$ couplings. For L3 limits from $LQ\overline{D}$ couplings, see ACCIARRI 01.

[73] HEISTER 02R search for signals of GMSB in the 189–209 GeV data. For the $\widetilde{\chi}_1^0$ NLSP scenario, they looked for topologies consisting of $\gamma\gamma\not{E}$ or a single γ not pointing to the interaction vertex. For the $\widetilde{\ell}$ NLSP case, the topologies consist of $\ell\ell\not{E}$ or $4\ell\not{E}$ (from $\widetilde{\chi}_1^0\widetilde{\chi}_1^0$) production), including leptons with large impact parameters, kinks, or stable particles. Limits are derived from a scan over the GMSB parameters (see their Table 5 for the ranges). The limits are valid whichever is the NLSP. The absolute mass bound on the $\widetilde{\chi}_1^0$ for any lifetime includes indirect limits from the chargino search, and from the slepton search HEISTER 02E preformed within the MSUGRA framework. A bound for any NLSP and any lifetime of 77 GeV has also been derived by using the constraints from the neutral Higgs search in HEISTER 02. Limits on the universal SUSY mass scale Λ are also derived in the paper. Supersedes the results from BARATE 00G.

[74] ABBIENDI 01 looked for final states with $\gamma\gamma\not{E}$, $\ell\ell\not{E}$, with possibly additional activity and four leptons + $\not{E}$ to search for prompt decays of $\widetilde{\chi}_1^0$ or $\widetilde{\ell}_1$ in GMSB. They derive limits in the plane ($m_{\widetilde{\chi}_1^0}$,$m_{\widetilde{\tau}_1}$), see Fig. 6, allowing either the $\widetilde{\chi}_1^0$ or a $\widetilde{\ell}_1$ to be the NLSP. Two scenarios are considered: tanβ=2 with the 3 sleptons degenerate in mass and tanβ=20 where the $\widetilde{\tau}_1$ is lighter than the other sleptons. Data taken at $\sqrt{s}$=189 GeV.

[75] ABREU 01D searches for multi-jet events, expected in the case of prompt decays from R-parity violating $\overline{UDD}$ couplings, using data from $\sqrt{s}$=189 GeV. Combined with the search for charginos, limits are obtained in the M_2 versus μ plane and a limit on the neutralino mass is derived from a scan over the parameters m_0 and tanβ. The weakest limit for $\widetilde{\chi}_1^0$ is reached for high m_0 and tanβ=1.

[76] ACCIARRI 01 searches for multi-lepton and/or multi-jet final states from $\not{R}$ prompt decays with $LL\overline{E}$, $LQ\overline{D}$, or $\overline{UDD}$ couplings at $\sqrt{s}$=189 GeV. The search is performed for direct and indirect decays of neutralinos, charginos, and scalar leptons, with the $\widetilde{\chi}_1^0$ or a $\widetilde{\ell}$ as LSP and assuming one coupling to be nonzero at a time. Mass limits are derived using simultaneously the constraints from the neutralino, chargino, and slepton analyses; and the Z^0 width measurements from ACCIARRI 00C in a scan of the parameter space assuming MSUGRA with gaugino and scalar mass universality. Updates and supersedes the results from ACCIARRI 99I.

[77] ADAMS 01 looked for neutral particles with mass > 2.2 GeV, produced by 900 GeV protons incident on a Beryllium oxide target and decaying through weak interactions into $\mu\mu$, μe, or $\mu\pi$ final states in the decay channel of the NuTeV detector (E815) at Fermilab. The number of observed events is 3 $\mu\mu$, 0 μe, and 0 $\mu\pi$ with an expected background of 0.069 ± 0.010, 0.13 ± 0.02, and 0.14 ± 0.02, respectively. The $\mu\mu$ events are consistent with the $\not{R}$ decay of a neutralino with mass around 5 GeV. However, they share several aspects with ν-interaction backgroundes. An upper limit on the differential production cross section of neutralinos in pp interactions as function of the decay length is given in Fig. 3.

[78] ABBIENDI,G 00D obtained an upper limit on the cross section for the process $e^+e^- \to \widetilde{G}\widetilde{\chi}_1^0$ followed by the prompt decay $\widetilde{\chi}_1^0 \to \gamma\widetilde{G}$ shown in Fig. 11. Data taken at $\sqrt{s}$=189 GeV. These limits include and update the results of ABBIENDI 99F.

[79] ABBIENDI,G 00D looked for $\gamma\gamma\not{E}$ final states at $\sqrt{s}$=189 GeV. The limit is for pure bino $\widetilde{B}$ NLSP and assumes $m_{\widetilde{e}_R} = 1.35 m_{\widetilde{\chi}_1^0}$ and $m_{\widetilde{e}_L} = 2.7 m_{\widetilde{\chi}_1^0}$. See Fig. 14 for the cross-section limits as function of $m_{\widetilde{\chi}_1^0}$. These limits include and update the results of ABBIENDI 99F.

[80] ABREU 00U searches for the production of charginos and neutralinos in the case of R-parity violation with $LL\overline{E}$ couplings, using data from $\sqrt{s}$=189 GeV. They investigate topologies with multiple leptons or jets plus leptons, assuming one coupling to be nonzero at the time and giving rise to direct or indirect decays. Limits are obtained in the M_2 versus μ plane and a limit on the neutralino mass is derived from a scan over the parameters m_0 and tanβ. The weakest limit for $\widetilde{\chi}_1^0$ is reached for high m_0 and tanβ=1. Supersedes the results of ABREU 00I.

[81] ABREU 00Z looks for $\gamma\not{E}$ final states using data from $\sqrt{s}$= 183–189 GeV. Assuming the decay $\widetilde{\chi}_1^0 \to \widetilde{G}\gamma$, limits on cross section are derived, see their Fig. 7.

[82] ABREU 00Z looks for diphoton +$\not{E}$ final states using data from $\sqrt{s}$= 130–189 GeV. The limit is derived for a pure bino $\widetilde{B}$ assuming the prompt decay $\widetilde{B} \to \widetilde{G}\gamma$ and $m_{\widetilde{e}_R} \gg m_{\widetilde{e}_R} = 2m_{\widetilde{B}}$. For long-lived neutralinos, cross-section limits are displayed in their Fig. 9. These results include and update limits from ABREU 99D.

[83] ABBIENDI 99T searches for the production of neutralinos in the case of R-parity violation with $LL\overline{E}$, $LQ\overline{D}$, or $\overline{UDD}$ couplings using data from $\sqrt{s}$=183 GeV. They investigate topologies with multiple leptons, jets plus leptons, or multiple jets, assuming one coupling at the time to be non-zero and giving rise to direct or indirect decays. Mixed decays (where one particle has a direct, the other an indirect decay) are also considered for the $\overline{UDD}$ couplings. Upper limits on the cross section are derived which, combined with the constraint from the Z^0 width, allow to exclude regions in the M_2 versus μ plane for any coupling. Limits on the neutralino mass are obtained for non-zero $LL\overline{E}$ couplings $> 10^{-5}$. The limit disappears for tanβ < 1.2 and it improves to 50 GeV for tan$\beta > 20$.

[84] ABE 99I looked for chargino and neutralino production, where the lightest neutralino in their decay products further decays into $\gamma\widetilde{G}$. The limit assumes the gaugino mass unification, and holds for $1 < \tan\beta < 25$, $M_2 < 200$ GeV, and all μ. ABE 99I is an expanded version of ABE 98L.

[85] ACCIARRI 99R searches for $\gamma\not{E}$ final states using data from $\sqrt{s}$=189 GeV. From limits on cross section times branching ratio, mass limits are derived in a no-scale SUGRA model, see their Fig. 5. Supersedes the results of ACCIARRI 98V.

[86] ACCIARRI 99R searches for $\gamma\not{E}$ final states using data from $\sqrt{s}$=189 GeV. From a scan over the GMSB parameter space, a limit on the mass is derived under the assumption that the neutralino is the NLSP. Supersedes the results of ACCIARRI 98V.

[87] BARATE 99E looked for the decay of gauginos via R-violating couplings $LQ\overline{D}$. The bound is significantly reduced for smaller values of m_0. Data collected at $\sqrt{s}$=130–172 GeV.

[88] ABBOTT 98 studied the chargino and neutralino production, where the lightest neutralino in their decay products further decays into $\gamma\widetilde{G}$. The limit assumes the gaugino mass unification.

[89] ABREU 98 uses data at $\sqrt{s}$=161 and 172 GeV. Upper bounds on $\gamma\gamma\not{E}$ cross section are obtained. Similar limits on $\gamma\not{E}$ are also given, relevant for $e^+e^- \to \widetilde{\chi}_1^0\widetilde{G}$ production.

[90] BARATE 98S looked for the decay of gauginos via R-violating coupling $LL\overline{E}$. The bound improves to 25 GeV if the chargino decays into neutralino which further decays into lepton pairs. Data collected at $\sqrt{s}$=130–172 GeV.

[91] ELLIS 97 reanalyzed the LEP2 ($\sqrt{s}$=161 GeV) limits of $\sigma(\gamma\gamma + E_{\text{miss}})$< 0.2 pb to exclude $m_{\widetilde{\chi}_1^0} < 63$ GeV if $m_{\widetilde{e}_L} = m_{\widetilde{e}_R} < 150$ GeV and $\widetilde{\chi}_1^0$ decays to $\gamma\widetilde{G}$ inside detector.

[92] CABIBBO 81 consider $\widetilde{\gamma} \to \gamma$ + goldstino. Photino must be either light enough (<30 eV) to satisfy cosmology bound, or heavy enough (>0.3 MeV) to have disappeared at early universe.

$\tilde{\chi}_2^0$, $\tilde{\chi}_3^0$, $\tilde{\chi}_4^0$ (Neutralinos) MASS LIMITS

Neutralinos are unknown mixtures of photinos, z-inos, and neutral higgsinos (the supersymmetric partners of photons and of Z and Higgs bosons). The limits here apply only to $\tilde{\chi}_2^0$, $\tilde{\chi}_3^0$, and $\tilde{\chi}_4^0$. $\tilde{\chi}_1^0$ is the lightest supersymmetric particle (LSP); see $\tilde{\chi}_1^0$ Mass Limits. It is not possible to quote rigorous mass limits because they are extremely model dependent; i.e. they depend on branching ratios of various $\tilde{\chi}^0$ decay modes, on the masses of decay products ($\tilde{e}$, $\tilde{\gamma}$, $\tilde{q}$, $\tilde{g}$), and on the $\tilde{e}$ mass exchanged in $e^+e^- \to \tilde{\chi}_i^0\tilde{\chi}_j^0$. Limits arise either from direct searches, or from the MSSM constraints set on the gaugino and higgsino mass parameters M_2 and μ through searches for lighter charginos and neutralinos. Often limits are given as contour plots in the $m_{\tilde{\chi}^0} - m_{\tilde{e}}$ plane vs other parameters. When specific assumptions are made, e.g. the neutralino is a pure photino ($\tilde{\gamma}$), pure z-ino ($\tilde{Z}$), or pure neutral higgsino ($\tilde{H}^0$), the neutralinos will be labelled as such.

Limits obtained from e^+e^- collisions at energies up to 136 GeV, as well as other limits from different techniques, are now superseded and have not been included in this compilation. They can be found in the 1998 Edition (The European Physical Journal **C3** 1 (1998)) of this Review.

VALUE (GeV)	CL%	DOCUMENT ID		TECN	COMMENT
> 55.9	95	[93] ABBIENDI	00H	OPAL	$\tilde{\chi}_2^0$, tanβ=1.5, Δm >10 GeV, all m_0
>106	95	[93] ABBIENDI	00H	OPAL	$\tilde{\chi}_3^0$, tanβ=1.5, Δm >10 GeV, all m_0
> 62.4	95	[94] ABREU	00W	DLPH	$\tilde{\chi}_2^0$, $1 \leq$ tan$\beta \leq 40$, all Δm_0, all m_0
> 99.9	95	[94] ABREU	00W	DLPH	$\tilde{\chi}_3^0$, $1 \leq$ tan$\beta \leq 40$, all Δm_0, all m_0
>116.0	95	[94] ABREU	00W	DLPH	$\tilde{\chi}_4^0$, $1 \leq$ tan$\beta \leq 40$, all Δm_0, all m_0
• • • We do not use the following data for averages, fits, limits, etc. • • •					
> 80.0	95	[95] ACHARD	02	L3	$\tilde{\chi}_2^0$, $\not{R}$, MSUGRA
>107.2	95	[95] ACHARD	02	L3	$\tilde{\chi}_3^0$, $\not{R}$, MSUGRA
		[96] ABREU	01B	DLPH	$e^+e^- \to \tilde{\chi}_i^0\tilde{\chi}_j^0$
> 68.0	95	[97] ACCIARRI	01	L3	$\tilde{\chi}_2^0$, $\not{R}$, all m_0, $0.7 \leq$ tan$\beta \leq 40$
> 99.0	95	[97] ACCIARRI	01	L3	$\tilde{\chi}_3^0$, $\not{R}$, all m_0, $0.7 \leq$ tan$\beta \leq 40$
> 50	95	[98] ABREU	00U	DLPH	$\tilde{\chi}_2^0$, $\not{R}$ ($LL\overline{E}$), all Δm_0, $1 \leq$ tan$\beta \leq 30$
	95	[99] ABREU	00Z	DLPH	$e^+e^- \to \tilde{\chi}_2^0\tilde{\chi}_2^0$ ($\tilde{\chi}_2^0 \to \tilde{\chi}_1^0\gamma$)
		[100] ABBIENDI	99F	OPAL	$e^+e^- \to \tilde{\chi}_2^0\tilde{\chi}_2^0$ ($\tilde{\chi}_2^0 \to \gamma\tilde{\chi}_1^0$)
		[101] ABBIENDI	99F	OPAL	$e^+e^- \to \tilde{\chi}_2^0\tilde{\chi}_2^0$ ($\tilde{\chi}_2^0 \to \gamma\tilde{\chi}_1^0$)
		[102] ACCIARRI	99R	L3	$e^+e^- \to \tilde{\chi}_2^0\tilde{\chi}_{2,1}^0$, $\tilde{\chi}_2^0 \to \tilde{\chi}_1^0\gamma$
		[103] ABBOTT	98C	D0	$p\overline{p} \to \tilde{\chi}_1^\pm\tilde{\chi}_2^0$
> 82.2	95	[104] ABE	98J	CDF	$p\overline{p} \to \tilde{\chi}_1^\pm\tilde{\chi}_2^0$
> 92	95	[105] ACCIARRI	98F	L3	$\tilde{H}_2^0$, tanβ=1.41, $M_2 < 500$ GeV
		[106] ACCIARRI	98V	L3	$e^+e^- \to \tilde{\chi}_2^0\tilde{\chi}_{1,2}^0$ ($\tilde{\chi}_2^0 \to \gamma\tilde{\chi}_1^0$)
> 53	95	[107] BARATE	98H	ALEP	$e^+e^- \to \tilde{\gamma}\tilde{\gamma}$ ($\tilde{\gamma} \to \gamma\tilde{H}^0$)
> 74	95	[108] BARATE	98J	ALEP	$e^+e^- \to \tilde{\gamma}\tilde{\gamma}$ ($\tilde{\gamma} \to \gamma\tilde{H}^0$)
		[109] ABACHI	96	D0	$p\overline{p} \to \tilde{\chi}_1^\pm\tilde{\chi}_2^0$
		[110] ABE	96K	CDF	$p\overline{p} \to \tilde{\chi}_1^\pm\tilde{\chi}_2^0$

[93] ABBIENDI 00H used the results of direct searches in the $e^+e^- \to \tilde{\chi}_1^0\tilde{\chi}_{2,3}^0$ channels, as well as the indirect limits from $\tilde{\chi}_1^0$ and $\tilde{\chi}_1^\pm$ searches, in the framework of the MSSM with gaugino and sfermion mass unification at the GUT scale. See the footnote to ABBIENDI 00H in the chargino Section for further details on the assumptions. Data collected at $\sqrt{s}$=189 GeV. The limits improve to 86.2 GeV ($\tilde{\chi}_2^0$) and 124 GeV ($\tilde{\chi}_3^0$) for tanβ=35. See their Table 6 for more details on the tanβ and m_0 dependence of the limits. Quoted values consistent with erratum published in ABBIENDI 00Y. Updates ABBIENDI 99G.

[94] ABREU 00W combines data collected at $\sqrt{s}$=189 GeV with results from lower energies. The mass limit is obtained by constraining the MSSM parameter space with gaugino and sfermion mass universality at the GUT scale, using the results of negative direct searches for neutralinos (including cascade decays and $\tilde{\tau}\,\tau$ final states) from ABREU 01, for charginos from ABREU 00J and ABREU 00T (for all Δm_+), and for charged sleptons from ABREU 01B. The results hold for the full parameter space defined by all values of M_2 and $|\mu| \leq 2$ TeV with the $\tilde{\chi}_1^0$ as LSP.

[95] ACHARD 02 searches for the production of sparticles in the case of $\not{R}$ prompt decays with $LL\overline{E}$ or $\overline{UDD}$ couplings at $\sqrt{s}$=189–208 GeV. The search is performed for direct and indirect decays, assuming one coupling at the time to be nonzero. The MSUGRA limit results from a scan over the MSSM parameter space with the assumption of gaugino and scalar mass unification at the GUT scale, imposing simultaneously the exclusions from neutralino, chargino, sleptons, and squarks analyses. The limit of $\tilde{\chi}_2^0$ holds for $\overline{UDD}$ couplings and increases to 84.0 GeV for $LL\overline{E}$ couplings. The same $\tilde{\chi}_3^0$ limit holds for both $LL\overline{E}$ and $\overline{UDD}$ couplings. For L3 limits from $LQ\overline{D}$ couplings, see ACCIARRI 01.

[96] ABREU 01B used data from $\sqrt{s}$=189 GeV to search for the production of $\tilde{\chi}_i^0\tilde{\chi}_j^0$. They looked for di-jet and di-lepton pairs with $\not{E}$ for events from $\tilde{\chi}_i^0\tilde{\chi}_j^0$ with the decay $\tilde{\chi}_j^0 \to f\overline{f}\tilde{\chi}_1^0$; multi-jet and multi-lepton pairs with or without additional photons to cover the cascade decays $\tilde{\chi}_j^0 \to f\overline{f}\tilde{\chi}_2^0$, followed by $\tilde{\chi}_j^0 \to f\overline{f}\tilde{\chi}_1^0$ or $\tilde{\chi}_j^0 \to \gamma\tilde{\chi}_1^0$; multi-tau final states from $\tilde{\chi}_2^0 \to \tilde{\tau}\,\tau$ with $\tilde{\tau} \to \tau\tilde{\chi}_1^0$. See Figs. 9 and 10 for limits on the (μ, M_2) plane for tanβ=1.0 and different values of m_0.

[97] ACCIARRI 01 searches for multi-lepton and/or multi-jet final states from $\not{R}$ prompt decays with $LL\overline{E}$, $LQ\overline{D}$, or $\overline{UDD}$ couplings at $\sqrt{s}$=189 GeV. The search is performed for direct and indirect decays of neutralinos, charginos, and scalar leptons, with the $\tilde{\chi}_1^0$ or a $\tilde{\ell}$ as LSP and assuming one coupling to be nonzero at a time. Mass limits are derived using simultaneously the constraints from the neutralino, chargino, and slepton analyses; and the Z^0 width measurements from ACCIARRI 00C in a scan of the parameter space assuming MSUGRA with gaugino and scalar mass universality. Updates and supersedes the results from ACCIARRI 99I.

[98] ABREU 00U searches for the production of charginos and neutralinos in the case of R-parity violation with $LL\overline{E}$ couplings, using data from $\sqrt{s}$=189 GeV. They investigate topologies with multiple leptons or jets plus leptons, assuming one coupling to be nonzero at the time and giving rise to direct or indirect decays. Limits are obtained in the M_2 versus μ plane and a limit on the neutralino mass is derived from a scan over the parameters m_0 and tanβ.

[99] ABREU 00Z looks for diphoton + $\not{E}$ final states using data from $\sqrt{s}$= 130–189 GeV. They obtain an upper bound on the cross section, see their Fig. 10 for limits in the $(m_{\tilde{\chi}_2^0}, m_{\tilde{\chi}_1^0})$ plane. Updates ABREU 99D.

[100] ABBIENDI 99F looked for $\gamma\not{E}$ final states at $\sqrt{s}$=183 GeV. They obtained an upper bound on the cross section for the production $e^+e^- \to \tilde{\chi}_2^0\tilde{\chi}_1^0$ followed by the prompt decay $\tilde{\chi}_2^0 \to \gamma\tilde{\chi}_1^0$ of 0.075–0.80 pb in the region $m_{\tilde{\chi}_2^0} + m_{\tilde{\chi}_1^0} > m_{Z^0}$, $m_{\tilde{\chi}_2^0}$=91–183 GeV, and $\Delta m_0 > 5$ GeV. See Fig. 7 for explicit limits in the $(m_{\tilde{\chi}_2^0}, m_{\tilde{\chi}_1^0})$ plane.

[101] ABBIENDI 99F looked for $\gamma\gamma\not{E}$ final states at $\sqrt{s}$=183 GeV. They obtained an upper bound on the cross section for the production $e^+e^- \to \tilde{\chi}_2^0\tilde{\chi}_2^0$ followed by the prompt decay $\tilde{\chi}_2^0 \to \gamma\tilde{\chi}_1^0$ of 0.08–0.37 pb for $m_{\tilde{\chi}_2^0}$=45–81.5 GeV, and $\Delta m_0 > 5$ GeV. See Fig. 11 for explicit limits in the $(m_{\tilde{\chi}_2^0}, m_{\tilde{\chi}_1^0})$ plane.

[102] ACCIARRI 99R searches for $\gamma\not{E}$ and $\gamma\gamma\not{E}$ final states using data from $\sqrt{s}$=189 GeV. Limits on the cross section for the processes $e^+e^- \to \tilde{\chi}_2^0\tilde{\chi}_{2,1}^0$ with the decay $\tilde{\chi}_2^0 \to \tilde{\chi}_1^0\gamma$ are derived, as shown in their Figs. 4 and 7. Supersedes the results of ACCIARRI 98V.

[103] ABBOTT 98C searches for trilepton final states (ℓ=e,μ). See footnote to ABBOTT 98C in the Chargino Section for details on the assumptions. Assuming a negligible decay rate of $\tilde{\chi}_1^\pm$ and $\tilde{\chi}_2^0$ to quarks, they obtain $m_{\tilde{\chi}_2^0} \gtrsim 103$ GeV.

[104] ABE 98J searches for trilepton final states (ℓ=e,μ). See footnote to ABE 98J in the Chargino Section for details on the assumptions. The quoted result for $m_{\tilde{\chi}_2^0}$ corresponds to the best limit within the selected range of parameters, obtained for $m_{\tilde{q}} > m_{\tilde{g}}$, tan$\beta$=2, and μ=− 600 GeV.

[105] ACCIARRI 98F is obtained from direct searches in the $e^+e^- \to \tilde{\chi}_{1,2}^0\tilde{\chi}_2^0$ production channels, and indirectly from $\tilde{\chi}_1^\pm$ and $\tilde{\chi}_1^0$ searches within the MSSM. See footnote to ACCIARRI 98F in the chargino Section for further details on the assumptions. Data taken at $\sqrt{s}$ = 130–172 GeV.

[106] ACCIARRI 98V looked for $\gamma(\gamma)\not{E}$ final states at $\sqrt{s}$=183 GeV. They obtained an upper bound on the cross section for the production $e^+e^- \to \tilde{\chi}_2^0\tilde{\chi}_{1,2}^0$ followed by the prompt decay $\tilde{\chi}_2^0 \to \gamma\tilde{\chi}_1^0$. See Figs. 4a and 6a for explicit limits in the $(m_{\tilde{\chi}_2^0}, m_{\tilde{\chi}_1^0})$ plane.

[107] BARATE 98H looked for $\gamma\gamma$ $\not{E}$ final states at $\sqrt{s}$ = 161,172 GeV. They obtained an upper bound on the cross section for the production $e^+e^- \to \tilde{\chi}_2^0\tilde{\chi}_2^0$ followed by the prompt decay $\tilde{\chi}_2^0 \to \gamma\tilde{\chi}_1^0$ of 0.4–0.8 pb for $m_{\tilde{\chi}_2^0}$ = 10–80 GeV. The bound above is for the specific case of $\tilde{\chi}_1^0 = \tilde{H}^0$ and $\tilde{\chi}_2^0 = \tilde{\gamma}$ and $m_{\tilde{e}_R}$ = 100 GeV. See Fig. 6 and 7 for explicit limits in the $(\tilde{\chi}_2^0, \tilde{\chi}_1^0)$ plane and in the $(\tilde{\chi}_2^0, \tilde{e}_R)$ plane.

[108] BARATE 98J looked for $\gamma\gamma$ $\not{E}$ final states at $\sqrt{s}$ = 161–183 GeV. They obtained an upper bound on the cross section for the production $e^+e^- \to \tilde{\chi}_2^0\tilde{\chi}_2^0$ followed by the prompt decay $\tilde{\chi}_2^0 \to \gamma\tilde{\chi}_1^0$ of 0.08–0.24 pb for $m_{\tilde{\chi}_2^0} < 91$ GeV. The bound above is for the specific case of $\tilde{\chi}_1^0 = \tilde{H}^0$ and $\tilde{\chi}_2^0 = \tilde{\gamma}$ and $m_{\tilde{e}_R}$ = 100 GeV.

[109] ABACHI 96 searches for 3-lepton final states. Efficiencies are calculated using mass relations and branching ratios in the Minimal Supergravity scenario. Results are presented as lower bounds on $\sigma(\tilde{\chi}_1^\pm\tilde{\chi}_2^0) \times$ B($\tilde{\chi}_1^\pm \to \ell\nu_\ell\tilde{\chi}_1^0$) × B($\tilde{\chi}_2^0 \to \ell^+\ell^-\tilde{\chi}_1^0$) as a function of $m_{\tilde{\chi}_1^0}$. Limits range from 3.1 pb ($m_{\tilde{\chi}_1^0}$ = 45 GeV) to 0.6 pb ($m_{\tilde{\chi}_1^0}$ = 100 GeV).

[110] ABE 96K looked for trilepton events from chargino-neutralino production. They obtained lower bounds on $m_{\tilde{\chi}_2^0}$ as a function of μ. The lower bounds are in the 45–50 GeV range for gaugino-dominant $\tilde{\chi}_2^0$ with negative μ, if tanβ <10. See paper for more details of the assumptions.

$\tilde{\chi}_1^\pm$, $\tilde{\chi}_2^\pm$ (Charginos) MASS LIMITS

Charginos are unknown mixtures of w-inos and charged higgsinos (the supersymmetric partners of W and Higgs bosons). A lower mass limit for the lightest chargino ($\tilde{\chi}_1^\pm$) of approximately 45 GeV, independent of the field composition and of the decay mode, has been obtained by the LEP experiments from the analysis of the Z width and decays. These results, as well as other now superseded limits from e^+e^- collisions at energies below 136 GeV, and from hadronic collisions, can be found in the 1998 Edition (The European Physical Journal **C3** 1 (1998)) of this Review.

Unless otherwise stated, results in this section assume spectra, production rates, decay modes and branching ratios as evaluated in the MSSM, with gaugino and sfermion mass unification at the GUT scale. These papers generally study production of $\tilde{\chi}_1^0\tilde{\chi}_2^0$, $\tilde{\chi}_1^+\tilde{\chi}_1^-$ and (in the case of hadronic collisions) $\tilde{\chi}_1^+\tilde{\chi}_2^0$ pairs, including the effects of cascade decays. The mass limits on $\tilde{\chi}_1^\pm$ are either direct, or follow indirectly from the constraints set by the non-observation of $\tilde{\chi}_2^0$ states on the gaugino and higgsino MSSM parameters M_2 and μ. For generic values of the MSSM parameters, limits from high-energy e^+e^- collisions coincide with the highest value of the mass allowed by phase-space, namely $m_{\tilde{\chi}_1^\pm} \lesssim \sqrt{s}/2$. At the time of this writing, preliminary and

unpublished results from the 2000 run of LEP2 at $\sqrt{s}$ up to $\simeq$ 209 GeV give therefore a lower mass limit of approximately 104 GeV valid for general MSSM models. The limits become however weaker in special regions of the MSSM parameter space where the detection efficiencies or production cross sections are suppressed. For example, this may happen when: (i) the mass differences $\Delta m_+ = m_{\widetilde{\chi}_1^\pm} - m_{\widetilde{\chi}_1^0}$ or $\Delta m_\nu = m_{\widetilde{\chi}_1^\pm} - m_{\widetilde{\nu}}$ are very small, and the detection efficiency is reduced; (ii) the electron sneutrino mass is small, and the $\widetilde{\chi}_1^\pm$ production rate is suppressed due to a destructive interference between s and t channel exchange diagrams. The regions of MSSM parameter space where the following limits are valid are indicated in the comment lines or in the footnotes.

VALUE (GeV)	CL%	DOCUMENT ID		TECN	COMMENT
> 89	95	[111] ABBIENDI	03H	OPAL	$0.5 \leq \Delta m_+ \leq 5$ GeV,higgsino-like, tanβ=1.5
> 97.1	95	[112] ABDALLAH	03M	DLPH	$\widetilde{\chi}_1^\pm$, $\Delta m_+ \geq 3$ GeV, $m_{\widetilde{\nu}} > m_{\widetilde{\chi}^\pm}$
> 75	95	[112] ABDALLAH	03M	DLPH	$\widetilde{\chi}_1^\pm$,higgsino,all Δm_+,$m_{\widetilde{f}} > m_{\widetilde{\chi}^\pm}$
> 70	95	[112] ABDALLAH	03M	DLPH	$\widetilde{\chi}_1^\pm$, all Δm_+, $m_{\widetilde{\nu}}$ >500 GeV, $M_2 \leq 2M_1 \leq 10M_2$
> 94	95	[113] ABDALLAH	03M	DLPH	$\widetilde{\chi}_1^\pm$, tan$\beta \leq 40$, $\Delta m_+ > 3$ GeV,all m_0
> 88	95	[114] HEISTER	02J	ALEP	$\widetilde{\chi}_1^\pm$, all Δm_+, large m_0
> 71.7	95	[115] ABBIENDI	00H	OPAL	tanβ=35, $\Delta m_+ > 5$ GeV, all m_0
> 67.7	95	[116] ACCIARRI	00D	L3	tan$\beta > 0.7$, all Δm_+, all m_0
> 69.4	95	[117] ACCIARRI	00K	L3	$e^+e^- \to \widetilde{\chi}^\pm\widetilde{\chi}^\mp$, all Δm_+, heavy scalars
• • • We do not use the following data for averages, fits, limits, etc. • • •					
>100	95	[118] ABDALLAH	03D	DLPH	$e^+e^- \to \widetilde{\chi}_1^\pm\widetilde{\chi}_1^\mp$ ($\widetilde{\chi}_1^\pm \to \widetilde{\tau}_1\nu_\tau$,$\widetilde{\tau}_1 \to \tau\widetilde{G}$)
>103	95	[119] HEISTER	03G	ALEP	$R\!\!\!/$ decays, $m_0 > 500$ GeV
>102.7	95	[120] ACHARD	02	L3	$R\!\!\!/$, MSUGRA
		[121] GHODBANE	02	THEO	
> 94.3	95	[122] ABREU	01C	DLPH	$\widetilde{\chi}^\pm \to \tau J$
> 94	95	[123] ABREU	01D	DLPH	$R(\overline{UDD})$, all Δm_0, $0.5 \leq \tan\beta \leq 30$
> 93.8	95	[124] ACCIARRI	01	L3	$R\!\!\!/$, all m_0, $0.7 \leq \tan\beta \leq 40$
>100	95	[125] BARATE	01B	ALEP	$R\!\!\!/$ decays, $m_0 > 500$ GeV
> 94	95	[126] ABREU	00U	DLPH	$R\!\!\!/$ ($LL\overline{E}$), all Δm_0, $1 \leq \tan\beta \leq 30$
> 91.8	95	[127] ABREU	00V	DLPH	$e^+e^- \to \widetilde{\chi}_1^\pm\widetilde{\chi}_1^\pm$ ($\widetilde{\chi}_1^\pm \to \widetilde{\tau}_1\nu_\tau$, $\widetilde{\tau}_1 \to \tau\widetilde{G}$)
		[128] CHO	00B	THEO	EW analysis
> 76	95	[129] ABBIENDI	99T	OPAL	$R\!\!\!/$, m_0=500 GeV
>120	95	[130] ABE	99I	CDF	$p\overline{p} \to \widetilde{\chi}\widetilde{\chi}$, $\widetilde{\chi}$=$\widetilde{\chi}_{1,2}^0$,$\widetilde{\chi}_1^\pm$, $\widetilde{\chi}_1^0 \to \gamma\widetilde{G}$
> 51	95	[131] MALTONI	99B	THEO	EW analysis, $\Delta m_+ \sim 1$ GeV
>150	95	[132] ABBOTT	98	D0	$p\overline{p} \to \widetilde{\chi}\widetilde{\chi}$, $\widetilde{\chi}$=$\widetilde{\chi}_{1,2}^0$,$\widetilde{\chi}_1^\pm$, $\widetilde{\chi}_1^0 \to \gamma\widetilde{G}$
		[133] ABBOTT	98C	D0	$p\overline{p} \to \widetilde{\chi}_1^\pm\widetilde{\chi}_2^0$
> 81.5	95	[134] ABE	98J	CDF	$p\overline{p} \to \widetilde{\chi}_1^\pm\widetilde{\chi}_2^0$
		[135] ACKERSTAFF	98K	OPAL	$\widetilde{\chi}^+ \to \ell^+ \not{E}$
> 65.7	95	[136] ACKERSTAFF	98L	OPAL	$\Delta m_+ > 3$ GeV, $\Delta m_\nu > 2$ GeV
		[137] ACKERSTAFF	98V	OPAL	light gluino
		[138] CARENA	97	THEO	$g_\mu - 2$
		[139] KALINOWSKI	97	THEO	$W \to \widetilde{\chi}_1^\pm\widetilde{\chi}_1^0$
		[140] ABE	96K	CDF	$p\overline{p} \to \widetilde{\chi}_1^\pm\widetilde{\chi}_2^0$

[111] ABBIENDI 03H used e^+e^- data at $\sqrt{s}$ = 188-209 GeV to search for chargino pair production in the case of small Δm_+. They select events with an energetic photon, large $\not{E}$ and little hadronic or leptonic activity. The bound applies to higgsino-like charginos with zero lifetime and a 100% branching ratio $\widetilde{\chi}_1^\pm \to \widetilde{\chi}_1^0 W^*$. The mass limit for gaugino-like charginos, in case of non-universal gaugino masses, is of 92 GeV for $m_{\widetilde{\nu}} = 1000$ GeV and is lowered to 74 GeV for $m_{\widetilde{\nu}} \geq 100$ GeV. Limits in the plane $(m_{\widetilde{\chi}_1^\pm}, \Delta m_+)$ are shown in Fig. 7. Exclusion regions are also derived for the AMSB scenario in the $(m_{3/2}, \tan\beta)$ plane, see their Fig. 9.

[112] ABDALLAH 03M searches for the production of charginos using data from $\sqrt{s}$= 192 to 208 GeV to investigate topologies with multiple leptons, jets plus leptons, multi-jets, or isolated photons. The first limit holds for tan$\beta \geq 1$ and is obtained at $\Delta m_+ = 3$ GeV in the higgsino region. For $\Delta m_+ \geq 10$ (5) GeV and large m_0, the limit improves to 102.7 (101.7) GeV. For the region of small Δm_+, all data from $\sqrt{s}$= 130 to 208 GeV are used to investigate final states with heavy stable charged particles, decay vertices inside the detector and soft topologies with a photon from initial state radiation. The second limit is obtained in the higgsino region, assuming gaugino mass universality at the GUT scale and $1 < \tan\beta < 50$. For the case of non-universality of gaugino masses, the parameter space is scanned in the domain $1 < \tan\beta < 50$ and, for $\Delta m_+ < 3$ GeV, for values of M_1, M_2 and μ such that $M_2 \leq 2M_1 \leq 10M_2$ and $|\mu| \geq M_2$. The third limit is obtained in the gaugino region. See Fig. 36 for the dependence of the low Δm_+ limits on Δm_+. These limits include and update the results of ABREU 00J and ABREU 00T.

[113] ABDALLAH 03M uses data from $\sqrt{s}$ = 192–208 GeV to obtain limits in the framework of the MSSM with gaugino and sfermion mass universality at the GUT scale. An indirect limit on the mass of charginos is derived by constraining the MSSM parameter space by the results from direct searches for neutralinos (including cascade decays), for charginos and for sleptons. These limits are valid for values of $M_2 < 1$ TeV, $|\mu| \leq 2$ TeV with the $\widetilde{\chi}_1^0$ as LSP. Constraints from the Higgs search in the M_h^{max} scenario assuming m_t=174.3 GeV are included. The quoted limit applies if there is no mixing in the third family or when $m_{\widetilde{\tau}_1} - m_{\widetilde{\chi}_1^0} > 6$ GeV. If mixing is included the limit degrades to 90 GeV. See Fig. 43 for the mass limits as a function of tanβ. These limits update the results of ABREU 00W.

[114] HEISTER 02J search for chargino production with small Δm_+ in final states with a hard isolated initial state radiation photon and few low-momentum particles, using 189–208 GeV data. This search is sensitive in the intermediate Δm_+ region. Combined with searches for $\not{E}$ topologies and for stable charged particles, the above bound is obtained for m_0 larger than few hundred GeV, $1 < \tan\beta < 300$ and holds for any chargino field contents. For light scalars, the general limit reduces to the one from the Z^0, but under the assumption of gaugino and sfermion mass unification the above bound is recovered. See Figs. 4–6 for the more general dependence of the limits on Δm_+. Updates BARATE 98X.

[115] ABBIENDI 00H data collected at $\sqrt{s}$=189 GeV. The results hold over the full parameter space defined by $0 \leq M_2 \leq 2$ TeV, $|\mu| \leq 500$ GeV, $m_0 \leq 500$ GeV, A=$\pm M_2$, $\pm m_0$, and 0. The results of slepton searches from ABBIENDI 00G were used to help set constraints in the region of small m_0. The limit improves to 78 GeV for tanβ=1.5. See their Table 5 and Fig. 4 for the tanβ and M_2 dependence of the limits. Updates ABBIENDI 99G.

[116] ACCIARRI 00D data collected at $\sqrt{s}$=189 GeV. The results hold over the full parameter space defined by $0.7 \leq \tan\beta \leq 60$, $0 \leq M_2 \leq 2$ TeV, $|\mu| \leq 2$ TeV $m_0 \leq 500$ GeV. The results of slepton searches from ACCIARRI 99W are used to help set constraints in the region of small m_0. See their Figs. 5 for the tanβ and M_2 dependence on the limits. See the text for the impact of a large B($\widetilde{\chi}^\pm \to \tau\widetilde{\nu}_\tau$) on the result. The region of small Δm_+ is excluded by the analysis of ACCIARRI 00K. Updates ACCIARRI 98F.

[117] ACCIARRI 00K searches for the production of charginos with small Δm_+ using data from $\sqrt{s}$=189 GeV. They investigate soft final states with a photon from initial state radiation. The results are combined with the limits on prompt decays from ACCIARRI 00D and from heavy stable charged particles from ACCIARRI 99L (see Heavy Charged Lepton Searches). The production and decay branching ratios are evaluated within the MSSM, assuming heavy sfermions. The parameter space is scanned in the domain $1 < \tan\beta < 50$, $0.3 < M_1/M_2 < 50$, and $0 < |\mu| < 2$ TeV. The limit is obtained in the higgsino region and improves to 78.6 GeV for gaugino-like charginos. The limit is unchanged for light scalar quarks. For light $\widetilde{\tau}$ or $\widetilde{\nu}_\tau$, the limit is unchanged in the gaugino-like region and is lowered by 0.8 GeV in the higgsino-like case. For light $\widetilde{\mu}$ or $\widetilde{\nu}_\mu$, the limit is unchanged in the higgsino-like region and is lowered by 0.9 GeV in the gaugino-like region. No direct mass limits are obtained for light $\widetilde{e}$ or $\widetilde{\nu}_e$.

[118] ABDALLAH 03D use data from $\sqrt{s}$= 183-208 GeV. They look for final states with two acoplanar leptons, expected in GMSB when the $\widetilde{\tau}_1$ is the NLSP and assuming a short-lived $\widetilde{\chi}_1^\pm$. Limits are obtained in the plane (m($\widetilde{\tau}$),m($\widetilde{\chi}_1^\pm$)) for different domains of m($\widetilde{G}$), after combining these results with the search for slepton pair production from the same paper. The limit above is valid if the $\widetilde{\tau}_1$ is the NLSP for all values of m($\widetilde{G}$) provided $m(\widetilde{\chi}_1^\pm) - m(\widetilde{\tau}_1) \geq 0.3$ GeV. For larger m($\widetilde{G}$) > 100 eV the limit improves to 102 GeV, see their Fig. 11. In the co-NLSP scenario, the limits are 96 and 102 GeV for all m($\widetilde{G}$) and m($\widetilde{G}$) > 100 eV, respectively. Supersedes the results of ABREU 01G.

[119] HEISTER 03G searches for the production of charginos prompt decays. in the case of $R\!\!\!/$ prompt decays with $LL\overline{E}$, $LQ\overline{D}$ or $\overline{UDD}$ couplings at $\sqrt{s}$=189–209 GeV. The search is performed for indirect decays, assuming one coupling at a time to be non-zero. The limit holds for tanβ = 1.41. Excluded regions in the (μ, M_2) plane are shown in their Fig. 3.

[120] ACHARD 02 searches for the production of sparticles in the case of $R\!\!\!/$ prompt decays with $LL\overline{E}$ or $\overline{UDD}$ couplings at $\sqrt{s}$=189–208 GeV. The search is performed for direct and indirect decays, assuming one coupling at the time to be nonzero. The MSUGRA limit results from a scan over the MSSM parameter space with the assumption of gaugino and scalar mass unification at the GUT scale, imposing simultaneously the exclusions from neutralino, chargino, sleptons, and squarks analyses. The limit of $\widetilde{\chi}_1^\pm$ holds for $\overline{UDD}$ couplings and increases to 103.0 GeV for $LL\overline{E}$ couplings. For L3 limits from $LQ\overline{D}$ couplings, see ACCIARRI 01.

[121] GHODBANE 02 reanalyzes DELPHI data at $\sqrt{s}$=189 GeV in the presence of complex phases for the MSSM parameters.

[122] ABREU 01C looked for τ pairs with $\not{E}$ at $\sqrt{s}$=183–189 GeV to search for the associated production of charginos, followed by the decay $\widetilde{\chi}^\pm \to \tau J$, J being an invisible massless particle. See Fig. 6 for the regions excluded in the (μ,M_2) plane.

[123] ABREU 01D searches for multi-jet events, expected in the case of prompt decays from R-parity violating $\overline{UDD}$ couplings, using data from $\sqrt{s}$=189 GeV. They investigate topologies with 6 or 10 jets, originating from direct or indirect decays. Limits are obtained in the M_2 versus μ plane and a limit on the chargino mass is derived from a scan over the parameters m_0 and tanβ.

[124] ACCIARRI 01 searches for multi-lepton and/or multi-jet final states from $R\!\!\!/$ prompt decays with $LL\overline{E}$, $LQ\overline{D}$, or $\overline{UDD}$ couplings at $\sqrt{s}$=189 GeV. The search is performed for direct and indirect decays of neutralinos, charginos, and scalar leptons, with the $\widetilde{\chi}_1^0$ or a $\widetilde{\ell}$ as LSP and assuming one coupling to be nonzero at a time. Mass limits are derived using simultaneously the constraints from the neutralino, chargino, and slepton analyses; and the Z^0 width measurements from ACCIARRI 00C in a scan of the parameter space assuming MSUGRA with gaugino and scalar mass universality. Updates and supersedes the results from ACCIARRI 99I.

[125] BARATE 01B searches for the production of charginos in the case of $R\!\!\!/$ prompt decays with $LL\overline{E}$, $LQ\overline{D}$, or $\overline{UDD}$ couplings at $\sqrt{s}$=189–202 GeV. The search is performed for indirect decays, assuming one coupling at a time to be nonzero. Updates BARATE 00H.

[126] ABREU 00U searches for the production of charginos and neutralinos in the case of R-parity violation with $LL\overline{E}$ couplings, using data from $\sqrt{s}$=189 GeV. They investigate topologies with multiple leptons or jets plus leptons, assuming one coupling to be nonzero at the time and giving rise to direct or indirect decays. Limits are obtained in the M_2 versus μ plane and a limit on the neutralino mass is derived from a scan over the parameters m_0 and tanβ. Supersedes the results of ABREU 00I.

[127] ABREU 00V use data from $\sqrt{s}$= 183–189 GeV. They look for final states with two acoplanar leptons, expected in GMSB when the $\widetilde{\tau}_1$ is the NLSP and assuming a short-lived $\widetilde{\chi}_1^\pm$. Limits are obtained in the plane $(m_{\widetilde{\tau}}, m_{\widetilde{\chi}_1^\pm})$ for different domains of $m_{\widetilde{G}}$, after combining these results with the search for slepton pair production in the SUGRA framework from ABREU 01 to cover prompt decays and on stable particle searches from ABREU 00Q. The limit above is valid for all values of $m_{\widetilde{G}}$.

[128] CHO 00B studied constraints on the MSSM spectrum from precision EW observables. Global fits favour charginos with masses at the lower bounds allowed by direct searches. Allowing for variations of the squark and slepton masses does not improve the fits.

[129] ABBIENDI 99T searches for the production of neutralinos in the case of R-parity violation with $LL\overline{E}$, $LQ\overline{D}$, or $\overline{UDD}$ couplings using data from $\sqrt{s}$=183 GeV. They investigate

topologies with multiple leptons, jets plus leptons, or multiple jets, assuming one coupling at the time to be non-zero and giving rise to direct or indirect decays. Mixed decays (where one particle has a direct, the other an indirect decay) are also considered for the $\overline{UDD}$ couplings. Upper limits on the cross section are derived which, combined with the constraint from the Z^0 width, allow to exclude regions in the M_2 versus μ plane for any coupling. Limits on the chargino mass are obtained for non-zero $LL\overline{E}$ couplings $> 10^{-5}$ and assuming decays via a W^*.

130 ABE 99I looked for chargino and neutralino production, where the lightest neutralino in their decay products further decays into $\gamma\,\widetilde{G}$. The limit assumes the gaugino mass unification, and holds for $1 < \tan\beta < 25$, $M_2 < 200$ GeV, and all μ. ABE 99I is an expanded version of ABE 98L.

131 MALTONI 99B studied the effect of light chargino-neutralino to the electroweak precision data with a particular focus on the case where they are nearly degenerate ($\Delta m_{\pm} \sim 1$ GeV) which is difficult to exclude from direct collider searches. The quoted limit is for higgsino-like case while the bound improves to 56 GeV for wino-like case. The values of the limits presented here are obtained in an update to MALTONI 99B, as described in MALTONI 00.

132 ABBOTT 98 studied the chargino and neutralino production, where the lightest neutralino in their decay products further decays into $\gamma\,\widetilde{G}$. The limit assumes the gaugino mass unification.

133 ABBOTT 98C searches for trilepton final states (ℓ=e,μ). Efficiencies are calculated using mass relations in the Minimal Supergravity scenario, exploring the domain of parameter space defined by $m_{\widetilde{\chi}_1^\pm}=m_{\widetilde{\chi}_2^0}$ and $m_{\widetilde{\chi}_1^\pm}=2m_{\widetilde{\chi}_1^0}$. Results are presented in Fig. 1 as upper bounds on $\sigma(p\overline{p} \to \widetilde{\chi}_1^\pm\widetilde{\chi}_2^0)\times B(3\ell)$. Assuming equal branching ratio for all possible leptonic decays, limits range from 2.6 pb ($m_{\widetilde{\chi}_1^\pm}$=45 GeV) to 0.4 pb ($m_{\widetilde{\chi}_1^\pm}$=124 GeV) at 95%CL. Assuming a negligible decay rate of $\widetilde{\chi}_1^\pm$ and $\widetilde{\chi}_2^0$ to quarks, this corresponds to $m_{\widetilde{\chi}_1^\pm} > 103$ GeV.

134 ABE 98J searches for trilepton final states (ℓ=e,μ). Efficiencies are calculated using mass relations in the Minimal Supergravity scenario, exploring the domain of parameter space defined by $1.1 < \tan\beta < 8$, $-1000 < \mu(\text{GeV}) < -200$, and $m_{\widetilde{q}}/m_{\widetilde{g}}$=1–2. In this region $m_{\widetilde{\chi}_1^\pm} \sim m_{\widetilde{\chi}_2^0}$ and $m_{\widetilde{\chi}_1^\pm} \sim 2m_{\widetilde{\chi}_1^0}$. Results are presented in Fig. 1 as upper bounds on $\sigma(p\overline{p} \to \widetilde{\chi}_1^\pm\widetilde{\chi}_2^0)\times B(3\ell)$. Limits range from 0.8 pb ($m_{\widetilde{\chi}_1^\pm}$=50 GeV) to 0.23 pb ($m_{\widetilde{\chi}_1^\pm}$=100 GeV) at 95%CL. The gaugino mass unification hypothesis and the assumed mass relation between squarks and gluinos define the value of the leptonic branching ratios. The quoted result corresponds to the best limit within the selected range of parameters, obtained for $m_{\widetilde{q}} > m_{\widetilde{g}}$, $\tan\beta$=2, and μ=−600 GeV. Mass limits for different values of $\tan\beta$ and μ are given in Fig. 2.

135 ACKERSTAFF 98K looked for dilepton+$\not{E}_T$ final states at $\sqrt{s}$=130–172 GeV. Limits on $\sigma(e^+e^- \to \widetilde{\chi}_1^+\widetilde{\chi}_1^-)\times B^2(\ell)$, with $B(\ell)=B(\chi^+ \to \ell^+\nu_\ell\chi_1^0)$ ($B(\ell)=B(\chi^+ \to \ell^+\overline{\nu}_\ell)$), are given in Fig. 16 (Fig. 17).

136 ACKERSTAFF 98L limit is obtained for $0 < M_2 < 1500$, $|\mu| < 500$ and $\tan\beta > 1$, but remains valid outside this domain. The dependence on the trilinear-coupling parameter A is studied, and found negligible. The limit holds for the smallest value of m_0 consistent with scalar lepton constraints (ACKERSTAFF 97H) and for all values of m_0 where the condition $\Delta m_{\widetilde{\nu}} > 2.0$ GeV is satisfied. $\Delta m_{\widetilde{\nu}} > 10$ GeV if $\widetilde{\chi}^\pm \to \ell\,\widetilde{\nu}_\ell$. The limit improves to 84.5 GeV for m_0=1 TeV. Data taken at $\sqrt{s}$=130–172 GeV.

137 ACKERSTAFF 98V excludes the light gluino with universal gaugino mass where charginos, neutralinos decay as $\widetilde{\chi}_1^\pm, \widetilde{\chi}_2^0 \to q\overline{q}\,\widetilde{g}$ from total hadronic cross sections at $\sqrt{s}$=130–172 GeV. See paper for the case of nonuniversal gaugino mass.

138 CARENA 97 studied the constraints on chargino and sneutrino masses from muon $g-2$. The bound can be important for large $\tan\beta$.

139 KALINOWSKI 97 studies the constraints on the chargino-neutralino parameter space from limits on $\Gamma(W \to \widetilde{\chi}_1^\pm\widetilde{\chi}_1^0)$ achievable at LEP2. This is relevant when $\widetilde{\chi}_1^\pm$ is "invisible," i.e., if $\widetilde{\chi}_1^\pm$ dominantly decays into $\widetilde{\nu}_\ell\ell^\pm$ with little energy for the lepton. Small otherwise allowed regions could be excluded.

140 ABE 96K looked for trilepton events from chargino-neutralino production. The bound on $m_{\widetilde{\chi}_1^\pm}$ can reach up to 47 GeV for specific choices of parameters. The limits on the combined production cross section times 3-lepton branching ratios range between 1.4 and 0.4 pb, for $45 < m_{\widetilde{\chi}_1^\pm}(\text{GeV}) < 100$. See the paper for more details on the parameter dependence of the results.

Long-lived $\widetilde{\chi}^\pm$ (Chargino) MASS LIMITS

Limits on charginos which leave the detector before decaying.

VALUE (GeV)	CL%		DOCUMENT ID		TECN	COMMENT
>102	95	141	ABBIENDI	03L	OPAL	$m_{\widetilde{\nu}}$ >500 GeV
none 2–93.0	95	142	ABREU	00T	DLPH	$\widetilde{H}^\pm$ or $m_{\widetilde{\nu}} > m_{\widetilde{\chi}^\pm}$
• • • We do not use the following data for averages, fits, limits, etc. • • •						
> 83	95	143	BARATE	97K	ALEP	
> 28.2	95		ADACHI	90C	TOPZ	

141 ABBIENDI 03L used e^+e^- data at $\sqrt{s}$ = 130-209 GeV to select events with two high momentum tracks with anomalous dE/dx. The excluded cross section is compared to the theoretical expectation as a function of the heavy particle mass in their Fig. 3. The bounds are valid for colorless fermions with lifetime longer than 10^{-6} s. Supersedes the results from ACKERSTAFF 98P.

142 ABREU 00T searches for the production of heavy stable charged particles, identified by their ionization or Cherenkov radiation, using data from $\sqrt{s}$= 130 to 189 GeV. These limits include and update the results of ABREU 98P.

143 BARATE 97K uses e^+e^- data collected at $\sqrt{s}$ = 130–172 GeV. Limit valid for $\tan\beta = \sqrt{2}$ and $m_{\widetilde{\nu}} > 100$ GeV. The limit improves to 86 GeV for $m_{\widetilde{\nu}} > 250$ GeV.

$\widetilde{\nu}$ (Sneutrino) MASS LIMIT

The limits may depend on the number, $N(\widetilde{\nu})$, of sneutrinos assumed to be degenerate in mass. Only $\widetilde{\nu}_L$ (not $\widetilde{\nu}_R$) is assumed to exist. It is possible that $\widetilde{\nu}$ could be the lightest supersymmetric particle (LSP).

We report here, but do not include in the Listings, the limits obtained from the final, but unpublished, fit of the final results obtained by the LEP Collaborations on the invisible width of the Z boson ($\Delta\Gamma_{\text{inv.}} < 2.0$ MeV, LEP 03): $m_{\widetilde{\nu}} > 43.7$ GeV ($N(\widetilde{\nu})$=1) and $m_{\widetilde{\nu}} > 44.7$ GeV ($N(\widetilde{\nu})$=3) .

VALUE (GeV)	CL%		DOCUMENT ID		TECN	COMMENT
> 94	95	144	ABDALLAH	03M	DLPH	$1 \leq \tan\beta \leq 40$, $m_{\widetilde{e}_R} - m_{\widetilde{\chi}_1^0} > 10$ GeV
> 84	95	145	HEISTER	02N	ALEP	$\widetilde{\nu}_e$, any Δm
> 37.1	95	146	ADRIANI	93M	L3	$\Gamma(Z \to$ invisible); $N(\widetilde{\nu})$=1
> 41	95	147	DECAMP	92	ALEP	$\Gamma(Z \to$ invisible); $N(\widetilde{\nu})$=3
> 36	95		ABREU	91F	DLPH	$\Gamma(Z \to$ invisible); $N(\widetilde{\nu})$=1
> 31.2	95	148	ALEXANDER	91F	OPAL	$\Gamma(Z \to$ invisible); $N(\widetilde{\nu})$=1
• • • We do not use the following data for averages, fits, limits, etc. • • •						
		149	ABDALLAH	03F	DLPH	$\widetilde{\nu}_{\mu,\tau}$, $\not{R}$ $LL\overline{E}$ decays
		150	ACOSTA	03E	CDF	$\widetilde{\nu}$, $\not{R}$, $LQ\overline{D}$ production and $LL\overline{E}$ decays
> 88	95	151	HEISTER	03G	ALEP	$\widetilde{\nu}_e$, $\not{R}$ decays, μ=−200 GeV, $\tan\beta$=2
> 65	95	151	HEISTER	03G	ALEP	$\widetilde{\nu}_{\mu,\tau}$, $\not{R}$ decays
		152	ABAZOV	02H	D0	$\not{R}$, λ'_{211}
> 95	95	153	ACHARD	02	L3	$\widetilde{\nu}_e$, $\not{R}$ decays, μ=−200 GeV, $\tan\beta=\sqrt{2}$
> 65	95	153	ACHARD	02	L3	$\widetilde{\nu}_{\nu,\tau}$, $\not{R}$ decays
>149	95	153	ACHARD	02	L3	$\widetilde{\nu}$, $\not{R}$ decays, MSUGRA
		154	HEISTER	02F	ALEP	$e\gamma \to \widetilde{\nu}_{\mu,\tau}\ell_k$, $\not{R}$ $LL\overline{E}$
		155	ABBIENDI	00	OPAL	$\widetilde{\nu}_{e,\mu}$, $\not{R}$, $LL\overline{E}$ or $LQ\overline{D}$ decays
none 100–264	95	156	ABBIENDI	00R	OPAL	$\widetilde{\nu}_{\mu,\tau}$, $\not{R}$, (s+t)-channel
none 100–200	95	157	ABBIENDI	00R	OPAL	$\widetilde{\nu}_\tau$, $\not{R}$, s-channel
		158	ABREU	00S	DLPH	$\widetilde{\nu}_\ell$, $\not{R}$, (s+t)-channel
> 76.5	95	159	ABREU	00U	DLPH	$\widetilde{\nu}_\ell$, $\not{R}$ ($LL\overline{E}$)
none 50–210	95	160	ACCIARRI	00P	L3	$\widetilde{\nu}_{\mu,\tau}$, $\not{R}$, s-channel
none 50–210	95	161	BARATE	00I	ALEP	$\widetilde{\nu}_{\mu,\tau}$, $\not{R}$, (s+t)-channel
none 90–210	95	162	BARATE	00I	ALEP	$\widetilde{\nu}_\tau$, $\not{R}$, s-channel
none 100–160	95	163	ABBIENDI	99	OPAL	$\widetilde{\nu}_e$, $\not{R}$, t-channel
$\neq m_Z$	95	164	ACCIARRI	97U	L3	$\widetilde{\nu}_\tau$, $\not{R}$, s-channel
none 125–180	95	164	ACCIARRI	97U	L3	$\widetilde{\nu}_\tau$, $\not{R}$, s-channel
		165	CARENA	97	THEO	$g_\mu - 2$
> 46.0	95	166	BUSKULIC	95E	ALEP	$N(\widetilde{\nu})$=1, $\widetilde{\nu} \to \nu\nu\ell\overline{\ell}'$
none 20–25000		167	BECK	94	COSM	Stable $\widetilde{\nu}$, dark matter
<600		168	FALK	94	COSM	$\widetilde{\nu}$ LSP, cosmic abundance
none 3–90	90	169	SATO	91	KAMI	Stable $\widetilde{\nu}_e$ or $\widetilde{\nu}_\mu$, dark matter
none 4–90	90	169	SATO	91	KAMI	Stable $\widetilde{\nu}_\tau$, dark matter

144 ABDALLAH 03M uses data from $\sqrt{s}$ = 192–208 GeV to obtain limits in the framework of the MSSM with gaugino and sfermion mass universality at the GUT scale. An indirect limit on the mass is derived by constraining the MSSM parameter space by the results from direct searches for neutralinos (including cascade decays) and for sleptons. These limits are valid for values of $M_2 < 1$ TeV, $|\mu| \leq 1$ TeV with the $\widetilde{\chi}_1^0$ as LSP. The quoted limit is obtained when there is no mixing in the third family. See Fig. 43 for the mass limits as a function of $\tan\beta$. These limits update the results of ABREU 00W.

145 HEISTER 02N derives a bound on $m_{\widetilde{\nu}_e}$ by exploiting the mass relation between the $\widetilde{\nu}_e$ and $\widetilde{e}$, based on the assumption of universal GUT scale gaugino and scalar masses $m_{1/2}$ and m_0 and the search described in the $\widetilde{e}$ section. In the MSUGRA framework with radiative electroweak symmetry breaking, the limit improves to $m_{\widetilde{\nu}_e} > 130$ GeV, assuming a trilinear coupling A_0=0 at the GUT scale. See Figs. 5 and 7 for the dependence of the limits on $\tan\beta$.

146 ADRIANI 93M limit from $\Delta\Gamma(Z)$(invisible)< 16.2 MeV.

147 DECAMP 92 limit is from Γ(invisible)/$\Gamma(\ell\ell) = 5.91 \pm 0.15$ ($N_\nu = 2.97 \pm 0.07$).

148 ALEXANDER 91F limit is for one species of $\widetilde{\nu}$ and is derived from Γ(invisible, new)/$\Gamma(\ell\ell)$ < 0.38.

149 ABDALLAH 03F looked for events of the type $e^+e^- \to \widetilde{\nu} \to \widetilde{\chi}^0\nu$, $\widetilde{\chi}^\pm\ell^\mp$ followed by $\not{R}$ decays of the $\widetilde{\chi}^0$ via λ_{1j1} (j = 2,3) couplings in the data at $\sqrt{s}$= 183-208 GeV. From a scan over the SUGRA parameters, they derive upper limits on the λ_{1j1} couplings as a function of the sneutrino mass, see their Figs. 5-8.

150 ACOSTA 03E search for $e\mu$, $e\tau$ and $\mu\tau$ final states, and sets limits on the product of production cross-section and decay branching ratio for a $\widetilde{\nu}$ in RPV models (see Fig. 3).

151 HEISTER 03G searches for the production of sneutrinos in the case of $\not{R}$ prompt decays with $LL\overline{E}$, $LQ\overline{D}$ or $\overline{UDD}$ couplings at $\sqrt{s}$=189–209 GeV. The search is performed for direct and indirect decays, assuming one coupling at a time to be non-zero. The limit holds for indirect $\overline{\nu}$ decays via $\overline{UDD}$ couplings and $\Delta m > 10$ GeV. Stronger limits are reached for ($\overline{\nu}_e$,$\overline{\nu}_{\mu,\tau}$) for $LL\overline{E}$ direct (100,90) GeV or indirect (98,89) GeV and for $LQ\overline{D}$ direct (−,79) GeV or indirect (91,78) GeV couplings. For $LL\overline{E}$ indirect decays, use is made of the bound $m(\widetilde{\chi}_1^0) > 23$ GeV from BARATE 98S. Supersedes the results from BARATE 01B.

152 ABAZOV 02H looked in 94 pb^{-1} of $p\overline{p}$ collisions at $\sqrt{s}$=1.8 TeV for events with at least 2 muons and 2 jets for s-channel production of $\widetilde{\mu}$ or $\widetilde{\nu}$ and subsequent decay via $\not{R}$ couplings $LQ\overline{D}$. A scan over the MSUGRA parameters is performed to exclude regions of the $(m_0, m_{1/2})$ plane, examples being shown in Fig. 2.

[153] ACHARD 02 searches for the associated production of sneutrinos in the case of $R\!\!\!/$ prompt decays with $LL\overline{E}$ or $\overline{UDD}$ couplings at $\sqrt{s}$=189–208 GeV. The search is performed for direct and indirect decays, assuming one coupling at the time to be nonzero. The limit holds for direct decays via $LL\overline{E}$ couplings. Stronger limits are reached for $(\tilde{\nu}_e,\tilde{\nu}_{\mu,\tau})$ for $LL\overline{E}$ indirect (99,78) GeV and for $\overline{UDD}$ direct or indirect (99,70) GeV decays. The MSUGRA limit results from a scan over the MSSM parameter space with the assumption of gaugino and scalar mass unification at the GUT scale, imposing simultaneously the exclusions from neutralino, chargino, sleptons, and squarks analyses. The limit holds for $\overline{UDD}$ couplings and increases to 152.7 GeV for $LL\overline{E}$ couplings.

[154] HEISTER 02F searched for single sneutrino production via $e\gamma \rightarrow \tilde{\nu}_j \ell_k$ mediated by $R\!\!\!/$ $LL\overline{E}$ couplings, decaying directly or indirectly via a $\tilde{\chi}_1^0$ and assuming a single coupling to be nonzero at a time. Final states with three leptons and possible $\not\!\!E_T$ due to neutrinos were selected in the 189–209 GeV data. Limits on the couplings λ_{1jk} as function of the sneutrino mass are shown in Figs. 10–14. The couplings λ_{233} and λ_{233} are not accessible and λ_{121} and λ_{131} are measured with better accuracy in sneutrino resonant production. For all tested couplings, except λ_{133}, the limits are significantly improved compared to the low-energy limits.

[155] ABBIENDI 00 searches for the production of sneutrinos in the case of R-parity violation with $LL\overline{E}$ or $LQ\overline{D}$ couplings, using data from $\sqrt{s}$=183 GeV. They investigate topologies with multiple leptons, jets plus leptons, or multiple jets, assuming one coupling at the time to be non-zero and giving rise to direct or indirect decays. For non-zero $LL\overline{E}$ couplings, they obtain limits on the electron sneutrino mass of 88 GeV for direct decays and of 87 GeV for indirect decays with a low mass χ_1^0. For non-zero $LQ\overline{D}$ couplings, the limits are 86 GeV for indirect decays of $\tilde{\nu}_e$ with a low mass χ_1^0 and 80 GeV for direct decays of $\tilde{\nu}_e$. There exists a region of small Δm, of varying size, for which no limit is obtained, see Fig. 20. It is assumed that tanβ=1.5 and μ=−200 GeV. For muon sneutrinos, direct decays via $LL\overline{E}$ couplings lead to a 66 GeV mass limit and via $LQ\overline{D}$ couplings to a 58 GeV limit.

[156] ABBIENDI 00R studied the effect of s- and t-channel τ or μ sneutrino exchange in $e^+e^- \rightarrow e^+e^-$ at $\sqrt{s}$=130–189 GeV, via the R-parity violating coupling $\lambda_{1i1}L_1L_if_1e_1$ (i=2 or 3). The limits quoted here hold for λ_{1i1} >0.13, and supersede the results of ABBIENDI 99. See Fig. 11 for limits on $m_{\tilde{\nu}}$ versus coupling.

[157] ABBIENDI 00R studied the effect of s-channel τ sneutrino exchange in $e^+e^- \rightarrow \mu^+\mu^-$ at $\sqrt{s}$=130–189 GeV, in presence of the R-parity violating couplings $\lambda_{ij3}L_iL_3e_j$ (i=1 and 2), with λ_{131}=λ_{232}. The limits quoted here hold for λ_{131} > 0.09, and supersede the results of ABBIENDI 99. See Fig. 12 for limits on $m_{\tilde{\nu}}$ versus coupling.

[158] ABREU 00S searches for anomalies in the production cross sections and forward-backward asymmetries of the $\ell^+\ell^-(\gamma)$ final states (ℓ=e,μ,τ) from e^+e^- collisions at $\sqrt{s}$=130–189 GeV. Limits are set on the s- and t-channel exchange of sneutrinos in the presence of $R\!\!\!/$ with $\lambda LL\overline{E}$ couplings. For points between the energies at which data were taken, information is obtained from events in which a photon was radiated. Exclusion limits in the $(\lambda,m_{\tilde{\nu}})$ plane are given in Fig. 5. These limits include and update the results of ABREU 99A.

[159] ABREU 00U searches for the pair production of sneutrinos with a decay involving R-parity violating $LL\overline{E}$ couplings, using data from $\sqrt{s}$=189 GeV. They investigate topologies with multiple leptons, assuming one coupling to be nonzero at the time and giving rise to direct or indirect decays. The limits, valid for each individual flavor, are determined by the indirect decays and assume a neutralino mass limit of 30 GeV, also derived in ABREU 00U. Better limits for specific flavors and for specific $R\!\!\!/$ couplings can be obtained and are discussed in the paper. Supersedes the results of ABREU 00I.

[160] ACCIARRI 00P use the dilepton total cross sections and asymmetries at $\sqrt{s}$=m_Z and $\sqrt{s}$=130–189 GeV data to set limits on the effect of $R\!\!\!/$ $LL\overline{E}$ couplings giving rise to μ or τ sneutrino exchange. See their Fig. 5 for limits on the sneutrino mass versus couplings.

[161] BARATE 00I studied the effect of s-channel and t-channel τ or μ sneutrino exchange in $e^+e^- \rightarrow e^+e^-$ at $\sqrt{s}$= 130–183 GeV, via the R-parity violating coupling $\lambda_{1i1}L_1L_ie_1^c$ (i=2 or 3). The limits quoted here hold for λ_{1i1} > 0.1. See their Fig. 15 for limits as a function of the coupling.

[162] BARATE 00I studied the effect of s-channel τ sneutrino exchange in $e^+e^- \rightarrow \mu^+\mu^-$ at $\sqrt{s}$= 130–183 GeV, in presence of the R-parity violating coupling $\lambda_{ij3}L_iL_3e_f^c$ (i=1 and 2). The limits quoted here hold for $\sqrt{|\lambda_{131}\lambda_{232}|}$ > 0.2. See their Fig. 16 for limits as a function of the coupling.

[163] ABBIENDI 99 studied the effect of t-channel electron sneutrino exchange in $e^+e^- \rightarrow \tau^+\tau^-$ at $\sqrt{s}$=130–183 GeV, in presence of the R-parity violating couplings $\lambda_{131}L_1L_3e_1^c$. The limits quoted here hold for λ_{131} > 0.6.

[164] ACCIARRI 97U studied the effect of the s-channel tau-sneutrino exchange in $e^+e^- \rightarrow e^+e^-$ at $\sqrt{s}$=m_Z and $\sqrt{s}$=130–172 GeV, via the R-parity violating coupling $\lambda_{131}L_1L_if_1e_1^c$. The limits quoted here hold for λ_{131} > 0.05. Similar limits were studied in $e^+e^- \rightarrow \mu^+\mu^-$ together with $\lambda_{232}L_2L_3e_2^c$ coupling.

[165] CARENA 97 studied the constraints on chargino and sneutrino masses from muon $g-2$. The bound can be important for large tanβ.

[166] BUSKULIC 95E looked for $Z \rightarrow \tilde{\nu}\tilde{\nu}$, where $\tilde{\nu} \rightarrow \nu\chi_1^0$ and χ_1^0 decays via R-parity violating interactions into two leptons and a neutrino.

[167] BECK 94 limit can be inferred from limit on Dirac neutrino using $\sigma(\tilde{\nu}) = 4\sigma(\nu)$. Also private communication with H.V. Klapdor-Kleingrothaus.

[168] FALK 94 puts an upper bound on $m_{\tilde{\nu}}$ when $\tilde{\nu}$ is LSP by requiring its relic density does not overclose the Universe.

[169] SATO 91 search for high-energy neutrinos from the sun produced by annihilation of sneutrinos in the sun. Sneutrinos are assumed to be stable and to constitute dark matter in our galaxy. SATO 91 follow the analysis of NG 87, OLIVE 88, and GAISSER 86.

CHARGED SLEPTONS

This section contains limits on charged scalar leptons ($\tilde{\ell}$, with ℓ=e,μ,τ). Studies of width and decays of the Z boson (use is made here of $\Delta\Gamma_{\rm inv}$ < 2.0 MeV, LEP 00) conclusively rule out $m_{\tilde{\ell}_R}$ < 40 GeV (41 GeV for $\tilde{\ell}_L$) , independently of decay modes, for each individual slepton. The limits improve to 43 GeV (43.5 GeV for $\tilde{\ell}_L$) assuming all 3 flavors to be degenerate. Limits on higher mass sleptons depend on model assumptions and on the mass splitting Δm= $m_{\tilde{\ell}} - m_{\tilde{\chi}_1^0}$. The mass and composition of $\tilde{\chi}_1^0$ may affect the selectron production rate in e^+e^- collisions through t-channel exchange diagrams. Production rates are also affected by the potentially large mixing angle of the lightest mass eigenstate $\tilde{\ell}_1$=$\tilde{\ell}_R$ sinθ_ℓ + $\tilde{\ell}_L$ cosθ_ℓ. It is generally assumed that only $\tilde{\tau}$ may have significant mixing. The coupling to the Z vanishes for θ_ℓ=0.82. In the high-energy limit of e^+e collisions the interference between γ and Z exchange leads to a minimal cross section for θ_ℓ=0.91, a value which is sometimes used in the following entries relative to data taken at LEP2. When limits on $m_{\tilde{\ell}_R}$ are quoted, it is understood that limits on $m_{\tilde{\ell}_L}$ are usually at least as strong.

Possibly open decays involving gauginos other than $\tilde{\chi}_1^0$ will affect the detection efficiencies. Unless otherwise stated, the limits presented here result from the study of $\tilde{\ell}^+\tilde{\ell}^-$ production, with production rates and decay properties derived from the MSSM. Limits made obsolete by the recent analyses of e^+e^- collisions at high energies can be found in previous Editions of this Review.

For decays with final state gravitinos ($\tilde{G}$), $m_{\tilde{G}}$ is assumed to be negligible relative to all other masses.

$\tilde{e}$ (Selectron) MASS LIMIT

VALUE (GeV)	CL%	DOCUMENT ID		TECN	COMMENT
> 97.5	95	[170] ABBIENDI	04	OPAL	$\tilde{e}_R$,Δm > 11 GeV, $\|\mu\|$ >100 GeV, tanβ=1.5
> 94.4	95	[171] ACHARD	04	L3	$\tilde{e}_R$,Δm > 10 GeV, $\|\mu\|$ >200 GeV, tan$\beta \geq$ 2
> 71.3	95	[171] ACHARD	04	L3	$\tilde{e}_R$, all Δm
none 30–94	95	[172] ABDALLAH	03M	DLPH	Δm >15 GeV, $\tilde{e}_R^+\tilde{e}_R^-$
> 94	95	[173] ABDALLAH	03M	DLPH	$\tilde{e}_R$,1 $\leq$ tan$\beta \leq$ 40, Δm >10 GeV
> 95	95	[174] HEISTER	02E	ALEP	Δm > 15 GeV, $\tilde{e}_R^+\tilde{e}_R^-$
> 73	95	[175] HEISTER	02N	ALEP	$\tilde{e}_R$, any Δm
>107	95	[175] HEISTER	02N	ALEP	$\tilde{e}_L$, any Δm
• • • We do not use the following data for averages, fits, limits, etc. • • •					
> 93	95	[176] HEISTER	03G	ALEP	$\tilde{e}_R$,$R\!\!\!/$ decays,μ=−200 GeV, tanβ=2
> 69	95	[177] ACHARD	02	L3	$\tilde{e}_R$, $R\!\!\!/$ decays, μ=−200 GeV, tanβ=$\sqrt{2}$
> 92	95	[178] BARATE	01	ALEP	Δm > 10 GeV, $\tilde{e}_R^+\tilde{e}_R^-$
> 72	95	[179] ABBIENDI	00	OPAL	$\tilde{e}_R^+\tilde{e}_R^-$, $R\!\!\!/$, light $\tilde{\chi}_1^0$
> 77	95	[180] ABBIENDI	00J	OPAL	Δm >5 GeV, $\tilde{e}_R^+\tilde{e}_R^-$
> 83	95	[181] ABREU	00U	DLPH	$\tilde{e}_R$, $R\!\!\!/$ ($LL\overline{E}$)
> 67	95	[182] ABREU	00V	DLPH	$\tilde{e}_R\tilde{e}_R$ ($\tilde{e}_R \rightarrow e\tilde{G}$), $m_{\tilde{G}}$ >10 eV
> 85	95	[183] BARATE	00G	ALEP	$\tilde{\ell}_R \rightarrow \ell\tilde{G}$, any $\tau(\tilde{\ell}_R)$
> 29.5	95	[184] ACCIARRI	99I	L3	$\tilde{e}_R$, $R\!\!\!/$, tan$\beta \geq$ 2
> 56	95	[185] ACCIARRI	98F	L3	Δm > 5 GeV, $\tilde{e}_R^+\tilde{e}_R^-$, tan$\beta \geq$ 1.41
> 77	95	[186] BARATE	98K	ALEP	Any Δm, $\tilde{e}_R^+\tilde{e}_R^-$, $\tilde{e}_R \rightarrow e\gamma\tilde{G}$
> 77	95	[187] BREITWEG	98	ZEUS	$m_{\tilde{q}}$=$m_{\tilde{e}}$, $m(\tilde{\chi}_1^0)$= 40 GeV
> 63	95	[188] AID	96C	H1	$m_{\tilde{q}}$=$m_{\tilde{e}}$, $m_{\tilde{\chi}_1^0}$=35 GeV

[170] ABBIENDI 04 search for $\tilde{e}_R\tilde{e}_R$ production in acoplanar di-electron final states in the 183–208 GeV data. See Fig. 13 for the dependence of the limits on $m_{\tilde{\chi}_1^0}$ and for the limit at tanβ=35 This limit supersedes ABBIENDI 00G.

[171] ACHARD 04 search for $\tilde{e}_R\tilde{e}_L$ and $\tilde{e}_R\tilde{e}_R$ production in single- and acoplanar di-electron final states in the 192–209 GeV data. Absolute limits on $m_{\tilde{e}_R}$ are derived from a scan over the MSSM parameter space with universal GUT scale gaugino and scalar masses $m_{1/2}$ and m_0, 1 $\leq$ tan$\beta \leq$ 60 and −2 $\leq \mu \leq$ 2 TeV. See Fig. 4 for the dependence of the limits on $m_{\tilde{\chi}_1^0}$. This limit supersedes ACCIARRI 99W.

[172] ABDALLAH 03M looked for acoplanar dielectron + $\not\!\!E$ final states at $\sqrt{s}$ = 189–208 GeV. The limit assumes μ=−200 GeV and tanβ=1.5 in the calculation of the production cross section and B($\tilde{e} \rightarrow e\tilde{\chi}_1^0$). See Fig. 15 for limits in the ($m_{\tilde{e}_R}$, $m_{\tilde{\chi}_1^0}$) plane. These limits include and update the results of ABREU 01

[173] ABDALLAH 03M uses data from $\sqrt{s}$ = 192–208 GeV to obtain limits in the framework of the MSSM with gaugino and sfermion mass universality at the GUT scale. An indirect limit on the mass is derived by constraining the MSSM parameter space by the results from direct searches for neutralinos (including cascade decays) and for sleptons. These limits are valid for values of M_2 < 1 TeV, $|\mu| \leq$ 1 TeV with the $\tilde{\chi}_1^0$ as LSP. The quoted limit is obtained when there is no mixing in the third family. See Fig. 43 for the mass limits as a function of tanβ. These limits update the results of ABREU 00W.

[174] HEISTER 02E looked for acoplanar dielectron + $\not\!\!E_T$ final states from e^+e^- interactions between 183 and 209 GeV. The mass limit assumes $\mu < -200$ GeV and tanβ=2 for the production cross section and B($\tilde{e} \rightarrow e\tilde{\chi}_1^0$)=1. See their Fig. 4 for the dependence of the limit on Δm. These limits include and update the results of BARATE 01.

[175] HEISTER 02N search for $\tilde{e}_R\tilde{e}_L$ and $\tilde{e}_R\tilde{e}_R$ production in single- and acoplanar di-electron final states in the 183–208 GeV data. Absolute limits on $m_{\tilde{e}_R}$ are derived from a scan over the MSSM parameter space with universal GUT scale gaugino and scalar masses $m_{1/2}$ and m_0, 1 $\leq$ tan$\beta \leq$ 50 and −10 $\leq \mu \leq$ 10 TeV. The region of small $|\mu|$, where cascade decays are important, is covered by a search for $\tilde{\chi}_1^0\tilde{\chi}_3^0$ in final states with leptons and possibly photons. Limits on $m_{\tilde{e}_L}$ are derived by exploiting the mass relation between the $\tilde{e}_L$ and $\tilde{e}_R$, based on universal m_0 and $m_{1/2}$. When the constraint from the mass limit of the lightest Higgs from HEISTER 02 is included, the bounds improve to $m_{\tilde{e}_R}$ >77(75) GeV and $m_{\tilde{e}_L}$ >115(115) GeV for a top mass of 175(180) GeV. In the MSUGRA framework with radiative electroweak symmetry breaking, the limits improve further to $m_{\tilde{e}_R}$ >95 GeV and $m_{\tilde{e}_L}$ >152 GeV, assuming a trilinear coupling A_0=0 at the GUT scale. See Figs. 4, 5, 7 for the dependence of the limits on tanβ.

[176] HEISTER 03G searches for the production of selectrons in the case of $R\!\!\!/$ prompt decays with $LL\overline{E}$, $LQ\overline{D}$ or $\overline{UDD}$ couplings at $\sqrt{s}$ = 189–209 GeV. The search is performed for direct and indirect decays, assuming one coupling at a time to be non-zero. The limit holds for indirect decays mediated by $LQ\overline{D}$ couplings with $\Delta m > 10$ GeV. Limits are also given for $LL\overline{E}$ direct ($m_{\tilde{e}_L R} > 96$ GeV) and indirect decays ($m_{\tilde{e}_L R} > 96$ GeV for $m(\tilde{\chi}^0_1) > 23$ GeV from BARATE 98S) and for $\overline{UDD}$ indirect decays ($m_{\tilde{e}_L R} > 94$ GeV with $\Delta m > 10$ GeV). Supersedes the results from BARATE 01B.

[177] ACHARD 02 searches for the production of selectrons in the case of $R\!\!\!/$ prompt decays with $LL\overline{E}$ or $\overline{UDD}$ couplings at $\sqrt{s}$=189–208 GeV. The search is performed for direct and indirect decays, assuming one coupling at the time to be nonzero. The limit holds for direct decays via $LL\overline{E}$ couplings. Stronger limits are reached for $LL\overline{E}$ indirect (79 GeV) and for $\overline{UDD}$ direct or indirect (96 GeV) decays.

[178] BARATE 01 looked for acoplanar dielectron + $\not{E}_T$ final states at 189 to 202 GeV. The limit assumes μ=−200 GeV and tanβ=2 for the production cross section and 100% branching ratio for $\tilde{e} \to e\tilde{\chi}^0_1$. See their Fig. 1 for the dependence of the limit on Δm. These limits include and update the results of BARATE 99Q.

[179] ABBIENDI 00 searches for the production of selectrons in the case of R-parity violation with $LL\overline{E}$ or $LQ\overline{D}$ couplings, using data from $\sqrt{s}$=183 GeV. They investigate topologies with multiple leptons, jets plus leptons, or multiple jets, assuming one coupling at the time to be non-zero and giving rise to direct or indirect decays. For non-zero $LL\overline{E}$ couplings, they obtain limits on the selectron mass of 84 GeV both for direct decays and for indirect decays with a low mass $\tilde{\chi}^0_1$. For non-zero $LQ\overline{D}$ couplings, the limits are 72 GeV for indirect decays of $\tilde{e}_R$ with a low mass $\tilde{\chi}^0_1$ and 76 GeV for direct decays of $\tilde{e}_L$. It is assumed that tanβ=1.5 and μ=−200 GeV.

[180] ABBIENDI 00J looked for acoplanar dielectron + $\not{E}_T$ final states at $\sqrt{s}$= 161–183 GeV. The limit assumes $\mu < -100$ GeV and tanβ=1.5 for the production cross section and decay branching ratios, evaluated within the MSSM, and zero efficiency for decays other than $\tilde{e} \to e\tilde{\chi}^0_1$. See their Fig. 12 for the dependence of the limit on Δm and tanβ.

[181] ABREU 00U studies decays induced by R-parity violating $LL\overline{E}$ couplings, using data from $\sqrt{s}$=189 GeV. They investigate topologies with multiple leptons, assuming one coupling at the time to be nonzero and giving rise to indirect decays. The limits assume a neutralino mass limit of 30 GeV, also derived in ABREU 00U. Updates ABREU 00I.

[182] ABREU 00V use data from $\sqrt{s}$= 130–189 GeV to search for tracks with large impact parameter or visible decay vertices. Limits are obtained as a function of $m_{\tilde{G}}$, from a scan of the GMSB parameters space, after combining these results with the search for slepton pair production in the SUGRA framework from ABREU 01 to cover prompt decays and on stable particle searches from ABREU 00Q. For limits at different $m_{\tilde{G}}$, see their Fig. 12.

[183] BARATE 00G combines the search for acoplanar dileptons, leptons with large impact parameters, kinks, and stable heavy-charged tracks, assuming 3 flavors of degenerate sleptons, produced in the schannel. Data collected at $\sqrt{s}$=189 GeV.

[184] ACCIARRI 99I establish indirect limits on $m_{\tilde{e}_R}$ from the regions excluded in the M_2 versus m_0 plane by their chargino and neutralino searches at $\sqrt{s}$=130–183 GeV. The situations where the $\tilde{\chi}^0_1$ is the LSP (indirect decays) and where a $\tilde{\ell}$ is the LSP (direct decays) were both considered. The weakest limit, quoted above, comes from direct decays with $\overline{UDD}$ couplings; $LL\overline{E}$ couplings or indirect decays lead to a stronger limit.

[185] ACCIARRI 98F looked for acoplanar dielectron+$\not{E}_T$ final states at $\sqrt{s}$=130–172 GeV. The limit assumes μ=−200 GeV, and zero efficiency for decays other than $\tilde{e}_R \to e\tilde{\chi}^0_1$. See their Fig. 6 for the dependence of the limit on Δm.

[186] BARATE 98K looked for $e^+e^-\gamma\gamma + \not{E}$ final states at $\sqrt{s}$= 161–184 GeV. The limit assumes μ=−200 GeV and tanβ=2 for the evaluation of the production cross section. See Fig. 4 for limits on the ($m_{\tilde{e}_R}$,$m_{\tilde{\chi}^0_1}$) plane and for the effect of cascade decays.

[187] BREITWEG 98 used positron+jet events with missing energy and momentum to look for $e^+q \to \tilde{e}\tilde{q}$ via gaugino-like neutralino exchange with decays into $(e\tilde{\chi}^0_1)(q\tilde{\chi}^0_1)$. See paper for dependences in $m(\tilde{q})$, $m(\tilde{\chi}^0_1)$.

[188] AID 96C used positron+jet events with missing energy and momentum to look for $e^+q \to \tilde{e}\tilde{q}$ via neutralino exchange with decays into $(e\tilde{\chi}^0_1)(q\tilde{\chi}^0_1)$. See the paper for dependences on $m_{\tilde{q}}$, $m_{\tilde{\chi}^0_1}$.

[189] ABBIENDI 04 search for $\tilde{\mu}_R\tilde{\mu}_R$ production in acoplanar di-muon final states in the 183–208 GeV data. See Fig. 14 for the dependence of the limits on $m_{\tilde{\chi}^0_1}$ and for the limit at tanβ=35. Under the assumption of 100% branching ratio for $\tilde{\mu}_R \to \mu\tilde{\chi}^0_1$, the limit improves to 94.0 GeV for $\Delta m > 4$ GeV. See Fig. 11 for the dependence of the limits on $m_{\tilde{\chi}^0_1}$ at several values of the branching ratio. This limit supersedes ABBIENDI 00G.

[190] ACHARD 04 search for $\tilde{\mu}_R\tilde{\mu}_R$ production in acoplanar di-muon final states in the 192–209 GeV data. Limits on $m_{\tilde{\mu}_R}$ are derived from a scan over the MSSM parameter space with universal GUT scale gaugino and scalar masses $m_{1/2}$ and m_0, $1 \leq$ tanβ ≤ 60 and $-2 \leq \mu \leq 2$ TeV. See Fig. 4 for the dependence of the limits on $m_{\tilde{\chi}^0_1}$. This limit supersedes ACCIARRI 99W.

[191] ABDALLAH 03M looked for acoplanar dimuon + $\not{E}$ final states at $\sqrt{s}$ = 189–208 GeV. The limit assumes B($\tilde{\mu} \to \mu\tilde{\chi}^0_1$) = 100%. See Fig. 16 for limits on the ($m_{\tilde{\mu}_R}$, $m_{\tilde{\chi}^0_1}$) plane. These limits include and update the results of ABREU 01.

[192] ABDALLAH 03M uses data from $\sqrt{s}$ = 192–208 GeV to obtain limits in the framework of the MSSM with gaugino and sfermion mass universality at the GUT scale. An indirect limit on the mass is derived by constraining the MSSM parameter space by the results from direct searches for neutralinos (including cascade decays) and for sleptons. These limits are valid for values of $M_2 < 1$ TeV, $|\mu| \leq 1$ TeV with the $\tilde{\chi}^0_1$ as LSP. The quoted limit is obtained when there is no mixing in the third family. See Fig. 43 for the mass limits as a function of tanβ. These limits update the results of ABREU 00W.

[193] HEISTER 02E looked for acoplanar dimuon + $\not{E}_T$ final states from e^+e^- interactions between 183 and 209 GeV. The mass limit assumes B($\tilde{\mu} \to \mu\tilde{\chi}^0_1$)=1. See their Fig. 4 for the dependence of the limit on Δm. These limits include and update the results of BARATE 01.

[194] HEISTER 03G searches for the production of smuons in the case of $R\!\!\!/$ prompt decays with $LL\overline{E}$, $LQ\overline{D}$ or $\overline{UDD}$ couplings at $\sqrt{s}$ = 189–209 GeV. The search is performed for direct and indirect decays, assuming one coupling at a time to be non-zero. The limit holds for direct decays mediated by $R\!\!\!/$ $LQ\overline{D}$ couplings and improves to 90 GeV for indirect decays (for $\Delta m > 10$ GeV). Limits are also given for $LL\overline{E}$ direct ($m_{\tilde{\mu}R} > 87$ GeV) and indirect decays ($m_{\tilde{\mu}R} > 96$ GeV for $m(\tilde{\chi}^0_1) > 23$ GeV from BARATE 98S) and for $\overline{UDD}$ indirect decays ($m_{\tilde{\mu}R} > 85$ GeV for $\Delta m > 10$ GeV). Supersedes the results from BARATE 01B.

[195] ABAZOV 02H looked in 94 pb^{-1} of $p\overline{p}$ collisions at $\sqrt{s}$=1.8 TeV for events with at least 2 muons and 2 jets for s-channel production of $\tilde{\mu}$ or $\tilde{\nu}$ and subsequent decay via $R\!\!\!/$ couplings $LQ\overline{D}$. A scan over the MSUGRA parameters is performed to exclude regions of the (m_0,$m_{1/2}$) plane, examples being shown in Fig. 2.

[196] ACHARD 02 searches for the production of smuons in the case of $R\!\!\!/$ prompt decays with $LL\overline{E}$ or $\overline{UDD}$ couplings at $\sqrt{s}$=189–208 GeV. The search is performed for direct and indirect decays, assuming one coupling at the time to be nonzero. The limit holds for direct decays via $LL\overline{E}$ couplings. Stronger limits are reached for $LL\overline{E}$ indirect (87 GeV) and for $\overline{UDD}$ direct or indirect (86 GeV) decays.

[197] BARATE 01 looked for acoplanar dimuon + $\not{E}_T$ final states at 189 to 202 GeV. The limit assumes 100% branching ratio for $\tilde{\mu} \to \mu\tilde{\chi}^0_1$. See their Fig. 1 for the dependence of the limit on Δm. These limits include and update the results of BARATE 99Q.

[198] ABBIENDI 00 searches for the production of smuons in the case of R-parity violation with $LL\overline{E}$ or $LQ\overline{D}$ couplings, using data from $\sqrt{s}$=183 GeV. They investigate topologies with multiple leptons, jets plus leptons, or multiple jets, assuming one coupling at the time to be non-zero and giving rise to direct or indirect decays. For non-zero $LL\overline{E}$ couplings, they obtain limits on the smuon mass of 66 GeV for direct decays and of 74 GeV for indirect decays with a low mass $\tilde{\chi}^0_1$. For non-zero $LQ\overline{D}$ couplings, the limits are 50 GeV for indirect decays of $\tilde{\mu}_R$ with a low mass $\tilde{\chi}^0_1$ and 64 GeV for direct decays of $\tilde{\mu}_L$. It is assumed that tanβ=1.5 and μ=−200 GeV.

[199] ABBIENDI 00J looked for acoplanar dimuon + $\not{E}_T$ final states at $\sqrt{s}$= 161–183 GeV. The limit assumes B($\tilde{\mu} \to \mu\tilde{\chi}^0_1$)=1. Using decay branching ratios derived from the MSSM, a lower limit of 65 GeV is obtained for $\mu < -100$ GeV and tanβ=1.5. See their Figs. 10 and 13 for the dependence of the limit on the branching ratio and on Δm.

[200] ABREU 00U studies decays induced by R-parity violating $LL\overline{E}$ couplings, using data from $\sqrt{s}$=189 GeV. They investigate topologies with multiple leptons, assuming one coupling at the time to be nonzero and giving rise to indirect decays. The limits, valid for each individual flavor, assume a neutralino mass limit of 30 GeV, also derived in ABREU 00U. Updates ABREU 00I.

[201] ABREU 00V use data from $\sqrt{s}$= 130–189 GeV to search for tracks with large impact parameter or visible decay vertices. Limits are obtained as function of $m_{\tilde{G}}$, after combining these results with the search for slepton pair production in the SUGRA framework from ABREU 01 to cover prompt decays and on stable particle searches from ABREU 00Q. For limits at different $m_{\tilde{G}}$, see their Fig. 12.

[202] BARATE 98K looked for $\mu^+\mu^-\gamma\gamma + \not{E}$ final states at $\sqrt{s}$= 161–184 GeV. See Fig. 4 for limits on the ($m_{\tilde{\mu}_R}$,$m_{\tilde{\chi}^0_1}$) plane and for the effect of cascade decays.

$\tilde{\mu}$ (Smuon) MASS LIMIT

VALUE (GeV)	CL%		DOCUMENT ID		TECN	COMMENT
>91.0	95	[189]	ABBIENDI	04	OPAL	$\Delta m > 3$ GeV, $\tilde{\mu}^+_R\tilde{\mu}^-_R$, $\lvert\mu\rvert > 100$ GeV, tanβ=1.5
>86.7	95	[190]	ACHARD	04	L3	$\Delta m > 10$ GeV, $\tilde{\mu}^+_R\tilde{\mu}^-_R$, $\lvert\mu\rvert >$200 GeV, tan$\beta \geq 2$
none 30–88	95	[191]	ABDALLAH	03M	DLPH	$\Delta m >$5 GeV, $\tilde{\mu}^+_R\tilde{\mu}^-_R$
>94	95	[192]	ABDALLAH	03M	DLPH	$\tilde{\mu}_R$,1 $\leq$ tan$\beta \leq$ 40, $\Delta m >$10 GeV
>88	95	[193]	HEISTER	02E	ALEP	$\Delta m >$ 15 GeV, $\tilde{\mu}^+_R\tilde{\mu}^-_R$
• • • We do not use the following data for averages, fits, limits, etc. • • •						
>81	95	[194]	HEISTER	03G	ALEP	$\tilde{\mu}_L$,$R\!\!\!/$ decays
		[195]	ABAZOV	02H	D0	$R\!\!\!/$, λ'_{211}
>61	95	[196]	ACHARD	02	L3	$\tilde{\mu}_R$, $R\!\!\!/$ decays
>85	95	[197]	BARATE	01	ALEP	$\Delta m >$ 10 GeV, $\tilde{\mu}^+_R\tilde{\mu}^-_R$
>50	95	[198]	ABBIENDI	00	OPAL	$\tilde{\mu}^+_R\tilde{\mu}^-_R$, $R\!\!\!/$, $\Delta m >$ 5 GeV
>65	95	[199]	ABBIENDI	00J	OPAL	$\Delta m >$2 GeV, $\tilde{\mu}^+_R\tilde{\mu}^-_R$
>83	95	[200]	ABREU	00U	DLPH	$\tilde{\mu}_R$, $R\!\!\!/$ ($LL\overline{E}$)
>80	95	[201]	ABREU	00V	DLPH	$\tilde{\mu}_R\tilde{\mu}_R$ ($\tilde{\mu}_R \to \mu\tilde{G}$), $m_{\tilde{G}} >$8 eV
>77	95	[202]	BARATE	98K	ALEP	Any Δm, $\tilde{\mu}^+_R\tilde{\mu}^-_R$, $\tilde{\mu}_R \to \mu\gamma\tilde{G}$

[203] ABBIENDI 04 OPAL $\Delta m > 6$ GeV, $\theta_\tau = \pi/2$, $|\mu| > 100$ GeV, tanβ=1.5

[204] ACHARD 04 L3 $\Delta m > 15$ GeV, $\theta_\tau = \pi/2$, $|\mu| >$200 GeV, tan$\beta \geq 2$

[205] ABDALLAH 03M DLPH $\Delta m >$15 GeV, all θ_τ

[205] ABDALLAH 03M DLPH $\Delta m > m_\tau$, all θ_τ

[206] HEISTER 02E ALEP $\Delta m >$ 15 GeV, $\theta_\tau = \pi/2$

[206] HEISTER 02E ALEP $\Delta m >$ 15 GeV, θ_τ=0.91

• • • We do not use the following data for averages, fits, limits, etc. • • •

[207] ABDALLAH 03D DLPH $\tilde{\tau}_R \to \tau\tilde{G}$, all $\tau(\tilde{\tau}_R)$

[208] HEISTER 03G ALEP $\tilde{\tau}_R$,$R\!\!\!/$ decay

[209] ACHARD 02 L3 $\tilde{\tau}_R$, $R\!\!\!/$ decays

[210] HEISTER 02R ALEP τ_1, any lifetime

[211] BARATE 01 ALEP $\Delta m >$ 10 GeV, $\theta_\tau = \pi/2$

[211] BARATE 01 ALEP $\Delta m >$ 10 GeV, θ_τ=0.91

$\tilde{\tau}$ (Stau) MASS LIMIT

VALUE (GeV)	CL%		DOCUMENT ID		TECN	COMMENT
>85.2	95	[203]	ABBIENDI	04	OPAL	$\Delta m > 6$ GeV, $\theta_\tau = \pi/2$, $\lvert\mu\rvert > 100$ GeV, tanβ=1.5
>78.3	95	[204]	ACHARD	04	L3	$\Delta m > 15$ GeV, $\theta_\tau = \pi/2$, $\lvert\mu\rvert >$200 GeV, tan$\beta \geq 2$
>81.9	95	[205]	ABDALLAH	03M	DLPH	$\Delta m >$15 GeV, all θ_τ
none m_τ − 26.3	95	[205]	ABDALLAH	03M	DLPH	$\Delta m > m_\tau$, all θ_τ
>79	95	[206]	HEISTER	02E	ALEP	$\Delta m >$ 15 GeV, $\theta_\tau = \pi/2$
>76	95	[206]	HEISTER	02E	ALEP	$\Delta m >$ 15 GeV, θ_τ=0.91
• • • We do not use the following data for averages, fits, limits, etc. • • •						
>82.5	95	[207]	ABDALLAH	03D	DLPH	$\tilde{\tau}_R \to \tau\tilde{G}$, all $\tau(\tilde{\tau}_R)$
>70	95	[208]	HEISTER	03G	ALEP	$\tilde{\tau}_R$,$R\!\!\!/$ decay
>61	95	[209]	ACHARD	02	L3	$\tilde{\tau}_R$, $R\!\!\!/$ decays
>77	95	[210]	HEISTER	02R	ALEP	τ_1, any lifetime
>70	95	[211]	BARATE	01	ALEP	$\Delta m >$ 10 GeV, $\theta_\tau = \pi/2$
>68	95	[211]	BARATE	01	ALEP	$\Delta m >$ 10 GeV, θ_τ=0.91

>66	95	[212] ABBIENDI	00	OPAL	$\tilde{\tau}_R^+\tilde{\tau}_R^-$, $\not{R}$, light $\tilde{\chi}_1^0$
>64	95	[213] ABBIENDI	00J	OPAL	Δm >10 GeV, $\tilde{\tau}_R^+\tilde{\tau}_R^-$
>83	95	[214] ABREU	00U	DLPH	$\tilde{\tau}_R$, $\not{R}$ ($LL\overline{E}$)
>84	95	[215] ABREU	00V	DLPH	$\tilde{\ell}_R\tilde{\ell}_R$ ($\tilde{\ell}_R \rightarrow \ell\tilde{G}$), $m_{\tilde{G}}>9$ eV
>73	95	[216] ABREU	00V	DLPH	$\tilde{\tau}_1\tilde{\tau}_1$ ($\tilde{\tau}_1 \rightarrow \tau\tilde{G}$), all $\tau(\tilde{\tau}_1)$
>52	95	[217] BARATE	98K	ALEP	Any Δm, θ_τ=$\pi/2$, $\tilde{\tau}_R \rightarrow \tau\gamma\tilde{G}$

[203] ABBIENDI 04 search for $\tilde{\tau}\tilde{\tau}$ production in acoplanar di-tau final states in the 183–208 GeV data. See Fig. 15 for the dependence of the limits on $m_{\tilde{\chi}_1^0}$ and for the limit at tanβ=35. Under the assumption of 100% branching ratio for $\tilde{\tau}_R \rightarrow \tau\tilde{\chi}_1^0$, the limit improves to 89.8 GeV for $\Delta m > 8$ GeV. See Fig. 12 for the dependence of the limits on $m_{\tilde{\chi}_1^0}$ at several values of the branching ratio and for their dependence on θ_τ. This limit supersedes ABBIENDI 00G.

[204] ACHARD 04 search for $\tilde{\tau}\tilde{\tau}$ production in acoplanar di-tau final states in the 192–209 GeV data. Limits on $m_{\tilde{\tau}_R}$ are derived from a scan over the MSSM parameter space with universal GUT scale gaugino and scalar masses $m_{1/2}$ and m_0, $1 \leq \tan\beta \leq 60$ and $-2 \leq \mu \leq 2$ TeV. See Fig. 4 for the dependence of the limits on $m_{\tilde{\chi}_1^0}$.

[205] ABDALLAH 03M looked for acoplanar ditaus + $\not{E}$ final states at $\sqrt{s}$ = 130–208 GeV. A dedicated search was made for low mass $\tilde{\tau}$s decoupling from the Z^0. The limit assumes B($\tilde{\tau} \rightarrow \tau\tilde{\chi}_1^0$) = 100%. See Fig. 20 for limits on the ($m_{\tilde{\tau}}$,$m_{\tilde{\chi}_1^0}$) plane and as function of the $\tilde{\chi}_1^0$ mass and of the branching ratio. The limit in the low-mass region improves to 29.6 and 31.1 GeV for $\tilde{\tau}_R$ and $\tilde{\tau}_L$, respectively, at $\Delta m > m_\tau$. The limit in the high-mass region improves to 84.7 GeV for $\tilde{\tau}_R$ and $\Delta m > 15$ GeV. These limits include and update the results of ABREU 01.

[206] HEISTER 02E looked for acoplanar ditau + $\not{E}_T$ final states from e^+e^- interactions between 183 and 209 GeV. The mass limit assumes B($\tilde{\tau} \rightarrow \tau\tilde{\chi}_1^0$)=1. See their Fig. 4 for the dependence of the limit on Δm. These limits include and update the results of BARATE 01.

[207] ABDALLAH 03D use data from $\sqrt{s}$= 130-208 GeV to search for tracks with large impact parameter or visible decay vertices and for heavy charged stable particles. Limits are obtained as function of m($\tilde{G}$), after combining these results with the search for slepton pair production in the SUGRA framework from ABDALLAH 03M to cover prompt decays. The above limit is reached for the stau decaying promptly, m($\tilde{G}$) < 6 eV, and is computed for stau mixing yielding the minimal cross section. Stronger limits are obtained for longer lifetimes, See their Fig. 9. Supersedes the results of ABREU 01G.

[208] HEISTER 03G searches for the production of staus in the case of $\not{R}$ prompt decays with $LL\overline{E}$, $LQ\overline{D}$ or $\overline{UDD}$ couplings at $\sqrt{s}$ = 189–209 GeV. The search is performed for direct and indirect decays, assuming one coupling at a time to be non-zero. The limit holds for indirect decays mediated by $\not{R}$ $\overline{UDD}$ couplings with $\Delta m > 10$ GeV. Limits are also given for $LL\overline{E}$ direct ($m_{\tilde{\tau}_R} > 87$ GeV) and indirect decays ($m_{\tilde{\tau}_R} > 95$ GeV for $m(\tilde{\chi}_1^0) > 23$ GeV from BARATE 98S) and for $LQ\overline{D}$ indirect decays ($m_{\tilde{\tau}_R} > 76$ GeV). Supersedes the results from BARATE 01B.

[209] ACHARD 02 searches for the production of staus in the case of $\not{R}$ prompt decays with $LL\overline{E}$ or $\overline{UDD}$ couplings at $\sqrt{s}$=189–208 GeV. The search is performed for direct and indirect decays, assuming one coupling at the time to be nonzero. The limit holds for indirect decays via $LL\overline{E}$ couplings. Stronger limits are reached for $LL\overline{E}$ indirect (86 GeV) and for $\overline{UDD}$ direct or indirect (75 GeV) decays.

[210] HEISTER 02R search for signals of GMSB in the 189–209 GeV data. For the $\tilde{\chi}_1^0$ NLSP scenario, they looked for topologies consisting of $\gamma\gamma\not{E}$ or a single γ not pointing to the interaction vertex. For the $\tilde{\ell}$ NLSP case, the topologies consist of $\ell\ell\not{E}$, including leptons with large impact parameters, kinks, or stable particles. Limits are derived from a scan over the GMSB parameters (see their Table 5 for the ranges). The limit remains valid whichever is the NLSP. The absolute mass bound on the $\tilde{\chi}_1^0$ for any lifetime includes indirect limits from the slepton search HEISTER 02E preformed within the MSUGRA framework. A bound for any NLSP and any lifetime of 77 GeV has also been derived by using the constraints from the neutral Higgs search in HEISTER 02. In the co-NLSP scenario, limits $m_{\tilde{e}_R} > 83$ GeV (neglecting t-channel exchange) and $m_{\tilde{\mu}_R} > 88$ GeV are obtained independent of the lifetime. Supersedes the results from BARATE 00G.

[211] BARATE 01 looked for acoplanar ditau + $\not{E}_T$ final states at 189 to 202 GeV. A slight excess (with 1.2% probability) of events is observed relative to the expected SM background. The limit assumes 100% branching ratio for $\tilde{\tau} \rightarrow \tau\tilde{\chi}_1^0$. See their Fig. 1 for the dependence of the limit on Δm. These limits include and update the results of BARATE 99Q.

[212] ABBIENDI 00 searches for the production of staus in the case of R-parity violation with $LL\overline{E}$ or $LQ\overline{D}$ couplings, using data from $\sqrt{s}$=183 GeV. They investigate topologies with multiple leptons, jets plus leptons, or multiple jets, assuming one coupling at the time to be non-zero and giving rise to direct or indirect decays. For non-zero $LL\overline{E}$ couplings, they obtain limits on the stau mass of 66 GeV both for direct decays and for indirect decays with a low mass χ_1^0. For non-zero $LQ\overline{D}$ couplings, the limits are 66 GeV for indirect decays of $\tilde{\tau}_R$ with a low mass χ_1^0 and 63 GeV for direct decays of $\tilde{\tau}_L$. It is assumed that tanβ=1.5 and μ=– 200 GeV.

[213] ABBIENDI 00J looked for acoplanar ditau + $\not{E}_T$ final states at $\sqrt{s}$= 161–183 GeV. The limit assumes B($\tilde{\tau} \rightarrow \tau\tilde{\chi}_1^0$)=1. Using decay branching ratios derived from the MSSM, a lower limit of 60 GeV at Δm >9 GeV is obtained for $\mu < -100$ GeV and tanβ=1.5. See their Figs. 11 and 14 for the dependence of the limit on the branching ratio and on Δm.

[214] ABREU 00U studies decays induced by R-parity violating $LL\overline{E}$ couplings, using data from $\sqrt{s}$=189 GeV. They investigate topologies with multiple leptons, assuming one coupling at the time to be nonzero and giving rise to indirect decays. The limits, valid for each individual flavor, assume a neutralino mass limit of 30 GeV, also derived in ABREU 00U. Updates ABREU 00I.

[215] ABREU 00V use data from $\sqrt{s}$= 130–189 GeV to search for tracks with large impact parameter or visible decay vertices. Limits are obtained as function of $m_{\tilde{G}}$, after combining these results with the search for slepton pair production in the SUGRA framework from ABREU 01 to cover prompt decays and on stable particle searches from ABREU 00Q. The above limit assumes the degeneracy of stau and smuon. For limits at different $m_{\tilde{G}}$, see their Fig. 12.

[216] ABREU 00V use data from $\sqrt{s}$= 130–189 GeV to search for tracks with large impact parameter or visible decay vertices. Limits are obtained as function of $m_{\tilde{G}}$, after combining these results with the search for slepton pair production in the SUGRA framework from ABREU 01 to cover prompt decays and on stable particle searches from ABREU 00Q. The above limit is reached for the stau mixing yielding the minimal cross section and decaying promptly. Stronger limits are obtained for longer lifetimes or for $\tilde{\tau}_R$; see their Fig. 11. For $10 \leq m_{\tilde{G}} \leq 310$ eV, the whole range $2 \leq m_{\tilde{\tau}_1} \leq 80$ GeV is excluded. Supersedes the results of ABREU 99C and ABREU 99F.

[217] BARATE 98K looked for $\tau^+\tau^-\gamma\gamma + \not{E}$ final states at $\sqrt{s}$= 161–184 GeV. See Fig. 4 for limits on the ($m_{\tilde{\tau}_R}$,$m_{\tilde{\chi}_1^0}$) plane and for the effect of cascade decays.

Degenerate Charged Sleptons

Unless stated otherwise in the comment lines or in the footnotes, the following limits assume 3 families of degenerate charged sleptons.

VALUE (GeV)	CL%	DOCUMENT ID		TECN	COMMENT
>93	95	[218] BARATE	01	ALEP	$\Delta m > 10$ GeV, $\tilde{\ell}_R^+\tilde{\ell}_R^-$
>70	95	[218] BARATE	01	ALEP	all Δm, $\tilde{\ell}_R^+\tilde{\ell}_R^-$
• • • We do not use the following data for averages, fits, limits, etc. • • •					
>88	95	[219] ABDALLAH	03D	DLPH	$\tilde{\ell}_R \rightarrow \ell\tilde{G}$, all $\tau(\tilde{\ell}_R)$
>82.7	95	[220] ACHARD	02	L3	$\tilde{\ell}_R$, $\not{R}$ decays, MSUGRA
>83	95	[221] ABBIENDI	01	OPAL	$e^+e^- \rightarrow \tilde{\ell}_1\tilde{\ell}_1$, GMSB, tan$\beta$=2
		[222] ABREU	01	DLPH	$\tilde{\ell} \rightarrow \ell\tilde{\chi}_2^0$, $\tilde{\chi}_2^0 \rightarrow \gamma\tilde{\chi}_1^0$, ℓ=e,μ
>68.8	95	[223] ACCIARRI	01	L3	$\tilde{\ell}_R$, $\not{R}$, $0.7 \leq \tan\beta \leq 40$
>84	95	[224,225] ABREU	00V	DLPH	$\tilde{\ell}_R\tilde{\ell}_R$ ($\tilde{\ell}_R \rightarrow \ell\tilde{G}$), $m_{\tilde{G}}>9$ eV

[218] BARATE 01 looked for acoplanar dilepton + $\not{E}_T$ and single electron (for $\tilde{e}_R\tilde{e}_L$) final states at 189 to 202 GeV. The limit assumes μ=– 200 GeV and tanβ=2 for the production cross section and decay branching ratios, evaluated within the MSSM, and zero efficiency for decays other than $\tilde{\ell} \rightarrow \ell\tilde{\chi}_1^0$. The slepton masses are determined from the GUT relations without stau mixing. See their Fig. 1 for the dependence of the limit on Δm.

[219] ABDALLAH 03D use data from $\sqrt{s}$= 130-208 GeV to search for tracks with large impact parameter or visible decay vertices and for heavy charged stable particles. Limits are obtained as function of m($\tilde{G}$), after combining these results with the search for slepton pair production in the SUGRA framework from ABDALLAH 03M to cover prompt decays The above limit is reached for prompt decays and assumes the degeneracy of the sleptons. For limits at different m($\tilde{G}$), see their Fig. 9. Supersedes the results of ABREU 01G.

[220] ACHARD 02 searches for the production of sparticles in the case of $\not{R}$ prompt decays with $LL\overline{E}$ or $\overline{UDD}$ couplings at $\sqrt{s}$=189–208 GeV. The search is performed for direct and indirect decays, assuming one coupling at the time to be nonzero. The MSUGRA limit results from a scan over the MSSM parameter space with the assumption of gaugino and scalar mass unification at the GUT scale and no mixing in the slepton sector, imposing simultaneously the exclusions from neutralino, chargino, sleptons, and squarks analyses. The limit holds for $LL\overline{E}$ couplings and increases to 88.7 GeV for $\overline{UDD}$ couplings. For L3 limits from $LQ\overline{D}$ couplings, see ACCIARRI 01.

[221] ABBIENDI 01 looked for final states with $\gamma\gamma\not{E}$, $\ell\ell\not{E}$, with possibly additional activity and four leptons + $\not{E}$ to search for prompt decays of $\tilde{\chi}_1^0$ or $\tilde{\ell}_1$ in GMSB. They derive limits in the plane ($m_{\tilde{\chi}_1^0}$,$m_{\tilde{\tau}_1}$), see Fig. 6, allowing either the $\tilde{\chi}_1^0$ or a $\tilde{\ell}_1$ to be the NLSP. Two scenarios are considered: tanβ=2 with the 3 sleptons degenerate in mass and tanβ=20 where the $\tilde{\tau}_1$ is lighter than the other sleptons. Data taken at $\sqrt{s}$=189 GeV. For tanβ=20, the obtained limits are $m_{\tilde{\tau}_1} > 69$ GeV and $m_{\tilde{e}_1,\tilde{\mu}_1} > 88$ GeV.

[222] ABREU 01 looked for acoplanar dilepton + diphoton + $\not{E}$ final states from $\tilde{\ell}$ cascade decays at $\sqrt{s}$=130–189 GeV. See Fig. 9 for limits on the (μ,M_2) plane for $m_{\tilde{\ell}}$=80 GeV, tanβ=1.0, and assuming degeneracy of $\tilde{\mu}$ and $\tilde{e}$.

[223] ACCIARRI 01 searches for multi-lepton and/or multi-jet final states from $\not{R}$ prompt decays with $LL\overline{E}$, $LQ\overline{D}$, or $\overline{UDD}$ couplings at $\sqrt{s}$=189 GeV. The search is performed for direct and indirect decays of neutralinos, charginos, and scalar leptons, with the $\tilde{\chi}_1^0$ or a $\tilde{\ell}$ as LSP and assuming one coupling to be nonzero at a time. Mass limits are derived using simultaneously the constraints from the neutralino, chargino, and slepton analyses; and the Z^0 width measurements from ACCIARRI 00C in a scan of the parameter space assuming MSUGRA with gaugino and scalar mass universality. Updates and supersedes the results from ACCIARRI 99I.

[224] ABREU 00V use data from $\sqrt{s}$= 130–189 GeV to search for tracks with large impact parameter or visible decay vertices. Limits are obtained as function of $m_{\tilde{G}}$, after combining these results with the search for slepton pair production in the SUGRA framework from ABREU 01 to cover prompt decays and on stable particle searches from ABREU 00Q. For limits at different $m_{\tilde{G}}$, see their Fig. 12.

[225] The above limit assumes the degeneracy of stau and smuon.

Long-lived $\tilde{\ell}$ (Slepton) MASS LIMIT

Limits on scalar leptons which leave detector before decaying. Limits from Z decays are independent of lepton flavor. Limits from continuum e^+e^- annihilation are also independent of flavor for smuons and staus. Selectron limits from e^+e^- collisions in the continuum depend on MSSM parameters because of the additional neutralino exchange contribution.

VALUE (GeV)	CL%	DOCUMENT ID		TECN	COMMENT
>98	95	[226] ABBIENDI	03L	OPAL	$\tilde{\mu}_R$, $\tilde{\tau}_R$
none 2–87.5	95	[227] ABREU	00Q	DLPH	$\tilde{\mu}_R$, $\tilde{\tau}_R$
>81.2	95	[228] ACCIARRI	99H	L3	$\tilde{\mu}_R$, $\tilde{\tau}_R$
>81	95	[229] BARATE	98K	ALEP	$\tilde{\mu}_R$, $\tilde{\tau}_R$

[226] ABBIENDI 03L used e^+e^- data at $\sqrt{s}$ = 130–209 GeV to select events with two high momentum tracks with anomalous dE/dx. The excluded cross section is compared to the theoretical expectation as a function of the heavy particle mass in their Fig. 3. The limit improves to 98.5 GeV for $\tilde{\mu}_L$ and $\tilde{\tau}_L$. The bounds are valid for colorless spin 0 particles with lifetimes longer than 10^{-6} s. Supersedes the results from ACKERSTAFF 98P.

[227] ABREU 00Q searches for the production of pairs of heavy, charged stable particles in e^+e^- annihilation at $\sqrt{s}$= 130–189 GeV. The upper bound improves to 88 GeV for $\tilde{\mu}_L$, $\tilde{\tau}_L$. These limits include and update the results of ABREU 98P.

[228] ACCIARRI 99H searched for production of pairs of back-to-back heavy charged particles at $\sqrt{s}$=130–183 GeV. The upper bound improves to 82.2 GeV for $\tilde{\mu}_L$, $\tilde{\tau}_L$.

[229] The BARATE 98K mass limit improves to 82 GeV for $\tilde{\mu}_L$,$\tilde{\tau}_L$. Data collected at $\sqrt{s}$=161–184 GeV.

$\tilde{q}$ (Squark) MASS LIMIT

For $m_{\tilde{q}} > 60$–70 GeV, it is expected that squarks would undergo a cascade decay via a number of neutralinos and/or charginos rather than undergo a direct decay to photinos as assumed by some papers. Limits obtained when direct decay is assumed are usually higher than limits when cascade decays are included.

Limits from e^+e^- collisions depend on the mixing angle of the lightest mass eigenstate $\tilde{q}_1 = \tilde{q}_R \sin\theta_q + \tilde{q}_L \cos\theta_q$. It is usually assumed that only the sbottom and stop squarks have non-trivial mixing angles (see the stop and sbottom sections). Here, unless otherwise noted, squarks are always taken to be either left/right degenerate, or purely of left or right type. Data from Z decays have set squark mass limits above 40 GeV, in the case of $\tilde{q} \to q\tilde{\chi}_1$ decays if $\Delta m = m_{\tilde{q}} - m_{\tilde{\chi}^0_1} \gtrsim 5$ GeV. For smaller values of Δm, current constraints on the invisible width of the Z ($\Delta\Gamma_{\rm inv} < 2.0$ MeV, LEP 00) exclude $m_{\tilde{u}_{L,R}} < 44$ GeV, $m_{\tilde{d}_R} < 33$ GeV, $m_{\tilde{d}_L} < 44$ GeV and, assuming all squarks degenerate, $m_{\tilde{q}} < 45$ GeV.

Limits made obsolete by the most recent analyses of e^+e^-, $p\overline{p}$, and ep collisions can be found in previous Editions of this *Review*.

VALUE (GeV)	*CL%*	*DOCUMENT ID*		*TECN*	*COMMENT*
> 99.5	95	[230] ACHARD	04	L3	$\Delta m > 10$ GeV, $e^+e^- \to \tilde{q}_{L,R}\bar{\tilde{q}}_{L,R}$
> 97	95	[230] ACHARD	04	L3	$\Delta m > 10$ GeV, $e^+e^- \to \tilde{q}_R\bar{\tilde{q}}_R$
>138	95	[231] ABBOTT	01D	D0	$\ell\ell$+jets+$\not\!\!E_T$, $\tan\beta < 10$, $m_0 <$ 300 GeV, $\mu < 0$, $A_0 = 0$
>255	95	[231] ABBOTT	01D	D0	$\tan\beta = 2$, $m_{\tilde{g}} = m_{\tilde{q}}$, $\mu < 0$, $A_0 = 0$, $\ell\ell$+jets+$\not\!\!E_T$
> 97	95	[232] BARATE	01	ALEP	$e^+e^- \to \tilde{q}\bar{\tilde{q}}$, $\Delta m > 6$ GeV
>250	95	[233] ABBOTT	99L	D0	$\tan\beta = 2$, $\mu < 0$, $A = 0$, jets+$\not\!\!E_T$
>224	95	[234] ABE	96D	CDF	$m_{\tilde{g}} \leq m_{\tilde{q}}$; with cascade decays, $\ell\ell$+jets+$\not\!\!E_T$
• • • We do not use the following data for averages, fits, limits, etc. • • •					
		[235] ADLOFF	03	H1	$e^\pm p \to \tilde{q}, \not{R}, L\overline{Q}\overline{D}$
>276	95	[236] CHEKANOV	03B	ZEUS	$\tilde{d} \to e^-u, \nu d, \not{R}, L\overline{Q}\overline{D}, \lambda > 0.1$
>260	95	[236] CHEKANOV	03B	ZEUS	$\tilde{u} \to e^+d, \not{R}, L\overline{Q}\overline{D}, \lambda > 0.1$
> 82.5	95	[237] HEISTER	03G	ALEP	$\tilde{u}_R, \not{R}$ decay
> 77	95	[237] HEISTER	03G	ALEP	$\tilde{d}_R, \not{R}$ decay
>240	95	[238] ABAZOV	02F	D0	$\tilde{q}, \not{R}\ \lambda'_{2jk}$ indirect decays, $\tan\beta = 2$, any $m_{\tilde{g}}$
>265	95	[238] ABAZOV	02F	D0	$\tilde{q}, \not{R}\ \lambda'_{2jk}$ indirect decays, $\tan\beta = 2$, $m_{\tilde{q}} = m_{\tilde{g}}$
		[239] ABAZOV	02G	D0	$p\overline{p} \to \tilde{g}\tilde{g}, \tilde{g}\tilde{q}$
none 80–121	95	[240] ABBIENDI	02	OPAL	$e\gamma \to \tilde{u}_L, \not{R}\ L\overline{Q}\overline{D}$, $\lambda = 0.3$
none 80–158	95	[240] ABBIENDI	02	OPAL	$e\gamma \to \tilde{d}_R, \not{R}\ L\overline{Q}\overline{D}$, $\lambda = 0.3$
none 80–185	95	[241] ABBIENDI	02B	OPAL	$e\gamma \to \tilde{u}_L, \not{R}\ L\overline{Q}\overline{D}$, $\lambda = 0.3$
none 80–196	95	[241] ABBIENDI	02B	OPAL	$e\gamma \to \tilde{d}_R, \not{R}\ L\overline{Q}\overline{D}$, $\lambda = 0.3$
> 79	95	[242] ACHARD	02	L3	$\tilde{u}_R, \not{R}$ decays
> 55	95	[242] ACHARD	02	L3	$\tilde{d}_R, \not{R}$ decays
>263	95	[243] CHEKANOV	02	ZEUS	$\tilde{u}_L \to \mu q, \not{R}, L\overline{Q}\overline{D}$, $\lambda = 0.3$
>258	95	[243] CHEKANOV	02	ZEUS	$\tilde{u}_L \to \tau q, \not{R}, L\overline{Q}\overline{D}$, $\lambda = 0.3$
>260	95	[244] ADLOFF	01B	H1	$e^+p \to \tilde{q}, \not{R}\ L\overline{Q}\overline{D}$, $\lambda = 0.3$
> 82	95	[245] BARATE	01B	ALEP	$\tilde{u}_R, \not{R}$ decays
> 68	95	[245] BARATE	01B	ALEP	$\tilde{d}_R, \not{R}$ decays
none 150–204	95	[246] BREITWEG	01	ZEUS	$e^+p \to \tilde{d}_R, \not{R}\ L\overline{Q}\overline{D}$, $\lambda = 0.3$
>200	95	[247] ABBOTT	00C	D0	$\tilde{u}_L, \not{R}, \lambda'_{2jk}$ decays
>180	95	[247] ABBOTT	00C	D0	$\tilde{d}_R, \not{R}, \lambda'_{2jk}$ decays
>390	95	[248] ACCIARRI	00P	L3	$e^+e^- \to q\overline{q}, \not{R}$, $\lambda = 0.3$
>148	95	[249] AFFOLDER	00K	CDF	$\tilde{d}_L, \not{R}\ \lambda'_{ij3}$ decays
>200	95	[250] BARATE	00I	ALEP	$e^+e^- \to q\overline{q}, \not{R}$, $\lambda = 0.3$
none 150–269	95	[251] BREITWEG	00E	ZEUS	$e^+p \to \tilde{u}_L, \not{R}, L\overline{Q}\overline{D}$, $\lambda = 0.3$
>240	95	[252] ABBOTT	99	D0	$\tilde{q} \to \tilde{\chi}^0_2 X \to \tilde{\chi}^0_1 \gamma X$, $m_{\tilde{\chi}^0_2} - m_{\tilde{\chi}^0_1} > 20$ GeV
>320	95	[252] ABBOTT	99	D0	$\tilde{q} \to \tilde{\chi}^0_1 X \to \tilde{G}\gamma X$
>243	95	[253] ABBOTT	99K	D0	any $m_{\tilde{g}}$, $\not{R}$, $\tan\beta = 2$, $\mu < 0$
>200	95	[254] ABE	99M	CDF	$p\overline{p} \to \tilde{q}\bar{\tilde{q}}, \not{R}$
none 80–134	95	[255] ABREU	99G	DLPH	$e\gamma \to \tilde{u}_L, \not{R}\ L\overline{Q}\overline{D}$, $\lambda = 0.3$
none 80–161	95	[255] ABREU	99G	DLPH	$e\gamma \to \tilde{d}_R, \not{R}\ L\overline{Q}\overline{D}$, $\lambda = 0.3$
>225	95	[256] ABBOTT	98E	D0	$\tilde{u}_L, \not{R}, \lambda'_{1jk}$ decays
>204	95	[256] ABBOTT	98E	D0	$\tilde{d}_R, \not{R}, \lambda'_{1jk}$ decays
> 79	95	[256] ABBOTT	98E	D0	$\tilde{d}_L, \not{R}, \lambda'_{1jk}$ decays
>202	95	[257] ABE	98S	CDF	$\tilde{u}_L, \not{R}\ \lambda'_{2jk}$ decays
>160	95	[257] ABE	98S	CDF	$\tilde{d}_R, \not{R}\ \lambda'_{2jk}$ decays
>140	95	[258] ACKERSTAFF	98V	OPAL	$e^+e^- \to q\overline{q}, \not{R}$, $\lambda = 0.3$
> 77	95	[259] BREITWEG	98	ZEUS	$m_{\tilde{q}} = m_{\tilde{e}}$, $m(\tilde{\chi}^0_1) = 40$ GeV
		[260] DATTA	97	THEO	$\tilde{\nu}$'s lighter than $\tilde{\chi}^\pm_1$, $\tilde{\chi}^0_2$
>216	95	[261] DERRICK	97	ZEUS	$ep \to \tilde{q}, \tilde{q} \to \mu j$ or τj, $\not{R}$
none 130–573	95	[262] HEWETT	97	THEO	$q\tilde{g} \to \tilde{q}, \tilde{q} \to q\tilde{g}$, with a light gluino
none 190–650	95	[263] TEREKHOV	97	THEO	$qg \to \tilde{q}\tilde{g}, \tilde{q} \to q\tilde{g}$, with a light gluino
> 63	95	[264] AID	96C	H1	$m_{\tilde{q}} = m_{\tilde{e}}$, $m_{\tilde{\chi}^0_1}$=35 GeV
none 330–400	95	[265] TEREKHOV	96	THEO	$ug \to \tilde{u}\tilde{g}, \tilde{u} \to u\tilde{g}$ with a light gluino
>176	95	[266] ABACHI	95C	D0	Any $m_{\tilde{g}} < 300$ GeV; with cascade decays
		[267] ABE	95T	CDF	$\tilde{q} \to \tilde{\chi}^0_2 \to \tilde{\chi}^0_1 \gamma$
> 90	90	[268] ABE	92L	CDF	Any $m_{\tilde{g}} < 410$ GeV; with cascade decay
>100		[269] ROY	92	RVUE	$p\overline{p} \to \tilde{q}\bar{\tilde{q}}$; $\not{R}$
		[270] NOJIRI	91	COSM	

[230] ACHARD 04 search for the production of $\tilde{q}\bar{\tilde{q}}$ of the first two generations in acoplanar di-jet final states in the 192–209 GeV data. Degeneracy of the squark masses is assumed either for both left and right squarks or for right squarks only, as well as $B(\tilde{q} \to q\tilde{\chi}^0_1) = 1$ See Fig. 7 for the dependence of the limits on $m_{\tilde{\chi}^0_1}$. This limit supersedes ACCIARRI 99V.

[231] ABBOTT 01D looked in $\sim 108\ pb^{-1}$ of $p\overline{p}$ collisions at $\sqrt{s}$=1.8 TeV for events with ee, $\mu\mu$, or $e\mu$ accompanied by at least 2 jets and $\not\!\!E_T$. Excluded regions are obtained in the MSUGRA framework from a scan over the parameters $0 < m_0 < 300$ GeV, $10 < m_{1/2} < 110$ GeV, and $1.2 < \tan\beta < 10$.

[232] BARATE 01 looked for acoplanar dijets + $\not\!\!E_T$ final states at 189 to 202 GeV. The limit assumes $B(\tilde{q} \to q\tilde{\chi}^0_1) = 1$, with $\Delta m = m_{\tilde{q}} - m_{\tilde{\chi}^0_1}$. It applies to $\tan\beta = 4$, $\mu = -400$ GeV. See their Fig. 2 for the exclusion in the $(m_{\tilde{q}}, m_{\tilde{g}})$ plane. These limits include and update the results of BARATE 99Q.

[233] ABBOTT 99L consider events with three or more jets and large $\not\!\!E_T$. Spectra and decay rates are evaluated in the framework of minimal Supergravity, assuming five flavors of degenerate squarks, and scanning the space of the universal gaugino ($m_{1/2}$) and scalar (m_0) masses. See their Figs. 2–3 for the dependence of the limit on the relative value of $m_{\tilde{q}}$ and $m_{\tilde{g}}$.

[234] ABE 96D searched for production of gluinos and five degenerate squarks in final states containing a pair of leptons, two jets, and missing E_T. The two leptons arise from the semileptonic decays of charginos produced in the cascade decays. The limit is derived for fixed $\tan\beta = 4.0$, $\mu = -400$ GeV, and $m_{H^+} = 500$ GeV, and with the cascade decays of the squarks and gluinos calculated within the framework of the Minimal Supergravity scenario.

[235] ADLOFF 03 looked for the s-channel production of squarks via $\not{R}\ L\overline{Q}\overline{D}$ couplings in 117.2 pb^{-1} of e^+p data at $\sqrt{s}$ = 301 and 319 GeV and of e^-p data at $\sqrt{s}$ = 319 GeV. The comparison of the data with the SM differential cross section allows limits to be set on couplings for processes mediated through contact interactions. They obtain lower bounds on the value of $m_{\tilde{q}}/\lambda'$ of 710 GeV for the process $e^+\tilde{u} \to \bar{d}^k$ (and charge conjugate), mediated by λ'_{11k}, and of 430 GeV for the process $e^+d \to \bar{u}^j$ (and charge conjugate), mediated by λ'_{1j1}.

[236] CHEKANOV 03B used 131.5 pb^{-1} of e^+p and e^-p data taken at 300 and 318 GeV to look for narrow resonances in the eq or νq final states. Such final states may originate from $L\overline{Q}\overline{D}$ couplings with non-zero λ'_{1j1} (leading to $\tilde{u}_j$) or λ'_{11k} (leading to $\tilde{d}_k$). See their Fig. 8 and explanations in the text for limits. The quoted mass bound assumes that only direct squark decays contribute.

[237] HEISTER 03G searches for the production of squarks in the case of $\not{R}$ prompt decays with $\overline{UDD}$ direct couplings at at $\sqrt{s} = 189$–209 GeV.

[238] ABAZOV 02F looked in 77.5 pb^{-1} of $p\overline{p}$ collisions at 1.8 TeV for events with $\geq 2\mu + \geq$ 4jets, originating from associated production of squarks followed by an indirect $\not{R}$ decay (of the $\tilde{\chi}^0_1$) via $L\overline{Q}\overline{D}$ couplings of the type λ'_{2jk} where j=1,2 and k=1,2,3. Bounds are obtained in the MSUGRA scenario by a scan in the range $0 \leq M_0 \leq 400$ GeV, $60 \leq m_{1/2} \leq 120$ GeV for fixed values $A_0 = 0$, $\mu < 0$, and $\tan\beta$=2 or 6. The bounds are weaker for $\tan\beta$=6. See Figs. 2,3 for the exclusion contours in $m_{1/2}$ versus m_0 for $\tan\beta$=2 and 6, respectively.

[239] ABAZOV 02G search for associated production of gluinos and squarks in 92.7 pb^{-1} of $p\overline{p}$ collisions at $\sqrt{s}$=1.8 TeV, using events with one electron, ≥ 4 jets, and large $\not\!\!E_T$. The results are compared to a MSUGRA scenario with $\mu < 0$, $A_0 = 0$, and $\tan\beta = 3$ and allow to exclude a region of the $(m_0, m_{1/2})$ shown in Fig. 11.

[240] ABBIENDI 02 looked for events with an electron or neutrino and a jet in e^+e^- at 189 GeV. Squarks (or leptoquarks) could originate from a $L\overline{Q}\overline{D}$ coupling of an electron with a quark from the fluctuation of a virtual photon. Limits on the couplings λ'_{1jk} as a function of the squark mass are shown in Figs. 8–9, assuming that only direct squark decays contribute.

[241] ABBIENDI 02B looked for events with an electron or neutrino and a jet in e^+e^- at 189–209 GeV. Squarks (or leptoquarks) could originate from a $L\overline{Q}\overline{D}$ coupling of an electron with a quark from the fluctuation of a virtual photon. Limits on the couplings λ'_{1jk} as a function of the squark mass are shown in Fig. 4, assuming that only direct squark decays contribute. The quoted limits are read off from Fig. 4. Supersedes the results of ABBIENDI 02.

[242] ACHARD 02 searches for the production of squarks in the case of $\not{R}$ prompt decays with UDD couplings at $\sqrt{s}$=189–208 GeV. The search is performed for direct and indirect decays, assuming one coupling at the time to be nonzero. The limit holds for indirect decays. Stronger limits are reached for ($\tilde{u}_R$,$\tilde{d}_R$) direct (80,56) GeV and ($\tilde{u}_L$,$\tilde{d}_L$) direct or indirect (87,86) GeV decays.

[243] CHEKANOV 02 search for lepton flavor violating processes $e^+p \to \ell X$, where $\ell = \mu$ or τ with high p_T, in 47.7 pb^{-1} of e^+p collisions at 300 GeV. Such final states may originate from $LQ\overline{D}$ couplings with simultaneously nonzero λ'_{1jk} and λ'_{ijk} (i=2 or 3). The quoted mass bound assumes that only direct squark decays contribute.

[244] ADLOFF 01B searches for squark exchange in 37 pb^{-1} of e^+p collisions, mediated by $\not{R}$ couplings $LQ\overline{D}$ and leading to several final states with leptons and jets from direct or indirect decays. The 7 decay topologies considered cover almost all branching fractions. Limits are derived on λ'_{1j1}, as a function of the squark mass from a scan over the parameters 70<M_2 <350 GeV, $-300 < \mu < 300$ GeV, assuming mass degeneracy for the squarks, a slepton mass of 90 GeV, and tanβ=2. Similar limits obtained under more constrained model assumptions are discussed in the paper. These results supersede AID 96.

[245] BARATE 01B searches for the production of squarks in the case of $\not{R}$ prompt decays with $LL\overline{E}$ indirect or $\overline{UDD}$ direct couplings at $\sqrt{s}$=189–202 GeV. The limit holds for direct decays mediated by $\not{R}$ $\overline{UDD}$ couplings. Limits are also given for $LL\overline{E}$ indirect decays ($m_{\tilde{u}_R} > 90$ GeV and $m_{\tilde{d}_R} > 89$ GeV). Supersedes the results from BARATE 00H.

[246] BREITWEG 01 searches for squark production in 47.7 pb^{-1} of e^+p collisions, mediated by $\not{R}$ couplings $LQ\overline{D}$ and leading to final states with $\tilde{\nu}$ and ≥ 1 jet, complementing the e^+X final states of BREITWEG 00E. Limits are derived on $\lambda'\sqrt{\beta}$, where β is the branching fraction of the squarks into e^+q+$\overline{\nu}q$, as function of the squark mass, see their Fig. 15. The quoted mass limit assumes that only direct squark decays contribute.

[247] ABBOTT 00C searched in $\sim$ 94 pb^{-1} of $p\overline{p}$ collisions for events with $\mu\mu$+jets, originating from associated production of leptoquarks. The results can be interpreted as limits on production of squarks followed by direct $\not{R}$ decay via $\lambda'_{2jk}L_2Q_jd^c_k$ couplings. Bounds are obtained on the cross section for branching ratios of 1 and of 1/2, see their Fig. 4. The former yields the limit on the $\tilde{u}_L$. The latter is combined with the bound of ABBOTT 99J from the $\mu\nu$+jets channel and of ABBOTT 98E and ABBOTT 98J from the $\nu\nu$+jets channel to yield the limit on $\tilde{d}_R$.

[248] ACCIARRI 00P studied the effect on hadronic cross sections of t-channel down-type squark exchange via R-parity violating coupling $\lambda'_{1jk}L_1Q_jd^c_k$. The limit here refers to the case j=1,2, and holds for λ'_{1jk}=0.3. Data collected at $\sqrt{s}$=130–189 GeV, superseding the results of ACCIARRI 98J.

[249] AFFOLDER 00K searched in $\sim$ 88 pb^{-1} of $p\overline{p}$ collisions for events with 2–3 jets, at least one being b-tagged, large $\not{E}_T$ and no high p_T leptons. Such $\nu\nu$+b-jets events would originate from associated production of squarks followed by direct $\not{R}$ decay via $\lambda'_{ij3}L_iQ_jd^c_3$ couplings. Bounds are obtained on the production cross section assuming zero branching ratio to charged leptons.

[250] BARATE 00I studied the effect on hadronic cross sections and charge asymmetries of t-channel down-type squark exchange via R-parity violating coupling $\lambda'_{1jk}L_1Q_jd^c_k$. The limit here refers to the case j=1,2, and holds for λ'_{1jk}=0.3. A 50 GeV limit is found for up-type squarks with k=3. Data collected at $\sqrt{s}$= 130–183 GeV.

[251] BREITWEG 00E searches for squark exchange in e^+p collisions, mediated by $\not{R}$ couplings $LQ\overline{D}$ and leading to final states with an identified e^+ and ≥ 1 jet. The limit applies to up-type squarks of all generations, and assumes B($\tilde{q} \to qe$)=1.

[252] ABBOTT 99 searched for $\gamma\not{E}_T + \geq 2$ jet final states, and set limits on $\sigma(p\overline{p} \to \tilde{q}$+X)·B($\tilde{q} \to \gamma\not{E}_T$X). The quoted limits correspond to $m_{\tilde{g}} \geq m_{\tilde{q}}$, with B($\tilde{\chi}^0_2 \to \tilde{\chi}^0_1\gamma$)=1 and B($\tilde{\chi}^0_1 \to \tilde{G}\gamma$)=1, respectively. They improve to 310 GeV (360 GeV in the case of $\gamma\tilde{G}$ decay) for $m_{\tilde{g}}$=$m_{\tilde{q}}$.

[253] ABBOTT 99K uses events with an electron pair and four jets to search for the decay of the $\tilde{\chi}^0_1$ LSP via $\not{R}$ $LQ\overline{D}$ couplings. The particle spectrum and decay branching ratios are taken in the framework of minimal supergravity. An excluded region at 95% CL is obtained in the (m_0,$m_{1/2}$) plane under the assumption that A_0=0, $\mu < 0$, tanβ=2 and any one of the couplings $\lambda'_{1jk} > 10^{-3}$ (j=1,2 and k=1,2,3) and from which the above limit is computed. For equal mass squarks and gluinos, the corresponding limit is 277 GeV. The results are essentially independent of A_0, but the limit deteriorates rapidly with increasing tanβ or $\mu > 0$.

[254] ABE 99M looked in 107 pb^{-1} of $p\overline{p}$ collisions at $\sqrt{s}$=1.8 TeV for events with like sign dielectrons and two or more jets from the sequential decays $\tilde{q} \to q\tilde{\chi}^0_1$ and $\tilde{\chi}^0_1 \to eq\overline{q}'$, assuming $\not{R}$ coupling $L_1Q_jD^c_k$, with j=2,3 and k=1,2,3. They assume five degenerate squark flavors, B($\tilde{q} \to q\tilde{\chi}^0_1$)=1, B($\tilde{\chi}^0_1 \to eq\overline{q}'$)=0.25 for both e^+ and e^-, and $m_{\tilde{g}} \geq$ 200 GeV. The limit is obtained for $m_{\tilde{\chi}^0_1} \geq m_{\tilde{q}}/2$ and improves for heavier gluinos or heavier χ^0_1.

[255] ABREU 99G looked for events with an electron or neutrino and a jet in e^+e^- at 183 GeV. Squarks (or leptoquarks) could originate from a $LQ\overline{D}$ coupling of an electron with a quark from the fluctuation of a virtual photon. Limits on the couplings λ'_{1jk} as a function of the squark mass are shown in Fig. 4, assuming that only direct squark decays contribute.

[256] ABBOTT 98E searched in $\sim$ 115 pb^{-1} of $p\overline{p}$ collisions for events with $e\nu$+jets, originating from associated production of squarks followed by direct $\not{R}$ decay via $\lambda'_{1jk}L_1Q_jd^c_k$ couplings. Bounds are obtained by combining these results with the previous bound of ABBOTT 97B from the ee+jets channel and with a reinterpretation of ABACHI 96B $\nu\nu$+jets channel.

[257] ABE 98S looked in $\sim$ 110 pb^{-1} of $p\overline{p}$ collisions at $\sqrt{s}$=1.8 TeV for events with $\mu\mu$+jets originating from associated production of squarks followed by direct $\not{R}$ decay via $\lambda'_{2jk}L_2Q_jd^c_k$ couplings. Bounds are obtained on the production cross section times the square of the branching ratio, see Fig. 2. Mass limits result from the comparison with theoretical cross sections and branching ratio equal to 1 for $\tilde{u}_L$ and 1/2 for $\tilde{d}_R$.

[258] ACKERSTAFF 98V and ACCIARRI 98J studied the interference of t-channel squark ($\tilde{d}_R$) exchange via R-parity violating $\lambda'_{1jk}L_1Q_jd^c_k$ coupling in $e^+e^- \to q\overline{q}$. The limit is for λ'_{1jk}=0.3. See paper for related limits on $\tilde{u}_L$ exchange. Data collected at $\sqrt{s}$=130–172 GeV.

[259] BREITWEG 98 used positron+jet events with missing energy and momentum to look for $e^+q \to \tilde{e}\tilde{q}$ via gaugino-like neutralino exchange with decays into ($e\tilde{\chi}^0_1$)($q\tilde{\chi}^0_1$). See paper for dependences in $m_{\tilde{e}}$, $m_{\tilde{\chi}^0_1}$.

[260] DATTA 97 argues that the squark mass bound by ABACHI 95C can be weakened by 10–20 GeV if one relaxes the assumption of the universal scalar mass at the GUT-scale so that the $\tilde{\chi}^\pm_1$,$\tilde{\chi}^0_2$ in the squark cascade decays have dominant and invisible decays to $\tilde{\nu}$.

[261] DERRICK 97 looked for lepton-number violating final states via R-parity violating couplings $\lambda'_{ijk}L_iQ_jd_k$. When $\lambda'_{11k}\lambda'_{ijk} \neq 0$, the process $eu \to \tilde{d}^*_k \to \ell_iu_j$ is possible. When $\lambda'_{1j1}\lambda'_{ijk} \neq 0$, the process $e\overline{d} \to \tilde{u}^*_j \to \ell_i\overline{d}_k$ is possible. 100% branching fraction $\tilde{q} \to \ell j$ is assumed. The limit quoted here corresponds to $\tilde{t} \to \tau q$ decay, with λ'=0.3. For different channels, limits are slightly better. See Table 6 in their paper.

[262] HEWETT 97 reanalyzed the limits on possible resonances in di-jet mode ($\tilde{q} \to q\tilde{g}$) from ALITTI 93 quoted in "Limits for Excited q (q^*) from Single Production," ABE 96 in "SCALE LIMITS for Contact Interactions: $\Lambda(qqqq)$," and unpublished CDF, DØ bounds. The bound applies to the gluino mass of 5 GeV, and improves for lighter gluino. The analysis has gluinos in parton distribution function.

[263] TEREKHOV 97 improved the analysis of TEREKHOV 96 by including di-jet angular distributions in the analysis.

[264] AID 96C used positron+jet events with missing energy and momentum to look for $e^+q \to \tilde{e}\tilde{q}$ via neutralino exchange with decays into ($e\tilde{\chi}^0_1$)($q\tilde{\chi}^0_1$). See the paper for dependences on $m_{\tilde{e}}$, $m_{\tilde{\chi}^0_1}$.

[265] TEREKHOV 96 reanalyzed the limits on possible resonances in di-jet mode ($\tilde{u} \to u\tilde{g}$) from ABE 95N quoted in "MASS LIMITS for g_A (axigluon)." The bound applies only to the case with a light gluino.

[266] ABACHI 95C assume five degenerate squark flavors with $m_{\tilde{q}_L} = m_{\tilde{q}_R}$. Sleptons are assumed to be heavier than squarks. The limits are derived for fixed tanβ = 2.0 μ = $-$250 GeV, and m_{H^+}=500 GeV, and with the cascade decays of the squarks and gluinos calculated within the framework of the Minimal Supergravity scenario. The bounds are weakly sensitive to the three fixed parameters for a large fraction of parameter space. No limit is given for m_{gluino} >547 GeV.

[267] ABE 95T looked for a cascade decay of five degenerate squarks into $\tilde{\chi}^0_2$ which further decays into $\tilde{\chi}^0_1$ and a photon. No signal is observed. Limits vary widely depending on the choice of parameters. For $\mu = -40$ GeV, tanβ = 1.5, and heavy gluinos, the range 50<$m_{\tilde{q}}$ (GeV)<110 is excluded at 90% CL. See the paper for details.

[268] ABE 92L assume five degenerate squark flavors and $m_{\tilde{q}_L} = m_{\tilde{q}_R}$. ABE 92L includes the effect of cascade decay, for a particular choice of parameters, $\mu = -250$ GeV, tanβ = 2. Results are weakly sensitive to these parameters over much of parameter space. No limit for $m_{\tilde{q}} \leq 50$ GeV (but other experiments rule out that region). Limits are 10–20 GeV higher if B($\tilde{q} \to q\tilde{\gamma}$) = 1. Limit assumes GUT relations between gaugino masses and the gauge coupling; in particular that for $|\mu|$ not small, $m_{\tilde{\chi}^0_1} \approx m_{\tilde{g}}/6$. This last relation implies that as $m_{\tilde{g}}$ increases, the mass of $\tilde{\chi}^0_1$ will eventually exceed $m_{\tilde{q}}$ so that no decay is possible. Even before that occurs, the signal will disappear; in particular no bounds can be obtained for $m_{\tilde{g}}$ >410 GeV. m_{H^+}=500 GeV.

[269] ROY 92 reanalyzed CDF limits on di-lepton events to obtain limits on squark production in R-parity violating models. The 100% decay $\tilde{q} \to q\tilde{\chi}$ where $\tilde{\chi}$ is the LSP, and the LSP decays either into $\ell q\overline{d}$ or $\ell\ell\overline{e}$ is assumed.

[270] NOJIRI 91 argues that a heavy squark should be nearly degenerate with the gluino in minimal supergravity not to overclose the universe.

Long-lived $\tilde{q}$ (Squark) MASS LIMIT

The following are bounds on long-lived scalar quarks, assumed to hadronise into hadrons with lifetime long enough to escape the detector prior to a possible decay. Limits may depend on the mixing angle of mass eigenstates: $\tilde{q}_1 = \tilde{q}_L\cos\theta_q + \tilde{q}_R\sin\theta_q$.

The coupling to the Z^0 boson vanishes for up-type squarks when θ_u=0.98, and for down type squarks when θ_d=1.17.

VALUE (GeV)	CL%	DOCUMENT ID		TECN	COMMENT
• • • We do not use the following data for averages, fits, limits, etc. • • •					
>95	95	[271] HEISTER	03H	ALEP	$\tilde{u}$
>92	95	[271] HEISTER	03H	ALEP	$\tilde{d}$
none 2–85	95	[272] ABREU	98P	DLPH	$\tilde{u}_L$
none 2–81	95	[272] ABREU	98P	DLPH	$\tilde{u}_R$
none 2–80	95	[272] ABREU	98P	DLPH	$\tilde{u}$, θ_u=0.98
none 2–83	95	[272] ABREU	98P	DLPH	$\tilde{d}_L$
none 5–40	95	[272] ABREU	98P	DLPH	$\tilde{d}_R$
none 5–38	95	[272] ABREU	98P	DLPH	$\tilde{d}$, θ_d=1.17

[271] HEISTER 03H use e^+e^- data at and around the Z^0 peak to look for hadronizing stable squarks. Combining their results on searches for charged and neutral R-hadrons with JANOT 03, a lower limit of 15.7 GeV on the mass is obtained. Combining this further with the results of searches for tracks with anomalous ionization in data from 183 to 208 GeV yields the quoted bounds.

[272] ABREU 98P assumes that 40% of the squarks will hadronise into a charged hadron, and 60% into a neutral hadron which deposits most of its energy in hadron calorimeter. Data collected at $\sqrt{s}$=130–183 GeV.

$\tilde{b}$ (Sbottom) MASS LIMIT

Limits in e^+e^- depend on the mixing angle of the mass eigenstate $\tilde{b}_1 = \tilde{b}_L\cos\theta_b + \tilde{b}_R\sin\theta_b$. Coupling to the Z vanishes for $\theta_b \sim 1.17$. As a consequence, no absolute constraint in the mass region $\lesssim 40$ GeV is available in the literature at this time from e^+e^- collisions. In the Listings below, we use $\Delta m = m_{\tilde{b}_1} - m_{\tilde{\chi}^0_1}$.

VALUE (GeV)	CL%	DOCUMENT ID		TECN	COMMENT
>95	95	[273] ACHARD	04	L3	$\tilde{b} \to b\tilde{\chi}^0_1, \theta_b$=0, Δm> 15–25 GeV
>81	95	[273] ACHARD	04	L3	$\tilde{b} \to b\tilde{\chi}^0_1$, all θ_b, Δm >15–25 GeV
>93	95	[274] ABDALLAH	03M	DLPH	$\tilde{b} \to b\tilde{\chi}^0$, θ_b=0, Δm >7 GeV
>76	95	[274] ABDALLAH	03M	DLPH	$\tilde{b} \to b\tilde{\chi}^0$, all θ_b, Δm >7 GeV
>85.1	95	[275] ABBIENDI	02H	OPAL	$\tilde{b} \to b\tilde{\chi}^0_1$, all$\theta_b$, Δm >10 GeV, CDF
>89	95	[276] HEISTER	02K	ALEP	$\tilde{b} \to b\tilde{\chi}^0_1$, all θ_b, Δm >8 GeV, CDF
none 3.5–4.5	95	[277] SAVINOV	01	CLEO	$\tilde{B}$ meson
none 80–145		[278] AFFOLDER	00D	CDF	$\tilde{b} \to b\tilde{\chi}^0_1$, $m_{\tilde{\chi}^0_1}$ <50 GeV
• • • We do not use the following data for averages, fits, limits, etc. • • •					
none 50–82	95	[279] ABDALLAH	03C	DLPH	$\bar{b} \to b\tilde{g}$, stable $\tilde{g}$, all θ_b, ΔM > 10 GeV
		[280] BERGER	03	THEO	
>71.5	95	[281] HEISTER	03G	ALEP	$\tilde{b}_L$,$\not{R}$ decay
>27.4	95	[282] HEISTER	03H	ALEP	$\tilde{b} \to b\tilde{g}$, stable $\tilde{g}$ or $\tilde{b}$
>48	95	[283] ACHARD	02	L3	$\tilde{b}_1$, $\not{R}$ decays
		[284] BAEK	02	THEO	
		[285] BECHER	02	THEO	
		[286] CHEUNG	02B	THEO	
		[287] CHO	02	THEO	
>72	95	[288] ABREU	01D	DLPH	$\not{R}(\overline{UDD})$, all Δm > 5 GeV, θ_b=0
		[289] BERGER	01	THEO	$p\overline{p} \to$ X+b-quark
none 52–115	95	[290] ABBOTT	99F	D0	$\tilde{b} \to b\tilde{\chi}^0_1$, $m_{\tilde{\chi}^0_1}$ < 20 GeV

[273] ACHARD 04 search for the production of $\tilde{b}\bar{\tilde{b}}$ in acoplanar b-tagged di-jet final states in the 192–209 GeV data. See Fig. 6 for the dependence of the limits on $m_{\tilde{\chi}^0_1}$. This limit supersedes ACCIARRI 99V.

[274] ABDALLAH 03M looked for $\tilde{b}$ pair production in events with acoplanar jets and $\not{E}$ at $\sqrt{s}$ = 189–208 GeV. The limit improves to 87 (98) GeV for all θ_b (θ_b = 0) for Δm > 10 GeV. See Fig. 24 and Table 11 for other choices of Δm. These limits include and update the results of ABREU,P 00D.

[275] ABBIENDI 02H search for events with two acoplanar jets and $\not{p}_T$ in the 161–209 GeV data. The limit assumes 100% branching ratio and uses the exclusion at large Δm from CDF (AFFOLDER 00D). For θ_b=0, the bound improves to > 96.9 GeV. See Fig. 4 and Table 6 for the more general dependence on the limits on Δm. These results supersede ABBIENDI 99M.

[276] HEISTER 02K search for bottom squarks in final states with acoplanar jets with b tagging, using 183–209 GeV data. The mass bound uses the CDF results from AFFOLDER 00D. See Fig. 5 for the more general dependence of the limits on Δm. Updates BARATE 01.

[277] SAVINOV 01 use data taken at $\sqrt{s}$=10.52 GeV, below the $B\overline{B}$ threshold. They look for events with a pair of leptons with opposite charge and a fully reconstructed hadronic D or D^* decay. These could originate from production of a light-sbottom hadron followed by $\tilde{B} \to D^{(*)}\ell^-\tilde{\nu}$, in case the $\tilde{\nu}$ is the LSP, or $\tilde{B} \to D^{(*)}\pi\ell^-$, in case of $\not{R}$. The mass range $3.5 \leq M(\tilde{B}) \leq 4.5$ GeV was explored, assuming 100% branching ratio for either of the decays. In the $\tilde{\nu}$ LSP scenario, the limit holds only for $M(\tilde{\nu})$ less than about 1 GeV and for the D^* decays it is reduced to the range 3.9–4.5 GeV. For the $\not{R}$ decay, the whole range is excluded.

[278] AFFOLDER 00D search for final states with 2 or 3 jets and $\not{E}_T$, one jet with a b tag. See their Fig. 3 for the mass exclusion in the $m_{\tilde{t}}$, $m_{\tilde{\chi}^0_1}$ plane.

[279] ABDALLAH 03C looked for events of the type $q\bar{q}R^{\pm}R^{\pm}$, $q\bar{q}R^{\pm}R^0$ or $q\bar{q}R^0R^0$ in e^+e^- interactions at $\sqrt{s} = 189 - 208$ GeV. The $R^{\pm}$ bound states are identified by anomalous dE/dx in the tracking chambers and the R^0 by missing energy due to their reduced energy loss in the calorimeters. Excluded mass regions in the $(m(\tilde{b}), m(\tilde{g}))$ plane for $m(\tilde{g}) > 2$ GeV are obtained for several values of the probability for the gluino to fragment into $R^{\pm}$ or R^0, as shown in their Fig. 19. The limit improves to 94 GeV for $\theta_b = 0$.

[280] BERGER 03 studies the constraints on a $\tilde{b}_1$ with mass in the 2.2–5.5 GeV region coming from radiative decays of Υ(nS) into sbottomonium. The constraints apply only if $\tilde{b}_1$ lives long enough to permit formation of the sbottomonium bound state. A small region of mass in the $m_{\tilde{b}_1} - m_{\tilde{g}}$ plane survives current experimental constraints from CLEO.

[281] HEISTER 03G searches for the production of $\tilde{b}$ pairs in the case of $\not{R}$ prompt decays with $LL\overline{E}$, $LQ\overline{D}$ or $\overline{UDD}$ couplings at $\sqrt{s}$ = 189–209 GeV. The limit holds for indirect decays mediated by $\not{R}$ $\overline{UDD}$ couplings. It improves to 90 GeV for indirect decays mediated by $\not{R}$ $LL\overline{E}$ couplings and to 80 GeV for indirect decays mediated by $\not{R}$ $LQ\overline{D}$ couplings. Supersedes the results from BARATE 01B.

[282] HEISTER 03H use their results on bounds on stable squarks, on stable gluinos and on squarks decaying to a stable gluino from the same paper to derive a mass limit on $\tilde{b}$, see their Fig. 13.

[283] ACHARD 02 searches for the production of squarks in the case of $\not{R}$ prompt decays with $\overline{UDD}$ couplings at $\sqrt{s}$=189–208 GeV. The search is performed for direct and indirect decays, assuming one coupling at the time to be nonzero. The limit is computed for the minimal cross section and holds for indirect decays and reaches 55 GeV for direct decays.

[284] BAEK 02 studies the constraints on a $\tilde{b}_1$ with mass in the 2.2–5.5 GeV region coming from precision measurements of Z^0 decays. It is noted that CP-violating couplings in the MSSM parameters relax the strong constraints otherwised derived from CP conservation.

[285] BECHER 02 studies the constraints on a $\tilde{b}_1$ with mass in the 2.2–5.5 GeV region coming from radiative B meson decays, and sets limits on the off-diagonal flavor-changing couplings $q\tilde{b}\tilde{g}$ (q=d,s).

[286] CHEUNG 02B studies the constraints on a $\tilde{b}_1$ with mass in the 2.2–5.5 GeV region and a gluino in the mass range 12–16 GeV, using precision measurements of Z^0 decays and e^+e^- annihilations at LEP2. Few detectable events are predicted in the LEP2 data for the model proposed by BERGER 01.

[287] CHO 02 studies the constraints on a $\tilde{b}_1$ with mass in the 2.2–5.5 GeV region coming from precision measurements of Z^0 decays. Strong constraints are obtained for CP-conserving MSSM couplings.

[288] ABREU 01D searches for multi-jet events, expected in the case of prompt decays from $\not{R}$ $\overline{UDD}$ couplings and indirect decays, using data from $\sqrt{s}$=189 GeV. Limits are obtained in the plane of the squark mass versus $m_{\tilde{\chi}^0_1}$. The mass limit is derived using the constraint on the neutralino mass from the same paper (see the section on unstable $\tilde{\chi}^0_1$). See Fig. 9 for other choices of Δm.

[289] BERGER 01 reanalyzed interpretation of Tevatron data on bottom-quark production. Argues that pair production of light gluinos ($m\sim$ 12–16 GeV) with subsequent 2-body decay into a light sbottom ($m\sim$ 2–5.5 GeV) and bottom can reconcile Tevatron data with predictions of perturbative QCD for the bottom production rate. The sbottom must either decay hadronically via a R-parity- and B-violating interaction, or be long-lived. Constraints on the mass spectrum are derived from the measurements of time-averaged B^0-$\overline{B}^0$ mixing.

[290] ABBOTT 99F looked for events with two jets, with or without an associated muon from b decay, and $\not{E}_T$. See Fig. 2 for the dependence of the limit on $m_{\tilde{\chi}^0_1}$. No limit for $m_{\tilde{\chi}^0_1} > 47$ GeV.

$\tilde{t}$ (Stop) MASS LIMIT

Limits depend on the decay mode. In e^+e^- collisions they also depend on the mixing angle of the mass eigenstate $\tilde{t}_1 = \tilde{t}_L\cos\theta_t + \tilde{t}_R\sin\theta_t$. The coupling to the Z vanishes when $\theta_t = 0.98$. In the Listings below, we use $\Delta m \equiv m_{\tilde{t}_1} - m_{\tilde{\chi}^0_1}$ or $\Delta m \equiv m_{\tilde{t}_1} - m_{\tilde{\nu}}$, depending on relevant decay mode. See also bounds in "$\tilde{q}$ (Squark) MASS LIMIT." Limits made obsolete by the most recent analyses of e^+e^- and $p\overline{p}$ collisions can be found in previous Editions of this *Review*.

VALUE (GeV)	CL%	DOCUMENT ID		TECN	COMMENT
> 90	95	[291] ACHARD	04	L3	$\tilde{t} \to c\tilde{\chi}^0_1$, all θ_t, Δm> 15–25 GeV
> 93	95	[291] ACHARD	04	L3	$\tilde{b} \to b\ell\tilde{\nu}$, all θ_t, Δm>15 GeV
> 88	95	[291] ACHARD	04	L3	$\tilde{b} \to b\tau\tilde{\nu}$, all θ_t,Δm>15 GeV
> 75	95	[292] ABDALLAH	03M	DLPH	$\tilde{t} \to c\tilde{\chi}^0$, θ_t=0, Δm >2 GeV
> 71	95	[292] ABDALLAH	03M	DLPH	$\tilde{t} \to c\tilde{\chi}^0$, all θ_t, Δm >2 GeV
> 96	95	[292] ABDALLAH	03M	DLPH	$\tilde{t} \to c\tilde{\chi}^0$,$\theta_t$=0,$\Delta m$ >10 GeV
> 92	95	[292] ABDALLAH	03M	DLPH	$\tilde{t} \to c\tilde{\chi}^0$,all θ_t,Δm >10 GeV
none 80–131	95	[293] ACOSTA	03C	CDF	$\tilde{t} \to b\ell\tilde{\nu}$, $m_{\tilde{\nu}} \leq$ 63 GeV
>144	95	[294] ABAZOV	02C	D0	$\tilde{t} \to b\ell\tilde{\nu}$, $m_{\tilde{\nu}}$=45 GeV
> 95.7	95	[295] ABBIENDI	02H	OPAL	$c\tilde{\chi}^0_1$, allθ_t, Δm >10 GeV
> 92.6	95	[295] ABBIENDI	02H	OPAL	$b\ell\tilde{\nu}$, allθ_t, Δm >10 GeV
> 91.5	95	[295] ABBIENDI	02H	OPAL	$b\tau\tilde{\nu}$, allθ_t, Δm >10 GeV
> 63	95	[296] HEISTER	02K	ALEP	any decay, any lifetime, all θ_t
> 92	95	[296] HEISTER	02K	ALEP	$\tilde{t} \to c\tilde{\chi}^0_1$, all θ_t, Δm >8 GeV, CDF
> 97	95	[296] HEISTER	02K	ALEP	$\tilde{t} \to b\ell\tilde{\nu}$, all θ_t, Δm >8 GeV, DØ
> 78	95	[296] HEISTER	02K	ALEP	$\tilde{t} \to b\tilde{\chi}^0_1 W^*$, all θ_t, Δm >8 GeV
• • • We do not use the following data for averages, fits, limits, etc. • • •					
none 50–87	95	[297] ABDALLAH	03C	DLPH	$\bar{t} \to c\bar{g}$, stable $\bar{g}$, all θ_t, ΔM > 10 GeV
		[298] CHAKRAB...	03	THEO	$p\overline{p} \to \tilde{t}\bar{t}^*$, RPV
> 71.5	95	[299] HEISTER	03G	ALEP	$\tilde{t}_L$,$\not{R}$ decay
> 80	95	[300] HEISTER	03H	ALEP	$\tilde{t} \to c\tilde{g}$, stable $\tilde{g}$ or $\tilde{t}$, all θ_t, all ΔM
> 77	95	[301] ACHARD	02	L3	$\tilde{t}_1$, $\not{R}$ decays
> 74	95	[302] ABREU	01D	DLPH	$\not{R}(\overline{UDD})$, all Δm > 5 GeV, θ_t=0
> 59	95	[302] ABREU	01D	DLPH	$\not{R}(\overline{UDD})$, all Δm > 5 GeV, θ_t=0.98
		[303] AFFOLDER	01B	CDF	$t \to \tilde{t}\chi^0_1$
> 76	95	[304] ABBIENDI	00	OPAL	$\not{R}$, $(\overline{UDD})$, all θ_t
> 61	95	[305] ABREU	00I	DLPH	$\not{R}$ $(LL\overline{E})$, θ_t=0.98, Δm > 4 GeV
none 68–119	95	[306] AFFOLDER	00D	CDF	$\tilde{t} \to c\tilde{\chi}^0_1$, $m_{\tilde{\chi}^0_1}$ <40 GeV
none 84–120	95	[307] AFFOLDER	00G	CDF	$\tilde{t}_1 \to b\ell\tilde{\nu}$, $m_{\tilde{\nu}}$ <45
> 59	95	[308] BARATE	00P	ALEP	Repl. by HEISTER 02K
>120	95	[309] ABE	99M	CDF	$p\overline{p} \to \tilde{t}_1\bar{\tilde{t}}_1$, $\not{R}$
none 61–91	95	[310] ABACHI	96B	D0	$\tilde{t} \to c\tilde{\chi}^0_1$, $m_{\tilde{\chi}^0_1}$ <30 GeV
none 9–24.4	95	[311] AID	96	H1	$ep \to \tilde{t}\bar{\tilde{t}}$, $\not{R}$ decays
>138	95	[312] AID	96	H1	$ep \to \tilde{t}$, $\not{R}$, $\lambda\cos\theta_t > 0.03$
> 45		[313] CHO	96	RVUE	B^0-$\overline{B}^0$ and ϵ, θ_t= 0.98, $\tan\beta$ <2
none 11–41	95	[314] BUSKULIC	95E	ALEP	$\not{R}$ $(LL\overline{E})$, θ_t=0.98
none 6.0–41.2	95	AKERS	94K	OPAL	$\tilde{t} \to c\tilde{\chi}^0_1$, θ_t=0, Δm >2 GeV
none 5.0–46.0	95	AKERS	94K	OPAL	$\tilde{t} \to c\tilde{\chi}^0_1$, θ_t=0, Δm >5 GeV
none 11.2–25.5	95	AKERS	94K	OPAL	$\tilde{t} \to c\tilde{\chi}^0_1$, θ_t=0.98, Δm >2 GeV
none 7.9–41.2	95	AKERS	94K	OPAL	$\tilde{t} \to c\tilde{\chi}^0_1$, θ_t=0.98, Δm >5 GeV
none 7.6–28.0	95	[315] SHIRAI	94	VNS	$\tilde{t} \to c\tilde{\chi}^0_1$, any θ_t, Δm >10 GeV
none 10–20	95	[315] SHIRAI	94	VNS	$\tilde{t} \to c\tilde{\chi}^0_1$, any θ_t, Δm > 2.5 GeV

[291] ACHARD 04 search in the 192–209 GeV data for the production of $\tilde{t}\bar{\tilde{t}}$ in acoplanar di-jet final states and, in case of $b\ell\tilde{\nu}$ ($b\tau\tilde{\nu}$) final states, two leptons (taus). The limits for θ_t=0 improve to 95, 96 and 93 GeV, respectively. All limits assume 100% branching ratio for the respective decay modes. See Fig. 6 for the dependence of the limits on $m_{\tilde{\chi}^0_1}$. These limits supersede ACCIARRI 99V.

[292] ABDALLAH 03M looked for $\tilde{t}$ pair production in events with acoplanar jets and $\not{E}$ at $\sqrt{s}$ = 189–208 GeV. See Fig. 23 and Table 11 for other choices of Δm. These limits include and update the results of ABREU,P 00D.

[293] ACOSTA 03C searched in 107 pb^{-1} of $p\bar{p}$ collisions at $\sqrt{s}$=1.8 TeV for pair production of $\tilde{t}$ followed by the decay $\tilde{t} \to b\ell\tilde{\nu}$. They looked for events with two isolated leptons (e or μ), at least one jet and $\not{E}_T$. The excluded mass range is reduced for larger $m_{\tilde{\nu}}$, and no limit is set for $m_{\tilde{\nu}} > 88.4$ GeV (see Fig. 2).

[294] ABAZOV 02C looked in 108.3pb^{-1} of $p\overline{p}$ collisions at $\sqrt{s}$=1.8 TeV for events with $e\mu\not{E}_T$, originating from associated production $\tilde{t}\bar{\tilde{t}}$. Branching ratios are assumed to be 100%. The bound for the $b\ell\tilde{\nu}$ decay weakens for large $\tilde{\nu}$ mass (see Fig. 3), and no limit is set when $m_{\tilde{\nu}} > 85$ GeV. See Fig. 4 for the limits in case of decays to a real $\tilde{\chi}^{\pm}_1$, followed by $\tilde{\chi}^{\pm}_1 \to \ell\tilde{\nu}$, as a function of $m_{\tilde{\chi}^{\pm}_1}$.

[295] ABBIENDI 02H looked for events with two acoplanar jets, $\not{p}_T$, and, in the case of $b\ell\tilde{\nu}$ final states, two leptons, in the 161–209 GeV data. The bound for $c\tilde{\chi}^0_1$ applies to the region where $\Delta m < m_W + m_b$, else the decay $\tilde{t}_1 \to b\tilde{\chi}^0_1 W^+$ becomes dominant. The limit for $b\ell\tilde{\nu}$ assumes equal branching ratios for the three lepton flavors and for $b\tau\tilde{\nu}$ 100% for this channel. For θ_t=0, the bounds improve to > 97.6 GeV ($c\tilde{\chi}^0_1$), > 96.0 GeV ($b\ell\tilde{\nu}$), and > 95.5 ($b\tau\tilde{\nu}$). See Figs. 5–6 and Table 5 for the more general dependence of the limits on Δm. These results supersede ABBIENDI 99M.

[296] HEISTER 02K search for top squarks in final states with jets (with/without b tagging or leptons) or long-lived hadrons, using 183–209 GeV data. The absolute mass bound is obtained by varying the branching ratio of $\tilde{t} \to c\tilde{\chi}^0_1$ and the lepton fraction in $\tilde{t} \to b\tilde{\chi}^0_1 f\overline{f}'$ decays. The mass bound for $\tilde{t} \to c\tilde{\chi}^0_1$ uses the CDF results from AFFOLDER 00D and for $\tilde{t} \to b\ell\tilde{\nu}$ the DØ results from ABAZOV 02C. See Figs. 2–5 for the more general dependence of the limits on Δm. Updates BARATE 01 and BARATE 00P.

[297] ABDALLAH 03C looked for events of the type $q\bar{q}R^{\pm}R^{\pm}$, $q\bar{q}R^{\pm}R^0$ or $q\bar{q}R^0R^0$ in e^+e^- interactions at $\sqrt{s} = 189 - 208$ GeV. The $R^{\pm}$ bound states are identified by anomalous dE/dx in the tracking chambers and the R^0 by missing energy, due to their reduced energy loss in the calorimeters. Excluded mass regions in the $(m(\tilde{t}), m(\tilde{g}))$ plane for $m(\tilde{g}) > 2$ GeV are obtained for several values of the probability for the gluino to fragment into $R^{\pm}$ or R^0, as shown in their Fig. 18. The limit improves to 90 GeV for $\theta_t = 0$.

[298] Theoretical analysis of $e^+e^- + 2$ jet final states from the RPV decay of $\tilde{t}\bar{\tilde{t}}^*$ pairs produced in $p\overline{p}$ collisions at $\sqrt{S} = 1.8$ TeV. 95%CL limits of 220 (165) GeV are derived for $B(\tilde{t} \to eq)$=1 (0.5).

[299] HEISTER 03G searches for the production of $\tilde{t}$ pairs in the case of $\not{R}$ prompt decays with $LL\overline{E}$, $LQ\overline{D}$ or $\overline{UDD}$ couplings at $\sqrt{s} = 189–209$ GeV. The limit holds for indirect decays mediated by $\not{R}$ $\overline{UDD}$ couplings. It improves to 91 GeV for indirect decays mediated by $\not{R}$ $LL\overline{E}$ couplings, to 97 GeV for direct (assuming $B(\tilde{t}_L \to q\tau) = 100\%$) and to 85 GeV for indirect decays mediated by $\not{R}$ $LQ\overline{D}$ couplings. Supersedes the results from BARATE 01B.

[300] HEISTER 03H use e^+e^- data from 183–208 GeV to look for the production of stop decaying into a c quark and a stable gluino hadronizing into charged or neutral R-hadrons. Combining these results with bounds on stable squarks and on a stable gluino LSP from the same paper yields the quoted limit. See their Fig. 13 for the dependence of the mass limit on the gluino mass and on θ_t.

[301] ACHARD 02 searches for the production of squarks in the case of $\not{R}$ prompt decays with $\overline{UDD}$ couplings at $\sqrt{s}$=189–208 GeV. The search is performed for direct and indirect decays, assuming one coupling at the time to be nonzero. The limit is computed for the minimal cross section and holds for both direct and indirect decays.

[302] ABREU 01D searches for multi-jet events, expected in the case of prompt decays from $\not{R}$ $\overline{UDD}$ couplings and indirect decays, using data from $\sqrt{s}$=189 GeV. Limits are obtained in the plane of the squark mass versus $m_{\tilde{\chi}^0_1}$. The mass limit is derived using the constraint on the neutralino mass from the same paper (see the section on unstable $\tilde{\chi}^0_1$). See Fig. 9 for other choices of Δm.

[303] AFFOLDER 01B searches for decays of the top quark into stop and LSP, in $t\bar{t}$ events. Limits on the stop mass as a function of the LSP mass and of the decay branching ratio are shown in Fig. 3. They exclude branching ratios in excess of 45% for SLP masses up to 40 GeV.

[304] ABBIENDI 00 searches for the production of stop in the case of R-parity violation with $\overline{UDD}$ or $LQ\overline{D}$ couplings, using data from $\sqrt{s}$=183 GeV. They investigate topologies with multiple leptons, jets plus leptons, or multiple jets, assuming one coupling at the time to be non-zero. For mass exclusion limits relative to $LQ\overline{D}$-induced decays, see their Table 5.

[305] ABREU 00I searches for the production of stop in the case of R-parity violation with $LL\overline{E}$ couplings, for which only indirect decays are allowed. They investigate topologies with jets plus leptons in data from $\sqrt{s}$=183 GeV. The lower bound on the stop mass assumes a neutralino mass limit of 27 GeV, also derived in ABREU 00I.

[306] AFFOLDER 00D search for final states with 2 or 3 jets and $\not{E}_T$, one jet with a c tag. See their Fig. 2 for the mass exclusion in the $(m_{\tilde{t}}, m_{\tilde{\chi}^0_1})$ plane. The maximum excluded $m_{\tilde{t}}$ value is 119 GeV, for $m_{\tilde{\chi}^0_1}$= 40 GeV.

[307] AFFOLDER 00G searches for $\tilde{t}_1\bar{\tilde{t}}^*_1$ production, with $\tilde{t}_1 \to b\ell\tilde{\nu}$, leading to topologies with ≥ 1 isolated lepton (e or μ), $\not{E}_T$, and ≥ 2 jets with ≥ 1 tagged as b quark by a secondary vertex. See Fig. 4 for the excluded mass range as a function of $m_{\tilde{\nu}}$. Cross-section limits for $\tilde{t}_1\bar{\tilde{t}}^*_1$, with $\tilde{t}_1 \to b\chi^{\pm}_1$ ($\chi^{\pm}_1 \to \ell^{\pm}\nu\tilde{\chi}^0_1$), are given in Fig. 2.

[308] BARATE 00P use data from $\sqrt{s}$= 189–202 GeV to explore the region of small mass difference between the stop and the neutralino by searching heavy stable charged particles or tracks with large impact parameters. For prompt decays, they make use of acoplanar jets from BARATE 99Q, updated up to 202 GeV. The limit is reached for Δm=1.6 GeV and a decay length of 1 cm. If the MSSM relation between the decay width and Δm is used, the limit improves to 63 GeV. It is set for Δm=1.9 GeV. tanβ=2.6, and $\theta_{\tilde{t}}$=0.98, and large negative μ.

[309] ABE 99M looked in 107 pb^{-1} of $p\overline{p}$ collisions at $\sqrt{s}$=1.8 TeV for events with like sign dielectrons and two or more jets from the sequential decays $\tilde{q} \to q\tilde{\chi}^0_1$ and $\tilde{\chi}^0_1 \to eq\overline{q}'$, assuming $\not{R}$ coupling $L_1 Q_j D^c_k$, with j=2,3 and k=1,2,3. They assume $B(\tilde{t}_1 \to c\tilde{\chi}^0_1)$=1, $B(\tilde{\chi}^0_1 \to eq\overline{q}')$=0.25 for both e^+ and e^-, and $m_{\tilde{\chi}^0_1} \geq m_{\tilde{t}_1}/2$. The limit improves for heavier $\tilde{\chi}^0_1$.

[310] ABACHI 96B searches for final states with 2 jets and missing E_T. Limits on $m_{\tilde{t}}$ are given as a function of $m_{\tilde{\chi}^0_1}$. See Fig. 4 for details.

[311] AID 96 considers photoproduction of $\tilde{t}\bar{\tilde{t}}$ pairs, with 100% R-parity violating decays of $\tilde{t}$ to eq, with q=d, s, or b quarks.

[312] AID 96 considers production and decay of $\tilde{t}$ via the R-parity violating coupling $\lambda' L_1 Q_3 d^c_1$.

[313] CHO 96 studied the consistency among the B^0-$\overline{B}^0$ mixing, ϵ in K^0-$\overline{K}^0$ mixing, and the measurements of V_{cb}, V_{ub}/V_{cb}. For the range 25.5 GeV$< m_{\tilde{t}_1} <$ $m_Z/2$ left by AKERS 94K for $\theta_t = 0.98$, and within the allowed range in M_2-μ parameter space from chargino, neutralino searches by ACCIARRI 95E, they found the scalar top contribution to B^0-$\overline{B}^0$ mixing and ϵ to be too large if tanβ <2. For more on their assumptions, see the paper and their reference 10.

[314] BUSKULIC 95E looked for $Z \to \tilde{t}\bar{\tilde{t}}$, where $\tilde{t} \to c\chi^0_1$ and χ^0_1 decays via R-parity violating interactions into two leptons and a neutrino.

[315] SHIRAI 94 bound assumes the cross section without the s-channel Z-exchange and the QCD correction, underestimating the cross section up to 20% and 30%, respectively. They assume m_c=1.5 GeV.

Heavy $\tilde{g}$ (Gluino) MASS LIMIT

For $m_{\tilde{g}} > 60–70$ GeV, it is expected that gluinos would undergo a cascade decay via a number of neutralinos and/or charginos rather than undergo a direct decay to photinos as assumed by some papers. Limits obtained when direct decay is assumed are usually higher than limits when cascade decays are included. Limits made obsolete by the most recent analyses of $p\overline{p}$ collisions can be found in previous Editions of this *Review*.

VALUE (GeV)	*CL%*	*DOCUMENT ID*		*TECN*	*COMMENT*
>195	95	[316] AFFOLDER	02	CDF	Jets+$\not{E}_T$, any $m_{\tilde{q}}$
>300	95	[316] AFFOLDER	02	CDF	Jets+$\not{E}_T$, $m_{\tilde{q}}$=$m_{\tilde{g}}$
>129	95	[317] ABBOTT	01D	DØ	$\ell\ell$+jets+$\not{E}_T$, tanβ < 10, m_0 < 300 GeV, μ < 0, A_0=0
>175	95	[317] ABBOTT	01D	DØ	$\ell\ell$+jets+$\not{E}_T$, tanβ=2, large m_0, μ < 0, A_0=0
>255	95	[317] ABBOTT	01D	DØ	$\ell\ell$+jets+$\not{E}_T$, tanβ=2, $m_{\tilde{g}}$=$m_{\tilde{q}}$, μ < 0, A_0=0
>168	95	[318] AFFOLDER	01J	CDF	$\ell\ell$+ Jets+$\not{E}_T$, tanβ=2, μ=− 800 GeV, $m_{\tilde{q}} \gg m_{\tilde{g}}$
>221	95	[318] AFFOLDER	01J	CDF	$\ell\ell$+ Jets+$\not{E}_T$, tanβ=2, μ=− 800 GeV, $m_{\tilde{q}}$=$m_{\tilde{g}}$
>190	95	[319] ABBOTT	99L	DØ	Jets+$\not{E}_T$, tanβ=2, μ <0, A=0
>260	95	[319] ABBOTT	99L	DØ	Jets+$\not{E}_T$, $m_{\tilde{g}}$=$m_{\tilde{q}}$
• • • We do not use the following data for averages, fits, limits, etc. • • •					
>224	95	[320] ABAZOV	02F	DØ	$\not{R}$ λ'_{2jk} indirect decays, tanβ=2, any $m_{\tilde{q}}$
>265	95	[320] ABAZOV	02F	DØ	$\not{R}$ λ'_{2jk} indirect decays, tanβ=2, $m_{\tilde{q}}$=$m_{\tilde{g}}$
		[321] ABAZOV	02G	DØ	$p\overline{p} \to \tilde{g}\tilde{g}$, $\tilde{g}\tilde{q}$
		[322] CHEUNG	02B	THEO	
		[323] BERGER	01	THEO	$p\overline{p} \to$ X+b-quark
>240	95	[324] ABBOTT	99	DØ	$\tilde{g} \to \tilde{\chi}^0_2 X \to \tilde{\chi}^0_1 \gamma X$, $m_{\tilde{\chi}^0_2} - m_{\tilde{\chi}^0_1} > 20$ GeV
>320	95	[324] ABBOTT	99	DØ	$\tilde{g} \to \tilde{\chi}^0_1 X \to \tilde{G}\gamma X$
>227	95	[325] ABBOTT	99K	DØ	any $m_{\tilde{q}}$, $\not{R}$, tanβ=2, μ < 0
>212	95	[326] ABACHI	95C	DØ	$m_{\tilde{g}} \geq m_{\tilde{q}}$; with cascade decays
>144	95	[326] ABACHI	95C	DØ	Any $m_{\tilde{q}}$; with cascade decays
		[327] ABE	95T	CDF	$\tilde{g} \to \tilde{\chi}^0_2 \to \tilde{\chi}^0_1 \gamma$
		[328] HEBBEKER	93	RVUE	e^+e^- jet analyses
>218	90	[329] ABE	92L	CDF	$m_{\tilde{q}} \leq m_{\tilde{g}}$; with cascade decay
>100		[330] ROY	92	RVUE	$p\overline{p} \to \tilde{g}\tilde{g}$; $\not{R}$
		[331] NOJIRI	91	COSM	
none 4–53	90	[332] ALBAJAR	87D	UA1	Any $m_{\tilde{q}} > m_{\tilde{g}}$
none 4–75	90	[332] ALBAJAR	87D	UA1	$m_{\tilde{q}} = m_{\tilde{g}}$
none 16–58	90	[333] ANSARI	87D	UA2	$m_{\tilde{q}} \lesssim$ 100 GeV

[316] AFFOLDER 02 searched in ~ 84 pb^{-1} of $p\overline{p}$ collisions for events with ≥ 3 jets and $\not{E}_T$, arising from the production of gluinos and/or squarks. Limits are derived by scanning the parameter space, for $m_{\tilde{q}} \geq m_{\tilde{g}}$ in the framework of minimal Supergravity, assuming five flavors of degenerate squarks, and for $m_{\tilde{g}} < m_{\tilde{g}}$ in the framework of constrained MSSM, assuming conservatively four flavors of degenerate squarks. See Fig. 3 for the variation of the limit as function of the squark mass. Supersedes the results of ABE 97K.

[317] ABBOTT 01D looked in ~ 108 pb^{-1} of $p\overline{p}$ collisions at $\sqrt{s}$=1.8 TeV for events with ee, $\mu\mu$, or $e\mu$ accompanied by at least 2 jets and $\not{E}_T$. Excluded regions are obtained in the MSUGRA framework from a scan over the parameters $0 < m_0 < 300$ GeV, $10 < m_{1/2} < 110$ GeV, and $1.2 <$ tanβ <10.

[318] AFFOLDER 01J searched in ~ 106 pb^{-1} of $p\overline{p}$ collisions for events with 2 like-sign leptons (e or μ), ≥ 2 jets and $\not{E}_T$, expected to arise from the production of gluinos and/or squarks with cascade decays into $\tilde{\chi}^{\pm}$ or $\tilde{\chi}^0_2$. Spectra and decay rates are evaluated

in the framework of minimal Supergravity, assuming five flavors of degenerate squarks and a pseudoscalar Higgs mass m_A=500 GeV. The limits are derived for tanβ=2, μ=−800 GeV, and scanning over $m_{\tilde{g}}$ and $m_{\tilde{q}}$. See Fig. 2 for the variation of the limit as function of the squark mass. These limits supersede the results of ABE 96D.

[319] ABBOTT 99L consider events with three or more jets and large $\not{E}_T$. Spectra and decay rates are evaluated in the framework of minimal Supergravity, assuming five flavors of degenerate squarks, and scanning the space of the universal gaugino ($m_{1/2}$) and scalar (m_0) masses See their Figs. 2–3 for the dependence of the limit on the relative value of $m_{\tilde{q}}$ and $m_{\tilde{g}}$.

[320] ABAZOV 02F looked in 77.5 pb^{-1} of $p\overline{p}$ collisions at 1.8 TeV for events with $\geq 2\mu + \geq$ 4jets, originating from associated production of squarks followed by an indirect $\not{R}$ decay (of the $\tilde{\chi}_1^0$) via $L\overline{Q}D$ couplings of the type λ'_{2jk} where j=1,2 and k=1,2,3. Bounds are obtained in the MSUGRA scenario by a scan in the range $0 \leq M_0 \leq 400$ GeV, $60 \leq m_{1/2} \leq 120$ GeV for fixed values A_0=0, $\mu < 0$, and tanβ=2 or 6. The bounds are weaker for tanβ=6. See Figs. 2,3 for the exclusion contours in $m_{1/2}$ versus m_0 for tanβ=2 and 6, respectively.

[321] ABAZOV 02G search for associated production of gluinos and squarks in 92.7 pb^{-1} of $p\overline{p}$ collisions at $\sqrt{s}$=1.8 TeV, using events with one electron, $\geq$ 4 jets, and large $\not{E}_T$. The results are compared to a MSUGRA scenario with $\mu < 0$, A_0=0, and tanβ=3 and allow to exclude a region of the (m_0,$m_{1/2}$) shown in Fig. 11.

[322] CHEUNG 02B studies the constraints on a $\tilde{b}_1$ with mass in the 2.2–5.5 GeV region and a gluino in the mass range 12–16 GeV, using precision measurements of Z^0 decays and e^+e^- annihilations at LEP2. Few detectable events are predicted in the LEP2 data for the model proposed by BERGER 01.

[323] BERGER 01 reanalyzed interpretation of Tevatron data on bottom-quark production. Argues that pair production of light gluinos ($m\sim$ 12–16 GeV) with subsequent 2-body decay into a light sbottom ($m\sim$ 2–5.5 GeV) and bottom can reconcile Tevatron data with predictions of perturbative QCD for the bottom production rate. The sbottom must either decay hadronically via a R-parity- and B-violating interaction, or be long-lived.

[324] ABBOTT 99 searched for $\gamma\not{E}_T + \geq 2$ jet final states, and set limits on $\sigma(p\overline{p} \to \tilde{g}+X)\cdot B(\tilde{g} \to \gamma\not{E}_T X)$. The quoted limits correspond to $m_{\tilde{q}} \geq m_{\tilde{g}}$, with B($\tilde{\chi}_2^0 \to \tilde{\chi}_1^0\gamma$)=1 and B($\tilde{\chi}_1^0 \to \tilde{G}\gamma$)=1, respectively. They improve to 310 GeV (360 GeV in the case of $\gamma\tilde{G}$ decay) for $m_{\tilde{g}}$=$m_{\tilde{q}}$.

[325] ABBOTT 99K uses events with an electron pair and four jets to search for the decay of the $\tilde{\chi}_1^0$ LSP via $\not{R}$ $L\overline{Q}D$ couplings. The particle spectrum and decay branching ratios are taken in the framework of minimal supergravity. An excluded region at 95% CL is obtained in the (m_0,$m_{1/2}$) plane under the assumption that A_0=0, $\mu < 0$, tanβ=2 and any one of the couplings $\lambda'_{1jk} > 10^{-3}$ (j=1,2 and k=1,2,3) and from which the above limit is computed. For equal mass squarks and gluinos, the corresponding limit is 277 GeV. The results are essentially independent of A_0, but the limit deteriorates rapidly with increasing tanβ or $\mu > 0$.

[326] ABACHI 95C assume five degenerate squark flavors with with $m_{\tilde{q}_L} = m_{\tilde{q}_R}$. Sleptons are assumed to be heavier than squarks. The limits are derived for fixed tanβ = 2.0 μ = −250 GeV, and m_{H^+}=500 GeV, and with the cascade decays of the squarks and gluinos calculated within the framework of the Minimal Supergravity scenario. The bounds are weakly sensitive to the three fixed parameters for a large fraction of parameter space.

[327] ABE 95T looked for a cascade decay of gluino into $\tilde{\chi}_2^0$ which further decays into $\tilde{\chi}_1^0$ and a photon. No signal is observed. Limits vary widely depending on the choice of parameters. For μ = −40 GeV, tanβ = 1.5, and heavy squarks, the range 50<$m_{\tilde{g}}$ (GeV)<140 is excluded at 90% CL. See the paper for details.

[328] HEBBEKER 93 combined jet analyses at various e^+e^- colliders. The 4-jet analyses at TRISTAN/LEP and the measured α_s at PEP/PETRA/TRISTAN/LEP are used. A constraint on effective number of quarks N=6.3 ± 1.1 is obtained, which is compared to that with a light gluino, N=8.

[329] ABE 92L bounds are based on similar assumptions as ABACHI 95C. Not sensitive to m_{gluino} <40 GeV (but other experiments rule out that region).

[330] ROY 92 reanalyzed CDF limits on di-lepton events to obtain limits on gluino production in R-parity violating models. The 100% decay $\tilde{g} \to q\overline{q}\tilde{\chi}$ where $\tilde{\chi}$ is the LSP, and the LSP decays either into $\ell q\overline{d}$ or $\ell\ell\overline{e}$ is assumed.

[331] NOJIRI 91 argues that a heavy gluino should be nearly degenerate with squarks in minimal supergravity not to overclose the universe.

[332] The limits of ALBAJAR 87D are from $p\overline{p} \to \tilde{g}\tilde{g}X$ ($\tilde{g} \to q\overline{q}\tilde{\gamma}$) and assume $m_{\tilde{q}} > m_{\tilde{g}}$. These limits apply for $m_{\tilde{\gamma}} \lesssim$ 20 GeV and $\tau(\tilde{g}) < 10^{-10}$ s.

[333] The limit of ANSARI 87D assumes $m_{\tilde{q}} > m_{\tilde{g}}$ and $m_{\tilde{\gamma}} \approx 0$.

Long-lived/light $\tilde{g}$ (Gluino) MASS LIMIT

Limits on light gluinos ($m_{\tilde{g}} < 5$ GeV), or gluinos which leave the detector before decaying.

VALUE (GeV)	CL%	DOCUMENT ID		TECN	COMMENT
• • • We do not use the following data for averages, fits, limits, etc. • • •					
none 2–18	95	[334] ABDALLAH	03C	DLPH	$e^+e^- \to q\overline{q}\tilde{g}\tilde{g}$, stable $\tilde{g}$
> 5		[335] ABDALLAH	03G	DLPH	QCD beta function
		[336] HEISTER	03	ALEP	Color factors
>26.9	95	[337] HEISTER	03H	ALEP	$e^+e^- \to q\overline{q}\tilde{g}\tilde{g}$
> 6.3		[338] JANOT	03	RVUE	$\Delta\Gamma_{had}$ <3.9 MeV
		[339] MAFI	00	THEO	$pp \to$ jets + $\not{E}_T$
		[340] ALAVI-HARATI	99E	KTEV	$pN \to R^0$, with $R^0 \to \rho^0\tilde{\gamma}$ and $R^0 \to \pi^0\tilde{\gamma}$
		[341] BAER	99	RVUE	Stable $\tilde{g}$ hadrons
		[342] FANTI	99	NA48	pBe $\to R^0 \to \eta\tilde{\gamma}$
		[343] ACKERSTAFF	98V	OPAL	$e^+e^- \to \tilde{\chi}_1^+\tilde{\chi}_1^-$
		[344] ADAMS	97B	KTEV	$pN \to R^0 \to \rho^0\tilde{\gamma}$
		[345] ALBUQUERQ...97		E761	$R^+(uud\tilde{g}) \to S^0(uds\tilde{g})\pi^+$, $X^-(ssd\tilde{g}) \to S^0\pi^-$
> 6.3	95	[346] BARATE	97L	ALEP	Color factors
> 5	99	[347] CSIKOR	97	RVUE	β function, $Z \to$ jets
> 1.5	90	[348] DEGOUVEA	97	THEO	$Z \to jjjj$
		[349] FARRAR	96	RVUE	$R^0 \to \pi^0\tilde{\gamma}$
none 1.9–13.6	95	[350] AKERS	95R	OPAL	Z decay into a long-lived $(\tilde{g}q\overline{q})^{\pm}$
< 0.7		[351] CLAVELLI	95	RVUE	quarkonia
none 1.5–3.5		[352] CAKIR	94	RVUE	$\Upsilon(1S) \to \gamma$+ gluinonium
not 3–5		[353] LOPEZ	93C	RVUE	LEP
≈ 4		[354] CLAVELLI	92	RVUE	α_s running
		[355] ANTONIADIS	91	RVUE	α_s running
> 1		[356] ANTONIADIS	91	RVUE	$pN \to$ missing energy
		[357] NAKAMURA	89	SPEC	R-Δ^{++}
> 3.8	90	[358] ARNOLD	87	EMUL	π^- (350 GeV). $\sigma \simeq A^1$
> 3.2	90	[358] ARNOLD	87	EMUL	π^- (350 GeV). $\sigma \simeq A^{0.72}$
none 0.6–2.2	90	[359] TUTS	87	CUSB	$\Upsilon(1S) \to \gamma$+ gluinonium
none 1 –4.5	90	[360] ALBRECHT	86C	ARG	$1\times10^{-11} \lesssim \tau \lesssim 1\times10^{-9}$ s
none 1–4	90	[361] BADIER	86	BDMP	$1\times10^{-10} < \tau < 1\times10^{-7}$ s
none 3–5		[362] BARNETT	86	RVUE	$p\overline{p} \to$ gluino gluino gluon
none		[363] VOLOSHIN	86	RVUE	lf (quasi) stable; $\tilde{g}uud$
none 0.5–2		[364] COOPER-...	85B	BDMP	For $m_{\tilde{q}}$=300 GeV
none 0.5–4		[364] COOPER-...	85B	BDMP	For $m_{\tilde{q}}$ <65 GeV
none 0.5–3		[364] COOPER-...	85B	BDMP	For $m_{\tilde{q}}$=150 GeV
none 2–4		[365] DAWSON	85	RVUE	$\tau > 10^{-7}$ s
none 1–2.5		[365] DAWSON	85	RVUE	For $m_{\tilde{q}}$=100 GeV
none 0.5–4.1	90	[366] FARRAR	85	RVUE	FNAL beam dump
> 1		[367] GOLDMAN	85	RVUE	Gluononium
>1–2		[368] HABER	85	RVUE	
		[369] BALL	84	CALO	
		[370] BRICK	84	RVUE	
		[371] FARRAR	84	RVUE	
> 2		[372] BERGSMA	83C	RVUE	For $m_{\tilde{q}}$ <100 GeV
		[373] CHANOWITZ	83	RVUE	$\tilde{g}u\overline{d}$, $\tilde{g}uud$
>2–3		[374] KANE	82	RVUE	Beam dump
>1.5–2		FARRAR	78	RVUE	R-hadron

[334] ABDALLAH 03C looked for events of the type $q\bar{q}R^{\pm}R^{\pm}$, $q\bar{q}R^{\pm}R^0$ or $q\bar{q}R^0R^0$ in e^+e^- interactions at 91.2 GeV collected in 1994. The $R^{\pm}$ bound states are identified by anomalous dE/dx in the tracking chambers and the R^0 by missing energy, due to their reduced energy loss in the calorimeters. The upper value of the excluded range depends on the probability for the gluino to fragment into $R^{\pm}$ or R^0, see their Fig. 17. It improves to 23 GeV for 100% fragmentation to $R^{\pm}$.

[335] ABDALLAH 03G used e^+e^- data at and around the Z^0 peak, above the Z^0 up to $\sqrt{s}$ = 202 GeV and events from radiative return to cover the low energy region. They perform a direct measurement of the QCD beta-function from the means of fully inclusive event observables. Compared to the energy range, gluinos below 5 GeV can be considered massless and are firmly excluded by the measurement.

[336] HEISTER 03 use e^+e^- data from 1994 and 1995 at and around the Z^0 peak to measure the 4-jet rate and angular correlations. The comparison with QCD NLO calculations allow $\alpha_S(M_Z)$ and the color factor ratios to be extracted and the results are in agreement with the expectations from QCD. The inclusion of a massless gluino in the beta functions yields $T_R/C_F = 0.15 \pm 0.06 \pm 0.06$ (expectation is $T_R/C_F = 3/8$), excluding a massless gluino at more than 95% CL. As no NLO calculations are available for massive gluinos, the earlier LO results from BARATE 97L for massive gluinos remain valid.

[337] HEISTER 03H use e^+e^- data at and around the Z^0 peak to look for stable gluinos hadronizing into charged or neutral R-hadrons with arbitrary branching ratios. Combining these results with bounds on the Z^0 hadronic width from electroweak measurements (JANOT 03) to cover the low mass region the quoted lower limit on the mass of a long-lived gluino is obtained.

[338] JANOT 03 excludes a light gluino from the upper limit on an additional contribution to the Z hadronic width. At higher confidence levels, $m_{\tilde{g}} > 5.3(4.2)$ GeV at $3\sigma(5\sigma)$ level.

[339] MAFI 00 reanalyzed CDF data assuming a stable heavy gluino as the LSP, with model for R-hadron-nucleon scattering. Gluino masses between 35 GeV and 115 GeV are excluded based on the CDF Run I data. Combined with the analysis of BAER 99, this allows a LSP gluino mass between 25 and 35 GeV if the probability of fragmentation into charged R-hadron P>1/2. The cosmological exclusion of such a gluino LSP are assumed to be avoided as in BAER 99. Gluino could be NLSP with $\tau_{\tilde{g}} \sim 100$ yrs, and decay to gluon gravitino.

[340] ALAVI-HARATI 99E looked for R^0 bound states, yielding $\pi^+\pi^-$ or π^0 in the final state. The experiment is sensitive to values of $\Delta m = m_{R^0} - m_{\tilde{\gamma}}$ larger than 280 MeV and 140 MeV for the two decay modes, respectively, and to R^0 mass and lifetime in the ranges 0.8–5 GeV and 10^{-10}–10^{-3} s. The limits obtained depend on B($R^0 \to \pi^+\pi^-$photino) and B($R^0 \to \pi^0$photino) on the value of $m_{R^0}/m_{\tilde{\gamma}}$, and on the ratio of production rates $\sigma(R^0)/\sigma(K_L^0)$. See Figures in the paper for the excluded R^0 production rates as a function of Δm, R^0 mass and lifetime. Using the production rates expected from perturbative QCD, and assuming dominance of the above decay channels over the suitable phase space, R^0 masses in the range 0.8–5 GeV are excluded at 90%CL for a large fraction of the sensitive lifetime region. ALAVI-HARATI 99E updates and supersedes the results of ADAMS 97B.

[341] BAER 99 set constraints on the existence of stable $\tilde{g}$ hadrons, in the mass range $m_{\tilde{g}} > 3$ GeV. They argue that strong-interaction effects in the low-energy annihilation rates could leave small enough relic densities to evade cosmological constraints up to $m_{\tilde{g}} < 10$ TeV. They consider jet+$\not{E}_T$ as well as heavy-ionizing charged-particle signatures from production of stable $\tilde{g}$ hadrons at LEP and Tevatron, developing modes for the energy loss of $\tilde{g}$ hadrons inside the detectors. Results are obtained as a function of the fragmentation probability P of the $\tilde{g}$ into a charged hadron. For P< 1/2, and for various energy-loss models, OPAL and CDF data exclude gluinos in the 3 <$m_{\tilde{g}}$(GeV)< 130 mass range. For P> 1/2, gluinos are excluded in the mass ranges 3 <$m_{\tilde{g}}$(GeV)< 23 and 50 <$m_{\tilde{g}}$(GeV)< 200.

[342] FANTI 99 looked for R^0 bound states yielding high P_T $\eta \rightarrow 3\pi^0$ decays. The experiment is sensitive to a region of R^0 mass and lifetime in the ranges of 1–5 GeV and 10^{-10}–10^{-3} s. The limits obtained depend on B($R^0 \rightarrow \eta\tilde{\gamma}$), on the value of $m_{R^0}/m_{\tilde{\gamma}}$, and on the ratio of production rates $\sigma(R^0)/\sigma(K^0_L)$. See Fig. 6–7 for the excluded production rates as a function of R^0 mass and lifetime.

[343] ACKERSTAFF 98V excludes the light gluino with universal gaugino mass where charginos, neutralinos decay as $\tilde{\chi}^{\pm}_1, \tilde{\chi}^0_2 \rightarrow q\overline{q}\tilde{g}$ from total hadronic cross sections at $\sqrt{s}$=130–172 GeV. See paper for the case of nonuniversal gaugino mass.

[344] ADAMS 97B looked for $\rho^0 \rightarrow \pi^+\pi^-$ as a signature of R^0=($\tilde{g}g$) bound states. The experiment is sensitive to an R^0 mass range of 1.2–4.5 GeV and to a lifetime range of 10^{-10}–10^{-3} sec. Precise limits depend on the assumed value of $m_{R^0}/m_{\tilde{\gamma}}$. See Fig. 7 for the excluded mass and lifetime region.

[345] ALBUQUERQUE 97 looked for weakly decaying baryon-like states which contain a light gluino, following the suggestions in FARRAR 96. See their Table 1 for limits on the production fraction. These limits exclude gluino masses in the range 100–600 MeV for the predicted lifetimes (FARRAR 96) and production rates, which are assumed to be comparable to those of strange or charmed baryons.

[346] BARATE 97L studied the QCD color factors from four-jet angular correlations and the differential two-jet rate in Z decay. Limit obtained from the determination of n_f = 4.24 ± 0.29 ± 1.15, assuming T_F/C_F=3/8 and C_A/C_F=9/4.

[347] CSIKOR 97 combined the α_s from $\sigma(e^+e^- \rightarrow$ hadron), τ decay, and jet analysis in Z decay. They exclude a light gluino below 5 GeV at more than 99.7%CL.

[348] DEGOUVEA 97 reanalyzed AKERS 95A data on Z decay into four jets to place constraints on a light stable gluino. The mass limit corresponds to the pole mass of 2.8 GeV. The analysis, however, is limited to the leading-order QCD calculation.

[349] FARRAR 96 studied the possible R^0=($\tilde{g}g$) component in Fermilab E799 experiment and used its bound B($K^0_L \rightarrow \pi^0\nu\overline{\nu}$) $\leq 5.8\times10^{-5}$ to place constraints on the combination of R^0 production cross section and its lifetime.

[350] AKERS 95R looked for Z decay into $q\overline{q}\tilde{g}\tilde{g}$, by searching for charged particles with dE/dx consistent with $\tilde{g}$ fragmentation into a state $(\tilde{g}q\overline{q})^{\pm}$ with lifetime $\tau > 10^{-7}$ sec. The fragmentation probability into a charged state is assumed to be 25%.

[351] CLAVELLI 95 updates the analysis of CLAVELLI 93, based on a comparison of the hadronic widths of charmonium and bottomonium S-wave states. The analysis includes a parametrization of relativisitic corrections. Claims that the presence of a light gluino improves agreement with the data by slowing down the running of α_s.

[352] CAKIR 94 reanalyzed TUTS 87 and later unpublished data from CUSB to exclude pseudo-scalar gluinonium $\eta_{\tilde{g}}(\tilde{g}\tilde{g})$ of mass below 7 GeV. it was argued, however, that the perturbative QCD calculation of the branching fraction $\Upsilon \rightarrow \eta_{\tilde{g}}\gamma$ is unreliable for $m_{\eta_{\tilde{g}}} < 3$ GeV. The gluino mass is defined by $m_{\tilde{g}}$=($m_{\eta_{\tilde{q}}}$)/2. The limit holds for any gluino lifetime.

[353] LOPEZ 93C uses combined restraint from the radiative symmetry breaking scenario within the minimal supergravity model, and the LEP bounds on the (M_2,μ) plane. Claims that the light gluino window is strongly disfavored.

[354] CLAVELLI 92 claims that a light gluino mass around 4 GeV should exist to explain the discrepancy between α_s at LEP and at quarkonia (Υ), since a light gluino slows the running of the QCD coupling.

[355] ANTONIADIS 91 argue that possible light gluinos (< 5 GeV) contradict the observed running of α_s between 5 GeV and m_Z. The significance is less than 2 s.d.

[356] ANTONIADIS 91 interpret the search for missing energy events in 450 GeV/c pN collisions, AKESSON 91, in terms of light gluinos.

[357] NAKAMURA 89 searched for a long-lived ($\tau \gtrsim 10^{-7}$ s) charge-(±2) particle with mass $\lesssim$ 1.6 GeV in proton-Pt interactions at 12 GeV and found that the yield is less than 10^{-8} times that of the pion. This excludes R-Δ^{++} (a $\tilde{g}uuu$ state) lighter than 1.6 GeV.

[358] The limits assume $m_{\tilde{q}} = 100$ GeV. See their figure 3 for limits vs. $m_{\tilde{\gamma}}$.

[359] The gluino mass is defined by half the bound $\tilde{g}\tilde{g}$ mass. If zero gluino mass gives a $\tilde{g}\tilde{g}$ of mass about 1 GeV as suggested by various glueball mass estimates, then the low-mass bound can be replaced by zero. The high-mass bound is obtained by comparing the data with nonrelativistic potential-model estimates.

[360] ALBRECHT 86C search for secondary decay vertices from $\chi_{b1}(1P) \rightarrow \tilde{g}\tilde{g}g$ where $\tilde{g}$'s make long-lived hadrons. See their figure 4 for excluded region in the $m_{\tilde{g}} - m_{\tilde{q}}$ and $m_{\tilde{g}} - m_{\tilde{q}}$ plane. The lower $m_{\tilde{g}}$ region below ~ 2 GeV may be sensitive to fragmentation effects. Remark that the $\tilde{g}$-hadron mass is expected to be ~ 1 GeV (glueball mass) in the zero $\tilde{g}$ mass limit.

[361] BADIER 86 looked for secondary decay vertices from long-lived $\tilde{g}$-hadrons produced at 300 GeV π^- beam dump. The quoted bound assumes $\tilde{g}$-hadron nucleon total cross section of 10 μb. See their figure 7 for excluded region in the $m_{\tilde{g}} - m_{\tilde{q}}$ plane for several assumed total cross-section values.

[362] BARNETT 86 rule out light gluinos (m = 3–5 GeV) by calculating the monojet rate from gluino gluino gluon events (and from gluino gluino events) and by using UA1 data from $p\overline{p}$ collisions at CERN.

[363] VOLOSHIN 86 rules out stable gluino based on the cosmological argument that predicts too much hydrogen consisting of the charged stable hadron $\tilde{g}uud$. Quasi-stable ($\tau > 1.\times10^{-7}$ s) light gluino of $m_{\tilde{g}} < 3$ GeV is also ruled out by nonobservation of the stable charged particles, $\tilde{g}uud$, in high energy hadron collisions.

[364] COOPER-SARKAR 85B is BEBC beam-dump. Gluinos decaying in dump would yield $\tilde{\gamma}$'s in the detector giving neutral-current-like interactions. For $m_{\tilde{q}} >$330 GeV, no limit is set.

[365] DAWSON 85 first limit from neutral particle search. Second limit based on FNAL beam dump experiment.

[366] FARRAR 85 points out that BALL 84 analysis applies only if the $\tilde{g}$'s decay before interacting, i.e. $m_{\tilde{q}} < 80 m_{\tilde{g}}^{1.5}$. FARRAR 85 finds $m_{\tilde{g}} < 0.5$ not excluded for $m_{\tilde{q}}$ = 30–1000 GeV and $m_{\tilde{g}} < 1.0$ not excluded for $m_{\tilde{q}}$ = 100–500 GeV by BALL 84 experiment.

[367] GOLDMAN 85 use nonobservation of a pseudoscalar $\tilde{g}$-$\tilde{g}$ bound state in radiative ψ decay.

[368] HABER 85 is based on survey of all previous searches sensitive to low mass $\tilde{g}$'s. Limit makes assumptions regarding the lifetime and electric charge of the lightest supersymmetric particle.

[369] BALL 84 is FNAL beam dump experiment. Observed no interactions of $\tilde{\gamma}$ in the calorimeter, where $\tilde{\gamma}$'s are expected to come from pair-produced $\tilde{g}$'s. Search for long-lived $\tilde{\gamma}$ interacting in calorimeter 56m from target. Limit is for $m_{\tilde{q}}$ = 40 GeV and production cross section proportional to $A^{0.72}$. BALL 84 find no $\tilde{g}$ allowed below 4.1 GeV at CL = 90%. Their figure 1 shows dependence on $m_{\tilde{q}}$ and A. See also KANE 82.

[370] BRICK 84 reanalyzed FNAL 147 GeV HBC data for R-$\Delta(1232)^{++}$ with $\tau > 10^{-9}$ s and $p_{\rm lab} >$2 GeV. Set CL = 90% upper limits 6.1, 4.4, and 29 microbarns in pp, π^+p, K^+p collisions respectively. R-Δ^{++} is defined as being $\tilde{g}$ and 3 up quarks. If mass = 1.2–1.5 GeV, then limits may be lower than theory predictions.

[371] FARRAR 84 argues that $m_{\tilde{g}} <$100 MeV is not ruled out if the lightest R-hadrons are long-lived. A long lifetime would occur if R-hadrons are lighter than $\tilde{\gamma}$'s or if $m_{\tilde{q}} >$100 GeV.

[372] BERGSMA 83C is reanalysis of CERN-SPS beam-dump data. See their figure 1.

[373] CHANOWITZ 83 find in bag-model that charged s-hadron exists which is stable against strong decay if $m_{\tilde{g}} <$1 GeV. This is important since tracks from decay of neutral s-hadron cannot be reconstructed to primary vertex because of missed $\tilde{\gamma}$. Charged s-hadron leaves track from vertex.

[374] KANE 82 inferred above $\tilde{g}$ mass limit from retroactive analysis of hadronic collision and beam dump experiments. Limits valid if $\tilde{g}$ decays inside detector.

LIGHT $\tilde{G}$ (Gravitino) MASS LIMITS FROM COLLIDER EXPERIMENTS

The following are bounds on light ($\ll$ 1 eV) gravitino indirectly inferred from its coupling to matter suppressed by the gravitino decay constant.

Unless otherwise stated, all limits assume that other supersymmetric particles besides the gravitino are too heavy to be produced. The gravitino is assumed to be undetected and to give rise to a missing energy ($\not{E}$) signature.

VALUE (eV)	CL%	DOCUMENT ID		TECN	COMMENT
• • • We do not use the following data for averages, fits, limits, etc. • • •					
$> 1.3\times10^{-5}$	95	[375]	HEISTER	03C ALEP	$e^+e^- \rightarrow \tilde{G}\tilde{G}\gamma$
$>11.7\times10^{-6}$	95	[376]	ACOSTA	02H CDF	
$> 8.7\times10^{-6}$	95	[377]	ABBIENDI,G	00D OPAL	$e^+e^- \rightarrow \tilde{G}\tilde{G}\gamma$
$>10.0\times10^{-6}$	95	[378]	ABREU	00Z DLPH	$e^+e^- \rightarrow \tilde{G}\tilde{G}\gamma$
$>11 \times10^{-6}$	95	[379]	AFFOLDER	00J CDF	$p\overline{p} \rightarrow \tilde{G}\tilde{G}$ +jet
$> 8.9\times10^{-6}$	95	[378]	ACCIARRI	99R L3	$e^+e^- \rightarrow \tilde{G}\tilde{G}\gamma$
$> 7.9\times10^{-6}$	95	[380]	ACCIARRI	98V L3	$e^+e^- \rightarrow \tilde{G}\tilde{G}\gamma$
$> 8.3\times10^{-6}$	95	[380]	BARATE	98J ALEP	$e^+e^- \rightarrow \tilde{G}\tilde{G}\gamma$

[375] HEISTER 03C use the data from $\sqrt{s}$= 189-209 GeV to search for $\gamma\not{E}_T$ final states.

[376] ACOSTA 02H looked in 87 pb^{-1} of $p\overline{p}$ collisions at $\sqrt{s}$=1.8 TeV for events with a high-E_t photon and $\not{E}_T$. They compared the data with a GMSB model where the final state could arise from $q\overline{q} \rightarrow \tilde{G}\tilde{G}\gamma$. Since the cross section for this process scales as $1/|F|^4$, a limit at 95% CL is derived on $|F|^{1/2} > 221$ GeV. A model independent limit for the above topology is also given in the paper.

[377] ABBIENDI,G 00D searches for $\gamma\not{E}$ final states from $\sqrt{s}$=189 GeV.

[378] ABREU 00Z, ACCIARRI 99R search for $\gamma\not{E}$ final states using data from $\sqrt{s}$=189 GeV.

[379] AFFOLDER 00J searches for final states with an energetic jet (from quark or gluon) and large $\not{E}_T$ from undetected gravitinos.

[380] Searches for $\gamma\not{E}$ final states at $\sqrt{s}$=183 GeV.

Supersymmetry Miscellaneous Results

Results that do not appear under other headings or that make nonminimal assumptions.

VALUE	DOCUMENT ID		TECN	COMMENT
• • • We do not use the following data for averages, fits, limits, etc. • • •				
	[381] AFFOLDER	02D CDF		$p\overline{p} \rightarrow \gamma b\,(\not{E}_T)$
	[382] AFFOLDER	01H CDF		$p\overline{p} \rightarrow \gamma\gamma X$
	[383] ABBOTT	00G D0		$p\overline{p} \rightarrow 3\ell + \not{E}_T$, R, $LL\overline{E}$
	[384] ABREU,P	00C DLPH		$e^+e^- \rightarrow \gamma + S/P$
	[385] ABACHI	97 D0		$\gamma\gamma X$
	[386] BARBER	84B RVUE		
	[387] HOFFMAN	83 CNTR		$\pi p \rightarrow n(e^+e^-)$

[381] AFFOLDER 02D looked in 85 pb^{-1} of $p\overline{p}$ collisions at $\sqrt{s}$=1.8 TeV for events with a high-E_T photon, and a b-tagged jet with or without $\not{E}_T$. They compared the data with models where the final state could arise from cascade decays of gluinos and/or squarks into $\tilde{\chi}^{\pm}$ and $\tilde{\chi}^0_2$ or direct associated production of $\tilde{\chi}^0_2\tilde{\chi}^{\pm}_2$, followed by $\tilde{\chi}^0_2 \rightarrow \gamma\tilde{\chi}^0_1$ or a GMSB model where $\tilde{\chi}^0_1 \rightarrow \gamma\tilde{G}$. It is concluded that the experimental sensitivity is insufficient to detect the associated production or the GMSB model, but some sensitivity may exist to the cascade decays. A model independent limit for the above topology is also given in the paper.

[382] AFFOLDER 01H searches for $p\overline{p} \rightarrow \gamma\gamma X$ events, where the di-photon system originates from sgoldstino production, in 100 pb^{-1} of data. Upper limits on the cross section times branching ratio are shown as function of the di-photon mass >70 GeV in Fig. 5. Excluded regions are derived in the plane of the sgoldstino mass versus the supersymmetry breaking scale for two representative sets of parameter values, as shown in Figs. 6 and 7.

[383] ABBOTT 00G searches for trilepton final states (ℓ=e,μ) with $\not{E}_T$ from the indirect decay of gaugino via $LL\overline{E}$ couplings. Efficiencies are computed for all possible production and decay modes of SUSY particles in the framework of the Minimal Supergravity scenario. See Figs. 1–4 for excluded regions in the $m_{1/2}$ versus m_0 plane.

[384] ABREU,P 00C look for the CP-even (S) and CP-odd (P) scalar partners of the goldstino, expected to be produced in association with a photon. The S/P decay into two photons or into two gluons and both the tri-photon and the photon + two jets topologies are investigated. Upper limits on the production cross section are shown in Fig. 5 and the excluded regions in Fig. 6. Data collected at $\sqrt{s}$= 189–202 GeV.

[385] ABACHI 97 searched for $p\overline{p} \rightarrow \gamma\gamma\not{E}_T + X$ as supersymmetry signature. It can be caused by selectron, sneutrino, or neutralino production with a radiative decay of their decay products. They placed limits on cross sections.

[386] BARBER 84B consider that $\tilde{\mu}$ and $\tilde{e}$ may mix leading to $\mu \rightarrow e\tilde{\gamma}\tilde{\gamma}$. They discuss mass-mixing limits from decay dist. asym. in LBL-TRIUMF data and e^+ polarization in SIN data.

[387] HOFFMAN 83 set CL = 90% limit $d\sigma/dt$ B(e^+e^-) $< 3.5 \times 10^{-32}$ cm^2/GeV^2 for spin-1 partner of Goldstone fermions with $140 < m < 160$ MeV decaying $\rightarrow e^+e^-$ pair.

REFERENCES FOR Supersymmetric Particle Searches

ABBIENDI 04 EPJ C32 453 G. Abbiendi *et al.* (OPAL Collab.)
ACHARD 04 PL B580 37 P. Achard *et al.* (L3 Collab.)
ABBIENDI 03H EPJ C29 479 G. Abbiendi *et al.* (OPAL Collab.)
ABBIENDI 03L PL B572 8 G. Abbiendi *et al.* (OPAL Collab.)
ABDALLAH 03C EPJ C26 505 J. Abdallah *et al.* (DELPHI Collab.)
ABDALLAH 03D EPJ C27 153 J. Abdallah *et al.* (DELPHI Collab.)
ABDALLAH 03F EPJ C28 15 J. Abdallah *et al.* (DELPHI Collab.)
ABDALLAH 03G EPJ C29 285 J. Abdallah *et al.* (DELPHI Collab.)
ABDALLAH 03M CERN-EP/2003-007 J. Abdallah *et al.* (DELPHI Collab.)
EPJ (accepted)
ACOSTA 03C PRL 90 251801 D. Acosta *et al.* (CDF Collab.)
ACOSTA 03E PRL 91 171602 D. Acosta *et al.* (CDF Collab.)
ADLOFF 03 PL B568 35 C. Adloff *et al.* (H1 Collab.)
AHMED 03 ASP 19 691 B. Ahmed *et al.* (UK Dark Matter Collab.)
BAER 03 JCAP 0305 006 H. Baer, C. Balazs
BERGER 03 PL B552 223 E. Berger *et al.*
BOTTINO 03 PR D68 043506 A. Bottino *et al.*
BOTTINO 03A PR D67 063519 A. Bottino, N. Fornengo, S. Scopel
CHAKRAB... 03 PR D68 015005 S. Chakrabarti, M. Guchait, N.K. Mondal
CHATTOPAD... 03 PR D68 035005 U. Chattopadhyay, A. Corsetti, P. Nath
CHEKANOV 03B PR D68 052004 S. Chekanov *et al.* (ZEUS Collab.)
ELLIS 03 ASP 18 395 J. Ellis, K.A. Olive, Y. Santoso
ELLIS 03B NP B652 259 J. Ellis *et al.*
ELLIS 03C PL B565 176 J. Ellis *et al.*
ELLIS 03D PL B573 162 J. Ellis *et al.*
HEISTER 03 EPJ C27 1 A. Heister *et al.* (ALEPH)
HEISTER 03C EPJ C28 1 A. Heister *et al.* (ALEPH Collab.)
HEISTER 03G EPJ C31 1 A. Heister *et al.* (ALEPH Collab.)
HEISTER 03H EPJ C31 327 A. Heister *et al.* (ALEPH Collab.)
HOOPER 03 PL B562 18 D. Hooper, T. Plehn
JANOT 03 PL B564 183 P. Janot
KLAPDOR-K... 03 ASP 18 525 H.V. Klapdor-Kleingrothaus *et al.*
LAHANAS 03 PL B568 55 A. Lahanas, D. Nanopoulos
LEP 03 SLAC-R-701, LEPEWWG/2003-02 (LEP Collabs.)
ALEPH, DELPHI, L3, OPAL, the LEP EWWG, and the SLD HFEW
TAKEDA 03 PL B572 145 A. Takeda *et al.*
ABAZOV 02C PRL 88 171802 V.M. Abazov *et al.* (D0 Collab.)
ABAZOV 02F PRL 89 171801 V.M. Abazov *et al.* (D0 Collab.)
ABAZOV 02G PR D66 112001 V.M. Abazov *et al.* (D0 Collab.)
ABAZOV 02H PRL 89 261801 V.M. Abazov *et al.* (D0 Collab.)
ABBIENDI 02 EPJ C23 1 G. Abbiendi *et al.* (OPAL Collab.)
ABBIENDI 02B PL B526 233 G. Abbiendi *et al.* (OPAL Collab.)
ABBIENDI 02H PL B545 272 G. Abbiendi *et al.* (OPAL Collab.)
Also 02J PL B548 258 (erratum) G. Abbiendi *et al.* (OPAL Collab.)
ABRAMS 02 PR D66 122003 D. Abrams *et al.* (CDMS Collab.)
ACHARD 02 PL B524 65 P. Achard *et al.* (L3 Collab.)
ACOSTA 02H PRL 89 281801 D. Acosta *et al.* (CDF Collab.)
AFFOLDER 02 PRL 88 041801 T. Affolder *et al.* (CDF Collab.)
AFFOLDER 02D PR D65 052006 T. Affolder *et al.* (CDF Collab.)
ANGLONER 02 ASP 18 43 G. Angloher *et al.* (CRESST Collab.)
ARNOWITT 02 hep-ph/0211417 R. Arnowitt, B. Dutta
BAEK 02 PL B541 161 S. Baek
BAER 02 JHEP 0207 050 H. Baer *et al.*
BECHER 02 PL B540 278 T. Becher *et al.*
BENOIT 02 PL B545 43 A. Benoit *et al.* (EDELWEISS Collab.)
CHEKANOV 02 PR D65 092004 S. Chekanov *et al.* (ZEUS Collab.)
CHEUNG 02B PRL 89 221801 K. Cheung, W.-Y. Keung
CHO 02 PRL 89 091801 G.-C. Cho
ELLIS 02 PL B525 308 J. Ellis, D.V. Nanopoulos, K.A. Olive
ELLIS 02B PL B532 318 J. Ellis, A. Ferstl, K.A. Olive
ELLIS 02C PL B539 107 J. Ellis, K.A. Olive, Y. Santoso
GHODBANE 02 NP B647 190 N. Ghodbane *et al.*
HEISTER 02 PL B526 191 A. Heister *et al.* (ALEPH Collab.)
HEISTER 02E PL B526 206 A. Heister *et al.* (ALEPH Collab.)
HEISTER 02F EPJ C25 1 A. Heister *et al.* (ALEPH Collab.)
HEISTER 02J PL B533 223 A. Heister *et al.* (ALEPH Collab.)
HEISTER 02K PL B537 5 A. Heister *et al.* (ALEPH Collab.)
HEISTER 02N PL B544 73 A. Heister *et al.* (ALEPH Collab.)
HEISTER 02R EPJ C25 339 A. Heister *et al.* (ALEPH Collab.)
KIM 02B JHEP 0212 034 Y.G. Kim *et al.*
LAHANAS 02 EPJ C23 185 A. Lahanas, V.C. Spanos
MORALES 02B ASP 16 325 A. Morales *et al.* (COSME Collab.)
MORALES 02C PL B532 8 A. Morales *et al.* (IGEX Collab.)
ABBIENDI 01 PL B501 12 G. Abbiendi *et al.* (OPAL Collab.)
ABBOTT 01D PR D63 091102 B. Abbott *et al.* (D0 Collab.)
ABREU 01 EPJ C19 29 P. Abreu *et al.* (DELPHI Collab.)
ABREU 01B EPJ C19 201 P. Abreu *et al.* (DELPHI Collab.)
ABREU 01C PL B502 24 P. Abreu *et al.* (DELPHI Collab.)
ABREU 01D PL B500 22 P. Abreu *et al.* (DELPHI Collab.)
ABREU 01G PL B503 34 P. Abreu *et al.* (DELPHI Collab.)
ACCIARRI 01 EPJ C19 397 M. Acciarri *et al.* (L3 Collab.)
ADAMS 01 PRL 87 041801 T. Adams *et al.* (NuTeV Collab.)
ADLOFF 01B EPJ C20 639 C. Adloff *et al.* (H1 Collab.)
AFFOLDER 01B PR D63 091101 T. Affolder *et al.* (CDF Collab.)
AFFOLDER 01H PR D64 092002 T. Affolder *et al.* (CDF Collab.)
AFFOLDER 01J PRL 87 251803 T. Affolder *et al.* (CDF Collab.)
BALTZ 01 PRL 86 5004 E. Baltz, P. Gondolo
BARATE 01 PL B499 67 R. Barate *et al.* (ALEPH Collab.)
BARATE 01B EPJ C19 415 R. Barate *et al.* (ALEPH Collab.)
BARATE 01C PL B499 53 R. Barate *et al.* (ALEPH Collab.)
BARGER 01C PL B518 117 V. Barger, C. Kao
BAUDIS 01 PR D63 022001 L. Baudis *et al.* (Heidelberg-Moscow Collab.)
BENOIT 01 PL B513 15 A. Benoit *et al.* (EDELWEISS Collab.)
BERGER 01 PRL 86 4231 E. Berger *et al.*
BERNABEI 01 PL B509 197 R. Bernabei *et al.* (DAMA Collab.)
BOTTINO 01 PR D63 125003 A. Bottino *et al.*
BREITWEG 01 PR D63 052002 J. Breitweg *et al.* (ZEUS Collab.)
CORSETTI 01 PR D64 125010 A. Corsetti, P. Nath
DJOUADI 01 JHEP 0108 55 A. Djouadi, M. Drees, J.L. Kneur
ELLIS 01B PL B510 236 J. Ellis *et al.*
ELLIS 01C PR D63 065016 J. Ellis, A. Ferstl, K.A. Olive
GOMEZ 01 PL B512 252 M.E. Gomez, J.D. Vergados
LAHANAS 01 PL B518 94 A. Lahanas, D.V. Nanopoulos, V. Spanos
ROSZKOWSKI 01 JHEP 0108 024 L. Roszkowski, R. Ruiz de Austri, T. Nihei
SAVINOV 01 PR D63 051101 V. Savinov *et al.* (CLEO Collab.)
ABBIENDI 00 EPJ C12 1 G. Abbiendi *et al.* (OPAL Collab.)
ABBIENDI 00G EPJ C14 51 G. Abbiendi *et al.* (OPAL Collab.)
ABBIENDI 00H EPJ C14 187 G. Abbiendi *et al.* (OPAL Collab.)
Also 00Y EPJ C16 707 (erratum) G. Abbiendi *et al.* (OPAL Collab.)
ABBIENDI 00J EPJ C12 551 G. Abbiendi *et al.* (OPAL Collab.)
ABBIENDI 00R EPJ C13 553 G. Abbiendi *et al.* (OPAL Collab.)
ABBIENDI 00Y EPJ C16 707 (erratum) G. Abbiendi *et al.* (OPAL Collab.)
ABBIENDI,G 00D EPJ C18 253 G. Abbiendi *et al.* (OPAL Collab.)
ABBOTT 00C PRL 84 2088 B. Abbott *et al.* (D0 Collab.)
ABBOTT 00G PR D62 071701R B. Abbott *et al.* (D0 Collab.)
ABREU 00I EPJ C13 591 P. Abreu *et al.* (DELPHI Collab.)
ABREU 00J PL B479 129 P. Abreu *et al.* (DELPHI Collab.)
ABREU 00Q PL B478 65 P. Abreu *et al.* (DELPHI Collab.)
ABREU 00S PL B485 45 P. Abreu *et al.* (DELPHI Collab.)
ABREU 00T PL B485 95 P. Abreu *et al.* (DELPHI Collab.)
ABREU 00U PL B487 36 P. Abreu *et al.* (DELPHI Collab.)
ABREU 00V EPJ C16 211 P. Abreu *et al.* (DELPHI Collab.)
ABREU 00W PL B489 38 P. Abreu *et al.* (DELPHI Collab.)
ABREU 00Z EPJ C17 53 P. Abreu *et al.* (DELPHI Collab.)
ABREU,P 00C PL B494 203 P. Abreu *et al.* (DELPHI Collab.)
ABREU,P 00D PL B496 59 P. Abreu *et al.* (DELPHI Collab.)
ABUSAIDI 00 PRL 84 5699 R. Abusaidi *et al.* (CDMS Collab.)
ACCIARRI 00C EPJ C16 1 M. Acciarri *et al.* (L3 Collab.)
ACCIARRI 00D PL B472 420 M. Acciarri *et al.* (L3 Collab.)
ACCIARRI 00K PL B482 31 M. Acciarri *et al.* (L3 Collab.)
ACCIARRI 00P PL B489 81 M. Acciarri *et al.* (L3 Collab.)
ACCOMANDO 00 NP B585 124 E. Accomando *et al.*
AFFOLDER 00D PRL 84 5704 T. Affolder *et al.* (CDF Collab.)
AFFOLDER 00G PRL 84 5273 T. Affolder *et al.* (CDF Collab.)
AFFOLDER 00J PRL 85 1378 T. Affolder *et al.* (CDF Collab.)
AFFOLDER 00K PRL 85 2056 T. Affolder *et al.* (CDF Collab.)
BARATE 00G EPJ C16 71 R. Barate *et al.* (ALEPH Collab.)
BARATE 00H EPJ C13 29 R. Barate *et al.* (ALEPH Collab.)
BARATE 00I EPJ C12 183 R. Barate *et al.* (ALEPH Collab.)
BARATE 00P PL B488 234 R. Barate *et al.* (ALEPH Collab.)
BERNABEI 00 PL B480 23 R. Bernabei *et al.* (DAMA Collab.)
BERNABEI 00C EPJ C18 283 R. Bernabei *et al.* (DAMA Collab.)
BERNABEI 00D NJP 2 15 R. Bernabei *et al.* (DAMA Collab.)
BOEHM 00B PR D62 035012 C. Boehm, A. Djouadi, M. Drees
BREITWEG 00E EPJ C16 253 J. Breitweg *et al.* (ZEUS Collab.)
CHO 00B NP B574 623 G.-C. Cho, K. Hagiwara
COLLAR 00 PRL 85 3083 J.I. Collar *et al.* (SIMPLE Collab.)
ELLIS 00 PR D62 075010 J. Ellis *et al.*
FENG 00 PL B482 388 J.L. Feng, K.T. Matchev, F. Wilczek
LAHANAS 00 PR D62 023515 A. Lahanas, D.V. Nanopoulos, V.C. Spanos
LEP 00 CERN-EP-2000-016 LEP Collabs. (ALEPH, DELPHI, L3, OPAL, SLD+)
MAFI 00 PR D62 035003 A. Mafi, S. Raby
MALTONI 00 PL B476 107 M. Maltoni *et al.*
MORALES 00 PL B489 268 A. Morales *et al.* (IGEX Collab.)
PDG 00 EPJ C15 1 D.E. Groom *et al.*
SPOONER 00 PL B473 330 N.J.C. Spooner *et al.* (UK Dark Matter Col.)
ABBIENDI 99 EPJ C6 1 G. Abbiendi *et al.* (OPAL Collab.)
ABBIENDI 99F EPJ C8 23 G. Abbiendi *et al.* (OPAL Collab.)
ABBIENDI 99G EPJ C8 255 G. Abbiendi *et al.* (OPAL Collab.)
ABBIENDI 99M PL B456 95 G. Abbiendi *et al.* (OPAL Collab.)
ABBIENDI 99T EPJ C11 619 G. Abbiendi *et al.* (OPAL Collab.)
ABBOTT 99 PRL 82 29 B. Abbott *et al.* (D0 Collab.)
ABBOTT 99F PR D60 031101 B. Abbott *et al.* (D0 Collab.)
ABBOTT 99J PRL 83 2896 B. Abbott *et al.* (D0 Collab.)
ABBOTT 99K PRL 83 4476 B. Abbott *et al.* (D0 Collab.)
ABBOTT 99L PRL 83 4937 B. Abbott *et al.* (D0 Collab.)
ABE 99I PR D59 092002 F. Abe *et al.* (CDF Collab.)
ABE 99M PRL 83 2133 F. Abe *et al.* (CDF Collab.)
ABREU 99A EPJ C11 383 P. Abreu *et al.* (DELPHI Collab.)
ABREU 99C EPJ C6 385 P. Abreu *et al.* (DELPHI Collab.)
ABREU 99D EPJ C6 371 P. Abreu *et al.* (DLEPHI Collab.)
ABREU 99F EPJ C7 595 P. Abreu *et al.* (DELPHI Collab.)
ABREU 99G PL B446 62 P. Abreu *et al.* (DELPHI Collab.)
ACCIARRI 99H PL B456 283 M. Acciarri *et al.* (L3 Collab.)
ACCIARRI 99I PL B459 354 M. Acciarri *et al.* (L3 Collab.)
ACCIARRI 99L PL B462 354 M. Acciarri *et al.* (L3 Collab.)
ACCIARRI 99R PL B470 268 M. Acciarri *et al.* (L3 Collab.)
ACCIARRI 99V PL B471 308 M. Acciarri *et al.* (L3 Collab.)
ACCIARRI 99W PL B471 280 M. Acciarri *et al.* (L3 Collab.)
ALAVI-HARATI 99E PRL 83 2128 A. Alavi-Harati *et al.* (FNAL KTeV Collab.)
AMBROSIO 99 PR D60 082002 M. Ambrosio *et al.* (Macro Collab.)
BAER 99 PR D59 075002 H. Baer, K. Cheung, J.F. Gunion
BARATE 99E EPJ C7 383 R. Barate *et al.* (ALEPH Collab.)
BARATE 99P EPJ C11 193 R. Barate *et al.* (ALEPH Collab.)
BARATE 99Q PL B469 303 R. Barate *et al.* (ALEPH Collab.)
BAUDIS 99 PR D59 022001 L. Baudis *et al.* (Heidelberg-Moscow Collab.)
BELLI 99C NP B563 97 P. Belli *et al.* (DAMA Collab.)
BERNABEI 99 PL B450 448 R. Bernabei *et al.* (DAMA Collab.)
FANTI 99 PL B446 117 V. Fanti *et al.* (CERN NA48 Collab.)
MALTONI 99B PL B463 230 M. Maltoni, M.I. Vysotsky
OOTANI 99 PL B461 371 W. Ootani *et al.*
ABBOTT 98 PRL 80 442 B. Abbott *et al.* (D0 Collab.)
ABBOTT 98C PRL 80 1591 B. Abbott *et al.* (D0 Collab.)
ABBOTT 98E PRL 80 2051 B. Abbott *et al.* (D0 Collab.)
ABBOTT 98J PRL 81 38 B. Abbott *et al.* (D0 Collab.)
ABE 98J PRL 80 5275 F. Abe *et al.* (CDF Collab.)
ABE 98L PRL 81 1791 F. Abe *et al.* (CDF Collab.)
ABE 98S PRL 81 4806 F. Abe *et al.* (CDF Collab.)
ABREU 98 EPJ C1 1 P. Abreu *et al.* (DELPHI Collab.)
ABREU 98P PL B444 491 P. Abreu *et al.* (DELPHI Collab.)
ACCIARRI 98F EPJ C4 207 M. Acciarri *et al.* (L3 Collab.)
ACCIARRI 98J PL B433 163 M. Acciarri *et al.* (L3 Collab.)
ACCIARRI 98V PL B444 503 M. Acciarri *et al.* (L3 Collab.)
ACKERSTAFF 98K EPJ C4 47 K. Ackerstaff *et al.* (OPAL Collab.)
ACKERSTAFF 98L EPJ C2 213 K. Ackerstaff *et al.* (OPAL Collab.)
ACKERSTAFF 98P PL B433 195 K. Ackerstaff *et al.* (OPAL Collab.)
ACKERSTAFF 98V EPJ C2 441 K. Ackerstaff *et al.* (OPAL Collab.)
BARATE 98H PL B420 127 R. Barate *et al.* (ALEPH Collab.)
BARATE 98J PL B429 201 R. Barate *et al.* (ALEPH Collab.)
BARATE 98K PL B433 176 R. Barate *et al.* (ALEPH Collab.)
BARATE 98S EPJ C4 433 R. Barate *et al.* (ALEPH Collab.)
BARATE 98X EPJ C2 417 R. Barate *et al.* (ALEPH Collab.)
BERNABEI 98 PL B434 195 R. Bernabei *et al.* (DAMA Collab.)
BERNABEI 98C PL B436 379 R. Bernabei *et al.* (DAMA Collab.)
BREITWEG 98 PL B434 214 J. Breitweg *et al.* (ZEUS Collab.)
ELLIS 98 PR D58 095002 J. Ellis *et al.*
ELLIS 98B PL B444 367 J. Ellis, T. Falk, K. Olive
PDG 98 EPJ C3 1 C. Caso *et al.*
ABACHI 97 PRL 78 2070 S. Abachi *et al.* (D0 Collab.)
ABBOTT 97B PRL 79 4321 B. Abbott *et al.* (D0 Collab.)
ABE 97K PR D56 R1357 F. Abe *et al.* (CDF Collab.)
ACCIARRI 97U PL B414 373 M. Acciarri *et al.* (L3 Collab.)
ACKERSTAFF 97H PL B396 301 K. Ackerstaff *et al.* (OPAL Collab.)
ADAMS 97B PRL 79 4083 J. Adams *et al.* (FNAL KTeV Collab.)
ALBUQUERQ... 97 PRL 78 3252 I.F. Albuquerque *et al.* (FNAL E761 Collab.)
BAER 97 PR D57 567 H. Baer, M. Brhlik
BARATE 97K PL B405 379 R. Barate *et al.* (ALEPH Collab.)
BARATE 97L ZPHY C76 1 R. Barate *et al.* (ALEPH Collab.)
BERNABEI 97 ASP 7 73 R. Bernabei *et al.* (DAMA Collab.)
CARENA 97 PL B390 234 M. Carena, G.F. Giudice, C.E.M. Wagner
CSIKOR 97 PRL 78 4335 F. Csikor, Z. Fodor (EOTV, CERN)
DATTA 97 PL B395 54 A. Datta, M. Guchait, N. Parua (ICTP, TATA)

DEGOUVEA	97	PL B400 117	A. de Gouvea, H. Murayama	
DERRICK	97	ZPHY C73 613	M. Derrick *et al.*	(ZEUS Collab.)
EDSJO	97	PR D56 1879	J. Edsjo, P. Gondolo	
ELLIS	97	PL B394 354	J. Ellis, J.L. Lopez, D.V. Nanopoulos	
HEWETT	97	PR D56 5703	J.L. Hewett, T.G. Rizzo, M.A. Doncheski	
KALINOWSKI	97	PL B400 112	J. Kalinowski, P. Zerwas	
TEREKHOV	97	PL B412 86	I. Terekhov	(ALAT)
ABACHI	96	PRL 76 2228	S. Abachi *et al.*	(D0 Collab.)
ABACHI	96B	PRL 76 2222	S. Abachi *et al.*	(D0 Collab.)
ABE	96	PRL 77 438	F. Abe *et al.*	(CDF Collab.)
ABE	96D	PRL 76 2006	F. Abe *et al.*	(CDF Collab.)
ABE	96K	PRL 76 4307	F. Abe *et al.*	(CDF Collab.)
AID	96	ZPHY C71 211	S. Aid *et al.*	(H1 Collab.)
AID	96C	PL B380 461	S. Aid *et al.*	(H1 Collab.)
ARNOWITT	96	PR D54 2374	R. Arnowitt, P. Nath	
BAER	96	PR D53 597	H. Baer, M. Brhlik	
BERGSTROM	96	ASP 5 263	L. Bergstrom, P. Gondolo	
CHO	96	PL B372 101	G.C. Cho, Y. Kizukuri, N. Oshimo	(TOKAH, OCH)
FARRAR	96	PRL 76 4111	G.R. Farrar	(RUTG)
LEWIN	96	ASP 6 87	J.D. Lewin, P.F. Smith	
TEREKHOV	96	PL B385 139	I. Terkhov, L. Clavelli	(ALAT)
ABACHI	95C	PRL 75 618	S. Abachi *et al.*	(D0 Collab.)
ABE	95N	PRL 74 3538	F. Abe *et al.*	(CDF Collab.)
ABE	95T	PRL 75 613	F. Abe *et al.*	(CDF Collab.)
ACCIARRI	95E	PL B350 109	M. Acciarri *et al.*	(L3 Collab.)
AKERS	95A	ZPHY C65 367	R. Akers *et al.*	(OPAL Collab.)
AKERS	95R	ZPHY C67 203	R. Akers *et al.*	(OPAL Collab.)
BEREZINSKY	95	ASP 5 1	V. Berezinsky *et al.*	
BUSKULIC	95E	PL B349 238	D. Buskulic *et al.*	(ALEPH Collab.)
CLAVELLI	95	PR D51 1117	L. Clavelli, P.W. Coulter	(ALAT)
FALK	95	PL B354 99	T. Falk, K.A. Olive, M. Srednicki	(MINN, UCSB)
LOSECCO	95	PL B342 392	J.M. LoSecco	(NDAM)
AKERS	94K	PL B337 207	R. Akers *et al.*	(OPAL Collab.)
BECK	94	PL B336 141	M. Beck *et al.*	(MPIH, KIAE, SASSO)
CAKIR	94	PR D50 3268	M.B. Cakir, G.R. Farrar	(RUTG)
FALK	94	PL B339 248	T. Falk, K.A. Olive, M. Srednicki	(UCSB, MINN)
SHIRAI	94	PRL 72 3313	J. Shirai *et al.*	(VENUS Collab.)
ADRIANI	93M	PRPL 236 1	O. Adriani *et al.*	(L3 Collab.)
ALITTI	93	NP B400 3	J. Alitti *et al.*	(UA2 Collab.)
CLAVELLI	93	PR D47 1973	L. Clavelli, P.W. Coulter, K.J. Yuan	(ALAT)
DREES	93	PR D47 376	M. Drees, M.M. Nojiri	(DESY, SLAC)
DREES	93B	PR D48 3483	M. Drees, M.M. Nojiri	
FALK	93	PL B318 354	T. Falk *et al.*	(UCB, UCSB, MINN)
HEBBEKER	93	ZPHY C60 63	T. Hebbeker	(CERN)
KELLEY	93	PR D47 2461	S. Kelley *et al.*	(TAMU, ALAH)
LOPEZ	93C	PL B313 241	J.L. Lopez, D.V. Nanopoulos, X. Wang	(TAMU, HARC+)
MIZUTA	93	PL B298 120	S. Mizuta, M. Yamaguchi	(TOHO)
MORI	93	PR D48 5505	M. Mori *et al.*	(KEK, NIIG, TOKY, TOKA+)
ABE	92L	PRL 69 3439	F. Abe *et al.*	(CDF Collab.)
BOTTINO	92	MPL A7 733	A. Bottino *et al.*	(TORI, ZARA)
Also	91	PL B265 57	A. Bottino *et al.*	(TORI, INFN)
CLAVELLI	92	PR D46 2112	L. Clavelli	(ALAT)
DECAMP	92	PRPL 216 253	D. Decamp *et al.*	(ALEPH Collab.)
LOPEZ	92	NP B370 445	J.L. Lopez, D.V. Nanopoulos, K.J. Yuan	(TAMU)
MCDONALD	92	PL B283 80	J. McDonald, K.A. Olive, M. Srednicki	(LISB+)
ROY	92	PL B283 270	D.P. Roy	(CERN)
ABREU	91F	NP B367 511	P. Abreu *et al.*	(DELPHI Collab.)
AKESSON	91	ZPHY C52 219	T. Akesson *et al.*	(HELIOS Collab.)
ALEXANDER	91F	ZPHY C52 175	G. Alexander *et al.*	(OPAL Collab.)
ANTONIADIS	91	PL B262 109	I. Antoniadis, J. Ellis, D.V. Nanopoulos	(EPOL+)
BOTTINO	91	PL B265 57	A. Bottino *et al.*	(TORI, INFN)
GELMINI	91	NP B351 623	G.B. Gelmini, P. Gondolo, E. Roulet	(UCLA, TRST)
GRIEST	91	PR D43 3191	K. Griest, D. Seckel	
KAMIONKOW...	91	PR D44 3021	M. Kamionkowski	(CHIC, FNAL)
MORI	91B	PL B270 89	M. Mori *et al.*	(Kamiokande Collab.)
NOJIRI	91	PL B261 76	M.M. Nojiri	(KEK)
OLIVE	91	NP B355 208	K.A. Olive, M. Srednicki	(MINN, UCSB)
ROSZKOWSKI	91	PL B262 59	L. Roszkowski	(CERN)
SATO	91	PR D44 2220	N. Sato *et al.*	(Kamiokande Collab.)
ADACHI	90C	PL B244 352	I. Adachi *et al.*	(TOPAZ Collab.)
GRIEST	90	PR D41 3565	K. Griest, M. Kamionkowski, M.S. Turner	(UCB+)
BARBIERI	89C	NP B313 725	R. Barbieri, M. Frigeni, G. Giudice	
NAKAMURA	89	PR D39 1261	T.T. Nakamura *et al.*	(KYOT, TMTC)
OLIVE	89	PL B230 78	K.A. Olive, M. Srednicki	(MINN, UCSB)
ELLIS	88D	NP B307 883	J. Ellis, R. Flores	
GRIEST	88B	PR D38 2357	K. Griest	
OLIVE	88	PL B205 553	K.A. Olive, M. Srednicki	(MINN, UCSB)
SREDNICKI	88	NP B310 693	M. Srednicki, R. Watkins, K.A. Olive	(MINN, UCSB)
ALBAJAR	87D	PL B198 261	C. Albajar *et al.*	(UA1 Collab.)
ANSARI	87D	PL B195 613	R. Ansari *et al.*	(UA2 Collab.)
ARNOLD	87	PL B186 435	R.G. Arnold *et al.*	(BRUX, DUUC, LOUC+)
NG	87	PL B188 138	K.W. Ng, K.A. Olive, M. Srednicki	(MINN, UCSB)
TUTS	87	PL B186 233	P.M. Tuts *et al.*	(CUSB Collab.)
ALBRECHT	86C	PL 167B 360	H. Albrecht *et al.*	(ARGUS Collab.)
BADIER	86	ZPHY C31 21	J. Badier *et al.*	(NA3 Collab.)
BARNETT	86	NP B267 625	R.M. Barnett, H.E. Haber, G.L. Kane	(LBL, UCSC+)
GAISSER	86	PR D34 2206	T.K. Gaisser, G. Steigman, S. Tilav	(BART, DELA)
VOLOSHIN	86	SJNP 43 495 Translated from YAF 43 779.	M.B. Voloshin, L.B. Okun	(ITEP)
COOPER-...	85B	PL 160B 212	A.M. Cooper-Sarkar *et al.*	(WA66 Collab.)
DAWSON	85	PR D31 1581	S. Dawson, E. Eichten, C. Quigg	(LBL, FNAL)
FARRAR	85	PRL 55 895	G.R. Farrar	(RUTG)
GOLDMAN	85	Physica 15D 181	T. Goldman, H.E. Haber	(LANL, UCSC)
HABER	85	PRPL 117 75	H.E. Haber, G.L. Kane	(UCSC, MICH)
BALL	84	PRL 53 1314	R.C. Ball *et al.*	(MICH, FIRZ, OSU, FNAL+)
BARBER	84B	PL 139B 427	J.S. Barber, R.E. Shrock	(STON)
BRICK	84	PR D30 1134	D.H. Brick *et al.*	(BROW, CAVE, IIT+)
ELLIS	84	NP B238 453	J. Ellis *et al.*	(CERN)
FARRAR	84	PRL 53 1029	G.R. Farrar	(RUTG)
BERGSMA	83C	PL 121B 429	F. Bergsma *et al.*	(CHARM Collab.)
CHANOWITZ	83	PL 126B 225	M.S. Chanowitz, S. Sharpe	(UCB, LBL)
GOLDBERG	83	PRL 50 1419	H. Goldberg	(NEAS)
HOFFMAN	83	PR D28 660	C.M. Hoffman *et al.*	(LANL, ARIZ)
KRAUSS	83	NP B227 556	L.M. Krauss	(HARV)
VYSOTSKII	83	SJNP 37 948 Translated from YAF 37 1597.	M.I. Vysotsky	(ITEP)
KANE	82	PL 112B 227	G.L. Kane, J.P. Leveille	(MICH)
CABIBBO	81	PL 105B 155	N. Cabibbo, G.R. Farrar, L. Maiani	(ROMA, RUTG)
FARRAR	78	PL 76B 575	G.R. Farrar, P. Fayet	(CIT)
Also	78B	PL 79B 442	G.R. Farrar, P. Fayet	(CIT)

Technicolor

DYNAMICAL ELECTROWEAK SYMMETRY BREAKING

Revised August 2003 by R.S. Chivukula and M. Narain (Boston University) and J. Womersley (Fermilab).

In theories of dynamical electroweak symmetry breaking, the electroweak interactions are broken to electromagnetism by the vacuum expectation value of a fermion bilinear. These theories may thereby avoid the introduction of fundamental scalar particles, of which we have no examples in nature. In this note, we review the status of experimental searches for the particles predicted in technicolor, topcolor, and related models. The limits from these searches are summarized in Table 1.

I. Technicolor

The earliest models [1,2] of dynamical electroweak symmetry breaking [3] include a new non-abelian gauge theory ("technicolor") and additional massless fermions ("technifermions") which feel this new force. The global chiral symmetry of the fermions is spontaneously broken by the formation of a technifermion condensate, just as the approximate chiral SU(2) $\times$ $SU(2)$ symmetry in QCD is broken down to SU(2) isospin by the formation of a quark condensate. If the quantum numbers of the technifermions are chosen correctly (*e.g.* by choosing technifermions in the fundamental representation of an SU(N) technicolor gauge group, with the left-handed technifermions being weak doublets and the right-handed ones weak singlets) this condensate can break the electroweak interactions down to electromagnetism.

The breaking of the global chiral symmetries implies the existence of Goldstone bosons, the "technipions" (π_T). Through the Higgs mechanism, three of the Goldstone bosons become the longitudinal components of the W and Z, and the weak gauge bosons acquire a mass proportional to the technipion decay constant (the analog of f_π in QCD). The quantum numbers and masses of any remaining technipions are model dependent. There may be technipions which are colored (octets and triplets) as well as those carrying electroweak quantum numbers, and some color-singlet technipions are too light [4,5] unless additional sources of chiral-symmetry breaking are introduced. The next lightest technicolor resonances are expected to be the analogs of the vector mesons in QCD. The technivector mesons can also have color and electroweak quantum numbers and, for a theory with a small number of technifermions, are expected to have a mass in the TeV range [6].

While technicolor chiral symmetry breaking can give mass to the W and Z particles, additional interactions must be introduced to produce the masses of the standard model fermions. The most thoroughly studied mechanism for this invokes "extended technicolor" (ETC) gauge interactions [4,7]. In ETC, technicolor, color and flavor are embedded into a larger gauge group which is broken to technicolor and color at an energy scale of 100s to 1000s of TeV. The massive gauge bosons associated with this breaking mediate transitions between quarks/leptons

and technifermions, giving rise to the couplings necessary to produce fermion masses. The ETC gauge bosons also mediate transitions among technifermions themselves, leading to interactions which can explicitly break unwanted chiral symmetries and raise the masses of any light technipions. The ETC interactions connecting technifermions to quarks/leptons also mediate technipion decays to ordinary fermion pairs. Since these interactions are responsible for fermion masses, one generally expects technipions to decay to the heaviest fermions kinematically allowed (though this need not hold in all models).

In addition to quark masses, ETC interactions must also give rise to quark mixing. One expects, therefore, that there are ETC interactions coupling quarks of the same charge from different generations. A stringent limit on these flavor-changing neutral current interactions comes from K^0–$\overline{K}^0$ mixing [4]. These force the scale of ETC breaking and the corresponding ETC gauge boson masses to be in the 100-1000 TeV range (at least insofar as ETC interactions of first two generations are concerned). To obtain quark and technipion masses that are large enough then requires an enhancement of the technifermion condensate over that expected naively by scaling from QCD. Such an enhancement can occur if the technicolor gauge coupling runs very slowly, or "walks" [8]. Many technifermions typically are needed to make the TC coupling walk, implying that the technicolor scale and, in particular, the technivector mesons may be much lighter than 1 TeV [3,9]. It should also be noted that there is no reliable calculation of electroweak parameters in a walking technicolor theory, and the values of precisely measured electroweak quantities [10] cannot directly be used to constrain the models. Recently, progress has been made in constructing a complete theory of fermion masses (including neutrino masses) in the context of extended technicolor [11].

In existing colliders, technivector mesons are dominantly produced when an off-shell standard model gauge-boson "resonates" into a technivector meson with the same quantum numbers [12]. The technivector mesons may then decay, in analogy with $\rho \to \pi\pi$, to pairs of technipions. However, in walking technicolor the technipion masses may be increased to the point that the decay of a technirho to pairs of technipions is kinematically forbidden [9]. In this case the decay to a technipion and a longitudinally polarized weak boson (an "eaten" Goldstone boson) may be preferred, and the technivector meson would be very narrow. Alternatively, the technivector may also decay, in analogy with the decay $\rho \to \pi\gamma$, to a technipion plus a photon, gluon, or transversely polarized weak gauge boson. Finally, in analogy with the decay $\rho \to e^+e^-$, the technivector meson may resonate back to an off-shell gluon or electroweak gauge boson, leading to a decay into a pair of leptons, quarks, or gluons.

When comparing the various results presented in this review, one should be aware that the more recent analyses [19,20] make use of newer calculations [13] of technihadron production and decay, as implemented in PYTHIA version 6.126

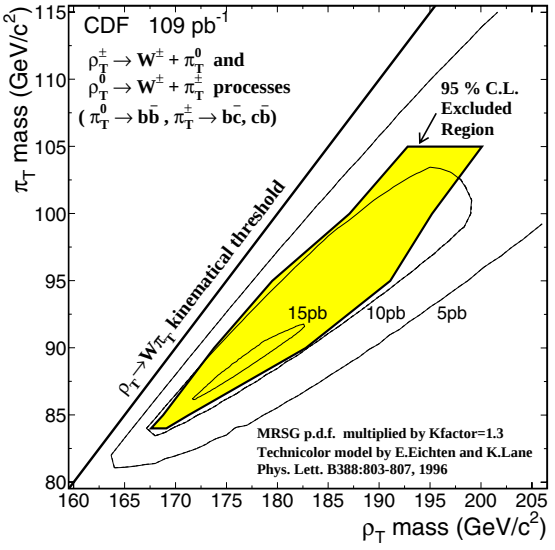

Figure 1: 95% CL exclusion region [16] for a light technirho decaying to $W^{\pm}$ and a π_T, and in which the π_T decays to two jets including at least one b quark. See full-color version on color pages at end of book.

and higher [14]. The results obtained with older cross section calculations are not always directly comparable.

If the dominant decay mode of the technirho is $W_L\pi_T$, promising signal channels [15] are $\rho_T^{\pm} \to W^{\pm}\pi_T^0$ and $\rho_T^0 \to W^{\pm}\pi_T^{\mp}$. If we assume that the technipions decay to $b\overline{b}$ (neutral) and $b\overline{c}$ (charged), then both channels yield a signal of $W(\ell\nu) + 2$jets, with one or more heavy flavor tags. The CDF collaboration has carried out a search in this final state [16] based on Run I data and using PYTHIA [17] version 6.1 for the signal simulation. The results are shown in Figure 1. We see that the search is sensitive to $\sigma \cdot B \gtrsim 10$ pb and that roughly $170 < m_{\rho_T} < 190$ GeV is excluded at the 95% confidence level, for $m_{\pi_T} \approx m_{\rho_T}/2$. For an integrated luminosity of 2 fb^{-1} in Run II, the 5σ discovery reach extends to $m_{\rho_T} = 210$ GeV and $m_{\pi_T} = 110$ GeV, while the 95% exclusion sensitivity will extend to $m_{\rho_T} = 250$ GeV and $m_{\pi_T} = 145$ GeV.

CDF has also searched [18] for the process $\omega_T^0 \to \gamma\pi_T^0$, yielding a signal of a hard photon plus two jets, with one or more heavy flavor tags. The sensitivity to $\sigma \cdot B$ is of order 1 pb. The excluded region is shown in Fig. 2 and is roughly $140 < m_{\omega_T} < 290$ GeV at the 95% level, for $m_{\pi_T} \approx m_{\omega_T}/3$. The analysis assumes four technicolors, $Q_D = Q_U - 1 = \frac{1}{3}$ and $M_T = 100$ GeV/c^2. Here Q_U and Q_D are the charges of the lightest technifermion doublet and M_T is a dimensionful

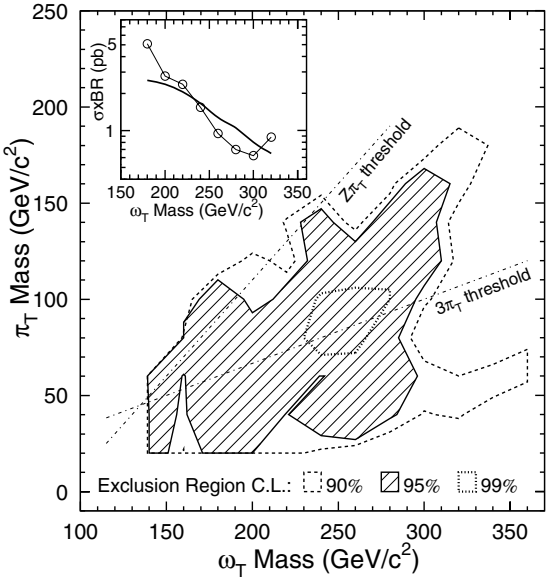

Figure 2: 95% CL exclusion region [18] for a light techniomega decaying to γ and a π_T, and in which the π_T decays to two jets including at least one b quark. (Inset: cross section limit for $m_{\pi_T} = 120$ GeV.)

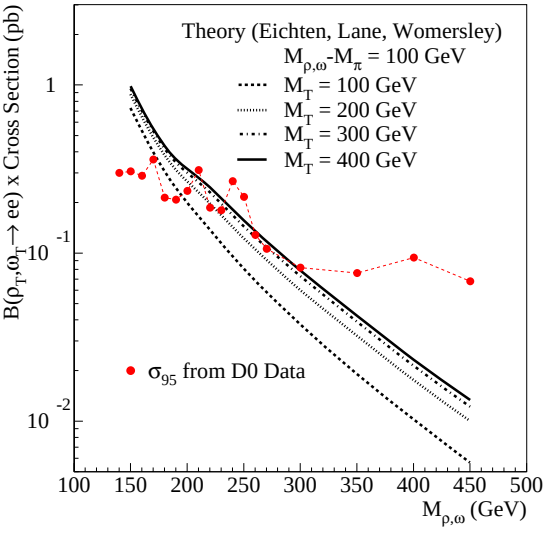

Figure 3: 95% CL cross-section limit [19] for a light techniomega and a light technirho decaying to $\ell^+\ell^-$. See full-color version on color pages at end of book.

parameter, of order 100 GeV/c^2, which controls the rate of $\rho_T, \omega_T \to \gamma\pi_T$.

The DØ experiment has searched [19] for low-scale technicolor resonances ρ_T and ω_T decaying to dileptons, using an inclusive e^+e^- sample from Run I. In the search, the ρ_T and ω_T are assumed to be degenerate in mass. The absence of structure in the dilepton invariant mass distribution is then used to set limits. Masses $m_{\rho_T} = m_{\omega_T} \lesssim 200$ GeV are excluded, provided either $m_{\rho_T} < m_{\pi_T} + m_W$, or $M_T > 200$ GeV (as shown in Fig. 3). With 2 fb^{-1} of data in Run II, the sensitivity will extend to $m_{\rho_T} = m_{\omega_T} \approx 500$ GeV.

DELPHI [20] has reported a search for technicolor production in 452 pb^{-1} of e^+e^- data taken between 192 and 208 GeV. The analysis combines searches for $e^+e^- \to \rho_T(\gamma)$ with $\rho_T \to W_L W_L$, $\rho_T \to$ hadrons ($\pi_T\pi_T$ or $q\overline{q}$), $\rho_T \to \pi_T\gamma$, and $e^+e^- \to \rho_T^* \to W_L\pi_T$ or $\pi_T\pi_T$. Technirho masses in the range $90 < m_{\rho_T} < 206.7$ GeV are excluded, while technipion masses $m_{\pi_T} < 79.8$ GeV are ruled out independent of the parameters of the technicolor model.

Searches have also been carried out at the Tevatron for colored technihadron resonances [21,22]. CDF has used a search for structure in the dijet invariant mass spectrum to set limits on a color-octet technirho ρ_{T8} produced by an off-shell gluon and decaying to two real quarks or gluons. As shown in Fig. 5 masses $260 < m_{\rho_{T8}} < 480$ GeV are excluded; in Run II the limits will improve to cover the whole mass range up to about 0.8 TeV [23].

The CDF second and third-generation leptoquark searches (see Refs. [24,25]) have also been interpreted in terms of the complementary ρ_{T8} decay mode: $p\overline{p} \to \rho_{T8} \to \pi_{LQ}\pi_{LQ}$. Here π_{LQ} denotes a color-triplet technipion carrying both color and lepton number, assumed to decay to $b\nu$ or $c\nu$ [25] or to a τ plus a quark [24]. The searches exclude technirho masses $m_{\rho_{T8}}$ less than 510 GeV ($\pi_{LQ} \to c\nu$), 600 GeV ($\pi_{LQ} \to b\nu$), and 465 GeV ($\pi_{LQ} \to \tau q$) for technipion masses up to $m_{\rho_{T8}}/2$. Figure 6 shows the $\pi_{LQ} \to b\nu$ exclusion region. (Leptoquark masses $m_{\pi_{LQ}}$ less than 123 GeV ($c\nu$), 148 GeV ($b\nu$), and 99 GeV (τq) are already ruled out by standard continuum-production leptoquark searches).

Recently, it has been demonstrated that there is substantial uncertainty in the theoretical estimate of the ρ_{T8} production cross section at the Tevatron and that the cross section may be as much as an order of magnitude lower than the naive vector meson dominance estimate [26]. To establish the range of allowed masses, these limits will need to be redone with a reduced theoretical cross section.

II. Top Condensate and Related Models

The top quark is much heavier than other fermions and must be more strongly coupled to the symmetry-breaking sector. It is natural to consider whether some or all of electroweak-symmetry breaking is due to a condensate of top quarks [3,27].

See key on page 323

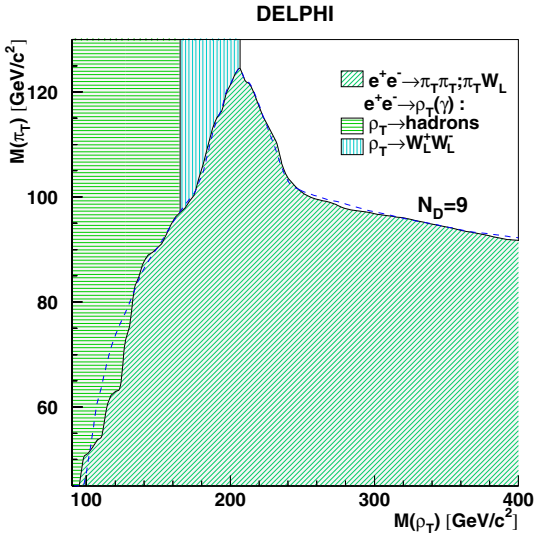

Figure 4: 95% CL exclusion region [20] in the technirho-technipion mass plane obtained from searches by the DELPHI collaboration at LEP 2, for nine technifermion doublets. The dashed line shows the expected limit for the 4-jet analysis. See full-color version on color pages at end of book.

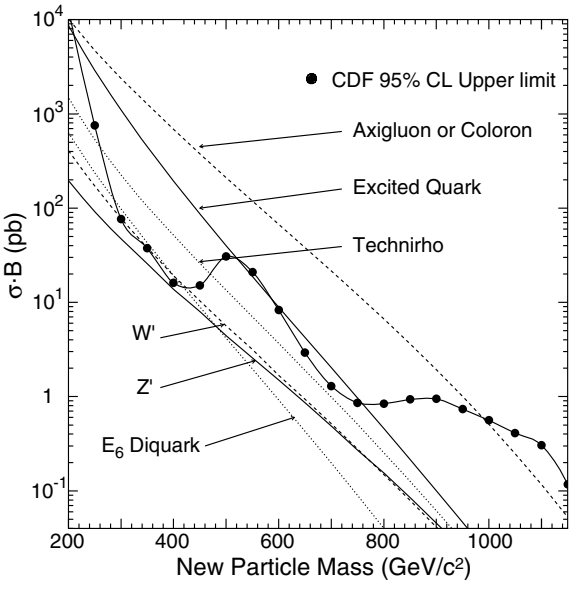

Figure 5: 95% CL Cross-section limits [22] for a technirho decaying to two jets at the Tevatron.

Top-quark condensation alone, without additional fermions, seems to produce a top-quark mass larger [28] than observed experimentally, and is therefore not favored. Topcolor assisted technicolor [29] combines technicolor and top-condensation. In addition to technicolor, which provides the bulk of electroweak symmetry breaking, top-condensation and the top quark mass arise predominantly from "topcolor," a new QCD-like interaction which couples strongly to the third generation of quarks. An additional, strong, U(1) interaction (giving rise to a topcolor Z') precludes the formation of a b-quark condensate.

CDF has searched [30] for the "topgluon," a massive color-octet vector which couples preferentially to the third generation, in the mode $p\overline{p} \to g_t \to b\overline{b}$. The results are shown in Fig. 7. Topgluon masses from approximately 0.3 to 0.6 TeV are excluded at 95% confidence level, for topgluon widths in the range $0.3m_{g_t} < \Gamma < 0.7m_{g_t}$. Results have also been reported by CDF [31] on a search for narrow resonances in the $t\overline{t}$ invariant mass distribution. The cross section limit is shown in Fig. 8 and excludes a leptophobic topcolor Z' with masses less than 480 (780) GeV/c^2, for the case where its width $\Gamma = 0.012(0.04)\, m_{Z'}$. (DØ has carried out a similar search, with greater sensitivity [32], but has not derived comparable Z' mass limits.) A broad topgluon could also be detected in the same final state, though no results are yet available. In Run II, the Tevatron [23] should be sensitive to topgluon and topcolor Z' masses up to of order 1 TeV in $b\overline{b}$ and $t\overline{t}$ final states. A detailed theoretical analysis of B–$\overline{B}$ mixing and light quark mass generation in top-color assisted technicolor shows that, at least in some models, the topgluon and Z' boson masses must be greater than about 5 TeV [33].

The top-quark seesaw model of electroweak symmetry breaking [34] is a variant of the original top-condensate idea which reconciles top-condensation with a lighter top-quark mass. Such a model can easily be consistent with precision electroweak tests, either because the spectrum includes a light composite Higgs [35] or because additional interactions allow for a heavier Higgs [36]. Such theories may arise naturally from gauge fields propagating in compact extra spatial dimensions [37].

A variant of topcolor-assisted technicolor is flavor-universal, in which the topcolor SU(3) gauge bosons, called colorons, couple equally to all quarks [38]. Flavor-universal versions of the seesaw model [39] incorporating a gauged flavor symmetry are also possible. In these models *all* left-handed quarks (and possibly leptons as well) participate in electroweak symmetry-breaking condensates with separate (one for each flavor) right-handed weak singlets, and the different fermion masses arise by adjusting the parameters which control the mixing of each fermion with the corresponding condensate.

A prediction of these flavor-universal models, is the existence of new heavy gauge bosons, coupling to color or flavor, at relatively low mass scales. The absence of an excess of high-E_T

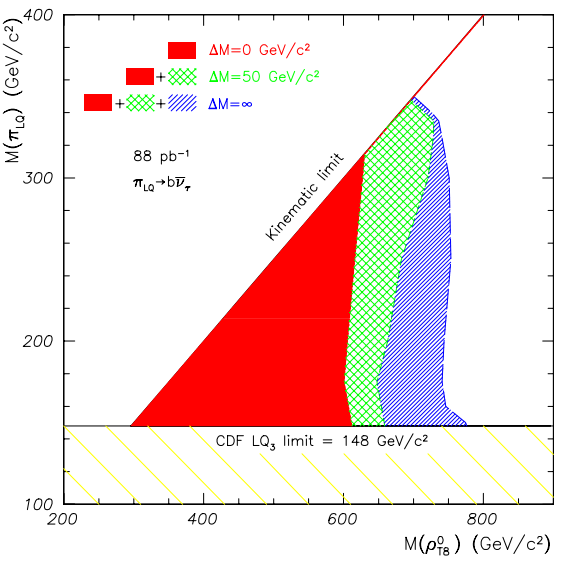

Figure 6: 95% CL exclusion region [25] in the technirho-technipion mass plane for pair produced technipions, with leptoquark couplings, decaying to $b\nu$. See full-color version on color pages at end of book.

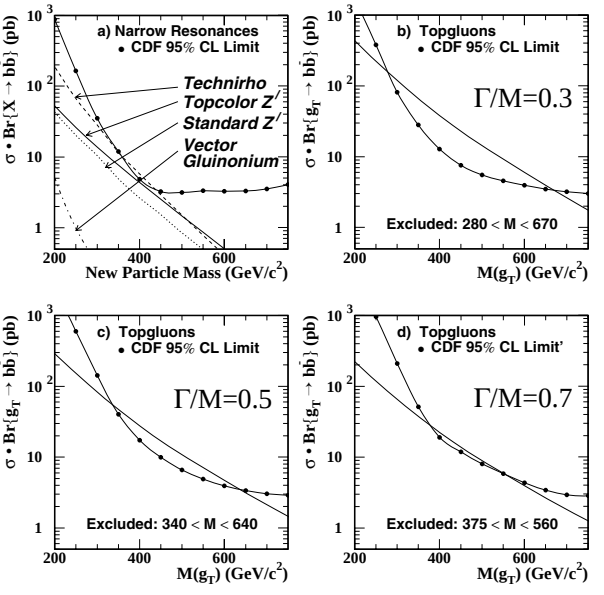

Figure 7: Tevatron limits [30] on new particles decaying to $b\bar{b}$: narrow resonances and topgluons for various widths.

jets in DØ data [40] has been used to constrain strongly-coupled flavor-universal colorons (massive color-octet bosons coupling to all quarks). A mass limit of between 0.8 and 3.5 TeV is set [41] depending on the coloron-gluon mixing angle. Precision electroweak measurements constrain [42] the masses of these new gauge bosons to be greater than 1–3 TeV in a variety of models, for strong couplings.

Recently a new class [43] of composite Higgs model [44], dubbed "Little Higgs Theory," has been developed which give rise to naturally light Higgs bosons without supersymmetry [46]. Inspired by discretized versions of higher-dimensional gauge theory [45], these models are based on the chiral symmetries of "theory space." The models involve extended gauge groups and novel gauge symmetry breaking patterns. The new chiral symmetries prevent large corrections to the Higgs boson mass, and allow the scale (Λ) of the underlying strong dynamics giving rise to the composite particles to be as large as 10 TeV. These models typically require new gauge bosons and fermions, and possibly additional composite scalars beyond the Higgs, in the TeV mass range.

Acknowledgments

We thank Tom Appelquist, Bogdan Dobrescu, Robert Harris, Chris Hill, Greg Landsberg, Kenneth Lane, and Elizabeth Simmons for help in the preparation of this article. *This work was supported in part by the Department of Energy under grant DE-FG02-91ER40676.*

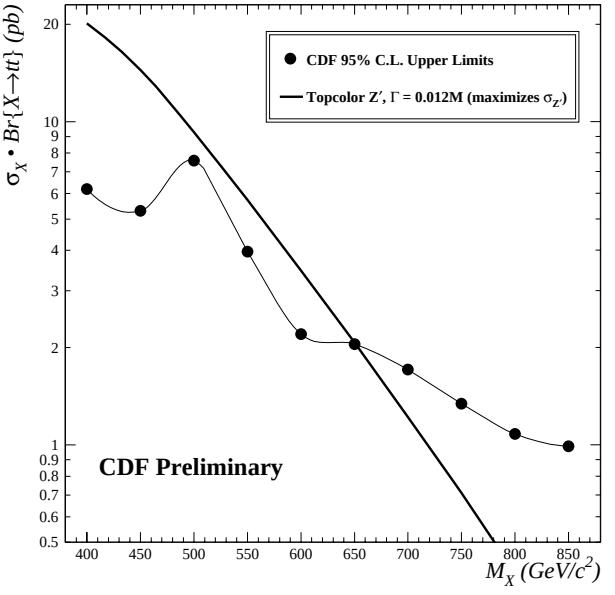

Figure 8: Cross-section limits for a narrow resonance decaying to $t\bar{t}$ [31] and expected cross section for a leptophobic topcolor Z' boson.

See key on page 323

Table 1: Summary of the mass limits. Symbols are defined in the text.

Process	Excluded mass range	Decay channels	Ref.
$p\overline{p} \to \rho_T \to W\pi_T$	$170 < m_{\rho_T} < 190$ GeV for $m_{\pi_T} \approx m_{\rho_T}/2$	$\rho_T \to W\pi_T$ $\pi_T^0 \to b\overline{b}$ $\pi_T^\pm \to b\overline{c}$	[16]
$p\overline{p} \to \omega_T \to \gamma\pi_T$	$140 < m_{\omega_T} < 290$ GeV for $m_{\pi_T} \approx m_{\omega_T}/3$ and $M_T = 100$ GeV	$\omega_T \to \gamma\pi_T$ $\pi_T^0 \to b\overline{b}$ $\pi_T^\pm \to b\overline{c}$	[18]
$p\overline{p} \to \omega_T/\rho_T$	$m_{\omega_T} = m_{\rho_T} < 203$ GeV for $m_{\omega_T} < m_{\pi_T} + m_W$ or $M_T > 200$ GeV	$\omega_T/\rho_T \to \ell^+\ell^-$	[19]
$e^+e^- \to \omega_T/\rho_T$	$90 < m_{\rho_T} < 206.7$ GeV $m_{\pi_T} < 79.8$ GeV	$\rho_T \to WW$, $W\pi_T$, $\pi_T\pi_T$, $\gamma\pi_T$, hadrons	[20]
$p\overline{p} \to \rho_{T8}$	$260 < m_{\rho_{T8}} < 480$ GeV	$\rho_{T8} \to q\overline{q}$, gg	[22]
$p\overline{p} \to \rho_{T8}$	$m_{\rho_{T8}} < 510$ GeV	$\pi_{LQ} \to c\nu$	[25]
$\to \pi_{LQ}\pi_{LQ}$	$m_{\rho_{T8}} < 600$ GeV	$\pi_{LQ} \to b\nu$	[25]
	$m_{\rho_{T8}} < 465$ GeV	$\pi_{LQ} \to \tau q$	[24]
$p\overline{p} \to g_t$	$0.3 < m_{g_t} < 0.6$ TeV for $0.3m_{g_t} < \Gamma < 0.7m_{g_t}$	$g_t \to b\overline{b}$	[30]
$p\overline{p} \to Z'$	$m_{Z'} < 480$ GeV for $\Gamma = 0.012m_{Z'}$ $m_{Z'} < 780$ GeV for $\Gamma = 0.04m_{Z'}$	$Z' \to t\overline{t}$	[31]

References

1. S. Weinberg, Phys. Rev. **D19**, 1277 (1979).
2. L. Susskind, Phys. Rev. **D20**, 2619 (1979).
3. For a recent review, see C.T. Hill and E.H. Simmons, Phys. Rept. **381**, 235 (2003).
4. E. Eichten and K. Lane, Phys. Lett. **90B**, 125 (1980).
5. For reviews, see E. Farhi and L. Susskind, Phys. Reports **74**, 277 (1981);
   R.K. Kaul, Rev. Mod. Phys. **55**, 449 (1983);
   R.S. Chivukula *et al.*, hep-ph/9503202.
6. S. Dimopoulos, S. Raby, and G.L. Kane, Nucl. Phys. **B182**, 77 (1981).
7. S. Dimopoulos and L. Susskind, Nucl. Phys. **B155**, 237 (1979).
8. B. Holdom, Phys. Rev. **D24**, 1441 (1981) and Phys. Lett. **150B**, 301 (1985);
   K. Yamawaki, M. Bando, and K. Matumoto, Phys. Rev. Lett. **56**, 1335 (1986);
   T.W. Appelquist, D. Karabali, and L.C.R. Wijewardhana, Phys. Rev. Lett. **57**, 957 (1986);
   T. Appelquist and L.C.R. Wijewardhana, Phys. Rev. **D35**, 774 (1987) and Phys. Rev. **D36**, 568 (1987).
9. E. Eichten and K. Lane, Phys. Lett. **B222**, 274 (1989).
10. J. Erler and P. Langacker, "Electroweak Model and Constraints on New Physics," in the section on Reviews, Tables, and Plots in this *Review*.
11. T.W. Appelquist, M. Piai, and R. Shrock, hep-ph/0308061.
12. E. Eichten, I. Hinchliffe, K.D. Lane, and C. Quigg, Rev. Mod. Phys. **56**, 579 (1984) and Phys. Rev. **D34**, 1547 (1986).
13. K. Lane, Phys. Rev. **D60**, 075007 (1999).
14. S. Mrenna, Technihadron production and decay at LEP2, Phys. Lett. **B461**, 352 (1999).
15. E. Eichten, K. Lane, and J. Womersley, Phys. Lett. **B405**, 305 (1997).
16. CDF Collaboration (T. Affolder *et al.*), Phys. Rev. Lett. **84**, 1110 (2000).
17. T. Sjostrand, Comp. Phys. Comm. **82**, 74 (1994).
18. CDF Collaboration (F. Abe *et al.*), Phys. Rev. Lett. **83**, 3124 (1999).
19. DØ Collaboration (V.M. Abazov *et al.*), Phys. Rev. Lett. **87**, 061802 (2001).
20. DELPHI Collaboration (J. Abdallah *et al.*), Eur. Phys. J. **C22**, 17 (2001).
21. K. Lane and M.V. Ramana, Phys. Rev. **D44**, 2678 (1991).
22. CDF Collaboration (F. Abe *et al.*), Phys. Rev. **D55**, R5263 (1997).
23. K. Cheung and R.M. Harris, hep-ph/9610382.
24. CDF Collaboration (F. Abe *et al.*), Phys. Rev. Lett. **82**, 3206 (1999).
25. CDF Collaboration (T. Affolder *et al.*), Phys. Rev. Lett. **85**, 2056 (2000).
26. A. Zerwekh and R. Rosenfeld, Phys. Lett. **B503**, 325 (2001);
    R.S. Chivukula, *et al.*, Boston Univ. preprint BUHEP-01-19.
27. V.A. Miransky, M. Tanabashi, and K. Yamawaki, Phys. Lett. **221B**, 177 (1989) and Mod. Phys. Lett. **4**, 1043 (1989);
    Y. Nambu, EFI-89-08 (1989);
    W.J. Marciano, Phys. Rev. Lett. **62**, 2793 (1989).
28. W.A. Bardeen, C.T. Hill, and M. Lindner, Phys. Rev. **D41**, 1647 (1990).
29. C.T. Hill, Phys. Lett. **B345**, 483 (1995);
    see also Phys. Lett. **266B**, 419 (1991).
30. CDF Collaboration (F. Abe *et al.*), Phys. Rev. Lett. **82**, 2038 (1999).
31. CDF Collaboration (F. Affolder *et al.*), Phys. Rev. Lett. **85**, 2062 (2000).
32. D0 Collaboration (V. Abazov *et al.*), Phys. Rev. Lett. **87**, 231801 (2001).
33. G. Burdman *et al.*, Phys. Lett. **B514**, 41 (2001).
34. B.A. Dobrescu and C.T. Hill, Phys. Rev. Lett. **81**, 2634 (1998).
35. R.S. Chivukula *et al.*, Phys. Rev. **D59**, 075003 (1999).
36. H. Collins, A. Grant, and H. Georgi, Phys. Rev. **D61**, 055002 (2000).
37. B.A. Dobrescu, Phys. Lett. **B461**, 99 (1999);
    H.-C. Cheng, *et al.*, Nucl. Phys. **B589**, 249 (2000).
38. E.H. Simmons, Nucl. Phys. **B324**, 315 (1989).
39. G. Burdman and N. Evans, Phys. Rev. **D59**, 115005 (1999).
40. DØ Collaboration (B. Abbott *et al.*), Phys. Rev. Lett. **82**, 2457 (1999).
41. I. Bertram and E.H. Simmons, Phys. Lett. **B443**, 347 (1998).
42. G. Burdman, R.S. Chivukula, and N. Evans, Phys. Rev. **D61**, 035009 (2000).
43. N. Arkani-Hamed, A. G. Cohen and H. Georgi, Phys. Lett. **B513**, 232 (2001).

44. D. B. Kaplan and H. Georgi, Phys. Lett. **B136**, 183 (1984) and Phys. Lett. **B145**, 216 (1984);
T. Banks, Nucl. Phys. **B243**, 123 (1984);
D. B. Kaplan, H. Georgi, and S. Dimopoulos, Phys. Lett. **B136**, 187 (1984);
M. J. Dugan, H. Georgi, and D. B. Kaplan, Nucl. Phys. **B254**, 299 (1985).

45. N. Arkani-Hamed, A. G. Cohen and H. Georgi, Phys. Rev. **D86**, 4757 (2001);
H. C. Cheng, C. T. Hill and J. Wang, Phys. Rev. **D64**, 095003 (2001).

46. See also review by P. Igo-Kemenes, "Searches for Higgs Bosons," in the Boson Listings in this *Review*.

MASS LIMITS for Resonances in Models of Dynamical Electroweak Symmetry Breaking

VALUE (GeV)	CL%	DOCUMENT ID		TECN	COMMENT
• • • We do not use the following data for averages, fits, limits, etc. • • •					
		[1] CHEKANOV	02B	ZEUS	color octet techni-π
>207	95	[2] ABAZOV	01B	D0	$\rho_T \to e^+e^-$
none 90–206.7	95	[3] ABDALLAH	01	DLPH	$e^+e^- \to \rho_T$
		[4] AFFOLDER	00F	CDF	color-singlet techni-ρ, $\rho_T \to W\pi_T$, $2\pi_T$
>600	95	[5] AFFOLDER	00K	CDF	color-octet techni-ρ, $\rho_{T8} \to 2\pi_{LQ}$
>480	95	[6] AFFOLDER	00L	CDF	top-color Z'
none 350–440	95	[7] ABE	99F	CDF	color-octet techni-ρ, $\rho_{T8} \to b\overline{b}$
>465	95	[8] ABE	99H	CDF	color-octet techni-ρ, $\rho_{T8} \to 2\pi_{LQ}$
		[9] ABE	99N	CDF	techni-ω, $\omega_T \to \gamma b\overline{b}$
none 260–480	95	[10] ABE	97G	CDF	color-octet techni-ρ, $\rho_{T8} \to$ 2jets

[1] CHEKANOV 02B search for color octet techni-π P decaying into dijets in ep collisions. See their Fig. 5 for the limit on $\sigma(ep \to eP X)\cdot B(P \to 2j)$.

[2] ABAZOV 01B searches for vector techni-resonances (ρ_T,ω_T) decaying to e^+e^-. The limit assumes $M_{\rho_T} = M_{\omega_T} < M_{\pi_T} + M_W$.

[3] The limit is independent of the π_T mass. See their Fig. 9 and Fig. 10 for the exclusion plot in the M_{ρ_T}–M_{π_T} plane. ABDALLAH 01 limit on the techni-pion mass is $M_{\pi_T} > 79.8$ GeV for N_D=2, assuming its point-like coupling to gauge bosons.

[4] AFFOLDER 00F search for ρ_T decaying into $W\pi_T$ or $\pi_T\pi_T$ with $W \to \ell\nu$ and $\pi_T \to \overline{b}b$, $\overline{b}c$. See Fig. 1 in the above Note on "Dynamical Electroweak Symmetry Breaking" for the exclusion plot in the M_{ρ_T}–M_{π_T} plane.

[5] AFFOLDER 00K search for the ρ_{T8} decaying into $\pi_{LQ}\pi_{LQ}$ with $\pi_{LQ} \to b\nu$. For $\pi_{LQ} \to c\nu$, the limit is $M_{\rho_{T8}}$ >510 GeV. See their Fig. 2 and Fig. 3 for the exclusion plot in the $M_{\rho_{T8}}$–$M_{\pi_{LQ}}$ plane.

[6] AFFOLDER 00L search for top-color $Z'_{\rm top}$ decaying into $\overline{t}t$. The quoted limit is for $Z'_{\rm top}$ with decay width Γ=0.012 $M_{Z'}$. For Γ=0.04 $M_{Z'}$ the limit becomes 780 GeV.

[7] ABE 99F search for a new particle X decaying into $b\overline{b}$ in $p\overline{p}$ collisions at $E_{\rm cm}$= 1.8 TeV. See Fig. 7 in the above Note on "Dynamical Electroweak Symmetry Breaking" for the upper limit on $\sigma(p\overline{p} \to X)\times B(X \to b\overline{b})$. ABE 99F also exclude top gluons of width Γ=0.3M in the mass interval 280 <M< 670 GeV, of width Γ=0.5M in the mass interval 340 <M< 640 GeV, and of width Γ=0.7M in the mass interval 375 <M< 560 GeV.

[8] ABE 99H search for the color-octet techni-ρ decaying into a pair of color-triplet technipions which subsequently decay into τ+ jet. See Fig. 6 in the above Note on "Dynamical Electroweak Symmetry Breaking" for the exclusion plot in the $M_{\rho_{T8}}$–$M_{\pi_{LQ}}$ plane.

[9] ABE 99N search for the techni-ω decaying into $\gamma\pi_T$. The technipion is assumed to decay $\pi_T \to b\overline{b}$. See Fig. 2 in the above Note on "Dynamical Electroweak Symmetry Breaking" for the exclusion plot in the M_{ω_T}–M_{π_T} plane.

[10] ABE 97G search for a new particle X decaying into dijets in $p\overline{p}$ collisions at $E_{\rm cm}$= 1.8 TeV. See Fig. 5 in the above Note on "Dynamical Electroweak Symmetry Breaking" for the upper limit on $\sigma(p\overline{p} \to X)\times B(X \to 2j)$.

REFERENCES FOR Technicolor

CHEKANOV	02B	PL B531 9	S. Chekanov *et al.*	(ZEUS Collab.)
ABAZOV	01B	PRL 87 061802	V.M. Abazov *et al.*	(D0 Collab.)
ABDALLAH	01	EPJ C22 17	J. Abdallah *et al.*	(DELPHI Collab.)
AFFOLDER	00F	PRL 84 1110	T. Affolder *et al.*	(CDF Collab.)
AFFOLDER	00K	PRL 85 2056	T. Affolder *et al.*	(CDF Collab.)
AFFOLDER	00L	PRL 85 2062	T. Affolder *et al.*	(CDF Collab.)
ABE	99F	PRL 82 2038	F. Abe *et al.*	(CDF Collab.)
ABE	99H	PRL 82 3206	F. Abe *et al.*	(CDF Collab.)
ABE	99N	PRL 83 3124	F. Abe *et al.*	(CDF Collab.)
ABE	97G	PR D55 R5263	F. Abe *et al.*	(CDF Collab.)

Quark and Lepton Compositeness, Searches for

SEARCHES FOR QUARK AND LEPTON COMPOSITENESS

Revised 2001 by K. Hagiwara (KEK), and K. Hikasa and M. Tanabashi (Tohoku University).

If quarks and leptons are made of constituents, then at the scale of constituent binding energies, there should appear new interactions among quarks and leptons. At energies much below the compositeness scale (Λ), these interactions are suppressed by inverse powers of Λ. The dominant effect should come from the lowest dimensional interactions with four fermions (contact terms), whose most general chirally invariant form reads [1]

$$L = \frac{g^2}{2\Lambda^2}\left[\eta_{LL}\,\overline{\psi}_L\gamma_\mu\psi_L\,\overline{\psi}_L\gamma^\mu\psi_L + \eta_{RR}\,\overline{\psi}_R\gamma_\mu\psi_R\,\overline{\psi}_R\gamma^\mu\psi_R + 2\eta_{LR}\,\overline{\psi}_L\gamma_\mu\psi_L\,\overline{\psi}_R\gamma^\mu\psi_R\right] . \quad (1)$$

Chiral invariance provides a natural explanation why quark and lepton masses are much smaller than their inverse size Λ. We may determine the scale Λ unambiguously by using the above form of the effective interactions; the conventional method [1] is to fix its scale by setting $g^2/4\pi = g^2(\Lambda)/4\pi = 1$ for the new strong interaction coupling and by setting the largest magnitude of the coefficients $\eta_{\alpha\beta}$ to be unity. In the following, we denote

$$\begin{aligned}
\Lambda &= \Lambda^\pm_{LL} \quad \text{for} \quad (\eta_{LL}, \eta_{RR}, \eta_{LR}) = (\pm1, 0, 0) ,\\
\Lambda &= \Lambda^\pm_{RR} \quad \text{for} \quad (\eta_{LL}, \eta_{RR}, \eta_{LR}) = (0, \pm1, 0) ,\\
\Lambda &= \Lambda^\pm_{VV} \quad \text{for} \quad (\eta_{LL}, \eta_{RR}, \eta_{LR}) = (\pm1, \pm1, \pm1) ,\\
\Lambda &= \Lambda^\pm_{AA} \quad \text{for} \quad (\eta_{LL}, \eta_{RR}, \eta_{LR}) = (\pm1, \pm1, \mp1) , \quad (2)
\end{aligned}$$

as typical examples. Such interactions can arise by constituent interchange (when the fermions have common constituents, *e.g.*, for $ee \to ee$) and/or by exchange of the binding quanta (whenever binding quanta couple to constituents of both particles).

Another typical consequence of compositeness is the appearance of excited leptons and quarks (ℓ^* and q^*). Phenomenologically, an excited lepton is defined to be a heavy lepton which shares leptonic quantum number with one of the existing leptons (an excited quark is defined similarly). For example, an excited electron e^* is characterized by a nonzero transition-magnetic coupling with electrons. Smallness of the lepton mass and the success of QED prediction for g–2 suggest chirality conservation, *i.e.*, an excited lepton should not couple to both left- and right-handed components of the corresponding lepton.

Excited leptons may be classified by SU(2)×U(1) quantum numbers. Typical examples are:

1. Sequential type

$$\begin{pmatrix}\nu^*\\ \ell^*\end{pmatrix}_L , \qquad [\nu^*_R] , \qquad \ell^*_R .$$

ν^*_R is necessary unless ν^* has a Majorana mass.

2. Mirror type

$$[\nu_L^*]\ , \qquad \ell_L^*\ , \qquad \begin{pmatrix}\nu^*\\ \ell^*\end{pmatrix}_R\ .$$

3. Homodoublet type

$$\begin{pmatrix}\nu^*\\ \ell^*\end{pmatrix}_L\ , \qquad \begin{pmatrix}\nu^*\\ \ell^*\end{pmatrix}_R\ .$$

Similar classification can be made for excited quarks.

Excited fermions can be pair produced via their gauge couplings. The couplings of excited leptons with Z are listed in the following table (for notation see Eq. (1) in "Standard Model of Electroweak Interactions"):

	Sequential type	Mirror type	Homodoublet type
V^{ℓ^*}	$-\frac{1}{2}+2\sin^2\theta_W$	$-\frac{1}{2}+2\sin^2\theta_W$	$-1+2\sin^2\theta_W$
A^{ℓ^*}	$-\frac{1}{2}$	$+\frac{1}{2}$	0
$V^{\nu_D^*}$	$+\frac{1}{2}$	$+\frac{1}{2}$	$+1$
$A^{\nu_D^*}$	$+\frac{1}{2}$	$-\frac{1}{2}$	0
$V^{\nu_M^*}$	0	0	—
$A^{\nu_M^*}$	$+1$	-1	—

Here ν_D^* (ν_M^*) stands for Dirac (Majorana) excited neutrino. The corresponding couplings of excited quarks can be easily obtained. Although form factor effects can be present for the gauge couplings at $q^2 \neq 0$, they are usually neglected.

In addition, transition magnetic type couplings with a gauge boson are expected. These couplings can be generally parameterized as follows:

$$\begin{aligned}\mathcal{L} = {} & \frac{\lambda_\gamma^{(f^*)} e}{2m_{f^*}}\,\overline{f}^*\sigma^{\mu\nu}(\eta_L\tfrac{1-\gamma_5}{2}+\eta_R\tfrac{1+\gamma_5}{2})f F_{\mu\nu} \\ & + \frac{\lambda_Z^{(f^*)} e}{2m_{f^*}}\,\overline{f}^*\sigma^{\mu\nu}(\eta_L\tfrac{1-\gamma_5}{2}+\eta_R\tfrac{1+\gamma_5}{2})f Z_{\mu\nu} \\ & + \frac{\lambda_W^{(\ell^*)} g}{2m_{\ell^*}}\,\overline{\ell}^*\sigma^{\mu\nu}\tfrac{1-\gamma_5}{2}\nu W_{\mu\nu} \\ & + \frac{\lambda_W^{(\nu^*)} g}{2m_{\nu^*}}\,\overline{\nu}^*\sigma^{\mu\nu}(\eta_L\tfrac{1-\gamma_5}{2}+\eta_R\tfrac{1+\gamma_5}{2})\ell\, W_{\mu\nu}^\dagger \\ & + \text{h.c.}\ , \end{aligned} \tag{3}$$

where $g = e/\sin\theta_W$, $F_{\mu\nu} = \partial_\mu A_\nu - \partial_\nu A_\mu$ is the photon field strength, $Z_{\mu\nu} = \partial_\mu Z_\nu - \partial_\nu Z_\mu$, *etc.* The normalization of the coupling is chosen such that

$$\max(|\eta_L|, |\eta_R|) = 1\ .$$

Chirality conservation requires

$$\eta_L \eta_R = 0\ . \tag{4}$$

Some experimental analyses assume the relation $\eta_L = \eta_R = 1$, which violates chiral symmetry. We encode the results of such analyses if the crucial part of the cross section is proportional to the factor $\eta_L^2 + \eta_R^2$ and the limits can be reinterpreted as those for chirality conserving cases $(\eta_L, \eta_R) = (1, 0)$ or $(0, 1)$ after rescaling λ.

These couplings in Eq. (3) can arise from SU(2)×U(1)-invariant higher-dimensional interactions. A well-studied model is the interaction of homodoublet type ℓ^* with the Lagrangian [2,3]

$$\mathcal{L} = \frac{1}{2\Lambda}\overline{L}^*\sigma^{\mu\nu}(g f\tfrac{\tau^a}{2}W_{\mu\nu}^a + g' f' Y B_{\mu\nu})\tfrac{1-\gamma_5}{2}L + \text{h.c.}\ , \tag{5}$$

where L denotes the lepton doublet (ν, ℓ), Λ is the compositeness scale, g, g' are SU(2) and U(1)$_Y$ gauge couplings, and $W_{\mu\nu}^a$ and $B_{\mu\nu}$ are the field strengths for SU(2) and U(1)$_Y$ gauge fields. The same interaction occurs for mirror-type excited leptons. For sequential-type excited leptons, the ℓ^* and ν^* couplings become unrelated, and the couplings receive the extra suppression of $(250\,\text{GeV})/\Lambda$ or m_{L^*}/Λ. In any case, these couplings satisfy the relation

$$\lambda_W = -\sqrt{2}\sin^2\theta_W(\lambda_Z\cot\theta_W + \lambda_\gamma)\ . \tag{6}$$

Additional coupling with gluons is possible for excited quarks:

$$\begin{aligned}\mathcal{L} = {} & \frac{1}{2\Lambda}\overline{Q}^*\sigma^{\mu\nu}\left(g_s f_s\tfrac{\lambda^a}{2}G_{\mu\nu}^a + g f\tfrac{\tau^a}{2}W_{\mu\nu}^a + g' f' Y B_{\mu\nu}\right) \\ & \times \tfrac{1-\gamma_5}{2}Q + \text{h.c.}\ , \end{aligned} \tag{7}$$

where Q denotes a quark doublet, g_s is the QCD gauge coupling, and $G_{\mu\nu}^a$ the gluon field strength.

It should be noted that the electromagnetic radiative decay of $\ell^*(\nu^*)$ is forbidden if $f = -f'$ ($f = f'$). These two possibilities ($f = f'$ and $f = -f'$) are investigated in many analyses of the LEP experiments above the Z pole.

Several different conventions are used by LEP experiments on Z pole to express the transition magnetic couplings. To facilitate comparison, we re-express these in terms of λ_Z and λ_γ using the following relations and taking $\sin^2\theta_W = 0.23$. We assume chiral couplings, *i.e.*, $|c| = |d|$ in the notation of Ref. 2.

1. ALEPH (charged lepton and neutrino)

$$\lambda_Z^{\text{ALEPH}} = \frac{1}{2}\lambda_Z \quad (1990\ \text{papers}) \tag{8a}$$

$$\frac{2c}{\Lambda} = \frac{\lambda_Z}{m_{\ell^*}\,[\text{or } m_{\nu^*}]} \quad (\text{for } |c| = |d|) \tag{8b}$$

2. ALEPH (quark)

$$\lambda_u^{\text{ALEPH}} = \frac{\sin\theta_W\cos\theta_W}{\sqrt{\frac{1}{4}-\frac{2}{3}\sin^2\theta_W+\frac{8}{9}\sin^4\theta_W}}\,\lambda_Z = 1.11\lambda_Z \tag{9}$$

3. L3 and DELPHI (charged lepton)

$$\lambda^{\text{L3}} = \lambda_Z^{\text{DELPHI}} = -\frac{\sqrt{2}}{\cot\theta_W - \tan\theta_W}\,\lambda_Z = -1.10\lambda_Z \tag{10}$$

4. L3 (neutrino)

$$f_Z^{\rm L3} = \sqrt{2}\lambda_Z \qquad (11)$$

5. OPAL (charged lepton)

$$\frac{f^{\rm OPAL}}{\Lambda} = -\frac{2}{\cot\theta_W - \tan\theta_W}\,\frac{\lambda_Z}{m_{\ell^*}} = -1.56\,\frac{\lambda_Z}{m_{\ell^*}} \qquad (12)$$

6. OPAL (quark)

$$\frac{f^{\rm OPAL}c}{\Lambda} = \frac{\lambda_Z}{2m_{q^*}} \quad ({\rm for}\,|c| = |d|) \qquad (13)$$

7. DELPHI (charged lepton)

$$\lambda_\gamma^{\rm DELPHI} = -\frac{1}{\sqrt{2}}\,\lambda_\gamma \qquad (14)$$

If leptons are made of color triplet and antitriplet constituents, we may expect their color-octet partners. Transitions between the octet leptons (ℓ_8) and the ordinary lepton (ℓ) may take place via the dimension-five interactions

$$\mathcal{L} = \frac{1}{2\Lambda}\sum_\ell \left\{ \overline{\ell}_8^\alpha\, g_S\, F_{\mu\nu}^\alpha\, \sigma^{\mu\nu}\left(\eta_L\,\ell_L + \eta_R\,\ell_R\right) + h.c.\right\} \qquad (15)$$

where the summation is over charged leptons and neutrinos. The leptonic chiral invariance implies $\eta_L\,\eta_R = 0$ as before.

References

1. E.J. Eichten, K.D. Lane, and M.E. Peskin, Phys. Rev. Lett. **50**, 811 (1983).
2. K. Hagiwara, S. Komamiya, and D. Zeppenfeld, Z. Phys. **C29**, 115 (1985).
3. N. Cabibbo, L. Maiani, and Y. Srivastava, Phys. Lett. **139B**, 459 (1984).

SCALE LIMITS for Contact Interactions: Λ(eeee)

Limits are for $\Lambda_{LL}^{\pm}$ only. For other cases, see each reference.

Λ_{LL}^{+}(TeV)	Λ_{LL}^{-}(TeV)	CL%	DOCUMENT ID		TECN	COMMENT
>8.3	**>10.3**	95	[1] BOURILKOV	01	RVUE	$E_{\rm cm}$= 192–208 GeV
• • • We do not use the following data for averages, fits, limits, etc. • • •						
>3.8	>5.6	95	ABBIENDI	00R	OPAL	$E_{\rm cm}$= 189 GeV
>4.4	>5.4	95	ABREU	00S	DLPH	$E_{\rm cm}$= 183–189 GeV
>4.3	>4.9	95	ACCIARRI	00P	L3	$E_{\rm cm}$= 130–189 GeV
>3.5	>3.2	95	BARATE	00I	ALEP	$E_{\rm cm}$= 130–183 GeV
>6.0	>7.7	95	[2] BOURILKOV	00	RVUE	$E_{\rm cm}$= 183–189 GeV
>3.1	>3.8	95	ABBIENDI	99	OPAL	$E_{\rm cm}$= 130–136, 161–172, 183 GeV
>2.2	>2.8	95	ABREU	99A	DLPH	$E_{\rm cm}$= 130–172 GeV
>2.7	>2.4	95	ACCIARRI	98J	L3	$E_{\rm cm}$= 130–172 GeV
>3.0	>2.5	95	ACKERSTAFF	98V	OPAL	$E_{\rm cm}$= 130–172 GeV
>2.4	>2.2	95	ACKERSTAFF	97C	OPAL	$E_{\rm cm}$= 130–136, 161 GeV
>1.7	>2.3	95	ARIMA	97	VNS	$E_{\rm cm}$= 57.77 GeV
>1.6	>2.0	95	[3] BUSKULIC	93Q	ALEP	$E_{\rm cm}$=88.25–94.25 GeV
>1.6		95	[3,4] BUSKULIC	93Q	RVUE	
	>2.2	95	BUSKULIC	93Q	RVUE	
	>3.6	95	[5] KROHA	92	RVUE	
>1.3		95	[5] KROHA	92	RVUE	
>0.7	>2.8	95	BEHREND	91C	CELL	$E_{\rm cm}$=35 GeV
>1.3	>1.3	95	KIM	89	AMY	$E_{\rm cm}$=50–57 GeV
>1.4	>3.3	95	[6] BRAUNSCH...	88	TASS	$E_{\rm cm}$=12–46.8 GeV
>1.0	>0.7	95	[7] FERNANDEZ	87B	MAC	$E_{\rm cm}$=29 GeV
>1.1	>1.4	95	[8] BARTEL	86C	JADE	$E_{\rm cm}$=12–46.8 GeV
>1.17	>0.87	95	[9] DERRICK	86	HRS	$E_{\rm cm}$=29 GeV
>1.1	>0.76	95	[10] BERGER	85B	PLUT	$E_{\rm cm}$=34.7 GeV

[1] A combined analysis of the data from ALEPH, DELPHI, L3, and OPAL.
[2] A combined analysis of the data from ALEPH, L3, and OPAL.
[3] BUSKULIC 93Q uses the following prescription to obtain the limit: when the naive 95%CL limit is better than the statistically expected sensitivity for the limit, the latter is adopted for the limit.
[4] This BUSKULIC 93Q value is from ALEPH data plus PEP/PETRA/TRISTAN data re-analyzed by KROHA 92.
[5] KROHA 92 limit is from fit to BERGER 85B, BARTEL 86C, DERRICK 86B, FERNANDEZ 87B, BRAUNSCHWEIG 88, BEHREND 91B, and BEHREND 91C. The fit gives $\eta/\Lambda_{LL}^2 = +0.230 \pm 0.206$ TeV^{-2}.
[6] BRAUNSCHWEIG 88 assumed $m_Z = 92$ GeV and $\sin^2\theta_W = 0.23$.
[7] FERNANDEZ 87B assumed $\sin^2\theta_W = 0.22$.
[8] BARTEL 86C assumed $m_Z = 93$ GeV and $\sin^2\theta_W = 0.217$.
[9] DERRICK 86 assumed $m_Z = 93$ GeV and $g_V^2 = (-1/2+2\sin^2\theta_W)^2 = 0.004$.
[10] BERGER 85B assumed $m_Z = 93$ GeV and $\sin^2\theta_W = 0.217$.

SCALE LIMITS for Contact Interactions: Λ(eeμμ)

Limits are for $\Lambda_{LL}^{\pm}$ only. For other cases, see each reference.

Λ_{LL}^{+}(TeV)	Λ_{LL}^{-}(TeV)	CL%	DOCUMENT ID		TECN	COMMENT
>6.6	**> 6.3**	95	ABREU	00S	DLPH	$E_{\rm cm}$= 183–189 GeV
> 8.5	>3.8	95	ACCIARRI	00P	L3	$E_{\rm cm}$= 130–189 GeV
• • • We do not use the following data for averages, fits, limits, etc. • • •						
>7.3	>4.6	95	ABBIENDI	00R	OPAL	$E_{\rm cm}$= 189 GeV
>4.0	>4.7	95	BARATE	00I	ALEP	$E_{\rm cm}$= 130–183 GeV
>4.5	>4.3	95	ABBIENDI	99	OPAL	$E_{\rm cm}$= 130–136, 161–172, 183 GeV
>3.4	>2.7	95	ABREU	99A	DLPH	$E_{\rm cm}$= 130–172 GeV
>3.6	>2.4	95	ACCIARRI	98J	L3	$E_{\rm cm}$= 130–172 GeV
>2.9	>3.4	95	ACKERSTAFF	98V	OPAL	$E_{\rm cm}$= 130–172 GeV
>3.1	>2.0	95	MIURA	98	VNS	$E_{\rm cm}$= 57.77 GeV
>2.4	>2.9	95	ACKERSTAFF	97C	OPAL	$E_{\rm cm}$= 130–136, 161 GeV
>1.7	>2.2	95	[11] VELISSARIS	94	AMY	$E_{\rm cm}$=57.8 GeV
>1.3	>1.5	95	[11] BUSKULIC	93Q	ALEP	$E_{\rm cm}$=88.25–94.25 GeV
>2.6	>1.9	95	[11,12] BUSKULIC	93Q	RVUE	
>2.3	>2.0	95	HOWELL	92	TOPZ	$E_{\rm cm}$=52–61.4 GeV
	>1.7	95	[13] KROHA	92	RVUE	
>2.5	>1.5	95	BEHREND	91C	CELL	$E_{\rm cm}$=35–43 GeV
>1.6	>2.0	95	[14] ABE	90I	VNS	$E_{\rm cm}$=50–60.8 GeV
>1.9	>1.0	95	KIM	89	AMY	$E_{\rm cm}$=50–57 GeV
>2.3	>1.3	95	BRAUNSCH...	88D	TASS	$E_{\rm cm}$=30–46.8 GeV
>4.4	>2.1	95	[15] BARTEL	86C	JADE	$E_{\rm cm}$=12–46.8 GeV
>2.9	>0.86	95	[16] BERGER	85	PLUT	$E_{\rm cm}$=34.7 GeV

[11] BUSKULIC 93Q and VELISSARIS 94 use the following prescription to obtain the limit: when the naive 95%CL limit is better than the statistically expected sensitivity for the limit, the latter is adopted for the limit.
[12] This BUSKULIC 93Q value is from ALEPH data plus PEP/PETRA/TRISTAN data re-analyzed by KROHA 92.
[13] KROHA 92 limit is from fit to BARTEL 86C, BEHREND 87C, BRAUNSCHWEIG 88D, BRAUNSCHWEIG 89C, ABE 90I, and BEHREND 91C. The fit gives $\eta/\Lambda_{LL}^2 = -0.155 \pm 0.095$ TeV^{-2}.
[14] ABE 90I assumed m_Z =91.163 GeV and $\sin^2\theta_W = 0.231$.
[15] BARTEL 86C assumed $m_Z = 93$ GeV and $\sin^2\theta_W = 0.217$.
[16] BERGER 85 assumed $m_Z = 93$ GeV and $\sin^2\theta_W = 0.217$.

SCALE LIMITS for Contact Interactions: Λ(eeττ)

Limits are for $\Lambda_{LL}^{\pm}$ only. For other cases, see each reference.

Λ_{LL}^{+}(TeV)	Λ_{LL}^{-}(TeV)	CL%	DOCUMENT ID		TECN	COMMENT
>3.9	**> 6.5**	95	ABBIENDI	00R	OPAL	$E_{\rm cm}$= 189 GeV
> 5.4	>4.7	95	ACCIARRI	00P	L3	$E_{\rm cm}$= 130–189 GeV
• • • We do not use the following data for averages, fits, limits, etc. • • •						
>5.2	>5.4	95	ABREU	00S	DLPH	$E_{\rm cm}$= 183–189 GeV
>3.9	>3.7	95	BARATE	00I	ALEP	$E_{\rm cm}$= 130–183 GeV
>3.8	>4.0	95	ABBIENDI	99	OPAL	$E_{\rm cm}$= 130–136, 161–172, 183 GeV
>2.8	>2.6	95	ABREU	99A	DLPH	$E_{\rm cm}$= 130–172 GeV
>2.4	>2.8	95	ACCIARRI	98J	L3	$E_{\rm cm}$= 130–172 GeV
>2.3	>3.7	95	ACKERSTAFF	98V	OPAL	$E_{\rm cm}$= 130–172 GeV
>1.9	>3.0	95	ACKERSTAFF	97C	OPAL	$E_{\rm cm}$= 130–136, 161 GeV
>1.4	>2.0	95	[17] VELISSARIS	94	AMY	$E_{\rm cm}$=57.8 GeV
>1.0	>1.5	95	[17] BUSKULIC	93Q	ALEP	$E_{\rm cm}$=88.25–94.25 GeV
>1.8	>2.3	95	[17,18] BUSKULIC	93Q	RVUE	
>1.9	>1.7	95	HOWELL	92	TOPZ	$E_{\rm cm}$=52–61.4 GeV
>1.9	>2.9	95	[19] KROHA	92	RVUE	
>1.6	>2.3	95	BEHREND	91C	CELL	$E_{\rm cm}$=35–43 GeV
>1.8	>1.3	95	[20] ABE	90I	VNS	$E_{\rm cm}$=50–60.8 GeV
>2.2	>3.2	95	[21] BARTEL	86	JADE	$E_{\rm cm}$=12–46.8 GeV

[17] BUSKULIC 93Q and VELISSARIS 94 use the following prescription to obtain the limit: when the naive 95%CL limit is better than the statistically expected sensitivity for the limit, the latter is adopted for the limit.

[18] This BUSKULIC 93Q value is from ALEPH data plus PEP/PETRA/TRISTAN data re-analyzed by KROHA 92.

[19] KROHA 92 limit is from fit to BARTEL 86C BEHREND 89B, BRAUNSCHWEIG 89C, ABE 90I, and BEHREND 91C. The fit gives $\eta/\Lambda^2_{LL} = +0.095 \pm 0.120$ TeV^{-2}.

[20] ABE 90I assumed m_Z =91.163 GeV and $\sin^2\theta_W = 0.231$.

[21] BARTEL 86 assumed m_Z = 93 GeV and $\sin^2\theta_W = 0.217$.

SCALE LIMITS for Contact Interactions: Λ(ℓℓℓℓ)

Lepton universality assumed. Limits are for $\Lambda^{\pm}_{LL}$ only. For other cases, see each reference.

Λ^+_{LL} (TeV)	Λ^-_{LL} (TeV)	CL%		DOCUMENT ID		TECN	COMMENT
>7.3	**> 7.8**	95		ABREU	00S	DLPH	E_{cm}= 183–189 GeV
> 9.0	>5.2	95		ACCIARRI	00P	L3	E_{cm}= 130–189 GeV
• • • We do not use the following data for averages, fits, limits, etc. • • •							
			[22]	BABICH	03	RVUE	
>6.4	>7.2	95		ABBIENDI	00R	OPAL	E_{cm}= 189 GeV
>5.3	>5.5	95		BARATE	00I	ALEP	E_{cm}= 130–183 GeV
>5.2	>5.3	95		ABBIENDI	99	OPAL	E_{cm}= 130–136, 161–172, 183 GeV
>4.4	>4.2	95		ABREU	99A	DLPH	E_{cm}= 130–172 GeV
>4.0	>3.1	95	[23]	ACCIARRI	98J	L3	E_{cm}= 130–172 GeV
>3.4	>4.4	95		ACKERSTAFF	98V	OPAL	E_{cm}= 130–172 GeV
>2.7	>3.8	95		ACKERSTAFF	97C	OPAL	E_{cm}= 130–136, 161 GeV
>3.0	>2.3	95	[23,24]	BUSKULIC	93Q	ALEP	E_{cm}=88.25–94.25 GeV
>3.5	>2.8	95	[24,25]	BUSKULIC	93Q	RVUE	
>2.5	>2.2	95	[26]	HOWELL	92	TOPZ	E_{cm}=52–61.4 GeV
>3.4	>2.7	95	[27]	KROHA	92	RVUE	

[22] BABICH 03 obtain a bound -0.175 TeV$^{-2} < 1/\Lambda^2_{LL} < 0.095$ TeV^{-2} (95%CL) in a model independent analysis allowing all of Λ_{LL}, Λ_{LR}, Λ_{RL}, Λ_{RR} to coexist.

[23] From $e^+e^- \to e^+e^-$, $\mu^+\mu^-$, and $\tau^+\tau^-$.

[24] BUSKULIC 93Q uses the following prescription to obtain the limit: when the naive 95%CL limit is better than the statistically expected sensitivity for the limit, the latter is adopted for the limit.

[25] This BUSKULIC 93Q value is from ALEPH data plus PEP/PETRA/TRISTAN data re-analyzed by KROHA 92.

[26] HOWELL 92 limit is from $e^+e^- \to \mu^+\mu^-$ and $\tau^+\tau^-$.

[27] KROHA 92 limit is from fit to most PEP/PETRA/TRISTAN data. The fit gives $\eta/\Lambda^2_{LL} = -0.0200 \pm 0.0666$ TeV^{-2}.

SCALE LIMITS for Contact Interactions: Λ(eeqq)

Limits are for $\Lambda^{\pm}_{LL}$ only. For other cases, see each reference.

Λ^+_{LL} (TeV)	Λ^-_{LL} (TeV)	CL%		DOCUMENT ID		TECN	COMMENT
>23.3	**>12.5**	95	[28]	CHEUNG	01B	RVUE	$(eeuu)$
>11.1	**>26.4**	95	[28]	CHEUNG	01B	RVUE	$(eedd)$
> 5.6	**>4.9**	95	[29]	BARATE	00I	ALEP	$(eebb)$
> 1.0	**>2.1**	95	[30]	ABREU	99A	DLPH	$(eecc)$
• • • We do not use the following data for averages, fits, limits, etc. • • •							
> 2.8	>1.6	95	[31]	ADLOFF	03	H1	$(eeqq)$
> 2.7	>2.7	95	[32]	ACHARD	02J	L3	$(eetc)$
> 5.5	>3.1	95	[33]	ABBIENDI	00R	OPAL	$(eeqq)$
> 4.9	>6.1	95	[33]	ABBIENDI	00R	OPAL	$(eeuu)$
> 5.7	>4.5	95	[33]	ABBIENDI	00R	OPAL	$(eedd)$
> 4.2	>2.8	95	[34]	ACCIARRI	00P	L3	$(eeqq)$
> 2.4	>1.3	95	[35]	ADLOFF	00	H1	$(eeqq)$
> 5.4	>6.2	95	[36]	BARATE	00I	ALEP	$(eeqq)$
			[37]	BREITWEG	00B	ZEUS	
> 4.4	>2.8	95	[38]	ABBIENDI	99	OPAL	$(eeqq)$
> 4.0	>4.8	95	[39]	ABBIENDI	99	OPAL	$(eebb)$
> 3.3	>4.2	95	[40]	ABBOTT	99D	D0	$(eeqq)$
> 2.4	>2.8	95	[30]	ABREU	99A	DLPH	$(eeqq)$ (d or s quark)
> 4.4	>3.9	95	[30]	ABREU	99A	DLPH	$(eebb)$
> 1.0	>2.4	95	[30]	ABREU	99A	DLPH	$(eeuu)$
> 4.0	>3.4	95	[41]	ZARNECKI	99	RVUE	$(eedd)$
> 4.3	>5.6	95	[41]	ZARNECKI	99	RVUE	$(eeuu)$
> 3.0	>2.1	95	[42]	ACCIARRI	98J	L3	$(eeqq)$
> 3.4	>2.2	95	[43]	ACKERSTAFF	98V	OPAL	$(eeqq)$
> 4.0	>2.8	95	[44]	ACKERSTAFF	98V	OPAL	$(eebb)$
> 9.3	>12.0	95	[45]	BARGER	98E	RVUE	$(eeuu)$
> 8.8	>11.9	95	[45]	BARGER	98E	RVUE	$(eedd)$
> 2.5	>3.7	95	[46]	ABE	97T	CDF	$(eeqq)$ (isosinglet)
> 2.5	>2.1	95	[47]	ACKERSTAFF	97C	OPAL	$(eeqq)$
> 3.1	>2.9	95	[48]	ACKERSTAFF	97C	OPAL	$(eebb)$
> 7.4	>11.7	95	[49]	DEANDREA	97	RVUE	$eeuu$, atomic parity violation
> 2.3	>1.0	95	[50]	AID	95	H1	$(eeqq)$ (u, d quarks)
1.7	>2.2	95	[51]	ABE	91D	CDF	$(eeqq)$ (u, d quarks)
> 1.2		95	[52]	ADACHI	91	TOPZ	$(eeqq)$ (flavor-universal)
	>1.6	95	[52]	ADACHI	91	TOPZ	$(eeqq)$ (flavor-universal)
> 0.6	>1.7	95	[53]	BEHREND	91C	CELL	$(eecc)$
> 1.1	>1.0	95	[53]	BEHREND	91C	CELL	$(eebb)$
> 0.9		95	[54]	ABE	89L	VNS	$(eeqq)$ (flavor-universal)
	>1.7	95	[54]	ABE	89L	VNS	$(eeqq)$ (flavor-universal)
> 1.05	>1.61	95	[55]	HAGIWARA	89	RVUE	$(eecc)$
> 1.21	>0.53	95	[56]	HAGIWARA	89	RVUE	$(eebb)$

[28] CHEUNG 01B is an update of BARGER 98E.

[29] BARATE 00I limits are from R_b and jet-charge asymmetry at 130–183 GeV.

[30] ABREU 99A limits are from flavor-tagged $e^+e^- \to q\overline{q}$ cross section at 130–172 GeV.

[31] ADLOFF 03 limits are from the $d\sigma/dQ^2$ measurement of $e^\pm p \to e^\pm X$.

[32] ACHARD 02J limit is from the bound on the $e^+e^- \to t\overline{c}$ cross section. $\Lambda_{LL} = \Lambda_{LR} = \Lambda_{RL} = \Lambda_{RR}$ and m_t = 175 GeV are assumed.

[33] ABBIENDI 00R limits are from $e^+e^- \to q\overline{q}$ cross section at $\sqrt{s}$= 130–189 GeV.

[34] ACCIARRI 00P limit is from $e^+e^- \to qq$ cross section at $\sqrt{s}$=130–189 GeV.

[35] ADLOFF 00 limits are from the Q^2 spectrum measurement of $e^+p \to e^+X$.

[36] BARATE 00I limits are from $e^+e^- \to q\overline{q}$ cross section and jet-charge asymmetry at 130–183 GeV.

[37] BREITWEG 00B limits are from Q^2 spectrum measurement of e^+p collisions. See their Table 3 for the limits of various models.

[38] ABBIENDI 99 limits are from $e^+e^- \to q\overline{q}$ cross section at 130–136, 161–172, 183 GeV.

[39] ABBIENDI 99 limits are from R_b at 130–136, 161–172, 183 GeV.

[40] ABBOTT 99D limits are from e^+e^- mass distribution in $p\overline{p} \to e^+e^-X$ at E_{cm}= 1.8 TeV.

[41] ZARNECKI 99 use data from HERA, LEP, Tevatron, and various low-energy experiments.

[42] ACCIARRI 98J limits are from $e^+e^- \to q\overline{q}$ cross section at E_{cm}= 130–172 GeV.

[43] ACKERSTAFF 98V limits are from $e^+e^- \to q\overline{q}$ at E_{cm}= 130–172 GeV.

[44] ACKERSTAFF 98V limits are from R_b measurements at E_{cm}= 130–172 GeV.

[45] BARGER 98E use data from HERA, LEP, Tevatron, and various low-energy experiments.

[46] ABE 97T limits are from e^+e^- mass distribution in $\overline{p}p \to e^+e^-X$ at E_{cm}=1.8 TeV.

[47] ACKERSTAFF 97C limits are from $e^+e^- \to q\overline{q}$ cross section at E_{cm} = 130–136 GeV and 161 GeV.

[48] ACKERSTAFF 97C limits are R_b measurements at E_{cm} = 133 GeV and 161 GeV.

[49] DEANDREA 97 limit is from atomic parity violation of cesium. The limit is eluded if the contact interactions are parity conserving.

[50] AID 95 limits are from the Q^2 spectrum measurement of $ep \to eX$.

[51] ABE 91D limits are from e^+e^- mass distribution in $p\overline{p} \to e^+e^-X$ at E_{cm} = 1.8 TeV.

[52] ADACHI 91 limits are from differential jet cross section. Universality of $\Lambda(eeqq)$ for five flavors is assumed.

[53] BEHREND 91C is from data at E_{cm} = 35–43 GeV.

[54] ABE 89L limits are from jet charge asymmetry. Universality of $\Lambda(eeqq)$ for five flavors is assumed.

[55] The HAGIWARA 89 limit is derived from forward-backward asymmetry measurements of D/D^* mesons by ALTHOFF 83C, BARTEL 84E, and BARINGER 88.

[56] The HAGIWARA 89 limit is derived from forward-backward asymmetry measurement of b hadrons by BARTEL 84D.

SCALE LIMITS for Contact Interactions: Λ(μμqq)

Λ^+_{LL} (TeV)	Λ^-_{LL} (TeV)	CL%		DOCUMENT ID		TECN	COMMENT
> 2.9	**> 4.2**	95	[57]	ABE	97T	CDF	$(\mu\mu qq)$ (isosinglet)
• • • We do not use the following data for averages, fits, limits, etc. • • •							
>1.4	>1.6	95		ABE	92B	CDF	$(\mu\mu qq)$ (isosinglet)

[57] ABE 97T limits are from $\mu^+\mu^-$ mass distribution in $\overline{p}p \to \mu^+\mu^-X$ at E_{cm}=1.8 TeV.

SCALE LIMITS for Contact Interactions: Λ(ℓνℓν)

VALUE (TeV)	CL%		DOCUMENT ID		TECN	COMMENT
>3.10	90	[58]	JODIDIO	86	SPEC	$\Lambda^{\pm}_{LR}(\nu_\mu\nu_e\mu e)$
• • • We do not use the following data for averages, fits, limits, etc. • • •						
>3.8		[59]	DIAZCRUZ	94	RVUE	$\Lambda^+_{LL}(\tau\nu_\tau e\nu_e)$
>8.1		[59]	DIAZCRUZ	94	RVUE	$\Lambda^-_{LL}(\tau\nu_\tau e\nu_e)$
>4.1		[60]	DIAZCRUZ	94	RVUE	$\Lambda^+_{LL}(\tau\nu_\tau \mu\nu_\mu)$
>6.5		[60]	DIAZCRUZ	94	RVUE	$\Lambda^-_{LL}(\tau\nu_\tau \mu\nu_\mu)$

[58] JODIDIO 86 limit is from $\mu^+ \to \overline{\nu}_\mu e^+\nu_e$. Chirality invariant interactions $L = (g^2/\Lambda^2)$ $[\eta_{LL}\ (\overline{\nu}_{\mu L}\gamma^\alpha\mu_L)\ (\overline{e}_L\gamma_\alpha\nu_{eL}) + \eta_{LR}\ (\overline{\nu}_{\mu L}\gamma^\alpha\nu_{eL}\ (\overline{e}_R\gamma_\alpha\mu_R)]$ with $g^2/4\pi = 1$ and $(\eta_{LL},\eta_{LR}) = (0,\pm1)$ are taken. No limits are given for $\Lambda^{\pm}_{LL}$ with $(\eta_{LL},\eta_{LR}) = (\pm1,0)$. For more general constraints with right-handed neutrinos and chirality nonconserving contact interactions, see their text.

[59] DIAZCRUZ 94 limits are from $\Gamma(\tau \to e\nu\nu)$ and assume flavor-dependent contact interactions with $\Lambda(\tau\nu_\tau e\nu_e) \ll \Lambda(\mu\nu_\mu e\nu_e)$.

[60] DIAZCRUZ 94 limits are from $\Gamma(\tau \to \mu\nu\nu)$ and assume flavor-dependent contact interactions with $\Lambda(\tau\nu_\tau\mu\nu_\mu) \ll \Lambda(\mu\nu_\mu e\nu_e)$.

SCALE LIMITS for Contact Interactions: Λ(eνqq)

VALUE (TeV)	CL%		DOCUMENT ID		TECN
>2.81	95	[61]	AFFOLDER	01I	CDF

[61] AFFOLDER 00I bound is for a scalar interaction $\overline{q}_R q_L \overline{\nu} e_L$.

SCALE LIMITS for Contact Interactions: $\Lambda(qqqq)$

Limits are for $\Lambda^{\pm}_{LL}$ with color-singlet isoscalar exchanges among u_L's and d_L's only, unless otherwise noted. See EICHTEN 84 for details.

VALUE (TeV)	CL%	DOCUMENT ID		TECN	COMMENT
>2.7	95	[62] ABBOTT	99C	D0	$p\overline{p} \to$ dijet mass. Λ^{+}_{LL}
• • • We do not use the following data for averages, fits, limits, etc. • • •					
>2.0	95	[63] ABBOTT	00E	D0	H_T distribution; Λ^{+}_{LL}
>2.1	95	[64] ABBOTT	98G	D0	$p\overline{p} \to$ dijet angl. Λ^{+}_{LL}
		[65] BERTRAM	98	RVUE	$p\overline{p} \to$ dijet mass
		[66] ABE	96	CDF	$p\overline{p} \to$ jets inclusive
>1.6	95	[67] ABE	96S	CDF	$p\overline{p} \to$ dijet angl.; Λ^{+}_{LL}
>1.3	95	[68] ABE	93G	CDF	$p\overline{p} \to$ dijet mass
>1.4	95	[69] ABE	92D	CDF	$p\overline{p} \to$ jets inclusive
>1.0	99	[70] ABE	92M	CDF	$p\overline{p} \to$ dijet angl.
>0.825	95	[71] ALITTI	91B	UA2	$p\overline{p} \to$ jets inclusive
>0.700	95	[69] ABE	89	CDF	$p\overline{p} \to$ jets inclusive
>0.330	95	[72] ABE	89H	CDF	$p\overline{p} \to$ dijet angl.
>0.400	95	[73] ARNISON	86C	UA1	$p\overline{p} \to$ jets inclusive
>0.415	95	[74] ARNISON	86D	UA1	$p\overline{p} \to$ dijet angl.
>0.370	95	[75] APPEL	85	UA2	$p\overline{p} \to$ jets inclusive
>0.275	95	[76] BAGNAIA	84C	UA2	Repl. by APPEL 85

[62] The quoted limit is from inclusive dijet mass spectrum in $p\overline{p}$ collisions at E_{cm}=1.8 TeV. ABBOTT 99C also obtain $\Lambda^{-}_{LL} > 2.4$ TeV. All quarks are assumed composite.

[63] The quoted limit for ABBOTT 00E is from H_T distribution in $p\overline{p}$ collisions at E_{cm}=1.8 TeV. CTEQ4M PDF and $\mu = E_T^{max}$ are assumed. For limits with different assumptions, see their Tables 2 and 3. All quarks are assumed composite.

[64] ABBOTT 98G limit is from dijet angular distribution in $p\overline{p}$ collisions at E_{cm}= 1.8 TeV. All quarks are assumed composite.

[65] BERTRAM 98 obtain limit on the scale of color-octet axial-vector flavor-universal contact interactions: $\Lambda_{A8} > 2.1$ TeV. They also obtain a limit $\Lambda_{V8} > 2.4$ TeV on a color-octet flavor-universal vectorial contact interaction.

[66] ABE 96 finds that the inclusive jet cross section for $E_T > 200$ GeV is significantly higher than the $\mathcal{O}(\alpha_s^3)$ perturbative QCD prediction. This could be interpreted as the effect of a contact interaction with $\Lambda_{LL} \sim 1.6$ TeV. However, ABE 96 state that uncertainty in the parton distribution functions, higher-order QCD corrections, and the detector calibration may possibly account for the effect.

[67] ABE 96S limit is from dijet angular distribution in $p\overline{p}$ collisions at E_{cm} = 1.8 TeV. The limit for Λ^{-}_{LL} is > 1.4 TeV. ABE 96S also obtain limits for flavor symmetric contact interactions among all quark flavors: $\Lambda^{+}_{LL} > 1.8$ TeV and $\Lambda^{-}_{LL} > 1.6$ TeV.

[68] ABE 93G limit is from dijet mass distribution in $p\overline{p}$ collisions at E_{cm} = 1.8 TeV. The limit is the weakest from several choices of structure functions and renormalization scale.

[69] Limit is from inclusive jet cross-section data in $p\overline{p}$ collisions at E_{cm} = 1.8 TeV. The limit takes into account uncertainties in choice of structure functions and in choice of process scale.

[70] ABE 92M limit is from dijet angular distribution for m_{dijet} >550 GeV in $p\overline{p}$ collisions at E_{cm}=1.8 TeV.

[71] ALITTI 91B limit is from inclusive jet cross section in $p\overline{p}$ collisions at E_{cm} = 630 GeV. The limit takes into account uncertainties in choice of structure functions and in choice of process scale.

[72] ABE 89H limit is from dijet angular distribution for $m_{dijet} > 200$ GeV at the Fermilab Tevatron Collider with E_{cm} = 1.8 TeV. The QCD prediction is quite insensitive to choice of structure functions and choice of process scale.

[73] ARNISON 86C limit is from the study of inclusive high-p_T jet distributions at the CERN $\overline{p}p$ collider (E_{cm} = 546 and 630 GeV). The QCD prediction renormalized to the low-p_T region gives a good fit to the data.

[74] ARNISON 86D limit is from the study of dijet angular distribution in the range 240 < m(dijet) < 300 GeV at the CERN $\overline{p}p$ collider (E_{cm} = 630 GeV). QCD prediction using EHLQ structure function (EICHTEN 84) with Λ_{QCD} = 0.2 GeV for the choice of $Q^2 = {p_T}^2$ gives the best fit to the data.

[75] APPEL 85 limit is from the study of inclusive high-p_T jet distributions at the CERN $\overline{p}p$ collider (E_{cm} = 630 GeV). The QCD prediction renormalized to the low-p_T region gives a good description of the data.

[76] BAGNAIA 84C limit is from the study of jet p_T and dijet mass distributions at the CERN $\overline{p}p$ collider (E_{cm} = 540 GeV). The limit suffers from the uncertainties in comparing the data with the QCD prediction.

SCALE LIMITS for Contact Interactions: $\Lambda(\nu\nu qq)$

Limits are for $\Lambda^{\pm}_{LL}$ only. For other cases, see each reference.

Λ^{+}_{LL} (TeV)	Λ^{-}_{LL} (TeV)	CL%	DOCUMENT ID		TECN	COMMENT
>5.0	**>5.4**	95	[77] MCFARLAND	98	CCFR	νN scattering

[77] MCFARLAND 98 assumed a flavor universal interaction. Neutrinos were mostly of muon type.

MASS LIMITS for Excited e (e*)

Most e^+e^- experiments assume one-photon or Z exchange. The limits from some e^+e^- experiments which depend on λ have assumed transition couplings which are chirality violating ($\eta_L = \eta_R$). However they can be interpreted as limits for chirality-conserving interactions after multiplying the coupling value λ by $\sqrt{2}$; see Note.

Excited leptons have the same quantum numbers as other ortholeptons. See also the searches for ortholeptons in the "Searches for Heavy Leptons" section.

Limits for Excited e (e*) from Pair Production

These limits are obtained from $e^+e^- \to e^{*+}e^{*-}$ and thus rely only on the (electroweak) charge of e^*. Form factor effects are ignored unless noted. For the case of limits from Z decay, the e^* coupling is assumed to be of sequential type. Possible t channel contribution from transition magnetic coupling is neglected. All limits assume a dominant $e^* \to e\gamma$ decay except the limits from $\Gamma(Z)$.

For limits prior to 1987, see our 1992 edition (Physical Review **D45**, 1 June, Part II (1992)).

VALUE (GeV)	CL%	DOCUMENT ID		TECN	COMMENT
>103.2	95	[78] ABBIENDI	02G	OPAL	$e^+e^- \to e^*e^*$ Homodoublet type
• • • We do not use the following data for averages, fits, limits, etc. • • •					
>102.8	95	[79] ACHARD	03B	L3	$e^+e^- \to e^*e^*$ Homodoublet type
>100.0	95	[80] ACCIARRI	01D	L3	$e^+e^- \to e^*e^*$ Homodoublet type
> 91.3	95	[81] ABBIENDI	00I	OPAL	$e^+e^- \to e^*e^*$ Homodoublet type
> 94.2	95	[82] ACCIARRI	00E	L3	$e^+e^- \to e^*e^*$ Homodoublet type
> 90.7	95	[83] ABREU	99O	DLPH	Homodoublet type
> 85.0	95	[84] ACKERSTAFF	98C	OPAL	$e^+e^- \to e^*e^*$ Homodoublet type
		[85] BARATE	98U	ALEP	$Z \to e^*e^*$
> 79.6	95	[86,87] ABREU	97B	DLPH	$e^+e^- \to e^*e^*$ Homodoublet type
> 77.9	95	[86,88] ABREU	97B	DLPH	$e^+e^- \to e^*e^*$ Sequential type
> 79.7	95	[86] ACCIARRI	97G	L3	$e^+e^- \to e^*e^*$ Sequential type
> 79.9	95	[86,89] ACKERSTAFF	97	OPAL	$e^+e^- \to e^*e^*$ Homodoublet type
> 62.5	95	[90] ABREU	96K	DLPH	$e^+e^- \to e^*e^*$ Homodoublet type
> 64.7	95	[91] ACCIARRI	96D	L3	$e^+e^- \to e^*e^*$ Sequential type
> 66.5	95	[91] ALEXANDER	96Q	OPAL	$e^+e^- \to e^*e^*$ Homodoublet type
> 65.2	95	[91] BUSKULIC	96W	ALEP	$e^+e^- \to e^*e^*$ Sequential type
> 45.6	95	ADRIANI	93M	L3	$Z \to e^*e^*$
> 45.6	95	ABREU	92C	DLPH	$Z \to e^*e^*$
> 29.8	95	[92] BARDADIN-...	92	RVUE	$\Gamma(Z)$
> 26.1	95	[93] DECAMP	92	ALEP	$Z \to e^*e^*$; $\Gamma(Z)$
> 46.1	95	DECAMP	92	ALEP	$Z \to e^*e^*$
> 33	95	[93] ABREU	91F	DLPH	$Z \to e^*e^*$; $\Gamma(Z)$
> 45.0	95	[94] ADEVA	90F	L3	$Z \to e^*e^*$
> 44.9	95	AKRAWY	90I	OPAL	$Z \to e^*e^*$
> 44.6	95	[95] DECAMP	90G	ALEP	$e^+e^- \to e^*e^*$
> 30.2	95	ADACHI	89B	TOPZ	$e^+e^- \to e^*e^*$
> 28.3	95	KIM	89	AMY	$e^+e^- \to e^*e^*$
> 27.9	95	[96] ABE	88B	VNS	$e^+e^- \to e^*e^*$

[78] From e^+e^- collisions at $\sqrt{s}$ = 183–209 GeV. $f = f'$ is assumed.

[79] From e^+e^- collisions at $\sqrt{s}$ = 189–209 GeV. $f = f'$ is assumed. ACHARD 03B also obtain limit for $f = -f'$: $m_{e^*} > 96.6$ GeV.

[80] From e^+e^- collisions at $\sqrt{s}$ = 192–202 GeV. f=f' is assumed. ACCIARRI 01D also obtain limit for f=$-f'$: $m_{e^*} > 93.4$ GeV.

[81] From e^+e^- collisions at $\sqrt{s}$=161–183 GeV. f=f' is assumed. ABBIENDI 00I also obtain limit for f=$-f'$ ($e^* \to \nu W$): $m_{e^*} > 86.0$ GeV.

[82] From e^+e^- collisions at $\sqrt{s}$=189 GeV. f=f' is assumed. ACCIARRI 00E also obtain limit for f=$-f'$ ($e^* \to \nu W$): $m_{e^*} > 92.6$ GeV.

[83] From e^+e^- collisions at $\sqrt{s}$= 183 GeV. f=f' is assumed. ABREU 99O also obtain limit for f=$-f'$ ($e^* \to \nu W$): $m_{e^*} > 81.3$ GeV.

[84] From e^+e^- collisions at $\sqrt{s}$=170–172 GeV. ACKERSTAFF 98C also obtain limit from $e^* \to \nu W$ decay mode: $m_{e^*} > 81.3$ GeV.

[85] BARATE 98U obtain limits on the form factor. See their Fig. 14 for limits in mass-form factor plane.

[86] From e^+e^- collisions at $\sqrt{s}$= 161 GeV.

[87] ABREU 97B also obtain limit from charged current decay mode $e^* \to \nu W$, $m_{e^*} > 70.9$ GeV.

[88] ABREU 97B also obtain limit from charged current decay mode $e^* \to \nu W$, $m_{e^*} > 44.6$ GeV.

[89] ACKERSTAFF 97 also obtain limit from charged current decay mode $e^* \to \nu W$, $m_{\nu_e^*} > 77.1$ GeV.

[90] From e^+e^- collisions at $\sqrt{s}$= 130–136 GeV.

[91] From e^+e^- collisions at $\sqrt{s}$= 130–140 GeV.

[92] BARDADIN-OTWINOWSKA 92 limit is independent of decay modes. Based on $\Delta\Gamma(Z)$<36 MeV.

[93] Limit is independent of e^* decay mode.

[94] ADEVA 90F is superseded by ADRIANI 93M.

[95] Superseded by DECAMP 92.

[96] ABE 88B limits assume $e^+e^- \to e^{*+}e^{*-}$ with one photon exchange only and $e^* \to e\gamma$ giving $ee\gamma\gamma$.

Limits for Excited e (e^*) from Single Production

These limits are from $e^+e^- \to e^*e$, $W \to e^*\nu$, or $ep \to e^*X$ and depend on transition magnetic coupling between e and e^*. All limits assume $e^* \to e\gamma$ decay except as noted. Limits from LEP, UA2, and H1 are for chiral coupling, whereas all other limits are for nonchiral coupling, $\eta_L = \eta_R = 1$. In most papers, the limit is expressed in the form of an excluded region in the $\lambda - m_{e^*}$ plane. See the original papers.

For limits prior to 1987, see our 1992 edition (Physical Review **D45,** 1 June, Part II (1992)).

VALUE (GeV)	CL%	DOCUMENT ID		TECN	COMMENT
>255	95	[97] ADLOFF	02B	H1	$ep \to e^*X$
• • • We do not use the following data for averages, fits, limits, etc. • • •					
>206	95	[98] ACHARD	03B	L3	$e^+e^- \to ee^*$
>208	95	[99] ABBIENDI	02G	OPAL	$e^+e^- \to ee^*$
>228	95	[100] CHEKANOV	02D	ZEUS	$ep \to e^*X$
>202		[101] ACCIARRI	01D	L3	$e^+e^- \to ee^*$
		[102] ABBIENDI	00I	OPAL	$e^+e^- \to ee^*$
		[103] ACCIARRI	00E	L3	$e^+e^- \to ee^*$
>223	95	[104] ADLOFF	00E	H1	$ep \to e^*X$
		[105] ABREU	99O	DLPH	$e^+e^- \to ee^*$
none 20–170	95	[106] ACCIARRI	98T	L3	$e\gamma \to e^* \to e\gamma$
		[107] ACKERSTAFF	98C	OPAL	$e^+e^- \to ee^*$
		[108] BARATE	98U	ALEP	$e^+e^- \to ee^*$
	109,110	ABREU	97B	DLPH	$e^+e^- \to ee^*$
	109,111	ACCIARRI	97G	L3	$e^+e^- \to ee^*$
		[112] ACKERSTAFF	97	OPAL	$e^+e^- \to ee^*$
		[113] ADLOFF	97	H1	Lepton-flavor violation
none 30–200	95	[114] BREITWEG	97C	ZEUS	$ep \to e^*X$
		[115] ABREU	96K	DLPH	$e^+e^- \to ee^*$
		[116] ACCIARRI	96D	L3	$e^+e^- \to ee^*$
		[117] ALEXANDER	96Q	OPAL	$e^+e^- \to ee^*$
		[118] BUSKULIC	96W	ALEP	$e^+e^- \to ee^*$
		[119] DERRICK	95B	ZEUS	$ep \to e^*X$
		[120] ABT	93	H1	$ep \to e^*X$
> 86	95	ADRIANI	93M	L3	$\lambda_\gamma > 0.04$
> 89	95	ADRIANI	93M	L3	$Z \to ee^*$, $\lambda_Z > 0.5$
		[121] DERRICK	93B	ZEUS	Superseded by DERRICK 95B
> 88	95	ABREU	92C	DLPH	$Z \to ee^*$, $\lambda_Z > 0.5$
> 86	95	ABREU	92C	DLPH	$e^+e^- \to ee^*$, $\lambda_\gamma > 0.1$
> 91	95	DECAMP	92	ALEP	$Z \to ee^*$, $\lambda_Z > 1$
> 88	95	[122] ADEVA	90F	L3	$Z \to ee^*$, $\lambda_Z > 0.5$
> 86	95	[122] ADEVA	90F	L3	$Z \to ee^*$, $\lambda_Z > 0.04$
> 87	95	AKRAWY	90I	OPAL	$Z \to ee^*$, $\lambda_Z > 0.5$
> 81	95	[123] DECAMP	90G	ALEP	$Z \to ee^*$, $\lambda_Z > 1$
> 50	95	ADACHI	89B	TOPZ	$e^+e^- \to ee^*$, $\lambda_\gamma > 0.04$
> 56	95	KIM	89	AMY	$e^+e^- \to ee^*$, $\lambda_\gamma > 0.03$
none 23–54	95	[124] ABE	88B	VNS	$e^+e^- \to ee^*$ $\lambda_\gamma > 0.04$
> 75	95	[125] ANSARI	87D	UA2	$W \to e^*\nu$; $\lambda_W > 0.7$
> 63	95	[125] ANSARI	87D	UA2	$W \to e^*\nu$; $\lambda_W > 0.2$
> 40	95	[125] ANSARI	87D	UA2	$W \to e^*\nu$; $\lambda_W > 0.09$

[97] ADLOFF 02B search for single e^* production in ep collisions with the decays $e^* \to e\gamma$, eZ, νW. $f = f' = \Lambda/m_{e^*}$ is assumed for the e^* coupling. See their Fig. 3 for the exclusion plot in the mass-coupling plane.

[98] ACHARD 03B result is from e^+e^- collisions at $\sqrt{s} = 189$–209 GeV. See their Fig. 4 for the exclusion plot in the mass-coupling plane.

[99] ABBIENDI 02G result is from e^+e^- collisions at $\sqrt{s} = 183$–209 GeV. $f = f' = \Lambda/m_{e^*}$ is assumed for e^* coupling. See their Fig. 4c for the exclusion limit in the mass-coupling plane.

[100] CHEKANOV 02D search for single e^* production in ep collisions with the decays $e^* \to e\gamma$, eZ, νW. $f = f' = \Lambda/m_{e^*}$ is assumed for the e^* coupling. See their Fig. 5a for the exclusion plot in the mass-coupling plane.

[101] ACCIARRI 01D result is from e^+e^- collisions at $\sqrt{s} = 192$–202 GeV. $f = f' = \Lambda/m_{e^*}$ is assumed for the e^* coupling. See their Fig. 4 for limits in the mass-coupling plane.

[102] ABBIENDI 00I result is from e^+e^- collisions at $\sqrt{s}$=161–183 GeV. See their Fig. 7 for limits in mass-coupling plane.

[103] ACCIARRI 00E result is from e^+e^- collisions at $\sqrt{s}$=189 GeV. See their Fig. 3 for limits in mass-coupling plane.

[104] ADLOFF 00E search for single e^* production in ep collisions with the decays $e^* \to e\gamma$, eZ, νW. $f = f' = \Lambda/m_{e^*}$ is assumed for the e^* coupling. See their Fig. 9 for the exclusion plot in the mass-coupling plane.

[105] ABREU 99O result is from e^+e^- collisions at $\sqrt{s}$= 183 GeV. See their Figs. 4 and 5 for the exclusion limit in the mass-coupling plane.

[106] ACCIARRI 98T search for single e^* production in quasi-real Compton scattering. The limit is for $|\lambda| > 1.0 \times 10^{-1}$ and non-chiral coupling of e^*. See their Fig. 7 for the exclusion plot in the mass-coupling plane.

[107] ACKERSTAFF 98C from e^+e^- collisions at $\sqrt{s}$=170–172 GeV. See their Fig. 11 for the exclusion limit in the mass-coupling plane.

[108] BARATE 98U is from e^+e^- collision at $\sqrt{s} = M_Z$. See their Fig. 12 for limits in mass-coupling plane

[109] From e^+e^- collisions at $\sqrt{s}$= 161 GeV.

[110] See Fig. 4a and Fig. 5a of ABREU 97B for the exclusion limit in the mass-coupling plane.

[111] See Fig. 2 and Fig. 3 of ACCIARRI 97G for the exclusion limit in the mass-coupling plane.

[112] ACKERSTAFF 97 result is from e^+e^- collisions at $\sqrt{s}$= 161 GeV. See their Fig. 3 for the exclusion limit in the mass-coupling plane.

[113] ADLOFF 97 search for single e^* production in ep collisions with the decays $e^* \to e\gamma$, eZ, νW. See their Fig. 4 for the rejection limits on the product of the production cross section and the branching ratio into a specific decay channel.

[114] BREITWEG 97C search for single e^* production in ep collisions with the decays $e^* \to e\gamma$, eZ, νW. $f = f' = 2\Lambda/m_{e^*}$ is assumed for the e^* coupling. See their Fig. 9 for the exclusion plot in the mass-coupling plane.

[115] ABREU 96K result is from e^+e^- collisions at $\sqrt{s}$= 130–136 GeV. See their Fig. 4 for the exclusion limit in the mass-coupling plane.

[116] ACCIARRI 96D result is from e^+e^- collisions at $\sqrt{s}$= 130–140 GeV. See their Fig. 2 for the exclusion limit in the mass-coupling plane.

[117] ALEXANDER 96Q result is from e^+e^- collisions at $\sqrt{s}$= 130–140 GeV. See their Fig. 3a for the exclusion limit in the mass-coupling plane.

[118] BUSKULIC 96W result is from e^+e^- collisions at $\sqrt{s}$= 130–140 GeV. See their Fig. 3 for the exclusion limit in the mass-coupling plane.

[119] DERRICK 95B search for single e^* production via $e^*e\gamma$ coupling in ep collisions with the decays $e^* \to e\gamma$, eZ, νW. See their Fig. 13 for the exclusion plot in the m_{e^*}–λ_γ plane.

[120] ABT 93 search for single e^* production via $e^*e\gamma$ coupling in ep collisions with the decays $e^* \to e\gamma$, eZ, νW. See their Fig. 4 for exclusion plot in the m_{e^*}–λ_γ plane.

[121] DERRICK 93B search for single e^* production via $e^*e\gamma$ coupling in ep collisions with the decays $e^* \to e\gamma$, eZ, νW. See their Fig. 3 for exclusion plot in the m_{e^*}–λ_γ plane.

[122] Superseded by ADRIANI 93M.

[123] Superseded by DECAMP 92.

[124] ABE 88B limits use $e^+e^- \to ee^*$ where t-channel photon exchange dominates giving $e\gamma(e)$ (quasi-real compton scattering).

[125] ANSARI 87D is at E_{cm} = 546–630 GeV.

Limits for Excited e (e^*) from $e^+e^- \to \gamma\gamma$

These limits are derived from indirect effects due to e^* exchange in the t channel and depend on transition magnetic coupling between e and e^*. All limits are for $\lambda_\gamma = 1$. All limits except ABE 89J and ACHARD 02D are for nonchiral coupling with $\eta_L = \eta_R = 1$. We choose the chiral coupling limit as the best limit and list it in the Summary Table.

For limits prior to 1987, see our 1992 edition (Physical Review **D45**, 1 June, Part II (1992)).

VALUE (GeV)	CL%	DOCUMENT ID		TECN	COMMENT
>310	95	ACHARD	02D	L3	$\sqrt{s}$= 192–209 GeV
>311	95	ABREU	00A	DLPH	$\sqrt{s}$= 189–202 GeV
• • • We do not use the following data for averages, fits, limits, etc. • • •					
>283	95	[126] ACCIARRI	00G	L3	$\sqrt{s}$= 183–189 GeV
>306	95	ABBIENDI	99P	OPAL	$\sqrt{s}$= 189 GeV
>231	95	ABREU	98J	DLPH	$\sqrt{s}$= 130–183 GeV
>194	95	ACKERSTAFF	98	OPAL	$\sqrt{s}$= 130–172 GeV
>227	95	ACKER...,K...	98B	OPAL	$\sqrt{s}$= 183 GeV
>250	95	BARATE	98J	ALEP	$\sqrt{s}$= 183 GeV
>160	95	[127] BARATE	98U	ALEP	
>210	95	[128] ACCIARRI	97W	L3	$\sqrt{s}$= 161, 172 GeV
>129	95	ACCIARRI	96L	L3	$\sqrt{s}$=133 GeV
>147	95	ALEXANDER	96K	OPAL	
>136	95	BUSKULIC	96Z	ALEP	$\sqrt{s}$=130, 136 GeV
>146	95	ACCIARRI	95G	L3	
		[129] BUSKULIC	93Q	ALEP	
>127	95	[130] ADRIANI	92B	L3	
>114	95	[131] BARDADIN-...	92	RVUE	
> 99	95	DECAMP	92	ALEP	
		[132] SHIMOZAWA	92	TOPZ	
>100	95	ABREU	91E	DLPH	
>116	95	AKRAWY	91F	OPAL	
> 83	95	ADEVA	90K	L3	
> 82	95	AKRAWY	90F	OPAL	
> 68	95	[133] ABE	89J	VNS	η_L=1, η_R=0
> 90.2	95	ADACHI	89B	TOPZ	
> 65	95	KIM	89	AMY	

[126] ACCIARRI 00G also obtain a limit on e^* with chiral coupling, $m_{e^*} > 213$ GeV.

[127] BARATE 98U is from e^+e^- collision at $\sqrt{s} = M_Z$. See their Fig. 5 for limits in mass-coupling plane

[128] ACCIARRI 97W also obtain a limit on e^* with chiral coupling, $m_{e^*} > 157$ GeV (95%CL).

[129] BUSKULIC 93Q obtain $\Lambda^+ > 121$ GeV (95%CL) from ALEPH experiment and $\Lambda^+ > 135$ GeV from combined TRISTAN and ALEPH data. These limits roughly correspond to limits on m_{e^*}.

[130] ADRIANI 92B superseded by ACCIARRI 95G.

[131] BARDADIN-OTWINOWSKA 92 limit from fit to the combined data of DECAMP 92, ABREU 91E, ADEVA 90K, AKRAWY 91F.

[132] SHIMOZAWA 92 fit the data to the limiting form of the cross section with $m_{e^*} \gg E_{cm}$ and obtain $m_{e^*} > 168$ GeV at 95%CL. Use of the full form would reduce this limit by a few GeV. The statistically unexpected large value is due to fluctuation in the data.

[133] The ABE 89J limit assumes chiral coupling. This corresponds to $\lambda_\gamma = 0.7$ for nonchiral coupling.

Indirect Limits for Excited e (e^*)

These limits make use of loop effects involving e^* and are therefore subject to theoretical uncertainty.

VALUE (GeV)	DOCUMENT ID		TECN	COMMENT
• • • We do not use the following data for averages, fits, limits, etc. • • •				
	[134] DORENBOS...	89	CHRM	$\overline{\nu}_\mu e \to \overline{\nu}_\mu e$ and $\nu_\mu e \to \nu_\mu e$
	[135] GRIFOLS	86	THEO	$\nu_\mu e \to \nu_\mu e$
	[136] RENARD	82	THEO	$g-2$ of electron

[134] DORENBOSCH 89 obtain the limit $\lambda_\gamma^2 \Lambda_{\rm cut}^2 / m_{e^*}^2 < 2.6$ (95% CL), where $\Lambda_{\rm cut}$ is the cutoff scale, based on the one-loop calculation by GRIFOLS 86. If one assumes that $\Lambda_{\rm cut} = 1$ TeV and $\lambda_\gamma = 1$, one obtains $m_{e^*} > 620$ GeV. However, one generally expects $\lambda_\gamma \approx m_{e^*}/\Lambda_{\rm cut}$ in composite models.

[135] GRIFOLS 86 uses $\nu_\mu e \to \nu_\mu e$ and $\overline{\nu}_\mu e \to \overline{\nu}_\mu e$ data from CHARM Collaboration to derive mass limits which depend on the scale of compositeness.

[136] RENARD 82 derived from $g-2$ data limits on mass and couplings of e^* and μ^*. See figures 2 and 3 of the paper.

MASS LIMITS for Excited μ (μ^*)

Limits for Excited μ (μ^*) from Pair Production

These limits are obtained from $e^+e^- \to \mu^{*+}\mu^{*-}$ and thus rely only on the (electroweak) charge of μ^*. Form factor effects are ignored unless noted. For the case of limits from Z decay, the μ^* coupling is assumed to be of sequential type. All limits assume a dominant $\mu^* \to \mu\gamma$ decay except the limits from $\Gamma(Z)$.

For limits prior to 1987, see our 1992 edition (Physical Review **D45,** 1 June, Part II (1992)).

VALUE (GeV)	CL%		DOCUMENT ID		TECN	COMMENT
>103.2	95	[137]	ABBIENDI	02G	OPAL	$e^+e^- \to \mu^*\mu^*$ Homodoublet type
• • • We do not use the following data for averages, fits, limits, etc. • • •						
>102.8	95	[138]	ACHARD	03B	L3	$e^+e^- \to \mu^*\mu^*$ Homodoublet type
>100.2	95	[139]	ACCIARRI	01D	L3	$e^+e^- \to \mu^*\mu^*$ Homodoublet type
> 91.3	95	[140]	ABBIENDI	00I	OPAL	$e^+e^- \to \mu^*\mu^*$ Homodoublet type
> 94.2	95	[141]	ACCIARRI	00E	L3	$e^+e^- \to \mu^*\mu^*$ Homodoublet type
> 90.7	95	[142]	ABREU	99O	DLPH	Homodoublet type
> 85.3	95	[143]	ACKERSTAFF	98C	OPAL	$e^+e^- \to \mu^*\mu^*$ Homodoublet type
		[144]	BARATE	98U	ALEP	$Z \to \mu^*\mu^*$
> 79.6	95	[145,146]	ABREU	97B	DLPH	$e^+e^- \to \mu^*\mu^*$ Homodoublet type
> 78.4	95	[145,147]	ABREU	97B	DLPH	$e^+e^- \to \mu^*\mu^*$ Sequential type
> 79.9	95	[145]	ACCIARRI	97G	L3	$e^+e^- \to \mu^*\mu^*$ Sequential type
> 80.0	95	[145,148]	ACKERSTAFF	97	OPAL	$e^+e^- \to \mu^*\mu^*$ Homodoublet type
> 62.6	95	[149]	ABREU	96K	DLPH	$e^+e^- \to \mu^*\mu^*$ Homodoublet type
> 64.9	95	[150]	ACCIARRI	96D	L3	$e^+e^- \to \mu^*\mu^*$ Sequential type
> 66.8	95	[150]	ALEXANDER	96Q	OPAL	$e^+e^- \to \mu^*\mu^*$ Homodoublet type
> 65.4	95	[150]	BUSKULIC	96W	ALEP	$e^+e^- \to \mu^*\mu^*$ Sequential type
> 45.6	95		ADRIANI	93M	L3	$Z \to \mu^*\mu^*$
> 45.6	95		ABREU	92C	DLPH	$Z \to \mu^*\mu^*$
> 29.8	95	[151]	BARDADIN-...	92	RVUE	$\Gamma(Z)$
> 26.1	95	[152]	DECAMP	92	ALEP	$Z \to \mu^*\mu^*$; $\Gamma(Z)$
> 46.1	95		DECAMP	92	ALEP	$Z \to \mu^*\mu^*$
> 33	95	[152]	ABREU	91F	DLPH	$Z \to \mu^*\mu^*$; $\Gamma(Z)$
> 45.3	95	[153]	ADEVA	90F	L3	$Z \to \mu^*\mu^*$
> 44.9	95		AKRAWY	90I	OPAL	$Z \to \mu^*\mu^*$
> 44.6	95	[154]	DECAMP	90G	ALEP	$e^+e^- \to \mu^*\mu^*$
> 29.9	95		ADACHI	89B	TOPZ	$e^+e^- \to \mu^*\mu^*$
> 28.3	95		KIM	89	AMY	$e^+e^- \to \mu^*\mu^*$

[137] From e^+e^- collisions at $\sqrt{s} = 183$–209 GeV. $f = f'$ is assumed.

[138] From e^+e^- collisions at $\sqrt{s} = 189$–209 GeV. $f = f'$ is assumed. ACHARD 03B also obtain limit for $f = -f'$: $m_{\mu^*} > 96.6$ GeV.

[139] From e^+e^- collisions at $\sqrt{s} = 192$–202 GeV. $f=f'$ is assumed. ACCIARRI 01D also obtain limit for $f=-f'$: $m_{\mu^*} > 93.4$ GeV.

[140] From e^+e^- collisions at $\sqrt{s}$=161–183 GeV. $f=f'$ is assumed. ABBIENDI 00I also obtain limit for $f=-f'$ ($\mu^* \to \nu W$): $m_{\mu^*} > 86.0$ GeV.

[141] From e^+e^- collisions at $\sqrt{s}$=189 GeV. $f=f'$ is assumed. ACCIARRI 00E also obtain limit for $f=-f'$ ($\mu^* \to \nu W$): $m_{\mu^*} > 92.6$ GeV.

[142] From e^+e^- collisions at $\sqrt{s}$= 183 GeV. $f=f'$ is assumed. ABREU 99O also obtain limit for $f=-f'$ ($\mu^* \to \nu W$): $m_{\mu^*} > 81.3$ GeV.

[143] From e^+e^- collisions at $\sqrt{s}$=170–172 GeV. ACKERSTAFF 98C also obtain limit from $\mu^* \to \nu W$ decay mode: $m_{\mu^*} > 81.3$ GeV.

[144] BARATE 98U obtain limits on the form factor. See their Fig. 14 for limits in mass-form factor plane.

[145] From e^+e^- collisions at $\sqrt{s}$= 161 GeV.

[146] ABREU 97B also obtain limit from charged current decay mode $\mu^* \to \nu W$, $m_{\mu^*} > 70.9$ GeV.

[147] ABREU 97B also obtain limit from charged current decay mode $\mu^* \to \nu W$, $m_{\mu^*} > 44.6$ GeV.

[148] ACKERSTAFF 97 also obtain limit from charged current decay mode $\mu^* \to \nu W$, $m_{\nu_\mu^*} > 77.1$ GeV.

[149] From e^+e^- collisions at $\sqrt{s}$= 130–136 GeV.

[150] From e^+e^- collisions at $\sqrt{s}$= 130–140 GeV.

[151] BARDADIN-OTWINOWSKA 92 limit is independent of decay modes. Based on $\Delta\Gamma(Z)$<36 MeV.

[152] Limit is independent of μ^* decay mode.

[153] Superseded by ADRIANI 93M.

[154] Superseded by DECAMP 92.

Limits for Excited μ (μ^*) from Single Production

These limits are from $e^+e^- \to \mu^*\mu$ and depend on transition magnetic coupling between μ and μ^*. All limits assume $\mu^* \to \mu\gamma$ decay. Limits from LEP are for chiral coupling, whereas all other limits are for nonchiral coupling, $\eta_L = \eta_R = 1$. In most papers, the limit is expressed in the form of an excluded region in the λ–m_{μ^*} plane. See the original papers.

For limits prior to 1987, see our 1992 edition (Physical Review **D45**, 1 June, Part II (1992)).

VALUE (GeV)	CL%		DOCUMENT ID		TECN	COMMENT
>190	95	[155]	ABBIENDI	02G	OPAL	$e^+e^- \to \mu\mu^*$
• • • We do not use the following data for averages, fits, limits, etc. • • •						
>180	95	[156]	ACHARD	03B	L3	$e^+e^- \to \mu\mu^*$
>178	95	[157]	ACCIARRI	01D	L3	$e^+e^- \to \mu\mu^*$
		[158]	ABBIENDI	00I	OPAL	$e^+e^- \to \mu\mu^*$
		[159]	ACCIARRI	00E	L3	$e^+e^- \to \mu\mu^*$
		[160]	ABREU	99O	DLPH	$e^+e^- \to \mu\mu^*$
		[161]	ACKERSTAFF	98C	OPAL	$e^+e^- \to \mu\mu^*$
		[162]	BARATE	98U	ALEP	$Z \to \mu\mu^*$
	163,164		ABREU	97B	DLPH	$e^+e^- \to \mu\mu^*$
	163,165		ACCIARRI	97G	L3	$e^+e^- \to \mu\mu^*$
		[166]	ACKERSTAFF	97	OPAL	$e^+e^- \to \mu\mu^*$
		[167]	ABREU	96K	DLPH	$e^+e^- \to \mu\mu^*$
		[168]	ACCIARRI	96D	L3	$e^+e^- \to \mu\mu^*$
		[169]	ALEXANDER	96Q	OPAL	$e^+e^- \to \mu\mu^*$
		[170]	BUSKULIC	96W	ALEP	$e^+e^- \to \mu\mu^*$
> 89	95		ADRIANI	93M	L3	$Z \to \mu\mu^*$, $\lambda_Z > 0.5$
> 88	95		ABREU	92C	DLPH	$Z \to \mu\mu^*$, $\lambda_Z > 0.5$
> 91	95		DECAMP	92	ALEP	$Z \to \mu\mu^*$, $\lambda_Z > 1$
> 85	95	[171]	ADEVA	90F	L3	$Z \to \mu\mu^*$, $\lambda_Z > 1$
> 75	95	[171]	ADEVA	90F	L3	$Z \to \mu\mu^*$, $\lambda_Z > 0.1$
> 87	95		AKRAWY	90I	OPAL	$Z \to \mu\mu^*$, $\lambda_Z > 1$
> 80	95	[172]	DECAMP	90G	ALEP	$e^+e^- \to \mu\mu^*$, $\lambda_Z = 1$
> 50	95		ADACHI	89B	TOPZ	$e^+e^- \to \mu\mu^*$, $\lambda_\gamma = 0.7$
> 46	95		KIM	89	AMY	$e^+e^- \to \mu\mu^*$, $\lambda_\gamma = 0.2$

[155] ABBIENDI 02G result is from e^+e^- collisions at $\sqrt{s} = 183$–209 GeV. $f = f' = \Lambda/m_{\mu^*}$ is assumed for μ^* coupling. See their Fig. 4c for the exclusion limit in the mass-coupling plane.

[156] ACHARD 03B result is from e^+e^- collisions at $\sqrt{s} = 189$–209 GeV. $f = f' = \Lambda/m_{\mu^*}$ is assumed. See their Fig. 4 for the exclusion plot in the mass-coupling plane.

[157] ACCIARRI 01D result is from e^+e^- collisions at $\sqrt{s} = 192$–202 GeV. $f=f'=\Lambda/m_{\mu^*}$ is assumed for the μ^* coupling. See their Fig. 4 for limits in the mass-coupling plane.

[158] ABBIENDI 00I result is from e^+e^- collisions at $\sqrt{s}$=161–183 GeV. See their Fig. 7 for limits in mass-coupling plane.

[159] ACCIARRI 00E result is from e^+e^- collisions at $\sqrt{s}$=189 GeV. See their Fig. 3 for limits in mass-coupling plane.

[160] ABREU 99O result is from e^+e^- collisions at $\sqrt{s}$= 183 GeV. See their Figs. 4 and 5 for the exclusion limit in the mass-coupling plane.

[161] ACKERSTAFF 98C from e^+e^- collisions at $\sqrt{s}$=170–172 GeV. See their Fig. 11 for the exclusion limit in the mass-coupling plane.

[162] BARATE 98U obtain limits on the $Z\mu\mu^*$ coupling. See their Fig. 12 for limits in mass-coupling plane

[163] From e^+e^- collisions at $\sqrt{s}$= 161 GeV.

[164] See Fig. 4a and Fig. 5a of ABREU 97B for the exclusion limit in the mass-coupling plane.

[165] See Fig. 2 and Fig. 3 of ACCIARRI 97G for the exclusion limit in the mass-coupling plane.

[166] ACKERSTAFF 97 result is from e^+e^- collisions at $\sqrt{s}$= 161 GeV. See their Fig. 3 for the exclusion limit in the mass-coupling plane.

[167] ABREU 96K result is from e^+e^- collisions at $\sqrt{s}$= 130–136 GeV. See their Fig. 4 for the exclusion limit in the mass-coupling plane.

[168] ACCIARRI 96D result is from e^+e^- collisions at $\sqrt{s}$= 130–140 GeV. See their Fig. 2 for the exclusion limit in the mass-coupling plane.

[169] ALEXANDER 96Q result is from e^+e^- collisions at $\sqrt{s}$= 130–140 GeV. See their Fig. 3a for the exclusion limit in the mass-coupling plane.

[170] BUSKULIC 96W result is from e^+e^- collisions at $\sqrt{s}$= 130–140 GeV. See their Fig. 3 for the exclusion limit in the mass-coupling plane.

[171] Superseded by ADRIANI 93M.

[172] Superseded by DECAMP 92.

Indirect Limits for Excited μ (μ^*)

These limits make use of loop effects involving μ^* and are therefore subject to theoretical uncertainty.

VALUE (GeV)	DOCUMENT ID		TECN	COMMENT
• • • We do not use the following data for averages, fits, limits, etc. • • •				
	[173] RENARD	82	THEO	$g-2$ of muon

[173] RENARD 82 derived from $g-2$ data limits on mass and couplings of e^* and μ^*. See figures 2 and 3 of the paper.

MASS LIMITS for Excited τ (τ^*)

Limits for Excited τ (τ^*) from Pair Production

These limits are obtained from $e^+e^- \to \tau^{*+}\tau^{*-}$ and thus rely only on the (electroweak) charge of τ^*. Form factor effects are ignored unless noted. For the case of limits from Z decay, the τ^* coupling is assumed to be of sequential type. All limits assume a dominant $\tau^* \to \tau\gamma$ decay except the limits from $\Gamma(Z)$.

For limits prior to 1987, see our 1992 edition (Physical Review **D45,** 1 June, Part II (1992)).

VALUE (GeV)	CL%	DOCUMENT ID		TECN	COMMENT
>103.2	95	[174] ABBIENDI	02G	OPAL	$e^+e^- \to \tau^*\tau^*$ Homodoublet type
• • • We do not use the following data for averages, fits, limits, etc. • • •					
>102.8	95	[175] ACHARD	03B	L3	$e^+e^- \to \tau^*\tau^*$ Homodoublet type
> 99.8	95	[176] ACCIARRI	01D	L3	$e^+e^- \to \tau^*\tau^*$ Homodoublet type
> 91.2	95	[177] ABBIENDI	00I	OPAL	$e^+e^- \to \tau^*\tau^*$ Homodoublet type
> 94.2	95	[178] ACCIARRI	00E	L3	$e^+e^- \to \tau^*\tau^*$ Homodoublet type
> 89.7	95	[179] ABREU	99O	DLPH	Homodoublet type
> 84.6	95	[180] ACKERSTAFF	98C	OPAL	$e^+e^- \to \tau^*\tau^*$ Homodoublet type
		[181] BARATE	98U	ALEP	$Z \to \tau^*\tau^*$
> 79.4	95	[182,183] ABREU	97B	DLPH	$e^+e^- \to \tau^*\tau^*$ Homodoublet type
> 77.4	95	[182,184] ABREU	97B	DLPH	$e^+e^- \to \tau^*\tau^*$ Sequential type
> 79.3	95	[182] ACCIARRI	97G	L3	$e^+e^- \to \tau^*\tau^*$ Sequential type
> 79.1	95	[182,185] ACKERSTAFF	97	OPAL	$e^+e^- \to \tau^*\tau^*$ Homodoublet type
> 62.2	95	[186] ABREU	96K	DLPH	$e^+e^- \to \tau^*\tau^*$ Homodoublet type
> 64.2	95	[187] ACCIARRI	96D	L3	$e^+e^- \to \tau^*\tau^*$ Sequential type
> 65.3	95	[187] ALEXANDER	96Q	OPAL	$e^+e^- \to \tau^*\tau^*$ Homodoublet type
> 64.8	95	[187] BUSKULIC	96W	ALEP	$e^+e^- \to \tau^*\tau^*$ Sequential type
> 45.6	95	ADRIANI	93M	L3	$Z \to \tau^*\tau^*$
> 45.3	95	ABREU	92C	DLPH	$Z \to \tau^*\tau^*$
> 29.8	95	[188] BARDADIN-...	92	RVUE	$\Gamma(Z)$
> 26.1	95	[189] DECAMP	92	ALEP	$Z \to \tau^*\tau^*$; $\Gamma(Z)$
> 46.0	95	DECAMP	92	ALEP	$Z \to \tau^*\tau^*$
> 33	95	[189] ABREU	91F	DLPH	$Z \to \tau^*\tau^*$; $\Gamma(Z)$
> 45.5	95	[190] ADEVA	90L	L3	$Z \to \tau^*\tau^*$
> 44.9	95	AKRAWY	90I	OPAL	$Z \to \tau^*\tau^*$
> 41.2	95	[191] DECAMP	90G	ALEP	$e^+e^- \to \tau^*\tau^*$
> 29.0	95	ADACHI	89B	TOPZ	$e^+e^- \to \tau^*\tau^*$

[174] From e^+e^- collisions at $\sqrt{s} = 183$–209 GeV. $f = f'$ is assumed.

[175] From e^+e^- collisions at $\sqrt{s} = 189$–209 GeV. $f = f'$ is assumed. ACHARD 03B also obtain limit for $f = -f'$: $m_{\tau^*} > 96.6$ GeV.

[176] From e^+e^- collisions at $\sqrt{s} = 192$–202 GeV. f=f' is assumed. ACCIARRI 01D also obtain limit for f=$-f'$: $m_{\tau^*} > 93.4$ GeV.

[177] From e^+e^- collisions at $\sqrt{s}$=161–183 GeV. f=f' is assumed. ABBIENDI 00I also obtain limit for f=$-f'$ ($\tau^* \to \nu W$): $m_{\tau^*} > 86.0$ GeV.

[178] From e^+e^- collisions at $\sqrt{s}$=189 GeV. f=f' is assumed. ACCIARRI 00E also obtain limit for f=$-f'$ ($\tau^* \to \nu W$): $m_{\tau^*} > 92.6$ GeV.

[179] From e^+e^- collisions at $\sqrt{s}$= 183 GeV. f=f' is assumed. ABREU 99O also obtain limit for f=$-f'$ ($\tau^* \to \nu W$): $m_{\tau^*} > 81.3$ GeV.

[180] From e^+e^- collisions at $\sqrt{s}$=170–172 GeV. ACKERSTAFF 98C also obtain limit from $\tau^* \to \nu W$ decay mode: $m_{\tau^*} > 81.3$ GeV.

[181] BARATE 98U obtain limits on the form factor. See their Fig. 14 for limits in mass-form factor plane.

[182] From e^+e^- collisions at $\sqrt{s}$= 161 GeV.

[183] ABREU 97B also obtain limit from charged current decay mode $\tau^* \to \nu W$, $m_{\tau^*} > 70.9$ GeV.

[184] ABREU 97B also obtain limit from charged current decay mode $\tau^* \to \nu W$, $m_{\tau^*} > 44.6$ GeV.

[185] ACKERSTAFF 97 also obtain limit from charged current decay mode $\tau^* \to \nu W$, $m_{\nu^*_\tau} > 77.1$ GeV.

[186] From e^+e^- collisions at $\sqrt{s}$= 130–136 GeV.

[187] From e^+e^- collisions at $\sqrt{s}$= 130–140 GeV.

[188] BARDADIN-OTWINOWSKA 92 limit is independent of decay modes. Based on $\Delta\Gamma(Z)$<36 MeV.

[189] Limit is independent of τ^* decay mode.

[190] Superseded by ADRIANI 93M.

[191] Superseded by DECAMP 92.

Limits for Excited τ (τ^*) from Single Production

These limits are from $e^+e^- \to \tau^*\tau$ and depend on transition magnetic coupling between τ and τ^*. All limits assume $\tau^* \to \tau\gamma$ decay. Limits from LEP are for chiral coupling, whereas all other limits are for nonchiral coupling, $\eta_L = \eta_R = 1$. In most papers, the limit is expressed in the form of an excluded region in the λ–m_{τ^*} plane. See the original papers.

VALUE (GeV)	CL%	DOCUMENT ID		TECN	COMMENT
>185	95	[192] ABBIENDI	02G	OPAL	$e^+e^- \to \tau\tau^*$
• • • We do not use the following data for averages, fits, limits, etc. • • •					
>180	95	[193] ACHARD	03B	L3	$e^+e^- \to \tau\tau^*$
>173	95	[194] ACCIARRI	01D	L3	$e^+e^- \to \tau\tau^*$
		[195] ABBIENDI	00I	OPAL	$e^+e^- \to \tau\tau^*$
		[196] ACCIARRI	00E	L3	$e^+e^- \to \tau\tau^*$
		[197] ABREU	99O	DLPH	$e^+e^- \to \tau\tau^*$
		[198] ACKERSTAFF	98C	OPAL	$e^+e^- \to \tau\tau^*$
		[199] BARATE	98U	ALEP	$Z \to \tau\tau^*$
		[200,201] ABREU	97B	DLPH	$e^+e^- \to \tau\tau^*$
		[200,202] ACCIARRI	97G	L3	$e^+e^- \to \tau\tau^*$
		[203] ACKERSTAFF	97	OPAL	$e^+e^- \to \tau\tau^*$
		[204] ABREU	96K	DLPH	$e^+e^- \to \tau\tau^*$
		[205] ACCIARRI	96D	L3	$e^+e^- \to \tau\tau^*$
		[206] ALEXANDER	96Q	OPAL	$e^+e^- \to \tau\tau^*$
		[207] BUSKULIC	96W	ALEP	$e^+e^- \to \tau\tau^*$
> 88	95	ADRIANI	93M	L3	$Z \to \tau\tau^*$, $\lambda_Z > 0.5$
> 87	95	ABREU	92C	DLPH	$Z \to \tau\tau^*$, $\lambda_Z > 0.5$
> 90	95	DECAMP	92	ALEP	$Z \to \tau\tau^*$, $\lambda_Z > 0.18$
> 88	95	[208] ADEVA	90L	L3	$Z \to \tau\tau^*$, $\lambda_Z > 1$
> 86.5	95	AKRAWY	90I	OPAL	$Z \to \tau\tau^*$, $\lambda_Z > 1$
> 59	95	[209] DECAMP	90G	ALEP	$Z \to \tau\tau^*$, λ_Z=1
> 40	95	[210] BARTEL	86	JADE	$e^+e^- \to \tau\tau^*$, λ_γ=1
> 41.4	95	[211] BEHREND	86	CELL	$e^+e^- \to \tau\tau^*$, λ_γ=1
> 40.8	95	[211] BEHREND	86	CELL	$e^+e^- \to \tau\tau^*$, λ_γ=0.7

[192] ABBIENDI 02G result is from e^+e^- collisions at $\sqrt{s} = 183$–209 GeV. $f = f' = \Lambda/m_{\tau^*}$ is assumed for τ^* coupling. See their Fig. 4c for the exclusion limit in the mass-coupling plane.

[193] ACHARD 03B result is from e^+e^- collisions at $\sqrt{s} = 189$–209 GeV. $f = f' = \Lambda/m_{\tau^*}$ is assumed. See their Fig. 4 for the exclusion plot in the mass-coupling plane.

[194] ACCIARRI 01D result is from e^+e^- collisions at $\sqrt{s} = 192$–202 GeV. f=f'=Λ/m_{τ^*} is assumed for the τ^* coupling. See their Fig. 4 for limits in the mass-coupling plane.

[195] ABBIENDI 00I result is from e^+e^- collisions at $\sqrt{s}$=161–183 GeV. See their Fig. 7 for limits in mass-coupling plane.

[196] ACCIARRI 00E result is from e^+e^- collisions at $\sqrt{s}$=189 GeV. See their Fig. 3 for limits in mass-coupling plane.

[197] ABREU 99O result is from e^+e^- collisions at $\sqrt{s}$= 183 GeV. See their Figs. 4 and 5 for the exclusion limit in the mass-coupling plane.

[198] ACKERSTAFF 98C from e^+e^- collisions at $\sqrt{s}$=170–172 GeV. See their Fig. 11 for the exclusion limit in the mass-coupling plane.

[199] BARATE 98U obtain limits on the $Z\tau\tau^*$ coupling. See their Fig. 12 for limits in mass-coupling plane

[200] From e^+e^- collisions at $\sqrt{s}$= 161 GeV.

[201] See Fig. 4a and Fig. 5a of ABREU 97B for the exclusion limit in the mass-coupling plane.

[202] See Fig. 2 and Fig. 3 of ACCIARRI 97G for the exclusion limit in the mass-coupling plane.

[203] ACKERSTAFF 97 result is from e^+e^- collisions at $\sqrt{s}$= 161 GeV. See their Fig. 3 for the exclusion limit in the mass-coupling plane.

[204] ABREU 96K result is from e^+e^- collisions at $\sqrt{s}$= 130–136 GeV. See their Fig. 4 for the exclusion limit in the mass-coupling plane.

[205] ACCIARRI 96D result is from e^+e^- collisions at $\sqrt{s}$= 130–140 GeV. See their Fig. 2 for the exclusion limit in the mass-coupling plane.

[206] ALEXANDER 96Q result is from e^+e^- collisions at $\sqrt{s}$= 130–140 GeV. See their Fig. 3a for the exclusion limit in the mass-coupling plane.

[207] BUSKULIC 96W result is from e^+e^- collisions at $\sqrt{s}$= 130–140 GeV. See their Fig. 3 for the exclusion limit in the mass-coupling plane.

[208] Superseded by ADRIANI 93M.

[209] Superseded by DECAMP 92.

[210] BARTEL 86 is at E_{cm} = 30–46.78 GeV.

[211] BEHREND 86 limit is at E_{cm} = 33–46.8 GeV.

MASS LIMITS for Excited Neutrino (ν^*)

Limits for Excited ν (ν^*) from Pair Production

These limits are obtained from $e^+e^- \to \nu^*\nu^*$ and thus rely only on the (electroweak) charge of ν^*. Form factor effects are ignored unless noted. The ν^* coupling is assumed to be of sequential type unless otherwise noted. All limits assume a dominant $\nu^* \to \nu\gamma$ decay except the limits from $\Gamma(Z)$.

VALUE (GeV)	CL%	DOCUMENT ID		TECN	COMMENT
>102.6	95	[212] ACHARD	03B	L3	$e^+e^- \to \nu^*\nu^*$ Homodoublet type
• • • We do not use the following data for averages, fits, limits, etc. • • •					
> 99.4	95	[213] ACCIARRI	01D	L3	$e^+e^- \to \nu^*\nu^*$ Homodoublet type
> 91.2	95	[214] ABBIENDI	00I	OPAL	$e^+e^- \to \nu^*\nu^*$ Homodoublet type
		[215] ABBIENDI,G	00D	OPAL	
> 94.1	95	[216] ACCIARRI	00E	L3	$e^+e^- \to \nu^*\nu^*$ Homodoublet type
		[217] ABBIENDI	99F	OPAL	
> 90.0	95	[218] ABREU	99O	DLPH	Homodoublet type
> 84.9	95	[219] ACKERSTAFF	98C	OPAL	$e^+e^- \to \nu^*\nu^*$ Homodoublet type
		[220] BARATE	98U	ALEP	$Z \to \nu^*\nu^*$
> 77.6	95	[221,222] ABREU	97B	DLPH	$e^+e^- \to \nu^*\nu^*$ Homodoublet type
> 64.4	95	[221,223] ABREU	97B	DLPH	$e^+e^- \to \nu^*\nu^*$ Sequential type
> 71.2	95	[221,224] ACCIARRI	97G	L3	$e^+e^- \to \nu^*\nu^*$ Sequential type

Searches Particle Listings

Quark and Lepton Compositeness

> 77.8	95	221,225	ACKERSTAFF	97	OPAL	$e^+e^- \to \nu^*\nu^*$ Homodoublet type
> 61.4	95	226,227	ACCIARRI	96D	L3	$e^+e^- \to \nu^*\nu^*$ Sequential type
> 65.0	95	228,229	ALEXANDER	96Q	OPAL	$e^+e^- \to \nu^*\nu^*$ Homodoublet type
> 63.6	95	226	BUSKULIC	96W	ALEP	$e^+e^- \to \nu^*\nu^*$ Sequential type
> 43.7	95	230	BARDADIN-...	92	RVUE	$\Gamma(Z)$
> 47	95	231	DECAMP	92	ALEP	
> 42.6	95	232	DECAMP	92	ALEP	$\Gamma(Z)$
> 35.4	95	233,234	DECAMP	90O	ALEP	$\Gamma(Z)$
> 46	95	234,235	DECAMP	90O	ALEP	

[212] From e^+e^- collisions at $\sqrt{s} = 189$–209 GeV. $f = -f'$ is assumed. ACHARD 03B also obtain limit for $f = f'$: $m_{\nu_e^*} > 101.7$ GeV, $m_{\nu_\mu^*} > 101.8$ GeV, and $m_{\nu_\tau^*} > 92.9$ GeV. See their Fig. 4 for the exclusion plot in the mass-coupling plane.

[213] From e^+e^- collisions at $\sqrt{s} = 192$–202 GeV. f=f' is assumed. ACCIARRI 01D also obtain limit for f=$-f'$: $m_{\nu_e^*} > 99.1$ GeV, $m_{\nu_\mu^*} > 99.3$ GeV, $m_{\nu_\tau^*} > 90.5$ GeV.

[214] From e^+e^- collisions at $\sqrt{s}$=161–183 GeV. f=$-f'$ (photonic decay) is assumed. ABBIENDI 00I also obtain limit for f=f' ($\nu^* \to \ell W$): $m_{\nu_e^*} > 91.1$ GeV, $m_{\nu_\mu^*} > 91.1$ GeV, $m_{\nu_\tau^*} > 83.1$ GeV.

[215] From e^+e^- collisions at $\sqrt{s}$= 189 GeV. ABBIENDI,G 00D obtain limit on $\sigma(e^+e^- \to \nu^*\nu^*)B(\nu^* \to \nu\gamma)^2$. See their Fig. 14. The limit ranges from 50 to 80 fb for $\sqrt{s}/2$= 95 GeV> m_{ν^*} >45 GeV.

[216] From e^+e^- collisions at $\sqrt{s}$=189 GeV. f=$-f'$ (photonic decay) is assumed. ACCIARRI 00E also obtain limit for f=f' ($\nu^* \to \ell W$): $m_{\nu_e^*} > 93.9$ GeV, $m_{\nu_\mu^*} > 94.0$ GeV, $m_{\nu_\tau^*} > 91.5$ GeV.

[217] From e^+e^- collisions at $\sqrt{s}$= 130–183 GeV, ABBIENDI 99F obtain limit on $\sigma(e^+e^- \to \nu^*\nu^*)$ B($\nu^* \to \nu\gamma)^2$. See their Fig. 13. The limit ranges from 0.094 to 0.14 pb for $\sqrt{s}/2 > m_{\nu^*} >$ 45 GeV.

[218] From e^+e^- collisions at $\sqrt{s}$= 183 GeV. f=$-f'$ is assumed. ABREU 99O also obtain limit for f=f': $m_{\nu_{e^*}} > 87.3$ GeV, $m_{\nu_{\mu^*}} > 88.0$ GeV, $m_{\nu_{\tau^*}} > 81.0$ GeV.

[219] From e^+e^- collisions at $\sqrt{s}$=170–172 GeV. ACKERSTAFF 98C also obtain limit from charged decay modes: $m_{\nu_e^*} > 84.1$ GeV, $m_{\nu_\mu^*} > 83.9$ GeV, and $m_{\nu_\tau^*} > 79.4$ GeV.

[220] BARATE 98U obtain limits on the form factor. See their Fig. 14 for limits in mass-form factor plane.

[221] From e^+e^- collisions at $\sqrt{s}$= 161 GeV.

[222] ABREU 97B also obtain limits from charged current decay modes, $m_{\nu^*} > 56.4$ GeV.

[223] ABREU 97B also obtain limits from charged current decay modes, $m_{\nu^*} > 44.9$ GeV.

[224] ACCIARRI 97G also obtain limits from charged current decay mode $\nu_e^* \to eW$, $m_{\nu^*} >$ 64.5 GeV.

[225] ACKERSTAFF 97 also obtain limits from charged current decay modes $m_{\nu_e^*} > 78.3$ GeV, $m_{\nu_\mu^*} > 78.9$ GeV, $m_{\nu_\tau^*} > 76.2$ GeV.

[226] From e^+e^- collisions at $\sqrt{s}$= 130–140 GeV.

[227] ACCIARRI 96D also obtain limit from $\nu^* \to eW$ decay mode: $m_{\nu^*} > 57.3$ GeV.

[228] From e^+e^- collisions at $\sqrt{s}$= 130–136 GeV.

[229] ALEXANDER 96Q also obtain limits from charged current decay modes: $m_{\nu_e^*} > 66.2$ GeV, $m_{\nu_\mu^*} > 66.5$ GeV, $m_{\nu_\tau^*} > 64.7$ GeV.

[230] BARDADIN-OTWINOWSKA 92 limit is for Dirac ν^*. Based on $\Delta\Gamma(Z)$<36 MeV. The limit is 36.4 GeV for Majorana ν^*, 45.4 GeV for homodoublet ν^*.

[231] Limit is based on B($Z \to \nu^*\overline{\nu}^*$)×B($\nu^* \to \nu\gamma)^2 < 5 \times 10^{-5}$ (95%CL) assuming Dirac ν^*, B($\nu^* \to \nu\gamma$) = 1.

[232] Limit is for Dirac ν^*. The limit is 34.6 GeV for Majorana ν^*, 45.4 GeV for homodoublet ν^*.

[233] DECAMP 90O limit is from excess $\Delta\Gamma(Z) < 89$ MeV. The above value is for Dirac ν^*; 26.6 GeV for Majorana ν^*; 44.8 GeV for homodoublet ν^*.

[234] Superseded by DECAMP 92.

[235] DECAMP 90O limit based on B($Z \to \nu^*\nu^*$)·B($\nu^* \to \nu\gamma)^2 < 7 \times 10^{-5}$ (95%CL), assuming Dirac ν^*, B($\nu^* \to \nu\gamma$) = 1.

Limits for Excited ν (ν^*) from Single Production

These limits are from $e^+e^- \to \nu\nu^*$, $Z \to \nu\nu^*$, or $ep \to \nu^*X$ and depend on transition magnetic coupling between ν/e and ν^*. Assumptions about ν^* decay mode are given in footnotes.

VALUE (GeV)	CL%	DOCUMENT ID		TECN	COMMENT
>190	95	[236] ACHARD	03B	L3	$e^+e^- \to \nu\nu^*$
• • • We do not use the following data for averages, fits, limits, etc. • • •					
none 50–150	95	[237] ADLOFF	02	H1	$ep \to \nu^*X$
>158	95	[238] CHEKANOV	02D	ZEUS	$ep \to \nu^*X$
>171	95	[239] ACCIARRI	01D	L3	$e^+e^- \to \nu\nu^*$
		[240] ABBIENDI	00I	OPAL	$e^+e^- \to \nu\nu^*$
		[241] ABBIENDI,G	00D	OPAL	
		[242] ACCIARRI	00E	L3	$e^+e^- \to \nu\nu^*$
>114	95	[243] ADLOFF	00E	H1	$ep \to \nu^*X$
		[244] ABBIENDI	99F	OPAL	
		[245] ABREU	99O	DLPH	$e^+e^- \to \nu\nu^*$
		[246] ACKERSTAFF	98C	OPAL	$e^+e^- \to \nu^*\nu^*$ Homodoublet type
		[247] BARATE	98U	ALEP	$Z \to \nu\nu^*$
		[248,249] ABREU	97B	DLPH	$e^+e^- \to \nu\nu^*$
		[250] ABREU	97I	DLPH	$\nu^* \to \ell W, \nu Z$
		[251] ABREU	97J	DLPH	$\nu^* \to \nu\gamma$
		[248,252] ACCIARRI	97G	L3	$e^+e^- \to \nu\nu^*$
		[253] ACKERSTAFF	97	OPAL	$e^+e^- \to \nu\nu^*$
		[254] ADLOFF	97	H1	Lepton-flavor violation
none 40–96	95	[255] BREITWEG	97C	ZEUS	$ep \to \nu^*X$
		[256] ACCIARRI	96D	L3	$e^+e^- \to \nu\nu^*$
		[257] ALEXANDER	96Q	OPAL	$e^+e^- \to \nu\nu^*$
		[258] BUSKULIC	96W	ALEP	$e^+e^- \to \nu\nu^*$
		[259] DERRICK	95B	ZEUS	$ep \to \nu^*X$
		[260] ABT	93	H1	$ep \to \nu^*X$
> 91	95	ADRIANI	93M	L3	$\lambda_Z > 1$, $\nu^* \to \nu\gamma$
> 89	95	ADRIANI	93M	L3	$\lambda_Z > 1$, $\nu_e^* \to eW$
> 87	95	ADRIANI	93M	L3	$\lambda_Z > 0.1$, $\nu^* \to \nu\gamma$
> 74	95	ADRIANI	93M	L3	$\lambda_Z > 0.1$, $\nu_e^* \to eW$
		[261] BARDADIN-...	92	RVUE	
> 91	95	[262] DECAMP	92	ALEP	$\lambda_Z > 1$
> 74	95	[262] DECAMP	92	ALEP	$\lambda_Z > 0.034$
> 91	95	[263,264] ADEVA	90O	L3	$\lambda_Z > 1$
> 83	95	[264] ADEVA	90O	L3	$\lambda_Z > 0.1$, $\nu^* \to \nu\gamma$
> 74	95	[264] ADEVA	90O	L3	$\lambda_Z > 0.1$, $\nu_e^* \to eW$
> 90	95	[265,266] DECAMP	90O	ALEP	$\lambda_Z > 1$
> 74.7	95	[265,266] DECAMP	90O	ALEP	$\lambda_Z > 0.06$

[236] ACHARD 03B result is from e^+e^- collisions at $\sqrt{s} = 189$–209 GeV. The quoted limit is for ν_e^*. $f = -f' = \Lambda/m_{\nu^*}$ is assumed. See their Fig. 4 for the exclusion plot in the mass-coupling plane.

[237] ADLOFF 02 search for single ν^* production in ep collisions with the decays $\nu^* \to \nu\gamma$, νZ, eW. The quoted limit assumes $f = -f' = \Lambda/m_{\nu^*}$. See their Fig. 1 for the exclusion plots in the mass-coupling plane.

[238] CHEKANOV 02D search for single ν^* production in ep collisions with the decays $\nu^* \to \nu\gamma$, νZ, eW. $f = -f' = \Lambda/m_{\nu^*}$ is assumed for the e^* coupling. CHEKANOV 02D also obtain limit for $f = f' = \Lambda/m_{\nu^*}$: $m_{\nu^*} >$135 GeV. See their Fig. 5c and Fig. 5d for the exclusion plot in the mass-coupling plane.

[239] ACCIARRI 01D search for $\nu\nu^*$ production in e^+e^- collisions at $\sqrt{s} = 192$–202 GeV with decays $\nu^* \to \nu\gamma$, $\nu^* \to eW$. f=$-f'$=Λ/m_{ν^*} is assumed for the ν^* coupling. See their Fig. 4 for limits in the mass-coupling plane.

[240] ABBIENDI 00I result is from e^+e^- collisions at $\sqrt{s}$=161–183 GeV. See their Fig. 7 for limits in mass-coupling plane.

[241] From e^+e^- collisions at $\sqrt{s}$= 189 GeV. ABBIENDI,G 00D obtain limit on $\sigma(e^+e^- \to \nu^*\nu^*)$B($\nu^* \to \nu\gamma)^2$. See their Fig. 11.

[242] ACCIARRI 00E result is from e^+e^- collisions at $\sqrt{s}$=189 GeV. See their Fig. 3 for limits in mass-coupling plane.

[243] ADLOFF 00E search for single ν^* production in ep collisions with the decays $\nu^* \to \nu\gamma$, νZ, eW. The quoted limit assumes f=$-f'$=Λ/m_{ν^*}. See their Fig. 10 for the exclusion plot in the mass-coupling plane.

[244] From e^+e^- collisions at $\sqrt{s}$= 130–183 GeV, ABBIENDI 99F obtain limit on $\sigma(e^+e^- \to \nu\nu^*)$ B($\nu^* \to \nu\gamma$). See their Fig. 8.

[245] ABREU 99O result is from e^+e^- collisions at $\sqrt{s}$= 183 GeV. See their Figs. 4 and 5 for the exclusion limit in the mass-coupling plane.

[246] ACKERSTAFF 98C from e^+e^- collisions at $\sqrt{s}$=170–172 GeV. See their Fig. 11 for the exclusion limit in the mass-coupling plane.

[247] BARATE 98U obtain limits on the $Z\nu\nu^*$ coupling. See their Fig. 13 for limits in mass-coupling plane

[248] From e^+e^- collisions at $\sqrt{s}$= 161 GeV.

[249] See Fig. 4b and Fig. 5b of ABREU 97B for the exclusion limit in the mass-coupling plane.

[250] ABREU 97I limit is from $Z \to \nu\nu^*$. See their Fig. 12 for the exclusion limit in the mass-coupling plane.

[251] ABREU 97J limit is from $Z \to \nu\nu^*$. See their Fig. 5 for the exclusion limit in the mass-coupling plane.

[252] See Fig. 2 and Fig. 3 of ACCIARRI 97G for the exclusion limit in the mass-coupling plane.

[253] ACKERSTAFF 97 result is from e^+e^- collisions at $\sqrt{s}$= 161 GeV, for homodoublet ν^*. See their Fig. 3 for the exclusion limit in the mass-coupling plane.

[254] ADLOFF 97 search for single e^* production in ep collisions with the decays $e^* \to e\gamma$, eZ, νW. See their Fig. 4 for the rejection limits on the product of the production cross section and the branching ratio.

[255] BREITWEG 97C search for single ν^* production in ep collisions with the decay $\nu^* \to \nu\gamma$. f=$-f'$=$2\Lambda/m_{\nu^*}$ is assumed for the ν^* coupling. See their Fig. 10 for the exclusion plot in the mass-coupling plane.

[256] ACCIARRI 96D result is from e^+e^- collisions at $\sqrt{s}$= 130–140 GeV. See their Fig. 2 for the exclusion limit in the mass-coupling plane.

[257] ALEXANDER 96Q result is from e^+e^- collisions at $\sqrt{s}$= 130–140 GeV for homodoublet ν^*. See their Fig. 3b and Fig. 3c for the exclusion limit in the mass-coupling plane.

[258] BUSKULIC 96W result is from e^+e^- collisions at $\sqrt{s}$= 130–140 GeV. See their Fig. 4 for the exclusion limit in the mass-coupling plane.

[259] DERRICK 95B search for single ν^* production via ν^*eW coupling in ep collisions with the decays $\nu^* \to \nu\gamma$, νZ, eW. See their Fig. 14 for the exclusion plot in the m_{ν^*}–$\lambda\gamma$ plane.

[260] ABT 93 search for single ν^* production via ν^*eW coupling in ep collisions with the decays $\nu^* \to \nu\gamma$, νZ, eW. See their Fig. 4 for exclusion plot in the m_{ν^*}–λ_W plane.

[261] See Fig. 5 of BARDADIN-OTWINOWSKA 92 for combined limit of ADEVA 90O, DECAMP 90O, and DECAMP 92.

[262] DECAMP 92 limit is based on B($Z \to \nu^*\overline{\nu}$)×B($\nu^* \to \nu\gamma) < 2.7 \times 10^{-5}$ (95%CL) assuming Dirac ν^*, B($\nu^* \to \nu\gamma$) = 1.

[263] Limit is either for $\nu^* \to \nu\gamma$ or $\nu^* \to eW$.

[264] Superseded by ADRIANI 93M.

[265] DECAMP 90O limit based on B($Z \to \nu\nu^*$)·B($\nu^* \to \nu\gamma) < 6 \times 10^{-5}$ (95%CL), assuming B($\nu^* \to \nu\gamma$) = 1.

[266] Superseded by DECAMP 92.

MASS LIMITS for Excited q (q^*)

Limits for Excited q (q^*) from Pair Production

These limits are obtained from $e^+e^- \to q^*\overline{q}^*$ and thus rely only on the (electroweak) charge of the q^*. Form factor effects are ignored unless noted. Assumptions about the q^* decay are given in the comments and footnotes.

VALUE (GeV)	CL%	DOCUMENT ID		TECN	COMMENT
>45.6	95	[267] ADRIANI	93M	L3	u or d type, $Z \to q^*q^*$
• • • We do not use the following data for averages, fits, limits, etc. • • •					
		[268] BARATE	98U	ALEP	$Z \to q^*q^*$
		[269] ADRIANI	92F	L3	$Z \to q^*q^*$
>41.7	95	[270] BARDADIN-...	92	RVUE	u-type, $\Gamma(Z)$
>44.7	95	[270] BARDADIN-...	92	RVUE	d-type, $\Gamma(Z)$
>40.6	95	[271] DECAMP	92	ALEP	u-type, $\Gamma(Z)$
>44.2	95	[271] DECAMP	92	ALEP	d-type, $\Gamma(Z)$
>45	95	[272] DECAMP	92	ALEP	u or d type, $Z \to q^*q^*$
>45	95	[271] ABREU	91F	DLPH	u-type, $\Gamma(Z)$
>45	95	[271] ABREU	91F	DLPH	d-type, $\Gamma(Z)$
>21.1	95	[273] BEHREND	86C	CELL	$e(q^*) = -1/3$, $q^* \to qg$
>22.3	95	[273] BEHREND	86C	CELL	$e(q^*) = 2/3$, $q^* \to qg$
>22.5	95	[273] BEHREND	86C	CELL	$e(q^*) = -1/3$, $q^* \to q\gamma$
>23.2	95	[273] BEHREND	86C	CELL	$e(q^*) = 2/3$, $q^* \to q\gamma$

[267] ADRIANI 93M limit is valid for $B(q^* \to qg) > 0.25$ (0.17) for up (down) type.

[268] BARATE 98U obtain limits on the form factor. See their Fig. 16 for limits in mass-form factor plane.

[269] ADRIANI 92F search for $Z \to q^*\overline{q}^*$ followed with $q^* \to q\gamma$ decays and give the limit $\sigma_Z \cdot B(Z \to q^*\overline{q}^*) \cdot B^2(q^* \to q\gamma) < 2$ pb at 95%CL. Assuming five flavors of degenerate q^* of homodoublet type, $B(q^* \to q\gamma) < 4\%$ is obtained for $m_{q^*} < 45$ GeV.

[270] BARDADIN-OTWINOWSKA 92 limit based on $\Delta\Gamma(Z) < 36$ MeV.

[271] These limits are independent of decay modes.

[272] Limit is for $B(q^* \to qg) + B(q^* \to q\gamma) = 1$.

[273] BEHREND 86C search for $e^+e^- \to q^*\overline{q}^*$ for $m_{q^*} > 5$ GeV. But $m < 5$ GeV excluded by total hadronic cross section. The limits are for point-like photon couplings of excited quarks.

Limits for Excited q (q^*) from Single Production

These limits are from $e^+e^- \to q^*\overline{q}$ or $p\overline{p} \to q^*X$ and depend on transition magnetic couplings between q and q^*. Assumptions about q^* decay mode are given in the footnotes and comments.

VALUE (GeV)	CL%	DOCUMENT ID		TECN	COMMENT
> 570, none 580–760 (CL = 95%) OUR EVALUATION					
none 200–520 and **580–760**	95	[274] ABE	97G	CDF	$p\overline{p} \to q^*X$, $q^* \to 2$ jets
none 80–570	95	[275] ABE	95N	CDF	$p\overline{p} \to q^*X$, $q^* \to qg$, $q\gamma$, qW
>288	90	[276] ALITTI	93	UA2	$p\overline{p} \to q^*X$, $q^* \to qg$
• • • We do not use the following data for averages, fits, limits, etc. • • •					
>205	95	[277] CHEKANOV	02D	ZEUS	$ep \to q^*X$
>188	95	[278] ADLOFF	00E	H1	$ep \to q^*X$
		[279] ABREU	99O	DLPH	$e^+e^- \to qq^*$
		[280] BARATE	98U	ALEP	$Z \to qq^*$
		[281] ADLOFF	97	H1	Lepton-flavor violation
none 40–169	95	[282] BREITWEG	97C	ZEUS	$ep \to q^*X$
		[283] DERRICK	95B	ZEUS	$ep \to q^*X$
none 80–540	95	[284] ABE	94	CDF	$p\overline{p} \to q^*X$, $q^* \to q\gamma$, qW
> 79	95	[285] ADRIANI	93M	L3	$\lambda_Z(L3) > 0.06$
		[286] ABREU	92D	DLPH	$Z \to qq^*$
		[287] ADRIANI	92F	L3	$Z \to qq^*$
> 75	95	[285] DECAMP	92	ALEP	$Z \to qq^*$, $\lambda_Z > 1$
> 88	95	[288] DECAMP	92	ALEP	$Z \to qq^*$, $\lambda_Z > 1$
> 86	95	[288] AKRAWY	90J	OPAL	$Z \to qq^*$, $\lambda_Z > 1.2$
		[289] ALBAJAR	89	UA1	$p\overline{p} \to q^*X$, $q^* \to qW$
> 39	95	[290] BEHREND	86C	CELL	$e^+e^- \to q^*\overline{q}$ ($q^* \to qg, q\gamma$), $\lambda_\gamma = 1$

[274] ABE 97G search for new particle decaying to dijets.

[275] ABE 95N assume a degenerate u^* and d^* with $f_s = f = f' = \Lambda/m_{q^*}$. See their Fig. 4 for the excluded region in $m_{q^*} - f$ plane.

[276] ALITTI 93 search for resonances in the two-jet invariant mass. The limit is for $f_s = f = f' = \Lambda/m_{q^*}$. u^* and d^* are assumed to be degenerate. If not, the limit for u^* (d^*) is 277 (247) GeV if $m_{d^*} \gg m_{u^*}$ ($m_{u^*} \gg m_{d^*}$).

[277] CHEKANOV 02D search for single q^* production in ep collisions with the decays $q^* \to q\gamma$, qZ, qW. $f_s = 0$ and $f = f' = \Lambda/m_{q^*}$ is assumed for the q^* coupling. See their Fig. 5b for the exclusion plot in the mass-coupling plane.

[278] ADLOFF 00E search for single q^* production in ep collisions with the decays $q^* \to q\gamma$, qZ, qW. $f_s = 0$ and $f = f' = \Lambda/m_{q^*}$ is assumed for the q^* coupling. See their Fig. 11 for the exclusion plot in the mass-coupling plane.

[279] ABREU 99O result is from e^+e^- collisions at $\sqrt{s} = 183$ GeV. See their Fig. 6 for the exclusion limit in the mass-coupling plane.

[280] BARATE 98U obtain limits on the Zqq^* coupling. See their Fig. 16 for limits in mass-coupling plane

[281] ADLOFF 97 search for single q^* production in ep collisions with the decay $q^* \to q\gamma$. See their Fig. 6 for the rejection limits on the product of the production cross section and the branching ratio.

[282] BREITWEG 97C search for single q^* production in ep collisions with the decays $q^* \to q\gamma$, qW. $f_s = 0$, and $f = -f' = 2\Lambda/m_{q^*}$ is assumed for the q^* coupling. See their Fig. 11 for the exclusion plot in the mass-coupling plane.

[283] DERRICK 95B search for single q^* production via $q^*q\gamma$ coupling in ep collisions with the decays $q^* \to qW$, qZ, qg, $q\gamma$. See their Fig. 15 for the exclusion plot in the $m_{q^*} - \lambda\gamma$ plane.

[284] ABE 94 search for resonances in jet-γ and jet-W invariant mass in $p\overline{p}$ collisions at $E_{cm} = 1.8$ TeV. The limit is for $f_s = f = f' = \Lambda/m_{q^*}$ and u^* and d^* are assumed to be degenerate. See their Fig. 4 for the excluded region in $m_{q^*} - f$ plane.

[285] Assumes $B(q^* \to qg) = 1$.

[286] ABREU 92D give $\sigma(e^+e^- \to Z \to q^*\overline{q}$ or $q\overline{q}^*) \times B(q^* \to q\gamma) < 15$ pb (95% CL) for $m_{q^*} < 80$ GeV.

[287] ADRIANI 92F search for $Z \to qq^*$ with $q^* \to q\gamma$ and give the limit $\sigma_Z \cdot B(Z \to qq^*) \cdot B(q^* \to q\gamma) < (2$–$10)$ pb (95%CL) for $m_{q^*} = (46$–$82)$ GeV.

[288] Assumes $B(q^* \to q\gamma) = 0.1$.

[289] ALBAJAR 89 give $\sigma(q^* \to W + \text{jet})/\sigma(W) < 0.019$ (90% CL) for $m_{q^*} > 220$ GeV.

[290] BEHREND 86C has $E_{cm} = 42.5$–46.8 GeV. See their Fig. 3 for excluded region in the $m_{q^*} - (\lambda_\gamma/m_{q^*})^2$ plane. The limit is for $\lambda_\gamma = 1$ with $\eta_L = \eta_R = 1$.

MASS LIMITS for Color Sextet Quarks (q_6)

VALUE (GeV)	CL%	DOCUMENT ID		TECN	COMMENT
>84	95	[291] ABE	89D	CDF	$p\overline{p} \to q_6\overline{q}_6$

[291] ABE 89D look for pair production of unit-charged particles which leave the detector before decaying. In the above limit the color sextet quark is assumed to fragment into a unit-charged or neutral hadron with equal probability and to have long enough lifetime not to decay within the detector. A limit of 121 GeV is obtained for a color decuplet.

MASS LIMITS for Color Octet Charged Leptons (ℓ_8)

$\lambda \equiv m_{\ell_8}/\Lambda$

VALUE (GeV)	CL%	DOCUMENT ID		TECN	COMMENT
>86	95	[292] ABE	89D	CDF	Stable ℓ_8: $p\overline{p} \to \ell_8\overline{\ell}_8$
• • • We do not use the following data for averages, fits, limits, etc. • • •					
		[293] ABT	93	H1	e_8: $ep \to e_8X$
none 3.0–30.3	95	[294] KIM	90	AMY	e_8: $e^+e^- \to ee +$ jets
none 3.5–30.3	95	[294] KIM	90	AMY	μ_8: $e^+e^- \to \mu\mu +$ jets
		[295] KIM	90	AMY	e_8: $e^+e^- \to gg$; R
>19.8	95	[296] BARTEL	87B	JADE	e_8, μ_8, τ_8: e^+e^-; R
none 5–23.2	95	[296] BARTEL	87B	JADE	μ_8: $e^+e^- \to \mu\mu +$ jets
		[297] BARTEL	85K	JADE	e_8: $e^+e^- \to gg$; R

[292] ABE 89D look for pair production of unit-charged particles which leave the detector before decaying. In the above limit the color octet lepton is assumed to fragment into a unit-charged or neutral hadron with equal probability and to have long enough lifetime not to decay within the detector. The limit improves to 99 GeV if it always fragments into a unit-charged hadron.

[293] ABT 93 search for e_8 production via e-gluon fusion in ep collisions with $e_8 \to eg$. See their Fig. 3 for exclusion plot in the m_{e_8}–Λ plane for $m_{e_8} = 35$–220 GeV.

[294] KIM 90 is at $E_{cm} = 50$–60.8 GeV. The same assumptions as in BARTEL 87B are used.

[295] KIM 90 result $(m_{e_8}\Lambda_M)^{1/2} > 178.4$ GeV (95%CL, $\alpha_s = 0.16$ used) is subject to the same restriction as for BARTEL 85K.

[296] BARTEL 87B is at $E_{cm} = 46.3$–46.78 GeV. The limits assume ℓ_8 pair production cross sections to be eight times larger than those of the corresponding heavy lepton pair production.

[297] In BARTEL 85K, R can be affected by $e^+e^- \to gg$ via e_q exchange. Their limit $m_{e_8} > 173$ GeV (CL=95%) at $\lambda = m_{e_8}/\Lambda_M = 1$ ($\eta_L = \eta_R = 1$) is not listed above because the cross section is sensitive to the product $\eta_L\eta_R$, which should be absent in ordinary theory with electronic chiral invariance.

MASS LIMITS for Color Octet Neutrinos (ν_8)

$\lambda \equiv m_{\ell_8}/\Lambda$

VALUE (GeV)	CL%	DOCUMENT ID		TECN	COMMENT
>110	90	[298] BARGER	89	RVUE	ν_8: $p\overline{p} \to \nu_8\overline{\nu}_8$
• • • We do not use the following data for averages, fits, limits, etc. • • •					
none 3.8–29.8	95	[299] KIM	90	AMY	ν_8: $e^+e^- \to$ acoplanar jets
none 9–21.9	95	[300] BARTEL	87B	JADE	ν_8: $e^+e^- \to$ acoplanar jets

[298] BARGER 89 used ABE 89B limit for events with large missing transverse momentum. Two-body decay $\nu_8 \to \nu g$ is assumed.

[299] KIM 90 is at $E_{cm} = 50$–60.8 GeV. The same assumptions as in BARTEL 87B are used.

[300] BARTEL 87B is at $E_{cm} = 46.3$–46.78 GeV. The limit assumes the ν_8 pair production cross section to be eight times larger than that of the corresponding heavy neutrino pair production. This assumption is not valid in general for the weak couplings, and the limit can be sensitive to its $SU(2)_L \times U(1)_Y$ quantum numbers.

MASS LIMITS for W_8 (Color Octet W Boson)

VALUE (GeV)	DOCUMENT ID		TECN	COMMENT
• • • We do not use the following data for averages, fits, limits, etc. • • •				
	[301] ALBAJAR	89	UA1	$p\overline{p} \rightarrow W_8 X$, $W_8 \rightarrow Wg$

[301] ALBAJAR 89 give $\sigma(W_8 \rightarrow W + \text{jet})/\sigma(W) < 0.019$ (90% CL) for $m_{W_8} > 220$ GeV.

REFERENCES FOR Searches for Quark and Lepton Compositeness

ACHARD 03B PL B568 23 P. Achard *et al.* (L3 Collab.)
ADLOFF 03 PL B568 35 C. Adloff *et al.* (H1 Collab.)
BABICH 03 EPJ C29 103 A.A. Babich *et al.*
ABBIENDI 02G PL B544 57 G. Abbiendi *et al.* (OPAL Collab.)
ACHARD 02D PL B531 28 P. Achard *et al.* (L3 Collab.)
ACHARD 02J PL B549 290 P. Achard *et al.* (L3 Collab.)
ADLOFF 02 PL B525 9 C. Adloff *et al.* (H1 Collab.)
ADLOFF 02B PL B548 35 C. Adloff *et al.* (H1 Collab.)
CHEKANOV 02D PL B549 32 S. Chekanov *et al.* (ZEUS Collab.)
ACCIARRI 01D PL B502 37 M. Acciarri *et al.* (L3 Collab.)
AFFOLDER 01I PRL 87 231803 T. Affolder *et al.* (CDF Collab.)
BOURILKOV 01 PR D64 071701 D. Bourilkov
CHEUNG 01B PL B517 167 K. Cheung
ABBIENDI 00I EPJ C14 73 G. Abbiendi *et al.* (OPAL Collab.)
ABBIENDI 00R EPJ C13 553 G. Abbiendi *et al.* (OPAL Collab.)
ABBIENDI,G 00D EPJ C18 253 G. Abbiendi *et al.* (OPAL Collab.)
ABBOTT 00E PR D62 031101 B. Abbott *et al.* (D0 Collab.)
ABREU 00A PL B491 67 P. Abreu *et al.* (DELPHI Collab.)
ABREU 00S PL B485 45 P. Abreu *et al.* (DELPHI Collab.)
ACCIARRI 00E PL B473 177 M. Acciarri *et al.* (L3 Collab.)
ACCIARRI 00G PL B475 198 M. Acciarri *et al.* (L3 Collab.)
ACCIARRI 00P PL B489 81 M. Acciarri *et al.* (L3 Collab.)
ADLOFF 00 PL B479 358 C. Adloff *et al.* (H1 Collab.)
ADLOFF 00E EPJ C17 567 C. Adloff *et al.* (H1 Collab.)
AFFOLDER 00I PR D62 012004 T. Affolder *et al.* (CDF Collab.)
BARATE 00I EPJ C12 183 R. Barate *et al.* (ALEPH Collab.)
BOURILKOV 00 PR D62 076005 D. Bourilkov
BREITWEG 00B EPJ C14 239 J. Breitweg *et al.* (ZEUS Collab.)
ABBIENDI 99 EPJ C6 1 G. Abbiendi *et al.* (OPAL Collab.)
ABBIENDI 99F EPJ C8 23 G. Abbiendi *et al.* (OPAL Collab.)
ABBIENDI 99P PL B465 303 G. Abbiendi *et al.* (OPAL Collab.)
ABBOTT 99C PRL 82 2457 B. Abbott *et al.* (D0 Collab.)
ABBOTT 99D PRL 82 4769 B. Abbott *et al.* (D0 Collab.)
ABREU 99A EPJ C11 383 P. Abreu *et al.* (DELPHI Collab.)
ABREU 99O EPJ C8 41 P. Abreu *et al.* (DELPHI Collab.)
ZARNECKI 99 EPJ C11 539 A.F. Zarnecki
ABBOTT 98G PRL 80 666 B. Abbott *et al.* (D0 Collab.)
ABREU 98J PL B433 429 P. Abreu *et al.* (DELPHI Collab.)
ACCIARRI 98J PL B433 163 M. Acciarri *et al.* (L3 Collab.)
ACCIARRI 98T PL B439 183 M. Acciarri *et al.* (L3 Collab.)
ACKERSTAFF 98 EPJ C1 21 K. Ackerstaff *et al.* (OPAL Collab.)
ACKERSTAFF 98C EPJ C1 45 K. Ackerstaff *et al.* (OPAL Collab.)
ACKERSTAFF 98V EPJ C2 441 K. Ackerstaff *et al.* (OPAL Collab.)
ACKER...K... 98B PL B438 379 K. Ackerstaff *et al.* (OPAL Collab.)
BARATE 98J PL B429 201 R. Barate *et al.* (ALEPH Collab.)
BARATE 98U EPJ C4 571 R. Barate *et al.* (ALEPH Collab.)
BARGER 98E PR D57 391 V. Barger *et al.*
BERTRAM 98 PRL 81 3447 I. Bertram, E.H. Simmons
MCFARLAND 98 EPJ C1 509 K.S. McFarland *et al.* (CCFR/NuTeV Collab.)
MIURA 98 PR D57 5345 M. Miura *et al.* (VENUS Collab.)
ABE 97G PR D55 R5263 F. Abe *et al.* (CDF Collab.)
ABE 97T PRL 79 2198 F. Abe *et al.* (CDF Collab.)
ABREU 97B PL B393 245 P. Abreu *et al.* (DELPHI Collab.)
ABREU 97I ZPHY C74 57 P. Abreu *et al.* (DELPHI Collab.)
Also 97L ZPHY C75 580 erratum P. Abreu *et al.* (DELPHI Collab.)
ABREU 97J ZPHY C74 577 P. Abreu *et al.* (DELPHI Collab.)
ACCIARRI 97G PL B401 139 M. Acciarri *et al.* (L3 Collab.)
ACCIARRI 97W PL B413 159 M. Acciarri *et al.* (L3 Collab.)
ACKERSTAFF 97 PL B391 197 K. Ackerstaff *et al.* (OPAL Collab.)
ACKERSTAFF 97C PL B391 221 K. Ackerstaff *et al.* (OPAL Collab.)
ADLOFF 97 NP B483 44 C. Adloff *et al.* (H1 Collab.)
ARIMA 97 PR D55 19 T. Arima *et al.* (VENUS Collab.)
BREITWEG 97C ZPHY C76 631 J. Breitweg *et al.* (ZEUS Collab.)
DEANDREA 97 PL B409 277 A. Deandrea (MARS)
ABE 96 PRL 77 438 F. Abe *et al.* (CDF Collab.)
ABE 96S PRL 77 5336 F. Abe *et al.* (CDF Collab.)
ABREU 96K PL B380 480 P. Abreu *et al.* (DELPHI Collab.)
ACCIARRI 96D PL B370 211 M. Acciarri *et al.* (L3 Collab.)
ACCIARRI 96L PL B384 323 M. Acciarri *et al.* (L3 Collab.)
ALEXANDER 96K PL B377 222 G. Alexander *et al.* (OPAL Collab.)
ALEXANDER 96Q PL B381 463 G. Alexander *et al.* (OPAL Collab.)
BUSKULIC 96W PL B385 445 D. Buskulic *et al.* (ALEPH Collab.)
BUSKULIC 96Z PL B384 333 D. Buskulic *et al.* (ALEPH Collab.)
ABE 95N PRL 74 3538 F. Abe *et al.* (CDF Collab.)
ACCIARRI 95G PL B353 136 M. Acciarri *et al.* (L3 Collab.)
AID 95 PL B353 578 S. Aid *et al.* (H1 Collab.)
DERRICK 95B ZPHY C65 627 M. Derrick *et al.* (ZEUS Collab.)
ABE 94 PRL 72 3004 F. Abe *et al.* (CDF Collab.)
DIAZCRUZ 94 PR D49 R2149 J.L. Diaz Cruz, O.A. Sampayo (CINV)
VELISSARIS 94 PL B331 227 C. Velissaris *et al.* (AMY Collab.)
ABE 93G PRL 71 2542 F. Abe *et al.* (CDF Collab.)
ABT 93 NP B396 3 I. Abt *et al.* (H1 Collab.)
ADRIANI 93M PRPL 236 1 O. Adriani *et al.* (L3 Collab.)
ALITTI 93 NP B400 3 J. Alitti *et al.* (UA2 Collab.)
BUSKULIC 93Q ZPHY C59 215 D. Buskulic *et al.* (ALEPH Collab.)
DERRICK 93B PL B316 207 M. Derrick *et al.* (ZEUS Collab.)
ABE 92B PRL 68 1463 F. Abe *et al.* (CDF Collab.)
ABE 92D PRL 68 1104 F. Abe *et al.* (CDF Collab.)
ABE 92M PRL 69 2896 F. Abe *et al.* (CDF Collab.)
ABREU 92C ZPHY C53 41 P. Abreu *et al.* (DELPHI Collab.)
ABREU 92D ZPHY C53 555 P. Abreu *et al.* (DELPHI Collab.)
ADRIANI 92B PL B288 404 O. Adriani *et al.* (L3 Collab.)
ADRIANI 92F PL B292 472 O. Adriani *et al.* (L3 Collab.)
BARDADIN-... 92 ZPHY C55 163 M. Bardadin-Otwinowska (CLER)
DECAMP 92 PRPL 216 253 D. Decamp *et al.* (ALEPH Collab.)
HOWELL 92 PL B291 206 B. Howell *et al.* (TOPAZ Collab.)
KROHA 92 PR D46 58 H. Kroha (ROCH)
PDG 92 PR D45, 1 June, Part II K. Hikasa *et al.* (KEK, LBL, BOST+)
SHIMOZAWA 92 PL B284 144 K. Shimozawa *et al.* (TOPAZ Collab.)
ABE 91D PRL 67 2418 F. Abe *et al.* (CDF Collab.)
ABREU 91E PL B268 296 P. Abreu *et al.* (DELPHI Collab.)
ABREU 91F NP B367 511 P. Abreu *et al.* (DELPHI Collab.)
ADACHI 91 PL B255 613 I. Adachi *et al.* (TOPAZ Collab.)
AKRAWY 91F PL B257 531 M.Z. Akrawy *et al.* (OPAL Collab.)
ALITTI 91B PL B257 232 J. Alitti *et al.* (UA2 Collab.)
BEHREND 91B ZPHY C51 143 H.J. Behrend *et al.* (CELLO Collab.)
BEHREND 91C ZPHY C51 149 H.J. Behrend *et al.* (CELLO Collab.)
Also 91B ZPHY C51 143 H.J. Behrend *et al.* (CELLO Collab.)
ABE 90I ZPHY C48 13 K. Abe *et al.* (VENUS Collab.)
ADEVA 90F PL B247 177 B. Adeva *et al.* (L3 Collab.)
ADEVA 90K PL B250 199 B. Adeva *et al.* (L3 Collab.)
ADEVA 90L PL B250 205 B. Adeva *et al.* (L3 Collab.)
ADEVA 90O PL B252 525 B. Adeva *et al.* (L3 Collab.)
AKRAWY 90F PL B241 133 M.Z. Akrawy *et al.* (OPAL Collab.)
AKRAWY 90I PL B244 135 M.Z. Akrawy *et al.* (OPAL Collab.)
AKRAWY 90J PL B246 285 M.Z. Akrawy *et al.* (OPAL Collab.)
DECAMP 90G PL B236 501 D. Decamp *et al.* (ALEPH Collab.)
DECAMP 90O PL B250 172 D. Decamp *et al.* (ALEPH Collab.)
KIM 90 PL B240 243 G.N. Kim *et al.* (AMY Collab.)
ABE 89 PRL 62 613 F. Abe *et al.* (CDF Collab.)
ABE 89B PRL 62 1825 F. Abe *et al.* (CDF Collab.)
ABE 89D PRL 63 1447 F. Abe *et al.* (CDF Collab.)
ABE 89H PRL 62 3020 F. Abe *et al.* (CDF Collab.)
ABE 89J ZPHY C45 175 K. Abe *et al.* (VENUS Collab.)
ABE 89L PL B232 425 K. Abe *et al.* (VENUS Collab.)
ADACHI 89B PL B228 553 I. Adachi *et al.* (TOPAZ Collab.)
ALBAJAR 89 ZPHY C44 15 C. Albajar *et al.* (UA1 Collab.)
BARGER 89 PL B220 464 V. Barger *et al.* (WISC, KEK)
BEHREND 89B PL B222 163 H.J. Behrend *et al.* (CELLO Collab.)
BRAUNSCH... 89C ZPHY C43 549 W. Braunschweig *et al.* (TASSO Collab.)
DORENBOS... 89 ZPHY C41 567 J. Dorenbosch *et al.* (CHARM Collab.)
HAGIWARA 89 PL B219 369 K. Hagiwara, M. Sakuda, N. Terunuma (KEK, DURH+)
KIM 89 PL B223 476 S.K. Kim *et al.* (AMY Collab.)
ABE 88B PL B213 400 K. Abe *et al.* (VENUS Collab.)
BARINGER 88 PL B206 551 P. Baringer *et al.* (HRS Collab.)
BRAUNSCH... 88 ZPHY C37 171 W. Braunschweig *et al.* (TASSO Collab.)
BRAUNSCH... 88D ZPHY C40 163 W. Braunschweig *et al.* (TASSO Collab.)
ANSARI 87D PL B195 613 R. Ansari *et al.* (UA2 Collab.)
BARTEL 87B ZPHY C36 15 W. Bartel *et al.* (JADE Collab.)
BEHREND 87C PL B191 209 H.J. Behrend *et al.* (CELLO Collab.)
FERNANDEZ 87B PR D35 10 E. Fernandez *et al.* (MAC Collab.)
ARNISON 86C PL B172 461 G.T.J. Arnison *et al.* (UA1 Collab.)
ARNISON 86D PL B177 244 G.T.J. Arnison *et al.* (UA1 Collab.)
BARTEL 86 ZPHY C31 359 W. Bartel *et al.* (JADE Collab.)
BARTEL 86C ZPHY C30 371 W. Bartel *et al.* (JADE Collab.)
BEHREND 86 PL B168 420 H.J. Behrend *et al.* (CELLO Collab.)
BEHREND 86C PL B181 178 H.J. Behrend *et al.* (CELLO Collab.)
DERRICK 86 PL B166 463 M. Derrick *et al.* (HRS Collab.)
Also 86B PR D34 3286 M. Derrick *et al.* (HRS Collab.)
DERRICK 86B PR D34 3286 M. Derrick *et al.* (HRS Collab.)
GRIFOLS 86 PL B168 264 J.A. Grifols, S. Peris (BARC)
JODIDIO 86 PR D34 1967 A. Jodidio *et al.* (LBL, NWES, TRIU)
Also 88 PR D37 237 erratum A. Jodidio *et al.* (LBL, NWES, TRIU)
APPEL 85 PL B160 349 J.A. Appel *et al.* (UA2 Collab.)
BARTEL 85K PL B160 337 W. Bartel *et al.* (JADE Collab.)
BERGER 85 ZPHY C28 1 C. Berger *et al.* (PLUTO Collab.)
BERGER 85B ZPHY C27 341 C. Berger *et al.* (PLUTO Collab.)
BAGNAIA 84C PL 138B 430 P. Bagnaia *et al.* (UA2 Collab.)
BARTEL 84D PL 146B 437 W. Bartel *et al.* (JADE Collab.)
BARTEL 84E PL 146B 121 W. Bartel *et al.* (JADE Collab.)
EICHTEN 84 RMP 56 579 E. Eichten *et al.* (FNAL, LBL, OSU)
ALTHOFF 83C PL 126B 493 M. Althoff *et al.* (TASSO Collab.)
RENARD 82 PL 116B 264 F.M. Renard (CERN)

Extra Dimensions

For explanation of terms used and discussion of significant model dependence of following limits, see the "Extra Dimensions Review." Limits are expressed in conventions of of Giudice, Rattazzi, and Wells as explained in the Review. Footnotes describe originally quoted limit. n indicates the number of extra dimensions.

Limits not encoded here are summarized in the "Extra Dimensions Review."

EXTRA DIMENSIONS

Written March 2002 by J. Hewett (SLAC) and J. March-Russell (CERN).

I. Introduction

The large separation between the weak scale $\sim 10^3$ GeV and the traditional scale of gravity—the Planck scale with $M_{\rm Pl} \sim 10^{19}$ GeV—is one of the most puzzling aspects of nature. The origin of this large ratio, as well as its stability under radiative corrections, demands explanation. This is known as the hierarchy problem. One theoretical means of solving this problem is to introduce Supersymmetry (see the "Note on Supersymmetry" in this Review). Alternatively one may hope to address the hierarchy by exploiting the geometry of space time. Specifically, recent theories involve the idea that the 3-spatial dimensions in which we live could be a 3-spatial-dimensional 'membrane' embedded in a much larger extra dimensional space, and that the hierarchy is generated by the geometry of the additional dimensions. Such ideas have led to extra dimensional theories which have verifiable consequences at the TeV scale.

See key on page 323

Our knowledge of the weak and strong forces extends down to scales of $\sim (100\ \text{GeV})^{-1}$ (or of order 10^{-15} mm). On the other hand, we have almost no knowledge of gravity at distances less than roughly a *millimeter*, as direct tests of the gravitational force at the smallest distances are based on torsion-balance experiments, which are mechanically limited. It is thus conceivable that gravity may behave quite differently from the 3-dimensional Newtonian theory at small distances.

This leads to the possibility that matter and non-gravitational forces are confined to our 3-dimensional subspace, whereas gravity may propagate throughout a higher dimensional volume. In this case, the gauge forces are trapped within our 3-dimensional space, unaware of the extra dimensions, and maintain their usual behavior. Gravity, on the other hand, would no longer follow the inverse-square force law at distances smaller than the size of the extra dimensions, as the gravitational equivalent of Gauss' Law mandates that the gravitational field spreads out into the full spatial volume.

Since Newton's Law must be reproduced at large distances, gravity must behave as if there were only three spatial dimensions for $r \gtrsim 1$ mm. This is achievable either by compactifying all the extra dimensions on circles, where the geometry of these dimensions is thus flat and the topology is that of a torus, or by using strong curvature effects in the extra dimensions. In the first case, Arkani-Hamed, Dimopoulos, and Dvali (ADD) [1,2] used this picture to generate the hierarchy by postulating a large volume for the extra dimensional space, building on earlier ideas in Refs. 3,4. In the latter case, the hierarchy can be established by a large curvature of the extra dimensions as demonstrated by Randall and Sundrum (RS) [5,6]. It is the relation of these models to the hierarchy which yields testable predictions at the TeV scale.

General Features of Models

More technically, our subspace of $(3+1)$ space-time dimensions is known as a '3-brane', where the terminology is derived from a generalization of a 2-dimensional membrane. This brane is embedded in a D-dimensional space-time, $D \equiv (3+\delta+1)$, known as the 'bulk'. It is usually assumed that all δ-dimensions transverse to the brane have a common size R. However, the brane can also have smaller extra dimensions associated with it, of size $r \ll R$, and through which it extends, leading to effects similar to a small finite thickness. The size and geometry of the bulk, as well as the types of particles which are allowed to propagate in the bulk and on the brane, vary between different models.

Upon compactification of the δ-additional dimensions, all fields which propagate in the bulk are Fourier expanded into a complete set of modes—the so-called Kaluza-Klein (KK) tower of states, with mode numbers $\vec{n} = (n_1, n_2, \ldots, n_\delta)$ labeling the KK excitations. Similar to a particle in a box, the momentum of the bulk field is quantized in the δ compactified dimensions, given by $\vec{p}_\delta{}^2 = \vec{n}\cdot\vec{n}/R^2$, where R is the compactification radius. From the 4d perspective of an observer on the brane, each allowed momentum in the compactified volume appears as a KK excitation of the bulk field with mass $m_{\vec{n}}^2 = \vec{p}_\delta{}^2$. This builds a KK tower of states where each KK excitation carries identical spin and gauge quantum numbers. Kaluza-Klein states are a generic feature of models with compactified dimensions. The above assumes that all additional dimensions are of the same size and are flat; in more complicated compactifications, the Fourier expansion must be generalized, and the mass formula no longer takes on the above simple form.

The many proposed scenarios may be divided into two categories, depending on whether they do or do not assume that the geometry of the full $(4+\delta)$-dimensional space time with metric G_{IJ} is of factorized form, where the $4d$ and δ-dimensional geometries are independent. In the factorized case, the metric can be put in the form

$$ds^2 = G_{IJ}dx^I dx^J = \eta_{\mu\nu}dx^\mu dx^\nu + h_{ij}(y)dy^i dy^j\ , \qquad (1)$$

where $I, J = (0, \ldots, 3+\delta)$, $\mu, \nu = (0, ..., 3)$ and $i, j = (1, \ldots, \delta)$. The metric h_{ij} for the extra dimensions is flat only if they are toroidal, as assumed in the ADD scenario. In general, however, the bulk geometry is curved, even in the factorized case, and this can have important consequences. In the non-factorizable case, where there is a function of y multiplying $\eta_{\mu\nu}dx^\mu dx^\nu$, the bulk geometry is automatically curved. This is sometimes referred to as a 'warped' geometry.

A further classification involves the field content assumed to be present in the bulk or confined to the brane. The latter may be accomplished via localization, where the field's wavefunction is narrowly peaked about the brane. The low-energy effective action for the bulk contains, at minimum, the higher-dimensional Einstein-Hilbert term

$$S = \int d^4x d^\delta y \sqrt{-\det G}\ \left\{\frac{\overline{M}_D^{(2+\delta)}}{2}\mathcal{R} + \ldots\right\} \qquad (2)$$

where $\mathcal{R}$ is the $(4+\delta)$-dimensional Ricci scalar. This expression defines the scale $\overline{M}_D$, which is the fundamental scale of the higher-dimensional theory, and is the analog of the 4-d reduced Planck mass, $\overline{M}_{\rm Pl} = 2.4 \times 10^{18}$ GeV. This theory is non-renormalizable, and thus, gravitational interactions grow with energy as $\sim (E/\overline{M}_D)^{(2+\delta)/2}$. Hence, as the energy in a process grows, the theory becomes strongly coupled, and $\overline{M}_D$ is the scale at which the low-energy description breaks down.

This bulk action is incomplete as it does not contain the dynamics that stabilize the extra dimensions at a given size [2,7,8]. This issue is very model-dependent and, with the exception of the warped scenario [5,9], no standard picture exists.

It is common practice to assume that the Standard Model (SM) fields are confined to the brane. A motivation for this assumption is that confinement of certain degrees of freedom (but not gravity in general) to branes is automatic [10] within string theory. However, if the extra dimensions are small enough, the SM fields are phenomenologically allowed to propagate in the

bulk, and this possibility allows for novel model-building techniques to address gauge coupling unification, Supersymmetry breaking, the neutrino mass spectrum, and the fermion mass hierarchy.

A general issue that can strongly affect the phenomenology of these scenarios is that branes can be of two types: 'rigid,' or flexible (see Refs. 7,8). If the brane is flexible, it can fluctuate in the extra dimensions, resulting in Nambu-Goldstone modes. These can have important phenomenological implications which are detailed below [11,12,13]. The other possibility is a rigid brane, which can be thought of as a boundary of the bulk space where gravity satisfies particular boundary conditions. In this case the Poincare invariance of the higher dimensional theory is *explicitly* broken and there are no Nambu-Goldstone modes. Due to the broken translational invariance, momentum in the transverse y^i directions is not conserved, and the production of a single bulk mode is allowed. Almost all studies to date consider this 'rigid brane' case.

II. Three scenarios

There are three principal scenarios with predictions at the TeV scale, each of which has a distinct phenomenology.

Large Extra Dimensions

In these theories [1,2], gravity alone propagates in the bulk, where it is assumed to become strong near the electroweak scale. Gauss' Law relates the (reduced) Planck scale of the effective 4d low-energy theory and the fundamental scale $\overline{M}_D$, through the volume of the compactified dimensions, V_δ, via

$$\overline{M}_{\rm Pl}^2 = V_\delta \overline{M}_D^{2+\delta} \ . \qquad (3)$$

(Here and below we use the conventions of [14].) $M_{\rm Pl}$ is thus no longer a fundamental scale as it is generated by the large volume of the higher dimensional space. If, following ADD, it is assumed that the extra dimensions are *flat*, and thus of toroidal form, then setting $\overline{M}_D \sim$ TeV to eliminate the hierarchy between $M_{\rm Pl}$ and the weak scale determines the compactification radius R of the extra dimensions. Under the simplifying assumption that all radii are of equal size, we can define $V_\delta = (2\pi R)^\delta$. R then ranges from a sub-millimeter to a few fermi for $\delta = 2$–6. The case of $\delta = 1$ is excluded as the corresponding dimension would directly alter Newton's law on solar-system scales. The large size of the additional dimensions forces the SM fields to be constrained to the brane. The bulk graviton expands into a KK tower of spin-2 states which have masses of $\sqrt{\vec{n}^2/R^2}$, where $\vec{n}$ labels the KK excitation level.

The interactions of the bulk graviton with matter and gauge fields are

$$S_{int} = -\frac{1}{\overline{M}_D^{\delta/2+1}} \int d^4x d^\delta y_i h_{AB}(x_\mu, y_i) T_{AB}(x_\mu, y_i) \ , \qquad (4)$$

where h_{AB} is the bulk graviton fluctuation, and T_{AB} is the symmetric conserved stress-energy tensor. Setting $T_{AB} = \eta_A^\mu \eta_B^\nu T_{\mu\nu} \delta(y_i)$ for fields on the brane, expanding h_{AB} into the KK tower, and integrating over $d^\delta y_i$ gives the interactions of the bulk KK gravitons with the SM fields on the brane. The Feynman rules governing these interactions are explicitly derived in Refs. 14,15. Each KK excitation state, G_n, couples universally to the Standard Model fields with a strength of $\overline{M}_{\rm Pl}^{-1}$. In addition, a scalar mode exists, which is the volume modulus or radion field representing the fluctuations of the compactification volume. This field couples to the trace of the stress-energy tensor. It is important to note that this description is an effective 4-dimensional theory, valid for energies below $\overline{M}_D$. The full theory above this scale is unknown.

TeV^{-1}-sized Extra Dimensions with SM Fields

The possibility of TeV^{-1}-sized extra dimensions arises in braneworld models [3]. It does not allow for a reformulation of the hierarchy problem. In this case, the Standard Model field content may propagate in the bulk. This allows for several model-building choices: (i) all, or only some, of the SM gauge fields are present in the bulk; (ii) the Higgs field(s) may be in the bulk or on the brane; (iii) the confinement of the SM fermions to the brane or to specific locales in the extra dimensions. If the Higgs field(s) propagate in the bulk, the vacuum expectation value (VEV) of the Higgs zero-mode, the $\vec{n} = 0$ KK state, generates spontaneous symmetry breaking. In this case, the gauge boson KK mass matrix is diagonal with the gauge excitation masses being given by $[M_0^2 + \vec{n} \cdot \vec{n}/R^2]^{1/2}$, where M_0 is the VEV-induced mass of the gauge zero-mode. However, if the Higgs is confined to the brane, its VEV induces off-diagonal elements in the mass matrix, generating mixing amongst the gauge KK states of order $(M_0 R)^2$. For the case of 1 extra dimension, the coupling strength of the bulk KK gauge states to the SM fermions is $\sqrt{2}g$, where g is the SM SU(2) coupling. The fermion fields may (a) be constrained to the rigid $(3+1)$-brane, in which case they are not directly affected by the extra dimensions; (b) be localized at specific points in the TeV^{-1} dimension, but not on a rigid brane. Here, the zero and excited-mode KK fermions obtain narrow Gaussian-like wave functions in the extra dimensions, with a width much smaller than R^{-1}. This possibility may suppress the rates for a number of dangerous processes such as proton decay [16]; (c) propagate in the bulk. This scenario is known as universal extra dimensions [17]. In this possibility, all fields propagate in the bulk, and thus, branes need not be present. $(4+\delta)$-dimensional momentum is then conserved at tree-level, and KK parity, $(-1)^n$, is conserved to all orders. The phenomenology is quite different for this brane-less theory.

Bulk KK gauge bosons within this context are also discussed in the section on Indirect Constraints on Kaluza-Klein Gauge Bosons in the Listings for "Searches for Heavy Bosons Other Than Higgs Bosons" in this *Review*.

Warped Extra Dimensions

In the simplest form of this scenario [5,6], known as RS1, gravity propagates in a 5d bulk of finite extent, with two rigid boundaries of dimensionality $(3+1)$. The Standard Model

fields are assumed to be constrained to one of these rigid $(3+1)$-branes. This configuration permits the metric

$$ds^2 = e^{-2ky}\eta_{\mu\nu}dx^\mu dx^\nu - dy^2\,, \qquad (5)$$

where the exponential function, or warp factor, multiplying the usual 4d Minkowski term, demonstrates the non-factorizable geometry, and $y \in [0, \pi R]$ is the coordinate of the extra dimension. Here, k describes the curvature scale, which together with $\overline{M}_D$ $(D = 5)$ is assumed [5,6] to be of order $\overline{M}_{\rm Pl}$, with

$$\overline{M}_{\rm Pl}^2 = \frac{\overline{M}_D^3}{k}(1 - e^{-2kR\pi})\,. \qquad (6)$$

Consistency of the low-energy description requires that the curvature be small, so $k/\overline{M}_{\rm Pl} \lesssim 0.1$ is assumed. Eq. (5) leads to the gravitational wavefunction being concentrated on the brane at $y = 0$. Moreover, the exponential dependence of proper length and energy scales with y implies that TeV scales are naturally realized and stabilized [9] on the second brane at $y = \pi R$, provided that $kR \simeq 10$. Therefore, the RS1 model [5] localizes the SM fields to this brane at $y = \pi R$. The scale $\Lambda_\pi = \overline{M}_{\rm Pl}e^{-kR\pi} \sim 1$ TeV describes the scale of all physical processes on this so-called 'TeV-brane' at $y = \pi R$. Note that since $kR \simeq 10$ and $k \sim 10^{18}$ GeV is assumed by Randall and Sundrum, this is *not* a model with a large extra dimension.

The 4d phenomenology is governed by the two parameters, Λ_π and $k/\overline{M}_{\rm Pl}$. The masses of the bulk graviton KK tower states on the TeV-brane are $m_n = x_n k e^{-kR\pi} = x_n \Lambda_\pi k/\overline{M}_{\rm Pl}$ with the x_n being the roots of the first-order Bessel function J_1. The KK states are thus not evenly spaced. For typical values of the parameters, the mass of the first graviton KK excitation is of order a TeV. The interactions of the bulk graviton KK tower with the SM fields are [18]

$$\Delta\mathcal{L} = -\frac{1}{M_{\rm Pl}}T^{\mu\nu}(x)h_{\mu\nu}^{(0)}(x) - \frac{1}{\Lambda_\pi}T^{\mu\nu}(x)\sum_{n=1}^{\infty}h_{\mu\nu}^{(n)}(x)\,. \qquad (7)$$

Experiments can determine or constrain the masses m_n and the coupling Λ_π. The couplings of the excitation states are inverse to TeV strength, which results in a different phenomenology than in the case of large extra dimensions.

Extensions of this basic model allow for the SM fields to propagate in the bulk [19,20] since R is small. In this case, the masses of the bulk fermion, gauge, and graviton KK states are related. A third parameter, associated with the fermion bulk mass, is introduced and governs the 4d phenomenology.

An alternate possibility is RS2 [6]; here the SM fields are assumed to live on the brane at $y = 0$, where the graviton zero mode is concentrated, and the second brane is taken off to infinity $R \to \infty$. In this case, there is *no* mass gap in the bulk KK modes, and their coupling to the SM fields on the $y = 0$ brane is much weaker than $1/M_{\rm Pl}$. The collider constraints are investigated in Ref. 21, and cosmological constraints in Ref. 22. Although this setup no longer provides a reformulation of the hierarchy problem, it allows for a modification of gravity, potentially giving signals in sub-mm gravitational force experiments.

III. Experimental constraints

Tests of the Gravitational Force Law

Deviations from the 4d inverse-square gravitational force law may be observable in the case of large flat (ADD) extra dimensions, or in the RS2 scenario. Gravity would obey Gauss' Law in $3+\delta$ spatial dimensions for distances $r < R$ with

$$V_{3+1+\delta}(r) = \frac{-1}{8\pi(2\pi)^\delta(\overline{M}_D)^{\delta+2}}\frac{m_1 m_2}{r^{\delta+1}}\,, \qquad (8)$$

while observing the usual $(\overline{M}_{\rm Pl}^2 r)^{-1}$ gravitational potential for distances $r > R$. The experimental bounds on such deviations [23] are displayed in Fig. 1, which shows the constraints on the general form for the gravitational potential

$$V(r) = -G_N\frac{m_1 m_2}{r}\left(1 + \alpha e^{-r/\lambda}\right)\,. \qquad (9)$$

$\delta = 2$ large extra dimensions predict $\alpha = 4$ for compactification on a torus, which leads to the bound $R < 218$ μm. For $\delta > 2$, R is too small for deviations, due to extra dimensional gravity to be detected in mechanical experiments.

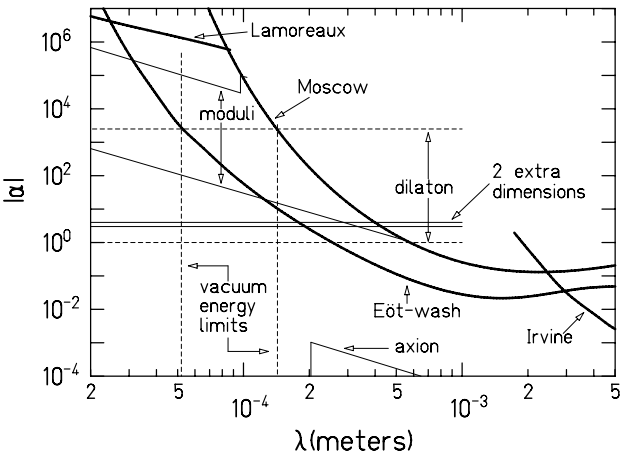

Figure 1: Constraints on deviations from Newton's gravitational force law. The allowed region is below the dark solid lines. From Ref. 23.

Astrophysical and Cosmological Constraints

As first analyzed in Ref. 2, astrophysical and cosmological considerations impose significant constraints on extra-dimensional theories. *Depending on the form of the spectrum of KK excitations of the bulk graviton*, these can imply stringent lower bounds on the gravitational scale $\overline{M}_D$, and corresponding upper bounds on the radii of the extra dimensions, given that

Newton's constant is correctly reproduced by Eq. (3). For extra dimensions of the ADD type, these constraints are significantly more stringent than those from direct collider or micro-gravity experiments for $\delta = 2$.

The spectrum of masses of the graviton KK modes sensitively depend on the topology and geometry of the extra dimensions. The spectral quantity of most direct importance for astrophysical and cosmological constraints is the mass gap between the bulk graviton zero mode and the first excited state. For flat (toroidal) extra dimensions of the type considered by ADD, the gap between the zero-mode and first excited state is given by $1/R$, where R is the (assumed common) radius of the extra dimensions, and the number density of KK modes grows as a power law $\rho(k) \sim V_\delta k^{\delta-1}$. Thus, in this case, the KK modes can be extremely light, *e.g.*, $m_n \geq nR^{-1} \geq n \times 10^{-4}$ eV, for $\delta = 2$, and numerous, $N_{KK} \simeq M_{\rm Pl}^2/\overline{M}_D^2 \leq 10^{32}$. As a result, even though these modes are individually only weakly coupled, with strength $1/M_{\rm Pl}$, they can be copiously produced by energetic processes on our brane.

However, such features are model-dependent. For curved extra dimensions, the spectral density of KK modes can possess a large gap, even approaching $\mathcal{O}(30$ GeV) in extreme cases [24]. Since the typical energy scale in astrophysical and cosmological conditions of interest is at most 100 MeV, the highly curved case avoids the constraints listed below with the exception of A2.

In the warped (RS1) case, these constraints are also avoided, as the scales k and $1/R$ are chosen to be close to the traditional Planck scale, and the resulting spectrum of KK modes has spacing of order a few hundred GeV or greater. In the warped RS2 case, the cosmological constraints are very mild even for $k \gtrsim 1$ mm)$^{-1}$ [22].

We now list the astrophysical and cosmological constraints for *flat extra dimensions* of toroidal type, and *involving solely the bulk graviton* and converted to the conventions of [14]. The constraints can depend upon, (A) only the production of bulk graviton KK modes, such as the case, in the anomalous supernova cooling and overclosure constraints, or (B) both the production and decay back to our brane of the bulk graviton KK modes, such as in the diffuse gamma ray background constraint. The model dependence of the constraints in class (A) is somewhat weaker than for class (B). All bounds become weak for $\delta \geq 4$.

A1 Anomalous cooling of red giants and supernovae due to bulk graviton emission. This was estimated by ADD [2] and calculated in Ref. 25 and further refined in Ref. 26. In particular, the observations of SN1987A place strong constraints on this energy loss mechanism, the dominant astrophysical uncertainty being the unknown core temperature $T_{\rm SN1987A}$ of SN1987A (estimates vary from 30 to 70 MeV). For the case of two flat extra dimensions, a bound of $\overline{M}_D \gtrsim 10$ TeV$(T_{\rm SN1987A}/30$ MeV$)^{1.375}$ is obtained, corresponding to a radius $R \lesssim 7.1 \times 10^{-4}$mm for $T_{\rm SN1987A} = 30$ MeV. For three extra dimensions $R \lesssim 8.5 \times 10^{-7}$mm, equivalent to $\overline{M}_D \gtrsim 0.78$ TeV$(T_{\rm SN1987A}/30$ MeV$)^{1.3}$, while for four or more dimensions the bounds can be extracted from [26], and are less than a TeV.

A2 In large extra dimension scenarios, there are severe limits on the maximum temperature (the 'normalcy temperature' T_*) above which the evolution of the universe must be non-standard [2]. This temperature is found by equating the rates for cooling by the usual process of adiabatic Hubble expansion, and by the new process of evaporation of KK gravitons into the bulk which becomes dominant at high temperatures. For $\overline{M}_D = 1$ TeV, [2] estimate that $T_* \lesssim 10$ MeV for $\delta = 2$, up to $T_* \lesssim 10$ GeV when $\delta = 6$. Since these temperatures are greater than that at big bang nucleosynthesis, there is no unavoidable constraint on $\overline{M}_D$. However, as the normalcy temperature is always below the electroweak phase transition temperature, many aspects of early universe cosmology, including baryogenesis and post-inflation reheating, must be carefully rethought.

B1 Distortion of the diffuse cosmic gamma-ray background due to decay on our brane of bulk gravitons to Standard Model states, and in particular two photons. As discussed above supernova cores will also emit large fluxes of KK gravitons, producing a cosmic background of these particles with energies and masses up to about 100 MeV. Radiative decays then give rise to a diffuse cosmic γ-ray background with $E_\gamma \sim 100$ MeV which is well in excess of the observations if more than 0.5–1% of the SN energy is emitted into the new channel [2]. This argument complements and tightens the cooling limit from the observed duration of the SN 1987A neutrino burst. For two extra dimensions a conservative bound [27] on their radius is $R \lesssim 0.9 \times 10^{-4}$ mm, while for three extra dimensions it is $R \lesssim 1.9 \times 10^{-7}$ mm. This corresponds to $\overline{M}_D \gtrsim 29$ TeV and $\overline{M}_D \gtrsim 1.9$ TeV, respectively.

B2 Anomalous heating of neutron stars by the decays of gravitationally trapped Kaluza-Klein graviton modes. In supernovae core collapse formation of neutron stars, massive KK gravitons would be produced with average velocities $\simeq 0.5c$, leading to many of them being gravitationally retained by the supernova core. Thus, every neutron star would have a halo of KK gravitons which decay into e^+e^-, $\gamma\gamma$, and $\nu\overline{\nu}$, on time scales $\simeq 10^9$ years. The EGRET γ-flux limits for nearby neutron stars then lead to the stringent constraint $\overline{M}_D \gtrsim 90$ TeV, for $\delta = 2$, and $\overline{M}_D \gtrsim 5$ TeV for $\delta = 3$ [28]. Even more stringent, the requirement that neutron stars are not excessively heated by KK decays implies $\overline{M}_D \gtrsim 280$ TeV for $\delta = 2$, and $\overline{M}_D \gtrsim 10$ TeV for $\delta = 3$ [28]. This translates into $R \lesssim 9.6 \times 10^{-7}$ mm and $R \lesssim 1.2 \times 10^{-8}$ mm, respectively.

B3 Over production of long-lived massive bulk gravitons leading to so-called overclosure of the universe [2,29]. This leads to a bound $\overline{M}_D > 2.2/\sqrt{h}$ TeV, or $R < 1.5h \times 10^{-5}m$ for 2 extra flat dimensions, where h is the current Hubble parameter in units of 100km/sMpc. Note that the diffuse gamma-ray background limit is more stringent than the

overclosure limit, so that the massive KK modes of the bulk graviton can not be the dark matter.

In principle, there are ways to evade the bounds that depend on decay back to our brane [7], even in the flat extra dimension case. For example, there may exist extra brane(s) in the bulk on which gravitons can decay, enhancing $\Gamma_{\rm inv}$. However, extreme parameter values are required.

If there are other fields in the bulk, such as right-handed neutrino states [30,31], then there are other potential astrophysical and cosmological constraints in addition to the ones listed above that must be considered [30,32]. This is particularly true of the scalar field that describes changes in the overall size of the extra dimensions (the 'radion') in the ADD case, as this field is, in all cases so far investigated, light with mass as small as 1 mm^{-1}. Moreover, this field has fixed couplings to the energy momentum tensor. Considerations of early universe cosmology typically lead to a severe radion 'moduli problem,' where coherent excitations of this degree of freedom overclose the universe [33]. Finally the extra spatial dimensions must be frozen in size from at least the big-bang nucleosynthesis epoch onwards, so any late motion of the radion is severely constrained, even if it slow enough to satisfy the overclosure constraint.

Constraints from Precision Electroweak Data

A precise description of the contributions to precision electroweak observables from bulk KK states requires a complete understanding of the underlying theory. Indirect contributions arise from the virtual exchange of KK states, and a summation over the entire KK tower must be performed. This summation diverges for $\delta > 1$ due to the non-renormalizability of the full $4+\delta$-dimensional field theory. In a fully consistent theory, such as string theory, the summation would be regularized and finite. Given our present lack of knowledge of the underlying theory, most authors choose to either terminate the summation with an explicit cut-off set to $\overline{M}_D$, or by invoking flexible branes to exponentially damp the sum [11]. These procedures yield naive estimates of the size of indirect KK contributions, and the resulting constraints are hence merely indicative [34].

Constraints in the special case of TeV^{-1} extra dimensions with $\delta = 1$ and rigid branes have been determined in Refs. 35,36. The contributions to the precision observables from tree-level KK gauge interactions, and from the mixing of the KK gauge states with the SM gauge bosons, have been computed, and a global fit to the data yields [35] a restriction on the compactification radius of $R^{-1} \gtrsim 4$ TeV. In addition, the contribution of the KK gauge states in the fit allow for the Higgs boson to be as heavy as ~ 320 GeV, which is larger than that allowed by the SM electroweak fit. These bounds on R^{-1} can be somewhat reduced in the case of flexible branes [12].

In the RS1 model with SM gauge fields in the bulk, the potential contributions to precision electroweak data depend on the placement of the fermions, on the brane or in the bulk. If the fermions are constrained to the TeV-brane, the couplings of the bulk KK gauge states to the SM fermions are large, being given by $\sqrt{2\pi k R}g \simeq 8.4g$. A global fit to the electroweak data, including bulk KK gauge tree-level and mixing contributions, yields [37] the bound $m_1 > 25$ TeV, which sets $\Lambda_\pi \gtrsim 100$ TeV. This constraint can be relaxed if the fermion fields are also placed in the bulk [19,38].

The contributions of bulk gauge KK states to the anomalous magnetic moment of the muon have been found to be small, whereas bulk fermion KK states can yield potentially sizable shifts in $g-2|_\mu$ in the RS scenario [39].

Graviton contributions to precision observables are notoriously problematic due to the non-renormalizability of the theory. Again, naive estimates on the size of such effects can be obtained in an effective field theory employing a cut-off to regulate the theory. In this approach, the cut-off dependent KK graviton contributions to the electroweak data set are found to be small for $\overline{M}_D \gtrsim 1$ TeV in ADD [40], and disfavor small values of $k/\overline{M}_{\rm Pl}$ in RS1 [19].

Collider Signals

Numerous collider searches have been performed which constrain each of the three scenarios. We limit our discussion to the case of low-energy effective Lagrangians, and note that new collider signatures may also be present in the context of string braneworld models, such as the resonant production of higher spin states [41,42].

Large Extra Dimensions: For the case of large flat extra dimensions, the reactions of individual bulk KK graviton states are not detectable, since they interact with the SM fields on the brane with $\overline{M}_{\rm Pl}^{-1}$ strength. However, the mass splittings between the bulk graviton KK states are given by $\Delta m \simeq 5 \times 10^{-4}$ eV, 20 KeV, and 7 MeV for $\delta = 2, 4$ and 6, respectively for $\overline{M}_D = 1$ TeV, and hence, their number density is large at collider energies. This results in observable signatures at the TeV scale. There are two classes of collider processes: (A) the direct production of bulk graviton KK states and (B) graviton KK production and subsequent decay to wall fields on our brane, *i.e.*, bulk graviton KK virtual exchange. Processes of type (A) are more model independent than those of type (B), but both classes are subject to the restrictions of the effective field theory description below $\overline{M}_D$.

The results of experimental searches for processes of both types are tabulated in the Listings.

A Direct Production of KK Gravitons

This class of collider tests is described by the emission of bulk graviton KK states in scattering processes [14,43] such as $e^+e^- \to \gamma/Z+G_n$, $p^{(}\bar{p}^{)} \to g+G_n$, and $Z \to f\bar{f}+G_n$. The graviton appears as missing energy in the detector, behaving as if it were a massive, non-interacting, stable particle. The cross section is computed for a single massive graviton KK state and then summed over the KK tower. This sum can be replaced by an integral weighted by the density of KK states which is cut off by the specific process kinematics. The produced G_n state appears to have a continuous mass

distribution corresponding to the probability of emitting KK gravitons with different extra dimensional momenta.

In e^+e^- collisions, the resulting γ/Z angular and energy distributions can be differentiated from those of the SM background reaction $e^+e^- \to \nu\overline{\nu}\gamma$. In addition, if bulk graviton KK emission is observed, then both parameters $\overline{M}_D$ and δ may be determined by measuring the production rate at different values of $\sqrt{s}$. The cross sections are lowered somewhat in the case of flexible branes [13].

Bulk graviton KK production at hadron colliders results in a mono-jet signal. The effective low-energy theory breaks down for some regions of parameter space, as the parton-level center of mass energy can exceed the value of $\overline{M}_D$. Experiment is then sensitive to the new physics present above this scale. Care must be exercised in interpreting experimental results/simulations, as the effective theory may not be valid over the whole search region.

B Virtual Exchange of KK Gravitons

This class of collider signals consists of bulk graviton KK exchange in all $2 \to 2$ scattering processes [14,44,45]. This results in deviations in cross sections and asymmetries in SM processes, as well as giving rise to new reactions which are not present at tree-level in the SM, such as $gg \to \ell^+\ell^-$. The signature is similar to that expected in the "Quark and Lepton Compositeness" Listings in this *Review*. The exchange process is governed by the effective Lagrangian

$$\mathcal{L} = i\frac{4\lambda}{M_H^4} T_{\mu\nu} T^{\mu\nu} \,. \qquad (10)$$

The amplitude is proportional to the sum over the propagators for the bulk graviton KK tower states which, as above, may be converted to an integral over the density of states. However, in this case, the integral is divergent for $\delta > 1$, and thus introduces a sensitivity to the unknown ultraviolet physics. Several approaches to regulate this integral have been employed: (i) a naive cut-off scheme [14,44], (ii) a flexible brane [11], or (iii) the inclusion of full weakly coupled TeV-scale string theory [42]. The most model independent approach is that of the naive cut-off, with the cut-off being set to $M_H \neq M_D$, to account for the uncertainties from the unknown ultraviolet physics. In addition, the parameter $\lambda = \pm 1$ is usually incorporated. Without a full specification of the UV theory, M_H must be treated as a new independent parameter: it cannot be reliably related to $\overline{M}_D$ and δ. Assuming that the integral is dominated by the lowest dimensional local operator results in a dimension-8 contact-type interaction limit. In the alternate notation of Ref. 14, the coefficient of this effective dimension-8 interaction is $(2/\pi)^{1/4}\Lambda_T = M_H|_{\lambda=+1}$. The resulting angular distributions for fermion pair production are quartic in $\cos\theta$, and thus provide a unique signal for spin-2 exchange.

The simultaneous observation of both classes of processes would signal the existence of large flat extra dimensions, as opposed to other new physics scenarios, as well as determine the parameters of the effective theory.

Once the center of mass energy reaches the scale $\overline{M}_D$, the extra-dimensional gravitational theory described by Eq. (2) becomes strongly coupled, and various exotic production processes might occur. One such possibility is black hole production. Black holes of Schwarzschild radius $R_s \lesssim R$ are substantially altered in the large extra dimension scenario [46], and may have much smaller masses, of order $\overline{M}_D$, than in traditional 4d theories of gravity. Discussions of black hole production at colliders are given in Ref. 47, and constraints on such scenarios from black-holes produced by cosmic rays in the atmosphere are estimated in Ref. 48. Finally, for small-angle elastic scattering, transplanckian collisions, $\sqrt{s} > \overline{M}_D$, can be reliably calculated from the low-energy effective theory and provide additional collider signatures [49].

TeV^{-1}-sized Extra Dimensions: In this scenario, the collider signatures consist of the direct production of the bulk gauge boson KK states at hadron colliders, or the indirect gauge boson KK exchange below production threshold in e^+e^- collisions [50]. This is in direct analogy to the standard signature of new gauge bosons from extended symmetry groups, and is discussed in detail in the extra gauge boson section. The distinction here is that the bulk gauge boson KK coupling strength to the Standard Model fermions is fixed to be $\sqrt{2}g$ for one extra dimension, where g is the SM gauge coupling strength, and the gluon, W, Z, and photon KK states are degenerate, modulo mixing effects. The bounds [35] on the first gauge KK excitation mass are $m_1 > 1.1$ TeV from Drell-Yan production at the Tevatron, and 3.1 TeV from $e^+e^- \to f\bar{f}$ at LEP II. These limits are eclipsed by the constraints from precision electroweak data. If the SM fermions are localized at specific points in the TeV^{-1} dimension, then the exchange of bulk gauge boson KK states in $2 \to 2$ scattering can be used to measure the fermion's wavefunction. The collider signatures of the universal extra dimensions scenario are varied and are discussed in Ref. [17].

Warped Extra Dimensions: In the scenario with warped extra dimensions, the first bulk graviton KK excitation state is of order a TeV, and has TeV^{-1} coupling strength. It can thus be produced as a spin-2 s-channel resonance at colliders. The constraints [18] on the simplest version of the RS model from Run I Tevatron data in the Drell-Yan and dijet resonance channels yield $m_1 \gtrsim 1100\,, 600\,, 200$ GeV for $k/\overline{M}_{\rm Pl} = 1.0\,, 0.1\,, 0.01$, respectively. Measurement of the first graviton KK excitation mass and width would determine the two parameters in this model. Higher energy accelerators may be able to directly observe several states of the bulk graviton KK spectrum; measurement of the mass splittings of the KK states would point to the presence of a warped geometry.

If the KK gravitons are too massive to be produced directly, their indirect exchange in fermion pair production results in a

contact-like interaction. Unlike ADD, the uncertainties associated with the introduction of a cut-off are avoided in this case, since there is only one additional dimension, and the sum over the KK states thus converges. The sensitivities [18] from LEPII data are $\Lambda_\pi = 4.0, 1.5, 0.4$ TeV, and those from Run I Tevatron searches are $\Lambda_\pi = 3.5, 1.0, 0.35$ TeV for $k/\overline{M}_{\rm Pl} = 0.01, 0.1, 1.0$, respectively.

The production rates for graviton KK states are drastically changed in the scenario where fermions are present in the bulk, and these limits are substantially weaker for some values of the fermion bulk mass parameter [19].

The radion, or graviscalar, is predicted to be the lightest new state in this scenario. Its coupling strength to SM fields is v/Λ_π. The signatures for its production and decay are similar to that of the SM Higgs and are examined in Ref. 51. It is allowed to mix with the SM Higgs, which can result in significant shifts in the properties of the Higgs [52].

References

1. N. Arkani-Hamed, S. Dimopoulos, and G.R. Dvali, Phys. Lett. **B429**, 263 (1998); I. Antoniadis *et al.*, Phys. Lett. **B436**, 257 (1998).
2. N. Arkani-Hamed, S. Dimopoulos, and G.R. Dvali, Phys. Rev. **D59**, 086004 (1999).
3. I. Antoniadis, Phys. Lett. **B246**, 377 (1990).
4. V.A. Rubakov and M.E. Shaposhnikov, Phys. Lett. **B125**, 139 (1983); Phys. Lett. **B125**, 136 (1983); M. Visser, Phys. Lett. **B159**, 22 (1985); J.D. Lykken, Phys. Rev. **D54**, 3693 (1996).
5. L. Randall and R. Sundrum, Phys. Rev. Lett. **83**, 3370 (1999).
6. L. Randall and R. Sundrum, Phys. Rev. Lett. **83**, 4690 (1999).
7. N. Arkani-Hamed, S. Dimopoulos, and J. March-Russell, Phys. Rev. **D63**, 064020 (2001).
8. R. Sundrum, Phys. Rev. **D59**, 085009 (1999).
9. W.D. Goldberger and M.B. Wise, Phys. Rev. Lett. **83**, 4922 (1999).
10. J. Polchinski, *String Theory, Vols. I, II*, Cambridge University Press, Cambridge, 1998.
11. M. Bando *et al.*, Phys. Rev. Lett. **83**, 3601 (1999).
12. T.G. Rizzo, Phys. Rev. **D61**, 055005 (2000).
13. H. Murayama and J.D. Wells, Phys. Rev. **D65**, 056011 (2002).
14. G.F. Giudice, R. Rattazzi, and J.D. Wells, Nucl. Phys. **B544**, 3 (1999).
15. T. Han, J.D. Lykken, and R.J. Zhang, Phys. Rev. **D59**, 105006 (1999).
16. N. Arkani-Hamed and M. Schmaltz, Phys. Rev. **D61**, 033005 (2000).
17. T. Appelquist, H.C. Cheng, and B.A. Dobrescu, Phys. Rev. **D64**, 035002 (2001).
18. H. Davoudiasl, J.L. Hewett, and T.G. Rizzo, Phys. Rev. Lett. **84**, 2080 (2000).
19. H. Davoudiasl, J.L. Hewett, and T.G. Rizzo, Phys. Rev. **D63**, 075004 (2001).
20. T. Gherghetta and A. Pomarol, Nucl. Phys. **B586**, 141 (2000).
21. D.J. Chung, L.L. Everett, and H. Davoudiasl, Phys. Rev. **D64**, 065002 (2001).
22. A. Hebecker and J. March-Russell, Nucl. Phys. **B608**, 375 (2001).
23. C.D. Hoyle *et al.*, Phys. Rev. Lett. **86**, 1418 (2001).
24. N. Kaloper *et al.*, Phys. Rev. Lett. **85**, 928 (2000).
25. S. Cullen and M. Perelstein, Phys. Rev. Lett. **83**, 268 (1999).
26. C. Hanhart *et al.*, Nucl. Phys. **B595**, 335 (2001).
27. S. Hannestad and G. Raffelt, Phys. Rev. Lett. **87**, 051301 (2001).
28. S. Hannestad and G.G. Raffelt, Phys. Rev. Lett. **88**, 071301 (2002).
29. L.J. Hall and D.R. Smith, Phys. Rev. **D60**, 085008 (1999).
30. N. Arkani-Hamed *et al.*, Phys. Rev. **D65**, 024032 (2002).
31. K.R. Dienes, E. Dudas, and T. Gherghetta, Nucl. Phys. **B557**, 25 (1999).
32. G.R. Dvali and A.Y. Smirnov, Nucl. Phys. **B563**, 63 (1999).
33. N. Arkani-Hamed *et al.*, Nucl. Phys. **B567**, 189 (2000).
34. R. Contino *et al.*, JHEP **0106**, 005 (2001).
35. T.G. Rizzo and J.D. Wells, Phys. Rev. **D61**, 016007 (2000).
36. M. Masip and A. Pomarol, Phys. Rev. **D60**, 096005 (1999); W.J. Marciano, Phys. Rev. **D60**, 093006 (1999).
37. H. Davoudiasl, J.L. Hewett, and T.G. Rizzo, Phys. Lett. **B473**, 43 (2000); A. Pomarol, Phys. Lett. **B486**, 153 (2000).
38. S. Chang *et al.*, Phys. Rev. **D62**, 084025 (2000).
39. P. Nath and M. Yamaguchi, Phys. Rev. **D60**, 116006 (1999); H. Davoudiasl, J.L. Hewett, and T.G. Rizzo, Phys. Lett. **B493**, 135 (2000); T.G. Rizzo, Phys. Rev. **D64**, 095010 (2001).
40. T. Han, D. Marfatia, and R.J. Zhang, Phys. Rev. **D62**, 125018 (2000).
41. E. Accomando, I. Antoniadis, and K. Benakli, Nucl. Phys. **B579**, 3 (2000); I. Antoniadis and K. Benakli, Int. J. Mod. Phys. A **15**, 4237 (2000).
42. E. Dudas and J. Mourad, Nucl. Phys. **B575**, 3 (2000); S. Cullen, M. Perelstein, and M.E. Peskin, Phys. Rev. **D62**, 055012 (2000).
43. E.A. Mirabelli, M. Perelstein, and M.E. Peskin, Phys. Rev. Lett. **82**, 2236 (1999).
44. J.L. Hewett, Phys. Rev. Lett. **82**, 4765 (1999).
45. T.G. Rizzo, Phys. Rev. **D59**, 115010 (1999).
46. P.C. Argyres, S. Dimopoulos, and J. March-Russell, Phys. Lett. **B441**, 96 (1998); R.C. Myers and M.J. Perry, Annals Phys. **172**, 304 (1986).
47. S.B. Giddings and S. Thomas, Phys. Rev. **D65**, 056010 (2002); S. Dimopoulos and G. Landsberg, Phys. Rev. Lett. **87**, 161602 (2001); R. Emparan, G.T. Horowitz, and R.C. Myers, Phys. Rev. Lett. **85**, 499 (2000); M.B. Voloshin, Phys. Lett. **B518**, 137 (2001).
48. J.L. Feng and A.D. Shapere, Phys. Rev. Lett. **88**, 021303 (2002);

R. Emparan, M. Masip, and R. Rattazzi, Phys. Rev. **D65**, 064023 (2002);
L.A. Anchordoqui *et al.*, hep-ph/0112247.

49. G.F. Giudice, R. Rattazzi, and J.D. Wells, Nucl. Phys. **B630**, 293 (2002).

50. I. Antoniadis and K. Benakli, Phys. Lett. **B326**, 69 (1994); I. Antoniadis, K. Benakli, and M. Quiros, Phys. Lett. **B331**, 313 (1994) and Phys. Lett. **B460**, 176 (1999).

51. G.F. Giudice, R. Rattazzi, and J.D. Wells, Nucl. Phys. **B595**, 250 (2001); W.D. Goldberger and M.B. Wise, Phys. Lett. **B475**, 275 (2000); K. Cheung, Phys. Rev. **D63**, 056007 (2001).

52. J.L. Hewett and T.G. Rizzo, hep-ph/0202155.

Limits on R from Deviations in Gravitational Force Law

This section includes limits on the size of extra dimensions from deviations in the Newtonian ($1/r^2$) gravitational force law at short distances. Deviations are parametrized by a gravitational potential of the form $V=-(G\ m\ m'/r^2)[1+\alpha\exp(-r/R)]$. For δ toroidal extra dimensions, $\alpha = 2\delta$.

VALUE (μm)	CL%	DOCUMENT ID		COMMENT
• • • We do not use the following data for averages, fits, limits, etc. • • •				
		[1] CHIAVERINI	03	Microcantilever
$\lesssim 200$	95	[2] LONG	03	Microcantilever
<190	95	[3] HOYLE	01	Torsion pendulum
		[4] HOSKINS	85	Torsion pendulum

[1] CHIAVERINI 03 search for new forces, probing α above 10^4 and λ down to 3μm, finding no signal. See their Fig. 4 for details on the bound. This bound does not place limits on the size of extra flat dimensions.
[2] LONG 03 search for new forces, probing α down to 3, and distances down to about 10μm. See their Fig. 4 for details on the bound.
[3] HOYLE 01 search for new forces, probing α down to 10^{-2} and distances down to 20μm. See their Fig. 4 for details on the bound.
[4] HOSKINS 85 search for new forces, probing distances down to 4 mm. See their Fig. 13 for details on the bound. This bound does not place limits on the size of extra flat dimensions.

Limits on R from On-Shell Production of Gravitons: $\delta = 2$

This section includes limits on on-shell production of gravitons in collider and astrophysical processes. Bounds quoted are on R, the assumed common radius of the flat extra dimensions, for $\delta = 2$ extra dimensions. Studies often quote bounds in terms of derived parameter; experiments are actually sensitive to the masses of the KK gravitons: $m_{\vec{n}} = |\vec{n}|/R$. See the Review on "Extra Dimensions" for details. Bounds are given in μm for δ=2.

VALUE (μm)	CL%	DOCUMENT ID		TECN	COMMENT
• • • We do not use the following data for averages, fits, limits, etc. • • •					
<610	95	[5] ABAZOV	03	D0	$\overline{p}p \to jG$
<0.96	95	[6] HANNESTAD	03		Supernova cooling
<0.096	95	[7] HANNESTAD	03		Diffuse γ background
<0.026	95	[8] HANNESTAD	03		Neutron star γ sources
<0.00016	95	[9] HANNESTAD	03		Neutron star heating
<300	95	[10] HEISTER	03C	ALEP	$e^+e^- \to \gamma G$
		[11] FAIRBAIRN	01		Cosmology
<0.66	95	[12] HANHART	01		Supernova cooling
<400	95	[13] ABREU	00Z	DLPH	$e^+e^- \to \gamma G$
		[14] CASSISI	00		Red giants
<460	95	[15] ACCIARRI	99R	L3	$e^+e^- \to \gamma G$
<1300	95	[16] ACCIARRI	99S	L3	$e^+e^- \to ZG$

Limits on R from On-Shell Production of Gravitons: $\delta \geq 3$

This section includes limits similar to those in the previous section, but for $\delta = 3$ extra dimensions. Bounds are given in nm for $\delta = 3$. Entries are also shown for papers examining models with $\delta > 3$.

VALUE (nm)	CL%	DOCUMENT ID		TECN	COMMENT
• • • We do not use the following data for averages, fits, limits, etc. • • •					
<6.1	95	[5] ABAZOV	03	D0	$\overline{p}p \to jG$
<1.14	95	[6] HANNESTAD	03		Supernova cooling
<0.025	95	[7] HANNESTAD	03		Diffuse γ background
<0.0072	95	[8] HANNESTAD	03		Neutron star γ sources
<0.0026	95	[9] HANNESTAD	03		Neutron star heating
<3.9	95	[10] HEISTER	03C	ALEP	$e^+e^- \to \gamma G$
		[17] ACOSTA	02H	CDF	$p\overline{p} \to \gamma G$
		[11] FAIRBAIRN	01		Cosmology
<0.8	95	[12] HANHART	01		Supernova cooling
		[13] ABREU	00Z	DLPH	$e^+e^- \to \gamma G$
		[14] CASSISI	00		Red giants
<5.1	95	[15] ACCIARRI	99R	L3	$e^+e^- \to \gamma G$
<18	95	[16] ACCIARRI	99S	L3	$e^+e^- \to ZG$

[5] ABAZOV 03 search for $p\overline{p} \to jG$ at $\sqrt{s}$=1.8 TeV to place bounds on M_D for 2 to 7 extra dimensions, from which these bounds on R are derived. See their paper for bounds on intermediate values of δ. We quote results without the approximate NLO scaling introduced in the paper.
[6] HANNESTAD 03 obtain a limit on R from graviton cooling of supernova SN1987a. Limits for all $\delta \leq 7$ are given in their Tables V and VI.
[7] HANNESTAD 03 obtain a limit on R from gravitons emitted in supernovae and which subsequently decay, contaminating the diffuse cosmic γ background. Limits for all $\delta \leq 7$ are given in their Tables V and VI. These limits supersede those in HANNESTAD 02.
[8] HANNESTAD 03 obtain a limit on R from gravitons emitted in two recent supernovae and which subsequently decay, creating point γ sources. Limits for all $\delta \leq 7$ are given in their Tables V and VI.
[9] HANNESTAD 03 obtain a limit on R from the heating of old neutron starts by the surrounding cloud of trapped KK gravitons. Limits for all $\delta \leq 7$ are given in their Tables V and VI. These limits supersede those in HANNESTAD 02.
[10] HEISTER 03C use the process $e^+e^- \to \gamma G$ at $\sqrt{s} = 189$–209 GeV to place bounds on the size of extra dimensions and the scale of gravity. See their Table 4 for limits with $\delta \leq 6$ for derived limits on M_D.
[11] FAIRBAIRN 01 obtains bounds on R from over production of KK gravitons in the early universe. Bounds are quoted in paper in terms of fundamental scale of gravity. Bounds depend strongly on temperature of QCD phase transition and range from $R<0.13\,\mu$m to 0.001 μm for δ=2; bounds for δ=3,4 can be derived from Table 1 in the paper.
[12] HANHART 01 obtain bounds on R from limits on graviton cooling of supernova SN 1987a using numerical simulations of proto-neutron star neutrino emission.
[13] ABREU 00Z use e^+e^- collisions at $\sqrt{s}$=189 GeV to look for on-shell production of gravitons in association with photons. Bounds are derived for δ=2,4,6.
[14] CASSISI 00 obtain rough bounds on M_D (and thus R) from red giant cooling for δ=2,3. See their paper for details.
[15] ACCIARRI 99R search for the reaction $e^+e^- \to \gamma G$ at $E_{\rm cm}$=189 GeV. Limits on the gravity scale are listed in their Table 4, for $\delta \leq 10$.
[16] ACCIARRI 99S search for $e^+e^- \to ZG$ at $\sqrt{s}$=189 GeV. Limits on the gravity scale are found in their Table 2, for $\delta \leq 4$.
[17] ACOSTA 02H uses the process $p\overline{p} \to \gamma G$ at $\sqrt{s} = 1.8$ TeV to place bounds on R for δ=4,6, and 8: $R<24$ pm, 55 fm, and 2.6 fm respectively. However the kinematics relevant to these bounds are probably outside the validity range of the effective theory.

Mass Limits on M_{TT}

This section includes limits on the cut-off mass scale, M_{TT}, of dimension-8 operators from KK graviton exchange in models of large extra dimensions. Ambiguities in the UV-divergent summation are absorbed into the parameter λ, which is taken to be $\lambda = \pm 1$ in the following analyses. Bounds for $\lambda = -1$ are shown in parenthesis after the bound for $\lambda = +1$, if appropriate. Different papers use slightly different definitions of the mass scale; some popular conventions, M_H and Λ_{TT}, are discussed in the above Review on "Extra Dimensions." All bounds scale as $\lambda^{1/4}$, unless otherwise stated.

VALUE (TeV)		CL%	DOCUMENT ID		TECN	COMMENT
• • • We do not use the following data for averages, fits, limits, etc. • • •						
>0.805	(>0.956)	95	[18] ABBIENDI	03D	OPAL	$e^+e^- \to \gamma\gamma$
>0.7	(>0.7)	95	[19] ACHARD	03D	L3	$e^+e^- \to ZZ$
>0.82	(>0.78)	95	[20] ADLOFF	03	H1	$ep \to eX$
>1.28	(>1.25)	95	[21] GIUDICE	03	RVUE	
>20.6	(>15.7)	95	[22] GIUDICE	03	RVUE	Dim-6 operators
>0.80	(>0.85)	95	[23] HEISTER	03C	ALEP	$e^+e^- \to \gamma\gamma$
>0.84	(>0.99)	95	[24] ACHARD	02D	L3	$e^+e^- \to \gamma\gamma$
>1.2	(>1.1)	95	[25] ABBOTT	01	D0	$p\overline{p} \to e^+e^-, \gamma\gamma$
>0.60	(>0.63)	95	[26] ABBIENDI	00R	OPAL	$e^+e^- \to \mu^+\mu$
>0.63	(>0.50)	95	[26] ABBIENDI	00R	OPAL	$e^+e^- \to \tau^+\tau^-$
>0.68	(>0.61)	95	[26] ABBIENDI	00R	OPAL	$e^+e^- \to \mu^+\mu$
			[27] ABREU	00A	DLPH	
>0.649	(>0.559)	95	[28] ABREU	00S	DLPH	$e^+e^- \to \mu^+\mu^-$
>0.564	(>0.450)	95	[28] ABREU	00S	DLPH	$e^+e^- \to \tau^+\tau^-$
>0.680	(>0.542)	95	[28] ABREU	00S	DLPH	$e^+e^- \to \mu^+\mu^-, \tau^+\tau^-$
>15–28		99.7	[29] CHANG	00B	RVUE	Electroweak
>0.98		95	[30] CHEUNG	00	RVUE	$e^+e^- \to \gamma\gamma$
>0.29–0.38		95	[31] GRAESSER	00	RVUE	$(g-2)_\mu$
>0.50–1.1		95	[32] HAN	00	RVUE	Electroweak
>2.0	(>2.0)	95	[33] MATHEWS	00	RVUE	$\overline{p}p \to jj$
>1.0	(>1.1)	95	[34] MELE	00	RVUE	$e^+e^- \to VV$
			[35] ABBIENDI	99P	OPAL	
			[36] ACCIARRI	99M	L3	
			[37] ACCIARRI	99S	L3	
>1.412	(>1.077)	95	[38] BOURILKOV	99		$e^+e^- \to e^+e^-$

[18] ABBIENDI 03D use e^+e^- collisions at $\sqrt{s}$=181–209 to place bounds on the ultraviolate scale M_{TT}, which is equivalent to their definition of M_s.
[19] ACHARD 03D look for deviations in the cross section for $e^+e^- \to ZZ$ from $\sqrt{s}$ = 200–209 GeV to place a bound on M_{TT}.
[20] ADLOFF 03 search for deviations in the differential cross section of $e^\pm p \to e^\pm X$ at $\sqrt{s}$=301 and 319 GeV to place bounds on M_{TT}.
[21] GIUDICE 03 review existing experimental bounds on M_{TT} and derive a combined limit.
[22] GIUDICE 03 place bounds on Λ_6, the coefficient of the gravitationally-induced dimension-6 operator $(2\pi\lambda/\Lambda_6^2)(\sum \overline{f}\gamma_\mu\gamma^5 f)(\sum \overline{f}\gamma^\mu\gamma^5 f)$, using data from a variety of experiments. Results are quoted for $\lambda=\pm 1$ and are independent of δ.
[23] HEISTER 03C use e^+e^- collisions at $\sqrt{s}$= 189–209 GeV to place bounds on the scale of dim-8 gravitational interactions. Their $M_s^\pm$ is equivalent to our M_{TT} with $\lambda=\pm 1$.
[24] ACHARD 02 search for s-channel graviton exchange effects in $e^+e^- \to \gamma\gamma$ at $E_{\rm cm}$ = 192–209 GeV.
[25] ABBOTT 01 search for variations in differential cross sections to e^+e^- and $\gamma\gamma$ final states at the Tevatron.
[26] ABBIENDI 00R uses e^+e^- collisions at $\sqrt{s}$= 189 GeV.

[27] ABREU 00A search for s-channel graviton exchange effects in $e^+e^- \to \gamma\gamma$ at E_{cm}= 189–202 GeV.

[28] ABREU 00S uses e^+e^- collisions at $\sqrt{s}$=183 and 189 GeV.

[29] CHANG 00B derive 3σ limit on M_{TT} of (28,19,15) TeV for δ=(2,4,6) respectively assuming the presence of a torsional coupling in the gravitational action. Highly model dependent.

[30] CHEUNG 00 obtains limits from anomalous diphoton production at OPAL due to graviton exchange. Original limit for δ=4. However, unknown UV theory renders δ dependence unreliable. Original paper works in HLZ convention.

[31] GRAESSER 00 obtains a bound from graviton contributions to $g-2$ of the muon through loops of 0.29 TeV for δ=2 and 0.38 TeV for δ=4,6. Limits scale as $\lambda^{1/2}$. However calculational scheme not well-defined without specification of high-scale theory. See the "Extra Dimensions Review."

[32] HAN 00 calculates corrections to gauge boson self-energies from KK graviton loops and constrain them using S and T. Bounds on M_{TT} range from 0.5 TeV (δ=6) to 1.1 TeV (δ=2); see text. Limits have strong dependence, $\lambda^{\delta+2}$, on unknown λ coefficient.

[33] MATHEWS 00 search for evidence of graviton exchange in CDF and DØ dijet production data. See their Table 2 for slightly stronger δ-dependent bounds. Limits expressed in terms of $M_S^4 = M_{TT}^4/8$.

[34] MELE 00 obtains bound from KK graviton contributions to $e^+e^- \to VV$ (V=γ,W,Z) at LEP. Authors use Hewett conventions.

[35] ABBIENDI 99P search for s-channel graviton exchange effects in $e^+e^- \to \gamma\gamma$ at E_{cm}=189 GeV. The limits $G_+ > 660$ GeV and $G_- > 634$ GeV are obtained from combined E_{cm}=183 and 189 GeV data, where $G_\pm$ is a scale related to the fundamental gravity scale.

[36] ACCIARRI 99M search for the reaction $e^+e^- \to \gamma G$ and s-channel graviton exchange effects in $e^+e^- \to \gamma\gamma$, W^+W^-, ZZ, e^+e^-, $\mu^+\mu^-$, $\tau^+\tau^-$, $q\overline{q}$ at E_{cm}=183 GeV. Limits on the gravity scale are listed in their Tables 1 and 2.

[37] ACCIARRI 99S search for the reaction $e^+e^- \to ZG$ and s-channel graviton exchange effects in $e^+e^- \to \gamma\gamma$, W^+W^-, ZZ, e^+e^-, $\mu^+\mu^-$, $\tau^+\tau^-$, $q\overline{q}$ at E_{cm}=189 GeV. Limits on the gravity scale are listed in their Tables 1 and 2.

[38] BOURILKOV 99 performs global analysis of LEP data on e^+e^- collisions at $\sqrt{s}$=183 and 189 GeV. Bound is on Λ_T.

Direct Limits on Gravitational or String Mass Scale

This section includes limits on the fundamental gravitational scale and/or the string scale from processes which depend directly on one or the other of these scales.

VALUE (TeV)	DOCUMENT ID	TECN	COMMENT
• • • We do not use the following data for averages, fits, limits, etc. • • •			
$\gtrsim$ 1–2	[39] ANCHORDOQ..02B	RVUE	Cosmic Rays
>0.49	[40] ACCIARRI 00P	L3	$e^+e^- \to e^+e^-$

[39] ANCHORDOQUI 02B derive bound on M_D from non-observation of black hole production in high-energy cosmic rays. Bound is stronger for larger δ, but depends sensitively on threshold for black hole production.

[40] ACCIARRI 00P uses e^+e^- collisions at $\sqrt{s}$= 183 and 189 GeV. Bound on string scale M_S from massive string modes. M_S is defined in hep-ph/0001166 by $M_S(1/\pi)^{1/8}\alpha^{-1/4} = M$ where $(4\pi G)^{-1} = M^{n+2}R^n$.

Limits on $1/R = M_c$

This section includes limits on $1/R = M_C$, the compactification scale in models with TeV extra dimensions, due to exchange of Standard Model KK excitations. See the "Extra Dimension Review" for discussion of model dependence.

VALUE (TeV)	CL%	DOCUMENT ID	TECN	COMMENT
• • • We do not use the following data for averages, fits, limits, etc. • • •				
>3.3	95	[41] CORNET 00	RVUE	Electroweak
> 3.3–3.8	95	[42] RIZZO 00	RVUE	Electroweak

[41] CORNET 00 translates a bound on the coefficient of the 4-fermion operator $(\overline{\ell}\gamma_\mu\tau^a\ell)(\overline{\ell}\gamma^\mu\tau^a\ell)$ derived by Hagiwara and Matsumoto into a limit on the mass scale of KK W bosons.

[42] RIZZO 00 obtains limits from global electroweak fits in models with a Higgs in the bulk (3.8 TeV) or on the standard brane (3.3 TeV).

Limits on Mass of Radion

This section includes limits on mass of radion, usually in context of Randall-Sundrum models. See the "Extra Dimension Review" for discussion of model dependence.

VALUE (GeV)	DOCUMENT ID	COMMENT
• • • We do not use the following data for averages, fits, limits, etc. • • •		
$\gtrsim$ 35	[43] MAHANTA 00	$Z \to$ radion $\ell\overline{\ell}$
>120	[44] MAHANTA 00B	$p\overline{p} \to$ radion $\to \gamma\gamma$

[43] MAHANTA 00 obtain bound on radion mass in the RS model. Bound is from Higgs boson search at LEP I.

[44] MAHANTA 00B uses $p\overline{p}$ collisions at $\sqrt{s}$= 1.8 TeV; production via gluon-gluon fusion. Authors assume a radion vacuum expectation value of 1 TeV.

REFERENCES FOR Extra Dimensions

ABAZOV	03	PRL 90 251802	V.M. Abazov *et al.* (D0 Collab.)
ABBIENDI	03D	EPJ C26 331	G. Abbiendi *et al.* (OPAL Collab.)
ACHARD	03D	PL B572 133	P. Achard *et al.* (L3 Collab.)
ADLOFF	03	PL B568 35	C. Adloff *et al.* (H1 Collab.)
CHIAVERINI	03	PRL 90 151101	J. Chiaverini *et al.*
GIUDICE	03	NP B663 377	G.F. Giudice, A. Strumia
HANNESTAD	03	PR D67 125008	S. Hannestad, G.G. Raffelt
HEISTER	03C	EPJ C28 1	A. Heister *et al.* (ALEPH Collab.)
LONG	03	Nature 421 922	J.C. Long *et al.*
ACHARD	02	PL B524 65	P. Achard *et al.* (L3 Collab.)
ACHARD	02D	PL B531 28	P. Achard *et al.* (L3 Collab.)
ACOSTA	02H	PRL 89 281801	D. Acosta *et al.* (CDF Collab.)
ANCHORDOQ..02B		PR D66 103002	L. Anchordoqui *et al.*
HANNESTAD	02	PRL 88 071301	S. Hannestad, G. Raffelt
ABBOTT	01	PRL 86 1156	B. Abbott *et al.* (D0 Collab.)
FAIRBAIRN	01	PL B508 335	M. Fairbairn
HANHART	01	PL B509 1	C. Hanhart *et al.*
HOYLE	01	PRL 86 1418	C.D. Hoyle *et al.*
ABBIENDI	00R	EPJ C13 553	G. Abbiendi *et al.* (OPAL Collab.)
ABREU	00A	PL B491 67	P. Abreu *et al.* (DELPHI Collab.)
ABREU	00S	PL B485 45	P. Abreu *et al.* (DELPHI Collab.)
ABREU	00Z	EPJ C17 53	P. Abreu *et al.* (DELPHI Collab.)
ACCIARRI	00P	PL B489 81	M. Acciarri *et al.* (L3 Collab.)
CASSISI	00	PL B481 323	S. Cassisi *et al.*
CHANG	00B	PRL 85 3765	L.N. Chang *et al.*
CHEUNG	00	PR D61 015005	K. Cheung
CORNET	00	PR D61 037701	F. Cornet, M. Relano, J. Rico
GRAESSER	00	PR D61 074019	M.L. Graesser
HAN	00	PR D62 125018	T. Han, D. Marfatia, R-J. Zhang
MAHANTA	00	PL B480 176	U. Mahanta, S. Rakshit
MAHANTA	00B	PL B483 196	U. Mahanta, A. Datta
MATHEWS	00	JHEP 0007 008	P. Mathews, S. Raychaudhuri, K. Sridhar
MELE	00	PR D61 117901	S. Mele, E. Sanchez
RIZZO	00	PR D61 016007	T.G. Rizzo, J.D. Wells
ABBIENDI	99P	PL B465 303	G. Abbiendi *et al.* (OPAL Collab.)
ACCIARRI	99M	PL B464 135	M. Acciarri *et al.* (L3 Collab.)
ACCIARRI	99R	PL B470 268	M. Acciarri *et al.* (L3 Collab.)
ACCIARRI	99S	PL B470 281	M. Acciarri *et al.* (L3 Collab.)
BOURILKOV	99	JHEP 08 006	D. Bourilkov
HOSKINS	85	PR D32 3084	J.K. Hoskins *et al.*

WIMPs and Other Particles Searches for

OMITTED FROM SUMMARY TABLE

WIMPS AND OTHER PARTICLE SEARCHES

Revised March 2002 by K. Hikasa (Tohoku University).

We collect here those searches which do not appear in any of the above search categories. These are listed in the following order:

1. Galactic WIMP (weakly-interacting massive particle) searches
2. Concentration of stable particles in matter
3. Limits on neutral particle production at accelerators
4. Limits on jet-jet resonance in hadron collisions
5. Limits on charged particles in e^+e^- collisions
6. Limits on charged particles in hadron reactions
7. Limits on charged particles in cosmic rays

Note that searches appear in separate sections elsewhere for Higgs bosons (and technipions), other heavy bosons (including W_R, W', Z', leptoquarks, axigluons), axions (including pseudo-Goldstone bosons, Majorons, familons), heavy leptons, heavy neutrinos, free quarks, monopoles, supersymmetric particles, and compositeness. We include specific WIMP searches in the appropriate sections when they yield limits on hypothetical particles such as supersymmetric particles, axions, massive neutrinos, monopoles, *etc.*

We omit papers on CHAMP's, millicharged particles, and other exotic particles. We no longer list for limits on tachyons and centauros. See our 1994 edition for these limits.

GALACTIC WIMP SEARCHES
Cross-Section Limits for Dark Matter Particles (X^0) on Nuclei

These limits are for weakly-interacting stable particles that may constitute the invisible mass in the galaxy. Unless otherwise noted, a local mass density of 0.3 GeV/cm^3 is assumed; see each paper for velocity distribution assumptions. In the papers the limit is given as a function of the X^0 mass. Here we list limits only for typical mass values of 20 GeV, 100 GeV, and 1 TeV. Specific limits on supersymmetric dark matter particles may be found in the Supersymmetry section.

For m_{X^0} = 20 GeV

VALUE (nb)	CL%	DOCUMENT ID		TECN	COMMENT
• • • We do not use the following data for averages, fits, limits, etc. • • •					
		[1] MIUCHI	03	BOLO	LiF
		[2] TAKEDA	03	BOLO	NaF
< 0.08	90	[3] ANGLOHER	02	CRES	Al
		[4] BENOIT	00	EDEL	Ge
< 0.04	95	[5] KLIMENKO	98	CNTR	^{73}Ge, inel.
< 0.8		ALESSAND...	96	CNTR	O
< 6		ALESSAND...	96	CNTR	Te
< 0.02	90	[6] BELLI	96	CNTR	^{129}Xe, inel.
		[7] BELLI	96C	CNTR	^{129}Xe
< 0.004	90	[8] BERNABEI	96	CNTR	Na
< 0.3	90	[8] BERNABEI	96	CNTR	I
< 0.2	95	[9] SARSA	96	CNTR	Na
< 0.015	90	[10] SMITH	96	CNTR	Na
< 0.05	95	[11] GARCIA	95	CNTR	Natural Ge
< 0.1	95	QUENBY	95	CNTR	Na
< 90	90	[12] SNOWDEN-...	95	MICA	^{16}O
< 4 × 10^3	90	[12] SNOWDEN-...	95	MICA	^{39}K
< 0.7	90	BACCI	92	CNTR	Na
< 0.12	90	[13] REUSSER	91	CNTR	Natural Ge
< 0.06	95	CALDWELL	88	CNTR	Natural Ge

[1] MIUCHI 03 give model-independent limit σ <35 pb (90%CL) for spin-dependent X^0-proton cross section.
[2] TAKEDA 03 give model-independent limit σ < 0.03 (0.6) nb (90%CL) for spin-dependent χ^0-proton (neutron) cross section.
[3] ANGLOHER 02 limit is for spin-dependent WIMP-Aluminum cross section.
[4] BENOIT 00 find four event categories in Ge detectors and suggest that low-energy surface nuclear recoils can explain anomalous events reported by UKDMC and Saclay NaI experiments.
[5] KLIMENKO 98 limit is for inelastic scattering $X^0\,^{73}$Ge → $X^0\,^{73}$Ge* (13.26 keV).
[6] BELLI 96 limit for inelastic scattering $X^0\,^{129}$Xe → $X^0\,^{129}$Xe*(39.58 keV).
[7] BELLI 96C use background subtraction and obtain σ < 150 pb (< 1.5 fb) (90%CL) for spin-dependent (independent) X^0-proton cross section. The confidence level is from R. Bernabei, private communication, May 20, 1999.
[8] BERNABEI 96 use pulse shape discrimination to enhance the possible signal. The limit here is from R. Bernabei, private communication, September 19, 1997.
[9] SARSA 96 search for annual modulation of WIMP signal. See SARSA 97 for details of the analysis. The limit here is from M.L. Sarsa, private communication, May 26, 1997.
[10] SMITH 96 use pulse shape discrimination to enhance the possible signal. A dark matter density of 0.4 GeV cm^{-3} is assumed.
[11] GARCIA 95 limit is from the event rate. A weaker limit is obtained from searches for diurnal and annual modulation.
[12] SNOWDEN-IFFT 95 look for recoil tracks in an ancient mica crystal. Similar limits are also given for ^{27}Al and ^{28}Si. See COLLAR 96 and SNOWDEN-IFFT 96 for discussion on potential backgrounds.
[13] REUSSER 91 limit here is changed from published (0.04) after reanalysis by authors. J.L. Vuilleumier, private communication, March 29, 1996.

For m_{X^0} = 100 GeV

VALUE (nb)	CL%	DOCUMENT ID		TECN	COMMENT
• • • We do not use the following data for averages, fits, limits, etc. • • •					
		[14] MIUCHI	03	BOLO	LiF
		[15] MIUCHI	03	BOLO	LiF
		[16] TAKEDA	03	BOLO	NaF
< 0.3	90	[17] ANGLOHER	02	CRES	Al
		[18] BELLI	02	RVUE	
		[19] BERNABEI	02C	DAMA	
		[20] GREEN	02	RVUE	
		[21] ULLIO	01	RVUE	
		[22] BENOIT	00	EDEL	Ge
< 0.004	90	[23] BERNABEI	00D		^{129}Xe, inel.
		[24] AMBROSIO	99	MCRO	
		[25] BRHLIK	99	RVUE	
< 0.008	95	[26] KLIMENKO	98	CNTR	^{73}Ge, inel.
< 0.08	95	[27] KLIMENKO	98	CNTR	^{73}Ge, inel.
< 4		ALESSAND...	96	CNTR	O
< 25		ALESSAND...	96	CNTR	Te
< 0.006	90	[28] BELLI	96	CNTR	^{129}Xe, inel.
		[29] BELLI	96C	CNTR	^{129}Xe
< 0.001	90	[30] BERNABEI	96	CNTR	Na
< 0.3	90	[30] BERNABEI	96	CNTR	I
< 0.7	95	[31] SARSA	96	CNTR	Na
< 0.03	90	[32] SMITH	96	CNTR	Na
< 0.8	90	[32] SMITH	96	CNTR	I
< 0.35	95	[33] GARCIA	95	CNTR	Natural Ge
< 0.6	95	QUENBY	95	CNTR	Na
< 3	95	QUENBY	95	CNTR	I
< 1.5 × 10^2	90	[34] SNOWDEN-...	95	MICA	^{16}O
< 4 × 10^2	90	[34] SNOWDEN-...	95	MICA	^{39}K
< 0.08	90	[35] BECK	94	CNTR	^{76}Ge
< 2.5	90	BACCI	92	CNTR	Na
< 3	90	BACCI	92	CNTR	I
< 0.9	90	[36] REUSSER	91	CNTR	Natural Ge
< 0.7	95	CALDWELL	88	CNTR	Natural Ge

[14] MIUCHI 03 give model-independent limit for spin-dependent X^0-proton and neutron cross sections. See their Fig. 5.
[15] MIUCHI 03 give model-independent limit σ <35 pb (90%CL) for spin-dependent X^0-proton cross section.
[16] TAKEDA 03 give model-independent limit σ < 0.04 (0.8) nb (90%CL) for spin-dependent χ^0-proton (neutron) cross section.
[17] ANGLOHER 02 limit is for spin-dependent WIMP-Aluminum cross section.
[18] BELLI 02 discuss dependence of the extracted WIMP cross section on the assumptions of the galactic halo structure.
[19] BERNABEI 02C analyze the DAMA data in the scenario in which X^0 scatters into a slightly heavier state as discussed by SMITH 01.
[20] GREEN 02 discusses dependence of extracted WIMP cross section limits on the assumptions of the galactic halo structure.
[21] ULLIO 01 disfavor the possibility that the BERNABEI 99 signal is due to spin-dependent WIMP coupling.
[22] BENOIT 00 find four event categories in Ge detectors and suggest that low-energy surface nuclear recoils can explain anomalous events reported by UKDMC and Saclay NaI experiments.
[23] BERNABEI 00D limit is for inelastic scattering $X^0\,^{129}$Xe → $X^0\,^{129}$Xe (39.58 keV).
[24] AMBROSIO 99 search for upgoing muon events induced by neutrinos originating from WIMP annihilations in the Sun and Earth.
[25] BRHLIK 99 discuss the effect of astrophysical uncertainties on the WIMP interpretation of the BERNABEI 99 signal.
[26] KLIMENKO 98 limit is for inelastic scattering $X^0\,^{73}$Ge → $X^0\,^{73}$Ge* (13.26 keV).
[27] KLIMENKO 98 limit is for inelastic scattering $X^0\,^{73}$Ge → $X^0\,^{73}$Ge* (66.73 keV).
[28] BELLI 96 limit for inelastic scattering $X^0\,^{129}$Xe → $X^0\,^{129}$Xe*(39.58 keV).
[29] BELLI 96C use background subtraction and obtain σ < 0.35 pb (< 0.15 fb) (90%CL) for spin-dependent (independent) X^0-proton cross section. The confidence level is from R. Bernabei, private communication, May 20, 1999.
[30] BERNABEI 96 use pulse shape discrimination to enhance the possible signal. The limit here is from R. Bernabei, private communication, September 19, 1997.
[31] SARSA 96 search for annual modulation of WIMP signal. See SARSA 97 for details of the analysis. The limit here is from M.L. Sarsa, private communication, May 26, 1997.
[32] SMITH 96 use pulse shape discrimination to enhance the possible signal. A dark matter density of 0.4 GeV cm^{-3} is assumed.
[33] GARCIA 95 limit is from the event rate. A weaker limit is obtained from searches for diurnal and annual modulation.
[34] SNOWDEN-IFFT 95 look for recoil tracks in an ancient mica crystal. Similar limits are also given for ^{27}Al and ^{28}Si. See COLLAR 96 and SNOWDEN-IFFT 96 for discussion on potential backgrounds.
[35] BECK 94 uses enriched ^{76}Ge (86% purity).
[36] REUSSER 91 limit here is changed from published (0.3) after reanalysis by authors. J.L. Vuilleumier, private communication, March 29, 1996.

For m_{X^0} = 1 TeV

VALUE (nb)	CL%	DOCUMENT ID		TECN	COMMENT
• • • We do not use the following data for averages, fits, limits, etc. • • •					
		[37] MIUCHI	03	BOLO	LiF
		[38] TAKEDA	03	BOLO	NaF
< 3	90	[39] ANGLOHER	02	CRES	Al
		[40] BENOIT	00	EDEL	Ge
		[41] BERNABEI	99D	CNTR	SIMP
		[42] DERBIN	99	CNTR	SIMP
< 0.06	95	[43] KLIMENKO	98	CNTR	^{73}Ge, inel.
< 0.4	95	[44] KLIMENKO	98	CNTR	^{73}Ge, inel.
< 40		ALESSAND...	96	CNTR	O
< 700		ALESSAND...	96	CNTR	Te
< 0.05	90	[45] BELLI	96	CNTR	^{129}Xe, inel.
< 1.5	90	[46] BELLI	96	CNTR	^{129}Xe, inel.
		[47] BELLI	96C	CNTR	^{129}Xe
< 0.01	90	[48] BERNABEI	96	CNTR	Na
< 9	90	[48] BERNABEI	96	CNTR	I
< 7	95	[49] SARSA	96	CNTR	Na
< 0.3	90	[50] SMITH	96	CNTR	Na
< 6	90	[50] SMITH	96	CNTR	I
< 6	95	[51] GARCIA	95	CNTR	Natural Ge
< 8	95	QUENBY	95	CNTR	Na
< 50	95	QUENBY	95	CNTR	I
< 7 × 10^2	90	[52] SNOWDEN-...	95	MICA	^{16}O
< 1 × 10^3	90	[52] SNOWDEN-...	95	MICA	^{39}K
< 0.8	90	[53] BECK	94	CNTR	^{76}Ge
< 30	90	BACCI	92	CNTR	Na
< 30	90	BACCI	92	CNTR	I
< 15	90	[54] REUSSER	91	CNTR	Natural Ge
< 6	95	CALDWELL	88	CNTR	Natural Ge

[37] MIUCHI 03 give model-independent limit $\sigma < 260$ pb (90%CL) for spin-dependent X^0-proton cross section.

[38] TAKEDA 03 give model-independent limit $\sigma < 0.15$ (4) nb (90%CL) for spin-dependent χ^0-proton (neutron) cross section.

[39] ANGLOHER 02 limit is for spin-dependent WIMP-Aluminum cross section.

[40] BENOIT 00 find four event categories in Ge detectors and suggest that low-energy surface nuclear recoils can explain anomalous events reported by UKDMC and Saclay NaI experiments.

[41] BERNABEI 99D search for SIMPs (Strongly Interacting Massive Particles) in the mass range 10^3–10^{16} GeV. See their Fig. 3 for cross-section limits.

[42] DERBIN 99 search for SIMPs (Strongly Interacting Massive Particles) in the mass range 10^2–10^{14} GeV. See their Fig. 3 for cross-section limits.

[43] KLIMENKO 98 limit is for inelastic scattering $X^0\,^{73}\mathrm{Ge} \rightarrow X^0\,^{73}\mathrm{Ge}^*$ (13.26 keV).

[44] KLIMENKO 98 limit is for inelastic scattering $X^0\,^{73}\mathrm{Ge} \rightarrow X^0\,^{73}\mathrm{Ge}^*$ (66.73 keV).

[45] BELLI 96 limit for inelastic scattering $X^0\,^{129}\mathrm{Xe} \rightarrow X^0\,^{129}\mathrm{Xe}^*$(39.58 keV).

[46] BELLI 96 limit for inelastic scattering $X^0\,^{129}\mathrm{Xe} \rightarrow X^0\,^{129}\mathrm{Xe}^*$(236.14 keV).

[47] BELLI 96C use background subtraction and obtain $\sigma < 0.7$ pb (< 0.7 fb) (90%CL) for spin-dependent (independent) X^0-proton cross section. The confidence level is from R. Bernabei, private communication, May 20, 1999.

[48] BERNABEI 96 use pulse shape discrimination to enhance the possible signal. The limit here is from R. Bernabei, private communication, September 19, 1997.

[49] SARSA 96 search for annual modulation of WIMP signal. See SARSA 97 for details of the analysis. The limit here is from M.L. Sarsa, private communication, May 26, 1997.

[50] SMITH 96 use pulse shape discrimination to enhance the possible signal. A dark matter density of 0.4 GeV cm^{-3} is assumed.

[51] GARCIA 95 limit is from the event rate. A weaker limit is obtained from searches for diurnal and annual modulation.

[52] SNOWDEN-IFFT 95 look for recoil tracks in an ancient mica crystal. Similar limits are also given for ^{27}Al and ^{28}Si. See COLLAR 96 and SNOWDEN-IFFT 96 for discussion on potential backgrounds.

[53] BECK 94 uses enriched ^{76}Ge (86% purity).

[54] REUSSER 91 limit here is changed from published (5) after reanalysis by authors. J.L. Vuilleumier, private communication, March 29, 1996.

CONCENTRATION OF STABLE PARTICLES IN MATTER

Concentration of Heavy (Charge +1) Stable Particles in Matter

VALUE	CL%	DOCUMENT ID		TECN	COMMENT
• • • We do not use the following data for averages, fits, limits, etc. • • •					
$< 4 \times 10^{-17}$	95	[55] YAMAGATA	93	SPEC	Deep sea water, M=5–1600 m_p
$< 6 \times 10^{-15}$	95	[56] VERKERK	92	SPEC	Water, $M = 10^5$ to 3×10^7 GeV
$< 7 \times 10^{-15}$	95	[56] VERKERK	92	SPEC	Water, $M = 10^4$, 6×10^7 GeV
$< 9 \times 10^{-15}$	95	[56] VERKERK	92	SPEC	Water, $M = 10^8$ GeV
$< 3 \times 10^{-23}$	90	[57] HEMMICK	90	SPEC	Water, $M = 1000 m_p$
$< 2 \times 10^{-21}$	90	[57] HEMMICK	90	SPEC	Water, $M = 5000 m_p$
$< 3 \times 10^{-20}$	90	[57] HEMMICK	90	SPEC	Water, $M = 10000 m_p$
$< 1. \times 10^{-29}$		SMITH	82B	SPEC	Water, M=30–400 m_p
$< 2. \times 10^{-28}$		SMITH	82B	SPEC	Water, M=12–1000 m_p
$< 1. \times 10^{-14}$		SMITH	82B	SPEC	Water, $M > 1000\ m_p$
$< (0.2\text{–}1.) \times 10^{-21}$		SMITH	79	SPEC	Water, M=6–350 m_p

[55] YAMAGATA 93 used deep sea water at 4000 m since the concentration is enhanced in deep sea due to gravity.

[56] VERKERK 92 looked for heavy isotopes in sea water and put a bound on concentration of stable charged massive particle in sea water. The above bound can be translated into into a bound on charged dark matter particle (5×10^6 GeV), assuming the local density, ρ=0.3 GeV/cm^3, and the mean velocity $\langle v \rangle$=300 km/s.

[57] See HEMMICK 90 Fig. 7 for other masses 100–10000 m_p.

Concentration of Heavy Stable Particles Bound to Nuclei

VALUE	CL%	DOCUMENT ID		TECN	COMMENT
• • • We do not use the following data for averages, fits, limits, etc. • • •					
$< 1.2 \times 10^{-11}$	95	[58] JAVORSEK	01	SPEC	Au, M= 3 GeV
$< 6.9 \times 10^{-10}$	95	[58] JAVORSEK	01	SPEC	Au, M= 144 GeV
$< 1 \times 10^{-11}$	95	[59] JAVORSEK	01B	SPEC	Au, M= 188 GeV
$< 1 \times 10^{-8}$	95	[59] JAVORSEK	01B	SPEC	Au, M= 1669 GeV
$< 6 \times 10^{-9}$	95	[59] JAVORSEK	01B	SPEC	Fe, M= 188 GeV
$< 1 \times 10^{-8}$	95	[59] JAVORSEK	01B	SPEC	Fe, M= 647 GeV
$< 4 \times 10^{-20}$	90	[60] HEMMICK	90	SPEC	C, $M = 100 m_p$
$< 8 \times 10^{-20}$	90	[60] HEMMICK	90	SPEC	C, $M = 1000 m_p$
$< 2 \times 10^{-16}$	90	[60] HEMMICK	90	SPEC	C, $M = 10000 m_p$
$< 6 \times 10^{-13}$	90	[60] HEMMICK	90	SPEC	Li, $M = 1000 m_p$
$< 1 \times 10^{-11}$	90	[60] HEMMICK	90	SPEC	Be, $M = 1000 m_p$
$< 6 \times 10^{-14}$	90	[60] HEMMICK	90	SPEC	B, $M = 1000 m_p$
$< 4 \times 10^{-17}$	90	[60] HEMMICK	90	SPEC	O, $M = 1000 m_p$
$< 4 \times 10^{-15}$	90	[60] HEMMICK	90	SPEC	F, $M = 1000 m_p$
$< 1.5 \times 10^{-13}$/nucleon	68	[61] NORMAN	89	SPEC	^{206}Pb X^-
$< 1.2 \times 10^{-12}$/nucleon	68	[61] NORMAN	87	SPEC	^{56,58}Fe X^-

[58] JAVORSEK 01 search for (neutral) SIMPs (strongly interacting massive particles) bound to Au nuclei. Here M is the effective SIMP mass.

[59] JAVORSEK 01B search for (neutral) SIMPs (strongly interacting massive particles) bound to Au and Fe nuclei from various origins with exposures on the earth's surface, in a satellite, heavy ion collisions, etc. Here M is the mass of the anomalous nucleus. See also JAVORSEK 02.

[60] See HEMMICK 90 Fig. 7 for other masses 100–10000 m_p.

[61] Bound valid up to $m_{X^-} \sim 100$ TeV.

LIMITS ON NEUTRAL PARTICLE PRODUCTION

Production Cross Section of Radiatively-Decaying Neutral Particle

VALUE (pb)	CL%	DOCUMENT ID		TECN	COMMENT
• • • We do not use the following data for averages, fits, limits, etc. • • •					
$< (0.043\text{–}0.17)$	95	[62] ABBIENDI,G	00D	OPAL	$e^+e^- \rightarrow X^0Y^0$, $X^0 \rightarrow Y^0\gamma$
$< (0.05\text{–}0.8)$	95	[63] ABBIENDI,G	00D	OPAL	$e^+e^- \rightarrow X^0X^0$, $X^0 \rightarrow Y^0\gamma$
$< (2.5\text{–}0.5)$	95	[64] ACKERSTAFF	97B	OPAL	$e^+e^- \rightarrow X^0Y^0$, $X^0 \rightarrow Y^0\gamma$
$< (1.6\text{–}0.9)$	95	[65] ACKERSTAFF	97B	OPAL	$e^+e^- \rightarrow X^0X^0$, $X^0 \rightarrow Y^0\gamma$

[62] ABBIENDI,G 00D associated production limit is for m_{X^0}= 90–188 GeV, m_{Y^0}=0 at E_{cm}=189 GeV. See also their Fig. 9.

[63] ABBIENDI,G 00D pair production limit is for m_{X^0} = 45–94 GeV, m_{Y^0}=0 at E_{cm}=189 GeV. See also their Fig. 12.

[64] ACKERSTAFF 97B associated production limit is for m_{X^0} = 80–160 GeV, m_{Y^0}=0 from 10.0 pb^{-1} at E_{cm} = 161 GeV. See their Fig. 3(a).

[65] ACKERSTAFF 97B pair production limit is for m_{X^0} = 40–80 GeV, m_{Y^0}=0 from 10.0 pb^{-1} at E_{cm} = 161 GeV. See their Fig. 3(b).

Heavy Particle Production Cross Section

VALUE (cm^2/N)	CL%	EVTS	DOCUMENT ID		TECN	COMMENT
• • • We do not use the following data for averages, fits, limits, etc. • • •						
			[66] ADAMS	97B	KTEV	m= 1.2–5 GeV
$< 10^{-36}$–10^{-33}	90		[67] GALLAS	95	TOF	m= 0.5–20 GeV
$< (4\text{–}0.3) \times 10^{-31}$	95		[68] AKESSON	91	CNTR	m = 0–5 GeV
$< 2 \times 10^{-36}$	90	0	[69] BADIER	86	BDMP	$\tau = (0.05\text{–}1.) \times 10^{-8}$ s
$< 2.5 \times 10^{-35}$		0	[70] GUSTAFSON	76	CNTR	$\tau > 10^{-7}$ s

[66] ADAMS 97B search for a hadron-like neutral particle produced in pN interactions, which decays into a ρ^0 and a weakly interacting massive particle. Upper limits are given for the ratio to K_L production for the mass range 1.2–5 GeV and lifetime 10^{-9}–10^{-4} s. See also our Light Gluino Section.

[67] GALLAS 95 limit is for a weakly interacting neutral particle produced in 800 GeV/c pN interactions decaying with a lifetime of 10^{-4}–10^{-8} s. See their Figs. 8 and 9. Similar limits are obtained for a stable particle with interaction cross section 10^{-29}–10^{-33} cm^2. See Fig. 10.

[68] AKESSON 91 limit is from weakly interacting neutral long-lived particles produced in pN reaction at 450 GeV/c performed at CERN SPS. Bourquin-Gaillard formula is used as the production model. The above limit is for $\tau > 10^{-7}$ s. For $\tau > 10^{-9}$ s, $\sigma < 10^{-30}$ cm^{-2}/nucleon is obtained.

[69] BADIER 86 looked for long-lived particles at 300 GeV π^- beam dump. The limit applies for nonstrongly interacting neutral or charged particles with mass >2 GeV. The limit applies for particle modes, $\mu^+\pi^-$, $\mu^+\mu^-$, $\pi^+\pi^-$X, $\pi^+\pi^-\pi^\pm$ etc. See their figure 5 for the contours of limits in the mass-τ plane for each mode.

[70] GUSTAFSON 76 is a 300 GeV FNAL experiment looking for heavy ($m > 2$ GeV) long-lived neutral hadrons in the M4 neutral beam. The above typical value is for $m = 3$ GeV and assumes an interaction cross section of 1 mb. Values as a function of mass and interaction cross section are given in figure 2.

Production of New Penetrating Non-ν Like States in Beam Dump

VALUE	DOCUMENT ID		TECN	COMMENT
• • • We do not use the following data for averages, fits, limits, etc. • • •				
	[71] LOSECCO	81	CALO	28 GeV protons

[71] No excess neutral-current events leads to σ(production) $\times$ σ(interaction)$\times$acceptance $< 2.26 \times 10^{-71}$ cm^4/nucleon^2 (CL = 90%) for light neutrals. Acceptance depends on models (0.1 to 4. $\times 10^{-4}$).

LIMITS ON JET-JET RESONANCES

Heavy Particle Production Cross Section in $p\overline{p}$

Limits are for a particle decaying to two hadronic jets.

Units(pb)	CL%	Mass(GeV)	DOCUMENT ID	TECN	COMMENT
• • • We do not use the following data for averages, fits, limits, etc. • • •					
			[72] ABE	99F CDF	1.8 TeV $p\overline{p} \rightarrow b\overline{b}$+ anything
			[73] ABE	97G CDF	1.8 TeV $p\overline{p} \rightarrow$ 2 jets
< 2603	95	200	[74] ABE	93G CDF	1.8 TeV $p\overline{p} \rightarrow$ 2jets
< 44	95	400	[74] ABE	93G CDF	1.8 TeV $p\overline{p} \rightarrow$ 2jets
< 7	95	600	[74] ABE	93G CDF	1.8 TeV $p\overline{p} \rightarrow$ 2jets

[72] ABE 99F search for narrow $b\overline{b}$ resonances in $p\overline{p}$ collisions at E_{cm}=1.8 TeV. Limits on $\sigma(p\overline{p} \rightarrow X+$ anything$)\times$B$(X \rightarrow b\overline{b})$ in the range 3–10^3 pb (95%CL) are given for m_X=200–750 GeV. See their Table I.

[73] ABE 97G search for narrow dijet resonances in $p\overline{p}$ collisions with 106 pb^{-1} of data at E_{cm} = 1.8 TeV. Limits on $\sigma(p\overline{p} \rightarrow X +$ anything$)\cdot$B$(X \rightarrow jj)$ in the range 10^4–10^{-1} pb (95%CL) are given for dijet mass m=200–1150 GeV with both jets having $|\eta| < 2.0$ and the dijet system having $|\cos\theta^*| < 0.67$. See their Table I for the list of limits. Supersedes ABE 93G.

[74] ABE 93G gives cross section times branching ratio into light (d, u, s, c, b) quarks for $\Gamma = 0.02\,M$. Their Table II gives limits for M = 200–900 GeV and $\Gamma = (0.02–0.2)\,M$.

LIMITS ON CHARGED PARTICLES IN e^+e^-

Heavy Particle Production Cross Section in e^+e^-

Ratio to $\sigma(e^+e^- \rightarrow \mu^+\mu^-)$ unless noted. See also entries in Free Quark Search and Magnetic Monopole Searches.

VALUE	CL%	EVTS	DOCUMENT ID		TECN	COMMENT
• • • We do not use the following data for averages, fits, limits, etc. • • •						
			[75] ACKERSTAFF	98P OPAL		Q=1,2/3, m=45–89.5 GeV
			[76] ABREU	97D DLPH		Q=1,2/3, m=45–84 GeV
			[77] BARATE	97K ALEP		Q=1, m=45–85 GeV
$<2 \times 10^{-5}$	95		[78] AKERS	95R OPAL		Q=1, m= 5–45 GeV
$<1 \times 10^{-5}$	95		[78] AKERS	95R OPAL		Q=2, m= 5–45 GeV
$<2 \times 10^{-3}$	90		[79] BUSKULIC	93C ALEP		Q=1, m=32–72 GeV
$<(10^{-2}–1)$	95		[80] ADACHI	90C TOPZ		Q = 1, m = 1–16, 18–27 GeV
$<7 \times 10^{-2}$	90		[81] ADACHI	90E TOPZ		Q = 1, m = 5–25 GeV
$<1.6 \times 10^{-2}$	95	0	[82] KINOSHITA	82 PLAS		Q=3–180, m <14.5 GeV
$<5.0 \times 10^{-2}$	90	0	[83] BARTEL	80 JADE		Q=(3,4,5)/3 2–12 GeV

[75] ACKERSTAFF 98P search for pair production of long-lived charged particles at E_{cm} between 130 and 183 GeV and give limits $\sigma <$(0.05–0.2) pb (95%CL) for spin-0 and spin-1/2 particles with m=45–89.5 GeV, charge 1 and 2/3. The limit is translated to the cross section at E_{cm}=183 GeV with the s dependence described in the paper. See their Figs. 2–4.

[76] ABREU 97D search for pair production of long-lived particles and give limits $\sigma <$(0.4–2.3) pb (95%CL) for various center-of-mass energies E_{cm}=130–136, 161, and 172 GeV, assuming an almost flat production distribution in cosθ.

[77] BARATE 97K search for pair production of long-lived charged particles at E_{cm} = 130, 136, 161, and 172 GeV and give limits $\sigma <$(0.2–0.4) pb (95%CL) for spin-0 and spin-1/2 particles with m=45–85 GeV. The limit is translated to the cross section at E_{cm}=172 GeV with the E_{cm} dependence described in the paper. See their Figs. 2 and 3 for limits on J = 1/2 and J = 0 cases.

[78] AKERS 95R is a CERN-LEP experiment with $W_{cm} \sim m_Z$. The limit is for the production of a stable particle in multihadron events normalized to $\sigma(e^+e^- \rightarrow$ hadrons). Constant phase space distribution is assumed. See their Fig. 3 for bounds for $Q = \pm 2/3$, $\pm 4/3$.

[79] BUSKULIC 93C is a CERN-LEP experiment with $W_{cm} = m_Z$. The limit is for a pair or single production of heavy particles with unusual ionization loss in TPC. See their Fig. 5 and Table 1.

[80] ADACHI 90C is a KEK-TRISTAN experiment with W_{cm} = 52–60 GeV. The limit is for pair production of a scalar or spin-1/2 particle. See Figs. 3 and 4.

[81] ADACHI 90E is KEK-TRISTAN experiment with W_{cm} = 52–61.4 GeV. The above limit is for inclusive production cross section normalized to $\sigma(e^+e^- \rightarrow \mu^+\mu^-)\cdot\beta(3-\beta^2)/2$, where $\beta = (1 - 4m^2/W_{cm}^2)^{1/2}$. See the paper for the assumption about the production mechanism.

[82] KINOSHITA 82 is SLAC PEP experiment at W_{cm} = 29 GeV using lexan and ^{39}Cr plastic sheets sensitive to highly ionizing particles.

[83] BARTEL 80 is DESY-PETRA experiment with W_{cm} = 27–35 GeV. Above limit is for inclusive pair production and ranges between $1. \times 10^{-1}$ and $1. \times 10^{-2}$ depending on mass and production momentum distributions. (See their figures 9, 10, 11).

Branching Fraction of Z^0 to a Pair of Stable Charged Heavy Fermions

VALUE	CL%	DOCUMENT ID		TECN	COMMENT
• • • We do not use the following data for averages, fits, limits, etc. • • •					
$<5 \times 10^{-6}$	95	[84] AKERS	95R OPAL		m= 40.4–45.6 GeV
$<1 \times 10^{-3}$	95	AKRAWY	90O OPAL		m = 29–40 GeV

[84] AKERS 95R give the 95% CL limit $\sigma(X\overline{X})/\sigma(\mu\mu) < 1.8\times10^{-4}$ for the pair production of singly- or doubly-charged stable particles. The limit applies for the mass range 40.4–45.6 GeV for $X^{\pm}$ and < 45.6 GeV for $X^{\pm\pm}$. See the paper for bounds for $Q = \pm 2/3$, $\pm 4/3$.

LIMITS ON CHARGED PARTICLES IN HADRONIC REACTIONS

Heavy Particle Production Cross Section

VALUE (nb)	CL%	EVTS	DOCUMENT ID		TECN	COMMENT
• • • We do not use the following data for averages, fits, limits, etc. • • •						
<0.05	95		[85] ABE	92J CDF		m=50–200 GeV
<30–130			[86] CARROLL	78 SPEC		m=2–2.5 GeV
<100		0	[87] LEIPUNER	73 CNTR		m=3–11 GeV

[85] ABE 92J look for pair production of unit-charged particles which leave detector before decaying. Limit shown here is for m=50 GeV. See their Fig. 5 for different charges and stronger limits for higher mass.

[86] CARROLL 78 look for neutral, $S = -2$ dihyperon resonance in $pp \rightarrow 2K^+X$. Cross section varies within above limits over mass range and p_{lab} = 5.1–5.9 GeV/c.

[87] LEIPUNER 73 is an NAL 300 GeV p experiment. Would have detected particles with lifetime greater than 200 ns.

Heavy Particle Production Differential Cross Section

VALUE ($cm^2 sr^{-1} GeV^{-1}$)	CL%	EVTS	DOCUMENT ID		TECN	CHG	COMMENT
• • • We do not use the following data for averages, fits, limits, etc. • • •							
$<2.6 \times 10^{-36}$	90	0	[88] BALDIN	76	CNTR	–	Q= 1, m=2.1–9.4 GeV
$<2.2 \times 10^{-33}$	90	0	[89] ALBROW	75	SPEC	±	Q= ±1, m=4–15 GeV
$<1.1 \times 10^{-33}$	90	0	[89] ALBROW	75	SPEC	±	Q= ±2, m=6–27 GeV
$<8. \times 10^{-35}$	90	0	[90] JOVANOV...	75	CNTR	±	m=15–26 GeV
$<1.5 \times 10^{-34}$	90	0	[90] JOVANOV...	75	CNTR	±	Q= ±2, m=3–10 GeV
$<6. \times 10^{-35}$	90	0	[90] JOVANOV...	75	CNTR	±	Q= ±2, m=10–26 GeV
$<1. \times 10^{-31}$	90	0	[91] APPEL	74	CNTR	±	m=3.2–7.2 GeV
$<5.8 \times 10^{-34}$	90	0	[92] ALPER	73	SPEC	±	m=1.5–24 GeV
$<1.2 \times 10^{-35}$	90	0	[93] ANTIPOV	71B	CNTR	–	Q=–, m=2.2–2.8
$<2.4 \times 10^{-35}$	90	0	[94] ANTIPOV	71C	CNTR	–	Q=–, m=1.2–1.7, 2.1–4
$<2.4 \times 10^{-35}$	90	0	BINON	69	CNTR	–	Q=–, m=1–1.8 GeV
$<1.5 \times 10^{-36}$		0	[95] DORFAN	65	CNTR		Be target m=3–7 GeV
$<3.0 \times 10^{-36}$		0	[95] DORFAN	65	CNTR		Fe target m=3–7 GeV

[88] BALDIN 76 is a 70 GeV Serpukhov experiment. Value is per Al nucleus at $\theta = 0$. For other charges in range -0.5 to -3.0, CL = 90% limit is $(2.6 \times 10^{-36})/|(\text{charge})|$ for mass range (2.1–9.4 GeV) $\times |(\text{charge})|$. Assumes stable particle interacting with matter as do antiprotons.

[89] ALBROW 75 is a CERN ISR experiment with E_{cm} = 53 GeV. θ = 40 mr. See figure 5 for mass ranges up to 35 GeV.

[90] JOVANOVICH 75 is a CERN ISR 26+26 and 15+15 GeV pp experiment. Figure 4 covers ranges Q = 1/3 to 2 and m = 3 to 26 GeV. Value is per GeV momentum.

[91] APPEL 74 is NAL 300 GeV pW experiment. Studies forward production of heavy (up to 24 GeV) charged particles with momenta 24–200 GeV (−charge) and 40–150 GeV (+charge). Above typical value is for 75 GeV and is per GeV momentum per nucleon.

[92] ALPER 73 is CERN ISR 26+26 GeV pp experiment. $p >$0.9 GeV, 0.2 < β <0.65.

[93] ANTIPOV 71B is from same 70 GeV p experiment as ANTIPOV 71C and BINON 69.

[94] ANTIPOV 71C limit inferred from flux ratio. 70 GeV p experiment.

[95] DORFAN 65 is a 30 GeV/c p experiment at BNL. Units are per GeV momentum per nucleus.

Long-Lived Heavy Particle Invariant Cross Section

VALUE (cm^2/GeV^2/N)	CL%	EVTS	DOCUMENT ID		TECN	CHG	COMMENT
• • • We do not use the following data for averages, fits, limits, etc. • • •							
$< 5 \times 10^{-35}$–7×10^{-33}	90	0	[96] BERNSTEIN	88	CNTR		
$< 5 \times 10^{-37}$–7×10^{-35}	90	0	[96] BERNSTEIN	88	CNTR		
$<2.5 \times 10^{-36}$	90	0	[97] THRON	85	CNTR	–	Q= 1, m=4–12 GeV
$<1. \times 10^{-35}$	90	1	[97] THRON	85	CNTR	+	Q= 1, m=4–12 GeV
$<6. \times 10^{-33}$	90	0	[98] ARMITAGE	79	SPEC		m=1.87 GeV
$<1.5 \times 10^{-33}$	90	0	[98] ARMITAGE	79	SPEC		m=1.5–3.0 GeV
		0	[99] BOZZOLI	79	CNTR	±	Q = (2/3, 1, 4/3, 2)
$<1.1 \times 10^{-37}$	90	0	[100] CUTTS	78	CNTR		m=4–10 GeV
$<3.0 \times 10^{-37}$	90	0	[101] VIDAL	78	CNTR		m=4.5–6 GeV

[96] BERNSTEIN 88 limits apply at x = 0.2 and p_T = 0. Mass and lifetime dependence of limits are shown in the regions: m = 1.5–7.5 GeV and $\tau = 10^{-8}$–2×10^{-6} s. First number is for hadrons; second is for weakly interacting particles.

[97] THRON 85 is FNAL 400 GeV proton experiment. Mass determined from measured velocity and momentum. Limits are for $\tau > 3 \times 10^{-9}$ s.

[98] ARMITAGE 79 is CERN-ISR experiment at E_{cm} = 53 GeV. Value is for x = 0.1 and p_T = 0.15. Observed particles at m = 1.87 GeV are found all consistent with being antideuterons.

[99] BOZZOLI 79 is CERN-SPS 200 GeV pN experiment. Looks for particle with τ larger than 10^{-8} s. See their figure 11–18 for production cross-section upper limits vs mass.

[100] CUTTS 78 is pBe experiment at FNAL sensitive to particles of $\tau > 5 \times 10^{-8}$ s. Value is for -0.3 <x<0 and p_T = 0.175.

[101] VIDAL 78 is FNAL 400 GeV proton experiment. Value is for x = 0 and p_T = 0. Puts lifetime limit of $< 5 \times 10^{-8}$ s on particle in this mass range.

Long-Lived Heavy Particle Production (σ(Heavy Particle) / $\sigma(\pi)$)

VALUE	EVTS	DOCUMENT ID		TECN	CHG	COMMENT
• • • We do not use the following data for averages, fits, limits, etc. • • •						
$<10^{-8}$		[102] NAKAMURA	89 SPEC		±	Q= (−5/3,±2)
	0	[103] BUSSIERE	80 CNTR		±	Q= (2/3,1,4/3,2)

[102] NAKAMURA 89 is KEK experiment with 12 GeV protons on Pt target. The limit applies for mass $\lesssim$ 1.6 GeV and lifetime $\gtrsim 10^{-7}$ s.

[103] BUSSIERE 80 is CERN-SPS experiment with 200–240 GeV protons on Be and Al target. See their figures 6 and 7 for cross-section ratio vs mass.

Production and Capture of Long-Lived Massive Particles

VALUE (10^{-36} cm^2)	EVTS	DOCUMENT ID		TECN	COMMENT
• • • We do not use the following data for averages, fits, limits, etc. • • •					
<20 to 800	0	[104] ALEKSEEV	76	ELEC	τ=5 ms to 1 day
<200 to 2000	0	[104] ALEKSEEV	76B	ELEC	τ=100 ms to 1 day
<1.4 to 9	0	[105] FRANKEL	75	CNTR	τ=50 ms to 10 hours
<0.1 to 9	0	[106] FRANKEL	74	CNTR	τ=1 to 1000 hours

[104] ALEKSEEV 76 and ALEKSEEV 76B are 61–70 GeV p Serpukhov experiment. Cross section is per Pb nucleus.
[105] FRANKEL 75 is extension of FRANKEL 74.
[106] FRANKEL 74 looks for particles produced in thick Al targets by 300–400 GeV/c protons.

Long-Lived Particle Search at Hadron Collisions

Limits are for cross section times branching ratio.

VALUE (pb/nucleon)	CL%	EVTS	DOCUMENT ID		TECN	COMMENT
• • • We do not use the following data for averages, fits, limits, etc. • • •						
<2	90	0	[107] BADIER	86	BDMP	$\tau = (0.05–1.) \times 10^{-8}$s

[107] BADIER 86 looked for long-lived particles at 300 GeV π^- beam dump. The limit applies for nonstrongly interacting neutral or charged particles with mass >2 GeV. The limit applies for particle modes, $\mu^+\pi^-$, $\mu^+\mu^-$, $\pi^+\pi^-$X, $\pi^+\pi^-\pi^\pm$ etc. See their figure 5 for the contours of limits in the mass-τ plane for each mode.

Long-Lived Heavy Particle Cross Section

VALUE (pb/sr)	CL%	DOCUMENT ID		TECN	COMMENT
• • • We do not use the following data for averages, fits, limits, etc. • • •					
<34	95	[108] RAM	94	SPEC	1015< $m_{X^{++}}$ <1085 MeV
<75	95	[108] RAM	94	SPEC	920< $m_{X^{++}}$ <1025 MeV

[108] RAM 94 search for a long-lived doubly-charged fermion X^{++} with mass between m_N and m_N+m_π and baryon number +1 in the reaction $pp \to X^{++}n$. No candidate is found. The limit is for the cross section at 15° scattering angle at 460 MeV incident energy and applies for $\tau(X^{++}) \gg 0.1\,\mu$s.

LIMITS ON CHARGED PARTICLES IN COSMIC RAYS

Heavy Particle Flux in Cosmic Rays

VALUE (cm^{-2}sr^{-1}s^{-1})	CL%	EVTS	DOCUMENT ID		TECN	CHG	COMMENT
• • • We do not use the following data for averages, fits, limits, etc. • • •							
$\sim 6 \times 10^{-9}$		2	[109] SAITO	90			$Q \simeq 14$, $m \simeq 370 m_p$
$< 1.4 \times 10^{-12}$	90	0	[110] MINCER	85	CALO		$m \geq 1$ TeV
			[111] SAKUYAMA	83B	PLAS		$m \sim 1$ TeV
$< 1.7 \times 10^{-11}$	99	0	[112] BHAT	82	CC		
$< 1. \times 10^{-9}$	90	0	[113] MARINI	82	CNTR	±	Q= 1, $m \sim 4.5 m_p$
2. $\times 10^{-9}$		3	[114] YOCK	81	SPRK	±	Q= 1, $m \sim 4.5 m_p$
		3	[114] YOCK	81	SPRK		Fractionally charged
3.0 $\times 10^{-9}$		3	[115] YOCK	80	SPRK		$m \sim 4.5\ m_p$
(4 ±1) $\times 10^{-11}$		3	GOODMAN	79	ELEC		$m \geq 5$ GeV
$< 1.3 \times 10^{-9}$	90		[116] BHAT	78	CNTR	±	m >1 GeV
$< 1.0 \times 10^{-9}$		0	BRIATORE	76	ELEC		
$< 7. \times 10^{-10}$	90	0	YOCK	75	ELEC	±	$Q > 7e$ or $< -7e$
$> 6. \times 10^{-9}$		5	[117] YOCK	74	CNTR		m >6 GeV
$< 3.0 \times 10^{-8}$		0	DARDO	72	CNTR		
$< 1.5 \times 10^{-9}$		0	TONWAR	72	CNTR		m >10 GeV
$< 3.0 \times 10^{-10}$		0	BJORNBOE	68	CNTR		m >5 GeV
$< 5.0 \times 10^{-11}$	90	0	JONES	67	ELEC		m=5–15 GeV

[109] SAITO 90 candidates carry about 450 MeV/nucleon. Cannot be accounted for by conventional backgrounds. Consistent with strange quark matter hypothesis.
[110] MINCER 85 is high statistics study of calorimeter signals delayed by 20–200 ns. Calibration with AGS beam shows they can be accounted for by rare fluctuations in signals from low-energy hadrons in the shower. Claim that previous delayed signals including BJORNBOE 68, DARDO 72, BHAT 82, SAKUYAMA 83B below may be due to this fake effect.
[111] SAKUYAMA 83B analyzed 6000 extended air shower events. Increase of delayed particles and change of lateral distribution above 10^{17} eV may indicate production of very heavy parent at top of atmosphere.
[112] BHAT 82 observed 12 events with delay $> 2. \times 10^{-8}$ s and with more than 40 particles. 1 eV has good hadron shower. However all events are delayed in only one of two detectors in cloud chamber, and could not be due to strongly interacting massive particle.
[113] MARINI 82 applied PEP-counter for TOF. Above limit is for velocity = 0.54 of light. Limit is inconsistent with YOCK 80 YOCK 81 events if isotropic dependence on zenith angle is assumed.
[114] YOCK 81 saw another 3 events with $Q = \pm 1$ and m about $4.5 m_p$ as well as 2 events with m >5.3m_p, $Q = \pm 0.75 \pm 0.05$ and m >2.8m_p, $Q = \pm 0.70 \pm 0.05$ and 1 event with $m = (9.3 \pm 3.)m_p$, $Q = \pm 0.89 \pm 0.06$ as possible heavy candidates.
[115] YOCK 80 events are with charge exactly or approximately equal to unity.
[116] BHAT 78 is at Kolar gold fields. Limit is for $\tau > 10^{-6}$ s.
[117] YOCK 74 events could be tritons.

Superheavy Particle (Quark Matter) Flux in Cosmic Rays

VALUE (cm^{-2}sr^{-1}s^{-1})	CL%	EVTS	DOCUMENT ID		TECN	COMMENT
• • • We do not use the following data for averages, fits, limits, etc. • • •						
$< 5 \times 10^{-16}$	90		[118] AMBROSIO	00B	MCRO	$m > 5 \times 10^{14}$ GeV
$< 1.8 \times 10^{-12}$	90		[119] ASTONE	93	CNTR	$m \geq 1.5 \times 10^{-13}$gram
$< 1.1 \times 10^{-14}$	90		[120] AHLEN	92	MCRO	$10^{-10} < m < 0.1$ gram
$< 2.2 \times 10^{-14}$	90	0	[121] NAKAMURA	91	PLAS	$m > 10^{11}$ GeV
$< 6.4 \times 10^{-16}$	90	0	[122] ORITO	91	PLAS	$m > 10^{12}$ GeV
$< 2.0 \times 10^{-11}$	90		[123] LIU	88	BOLO	$m > 1.5 \times 10^{-13}$ gram
$< 4.7 \times 10^{-12}$	90		[124] BARISH	87	CNTR	$1.4 \times 10^8 < m < 10^{12}$ GeV
$< 3.2 \times 10^{-11}$	90	0	[125] NAKAMURA	85	CNTR	$m > 1.5 \times 10^{-13}$gram
$< 3.5 \times 10^{-11}$	90	0	[126] ULLMAN	81	CNTR	Planck-mass 10^{19}GeV
$< 7. \times 10^{-11}$	90	0	[126] ULLMAN	81	CNTR	$m \leq 10^{16}$ GeV

[118] AMBROSIO 00B searched for quark matter ("nuclearites") in the velocity range $(10^{-5}–1)\,c$. The listed limit is for $2 \times 10^{-3}\,c$.
[119] ASTONE 93 searched for quark matter ("nuclearites") in the velocity range $(10^{-3}–1)\,c$. Their Table 1 gives a compilation of searches for nuclearites.
[120] AHLEN 92 searched for quark matter ("nuclearites"). The bound applies to velocity $< 2.5 \times 10^{-3}\,c$. See their Fig. 3 for other velocity/c and heavier mass range.
[121] NAKAMURA 91 searched for quark matter in the velocity range $(4 \times 10^{-5}–1)\,c$.
[122] ORITO 91 searched for quark matter. The limit is for the velocity range $(10^{-4}–10^{-3})\,c$.
[123] LIU 88 searched for quark matter ("nuclearites") in the velocity range $(2.5 \times 10^{-3}–1)c$. A less stringent limit of 5.8×10^{-11} applies for $(1–2.5) \times 10^{-3}c$.
[124] BARISH 87 searched for quark matter ("nuclearites") in the velocity range $(2.7 \times 10^{-4}–5 \times 10^{-3})c$.
[125] NAKAMURA 85 at KEK searched for quark-matter. These might be lumps of strange quark matter with roughly equal numbers of u, d, s quarks. These lumps or nuclearites were assumed to have velocity of $(10^{-4}–10^{-3})\,c$.
[126] ULLMAN 81 is sensitive for heavy slow singly charge particle reaching earth with vertical velocity 100–350 km/s.

Highly Ionizing Particle Flux

VALUE (m^{-2}yr^{-1})	CL%	EVTS	DOCUMENT ID	TECN	COMMENT
• • • We do not use the following data for averages, fits, limits, etc. • • •					
<0.4	95	0	KINOSHITA	81B PLAS	Z/β 30–100

REFERENCES FOR Searches for WIMPs and Other Particles

MIUCHI 03 ASP 19 135 K. Miuchi *et al.*
TAKEDA 03 PL B572 145 A. Takeda *et al.*
ANGLOHER 02 ASP 18 43 G. Angloher *et al.* (CRESST Collab.)
BELLI 02 PR D66 043503 P. Belli *et al.*
BERNABEI 02C EPJ C23 61 R. Bernabei *et al.* (DAMA Collab.)
GREEN 02 PR D66 083003 A.M. Green
JAVORSEK 02 PR D65 072003 D. Javorsek II *et al.*
JAVORSEK 01 PR D64 012005 D. Javorsek II *et al.*
JAVORSEK 01B PRL 87 231804 D. Javorsek II *et al.*
SMITH 01 PR D64 043502 D. Smith, N. Weiner
ULLIO 01 JHEP 0107 044 P. Ullio, M. Kamionkowski, P. Vogel
ABBIENDI,G 00D EPJ C18 253 G. Abbiendi *et al.* (OPAL Collab.)
AMBROSIO 00B EPJ C13 453 M. Ambrosio *et al.* (MACRO Collab.)
BENOIT 00 PL B479 8 A. Benoit *et al.* (EDELWEISS Collab.)
BERNABEI 00D NJP 2 15 R. Bernabei *et al.* (DAMA Collab.)
ABE 99F PRL 82 2038 F. Abe *et al.* (CDF Collab.)
AMBROSIO 99 PR D60 082002 M. Ambrosio *et al.* (Macro Collab.)
BERNABEI 99 PL B450 448 R. Bernabei *et al.* (DAMA Collab.)
BERNABEI 99D PRL 83 4918 R. Bernabei *et al.* (DAMA Collab.)
BRHLIK 99 PL B464 303 M. Brhlik, L. Roszkowski
DERBIN 99 PAN 62 1886 A.V. Derbin *et al.*
Translated from YAF 62 2034.
ACKERSTAFF 98P PL B433 195 K. Ackerstaff *et al.* (OPAL Collab.)
KLIMENKO 98 JETPL 67 875 A.A. Klimenko *et al.*
Translated from ZETFP 67 835.
ABE 97G PR D55 R5263 F. Abe *et al.* (CDF Collab.)
ABREU 97D PL B396 315 P. Abreu *et al.* (DELPHI Collab.)
ACKERSTAFF 97B PL B391 210 K. Ackerstaff *et al.* (OPAL Collab.)
ADAMS 97B PRL 79 4083 J. Adams *et al.* (FNAL KTeV Collab.)
BARATE 97K PL B405 379 R. Barate *et al.* (ALEPH Collab.)
SARSA 97 PR D56 1856 M.L. Sarsa *et al.* (ZARA)
ALESSAND... 96 PL B384 316 A. Alessandrello *et al.* (MILA, MILAI, SASSO)
BELLI 96 PL B387 222 P. Belli *et al.* (DAMA Collab.)
Also 96B PL B389 783 (erratum) P. Belli *et al.* (DAMA Collab.)
BELLI 96C NC 19C 537 P. Belli *et al.* (DAMA Collab.)
BERNABEI 96 PL B389 757 R. Bernabei *et al.* (DAMA Collab.)
COLLAR 96 PRL 76 331 J.I. Collar (SCUC)
SARSA 96 PL B386 458 M.L. Sarsa *et al.* (ZARA)
Also 97 PR D56 1856 M.L. Sarsa *et al.* (ZARA)
SMITH 96 PL B379 299 P.F. Smith *et al.* (RAL, SHEF, LOIC+)
SNOWDEN-... 96 PRL 76 332 D.P. Snowden-Ifft, E.S. Freeman, P.B. Price (UCB)
AKERS 95R ZPHY C67 203 R. Akers *et al.* (OPAL Collab.)
GALLAS 95 PR D52 6 E. Gallas *et al.* (MSU, FNAL, MIT, FLOR)
GARCIA 95 PR D51 1458 E. Garcia *et al.* (ZARA, SCUC, PNL)
QUENBY 95 PL B351 70 J.J. Quenby *et al.* (LOIC, RAL, SHEF+)
SNOWDEN-... 95 PRL 74 4133 D.P. Snowden-Ifft, E.S. Freeman, P.B. Price (UCB)
Also 96 PRL 76 331 J.I. Collar (SCUC)
Also 96 PRL 76 332 D.P. Snowden-Ifft, E.S. Freeman, P.B. Price (UCB)
BECK 94 PL B336 141 M. Beck *et al.* (MPIH, KIAE, SASSO)
RAM 94 PR D49 3120 S. Ram *et al.* (TELA, TRIU)
ABE 93G PRL 71 2542 F. Abe *et al.* (CDF Collab.)
ASTONE 93 PR D47 4770 P. Astone *et al.* (ROMA, ROMAI, CATA, FRAS)
BUSKULIC 93C PL B303 198 D. Buskulic *et al.* (ALEPH Collab.)
YAMAGATA 93 PR D47 1231 T. Yamagata, Y. Takamori, H. Utsunomiya (KONAN)
ABE 92J PR D46 R1889 F. Abe *et al.* (CDF Collab.)
AHLEN 92 PRL 69 1860 S.P. Ahlen *et al.* (MACRO Collab.)
BACCI 92 PL B293 460 C. Bacci *et al.* (Beijing-Roma-Saclay Collab.)
VERKERK 92 PRL 68 1116 P. Verkerk *et al.* (ENSP, SACL, PAST)
AKESSON 91 ZPHY C52 219 T. Akesson *et al.* (HELIOS Collab.)
NAKAMURA 91 PL B263 529 S. Nakamura *et al.*
ORITO 91 PRL 66 1951 S. Orito *et al.* (ICEPP, WASCR, NIHO, ICRR)
REUSSER 91 PL B255 143 D. Reusser *et al.* (NEUC, CIT, PSI)
ADACHI 90C PL B244 352 I. Adachi *et al.* (TOPAZ Collab.)
ADACHI 90E PL B249 336 I. Adachi *et al.* (TOPAZ Collab.)

AKRAWY	90O	PL B252 290	M.Z. Akrawy *et al.*	(OPAL Collab.)
HEMMICK	90	PR D41 2074	T.K. Hemmick *et al.*	(ROCH, MICH, OHIO+)
SAITO	90	PRL 65 2094	T. Saito *et al.*	(ICRR, KOBE)
NAKAMURA	89	PR D39 1261	T.T. Nakamura *et al.*	(KYOT, TMTC)
NORMAN	89	PR D39 2499	E.B. Norman *et al.*	(LBL)
BERNSTEIN	88	PR D37 3103	R.M. Bernstein *et al.*	(STAN, WISC)
CALDWELL	88	PRL 61 510	D.O. Caldwell *et al.*	(UCSB, UCB, LBL)
LIU	88	PRL 61 271	G. Liu, B. Barish	
BARISH	87	PR D36 2641	B.C. Barish, G. Liu, C. Lane	(CIT)
NORMAN	87	PRL 58 1403	E.B. Norman, S.B. Gazes, D.A. Bennett	(LBL)
BADIER	86	ZPHY C31 21	J. Badier *et al.*	(NA3 Collab.)
MINCER	85	PR D32 541	A. Mincer *et al.*	(UMD, GMAS, NSF)
NAKAMURA	85	PL 161B 417	K. Nakamura *et al.*	(KEK, INUS)
THRON	85	PR D31 451	J.L. Thron *et al.*	(YALE, FNAL, IOWA)
SAKUYAMA	83B	LNC 37 17	H. Sakuyama, N. Suzuki	(MEIS)
Also	83	LNC 36 389	H. Sakuyama, K. Watanabe	(MEIS)
Also	83D	NC 78A 147	H. Sakuyama, K. Watanabe	(MEIS)
Also	83C	NC 6C 371	H. Sakuyama, K. Watanabe	(MEIS)
BHAT	82	PR D25 2820	P.N. Bhat *et al.*	(TATA)
KINOSHITA	82	PRL 48 77	K. Kinoshita, P.B. Price, D. Fryberger	(UCB+)
MARINI	82	PR D26 1777	A. Marini *et al.*	(FRAS, LBL, NWES, STAN+)
SMITH	82B	NP B206 333	P.F. Smith *et al.*	(RAL)
KINOSHITA	81B	PR D24 1707	K. Kinoshita, P.B. Price	(UCB)
LOSECCO	81	PL 102B 209	J.M. LoSecco *et al.*	(MICH, PENN, BNL)
ULLMAN	81	PRL 47 289	J.D. Ullman	(LEHM, BNL)
YOCK	81	PR D23 1207	P.C.M. Yock	(AUCK)
BARTEL	80	ZPHY C6 295	W. Bartel *et al.*	(JADE Collab.)
BUSSIERE	80	NP B174 1	A. Bussiere *et al.*	(BGNA, SACL, LAPP)
YOCK	80	PR D22 61	P.C.M. Yock	(AUCK)
ARMITAGE	79	NP B150 87	J.C.M. Armitage *et al.*	(CERN, DARE, FOM+)
BOZZOLI	79	NP B159 363	W. Bozzoli *et al.*	(BGNA, LAPP, SACL+)
GOODMAN	79	PR D19 2572	J.A. Goodman *et al.*	(UMD)
SMITH	79	NP B149 525	P.F. Smith, J.R.J. Bennett	(RHEL)
BHAT	78	Pramana 10 115	P.N. Bhat, P.V. Ramana Murthy	(TATA)
CARROLL	78	PRL 41 777	A.S. Carroll *et al.*	(BNL, PRIN)
CUTTS	78	PRL 41 363	D. Cutts *et al.*	(BROW, FNAL, ILL, BARI+)
VIDAL	78	PL 77B 344	R.A. Vidal *et al.*	(COLU, FNAL, STON+)
ALEKSEEV	76	SJNP 22 531 Translated from YAF 22 1021.	G.D. Alekseev *et al.*	(JINR)
ALEKSEEV	76B	SJNP 23 633 Translated from YAF 23 1190.	G.D. Alekseev *et al.*	(JINR)
BALDIN	76	SJNP 22 264 Translated from YAF 22 512.	B.Y. Baldin *et al.*	(JINR)
BRIATORE	76	NC 31A 553	L. Briatore *et al.*	(LCGT, FRAS, FREIB)
GUSTAFSON	76	PRL 37 474	H.R. Gustafson *et al.*	(MICH)
ALBROW	75	NP B97 189	M.G. Albrow *et al.*	(CERN, DARE, FOM+)
FRANKEL	75	PR D12 2561	S. Frankel *et al.*	(PENN, FNAL)
JOVANOV...	75	PL 56B 105	J.V. Jovanovich *et al.*	(MANI, AACH, CERN+)
YOCK	75	NP B86 216	P.C.M. Yock	(AUCK, SLAC)
APPEL	74	PRL 32 428	J.A. Appel *et al.*	(COLU, FNAL)
FRANKEL	74	PR D9 1932	S. Frankel *et al.*	(PENN, FNAL)
YOCK	74	NP B76 175	P.C.M. Yock	(AUCK)
ALPER	73	PL 46B 265	B. Alper *et al.*	(CERN, LIVP, LUND, BOHR+)
LEIPUNER	73	PRL 31 1226	L.B. Leipuner *et al.*	(BNL, YALE)
DARDO	72	NC 9A 319	M. Dardo *et al.*	(TORI)
TONWAR	72	JPA 5 569	S.C. Tonwar, S. Naranan, B.V. Sreekantan	(TATA)
ANTIPOV	71B	NP B31 235	Y.M. Antipov *et al.*	(SERP)
ANTIPOV	71C	PL 34B 164	Y.M. Antipov *et al.*	(SERP)
BINON	69	PL 30B 510	F.G. Binon *et al.*	(SERP)
BJORNBOE	68	NC B53 241	J. Bjornboe *et al.*	(BOHR, TATA, BERN+)
JONES	67	PR 164 1584	L.W. Jones	(MICH, WISC, LBL, UCLA, MINN+)
DORFAN	65	PRL 14 999	D.E. Dorfan *et al.*	(COLU)

INDEX

Greek letters are alphabetized by their English-language spelling. Bold page numbers signify entries in the Particle Properties Summary Tables.

Greek letters are alphabetized by their English-language spelling. Bold page numbers signify entries in the Particle Properties Summary Tables.

Greek letters are alphabetized by their English-language spelling. Bold page numbers signify entries in the Particle Properties Summary Tables.

Greek letters are alphabetized by their English-language spelling. Bold page numbers signify entries in the Particle Properties Summary Tables.

Greek letters are alphabetized by their English-language spelling. Bold page numbers signify entries in the Particle Properties Summary Tables.

Greek letters are alphabetized by their English-language spelling. Bold page numbers signify entries in the Particle Properties Summary Tables.

Greek letters are alphabetized by their English-language spelling. Bold page numbers signify entries in the Particle Properties Summary Tables.

Greek letters are alphabetized by their English-language spelling. Bold page numbers signify entries in the Particle Properties Summary Tables.

Greek letters are alphabetized by their English-language spelling. Bold page numbers signify entries in the Particle Properties Summary Tables.

Greek letters are alphabetized by their English-language spelling. Bold page numbers signify entries in the Particle Properties Summary Tables.

Greek letters are alphabetized by their English-language spelling. Bold page numbers signify entries in the Particle Properties Summary Tables.

Greek letters are alphabetized by their English-language spelling. Bold page numbers signify entries in the Particle Properties Summary Tables.

Greek letters are alphabetized by their English-language spelling. Bold page numbers signify entries in the Particle Properties Summary Tables.

Greek letters are alphabetized by their English-language spelling. Bold page numbers signify entries in the Particle Properties Summary Tables.

Greek letters are alphabetized by their English-language spelling. Bold page numbers signify entries in the Particle Properties Summary Tables.

Greek letters are alphabetized by their English-language spelling. Bold page numbers signify entries in the Particle Properties Summary Tables.

COLOR FIGURES

Electroweak model and constraints on new physics (p.122)

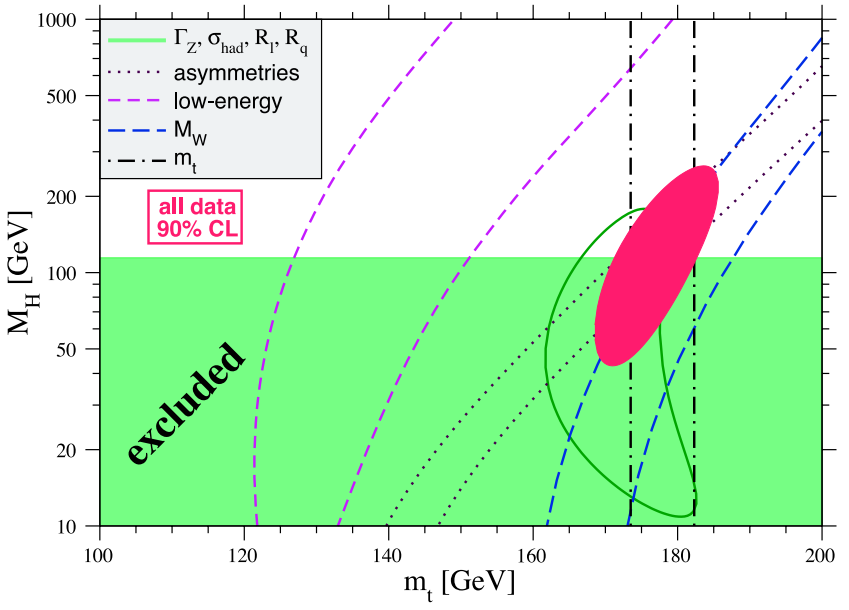

Figure 10.1: One-standard-deviation (39.35%) uncertainties in M_H as a function of m_t for various inputs, and the 90% CL region ($\Delta\chi^2 = 4.605$) allowed by all data. $\alpha_s(M_Z) = 0.120$ is assumed except for the fits including the Z-lineshape data. The 95% direct lower limit from LEP 2 is also shown.

Electroweak model and constraints on new physics (p.123)

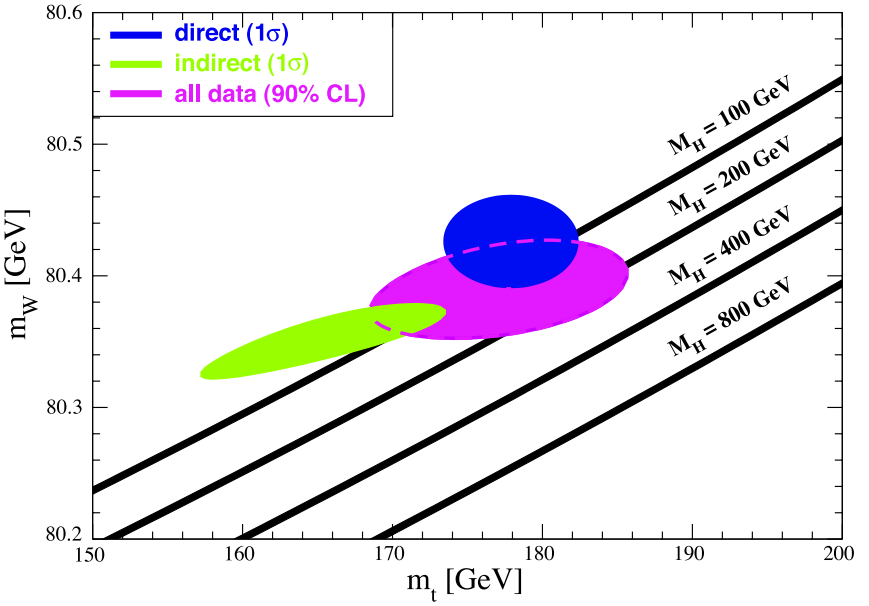

Figure 10.2: One-standard-deviation (39.35%) region in M_W as a function of m_t for the direct and indirect data, and the 90% CL region ($\Delta\chi^2 = 4.605$) allowed by all data. The SM prediction as a function of M_H is also indicated. The widths of the M_H bands reflect the theoretical uncertainty from $\alpha(M_Z)$.

Electroweak model and constraints on new physics (p.125)

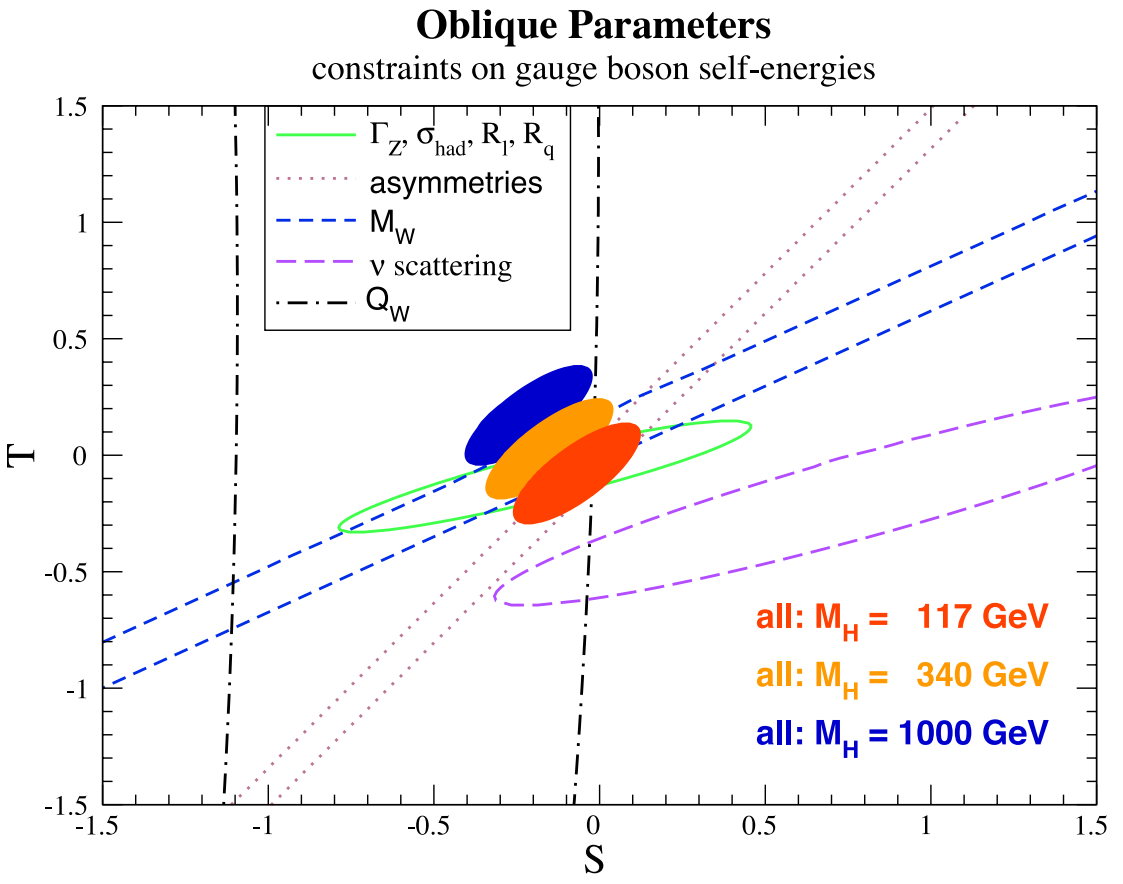

Figure 10.3: 1 σ constraints (39.35%) on S and T from various inputs. S and T represent the contributions of new physics only. (Uncertainties from m_t are included in the errors.) The contours assume $M_H = 117$ GeV except for the central and upper 90% CL contours allowed by all data, which are for $M_H = 340$ GeV and 1000 GeV, respectively. Data sets not involving M_W are insensitive to U. Due to higher order effects, however, $U = 0$ has to be assumed in all fits. α_s is constrained using the τ lifetime as additional input in all fits.

CKM quark-mixing matrix (p.133)

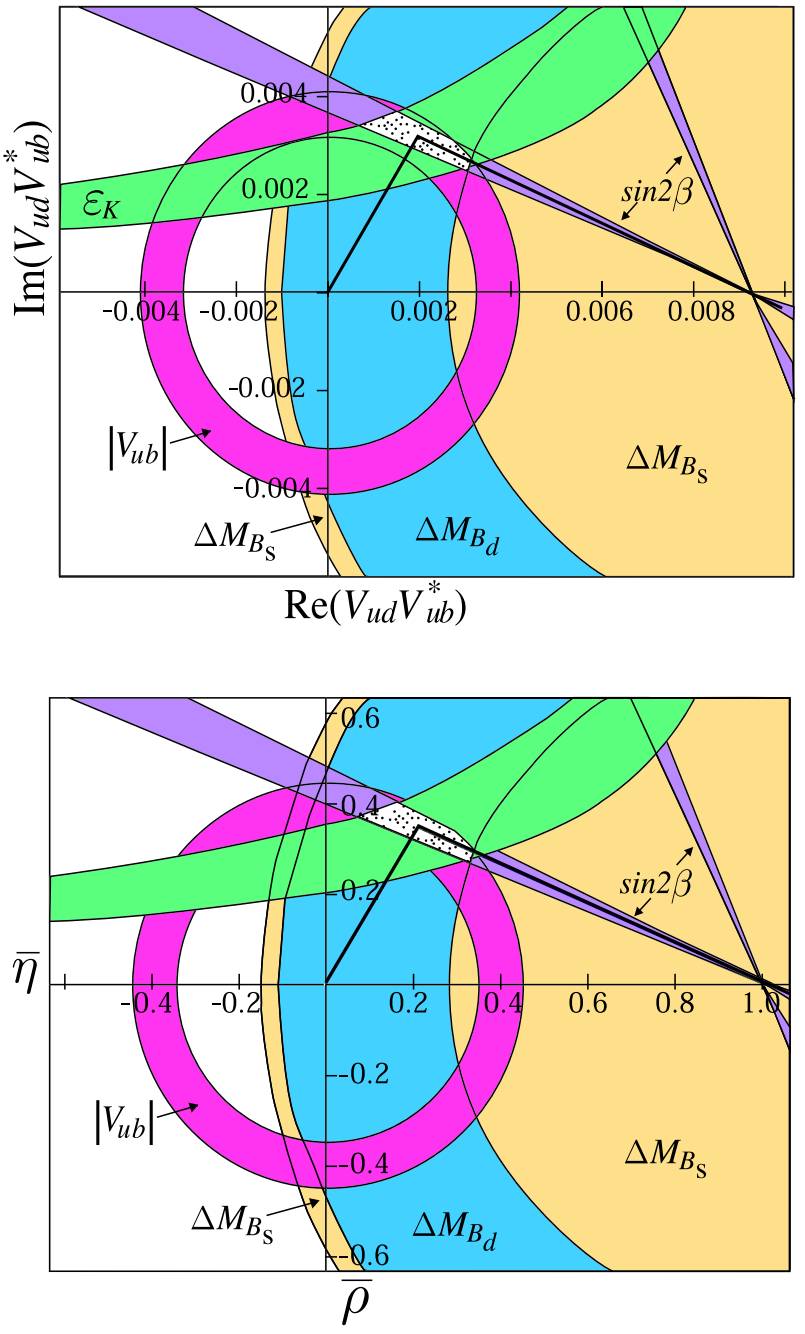

Figure 11.2: Constraints from the text on the position of the apex, A, of the unitarity triangle following from $|V_{ub}|$,B mixing, ϵ, and $\sin 2\beta$. A possible unitarity triangle is shown with A in the preferred region.

Neutrino mixing (p.148)

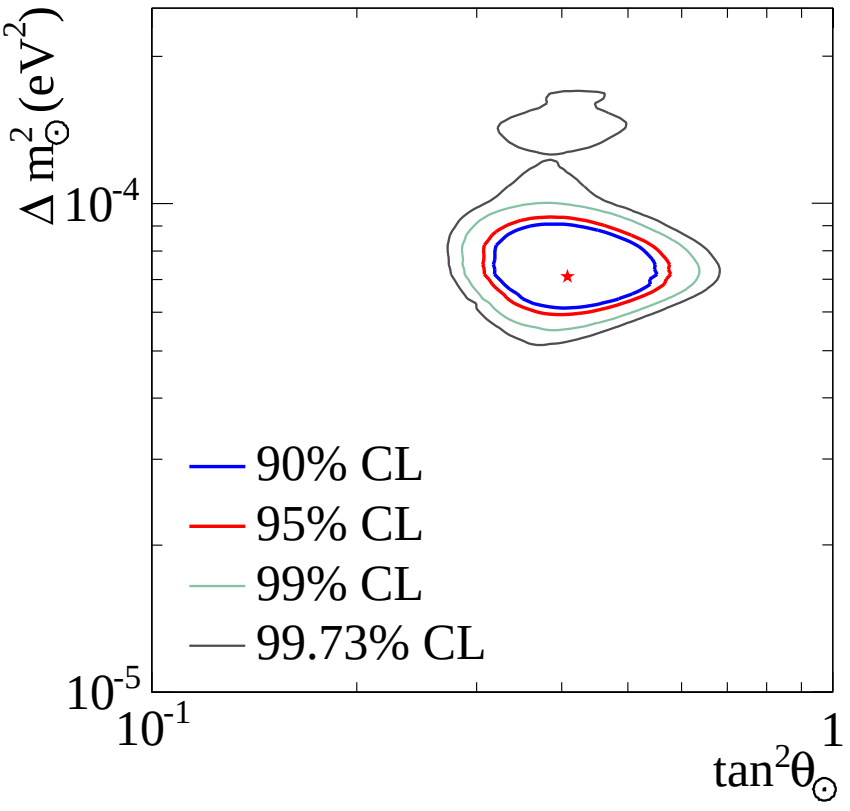

Figure 13.1: The region allowed for the neutrino parameters $\Delta m^2_\odot$ and $\theta_\odot$ by the solar and KamLAND data. The best-fit point, indicated by the star, is $\Delta m^2_\odot = 7.1 \times 10^{-5}\,\mathrm{eV}^2$ and $\theta_\odot = 32.5°$.

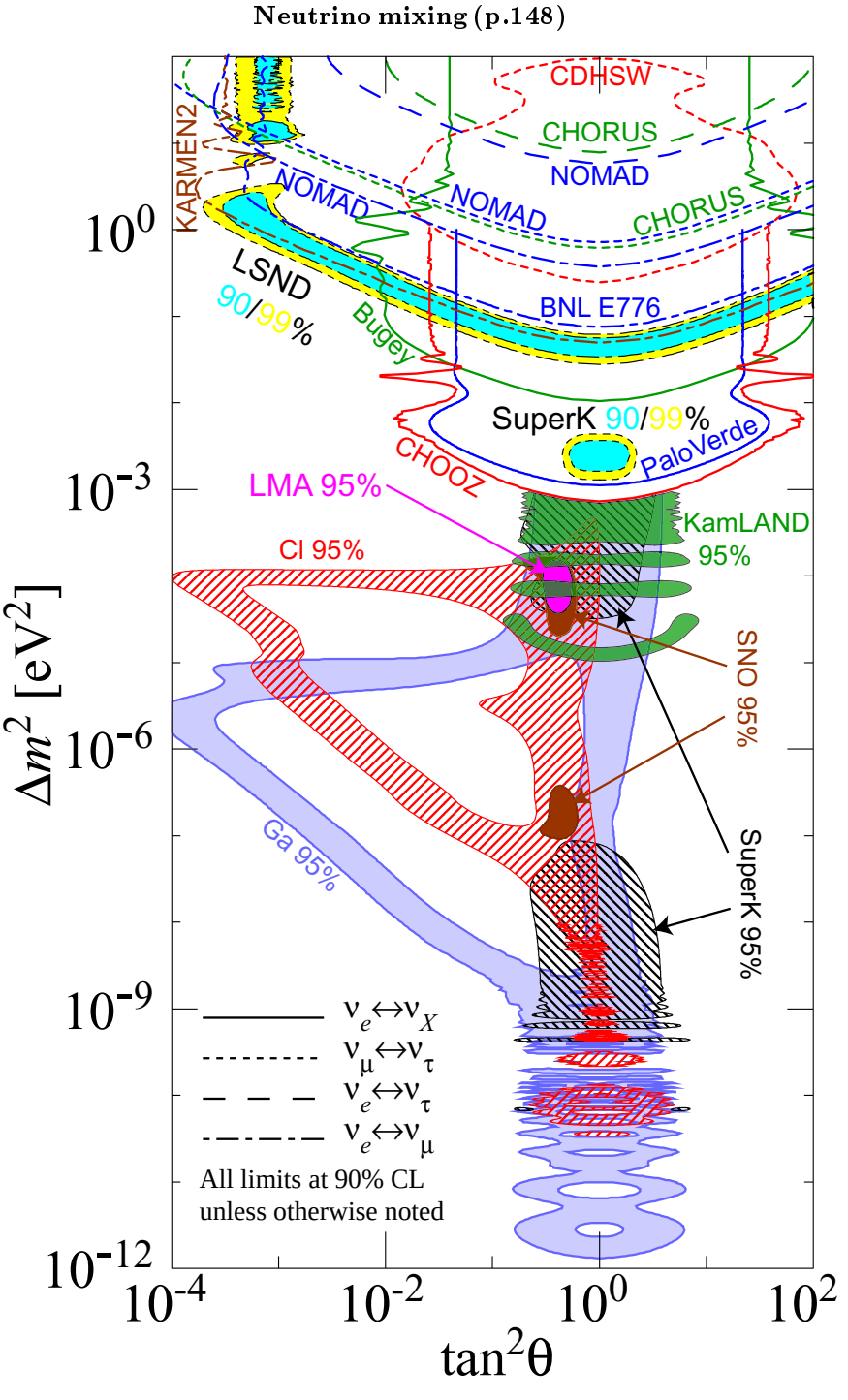

Figure 13.2: The regions of squared-mass splitting and mixing angle favored or excluded by various experiments. This figure was contributed by H. Murayama (University of California, Berkeley). References to the data used in the figure can be found at `http://hitoshi.berkeley.edu/neutrino/ref.html`.

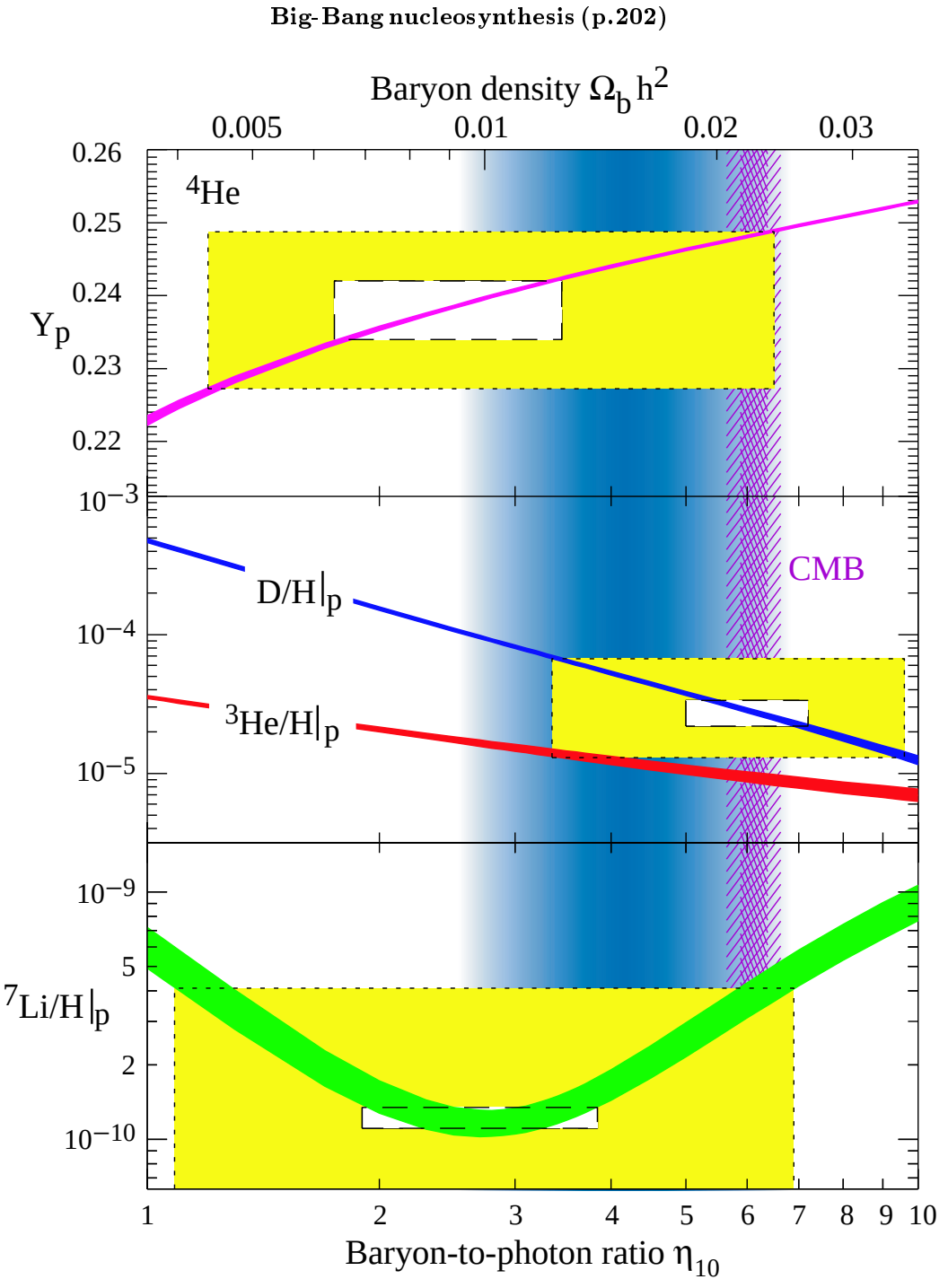

Figure 20.1: The abundances of ^{4}He, D, ^{3}He and ^{7}Li as predicted by the standard model of big-bang nucleosynthesis. Boxes indicate the observed light element abundances (smaller boxes: 2σ statistical errors; larger boxes: $\pm 2\sigma$ statistical and systematic errors added in quadrature). The narrow vertical band indicates the CMB measure of the cosmic baryon density.

The Cosmological Parameters (p.210)

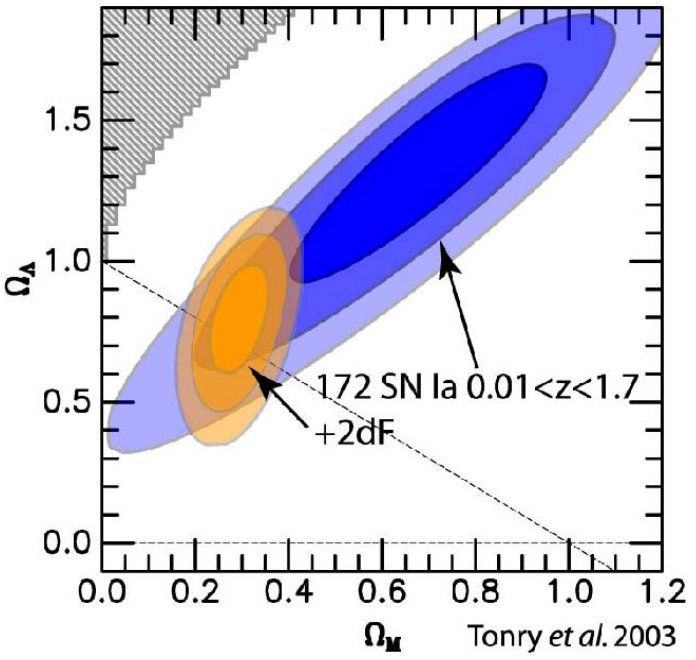

Figure 21.1: This shows the preferred region in the Ω_m–Ω_Λ plane from a study of 172 supernovae, and also how the constraints tighten when the 2dF galaxy redshift survey power spectrum is added as an additional constraint. [Reproduced with permission from Tonry *et al.* [16].]

The Cosmological Parameters (p.213)

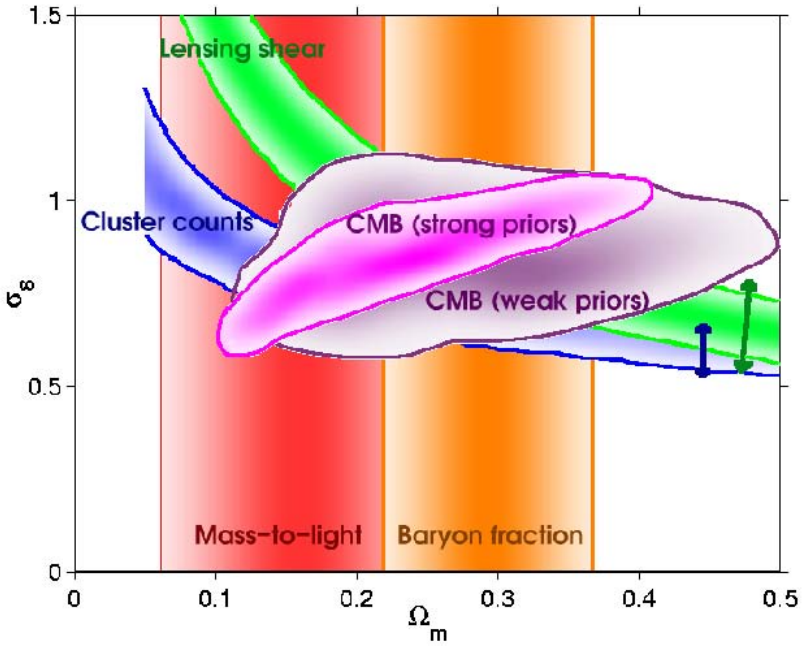

Figure 21.4: Various constraints shown in the Ω_m–σ_8 plane. [Figure provided by Sarah Bridle; see also Ref. 42.]

The Mass of the W boson (p.336)

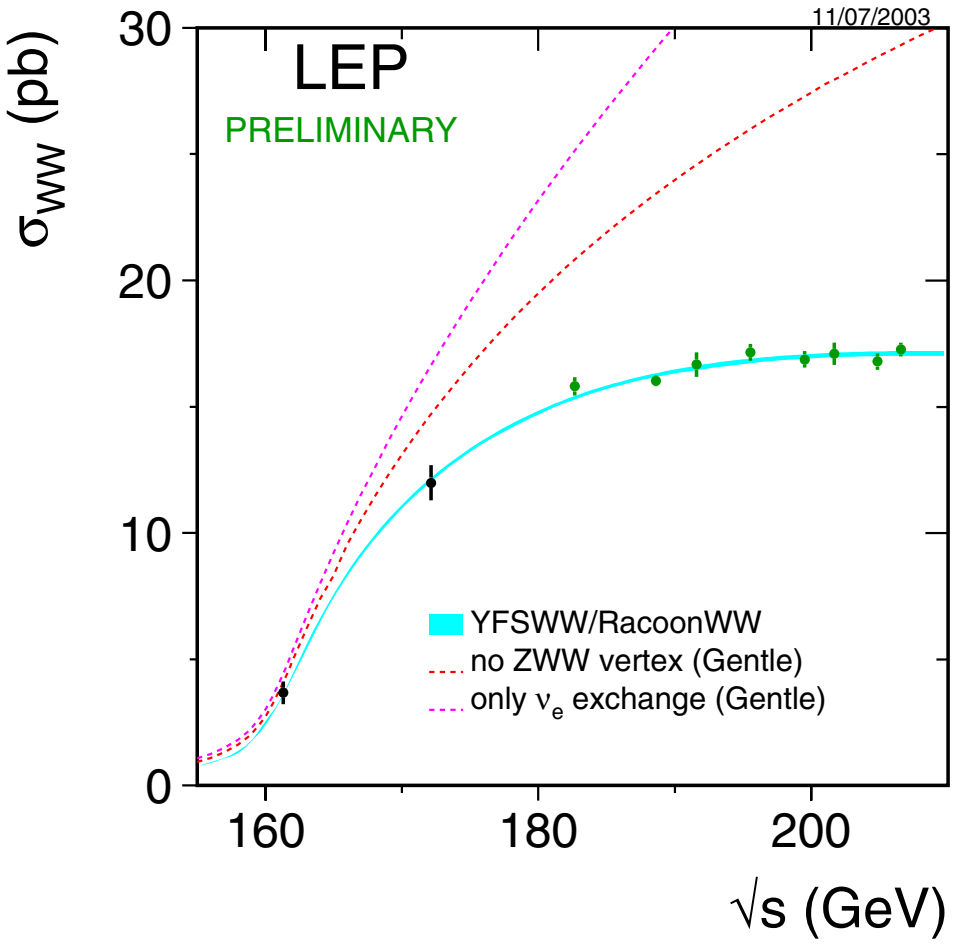

Figure 1: The W–pair cross section as a function of the center–of–mass energy. The data points are the LEP averages. The solid lines are predictions from different models of WW production. For comparison the figure contains also the cross section if the ZWW coupling did not exist (dashed line), or if only the t–channel ν_e exchange diagram existed (dotted-dashed line). (Figure from `http://lepewwg.web.cern.ch/LEPEWWG/lepww/4f/Summer03/wwxsec/nocouplings/2003.eps`)

Searches for Higgs Bosons (p.366)

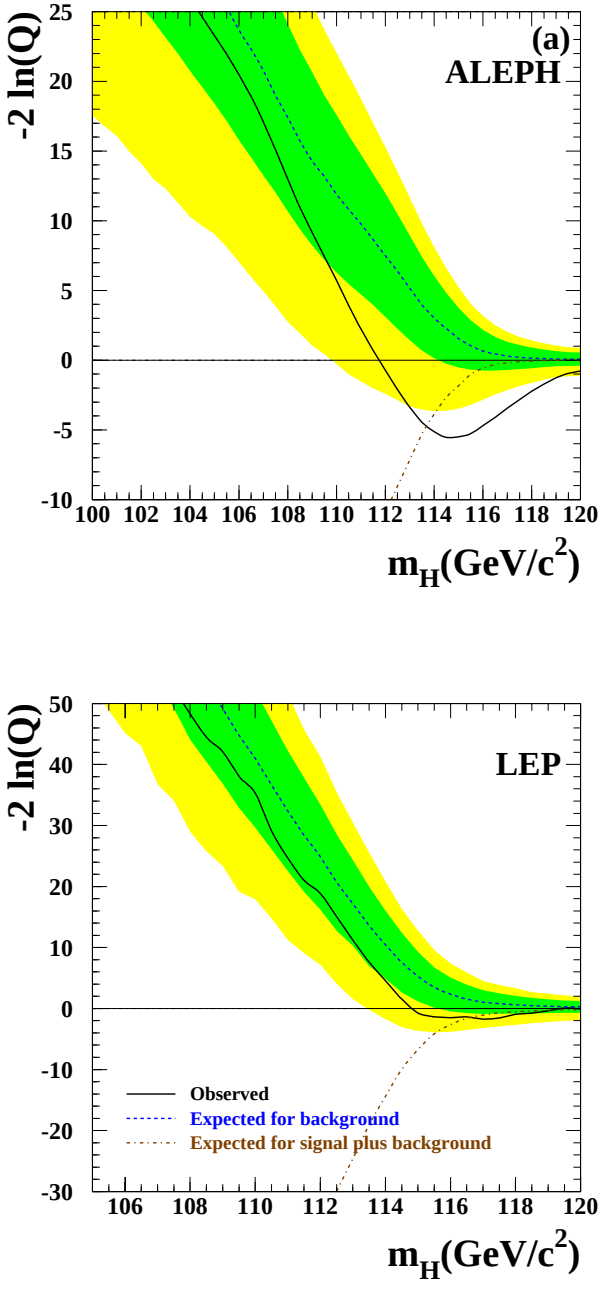

Figure 2: Observed (solid line), and expected behaviors of the test statistic $-2\ln Q$ for the background (dashed line), and the signal + background hypothesis (dash-dotted line) as a function of the test mass m_H. Top: ALEPH data alone; bottom: LEP data combined [27]. The dark and light shaded areas represent the 68% and 95% probability bands about the background expectation.

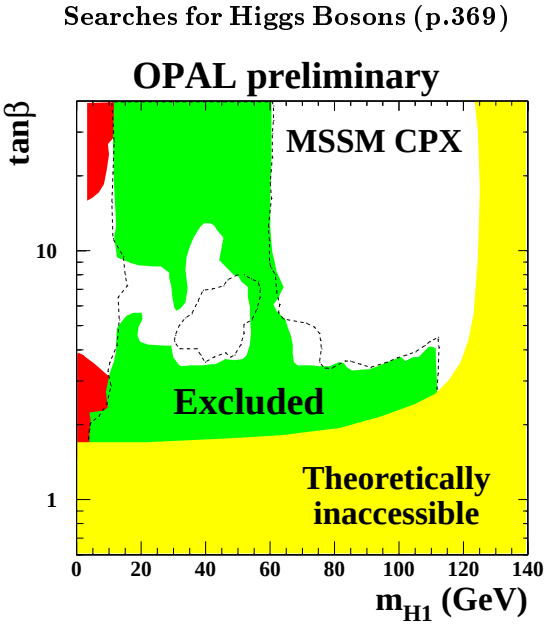

Figure 4: The 95% CL bounds on m_{H_1} and $\tan\beta$ in the CPX MSSM scenario with $\mu = 2$ TeV and $M_{\rm SUSY} = 500$ GeV, from a preliminary OPAL analysis [36]. The shaded areas are excluded either by the model or by the experiment. The areas delimited by the dashed lines are expected to be excluded on the basis of Monte Carlo simulations. The top mass is fixed to 174.3 GeV.

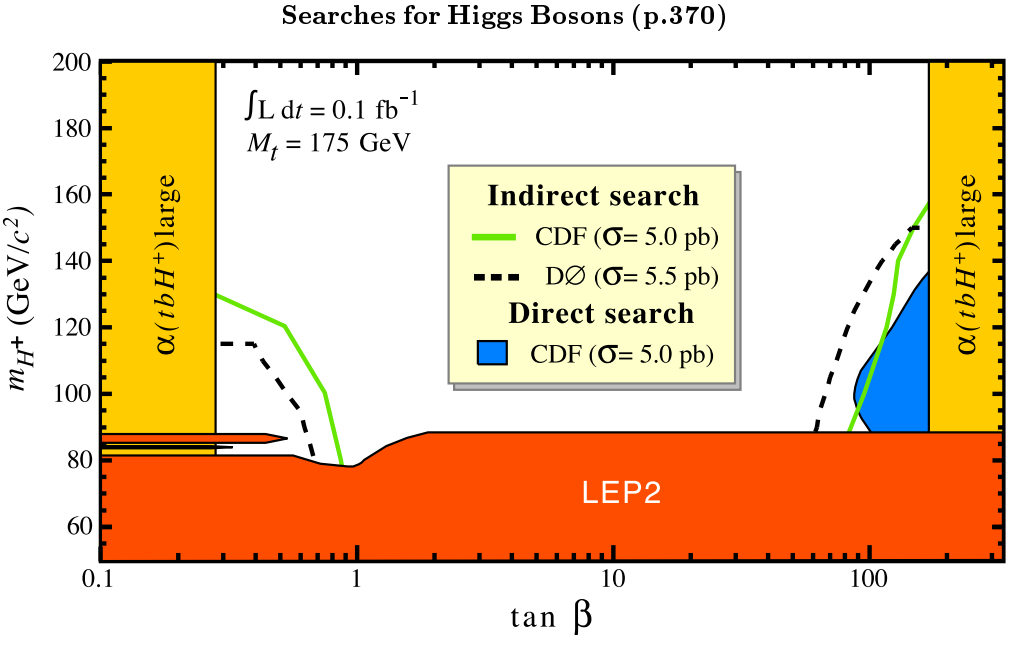

Figure 5: Summary of the 95% CL exclusions in the (m_{H^+}, $\tan\beta$) plane from DØ [45] and CDF [47], using various indirect and direct observation techniques (the regions below the curves are excluded). The two experiments use slightly different theoretical $t\bar{t}$ cross sections, as indicated. The shaded domains at extreme values of $\tan\beta$ are not considered in these searches, since there the tbH^+ coupling becomes large and perturbative calculations do not apply. The dark region labeled LEP2 is excluded by LEP [42].

Understanding two-flavor oscillation parameters and limits (p.451)

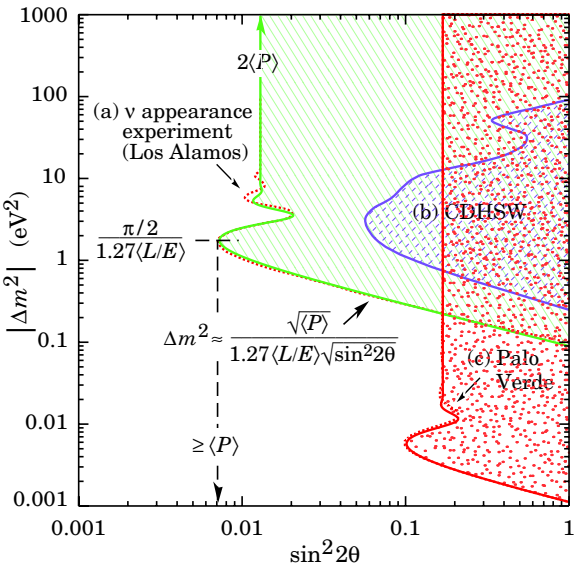

Figure 1: Neutrino oscillation parameter ranges excluded by three experiments. The dotted line in (a) is from an older Los Alamos appearance experiment (DURKIN 88), while the solid line is obtained from Eq. (2) using the parameters $\langle P\rangle = 0.0065$, $\Delta m^2 = 0.095$ eV^2 at $\sin^2 2\theta = 1$, and $\sigma_b/b_0 = 0.23$; (b) is a disappearance experiment with the flux obtained from the data in a long detector (DYDAK 84); and for (c) the Palo Verde reactor experiment result (BOEHM 01) is shown by the dotted line. In this experiment the flux at production is known. The solid line is calculated from Eq. (2) using $\langle P\rangle = 0.084$, $\Delta m^2 = 0.0011$ eV^2 at $\sin^2 2\theta = 1$, and $\sigma_b/b_0 = 0.3$. The experiments have been chosen for illustrative purposes, and none represents a current best limit.

Solar neutrinos (p.460)

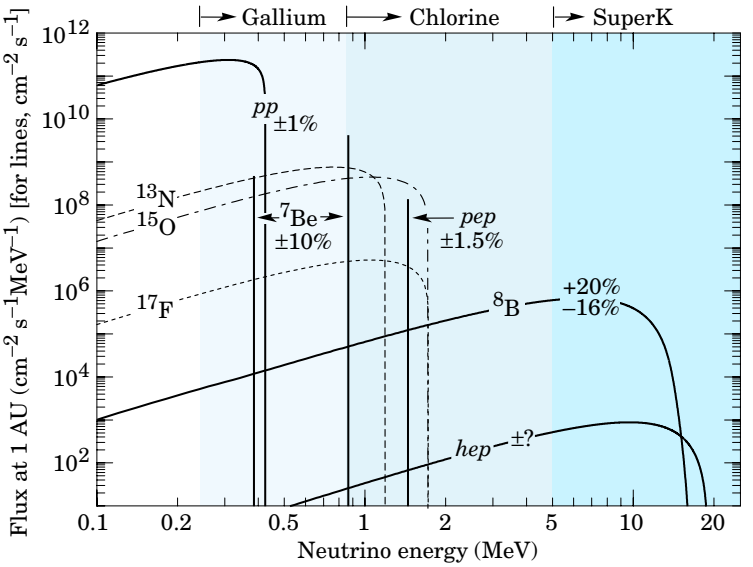

Figure 1: The solar neutrino spectrum predicted by the standard solar model. The neutrino fluxes from continuum sources are given in units of number cm^{-2}s^{-1}MeV^{-1} at one astronomical unit, and the line fluxes are given in number cm^{-2}s^{-1}. Spectra for the *pp* chain, shown by the solid curves, are courtesy of J.N. Bahcall (2001). Spectra for the CNO chain are shown by the dotted curves, and are also courtesy of J.N. Bahcall (1995).

Solar neutrinos (p.462)

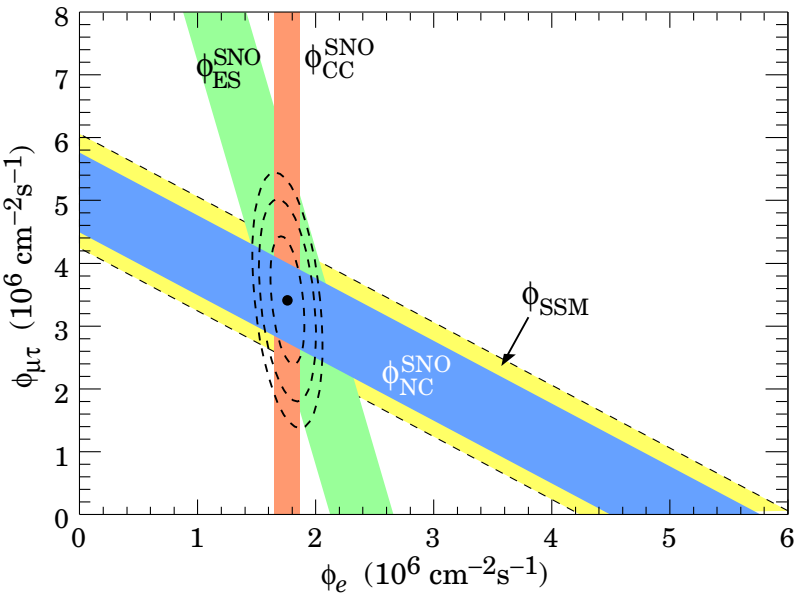

Figure 2: Fluxes of ^{8}B solar neutrinos, $\phi(\nu_e)$, and $\phi(\nu_{\mu \text{ or } \tau})$, deduced from the SNO's charged-current (CC), ν_e elastic scattering (ES), and neutral-current (NC) results for pure D_2O. The standard solar model prediction [9] is also shown. The bands represent the 1σ error. The contours show the 68%, 95%, and 99% joint probability for $\phi(\nu_e)$ and $\phi(\nu_{\mu \text{ or } \tau})$. This figure is courtesy of K.T. Lesko (LBNL).

Solar neutrinos (p.464)

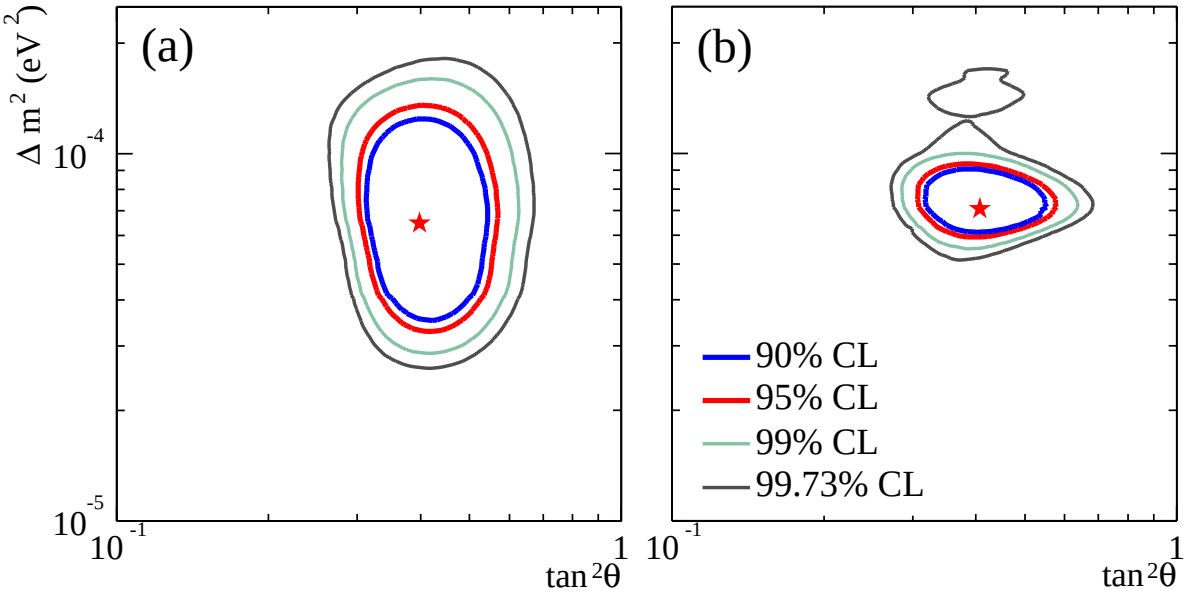

Figure 4: Global neutrino oscillation contours given by the SNO Collaboration assuming that the ^{8}B neutrino flux is free and the *hep* neutrino flux is fixed. (a) Solar global analysis. (b) Solar global + KamLAND. For details, see Ref. [8].

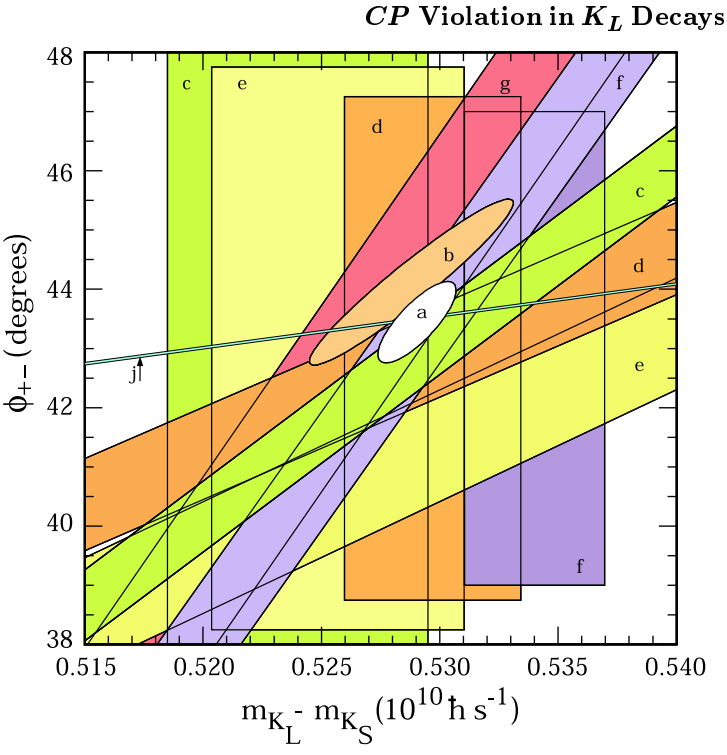

Figure 1: ϕ_{+-} vs Δm for experiments which do not assume CPT invariance. Δm measurements appear as vertical bands spanning $\Delta m \pm 1\sigma$, cut near the top and bottom to aid the eye. Most ϕ_{+-} measurements appear as diagonal bands spanning $\phi_{+-} \pm \sigma_\phi$. Data are labeled by letters: "b"–FNAL KTeV, "c"–CERN CPLEAR, "d"–FNAL E773, "e"–FNAL E731, "f"–CERN, "g"–CERN NA31, and are cited in Table 1. The narrow band "j" shows ϕ_{SW}. The ellipse "a" shows the $\chi^2 = 1$ contour of the fit result.

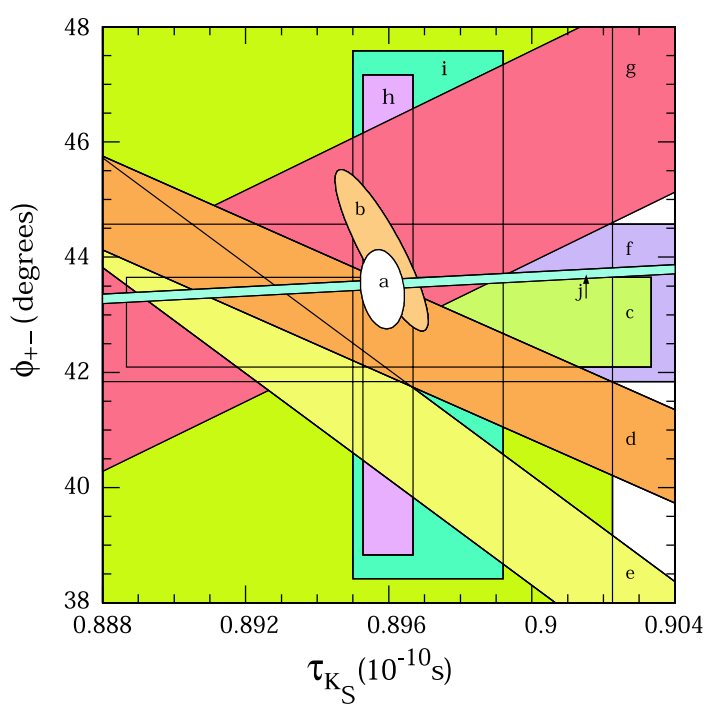

Figure 2: ϕ_{+-} vs τ_s. τ_s measurements appear as vertical bands spanning $\tau_s \pm 1\sigma$, some of which are cut near the top and bottom to aid the eye. Most ϕ_{+-} measurements appear as diagonal or horizontal bands spanning $\phi_{+-} \pm \sigma_\phi$. Data are labeled by letters: "b"–FNAL KTeV, "c"–CERN CPLEAR, "d"–FNAL E773, "e"–FNAL E731, "f"–CERN, "g"–CERN NA31, "h"–CERN NA48, "i"–CERN NA31, and are cited in Table 1. The narrow band "j" shows ϕ_{SW}. The ellipse "a" shows the fit result's $\chi^2 = 1$ contour.

D^0–$\overline{D}^0$ Mixing (p.679)

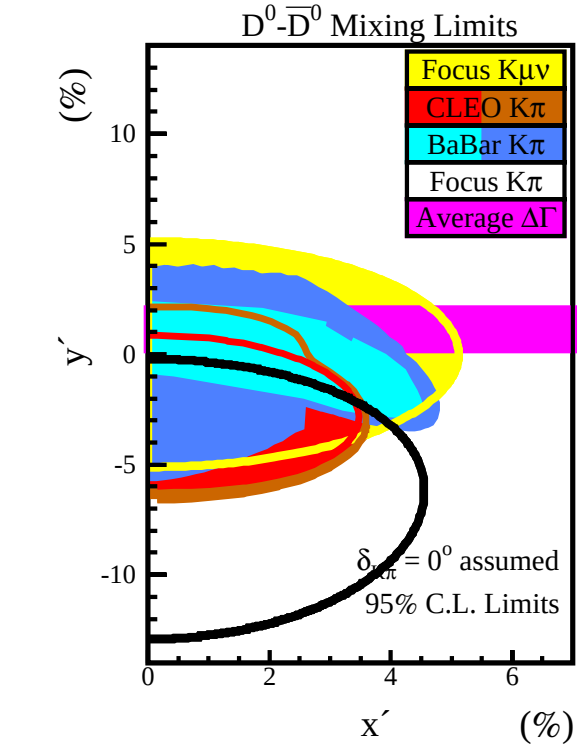

Figure 1: Current allowed regions in the plane of y' versus x'. The regions for CLEO and BaBar allow CP violation in the decay amplitude, in the mixing amplitude, and in the interference between these two processes. The FOCUS result does not allow CP violation. The allowed region for $\Delta\Gamma$ is the average of the y_{CP} [26, 28–31] results and the BABAR measurement of $y\cos\phi$ [27] and does not include $y = 0$. We assume $\delta = 0$ to place the $\Delta\Gamma$ results. A non-zero value for δ would rotate this confidence region clockwise about the origin by an angle δ.

B^0–$\overline{B}^0$ Mixing (p.763)

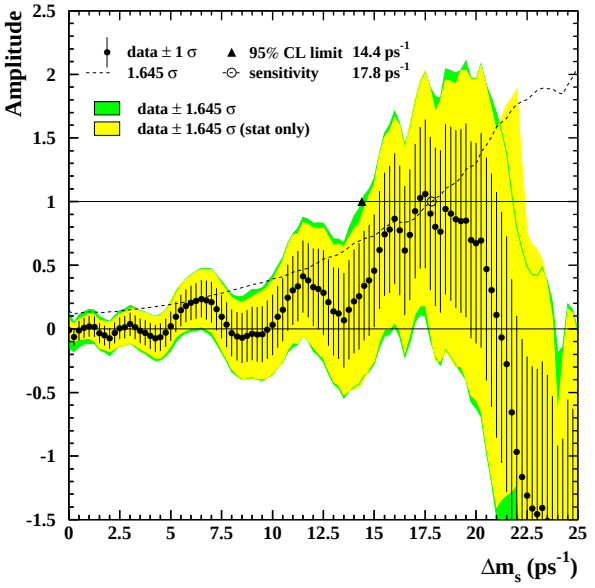

Figure 2: Combined measurements of the B_s^0 oscillation amplitude as a function of Δm_s, including all results published by November 2003. The measurements are dominated by statistical uncertainties. Neighboring points are statistically correlated.

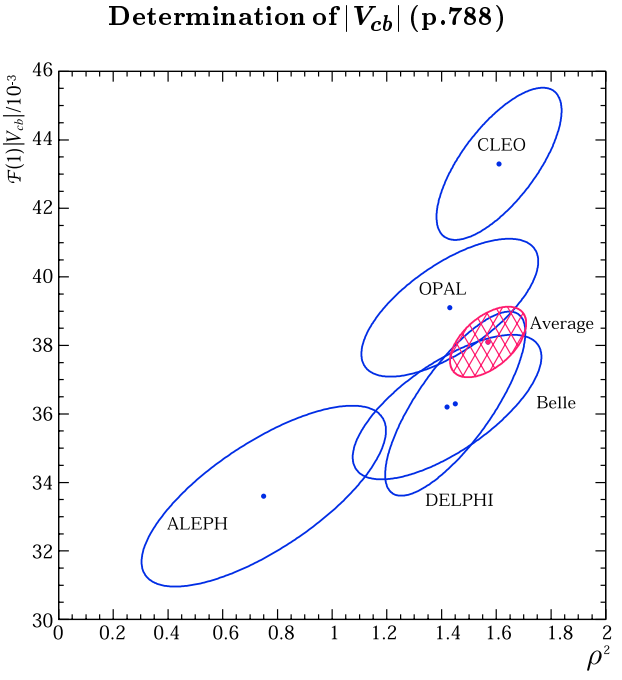

Figure 1: The error ellipses for the corrected measurements and world average for $\mathcal{F}(1)|V_{cb}|$ vs ρ^2. The ellipses are the product between the 1 σ error of $\mathcal{F}(1)|V_{cb}|$, ρ^2, and the correlation between the two.

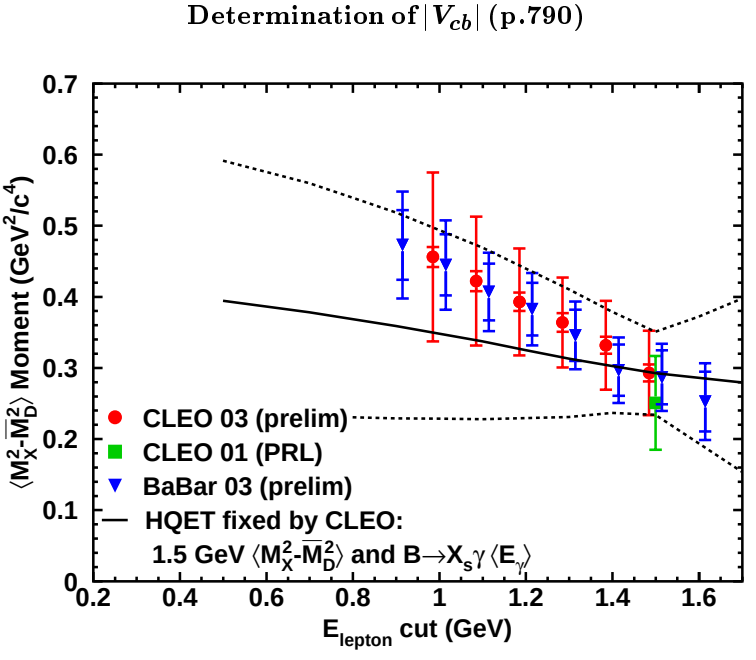

Figure 2: The results of the recent CLEO analysis [59] compared to previous measurements [55,60] and the HQET prediction. The theory bands shown in the figure reflect the variation of the experimental errors on the two constraints, the variation of the third-order HQET parameters by the scale $(0.5\ \mathrm{GeV})^3$, and variation of the size of the higher order QCD radiative corrections [56].

Supersymmetry, Part II (Experiment, p.1016)

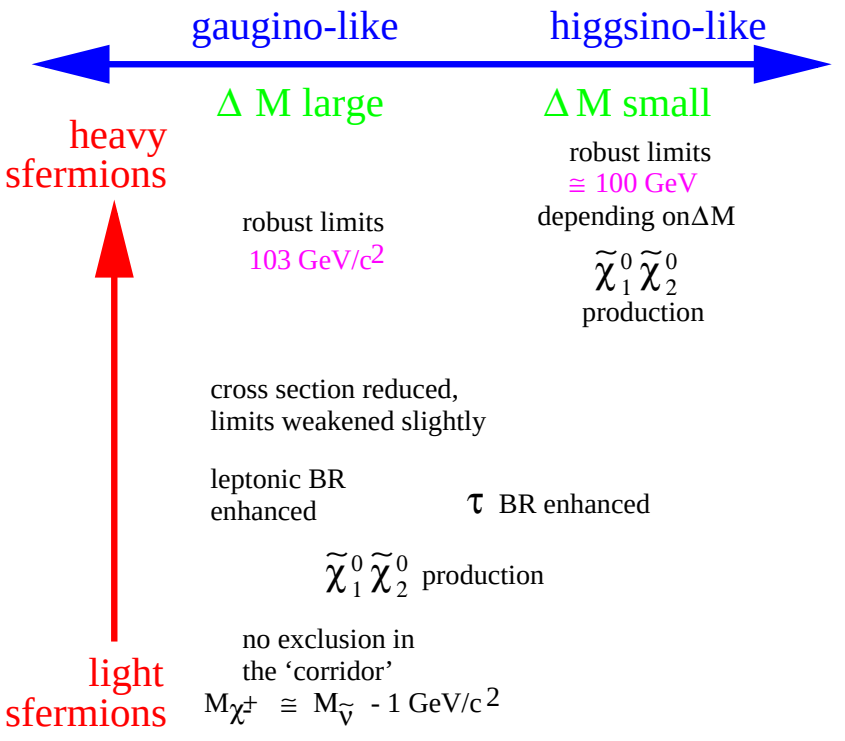

Figure 1: Heuristic diagram of the interplay of chargino field content and sfermion masses.

Supersymmetry, Part II (Experiment, p.1019)

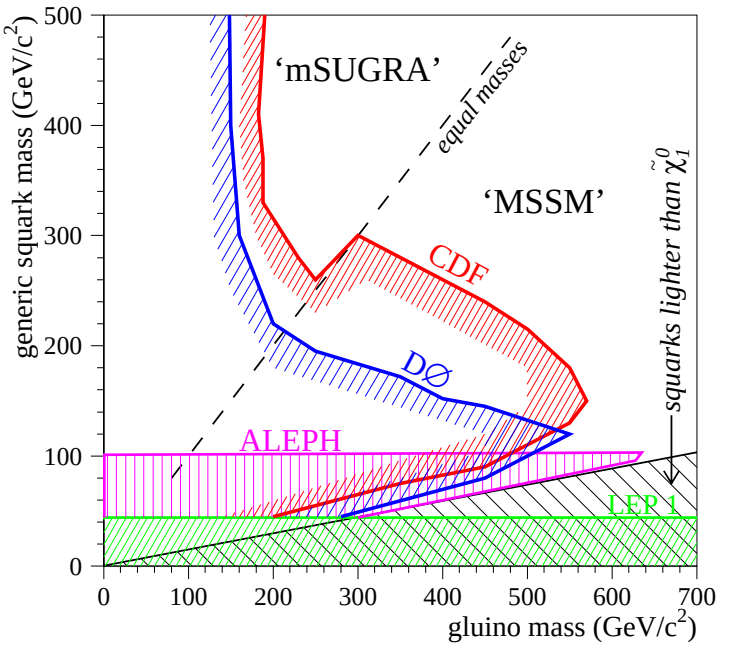

Figure 2: Regions in the $M_{\tilde{g}}$-$M_{\tilde{q}}$ plane excluded by searches for jets and missing energy at CDF, DØ, and LEP.

Supersymmetry, Part II (Experiment, p.1020)

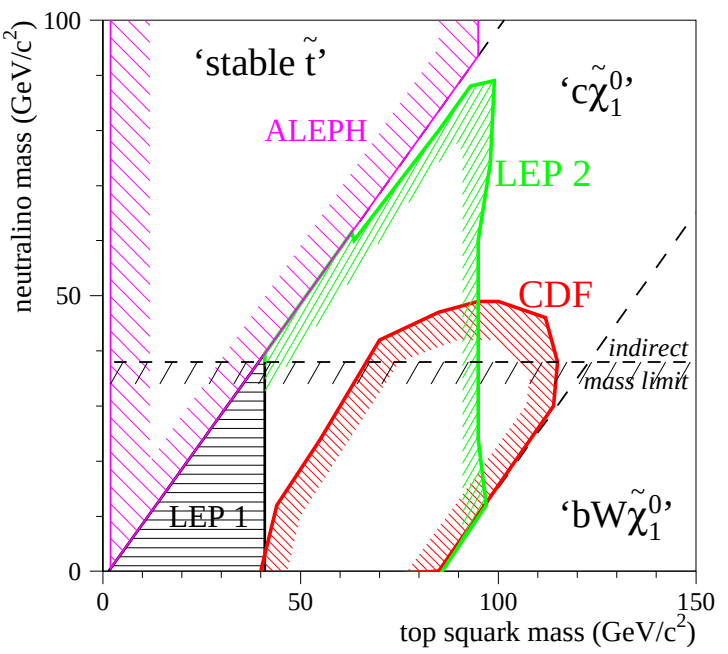

Figure 3: Regions excluded in the ($M_{\tilde{t}_1}$,$M_{\tilde{\chi}}$) plane. The results for the $c\tilde{\chi}_1^0$ decay mode are displayed from LEP and CDF. A DELPHI result for stable stops is indicated for $M_{\tilde{t}_1} < M_{\tilde{\chi}}$. Finally, the indirect limit on $M_{\tilde{\chi}}$ is also shown. There is effectively no exclusion in the region where $\tilde{t}_1 \to bW\tilde{\chi}_1^0$.

Dynamical Electroweak Symmetry Breaking (p.1041)

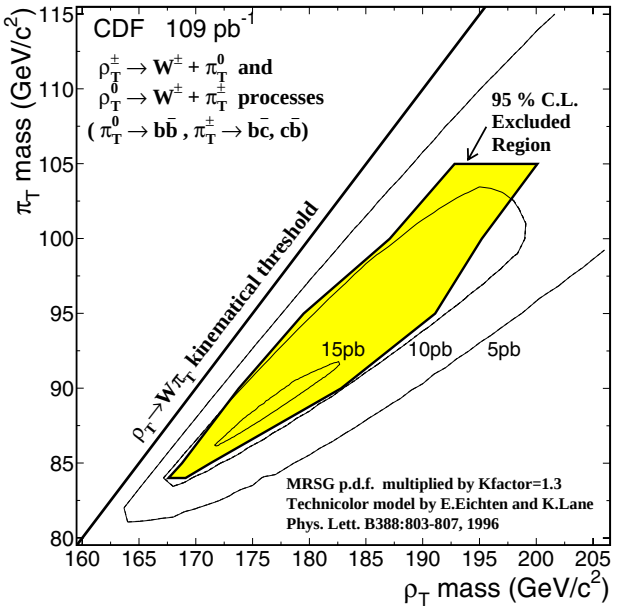

Figure 1: 95% CL exclusion region [16] for a light technirho decaying to $W^{\pm}$ and a π_T, and in which the π_T decays to two jets including at least one b quark.

Dynamical Electroweak Symmetry Breaking (p.1042)

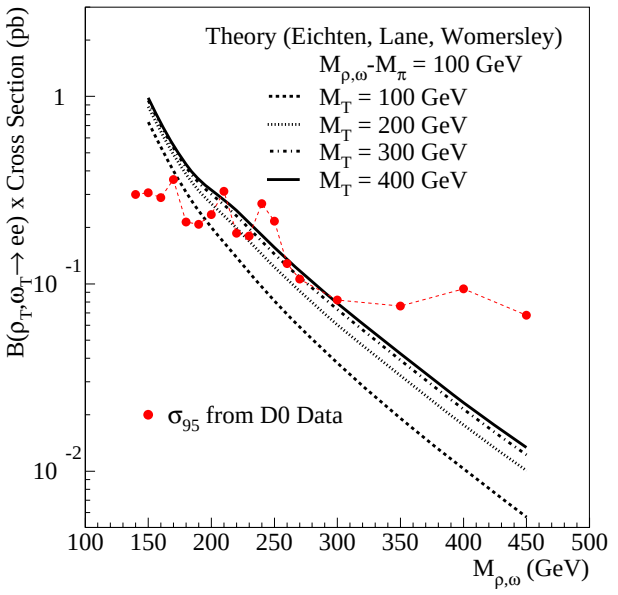

Figure 3: 95% CL cross-section limit [19] for a light techniomega and a light technirho decaying to $\ell^+\ell^-$.

Dynamical Electroweak Symmetry Breaking (p.1043)

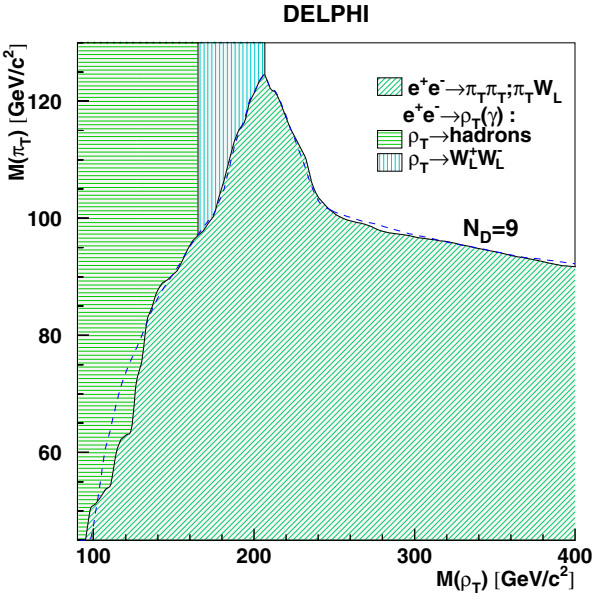

Figure 4: 95% CL exclusion region [20] in the technirho-technipion mass plane obtained from searches by the DELPHI collaboration at LEP 2, for nine technifermion doublets. The dashed line shows the expected limit for the 4-jet analysis.

Dynamical Electroweak Symmetry Breaking (p.1044)

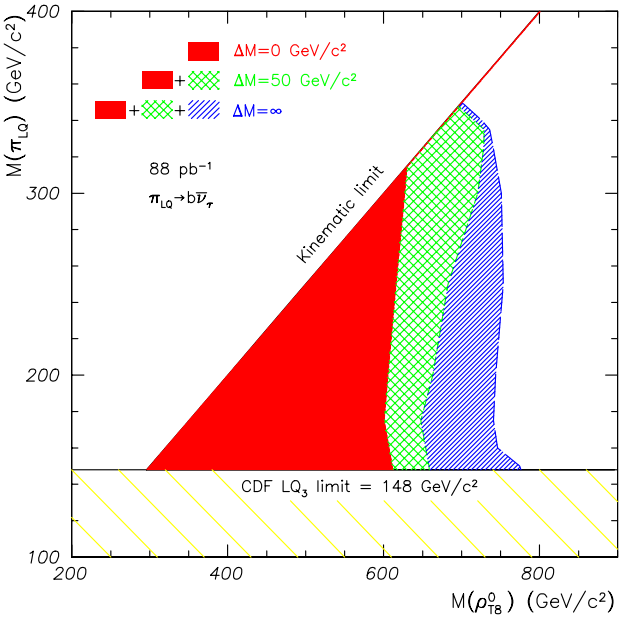

Figure 6: 95% CL exclusion region [25] in the technirho-technipion mass plane for pair produced technipions, with leptoquark couplings, decaying to $b\nu$.